REVIEW

General Characteristics of *Pinus* spp. Seed Fatty Acid Compositions, and Importance of Δ5-Olefinic Acids in the Taxonomy and Phylogeny of the Genus

Robert L. Wolff[a,]*, Frédérique Pédrono[a], Elodie Pasquier[a], and Anne M. Marpeau[b]

[a]ISTAB and [b]LCSV, Institut du Pin, Université Bordeaux 1, Talence, France

ABSTRACT: The Δ5-unsaturated polymethylene-interrupted fatty acid (Δ5-UPIFA) contents and profiles of gymnosperm seeds are useful chemometric data for the taxonomy and phylogeny of that division, and these acids may also have some biomedical or nutritional applications. We recapitulate here all data available on pine (*Pinus*; the largest genus in the family Pinaceae) seed fatty acid (SFA) compositions, including 28 unpublished compositions. This overview encompasses 76 species, subspecies, and varieties, which is approximately one-half of all extant pines officially recognized at these taxon levels. Qualitatively, the SFA from all pine species analyzed so far are identical. The genus *Pinus* is coherently united—but this qualitative feature can be extended to the whole family Pinaceae—by the presence of Δ5-UPIFA with C_{18} [taxoleic (5,9-18:2) and pinolenic (5,9,12-18:3) acids] and C_{20} chains [5,11-20:2, and sciadonic (5,11,14-20:3) acids]. Not a single pine species was found so far with any of these acids missing. Linoleic acid is almost always, except in a few cases, the prominent SFA, in the range 40–60% of total fatty acids. The second habitual SFA is oleic acid, from 12 to 30%. Exceptions, however, occur, particularly in the *Cembroides* subsection, where oleic acid reaches *ca.* 45%, a value higher than that of linoleic acid. α-Linolenic acid, on the other hand, is a minor constituent of pine SFA, almost always less than 1%, but that would reach 2.7% in one species (*P. merkusii*). The sum of saturated acids [16:0 (major) and 18:0 (minor) acids principally] is most often less than 10% of total SFA, and *anteiso*-17:0 acid is present in all species in amounts up to 0.3%. Regarding C_{18} Δ5-UPIFA, taxoleic acid reaches a maximum of 4.5% of total SFA, whereas pinolenic acid varies from 0.1 to 25.3%. The very minor coniferonic (5,9,12,15-18:4) acid is less than 0.2% in all species. The C_{20} elongation product of pinolenic acid, bishomo-pinolenic (7,11,14-20:3) acid, is a frequent though minor SFA constituent (maximum, 0.7%). When considering C_{20} Δ5-UPIFA, a difference is noted between the subgenera *Strobus* and *Pinus*. In the former subgenus, 5,11-20:2 and sciadonic acids are ≤0.3 and ≤1.9%, respectively, whereas in the latter subgenus, they are most often ≥0.3 and ≥2.0%, respectively. The highest values for 5,11-20:2 and sciadonic acids are 0.5% (many species) and 7.0% (*P. pinaster*). The 5,11,14,17-20:4 (juniperonic) acid is present occasionally in trace amounts. The highest level of total Δ5-UPIFA is 30–31% (*P. sylvestris*), and the lowest level is 0.6% (*P. monophylla*). Uniting as well as discriminating features that may complement the knowledge about the taxonomy and phylogeny of pines are emphasized.

Paper no. L8356 in *Lipids 35,* 1–22 (January 2000).

The Coniferophytinae (the conifers, in the broadest sense) is the largest and most diverse subdivision of living gymnosperms. They include two classes, Ginkgoatae and Pinatae. The first class is limited to a single extant family, Ginkgoaceae, with only one living representative, *Ginkgo biloba*. The second class encompasses 8–9 families, Taxaceae and Cephalotaxaceae (the limits between these two families are uncertain), Phyllocladaceae, Podocarpaceae, Araucariaceae, Sciadopityaceae, Cupressaceae, Taxodiaceae (distinction of these families appears artificial and only the family Cupressaceae, including Taxodiaceae, should be recognized), and Pinaceae (1). The latter family is the most important group of conifers in the Northern Hemisphere when considering its phytogeographical distribution, its biomass, its number of species, and its economical importance.

The family Pinaceae contains a total of 11 accepted genera: *Abies*, *Cathaya*, *Cedrus*, *Keteleeria*, *Larix*, *Nothotsuga*, *Picea*, *Pinus*, *Pseudolarix*, *Pseudotsuga*, and *Tsuga*. A twelfth genus, *Hesperopeuce*, has been suggested recently (2). Among these genera, *Pinus* is the largest and most heteromorphic genus, almost exclusively distributed in the Northern Hemisphere (one exception, *P. merkusii*, is known to cross the equator in northern Sumatra). This genus is ecologically versatile, "ranging from the tundra line in Eurasia to tropical coastal savannas in Nicaragua and from the salt spray zone of the Pacific coast to the alpine tree line in Europe and western U.S.A." (2). Some species are also broadly distributed in semiarid regions (e.g., southwestern United States and Mexico).

Morphologists, anatomists, physiologists, embryologists, paleobotanists, biochemists, and more recently, molecular biologists, have tried for almost one century and still continue to try to understand the phylogenetic interrelationships in conifers, because they are the most prominent components of

*To whom correspondence should be addressed at ISTAB, Université Bordeaux 1, avenue des Facultés, 33405 Talence Cedex, France.
E-mail: r.wolff@istab.u-bordeaux.fr

Abbreviations: *anteiso*-17:0, 14-methylhexadecanoic; FAME, fatty acid methyl ester; GLC, gas–liquid chromatography; SFA seed fatty acid; UPIFA, unsaturated polymethylene-interrupted fatty acid.

the extant flora, with a very long history and particularly rich fossil record, beginning in pre-Permian time (3). Most of the essential features of the modern *Pinus* cone had evolved by the Early Cretaceous period (130 million yr), with a significant history of the family Pinaceae prior to the Late Triassic period (180 million yr) (4). As we were involved in the systematic study of conifer and, more generally, gymnosperm seed fatty acid (SFA) compositions, essentially for nutritional applications, we noted that these data could be of some use as new, original, and supplementary chemometric markers for the taxonomy of this plant division (5–7).

Conifer SFA contain a series of constituents that were considered until recently as "unusual" (8), or as presenting an unusual structure, the Δ5-unsaturated polymethylene-interrupted fatty acids (Δ5-UPIFA), that have been shown in the meantime not only to be common constituents of seed oils from all Coniferophyte families but also to be characteristic of some Cycadophyte families (9), and likely of great antiquity on a geological time scale [estimated 300 million yr (9)]. In gymnosperms (Coniferophytes and Cycadophytes), Δ5-UPIFA have the following structures: 5,9-18:2 (taxoleic); 5,11-18:2 (ephedrenic); 5,9,12-18:3 (pinolenic); 5,9,12,15-18:4 (coniferonic); 5,11-20:1; 5,11,14-20:3 (sciadonic); and 5,11,14,17-20:4 (juniperonic) acids, all ethylenic bonds being in the *cis* configuration. In addition to seeds, these fatty acids also occur in the leaf and wood lipids of Coniferophytes and likely of some Cycadophytes (10). Considering the importance of gymnosperms, and particularly of conifers in the land plant biomass, it was recently observed that one or two of these Δ5-UPIFA, i.e., sciadonic and juniperonic acids, are probably the most abundant C_{20} polyunsaturated acids in land plants (10).

The chemical structures of Δ5-UPIFA have been repeatedly established since the 1960s through more or less complicated analytical procedures, and recently by gas–liquid chromatography (GLC) coupled with mass spectrometry of the easily prepared picolinyl ester and 4,4-dimethyloxazoline derivatives (9,11–14). Also, ^{13}C nuclear magnetic resonance spectroscopy allowed confirmation of GLC data regarding the total Δ5-UPIFA content of many gymnosperm seed oils (9,13,15,16).

The positions of ethylenic bonds along the hydrocarbon chains and the number of carbon atoms in Δ5-UPIFA have allowed construction of possible biosynthetic pathways of these acids (9,14,17,18). Briefly, individual Δ5-UPIFA fall inside the classical n-9, n-6, and n-3 series [except for the rare 5,11-18:2 (ephedrenic) acid (9,12), likely derived from palmitoleic acid *via cis*-vaccenic acid and thus belonging to the n-7 series], being possibly synthesized by Δ5-desaturation of oleic, linoleic, or α-linolenic acids, or by Δ5-desaturation of their elongation products (11-20:1, 11,14-20:2, or 11,14,17-20:3 acids, respectively). Only one elongation product of Δ5-UPIFA has been characterized so far, the 7,11,14-20:3 (bishomopinolenic) acid, which is apparently restricted to species of the Pinaceae family (19).

In this study, a compilation of data available on pine SFA is made, including 28 unpublished pine SFA compositions corresponding mainly to *Pinus* species that were not screened earlier for their seed Δ5-UPIFA content, or for which only partial data were available. This allows conclusions to be drawn on general features of the quantitative distribution of Δ5-UPIFA and other constituent SFA in this genus. The purpose of the present overview is not to propose another classification that would only add to the sufficiently confusing literature on this topic. We merely wish, when possible, to emphasize some features that unite a given group or that significantly distinguish a species or a group of species from others.

Another purpose of this study is to help find sources of individual Δ5-UPIFA, some of which are considered to have potential biomedical or nutritional applications or to be efficient tools to study lipid metabolism in animal experiments (20–31).

EXPERIMENTAL PROCEDURES

Seeds, oil extraction, and fatty acid methyl ester (FAME) preparation. Most pine seeds were purchased from Lawyer Nursery, Inc. (Plains, MT), F.W. Schuhmacher Co., Inc. (Sandwich, MA), and Sandeman Seeds (Pulborough, Great Britain). *Pinus sylvestris* seeds from different French orchards and indigenous stands were kindly donated by Vilmorin S.A. (La Ménitré, France). *Pinus pinaster* seeds were taken from three important lots of seeds collected in the Landes (southwest of France) for reforestation purposes and kindly donated by D'a Noste S.A.R.L. (Vendays-Montalivet, France). Seeds were kept at 4°C until used. Lipid extraction, always performed starting with 10-g samples taken from 20 ± 5 g of powdered seeds, and FAME preparation were performed as described in detail elsewhere for other gymnosperm seeds (5–7). All FAME preparations were done in duplicate, and each preparation was analyzed at least once by GLC. Generally, FAME were prepared within 24 h after lipid extraction and immediately analyzed, thus alleviating the use of antioxidants that may give rise to artifacts during methylation.

Analytical GLC. FAME were analyzed in a Carlo Erba 4130 chromatograph (Carlo Erba, Milano, Italy) equipped with a DB-Wax column (30 m × 0.32 mm i.d., 0.5 µm film; J&W Scientific, Folsom, CA). The oven temperature was 190°C, and the inlet pressure of the carrier gas (helium) was 140 kPa (*ca.* 30 m/min at the outlet). Occasionally, to confirm some identifications, a CP-Sil 88 column (50 m × 0.25 mm i.d., 0.2 µm film; Chrompack, Middelburg, The Netherlands) was operated with temperature programming in a Carlo Erba HRGC chromatograph from 150 to 185°C at 4°C/min with H_2 at 100 kPa. The injector (split mode) and flame-ionization detector were maintained at 250°C for both columns. Quantitative data were calculated by an SP 4290 integrator (Spectra Physics, San Jose, CA).

Identification of FAME peaks. The seed lipids from selected conifer species (11) were used as a source of Δ5-olefinic acid methyl esters with known structures to identify

fatty acids from pine seed lipids by GLC, either by coinjection, comparison of the equivalent chain lengths (DB-Wax column), or retention times (CP-Sil 88 column).

RESULTS AND DISCUSSION

Comments on the GLC analysis of Δ5-UPIFA and other fatty acids. The structures, as well as the formulas and trivial names of Δ5-UPIFA, are given in Figure 1. To date, no Δ5-monoenoic acids, such as those found in some rare angiosperms (32), have been detected in Pinaceae seeds, at least under routine analytical conditions. On columns coated with a polyethylene-glycol stationary phase (e.g., DB-Wax), as well as on more polar columns (e.g., CP-Sil 88, or Silar 5), these monoenes elute earlier than the corresponding Δ9-isomers, with a good resolution (32,33; Wolff, R.L., unpublished data). Among gymnosperms, however, a 5-18:1 isomer was tentatively identified in *Ephedra sinica* dried stalks (33), but this could not be confirmed in *Ephedra* spp. seed lipids (9). On the other hand, ephedrenic acid is a rather abundant fatty acid only in *G. biloba* (12) and *Ephedra* spp. (9) seeds, apparently associated with high levels of *cis*-vaccenic (11-18:1) acid. In most studies reported here, this dienoic acid may have been masked by taxoleic acid, from which it is poorly resolved on polyethylene glycol-coated columns (9,12). However, taxoleic and ephedrenic acids are fully separated on the CP-Sil 88 and Silar 5 capillary columns. Because no authors reported on this acid in Pinaceae and because the *cis*-vaccenic acid percentage is always low in this family, it is inferred that if present in *Pinus* seeds, ephedrenic acid can only reach trace levels. Otherwise, as illustrated in Figure 2, all fatty acids reported here, including Δ5-UPIFA, are base-line resolved. A minor exception is *cis*-vaccenic acid, not completely resolved from the isomeric oleic acid.

Juniperonic acid does not seem to occur in any significant amounts in *Pinus* SFA when total, neutral, or polar (33) lipids are analyzed. Minor amounts (<0.1%) of this fatty acid would however occur in some instances. Finally, no arachidonic or eicosapentaenoic acids, recently characterized in the seeds of a few species of the Araucariaceae family (14), were observed in pine seed lipids. It should however be noted that arachidonic acid was reported [cited in Ref. 34 (original paper in Russian)] to be present in the cambium zone of *L. sibirica* (Siberian larch) that belongs to another genus of the Pinaceae family.

The minor 14:0 and 15:0 acids, visible in Figure 2, are not reported individually in the present study and are included in the category "others" in the tables. On the other hand, the *anteiso*-17:0 (14-methylhexadecanoic) and 17:1 acids (likely the Δ9 isomer) are included in this study. These acids may correspond respectively to the 16:2n-6 and 16:3n-3 acids tentatively identified by Takagi and Itabashi (33) in several gymnosperm seeds. In conifer leaves, *anteiso*-17:0, 17:1, 16:2n-6, and 16:3n-3 acids occur together, along with the additional *trans*-3 16:1 acid (35; Pasquier, E., Destaillats, F., and Wolff, R.L., unpublished observations). Although *anteiso*-17:0 acid was unambiguously characterized by mass spectrometry in pine seed lipids (36), it cannot be excluded that trace amounts of 16:2n-6 and 16:3n-3 acids may coelute with *anteiso*-17:0

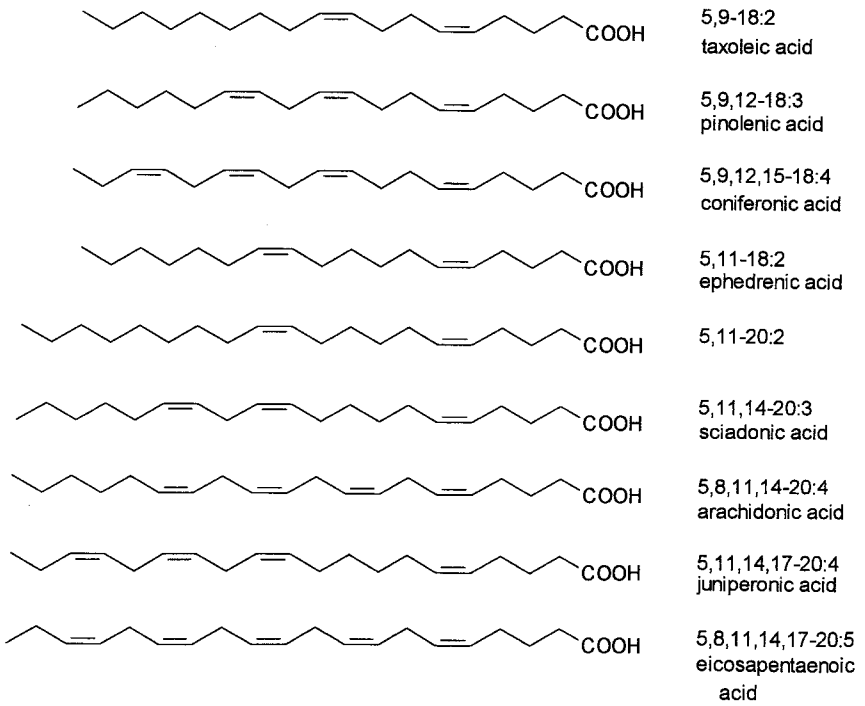

FIG. 1. Δ5-Unsaturated polymethylene- and methylene-interrupted fatty acids that may occur in the seed lipids from gymnosperms, and their trivial names. Generally, not all fatty acids occur together in a given species.

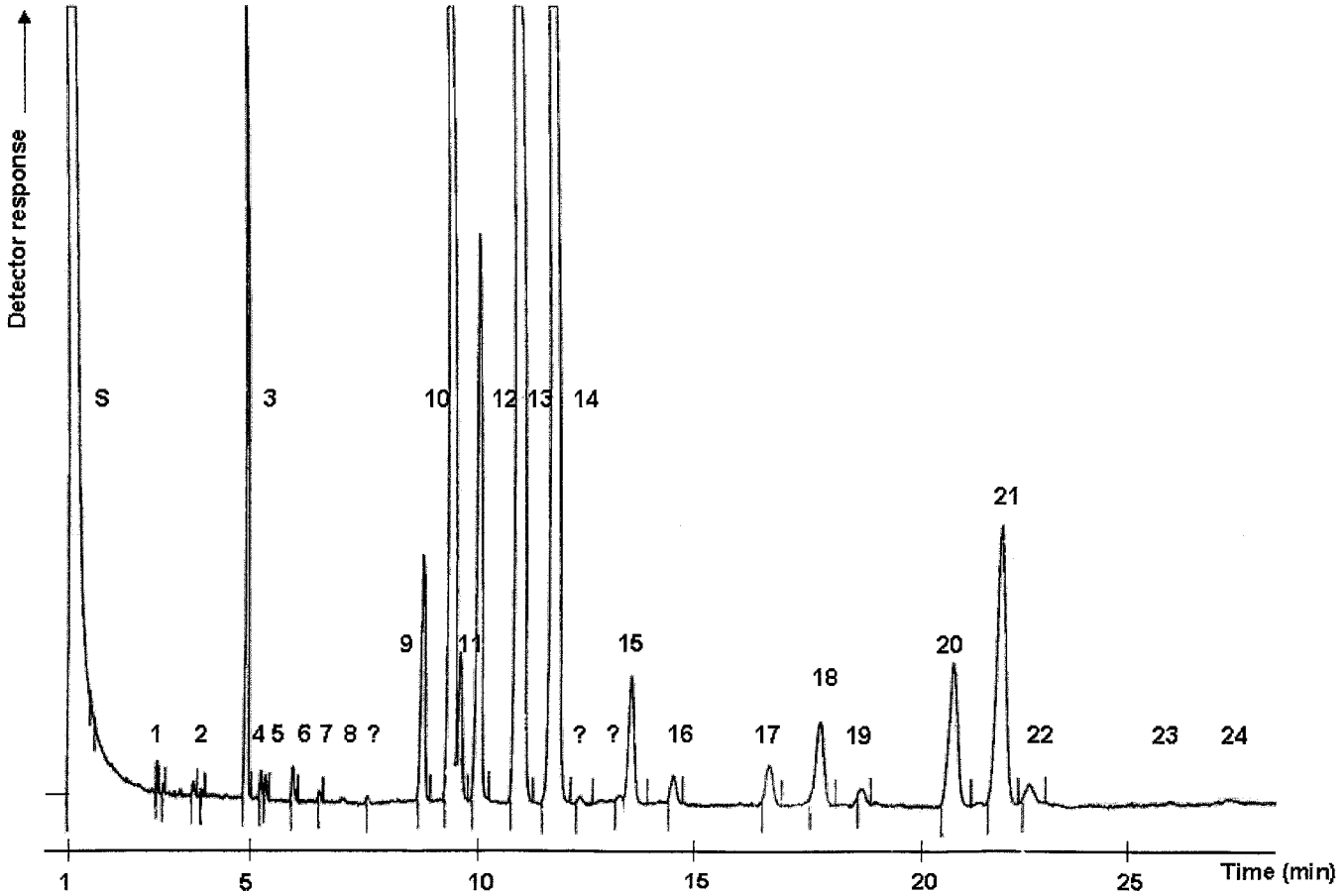

FIG. 2. Typical gas–liquid chromatogram of fatty acid methyl esters prepared from the seed lipids of *Pinus resinosa* and analyzed on a polyethylene glycol-coated capillary column (30 m) at 190°C (carrier gas, He, at 140 kPa). Identification of peaks: S, solvent (hexane); **1**, 14:0; **2**, 15:0; **3**, 16:0; **4**, 7-16:1; **5**, 9-16:1; **6**, *anteiso*-17:0; **7**, 17:0; **8**, 17:1; **9**, 18:0; **10**, 9-18:1; **11**, 11-18:1; **12**, 5,9-18:2; **13**, 9,12-18:2; **14**, 5,9,12-18:3; **15**, 9,12,15-18:3; **16**, 5,9,12,15-18:4; **17**, 20:0; **18**, 11-20:1; **19**, 5,11-20:2; **20**, 11,14-20:2; **21**, 5,11,14-20:3; **22**, 7,11,14-20:3; **23**, 11,14,17-20:3; **24**, 5,11,14,17-20:4 acids. Peaks with a question mark are unidentified; 22:0 acid, not shown, starts eluting at 30.7 min.

and 17:1 acids, respectively, owing to their similar GLC behavior. Some minor unidentified peaks with constant retention times, in amounts apparently species-dependent, occasionally appear on chromatograms between pinolenic and α-linolenic acid methyl esters (Fig. 2). No polyunsaturated C_{22} acids have been reported in pine seed lipids.

Remarks on Pinus *classification*. Only the basic division of pines at the subgenera level, *Strobus* (*Haploxylon*, or soft or white pines) and *Pinus* (*Diploxylon*, or hard pines), is widely accepted. Subdivisions of these subgenera into sections and subsections, and taxonomic ranking at the species, subspecies, or variety levels, as employed here (Table 1), may not appear satisfactory, as they are rather controversial and still disputed (37–43). DNA- and RNA-based investigations (44–46), though themselves having limitations, will certainly help in clarifying this situation. Regarding the nomenclature of the species employed here, it is important to quote A. Farjon's estimate (2) for the ratio of accepted names/synonyms/uncertain names at the species rank and below in the genus *Pinus*: 157/1071/27. For the sole species *P. sylvestris*, the most widespread pine species in Eurasia and possibly in the world, almost 150 variants have been described (47), of which only three are "officially" recognized as varieties (2). Within the polymorphic *P. mugo* complex (48), alternately known as *P. montana* (39), of more limited geographical distribution than *P. sylvestris*, the situation is equally complicated, with sometimes as many as four infraspecific taxa recognized, not to mention hybrids with *P. sylvestris* and nothotaxa (48). However, a study of the seed oil from *P. sylvestris* from 10 distinct locations in France (Marpeau, A.M., and Wolff, R.L., unpublished data), compared to similar data for Finland (49), showed that variations in the fatty acid percentages most often affect figures at the first decimal place, with little or no statistical significance. This observation would indicate that visible morphological differences will hardly affect the SFA composition within variants of a given species. With few exceptions, data in Table 1 (6,7,18,33,49–58) do not refer to infraspecific taxa because of obvious difficulties in getting information from tree-seed sellers, or correctly identifying infraspecific taxa.

SFA compositions in the Strobus *subgenus*. This subgenus encompasses two sections, *Strobus* and *Parrya* (Tables 2–4).

TABLE 1
List of *Pinus* Species for Which the Seed Fatty Acid Compositions Have (or have not yet) Been Described (including species analyzed in the present study)

Subgenus[a]	Section	Subsection	Species[b]	Trivial name[c]	References[d]
Strobus	*Strobus*	*Strobi*	1. *P. strobus* var. *strobus*	Eastern white pine	5
			2. *P. strobus* var. *chiapensis*	—	—[e]
			3. *P. peuce*	Balkan white pine	6
			4. *P. parviflora*	Japanese white pine	6,33
			5. *P. morrisonicola*	Taiwan white pine	—
			6. *P. fenzeliana*	—	-—
			7. *P. dalatensis*	—	52
			8. *P. lambertiana*	Sugar pine	6
			9. *P. wallichiana*	Himalayan (blue) pine	55
			10. *P. ayacahuite*	Mexican white pine	This study
			11. *P. monticola*	Western white pine	6
			12. *P. strobiformis*	Southwestern white pine	This study
			13. *P. wangii*	—	—
			14. *P. armandii*	Armand pine	51, this study
			15. *P. amamiana*	—	—
			16. *P. bhutanica*	—	—
		Flexiles	17. *P. flexilis* var. *flexilis*	Limber pine	50
			18. *P. flexilis* var. *reflexa*	—	—
		Cembrae	19. *P. cembra*	Swiss stone pine	5,51
			20. *P. sibirica*	Russian cedar	5,52
			21. *P. coronans*	Siberian cedar	—
			22. *P. pumila*	Japanese stone pine	This study
			23. *P. koraiensis*	Korean pine	51,57,58
			24. *P. albicaulis*	Whitebark pine	(possible, L)[f]
	Parrya	*Cembroides*	25. *P. cembroides* ssp. *cembroides*	Mexican pinyon	—
			26. *P. cembroides* ssp. *orizabensis*	—	—
			27. *P. cembroides* ssp. *lagunae*	—	—
			28. *P. culminicola*	Potosi pinyon	—
			29. *P. maximartinezii*	Martinez pinyon	50
			30. *P. edulis*	Colorado pinyon	56
			31. *P. discolor*	Border pinyon	—
			32. *P. californiarum*	—	—
			33. *P. johannis*	—	—
			34. *P. remota*	Papershell pinyon	—
			35. *P. monophylla*	Singleleaf pinyon	50
			36. *P. quadrifolia*	Parry pinyon, four-leaf pinyon	—
			37. *P. pinceana*	Pince pinyon	—
			38. *P. nelsonii*	Nelson pinyon	50
		Rzedowskiae	39. *P. rzedowskii*	—	—
		Balfourianae	40. *P. balfouriana* ssp. *balfouriana*	Foxtail pine	(possible, L)
			41. *P. balfouriana* ssp. *austrina*	—	—
			42. *P. aristata*	Bristlecone pine	6
			43. *P. longaeva*	Intermountain bristlecone pine	—
		Gerardianae	44. *P. bungeana*	Lacebark pine	54, this study
			45. *P. gerardiana*	Chilgoza pine	50
Pinus	*Pinus*	*Sylvestres*	46. *P. sylvestris* var. *sylvestris*	Scots pine	49,55, this study
			47. *P. sylvestris* var. *mongolica*	—	This study
			48. *P. sylvestris* var. *hamata*	—	—
			49. *P. koekelare* (hyb.)	—	5
			50. *P. nigra* ssp.*salzmannii*	Salzmann pine	5
			51. *P. nigra* ssp. *laricio*	Calabrian black pine	5, this study
			52. *P. nigra* ssp. *nigra*	Austrian pine	6
			53. *P. nigra* ssp. *pallasiana*	Crimean pine	This study
			54. *P. uncinata*	—	5
			55. *P. mughus*	Swiss Mountain pine	55
			56. *P. pumilio*	Dwarf Mugo pine	5
			57. *P. leucodermis*	Palebark pine	(possible, S)
			58. *P. heldreichii*	Bosnian (Balkan) pine	(possible, S)
			59. *P. densiflora*	Japanese red pine	33,54
			60. *P. densata*	—	—
			61. *P. tabuliformis*	Chinese pine	54, this study

(continued)

TABLE 1 (continued)

Subgenus[a]	Section	Subsection	Species[b]	Trivial name[c]	References[d]
			62. *P. thunbergii*	Japanese black pine	5,33,53,54
			63. *P. massoniana*	Masson pine	6,52,54
			64. *P. henryi*	—	54
			65. *P. mukdensis*	—	—
			66. *P. yunnanensis*	Yunnan pine	This study
			67. *P. sylvestriformis*	—	—
			68. *P. hwangshanensis*	Hwangshan pine	—
			69. *P. luchuensis*	Okinawa (Luchu) pine	—
			70. *P. taiwanensis*	Taiwan red pine	54, this study
			71. *P. latteri*	—	—
			72. *P. merkusii*	Merkus pine	52, this study
			73. *P. kesiya (khasya)*	Khasya pine, Benguet pine	52, this study
			74. *P. insularis*	Luzon pine	—
			75. *P. resinosa*	Norway pine, Red pine	6
			76. *P. tropicalis*	Tropical pine	—
			77. *P. pinaster*	Cluster pine, Maritime pine	7,55
			78. *P. halepensis*	Aleppo pine	5
			79. *P. brutia*	Calabrian pine	5
			80. *P. pithyusa*	Pitsunda pine	(possible, L, S)
			81. *P. stankewiczii*	—	—
			82. *P. eldarica*	Afghan pine	7
		Ponderosae	83. *P. ponderosa* var. *ponderosa*	Ponderosa pine	5
			84. *P. ponderosa* var. *scopulorum*	—	—
			85. *P. arizonica* var. *storrmiae*	—	—
			86. *P. arizonica* var. *arizonica*	Arizona pine	—
			87. *P. arizonica* var. *cooperi*	Pino amarillo (Cooper pine)	—
			88. *P. engelmannii*	Apache pine	—
			89. *P. jeffreyi*	Jeffrey pine	7
			90. *P. whashoensis*	Whashoe pine	—
			91. *P. devoniana (michoacana)*	Michoacan pine	7
			92. *P. hartwegii*	Hartweg pine	—
			93. *P. montezumae*	Montezuma pine	(possible, L, S)
			94. *P. durangensis*	Durango pine	—
			95. *P. pseudostrobus* var. *pseudostrobus*	Smooth-bark Mexican pine	This study
			96. *P. pseudostrobus* var. *protuberens*	—	—
			97. *P. pseudostrobus* var. *apulcensis*	Oaxaca pine	—
			98. *P. maximinoi*	—	This study
			99. *P. douglasiana*	—	—
			100. *P. lawsonii*	Lawson pine	—
			101. *P. teocote*	Teocote, Aztec pine	—
			102. *P. herrerae*	—	—
		Contortae	103. *P. banksiana*	Jack pine	7
			104. *P. contorta* var. *contorta*	Shore pine	7
			105. *P. contorta* var. *latifolia*	Lodgepole pine	(possible, L, S)
			106. *P. contorta* var. *murrayana*	Lodgepole pine	(possible, L)
			107. *P. virginiana*	Virginia pine	(possible, L, S)
			108. *P. clausa*	Sand pine	-—
		Australes	109. *P. rigida*	Pitch pine	53, this study
			110. *P. palustris*	Longleaf pine	7
			111. *P. elliottii* var. *elliotti*	Slash pine	7
			112. *P. elliottii* var. *densa*	—	—
			113. *P. caribaea* var. *caribaea*	Caribbean pine	7,52
			114. *P. caribaea* var. *hondurensis*	Honduran pine	This study
			115. *P. taeda*	Loblolly pine	7
			116. *P. echinata*	Shortleaf pine	7
			117. *P. glabra*	Spruce pine	This study
			118. *P. serotina*	Pond pine	This study
			119. *P. pungens*	Table-Mountain pine	—
			120. *P. occidentalis*	West Indian pine	7
			121. *P. cubensis*	Cuban pine	—
		Oocarpae	122. *P. pringlei*	Pringle pine	—
			123. *P. patula*	Mexican weeping (yellow) pine	6

(continued)

TABLE 1 (continued)

Subgenus[a]	Section	Subsection	Species[b]	Trivial name[c]	References[d]
			124. *P. oocarpa*	Oocarpa pine	This study
			125. *P. greggii*	Gregg pine	(possible, L, S)
			126. *P. attenuata*	Knobcone pine	7
			127. *P. muricata*	Bishop pine	7
			128. *P. radiata*	Monterey pine	5
			129. *P. tecunumanii*	—	—
			130. *P. jaliscana*	—	—
			131. *P. praetermissa*	—	—
		Sabinianae	132. *P. coulteri*	Big cone pine	This study
			133. *P. sabiniana*	Digger pine	50
			134. *P. torreyana*	Torrey pine	(possible, L, S)
		Leiophyllae	135. *P. leiophylla* var. *leiophylla*	Pino chino	—
			136. *P. leiophylla* var. *chihuahuana*	Chihuahua pine	—
			137. *P. lumholtzii*	Lumholtz pine	—
	Pinea	*Canarienses*	138. *P. canariensis*	Canary Island pine	6
			139. *P. roxburghii*	Chir pine	This study
		Pineae	140. *P. pinea*	Italian stone pine	55
Ducampopinus	*Ducampopinus*	*Krempfianae*	141. *P. krempfii*	—	52
Miscellaneous[g]			142. *P. hakkodensis*	—	—
			143. *P. shenkanensis*	—	This study
			144. *P. szemaoensis*	—	This study

[a]The classification adopted here is essentially that suggested by Little and Critchfield (37). For both subgenera *Strobus* (soft pines) and *Pinus* (hard pines), other classifications have been proposed [*cf.* Debazac (38), Mirov (39), Critchfield (40), Klaus (41), or Farjon and Styles (42)]. However, molecular phylogeny of the *Pinus* genus will likely still modify these classifications (43–45). Subspecies (ssp.) or varieties (var.) (spontaneous, horticultural, geographical) are not systematically reported here. On the other hand, some species reported as such may be hybrids (hyb.), and ill-defined species may as well be described under two different names. However, synonyms were tentatively excluded, or grouped under a single accepted name where possible according to Farjon's *World Checklist and Bibliography of Conifers* (2). A few exceptions are for different spellings or names still most often used. Some uncertainties, however, still remain, owing to the lack of author references in the seed-sellers' price lists.

[b]The bulk of species mentioned in the table are from a compilation of descriptions in References 2, 37, 38, and 39 (156, *ca*. 110, 94, and 92 species described, respectively, including nothospecies, subspecies, etc.).

[c]Trivial names are mainly those given by Little and Critchfield (37), Mirov (39), and secondarily by Debazac (38), and those used by U.S. tree-seed sellers (in particular, Lawyer Nursery, Inc., Plains, MT, and F.W. Schuhmacher Co., Inc., Sandwich, MA).

[d]Reference 57 is a review on *P. koraiensis* seed oil fatty acids, including references not cited here.

[e]Seed fatty acid compositions not yet described and not available from the tree-seed sellers known by the authors.

[f]Seeds available from tree-seed sellers, for which the fatty acid composition has not been established in detail, or not at all (L, Lawyer Nursery, Inc.; S, Sandeman Seeds, Pulborough, United Kingdom).

[g]This part of the table lists some species mentioned in the literature, or available from tree-seed sellers, that the authors could not classify correctly (see text however).

Within the *Strobus* section, only the *Flexiles* subsection appears as quite distinct from the two other subsections, *Strobi* and *Cembrae*. *Pinus flexilis* (unknown variety) has a significantly higher level of oleic acid (34.9%) than any other species of the same section (≤27.3%), counterbalanced by the lowest taxoleic (0.3% vs. ≥1.5%) and pinolenic (1.6% vs. ≥7.7%) acid percentages. We will not discuss here the significance of that observation, because the status of species retained here in the *Flexiles* subsection (Table 1) is variously treated to relate to *P. strobiformis*, *P. armandii*, and *P. albicaulis*. Though the latter species has not yet been analyzed for its SFA, data for the former two species show completely different Δ5-UPIFA profiles (Table 2), and indeed, the completely original status of *P. flexilis* could justify maintaining the *Flexiles* subsection as distinct from both subsections *Strobi* and *Cembrae*. The single component that allows distinction of all species of a given subsection as compared to the other subsection is the level of sciadonic acid, being ≤1.1% in the *Cembrae* subsection and ≥1.3% in the *Strobi* subsection, except possibly in a variety of *P. parviflora*, reported as *P. pentaphylla*, and in *P. lambertiana*, 1.1%. However, *P. lambertiana* appears atypical regarding its level of total Δ5-UPIFA: 10.9%, instead of 17.5–29.7% as in other species of subsections *Strobi* and *Cembrae*. Incidentally, one should note the remarkable similitude of results for *P. parviflora* and *P. pentaphylla* (a variety, or synonym of *P. parviflora*) (Table 2), despite the fact that they were established with seeds from different origins, and by different authors using different analytical procedures, at about 15 years' interval. The same holds true for *P. armandii* SFA compositions, which indicate that each pine species has a constant SFA omposition, a prerequisite for its use as chemometric markers.

Within the *Cembrae* section, it should be pointed out that *P. cembra* and *P. sibirica* are two closely related species in spite of their geographical separation (Alps and Carpathians, and Siberia, respectively). Indeed, these two species can hardly be distinguished, or not at all, if one considers their SFA compositions, which are nearly identical (Table 3). However, their turpentine chemical compositions would considerably differ (39). *Pinus pumila* is a dwarf species diversely regarded as related to either *P. sibirica* (38,39) or *P. parviflora*

TABLE 2
Fatty Acid Composition (weight % of total fatty acids) of the Seed Lipids from Pines of the Subgenus *Strobus*, Section *Strobus*, Subsection *Strobi*

Number[a]	Species	16:0	16:1[b]	*aiso*-17:0[c]	17:0	9-17:1	18:0	9-18:1	11-18:1	9,12-18:2	9,12,15-18:3	20:0	11-20:1
1	*P. strobus*	3.85	0.11	0.06	0.05	0.03	1.94	13.75	0.36	46.74	0.24	0.29	1.24
3	*P. peuce*	3.84	0.10	0.08	0.05	—	2.41	13.41	0.37	47.98	0.30	0.31	0.82
4	*P. parviflora*	4.41	0.13	0.07	0.05	0.03	2.53	19.85	0.44	47.35	0.27	0.30	0.74
4	*P. pentaphylla*[h]	4.09	0.14	—	0.03	—	2.13	20.74	Trace[d]	47.75	0.25	0.27	0.73
7	*P. dalatensis*	7.1	0.5	—	—	—	1.8	20.7	1.4	47.4	0.4	0.4	0.8
8	*P. lambertiana*	5.73	0.16	0.10	0.04	0.03	2.08	24.46	0.53	53.78	0.18	0.33	0.81
9	*P. wallichiana*	4.71	0.15	0.15	0.05	0.02	2.58	17.15	0.48	46.44	0.30	0.40	0.61
10	*P. ayacahuite*	4.11	0.14	0.09	0.05	0.04	1.78	19.43	0.40	49.01	0.31	0.29	1.00
11	*P. monticola*	3.80	0.09	0.12	0.04	0.02	2.14	14.36	0.36	50.92	0.34	0.34	0.93
12	*P. strobiformis*	4.40	0.11	0.07	0.03	0.03	1.99	21.57	0.42	48.33	0.33	0.34	0.84
14	*P. armandii*	4.6	—	—	—	—	2.0		23.8[i]	45.8	0.2	0.4	1.4
14	*P. armandii*	4.49	0.13	0.04	0.03	0.02	1.90	23.86	0.47	46.03	0.23	0.36	0.90

Number	Species	11,14-20:2	22:0	5,9-18:2	5,9,12-18:3	5,9,12,15-18:4	5,11-20:2	5,11,14-20:3	7,11,14-20:3	5,11,14,17-20:4	∑Δ5[d]	Others[e]	Reference
1	*P. strobus*	1.21	0.13	1.74	25.29	0.05	0.21	1.93	0.47	—[f]	29.69	0.31	5
3	*P. peuce*	0.87	Trace[g]	2.04	25.18	Trace	0.19	1.59	0.39	—	29.39	0.07	6
4	*P. parviflora*	0.72	Trace	3.47	18.18	Trace	0.10	1.31	0.13	—	23.19	0.00	6
4	*P. pentaphylla*	0.64	—	3.54	18.10	0.03	0.11	1.11	—	0.08	22.97	0.26	33
7	*P. dalatensis*	0.7	—	2.8	12.2	—	0.4	1.9	—	—	17.3	1.5	52
8	*P. lambertiana*	0.77	0.13	2.00	7.69	0.03	0.14	1.08	0.04	—	10.91	0.09	36
9	*P. wallichiana*	0.61	0.14	2.44	21.69	0.05	0.14	1.40	0.16	—	25.88	0.33	55
10	*P. ayacahuite*	0.68	0.07	1.98	18.27	0.03	0.25	1.70	0.13	—	22.36	0.24	This study
11	*P. monticola*	0.99	Trace	2.62	20.83	—	0.20	1.57	0.21	—	25.43	0.12	6
12	*P. strobiformis*	0.71	0.05	2.22	16.59	0.02	0.18	1.40	0.11	—	20.52	0.46	This study
14	*P. armandii*	0.6	—	3.8	15.8	—	—	1.5	—	—	21.1	0.1	51
14	*P. armandii*	0.57	0.13	3.39	15.98	Trace	0.12	1.31	0.06	—	20.76	0.08	This study

[a]Same numbering of species as in Table 1. In the absence of any precisions on the subspecies or the variety, the number given here is the number occurring first in Table 1 for a given species.
[b]Two isomers, 7- and 9-16:1 acids.
[c]14-Methylhexadecanoic, or *anteiso*-17:0 acid.
[d]Sum of Δ5-olefinic acids, including the 7,11,14-20:3 acid.
[e]Minor and unidentified components.
[f]Not detected or not reported.
[g]Trace amounts.
[h]A variety of *P. parviflora*.
[i]Isomers not given separately.

TABLE 3
Fatty Acid Composition (weight % of total fatty acids) of the Seed Lipids from Pines of the Subgenus *Strobus*, Section *Strobus*, Subsections *Flexiles* and *Cembrae*

Number[a]	Species	16:0	16:1[b]	*aiso*-17:0[c]	17:0	9-17:1	18:0	9-18:1	11-18:1	9,12-18:2	9,12,15-18:3	20:0	11-20:1
17	*P. flexilis*	6.68	0.12	0.04	0.04	0.03	3.22	34.93	0.43	50.56	0.31	0.37	0.36
19	*P. cembra*	4.30	0.06	0.09	0.05	0.03	2.67	23.22	0.27	44.66	0.26	0.31	1.17
19	*P. cembra*	4.6	—	—	—	—	2.4	24.9[h]		44.6	0.3	0.3	1.3
20	*P. sibirica*	4.31	0.06	—	—	—	2.38	25.07	0.30	43.71	0.20	0.27	1.24
20	*P. sibirica*	4.4	0.1	—	—	—	2.6	25.1	0.5	43.2	0.2	0.3	1.3
22	P. pumila	3.95	0.08	0.09	0.05	0.03	1.97	21.92	0.35	46.04	0.24	0.26	1.10
22	*P. pumila*	3.93	0.08	0.07	0.05	0.03	2.26	22.97	0.29	44.70	0.22	0.29	1.10
23	*P. koraiensis*	4.7	0.05	0.06	0.04	—	2.10	27.29	1.11	44.70	0.10	0.40	1.20
23	*P. koraiensis*	5.0	—	—	—	—	2.3	27.0		45.5	0.2	0.3	1.3
23	*P. koraiensis*	4.9	0.1	—	0.1	—	2.0	26.9	—	45.0	0.2	0.3	1.2
23	*P. koraiensis*	4.94	0.10	—	0.04	—	1.98	26.29	0.17	46.70	0.14	0.30	1.01
23	*P. koraiensis*	5.0	0.1	—	—	—	2.7	28.1	0.5	44.1	0.1	0.5	1.3

Number	Species	11,14-20:2	22:0	5,9-18:2	5,9,12-18:3	5,9,12,15-18:4	5,11-20:2	5,11,14-20:3	7,11,14-20:3	5,11,14,17-20:4	∑Δ5[d]	Others[e]	Reference
17	*P. flexilis*	0.21	0.13	0.28	1.60	—[f]	0.04	0.38	trace[g]	—	2.30	0.27	50
19	*P. cembra*	0.60	0.10	1.67	19.19	0.03	0.12	1.07	0.14	—	22.22	0.00	5
19	*P. cembra*	0.6	—	1.4	18.6	—	—	1.0	—	—	21.0	0.0	51
20	*P. sibirica*	0.55	—	1.98	18.49	—	0.13	1.03	0.10	—	21.73	0.18	5
20	*P. sibirica*	0.6	—	1.7	18.1	—	0.1	0.9	—	—	20.8	0.9	52
22	*P. pumila*	0.57	0.11	2.44	19.46	0.03	0.17	0.88	0.15	—	23.24	0.08	This study[i]
22	*P. pumila*	0.47	0.11	2.85	19.40	0.04	0.17	0.82	0.09	—	23.37	0.06	This study[i]
23	*P. koraiensis*	0.50	0.20	2.00	14.50	—	0.10	0.90	—	—	17.50	0.05	57
23	*P. koraiensis*	0.6	—	1.9	14.7	—	—	1.1	—	—	17.7	0.1	51
23	*P. koraiensis*	0.8	0.2	2.2	14.6	—	(0.1)[j]	1.0	—	—	17.9	0.6	53
23	*P. koraiensis*	0.47	—	1.87	15.04	Trace	0.08	0.79	—	—	17.78	0.08	33
23	*P. koraiensis*	0.5	—	2.2	13.9	—	0.1	0.4	0.4	—	17.0	0.0	58

[a]Same numbering of species as in Table 1.
[b]Two isomers, 7- and 9-16:1 acids.
[c]14-Methylhexadecanoic, or *anteiso*-17:0 acid.
[d]Sum of Δ5-olefinic acids, including the 7,11,14-20:3 acid.
[e]Minor and unidentified components.
[f]Not detected or not reported.
[g]Trace amounts.
[h]Isomers not given separately.
[i]For this species, two lots of seeds from two different tree-seed sellers.
[j]Reported as 13-20:1 acid.

TABLE 4

Fatty Acid Composition (weight % of total fatty acids) of the Seed Lipids from Pines of the Subgenus *Strobus*, Section *Parrya*, Subsections *Cembroides*, *Balfourianae*, and *Gerardianae*

Number[a]	Species	16:0	16:1[b]	*aiso*-17:0[c]	17:0	9-17:1	18:0	9-18:1	11-18:1	9,12-18:2	9,12,15-18:3	20:0	11-20:1
29	*P. maximartinezii*	9.20	0.23	0.05	0.07	0.03	3.07	31.70	0.39	52.46	0.31	0.26	0.36
30	*P. edulis*	7.05	0.18	0.02	0.03	0.04	2.27	46.85	0.61	40.70	0.19	0.47	0.53
35	*P. monophylla*	6.92	0.11	—	0.03	—	3.25	46.13	0.42	41.15	0.18	0.37	0.47
38	*P. nelsonii*	6.83	0.18	Trace	0.05	0.04	3.63	44.80	0.45	41.40	0.18	0.38	0.55
42	*P. aristata*	3.73	0.11	0.09	0.02	0.02	2.39	19.51	0.45	55.90	0.29	0.36	0.58
44	*P. bungeana*	8.1	—	—	—	-	5.8	28.0[h]		39.1	—	1.5	—
44	*P. bungeana*	4.64	0.14	0.07	0.02	0.02	3.10	24.40	0.42	52.26	0.18	0.49	0.75
45	*P. gerardiana*	5.21	0.12	0.09	0.05	0.05	1.61	36.85	0.39	51.25	0.46	0.43	0.64

Number	Species	11,14-20:2	22:0	5,9-18:2	5,9,12-18:3	5,9,12,15-18:4	5,11-20:2	5,11,14-20:3	7,11,14-20:3	5,11,14,17-20:4	∑Δ5[d]	Others[e]	Reference
29	*P. maximartinezii*	0.34	0.06	0.17	0.35	—[f]	0.07	0.46	—	—	1.05	0.42	50
30	*P. edulis*	0.24	Trace[g]	0.14	0.36	—	—	0.29	—	—	0.79	0.03	56
35	*P. monophylla*	0.23	0.02	0.03	0.13	—	0.07	0.34	—	—	0.57	0.15	50
38	*P. nelsonii*	0.45	0.05	0.12	0.43	—	Trace	0.39	—	—	0.94	0.07	50
42	*P. aristata*	0.51	Trace	2.39	12.44	Trace	0.31	0.84	Trace	—	15.98	0.08	6
44	*P. bungeana*	2.5	—	3.8	8.6	—	—	—	—	—	12.4	2.6	54
44	*P. bungeana*	0.62	0.08	2.77	8.62	—	0.13	0.69	—	—	12.21	0.60	This study
45	*P. gerardiana*	0.24	0.19	0.42	0.83	—	0.11	0.23	—	—	1.62	0.60	50

[a]Same numbering of species as in Table 1. In the absence of any precisions on the subspecies or the variety, the number given here is the number occurring first in Table 1 for a given species.
[b]Two isomers, 7- and 9-16:1 acids.
[c]14-Methylhexadecanoic, or *anteiso*-17:0 acid.
[d]Sum of Δ5-olefinic acids, including the 7,11,14-20:3 acid.
[e]Minor and unidentified components.
[f]Not detected or not reported.
[g]Trace amounts.
[h]Isomers not given separately.

(59). Its geographical distribution is indeed intermediate between those of the latter two species (roughly, from eastern Siberia to Japan). In many respects, the SFA of *P. pumila* resembles those of both *P. sibirica* (Table 3) and *P. parviflora* (Table 2), as well as *P. cembra* (Table 3). This does not indicate any particular relationships with one or more species, or conversely, may be indicative of close relationships between the four species.

Pinus lambertiana, an "archetypal white pine" (40), does not successfully cross with other species of the same subsection *Strobi*, with the exception of *P. armandii* (of uncertain taxonomic position), whereas it hybridizes with *P. koraiensis*, an Asian species of subsection *Cembrae* (40). *Pinus flexilis* also crosses with species of subsection *Strobi* (40). Clearly, relationships between subsections within section *Strobus* are not well understood. Except for *P. lambertiana*, this section however appears united by many features of their SFA composition, e.g., by their 9,12-18:2 acid content, in the narrow range 44–51%, that contrasts with that in pines of section *Parrya*, with higher or lower linoleic acid contents (see below).

Subsections *Cembroides*, *Balfourianae*, and *Gerardianae* of section *Parrya* (Table 4) display species with SFA profiles, in a general manner, quite distinct from those of the *Strobus* and *Cembrae* subsections (Tables 2 and 3). However, section *Parrya* and even some of its subsections, e.g., the highly complex *Cembroides* subsection, are not considered "natural" groups (43). From our SFA analyses of a single representative of the *Balfourianae* subsection, *P. aristata*, and of *P. bungeana* from the *Gerardianae* subsection, it would appear that these species are closer to species of section *Strobi* than to species of the *Cembroides* subsection. Among the *Cembroides* species analyzed so far, three are very similar (*P. edulis*, *P. monophylla*, and *P. nelsonii*), whereas the fourth one (*P. maximartinezii*) shows some significantly distinctive features. The four species are united in having the lowest total Δ5-UPIFA inside the subgenus *Strobus* (0.6–1.0%). They differ, however, in their prominent fatty acid, oleic acid in the *P. edulis-monophylla-nelsonii* group (44.8 to 46.8%) and linoleic acid in *P. maximartinezii* (52.5%). Apparently, all of these species show considerably low Δ5-desaturase activities, but the *P. edulis-monophylla-nelsonii* group would additionally present a somewhat reduced Δ12-desaturase activity, leading to an unusual accumulation of oleic acid in the seeds from this group. Specialists of the single-needle pinyons (60) regard *P. cembroides* as a species complex including among others, *P. monophylla* and its several subspecies. Seed fatty acid compositions for these subspecies have been published [(59); not included in Table 4], and despite some inconsistencies with our own data (50), very low Δ5-UPIFA (the C_{18} Δ5-UPIFA are likely those fatty acids reported as linolelaidic and β-eleostearic acids), and exceptionally high oleic acid levels (>42%) were established. Another report (61) on the fatty acid composition of "nuts from three seed coat phenotypes" of *P. cembroides* also indicates high oleic acid levels (range, 37–47%), and as no Δ5-UPIFA are reported, probably low amounts of such acids (data not reported in Table 4). As *P. monophylla* hybridizes with *P. edulis* (two-needle pinyon), not surprisingly SFA compositions for both species are almost indistinguishable (Table 4).

The two species constitutive of the *Gerardianae* subsection (Table 4) are quite distinct from one another, with relatively low (*P. bungeana*) or very low (*P. gerardiana*) levels of total Δ5-UPIFA (12.2 and 1.6%, respectively). Regarding its main SFA, *P. maximartinezii* is closer to *P. gerardiana* (*Gerardianae*) than to other members of subsection *Cembroides*, which is in line with a common rooting of these species as suggested by Malusa (43). However, *P. nelsonii*, also grouped with *P. maximartinezii* by Malusa (43), is hardly distinguishable from *P. edulis* and *P. monophylla* (grouped apart as "true pinyons") when considering their SFA compositions. The suggestion to segregate subsection *Cembroides* into three "groups" (62), *Pinceanae* (*P. maximartinezii* and *P. pinceana*, the latter species not yet analyzed), *Nelsoniae* (*P. nelsonii*), and *Cembroidae* (the remaining species of subsection *Cembroides*, including *P. edulis* and *P. monophylla*, analyzed for their SFA), is not incompatible with SFA compositions reported here.

SFA compositions in the Pinus *subgenus*. Within this subgenus, species from subsection *Sylvestres* are particularly well-documented (Tables 5–7), and deserve some comments. They are mostly Eurasian or Asian, with only *P. resinosa* (analyzed) and *P. tropicalis* (not analyzed) being native to North America. The first remark relates to the small variability inside the species *P. sylvestris*, despite its numerous variants or varieties. To support this observation, we established the fatty acid compositions from seeds collected in 10 different French stands (two lots in each case, two preparations of FAME per lot, totalling 40 GLC analyses), in Ukraine and in Mongolia, and compared them with a similar analysis of seeds collected in 10 different locations in Finland (49). As can be noted from Table 5, small variations occur, some of which are statistically significant, e.g., a decrease eastward of C_{20} fatty acids, particularly of sciadonic acid: from *ca*. 5.0% in France-Finland to 3.6% in Mongolia. Part of these variations, however, may be attributable to analytical causes or sampling as well. At least for the 10 French stands, no statistically significant differences could be established (results not shown). Moreover, an obvious limitation in SFA analysis is the history of the seeds (mainly authentification, perhaps storage conditions, e.g., duration and temperature), which is generally not known, though seeds were purchased from national (France) or reputable major (France, United States, and the United Kingdom) tree-seed sellers, and thus supposed to be viable and suited for plantation. The same limited variability can be observed in the *P. nigra* complex (Table 5).

All *Sylvestres* species have seed oils in which the major fatty acid is linoleic acid, with a mean in the narrow range 43.5 to 48.3% (52.0%, however, in *P. merkusii*), with the exception of data for *P. pinaster*, along with the circum-Mediterranean species alternately grouped in a *Halepenses* subsection (38,41), *P. halepensis*, *P. brutia*, and *P. eldarica*. For

TABLE 5
Fatty Acid Composition (weight % of total fatty acids) of the Seed Lipids from Pines of the Subgenus *Pinus*, Section *Pinus*, Subsection *Sylvestres*, Part 1

Number[a]	Species[b]	16:0	16:1[c]	*aiso*-17:0[d]	17:0	9-17:1	18:0	9-18:1	11-18:1	9,12-18:2	9,12,15-18:3	20:0	11-20:1
46	*P. sylvestris*	3.36	0.23	0.11	0.05	—[g]	1.78	14.36	0.77	44.84	0.38	0.20	1.14
46	*P. sylvestris* (France)[h]	3.32	0.20	0.19	0.04	—	1.77	14.53	0.75	45.44	0.35	0.40	1.16
46	*P. sylvestris* (Finland)[i]	2.70	0.09	—	—	—	1.68	13.10	0.57	47.23	0.34	0.44	1.46
46	*P. sylvestris* (Ukraine)	4.33	0.28	0.21	0.05	Trace[k]	1.76	14.42	0.75	46.22	0.37	0.23	0.73
47	*P. sylvestris* (Mongolia)	4.01	0.29	0.19	0.04	Trace	1.56	14.36	0.83	46.64	0.36	0.21	0.68
49	*P. koekelare*	4.66	0.22	0.11	0.05	0.02	1.96	17.18	0.57	46.17	0.56	0.31	0.95
50	*P. nigra* ssp. *salzmannii*	4.43	0.24	0.13	0.05	0.02	1.85	17.81	0.66	45.45	0.51	0.32	0.80
51	*P. nigra* ssp. *laricio* (Cal.)	4.62	0.23	0.13	0.05	0.02	2.01	15.87	0.54	47.10	0.60	0.35	0.71
51	*P. nigra* ssp. *laricio* (Cor.)	4.72	0.25	0.15	0.05	0.02	1.89	17.80	0.53	44.78	0.70	0.36	0.88
52	*P. nigra* ssp. *nigra* (Aust.)	4.43	0.24	0.13	0.05	0.02	1.95	17.24	0.63	46.44	0.70	0.32	0.91
53	*P. nigra* ssp. *pallasiana*	4.37	0.24	0.10	0.04	0.02	1.96	16.94	0.70	46.43	0.53	0.38	0.93
50	*P. nigra* (Bulgaria)	4.54	0.25	0.11	0.05	0.02	1.87	16.92	0.67	46.31	0.62	0.31	0.94
50	*P. nigra*	4.16	0.18	0.14	0.05	—	1.94	17.64	0.72	45.00	0.62	0.27	0.97
54	*P. uncinata*	3.39	0.16	0.16	0.04	0.02	1.52	17.07	0.49	46.62	0.29	0.34	1.23
55	*P. mughus*	3.27	0.13	0.07	0.05	—	1.60	18.02	0.51	45.81	0.33	0.22	1.37
56	*P. pumilio*	3.13	0.13	0.15	0.03	0.02	1.47	19.28	0.40	46.45	0.30	0.36	1.42

Number	Species	11,14-20:2	22:0	5,9-18:2	5,9,12-18:3	5,9,12,15-18:4	5,11-20:2	5,11,14-20:3	7,11,14-20:3	5,11,14,17-20:4	∑Δ5[e]	Others[f]	Reference
46	*P. sylvestris*	0.99	0.17	2.70	21.65	0.06	0.50	5.46	0.65	—	31.08	0.54	55
46	*P. sylvestris* (France)	0.96	0.12	2.59	21.47	0.04	0.51	5.13	0.59	—	30.33	0.44	This study
46	*P. sylvestris* (Finland)	1.15	0.12	2.27	21.66	—	0.53	5.00	(0.76)[j]	—	30.22	0.92	49
46	*P. sylvestris* (Ukraine)	0.77	Trace	2.64	22.37	0.03	0.37	3.81	0.45	—	29.67	0.21	This study
47	*P. sylvestris* (Mongolia)	0.75	—	2.65	22.82	0.04	0.33	3.57	0.39	—	29.80	0.28	This study
49	*P. koekelare*	0.76	0.10	3.32	18.97	0.07	0.32	3.27	0.35	—	26.30	0.08	5
50	*P. nigra* ssp. *salzmannii*	0.55	0.08	3.91	19.54	0.06	0.32	2.87	0.31	—	27.01	0.09	5
51	*P. nigra* ssp. *laricio* (Cal.)	0.71	0.07	3.05	19.34	0.07	0.41	3.55	0.34	—	26.76	0.23	This study
51	*P. nigra* ssp. *laricio* (Cor.)	0.59	0.09	3.75	19.44	0.09	0.33	3.21	0.30	—	27.12	0.07	5
52	*P. nigra* ssp. *nigra* (Aust.)	0.77	0.09	3.32	18.76	0.09	0.31	3.07	0.32	0.04	25.91	0.17	6
53	*P. nigra* ssp. *pallasiana*	0.77	0.09	3.22	18.81	0.05	0.32	3.56	0.37	—	26.33	0.17	This study
50	*P. nigra* (Bulgaria)	0.84	0.08	3.15	19.06	0.08	0.31	3.34	0.43	—	26.37	0.10	This study
50	*P. nigra*	0.87	0.13	3.62	18.89	0.08	0.34	3.42	0.42	—	26.77	0.54	55
54	*P. uncinata*	0.78	0.02	2.74	20.44	0.04	0.46	3.66	0.42	—	27.76	0.11	5
55	*P. mughus*	0.84	0.14	2.84	19.55	0.06	0.51	3.73	0.36	—	27.05	0.59	10
56	*P. pumilio*	0.82	0.11	3.02	18.74	0.04	0.45	3.19	0.32	—	25.76	0.17	55

[a]Same numbering of species as in Table 1. In the absence of any precisions on the subspecies or the variety, the number given here is the number occurring first in Table 1 for a given species.
[b]Initial nomenclature modified to fit recent recommendations. Origin of seeds between parentheses (abbreviations: Cal., Calabria; Cor., Corsica; Aust., Austria).
[c]Two isomers, 7- and 9-16:1 acids.
[d]14-Methylhexadecanoic, or *anteiso*-17:0 acid.
[e]Sum of Δ5-olefinic acids, including the 7,11,14-20:3 acid.
[f]Minor and unidentified components.
[g]Not detected or not reported.
[h]Means of duplicate analyses of two seed lots from 10 different locations in France (n = 40).
[i]Mean values for seed lots from 10 different locations in Finland. Recalculated in weight % from data originally expressed in mol%.
[j]Reported as 20:3n-6.
[k]Trace amounts.

TABLE 6
Fatty Acid Composition (weight % of total fatty acids) of the Seed Lipids from Pines of the Subgenus *Pinus*, Section *Pinus*, Subsection *Sylvestres*, Part 2

Number[a]	Species	16:0	16:1[b]	*aiso*-17:0[c]	17:0	9-17:1	18:0	9-18:1	11-18:1	9,12-18:2	9,12,15-18:3	20:0	11-20:1
59	*P. densiflora*	5.8	—[f]	—	—	—	2.0	16.0[g]		50.8	—	0.2	0.6
59	*P. densiflora*	4.92	0.17	0.06	0.04	0.06	1.82	19.55	0.19	45.12	0.34	0.28	0.63
61	*P. tabuliformis*	8.3	—	—	—	—	2.2	22.2		51.9	—	0.1	1.2
61	*P. tabuliformis*	4.56	0.23	0.10	0.03	0.01	1.97	20.86	0.70	43.44	0.35	0.26	0.89
62	*P. thunbergii*	5.02	0.18	0.12	0.05	0.02	1.90	17.43	0.40	46.49	0.64	0.24	0.64
62	*P. thunbergii*	3.2	0.1	—	0.1	—	1.5	18.1		45.2	0.7	0.3	0.9
62	*P. thunbergii*	3.6	—	—	—	—	1.7	18.6		54.6	0.6	0.2	—
62	*P. thunbergii*	4.73	0.17	—	0.04	—	1.61	17.13	0.12	48.27	0.64	0.18	0.49
63	*P. massoniana*	3.99	0.30	0.12	0.05	Trace	1.80	17.65	0.70	47.00	0.42	0.24	0.28
63	*P. massoniana*	4.1	0.4	—	—	—	1.8	17.0	0.8	47.4	0.4	0.2	0.3
63	*P. massoniana*	3.4	—	—	—	—	2.1	14.4		57.5	—	0.1	—
64	*P. henryi*	8.3	—	—	—	—	3.4	30.5		37.1	—	0.6	—

Number	Species	11,14-20:2	22:0	5,9-18:2	5,9,12-18:3	5,9,12,15-18:4	5,11-20:2	5,11,14-20:3	7,11,14-20:3	5,11,14,17-20:4	∑Δ5[d]	Others[e]	Reference
59	*P. densiflora*	0.6	—	2.7	16.5	—	—	4.8	—	—	24.00	0.00	54
59	*P. densiflora*	0.71	—	2.91	19.06	Trace[h]	0.29	3.42	—	Trace	25.68	0.43	33
61	*P. tabuliformis*	0.3	—	<0.1[i]	12.5	—	—	2.7	—	—	15.2	0.00	54
61	*P. tabuliformis*	0.85	0.07	4.00	17.15	0.02	0.40	3.73	0.26	Trace	25.30	0.12	This study
62	*P. thunbergii*	1.03	0.02	2.82	17.80	0.06	0.31	4.36	0.21	—	25.35	0.49	5
62	*P. thunbergii*	1.6	0.2	2.8	18.1	0.1	(0.5)	5.8	(0.3)	—	27.3	0.50	53
62	*P. thunbergii*	3.6	—	3.0	12.8	—	—	4.1	—	—	19.9	0.00	54
62	*P. thunbergii*	0.90	0.04	2.65	18.15	0.06	0.25	3.94	(0.17)	0.08	25.13	0.38	33
63	*P. massoniana*	0.47	Trace	4.46	18.20	Trace	0.48	3.49	0.14	—	26.63	0.21	6
63	*P. massoniana*	0.6	—	4.5	18.4	—	0.4	3.1	(0.2)	—	26.4	0.4	52
63	*P. massoniana*	0.7	—	2.5	14.4	—	—	3.5	—	—	20.4	1.4	54
64	*P. henryi*	1.3	—	4.9	12.6	—	—	0.8	—	—	18.3	0.5	54

[a]Same numbering of species as in Table 1. In absence of any precisions on the subspecies or the variety, the number given here is the number occurring first in Table 1 for a given species.
[b]Two isomers, 7- and 9-16:1 acids.
[c]14-Methylhexadecanoic, or *anteiso*-17:0 acid.
[d]Sum of Δ5-olefinic acids, including the 7,11,14-20:3 acid.
[e]Minor and unidentified components.
[f]Not detected or not reported.
[g]Isomers not given separately.
[h]Trace amounts.
[i]A Chinese ideogram in the original table, likely "trace amounts" as compared to other data in that table.

TABLE 7

Fatty Acid Composition (weight % of total fatty acids) of the Seed Lipids from Pines of the Subgenus *Pinus*, Section *Pinus*, Subsections *Sylvestres*, Part 3, and *Halepenses* (not generally recognized as independent from subsection *Sylvestres*)

Number[a]	Species[b]	16:0	16:1[c]	*aiso*-17:0[d]	17:0	9-17:1	18:0	9-18:1	11-18:1	9,12-18:2	9,12,15-18:3	20:0	11-20:1
66	*P. yunnanensis*	4.27	0.28	0.15	0.03	Trace[g]	1.51	17.68	0.69	44.92	0.41	0.19	0.58
70	*P. taiwanensis*	3.1	—	—	—	—	1.6	15.8[i]		62.4	—	0.2	—
70	*P. taiwanensis*	4.83	0.20	0.11	0.05	0.02	1.96	18.24	0.49	45.06	0.49	0.23	0.65
72	*P. merkusii*	5.3	0.2	—	—	—	4.6	16.5	0.5	54.9	1.3	0.4	0.4
72	*P. merkusii*	8.38	0.11	0.09	0.09	—	2.88	12.33	0.43	52.01	2.65	0.26	0.43
73	*P. kesiya*	5.5	0.2	0.09	—	—	1.4	18.7	0.7	43.6	0.3	0.3	0.8
73	*P. kesiya*	5.65	0.33	0.13	0.03	0.02	1.47	18.78	0.75	43.43	0.38	0.20	0.78
75	*P. resinosa*	2.73	0.17	0.20	0.03	Trace	1.29	18.23	0.82	44.37	0.98	0.38	0.75
77	*P. pinaster*[k]	4.61	0.17	0.11	0.05	—	2.70	18.92	0.38	52.23	1.37	0.31	1.15
77	*P. pinaster*	3.60	0.24[l]		0.05	—	2.39	17.87	0.22	55.85	1.30	(0.27)	1.01
78	*P. halepensis*	4.51	0.09	0.09	0.06	Trace	3.67	23.68	0.36	55.49	0.69	0.50	0.53
79	*P. brutia* (Greece)	4.73	0.09	0.08	0.05	0.02	3.54	18.81	0.32	60.45	0.66	0.50	0.87
79	*P. brutia* (Turkey)	4.77	0.08	0.07	0.06	Trace	3.32	18.26	0.32	60.53	0.60	0.47	0.90
82	*P. eldarica*	3.97	0.05	0.05	trace	3.32	19.94	0.28	57.61	0.70	0.49	0.87	

Number	Species	11,14-20:2	22:0	5,9-18:2	5,9,12-18:3	5,9,12,15-18:4	5,11-20:2	5,11,14-20:3	7,11,14-20:3	5,11,14,17-20:4	∑Δ5[e]	Others[f]	Reference
66	*P. yunnanensis*	0.86	—[h]	2.19	20.58	0.04	0.39	4.84	0.35	—	28.39	0.04	This study
70	*P. taiwanensis*	0.7	—	3.1	10.2	—	—	2.8	—	—	16.10	0.10	54
70	*P. taiwanensis*	0.82	Trace	3.11	18.64	0.05	0.37	4.32	0.30	Trace	26.79	0.06	This study
72	*P. merkusii*	0.8	—	1.7	10.3	—	0.3	2.6	—	—	14.90	0.20	52
72	*P. merkusii*	1.68	—	1.28	11.40	0.15	0.50	4.25	0.19	—	18.37	0.38	This study
73	*P. kesiya*	1.0	—	2.7	18.2	—	0.5	5.2	(0.5)[j]	—	27.10	0.31	52
73	*P. kesiya*	0.87	0.07	3.05	17.83	0.04	0.50	5.00	0.31	—	26.73	0.42	This study
75	*P. resinosa*	1.59	0.07	3.36	21.09	0.19	0.13	3.33	0.20	—	28.30	0.09	6
77	*P. pinaster*	0.87	0.07	0.90	7.90	0.07	0.85	6.97	0.18	—	16.87	0.19	This study
77	*P. pinaster*	0.85	—	0.74	7.13	—	0.76	7.09	—	—	15.72	0.63	55
78	*P. halepensis*	0.53	0.12	0.95	4.02	0.02	0.51	3.60	0.04	—	9.14	0.54	5
79	*P. brutia* (Greece)	0.87	0.12	0.50	3.14	—	0.38	4.60	0.04	—	8.66	0.23	5
79	*P. brutia* (Turkey)	0.90	0.09	0.50	3.12	0.04	0.45	5.13	0.05	—	9.29	0.34	5
82	*P. eldarica*	1.09	0.08	0.74	4.42	—	0.53	5.38	Trace	—	11.07	0.48	7

[a]Same numbering of species as in Table 1. In the absence of any precisions on the subspecies or the variety, the number given here is the number occurring first in Table 1 for a given species.
[b]Origin of seeds between parentheses.
[c]Two isomers, 7- and 9-16:1 acids.
[d]14-Methylhexadecanoic, or *anteiso*-17:0 acid.
[e]Sum of Δ5-olefinic acids, including the 7,11,14-20:3 acid.
[f]Minor and unidentified components.
[g]Trace amounts.
[h]Not detected or not reported.
[i]Isomers not given separately.
[j]Reported as 20:3n-6.
[k]Duplicate analyses of 10 lipid extracts of each from three important seed lots for reforestation use (total, $n = 60$).
[l]16:1 isomers plus *aiso*-17:0.

these species, linoleic acid is definitely higher than in species of the remainder of the *Sylvestres* subsection (means, 45.8 ± 1.2%), from 52.2% in *P. pinaster* (n = 60) to 55.5–60.5% in the other three pine species. Data from Reference 9 are excluded from the present calculations and discussion because they do not correspond to data from other authors when available for the corresponding species (e.g., *P. densiflora*, *P. thunbergii*, *P. massoniana*; Table 6). Oleic acid also shows rather small variations within the *Sylvestres* subsection, in the range 14.4–20.9%, except for *P. merkusii* and *P. halepensis*, which present slightly lower (12.3%) or higher values (23.7%), respectively.

The content and distribution profile of Δ5-UPIFA in the seed lipids from pines of the *Sylvestres* subsection also appear homogenous, here too after exclusion of *P. pinaster*, *P. merkusii*, and the *Halepenses* pines. The total Δ5-UPIFA percentage varies from a low of 25.4% to a high of *ca*. 30%, essentially distributed between taxoleic (2.2–4.5%), pinolenic (17.2–22.8%), and sciadonic (2.9–5.5%) acids. The specific case of *P. pinaster* has been discussed elsewhere (7), and we will comment here only on the distinctive features of the *Halepenses* pines, and of *P. merkusii* (Table 7). However, concerning the present data for *P. pinaster*, regardless of numerous analyses (duplicate analyses from 30 extracts of seeds from the Landes region in France), no significant statistical differences in SFA compositions could be established between the different lots analyzed (data not presented).

In addition to the above mentioned points, the *Halepenses* pines differ from other *Sylvestres* species by their higher level of 18:0 acid (≥3.3% instead of ≤2.0%, respectively), but the most conspicuous feature lies in individual C_{18} Δ5-UPIFA, taxoleic and pinolenic acids being less than 1.0 and 4.4%, respectively. This results in rather low total Δ5-UPIFA, between 9.1 and 11.1%. Two additional salient points that characterize *P. merkusii* SFA are their extreme 16:0 and 18:3n-3 acid levels, 8.4 and 2.6%, respectively, and as noted previously, their low oleic acid content, the lowest among all pine seeds analyzed so far. Finally, it should be pointed out that no obvious characteristics in its SFA profile can distinguish the North American *Sylvestres* species *P. resinosa* from its Eurasian and Asian relatives. In European *Sylvestres* pines, average total Δ5-UPIFA accounts for 30.1% of total SFA, slightly less in *P. nigra* and in the complex *P. uncinata-mughus-pumilio*, 26.7%, whereas corresponding values for Asian *Sylvestres* pines are in the range 25.7–28.4%, and 28.3% in the North American *P. resinosa*. Data for *Sylvestres* species indicate that only slight variations occurred in SFA compositions during the relatively recent differentiation of this subsection.

The four following subsections (Tables 8–10), *Ponderosae*, *Contortae*, *Australes*, and *Oocarpae*, taken as a whole, are hardly distinguishable one from another at first glance, except for *P. jeffreyii* (*Ponderosae* subsection; Table 8), which will be discussed separately. These subsections were grouped in Debazac's (38) description of pines in a *Ponderosa-Banksiana* section, also including *P. pinaster*, that we studied recently (7), and where most of the following observations were made. The major SFA is linoleic acid, from 43.3 to 49.5%, which is a somewhat broader range than that observed in the *Sylvestres* subsection. The second common fatty acid is oleic acid, in the range 15.4–21.8%, which compares well with the corresponding values established for the *Sylvestres* subsection. Concerning Δ5-UPIFA, the range of their total, 22.8–29.2%, is very similar to that presented by most species of subsection *Sylvestres*, a situation also observable at the level of individual C_{18} Δ5-UPIFA: taxoleic acid, 1.6–3.2%; pinolenic acid, 17.5–22.9%; and C_{20} Δ5-UPIFA: sciadonic acid, 1.6–4.4%. Older data for *P. taeda* (63) and *P. elliottii* (64) (not presented in Table 9) have also been reported, and at least for major components, are in the ranges reported here.

Pinus jeffreyi does not fit the general pattern of the *Sylvestres-Ponderosae-Contortae-Australes-Oocarpae* group. In particular, it shows a SFA composition with a higher level of oleic and taxoleic acids and a lower content of pinolenic and sciadonic acids. This might be indicative of a tendency in that species to a reduced Δ12-desaturase activity accompanied by a lower Δ5-desaturase activity of linoleic acid as compared to other species. Interestingly, Mirov (39), basing his conclusions on the chemistry of *P. jeffreyi* turpentine (presence of *n*-heptane), and on its natural and fertile hybridization with *P. coulteri*, suggested its inclusion in a "*Macrocarpae* group," here the *Sabinianae* subsection augmented with *P. oaxana*. However, *P. jeffreyi* would also be related to a variety of *P. ponderosa* (not analyzed) through the same crossability and turpentine composition criteria. Indeed, the total Δ5-UPIFA in *P. jeffreyi* (17.0%) is intermediary between that in *P. coulteri* (14.5%) and the bulk of species from the *Banksiana-Ponderosa* section (corresponding here to section *Pinus* without subsections *Sabinianae* and *Leiophyllae*; Tables 8–10) (23.0–29.2%).

The two species from the *Sabinianae* subsection analyzed so far (Table 10; *P. torreyana* does not seem to have been analyzed so far) reveal an apparent heterogeneity in this subsection. As mentioned above, *P. coulteri* is closer to *P. jeffreyi* than to any other species of the preceding subsections, whereas *P. sabiniana* displays a unique and quite distinct SFA profile. Regarding *P. coulteri*, the similitude with *P. jeffreyi* is unlikely to be coincidental, especially when considering the chemical point of view of Mirov (39). On the other hand, the SFA composition of *P. sabiniana* resembles that of many *Cembroides* species that belong to the *Strobus* subgenus, and not to species of the *Pinus* subgenus.

The *Canarienses* subsection (Table 11) embraces only two species, one native to the Canary Islands (*P. canariensis*) and the other to the Himalayas (*P. roxburghii*). Despite this geographical remoteness, the SFA compositions of both species are remarkably similar, with only minor differences. Among these is the content of α-linolenic acid, exceptionally high in *P. canariensis* (1.9%). Otherwise, both species have low C_{18} Δ5-UPIFA contents, relatively high levels of sciadonic acid, and general SFA profiles not very different from that of *P. halenpensis*.

TABLE 8
Fatty Acid Composition (weight % of total fatty acids) of the Seed Lipids from Pines of the Subgenus *Pinus*, Section *Pinus*, Subsections *Ponderosae* and *Contortae*

Number[a]	Species	16:0	16:1[b]	*aiso*-17:0[c]	17:0	9-17:1	18:0	9-18:1	11-18:1	9,12-18:2	9,12,15-18:3	20:0	11-20:1
83	*P. ponderosa*	3.97	0.09	0.16	0.03	0.02	2.18	21.81	0.38	45.44	0.58	0.42	0.89
89	*P. jeffreyi*	5.04	0.11	0.16	0.04	0.02	1.49	30.88	0.54	42.50	0.52	0.45	0.88
91	*P. devoniana*[g]	3.48	0.11	0.15	0.05	0.02	1.60	16.74	0.52	48.55	0.64	0.41	1.23
95	*P. pseudostrobus*	5.93	0.12	0.30	0.10	trace	2.34	18.79	0.55	44.75	1.21	0.49	1.45
98	*P. maximinoi*	3.75	0.07	0.14	0.04	trace	2.03	17.02	0.51	49.45	0.57	0.31	1.07
103	*P. banksiana*	3.65	0.13	0.17	0.04	0.02	1.55	16.73	0.94	44.73	0.46	0.39	0.95
104	*P. contorta*	3.21	0.16	0.23	0.03	—	1.62	15.35	1.69	44.75	0.58	0.59	1.22

Number	Species	11,14-20:2	22:0	5,9-18:2	5,9,12-18:3	5,9,12,15-18:4	5,11-20:2	5,11,14-20:3	7,11,14-20:3	5,11,14,17-20:4	$\sum\Delta5^{d}$	Others[e]	Reference
83	*P. ponderosa*	0.45	0.02	2.92	18.36	0.07	0.26	1.62	0.20	—[f]	23.43	0.13	5
89	*P. jeffreyi*	0.29	0.05	3.88	11.28	0.07	0.34	1.41	0.05	—	17.03	0.00	7
91	*P. devoniana*	0.80	trace[h]	2.32	18.76	0.10	0.43	3.83	0.24	—	25.68	0.02	7
95	*P. pseudostrobus*	1.15	trace	2.11	16.60	0.13	0.39	3.37	0.22	—	22.82	0.00	This study
98	*P. maximinoi*	0.89	0.07	2.87	17.50	0.07	0.31	2.92	0.22	—	23.89	0.17	This study
103	*P. banksiana*	0.84	0.14	2.37	22.90	0.07	0.29	2.87	0.56	—	29.06	0.20	7
104	*P. contorta*	0.82	0.15	1.87	22.75	0.11	0.35	3.46	0.68	—	29.22	0.38	7

[a]Same numbering of species as in Table 1. In the absence of any precisions on the subspecies or the variety, the number given here is the number occurring first in Table 1 for a given species.
[b]Two isomers, 7- and 9-16:1 acids.
[c]14-Methylhexadecanoic, or *anteiso*-17:0 acid.
[d]Sum of Δ5-olefinic acids, including the 7,11,14-20:3 acid.
[e]Minor and unidentified components.
[f]Not detected or not reported.
[g]Reported as *P. michoacana*.
[h]Trace amounts.

The *Pineae* subsection (Table 11) is monospecific, with the single *P. pinea* of circum-Mediterranean distribution. Its SFA composition closely resembles that of *P. gerardiana* (subgenus *Strobus*, Table 4), with, however, a sciadonic acid percentage typical of subgenus *Pinus*. Data on the SFA composition of *P. pinea* (not included in Table 11) showing similar levels of oleic and linoleic acids have been reported (65), but apparently no Δ5-UPIFA were detected, likely indicating their scarcity in *P. pinea* seeds.

Pinus krempfii (Table 11), a rare Vietnamese species, is the unique species of the third subgenus *Ducampopinus*, possibly artificial. For example, some observations indicate that *P. krempfii* would fit equally well in the subgenus *Strobus* (66), section *Parrya* (42,44), being even qualified a "*Geradianae*-like species" (44). Indeed, the level of sciadonic acid in the SFA from *P. krempfii* (1.3%) is in the range observed for pines of the *Strobus* subgenus (0.2–1.9%), and the whole SFA composition of *P. krempfii* shares many points in common with that of *P. bungeana*, of the *Parrya* section (subsection *Gerardianae*, Table 4), in particular the total Δ5-UPIFA content (*ca*. 12.2% in both cases).

The unclassified species, *P. shenkanensis* and *P. szemaoensis* (Table 11), may be Asian species or varieties of pines of the *Sylvestres* subsection, as deduced from their SFA compositions (related, e.g., to *P. tabuliformis* or *P. thunbergii*), or even hybrids. *Pinus szemaoensis* would thus present the highest sciadonic acid content (6.0%) after *P. pinaster* in subsection *Sylvestres*, provided its *Sylvestres* nature is confirmed.

General characteristics of Pinus *SFA compositions*. The pine species analyzed so far for their SFA composition (including species from this study) encompass 76 species (and some subspecies or varieties), which is approximately one-half the total number of extant species (Table 1). Regarding the fatty acid compositions of species analyzed in the present study, no other components than those previously described for other pine species were found. This does not exclude the possibility of characterizing in the future traces of fatty acids not observable under routine analytical conditions. A discussion of results on pine SFA compositions in general terms is made.

The major unsaturated fatty acids also common to most seed plants are linoleic acid, from 39.4% (*P. coulteri*) to 60.5% (*P. brutia*), and oleic acid [in the range 13.8 (*P. strobus*)–46.8% (*P. edulis*)], always accompanied by small amounts of *cis*-vaccenic acid (most often <1%, but that can reach 2.0% in *P. pinea*). Generally, linoleic acid predominates over oleic acid, except for some species principally from the *Cembroides* subsection. Though no clear relationships could be established between the two preceding fatty acids and C_{18} Δ5-UPIFA, it would however appear that oleic acid predominates over linoleic acid in those species with the lowest levels of Δ5-UPIFA, particularly, but not exclusively, in species of the *Cembroides* subsection. In no species could we observe α-linolenic acid at levels higher than 1.9% [in *P. canariensis*; otherwise, always less than 1.0%; data for *P. merkusii* are contradictory (Table 7)], and at least under routine analytical

TABLE 9
Fatty Acid Composition (weight % of total fatty acids) of the Seed Lipids from Pines of the Subgenus *Pinus*, Section *Pinus*, Subsection *Australes*

Number[a]	Species	16:0	16:1[b]	*aiso*-17:0[c]	17:0	9-17:1	18:0	9-18:1	11-18:1	9,12-18:2	9,12,15-18:3	20:0	11-20:1
109	*P. rigida*	3.5	0.2	—[f]	0.2	—	1.5		21.6[g]	40.8	0.6	0.6	1.2
109	*P. rigida*	4.22	0.14	0.18	0.04	0.02	1.66	17.80	0.53	45.39	0.45	0.33	0.84
110	*P. palustris*	5.09	0.10	0.16	0.06	0.03	1.66	19.66	0.46	43.43	0.57	0.42	0.81
111	*P. elliottii*	5.14	0.08	0.17	0.05	0.02	2.07	18.95	0.50	44.96	0.43	0.52	1.11
113	*P. caribaea*	5.4	0.2	—	—	—	2.0	19.3	0.7	46.0	0.3	0.4	0.7
113	*P. caribaea*	5.82	0.10	0.18	0.05	Trace[k]	2.65	19.11	0.51	45.02	0.30	0.55	1.19
114	*P. caribaea* var. *hondurensis*	5.63	0.13	0.18	0.05	0.03	2.26	19.96	0.57	44.53	0.42	0.54	1.14
115	*P. taeda*	4.02	0.06	0.15	0.06	0.02	1.84	17.62	0.48	48.25	0.40	0.44	1.06
116	*P. echinata*	5.40	0.07	0.16	0.06	0.02	2.25	19.12	0.50	45.52	0.40	0.55	1.19
117	*P. glabra*	4.29	0.12	0.14	0.07	Trace	2.30	20.96	0.58	45.25	0.35	0.53	0.98
118	*P. serotina*	3.76	0.11	0.15	0.06	0.03	2.05	17.97	0.63	45.10	0.38	0.47	1.14
120	*P. occidentalis*[l]	5.28	0.07	0.12	0.04	Trace	2.41	19.54	0.60	45.32	0.32	0.47	0.92

Number	Species	11,14-20:2	22:0	5,9-18:2	5,9,12-18:3	5,9,12,15-18:4	5,11-20:2	5,11,14-20:3	7,11,14-20:3	5,11,14,17-20:4	∑Δ5[d]	Others[e]	Reference
109	*P. rigida*	0.6	0.3	4.2	20.3	0.2	(0.5)[h]	2.8	(0.7)[i]	—	28.7	0.20	53
109	*P. rigida*	0.61	0.07	2.81	21.55	0.06	0.28	2.33	0.52	—	27.55	0.17	This study
110	*P. palustris*	0.56	0.10	3.20	19.93	0.06	0.35	2.42	0.34	—	24.30	0.59	7
111	*P. elliottii*	0.90	0.22	2.50	18.47	0.06	0.34	2.89	0.37	—	24.63	0.25	7
113	*P. caribea*	0.6	—	2.5	18.3	—	0.3	2.5	(0.3)[j]	—	23.90	0.50	52
113	*P. caribea*	0.88	—	2.25	17.71	0.08	0.23	2.42	0.33	—	23.02	0.62	7
114	*P. caribaea* var. *hondurensis*	0.87	0.18	2.02	17.40	0.05	0.33	3.33	0.31	—	23.44	0.07	This study
115	*P. taeda*	0.76	Trace	2.19	18.34	Trace	0.42	3.37	0.32	—	24.64	0.20	7
116	*P. echinata*	0.76	0.15	2.69	18.18	0.05	0.25	2.31	0.28	—	23.76	0.09	7
117	*P. glabra*	0.80	0.20	2.79	17.84	—	0.31	2.24	0.26	—	23.44	0.00	This study
118	*P. serotina*	0.65	0.17	2.60	20.48	0.06	0.50	3.18	0.48	—	27.30	0.04	This study
120	*P. occidentalis*	0.71	0.08	2.57	18.50	Trace	0.31	2.35	0.22	—	23.95	0.17	7

[a]Same numbering of species as in Table 1. In the absence of any precisions on the subspecies or the variety, the number given here is the number occurring first in Table 1 for a given species.
[b]Two isomers, 7- and 9-16:1 acids.
[c]14-Methylhexadecanoic, or *anteiso*-17:0 acid.
[d]Sum of Δ5-olefinic acids, including the 7,11,14-20:3 acid.
[e]Minor and unidentified components.
[f]Not detected or not reported.
[g]Isomers not given separately.
[h]Reported as 13-20:1.
[i]Reported as 20:3n-3.
[j]Reported as 20:3n-6.
[k]Trace amounts.
[l]Sold under the confusing name "*P. cubensis (occidentalis)*."

TABLE 10

Fatty Acid Composition (weight % of total fatty acids) of the Seed Lipids from Pines of the Subgenus *Pinus*, Section *Pinus*, Subsections *Oocarpae* and *Sabinianae*

Number[a]	Species	16:0	16:1[b]	*aiso*-17:0[c]	17:0	9-17:1	18:0	9-18:1	11-18:1	9,12-18:2	9,12,15-18:3	20:0	11-20:1
123	*P. patula*	4.29	0.05	0.20	0.06	Trace[f]	1.58	16.26	0.44	46.85	0.54	0.39	1.23
124	*P. oocarpa*	5.39	0.13	0.31	0.07	0.03	1.65	17.24	0.69	46.12	0.46	0.45	0.84
126	*P. attenuata*	3.63	0.13	0.11	0.05	0.04	1.85	20.25	0.63	45.41	0.36	0.39	0.84
127	*P. muricata*	3.39	0.07	0.16	0.05	Trace	1.55	18.00	0.33	44.63	0.45	0.31	1.08
128	*P. radiata*	3.62	0.15	0.11	0.04	0.04	1.48	19.40	0.97	43.60	0.37	0.24	0.67
132	*P. coulteri*	4.92	0.12	0.13	0.03	0.02	1.54	36.46	0.67	39.36	0.28	0.43	0.86
133	*P. sabiniana*	5.92	0.11	0.11	0.04	Trace	2.20	40.97	0.61	45.38	0.30	0.73	0.80

Number	Species	11,14-20:2	22:0	5,9-18:2	5,9,12-18:3	5,9,12,15-18:4	5,11-20:2	5,11,14-20:3	7,11,14-20:3	5,11,14,17-20:4	∑Δ5[d]	Others[e]	Reference
123	*P. patula*	1.05	Trace	1.65	19.96	—[g]	0.37	4.35	0.44	—	26.77	0.29	6
124	*P. oocarpa*	0.83	0.18	1.65	18.96	0.08	0.38	3.62	0.41	0.05	25.15	0.46	This study
126	*P. attenuata*	0.57	0.05	2.55	20.33	0.20	0.28	2.01	0.32	—	25.69	0.00	7
127	*P. muricata*	0.96	0.08	2.02	22.80	0.07	0.36	3.00	0.46	—	28.71	0.23	7
128	*P. radiata*	0.56	0.08	2.98	22.34	0.04	0.31	1.82	0.27	—	27.76	0.91	5
132	*P. coulteri*	0.25	0.19	4.44	8.75	Trace	0.33	1.01	Trace	—	14.53	0.21	This study
133	*P. sabiniana*	0.25	0.23	0.43	0.93	—	0.13	0.78	—	—	2.27	0.08	50

[a]Same numbering of species as in Table 1. In absence of any precisions on the subspecies or the variety, the number given here is the number occurring first in Table 1 for a given species.
[b]Two isomers, 7- and 9-16:1 acids.
[c]14-Methylhexadecanoic, or *anteiso*-17:0 acid.
[d]Sum of Δ5-olefinic acids, including the 7,11,14-20:3 acid.
[e]Minor and unidentified components.
[f]Trace amounts.
[g]Not detected or not reported.

TABLE 11

Fatty Acid Composition (weight % of total fatty acids) of the Seed Lipids from Pines of the Subgenus *Pinus*, Section *Pinea*, Subsections *Canarienses* and *Pineae*, from *P. krempfii* (subgenus *Ducampopinus*), and from Unclassified Species

Number[a]	Species	16:0	16:1[b]	*aiso*-17:0[c]	17:0	9-17:1	18:0	9-18:1	11-18:1	9,12-18:2	9,12,15-18:3	20:0	11-20:1
138	*P. canariensis*	5.07	0.08	0.04	0.06	Trace[f]	3.86	23.11	0.28	57.05	1.89	0.57	0.87
139	*P. roxburghii*	5.00	0.13	0.06	0.05	0.02	4.53	24.92	0.35	55.14	0.33	0.60	1.20
140	*P. pinea*	5.55	0.08	0.08	0.05	—	3.20	36.34	2.03	47.19	0.63	0.49	0.71
141	*P. krempfii*	6.1	0.2	—	—	—	2.2	24.3	0.4	51.1	0.4	0.4	0.6
143	*P. shenkanensis*	4.33	0.20	0.10	0.04	0.03	1.68	19.60	0.53	45.19	0.42	0.24	0.78
144	*P. szemaoensis*	4.65	0.30	0.14	0.05	0.02	1.36	17.44	0.72	44.15	0.34	0.23	0.70

Number	Species	11,14-20:2	22:0	5,9-18:2	5,9,12-18:3	5,9,12,15-18:4	5,11-20:2	5,11,14-20:3	7,11,14-20:3	5,11,14,17-20:4	∑Δ5[d]	Others[e]	Reference
138	*P. canariensis*	0.96	Trace	0.30	1.49	Trace	0.36	3.90	—[g]	—	6.05	0.11	This study
139	*P. roxburghii*	1.44	0.08	0.05	1.40	—	0.29	4.02	—	—	5.76	0.39	55
140	*P. pinea*	0.51	—	0.14	0.35	—	0.14	2.47	—	—	3.10	0.04	55
141	*P. krempfii*	0.7	—	3.3	7.3	—	0.1	1.3	(0.2)[h]	—	12.20	1.40	52
143	*P. shenkanensis*	0.90	0.07	3.79	17.48	0.05	0.42	3.78	0.22	0.01	25.75	0.14	This study
144	*P. szemaoensis*	0.95	0.07	2.60	18.92	0.03	0.53	6.02	0.55	—	28.65	0.23	This study

[a]Same numbering of species as in Table 1.
[b]Two isomers, 7- and 9-16:1 acids.
[c]14-Methylhexadecanoic, or *anteiso*-17:0 acid.
[d]Sum of Δ5-olefinic acids, including the 7,11,14-20:3 acid.
[e]Minor and unidentified components.
[f]Trace amounts.
[g]Not detected or not reported.
[h]Reported as 20:3n-6.

conditions, its elongation product (11,14,17-20:3 acid) was not observed. Its presence at subtrace levels cannot be excluded, as juniperonic acid occasionally occurs in trace amounts (e.g., in *P. pentaphylla*). Among other detectable monoenes are 11-20:1 (up to 1.4% in *P. pumilio*), 7-16:1 plus 9-16:1, and 9-17:1 acids, totaling a maximum of 0.3% each. The intermediate metabolite between linoleic and sciadonic acids, 11,14-20:2 acid, is present in all species and can reach 1.6% in *P. resinosa*.

The principal saturated acids are 16:0 (3.1 to 9.2%, in *P. pumilio* and *P. maximartinezii*, respectively) and 18:0 acids (1.4%, in a few *Sylvestres* pines, to 4.5% in *P. roxburghii*). Eicosanoic acid is less than 0.6%, and minor even and odd linear saturated acids including 14:0, 15:0 (not reported here), and 17:0 acids are less than 0.1% each. The *anteiso*-17:0 acid, always observable, may reach 0.3%, and the 22:0 acid is always less than 0.25%. Thus, pine seed lipids have total SFA most often less than 10%, and slightly more in a few cases only (e.g., *P. merkusii* and species of subsection *Cembroides*).

Apart from the fatty acids described above, pine seed lipids contain taxoleic and pinolenic acids as main C_{18} Δ5-UPIFA (minor, 5,9,12,15-18:4 acid), and sciadonic acid as a main C_{20} Δ5-UPIFA [minor, 5,11-20:2 acid, and the Δ5-related 7,11,14-20:3 (bishomopinolenic) acid]. A compilation of data available (Tables 2–11) indicates that the highest percentage of pinolenic acid (25.3%) is found in *P. strobus*, whereas this acid represents only 0.13% in *P. monophylla*. Taxoleic acid apparently is always less than 4.5% (*P. coulteri*, *P. massoniana*) and sometimes present in trace amounts only (<0.05%; *P. roxburghii*, *P. monophylla*). The upper limits of coniferonic acid, and of the elongation product of pinolenic acid, bishomopinolenic acid, would be 0.2% (*P. attenuata, P. resinosa*) and 0.7% (*P. contorta*, *P. sylvestris*), respectively. Regarding C_{20} Δ5-UPIFA, the maximum level of sciadonic acid that can be reached is observed in *P. pinaster* (7%). The 5,11-20:2 acid is seldom higher than 0.5%. However, this acid allows distinction between species of the *Strobus* and *Pinus* subgenera, being less than 0.2% in the former (with however a slightly higher value in *P. aristata*) and presenting a generally higher value in the latter subgenus. A similar limit for sciadonic acid allows separation of the two subgenera at *ca*. 1.9%, lower values occurring mostly in the *Strobus* subgenus. Except for *P. ponderosa*, *P. jeffreyi*, and the two *Sabinianae* species, sciadonic acid levels in species from subgenus *Pinus* are equal to or higher than 2.0%. Total Δ5-UPIFA are in the range 0.6 (*P. monophylla*) to 30–31% (*P. sylvestris*).

The primeval status in pine seeds: low, or high Δ5-desaturase activities? Cladistic and phylogenetic studies based on restriction fragment analyses of either total genomic or chloroplastic DNA (45,46) have shown that the soft pines in section *Parrya* represented by species of subsections *Cembroides* (*P. edulis*, *P. monophylla*), *Balfourianae* (*P. aristata*, *P. longaeva*), and *Gerardiana* (*P. gerardiana, P. bungeana*) constitute the group closest to the hypothesized root of the genus *Pinus*. Except for *P. longaeva*, SFA compositions are fortunately available for the other species and show that most of these species are "united" by low to very low levels of total Δ5-UPIFA, i.e., *P. edulis*, *P. monophylla*, and *P. gerardiana*, less than 1.6% of total fatty acids. This also occurs in other *Cembroides* species, but *P. aristata* and *P. bungeana* have higher total Δ5-UPIFA percentages (up to 16%). On the other hand, all other species examined by DNA-fragment analyses appeared rather homogenous, suggesting a more recent radiation (44,45). Coincidentally, these species have higher total Δ5-UPIFA contents, from 17.0 to 29.7%.

Within diploxyl species (subgenus *Pinus*), *P. pinea* and *P. canariensis* would also form a clade, possibly along with *P. sabiniana*, near the base of the subgenus (44). Here too, *P. pinea* and *P. sabiniana* have SFA containing no more than 3.1% of total Δ5-UPIFA, whereas the corresponding value for the two *Canarienses* species is less than 6%. It is worth mentioning at this point the relationships suggested by Klaus (41) among "coast and island Mediterranean pines," based on morphological characters. This author has emphasized possible links between haploxyl ancestors of the *Parrya* section through the subsection *Canarienses*, to more advanced diploxyl species of the *Pineae* and *Halepenses* subsections, and also in some manner to *P. pinaster*. Data presented here would support this point of view in that all species from this "Mediterranean group" display total Δ5-UPIFA in their SFA that are the lowest, or among the lowest, in all sections. A low Δ5-desaturation activity might thus have been the primeval status in the genus *Pinus.*

Contradicting this possibility is the fact that a high Δ5-UPIFA content in SFA (largely contributed to by pinolenic acid) is also the rule in some other Pinaceae genera, i.e., *Picea*, *Larix*, *Tsuga*, and *Pseudotsuga* (5,18). Though relationships between these genera are diversely interpreted, depending on the characters considered (67–71), a common rooting is largely admitted (46). This view is supported by the striking resemblance of the overall SFA composition of the latter genera with "high Δ5-UPIFA" pine species (5,18). In a multiple-component analysis of their SFA compositions (5), *Picea* spp. were indistinguishable from *Larix* spp., whereas *Tsuga* spp. and *Pseudotsuga menziesii* were slightly outlying within the bulky *Pinus* spp. group. *Abies* spp., *Cedrus* spp. (5,18), and *Keteleeria davidiana* (unpublished data by the authors), though presenting the same individual Δ5-UPIFA and other common fatty acids in their seed lipids as all other Pinaceae genera, have however distinct quantitative distributions of these fatty acids that allow their distinction as individual groups upon multiple component analysis (5,18). However, they also can be considered as "high Δ5-UPIFA" species as their total Δ5-UPIFA content is generally higher than 20% (except for *K. davidiana*). It would thus be reasonable to consider that "low Δ5-UPIFA" species coexisted with "high Δ5-UPIFA" species in the early history of pines, perhaps to accommodate for different edaphic or climatic conditions, before other Pinaceae genera differentiated. Alternately, extant "low Δ5-UPIFA" pine species might be the descendants of extinct "high Δ5-UPIFA" species, and in this case too, a "high Δ5-UPIFA" content could have been the primeval status.

Though no precise physiological roles have been attributed to Δ5-UPIFA in gymnosperms, their possible evolutionary origin however has been discussed (14). The C_{20} Δ5-UPIFA sciadonic and juniperonic acids might be relict fatty acids resulting from modifications of the metabolic pathways that lead, in vegetables of lower phyletic rank, e.g., ferns and fern allies (Pteridophytes), to arachidonic and eicosapentaenoic acids. In the same way, it was suggested that pinolenic acid might be the equivalent of γ-linolenic acid, an intermediate in the biosynthesis of arachidonic acid, following a change of a C_{18} Δ6- (in pteridophytes) to a C_{18} Δ5-desaturase activity (in gymnosperms). Also, some arguments, mostly based on the stereospecific acylation of Δ5-UPIFA to triacylglycerols, were given (9) regarding a different biochemical origin for Δ5-UPIFA occurring in most gymnosperms [all Coniferophyte families, and several Cycadophyte families (10)] on the one hand, and in some rare angiosperms [especially in the archaic family Ranunculaceae (72)] on the other hand.

Some practical considerations. Regarding potential biomedical and nutritional applications of Δ5-UPIFA (20–31, 73), our systematic study of gymnosperm seed oils indicates that numerous pine species may be a source of Δ5-UPIFA. However, the Δ5-UPIFA percentage in the oil may considerably vary from one species to another species, and inside this particular class of fatty acids, the percentage of individual Δ5-UPIFA also is variable. Among pines, the best sources of sciadonic acid are to be found in the subgenus *Pinus*, mostly in species from the *Sylvestres* (generally in the range 2.9–5.5%, but *ca*. 7% in the particular case of *P. pinaster*), *Halepenses* (3.6–5.4%), and *Canarienses* (*ca*. 4.0%) subsections (all species but two of Eurasian location). In contrast, only few North and Central American hard pines have sciadonic acid contents equal to or higher than 3.5%: *P. devoniana*, *P. contorta* (subsections *Ponderosae* and *Contortae*, respectively), *P. taeda* (subsection *Australes*), *P. patula*, and *P. oocarpa* (both from subsection *Oocarpae*). On the other hand, species from the *Strobus* subgenus may not be as interesting, for the maximum level that is reached is at most 1.9% (in *P. strobus*). Good sources of pinolenic are easier to select, as most common pine species from both subgenera contain levels of pinolenic acid equal to or higher than 15% of total fatty acids, being limited to an apparent maximum of 25%. In this regard, however, a Russian report (74) indicates that *P. sibirica* seed oil would contain up to 30% of pinolenic acid, which appears exceptional.

In conclusion, the most common and widespread pine species have been described regarding their SFA compositions. The problem now is to get seeds from less common species, subspecies, or varieties not easily available from tree-seed sellers, nurseries, or botanical gardens. Obviously, SFA compositions alone, as is generally the case for other individual characters, cannot solve the problem of pine phylogeny, as extant species represent at most a small proportion of all species that have existed. Even when the remainder of species not yet studied are described regarding their SFA compositions, the problem may not be solved. However, our original approach has shown that Δ5-UPIFA in pine seeds are highly conservative biochemical characters, in most instances tightly associated with taxonomic groups otherwise recognized as such on the basis of different botanical criteria. As uniting or separative characters, pine SFA compositions, that are technically relatively easy to establish provided the seeds are available, should be considered a complement to be associated with studies on pine taxonomy and phylogeny.

ACKNOWLEDGMENTS

Authors R.L. Wolff and A.M. Marpeau would be most grateful to receive authenticated seeds from any Pinaceae species not already analyzed, more usefully rare ones, for further studies. Prof. Mike Powell, Sul Ross State University, Alpine, Texas, provided some trivial names. This is contribution No. 50 by R.L. Wolff to AOCS Press.

REFERENCES

1. Page, C.N. (1990) Gymnosperms: Coniferophytina (Conifers and Ginkgoids), in *The Families and Genera of Vascular Plants* (Kubitzki, K., ed.), Vol. 1, pp. 279–361, *Pteridophytes and Gymnosperms* (Kramer, K.U., and Green, P.S., eds.), Springer-Verlag, Berlin, Heidelberg.
2. Farjon, A. (1998) *World Checklist and Bibliography of Conifers*, The Royal Botanic Gardens, Kew, United Kingdom.
3. Rothwell, G.W. (1982) New Interpretations of the Earliest Conifers, *Rev. Palaeobot. Palynol. 37*, 7–29.
4. Miller, C.N., Jr. (1976) Early Evolution in the Pinaceae, *Rev. Palaeobot. Palynol. 21*, 101–117.
5. Wolff, R.L., Deluc, L.G., Marpeau, A.M., and Comps, B. (1997) Chemotaxonomic Differentiation of Conifer Families and Genera Based on the Seed Oil Fatty Acid Compositions: Multivariate Analyses, *Trees 12*, 57–65.
6. Wolff, R.L., Comps, B., Marpeau, A.M., and Deluc, L.G. (1997) Taxonomy of *Pinus* Species Based on the Seed Oil Fatty Acid Compositions, *Trees 12*, 113–118.
7. Wolff, R.L., Comps, B., Deluc, L.G., and Marpeau, A.M. (1997) Fatty Acids of the Seeds from Pine Species of the *Ponderosa-Banksiana* and *Halepensis* Sections. The Peculiar Taxonomic Position of *Pinus pinaster*, *J. Am. Oil Chem. Soc. 74*, 45–50.
8. Wolff, R.L. (1997) Discussion of the Term "Unusual" When Discussing Δ5-Olefinic Acids in Plant Lipids, *J. Am. Oil Chem. Soc. 74*, 619.
9. Wolff, R.L., Christie W.W., Pédrono, F., Marpeau, A.M., Tsevegsüren, N., Aitzetmüller, K., and Gunstone, F.D. (1999) Δ5-Olefinic Acids in the Seed Lipids from Four *Ephedra* Species and Their Distribution Between the α- and β-Positions of Triacylglycerols. Characteristics Common to Coniferophytes and Cycadophytes, *Lipids 34*, 855–864.
10. Wolff, R.L. (1999) The Phylogenetic Significance of Sciadonic (all-*cis* 5,11,14-20:3) Acid in Gymnosperms and Its Quantitative Significance in Land Plants, *J. Am. Oil Chem. Soc. 76*, 1515–1516.
11. Berdeaux, O., and Wolff, R.L. (1996) Gas–Liquid Chromatography–Mass Spectrometry of the 4,4-Dimethyloxazoline Derivatives of Δ5-Unsaturated Polymethylene-Interrupted Fatty Acids from Conifer Seed Oils, *J. Am. Oil Chem. Soc. 73*, 1323–1326.
12. Wolff, R.L., Christie, W.W., and Marpeau, A.M. (1999) Reinvestigation of the Polymethylene-Interrupted 18:2 and 20:2 Acids of *Ginkgo biloba* Seed Lipids, *J. Am. Oil Chem. Soc. 76*, 273–276.
13. Wolff, R.L., Pédrono, F., Marpeau, A.M., and Gunstone, F.D. (1999) The Seed Fatty Acid Composition and the Distribution

of Δ5-Olefinic Acids in the Triacylglycerols of Some Taxares (*Cephalotaxus* and *Podocarpus*), *J. Am. Oil Chem. Soc. 76*, 469–473.
14. Wolff, R.L., Christie W.W., Pédrono, F., and Marpeau, A.M. (1999) Arachidonic, Eicosapentaenoic, and Biosynthetically Related Fatty Acids in the Seed Lipids from a Primitive Gymnosperm, *Agathis robusta*, *Lipids 34*, 1083–1097.
15. Gunstone, F.D., Seth, S., and Wolff, R.L. (1995) The Distribution of Δ5 Polyene Acids in Some Pine Seed Oils Between the α- and β-Chains by ^{13}C-NMR Spectroscopy, *Chem. Phys. Lipids 78*, 89–96.
16. Gunstone, F.D., and Wolff, R.L. (1997) Conifer Seed Oils: Distribution of Δ5 Acids Between α-and β-Chains by ^{13}C Nuclear Magnetic Resonance Spectroscopy, *J. Am. Oil Chem. Soc. 73*, 1611–1613.
17. Itabashi, Y., and Takagi, T. (1982) *Cis*-5-Olefinic Nonmethylene-Interrupted Fatty Acids in Lipids of Seeds, Arils, and Leaves of Japanese Yew, *Yukagaku 31*, 574–579.
18. Wolff, R.L., Deluc, L.G., and Marpeau, A.M. (1996) Conifer Seeds: Oil Content and Fatty Acid Distribution, *J. Am. Oil Chem. Soc. 73*, 765–771.
19. Wolff, R.L., Christie, W.W., and Coakley, D. (1997) Bishomopinolenic (7,11,14-20:3) Acid in Pinaceae Seed Oils, *J. Am. Oil Chem. Soc. 74*, 1583–1586.
20. Berger, A., and German, J.B. (1991) Extensive Incorporation of Dietary Δ-5,11,14 Eicosatrienoate into the Phosphatidylinositol Pool, *Biochim. Biophys. Acta 1085*, 371–376.
21. Ikeda, I., Oka, T., Koba, K., Sugano, M., and Lie Ken Jie, M.S.F. (1992) 5*c*,11*c*,14*c* Eicosatrienoic and 5*c*,11*c*,14*c*,17*c*-Eicosatetraenoic Acid of *Biota orientalis* Seed Oil Affect Lipid Metabolism in the Rat, *Lipids* 27, 500–504.
22. Sugano, M., Ikeda, I., and Lie Ken Jie, M.S.F. (1992) Polyunsaturated Fatty Acid Regulation of Cholesterol Metabolism and Eicosanoid Production in Rats: Effects of Uncommon Fatty Acids, in *Essential Fatty Acids and Eicosanoids: Invited Papers from the Third International Congress* (Sinclair, A., and Gibson, R., eds.), pp. 268–270, American Oil Chemists' Society, Champaign.
23. Berger, A., Fenz, R., and German, J.B. (1993) Incorporation of Dietary 5,11,14-Icosatrienoate into Various Mouse Phospholipid Classes and Tissues, *J. Nutr. Biochem. 4*, 409–420.
24. Sugano, M., Ikeda, I., Wakamatsu, K., and Oka, T. (1994) Influence of Korean Pine (*Pinus koraiensis*)-Seed Oil Containing *cis*-5,*cis*-9,*cis*-12-Octadecatrienoic Acid on Polyunsaturated Fatty Acid Metabolism, Eicosanoid Production and Blood Pressure of Rats, *Br. J. Nutr. 72*, 775–783.
25. Lai, L.T., Naiki, M., Yoshida, S.H., German, J.B., and Gerschwin, M.E. (1994) Dietary *Platycladus orientalis* Seed Oil Suppresses Anti-Erythrocyte Autoantibodies and Prolongs Survival of NZB Mice, *Clin. Immunol. Immunopathol. 71*, 293–302.
26. Matsuo, N., Osada, K., Kodama, T., Lim, B.O., Nakao, A., Yamada, K., and Sugano, M. (1996) Effects of Gamma-Linolenic Acid and Its Positional Isomer Pinolenic Acid on Immune Parameters of Brown-Norway Rats, *Prostaglandins Leukotrienes Essent. Fatty Acids 55*, 223–229.
27. Yoshida, S.H., Siu, J., Griffey, S.M., German, J.B., and Gerschwin, M.E. (1996) Dietary *Juniperis virginiensis* (*sic*) Seed Oil Decreased Pentobarbital-Associated Mortalities Among DBA/1 Mice Treated with Collagen-Adjuvant Emulsions, *J. Lipid Mediat. Cell. Signal. 13*, 283–293.
28. Chavali, S.R., Weeks, C.E., Zhong, W.W., and Forse, R.A. (1998) Increased Production of TNF-α and Decreased Levels of Dienoic Eicosanoids, IL-6 and IL-10 in Mice Fed Menhaden Oil and Juniper Oil Diets in Response to an Intraperitoneal Lethal Dose of LPS, *Prostaglandins Leukotrienes Essent. Fatty Acids 59*, 89–93.
29. Asset, G., Staels, B., Wolff, R.L., Baugé, E., Fruchart, J.C., and Dallongeville, J. (1999) Effects of *Pinus pinaster* and *Pinus koraiensis* Seed Oil Supplementation on Lipoprotein Metabolism in Rats, *Lipids 34*, 39–44.
30. Wolff, R.L. (1997) New Tools to Explore Lipid Metabolism, *INFORM 8*, 116–119.
31. Wolff, R.L., Marpeau, A.M., Gunstone, F.D., Bézard, J., Farines, M., Martin, J.C., and Dallongeville, J. (1997) Particularités Structurales et Physiologiques d'Huiles Nouvelles, les Huiles de Graines de Conifères, *Oléagineux 4*, 65–70 (in French).
32. Aitzetmüller, K. (1998) *Komaroffia* Oils—An Excellent New Source of Δ5-Unsaturated Fatty Acids, *J. Am. Oil Chem. Soc. 75*, 1897–1899.
33. Takagi, T., and Itabashi, Y. (1982) *cis*-5 Olefinic Unusual Fatty Acids in Seed Lipids of Gymnospermae and Their Distribution in Triacylglycerols, *Lipids 17*, 716–723.
34. Groenewald, E.G., and van der Westhuizen, J. (1997) Prostaglandins and Related Substances in Plants, *Bot. Rev. 63*, 199–220.
35. Jamieson, G.R., and Reid, E.H. (1972) The Leaf Lipids of Some Conifer Species, *Phytochemistry 11*, 269–275.
36. Wolff, R.L., Christie, W.W., and Coakley, D. (1997) The Unusual Occurrence of 14-Methylhexadecanoic Acid in Pinaceae Seed Oils Among Plants, *Lipids 32*, 971–973.
37. Little, E.L., Jr., and Critchfield, W.B. (1969) *Subdivision of the Genus* Pinus *(Pines)*, U.S. Department of Agriculture, Forest Service, Miscellaneous Publication No. 1144, Washington, DC, 51 pp.
38. Debazac, E.B. (1964) *Manuel des Conifères*, Ecole Nationale des Eaux et Forêts, Nancy, pp. 23–112 (in French).
39. Mirov, N.T. (1961) *Composition of Gum Turpentines of Pines*, U.S. Department of Agriculture, Forest Service Technical Bulletin No. 1239, Washington, DC, 158 pp.
40. Critchfield, W.B. (1986) Hybridization and Classification of the White Pines (*Pinus* Section *Strobus*), *Taxon 35*, 647–656.
41. Klaus, W. (1989) Mediterranean Pines and Their History, *Plant Syst. Evol. 162*, 133–163.
42. Farjon, A., and Styles, B. (1997) Pinus *L. (Pinaceae)*, *Flora Neotropica* Monograph 75, New York Botanical Garden, Bronx, New York.
43. Malusa, J. (1992) Phylogeny and Biogeography of the Pinyon Pines (*Pinus* subsect. *Cembroides*), *Syst. Bot. 17*, 42–66.
44. Strauss, S.H., and Doerksen, A.H. (1990) Restriction Fragment Analysis of Pine Phylogeny, *Evolution 44*, 1081–1096.
45. Wang, X.-R., and Szmidt, A.I. (1993) Chloroplast DNA-Based Phylogeny of Asian *Pinus* Species (*Pinaceae*), *Plant Syst. Evol. 188*, 197–211.
46. Chaw, S.-M., Zharkikh, A., Sung, H.-M., Lau, T.-C., and Li, W.-H. (1997) Molecular Phylogeny of Extant Gymnosperms and Seed Plant Evolution: Analysis of Nuclear 18S rRNA Sequences, *Molec. Biol. Evol. 14*, 56–60.
47. Carlisle, A. (1958) A Guide to the Named Variants of Scots Pine (*Pinus sylvestris* Linnaeus), *Forestry (Oxford) 31*, 203–224.
48. Christensen, K.I. (1987) Taxonomic Revision of the *Pinus mugo* Complex and *P. × rhaetica* (*P. mugo × sylvestris*) (*Pinaceae*), *Nord. J. Bot. 7*, 383–408.
49. Tillman-Sutela, E., Johanson, A., Laakso, R., Mattila, T., and Kallio, H. (1995) Triacylglycerols in the Seeds of Northern Scots Pine, *Pinus sylvestris* L. and Norway Spruce, *Picea abies* (L.) Karst, *Trees 10*, 40–45.
50. Wolff, R.L., Pédrono, F., and Marpeau, A.M. (1999) Fatty Acid Composition of Edible Pine Seeds with Emphasis on North American and Mexican Pines of the *Cembroides* Subsection, *Oléagineux 6*, 107–110.
51. Hirata, Y., Sekiguchi, R., Saitoh, M., Kubota, K., and Kayama,

M. (1994) Components of Pine Seed Lipids, *Yukagaku 43*, 579–582 (in Japanese).
52. Imbs, A.B., and Pham, L.Q. (1996) Fatty Acids and Triacylglycerols in Seeds of Pinaceae Species, *Phytochemistry 42*, 1051–1053.
53. Kim, S.-J., Kim, G.-S., Yi, M.-O., and Joh, Y.-G. (1992) Fatty Acid Compositions of Some Seed Oils from the *Pinaceae* Family, *J. Korean Oil Chem. Soc. 9*, 149–156 (in Korean).
54. Hu, Z.-L., Li, X.-P., and Bao, H. (1992) Distribution of Fatty Acids from the *Pinus* Seed Oils and the Chemotaxonomic Survey, *J. Plant Res. Environ. (Zhiwu Ziyuan Yu Huanjing) 1*, 15–18 (in Chinese).
55. Wolff, R.L., and Bayard, C.C. (1995) Fatty Acid Composition of Some Pine Seed Oils, *J. Am. Oil Chem. Soc. 72*, 1043–1046.
56. Wolff, R.L., and Marpeau, A.M. (1997) Δ5-Olefinic Acids in the Edible Seeds of Nut Pine (*Pinus cembroides edulis*) from the United States, *J. Am. Oil Chem. Soc. 74*, 613–614.
57. Wolff, R.L. (1998) A Practical Source of Δ5-Olefinic Acids for Identification Purposes, *J. Am. Oil Chem. Soc. 75*, 891–892.
58. Imbs, A.B., Nevshupova, N.V., and Pham, L.Q. (1998) Triacyl Composition of *Pinus koraiensis* Seed Oil, *J. Am. Oil Chem. Soc. 75*, 865–870.
59. De Ferré, Y. (1966) Validité de l'Espèce *Pinus pumila* et Affinités Systématiques, *Bull. Soc. Hist. Nat. Toulouse 102*, 351–356 (in French).
60. Zavarin, E., Snajberk, K., and Cool, L. (1990) Chemical Differentiation in Relation to the Morphology of the Single-Needle Pinyons, *Biochem. Syst. Ecol. 18*, 125–137.
61. Sagrero-Nieves, L. (1992) Fatty Acid Composition of Mexican Nut (*Pinus cembroides*) from Three Seed Coat Phenotypes, *J. Sci. Food Agric. 59*, 413–414.
62. Zavarin, E. (1987) Taxonomy of Pinyon Pines, in *Proceedings of Il Simposio Nacional sobre Pinos Piñoneros* (Passini, M.F., Tovar, D.C., and Eguiluz Piedra, T., eds.), pp. 29–40, CEMCA, Mexico City, Mexico.
63. Janick, J., Cabral Velho, C., and Whipkey, A. (1991) Developmental Changes in Seeds of Loblolly Pine, *J. Am. Soc. Hort. Sci. 116*, 297–301.
64. Laseter, J.L., Lawler, G.C., Walkinshaw, C.H., and Weete, J.D. (1972) Fatty Acids of *Pinus elliottii* Tissues, *Phytochemistry 12*, 817–821.
65. Yazicioglu, T., and Karaali, A. (1983) On the Fatty Acid Composition of Turkish Vegetable Oils, *Fette Seifen Anstrichm. 85*, 23–29.
66. Ickert-Bond, S.M. (1997) *Pinus krempfii* Lec.—A Vietnamese Conifer with Problematic Affinities, *Am. J. Bot. 84*, 203 (abstract).
67. Frankis, M.P. (1988) Generic Inter-Relationships in Pinaceae, *Notes RBG Edinb. 45*, 527–548.
68. Hart, J.A. (1987) A Cladistic Analysis of Conifers: Preliminary Results, *J. Arnold Arbor. 68*, 269–307.
69. Price, R.A., and Olsen-Stojkovich, J. (1987) Relationships Among the Genera of Pinaceae: An Immunological Comparison, *Syst. Bot. 12*, 91–97.
70. Prager, E.M., Fowler, D.P., and Wilson, A. (1976) Rates of Evolution in Conifers (Pinaceae), *Evolution 30*, 637–649.
71. Suzuki, M. (1979) The Course of Resin Canals in the Shoots of Conifers. III. Pinaceae and Summary Analysis, *Bot. Mag. Tokyo 92*, 333–353.
72. Aitzetmüller, K., and Tsevegsüren, N. (1994) Seed Fatty Acids, "Front-End"-Desaturases and Chemotaxonomy—A Case Study in the Ranunculaceae, *J. Plant Physiol. 143*, 538–543.
73. Berger, J.J. (1999) Additif Alimentaire, Composition Cosmétique et Médicament à Base d'Huile de Graines de Pin, French Patent 96 14794.
74. Medvedev, F.A., Kilakova, S.J., and Levatchev, M.M. (1992) Characteristics of Fatty Acid Composition of Pine Kernels in Siberia and Far East, *Voprosy Pitania 2*, 70–71 (in Russian).

[Received September 21, 1999, and in final revised form December 7, 1999; revision accepted December 8, 1999]

ARTICLE

The Biosynthesis of Oxylipins of Linoleic and Arachidonic Acids by the Sewage Fungus *Leptomitus lacteus*, Including the Identification of 8*R*-Hydroxy-9*Z*,12*Z*-octadecadienoic Acid

Simon R. Fox*, Arzu Akpinar[1], Asmita A. Prabhune[2], John Friend, and Colin Ratledge

University of Hull, Department of Biological Sciences, Hull HU6 7RX, United Kingdom

ABSTRACT: When the sewage fungus *Leptomitus lacteus* was grown in liquid culture aerobically and then transferred to medium containing long-chain fatty acids, it produced a number of oxygenated fatty acids. From linoleic acid (18:2n-6), the major metabolite produced was *R*-8-hydroxy-9*Z*,12*Z*-octadecadienoic acid (8*R*-HODE), with additional quantities of 8,11-di-HODE, 11,16-di-HODE, and 11,17-di-HODE. Other fatty acid derivatives identified included 7-HODE, 10-HODE, and 13-hydroxy-octadecamonoenoic acid. Arachidonic acid (20:4n-6) was metabolized primarily to 18- and 19-hydroxy-eicosatetraenoic acids (18- and 19-HETE) also as *R* enantiomers, along with smaller quantities of 17-HETE, 9-HETE, 14,15-dihydroxy-eicosatrienoic acid and 11,12,19-trihydroxy-eicosatrienoic acid. The oxygenated products of long-chain fatty acids, in particular the biosynthesis of 8*R*-HODE, a compound classified as a precocious sporulation inducer, were similar to those produced by an unrelated fungal species in the Ascomycota, the take-all fungus *Gaeumannomyces graminis.* As in *G. graminis*, the biotransformation of linoleate to 8*R*-HODE was not significantly inhibited by exposure of the organism to CO. This indicated that the enzyme responsible for 8*R*-HODE biosynthesis in *Leptomitus* could be similar to that of *G. graminis*; yet we did not detect 7,8-di-HODE as a product of 18:2n-6 metabolism as in *G. graminis*. CO did inhibit the biosynthesis of 14,15-di-HETE, 18-HETE, and 19-HETE in *L. lacteus*, which suggested the involvement of a cytochrome P_{450}-type monooxygenase. The biosynthesis of 8*R*-HODE from 18:2n-6 was found to occur in certain cell lysates, specifically in low speed (15,000 × *g*) supernatant, following cell disruption.

Paper no. L8339 in *Lipids 35*, 23–30 (January 2000).

Oxygenated long-chain fatty acids, known as oxylipins, are increasingly being identified as products of fungal fatty acid metabolism, and some evidence suggests that their biosynthesis may be associated with important features of the fungal life cycle such as changes from asexual to sexual reproduction (1). Some unusual oxylipins have been isolated from *Gaeumannomyces graminis*, a pathogen of agricultural crops, and these compounds have been implicated in the pathogenicity of this fungus (2). One of these fatty acids is 8-hydroxy-octadecadienoic acid (8*R*-HODE); this compound has some potent effects and is one of several sporulation factors in the ascomycete *Aspergillus nidulans* (3; 8*R*-HODE is categorized as a psi, otherwise known as a precocious sporulation inducer). The compound is secreted by the basidiomycete fungus *Laetisaria arvalis* and is fungicidal to some plant pathogenic strains of *Pythium ultimum* (4). This effect was later shown not to be affected by the enantiomeric composition of the 8-HODE.

Oomycetes are mostly aquatic fungi and characteristically contain eicosanoids. The oxygenated derivatives of C_{20} fatty acids have been extensively studied in mammalian tissues where they participate in a multitude of physiological processes (5). Among the Oomycetes, species such as *Saprolegnia parasitica* and *S. diclina* possess a 15-lipoxygenase, and in both fungi this results in the biosynthesis of significant quantities of oxygenated fatty acids during vegetative growth (6; Akpinar, A., Fox, S.R., Friend, J., and Ratledge, C., unpublished results).

*To whom correspondence should be addressed at Department of Brassica and Oilseeds Research, John Innes Centre, Norwich Research Park, Norwich, NR4 7UH, United Kingdom.
E-mail: Simon.Fox@bbsrc.ac.uk.
[1]Current address: Department of Food Engineering, The University of Uludag, Bursa, Turkey.
[2]Current address: Department of Biotechnology, The National Chemical Laboratory, Pune 4110088, India.

Abbreviations: 16:0, palmitic acid; 18:1n-6, 9*Z*-oleic acid; 18:2n-6, 9*Z*,12*Z*-linoleic acid; 20:4n-6, 5*Z*,8*Z*,11*Z*,14*Z*-eicosatetraenoic acid; EI, electron impact; GC–MS, gas chromatography–mass spectrometry; 9-HETE, 9-hydroxy-5*Z*,7*Z*,11*Z*,14*Z*-eicosatetraenoic acid; 17-HETE, 17-hydroxy-5*Z*,8*Z*,11*Z*,14*Z*-eicosatetraenoic acid; 18-HETE, 18-hydroxy-5*Z*,8*Z*,11*Z*,14*Z*-eicosatetraenoic acid; 19-HETE, 19-hydroxy-5*Z*,8*Z*,11*Z*,14*Z*-eicosatetraenoic acid; 14,15-HETriE, 14,15-dihydroxy-5*Z*,8*Z*,11*Z*-eicosatrienoic acid; 11,12,19-HETriE, 11,12,19-trihydroxy-5*Z*,8*Z*,14*Z*-eicosatrienoic acid; 7-HODE, 7-hydroxy-9*Z*,12*Z*-octadecadienoic acid; 8-HODE, 8-hydroxy-9*Z*,12*Z*-octadecadienoic acid; 10-HODE, 10-hydroxy-8*Z*,12*Z*-octadecadienoic acid; 16-HODE, 16-hydroxy-9*Z*,12*Z*-octadecadienoic acid; 8,11-di-HODE, 8,11-dihydroxy-9*Z*,12*Z*-octadecadienoic acid; 11,16-di-HODE, 11,16-dihydroxy-9*Z*,12*Z*-octadecadienoic acid; 11,17-di-HODE; 11,17-dihydroxy-9*Z*,12*Z*-octadecadienoic acid; 13-HOME, 13-hydroxy-9*Z*-octadecamonoenoic acid; 9,10-di-HOME; 9,10-dihydroxy-12*Z*-octadecamonoenoic acid; 12,13-di-HOME, 12,13-dihydroxy-9*Z*-octadecamonoenoic acid; HPLC, high-performance liquid chromatography; LDS, linoleate diol synthase; MS, mass spectrometry; NDGA, nordihydroguaiaretic acid; sp. act., specific activity; TLC, thin-layer chromatography; TMSO, trimethyl silyl ester.

Achlya ambisexualis, also in the same family, accumulates cyclooxygenase-type products in both vegetative and sexual stages of development (7); but despite the capacity for oxylipin biosynthesis by fungi, little is known about the potential physiological roles that such compounds might play in fungal life cycles. *Leptomitus lacteus*, classified as another Oomycete, is a member of a small order, the Leptomitales, and is found in large rivers and lakes, especially those with a high acid content where there tends to be sewage contamination (8,9). As part of a survey of secondary fatty acid metabolism in the Oomycetes, we have carried out an investigation into the capacity of *L. lacteus* to biotransform long-chain fatty acids.

MATERIALS AND METHODS

Growth conditions. *Leptomitus lacteus* (IMI 308.102) was obtained from The International Mycological Institute, (Surrey, United Kingdom). The organism was purified from bacterial contamination and maintained on Rose Bengal agar at 10°C. Stock cultures were kept on potato/dextrose/agar slants and subcultured every 2–3 mon. Inocula were taken from mycelial mats and grown for 48 h to the late stationary phase in 250-mL conical flasks. Each flask contained 50 mL of growth medium comprising: (g/L) glucose, 10; KH_2PO_4, 7; Na_2HPO_4, 2; defatted yeast extract, 1.5; diammonium tartrate, 2; $CaCl_2{\cdot}H_2O$, 0.5; $FeSO_4{\cdot}7H_2O$, 0.1; $ZnSO_4{\cdot}7H_2O$, 0.01; $MnSO_4{\cdot}2H_2O$, 0.001; $CuSO_4{\cdot}5H_2O$, 0.0005; pH 6. A starter culture was used to inoculate (at 2% vol/vol) conical flasks (1 L) containing 500 mL growth medium (as described) or an identical medium containing safflower oil (10 g/L) instead of glucose. In all experiments, *L. lacteus* cultures were routinely maintained under aerobic conditions at 10°C and 160 rev/min.

Addition of fatty acids. After 48 h growth in liquid culture, cells were separated from the growth medium by filtration and washed with 100–200 mL sterile water. The resulting mycelial mat (5 g wet wt) was reinoculated into 50 mL Tris/HCl buffer (50 mM), pH 7.5. Cultures received 10 mg linoleic acid (18:2n-6, Na salt) or 10 mg arachidonic acid (5*Z*,8*Z*,11*Z*,14*Z*-eicosatetraenoic acid, Na salt) in 200 µL ethanol. The cultures were then incubated for 1 h before extraction of oxygenated fatty acids.

Addition of inhibitors. In the first series of experiments, aimed at inhibiting potential enzymes of oxylipin biosynthesis, aspirin, indomethacin, aesculetin and nordihydroguaiaretic acid (NDGA) were individually included at 1 mM with either 10 mg 18:2n-6 (containing 3.7 kBq [1-^{14}C]18:2n-6, sp. act. 2.04 GBq/mmol), (all isotopes were obtained from Amersham International, Buckinghamshire, United Kingdom), or 10 mg arachidonic acid (20:4n-6) (containing 3.7 kBq [1-^{14}C]20:4n-6, sp. act. 2.04 GBq/mmol) and incubated for 1 h before extraction of fatty acid derivatives (see below). Control experiments were carried out using hyphae which had been boiled in 50 mM Tris/HCl, pH 7.5 for 10 min prior to incubation with [1-^{14}C]18:2n-6 or [1-^{14}C]20:4n-6. In a second series of inhibitor experiments, after the addition of 10 mg [1-^{14}C]18:2n-6 (as above) or similarly 10 mg [1-^{14}C]20:4n-6, carbon monoxide (CO) was bubbled through the cultures (at 1 mL min^{-1}) for either 1 or 10 min. Cultures were then removed from the CO chamber and incubated as before for 30 min before extraction of labeled fatty acid derivatives.

Extraction of fatty acids. Cells were separated from the buffer and fatty acid by filtration through Whatman No. 1 paper and weighed (wet weight). They were then resuspended in ethanol (8 parts ethanol/1 part cells, vol/vol) and homogenized in an Atomix blender (MSE; Fisher Scientific, Loughborough, United Kingdom) for 3 min. The slurry was stirred at 4°C for 24 h after which the mixture was filtered, and the resulting ethanolic solution was concentrated to dryness. The residue was saponified by resuspension in 10 mL 4 M NaOH and left at room temperature overnight (10). The hydrolyzed solution was subsequently adjusted to pH 1 with 6 M HCl and the fatty acids were extracted into 40 mL chloroform. The chloroform phase was concentrated to form the cell extract.

The Tris/HCl buffer in which *L. lacteus* had been incubated with fatty acids (from which cells had been removed by filtration) was adjusted to pH 3.0 with 0.14 M formic acid, and the fatty acids were extracted into an equal volume of chloroform. The chloroform phase was evaporated and the residue saponified (as described above), forming the medium extract.

The chloroform-extracted material from both the cell and culture medium extracts was methylated with diazomethane and also derivatized to methyl silyl ethers (11). Qualitative analysis of fatty acids was carried out using a Finnegan series 1020 automated gas chromatograph–mass spectrometer (GC–MS) operating in the electron impact (EI) mode. The GC parameters were: HP-1 30 m fused-silica capillary column (Hewlett-Packard, Palo Alto, CA), 0.25 mm i.d., 0.25 µm coating; helium carrier gas at 5.06×10^5 Pa head pressure; 10:1 split; injector temperature, 240°C; initial temperature, 220°C; initial time, 5 min; ramp rate, 5°C min^{-1}; final temperature, 280°C; final time, 10 min; injection volume, 1 µL. MS parameters were: source temperature, 240°C; manifold temperature, 100°C; ionization current, 0.30 A.

Chiral analysis. The cell and medium extracts containing fatty acids in chloroform were purified on amino-propyl Sep-Pak cartridges (500 mg) (Millipore Corp., Milford, MA). The cartridges were equilibrated with 5 mL hexane, and the cell or culture medium fatty acid extracts were applied in 200 µL chloroform. After an initial wash with 10 mL chloroform/propan-2-ol (2:1, vol/vol), monohydroxylated and unsubstituted fatty acids were eluted with 10 mL diethyl ether (containing 2% acetic acid by volume). Di- and trihydroxylated fatty acids were eluted with 10 mL methanol. The ethereal phases from the Sep-Pak cartridges were concentrated to dryness before resuspension of the residues in 50% aqueous acetonitrile. Monohydroxylated fatty acids were purified by high-performance liquid chromatography (HPLC) on a semipreparative LiChroprep 25-40 RP C18 column (250 × 10 mm; Chrompack International, Middelburg, The Netherlands). HPLC conditions comprised an isocratic gradient of 0.017 M H_3PO_4/acetonitrile (1:1, vol/vol) at a flow rate of 2 mL min^{-1}; hydroxylated fatty acids were monitored at 192 nm and fractions collected.

The chirality of 8-HODE was determined by Dr. M. Ham-

berg at the Karolinska Institute, Stockholm, Sweden. In short, the methyl ester of 8-HODE was derivatized to its (−)-menthoxycarbonyl analog, subjected to oxidative ozonolysis, and methylated (12,13). The corresponding racemic standard was then separated into *R* and *S* enantiomers by GC and compared with derivatized 8-HODE from *L. lacteus*.

Chiral analysis of certain monohydroxylated derivatives of 20:4n-6 was carried out by derivatization to naphthyl ester methyl esters (14). The enantiomers were separated by HPLC on an Apex Chiral AU 50 column (4.6 × 250 mm; Jones Chromatography, Glamorgan, United Kingdom). HPLC conditions comprised an isocratic gradient of 1% propan-2-ol in *n*-hexane with a flow rate of 1.0 mL/min and detection of peaks at 192 nm. In this system, the *R* enantiomers elute before *S* enantiomers (14). This was confirmed in the current study by using a standard naphthyl ester methyl ester of 3-hydroxyeicosatetraenoic acid (3-HETE), where chirality was previously established as an enantiomeric ratio of 95:5 (*R*/*S*) (Hamberg, M., personal communication); 3-HETE was purified from cultures of the yeast *Dipodascopsis uninucleata* metabolizing 20:4n-6 (15).

Quantitative analysis of oxylipins. In experiments in which [1-^{14}C]18:2n-6 or [1-^{14}C]20:4n-6 was used, fatty acids from the diethyl ether and methanol fractions of amino-propyl Sep-Pak cartridges were separated by thin-layer chromatography (TLC). Quantitative determinations of ^{14}C-labeled oxylipins were made using a Bioscan Autochanger 4000 (Bioscan Inc., Washington, DC). ^{14}C-monohydroxylated fatty acids were detected by running the diethyl ether fractions on silica gel plates (Autofolien, Kieselgel 60; Merck, Darmstadt, Germany) developed with petroleum ether (60–80°C)/diethyl ether/acetic acid (50:50:1, by vol). [1-^{14}C]Di- and trihydroxy fatty acids were detected by running the methanol fractions on silica gel TLC plates developed with the organic phase of ethyl acetate/2,2,4; trimethylpentane/acetic acid/water (110:50:20:100, by vol).

Preparation of cell lysates and microsomes. The fungus was separated from the medium of safflower oil-grown cultures and rinsed with Tris/HCl buffer (50 mM, pH 7.5). The cells were weighed and resuspended in two parts of the buffer (wet wt/vol). Cell rupture was achieved by two passages through a precooled French pressure cell. The homogenate was centrifuged at 15,000 × *g* for 30 min to precipitate whole cells, cell debris, and unwanted organelles. The low-speed supernatant (the cytosolic fraction) was centrifuged at 100,000 × *g* for 60 min to obtain microsomes and a high-speed supernatant (solubilized membrane components); the microsomes were dissolved in 2 mL 50 mM Tris/HCl pH 7.5. The cytosolic fraction, the microsomes, and the high-speed supernatant were each incubated with 0.1 mg 18:2n-6 or 0.1 mg 20:4n-6 (all in a final volume of 2 mL) in the presence and absence of 1 mM NADPH for 20 min. Reactions were terminated by adding ethanol (4 vol) and fatty acids extracted as before. The fatty acid derivatives were identified by GC–MS.

RESULTS AND DISCUSSION

Growth of Leptomitus. *Leptomitus lacteus* produced only vegetative structures on both the glucose and the safflower media. We did not observe oogonium formation in any culture, even when we monitored growth over longer periods of time of up to 4–5 wk. The formation of sexual structures, as far as we are aware, is unknown in this fungus. The hyphae appeared septate but they were, in fact, pseudoseptate; cellulin plugs cause the constrictions, which is a characteristic feature of this organism (16). The fungus grew more vigorously on safflower oil (5–10 g cells/L) than on glucose-based medium (<1 g cells/L). This led us to use *L. lacteus* cultured on safflower oil for experiments investigating oxylipin biosynthesis from exogenously added fatty acids. In a previous report (8), sugars were found to be unable to support growth of *L. lacteus*. Our findings were to the contrary, but we have no explanation for this other than the composition of the nutrient medium we used may have been different or perhaps different strains of *L. lacteus* exist.

Biotransformation of fatty acids. The following oxygenated fatty acids were all extracted from the medium extracts and qualitative determination made by GC–MS. The ion fragments of fatty acids are listed with our interpretation of likely structures.

Oxylipins of 18:2n-6. (i) 8-HODE. Scan no. 650 (scan nos. for 18:2n-6 refer to Fig. 1). The most abundant peak of the total ion chromatogram, the mass spectrum of the compound (Fig. 2) produced ions at *m*/*z* 382 [M^+], 367 [$M^+ - 15$; loss of a methyl group on the silyl derivative], 351 [$M^+ - 31$], 335 [possibly $(M^+ + 1) - 48$; loss of OCH–CH_2–CH_3], 311 [$M^+ - 71$; loss of $(CH_2)_4$–CH_3], 292 [$M^+ - 90$; loss of silyl group], 284 [possibly $(M^+ - 1) - 97$; loss of CH=CH–$(CH_2)_4$–CH_3], 271 [possibly a split at C_{10} representing CH=CH–$(CH_3)_3SiO^+$ =CH–$(CH_2)_6$–$COOCH_3$], 261 [possibly $M^+ - (31 + 90)$], 245 [split between C_8 and C_9; $(CH_3)_3SiO^+$=CH–$(CH_2)_6$–$COOCH_3$], 239 [fragmentation between C_7 and C_8 with the loss of CH–[OSi-$(CH_3)_3$]CH=CH–CH_2–CH=CH–$(CH_2)_4$–CH_3; indicative of a hydroxyl group at C_8], and 149 (possibly 239 − 90). The base ion, as in all mass spectra reported, was 73. The mass spectrum and abundance of ions were similar to that for 8*R*-HODE (8-hydroxy-9*Z*,12*Z*-octadecadienoic acid) from *G. graminis* (2). The conversion of exogenously supplied 18:2n-6 to 8-HODE was in the region of 10% as judged from the total ion chromatogram (result not shown).

(ii) 10-HODE. Scan no. 673. *m*/*z* 382 [M^+], 367 [$M^+ -15$], 311 [$M^+ -71$], 271 [the major fragment, representing cleavage from C_{10} to C_1 with hydroxyl group at C_{10} and the double bond shifting to C_8], 261 [$M^+ - (31 + 90)$], 239 [$M^+ - 143$; representing CH=CH–CH(OSi$(CH_3)_3$–CH_2–CH=CH–$(CH_2)_4$–CH_3], 181 [271 − 90], 149 [239 − 90], 129 [possibly $(CH_3)_3SiO^+$= CH–CH=CH_2], and 111 [$M^+ - 271$].

(iii) 7-HODE. Scan no. 697. *m*/*z* 382 [M^+], 367 [$M^+ - 15$], 334 [$M^+ - 48$], 311 [$M^+ - 71$], 292 [$M^+ - 90$], 284 [possibly $(M^+ - 1) - 97$], 261 [$M^+ - (31 + 90)$, 253 [split between C_6 and C_7 representing $(CH_3)_3SiO^+$=CH–CH_2–CH=CH–CH_2–CH= CH–$(CH_2)_4$–CH_3], 231 [split between C_7 and C_8; $(CH_3)_3SiO^+$= CH–$(CH_2)_5COOCH_3$; indicates hydroxyl group at C_7], and 151 [$M^+ - 231$]. The mass spectrum contained several ions we were not able to assign, notably *m*/*z* 225.

(iv) 13-Hydroxy-9Z-octadecamonoenoic acid (13-HOME).

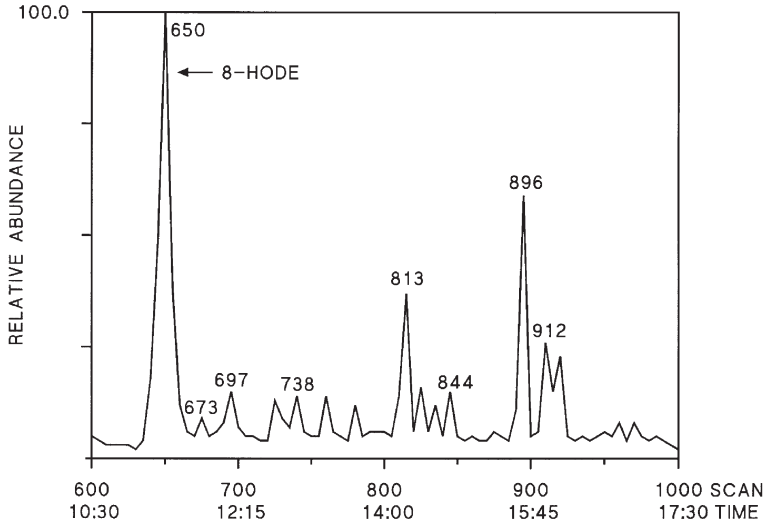

FIG. 1. Partial total ion current chromatogram (with scan numbers) of methyl and silyl derivatives of 18:2n-6 extracted from cultures of *Leptomitus lacteus*. 8-HODE, 8-hydroxy-9*Z*,12*Z*-octadecadienoic acid.

Scan no. 724. *m/z* 384 [M^+], 369 [$M^+ - 15$], 294 [$M^+ - 90$], 313, [$(CH_3)_3SiO^+$=CH–$(CH)_2$–CH=CH–$(CH_2)_7$–$COOCH_3$; cleavage from C_1 to C_{13} indicating a hydroxyl group at C_{13}], 294 [$M^+ - 90$], 223 [$M^+ - (90 + 71)$, 211 [split between C_{12} and C_{13} with loss of $(CH_2)_2$–CH=CH–$(CH_2)_7COOCH_3$], 187 [possibly 173 + CH_2], and 173 [the major ion fragment with cleavage from C_{13} to C_{18} representing $(CH_3)_3SiO^+$=CH–$(CH_2)_4$–CH_3].

(v) 16-HODE. Scan no. 738. *m/z* 382 [M^+], 367 [$M^+ - 15$], 353 [cleavage between C_1 and C_{16} with hydroxyl group at C_{16}; $(CH_3)_3SiO^+$=CH–$(CH_2)_2$–CH=CH–CH_2–CH=CH–$(CH_2)_7$–$COOCH_3$], 292 [$M^+ - 90$], 251 [loss of C_{16} to C_{18}; $(CH_3)_3SiO^+$=CH–CH_2–CH_3], and 131 [the major ion fragment with cleavage from C_{16} to C_{18}]

(vi) 8,11-di-HODE. Scan no. 813. *m/z* 470 [M^+], 455 [$M^+ - 15$], 439 [$M^+ - 31$], 399 [$M^+ - 71$], 380 [$M^+ - 90$], 373 [cleavage between C_{11} and C_{12}], 327 [$M^+ - 143$; cleavage between C_7 and C_8 with loss of $(CH_2)_6$–$COOCH_3$], 309 [$M^+ - (71 + 90)$], 271 [cleavage between C_{10} and C_{11} with hydroxyl group at C_8; CH=CH–CH(OSi$(CH_3)_3$)–$(CH_2)_6COOCH_3$], 245 [cleavage at C_8 to C_1 with the loss of $(CH_3)_3SiO^+$=CH–$(CH_2)_6$–$COOCH_3$; indicated a hydroxyl group at C_8], 237 [possibly 327–90], 225 [C_9 to C_{18} fragment], 199 [$M^+ - 271$], and 147 [possibly 237 – 90].

(vii) 9,10-di-HOME. Scan no. 832. *m/z* 472 [M^+], 457 [$M^+ - 15$], 441 [$M^+ - 31$], 382 [$M^+ - 90$], 361 [possible cleavage from C_{10} to C_1 with loss of $(CH_3)_3SiO^+$=CH–CH(OSi$(CH_3)_3$–$(CH_2)_7$–$COOCH_3$, indicating the existence of two hydroxyl groups between C_1 and C_{10}], 271 [361 – 90], 259 [cleavage at C_9 to C_1; $(CH_3)_3SiO^+$=CH–$(CH_2)_7$–$COOCH_3$, indicating a hydroxyl group at C_9], 213 [$M^+ - 259$], and 111 [$M^+ - 361$].

(viii) 12,13-di-HOME. Scan no. 844. *m/z* 472 [M^+], 457 [$M^+ - 15$], 382 [$M^+ - 90$], 299 [cleavage from C_{12} to C_1 with hydroxyl group at C_{12}; $(CH_3)_3SiO^+$=CH–CH_2–CH=CH–$(CH_2)_7$–$COOCH_3$], 275 [loss of fragment C_{12} to C_{18}; $(CH_3)_3SiO^+$=CH–CH(OSi$(CH_3)_3$)–$(CH_2)_4$–CH_3], and 173 [loss of fragment C_{13} to C_{18} with hydroxyl group at C_{13}; $(CH_3)_3SiO^+$=CH–$(CH_2)_4$–CH_3].

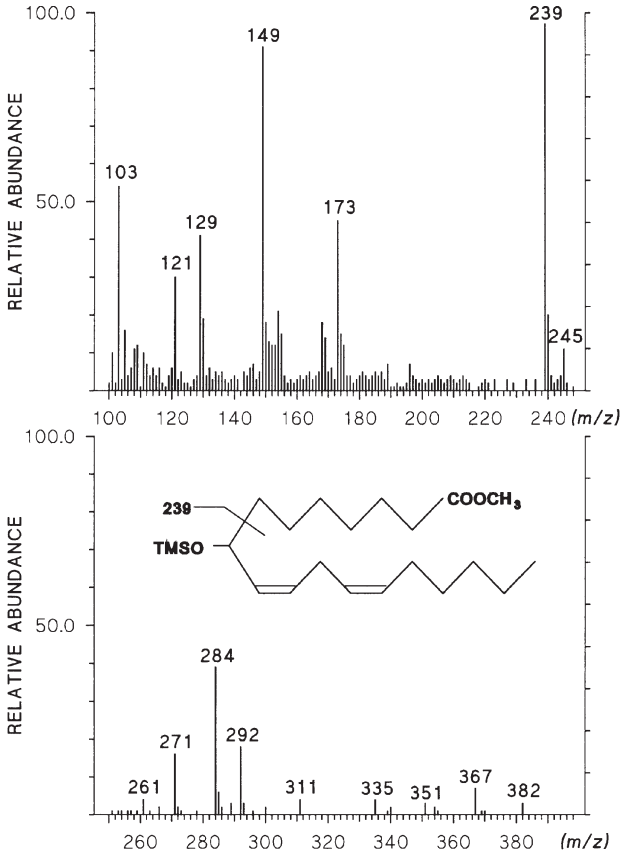

FIG. 2. Electron impact mass spectrum of the methyl ester silyl ether of 8-HODE from cultures of *L. lacteus* metabolizing 18:2n-6. TMSO, trimethyl silyl ester; see Figure 1 for other abbreviations.

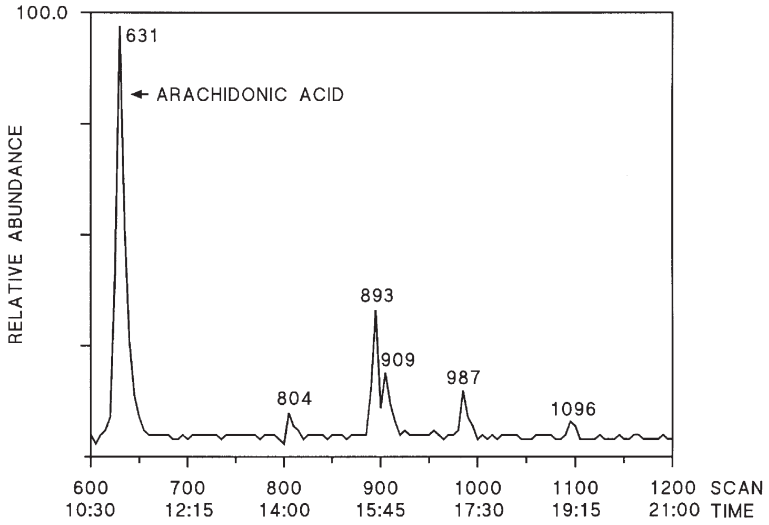

FIG. 3. Partial total ion current chromatogram of methyl ester silyl ethers of mono-, di-, and trihydroxylated derivatives of 20:4n-6 extracted from cultures of *Leptomitus lacteus.*

(ix) 11,16-di-HODE. Scan no. 896. *m/z* 470 [M^+], 455 [$M^+ - 15$], 441 [$M^+ - 29$], 439 [$M^+ - 31$], 380 [$M^+ - 90$], 287 [cleavage at C_{11} to C_{18}], 285 [possible cleavage at C_{11} to C_1; $(CH_3)_3SiO^+$=CH–CH=CH–$(CH_2)_7$–$COOCH_3$; a prominent fragment for a hydroxyl group at C_{11}], 183 [$M^+ - 287$], and 131 (cleavage from C_{16} to C_{18}; $(CH_3)_3SiO^+$=CH–CH_2–CH_3].

(x) 11,17-di-HODE. Scan no. 912. *m/z* 470 [M^+], 455 [$M^+ - 15$], 365 [possibly $M^+ - (15 + 90)$], 287 [possible cleavage between C_{10} and C_{11} with the loss of $(CH_3)_3SiO^+$=CH–CH=CH–$(CH_2)_3$–CH[OSi–$(CH_3)_3$]–CH_3], 285 [cleavage from C_{11} to C_1], 183 [$M^+ - 287$] and 117 [loss of fragment C_{17} to C_{18} with hydroxyl group at C_{17}; $(CH_3)_3SiO^+$=CH-CH_3].

Oxylipins of 20:4n-6. (i) 18-HETE. The main compound (Fig. 2, scan no. 893) produced ions at *m/z* 407 [$M^+ + 1$], 391 [$M^+ - 15$], 377 [$M^+ - 29$], 375 [$M^+ - 31$], 348 [$M^+ - 58$, possible loss of OCH-CH_2-CH_3 with migration of $(CH_3)_3SiO^+$ to the carboxyl group], 316 [$M^+ - 90$], 285 [375 – 90] and 131 [hydroxyl group at C_{18} with loss of $(CH_3)_3SiO^+$=CH–CH_2–CH_3].

(ii) 19-HETE. Scan no. 909. *m/z* 406 [M^+], 391 [$M^+ - 15$], 375 [$M^+ - 31$], 316 [$M^+ - 90$], 289 [$M^+ - 117$; cleavage between C_{18} and C_{19}], 285 [375 – 90], 254 [285 – 31], 220 [289 – 69, loss of CH_2–CH=CH–CH_2–CH_3], and 117 [hydroxyl group at C_{19} with loss of $(CH_3)_3SiO^+$=CH–CH_3]. The percentage conversion of 20:4n-6 to 18- and 19-HETE was in the region of 5%, as judged from the total ion chromatogram (Fig. 2).

(iii) 17-HETE. Scan no. 878. *m/z* 406 [M^+], 391 [$M^+ - 15$], 375 [$M^+ - 31$], 316 [$M^+ - 90$], 285 [375 – 90], 275 [$M^+ - 131$; cleavage at C_{17} to C_{18}], and 145 [$(CH_3)_3SiO^+$=CH–$(CH_2)_2$–CH_3; indicating a hydroxyl group at C_{17}].

(iv) 9-HETE. Scan no. 804. *m/z* 406 [M^+], 391 [$M^+ - 15$], 375 [$M^+ - 31$], 316 [$M^+ - 90$], 255 [a major fragment, cleavage from C_9 to C_{10} with the double bond shifting to C_7, representing $(CH_3)_3SiO^+$=CH–CH=CH–CH=CH–$(CH_2)_3$–$COOCH_3$], 183 [possibly 255 – 72] and 143 [possibly 255 – (90 + 43)].

(v) 14,15-Dihydroxy-5Z,8Z,11Z-eicosatrienoic acid (14,15-di-HETriE). Scan no. 987. *m/z* 496 [M^+], 481 [$M^+ - 15$], 424 [cleavage at C_{15} to C_{16} representing $(CH_3)_3SiO^+$=CH–$(OSi(CH_3)_3)$–CH_2–CH=CH–CH_2–CH=CH–CH_2–CH=CH–$(CH_2)_3COOCH_3$], 396 [$M^+ - 100$], 275 [cleavage from C_{14} to C_{20} with loss of $(CH_3)_3SiO^+$=CH–CH$(OSi(CH_3)_3)$–$(CH_2)_4$–CH_3], and 173 [cleavage from C_{15} to C_{20}].

(vi) 11,12,19-Trihydroxy-5Z,8Z,14Z-eicosatrienoic acid (11,12,19-tri-HETriE). Scan no. 1149. *m/z* 585 [$M^+ + 1$], 569 [$M^+ - 15$], 403 [$M^+ - 181$; cleavage between C_{10} and C_{11} with the loss of $(CH_2$–CH=CH$)_2$–$(CH_2)_3$–$COOCH_3$], 385 [cleavage between C_{12} and C_{13} with the loss of $(CH_3)_3SiO^+$=CH–CH$(OSi(CH_3)_3)$–$(CH_2$–CH=CH$)_2$–$(CH_2)_3$–$COOCH_3$], 313 [385 – 72 (possibly $(CH_3)_3Si - 1$)]; 295 [385 – 90]; 283 [cleavage at C_{11} to C_{12} with loss of $(CH_3)_3SiO^+$=CH–$(CH_2$–CH=CH$)_2$–$(CH_2)_3$–$COOCH_3$]; 223 [295 – 72]; 191 [295– (72 + 32)], and 117 [$(CH_3)_3SiO^+$=CH–CH_3].

The controls did not produce oxygenated derivatives of either 18:2n-6 or 20:4n-6. During the growth of *L. lacteus* on safflower oil, the major oxygenated fatty acid recoverable from the medium was 8-HODE, as expected. The same appeared to be the case with glucose-grown cells, until it became apparent that the 8-HODE was the product of the oxygenation of fatty acids present in the yeast extract added to the growth medium. To overcome any ambiguities this may have caused when determining the origin of fungal oxylipins, we then switched to using yeast extract which had been defatted by repeated washing with chloroform prior to its addition to the growth medium.

After the addition of exogenous fatty acids, only trace amounts of the oxylipins of 18:2n-6 or 20:4n-6 were recovered in the cell extracts. One of two explanations may account for this: either the oxylipins were exported from the cells during the metabolism of 18:2n-6 and 20:4n-6 or the enzyme responsible for 8-HODE biosynthesis and derivatives of 20:4n-6 were secreted by the cells into the growth medium. The secretion in large quantities of an enzyme of this nature, a manganese-con-

taining lipoxygenase that results in the biosynthesis of oxylipins of linoleic acid, has been reported from the take-all fungus, *G. graminis* (17).

Unusually for an organism classified as an Oomycete and for an aquatic species, eicosanoids amounted to only a small proportion of the total cellular lipids in *L. lacteus*; 20:4n-6 accounted for 0.3% of the total cellular fatty acid. The major fatty acids were 18:2n-6, constituting 40% of cellular fatty acid; 18:1n-6, constituting 35%; and 16:0, constituting 30%.

Chiral analysis. The enantiomeric composition of 8-HODE was 98% *R* and 2% *S* (Hamberg, M., personal communication). The compound thus has the same chirality as 8*R*-HODE produced by *G. graminis* (18).

The most abundant oxylipins of 20:4n-6 were 18-HETE and 19-HETE which, when converted to their naphthyl ester methyl ester derivatives, displayed two peaks by HPLC; the first to be eluted was the *R* enantiomer (e.g., 18-HETE, Fig. 4). The enantiomeric distribution was 86% *R*/14% *S* for 18-HETE and 90% *R*/10% *S* for 19-HETE. The monohydroxylated oxylipins produced by *Leptomitus* are therefore formed stereospecifically.

Inhibition of oxylipin biosynthesis. Aspirin, an inhibitor of cyclooxygenase enzymes (19), indomethacin and aesculetin, inhibitors of lipoxygenases (20), all brought about a small decrease of 12–18% in the biotransformation of 18:2n-6 to 8*R*-HODE (Table 1); this was calculated in comparison to controls in which no inhibitors were added. 8*R*-HODE, for these experiments, was detected radiochemically by TLC and ran to an R_f of 0.40. The relatively small inhibition recorded with these compounds did not seem to represent firm evidence that 8*R*-HODE was produced by a cyclooxygenase or lipoxygenase-type enzyme. The extent of the inhibition of 8*R*-HODE biosynthesis with NDGA (30%) was significantly higher and may indicate that 8*R*-HODE was synthesized by a lipoxygenase-type enzyme. NDGA, however, possesses general antioxidative properties, and so caution is necessary in interpreting this result; NDGA has been shown to inhibit certain reactions catalyzed by cytochrome P_{450} monooxygenases in rat tissues (21). These experiments were carried out using whole cells, and it may be that some of the inhibitors could have become inactivated during the incubation.

Exposure of *L. lacteus* to CO, for either 1 or 10 min, had little effect on the ability of the organism to oxygenate 18:2n-6 to 8*R*-HODE. This appeared to rule out the involvement of a cytochrome P_{450}-type enzyme in the biosynthesis of this molecule, as it is well established that enzymes of this kind are inactivated by irreversible binding of CO to the catalytic site of the enzyme. The relative insensitivity of the enzyme responsible for 8*R*-HODE biosynthesis to CO is a feature shared by the enzyme isolated from *G. graminis* and characterized as linoleate diol synthase (LDS) (22). However, the similarities between the two enzymes may end there because LDS in *G. graminis* produces 7,8-di-HODE as a major metabolite of linoleic acid, a compound that was not detected in this study. The small amount of 8*R*-HODE which was synthesized by *G. graminis* appeared to be the result of the presence of heme in the LDS, which caused the reduction of some of the 8-hydroperoxylinoleic acid to 8*R*-HODE (22), while the remainder was metabolized to 7,8-di-HODE. Clearly, more detailed experiments are required, involving purification of the enzyme, before it can be established that a dioxygenase is responsible for the biosynthesis of 8*R*-HODE in *L. lacteus*. For example, we have yet to prove that a hydroperoxide is formed as a precursor to 8*R*-HODE biosynthesis.

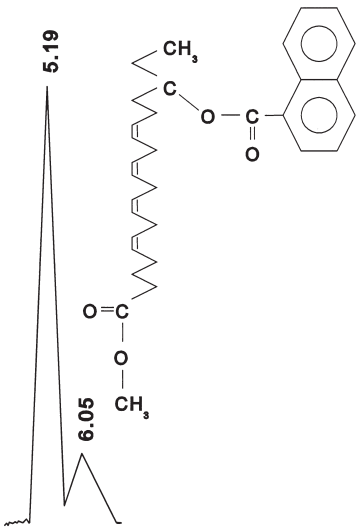

FIG. 4. Partial HPLC chromatogram (with retention times) showing the separation of the *R* (first peak) and *S* enantiomers of the naphthyl ester methyl ester derivatives of 18-hydroxy-5*Z*,8*Z*,11*Z*,14*Z*-eicosatetraenoic acid from *Leptomitus lacteus.*

Exposure of *L. lacteus* to CO for 1 min decreased the oxygenation of [1-^{14}C]20:4n-6 to 18-HETE, 19-HETE, and 14,15-di-HETE by 37% (Table 1). This value rose to 62% when the exposure of the organism to CO was increased to 10 min. Neither aspirin nor indomethacin inhibited the oxygenation of 20:4n-6 to these mono- and di-HETE to any significant extent and the inhibition with aesculetin, at 14%, was also not significant. In contrast, NDGA decreased biosynthesis of mono- and di-HETE by 82%, but as with the biotransformation of 18:2n-6 to 8*R*-HODE, this may represent a general antioxidative effect of the drug.

TABLE 1
Inhibition of the Biosynthesis of 8-HODE from 18:2n-6 and Mono- and Di-HETE of 20:4n-6 in *Leptomitus lacteus*

	Inhibition in the biosynthesis of oxylipins of 18:2n-6 and 20:4n-6[a] (%)	
Inhibitor added	8-HODE	Mono/di-HETE
Aspirin (1 mM)	12	2
Indomethacin (1 mM)	18	2
Aesculetin (1 mM)	12	14
NDGA (1 mM)	30	82
CO (1 min)	2	37
CO (10 min)	2	62

[a]Calculated in comparison to controls where no inhibitors were added. 8-HODE, 8-hydroxy-9*Z*,12*Z*-octadecadienoic acid; mono-/di-HETE, 18-hydroxy-5*Z*,8*Z*,11*Z*,14*Z*-eicosatetraenoic acid (HETE) + 19-HETE + 14,15-di-HETE; NDGA, nordihydroguaiaretic acid.

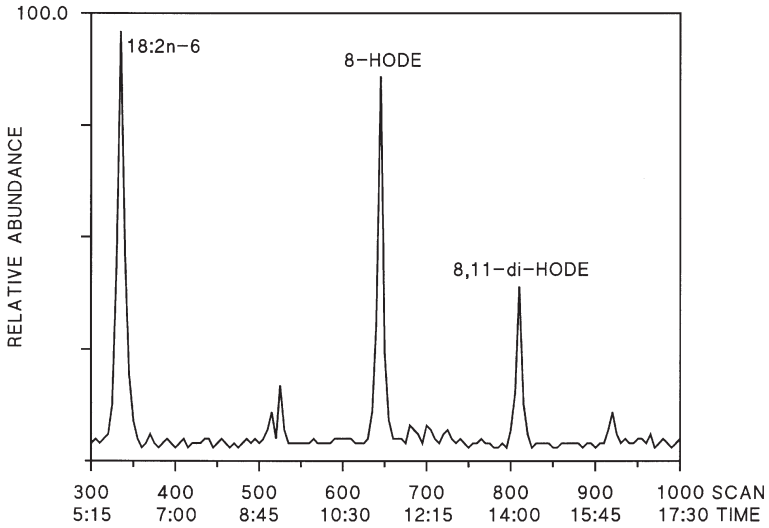

FIG. 5. Partial total ion current chromatogram of methyl and silyl derivatives of fatty acids extracted from a cell lysate low-speed supernatant (15,000 × *g*) of *Leptomitus lacteus* incubated with 18:2n-6. For abbreviation see Figure 1.

The susceptibility of the organism to CO with respect to the formation of 18-HETE, 19-HETE, and 14,15-di-HETE, as opposed to the biosynthesis of 8*R*-HODE, suggested that these reactions were catalyzed by a cytochrome P_{450} oxygenase.

Cell-free incubations. The 8*R*-HODE biosynthesis was found to occur in the supernatant from the initial centrifugation step (i.e., the cytosolic fraction; Fig. 5). The total yield of 8*R*-HODE under our incubation conditions was variable, but could be as high as 40–50%; the synthesis of 8*R*-HODE was unaffected by addition of NADPH. Other derivatives of 18:2n-6 were also produced, notably 8,11-di-HODE, as well as some uncharacterized derivatives. It therefore appeared that the enzyme synthesizing 8*R*-HODE in *L. lacteus* was probably soluble.

Our initial attempts at demonstrating cell-free 8*R*-HODE biosynthesis were unsuccessful; this may in part have been due to the presence of the widely used protease inhibitor PMSF (phenylmethanesulfonyl fluoride) in our extraction buffer (which we later eliminated). Some protease inhibitors have been reported to inhibit the biosynthesis of 7,8-di-HODE in *G. graminis* (23). 8*R*-HODE biosynthesis was not detected in either microsomes or a high-speed supernatant. We are at present unclear as to why enzyme activity for 8*R*-HODE biosynthesis was lost in our high-speed supernatant. The fact that 8*R*-HODE biosynthesis was achieved in soluble enzyme extracts may allow further characterization of this enzyme.

The fatty acid derivatives of 20:4n-6 we found were 18- and 19-HETE and uncharacterized di-HETE (results not shown). In this case, the compounds were only detected when the cytosolic fraction was incubated with NADPH, but the total yields of 18- and 19-HETE were less than 0.5%. This implied that the cytochrome P_{450} enzymes involved in the biotransformation of 20:4n-6 were, like that for 8*R*-HODE biosynthesis, probably cytosolic.

In conclusion, *L. lacteus* possesses several enzymes capable of oxygenating long-chain fatty acids; it remains to be discovered what role these enzymes play in the life cycle and biochemistry of the organism.

ACKNOWLEDGMENTS

S.R.F. was funded by a grant awarded to J.F. and C.R. from the Biotechnology and Biological Sciences Research Council, United Kingdom. The University of Uludag, Bursa, Turkey, funded A.A., and The National Chemical Laboratory, Pune, India, funded A.A.P. The authors extend their gratitude to Dr. Mats Hamberg for determining the chirality of 8-HODE and to Mr. Alan Roberts for help with the GC–MS.

REFERENCES

1. Herman, R.P., and Luchini, M.M. (1989) Lipoxygenase Activity in Oomycete *Saprolegnia* Is Dependent on Environmental Cues and Reproductive Competence, *Exp. Mycol. 13*, 372–379.
2. Brodowsky, I.D., and Oliw, E.H. (1992) Metabolism of 18-2n-6, 18-3n-3, 20-4n-6 and 20-5n-3 by the Fungus *Gaeumannomyces graminis*—Identification of Metabolites formed by 8-Hydroxylation and by ω2 and ω3 Oxygenation, *Biochim. Biophys. Acta 1124*, 59–65.
3. Mazur, P., Meyers, H.V., Nakanishi, K., ElZayat, A.A.E., and Champe, S.P. (1990) Structural Elucidation of Sporogenic Fatty-Acid Metabolites from *Aspergillus nidulans, Tetrahedron Lett. 31*, 3837–3840.
4. Bowers, W.S., Hoch, H.C., Evans, P.H., and Katayama, M. (1986) Thallophytic Allelopathy—Isolation and Identification of Laetisaric Acid, *Science 232*, 105–106.
5. Needleman, P., Turk, J., Jakschik, B.A., Morrison, A.R., and Lefkowith, J.B. (1986) Arachidonic Acid Metabolism, *Annu. Rev. Biochem. 55*, 69–102.
6. Hamberg, M. (1986) Isolation and Structures of Lipoxygenase Products from *Saprolegnia parasitica, Biochim. Biophys. Acta 876*, 688–692.

7. Herman, R.P., and Herman, C.A. (1985) Prostaglandins or Prostaglandin-Like Substances Are Implicated in Normal Growth and Development in Oomycetes, *Prostaglandins 29*, 819–830.
8. Schade, A.L. (1940) The Nutrition of *Leptomitus, Am. J. Bot. 27*, 376–384.
9. Willoughby, L.G., and Roberts, R.J. (1991) Occurrence of the Sewage Fungus *Leptomitus-lacteus*, a Necrotroph on Perch (*Perca-fluviatilis*), in Windermere, *Mycol. Res. 95*, 755–768.
10. Luthria, D.L., Baykousheva, S.P., and Sprecher, H. (1995) Double Bond Removal from Odd-Numbered Carbons During Peroxisomal β-Oxidation of Arachidonic Acid, *J. Biol. Chem. 270*, 13771–13778.
11. MacLouf, J., and Rigaud, M. (1982) Open Tubular Glass Capillary Gas Chromatography for Separating Eicosanoids, *Methods Enzymol. 86*, 612–631.
12. Hamberg, M. (1971) Steric Analysis of Hydroperoxides Formed by Lipoxygenase Oxygenation of Linoleic Acid, *Anal. Biochem. 43*, 515–526.
13. Oliw, E.H., Fahlstadius, P., and, Hamberg, M. (1986) Isolation and Biosynthesis of 20-Hydroxy Prostaglandins-E_1 and 20-Hydroxy Prostaglandin-E_2 in Ram Seminal Fluid, *J. Biol. Chem. 261*, 9216–9221.
14. Hawkins, D.J., Kuhn, H., Petty, E.H., and Brash, A.R. (1988) Resolution of Enantiomers of Hydroxyeicosatetraenoate Derivatives by Chiral Phase High-Pressure Liquid Chromatography, *Anal. Biochem. 173*, 456–462.
15. Fox, S.R., Friend, J., and Ratledge, C. (1997) Optimisation of 3-Hydroxyeicosanoid Biosynthesis by the Yeast *Dipodascopsis uninucleata, Biotechnol. Lett. 19*, 155–158.
16. Butcher, R.W. (1932) Contribution to Our Knowledge of the Ecology of Sewage Fungus, *Transactions Brit. Mycolog. Soc. 17*, 12–124.
17. Su, C., and Oliw, E.H. (1998) Manganese Lipoxygenase: Purification and Characterization, *J. Biol. Chem. 273,* 13072–13079.
18. Brodowsky, I.D., Hamberg, M., and Oliw, E.H. (1992) A Linoleic Acid (8*R*)-Dioxygenase and Hydroperoxide Isomerase of the Fungus *Gaeumannomyces graminis*, *J. Biol. Chem. 267*, 14738–14745.
19. Smith, W.L., and Lands, W.E.M. (1971) Stimulation and Blockade of Prostaglandin Biosynthesis, *J. Biol. Chem. 246*, 6700–6702.
20. Hamasaki, Y., and Tai, H.H. (1985) Gossypol, a Potent Inhibitor of Arachidonate 5-Lipoxygenase and 12-Lipoxygenase, *Biochim. Biophys. Acta 834*, 37–41.
21. Agarwal, R., Wang, Z.Y., and Mukhtar, H. (1991) Nordihydroguaiaretic Acid, an Inhibitor of Lipoxygenase, Also Inhibits Cytochrome-P_{450}-Mediated Monooxygenase Activity in Rat Epidermal and Hepatic Microsomes, *Drug Metab. Dispos. 19*, 620–624.
22. Su, C., and Oliw, E.H. (1996) Purification and Characterization of Linoleate 8-Dioxygenase from the Fungus *Gaeumannomyces graminis* as a Novel Hemoprotein, *J. Biol. Chem. 271*, 14112–14118.
23. Su, C., Brodowsky, I.D., and Oliw, E.H. (1995) Studies on Linoleic Acid 8*R*-Dioxygenase and Hydroperoxide Isomerase of the Fungus *Gaeumannomyces graminis, Lipids 30*, 43–50.

[Received August 24, 1999, and in final revised form December 2, 1999; revision accepted December 9, 1999]

Fatty Acid Transport Across Lipid Bilayer Planar Membranes

L.G. Romano-Fontes, R. Curi, C.M. Peres, A. Nishiyama-Naruke, K. Brunaldi, F. Abdulkader, and J. Procopio*

Departamento de Fisiologia e Biofísica, Instituto de Ciencias Biomédicas, Universidade de São Paulo, Brazil

ABSTRACT: The transport of palmitic acid (PA) across planar lipid bilayer membranes was measured using a high specific activity [^{14}C]palmitate as tracer for PA. An all-glass *trans* chamber was employed in order to minimize adsorbance of PA onto the surface. Electrically neutral (diphytanoyl phosphatidylcholine) and charged (Azolectin) planar bilayers were maintained at open electric circuit. We found a permeability to PA of (8.8 ± 1.9) × 10^{-6} cm s^{-1} (n = 15) in neutral and of (10.3 ± 2.2) × 10^{-6} cm s^{-1} (n = 5) in charged bilayers. These values fall within the order of magnitude of those calculated from desorption constants of PA in different vesicular systems. Differences between data obtained from planar and vesicular systems are discussed in terms of the role of solvent, radius of curvature, and pH changes.

Paper no. L8056 in *Lipids 35,* 31–34 (January 2000).

Nonesterified fatty acids (FA) have a central role in cellular processes, such as cell signaling (1), K^+ channel activation (2), Na^+/Ca^{2+} exchange (3), uptake modulation of plasmatic lipoproteins (4), and uncoupling of oxidative phosphorylation (5), among others. Furthermore, recent studies suggest that FA may function as proton carriers across the cell membrane (6).

A crucial question in the physiology of FA refers to their mechanism of entry into and export from cells.

Studies of intravesicular acidification of unilamellar vesicles (UV) (6,7) have shown a very fast FA flip-flop rate in bilayers following pulses of FA on the bath. On the other hand, more recent studies (8) suggest the flip-flop is the limiting process in FA transfer across UV.

Furthermore, studies of FA transport across planar bilayer membranes (PBM) are scant and have provided mainly indirect evidence (9) of FA flip-flop.

The availability of [^{14}C]palmitic acid (PA) at a very high specific activity prompted us to investigate directly the transfer of this FA across planar bilayers and provided direct evidence that its translocation across the membrane occurs at a reasonably fast rate, comparable to that described for vesicular systems.

*To whom correspondence should be addressed at Av. Prof. Lineu Prestes 1524, CEP 05508-900, São Paulo, SP, Brazil.
E-mail: Procopio@fisio.icb.usp.br

Abbreviations: cpm, counts per minute; DPPC, diphytanoyl phosphatidylcholine; FA, fatty acid; GUV, giant unilamellar vesicle; LUV, large unilamellar vesicle; PA, palmitic acid; PBM, planar bilayer membranes; SUV, small unilamellar vesicle; Trizma, tris(hydroxymethyl)aminomethane; UV, unilamellar vesicles.

MATERIALS AND METHODS

PA transfer across PBM was measured by tracer flow using ^{14}C-labeled ([U-^{14}C]palmitic acid, with a specific activity of 850 Ci mol^{-1}; DuPont, Boston, MA). Quantities of the tracer in the *cis* (hot) side ranged from 200,000–1,000,000 counts per minute cm^{-3}, giving a maximal PA concentration of 0.5 μmol L^{-1}.

Experiments were carried out under conditions of open electric circuit, with no attached electronics. Owing to the known adsorbance of FA to plastics (10), we employed an all-glass chamber as *trans* compartment. Also, samples from the *trans* (cold) side had no contact with plastics. To check for FA escape from the bilayer material, samples of aqueous solutions bathing the bilayers were run on high-performance liquid chromatography. Levels of FA contaminants were undetectable.

Electrically neutral PBM were formed from diphytanoyl phosphatidylcholine (DPPC) from Avanti Polar Lipids (Alabaster, AL), and negatively charged membranes were formed from soybean lecithin (Azolectin; Sigma Chemical Co., St. Louis, MO), which contains about 10% of charged phospholipids, mainly phosphatidylglycerol (11). The phospholipids were dissolved in *n*-decane (2.5 mg lipid/100 μl *n*-decane). Surface potentials of charged membranes in 5 mM KCl–5 mM Trizma [tris(hydroxymethyl)aminomethane] were determined, according to a modification of the method described by McLaughlin *et al.* (12), by measuring the ratio of the valinomycin-doped membrane conductances before and after addition of Ba^{2+} to the bath.

Bilayers were formed, using the technique of Mueller *et al.* (13), across a hole (1- to 2-mm diameter) in the lateral wall of a cylindrical glass vial. The hole was made using the procedure described by Procopio *et al.* (14). Both *trans* and *cis* sides were adequately stirred. Solutions had the same composition and had volumes between 2 and 3 mL. In experiments using neutral bilayers, solutions were 150 mM NaCl + Trizma base 20 mM, titrated to pH 7.4. Solutions used for charged membranes were KCl 5 mM + Trizma 5 mM, pH 7.2, in order to maintain low ionic strength and enhance the negative surface potential. Surface pH is lower than bulk pH in this condition; this difference increases FA partitioning into the membrane phase (see Ref. 15 for example and discussion).

Samples of 200 μL were drawn from the *trans* (cold) side at 15 and at 30 or 45 min after introduction of labeled palmi-

tate into the *cis* side. The use of these time intervals was dictated by the geometry of the system and bilayer permeability: 15 min was the minimum for obtaining statistically significant cpm on the trans (cold) side, and 45 min was the maximal membrane lifetime on average. A single 50-µL sample was obtained from the *cis* (hot) side. Samples were diluted in Universol™ from ICN Biomedicals (Costa Mesa, CA) and counted in a Beckman counter for β^- emission, from 20 kEV upwards.

Since the sampling procedure removes a significant number of cpm from the cold side, a correction was done for cpm withdrawal during multiple samplings, according to the procedure described in Figure 1. We also checked, using ink, that the mixing time in the solutions was below 1 min.

RESULTS

Figure 1 depicts a typical time evolution of the isotopic activity on the cold side, in a three-samples experiment. Thanks to the enormous $t_{1/2}$ (see Eq. A-12 in the Appendix) of the process during the first few hours after the tracer addition to the *cis* side, the following assumptions can safely be made: (i) The *cis* (hot) side isotopic activity is constant, and (ii) the increase in isotopic activity in the *trans* (cold) side is linear with time.

Indeed, in preliminary experiments, we did not identify any tendency of the cold-side activity vs. time plots to deviate from linearity.

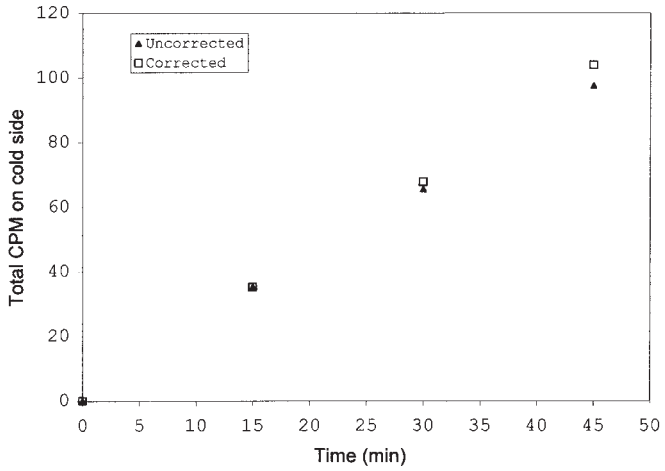

FIG. 1. Plot of total counts per minute (cpm) on the cold side as function of time for a typical 3-sample experiment. The point at time zero corresponds to a blank and has zero cpm by definition. Correction for cpm withdrawal during samplings was done according to the equation exemplifying the correction for Sample #3:

$$\text{total cpm}_3 = (\text{cpm}_3 - \text{cpm}_{\text{blank}})\ \frac{\text{CSV}}{\text{CSAV}} + (\text{cpm}_2 - \text{cpm}_{\text{blank}}) + (\text{cpm}_1 - \text{cpm}_{\text{blank}})$$

where total cpm_3 = total corrected cpm on cold side in sampling #3, at 45 min; $\text{cpm}_{\text{blank}}$ = average cpm of two blanks; cpm_1, cpm_2, and cpm_3 = counted cpm in samples #1, #2, and #3 respectively, at 15, 30, and 45 min; CSV = volume of cold side (variable); and CSAV = volume of aliquot taken from cold side (200 µL).

Table 1 shows the bilayer permeability to PA obtained in our study, compared with those calculated from the literature, in unilamellar vesicles. Permeability coefficients for [^{14}C]palmitic acid across PBM were calculated as follows:

$$\text{permeability to [}^{14}\text{C]palmitic acid} = \frac{\text{flow of cpm}}{[\text{cpm}]_{cis}} \quad [1]$$

where the flow of cpm is expressed as cpm s^{-1} cm^{-2} and $[\text{cpm}]_{cis}$ is cpm cm^{-3},

$$\text{flow of cpm} = \frac{\text{average difference in total cpm betwen 2 successive } \textit{trans} \text{ samples}}{\text{time difference} \times \text{membrane area}} \quad [2]$$

$[\text{cpm}]_{cis}$ counts for samples taken from the *cis* (hot) side,

$$\text{total cpm} = (\text{cpm in } \textit{trans} \text{ sample}) \times \frac{\textit{trans} \text{ volume}}{\text{sample volume}} + \Sigma \text{ cpm in previous } \textit{trans} \text{ samples} \quad [3]$$

Permeabilities to palmitic acid of UV membranes, used for comparison, were estimated from literature values (8,16) of the desorption rate contants (k_{off}), using Equation 4 (derived in the Appendix as Eq. A-12),

$$\text{permeability} = k\ \frac{\text{vesicular radius}}{3} \quad [4]$$

DISCUSSION

Our results indicate a permeability of planar bilayers to PA of about the same order of magnitude as those calculated for large unilamellar vesicles (LUV) and giant unilamellar vesicles (Table 1). The present comparison needs careful interpretation because of the present controversy as to the rate-limiting step for FA transfer across bilayers and the extremely

TABLE 1
Comparison Between PBM and UV Data on Palmitic Acid Permeability[a]

Planar bilayers (this paper) (T = 22–24°C) (mean ± SEM)	SUV (diam. ≈ 25 nm) (Ref. 16) (T = 24 ± 1°C) (k_{off} = 8.22 s^{-1})	GUV (diam. ≈ 200 nm) (Ref. 8) (T = 20°C) (k_{off} ≈ 0.5 s^{-1})
DPPC (neutral) (8.8 ± 1.9) × 10^{-6} (n = 15)	2.7 × 10^{-6}	1.7 × 10^{-6}
Soybean lecithin (charged) (10.3 ± 2.2) × 10^{-6} (n = 5)		

[a]Permeabilities (cm s^{-1}) of small unilamellar vesicles (SUV) and giant unilamellar vesicles (GUV) were calculated from Equation 2 (see Results section), based on reported rate constants for palmitic acid, k_{off}. DPPC, diphytanoyl phosphatidylcholine.

diverse geometry of these membrane systems. Our experiments measure a "lumped" transfer parameter which includes the three essential steps in FA translocation, i.e., adsorption, flip-flop, and desorption. It is generally assumed that the adsorption step is very fast compared either to flip-flop or desorption, but controversy still remains (8) regarding the difference between flip-flop and desorption rates. Table 1 compares the permeability of PBM to PA and permeability coefficients estimated from the reported desorption rates of PA from vesicles, assuming the limiting step is desorption. In Table 1, permeability values calculated from such diverse systems as PBM and UV fall within one order of magnitude of each other.

In the group of charged membranes, we determined the surface potential in KCl 5 mM + Trizma 5 mM as Ψ_o = –112.4 ± 11 mV (SEM) (n = 4) (see Materials and Methods section), which corresponds to an increase of surface apparent pK (17) given by:

$$\Delta pK_a = \frac{F}{2.3RT}\Psi_o = 2 \text{ units} \qquad [5]$$

thus favoring the protonated form of PA in the membrane vicinity. This effect supposedly increases the FA partitioning into the bilayer matrix. The finding of only a small increase in permeability in going from neutral to charged membranes favors the idea that the limiting step for FA passage is indeed desorption.

Differences between the PA permeability in UV and PBM might occur by the presence of solvent in the planar membranes (and absence in UV) and the small radius of curvature of UV. The extremely small radius of curvature of small unilamellar vesicles (SUV) and LUV may create mismatch between the areas of the inner and outer vesicular bilayer leaflets, increasing the probability of defects and leading to facilitation of FA flip-flop (8). This latter effect, however, may be rendered unnoticeable by the slower transfer imposed by desorption.

By having both compartments at a fixed pH (in our case, 7.4 and 7.2), we avoided the inherent pH decrease of the *trans* side observed in UV studies, due to FA entry. This decrease in pH was associated with the build-up of diffusion potentials (16) that could counteract proton passage.

APPENDIX

Derivation of kinetic parameters of FA transfer relating data on planar bilayers and vesicles. We analyzed the washout [uptake gives a similar result] of FA from a spherical compartment with volume V (*cis* side) across an area A and to an infinite external reservoir (*trans* side), with a rate constant k:

$$\text{FA } (cis) \xrightarrow{k \text{ (membrane)}} \text{FA } (trans) \qquad [A\text{-}1]$$

From the definition of the rate k, we have

$$-\frac{d[\text{FA}]_{cis}}{dt} = k[\text{FA}]_{cis} \qquad [A\text{-}2]$$

Rearranging and integrating Equation A-2, we obtain

$$\int \frac{d[\text{FA}]_{cis}}{[\text{FA}]_{cis}} = -kt \qquad [A\text{-}3]$$

giving, finally, the FA concentration (in the *cis* side) as a function of time as:

$$[\text{FA}]^t_{cis} = [\text{FA}]^0_{cis} e^{-kt} \qquad [A\text{-}4]$$

where $[\text{FA}]^0$ and $[\text{FA}]^t$ are the concentrations of FA at time zero and at time t in the *cis* compartment.

Multiplying both sides of Equation A-2 by the volume V and dividing by the area A, we obtain the flow of FA molecules (in mol s^{-1} cm^{-2}) from the internal (*cis*) compartment to the infinite external reservoir,

$$\text{flow of FA} = -\frac{d[\text{FA}]_{cis}}{dt}\left(\frac{V}{A}\right) = k\left(\frac{V}{A}\right)[\text{FA}]_{cis} \qquad [A\text{-}5]$$

But, since the relation between flow and concentration difference of a substance S across a membrane is the membrane permeability coefficient (P) to S we can write, from Equation A-5,

$$\text{flow of FA} = k\left(\frac{V}{A}\right)[\text{FA}]_{cis} = P[\text{FA}]_{cis} \qquad [A\text{-}6]$$

from which we obtain that:

$$P = k\frac{V}{A} \qquad [A\text{-}7]$$

Since k and $t_{1/2}$ are related by

$$t_{1/2} = \frac{0.693}{k} \qquad [A\text{-}8]$$

we obtain:

$$t_{1/2} = 0.693\,\frac{V}{P\,A} \qquad [A\text{-}9]$$

which is valid for any geometry.

For the particular case of a spherical vesicle we have:

$$\text{volume} = (4/3)\pi R^3 \qquad [A\text{-}10]$$

$$\text{area} = 4\pi R^2 \qquad [A\text{-}11]$$

from which we obtain the relation between the rate constant and permeability for a vesicular structure as

$$\text{permeability} = k\,\frac{\text{vesicular radius}}{3} \qquad \text{[A-12]}$$

Applying Equation A-9 to the case of a planar bilayer with area = 3×10^{-2} cm^2 separating an outer reservoir with large volume from an inner reservoir with 2-mL volume, we obtain (using our tracer-measured permeability for FA = 8.8×10^{-6} cm s^{-1})

$$t_{1/2} = 0.693\,\frac{V}{P\,A} = 0.693\,\frac{2}{(8.8 \times 10^{-6})(3 \times 10^{-2})} = 5.25 \times 10^{6}\ \text{s} = 60\ \text{d} \qquad \text{[A-13]}$$

which, of course, precludes the use of this system for determination of kinetic studies based on half-time determination for FA and justifies the use of tracer flow protocols.

ACKNOWLEDGMENTS

This work was supported by the following grants from Fundação de Amparo a Pesquisa do Estado de São Paulo: 93/3498-4, 96/4581-0, 97/5683-4, 95/9015-0, 98/13269-6.

REFERENCES

1. Hannigan, G.E., and Williams, B.R.G. (1991) Signal Transduction by Interferon-α Through Arachidonic Acid Metabolism, *Science 251*, 204–207.
2. Ordway, R.W., Walsh, J.V., Jr., and Singer, J.J. (1989) Arachidonic Acid and Other Fatty Acids Directly Activate Potassium Channels in Smooth Muscle Cells, *Science 244*, 1176–1179.
3. Philipson, K.D., and Ward, R. (1985) Effects of Fatty Acids on Na^+-Ca^{2+} Exchange and Ca^{2+} Permeability of Cardiac Sarcolemmal Vesicles, *J. Biol. Chem. 256*, 9666–9671.
4. Bihain, B.E., Deckelbaum, R.J., Yen, F.T., Gleeson, A.M., Carpentier Y.A., and White, L.D. (1989) Unesterified Fatty Acids Inhibit the Binding of Low Density Lipoproteins to the Human Fibroblast Low Density Lipoprotein Receptor, *J. Biol. Chem. 264*, 17316–17323.
5. Skulachev, V.P. (1991) Fatty Acid Circuit as a Physiological Mechanism of Uncoupling of Oxidative Phosphorylation. Review, *FEBS Lett. 294*, 158–162.
6. Kamp, F., and Hamilton, J.A. (1993) Movement of Fatty Acids, Fatty Acid Analogues, and Bile Acids Across Phospholipid Bilayers, *Biochemistry 32*, 11074–11086.
7. Kamp, F., Zakim,D., Zhang, F., Noy, N., and Hamilton, J.A. (1995) Fatty Acid Flip-Flop in Phospholipid Bilayers is Extremely Fast, *Biochemistry 34*, 11928–11937.
8. Kleinfeld, A.M., Chu, P., and Romero, C. (1997) Transport of Long-Chain Fatty Acids Across Lipid Bilayer Membranes Indicates That Transbilayer Flip-Flop Is Rate Limiting, *Biochemistry 36*, 14146-14158.
9. Gutknecht, J. (1988) Proton Condutance Caused by Long-Chain Fatty Acids in Phospholipid Bilayer Membranes, *J. Membrane Biol. 106*, 83–93.
10. Mailman, D., and Rose, C. (1990) Binding and Solubility of Oleic Acid to Laboratory Materials: a Possible Artifact, *Life Sci. 47*, 1737–1744.
11. Kagawa, Y., and Racker, E. (1966) Partial Resolution of the Enzymes Catalyzing Oxidative Phosphorylation IX. Reconstruction of Oligomycin-Sensitive Adenosine Triphosphatase, *J. Biol. Chem. 241*, 2467–2474.
12. McLaughlin, S.G.A., Szabo, G., and Eisenman, G. (1971) Divalent Ions and the Surface Potential of Charged Phospholipid Membranes, *J. Gen. Physiol. 58*, 667–687.
13. Mueller, P., Rudin, H.T., Tien, T., and Wescott, W.C. (1963) Methods for the Formation of Single Bimolecular Lipid Membranes in Aqueous Solutions, *J. Phys. Chem. 67*, 534–535.
14. Procopio, J., Varanda, W.A., and Fornes, J.A. (1982) A Quartz Cell for Studying Planar Lipid Bilayers, *Biochim. Biophys. Acta 688*, 808–810.
15. Hamilton, J.A. (1998) Fatty Acid Transport: Difficult or Easy? *J. Lipid Res. 39*, 467–481.
16. Zhang, F., Kamp, F., and Hamilton, J.A. (1996) Dissociation of Long and Very Long Chain Fatty Acids from Phospholipid Bilayers, *Biochemistry 35*, 16055–16060.
17. Cevc, G., and Marsh, D. (1987) *Phospholipid Bilayers: Physical Principles and Models*, Vol. 5 of *Cell Biology: A Series of Monographs* (Bittar, E.E., ed.), pp. 182–183, John Wiley & Sons, New York.

[Received November 10, 1998 and in final revised form October 29, 1999; revision accepted December 8, 1999]

Coordinate Packaging of Newly Synthesized Phosphatidylcholine and Phosphatidylglycerol in Lamellar Bodies in Alveolar Type II Cells

Avinash Chander*, Namita Sen, Sandra Wadsworth, and Alan R. Spitzer

Division of Neonatology, Department of Pediatrics, Jefferson Medical College, Thomas Jefferson University, Philadelphia, Pennsylvania

ABSTRACT: Methylamine, a weak base, inhibits packaging of newly synthesized phosphatidylcholine (PC) in lamellar bodies in 20–22 h cultured alveolar type II cells, suggesting a role for acidic pH of lamellar bodies. In this study, we tested if (i) the packaging of PC is similarly regulated in freshly isolated type II cells and (ii) methylamine also inhibits the packaging of other surfactant phospholipids, particularly, phosphatidylglycerol (PG). The latter would suggest coordinated packaging so as to maintain the phospholipid composition of lung surfactant. During the short-term metabolic labeling experiments in freshly isolated type II cells, methylamine treatment decreased the incorporation of radioactive precursors into PC, disaturated PC (DSPC), and PG of lamellar bodies but not of the microsomes, when compared with controls. The calculated packaging (the percentage of microsomal lipid packaged in lamellar bodies) of each phospholipid was similarly decreased (~50%) in methylamine-treated cells, suggesting coordinated packaging of surfactant phospholipids in lamellar bodies. Equilibrium-labeling studies with freshly isolated type II cells (as is routinely done for studies on surfactant secretion) ± methylamine showed that in methylamine-treated cells, the secretion of PC and PG was decreased (possibly due to decreased packaging), but the phospholipid composition of released surfactant (measured by radioactivity distribution) was unchanged; and the PC content (measured by mass or radioactivity) of lamellar bodies was lower, but the PC composition (as percentage of total phospholipids) was unchanged when compared with control cells. We speculate that the newly synthesized surfactant phospholipids, PC, DSPC, and PG, are coordinately transported into lamellar bodies by a mechanism requiring the acidic pH, presumably, of lamellar bodies.

Paper no. L8341 in *Lipids 35*, 35–43 (January 2000).

Pulmonary surfactant is a lipoprotein-like substance that lines the alveolar epithelium. It maintains alveolar stability during end-expiration by lowering the surface tension at the air–liquid interface (reviewed in 1,2). Various lipid and protein components of lung surfactant are synthesized and secreted by lung epithelial type II cells (reviewed in 2,3). The major phospholipids of lung surfactant, phosphatidylcholine (PC), disaturated PC (DSPC), and phosphatidylglycerol (PG) are stored in the lamellar bodies and secreted by exocytosis of lamellar body contents into alveolar lumen. Various agents can increase the secretion and clearance of lung surfactant to maintain its alveolar pool size (reviewed in 3,4). Although not investigated, any alteration in the packaging of one or more surfactant phospholipids has the potential to affect the quantity and quality of alveolar surfactant pool.

Various models have been suggested for phospholipids trafficking from their site of synthesis to target membranes (5,6). One of these involves molecular transfer of phospholipids through phospholipid transfer proteins (5), which also are present in type II cells, where they are suggested to mediate transfer of PC, DSPC, and PG to lamellar bodies (reviewed in Ref. 7). Another mechanism for transfer of phospholipids (and proteins) may involve vesicle trafficking from the site of synthesis to the targeted membrane (8–10). The phospholipid composition of lung surfactant is maintained within a narrow range, suggesting coordinated packaging of surfactant phospholipids in lamellar bodies. Such coordination can be exerted by controlling the activities of different phospholipid transfer proteins toward each of the surfactant phospholipids or by transport of surfactant phospholipids through vesicles, which may fuse with small or growing lamellar bodies.

The lamellar bodies are unique organelles in type II cells that are rich in phospholipids and hydrophobic proteins (11), contain lysosomal enzymes (12–14), and maintain an internal acidic pH by a vacuolar type H^+-ATPase (15–17). The intralamellar body pH can be increased with membrane-permeable weak bases (12,15). The function of the acidic pH is unclear, but may be necessary for the packaging of *de novo* synthesized surfactant PC (16), processing of surfactant protein B (18) or C (19), or the function of surfactant protein A (20).

For this study, we used methylamine treatment as a tool to investigate the mechanism of surfactant phospholipid trafficking from endoplasmic reticulum to lamellar bodies. Our previous study in 20–22 h cultured type II cells showed that methylamine inhibited the packaging of PC and DSPC in lamellar

*To whom correspondence should be addressed at Jefferson Medical College, 1025 Walnut St., Philadelphia, PA 19107.
E-mail: Avinash.Chander@mail.tju.edu

Abbreviations: ANOVA, Analysis of variance; CL, cardiolipin; DPPC, dipalmitoyl phosphatidylcholine; DSPC, disaturated phosphatidylcholine; MEM, minimum essential medium; PMA, phorbol 12-myristate 13-acetate; PC, phosphatidylcholine; PG, phosphatidylglycerol; PI, phosphatidylinositol; PS, phosphatidylserine; PL, phospholipid; Sph, sphingomyelin; TLC, thin-layer chromatography.

bodies (16). Since lung epithelial type II cells show altered morphologic and metabolic characteristics during cell culture (21,22), we conducted metabolic studies in freshly isolated type II cells to test the following hypotheses: (i) Methylamine inhibits the packaging of PC in lamellar bodies in freshly isolated type II cells, which will suggest that the pH regulation of PC packaging is intrinsic to type II cells and is not an artifact of cell culture, and (ii) the acidic pH also regulates the packaging of PG, the third major surfactant phospholipid after DSPC and unsaturated PC. Such regulation of PG, DSPC, and unsaturated PC would suggest that the phospholipids of lung surfactant are transported in a coordinated manner so as to maintain the phospholipid composition of lung surfactant. We tested these hypotheses by conducting metabolic labeling studies in freshly isolated type II cells and found that freshly isolated type II cells packaged a higher percentage of microsomal PC in lamellar bodies when compared with 20–22 h cultured cells (16). Methylamine treatment inhibited PC and DSPC packaging in lamellar bodies in freshly isolated type II cells. Furthermore, methylamine also inhibited the packaging of PG in lamellar bodies but did not alter the phospholipid composition of secreted surfactant, supporting the concept of coordinated packaging of lung surfactant phospholipids in lamellar bodies. As in the previous study (16), the packaging of a phospholipid in lamellar bodies is defined as the ratio of incorporation into a lamellar body lipid to that in the microsomal lipid.

MATERIALS AND METHODS

Materials. [^{3}H-methyl]Choline, [9,10-^{3}H]palmitic acid, and [^{14}C]dipalmitoyl PC (DPPC) were obtained from Amersham Corp. (Arlington Heights, IL). Tissue culture plastic dishes were obtained from Corning (Corning, NY). Bacteriological plates were purchased from Becton Dickinson (Franklin Lakes, NJ). All other tissue culture supplies were obtained from Gibco/BRL (Grand Island, NY). Porcine elastase was obtained from Worthington Biochemicals (Freehold, NJ). Terbutaline, methylamine, phorbol 12-myristate 13-acetate (PMA), vanadate-free adenosine triphosphate (ATP), and all other chemicals were purchased from Sigma Chemical Co. (St. Louis, MO). All phospholipids were obtained from Avanti Polar Lipids, Inc. (Alabaster, AL). All chemicals were added at the indicated final concentrations.

Isolation of type II cells. Sprague-Dawley rats (180–200 g body weight) were used for isolation of alveolar type II cells according to Dobbs *et al.* (23), as described previously (24). Briefly, lungs of anesthetized and exsanguinated rats were visibly cleared of blood, and intratracheally treated (×3) with porcine elastase (3 units/mL). The lung tissue was then minced on a tissue chopper, and free cells were sequentially filtered through nylon filters of various sizes. The free cells were incubated for 1 h on rat IgG-coated bacteriological plates. Thereafter, the free cells were collected by "panning." Staining with phosphine showed that >85% of these cells were type II cells and >90% of cells excluded vital dye, erythrosin B. These cells were termed as freshly isolated type II cells.

Short-term labeling of freshly isolated cells: About 4×10^7 cells were taken up in 3.0 mL of fresh minimum essential medium (MEM) and incubated for 15 min in air containing 5% CO_2 at 37°C in a shaking water bath at 75 cycles/min. The radioactive substrate of interest, [^{3}H-methyl]choline or [9,10-^{3}H]palmitic acid, was added at a final concentration of 0.1 mM. In these experiments, [^{3}H]palmitic acid was complexed with fatty acid-poor bovine serum albumin (fatty acid to bovine serum albumin ratio 6:1; mol/mol) before addition to the cells. The incubations were continued for another 60 min after addition of 5 mM methylamine to experimental tubes. The labeling was terminated by addition of 10 mL of ice-cold MEM and the cells separated by centrifugation for 10 min at $300 \times g$. The cells were washed with fresh MEM and then processed for isolation of subcellular fractions as described below.

Long-term labeling of type II cells: In these studies, cells were incubated for 20–22 h in the presence of indicated radioactive substrate (as is routinely done for surfactant secretion studies) and ± methylamine. Preliminary studies indicated that >2.5 mM methylamine interfered with attachment of cells to tissue culture plastic dishes during 20–22 h incubation, although cells already attached to plastic were unaffected by up to 10 mM methylamine (16). Therefore, all long-term labeling studies employed 2.5 mM or lower concentrations of methylamine. Freshly isolated cells were plated in MEM containing 10% fetal bovine serum (1.5×10^6 cells/35 mm plate or 10^7 cells/100 mm plate at 10^6 cells per mL) for 20–22 h in tissue culture plastic dishes and in the presence of 0.25 μCi/mL of [^{3}H-methyl]choline (36 Ci/mol) or 2.5 μCi/mL of [9,10-^{3}H]palmitic acid (54 Ci/mmol). The latter was added from a stock solution in ethanol. The final concentration of ethanol was 0.25%. Where indicated, methylamine or NH_4Cl was added at the start of this incubation period. At the end of this culture period, cells attached to plastic dishes were routinely found to be >93% type II cells, as evaluated by fluorescence staining with phosphine, and >95% of these cells excluded vital dye, erythrosin B. These cells were then processed for isolation of subcellular fractions, surfactant secretion studies, or for distribution of [9,10-^{3}H]palmitic acid radioactivity into various phospholipid classes in the cells and the medium.

Secretion of PC and PG. To evaluate if decreased packaging of surfactant components is reflected in decreased secretion, we measured PC and PG secretion in type II cells that were labeled in the absence or presence of methylamine. Isolated type II cells were labeled for 20–22 h (the cells also attach to plastic dishes during this period) with either [^{3}H-methyl]choline or [9,10-^{3}H]palmitic acid and in the absence or presence of 2.5 mM methylamine. These cells were evaluated for surfactant secretion in the absence of methylamine. The protocol for measuring surfactant secretion has been described previously (24). Briefly, after the labeling period of 20–22 h, the cells were washed (5×) with MEM. Fresh MEM was plated, and the cells were equilibrated for 30 min in 5% CO_2 in air. At the end of this incubation period, secretagogues were added from appropriate stock solution in <1% volume, and the incubation continued for another 2 h. ATP and terbutaline were pre-

pared fresh in water at 100-fold higher concentrations. Stock solution of PMA was prepared in ethanol and diluted 100-fold before addition to the incubation medium so that the final concentration of ethanol was 0.01%. At the end of 2 h of incubation, the medium from each plate was collected, and centrifuged for 10 min at 300 × *g* to sediment any free cells that may have come off during the incubation. The cells on the plate were pooled with those recovered after centrifugation of the medium. Aliquots of cells and medium from each sample were processed for lipid extraction (25) after addition of 0.4 mg of egg PC and [^{14}C]DPPC as a tracer to assess the recovery of PC. In some experiments, lipid mixture containing major surfactant lipids was added as carrier lipids so as to facilitate recovery and separation of surfactant phospholipids. For this purpose, rat lung surfactant was purified (26) and extracted for lipids (25). All results on radioactivity measurement for secretion were corrected for recovery of [^{14}C]DPPC. Secretion of PC in the medium was expressed as a percentage of that in the medium plus cells.

Isolation of lamellar bodies and microsomes. Freshly isolated cells, or 20–22 h-cultured type II cells, harvested by gentle scraping of petri dishes, were suspended in 1 M sucrose solution and disrupted by sonication (3 × 15 s) with a probe sonicator set at 10% of maximum output (Cell Disrupter, Model 50; Fisher Scientific Co., Philadelphia, PA). The lamellar body and microsomal fractions were isolated as described previously (16).

Isolation of membranes and "residual" fractions from lamellar bodies. The isolated lamellar bodies were resuspended in 0.05 M sucrose solution containing 5 μg/mL each of aprotinin, leupeptin, and pepstatin. The suspension was mixed well with a pasteur pipette, layered on 0.5 M sucrose, and centrifuged for 1 h at 80,000 × *g* to recover membrane fraction in the pellet (27). At the end of this centrifugation, a band present at the interface of 0.05/0.5 M sucrose was also collected and was termed the "residual" fraction.

Analytical. Proteins were measured by reaction with the protein-binding dye-reagent (Bio-Rad Laboratories, Richmond, VA) using bovine-γ-globulin as standard (28). DSPC was separated after oxidation of lipid extract with OsO_4 followed by chromatography on neutral alumina column (29). PC in lipid extracts was separated by thin-layer chromatography (TLC) on boric acid-impregnated plates (30). In experiments aiming to measure distribution of [9,10-^{3}H]palmitic acid radioactivity, the phospholipids were separated by two-dimensional TLC on boric acid-impregnated silica gel G plates (31). This method, however, could not be used for experiments that required determinations of mass and radioactivity in PC and PG because of problems with Pi measurements in eluates from scrapings of boric acid-impregnated silica gel plates. Therefore, in experiments aiming to measure both the mass and radioactivity in PG, we first chromatographed lipid extracts on prepackaged silica gel-bonded aminopropyl columns (LC-NH_2, Supelco; St. Louis, MO) and separated phospholipids into neutral polar lipids (PC, phosphatidylethanolamine, and sphingomyelin) and acidic polar lipids (phosphatidylglycerol, phosphatidylinositol, and phosphatidylserine), according to Alvarez and Touchstone (32). Individual phospholipids in these two fractions were separated by one-dimensional TLC on silica gel G plates (33). The phospholipids on TLC plates were visualized by exposure to I_2 vapors and identified by co-migration of authentic phospholipid. The phospholipid spots were scraped and processed for measurement of phospholipid phosphorus and/or radioactivity. Phospholipid phosphorus was measured by reaction with 1,2,4-amino naphthol sulfonic acid (34) as described previously (35). Radioactive samples were counted in a scintillation counter, and the counts were corrected for quenching using computer-generated quench curves.

All secretion experiments were carried out in duplicate and the results averaged to yield single data points. Results were evaluated for statistical significance by Students' *t*-test for experiments unpaired or paired with respect to the cell preparation. Comparison between multiple groups was carried out by analysis of variance (ANOVA) followed by Tukey's post-hoc test. Differences were considered significant at $P < 0.05$.

RESULTS

Short-term labeling in freshly isolated cells. The effects of 5 mM methylamine on labeling of PC in cell homogenate, and the microsomal and lamellar body fractions are shown in Table 1. In control cells, the labeling of cellular and microsomal PC from [^{3}H-methyl]choline was similar to that previously reported in 20–22 h cultured cells (16). As demonstrated before, as well as in this study, the methylamine treatment did not affect choline incorporation into PC or DSPC in the cell homogenate or in the microsomal fraction. Methylamine, however, decreased the labeling of lamellar body PC and DSPC by almost 60% when compared with controls.

Next, we evaluated the incorporation of [9,10-^{3}H]palmitic acid into PC and PG in the absence or presence of 5 mM methylamine (Table 2). Compared to controls, methylamine decreased the incorporation of [9,10-^{3}H]palmitic acid into lamellar body PG, but not into PG of cell homogenate or microsomal fraction. As observed with the choline incorporation

TABLE 1
Effect of Methylamine (MA) on [^{3}H]Choline Incorporation in Phosphatidylcholine (PC) and Disaturated Phosphatidylcholine (DSPC) During Short-Term Labeling in Freshly Isolated Type II Cells and in Subcellular Fractions[a]

	Choline incorporation (nmol/μg Pi)	
	PC	DSPC
Cells (8)		
Control	2.06 ± 0.15	2.45 ± 0.33
MA	1.65 ± 0.17	2.06 ± 0.36
Microsomes (4)		
Control	3.89 ± 0.42	4.32 ± 0.52
MA	3.48 ± 0.49	3.69 ± 0.65
Lamellar bodies (4)		
Control	0.79 ± 0.13	0.98 ± 0.19
MA	0.31 ± 0.04*	0.40 ± 0.05*

[a]Alveolar epithelial type II cells in suspension were incubated for 60 min with 0.1 mM [^{3}H]choline ± 5 mM MA. Results are means ± SE of experiments indicated in parentheses. *$P < 0.05$ when compared with corresponding control.

TABLE 2
Palmitic Acid Incorporation in Phosphatidylglycerol and PC in Freshly Isolated Type II Cells and in Subcellular Fractions[a]

	Palmitic acid incorporation (nmol/μg Pi)	
	Control	MA
Phosphatidylglycerol		
Cell homogenate	5.19 ± 0.82	6.34 ± 1.38
Microsomes	7.24 ± 1.30	7.33 ± 1.42
Lamellar bodies	3.18 ± 0.38	1.64 ± 0.20*
PC		
Cell homogenate	6.05 ± 0.19	5.94 ± 0.44
Microsomes	12.73 ± 0.71	13.84 ± 1.32
Lamellar bodies	3.04 ± 0.36	1.41 ± 0.63*

[a]Alveolar epithelial type II cells in suspension were incubated for 60 min with 0.1 mM [^{3}H]palmitic acid ± 5 mM MA. Results are means ± SE of four separate experiments. *$P < 0.05$ when compared with corresponding control. See Table 1 for abbreviations.

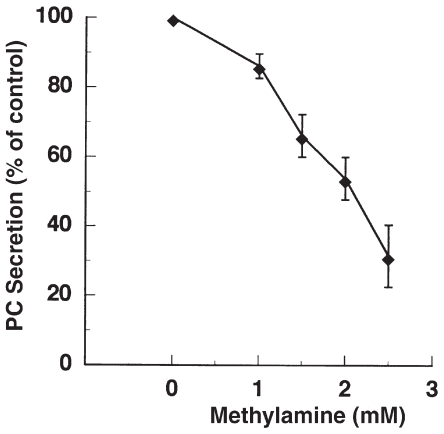

FIG. 2. Concentration-dependence of methylamine effect on packaging and secretion of surfactant PC. Isolated type II cells were labeled for 20–22 h with [^{3}H-methyl]choline in the absence or presence of indicated concentrations of methylamine. Thereafter, cells were washed and evaluated for PMA-stimulated secretion of PC. Results are means ± SE of experiments with four cell preparations and are expressed as percentage of phorbol 12-myristate 13-acetate (PMA)-stimulated secretion of PC (6.8 ± 0.8%) in untreated cells. See Figure 1 for other abbreviation.

(Table 1), methylamine also decreased the incorporation of [9,10-^{3}H]palmitic acid into PC of lamellar bodies but not of cell homogenate or the microsomal fraction. Using the incorporation results in Tables 1 and 2, we calculated the packaging of each phospholipid (PC, DSPC, and PG) into lamellar bodies. We specifically did not calculate the percentage incorporation of cellular lipid label into the lamellar bodies because of possible variations in the recovery of lamellar bodies, which would affect such calculations and, which cannot be corrected for recoveries because of lack of a specific lamellar body marker. As shown in Figure 1, the calculated percentage packaging (100 × labeling of lamellar body lipid per unit mass/labeling of microsomal lipid per unit mass) in control cells was higher for PG when compared with that of PC (49% PG and 23% PC). This difference in percentage packaging is possibly due to different PC pools in the endoplasmic reticulum, which is the site of synthesis of PC targeted for different subcellular compartment. Phosphatidylcholine is a major phospholipid class of most subcellular membranes while the microsomal PG pool may be intended mostly for the lamellar bodies. Compared to control cells, methylamine treatment decreased the packaging of all three phospholipids, DSPC, PC and PG, in the lamellar body fraction. The packaging of each phospholipid was decreased to the same extent (~50%) when compared with the corresponding controls. These results indicate that all three phospholipids are processed through a methylamine (or acidic pH)-sensitive step, suggesting coordinated packaging of surfactant phospholipids in lamellar bodies.

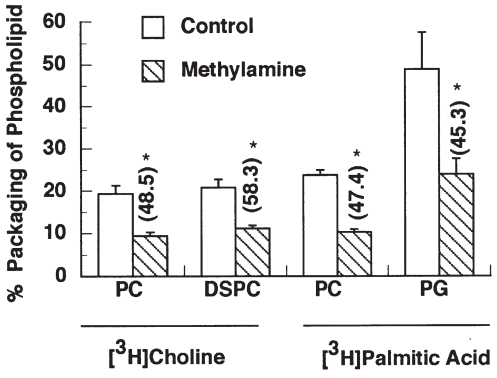

FIG. 1. Calculated percentage packaging of phosphatidylcholine (PC), disaturated phosphatidylcholine (DSPC), and phosphatidylglycerol (PG) in lamellar bodies of freshly isolated type II cells labeled with [^{3}H]choline or [^{3}H]palmitate in the absence (control) or presence of 5 mM methylamine. Percentage packaging was calculated from results given in Tables 1 and 2. *$P < 0.05$ when compared with corresponding controls. The numbers in parentheses indicate percentage inhibition of packaging of each phospholipid in methylamine-treated cells when compared with that in control cells.

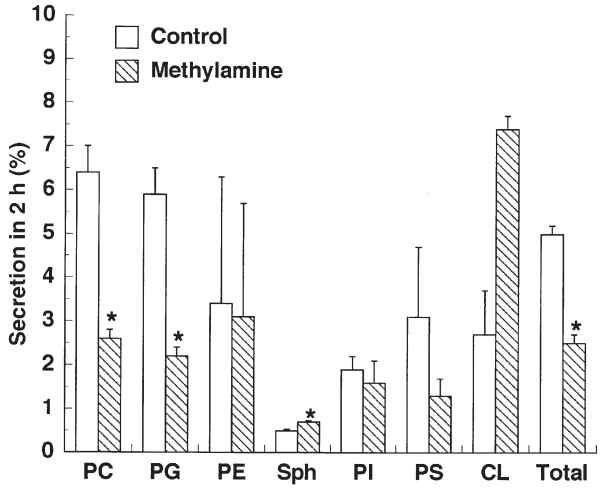

FIG. 3. PMA-stimulated secretion in cells labeled for 20–22 h with [^{3}H]palmitic acid and ± 2.5 mM methylamine. Results are means ± SE of three separate experiments except in case of PI and CL. *$P < 0.05$ when compared with control cells. CL, cardiolipin; PE, phosphatidylethanolamine; PI, phosphatidylinositol; PS, phosphatidylserine; Sph, sphingomyelin. See Figures 1 and 2 for other abbreviations.

TABLE 3
Effect of MA on [^{3}H]Choline Incorporation in PC in Type II Cells During Long-Term Labeling

	Cells	Microsomes	Lamellar bodies
	Specific Activity (x 105 dpm/mg Pi)		
Control	3.3 ± 0.1	3.0 ± 0.4	3.2 ± 0.3
MA	2.7 ± 0.1*	3.1 ± 0.4	2.4 ± 0.2*
	Recovery of PC (% of cell PC)		
Mass			
Control	100	3.2 ± 0.3	26.7 ± 2.3
MA	100	3.2 ± 0.3	16.3 ± 1.0*
Radioactivity			
Control	100	2.9 ± 0.3	26.0 ± 2.8
MA	100	4.2 ± 0.4**	14.3 ± 1.3*

[a]Cells were labeled for 20–22 h with [^{3}H-methyl]choline in the absence (control) or presence of 2.5 mM MA. Results are means ± SE of experiments with four cell preparations. *$P < 0.05$ compared to corresponding controls. **$P < 0.05$ compared to corresponding control by *t*-test for experiments paired with respect to cell preparation. See Table 1 for abbreviations.

The effects of methylamine are unlikely due to cellular toxicity of this drug. We have previously shown that 10 mM methylamine did not increase the uptake of a vital dye, erythrosin B, or the lactate dehydrogenase release in type II cells (16). In this study also, the cell viability, as judged by exclusion of erythrosin B, was not different in cells incubated in the absence or presence of 5 mM methylamine (not shown). The results on the incorporation of [^{3}H]choline or [^{3}H]palmitic acid into the cellular or microsomal phospholipids would also suggest that the methylamine treatment is not toxic to type II cells.

Long-term labeling studies. Since the lamellar body contents are released by exocytosis during surfactant secretion, the decreased packaging of surfactant components in lamellar bodies would likely reflect decreased PC secretion in methylamine-treated cells. However, such inhibition of packaging would not alter the phospholipid composition of the released surfactant if these phospholipids were coordinately transported to the lamellar bodies. During standard protocol for surfactant secretion, type II cells are labeled for 20–22 h with a radioactive precursor. In these experiments, we also added 2.5 mM or lower concentrations of methylamine during this labeling period. Results from such experiments are shown in Tables 3–7 and Figures 2 and 3. In control cells, the incorporations into PC (specific activity, dpm/μg PC phosphorus) in the cell homogenate and the lamellar body and microsomal fractions were similar (Table 3), suggesting equilibrium labeling of PC in different subcellular compartments. In comparison, the specific activity of PC was decreased by 18% in the cell homogenate and by 25% in the lamellar body fraction in methylamine-treated cells. The decrease in the specific activity of cell PC was likely due to decreased labeling of lamellar body PC since it comprised a significant part of cell PC. In control cells, we recovered almost 27% of the cell PC pool in the lamellar bodies. Such recovery agrees well with the 15 times higher phospholipid-to-protein ratio of the lamellar body fraction when compared with the cell homogenate (Table 4). In methylamine-treated cells, we recovered only 16% of cell PC pool in lamellar bodies from methylamine-treated cells, a decrease of 39% when compared with the control group. As a result of decreased mass and specific activity of PC in lamellar bodies, the percentage recovery of total cell PC radioactivity (mass × specific activity) in the lamellar bodies was lower. The recovery of radioactive PC in the microsomal fraction accounted for only a small percentage of cellular PC, but was higher (44%) in methylamine-treated cells when compared with the control group (Table 3).

TABLE 4
Effect of MA on PC of Subcellular Fractions in Type II Cells[a]

	Cells	Microsomes	Lamellar bodies
	PL/protein (mg/mg)		
Control	0.39 ± 0.08	0.24 ± 0.01	6.00 ± 0.38
MA	0.33 ± 0.05	0.22 ± 0.01	4.60 ± 0.75
	PC percentage (% of total PL)		
Control	57.3 ± 2.1	31.5 ± 2.9	66.7 ± 5.5
MA	58.3 ± 2.5	33.9 ± 3.3	65.0 ± 5.5

[a]Cells were incubated for 20–22 h in the absence (control) or presence of 2.5 mM MA. Results are means ± SE of experiments in four cell preparations. PL, phospholipids. See Table 1 for other abbreviations.

The lamellar body fraction was enriched in phospholipids, and the PC accounted for a significant proportion of total phospholipids (Table 4). In methylamine-treated cells, the phospholipid-to-protein ratio was unchanged in cell homogenate or in either subcellular fraction, although it had a tendency to be lower in the lamellar body fraction when compared with the control group ($P = 0.14$). Surprisingly, although the PC mass in lamellar bodies was decreased by almost 40% (Table 3), the PC composition of lamellar bodies was unchanged in methylamine-treated cells (Table 4), suggesting a parallel decrease in packaging of other surfactant phospholipids in lamellar bodies of methylamine-treated cells.

In the experiments described above, we also isolated the lamellar body membrane fraction, which was previously characterized extensively (27), and another fraction, which is lighter in density and was termed the "residual" fraction. We are yet to characterize the latter extensively but suspect it to be more like the alveolar surfactant with respect to the phospholipid composition. Some of its characteristics are described here. The "residual" fraction showed a high phospholipid-to-protein ratio (control, 8.4 ± 1.8; methylamine 8.1 ± 2.1, $n = 4$, $P > 0.05$), and the recovery of phospholipids in this fraction was seven times higher than in the membrane fraction (not shown). The PC (percentage of total phospholipid) in "residual" fraction was also higher when compared with the membrane fraction (Table 5). On the basis of phospholipid-to-protein ratio, recovery of PC, and the PC composition, we assume that the "residual" fraction represents the lamellar body contents. In methylamine-treated cells, the recovery of PC mass, radioactivity, and the specific activity of PC in the "residual" fraction were lower when compared with those in the "residual" fraction in control cells (Table 5). However, the percentage PC was unchanged, similar to that observed in the lamellar bodies.

Next, we evaluated PC secretion in type II cells that were labeled with [^{3}H-methyl]choline for 20–22 h in the absence or presence of 2.5 mM methylamine. The secretion was measured

TABLE 5
Effect of MA on PC Composition and Labeling in Sublamellar Body Fractions During Labeling with [^{3}H]Choline[a]

	Membranes		"Residual" fraction	
	Control	MA	Control	MA
PC (% of total PL)	40.1 ± 4.8	44.1 ± 6.4	72.1 ± 1.8	70.0 ± 3.0
Specific activity ($\times 10^5$ dpm/μg Pi)	3.5 ± 0.4	2.7 ± 0.7	3.3 ± 0.2	2.2 ± 0.1*
Recovery (% of cell PC)				
PC mass	1.4 ± 0.4	1.3 ± 0.1	20.2 ± 2.2	11.3 ± 0.8*
PC radioactivity	1.4 ± 0.4	1.2 ± 0.3	20.1 ± 1.5	9.7 ± 0.4*

[a]Lamellar bodies were isolated from type II cells labeled for 20–22 h with 0.1 mM [^{3}H-methyl]choline ± 2.5 mM MA, disrupted in hypotonic sucrose solution, and the membranes and the "residual" fractions were isolated. *$P < 0.05$ compared to corresponding controls. See Tables 1 and 4 for abbreviations.

in the absence of methylamine. As demonstrated previously (24), in control cells, the secretion of PC was higher with each of the agonists when compared with the basal secretion (Table 6). The secretagogue-stimulated secretion of PC was 414% (with ATP), 257% (with terbutaline), and 371% (with PMA) of basal secretion. In comparison, in cells labeled in the presence of methylamine, the absolute secretion was lower (40–50%) under basal and stimulated conditions (Table 6). However, the stimulation of PC secretion with each agonist was similar to that observed in control cells (ATP, 340%, terbutaline, 200%, and PMA, 360%). We also evaluated the dose-dependence of methylamine (added during the 20–22 h labeling period) effect on PMA-stimulated PC secretion. The absolute decrease in PMA-stimulated secretion was dependent on the methylamine concentration employed during the labeling period. The decrease was ~15% at the lowest (1 mM), and was ~70% at the highest (2.5 mM) concentration used in this study (Fig. 2).

In another set of experiments, we evaluated the effects of another weak base, NH_4Cl, on PMA-stimulated secretion. In these experiments, the PMA-stimulated PC secretion during the 2-h period was lower in cells labeled in the presence of 2.5 mM NH_4Cl or 2.5 mM methylamine (control, 5.85 ± 0.37%, $n = 7$; methylamine, 2.75 ± 0.32, $n = 6$; NH_4Cl, 2.07 ± 0.19, $n = 5$; $P < 0.05$ by ANOVA when control cells were compared with methylamine- or NH_4Cl-treated cells). In control cells, the addition of methylamine or NH_4Cl during the 2-h incubation period for measuring surfactant secretion did not affect the PMA-stimulated secretion (not shown). Since methylamine and NH_4Cl dissipate pH gradients across membranes of acidic compartments including lamellar bodies (16,17), the results of the secretion studies suggest that these two weak bases exert their effect on surfactant phospholipid packaging by raising the pH of acidic compartments, most likely, the lamellar bodies.

Similar effects on secretion of PC and PG in cells labeled for 20–22 h with [9,10-^{3}H]palmitic acid and ± 2.5 mM methylamine provide further support for coordinated packaging of surfactant phospholipids in lamellar bodies. In this study, we evaluated only PMA-stimulated secretion (Fig. 3). In control cells, the PMA-dependent secretions of PC and PG were approximately similar. In methylamine-treated cells, the PMA-dependent secretions for both PC and PG were decreased to about the same extent, suggesting that methylamine similarly affected the packaging of these two (and possibly other) surfactant phospholipids.

The surfactant released after PMA-stimulation of cells that were labeled with [9,10-^{3}H]palmitic acid and ± methylamine was evaluated for distribution of palmitate radioactivity in different phospholipid classes. In surfactant released from control cells, most of the palmitate radioactivity was present in PC and PG fractions (Table 7). In surfactant from methylamine-treated

TABLE 6
Surfactant Secretion in Type II Cells Labeled for 20–22 h in the Presence of MA[a]

		[^{3}H]PC Secretion in 2 h (%)	
		Control	MA*
Basal	(5)	1.4 ± 0.3	0.5 ± 0.1
ATP (1 mM)	(4)	5.8 ± 0.5	1.7 ± 0.4
Terbutaline (0.1 mM)	(3)	3.6 ± 0.8	1.0 ± 0.1
PMA (80 nM)	(3)	5.2 ± 0.5	1.8 ± 0.2

[a]Isolated type II cells were labeled for 20–22 h with [^{3}H-methyl]choline ± 2.5 mM MA. Secretion of PC ± indicated secretagogues was followed for 2 h according to standard protocol in the absence of MA. Results are means ± SE of experiments indicated in parentheses. *Labeling in the presence of MA significantly decreased the secretion of PC under each condition. PMA, phorbol 12-myristate 13-acetate.

TABLE 7
Distribution of [^{3}H]Palmitic Acid-Labeled PL in Surfactant Released by Type II Cells Labeled in the Presence of MA[a]

	[^{3}H]-Palmitic acid-labeled PL (%)	
PL	Control	MA
PC	94.4 ± 0.2	93.4 ± 0.1
Phosphatidylglycerol	4.09 ± 0.48	3.53 ± 0.34
Phosphatidylethanolamine	0.39 ± 0.14	0.89 ± 0.28
Sphingomyelin	0.22 ± 0.03	0.75 ± 0.03*
Phosphatidylserine	0.15 ± 0.06	0.20 ± 0.05
Phosphatidylinositol	0.30 ± 0.15	0.20 ± 0.07
Cardiolipin	0.32 ± 0.24	1.35 ± 0.32

[a]Freshly isolated type II cells were labeled for 20–22 h with [^{3}H]-palmitic acid ± 2.5 mM MA. Cells were then stimulated for 2 h with 80 nM PMA and the media analyzed for palmitic acid label in indicated PL. Results are means ± SE of three experiments in each case except for phosphatidylinositol and cardiolipin, which are means ± range of two experiments. * $P < 0.05$ when compared with corresponding control. See Tables 1, 4, and 6 for abbreviations.

cells also, most of the palmitate radioactivity was present in PC and PG. Thus, methylamine treatment did not affect the distribution of palmitate radioactivity in different phospholipid classes, suggesting that various phospholipids of lung surfactant follow a common pathway during packaging in the lamellar bodies.

DISCUSSION

Although lamellar bodies have long been recognized as surfactant storage organelles, there has been relatively little progress in understanding the mechanisms that regulate packaging of lung surfactant phospholipids and proteins in lamellar bodies. Using 20–22 h cultured type II cells, we have previously suggested that the acidic pH, presumably in lamellar bodies, might regulate the packaging of newly synthesized PC and DSPC in lamellar bodies (16). In the current study, our goal was to show that the acidic pH is also important in regulating the packaging of PC and DSPC in lamellar bodies in freshly isolated type II cells and that our previous observations on PC packaging were not an artifact of culture of these cells. However, the 20–22 h cultured cells demonstrate lower packaging (14), when compared with the freshly isolated cells (current study). Thus, it may be more useful to utilize freshly isolated cells for acute metabolic studies investigating surfactant phospholipid packaging.

The second major goal of this study was to understand the mechanism of surfactant phospholipid transport to the lamellar bodies. Specifically, we wished to determine if methylamine also inhibited the packaging of PG in lamellar bodies. Such inhibition would suggest that type II cells exercise some degree of coordination during the transport of different surfactant phospholipids to the lamellar bodies. Our short- and long-term metabolic labeling studies in freshly isolated type II cells show that methylamine also inhibited the packaging of PG in lamellar bodies. Thus, the acidic pH is important for packaging of all three phospholipids (PC, DSPC, and PG) and possibly other minor components of lung surfactant in lamellar bodies. It is unlikely that methylamine affects a specific metabolic pathway (e.g., remodeling) in type II cells, because (i) it similarly inhibited the labeling of the unsaturated PC and DSPC in lamellar bodies (16) and (ii) its effect on the labeling of lamellar body PC with choline or palmitic acid was similar (Tables 1 and 2, Fig. 1). An inhibition of PC remodeling should inhibit the palmitic acid, but not the choline, incorporation in lamellar body PC. Also, it should not affect the palmitic acid incorporation into lamellar body PG. Thus, the effects of methylamine appear to be on the packaging of PC, DSPC, and PG. Because the inhibition of packaging is of similar magnitude for each phospholipid, the phospholipid composition of the released surfactant remains unaltered. These findings suggest that type II cells exercise some degree of coordination in the transfer and packaging of surfactant phospholipids.

The mechanisms for phospholipid trafficking from the site of synthesis (endoplasmic reticulum) to the lamellar bodies are not known. However, several mechanisms for intermembrane transfer of lipids have been postulated in other cell types. One mechanism for intracellular transport of phospholipids involves the phospholipid transfer proteins, which, under specialized conditions, facilitate molecular transfer or exchange of individual phospholipids between the donor and acceptor organelles (5). These proteins are possibly present in soluble form although their association with membranes or specific organelles cannot be excluded. In type II cells also, several proteins have been postulated to mediate transfer of surfactant phospholipids, PC, DSPC, and PG, to lamellar bodies (7,36). Because methylamine decreased the packaging of all three phospholipids to a similar extent (Fig. 1), the transfer and packaging of all three surfactant phospholipids would proceed at rates comparable with their relative distribution. If several transfer proteins mediate the transfer of different surfactant phospholipids, then all these proteins may be similarly sensitive to methylamine to cause similarly decreased packaging of individual phospholipids. Alternately, a single protein with above-described characteristics may facilitate the transfer of PC, DSPC, and PG (and possibly other surfactant phospholipids) type II cells. A phospholipid transfer protein with these characteristics is yet to be described in type II cells or in any other system.

Bulk transfer of lipids can be one mechanism for the coordinated trafficking of several phospholipids to a target site. In other cell types, various investigators have suggested that bulk transfer of phospholipids and proteins involves vesicle budding, translocation, and fusion with the target membrane (9). Several systems have been described for the study of PC, cholesterol, or PS trafficking to intracellular membranes (8–10). In the liver (37), the transfer of PC from the endoplasmic reticulum to the Golgi apparatus is suggested to occur by transitional vesicles (~60 nm in diameter), which bud and pinch off from the transitional elements of endoplasmic reticulum (part rough and part smooth). PC comprises ~70% of total phospholipids in these vesicles (38). Previous ultrastructural and radioautographic studies in mouse lungs have reported the presence of small vesicles in close vicinity of lamellar bodies (39). It is likely that these vesicles contain surfactant lipids. By analogy with other systems, the transfer of lipids from these vesicles could occur after their fusion with the small or growing lamellar bodies, which would deliver the contents to the lamellar body interior (the "residual" fraction). These vesicles (possibly containing all phospholipids of lung surfactant) could also mediate some degree of coordination since any change in the transfer efficiency would similarly influence packaging of all surfactant phospholipids. If methylamine inhibits such transfer then it would not affect the percentage PC in lamellar bodies (or "residual" fraction) or the phospholipid composition of released surfactant (Tables 3–5, 7).

The acidic pH, possibly of lamellar bodies, which is increased with methylamine or other weak bases (15–17), appears to regulate the phospholipid packaging. One possibility is that the acidic pH facilitates the fusion of hypothesized vesicles with the lamellar bodies. *In vitro* studies on vesicle fusion have demonstrated that the internal pH of vesicles can affect the phospholipid distribution in the bilayer and the fusion of vesicles (40,41). Various studies have suggested that annexins

(42,43) or surfactant protein B (44) can facilitate vesicle fusion under appropriate conditions. However, the nature of surfactant-carrying vesicles and the proteins that mediate fusion of these vesicles with growing lamellar bodies are not known at present.

The inhibition of surfactant secretion under basal or stimulated conditions also appears to be due to decreased packaging of surfactant in the lamellar bodies. The secretion, in response to various secretagogues (Table 6), which act through different receptors or protein kinases, was similarly decreased in methylamine-pretreated cells. It is unlikely that all of these pathways are similarly affected in methylamine-treated cells. Nevertheless, our studies cannot exclude the possibility that methylamine treatment influences the signal-transduction pathway in type II cells.

In summary, we have shown that weak bases (methylamine and NH_4Cl) inhibit packaging of *de novo* synthesized PG, DSPC, or PC (and possibly other phospholipids) in lamellar bodies in freshly isolated type II cells, suggesting the significance of acidic pH in subcellular compartments (presumably lamellar bodies). Our results showing similar decrease in the packaging of three surfactant phospholipids and the unaltered composition of released surfactant lead us to suggest that the type II cells excercise coordination in the trafficking of different surfactant phospholipids to the lamellar bodies. We speculate that the coordinated tranport occurs through surfactant-phospholipid-containing vesicles. These surfactant-containing transport vesicles are yet to be described in type II cells although vesicles containing high PC content (~70%) have been described in the liver. However, we cannot exclude an alternate mechanism(s) involving novel phospholipid transfer protein(s), which is (are) yet to be described in any system.

ACKNOWLEDGMENTS

This work was supported by grant HL 49959 from National Heart Lung and Blood Institute. The authors acknowledge the technical assistance of Ai-Min Wu and Graham Vigliotta. Parts of these studies were presented at the Experimental Biology meeting held in April 1995 in Atlanta, Georgia, and in April 1997 held in New Orleans, Louisiana and were published in abstract forms (*FASEB J. 9*: A860, 1995; *FSEB J. 11*: A558, 1997).

REFERENCES

1. Batenburg, J.J. (1992). Surfactant Phospholipids: Synthesis and Storage, *Am. J. Physiol. 262*, L367–L385.
2. Rooney, S.A., Young, S.L., and Mendelson, C.R. (1993) Molecular and Cellular Processing of Lung Surfactant, *FASEB J. 8*, 957–967.
3. Chander, A., and Fisher, A.B. (1990) Regulation of Lung Surfactant Secretion, *Am. J. Physiol. 258*, L241–L253.
4. Wright, J.R. (1990) Clearance and Recycling of Pulmonary Surfactant, *Am. J. Physiol. 259*, L1–L12.
5. Helmkamp, G.M. (1986) Phospholipids Transfer Proteins: Mechanism of Action, *J. Bioenerg. Biomembr. 18*, 71–91.
6. Vance, J.E., Aasman, E.J., and Szarka, R. (1991) Brefeldin A Does Not Inhibit the Movement of Phosphatidylethanolamine from Its Site of Synthesis to the Cell Surface, *J. Biol. Chem. 266*, 8241–8247.
7. Lumb, R.H. (1989) Phospholipid Transfer Proteins in Mammalian Lung, *Am. J. Physiol. 257*, L190–L194.
8. Moreau, P., and Cassagne, C. (1994) Phospholipid Trafficking and Membrane Biogenesis, *Biochim. Biophys. Acta 1197*, 257–290.
9. Pfeffer, S.R., and Rothman, J.E. (1987) Biosynthetic Protein Transport and Sorting by the Endoplasmic Reticulum and Golgi, *Annu. Rev. Biochem. 56*, 829–852.
10. Trotter, P.J., and Voelker, D.R. (1994) Lipid Transport in Eukaryotic Cells, *Biochim. Biophys. Acta 1213*, 241–262.
11. Phizackerly, P.J.R., Town, M.H., and Newman, G.E. (1979) Hydrophobic Proteins of Lamellated Osmiophillic Bodies Isolated from Pig Lung, *Biochem. J. 183*, 731–736.
12. Chander, A., Dodia, C.R., Gil, J., and Fisher, A.B. (1983) Isolation of Lamellar Bodies from Rat Granular Pneumocytes in Primary Culture, *Biochim. Biophys. Acta 753*, 119–129.
13. DiAugustine, R.P. (1974) Lung Concentric Laminar Organelle, *J. Biol. Chem. 249*, 584–593.
14. Hook, G.E.R., and Gilmore, L.B. (1982) Hydrolases of Pulmonary Lysosomes and Lamellar Bodies, *J. Biol. Chem. 257*:9211–9220.
15. Chander, A., Johnson, R.G., Reicherter, J., and Fisher, A.B. (1986). Lung Lamellar Bodies Maintain an Acidic Internal pH, *J. Biol. Chem. 261*, 6126–6131.
16. Chander, A., Sen, N., Wu, A.-I., Higgins, S., Wadsworth, S., and Spitzer, A. (1996) Methylamine Decreases Trafficking and Packaging of Newly Synthesized Phosphatidylcholine in Lamellar Bodies in Alveolar Type II Cells, *Biochem. J. 318*, 271–278.
17. Wadsworth, S.J., Spitzer, A.R., and Chander, A. (1997) Ionic Regulation of Proton Chemical (pH) and Electrical Gradients in Lung Lamellar Bodies, *Am. J. Physiol. 273*, L427–L436.
18. Voorhout, W.F.T., Veenendaal, T., Haagsman, H.P., Weaver, T.E., Whitsett, J.A., VanGolde, L.M.G., and Geuze, H.J. (1992) Intracellular Processing of Pulmonary Surfactant Protein B in an Endosomal/Lysosomal Compartment, *Am. J. Physiol. 263*, L479–L486.
19. Beers, M.F. (1996) Inhibition of Cellular Processing of Surfactant Protein C by Drugs Affecting Intracellular pH Gradients, *J. Biol. Chem. 271*, 14361–14370.
20. Ruano, M.L.F., Perez-Gil, J., and Casals, C. (1998) Effect of Acidic pH on the Structure and Lipid Binding Properties of Porcine Surfactant Protein A. Potential Role of Acidification Along Its Exocytic Pathway, *J. Biol. Chem. 273*, 15183–15191.
21. Shannon, J.M., Mason, R.J., and Jennings, S.D. (1987) Functional Differentiation of Alveolar Type II Epithelial Cells *in vitro*: Effects of Cell-Shape, Cell-Matrix Interactions and Cell-Cell Interactions, *Biochim. Biophys. Acta 931*, 143–156.
22. Suwabe, A., Mason, R.J., and Voelker, D.R. (1991) Temporal Segregation of Surfactant Secretion and Lamellar Body Biogenesis in Primary Cultures of Rat Alveolar Type II Cells, *Am. J. Respir. Cell Mol. Biol. 5*, 80–86.
23. Dobbs, L.G., Gonzales, R., and Williams, M.C. (1986) An Improved Method for Isolating Type II Cells in High Purity and Yield, *Am. Rev. Respir. Dis. 134*, 141–145.
24. Chander, A., and Sen, N. (1993) Inhibition of Phosphatidylcholine Secretion by Stilbene Disulfonates in Alveolar Type II Cells, *Biochem. Pharmacol. 45*, 1905–1912.
25. Bligh, E.G., and Dyer, W.J. (1959) A Rapid Method of Total Lipid Extraction and Purification, *Canad. J. Biochem. Physiol. 37*, 911–917.
26. Katyal, S.L., Estes, W., and Lombardi, B. (1977) Method for the Isolation of Surfactant from Homogenates and Lavages of Adult, Newborn, and Fetal Rats, *Lab. Invest. 36*, 585–592.
27. Chander, A. (1992) Dicyclohexylcarbodiimide and Vanadate Sensitive ATPase of Lung Lamellar Bodies, *Biochim. Biophys. Acta 1123*:198–206.
28. Bradford, M.M. (1976) A Rapid and Sensitive Method for

Quantitation of Microgram Quantities of Proteins Utilizing the Principle of Protein Dye Binding, *Anal. Biochem. 72*, 248–254.
29. Mason, R.J., Nellenbogen, J., and Clements, J.A. (1976). Isolation of Disaturated Phosphatidylcholine with Osmium Tetraoxide, *J. Lipid Res. 17*, 281–284.
30. Fine, J.B. and Sprecher, H. (1982) Unidimensional Thin-Layer Chromatography of Phospholipids on Boric Acid Impregnated Plates, *J. Lipid Res. 23*, 660–663.
31. Poorthuis, B.J.H., Yazaki, P.J., and Hostetler, K. (1976) An Improved Two-Dimensional Thin-Layer Chromatography System for Separation of Phosphatidylglycerol and Its Derivatives, *J. Lipid Res. 17*, 433–437.
32. Alvarez, J.G., and Touchstone, J.C. (1992) Separation of Acidic and Neutral Lipids by Aminopropyl-Bonded Silica Gel Column Chromatography, *J. Chromatogr. 577*, 142–145.
33. Abramson, D., and Blecher, M. (1964) Quantitative Two-Dimensional Thin-Layer Chromatography of Naturally Occurring Phospholipids, *J. Lipid Res. 5*, 628–631.
34. Marinetti, G.V. (1962) Chromatographic Separation, Identification, and Analysis of Phosphatides, *J. Lipid Res. 3*, 1–20.
35. Chander, A., Fisher, A.B., and Strauss III, J.F. (1982) Role of an Acidic Compartment in Synthesis of Disaturated Phosphatidylcholine by Rat Granular Pneumocytes, *Biochem. J. 208*, 651–658.
36. Read, R.J., and Funkhouser, J.D. (1984) Acyl-Chain Specificity and Membrane Fluidity. Factors Which Influence the Activity of a Purified Phospholipid-Transfer Protein from Lung, *Biochim. Biophys. Acta 794*, 9–17.
37. Paulik, M., Nowack, D.D., and Morre, D.J. (1988) Isolation of a Vesicular Intermediate in the Cell-Free Transfer of Membrane from Transitional Elements of the Endoplasmic Reticulum to Golgi Apparatus Cisternae of Rat Liver, *J. Biol. Chem. 263*, 17738–17748.
38. Moreau, P., Cassagne, C., Keenan, T.W., and Morre, J.D. (1993) Ceramide Excluded from Cell-Free Vesicular Lipid Transfer from Endoplasmic Reticulum to Golgi Apparatus. Evidence for Lipid Sorting, *Biochim. Biophys. Acta 1146*, 9–16.
39. Chevalier, G., and Collet, A.J. (1972) *In Vivo* Incorporation of Choline-^{3}H, Leucine-^{3}H, and Galactose-^{3}H in Alveolar Type II Pneumocytes in Relation to Surfactant Synthesis. A Quantitative Radioautographic Study in Mouse by Electron Microscopy, *Anat. Rec. 174*, 289–310.
40. Hope, M.J., Redelmeier, T.E., Fong, K.F., Rodrigueza, W., and Cullis, P.R. (1989) Phospholipid Asymmetry in Large Unilamellar Vesicles Induced by Transmembrane pH Gradients, *Biochemistry 28*, 4181–4187.
41. Murata, M., Takahashi, S., Kagiwada, S., Suzuki, A., and Ohnishi, S.-I. (1992) pH-Dependent Membrane Fusion and Vesiculation of Phospholipids Large Unilamellar Vesicles Induced by Amphiphillic and Cationic Peptides, *Biochemistry 31*, 1986–1992.
42. Chander, A., and Wu, R.-D. (1991) *In Vitro* Fusion of Lung Lamellar Bodies and Plasma Membrane Is Augmented by Lung Synexin, *Biochim. Biophys. Acta 1086*, 157–166.
43. Tsao, F.H.C. (1990) Purification and Characterization of Two Rabbit Lung Ca^{2+}-Dependent Phospholipid Binding Proteins, *Biochim. Biophys. Acta 1045*: 29–39.
44. Shiffer, K., Hawgood, W., Duzugens, N., and Goerke, J. (1988) Interactions of Low Molecular Weight Group of Surfactant-Associated Proteins (5–18) with Pulmonary Surfactant Lipids, *Biochemistry 27*, 2689–2695.

[Received August 25, 1999, and in final revised form November 22, 1999; revision accepted December 8, 1999]

Protective Effect of Oleuropein, an Olive Oil Biophenol, on Low Density Lipoprotein Oxidizability in Rabbits

E. Coni[a,*], R. Di Benedetto[a], M. Di Pasquale[a], R. Masella[b], D. Modesti[b], R. Mattei[c], and E.A. Carlini[c]

[a]Food Department and [b]Metabolism and Pathological Biochemistry Department, Istituto Superiore di Sanità, 00161 Rome, Italy, and [c]Psychobiology Department, Universidade Federal de Saõ Paulo, 04023-062 Saõ Paulo, Brazil

ABSTRACT: On the basis of the results obtained with pilot studies conducted *in vitro* on human low density lipoprotein (LDL) and on cell cultures (Caco-2), which had indicated the ability of certain molecules present in olive oil to inhibit prooxidative processes, an *in vivo* study was made of laboratory rabbits fed special diets. Three different diets were prepared: a standard diet for rabbits (diet A), a standard diet for rabbits modified by the addition of 10% (w/w) extra virgin olive oil (diet B), a modified standard diet for rabbits (diet C) differing from diet B only in the addition of 7 mg kg^{-1} of oleuropein. A series of biochemical parameters was therefore identified, both in the rabbit plasma and the related isolated LDL, before and after Cu-induced oxidation. The following, in particular, were selected: (i) biophenols, vitamins E and C, uric acid, and total, free, and ester cholesterol in the plasma; (ii) proteins, triglycerides, phospholipids, and total, free, and ester cholesterol in the native LDL (for the latter, the dimensions were also measured); (iii) lipid hydroperoxides, aldehydes, conjugated dienes, and relative electrophoretic mobility (REM) in the oxidized LDL (ox-LDL). In an attempt to summarize the results obtained, it can be said that this investigation has not only verified the antioxidant efficacy of extra virgin olive oil biophenols and, in particular, of oleuropein, but has also revealed a series of thus far unknown effects of the latter on the plasmatic lipid situation. In fact, the addition of oleuropein in diet C increased the ability of LDL to resist oxidation (less conjugated diene formation) and, at the same time, reduced the plasmatic levels of total, free, and ester cholesterol (–15, –12, and –17%, respectively), giving rise to a redistribution of the lipidic components of LDL (greater phospholipid and cholesterol amounts) with an indirect effect on their dimensions (bigger by about 12%).

Paper no. L8329 in *Lipids 35*, 45–54 (January 2000).

In recent years, considerable evidence has accumulated that shows free radicals play a key role in the etiopathogenesis of atherosclerosis (1). It has, in fact, been demonstrated that the main cause of changes in the conformation of both low density lipoproteins (LDL) and high density lipoproteins (HDL) is lipid peroxidation, and that these oxidized lipoproteins (ox-LDL, ox-HDL) are among the main causes of the formation of atherosclerotic lesions. This theory is amply supported by data derived from biochemical studies, experiments on animal models, and epidemiological and clinical investigations (1–7). Much of the recent attention given to the pathogenic role of ox-LDL in the onset of atherosclerosis is a result of the increasing indications that ox-LDL are capable of causing both the migration of monocytes in the intima of the artery and their subsequent conversion into foam cells (8,9).

It is also important to remember that both ox-LDL and -HDL contain high concentrations of highly cytotoxic lipoperoxides in their hydrophobic region (2). Once ox-LDL and -HDL have been deposited on artery walls, they can release these endothelial toxins, which promote a state of irritation among the cells of the arterial wall, causing a series of side effects that certainly contribute to the further development of degenerative lesions. For example, it is known that oxidized lipoproteins inhibit the relaxation of smooth muscle cells induced by the endothelial release factor (EDRF), now identified as nitrogen monoxide (NO) freed from arginine by NO synthetase. This inhibition is able to induce a state of hypertension that can in turn contribute to increasing the gravity of the lesion.

Furthermore, ox-LDL are capable of promoting other proatherogenic lesions by setting off an immune-type inflammatory reaction and stimulating the endothelial cells into releasing a whole series of biologically active substances that promote the endothelial adhesion of leukocytes and stimulate the growth of monocytes (2,6,9).

Lastly, oxidized lipoproteins can modulate transcription factors such as API and NFkβ and modify the homeostasis of prostanoids (thromboxanes and leukotrienes), favoring platelet aggregation. The vast spectrum of direct and indirect actions of ox-LDL is thus extremely complex (2).

The above being said, it should be recalled that humans have efficient endogenous systems of protection against radi-

*To whom correspondence should be addressed at Food Dept., Istituto Superiore di Sanità, viale Regina Elena 299, 00161 Rome, Italy.

E-mail: e.coni@iss.it

Abbreviations: EDRF, endothelial release factor; 4-HNE, 4-hydroxy-2(*E*)-nonenal; HPLC, high-performance liquid chromatography; LDL, low density lipoprotein; MDA, malondialdehyde; ox-LDL, oxidized LDL; PBS, phosphate-buffered saline; PGGE, polyacrylamide gradient gel electrophoresis, REM, relative electrophoretic mobility.

cal oxidative reactions able to reduce the reactivity and/or concentration of prooxidant species. Also exogenous compounds of dietary origin (i.e., free radical scavengers), can play an important role (10). Some studies have shown that inhibitors of lipid oxidation, such as vitamins E and C, carotene, and flavonoids, reduce the oxidation of LDL and diminish their catabolism by means of macrophages (11–15). The diet can therefore influence the oxidative processes that take place in the human body by regulating the supply of exogenous prooxidants and antioxidants or modulating the synthesis of endogenous antioxidants. In this context, the antioxidant potential of some biophenols contained, for example, in green tea and red wine has been recognized. These compounds have been evaluated, in both *in vitro* and *in vivo* models, as free radical scavengers and, consequently, as regulators of lipid metabolism or as protective factors against the induction of certain tumors, particularly cutaneous ones (16–18). The results obtained have been particularly encouraging and have suggested the extension of the studies in order to evaluate whether other components of the diet can, thanks to their biophenol content, contribute to biological defenses against cell aging and carcinogenesis.

In recent years, researchers have been focusing their attention on a typical item of the Mediterranean diet—olive oil. However, most experiments carried out so far on the biophenols of olive oil have been aimed at checking and, where possible, quantifying their antioxidant power only in relation to the stabilizing activity exercised on the oil itself (19–22). Not many studies have been made that evaluate the protective role of the biophenols contained in olive oil in biological systems, and very few have been done on animal models (23–26). The reason for this lack of information is due to the fact that planning studies on *in vivo* experimental models is very complicated and expensive. On the other hand, this type of study recognizes the real mechanisms of biophenols action and consequently makes a clearer indication of its antioxidant activity.

On the basis of data obtained from pilot studies conducted *in vitro* on human LDL and on cell cultures (Caco-2) (26,27) that had indicated the ability of certain molecules present in olive oil to inhibit prooxidative processes even at extremely low concentrations, an *in vivo* study was undertaken on laboratory rabbits fed special diets. Oleuropein was chosen for this study because of its peculiar presence in olives, its antibacterial, antifungal, and antioxidant effects, and because, to the best of our knowledge, its protective role in biological systems has not yet been tested on animal models. The chemical structure of oleuropein is shown in Scheme 1.

Particular attention was paid to the selection of indices, related both to rabbit plasma and isolated LDL, which could better define the influence of biophenols on peroxidative processes. The following biochemical parameters were selected: (i) biophenols, vitamins E and C, uric acid, and total, free, and ester cholesterol in the plasma; (ii) proteins, triglycerides, phospholipids, and total, free, and ester cholesterol in native LDL (for the latter, the dimensions, lipid hydroperoxides, and aldehydes were also measured); and (iii) conjugated dienes, lipid hydroperoxides, aldehydes, and relative electrophoretic mobility (REM) in ox-LDL.

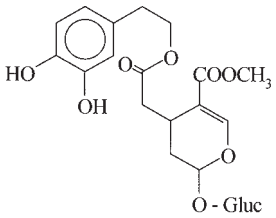

OLEUROPEIN

SCHEME 1

EXPERIMENTAL PROCEDURES

Animals and diets. Twenty-four female New Zealand White rabbits, 8–10 wk old (Charles River S.p.A., Como, Italy), were used for the investigation. Upon their arrival, the animals were transferred into single cages put in a room where the environmental requirements (ventilation, temperature, humidity, illumination, and noise) complied with those required by Italian legislative decree 116 of 1992 (28). Food and water were available *ad libitum* during the whole study, and the health state of animals was verified every day.

Three different diets were prepared by Mucedola S.r.l. (Settimo Milanese, Italy): a standard diet (2RB 15) for rabbits (diet A); a standard diet for rabbits modified by the addition of 10% (w/w) extra virgin olive oil (diet B); and a modified standard diet for rabbits (diet C) differing from diet B only in the addition of 7 mg kg^{-1} of oleuropein (Extrasynthese S.A., Genay, France). This dose [corresponding to about 0.4 mg kg^{-1} rabbit body weight (b.w.) day^{-1}] was selected because it is comparable to the average daily biophenol intake per kilogram of human b.w. from olive oil in a Mediterranean diet.

The olive oil addition was carried out by replacing part of specific ingredients (i.e., dehydrated alfalfa and grass meal) in a standard diet so as not to change the content of some nutrients, such as water, elements and vitamins, that could be involved in oxidative processes occurring both in the feedstuffs and in rabbits. Since the replacement of dehydrated alfalfa and grass meal with extra virgin olive oil resulted in a vitamin E increase in diets B and C, a greater amount of vitamin E was supplemented in diet A. The nutritional composition of the three diets, experimentally assessed, is shown in Table 1, while in Table 2, the vitamin E and biophenol content of the extra virgin olive oil added to diets B and C is reported. The data shown in this latter table also provide information about the biophenol content of the diet supplemented with extra virgin olive oil. In fact, it is easy to estimate the biopherol contribution of the oil to diets B and C, considering its addition at 10%.

The group of rabbits fed standard diet A was included in the experimental protocol to verify in which manner the plasmatic lipid composition was influenced by the six-times-higher lipid content of diets B and C.

TABLE 1
Nutritional Composition of the Three Diets (% w/w on wet weight)[a]

Component	Diet A	Diet B	Diet C
Experimental data[b]			
Water	12.08 ± 0.34	11.97 ± 0.41	12.07 ± 0.28
Carbohydrates[c]	41.76	36.16	36.29
Protein	13.51 ± 0.78	12.21 ± 0.69	12.18 ± 0.87
Fat	2.13 ± 0.35	11.10 ± 0.27	11.04 ± 0.33
Saturated fatty acids	0.40 ± 0.05	1.76 ± 0.22	1.81 ± 0.32
Monounsaturated fatty acids	1.05 ± 0.16	8.16 ± 0.53	8.09 ± 0.64
Polyunsaturated fatty acids	0.53 ± 0.09	1.06 ± 0.22	1.08 ± 0.19
Cholesterol	$4.0 \cdot 10^{-5}$	$3.3 \cdot 10^{-5}$	$3.3 \cdot 10^{-5}$
Fiber	22.04 ± 0.98	20.11 ± 1.02	19.96 ± 1.21
Minerals	8.42 ± 078	8.39 ± 0.86	8.40 ± 0.66
Vitamin E[d]	0.078 ± 0.021	0.073 ± 0.019	0.074 ± 0.016
Manufacturer's data			
Vitamin integration[e]	0.060	0.058	0.058
Mineral integration	0.028	0.028	0.028

[a]Diet A, standard rabbit food; diet B, standard food modified by the addition of 10% (w/w) extra virgin olive oil; diet C, same as diet B but with 7 mg kg^{-1} oleuropein.
[b]Values are expressed as mean ± SD (n = 5).
[c]Calculated for difference.
[d]Expressed as % α-tocopherol; calculated using activity coefficients for individual tocopherols (51).
[e]The value related to diet A is greater because it provides for higher vitamin E supplementation.

Before starting the experiment, the animals were acclimatized for a period of 15 d during which they all received the same food (standard diet A). Subsequently, the rabbits were randomly divided into three groups of eight animals each. One group continued to be fed standard diet A, while the other two groups were gradually adapted to diets B and C, respectively. This period of adaptation has been believed necessary considering the high lipid content of these last two diets compared with that of a standard diet for rabbits. The entire feeding design is reported in Table 3. Food consumption was checked daily and the animals were weighed every week.

Preparation of plasma and isolation of LDL. After 6 wk on the special diets, 30 mL of blood from rabbits that had been fasted for 12 h was taken by intracardiac injection and collected in test tubes containing 30 mg of EDTA. The plasma was immediately separated by centrifugation at 500 × g for 15 min at ambient temperature and divided into two aliquots. The first was immediately tested to determine biophenol, vitamins E and C, uric acid, and total, free, and ester cholesterol contents, while the second was used to isolate LDL.

LDL were isolated by sequential ultracentrifugation (UL-70 ultracentrifuge Beckman fitted with a 60 Ti rotor; Fullerton, CA) in the density range 1.015–1.063 mg mL^{-1}, at 140,000 × g for 22 h (two times) at a temperature of 15°C according to the method proposed by Havel *et al.* (29). After measuring the protein in the LDL, using the method of Lowry *et al.* (30), the LDL fraction was diluted with a phosphate-buffered saline (PBS) solution (150 mM sodium phosphate, 150 mM NaCl, pH 7.2) until a final concentration of 0.2 mg LDL protein/mL was obtained. This fraction was then dialyzed against NaCl (0.9%, wt/vol) in a proportion of 1:500.

Analysis of plasma and native LDL. The methodology used for analyzing the biophenol concentration in the plasma was based on the extraction of these compounds from the matrix, then purification and extraction by high-performance liquid chromatography (HPLC). The procedure is similar to that described by Papadopoulus and Tsimidou (31) except for some changes in the extraction procedure and the chromatographic conditions. These changes were ascribed to the fact that the above mentioned method refers solely to olive oil matrix, whereas in the present study it was also applied to plasma matrix. Briefly, SPE (Spe-ed SPE C_{18} 500 mg-6 mL, Applied Separations, Allentown, PA) cartridges, previously conditioned by passing 2 mL of an *n*-hexane/ethyl ether solution (98:2, vol/vol), were used for the extraction and purification of the biophenols. One milliliter of sample was then deposited on the top of the cartridge, which was subsequently washed

TABLE 2
Biophenol and Vitamin E Contents of the Extra Virgin Olive Oil Added to Diets[a] B and C

Component	mg L^{-1}[b]
Vitamin E[c]	11.9 ± 0.9
Total biophenols[d]	238 ± 54
Oleuropein	2.04 ± 0.78
Oleuropein aglycone	18.64 ± 3.36
3,4-Dihydroxyphenylethanol	1.62 ± 0.25
p-Hydroxyphenylethanol (tyrosol)	4.68 ± 0.77
Gallic acid	0.82 ± 0.18
Protocatechuic acid	1.83 ± 0.56
Vanillic acid	1.15 ± 0.39
Caffeic acid	0.04 ± 0.02
p-Cumaric acid	0.32 ± 0.09
o-Cumaric acid	0.07 ± 0.03
Ferulic acid	0.34 ± 0.10

[a]See Table 1 for information regarding diets.
[b]Values are expressed as mean ± SD (n = 5).
[c]Expressed as mg α-tocopherol calculated using activity coefficients for individual tocopherols (51).
[d]Expressed as tyrosol concentration.

TABLE 3
Feeding Protocol for the Three Rabbit Groups

Time	Feedstuffs[a] Group 1 (*n* = 8)	Group 2 (*n* = 8)	Group 3 (*n* = 8)
1st wk	100% Diet A	75% Diet A + 25% Diet B	75% Diet A + 25% Diet C
2nd wk	100% Diet A	50% Diet A + 50% Diet B	50% Diet A + 50% Diet C
3rd wk	100% Diet A	25% Diet A + 75% Diet B	25% Diet A + 75% Diet C
4th–9th wk	100% Diet A	100% Diet B	100% Diet C

[a]See Table 1 for information regarding diets.

with 10 mL of the conditioning solution. The biophenol fraction was then eluted with 8 mL of methanol, filtered through disposable Teflon filters, and evaporated in a Rotavapor at 35°C. The dry residue was then dissolved in 0.5 mL of methanol and 10 μL of this solution was injected into a high-performance liquid chromatograph (Waters, Milford, MA) fitted with a Lichrosorb (Merck, Darmstadt, Germany) column (RP18 250 × 4.6 mm, 5 μm) and an ultraviolet/visible light (UV-Vis) detector set at 280 nm. The eluants were: (A) acetonitrile/methanol (50:50 vol/vol) and (B) phosphoric acid/water (1:99 vol/vol). The gradient was: t = 0 min, 4% A; t = 20 min, 20% A; t = 40 min, 50% A; t = 50 min, 60% A; t = 60 min, 100% A. For the sake of completeness, mention should be made of the fact that during HPLC–UV-Vis method validation, mass spectrometry was used for phenol identification.

The plasmatic content of vitamin E (α-, β-, δ-, and γ-tocopherols) was determined by extracting the analyte from the matrix and then separating it in a high-performance liquid chromatograph as reported by Cavina *et al.* (32).

An analytical methodology based on the use of an HPLC, as described by Ross (33), also was used for determining vitamin C and uric acid in the plasma.

Enzymatic spectrophotometric methods, involving the use of kits such as Chol MPR 1 (CHOD-PAP method), F-Chol MPR 1 (CHOD-PAP method), TG (GPO-PAP method), and PL MPR 2, all supplied by Boehringer Mannheim (Mannheim, Germany), were employed for determining, the total and free cholesterol in the plasma and native LDL and the triglycerides and phospholipids in the native LDL, respectively. The cholesteryl esters were calculated by the difference between total and free cholesterol multiplied by a factor of 1.68.

Lastly, polyacrylamide gradient gel electrophoresis (PGGE) (Pharmacia LKB Biotechnology, Uppsala, Sweden) was used to measure the dimensions of the native LDL (34). The diameter of the dominant LDL fraction was computed by interpolation from a plot of the logarithm of the diameter of three standards (i.e., apoferritin, thyroglobulin, and latex beads) vs. the migration length of the same standards, as reported by Coresh *et al.* (35).

Studies on ox-LDL. As far as ox-LDL are concerned, their susceptibility to Cu-induced oxidation was preliminarily evaluated by a test of the conjugated dienes (36,37). For this purpose, 250 μL of dialyzed LDL (0.2 mg of LDL protein mL^{-1}) was pipetted into 1-cm quartz cuvettes and brought to a volume of 1 mL with PBS, and then 10 μL of 1 mM $CuSO_4$ was added so that the final concentration of Cu^{2+} was 10 μM. Shortly after, measurements of absorbance at 234 nm were taken, at 10-min intervals for 8 h. A Beckman Instruments DU-640 UV-Vis spectrophotometer, equipped with an automatic cell exchanger and a thermostat set at 30°C, was used. The instrument was connected to a computer for automatic acquisition of the data. The oxidation kinetics of every LDL sample was graphically represented as absolute absorbance against time, and the lag phase was measured as indicated by Puhl *et al.* (37).

TABLE 4
Biophenol Content in the Plasma of Rabbits Fed Different Diets[a]

Biophenol	mg L^{-1}[b] Diet A standard	Diet B modified	Diet C modified
Total biophenols	0.15 ± 0.06	1.93 ± 0.20[c]	2.73 ± 0.34[c,d]
Oleuropein	ND	0.008 ± 0.002	0.143 ± 0.022[c,d]
Oleuropein aglycone	ND	0.482 ± 0.086	0.501 ± 0.072
3,4-Dihydroxyphenylethanol	ND	0.059 ± 0.011	0.051 ± 0.009
p-Hydroxyphenylethanol (tyrosol)	ND	0.153 ± 0.020[c]	0.175 ± 0.021[c]
Gallic acid	0.041 ± 0.019	0.132 ± 0.015[c]	0.143 ± 0.021[c]
Protocatechuic acid	ND	0.062 ± 0.025[c]	0.094 ± 0.036[c]
Vanillic acid	ND	0.030 ± 0.013[c]	0.027 ± 0.010[c]
Caffeic acid	0.001 ± 0.0004	0.018 ± 0.007[c]	0.025 ± 0.011[c]
p-Cumaric acid	0.001 ± 0.0006	0.007 ± 0.002[c]	0.010 ± 0.004[c]
o-Cumaric acid	0.001 ± 0.005	0.011 ± 0.006[c]	0.013 ± 0.007[c]
Ferulic acid	0.002 ± 0.001	0.089 ± 0.034[c]	0.081 ± 0.025[c]

[a]See Table 1 for information regarding diets. ND, not detected.
[b]Values are expressed as mean ± SD (n = 8 per group). Total biophenols are expressed as tyrosol concentration.
[c]$P < 0.05$ vs. diet A, as found by analysis of variance (ANOVA).
[d]$P < 0.05$ vs. diet B, as found by ANOVA.

In order to assess the resistance of LDL to Cu-induced oxidation by means of other tests, i.e., determination of lipid hydroperoxides, malondialdehyde (MDA), and 4-hydroxy-2(*E*)-nonenal (4-HNE), and the measurement of relative electrophoretic mobility, preliminary *in vitro* oxidation of the LDL of rabbits fed the three different diets was necessary. For this purpose, the dialyzed LDL solutions (0.2 mg of LDL protein mL^{-1}) were oxidized by incubating for 3 h with 20 μM $CuSO_4$ at 37°C.

The concentration of lipid hydroperoxides was calculated iodometrically according to the method proposed by El-Saadani *et al.* (38), with the reaction time changed from 30 to 60 min.

MDA and 4-HNE determination was done by an enzymatic spectrophotometric method, using a Bioxytech LPO-586 kit (Oxis International Inc., Portland, OR).

Electrophoresis of ox-LDL was done as described by Morel *et al.* (39), using a Beckman Paragon LIPO electrophoretic kit (Beckman Instruments Inc., Fullerton, CA).

Statistical analyses. The results obtained from each group of rabbits were subjected to both parametrical and nonparametrical statistical analysis. Furthermore, in order to evaluate the significance of the differences noted between the biochemical parameters of the groups fed different diets, multifactor analysis of variance (ANOVA) was applied. Statgraphics software (V. 7 for DOS, Manugistic, Rockville, MD) was used for processing.

RESULTS AND DISCUSSION

No statistically significant differences were noted in terms of increased body weight and consumption of food between the rabbits fed the three different diets (data not shown).

The results related to the determination of the parameters for plasma and native LDL are set out in Tables 5 and 6, while those related to the study of the parameters for ox-LDL are set out in Table 7.

Plasmatic parameters. The data clearly show that biophenols, derived from the diets, are present as such in the plasma and are therefore capable of exerting their functional activity on plasmatic components such as LDL. Previous studies have proven that very low concentrations of some phenolic compounds also have this antioxidant activity (24,40).

It appears equally evident that the inclusion of extra virgin olive oil in diets B and C had a clear influence on the total biophenol content. As expected, the addition of oleuropein in diet C further increased that content. It is also interesting to point out that a very small quantity of oleuropein was present in the plasma of rabbits fed diet B, whereas the plasma of rabbits fed diet C, to which the molecule had been added, showed a decidedly higher concentration. This confirms what has, in any case, already been amply proved (41): while the olives are ripening, and during processing for oil production, the oleuropein, in part, undergoes enzymatic hydrolysis, forming 3,4-dihydroxy-phenylethanol and enolic acid of 3,4-dihydroxy-phenylethanol, which are, in their turn, efficacious antioxidants. Obviously, the considerations above refer only to the most significant olive oil biophenols, as analytical determination in plasma was limited to these last. In reality, the rabbit diets supplied many other biophenols, but the investigation was focused on those of olive oil and, in particular, on their capacity to enter the blood stream as such. The differences found in plasma samples between the total phenol content and the sum of the analyzed individual phenols (see Table 4) corroborate the fact that other components of the rabbit diet contribute to the total phenol intake.

The average concentration of vitamin E measured in the plasma of the rabbits fed diet C was not much higher than that found in rabbits fed diet B (4%). However, as can be seen in Table 5, diets B and C, had a vitamin E content nearly doubled that of diet A (increases of 76 and 83%, respectively). In this connection it should be pointed out that diets B and C, in spite of the addition of extra virgin olive oil, had the same vitamin E content as diet A (Table 1). This is because, as mentioned before, it had expressly been requested that the manufacturer add more vitamin E to diet A. Therefore, the higher concentration found in the plasma of the rabbits fed diets B

TABLE 5
Results Related to the Determination of the Plasmatic Parameters[a]

Parameter[b]	Diet A standard	Diet B modified	Diet C modified
Total biophenols (μg mL^{-1})	0.15 ± 0.06	1.93 ± 0.20[c]	2.73 ± 0.34[c,d]
Vitamin E (μg mL^{-1})	2.9 ± 0.9	5.1 ± 0.8[c]	5.3 ± 0.8[c]
Vitamin C (μg mL^{-1})	4.1 ± 0.7	2.3 ± 0.5[c]	2.8 ± 0.4[c]
Uric acid (μg mL^{-1})	3.5 ± 0.9	2.7 ± 0.4[c]	2.7 ± 0.7[c]
Cholesterol (mg/100 mL)			
Total	69.9 ± 6.9	83.5 ± 11.5[c]	70.6 ± 13.9[d]
Free	32.8 ± 5.7	29.7 ± 5.7	26.1 ± 2.8[c]
Esters	62.3 ± 7.4	90.4 ± 9.1[c]	74.8 ± 13.3[c,d]

[a]See Table 1 for information regarding diets.
[b]Values are expressed as mean ± SD (n = 8 per group). Total biophenols are expressed as tyrosol concentration.
[c]$P < 0.05$ vs. diet A, as found by ANOVA.
[d]$P < 0.05$ vs. diet B, as found by ANOVA. See Table 4 for abbreviation.

TABLE 6
Results Related to the Determination of the Native LDL Parameters[a]

Parameter[a]	Diet A standard	Diet B modified	Diet C modified
	mg mg^{-1} of LDL protein		
Triglycerides[c]	0.69 ± 0.12 (19.2%)	0.92 ± 0.31[d] (21.6%)	0.89 ± 0.37[d] (14.9%)
Phospholipids[c]	1.0 ± 0.1 (27.8%)	1.1 ± 0.5 (25.9%)	1.9 ± 0.5[d,e] (31.9%)
Cholesterol			
Total	1.3 ± 0.4	1.5 ± 0.3d	2.1 ± 0.3[d,e]
Free[c]	0.40 ± 0.10 (11.1%)	0.42 ± 0.05 (9.9%)	0.54 ± 0.05[d,e] (9.1%)
Esters[c]	1.51 ± 0.2 (42.0%)	1.81 ± 0.3 (42.6%)	2.62 ± 0.5[d,e] (44.0%)
	nmoles mg^{-1} of LDL protein		
MDA and 4-HNE	0.003 ± 0.0005	0.005 ± 0.001	0.005 ± 0.001
Lipid hydroperoxides	0.006 ± 0.002	0.010 ± 0.003	0.006 ± 0.001
Size (nm)	22.3 ± 0.6	23.3 ± 0.4	26.1 ± 0.5[c,d]

[a]See Table 1 for information regarding diets.
[b]Values are expressed as mean ± SD (n = 8 per group). MDA, malondialdehyde; 4-HNE, 4-hydroxy-2(*E*)-nonenal.
[c]Average percentage of the compound in lipidic fraction of native low-density lipoprotein (LDL) is reported in parentheses. Measured in mg mg^{-1} of LDL protein.
[d]$P < 0.05$ vs. diet A, as found by ANOVA.
[e]$P < 0.05$ vs. diet B as found by ANOVA. See Table 4 for abbreviation.

and C does not correlate to a greater vitamin intake. Presumably, as reported by some authors (42), an increase of polyunsaturated fatty acids (PUFA) in the plasma induced by a diet rich in such acids gives rise to a subsequent increase in vitamin E. This phenomenon is probably caused by a redistribution of the vitamin from the reserves, which would compensate for the increased oxidizability of the PUFA-rich lipoproteins that are more easily open to attack by radicals. Furthermore, it can be reasonably supposed that, by an exchange action, the contemporaneous presence of the olive oil biophenols in the plasma prevents vitamin E oxidation by increasing its plasmatic levels. This hypothesis was confirmed for other biophenols in earlier studies (10).

Both diets B and C caused a reduction in the levels of vitamin C and uric acid in the plasma of rabbits, evaluated at around 30–40% for vitamin C and 20% for uric acid. In this case, it is presumed that the increased presence of other water-soluble antioxidants with the same function, like the olive oil biophenols, depress the metabolic synthesis of vitamin C and modulate the excretion of uric acid (23).

The most noticeable differences deducible from the analysis of the plasma of rabbits fed diet C compared to those fed diet B concern cholesterol content (Table 5). Administration of diet C led to a 15% reduction in total cholesterol, which affected fairly uniformly both free and ester cholesterol (reductions of 12 and 17%, respectively). This fact appears ex-

TABLE 7
Results Related to the Determination of the ox-LDL Parameters[a]

ox-LDL parameter[b]	Diet A standard	Diet B modified	Diet C modified
Conjugated diene formation			
Lag phase (min)	150 ± 45	345 ± 94[c]	350 ± 86[c]
Maximum of oxidation rate (μM min^{-1})	1.55 ± 0.18	0.52 ± 0.09[c]	0.47 ± 0.08[c]
Maximum amount of dienes (μM)	51.0 ± 9.3	25.8 ± 4.1[c]	19.8 ± 3.9[c,d]
REM	1.7 ± 0.3	1.1 ± 0.2[c]	1.1 ± 0.3[c]
MDA and 4-HNE[e]	0.138 ± 0.008	0.014 ± 0.005[c]	0.013 ± 0.005[c]
Lipid hydroperoxides[e]	0.247 ± 0.21	0.029 ± 0.02[c]	0.035 ± 0.02[c]

[a]See Table 1 for information on diets. ox-=LDL, oxidized low density lipoprotein.
[b]Values are expressed as mean ± SD (n = 8 per group). Relative electrophoretic mobility (REM) is given as the change relative to native LDL (= 1). See Table 6 for abbreviations.
[c]$P < 0.05$ vs. diet A as found by ANOVA.
[d]$P < 0.05$ vs. diet B as found by ANOVA. See Table 4 for abbreviations.
[e]Given as nmoles mg^{-1} of LDL protein.

tremely significant seeing that the composition of diets B and C was the same both from a quantitative and qualitative point of view (see Table 1). Therefore, the addition of oleuropein in diet C had a markedly different effect on the cholesterolemic situation of the plasma. As far as the comparison with diet A is concerned, there was a percentage increase of about 19% of total cholesterol in the plasma of rabbits fed diet B, but, no statistically significant variation in total cholesterol was found in the plasma of rabbits fed diet C. It is also interesting to note that free cholesterol content was lower in the plasma of rabbits fed diets B and C (Table 5). The percentage decreases were 9 and 20%, respectively, compared to the value found in the plasma of the control rabbits (diet A). Consequently there was an increase in cholesteryl esters in the plasma of rabbits fed diets B and C. In particular, the increase assessed was 45% in the first case and 20% in the second.

Parameters on native LDL. As was expected, given the higher number of calories supplied by the lipids in diets B and C as compared to diet A, there was an increase in the concentration of triglycerides both in the case of rabbits fed diet B and those fed diet C. The increase was about 33 and 29%, respectively. When diet C was compared with diet B, the variation in the triglyceride content of the respective LDL was not statistically significant.

The behavior of phospholipids was different; there was a significant increase (73%) in the LDL of rabbits fed diet C compared to those fed diet B. With regard to diet A, the data collected showed a moderate increase of about 10% in the concentration of phospholipids in the LDL of rabbits fed diet B, while there was a marked increase in rabbits fed diet C (90%). This confirms the remarks already made about the influence of the addition of oleuropein (diet C) on the plasmatic lipidic components.

Further confirmation of this influence comes from an analysis of the data related to the total cholesterol content, which increased sharply (40%) in the LDL of rabbits fed diet C compared to those fed diet B. This increase is to a large extent attributable to the increase in cholesteryl esters (45%) and, to a lesser extent, free cholesterol (29%). A comparison with diet A shows that, in the LDL of rabbits fed diet B, there was an increase in total cholesterol (about 15%), which had a marked influence on the levels of cholesteryl esters (increase of 20%) and, to a much lesser extent, on free cholesterol (percentage increase of 5%). The situation for the LDL of rabbits fed diet C was qualitatively similar, but quantitatively more marked. In the latter case, the levels of total, free, and ester cholesterol increased by 61, 35, and 73%, respectively. Considering that the data obtained for the plasma showed a different pattern, particularly for the plasma of rabbits fed diet C—where there was a statistically insignificant increase in total cholesterol, an increase in cholesteryl esters, and a decrease in free cholesterol—the influence of the oleuropein added to diet C on the lipidic component of plasma is confirmed once again. The significant increase in free cholesterol found in the LDL of rabbits fed diet C is of particular interest considering that some authors (43) have shown how this lipid can contribute, although the action mechanisms are not quite clear, to the resistance of LDL to oxidation. In particular, it has been suggested that free cholesterol limits propagation of the peroxidative processes outside the core of the LDL because the molecule present on the surface of the LDL interacts with the radicals and causes the formation of oxycholesterol, which participates less reactively in the propagation reactions than the lipidic hydroperoxides (44).

It may be supposed that the biophenols induce a redistribution of the various plasmatic components, with an indirect effect on the size and composition of the LDL. To better clarify the events observed, Table 6 shows the average values of the diameter of the native LDL found in the three groups of rabbits. Going from diet B to diet C, there was an increase of 12%. Compared to diet A, the increase was 5% for diet B, and 17% for C.

At the same time, Table 6 shows the average chemical compositions, relative to lipidic component, characterizing the LDL of the rabbits fed the three different diets. The observed variations are extremely significant from the metabolic point of view for two reasons. The first relates to the fact that, as suggested by some authors (43,45–47), larger LDL have greater resistance to peroxidative processes and the fluidity of the lipoproteins is increased. The second, concerns the chemical composition of the LDL. In this connection, it has been known for some time that phospholipids act as blockers of the free cholesterol and this effect is easy to understand from the chemical point of view, since the two compounds are capable of forming a molecular association with a ratio of 1:1. Considering this ratio, the state of saturation between the two compounds is given by a value exactly equal to 1. In addition to the characteristic of forming molecular associations with cholesterol, phospholipids are also agents with a strong emulsifying action capable of solubilizing lipophilic molecules (including cholesterol) by forming micelles. It is therefore clear that in any system—LDL, for example—when the molar ratio between phospholipids and free cholesterol is greater than 1, the affinity of the system for free cholesterol is stronger as the ratio increases (48). Taking into account the fact that, even though still under discussion, many authors believe levels of plasmatic cholesterol are closely linked to the onset of atherosclerosis (6,49), it seems clear how important it is for the phospholipids/free cholesterol ratio in LDL to be as high as possible. This is exactly what happens with the LDL of the rabbits fed diet C, where the increase in phospholipids is higher than that found for free cholesterol and is therefore a considerable increase in that ratio, from 2.5 (rabbits fed diet A) to 3.5.

Parameters on ox-LDL. It can be seen from the oxidation kinetics that the lag phase, which represents a significant index of the summation of all the antioxidants contained in the LDL, which should obviously become exhausted before the peroxidative processes can proceed in a quantitatively relevant manner (3,36), was markedly different for the LDL of the three groups of rabbits. Figure 1 shows the average curves

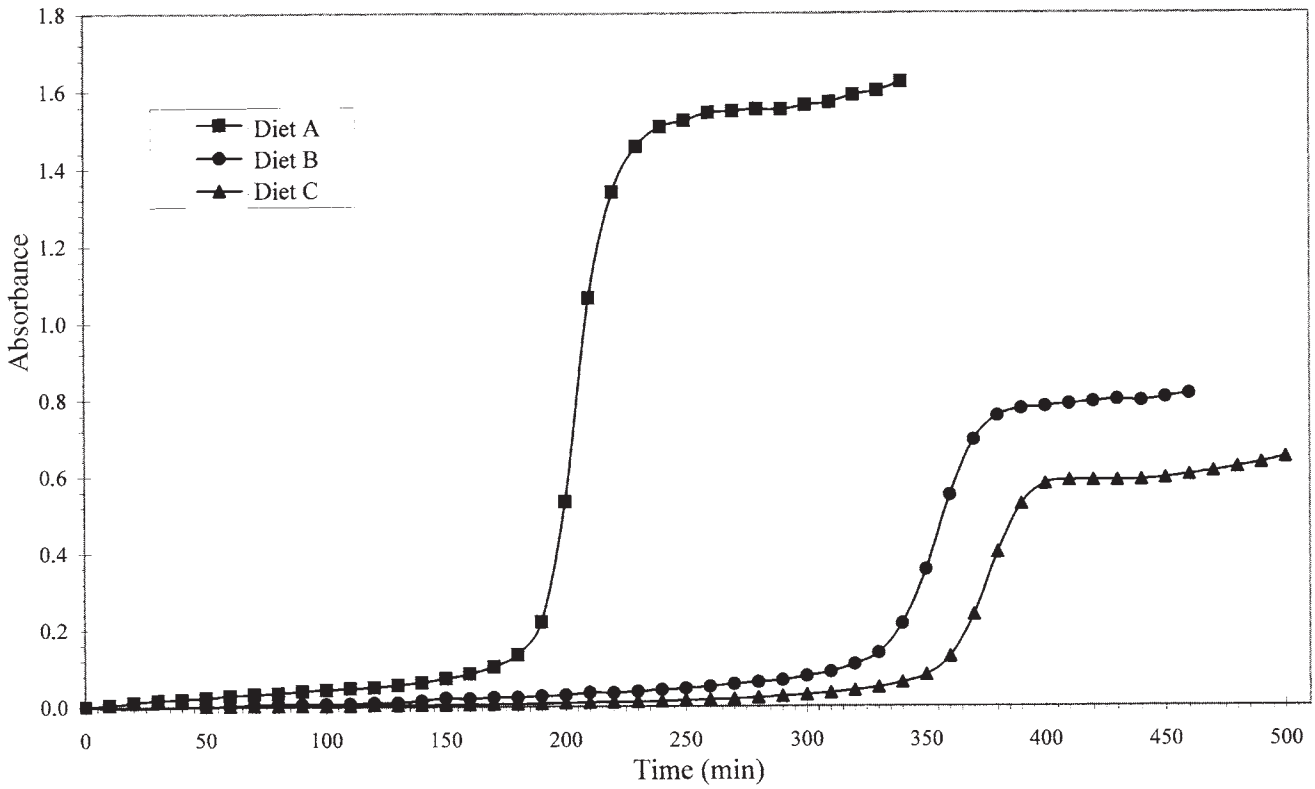

FIG. 1. Effect of the three different diets (A, standard; B, modified with 10% extra virgin olive oil; C, same as B, but with 7 mg kg^{-1} oleuropein) on Cu^{2+}-stimulated low density lipoprotein (LDL) conjugated diene formation *in vitro*. Each point represents the average value (n = 8 per group).

related to the kinetics of oxidation measured for the LDL of the rabbits. In particular, it was found that the lag phases associated with the LDL of rabbits fed diets B and C were noticeably longer than those for the LDL of the group fed diet A (345 and 350 min, respectively, as compared with 150 min). Furthermore, the maximal rate of the propagation reactions, easily calculable from the slopes of the tangents to the sigmoid or by means of the differential $\Delta A/\Delta t \times 33.8$ (where ΔA is the difference of absorbance measured at the end and beginning of the propagation reaction and Δt is the reaction time) also differed in a statistically significant way (see Table 7). Since the concentration of the LDL solutions was always equal to 0.1 μM on the spectrophotometer, it was also possible to calculate the number of molecules of dienes that formed every minute in each LDL at the maximal rate of propagation reaction (37). The count for the LDL of rabbits fed diets A, B, and C gave values of 15.5, 5.2, and 4.7 molecules min^{-1}, respectively. Lastly, a final remark concerns the absorbance measured at the end of the oxidation process which, in the case of the LDL of the group of rabbits fed diet A, was decidedly higher, showing a greater presence of conjugated dienes and therefore of lipidic radicals (see Table 7). Still, with regard to the total number of diene molecules formed for each LDL, it can be said that in the case of diet A, the number at the end of the reaction was 510, 258 for diet B, and 198 for diet C.

In the ox-LDL of rabbits fed diets B and C, the concentration of lipidic hydroperoxides was found to be less by about one order of magnitude to that measured for the ox-LDL of the rabbits treated with diet A (control).

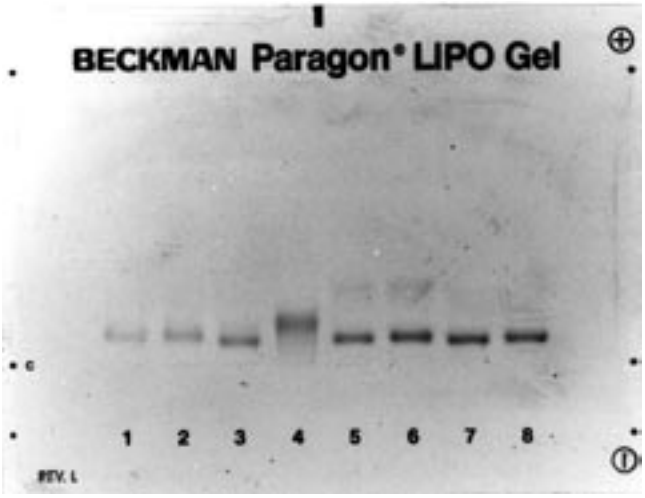

FIG. 2. Effect of the three different diets on relative electrophoretic mobility of Cu^{2+} oxidized LDL (ox-LDL). Number sequence: (1), native LDL (diet B); (2), ox-LDL (diet B); (3), native LDL (diet A); (4), ox-LDL (diet A); (5), native LDL (diet B); (6), ox-LDL (diet B); (7), native LDL (diet C); (8), ox-LDL (diet C). See Figure 1 for abbreviation and information on diets.

Similar results were obtained for the concentration of the two oxidation products MDA and 4-HNE. This last fact, combined with the results obtained from the test on the dienes (see the A_{max} values in Table 7), suggests that the action of the olive oil biophenols on peroxidative processes does not merely consist of slowing down the oxidation kinetics, but also increasing the resistance of the native LDL to oxidation.

A further confirmation of the diminished oxidizability of the LDL of rabbits fed diets B and C comes from the results of the electrophoretic test that are shown in Figure 2. The LDL of the rabbits in the group fed diet A, after Cu-induced stress, showed a much higher migration speed than that shown by the LDL of the other two groups.

Furthermore, the electrophoretic migration of the ox-LDL related to diet A causes the formation of more dispersed bands, probably because there has been fragmentation of the apolipoprotein B and/or aggregation of the LDL (50).

In an attempt to sum up the results obtained, it can be said that the investigation has not only verified the antioxidant efficacy of the biophenols contained in olive oil but also revealed a series of so far unknown effects of a specific biophenol on the plasmatic lipid situation. In fact, the addition of oleuropein in diet C not only increased the ability of LDL to resist oxidation but also reduced the plasmatic levels of total, free, and ester cholesterol and caused a redistribution of the lipidic components of the LDL with an indirect effect on their dimensions (greater).

The results of this investigation indicate that there is a need to plan *in vitro* and *in vivo* metabolic studies to verify the mechanisms of action by which the biophenols of olive oil exert their effect on the plasmatic lipid distribution.

The confirmation of certain theories would certainly have implications for the dietetics and pharmacological fields and might justify the recovery of olive oil processing residues, which are costly to eliminate.

REFERENCES

1. Witzum, J.L. (1994) The Oxidative Hypothesis of Atherosclerosis, *Lancet 344*, 793–795.
2. Berliner, J.A., Mohamad, N., Fogelman, A.M., Frank, J.S., Demer, L.L., Edwards, P.A., Watson A.D., and Lusis A.J. (1995) Atherosclerosis: Basic Mechanisms. Oxidation, Inflammation, and Genetics, *Circulation 91*, 2488–2496.
3. Esterbauer, H., Gebicki, J., Puhl, H., and Jürgens, G. (1992) The Role of Lipid Peroxidation and Antioxidants in Oxidative Modification of LDL, *Free Radical Biol. Med. 13*, 341–390.
4. Esterbauer, H., Schmidt, R., and Hayn, M. (1997) Relationships Among Oxidation of Low-Density Lipoprotein, Antioxidant Protection, and Atherosclerosis, *Adv. Pharmacol. 38*, 425–456.
5. Holvoet, P., and Collen, D. (1998) Oxidation of Low Density Lipoproteins in the Pathogenesis of Atherosclerosis, *Atherosclerosis 137* (Suppl.), S33–S38.
6. Ross, R. (1993) The Pathogenesis of Atherosclerosis: A Perspective for the 1990s, *Nature 362*, 801–809.
7. Witzum, J.L., and Steinberg, D. (1991) Role of Oxidized Low-Density Lipoproteins in Atherogenesis, *J. Clin. Invest. 88*, 1785–1792.
8. Quinn, M.T., Parthasarathy, S., Fong, L.G., and Steinberg, D. (1987) Oxidatively Modified Low Density Lipoproteins: A Potential Role in Recruitment and Retention of Monocyte/Macrophages During Atherogenesis, *Proc. Natl. Acad. Sci. USA 84*, 2995–2998.
9. Berliner, J., Territo, M., Sevanian, A., Ramin, S., Kim, J.A., Bamshad, B., Esterson, M., and Fogelman, A.M. (1990) Minimally Modified Low Density Lipoprotein Stimulates Monocytes Endothelial Interaction, *J. Clin. Invest. 85*, 1260–1266.
10. Rice-Evans, C., Miller, N., and Paganga, G. (1996) Structure–Antioxidant Activity Relationships of Flavonoids and Phenolic Acids, *Free Radical Biol. Med. 20*, 933–956.
11. Machlin, L., and Bendich, A. (1987) Free Radical Tissue Damage: Protective Role of Antioxidant Nutrients, *FASEB J. 1*, 444–445.
12. Martin, A., Wu, D., Meydani, S.N., Blumberg, J.B., and Meydani, M. (1998) Vitamin E Protects Human Aortic Endothelial Cells from Cytotoxic Injury Induced by Oxidized LDL *in vitro*, *J. Nutr. Biochem. 9*, 201–208.
13. Jialal, I., and Grundy, S.M. (1992) The Effect of Dietary Supplementation with α-Tocopherol in the Oxidative Modification of LDL, *J. Lipid Res. 33*, 899–906.
14. Abbey, M., Nestel, P.J., and Baghurst, P.A. (1993) Antioxidant Vitamins and Low Density Lipoprotein Oxidation, *Am. J. Clin. Nutr. 58*, 525–532.
15. Sato, K., Niki, E., and Shimasaki, H. (1990) Free Radical-Mediated Chain Oxidation of Low Density Lipoprotein and Its Synergistic Inhibition by Vitamin E and Vitamin C, *Arch. Biochem. Biophys. 279*, 402–405.
16. Jang, M., Cai, L., Udeani, G.O., Slowing, K.V., Thomas, C.F., Beecher, C.W.W., Fong, H.H.S., Farnsworth, N.R., Kinghorn, A.D., Mehta, R.G., Moon, R.C., and Pezzuto, J.M. (1997) Cancer Chemopreventive Activity of Resveratrol, a Natural Product Derived from Grapes, *Science 275*, 218–220.
17. Tijburg, L.B.M., Wiseman, S., Meijer, G.W., and Weststrate, J.A. (1997) Effects of Green Tea, Black Tea and Lipophilic Antioxidants on LDL Oxidability and Atherosclerosis of Hypercholesterolaemic Rabbits, *Atherosclerosis 135*, 37–47.
18. Serafini, M., Maiani, G., and Ferro-Luzzi, A. (1998) Alcohol-Free Red Wine Enhances Plasma Antioxidant Capacity in Humans, *J. Nutr. 128*, 1003–1007.
19. Baldioli, M., Servili, M., Perretti, G., and Montedoro, G.F. (1996) Antioxidant Activity of Tocopherols and Phenolic Compounds in Virgin Olive Oil, *J. Am. Oil. Chem. Soc. 73*, 1589–1593.
20. Montedoro, G., Servili, M., Baldioli, M., and Miniati, E. (1992) Simple and Hydrolyzable Phenolic Compounds in Virgin Olive Oil. 1. Their Extraction, Separation, and Quantitative and Semiquantitative Evaluation by HPLC, *J. Agric. Food Chem. 40*, 1571–1576.
21. Graciani Constante, E., and Vasquez Rocero, A. (1980) Estudio de los componentes del aceite de oliva por cromatografia liquida de alta eficacia (HPLC). II. Cromatografia en fase inversa, *Grasa Aceites 31*, 237–243.
22. Papadopoulos, G., and Boskou, D. (1991) Antioxidant Effect of Natural Phenols on Olive Oil, *J. Am. Oil Chem. Soc. 68*, 669–671.
23. Wiseman, S.A., Mathot, J.N.N.J., de Fouw N.J., and Tijburg, L.B.M. (1996) Dietary Non-Tocopherol Antioxidants Present in Extra Virgin Olive Oil Increase the Resistance of Low Density Lipoproteins to Oxidation in Rabbits, *Atherosclerosis 120*, 15–23.
24. Nardini, M., Natella, F., Gentili, V., Di Felice, M., and Scaccini, C. (1997) Effect of Caffeic Acid Dietary Supplementation on the Antioxidant Defense System in Rat: An *in vivo* Study, *Arch. Biochem. Biophys. 342*, 157–160.
25. Visioli, F., and Galli, C. (1994) Oleuropein Protects Low Density Lipoproteins from Oxidation, *Life Sci. 55*, 1965–1971.

26. Masella, R., Cantafora, A., Modesti, D., Cardilli, A., Gennaro, L., Bocca, A., and Coni, E. (1999) Antioxidant Activity of 3,4-DHPEA-EA and Protocatecuic Acid: A Comparative Assessment with Other Olive Oil Biophenols, *Redox Rep. 4*, 113–121.
27. Giovannini, C., Straface, E., Modesti, D., Coni, E., Cantafora, A., De Vincenzi, M., Malorni, W., and Masella, R. (1999) Tyrosol, the Major Olive Oil Biophenol, Protects Against Oxidized-LDL-Induced Injury in Caco-2 Cells, *J. Nutr. 129*, 1269–1277.
28. Italian Legislative Decree n. 116 (1992) Suppl. Ord. G.U. n. 40, 18.2.1992.
29. Havel, R.J., Eder H.A., and Bragdon, J.K. (1955) The Distribution and Chemical Composition of Ultracentrifugally Separated Lipoproteins in Human Serum, *J. Clin. Invest. 34*, 1345–1353.
30. Lowry, O.H., Rosebrough, N.J., Farr, A.L., and Randall, R.J. (1951) Protein Measurement with the Folin Phenol Reagent, *J. Biol. Chem. 193*, 265–275.
31. Papadopoulos, G.F., and Tsimidou, M. (1992) Rapid Method for the Isolation of Phenolic Compounds from Virgin Olive Oil Using Solid Phase Extraction, XVI International Conference Group Polyphenols, July, 13–16.
32. Cavina, G., Gallinella, B., Porrà, R., Pecora, P., and Suraci, C. (1988) Carotenoids, Retinoids and α-Tocopherol in Human Serum: Identification and Determination by Reversed-Phase HPLC, *J. Pharmaceut. Biomed. Anal. 6*, 259–269.
33. Ross, M.A. (1994) Determination of Ascorbic Acid and Uric Acid in Plasma by High-Performance Liquid Chromatography, *J. Chromatogr. B 657*, 197–200.
34. Krauss, R.M., and Burke, D.J. (1982) Identification of Multiple Subclasses of Plasma Low Density Lipoproteins in Normal Humans, *J. Lipid Res. 23*, 97–104.
35. Coresh, J., Kwiterovich, P.O., Smith, J.H., and Bachorik, P.S. (1993) Association of Plasma Triglyceride Concentration and LDL Particle Diameter, Density, and Chemical Composition with Premature Coronary Artery Disease in Men and Women, *J. Lipid Res. 34*, 1687–1697.
36. Esterbauer, H., Striegl, G., Puhl, H., and Dieber-Rotheneder, M. (1989) Continuous Monitoring of *in vitro* Oxidation of Human Low Density Lipoprotein, *Free Radical Res. Com. 6*, 67–75.
37. Puhl, H., Waeg, G., and Esterbauer, H. (1994) Methods to Determine Oxidation of Low Density Lipoprotein, *Methods Enzymol. 233*, 425–441.
38. El-Saadani, M., Esterbauer, H., El-Sayed, M., Goher, M., Nassar, A.Y., and Yurgens, G. (1989) A Spectrophotometric Assay for Lipid Peroxides in Serum Lipoproteins Using a Commercially Available Reagent, *J. Lipid Res. 30*, 627–630.
39. Morel, D.W., Hessler, J.R., and Chisolm, G.M. (1976) Low Density Lipoprotein Cytotoxicity Induced by Free Radical Peroxidation of Lipids, *J. Lipid Res. 24*, 1070–1076.
40. Hollman, P.C.H., Van der Gaag, M., Mengelers, M.J.B., Van Trijp, J.M.P., De Vries, J.H.M., and Katan, M.B. (1996) Absorption and Disposition Kinetics of the Dietary Antioxidant Quercetin in Man, *Free Radical Biol. Med. 21*, 703–707.
41. Servili, M., Baldioli, M., Miniati, E., and Montedoro, G. (1996) Antioxidant Activity of New Phenolic Compounds Extracted from Virgin Olive Oil and Their Interaction with α-Tocopherol and β-Carotene, *Riv. It. Sost. Grasse 73*, 55–59.
42. Esterbauer, H., Dieber-Rotheneder, M., Striegl, G., and Waeg, G. (1991) Role of Vitamin E in Preventing the Oxidation of Low Density Lipoprotein, *Am. J. Clin. Nutr. 53*, 314S–321S.
43. Tribble, D.L. (1995) Lipoprotein Oxidation in Dyslipidemia: Insights into General Mechanisms Affecting Lipoprotein Oxidative Behaviour, *Curr. Opin. Lipidol. 6*, 196–208.
44. Smith, L.L. (1991) Another Cholesterol Hypothesis: Cholesterol as an Antioxidant, *Free Radical Biol. Med. 11*, 47–61.
45. Dejager, S., Bruckert, E., and Chapman, M.J. (1993) Dense Low Density Lipoprotein Subspecies with Diminished Oxidative Resistance Predominate in Combined Hyperlipidemia, *J. Lipid Res. 34*, 295–308.
46. Hirano, T., Naito, H., Kurokawa, M., Ebara, T., Nagano, S., Adachi, M., and Yoshino, G. (1996) High Prevalence of Small LDL Particles in Non-Insulin-Dependent Diabetic Patients with Nephropathy, *Atherosclerosis 123*, 57–72.
47. Chapman, M.J., Guèrin, M., and Bruckert, E. (1998) Atherogenic, Dense Low-Density Lipoproteins. Pathophysiology and New Therapeutic Approaches, *Eur. Heart J. 19 (Suppl. A)*, A24–A30.
48. Bourne, G.H. (1985) *World Review of Nutrition and Dietetics*, Vol. 46, Karger, Basel, pp. 219–251.
49. Nenster, M.S., Gudmundsen, O., Malterud, K.E., Berg, T., and Drevon, C.A. (1994) Effect of Cholesterol Feeding of Susceptibility of Lipoprotein to Oxidative Modification, *Biochim. Biophys. Acta 1213*, 207–214.
50. Chang, Y.H., Abdalla, D.S.P., and Sevanian, A. (1997) Characterization of Cholesterol Oxidation Products Formed by Oxidative Modification of Low Density Lipoprotein, *Free Radical Biol. Med. 23*, 202–214.
51. McLaughin, P.J., and Weihrauch, J.L. (1979) Vitamin E Content of Foods, *J. Am. Diet. Assoc. 75*, 647–665.

[Received August 3, 1999, and in revised form November 15, 1999; revision accepted November 24, 1999]

Lipoproteins Modify the Macrophage Uptake of Triacylglycerol Emulsion and of Zymosan Particles by Similar Mechanisms

Márcia D.T. Carvalho[a], Vanessa E. Tobias[a], Célia M.V. Vendrame[b], Alice F. Shimabukuro[a], Magnus Gidlund[c], and Eder C.R. Quintão[a,*]

[a]Lipids Laboratory (LIM/10), [b]Schistosomiasis Immunopathology Laboratory (LIM/06), and [c]Department of Pathology, University of São Paulo Medical School, São Paulo, 01246-903, Brazil

ABSTRACT: The uptake of lipids and formation of foam cells are key events in atherosclerosis and in eruptive xanthomata formation in primary hyperchylomicronemia. Here we have compared the influence of low density lipoprotein (LDL), oxidized LDL (oxLDL), high density lipoprotein (HDL), and delipidated HDL (apoHDL) on the uptake by macrophages of zymosan (an insoluble fraction of yeast cell walls) and of triglyceride-rich emulsion (EM) particles that resemble chylomicrons, but, like zymosan, are equally devoid of protein components. Zymosan internalization is known to occur through unspecific phagocytosis, whereas natural chylomicrons are taken up by several specific lipoprotein receptors. We found that phagocytosis is not promoted as much by oxLDL as by normal LDL. HDL-coated zymosan was found to be inert and apoHDL slightly enhanced phagocytosis. LDL and apoHDL promoted the uptake of EM while oxLDL and HDL significantly inhibited the uptake. Therefore, the data support that HDL, and not apoHDL, particles inhibit EM uptake. We concluded that by using lipoprotein-coated zymosan particles, we could demonstrate different biological effects of LDL, oxLDL, HDL, and apoHDL on macrophage phagocytosis and that this method could be useful to delineate components of the various lipoproteins important for the propagation or inhibition of the formation of foam cells.

Paper no. L8302 in *Lipids 35,* 55–59 (January 2000).

The phagocytic process in monocyte macrophages represents a fundamental biological mechanism whereby lipoprotein molecules are rapidly taken up (1,2). In most cases, this is beneficial for the organism, but in some cases it may contribute and constitute a fundamental component of the pathogenic mechanism of a disease. A key event in atherosclerosis and in the formation of eruptive xanthomata in familial hyperchylomicronemia is the formation of lipid-laden foam cells resulting from the uptake of lipoproteins by skin and arterial intima resident macrophages (1).

Elevated plasma concentration of low density lipoprotein (LDL) is considered a major risk factor for atherosclerosis. This is true for LDL subjected to chemical modification, including acetylation, methylation, glycation, and oxidation (3–5). Besides oxidized LDL (oxLDL), epidemiological surveys strongly suggest that triacylglycerol (TG)-rich lipoproteins like very low density lipoprotein (VLDL) (6,7), as well as intestinally derived chylomicrons, contribute to atherogenesis, and their remnants drawn from patients with severe familial hyperchylomicronemia are also atherogenic (8,9). By contrast, several studies suggest that high density lipoprotein (HDL) is antiatherogenic as it removes cell cholesterol (10,11).

Although the function of various lipoprotein fractions in atherogenesis is under investigation (12,13), the interaction between these components in phagocytosis is less well studied (14).

To study the mechanisms of mouse peritoneal macrophage uptake, we used an assay whereby LDL, oxLDL, HDL, and delipidated HDL (apoHDL), which are known to interact with specific cell receptors, either were utilized to coat inert zymosan (an insoluble fraction of yeast cell walls) particles or were coincubated with TG-rich emulsions (EM) that resemble natural chylomicrons (15).

EXPERIMENTAL PROCEDURES

Lipoprotein isolation, delipidation of HDL, and oxidation of LDL. LDL (d = 1.006–1.063 g/mL) and HDL (d = 1.063–1.21 g/mL) from the plasma of healthy volunteer blood donors was isolated by sequential preparative ultracentrifugation (16) utilizing a 50 Ti rotor in an L-8 Beckman ultracentrifuge (Beckman Instruments, Palo Alto, CA). HDL was 96% delipidated by extraction with precooled (–20°C) diethyl ether/ethanol (3:2, vol/vol) (17), and the precipitated apolipoproteins were washed twice with ice-cold ether and then partially dried

*To whom correspondence should be addessed at Lipids Laboratory (LIM/10), University of São Paulo Medical School, São Paulo, Brazil, Av. Dr. Arnaldo 455, s/3317, CEP 01246-903, São Paulo, Brazil.
E-mail: lipideq@usp.br

Abbreviations: apoHDL, delipidated high density lipoprotein; DMEM, Dulbecco's modified Eagle's medium; EM, chylomicron-like triglyceride-rich emulsions; FCS, fetal calf serum; HDL, high density lipoprotein; IgG, immunoglobulin G; LDL, low density lipoprotein; oxLDL, oxidized LDL; PBS, phosphate-buffered saline; TG, triacylglycerol; VLDL, very low density lipoprotein; [^{3}H]-COE, [1α,2α,(N)-^{3}H]-cholesteryl oleoyl ether.

under a stream of N_2. LDL was oxidized with 1 µM $CuSO_4$ according to the method of Heinecke *et al.* (18). Total cholesterol and TG concentrations of the LDL and HDL preparations were measured by commercially available enzymatic kits, and the total protein concentration was by the method of Lowry *et al.* (19).

Mouse peritoneal macrophages. This experiment was approved by the Ethics Committee of the Hospital of the University of São Paulo Medical School. Resident peritoneal exudate cells were harvested from mice in phosphate-buffered saline (PBS), pH 7.4, washed twice in PBS, and had the final concentration of cells adjusted as indicated in RPMI 1640 medium (Sigma Chemical Co., St. Louis, MO) containing 10% (vol/vol) fetal calf serum (FCS), penicillin (100 IU/mL), streptomycin (100 IU/mL), and fungizone (2.5 µg/mL) (5).

Phagocytosis assay. Phagocytosis assay was done according to the method described by Miller (20). Briefly, 10^6 cells in 1 mL RPMI 1640 medium were cultured in Leighton tubes on micro-coverslips and maintained at 37°C for 30 min in a humid, 5% CO_2 atmosphere. The micro-coverslips were then washed in RPMI 1640 medium. Meanwhile, 10^7 zymosan particles [average diameter about 3 µm (21)] in 1 mL RPMI 1640 medium were incubated at 37°C for 30 min with either 10 mg protein/mL of HDL or apoHDL, or 0.25 mg protein/mL of LDL or oxLDL. Lipoprotein-coated zymosan suspension was added to each tube with micro-coverslips with adhered cells and incubated at 37°C for an additional 30 min in a humid, 5% CO_2 atmosphere. Then the micro-coverslips were washed in RPMI 1640 medium and stained with Leishman solution. The criterion for phagocytosis was that cells took up three or more coated or control uncoated zymosan particles. The results were expressed as a phagocytic index and calculated as [(number of macrophages with phagocytosis of coated zymosan particles/number of macrophages with phagocytosis of control uncoated zymosan particles) – 1]. At least 100 cells were counted on each coverslip.

Determination of zymosan-bound proteins. Particles (10^8) of zymosan in 1 mL RPMI 1640 medium were incubated with either 10 mg protein/mL of HDL or apoHDL, or 0.25 mg protein/mL of native or oxLDL at 37°C for 30 min, washed twice, and the pellets resuspended in 0.5 mL of RPMI 1640 medium for protein determination by the method of Lowry *et al.* (19). Proper blank controls containing zymosan were introduced in the method. The results were expressed as g protein bound/10^8 zymosan particles.

TG-rich EM. Cholesterol, cholesteryl oleate, triolein (Nu-Chek-Prep, Elysian, MN), and phosphatidylcholine (egg lecithin; Lipid Products, Surrey, United Kingdom) were dissolved in chloroform/methanol solution (2:1, vol/vol) and mixed in the following proportions, respectively, 2, 6, 69, and 23% (% by weight), together with 30 µCi of [1α,2α,(N)-^{3}H]-cholesteryl oleoyl ether ([^{3}H]-COE), specific activity 75 mCi/mg (Amersham Life Science, Buckinghamshire, United Kingdom). The solvent was evaporated under a nitrogen stream and the lipids were maintained at 4°C for 12 h in a vacuum chamber to eliminate the residual solvent. The lipid mixture was sonicated in a NaCl solution (d = 1.101 g/mL, pH 7.3) utilizing a Branson Cell Disruptor (model 450, Branson Sonifier, Danbury, CT), with a 1-cm probe, at 70–80 W for 30 min under nitrogen flow. TG-rich EM were purified after discontinuous gradient ultracentrifugation as previously described (15,22), and their particle size was about 0.1 µm.

Uptake of [^{3}H]-COE-EM by peritoneal macrophages. Peritoneal exudate cells (5×10^6) in 4 mL RPMI 1640 medium containing 10% FCS were cultured in Petri dishes in a humid 5% CO_2 atmosphere at 37°C for 12 h. Thereafter, each plate was washed twice with RPMI 1640 medium to remove nonadherent cells (5). Adherent cells were incubated in Dulbecco's modified Eagle's medium (DMEM, Sigma Chemical Co.) with [^{3}H]-COE-EM either alone (as control) or with HDL, apoHDL, LDL, or oxLDL (0.6 µg of protein/µg TG of EM) for 4 h at 37°C in a humid 5% CO_2 atmosphere. The cells were then washed in PBS and solubilized in 0.2 N NaOH for the measurement of the cell-associated radioactivity in a beta counter Beckman LS-6000 TA (Beckman Instruments, Palo Alto, CA). Cell protein content was measured by the method of Lowry *et al.* (19). Cellular EM uptake was defined as the percentage of radioactivity taken up by the cells from the medium. These values were subtracted from blank values found in Petri dishes incubated with radiolabeled emulsions without cells. Results of cellular EM uptake were expressed as an index: [(percentage of [^{3}H]-COE × mg of cell protein^{-1} in the presence of lipoprotein/percentage of [^{3}H]-COE × mg of cell protein^{-1} in the absence of lipoprotein as the experimental control) – 1].

Statistical analysis. The amount of protein bound to the zymosan particles was compared by Student's *t*-test. The Mann-Whitney test was used for statistical comparison of the phagocytic index of zymosan particles and of the uptake index of [^{3}H]-COE-EM by macrophages; a level of confidence of 0.05 was considered significant.

RESULTS

Initially, we analyzed the difference in the uptake by mouse peritoneal macrophages of zymosan particles coated with LDL or with the copper-oxidized form of the same preparation. The data in Table 1, presented as relative increase, demonstrate that LDL greatly enhances the ability of the zymosan to be recognized and phagocytized by macrophages. If the same LDL preparation were subjected to oxidative modification, it would lead to an approximately sixfold reduction in the number of cells able to ingest these particles. The data also show that this reduction was not due to an inability of the zymosan particle to be coated with oxLDL since the zymosan particles showed an equal degree of protein binding with both LDL and oxLDL. Table 1 also compares the phagocytosis of zymosan particles coated with either HDL or apoHDL. Most interestingly, while HDL was unable to modify the ability of the zymosan particle to be phagocytized, the removal of the lipid part of HDL, i.e., using apoHDL, significantly enhanced phagocytosis of the particle. Part of this effect could be due

TABLE 1
Phagocytic Index of Mouse Peritoneal Macrophage Exposed to Zymosan Particles Coated with LDL, oxLDL, HDL, or apoHDL

Coated with lipoproteins[a]	Phagocytic index[b]	Protein binding (μg/10^8 particles)[e]
LDL	6.1 (5.1–7.3)	23.7 ± 1.1
oxLDL	1.1 (0.9–1.7)[c]	26.4 ± 1.7
HDL	0.0 (–0.2–0.2)	10.1 ± 2.2
apoHDL	0.7 (0.7–0.8)[d]	18.7 ± 3.6[f]

[a]Zymosan particles were coated with indicated lipoprotein mixture and incubated with mouse peritoneal macrophages as described in the Materials and Methods section. LDL, low density lipoprotein; oxLDL, oxidized LDL; HDL, high density lipoprotein; apoHDL, delipidated HDL.
[b]Calculated as [(number of macrophages that took up three or more zymosan particles coated with lipoprotein mixture/number of macrophages that took up three or more uncoated zymosan particles) – 1]. Values are expressed as median (range) for each experimental group, which included five experiments each. Studies on LDL and oxLDL and those with HDL and apoHDL were carried out at different occasions.
[c]LDL × oxLDL: $P < 0.01$ by the Mann-Whitney test.
[d]HDL × apoHDL: $P < 0.05$ by the Mann-Whitney test.
[e]The mean amounts of LDL, oxLDL, HDL, and apoHDL protein that coated zymosan particles were obtained by the method of Lowry *et al.* (19) as presented in the Materials and Methods section. Values are expressed as mean ± SD for each experimental group, which included five experiments each.
[f]HDL × apoHDL: $P < 0.05$ by the *t*-test.

to the slight increase in the protein content of the apoHDL particle.

Finally, we analyzed to what extent LDL, oxLDL, HDL, and apoHDL could affect the uptake of chylomicron-like TG-rich EM labeled with [^{3}H]-COE. The results clearly demonstrate that the cellular uptake of the [^{3}H]-COE-EM was greatly stimulated by LDL if compared to oxLDL, and by apoHDL if compared to HDL (Fig. 1).

DISCUSSION

Two general mechanisms are involved in the macrophage uptake of large amounts of lipids: receptor-mediated endocytosis of plasma lipoproteins either in solution or forming complexes with other tissue constituents (3); or phagocytosis of whole cells, fragments of membranes containing cholesterol, or as aggregated LDL (2). These mechanisms may be involved in the lipid accumulation in the atherosclerotic lesions and in the formation of eruptive xanthomata of the primary hyperchylomicronemia (8,9). In other words, to study the influence of several lipoproteins in the receptor-mediated endocytosis, we have utilized EM, whereas zymosan was utilized to investigate the influence of these lipoproteins in phagocytosis.

The formation of lipid-laden foam cells *via* internalization of lipoproteins represents a key event in the formation of atherosclerotic lesions (1) and of the eruptive xanthomata of primary hyperchylomicronemia, but the mechanisms of cell uptake of these large particles are poorly understood (23). In the present study, we have analyzed whether LDL, oxLDL, HDL, or apoHDL can modify the uptake by macrophages of inert zymosan particles as compared to a known atherogenic lipoprotein, the intact chylomicron-like large EM. The uptake of zymosan particles (yeast cell walls) by macrophages is classified as unspecific phagocytosis, and this fact had previously been used to study the receptor-mediated uptake of ligands such as immunoglobulin G (IgG) or its complement (24). The interaction of coated zymosan particles with cells also promotes a number of important biological functions, such as superoxide generation, release of a variety of enzymes, and phagocytosis (25).

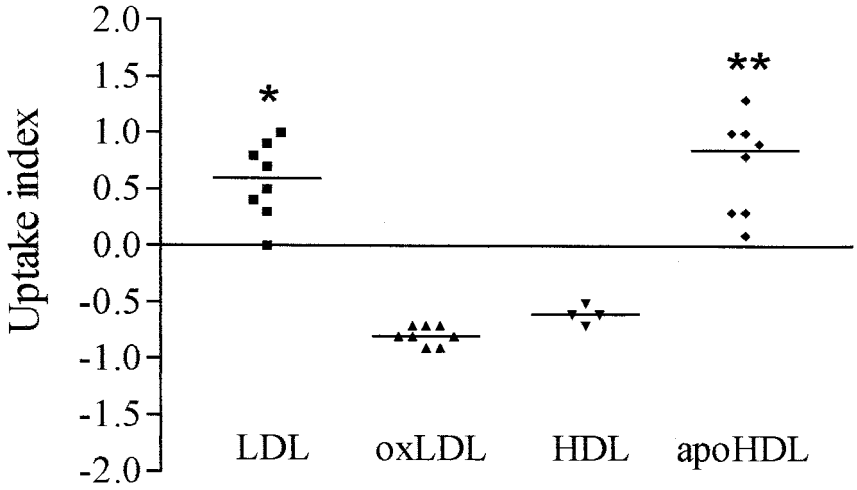

FIG. 1. Uptake index of [1α,2α(N)-^{3}H]-cholesteryl oleoyl ether from chylomicron-like triglyceride (TG)-rich emulsions (EM) by mouse peritoneal macrophages in the absence or presence of low density lipoprotein (LDL), oxidized LDL (oxLDL), as well as of high density lipoprotein (HDL) and delipidated HDL (apoHDL) (0.6 μg of protein/μg of TG of EM) during 4-h incubation periods. Studies on LDL and oxLDL and those with HDL and apoHDL were carried out on different occasions. Values are expressed as median (range) for each experimental group. Mann-Whitney test, $P < 0.001$: *LDL ($n = 8$ experiments) vs. oxidized LDL ($n = 8$ experiments), $P < 0.01$: **apoHDL ($n = 8$ experiments) vs. HDL ($n = 4$ experiments).

We showed that zymosan particles coated with LDL were efficiently and rapidly taken up by mouse peritoneal macrophages. This enhanced uptake could have occurred *via* specific receptors, such as through the LDL receptor, or by induction of phagocytosis. According to Bigler *et al.* (26), LDL promotes the expression of the Fc receptor, a known mediator of phagocytosis, and thus could explain the high macrophage phagocytic index of the LDL-coated zymosan. This process could also be influenced by several other factors, such as modification of surface charge, unspecific interactions of lipid or of protein components.

The oxidation of the LDL particle led, on the other hand, to a substantial loss of the ability of zymosan to be phagocytized, possibly because of competition toward the scavenger receptor. On the other hand, we noticed that, as opposed to the normal LDL, oxLDL facilitated the adherence to the macrophage surface of zymosan but not necessarily its internalization, a fact that had also been observed in regard to erythrocytes coated by oxLDL (27). Therefore, zymosan cell binding does not by itself define the process of phagocytosis, which in fact was severalfold lower when compared to phagocytosis elicited by coating of zymosan with nonoxidized LDL. In this regard, Sambrano *et al.* (28) had shown that oxLDL competed with oxidized erythrocytes for binding to macrophages. This suggests that the receptors described for oxLDL, including the scavenger receptor and the CD36 molecules (5,13,29), are involved in the attachment of zymosan to the cell, without, nonetheless, promoting internalization. Seemingly, the latter depends on other cell surface receptors, such as the Fc receptor.

Coating with HDL did not interfere with zymosan phagocytosis. However, coating with apoHDL, obtained through delipidation of HDL, resulted in a slightly increased ability of zymosan to be phagocytized. Even though the coating with apoHDL resulted in particles with slightly increased protein content, the data suggest that the lipid part of the HDL is not important for the phagocytosis of zymosan. According to previous reports, HDL_3, a fraction relatively richer in apolipoprotein than bulk HDL, although less efficiently than LDL, also mediates the expression of the phagocytic Fc receptor (26). Therefore, the enhanced phagocytosis elicited by apoHDL could be attributed to the protein component of HDL.

In the second part of this study, we analyzed the effect of the same lipoprotein fractions on the uptake of EM. EM are considered to closely resemble the metabolism of chylomicrons (15). Similarly to what occurred in regard to the zymosan particles, LDL increased while oxLDL inhibited the uptake of EM (Fig. 1). Since the uptake of EM particles also was considerably stimulated by LDL, phagocytosis seems to have taken part in the uptake of EM as suggested by others (9,30). This may have occurred because LDL particles are known to aggregate *in vitro* and *in vivo* (31) and thus could have adhered to the EM forming larger complexes or else LDL could have promoted the expression of the Fc receptor (26). Thus, the LDL-EM interaction brings on the formation of foam cells (32) due to production of much larger particles that facilitate EM phagocytosis, similar to what occurs with zymosan.

On the other hand, because oxLDL is atherogenic, the decrease of uptake by oxLDL that occurred with both zymosan and EM seems paradoxical in regard to atherogenesis. Accordingly, oxLDL would contribute to make the large triglyceride-rich particles that are abundant in hyperchylomicronemia less atherogenic (23). However, oxLDL itself remains highly atherogenic since it could compete with the other particles for the scavenger receptor.

A significant reduction of the uptake of EM by macrophages occurred in the presence of HDL. This was further confirmed by the fact that the HDL-zymosan particle was not phagocytized. On the other hand, apoHDL derived from the delipidation of HDL resulted in an increased uptake of EM, similarly to what occurred in regard to the zymosan particles. Thus, HDL facilitates, whereas apoHDL inhibits the metabolism of the large EM by macrophages. ApoHDL is the most abundant lipoprotein-derived component in the interstice and thus may contribute to formation of eruptive xanthomata and to the atherogenic role of chylomicrons in familial primary hyperchylomicronemia (23).

We thus conclude that by using coated zymosan particles and TG-rich EM we demonstrate different biological effects of LDL, oxLDL, HDL, and apoHDL on phagocytosis by macrophage and that this method could be used to identify the various lipoproteins, including other forms of hyperlipidemia, important for the propagation or inhibition of the formation of foam cells and the mechanisms involved.

ACKNOWLEDGMENTS

The authors would like to thank Santa Poppe, Lila Mina Harada, and Isac Castro for excellent and invaluable assistence and Hiro Goto for helpful suggestions. Zymosan was a gift from Allergy and Immunopathology Laboratory, São Paulo Medical School, Brazil. This work was supported in part by FAPESP (MG 99/00 158-4).

REFERENCES

1. Ross, R. (1999) Atherosclerosis—An Inflammatory Disease, *N. Engl. J. Med. 340*, 115–126.
2. Khoo, J.C., Miller, E., Pio, F., Steinberg, D., and Witztum, J.L. (1992) Monoclonal Antibodies Against LDL Further Enhance Macrophage Uptake of LDL Aggregates, *Arterioscler. Thromb. 12*, 1258–1266.
3. Goldstein, J.L., Ho, Y.K., Basu, S.K., and Brown, M.S. (1979) Binding Sites of Macrophages That Mediate Uptake and Degradation of Acetylated Low Density Lipoprotein, Producing Massive Cholesterol Depositon, *Proc. Natl. Acad. Sci. USA 76*, 333–337.
4. Dobrian, A., Lazar, V., Tirziu, D., and Simionescu, M. (1996) Increased Macrophage Uptake of Irreversibly Glycated Albumin Modified-Low Density Lipoprotein of Normal and Diabetic Subjects Is Mediated by Non-Saturable Mechanisms, *Biochim. Biophys. Acta 1317*, 5–14.
5. Sparrow, C.P., Parthasarathy, S., and Steinberg, D. (1989) A Macrophage Receptor That Recognizes Oxidized Low Density Lipoprotein but Not Acetylated Low Density Lipoprotein, *J. Biol. Chem. 264*, 2599–2604.

6. Karpe, F., Steiner, G., Uffelman, K., Olivecrona, T., and Hamsten, A. (1994) Postprandial Lipoproteins and Progression of Coronary Atherosclerosis, *Atherosclerosis 106*, 83–97.
7. Patsch, J.R., Miesenbock, G., Hopferwieser, T., Muhlberger, V., Knapp, E., Dunn, J.K., Gotto, A.M., Jr., and Patsch, W. (1992) Relation of Tryglyceride Metabolism and Coronary Artery Disease. Studies in Postprandial State, *Arteroscler. Thomb. 12*, 1336–1345.
8. Fisher, R.M., Humphries, S.E., and Talmud, P.J. (1997) Common Variation in the Lipoprotein Lipase Gene: Effects on Plasma Lipids and Risk of Atherosclerosis, *Atherosclerosis 135*, 145–159.
9. Yu, K.C.-W., Smith, D., Yamamoto, A., Kawguchi, A., Harada-Shiba, M., Yamamura, T., and Mamo, J.C.L. (1997) Phagocytic Degradation of Chylomicron Remnants by Fibroblasts from Subjects with Homozygous Familial Hypercholesterolaemia, *Clin. Sci. 92*, 197–203.
10. Kruth, H.S., Skarlatos, S.I., Gaynor, P.M., and Gamble, W. (1994) Production of Cholesterol-Enriched Nascent High Density Lipoprotein by Human Monocyte-Derived Macrophages Is a Mechanism That Contributes to Macrophage Cholesterol Efflux, *J. Biol. Chem. 269*, 24511–24518.
11. Atger, V., Giral, P., Simon, A., Cambillau, M., Leveson, J., Gariepy, J., Megnien, J.L., and Moatti, N. (1995) High-Density Subfractions as Markers of Early Atherosclerosis, *Am. J. Cardiol. 75*, 127–131.
12. Steinberg, D., Parthasarathy, S., Carew, T.E., Khoo, J.C., and Witztum, J.L. (1989) Beyond Cholesterol. Modifications of Low Density Lipoprotein That Increase Its Atherogenicity, *N. Engl. J. Med. 320*, 915–924.
13. Schneider, W.J. (1997) Novel Members of the Low Density Lipoprotein Receptor Superfamily and Their Potential Roles in Lipid Metabolism, *Curr. Opin. Lipidol. 8*, 315–319.
14. Hoff, H.F., Whitaker, T.E., and O'Neil, J. (1992) Oxidation of Low Density Lipoprotein Leads to Particle Aggregation and Altered Macrophage Recogniton, *J. Biol. Chem. 267*, 602–609.
15. Oliveira, H.C.F., Hirata, M.H., Redgrave, T.G., and Maranhão, R.C. (1998) Competition Between Chylomicrons and Their Remnants for Plasma Removal: a Study with Artificial Emulsion Models of Chylomicrons, *Biochim. Biophys. Acta 958*, 211–217.
16. Kesaniemi, Y.A., Witztum, J.L., and Steimbrecher, U.P. (1983) Receptor-Mediated Catabolism of Low Density Lipoprotein in Man. Quantitation Using Glycosylated Low Density Lipoprotein, *J. Clin. Invest. 71*, 950–959.
17. Koizumi, J., Kano, M., Okabauashi, A.J., and Thompson, G.R. (1988) Behavior of Human Apolipoprotein A-I: Phospholipid ApoHDL: Phospholipid Complexes *in Vitro* and After Injection into Rabbits, *J. Lipid Res. 29*, 1405–1415.
18. Heinecke, J.W., Rosen, H., and Chait, A. (1984) Iron and Copper Promote Modification of Low Density Lipoprotein by Human Arterial Smooth Muscle Cells in Culture, *J. Clin. Invest. 74*, 1890–1894.
19. Lowry, O.H., Rosebrough, N.J., Farr, A.L., and Randall, R.J. (1951) Protein Measurement with the Folin Phenol Reagent, *J. Biol. Chem. 193*, 265–275.
20. Miller, M.E. (1969) Phagocytosis in the Newborn Infant: Humoral and Cellular Factors, *J. Pediatr. 74*, 255–259.
21. Di Carlo, F.J., and Fiore, J.V. (1958) On the Composition of Zymosan, *Science 127*, 756–757.
22. Zerbinatti, C.V., Oliveira, H.C.F., Wechster, S., and Quintão, E.C.R. (1991) Independent Regulation of Chylomicron Lipolysis and Particle Removal Rates: Effects of Insulin and Thyroid Hormones on the Metabolism of Artificial Chylomicrons, *Metabolism 40*, 1122–1127.
23. Benlian, P., Gennes, J.L., Foubert, L., Zhang, H., Gagné, S.E., and Hayden, M. (1996) Premature Atherosclerosis in Patients with Familial Chylomicronemia Caused by Mutations in the Lipoproteins Lipase Gene, *N. Engl. J. Med. 335*, 848–854.
24. Sung, S.J., Nelson, R.S., and Silverstein, S.C. (1983) Yeast Mannans Inhibit Binding and Phagocytosis of Zymosan by Mouse Peritoneal Macrophages, *J. Cell. Biol. 96*, 160–166.
25. Melamed, J., Medicus, R.G., Arnaout, M.A., and Colten, H.R. (1983) Induction of Granulocyte Histaminase Release by Particle Bound Complement C3 Cleavage Products (C3b, C3bi) and IgG, *J. Immunol. 131*, 439–444.
26. Bigler, R.D., Khoo, M., Lund-Katz, S., Scerbo, L., and Esfahani, M. (1990) Identification of Low Density Lipoprotein as a Regulator of Fc Receptor-Mediated Phagocytosis, *Proc. Nat. Acad. Sci. USA 87*, 4981–4985.
27. Beppu, M., Hora, M., and Kikugawa, K. (1994) A Simple Method for the Assessment of Macrophage Scavenger Receptor–Ligand Interaction: Adherence of Erythrocytes Coated with Oxidized Low Density Lipoprotein and Modified Albumin to Macrophages, *Biol. Pharm. Bull. 17*, 39–46.
28. Sambrano, G.R., Parthasarathy, S., and Steinberg, D. (1994) Recognition of Oxidatively Damaged Erythrocytes by a Macrophage Receptor with Specificity for Oxidized Low Density Lipoprotein, *Proc. Natl. Acad. Sci. USA 91*, 3265–3269.
29. Gruarin, P., Stia, R., and Alessio, M. (1997) Formation of One or More Intrachain Disulphide Bonds Is Required for the Intracellular Processing and Transport of CD36, *Biochem. J. 328*, 635–642.
30. Mamo, J.C.L., Elsegood, C.L., Gennat, H.C., and Yu, K.C.-W. (1996) Degradation of Chylomicron Remnants by Macrophages Occurs *Via* Phagocytosis, *Biochemistry 35*, 10210–10214.
31. Zhang, W.-Y., Gaynor, P.M., and Kruth, H.S. (1997) Aggregated Low Density Lipoprotein Induces and Enters Surface-Connected Compartments of Human Monocyte-Macrophages. Uptake Occurs Independently of the Low Density Lipoprotein Receptor, *J. Biol. Chem. 272*, 31700–31706.
32. Yu, K.C.-W., and Mamo, J.C.L. (1997) Regulation of Cholesterol Synthesis and Esterification in Primary Cultures of Macrophages Following Uptake of Chylomicron Remnants, *Biochem. Mol. Biol. Int. 41*, 33–39.

[Received July 2, 1999 and in revised form November 23, 1999; revision accepted January 4, 2000]

Dietary Docosahexaenoic Acid Suppresses Inflammation and Immunoresponses in Contact Hypersensitivity Reaction in Mice

Yoko I. Tomobe[a], Kazuya Morizawa[b], Mamoru Tsuchida[a], Hidehiko Hibino [b], Yoshio Nakano[a], and Yukihisa Tanaka[a,*]

[a]Tsukuba Research Laboratory, NOF Corporation, Tsukuba Ibaraki, 300-2635, Japan, and [b]Food Research Laboratory, NOF Corporation, Kita Tokyo 224-0003, Japan

ABSTRACT: This study was designed to examine the immunomodulatory effects of dietary docosahexaenoic acid (DHA) in the absence of eicosapentaenoic acid (EPA). We investigated the effects of feeding dietary DHA ethyl ester (DHA-Et) (97% pure) at levels of 4.8 wt% of the total diet and of feeding EPA ethyl ester (EPA-Et) (99% pure) at 4.8 wt% on the inflammatory response in the challenge phase of the contact hypersensitivity reaction (CHR) in the ears of mice sensitized with 2,4-dinitro-1-fluorobenzene (DNFB). The effect of DHA-Et on T lymphocytes at the CHR site was examined using anti-CD4 antibodies. Furthermore, we examined the cytokines formed at the CHR site on the mRNA level. It was found that 24 h after the challenge, DHA-Et but not EPA-Et reduced the ear swelling. Infiltration of inflammatory cells, in particular, CD4-positive T lymphocytes, into the ears in the challenge phase of CHR was observed. DHA-Et reduced the infiltration of CD4-positive T lymphocytes into the ears. DHA-Et also decreased the expression of interferon-γ, interleukin (IL)-6, IL-1β , and IL-2 mRNA in ears. These observations suggest that DHA, but not EPA, may exert an antiinflammatory and immunosuppressive effect. The immunosuppressive effectiveness of fish oil may be attributed mainly to DHA.

Paper no. L8225 in *Lipids 35,* 61–69 (January 2000).

Many researchers have reported that intake of polyunsaturated fatty acids (PUFA), especially n-3 PUFA, have a beneficial role in the prevention of cardiovascular diseases (1,2), at least in part because of reduced arteriosclerosis (3). Eicosapentaenoic acid (EPA) in particular has been demonstrated to prevent hypertriglyceridemia (4) and osteoporosis (5). In the last decade, there has been great interest in the effects of different types of dietary PUFA upon the immune system (6). The reason for the interest in the immunomodulatory effects of fatty acids is that epidemiological studies have shown that people such as the Inuit, who consume large quantities of fish oil rich in n-3 PUFA EPA (20:5n-3) and docosahexaenoic acid (DHA; 22:6n-3), have a very low incidence of inflammatory and autoimmune diseases (6).

Further, many clinical studies have reported that fish oil supplementation of the human diet has several beneficial effects in acute and chronic inflammatory conditions (7–13). Feeding laboratory animals diets rich in n-3 PUFA (canola, linseed, fish oils), particularly diets rich in fish oil, has resulted in immunosuppression (14–18). Arm *et al.* (19) reported fish oil supplementation ameliorated the condition of asthmatic subjects. However, the consumption of diets that contained n-3 PUFA aided immunosuppression, whereas those rich in n-6 PUFA were less suppressive (14–18).

Most of the studies cited investigated the effects of large amounts of n-3 or n-6 PUFA. The amounts used in many cases could not be achieved in the human diet. There is little information on how much n-3 PUFA needs to be present to bring about the beneficial effects of fish oil. Fish oil contains variable amounts of EPA and DHA, along with many other fatty acids, cholesterol, heavy metals, and chlorinated hydrocarbons. It is not known if the decline in immune response caused by fish oils is due to EPA or DHA, to both, or to some other factor. Purified esters of EPA lowered several aspects of the immune response in humans (20–22). *In vitro* studies conducted with human (23) and rat lymphocytes (24) and *in vivo* studies in rats (25) showed that DHA esters/salts also inhibit immune cell functions.

Kelley *et al.* (26) reported that when total fat intake was low and held constant, DHA consumption did not inhibit many of the lymphocyte functions that have been reported to be inhibited by fish oil consumption in young healthy men.

Bjørneboe *et al.* (27) reported improvement in the condition of atopic dermatitis patients with the treatment of Max-Epa (18% EPA and 12% DHA). In atopic dermatitis, the mechanism underlying skin lesion formation has remained unclear

*To whom correspondence should be addressed at Tsukuba Research Laboratory, NOF Corporation, 5-10 Tokodai, Tsukuba, Ibaraki, 300-2635, Japan. E-mail: KYF00305@nifty.ne.jp

Abbreviations: AA, arachidonic acid; CHR, contact hypersensitivity reaction; DHA, docosahexaenoic acid; DHA-Et, DHA ethyl ester; DNFB, 2,4-dinitro-1-fluorobenzene; EPA, eicosapentaenoic acid; EPA-Et, EPA ethyl ester; G3PDH, glyceraldehyde 3-phosphate dehydrogenase; ICAM-1, intercellular adhesion molecule-1; IFN, interferon; Ig, immunoglobulin; IL, interleukin; LT, leukotrienes; MAb, monoclonal antibody; PAF, platelet-activating factor; PBS, phosphate-buffered saline; PCR, polymerase chain reaction; PG, prostaglandin; PUFA, polyunsaturated fatty acid; RT, room temperature; Th cells, T-helper cells; TNF, tumor necrosis factor; VCAM-1, endothelial leucocyte adhesion molecule.

except for instances of delayed hypersensitivity reaction against environmental substances (28–30) or immunoglobulin E (IgE)-mediated immediate hypersensitivity reaction against food or inhalant allergens (31–33). Eczematous skin lesions in atopic dermatitis patients contain cytokine-producing CD4-positive T cells (34,35). CD4-positive T cells or T-helper cells (Th cells) have been divided into two subclasses depending on their cytokine secretion pattern: The Th1-like subtype, which is characterized by predominant production of interferon (IFN)-γ and interleukin (IL)-2, and the Th2-like subtype, which typically synthesizes IL-4 (36). In previous studies, 85% of skin samples obtained from chronic eczematous lesions of atopic dermatitis patients were found to contain increased levels of IFN-γ mRNA, whereas increased IL-4 mRNA expression could be observed in only 25 to 30% (33). In addition, in those atopic dermatitis patients whose skin disease responded to treatment, increased IFN-γ mRNA but not increased IL-4 mRNA levels were down-regulated. These studies indicate that the Th1-like cytokine IFN-γ plays a major role in the maintenance of chronic eczematous lesions in atopic dermatitis patients. It has already been reported that the expression of IFN-γ among several Th1 types of cytokine is especially important for the formation of contact hypersensitivity reaction (CHR) (37). Although there are limitations in the use of mouse CHR as a model for chronic atopic dermatitis, it is one approach for studying the late phase of this disease.

In our study, we investigated the immunomodulatory effects of dietary DHA ethyl ester (DHA-Et) fed at a level of 4.8 wt% of total diet and of EPA ethyl ester (EPA-Et) also fed at 4.8 wt% on the inflammatory response in the challenge phase of CHR in the ears of mice sensitized with 2,4-dinitro-1-fluorobenzene (DNFB). We used a 4.8 wt% corn oil diet as control. We show here that DHA-Et reduced the ear swelling and the expression of Th1 type cytokines and decreased the infiltration of inflammatory cells into the ears in the challenge phase of CHR.

MATERIALS AND METHODS

Diet. The low-fat (basal) diet was obtained from Clea Japan Inc. (Yokohama, Japan). Its composition, in weight percentages, was as follows: milk casein, 26.1; corn starch, 48.4; crystallized cellulose, 10.6; cellulose powder, 3.2; sugar, 2.1; potato α-starch, 1.1; vitamine mixture, 1.1; mineral mixture, 7.4. Each diet contained 94.0 wt% of basal diet and 1.2 wt% of safflower oil, to supply the essential fatty acid linoleic acid. The rest of the diet constituted the experimental lipid. The EPA-Et, DHA-Et, and control diets contained 4.8 wt% of EPA-Et (99% purity; NOF Corp., Tokyo, Japan), DHA-Et (97% purity; NOF Corp.), and corn oil, respectively. All lipids contained 0.2 wt% of α-tocopherol as an antioxidant. The fatty acid composition of experimental lipids that were added in the basal diet were shown in Table 1. Saibokuto (1.0 wt%; Tsumura Inc., Tokyo, Japan) was added in a control diet as a positive control diet (Saibokuto diet). Saibokuto is an antiinflammatory Chinese medicine that suppresses the production of leukotriene (LT) C_4 and platelet-activated factor (PAF). The diets were divided into small packages and stored at 4°C. To minimize lipid peroxidation, fresh diets were provided to the mice every day.

TABLE 1
Fatty Acid Composition of Experimental Lipids[a]

	Control, Saibokuto	DHA-Et	EPA-Et
16:0	11.5	—	—
16:1	0.2	—	—
18:0	2.1	—	—
18:1	28.1	—	—
18:2 (n-6)	57.6	—	—
20:5 (EPA)	—	2.8	99.0
22:6 (DHA)	—	97.1	—

[a]DHA, docosahexaenoic acid; DHA-Et, DHA ethyl ester; EPA, eicosapentaenoic acid; EPA-Et, EPA ethyl ester; —, not detected.

Feed design and induction of CHR. The use of animals in all of our experiments was in accordance with guidelines of the Tsukuba Research Laboratory, NOF Corporation. Four-week-old female ddy mice (this strain came to Japan from Germany in the early 1900s and has been kept in a closed colony since) were obtained from Charles River Japan Inc. (Tokyo, Japan). After a 1-wk accommodation period, the mice were divided into four groups (n = 12). Their body weights were measured twice a week. After 23 d of feeding the described diets, the fur on the backs of the mice was shaved off. The next day, to induce the inflammatory reaction, the mice were treated with 0.1 mL of 0.5% DNFB diluted with an acetone/olive oil mixture (4:1 vol/vol) on their backs (induction). Five days after induction, 20 μL of the same DNFB mixture as in the induction treatment was applied to both ears of the sensitized mice (challenge). Before the challenge and at 6 and 24 h afterward, the thicknesses of the mice ears were measured using a thickness gauge (Ozaki Mfg. Co. Ltd., Tokyo, Japan).

Increase in thickness is defined as ear swelling. DNFB solution was painted on both ears. The average for both ears of each animal was taken as the individual mouse ear swelling.

Histopathological analysis. Twenty-four hours after the challenge, the mice were sacrificed. Their ears were then removed, embedded in Tissue-Tek OCT (Miles, Elkhart, IN), and frozen with dry ice/acetone. Serial 6-μm sections were cut on a cryostat and placed on poly-L-lysine-coated slides (two sections per slide). The slides of the frozen sections were defrosted and dried at room temperature (RT) for an hour. After fixation in 5% paraformaldehyde, the sections were stained with hematoxylin-eosin solution.

Infiltration of inflammatory cells into the epidermis and the severity of edema were observed and the degree ranked in five levels. Rank 1 indicated very slight; rank 2, slight; rank 3, middle; rank 4, severe; rank 5, most severe.

Immunohistochemistry. Serial 8-μm sections were cut on a cryostat and placed on poly-L-lysine-coated slides (two sections per slide). Slides with frozen sections were defrosted and dried at RT for an hour. After fixation in cold acetone (10 min), they were allowed to dry at RT (10 min). After washing in phosphate-buffered saline (PBS) (5 min × 3), nonspecific

binding sites were blocked with block ace (Dainippon Seiyaku, Osaka, Japan). Excess solution was removed; the sections were then circled with a waterproof pen (Dako; Glosstrup, Denmark), and incubated with the primary monoclonal antibody (MAb), anti-mouse CD4 (L3/T4)(Cedarlane Laboratory Ltd., Canada) or anti-mouse CD8α (KT 15) (Serotec Ltd., Oxford, England) at 37°C for an hour. All MAb against mouse antigens were rat immunoglobulin G (IgG). Diluent was 10% block ace. Negative control slides were incubated in the diluent alone. After washing in PBS, the slides were incubated with biotinylated rabbit antirat IgG preadsorbed with mouse liver powder, followed by avidin-biotinylated horseradish peroxidase complex and diaminobenzidine according to the Vectastain protocol (Vector, Burlingame, CA). For individual slides, the nuclei were counterstained with methyl green (Vector).

Expression of cytokines. Cytokine mRNA expression was measured by reverse transcription-polymerase chain reaction (PCR). The ears were taken from mice 24 h after the challenge. The specimens were homogenized with 1.0 mL of 4 M guanidium isothiocyanate buffer. After this, the total RNA was extracted and reverse transcribed to cDNA using Moloney Murine Leukemia Virus (M-MuLV) Reverse Transcriptase and a random primer [pd $(N)_6$] (Amersham Pharmacia Biotech, Uppsala, Sweden). Identical amounts of cDNA were subjected to 35 PCR cycles with primers of cytokines (Clontec Inc., Palo Alto, CA). The products were subjected to electrophoresis on a 1.0% agarose gel and visualized by ethidium bromide staining. For the estimation of similar amounts of cDNA used for PCR, the samples were screened for the expression of glyceraldehyde 3-phosphate dehydrogenase (G3PDH) as the housekeeping gene. The relative amounts of cDNA of each sample to be inserted into PCR were calculated to yield similar amounts of G3PDH PCR products by using the computer software Bioimage Version 0.81 (Bioimage Japan Inc., Tokyo, Japan).

Data analysis. The data were expressed as the mean ± SD of four mice fed each diet. The data were analyzed by analysis of variance and Bonferroni's test. A P value of less than 0.05 was considered to be statistically significant.

RESULTS

Mouse growth. The final body weights, and therefore the total growth, were not found to differ among the mice fed on the different diets (data not shown). No side effects were observed among mice fed on the diets described in the Materials and Methods section.

Ear swelling. Ear swelling of mice fed the control diet was measurable 6 h after the challenge. The differences in ear thickness (mean ± SD) before the challenge and 6 and 24 h afterward (ear swelling) are shown in Figure 1. In the early and late phases (6 and 24 h after the challenge, respectively), the ear swelling of the mice fed the DHA-Et diet was significantly suppressed compared to that of those fed the control diet and the EPA-Et diet ($P < 0.01$). The ear swelling of the mice fed

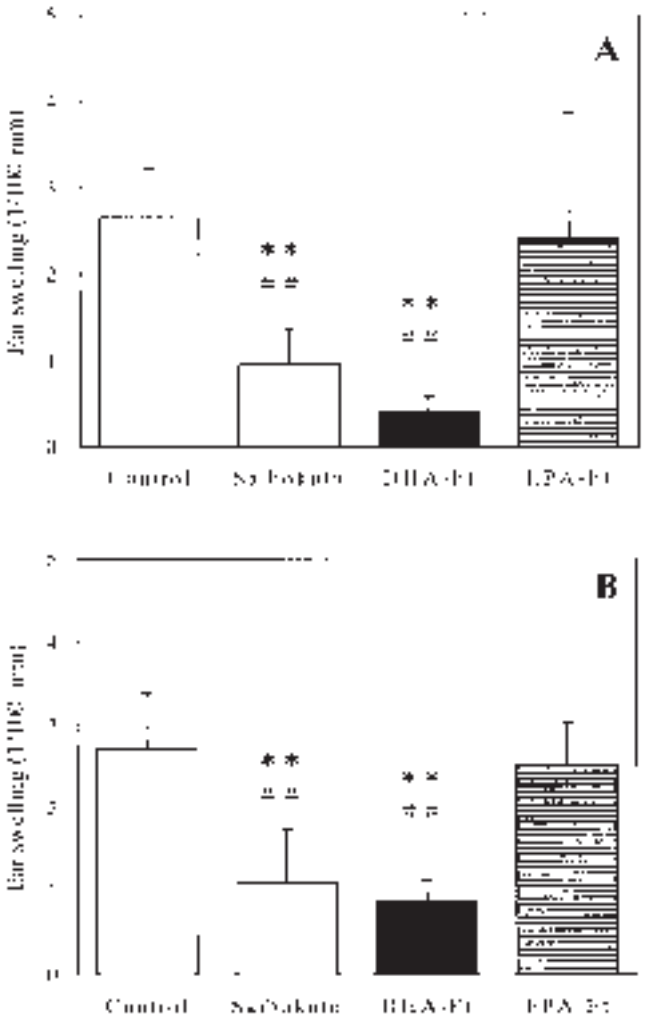

FIG. 1. Ear swelling of mice fed several kinds of diets (A) 6 h and (B) 24 h after the challenge. Control,Control diet; DHA-Et, docosahexaenoic acid ethyl ester diet; EPA-Et, eicosapentaenoic acid ethyl ester diet; Saibokuto, control diet to which was added 1.0 wt% Saibokuto. Six and 24 h after the challenge, ear swelling of mice fed on the DHA-Et diet was significantly suppressed compared with those fed on control diet ($P < 0.01$). Ear swelling of mice fed EPA-Et diet was not different from that of mice fed control diet. Six hours after the challenge, ear swelling of mice fed Saibokuto diet was also suppressed compared with that of mice fed control diet from. $^{**}P < 0.01$, significantly different from the control diet group. $\#\#P < 0.01$, significantly different from the EPA-Et diet group (one-way analysis of variance followed by Bonferroni's test). The data are expressed as the mean ± SD.

EPA-Et diet was found not to be different from that of the mice fed the control diet. The ear swelling of mice fed the saibokuto diet was also significantly suppressed compared to that of those fed the control diet and the EPA-Et diet ($P < 0.01$).

Histopathological analysis. On histological examination 24 h after the challenge, spongiosis (paracytic edema of the epidermis and corium) and mononuclear cell infiltration into the epidermis were observed in the ear tissues from the mice fed the control diet. Significant filtration of the lymphocytes (mostly monocytes) was also observed at the stratum reticular. Typical photomicrographs are shown in Figures 2A and

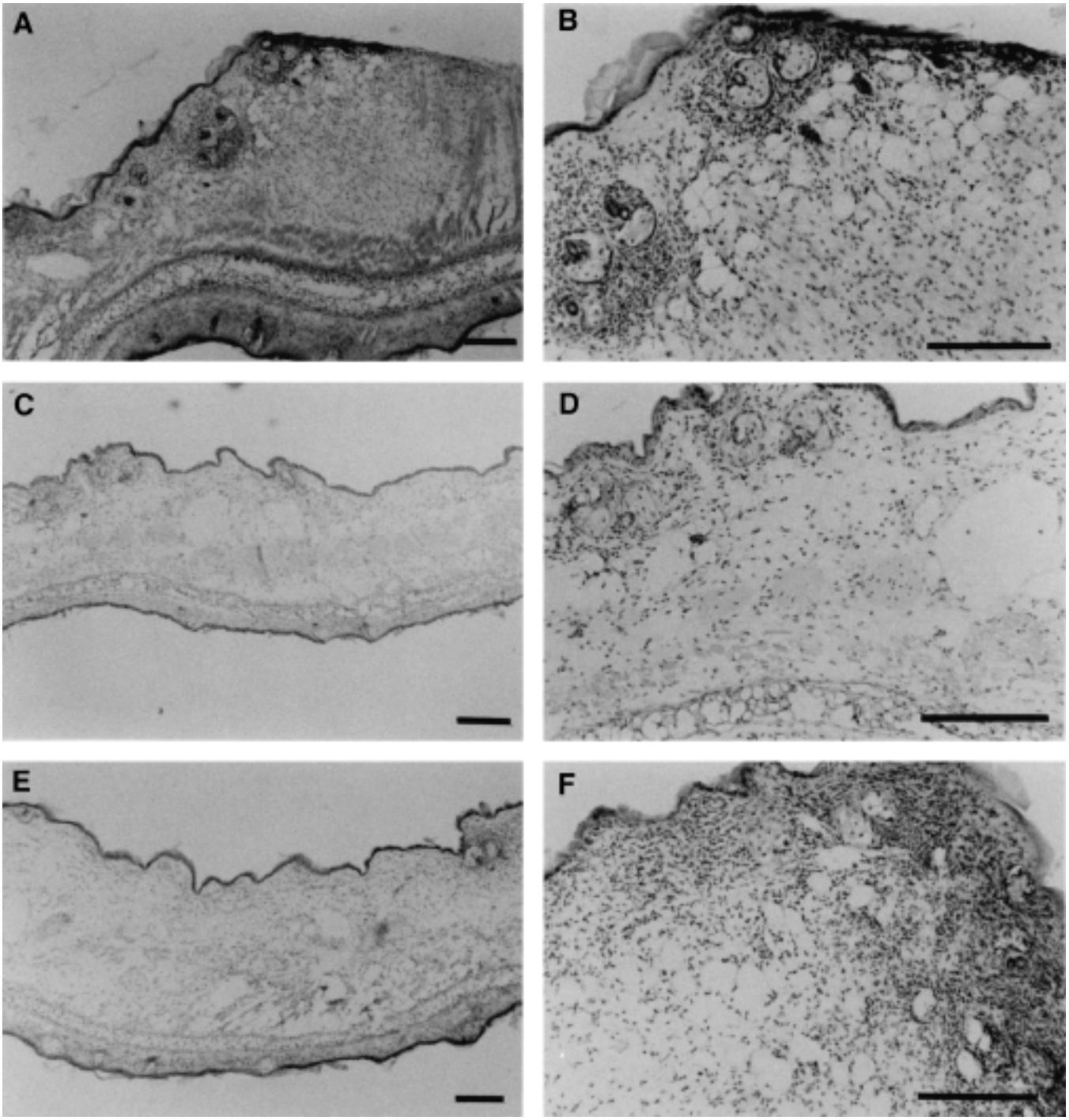

FIG. 2. Photomicrographs of mouse ear stained with hematoxyline and eosin. (A,B) Ear of a mouse fed the control diet, 24 h after challenge. Note spongiosis (paracytic edema of epidermis and corium) and mononuclear cell infiltration into the epidermis. (C,D) DHA-Et decreased the number of infiltrated inflammatory cells in the epidermis in comparison with control. (E,F) EPA-Et did not ameliorate the severity of spongiosis and did not decrease the number of filtrated inflammatory cells into the epidermis. Photomicrographs of B, D, and F are magnifications (10×) of A, C, and E, respectively. Each bar represents 200 μm. For abbreviations see Figure 1.

2B. The number of infiltrated inflammatory cells in the ear tissues from the mice fed the DHA-Et diet was reduced (Figs. 2C and 2D), while in the tissues from the mice fed the EPA-Et diet, the severity of spongiosis and the infiltration of inflammatory cells into the epidermis were almost the same as in the control diet (Figs. 2E and 2F).

The severity of the ear tissue damage in the mice fed each diet is shown in Table 2. Less edema was observed in ear tissues from mice fed the DHA-Et diet than in tissues from mice fed the EPA-Et and the control diet ($P < 0.01$). Focal granulation tissue formation in the dermis was not observed in the ear tissues from the mice 24 h after the challenge.

TABLE 2
Histopathological Findings

	Inflammatory cell infiltration	Edema
Nontreated	—	—
Control	4.0 ± 0.0	4.0 ± 0.0
Saibokuto	3.0 ± 0.0	3.8 ± 0.5
DHA-Et	*2.8 ± 0.5	* **2.5 ± 0.6
EPA-Et	3.0 ± 0.0	4.0 ± 0.0

[a]Scoring: —, no change; 1, very slight; 2, slight; 3, middle; 4, severe; 5, most severe. Data represent the mean of four specimens. *$P < 0.01$, significantly different from the control diet group. **$P < 0.01$, significantly different from the EPA-Et diet group. For abbreviations see Table 1.

Immunohistological study. Twenty-four hours after the challenge, infiltration of CD4-positive cells into the corium was observed in the ear tissues from the mice fed the control diet (Figs. 3A and 3B). The number of CD4-positive cells in the tissues from the mice fed DHA-Et was less than those from the control diet mice (Figs. 3C and 3D). CD4-positive cells in the tissues from the mice fed EPA-Et were not different from those in the mice fed the control diet (Figs. 3E and 3F).

Twenty-four hours after the challenge, infiltration of CD8-positive cells into the corium was also observed in the ear tissues from the mice fed the control diet, although the number of CD8-positive cells was less than that of CD4-positive cells. The number of CD8-positive cells in the tissues from the mice fed DHA-Et was not significantly less than that in the control diet (data not shown).

Expression of cytokines in the ear tissues from mice in the challenge phase of CHR. We examined the cytokine mRNA expressed at the CHR sites. At 24 h after the challenge, IL-1β, IL-2, IL-6, and IFN-γ mRNA were expressed in the ear tissues from the mice fed the control diet, but IL-4, IL-3, and TNF-α mRNA were not. The expression of IL-2, IL-6, and IFN-γ mRNA was decreased significantly in the tissues from the mice fed the DHA-Et diet compared with that from the mice fed the control diet (Fig. 4). The expression of IL-1β was decreased, but not significantly. In contrast, no decrease of the expression of IL-1β, IL-6, IFN-γ, and IL-2 mRNA in the tissues from the mice fed the EPA-Et diet was observed (Fig. 4).

Under these conditions, G3PDH mRNA was not seen to change.

DISCUSSION

In this study we compared DHA-Et with EPA-Et for their antiinflammatory and immunosuppressive effects in a rodent CHR model. Generally, inflammatory mediators are thought to convert from PUFA through an arachidonate cascade and play important roles in the development of the inflammatory process. Arachidonic acid (AA) is converted to 2-series prostaglandins (PG) and 4-series leukotrienes (LT), all of which are mediators of inflammation. In particular 4-series LT intensify neutrophil chemotactic responsiveness in the development of the inflammatory process. On the other hand, EPA displaces AA from macrophage phospholipids and effectively competes with AA for cyclooxygenase and lipoxygenase binding sites to foster formation of eicosanoids with relatively lower inflammatory properties (38), e.g., thromboxane A_3, LT B_5 and PGE_1, than those generated from AA (e.g., thromboxane A_2 and LT B_4). Palombo *et al.* (39) reported that short-time (i.e., 3 d) continuous enteral feeding of diets containing EPA and γ-linolenic acid to endotoxemic rats reduces the levels of AA and linoleic acid in alveolar macrophage and liver Kupffer and endothelial cell phospholipids with attendant decreases in PG formation by these cells *in vitro*. The suppression of inflammatory responses by EPA might be due to some adverse effect on the arachidonate cascade whereas DHA is thought not to be a substrate of the enzymes in the arachidonate cascade nor to be converted to eicosanoid products. Krokan *et al.* (40) reported that, since substituting DHA for AA in the phospholipids of the cell membrane was more difficult than substituting EPA for AA, the suppressive effect of DHA on the arachidonate cascade was less than for EPA. In contrast, Corey *et al.* (41) reported that DHA inhibited AA conversion to PGE_2 in an *in vitro* experiment. Nakamura *et al.* (42) reported that the inflammatory effects of DHA and EPA in carrageenan-induced edema in rats were essentially same. DHA suppressed the production of the PAF after stimulation of cultured Eol-1 cell by calcium ionophore A23187 (43). Matsumoto *et al.* (44) reported 1-oleic-2-docosahexaenoic phosphatidylcholine inhibited 5-lipoxygenase activity. These results lead to the conclusion that DHA may also suppress the inflammatory response through the modulation of the arachidonate cascade in a similar way to EPA.

Danno *et al.* (45) reported that (i) EPA did not suppress DNFB-induced ear edema (they did not examine DHA treatment), and (ii) EPA, but not DHA, suppresses AA-induced acute inflammation reaction in mice. They concluded that only EPA was able to inhibit AA conversion to 4-series LT and 2-series PG; DHA was not able to inhibit LT biosynthesis

Our results showed that ear swelling in CHR mice fed DHA-Et but not EPA-Et was significantly suppressed compared with that in the control diet in the early and late phases of CHR. We suggested in our report the inhibition of the arachidonate cascade by DHA is unlikely to be the mechanism through which DHA suppresses CHR. Although arachidonate casacade inhibition may be one of several antiinflammatory effects of DHA in CHR, DHA may be acting through the AA-independent mechanism.

In atopic dermatitis, the mechanism underlying skin lesion formation has remained unclear except for the possibility of a delayed hypersensitivity reaction against environmental pollutants (28,29,46) or an IgE-mediated immediate hypersensitivity reaction against food or inhalant allergens (30–32). Atopic eczema is thought to be caused by skin-infiltrating CD4 T cells of Th1- and/or Th2-like subtype, resulting in chronic inflammation of the skin. A dysregulated, cytokine-mediated response for the immune system to environmental, in particular inhalant, allergens is thought to be an important pathogenic factor (47). It has been reported that IFN-γ (Th1-like cytokine) mRNA expression is linked to the clinical

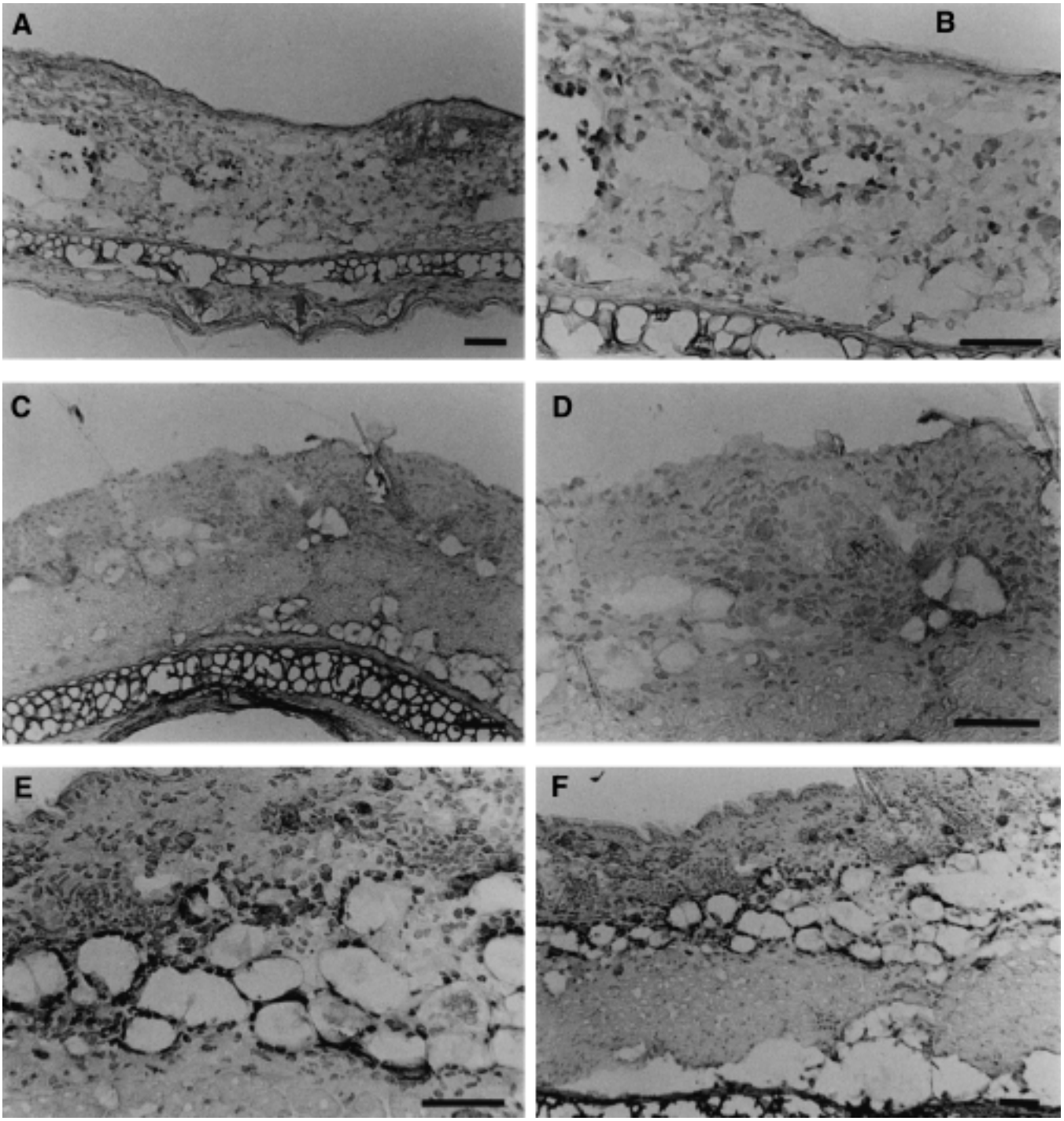

FIG. 3. Immunohistochemical analysis. (A,B) CD4-positive cells in ear from mouse fed control diet, 24 h after challenge. Determined using avidin-biotinylated horseradish peroxidase complex method. Note infiltration of CD4-positive cells into corium. (C,D) DHA-Et decreased the number of the infiltrated CD4-positive cells in inflammatory sites in comparison with control. (E,F) The level of CD4-positive cells in ear from mouse fed EPA-Et was not different from those of the control diet. Photomicrographs of B, D and F were are magnifications (10×) of A, C and E, respectively. Each bar represents 100 μm. For abbreviations see Figure 1.

course of atopic eczema since it was down-regulated after successful therapy but was unaltered in nonresponders (33). Lesional atopic skin clinically and histologically resembles allergic contact dermatitis, which may be mediated by a predominant expression of the Th1-like cytokine IFN-γ (48), and a potential role for IFN-γ in atopic dermatitis is further supported by the observation that the intercellular adhesion molecule-1 (ICAM-1), which is strongly inducible by IFN-γ, is expressed on keratinocytes in lesional atopic skin (49). To clarify the immunosuppressive effect of DHA, we used the

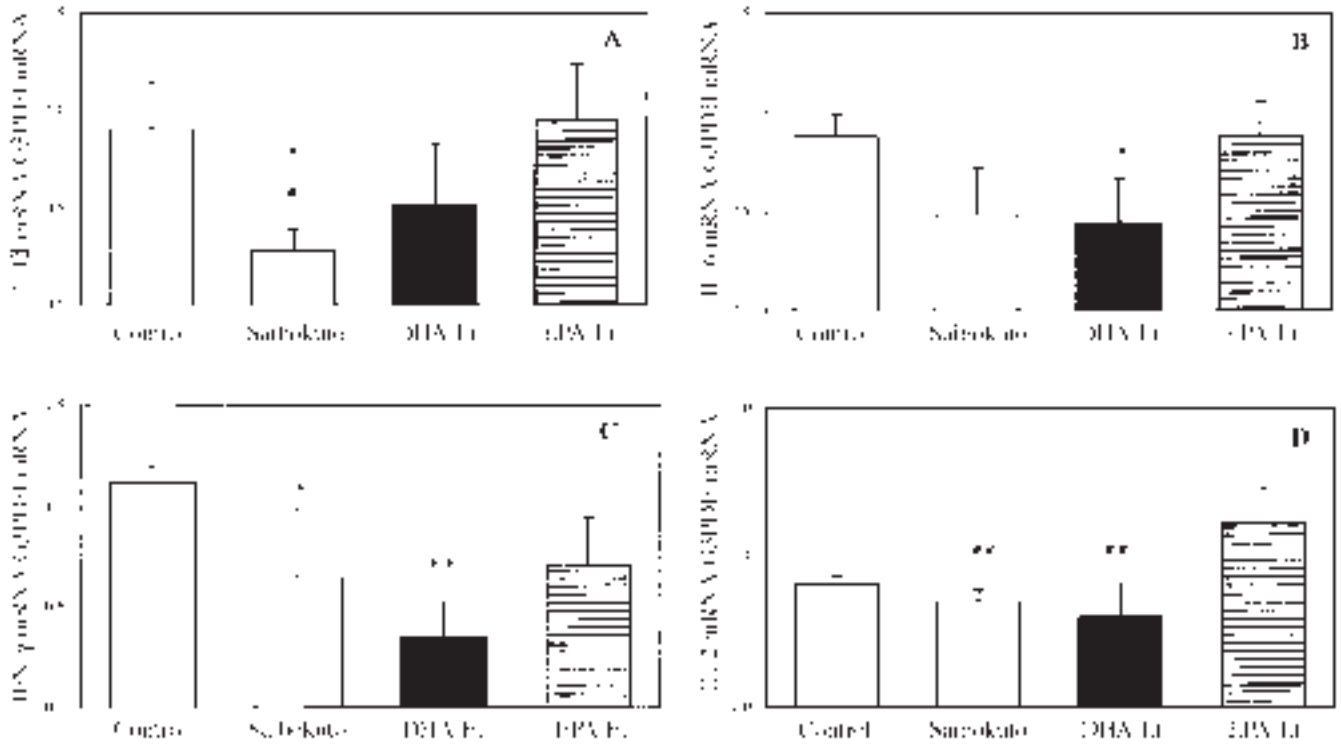

FIG. 4. Expression of cytokine mRNA in the ear of a mouse fed several diets 24 h after challenge. (A) Expression of IL-1β mRNA. (B) Expression of IL-6 mRNA. (C) Expression of IFN-γ mRNA. (D) Expression of IL-2 mRNA. The total RNA (2 μg) from each sample was used and subjected to reverse transcription-polymerase chain reaction (PCR) analysis. For the estimation of similar amounts of cDNA used for the PCR, samples were screened for the expression of glyceraldehyde 3-phosphate dehydrogenase (G3PDH) as the housekeeping gene. The relative amounts of cDNA of each sample to be inserted into the PCR were calculated to yield similar amounts of GAPDH PCR products by using the computer software Bioimage Version 0.81 (Bioimage Japan Inc., Tokyo, Japan). $^{*}P < 0.05$, $^{**}P < 0.01$, significantly different from the control diet group. $\#P < 0.05$, $\#\#P < 0.01$, significantly different from the EPA-Et diet group (one-way anaylsis of variance followed by Bonferroni's test). The data are expressed as the mean ± SD. For abbreviation see Figure 1.

mouse CHR model induced with DNBF. It was reported that ear swelling became worse after about 24 h and was ameliorated 48 h after the challenge, so this reaction in a mouse is based on a chronic delayed-type hypersensitivity (type IV hypersensitivity) (37). It was reported that 24 h after the challenge, IFN-γ, IL-6, and IL-1β mRNA were expressed in the ear tissues in the mice and 48 h after the challenge, IL-2, IL-4, and TNF-α mRNA were expressed in addition to these cytokines (37). Moreover, Yamazaki *et al.* (37) suggested that the expression of IFN-γ among several Th1 types of cytokine is especially important for the formation of CHR by analysis of IFN-γ knock-out mice and using anti-IFN-γ antibody (37). As in the previous study, 24 h after the challenge we found that ear swelling, the number of infiltrated CD4-positive cells into lesion sites, and the expression of IL-1β, IL-6, IFN-γ, and IL-2 mRNA were decreased in the ear lesion sites in mice fed DHA-Et not but EPA-Et compared with those in mice fed the control diet. It was suggested that decreased expression of these cytokines, in particular IFN-γ, might suppress the progression of ear swelling.

Inflammatory reaction was induced by the adhesion of circulating leukocytes into the endothelium and their subsequent transendothelial migration. This process depends on the endothelial expression of the endothelial leukocyte adhesion molecules (50,51). De Caterina *et al.* (52) reported DHA inhibited cytokine-stimulated expression of the endothelial leukocyte adhesion molecule VCAM-1 and two other cytokine-induced secretable products, IL-6 and IL-8, from human endothelial cells in culture. They found that the adhesion of cytokine-stimulated monocyte-like cells to activated endothelial cells was decreased with DHA not but EPA treatment. Their study suggested that dietary DHA might decrease the level of VCAM-1 mRNA, consistent with the protein expression; therefore, the infiltration and chemotaxis of T cells, monocytes, and neutrophiles into endothelial cells might be also decreased. It is unclear why DHA but not EPA reduced cytokine-induced leukocyte adhesion molecule expression in endothelial cells. An effect of DHA on cytokine-induced nuclear translocation of specific transcription factors (e.g., nuclear factor-κB) is a likely possibility (53). Several recent reports have described properties of DHA not shared by EPA (43,54–57).

Grewe *et al.* (33) showed the levels of ICAM-1 mRNA on keratinocytes in lesional atopic skin were also up-regulated to more than that in normal skin. The expression of IFN-γ could be linked to clinical treatment of a lesion of atopic skin

because it was down-regulated after successful therapy. Decreased *in-situ* expression of IFN-γ in the responders was paralleled by a reduced expression of ICAM-1 inducible by IFN-γ on keratinocytes, which suggests a functional relevance. In a chronic dermatitis phase, Th1-type cytokines, such as IFN-γ, predominate, which may be critical for the induction of keratinocyte ICAM-1 expression and subsequent accumulation of inflammatory cells in lesional skin (37).

Th1-like cytokine IFN-γ has been reported to play a major role in the maintenance of chronic eczematous lesions in atopic dermatitis patients (37). In this study, the level of IFN-γ mRNA was decreased in the ear tissues in the mice treated with DHA-Et. Because this effect is important for amelioration of the inflammatory response in lesional skin, it was expected that the DHA-Et treatment might improve on the severity in chronic atopic dermatitis. Jenski *et al.* (58) reported that concanavalin A-stimulated proliferation of T lymphocytes and the development of an immunologic memory, as modeled by the secondary mixed lymphocyte reaction, were severely decreased by DHA. They suggested that DHA might be used to modulate immune responses selectively, e.g., to suppress undesired autoimmunity while maintaining protective immunity. In our study, the results from immunohistochemical observation also showed that the infiltration of the inflammatory cells (especially CD4-positive cells) into lesional sites in mice fed DHA-Et diet 24 h after the challenge (late phase of the reaction) was suppressed compared with those in the control diet.

In this report the authors have shown DHA-Et, but not EPA-Et, suppresses ear swelling 24 h after the challenge with DNBF, the expression of Th1-type cytokines such as IFN-γ, and infiltration of inflammatory cells, in particular CD4-positive cells, into the lesion sites. Overall, our data suggest that DHA may ameliorate the inflammation and immune response in the late phase of atopic dermatitis.

ACKNOWLEDGMENT

We thank Dr. Terada (Kitasato University, Sagamihara Japan), who passed away in the winter of 1997, for his many useful suggestions. We pray for the repose of his soul.

REFERENCES

1. Kristensen, S.D., De Caterina, R., Schmit, E.B., and Endres, S. (1993) Fish Oil and Ischaemic Heart Diseases, *Br. Heart J. 70,* 212–214.
2. Goodnight, S.H. (1993) The Effects of n-3 Fatty Acids on Arteriosclerosis and the Vascular Response to Injury, *Arch. Pathol. Lab. Med. 117,* 102–106.
3. Newman, W., Middaugh, J., Prost, M., and Rogers, D. (1993) Arteriosclerosis in Alaska Natives and Non-natives, *Lancet 341,* 1056–1057.
4. Harris, W.C., Rothrock, D.W., Fanning, A., Inkeles, S.B., Goodnight, S.H., Jr., Illingworth, D.W., and Connor, W.E. (1990) Fish Oils in Hypertriglyceridemia, A Dose Response Study, *Am. J. Clin. Nutr. 51,* 399–406.
5. Sakaguchi, K., Morita, I., and Murota, S. (1994) Eicosapentaenoic Acid Inhibits Bone Loss Due to Ovariectomy in Rats, *Prostaglandins Leukotrienes Essent. Fatty Acids 50,* 81–84.
6. Kromann, N., and Green, A. (1980) Epidemiological Studies in the Upernavik District, Greenland, *Acta Med. Scand. 208,* 401–406.
7. Kremer, J.M., Lawrence, D.A., Jubiz, W., Di Giacomo, R., Rynes, K., Bartholomew, L.E., and Sherman, M. (1990) Dietary Fish Oil and Olive Oil Supplementation in Patients with Rheumatoid Arthritis, *Arthritis Rheum. 33*, 810–820.
8. Sperling, R.I., Lewis, R.A., and Austen, K.F. (1987) Effects of Dietary Supplimentation with Marine Fish Oil on Leukocyte Lipid Mediator Generation and Function in Rheumatoid Arthritis, *Arthritis Rheum. 30,* 987–988.
9. Cleland, L.G., French, J.K., Betts, W.H., Murphy, G.A., and Elliott, M.J. (1988) Clinical and Biochemical Effects of Dietary Fish Oil Supplements in Rheumatoid Arthritis, *J. Rheumatol. 15,* 1471–1475.
10. Ziboh, V.A., Cohen, K.A., Ellis, C.N., Miller, C., Hamilton, T.A., Kragballe, K., Hydrick, C.R., and Voorhees, J.J. (1986) Effects of Dietary Supplementation of Fish Oils on Neutrophil and Epidermal Fatty Acids: Modulation of Clinical Course of Psoriatic Lesions, *Arch. Dermatol. 122*, 1277–1282.
11. Das, U.N. (1994) Beneficial Effects of Eicosapentaenoic and Docosahexaenoic Acids in the Management of Systemic Lupus Erythematosus and Its Relationship to the Cytokine Network, *Prostaglandins Leukotrienes Essent. Fatty Acids 51*, 207–213.
12. Hawthorne, A.B., Daneshmend, T.K., Hawkey, C.J., Belluzzi, A., Everitt, S.J., Holmes, G.K.T., Malkinson, C., Shaheen, M.Z., and Willars, J.E. (1992) Treatment of Ulcerative Colitis with Fish Oil Supplementation: A Prospective 12 Month Randomized Controlled Trial, *Gut 33,* 922–928.
13. Belluzzi, A., Brignola, C., Campieri, M., Pera, A., Boschi., and Miglioloi, M. (1996) Effect of an Enteric-Coated Fish Oil Preparation on Relapses in Crohn's Disease, *New Engl. J. Med. 334,* 1557–1560.
14. Calder, P.C. (1995) Fatty Acids, Dietary Lipids and Lymphocyte Function, *Biochem. Soc. Trans. 23,* 302–309.
15. Calder, P.C. (1996) Can n-3 Polyunsaturated Fatty Acids Be Used as Immunomodulatory Agents? *Biochem. Soc. Trans. 24,* 211–220.
16. Calder, P.C. (1996) Effects of Fatty Acids and Dietary Lipids on Cells of the Immune System, *Proc. Nutr. Soc. 55,* 127–150.
17. Calder, P.C. (1996) Immunomodulatory and Anti-Inflammatory Effects of Omega-3 Polyunsaturated Fatty Acid, *Proc. Nutr. Soc. 55,* 737–774.
18. Calder, P.C. (1998) Dietary Fatty Acids and the Immune System, *Nutr, Rev. 56,* S70–S83.
19. Arm, J.P., Horton, C.E., Mencia-Huerta, J.M., House, F., Eiser, M.N., Clark, T.J.H., Spur, B.W., and Lee, T.H. (1988) Effects of Dietary Supplementation with Fish Oil Lipids on Mild Asthma, *Thorax 43,* 84–92.
20. Payan, D.G., Wong, M.Y.S., Chernov-Rogan, T., Valone, F.H., Pickett, W.C., Blake, V., and Gold, W.M. (1986) Alteration in Human Leukocyte Function Induced by Ingestion of Eicosapentaenoic Acid, *J. Clin. Immunol. 6,* 402–410.
21. Virella, G., Kilpatrick, J.M., Rugeles, M.T., Hyman, B., and Russell, R. (1989) Depression of Humoral Responses and Phagocytic Functions *in vivo* and *in vitro* by Fish Oil and Eicosapentaenoic Acid, *Clin. Immunol. Immunopathol. 52,* 257–270.
22. Yamashita, N., Maruyama, M., Yamazaki, K., Hamazaki, T., and Yano, S. (1991) Effect of Eicosapentaenoic Acid and Docosahexaenoic Acid on Natural Killer Cell Activity in Human Peripheral Blood Lymphocytes, *Clin. Immunol. Immunopathol. 59*, 335–345.
23. Khalfoun, B., Thibault, G., Lacord, M., Bardos, P., and Lebranchu, Y. (1996) Docosahexaenoic and Eicosapentaenoic Acids Inhibit Human Lymphoproliferative Responses *in vitro* but Not the Expression of T Cell Surface Markers, *Scand. J. Immunol. 43,* 248–256.

24. Lim, B.O., Yamada, K., Hung, P., Watanabe, T., Taniguchi, S., and Sugano M. (1996) Effects of n-3 Polyunsaturated Fatty Acids and Lectins on Immunoglobulin Production by Spleen Lymphocytes of Sprague-Dawley Rats, *Biosci. Biotechnol. Biochem. 60,* 1025–1027.
25. Jolly, C., Jiang Y.H., Chapkin, R.S., and McMurry, D. (1997) Dietary n-3 Polyunsaturated Fatty Acids Suppress Murine Lymphoproliferation, Interleukin 2 Secretion, and the Formation of Diacylglycerol and Ceramide. *J. Nutr. 127,* 37–43.
26. Kelley, D.S., Taylor, P.C., Nelson, G.J., and Mackey, B.E. (1998) Dietary Docosahexaenoic Acid and Immunocompetence in Young Healthy Men, *Lipids 33*, 559–566.
27. Bjørneboe, A., Søyland, E., Bjørneboe, G.-E.A., Rajaka, G., and Drevon, C.A. (1987) Effect of Dietary Supplementation with Eicosapentaenoic Acid in the Treatment of Atopic Dermatitis, *Br. J. Dermatol. 117,* 463–469.
28. Uehara, M., and Ofuji, S. (1976) Patch Test Reactions to Human Skin Dander in Atopic Dermatitis, *Arch. Dermatol. 112,* 951.
29. Adinoff, A.D., Tellez, P., and Clark, A.F. (1988) Atopic Dermatitis and Aeroallergen in Contact Sensitivity, *J. Allergy Clin. Immunol. 81,* 736–742.
30. Atherton, D.J., Sewell, M., Soothill, J.F., and Wells, R.S. (1978) A Double Blind Controlled Crossover Trial of an Antigen Avoidance Diet in Atopic Eczema, *Lancet 1,* 401-403.
31. Sampson, H.A. (1988) The Role of Food Allergy and Mediator Release in Atopic Dermatitis, *J. Allergy Clin. Immunol. 81,* 635–645.
32. Rajka, G. (1989) Pathomechanism: Genetic and Immunological Factors, in *Essential Aspects of Atopic Dermatitis,* pp. 108–111, Tokyo, Springer-Verlag.
33. Grewe, M., Gyufko, K., Schopf, E., and Krutmann, J. (1994) Lesional Expression of Interferon-γ in Atopic Eczema, *Lancet 343,* 25–26.
34. Braathen, L.R., Forre, O., Natvig, J.B., and Eeg-Larsen, T. (1987) Predominance of T Lymphocytes in the Dermal Infiltrate of Atopic Dermatitis, *Br. J. Dermatol. 100,* 511–514.
35. Zachary, G.B., Allen, M.H., and MacDonald, D.M. (1985) In Situ Quantification of T-Lymphocyte Subsets and Langerhans Cells in the Inflammatory Infiltrate of Atopic Eczema, *Br. J. Dermatol. 112,* 149–155.
36. Mosman, T.R., and Coffman, R.L. (1989) TH1 and TH2 Cells: Different Patterns of Lymphokine Secretion Lead to Different Functional Properties, *Annu. Rev. Immunol. 7,* 145–149.
37. Yamazaki, S., Kumahara, H., and Kakishima, H. (1997) Analysis of Contact Dermatitis by Cytokines. I, *Yakugaku Zasshi 117,* 155–161 (in Japanese).
38. Kinsella, J.E., Broughton, K.S., and Whelan, J.W. (1990) Dietary Unsaturated Fatty Acids: Interactions and Possible Needs in Relation to Eicosanoid Synthesis, *J. Nutr. Biochem. 1,* 123–142.
39. Palombo, J.D., DeMichele, S.J., Boyce, P.J., Noursalehi, M., Forse, R.A., and Bistrian, B.R. (1998) Metabolism of Dietary α-Linolenic Acid vs. Eicosapentaenoic Acid in Rat Immune Cell Phospholipids During Endotoxemia, *Lipids 33,* 1099–1105.
40. Krokan, H.E., Bjerve, K.S., and Mørk, E. (1993) The Enteral Bioavailability of Eicosapentaenoic Acid and Docosahexaenoic Acid Is as Good from Ethyl Esters as from Glyceryl Esters in Spite of Lower Hydrolytic Rates by Pancreatic Lipase *in vitro*, *Biochim. Biophys. Acta. 1168,* 59–67.
41. Corey, E.J., Shin, C., and Cashman, J.R. (1983) Docosahexaenoic Acid Is a Strong Inhibitor of Prostaglandin but Not Leukotriene Biosynthesis, *Proc. Natl. Acad. Sci. USA 80,* 3581–3584.
42. Nakamura N., Hamazaki T., Kobayashi, M., and Yazawa, K. (1994) The Effect of Oral Administration of Eicosapentaenoic and Docosahexaenoic Acids on Acute Inflammation and Fatty Acid Composition in Rats, *J. Nutr. Sci. Vitaminol. 40,* 161–170.
43. Shikano, M., Masuzawa, Y., and Yazawa, K. (1993) Effect of Docosahexaenoic Acid on the Generation of Platelet-Activation Factor by Eosinophilic Leukemia Cells, Eol-1, *J. Immunol. 150,* 3525–3533.
44. Matsumoto, K., Morita, I., Hibino, H., and Murota, S. (1993) Inhibitory Effect of Docosahexaenoic Acid-Containing Phospholipids on 5-Lipoxygenase in Rat Basophilic Leukemia Cells, *Prostaglandins Leukotrienes Essent. Fatty Acids 49,* 861–866.
45. Danno, K., Ikai, K., and Imamura, S. (1993) Anti-inflammatory Effects of Eicosapentaenoic Acid on Experimental Skin Inflammation Models, *Arch. Dermatol. Res. 285,* 432–435.
46. Mitchell, E.B., Chapman, M.D., Pope, F.M., Crow, J., Jouhal, S.S., and Platts-Mills, T.A.E. (1982) Basophils in Allergen Induced Patch Test Sites in Atopic Dermatitis, *Lancet 1,* 127–130.
47. Bos, J.D., Wierenga, E.A., Smitt, J.H.S., van der Heijden, F.L., and Kapsenberg, M.L. (1992) Immune Dysregulation in Atopic Eczema, *Arch. Dermatol. 128,* 1509–1512.
48. Romagnani, S. (1991) Human Th1 and Th2 Subsets: Doubt No More, *Immunol. Today 12,* 256–257.
49. Krutmann, J. (1994) Regulatory Interactions Between Epidermal Cell Adhesion Molecules and Cytokines, in *Epidermal Cytokines and Growth Factors* (Lunger, T.A., and Schwarz, T., eds.), pp. 415–432, Marcel Dekker, New York.
50. Bevilacqua, M., Mendrick, P.J., Cortran, R., and Gimbrone, M.J. (1987) Identification of an Inducible Endothelial-Leukocyte Adhesion Molecule, *Proc. Natl. Acad. Sci. USA 84,* 9238–9242.
51. Springer, T. (1990) Adhesion Receptors of the Immune System, *Nature 346,* 425–434.
52. DeCaterin, R., Cybulsky, M.I., Clinton, S.K., Gimbrone, M.A., Jr., and Libby, P. (1994) The Omega-3 Fatty Acid Docosahexaenoate Reduces Cytokine-Induced Expression of Proarteriogenic and Proinflammatory Proteins in Human Endothelial Cells, *Arterioscler. Thromb. 14,* 1829–1836.
53. Collins, T. (1993) Endothelial Nuclear Factor-κB and the Initiation of the Arteriosclerotic Lesion, *Lab. Invest. 68,* 499–508.
54. Weber, C., Aepfelbacher, M., Lux, I., Zimmer, B., and Weber, P. (1991) Docosahexaenoic Acid Inhibits PAF and LT_4 Stimulated [Ca^{2+}] Increase in Differentiated Monocytic U937 Cells, *Biochim. Biophys. Acta 1133,* 38–45.
55. Hrelia, S., Biagi, P., Turchetto, E., Rossi, C., and Bordoni, A. (1992) Protein Kinase C Activity in Neonatal Cultured Rat Cardiomyocytes Supplemented with Docosahexaenoic Acid, *Biochem. Biophys. Res. Commun. 183,* 893–898.
56. Scheurlen, M., Kirchner, M., Clemens, M., and Jaschonek, K. (1993) Fish Oil Preparations Rich in Docosahexaenoic Acid Modify Platelet Responsiveness to Prostaglandin-Endoperoxide/Thromboxane A_2 Receptor Agonists, *Biochem. Pharmacol. 46,* 245–249.
57. Willumsen, N., Hexeberg, S., Skorve, J., Lundquist, M., and Berge, R. (1993) Docosahexaenoic Acid Shows No Triglyceride-Lowering Effects but Increases the Peroxisomal Fatty Acid Oxidation in Liver of Rats, *J. Lipid. Res. 34,* 13–22.
58. Jenski, L.J., Scherer, J.M., Caldwell, L.D., Ney, V.A., and Stillwell, W. (1998) The Triggering Signaal Dictates the Effect of Docosahexaenoic Acid on Lymphocyte Function *in vitro, Lipids 33,* 869–878.

[Received July 1, 1999, and in final revised form November 10, 1999; revision accepted December 3, 1999]

The Metabolism and Distribution of Docosapentaenoic Acid (n-6) in Rats and Rat Hepatocytes

Phyllis S.Y. Tam[a], Rumi Umeda-Sawada[a,*], Toshiaki Yaguchi[b], Kengo Akimoto[b], Yoshinobu Kiso[b], and Osamu Igarashi[a]

[a]Institute of Environmental Science for Human Life, Ochanomizu University, Tokyo 112-8610, Japan, and [b]Institute for Fundamental Research, Suntory Limited, Osaka 618-8503, Japan

ABSTRACT: In this study, a new marine oil that contains 45% docosahexaenoic acid (DHA, 22:6n-3) and 13% docosapentaenoic acid (DPA, 22:5n-6) was administered to rats. The metabolism and distribution of DPA in rats was investigated. In experiment 1, the effects of DHA and n-6 fatty acids (linoleic acid, LA; arachidonic acid, AA; and DPA) on AA contents were investigated *in vivo*. LA group: LA 25%, DHA 30%; LA-DPA group: LA 15%, DPA 10%, DHA 35%; LA-AA-DPA group: LA 10%, AA 5%, DPA 10%, DHA 35% were administered to rats for 4 wk. In the liver, the AA content in the LA-DPA and LA-AA-DPA groups was significantly higher than in the LA group. The decreased AA contents in the LA group might be caused by DHA administration. Although DHA also was administered in the LA-DPA and LA-AA-DPA groups, the AA contents in these two groups did not decrease. These results suggested that DPA retroconverted to AA, blunting the decrease in AA content caused by DHA administration. To conduct a detailed investigation on DPA metabolism and its relation with AA and DHA, rat hepatocytes were cultured with purified DPA and DHA for 24 h. We discovered the retroconversion of DPA to AA occurred only when AA content was decreased by a high DHA administration; it did not occur when AA content was maintained at a normal level.

Paper no. L8212 in *Lipids 35*, 71–75 (January 2000).

Recently, a marine microbe was isolated by a screening test for polyunsaturated fatty acids (PUFA) and was found to accumulate lipids that contain docosahexaenoic acid (DHA, 22:6n-3) and docosapentaenoic acid (DPA,22:5n-6) (1). A new marine oil, DPA-DHA oil, containing 45% DHA and 13% DPA, is therefore available for study. Among n-3 PUFA, DHA has specific functions in the brain and retina (2–5). A recent trend in DHA research focuses on the relation between DHA and the immune system (6). Regarding DPA, its content in most organisms is low, and the n-3 isomer of DPA in most fish oils is at higher levels than is the n-6 isomer (7). It is also known that n-6 DPA is β-oxidized to arachidonic acid (AA, 20:4n-6) (8–11), and that the deficiency of n-3 essential fatty acids (EFA) in animals causes a compensatory rise in the n-6 DPA level in the brain/retina (12,13), but the physiological function of n-6 DPA itself has not yet been clarified.

AA is important in cell membrane phospholipids and serves as the precursor of eicosanoids. AA is maintained at a constant level under normal conditions *in vivo*. It was recently shown that breast milk contains AA that contributes to infant development (14). Moreover, Carlson *et al.* (15) reported that a condition of AA deficiency in preterm infants may lead to impaired growth over the first year of life. In the studies of DHA supplementation, however, high dietary intake of DHA resulted not only in an increase of DHA content but also in a decrease in AA content (16,17). The decrease in AA has been proposed to relate to the inhibition of Δ6 desaturases, reducing synthesis of AA from linoleic acid (LA, 18:2n-6). Both DHA and AA are essential components of the infant central nervous system, and a lack in either may lead to impaired growth. Therefore, an AA decline because of DHA supplementation is a problem that still must be addressed.

In this study, DPA-DHA oil was administered to rats, and its metabolism and distribution were investigated. In experiment 1, the effects of DPA-DHA oil on EFA metabolism was examined with a focus on the interaction and change in the composition of n-6 and n-3 fatty acids *in vivo*. In the second part of this study, primary cultured rat hepatocytes were used to conduct a more detailed investigation of the metabolism of n-6 DPA and its relations with other PUFA, especially DHA and AA.

MATERIALS AND METHODS

Materials. The DPA-DHA oil prepared from a single-cell marine microbe was donated by Suntory Ltd. (Osaka, Japan). DPA ethyl esters (purity >99%), DHA ethyl esters (purity >99%), and AA ethyl esters (purity <95%) also were donated by Suntory Ltd. (Osaka, Japan). Soybean oils, safflower oils, and rapeseed oils were provided by Ajinomoto Co., Inc. (Tokyo, Japan). The standard basal diet was purchased from Eisai Co., Ltd. (Tokyo, Japan). Collagenase (Lot. LEL7202) and L-glutamine were purchased from Wako Pure Chemical Industries, Ltd. (Tokyo, Japan). Trypsin inhibitor (from soybean, Lot. 40H8200)

*To whom correspondence should be addressed at Institute of Environmental Science for Human Life, Ochanomizu University, 2-2-1, Otsuka, Bunkyo-ku, Tokyo 112-8610, Japan. E-mail: sawada@cc.ocha.ac.jp

Abbreviations: AA, arachidonic acid; BSA, bovine serum albumin; DHA, docosahexaenoic acid; DPA, docosapentaenoic acid; EFA, essential fatty acid; EPA, eicosapentaenoic acid; GLC, gas–liquid chromatography; LA, linoleic acid; PUFA, polyunsaturated fatty acid.

and bovine serum albumin (BSA, essentially fatty acid-free, Lot. 122H9318) were purchased from Sigma Chemical Co. (St. Louis, MO). Dulbecco's modified Eagle medium (DME) and phosphate-buffered saline (PBS) were purchased from Sankoh Pure Chemical Co. (Tokyo, Japan); 8.4% $NaHCO_3$ was purchased from Ohtsuka Pharmaceutical Co. (Tokyo, Japan).

Animals and diets. All experiments were approved by the Animal Experiment Ethics Committee of Ochanomizu University. Four-week-old male Wistar rats were initially fed a commercial diet (CE-2; Nippon Clea Co., Tokyo, Japan) for 1 wk. The animals were then divided into four groups of 5–6 animals each and fed experimental diets for 4 wk. These diets were prepared by mixing 5% (w/w) experimental oil mixtures with the basal diet. The basal diet, prepared according to the standards given by the American Institute of Nutrition (AIN) (18), was provided by Eisai Co. and contained the following percentage of ingredients according to weight: casein 20; glucose 25; sucrose 25; cornstarch 15; filter paper 5; AIN mineral mixture 3.5; AIN vitamin mixture; 1; choline bitartrate 0.2; and DL-methionine 0.3. In experiment 1, the oil mixtures were prepared as follows: (i) LA group: (rapeseed oil/soybean oil, 1:1)/DHA ethyl esters, 65:35; (ii) LA-DPA group: DPA-DHA oil/safflower oil, 4:1; (iii) LA-AA-DPA group: safflower oil AA ethyl esters/ DPA-DHA oil, 15:5:80. The fatty acid compositions of dietary oils are shown in Table 1.

Preparation of rat hepatocytes. Rat hepatocytes were prepared and cultured by the methods described previously (19). Hepatocytes were used for experiments after 17 h of incubation. DPA and DHA ethyl esters were dissolved in 10% BSA solution and added to the culture medium at a final concentration of 0.5 and 0.25 mM, respectively. Hepatocytes were incubated with fatty acids (DPA and/or DHA) for 24 h.

Lipids analyses. Lipids were extracted from the livers, testis, and brains of the rats in experiment 1 and the rat hepatocytes of the rats in experiment 2 by the method used by Folch *et al.* (20). Margaric acid (17:0) was added to the lipid extracts as an internal standard. The lipid extract was then methylated by using HCl/methanol to measure the content of fatty acids. The fatty acid methyl esters were measured by gas–liquid chromatography (GLC) (PerkinElmer Auto system GLC, Palo Alto, CA) on a Rascot Siller 5CP capillary column (0.25 mm × 50 m; Nihon Chromato Works Ltd., Tokyo, Japan), with conditions as described in detail previously (19). Protein was measured by the method of Lowry *et al.* (21).

Statistical analyses. All results are shown as means ± SD. The significance of differences in mean values was evaluated by analysis of variance (ANOVA). After ANOVA, a Bonferroni-Dunn *post-hoc* test was used. Analyses were performed by using a StatView (System 4.02) computer package (Abacus Concepts, Inc., Berkeley, CA).

RESULTS AND DISCUSSIONS

Experiment 1. DHA content in dietary oils was adjusted to 30 to 35% in all groups. The content of total n-6 fatty acids, LA, AA, and DPA was adjusted to about 25%. The concentration of main fatty acids in the different groups was: LA 25% and DHA 30% in the LA group; LA 15, DPA 10, and DHA 35% in the LA-DPA group; and LA 10, AA 5, DPA 10, and DHA 35% in the LA-AA-DPA group. The fatty acid composition of the diet is shown in Table 1.

Results from experiment 1 are shown in Tables 2, 3, and 4. The total fatty acid composition in liver is shown in Table 2. The AA content in the LA-DPA and LA-AA-DPA groups was significantly higher than in the LA group despite the similar total amount of n-6 fatty acids in the diet. The decrease in AA content in the LA group may be due to the high intake of DHA owing to the inhibition of Δ6 desaturation enzymatic reaction from LA to AA. However, a similar amount of DHA administered in the LA-DPA and LA-AA-DPA groups resulted in a much higher AA content. These results suggest that DPA retroconverted to AA to cover the decreased AA content caused by high DHA intake. On the other hand, the AA content in the LA-AA-DPA group was significantly higher than in the LA-DPA group and shows the direct effect of AA administration in the diet.

DPA (n-6) was observed in the LA-DPA and LA-AA-DPA groups, but no significant amount was detected in the LA group. Low DPA (n-3) and 22:4n-6 content was observed in all groups, but no significant difference was observed.

Eicosapentaenoic acid (EPA, 20:5n-3) contents in the LA-DPA and LA-AA-DPA groups were significantly lower than in the LA group. No significant difference was found between the EPA content of the LA-DPA and LA-AA-DPA groups. EPA, which may result from the retroconversion of DHA, was observed in low amounts in the two groups fed DPA and DHA, but not in the group that was fed only DHA. It may imply the occurrence of the retroconversion of DPA to AA (n-6) inhibits the similar retroconversion of DHA to EPA (n-3) in the LA-DPA and LA-AA-DPA groups. A similar fatty acid profile was found in liver phospholipids (phosphatidylcholine and phosphatidylethanolamine) (data not shown).

Table 1
Fatty Acid Composition of Dietary Oils[a]

	16:0	18:0	18:1n-9	18:2n-6	18:3n-3	AA 20:4n-6	EPA 20:5n-3	DPA 22:5n-6	DHA 22:6n-3
LA	5.5	2.4	29.0	26.4	6.0	0.0	0.0	0.0	30.7
LA-DPA	31.4	2.0	3.9	16.9	0.0	0.0	0.0	10.2	35.7
LA-AA-DPA	33.7	1.7	2.4	11.2	0.0	5.1	0.0	10.2	35.8

[a]Values are expressed as percentage of weight. AA, arachidonic acid; EPA, eicosapentaenoic acid; DPA, docosapentaenoic acid; DHA, docosahexaenoic acid; LA, linoleic acid.

TABLE 2
Effect of Dietary Oils on Fatty Acid Composition in Liver[a]

	LA	LA-DPA	LA-AA-DPA
18:0	24.8 ± 1.19	25.0 ± 2.15	24.2 ± 4.18
18:1n-9	20.7 ± 6.08	16.2 ± 2.64	23.7 ± 3.63
18:2n-6	20.2 ± 1.74[a]	13.0 ± 1.75[b]	11.0 ± 3.44[b]
18:3n-3	1.19 ± 0.17[a]	0.05 ± 0.11[b]	0.20 ± 0.06[b]
20:4n-6	8.60 ± 1.36[a]	20.8 ± 1.84[b]	29.9 ± 3.73[c]
20:5n-3	4.27 ± 0.64[a]	2.16 ± 0.62[b]	1.97 ± 0.70[b]
22:4n-6	0.11 ± 0.01	0.99 ± 0.07	0.34 ± 0.54
22:5n-6	ND	6.94 ± 1.96	8.31 ± 2.51
22:5n-3	0.63 ± 0.50	0.68 ± 0.12	2.06 ± 3.12
22:6n-3	43.9 ± 7.68	44.9 ± 9.38	55.0 ± 10.9

[a]Results are expressed as μmol/g tissue and means ± SD (n = 5–6). ND, not detected. The significance of differences between dietary treatments was analyzed by analysis of variance (ANOVA). Values not sharing a common roman letter are significantly different. See Table 1 for abbreviations.

TABLE 3
Effect of Dietary Oils on Fatty Acid Composition in Testis[a]

	LA	LA-DPA	LA-AA-DPA
18:0	4.18 ± 0.41[a]	4.29 ± 0.51[a]	3.33 ± 0.15[b]
18:1n-9	6.85 ± 0.68	11.4 ± 6.36	6.96 ± 1.91
18:2n-6	3.49 ± 0.45	4.92 ± 3.53	1.85 ± 0.69
18:3n-3	ND	0.11 ± 0.16	ND
20:4n-6	6.48 ± 0.76	7.13 ± 0.36	6.50 ± 0.21
20:5n-3	0.20 ± 0.04	0.24 ± 0.21	0.12 ± 0.03
22:4n-6	0.06 ± 0.01	0.06 ± 0.01	0.08 ± 0.11
22:5n-6	7.86 ± 0.95[a,b]	8.95 ± 0.65[a]	7.39 ± 0.27[b]
22:5n-3	0.10 ± 0.02	0.09 ± 0.03	0.09 ± 0.02
22:6n-3	1.88 ± 0.33	3.38 ± 1.44	2.34 ± 0.92

[a]Results are expressed as μmol/g tissue and means ± SD (n = 5–6). The significance of differences between dietary treatments was analyzed by ANOVA. Values not sharing a common roman letter are significantly different. See Tables 1 and 2 for abbreviations.

The fatty acid content in the testis is shown in Table 3. DPA content in all groups was high compared with that in the liver or brain (Tables 2 and 4). We may assume that DPA accumulates the most in testis, although the physiological function of DPA in the testis still needs to be clarified.

Table 4 shows the total fatty acid composition in the brain. DHA, which is essential in the brain, has a high content in all groups.

The fatty acid profiles in the lung, heart, and kidneys of the different dietary groups were similar to the liver (data not shown).

Experiment 2. Highly purified DPA (>99%) and DHA (>95%) ethyl esters were used to conduct a more detailed investigation on the metabolism of DPA. The retroconversion of DPA to blunt the decreased AA content caused by DHA supplementation was also examined *in vitro*. The total fatty acid content of cultured rat hepatocytes is shown in Table 5.

TABLE 4
Effect of Dietary Oils on Fatty Acid Composition in Brain[a]

	LA	LA-DPA	LA-AA-DPA
18:0	28.3 ± 1.73[a]	31.7 ± 4.80[a]	22.1 ± 1.05[b]
18:1n-9	28.7 ± 4.32[a]	30.3 ± 3.76[a]	16.3 ± 3.87[b]
18:2n-6	1.03 ± 0.14[a]	0.67 ± 0.11[b]	0.33 ± 0.08[c]
18:3n-3	ND	0.06 ± 0.03	0.02 ± 0.02
20:4n-6	9.86 ± 0.92[a]	12.5 ± 2.05[b]	9.31 ± 0.68[a]
20:5n-3	0.62 ± 0.34[a]	0.03 ± 0.05[b]	ND
22:4n-6	0.24 ± 0.06	0.21 ± 0.06	0.17 ± 0.08
22:5n-6	3.30 ± 0.55[a]	3.84 ± 1.48[a]	0.70 ± 0.09[b]
22:5n-3	0.80 ± 0.11[a]	1.08 ± 0.13[b]	0.81 ± 0.26[a]
22:6n-3	17.5 ± 1.26[a,b]	19.7 ± 2.68[a]	14.2 ± 0.92[b]

[a]Results are expressed as μmol/g tissue and means ± SD (n = 5–6). The significance of differences between dietary treatments was analyzed by ANOVA. Values not sharing a common roman letter are significantly different. See Tables 1 and 2 for abbreviations.

TABLE 5
Effect of DPA and DHA on Fatty Acids of Cultured Rat Hepatocytes[a]

	Control	DPA	DHA	DPA–DHA
18:0	139.2 ± 12.8[a]	192.5 ± 70.3[a,b]	126.7 ± 12.6[a]	229.7 ± 13.1[b]
18:1n-9	55.3 ± 8.61[a]	79.3 ± 33.9[a,b]	48.2 ± 5.63[a]	107.1 ± 5.88[b]
18:2n-6	50.8 ± 3.35[a]	51.4 ± 8.04[a]	46.6 ± 6.36[a]	67.3 ± 1.86[b]
18:3n-3	0.56 ± 0.52	0.24 ± 0.41	ND	1.12 ± 0.84
20:4n-6	58.5 ± 4.62[a]	57.3 ± 4.58[a,c]	41.8 ± 5.37[b]	50.3 ± 1.50[c]
20:5n-3	0.19 ± 0.33	0.08 ± 0.14	3.00 ± 2.03	2.04 ± 0.59
22:4n-6	0.03 ± 0.003[a]	0.03 ± 0.002[a]	0.02 ± 0.001[b]	0.03 ± 0.001[a]
22:5n-6	ND	6.97 ± 2.69[a]	ND	2.51 ± 0.51[b]
22:5n-3	0.06 ± 0.01	0.06 ± 0.01	0.06 ± 0.01	0.06 ± 0.01
22:6n-3	7.74 ± 7.88	12.3 ± 1.21	18.8 ± 8.14	19.4 ± 2.09

[a]Hepatocytes were cultured in the presence of 0.5 mM DPA in the DPA group or 0.25 mM DHA in the DHA group, or of both in the DPA-DHA group. Control means no addition of any fatty acid in medium. Results are expressed as nmol/mg protein and means ± SD (n = 3–4). The significance of differences between dietary treatments was analyzed by ANOVA. Values not sharing a common roman letter are significantly different. See Tables 1 and 2 for abbreviations.

The AA contents in the control and the DPA groups were similar. This shows that DPA supplementations did not lead to increased AA content. Thus, the retroconversion of DPA to AA is not active when the AA content is maintained at a normal level. On the other hand, the AA content in the DHA group was significantly lower than the control and DPA groups, suggesting that the decline of AA was caused by the presence of DHA. No significant difference was found between the AA content of the control and DPA-DHA group. These results indicate that the decreased AA content associated with DHA supplementation was blocked by DPA through its retroconverison to AA.

The 22:4n-6 content in the DHA group was significantly lower than in the other three groups. The AA content in the DHA group was lowered by DHA, and 22:4n-6, thought to be the elongation product of AA, was thus also decreased. The 22:4n-6 content in the DPA-DHA group, however, did not decrease despite the addition of DHA. This result suggests that retroconversion of DPA to AA was also associated with increased accumulation of 22:4n-6.

The DPA content in the DPA-DHA group was significantly lower than in the DPA group, and this difference in DPA content between the DPA and DPA-DHA groups suggests that DPA is converted to AA by retroconversion in the DPA-DHA group. From the results of experiment 2, we can conclude that the retroconversion of DPA to AA is active when the AA content is rapidly decreased by DHA and is not active when the AA content is maintained at a normal level.

From the results in this study, the following conclusions could be made: DPA (22:5n-6) is found to be extraordinarily high in testis. The most important finding in this study is the retroconversion of DPA to AA both *in vivo* and *in vitro*. The *in vitro* investigation also showed that the retroconversion of DPA occurred only when the AA content was decreased by high DHA administration, but it did not occur when AA content was maintained at a normal level. At present, there are some reports on the retroconversion of DPA to AA (8–11). However, a study on the condition for the occurrence of DPA to AA retroconversion has not been reported. This study may be the first report to suggest that the retroconversion of DPA to AA occurs only when AA content is decreased. Therefore, it is possible to increase DHA content without causing a rapid decrease in AA by administering DHA with DPA. This finding may suggest a solution to the problem of high DHA administration decreasing AA content. Moreover, DPA-DHA oil may be an appropriate oil for administing DHA *in vivo* without decreasing AA content.

REFERENCES

1. Nakahara, T., Yokochi, T., Higashihara, T., Tanaka, S., Yaguchi, T., and Honda, D. (1996) Production of Docosahexaenoic and Docosapentaenoic Acids by *Schizochytrium* sp. Isolated from Yap Islands, *J. Am. Oil Chem. Soc. 73*, 1421–1426.
2. Nuringer, M., Conner, W.E., Petten, C.V., and Barstad, L. (1984) Dietary Omega-3 Fatty Acid Deficiency and Visual Loss in Infant Rhesus Monkeys, *J. Clin. Invest. 73*:272–276.
3. Bazan, N.G., Reddy, R.S., Bazan, H.E.P., and Birkle, D.L. (1986) Metabolism of Arachidonic and Docosahexaenoic Acids in the Retina, *Prog. Lipid Res. 25*:595–606.
4. Uauy, R.D., Birch, D.G., Tyson, J.E., and Hoffman, D.R. (1990) Effect of Dietary Omega-3 Fatty Acids on Retinal Function of Very-Low-Birth-Weight Neonates, *Pediatr. Res. 28*:485–492.
5. Sandra, N., Gharib, A., Croset, M., Moliere, P., and Lagarde, M. (1991) Fatty Acid Composition of the Rat Pineal Gland. Dietary Modifications, *Biochim. Biophys. Acta 1081*:75–78.
6. Bourre, G.M., Durand, G., Pascal, G., and Youyou, A. (1989) Brain Cell and Tissue Recovery in Rats Made Deficient in n-3 Fatty Acid by Alteration of Dietary Fat, *J. Nutr. 119*, 15–22.
7. Gunstone, F.D., Harwood, J.L., and Padley, F.B. (1994) *The Lipid Handbook*, pp. 173–175, Chapman & Hall, London.
8. Verdino, B., Blank, M.L., Privett, O.S., and Lundberg, W.O. (1964) Metabolism of 4,7,10,13,16-Docosapentaenoic Acid in the Essential Fatty Acid-Deficient Rat, *J. Nutr. 83*, 234–236.
9. Schlenk, H., Gellerman, J.L., and Sand, D.M. (1967) Retroconversion of Polyunsaturated Fatty Acids *in vivo* by Partial Degradation and Hydrogenation, *Biochim. Biophys. Acta 137*, 420–425.
10. Kunau, W.H. (1968) Uber dei Synthese der an allen doppelbindungen tritiummarkierten 4.7.10.13.16-docosapentaensaure und ihre Umwandlung in 5.8.11.14-eicosatetraensaure bei fettfrei ernahrten ratten, *Z. Physiol. Chem. 349*, 333–336.

11. Bridges, R.B., and Coniglio, J.G. (1970) The Metabolism of 4,7,10,13,16-[5-^{14}C]Docosapentaenoic Acid in the Testis of the Rat, *Biochim. Biophys. Acta 218*, 29–35.
12. Homayoun, P.G., Durand, G., Pascal, G., and Bourre, J.M. (1988) Alteration of Fatty Acid Composition of Adult Rat Brain Capillaries and Choroid Plexus Induced by a Diet Deficient in n-3 Fatty Acids: Slow Recovery After Substitution with a Non-deficient Diet, *J. Neurochem.* 5*1*, 45–48.
13. Guesnet, P., Pasval, G., and Durand, G. (1988) Effects of Dietary Alpha-Linolenic Acid Deficiency During Pregnancy and Lactation on Lipid Fatty Acid Composition of Liver and Serum in the Rat, *Reprod. Nutr. Dev. 28*, 275–292.
14. Sanjurjo, P., Rodriguez-Alarcon, J., and Rodriguez-Soriano, J. (1988) Plasma Fatty Acid Composition During the First Week of Life Following Feeding with Human Milk or Formula, *Acta Paediatr. Scand. 77*, 202–209.
15. Carlson, S.E., Werkman, S.H., Peeples, J.M., Cooke, R.J., and Tolley, E.A. (1993) Arachidonic Acid Status Correlates with First Year Growth in Preterm Infants, *Proc. Natl. Acad. Sci. USA 90*, 1073–1077.
16. Cao, J.M., Blond, J.P., Juaneda, P., Durand, G., and Bezard, J. (1995) Effect of Low Levels of Dietary Fish Oils on Fatty Acid Desaturation and Tissue Fatty Acids in Obese and Lean Rats, *Lipids 30*, 825–832.
17. Suarez, A., Faus, M.J., and Gil, A. (1996) Dietary Long-Chain Polyunsaturated Fatty Acids Modify Heart, Kidney, and Lung Fatty Acid Composition in Weanling Rats, *Lipids 31*, 345–348.
18. American Institute of Nutrition (1977) Report of the American Institute of Nutrition *ad hoc* Committee on Standards for Nutritional Studies, *J. Nutr. 107,* 1340–1348.
19. Fujiyama-Fujiwara, Y., Ohmori, C., and Igarashi, O. (1989) Metabolism of γ-Linolenic Acid in Primary Cultures of Rat Hepatocytes and in HepG2 Cells, *J. Nutr. Sci. Vitaminol. 35*, 591–611.
20. Folch, J., Lees, M., and Sloane-Stanley, G.H. (1957) A Simple Method for the Isolation and Purification of Total Lipids from Animal Tissues, *J. Biol. Chem. 266*, 497–509.
21. Lowry, O.H., Rosebrough, N.J., Farr, A.L., and Randall, R.J. (1951) Protein Measurement with the Folin Phenol Reagent, *J. Biol. Chem. 193*, 265–275.

[Received March 22, 1999, and in revised form November 22, 1999; revision accepted December 20, 1999]

Relationships Between the Fatty Acid Composition of Muscle and Erythrocyte Membrane Phospholipid in Young Children and the Effect of Type of Infant Feeding

Louise A. Baur[a,*], Janice O'Connor[a], David A. Pan[b], Ben J. Wu[c], Marcus J. O'Connor[d], and Leonard H. Storlien[c]

[a]Department of Paediatrics and Child Health, University of Sydney NSW 2006, Australia,
[b]Department of Botany and Plant Pathology, Michigan State University, Michigan 48824,
[c]Metabolic Research Centre, Faculty of Health and Behavioural Sciences, University of Wollongong, Wollongong NSW 2522, Australia, and [d]School of Information Systems, Technology and Management, University of New South Wales, Sydney NSW 2052, Australia

ABSTRACT: Muscle membrane fatty acid (FA) composition is linked to insulin action. The aims of this study were to compare the FA composition of muscle and erythrocyte membrane phospholipid in young children; to investigate the effect of diet on these lipid compositions; and to investigate differential incorporation of FA into muscle, erythrocyte and adipose tissue membrane phospholipid, and adipose tissue triglyceride. Skeletal muscle biopsies and fasting blood samples were taken from 61 normally nourished children (45 males and 16 females), less than 2 yr old (means ± SE, 0.80 ± 0.06 yr), undergoing elective surgery. Adipose tissue samples were taken from 15 children. There were significant positive correlations between muscle and erythrocyte docosahexaenoic acid (DHA) ($r = 0.44$, $P < 0.0001$), total n-3 polyunsaturated fatty acids (PUFA) ($r = 0.39$, $P = 0.002$), and the n-6/n-3 PUFA ratio ($r = 0.39$, $P = 0.002$). Adipose tissue triglyceride had lower levels of long-chain PUFA, especially DHA, than muscle and erythrocytes (0.46 ± 0.18% vs. 2.44 ± 0.26% and 3.17 ± 0.27%). Breast-fed infants had higher levels of DHA than an age-matched group of formula-fed infants in both muscle (3.91 ± 0.21% vs. 1.94 ± 0.18%) and erythrocytes (3.81 ± 0.40% vs. 2.65 ± 0.23%). The results of this study show that (i) erythrocyte FA composition is a reasonable index of muscle DHA, total n-3 PUFA, and the n-6/n-3 PUFA ratio; (ii) breast feeding has a potent effect on the FA composition of all these tissues; and (iii) there is a wide range in long-chain PUFA levels in muscle, erythrocytes, and adipose tissue.

Paper no. L8284 in *Lipids 35,* 77–82 (January 2000).

Lipids have many important functions in the body: as a major metabolic fuel, as essential components of all cell membranes, as gene regulators, and as precursors of locally acting metabolites. Knowledge of the fatty acid (FA) composition of lipid in various tissues in the body can give an indication of the level of function of the tissue and also the degree of risk for development of certain diseases.

*To whom correspondence should be addressed at Department of Paediatrics and Child Health, The Royal Alexandra Hospital for Children, P.O. Box 3515, Parramatta NSW 2124, Australia. E-mail: louiseb3@nch.edu.au

Abbreviations: DHA, docosahexaenoic acid; FA, fatty acid; LCPUFA, long-chain polyunsaturated fatty acids; PUFA, polyunsaturated fatty acid.

Work in rodents and humans has shown that dietary FA profiles strongly influence the FA composition of muscle phospholipid (the major structural lipid in membranes) (1). In turn, a higher proportion of long-chain (20 and 22 carbon) polyunsaturated fatty acids (LCPUFA) and a low n-6/n-3 PUFA ratio in muscle membrane are associated with enhanced insulin action (2,3). Since muscle is the major site of insulin-stimulated glucose uptake in the body, this translates to improved whole-body insulin action (4). Insulin resistance (the relative failure of insulin action) is strongly linked to a cluster of prevalent diseases including noninsulin-dependent diabetes mellitus, coronary heart disease, various dyslipidemias, hypertension, and central obesity (5–7).

Currently, the most direct measure of muscle FA composition is a muscle biopsy. However it would be highly advantageous to be able to obtain an index of the FA composition of lipid in muscle without the need to use an invasive method. To our knowledge, no studies have compared the FA composition of erythrocytes and muscle from the same human subjects. The aim of this study was to compare the FA composition of these tissues in young children and to investigate the effect of diet in infancy. In addition, little is known about the incorporation of FA into membrane structural lipid of different tissues. In the current study, we compared the FA composition of erythrocyte and muscle membrane and adipose tissue membrane and triglyceride to investigate whether there was evidence of differential incorporation of FA in these tissues.

METHODS

Participants. Sixty-one children (45 males and 16 females), less than 2 yr old, who were undergoing elective surgery at The Royal Alexandra Hospital for Children (Sydney, Australia) were recruited into the study. These children had no history of poor weight gain, significant systemic disease, major congenital malformations, or previous surgery. The types of elective surgery were correction of congenital talipes and several forms of cardiovascular, urological, or abdominal surgery. The muscle groups obtained were abductor hallucis

(n = 29), rectus abdominis (n = 14), latissimus dorsi (n = 4), and external oblique (n = 14). The study protocol was approved by the Ethics Committee of The Royal Alexandra Hospital for Children.

Protocol. Part of the protocol for this study has been described elsewhere (8). Briefly, patients were admitted to the hospital in the afternoon prior to the day of elective surgery. At this time, written, informed consent was obtained from their parents. The children were weighed, their length was measured, and a detailed diet history was obtained, focusing on duration of breast and/or formula feeding and time of introduction of solid foods.

A fasting blood sample (1.5–2.0 mL) was obtained at the time of insertion of an intravenous line directly after halothane induction of anesthesia. Blood was collected in tubes containing lithium heparin. After removal of plasma, erythrocytes were washed three times with cold isotonic saline containing 0.01% butylated hydroxytoluene and stored at −70°C.

Biopsies of muscle (40–200 mg; n = 61) and subcutaneous fat (40–300 mg; n = 15) were obtained in the operating theater at the time of surgery and immediately freeze-clamped in liquid nitrogen. The samples were stored at −70°C for later analysis of phospholipid and triglyceride (for adipose tissue only) FA composition.

Analytical methods. The extraction and derivatization of the FA components of muscle, erythrocyte, and adipose tissue phospholipids and triglycerides have been described elsewhere (9). Phospholipid is almost exclusively associated with membrane, but our analysis does not differentiate between cellular membranes, e.g., sarcoplasmic reticulum, plasma, and mitochondrial. In brief, tissue was homogenized in 2:1 (vol/vol) chloroform/methanol and total lipid extracts prepared according to Folch *et al.* (10). Phospholipids and triglycerides were separated by solid-phase extraction on Sep-pak silica cartridges (Waters, Milford, MA). Briefly, triglycerides were eluted with 30 mL of dichloromethane followed by 30 mL of ethyl acetate. Phospholipids were then eluted with 30 mL methanol. This procedure gave 100% separation and >95% recovery of [^{14}C]triolein and [^{14}C]phosphatidylcholine added to the $CHCl_3$–methanol fraction. Triglyceride and phospholipid fractions were transmethylated with 140 g/L boron trifluoride (Sigma, St. Louis, MO) at 85°C for 1 h. Methyl esters were extracted into hexane and passed through Sep-pak florisil cartridges (Waters) to remove cholesterol esters and polar contaminants. The methyl FA were separated, identified, and quantitated by gas chromatography. The content of individual FA in the phospholipids and triglyceride was expressed as a percentage of the total FA. Identified minor FA peaks (<0.5 percentage of the total) were excluded from the calculation.

Data analysis. The content of individual FA in phospholipids and triglyceride was expressed as a percentage of the total FA identified. Results for the different muscle groups were pooled because there were no major differences between them. Several FA indices were derived from the primary data: the total percentage of 20–22 LCPUFA (the sum of the individual LCPUFA 20:2n-6, 20:3n-9, 20:3n-6, 20:3n-3, 20:4n-6, 20:5n-3, 22:2n-6, 22:4n-6, 22:5n-6, 22:5n-3, and 22:6n-3) and the average degree of FA unsaturation (the unsaturation index), which was calculated as the average number of double bonds per FA residue multiplied by 100.

Length and weight measurements of the children were compared with the National Center for Health Statistics reference population (11). These measurements were normalized by being expressed as SD scores (12).

Diet histories were analyzed using Australian food composition tables (13) extended to specifically index LCPUFA intake.

In investigating the effect of infant feeding on FA composition, comparisons were made using results from infants who were either currently breast-fed or formula-fed (i.e., breast-fed for less than 4 wk). Note that breast milk contains significant quantities of LCPUFA, especially docosahexaenoic acid (DHA), whereas at the time of this study, commercially available infant formulas contained negligible quantities of LCPUFA (14,15).

Statistical analysis. All data are expressed as means ± SE. Statistical analyses were performed using SPSS/PC version 8.0 (SPSS Inc., Chicago, IL). The level of significance was set at $P < 0.05$. Multiple analysis of variance was used to examine differences between the FA composition of (i) muscle and erythrocyte membrane; (ii) muscle and erythrocyte membrane of breast-fed and formula-fed infants; (iii) muscle and erythrocyte membrane and adipose tissue triglyceride; and (iv) adipose tissue membrane and adipose tissue triglyceride. Simple correlation was used to investigate relationships between the FA composition of (i) erythrocyte and muscle membrane; (ii) adipose tissue triglyceride and muscle membrane; (iii) adipose tissue triglyceride and erythrocyte membrane; and (iv) adipose tissue membrane and adipose tissue triglyceride. Two-factor multiple analysis of variance was used to examine whether there was an interaction between tissue type (muscle and erythrocyte) and type of infant feeding. A nonparametric test (Kruskal-Wallis) was used to investigate differences in adipose triglyceride FA composition between breast-fed and formula-fed children because of the small numbers and inequality of variance in the groups.

RESULTS

Characteristics of children. The mean age ± SE of the 61 children (45 males/16 females) in the study was 0.80 ± 0.06 yr, range 0.20–1.93 yr. The mean SD scores for both weight (0.39 ± 0.11) and length (0.43 ± 0.12) were significantly different from zero, indicating that the children were slightly heavier (P = 0.001) and longer (P = 0.001) than the reference population.

The duration of breast-feeding for the 61 children ranged from 0–21 mon (means ± SE, 4.8 ± 0.6 mon). In this study, breast-feeding duration was calculated as the actual duration of breast feeding, whether sole (no food given other than breast milk) or partial (some solid foods and/or complementary formula feeds offered concurrently with breast feeding). None of the infant formulas consumed by children in this study contained added LCPUFA. Further dietary analysis

showed that major food sources of LCPUFA (e.g., fish, egg yolk, lamb brains, and liver) were consumed in negligible amounts in the diets of children of this study.

The length of time since breast feeding ceased ranged from 0 mon (still being breast-fed at the time of surgery) to 19 mon (mean ± SE, 4.8 ± 0.7).

Comparison of the FA composition of muscle and erythrocytes. Table 1 shows the FA composition of muscle and erythrocyte membrane. The pattern of FA composition suggests that erythrocytes have a higher percentage of total saturates (but similar 14:0% and 18:0%) and a higher percentage of monounsaturates than muscle. However erythrocytes have a lower percentage of total n-6 PUFA, in particular a lower percentage of 18:2n-6 than muscle. The pattern of n-3 PUFA in erythrocytes reflects that of muscle and the percentages of 20–22 PUFA are not significantly different in these two tissues.

Relationships between the FA composition of erythrocytes and muscle. Simple correlations between FA and FA indices of structural lipid in erythrocytes and muscle are also shown in Table 1. There was a significant positive correlation between muscle and erythrocyte DHA (22:6n-3, $r = 0.44$, $P < 0.0001$), sum of the n-3 PUFA ($r = 0.39$, $P = 0.002$), and the n-6/n-3 PUFA ratio ($r = 0.39$, $P = 0.002$), but a significant inverse correlation between these two tissues for 22:4n-6.

TABLE 1
Fatty Acid Composition[a] of Muscle and Erythrocytes of 61 Young Children (means ± SE)

Fatty acid	Muscle	Erythrocyte	Correlation
Saturated	30.84 ± 0.32	37.26 ± 0.73	0.13
14:0	0.66 ± 0.04[b]	0.72 ± 0.05[b]	0.08
16:0	14.94 ± 0.21	20.82 ± 0.41	0.13
18:0	14.92 ± 0.18[b]	14.48 ± 0.46[b]	0.17
Monounsaturated	14.54 ± 0.33	21.43 ± 0.53	–0.11
14:1	0.76 ± 0.08	0.41 ± 0.03	–0.08
16:1	0.65 ± 0.03	1.76 ± 0.09	–0.04
18:1	13.13 ± 0.31	19.25 ± 0.50	–0.10
n-6 Polyunsaturated	46.55 ± 0.51	29.51 ± 0.86	–0.02
18:2n-6	24.67 ± 0.56	9.07 ± 0.30	0.04
20:3n-6	2.15 ± 0.06	1.54 ± 0.06	0.19
20:4n-6	17.69 ± 0.29	15.49 ± 0.62	0.17
22:4n-6	1.10 ± 0.04	1.89 ± 0.10	–0.31[c]
22:5n-6	0.83 ± 0.04	1.11 ± 0.06	0.16
n-3 Polyunsaturated	5.18 ± 0.20	5.74 ± 0.25	0.39[d]
18:3n-3	0.19 ± 0.01	0.36 ± 0.03	0.19
20:5n-3	0.40 ± 0.03	0.93 ± 0.06	0.06
22:5n-3	1.55 ± 0.07	1.11 ± 0.09	0.20
22:6n-3	2.72 ± 0.15	3.23 ± 0.18	0.44[e]
Derived indices			
20–22 PUFA[f]	27.78 ± 0.45[b]	26.39 ± 0.93[b]	0.19
Unsaturation index[g]	181.58 ± 1.28	158.43 ± 3.56	0.22
n-6/n-3 PUFA ratio	9.99 ± 0.48	5.61 ± 0.24	0.39[d]

[a]Individual fatty acids (FA) are expressed as the percentage of total FA identified.
[b]Comparison of FA composition of muscle and erythrocytes: means of corresponding FA in muscle and erythrocytes not significantly different by multivariate analysis of variance.
[c–e]Significant correlations between corresponding FA in muscle and erythrocytes: [c]$P < 0.02$, [d]$P = 0.002$, [e]$P < 0.0001$.
[f]Calculated as the sum of the percentage of the polyunsaturated fatty acids (PUFA) 20:2n-6, 20:3n-9, 20:3n-6, 20:3n-3, 20:4n-6, 20:5n-3, 22:2n-6, 22:4n-6, 22:5n-6, 22:5n-3, and 22:6n-3. Minor FA (i.e., <0.5% of total FA) not shown in table.
[g]Calculated as the mean number of double bonds per FA residue multiplied by 100.

Relationship between the type of feeding and membrane FA composition in erythrocytes and muscle. We investigated the relationship between the type of infant feeding and membrane FA composition. Only infants less than 1 yr old were included, to allow age-matching. The formula-fed group ($n = 17$) consisted of children who were breast-fed for less than 4 wk (mean time since breast feeding ceased was 5.3 ± 0.5 mon), and the breast-fed group ($n = 19$) consisted of children who were still being breast fed at the time of surgery. There was no significant difference in age, weight SD score, or length SD score between the two groups.

Table 2 shows the results of mulitvariate analysis of variance on the FA composition of erythrocytes and muscle of infants fed either breast milk or formula milk as a primary energy source. In erythrocytes, the breast-fed infants had significantly greater proportions of DHA and n-3 PUFA, but lower proportions of 16:1 and the n-6/n-3 PUFA ratio, in comparison to the formula-fed infants. In muscle, breast-fed infants had greater proportions of 16:1, 20:4n-6, 22:5n-3, DHA, n-3 PUFA, 20–22 PUFA and the unsaturation index, but lower proportions of 18:2n-6 and 22:4n-6.

Two-factor multivariate analysis of variance was used to investigate whether there was an interaction between type of feeding and tissue type. There was a significant effect [$F = 2.45$, df (1,68), $P = 0.023$] when the major indicators of n-6 and n-3 PUFA (i.e., sum n-3 PUFA, sum n-6 PUFA, n-6/n-3 PUFA ratio, unsaturation index, 20–22 PUFA) were used as the dependent variables. Examination of the means indicated that the n-6/n-3 PUFA ratio was the most important variable and univariate ANOVA showed that it was significant at the 0.008 level [$F = 7.42$, df (1,68)]. Figure 1 shows graphically that, for the n-6/n-3 PUFA ratio, the effect of type of infant feeding is greater in muscle than in erythrocytes.

Comparison with adipose tissue triglyceride FA. We were only able to analyze adipose tissue triglyceride FA composition from 15 children (Table 3). In comparison with muscle and erythrocyte membrane FA composition, adipose tissue triglyceride had significantly greater proportions of monounsaturates (especially 18:1), but lower proportions of n-6 PUFA (especially 20:4n-6), 20–22 PUFA, the unsaturation index, and n-3 PUFA (particularly DHA). Multivariate analysis of variance showed that there was a significant difference between means of adipose triglyceride and both muscle and erythrocytes for all variables with the exception of the sum of the saturates, 20:5n-3 and the n-6/n-3 ratio for muscle membrane and adipose triglycerides. The only significant intercorrelations were for 18:0 (with muscle; $r = –0.58$, $P = 0.02$) and 18:2n-6 (with erythrocytes; $r = 0.56$, $P = 0.03$).

Comparison of adipose tissue triglyceride FA composition between currently breast-fed ($n = 6$) and formula-fed ($n = 4$) children using a nonparametric test (Kruskal-Wallis) showed significantly higher levels of DHA (0.64 ± 0.38% vs. 0.12 ± 0.03%, $P = 0.05$) and lower levels of n-6 PUFA (12.44 ± 0.34% vs. 16.08 ± 1.24%, $P = 0.023$) with breast feeding. There was a nonsignificant trend toward higher n-3 PUFA in

TABLE 2
Fatty Acid Composition[a] of Tissues of 36 Infants Fed Either Breast Milk or Formula Milk as a Primary Energy Source: Comparison of Breast-Fed and Formula-Fed Groups[b]

Fatty acid	Muscle breast-fed (n = 19)	Muscle formula-fed (n = 17)	Erythrocyte breast-fed (n = 19)	Erythrocyte formula-fed (n = 17)
Saturated	31.39 ± 0.50	30.73 ± 0.56	37.26 ± 0.99	37.92 ± 1.64
Monounsaturated	14.36 ± 0.74	14.71 ± 0.65	22.34 ± 1.17	22.09 ± 1.01
n-6 Polyunsaturated	44.60 ± 1.13	46.67 ± 0.70	27.90 ± 1.50	28.59 ± 1.83
18:2n-6	21.73 ± 1.05[a]	25.73 ± 0.94[a]	8.04 ± 0.49	9.49 ± 0.75
20:3n-6	2.23 ± 0.11	2.25 ± 0.12	1.34 ± 0.09	1.62 ± 0.13
20:4n-6	18.65 ± 0.36[a]	16.42 ± 0.59[a]	15.14 ± 1.19	14.04 ± 0.96
22:4n-6	1.13 ± 0.08[b]	1.32 ± 0.04[b]	1.72 ± 0.18	1.87 ± 0.24
22:5n-6	0.77 ± 0.05	0.85 ± 0.06	1.21 ± 0.13	1.08 ± 0.09
n-3 polyunsaturated	6.50 ± 0.30[c]	4.22 ± 0.30[c]	6.30 ± 0.52[d]	4.76 ± 0.38[d]
18:3n-3	0.15 ± 0.02	0.20 ± 0.02	0.36 ± 0.07	0.39 ± 0.05
20:5n-3	0.35 ± 0.04	0.37 ± 0.05	0.98 ± 0.14	0.77 ± 0.10
22:5n-3	1.85 ± 0.11[b]	1.42 ± 0.17[b]	1.12 ± 0.17	0.84 ± 0.16
22:6n-3	3.91 ± 0.21[c]	1.94 ± 0.18[c]	3.81 ± 0.40[d]	2.65 ± 0.23[d]
Derived indices				
20–22 PUFA	30.26 ± 0.51[c]	26.20 ± 0.88[c]	26.26 ± 1.73	23.97 ± 1.59
Unsaturation index	186.89 ± 1.58[a]	175.71 ± 2.54[a]	158.91 ± 6.31	149.41 ± 6.50
n-6/n-3 PUFA ratio	7.26 ± 0.51[c]	12.10 ± 1.00[c]	4.85 ± 0.40[d]	6.31 ± 0.44[d]

[a]Individual FA are expressed as the percentage of the total FA identified.
[b]Results of multivariate analysis of variance: significant differences between FA composition of breast-fed and formula-fed infants in muscle ([a]$P < 0.008$, [b]$P < 0.05$, [c]$P < 0.0001$) and erythrocytes ([d]$P < 0.03$). See Table 1 for abbreviations.

breast-fed children compared with those who were formula-fed (1.41 ± 0.44% vs. 1.07 ± 0.15%).

We also compared the FA composition of adipose tissue membrane phospholipid with that of adipose tissue triglyceride in these 15 children by multivariate analysis of variance (Table 3). There was a significant difference between all means except for 16:0, 14:1, 18:3n-3, and the n-6/n-3 PUFA ratio. Interestingly, the only significant intercorrelations between FA were with 16:0, 18:2n-6, 20:3n-6, and the n-6/n-3 PUFA ratio.

DISCUSSION

This study shows that there are significant differences in the FA composition of muscle and erythrocyte phospholipid and adipose tissue triglyceride and phospholipid of young children. In particular, erythrocyte phospholipid has lower levels of n-6 PUFA (especially 18:2n-6) than muscle and a correspondingly lower n-6/n-3 PUFA ratio. Adipose tissue triglyceride has lower levels of n-6 and n-3 PUFA but higher total monounsaturated FA (especially 18:1) than both erythrocytes and muscle. However, despite these differences in FA composition between tissues, there are significant positive correlations between erythrocyte and muscle n-3 PUFA, in particular DHA, and the n-6/n-3 PUFA ratio.

A significant environmental factor in our study that influenced availability of FA for incorporation into different tissues was the type of infant feeding. Our results are in keeping with the known differences in FA composition between infant formulas and breast milk (14,15). Infant formulas contain the precursor FA linoleic acid (18:2n-6) and α-linolenic acid (18:3n-3), but lack important LCPUFA such as DHA (22:6n-3) (15). Likewise, infant-weaning foods supply a negligible amount of LCPUFA, especially DHA (16). However breast milk contains a range of LCPUFA (14). In the current study, as a reflection of diet, breast-fed infants had more DHA and a lower n-6/n-3 PUFA ratio than formula-fed infants in both muscle and erythrocytes; in adipose tissue triglyceride, breast-fed children had a higher level of DHA and lower level of n-6 PUFA than formula-fed children. In addition, the influence of type of feeding on the n-6/n-3 PUFA ratio was significantly greater in muscle than in erythrocyte membrane phospholipid. This latter result suggests that dietary availability of particular FA is not the only factor influencing incorporation of FA into muscle and erythrocyte membranes.

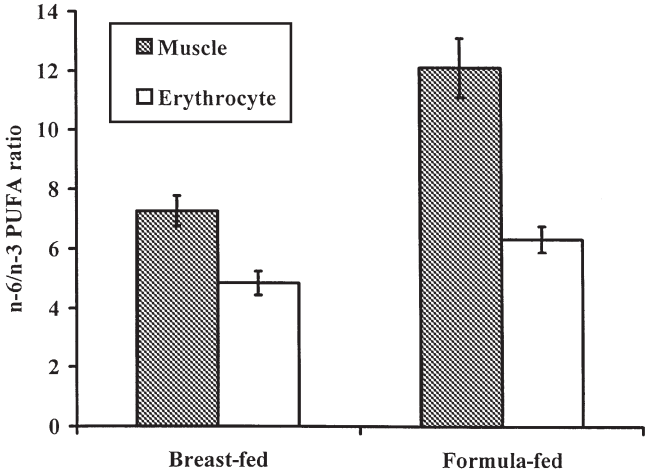

FIG. 1. The effect of type of feeding on the n-6/n-3 polyunsaturated fatty acid (PUFA) ratio in two different tissues: a significantly greater effect in muscle than in erythrocytes.

TABLE 3
The Fatty Acid Composition[a] of Muscle, Erythrocyte, and Adipose Tissue Membrane Phospholipid and Adipose Tissue Triglyceride in 15 Children[b]

Fatty acid	Muscle	Erythrocytes	Adipose tissue phospholipid	Adipose tissue triglyceride
Saturated	29.51 ± 0.59	35.24 ± 1.09	35.81 ± 0.59	30.51 ± 1.66
14:0	0.57 ± 0.07	0.75 ± 0.07	2.09 ± 0.22	4.20 ± 0.41
16:0	14.03 ± 0.32	20.37 ± 0.48	23.90 ± 0.74[a]	21.73 ± 0.99[a]
18:0	14.54 ± 0.34[b]	12.39 ± 0.91	8.81 ± 0.40	4.20 ± 0.60[b]
Monounsaturated	16.43 ± 0.53	24.52 ± 0.36	33.25 ± 0.89	54.68 ± 1.37
14:1	0.70 ± 0.10	0.42 ± 0.04	0.73 ± 0.07	1.00 ± 0.16
16:1	0.58 ± 0.06	1.84 ± 0.19	1.62 ± 0.16	6.95 ± 0.98
18:1	12.82 ± 0.45	16.69 ± 0.42	28.70 ± 0.83	44.41 ± 1.32
n-6 Polyunsaturated	48.31 ± 0.98	33.88 ± 0.98	27.48 ± 1.21	13.17 ± 0.65
18:2 n-6	25.69 ± 0.94	9.92 ± 0.39[c]	15.81 ± 0.70[a]	12.26 ± 0.68[a,c]
20:3 n-6	2.15 ± 0.12	1.69 ± 0.07	1.47 ± 0.15[a]	0.18 ± 0.02[a]
20:4 n-6	18.54 ± 0.64	18.43 ± 1.10	9.18 ± 0.67	0.35 ± 0.04
22:4 n-6	1.00 ± 0.07	2.19 ± 0.13	0.44 ± 0.05	0.17 ± 0.07
22:5 n-6	0.83 ± 0.07	1.18 ± 0.07	0.24 ± 0.04	0.06 ± 0.02
n-3 Polyunsaturated	5.02 ± 0.37	5.90 ± 0.33	3.00 ± 0.27	1.42 ± 0.24
18:3 n-3	0.20 ± 0.02	0.42 ± 0.07	0.68 ± 0.13	0.61 ± 0.07
20:5 n-3	0.40 ± 0.05	0.97 ± 0.12	1.07 ± 0.10	0.25 ± 0.09
22:5 n-3	1.48 ± 0.16	1.25 ± 0.11	0.20 ± 0.03	0.11 ± 0.02
22:6 n-3	2.44 ± 0.26	3.17 ± 0.27	1.05 ± 0.20	0.46 ± 0.18
Derived indices				
20–22 PUFA	28.27 ± 0.95	30.26 ± 1.31	14.10 ± 0.87	1.80 ± 0.36
Unsaturation index	185.04 ± 2.76	172.23 ± 5.00	125.98 ± 3.25	89.20 ± 2.91
n-6/n-3 PUFA ratio	10.60 ± 1.05	6.00 ± 0.37	10.23 ± 1.02[a]	11.65 ± 1.24[a]

[a]Individual FA are expressed as the percentage of the total FA identified.
[b]Significant correlations ($P < 0.05$) between: [a]adipose phospholipid and adipose triglyceride, [b]muscle and adipose triglyceride, [c]erythrocytes and adipose triglyceride. See Table 1 for abbreviation.

A closer examination of the FA composition of muscle and erythrocyte membranes showed that there were no significant differences between the two feeding groups in levels of total saturates, monounsaturated FA, or n-6 PUFA. The major effects of feeding were on levels of n-3 PUFA (especially DHA) and the n-6/n-3 PUFA ratio and were more marked in muscle than in erythrocytes. In a subset of 15 infants from whom stored triglyceride was obtained, there was a much lower proportion of DHA stored in adipose tissue compared to both muscle and erythrocytes. Interestingly, an effect of type of feeding was again noticed in that there was a fivefold difference in adipose tissue DHA between breast-fed and formula-fed infants. Farquharson *et al.* (17) found that levels of DHA in adipose tissue of formula-fed infants were lower than those of breast-fed infants and decreased rapidly from birth. The current study suggests that DHA stored in the adipose tissue of breast-fed infants may provide a reasonable reserve of this FA that is so critical for nervous system development (18). If we calculate the DHA content of adipose tissue triglyceride for a child of mean age 0.8 yr in our study group, using available reference data (19) for total body fat in infants, then the breast-fed infants have 14 g of DHA while the formula-fed infants have 3 g. The lower reserves of adipose tissue DHA in formula-fed infants may represent a potential endogenous supply problem.

There are two possible explanations for the wide variation in DHA and n-3 LCPUFA in different tissue types. Firstly, in muscle and erythrocyte membranes and in adipose tissue stores, there may be a tight regulation of the relative levels of saturates, monounsaturates, and n-6 PUFA, whereas the proportion of n-3 LCPUFA appears to vary and may be highly influenced by availability in the diet. Alternatively, there may be such an avidity for n-3 LCPUFA in membranes that even with very low availability in the diet (e.g., formula feeding), the endogenous cellular mechanisms of desaturation and elongation are upregulated to increase the production of n-3 LCPUFA which are then retained assiduously. The low levels of DHA stored in adipose tissue reserves add more weight to the view that n-3 LCPUFA are avidly incorporated into muscle and erythrocyte membranes of formula-fed infants against very low availability in triglyceride stores or in the diet. This may be a function of alteration in facilitated transport of PUFA across membranes (20).

Studies have shown that lower proportions of the LCPUFA, especially n-3 PUFA, in muscle membrane phospholipid are associated with insulin resistance and obesity (3,4,21). Insulin resistance is a key etiological factor in the development of a cluster of prevalent diseases including non-insulin dependent diabetes mellitus, obesity, the dyslipidemias, hypertension, and coronary heart disease (5–7). Thus, the level of muscle membrane n-3 LCPUFA may be a key indicator of metabolic health. There is increasing interest in using circulating levels of n-3 PUFA and LCPUFA as potential markers of insulin resistance and risk of coronary heart disease (22,23). For example, in a population-based case-control study in the United States, Siscovick *et al.* (23) found that a red blood cell n-3 PUFA level of 5.0% of total FA was associated with a 70% reduction in the

risk of primary cardiac arrest compared with a red blood cell n-3 PUFA level of 3.3% (22). Such markers could be of use at both a clinical level and in population studies.

The results of the current study show that it is valid to use erythrocyte FA composition to give an index of the level of DHA, total n-3 PUFA, and the n-6/n-3 PUFA ratio in muscle, at least on a population basis. A test requiring 1.0–2.0 mL of blood is much less invasive and has fewer ethical problems than the procedure for biopsy of muscle tissue. The study also shows the potent effects of breast feeding on the n-3 LCPUFA composition of muscle and erythrocytes. These findings are important for those who are designing studies aimed at estimating risk for future development of diseases associated with metabolic syndrome and also for testing new therapeutic approaches to the prevention of these prevalent diseases. Further studies are required to extend these observations to older children and adults. However, current medical opinion emphasizes the need to determine level of risk of these costly lifestyle diseases at a young age in order to institute early intervention before significant morbidity occurs.

ACKNOWLEDGMENTS

Supported by The Children's Hospital Fund, Hoechst Diabetes Research and Development, the Diabetes Australia Research Trust, the National Health and Medical Research Council (Australia), and a Lilly Diabetes Fellowship (Dr. Baur). Dr. Pan is a Lilly Fellow of the Life Sciences Research Foundation. We are very grateful for the assistance of the anesthetists and surgeons of The Royal Alexandra Hospital for Children for supplying blood samples and muscle and adipose tissue biopsies. Their enthusiasm and cooperation have been greatly appreciated. We also wish to thank the theater staff and surgical nursing staff for their help in this study. Finally our thanks to Dr. Jenny Peat for her advice on statistical analysis for this study.

REFERENCES

1. Storlien, L.H., Pan, D.A., Kriketos, A.D., O'Connor, J., Caterson, I.D., Cooney, G.J., Jenkins, A.B., and Baur, L.A. (1996) Skeletal Muscle Membrane Lipids and Insulin Resistance, *Lipids 31*, S261–S265.
2. Storlien, L.H., Jenkins, A.B., Chisholm, D.J., Pascoe, W.S., Khouri, S., and Kraegen, E.W. (1991) Influence of Dietary Fat Composition on Development of Insulin Resistance in Rats. Relationship to Muscle Triglyceride and ω-3 Fatty Acids in Muscle Phospholipids, *Diabetes 40*, 280–289.
3. Borkman, M.B., Storlien, L.H., Pan, D.A., Jenkins, A.B., Chisholm, D.J., and Campbell, L.V. (1993) The Relation Between Insulin Sensitivity and the Fatty-Acid Composition of Skeletal-Muscle Phospholipids, *N. Engl. J. Med. 328*, 238–244.
4. Pan, D.A., Lillioja, S., Milner, M.R., Kriketos, A.D., Baur, L.A., Bogardus, C., and Storlien, L.H. (1995) Skeletal Muscle Membrane Lipid Composition Is Related to Adiposity and Insulin Action, *J. Clin. Invest. 96*, 2802–2808.
5. Reaven, G.M. (1988) Banting Lecture: Role of Insulin Resistance in Human Disease, *Diabetes 37*, 1595–1607.
6. Reaven, G.M. (1993) Role of Insulin Resistance in Human Disease (Syndrome X): An Expanded Definition, *Ann. Rev. Med. 44*, 121–131.
7. Björntorp, P. (1991) Visceral Fat Accumulation: The Missing Link Between Psychosocial Factors and Cardiovascular Disease? *J. Int. Med. 230*, 195–201.
8. Baur, L.A., O'Connor, J., Pan, D.A., Kriketos, A.D., and Storlien, L.H. (1998) The Fatty Acid Composition of Skeletal Muscle Membrane Phospholipid: Its Relationship with the Type of Feeding and Plasma Glucose Levels in Young Children, *Metabolism 47*, 106–112.
9. Pan, D.A., and Storlien, L.H. (1993) Dietary Lipid Profile Is a Determinant of Tissue Phospholipid Fatty Acid Composition and Rate of Weight Gain in Rats, *J. Nutr. 123*, 512–519.
10. Folch, J., Lees, M., and Sloane-Stanley, G.H. (1957) A Simple Method for the Isolation and Purification of Total Lipids from Animal Tissues, *J. Biol. Chem. 226*, 497–509.
11. World Health Organization (1983) Measuring Change in Nutritional Status, Geneva, *World Health Organization,* pp. 61–101.
12. Dibley, M.J., Staehling, N.W., Nieburg, P., and Trowbridge, F.L. (1987) Interpretation of Z-score Anthropometric Indicators Derived from the International Growth Reference, *Am. J. Clin. Nutr. 46*, 749–762.
13. National Food Authority (1991) NUTTAB91-19: Nutrient Data Table for Use in Australia, *A.G.P.S.,* Canberra.
14. Makrides, M., Simmer, K., Neumann, M.A., and Gibson, R.A. (1995) Changes in the Polyunsaturated Fatty Acids of Breast Milk from Mothers of Full-Term Infants over 30 Weeks of Lactation, *Am. J. Clin. Nutr. 61*, 1231–1233.
15. Koletzko, B., and Bremer, H.J. (1989) Fat Content and Fatty Acid Composition of Infant Formulas*, Acta Paediatr. Scand. 78*, 513–521.
16. Jackson, K.A., and Gibson, R.A. (1989) Weaning Foods Cannot Replace Breast Milk as Sources of Long-Chain Polyunsaturated Fatty Acids, *Am. J. Clin. Nutr. 50,* 980–982.
17. Farquharson, J., Cockburn, F., Patrick, W.A., Jamieson, E.C., and Logan, R.W. (1992) Infant Cerebral Cortex Phospholipid Fatty-Acid Composition and Diet, *Lancet 340,* 810–813.
18. Crawford, M.A (1993) The Role of Essential Fatty Acids in Neural Development: Implications for Perinatal Nutrition, *Am. J. Clin. Nutr. 57,* 703S–710S.
19. Fomon, S.J., Haschke, F., Ziegler, E.E., and Nelson, S.E. (1982) Body Composition of Reference Children from Birth to Age 10 Years, *Am. J. Clin. Nutr. 35,* 1169–1175.
20. Aitman, T.J., Glazier, A.M., Wallace, C.A., Cooper, L.D., Norsworthy, P.J., Wahid, F.N., Al-Majali, K.M., Trembling, P.M., Mann, C.J., Shoulders, C.C., Graft, D., St Lezin, E., Kurtz, T.W., Kren, V., Pravenec, M., Ibrahimi, A., Abumrad, N.A., Stanton, L.W., and Scott, J. (1999) Identification of Cd36(Fat) as an Insulin-Resistance Gene Causing Defective Fatty Acid and Glucose Metabolism in Hypertensive Rats, *Nature Genetics 21*, 76–83.
21. Vessby, B., Tengblad, S., and Lithell, H. (1994) Insulin Sensitivity Is Related to the Fatty Acid Composition of Serum Lipids and Skeletal Muscle Phospholipids in 70-Year-Old Men, *Diabetologia 37,* 1044–1050.
22. Hojo, N., Fukushima, T., Isobe, A., Gao, T., Shiwaky, K., Ishida, K., Ohta, N., and Yamane, Y. (1998) Effect of Serum Fatty Acid Composition on Coronary Atherosclerosis in Japan, *Int. J. Cardiol. 66*, 31–38.
23. Siscovick, D.S., Raghunathan, T.E., King, I., Weinmann, S., and Wicklund, K.G. (1995) Dietary Intake and Cell Membrane Levels of Long-Chain n-3 Polyunsaturated Fatty Acids and the Risk of Primary Cardiac Arrest, *JAMA 274*, 1363–1367.

[Received June 18, 1999, and in final revised form October 26, 1999; revision accepted December 10, 1999]

Effects of Different Medium-Chain Fatty Acids on Intestinal Absorption of Structured Triacylglycerols[1]

Huiling Mu* and Carl-Erik Høy

Department of Biochemistry & Nutrition, Center for Advanced Food Study, Technical University of Denmark, DK-2800 Lyngby, Denmark

ABSTRACT: To study the effect of the chain length of medium-chain fatty acids on the intestinal absorption of long-chain fatty acids, we examined the lymphatic transport of fat following administration of five purified structured triacylglycerols (STAG) containing different medium-chain fatty acids in the *sn*-1,3 positions and long-chain fatty acids in the *sn*-2 position in a rat model. Significant amounts of medium-chain fatty acids were found in lymph samples after intragastric administration of 1,3-dioctanoyl-2-linoleyl-*sn*-glycerol (8:0/18:2/8:0), 1,3-didecanoyl-2-linoleyl-*sn*-glycerol, and 1,3-didodecanoyl-2-linoleyl-*sn*-glycerol. The accumulated lymphatic transport of medium-chain fatty acids increased with increasing carbon chain length. The recoveries of caprylic acid (8:0), capric acid (10:0), and lauric acid (12:0) were 7.3 ± 0.9, 26.3 ± 2.4, and 81.7 ± 6.9%, respectively. No significant differences were observed for the maximal intestinal absorption of linoleic acid (18:2n-6) when the chain length of medium-chain fatty acids at the primary positions was varied, and the absorption of 18:2 and oleic acid (18:1) from 8:0/18:2/8:0 and 1,3-dioctanoyl-2-oleyl-*sn*-glycerol was similar. We conclude that the chain length of the medium-chain fatty acids in the primary positions of STAG does not affect the maximal intestinal absorption of long-chain fatty acids in the *sn*-2 position in the applied rat model, whereas the distribution of fatty acids between the lymphatics and the portal vein reflects the chain length of the fatty acids.

Paper no. L8321 in *Lipids 35,* 83–89 (January 2000).

In the intestine, normal long-chain triacylglycerols (LCT), such as those from vegetable oils, animal fats or fish oils, are hydrolyzed by several enzymes into monoacylglycerols and free fatty acids and incorporated into mixed micelles with bile acid and absorbed (1–3). Medium-chain triacylglycerols (MCT) have been suggested to undergo nearly complete hydrolysis to be absorbed predominantly as free fatty acids due to low activation to CoA esters and transported *via* the portal vein to the liver where they undergo preferentially oxidation by a carnitine-independent pathway (4,5). In the absence or deficiency of pancreatic lipase, previous studies have indicated that a large fraction of MCT can be absorbed as triacylglycerols, whereas LCT are not absorbed (4). Therefore, MCT have been used for certain groups of patients or infants based on their rapid digestion and fast energy supplement (4,6–8). However, an obvious problem with the use of MCT is the lack of the essential fatty acids (9,10), and a high dose of MCT also has caused certain toxic effects in the animal experiments (11). Therefore, alternative triacylglycerols have been used in absorption studies, such as physical blends of MCT and LCT, interesterified lipids with random triacylglycerol structure or specific triacylglycerol structure (12–18).

A physical blend of MCT and LCT does not improve the absorption of long-chain fatty acids since each of the individual triacylglycerols maintains its original absorption rate; the long-chain fatty acids in the primary positions of randomized triacylglycerols also have a slower rate of hydrolysis. However, structured triacylglycerols (STAG) containing long-chain fatty acids in the *sn*-2 position and medium-chain fatty acids in the primary positions have improved metabolic benefits in comparison with randomized triacylglycerols (12,13) and physical blends (13). Therefore, MLM (M, medium-chain fatty acid; L, long-chain fatty acid)-type STAG have potential advantages for providing polyunsaturated fatty acids.

Even though several studies have shown the metabolic benefits of STAG (12–14,19), still no systematic data are available comparing the intestinal absorption of different MLM-type STAG *in vivo*. In the present study, we studied the lymphatic transport of fatty acids from specific STAG containing different medium-chain fatty acids varying from caprylic acid (8:0) to lauric acid (12:0) in the *sn*-1,3 positions and long-chain fatty acids in the *sn*-2 position to investigate the effect of chain length of medium-chain fatty acids on the absorption of long-chain fatty acids and the distributions of medium-chain fatty acids between the portal vein and lymphatics in rats with normal fat absorption.

EXPERIMENTAL PROCEDURES

Preparation of the STAG. The STAG were produced by lipase-catalyzed interesterification of safflower oil (Róco, Copenhagen, Denmark) or high-oleic sunflower oil (Århus Olie A/S

[1]Presented in part at the 3rd ISSFAL Conference, Lyon, France, June 1–5, 1998.

*To whom correspondence should be addressed at Department of Biochemistry and Nutrition, Building 224, Technical University of Denmark, DK-2800 Lyngby, Denmark. E-mail: mu@mimer.be.dtu.dk

Abbreviations: ANOVA, analysis of variance; GLC, gas–liquid chromatography; HPLC, high-performance liquid chromatography; LCT, long-chain triacylglycerol; MCT, medium-chain triacylglycerol; STAG, structured triacylglycerol; 8:0/18:2/8:0, 1,3-dioctanoyl-2-linoleyl-*sn*-glycerol; 10:0/18:2/10:0, 1,3-didecanoyl-2-linoleyl-*sn*-glycerol; 10:0/18:2/18:2, 1,2(2,3)-dilinoleyl-(1)3-decanoyl-*sn*-glycerol; 12:0/18:2/12:0, 1,3-didodecanoyl-2-linoleyl-*sn*-glycerol; 8:0/18:1/8:0, 1,3-dioctanoyl-2-oleyl-*sn*-glycerol.

(Århus, Denmark) and medium-chain fatty acids (caprylic, capric, and lauric acids from Sigma Chemical Co., St. Louis, MO) in a packed-bed reactor (20). The interesterification parameters and the yield of the STAG are listed in Table 1 (21). The interesterified products are mixtures of triacylglycerols, diacylglycerols, and free fatty acids; therefore, the required STAG were isolated from interesterified products with preparative high-performance liquid chromatography (HPLC). A Waters Delta Prep 3000 HPLC (Millipore Corporation, Milford, MA) was equipped with a Delta-Pak C18 column (47 × 300 mm, 15 μm particle size, and 100Å pore size; Waters Corporation, Milford, MA). Lambda-Max model 481 LC spectrophotometer (Waters Corporation) was used as the detector at 210 nm. The column was maintained at ambient temperature with a flow rate of 60 mL/min. A binary solvent system was applied; solvent A was acetonitrile and solvent B was isopropanol/hexane (2:1, vol/vol). All solvents were of HPLC grade (BDH Laboratory Supplies, Poole, England). The gradient of solvent was changed according to the composition of interesterified products. Two milliliters of the product solution at a concentration of 0.5 g/mL was injected, and the required STAG were collected.

The composition of the purified STAG was determined by gas–liquid chromatography (GLC) after methylation with 2 M KOH in methanol (Table 2). The fatty acid in the *sn*-2 position of the STAG was determined by Grignard degradation (22). In short, 30 mg of the STAG was dissolved in 10 mL diethylether. The reaction started after adding 0.3 mL allylmagnesium bromide (1 M in diethyl ether) and lasted for 1 min. It was then stopped by adding acid buffer (0.27 M HCl in 0.4 M boric acid). The organic phase was washed twice with 0.4 M boric acid and dried with anhydrous sodium sulfate and evaporated under nitrogen. The lipid residua were separated on a TLC plate that was precoated with boric acid, and the 2-monoacylglycerol fraction was scraped off and extracted with diethylether. After methylation with 2M KOH in methanol, the fatty acid methyl esters were analyzed by GLC.

Animal experiments. Male albino Wistar rats were obtained from Møllegård Breeding Center (Ll. Skensved, Denmark) and caged in groups of four. The light was regulated to a 12/12 h light-dark cycle, at 21°C, and 50% humidity. The animals were fed standard rat chow diet (Chr. Petersen A/S, Ringsted, Denmark) until surgery.

The animals weighed 250–300 g at the time of surgery and were anesthetized i.m. with 0.06 mL Zoletilmixture (The Royal Veterinary and Agricultural University, Frederiksburg, Denmark) per 100 g body weight. The mesenteric lymph duct was cannulated with a clear vinyl tubing (0.8 mm o.d., 0.5 mm i.d.; Critchley Electrical Products Pty. Ltd., NSW, Australia). A silicon tube (3.0 mm o.d., 1.0 mm i.d.; Polystan, Værløse, Denmark) was inserted into the stomach and secured in the stomach *via* a purse-string suture. Following surgery, the rats were placed in individual restraining cages in a room with 24-h light. They had free access to tap water and were kept hydrated by infusion of physiological saline (0.9% NaCl, 2 mL/h) through a gastrostomy feeding tube.

The lymph collection was initiated the next day 1 h prior to the administration of lipids to obtain a baseline level of intestinal absorption of fat. It was performed at room temperature. A fat emulsion containing 300 μL of STAG or safflower oil and 300 μL 20 mM sodium taurocholate (98%, Sigma Chemical Co.) and 10 mg/mL choline (99%, Sigma Chemical Co.) was prepared in an ice-water bath. A fat emulsion was administered through the feeding tube followed by 0.5 mL of physiological saline, and the infusion of saline was continued at a rate of 2 mL/min. The lymph was collected in 1-h fractions for the first 8 h, one fraction from 8–24 h postinjection. The collection tubes contained 100 μL of 10% EDTA (Titriplex III GR, Merck, Darmstadt, Germany) in 1-h fractions and 700 μL

TABLE 1
Interesterification Parameters (packed-bed reactor) and Yield of the Specific Structured Triacylglycerols (STAG)[a]

STAG	Oil	MCFA	*R*	*T* (°C)	*t* (h)	*Y* (%)
8:0/18:2/8:0	Safflower	8:0	1:6	60	6	35.0
8:0/18:1/8:0	HO sunflower[b]	8:0	1:6	60	9	49.6
10:0/18:2/10:0	Safflower	10:0	1:6	60	6	34.5
10:0/18:2/18:2	Safflower	10:0	1:6	60	6	37.1
12:0/18:2/12:0	Safflower	12:0	1:4	60	6	27.6

[a]MCFA, medium-chain fatty acid; *R*, molar ratio between the oil and the medium-chain fatty acid; *T*, reactor temperature; *t*, reaction time; *Y*, yield of the STAG expressed as percentages after normalization. The triacylglycerols were determined by high-performance liquid chromatography with evaporative light scattering detector (*c.f.* Ref. 21).
[b]High-oleic sunflower oil.

TABLE 2
The Main Fatty Acid Composition (mol%) of Oils and Different STAG[a]

	Safflower oil		HO sunflower oil		8:0/18:2/8:0		10:0/18:2/10:0		10:0/18:2/18:2		12:0/18:2/12:0		8:0/18:1/8:0	
	TAG	*sn*-2	TAG	*sn*-2	TAG	*sn*-2	TAG	*sn*-2	TAG	*sn*-2	TAG	*sn*-2	TAG	*sn*-2
8:0					64.4	2.6							69.7	0.5
10:0							60.7	1.9	33.4	1.2				
12:0											65.8	6.3		
16:0	7.1	0.3	4.5	0.3	0.1	0.2	2.4	0.1	0.2	0.5			0.3	
18:0	2.4	0.1	4.7	0.2			1.3							
18:1(n-9)	11.2	10.9	77.0	89.9	0.1	0.2	2.3	0.2	0.6	1.4			29.6	97.4
18:2	75.5	85.6	6.4	6.8	35.1	94.4	31.8	94.7	64.9	90.8	33.4	87.4	0.3	0.9
Others	3.8	3.1	7.4	2.8	0.3	2.6	7.5	3.4	1.7	8.0	0.8	6.3	0.1	1.2

[a]The fatty acids were analyzed and quantified by gas–liquid chromatography using internal standard. The fatty acids with lower concentration (<0.1%) are not listed in the table. TAG, triacylglycerol; see Table 1 for other abbreviation.

of EDTA (10%) in the final fraction. The lymph fractions were frozen at −20°C until further processing.

Experimental design. Six groups of rats (six rats in each group) were administered with five different STAG: 1,3-dioctanoyl-2-linoleyl-*sn*-glycerol (8:0/18:2/8:0); 1,3-didecanoyl-2-linoleyl-*sn*-glycerol (10:0/18:2/10:0); 1,2(2,3)-dilinoleyl-(1)3-decanoyl-*sn*-glycerol (10:0/18:2/18:2); 1,3-didodecanoyl-2-linoleyl-*sn*-glycerol (12:0/18:2/12:0); and 1,3-dioctanoyl-2-oleyl-*sn*-glycerol (8:0/18:1/8:0); and a control group was given safflower oil (75.5% 18:2n-6).

Analytical procedure. The total lipids from lymph samples were extracted with chloroform and methanol (12). The fatty acids in the purified STAG and the lipids from lymph samples were methylated to fatty acid methyl esters with 2 M KOH solution (in methanol). This procedure would not methylate free fatty acids. The fatty acid methyl esters were determined with an HP 6890 series gas–liquid chromatograph (Hewlett-Packard, Waldbronn, Germany) equipped with a fused-silica capillary column (SP-2380, 60 m × 0.25 mm i.d.; Supelco Inc., Bellefonte, PA). Oven temperature was programmed from 70 to 160°C at a rate of 15°C /min, followed by an increase to 180°C at a rate of 1°C/min, then to 185°C at a rate of 0.5°C/min, and finally to 200°C at a rate of 20°C/min and held for 10 min. A flame-ionization detector was used at 280°C, and the injector temperature was 250°C. The injector was used in split mode with a ratio 1:16. Carrier gas was helium with a column flow of 2 mL/min. The fatty acid methyl esters were identified by comparing their retention times with authentic standards (Sigma Chemical Co.), and the resulting compositions were calculated using the actual response factors for each fatty acid.

Calculation. The amount of fatty acids in lymph samples (FA_{lym}) was calculated using Equation 1,

$$FA_{lym} = \frac{FA_R \times FA_{RF}}{IS_R \times IS_{RF}} \times \frac{IS_W \times F_{lym}}{FA_{MW} \times W_{lym}} \quad [1]$$

where FA_R, FA_{RF}, and FA_{MW} are the GLC response, response factor, and molecular weight of the fatty acid, respectively; IS_R, IS_{RF}, and IS_W are the GLC response, response factor, and the amount of the internal standard, respectively; and F_{lym} and W_{lym} are the lymph flow and the amount of lymph used in the extraction, respectively.

The amount of intestinal absorbed fatty acids (FA_{abs}) was expressed as mole percentage. It was calculated from the amount of fatty acids found in lymph by reference to the amount of the FA in the intragastric administrated STAG (FA_{adm}):

$$FA_{abs} = \frac{FA_{lym}}{FA_{adm}} \times 100 \quad [2]$$

Statistical methods. The statistical program InStat (GraphPad Software Inc., San Diego, CA) was used in the calculation. A two-way repeated analysis of variance (ANOVA) was applied in the analysis of differences among groups for each hour of lymph collection and among different lymph fractions within each group. Paired *t* tests were used to evaluate the statistical significance.

RESULTS

Lymph flow. There were significant differences in lymph flow as a function of time for all 36 rats (Fig.1). The baseline lymph flow rate was 1.6 ± 0.1 g/h (all rats pooled). Two hours after the administration of STAG or safflower oil, it increased to 2.7 ± 0.1 g/h, and after 24 h, it was close to the baseline again (1.7 ± 0.1 g/h). There were no significant differences between different groups for each fraction, except that the baseline fraction of the 10:0/18:2/10:0 was significantly lower than other groups because of clotting of the lymph.

Lymphatic transport of medium-chain fatty acids. A portion of the medium-chain fatty acids was transported through the mesenteric lymph duct, and in studying lipid fractions of

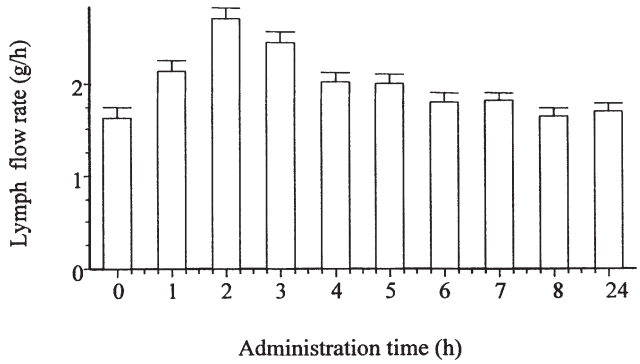

FIG. 1. The lymph flow of different fractions of all 36 animals (6 rats in each group and 6 groups), expressed as mean and standard error.

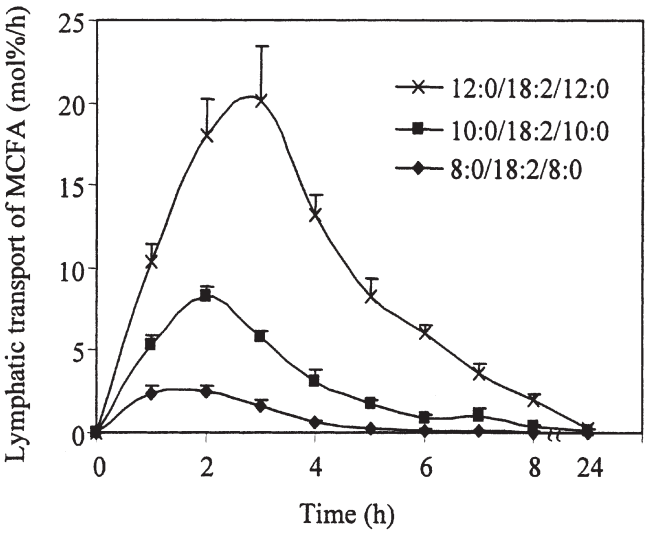

FIG. 2. The lymphatic transport of medium-chain fatty acids (MCFA) after intragastric administration of structured triacylglycerol (STAG) 1,3-dioctanoyl-2-linoleyl-*sn*-glycerol (8:0/18:2/8:0), 1,3-didecanoyl-2-linoleyl-*sn*-glycerol (10:0/18:2/10:0), and 1,3-dodecanoyl-2-linoleyl-*sn*-glycerol (12:0/18:2/12:0), expressed as molar percentage of the administered MCFA (mean ± SEM of 6 rats).

two samples, capric acid was detected only in the triacylglycerol fraction. A maximal lymphatic transport of medium-chain fatty acids was obtained after 2 or 3 h (Fig. 2), and there was a significant difference ($P = 0.0005$) between the maximal transport levels of the medium-chain fatty acids. From Figure 2, we also observe that the time needed to reach the maximal absorption of medium-chain fatty acids increased with increasing chain length, i.e., 8:0 reached maximal absorption sooner than 10:0, and 10:0 reached the maximal absorption sooner than 12:0.

The accumulated lymphatic transport level of medium-chain fatty acids increased significantly with increasing carbon chain length (Fig. 3). For lauric acid, 81.7 ± 6.9% was recovered in the lymph after administration of 12:0/18:2/12:0, whereas only 7.3 ± 0.9% of caprylic acid was recovered after administration of 8:0/18:2/8:0.

Lymphatic transport of linoleic acid. Maximal lymphatic transport of linoleic acid (25.6 ± 1.5%) was observed 2 or 3 h after administration of the lipids (Fig. 4). There was no significant difference for the maximal lymphatic transport of linoleic acid between the STAG and the safflower oil or between the individual STAG, even though they contained different medium-chain fatty acids.

Apparent higher accumulated lymphatic transport of linoleic acid was observed for 10:0/18:2/10:0, 10:0/18:2/18:2, and 12:0/18:2/12:0 in comparison with safflower oil, whereas lower value was observed for the 8:0/18:2/8:0 (Fig. 5). However, the differences between the accumulated lymphatic transport of linoleic acid were not significant, except the 10:0/18:2/10:0 had a significant higher value than safflower oil ($P = 0.034$).

Comparison of lymphatic transport of different long-chain fatty acids. The lymphatic transport of oleic acid and linoleic acid was compared by intragastric administration of STAG 8:0/18:1/8:0 and 8:0/18:2/8:0. Maximal transport of long-chain fatty acids was observed after 2 h of administration of lipids for both STAG; they were 20.5 ± 1.5 and 18.2 ± 3.1% for linoleic acid and oleic acid, respectively. The difference between the maximal transport level was not significant ($P = 0.49$).

The accumulated lymphatic transport of linoleic acid and oleic acid was 97.3 ± 5.0% and 91.0 ± 8.3%, respectively. There was no significant ($P = 0.46$) difference between the accumulated lymphatic transport of oleic acid and linoleic acid either.

The recovery of caprylic acid was 5.7 ± 0.6% in the lymph after intragastric administration of the 8:0/18:1/8:0. In the comparison of intestinal absorption of caprylic acid from 8:0/18:1/8:0 and 8:0/18:2/8:0, no significant difference was found between the maximal intestinal absorption of caprylic acid ($P = 0.56$), or between the accumulated lymphatic transport ($P = 0.22$).

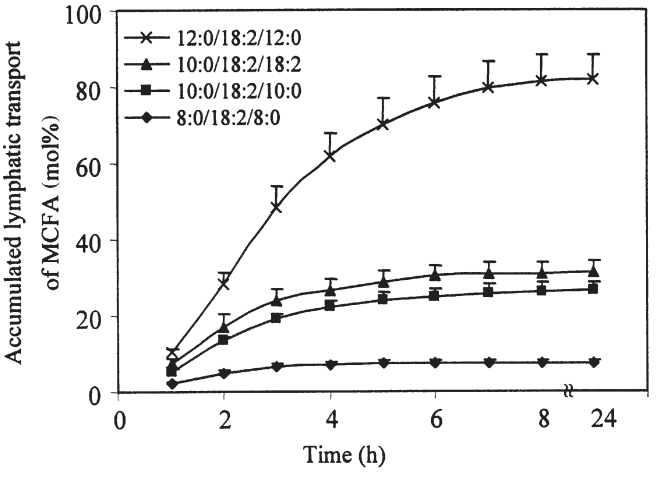

FIG. 3. Accumulated lymphatic transport of MCFA after intragastric administration of STAG 8:0/18:2/8:0, 10:0/18:2/10:0, 1,2(2,3)-dilinoleyl-(1)3-decanoyl-*sn*-glycerol (10:0/18:2/18:2), and 12:0/18:2/12:0, expressed as molar percentage of the administered MCFA (mean ± SEM of 6 rats). See Figure 2 for abbreviations.

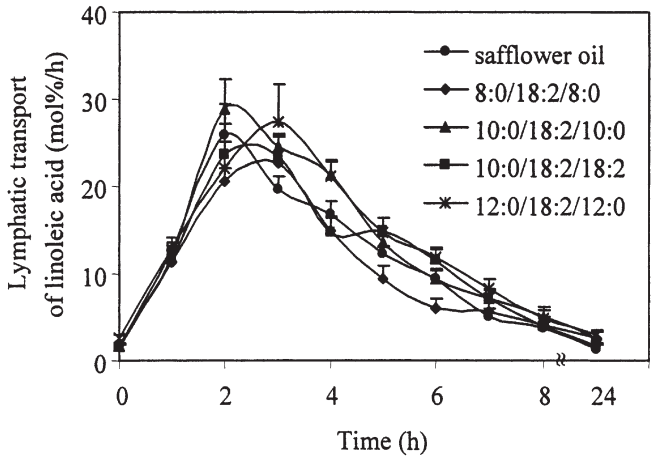

FIG. 4. The lymphatic transport of linoleic acid after intragastric administration of STAG 8:0/18:2/8:0, 10:0/18:2/10:0, 10:0/18:2/18:2, 12:0/18:2/12:0, and safflower oil, expressed as molar percentage of the administered linoleic acid (mean ± SEM of 6 rats). See Figures 2 and 3 for abbreviations.

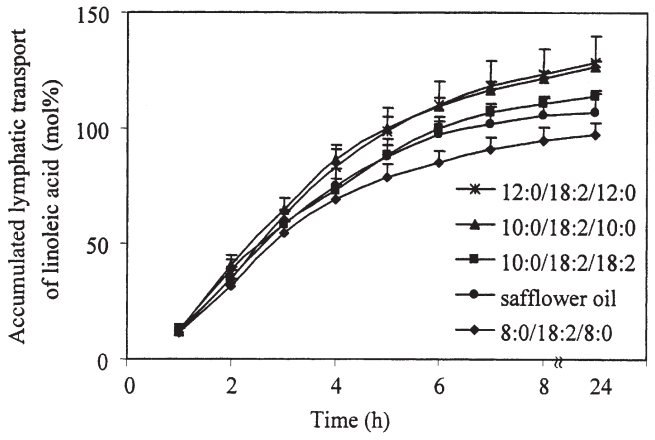

FIG. 5. Accumulated lymphatic transport of linoleic acid after intragastric administration of STAG 8:0/18:2/8:0, 10:0/18:2/10:0, 10:0/18:2/18:2, 12:0/18:2/12:0, and safflower oil, expressed as molar percentage of the administered linoleic acid (mean ± SEM of 6 rats).

DISCUSSION

Pancreatic lipase catalyzes the intestinal hydrolysis of the emulsified triacylglycerols in the presence of colipase, resulting in *sn*-2-monoacylglycerols and free fatty acids (released from the primary positions), which form the mixed micelles and diffuse through both the stagnant water layer and the brush border membrane into the enterocytes (23). The fatty acids located in the *sn*-2 positions in the dietary fat are thus conserved during absorption (24). Long-chain fatty acids are activated to their CoA derivatives through the action of fatty acyl-CoA ligase in the endoplasmic reticulum and resynthesized to triacylglycerols together with monoacylglycerol by acyltransferase, whereas medium-chain fatty acids are predominantly transported through the portal vein, since the ligase has low activity toward medium-chain fatty acids (25). The fatty acyl synthetase responsible for triacylglycerol reesterification is most effective with fatty acids of 14 or more carbons (5). In previous studies of absorption of STAG, medium-chain fatty acids have been found in lymph samples, and the medium-chain fatty acids esterified in the *sn*-2 position of a triacylglycerol are transported to a larger extent by the lymphatics than these medium-chain fatty acids esterified in the primary positions (12,14,24). However, the variation of the extent of the intestinal absorption of medium-chain fatty acids with chain length has not been systematically investigated yet. Therefore, we compared the intestinal absorption of different medium-chain fatty acids in the MLM-type STAG. We estimated the intestinal absorption of five STAG containing one long-chain fatty acid in the *sn*-2 position and one medium-chain fatty acid and one long-chain fatty acid or two medium-chain fatty acids in the primary positions.

LCT (18:2/18:2/18:2) has been used as the reference compound in previous studies, and Ikeda *et al.* (14) found higher lymphatic transport of linoleic acid from 10:0/18:2/10:0 than from 18:2/18:2/18:2. In the present study, safflower oil, which has been used in the production of the STAG, was selected as the reference oil.

Similar to the results of Tso *et al.* (16), we found that the intestinal lymph flow responded to a lipid meal. The lymph flow increased significantly as a result of intragastric administration of lipids in all groups, and maximal intestinal absorption was reached 2 or 3 h after administration. Although the lymph flow varied between different animals, there was no significant difference between different groups for each fraction (except the baseline fraction of 10:0/18:2/10:0). Therefore, the lymphatic transport of different STAG and the oil can be compared.

We found high recovery of medium-chain fatty acids in the rats' lymphatic ducts after intragastric administration of fat emulsions containing STAG, and the maximal intestinal absorption level increased significantly with increasing carbon chain length (Fig. 2). Most of the caprylic acid in 8:0/18:2/8:0 and 8:0/18:1/8:0 was probably transported through the portal vein after hydrolysis by pancreatic lipase, since only 6–7% of caprylic acid was transported *via* lymphatics. In lymph 26 and 31% of capric acid were recovered after administration of 10:0/18:2/10:0 and 10:0/18:2/18:2, respectively, whereas up to 82% of lauric acid was transported through lymphatics after administration of 12:0/18:2/12:0, and only a minor part of lauric acid was therefore transported through the portal vein. The large variation between the accumulated lymphatic transport of medium-chain fatty acids in different STAG suggests that the absorption pathway of medium-chain fatty acids differs significantly. The distribution of fatty acids between the lymphatics and the portal vein reflected the chain length of the fatty acids. Similar results for free fatty acids have been reported by McDonald *et al.* (26,27) and Bloom *et al.* (28), who studied the route of transport of free fatty acids from the rat intestine and found that the lymphatic recovery of infused fatty acids increased with the increase of carbon chain length for saturated fatty acids. Comparing our results with the results reported by the others, we find a similar tendency for the effects of carbon chain length on the intestinal absorption of triacylglycerols and free fatty acids, the absorption level increases with the increase of chain length of fatty acids (in both free acid form or as an acyl group in the STAG).

Comparing the level of lymphatic transport of lauric acid in our study with the studies reported by the others, it is rather clear that more medium-chain fatty acids can be transported *via* lymphatics from MLM-type STAG than from free fatty acid. McDonald *et al.* (26) reported that 72% of lauric acid bypassed the lymphatic pathway when it was infused intraduodenally in the form of free fatty acids; Bloom *et al.* (28) also found that only 15–55% of absorbed lauric acid was transported in the chyle when it was fed in the form of free fatty acid, whereas we found up to 82% of lauric acid in lymph. Since the level of lauric acid is very low in adipose tissue, we may exclude that the high recovery of lauric acid reflects mobilization of endogenous fatty acids. Comparing the concentration of medium-chain fatty acids in the *sn*-2 position of the STAG (Table 2) with the recovery of medium-chain fatty acids in the lymph (Fig. 3), the concentration of positional isomers of the STAG was much lower than the lymphatic transport of medium-chain fatty acids. Therefore, the large part of the medium-chain fatty acids was not transported through lymphatics in the form of monoacylglycerols after hydrolysis and resynthesized to triacylglycerols in the intestinal mucosa, although it cannot be excluded that some isomerization may have occurred during hydrolysis and absorption. Since the recovery of medium-chain fatty acids in the lymphatics was much higher in the form of MLM-type STAG than in the form of free fatty acids (26,28), it is most likely that the enterocytes have the ability to activate and reacylate medium-chain fatty acids into triacylglycerols, especially for lauric acid. However, the metabolic pathways of medium-chain fatty acids in the enterocytes are not clear at present.

In a study of *in vitro* lipase digestion, Jandacek *et al.* (19) reported that the triacylglycerols with medium-chain fatty acids in the 1- and 3-positions and a long-chain fatty acid in the 2-position could be hydrolyzed faster than the triacylglyc-

erols constituting all long-chain fatty acids. In our present study, we found an apparent delay for lauric acid to reach maximal absorption compared to capric acid and caprylic acid, which may indicate the differences of the hydrolysis rate between medium-chain fatty acids in the MLM-type STAG. The delay was correlated with the chain length, so the hydrolysis rate of medium-chain fatty acids might decrease with the increase of chain length. However, these data show a poor correlation with the maximal lymphatic transport of linoleic acid, i.e., there were no significant differences in the absorption of linoleic acid (located in the *sn*-2 position) between different STAG. This may reflect that the hydrolysis of medium-chain fatty acids was not the rate-limiting step for the absorption of linoleic acid, but rather the diffusion and the following activation of fatty acids before triacylglycerol synthesis. If the diffusion rate of the monoacylglycerol-containing linoleic acid is slower than the hydrolysis rate of medium-chain fatty acids in the STAG, the absorption of linoleic acid from different MLM-type STAG will be similar.

There was no significant difference between the recovery of capric acid in lymph from 10:0/18:2/10:0 and 10:0/18:2/18:2, although the absorbed capric acid (mmol) from 10:0/18:2/10:0 was two times of that from 10:0/18:2/18:2. Therefore, the different hydrolysis rate of medium-chain fatty acids and long-chain fatty acids does not affect the intestinal absorption of medium-chain fatty acids in MLM- or MLL-type STAG in rats with normal level of pancreatic enzymes.

Ikeda *et al.* (14) have declared that MLM-type STAG can be used both as a fast energy source and as a source of essential fatty acids. Our results have certain practical implications for the design of the MLM-type STAG. Since the chain length of medium-chain fatty acids does not affect the maximal intestinal absorption of the long-chain fatty acids at the *sn*-2 position, the selection of medium-chain fatty acids in MLM-type STAG can be based on the clinical and nutritional requirements. When STAG is used as fast energy source, the MLM-type STAG containing lauric acid can provide more energy than caprylic acid. If lauric acid is incorporated into chylomicrons, it can be used for oxidation in the muscle or it may be deposited in the adipose tissue. On the other hand, caprylic acid and capric acid will be directed preferentially toward the hepatic tissue for immediate oxidation and therefore have a protein-sparing effect. However, the effect of saturated fatty acids on cholesterol-raising properties in low density lipoproteins (LDL) and cardiovascular risk has been subject to much debate. Lauric acid has been reported as a hypercholesterolemic saturated fatty acid (29–31). Diverse results have been reported for the effects of caprylic and capric acid (30,32–34). In the latest review on dietary saturated fats and their effect on LDL concentrations and metabolism, Nicolosi (34) stated that caprylic and capric acid are neutral with respect to their LDL-cholesterol-raising properties and their ability to modulate LDL metabolism. Therefore, caprylic acid and capric acid may be the preferred choice in the production of MLM-type STAG.

We also studied the effect of medium-chain fatty acids on the lymphatic transport of different long-chain fatty acids by intragastric administration of 8:0/18:1/8:0 and 8:0/18:2/8:0. Similar intestinal absorption of oleic acid and linoleic acid was observed, indicating no significant difference between the intestinal absorption of long-chain fatty acids in MLM-type STAG. This result suggests that we may use similar type STAG to provide different long-chain fatty acids according to the clinical demand.

Our present study shows that the chain length of medium-chain fatty acids located in the primary positions does not affect the lymphatic transport of long-chain fatty acids in the *sn*-2 position. Similar intestinal absorption of different long-chain fatty acids can be expected in the MLM-type STAG. It is therefore possible by manufacturing STAG with different medium-chain fatty acids to direct the fatty acids from the *sn*-1,3 positions toward the liver through the portal vein or toward the muscle or adipose tissues through formation of chylomicrons without affecting the transport of the long-chain fatty acid in the *sn*-2 position.

ACKNOWLEDGMENTS

We thank Tina Dahl and Karen Jensen for their technical assistance, Xuebing Xu for producing some of the structured triacylglycerols, Ellen Marie Straarup and Trine Porsgaard for their help and valuable discussions on the animal experiments. This work was supported by the Center for Advanced Food Study.

REFERENCES

1. Small, D.M. (1991) The Effects of Glyceride Structure on Absorption and Metabolism, *Annu. Rev. Nutr. 11*, 413–434.
2. Mattson, F.H., and Volpenhein, R.A. (1964) The Digestion and Absorption of Triglycerides, *J. Biol. Chem. 239*, 2772–2777.
3. Kayden, H.J., Senior, J.R., and Mattson, F.H. (1967) The Monoglyceride Pathway of Fat Absorption in Man, *J. Clin. Invest. 46*, 1695–1702.
4. Bach, A.C., and Babayan, V.K. (1982) Medium-Chain Triglycerides: An Update, *Am. J. Clin. Nutr. 36*, 950–962.
5. Papamandjaris, A.A., MacDougall, D.E., and Jones, P.J.H. (1998) Medium Chain Fatty Acid Metabolism and Energy Expenditure: Obesity Treatment Implications, *Life Sci. 62*, 1203–1215.
6. Babayan, V.K. (1987) Medium Chain Triglycerides and Structured Lipids, *Lipids 22*, 417–420.
7. Mascioli, E.A., Bistrian, B.R., Babayan, V.K., and Blackburn, G.L. (1987) Medium Chain Triglycerides and Structured Lipids as Unique Nonglucose Energy Sources in Hyperalimentation, *Lipids 22*, 421–423.
8. Merolli, A., Lindemann, J., and Vecchio, A.J.D. (1997) Medium-Chain Lipids: New Sources, Uses, *INFORM 8*, 597–603.
9. Heird, W.C., Grundy, S.M., and Hubbard, V.S. (1986) Structured Lipids and Their Use in Clinical Nutrition, *Am. J. Clin. Nutr. 43*, 320–324.
10. Jeppesen, P.B., Christensen, M.S., Høy, C.E., and Mortensen, P.B. (1997) Essential Fatty Acid Deficiency in Patients with Severe Fat Malabsorption, *Am. J. Clin. Nutr. 65*, 837–843.
11. Henwood, S., Wilson, D., White, R., and Trimbo, S. (1997) Developmental Toxicity Study in Rats and Rabbits Administered an Emulsion Containing Medium Chain Triglycerides as an Alternative Caloric Source, *Fundam. Appl. Toxicol. 40*, 185–190.

12. Christensen, M.S., Høy, C.E., Becker, C.C., and Redgrave, T.G. (1995) Intestinal Absorption and Lymphatic Transport of Eicosapentaenoic (EPA), Docosahexaenoic (DHA), and Decanoic Acids: Dependence on Intramolecular Triacylglycerol Structure, *Am. J. Clin. Nutr. 61*, 56–61.
13. Christensen, M.S., Müllertz, A., and Høy, C.E. (1995) Absorption of Triglycerides with Defined or Random Structure by Rats with Biliary and Pancreatic Diversion, *Lipids 30*, 521–526.
14. Ikeda, I., Tomari, Y., Sugano, M., Watanabe, S., and Nagata, J. (1991) Lymphatic Absorption of Structured Glycerolipids Containing Medium-Chain Fatty Acids and Linoleic Acid, and Their Effect on Cholesterol Absorption in Rats, *Lipids 26*, 369–373.
15. Jensen, G.L., McGarvey, N., Taraszewski, R., Wixson, S.K., Seidner, D.L., Pai, T., Yeh, Y.Y., Lee, T.W., and DeMichele, S.J. (1994) Lymphatic Absorption of Enterally Fed Structured Triacylglycerol vs. Physical Mix in a Canine Model, *Am. J. Clin. Nutr. 60*, 518–524.
16. Tso, P., Karlstad, M.D., Bistrian, B.R., and DeMichele, S.J. (1995) Intestinal Digestion, Absorption, and Transport of Structured Triglycerides and Cholesterol in Rats, *Am. J. Physiol. 268*, G568–G577.
17. Sakono, M., Takagi, H., Sonoki, H., Yoshida, H., Iwamoto, M., Ikeda, I., and Imaizumi, K. (1997) Absorption and Lymphatic Transport of Interesterified or Mixed Fats Rich in Saturated Fatty Acids and Their Effect on Tissue Lipids in Rats, *Nutr. Res. 17*, 1131–1141.
18. Hubbard, V.S., and McKenna, M.C. (1987) Absorption of Safflower Oil and Structured Lipid Preparations in Patients with Cystic Fibrosis, *Lipids 22*, 424–428.
19. Jandacek, R.J., Whiteside, J.A., Holcombe, B.N., Volpenhein, R.A., and Taulbee, J.D. (1987) The Rapid Hydrolysis and Efficient Absorption of Triglycerides with Octanoic Acid in the 2 Position, *Am. J. Clin. Nutr. 45*, 940–945.
20. Mu, H., Xu, X., and Høy, C.E. (1998) Production of Specific Structured Triacylglycerols by Lipase-Catalyzed Interesterification in a Laboratory Scale Continuous Reactor, *J. Am. Oil Chem. Soc. 75*, 1187–1193.
21. Mu, H., Kalo, P., Xu, X., and Høy, C.-E. (2000) Chromatographic Methods in the Monitoring of Lipase-Catalyzed Interesterification, *Fett/Lipid,* In press.
22. Becker, C.C., Rosenquist, A., and Hølmer, G. (1993) Regiospecific Analysis of Triacylglycerols Using Allyl Magnesium Bromide, *Lipids 28*, 147–149.
23. Thomson, A.B.R., Keelan, M., Garg, M.L., and Clandinin, M.T. (1989) Intestinal Aspects of Lipid Absorption: in Review, *Can. J. Physiol. Pharmacol. 67*, 179–191.
24. Åkesson, B., Gronowitz, S., Herslöf, B., and Ohlson, R. (1978) Absorption of Synthetic, Stereochemically Defined Acylglycerols in the Rat, *Lipids 13*, 338–343.
25. Mead, J.F., Alfin-Slater, R.B., Howton, D.R., and Popják, G. (1986) *Digestion and Absorption of Lipids*, pp. 255–272*,* Plenum Press, New York.
26. McDonald, G.B., Saunders, D.R., Weidman, M., and Fisher, L. (1980) Portal Venous Transport of Long-Chain Fatty Acids Absorbed from Rat Intestine, *Am. J. Physiol. 239*, G141–G150.
27. McDonald, G.B., and Weidman, M. (1987) Partitioning of Polar Fatty Acids into Lymph and Portal Vein After Intestinal Absorption in the Rat, *Q. J. Exp. Physiol. 72*, 153–159.
28. Bloom, B., Chaikoff, I.L., and Reinhardt, W.O. (1951) Intestinal Lymph as Pathway for Transport of Absorbed Fatty Acids of Different Chain Lengths, *Am. J. Physiol. 166*, 451–455.
29. Temme, E.H., Mensink, R.P., and Hornstra, G. (1996) Comparison of the Effects of Diets Enriched in Lauric, Palmitic, or Oleic Acids on Serum Lipids and Lipoproteins in Healthy Women and Men, *Am. J. Clin. Nutr. 63*, 897–903.
30. Grundy, S.M. (1994) Influence of Stearic Acid on Cholesterol Metabolism Relative to Other Long-Chain Fatty Acids, *Am. J. Clin. Nutr. 60*, 986S–990S.
31. Woollett, L.A., Spady, K.K., and Dietschy, J.M. (1992) Regulatory Effects of the Saturated Fatty Acids 6:0 Through 18:0 on Hepatic Low Density Lipoprotein Receptor Activity in the Hamster, *J. Clin. Invest. 89*, 1133–1141.
32. Cater, N.B., Heller, H.J., and Denke, M.A. (1997) Comparison of the Effects of Medium-Chain Triacylglycerols, Palm Oil, and High Oleic Acid Sunflower Oil on Plasma Triacylglycerol Fatty Acids and Lipid and Lipoprotein Concentrations in Humans, *Am. J. Clin. Nutr. 64*, 41–45.
33. Wardlaw, G.M., Snook, J.T., Park, S., Patel, P.K., Pendley, F.C., Lee, M.S., and Jandacek, R. (1995) Relative Effects on Serum Lipids and Apolipoproteins of a Caprenin-rich Diet Compared with Diets Rich in Palm Oil/Palm-Kernel Oil or Butter, *Am. J. Clin. Nutr. 61*, 535–542.
34. Nicolosi, R.J. (1997) Dietary Fat Saturation Effects on Low-Density-Lipoprotein Concentrations and Metabolism in Various Animal Models, *Am. J. Clin. Nutr. 65*, 1617S–1627S.

[Received July 28, 1999, and in revised form and accepted December 28, 1999]

Effects of Conjugated Linoleic Acid Isomers on Lipid-Metabolizing Enzymes in Male Rats

Jean-Charles Martin[a,*], Stéphane Grégoire[a], Marie-Hélène Siess[b], Martine Genty[a], Jean-Michel Chardigny[a], Olivier Berdeaux[a], Pierre Juanéda[a], and Jean-Louis Sébédio[a]

I.N.R.A., [a]Unité de Nutrition Lipidique and [b]Laboratoire de Toxicologie Nutritionnelle, 21034 Dijon Cedex, France

ABSTRACT: Male weanling Wistar rats (n = 15), weighing 200–220 g, were allocated for 6 wk to diets containing 1% (by weight) of conjugated linoleic acid (CLA), either as the 9*c*,11*t*-isomer, the 10*t*,12*c*-isomer, or as a mixture containing 45% of each of these isomers. The five rats of the control group received 1% of oleic acid instead. Selected enzyme activities were determined in different tissues after cellular subfractionation. None of the CLA-diet induced a hepatic peroxisome-proliferation response, as evidenced by a lack of change in the activity of some characteristic enzymes [i.e., acyl-CoA oxidase, CYP4A1, but also carnitine palmitoyltransferase-I (CPT-I)] or enzyme affected by peroxisome-proliferators (glutathione *S*-transferase). In addition to the liver, the activity of the rate-limiting β-oxidation enzyme in mitochondria, CPT-I, did not change either in skeletal muscle or in heart. Conversely, its activity increased more than 30% in the control value in epididymal adipose tissue of the animals fed the CLA-diets containing the 10*t*,12*c*-isomer. Conversely, the activity of phosphatidate phosphohydrolase, a rate-limiting enzyme in glycerolipid neosynthesis, remained unchanged in adipose tissue. Kinetic studies conducted on hepatic CPT-I and peroxisomal acyl-CoA oxidase with CoA derivatives predicted a different channeling of CLA isomers through the mitochondrial or the peroxisomal oxidation pathways. In conclusion, the 10*t*,12*c*-CLA isomer seems to be more efficiently utilized by the cells than its 9*c*,11*t* homolog, though the Wistar rat species appeared to be poorly responsive to CLA diets for the effects measured.

Paper no. L8294 in *Lipids 35*, 91–98 (January 2000).

The collective term conjugated linoleic acids (CLA), describing positional and geometrical isomers of linoleic acid, has been receiving more attention in the last decade because of CLA pleiotropic biological activities. For instance, these fatty acids are effective anticarcinogens, antiatherosclerotic agents, fat reducers, and potent modulators of the immune function (see reviews 1–7). However, little is known about their mechanisms of action. Regarding the effects associated with fat utilization, CLA can, some authors found, induce a peroxisome-proliferation response in mice (8), although the issue seems to be less clear in the rat (9). Also, associated with their fat reduction properties, CLA increase the *in vitro* 3T3 adipose cells lipolysis and decrease the heparin-releasable lipoprotein lipase activity in mice (10,11). In addition, they potentially enhance the channeling of the fatty acids into the mitochondrial β-oxidation pathway in mice through an increase of the carnitine palmitoyltransferase (CPT) activity, both in the adipose tissue of the fed animal and in the skeletal muscle of the fasted mice (10). These effects may have collectively contributed to the observed reduction in the fat body mass of animals consuming CLA (10,12,13). However, most of these experimental results were obtained by using different brands of CLA mixtures obtained after alkali-isomerization of linoleic acid, which may greatly differ in their CLA isomer distribution and complexity (14–16). Therefore, it is generally not possible to date to determine whether one isomer is more potent than the others for any of the biological activities depicted. Nonetheless, one study demonstrated a significant effect of the 10*t*,12*c*-isomer on some biochemical mechanisms associated with fat reduction in mice (11).

Another important issue is how the different CLA isomers may be metabolized once absorbed, and especially how they are channeled toward the esterification or the oxidation pathways. This is of great importance since these pathways determine the availability of CLA to elicit their biological effects. In that instance, the determination of the kinetic parameters of CPT-I with selected acyl-CoA derivatives *in vitro* (17) generally gives a good prediction of their oxidative breakdown *in vivo* (18).

This study reports the relative impact of diets supplemented with different CLA isomers toward selected enzymes involved in lipid metabolism. In addition, the apparent kinetic parameters of two rate-limiting enzymes of fatty acid oxidation, i.e., CPT-I and acyl-CoA oxidase (ACO), were determined using CLA as their CoA derivatives.

EXPERIMENTAL PROCEDURES

Chemicals. The solvents were provided by SDS (Peypin, France) and were distilled before use (except diethylether). [1-^{14}C]Lauric acid (52 μCi/mmol) was purchased from Amersham (Amersham, Les Ulis, France). All the other chemicals

*To whom correspondence should be addressed at Laboratoire de Physiologie de la Nutrition, Université de Paris Sud, 91405 Orsay, France.
E-mail: jean-charles.martin@ibaic.u-psud.fr.

Abbreviations: ACO, acyl-CoA oxidase; CLA, conjugated linoleic acid; CPT, carnitine palmitoyl transferase; CYP, cytochrome P450; OD, optical density; PAP, phosphatidate phosphohydrolase.

were provided by Sigma-Aldrich (Sigma-Aldrich Co., L'Isle d'Abeau-Chêne, France).

Animals and diet. Male Wistar rats, weighing 200–220 g, were provided by the Centre d'élevage DEPRE (Saint Doulchard, France). They were housed individually and at a constant humidity and temperature with a 12-h light/dark cycle throughout the experiment. They had free access to water and received the same amount of the semisynthetic diet daily and were starved 12 h before killing. Rats used for the determination of the enzyme kinetic constants were fed with a commercial chow diet.

The CLA-diet composition is featured in Table 1. Rats were divided into four groups of five animals each and were fed for 6 wk with a 6% fat diet (by weight), containing 5% of fat as a mixture of high-oleic sunflower oil and linseed oil (98:2, w/w) and 1% of either 9*c*,11*t*-octadecadienoate (87% pure), 10*t*,12*c*-octadecadienoate (92% pure), or a mixture of both isomers (CLA 90) (43% of 9*c*,11*t*-isomer, 44.5% of 10*t*,12*c*-isomer), all of them being in the form of free acids. The control group received the same oil-mixture-based diet, except the CLA were replaced by oleic acid (89.4% pure).

The CLA 90 mixture was kindly provided by Natural Lipids (Hovdebygda, Norway). Its CLA isomer composition was determined by gas chromatography/mass spectrometry after conversion into dimethyloxazoline derivatives (19) as well as 4-methyl-1,2,4-triazoline-3,5-dione derivatives (20). Oleic acid was purchased from Sigma (Sigma-Aldrich Co.). The 9*c*,11*t*-octadecadienoic acid isomer was synthesized from castor oil (21), and the 10*t*,12*c*-octadecadienoic acid isomer was obtained by low-temperature crystallization from a mixture of CLA isomers obtained by alkali isomerization of linoleic acid (22). These fatty acids were then incorporated into the experimental diets.

TABLE 1
Composition of the Experimental Diets (in g per kg)

Casein	180
Sucrose	220
Corn starch	420
Cellulose	20
Mineral mixture[a]	50
Vitamin mixture[b]	10
Oil[c]	5
Free fatty acids[d]	1

[a]Contained $CaCO_3$ (12 g), K_2HPO_4 (10.75 g), $CaHPO_4$ (10.75 g), MgSO4·7H_2O (5 g), NaCl (3 g), MgO (2 g), $FeSO_4·7H_2O$ (400 mg), $ZnSO_4·7H_2O$ (350 mg), $MnSO_4·H_2O$ (100 mg), $CuSO_4·5H_2O$ (50 mg), $Na_2SiO_7·3H_2O$ (25 mg), $AlK(SO_4)_2·12H_2O$ (10 mg), K_2CrO_4 (7.5 mg), NaF (5 mg), $NiSO_4·6H_2O$ (5 mg), H_3BO_3 (5 mg), $CoSO_4·7H_2O$ (2.5 mg), KIO_3 (2 mg), $(NH_4)_6Mo_7O_{24}·4H_2O$ (1 mg), LiCl (0.75 mg), Na_2SeO_3 (0.75 mg), NH_4VO_3 (0.5 mg).

[b]Contained retinol acetate (5000 IU), cholecalciferol (1250 IU), DL-α tocopherol acetate (100 IU), phylloquinone (1 mg), thiamine chlorhydrate (10 mg), riboflavin (10 mg), nicotinic acid (50 mg), Ca-pantothenate (25 mg), pyridoxin chlorhydrate (10 mg), D-biotin (0.2 mg), folic acid (2 mg), cyanocobalamin (25 μg), choline chlorhydrate (1 g), DL-methionine (2 g), *p*-aminobenzoic acid (50 mg), inositol (100 mg).

[c]Contained 98% high-oleic sunflower oil and 2% linseed oil.

[d]Contained either 1% of oleic acid (89.4% pure), 9*c*,11*t*-octadecadienoate (87% pure), 10*t*,12*c*-octadecadienoate (92% pure), or a mixture of both isomers (CLA 90) (43% of 9*c*,11*t*-isomer, 44.5% of 10*t*,12*c*-isomer).

Tissue fractionation. After the end of the experimental diets, the starved animals were anesthetized with diethylether between 9 and 10.00 A.M. They were killed by exsanguination, and their blood was withdrawn at the abdominal artery. The organs, the epididymal adipose tissue, and the gastrocnemian muscle were removed, weighed and rinsed with cold saline prior to further analyses. Half of the liver, 0.9–1.2 g of the gastrocnemian muscle, 2.2–5.0 g of the epididymal adipose tissue, and 0.18–0.20 g of the heart (apex) were subsequently used for the cellular subfractionation which was carried out at 0°C. The tissues were first homogenized in a Tris buffer (10 mM, pH 7.4, 1 mM EDTA) containing 25 mM sucrose (muscle and adipose tissues) or 75 mM sucrose and 0.225 mM mannitol (heart), or a 0.25 M sucrose and 50 mM phosphate buffer (liver tissues). The homogenized tissues were then centrifuged at $1,000 \times g$ for 10 min to remove the cell debris. The gauze-filtered supernatants were subsequently spun at $12,000 \times g$ for 15 min. The peroxisome/mitochondrial pellet was then recovered and diluted with 3–5 mL of a 2 mM HEPES buffer for the heart, muscle, and adipose tissue fractions (pH 7.4, 70 mM sucrose, 220 mM mannitol, 1 mM EDTA), or 3–5 mL of a 50 mM phosphate buffer (pH 7.4, 250 mM sucrose) for the liver. The supernatants obtained from the $12,000 \times g$ centrifugation were further ultracentrifuged (two times 1 h at $105,000 \times g$) to yield the microsomal pellet and the cytosolic fraction. All the liver fractions were then stored at −80°C prior to analysis.

Enzymatic activities. The peroxisomal acyl-CoA oxidase and mitochondrial CPT activities were both assessed in the peroxisomal/mitochondrion fractions. The ACO activity, determined according to Lazarow (23), was assessed only in the liver. The peroxisomal fraction (≤0.3 mg protein) was mixed to the incubation medium (pH 8.3) containing CoA (0.075 mM), NAD (0.555 mM), nicotinamide (0.141 mM), dithiothreitol (4.4 mM), KCN (3 mM), and BSA (0.225 mg/mL) in Tris (60 mM), along with 20–100 μL of Triton X-100 (1% in Tris 60 mM), 20 μL of FAD (18 mM in Tris 60 mM) (final volume 3 mL). After incubation for 4 min at 37°C, 20 μL of palmitoyl-CoA (7.5 mM in Tris 60 mM) was added, and the reaction was monitored at 340 nm against the same medium without palmitoyl-CoA (ε for NADH = 6.22 mM^{-1} cm^{-1}) (Uvikon spectrophotometer, Basel, Switzerland).The activity of the liver peroxisomal acyl-CoA oxidase toward the different CLA preparation was determined by replacing palmitoyl-CoA with the respective conjugated linoleoyl-CoA (CLA-CoA) at different concentrations (5, 10, 20, 50 μM), as well as linoleoyl-CoA as a second reference. These acyl-CoA were chemically prepared by condensing the free fatty acids to the free CoASH, as described by Kawaguchi *et al*. (24).

CPT activity was determined in the liver, adipose tissue, heart, and gastrocnemian muscle according to the method of Bieber *et al*. (25). The incubation medium (pH 8.0, room temperature) contained (in mM), Tris (116), Na_2EDTA (1.1), palmitoyl-CoA, (0.035), 5-thio-2-nitrobenzoate (0.12), L(−)-carnitine (1.1) (experimental) or D(−)-carnitine (11) (blank). The reaction was initiated by adding 10–50 μL of the mitochondrion fraction (2 mg) and the change in optical density (OD) was monitored at

412 nm for 2–4 min (ε for 5-thio-2-nitrobenzoate = 13.6 $mM^{-1}cm^{-1}$). The kinetic parameters for the liver CPT-I were examined similarly, but using different kinds of acyl-CoA (16:0-, 18:2-, octadeca-9*c*11*t*-dienoyl-, octadeca-10*t*,12*c*-dienoyl-, and a mixture of CLA-CoA isomers) at several concentrations each (5, 10, 20, 40 μM).

The n- and (n-1)-laurate hydroxylation were determined as a marker of the cytochrome P4504A1 and cytochrome P4502E1 activities, respectively (26,27). Measurements were determined in the microsomal fraction according to Orton and Parker (28) and modified by Laignelet *et al.* (29). The microsomal protein concentration was adjusted at 1 mg/mL with a Tris buffer (pH 7.4, 66 mM, final volume 500 μL/assay). This medium was then incubated for 3 min at 37°C, with 1.5 mL in the same buffer containing [1-^{14}C]lauric acid (52 mCi/mmol, 1.1 μCi per assay). The reaction was initiated by adding 100 μL of NADPH (34 mM in Tris 66 mM, pH 7.4) and stopped with 0.1 mL HCl (1 N) after 15 min at 37°C. The reaction products were extracted with diethylether, separated by reversed-phase high-performance liquid chromatography, and quantified with a radiochromatographic detector Flo-one β (series A-100; Radiomatic Instruments, Tampa, FL) by peak integration high-performance liquid chromatography conditions: ODS column 25 cm length × 4.6 mm i.d., scintillation solution of Floscint II, 2:1, vol/vol). The mobile phase was made up of ammonium acetate (A, 27%), acetonitrile (B, 32%), and H_2O (C, 41%) and the samples were eluted with this mixture for 4 min. The mobile phase was then switched in 2 min to A (10%) and B (90%) and held for a further 4.5 min.

The phosphatidate phosphohydrolase (PAP) total activity (i.e., Mg^{2+}-dependent and Mg^{2+}-independent) was assessed in the microsomal fraction of the epididymal adipose tissue, essentially as described by Walton and Possmayer (30) and modified by Surette *et al.* (31). The reaction mixture contained 0.05 M Tris (pH 7.0), 1 mM phosphatidic acid, and 1 mM phosphatidylcholine prepared by sonication in 0.9% NaCl (at maximal frequency with a microprobe for 10 min with a model VC-500 sonicator; Sonics & Materials, Danbury, CT), Na_2-EDTA (1.25 mM), 50 to 100 μg microsomal or cytosolic protein, and 3.25 mM $MgCl_2$ (final volume of 0.2 mL). The mixtures were incubated at 37°C for 15 min, and the reaction was terminated by adding 0.8 mL of a solution containing 0.13% sodium dodecyl sulfate, 1.25% ascorbic acid, 0.32% $(NH_4)_6Mo_7O_{24}{\cdot}4H_2O$ and 0.375 M H_2SO_4. The phosphomolybdate color was developed at 45°C for 20 min, and the OD was determined at 820 nm (Uvikon spectrophotometer).

The glutathione *S*-transferase activity was determined in the cytosolic fraction of the hepatocytes according to Habig *et al.* (32). Glutathione (1 mM) was incubated at 30°C in a phosphate buffer (pH 6.5) with cytosolic protein (0.01 to 0.02 mg/mL), and the OD was followed at 340 nm for 3 min in presence of 1 mM of 1-chloro-2,4-dinitrobenzene (ε for the 1-chloro-2,4-dinitrobenzene/glutathione complex = 10 $mM^{-1}{\cdot}cm^{-1}$).

Statistics. The results were computed with Excel (Microsoft®). Comparison was made using the one-way analysis of variance (ANOVA) or the ANOVA on ranks (Jandel Scientific, San Rafael, CA) when the normality test failed. Student-Newman-Keuls test was used as soon as heterogeneity between groups was demonstrated. The level of significance was set at $P \leq 0.05$. Kinetic constants were derived by nonlinear regression of initial velocity data fitting a Michaelis-Menten plot as described by Sagnella (33), thereby allowing calculation of an apparent V_{max} ($V_{app\ max}$) and K_m ($K_{app\ m}$) (17).

RESULTS

Dietary treatment and enzymatic activities. The weight of the rats and the food efficiency did not differ between the animals throughout the experiment (Table 2). In addition, no liver enlargement was noticed in any of the dietary groups (Table 2). Independently of diet treatment, the activity of CPT-I differed among the mitochondrion fraction isolated from the four different tissues (hepatic, heart, skeletal muscle, and epididymal fat pad) (Table 3). Overall, this activity was the highest in mitochondrion of the heart tissue, then in decreasing order, in the fat pads, in the skeletal muscle and in the liver. No diet effect was detected, except in the adipose tissue where the activity was 25.5 to 31.6% higher in the CLA groups than in the oleic acid control group. However, the difference reached the statistical significance only in the 10*t*,12*c*- isomer group and the CLA 90 group ($P < 0.05$).

In the liver, the dietary treatment did not influence the acyl-CoA oxidase activity of the peroxisome either (Table 3), and the activity ranged from 12.5 to 14.3 nmol/min/mg of protein ($P > 0.05$). Also, the microsomal CYP4A1 activity, which is usually associated with the ACO activity, did not change with the type

TABLE 2
Liver and Body Weights After Dietary Treatment[a]

Dietary groups	Control	9*c*,11*t*	10*t*,12*c*	CLA90	Statistical difference[b]
Body weight (g)	304.1 ± 11.7	313.2 ± 29.3	318.0 ± 6.9	320.9 ± 7.0	NS
Liver weight (g)	9.3 ± 0.7	9.3 ± 0.3	10.6 ± 0.7	10.0 ± 0.5	NS
% Liver/body weight	3.1 ± 0.1	3.0 ± 0.1	3.3 ± 0.1	3.1 ± 0.1	NS
Food efficiency[c]	4.1 ± 0.2	3.9 ± 0.1	4.0 ± 0.2	4.0 ± 0.2	NS

[a]Expressed as means ± SEM; *n* = five animals per group.
[b]NS, not significant [one-way analysis of variance (ANOVA)].
[c]Expressed as [body weight gain (g)/food intake (g)] × 100.

TABLE 3
Selected Enzyme Activities in Different Organs of 12-h Fasted Rats[a]

Dietary groups	Control	9*c*,11*t*	10*t*,12*c*	CLA90
Carnitine palmitoyltransferase-I				
Liver	6.1 ± 1.2	5.4 ± 1.2	5.4 ± 0.9	5.4 ± 0.6
Heart	15.5 ± 1.1	17.0 ± 1.1	16.9 ± 1.3	17.9 ± 0.3
Skeletal muscle	8.4 ± 0.7	7.4 ± 1.2	8.5 ± 1.3	7.6 ± 0.7
Fat pad	8.9 ± 0.9[b]	11.9 ± 1.7[b,c]	12.2 ± 1.1[c]	13.0 ± 1.9[c]
Other enzymes in liver				
Acyl-CoA oxidase	13.8 ± 1.3	12.5 ± 2.9	14.3 ± 0.6	12.9 ± 1.3
CYP4A1	6.0 ± 0.5	6.1 ± 0.4	6.4 ± 0.4	5.6 ± 0.5
CYP2E1	6.3 ± 0.3	6.5 ± 0.5	7.0 ± 0.9	5.5 ± 0.1
Glutathione *S*-tranferase	1167 ± 87	1055 ± 47	1166 ± 80	1118 ± 51
Epididymal fat pad				
Phosphatidate phosphohydrolase	69.2 ± 11.3	68.0 ± 12.1	81.5 ± 6.6	67.1 ± 9.5

[a]All results are expressed as means ± SEM in nmol/min/mg of proteins (*n* = four to five animals per group).
[b,c]Denote a significant difference with the other numbers in the same row ($P < 0.05$).

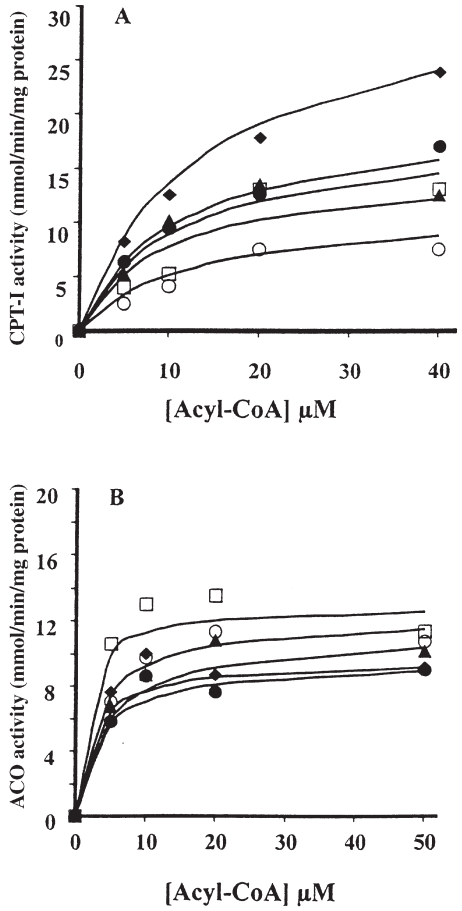

FIG. 1. (A) Initial rates of CoASH formation by carnitine palmitoyl transferase-I (CPT-I) while increasing the concentration of acyl-CoA substrates. Each data point represents the mean value obtained from five animals. (B) Initial rate of NADH reduction as a measure of acyl-CoA oxidase (ACO) activity while increasing the concentration of acyl-CoA substrates. Each data point represents the mean value obtained from four animals. Curves were generated from the apparent V_{max} and K_m values calculated by nonlinear regression. ◆ 18:2-CoA, ● 9*c*,11*t*-CoA, □ 10*t*,12*c*-CoA, ○ CLA90-CoA, ▲ 16:0-CoA.

of diet. In addition, the (n-1)-laurate hydroxylase activity, another phase-I detoxifying enzyme which reflects the CYP2E1 activity, did not differ with respect to the diet and was as high as the CYP4A1 activity (a range of 6.0 to 7.0 nmol/min/mg protein). The activity of the glutathione *S*-transferase was also determined in the cytosolic fraction of the hepatocytes. This activity ranged from 1.055 to 1.167 µmol/min/mg protein and did not significantly differ between the four experimental groups, as depicted in Table 3. Finally, the activity of the PAP, one of the rate-limiting enzymes involved in the *de novo* synthesis of triacylglycerols in the adipocytes, did not change with one diet or the other (Table 3).

CPT and ACO activities using hexadecanoic- and octadecadienoic-CoA as substrates. The mean activities of the mitochondrial CPT-I toward the different substrates and the kinetic constants derived from these activities are presented in Figure 1A and Table 4. The $V_{app\ max}$ differed ($P < 0.05$) between the substrates tested and was in decreasing order: 18:2-CoA, 16:0-CoA, 9*c*,11*t*-CoA, 10*t*,12*c*-CoA = CLA90-CoA. Conversely, no significant differences were observed between the corresponding $K_{app\ m}$ values. Comparison of the acyl-CoA substrates' efficiency for the enzyme based on the $V_{app\ max}/K_{app\ max}$ ratio showed lower values with the CLA mixture (Table 4, $P < 0.05$). This indicated that the conjugated linoleate CoA derivatives were not as good substrates for CPT-I as the linoleate homolog when given as a mixture (CLA 90).

The peroxisomal ACO activity toward the different acyl-CoA is displayed in Figure 1B and Table 4. No statistical differences were observed for $V_{app\ max}$ or $K_{app\ m}$ using either of the acyl-CoA substrates. In contrast, comparison of the $V_{app\ max}/K_{app\ m}$ indicated that the 10*t*,12*c*-CoA derivative was by far the best substrate for the enzyme (2.7 to 3.7 times more efficient) (Table 4). The $V_{app\ max}$ were significantly lower than the corresponding values found for CPT-I ($P < 0.05$), except for CLA90- and 10*t*,12*c*-CoA. The $K_{app\ m}$ were also consistently lower. As a result, in contrast to all the other acyl-CoA derivatives, both the CLA90- and 10*t*,12*c*-CoA were better substrates for ACO than for CPT-I, as indicated by their significantly higher $V_{app\ max}/K_{app\ m}$ for ACO than for CPT-I ($P < 0.05$, Table 4).

TABLE 4
Liver Carnitine Palmitoyltransferase-I (CPT-I) and Acyl-CoA Oxidase (ACO) Apparent Kinetic Constants Calculated from the Different Acyl-CoA *in vitro*[a]

	CPT-I			ACO		
Acyl-CoA	$V_{app\ max}$ (nmol/min/mg)	$K_{app\ m}$ (μM)	$V_{app\ max}/K_{app\ m}$	$V_{app\ max}$ (nmol/min/mg)	$K_{app\ m}$ (μM)	$V_{app\ max}/K_{app\ m}$
18:2	32.5 ± 6.2[b]	13.9 ± 5.2	2.3 ± 0.6[b]	9.6 ± 0.3[b,d]	2.6 ± 0.2[d]	3.9 ± 0.3[b]
16:0	20.1 ± 4.2[b,c]	11.2 ± 5.7	1.8 ± 0.8[b]	11.3 ± 1.3[b,d]	4.7 ± 1.9[d]	2.4 ± 0.9[b]
9*c*,11*t*	18.6 ± 2.8[b,c]	11.2 ± 2.9	1.7 ± 0.3[b]	9.5 ± 0.8[b,d]	3.5 ± 0.6[d]	2.7 ± 0.6[b]
10*t*,12*c*	15.1 ± 2.8[c]	9.7 ± 1.8	1.6 ± 0.3[b]	12.9 ± 1.3[b]	1.5 ± 0.4[d]	8.8 ± 3.0[c,d]
CLA 90	11.4 ± 3.0[c]	12.6 ± 3.2	0.9 ± 0.1[c]	12.2 ± 1.0[b]	3.3 ± 0.9[d]	3.7 ± 1.2[b,d]

[a]Kinetic constants are calculated from nonlinear regression (coefficients for the nonlinear regression fit range from 0.81 to 0.91 for CPT-I, and from 0.79 to 0.95 for ACO; $P < 0.0001$ for all r; $n = 15$ to 25 data points).
[b,c]Numbers in the same column not sharing a common superscript are significantly different ($P < 0.05$; one-way ANOVA) (expressed as means ± SEM, $n = 4$ to 5 animals).
[d]Indicates a significant difference ($P < 0.05$; one-way ANOVA) between the ACO value and its CPT-I counterpart in the same row. See Table 2 for other abbreviation.

DISCUSSION

The present study examined the influence of two isomers of CLA (individually or in combination) in the diet upon selected enzymes associated with lipid metabolism. In addition, as the biological activity of CLA is obviously dependent on their cellular metabolism, the other goal of that experiment was to predict to which extent these conjugated fatty acids can be channeled and eventually degraded through β-oxidation. For that purpose, we measured the activity of two important rate-limiting enzymes toward CLA, namely, the mitochondrial CPT-I and the peroxisomal ACO, which govern the flux of the fatty acids through the β-oxidation pathway. The depicted CPT activities mainly reflect the activity of the mitochondrion enzyme (34).

Effects of on lipid-related metabolizing enzymes. Belury *et al.* (8) found a peroxisome-proliferator response in the liver of female SENCAR mice fed a commercial mixture of CLA. This conclusion was supported by examining the mRNA levels encoding for different proteins accompanying the peroxisome proliferation, such as CYP4A1, fatty acid-binding protein and ACO, as well as the ACO protein expression—an important issue since peroxisome proliferation is usually accompanied by a pleiotropic cellular response associated with gene regulation (35–38), whether potentially beneficial (hypolipemia) or pathological (hepatotoxicity). However, at the time the present manuscript was written, the same authors published another report in which they contradicted this observation, but female and male Sprague-Dawley rats were used instead of female SENCAR mice (9). Consistent with this latter report, our results also confirm the lack of a peroxisome proliferation effect in our male rats (strain Wistar), though using another method. We thus measured the enzyme activity and not the mRNA induction of target enzymes which are generally increased during peroxisome proliferation (36,37). For instance, the peroxisomal ACO activity and the microsomal CYP4A1 activity remained unchanged (Table 3). Additionally, in peroxisome proliferation, the mitochondrion CPT-I activity is also often increased (35,39), and the cytosolic glutathione *S*-transferase activity is decreased (40–42). These activities were not modified after dietary intake of any of the CLA isomers (Table 3). Therefore, by using a complementary approach (phenotypic), our findings extend and confirm the former rat study (genotypic) (9) and point out that great care should be exercised in interpreting data of CLA experiments obtained in different species. The question should thus be raised: Which animal model, i.e., rats or mice (or others), would best mimic the human situation for that aspect (and other aspects) of fat metabolism during CLA feeding? Interesting to note and as formulated above, the activity of the cytosolic glutathione *S*-transferase is not impaired along with CLA intake (Table 3). This phase-II detoxifying enzyme has a critical role in cellular protection, and its activity might be induced during a chemical stress or by chemoprotective agents (43), or declined with peroxisome proliferator molecules (40–42). Therefore, in addition to the two phase-I enzymes presently studied (CYP4A1 and CYP2E1), the CLA diets caused no impairment of this glutathione-dependent detoxication activity either (phase II enzyme). This can be seen as a lack of a detrimental effect and would additionally argue for the absence of toxicity of CLA in this species, as it also has been documented by others but while examining histopathological and hematological parameters (44).

Mixtures of CLA are potent in reducing the fat body mass in different species (10,12,13,45) including rats. Among the identified causes, a greater channeling of fatty acids toward β-oxidation (higher CPT-I activity) (10), a lower adipose fatty acid uptake (10,11), a greater adipose tissue lipolysis (10,11), and an overall increased metabolic rate (13) are responsible for body fat reduction in mice. A possible impairment of triacylglycerol synthesis in the adipocyte can not be ruled out as well. However, our results did not suggest that a reduced lipid synthesis in the adipose tissue occurs in male Wistar rats, as the activity of PAP, a rate-limiting enzyme in the glycerolipid synthesis, remained unchanged in the epididymal adipose tissue (Table 3). Nonetheless, consistent with others (10), our data suggest that part of the body fat reduction induced by CLA can be ascribed to a greater β-oxidation rate of fatty acids in the adipose tissue, as evidenced by a higher CPT-I activity in the adipocyte (Table 3). Our findings also indicate that the two diets containing the

10*t*,12*c*-isomer elicited a larger effect when compared to the control group, a result consistent with the identified role of that isomer in body composition changes (11). In contrast to fasted mice (10), no changes of the β-oxidative capabilities (CPT-I activities) were detected in skeletal muscle of our fasted rats with one or the other CLA isomers (Table 3). This observation additionally underlines the differences between these two rodent species in response to CLA feeding.

Kinetic parameters of CPT and ACO using CLA as their CoA derivatives. Individual CLA-CoA isomers have comparable CPT-I $V_{app\ m}$ and $K_{app\ m}$ as palmitoyl-CoA, but a lower $V_{app\ m}$ value than linoleoyl-CoA (Table 4, Fig. 1A). Hence, besides the double-bond geometry (46), CPT-I is also able to discriminate between a methylene-interrupted (linoleate) and a conjugated double-bond system, especially when located in the Δ10,12 position. On the other hand, both the 9*c*,11*t*- and 10*t*,12*c*-isomers have comparable kinetic constants and identical $V_{app\ m}/K_{app\ m}$ ratios, suggesting that the enzyme cannot differentiate positional isomers of conjugated linoleates. This would also suggest that both isomers, as their CoA derivatives, are equally degraded through β-oxidation within the mitochondria. Thus, the preferential accumulation of the 9*c*,11*t*-CLA isomer over the 10*t*,12*c*- that is usually observed in tissue lipids (1,47) cannot be explained based on a better substrate specificity for the liver mitochondrial CPT-I. Indeed, based on the geometrical and positional arrangements of the conjugated double-bond system and on the enzymatic sequence involved in the β-oxidation spiral, one would expect that the 10*t*,12*c*-isomer would be more efficiently oxidized in the mitochondrion matrix than the 9*c*,11*t*-homolog: the 10*t*,12*c*-isomer would escape four enzymatic steps that may be potentially rate-limiting (i.e., enoyl-CoA isomerase, 2-*trans*-enoyl-CoA hydratase, β-hydroxyacyl-CoA dehydrogenase, and acyl-CoA dehydrogenase), while the 9*c*,11*t*-isomer would bypass only two (acyl-CoA dehydrogenase and 2,4-dienoyl-CoA reductase). Such a potentially facilitating metabolism could preferentially drive the 10*t*,12*c*-isomer through the β-oxidation pathway compared to the 9*c*,11*t*-homolog, and give some rationale to the lower amount in the 10*t*,12*c*-isomer found in the tissue lipids. Oxidation studies carried out with mitochondrial preparations using CoA derivatives and oxygen electrodes such as described elsewhere (48–50) would give a more precise feature as to the relative importance of the β-oxidation pathway toward each of the individual CLA isomers. Differences in the activation of the CLA isomers into their respective CoA by the acyl-CoA synthase, whether in the mitochondria or in the endoplasmic reticulum, would also offer an explanation as to the differences in their content in tissue lipids, as observed with long-chain n-3 fatty acids (51). Interestingly, we found a lower $V_{app\ m}$ and a lower $V_{app\ m}/K_{app\ m}$ ratio with the mixture of CLA-CoA (made up of equal amounts of both the 9*c*,11*t*- and 10*t*,12*c*-isomers) compared to the individual isomers situation (Table 4). If it is possible to extend this observation to the *in vivo* situation, it would mean that to give CLA as a mixture of isomers would spare them from β-oxidation to a greater extent than to give them separately. They would be therefore potentially more available for other metabolic purposes.

In a normal situation, the overall peroxisomal β-oxidation is quantitatively less compared to the mitochondrial β-oxidation. However, it may efficiently contribute to channeling certain fatty acids into the β-oxidative pathways (52–54). Especially, the availability for the peroxisome β-oxidation seems to be greater for the 10*t*,12*c*-isomer than for the 9*c*,11*t*-isomer since the former had higher $V_{app\ m}/K_{app\ m}$ ratio for ACO than the latter (Table 4). In addition, since peroxisomal β-oxidation is not complete in contrast to mitochondrial β-oxidation (55), it is therefore not surprising that a 16-carbon conjugated retroconverted product arising from the 10*t*,12*c*-CLA isomer and not from the 9*c*,11*t*-isomer was detected in the glycerolipids of rats fed with CLA (either as a mixture or as separate isomers) (56). This better channeling into the peroxisome oxidative pathway would also explain why the 10*t*,12*c*-isomer is generally found at a lower level than the 9*c*,11*t*-isomer in most tissue lipids (1,47).

In conclusion, the present study confirms and extends the observation made by others (9) as to a lack of a peroxisome-proliferator response elicited by either the 9*c*,11*t*- or 10*t*,12*c*-CLA isomer in the liver of rats. Our results also indicate that the *β*-oxidation activity in highly oxidative tissues, i.e., skeletal and cardiac muscles, was not modified with any of the CLA diet used. This was not the case in the epididymal adipose tissue where the CLA diets and especially the 10*t*,12*c*-isomer diet brought about a 30% increase of the mitochondrial CPT-I activity. Kinetic data obtained with CPT-I and ACO using a pure preparation of CLA isomers as their CoA derivatives suggested a greater availability of the 10*t*,12*c*-isomer for the peroxisomal β-oxidation pathways, which in turn would potentially lower its bioavailability and further its biological efficiency. Comparison of our rat results with mice studies, especially with those related to peroxisome proliferation and CPT-I, underlines species differences in response to CLA feeding and raises the question of which animal species would be preferred to mimic the human model.

ACKNOWLEDGMENT

This work was in part financially supported by the French ministry of research, Contrat MENRT 98G005.

REFERENCES

1. Banni, S., and Martin, J.C. (1998) Conjugated Linoleic Acid and Metabolites, in Trans *Fatty Acids in Human Nutrition* (Christie, W.W., and Sébédio, J.L., eds.), Vol. 9, pp. 261–302, The Oily Press Ltd., Dundee.
2. Parodi, P.W. (1997) Milk Fat Conjugated Linoleic Acid: Can It Help Prevent Breast Cancer? in *Proceedings of the Nutrition Society of New Zealand* (Savage, G.P., ed.), pp. 137–149, Nutrition Society of New Zealand, Canterbury.
3. Belury, M.A. (1995) Conjugated Dienoic Linoleate: A Polyunsaturated Fatty Acid with Unique Chemoprotective Properties, *Nutr. Rev. 53*, 83–89.
4. Ip, C., Scimeca, J.A., and Thompson, H.J. (1994) Conjugated Linoleic Acid. A Powerful Anticarcinogen from Animal Fat Sources, *Cancer 74*, 1050–1054.
5. Doyle, E. (1998) Scientific Forum Explores CLA Knowledge, *INFORM 9*, 69–72.

6. Haumann, B.F. (1996) Conjugated Linoleic Acid Offers Research Promise, *INFORM 7*, 152–159.
7. Fritsche, J., and Steinhart, H. (1998) Analysis, Occurrence, and Physiological Properties of *trans* Fatty Acids (TFA) with Particular Emphasis on Conjugated Linoleic Acid Isomers (CLA)—A Review, *Fett–Lipid 100*, 190–210.
8. Belury, M.A., Moya-Camarena, S.Y., Liu, K.L., and Heuvel, J.P.V. (1997) Dietary Conjugated Linoleic Acid Induces Peroxisome-Specific Enzyme Accumulation and Ornithine Decarboxylase Activity in Mouse Liver, *J. Nutr. Biochem. 8*, 579–584.
9. Moya-Camarena, S.Y., Vanden Heuvel, J.P., and Belury, M.A. (1999) Conjugated Linoleic Acid Activates Peroxisome Proliferator-Activated Receptor α and β Subtypes but Does Not Induce Hepatic Peroxisome Proliferation in Sprague-Dawley Rats, *Biochim. Biophys. Acta 1436*, 331–342.
10. Park, Y., Albright, K.J., Liu, W., Storkson, J.M., Cook, M.E., and Pariza, M.W. (1997) Effect of Conjugated Linoleic Acid on Body Composition in Mice, *Lipids 32*, 853–858.
11. Park, Y., Storkson, J.M., Albright, K.J., Liu, W., and Pariza, M.W. (1999) Evidence That the *trans*-10,*cis*-12 Isomer of Conjugated Linoleic Acid Induces Body Changes in Mice, *Lipids 34*, 235–241.
12. Pariza, M., Park, Y., Cook, M., Albright, K., and Liu, W. (1996) Conjugated Linoleic Acid (CLA) Reduces Body Fat, *FASEB J. 11,* 3227.
13. West, D.B., Delany, J.P., Camet, P.M., Blohm, F., Truett, A.A., and Scimeca, J. (1998) Effects of Conjugated Linoleic Acid on Body Fat and Energy Metabolism in the Mouse, *Am. J. Physiol. 44*, R667–R672.
14. Christie, W.W., Dobson, G., and Gunstone, F.D. (1997) Isomers in Commercial Samples of Conjugated Linoleic Acid, *Lipids 32,* 1231.
15. Ackman, R.G. (1998) Laboratory Preparation of Conjugated Linoleic Acids, *J. Am. Oil Chem. Soc. 75*, 1227.
16. Sehat, N., Yurawecz, M.P., Roach, J.A.G., Mossoba, M.M., Kramer, J.K.G., and Ku, Y. (1998) Silver-Ion High-Performance Chromatographic Separation and Identification of Conjugated Linoleic Acid Isomers, *Lipids 33*, 217–221.
17. Gavino, G.R., and Gavino, V.C. (1991) Rat Liver Outer Mitochondrial Carnitine Palmitoyltransferase Activity Towards Long-Chain Polyunsaturated Fatty Acids and Their CoA Esters, *Lipids 26*, 266–270.
18. Leyton, J., Drury, P.J., and Crawford, M.A. (1987) Differential Oxidation of Saturated and Unsaturated Fatty Acids *in vivo* in the Rat, *Br. J. Nutr. 58*, 383–393.
19. Lavillonnière, F., Martin, J.C., Bougnoux, P., and Sébédio, J.L. (1998) Analysis of Conjugated Linoleic Acid Isomers and Content in French Cheeses, *J. Am. Oil Chem. Soc. 75*, 343–352.
20. Dobson, G. (1998) Identification of Conjugated Fatty Acids by Gas Chromatography–Mass Spectrometry of 4-Methyl-1,2,4-triazoline-3,5-dione Adducts, *J. Am. Oil Chem. Soc. 75*, 137–142.
21. Berdeaux, O., Christie, W.W., Gunstone, F.D., and Sébédio, J.L. (1997) Large-Scale Synthesis of Methyl *cis*-9,*trans*-11-Octadecadienoate from Methyl Ricinoleate, *J. Am. Oil Chem. Soc. 74*, 1011–1015.
22. Berdeaux, O., Voinot, L., Angioni, E., Juanéda, P., and Sébédio, J.L. (1998) A Simple Method of Preparation of Methyl *trans*-10,*cis*-12- and *cis*-9,*trans*-11-Octadecadienoates from Methyl Linoleate, *J. Am. Oil Chem. Soc. 75*, 1749–1755.
23. Lazarow, P.B. (1976) Assay of Peroxisomal Beta-Oxidation of Fatty Acids, in *Methods in Enzymology*, Vol. 72, pp. 315–319, Academic Press, New York.
24. Kawaguchi, A., Yoshimura, T., and Okuda, S. (1981) A New Method for the Preparation of Acyl-CoA Thioesters, *J. Biochem. 89*, 337–339.
25. Bieber, L.L., Abraham, T., and Helmrath, T. (1972) A Rapid Spectrometric Assay for Carnitine Palmitoyltransferase, *Anal. Biochem. 50*, 509–518.
26. Pacot, C., Petit, M., Caira, F., Rollin, M., Behechti, N., Grégoire, S., Cherkaoui Malki, M., Cavatz, C., Moisant, M., Moreau, C., Thomas, C., Descotes, G., Gallas, J.F., Deslex, P., Althoff, J., Zahnd, J.P., Lhuguenot, J.C., and Latruffe, N. (1993) Response of Genetically Obese Zucker Rats to Ciprofibrate, a Hypolipidemic Agent, with Peroxisome Proliferation Activity as Compared to Zucker Lean and Sprague-Dawley Rats, *Biol. Cell 77*, 27–35.
27. Amet, Y., Berthou, F., Goasduff, T., Salaun, J.P., Le Breton, L., and Menez, J.F. (1994) Evidence That Cytochrome P450 2E1 Is Involved in the (ω-1)-Hydroxylation of Lauric Acid in Rat Liver Microsomes, *Biochem. Biophys. Res. Commun. 203*, 1168–1174.
28. Orton, T.C., and Parker, G.L. (1982) The Effect of Hypolipidemic Agents on the Hepatic Microsomal Drug-Metabolizing Enzyme System of the Rat. Induction of Cytochrome(s) P-450 with Specificity Toward Terminal Hydroxylation of Lauric Acid, *Drug. Metab. Dispos. 10*, 10110–10115.
29. Laignelet, L., Narbonne, J.F., Lhuguenot, J.C., and Riviere, J.L. (1989) Induction and Inhibition of Rat Liver Cytochrome(s) P-450 by an Imidazole Fungicide (prochloraz), *Toxicology 59*, 271–284.
30. Walton, P.A., and Possmayer, F. (1985) Mg^{2+}-Dependent Phosphatidate Phosphohydrolase of Rat Lung: Development of an Assay Employing a Defined Chemical Substrate Which Reflects the Phosphohydrolase Activity Measured Using Membrane-Bound Substrate, *Anal. Biochem. 151*, 479–486.
31. Surette, M.E., Whelan, J., Broughton, K.S., and Kinsella, J.E. (1992) Evidence of Mechanisms of the Hypotriglyceridemic Effect of n-3 Polyunsaturated Fatty Acids, *Biochim. Biophys. Acta 1126*, 199–205.
32. Habig, W.H., Pabst, M.J., and Jakoby, W.B. (1974) Glutathione *S*-Transferases. The First Enzymatic Step in Mercapturic Acid Formation, *J. Biol. Chem. 249*, 7130–7139.
33. Sagnella, G.A. (1985) Model Fitting, Parameter Estimation, Linear and Non-Linear Regression, *Trends Biol. Sci. 10*, 100–103.
34. Derrick, J.P., and Ramsay, R.R. (1989) L-Carnitine Acyltransferase in Intact Peroxisomes Is Inhibited by Malonyl-CoA, *Biochem. J. 262*, 801–806.
35. Hawkins, J.M., Jones, W.E., Bonner, F.W., and Gibson, G.G. (1987) The Effect of Peroxisome Proliferators on Microsomal, Peroxisomal, and Mitochondrial Enzyme Activities in the Liver and Kidney, *Drug Metab. Rev. 18*, 441–515.
36. Bentley, P., Calder, I., Elcombe, C., Grasso, D., Stringer, D., and Wiegand, H.-J. (1993) Hepatic Peroxisome Proliferation in Rodents and Its Significance for Humans, *Food Chem. Toxicol. 31*, 857–907.
37. Schoonjans, K., Staels, B., and Auwerx, J. (1996) Role of the Peroxisome Proliferator-Activated Receptor (PPAR) in Mediating the Effects of Fibrates and Fatty Acids on Gene Expression, *J. Lipid Res. 37*, 907–925.
38. Master, C., and Crane, D. (1998) On the Role of Peroxisome in Cell Differentiation and Carcinogenesis, *Mol. Cell. Biochem. 187*, 85–97.
39. Mannaerts, G.P., Debeer, L.J., Thomas, J., and De Schepper, P.J. (1979) Mitochondrial and Peroxisomal Fatty Acid Oxidation in Liver Homogenates and Isolated Hepatocytes from Control and Clofibrate-Treated Rats, *J. Biol. Chem. 254*, 4585–4595.
40. Fleischner, G., Meijer, D.K.F., Levine, W.G., Gatmaitan, Z., Gluck, R., and Arias, I.M. (1975) Effect of Hypolipidemic Drugs, Nafenopin and Clofibrate, on the Concentration of Ligandin and Z Protein in Rat Liver, *Biochem. Biophys. Res. Commun. 67*, 1401–1407.
41. Awasthi, Y.C., Singh, S.V., Goel, S.K., and Reddy, J.K. (1984)

Irreversible Inhibition of Hepatic Glutathione *S*-Transferase by Ciprofibrate, a Peroxisome Proliferator, *Biochem. Biophys. Res. Commun. 123*, 1012–1018.
42. Foliot, A., Touchard, D., and Celier, C. (1984) Impairment of Hepatic Glutathione *S*-Transferase Activity as a Cause of Reduced Biliary Sulfobromophthalein Excretion in Clofibrate-Treated Rats, *Biochem. Pharmacol. 33*, 2829–2834.
43. Wilkinson, J., and Clapper, M.L. (1997) Detoxication Enzymes and Chemoprevention, *Proc. Soc. Exp. Biol. Med. 216*, 192–200.
44. Scimeca, J.A. (1998) Toxicological Evaluation of Dietary Conjugated Linoleic Acid in Male Fischer 344 Rats, *Food Chem. Toxicol. 36*, 391–395.
45. Dugan, M.E.R., Aalhus, J.L., Schaefer, A.L., and Kramer, J.K.G. (1997) The Effect of Conjugated Linoleic Acid on Fat to Lean Repartitioning and Feed Conversion in Pigs, *Can. J. Anim. Sci. 77*, 723–725.
46. Ide, T., Watanabe, M., Sugano, M., and Yamamoto, I. (1987) Activities of Liver Mitochondrial and Peroxisomal Fatty Acid Oxidation Enzymes in Rats Fed *trans* Fat, *Lipids 22*, 6–10.
47. Park, Y., Albright, K.J., Liu, W., Cook, M.E., and Pariza, M.W. (1999) Changes in Body Composition in Mice During Feeding and Withdrawal of Conjugated Linoleic Acid, *Lipids 34*, 243–248.
48. Estabrook, R.W. (1967) Mitochondrial Respiratory Control and the Polarographic Measurement of ADP/O Ratios, *Meth. Enzymol. 10*, 41–47.
49. Lawson, L.D., and Holman, R.T. (1981) β-Oxidation of the Geometric and Positional Isomers of Octadecenoic Acid by Rat Heart and Liver Mitochondria, *Biochim. Biophys. Acta 665*, 60–65.
50. Osmundsen, H., Braud, H., Beauseigneur, F., Gresti, J., Tsoko, M., and Clouet, P. (1998) Effects of Dietary Treatment of Rats with Eicosapentaenoic Acid or Docosahexaenoic Acid on Hepatic Lipid Metabolism, *Biochem. J. 331*, 153–160.
51. Madsen, L., Froyland, L., Dyroy, E., Helland, K., and Berge, R.K. (1998) Docosahexaenoic and Eicosapentaenoic Acids Are Differently Metabolized in Rat Liver During Mitochondria and Peroxisome Proliferation, *J. Lipid Res. 39*, 583–593.
52. Alexson, S.E.H., and Cannon, B. (1984) A Direct Comparison Between Peroxisomal and Mitochondrial Preferences for Fatty-Acyl β-Oxidation Predicts Channelling of Medium-Chain and Very-Long-Chain Unsaturated Fatty Acids to Peroxisomes, *Biochim. Biophys. Acta 796*, 1–10.
53. Yamada, J., Ogawa, S., Horie, S., Watanabe, T., and Suga, T. (1987) Participation of Peroxisomes in the Metabolism of Xenobiotic Acyl Compounds: Comparison Between Peroxisomal and Mitochondrial β-Oxidation of ω-Phenyl Fatty Acids in Rat Livers, *Biochim. Biophys. Acta 921*, 292–301.
54. Guzman, M., Klein, W., Gomez Del Pulgar, T., and Geelan, M. (1999) Metabolism of *trans* Fatty Acids by Hepatocytes, *Lipids 34*, 381–386.
55. Osmundsen, H., Breler, J., and Pedersen, J.I. (1991) Metabolic Aspects of Peroxisomal β-Oxidation, *Biochim. Biophys. Acta 1085*, 141–158.
56. Sébédio, J.L., Grégoire, S., Juanéda, P., Angioni, E., Chardigny, J.M., Martin, J.C., and Berdeaux, O. (1999) 9*c*,11*t* and 10*t*,12*c* Do Not Influence Similarly Fatty Acid Composition of Rat Tissue Lipids, presented at the 90th American Oil Chemists' Society Meeting & Expo, May 1999, Orlando.

[Received June 28, 1999, and in final revised form November 23, 1999; revision accepted December 1, 1999]

Apolipoprotein E Polymorphism: Automated Determination of Apolipoprotein E2, E3, and E4 Isoforms

Claudia Wiebe, Guido Holzem, Klaus Wielckens, and Karl Rolf Klingler*

Institut für Klinische Chemie, Universität zu Köln, Cologne, Germany

ABSTRACT: Apolipoprotein E (apo E) plays an essential role in lipoprotein metabolism, where it is involved in the clearance of chylomicrons and very low density lipoproteins. Apart from some rare variants, apo E exists in three common isoforms (E2, E3, and E4). The different isoforms have not only been associated with different plasma lipid levels but have also been correlated with certain pathological conditions, such as lipid disorders (dysbetalipoproteinemia, hypercholesterolemia), cardiovascular diseases, and Alzheimer's disease. Here we describe a rapid, automated test for the determination of the most frequent polymorphisms (E2, E3, and E4). This polymerase chain reaction-based test allows the reliable discrimination of all six genotypes. The assay has been developed especially for the nonspecialized routine clinical laboratory by employing an analyzer and chemistry often present in this type of laboratory. Because of its low costs and easy handling, the assay can be performed on a daily basis.

Paper no. L8369 in *Lipids 35,* 99–104 (January 2000).

Apolipoprotein E (apo E) plays a central role in the receptor-mediated uptake of chylomicrons and very low density lipoprotein remnants by the liver. Apo E is one of the major proteins of these particles and acts as the ligand to the low density lipoprotein (LDL) receptor and to other receptors of this receptor family (reviewed in 1). Apo E is polymorphic; it exists in three common isoforms (E2, E3, E4) (2,3) and in some rare variants (4,5). The major isoforms differ from each other only by single amino acid substitutions at two sites. The isoforms are associated with certain diseases: apo E2 homozygosity plays an important role in the development of type III hyperlipoproteinemia (6–8) and atherosclerosis (9), because apo E2 is defective in its ability to bind to lipoprotein receptors (10,11); apo E4, apart from being associated with elevated LDL concentrations, increases—in a dose-dependent manner—the likelihood of developing Alzheimer's disease (12,13).

Several methods have been employed for the determination of apo E isoforms. Basically, these methods can be divided into two groups: methods of the first group focus on the separation of the lipoprotein isoforms by isoelectric focusing with subsequent immunoblotting using an anti-apo E antibody (14,15) or by direct immunofixation (16). A second group of methods is based on the polymerase chain reaction (PCR) technique and therefore determines the patient's genetic status directly. Most of these methods employ restriction endonucleases followed by the analysis of the restriction fragment length polymorphism, which can be detected by separating the fragments on agarose or polyacrylamide gels (17–19), or even by employing microplate array diagonal gel electrophoresis (20). Others employ single-strand conformation polymorphism (21) or oligonucleotide binding (22).

Although all of these methods are certainly capable of determining a patient's apo E isoform status, most of them were developed in, and for, research laboratories and are, as such, time-consuming and laborious. It is therefore necessary to establish methods that especially meet the needs of a routine laboratory, i.e., are easy to perform, allow for a high throughput, require less hands-on time, are reliable, fast, and cost effective.

Here we describe a rapid, automated PCR-based method for the determination of the apo E isoforms that uses electrochemiluminescence (ECL) as detection technology, employs off-the-shelf chemistry, and uses the automated detection process of an immunoassay analyzer that is present in many clinical laboratories, thus avoiding an additional investment for more specialized equipment.

MATERIAL AND METHODS

DNA isolation. Genomic DNA was isolated from 10 μL of anticoagulated whole blood (EDTA, citrate, or Li-heparin), which we obtained for routine analysis from our hospital, using the Dynabeads DNA DIRECT™ kit from DYNAL (Oslo, Norway). DNA was dissolved in 30 μL of Tris-EDTA buffer and stored at –20°C until use.

All primers were designed according to the sequence published by Hixson and Vernier (17). The currently available version of the apo E sequence from GenBank (accession number M10065) shows a few differences that are marked by underlining the respective bases.

PCR. Two fragments, separated only by 22 bp, within exon 3 of the apo E gene were amplified (Fig. 1). Each fragment covers a single, diagnostic restriction site for the enzyme *Hin 6 I.* Fragment A (89 bp, GenBank: position 3914–4002), was

*To whom correspondence should be addressed at Institut für Klinische Chemie, Joseph-Stelzmann-Straße 9, 50925 Köln, Germany.

Abbreviations: apo, apolipoprotein; dNTP, deoxynucleotide triphosphates; ECL, electrochemiluminescence; LDL, low density lipoprotein; PCR, polymerase chain reaction.

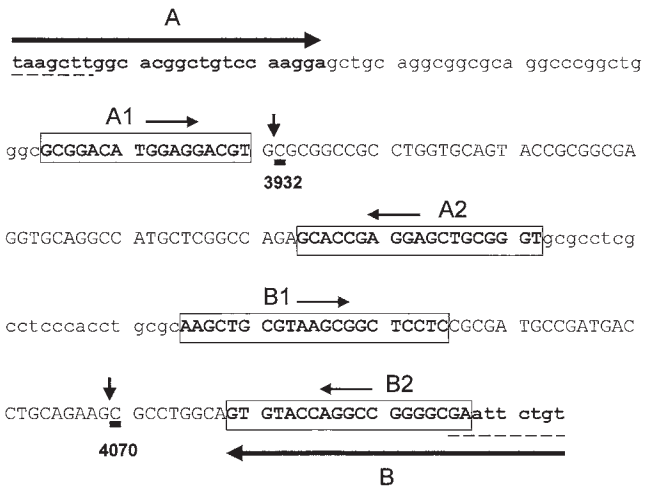

FIG. 1. Apolipoprotein E (apo E) polymerase chain reaction. Sequence of the 244-bp-long amplified fragment within exon 3 of the human apo E gene (GenBank accession number M10065, position 3861–4104), which was amplified with primer A and B. Dotted line: mismatch between GenBank sequence and primer sequences published by Hixson and Vernier (17). Primers A1 and A2 were used to generate fragment A, which includes the recognition sequence for *Hin 6 I* at position 3931–3934. Apo E isoforms E2 and E3 display "T" instead of "C" at position 3932 and by this destroy the recognition sequence of *Hin 6 I*. Primers B1 and B2 were used to generate fragment B, which includes the recognition sequence for *Hin 6 I* at position 4069–4072. Apo E isoform E2 carries "T" instead of "C" at position 4070 and by this destroys the recognition sequence for *Hin 6 I*. Down arrows indicate *Hin 6 I* cleavage sites in fragments A and B.

amplified using primer A1: 5′-ruthenium-GCG GAC ATG GAG GAC GT-3′ and primer A2: 5′-biotin-ACC CGC AGC TCC TCG GTG C-3′ (synthesized by MWG-Biotech-AG, Ebersberg, Germany). DNA (5 µL) was added to 45 µL of PCR mastermix containing 300 nM of each primer and 250 µM of each deoxynucleotide triphosphates (dNTP) (Promega, Madison, WI), 2% (vol/vol) dimethylsulfoxide (Sigma, St. Louis, MO), 10 mM Tris HCl (pH 8.3), 50 mM KCl, 1.5 mM $MgCl_2$, 1 unit Taq-polymerase (Sigma), 7% (vol/vol) glycerol (Merck, Darmstadt, Germany), and 27 µL of sterile water. The samples were then subjected to the following cycling conditions: 96°C for 2 min; cycles 1–4: 96°C for 1 min, 61°C for 50 s, and 72°C for 1 min; cycles 5–32: 91°C for 1 min, 61°C for 50 s, and 72°C for 1 min.

Fragment B (73 bp, GenBank: position 4025–4097) was amplified using primer B1: 5′-ruthenium-AAG CTG CGT AAG CGG CTC CTC-3′ and primer B2: 5′-Biotin-TCG CCC CGG CCT GGT ACA C-3′ (synthesized by MWG-Biotech-AG). DNA (5 µL) was added to 45 µL of PCR mastermix containing 250 µM of each dNTP, 2% (vol/vol) formamide (Merck), 10 mM Tris HCl (pH 8.3), 50 mM KCl, 1.5 mM $MgCl_2$, 1 unit Taq-polymerase (Sigma) 10% (vol/vol) glycerol (Merck) containing 300 nM of each primer. The samples were then subjected to the following cycling conditions: 96°C for 1 min, then cycles 1–5: 96°C for 1 min, 53°C for 50 s, and 72°C for 1 min; cycles 6–34: 90°C for 1 min, 53°C for 50 s, and 72°C for 1 min.

Hin 6 I *digestion.* Both PCR products were digested independently. Fifteen microliters from each PCR product was added to 5 µL of a digestion mastermix, containing 20 units *Hin 6 I* (FERMENTAS, Vilnius, Lithuania) and 3 µL of buffer "Y-Tango," supplied with the enzyme. The samples were digested for 40 min at 37°C.

DNA sequencing. A 244 bp (GenBank: position 3861–4104) within exon 3 of the apo E gene (Fig. 1), spanning fragments A and B, was amplified using primer A: 5′-TAA GCT TGG CAC GGC TGT CCA AGG A- 3′ and primer B: 5′-ACA GAA TTC GCC CCG GCC TGG TAC AC-3′ (MWG-Biotech-AG).The amplified DNA was sequenced with the Big-Dye™ DNA sequencing kit of PE-Applied Biosystems (Warrington, United Kingdom) on a 377 DNA Sequencer (PE-Applied Biosystems, Weiterstadt, Germany).

Detection. We used a modified Elecsys system 1010 ("Molecsys"), especially suited for molecular biology tests (not commercially available, Roche Diagnostics, Mannheim, Germany) in conjunction with the reagents (buffers, microbeads) supplied with the normal test kits by Roche Diagnostics. The system is a fully automated random access analyzer; its underlying principles have been described in great detail elsewhere (23). In principle, the system employs ECL for detection, which utilizes $Ru^{2+}(bipy)_3$-chelates as a label in combination with universal streptavidin-coated paramagnetic micro particles.

RESULTS

The basic principle of the assay is outlined in Figures 2 and 3. Briefly, two DNA fragments, spanning either of the diagnostic restriction sites, are amplified independently, using a pair of a biotin-labeled 3′ primer and a ruthenium-labeled 5′ primer for each fragment. After amplification, each of the two samples is split into two aliquots. One aliquot is incubated with the restriction enzyme *Hin 6 I*. If the restriction site is present, the ruthenium-labeled 5′ part of the fragment is removed from the biotinylated 3′ part. The other aliquot remains unaltered. Biotinylated DNA binds *via* streptavidin to paramagnetic beads, which keep the biotinylated DNA in the detection chamber of the analyzer while all other components are washed away. The amount of ruthenium bound to the biotinylated DNA is determined for both samples by measuring the ECL signal generated by the ruthenium complex in the detection chamber. The genotype is determined by calculating the ratio between the signals from the digested and the undigested aliquot for both fragments.

DNA preparation. We decided to use the Dynabeads DNA DIRECT™ kit, which allows the preparation of 10 samples within 15 min from blood samples anticoagulated with heparin, citrate, or EDTA. In almost all cases, blood samples reach the laboratory without being cooled or frozen during transport; thus DNA may degrade quite rapidly during transportation. Using the Dynabeads DNA DIRECT™ kit, we were able to obtain DNA from samples that had been stored up to 4 d at room temperature.

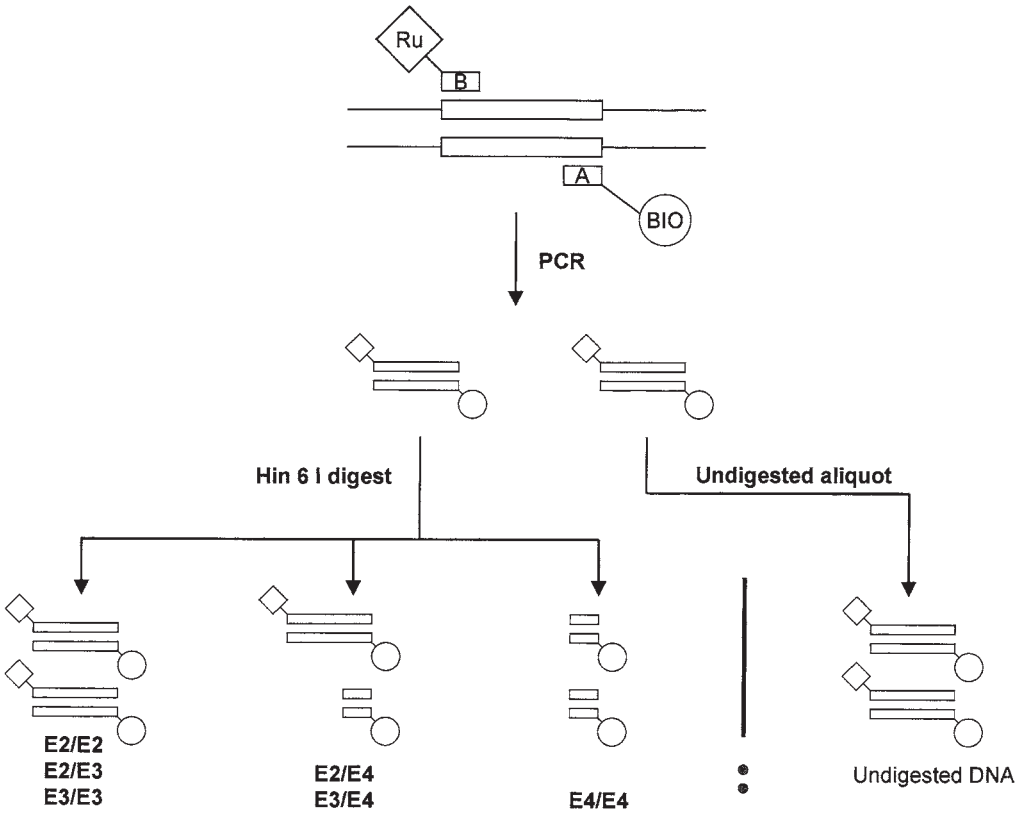

FIG. 2. The Apo E assay. After amplification, each sample is split into two aliquots. One of the two aliquots is incubated with the restriction enzyme *Hin 6 I*. If the restriction site is present, the ruthenium-labeled 5' part of the fragment is separated from the biotinylated 3' part. The other aliquot remains unaltered. Biotinylated DNA binds *via* streptavidin to paramagnetic beads, which keep the biotinylated DNA in the detection chamber of the analyzer while all other components are washed away. The amount of ruthenium bound to the biotinylated DNA is determined for both aliquots by measuring the electrochemiluminescence signal, which is generated by the ruthenium complex in the detection chamber. The apo E isoform is determined by calculating the ratios between the signals from the digested and the undigested aliquots for fragments A and B. Figure 2 represents the situation for fragment A. For abbreviation see Figure 1.

Validity of the new method. The assay is based on the presence of a single diagnostic *Hin 6 I* restriction site in each of the two short (89 and 73 bp) fragments (Fig. 3A) that were amplified by PCR. Depending on the genotype, the site is present in all, none, or one of the two fragments leading to a unique pattern of two distinctive ratios for each isoform (Fig. 3B; Table 1).

To demonstrate the validity of our method, we analyzed samples that had already been sequenced. For each of the six possible genotypes, we analyzed 10 samples (with the exception of E2/2: nine samples). The results are listed in Table 1, demonstrating total agreement of our method with the independently obtained results. Combination of the two ratios for fragments A and B allows for an unambiguous determination of the genotype; each analyzed sample falls into one of six nonoverlapping groups (Fig. 4).

The mean ratio of the heterozygous samples is significantly higher than theoretically expected (0.63–0.67 vs. 0.5). This is due to the formation of heteroduplex DNA during PCR amplification: a single strand of wild-type DNA and a single strand of mutated DNA form double-stranded DNA (heteroduplex DNA). This DNA cannot be cut by the restriction enzyme, thus leading to a ratio >0.5. Nevertheless, this does not hamper the ability of the test to distinguish clearly among all six genotypes.

Intra-assay and interassay imprecision. Following the procedure described here, we independently determined, for each of the two fragments, intra-assay and interassay imprecision. For each genotype, DNA from a single sample was split into 10 aliquots that were subsequently amplified by PCR and analyzed by the standard procedure: each sample was split into two secondary aliquots, and one of these secondary aliquots was incubated with the respective restriction enzyme. All 20 secondary aliquots were measured on the analyzer in the same run and the ratios were calculated. From these data, intra-assay imprecision was calculated. Further, DNA from a single sample was split into 10 aliquots that were subsequently amplified by PCR and stored at –20°C. For 10 d within a 14-d period, a

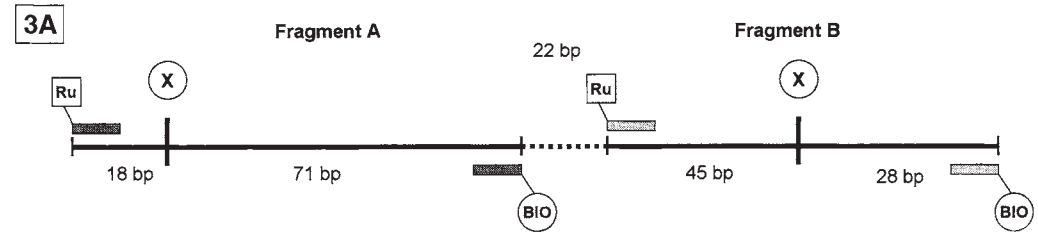

3A

	Fragment A	Ratio	Fragment B	Ratio
E2/E2	E2 / E2	1	E2 / E2	1
E2/E3	E2 / E3	1	E2 / E3	0.5
E2/E4	E2 / E4	0.5	E2 / E4	0.5
E3/E3	E3 / E3	1	E3 / E3	0
E3/E4	E3 / E4	0.5	E3 / E4	0
E4/E4	E4 / E4	0	E4 / E4	0

FIG. 3. Apo E isoforms and *Hin 6 I* restriction pattern. Restriction endonuclease *Hin 6 I* generates unique restriction patterns of fragments A and B which, together, allow the unambiguous identification of the respective apo E isoform. (A) In the case of E4, each fragment carries a single "diagnostic" restriction site (**X**) for *Hin 6 I*. In the case of the E2 and E3 isoforms, the recognition sequence in one or both fragments is destroyed, and *Hin 6 I* will not cut the DNA. (B) The pattern of DNA fragments generated by *Hin 6* and the corresponding results with the new assay as a ratio between the signals from the digested and the undigested aliquots is shown for each isoform combination.

single aliquot was thawed and two secondary aliquots were generated and analyzed ± digestion with the *Hin 6 I* restriction enzyme. These data were used to calculate interassay imprecision. The results are summarized in Table 2.

Costs. Since our intention was to design an assay for the average clinical laboratory, we not only focused on handling and reliability but also looked at cost effectiveness as well. Apart from a thermal cycler, no special equipment is needed. The costs of the consumables (enzymes, reagents, and plasticware) for one blood sample (both mutations) are less than $5 (U.S.).

DISCUSSION

A large variety of assays for the detection of point mutations in general and for the determination of apo E isoforms already exists. Our intention was to focus strictly on the development of an assay that is truly suited for use under the conditions and restraints present in the setting of an average clinical laboratory.

To reach this goal, chemicals and equipment usually available in such laboratories have to be integrated into the analytical procedure, and manual work has to be avoided whenever

TABLE 1
Comparison of Expected Ratios (based on DNA sequencing) and the Ratios That Were Obtained with the New Method

Genotype	E2/E2	E2/E3	E2/E4	E3/E3	E3/E4	E4/E4
Fragment A						
Expected ratio	1	1	0.5	1	0.5	0
Obtained ratio, mean	1.05	0.99	0.63	0.98	0.67	0.02
Range	1.01–1.08	0.93–1.06	0.53–0.72	0.92–1.03	0.58–0.72	0.01–0.04
Fragment B						
Expected ratio	1	0.5	0.5	0	0	0
Obtained ratio, mean	1.02	0.66	0.67	0.02	0.01	0.02
Range	0.94–1.1	0.56 -0.75	0.52–0.73	0.01–0.04	0.01–0.03	0.01–0.06

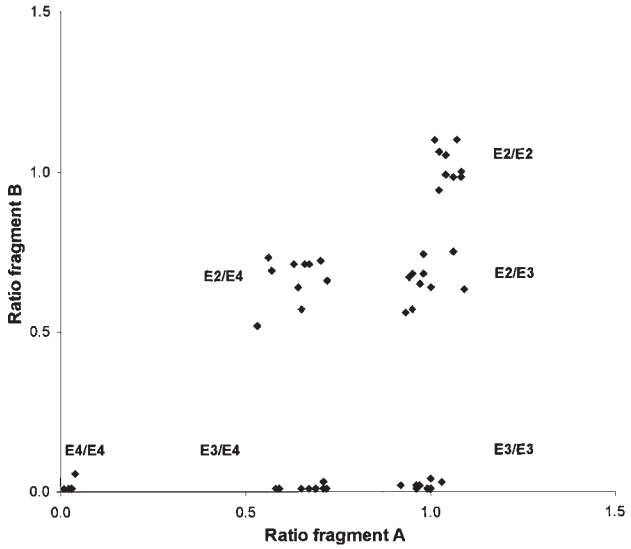

FIG. 4. Ratio distribution. Combination of the two ratios for fragments A and B allows for an unambiguous determination of the genotype: 10 samples for each of the six possible genotypes (E2/E2: nine samples) were analyzed by this method. Each analyzed sample falls into one of six nonoverlapping groups.

possible. Therefore, DNA sequencing or procedures requiring high-purity DNA were not options since these methods require the use of toxic chemicals and extensive manual labor, thereby increasing the costs.

Consequently we decided to use a DNA preparation method that yields DNA of only average purity but that is very quick and allows the handling of several samples simultaneously. For the same reason any quantification of DNA or cells was omitted. Instead, we decided to split every sample and carry the undigested sample through the whole assay, allowing on one hand control of all assay steps and on the other hand avoiding any quantification steps after DNA preparation and after PCR amplification. In addition, the undigested sample is the 100% base for the calculation of the ratio of each sample, thus avoiding extra handling steps and additional reagents or the necessity of comparing the result with an external 100% standard. These procedures do not compromise quality and reliability.

For the detection of the PCR product itself, we used an Elecsys system from Roche Diagnostics, because this type of instrument is widely distributed, thereby taking advantage of the possibility of using shelf reagents. Moreover, this analytical system allows the determination of the genotype with high reliability and low costs. The system employs ECL for detection, which is very sensitive and, since detection is linear over almost five orders of magnitude, allows the simultaneous processing of samples with varying amounts of amplified DNA.

The reliable identification of patients who are heterozygous for a mutation is often a problem and therefore was of primary importance for the assay design. The results prove that the "heterozygous" genotypes (leading to a ratio of ~0.65) can be reliably distinguished from the homozygous genotypes. In addition, the assay is fast enough to allow same-day reporting.

Nowadays, almost all clinical laboratories feel increasingly the impact of a tight budget. The fact that this assay, apart from the PCR step, does not require any specialized equipment, since the instrumentation is available in many laboratories, keeps the costs to less than $5 (U.S.) and avoids any major upfront investment in hardware.

The recently described fluorescence-based PCR method (LightCycler™) (24) is faster than the method described here, but it requires an analyzer exclusively dedicated to PCR-based testing, which represents an additional investment of $40,000 to $50,000 (U.S.). In a large percentage of clinical laboratories, this investment cannot be justified owing to low sample numbers. The only option left to most of these laboratories is to use equipment already present in conjunction with tests such as the one described here.

Assays, comparable to this test, may help genetic analyses in the future to become an affordable part of the daily workload of an average clinical laboratory.

ACKNOWLEDGMENTS

We thank Dr. Juergen Geisel, University Hospital, Homburg/Saar, for providing DNA samples. We gratefully acknowledge the support of Roche Diagnostics, Mannheim, Germany, which supplied the modified Elecsys 1010 system.

REFERENCES

1. Siest, G., Pillot, T., Regis-Bailly, A., Leininger-Muller, B., Steinmetz, J., Galteau, M.M., and Visvikis, S. (1995)

TABLE 2
Intra- and Interassay Imprecision

Genotype	E2/E2		E2/E3		E2/E4		E3/E3		E3/E4		E4/E4	
expected ratio	A: 1	B: 1	A: 1	B: 0.5	A: 0.5	B: 0.5	A: 1	B: 0	A: 0.5	B: 0	A: 0	B: 0
Intra-assay imprecision												
Mean	1.05	1.1	1.04	0.71	0.64	0.71	1.02	0.02	0.67	0.02	0.02	0.03
SD	0.07	0.06	0.06	0.03	0.04	0.05	0.05	0.01	0.04	0.01	0.01	0.01
CV (%)	6.8	5.4	5.9	4.4	6.5	7.4	5	31	6	43	35	26
Interassay imprecision												
Mean	0.98	0.98	1.01	0.76	0.61	0.66	0.99	0.02	0.58	0.02	0.02	0.02
SD	0.07	0.08	0.08	0.04	0.07	0.07	0.08	0.01	0.06	0.01	0.01	0.01
CV (%)	7.5	7.8	8.1	5.5	11.5	10.3	7.7	61.5	9.5	33.3	39.6	39.1

Apolipoprotein E: An Important Gene and Protein to Follow in Laboratory Medicine, *Clin. Chem. 41*, 1068–1086.
2. Zannis, V.I., and Breslow, J.L. (1981) Human Very Low Density Lipoprotein Apolipoprotein E Isoprotein Polymorphism Is Explained by Genetic Variation and Posttranslational Modification, *Biochemistry 20*, 1033–1041.
3. Weisgraber, K.H., Rall, S.C., Jr., and Mahley, R.W. (1981) Human E Apoprotein Heterogeneity: Cysteine–Arginine Interchanges in the Amino Acid Sequence of the Apo-E Isoforms, *J. Biol. Chem. 256*, 9077–9083.
4. Matsunaga, A., Sasaki, J., Moriyama, K., Arakawa, F., Takada, Y., Nishi, K., Hidaka, K., and Arakawa, K. (1995) Population Frequency of Apolipoprotein E5 (Glu3→Lys) and E7 (Glu244→Lys, Glu245→Lys) Variants in Western Japan, *Clin. Genet. 48*, 93–99.
5. Hoffer, M.J., Niththyananthan, S., Naoumova, R.P., Kibirige, M.S., Frants, R.R., Havekes, L.M., and Thompson, G.R. (1996) Apolipoprotein E1-Hammersmith (Lys146→Asn; Arg147→Trp), Due to a Dinucleotide Substitution, Is Associated with Early Manifestation of Dominant Type III Hyperlipoproteinaemia, *Atherosclerosis 124*, 183–189.
6. Utermann, G., Jaeschke, M., and Menzel, J. (1975) Familial Hyperlipoproteinemia Type III: Deficiency of a Specific Apolipoprotein (apo E-III) in the Very-Low-Density Lipoproteins, *FEBS Lett. 56*, 352–355.
7. Utermann, G., Hees, M., and Steinmetz, A. (1977) Polymorphism of Apolipoprotein E and Occurrence of Dysbetalipoproteinaemia in Man, *Nature 269*, 604–607.
8. März, W., Hoffmann, M.M., Scharnagl, H., Fisher, E., Chen, M., Nauck, M., Feussner, G., and Wieland, H. (1998) Apolipoprotein E2 (Arg136→Cys) Mutation in the Receptor Binding Domain of Apo E Is Not Associated with Dominant Type III Hyperlipoproteinemia, *J. Lipid Res. 39*, 658–669.
9. Davignon, J., Gregg, R.E., and Sing, C.F. (1988) Apolipoprotein E Polymorphism and Atherosclerosis, *Arteriosclerosis 8*, 1–21.
10. Schneider, W.J., Kovanen, P.T., Brown, M.S., Goldstein, J.L., Utermann, G., Weber, W., Havel, R.J., Kotite, L., Kane, J.P., Innerarity, T.L., and Mahley, R.W. (1981) Familial Dysbetalipoproteinemia. Abnormal Binding of Mutant Apoprotein E to Low Density Lipoprotein Receptors of Human Fibroblasts and Membranes from Liver and Adrenal of Rats, Rabbits, and Cows, *J. Clin. Invest. 68*, 1075–1085.
11. Lalazar, A., Weisgraber, K.H., Rall, S.C., Jr., Giladi, H., Innerarity, T.L., Levanon, A.Z., Boyles, J.K., Amit, B., Gorecki, M., Mahley, R.W., and Vogel, T. (1988) Site-Specific Mutagenesis of Human Apolipoprotein E. Receptor Binding Activity of Variants with Single Amino Acid Substitutions, *J. Biol. Chem. 263*, 3542–3545.
12. Corder, E.H., Saunders, A.M., Strittmatter, W.J., Schmechel, D.E., Gaskell, P.C., Small, G.W., Roses, A.D., Haines, J.L., and Pericak-Vance, M.A. (1993) Gene Dose of Apolipoprotein E Type 4 Allele and the Risk of Alzheimer's Disease in Late Onset Families, *Science 261*, 921–923.
13. Ohm, T.G., Kirca, M., Bohl, J., Scharnagl, H., Gross, W., and März, W. (1995) Apolipoprotein E Polymorphism Influences Not Only Cerebral Senile Plaque Load but Also Alzheimer-Type Neurofibrillary Tangle Formation, *Neuroscience 66*, 583–587.
14. Havekes, L.M., de Knijff, P., Beisiegel, U., Havinga, J., Smit, M., and Klasen, E. (1987) A Rapid Micromethod for Apolipoprotein E Phenotyping Directly in Serum, *J. Lipid Res. 28*, 455–463.
15. Kataoka, S., Paidi, M., and Howard, B.V. (1994) Simplified Isoelectric Focusing/Immunoblotting Determination of Apoprotein E Phenotype, *Clin. Chem. 40*, 11–13.
16. Hackler, R., Schafer, J.R., Motzny, S., Brand., S., Kleine, T.O., Kaffarnik, H., and Steinmetz, A. (1994) Rapid Determination of Apolipoprotein E Phenotypes from Whole Plasma by Automated Isoelectric Focusing Using PhastSystem and Immunofixation, *J. Lipid Res. 35*, 153–158.
17. Hixson J.E., and Vernier, D.T. (1990) Restriction Isotyping of Human Apolipoprotein E by Gene Amplification and Cleavage with HhaI, *J. Lipid Res. 31*, 545–548.
18. Lagarde, J.P., Benlian, P., Zekraoui, L., and Raisonnier, A. (1995) Genotyping of Apolipoprotein E (alleles epsilon 2, epsilon 3 and epsilon 4) from Capillary Blood, *Ann. Biol. Clin. (Paris) 53*, 15–20.
19. Dallinga-Thie, G.M., van Linde-Sibenius Trip, M., Kock, L.A., and De Bruin, T.W. (1995) Apolipoprotein E2/E3/E4 Genotyping with Agarose Gels, *Clin. Chem. 41*, 73–75.
20. Bolla, M.K., Haddad, L., Humphries, S.E., Winder, A.F., and Day, I.N. (1995) High-Throughput Method for Determination of Apolipoprotein E Genotypes with Use of Restriction Digestion Analysis by Microplate Array Diagonal Gel Electrophoresis, *Clin. Chem. 41*, 1599–1604.
21. Aozaki, R., Kawaguchi, R., Ogasa, U., Hikiji, K., Kubo, N., and Sakurabayashi, I. (1994) Rapid Identification of the Common Apo E Isoform Genotype Using Polymerase Chain Reaction–Single Strand Conformation Polymorphism (PCR–SSCP), *Mol. Cell. Probes 8*, 51–54.
22. Houlston, R.S., Wenham, P.R., and Humphries, S.E. (1990) Detection of Apolipoprotein E Polymorphisms Using PCR/ASO Probes and Southern Transfer: Application for Routine Use, *Clin. Chim. Acta 189*, 153–157.
23. Erler, K. (1998) Elecsys® Immunoassay Systems Using Electrochemiluminescence Detection, *Wien. Klin. Wochenschr. 110*, 5–10 (supplement 3).
24. Aslanidis, C., and Schmitz, G. (1999) High-Speed Apolipoprotein E Genotyping and Apolipoprotein B3500 Mutation Detection Using Real-Time Fluorescence PCR and Melting Curves, *Clin. Chem. 45*, 1094–1097.

[Received October 13, 1999, and in revised form December 14, 1999; revision accepted December 20, 1999]

COMMENTARY

Breast-Fed Infants Achieve a Higher Rate of Brain and Whole Body Docosahexaenoate Accumulation Than Formula-Fed Infants Not Consuming Dietary Docosahexaenoate

Stephen C. Cunnane[a,*], Valerie Francescutti[a], J. Thomas Brenna[b], and Michael A. Crawford[c]

[a]Department of Nutritional Sciences, University of Toronto, Toronto, Canada M5S 3E2, [b]Division of Nutritional Sciences, Cornell University, Ithaca, New York, and [c]University of North London, London N7 8DB, England

ABSTRACT: Docosahexaenoate (DHA) has been increasingly recognized as an important fatty acid for neural and visual development during the first 6 mon of life. One important point of controversy that remains is the degree to which adequate levels of DHA can be acquired from endogenous synthesis in infants vs. what should be provided as dietary DHA. We have approached this problem by a retrospective analysis of published body composition data to estimate the actual accumulation of DHA in the human infant brain, liver, adipose tissue, remaining lean tissue, and whole body. Estimating whether infants can synthesize sufficient DHA required comparison to and extrapolation from animal data. Over the first 6 mon of life, DHA accumulates at about 10 mg/d in the whole body of breast-fed infants, with 48% of that amount appearing in the brain. To achieve that rate of accumulation, breast-fed infants need to consume a minimum of 20 mg DHA/d. Virtually all breast milk provides a DHA intake of at least 60 mg/d. Despite a store of about 1,050 mg of DHA in body fat at term birth and an intake of about 390 mg/d α-linolenate (α-LnA), the brain of formula-fed infants not consuming DHA accumulates half the DHA of the brain of breast-fed infants while the rest of the body actually loses DHA over the first 6 mon of life. No experimental data indicate that formula-fed infants not consuming DHA are able to convert the necessary 5.2% of α-LnA intake to DHA to match the DHA accumulation of breast-fed infants. We conclude that dietary DHA should likely be provided during at least the first 6 mon of life.

Paper no. L8211 in *Lipids 35,* 105–111 (January 2000).

Whether there is a need for dietary docosahexaenoate (DHA, 22:6n-3) to achieve optimal postnatal visual and cognitive development in human infants is controversial. Reasons for adding DHA to milk formulas include (i) the presence of DHA in human milk irrespective of maternal DHA intake (1); (ii) the lower brain DHA levels in human infants when preformed DHA is not provided (2,3); and (iii) the improvement in vision and/or neurodevelopment when DHA is provided in the milk formula (4–8). Reasons for not adding DHA to milk formula include (i) a lack of improvement in cognitive or motor development over the first 18 mon of life in a large study of term infants given a formula containing DHA and arachidonate (9), (ii) a similar level of visual and neural development in formula-fed term infants not receiving supplemental DHA as in breast-fed infants (10,11), and (iii) potentially impaired development when supplemental DHA is given without added arachidonate (12). One of the problems in achieving consensus on this issue relates to having a large enough sample size studied for long enough (13). This problem has been addressed recently (9) but other potential confounders remain, including the relatively low DHA intake of breast-fed infants in some studies.

Among a number of investigators, measurement of percentage DHA in fatty acid profiles has developed into a surrogate for functional indicators of DHA adequacy. Such data rely predominantly on percentage DHA in plasma total or phospholipid fatty acids which certainly reflects differences in intake of n-3 polyunsaturates but for which no "desirable" normal range has been established for infants. A higher percentage DHA in plasma fatty acids is usually encouraged because it suggests that more DHA is available for the brain. However, even detailed animal data do not clearly establish a relation between plasma or erythrocyte DHA and brain DHA (14). Indeed, one could argue that there should be no relation between blood and brain DHA because the brain presumably has a more rigid DHA requirement whereas the plasma is a transport medium that reflects a balance between intake and utilization of DHA but has no DHA requirement *per se*.

Thus, the limits may have been reached of what can be inferred from fatty acid profiles as a measure of DHA status. Practical and ethical restrictions may make it difficult to design and complete unambiguous clinical studies assessing DHA effects on neurodevelopment. Nevertheless, published data on DHA intake and its levels in organs of human infants are available that are relevant to this issue but have not been applied toward estimating whole-body DHA accumulation by the human infant. In an effort to contribute to the dialogue on the possible need for dietary DHA in human infants, the published literature on growth and fatty acid profiles of various organs was reviewed with an emphasis on determining the net accumulation of DHA in the term infant, particularly in the brain. DHA accumulation was compared to an estimate of ca-

*To whom correspondence should be addressed.
E-mail: s.cunnane@utoronto.ca

Abbreviations: DHA, docosahexaenoate; α-LnA, α-linolenate.

pacity to provide DHA from breast milk, body fat stores, or synthesis from α-LnA.

The premise for this analysis was that if the combination of DHA synthesis and body stores of preformed DHA appears adequate to meet the rate of DHA accumulation in breast-fed infants for at least 6 mon, then it would not be necessary to provide DHA in milk formulas. Conversely, if DHA stores and synthesis are inadequate to match brain DHA accumulation of breast-fed infants over 6 mon then we would propose that there is a need for dietary DHA. The period from birth to 6 mon was chosen because few data on infant body composition and organ fatty acid profiles exist beyond this period and because exclusive breast or formula feeding is uncommon beyond this age.

COMPONENTS OF GROWTH AND DHA ACCUMULATION

All the data presented here are from literature values that have been previously reported elsewhere but have not been compiled to determine fatty acid accumulation. Changes in organ weights were assumed to be the same for breast- and formula-fed infants because most studies do not distinguish or else combine the data. Data on DHA concentration in the brain, liver, and body fat are in the literature; DHA in the remaining lean tissue of the body was estimated from animal data referenced against liver values (15). Brain and whole-body DHA accumulation data were then compared to DHA intake and bioavailability from breast milk. In essence, this is an analysis of whole-body docosahexaenoate balance comparing the breast- and formula-fed infant. No data on the DHA content of tissues are available for infants given formulas containing DHA, so a comparison cannot be made here.

Data from two papers reporting brain fatty acid profiles in infants (2,3) are central to the present analysis, so a brief description of those two studies is relevant. Farquharson *et al.* (2) reported phospholipid fatty acid profiles for parietal cortex samples from 20 infants who died of sudden infant death syndrome at 1–43 wk. Five infants were exclusively breast-fed and the remaining 15 received milk formulas providing a linoleate/α-LnA ratio of 10:1 ($n = 5$) or 40:1 ($n = 10$). Makrides *et al.* (3) reported fatty acid profiles for frontal cortex total lipids from 15 infants breast-fed for an average of 16 wk, and from 20 formula-fed infants. Most of the deaths in this study were also attributed to sudden infant death syndrome. The formula-fed infants consumed a linoleate/α-LnA ratio of about 10:1.

Over the first 6 mon of life, body weight increases by an average of 4,350 g (Table 1). Brain weight increases by 250 g, liver by 80 g, body fat by 1,440 g, and remaining lean tissue by 2,580 g. The concentration of DHA in the whole brain of a breast-fed infant increases by 39% (1.8 to 2.5 mg/g) from term to 6 mon (16). By extrapolating from the combined average of data reported by Farquharson *et al.* (2) and Makrides *et al*. (3), brain DHA concentration does not increase from birth over the first 6 mon in formula-fed infants not consuming DHA. Thus, the gain in whole brain DHA over the first 6 mon is about 905 mg in breast-fed infants, but is 450 mg in the formula-fed infant receiving no dietary DHA (Table 1).

In the liver, total DHA increases slightly in the breast-fed infant with a gain of 24 mg over 6 mon, but decreases by 136 mg in the formula-fed infant (Table 1). DHA is present in body fat at a higher concentration at term (0.4 wt% of total fatty acids) than after 6 mon of breast-feeding (0.1 wt%), but was not detectable in body fat of formula-fed infants (17). Hence, in absolute terms, body fat as a whole in breast-fed infants accumulates a small amount of DHA over 6 mon (147 mg), but appears to lose all its DHA if the infant is given a formula without DHA. These data assume that total body fat does not differ between breast- and formula-fed infants. They also take into account the lower amount of triglyceride (actual fat) in adipose tissue at birth (47% of total fat weight; 18), a value that we assumed rose to 60% by 6 mon of age, on its way to a mean of 82% in adults (19). DHA in lean tissues of the remaining body was estimated by extrapolation from animal data showing that DHA in skeletal muscle and viscera is about 25% of that in the liver (15). On that basis, and assuming that the DHA concentration of the remaining lean tissue changes in parallel to the DHA in the liver, the remaining lean tissue of breast-fed infants accumulates about 806 mg of DHA over the first 6 mon of life compared to a loss of about 194 mg of DHA if the infant consumes a formula without DHA (Table1).

Summing the DHA in each of these compartments gives a net whole-body content of DHA at term birth of about 3,800 mg. There is a gain of 1,882 mg or 10.3 mg/d of DHA in the whole body over 6 mon for the breast-fed infant. On the other hand, the whole body of the formula-fed infant loses 993 mg DHA over 6 mon or 5.1 mg/d (Table 1). In the breast-fed infant, 48% (5.0 mg/d) of the gain in whole-body DHA is in the brain and 43% (4.4 mg/d) is in lean tissue excluding the liver. In the breast-fed infant, the liver and body fat seem to be largely DHA "neutral" over the first 6 mon of life (jointly gaining <1 mg/d DHA as a whole). By contrast, only the brain gains DHA in the formula-fed infant (at 2.5 mg/d or half the rate in breast-fed infants), while the rest of the body undergoes a net loss of 7.6 mg/d (Table 1).

MEETING THE ESTIMATED RATE OF DHA ACCUMULATION

To achieve the rate of DHA accumulation calculated for breast-fed infants (about 10 mg/d), a higher DHA intake is needed, thereby allowing for obligate losses before and after absorption. Absorption of DHA from the gut of formula-fed term infants is above 95% (20); we are unaware of similar data for breast-fed infants, but it is likely to be the same. Oxidation is the main postabsorptive route of DHA catabolism. The amount of DHA that is catabolized in humans is unknown but can be estimated from a mixture of primate and rat data. In the liver, brain, and eye of the infant baboon, about 30% of a single dose of preformed isotopically labeled DHA is lost *via* carbon recycling into saturated and monounsaturated fatty acids synthesized *de novo* (21). Losses of DHA due to carbon recycling into cholesterol or

TABLE 1
Accumulation of Docosahexaenoate (DHA) in Breast-Fed or Formula-Fed Term Infants from Birth to 6 mon[a]

	Term	6 mon	Change	Accumulation of DHA (mg/d)[a]
Brain (g)	400[c]	650[c]		
DHA (mg/g)	1.8[d]	2.5[d] (1.8[e])		
DHA (mg/brain)	720	1,625 (1,170)	+905 (+450)	5.0 (2.5)
Liver (g)	120[f]	200[f]		
DHA (mg/g)	2.8[g]	1.8[g] (1.0[g])		
DHA (mg/liver)	336	360 (200)	+24 (–136)	0.1 (–0.7)
Body fat (g)	560[h,i]	2000[h,i]		
Actual fat (wt%)	47[j]	60[k]		
DHA (%)	0.4[l]	0.1[l] (ND[l])		
DHA (mg/total fat)	1,053	1,200 (0)	+147 (–1053)	0.8 (–5.8)
Remaining lean (g)	2,420[h]	5,000[h]		
DHA (mg/g)	0.7[m]	0.5[m] (0.3[m])		
DHA (mg/total lean)	1,694	2,500 (1,500)	+806 (–194)	4.4 (–1.1)
Total body (g)	3,500[n]	7,850[n]		
DHA (mg/body)	3,803[o]	5,685[o] (2,870[o])	+1,882 (–933)	10.3 (–5.1)

[a]Data for formula-fed infants are shown in parentheses.
[b]Change over 6 mon/182 d.
[c]Muhlman (34).
[d]Martinez (16).
[e]An average of the data reported by Farquharson *et al.* (2) and Makrides *et al.* (3), which, when combined, shows no net change from birth in percent DHA in fatty acids of the cerebral cortex of formula-fed infants. The percent DHA values were converted to mg/g using Martinez's (16) data for forebrain in term infants. The proportion of whole brain that is forebrain was determined from Reference 35.
[f]An average of data from Clandinin *et al.* (36) and Coppeletta and Wolbach (37).
[g]Farquharson *et al.* (38).
[h]de Bruin *et al.* (39).
[i]Widdowson (40).
[j]Baker (18).
[k]Estimated to be 60% by extrapolation from 47% at birth (18) and 82% in adults (19).
[l]Farquharson *et al.* (17).
[m]The average DHA concentration of rat skeletal muscle and viscera is 25% of that in rat liver (15) so this proportion was used to convert the value for DHA in infant liver at birth (2.8 mg/g) to 0.7 mg/g in lean tissue at birth.
[n]Sum of compartments, which yields a similar value to whole body data published by Soriguer Escofet *et al.* (41).
[o]Sum of DHA values for brain + liver + body fat + remaining lean tissue.

by oxidation to CO_2 were not reported in that study. However, in rat studies examining metabolism of other polyunsaturates, oxidation to CO_2 is equivalent in magnitude to the carbon recycling to *de novo* fatty acid synthesis (22,23). Thus, oxidation to CO_2 and carbon recycling into *de novo* lipogenesis would at least double the 30% loss of DHA to fatty acid synthesis alone. Hence, obligatory losses of dietary DHA in infants appear to be on the order of at least 50–60% of that consumed so, to achieve a whole-body DHA accumulation rate of 10 mg/d, at least double (20 mg/d) would have to be provided. This may be a conservative estimate of the amount of DHA needed to achieve the observed accumulation rates but no published data were found that support adjusting this estimate to a higher value.

We believe that it is important to be able to estimate the actual whole-body accumulation of DHA and the amount of dietary DHA or DHA precursors that is necessary to achieve the estimated DHA accumulation rate. However, we do not intend that the estimated accumulation rate for DHA in infants should be viewed as a DHA requirement *per se* because we have no proof that 20 mg/d achieves a desirable functional outcome, only that it approximates the amount of DHA needed to achieve the estimated rate of DHA accumulation in breast-fed infants. Furthermore, the source of the DHA (dietary or synthesized endogenously) to meet this accumulation estimate is also undefined. Once a measurable functional outcome dependent on DHA intake is defined, it will be possible to estimate DHA requirement.

DHA IN MILK RELATIVE TO ITS ACCUMULATION IN THE BREAST-FED INFANT

Over the first 6 mon of life, breast milk intake averages 750 mL/d (24,25). It contains about 4 g/dL fat and DHA at about 0.2 wt% of total fatty acids. This would provide about 60 mg/d of DHA to the breast-fed infant. A value of 0.2 wt% DHA in breast milk fatty acids seems to be more typical of North American and some European milk than of the rest of the world where it tends to be higher (1). Hence, breast milk typically provides about three times more DHA than appears to be needed by the whole infant between term birth and 6 mon of age.

The brain accounts for 48% of the whole body DHA accumulation during the first 6 mon of life (Table 1). By taking into account an obligatory loss of 50% of dietary DHA, the infant brain's accumulation of DHA is equivalent to about 16% of the average DHA intake from breast milk (5 of 30 mg/d available DHA). These calculations ignore both DHA stores (17) and the known capability of the neonate to synthesize DHA (26–28), which suggest that, normally, <16% of the available DHA is used by the developing brain of a breast-fed infant. Furthermore, if DHA intake is higher than 0.2% of milk fatty acids, the proportion of consumed DHA being used by the brain will decrease further. Hence, in using a conservative estimate of DHA in breast milk and disregarding DHA stores and synthesis, the average breast-fed term infant appears to have access to a surplus of preformed DHA.

DHA SYNTHESIS IN THE FORMULA-FED INFANT

The formula-fed infant consuming no dietary DHA must acquire its DHA from body stores or from endogenous synthesis, the latter primarily from α-LnA. α-LnA in milk formulas varies but, on average, is currently present at 1.5% of total fatty acids (6,11). Most formulas contain about 3.5 g/dL fat, so assuming a similar average fluid intake over 6 mon as in the breast-fed infant (750 mL/d; 24,25), this provides about 390 mg/d of α-LnA to the healthy term infant. To meet the brain's DHA accumulation rate alone, the conversion of α-LnA to DHA in human infants needs to be about 2.6% (10 out of 390 mg/d). For the whole body, the conversion of α-LnA needed to make 20 mg/d of DHA would have to be 5.2%. This conversion estimate takes into account the calculated obligate losses of DHA.

How feasible is it for human infants to convert 5.2% of α-LnA intake to DHA? There are several reports on desaturation and chain elongation of α-LnA to DHA by human infants (26–28). In each case, labeled α-LnA was given by mouth and the appearance of labeled metabolites such as DHA in plasma was compared to the amount of tracer given. However, this does not represent actual conversion of α-LnA to DHA because tracer accumulation by the tissues remains unknown in these studies. Hence, to date, we are aware of no study that has reported the actual quantitative capacity to convert α-LnA to DHA in infant or adult humans. This can probably only be achieved by whole-body fatty acid balance methods (15), which are inevitably restricted to animal studies.

Without being able to make direct measurements in humans, the remaining option is to extrapolate from tracer and/or fatty acid balance studies in animals as to whether is it likely that human infants can convert 5.2% of α-LnA intake to whole body DHA or 2.6% of α-LnA intake to brain DHA. Only one directly relevant study in an animal model similar to human infants appears to have been published. By using a stable isotope approach, formula-fed neonatal baboons not consuming DHA have been reported to convert 0.23% of an oral tracer dose of ^{13}C-α-LnA to brain DHA; whole-body conversion of α-LnA to DHA was not reported in that study (29). A commercially available human infant formula containing a linoleate to α-LnA ratio of about 10:1 was used in that study. Hence, baboon infants consuming a similar formula to those used for human infants achieved a rate of conversion of α-LnA to DHA that was 9% of that needed by human infants.

Whole-body fatty acid balance analysis of α-LnA conversion to DHA in growing rats not consuming DHA shows that the overall desaturation/chain elongation of α-LnA to DHA is about 1.4% (15) or 27% of that needed by human infants. The seemingly low conversion rate in rats and baboon infants is supported by the fact that some α-LnA is stored but 70–80% of α-LnA intake is completely β-oxidized. In addition, in the suckling rat, tracer studies show that recycling of α-LnA carbon into newly synthesized brain lipids consumes 30–50 times more ^{13}C-α-LnA than is converted into brain ^{13}C-DHA (22). Thus, carbon recycling consumes a significant additional amount of carbon from α-LnA beyond that which is oxidized to CO_2.

The rat is considered to have a relatively high capacity to desaturate and chain elongate α-LnA, while the baboon is an omnivorous primate that is close in many respects to the development of human infants. In both the primate and rodent models, the available conversion estimates are still well short of the apparent minimum value of 2.6% for the human brain, let alone the overall 5.2% conversion needed for the whole body. At present, no experimental or theoretical data support a capacity to achieve 5.2% conversion of α-LnA to DHA in human infants. Even if α-LnA intake was above 2 wt% of the fatty acids in a formula, as has been recommended (10), i.e., 2.5 wt% would provide 656 mg/d α-LnA, the brain alone would require 1.5% conversion efficiency (10 mg/d of the 656 mg/d consumed). This is still 6.5 times more than the reported capacity in baboon infants (29). Hence, in the absence of dietary DHA, it doesn't seem plausible that sufficient DHA synthesis from dietary α-LnA occurs in the human infant to achieve brain DHA accumulation equivalent to that of the breast-fed term infant.

DHA AND α-LNA IN BODY FAT STORES

Compared to adult humans, there is a relatively high proportion of DHA in adipose tissue at term birth. Regardless of breast or formula feeding, the proportion of DHA in adipose tissue DHA decreases postnatally but more so if the infant consumes a milk formula without DHA, in which case it decreases to an undetectable level during the first 6 mon of life (Table 1; 17). This decrease in percentage DHA in adipose tissue occurred regardless of α-LnA intake which varied between 0.4 and 1.5% of fatty acids in the three formulas used in that study. There is about 1,050 mg DHA in body fat at term, which, if exclusively available to the brain of the formula-fed infant not receiving DHA, would eliminate the need to synthesize DHA destined for the brain for about 3 mon (Table 1). This would reduce the necessary conversion of α-LnA for the brain alone from 10 mg/d to about 5 mg/d or to about 1.2% of the consumed α-LnA over the first 6 mon of

life. Such a value is still five times the 0.23% conversion of α-LnA to DHA achieved by baboon infants (29).

There are two crucial points indicating that, in a net sense, DHA in adipose tissue is probably inaccessible to the developing brain: (i) despite the decreasing percentage DHA in adipose tissue, the actual amount of DHA increases slightly in breast-fed infants (+147 mg over 6 mon; Table 1), and (ii) brain DHA accumulation in formula-fed infants is still significantly lower compared to equivalent breast-fed infants (2,3). Thus, the store of DHA in body fat does not prevent significantly lower accumulation of DHA in the brain when there is no dietary DHA. Indeed, it is possible that brain DHA of formula fed infants not getting dietary DHA might be even lower if DHA was not present in body fat stores at birth. This is clearly speculative but the point is that, if substantiated, these reports (2,3) clearly expose the fundamental problem that brain DHA accumulation is reduced when dietary DHA is not provided and they highlight an apparent need for a dietary source of DHA in human neonates. Furthermore, in low birth weight or premature infants, who are at higher risk of impaired neurodevelopment (4), total body fat is greatly reduced so the amount of DHA stored in body fat, whether available to the brain or not, would be substantially less than in healthy term infants.

The total amount of α-LnA present in body fat at term (0.1 wt% of fatty acids or about 260 mg in total; 17) is less than the amount of α-LnA consumed daily by the formula-fed infant so it would not have a significant impact on these estimates. We are unaware of data for n-3 polyunsaturated fatty acid intermediates between α-LnA and DHA that are presumably present in body fat stores and liver and which would somewhat reduce the necessary conversion of dietary α-LnA to DHA. However, their levels in fat are likely to be lower than those of α-LnA.

THE NEED FOR SURPLUS DHA

The apparent surplus of DHA intake in the healthy, breast-fed term infant is needed because the requirement for all nutrients, especially those that can be β-oxidized, must provide for potentially increased losses during disease, infection, surgery, undernutrition, or other conditions adversely affecting metabolism. These adverse conditions often involve voluntary or involuntary food restriction which, in addition to increasing fatty acid β-oxidation, impairs synthesis of DHA and arachidonate by inhibiting the desaturation chain elongation pathway (30). Hence, the apparent dietary surplus of DHA with breast-feeding could provide insurance against depletion in disease states or undernutrition.

Long-chain polyunsaturated fatty acids, especially DHA, are traditionally viewed as fatty acids with a "structural" role in membranes. However, they are not exempt from β-oxidation. In fact, the body content of long-chain polyunsaturates is more rapidly depleted by fasting or semistarvation than by dietary deficiency alone and was frequently used to accelerate linoleate deficiency (31). A substantial amount of β-oxidation and carbon recycling to *de novo* lipid synthesis seems to be a prominent pathway for polyunsaturates including DHA (21,22) and normally consumes the overwhelming majority of linoleate (18:2n-6) and α-LnA intake (15). Even an intentionally deficient linoleate intake does not prevent significant losses of linoleate to β-oxidation and carbon recycling, demonstrating that this is an obligatory pathway (23) that, with undernutrition, can readily consume the entire dietary intake and reduce body stores of linoleate and α-LnA (32).

Thus, a combination of increased β-oxidation and impaired desaturation–chain elongation during adverse nutritional or metabolic conditions (30,32) is an important reason for providing an apparent surplus of pre-formed DHA because α-LnA cannot be relied upon to be available for DHA synthesis when fatty acid oxidation increases. This diversion of α-LnA toward oxidation and impairment of desaturation-chain elongation (30) may contribute to the DHA deficit in the brain when dietary DHA is not provided. Hence, dietary DHA is not effectively replaced by DHA from endogenous stores or synthesis, both of which appear inadequate to meet the DHA needs of the formula-fed infant not receiving dietary DHA.

LIMITATIONS OF THIS ANALYSIS

The present analysis is subject to the constraints imposed by collecting and combining data from multiple sources published over several decades. In several instances, extrapolation from animal data also was necessary, though this was kept to a minimum and relevant primate data were used where available. The DHA data for body fat and liver were derived from single reports while the DHA values for the remaining lean tissue were estimated from animal data referenced to the liver. Nevertheless, most of the organ weight and fatty acid data are directly or indirectly substantiated by other reports. Similar to the present data but using less complete information, Farquharson *et al.* (17) estimated a DHA requirement in infants of about 30 mg/d. Clandinin *et al.* (33) reported that total n-3 polyunsaturates accumulated at about 3 mg/d in the fetal brain during the third trimester which is close to, but predictably lower than, the 5 mg/d calculated here for the early postnatal period. Hence, the present estimates fit with the limited literature in this area.

The estimated need to convert 5.2% of α-LnA intake to obtain sufficient DHA for the whole human infant has no clear comparison in the literature because fatty acid balance data for the rat (15) did not address a period when brain growth was rapid while the tracer data in baboon infants (29) were for the brain only. Microsomal desaturase activity is generally more rapid in rats than in other species but the baboon infant data should, in principle, be in a similar range to human rates of α-LnA conversion to DHA. In either case, the estimated accumulation of DHA by the human infant brain alone relative to its accumulation after conversion from α-LnA is about 10 times greater than the reported capacity in primates (2.6 vs. 0.23%; 29); the whole-body conversion needed is 3.7 times higher than that achieved by rats (5.2 vs.

1.4%; 15). Furthermore, and most importantly, human brain DHA levels are significantly lower without dietary DHA (2,3). Thus, to some extent, whether estimates of DHA synthesis from α-LnA or lean tissue DHA accumulation are correct is of secondary importance to the biological implications of the brain composition data.

CONCLUSION

From the current data, DHA stores and synthesis alone appear inadequate to meet the rate of DHA accumulation of breast-fed term infants. Therefore, a need for dietary DHA in infant formula seems to exist if the rate of DHA accumulation in breast-fed infants is to be achieved. Formulas containing both arachidonate and DHA are commercially available in some countries and it seems likely that DHA accumulation in infants given such formulas would more closely approximate that of breast-fed infants. The present analysis focuses on DHA, but current evidence suggests that arachidonate should be concurrently supplemented in formulas containing DHA (7). Further studies involving autopsy material are also needed to determine whether provision of a formula containing at least 0.2% DHA (providing 60 mg/d DHA) permits equivalent brain DHA accumulation to that of breast-fed infants.

ACKNOWLEDGMENTS

NSERC supported this study financially. Dr. Norman Salem provided a helpful critique and Dr. Robert Jensen provided information on breast milk fatty acids.

REFERENCES

1. Hamosh, M., and Salem, N. (1998) Long Chain Polyunsaturated Fatty Acids, *Biol. Neonate 74*, 106–120.
2. Farquharson, J., Cockburn, F., Patrick, W.A., Jamieson, E.C., and Logan, R.W. (1992) Infant Cerebral Cortex Phospholipid Fatty Acid Composition and Diet, *Lancet 340*, 810–813.
3. Makrides, M., Neumann, M.A., Byard, R.W., Simmer, K., and Gibson, R.A. (1994) Fatty Acid Composition of Brain, Retina and Erythrocytes in Breast- and Formula-Fed Infants, *Am. J. Clin. Nutr. 60*, 189–194.
4. Crawford, M.A. (1993) The Role of Essential Fatty Acids in Neural Development: Implications for Perinatal Nutrition, *Am. J. Clin. Nutr. 57 (suppl.)*, 703S–710S.
5. Agostoni, C., Trojan, S., Bellu, R., Riva, E., and Giovannini, M. (1995) Neurodevelopmental Quotient of Healthy Term Infants at 4 Months and Feeding Practice: The Role of Long-Chain Polyunsaturated Fatty Acids, *Pediatr. Res. 38*, 262–266.
6. Makrides, M., Neumann, M., Simmer, K., Pater, J., and Gibson, R.A. (1995) Are Long Chain Polyunsaturated Fatty Acids Essential Nutrients in Infancy? *Lancet 345*, 1463–1468.
7. Birch, E.E., Hoffman, D.R., Uauy, R., Birch, D.G., and Prestidge, C. (1998) Visual Acuity and the Essentiality of Docosahexaenoic Acid and Arachidonic Acid in the Diet of Term Infants, *Pediatr. Res. 44*, 201–209.
8. Willatts, P., Forsyth, J.S., DiModugno, M.K., Varma, S., and Colvin, M. (1998) Influence of Long-chain Polyunsaturated Fatty Acids on Infant Cognitive Function, *Lipids 33*, 973–980.
9. Lucas, A., Stafford, M., Morley, R., Abbott, R., Stephenson, T., MacFayden, U., Elias-Jones, A., and Clements, H. (1999) Efficacy and Safety of Long Chain Polyunsaturated Fatty Acid Supplementation of Infant Formula Milk. A Randomized Trial, *Lancet 354*, 1948–1954.
10. Innis, S.M., Nelson, C.M., Lwanga, D., Rioux, F.M., and Waslen, P. (1996) Feeding Formula Without Arachidonic Acid and Docosahexaenoic Acid Has No Effect on Preferential Looking Acuity or Recognition Memory in Healthy Full-Term Infants at 9 Months of Age, *Am. J. Clin. Nutr. 64*, 40–46.
11. Auestad, N., Montalto, M.B., Hall, R.T., Fitzgerald, K.M., Wheeler, R.E., Connor, W.E., Neuringer, M., Connor, S.L., Taylor, J.A., and Hartmann, E.E. (1997) Visual Acuity, Erythrocyte Fatty Acid Composition, and Growth in Term Infants Fed Formulas with Long Chain Polyunsaturated Fatty Acids for One Year, *Pediatr. Res. 41*, 1–10.
12. Carlson, S.E., Werkman, S., and Tolley, E. (1996) Effect of Long Chain n-3 Supplementation on Visual Acuity and Growth in Preterm Infants With and Without Bronchopulmonary Dysplasia, *Am. J. Clin. Nutr. 63*, 687–697.
13. Morley, R. (1998) Nutrition and Cognitive Development, *Nutrition 14*, 752–754.
14. Innis, S.M. (1992) Plasma and Red Blood Cell Fatty Acid Values as Indexes of Essential Fatty Acids in the Developing Organs of Infants Fed with Milk or Formulas, *J. Pediatr. 120*, S78–86.
15. Cunnane, S.C., and Anderson, M.J. (1997) The Majority of Dietary Linoleate in Growing Rats Is β-Oxidized or Stored in Visceral Fat, *J. Nutr. 127*, 146–151.
16. Martinez, M. (1992) Abnormal Profiles of Polyunsaturated Fatty Acids in the Brain Liver, Kidney and Retina of Patients with Peroxisomal Disorders, *Brain Res. 583*, 171.
17. Farquharson, J., Cockburn, F., Patrick, W.A., Jamieson, E.C., and Logan, R.W. (1993) Effect of Diet on Infant Subcutaneous Tissue Triglyceride Fatty Acids, *Arch. Dis. Child. 69*, 589–593.
18. Baker, G.L. (1969) Human Adipose Tissue Composition and Age, *Am. J. Clin. Nutr. 22*, 829–835.
19. Bannister, J.L. (1996) Linoleate Balance in Obese Humans Undergoing Weight Loss, M.Sc. Thesis, University of Toronto, p. 61.
20. Morgan, C., Davies, L., Corcoran, F., Stammers, J., Colley, J., Spencer, S.A., and Hull, D. (1998) Fatty Acid Balance in Term Infants Fed Formula Milk Containing Long Chain Fatty Polyunsaturated Fatty Acids, *Acta Paediatr. 87*, 136–142.
21. Sheaff-Greiner, R.C., Zhang, Q., Goodman, K.J., Guissani, D.A., Nathanielsz, P.W., and Brenna, J.T. (1996) Linoleate, α-Linolenate and Docosahexaenoate Recycling into Saturated and Monounsaturated Fatty Acids Is a Major Pathway in Pregnant or Lactating Adults and Fetal or Infant Rhesus Monkeys, *J. Lipid Res. 137*, 243–254.
22. Menard, C.R., Goodman, K.J., Corso, T., Brenna, J.T., and Cunnane, S.C. (1998) Recycling of Carbon into Lipids Synthesized *de novo* Is a Quantitatively Important Pathway of [U-^{13}C]-α-Linolenate Utilization in the Developing Rat Brain, *J. Neurochem. 71*, 2151–2158.
23. Cunnane, S.C., Belza, K., Anderson, M.J., and Ryan, M.A. (1998) Substantial Carbon Recycling from Linoleate into Products of *de novo* Lipogenesis Occurs in Rat Liver Even Under Conditions of Extreme Linoleate Deficiency, *J. Lipid Res. 39*, 2271–2276.
24. Demmelmair, H., Baumheuer, M., Koletzko, B., Dokoupil, K., and Kratl, G. (1996) Metabolism of U-^{13}C-Labelled Linoleic Acid in Lactating Women, *J. Lipid Res. 39*, 1389–1396.
25. Montandon, C.M., Wills, C., Garza, C., Edith, E.O., and Nichols, B.L. (1986) Formula Intake of 1- and 4-month Old Infants, *J. Pediatr. Gastroenterol. Nutr. 5*, 434–438.
26. Carnielli, V.P., Wattimena, D.J.L., Luijendijk, I.H.T., Boerlage, A., Degenhart, H.J., and Sauer, P.J.J. (1996) The Very Low Birth Weight Premature Infant Is Capable of Synthesizing Arachidonic and Docosahexaenoic Acid from Linoleic and α-Linolenic Acids, *Pediatr. Res. 40*, 169–171.

27. Salem, N., Jr., Wegher, B., Mena, P., and Uauy, R. (1996) Arachidonic and Docosahexaenoic Acids Are Biosynthesized from Their 18 Carbon Precursors in Human Infants, *Proc. Natl Acad. Sci. USA 93*, 49–54.
28. Sauerwald, T.V., Hachey, D.L., and Jensen, C. (1997) Intermediates in Endogenous Synthesis of 22:6n-3 and 20:4n-6 by Term and Preterm Infants, *Pediatr. Res. 41*, 183.
29. Su, H.-M., Bernardo, L., Mirmiran, M., Ma, X.H., Corso, T.N., Nathanielsz, P.W., and Brenna, J.T. (1999) Bioequivalence of Dietary α-Linolenic and Docosahexaenoic Acids as Sources of Docosahexaenoate Accretion in Brain and Associated Organs of Neonatal Baboons, *Pediatr. Res. 45*, 1–7.
30. Brenner, R.R. (1974) The Oxidative Desaturation of Unsaturated Fatty Acids in Animals, *Mol. Cell. Biochem. 3*, 41–52.
31. Holman, R.T. (1971) Essential Fatty Acid Deficiency, *Progr. Chem. Fats Other Lipids 9*, 275–348.
32. Cunnane, S.C., Yang, J., and Chen, Z.-Y. (1993) Low Zinc Intake Increases Apparent Oxidation of Linoleic and α-Linolenic Acids in the Pregnant Rat, *Can. J. Physiol. Pharmacol. 71*, 1246–1252.
33. Clandinin, M.T., Chappell, J.E., Leong, S., Heim, T., Swyer, P.R., and Chance, G.W. (1980) Intrauterine Fatty Acid Accretion Rates in Human Brain: Implications for Fatty Acid Requirements, *Early Hum. Develop. 4*, 121–129.
34. Glezer, I. (1968) Weight, Volume and Linear Dimensions of the Brain, in *The Human Brain in Figures and Tables: A Quantitative Handbook* (Blinkov, S.M., and Glezer, I., eds.), pp. 123–136, Plenum, New York.
35. Glezer, I. (1968) Table 120, in *The Human Brain in Figures and Tables: A Quantitative Handbook* (Blinkov, S.M., and Glezer, I., eds.), p. 336, Plenum, New York.
36. Clandinin, M.T., Chappell, J.E., Heim, T., Swyer, P.R., and Chance, G.W. (1981) Fatty Acid Accretion in Fetal and Neonatal Liver: Implications for Fatty Acid Requirements, *Early Hum. Develop. 5*, 7–14.
37. Coppeletta, J.M., and Wolbach, S.B. (1933) Body Length and Organ Weights of Infants and Children, *Am. J. Pathol. 9*, 55–70.
38. Farquharson, J., Jamieson, E.C., Logan, R.W., Patrick, W.A., Howatson, A.G., and Cockburn, F. (1995) Age- and Dietary-Related Distributions of Hepatic Arachidonic and Docosahexaenoic Acid in Early Infancy, *Pediatr. Res. 38*, 361–365.
39. de Bruin, N.C., van Velthoven, K.A.M., de Ridder, M., Stijnen, T., Juttmann, R.E., Degenhart, H.J., and Visser, H.K.A. (1996) Standards for Total Body Fat and Fat-free Mass in Infants, *Arch. Dis. Child. 74*, 386–399.
40. Widdowson, E.M. (1974) Changes in Body Proportion and Composition During Growth, in *Scientific Foundations of Pediatrics* (Davies, J.A., and Dobbing, J., eds.), pp. 153–163, William Heinemann Medical Books, London.
41. Soriguer Escofet, F.J.C., Esteva de Antonio, I., Tinahones, F.J., and Pareja, A. (1996) Adipose Tissue Fatty Acids and Size and Number of Fat Cells from Birth to 9 Years of Age—a Cross-sectional Study in 96 Boys, *Metabolism 45*, 1395–1401.

[Received March 22, 1999; and in final revised form and accepted December 15, 1999]

REVIEW

Lipids and Retroviruses

Jeanine Raulin*

Université Denis Diderot (Paris 7), 75251 Paris 05, France

ABSTRACT: The role that lipids may play in enveloped viruses is reviewed. Small lipid molecules can influence retrovirus binding to cell receptors, plasma membrane fusion, and transcription. Palmitoylation following myristoylation of viral glycoproteins is required at the transmembrane level for signal transduction as well as for virion budding and maturation. Cholesterol, ether lipids, phospholipids, platelet-activating factor, phosphatidic acids, diacylglycerols, and several analogs and derivatives influence human immunodeficiency virus (HIV) activity; when conjugated with inhibitors of the viral reverse transcriptase (RT) or aspartyl protease these compounds increase drug effectiveness. On the other hand, L-carnitine, in association with the mitochondrial cardiolipins, inhibits myopathy due to continued prescription of drugs [AZT (zidovudine), ddI (didanoside), or ddC (zalcitabine)], and the redox couple of α-lipoic-dihydrolipoic acid prevents production of the reactive oxygen species that trigger apoptosis of infected cells, with sphingomyelin breakdown to ceramides. Retroviral infection induces a shift from phospholipid to neutral fat synthesis in host cells, and a long antiviral, i.e., antiprotease, treatment may lead to lipodystrophy. Multitherapy involving lipids and their analogs in association with anti-RT and antiproteases might enhance the inhibition of growth and proliferation of retroviruses.

Paper no. L8336 in *Lipids 35,* 123–130 (February 2000).

Initial studies indicated that, like other retroviruses, human immunodeficiency virus (HIV) is enclosed in an envelope that is similar in composition to host cell plasma membranes and similar to those of other enveloped viruses. Like other biological membranes, the retroviral envelope is built of a phospholipid bilayer enclosed between two leaflets of proteins and glycoproteins. Further observations showed that the HIV envelope has a lower lipid-to-protein molar ratio than host cells and, in virtually every case, the cholesterol-to-phospholipid molar ratio (C/P) of the viral envelope is higher than in plasma membranes isolated from the host cells. C/P in infected cells is low compared with uninfected cells. Moreover, purified host cell membranes and retrovirus envelopes showed differences in their phospholipid bilayers. In comparison with lipids of plasma membranes, phosphatidylcholine (PC) and phosphatidylinositol (PI) are diminished by 50 and 80%, respectively, sphingomyelin (SM) is enriched threefold, and phosphatidylserine is elevated by 40% in HIV-1 and HIV-2 (1–3).

The above results imply that retrovirions select those regions of the host cell membranes through which they emerge during budding and maturation, i.e., the phospholipid and cholesterol domains through which virions evaginate. Such domains are presumed to be passive (pre-existing) or dynamic when induced by insertion of viral peptides into the inner monolayer of the plasma membrane. Lipid composition of the virus envelope plays a critical role in the course of virus infection and fusion between infected and uninfected cells. The capacity of cholesterol to modulate virus binding to cell receptors and cell fusion may reflect the requirement for a certain degree of membrane viscosity for successful infection (4,5).

In contrast to the huge number of studies on the genome and glycoproteins, retroviral lipids have rarely been investigated. The absence of genes for lipid-metabolizing enzymes in animal retroviruses implies their inaptitude for autonomous lipid synthesis and may explain this lack of interest. However, the clear differences between viral and host cell lipids obviously result from an influence of viral glycoproteins on cellular metabolism. Retroviruses either have to select preformed cellular lipids, or initiate the formation of new lipids or both, although appropriate pathways have yet to be described.

SIGNAL TRANSDUCTION, INFECTION, AND RETROVIRUS MATURATION

CD4, a transmembrane glycoprotein present in T-helper cells, serves as a receptor for major histocompatibility complex antigens and also for the HIV-1 viral coat protein gp120. The cytoplasmic tail of CD4 is coupled to the protein-tyrosine kinase p56 (PTK), an interaction necessary for an optimal response of T-cells to antigen. This process generates intracellular signals and other interactions with various downstream molecules. One such target is the PI 3-kinase (PI 3-K), which phosphorylates the third position of the inositol ring of PI, PI 4-phosphate, and PI 4,5 bisphosphate. CD4-p56 also associates with another lipid kinase, the PI 4-kinase (PI 4-K). The binding of PI 3- and PI 4-K to the CD4-

*Address correspondence at 22 rue Poliveau, 75005 Paris, France. E-mail: craulin@aol.com

Abbreviations: 12MO, 12-methoxydodecanoic acid; AIDS, acquired immune deficiency syndrome; AZT, zidovudine; CD4, a transmembrane glycoprotein present in T-helper cells; CEM, human T-lymphocytes; CER, ceramide; C/P, cholesterol to phospholipid molar ratio; CP-51, 1-octadecanamido-2-ethyoxypropyl-*rac*-3-phosphocholine; CTK, cytotoxic T-lymphocyte; DAG, diacylglycerol; ddC, zalcitabine; ddI, didanosine; EL, ether lipid; GPI, glycan phosphatidylinositol; HIV, human immunodeficiency virus; NB-kB, transcription factor; NMT; N-myristoylCoA transferase; ODG, 1-*O*-octadecyl-*sn*-glycerol; PA, phosphatidic acid; PAF, platelet-activating factor; PC, phosphatidylcholine; PFA, phosphonoformate; PGE2, prostaglandin E2; PLC, phospholipase-C; PI, phosphatidylinositol; PI 3-K, phosphatidylinositol 3-kinase; PI 4-K, phosphatidylinositol 4-kinase; PKC, protein kinase C; PTK, protein-tyrosine kinase; ROS, reactive oxygen species; RT, reverse transcriptase; SM, sphinogmyelin; SUgp120, virus surface glycoprotein.

p56 complex contributes to activation of T-cells and has important implications to the pathogenesis of HIV-1 infection (6).

N-Palmitoylation of PTK by N-palmitoylacyl transferase (PAT), which palmitoylates proteins of the PTK family containing the N-terminal sequence "myrGlyCys," occurs on cysteine residues. This reversible modification, along with amino-terminal myristoylation of glycine, is critical for PTK association with GPI (glycan phosphatidylinositol)-anchored proteins. GPI-anchored protein subdomains are enriched in lipids, and PTK palmitoylation together with myristoylation are needed for PTK localization in the same membrane subdomains (7–10).

This cell activation cascade involves the production of lipid messengers, i.e., (i) platelet-activating factor (PAF), which plays an important role in HIV pathogenesis and can be inactivated by PAF-acetyl hydrolase, the specific hydrolase of the phospholipase A2 subfamily (11); (ii) phosphatidic acids (PA), generated from GPI hydrolyzed by a specific phospholipase D. PA production can be suppressed *in vitro* with CT-2576 [1-(11-octylamino-10-hydroxyundecyl)-3,7-dimethylxanthine] (12); and (iii) ceramides (CER): SM are hydrolyzed into CER by a specific sphingomyelinase, a process that stimulates a CER-activated protein kinase (13).

Initiation of HIV genome transcription, after integration of HIV proviruses into the host cell DNA, is determined by transcription factors interacting with long terminal repeats. For this event to occur and HIV transcription to be initiated, transcription factor (NF-κB) must be activated and translocated from the cytoplasm to the nucleus. In human monocytes and T-lymphocytes, PC hydrolysis into diacylglycerol (DAG), the potent second messenger, by a specific phospholipase C (PLC) is the major activation pathway leading to the induction of HIV enhancers (14).

Structural nucleocapsid proteins of most mammalian retroviruses including HIV-1 are specifically cleaved from a myristoylated polyprotein precursor. HIV-1 encodes the Pr*55gag*, normally processed by viral protease to the structural proteins found in mature virus particles. Pr*55gag* is myristoylated as well as p17 matrix protein, produced by proteolytic cleavage from the N-terminal end of Pr*55gag*. Myristoylation is required for virus assembly and production of infectious particles, whereas without the myristoyl moiety Pr*55gag* accumulates in infected cells and processing into mature virion structures is prevented. Myristoylation by N-myristoylCoA transferase (NMT) is an irreversible process specific to the N-terminal amino acid glycine of the proteins, part of a chain of events that drives proteins to their functional site (8–10,15–17) (see Fig. 1).

LIPID ANALOGS AND PRODRUGS ACT ON RETROVIRUS INFECTION

Cytotoxic T-lymphocyte (CTL) response. Possible mechanisms whereby HIV causes CD4+ T-cell depletion, as well as the influence of host cell factors on the disease process have been extensively debated (18), although the role of lipids is rarely documented. However, the ability of SUgp120 (virus surface glycoprotein) to transduce an activation signal directly in monocytes, resulting in the production of polyunsaturated acid metabolites, may affect the immune system. Prostaglandin E2 (PGE2), an arachidonic acid metabolite, is a suppressor of immune function, as demonstrated *in vitro* by its ability to inhibit the lymphokine production and the natural killer CTL proliferation (19). Conjugated linoleic acid-supplemented mice have higher splenocyte interleukin-2 production than those fed a control diet (20).

Subunits of purified SUgp120 peptides are inducers of antibody response but are less immunogenic unless associated with lipids. Generation of a long CTL response in mice is obtained by injecting lipopeptides of different amino acid sequences in association with 2-amino-hexadecanoic acid. CTL response of long duration can also be obtained from SUgp120 peptides injected in association with DAG derivatives, suggesting that DAG derivatives enhance the production of peptide-specific antibodies (21–23).

Stimulation of anti-HIV activity.

(i) Inhibition of the viral reverse transcriptase (RT). Zidovudine (AZT), didanosine (ddI), zalcitabine (ddC), and several other nucleosides are reference RT inhibition therapies. Certain lipid molecules strengthen their activity.

Ether lipids (EL) inhibitors of CD4 receptor phosphorylation. EL are membrane-targeted therapeutic agents that inhibit the production of infectious viruses. The lipophilic nature of EL-AZT conjugates permits large amounts of anti-RT to penetrate cells and be active, while the EL portion hinders phosphorylation of CD4 receptors by inhibiting protein kinase C (PKC). This results from a fall in DAG, the PKC activators, by inhibition of the PI-PLC. The replacement of long alkyl chains with aromatic groups in oxyalkyl ether phospholipid-AZT conjugates leads to even more potent compounds, less toxic than AZT for human T-lymphocytes (CEM) in culture. INK 14, a lipid-AZT conjugate in which AZT replaces choline in INK-3, a PC with two medium-chain fatty acids (12 and 8 carbon atoms), gives the highest selective index of activity against HIV-1 replication in CEM cells and also in a clinical isolate of peripheral blood leukocytes (24–26).

Phospholipid analogs as inhibitors of syncytium formation. CP-51 (1-octadecanamido-2-ethoxypropyl-*rac*-3-phosphocholine), one of the membrane interactive phospholipids, inhibits SUgp120 binding to CD4 receptors, bringing about an alteration of surface membranes. CP-92, the CP-51 covalent conjugate to AZT (1-octadecanamido-2-ethoxypropyl-*rac*-3-phospho-3′-azido-3′-deoxythymidine), combines the effects of AZT and the phospholipid analog and has greater potency than the free drug on inhibition of syncytium formation in infected cells (27).

Lipids and vitamins that increase anti-RT activity of the Cordycepin trimer. The 3′-deoxyadenosine (cordycepin) is extracted from *Cordyceps militaris,* and its d3 trimer core (A2′p5′A2′p5′A) provokes RT inhibition. The 2′-O- and 5′-O-cholesterol conjugates of (2′-5′)d3(A-A-A) display a highly increased (× 1000) anti-HIV-1 activity. Covalent conjugation of vitamin A, D_2, or E and palmitoyl or hexadecyl lipids to the 2′- or 5′-OH group of the trimer core supplies

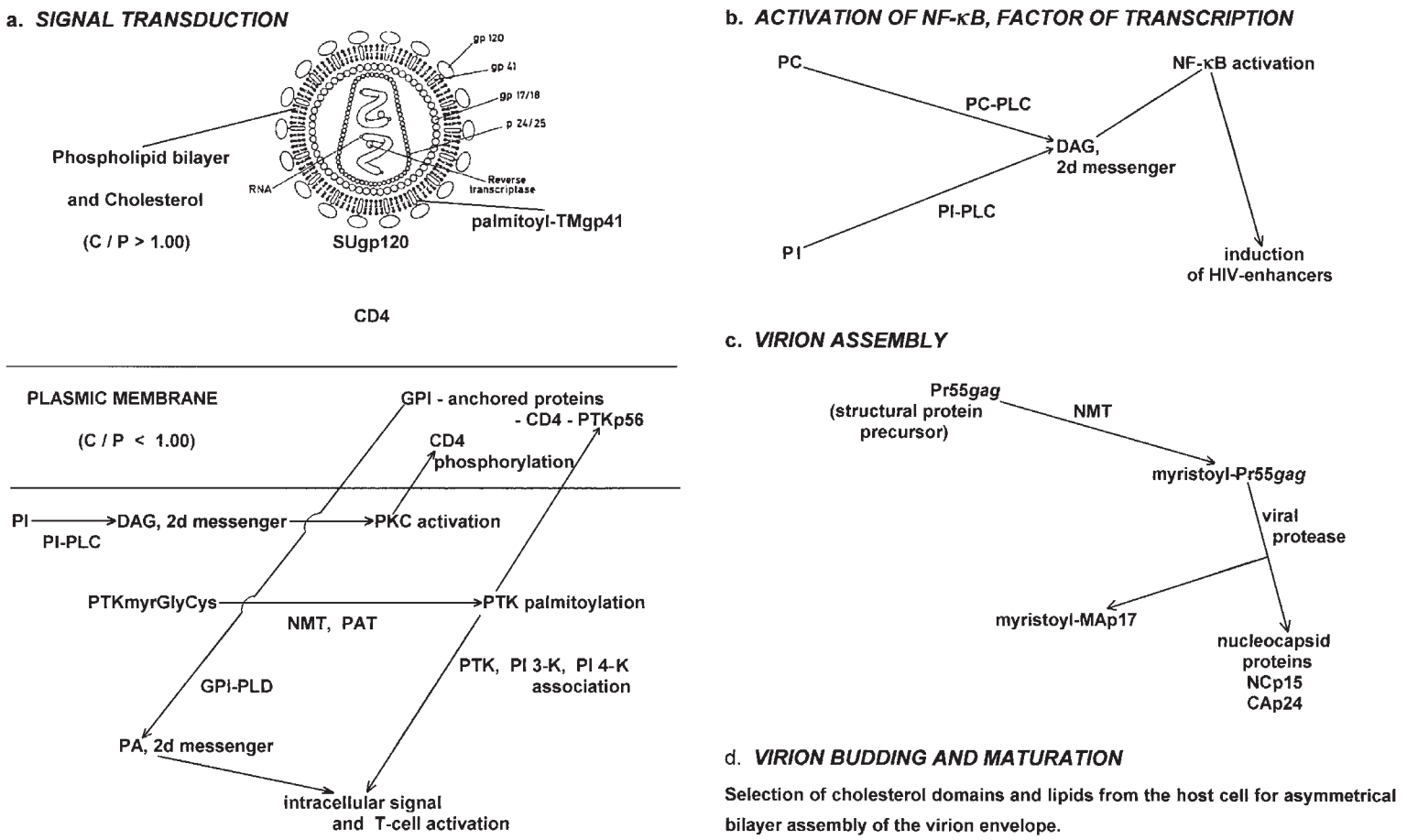

FIG. 1. Retroviruses and host cell lipid metabolism. The schematic representation of an enveloped virus particle and the accompanying legend were published by Hoestra, D., and de Lima, M.C.P. (1992) in *Membrane Interactions of HIV* (Aloia, R.C., and Curtain, C.C., eds.). Reprinted by permission of Wiley-Liss, Inc., a subsidiary or John Wiley & Sons, Inc. The structure of an HIV particle is shown in cross section. In general, the viral envelope consists of a lipid bilayer, commonly containing very few virus-specific membrane glycoproteins. These proteins can be distinguished by the electron microscope as "spikes." For HIV, this spike consists of protein gp160, which is composed of two subunits, gp120 (the knob of the spike) and gp41, the transmembrane part that anchors the protein to the membrane. Abbreviations: (a) C/P, cholesterol/phospholipid molar ratio; CD4, transmembrane glycoprotein, present in T-helper cells; DAG, diacylglycerol, second messenger; GPI, glycan phosphatidylinositol; PA, phosphatidic acid, second messenger; PC, phosphatidylcholine; PI, phosphatidylinositol; SUgp120, virus surface glycoprotein. (b) GPI-PLD, glycosyl phosphatidylinositol-phospholipase D—production of PA from GPI; HIV, human immunodeficiency virus; NF-κB, transcription factor: after activation and translocation from cytoplasm to nucleus, interacts with long terminal repeats and determines initiation of provirus transcription into the host cell DNA; NMT, N-myristoylCoA transferase: irreversible process specific to N-terminal amino-acid glycine of proteins, critical for PTK association with GPI-anchored proteins; PAT, N-palmitoylacyl transferase: reversible modification along with amino-terminal of glycine; PC-PLC, phosphatidylcholine phospholipase C: production of DAG from PC; PI 3-K, phosphatidylinositol 3-kinase; PI 4-K, phosphatidylinositol 4-kinase; PI-PLC, phosphatidylinositol phospholipase C; PKC, protein kinase C—phosphorylation of CD4 receptors; PTKp56, protein tyrosine kinase C; PTKmyr GlyCys, palmitoylation of PTKp56 on N-terminal cysteine residues after myristoylation on N-terminal glycine residues.

new series of inhibitors, active both on syncytium virus-induced formation and HIV-1 replication (28).

(ii) Inhibition of the viral polymerase. Phosphonoformate (PFA), a viral polymerase inhibitor, displays much greater anti-HIV-1 activity when coupled to *sn*-3-hydroxyl of the 1-*O*-octadecyl-*sn*-glycerol (ODG). Twenty-four hours after the addition of ODG-PFA, drug uptake by cells in culture is greater than after the addition of free PFA, while the antiviral effect is much increased. The marked increase in antiviral activity (43- to 93-fold) was observed on a large panel of viruses and retroviruses. Further studies are required to establish whether the lipid prodrug can significantly reduce PFA toxicity (29–31).

(iii) Inhibition of the viral aspartyl protease. Aspartyl protease of HIV is an important target for chemotherapeutic intervention, given its key role in cleaving the surface polyprotein during retrovirion assembly and budding. Antiprotease drugs are efficiently used in multitherapy.

Phospholipids—pentapeptide antiprotease prodrugs. C-terminal or N-terminal derivatization of the antiprotease Nr. *7194* pentapeptide, with a phosphatidylethanolamine to make the Nr. *7196* prodrug, does not interfere with pentapeptide activity *in vitro* (32). Cellular phospholipases A and/or C and phosphodiesterases catalyze the breakdown of the lipid portion, freeing the peptide to interact with the viral protease. Its slow removal from circulation suggests that phospholipid derivatives provide high levels of available material and may provide advantageous distribution *in vivo* (32).

Substituted myristic acid and 12-methoxydodecanoic acid (12MO)-AZT. Heteroatom analogs of myristic acid, containing oxygen or sulfur substituted for an alkyl methylene group,

have been reported to exhibit potent activity against HIV replication in infected cells. The compound 12MO is easily incorporated into host cell and retroviral proteins, bringing about inhibition of HIV polyprotein proteolysis. The potent anti-HIV activity of such myristic acid analogs can last for several days. L-AC2, a PC containing two 12MO, is synergistic with AZT, owing to the combined effects on the proteolytic processing and RT activity. On the other hand, the half-life of D-AC2 is higher than the half-life of its L-AC2 isomer, while yielding the same antiviral activity. Moreover, since phospholipase A2 cannot be active on D-isomers, D-AC2 does not undergo rapid degradation *in vivo*, and oral prescription of such conjugates might be considered (33–35) (Table 1).

CARDIOLIPIN–CARNITINE ASSOCIATION PRESERVES MITOCHONDRIA FROM MYOPATHY DUE TO LONG-TERM ANTIVIRAL THERAPY

Patients with acquired immune deficiency syndrome (AIDS) under long-term antiviral therapy incur the risk of mitochondrial myopathy. Mitochondria are structurally abnormal and functionally impaired, uncoupled and with lesser mtDNA and cytochromes. Human muscle cells exposed *in vitro* to AZT, ddI, or ddC show decreased proliferation and differentiation, lipid droplet and lysosome accumulation, increased lactate production, and decreased cytochrome c oxidase and succinate dehydrogenase. Added L-carnitine interacts with cardiolipins and preserves mitochondria (36–40). Besides the improvement of long-chain fatty acylCoA transport, protein synthesis is reinduced in cells, while lipid droplets disappear. Moreover, the number of lysosomes is reduced and the muscle cell proliferation and functions are restored *in vitro* (36–40).

TRANSPORT OF INHIBITORS

Liposomes are taken up by macrophages, the reservoirs for dissemination of HIV in the immune system, and they function as a carrier matrix in which HIV inhibitors are targeted to infected cells. Therefore, encapsulation in liposomes can improve anti-HIV drug delivery within cells that play a central role in HIV pathogenesis. Liposomal ddC, containing dipalmitoyl-PC/dicetylphosphate/cholesterol in a molar ratio of 4:1:5, is rapidly taken up by macrophages, whereas free ddC accumulates more slowly. HIV-1-induced cell fusion is critically dependent on liposome composition (41). The highest rate and extent are obtained with pure cardiolipin liposomes; pretreatment with cardiolipin liposomes much reduces HIV-1 infectivity. Liposomes appear to be an effective means of delivering an HIV inhibitor such as L-689,502 (42), since HIV protease acts at the membrane level during the last stages of the virion formation (43).

ALTERATION OF CELLULAR LIPIDS DUE TO THE RETROVIRUS INFECTION

Enhanced synthesis of neutral lipids is the primary effect of HIV infection and a consequence of diminished cell viability. Changes in cellular lipid composition have been characterized by a shift from phospholipid synthesis to neutral lipid synthesis. Prior to virus progeny production, during the eclipse period, host cell lipid synthesis is unaltered but is significantly changed when new viral proteins are detectable. In stages II and III of infection, all the metabolic routes are abnormal, and the metabolic indicators can be correlated with changes in the production of cytokines and steroid hormones. The resulting hypertriglyceridemia is one of the causes of cachexia and dementia, also facilitated by changes in cholesterol metabolism (44–46).

Phospholipids are especially susceptible to peroxidation in HIV-infected human T-cells. PGE2 and leukotriene B4 are products of eicosanoid metabolism, either through the cyclooxygenase or lipoxygenase pathway. Cyclooxygenase products of arachidonic acid are produced in excess by HIV-infected cells, and increased amounts of PGE2 are released by monocytes from HIV-1 infected patients, which lends support to the relevance of this lipid mediator in HIV infection (19,47–49). Moreover, there is a correlation between retroviral gene expression and the decreased level of antioxidants

TABLE 1
Alteration by Lipid Compounds of Cellular and Retroviral Enzyme Pathways. Stimulation of Drug Effectiveness[a]

Lipid compounds	Target	Impact	Inhibition of cellular enzyme activity
Ether lipids with alkyl or aryl group	PI-PLC	DAG generation	PKC activation, CD4 phosphorylation
Substituted myristic acid	GPI-PLD	PA generation	Signaling
	NMT, and PAT	PTK palmitoylation	CD4-PTK-GPI anchored protein complex
	NMT	Pr55*gag* myristoylation	Cleavage and maturation of structural proteins
			Enhancement of antiviral enzyme inhibition
Phospholipid analogs, ether lipids, cholesterol, fatty acyl-, vitamine A,E,D			Anti-RT nucleosides (AZT, ddC, ddI, Cordycepin)
sn-3-OH of 1-*O*-octadecyl-*sn*-glycerol			Anti-polymerase phosphonoformate
Phosphatidylethanolamine			Antiprotease
12MO (substituted myristic acid) incorporation into phosphatidylcholine			Antiprotease and synergism with anti-RT (AZT)

[a]Abbreviations: PI-PLC, phosphatidylinositol-phospholipase C; DAG, diacylglycerol; PKC, protein kinase C; CD4, a transmembrane glycoprotein present in T-helper cells; GPI-PLD, glycan phosphatidylinositol-phospholipase D; PA, phosphatidic acid; NMT, N-myristoylCoA transferase; PAT, N-palmitoylacyl transferase; PTK, protein-tyrosine kinase; RT, reverse transcriptase; AZT, zidovudine; ddC, zalcitabine; ddI,didanosine; Cordycepin, 3′-deoxyadenosine; 12MO, 12-methoxydodecanoic acid.

thioredoxin, superoxide dismutase, and catalase. In response to extracellular stimuli, reactive oxygen species (ROS) accumulate in cells. T-cells localized in, or passing through infected lymphoid tissues, are exposed to ROS released by activated phagocytic and inflammatory cells. The formation of lipid peroxides may trigger "activation-induced death" of HIV-infected, antioxidant-deficient T-cells (50,51). One of the primary signals for both the inflammatory response and T-cell susceptibility to apoptosis is the rapid breakdown of SM to CER (52–54).

On the other hand, one of the unsaturated fatty acid derivatives, the redox couple α-lipoic-dihydrolipoic acids (55,56), prevents activation of the NF-κB transcription factor and HIV replication, which are regulated by oxidative stress, in infected cells (57). In a pilot study conducted on HIV-positive men receiving oral doses of α-lipoate, plasmatic factors were improved and the number of T-helper cells was increased (57).

DISCUSSION

Control of genetic expression by exogenous lipids has been described for a long time in animals (58,59). Although nothing identical has been described for retroviruses, lipid compounds, analogs, and derivatives affect the retrovirus life cycle and infectivity. Given their structural and dynamic roles, lipids exert control on syncytium formation between infected and uninfected cells (27). Lipid control is observed at various levels: cytokine production by host cells (20,60), inhibition of viral RT (24–26), polymerase (29–31), and protease (32). Interestingly, the HIV-RT inhibitory effect is obtained from the diether sulfated glycolipid KN-208, the major component of the archaebacterium cell membrane (61).

The cell activation cascade during infection involves lipid messengers (11–13) including PAF, PA, CER, DAG, and small lipid derivatives, such as the redox couple α-lipoic-dihydrolipoic acid (55,56) that prevents oxidative stress due to virus infection and then, inhibits activation of NF-κB transcription factor (57). On the other hand, subunits of SUgp120 peptides, inducers of antibody response, bring about longer CTL response in mice when injected along with lipopeptides prepared from DAG derivatives (21–23).

In their huge role in the tissues, including brain (62), lipid kinases and transferases actually participate in retrovirus infectivity (6–10). Palmitoylation of amino-terminal cysteine residues by PAT, together with myristoylation of amino-terminal glycine residues by NMT, enables the association of PTK with GPI-anchored proteins. Viral Pr55*gag* is myristoylated, as is p17 matrix protein that has been proteolytically cleaved from N-terminal end of Pr55*gag*. Myristoylation is required for virion assembly and production of infectious particles. Without the myristoyl moiety, processing into mature virion structures is prevented. Given the importance of acylating steps in retrovirus replication, the development of specific inhibitors of protein acylation appears desirable. Fortunately, myristic acid analogs, well incorporated both in the virion and cell membranes, have already been prepared (33–35).

Apart from the improved transport when an antiviral drug is enclosed in liposomes, and especially in cardiolipin liposomes conjugated with anti-RT or antiprotease (41–43), a number of lipid molecules enhance antiviral effectiveness. This was shown with phospholipids and analogs (27,32), ether lipids (24–26), oxysterols (63), fatty acyl-CoA, vitamins (28), lipid prodrugs of phosphonoacids (29–31), and substituted or heteroatom analogs of myristic acid (33–35). However, a long-term antiviral treatment can induce mitochondrial myopathy. *In vitro*, the addition of L-carnitine to cultures of human myotubes reduces, and even prevents this side effect. The cardiolipin–carnitine association preserves mitochondrial functions and acts in protein synthesis and myotube proliferation (36–40).

As enhanced retrovirus replication is associated with an increased level in CER, therapeutic strategies aimed at down-modulating intracellular CER may slow the progression of HIV infection (64). On the other hand, a glycolipid (GalAAG) related but not identical to galactosylCER has been described at the surface membrane of human spermatozoa, despite plasmatic suppression of HIV-1 RNA. This glycolipid, able to bind gp120, could function as an alternative receptor for HIV and might be an additional target for multitherapy (65–67).

There is a need for new inhibitors of retrovirus infectivity with less toxicity and without such side effects as lipodystrophy, as recently described (68–71). Therefore, further studies should help to elucidate mechanisms of the lipid and cholesterol incorporation into the retroviral envelopes and their control.

ACKNOWLEDGMENTS

The author wishes to express warm thanks to Dr. Joyce L. Beare-Rogers, Department of Health and Welfare, Ottawa, Ontario, Canada, for her comments and for the scrupulous reviewing of the manuscript.

APPENDIX (SEE ALSO REF. 77)

Retroviruses, a single-stranded RNA virus subfamily: Lentiviruses (including HIV), oncoviruses, and spumaviruses.

Organization: 62% proteins (p) and glycoproteins (gp), 3% nucleic acids (dimer RNA), and 35% lipids (mostly phospholipid bilayer and cholesterol in the retrovirus envelope).

Protein and glycoprotein nomenclature: SUgp120 (surface), TMgp41 (transmembrane), MAp17 (matrix), NCp15 (nucleocapsid), CAp24 (capsid), and enzymes: RTp66 (reverse transcriptase), PRp12 (protease), INp32 (integrase).

RT activities: Reverse transcriptase, RNA and DNA matrix recognition, tRNA Lys3 primer recognition, DNA- and RNA-dependent DNA polymerase, endo- and exo-RNaseH, and double-helix denaturation.

Virion budding and maturation: After SUgp120 binding to T-lymphocyte CD4 receptors and fusion of membranes, the viral core is delivered into cell cytoplasm. Retroviral DNA is synthesized (RT and polymerase activity) using viral RNA as a matrix, and hydrolyzed afterward (RNase activity). Provirion (retroviral DNA) is then integrated into a host cell's chromo-

some (IN activity) and retranscripted to genomic RNA and mRNA, thus generating new viral proteins. Virion leaves the host cell by budding, after maturation of various structural proteins (protease), assemblage at the plasma membrane, and wrapped in its envelope (see also Ref. 77).

REFERENCES

1. Barré-Sinoussi, F., Chermann, J.C., Rey, F., Nugeyre, M.T., Chamaret, S., Gruest, J., Dauguet,C., Axler-Blin, C., Vésinet-Brun, F., Rouzioux, C., Rozenbaum, W., and Montagnier, L. (1983) Isolation of a T-lymphotropic Retrovirus from a Patient at Risk for Acquired Immune Deficiency Syndrome (AIDS), *Science 220*, 868–871.
2. Darlix, J.-L. (1991) Eléments de Structure et de Variabilité du Rétrovirus Humain HIV-1, *Bull. Inst. Pasteur 89*, 211–242.
3. Aloia, R.C., Curtan, C.C., and Jensen, F.C. (1992) Membrane Cholesterol and Human Immunodeficiency Virus Infectivity, in *Membrane Interactions of HIV* (Aloia, R.C., and Curtain, C.C., eds.), pp. 283–303, Wiley-Liss Inc., New York.
4. Patel, R.A., and Crews, F. (1992) Membrane Lipids and Dynamics in the Enveloped Virus Life Cycle, in *Membrane Interactions of HIV* (Aloia, R.C., and Curtain, C.C., eds.), pp. 237–253, Wiley-Liss Inc., New York.
5. Aloia, R.C., Tian, H., and Jensen, F.C. (1993) Lipid Composition and Fluidity of the Human Immunodeficiency Virus Envelope and Host Cell Plasma Membranes, *Proc. Natl Acad. Sci. USA 90,* 5181–5185.
6. Prasad, K.V.S., Kapeller, R., Janssen, O., Repke, H., Duke-Cohan, J.S., Cantley, L.C., and Rudd, C.E. (1993) Phosphatidylinositol (PI) 3-Kinase and PI 4-Kinase Binding to the CD4-p56(lck) Complex: the p56(lck) SH3 Domain Binds to PI 3-Kinase but not PI 4-Kinase, *Mol. Cell. Biol. 13,* 7708–7717.
7. Shenoy-Scaria, A.M., Timson-Gauen, L.K., Kwong, J., Shaw, A.S., and Lublin, D.M. (1993) Palmitoylation of an Amino-Terminal Motif of Protein Tyrosine Kinase p56lck and p59fyn Mediates Interaction with Glycosyl-Phosphatidylinositol-anchored Proteins. *Mol. Cell. Biol. 13,* 6385–6392.
8. Johnson, D.R., Bhatnagar, R.S., Knoll, L.J., and Gordon, J.I. (1994) Genetic and Biochemical Studies of Protein N-Myristoylation, *Annu. Rev. Biochem. 63*, 869–914.
9. Berthiaume, L., and Resh, M.D. (1995) Biochemical Characterization of a Palmitoyl Acyltransferase Activity that Palmitoylates Myristoylated Proteins, *J. Biol. Chem. 270*, 22399–22405.
10. Boutin, J.A. (1997) Myristoylation. Review, *Cell. Signal. 9,* 15–35.
11. Ho, Y.S., Swenson, L., Derewenda, U., Serre, L., Wei, Y., Dauter, Z., Hattori, M., Adachi, T., Aoki, J., Arai, H., Inoue, K., and Derewenda, Z.S. (1997) Brain Acetylhydrolase that Inactivates Platelet-Activating Factor Is a G-Protein-like Trimer, *Nature 385*, 89–93.
12. Leung, D.W., Peterson, P.K., Weeks, R., Gekker, .G., Chao, C.C., Kaplan, A.H., Balantac, N., Tompkins, C., Underiner, G.E., Bursten, S., Harris, W., Bianco, J.A., and Singer, J. (1995) CT-2576, an Inhibitor of Phospholipid Signaling, Suppresses Constitutive and Induced Expression of Human Immunodeficiency Virus, *Proc. Natl. Acad. Sci. USA 92,* 4813–4817.
13. Yao, B., Zhang, Y., Delikat, S., Mathias, S., Basu, S., and Kolesnick, R. (1995) Phosphorylation of Raf by Ceramide-Activated Protein Kinase, *Nature 378*, 307–310.
14. Arenzana-Seisdedos, F., Fernandez, B., Dominguez, I., Jacqué, J.-M., Thomas, D., Diaz-Meco, M.-T., Moscat, J., and Virelizier, J.-L. (1993) Phosphatidylcholine Hydrolysis Activates NF-κB and Increases Human Immunodeficiency Virus Replication in Human Monocytes and T Lymphocytes, *J. Virol. 67,* 6596–6604.
15. Göttlinger, H.G., Sodroski, J.G., and Haseltine, W.A. (1989) Role of Capsid Precursor Processing and Myristoylation in Morphogenesis and Infectivity in Human Immunodeficiency Virus Type 1, *Proc. Natl. Acad. Sci. USA 86*, 5781–5785.
16. Bryant, M.L., and Ratner, L. (1990) Myristoylation-Dependent Replication and Assembly of Human Immunodeficiency Virus 1, *Proc. Natl. Acad. Sci. USA 87*, 523–527.
17. Peitzsch, R.M., and McLaughlin, S. (1993) Binding of Acylated Peptides and Fatty Acids to Phospholipid Vesicles: Pertinence to Myristoylated Proteins, *Biochemistry 32*, 10436–10443.
18. Pantaleo, G. (1997) Immunology of HIV Infection, *Res. Immunol.* (*Imm. System Mol. Cell. Comp.) 148,* 417–419.
19. Wahl, L.M., Corcoran, M.L., Pyle, S.W., Arthur, L.O., Harel-Bellan, A., and Farrar, W.L. (1989) Human Immunodeficiency Virus Glycoprotein (gp120) Induction of Monocyte Arachidonic Acid Metabolites and Interleukin 1, *Proc. Natl. Acad. Sci. USA 86*, 621–625.
20. Hayek, M.G., Han, S.N., Wu, D.Y., Watkins, B.A., Meydani, M., Dorsey, J.L., Smith, D.E. and Meydani, S.N. (1999) Dietary Conjugated Linoleic Acid Influences the Immune Response of Young and Old C57BL/6NCrlBR Mice, *J. Nutr. 129*, 32–38.
21. Martinon, F., Cras-Masse, H., Boutillon, C., Chirat, F., Deprez, B., Guillet, J.-G., Gomard, E., Tartar, A., and Lévy, J.-P. (1992) Immunization of Mice with Lipopeptides Bypasses the Prerequisite for Adjuvant. Immune Response of BALB/c Mice to HIV Envelope Glycoprotein, *J. Immunol. 149,* 3416–3422.
22. Sauzet, J.-P., Déprez, B., Martinon, F., Guillet, J.-G., Gras-Masse, H., and Gomard, E. (1995) Long-Lasting Anti-Viral Cytotoxic T Lymphocytes Induced *in vivo* with Chimeric-Multirestricted Lipopeptides, *Vaccine 13,* 1339–1345.
23. Shimizu, T., Iwamoto, Y., Yanagihara, Y., Ryoyama, K., Maruyama, Y., and Achiwa, K. (1996) Antibody-Producing Effects in Mice by Synthetic Immunoreactive Lipopeptides with the Conjugated Amino Acid Sequence of gp120 in Human Immunodeficiency Virus, *Biol. Pharm. Bull. 19,* 1271–1274.
24. Kucera, L.S., Piantadosi, C., and Modest, E.J. (1992) Novel Membrane Interactive Ether Lipids with Anti-Human Immunodeficiency Virus Activity, in *Membrane Interactions of HIV* (Aloia, R.C., and Curtain, C.C., eds.), pp. 329–350, Wiley-Liss, Inc., New York.
25. Calogeropoulou, T., Koufaki, M., Tsotinis, A., Balzarini, J., De Clercq, E., and Makriyannis, A. (1995) Synthesis and Anti-HIV Evaluation of Alkyl and Alkoxyethyl Phosphodiester AZT Derivatives, *Antivir. Chem. Chemother. 6,* 43–49.
26. Kucera, L.S., Iyer, N., Morrinatschke, S.L., Chen, S.Y., Gumus, F., Ishaq, K., and Herrmann, D.B.J. (1998) *In vitro* Evaluation and Characterization of Newly Designed Alkylamidophospholipid Analogues as Anti-Human Immunodeficiency Virus Type 1 Agents, *Antivir. Chem. Chemother. 9,* 157–165.
27. Krugner-Higby, L., Goff, D., Edwards, T., Iyer, N., Neufeld, J., Kute, T., Morris-Natschke, S., Ishaq, K., Piantadosi, C., and Kucera, L.S. (1995) Membrane-Interactive Phospholipids Inhibit HIV Type 1-Induced Cell Fusion and Surface gp160/gp120 Binding to Monoclonal Antibody, *AIDS Res. Hum. Retrovir. 11,* 705–712.
28. Wasner, M., Suhadolnik, R.J., Horvath, S.E., Adelson, M.E., Kon, N., Guan, M.-X., Henderson, E.E., and Pfleiderer, W. (1996) Synthesis and Characterization of Cordycepin-Trimer-vitamin and Lipid Conjugates Potential Inhibitors of HIV-1 Replication, *Helv. Chim. Acta 79*, 619–633.
29. Hostetler, K.Y., Kini, G.D., Beadle, J.R., Aldern, K.A., Gardner, M.F., Border, R., Kumar, R., Barshak, L., Sridhar, C.N., Wheeler, C.J., and Richman, D.D. (1996) Lipid Prodrugs of Phosphono-Acids: Greatly Enhanced Antiviral Activity of 1-O-Octadecyl-*sn*-Glycero-3-Phosphonoformate in HIV-1, HSV-1 and HCMV-Infected Cells, *in vitro*, *Antivir. Res. 31*, 59–67.
30. Patent Evaluation Anti-infectives (1996) Phosphonic Acid Prodrugs with Improved Antiviral Activity, University of California: WO 9615132, *Exp. Opin. Ther. Patents 6,* 1331–1333.

31. Kini, G.D., Hostetler, K.Y., Beadle, J.R., and Aldern, K.A. (1997) Synthesis and Antiviral Activity of 1-*O*-Octadecyl-2-*O*-Alkyl-*sn*-Glycero-3-Foscarnet Conjugates in Human Cytomegalovirus-Infected Cells, *Antivir. Res. 36*, 115–124.
32. Hostetler, K.Y., Richman, D.D., Forssen, E.A., Selk, L., Basava, R., Gardner, M.F., Parker, S., and Basava, C. (1994) Phospholipid Prodrug Inhibitors of the HIV Protease. Antiviral Activity and Pharmacokinetics in Rats, *Biochem. Pharm. 48,* 1399–1404.
33. Bryant, M.L., Heuckeroth, R.O., Kimata, J.T., Ratner, L., and Gordon, J.I. (1989) Replication of Human Immunodeficiency Virus1 and Moloney Murine Leukemia Virus Is Inhibited by Different Heteroatom-Containing Analogs of Myristic Acid, *Proc. Natl Acad. Sci. USA 86*, 8655–8659.
34. Pidgeon, C., Markovich, R.J., Liu, M.D., Holzer, T.J., Novak, R.M., and Keyer, K.A. (1993) Antiviral Phospholipids. Anti-HIV Drugs Conjugated to the Glycerobackbone of Phospholipids, *J. Biol. Chem. 268,* 7773–7778.
35. Parang, K., Wiebe, L.I., Knaus, E.E., Huang, J.S., Tyrell, D.L., and Csizmadia, F. (1997) *In vitro* Antiviral Activities of Myristic Acid Analogs Against Human Immunodeficiency and Hepatitis B Viruses, *Antivir. Res. 34,* 75–90.
36. Battelli, D., Bellei, M., Arrigoni-Martelli, E., Muscatello, U., and Bobyleva, V. (1992) Interaction of Carnitine with Mitochondrial Cardiolipin, *Biochim. Biophys. Acta 1117*, 33–36.
37. Dalakas, M.C., Leon-Monzon, M.E., Bernardini, I., Gahl, W.A., and Jay, C.A. (1994) Zidovudine-Induced Mitochondrial Myopathy Is Associated with Muscle Carnitine Deficiency and Lipid Storage, *Ann. Neurol. 35,* 482–486.
38. Semino-Mora, M.C., Leon-Monzon, M.E., and Dalakas, M.C. (1994) Effect of L-Carnitine on the Zidovudine-Induced Destruction of Human Myotubes. Part I: L-Carnitine Prevents the Myotoxicity of AZT *in Vitro, Lab. Invest. 71(1),* 102–112.
39. Semino-Mora, M.C., Leon-Monzon, M.E., and Dalakas M.C. (1994) The Effect of L-Carnitine on the AZT-induced Destruction of Human Myotubes. Part II: Treatment with L-Carnitine Improves the AZT-Induced Changes and Prevents Further Destruction, *Lab. Invest. 71,* 773–781.
40. Benbrik, E., Chariot, P., Bonavaud, S., Ammi-Saïd, M., Frisdal, E., Rey, C., Gherardi, R., and Barlovatz-Meimon, G. (1997) Cellular and Mitochondrial Toxicity of Zidovudine (AZT), Didanosine (ddI) and Zalcitabine (ddC) on Cultured Human Muscle Cells, *J. Neurol. Sci. 149*, 19–25.
41. Düzgünes, N., Larsen, C.E., Stamatatos, L., and Konopka, K. (1992) Fusion of Immunodeficiency Viruses with Liposomes and Cells: Inhibition of Human Immunodeficiency Virus Type 1 Infectivity by Cardiolipin Liposomes, in *Membrane Interactions of HIV* (Aloia, R.C., and Curtain, C.C., eds.), pp. 317–327, Wiley-Liss Inc., New York.
42. Flasher, D., Konopka, K., Chamow, S.M., Dazin, P., Ashkenazi, A., Pretzer, E., and Düzgünes, N. (1994) Liposome Targeting to Human Immunodeficiency Virus Type 1-Infected Cells *via* Recombinant Soluble CD4 and CD4 Immunoadhesin (CD4-IgG), *Biochim. Biophys. Acta 1194,* 185–196.
43. Makabi-Panzu, B., Lessard, C., Beauchamp, D., Désormeaux, A., Poulin, L., Tremblay, M., and Bergeron, M.G. (1995) Uptake and Binding of Liposomal 2′,3′-Dideoxycytidine by RAW 264.7 Cells: a Three-Step Process, *J. Acq. Imm. Def. Syndr. Hum. Retrovir. 8*, 227–235.
44. Nunez, E.A., and Christeff, N. (1994) Steroid Hormone, Cytokine, Lipid and Metabolic Disturbances in HIV Infection, *Baillière's Clin. Endocr. Metab. 8,* 803–824.
45. Keréveur, A., Cambillau, M., Kazatchkine, M., and Moatti, N. (1996) Anomalies Lipoprotéiniques au Cours de l'Infection par le VIH, *Ann. Med. Int. 147,* 333–343.
46. Vicenzi, E., Biswas, P., Mengozzi, M., and Poli, G. (1997) Role of Pro-inflammatory Cytokines and Beta-Chemokines in Controlling HIV Replication, *J. Leukocyte Biol. 62,* 34–40.
47. Skot, J., Kabrit, P., Hansen, J.-E.S., Nielsen, J.O., Nielsen, L., and Lundgren, J.D. (1994) Tumour Necrosis Factor and Eicosanoid Production from Monocytes Exposed to HIV *in vitro, APMIS 102*, 603–611.
48. Genis, P., Jett, M., Bernton, E.W., Boyle, T., Gelbard, H.A., Dzenko, K., Keane, R.W., Resnick, L., Mizrachi, Y., Volsky, D.J., Epstein, L.G., and Gendelman, H.E. (1992) Cytokines and Arachidonic Metabolites Produced During Human Immunodeficiency Virus (HIV)-Infected Macrophage-Astroglia Interactions: Implication for the Neuropathogenesis of HIV Disease, *J. Exp. Med. 176*, 1703–1718.
49. Foley, P., Kazazi, F., Biti, R., Sorrell, T.C., and Cunningham, A.L. (1992) HIV Infection of Monocytes Inhibits the T-Lymphocyte Proliferative Response to Recall Antigens, *via* Production of Eicosanoids, *Immunology 75*, 391–397.
50. Sandstrom, P.A., Tebbey, P.W., Van Cleave, S., and Buttke, T.M. (1994) Lipid Hydroperoxides Induce Apoptosis in T Cells Displaying a HIV-Associated Glutathione Peroxidase Deficiency, *J. Biol. Chem. 269,* 798–801.
51. Piedimonti, G., Guetard, D., Magnani, M., Corsi, D., Picerno, I., Spataro, P., Kramer, L., Montroni, M., Silvestri, G., Roca, J.F.T., and Montagnier, L. (1997) Oxidative Protein Damage and Degradation in Lymphocytes from Patients Infected with Human Immunodeficiency Virus, *J. Infect. Dis. 176,* 655–664.
52. Skowronski, E.W., Kolesnick, R.N., and Green, D.R. (1996) Fas-Mediated Apoptosis and Sphingomyelinase Signal Transduction: The Role of Ceramide as a Second Messenger for Apoptosis, *Death Differentiation 3*, 171–176.
53. Moretti, S., Alesse, E., Di Marzio, L., Zazzeroni, F., Ruggeri, B., Marcellini, S., Famularo, G., Steinberg, S.M., Boschini, A., Cifone, M.G., and De Simone, C. (1998) Effect of L-Carnitine on Human Immunodeficiency Virus-1 Infection-Associated Apoptosis: A Pilot Study, *Blood 91,* 3817–3824.
54. Liles, W.C. (1997) Apoptosis. Role in Infection and Inflammation (review), *Curr. Op. Infect. Dis. 10,* 165–170.
55. Carreau, J.-P., Lapous, D., and Raulin, J. (1977) Signification des Acides Gras Essentiels dans le Métabolisme Intermédiaire. Hypothèses sur la Synthèse de l'Acide Lipoïque, *Biochimie 59*, 487–496.
56. Carreau, J.-P. (1979) Biosynthesis of Lipoic Acid *via* Unsaturated Fatty Acids, in *Methods in Enzymology (*Colowick, S.P., and Kaplan, N.O., eds.). *Vitamins & Coenzymes* (Part D: McCormick, D.B., and Wright, L.D., eds.), pp. 152–158, Academic Press, New York.
57. Packer, L., Witt, E.H., and Tritschler, H.J. (1995) Alpha-Lipoic Acid as a Biological Antioxidant. Review Article, *Free Radical Biol. Med. 19,* 227–250.
58. Goureau-Counis, M.-F., Fichot, O., Raulin, J., and De Recondo, A.-M. (1974) Phospholipid Configuration and Template Capacity of Liver Nuclei and Purified Chromatin in Presence or Absence of Hepatic DNA Polymerase, *Physiol. Chem. Phys. 6*, 379–392
59. Launay, M., Lapous, D., and Raulin, J. (1982) Control of Replication by Dietary Lipids and Namely by Linoleic Acid in Liver and Adipose Tissue of Developing Rats, *Progr. Lipid Res. 20*, 331–338.
60. Xi, S., Cohen, D., and Chen, L.H. (1998) Effects of Fish Oil on Cytokines and Immune Functions of Mice with Murine AIDS, *J. Lipid Res. 39*, 1677–1687.
61. Okawa, A., Murate, T., Izuta, S., Takemura, M., Furuta, K., Kobayashi, J., Kamikawa, T., Nimura, Y., and Yoshida, S. (1998) Sulfated Glycoglycerolipid from *Archaebacterium* Inhibits Eukaryotic DNA Polymerase Alpha, Beta and Retroviral Reverse Transcriptase and Affects Methyl Methane Sulfonate Cytotoxicity, *Int. J. Cancer 76,* 512–518.
62. Vourc'h, C., Eychenne, B., Jo, D.-H., Raulin, J., Lapous, D., Baulieu, E.-E., and Robel, P. (1992) Delta 5-3 Beta-Hydroxysteroid Acyl Transferase Activity in the Rat Brain, *Steroids 57*, 210–214.

63. Moog, C., Aubertin, A.M., Kirn, A., and Luu, B. (1998) Oxysterols, but Not Cholesterol, Inhibit Human Immunodeficiency Virus Replication *in vitro*, *Antivir. Chem. Chemother. 9,* 491–496.
64. De Simone, C., Famularo, G., Cifone, G., and Mittsuya, H. (1998) HIV-1 Infection and Cellular Metabolism, *Trends Immunol. Today*, *17,* 256–258.
65. Brogi, A., Presentini, R., Piomboni, P., Collodel, G., Strazza, M., and Constantino-Ceccarini, E. (1995) Human Sperm and Spermatogonia Express a Galactoglycerolipid Which Interacts with gp120, *J. Submicr. Cytol. Pathol. 27,* 565–571.
66. Brogi, A., Presentini, R., Solazzo, D., Piomboni, P., and Constantino-Ceccarini, E. (1996) Interaction of Human Immunodeficiency Virus Type 1 Envelope Glycoprotein gp120 with a Galactoglycerolipid Associated with Human Sperm, *AIDS Res. Hum. Retrovir. 12,* 483–489.
67. Zhang, H., Dornadula, G., Beumont, M., Livornese, L., van Uitert, B., Henning, K., and Pomerantz, R.J. (1998) Human Immunodeficiency Virus Type 1 in the Semen of Men Receiving Highly Active Antiviral Therapy, *N. Engl. J. Med. 339,* 1803–1809.
68. Lipsky, J.J. (1998) Abnormal Fat Accumulation in Patients with HIV-1 Infection, *Lancet 351*, 847–848.
69. Lo, J.C., Mulligan, K., Tai, V.W., Algren, H., and Schambelan, M. (1998) "Buffalo Hump" in Men with HIV-1 Infection, *Lancet 351*, 867–870.
70. Miller, K.D., Jones, E., Yanovski, J.A., Shankar, R., Feuerstein, I., and Falloon, J. (1998) Visceral Abdominal-Fat Accumulation Associated with Use of Indinavir, *Lancet 351*, 871–875.
71. Duncombe, C., Bloch, M., Austin, D., and Quan, D. (1998) Reversal of Hyperlipidemia and Lipodystrophy in Patients Switching Therapy to Nelfinavir, *12th World AIDS Conference,* Genève, July 1998 (Int. Abstract Review Committee, ed.), Abstract 12287, p. 70, Marathon International, Hoorn, Holland.
72. Bonnet, E., Cuzin, L., Sailler, L., Obadia, M., Marchou, B., Caron, P., and Massip, P. (1998) Associated Lipodystrophy Metabolic Disorders Due to Protease Inhibitor-Containing Regimens, *12th World AIDS Conference,* Genève, July 1998 (Int. Abstract Review Committee, ed.), Abstract 12299, p. 72, Marathon International, Hoorn, Holland.
73. Henry, K. (1998) Lipid Abnormalities Associated with the Use of Protease Inhibitors: Prevalance, Clinical Sequelae and Treatment, *12th World AIDS Conference,* Genève, July 1998 (Int. Abstract Review Committee, ed.), Abstract 122319, p. 77, Marathon International, Hoorn, Holland.
74. Chang, E., Deleo, M., Liu, Y.T., Tetreault, D., and Beall, G. (1998) The Effect of Antiretroviral Protease Inhibitors (PIs) on Serum Lipids and Glucose in HIV-Infected Patients, *12th World AIDS Conference,* Genève, July 1998 (Int. Abstract Review Committee, ed.), Abstract 12381, pp. 89–90, Marathon International, Hoorn, Holland.
75. Boix, V., Reus, S., Priego, M., Merino, E., Roman, F., Climent, E., and Portilla, J. (1998) Expanding the Spectrum of Protease Inhibitors-Induced Lipodystrophy, *12th World AIDS Conference,* Genève, July 1998 (Int. Abstract Review Committee, ed.), Abstract 12398, p. 93, Marathon International, Hoorn, Holland.
76. Papadopoulos, A.I., Evangelopoulou, E.P., Nicolaidi, N.A., Zolatas, Z.N., Groutsis, G.T., Montsenigos, M.T., and Stergiou, S.G.D. (1998) Serum Lipids Changes in HIV-Infected Patients Under Combination Therapy Containing a Protease Inhibitor, *12th World AIDS Conference,* Genève, July 1998 (Int. Abstract Review Committee, ed.), Abstract 50118, p. 1021, Marathon International, Hoorn, Holland.
77. Pomerantz, R.J., and Trono, D. (1995) Genetic Therapies for HIV Infections: Promise for the Future, *AIDS 9,* 985–993.

[Received August 24, 1999, and in revised form January 18, 2000; revision accepted January 31, 2000]

Biosynthesis of Conjugated Linoleic Acid in Humans

R.O. Adlof[a,*], S. Duval[a], and E.A. Emken[b]

[a]Food Quality and Safety Research, NCAUR, USDA, ARS, Peoria, Illinois 61604, and [b]Midwest Research Consultants, Princeville, Illinois

ABSTRACT: This paper deals with the reanalysis of serum lipids from previous studies in which deuterated fatty acids were administered to a single person. Samples were reanalyzed to determine if the deuterated fatty acids were converted to deuterium-labeled conjugated linoleic acid (CLA, 9*c*,11*t*-18:2) or other CLA isomers. We found 11-*trans*-octadecenoate (fed as the triglyceride) was converted (Δ9 desaturase) to CLA, at a CLA enrichment of *ca.* 30%. The 11-*cis*-octadecenoate isomer was also converted to 9*c*,11*c*-18:2, but at <10% the concentration of the 11*t*-18:1 isomer. No evidence (within our limits of detection) for conversion of 10-*cis*- or 10-*trans*-octadecenoate to the 10,12-CLA isomers (Δ12 desaturase) was found. No evidence for the conversion of 9-*cis*,12-*cis*-octadecadienoate to CLA (*via* isomerase enzyme) was found. Although these data come from four single human subject studies, data from some 30 similar human studies have convinced us that the existence of a metabolic pathway in one subject may be extrapolated to the normal adult population.

Paper no. L8342 in *Lipids 35,* 131–135 (February 2000).

Conjugated linoleic acid (CLA; 9-*cis*,11-*trans*-octadecadienoic acid; 9*c*,11*t*-18:2) has been associated with the reduction of chemically induced cancers in mice and rats and the suppression of atherosclerosis in rats (1–3). Whereas commercially available samples of CLA usually contain a mixture of conjugated fatty acid (FA) isomers (4,5), the 9-*cis*,11-*trans*-octadecadienoic acid isomer is considered to be the active constituent (6). Rats fed 11*t*-18:1 were shown to have increased levels of CLA in their tissues (7), and the presence of a similar metabolic pathway (11*t*-18:1 → 9*c*,11*t*-18:2 *via* Δ9 desaturase enzyme) has been suggested to occur in humans (8–11). Furthermore, Chin *et al.* (12) demonstrated that both the 9*c*,11*t*- and 10*t*,12*c*-18:2 FA isomers are produced in conventional, but not germ-free, rats fed linoleic acid and described the conversion of 9*c*,12*c*-18:2 to 9*c*,11*t*-18:2. (See Reference 13 for an extensive review of CLA biosynthesis.)

This study was undertaken to determine if, as postulated, detectable amounts [defined as present at >2 ng fatty acid methyl esters (FAME)/mL plasma] of the previously mentioned FA are actually converted to CLA or CLA isomers (i.e., 10*t*,12*c*-18:2) in humans. Samples from human metabolism studies in which deuterium-labeled fats were fed as triglycerides (TG) were reanalyzed for evidence of the following conversions: (i) 11*c*-18:1 to 9*c*,11*c*-18:2, (ii) 11*t*-18:1 to 9*c*,11*t*-18:2, (iii) 10*c*-18:1 to 10*c*,12*c*-18:2, (iv) 10*t*-18:1 to 10*t*,12*c*-18:2, and (v) 9*c*,12*c*-18:2 to 9*c*,11*t*-18:2. [The deuterium label is nonradioactive; thus deuterium-labeled fats can be safely fed to human volunteers (14–16).] Since conjugated 18:2 FAME isomers tend to elute by gas chromatography (GC) later than their methylene-interrupted analogs, the time windows set for selective ion monitoring in the original GC/mass spectrometry (MS) studies (Table 1) were not set to detect the CLA ions. By reanalysis of relevant samples, we were able to demonstrate the existence or absence of these biosynthetic pathways in humans. It must again be emphasized that each study is limited to a single human subject.

EXPERIMENTAL PROCEDURES

Materials. All reagents used were analytical grade or better.

Procedures/equipment. (i) Protocol of original studies. Complete details may be found in References 17–21. In these studies (designated I, II, III, and IV in Table 1), subjects were fed milkshakes containing a mixture of 8–10 g (studies I, II, III) or 2.5 g (study IV) each of 3–5 deuterium-labeled FA. The labeled fats were fed as homogeneous TG. (See Table 1 for spe-

TABLE 1
Deuterium-Labeled Fatty Acid Contents of Triglyceride Mixtures Fed

Study	Date	No. subjects	Fed	Reference(s)
I	1978	1	9*c*-18:1-9,10-d_2 11*t*-18:1-15,15,16,16-d_4 11*c*-18:1-14,14,15,15,17,18-d_6	17
II	1979	1	9*c*-18:1-14,14,15,15,17,18-d_6 10*t*-18:1-9,10-d_2 10*c*-18:1-15,15,16,16-d_4	18
III	1980	1	9*c*-18:1-14,14,15,15,17,18-d_6 10*t*-18:1-15,15,16,16-d_4 10*c*-18:1-9,10-d_2	18
IV	1988	1	16:0-9,10-d_2 18:0-9,10-d_2 9*c*-18:1-14,14,15,15,17,18-d_6 9*c*,12*c*-18:2-15,15,16,16-d_4 9*c*,12*c*,15*c*-18:3-9,10-d_2	19–21

*To whom correspondence should be addressed at Food Quality and Safety Research, NCAUR, USDA, ARS, 1815 N. University St., Peoria, IL 61604.

Abbreviations: CLA, conjugated linoleic acid; 9-*cis*,11-*trans*-octadecadienoic acid; 9c,11t-18:2, EE, ethyl ether; FA, fatty acid(s), FAME, fatty acid methyl ester(s), GC, gas chromatography, GC/MS, gas chromatography/mass spectrometry, PE, petroleum ether; PL phospholipid(s); TG triglyceride(s); TLC, thin-layer chromatography.

E-mail: adlofro@mail.ncaur.usda.gov

cific fats fed.) Blood samples were collected by venipuncture at specified intervals (i.e., 0, 2, 4, 8, 12, 15, 24, 48 h), and the red blood cells were removed by centrifugation. One portion of the blood plasma was extracted with $CHCl_3$/methanol to obtain total plasma lipids, from which the neutral and phospholipid (PL) classes were separated by preparative thin-layer chromatography (TLC). An internal standard (17:0) was added to each fraction. The lipids in each fraction were converted to FAME with HCl/methanol (22), and each fraction was analyzed by GC to obtain total lipid composition and by GC/MS [chemical ionization conditions with isobutane as the reagent gas and selective ion monitoring (23,24)] to determine the deuterium-labeled FA composition. The blood lipid FAME samples were stored in isooctane under nitrogen gas in 1-dram vials (aluminum foil-lined caps) at 0°C (in the dark).

(ii) Sample selection. To maximize GC/MS sensitivity, samples were taken from studies in which the fats of interest fed were labeled with four or more deuterium atoms. The carbon-13 isotope contribution to the MS data for FA labeled with two deuterium atoms must be calculated, resulting in some loss of sensitivity. Given the low (0.1–0.3%) levels of CLA isomers present, the authors felt the highest sensitivity/accuracy would be obtained by analyzing for fats labeled with four or more deuterium atoms. A representative grouping of 4–6 blood lipid samples (plasma TG/PL or chylomicron TG/PL) from each of four different human metabolism studies were retrieved. The date of the study, the FA fed and pertinent publications resulting from these studies are listed in Table 1.

(iii) Sample preparation. Each sample was eluted through a Sep- Pak cartridge (Waters, Inc., Milford, MA) with 10 mL 10% ethyl ether (EE) in petroleum ether (PE; vol/vol) as solvent. The eluant was concentrated to 0.5 mL under a stream of inert gas and analyzed by TLC (Silica gel 60A, Whatman, Inc., Clifton, NJ), using 15% EE/85% PE as solvent and with I_2 visualization. The remaining solvents were removed by a stream of inert gas, and the residue was transferred to a sample vial with a minimal volume of isooctane for analysis by GC.

(iv) Blood lipid fraction analysis by GC. Samples (as FAME) were initially analyzed on a Varian 3400 GC (Varian Instruments, Palo Alto, CA) to obtain a total lipid profile. The GC was equipped with a 100 m × 0.32 mm SP2380 (Supelco, Inc., Bellefonte, PA) capillary column and flame-ionization detector (FID). Helium was utilized as carrier gas. Unknown peaks were identified by comparison with standard FAME mixtures of known composition. The extent of sample oxidation was estimated by comparing saturated and polyunsaturated FA compositions from our GC results with the original published data.

(v) GC/MS analysis of blood lipid fractions. GC/MS was utilized to determine the presence (or absence) of deuterium-labeled CLA and other deuterium-labeled metabolites. Analyses were made on a Hewlett-Packard model 5890/5988a GC/MS (quadrapole; positive chemical ionization mode; isobutane as ionizing gas; Palo Alto, CA) equipped with a 30 m × 0.25 mm Omegawax 10 fused-silica capillary column (Supelco, Inc.), Data collection and processing have been described previously (23). The isomerization of conjugated FA during their conversion to FAME by acidic catalysts such as HCl or BF_3 in methanol has been well documented (5,25). Since 5% HCl in methanol (at 50°C) had initially been used to convert the blood lipids to FAME (22), the 9*c*,11*t*- and 9*t*,11*t*-18:2-d_4 and -d_0 peak areas were combined to calculate total concentrations of labeled and unlabeled CLA, respectively. If deuterium-labeled CLA was detected, additional samples from that study were retrieved and prepared for analysis by GC and GC/MS as described previously.

RESULTS

Only in study I (in which 11*c*-18:1-d_6 and 11*t*-18:1-d_4 were fed) were deuterium-labeled CLA isomers detected in measurable (>2 ng FAME/mL plasma) quantities. Four samples (0-, 4-, 8-, and 15-h) of blood plasma TG (as FAME) were retrieved and reanalyzed by GC and GC/MS to provide the data presented in this study. A portion of a gas chromatogram (100 m SP2380 capillary column) containing the CLA isomers is shown in Figure 1. Peaks have been identified by coinjection with known standards or marked as "unknown."

The percentage of 9*t*,11*t*-18:2 formed during conversion (HCl/methanol) of the blood TG fractions to FAME varied significantly (from 10 to *ca.* 50% of total CLA concentration) from sample to sample. This amount of isomerization is typical when HCl/methanol or BF_3/methanol and 50°C are used to convert CLA-containing TG, PL, or free FA to FAME. The two peak areas were combined to calculate total % CLA. A representative GC/MS chromatogram, with the peaks of interest labeled, of the CLA region for the 4-h plasma TG sample is presented in Figure 2. As we demonstrate in Figure 2, the presence of deuterium-labeled CLA and CLA isomers may readily be detected by our methodology. The 9*c*,11*c*-18:2 isomer is also present, but at <0.01%. We also characterized the separation

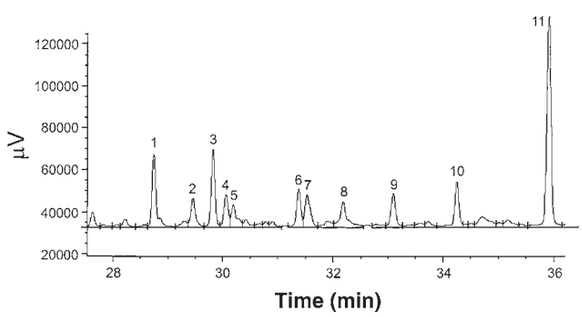

FIG. 1. Portion of gas chromatography trace (100 m SP2380 capillary column; Supelco Inc., Bellefonte, PA) with conjugated linoleic acid (CLA) and other minor (<1% each by weight total lipids) fatty acid methyl esters marked. (See Experimental Procedures section for details.) Designations: peak no. 1 = 6*c*,9*c*,12*c*-18:3; peak no. 2 = 11*c*-20:1, peak no. 3 = 9*c*,12*c*,15*c*-18:3; peak no. 4 = 9*c*,11*t*-18:2; peak no. 5 = 21:0; peak no. 6 = 9*t*,11*t*-18:2; peak no. 7 = unknown (8*c*,11*c*-20:2?); peak no. 8 = 11*c*,14*c*-20:2; peak no. 9 = 22:0; peak no. 10 = 8*c*,11*c*,14*c*-20:3; peak no. 11 = 5*c*,8*c*,11*c*,14*c*-20:4.

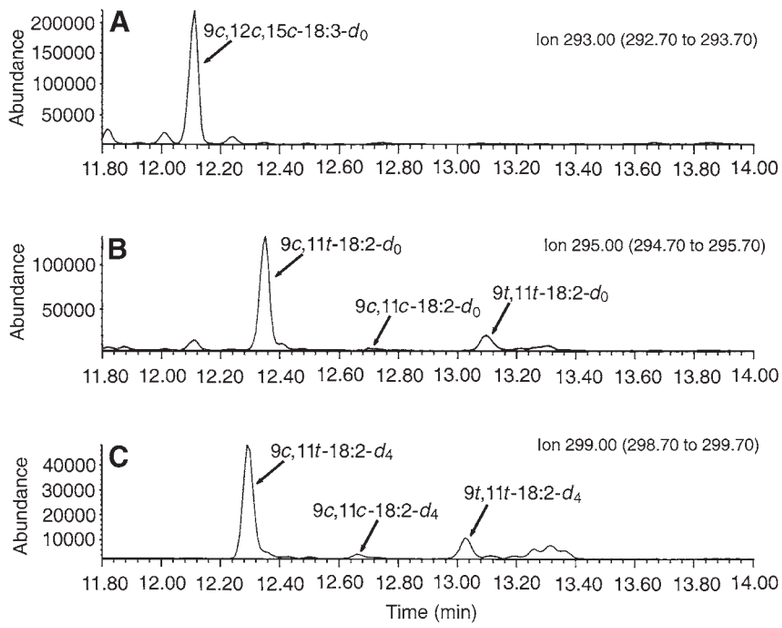

FIG. 2. Portion of gas chromatography/mass spectrometry chromatogram illustrating selective ion monitoring at molecular weights 292, 294, and 298 (molecular ions of 293, 295, and 299), corresponding to 18:3n-3-d_0, 9*c*,11*t*-18:2-d_0, and 9*c*,11*t*-18:2-d_4, respectively. (See Experimental Procedures section for details.)

capabilities of the Omegawax GC column by injecting a mixture of 9,11- and 10,12-18:2 FAME isomers. Under the GC conditions employed (see the Experimental Procedures section), we found the Omegawax column capable of achieving baseline separation of 9*c*,11*t*-18:2 and 10*t*,12*c*-18:2, the 9*c*-isomer eluting before the 10*t*-isomer. The 9*c*,11*c*-18:2 and 10*c*,12*c*-18:2 were only slightly resolved, with the 9*c*-isomer eluting first. The 9*t*,11*t*-18:2 and 10*t*,12*t*-18:2 isomer pair was not resolved.

The incorporation of 11*t*-18:1-d_4 and its conversion to CLA-d_4 and 9*t*-16:1-d_4 (formed by β-oxidation of 11*t*-18:1-d_4) are plotted (as enrichment data) in Figure 3. A small amount of 9*c*,11*c*-18:2-d_6 (from 11*c*-18:1-d_6 *via* Δ9 desaturase) was also detected at *ca.* 10% of the CLA-d_4 concentration. The total weight percentages of the isomers (labeled and unlabeled) plotted in Figure 3 are presented in Table 2.

DISCUSSION

After 10–20 yr in storage, some oxidation of the lipid samples was expected. Although some loss (2–5%) of polyunsaturated FA was noted, the overall lipid compositions were found to compare favorably with the original lipid data obtained by packed column GC (data not shown). A more limited selection of samples from studies II, III and IV was also analyzed for extent of oxidation. Since the oxidative stability of CLA has been reported to lie between arachidonic and docosahexaenoic acids (26), the 20:4 FA concentration was chosen as another marker for oxidation. The low concentration of this FA (0.8–2.2%), however, limited this approach. The formation of methoxy artifacts during the FAME preparation or the presence of plasticizers was also studied. By use of internal standards, we found methoxy artifacts to be formed at a total concentration of <0.5% during our HCl/methanol procedure. Plasticizers were also detected during our GC analyses, but at a total concentration of <0.01%. Any possible interference(s) due to methoxy artifacts or plasticizers were eliminated by use of selective ion monitoring (Fig. 2).

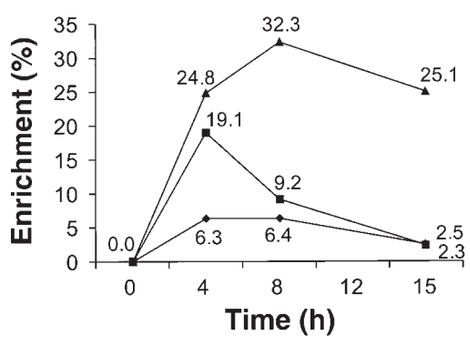

FIG. 3. Uptake and disappearance in plasma triglycerides of 11*t*-18:1-d_4 (■) related to formation and disappearance of 9*c*,11*t*-18:2-d_4 (▲) and 9*t*-16:1-d_4 (◆). Data plotted as percent isotopic enrichment within each individual fatty acid methyl ester.

TABLE 2
Study I: Compositions (percentage by weight) for Fatty Acids Plotted in Figure 3

	Hour			
Fatty acid[a]	0	4	8	15
9*t*-16:1	2.0	1.5	1.5	1.5
11*t*-18:1	1.4	11.4	4.5	2.5
CLA	0.07	0.19	0.32	0.14

[a]Total (deuterium-labeled and unlabeled) percentage of fatty acids. CLA, conjugated linoleic acid.

The only readily identifiable metabolic pathway for the biosynthesis of CLA in humans utilizes the Δ11-18:1 FA as precursors and, presumably, the Δ9 desaturase enzyme (10). As we demonstrated in study I (17), both the 9*c*-18:1 and the Δ11-18:1 isomers are equally well-absorbed in humans. The total percentage of CLA in blood plasma lipids 8 h after ingestion of more than 8 g of 11*t*-18:1 (fed as a homogeneous TG) was found to be only 0.3% by weight of total blood lipids. This number (0.3%) falls within the percentage composition ranges listed for CLA in blood lipids by Ackman (27) and Jiang *et al.* (28). At 33% enrichment, the CLA-d_4 was present at a maximum of only 0.1% (by weight) of total lipids. The presence of 9*c*,11*c*-18:2-14,14,15,15,17,18-d_6 at *ca.* 0.01% by weight suggests the existence of a similar, but less utilized, biosynthetic pathway for conversion of the 11*c*-18:1 isomer. No CLA-d_4 metabolites (6*c*,9*c*,11*t*-18:3-d_4 or 5*c*,8*c*,11*c*,13*t*-20:4-d_4) were detected. [In the original study (17), no metabolites of the Δ11-18:1 isomers were found (0.001% listed then as limit of detectability)].

It should again be stressed that a single human male was used in each of the feeding studies listed in Table I; the data thus cannot be statistically evaluated as representative of the normal population. The amounts of CLA formed from the 11*t*-18:1 isomer are expected to vary between individuals, but data from some 30 human studies have convinced us (17) that the existence of a metabolic pathway in one subject may be safely extrapolated to the normal adult population. Our results also agree with previous findings which show 9*c*,11*t*-18:1 to be "practically the only one of the CLA isomers found in humans" (10). Other postulated pathways for the biosynthesis of CLA isomers in humans (10*t*,12*c*-18:2 from 10*t*-18:1 or 10*c*,12*c*-18:2 from 10*c*-18:1, both by Δ12 desaturase) are still feasible but, if these isomers were formed, they were formed below the detection limits (again defined as <2 ng FAME/mL plasma) of our methodologies.

The conversion of 9*c*,12*c*-18:2 to CLA *via* an isomerase enzyme generated by bacteria in the human intestinal tract [as noted by Chin *et al.* in mice (12)] also remains a possibility, but any deuterium-labeled CLA formed in the human colon would be expected to be as poorly absorbed in the lower intestine of animals as are methylene-interrupted polyunsaturated FA (8). Previous studies in humans (19,29) have shown ingested 9*c*,12*c*-18:2 (as TG) to be >96% absorbed. Only a very small percentage of the labeled 9*c*,12*c*-18:2 fed would thus be available to bacteria in the intestine. Any metabolites formed *via* isomerization of 9*c*,12*c*-18:2 and absorbed in the lower intestine would again be present at levels below our limits of detection.

All other sources/pathways to explain the presence of deuterium-labeled CLA isomers (impurities in the fed materials, oxidation, etc.) in study I samples have been examined and eliminated. Utilizing isotopically labeled FA, we thus demonstrate the existence, in human(s), of a metabolic pathway for the biosynthesis of CLA. Since some oxidation may have occurred during storage, the concentrations of CLA presented in this manuscript should be considered at the low end of possible CLA levels in human plasma. The relatively large (>8 g) quantity of 11*t*-18:1 ingested also resulted in a relatively small increase in plasma CLA concentration (from 0.1 to 0.3% total lipids). Whether the amount of CLA formed from increased levels of 11*t*-18:1 in the diet will result in "positive health benefits" and a situation where "*trans* FA in dairy products represent a complete opposite situation to the possible adverse health effects of *trans* FA isomers from partially hydrogenated plant oils" (30) remains to be seen.

ACKNOWLEDGMENTS

To Teresa Lamm, Lynne Copes, and Erin Walter for technical assistance.

REFERENCES

1. Steinhart, C. (1996) Conjugated Linoleic Acid—The Good News About Animal Fat, *J. Chem. Educ. 73*, A302–A303.
2. Ip, C., Briggs, S.P., Haegele, A.D., Thompson, H.J., Storkson, J., and Scimeca, J.A. (1996) The Efficacy of Conjugated Linoleic Acid in Mammary Cancer Prevention Is Independent of the Level or Type of Fat in the Diet, *Carcinogenesis 17*, 1045–1050.
3. Belury, M.A. (1995) Conjugated Dienoic Linoleate: A Polyunsaturated Fatty Acid with Unique Chemoprotective Properties, *Nutr. Rev. 53*, 83–89.
4. Christie, W.W. (1997) The Analysis of Conjugated Fatty Acids, *Lipid Technol.* (May), 73–75.
5. Kramer, J.K.G., Fellner, V., Dugan, M.E.R., Sauer, S.D., Mossoba, M.M., and Yurawecz, M.P. (1997) Evaluating Acid and Base Catalysts in the Methylation of Milk and Rumen Fatty Acids with Special Emphasis on Conjugated Dienes and Total *trans* Fatty Acids, *Lipids 32*, 1219–1228.
6. Ha, Y.L., Storkson, J., and Pariza, M.W. (1990) Inhibition of Benzo(a)Pyrene-Induced Mouse Forestomach Neoplasia by Conjugated Dienoic Derivatives of Linoleic Acid, *Cancer Res. 50*, 1097–1101.
7. Sebedio, J.L., Juaneda, P., Dobson, G., Ramilison, I., Martin, J.C., Chardigny, J.M., and Christie, W.W. (1997) Metabolites of Conjugated Isomers of Linoleic Acid (CLA) in the Rat, *Biochim. Biophys. Acta 1345*, 5–10.
8. Fogerty, A.C., Ford, G.L., and Svoronos, D. (1988) Octadeca-9,11-dienoic Acid in Foodstuffs and in the Lipids of Human Blood and Breast Milk, *Nutr. Rep. Int. 38*, 937–944.
9. Pollard, M.R., Gunstone, F.D., James, A.T., and Morris, L.J. (1980) Desaturation of Positional and Geometric Isomers of Monoenoic Fatty Acids by Microsomal Preparations from Rat Liver, *Lipids 15*, 306–314.
10. Salminen, M.M., Mutanen, M., Jauhiainen, M., and Aro, A. (1998) Dietary *trans* Fatty Acids Increase Conjugated Linoleic Acid Levels in Human Serum, *Nutr. Biochem. 9*, 93–98.

11. Aro, A., and Salminen, I. (1998) Difference Between Animal and Vegetable *trans* Fatty Acids, *Am. J. Clin. Nutr. 68*, 918–919.
12. Chin, S.F., Liu, W., Storkson, J.M., Ha, Y.L., and Pariza, M.W. (1992) Dietary Sources of Conjugated Dienoic Isomers of Linoleic Acid, a Newly Recognized Class of Anticarcinagens, *J. Food Comp. Anal. 5*, 185–197.
13. Griinari, J.M., and Bauman, D.E. (1999) Biosynthesis of Conjugated Linoleic Acid and Its Incorporation into Meat and Milk in Ruminants, in *Advances in Conjugated Linoleic Acid Research*, Vol. 1 (Yurawecz, M.P., Mossoba, M.M., Kramer, J.K.G., Pariza, M.W., and Nelson, G.J., eds.), pp. 180–200, AOCS Press, Champaign.
14. Emken, E.A. (1979) Utilization and Effects of Isomeric Fatty Acids in Humans, in *Geometrical and Positional Fatty Acid Isomers* (Emken, E.A., and Dutton, H.J., eds.), pp. 99–129, American Oil Chemists' Society, Champaign.
15. Demmelmair, H., Sauerwald, T., Koletzko, B., and Richter, T. (1997) New Insights into Lipid and Fatty Acid Metabolism *via* Stable Isotopes, *Europ. J. Ped. 156* (suppl. 1), S70–S74.
16. Descomps, B. (1995) Utilization of Stable Isotopes to Study Lipid Metabolism in Humans, in *New Trends in Lipid and Lipoprotein Analyses* (Sebedio, J.L., and Perkins, E.G., eds.), pp. 299–316, AOCS Press, Champaign.
17. Emken, E.A., Rohwedder, W.K., Adlof, R.O., DeJarlais, W.J., and Gulley, R.M. (1986) Absorption and Distribution of Deuterium-Labeled *trans*- and *cis*-11-Octadecenoic Acid in Human Plasma and Lipoprotein Lipids, *Lipids 21*, 589–595.
18. Emken, E.A., Rohwedder, W.K., Adlof, R.O., DeJarlais, W.J., and Gulley, R.M. (1985) *In vivo* Distribution and Turnover of *trans*- and *cis*-10-Octadecenoic Acid Isomers in Human Plasma Lipids, *Biochim. Biophys. Acta 836*:233–245.
19. Emken, E.A., Adlof, R.O., Rakoff, H., and Rohwedder, W.K. (1988) Metabolism of Deuterium-Labeled Linolenic, Linoleic, Oleic, Stearic and Palmitic Acid in Human Subjects, in *Synthesis and Applications of Isotopically Labelled Compounds* (Baillie, T.A., and Jones, J.R. eds.), pp. 713–716, Elsevier Science Publishers, Amsterdam.
20. Emken, E.A., Adlof, R.O., Rakoff, H., Rohwedder, W.K., and Gulley, R.M. (1990) Metabolism *in vivo* of Deuterium-Labelled Linolenic and Linoleic Acids in Humans, *Biochem. Soc. Trans. 18*:766–769.
21. Emken, E.A., Adlof, R.O., Rohwedder, W.K., and Gulley, R.M. (1992) Comparison of Linolenic and Linoleic Acid Metabolism in Man: Influence of Dietary Linoleic Acid, in *Essential Fatty Acids and Eicosanoids* (Sinclair, A., and Gibson, R., eds.) pp. 23–25, American Oil Chemists' Society, Champaign.
22. Christie, W.W. (1973) *Lipid Analysis*, pp. 85–102, Pergamon Press, New York.
23. Rohwedder, W.K. (1975) Mass Spectrometry of Lipids, in *Analysis of Lipids and Lipoproteins* (Perkins, E.G., ed.), pp. 170–182, American Oil Chemists' Society, Champaign.
24. Rohwedder, W.K., Emken, E.A., and Wolf, D.J. (1985) Analysis of Deuterium Labeled Blood Lipids by Chemical Ionization Mass Spectrometry, *Lipids 20*, 303–310.
25. Christie, W.W. (1994) Why I Dislike Boron Trifluoride/Methanol, *Lipid Technol*. (May/June), 66–68.
26. Zhang, A., and Chen., Z.Y. (1997) Oxidative Stability of Conjugated Linoleic Acids Relative to Other Polyunsaturated Fatty Acids, *J. Am. Oil Chem. Soc. 74*, 1611–1613.
27. Ackman, R.G., (1997) Has Evolution and Long-term Coexistence Adapted Us to Cope with *trans* Fatty Acids? *J. Food Lipids 4*:295–318.
28. Jiang, J., Wolk, A., and Vessby, B. (1998) Relationship Between the Intake of Milk Fat and the Occurrence of Conjugated Linoleic Acid in Human Adipose Tissue, Ph. D. Thesis, Swedish University of Agricultural Sciences, Uppsala, Sweden, III: 1–18.
29. Emken, E.A., Adlof, R.O., and Gulley, R.M. (1994) Dietary Linoleic Acid Influences Desaturation and Acylation of Deuterium-Labeled Linoleic and Linolenic Acids in Young Adult Males, *Biochim. Biophys. Acta 1213*, 277–288.
30. Bauman, D.E., Corl, B.A., Baumgard, L.H., and Griinari, J.M., (1998) *trans* Fatty Acids, Conjugated Linoleic Acid and Milk Fat Synthesis, *Proceedings of the Cornell Nutrition Conference-for Feed Manufacturers*, Rochester, NY, Oct. 20–22, pp. 95–103, Cornell University Press, Ithaca.

[Received August 25, 1999, and in revised form and accepted January 10, 2000]

Effects of Dietary α-Linolenic Acid on the Conversion and Oxidation of ^{13}C-α-Linolenic Acid

Susanne H.F. Vermunt, Ronald P. Mensink*, Marianne M.G. Simonis, and Gerard Hornstra

Department of Human Biology, Maastricht University, 6200 MD, Maastricht, The Netherlands

ABSTRACT: The effects of a diet rich in α-linolenic acid vs. one rich in oleic acid on the oxidation of uniformly labeled ^{13}C-α-linolenic acid and its conversion into longer-chain polyunsaturates (LCP) were investigated *in vivo* in healthy human subjects. Volunteers received a diet rich in oleic acid (n = 5) or a diet rich in α-linolenic acid (n = 7; 8.3 g/d) for 6 wk before and during the study. After 6 wk, subjects were given 45 mg of ^{13}C-α-linolenic acid dissolved in olive oil. Blood samples were collected at t = 0, 5, 11, 24, 96, and 336 h. Breath was sampled and CO_2 production was measured each hour for the first 12 h. The mean (± SEM) maximal absolute amount of ^{13}C-eicosapentaenoic acid (EPA) in plasma total lipids was 0.04 ± 0.01 mg in the α-linolenic acid group, which was significantly lower (P = 0.01) than the amount of 0.12 ± 0.03 mg ^{13}C-EPA in the oleic acid group. Amounts of ^{13}C-docosapentaenoic acid (DPA) and ^{13}C-docosahexaenoic acid (DHA) tended to be lower as well. The mean proportion of labeled α-linolenic acid (ALA) recovered as $^{13}CO_2$ in breath after 12 h was 20.4% in the ALA and 15.7% in the oleic acid group, which was not significantly different (P = 0.12). The cumulative recovery of ^{13}C from ^{13}C-ALA in breath during the first 12 h was negatively correlated with the maximal amounts of plasma ^{13}C-EPA (r = –0.58, P = 0.047) and ^{13}C-DPA (r = –0.63, P = 0.027), but not of ^{13}C-DHA (r = –0.49, P = 0.108). In conclusion, conversion of ^{13}C-ALA into its LCP may be decreased on diets rich in ALA, while oxidation of ^{13}C-ALA is negatively correlated with its conversion into LCP. In a few pilot samples, low ^{13}C enrichments of n-3 LCP were observed in a diet rich in EPA/DHA as compared to oleic acid.

Paper no. L8240 in *Lipids 35*, 137–142 (February 2000).

Eicosapentaenoic acid (EPA; 20:5n-3) and docosahexaenoic acid (DHA; 22:6n-3) are important structural membrane components and play a major role in many physiological processes (1). These longer-chain polyunsaturated fatty acids (LCP) are not only provided by the diet, but can also be formed by alternate desaturation and elongation of α-linolenic acid (ALA; 18:3n-3), the parent essential fatty acid from the n-3 family. However, it is largely unknown to what extent this happens in humans.

From *in vitro* and rat studies with radioactive isotopes, it has been suggested that the conversion of ALA is positively related to the amount of substrate (ALA), but negatively to that of their LCP (EPA and DHA) (2,3). These results, however, have not been confirmed by others (4,5).

In humans, EPA and docosapentaenoic acid (DPA) concentrations increase after ALA consumption (6,7), while DHA concentrations are hardly affected (8). Fatty acid compositions of tissues, however, give no information about the origin of the fatty acids or their availability for conversion reactions. The introduction of stable isotopes has now created better opportunities to examine the *in vivo* metabolism of essential fatty acids in humans. So far, a few studies with deuterated ALA in adults (9–11) and infants (12), and some studies with ^{13}C labeled ALA in infants (13–15) have been carried out. These studies, however, only focused on the chain elongation and desaturation of ALA, although it is also possible to measure oxidation at the same time ^{13}C labeled fatty acids are used.

In the present study, we have therefore investigated the *in vivo* conversion of uniformly labeled ^{13}C-ALA into its LCP and its oxidation in healthy adults. In particular, the effects of a diet rich in ALA vs. a diet rich in oleic acid on ^{13}C-ALA metabolism have been examined. Finally, the relationship between the oxidation of ^{13}C-ALA and the conversion into LCP was studied. The effects of dietary EPA plus DHA on ^{13}C-ALA metabolism were examined in a pilot study.

EXPERIMENTAL PROCEDURES

Subjects. Fifteen subjects, both men and women (ages between 21 and 66 yr), who participated in an intervention trial on the effects of ALA and EPA/DHA on various cardiovascular risk markers (16), were asked to participate in this study. All subjects were healthy as indicated by a medical questionnaire and had fasting serum total cholesterol concentrations below 7.5 mmol/L and serum triacylglycerols below 3.0 mmol/L. None of the volunteers used medication or a diet known to affect fatty acid metabolism. Five of the participants smoked. Three younger women used oral contraceptives, while the elderly women were postmenopausal. The protocol had been approved by the local ethical committee and informed written consent was obtained from each volunteer.

Diets and experimental design. After a run-in period of 3 wk, in which all subjects consumed an oleic acid-rich diet,

*To whom correspondence should be addressed at Maastricht University, Dept. of Human Biology, P.O. Box 616, 6200 MD Maastricht, The Netherlands. E-mail: R.Mensink@HB.UNIMAAS.NL

Abbreviations: ALA, α-linolenic acid; DHA, docosahexaenoic acid; DPA, docosapentaenoic acid; EPA, eicosapentaenoic acid; FAME, fatty acid methyl esters; GC–C–IRMS, gas chromatography–combustion-isotope ratio mass spectrometer; GC–FID, gas chromatography–flame-ionization detector; LCP, long-chain polyunsaturated fatty acids.

the subjects were randomly allocated to three groups. The first group received for the following 7 wk the same diet they were given during the run-in period (n = 5); the second group received a diet rich in ALA (n = 7), while the third group received a diet rich in EPA plus DHA (n = 3). ALA and EPA/DHA replaced oleic acid. Fatty acids were provided as margarine from which pies, cakes, and chocolate paste were prepared. Subjects had to consume 30 g of the experimental fat daily. In order not to change energy intakes, the volunteers were required to replace their usual margarine, pastries, and sandwich spread with the experimental products provided in this study. Subjects in the oleic acid and ALA groups were not allowed to consume fatty fish during the whole study. Furthermore, subjects were urged not to change their background diets. The fatty acid compositions of the experimental margarines, which were prepared by Unilever Research (Vlaardingen, The Netherlands), have been presented elsewhere (16).

During the run-in and the experimental period, subjects recorded their food intake during the whole day for three consecutive days, one weekend, and two weekdays. After the food diary had been checked by a dietitian, foods were coded, and energy and nutrient intakes were calculated using the Dutch food composition table (17).

At wk 9, subjects came to the department at 8.00 A.M. after a fasting period of 12 h. First, a 10-mL blood sample was taken, whereafter 45 mg of uniformly labeled ^{13}C-ALA (isotopic purity >95% ^{13}C18:3n-3) was given as a methylester (Martek Biosciences Corp., Columbia, MD) dissolved in 8 g olive oil. Subjects were then given a breakfast, which consisted of 2 slices of white bread with jam. Two hours after ^{13}C-ALA intake, a second blood sample was taken, after which the subjects were allowed to eat and drink according to their respective dietary regimes. During the day, subjects stayed at the department and food was provided for the whole day. Other nonfasting blood samples were collected 2, 4, 6, 8, 10 and 12 h after the intake of labeled ALA, while fasting samples were taken after 24, 48, 72, 96, and 168 h. Subjects then returned to their usual diets and 1 wk later, a final fasting blood sample was taken at t = 336 h. At the same time points of blood sampling (except at t = 336 h and during the first day at t = 3, 5, 7, 9 and 11 h), a breath sample was taken. For this, subjects breathed for 5 min into a SensorMedics analyzer (SensorMedics 2900 analyzer, Anaheim, CA) in order to stabilize their breathing. For the next 5 min, CO_2 production was registered, after which a breath sample was taken. Breath samples were stored in vacutainers (Becton & Dickinson, Meylan, France).

Blood sampling and analysis. Until 12 h after ^{13}C-ALA administration, blood (10 mL) was sampled in an EDTA tube through a Teflon catheter (Baxter Quick Cath, Dupont, Ireland) or a vacuum tube using a 1.2-mm needle (Strauss Kanule; Luer, Wächtersbach, Germany) with the volunteer in a recumbent position. The catheter was flushed every hour with 1 mL heparin solution (0.5 IU heparin-sodium; Leo Pharmaceutical Products BV, Weesp, The Netherlands). The next fasting blood samples were taken with a vacuum tube. Plasma for ^{13}C enrichment analyses and analyses of fatty acid composition of total plasma lipids were obtained by centrifugation at 2,000 × g for 15 min at 4°C, within 1 h of venipuncture. Plasma samples were snap-frozen and stored at –80°C.

Lipids from plasma were extracted (18), using triheptadecanoate (17:0) as an internal standard. Thereafter, lipid extracts were hydrolyzed and the resulting fatty acids methylated (19). The absolute fatty acid composition in plasma total lipids was analyzed using a gas chromatograph with a flame-ionization detector (GC–FID) (PerkinElmer Autosystem, Norwalk, CT). Fatty acid methyl esters (FAME) were separated using a 50-m column (CP-SIL88, 0.25 mm, 0.20-μm film thickness; Chrompack, Middelburg, The Netherlands) with an injection temperature of 300°C. Helium gas was used as a carrier (injector inlet pressure 130 kPa). The oven was programmed from 160°C to 230°C in three temperature steps (160°C for 10 min, rise of 3.2°C min^{-1}, 190°C for 15 min, rise of 5°C min^{-1}, 230°C for 37 min).

^{13}C enrichments of individual FAME in total lipids from plasma and of CO_2 in breath were analyzed with a GC (Varian 3400) coupled to an isotope ratio mass spectrometer (IRMS; Finnigan MAT 252, Bremen, Germany) *via* a combustion interface. Samples were injected on a 50-m column (BPX70, 0.33 mm, 0.25-μm film thickness; SGE, Austin, TX) at a temperature of 250°C. Helium gas was used as a carrier (injector inlet pressure 124 kPa). For complete separation of the peaks, enrichments of the FAME were determined in two separate runs, as shown in the chromatograms in Figure 1. For 18:3n-3, 20:5n-3, and 22:6n-3, the oven was programmed from 185°C for 35 min (rise of 30°C min^{-1}) to 260°C for 33 min (Fig. 1A), and for 22:5n-3 from 205°C for 20 min (rise of 30°C min^{-1}) to 260°C for 25 min (Fig. 1B). The ^{13}C/^{12}C ratios were deter-

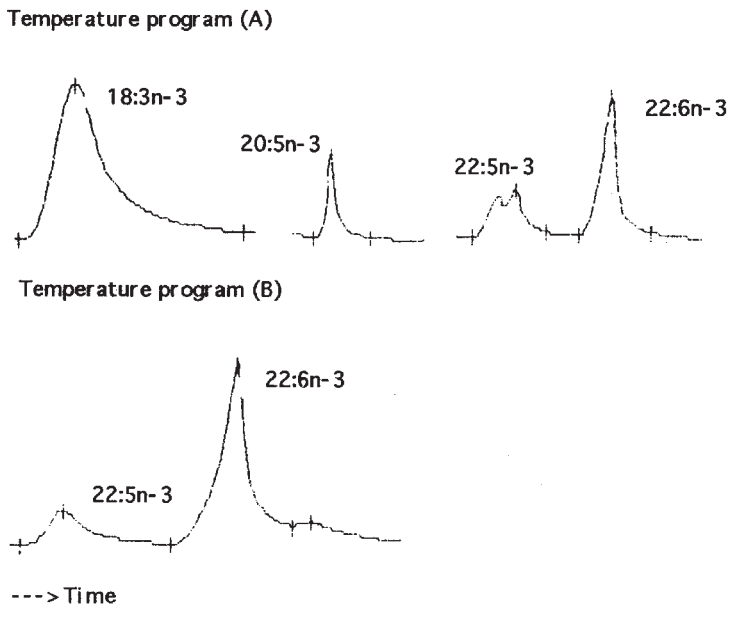

FIG. 1. Chromatograms showing the complete separation of the 18:3n-3, 20:5n-3, 22:5n-3, and 22:6n-3 peaks using gas chromatography–combustion-isotope ratio mass spectrometer. Temperature program (A): from 185°C for 35 min (rise of 30°C min^{-1}) to 260°C for 33 min for separation of 18:3n-3, 20:5n-3, and 22:6n-3; temperature program (B): from 205°C for 20 min (rise of 30°C min^{-1}) to 260°C for 25 min for separation of 22:5n-3.

mined with a precision of δ_{PDB}<1‰, while the reproducibility of the standard was δ_{PDB}<1‰.

Calculations. The difference between the $^{13}C/^{12}C$ ratio of the samples and a known reference standard was expressed as the delta ($\delta^{13}C$). The true ratio of the sample was then calculated by normalizing the isotopic enrichment ($\delta^{13}C$), against the international standard Pee Dee Belemate limestone (PDB), which has a $^{13}C/^{12}C$ ratio of 0.0112372. The concentration of a ^{13}C labeled fatty acid was calculated by correction for the plasma concentration of this particular fatty acid. It was assumed that during fatty acid elongation the two carbon-atom fragments added after elongation were not enriched above background. Absolute amounts of fatty acids were calculated based on a plasma volume of 4.5% of body weight (20).

Oxidation of ^{13}C-ALA was calculated from the $^{13}C/^{12}C$ ratio in breath and the absolute CO_2 production. From the second day after intake of ^{13}C-ALA onward, the CO_2 production was estimated only once a day. Since the determination of total $^{13}CO_2$ production during the day requires regular measurements of both ^{13}C enrichment and CO_2 production throughout the day, $^{13}CO_2$ production was calculated for the first 12 h only.

Statistical analyses. Results for the EPA/DHA group were not statistically analyzed as plasma ^{13}C-enrichments in n-3 fatty acids of only two subjects could be measured. Values of subjects within the other groups were averaged, and presented as means ± standard errors. For each subject, changes were calculated by subtracting baseline values ($t = 0$). Differences between the oleic acid group and the ALA group were tested with the Mann Whitney *U*-test. Spearman correlation coefficients were calculated to examine the relationship between the cumulative recovery of $^{13}CO_2$ in breath, derived from ^{13}C-ALA, and the maximal amount of plasma ^{13}C-labeled n-3 fatty acids. *P*-values are two-tailed, and differences were considered statistically significant when $P < 0.05$.

RESULTS

The mean daily energy and nutrient intakes are shown in Table 1. The mean supplemented daily ALA intake was significantly higher in the ALA (8.3 ± 1.3 g; 3.1 ± 0.4 energy%) as compared to the oleic acid group. Furthermore, the intake of protein and total polyunsaturated fatty acids differed between the groups.

First, plasma ^{13}C enrichments of all 13 plasma samples of four randomly chosen subjects, one or two from each intervention group, were analyzed. Results of one subject from the ALA group and one of the oleic acid group are shown in Figure 2. For ALA, results are presented for the first 24 h only, because values had nearly returned to baseline within 1 d. Results of EPA, DPA, and DHA are presented for 336 h. Based on these results, it was decided to analyze only samples from $t = 0$, 24, 96, and 336 h for the other 11 subjects so as to reduce the number of analyses to a more manageable quantity. In addition, samples from $t = 4$ and $t = 6$, and from $t = 10$ and $t = 12$ were pooled and analyzed. These samples are denoted as $t = 5$ and $t = 11$. In order to compare the results of the first four subjects with the others, the data from $t = 4$ and $t = 6$, and from $t = 10$ and $t = 12$ were averaged.

TABLE 1
Energy and Nutrient Intake at Baseline on Diets Rich in Oleic Acid or α-Linolenic Acid[a]

	Oleic acid group ($n = 5$)	ALA group ($n = 7$)
Energy (MJ/d)	9.5 ± 1.1	9.9 ± 0.6
Protein (En%)	15.0 ± 0.5	12.4 ± 0.8[b]
Fat (En%)	36.0 ± 2.7	38.3 ± 0.8
SAFA	12.1 ± 1.2	12.1 ± 0.5
MUFA	15.5 ± 1.6	14.5 ± 0.7
PUFA	6.0 ± 0.7	8.8 ± 0.7[b]
Linoleic acid	4.1 ± 0.7	4.5 ± 0.9
Carbohydrates (En%)	43.1 ± 3.1	46.9 ± 1.6
Alcohol (En%)	6.1 ± 1.5	2.5 ± 0.7
Cholesterol (mg/MJ)	16.1 ± 2.1	16.8 ± 3.1
Dietary fiber (g/MJ)	2.6 ± 0.5	1.8 ± 0.2

[a]Values are presented as mean ± SEM. Abbreviations: ALA, α-linolenic acid; SAFA, saturated fatty acids; MUFA, monounsaturated fatty acids; PUFA, polyunsaturated fatty acids.
[b]Denotes a significant difference between groups: $P < 0.05$.

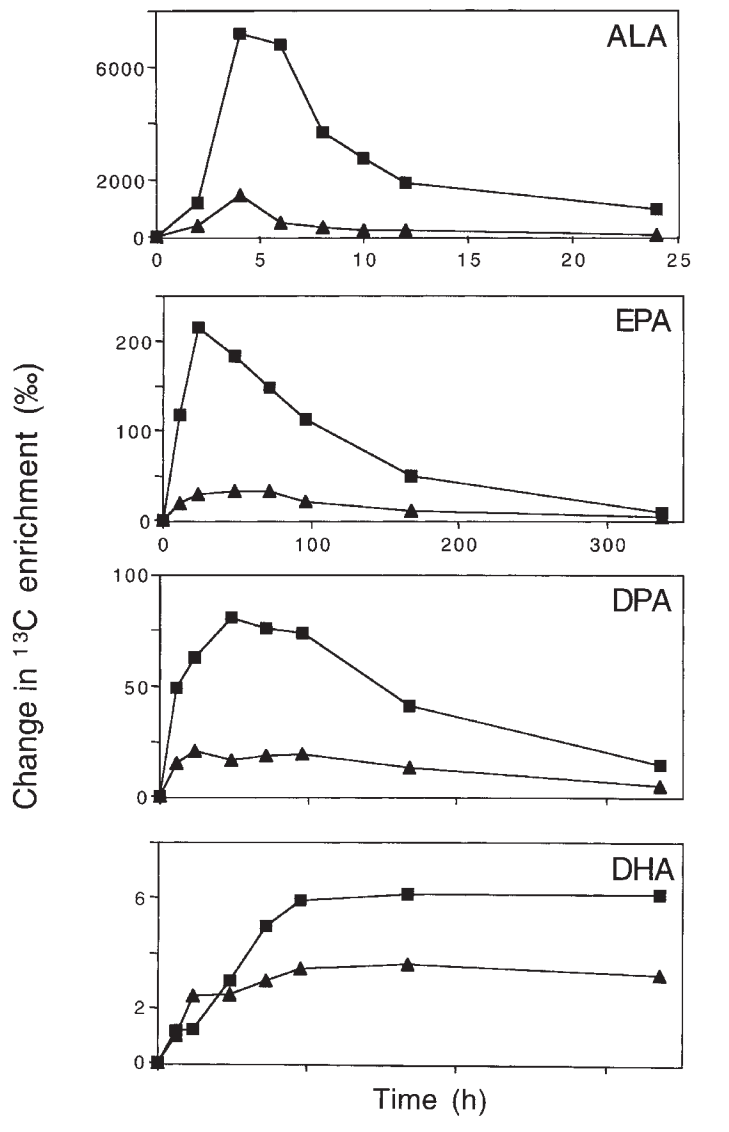

FIG. 2. Changes in plasma ^{13}C enrichments of ALA, EPA, DPA, and DHA after intake of a single dose of ^{13}C-ALA on diets rich in oleic acid (■) or ALA (▲) of two randomly chosen volunteers. Abbreviations: ALA, α-linolenic acid; EPA, eicosapentaenoic acid; DPA, docosapentaenoic acid; DHA, docosahexaenoic acid.

Enrichments. The changes in ^{13}C enrichments of ALA, EPA, DPA, and DHA are shown in Figure 3. Maximum changes in ^{13}C enrichment of ALA were reached after 5 h, followed by a rapid decrease. After 24 h, changes in ^{13}C enrichment were still about 15% of the maximal changes. Values had returned to baseline after 336 h (data not shown). The mean maximum ^{13}C enrichment of ALA relative to baseline in the ALA group was only 37% of that in the oleic acid diet. The ^{13}C enrichment peaks of EPA relative to baseline were much lower and were reached 19 h later than those of ALA. In the ALA group, maximal changes in ^{13}C enrichments of EPA were 43% of those in the oleic acid group. The ^{13}C enrichments of DPA hardly changed between 24 and 96 h in the ALA group. As compared to the oleic acid group, maximal changes in ^{13}C enrichment were 40% in the ALA group. After 336 h, ^{13}C enrichments of EPA and DPA had nearly returned to baseline values in both groups. Ninety-one hours after the ^{13}C enrichment peak of ALA, ^{13}C enrichment of DHA plateaued in both groups until after 336 h. The order of appearance of ^{13}C-labeled ALA, EPA, DPA, and DHA in plasma was thus in accordance with the conversion of ^{13}C ALA into its LCP.

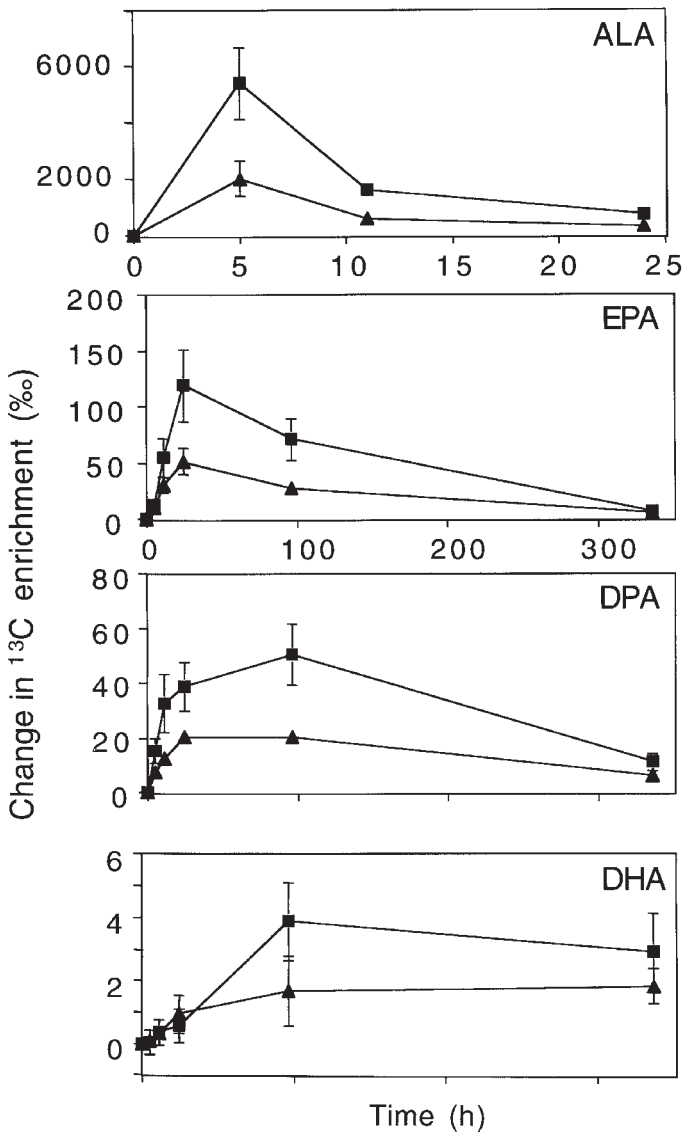

FIG. 3. Mean (± SEM) changes in plasma ^{13}C enrichments of ALA, EPA, DPA, and DHA after intake of a single dose of ^{13}C-ALA in diets rich in oleic acid (■) or ALA (▲). For abbreviations see Figure 2.

Plasma total fatty acid concentrations. Proportions of total ALA in plasma total lipids at baseline were 0.91 ± 0.35% of total fatty acids in the oleic acid group and 1.12 ± 0.17% of total fatty acids in the ALA group. Plasma total EPA, DPA, and DHA concentrations were 0.77 ± 0.12, 0.55 ± 0.06, and 1.61 ± 0.12% of total fatty acids for the oleic acid group and 0.63 ± 0.11, 0.48 ± 0.07, and 1.37 ± 0.13% of total fatty acids for the ALA group, respectively.

Absolute amounts of plasma-labeled fatty acids. Figure 4 shows the individual maximal absolute amounts of plasma ^{13}C n-3 fatty acids. The mean maximal amounts of plasma ^{13}C-ALA were 4.4 ± 0.7 mg (9.8% of the given dose) on the oleic acid diet and 2.8 ± 0.6 mg (6.2%) on the ALA diet ($P = 0.22$). Mean maximal amounts of ^{13}C-EPA were significantly lower in the ALA group (0.04 ± 0.01 mg) as compared to the oleic acid group (0.12 ± 0.03 mg) ($P = 0.01$). Values of ^{13}C-DPA and ^{13}C-DHA were very low, and were somewhat lower on the ALA-rich diet compared to the oleic acid-rich diet ($P = 0.17$ and $P = 0.17$, respectively).

Oxidation. During the first 12 h, maximum ^{13}C enrichments in breath were 11.2 ± 2.5‰ in the oleic acid group and 12.6 ± 1.7‰ in the ALA group, and were reached after about 5 h. Thereafter, ^{13}C enrichment decreased, until 3.8 ± 0.5‰ and 4.7 ± 0.9‰, respectively after 12 h (data not shown). The cumulative recovery of ^{13}C in breath derived from ^{13}C-ALA during the first 12 h after intake is presented in Figure 5. After 12 h, the mean recovery of ^{13}C was not significantly different on the ALA-rich diet (20.4 ± 0.8%) as compared to the oleic acid-rich diet (15.7 ± 2.3%) ($P = 0.12$).

Correlations. Spearman correlation coefficients were calculated between the cumulative recovery of ^{13}C in breath derived from ^{13}C-ALA during the first 12 h after tracer intake and the maximal amount of plasma ^{13}C-labeled n-3 fatty acids for all subjects. The cumulative recovery of $^{13}CO_2$ in breath was neg-

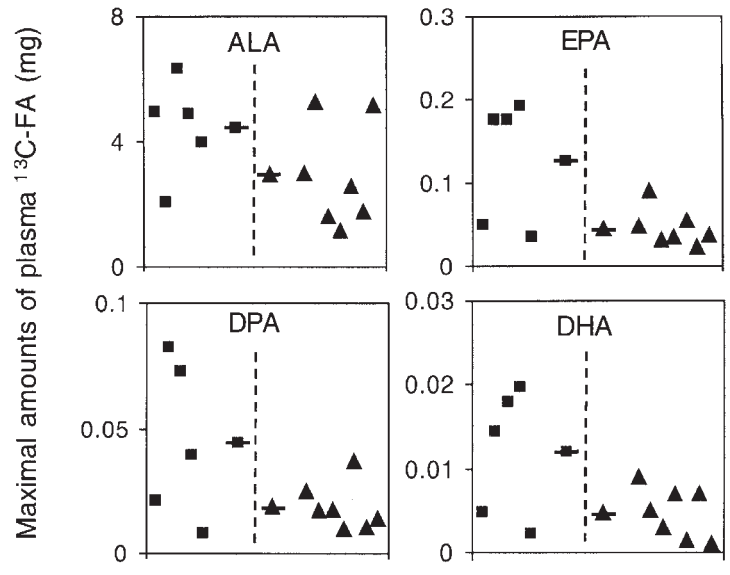

FIG. 4. Individual absolute amounts of plasma ^{13}C-labeled ALA, EPA, DPA, and DHA after intake of a single dose of ^{13}C-ALA in diets rich in oleic acid (■; mean ▬) or ALA (▲; mean ▲). For abbreviations see Figure 2.

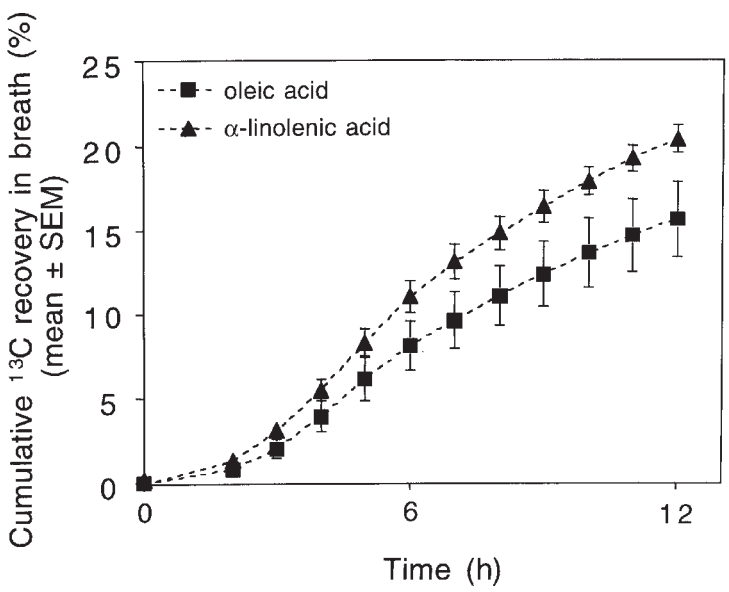

FIG. 5. Cumulative recovery of $^{13}CO_2$ in breath derived from ALA (mean ± SEM) after intake of a single dose of ^{13}C-ALA on diets rich in oleic acid (n = 5) or ALA (n = 7). For abbreviations see Figure 2.

atively correlated with plasma ^{13}C-EPA (r = –0.58, P = 0.047) and ^{13}C-DPA (r = –0.63, P = 0.027), but not with ^{13}C-ALA (r = 0.05, P = 0.888) and ^{13}C-DHA (r = –0.49, P = 0.108). The maximal amounts of plasma ^{13}C-ALA, ^{13}C-EPA, ^{13}C-DPA, and ^{13}C-DHA did not correlate with each other.

EPA/DHA group. The daily supplemented intake in the EPA/DHA group was 0.9 g (0.5 energy %) for EPA and 0.5 g (0.3 energy %) for DHA.

Conversion of ^{13}C-ALA could not be measured in one woman of the EPA/DHA group due to problems during preparation of FAME. Maximal changes in ^{13}C enrichment of ALA (2427‰) and EPA (5.1‰) were reached at the same time as in the ALA and oleic acid group, while changes were lower for EPA. Values had returned to baseline after 336 h. Changes in ^{13}C enrichments of DPA were very low (2.8‰), and that of DHA were zero.

The proportions of total ALA, EPA, DPA, and DHA in plasma total lipids at baseline were 0.56, 3.09, 0.71, and 2.40%, respectively. Maximal amounts of ^{13}C-ALA, ^{13}C-EPA, and ^{13}C-DPA were 2.1 mg, $3.4 \cdot 10^{-2}$ mg, and $5.1 \cdot 10^{-3}$ mg, respectively. The cumulative recovery of ^{13}C-ALA in breath during the first 12 h after intake was 24.8%.

DISCUSSION

In this study with healthy adults, maximal absolute amounts of labeled EPA in plasma were significantly lower in the ALA group as compared to the oleic acid group, after intake of a single oral dose of uniformly labeled ^{13}C-ALA. Although maximal absolute amounts of labeled DPA and DHA were not lowered on the ALA rich diet, our conversion data may suggest that the metabolism of dietary ALA depends on its intake.

Effects of ALA on the conversion of ALA *in vivo* have never been reported in humans before. Dietary linoleic acid, however, inhibits the conversion of deuterated linoleic acid (9), while a diet rich in arachidonic acid has no significant effect on the conversion of deuterated linoleic acid into arachidonic acid (21). This suggests that the reduced conversion of deuterated linoleic acid is caused by linoleic acid from the diet.

ALA is converted into 18:4n-3 by Δ6 desaturation, subsequently elongated into 20:4n-3, from which EPA can be formed by Δ5 desaturation. EPA is converted into DHA *via* two elongation steps, followed by another Δ6 desaturation step and one cycle of β-oxidation (22). The Δ6 desaturation has been suggested to be the rate limiting step in the conversion of ALA. We are unable to decide whether or not ALA affects the Δ6 or Δ5 desaturase activity, because plasma concentrations of 18:4n-3 and 20:4n-3 were too low to detect ^{13}C enrichments.

Our experimental design did not allow to quantify the conversion of ALA. One commonly used method is to calculate area under the curves (21). We think, however, that this method is not applicable in our study, since after administration of a single dose of ^{13}C-labeled ALA, the distribution of ^{13}C-n-3 fatty acids over the various tissue lipids did not reach a steady state. In addition, the slow appearance and disappearance rates of the tracer in plasma may indicate that these processes are not sequential, but overlap. Therefore, the area under the curve does not reflect the amount of ^{13}C-labeled fatty acids converted (23).

From rat studies, it is known that the activity of enzymes involved in the mitochondrial and peroxisomal fatty acid oxidation are increased by dietary EPA (24). The effects of dietary ALA on ALA oxidation in humans are, however, not known. In the present study, the mean proportion of labeled ALA recovered as $^{13}CO_2$ in breath after 12 h was slightly, although not significantly, higher in the ALA group compared to the oleic acid group, suggesting that the oxidation of ALA may not be inhibited by dietary ALA.

We hardly found any ^{13}C enrichment of n-3 LCP in a diet rich in EPA/DHA. However, the plasma total EPA and DHA concentrations were increased in an EPA/DHA-rich diet as compared to values on an oleic acid- or ALA rich diet. This suggests that plasma EPA and DHA were mainly derived from dietary sources. Absolute amounts of ^{13}C-LCP were very low, suggesting that conversion of ^{13}C-ALA may be lowered on dietary EPA/DHA. As suggested before (25), the conversion of ^{13}C-ALA may be inhibited by dietary EPA plus DHA. However, because of the small number of subjects in this group, results should be interpreted with caution. Recently, our suggestion was confirmed by Emken *et al.*, who found decreased accumulation of deuterated n-3 LCP in a diet enriched in DHA (11).

We observed negative correlations between the recovery in breath of $^{13}CO_2$ derived from ^{13}C-ALA after 12 h and the maximal amounts of plasma ^{13}C-EPA and ^{13}C-DPA in plasma total lipids. The correlation between the $^{13}CO_2$ recovery and ^{13}C-DHA amounts failed to reach statistical significance. If results of the EPA/DHA group are, however, also incorporated into the analysis, the negative correlations between the oxidation and conversion of ^{13}C-ALA become stronger. Even ^{13}C-DHA is now significantly correlated with the $^{13}CO_2$ recovery (r = –0.63; P = 0.008). The lack of significantly lower amounts of ^{13}C-DPA and ^{13}C-DHA on the ALA group as com-

pared to the oleic acid group, could also be due to the limited number of subjects.

Except for ALA, differences in energy and nutrient intakes between the treatment groups were small. We, therefore, suggest that conversion of ^{13}C-ALA into LCP may be lowered by dietary ALA, while oxidation of ^{13}C-ALA is negatively correlated with its conversion into LCP. The preliminary results of an EPA/DHA-rich diet showed very low amounts of ^{13}C-LCP, suggesting that conversion of ^{13}C-ALA may also be lowered on dietary EPA/DHA. Therefore, it seems it would be very interesting to examine this issue in more detail in further studies.

ACKNOWLEDGMENTS

We gratefully acknowledge Dr. David Kyle of Martek Biosciences Corporation (Columbia, MD) for providing stable isotopes. We thank the volunteers for their cooperation.

REFERENCES

1. Kinsella, J.E. (1991) α-Linolenic Acid: Functions and Effects on Linoleic Acid Metabolism and Eicosanoid-Mediated Reactions, in *Advances In Food And Nutrition Research* (Kinsella, J.E. ed.), pp. 1–184, Academic Press, San Diego.
2. Bordoni, A., Lopez-Jimenez, J.A., Spanò, C., Biagi, P., Horrobin, D.F., and Hrelia, S. (1996) Metabolism of Linoleic and α-Linolenic Acids in Cultured Cardiomyocytes: Effect of Different n-6 and n-3 Fatty Acid Supplementation, *Mol. Cell. Biochem 157*, 217–222.
3. Christiansen, E.N., Lund, J.S., Rortveit, T., and Rustan, A.C. (1991) Effect of Dietary n-3 and n-6 Fatty Acids on Fatty Acid Desaturation in Rat Liver, *Biochim. Biophys. Acta 1082*, 57–62.
4. de Alaniz , M.J.T., and de Gómez Dumm, I.N.T. (1990) Role of Fatty Acids of (n-3) and (n-6) Series on α-Linolenic Acid Desaturation and Chain Elongation in HTC Cells, *Mol. Cell. Biochem. 93*, 77–85.
5. Cao, J.-M., Blond, J.P., Juaneda, P., Durand, G., and Bézard, J. (1995) Effect of Low Levels of Dietary Fish Oil on Fatty Acid Desaturation and Tissue Fatty Acids in Obese and Lean Rats, *Lipids 30*, 825–832.
6. Chan, J.K., McDonald, B.E., Gerrard, J.M., Bruce, V.M., Weaver, B.J., and Holub, B.J. (1993) Effect of Dietary α-Linolenic Acid and Its Ratio to Linoleic Acid on Platelet and Plasma Fatty Acids and Thrombogenesis, *Lipids 28*, 811–817.
7. Mantzioris, E., James, M.J., Gibson, R.A., and Cleland, L.G. (1995) Differences Exist in the Relationships Between Dietary Linoleic and α-Linolenic Acids and Their Respective Long-Chain Metabolites, *Am. J. Clin. Nutr. 61*, 320–324.
8. Gerster, H. (1998) Can Adults Adequately Convert α-Linolenic Acid (18:3n-3) to Eicosapentaenoic Acid (20:5n-3) and Docosahexaenoic Acid (22:6n-3)? *Int. J. Vit. Nutr. Res. 68*, 159–173.
9. Emken, E.A., Adlof, R.O., and Gulley, R.M. (1994) Dietary Linoleic Acid Influences Desaturation and Acylation of Deuterium-Labeled Linoleic and Linolenic Acids in Young Adult Males, *Biochim. Biophys. Acta 1213*, 277–288.
10. Salem, N., Pawlosky, R., Wegher, B., and Hibbeln, J. (1999) *In vivo* Conversion of Linoleic Acid to Arachidonic Acid in Human Adults, *Prostaglandins Leukotrienes Essent. Fatty Acids 60*, 407–410.
11. Emken, E.A., Adlof, R.O., Duval, S.M., and Nelson, G.J. (1999) Effect of Dietary Docosahexaenoic Acid on Desaturation and Uptake *in vivo* of Isotope-Labeled Oleic, Linoleic, and Linolenic Acids by Male Subjects, *Lipids 34*, 785–791.
12. Salem, N., Wegher, B., Mena, P., and Uauy, R. (1996) Arachidonic and Docosahexaenoic Acids Are Biosynthesized from Their 18-Carbon Precursors in Human Infants, *Proc. Natl. Acad. Sci. Usa 93*, 49–54.
13. Carnielli, V.P., Wattimena, D.J.L., Luijendijk, I.H.T., Boerlage, A., Degenhart, H.J., and Sauer, P.J.J. (1996) The Very Low Birth Weight Premature Infant Is Capable of Synthesizing Arachidonic and Docosahexaenoic Acids from Linoleic and Linolenic Acids, *Pediatr. Res. 40*, 169–174.
14. Sauerwald, T.U., Hachey, D.L., Jensen, C.L., Huiming, C., Anderson, R.E., and Heird, W.C. (1996) Effect of Dietary α-Linolenic Acid Intake on Incorporation of Docosahexaenoic and Arachidonic Acids into Plasma Phospholipids of Term Infants, *Lipids 31*, 131–135.
15. Sauerwald, T.U., Hachey, D.L., Jensen, C.L., Chen, H., Anderson, R.E., and Heird, W.C. (1997) Intermediates in Endogenous Synthesis of C22:6ω3 and C20:4ω6 by Term and Preterm Infants, *Pediatr. Res. 41*, 183–187.
16. Wensing, A.G.C.L., Mensink, R.P., and Hornstra, G. (1999) Effects of Dietary n-3 Polyunsaturated Fatty Acids from Plant and Marine Origin on Platelet Aggregation in Healthy Elderly Subjects, *Br. J. Nutr. 82*, 183–191.
17. Stichting NEVO (1989) NEVO tabel, Nederlands voedingsstoffenbestand (Dutch food composition table), Voorlichtingsbureau voor de Voeding, Den Haag, Nederlands.
18. Folch, J., Lees, M., and Sloane Stanley, G.H. (1957) A Simple Method for the Isolation and Purification of Total Lipids from Animal Tissues, *J. Biol. Chem. 226*, 497–509.
19. Lepage, G, and Roy, C.C. (1986) Direct Transesterification of All Classes of Lipids in a One-Step Reaction, *J. Lipid Res. 27*, 114–120.
20. Gregersen, M.I., and Rawson, R.A. (1959) Blood Volume, *Physiol. Rev. 39*, 307–342.
21. Emken, E.A., Adlof, R.O., Duval, S.M., and Nelson, G.J. (1998) Effect of Dietary Arachidonic Acid on Metabolism of Deuterated Linoleic Acid by Adult Male Subjects, *Lipids 33*, 471–480.
22. Voss, A., Reinhart, M., Sankarappa, S., and Sprecher H. (1991) The Metabolism of 7,10,13,16,19-Docosapentaenoic Acid to 4,7,10,13,16,19-Docosahexaenoic Acid in Rat Liver Is Independent of a 4-Desaturase, *J. Biol. Chem. 266*, 19995–20000.
23. Demmelmair, H., Iser, B., Rauh-Pfeiffer, A., and Koletzko, B. (1999) Comparison of Bolus Versus Fractionated Oral Applications of [^{13}C]-Linoleic Acid in Humans, *Eur. J. Clin. Invest. 29*, 603–609.
24. Aarsland, A., Lundquist, M., Borretsen, B., and Berge, R.K. (1990) On the Effect of Peroxisomal β-Oxidation and Carnitine Palmitoyltransferase Activity by Eicosapentaenoic Acid in Liver and Heart from Rats, *Lipids 25*, 546–548.
25. Vermunt, S.H.F., Mensink, R.P., Simonis, A.M.G., and Hornstra, G. (1999) Effects of Age and Dietary n-3 Fatty Acids on the Metabolism of [^{13}C]-α-Linolenic Acid, *Lipids 34*, S127.

[Received April 21, 1999, and in revised form January 6, 2000; revision accepted January 26, 2000]

A High-Fat Diet Induces and Red Wine Counteracts Endothelial Dysfunction in Human Volunteers

Ada M. Cuevas[a], Viviana Guasch[b], Oscar Castillo[a], Veronica Irribarra[a], Claudio Mizon[a], Alejandra San Martin[b], Pablo Strobel[b], Druso Perez[b], Alfredo M. Germain[c], and Federico Leighton[b,*]

Departments of [a]Nutrition, Metabolism & Diabetes and [c]Obstetrics & Gynecology, School of Medicine, and [b]Biochemical Cytology and Lipids Laboratory, Faculty of Biological Sciences, Pontificia Universidad Católica de Chile, Santiago, Chile

ABSTRACT: Endothelial dysfunction is associated with atherogenesis and oxidative stress in humans. In rat and rabbit blood vessels, wine polyphenol antioxidants induce vascular relaxation *in vitro* through the NO-cGMP pathway. To assess the effect of a regular high-fat diet (HFD) and moderate red wine consumption on endothelial function (EF), a study was performed in healthy male volunteers. EF was measured as flow-mediated dilatation of the brachial artery, employing high-resolution ultrasound after an overnight fast. Other clinical and biochemical parameters related to EF were also measured. Six volunteers received a control diet, rich in fruits and vegetables (27% calories as fat) and five volunteers received an HFD (39.5% calories as fat). Measurements were done twice on each volunteer: after a period of 30 d with diet plus 240 mL of red wine/d, and after a period of 30 d with diet, without wine. In the absence of wine, there is a reduction of EF with HFD when compared to the control diet ($P = 0.014$). This loss of EF is not seen when both diets are supplemented with wine for 30 d ($P = 0.001$). Plasma levels of *n*-3 fatty acids ($R^2 = 0.232$, $P = 0.023$) and lycopene ($R^2 = 0.223$, $P = 0.020$) show a positive correlation with individual EF measurements, but they do not account for the significant differences observed among dietary groups or after wine supplementation. These results help elucidate the deleterious effect of a high-fat diet and the protective role of wine, n-3 fatty acids and dietary antioxidants in cardiovascular disease.

Paper no. L8349 in *Lipids 35*, 143–148 (February 2000).

Normal endothelium-dependent vasomotor function or endothelial function (EF) is a physiological response, mediated by nitric oxide (NO), that appears to play a key role in the prevention or reduction of the risk of atherosclerosis (1,2). Endothelial dysfunction is associated with risk factors for coronary heart disease such as hypercholesterolemia, hypertension, cigarette smoking, hyperhomocysteinemia and diabetes mellitus and is detectable before anatomical vascular signs of atherosclerosis appear, supporting a pathogenic role of endothelial dysfunction in atherogenesis (3–5). Young healthy subjects with a family history of premature coronary disease and no other apparent risk factor also show impaired EF (6).

Hypercholesterolemia (7), genetic hyperlipidemias (8), or a single high-fat meal (9) decrease EF, suggesting that a regular high-fat diet (HFD) might lead to endothelial dysfunction. Ingestion of the antioxidant vitamins C and E (1,5,8,10,11) partially blocks the decrease in EF *in vivo*, a phenomenon attributed to protection of NO from inactivation by free radicals.

Vegetables and moderate wine consumption have been associated with a decreased risk of coronary disease (12,13), an effect related, at least in part, to their high content in flavonoids and other polyphenol antioxidants (14,15). Also, it has been shown that wine polyphenols exert vasorelaxing activity in rat and rabbit aortic rings and human coronary arteries rings (16–19). Plant polyphenols from other sources show a similar activity (20). Moderate wine consumption and a high intake of fruits and vegetables characterize Mediterranean diets (21,22). Therefore, plant polyphenol antioxidants could account, at least in part, for the cardiovascular health benefits associated with Mediterranean diets and moderate wine consumption.

The present study evaluates EF employing a noninvasive ultrasound detection method (23) in human volunteers on either an HFD or a control diet (CD) rich in fruits and vegetables, with and without moderate red wine consumption.

EXPERIMENTAL PROCEDURES

Study design. The experimental protocol employed was approved by the Ethics Committee of the Faculty of Medicine, Catholic University of Chile. Subjects were randomly selected from a larger group of volunteers participating in a diet and wine intervention study. For 90 d they received either an HFD ($n = 5$) or a CD ($n = 6$). From day 31 to 60 the diet was isocalorically supplemented with 240 mL/d of red wine (cabernet sauvignon). No other alcoholic beverage was allowed during the 3 mon of the study. EF, as well as the other measurements reported here, were performed at days 60 and 90.

*To whom correspondence should be addressed at Department of Cellular and Molecular Biology, Faculty of Biological Sciences, Pontificia Universidad Católica de Chile, Casilla 114-D, Santiago, Chile.
E-mail: fleighto@genes.bio.puc.cl

Abbreviations: ANOVA, analysis of variance; CD, control diet; cGMP, guanosine 3′:5′-cyclic monophosphate; DHA, docosahexaenoic acid; DPA, docosapentaenoic acid; EDRF, endothelium-derived vascular relaxing factor; EF, endothelial function; γ-GT, γ-glutamyl transferase; HFD, high-fat diet; HPLC, high-performance liquid chromatography; NO, nitric oxide; PUFA, polyunsaturated fatty acids; SFA, saturated fatty acids; VLCn-3, very long-chain n-3-fatty acids.

Subjects. Subjects were healthy males, aged 20–28 yr, undergraduate or graduate students from the Faculty of Medicine, who signed an informed consent form and were well informed about the project procedures and objectives. They were randomly selected from a larger group of 42 subjects. The smaller size of the groups for EF measurement was determined both by the chronogram of biological sampling defined for the larger study, and limitations in the access to the ultrasound imaging equipment, since the volunteers were required to fast overnight. Criteria for inclusion were absence of clinical disease, body mass index 20–25 kg/m^2, and normal values for serum lipids, blood pressure, and blood glucose. They were normally active, nonsmokers, and were not taking any medication or vitamin supplementation. Clinical interview, physical examination, and laboratory evaluation were done every 30 d. Blood pressure values correspond to the mean of two measurements, separated 5 min, with the subject in a sitting position.

Diets. HFD and CD were prepared by a catering company, with daily supervision by a nutritionist and a food microbiologist working for the project. Diets were delivered at the work place, or at home at night and weekends, in isolated personalized boxes. The average daily caloric supply was 2,565 kcal. Proteins supplied 17.6% of calories for both diets. Fats, as detailed in Table 1 supplied 27.3 or 39.9% of calories for CD and HFD, respectively. Diet composition was calculated employing Food Processor II (Esha Research, Salem, OR). Fruits and vegetables consumption was an average of 675 g/d for CD and 246 g/d for HFD. HFD used preferentially red meats and was low in fish; CD used predominantly fish and white meat. On the whole, HFD resembled a regular Western or U.S. diet from the last decades (24,25) and CD a Mediterranean-style diet (21,22).

Biochemical analysis. Plasma glucose, serum enzymes, total cholesterol, low density lipoprotein cholesterol, and triglycerides were measured following routine clinical laboratory procedures. Fatty acids were measured by gas chromatography as follows: plasma lipids were extracted according to Bligh and Dyer (26) using chloroform/methanol (2:1, vol:vol) containing butylated hydroxytoluene (0.01%). Total fatty acids were transesterified with methanolic-HCl (1 N) overnight at room temperature; after extraction with *n*-hexane, the methyl esters were quantified by gas–liquid chromatography employing a capillary column (50 m × 0.25 mm, SGE BPX-70) with hydrogen as carrier gas and a temperature program of 5°/min from 110 to 230°C. Vitamin E (as α-tocopherol), β-carotene, and lycopene were determined by high-performance liquid chromatography (HPLC) with electrochemical detection (LC-4C, Bioanalytical Systems Inc., W. Lafayette, IN) (27). Serum vitamin C was detected by a procedure based on the reduction of ferric chloride (28); the accuracy of these measurements was checked by HPLC. Folate and vitamin B_{12} in serum were determined by ion capture and microparticle immunoassay, respectively (IMX® Folate and AxSYM B_{12}; Abbott Labs, Abbott Park, IL). Plasma homocysteine was measured by HPLC with fluorometric detection, employing a commercial kit (Chromsystems, München, Germany).

TABLE 1
Daily Intake of Fats and Fatty Acids[a]

	High fat diet (g/d)	Control diet (g/day)
Total fat	112.7 ± 12.9	77.0 ± 2.6
SFA	35.8 ± 9.6	22.7 ± 2.3
MUFA	35.3 ± 4.2	37.9 ± 2.5
PUFA	32.0 ± 4.5	9.6 ± 1.4
VLCn-3	0.12 ± 0.04	0.38 ± 0.13
Cholesterol	0.61 ± 0.12	0.29 ± 0.09

[a]Mean values ± SD. Abbreviations: SFA, saturated fatty acids; MUFA, monounsaturated fatty acids; PUFA, polyunsaturated fatty acids; VLCn-3, very long-chain n-3 fatty acids = eicosapentaenoic acid + docosapentaenoic acid + docosahexaenoic acid.

EF. EF was assessed twice for each volunteer: on day 60, at the end of the 30-d wine supplementation period; and at day 90, after a period of 30 d without wine, only with diet. Measurement were made at 8–9 A.M., with an overnight fast. The noninvasive procedure employs 7.5 MHz ultrasound imaging (GAIA 8800, Medison, Seoul, Korea) and has been validated by Celermajer *et al.* (23). The measurements were performed essentially as described by Plotnick *et al.* (10). The brachial artery was longitudinally imaged approximately 5 cm proximal to the antecubital crease, twice at baseline and then 1, 3, and 5 min after release of 5 min arterial occlusion with a blood pressure cuff, 12.5-cm wide, placed on the forearm, kept at 200 mm Hg. Results are expressed as percent dilation at minute 1 after flow reestablishment. Two independent investigators, unaware of subject identity and dietary status, performed the measurements of end-diastolic brachial artery diameter in the video recordings obtained. Following flow-mediated reactivity measurement, after 15 min rest, volunteers received 300 μg nitroglycerin sublingually to control the dilatation response 3 min after nitroglycerin administration.

Statistical procedures Data are expressed as mean ± SD. The measurements within the same dietary group, at different times, were compared by analysis of variance (ANOVA) for repeated measures and paired *t* test with Bonferroni adjustment. To determine if wine supplementation to both dietary groups modifies the variables in the same direction, ANOVA for repeated measures with interaction between diet and wine was applied. For comparisons among the two dietary groups, the Student *t* test for independent samples was employed. Bivariant correlation analysis was performed according to Pearson. *P* values <0.05 were considered statistically significant.

RESULTS

The relative increase in brachial artery diameter that follows the reestablishment of circulation constitutes the basis of the noninvasive procedure to quantitate EF. The kinetics of the relative change in mean arterial diameter values for the two experimental conditions are shown in Figure 1. In the HFD maximal response occurs after 1 min of flow reestablishment, whereas for CD the vasodilation response apparently is slower. The difference observed with wine was maximal after 1 min for both dietary groups. In fact, this time interval is routinely em-

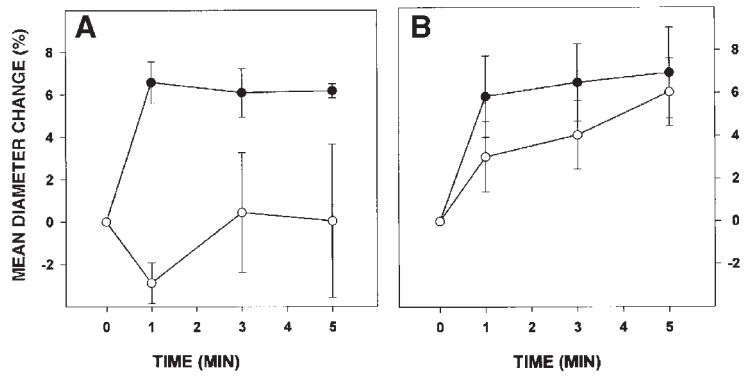

FIG. 1. Effect of diet and wine on endothelium-dependent brachial artery vasoactivity. Flow-mediated brachial artery vasoactivity, expressed as percent change in arterial diameter, was measured with high-resolution ultrasound, before and at various times after releasing the circulatory arrest imposed by an inflated cuff in the forearm. The measurements were made after 12 h without food and wine, and correspond to the mean values ± standard error, from (A) 5 subjects under a high-fat diet or (B) 6 subjects under a control diet rich in fruits and vegetables, with (●) or without (○) supplementation with red wine (240 mL/d). The change in diameter is expressed relative to the diameter before circulatory arrest.

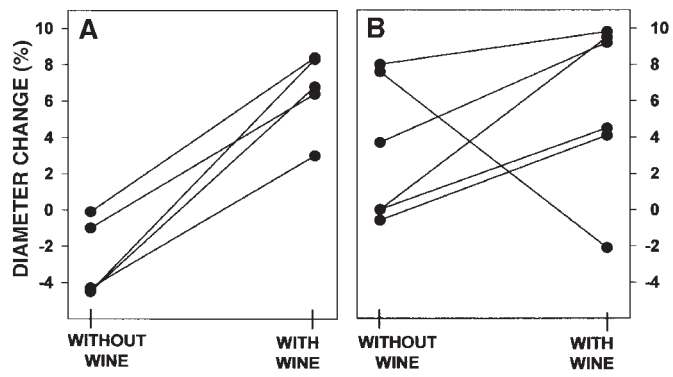

FIG. 2. Effect of wine supplementation on endothelium-dependent flow-mediated brachial artery vasoactivity, expressed as percent change in arterial diameter for each experimental subject consuming a high-fat (A) or a control (B) diet. Values represented correspond to individual measurements, 1 min after releasing the arterial flow, obtained during the observations summarized in Figure 1.

ployed in the standard procedure to evaluate EF. The individual EF values with and without wine, for the five HFD and the six CD volunteers, are shown in Figure 2. A striking result is the consistent increase of EF in the HFD subjects when wine is present in the diet. The average percent diameter change varies from –2.9 ± 2.1 without wine to 6.6 ± 2.2 with wine ($P = 0.001$ for paired data analysis). It can also be seen that in the absence of wine, HFD values are significantly lower than those for CD, average 3.1 ± 3.9 ($P = 0.014$). The effect of wine, clearly seen for HFD, is not evident with CD; 3.1 ± 3.9 is the average percent diameter change without wine supplementation and 5.8 ± 4.6 with wine supplementation ($P = 0.358$ for paired samples), yet ANOVA for repeated measurements with interaction among diet and wine shows a parallel behavior for HFD and CD, i.e., both groups change with wine in the same direction. Unexpectedly, one CD volunteer showed decreased EF in the wine supplementation period, a result for which we do not have a more precise explanation than biological variability.

Nitroglycerin-induced percent dilation values for HFD were 19.1 ± 10.3 and 26.5 ± 2.9 without and with wine supplementation; and for CD 21.4 ± 5.3 and 20.9 ± 3.5, without and with wine supplementation. These values suggest an increase in the nitroglycerin-induced dilatation for the HFD group after wine supplementation, but the difference is not statistically significant for the HFD group ($P = 0.262$ for paired samples).

The diets employed had either 39.5 (HFD) or 27% (CD) of total calories as fat. As shown in Table 1, both provided almost the same amount of monounsaturated fatty acids; in contrast, HFD supplied three times more polyunsaturated fatty acids (PUFA) and 1.6 times the saturated fatty acids (SFA) of CD. For CD, SFA amount to 8.7% of total energy consumption. For fruits and vegetables the supply was almost three times higher in CD.

The average values for some plasma biochemical parameters in both dietary groups, with and without wine, are shown in Table 2. The plasma fatty acid profiles apparently reflect the dietary pattern; nevertheless, statistically significant differences among diets are seen only in PUFA and very long chain n-3 fatty acids (VLCn-3) values after wine supplementation. Total and low density lipoprotein cholesterol values as well as triglycerides apparently reflect the diet composition, but the changes are not statistically significant, most probably as a consequence of the relatively small number of subjects evaluated. Other biochemical parameters known to influence EF do not show variations that could account for the changes in EF observed with diet and wine: homocysteine and vitamin B_{12} remain constant, and folic acid increases with the diet rich in fruits and vegetables, but without correlation with homocysteine levels. A consistent change observed with both diets is a statistically significant 14% decrease in plasma vitamin E (α-tocopherol) at the end of the wine supplementation period. Lycopene mean values do not show statistically significant variations within or among diets, yet there is a positive correlation among all individual lycopene values and EF values expressed as percent dilation of the brachial artery ($R^2 = 0.223$, $P = 0.020$). A similar correlation is seen among VLCn-3 mass plasma levels and EF ($R^2 = 0.232$, $P = 0.023$). This positive and statistically significant correlation of EF with n-3 fatty acids is mainly due to docosapentaenoic acid (DPA) ($R^2 = 0.504$, $P = 0.017$) and docosahexaenoic acid (DHA) ($R^2 = 0.437$, $P = 0.042$). A significant increase in VLCn-3 plasma concentration, in the presence of wine supplementation, is seen only in CD; in contrast, the most striking change in EF is seen with the HFD, when wine is added. In HFD, VLCn-3 plasma levels do not change with wine, in contrast to the striking effect of wine on EF. This probably means that lycopene and VLCn-3 plasma levels influence the absolute value for each EF measurement, while the relative changes observed with wine apparently are independent of lycopene or VLCn-3 concentration changes.

As part of the biochemical monitoring procedure, (γ-glutamyl transferase), serum glutamic-oxalacetic transaminase, and alkaline phosphatase levels in serum were measured (Table 3). The main change observed, a 40% increase in γ-GT in HFD

TABLE 2
Biochemical Measurements in Plasma[a]

Plasma variable	High-fat diet		Control diet	
	Without wine	With wine	Without wine	With wine
Glucose (mg/dL)	82.0 ± 3.3	83.0 ± 5.5	81.2 ± 5.5	87.3 ± 6.4
Total cholesterol (mg/dL)	177 ± 33	185 ± 33	155 ± 24	150 ± 19
LDL (mg/dL)	102 ± 24	111 ± 28	89 ± 21	88 ± 18
Triglycerides (mg/dL)	137 ± 128	127 ± 89	88 ± 41	68 ± 31
SFA (μg/mL)	622 ± 136	737 ± 180	559 ± 60	525 ± 14
MUFA (μg/mL)	404 ± 182	537 ± 214[a]	377 ± 81	421 ± 83
PUFA (μg/mL)	896 ± 116	1,166 ± 252[a]	776 ± 176	756 ± 90[b]
VLCn-3 (μg/mL)	80.2 ± 36.2	91.0 ± 16.0	80.8 ± 25.7	137 ± 18.9[a,b]
Vitamin E (μmol/L)	27.4 ± 10.5	23.6 ± 9.5[a]	19.9 ± 4.7	17.0 ± 3.9[a]
Vitamin C (μmol/L)	32.5 ± 23.4	25.8 ± 6.8	54.1 ± 7.2	58.3 ± 11.7[b]
Lycopene (nmol/L)	156 ± 63	318 ± 130	167 ± 62	245 ± 105
Folic acid (ng/mL)	3.96 ± 1.29	3.88 ± 0.62	5.82 ± 2.03	6.35 ± 2.19[b]
Vitamin B_{12} (pg/mL)	376 ± 177	334 ± 164	423 ± 173	381 ± 142
Homocysteine (μmol/L)	16.5 ± 6.1	15.3 ± 4.9	14.7 ± 2.4	11.8 ± 2.2

[a]Mean values ± SD. [a]Significant difference, within the same diet, with wine supplementation; Student *t* test for paired samples. [b]Significant difference among different diets; Student *t* test for independent samples. LDL, low density lipoprotein; for other abbreviations, see Table 1.

when compared to CD, was apparently due to the diet and not to wine supplementation. Wine supplementation induced only a slight, statistically significant, reduction in alkaline phosphatase in the CD group.

DISCUSSION

The results presented indicate that normal subjects experience a marked decrease or impairment of EF, under a usual western-style diet rich in fats. Strikingly, after moderate wine consumption vascular reactivity or EF is preserved. The EF measurements were done after an overnight fast, 12 h without food and wine; therefore, the changes induced by wine and diet do not correspond to a transient or acute postprandial response but rather to a stable change associated with the specific dietary condition.

The noninvasive procedure employed to measure EF has been validated (29–31). It has been applied to detect the consequences of an acute overload with fat (8) and the effect of antioxidant vitamins (1,5,8,10,11). The mechanism through which fats interfere with EF is apparently linked to free radical generation, since antioxidant vitamins prevent the effect. In the presence of free radicals NO is inactivated (32) and the reaction with superoxide leads to the formation of peroxynitrite. Therefore, as much as fats can lead to increased levels of free radicals and reactive oxygen species, it is not surprising that NO-mediated processes will be slowed, unless an adequate antioxidant defense is present. The initial *in vitro* observations with wine polyphenols (16) and the present work in humans suggest that wine polyphenols constitute an adequate source of antioxidants, readily available *in vivo*, capable of protecting NO function.

The finding that VLCn-3 plasma levels correlate with the degree of flow-mediated vasodilation is in agreement with previous findings. Dietary supplementation with fish oil, not necessarily with purified n-3 fatty acids, has been shown to augment endothelium-dependent vasodilation in human peripheral and coronary arteries, in a process apparently mediated by increased NO production (33,34). This effect of n-3 fatty acids is an example of the difficulties experienced when attributing to fats or fatty acids in general a specific biological effect: elevated lipid levels will favor free radical generation and oxidative stress, yet n-3 fatty acids protect EF and are antiatherogenic (35,36) in spite of their high degree of unsaturation, which makes them most susceptible to oxidation. The reduced EF observed with HFD might correlate with the three fold increase in PUFA, mostly 18:2n-6, when compared with CD. In fact, a diet rich in linoleic acid is expected to cause oxidative stress, and the mass or amount of linoleic acid supplied by the HFD is 100-fold or more higher than the amount of VLCn-3.

The present results most likely are the consequence of the

TABLE 3
Serum Enzyme Levels: Glutamate-Oxaloacetate Transaminase (SGOT), γ-Glutamyl Transferase (γ-GT), and Alkaline Phosphatase (ALP)[a]

Enzyme	High-fat diet		Control diet	
	Without wine	With wine	Without wine	With wine
SGOT (U/L)	23.3 ± 4.2	24.2 ± 4.1	18.5 ± 3.4	20.8 ± 6.4
γ-GT (U/L)	26.6 ± 5.6	27.0 ± 7.8	16.0 ± 4.7	19.3 ± 6.3[a]
ALP (U/L)	92.2 ± 25.2	87.0 ± 27.9	95.8 ± 12.7	85.3 ± 11.6[b]

[a]Mean value ± SD. [a]Significant among different diets; Student *t* test for independent samples. [b]Significant difference, within the same diet, with wine supplementation; Student *t* test for paired samples.

antioxidant properties of wine and the prooxidant effect of a HFD (37). We found no evidence in favor of other mechanisms. It has been observed that homocysteine plasma levels inversely correlate with EF values, and that the administration of antioxidants counteracts the homocysteine-induced inhibition of EF (5); however, in the present observations homocysteine levels did not correlate with EF changes. The supply of arginine in the diet (data not shown) was also unrelated to the changes observed in EF.

In our observations, among established plasma antioxidants, only lycopene levels correlate with vascular reactivity. This probably means that lycopene is particularly effective at this level, or that it is a marker for other antioxidants present in tomatoes (38), or that wine polyphenols from the diet exert a sparing or protective effect on plasma lycopene.

ACKNOWLEDGMENTS

We thank Dr. Diego Mezzano for constructive criticism of this work and Mr. Eduardo Aranda for the homocysteine measurements, at the Department of Hematology-Oncology, School of Medicine, Pontificia Universidad Católica de Chile. This work was supported by the Molecular Basis of Chronic Diseases Program at the Pontificia Universidad Católica de Chile (PUC-PBMEC98)

REFERENCES

1. Wilkinson, I.B., and Cockcroft, J.R. (1998) Cholesterol, Endothelial Function and Cardiovascular Disease, *Curr. Opin. Lipidol. 9*, 237–242.
2. Vogel, R.A., Corretti, M.C., and Gellman, J. (1998) Cholesterol, Cholesterol Lowering, and Endothelial Function, *Prog. Cardiovasc. Dis. 41*, 117–136.
3. Celermajer, D.S., Sorensen, K.E., Bull, C., Robinson, J., and Deanfield, J.E. (1994) Endothelium-Dependent Dilation in the Systemic Arteries of Asymptomatic Subjects Relates to Coronary Risk Factors and Their Interaction, *J. Am. Coll. Cardiol. 24*, 1468–1474 .
4. Vogel, R.A. (1997) Coronary Risk Factors, Endothelial Function and Atherosclerosis: A Review, *Clin. Cardiol. 20*, 426–432.
5. Chambers, J.C., McGregor, A., Jean-Marie, J., Obeid, O.A., and Kooner, J.S. (1999) Demonstration of Rapid Onset Vascular Endothelial Dysfunction After Hyperhomocysteinemia: An Effect Reversible with Vitamin C Therapy, *Circulation 99*, 1156–1160.
6. Clarkson, P., Celermajer, D.S., Powe, A.J., Donald, A.E., Henry, R.M., and Deanfield, J.E., (1997) Endothelium-Dependent Dilatation Is Impaired in Young Healthy Subjects with a Family History of Premature Coronary Disease, *Circulation 96*, 3378–3383.
7. Seiler, C., Hess, O.M., Buechi, M., Suter, T.M., and Kayenbuehl, H.P. (1993) Influence of Serum Cholesterol and Other Coronary Risk Factors on Vasomotion of Angiographically Normal Coronary Arteries, *Circulation 88*, 2139–2148.
8. Mietus-Snyder, M., and Malloy, M.J. (1998) Endothelial Dysfunction Occurs in Children with Two Genetic Hyperlipidemias: Improvement with Antioxidant Vitamin Therapy, *J. Pediatr. 133*, 35–40.
9. Vogel, R.A., Corretti, M.C., and Plotnick, G.D. (1997) Effect of a Single High-Fat Meal on Endothelial Function in Healthy Subjects, *Am. J. Cardiol. 79*, 350–354.
10. Plotnick, G.D., Corretti, M.C., and Vogel, R.A. (1997) Effect of Antioxidant Vitamins on the Transient Impairment of Endothelium-Dependent Brachial Artery Vasoactivity Following a Single High-Fat Meal, *J. Amer. Med. Assoc. 278*, 1682–1686.
11. Motoyama, T., Kawano, H., Kugiyama, K., Hirashima, O., Ohgushi, M., Yoshimura, M., Ogawa, H., and Yasue, H. (1997) Endothelium-Dependent Vasodilation in the Brachial Artery Is Impaired in Smokers: Effect of Vitamin C, *Am. J. Physiol. 273*, H1644–H1650.
12. Renaud, S., and De Lorgeril, M. (1992) Wine, Alcohol, Platelets, and the French Paradox for Coronary Heart Disease, *Lancet 339*, 1523–1526.
13. Gronbaek, M., Deis, A., Sorensen, T.I., Becker, U., Schnohr, P., and Jensen, G.(1995) Mortality Associated with Moderate Intakes of Wine, Beer or Spirits, *Br. Med. J. 310*, 1165–1169.
14. Frankel, E.N., Kanner, J., German, J.B., Parks, E., and Kinsella, J.E. (1993) Inhibition of Oxidation of Human Low-Density Lipoprotein by Phenolic Substances in Red Wine, *Lancet 341*, 454–457.
15. Hertog, M.G., Feskens, E.J., Hollman, P.C., Katan, M.B., and Kromhout, D. (1993) Dietary Antioxidant Flavonoids and Risk of Coronary Heart Disease: the Zutphen Elderly Study, *Lancet 342*, 1007–1011.
16. Fitzpatrick, D.F., Hirschfield, S.L., and Coffey, R.G. (1993) Endothelium-Dependent Vasorelaxing Activity of Wine and Other Grape Products, *Am. J. Physiol. 265*, H774–H778.
17. Cishek, M.B., Galloway, M.T., Karim, M., German, J.B., and Kappagoda, C.T. (1997) Effect of Red Wine on Endothelium-Dependent Relaxation in Rabbits, *Clin. Sci. 93*, 507–511.
18. Andriambeloson, E., Kleschyov A.L., Muller, B., Beretz, A., Stoclet, J.C., and Adriantsitohaina, R. (1997) Nitric Oxide Production and Endothelium-Dependent Vasorelaxation Induced by Wine Polyphenols in Rat Aorta, *Br. J. Pharmacol. 120*, 1053–1058.
19. Flesch, M., Schwarz, A., and Bohm, M. (1998) Effects of Red and White Wine on Endothelium-Dependent Vasorelaxation of Rat Aorta and Human Coronary Arteries, *Am. J. Physiol. 275*, H1183–H1190.
20. Andriambeloson, E., Magnier, C., Haan-Archipoff, G., Lobstein, A., Anton, R., Beretz, A., Stoclet, J.C., and Andriantsitohaina, R. (1998) Natural Dietary Polyphenolic Compounds Cause Endothelium-Dependent Vasorelaxation in Rat Thoracic Aorta, *J. Nutr. 128*, 2324–2333.
21. Ferro-Luzzi, A., and Branca, F. (1995) Mediterranean Diet, Italian-Style: Prototype of a Healthy Diet, *Am. J. Clin. Nutr. 61*,1338S–1345S.
22. Helsing, E. (1995) Traditional Diets and Disease Patterns of the Mediterranean, Circa 1960, *Am. J. Clin. Nutr. 61*, 1329S–1337S.
23. Celermajer, D.S., Sorensen, K.E., Gooch, V.M., Spiegelhalter, D.J., Miller, O.I., Sullivan, I.D., Lloyd, J.K., Deanfield, J.E. (1992) Non-Invasive Detection of Endothelial Dysfunction in Children and Adults at Risk of Atherosclerosis, *Lancet 340*, 1111–1115.
24. Lichtenstein, A.H., Kennedy, E., Barrier, P., Danford, D., Ernst, N.D., Grundy, S.M., Leveille, G.A., Van Horn, L., Williams, C.L., and Booth, S.L. (1998) Dietary Fat Consumption and Health, *Nutr. Rev. 56*, S3–S19, Discussion S19–S28.
25. Browner, W.S., Westenhouse, J., and Tice, J.A. (1991) What If Americans Ate Less Fat? A Quantitative Estimate of the Effect on Mortality, *JAMA 265*, 3285–3291.
26. Bligh, E.G., and Dyer, W.J. (1959) A Rapid Method of Total Lipid Extraction and Purification, *Can. J. Biochem. Physiol. 37*, 911–917.
27. Motchnik, P.A., Frei, B., and Ames, B.N. (1994) Measurement of Antioxidants in Human Blood Plasma, *Methods Enzymol. 234*, 269–279.
28. Day, B.R., Williams, D.R., and Marsh, C.A. (1979) A Rapid Manual Method for Routine Assay of Ascorbic Acid in Serum and Plasma, *Clin. Biochem. 12*, 22–26.

29. Atkov, O.Y., Balahonova, T.V., and Pogorelova, O.A. (1998) Non-Invasive Ultrasound Detection of Endothelial Dysfunction, *Eur. J. Ultrasound 7*, 37–45.
30. Celermajer, D.S. (1998) Testing Endothelial Function Using Ultrasound, *J. Cardiovasc. Pharmacol. 32*, S29–S32.
31. Playford, D.A., and Watts, G.F. (1998) Special Article: Non-Invasive Measurement of Endothelial Function, *Clin. Exp. Pharmacol. Physiol. 25*, 640–643.
32. Gryglewski, R.J., Palmer, R.M., and Moncada, S. (1986) Superoxide Anion Is Involved in the Breakdown of Endothelium-Derived Vascular Relaxing Factor, *Nature 320*, 454–456.
33. Chin, J.P., and Dart, A.M. (1994) HBPRCA Astra Award. Therapeutic Restoration of Endothelial Function in Hypercholesterolaemic Subjects: Effect of Fish Oils, *Clin. Exp. Pharmacol. Physiol. 21*, 749–755.
34. Harris, W.S., Rambjor, G.S., Windsor, S.L., and Diederich, D. (1997) n-3 Fatty Acids and Urinary Excretion of Nitric Oxide Metabolites in Humans, *Am. J. Clin. Nutr. 65*, 459–64.
35. Dyerberg, J., and Bang, H.O. (1979) Lipid Metabolism, Atherogenesis, and Haemostasis in Eskimos: The Role of the Prostaglandin-3 Family, *Haemostasis 8*, 227–233.
36. Kinsella, J.E., Lokesh, B., and Stone, R.A. (1990) Dietary n-3 Polyunsaturated Fatty Acids and Amelioration of Cardiovascular Disease: Possible Mechanisms, *Am. J. Clin. Nutr. 52*, 1–28.
37. Loft, S., Thorling, E.B., and Poulsen, H.E. (1998) High Fat Diet Induced Oxidative DNA Damage Estimated by 8-Oxo-7,8-dihydro-2-deoxyguanosine Excretion in Rats, *Free Radical. Res. 29*, 595–600.
38. Crozier, A., Lean, M.E.J., McDonald, M.S., and Black, C. (1997) Quantitative Analysis of the Flavonoid Content of Commercial Tomatoes, Onions, Lettuce, and Celery, *J. Agric. Food Chem. 45*, 590–595.

[Received September 7, 1999, and in revised form and accepted January 10, 2000].

Effect of DHA Supplementation on DHA Status and Sperm Motility in Asthenozoospermic Males

Julie A. Conquer[a,]*, James B. Martin[b], Ian Tummon[b], Lynn Watson[b], and Francis Tekpetey[b]

[a]Human Nutraceutical Research Unit and Department of Human Biology and Nutritional Sciences, University of Guelph, Guelph, Ontario, Canada N1G 2W1, and [b]London Health Sciences Centre and Department of Obstetrics and Gynecology, University of Western Ontario, London, Ontario, Canada N6A 5A5

ABSTRACT: The effects of supplementation with docosahexaenoic acid (DHA) on DHA levels in serum, seminal plasma, and sperm of asthenozoospermic men as well as on sperm motility were examined in a randomized, double-blind, placebo-controlled manner. Asthenozoospermic men (n = 28; ≤50% motility) were supplemented with 0, 400, or 800 mg DHA/d for 3 mon. Sperm motility and the fatty acid composition of serum, seminal plasma, and sperm phospholipid were determined before and after supplementation. In serum, DHA supplementation resulted in decreases in 22:4n-6 (–30% in the 800-mg DHA group only) and total n-6 (–6 and –12% in the 400- and 800-mg DHA groups, respectively) fatty acids. Increases were noted in DHA (71 and 131% in the 400- and 800-mg DHA groups, respectively), total n-3 fatty acids (42 and 67% in the 400- and 800-mg DHA groups, respectively), and the n-3/n-6 ratio (50 and 93% in the 400- and 800-mg DHA groups, respectively). In seminal plasma, DHA supplementation resulted in a decrease in 22:4n-6 (–31% in the 800-mg DHA group only) and an increase in the ratio of n-3 to n-6 (35 and 33% in the 400- and 800-mg DHA groups, respectively). There were insignificant increases in DHA and total n-3 fatty acids. In sperm, decreases were noted in 22:4n-6 (–37 and –31% in the 400- and 800-mg DHA groups, respectively). There were no other changes. There was no effect of DHA supplementation on sperm motility. The results show that dietary DHA supplementation results in increased serum—and possibly seminal plasma—phospholipid DHA levels, without affecting the incorporation of DHA into the spermatozoa phospholipid in asthenozoospermic men. This inability of DHA to be incorporated into sperm phospholipid is most likely responsible for the observed lack of effect of DHA supplementation on sperm motility.

Paper no. L8322 in *Lipids 35,* 149–154 (February 2000).

The motility patterns of spermatozoa correlate closely with the rate of natural pregnancy (1) as well as pregnancy induced by *in vitro* fertilization (2). It is not clear which compounds in seminal plasma or spermatozoa may be involved in the regulation of sperm motility. Various compounds found naturally in the spermatozoa or seminal plasma, for example, levels and/or types of antioxidant enzymes (e.g., glutathione peroxidase, superoxide dismutase), oxidants (e.g., nitric oxide, hydrogen peroxide, singlet oxygen), and lipids (e.g., cholesterol, phospholipids, individual fatty acids), may all play a role (3–10). All of the factors controlling sperm motility in humans are as yet unknown.

Previous studies suggested that the level of docosahexaenoic acid (DHA; 22:6n-3) in human ejaculate and sperm is correlated with sperm motility (11,12). Furthermore, DHA levels have been shown to be lower in the total ejaculate (11,12), sperm (13,14), and seminal plasma (14) of asthenozoospermic men (men with ≤50% sperm motility) vs. normozoospermic men. It is unclear how DHA may be involved in regulating sperm motility in humans: it may be involved in the regulation of free fatty acid utilization by sperm (15,16) or it can be metabolized to other lipid-like compounds (19,20-dihydroxy-4,7,10,13,16-docosapentaenoic acid), as has been reported in monkey seminal vesicles (17). It is most likely that the biophysical properties of DHA contribute to the membrane fluidity and flexibility demanded by the motility of the tail (18).

Despite recent advances in treatments for female infertility, the ability to provide simple, effective treatment for male-factor infertility patients remains poor. The effect of dietary supplementation with various compounds on sperm motility has been investigated. In 1996, Suleiman *et al.* (19) determined that treatment of asthenozoospermic patients with oral vitamin E (100 mg; 6 mon), significantly decreased the malondialdehyde (MDA) concentration in spermatozoa, improved sperm motility, and increased the patient's chances of impregnating his spouse. In 1990, Knapp (20) fed 50 mL of menhaden oil [containing DHA + eicosapentaenoic acid (EPA, 20:5n-3)] per day to 10 normal male subjects for 4 wk. There was no effect on sperm motility, but semen phospholipids were enhanced in EPA. DHA also was increased in both the phosphatidylcholine (PC) and phosphatidylethanolamine (PE) fractions. In 1997, in two separate studies, male birds were supplemented with fish oil (rich in EPA and DHA; 21) or linseed oil [rich in α-linolenic acid (α-LNA); 22]. After 30 wk of supplementation with fish oil, sperm DHA levels increased in total phospholipid as well as in PC and PE fractions. α-LNA supplementation resulted in a decrease in sperm 22:4n-6 and an increase in docosapentaenoic acid (DPA; 22:5n-3) but had little effect on the concentration of DHA. The small increase

*To whom correspondence should be addressed. E-mail: jconquer@uoguelph.ca

Abbreviations: DHA, docosahexaenoic acid; DPA, docosapentaenoic acid; EPA, eicosapentaenoic acid; GLM, general linear model; α-LNA, α-linolenic acid; MDA, malondialdehyde; PC, phosphatidylcholine; PE, phosphatidylethanolamine.

in n-3 (as DPA) resulted in enhanced semen fertility. In a third study in broiler breeder roosters, fish oil supplementation increased DHA and total n-3 fatty acid levels in the sperm (23). In 1995, Paulenz *et al.* (24) reported that supplementation of fertile boars with 75 mL of cod liver oil (rich in EPA + DHA) every day for 9 wk resulted in increases in sperm phospholipid levels of DHA. EPA (nondetectable) and DPA levels did not change. In humans, there is evidence to suggest that the synthesis of DHA is reduced in infertile men (25) and that the intake of preformed DHA in the diet, in the presence of EPA, is associated with poorer sperm parameters. The effect of supplementation with an EPA-free DHA source on sperm function and DHA status has not been investigated.

In the present study, the responsiveness of blood serum phospholipid-, seminal plasma phospholipid- and sperm phospholipid-DHA status to supplementation with dietary DHA (EPA-free) was investigated in a group of asthenozoospermic men. The effect of DHA supplementation on sperm motility was studied as well.

MATERIALS AND METHODS

Subjects and experimental design. The subjects were 28 healthy asthenozoospermic individuals who were patients of the Reproductive Endocrinology and Infertility Program at the London Health Sciences Centre (London, Ontario, Canada). Approval for this study was granted by the Human Ethics Committee of the London Health Sciences Centre and the University of Western Ontario, and written informed consent was obtained from each subject. Subjects were determined to be asthenozoospermic after analysis of sperm motility for each individual. The sperm motility criteria applied to the asthenozoospermic individuals was ≤50% (of total sperm), based on the recommendation of Mortimer (26). The 28 subjects were randomly assigned to two DHA supplementation groups (400 or 800 mg/d) or to a placebo group. The DHA-enriched encapsulated triglyceride oil, Neuromins™, and the encapsulated placebo (corn oil/soy oil), were kindly provided by Martek Biosciences Corporation (Columbia, MD). Fatty acid analysis of Neuromins™ and placebo are as published by Conquer and Holub (27). Each group consumed the capsules for a period of 3 mon. Semen and blood samples were collected prior to and after the 3-mon supplementation.

Semen analysis. Semen samples (before and after supplementation) were produced on site by masturbation into a sterile container and allowed to liquefy for 30 min before analysis. Measurements of ejaculate volume, sperm motility, and sperm concentration using hemacytometer count were performed by an experienced technician, in accordance with the recommendations of the World Health Organization (28). Following the assessment, 0.5 or 1.0 mL aliquots of each sample were placed into an Eppendorf tube (1.5 mL capacity) and centrifuged at high speed (15,000 rpm) for 15 min to pellet the sperm. The supernatant seminal plasma was then carefully removed and transferred to a separate container. Both sperm and seminal plasma fractions were stored at –70°C until fatty acid analysis of total phospholipid.

Blood collection. Blood was collected from each subject (before and after supplementation) by antecubital venipuncture into siliconized tubes and centrifuged at 1200 × *g* for 10 min to obtain serum. Serum was stored at –70°C until analysis of the fatty acid composition of total serum phospholipid.

Fatty acid analysis of phospholipid of serum, seminal plasma, and sperm. The fatty acid composition of total phospholipid from serum, seminal plasma, and sperm was determined following lipid extraction, thin-layer chromatography, transmethylation, and gas–liquid chromatography as previously described (14). Gas–liquid chromatography of the fatty acid methyl esters was performed using a Varian 4000 gas chromatograph (Palo Alto, CA) with a 30-m DB-23 capillary column (0.32-mm internal diameter).

Statistical analysis. All data are reported as mean (SEM). Data were analyzed by the general linear model (GLM) procedure on least squared means (for between-group subject characteristics), or repeated measures GLM on least squared means (for fatty acid analyses and sperm characteristics), using the SAS system (SAS Institute, Cary, NC). Specific differences between groups, as well as before and after supplementation, were examined and reported only if $P < 0.05$.

RESULTS

Table 1 shows the subject characteristics for each group. There were no significant differences in height, weight, or body mass index between the groups ($P > 0.05$). Age was significantly higher in the group supplemented with 400 vs. 800 mg DHA/d. This was not considered to interfere with the outcome of this study.

The fatty acid compositions of the serum total phospholipid of asthenozoospermic individuals supplemented with placebo or DHA are given in Table 2 (SEM wt%). The fatty acid profiles of total serum phospholipid at entry were similar among the three groups. The levels of total saturated, monounsaturated, and polyunsaturated fatty acids, as well as total phospholipid, n-6 levels, and the ratio of n-3/n-6 fatty acids, were also similar among the three groups at entry. Supplementation of asthenozoospermic individuals with placebo did not result in the modification of fatty acid composition of serum. Supplementation with 400 and 800 mg DHA/d resulted in an increased DHA content (by 71 and 131% above pre-entry levels, respectively). This was coupled with a rise

TABLE 1
Subject Characteristics of Asthenozoospermic Men Supplemented with DHA or Placebo[a]

Characteristics	Placebo (n = 9)	400 mg DHA/d (n = 9)	800 mg DHA/d (n = 10)
Height (m)	1.8 (0.0)	1.8 (0.0)	1.8 (0.0)
Weight (kg)	83.6 (2.5)	86.1 (2.4)	86.1 (2.4)
BMI (kg/m^2)	27.2 (0.7)	27.2 (0.6)	27.2 (0.6)
Age (yr)	35.2 (1.1)[a,b]	38.3 (1.2)[a]	34.4 (1.0)[b]

[a]DHA, docosahexaenoic acid; BMI, body mass index. Values are reported as mean (SEM) for a total of 28 asthenozoospermic men. [a,b]Values not sharing a superscript within the same row are significantly different ($P < 0.05$).

TABLE 2
Effect of DHA Supplementation on Fatty Acid Analysis of Serum Phospholipid in Asthenozoospermic Men[a]

	Placebo (n = 9)		400 mg DHA/d (n = 9)		800 mg DHA/d (n = 10)	
Fatty acids (wt%)	Pre	Post	Pre	Post	Pre	Post
16:0	27.4 (0.6)	25.7 (0.8)	27.5 (0.5)	26.2 (0.4)	27.3 (0.4)	26.4 (0.6)
18:0	13.9 (0.3)	13.8 (0.4)	14.4 (0.3)	14.3 (0.3)	14.3 (0.3)	14.1 (0.1)
18:1	12.4 (0.6)	13.9 (0.7)	11.9 (0.5)	12.8 (0.5)	12.6 (0.5)	13.2 (0.4)
18:2n-6	19.8 (0.7)	20.6 (0.8)	20.5 (1.3)	19.9 (0.8)	20.5 (0.6)	18.7 (1.1)
18:3n-3	0.19 (0.01)	0.20 (0.02)	0.19 (0.03)	0.19 (0.02)	0.23 (0.02)	0.26 (0.05)
20:3n-6	3.0 (0.2)	2.8 (0.2)	2.9 (0.3)	2.8 (0.2)	3.0 (0.1)	2.7 (0.2)
20:4n-6	11.6 (0.4)	10.6 (0.5)	11.9 (0.6)	10.5 (0.5)	10.9 (0.4)	9.0 (0.5)
20:5n-3	0.90 (0.10)	0.85 (0.09)	0.66 (0.09)	0.85 (0.11)	0.91 (0.13)	0.96 (0.12)
22:4n-6	0.30 (0.05)^{a,b}	0.37 (0.03)^{a,b}	0.39 (0.06)^{a}	0.32 (0.02)^{a,b}	0.40 (0.04)^{a}	0.28 (0.02)^{b}
22:5n-3	1.07 (0.05)	0.95 (0.04)	1.03 (0.07)	0.79 (0.06)	1.10 (0.06)	0.77 (0.05)
22:6n-3 (DHA)	2.8 (0.4)^{a}	2.6 (0.3)^{a}	2.4 (0.2)^{a}	4.1 (0.2)^{b}	2.6 (0.2)^{a}	6.0 (0.3)^{c}
Total saturated	44.7 (0.4)	43.3 (0.7)	45.4 (0.4)	44.3 (0.3)	44.9 (0.2)	44.3 (0.8)
Total MUFA	15.2 (0.5)	17.2 (0.7)	14.2 (0.6)	15.6 (0.5)	15.0 (0.5)	16.4 (0.4)
Total PUFA	40.1 (0.7)	39.6 (0.5)	40.5 (0.7)	40.1 (0.5)	40.2 (0.6)	39.3 (0.7)
Total n-3	5.0 (0.4)^{a}	4.8 (0.3)^{a}	4.3 (0.2)^{a}	6.1 (0.2)^{b}	4.9 (0.3)^{a}	8.2 (0.4)^{c}
Total n-6	35.1 (0.5)^{a,b}	34.8 (0.3)^{a,b}	36.2 (0.8)^{a}	34.0 (0.5)^{b}	35.2 (0.7)^{a,b}	31.1 (0.9)^{c}
n-3/n-6	0.14 (0.01)^{a}	0.14 (0.01^{a}	0.12 (0.01)^{a}	0.18 (0.01)^{b}	0.14 (0.01)^{a}	0.27 (0.02)^{c}
Total PL (mg/dL)	202.8 (10.6)	199.3 (9.9)	234.1 (27.7)	240.3 (21.7)	213.3 (15.1)	240.6 (20.6)

[a]MUFA, monounsaturated fatty acid; PUFA, polyunsaturated fatty acid; PL, phospholipid. See Table 1 for other abbreviations. Values are reported as means (SEM) for a total of 28 individuals. [a,b,c]Values not sharing a superscript within the same row are significantly different ($P < 0.05$).

in the total n-3 fatty acid levels (by 42 and 67% in the 400 and 800 mg DHA groups, respectively) and the ratio of n-3/n-6 fatty acids (by 50 and 93% in the 400 and 800 mg DHA groups, respectively). Decreases were noted in 22:4n-6 (–30% in the 800 mg/d group) and the total levels of n-6 (–6 and –12%, respectively). Insignificant decreases were noted in arachidonic acid (20:4n-6) (–12 and –17%, respectively) and 22:5n-3 (–23 and –30%, respectively).

TABLE 3
Effect of DHA Supplementation on Fatty Acid Analysis of Seminal Plasma Phospholipid of Asthenozoospermic Men[a]

	Placebo (n = 9)		400 mg DHA/d (n = 9)		800 mg DHA/d (n = 10)	
Fatty acids (wt%)	Pre	Post	Pre	Post	Pre	Post
16:0	27.5 (0.5)	27.7 (0.9)	28.4 (0.3)	28.2 (0.3)	28.1 (0.6)	27.1 (0.5)
18:0	15.0 (0.3)	14.1 (0.5)	15.0 (0.1)	13.6 (0.2)	14.7 (0.2)	13.9 (0.1)
18:1	18.7 (0.7)	17.1 (0.8)	19.6 (0.7)	17.9 (0.7)	18.7 (0.5)	18.0 (0.5)
18:2n-6	2.5 (0.3)	2.6 (0.3)	2.3 (0.1)	2.2 (0.2)	2.3 (0.1)	2.9 (0.2)
20:0	5.9 (0.4)	6.1 (0.3)	5.9 (0.3)	5.5 (0.2)	6.0 (0.2)	5.9 (0.3)
20:1	1.1 (0.1)	1.4 (0.1)	1.2 (0.1)	1.4 (0.1)	1.1 (0.1)	1.3 (0.1)
20:3n-6	2.2 (0.3)	2.0 (0.2)	1.9 (0.1)	1.9 (0.2)	1.9 (0.1)	1.9 (0.2)
20:4n-6	3.1 (0.2)	3.2 (0.2)	3.3 (0.1)	3.2 (0.1)	2.9 (0.1)	2.9 (0.1)
22:0	7.8 (0.5)^{a}	7.9 (0.4)^{a}	7.0 (0.5)^{b}	7.5 (0.3)^{a}	7.9 (0.3)^{a}	7.9 (0.3)^{a}
22:1	0.35 (0.03)	0.47 (0.11)	0.31 (0.13)	0.58 (0.11)	0.41 (0.06)	0.60 (0.07)
22:4n-6	0.42 (0.03)^{a,b,c}	0.38 (0.04)^{a}	0.43 (0.04)^{b,c}	0.38 (0.04)^{a,b,d}	0.48 (0.04)^{c}	0.33 (0.02)^{d}
22:5n-3	0.43 (0.06)	0.42 (0.08)	0.43 (0.06)	0.53 (0.05)	0.47 (0.05)	0.50 (0.05)
22:6n-3 (DHA)	3.1 (0.5)	3.3 (0.5)	3.0 (0.3)	4.1 (0.7)	3.0 (0.2)	4.2 (0.3)
24:0	6.0 (0.3)	5.6 (0.6)	6.3 (0.3)	5.9 (0.3)	6.3 (0.2)	6.2 (0.2)
24:1	2.7 (0.1)	3.3 (0.4)	3.0 (0.2)	2.9 (0.2)	3.1 (0.2)	3.1 (0.2)
Total saturated	64.1 (0.9)	63.4 (1.0)	63.2 (0.5)	62.5 (0.9)	64.5 (0.6)	62.5 (0.7)
Total MUFA	23.6 (0.8)	24.0 (0.8)	24.8 (0.6)	24.6 (0.8)	24.1 (0.7)	25.1 (0.6)
Total PUFA	12.4 (1.1)	12.5 (1.2)	12.0 (0.4)	12.8 (1.0)	11.4 (0.4)	12.4 (0.6)
Total n-3	3.8 (0.5)	3.9 (0.6)	3.6 (0.4)	4.8 (0.8)	3.7 (0.2)	4.8 (0.3)
Total n-6	8.6 (0.8)	8.6 (0.7)	8.4 (0.2)	8.1 (0.4)	7.7 (0.3)	7.6 (0.4)
n-3/n-6	0.45 (0.06)^{a}	0.45 (0.05)^{a}	0.43 (0.04)^{a}	0.58 (0.07)^{b}	0.48 (0.03)^{a}	0.64 (0.05)^{b}
Total PL (mg/dL)	30.0 (2.4)	28.6 (1.8)	33.1 (4.7)	36.5 (4.8)	33.1 (3.7)	36.7 (6.0)

[a]See Tables 1 and 2 for abbreviations. Values are reported as means (SEM) for a total of 28 individuals. [a,b,c,d]Values not sharing a superscript within the same row are significantly different ($P < 0.05$).

Table 3 shows the levels of fatty acids in the total phospholipid of human seminal plasma. The fatty acid profiles of total seminal plasma phospholipid at entry were similar among the three groups except for differences in 22:0 (lower in the group that was to receive 400 mg DHA/d). The levels of total saturated, monounsaturated, and polyunsaturated fatty acids, as well as total phospholipid, n-3, and n-6 levels and the ratio of n-3/n-6 fatty acids also were similar among the three groups at entry. DHA supplementation resulted in a significant decrease in 22:4n-6 (–31%) in the 800 mg group only, and a significant increase in the ratio of n-3 to n-6 fatty acids in the 400 and 800 mg supplemented groups (34.9 and 33.3%, respectively). DHA (37 and 40% in the 400 and 800 mg DHA groups, respectively) and total n-3 fatty acids (33 and 30% in the 400 and 800 mg DHA groups, respectively) tended to be slightly increased or unchanged compared to levels found prior to supplementation. There was no change in DPA.

The fatty acid composition of sperm total phospholipid is given in Table 4. Other than a difference in the initial concentration of 22:4n-6, there were no differences in concentrations of the various fatty acids among the three groups at entry; nor were there differences in total polyunsaturated, monounsaturated, or saturated fatty acids, total n-3 fatty acids, total n-6 fatty acids, the n-3/n-6 fatty acid ratio, or total phospholipid levels. DHA supplementation (400 or 800 mg per day) was associated with decreases in the 22:4n-6 content of the sperm phospholipid (–36.8 and –30.8% in the 400 and 800 mg DHA per day groups, respectively), but did not result in any other sperm phospholipid fatty acid composition modification. Slight decreases in 20:2n-6 and total n-6 fatty acids and an insignificant increase in the n-3/n-6 fatty acid ratio were noted.

Table 5 shows the effect of DHA supplementation on sperm motility and sperm concentration in the asthenozoospermic men. DHA supplementation had no effect on sperm motility or concentration (as measured by repeated GLM). Removing subjects with the highest (50%) or lowest (<10%) sperm motility values had no effect on this outcome.

DISCUSSION

This is the first study to examine the effect of supplementation with dietary DHA on DHA status and sperm motility in asthenozoospermic men. Serum n-3 fatty acid status, including DHA status, represents n-3 dietary intake (29–31). The effect of DHA supplementation on serum DHA status was used as a control. Previous studies in our laboratory have shown that dietary supplementation with DHA (from 800 to 1,620 mg per day) for 6 wk resulted in an increase in DHA content from 167 to 247%, depending on the amount of supplemented DHA (27,32,33). In the present study, the increase in serum DHA in the 800 mg

TABLE 4
Effect of DHA Supplementation on Fatty Acid Analysis of Sperm Phospholipid of Asthenozoospermic Men[a]

	Placebo (n = 9)		400 mg DHA/d (n = 9)		800 mg DHA/d (n = 10)	
Fatty acids (wt%)	Pre	Post	Pre	Post	Pre	Post
14:0	1.3 (0.1)	1.4 (0.1)	1.3 (0.1)	1.3 (0.1)	1.3 (0.1)	1.4 (0.1)
14:1	1.2 (0.1)	1.2 (0.1)	1.4 (0.1)	1.6 (0.1)	1.4 (0.0)	1.5 (0.2)
15:0	0.42 (0.05)	0.44 (0.08)	0.41 (0.04)	0.43 (0.04)	0.35 (0.04)	0.48 (0.05)
16:0	31.6 (0.6)	29.3 (0.6)	31.9 (0.9)	31.3 (1.0)	32.2 (0.8)	31.1 (1.1)
16:1	0.51 (0.14)	0.40 (0.10)	0.33 (0.06)	0.39 (0.11)	0.37 (0.09)	0.39 (0.09)
18:0	13.8 (0.3)	14.2 (0.3)	13.9 (0.4)	15.6 (0.4)	14.9 (0.5)	15.4 (0.7)
18:1	14.4 (0.6)	15.3 (0.7)	14.1 (0.9)	15.1 (1.1)	12.6 (0.6)	14.0 (0.9)
18:2n-6	2.9 (0.4)	3.4 (0.4)	2.7 (0.1)	2.8 (0.2)	2.9 (0.2)	3.0 (0.3)
20:0	4.7 (0.3)	4.5 (0.4)	4.1 (0.3)	4.0 (0.4)	3.7 (0.3)	3.7 (0.3)
20:1	0.92 (0.08)	1.08 (0.10)	0.93 (0.10)	1.12 (0.15)	0.77 (0.08)	0.86 (0.11)
20:2n-6	0.44 (0.05)	0.45 (0.03)	0.53 (0.07)	0.48 (0.03)	0.50 (0.04)	0.42 (0.06)
20:3n-6	2.7 (0.6)	2.7 (0.4)	2.5 (0.2)	2.0 (0.2)	2.8 (0.3)	2.4 (0.4)
20:4n-6	2.7 (0.4)[a,b]	3.1 (0.3)[a,c]	2.8 (0.2)[b,c]	2.4 (0.2)[b]	2.3 (0.2)[b]	2.1 (0.2)[b]
22:0	6.0 (0.4)	5.7 (0.5)	5.0 (0.7)	5.2 (0.5)	4.6 (0.3)	4.6 (0.3)
22:1	0.65 (0.12)	0.49 (0.11)	0.72 (0.10)	0.47 (0.07)	0.38 (0.07)	0.45 (0.08)
22:4n-6	0.38 (0.05)[a]	0.38 (0.04)[a]	0.49 (0.05)[b]	0.31 (0.03)[a,c]	0.39 (0.04)[a,b]	0.27 (0.03)[c]
22:5n-3	0.62 (0.10)	0.83 (0.08)	0.80 (0.13)	0.72 (0.07)	0.82 (0.12)	0.83 (0.08)
22:6n-3 (DHA)	6.4 (1.3)	8.2 (1.1)	7.7 (1.3)	8.0 (1.4)	10.6 (1.4)	10.7 (1.3)
24:0	4.7 (0.4)	4.1 (0.4)	4.4 (0.3)	4.2 (0.3)	3.8 (0.3)	3.8 (0.2)
24:1	2.5 (0.2)	2.5 (0.2)	2.5 (0.1)	2.4 (0.1)	2.5 (0.2)	2.3 (0.2)
Total saturated	62.4 (1.3)	59.6 (1.1)	60.9 (1.7)	62.1 (1.2)	60.9 (1.2)	60.5 (1.7)
Total MUFA	20.2 (0.9)	21.0 (0.8)	19.9 (0.9)	21.0 (1.2)	18.0 (0.7)	19.5 (0.9)
Total PUFA	17.2 (1.9)	19.3 (1.6)	19.0 (2.1)	16.9 (1.8)	21.0 (1.6)	20.0 (1.8)
Total n-3	7.4 (1.3)	9.2 (1.2)	9.2 (1.5)	8.8 (1.4)	11.6 (1.4)	11.7 (1.3)
Total n-6	9.8 (1.2)	10.2 (1.1)	9.9 (0.6)	8.1 (0.4)	9.4 (0.6)	8.4 (0.7)
n-3/n-6	0.81 (0.15)	0.95 (0.13)	0.89 (0.11)	1.06 (0.14)	1.25 (0.15)	1.41 (0.12)
Total PL (mg/dL)	18.0 (1.8)	21.9 (2.6)	24.1 (3.5)	27.6 (5.3)	24.5 (2.6)	32.9 (9.2)

[a]See Tables 1 and 2 for abbreviations. Values are reported as means (SEM) for a total of 28 individuals. [a,b,c]Values not sharing a superscript within the same row are significantly different ($P < 0.05$).

TABLE 5
Effect of DHA Supplementation on Sperm Characteristics in Asthenozoospermic Men[a]

	Placebo (n = 9)		400 mg DHA/d (n = 9)		800 mg DHA/d (n = 10)	
Fatty acids (wt%)	Pre	Post	Pre	Post	Pre	Post
Sperm motility (% total sperm)	41.1 (3.1)	47.2 (6.2)	26.7 (4.2)	39.4 (8.1)	25.3 (4.5)	32.0 (5.1)
Sperm concentration (M/mL)	34.9 (8.5)	43.1 (13.5)	31.6 (9.8)	37.8 (12.3)	57.0 (17.6)	44.6 (13.0)

[a]See Table 4 for abbreviations. Values are reported as means (SEM) for a total of 28 individuals. There were no significant differences as measured.

DHA/d group (2.6 to 6.0% DHA) was consistent with that observed in an earlier study in our laboratory (2.4 to 6.4% DHA). DHA supplementation of asthenozoospermic men resulted in serum levels of this fatty acid that were much higher than the baseline levels observed in normozoospermic men (14).

The amount of DHA consumed in this study (400 to 800 mg/d) was not sufficient to cause a decrease in DPA levels or an increase in EPA levels, which are often reported in DHA supplementation studies (27,32,33). Insignificant increases in EPA and decreases in DPA, however, were noted in this study. The decreases observed in n-6 fatty acids in this study were also not as great as those observed in earlier studies. Again, this may have resulted from the smaller amount of supplemented DHA consumed by the subjects in this study (27,32,33). Interestingly, DHA appeared to decrease the elongation of 20:4n-6 to 22:4n-6, as indicated by the decrease in 22:4n-6 with DHA supplementation.

Previous work in our laboratory suggests that seminal plasma phospholipid DHA levels are lower in asthenozoospermic men than normozoospermic men (14). Supplementation with DHA in asthenozoospermic individuals resulted in decreases in 22:4n-6 but had no significant effect on other individual n-6 or n-3 fatty acids. As in serum, DHA incorporation may inhibit the elongation of 20:4n-6 to 22:4n-6 and/or inhibit the incorporation of 22:4n-6 into seminal plasma phospholipid. Although the increase in DHA and total n-3 fatty acids in the DHA-supplemented groups was not marked, only one subject in the 800 mg DHA/d supplemented group did not exhibit a rise in DHA levels. Interestingly, this subject did exhibit a marked rise in serum DHA, with DHA supplementation. Furthermore, all subjects exhibited a marked rise in the ratio of n-3 to n-6 fatty acids. This suggests that DHA supplementation will enhance levels of this fatty acid in the seminal plasma of most asthenozoospermic subjects. It is possible that high oxidant levels and/or low antioxidant levels (34–37) may be responsible for the lack of DHA accumulation in some subjects. It is also clear that DHA supplementation increases levels of this fatty acid in seminal plasma (4.2%) to levels comparable with those reported previously in normozoospermic men (3.7%) (14).

The levels of DHA in the sperm of asthenozoospermic men (average baseline 8.5%) were much lower than those of normozoospermic men (average 13.8%), as previously shown (14). Although DHA supplementation did modify levels of this fatty acid in serum and seminal plasma, supplementation had no effect on DHA levels in the spermatozoa. Although it is possible that higher concentrations of supplemented DHA may have resulted in increased DHA levels of spermatozoa, it is more likely that this was related to an inability of the sperm to take up preformed DHA. Indeed, one study in normozoospermic humans (20) suggests that DHA levels rise with supplementation by fish oil (a source of EPA + DHA). Christophe *et al.* (25) suggest that α-LNA intake may be more important in terms of sperm function and DHA status. The effect of DHA supplementation in the absence of EPA on DHA levels in the sperm of normozoospermic or asthenozoospermic men has never been published. Thus, it is difficult to know if the low DHA uptake by sperm from the men in our study could be attributed to limited supplies of the n-3 fatty acids and/or their protective antioxidants, or to fundamental structural/functional changes in the asthenozoospermic men (34–37). It would be interesting to know whether DHA supplementation would increase DHA levels in the sperm of normozoospermic patients, as well as in retinitis pigmentosa patients, who have decreased levels of DHA in their serum and sperm as well as decreased sperm motility (38).

DHA supplementation had no effect on sperm motility in the asthenozoospermic men. It is possible that the increased DHA levels in seminal plasma and concomitant decrease in 22:4n-6 in the seminal plasma and sperm, as observed with DHA supplementation, was not sufficient to increase sperm motility. These results, along with the correlation of sperm phospholipid DHA levels and sperm motility (14), further support the hypothesis that it is DHA itself, and not other fatty acids such as 22:4n-6, in the sperm phospholipid that may be involved in the regulation of sperm motility.

In conclusion, this study suggests that DHA supplementation in asthenozoospermic men increases DHA levels in serum, and possibly seminal plasma. However, DHA supplementation had little effect on DHA levels in sperm and had no effect on sperm motility. It would be interesting to determine the effect of supplementation with DHA precursors (for example α-LNA) and/or antioxidants on DHA levels in sperm as well as on sperm motility.

ACKNOWLEDGMENTS

We would like to thank Martek Biosciences Corporation for funding this investigation. In addition, special thanks go to Dr. Bruce Holub for his input in all aspects of this investigation and to Dr. Diana Philbrick for reading the manuscript.

REFERENCES

1. Beauchamp, P.J., Galle, P.C., and Blasco, L. (1984) Human Sperm Velocity and Post Insemination Cervical Mucous Test in the Evaluation of Infertile Couple, *Arch. Androl. 13,* 107–112.
2. Bongso, T.A., Ng, S.C., Mok, H., Lim, M.N., Teo, H.L., Wong, P.C., and Ratnam, S.S. (1989) Effect of Sperm Motility on Human *in vitro* Fertilization, *Arch. Androl. 22,* 185–190.
3. Nissen, H.P., and Kreysel, H.W. (1983) Superoxide Dismutase in Human Semen, *Klin. Wochensch. 61,* 63–65.
4. Alvarez, J.G., and Storey, B.T. (1983) Role of Superoxide Dismutase in Protecting Rabbit Spermatozoa from O_2 Toxicity Due to Lipid Peroxidation, *Biol. Reprod. 28,* 1129–1136.
5. Alvarez, J.G., and Storey, B.T. (1992) Evidence for Increased Lipid Peroxidative Damage and Loss of Superoxide Dismutase Activity as a Mode of Sublethal Cryo-Damage to Human Sperm During Cryopreservation, *J. Androl. 13,* 232–241.
6. Weinberg, J.B., Doty, E., Bonaventura, J., and Haney, A.F. (1995) Nitric Oxide Inhibition of Human Sperm Motility, *Fertil. Steril. 64,* 408–413.
7. Griveau, J.F., and Le Lannou, D. (1997) Reactive Oxygen Species and Human Spermatozoa: Physiology and Pathology, *Int. J. Androl. 20,* 61–69.
8. Tanphaichitr, N., Zheng, Y.S., Kates, M., Abdullah, N., and Chan, A. (1996) Cholesterol and Phospholipid Levels of Washed and Percoll Gradient Centrifuged Mouse Sperm: Presence of Lipids Possessing Inhibitory Effects on Sperm Motility, *Mol. Reprod. Devel. 43,* 187–195.
9. Hula, N.M., Tron'ko, M.D., Volkov, H.L., and Marhitych, V.M. (1993) Phospholipids of Human Seminal Plasma and Their Role in Ensuring Fertility, *Ukr. Biokhim. Zh. 65,* 75–78.
10. Hong, C.Y., Shieh, C.C., Wu, P., Huang, J.J., and Chiang, B.N. (1986) Effect of Phosphatidylcholine, Lysophosphatidylcholine, Arachidonic Acid and Docosahexaenoic Acid on the Motility of Human Sperm, *Int. J. Androl. 9,* 118–122.
11. Nissen, H.P., and Kreysel, H.W. (1983) Polyunsaturated Fatty Acids in Relation to Sperm Motility, *Andrologia 15*, 264–269.
12. Gulaya, N.M., Tronko, M.D., Volkov, G.L., and Margitich, M. (1993) Lipid Composition and Fertile Ability of Human Ejaculate, *Ukr. J. Biochem. 65*, 64–70.
13. Zalata, A.A., Christophe, A.B., Depuydt, C.E., Schoonjans, F., and Comhaire, F.H. (1998) The Fatty Acid Composition of Phospholipids of Spermatozoa from Infertile Patients, *Mol. Hum. Reprod. 4*, 111–118.
14. Conquer, J., Martin, J.B., Tummon, I., Watson, L., and Tekpetey, F. (1999) Fatty Acid Analysis of Blood Serum, Seminal Plasma and Spermatozoa of Normozoospermic vs. Asthenozoospermic Males, *Lipids 34,* 793–799.
15. Jones, R.E., and Plymate, S.R. (1993) Synthesis of Docosahexaenoyl Coenzyme A in Human Spermatozoa, *J. Androl. 14*, 428–432.
16. Jones, R.E., and Plymate, S.R. (1988) Evidence for the Regulation of Fatty Acid Utilization in Human Sperm by Docosahexaenoic Acid, *Biol. Reprod. 39*, 76–80.
17. Oliw, E.H., and Sprecher, H.W. (1991) Metabolism of Polyunsaturated (n-3) Fatty Acids by Monkey Seminal Vesicles: Isolation and Biosynthesis of n-3 Epoxides, *Biochim. Biophys. Acta 1086*, 287–294.
18. Connor, W.E., Lin, D.S., Wolf, D.P., and Alexander, M. (1998) Uneven Distribution of Desmosterol and Docosahexaenoic Acid in the Heads and Tails of Monkey Sperm, *J. Lipid Res. 39,* 1404–1411.
19. Suleiman, S.A., Elamin Ali, M., Zaki, M.S., El-Malik, E.M.A., and Nasr, M.A. (1996) Lipid Peroxidation and Human Sperm Motility: Protective Role of Vitamin E, *J. Androl. 17:*530-537.
20. Knapp, H.R. (1990) Prostaglandins in Human Semen During Fish Oil Ingestion: Evidence for *In Vivo* Cyclooxygenase Inhibition and Appearance of Novel Trienoic Compounds, *Prostaglandins 39,* 407–423.
21. Kelso, K.A., Cerolini, S., Noble, R.C., Sparks, N.H.C., and Speake, B.K. (1997) The Effects of Dietary Supplementation with Docosahexaenoic Acid on the Phospholipid Fatty Acid Composition of Avian Spermatozoa, *Comp. Biochem. Physiol. 118B,* 65–69.
22. Kelso, K.A., Cerolini, S., Speake, B.K., Cavalchini, L.G., and Noble, R.C. (1997) Effects of Dietary Supplementation with Alpha-Linolenic Acid on the Phospholipid Fatty Acid Composition and Quality of Spermatozoa in Cockerel from 24 to 72 Weeks of Age, *J. Reprod. Fertil. 10,* 53–59.
23. Blesbois, E., Lessire, M., Grasseau, I., Hallouis, J.M., and Hermier, G. (1997) Effect of Dietary Fat on the Fatty Acid Composition and Fertilizing Ability of Fowl Semen, *Biol. Reprod. 56,* 1216–1220.
24. Paulenz, H., Taugbol, O., Hofmo, P.O., and Saarem, K. (1995) A Preliminary Study on the Effect of Dietary Supplementation with Cod Liver Oil on the Polyunsaturated Fatty Acid Composition of Boar Semen, *Vet. Res. Commun. 19,* 273–284.
25. Christophe, A., Zalata, A., Mahmoud, A., and Combaire, F. (1998) Fatty Acid Composition of Sperm Phospholipids and Its Nutritional Implications, *Middle East Fertil. Soc. J. 3,* 46–53.
26. Mortimer, D. (1985) The Male Factor in Infertility Part II. Sperm Function Testing, *Curr. Prob. Obstet. Gynecol. Fertil. 8*, 75 pp. Year Book Medical Publishers, Chicago.
27. Conquer, J.A., and Holub, B.J. (1997) Effect of Supplementation with DHA on Lipid/Lipoprotein Levels in Subjects of Asian Indian Background, *J. Lipid Res. 39,* 286–292.
28. World Health Organization (1992) *WHO Laboratory Manual for the Examination of Human Semen and Semen–Cervical Mucus Interactions*, pp. 9–15, Cambridge University Press, Cambridge.
29. Ma, J., Folsom, A.R., Eckfeldt, J.H., Lewis, S.L., and Chambless, L.E. (1995) Short- and Long-Term Repeatability of Fatty Acid Composition of Human Plasma Phospholipids and Cholesterol Esters, *Am. J. Clin. Nutr. 62*, 572–578.
30. Bonaa, K.H., Bjerve, K.S., and Nordoy, A. (1992) Habitual Fish Consumption, Plasma Phospholipid Fatty Acids, and Serum Lipids: The Tromsø Study, *Am. J. Clin. Nutr. 55*, 1126–1134.
31. Nikkari, T., Luukkainen, P., Pietinen, P., and Buska, P. (1995) Fatty Acid Composition of Serum Lipid Fractions in Relation to Gender and Quality of Dietary Fat, *Ann. Med. 27*:491–498.
32. Conquer, J.A., and Holub, B.J. (1997) Dietary Docosahexaenoic Acid as a Source of Eicosapentaenoic Acid in Vegetarians and Omnivores, *Lipids 32,* 341–345.
33. Conquer, J.A., and Holub, B.J. (1996) Effect of Supplementation with an Algae Source of Docosahexaenoic Acid on n-3 Status and Risk Factors for Heart Disease in Vegetarians. *J. Nutr. 126,* 3032–3039.
34. Aitken, R.J. (1995) Free Radicals, Lipid Peroxidation and Sperm Function, *Reprod. Fertil. Dev. 7,* 659–668.
35. Mitropoulos, D., Deliconstantinos, G., Zervas, A., Villiotou, V., Dimopoulos, C., and Stavrides, J. (1996) Nitric Oxide Synthase and Xanthine Oxidase Activities in the Spermatic Vein of Patients with Varicocele: A Potential Role for Nitric Oxide and Peroxynitrite in Sperm Dysfunction, *J. Urol. 156,* 1952–1958.
36. Alkan, I., Simsek, F., Goncagul, H., Kervancioglu, E., Ozveri, H., Yalcin, S., and Akdas, A. (1997) Reactive Oxygen Species Production by the Spermatozoa of Patients with Idiopathic Infertility: Relationship to Seminal Plasma Antioxidants, *J. Urol. 157,* 140–143.
37. Lewis, S.E.M., Sterling, E.S.L., Young, I.S., and Thompson, W. (1997) Comparison of Individual Antioxidants of Sperm and Seminal Plasma in Fertile and Infertile Men, *Fertil. Steril. 67,* 142–147.
38. Connor, W.E., Weleber, R.G., DeFrancesco, C., Lin, D.S., and Wolf, D.P. (1997) Sperm Abnormalities in Retinitis Pigmentosa, *Invest. Opthmol. Vis. Sci. 38,* 2619–2628.

[Received July 28, 1999, and in final revised form December 10, 1999; revision accepted December 14, 1999]

Effects of Dietary Conjugated Linoleic Acids on Hepatic and Muscle Lipids in Hybrid Striped Bass

Ronald G. Twibell[a], Bruce A. Watkins[b], Laura Rogers[b], and Paul B. Brown[a,*]

Purdue University, [a]Department of Forestry and Natural Resources, and [b]Department of Food Science, Lipid Chemistry and Molecular Biology Laboratory, West Lafayette, Indiana 47907-1159

ABSTRACT: Conjugated linoleic acids (CLA) are the focus of numerous studies, yet the effects of these isomers of octadecadienoic acids have not been evaluated in many species of fish. In this study, graded amounts of CLA—0, 0.5, 0.75, or 1.0% of the diet—were fed to juvenile hybrid striped bass for 8 wk. Dietary treatments were fed to apparent satiation twice daily to triplicate groups of fish initially weighing 13.4 g/fish. Feed intake and weight gain of fish fed 1.0% CLA were significantly reduced compared to fish fed no CLA. Fish fed 0.5 and 0.75% CLA exhibited reduced feed intake similar to fish fed 1.0% CLA, but had growth rates that were not significantly different from those of fish fed no CLA. Feed efficiency improved significantly in fish as dietary CLA concentrations increased. Total liver lipid concentrations were significantly reduced in fish fed the diets containing CLA compared to those of fish fed the control diet, and intraperitoneal fat ratio was significantly lower in fish fed 1.0% CLA compared to fish fed no CLA. Fish fed dietary CLA exhibited significant increases in hepatosomatic index and moisture content of muscle and carcass. The CLA isomers were detected in liver and muscle of fish fed the diets containing CLA, while a low concentration of one isomer was detected in liver and muscle of fish fed the control diet. Dietary CLA resulted in a significant increase in 18:2(*c*-9,*c*-12) concentration in liver and muscle, but a significant reduction in 18:1n-7 in these tissues. Furthermore, feeding CLA resulted in a significant increase in the concentration of 20:5n-3 and 22:6n-3 in liver, but a reduction of these fatty acids in muscle. This study showed that feeding CLA elevated tissue concentrations of these fatty acid isomers, reduced tissue lipid contents, improved feed efficiency, and altered fatty acid concentrations in liver and muscle of fish.

Paper no. L8309 in *Lipids 35*, 155–161 (February 2000).

Conjugated linoleic acids (CLA) are an isomeric mixture of octadecadienoic fatty acids lacking a methylene group between double bonds. Research with CLA indicates that these fatty acids have anticarcinogenic, antiatherosclerotic, antioxidative, immunomodulative, and antibacterial properties (1–7). The CLA occur naturally in a wide variety of food products, including meat, poultry, seafood, cheese, butter, milk, and vegetable oils (8). Fats and meats from ruminant species are the richest natural sources of CLA.

*To whom correspondence should be addressed at Purdue University, 1159-Forestry Bldg., West Lafayette, IN 47907-1159. E-mail: pb@fnr.purdue.edu

Abbreviations: CLA, conjugated linoleic acids; E/P, energy/protein; FAME, fatty acid methyl ester; HSI, hepatosomatic index; IPF, intraperitoneal fat.

Dietary CLA improved feed efficiency and reduced body fat in growing pigs, rats, mice, rabbits, and chickens (1,2,3,9–12), but not in fish (13). Nutritional studies with CLA have shown that the isomeric fatty acids were incorporated into different animal organs and tissues, and enriched both neutral and polar lipid fractions (3,11,14–16). Moreover, CLA may affect the fatty acid composition of animal tissues and cultured cells (11).

Several hybrids of fish are being evaluated as new aquaculture species in the United States. Most of the interest in aquaculture arose from restrictions on harvest of wild fishes and increased consumption of seafoods (17). Fish are important sources of food protein and beneficial fatty acids and serve as an important link between n-3 fatty acid intake and reduced incidence of atherosclerosis (18,19).

One of the lingering concerns with hybrid striped bass (*Morone saxatilis* × *M. chrysops*) has been the macro- and microvesicular degeneration seen in hepatic samples of fish fed any commercial or experimental diet (20), resulting from accumulation of glycogen and lipid in hepatocytes. Regardless of the laboratory or diet, hepatic samples from hybrid striped bass consistently demonstrate these lesions and some pathologists consider this the normal liver. Hybrid striped bass also accumulate relatively high levels of fat in the visceral cavity, which increases production costs and reduces market value. The purpose of the present investigation was to examine the effects of feeding graded levels of CLA on growth, liver lipids, and fatty acid composition of hybrid striped bass.

MATERIALS AND METHODS

Fish and diets. Juvenile hybrid striped bass (male *Morone saxatilis* × female *M. chrysops*) were obtained from a commercial producer (Keo Fish Farms, Keo, AR) and transported to the Purdue University Aquaculture Research Facility. All fish were acclimated to laboratory conditions for 5 wk prior to initiation of the experiment. Procedures used during transport, quarantine, and experimental period were approved by the Purdue Animal Care and Use Committee (PACUC No. 89-060-98, "Nutritional Studies with Aquatic Animals," Principal Investigator Qualification No. BRO-249).

The closed recirculating system contained 24 individual 38-L aquaria and was equipped with two submerged filtration tanks for solid material removal and denitrification of the water.

Water was pumped through a sand filter to each aquarium at a rate of ~1 L/min and was maintained at 28 ± 1°C throughout the experiment. The diurnal light/dark cycle of the aquaculture facility remained at 16 h light/8 h dark throughout the study.

Groups of 20 randomly chosen fish were stocked into each of 12 aquaria. Fish were acclimated to the experimental system and their respective diets for 3 wk prior to the experiment. Following the acclimation period, the number of fish in each tank was reduced to 12 so that the total weight of fish in each tank was 160.0 ± 5.0 g. Dietary treatments were randomly assigned to triplicate aquaria. Upon initiation of the experiment, fish were fed to apparent satiation twice daily for 8 wk. Water quality was monitored daily and was within acceptable limits throughout the study. Dissolved oxygen concentrations were not below 5.0 mg/L at any time. Ammonia-N and nitrite-N concentrations did not exceed 0.25 and 0.20 mg/L, respectively.

The basal diet was formulated to provide 34.6% crude protein (Table 1). Casein and gelatin provided a total of 10.1% crude protein, while the remaining 24.5% crude protein was supplied by an L-amino acid mixture (Table 1). The L-amino acid mixture was formulated so that the diets contained 1.55% arginine (21), 1.40% lysine (22), and 0.73% total sulfur amino acids (23), thus meeting the dietary requirement of hybrid striped bass for these amino acids. The remaining dietary essential amino acid concentrations met or exceeded the highest known requirements for fish (24). All diets contained 500 mg choline/kg diet, provided as choline chloride (25). The basal diet contained 6.0% lipid (menhaden oil) and 25.0% carbohydrate (dextrin). The energy/protein (E/P) ratio of the basal diet was calculated as 8.5 kcal/g crude protein using physiological fuel values of 4.0, 4.0, and 9.0 kcal/g for protein, carbohydrate, and lipid, respectively. An E/P ratio of 8 kcal/g protein is nearly optimal for growth of hybrid striped bass (26).

TABLE 1
Composition of Basal Diet Fed to Juvenile Hybrid Striped Bass

Ingredient	Amount (g/kg dry mixture)
Casein	90.0
Gelatin	18.0
Amino acid mixture[a]	249.0
Dextrin	250.0
Mineral premix[b]	80.0
Vitamin premix[c]	3.3
STAY-C 25[d]	2.0
Choline chloride	0.7
Carboxymethylcellulose	20.0
Cellulose	227.1
Menhaden oil	60.0

[a]Amino acid mixture was formulated so that diets contained (g L-amino acid/kg dry diet): arginine, 15.5; histidine, 9.5; isoleucine, 19.3; leucine, 31.9; lysine, 14.0; methionine, 4.7; cyst(e)ine, 2.6; phenylalanine, 21.0; tyrosine, 20.0; threonine, 18.2; tryptophan, 4.9; valine, 23.5; aspartic acid, 21.9; proline, 21.9; glutamic acid, 21.8; serine, 21.8; glycine, 21.6.

[b]Mineral premix consisted of (g/kg of premix): Na_2SeO_3, 0.4; $CaCO_3$, 350; $NaH_2PO_4 \cdot H_2O$, 200; KH_2PO_4, 200; $MgSO_4 \cdot 7H_2O$, 10; $MnSO_4 \cdot H_2O$, 2; $CuCl_2 \cdot 2H_2O$, 1; $ZnSO_4 \cdot 7H_2O$, 2; $FeSO_4 \cdot 7H_2O$, 2; NaCl, 12; KI, 0.1; $CoCl_2 \cdot 6H_2O$, 0.1; $Na_2MoO_4 \cdot 2H_2O$, 0.5; $AlCl_3 \cdot 6H_2O$, 1; and KF, 1.

[c]Vitamin premix supplied the diets with (mg/kg dry diet): retinyl acetate, 40; cholecalciferol, 0.1; DL-α-tocopheryl acetate, 80; menadione, 15; niacin, 168; riboflavin, 22; pyridoxine HCl, 40; thiamine mononitrate, 45; D-Ca pantothenate, 102, biotin, 0.4; folic acid, 10; vitamin B-12, 0.04; and inositol, 450.

[d]Contained 25% ascorbic acid equivalents, as L-ascorbyl 2-polyphosphate.

Vitamins (with the exception of ascorbic acid and choline chloride) and minerals were added to the diets as nutritionally complete premixes (Table 1). Menhaden oil and reagent-grade minerals were obtained from commercial suppliers (Omega Protein, Reedville,VA, and Sigma Chemical Co., St. Louis, MO, respectively). Vitamins (with the exception of ascorbic acid), casein, gelatin, dextrin, carboxymethylcellulose, crystalline L-amino acids, and cellulose were acquired from U.S. Biochemical (Cleveland, OH). Ascorbic acid, as L-ascorbyl 2-polyphosphate, was obtained from Roche Inc. (Nutley, NJ). CLA were provided by Saskatchewan Wheat Pool (Saskatoon, Canada). Analysis of the supplement revealed that the total CLA isomers were 66.9% of the fatty acids [24.9% 18:2(*c*-9,*t*-11), 35.2% 18:2(*t*-10,*c*-12), 4.6% 18:2(*c*-9,*c*-11), and 2.2% 18:2(*t*-10,*t*-12)].

The dietary treatments were formulated to contain CLA at concentrations of 0, 0.5, 0.75, or 1.0% of the dry diet. Based on analyzed content, the diets supplemented with CLA at 0.75 and 1.0% contained 0.49 and 0.64% total isomers, respectively. The CLA supplement was added to the diets at the expense of menhaden oil to maintain a constant energy level among all dietary treatments.

Dry ingredients were thoroughly mixed in a twin-shell V-mixer (Patterson-Kelly, East Stroudsburg, PA). Diets were then transferred to a Hobart mixer (Hobart Corp., Troy, OH). Water, lipid, and CLA were then added to the dry ingredients and mixed. Diets were adjusted to pH 7.0 ± 0.2 with saturated NaOH (27) and pelleted. The diets were air-dried for 48 h, then stored under air-tight conditions at –20°C until needed.

Sample collection and analysis. All fish were anesthetized (tricaine methanesulfonate, Argent Chemical, Redmond, WA) and weighed 24 h after the final feeding. Three randomly chosen fish were collected from each dietary replicate group and frozen at –20°C for subsequent carcass proximate analysis. Fillets were obtained from an additional group of three randomly chosen fish and were also frozen at –20°C for subsequent proximate analysis. Both whole fish and fillet samples were pooled into one sample per replicate. Moisture concentration was determined by drying whole fish or muscle for 24 h in a forced-air oven maintained at 100°C. Crude protein was estimated from whole-body and muscle nitrogen values, which were determined in an elemental nitrogen analyzer (LECO Corp., St. Joseph, MI). Ash content was determined by incinerating samples at 600°C for 24 h in a muffle furnace. Lipid concentration of carcass and muscle was determined as described by Folch *et al.* (28).

Livers from three randomly chosen fish in each dietary replicate group were removed and weighed for calculation of hepatosomatic index (HSI) (liver weight × 100/body weight). The livers were then pooled and frozen at –20°C for subsequent determination of total lipids. Visceral fat was also removed from these same fish for calculation of intraperitoneal fat (IPF) ratio (IPF × 100/body weight).

Analysis of fatty acids. Liver and muscle samples were obtained from one randomly chosen fish in each dietary replicate group for determination of fatty acid composition. Individual samples were extracted with chloroform/methanol (2:1, vol/vol) and fatty acid methyl esters (FAME) prepared using 0.5 M sodium methoxide in anhydrous methanol following procedures described by Li and Watkins (11). Samples of diet also were subjected to lipid extraction, and FAME were produced (11). The FAME were quantified using a gas chromatograph (HP 5890 series II, autosampler 7673, HP 3365 ChemStation; Hewlett-Packard Co., Avondale, PA) equipped with a DB23 column (30 m, 0.53 mm i.d., 0.5 μm film thickness; J&W Scientific Co., Folsom, CA) and operated at 140°C for 2 min, temperature programmed 1.5°C/min to 198°C and held for 7 min (11). The injector and flame-ionization detector temperatures were held at 225 and 250°C, respectively. FAME were identified by comparison of retention times with authentic standards [GLC-422, CLA (UC-59-A and UC-59-M), Nu-Chek-Prep, Elysian, MN; CLA (Cat# 1245, *c*-9, *t*-11 and Cat# 1181, *t*-9, *t*-11), Matreya Inc., Pleasant Gap, PA] and with FAME prepared from menhaden oil (Matreya Inc.).

Statistical analyses. Weight gain, feed intake, feed efficiency, HSI, total liver lipid concentrations, IPF ratio, whole body and muscle proximate composition, and liver and muscle fatty acid concentrations were analyzed as a completely randomized design using each aquarium as an experimental unit. The data were subjected to one-way analysis of variance (ANOVA) using the Statistical Analysis System (SAS Users' Guide: Statistics, SAS Institute Inc., Cary, NC). Analyses were conducted with dietary treatment as the independent variable. Student-Neuman-Keuls test separated mean values when significant differences were detected by ANOVA. Accepted level of significance was 0.05.

RESULTS

There were no significant differences in weight gain between groups of fish fed 0, 0.5, or 0.75% CLA; however, growth rates of fish fed 1.0% CLA were significantly lower than those of fish fed the control diet (Table 2). Feed intake was significantly reduced in fish fed CLA compared to fish fed the control diet (0% CLA). Feed efficiencies improved significantly as dietary CLA concentrations increased. HSI increased and total liver lipid concentration decreased significantly with increasing dietary CLA concentrations (Table 2). Fish fed 1.0% CLA exhibited a 2.5-fold reduction in liver lipid concentration compared to fish fed the control diet.

IPF ratio was significantly reduced in fish fed 1.0% CLA compared to fish fed no CLA (Table 3). Moisture content of carcass and muscle increased significantly in fish fed increasing concentrations of CLA (Table 3). There were no significant differences in crude protein, fat, or ash concentrations in carcass or muscle of fish fed any of the dietary treatments.

Only one CLA isomer, 18:2(*c*-9,*t*-11) was detected in liver of fish fed the control diet (Table 4). Based on the retention time of the 18:2(*c*-9,*t*-11) standard, this peak immediately followed 18:4n-3 and was resolved at baseline. Four CLA isomers, 18:2(*c*-9,*t*-11/*c*-9,*c*-11) and 18:2(*t*-10,*c*-12/*t*-10,*t*-12), were detected in liver of fish fed 0.5, 0.75, and 1.0% dietary CLA. The highest concentrations were observed in fish fed 1.0% CLA. Total liver CLA concentrations in fish fed 0.5, 0.75, and 1.0% CLA were 2.8, 2.5, and 5.8% of fatty acids, respectively.

Significant differences were detected in fatty acid composition of liver between fish fed the control diet and those fed the diets containing CLA (Table 4). Fish fed 0.5% CLA and higher levels exhibited significantly greater concentrations of 14:0, 18:0, and 18:2(*c*-9,*c*-12), but significantly lower concentrations of 18:1n-7, 18:2(*t*-9,*t*-12) and 20:1n-9 in liver compared to fish fed the control diet. Furthermore, fish fed 1.0% CLA exhibited significantly higher liver concentrations of 20:4n-6, 20:5n-3, 22:5n-3, and 22:6n-3, but significantly lower concentrations of 18:1n-9 compared to fish fed 0, 0.5, or 0.75% CLA.

Similar to the liver fatty acid composition, 18:2(*c*-9,*t*-11) was the only CLA isomer detected in muscle of fish fed the control diet (Table 5). Three CLA isomers, 18:2(*c*-9,*t*-11) and 18:2(*t*-10,*c*-12/*t*-10,*t*-12), were detected in muscle of fish fed 0.5, 0.75, and 1.0% dietary CLA, while the 18:2(*c*-9,*c*-11) isomer was detected only in muscle of fish fed 0.75 and 1.0% CLA. Total muscle CLA concentrations in fatty acids of fish fed 0.5, 0.75, and 1.0% CLA were 3.4, 4.4, and 8.1%, respectively.

TABLE 2
Mean Initial Weight/Fish, Weight Gain (% increase from initial weights), Feed Efficiency, Feed Intake/Fish, Hepatosomatic Index, and Total Liver Lipid Concentration of Hybrid Striped Bass Fed Conjugated Linoleic Acids (CLA)[a]

Dietary CLA (%)	Initial weight (g/fish)	Weight gain (% initial weight)	Feed efficiency (g gain/g dry feed)	Feed intake (g dry feed/fish)	Hepatosomatic index[b]	Total liver lipids[b] (% dry liver)
0	13.4	320.9*	0.60[#]	71.3*	3.1[#]	25.9*
0.5	13.5	292.1*,[†]	0.64[†]	61.1[†]	4.1[†]	13.9[†]
0.75	13.4	297.6*,[†]	0.66[†]	60.7[†]	4.2[†]	12.2[†]
1.0	13.3	271.5[†]	0.69*	52.1[†]	4.8*	9.9[†]
Pooled SEM	0.1993	9.7065	0.0090	2.5387	0.1604	1.8679
Probability[c]	0.9392	0.0424	0.0005	0.0050	0.0001	0.0001

[a]Means in the same column with the same superscript were not significantly different ($P < 0.05$).
[b]Hepatosomatic index (liver weight × 100/body weight) and all other variables were means of three replications.
[c]Probability (Pr > F) of treatment differences as determined by analysis of variance (ANOVA).

TABLE 3
Carcass and Muscle Composition of Juvenile Hybrid Striped Bass Fed CLA[a,b]

Dietary CLA (%)	Intraperitoneal fat ratio[c] (% wet body weight)	Carcass				Muscle			
		Moisture (%)	Protein (% dry weight)	Fat (% dry weight)	Ash (% dry weight)	Moisture (%)	Protein (% dry weight)	Fat (% dry weight)	Ash (% dry weight)
0	5.8*	64.8†	51.9	36.0	13.9	75.3†	79.5	18.2	5.2
0.5	5.0*,†	66.5*	53.1	33.1	14.5	75.8*,†	80.4	15.6	4.7
0.75	4.9*,†	66.5*	52.0	33.8	13.5	76.3*,†	79.9	14.3	3.9
1.0	4.0†	67.1*	52.7	32.6	15.0	76.7*	78.2	15.0	4.2
Pooled SEM	0.2919	0.4282	0.5538	1.1307	0.6581	0.3369	1.1516	1.3135	0.3989
Probability[d]	0.0021	0.0071	0.3422	0.1936	0.4077	0.0279	0.5678	0.1903	0.1762

[a]Means in the same column with the same roman letter designation were not significantly different ($P < 0.05$).
[b]Values are means of three replications.
[c]Intraperitoneal fat (IPF) ratio was calculated as (IPF × 100/body weight).
[d]Probability (Pr > F) of treatment differences as determined by ANOVA. For other abbreviations see Table 2.

Significant differences in muscle fatty acid composition were detected between fish fed the control diet and those fed the diets containing CLA (Table 5). For example, fish fed 0.5% CLA and higher levels exhibited significant reductions in muscle 18:2(*t*-9,*t*-12) concentrations compared to fish fed the control diet. Fish fed 1.0% dietary CLA exhibited significantly higher concentrations of 18:2(*c*-9,*c*-12) in muscle compared to fish fed the control diet. Muscle concentrations of 20:5n-3 and 22:6n-3 were significantly decreased in fish fed 1.0% CLA compared to fish fed 0, 0.5, or 0.75% dietary CLA.

DISCUSSION

Research with terrestrial animals has demonstrated that dietary CLA elicit several positive responses, including reduced tumorigenesis (29), reduced atherosclerosis (6), enhanced immune response (5), increased feed efficiency (1,11), and reduced body fat (12,30). The implications of these findings for improved human health are obvious. Perhaps less obvious are the possible beneficial effects of dietary CLA on the production of food animals. Enhanced immune response and feed ef-

TABLE 4
Fatty Acid Composition (wt%) of Liver from Hybrid Striped Bass Fed CLA[a,b]

Fatty acid	Dietary treatment				Pooled SEM	ANOVA (P value[c])
	Control	0.5% CLA	0.75% CLA	1.0% CLA		
14:0	3.2 ± 0.2#	3.8 ± 0.3†	3.9 ± 0.4†	4.5 ± 0.2*	0.15	0.002
15:0	0.1 ± 0.04	0.2 ± 0.03	0.1 ± 0.03	0.2 ± 0.02	0.02	0.050
16:0	19.2 ± 1.2	17.0 ± 1.6	18.0 ± 0.8	17.3 ± 0.7	0.66	0.155
16:1n-7	8.7 ± 1.4	8.2 ± 1.9	8.1 ± 0.7	6.7 ± 0.3	0.72	0.316
17:0	0.3 ± 0.02	0.3 ± 0.06	0.3 ± 0.04	0.4 ± 0.04	0.02	0.098
18:0	5.6 ± 1.0†	8.9 ± 2.1*	8.8 ± 0.7*	9.5 ± 0.2*	0.71	0.017
18:1n-9	38.4 ± 2.9*	32.8 ± 4.1*	36.1 ± 3.0*	24.4 ± 2.0†	1.78	0.003
18:1n-7	3.2 ± 0.3*	2.7 ± 0.2†	2.4 ± 0.1†	2.3 ± 0.07†	0.12	0.003
18:2(*t*-9,*t*-12)[d]	2.1 ± 0.3*	0.9 ± 0.1†	0.4 ± 0.4†	0.7 ± 0.08†	0.16	0.0003
18:2(*c*-9,*c*-12)	0.6 ± 0.2#	1.1 ± 0.1†	1.0 ± 0.1†	1.4 ± 0.09*	0.08	0.001
18:3n-6	0.2 ± 0.06	0.2 ± 0.03	0.1 ± 0.01	0.2 ± 0.01	0.02	0.255
18:3n-3	0.2 ± 0.1	0.3 ± 0.08	0.3 ± 0.07	0.4 ± 0.03	0.05	0.258
18:2(*c*-9,*t*-11)	0.1 ± 0.1#	1.0 ± 0.2†	1.0 ± 0.3†	2.1 ± 0.1*	0.11	0.0001
18:2(*t*-10,*c*-12)	0c	1.2 ± 0.3†	1.1 ± 0.3†	2.6 ± 0.2*	0.14	0.001
18:2(*c*-9,*c*-11)	0c	0.2 ± 0.1†	0.2 ± 0.1†	0.6 ± 0.05*	0.05	0.0002
18:2(*t*-10,*t*-12)	0c	0.4 ± 0.04†	0.3 ± 0.04†	0.5 ± 0.06*	0.02	0.0001
18:4n-3	0.4 ± 0.1	0.5 ± 0.1	0.4 ± 0.1	0.5 ± 0.02	0.06	0.531
20:1n-9	2.9 ± 0.2*	1.7 ± 0.2†	1.7 ± 0.2†	1.5 ± 0.1†	0.10	0.0001
20:2n-6	0	0	0	0.04 ± 0.08	0.02	0.441
20:3n-6	0	0	0	0.1 ± 0.1	0.03	0.053
20:4n-6	0.5 ± 0.04†	0.7 ± 0.1†	0.6 ± 0.04†	1.0 ± 0.1*	0.05	0.0005
20:5n-3	4.4 ± 0.8†	6.1 ± 1.1†	5.0 ± 0.5†	8.6 ± 0.7*	0.47	0.0011
22:1n-9	0.1 ± 0.08	0	0	0.1 ± 0.1	0.05	0.388
22:4n-6	0.1 ± 0.08	0.2 ± 0.07	0.2 ± 0.04	0.2 ± 0.1	0.05	0.300
22:5n-3	0.7 ± 0.3†	0.9 ± 0.2†	0.7 ± 0.1†	1.4 ± 0.2*	0.13	0.012
22:6n-3	4.5 ± 0.6†	5.8 ± 1.3*,†	4.5 ± 0.3†	7.6 ± 1.3*	0.58	0.015

[a]Means in the same row with the same superscript were not significantly different ($P < 0.05$).
[b]Values are means of three replications.
[c]Probability (Pr > F) of treatment differences as determined by ANOVA.
[d]Tentative identification. For abbreviations see Table 2.

TABLE 5
Fatty Acid Composition (wt%) of Muscle from Hybrid Striped Bass Fed CLA[a,b]

Fatty acid	Dietary treatment				Pooled SEM	ANOVA (*P* value[c])
	Control	0.5% CLA	0.75% CLA	1.0% CLA		
14:0	4.4 ± 0.5	4.8 ± 0.2	4.4 ± 0.3	5.0 ± 0.5	0.22	0.216
15:0	0.3 ± 0.02	0.3 ± 0.01	0.3 ± 0.01	0.2 ± 0.2	0.05	0.421
16:0	19.8 ± 0.4	19.3 ± 0.5	19.7 ± 0.4	19.2 ± 1.1	0.40	0.694
16:1n-7	8.6 ± 0.6	8.1 ± 0.4	7.5 ± 0.3	8.3 ± 1.0	0.38	0.303
17:0	0.3 ± 0.02	0.3 ± 0.005	0.4 ± 0.01	0.5 ± 0.3	0.09	0.479
18:0	4.1 ± 0.5†	4.9 ± 0.3*,†	5.4 ± 0.2*	5.2 ± 0.7*,†	0.28	0.048
18:1n-9	22.3 ± 1.1	22.9 ± 0.5	23.0 ± 0.9	24.4 ± 1.4	0.60	0.182
18:1n-7	3.1 ± 0.1*	2.8 ± 0.1†	2.6 ± 0.1†	2.7 ± 0.1†	0.07	0.006
18:2(*t*-9,*t*-12)[d]	0.9 ± 0.1*	0.5 ± 0.02†	0.5 ± 0.02†	0.3 ± 0.3†	0.09	0.009
18:2(*c*-9,*c*-12)	1.5 ± 0.1†	1.7 ± 0.06†	1.8 ± 0.03†	2.2 ± 0.4*	0.13	0.023
18:3n-6	0.3 ± 0.08	0.2 ± 0.006	0.2 ± 0.06	0.3 ± 0.2	0.08	0.928
18:3n-3	0.7 ± 0.03	0.7 ± 0.03	0.6 ± 0.008	0.5 ± 0.2	0.06	0.286
18:2 (*c*-9,*t*-11)	0.5 ± 0.5$^{\#}$	1.5 ± 0.05†	1.8 ± 0.1†	3.2 ± 0.3*	0.17	0.0001
18:2(*t*-10,*c*-12)	0‡	1.6 ± 0.06$^{\#}$	2.2 ± 0.2†	4.1 ± 0.3*	0.12	0.0001
18:2(*c*-9,*c*-11)	0	0	0.1 ± 0.1	0.4 ± 0.4	0.12	0.104
18:2(*t*-10,*t*-12)	0	0.3 ± 0.2	0.3 ± 0.3	0.4 ± 0.4	0.15	0.313
18:4n-3	1.1 ± 0.06	1.0 ± 0.06	0.9 ± 0.01	0.9 ± 0.1	0.04	0.065
20:1n-9	2.1 ± 0.2	1.8 ± 0.3	1.7 ± 0.3	1.8 ± 0.3	0.16	0.295
20:2n-6	0	0	0.1 ± 0.1	0.1 ± 0.1	0.05	0.596
20:3n-6	0	0	0.1 ± 0.1	0.1 ± 0.1	0.04	0.596
20:4n-6	1.1 ± 0.1	1.0 ± 0.1	1.0 ± 0.01	0.8 ± 0.05	0.05	0.137
20:5n-3	11.2 ± 0.6*	10.1 ± 0.4*	9.8 ± 0.2*	7.6 ± 0.9†	0.34	0.005
22:1n-9	0	0	0	0	—	—
22:4n-6	0	0	0	0.04 ± 0.07	0.02	0.441
22:5n-3	2.1 ± 0.2	2.1 ± 0.04	1.9 ± 0.1	2.1 ± 0.1	0.07	0.381
22:6n-3	9.5 ± 0.8*	8.7 ± 0.4*	8.4 ± 0.6*	4.6 ± 1.3†	0.49	0.0004

[a]Means in the same row with the superscript were not significantly different ($P < 0.05$).
[b]Values are means of three replications.
[c]Probability (Pr > F) of treatment differences as determined by ANOVA.
[d]Tentative identification. For abbreviations see Table 2.

ficiency and reduced tissue lipids are desirable traits for food animals, including fish. However, CLA concentrations ≥1.0% of the diet have been shown to reduce growth rates in some experiments (5,13,14,30).

In the present study, hybrid striped bass fed 1.0% dietary CLA exhibited reduced feed intake and weight gain compared to control animals. Reduced growth rates have also been reported for mice fed dietary CLA at 1.0–1.5% of the dry diet (5,13,30), for tilapia and rockfish fed greater than 1.0% CLA, and for carp fed 10.0% CLA (13). Among the fishes examined to date, only the hybrid striped bass exhibited significantly lower weight gain when fed 1.0% dietary CLA.

Dietary CLA concentrations of less than 1.0% appear to have no significant effect on growth rates when compared to control animals. For example, growth rates of mice and rats fed 0.5% dietary CLA were not significantly different from those of animals fed no CLA (12,14,31), and hybrid striped bass fed 0.5 and 0.75% dietary CLA exhibited weight gains that were not significantly different from fish fed no CLA. Fish fed all dietary CLA concentrations evaluated exhibited significantly improved feed efficiencies compared to control animals. These results are consistent with studies conducted with rats (11). However, mice fed dietary CLA concentrations of 0.5, 1.0, and 1.5% exhibited reduced feed efficiencies compared to mice fed no CLA (14). Carp fed 5.0 or 10.0% dietary CLA exhibited reduced feed efficiencies compared to control animals, tilapia feed efficiency values were lower when fed 2.5% dietary CLA and higher concentrations, and feed efficiency values for rockfish were lower when fed 1.0% dietary CLA and higher concentrations (13).

Significant reductions in total liver lipid concentration and intraperitoneal fat ratio were observed in hybrid striped bass fed dietary CLA. Liver lipid concentration of fish fed 1.0% CLA was 2.5-fold lower than that observed in control fish. Dietary CLA have also been shown to modify body composition of rodents. Mice fed 0.5% CLA exhibited a significant reduction in body fat and a significant increase in body protein (12). In that experiment, carnitine palmitoyltransferase activity was significantly increased in fat pad and skeletal muscle of mice fed CLA, which indicates an increase in β-oxidation of fatty acids in response to dietary CLA. Furthermore, CLA caused a significant reduction in triglyceride concentration and lipoprotein lipase activity (consistent with reduced uptake of free fatty acids) in cultured 3T3-L1 adipocytes (12). In contrast to the significant reduction in lipid concentration of extrahepatic tissues, Belury and Kempa-Steczko (14) observed a two fold increase in liver lipid concentrations of mice fed 1.0 or 1.5% CLA. Similarly, rats fed 1.5% CLA exhibited a significant in-

crease in liver lipid concentration (32). Such differences in liver lipid accumulation between rodents and fish indicate that the effects of dietary CLA on lipid metabolism are likely to vary across species.

Four isomers of CLA were identified in both liver and muscle of hybrid striped bass fed dietary CLA, while only one isomer was identified in fish fed no CLA (Tables 4 and 5). In fish fed 0 CLA, mean values of 18:2(*c*-9,*t*-11) were 0.1 and 0.5% in liver and muscle, respectively, and both standard deviations were the same as the mean values. It seems unlikely the CLA was supplied in the experimental diets used in these studies, as the 9,11 isomers constituted only 29.5% of the supplement and only one isomer was identified. It is more probable that the CLA identified in control fish fed CLA in our studies was provided by previous diets fed to the experimental fish prior to acquisition. Those diets are proprietary, but it is common practice to include whey as an ingredient in diets of this type when price warrants inclusion.

Muscle CLA concentrations were as high as 7.97% of fatty acids in fish fed the highest dietary concentration (1.0% CLA) and 3.35% in fish fed the lowest concentration of CLA (0.5%). Regardless of the dietary level of CLA, the sum of the 10,12 isomers was slightly higher than the sum of the 9,11 isomers. Further, both sets of isomers constituted a relatively stable percentage of the total CLA across all treatments and in both tissues. The percentage of 10,12 isomers ranged from 53–57% of total CLA, and the 9,11 isomers were 43–46% of the total. These values are similar to the percentages of isomers in the diets (55.9% of 10,12 and 44.1% of 9,11). Thus, it appears CLA isomers are retained in tissues in similar proportions found in diets fed to fish. However, both 18:2(*c*-9,*t*-11) and 18:2(*t*-10,*c*-12) were retained in higher percentages than either all-*cis* or all-*trans* CLA. Further evaluation of these differences might be beneficial.

Muscle CLA concentrations in carp, tilapia, and rockfish fed 1.0% dietary CLA were 13.0, 4.1, and 5.1% of fatty acids, respectively (13). Those results indicate the ability of fish to accumulate CLA in muscle varies among species. Levels of CLA in those animals that naturally produce the fatty acid and its isomers are 0.27–0.56 g of CLA per 100 g of fatty acid (1). Cheese and milk fat contain 0.3–0.6 g of CLA per g of fatty acid (8). Thus, of the animals evaluated, fish appear to possess the ability to accumulate higher concentrations of CLA than other vertebrates. Additionally, there appears to be an interaction between CLA and long-chain n-3 fatty acids considered essential in this fish (20:5n-3 and 22:6n-3) (33) and beneficial for human health.

As dietary concentration of CLA increased, the concentration of 18:3n-3 was not significantly different in either liver or muscle, but the longer-chain n-3 fatty acids were significantly different across dietary treatments. In liver, 20:5n-3, 22:5n-3, and 22:6n-3 were significantly higher in fish fed 1.0% CLA, but were not significantly different in fish fed other levels of CLA or those in fish fed no CLA. Muscle concentrations of 20:5n-3 and 22:6n-3 were significantly lower in muscle of fish accumulating increasing levels of CLA and 18:2(*c*-9,*c*-12). Thus, as dietary concentrations and intake of CLA increased in hybrid striped bass, long-chain n-3 fatty acids appeared to be sequestered in liver resulting in decreasing concentrations in muscle, while 22:5n-3 concentrations were not significantly affected. At the same time, liver lipid concentrations dramatically decreased, and there were no clear distinctions regarding which fatty acids led to the decreased liver lipid concentrations. Since total liver lipid decreased and individual fatty acids remain somewhat constant as a percentage of the total, dietary CLA clearly affected hepatic lipid metabolism in hybrid striped bass.

Fish remain an important route of ingestion of beneficial fatty acids, and CLA is an important new component of fatty acid metabolism in humans. In this study, we demonstrated that the hybrid striped bass is capable of absorbing and retaining dietary CLA in liver and muscle and that the concentrations in muscle are higher than recorded for other vertebrates. Thus, fish appear to be a potential route of increased ingestion of CLA in humans.

ACKNOWLEDGMENTS

The authors thank Paul D. Adelizi (Saskatchewan Wheat Pool, Saskatoon, Canada) for providing the conjugated linoleic acid supplement. This research was partially supported by the Purdue University Agricultural Research Programs and is technical manuscript #16042.

REFERENCES

1. Haumann, B.F. (1996) Conjugated Linoleic Acid Offers Research Promise, *INFORM 7*, 152–159.
2. Parodi, P.W. (1996) Milk Fat Components: Possible Chemopreventive Agents for Cancer and Other Diseases, *Aust. J. Dairy Technol. 51*, 24–32.
3. Sugano, M., Tsujita, A., Yamasaki, M., Yamada, K., Ikeda, I., and Kritchevsky, D. (1997) Lymphatic Recovery, Tissue Distribution, and Metabolic Effects of Conjugated Linoleic Acid in Rats, *J. Nutr. Biochem. 8*, 38–43.
4. Decker, E.A. (1995) The Role of Phenolics, Conjugated Linoleic Acid, Carnosine, and Pyrroloquinoline Quinone as Nonessential Dietary Antioxidants, *Nutr. Rev. 53*, 49–58.
5. Hayek, M.G., Han, S.N., Wu, D., Watkins, B.A., Meydani, M., Dorsey, J.L., Smith, D.E., and Meydani, S.N. (1999) Dietary Conjugated Linoleic Acid Influences the Immune Response of Young and Old C57BL/6NCrlBR Mice, *J. Nutr. 129*, 32–38.
6. Lee, K.N., Kritchevsky, D., and Pariza, M.W. (1994) Conjugated Linoleic Acid and Atherosclerosis in Rabbits, *Atherosclerosis 108*, 19–25.
7. Scimeca, J.A., Thompson, H.J., and Ip, C. (1994) Effects of Conjugated Linoleic Acid on Carcinogenesis, in *Diet and Breast Cancer* (Weisburger, E.K., ed.), Plenum Press, New York, pp. 59–65.
8. Ip, C. (1994) Conjugated Linoleic Acid in Cancer Prevention Research: a Report of Current Status and Issues, Special Report Prepared for the National Livestock and Meat Board, Research Report No. 100-104, Washington, DC.
9. Chin, S.F., Storkson, J.M., Albright, K.J., Cook, M.E., and Pariza, M.W. (1994) Conjugated Linoleic Acid Is a Growth Factor for Rats as Shown by Enhanced Weight Gain and Improved Feed Efficiency, *J. Nutr. 124*, 2344–2349.
10. Cook, M.E., Miller, C.C., Park, Y., and Pariza, M. (1993) Immune Modulation by Altered Nutrient Metabolism: Nutritional Control of Immune-Induced Growth Depression, *Poult. Sci. 72*, 1301–1305.

11. Li, Y., and Watkins, B.A. (1998) Conjugated Linoleic Acids Alter Bone Fatty Acid Composition and Reduce *ex vivo* Prostaglandin E_2 Biosynthesis in Rats Fed n-6 or n-3 Fatty Acids, *Lipids 33*, 417–425.
12. Park, Y., Albright, K.J., Liu, W., Storkson, J.M., Cook, M.E., and Pariza, M.W. (1997) Effect of Conjugated Linoleic Acid on Body Composition in Mice, *Lipids 32*, 853–858.
13. Choi, B.-D., Kang, S.-J., Ha, Y.-L., and Ackman, R.G. (1999) Accumulation of Conjugated Linoleic Acid (CLA) in Tissues of Fish Fed Diets Containing Various Levels of CLA, in *Quality Attributes of Muscle Foods* (Xiong, Y.L., Ho, C.-T., and Shahidi, F., eds.), pp. 61–71, Kluwer Academic/Plenum Publishers, New York.
14. Belury, M.A., and Kempa-Steczko, A. (1997) Conjugated Linoleic Acid Modulates Hepatic Lipid Composition in Mice, *Lipids 32*, 199–204.
15. Kramer, J.K.G., Sehat, N., Dugan, M.E.R., Mossoba, M.M., Yurawecz, M.P., Roach, J.A.G., Eulitz, K., Aalhus, J.L., Schaefer, A.L., and Ku, Y. (1998) Distributions of Conjugated Linoleic Acid (CLA) Isomers in Tissue Lipid Classes of Pigs Fed a Commercial CLA Mixture Determined by Gas Chromatography and Silver Ion–High-Performance Liquid Chromatography, *Lipids 33*, 549–558.
16. Sebedio, J.L., Juaneda, P., Dobson, G., Ramilison, I., Martin, J.C., Chardigny, J.M., and Christie, W.W. (1997) Metabolites of Conjugated Isomers of Linoleic Acid (CLA) in the Rat, *Biochim. Biophy. Acta 1345*, 5–10.
17. New, M.B. (1997) Aquaculture and the Capture Fisheries—Balancing the Scales, *World Aquacult. 28*, 11–30.
18. Mortensen, A., Hansen, B.F., Hansen, J.F., Frandsen, H., Bartnikowska, E., Andersen, P.S., and Bertelsen, L.S. (1998) Comparison of the Effects of Fish Oil and Olive Oil on Blood Lipids and Aortic Atherosclerosis in Watanabe Heritable Hyperlipidaemic Rabbits, *Br. J. Nutr. 80*, 565–573.
19. Uauy-Dagach, R., and Valenzuela, A. (1996) Marine Oils: the Health Benefits of n-3 Fatty Acids, *Nutr. Rev. 54*, S102–S108.
20. Brown, P.B., Griffin, M.E., and White, M.R. (1993) Experimental and Practical Diet Evaluations with Juvenile Hybrid Striped Bass, *J. World Aquacult. Soc. 24*, 80–89.
21. Griffin, M.E., Wilson, K.A., and Brown, P.B. (1994) Dietary Arginine Requirement of Juvenile Hybrid Striped Bass, *J. Nutr. 124*, 888–893.
22. Griffin, M.E., Brown, P.B., and Grant, A. (1992) Dietary Lysine Requirement of Juvenile Hybrid Striped Bass, *J. Nutr. 122*, 1332–1337.
23. Griffin, M.E., White, M.R., and Brown, P.B. (1994) Total Sulfur Amino Acid Requirement and Cysteine Replacement Value for Juvenile Hybrid Striped Bass (*Morone saxatilis* × *M. chrysops*), *Comp. Biochem. Phys. 108A*, 423–429.
24. NRC (National Research Council) (1993) *Nutrient Requirements of Fish*, National Academy Press, Washington, DC.
25. Griffin, M.E., Wilson, K.A., White, M.R., and Brown, P.B. (1994) Dietary Choline Requirement of Juvenile Hybrid Striped Bass, *J. Nutr. 124*, 1685–1689.
26. Nematipour, G.R., Brown, M.L., and Gatlin, D.M. (1992) Effects of Dietary Energy:Protein Ratio on Growth Characteristics and Body Composition of Hybrid Striped Bass, *Morone chrysops* × *M. saxatilis*, *Aquaculture 107*, 359–368.
27. Wilson, R.P., Harding, D.E., and Garling, D.L. (1977) Effect of Dietary pH on Amino Acid Utilization and the Lysine Requirement of Fingerling Channel Catfish, *J. Nutr. 107*, 166–170.
28. Folch, J., Lees, M., and Sloan Stanley, G.H. (1957) A Simple Method for the Isolation and Purification of Total Lipides from Animal Tissues, *J. Biol. Chem. 226*, 497–509.
29. Ip, C., Chin, S.F., Scimeca, J.A., and Pariza, M.A. (1991) Mammary Cancer Prevention by Conjugated Derivatives of Linoleic Acid, *Cancer Res. 51*, 6118–6124.
30. West, D.B., Delany, J.P., Camet, P.M., Blohm, F., Truett, A.A., and Scimeca, J. (1998) Effects of Conjugated Linoleic Acid on Body Fat and Energy Metabolism in the Mouse, *Am. J. Physiol. 275*, R667–R672.
31. Sisk, M., Azain, M.J., and Hausman, D.B. (1998) Effect of Conjugated Linoleic Acid on Fat Pad Weights and Cellularity in Sprague-Dawley and Zucker Rats, *FASEB J. 12*, A536 (abs.).
32. Moya-Camarena, S.Y., Vanden Heuvel, J.P., and Belury, M.A. (1999) Conjugated Linoleic Acid Activates Peroxisome Proliferator-Activated Receptor α and β Subtypes but Does Not Induce Hepatic Peroxisome Proliferation in Sprague-Dawley Rats, *Biochim. Biophy. Acta 1436*, 331–342.
33. Nematipour, G.R., and Gatlin, D.M. (1993) Requirement of Hybrid Striped Bass for Dietary (n-3) Highly Unsaturated Fatty Acids, *J. Nutr. 123*, 744–753.

[Received July 12, 1999, and in final revised form January 28, 2000; revision accepted January 31, 2000]

Effects of Various Tocopherol-Containing Diets on Tocopherol Secretion into Bile

Kanae Yamashita*, Noriko Takeda, and Saiko Ikeda

Department of Food and Nutrition, School of Life Studies, Sugiyama Jogakuen University, Nagoya, 464-8662 Japan

ABSTRACT: γ-Tocopherol is abundant in common vegetable oil, but its concentration in plasma and liver is much lower than that of α-tocopherol. Discrimination between different forms of tocopherol is thought to take place *via* the hepatic α-tocopherol transfer protein (α-TTP). γ-Tocopherol, with a low binding capacity to α-TTP, is thought to be excreted *via* the bile. Our previous studies showed that γ-tocopherol administered with sesame seed exhibits significantly higher concentrations in the plasma and liver of rats than γ-tocopherol alone. Thus, we attempted to confirm whether a much higher amount of γ-tocopherol rather than α-tocopherol would be secreted in the bile, and whether sesame seed would suppress the secretion of γ-tocopherol. In one experiment, we examined the concentrations of α- or γ-tocopherol in the plasma, liver, and bile of rats fed diets containing 300 mg/kg of α-tocopherol, 300 mg/kg of γ-tocopherol, or 300 mg/kg each of α-tocopherol + γ-tocopherol, and in the other experiment, we compared the γ-tocopherol concentrations of rats fed a diet of γ-tocopherol alone to those of rats fed a γ-tocopherol + sesame seed diet (each diet contained 300 mg/kg γ-tocopherol). The bile collection was done over 6 h. The γ-tocopherol concentration in the bile was markedly lower than that of α-tocopherol, paralleling the concentrations in the plasma and liver. Intake of α-tocopherol and γ-tocopherol together further lowered the concentration of γ-tocopherol in the bile as well as in the plasma and liver, compared to the intake of γ-tocopherol alone. The γ-tocopherol concentration in the bile, as well as in the plasma and liver, was markedly higher in the sesame seed-fed group than in the γ–tocopherol alone group. We found that the concentrations of α- or γ-tocopherol in the bile showed a good correlation with the concentrations of α- or γ-tocopherol in the liver, though the concentrations in the bile were substantially lower than those in the liver. These findings suggest that secretion into the bile is not a major metabolic route of α- or γ-tocopherol.

Paper no. L8099 in *Lipids 35*, 163–170 (January 2000).

Among the eight structural forms of vitamin E, α-tocopherol is found in the highest concentrations in human plasma and tissue and shows the highest physiological activity. γ-Tocopherol is abundant in common vegetable oil, but its biological activity is estimated to be only 6 to 16% that of α-tocopherol (1,2). According to recent studies using various forms of vitamin E, no discrimination exists between α-tocopherol and γ-tocopherol during absorption (3,4), but following uptake by the liver, only *RRR*-α-tocopherol is preferentially bound to the α-tocopherol transfer protein (α-TTP) and secreted in nascent very low density lipoprotein (VLDL) (5–9). Thus, it is thought that discrimination between forms of tocopherol may occur in hepatic α-TTP. Tocopherols such as γ-tocopherol, which possess a low binding capacity to α-TTP, are thought to be excreted *via* the bile (6,9). Our previous studies have examined the antiaging effect of sesame seed. Sesame seed has long been used as a health food with purported antiaging effects, but contains only γ-tocopherol and negligible amount of α-tocopherol, which suggests low physiological vitamin E activity. Our experiments compared the *in vivo* concentrations of α- and γ-tocopherol in rats fed α-tocopherol, γ-tocopherol, or sesame seed-containing diets (50 mg/kg concentrations in all diets) (10,11). Sesame seed-fed rats showed almost the same concentration of γ-tocopherol in the plasma and tissue as α-tocopherol in rats fed the α-tocopherol-containing diet, but the γ-tocopherol concentration in rats fed a diet containing γ-tocopherol alone was very low in the plasma and tissue. In other words, γ-tocopherol administered with sesame seed exhibits significantly higher concentrations in the plasma and liver of rats than γ-tocopherol alone. One possibility we considered was that the biliary secretion of γ-tocopherol in rats fed sesame seed might be suppressed. Under this assumption, our preliminary investigation examined γ-tocopherol secretion in the bile of rats fed diets containing γ-tocopherol or sesame seed as the source of vitamin E. We found a higher γ-tocopherol concentration in the bile of rats fed the sesame seed-containing diet, though these rats showed higher γ-tocopherol concentrations in the plasma and liver than those of rats fed γ-tocopherol alone. Accordingly, we suspected that α-tocopherol, with concentrations higher than γ-tocopherol in the plasma and liver, might also be higher in the bile. Thus, we determined the investigation of biliary secretion of α- or γ-tocopherol in rats fed diets containing α- or γ-tocopherol as the vitamin E source. An additional consideration was that, when α-tocopherol and γ-tocopherol are administered together, the *in vivo* concentration of γ-tocopherol is substantially lower with administration of α-tocopherol

*To whom correspondence should be addressed at Department of Food and Nutrition, School of Life Studies, Sugiyama Jogakuen University, 17-3 Hoshigaoka Motomachi, Chikusa-ku, Nagoya, 464-8662, Japan.
E-mail: kanaey@food.sugiyama-u.ac.jp.

Abbreviations: ANOVA, analysis of variance; α-CEHC, 2,5,7,8-tetramethyl-2(2′-carboxyethyl)-6-hydroxychroman; γ-CEHC, 2,7,8-trimethyl-2(2′-carboxyethyl)-6-hydroxychroman; α-TTP, α-tocopherol transfer protein; HPLC, high-performance liquid chromatography; PMC, 2,2,5,7,8-pentamethyl-6-chromanol; VLDL, very low density lipoprotein.

(12–16). This indicates that α-tocopherol promotes γ-tocopherol elimination. It was necessary to determine whether the biliary concentration of γ-tocopherol would be high or low in this case. Therefore, in the first of the present experiments, we examined the secretion of tocopherol into the bile in rats fed diets containing α-tocopherol, γ-tocopherol, or α- + γ-tocopherol. In the second experiment, we examined in more detail γ-tocopherol secretion into the bile in rats fed diets containing γ-tocopherol or γ-tocopherol with sesame seed as the source of vitamin E.

MATERIALS AND METHODS

Materials. α-Tocopherol, γ-tocopherol, and vitamin E homologs used for biochemical analysis were gifts of Eisai Co. (Tokyo, Japan). Vitamin E-stripped corn oil was purchased from Funahasi Nougyou Co. (Chiba, Japan). A vitamin E-free vitamin and mineral mixtures were both made according to AIN-76 formulation (17) by Nihon Hosan Kogyo (Yokohama, Japan). The white roasted sesame seed (donated by the Shinsei Co., Aichi, Japan) was ground finely in a mixer. The seed from the same batch was used throughout this investigation. Solvents used for chromatography were high-performance liquid chromatography (HPLC) grade from Katayama Chemicals Co., Ltd. (Osaka, Japan).

Animals and diets. Male Wistar rats, each weighing about 250 g (Japan SLC Inc., Shizuoka, Japan), were housed individually in stainless-steel wire-mesh cages at 24.5°C and 55% humidity, with a 12-h light/dark cycle. Rats were maintained in accordance with the Guidelines for Animal Experimentation of Nagoya University. They were allowed free access to a vitamin E-free diet (Table 1) for 7 d to standardize the *in vivo* conditions, and then given the experiment diets *ad libitum* for 1, 3, and 7 d. The experimental diets were in accordance with AIN-76 formulation (17) and consisted of 20% protein, 10% fat, vitamins excluding vitamin E, and minerals, as shown in Table 1. Tocopherol content in the diets was 300 mg/kg because we expected the high dose of tocopherols to produce a higher concentration of tocopherols in the body. In Experiment 1, a vitamin E-free diet, α-tocopherol alone diet, γ-tocopherol alone diet, and α- + γ-tocopherol combined diet were used. The amount of tocopherol was 300 mg/kg in the α-tocopherol and γ-tocopherol diets, and the amounts of α-tocopherol and γ-tocopherol were each 300 mg/kg in the α + γ diet. In Experiment 2, a vitamin E-free diet, γ-tocopherol diet, and sesame seed diet containing 20% ground white sesame seed (all diets contained a negligible amount of α-tocopherol) were used. The amount of γ-tocopherol in the γ-tocopherol diet was 300 mg/kg, and in the sesame seed diet (which already contained ~ 50 mg/kg of γ-tocopherol), it was adjusted to 300 mg/kg by the addition of γ-tocopherol. The concentration of tocopherol in the diets was confirmed by assay immediately after formulation. Diets were stored at –20°C until use. After the end of the experimental feeding, at 9:00 A.M. the next morning, rats were anesthetized with Nembutal (pentobarbital Na), and a laparotomy was performed to collect the bile, which was done for 6 h. Then rats were anesthetized again (at about 3:30 P.M.), blood was collected from the heart, and the liver was excised after perfusion with physiological saline. The concentrations of tocopherol in the plasma, liver, and bile were measured by HPLC according to the method developed by Ueda and Igarashi (18). The

TABLE 1
Composition of Diets (Experiments 1 and 2)

	Experiment 1 Control (–E)	α-Tocopherol	γ-Tocopherol	α- + γ-Tocopherol
		g/kg diet		
Casein (–E)	200	200	200	200
Mineral mixture (AIN-76)	35	35	35	35
Vitamin mixture [AIN-76 (–E)]	10	10	10	10
Corn starch (–E)	655	655	655	655
Stripped corn oil[a]	100	99.7	99.7	99.4
α-Tocopherol[b]		0.3		0.3
γ-Tocopherol[b]			0.3	0.3

	Experiment 2 Control (–E)	γ-Tocopherol	Sesame
		g/kg diet	
Casein (–E)	200	200	160
mineral mixture (AIN-76)	35	35	35
Vitamin mixture [AIN-76 (–E)]	10	10	10
Corn starch (–E)	655	655	585
Stripped corn oil[a]	110	109.7	9.75
Crushed sesame seed			200
α-Tocopherol[b]			
γ-Tocopherol[b]		0.3	0.25

[a]In tocopherol- and sesame seed-containing diets, stripped corn oil was reduced, depending on the concentrations of tocopherol and sesame seed oil, which were calculated to be 50 g/100 g in the seed.
[b]Tocopherols were added dissolved in stripped corn oil. In sesame seed-containing diet, sesame seeds contained 23.5 mg/100 g of γ-tocopherol and negligible amounts of α-tocopherol.

plasma (0.15 mL) and the bile (0.5 mL) were pipetted into 10-mL centrifuge tubes with caps, and ethanol (1 mL), distilled water (0.5 mL), *n*-hexane (5 mL), and an hexanolic solution of 2,2,5,7,8-pentamethyl-6-chromanol (PMC) as an internal standard (0.2 mL) were added. The whole media were mixed vigorously for 1 min, and tocopherols were extracted in hexane. After centrifuging for 5 min at 1,000 rpm, the hexane layer was moved into the test tubes for the evaporation. Extraction with 5 mL *n*-hexane was repeated once more. The combined hexane layer was evaporated by the centrifugal vaporizer, redissolved in *n*-hexane (200 μL), and injected into the HPLC system. The liver (0.5 g) was homogenized with distilled water (1 mL). The homogenate (1 mL) was pipetted into a 25-mL test tube with a cap and 6% ethanolic pyrogallol (1 mL) and ethanolic solution of PMC (1 mL) were added. A 60% KOH solution (0.2 mL) was added and saponified at 70ºC for 30 min. After adding 2% NaCl solution (4.5 mL), the whole media were extracted with 10% ethylacetate in *n*-hexane (3 mL). After centrifuging, a portion of the hexane layer was evaporated, redissolved in *n*-hexane (200 μL), and injected into the HPLC system. Instrumentation used for HPLC was a Shimadzu Model LC-9A (Shimadzu, Kyoto, Japan) with a Shimadzu RF-535 fluorescence detector (Ex: 298 nm, Em: 325 nm). The analytical column used was a Nucleosil 5 NH_2 (4.6 Φ × 150 mm; Shinwa Chemical Industries, Ltd., Kyoto, Japan). The mobile phase was *n*-hexane/isopropylalcohol (99:1, vol/vol) at a flow rate of 1 mL/min.

Statistical analysis. Data are expressed as means ± SEM. Statistical analysis was performed using one-way analysis of variance (ANOVA) in SPSS Base 9.0 (Chicago, IL). When one-way ANOVA revealed $P < 0.05$, the data were further analyzed using Duncan's multiple comparison test (19). Differences were considered statistically significant at $P < 0.05$.

RESULTS AND DISCUSSION

(i) Concentrations of α-tocopherol and γ-tocopherol in plasma, liver, and bile (Experiment 1). In Experiment 1, rats were divided into four experimental groups: vitamin E-free, α-tocopherol (300 mg), γ-tocopherol (300 mg), and α- + γ-tocopherol (300 mg α-tocopherol + 300 mg γ-tocopherol). The results of body weight, liver weight, food intake, and amount of bile are shown in Table 2. The amount of bile collected during the 6-h period from 9:30 A.M. ranged from 1.8 to 4.9 mL, but was mostly in the range 3.0–3.5 mL. The concentrations of tocopherol in the plasma, liver, and bile of rats fed the experimental

TABLE 2
Body Weight, Liver Weight, Food Intake, and Bile Volume of Rats in Experiments 1 and 2[a]

Group	Body weight	Liver weight	Food intake	Bile volume[b]
Experiment 1	(g)	(g)	(g)	(mL)
Vitamin E-free (d)				
1	280.3 ± 6.8^{a,b}	9.66 ± 0.22^{a,b,c}	14.12 ± 0.42	3.2 ± 0.3^{a,b,c}
3	276.5 ± 4.1^{a,b}	9.28 ± 0.14^{a,b,c}	38.55 ± 0.75	3.0 ± 0.2^{a,b,c}
7	298.4 ± 2.8^{c}	9.51 ± 0.22^{a,b,c}	87.57 ± 1.34	3.4 ± 0.1^{b,c}
α-Tocopherol (d)				
1	282.3 ± 6.4^{a,b}	9.95 ± 0.25^{c}	15.1 ± 0.88	2.9 ± 0.2^{a,b}
3	283.1 ± 5.0^{a,b,c}	9.47 ± 0.34^{a,b,c}	40.65 ± 1.36	3.4 ± 0.2^{b,c}
7	297.7 ± 4.5^{c}	9.45 ± 0.34^{a,b,c}	89.40 ± 3.33	3.4 ± 0.1^{b,c}
γ-Tocopherol (d)				
1	271.4 ± 3.8^{a}	9.53 ± 0.19^{a,b,c}	13.7 ± 0.38	3.0 ± 0.2^{a,b,c}
3	278.4 ± 5.1^{a,b}	9.31 ± 0.27^{a,b,c}	36.75 ± 2.20	3.5 ± 0.1^{c}
7	292.2 ± 1.6^{b,c}	9.08 ± 0.05^{a,b}	84.16 ± 1.84	3.0 ± 0.2^{a,b,c}
α- + γ-Tocopherol (d)				
1	278.4 ± 5.3^{a,b}	9.85 ± 0.25^{b,c}	14.9 ± 0.65	2.7 ± 0.1^{a}
3	278.6 ± 4.5^{a,b}	9.10 ± 0.18^{a,b}	40.91 ± 3.12	3.3 ± 0.2^{b,c}
7	292.1 ± 4.8^{b,c}	9.00 ± 0.30^{a}	87.75 ± 4.25	3.2 ± 0.2^{a,b,c}
Experiment 2				
Vitamin E-free (d)				
1	280.0 ± 2.5^{a,b,c}	9.89 ± 0.29^{c}	14.69 ± 0.39	3.4 ± 0.2^{b,c}
3	283.1 ± 4.4^{b,c}	8.86 ± 0.31^{a,b}	41.21 ± 1.66	2.5 ± 0.2^{a}
7	299.4 ± 6.9^{d}	9.74 ± 0.22^{b,c}	92.59 ± 2.37	3.1 ± 0.2^{a,b,c}
γ-Tocopherol (d)				
1	272.8 ± 3.2^{a,b}	9.23 ± 0.19^{a,b,c}	14.94 ± 0.56	2.7 ± 0.3^{a,b}
3	287.2 ± 4.7^{c}	9.17 ± 0.31^{a,b,c}	42.69 ± 2.45	3.0 ± 0.3^{a,b,c}
7	302.3 ± 3.3^{d}	9.85 ± 0.42^{c}	95.35 ± 1.41	3.5 ± 0.1^{c}
Sesame (d)				
1	269.6 ± 3.9^{a}	8.50 ± 0.14^{a}	13.36 ± 0.52	3.2 ± 0.2^{a,b,c}
3	286.1 ± 3.1^{c}	9.16 ± 0.33^{a,b,c}	40.43 ± 1.65	3.0 ± 0.3^{a,b,c}
7	311.6 ± 4.9^{d}	10.07 ± 0.30^{c}	97.44 ± 4.44	4.2 ± 0.3^{d}

[a]Values are presented as means ± SEM of six rats. Statistical analysis was performed combining all groups and times (12 in Experiment 1, and 9 in Experiment 2). Values not bearing the same superscript letter are significantly different at $P < 0.05$.
[b]The bile collection was performed for 6 h from 9:30 A.M.

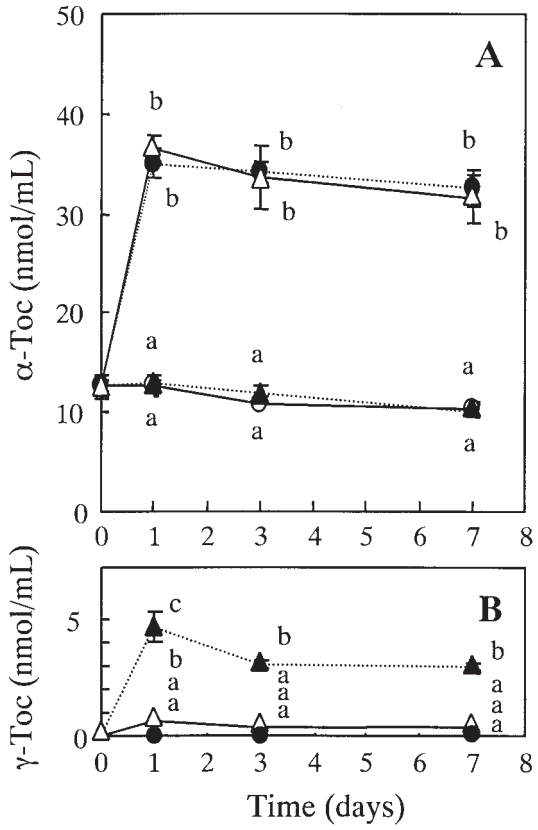

FIG. 1. α-Tocopherol (α-Toc) (A) and γ-tocopherol (γ-Toc) (B) concentrations in the plasma of rats fed a α-tocopherol diet, γ-tocopherol diet, and α- + γ-tocopherol diet in Experiment 1. After being fed a vitamin E-free diet for 7 d, rats were fed vitamin E-free diet, α-tocopherol diet (300 mg/kg), γ-tocopherol diet (300 mg/kg), or α- + γ-tocopherol diet (containing 300 mg/kg α-tocopherol and 300 mg/kg γ–tocopherol) for 1, 3, or 7 d. Each point represents the mean ± SE of six rats. Values not bearing the same superscript letter are significantly different at $P < 0.05$. ⅄ control (–E); ⅂ α-tocopherol; ⅁, γ-tocopherol; ⅋, α- + γ-tocopherol.

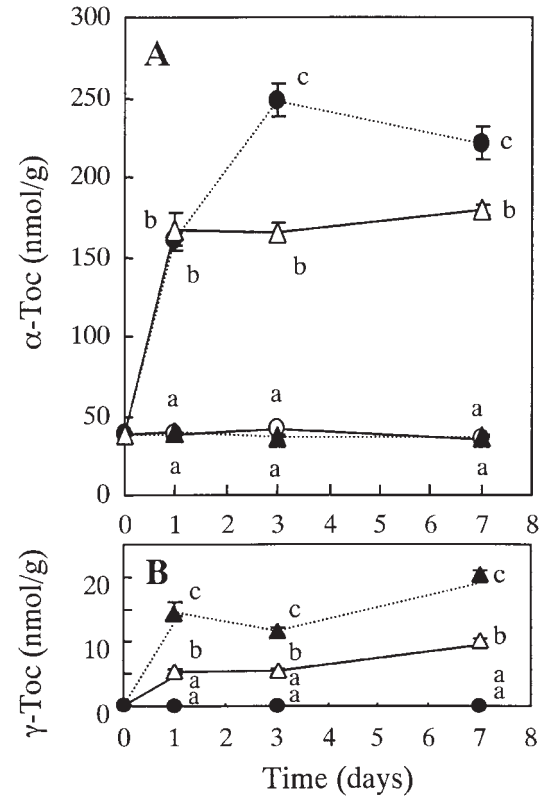

FIG. 2. α-Toc (A) and γ-Toc (B) concentrations in the liver of rats fed α-tocopherol diet, γ-tocopherol diet, and α- + γ-tocopherol diet in Experiment 1. See Figure 1 for abbreviations and point and symbol details.

diet for 1, 3, and 7 d are shown in Figures 1, 2, and 3. As shown in the figures, the concentrations of α-tocopherol and γ-tocopherol in the plasma, liver, and bile reached a plateau with only 1 d repletion of α- or γ-tocopherol after 1 wk of feeding with the vitamin E-free diet, with the exception of the liver in the α-tocopherol alone group which reached a plateau with 3 d repletion. Clement *et al.* (12) reported that α- or γ-tocopherol concentrations in the serum and liver reached a plateau after 8 d of repletion with *RRR*-α- or γ-tocopherol. Their experimental conditions differed in the acclimation period of the vitamin E-deficient diet (8 wk as opposed to our 1 wk) and in the quantity of repletion with tocopherol (they used a 30 mg/kg diet as opposed to our 300 mg/kg diet). Traber *et al.* (20) estimated that the binding capacity of α-TTP to α-tocopherol would be so large that it could bind an amount of α-tocopherol a few times larger than the apparent amount in the liver. Thus, the larger amount of feeding (300 mg/kg diet) caused the plateau to come sooner. We anticipated that a large amount of feeding would cause a large amount to be retained in the body, with a large amount secreted into the bile, thus providing us with clear-cut results. Our previous experiment showed that a large amount (250 mg/kg) of feeding produced 92.4 ± 3.5 μmol/g of α-tocopherol in the liver in comparison to 50 mg/kg feeding

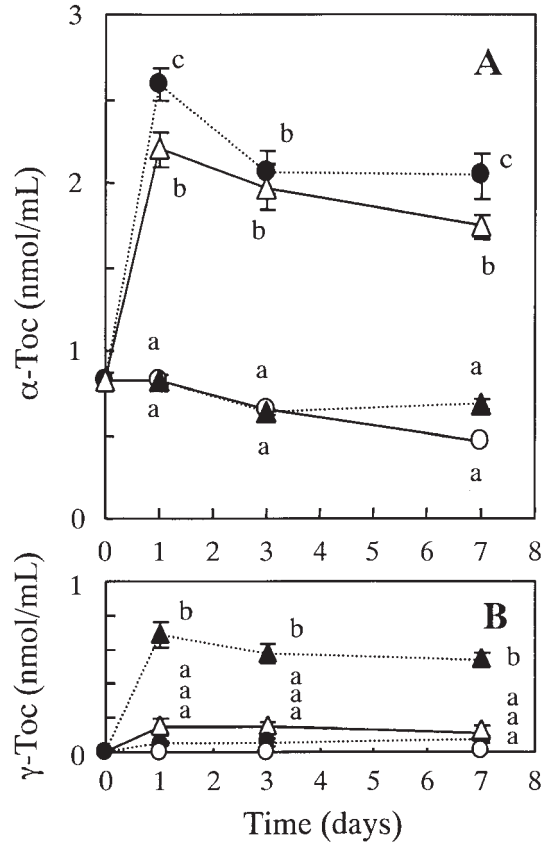

FIG. 3. α-Toc (A) and γ-Toc (B) concentrations in the bile of rats fed α-tocopherol diet, γ-tocopherol diet, and α- + γ-tocopherol diet in Experiment 1. Bile was collected for 6 h at the end of experimental feeding, starting at 9:30 the following morning. See Figure 1 for abbreviations and point and symbol details.

with 36.0 ± 1.4 μmol/g (11). Further, Traber *et al.* (20) showed with rats with cannulated thoracic lymph ducts that a large dose of α-tocopherol caused a lower percentage of tocopherol to be absorbed but the amount of tocopherol absorbed was large (4).

The α-tocopherol concentration in all rats was higher than γ-tocopherol not only in the plasma and liver but also in the bile. α-Tocopherol concentrations were high in the α-tocopherol and α + γ groups that took α-tocopherol. The concentrations of α-tocopherol in the plasma were similar in the α-tocopherol and α + γ groups, but those in the liver were slightly lower than in the α-tocopherol group on days 3 and 7. The large (300 mg) intake of γ-tocopherol apparently acts to lower the concentration of α-tocopherol in the liver. Behrens and Madere (15) reported on α- and γ-tocopherol concentrations in plasma and tissue in rats dosed of a large amount of *RRR*-α- and/or *d*-γ-tocopherol. They claimed that α-tocopherol levels in the plasma and tissue showed no significant difference between the α-tocopherol alone group and the α-tocopherol with γ-tocopherol group, but the data showed a tendency toward a slightly lower concentration of α-tocopherol in the α- + γ-tocopherol group than in the α-tocopherol alone group. Thus, the α-tocopherol concentration in the liver might become low due to the large accompanying dose of γ-tocopherol. It is not clear that a large dose of γ-tocopherol suppresses α-tocopheol absorption or promotes elimination of α-tocopherol from the liver. We initially thought that a large, simultaneously ingested amount of γ-tocopherol would promote secretion of α-tocopherol into the bile, with the concentration of α-tocopherol in the liver becoming subsequently low. However, the opposite result was achieved. The concentration of α-tocopherol in the bile was lower in α + γ combined group than in α-tocopherol alone group. On the other hand, we observed fairly large amounts of α-tocopherol in the vitamin E-free and γ-tocopherol groups, which consumed no α-tocopherol. The depletion of α-tocopherol from plasma and tissue takes over 8 wk. As the period of acclimation with the α-tocopherol-free diet was only 1 wk in the present experiment, we detected a rather large amount of α-tocopherol in the plasma, liver, and bile of the vitamin E-free and γ-tocopherol groups. Of course, the concentrations of α-tocopherol in the vitamin E-free control and γ-tocopherol groups were low in the bile as well as in the plasma and liver as compared with the α-tocopherol-fed groups. Thus, it was shown that the groups with a high concentration α-tocopherol in the liver were also high in the bile.

On the other hand, γ-tocopherol was detected in the plasma and liver only in the γ-tocopherol and α + γ combined groups that had been given γ-tocopherol. Furthermore, the γ-tocopherol was detected at extremely low concentrations in spite of the large nonphysiological dose (300 mg /kg), and the γ-tocopherol concentration in the plasma and liver of the α + γ combined group was lower than that in the γ-tocopherol group, which is in agreement with previous reports (12–15). Further, in the α-tocopherol and vitamin E-free groups, no γ-tocopherol was detected in the plasma and liver. The fact that γ-tocopherol is low in the plasma and tissue is caused by the low affinity of γ-tocopherol to α-TTP, though it is said that α- and γ-tocopherol are absorbed at the same rate (3,4). γ-Tocopherol, which does not bind to α-TTP, should have been secreted into the bile at the time we started this experiment (6,9,21). Thus, we anticipated that the large dose of γ-tocopherol would cause a larger amount of γ-tocopherol than α-tocopherol to be secreted into bile, and further that α-tocopherol in the α + γ combined group would also cause a larger amount of γ-tocopherol to be secreted into the bile. We expected the largest amount of γ-tocopherol in the α + γ combined group and next largest in the γ-tocopherol group. However, we obtained quite the opposite results. The concentration of γ-tocopherol in the bile was lower than that of α-tocopherol, and the concentration of γ-tocopherol in the γ-tocopherol group was lower than that of α-tocopherol in the α-tocopherol group and higher than that of γ-tocopherol in the α + γ combined group. These results suggest that γ-tocopherol is not simply excreted into the bile but instead that the elimination of γ-tocopherol from the animal body is effected by a different mechanism. Recently, metabolites of α- and γ-tocopherol have been found in the urine of humans and rats (22–26) and we discuss these factors below.

(ii) Effect of sesame seed on γ-tocopherol concentration in plasma, liver, and bile (Experiment 2). Sesame seed contains about 25 mg/100 g γ-tocopherol and negligible amounts of α-tocopherol. Thus, none of the three diets used in this experiment (vitamin E-free, γ-tocopherol, and sesame seed) contained α-tocopherol. As shown in Table 2, there were no significant differences among the three dietary groups in rat body weight and the amount of bile collected during the 6 h. The α- and γ-tocopherol concentrations in the plasma, liver, and bile in the rats fed the vitamin E-free, γ-tocopherol, and sesame diets for 1, 3, and 7 d are shown in Figures 4, 5, and 6. None of the rats in the vitamin E-free, γ-tocopherol, or sesame groups consumed α-tocopherol, but fairly large amounts of α-tocopherol were detected in all groups. The reason is described above. With the extension of the diet-feeding period, α-tocopherol in the plasma decreased slightly, but that in the liver and bile scarcely changed. Although statistically significant differences in the plasma and liver α-tocopherol concentrations were observed among the dietary groups, the result did not show a fixed tendency. Therefore, the amount of α-tocopherol stored should be similar in all three groups as a whole. The amount of α-tocopherol secreted into the bile tended to be low in the vitamin E-free group on days 1, 3, and 7, but generally, the intake of γ-tocopherol or sesame seed seemed to have a little effect on the amount of α-tocopherol secreted into the bile.

On the other hand, the concentration of γ-tocopherol in the plasma, liver, and bile greatly differed from group to group. In the vitamin E-free group, γ-tocopherol was not detected in the plasma, liver, or bile (as in Experiment 1). γ-Tocopherol and sesame groups consumed almost the same amount of γ-tocopherol, but showed a great difference in the concentration of γ-tocopherol in the plasma, liver and bile, the value in the sesame group being very high. For example, γ-tocopherol concentrations in the plasma on 1-d feeding of γ-tocopherol or sesame seed were 5.96 ± 1.27 μmol/mL and 37.28 ± 3.07 μmol/mL, respectively. Previously, we reported that the plasma and liver concentrations of γ-tocopherol increased with the administra-

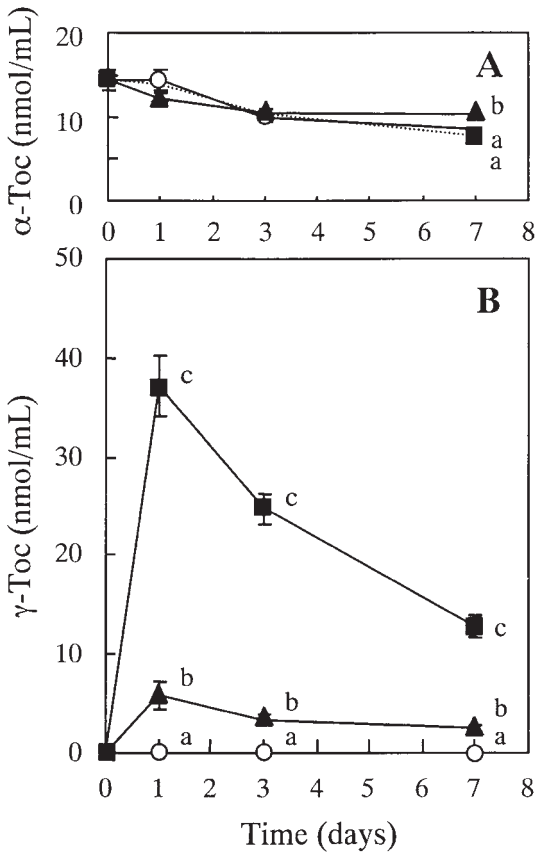

FIG. 4. The effect of sesame seed on α-Toc (A) and γ-Toc (B) concentrations in the plasma of rats in Experiment 2. After being fed a vitamin E-free diet for 7 d, the rats were fed vitamin E-free diet, γ–tocopherol (containing 300 mg/kg γ–tocopherol), or sesame seed diet (containing 300 mg/kg γ–tocopherol including γ–tocopherol in 20% sesame seed) for 1, 3, or 7 d. See Figure 1 for abbreviations and point and symbol details.

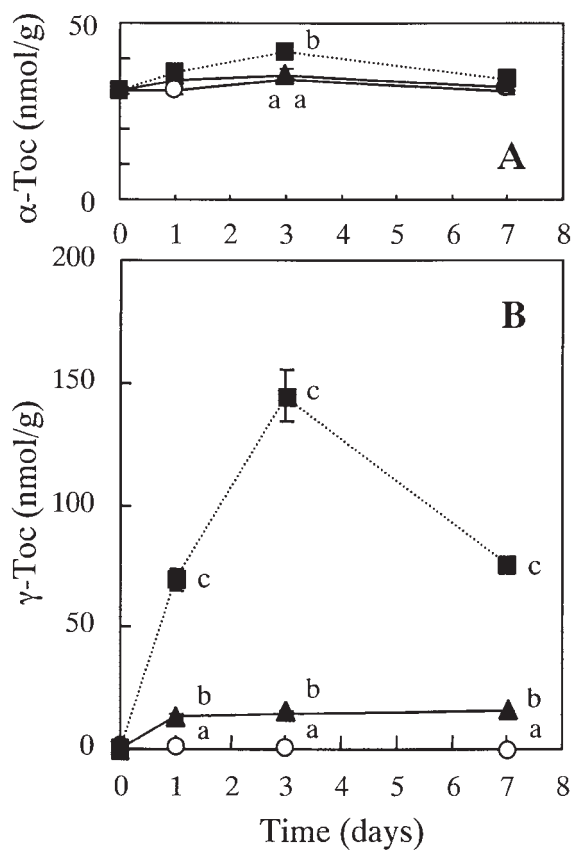

FIG. 5. Effect of sesame seed on α-Toc (A) and γ-Toc (B) concentrations in the liver of rats in Experiment 2. See Figure 1 for abbreviations and point and symbol details.

tion of sesame seed (10,11,16). The present experiment showed that the intake of sesame seed even for 1 d is greatly effective. The purpose of this experiment at the beginning was to clarify why sesame seed causes high concentrations of γ-tocopherol. Thus, this experiment was conducted under the assumption that a high concentration of γ-tocopherol is maintained in rats fed sesame seed due to the suppression of γ-tocopherol elimination into the bile. However, the concentration of γ-tocopherol in the bile was higher in the sesame seed group than in the γ-tocopherol group, contrary to our expectations. The increase of the plasma and liver concentrations of γ-tocopherol by sesame seed intake cannot be explained by the suppression of secretion into the bile. The explanation that γ-tocopherol, with a weak binding affinity to α-TTP, secretes into the bile quickly was too simple. The original data by Traber and Kaden (6), who proposed this idea, showed that a larger amount of γ-tocopherol than α-tocopherol was secreted into bile for the first 8 h after ingestion of a single dose (300 mg each), but that secretion into the bile from 12 to 24 h was higher in α-tocopherol than γ-tocopherol. The pattern of change in concentration in the bile was similar to that in the liver. Thus, plotting the α- and γ-tocopherol concentrations in the bile against those of the liver in all the rats combining the results in Experiments 1 and 2 showed that changes of α- and γ-tocopherol in the bile were linearly correlated with their liver

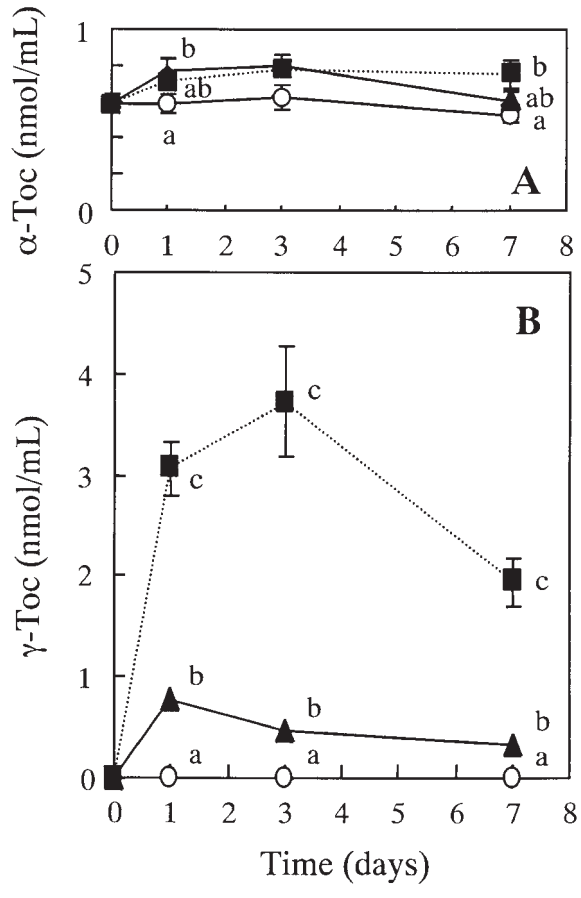

FIG. 6. Effect of sesame seed on α-Toc (A) and γ-Toc (B) concentrations in the bile of rats in Experiment 2. Bile was collected at the end of experimental feeding for 6 h, starting at 9:30 the following morning. See Figure 1 for abbreviations and point and symbol details.

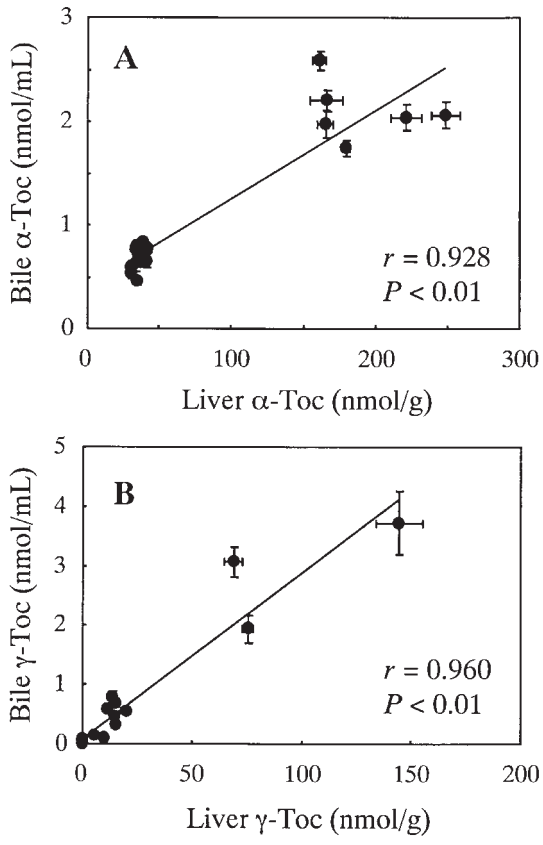

FIG. 7. Correlations between biliary concentrations of α-Toc (A) and γ-Toc (B) and those in the liver. See Figure 1 for abbreviations.

counterparts (Fig. 7). The strong correlation between the liver and the bile suggests that α- or γ-tocopherol in the liver leaked into the bile in proportion to the concentration in the liver. In addition, the amounts of α- or γ-tocopherol in the bile were very slight. We roughly calculated how much tocopherol in the liver was secreted into the bile over 6 h. The percentages of secreted tocopherol in the bile to α- and γ-tocopherol concentration in the liver were 0.3–0.7% of α-tocopherol and 0.3–1.7% of γ-tocopherol. An example of the calculation as shown in the rats fed α-tocopherol diet for 1 d is as follows. As the liver weight was 9.95 g and the concentration of α-tocopherol was 161 μmol/g, the total tocopherol in the liver became 1,604 μmol. The bile volume was 2.9 mL and its concentration of α-tocopherol was 2.56 μmol/mL; then the α-tocopherol in bile became 7.44 μmol/6 h. Thus, the percentage of α-tocopherol in bile to α-tocopherol in liver for 6 h came to 0.4%. Further, Bjorneboe *et al.* (27) determined the appearance of radioactivity in the bile duct after injection of α-[^{3}H]tocopherol. They recovered 14.2% of the given dose of radioactivity by draining the bile duct for 24 h. Only 13.5% of the radioactivity in the bile emerged with α-tocopherol. That means only 2% of the dose of α-tocopherol has recovered as α-tocopherol in the bile over 24 h. Our results as well as those of Bjorneboe *et al.* show that very slight quantities of α- and γ-tocopherol are secreted into the bile.

Recently, a urinary metabolite of α-tocopherol, α-CEHC [2,5,7,8-tetramethyl-2(2′-carboxyethyl)-6-hydroxychroman], was shown to be the major metabolite of α-tocopherol, which conjugates with glucuronic acid or sulfilic acid and is eliminated into urine. Schultz *et al.* (22) reported that urinary α-CEHC was an indicator of an adequate α-tocopherol supply. Traber *et al.* (24) reported that there was more α-CEHC from all-rac-α-tocopherol, which has lower biologic activity, than from *RRR*-α-tocopherol, which has higher biologic activity, and that γ-CEHC, a major metabolite of γ-tocopherol, was more prevalent than α-CEHC in human urine. Further, Swanson *et al.* (25) described that given an estimated mean intake of γ-tocopherol of 20 mg/d, the catabolism of γ-tocopherol to γ-CEHC, followed by glucuronide conjugation and urinary excretion, is a major pathway for elimination of γ-tocopherol in humans. Initially, γ-CEHC was reported by Wechter *et al.* (23) to be a new endogenous natriuretic factor, LLU-α. If γ-CEHC is a major metabolite for γ-tocopherol, its concentration would fluctuate greatly depending on the γ-tocopherol intake, that is, by dietary habit. However, Swanson *et al.* (25) observed in their paper that most γ-CEHC was eliminated as glucuronide conjugate and the quantity of free γ -CEHC, which might act as a similar hormone, would be slight. These results were shown using human subjects. However, CEHC derivative was first described as δ-CEHC, a δ-tocopherol metabolite in urine, by Chiku *et al.* (26) using rats. In our study, one of the reasons γ-tocopherol is high in rats fed sesame seed is that sesame lignans, characteristic compounds of sesame seed, might inhibit the enzymes that convert γ-tocopherol to γ-CEHC. It is necessary to further investigate this possibility.

Biliary secretion of small quantities of α- or γ-tocopherol does take place correlating with the concentrations in the liver, but these tocopherols in the bile might be recirculated from the small intestine to the liver as Lee-Kim *et al.* (28) have shown. However, the present findings suggest that secretion into bile is not a major metabolic route of α- or γ-tocopherols.

ACKNOWLEDGMENTS

This study was supported by a grant-in-aid for scientific research (C) from the Ministry of Education, Science, and Culture and the Science Research Promotion Fund from the Japan Private School Promotion Foundation.

REFERENCES

1. Bieri, J.G., and Evarts, R.P. (1974) Vitamin E Activity of γ-Tocopherol in the Rat, Chick and Hamster, *J. Nutr. 104*, 850–857.
2. Bieri, J.G., and Evarts, R.P. (1974) Gamma Tocopherol: Metabolism, Biological Activity, and Significance in Human Vitamin E Nutrition, *Am. J. Clin. Nutr. 27*, 980–986.
3. Peake, I.R., Windmueller, H.G., and Bieri, J.G. (1972) A Comparison of the Intestinal Absorption, Lympa and Plasma and Tissue Uptake of Alpha and Gamma Tocopherols in the Rat, *Biochim. Biophys. Acta 260*, 679–688.
4. Traber, M.G., Kayden., H.J., Green, J.B., and Green, M.H. (1986) Absorption of Water-Miscible Forms of Vitamin E in a Patient with Cholestasis and in Thoracic Duct-Cannulated rats, *Am. J. Clin. Nutr. 44*, 914–923.
5. Catignani, G.L., and Bieri, J.G. (1977) Rat Liver α-Tocopherol Binding Protein, *Biochim. Biophys. Acta 497*, 349–357.
6. Traber, M.G. and Kaden H.J. (1989) Preferential Incorporation of α-Tocopherol vs. γ-Tocopherol in Human Lipoproteins, *Am. J. Clin. Nutr. 49*, 518–526.
7. Sato, Y., Hagiwara, K., Arai, H., and Inoue, K. (1991) Purifica-

tion and Characterization of the α-Tocopherol Transfer Protein from Rat Liver, *FEBS Lett.* 288, 41–45.
8. Yoshida, H., Yusin, M., Kuhlenkamp, J., Hirano, A., Stolz, A., and Kaplowitz, N. (1992) Identification, Purification, and Immunochemical Characterization of a Tocopherol-Binding Protein in Rat Liver Cytosol, *J. Lipid Res. 33*, 343–350.
9. Kaden, H.J., and Traber, M.G. (1993) Absorption, Lipoprotein Transport, and Regulation of Plasma Concentrations of Vitamin E in Humans, *J. Lipid Res. 34*, 343–358.
10. Yamashita, K., Nohara, Y., Katayama, K., and Namiki, M. (1992) Sesame Seed Lignans and γ-Tocopherol Act Synergistically to Produce Vitamin E Activity in Rats, *J. Nutr. 122*, 2440–2446.
11. Imai, T., Iizuka, Y., Namiki, M., and Yamashita, K. (1995) Marked Increase of α-Tocopherol Concentration in Rats Fed Sesame Seed, *J. Home Econ. Jpn. 46*, 627–633.
12. Clement, M., Dinh, L., and Bourre, J.-M. (1995) Uptake of Dietary *RRR*-α- and *RRR*-γ-Tocopherol by Nervous Tissues, Liver, and Muscle in Vitamin-E-Deficient Rats, *Biochim. Biophys. Acta 1256*, 175–180.
13. Handelman, G.J., Machlin, L.J., Fitch, K., Weiter J.J., and Dratz, E.A. (1985) Oral α-Tocopherol Supplements Decrease Plasma γ-Tocopherol Levels in Humans, *J. Nutr. 115*, 807–813.
14. Baker, H., Handelman, G.J., Short, S., Machlin, L.J., Bhagavan, H.N., Dratz, E.A., and Frank, O. (1986) Comparison of Plasma α and γ-Tocopherol Levels Following Chronic Oral Administration of Either all-rac-α-Tocopheryl Acetate or *RRR*-α-Tocopheryl Acetate in Normal Adult Male Subjects, *Am. J. Clin. Nutr. 43*, 382–387.
15. Behrens, W.A., and Madere, R. (1987) Mechanisms of Absorption, Transport, and Tissue Uptake of *RRR*-α-Tocopherol and d-γ-Tocopherol in the White Rat, *J. Nutri 177*, 1562–1569.
16. Yamashita, K., Iizuka, Y., Imai, T., and Namiki, M. (1995) Sesame Seed and Its Lignans Produce Marked Enhancement of Vitamin E Activity in Rats Fed a Low α-Tocopherol Diet, *Lipids 30*, 1019–1028.
17. American Institute of Nutrition (1997) Report of the American Institute of Nutrition Ad Hoc Committee on Standards for Nutritonal Studies, *J. Nutr. 107*, 1340–1348.
18. Ueda, T., and Igarashi, O. (1987) New Solvent System for Extraction of Tocopherols from Biological Specimens for HPLC Determination and the Evaluation of 2,2,5,7,8,-Pentamethyl-6-Chromanol as an Internal Standard, *J. Micronutr. Anal. 3*, 185–198.
19. Duncan, D.B. (1957) Multiple Range Tests for Correlated and Heteroscedastic Means, *Biometrics 13*, 164–176.
20. Traber, G.M., Ramakrishnan, R., and Kayden, H.J. (1994) Human Plasma Vitamin E Kinetics Demonstrate Rapid Recycling of Plasma *RRR*-α-Tocopherol, *Proc. Natl. Acad. Sci. USA 91*, 10005–10008.
21. Bjorneboe, A., Bjorneboe, G.-E. A., and Drevon, C.A. (1990) Absorption, Transport and Distribution of Vitamin E, *J. Nutr. 120*, 233–242.
22. Schultz, M., Leist, M., Petrzika, M. Gassmann, B., and Brigelius-Flohe, R. (1995) Novel Urinary Metabolite of α-Tocopherol, 2,5,7,8-Tetramethyl-2 (2′-Carboxyethyl)-6-Hydroxychroman, as an Indicator of an Adequate Vitamin E Supply? *Am. J. Clin. Nutr. 62 (suppl.)*, 1527S–1534S.
23. Wechter, W.J., Kantoci, D., Murray, E.D. Jr., D'Amico, D.C., Jung, M.E., and Wang, W.-H. (1996) A New Endogenous Natriuretic Factor: LLU-α, *Biochemistry 93*, 6002–6007.
24. Traber, M.G., Elsner, A., and Brigelius-Flohe, R. (1998) Synthetic as Compared with Natural Vitamin E Is Preferentially Excreted as α-CEHC in Human Urine: Studies Using Deuterated α-Tocopheryl Acetates, *FEBS Lett. 437*, 145–148.
25. Swanson, J.E., Ben, R.N., Burton, G.W., and Parker, R.S. (1999) Urinary Excretion of 2,7,8,-Trimethyl-2-(β-carboxyethyl)-6-Hydroxychroman Is a Major Route of Elimination of γ-Tocopherol in Humans, *J. Lipid Res. 40*, 665–671.
26. Chiku, S., Hamamura, K., and Nakamura, T. (1984) Novel Urinary Metabolite of *d*-δ-Tocopherol in Rats, *J. Lipid Res. 25*, 40–48.
27. Bjorneboe, A., Bjorneboe, G.-E.A., and Drevon, C.A. (1987) Serum Half-Life, Distribution, Hepatic Uptake and Biliary Excretion of α-Tocopherol in Rats, *Biochim. Biophys. Acta 921*, 175–181.
28. Lee-Kim, Y.C., Meydani, M., Kassarjian, Z., Blumberg, J.B., and Russell, R.M. (1988) Enterohepatic Circulation of Newly Administered α-Tocopherol in the Rat, *Int. J. Vit. Nutr. Res. 58*, 284–291.

[Received January 11, 1999, and in final revision form October 27, 1999; revision accepted December 3, 1999]

Antiproliferative and Apoptotic Effects of Tocopherols and Tocotrienols on Normal Mouse Mammary Epithelial Cells

Barry S. McIntyre[a], Karen P. Briski[a], Mark A. Tirmenstein[b], Marc W. Fariss[b], Abdul Gapor[c], and Paul W. Sylvester[a,*]

Colleges of Pharmacy, [a]University of Louisiana, Monroe, Louisiana 71209-0470 and [b]Washington State University, Pullman Washington 99164, and [c]Palm Oil Research Institute of Malaysia, Kuala Lumpur 50720, Malaysia

ABSTRACT: Studies were conducted to determine the comparative effects of tocopherols and tocotrienols on normal mammary epithelial cell growth and viability. Cells isolated from midpregnant BALB/c mice were grown within collagen gels and maintained on serum-free media. Treatment with 0–120 μM α- and γ-tocopherol had no effect, whereas 12.5–100m μM tocotrienol-rich fraction of palm oil (TRF), 100–120 μM δ-tocopherol, 50–60 μM α-tocotrienol, and 8–14 μM γ- or δ-tocotrienol significantly inhibited cell growth in a dose-responsive manner. In acute studies, 24-h exposure to 0–250 μM α-, γ-, and δ-tocopherol had no effect, whereas similar treatment with 100–250 μM TRF, 140–250 μM α-, 25–100 μM γ- or δ-tocotrienol significantly reduced cell viability. Growth-inhibitory doses of TRF, δ-tocopherol, and a-, γ-, and δ-tocotrienol were shown to induce apoptosis in these cells, as indicated by DNA fragmentation. Results also showed that mammary epithelial cells more easily or preferentially took up tocotrienols as compared to tocopherols, suggesting that at least part of the reason tocotrienols display greater biopotency than tocopherols is because of greater cellular accumulation. In summary, these findings suggest that the highly biopotent γ- and δ-tocotrienol isoforms may play a physiological role in modulating normal mammary gland growth, function, and remodeling.

Paper no. L8332 in *Lipids 35,* 171–180 (February 2000).

During the past decade a large volume of literature has accumulated indicating that dietary supplementation of the vitamin E isoform α-tocopherol (α-T) may have significant health benefits in preventing a variety of diseases (1–3). It is well established that α-T is an important antioxidant that regulates peroxidation reactions and free-radical production (1). Uncontrolled or excessive free-radical production can ultimately lead to cellular damage, dysfunction, or death (1). However, α-T and other vitamin E isoforms also have been shown to play an important role in modulating several intracellular signaling pathways involved with mitogenesis (4–7) and apoptosis (8–12).

Vitamin E is a generic term that represents a family of chemically related compounds that is subdivided into two subgroups called tocopherols and tocotrienols. Tocopherols are commonly found in high concentrations in a wide variety of foods, whereas tocotrienols are relatively rare and found in appreciable levels in only a few specific vegetable fats, such as palm oil (13,14). Previous studies have demonstrated that high dietary intake of crude palm oil, in contrast to other high-fat diets, suppressed carcinogen-induced mammary tumorigenesis in experimental animals (14–17). Furthermore, if tocotrienols are removed from palm oil, the protective effects of high palm oil diets are no longer observed (17). Similarly, tocotrienol treatment has been associated with beneficial effects in a variety of *in vivo* and *in vitro* experimental models, and the majority of these studies showed that specific tocotrienol isoforms are significantly more potent than corresponding tocopherol isoforms (18–23).

The exact reason why tocotrienols display greater bioactivity than tocopherols is still under investigation. Tocopherols and tocotrienols have the same basic chemical structure characterized by a long phytyl chain attached at the 1-position of a chromane ring (Scheme 1). However, tocopherols have a saturated, whereas tocotrienols have an unsaturated phytyl chain (Scheme 1). Individual isoforms of tocopherols and tocotrienols differ from each other based on the number of methyl groups bound to their chromane ring. Tocopherol and tocotrienol α-isoforms contain methyl groups on the 5-, 7-, and 8-positions, while their γ-isoforms lack the methyl group at the 5-position, and their δ-isomers lack methyl groups on the 5- and 7-positions on the chromane ring (Scheme 1). It is possible that the level of phytyl chain saturation and/or chromane ring methylation may be critical in determining the antiproliferative and apoptotic activity of individual tocopherol and tocotrienol isoforms.

At present, little information is available regarding the effects of specific vitamin E isoforms on the growth and viabil-

*To whom correspondence should be addressed.
E:mail: pysylvester@alpha.ulm.edu

Abbreviations: BSA, bovine serum albumin; DMEM, Dulbecco's modified Eagle's medium; EGF, epidermal growth factor; HPLC, high-performance liquid chromatography; IC_{50}, treatment dose that induces 50% growth inhibition; LD_{50}, treatment dose that induces 50% cell death; MTT, 3-(4,5-dimethylthiazol-2yl)-2,5-diphenyl tetrazolium bromide; α-T, α-tocopherol; γ-T, γ-tocopherol; δ-T, δ-tocopherol; α-T^3, α-tocotrienol; γ-T^3, γ-tocotrienol; δ-T^3, δ-tocotrienol; TGF, transforming growth factor; TRF, tocotrienol-rich fraction.

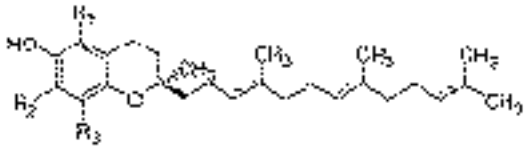

Compound	R_1	R_2	R_3	Phytyl Chain
α-tocopherol	CH_3	CH_3	CH_3	Saturated
γ-tocopherol	H	CH_3	CH_3	Saturated
δ-tocopherol	H	H	CH_3	Saturated
α-tocotrienol	CH_3	CH_3	CH_3	Unsaturated
γ-tocotrienol	H	CH_3	CH_3	Unsaturated
δ-tocotrienol	H	H	CH_3	Unsaturated

SCHEME 1

ity of normal cells. Therefore, the following studies were conducted to characterize the antiproliferative and apoptotic effects of specific tocopherol and tocotrienol isoforms on normal mouse mammary epithelial cells grown in primary culture and maintained in serum-free media. Additional studies were conducted to determine the relationship between biopotency and the magnitude of cellular accumulation for the various tocopherol and tocotrienol isoforms.

EXPERIMENTAL PROCEDURES

Isolation and culture of mammary epithelial cells. All procedures involving animals were approved by the institutional animal use and care committees at the University of Louisiana at Monroe and Washington State University. Mammary epithelial cells were isolated and prepared for culture, as previously described (24–27). All materials were purchased from Sigma Chemical Co. (St. Louis, MO), unless otherwise stated. Briefly, mammary glands from midpregnant BALB/c mice were removed, minced, and subjected to collagenase followed by pronase E (Type XIV bacterial from *Streptomyces griseus*) digestion. Mammary epithelial cells isolated from midpregnant mice were selected for experimentation because these cells are highly responsive to EGF-induced mitogenesis (28). Mammary epithelial cell organoids were isolated by a series of filtrations through sterile 250- and 48-μm nitex filters (Tetko Inc., Briarcliff Manor, NY), plated within rat tail collagen gels at a density of 2.2×10^7 cells/8 mL of collagen in 100 mm plastic plates, and fed 10 mL of growth media [Dulbecco's modified Eagle's medium (DMEM)/Ham's F-12 medium, 1:1, insulin 10 μg/mL, penicillin 100 U/mL, streptomycin 100 μg/mL, 10% bovine calf serum (Hyclone, Logan, UT)]. Plates were then placed in a humidified incubator at 37°C in an environment of 95% air and 5% CO_2. After a 2-d incubation period, mammary epithelial cell organoids were again isolated by collagenase digestion and filtration. This double isolation procedure provides isolated mammary epithelial cell organoids ready for experimentation that are devoid of fibroblast and adipocyte contaminants (29). Mammary epithelial cells were then plated within collagen gels at a density of 2×10^5 cells/0.5 mL collagen in 24-well tissue culture plates (growth studies) or 1×10^7 cells/8 mL collagen in 100-mm culture plates (DNA isolation studies). Cells were divided into different treatment groups and fed serum-free control or treatment media every other day, consisting of DMEM/F12 containing 5 mg/mL bovine serum albumin (BSA), 10 μg/mL transferrin, 100 U/mL soybean trypsin inhibitor, 100 U/mL penicillin, 0.1 mg/mL streptomycin, 10 ng/mL EGF, and 10 μg/mL insulin.

Medium vitamin E supplementation and experimental treatments. Tocopherol and tocotrienol isoforms were conjugated to BSA as previously described (24). Briefly, an appropriate amount of α-T, γ- and δ-tocopherol (γ-T and δ-T), α-, γ-, δ-tocotrienol (α-T^3, γ-T^3, and δ-T^3) or tocotrienol-rich fraction of palm oil (TRF) was placed into a 1.5-mL screw top glass vial and dissolved in 100 μL of 100% ethanol. Once dissolved, this ethanol solution was added to a small volume of sterile 10% BSA in water and incubated overnight at 37°C. The resulting sterile stock solutions of TRF, and individual tocopherol and tocotrienol isoforms conjugated to BSA, was then used to prepare various concentrations (0–250 μM) of tocopherol-, tocotrienol-, or TRF-supplemented treatment media. Ethanol was added to all treatment media so that the final ethanol concentration was the same in all treatment groups within a given experiment and was always less than 0.1%.

Measurement of viable cell number. Mammary epithelial cell number was determined in 24-well culture plates (6 wells/group) by the 3-(4,5-dimethylthiazol-2yl)-2,5-diphenyl

tetrazolium bromide (MTT) colorimetric assay as described previously (24–27). On the day of assay, treatment medium was replaced with fresh growth medium containing 0.83 mg/mL MTT, and cells were returned to the incubator for 4 h. Afterward, gels were removed from the culture plates, placed in 12 × 75 mm test tubes, and dissolved in 0.5 mL of 25% acetic acid. MTT crystals were pelleted by centrifugation, and the MTT crystals dissolved in 1 mL of 2-propanol. Optical density of each sample was read on a microplate reader (model 7520 Cambridge Technology, Inc., Watertown, MA) at 570 nm against a blank prepared from cell-free collagen gels. The number of cells/well was calculated against a standard curve prepared by plating various concentrations of cells, as determined by hemacytometer, at the start of each experiment (24–27). In separate control studies, various doses (0–250 μM) of TRF or specific tocopherol or tocotrienol subtypes were not found to affect the specific activity of the MTT colorimetric assay.

Apoptosis as determined by DNA fragmentation and nuclear condensation assays. Cells in each treatment group were grown in 100-mm plates (2–3 plates/group) and treated with various doses of specific tocopherols, tocotrienols, or TRF for 0–48 h. To determine treatment-induced programmed cell death, as indicated by DNA fragmentation, cells were isolated from collagen gels by collagenase digestion, rinsed three times, and pooled; DNA was then isolated from cells within each treatment group by phenol/chloroform extractions (30). Isolated DNA was then fractionated on a 1.2% Tris/acetic acid/EDTA agarose gel and visualized with an ultraviolet transluminator. Treatment-induced apoptosis was also determined *in situ* by visualization of treatment effects on nuclear condensation in mammary epithelial cells grown in primary culture. In these studies, cells were cultured within collagen gels for 5 d and then exposed for 24 h to 25 or 110 μM TRF. Ethidium bromide (10 μg/mL) was then added directly to the culture media and 30 min later, bright-field and epifluorescence photomicrographs of the same field were taken of mammary epithelial cell cultures in each treatment group. Cells undergoing apoptosis were characterized by enhanced nuclear epifluorescence intensity, an indication of increased nuclear accumulation of ethidium bromide (31).

Cellular accumulation of tocopherols and tocotrienols. Mammary epithelial cells were cultured in control media for 5 d and then treated with various doses of tocopherols, tocotrienols, or TRF for 0, 15 min, 6 h, 12 h, or 24 h. Cells within each treatment group were isolated from collagen gels by collagenase digestion, rinsed three times, and then extracted for assay of tocopherol and tocotrienol content as determined by reversed-phase high-performance liquid chromatography (HPLC) with fluorometric detection using a modification of the methods previously described (32,33). Briefly, aliquots of internal standard (1.6 nmol of α-T for determination of δ-T levels or 1.6 nmol of δ-T for quantification of all other tocopherol and tocotrienol isoforms) was added to the appropriate treatment group of isolated mammary epithelial cells. The same amount of the corresponding internal standard (1.6 nmol) was also added to the appropriate tocopherol and tocotrienol isoform standards. Cells in each treatment group were then resuspended by sonication in 0.3 mL of 1% asorbate in 0.1 M sodium dodecyl sulfate and 0.45 mL 100% ethanol. Hexane (0.8 mL) was next added to each sample, and then each sample/hexane mixture was vortexed for 30 s; the resulting hexane extracts were dried under nitrogen. The dried extracts were then resuspended in 1 mL methanol containing 2.5% ascorbate. Extracted and nonextracted standards of each tocopherol and tocotrienol isoform (0.05 to 5 nmol/sample) were run with each assay, and results were expressed as nmol/mg. Samples were injected on a Hewlett-Packard 1050 HPLC equipped with an autosampler, Chem Station software, McPherson 749 fluorescence detector, and Spherisorb ODS II column (250 × 4.6 mm i.d., 5 μm; Alltech, Avondale, PA). The mobile phase was 96% methanol, which was run isocratically at a flow rate of 1.8 mL/min. Excitation and emission wavelengths of 210 and 300 nm, respectively, were used for all tocopherol and tocotrienol isoform determinations. Samples and standards were assayed by HPLC on the same day of extraction. Cellular concentrations was expressed as the average of four replicates in each treatment group. TRF was assayed by HPLC prior to use in experimentation and determined to be composed of 20.2% α-T, 16.8% α-T[3], 44.9% γ-T[3], 14.8% δ-T[3], and 3.2% of a nonvitamin E lipid soluble contaminant. Treatment doses of TRF were then calculated based on the percent composition and molecular weights of individual vitamin isoforms within TRF.

Statistical analysis. Differences among the various treatment groups were determined by analysis of variance, followed by Duncan's multiple range test. A difference of $P < 0.05$ was considered to be significant, as compared to controls or as defined in the figure legends. Linear regression analysis of treatment effects on viable cell number in growth and cytotoxicity studies was used to determine the 50% growth inhibition concentration (IC_{50}) and 50% lethal dose (LD_{50}) for individual treatments.

RESULTS

The effects of various doses of TRF on normal mammary epithelial cell growth in primary culture are shown in Figure 1. Cells grown in serum-free control media displayed more than a twofold increase in viable cell number over the 5-d culture period (Fig. 1). Supplementation of culture medium with 12.5–50 μM TRF significantly inhibited EGF-induced cell proliferation in a dose-responsive manner as compared to controls (Fig. 1). The highest dose of TRF (100 μM) appeared to be cytotoxic since viable cell number after 5 d of culture was less than that initially plated at the start of experimentation (Fig. 1).

Since TRF contains a number of vitamin E isoforms, it was not possible to determine if one or all of these isoforms were responsible for mediating the growth inhibitory effects of TRF described in Figure 1. Additional studies were conducted to determine the antiproliferative effects of specific tocopherol and tocotrienol isoforms on EGF-induced mammary epithelial cell proliferation in primary culture (Fig. 2). After

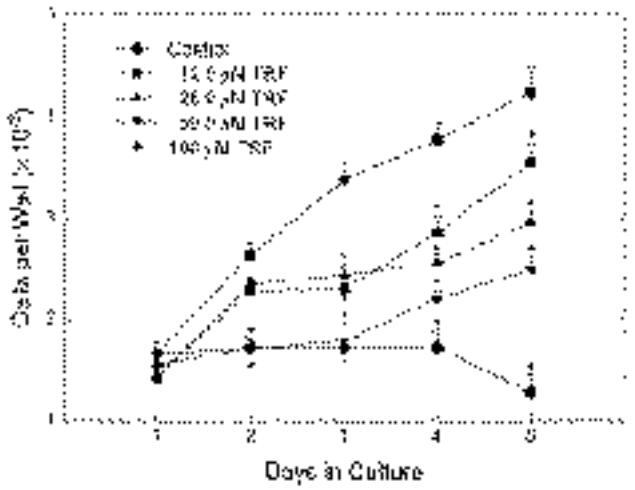

FIG. 1. Effects of various doses of tocotrienol-rich fraction (TRF) on normal mammary epithelial cell proliferation in primary culture. Data points indicate the mean cell count/well ± SEM for six replicates in each treatment group during the 5-d culture period. $^*P < 0.05$, as compared to controls.

5 d of culture, treatment with 0–120 μM α-T or γ-T had no effect (Fig. 2A and B), whereas treatment with 100–120 μM δ-T significantly inhibited mammary epithelial cell growth as compared to controls (Fig. 2C). Treatment with 50–60 μM α-T^3 (Fig. 2D), 8–14 μM γ-T^3 (Fig. 2E) or δ-T^3 (Fig. 2F) was also found to significantly inhibit mammary epithelial cell growth as compared to controls.

TABLE 1
Effects of Various Vitamin E Compounds on Mammary Epithelial Cell Growth (IC_{50}) and Viability (LD_{50})[a]

Vitamin E	IC_{50} (μM)	LD_{50} (μM)
TRF	25	110
α-Tocopherol	>120	>250
γ-Tocopherol	>120	>250
δ-Tocopherol	94	>250
α-Tocotrienol	45	238
γ-Tocotrienol	8	46
δ-Tocotrienol	7	36

[a]IC_{50}, treatment dose that induces 50% growth inhibition; LD_{50}, treatment dose that induces 50% cell death; TRF, tocotrienol-rich fraction.

The effects of a 24 h treatment exposure to various concentrations of tocopherols, tocotrienols, or TRF on viable cell number are shown in Figure 3. Acute treatment with 0–250 μM of α-T, γ-T, or δ-T had no significant affect on mammary epithelial cell viability (Fig. 3). In contrast, 24-h exposure to 100–250 μM TRF, 140–250 μM α-T^3, 25–100 μM γ-T^3, or 25–100 μM δ-T^3 caused a significant dose-responsive decrease in viable cell number, with 100 μM γ-T^3 and 60–100 μM δ-T^3 reducing viable cell number to undetectable levels (Fig. 3).

Table 1 summarizes the relative potencies of TRF and specific tocopherol and tocotrienol isoforms on normal mammary epithelial cell growth and viability. TRF was found to have an IC_{50} of 25 μM and LD_{50} of 110 μM (Table 1). Over

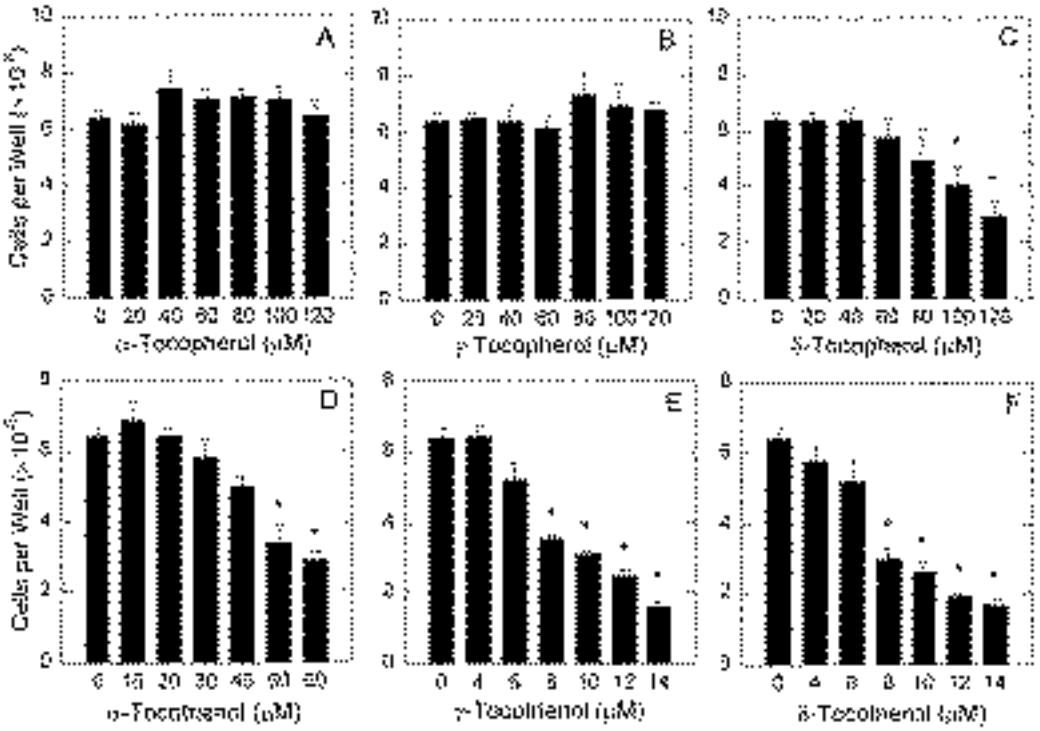

FIG. 2. Effects of various doses of individual tocopherol and tocotrienol isoforms on normal mammary epithelial cell proliferation in primary culture. Vertical bars represent mean cell count/well ± SEM for six replicates in each treatment group after 5 d in culture. $^*P < 0.05$, as compared to controls.

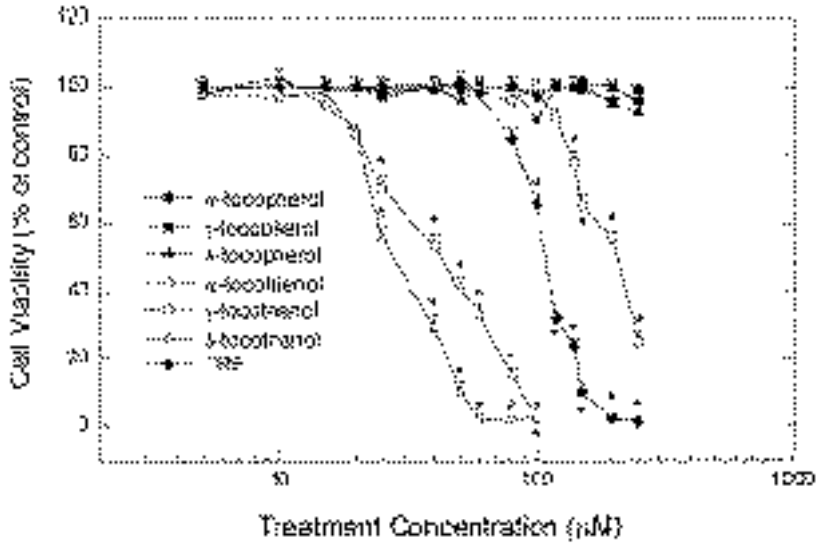

FIG. 3. Mammary epithelial cell viability after a 24-h exposure period to various doses of TRF or individual tocopherol and tocotrienol isoforms. Cells in each treatment group were grown in primary culture and maintained on control media for 5 d prior to exposure to their respective treatments. Data points indicate the percentage of viable cells/well ± SEM for six replicates in each treatment group, as compared to controls. $^*P < 0.05$, as compared to controls. For abbreviation see Figure 1.

the 0–250 μM dose range tested, α-T and γ-T were not found to alter cell growth or viability. Therefore, IC_{50} and LD_{50} doses were not determined for these compounds (Table 1). The IC_{50} for δ-T was calculated to be 94 μM, but the LD_{50} could not be determined over the dose range tested for this compound (Table 1). In contrast, α-T^3, γ-T^3, or δ-T^3 displayed IC_{50} doses of 45, 8, and 7 μM, and LD_{50} doses of 235, 46, and 36 μM, respectively (Table 1).

DNA isolated from untreated mammary epithelial cells grown in primary culture for 5 d did not show appreciable levels of fragmentation (Fig. 4). Following exposure to 25 μM TRF (IC_{50}) mammary epithelial cells displayed detectable levels of DNA fragmentation 48 h after the start of treatment (Fig. 4). In contrast, exposure to 110 μM TRF (LD_{50}) resulted in a rapid and intense DNA laddering response within 12 h and continuing for 48 h after the start of treatment (Fig. 4).

The effects of a 24-h exposure to IC_{50} or maximal doses previously tested for individual tocopherols and tocotrienols on DNA fragmentation in mammary epithelial cells grown in primary culture for 5 d are shown in Figure 5. DNA isolated from untreated controls showed little fragmentation or laddering (Fig. 5, lane C), and treatment for 24 h with 120 μM α-T or γ-T had little effect on DNA fragmentation in these cells (Fig. 5, lanes α-T and γ-T, respectively). Similar treatments with 94 μM δ-T, 45 μM α-T^3, 8 μM γ-T^3, or 7 μM δ-T^3 induced intense DNA fragmentation in mammary epithelial cells (Fig. 5, lanes δ-T, α-T^3, γ-T^3, and δ-T^3, respectively).

The effects of 24-h treatment with 0 (controls), 25 (IC_{50}), or 110 μM (LD_{50}) TRF on *in situ* nuclear condensation, as determined by ethidium bromide epifluorescence staining, in mammary epithelial cells are shown in Figure 6. Brightfield photomicrographs of untreated control mammary epithelial cell organoids were characterized by duct-like branching that extended throughout the collagen gel (Fig. 6A). Epifluorescence photomicrographs of the same field showed a small amount of epifluorescence staining (Fig. 6B). Cells grown in primary culture have a finite life span, and it is expected that some portions of these cells are undergoing apoptosis. Treat-

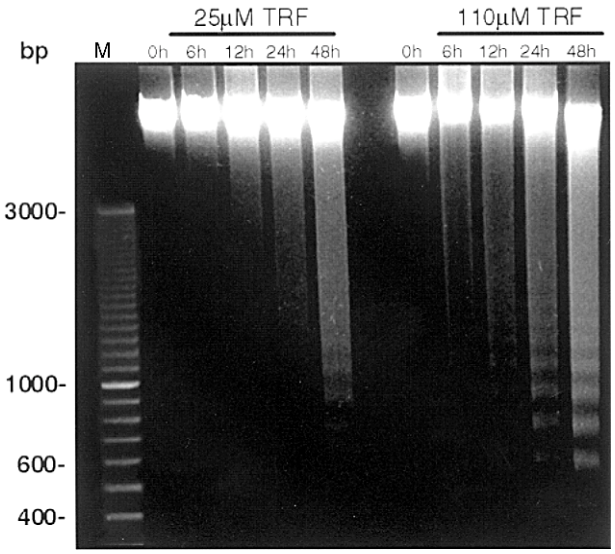

FIG. 4. Mammary epithelial cell internucleosomal DNA fragmentation during a 48-h period following exposure to either 25 [IC_{50} (treatment doese that induces 50% growth inhibition)] or 110 μM [LD_{50} (treatment dose that induces 50% cell death)] TRF. Cells were cultured in control media for 5 d and then exposed to their respective treatments. Lane M contains DNA laddering markers. For other abbreviation see Figure 1.

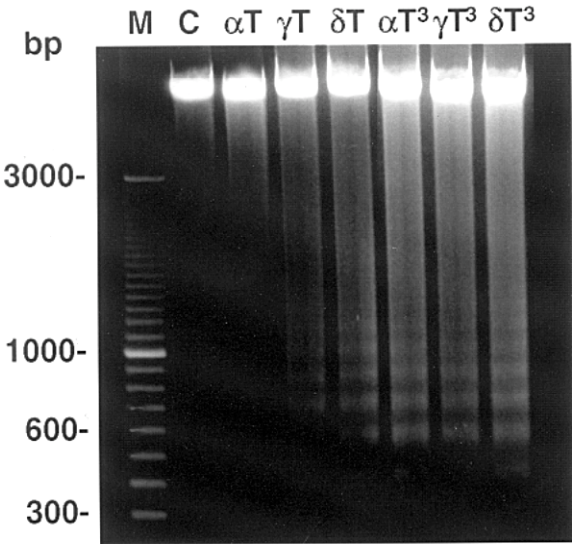

FIG. 5. Mammary epithelial cell internucleosomal DNA fragmentation following a 24-h exposure period to control media (lane C), 120 μM α-tocopherol (lane αT), 120 μM γ-tocopherol (lane γT), 94 μM δ-tocopherol (lane δT), 45 μM α-tocotrienol (lane αT^3), 8 μM γ-tocotrienol (lane γT^3), or 7 μM δ-tocotrienol (lane δT^3). Lane M contains DNA laddering markers.

ment for 24 h with 25 μM TRF (IC_{50}) resulted in a noticeable change in mammary epithelial cell organoid morphology that was characterized by a slight fragmentation in ductal branching in brightfield photomicrographs (Fig. 6C), and an increase in epifluorescence intensity (Fig. 6D). Brightfield photomicrographs of mammary epithelial cell organoids treated for 24 h with 110 μM TRF (LD_{50}) were characterized by severe fragmentation in ductal morphology (Fig. 6E) and a corresponding large increase in epifluorescence intensity (Fig. 6F).

Figure 7 shows cellular accumulation of specific tocopherol and tocotrienol isoforms in mammary epithelial cells treated for 24 h with 25 (IC_{50}) or 110 μM (LD_{50}) TRF. Cellular levels of α-T and α-T^3, γ-T^3, and δ-T^3 were undetectable 15 min after exposure to 25 or 110 μM TRF (Fig. 7). However, a dose- and time-responsive increase in cellular levels of these compounds was observed over the 24-h treatment period (Fig. 7). The relative magnitude of cellular accumulation of tocotrienol isoforms was greater than α-T, even though the concentration of α-T present in the TRF treatment media was higher than the concentrations of α-T^3 and δ-T^3 (Fig. 7).

Cellular accumulation of specific tocopherol and tocotrienol isoforms throughout the 24-h treatment period is

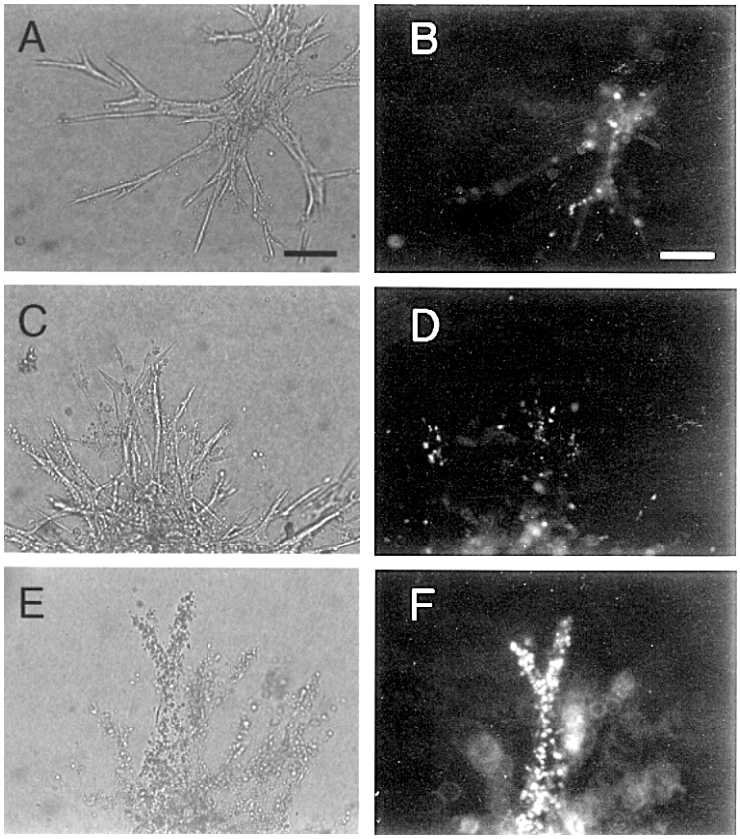

FIG. 6. Effects of TRF organoid morphology and DNA condensation in normal mammary epithelial cells grown in primary culture. Cells were cultured for 5 d in control media and then exposed to either 0 (Control), 25 (IC_{50}), or 110 μM (LD_{50}) TRF. Phase contrast and epifluorescence micrographs of the same field 24 h after treatment exposure are shown for Control (A and B), 25 μM TRF (C and D), and 110 μM TRF (E and F), respectively. Magnification for each photograph is 100× and the bar in A and B represents 10 μm in length. For abbreviations see Figures 1 and 4.

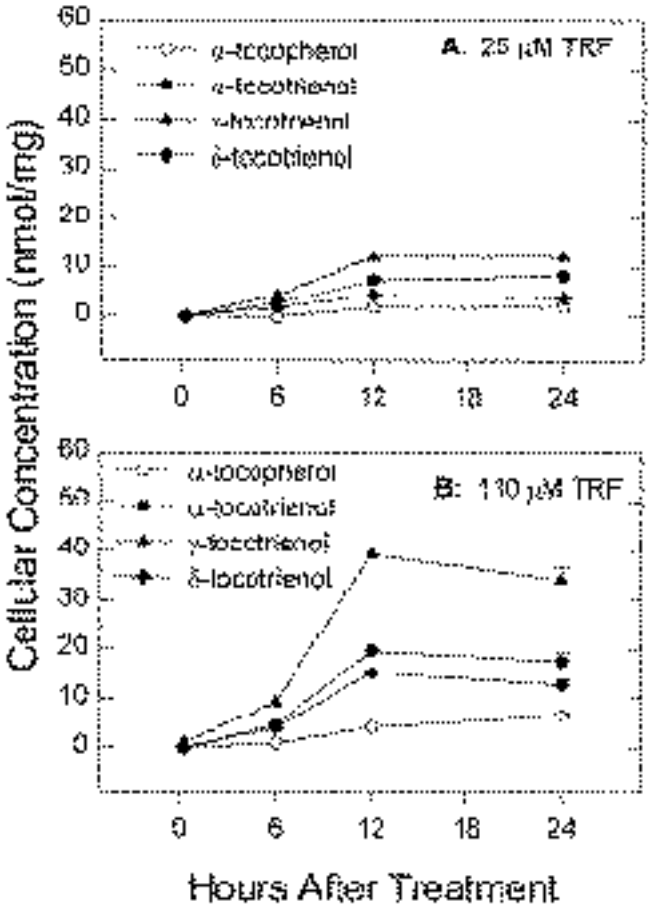

FIG. 7. Cellular accumulation of individual tocopherol and tocotrienol isoforms in normal mammary epithelial cells grown in primary culture during a 24-h exposure to either 25 (A) or 110 μM (B) TRF. Data points indicate mean cellular concentration ± SEM for four replicates in each treatment group containing 1×10^7 cells per each time point. For abbreviation see Figure 1.

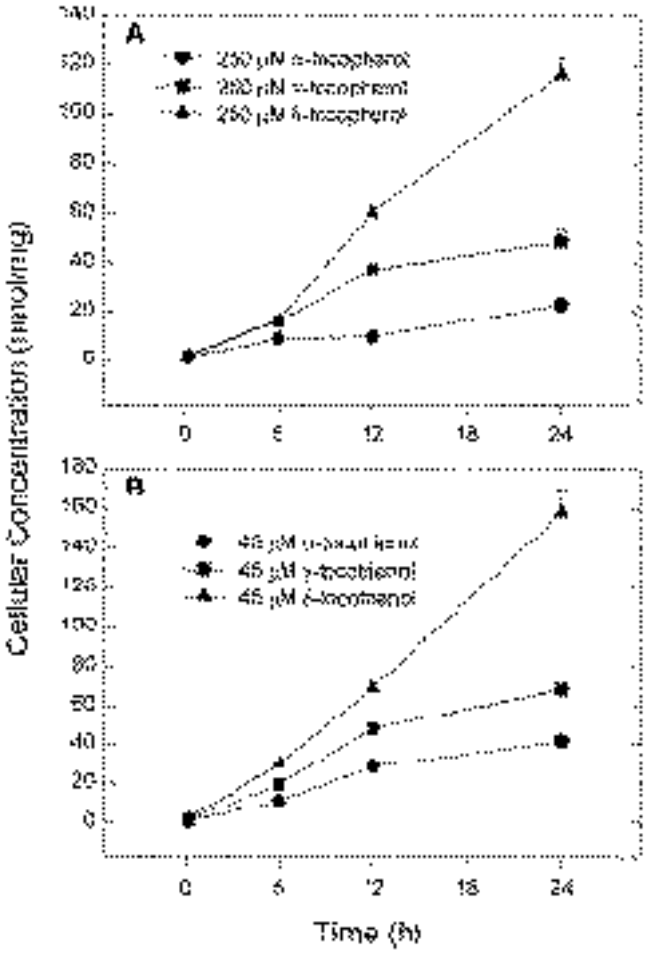

FIG. 8. Cellular accumulation of individual tocopherol and tocotrienol isoforms in normal mammary epithelial cells grown in primary culture during a 24-h exposure to either (A) 250 μM α-, γ-, or δ-tocopherol or 45 μM α-, γ-, or δ-tocotrienol. Data points indicate mean cellular concentration ± SEM for four replicates in each treatment group containing 1×10^7 cells per each time point.

shown in Figure 8. Treatment with 250 μM α-T, γ-T, or δ-T resulted in a time- and dose-dependent increase in cellular levels during the 24 h exposure period (Fig. 8A). However, cellular accumulation of individual tocopherol isoforms was not equal and characterized as δ > γ > α (Fig. 8A). Similarly, exposure to 45 μM α-T^3, γ-T^3, and δ-T^3 also showed a time- and dose-dependent increase in cellular accumulation, and a greater cellular accumulation of individual tocotrienol isoforms characterized as δ > γ > α (Fig. 8B).

DISCUSSION

These results demonstrate that individual tocopherols and tocotrienols display differential potencies in regard to their antiproliferative and apoptotic activity in normal mammary epithelial cells grown in primary culture. Direct comparisons between the two vitamin E subclasses show that tocotrienols are significantly more potent than tocopherols. Furthermore, the biopotency of specific isoforms displayed a consistent relationship corresponding to δ-T^3 ≥ γ-T^3 > α-T^3 > δ-T ≥ γ-T and α-T. Although the exact intracellular mechanism mediating the antiproliferative effects of tocotrienols is currently unknown, tocotrienol-induced reductions in cellular viability result from the induction of apoptosis, as indicated by DNA fragmentation. It was also shown that the biopotency of individual tocotrienol and tocopherol isoforms is directly related to the ease and/or preference with which these compounds accumulate within mammary epithelial cells.

Previous investigations have shown that very high treatment doses of α-T (millimolar) can induce antiproliferative and apoptotic effects in various cell types (11,34), but the physiological significance of these findings is unclear. Therefore, the exact IC_{50} and LD_{50} dose for individual tocopherols was not determined because the primary objective of the present study was to contrast the very high relative biopotency of tocotrienols vs. tocopherols. Although chronic treatment with 120 μM or acute treatment with 250 μM α-T and γ-T was not found to have significant effects on cell growth or viability, respectively, it should not be concluded that these compounds are devoid of bioactivity in normal mammary ep-

ithelial cells. Experimental results show that treatment with 120 μM of α-T or γ-T induced a small amount of DNA fragmentation as compared to untreated controls (Fig. 5), even though these effects were not of great enough magnitude to cause a corresponding reduction in mammary epithelial cell proliferation or viability. These findings indicate that both tocopherols and tocotrienols induce antiproliferative and apoptotic effects in normal mammary epithelial cells, but specific tocotrienol isoforms are significantly more potent than corresponding tocopherol isoforms.

EGF-dependent mitogenesis in normal mammary epithelial cells grown in primary culture is associated with the activation of phospholipid-dependent protein kinase C and cyclic AMP-dependent proteins (24,28,35–38). It has been established that treatments that enhance protein kinase C and cyclic AMP activation stimulate, whereas treatments that inhibit protein kinase C and cyclic AMP activation inhibit, EGF-induced mammary epithelial cell proliferation (24,28,35–38). Tocopherols and tocotrienols have also been shown to inhibit protein kinase C (4,5,7), adenylate cyclase and cyclic AMP-dependent protein activation (39,40). Therefore, it is possible that the antiproliferative effects of tocopherols and tocotrienols in mammary epithelial cells may result from an inhibition of these mitogenic-signaling pathways.

Various signaling pathways also have been suggested for mediating vitamin E-dependent apoptosis (8–12). Nevertheless, it remains unclear whether the antiproliferative and apoptotic effects of tocopherol and tocotrienol isoforms are mediated through similar or independent intracellular mechanisms. Dose-response studies showed that IC_{50} doses of individual tocotrienol isoforms were 5–6 times lower than their corresponding LD_{50} doses. These data might indicate that the antiproliferative and apoptotic effects of tocotrienols are mediated through different mechanisms. However, subsequent studies showed that IC_{50} doses for TRF, δ-T, and α-T^3, γ-T^3, and δ-T^3 induced substantially large amounts of DNA fragmentation within 24 h after exposure. Similar results were also observed *in situ*. Primary culture of normal mammary epithelial cells in collagen gels is characterized as multicellular organoids with duct-like branching similar in appearance to that of the intact mammary gland (25). Controls displayed a modest amount of epifluorescence staining, an indication of DNA condensation and programmed cell death occurring in some of these cells (31). Since mammary epithelial cells grown in primary culture have a limited life span (25), it is not surprising that portions of these cells are undergoing apoptosis. However, 24-h exposure to 25 (IC_{50}) and 110 μM (LD_{50}) TRF resulted in a dose-dependent increase in the deterioration of organoid morphology and epifluorescence intensity in these cells. These findings raise the possibility that the growth-inhibitory effects of vitamin E isoforms could result from an increase in the total number of cells undergoing programmed cell death. Additional studies are required to clarify if the growth-inhibitory effects of vitamin E result simply from a greater proportion of cells undergoing apoptosis or if they also involve a reduction in EGF-dependent mitogenic responsiveness in these cells.

Previous investigations have shown that vitamin E-dependent apoptosis is mediated through different intracellular mechanisms in different cell types (8–12). Furthermore, apoptosis in normal mammary epithelial cells can be initiated through more than one pathway (41–44). It has been established that mitogen-starved mammary epithelial cells will undergo apoptosis approximately 15 h after mitogen has been removed from the culture medium (43). Various mitogens such as EGF or transforming growth factor α (TGFα) have been shown to induce high cytosolic levels of Bcl-x_L, a protein that inhibits apoptosis (43). In the absence of mitogens, Bcl-x_L levels become significantly reduced, ultimately leading to the induction of apoptosis in these cells (43). Alternatively, activation of specific membrane-bound receptors by their ligands, such as TGFβ or Fas, can also induce apoptosis in mammary epithelial cells even in the presence of high levels of mitogens (43). Studies have also shown that TGFβ- and Fas-receptor signaling pathways appear to play a role in mediating vitamin E-induced apoptosis in some cell types (12,43). Therefore, it is possible that vitamin E-induced programmed cell death in normal mammary epithelial cells might involve the activation of more than one apoptotic signaling pathway. Studies are currently underway to investigate this possibility.

Another factor that may be important in determining tocopherol and tocotrienol isoform biopotency is the ease or preference with which these compounds are taken up by mammary epithelial cells. Prior to treatment, tocopherol and tocotrienol isoform levels were undetectable in mammary epithelial cells. The lack of detectable levels of tocopherols and tocotrienols prior to treatment is not unexpected since these cells were grown for 7 d (2 d preculture plus 5 d experimental culture) in vitamin E-free control media and tissue vitamin E turnover is very rapid (1). Exposure to tocopherol and tocotrienol treatment resulted in a time- and dose-responsive increase in cellular levels of these compounds. However, cellular accumulation of tocotrienols was much greater than that of tocopherols. It is possible that specific structural characteristics are responsible for a less restricted passage of tocotrienols through the mammary epithelial cell membrane. Tocotrienols differ from tocopherols in that they contain an unsaturated phytyl chain. The presence of double bonds in the tocotrienol phytyl chain would create a less planar molecular conformation that could allow for enhanced interaction and uptake at the surface of the cell membrane. Nevertheless, since mammary epithelial cells take up tocotrienols preferentially over tocopherols, higher levels of these compounds are present at their intracellular sites of action and are thereby able to induce a greater biological response.

In addition to enhanced cellular uptake, experimental evidence also indicates that tocotrienols are inherently more potent than tocopherols in regard to their antiproliferative and apoptotic activity. Results showed that similar cellular levels of corresponding tocopherol and tocotrienol isoforms could

be obtained in mammary epithelial cells with 250 μM α-T, γ-T, and δ-T and 45 μM of α-T^3, γ-T^3, and δ-T^3. However, treatment doses that produced similar intracellular levels of tocopherols and tocotrienols did not cause the same antiproliferative and apoptotic response in these cells. These findings indicate that tocotrienol isoforms are more potent than their corresponding tocopherol isoforms in activating the intracellular mechanisms responsible for inhibiting growth and inducing apoptosis in normal mammary epithelial cells.

It was also observed that different isoforms within each tocopherol and tocotrienol subgroup displayed differences in cellular accumulation and biopotency. Specifically, α-isoforms of tocopherols and tocotrienols are more highly methylated than their corresponding γ- or δ-isoforms, and cellular accumulation and biopotency of α-T and α-T^3 were less than their respective γ- and δ-isoforms. Since a decrease in the level of chromane ring methylation results in a corresponding decease in the partition coefficient of these compounds, cellular accumulation and biopotency displayed an inverse relationship with tocopherol and tocotrienol lipophilicity. The suggestion that less lipophilic tocopherol and tocotrienol isoforms are more easily taken up by mammary epithelial cells is supported by the findings that α-tocopheryl succinate or hemisuccinate, less lipophilic derivatives of α-T, display significantly greater cellular accumulation and bioactivity than α-T (33,45). It has not yet been determined if succinate or other less lipophilic derivatives of tocotrienol isoforms also display significantly greater cellular accumulation and biopotency than their parent compounds. In addition, these data suggest that cellular uptake of tocopherols and tocotrienols is most likely determined by nonspecific factors such as molecular conformation and lipid solubility rather than selective uptake mechanisms involving specific transporter or carrier proteins.

In conclusion, tocotrienols display greater biopotency than tocopherols, at least in part because of their greater cellular uptake and enhanced ability to activate the antiproliferative and/or apoptotic signaling pathways. Nevertheless, it is well established that the plasma concentration of individual tocopherol and tocotrienol isoforms is limited by the specificity and saturability of specific transfer proteins and transport mechanisms within the body that display significant preference for α-T (46). Although it remains to be determined whether the high biopotency displayed by individual tocotrienol isoforms *in vitro* is also evident in the intact mammary gland, the present findings provide evidence to suggest that the highly biopotent γ-T^3 and δ-T^3 isoforms may play a physiological role in modulating normal mammary gland growth, function, and remodeling.

ACKNOWLEDGMENTS

The authors thank the Palm Oil Research Institute of Malaysia (PORIM) for generously providing TRF, α-T^3, γ-T^3, and δ-T^3 for use in these experiments, and Dr. Michael Crider for his helpful discussion during the preparation of this manuscript. This work was supported by AICR Grant 96B053.

REFERENCES

1. Packer, L. (1991) Protective Role of Vitamin E in Biological Systems, *Am. J. Clin. Nutr. 53,* 1050S–1055S.
2. Elson, C.E. (1992) Tropical Oils: Nutritional and Scientific Issues, *Crit. Rev. Food Sci. Nutr. 31,* 79–102.
3. Kimmick, G.G., Bell, R.A., and Bostick, R.M. (1997) Vitamin E and Breast Cancer: A Review, *Nutr. Cancer 27,* 109–117.
4. Chatelain, E., Boscoboinik, D.O., Bartoli, G.-M., Kagan, V.E., Gey, F.K., Packer, L., and Azzi, A. (1993) Inhibition of Smooth Muscle Cell Proliferation and Protein Kinase C Activity by Tocopherols and Tocotrienols, *Biochim. Biophys. Acta 1176,* 83–89.
5. Stauble, B., Boscoboinik, D., Tasinato, A., and Azzi, A. (1994) Modulation of Activator Protein-1 (AP-1) Transcription Factor and Protein Kinase C by Hydrogen Peroxide and D-α-Tocopherol in Vascular Smooth Muscle Cells, *Eur. J. Biochem. 226,* 393–402.
6. Turley, J.M., Ruscetti, F.W., Kim, S.J., Fu, T., Gou, F.V., and Birchenall-Roberts, M.C. (1997) Vitamin E Succinate Inhibits Proliferation of BT-20 Human Breast Cancer Cells: Increased Binding of Cyclin A Negatively Regulates E2F Transactivation Activity, *Cancer Res. 57,* 2668–2675.
7. Fazzio, A., Marilley, D., and Azzi, A. (1997) The Effect of α-Tocopherol and β-Tocopherol on Proliferation, Protein Kinase C Activity and Gene Expression in Different Cell Lines, *Biochem. Mol. Biol. Int. 41,* 93–101.
8. Turley, J.M., Fu, T., Ruscetti, F.W., Mikovits, J.A., Bertolette, D.C., III, and Birchenall-Roberts, M.C. (1997) Vitamin E Succinate Induces Fas-mediated Apoptosisin Estrogen Receptor-negative Human Breast Cancer Cells. *Cancer Res. 57,* 881–890.
9. Zhao, B., Yu, W., Qian, M., Simmons-Menchaca, M., Brown, P., Birrer, M.J., Sanders, B.G., and Kline, K. (1997) Involvement of Activator Protein-1 (AP-1) in Induction of Apoptosis by Vitamin E Succinate in Human Breast Cancer Cells, *Mol. Carcinog. 19,* 180–190.
10. Yu, W., Sanders, B.G., and Kline, K. (1997) *RRR*-α-Tocopheryl Succinate Inhibits El4 Thymic Lymphoma Cell Growth by Inducing Apoptosis and DNA Synthesis Arrest, *Nutr. Cancer 27,* 92–101.
11. Sigounas, G., Anagnostou, A., and Steiner, M. (1997) DL-α-Tocopherol Induces Apoptosis in Erythroleukemia, Prostate, and Breast Cancer Cells, *Nutr. Cancer 28,* 30–35.
12. Yu, W., Israel, K., Liao, Q.Y., Aldaz, C.M., Sanders, B.G., and Kline, K. (1999) Vitamin E Succinate (VES) Induces Fas Sensitivity in Human Breast Cancer Cells: Role for M_r 43,000 Fas in VES-Triggered Apoptosis, *Cancer Res. 59,* 953–961.
13. Cottrell, R.C. (1991) Introduction: Nutritional Aspects of Palm Oil, *Am. J. Clin. Nutr. 53,* 989S–1009S.
14. Sundram, K., Khor, H.T., Ong, A.S.H., and Pathmanathan, R. (1989) Effects of Dietary Palm Oils on Mammary Carcinogenesis in Female Rats Induced by 7,12-Dimethylbenz(a)anthracene, *Cancer Res. 49,* 1447–1451.
15. Sylvester, P.W., Russell, M., Ip, M.M., and Ip, C. (1986) Comparative Effects of Different Animal and Vegetable Fats Fed Before and During Carcinogen Administration on Mammary Tumorigenesis, Sexual Maturation, and Endocrine Function in Rats, *Cancer Res. 46,* 757–762
16. Gould, M.N., Haag, J.D., Kennan, W.S., Tanner, M.A., and Elson, C.E. (1991) A Comparison of Tocopherol and Tocotrienol for the Chemoprevention of Chemically Induced Rat Mammary Tumors, *Am. J. Clin. Nutr. 53,* 1068S–1070S.
17. Nesaretnam, K., Khor, H.T., Ganeson, J., Chong, Y.H., Sundram, K., and Gapor, A. (1992). The Effect of Vitamin E Tocotrienols from Palm Oil on Chemically Induced Mammary Carcinogenesis in Female Rats, *Nutr. Res. 12,* 879–892.
18. Zurinah, W., Ngah, W., Jarien, Z., San, M.M., Marzuki, A., Top,

G.D., Shamaan, N.A., and Kadir, K.A. (1991) Effect of Tocotrienols on Hepatocarcinogenesis Induced by 2-Acetylaminofluorene in Rats, *Am. J. Clin. Nutr. 53,* 1076S–1081S.
19. Goh, S.H., Hew, N.F., Norhanom, A.W., and Yadav, M. (1994) Inhibition of Tumour Promotion by Various Palm-Oil Tocotrienols, *Int. J. Cancer 57,* 529–531.
20. Nesaretnam, K., Guthrie, N., Chambers, A.F., and Carroll, K.K. (1995) Effect of Tocotrienols on the Growth of a Human Breast Cancer Cell Line in Culture, *Lipids 30,* 1139–1143.
21. He, L., Mo, H., Hadisusilo, S., Qureshi, A.A., and Elson, C.E. (1997) Isoprenoids Suppress the Growth of Murine B16 Melanomas *in vitro* and *in vivo, J. Nutr. 127,* 668–674.
22. Guthrie, N., Gapor, A., Chambers, A.F., and Carroll K.K. (1997) Inhibition of Proliferation of Estrogen Receptor-Negative MDA-MB-435 and -Positive MCF-7 Human Breast Cancer Cells by Palm Oil Tocotrienols and Tamoxifen, Alone and in Combination, *J. Nutr. 127,* 544S–548S.
23. Nesaretnam, K., Stephen, R., Dils, R., and Darbre, P. (1998) Tocotrienols Inhibit the Growth of Human Breast Cancer Cells Irrespective of Estrogen Receptor Status, *Lipids 33,* 461–469.
24. Sylvester, P.W., Birkenfeld, H.P., Hosick, H.L., and Briski, K.P. (1994) Fatty Acid Modulation of Epidermal Growth Factor-Induced Mouse Mammary Epithelial Cell Proliferation *in vitro, Exp. Cell Res. 214,* 145–153.
25. McIntyre, B.S., Birkenfeld, H.P., and Sylvester, P.W. (1995) Relationship Between Epidermal Growth Factor Receptor Levels, Autophosphorylation and Mitogenic-Responsiveness in Normal Mouse Mammary Epithelial Cells *in vitro, Cell Prolif. 28,* 45–56.
26. McIntyre, B.S., and Sylvester, P.W. (1998) Genistein and Erbstatin Inhibition of Normal Mammary Epithelial Cell Proliferation Is Associated with EGF-Receptor Down-regulation, *Cell Prolif. 31,* 35–46.
27. McIntyre, B.S., Briski, K.P., Hosick, H.L., and Sylvester, P.W. (1998) Effects of Protein Tyrosine Phosphatase Inhibitors on EGF- and Insulin-Dependent Mammary Epithelial Cell Growth, *Proc. Exp. Biol. Med. 217,* 180–187.
28. Imagawa, W., Bandyopadhyay, G.K., and Nandi, S. (1990) Regulation of Mammary Epithelial Cell Growth in Mice and Rats, *Endocr. Rev. 11,* 494–523.
29. Jones, W., Challowes, R.C., Choongkittaworn, N., Hosick, H.L., and Dils, R. (1983) Isolation of the Epithelial Subcomponents of the Mouse Mammary Gland for Tissue-Level Culture Studies, *J. Tissue Cult. Methods 8,* 17–25.
30. Tepper, C.G., and Studzinski, G.P. (1992) Teniposide Induces Nuclear But Not Mitochondrial DNA Degradation, *Cancer Res. 52,* 3384–3390.
31. Tsangaris, G.T., Moschovi, M., Mikraki, V., Vrachnou, E., and Tzortzatou-Stathopoulou, F. (1996) Study of Apoptosis in Peripheral Blood of Patients with Acute Lymphoblastic Leukemia During Induction Therapy, *Anticancer Res. 16,* 3133–3140.
32. Fariss, M.W., Pascoe, G.A., and Reed, D.J. (1985) Vitamin E Reversal of the Effect of Extracellular Calcium on Chemically Induced Toxicity in Hepatocytes, *Science 227,* 751–754.
33. Tirmenstein M.A., Watson B.W., Haar, N.C., and Fariss, M.W. (1998) Sensitive Method for Measuring Tissue α-Tocopherol and α-Tocopheryloxybutyric Acid by High-Performance Liquid Chromatography with Fluorometric Detection, *J. Chromatogr. B. Biomed. Sci. Appl. 707,* 308–311.
34. Schwartz, J., and Shklar, G. (1992) The Selective Cytotoxic Effects of Carotenoids and Alpha-Tocopherol on Human Cancer Cell Lines *in vitro, J. Oral Maxillofac. Surg. 50,* 367–373.
35. Birkenfeld, H.P., McIntyre, B.S., Briski, K.P., and Sylvester, P.W. (1996) Role of Protein Kinase C in Modulating Epidermal Growth Factor- and Phorbol Ester-Induced Mammary Epithelial Cell Growth *in vitro, Exp. Cell Res. 223,* 183–191.
36. Birkenfeld, H.P., McIntyre, B.S., Briski, K.P., and Sylvester, P.W. (1996) Protein Kinase C Isoenzyme Expression in Normal Mammary Epithelial Cells Grown in Primary Culture, *Proc. Exp. Biol. Med. 213,* 65–70.
37. Bandyopadhyay, G.K., Hwang, S., Imagawa, W., and Nandi, S. (1993) Role of Polyunsaturated Fatty Acids as Signal Transducers: Amplification of Signals from Growth Factor Receptors by Fatty Acids in Mammary Epithelial Cells, *Prostaglandins Leukotrienes Essent. Fatty Acids 48,* 71–78.
38. Bandyopadhyay, G.K., Imagawa, W., and Nandi, S. (1995) Role of GTP-Binding Proteins in the Polyunsaturated Fatty Acid Stimulated Proliferation of Mouse Mammary Epithelial Cells, *Prostaglandins Leukotrienes Essent. Fatty Acids* 52, 151–158.
39. Torelli, S., Masoudi, F., and Prasad, K.N. (1988) Effect of α-Tocopherol Succinate on Cyclic AMP-Dependent Protein Kinase Activity in Murine B-16 Melanoma Cells in Culture, *Cancer Lett. 39,* 129–136.
40. Ottino, P., and Duncan, J.R. (1997) Prostaglandin Levels in BL6 Melanoma Cells Cultured *in vitro*: The Effect of Vitamin E Succinate Supplementation, *Prostaglandins Leukotrienes Essent. Fatty Acids 56,* 143–149.
41. Hockenbery, D.M., Nunez, G., Milliman, C., Schreiber, R.D., and Korsmeyer, S.J. (1990) BcL-2 Is an Inner Mitochondrial Membrane Protein That Blocks Programmed Cell Death, *Nature 348,* 334–336.
42. Oltvai, Z.N., and Korsmeyer, S.J. (1994) Checkpoints of Dueling Dimers Foil Death Wishes, *Cell 79,* 189–192.
43. Nass, S.J., Li, M., Amundadottir, L.T., Furth, P.A., and Dickson, R.B. (1996) Role for Bcl-x_L in Regulation of Apoptosis by EGF and TGFβ1 in c-myc Overexpressing Mammary Epithelial Cells, *Biochem. Biophys. Res. Comm. 227,* 248–256.
44. Heermeier, K., Benedict, M., Li, M., Furth, P., Nunez, G., and Hennighausen, L. (1996) Bas and Bcl-x_s Are Induced at the Onset of Apoptosis in Involuting Mammary Epithelial Cells, *Mech. Dev. 56,* 197–207.
45. Fariss, M.W., Fortuna, M.B., Everett, C.K, Smith J.D., Trent, D.F., and Djuric, Z. (1994) The Selective Antiproliferative Effects of α-Tocopheryl Hemisuccinate and Cholesteryl Hemisuccinate on Murine Leukemia Cells Result from the Action of the Intact Compounds, *Cancer Res. 54,* 3346–3351.
46. Hosomi, A., Arita, M., Sato, Y., Kiyose, C., Ueda, T., Igarashi, O., Arai, H., and Inoue, D. (1997) Affinity for α-Tocopherol Transfer Protein as a Determinant of the Biological Activities of Vitamin E Analogs, *FEBS Lett. 409,* 105–108.

[Received August 18, 1999, and in revised form November 4, 1999; revision accepted December 8, 1999]

Incorporation of Polyunsaturated Fatty Acids into CT-26, a Transplantable Murine Colonic Adenocarcinoma

Daniel P. Gaposchkin[a,b], Raphael A. Zoeller[b], and Selwyn A. Broitman[c,*]

The Departments of [a]Pathology and Laboratory Medicine, [b]Biophysics, and [c]Microbiology, Boston University School of Medicine, Boston, Massachusetts 02118

ABSTRACT: Previous studies in our laboratory have shown that marine oils, with high levels of eicosapentaenoic (EPA, 20:5n-3) and docosahexaenoic acids (DHA, 22:6n-3), inhibit the growth of CT-26, a murine colon carcinoma cell line, when implanted into the colons of male BALB/c mice. An *in vitro* model was developed to study the incorporation of polyunsaturated fatty acids (PUFA) into CT-26 cells in culture. PUFA-induced changes in the phospholipid fatty acid composition and the affinity with which different fatty acids enter the various phospholipid species and subspecies were examined. We found that supplementation of cultured CT-26 cells with either 50 μM linoleic acid (LIN, 18:2n-6), arachidonic acid (AA, 20:4n-6), EPA, or DHA significantly alters the fatty acid composition of CT-26 cells. Incorporation of these fatty acids resulted in decreased levels of monounsaturated fatty acids, while EPA and DHA also resulted in lower levels of AA. While significant elongation of both AA and EPA occurred, LIN remained relatively unmodified. Incorporation of radiolabeled fatty acids into different phospholipid species varied significantly. LIN was incorporated predominantly into phosphatidylcholine and had a much lower affinity for the ethanolamine phospholipids. DHA had a higher affinity for plasmenylethanolamine (1-*O*-alk-1′-enyl-2-acyl-*sn*-glycero-3-phosphoethanolamine) than the other fatty acids, while EPA had the highest affinity for phosphatidylethanol-amine (1,2-diacyl-*sn*-glycero-3-phosphoethanolamine). These results demonstrate that, *in vitro*, significant differences are seen between the various PUFA in CT-26 cells with respect to metabolism and distribution, and these may help to explain differences observed with respect to their effects on tumor growth and metastasis in the transplantable model.

Paper no. L8155 in *Lipids 35*, 181–186 (February 2000).

The n-3 polyunsaturated fatty acids (PUFA) have been found to inhibit chemical-induced colon cancer in a number of animal models (1–3), and higher dietary n-3 PUFA intake has been associated with lower risk of colon and breast cancer in humans (4). Studies by Cannizzo and Broitman (5) have shown that marine oil diets containing eicosapentaenoic acid (EPA, 20:5n-3) and docosahexaenoic acid (DHA, 22:6n-3), compared to safflower oil diets [predominantly linoleic acid (LIN; 18:2n-6)], inhibit the growth of CT-26, a BALB/c mouse colonic adenocarcinoma, implanted into the descending colon of syngeneic mice. Tumors in marine oil-fed mice were significantly smaller 21 d after implantation (5). Studies by Iigo *et al.* (6) have recently demonstrated that DHA alters the membrane characteristics and reduces the ability of CT-26 to metastasize.

Although n-3 fatty acids affect tumor development and growth (7–9), the mechanism by which this occurs is uncertain. Fish oil fatty acids may exert their effect on tumor growth once they are released by phospholipases and converted to oxygenated derivatives (10). Different types and proportions of such derivatives are produced from different PUFA. A number of phospholipase A_2 activities have been shown to cleave fatty acids from phospholipids bearing specific headgroups, fatty acids, or vinyl-ether linkages at the *sn*-1 position (11).

Incorporation of PUFA into CT-26 *in vitro* has not been examined even though PUFA have been shown to influence the rate of growth and metastatic potential of these cells *in vivo* (5,6). We have therefore studied the effects of supplementation of LIN, arachidonic acid (AA), EPA, and DHA on the phospholipid fatty acid composition of cultured CT-26 cells over a 24-h period. We also have studied the incorporation of radiolabeled fatty acids and determined into which phospholipid species and subspecies they are incorporated. These studies characterizing the behavior of PUFA in CT-26 cells further our understanding of potential anticancer effects and provide important background data for future studies examining the effects of n-3 fatty acids on colon tumor cell growth in this transplantable tumor system.

MATERIALS AND METHODS

Tissue culture. CT-26 cells were maintained in 75- or 150-mm^2 flasks (Falcon, Lincoln Park, NJ; or Corning, Corning, NY) in RPMI 1640 with 1% penicillin/streptomycin, 1% glutamine, and 2.5% fetal bovine serum (FBS; Sigma, St. Louis, MO). Cells were maintained at 37°C in a humidified atmosphere of 5% CO_2/95% air.

*To whom correspondence should be addressed at Dept. of Microbiology, Boston University School of Medicine, 715 Albany St., Boston, MA 02118-2526. E-mail: essaybee@bu.edu

Abbreviations: AA, arachidonic acid; BSA, bovine serum albumin; DHA, docosahexaenoic acid; EPA, eicosapentaenoic acid; FAME, fatty acid methyl ester; FBS, fetal bovine serum; LIN, linoleic acid; PUFA, polyunsaturated fatty acid; TLC, thin-layer chromatography.

Fatty acid analysis of supplemented cells. LIN, AA, EPA, and DHA sodium salts (Sigma) were conjugated to fatty acid-free bovine serum albumin (BSA; Sigma) at a 3:1 molar ratio prior to addition to cultured cells. The growth rate of cultured CT-26 cells was not affected over a 24-h time period when n-6 or n-3 fatty acids (LIN, AA, EPA) were added to the medium in this way at concentrations as high as 100 μM (Broitman, S.A., and Kosakolsky-Singer, C., unpublished data). Cells (2×10^6) were plated into 100-mm dishes (Falcon). The next day, medium was removed, and growth medium containing the fatty acid/BSA mixtures was added to cells (this was considered time zero). At designated times, medium was removed and the dishes were washed twice with ice-cold phosphate-buffered saline (PBS); cells were harvested by scraping, and were then resuspended in 2 mL PBS. Cell suspensions were transferred to glass culture tubes and a phospholipid standard (diheptadecanoyl L-α-phosphatidylcholine; Sigma) was added to each sample. The lipids were extracted by the method of Folch *et al.* (12). Samples were dried under a stream of nitrogen and spotted on silica gel G thin-layer chromatography (TLC) plates (Analtech, Newark, DE). TLC plates were developed using hexane/diethylether/acetic acid (70:30:1, by vol), and were visualized with diphenyl-hexatriene (Sigma) under long-wave ultraviolet light. The origins, containing the phospholipids, were scraped into glass culture tubes, and fatty acid methyl esters (FAME) were generated by transesterification using boron trifluoride–methanol (1 mL of a 14% solution in methanol) for 1 h at 80°C. The reaction was stopped by addition of 1 mL of distilled H_2O. FAME were extracted twice, using 4 mL of hexane. Solvent was evaporated using a stream of nitrogen gas and resuspended in chloroform. Samples were injected into a Shimadzu 14A gas chromatograph (Kyoto, Japan) with a flame-ionization detector (FID) connected to a Shimadzu Chromatopac CR-501 data-processing system. The gas chromatograph was equipped with an SP-2330 fused-silica capillary column, 30 m × 25 mm i.d., 0.20-mm film (Supelco, Bellefonte, PA). Hydrogen was used for the FID mixed with compressed breathing air, zero grade (<10 ppm hydrocarbons). Helium, ultra-high purity, was used as the carrier gas as well as the makeup gas. Injector and detector temperatures were 240°C. The column initial temperature was 150°C, where it remained for 2 min and then increased at the rate of 5.0°C/min until 240°C. The column then remained at 240°C for 4 min. Chromatograms were analyzed by comparison of peak retention times to that of a standard (Matreya, Pleasant Gap, PA) containing FAME of interest.

Phospholipid composition. The phospholipid composition of CT-26 cells was determined using long-term ^{32}P labeling. This technique has been shown to provide similar results to phosphorus determination when performed side by side (13). Cells were plated to sterile glass scintillation vials (10^5 cells), to which they adhered and radioactive inorganic phosphate ($^{32}P_i$) was added, (5 μCi/mL). After 48 h of incubation at 37°C, the medium was aspirated and fresh medium containing [$^{32}P_i$] (5 μCi/mL) was added to the cells. The cells were incubated for an additional 24 h, washed twice with ice-cold PBS, and the lipids extracted by the method of Bligh and Dyer (14). Samples were dried under a stream of nitrogen gas and spotted onto silica gel 60 (20 × 20 cm, 250-μm thick) TLC plates. Phospholipids were separated by two-dimensional TLC (15). Samples were developed using chloroform/methanol/acetic acid/water (25:15:3:1.5, by vol) in the first dimension and chloroform/methanol/formic acid (65:25:10, by vol) in the second dimension. Between dimensions, plates were sprayed with 10 mM mercuric chloride in acetic acid to cleave vinyl ethers associated with plasmalogens and then dried. In this way, the resulting *sn*-1-lysophospholipid generated from the plasmalogen could be separated from the diacyl and 1-alkyl species in the second dimension. The phospholipid species were localized using autoradiography, and the different lipids were scraped into scintillation vials containing 1 mL of methanol. Scintillation cocktail (8 mL; National Diagnostics, Atlanta, GA) was added and the radioactivity quantitated by liquid scintillation spectroscopy.

Labeling cells with radioactive fatty acids. Cells (2.5×10^5) were plated to sterile glass scintillation vials in 1 mL of medium containing 2 μCi [4,5-^{3}H]DHA [58 Ci/mmol; New England Nuclear (NEN), Boston, MA], 2 μCi [5,6,8,9,11,12,14,15-^{3}H]AA (100 Ci/mmol; NEN), 2 μCi, [5,6,8,9,11,12,14,15,17,18-^{3}H] EPA (100 Ci/mmol; American Radiolabeled Chemicals, St. Louis, MO), or 1 μCi [1-^{14}C]LIN (50 mCi/mmol; NEN). Final concentration of all fatty acids in the labeling media was 50 μM. Fatty acids were added as fatty acid/BSA (3:1) complexes. Cells were incubated for 24 h at 37°C, after which the cells were washed twice with 3 mL of ice-cold RPMI medium containing 2.5% FBS. The lipids were extracted by the method of Bligh and Dyer and two-dimensional TLC performed as described above. TLC plates were sprayed with EN^{3}HANCE (NEN) and exposed to X-ray film (GBX-2; Eastman Kodak, Rochester, NY) at –80°C. Labeled phospholipid species were scraped and the radioactivity quantitated by liquid scintillation spectroscopy as described above.

Statistics. Data were analyzed by analysis of variance (ANOVA) and Tukey's *post-hoc* comparison using NCSS 6.0 statistics software program (Kaysville, UT).

RESULTS

Fatty acid analysis. All four PUFA studied were readily incorporated into cellular phospholipids, significantly altering the membrane fatty acid composition over a 24-h period (Table 1). Vehicle alone (medium and 16 μM BSA) had no effect on the fatty acid profile of CT-26 phospholipids (data not shown). Incorporation of 50 μM PUFA (LIN, AA, EPA, or DHA) for 24 h resulted in a reduction of the monounsaturated fatty acids (16:1 and 18:1) from approximately 40 to 20% of total phospholipid fatty acid. Addition of the n-3 PUFA, EPA and DHA, also resulted in significant decreases of AA levels from 10.9 to 4.3 and 3.1%, respectively.

The 20-carbon fatty acids, AA and EPA, were substantially elongated, although to different extents. Supplementation

TABLE 1
Phospholipid Fatty Acid Composition of CT-26 Cells Supplemented with Various Fatty Acids for 24 h

	Total fatty acid mass (weight %)[a]				
Fatty acid	Control	LIN	AA	EPA	DHA
Saturates					
14:0	2.3 ± 0.4	1.5 ± 0.7	1.2 ± 0.2	1.0 ± 0.2	1.7 ± 0.8
16:0	19.9 ± 0.9	19.8 ± 3.6	23.0 ± 0.5	22.4 ± 1.6	26.5 ± 1.8*
18:0	15.1 ± 0.7	16.2 ± 2.9	13.9 ± 0.4	15.3 ± 0.6	19.3 ± 1.6*
Monounsaturates					
16:1	6.6 ± 0.2	2.3 ± 0.5*	2.6 ± 0.4*	2.7 ± 0.1*	2.8 ± 0.5*
18:1	35.6 ± 0.7	15.5 ± 0.4*	18.6 ± 0.2*	20.9 ± 0.5*	19.9 ± 1.0*
Polyunsaturates (n-6)					
18:2	2.2 ± 0.2	27.8 ± 4.0*	1.9 ± 0.3	1.7 ± 0.1	1.3 ± 0.2
20:3	1.2 ± 0.1	1.4 ± 0.2	0.4 ± 0.3*	0.7 ± 0.0	0.4 ± 0.3*
20:4	10.9 ± 0.5	10.0 ± 1.1*	26.5 ± 0.6*	4.3 ± 0.2*	3.1 ± 0.9*
22:4	0.7 ± 0.6	1.7 ± 0.2*	10.0 ± 0.2*	0.8 ± 0.1	0.2 ± 0.3
Polyunsaturates (n-3)					
20:5	0.3 ± 0.5	ND	ND	15.2 ± 0.7*	0.9 ± 0.4
22:5	2.0 ± 0.0	1.3 ± 0.3	1.0 ± 0.1*	14.1 ± 0.7*	0.7 ± 0.2*
22:6	2.7 ± 0.1	1.0 ± 0.9	0.9 ± 0.0	1.1 ± 0.1	22.6 ± 2.5*
Totals					
Monoenes	42.7 ± 0.8	17.7 ± 0.7*	21.2 ± 0.6*	23.6 ± 0.4*	22.6 ± 1.4*
n-6	12.8 ± 0.5	13.0 ± 1.1	36.9 ± 0.8*	5.7 ± 0.3*	4.3 ± 1.0*
n-3	5.0 ± 0.5	2.3 ± 1.1	1.9 ± 0.1	30.4 ± 1.4*	24.2 ± 2.8*
n-6/n-3	2.6 ± 0.3	7.1 ± 4.1	19.2 ± 1.0*	0.2 ± 0.0	0.2 ± 0.0

[a]Values represent the mean ± standard deviation of three samples. Control groups were exposed to bovine serum albumin (16.6 μM) in medium. ND, not detectable. Asterisk indicates value is significantly different from control group ($P < 0.05$). LIN, linoleic acid; AA, arachidonic acid; EPA, eicosapentaenoic acid; DHA, docosahexaenoic acid.

with 50 μM AA for 24 h resulted in an increase in AA from about 7% of total phospholipid to more than 26% and a greater than 10-fold increase in docosatetraenoic acid (22:4n-6) from 0.7 to 10.0%. There were no changes in LIN levels, suggesting that there was no significant retroconversion of AA to this fatty acid. Addition of EPA (50 μM) led to increases in both EPA, from 0.3 to 15.2%, and its elongation product, docosapentaenoic acid (22:5n-3), from 2.0 to 15.1%, although there was no accumulation of DHA.

Addition of LIN resulted in increased levels of LIN from 2.2% of the phospholipid fatty acids to 27.8% of total phospholipid fatty acid within 24 h. Surprisingly, there was relatively little desaturation or elongation of LIN with no significant changes in the levels of AA.

Addition of 50 μM DHA resulted in increased levels of DHA from 2.7 to 22.6%. There were no changes in the other long-chain n-3 fatty acids, suggesting that there is no significant retroconversion of DHA to 22:5n-3 or 20:5n-3. There was an increase in the levels of the saturated fatty acid palmitate (16:0) in cells supplemented with DHA.

Phospholipid composition. To better define the membrane phospholipid composition of CT-26 cells, we performed long-term labeling with $^{32}P_i$ to determine the phospholipid composition of CT-26 (Table 2, right-hand column). The predominant phospholipid head group class was choline (53.1% of total) while approximately 18% of the phospholipids contained the ethanolamine headgroup. More than 40% of ethanolamine phospholipids were plasmalogens (plas-

TABLE 2
Distribution of Labeled Fatty Acids in Different Phospholipid Species and Subspecies in CT-26 Cells. Comparison to the Phospholipid Composition

	Total label recovered (%)[a]				
	LIN	ARA	EPA	DHA	PL composition
Lyso-species	ND	ND	ND	ND	0.9 ± 0.1
Sphingomyelin	1.0 ± 0.2^{a,e,d}	ND	ND	ND	4.8 ± 0.5
Plasmenylcholine	1.5 ± 0.1^{d,a}	1.8 ± 0.1^{d,l}	1.4 ± 0.2^{d}	2.4 ± 0.2^{l,a,e}	2.2 ± 0.0
Phosphatidylcholine	60.4 ± 0.4^{a,e,d}	44.2 ± 0.9^{l,e,d}	37.6 ± 1.1^{l,a}	37.8 ± 1.3^{l,a}	53.1 ± 0.7
Phosphatidylinositol	6.3 ± 1.0^{a,e,d}	12.9 ± 0.1^{l,d}	13.2 ± 0.4^{l,d}	9.8 ± 0.6^{l,a,e}	9.9 ± 0.4
Phosphatidylserine	5.6 ± 1.2	4.8 ± 0.2^{e}	7.5 ± 0.6^{a}	5.7 ± 0.2	4.6 ± 0.6
Plasmenylethanolamine	2.9 ± 0.2^{a,e,d}	10.1 ± 0.4^{l,d,*}	9.1 ± 0.2^{l,d,*}	14.3 ± 0.3^{l,a,e}	7.5 ± 0.9
Phosphatidylethanolamine	13.0 ± 0.3^{a,e,d}	17.9 ± 0.2^{l,e}	24.0 ± 0.1^{l,a,d}	17.8 ± 0.8^{l,e}	10.8 ± 0.5
Other	9.3 ± 1.0^{d}	8.4 ± 1.2^{d}	7.3 ± 0.2^{d}	12.4 ± 0.3^{l,a,e}	6.1 ± 0.4

[a]Values represent the mean ± standard deviation of three samples. Other fatty acids include cardiolipin, phosphatidic acid, phosphatidylglycerol, and neutral lipids (in labeled fatty acids only). Superscript letters indicate values are significantly different (at $P < 0.01$) than the fatty acid indicated: l, linoleic acid, a, arachidonic acid, e, eicosapentaenoic acid d, docosahexaenoic acid, and *two values are significantly different at $P < 0.05$. See Table 1 for other abbreviations.

menylethanolamine, 1-*O*-alk-1′-enyl-2-acyl-*sn*-3-glycerophosphoethanolamine) while less than 4% of choline phospholipids were plasmalogens (plasmenylcholine, 1-*O*-alk-1′-enyl-2-acyl-*sn*-3-glycero-phosphocholine). Phosphatidylinositol constituted roughly 10% of the phospholipids, while phosphatidylserine, sphingomyelin, the lysophospholipid species, and other (cardiolipin, phosphatidic acid, phosphatidylglycerol), accounted for the remaining phospholipids in CT-26.

Incorporation of labeled fatty acids into phospholipids. Cells were labeled with the radioactive fatty acids to determine their distribution after 24 h among the different phospholipid species. Linoleate's pattern of labeling, for the most part, reflected the relative amounts of each phospholipid species (Table 2) with the majority of the label found associated with the most abundant phospholipid, phosphatidylcholine. There was, however, a reduced affinity for labeling of the plasmalogen, plasmenylethanolamine, when using LIN. The other fatty acids (AA, EPA, and DHA) displayed a preference for incorporation into inositol and ethanolamine phospholipids. This was most apparent in the cases of EPA and DHA; approximately one-third of the label was found in the ethanolamine phospholipids, while this head group class accounts for only 18.3% of the total phospholipid. The distribution of the label between plasmenylethanolamine and phosphatidylethanolamine favored the latter species when using either AA or EPA, but DHA showed a minor preference for the plasmenyl species. This preference was determined by dividing the percentage of fatty acid incorporated into a phospholipid species (percentage of total label recovered in phospholipids) by the percentage that the species contribute to the total phospholipid mass (see "phospholipid composition" in Table 2), such that a value greater than 1.0 indicates specificity. The greatest affinities observed are for DHA incorporation into plasmenylethanolamine (1.9) and EPA incorporation into phosphatidylethanolamine (2.2). A greater portion of the DHA label was also recovered in the fraction containing cardiolipin and phosphatidic acid (other phospholipids). As expected, there was little or no labeling of sphingomyelin or the lysophospholipids.

A significantly greater percentage of the n-6 fatty acids, LIN and AA, were recovered in phosphatidylcholine as compared to the n-3 fatty acids, EPA and DHA. This was the only phospholipid class that displayed this preference for n-6 PUFA.

DISCUSSION

A number of studies have found that, unlike the n-6 PUFA (16,17), EPA and DHA can inhibit the growth or metastasis of tumor cells within the host (4–9,18), as well as in culture (19,20); however, the mechanism behind these effects is still unclear. The physical properties of cell membranes can be altered by dietary PUFA (21,22), and these changes may affect the growth and/or the metastatic potential of tumor cells. Other evidence points toward a role for the n-3 PUFA in altering eicosanoid production in tumor cells (19,20,23); highly metastatic tumor cells contained higher levels of prostag-landins than similar less metastatic cells (23), and cyclooxygenase inhibitors have been shown to suppress the stimulatory effects seen with n-6 fatty acid supplementation in some cells (19,20). The n-3 fatty acids may exert their tumor-inhibiting effects by decreasing the synthesis of eicosanoids derived from n-6 fatty acids or by increasing the production of n-3 eicosanoid analogs, which counteract the n-6 eicosanoid's effects.

Our laboratory has previously demonstrated that CT-26 cells are nutritionally responsive to PUFA when implanted into the colons of male BALBc mice (5), growing more slowly in mice fed diets containing n-3 lipids than those fed n-6 lipids. The purpose of the present study was to develop an *in vitro* model to determine the effects of both n-6 and n-3 PUFA on phospholipid fatty acid composition. To this end, we have begun to determine the ability of these cells to assimilate both n-6 and n-3 PUFA into the phospholipid pool and to characterize the effects this has on the fatty acid composition of the membrane lipids.

There is a wide variation in the ability of different culture cells to incorporate and convert of fatty acids *via* desaturation and elongation (24). The present study demonstrated that *in vitro* all of the PUFA were incorporated readily into the phospholipids of CT-26 cells. Addition of LIN, AA, and EPA resulted in comparable incorporation of these fatty acids. Over a 24-h treatment period, these exogenous PUFA represented 26–28% of total phospholipid fatty. The increase of PUFA attributable to exogenous DHA, however, was less (20%). Several possibilities exist for this difference: DHA might be metabolized at a higher rate than the other fatty acids, resulting in its breakdown and loss from the phospholipids, or it may be shunted into nonphospholipid pools at a greater rate than the other fatty acids examined.

In all cases, incorporation of PUFA led to a corresponding decrease in the proportion of monounsaturated fatty acids. The monounsaturates 16:1 and 18:1, which originally constituted about 40% of phospholipid fatty acids, were reduced to about 20% after 24 h of supplementation with any of the fatty acids. This is consistent with studies by Tebbey and Butke (25), who observed that as AA levels increased in cultured murine lymphocytes, there was a 30% decrease in the amount of oleic acid. They further showed that AA regulates stearoyl-CoA desaturase gene expression by inhibiting transcription. Addition of LIN, AA, and EPA did not alter the levels of the saturated fatty acids in any consistent manner. However, addition of DHA did raise the level of palmitate slightly. It is possible that the addition of such a highly unsaturated fatty acid as DHA requires an increase in saturated fatty acids to maintain the membrane fluidity within a critical range.

Studies using an implanted tumor cell line, derived from CT-26 cells, resulted in similar trends as those observed in this study (6). When mice bearing these cells were fed PUFA, there was a marked increase in the PUFA levels in the phospholipids as well as elongation of AA and EPA. However, the changes were not as rapid and not of the same magnitude as observed when using cells in culture. This was probably due to the fact that, in culture, the cells are exposed directly to free

fatty acid, while in the host animal, the dietary fatty acids reach the tumor cells esterified to complex lipids and found within lipoprotein complexes. The free fatty acids are more readily taken up and activated for acylation. Also, in the *in vivo* studies (6), increased PUFA levels did not result in a reduction in the monounsaturated fatty acids.

Several studies have suggested that the effects observed with n-3 fatty acids occur because they displace AA from phospholipids (8). Our studies confirm that addition of EPA or DHA leads to a reduction of phospholipid AA levels; EPA and DHA reduced AA levels by approximately 40 and 60%, respectively. Two of the fatty acids, AA (20:4n-6) and EPA (20:5n-3), were significantly modified by elongation, to 22:4 n-6 and 22:5n-3, respectively. The process of elongation is thought to occur in all mammalian cells (24); however, the extent to which a cell elongates long-chain PUFA varies. These studies allowed us to observe the changes in mass of the elongation products of AA and EPA in CT-26. EPA was elongated more extensively than AA after 24 h; approximately 30% of the AA present had been elongated to 22:4n-6, while around 50% of EPA was elongated. Even at earlier time periods after addition of the fatty acid (1–3 h), EPA is elongated while AA appears to be elongated only after significant levels accumulate (data not shown). It was unclear whether this was due to a decreased elongation of AA or the reluctance of the phospholipids to incorporate the elongation product 22:4n-6. It seems likely that the former is true: umbilical vein endothelial cells, rat liver cells, and human skin fibroblasts have been shown to elongate EPA more readily than AA (24). Banerjee and Rosenthal (26) reported that AA was only elongated when there was a relative excess of this crucial fatty acid, however, EPA was elongated even when present at low concentrations, and was elongated to a greater extent. It has been suggested that this increased elongation of EPA functions as a mechanism to reduce the amount of EPA that can compete with AA for entry into cyclooxygenase or lipoxygenase pathways (24).

We could find no evidence that LIN was modified in these cells. LIN (18:2n-6) is converted by many cells to AA (20:4n-6) through a sequence of desaturation and elongation steps. We found no accumulation of AA or any of the intermediates of this process. These data are consistent, however, with the observations that certain tumors or tumor cell lines are deficient in the Δ6-desaturase activity, the first step in this process (24). Reduced Δ6-desaturase activity could also explain the inability of the cells to convert EPA to DHA. Conversion of EPA to DHA is presently believed to occur *via* two successive elongations (to 24:5n-3), insertion of a double bond *via* Δ6 desaturase (forming 24:6n-3), followed by one round of peroxisomal β-oxidation forming 22:6n-3. Isotopic conversion studies would be required to confirm this.

The present study demonstrated significant differences in the affinity of labeled fatty acids for the different phospholipid species. Studies by Hatala *et al.* (27) examining the incorporation of LIN and EPA into breast cancer cells found that 65% of [^{14}C]LIN was recovered in phosphatidylcholine after 24 h. This is very similar to the 60% we observed with [^{3}H]LIN in CT-26 cells after the same period of time. Their studies were different with respect to incorporation of [^{14}C]EPA: they found 58% in phosphatidylethanolamine, whereas we see considerably less EPA recovered in the ethanolamine phospholipids. It has been speculated that plasmalogen phospholipids serve as a sink for PUFA (28–30). Some studies have demonstrated increased selectivity of n-3 fatty acids for plasmalogens (31–33), while others have found incorporation to be dependent on chain length and degree of unsaturation (34). Our studies demonstrate that, in CT-26 cells in culture, chain length influences incorporation into plasmalogens, since DHA incorporation into plasmenylethanolamine is greater than AA and EPA, which in turn are greater than LIN. However, incorporation of AA into plasmalogen species was greater than EPA. This is in contrast to some studies, which showed increased incorporation with increasing unsaturation (34).

Prostaglandins, which are derived from membrane phospholipids, affect the rate of growth as well as the ability of tumors to metastasize (35,36). It is believed that ethanolamine plasmalogens are involved in the release of PUFA to form oxidized fatty acid derivatives such as leukotrienes and prostaglandins (37). Our data indicate that, in CT-26, DHA has a higher affinity for plasmenylethanolamine than the other PUFA studied. Other studies also have demonstrated that plasmalogens contain high levels of DHA (29,38). Certain tumors, including colon tumors, contain altered levels of plasmalogens (39). It is possible that n-3 fatty acids compete with arachidonic acid for incorporation into plasmalogens and, once incorporated, these cells produce fewer or different prostaglandins resulting in a reduced rate of cell growth and metastasis.

ACKNOWLEDGMENTS

This work was supported by NIH grant CA57684 (SAB), American Institute for Cancer Research grant 93-B34 (SAB), and NIH grant GM 50571 (RAZ).

REFERENCES

1. Reddy, B.S., and Maruyama, H. (1986) Effect of Dietary Fish Oil on Azoxymethane-Induced Colon Carcinogenesis in Male F344 Rats, *Cancer Res. 46*, 3367–3370.
2. Latham, P., Lund, E.K., and Johnson, I.T. (1999) Dietary n-3 PUFA Increases the Apoptotic Response to 1,2-Dimethylhydrazine, Reduces Mitosis and Suppresses the Induction of Carcinogenesis in the Rat Colon, *Carcinogenesis 20*, 645–650.
3. Reddy, B.S., Burill, C., and Rigotty, J. (1991) Effect of Diets High in Omega-3 and Omega-6 Fatty Acids on Initiation and Postinitiation Stages of Colon Carcinogenesis, *Cancer Res. 51*, 487–491.
4. Caygill, C.P., and Hill, M.J. (1995) Fish n-3 Fatty Acids and Human Colorectal and Breast Cancer Mortality, *Eur. J. Cancer Prev. 4*, 329–332.
5. Cannizzo, F., and Broitman, S.A. (1989) Postpromotional Effects of Dietary Marine or Safflower Oils on Large Bowel or Pulmonary Implants of CT-26 in Mice, *Cancer Res. 49*, 4289–4294.

6. Iigo, M., Nakagawa, T., Ishikawa, Y., Asamoto, M., Kazawa, K., Araki, E., and Tsuda, H. (1997) Inhibitory Effects of Docosahexaenoic Acid on Colon Carcinoma 26 Metastasis to the Lung, *Br. J. Cancer 75*, 650–655.
7. Reddy, B.S., (1992) Dietary Fat and Colon Cancer: Animal Model Studies, *Lipids 27*, 807–813.
8. Jurkowski, J.J., and Cave, W.T., Jr. (1985) Dietary Effects of Menhaden Oil on the Growth and Membrane Lipid Composition of Rat Mammary Tumors, *J. Natl. Cancer Inst. 74*, 1145–1150.
9. Lindner, M.A. (1991) A Fish Oil Diet Inhibits Colon Cancer in Mice, *Nutr. Cancer 15*, 1–11.
10. Marshall, L.A., and Jonston, P.V. (1982) Modulation of Tissue Prostaglandin Synthesizing Capacity by Increased Ratios of Dietary Alpha-Linolenic Acid to Linoleic Acid, *Lipids 17*, 905–913.
11. Bilsen, M.V., and Van der Vusse, G.J. (1995) Phospholipase-A2-Dependent Signalling in the Heart, *Cardiovasc. Res. 30*, 518– 529.
12. Folch, J., Lees, M., and Sloane-Stanley, G.H. (1957) A Simple Method for the Isolation and Purification of Total Lipids, *J. Biol. Chem. 226*, 497–507.
13. Esko, J., Nishijima, M., and Raetz, C.R.H. (1982) Animal Cells Dependent on Exogenous Phosphatidylcholine for Membrane Biogenesis, *Proc. Natl. Acad. Sci. USA 79*, 1698–1702.
14. Bligh, E.G., and Dyer, W.J. (1959) A Rapid Method of Total Lipid Extraction and Purification, *Can. J. Biochem. Physiol. 37*, 911– 917.
15. Esko, J.D., and Raetz, C.R.H. (1980) Mutants of Chinese Hamster Ovary Cells with Altered Membrane Phospholipid Composition. Replacement of Phosphatidylinositol by Phosphatidylglycerol in a Myo-inositol Auxotroph, *J. Biol. Chem. 255*, 4474–4480.
16. Chen, Y.Q., Liu, B., Tang, D.G., and Honn, K.V. (1992) Fatty Acid Modulation of Tumor Cell-Platelet–Vessel Wall Interaction, *Cancer Metastasis Rev. 11*, 389–409
17. Rose, D.P., and Hatala, M.A. (1994) Dietary Fatty Acids and Breast Cancer Invasion and Metastasis, *Nutr. Cancer 21*, 103–111.
18. Kort, W.J., Weijma, I.M., Bijma, A.M., van Schalkwijk, W.P., Vergroesen, A.J., and Westbroek, D.L. (1987) Omega-3 Fatty Acids Inhibiting the Growth of a Transplantable Rat Mammary Adenocarcinoma, *J. Natl. Cancer Inst. 79*, 593–599.
19. Connolly, J.M., and Rose, D.P. (1993) Effects of Fatty Acids on Invasion Through Reconstituted Basement Membrane ('Matrigel') by a Human Breast Cancer Cell Line, *Cancer Lett. 75*, 137–142.
20. Rose, D.P., and Connolly, J.M. (1991) Effects of Fatty Acids and Eicosanoid Synthesis Inhibitors on the Growth of Two Human Prostate Cancer Cell Lines, *Prostate 18*, 243–254.
21. Mengeaud, V., Nano, J.L., Fournel, S., and Rampal, P. (1992) Effects of Eicosapentaenoic Acid, Gamma-linolenic Acid and Prostaglandin E1 on Three Human Colon Carcinoma Cell Lines, *Prostaglandins Leukotrienes Essen. Fatty Acids 47*, 313–319.
22. Sobajima, T., Tamiya-Koizumi, K., Ishihara, H., and Kojima, K. (1986) Effects of Fatty Acid Modification of Ascites Tumor Cells on Pulmonary Metastasis in Rat, *Jpn. J. Cancer Res. 77*, 657–663.
23. Fulton, A.M., and Hepner, G.H. (1985) Relationships of Prostaglandin E and Natural Killer Sensitivity to Metastatic Potential in Murine Mammary Adenocarcinomas, *Cancer Res. 45*, 4779–4784.
24. Rosenthal, M.D. (1987) Fatty Acid Metabolism of Isolated Mammalian Cells, *Prog. Lipid Res. 26*, 87–124.
25. Tebbey, P.W., and Butke, T.M. (1984) Arachidonic Acid Regulates Unsaturated Fatty Acid Synthesis in Lymphocytes by Inhibiting Stearoyl-CoA Desaturase Gene Expression, *Biochim. Biophys. Acta 796*, 205–217.
26. Banerjee, N., and Rosenthal, M.D. (1986) Elongation of C20 Polyunsaturated Fatty Acids by Human Skin Fibroblasts, *Biochim. Biophys. Acta 878*, 404–411.
27. Hatala, M.A., Rayburn, J., and Rose, D.P. (1994) Comparison of Linoleic Acid and Eicosapentaenoic Acid Incorporation into Human Breast Cancer Cells, *Lipids 29*, 831–837.
28. Ford, D.A., and Gross, R.W. (1994) The Discordant Rates of *sn*-1 Aliphatic Chain and Polar Head Group Incorporation into Plasmalogen Molecular Species Demonstrate the Fundamental Importance of Polar Head Group Remodeling in Plasmalogen Metabolism in Rabbit Myocardium, *Biochemistry 33*, 1216–1222.
29. Gaposchkin, D.P., and Zoeller, R.A. (1999) Plasmalogen Status Influences Docosahexaenoic Acid Levels in a Macrophage Cell Line: Insights Using Ether Lipid-Deficient Variants, *J. Lipid Res. 40,* 495–503.
30. Horrocks, L.A., and Sharma, M. (1982) Plasmalogens and *O*-Alkyl Glycerophospholipids, in *Phospholipids* (Hawthorne, J.N., and Ansell, G.B., eds.), pp. 51–93, Elsevier Biomedical Press, New York.
31. Blank, M.L., Smith, Z.L., Joseph Lee, Y., and Snyder, F. (1989) Effects of Eicosapentaenoic and Docosahexaenoic Acid Supplements on Phospholipid Composition and Plasmalogen Biosynthesis in P388D1 Cells, *Arch. Biochem. Biophys. 269*, 603–611.
32. Robinson, D.R., Xu, L., Knoell, T., Tateno, S., and Olesiak, W. (1993) Modification of Spleen Phospholipid Fatty Acid Composition by Dietary Fish Oil and by n-3 Fatty Acid Ethyl Esters, *J. Lipid Res. 34*, 1423–1434.
33. Blank, M.L., Smith, Z.L., Cress, E.A., and Snyder, F. (1994) Molecular Species of Ethanolamine Plasmalogens and Transacylase Activity in Rat Tissues Are Altered by Fish Oil Diets, *Biochim. Biophys. Acta 1214*, 295–302.
34. Thomas, S.E., Byers, D.M., Palmer, F.B., Spence, M.W., and Cook, H.W. (1990) Incorporation of Polyunsaturated Fatty Acids into Plasmalogens, Compared to Other Phospholipids of Cultured Glioma Cells, Is More Dependent on Chain Length Than on Selectivity Between (n-3) and (n-6) Families, *Biochim. Biophys. Acta 1044*, 349–356.
35. Bennett, A., Houghton, J., Leaper, D.J., and Stamford, I.F. (1978) Tumor Growth and Response to Treatment: Beneficial Effect of the Prostaglandin Synthesis Inhibitor Flurbiprofen, *Br. J. Pharmacol. 63*, 356P–357P.
36. Lunch, N.R., and Salomon, J-C. (1979) Tumor Growth Inhibition and Potentiation of Immunotherapy by Indomethacin in mice, *J. Natl. Cancer Inst. 62*, 117–121.
37. Farooqui, A.A., Yang, H.C., and Horrocks, L.A. (1995) Plasmalogens, Phospholipases A2 and Signal Transduction, *Brain Res. Rev. 21*, 152–162.
38. Favreliere, S., Barrier, L., Durand, G., Chalon, S., and Tallineau, C. (1998) Chronic Dietary n-3 Polyunsaturated Fatty Acids Deficiency Affects the Fatty Acid Composition of Plasmenylethano-lamine and Phosphatidylethanolamine Differently in Rat Frontal Cortex, Striatum, and Cerebellum, *Lipids 33*, 401–407.
39. Dueck, D.A., Chan, M., Tran, K., Wong, J.T., Jay, F.T., Littman, C., Stimpson, R., and Choy, P.C. (1996) The Modulation of Choline Phosphoglyceride Metabolism in Human Colon Cancer, *Mol. Cell. Biochem. 162*, 97–103.

[Received February 15, 1999, and in final revised form and accepted January 13, 2000]

Accumulation of Docosahexaenoic Acid in Phosphatidylserine Is Selectively Inhibited by Chronic Ethanol Exposure in C-6 Glioma Cells

Hee-Yong Kim* and Jillonne Hamilton

Section of Mass Spectrometry, Laboratory of Membrane Biochemistry and Biophysics, National Institute on Alcohol Abuse and Alcoholism, National Institutes of Health, Rockville, Maryland 20852

ABSTRACT: Neuronal membranes are highly enriched with docosahexaenoic acid (22:6n-3), and its content can be altered by ethanol consumption. We have previously reported that the 22:6n-3 status in membrane affects the biosynthesis of phosphatidylserine (PS), a phospholipid class which contains an exceptionally high proportion of 22:6n-3. The aim of the present study is to investigate the effect of chronic ethanol exposure on PS accumulation in relation to the 22:6n-3 status. C-6 glioma cells were enriched with 25 μM 22:6n-3 for 48 h and the PS accumulation was first evaluated in comparison to nonenriched cells as well as cells enriched with arachidonic acid (20:4n-6). Electrospray liquid chromatography–mass spectrometry analysis revealed that cells treated with 22:6n-3 showed significantly higher accumulation of PS in comparison to nonenriched or 20:4n-6-enriched cells, primarily due to an increase of 1-stearoyl-2-docosahexaenoyl-glycerophosphoserine (18:0,22:6-PS). Chronic ethanol exposure selectively affected the accumulation of PS in 22:6n-3-enriched cells. After cells were exposed to 20 or 50 mM ethanol for 4 wk, accumulation of 18:0,22:6-PS upon 22:6n-3 supplementation was significantly lower, resulting in a drastic reduction of total PS. Concomitantly, ethanol-treated cells showed lower incorporation of serine in comparison to control cells. From these data, it was concluded that supplementation of cells with 22:6n-3 promotes the accumulation of PS and chronic ethanol treatment diminishes this effect at least in part through impaired serine incorporation processes. Attenuated accumulation of 22:6n-3 in PS and the reduction of PS thus may have significant implications in pathophysiological effects of ethanol, especially in tissues with abundant 22:6n-3.

Paper no. L8334 in *Lipids 35,* 187–195 (February 2000).

*To whom correspondence should be addressed at Section of Mass Spectrometry, LMBB, NIAAA, NIH, 12420 Parklawn Dr., Rm. 114, Rockville, MD 20852. E-mail: hykim@nih.gov

Abbreviations: 22:6n-3, docosahexaenoic acid; 20:4n-6, arachidonic acid; 22:4n-6, adrenic acid; DMEM, Dulbecco's modified Eagle's medium; FBS, fetal bovine serum; GC, gas chromatography; HPLC, high-performance liquid chromatography; PS, phosphatidylserine; PC, phosphatidylcholine; PE, phosphatidylethanolamine; PLE, plasmalogen; PI, phosphatidylinositol; 18:0,22:6-PS, 1-stearoyl-2-docosahexaenoyl-glycerophosphoserine; 18:0,20:4-PC, 1-stearoyl-2-arachidonyl-glycerophosphocholine; 16:0,20:4-PC, 1-palmitoyl-2-arachidonyl-glycerophosphocholine; 16:0,22:6-PE, 1-palmitoyl-2-docosahexaenoyl-glycerophosphoethanolamine; TLC, thin-layer chromatography.

Docosahexaenoic acid (22:6n-3) is highly concentrated in neuronal membranes (1,2). Normal brain development, visual acuity, and retinal function have been suggested to correlate with the enrichment of 22:6n-3 in neuronal tissues (1–5). This fatty acid represents a particularly high proportion in phosphatidylserine (PS) (1,2). In mammalian cells, PS is synthesized from phosphatidylethanolamine (PE) or phosphatidylcholine (PC) by base exchange reaction (6). Conversely, PS can be metabolized to PE or PC by base exchange reaction or to PE by PS decarboxylation (7). Recently, we have shown that the status of membrane 22:6n-3 affects PS biosynthesis in brain microsomes and C-6 glioma cells, implying 22:6n-3 is a modulator of PS accumulation (8). Involvement of PS in the activation of protein kinases (9,10) suggests that alteration in PS accumulation in cell membranes may have significant implication in cell signaling.

High levels of 22:6n-3 appear to be well maintained in neuronal cells. Maintenance of the membrane lipid profile is thought to be achieved through dynamic but tightly regulated biosynthetic and remodeling processes, including acylation, deacylation, and base exchange reactions. Ethanol is believed to exert its effect through the perturbation of structure and function of cell membranes. The results regarding the effect of ethanol on the membrane polyunsaturate content have been inconsistent (11), primarily due to differences in animal models and experimental conditions employed. Nevertheless, it has been reported that ethanol can alter the lipid composition in neuronal membranes with possible detrimental consequences in neuronal function. The decrease of polyunsaturates, especially 22:6n-3, has been demonstrated in the rodent brain (12) as well as its subcellular fractions including microsomes (13), synaptosomes (14,15), synaptic plasma membranes (16,17), and mitochondria (18). It has been also reported that *in utero* ethanol exposure decreased PS biosynthesis in rat pup cerebellum (19). While it is often difficult to find any significant effect of ethanol on the total lipid content, it may be possible to observe the effect of ethanol associated with particular phospholipid molecular species. The demonstration that PS biosynthetic activity is influenced both by the 22:6n-3 status (8) and by ethanol (19) and that ethanol can

deplete 22:6n-3 from neuronal membranes presents a possibility that the effect of ethanol may be indicated more prominently in PS molecular species.

In this study, we investigated the effect of chronic ethanol exposure in relation to the 22:6n-3 status using C-6 cells as a model system. Since cells under the normal culture conditions are deficient in 22:6n-3 fatty acids, cells were enriched with 22:6n-3 and the effect of enrichment on the phospholipid profile was first examined using reversed-phase liquid chromatography/electrospray mass spectrometry. The effect of ethanol on the accumulation of individual molecular species was subsequently evaluated. We report here that the accumulation of PS is considerably enhanced by 22:6n-3 in comparison to nonenriched or arachidonic acid (20:4n-6)-enriched cells and that long-term exposure to ethanol diminishes the effect of 22:6n-3 on PS accumulation. Ethanol treatment concomitantly decreased serine incorporation, providing it as a mechanism for the observed PS reduction.

EXPERIMENTAL PROCEDURES

Materials. Deuterium-labeled or nonlabeled phospholipid standards were either purchased from or custom-synthesized by Avanti Polar Lipids (Alabaster, AL). [^{3}H]Serine (100 Ci/mmol) was obtained from New England Nuclear (Wilmington, DE). Dulbecco's modified Eagle's medium (DMEM), fetal bovine serum (FBS), and other tissue culture reagents were purchased from Gibco Life Technologies Laboratories (Grand Island, NY). Silica gel 60 plates were obtained from Analtech (Newark, DE). All the solvents were high-performance liquid chromatography (HPLC) grade purchased from EM Scientific (Gibbstown, NJ). The phospholipid standards were calibrated by phosphorus assay (20) or gas chromatography (GC) analysis as described earlier (21).

Cell culture conditions. The rat C-6 glioma cell line was obtained from the American Type Cell Culture (ATCC CCL-107; Rockville, MD) and maintained in a culture medium consisting of DMEM supplemented with 10% FBS. Cells were grown in 20 mL of this culture medium in 75-cm^2 Corning culture flasks in a humidified environment of 5% CO_2, 95% air at 37°C. To investigate the effect of long-term exposure to ethanol, the medium was replaced daily with fresh medium containing ethanol at 20 or 50 mM concentrations for 4 wk as described earlier (22). During this period, cells were subcultured every 3–4 d upon confluency. Control cells received the same treatment with ethanol-free medium.

Incubation with polyunsaturated fatty acids. C-6 glioma cells were cultured in DMEM containing 10% FBS and 0, 20, or 50 mM ethanol by changing the medium daily. After 4 wk of ethanol treatment, 4×10^5 cells/well were subcultured in six-well plates for 24 h and then incubated with DMEM containing 10% FBS and 25 μM (final concentration) 22:6n-3 or 20:4n-6 for 48 h in the presence of 40 μM vitamin E as an antioxidant. The media with 10% FBS alone contained 9 μM 20:4n-6 and 4 μM 22:6n-3. At the end of the incubation period, unincorporated fatty acids were washed off with DMEM containing 2% bovine serum albumin and the cells were scraped on ice to minimize the free fatty acid release by mechanical disturbance (23). Aliquots were taken from the cell suspension for protein assay using bicinchoninic acid method (24) and for counting cell numbers using a hemacytometer. Lipids were extracted according to Bligh and Dyer (25) in the presence of tricosanoic acid (23:0) for GC analysis or deuterium-labeled phospholipid standards for phospholipid analysis by electrospray mass spectrometry. Separately, cells were incubated with 0.5 μCi of [^{3}H]20:4n-6 or [1-^{14}C]22:6n-3 (at the final concentration adjusted to 25 μM) under the same condition described above. At 5, 11, 24, and 48 h, cells were harvested and cell lipids were extracted. Aliquots were taken for measurement of radioactivity. Lipid extracts were subjected to thin-layer chromatography (TLC) using a solvent system containing hexane/diethylether/formic acid (90:60:4, by vol). Separated lipids were identified by comparison with standards visualized by exposure to iodine. Radioactivity for each lipid class was determined by liquid scintillation after scraping off the individual TLC spots.

Phospholipid molecular species analysis. Phospholipid molecular species were separated and determined using reversed-phase HPLC/electrospray mass spectrometry using similar conditions described previously (8,26). A C-18 column (Phenomenex, Torrance, CA; 5 μ, 2.0 mm i.d. × 15 cm) was used with mobile phase containing water/0.5% ammonium hydroxide in methanol/hexane changing from 12:88:0 to 0:88:12 in 17 min after holding at the initial composition for 3 min at a flow rate of 0.4 mL/min (27). A Hewlett-Packard (Palo Alto, CA) HPLC–MS series 1100 MSD instrument was employed to detect the separated phospholipid molecular species. For electrospray ionization, the capillary temperature was set at 350°C while the capillary exit voltage was set at 200 V. The drying gas flow rate and the nebulizing gas pressure were set at 13 L/min and 32 psi, respectively. Quantitation was performed in the presence of d_{35}-1-stearoyl-2-arachidonyl-glycerophosphocholine (18:0,20:4-PC), PE, and d_{35}-1-stearoyl-2-docosahexaenoyl-glycerophosphoserine (18:0,22:6-PS) as internal standards. The amount of phospholipid species was obtained based on the area ratio calculated against the standard of the same class.

Fatty acid analysis. Lipid extract was transmethylated according to Morrison and Smith (28) and analyzed using a Hewlett-Packard gas chromatograph and a J&W (Folsom, CA) DB-FFAP capillary column (30 m × 0.25 mm i.d., with a 0.25 μm film thickness) with hydrogen gas as the carrier gas (55 cm/s), as described earlier (21). The oven temperature was programmed from 130 to 175°C at 4°C/min and then raised to 240°C at 30°C/min. The injector and detector temperatures were set at 240°C. The mixture of transmethylation reagent (BF_3-methanol) and lipid extract was purged with argon prior to heating. Under this condition, BF_3-transmethylation did not affect the 22:6n-3 recovery (99 ± 0.3%) determined by re-transmethylating 22:6n-3 methylester in the presence of 23:0. Under the nitrogen atomosphere, the recovery of 22:6n-3 was 96 ± 0.5%.

Serine incorporation. Control and ethanol-treated C-6 glioma cells (4×10^5 cells/well) were incubated with [^{3}H]serine (0.5 μCi) in DMEM with 10% FBS for 48 h in the presence or absence of 25 μM 22:6n-3. At the end of incubation, the medium was discarded and cells were washed with DMEM containing 2% bovine serum albumin. The cells were scraped in 1 mL of BHT/methanol and the incorporated radioactivity was determined after the extraction of total cell lipids. Cell lipids were separated using a slightly modified two-step TLC method by Smith and Waite (29). The plates were chromatographed halfway up in a phospholipid system containing chloroform/(methanol with 50 μg/mL BHT)/glacial acetic acid/water (100:75:7:4, by vol), taken out and dried briefly under a stream of nitrogen. The plates were then developed again completely in a solvent system containing hexane/diethylether/formic acid (90:60:4, by vol). Radioactivity for each lipid class was determined by liquid scintillation after scraping off the individual TLC spots.

RESULTS

Incorporation of 22:6n-3 and 20:4n-6. C-6 glioma cells quickly incorporated both 22:6n-3 and 20:4n-6 fatty acids at 25 μM with no apparent toxic effect on cell survival as evaluated by trypan blue staining. The total incorporation of radioactive fatty acids steadily increased during 24 h of incubation and leveled off thereafter (data not shown) as has been reported previously (30). Both fatty acids were initially incorporated into neutral lipids, but gradually remodeled into the phospholipid fraction so that after 24 h over 90% of the total incorporated polyunsaturated fatty acids was found in phospholipids. After 48 h of incubation, 92.7 ± 0.8 or 92.3 ± 0.4% of total cellular radioactivity from 20:4n-6 or 22:6n-3 was found in phospholipid fraction, respectively. Incubation of cells with 22:6n-3 for 48 h increased the composition of 22:6n-3 in total lipids from 1.4 ± 0.1 to 10.9 ± 0.2% while 20:4n-6 increased from 4.0 ± 0.1 to 12.4 ± 0.2% after supplementation with 20:4n-6 (Table 1). Under the conditions employed, a significant proportion of 20:4n-6 was found to be chain-elongated to adrenic acid (22:4n-6), and the total content of 22:4n-6 reached 6.3 ± 0.2%. Concomitant decreases of 18:1n-9 compensated the increase of polyunsaturated fatty acids in cells treated with polyunsaturated fatty acids. Except for slight increases in 22:5n-3 and 20:5n-3 in 22:6n-3-treated cells, the composition of other fatty acids was not affected significantly.

Phospholipid molecular species analysis. Phospholipid molecular species analysis was performed using electrospray mass spectrometry as described earlier (8,26). It was found that 22:6n-3 was mostly incorporated into 18:0,22:6-PS followed by 18:0,22:6-PE plasmalogen, 1-palmitoyl-2-docosahexanoyl-glycerophosphocholine (16:0,22:6-PC), 18:0,22:6-PE and 16:0,22:6-PE plasmalogen and PE, in descending order (Fig. 1A). In contrast, 20:4n-6 was particularly enriched in 1-palmitoyl-2-arachidonyl-glycerophosphocholine (16:0,20:4-PC) followed by 18:0,20:4-PE, PC and PS, 16:0,20:4-PE and 18:1,20:4-PE species (Fig. 1B). In comparison to control cells, higher plasmalogen contents also were observed after enrichment with 20:4n-6. The content of 16:0,20:4- and 18:0,20:4-PE plasmalogen was raised from 1.2 ± 0.01 and 1.8 ± 0.2 pmol/μg protein to 2.2 ± 0.2 and 2.2 ± 0.2 pmol/μg protein, respectively. In addition, 22:4n-6, an elongation product of 20:4n-6, appeared in PE plasmalogen as 18:0,22:4 species (from the nondetectable level to 2.4 ± 0.7 pmol/μg protein).

Enrichment of cells with polyunsaturated fatty acids affected the distribution of glycerophospholipid classes although the absolute levels of total glycerophospholipids did not alter significantly (Fig. 2). The absolute level (Fig. 2A) as well as the mole percentage (Fig. 2B) of PS was higher after the supplementation with 20:4n-6 or 22:6n-3. In the cells enriched with 22:6n-3 in particular, the total PS content was more than twice as high in comparison to nonenriched cells (Table 2). The elevated level of total PS with 22:6n-3 enrichment was primarily due to the marked accumulation of 18:0,22:6-PS as this species changed from 0.67 to 8.00 pmol/μg protein. The observed higher PS content appeared to be compensated by slightly but significantly reduced total PC contents (Fig. 2), mainly due to lower accumulation of the PC

TABLE 1
Fatty Acid Distribution in Total Lipids After Enrichment with Polyunsaturated Fatty Acids for 48 h[a]

Fatty acids	Nonenriched	+20:4n-6	+22:6n-3
18:1n-9	31.7 ± 0.7	16.9 ± 0.4***	21.2 ± 1.3**
20:4n-6	4.0 ± 0.1	12.4 ± 0.2***	3.4 ± 0.1*
22:4n-6	0.8 ± 0.1	6.3 ± 0.2***	0.5 ± 0.1*
22:6n-3	1.4 ± 0.1	1.5 ± 0.1	10.9 ± 0.2***
22:5n-3	1.2 ± 0.1	1.5 ± 0.1*	2.7 ± 0.1***
20:5n-3	ND	ND	3.0 ± 0.1***

[a]Total fatty acid profile after enrichment of C-6 cells with 25 μM 20:4n-6 or 22:6n-3 for 48 h. ND = not detected. Data are the mean of three determinations ± SD. Asterisks denote that the values are significantly different from values of nonenriched control; **$P < 0.01$ and ***$P < 0.001$. The profile of other fatty acids was not significantly altered after the enrichment.

TABLE 2
Effect of Fatty Acid Enrichment on Phosphatidylserine (PS) Molecular Species[a]

PS	Nonenriched	+20:4n-6	+22:6n-3
16:0/18:1	0.60 ± 0.01	0.49 ± 0.04*	0.55 ± 0.04
18:0/18:1	3.14 ± 0.03	2.01 ± 0.10**	1.40 ± 0.22*
16:0/20:4	0.14 ± 0.02	ND**	ND**
18:0/20:4	0.66 ± 0.19	3.42 ± 0.34**	1.00 ± 0.08
16:0/22:6	ND	ND	0.73 ± 0.11*
18:0/22:6	0.67 ± 0.08	1.06 ± 0.25	8.00 ± 0.03***
16:0/22:4	ND	ND	ND
18:0/22:4	ND	1.04 ± 0.13**	ND
Total PS	5.21 ± 0.43	8.04 ± 0.62*	11.68 ± 0.05***

[a]Phosphatidylserine molecular species observed after the enrichment of C-6 glioma cells with 25 μM 20:4n-6 or 22:6n-3 for 48 h. The figures represent pmol/μg protein (mean ± SD). Statistical analysis was performed in comparison to values from nonenriched control cells using Student's *t*-test: *$P < 0.05$; **$P < 0.01$; ***$P < 0.001$.

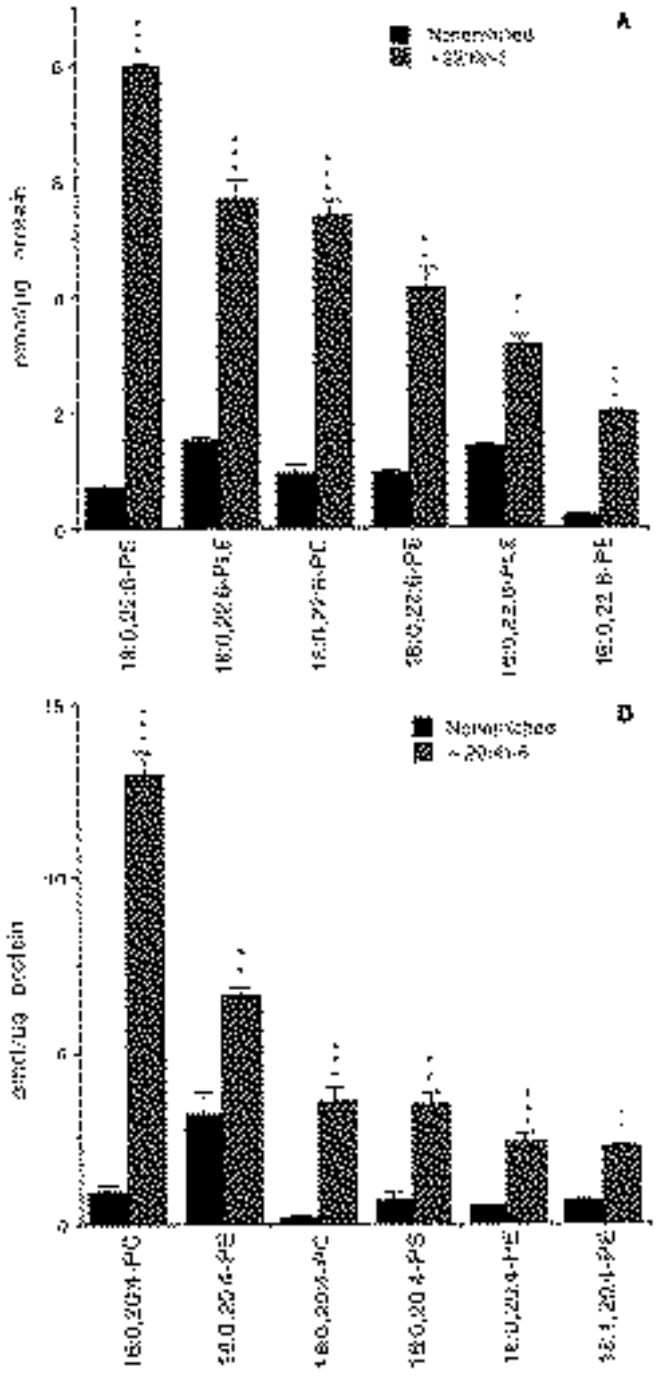

FIG. 1. The major molecular species observed after supplementation of cells with 25 μM (A) 22:6n-3 or (B) 20:4n-6 for 48 h. The phospholipid molecular species were determined by reversed phase high-performance liquid chromatography (HPLC)/electrospray mass spectrometry. The results are the mean ± SD of triplicates. Statistical analysis was performed in comparison to values from nonenriched control cells using Student's *t*-test: $^{**}P < 0.01$; $^{***}P < 0.001$. PS, phosphatidylserine; PE, phosphatidylethanolamine; PC, phosphatidylcholine; PLE, plasmalogen.

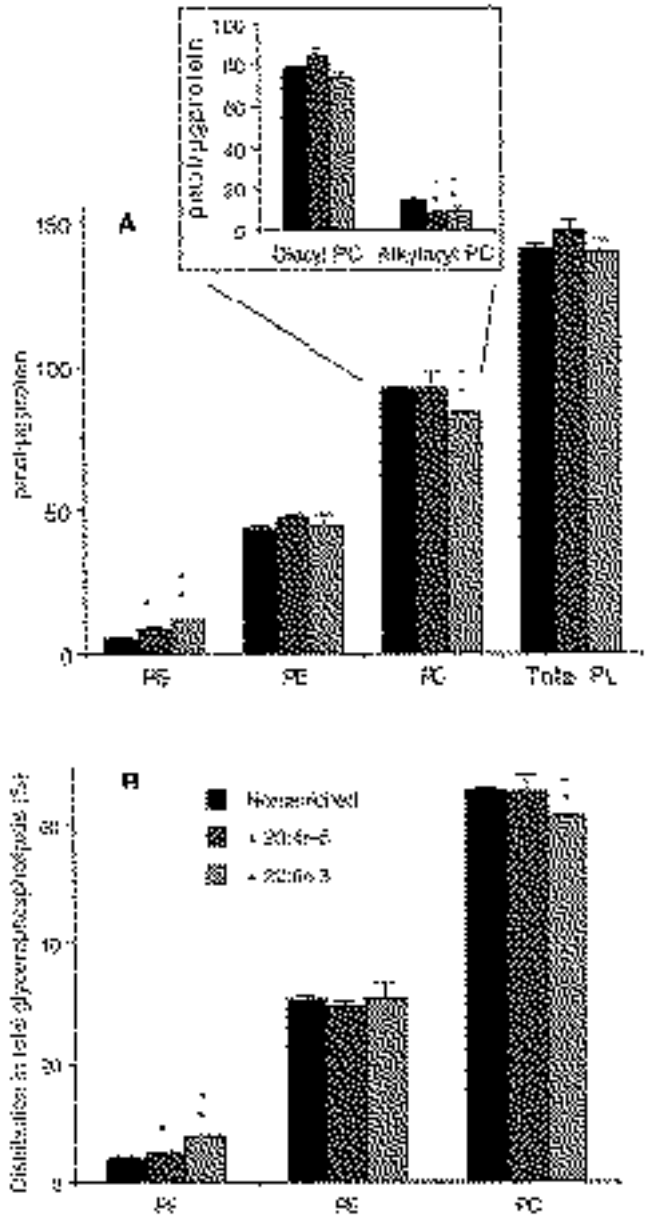

FIG. 2. Effect of supplementation on the phospholipid class distribution. C-6 cells were enriched with 25 μM 20:4n-6 or 22:6n-3 for 48 h and the phospholipid (PL) molecular species were determined by reversed-phase HPLC/electrospray mass spectrometry. The results are the mean ± SD of triplicates and presented as (A) pmol/μg protein and (B) percentage of total glycerophospholipids. Statistical analysis was performed in comparison to values from nonenriched control cells using Student's *t*-test: $^{*}P < 0.05$; $^{**}P < 0.01$. The effect of fatty acid supplementation on phosphatidylcholine subclasses is shown in the inset. See Figure 1 for abbreviation.

species containing 18:1n-9. In cells enriched with 20:4n-6, elevation of 18:0,20:4 and 18:0,22:4 species was the major cause for the slight increase of total PS. Supplementation of cells with 20:4n-6 or 22:6n-3 decreased 18:0,18:1-PC from 32 ± 2 to 17 ± 2 or 18 ± 2 pmol/μg protein and 16:0,18:1-alkylacyl PC from 14 ± 1 to 7 ± 1 or 8 ± 1 pmol/μg protein, respectively. Since incorporation of 22:6n-3 into PC was considerably less than that of 20:4n-6, the total PC content was significantly lower with 22:6n-3 enrichment but did not change significantly in 20:4n-6-treated cells. The content of

total alkylacyl-PC species, where 18:1n-9 is the major component, was also significantly lower after the enrichment with 20:4n-6 or 22:6n-3 (Fig. 2A inset).

Effect of ethanol on the accumulation of polyunsaturated species. The treatment of cells with ethanol at 20 or 50 mM for 4 wk showed lower long-chain polyunsaturate contents in 20:4n-6- or 22:6n-3-enriched cells in comparison to non-ethanol-treated cells while much less change was observed in nonenriched cells (Fig. 3). The 18:1n-9 content was raised concomitantly in ethanol-treated cells, as has been observed frequently after chronic ethanol exposure (18).

The observed higher levels of 18:1n-9 after ethanol exposure were reflected by a slight elevation of PC, especially due to the higher levels of 18:0,18:1- and 18:1,18:1-PC and 16:0,18:1-alkylacyl PC (data not shown). The decreased content of 22:6n-3 by ethanol was associated with specific phospholipid molecular species in 22:6n-3-enriched cells. Conversely, in 20:4n-6-treated cells, 20:4n-6-containing species either were decreased or remained unchanged by ethanol. Since the majority of phospholipid species containing either 22:6n-3 or 20:4n-6 were coupled to either 18:0 or 16:0 fatty acid at the *sn*-1 position, only these species are presented in

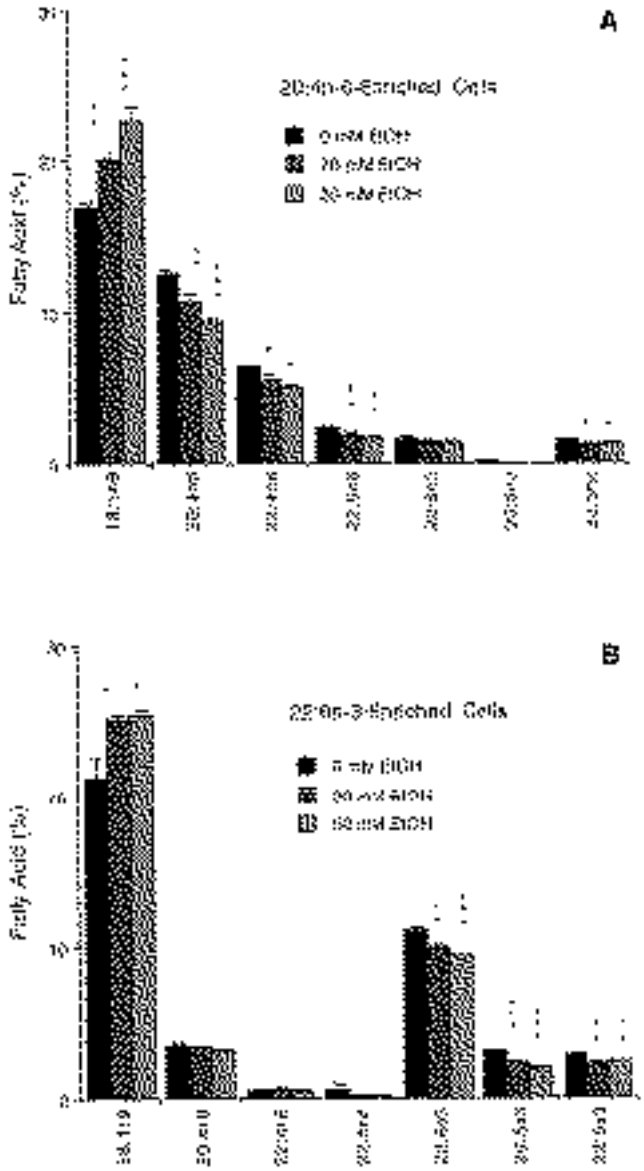

FIG. 3. Effect of long-term ethanol exposure on the incorporation of (A) 22:6n-3 and (B) 20:4n-6 into C-6 glioma cells. Cells were exposed to 0, 20, or 50 mM ethanol for 4 wk, and the incorporation of 25 μM (A) 20:4n-6 or (B) 22:6n-3 was monitored for 48 h as described in the Experimental Procedures section. The fatty acid distribution in total lipids are presented as the mean ± SD of triplicates. Statistical analysis was performed in comparison to values from control cells (0 mM ethanol) using Student's *t*-test: $^{*}P < 0.05$; $^{**}P < 0.01$; $^{***}P < 0.001$.

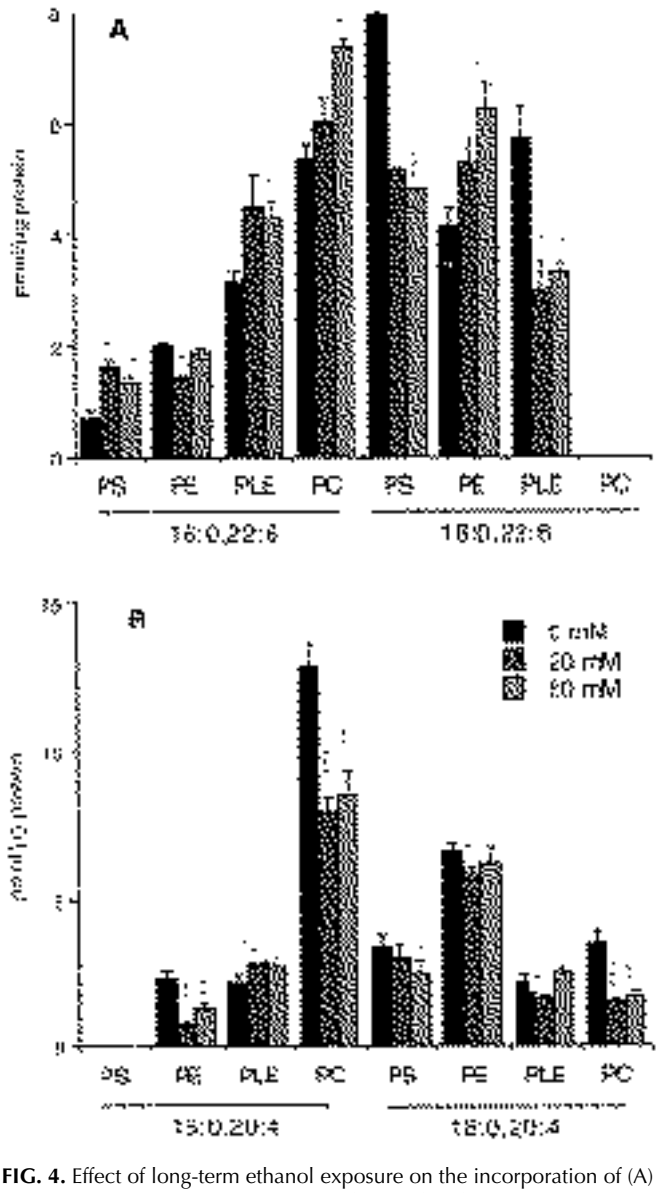

FIG. 4. Effect of long-term ethanol exposure on the incorporation of (A) 22:6n-3 or (B) 20:4n-6 into major phospholipid molecular species. Cells were exposed to 0, 20, or 50 mM ethanol for 4 wk and further incubated with 25 μM (A) 22:6n-3 or (B) 20:4n-6 for 48 h. Phospholipid molecular species were determined by reversed-phase HPLC/electrospray mass spectrometry. The results are the mean ± SD of triplicates. Statistical analysis was performed in comparison to values from control cells (0 mM ethanol) using Student's *t*-test: $^{*}P < 0.05$; $^{**}P < 0.01$; $^{***}P < 0.001$. See Figure 1 for abbreviations.

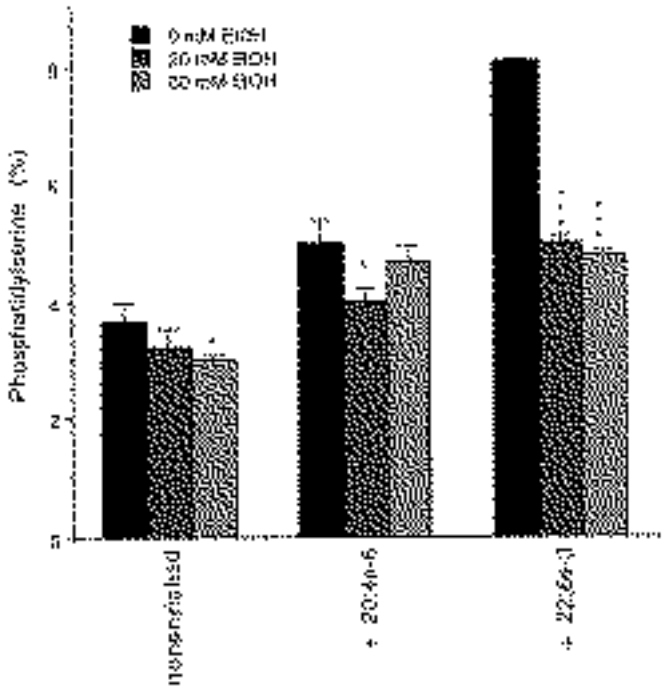

FIG. 5. Effect of long-term ethanol exposure on phosphatidylserine accumulation. Cells were exposed to 0, 20, or 50 mM ethanol for 4 wk and further incubated with 25 μM 20:4n-6 or 25 μM 22:6n-3 for 48 h. Phospholipid molecular species were determined by reversed-phase HPLC/electrospray mass spectrometry. The results are the mean ± SD of triplicates. Statistical analysis was performed in comparison to values from control cells (0 mM ethanol) using Student's *t*-test: $*P < 0.05$; $***P < 0.001$. See Figure 1 for abbreviation.

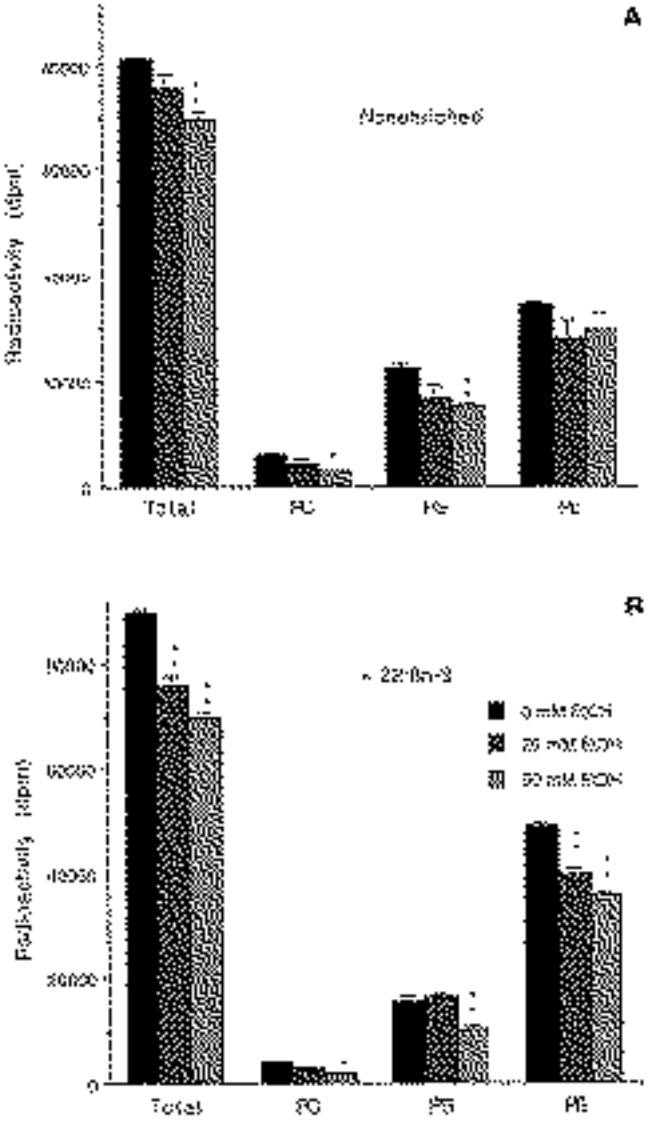

FIG. 6. Effect of long-term ethanol exposure on serine incorporation. Cells were exposed to 0, 20, or 50 mM ethanol for 4 wk. Control (0 mM ethanol) and ethanol-treated C-6 glioma cells were incubated with [^{3}H]serine (0.5 μCi) for 48 h in the (A) absence or (B) presence of 25 μM 22:6n-3. The total incorporated radioactivity was counted after extraction of the cell lipids. The radioactivity associated with individual phospholipid classes was counted after further separation of total cell lipids by thin-layer chromatography. The results are the mean ± SD of triplicates. Statistical analysis was performed in comparison to values from control cells using Student's *t*-test: $*P < 0.05$; $**P < 0.01$. See Figure 1 for abbreviations.

Figure 4. The most drastic effect of ethanol was the decreased accumulation of 18:0,22:6-PS and 18:0,22:6-PE plasmalogen in 22:6n-3 treated cells, as these species were reduced by approximately 40% (Fig. 4A). In contrast, ethanol increased 18:0,22:6-PE and 16:0,22:6-PC. In 20:4n-6-treated cells, 16:0,20:4- and 18:0,20:4-PC decreased most extensively (Fig. 4B). Although 18:0,20:4-PS also showed a decreasing trend after ethanol exposure, the reduction was not as significant as 18:0,22:6-PS in 22:6n-3-treated cells.

Altered accumulation of specific PS molecular species after ethanol exposure was reflected in the total PS content. As shown in Figure 5, there was a trend of decreasing PS by ethanol although the effect of ethanol on PS accumulation in nonenriched or 20:4n-6-enriched cells was not consistently significant. The effect of ethanol was most prominent for 22:6n-3-treated cells as the mole fraction of PS decreased by more than 40% from 8.3% to 5.0 or 4.8% after the exposure of cells to 20 or 50 mM ethanol, respectively. This decrease was primarily due to the dramatic reduction of 18:0,22:6-PS (Fig. 4A), indicating that preferential accumulation of PS caused by 22:6n-3 (Fig. 2) was prevented by ethanol exposure.

Effect of ethanol on the serine base exchange reaction. As indicated above, the negative effect of ethanol on polyunsaturated fatty acid incorporation was prominently shown for PS. In the mammalian system, PS is biosynthesized by serine base exchange reaction (6). In order to test whether PS biosynthetic activity was modified after the ethanol exposure, the cells treated with 0, 20, or 50 mM ethanol for 4 wk were incubated with ^{3}H-serine for 48 h. The total incorporation of serine into C-6 glioma cells pretreated with ethanol was much less than that observed with control cells, especially in the presence of 22:6n-3. The effect of ethanol on serine incorporation appeared to be ethanol-concentration dependent

(Fig. 6). A similar ethanol effect was also observed in the absence of 22:6n-3, although at a lesser extent. Further analysis of phospholipid classes by TLC showed that most radioactivity of the incorporated serine appeared in PE, then in PS and to a lesser extent in PC, indicating that remodeling of phospholipids, especially decarboxylation of PS to PE, actively occurs in C-6 glioma cells. The incorporation of the radioactivity derived from serine into all phospholipid classes showed a decreasing trend with ethanol exposure. The extent of conversion from PS to PE or PC in ethanol-treated cells was not significantly different from that in control cells, suggesting that decarboxylation of PS to PE and then methylation to PC may not be affected significantly by ethanol in this system. These data suggest that the reduced accumulation of polyunsaturates in PS by chronic ethanol exposure may be at least partly due to impaired PS biosynthetic activity. Since 22:6n-3 prefers the accumulation in PS, attenuated PS biosynthetic activity after the ethanol exposure may affect the accumulation of PS with a greater extent in 22:6n-3-treated cells in comparison to nonenriched cells.

DISCUSSION

Many investigators have demonstrated that chronic ethanol exposure can alter the content of polyunsaturates (6,11–18). Both polyunsaturate status (8) and ethanol (19) have been shown to modulate PS biosynthetic activity. These findings suggest that ethanol may specifically affect the accumulation of PS in cell membranes. In the present study, we examined the effect of ethanol on the accumulation of PS under different polyunsaturate status, using C-6 glioma cells as the model system. By using reversed-phase chromatography coupled to electrospray mass spectrometry, separation and detection of individual phospholipid molecular species from C-6 glioma cell extracts were achieved. The presence of deuterium-labeled internal standards facilitated reliable quantitation of targeted molecular species in cell lipids.

Enrichment of cells with polyunsaturated fatty acids increased PS accumulation without altering the total phospholipid content significantly (Fig. 2). Supplementation with 22:6n-3, in particular, resulted in the most significant increase of PS, as has been suggested with PS biosynthetic activity in our previous report (8). While the absolute changes observed seem small, PS accumulation was doubled in these cells (Table 2). This observation is consistent with the fact that neuronal cells, which are enriched with 22:6n-3, carry a higher PS proportion in comparison to cells of nonneuronal origin (31,32).

As cells in culture are generally deficient in polyunsaturates, especially n-3 fatty acids, supplementation with 22:6n-3 was necessary to accomplish the enrichment of this fatty acid to the level that is normally found in brain cells. Although exposing cells to 25 μM free fatty acid may not be physiological, we have observed that 22:6n-3 is incorporated in a concentration-dependent manner up to 40 μM without affecting cell viability (8).

The most prominent accumulations of molecular species found after incubation with either 20:4n-6 or 22:6n-3 were different. Whereas 20:4n-6 was mainly incorporated into PC, 22:6n-3 was incorporated mostly into PS and PE. As a single molecular species, 18:0,22:6-PS was the most abundant 22:6n-3-containing species observed after enrichment with 22:6n-3. The level of 18:0,22:6-PS was approximately 10 times higher than that of 16:0,22:6-PS, suggesting that PS synthesis may be preferred for species containing 18:0 at the *sn*-1 position as has been reported earlier (33). Enrichment of 22:6n-3 into 18:0-containing PS species is consistent with the fatty acyl composition observed in neuronal tissues (34). Our present finding that 16:0,20:4-PC was the most enriched species after 20:4n-6 enrichment is not consistent with the previous report by Sun *et al.* (35) where the greatest incorporation of [^{14}C]20:4n-6 was indicated in plasmalogen PE. The discrepancy may be due to the fact that radioactivity distribution may not reflect the resulting lipid profile as radioactivity enrichment depends on the turnover rates as well as the specific activities of lipid molecules involved in the turnover process. Alternatively, the different fatty acid concentration used (0.37 μM vs. 25 μM) may have contributed to the apparent discrepancy.

A few reports indicated that ethanol affects serine incorporation (19,36–38). Acute ethanol exposure of hepatocytes *in vitro* has been reported to increase the incorporation of radioactive serine (36). Hepatocytes isolated from rats treated with ethanol chronically also showed enhanced incorporation of radioactive serine (37). It has also been reported that NG108-15 cells showed higher serine incorporation after treatment with 100 mM ethanol for 2 d (38). Conversely, it has been reported that *in utero* exposure to ethanol decreased PS biosynthesis in rat pup cerebra (19), where it is known to have a high 22:6n-3 content. Our present findings indicated that long-term (4 wk) exposure of C-6 glioma cells to ethanol at 20 mM, which is below the legal intoxication concentration of ethanol (22.5 mM), the serine incorporation is considerably inhibited, particularly in cells where 22:6n-3 is highly enriched. This finding was corroborated by the marked reduction in the accumulation of 18:0,22:6-PS and total PS in 22:6n-3-treated cells by ethanol (Figs. 4 and 5). The significant decrease of 18:0,22:6-PS by ethanol observed in this study is consistent with previous reports that 22:6n-3 was depleted from PS of rat brain mitochondria (18) or mouse brain synaptic plasma membranes (16) after chronic ethanol exposure.

The inhibited incorporation of [^{3}H]serine into the lipid fraction observed in ethanol-treated cells may not directly represent the reduced serine base exchange reaction. Impaired [^{3}H]serine uptake into the endogenous pool by long-term ethanol exposure or changes in the serine pool size may also cause the decreased radioactive label in total lipids as well as in PS. It has been reported, however, that long-term ethanol exposure did not change the serine levels in human blood (39) and mouse brain (40) while several amino acid levels were affected significantly, suggesting that the serine pool size may

not be sensitive to ethanol exposure. Besides, attenuated total serine incorporation by ethanol was accompanied by the decrease in the PS content, suggesting that PS biosynthetic activity, whether it is serine uptake or the serine base exchange reaction itself, may have been compromised in ethanol-treated cells. Alternatively, the attenuated PS accumulation observed in ethanol-treated cells may have resulted from altered PS degradation by base exchange reaction or PS decarboxylation, although the distribution of the radiolabel from [^{3}H]serine into major phospholipid classes was not significantly affected by the ethanol exposure (Fig. 6).

The decrease of 18:0,22:6 or 18:0,20:4-PS by ethanol was not quantitatively compensated by the increase of the corresponding PC or PE species (Fig. 4). In addition, the effect of ethanol on the incorporation of serine radioactivity into PS (Fig. 6) did not simply correlate with that of the PS accumulation (Fig. 5). These results suggest that the decreased polyunsaturated PS is not the mere consequence of inhibited base exchange reaction. Rapid redistribution of radioactivity from serine into PE suggests that decarboxylation of PS may influence significantly the accumulation of polyunsaturated PS and PE in C-6 glioma. In a recent report, it has been suggested that chronic ethanol exposure can alter PE levels, depending on the biosynthetic pathway from which PE was originally derived (41). It has also been shown that ethanol exhibited a differential effect at higher concentrations (200–750 mM), inhibiting acylation of oleic acid in PE and PC, but stimulating acylation in PA and DG (42). Obviously, it is not easy to discern various overlapping metabolic pathways involved in the accumulation of certain molecular species in living cells. Nevertheless, our data does suggest that inhibited PS biosynthesis is involved, although it is not the only mechanism that is accountable for the reduction of polyunsaturated PS species.

In this report, we demonstrate that the 22:6n-3 status positively affects the accumulation of PS and that chronic ethanol exposure can inhibit PS accumulation. The preferential accumulation of PS in the presence of 22:6n-3 is consistent with the fact that tissues containing abundant 22:6n-3 show high proportions of PS as is observed in neuronal membranes (1,31,32). We found that chronic ethanol exposure at or near physiologically relevant concentrations (20–50 mM) inhibited the accumulation of PS promoted by 22:6n-3 in as little as 4 wk. Since the brain is particularly enriched with 22:6n-3, our findings imply that ethanol may exert greater influence on PS accumulation in brain cells. Considering the involvement of PS in various signal transduction events, such as the recruitment of protein kinase (9) or Raf-1 kinase to cell membranes (10), the effect of ethanol on the accumulation of PS may have a significant implication in pathophysiological effects of ethanol, especially in the brain.

ACKNOWLEDGMENT

The technical assistance in cell preparation by Brian Nardini is greatly appreciated.

REFERENCES

1. Salem, N., Jr. (1989) Omega-3 Fatty Acids: Molecular and Biochemical Aspects, in *New Protective Roles for Selected Nutrients* (Spiller, G., and Scala, J., eds.), pp. 109–228, Alan R. Liss, New York.
2. Salem, N., Jr., Kim, H.Y., and Yergey, Y.J. (1986) Docosahexaenoic Acid: Membrane Function and Metabolism, in *Health Effect of Polyunsaturated Fatty Acids in Seafoods* (Simopoulos, A.P., Kifer, R.R., and Martin, R.E., eds.), pp. 263–317, Academic Press, New York.
3. Neuringer, M., and Connor, W.E. (1986) ω-3 Fatty Acids in the Brain and Retina: Evidence for Their Essentiality, *Nutr. Rev. 44*, 285–294.
4. Uauy, R., Birch, E., Birch, D., and Peirano, P. (1992) Visual and Brain Function Measurements in Studies of ω3 Fatty Acid Requirements of Infants, *J. Pediatr. 120*, S168–S180.
5. Mills, D.E., Ward, R.P., and Young, C. (1988) Effects of Prenatal and Early Postnatal Fatty Acid Supplementation on Behavior, *Nutr. Res. 8,* 273–286.
6. Kanfer, J.N. (1980) The Base Exchange Enzymes and Phospholipase D of Mammalian Tissue, *Can. J. Biochem 58,* 1370–1380.
7. Dowhan, W. (1997) Molecular Basis for Membrane Phospholipid Diversity: Why Are There So Many Lipids? *Annu. Rev. Biochem. 66*, 199–232.
8. Garcia, M.C., Ward, G., Ma, Y.C., Salem, N., Jr., and Kim, H.Y. (1998) Effect of Docosahexaenoic Acid on the Synthesis of Phosphatidylserine in Rat Brain in Microsomes and C6 Glioma Cells, *J. Neurochem. 70*, 24–30.
9. Bell, R.M., and Burns, D. (1991) Lipid Activation of Protein Kinase C, *J. Biol. Chem. 266*, 4661–4664.
10. Ghosh, S., Strum, J.C., Sciorra, V.A., Daniel, L., and Bell, R.M. (1996) Raf-1 Kinase Possesses Distinct Binding Domains for Phosphatidylserine and Phosphatidic Acid, *J. Biol. Chem. 271*, 8472–8480.
11. Salem, N., Jr., and Ward, G. (1993) The Effect of Ethanol on Polyunsaturated Fatty Acid Composition, in *Alcohol, Cell Membranes, and Signal Transduction in Brain* (Alling, C., ed.), pp. 33–46, Plenum Press, New York.
12. Burdge, G.C., and Postle, A.D. (1995) Effect of Maternal Ethanol Consumption During Pregnancy on the Phospholipid Molecular Species Composition of Fetal Guinea-Pig Brain, Liver and Plasma, *Biochim. Biophys. Acta 1256*, 346–352.
13. Aloia, R.C., Paxton, J., Daviau, J.S., Van Gelb, O., Mlekusch, W., Truppe, W., Meyer, J.A., and Braver, F.S. (1985) Effect of Chronic Alcohol Consumption on Rat Brain Microsome Lipid Composition, Membrane Fluidity and Na^+, K^+-ATPase Activity, *Life Sci. 36*, 1003–1017.
14. Corbett, R., Berthou, F., Leonard, B.E., and Menez, J.-F. (1992) The Effects of Chronic Administration of Ethanol on Synaptosomal Fatty Acid Composition: Modulation by Oil Enriched with Gamma-Linolenic Acid, *Alcohol Alcoholism, 27*, 11–14.
15. Alling, C., Liljequist, S., and Engel. J. (1982) The Effect of Chronic Ethanol Administration on Lipids and Fatty Acids in Subcellular Fractions of Rat Brain, *Med. Biol. 60*, 149–154.
16. Harris, R.A., Baxter, D.M., Mitchell, M.A. and Hitzemann, R.J. (1984) Physical Properties and Lipid Composition of Brain Membranes from Ethanol Tolerant-Dependent Mice, *Mol. Pharmacol. 25*, 401–409.
17. Zerouga, M., Beauge, F., Niel, E., Durand, G., and Bourre, J.M. (1991) Interactive Effects of Dietary (n-3) Polyunsaturated Fatty Acids and Chronic Ethanol Intoxication on Synaptic Membrane Lipid Composition and Fluidity in Rats, *Biochim. Biophys. Acta 1086*, 295–304.
18. Gustavsson, L., and Alling, C. (1989) Effect of Chronic Ethanol Exposure on Fatty Acids of Rat Brain Glycerophospholipids, *Alcohol 6*, 139–146.

19. Hu, Z., Sun, G.Y., and Rhodes, P.G. (1992) *In utero* Ethanol Exposure Decreases the Biosynthesis of Phosphatidylserine in Rat Pup Cerebrum, *Alcohol. Clin. Exp. Res. 16,* 432–435.
20. Bartlett, G. (1959) Phosphorus Assay in Column Chromatography, *J. Biol. Chem. 234,* 466–468.
21. Kim, H.Y., and Salem, N., Jr. (1990) Separation of Lipid Classes by Solid Phase Extraction, *J. Lipid Res. 31,* 2285–2290.
22. Garcia, M.C., Kim, K.Y., Hough, C., and Kim, H.Y. (1997) Effects of Chronic Ethanol on the Mobilization of Arachidonate and Docosahexaenoate Stimulated by the Type 2A Serotonin Receptor Agonist (±)-2,5-Dimethoxy-4-iodoamphetamine Hydrochloride in C6 Glioma Cells, *Alcohol. Clin. Exp. Res. 21,* 1465–1470.
23. Demediuk, P., Anderson, D.K., Horrocks, L.A., and Means, E.D. (1985) Mechanical Damage to Murine Neuronal-Enriched Cultures During Harvesting: Effects on Free Fatty Acids, Diglycerides, Na^+K^+-ATPase, and Lipid Peroxidation, *In Vitro Cell Dev. Biol. 21,* 569–574.
24. Smith, P.K., Krohn, R.I., Hermanson, G.T., Mallia, A.K., Gartner, F.H., Provenzano, M.D., Fujimoto, E.K., Goeke, N.M., Olson, B.J., and Klenk, D.C. (1985) Measurement of Protein Using Bicinchoninic Acid, *Anal. Biochem. 150*, 76–85.
25. Bligh, E.G., and Dyer, W.J. (1959) A Rapid Method of Total Lipid Extraction and Purification, *Can. J. Biochem. Physiol. 37*, 911–917.
26. Kim, H.Y., Wang, T.C., and Ma, Y.C. (1994) Liquid Chromatography/Mass Spectrometry of Phospholipids Using Electrospray Ionization, *Anal. Chem. 66*, 3977–3982.
27. Ma, Y.C., and Kim, H.Y. (1995) Development of the On-Line High-Performance Liquid Chromatography/Thermospray Mass Spectrometry Method for the Analysis of Phospholipid Molecular Species in Rat Brain, *Anal. Biochem. 226*, 293–301.
28. Morrison, W.R., and Smith, L.M. (1961) Preparation of Fatty Acid Methyl Esters and Dimethylacetals from Lipids with Boron Fluoride-Methanol, *J. Lipid Res. 35*, 600–608.
29. Smith, D.M., and Waite, M. (1986) Phospholipid Metabolism in Human Neutrophil Subfractions, *Arch. Biochem. Biophys. 246*, 263–273.
30. Garcia, M.C., and Kim, H.Y. (1997) Mobilization of Arachidonate and Docosahexaenoate by Stimulation of the 5-HT2A Receptor in Rat C6 Glioma Cells, *Brain Res. 768*, 43–48.
31. Rouser, G., Yamamoto, A., and Kritchevsky, G. (1971) Cellular Membranes, *Arch. Intern. Med. 127*, 1105–1121.
32. White, D.A. (1973) The Phospholipid Composition of Mammalian Tissues, in *Form and Function of Phospholipids* (Ansell, G.B., Hawthorne, J.N., and Dawson, R.M.C., eds.), pp. 441–482, Elsevier Scientific Co., Amsterdam, The Netherlands.
33. Ellingson, J.S., and Seenaiah, B. (1994) The Selective Use of Stearoyl-Polyunsaturated Molecular Species of Phosphatidylcholine and Phosphatidylethanolamine for the Synthesis of Phosphatidylserine, *Biophys. Biochim. Acta 1213,* 113–117.
34. Hitzemann, R. (1981) Developmental Changes in the Fatty Acids of Synaptic Membrane Phospholipids: Effect of Protein Malnutrition, *Neurochem. Res. 6*, 935–946.
35. Sun, G.Y., Aradottir, S., Gustavsson, L., and Alling, C. (1989) Ethanol Alters the Transfer of Arachidonic Acid to Ethanolamine Plasmalogens in C-6 Glioma Cells, *J. Neurosci. Res. 24*, 268–275.
36. Carrasco, M.P., Sanchez-Amate, M.C., Marco, C., and Segovia, J.L. (1996) Evidence of Differential Effects Produced by Ethanol on Specific Phospholipid Biosynthetic Pathways in Rat Hepatocytes, *Br. J. Pharmacol. 119*, 233–238.
37. Carrasco, M.P., Sanchez-Amate, M.C., Segovia, J.L., and Marco, C. (1996) Studies on Phospholipid Biosynthesis in Hepatocytes from Alcoholic Rats by Using Radiolabeled Exogenous Precursors, *Lipids 31*, 393–397.
38. Rodriguez, F.D., Alling, C., and Gustavsson, L. (1996) Ethanol Potentiates the Uptake of [^{14}C]Serine into Phosphatidylserine by Base-Exchange Reaction in NG 108-15 Cells, *Neurochem. Res.* 21, 305–311.
39. Loguercio, C., Blanco, F.D., De Girolamo, V., Disalvo, D., Nardi, G., Parente, A., and Blanco, C.D. (1999) Ethanol Consumption, Amino Acid and Glutathione Blood Levels in Patients With and Without Chronic Liver Disease, *Alcohol. Clin. Exp. Res. 23*, 1780–1784.
40. Griffiths, P.J., and Littleton, J.M. (1977) Concentrations of Free Amino Acids in Brains of Mice During the Induction of Physical Dependence on Ethanol and During the Ethanol Withdrawal Syndrome, *Br. J. Exp. Path. 58*, 19–27.
41. Seenaiah, B., Bichenkov, E., and Ellingson, J.S. (1998) The Effects of Chronic Ethanol Consumption on the Formation of Phosphatidylethanolamine Molecular Species and Their Appearance at the Plasma Membrane, *Alcohol. Clin. Exp. Res. 22*, 1245–1254.
42. Petit-Thevenin, J.L., Nobili, O., Verine, A., and Boyer, J. (1995) Differential *in vitro* Effect of Ethanol on Glycerolipid Acylation and Biosynthesis in Rat Reticulocytes, *Biophys. Biochim. Acta 1257*, 103–110.

[Received August 24, 1999, and in revised form January 12, 2000; revision accepted January 28, 2000]

Inhibition of Cholesterol Biosynthesis by Organosulfur Compounds Derived from Garlic

Lijuan Liu and Yu-Yan Yeh*

Graduate Program in Nutrition, The Pennsylvania State University, University Park, Pennsylvania 16802

ABSTRACT: The study was undertaken to test the inhibitory potential on cholesterogenesis of organosulfur compounds derived from garlic. The primary rat hepatocytes maintained in Dulbecco's modified Eagle's medium were treated with [2-^{14}C]-acetate as substrate for cholesterol synthesis in the presence or absence of test compounds at 0.05 to 4.0 mmol/L. Eleven water-soluble and six lipid-soluble compounds of garlic were tested. Among water-soluble compounds, *S*-allyl cysteine (SAC), *S*-ethyl cysteine (SEC), and *S*-propyl cysteine (SPC) inhibited [2-^{14}C]acetate incorporation into cholesterol in a concentration-dependent manner, achieving 42 to 55% maximal inhibition. γ-Glutamyl-*S*-allyl cysteine, γ-glutamyl-*S*-methyl cysteine, and γ-glutamyl-*S*-propyl cysteine were less potent, exerting only 16 to 29% maximal inhibitions. Alliin, *S*-allyl-*N*-acetyl cysteine, *S*-allylsulfonyl alanine, and *S*-methyl cysteine had no effect on cholesterol synthesis. Of the lipid-soluble compounds, diallyl disulfide (DADS), diallyl trisulfide (DATS), and dipropyl disulfide (DPDS) depressed cholesterol synthesis by 10 to 25% at low concentrations (0. 5 mmol/L), and abolished the synthesis at high concentrations (1. 0 mmol/L). Diallyl sulfide, dipropyl sulfide, and methyl allyl sulfide slightly inhibited [2-^{14}C]acetate incorporation into cholesterol only at high concentrations. The complete depression of cholesterol synthesis by DADS, DATS, and DPDS was associated with cytotoxicity as indicated by marked increase in cellular LDH release. There was no apparent increase in LDH secretion by water-soluble compounds except *S*-allyl mercaptocysteine, which also abolished cholesterol synthesis. Judging from maximal inhibition and IC_{50} (concentration required for 50% of maximal inhibition), SAC, SEC, and SPC are equally potent in inhibiting cholesterol synthesis.

Paper no. L8348 in *Lipids 35,* 197–203 (February 2000).

Garlic has been recognized for its medicinal potentials since ancient times, but only recently has evidence emerged that garlic may decrease hypercholesterolemia (1,2) and reduce cancer risk (3). Extensive studies have been conducted to test anticarcinogenic and antitumorigenic properties of garlic and garlic components (4–9). It has been shown that *S*-allyl cysteine (SAC) and *S*-propyl cysteine (SPC) effectively blocked *N*-nitrosomorpholine (NMOR, a liver carcinogen) formation, and SAC and diallyl disulfide (DADS) reduced NMOR mutagenicity (10). Diallyl sulfides, such as diallyl sulfide (DAS), DADS, and diallyl trisulfide (DATS), also have been found to prevent benzo(a)pyrene-induced cancer in mice (11). However, less is known about garlic ingredients responsible for reducing plasma level of cholesterol.

Studies have shown that garlic can decrease plasma lipids, especially total cholesterol and low density lipoprotein cholesterol in humans and animals (1,2,12–17). The hypocholesterolemic effects were confirmed by meta-analyses showing a reduction of plasma cholesterol concentration between 9 and 12% in subjects treated with garlic as compared to a placebo group (18,19). A recent clinical study reported that garlic supplementation significantly reduced total serum cholesterol and triglycerides and increased high density lipoprotein-cholesterol in patients with coronary artery disease (20). However, the most recent studies of Berthold *et al*. (21), Isaacsohn *et al*. (22) and Simons *et al*. (23) failed to confirm such a beneficial effect of garlic. Despite the discrepancy in these studies, garlic has been shown to decrease hepatic cholesterol synthesis (24–27), which may explain in part the hypocholesterolemic effect of garlic in humans and animals (1,14,16,20). We recently have shown that water extract of garlic and a water-soluble component of garlic, SAC, depressed cholesterol synthesis in rat hepatocyte culture (27). Similarly, lipid-soluble sulfur compounds of garlic, such as DADS, allicin, and its derivative (ajoene), have been found to be potent inhibitors of cholesterol synthesis (26,28). However, since a wide variety of organosulfur compounds has been identified and isolated from different garlic preparations (29,30), it is essential to characterize the active ingredient(s) responsible for the cholesterol-lowering effect of garlic (30).

The present study was undertaken to identify the active compounds and their inhibitory potency of cholesterol

*To whom correspondence should be addressed at 129 South Henderson Bldg., Nutrition Dept., The Pennsylvania State University, University Park, PA 16802. E-mail: yyy1@psu.edu

Abbreviations: ANOVA, analysis of variance; DADS, diallyl disulfide; DAS, diallyl sulfide; DATS, diallyl trisulfide; DMEM, Dulbecco's modified Eagle's medium; DMSO, dimethyl sulfoxide; DPDS, dipropyl disulfide; DPS, dipropyl sulfide; FBS, fetal bovine serum; GSAC, γ-glutamyl-*S*-allyl cysteine; GSMC, γ-glutamyl-*S*-methyl cysteine; GSPC, γ-glutamyl-*S*-propyl cysteine; IC_{50}, concentration required for 50% of maximal inhibition; LDH, lactate dehydrogenase; MAS, methyl allyl sulfide; NMOR, *N*-nitrosomorpholine; SAC, *S*-allyl cysteine; SAMC, *S*-allyl mercaptocysteine; SANC, *S*-allyl-*N*-acetyl cysteine; SASA, *S*-allylsulfonyl alanine; SEC, *S*-ethyl cysteine; SMC, *S*-methyl cysteine; SPC, *S*-propyl cysteine.

biosynthesis in cultured rat hepatocytes. Additionally, the cytotoxicity of these compounds was determined and correlated to the cholesterol-lowering effect of the compounds.

MATERIALS AND METHOD

Chemicals. [2-^{14}C]Acetate was purchased from Amersham Corp. (Arlington Heights, IL). Collagenase D was obtained from Boehringer Mannheim Corp. (Indianapolis, IN). Culture media, fetal bovine serum (FBS), penicillin, and streptomycin were from Gibco (Gaithersburg, MD). Organosulfur compounds tested in this study included 11 water-soluble compounds, SAC, SEC, *S*-methyl cysteine (SMC), SPC, γ-glutamyl-*S*-allyl cysteine (GSAC), γ-glutamyl-*S*-methyl cysteine (GSMC), γ-glutamyl-*S*-propyl cysteine (GSPC), *S*-allyl cysteine sulfoxide (i.e., alliin), *S*-allyl-*N*-acetyl cysteine (SANC), *S*-allyl-mercaptocysteine (SAMC), and *S*-allylsulfonyl alanine (SASA), and six lipid-soluble compounds: DAS, DADS, DATS, dipropyl sulfide (DPS), dipropyl disulfide (DPDS), and methyl allyl sulfide (MAS). All the water-soluble compounds were provided by Wakunaga of America Co., Ltd. (Mission Viejo, CA). Of the six lipid-soluble compounds tested, DAS, DADS, DPS, and DPDS were purchased from Fluka Chemika (Ronkonkoma, NY). MAS was obtained from Aldrich Chemical Co. (Milwaukee, WI). DATS was a generous gift from Dr. John Milner's lab (The Pennsylvania State University, University Park, PA). All other chemicals of reagent grade were purchased from Sigma Chemical Co. (St. Louis, MO).

Animals. Male Sprague-Dawley rats (200–300 g) were obtained from Harlan Sprague-Dawley Co. (Indianapolis, IN) and fed a nonpurified diet (Purina Rat Chow, Ralston Purina, St. Louis, MO). The animals were housed individually in stainless-steel cages at approximately 24°C and 50% relative humidity on a 12-h light/dark cycle (0600–1800). The animal protocol was approved by The Pennsylvania State University Institutional Animal Care and Use Committee.

Hepatocyte culture. Liver cells were isolated from rats according to the method of Berry and Friend (31), as modified by Seglen (32). Briefly, rats were anesthetized with Nembutal (5 mg/100 g body weight), and the hepatic portal vein was cannulated for perfusion with buffer (NaCl, 142 mmol/L; KCl, 6.7 mmol/L; HEPES, 10 mmol/L; NaOH, 5.5mmol/L; pH 7.4) for 15 min. Immediately after perfusion *in situ*, the liver was carefully excised and perfused with collagenase buffer (NaCl, 67 mmol/L; KCl, 6.7 mmol/L; HEPES, 100 mmol/L; $CaCl_2 \cdot H_2O$, 5.4 mmol/L; NaOH, 66 mmol/L; pH 7.6; 50 mg collagenase D/100 mL) for 10–15 min. The enzyme-treated liver was then subjected sequentially to mincing, incubation, filtration, and centrifugation for cell isolation and purification. From each liver, 100–250 × 10^6 cells were obtained with a viability of 92–94%, as judged by trypan blue exclusion. The cells were resuspended in Dulbecco's modified Eagle's medium (DMEM) supplemented with 10% FBS and antibiotics (100 units penicillin/mL, and 100 μg streptomycin/mL) to obtain 0.5–0.8 × 10^6 cells/mL of suspension. Two-milliliter aliquots of the suspension were plated per well in a six-well culture plate (Becton Dickinson Labware, Lincoln, NJ) and incubated at 37°C under an atmosphere of 95% air and 5% CO_2. After 4 h of incubation, nonadhering cells were removed and discarded. Hepatocytes that adhered to the culture plate were refed with DMEM and incubated for 16 h.

Metabolic studies. At the end of 20 h of incubation, cells were washed three times with 2 mL of FBS-free DMEM, followed by incubation with 2 mL of the same medium containing sodium salt of [2-^{14}C]acetate (specific activity, 37 MBq/mmol) and 0.5 mmol/L nonlabeled sodium acetate in the presence or absence of organosulfur compounds. The lipid-soluble organosulfur compounds were dissolved in dimethyl sulfoxide (DMSO) and then in DMEM. The final concentrations of DMSO did not exceed 2%, and appropriate controls containing DMSO were run. A preliminary study has established a linear rate of [2-^{14}C]acetate incorporation into cholesterol between 4- and 12-h incubation of hepatocytes. Thus, throughout the study, cells were incubated for 4 h. After the incubation, the medium was collected and cells were harvested with 1.3 mL of ice-cold water by scraping with a cell scraper.

Lipid analysis. The harvested cells were mixed with 20 mL of chloroform/methanol (2:1, vol/vol) to extract lipids according to the method of Folch *et al.* (33). For measurement of [2-^{14}C]acetate incorporation into cholesterol, the lipid extract was saponified in 6 mL of 3.75% methanolic KOH at 90°C for 4 h. Nonsaponifiable lipids were extracted with petroleum ether (b.p. 35–60°C), and cholesterol was precipitated with digitonin (34). Briefly, nonsaponifiable lipid fraction was evaporated to dryness under nitrogen stream and dissolved in acetone/ethanol (1:1, vol/vol). After the addition of 1% digitonin solution (in 50% ethanol and 1% acetic acid), the sample was allowed to stand overnight for digitonide formation. For further purification, digitonide was washed with acetone/ethyl ether (1:1, vol/vol), followed by a final wash with ethyl ether alone. The radioactivity of ^{14}C-labeled sterol digitonide was taken as a measure of cholesterol derived from [2-^{14}C]acetate. The radioactivity was determined by liquid scintillation counting (Beckman model LS 3801; Beckman Instruments, Fullerton, CA). The specific activity of cholesterol synthesis was expressed as pmol acetate incorporated into cholesterol/mg cellular protein. Cellular protein was determined by the procedure of Lowry *et al.* (35). The relative rate of cholesterol synthesis by cells treated with organosulfur compounds was expressed as percentage of control calculated by specific activity of treatment group/specific activity of control nontreatment group × 100. IC_{50} (concentration required for 50% of maximal inhibition) was calculated by regression and correlation analysis between substrate concentration and inhibition percentage.

Determination of cytotoxicity. Cytotoxicity of hepatocytes was determined by measuring release of cellular lactate dehydrogenase (LDH) into the culture medium. The percentage of LDH released was estimated by dividing the activity in the medium by the sum of LDH activity in cells and medium × 100. Hepatocytes were lysed with 0.2% Triton X-100. LDH

activity was measured according to the method of Chao *et al.* (36) with modification as follows: the reaction mixture contained 2.55 mL of potassium phosphate buffer (0.1 M, pH 7.4) and 0.1mL of NADH (4.5 mM). The cell lysate (0.05 mL) was added and mixed. At time zero, the reaction was initiated by adding 0.1 mL of 20 mM sodium pyruvate solution. The rate of decreasing absorbance at 340 nm was monitored at 25°C with a Beckman DU®-50 LS 5801 spectrophotometer (Beckman Instruments). The specific activity of the enzyme measured in hepatocytes of untreated group ranged from 1 to 2 μmol of substrate used /min/well.

Statistics. Data are presented as means ± SEM. The comparisons of the test compounds were analyzed by analysis of variance (ANOVA). When statistical significance was indicated by ANOVA, Fisher's multiple test was applied to identify the significant difference between the groups at $P < 0.05$.

RESULTS

Incorporation of [2-^{14}C]acetate into cholesterol was measured in hepatocytes treated with or without organosulfur compounds at various concentrations (0.05–4.0 mmol/L) throughout the study. As shown in Figure 1, the rate of [2-^{14}C]acetate incorporation into cholesterol in the untreated group was arbitrarily defined as 100%. The rates of incorporation expressed as pmol acetate/mg cellular protein/4 h for the control varied from one experiment to another, but ranged from 868 to 1,396 pmol acetate/mg cellular protein. Among *S*-alk(en)yl cysteines, SAC, SEC and SPC but not SMC inhibited [2-^{14}C]acetate incorporation into cholesterol in a concentration-dependent manner with a maximal inhibition of 42–55%. The inhibition was apparent at a concentration as low as 0.05 mmol/L for SEC and SPC, and 0.1 mmol/L for SAC. All γ-glutamyl *S*-alk(en)yl cysteines (i.e., GSAC, GSMC, and GSPC) inhibited the rate of cholesterol synthesis to a maximum of 16–30% (Fig. 2). The inhibition was not seen at concentrations lower than 2.0 mmol/L for GSAC and GSPC, while a significant inhibition was noted at 0.5 mmol/L for GSMC. SAMC, a disulfur containing *S*-allyl cysteine derivative, inhibited the [2-^{14}C]acetate incorporation into cholesterol by 7–17% at 0.05 and 0.5 mmol/L and diminished the incorporation into cholesterol at 2.0 and 4.0 mmol/L (Fig. 3).

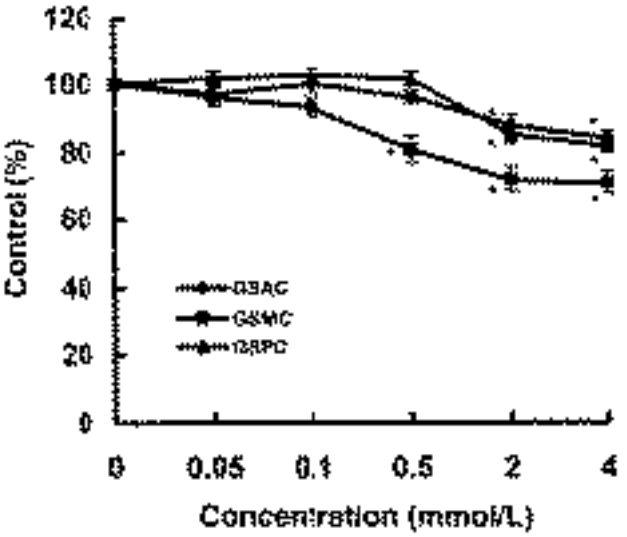

FIG. 2. Inhibition of [2-^{14}C]acetate incorporation into cholesterol by γ-glutamyl-*S*-allyl cysteine (GSAC), γ-glutamyl-*S*-methyl cysteine (GSMC), and γ-glutamyl-*S*-propyl cysteine (GSPC) in primary hepatocyte culture. Data are expressed as percentage of the control and represent means ± SEM of eight samples. *Statistically different from controls, $P < 0.05$.

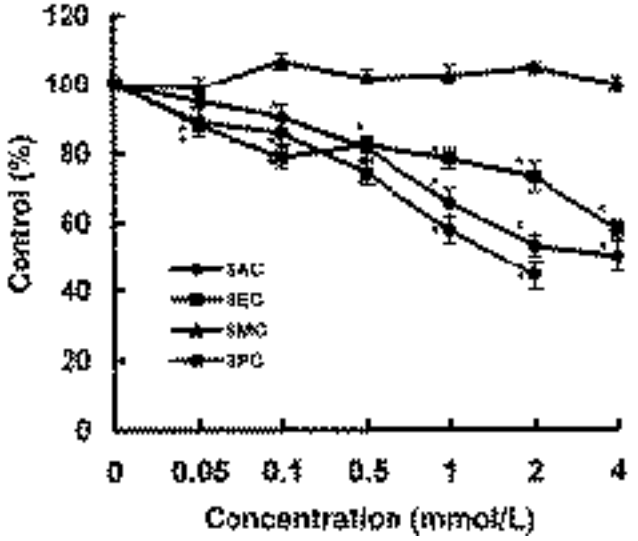

FIG. 1. Inhibition of [2-^{14}C]acetate incorporation into cholesterol by *S*-allyl cysteine (SAC), *S*-ethyl cysteine (SEC), *S*-methyl cysteine (SMC), and *S*-propyl cysteine (SPC) in primary hepatocyte culture. Data are expressed as percentage of the control and represent means ± SEM of eight samples. *Statistically different from controls, $P < 0.05$.

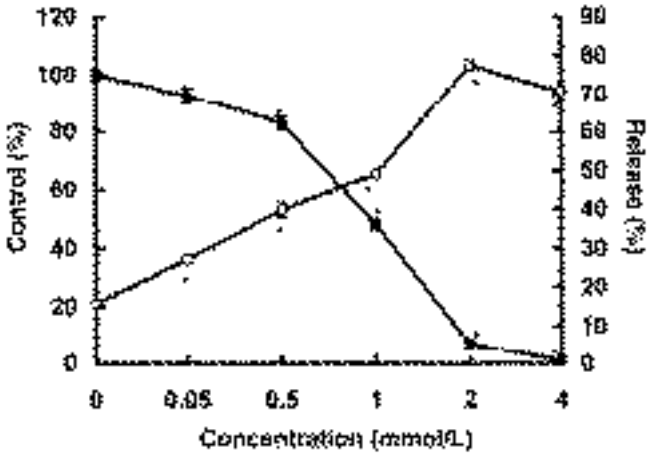

FIG. 3. Inhibition of [2-^{14}C]acetate incorporation into cholesterol and lactate dehydrogenase (LDH) release into the medium by *S*-allyl mercaptocysteine (SAMC) in primary hepatocyte culture. Data are expressed as a percentage of the control for [2-^{14}C]acetate incorporation into cholesterol (●) and a percentage of LDH activity in medium relative to total activity in cells and medium (○). The data represent means ± SEM of eight samples. *Statistically different from controls, $P < 0.05$.

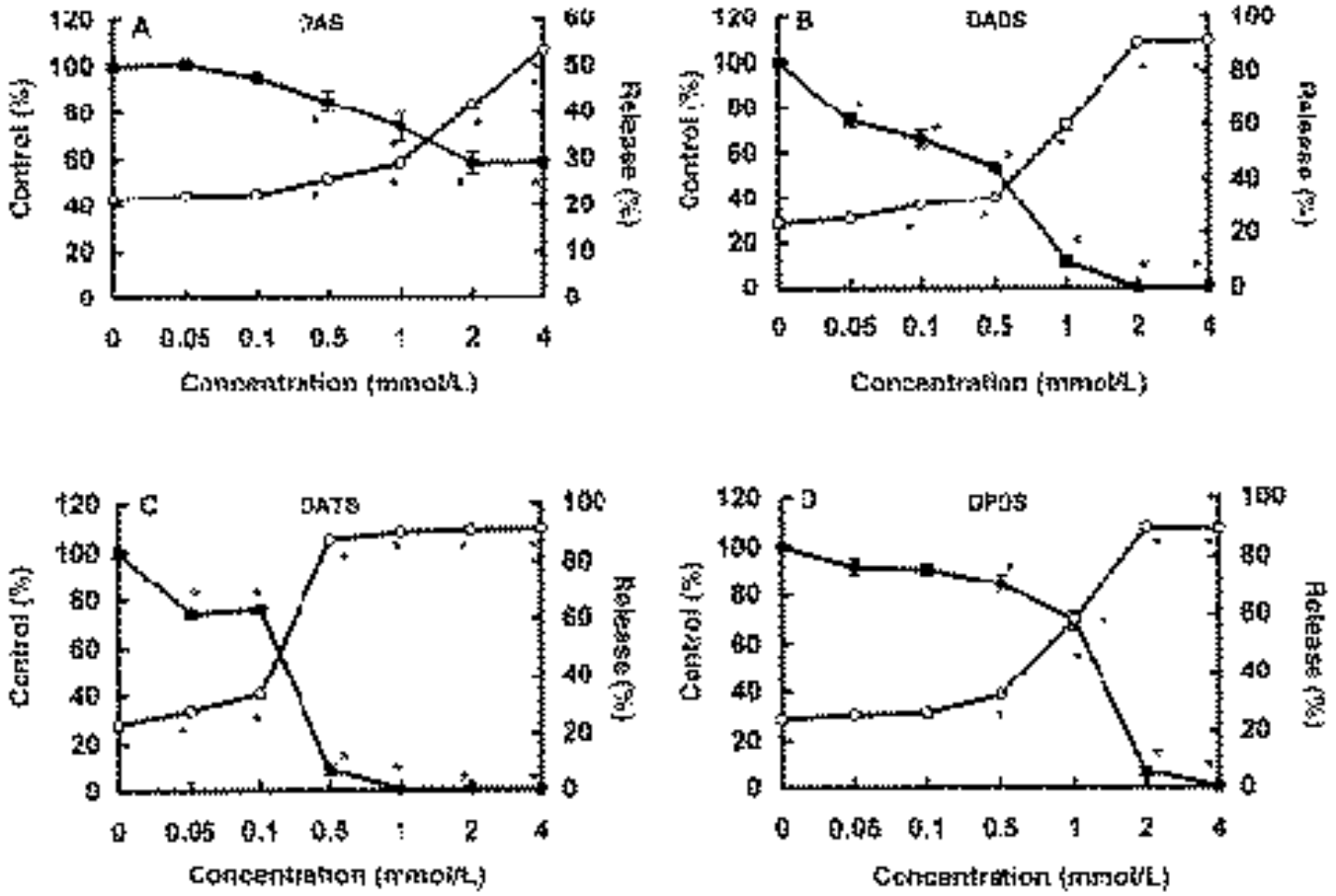

FIG. 4. Inhibition of [2-^{14}C]acetate incorporation into cholesterol and LDH release into the medium by diallyl sulfide (DAS), diallyl disulfide (DADS), diallyl trisulfide (DATS), and dipropyl disulfide (DPDS) in primary hepatocyte culture. Data are expressed as percentage control of [2-^{14}C]acetate incorporation into cholesterol (●) and percentage of LDH activity in medium relative to total activity in cells and medium (○), and represent means ± SEM of eight samples. *Statistically different from controls, $P < 0.05$. See Figure 3 for other abbreviation.

Other water-soluble compounds (i.e., alliin, SANC, and SASA) at concentrations from 0.05 to 4.0 mmol/L did not alter the rate of [2-^{14}C]acetate incorporation into cholesterol (data not shown).

The inhibition of cholesterol synthesis by lipid-soluble compounds was determined in subsequent experiments. Of three sulfur-containing diallyl compounds, DAS (monosulfide) exhibited the least effect with a maximal inhibition of 40% observed at 4.0 mmol/L concentration (Fig. 4A). The rate of cholesterol synthesis was decreased by 25% by both DADS and DATS (polysulfides) at 0.05 mmol/L (Fig. 4B and C). The synthesis was completely diminished by DATS and DADS at 1.0 and 2.0 mmol/L, respectively. The inhibition pattern by sulfur-containing dipropyl compounds resembled that of DAS and DADS. A maximum of 17% inhibition was achieved by DPS at 4.0 mmol/L (data not shown), while the synthesis was abolished by DPDS at the same concentration (Fig. 4D). An inhibition (by 15%) was apparent beginning at 0.5 mmol/L for DPDS. The synthesis was inhibited 15% maximally by MAS, a sulfide containing two different alk(en)yl groups, i.e., methyl and allyl moieties (data not shown).

In order to determine whether the inhibitory effect of sulfur compounds on cholesterogenesis could also be attributed to cytotoxicity, cellular release of LDH into the medium was measured. Increased release of lactate dehydrogenase (LDH) by hepatocytes into culture medium is widely used as an index of cytotoxicity (36,37). For hepatocytes treated without water-soluble compounds, the amount of LDH activity recovered in the medium accounted for 13–16% of total cellular LDH activity (Table 1). The treatment of cells with *S*-alk(en)yl cysteines and γ-glutamyl *S*-alk(en)yl cysteines except GSPC did not increase LDH release at 4.0 mmol/L (Table 1). However, GSPC did not alter the percentage of LDH release at 2.0 mmol/L (data not shown). Unlike these findings, SAMC increased LDH release in a concentration-dependent fashion and reached 70–78% at higher concentrations (2.0 and 4.0 mmol/L) (Fig. 3).

Since lipid-soluble compounds were dissolved in DMSO to a final concentration of less than 2%, cells in the control group were incubated in the presence of DMSO at the same concentration. LDH release into the medium of the control ranging from 21–24% was higher than that observed in the cells not treated with DMSO (Fig. 4 and Table 1). Incubation of cells with DAS and DPDS significantly increased percent-

TABLE 1
Release of Cellular LDH into Medium of Water-Soluble Compounds in Primary Hepatocyte Culture[a]

Compounds	Concentration (mmol/L)	
	0	4
SAC	13.39 ± 0.94	14.50 ± 0.36
SEC	14.71 ± 1.08	15.43 ± 0.31
SPC	14.38 ± 1.96	14.09 ± 0.67
GSAC	14.72 ± 0.73	15.96 ± 0.91
GSMC	14.72 ± 0.73	14.96 ± 0.72
GSPC	15.82 ± 0.31	17.72 ± 1.03*

[a]Data are expressed as percentage of activity in medium relative to total activity in cells and medium, and represent means ± SD of eight samples. *Statistically different from controls, $P < 0.05$. SAC, *S*-allyl cysteine; SEC, *S*-ethyl cysteine; SPC, *S*-propyl cysteine; GSAC, γ-glutamyl-*S*-allyl cysteine; GSMC, γ-glutamyl-*S*-methyl cysteine; GSPC, γ-glutamyl-*S*-propyl cysteine; LDH, lactate dehydrogenase.

TABLE 2
Maximal Inhibition and Calculated IC_{50} of Water-Soluble Compounds on Cholesterol Synthesis[a]

Compounds	IC_{50} (mmol/L)	Maximal inhibition (%)
SAC	0.61	50
SEC	0.58	42
SPC	0.72	55
GSAC	1.66	16
GSMC	1.12	29
GSPC	1.92	18

[a]IC_{50}, concentration required for 50% of maximal inhibition. See Table 1 for other abbreviations.

age release of LDH at 0.5 mmol/L (Fig. 4A and D). The increase was noted for DATS at 0.05 mmol/L and for DADS at 0.1 mmol/L (Fig. 4B and C). Increasing the concentration to 1.0 mmol/L of DATS, 2.0 mmol/L of DADS, and 2.0 mmol/L of DPDS further increased LDH release to approximately 90%. At 4.0 mmol/L, DADS, DATS and DPDS did not further increase LDH release. DAS also elevated LDH release, but only up to 50%. DPS, another monosulfur compound, increased LDH release to 33% only at 4.0 mmol/L, whereas MAS had no effect on the release (data not shown).

Table 2 shows maximal inhibition and IC_{50} for water-soluble compounds that exhibited concentration-dependent inhibition on cholesterol synthesis. The maximal inhibition was the highest for SPC followed in increasing order by SAC > SEC > GSMC > GSPC > GSAC, while the calculated IC_{50} was the lowest for SEC followed in decreasing order by SAC < SPC < GSMC < GSAC < GSPC.

DISCUSSION

Previous studies from our laboratory (27) and that of Gebhardt *et al.* (26,28) have reported inhibitory effects of some garlic constituents on cholesterol biosynthesis *in vitro*. The present study not only confirmed the earlier findings but also expanded to test 11 water-soluble and 6 lipid-soluble compounds derived from garlic. When incubated with hepatocytes in culture, most water-soluble compounds were effective in decreasing [2-^{14}C]acetate incorporation into cholesterol. All *S*-alk(en)yl cysteines except SMC inhibited cholesterol synthesis to various degrees. The differences among the *S*-alk(en)yl cysteines are the numbers of carbon and/or the number of double bonds. The potency of inhibition on cholesterol synthesis increased with increasing carbon number. SMC containing only one carbon (CH_3–) in the alk(en)yl group was ineffective, while SEC containing two carbons (CH_3CH_2–) inhibited the rate of [2-^{14}C]acetate incorporation into cholesterol. A greater inhibition was noted by SAC and SPC, both containing three carbons, but with a double bond (CH_2=$CHCH_2$–) in SAC and none (CH_3CH_2 CH_2–) in SPC. Glutamylated products of *S*-alk(en)yl cysteines, i.e., GSAC, GSMC, and GSPC, were less potent than SAC, SEC, and SPC in inhibiting cholesterogenesis. However, unlike SMC, GSMC reduced [2-^{14}C]acetate incorporation into cholesterol and was more effective than GSAC and GSPC. Interestingly, SAMC, which contains one more sulfur atom than SAC, was more potent than the latter in inhibiting [2-^{14}C]acetate incorporation into cholesterol.

All six lipid-soluble compounds except MAS appeared to exert greater inhibition on [2-^{14}C]acetate incorporation into cholesterol than water-soluble compounds. The degree of inhibition was associated with the number of sulfur atoms in the molecules. At concentrations of 1.0 mmol/L or higher, the percentage of inhibition was in order of DATS > DADS > DAS. This is consistent with inhibition on the growth of canine mammary tumor cells in culture (8). Similarly, DPDS, a polysulfide compound, exerted a greater inhibition than a single sulfur-containing DPS. However, it should be stressed that the marked decrease of [2-^{14}C]acetate incorporation into cholesterol by the lipid-soluble compounds was closely associated with the extensive cytotoxicity as indicated by markedly increased release of cellular LDH into the medium.

For determination of cytotoxicity, LDH released into culture medium was measured in cells treated with the test compounds. In the presence of water-soluble compounds, percentage release of LDH remained unchanged from that seen in control group (i.e., 13–16%). It should be noted that the control values were consistent with the range observed by other investigators (37–40), although values as low as 10% and as high as 30% have been reported (41). DMSO added to the incubation medium alone at a final concentration of 2% or less augmented LDH release to 21–24%. Nonetheless, in the presence of DMSO, most lipid-soluble compounds further increased LDH release in a concentration-dependent manner, especially for those containing at least two sulfur atoms, e.g., DADS, DATS, and DPDS. Overall, the degree of LDH release was the greatest with DATS, followed in order by DADS, DPDS, and DAS. The results therefore revealed that the more sulfur atoms in the molecule, the higher the cytotoxicity of the compounds. Consistent with this notion, SAMC, the only water-soluble compound with two sulfur atoms in the molecule, was also highly cytotoxic.

It should be pointed out that an earlier study by Gebhardt

and Beck (28) showed that treatment of hepatocytes with DADS even at 10 mmol/L did not increase LDH release. The reason for the discrepancy observed between the studies is not known. However, it is worth noting that in the latter study (28), the cells were pretreated with the compound for 2 h in the culture medium. The medium was then replaced by new medium containing labeled acetate and incubated again for measurements of cholesterol synthesis and LDH release (28). In the present study, sulfur compounds were added directly to the culture medium and LDH release measured 4 h after incubation (27). Whether these different experimental conditions account for the observed difference warrants further investigation. At this juncture, it is interesting to note that the study of Abdul-Hussain and Mehendale (41) demonstrated that the degree of LDH leakage through the hepatocyte membrane was dependent on the duration of cell incubation in the medium (41).

The inverse relationship between cholesterol synthesis and LDH release led us to conclude the inhibition on cholesterogenesis by lipid-soluble compounds at concentrations higher than 0.5 mmol/L was likely due to cytotoxicity rather than impairment in the metabolic pathway of cholesterol synthesis. Similarly, the marked inhibition by SAMC was associated with cytotoxic effect. The unaltered percentage of LDH release associated with most water-soluble compounds therefore strongly suggests that inhibition of cholesterol synthesis by these compounds likely results from impairment of specific enzyme(s) of cholesterogenic pathway.

A comparison of cytotoxicity and cholesterol inhibition potency of various compounds suggests that water-soluble compounds of garlic may be of more potential than lipid-soluble compounds in lowering plasma concentration of cholesterol. In fact, in a recent clinical trial (21), garlic oil rich in polysulfides (42) given to patients with moderate hypercholesterolemia was ineffective in lowering serum cholesterol. On the other hand, aged garlic extract consisting mostly of water-soluble sulfur compounds supplemented to the diet of hypercholesterolemic patients decreased by plasma concentrations of total cholesterol and LDL-cholesterol 6–9% (1,2). It is apparent from the present study that three *S*-alk(en)yl cysteines (i.e., SAC, SPC, and SEC) effectively depressed hepatic cholesterogenesis at a low concentration and without a sign of cytotoxicity. However, SAC may be the most important contributor to the hypocholesterolic effect of aged garlic extract (1,2) because SAC is a major sulfur-containing amino acid derivative in garlic, especially in aged garlic extract (43). Aged garlic extract is known to contain 456 μg/g of SAC/g of dry powder (44).

The mechanisms underlying the inhibitory action of garlic compounds on cholesterol synthesis have not been fully elucidated. However, animal studies have suggested that garlic-supplemented diets decreased the cholesterogenic enzyme, 3-hydroxy-3-methyl-glutaryl-CoA reductase (16,45). Sulfur compounds of garlic such as allicin have been shown to inhibit the activity of acetyl-CoA synthetase (46). Since [2-^{14}C]acetate was used as a substrate in the present study, the activation of acetate to acetyl-CoA by the synthetase must also play a role in its incorporation into cholesterol.

In conclusion, although lipid-soluble compounds appeared to abolish cholesterol synthesis, the inhibition may be due to cytotoxicity. Water-soluble components of garlic, especially SAC, appears to be most responsible for the reduction of cholesterol synthesis. Furthermore, the results suggest that the hypocholesterolemic effect of garlic results in part from impaired cholesterol synthesis.

ACKNOWLEDGMENT

The authors are grateful to the expert technical assistance provided by Shaw-Mei Yeh. This work was supported in part by Wakunaga of America Company.

REFERENCES

1. Steiner, M., Khan, A.H., Holbert, D., and Lin, R.I. (1996) A Double-Blind Crossover Study in Moderately Hypercholesterolemic Men That Compared the Effect of Aged Garlic Extract and Placebo Administration on Blood Lipids, *Am. J. Clin. Nutr. 64,* 866–870.
2. Yeh, Y.-Y., Lin, R.I., Yeh, S.-M., and Evens, S. (1997) Garlic Reduces Plasma Cholesterol in Hypercholesterolemic Men Maintaining Habitual Diets, in *Food Factors for Cancer Prevention* (Ohigashi, H., Osawa, T., Terao, J., Watanabe, S., and Toshikawa, T., eds.), pp. 226–230, Springer, Tokyo.
3. Milner, J.A. (1996) Garlic: Its Anticarcinogenic and Antitumorigenic Properties, *Nutr. Rev. 54,* S82–S86.
4. Dirsch, V.M., Gerbes, A.L., and Vollmar, A.M. (1998) Ajoene, a Compound of Garlic, Induces Apoptosis in Human Promyeloleukemic Cells, Accompanied by Generation of Reactive Oxygen Species and Activation of Nuclear Factor κB, *Mol. Pharmacol. 53,* 402–407.
5. Lin, X.Y., Liu, J.Z., and Milner, J.A. (1994) Dietary Garlic Suppresses DNA Adducts Caused by *N*-Nitroso Compounds, *Carcinogenesis 15,* 349–352.
6. Sakamoto, K., Lawson, L.D., and Milner, J.A. (1997) Allyl Sulfides from Garlic Suppress the *in vitro* Proliferation of Human A549 Lung Tumor Cells, *Nutr. Cancer 29,* 152–156.
7. Schaffer, E.M., Liu, J.Z., Green, J., Dangler, C.A., and Milner, J.A. (1996) Garlic and Associated Allyl Sulfur Components Inhibit *N*-Methyl-*N*-nitrosourea Induced Rat Mammary Carcinogenesis, *Cancer Lett. 102,* 199–204.
8. Sundaram, S.G., and Milner, J.A. (1993) Impact of Organosulfur Compounds in Garlic on Canine Mammary Tumor Cells in Culture, *Cancer Lett. 74,* 85–90.
9. Sundaram, S.G., and Milner, J.A. (1996) Diallyl Disulfide Inhibits the Proliferation of Human Tumor Cells in Culture, *Biochim. Biophys. Acta 1315,* 15–20.
10. Dion, M.E., Agler, M., and Milner, J.A. (1997) *S*-Allyl Cysteine Inhibits Nitrosomorpholine Formation and Bioactivation, *Nutr. Cancer 28,* 1–6.
11. Srivastava, S.K., Hu, X., Xia, H., Zaren, H.A., Chatterjee, M.L., Agarwal, R., and Singh, S.V. (1997) Mechanism of Differential Efficacy of Garlic Organosulfides in Preventing Benzo(a)-pyrene-Induced Cancer in Mice, *Cancer Lett. 118,* 61–67.
12. Auer, W., Eiber, A., Hertkorn, E., Hoehfeld, E., Koehrle, U., Lorenz, A., Mader, F., Merx, W., Otto, G., and Schmid-Otto, B. (1990) Hypertension and Hyperlipidaemia: Garlic Helps in Mild Cases, *Br. J. Clin. Pract. Suppl. 69,* 3–6.
13. Brosche, T., Platt, D., and Dorner, H. (1990) The Effect of a Garlic Preparation on the Composition of Plasma Lipoproteins

and Erythrocyte Membranes in Geriatric Subjects, *Br. J. Clin. Pract. Suppl. 69,* 12–19.
14. Jain, A.K., Vargas, R., Gotzbowsky, S., and McMahon, F.G. (1993) Can Garlic Reduce Levels of Serum Lipids? *Am. J. Med. 94,* 632–635.
15. Lau, B.H.S., Sam, F., and Wang-Cheng, R. (1987) Effect of an Odor-Modified Garlic Preparation on Blood Lipids, *Nutr. Res. 7,* 139–149.
16. Qureshi, A.A., Abuirmeileh, N., Din, Z.Z., Elson, C.E., and Burger, W.C. (1983) Inhibition of Cholesterol and Fatty Acid Biosynthesis in Liver Enzymes and Chicken Hepatocytes by Polar Fractions of Garlic, *Lipids 18,* 343–348.
17. Vorberg, G., and Schneider, B. (1990) Therapy with Garlic: Results of a Placebo-Controlled, Double-Blind Study, *Br. J. Clin. Pract. Suppl. 69,* 7–11.
18. Silagy, C., and Neil, A. (1994) Garlic as a Lipid Lowering Agent—A Meta-Analysis, *J.R. Coll. Physicians Lond. 28,* 39–45.
19. Warshafsky, S., Kamer, R.S., and Sivak, S.L. (1993) Effect of Garlic on Total Serum Cholesterol. A Meta-Analysis, *Ann. Intern. Med. 119,* 599–605.
20. Bordia, A., Verma, S.K., and Srivastava, K.C. (1998) Effect of Garlic *(Allium sativum)* on Blood Lipids, Blood Sugar, Fibrinogen and Fibrinolytic Activity in Patients with Coronary Artery Disease, *Prostaglandins Leukotrienes Essent. Fatty Acids 58,* 257–263.
21. Berthold, H.K., Sudhop, T., and von Bergmann, K. (1998) Effect of a Garlic Oil Preparation on Serum Lipoproteins and Cholesterol Metabolism: A Randomized Controlled Trial, *JAMA 279,* 1900–1902.
22. Isaacsohn, J.L., Moser, M., Stein, E.A., Dudley, K., Davey, J.A., Liskov, E., and Black, H.R. (1998) Garlic Powder and Plasma Lipids and Lipoproteins: A Multicenter, Randomized, Placebo-Controlled Trial, *Arch. Intern. Med. 158,* 1189–1194.
23. Simons, L.A., Balasubramaniam, S., von Konigsmark, M., Parfitt, A., Simons, J., and Peters, W. (1995) On the Effect of Garlic on Plasma Lipids and Lipoproteins in Mild Hypercholesterolaemia, *Atherosclerosis 113,* 219–225.
24. Gebhardt, R. (1991) Inhibition of Cholesterol Biosynthesis by a Water-Soluble Garlic Extract in Primary Cultures of Rat Hepatocytes, *Arzneim. Forsch. 41,* 800–804.
25. Gebhardt, R. (1993) Multiple Inhibitory Effects of Garlic Extracts on Cholesterol Biosynthesis in Hepatocytes, *Lipids 28,* 613–619.
26. Gebhardt, R., Beck, H., and Wagner, K.G. (1994) Inhibition of Cholesterol Biosynthesis by Allicin and Ajoene in Rat Hepatocytes and HepG2 Cells, *Biochim. Biophys. Acta 1213,* 57–62.
27. Yeh, Y.-Y., and Yeh, S.-M. (1994) Garlic Reduces Plasma Lipids by Inhibiting Hepatic Cholesterol and Triacylglycerol Synthesis, *Lipids 29,* 189–193.
28. Gebhardt, R., and Beck, H. (1996) Differential Inhibitory Effects of Garlic-Derived Organosulfur Compounds on Cholesterol Biosynthesisin Primary Rat Hepatocyte Cultures, *Lipids 31,* 1269–1276.
29. Lawson, L.D. (1993) Bioactive Organosulfur Compounds of Garlic and Garlic Products, in *Human Medicinal Agents from Plants* (Kinghorn, A.D., and Balandrin, M.F., eds.), pp. 307–330, American Chemical Society, Washington, DC.
30. Agarwal, K.C. (1996) Therapeutic Actions of Garlic Constituents, *Med. Res. Rev. 16,* 111–124.
31. Berry, M.N., and Friend, D.S. (1969) High-Yield Preparation of Isolated Rat Liver Parenchymal Cells: A Biochemical and Fine Structural Study, *J. Cell Biol. 43,* 506–520.
32. Seglen, P.O. (1973) Preparation of Rat Liver Cells. 3. Enzymatic Requirements for Tissue Dispersion, *Exp. Cell Res. 82,* 391–398.
33. Folch, J., Lees, M., and Sloane-Stanley, G.H. (1957) A Simple Method for the Isolation and Purification of Total Lipids from Animal Tissues, *J. Biol. Chem. 226,* 497–510.
34. Kabara, J.J. (1957) A Quantitative Micromethod for Isolation and Liquid Scintillation Assay of Radioactive Free and Ester Cholesterol, *J. Lab. Clin. Med. 50,* 146–151.
35. Lowry, O.H., Rosebrough, N.J., Farr, A.L., and Randall, R.J. (1951) Protein Measurement with the Folin Phenol Reagent, *J. Biol. Chem. 193,* 265–275.
36. Chao, E.S., Dunbar, D., and Kaminsky, L.S. (1988) Intracellular Lactate Dehydrogenase Concentration as an Index of Cytotoxicity in Rat Hepatocyte Primary Culture, *Cell Biol. Toxicol. 4,* 1–11.
37. Jauregui, H., Hayner, N.T., Driscoll, J.L., Williams-Holland, R., Lipsky, M.H., and Galletti, P.M. (1981) Trypan Blue Dye Uptake and Lactate Dehydrogenase in Adult Rat Hepatocytes—Freshly Isolated Cells, Cell Suspensions, and Primary Monolayer Cultures, *In Vitro 81,* 1100–1110.
38. Houck, H.E, Lipsky, M.M., Marzella, L., and Burnett, J.V. (1996) Toxicity of Sea Nettle *(Chrysaora quinquecirrha)* Fishing Tentacle Nematocyst Venom in Cultured Rat Hepatocytes, *Toxicon 34,* 771–778.
39. McMillan, J.M., and Jollow, D.J. (1995) Macrophage Enhancement of Galactosamine Hepatotoxicity Using a Rat Hepatocyte Culture System, *Res. Commun. Mol. Pathol. Pharmacol. 88,* 327–338.
40. Zurlo, J., and Arterburn, L.M. (1996) Characterization of a Primary Hepatocyte Culture System for Toxicological Studies, *In Vitro Cell Dev. Biol. 32,* 211–220.
41. Abdul-Hussain, S.K., and Mehendale, H.M. (1991) Studies on the Age-Dependent Effects of Galactosamine in Primary Rat Hepatocyte Cultures, *Toxicol. Appl. Pharmacol. 107,* 504–513.
42. Augusti, K.T. (1996) Therapeutic Values of Onion (*Allium cepa* L.) and Garlic (*Allium sativum* L.), *Indian J. Exp. Biol. 34,* 634–640.
43. Imai, J., Ide, N., Nagae, S., Moriguchi, T., Matsuura, H., and Itakura, Y. (1994) Antioxidant and Radical Scavenging Effects of Aged Garlic Extract and Its Constituents, *Planta Med. 60,* 417–420.
44. Amagase, H., and Milner, J.A. (1993) Impact of Various Sources of Garlic and Their Constituents on 7,12-Dimethylbenz[a]anthracene Binding to Mammary Cell DNA, *Carcinogenesis 14,* 1627–1631.
45. Qureshi, A.A., Crenshaw, T.D., Abuirmeileh, N., Peterson, D.M., and Elson, C.E. (1987) Influence of Minor Plant Constituents on Porcine Hepatic Lipid Metabolism. Impact on Serum Lipids, *Atherosclerosis 64,* 109–115.
46. Focke, M., Feld, A., and Lichtenthaler, K. (1990) Allicin, a Naturally Occurring Antibiotic from Garlic, Specifically Inhibits Acetyl-CoA Synthetase, *FEBS Lett. 261,* 106–108.

[Received September 7, 1999, and in final revised form January 19, 2000; revision accepted January 31, 2000]

Mechanisms of Tubulin Modification by Phosphatidylcholine Hydroperoxides

Misako Kawakami[a,*], Larry Ward[b], and Hiroshi Doi[a]

[a]Department of Food Science and Nutrition, Mukogawa Women's University, Nishinomiya, Hyogo 663-8558, Japan and [b]AMRAD Operations, Richmond, Victoria 3121, Australia

ABSTRACT: The interaction of lipid peroxides with cellular proteins has been postulated to contribute to cellular aging. A potential target for such effects is tubulin, the building block of microtubules. We examined the concentration-dependent effects of phosphatidylcholine hydroperoxides on the ability of tubulin to polymerize into microtubules. The results demonstrated that even very low concentrations of peroxides were sufficient to interfere with the tubulin and, therefore, the microtubule function. Decreased tubulin activity (as measured by tubulin GTPase activity) showed correlation with the modification of methionine and cysteine in tubulin and a change in the tubulin conformational state as indicated by fluorescence and ultraviolet spectroscopic measurements. As no effect on electric conductivity was observed, indicating that modulation of ionic binding was not involved, the interaction mechanism may be a hydrophobic one.

Paper no. L8235 in *Lipids 35,* 205–211 (February 2000).

Lipid hydroperoxides, which display deleterious effects upon protein structure and function and consequently the cellular function of lipid hydroperoxides, may contribute to cellular aging (1–5). What remains to be clarified is the molecular mechanism at the level of individual cellular proteins. Dietary lipid peroxidation products have been shown to be toxic to cells (6). Similarly, oxygen-free radicals can trigger human disease by causing functional and morphologic disturbances in cells (7). These effects are thought to be due to the accumulation of cellular lipid peroxidation products resulting in interference of normal cellular functions (8,9). The primary site of action of oxygen-free radicals is the plasma membrane, as lipids are easily oxidized into phospholipid hydroperoxides. A potential target for some of the observed effects of lipid peroxides on cellular function is microtubules, which are intrinsic to a variety of cellular functions including maintenance of cell form, motility, movement, and division (10–12).

The aging phenomenon is postulated to be affected by microtubule-related activities because the rate of microtubule formation has been found to be slow in old rats compared with young animals (13) and hydroperoxides produced in the cells eventually cause their death (14).

We have previously demonstrated with an *in vitro* system of microtubule assembly that lipid hydroperoxides interfere with microtubule formation. This system utilized an assay of tubulin GTPase activity, with tubulin being the protein building block of microtubules (15,16).

In the present study, we examined the mechanism at the structural level of tubulin by lipid peroxidation to further the understanding of this process. We also tried to determine the sensitivity of tubulin to lipid peroxidation in order to gauge whether long-term exposure to low concentrations of hydroperoxides could interfere with tubulin function. Previous studies have utilized strong oxidizing conditions (15–18), and this is the first work using weak oxidizing conditions, which more accurately simulate the *in vivo* state.

MATERIALS AND METHODS

Tubulin. Tubulin was prepared from bovine brain by the modified procedure of Lee *et al.* described previously (19,20). Bovine brain, obtained from a freshly slaughtered animal, was kept on ice and used within 30 min of slaughter. All steps were performed at 4°C as rapidly as possible. After purification, protein aliquots were stored at –80°C in 10 mM phosphate buffer, pH 7.0, containing 1 M sucrose, 0.1 mM GTP, and 0.5 mM $MgCl_2$. Prior to each experiment, the bulk of the sucrose was removed from the tubulin solution by a Sephadex (Pharmacia Biotech, Uppsala, Sweden) G-25 batch procedure (21). The resulting protein solution was cleared of aggregates by centrifugation at 20,000 × *g* for 30 min at 4°C. The final equilibration of the protein solution with the desired buffer was done by gel chromatography on a Sephadex G-25 column (10 × 10 cm; Pharmacia Biotech). Protein concentration was determined in 6M guanidine hydrochloride with an absorptivity value of 1.09 $mL \cdot mg^{-1} \cdot cm^{-1}$ at 275 nm (22).

Phosphatidylcholine hydroperoxides (PCOOH). Because the cell membrane is primarily composed of phospholipids, soybean phosphatidylcholine (PC) was used as the starting material for the generation of PCOOH. The PC was lipoid S-100 of soybean origin, obtained from Nisshin Oil Mills Ltd. (Tokyo, Japan). Lipoid S-100 is essentially pure PC. Photo-

*To whom correspondence should be addressed.
E-mail: misakoka@mwu.mukogawa-u.ac.jp

Abbreviations: ECD, electrochemical detection; HPLC, high-performance liquid chromatography; PC, phosphatidylcholine; PCOOH, phosphatidylcholine hydroperoxides; UV, ultraviolet.

sensitized oxidation was carried out in methanol, with methylene blue being added to the PC-methanol solution as a sensitizer. The final concentrations of methylene blue and PC were 0.004% and 10 mg/mL, respectively. PC was photooxidized by irradiation with a 30-W tungsten projection lamp, which was positioned 40 cm above the reaction mixture for 20 h at 4°C. Upon completion of the reaction, methylene blue was removed using a Disposil SL gel column (Nacalai Tesque, Kyoto, Japan), and methanol was removed by evaporation. Aliquots (50 μL) of the generated lipid peroxides were added to the protein solution to a final concentration of 0.1 mg/mL. For the control samples, no sensitizer was added and no irradiation was performed.

Other reagents. GTP was purchased from Sigma Chemical Co. (St. Louis, MO). Tetrabutyl ammonium dihydrogenphosphate (TBAP) was obtained from Nacalai Tesque Inc. All other chemicals were of reagent grade.

Characterization of the generated PCOOH. PC oxidation products were diluted with methanol, prior to measurement of ultraviolet (UV) absorption spectra in the wavelength range from 200 to 300 nm. This was to confirm the induction of conjugated diene formation by hydroperoxides which have characteristic absorption at 233 nm (23). Native lecithin was similarly diluted with methanol and the UV absorption spectrum was measured. The production of PCOOH was verified by reversed-phase high-performance liquid chromatography (HPLC) in a Tosoh (Tokyo, Japan) system composed of a CCPS pump, a UV-8020 UV absorption detector and a Chromatocorder 21 integrator, attached to an Irika Σ985 electrochemical detector (ECD) (Kyoto, Japan), and another Chromatocorder 21 integrator. The column was a packed octadecyl silica gel (ODS) column (4.6 i.d. × 150 mm) from YMC (Kyoto, Japan). The mobile phase solution was a mixture of methanol/water (95:5, vol/vol) containing 30 mM lithium acetate. The flow rate of the mobile phase was 1.0 mL/min. To detect PCOOH, the eluent was monitored at 210 nm with the UV detector and at –300 mV vs. Ag/AgCl with the ECD (24). The relationship between absorbance at 233 nm and the ratio of PCOOH to total native PC was also determined.

Assay of tubulin GTPase activity. Tubulin GTPase activity was measured as the indicator of tubulin function, with the tubulin GTPase activity being diagnostic of the microtubule assembly (15,16).

Measurement of enzyme activity was carried out as described previously by Seckler *et al.* (25). The total volume of the assay system was 250 μL in a microtube. Assays were performed in 10 mM phosphate buffer, pH 7.0, containing 0.1 mM GTP, 3.4 M glycerol, and 10 mM $MgCl_2$ with native PC or PCOOH at a final concentration of 0.1 mg/mL. The assay solution was constituted by successive addition of $MgCl_2$, the basic buffer (10 mM phosphate buffer, pH 7.0, containing 0.1 mM GTP, 3.4 M glycerol, and 0.5 mM $MgCl_2$), PCOOH, and tubulin (16). The lipid used in this interaction study with tubulin was a mixture of native and hydroperoxides of PC because the purification was too complicated and difficult to do. The reaction was terminated after 30 min (26) as this incubation time has been shown to be sufficient to measure steady-state tubulin GTPase activity. This activity was measured on the basis of GDP formation, with the GDP concentration being determined by reversed-phase HPLC using a Tosoh HPLC system which consisted of a CCPS pump and a UV-8020 UV absorption detector and a Chromatocorder 21 integrator. A packed ODS column (4.6 × 250 mm) obtained from Nacalai Tesque was used for all assays, with the flow rate set at 1.0 mL/min and the detection wavelength at 253 nm.

The GTPase activity was calculated from the amount of GDP obtained by comparing the area obtained with a Chromatocoder 21 integrator with that of a standard GTP solution. An extinction coefficient at 253 nm of 13,700 $M^{-1}\cdot cm^{-1}$ was used for both GTP and GDP (27).

Fluorescence spectroscopy. The effect of PCOOH on tubulin structure was monitored by fluorescence spectroscopy. A concentration of 0.1 mg/mL was utilized for PCOOH and tubulin in all cases. PCOOH was added to the basic buffer (10 mM phosphate buffer (pH 7.0) containing 3.4 M glycerol, 0.1 mM GTP and 0.5 mM $MgCl_2$) prior to ultrasonication. Tubulin and PCOOH were mixed in the fluorescence cuvette for 15 min prior to measurement of the fluorescence spectra. Excitation spectra were obtained at the emission wavelength of 330 nm, with the excitation being measured between 200 and 300 nm. For emission spectra, an excitation wavelength at 278 nm was utilized, and the emission was measured between 290 and 450 nm. The temperature was 20°C for all assays. A Shimadzu PF-540 spectrofluorophotometer (Kyoto, Japan), with an attached Shimadzu DR-3 data recorder was used for all fluorescence measurements.

UV difference spectra. In order to detect small changes in the conformation of tubulin induced by reaction with PCOOH, UV difference spectroscopy was utilized. The temperature of the reaction mixture was increased from 0 to 37°C, and the difference spectrum measured after 20 min. As tubulin polymerizes in the presence of a high concentration of glycerol (28), a buffer (10 mM phosphate buffer, pH 7.0, containing 0.1 mM GTP, and 0.5 mM $MgCl_2$) without glycerol was used. Because lipid hydroperoxides have an absorption maximum at 233 nm and GTP has one at 253 nm, the total absorption of the reaction mixture is potentially very high. Therefore, in order to minimize experimental and instrumental problems due to high absorbance, the PCOOH concentration was kept to a minimum. Difference spectra were obtained with a cell having a 1-mm partition in the reference cuvette. PCOOH (0.1 mg/mL) was added to one compartment and tubulin (1.0 mg/mL) to another of the reference cuvette.

Tubulin and PCOOH were mixed in the sample cell at concentrations equivalent to those in to the sample cells taking into account the thickness of the cell partition. The concentrations of PCOOH and tubulin in the sample cell were 0.045 and 0.45 mg/mL, respectively. A Shimadzu UV-2000 spectrophotometer, with an attached Neslab RTE-110 incubator (Portsmouth, NH) was used in all cases.

Measurement of electric conductivity. In order to monitor the binding state of tubulin with PCOOH, electric conductivity measurements were performed. The assay buffer (0.1 mM GTP and 0.5 mM $MgCl_2$ in 10 mM phosphate buffer, pH 7.0) did not contain glycerol. The concentration of tubulin was 0.1 mg/mL. This is lower than in other experiments due to the large volume of solution required in conductivity experiments and the known difficulty of purifying large amounts of tubulin from bovine brain. Glycerol was not included in the assay mixture as it has no electric charge and a high viscosity, which can result in an unstable conductivity signal. The concentration of PC or PCOOH was 0.1 mg/mL and the volume of the assay solution was 10 mL in all cases. Conductivity measurements were performed as follows. After each sample had been placed in a test tube, it was stirred using a test tube mixer (Koike Precision Instruments, Hyogo, Japan) for 10 s. The reaction mixture was then ultrasonicated for 30 s, the reaction temperature was brought to 25°C by being placed in an incubator and the reaction was allowed to take place for 20 min. The electric conductivity was then measured 30 s after the cells had been dipped into the sample. The electric conductivity meter was a model CM-15 meter from Kyoto Electronics Manufacturing Corp. (Kyoto, Japan).

Amino acid analysis. The effect of PCOOH on individual amino acids in tubulin was monitored using amino acid analysis. To prepare samples, mixtures of tubulin with PC or PCOOH in 10 mM phosphate buffer, pH 7.0, containing 0.1 mM GTP and 10 mM $MgCl_2$ in the presence or absence of 3.4 M glycerol were incubated at 37°C for 30 min or 5 h. The concentrations of tubulin and PC or PCOOH were 1.0 mg/mL and 0.1 mg/mL, respectively. Excess PC or PCOOH was removed by batch gel filtration (1.0 × 7 cm column) with Sephadex G-25 (m). Samples were hydrolyzed in 6 M HCl at 110°C for 24 h after removing oxygen by flushing with nitrogen gas. Cysteine was oxidized in 0.01 M NaOH for 5 h after hydrolysis. The instrument was a Hitachi 835 amino acid analyzer (Tokyo, Japan).

RESULTS AND DISCUSSION

Production of PCOOH. The formation of PCOOH was confirmed using ultraviolet absorption spectroscopy. Photooxidation of Lipoid S-100 resulted in an increase in absorbance at 233 nm attributable to the formation of hydroperoxides. Four main peaks, observed on analysis of the Lipoid S-100 by HPLC (Fig. 1), presumably are due to distinct molecular species. After photooxidation, four new peaks detectable by both UV absorption and ECD were observed (Fig. 1). ECD detects hydroperoxides and hydroxides (24). Monohydroperoxide was detected by mass spectrometry of photooxidized PC in our preliminary experiment (data not shown). The mass spectrum indicated two important peaks of MW = 782 due to dilinoleoyl-PC and of MW = 814 due to its monohydroperoxide. Linoleic acid (64.8%) is the most common fatty acid in soybean PC. Also, dilinoleoyl-PC accounts for the largest portion (31.1%) of the principal molecular species of soybean PC (29). These results indicate that the molecular species cor-

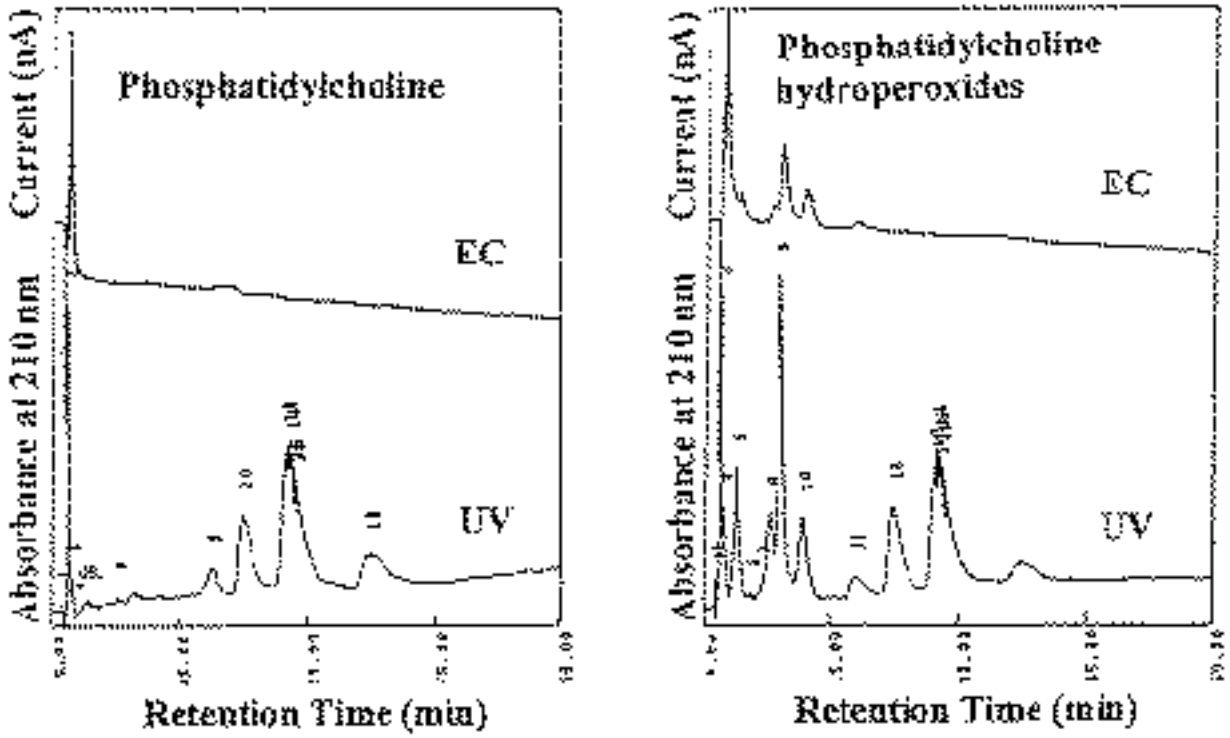

FIG. 1. High-performance liquid chromatography analyses of phosphatidylcholine (PC) and phosphatidylcholine hydroperoxides (PCOOH). PC, 25 µL (1.0 mg/mL); PCOOH, 25 µL (1.0 mg/mL). UV, ultraviolet; EC, electrochemical.

responding to the new peaks are hydroperoxides produced by photooxidation of PC. We can detect almost all compounds by the absorbance at 210 nm in HPLC. On the other hand, the increase of absorbance at 233 nm is due to conjugated hydroperoxides. Therefore, examining the relationship with the area of absorbance at 233 nm can provide information on the generation of secondary products.

Figure 2 shows the relationship between the observed absorbance at 233 nm and the integrated area of the peaks assigned to hydroperoxides in HPLC. The correlation coefficient was 0.945, indicating that the photooxidation in this experiment produced monohydroperoxides of PC but no secondary products. As 50% each of the conjugated and nonconjugated hydroperoxides are produced by photooxidation (30,31), twice the amount of hydroperoxides was used in this study compared the amount calculated from the UV absorbance at 233 nm.

We should be able to obtain the same results even if conjugated and nonconjugated dienes are used independently because the interaction between tubulin and lipid peroxides was due to a hydrophobic interaction as described below on the bases of photospectroscopy and electric conductivity measurements.

Tubulin GTPase activity. PCOOH clearly lowered tubulin GTPase activity, as shown in Figure 3. It is confirmed in the preliminary experiment that PC had no effect on tubulin GTPase activity. We reported previously that PCOOH acted directly on tubulin and that its ability to polymerize into microtubules was reduced (14,15).

Figure 4 shows the relationship between tubulin GTPase activity and the concentration of added PCOOH. There is a direct linear correlation between the reduction in tubulin GTPase activity (and therefore polymerization ability) and the concentration of conjugated PCOOH, the correlation efficient being –0.959. The concentration of conjugated PCOOH was calculated from the absorbance at 233 nm (23). The concentration of hydroperoxides can double when conjugated and nonconjugated hydroperoxides exist at equal concentration. These results emphasize that prolonged exposure of even low concentrations of lipid hydroperoxides to tubulin in a living cell will adversely affect the tubulin and therefore the microtubule function.

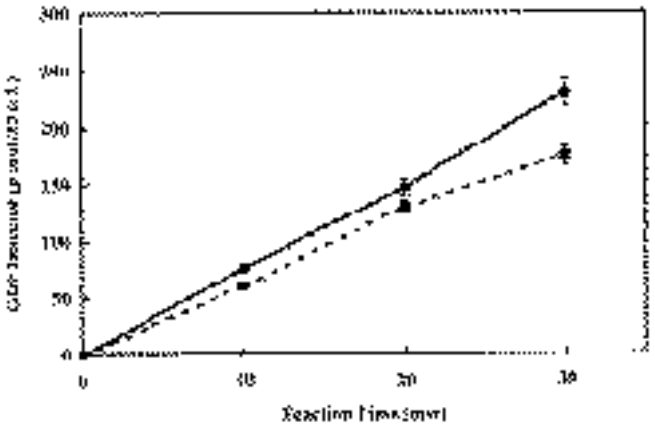

FIG. 3. Effect of PCOOH on tubulin GTPase activity. (●) Control (tubulin: 1.0 mg/mL); (■) PCOOH (84.3 μM) added. See Figure 1 for abbreviation.

Measurement of the fluorescence spectrum of tubulin. Figure 5 shows a typical fluorescence emission spectrum of tubulin in the absence and presence of PCOOH. PC had no effect on a fluorescence spectrum of tubulin in our preliminary experiment. When excited at 278 nm, the emission maxima of tubulin in the absence and presence of PCOOH were 326.4 and 330 nm, respectively. In addition, the emission intensity increased by about 15%. The fluorescence spectrum of tryptophan residue in protein shifts to the red region on contact with water (32). The red shift in the emission maximum indicates that the fluorescent aromatic amino acids become easier to dissolve on reaction with PCOOH. These results indicate a significant conformational change upon reaction with PCOOH.

Ultraviolet difference spectrum measurement. Figure 6 shows the UV difference spectrum of tubulin in the absence and presence of PCOOH. The UV spectra of protein in the re-

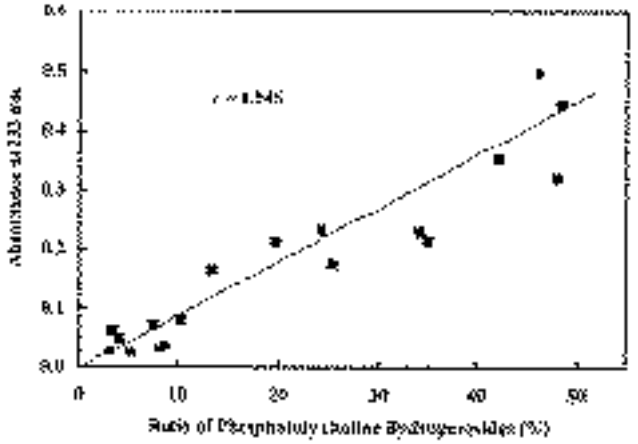

FIG. 2. Relationship between absorbance at 233 nm and ratio of PCOOH to total PC. See Figure 1 for abbreviations.

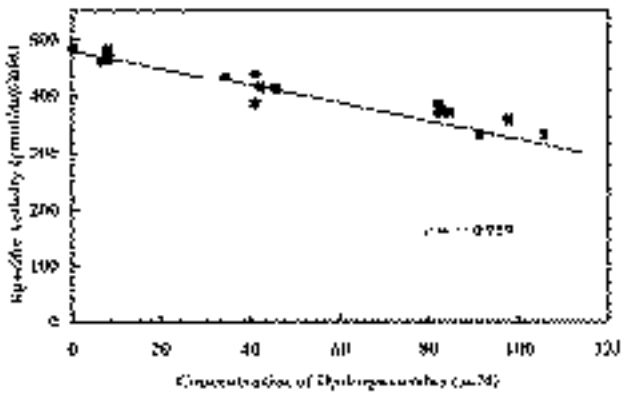

FIG. 4. Relationship between tubulin GTPase activity and PCOOH concentration. See Figure 1 for abbreviation.

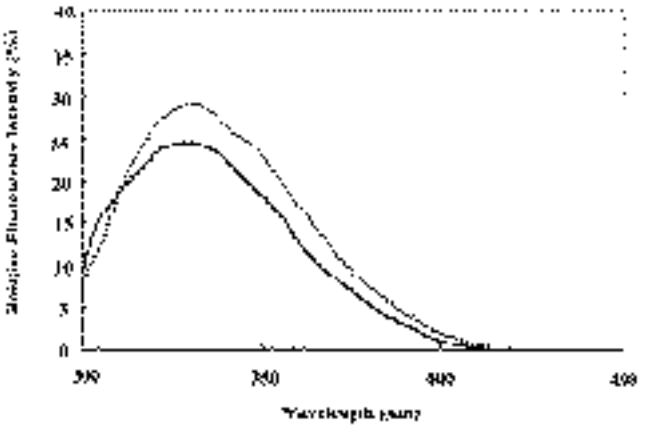

FIG. 5. Fluorescence spectra of tubulin in the presence and absence of PCOOH. ——, tubulin in the absence of PC; ·····, tubulin and PCOOH. See Figure 1 for abbreviations.

gion of 280 nm are dominated by the aromatic amino acids. Close scrutiny of the spectra in this region shows a reproducible decrease in the absorbance upon reaction with PCOOH. The differences are, however, much less obvious than the fluorescence measurement which presumably reflects the greater sensitivity of tryptophan fluorescence relative to its absorbance characteristics on the conformational state of the protein.

Electric conductivity measurement. Table 1 shows the electric conductivity of tubulin solution in the absence and presence of PCOOH. The electric conductivities of the tubulin and buffer solutions were 1.407 and 1.386 mS/cm, respectively.

The difference is due to the presence of charged tubulin. No difference was observed between the electric conductivities for the buffer and PC solution, indicating the PC has no charge under these experimental conditions. The electric conductivity increased from 1.386 to 1.395 mS/cm upon addition of PCOOH, reflecting a slight ionic dissociation of PCOOH in solution.

The electric conductivities measured for tubulin in the presence or absence of PC were almost identical. The conductivity measured for tubulin in the presence of PCOOH (1.417 mS/cm) is very close (1.416 mS/cm) to the calculated value obtained by adding the conductivity of tubulin solution (1.407 mS/cm) and the difference (0.009 mS/cm) between that of PCOOH solution (1.395 mS/cm) and buffer (1.386 mS/cm). These results indicate no change in the charge states of either tubulin or PCOOH. This supports the interpretation that the interaction is of a hydrophobic nature and does not involve a change in the net charge of the individual amino acids.

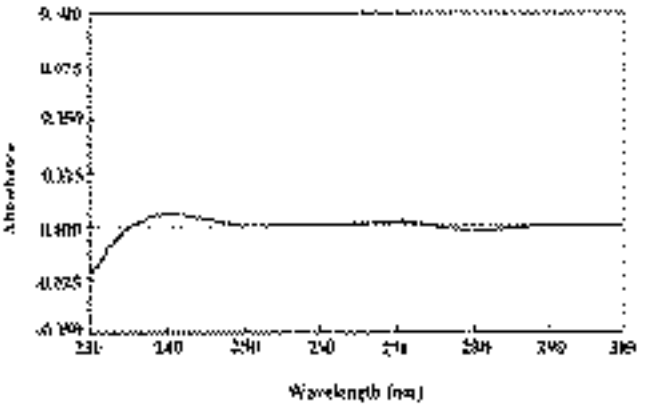

FIG. 6. Difference spectrum of tubulin in the presence and absence of PC or PCOOH. See Figure 1 for abbreviations.

TABLE 1
Electric Conductivities of Tubulin Solution in the Presence and Absence of Phosphatidylcholine or Phosphatidylcholine Hydroperoxides

Sample	(mS/cm)[a]
Tubulin	1.407 ± 0.0079
PC	1.386 ± 0.0087
PCOOH	1.395 ± 0.0111
Tubulin + PC	1.403 ± 0.0075
Tubulin + PCOOH	1.417 ± 0.0124
Buffer	1.386 ± 0.0078

[a]Values are expressed as means ± SE of seven independent determinations. PC, phosphatidylcholine; PCOOH, phosphatidylcholine hydroperoxide.

Amino acid analysis. The potential covalent modification of individual amino acids by lipid peroxides was examined using amino acid compositional analysis. Table 2 summarizes the results of amino acid analysis of tubulin when treated with PC or PCOOH in the presence or absence of glycerol. The presence of PC had no effect on the amino acid composition of tubulin either in the absence or presence of glycerol. However, a small reproducible effect of PCOOH on the observed methionine and cysteine contents was detected in the presence of glycerol. This decrease was clearly time dependent (Table 2). Many amino acids (Met, Cys, Tyr, His, Arg, and Trp) are susceptible to lipid peroxides in papers described below.

Soluble tubulin has been reported to interact with PC vesicles (33,34). However, these interactions were presumably noncovalent. The nature of the interaction of tubulin with phospholipid oxidation products has not been characterized, although it is known that membrane lipid is peroxidized (35), and that PCOOH is present in human plasma (36).

The nature of the modification of particular amino acids by lipid peroxides has yielded seemingly contradictory results. Crawford *et al.* (37) reported the interaction of glycine with malonaldehyde, which is one of the secondary products of lipid peroxidation. Chio and Tappel (38) reported that malonaldehyde formed a Schiff base with various amino acids and that the final product displayed fluorescence with an emission maximum at 450 nm excited at 370 nm. However, Kikugawa and Ido (39) examined in detail the formation of dihydropyridine from malonaldehyde and primary amines under mild conditions. Shimasaki *et al.* (40) have also reported the interaction of lipid with glycine in the presence of ascorbic acid. A decrease of methionine and lysine residues

TABLE 2
Changes of Amino Acid Composition of Tubulin Exposed to by PC or PCOOH (mol%)[a]

	In the presence of glycerol				In the absence of glycerol			
		Tb + PC	Tb + PCOOH			Tb + PC	Tb + PCOOH	
	Tb only	5 h	0.5 h	5 h	Tb only	5 h	0.5 h	5 h
ASp	11.06	10.92	11.39	10.83	10.45	10.54	10.54	10.53
Thr	6.83	6.63	6.95	6.69	6.45	6.49	6.49	6.43
Ser	5.92	5.86	6.00	5.90	5.47	5.61	5.63	5.74
Glu	11.90	12.74	12.28	12.98	13.33	13.47	13.47	13.47
Pro	4.68	4.70	4.91	4.91	4.85	4.74	4.66	4.67
Gly	8.77	8.85	8.87	8.83	8.39	8.52	8.48	8.70
Ala	7.90	7.93	8.21	7.83	7.62	7.61	7.58	7.55
Cys	1.23	1.42	1.12	0.95	1.45	1.57	1.56	1.35
Val	7.00	6.94	7.00	6.87	6.68	6.64	6.64	6.69
Met	2.65	2.60	2.09	1.79	2.87	2.85	2.71	2.67
Ile	4.95	4.93	5.05	4.85	4.79	4.70	4.72	4.75
Leu	7.85	7.79	8.06	7.70	7.55	7.46	7.55	7.43
Tyr	3.01	2.79	3.30	3.38	3.75	3.71	3.73	3.68
Phe	5.15	5.08	5.51	4.97	4.79	4.68	4.77	4.73
Lys	4.23	4.25	4.48	4.19	3.99	3.98	4.00	4.02
His	2.87	2.72	2.87	2.70	2.63	2.57	2.60	2.63
Arg	4.00	3.82	2.96	4.63	4.94	4.88	4.91	4.91

[a]Tb, tubulin; see Table 1 for other abbreviations.

has been observed during the autooxidation process between linoleic acid and casein (5).

As described above, the interaction of lipid peroxides with protein is very complicated at the mechanistic level and not easily interpretable. In this experiment, we observed that the molar concentration of methionine in tubulin decreases with the time of reaction with hydroperoxides.

As tubulin GTPase activity decreases in a similar time-dependent manner, it can be postulated that chemical modific ation of methionine leads to a decrease in the specific activity of the modified tubulin. Whether this effect is due to direct steric hindrance of the tubulin–tubulin contacts in the microtubule or to conformationally induced changes is unclear. Fluorescence spectra indicated clear conformational changes on lipid peroxidation, which probably were not due to global unfolding as they only involved a small red shift in the fluorescence spectra. Reinforcing this interpretation is the observation that there was only a very small change in UV spectra observed on peroxidation of tubulin. We previously examined the effect of strongly oxidized lipid on tubulin GTPase activity to examine the effect of one of the lipid peroxides on the cytoskeleton protein, tubulin. We observed a strong interaction between them, with the activity being inhibited during the assay, when strongly oxidized lipid was used (16–18). However, lipid may not be strongly oxidized in living cells which are known to contain hydroperoxides. We therefore decided that there was a need to study the effect of mildly oxidized lipid to clarify the interaction with protein. Although the conformational damage of protein *in vivo* may be small, the effect on cell functions can be expected to be large. In this paper, we have tried to clarify the effect of a small amount of lipid peroxides by examining the concentration dependence of mildly oxidized lipids and the change of protein structure, although the change was small. Our findings suggest that the binding style between lipid hydroperoxides and protein may be a hydrophobic one.

ACKNOWLEDGMENT

This work was supported in part by a grant-in-aid for Encouragement of Young Scientists from the Ministry of Education, Science and Culture of Japan (to MK) (No. 09780019).

REFERENCES

1. Kanazawa, K., Ashida, H., Minamoto, S., and Natake, M. (1986) The Effect of Orally Administrated Secondary Autoxidation Products of Linoleic Acid on the Activity of Detoxifying Enzymes in the Rat Liver, *Biochim. Biophys. Acta 879,* 36–43.
2. Ashida, H., Kanazawa, K., and Natake, M. (1987) Decrease of the NADPH Level in Rat Liver on Oral Administration of Secondary Autoxidation Products of Linoleic Acid, *Agric. Biol. Chem. 51,* 2951–2957.
3. Chiba, H., Doi, H., Yoshikawa, M., and Sugimoto, E. (1976) Deterioration of Casein Components by Malonaldehyde, *Agric. Biol. Chem. 40,* 1001–1010.
4. Shimasaki, H., Ueta, N., and Privett, O.S. (1982) Covalent Binding of Peroxidized Linoleic Acid to Protein and Amino Acids as Models for Lipofuscin Formation, *Lipids 17,* 878–883.
5. Kanazawa, K., Ashida, H., and Natake, M. (1987) Autoxidizing Process Interaction of Linoleic Acid with Casein, *J. Food Sci. 52,* 475–478.
6. Kubow, S. (1990) Toxicity of Dietary Lipid Peroxidation Products, *Trends Food Sci. Technol. 9,* 67–71.
7. Martinez-Cayuela, M. (1995) Oxygen Free Radicals and Human Disease, *Biochimie 77,* 147–161.
8. Steinbrecher, U.P., Parthasarathy, S., Leake, D.S., Witztum, J.L., and Steinberg, D. (1984) Modification of Low Density Lipoprotein by Endothelial Cells Involves Lipid Peroxidation and Degradation of Low Density Lipoprotein Phospholipids, *Proc. Natl. Acad. Sci. USA 81,* 3883–3887.

9. Yu, B.P., Chen, J.J., Kang, C.M., Choe, M., Maeng, Y.S., and Kristal, B.S. (1996) Mitochondrial Aging and Lipoperoxidative Products, *Ann. New York Acad. Sci. 786,* 44–56.
10. Purich, D.L., and Kristofferson, D. (1984) Microtubule Assembly: A Review of Progress, Principles, and Perspectives, in *Advances in Protein Chemistry* (Anifinsen, C.B., Edsall, J.T., and Richards F.M., ed.), Vol. 36, pp. 133–212, Academic Press, Orlando.
11. Luduena, R., Shooter, M.E., and Wilson, L. (1977) Structure of the Tubulin Dimer, *J. Biol. Chem. 252,* 7006–7014.
12. Ponstingl, H., Little, M., and Krauhs, E. (1984) Tubulins, in *Peptide and Protein Reviews* (Hearn, M.T.W., ed.), Vol. 2, pp. 1–81, Marcel Dekker, New York.
13. Qian, A., Burton, P.R., and Himes, R.H. (1993) A Comparison of Microtubule Assembly in Brain Extracts from Young and Old Rats, *Mol. Brain Res. 18,* 100–106.
14. Miyazawa, T., Suzuki, T., Fujimoto, K., and Kaneda, T. (1990) Phospholipid Hydroperoxide Accumulation in Liver of Rats Intoxicated with Carbon Tetrachloride and Its Inhibition by Dietary α-Tochopherol, *J. Biochem. 107,* 689–693.
15. Kawakami, M., Hasegawa, K., and Doi, H. (1994) Effect of Phospholipid Peroxides on GTPase Activity of Tubulin, *Bull. Mukogawa Women's Univ. Nat. Sci. 42,* 17–23.
16. Kawakami, M., Kanazawa, K., and Doi, H. (1993) Effects of Lecithin Peroxides on Microtubule Assembly of Tubulin, *J. Jpn. Soc. Nutr. Food Sci. 46,* 89–91.
17. Doi, H., Imanishi, T., Iwami, K., and Ibuki, F. (1991) Is Microtubule Assembly Not Associated with GTP Hydrolysis? *Agric. Biol. Chem. 55,* 245–246.
18. Kawakami, M., Ward, L., and Doi, H. (1998) Inhibition of Tubulin Guanosine-5′-triphosphatase by Lipid Peroxides: Protective Effects of Vitamin A Derivatives, *J. Am. Oil Chem. Soc. 75,* 635–641.
19. Weisenberg, R.C., and Timasheff, S.N. (1970) Aggregation of Microtubule Subunit Protein. Effects of Divalent Cations Colchicine and Vinblastine, *Biochemisty 9,* 4110–4116.
20. Lee, J.C., Frigon, R.P., and Timasheff, S.N. (1973) The Chemical Characterization of Calf Brain Microtubule Protein Subunits, *J. Biol. Chem. 248,* 7253–7262.
21. Na, G.C., and Timasheff, S.N. (1981) Interaction of Calf Brain Tubulin with Glycerol, *J. Mol. Biol. 151,* 165–178.
22. Andreu, J.M., and Timasheff, S.N. (1982) Conformational States of Tubulin Liganded to Colchicine, Tropolone Methyl Ester, and Podophyllotoxin, *Biochemistry 21,* 6465–6478.
23. Little, C., and O'Brien, P.J. (1968) The Effectiveness of Lipid Peroxide in Oxidizing Protein and Non-Protein Thiols, *Biochem. J. 106,* 419–423.
24. Terao, J., Shibata, S., and Matsushita, S. (1988) Selective Quantification of Arachidonic Acid Hydroperoxides and Their Hydroxy Derivatives in Reverse Phase High-Performance Liquid Chromatography, *Anal. Biochem.* 169, 415–423.
25. Seckler, R., Wu, G.-M., and Timasheff, S.N. (1990) Interactions of Tubulin with Guanylyl-(β-γ-methylene)Diphosphonate. Formation and Assembly of a Stoichiometric Complex, *J. Biol. Chem. 265,* 7655–7661.
26. Doi, H. (1987) Calcium Binding to Tubulin (tubulin-colchicine complex), *J. Biochem. Soc. Jpn. 59,* 284–289.
27. Bock, R.M., Ling, N.-S., Morell, S.A., and Lipton, S.H. (1956) Ultraviolet Absorption Spectra of Adenosine-5′-triphosphate and Related 5′-Ribonucleotides, *Arch. Biochem. Biophys. 62,* 253–264.
28. Lee, J.C., and Timasheff, S.N. (1975) The Reconstitution of Microtubules from Purified Calf Brain Tubulin, *Biochemistry 14,* 5183–5187.
29. Rawls H.R., and Santen, P.J.V. (1970) A Possible Role for Singlet Oxygen in the Initiation of Fatty Acid Autoxidation, *J. Am. Oil Chem Soc. 47,* 121–125.
30. Chan, H.W.-S., Frank, A.A., and Swoboda, P.A.T. (1976) Thermal Decomposition of Individual Positional Isomers of Methyl Linoleate Hydroperoxide: Evidence of Carbonoxygen Bond Scission, *J. Am. Oil Chem Soc. 53,* 572–576.
31. Terao, J., Hirota, Y., Kawakatsu, M., and Matsushita, M. (1981) Structural Analysis of Hydroperoxides Formed by Oxidation of Phosphatidylcholine with Singlet Oxygen, *Lipids 16,* 427–432.
32. Kronman, M.J., and Holmes, L.G. (1971) The Fluorescence of Native, Denatured and Reduced-Denatured Proteins, *Photochem. Photobiol. 14,* 113–134.
33. Casron, J.M., and Berlin, R.D. (1979) Interaction of Microtubule Proteins with Phospholipid Vesicles, *J. Cell Biol. 81,* 665–671.
34. Klausner, R.D., Kumar, N., Weinstein, J.N., Blumenthal, R., and Flavin, M. (1981) Interaction of Tubulin with Phospholipid Vesicles. I. Association with Vesicles at the Phase Transition, *J. Biol. Chem. 256,* 5879–5885.
35. Mead, J.F. (1980) Membrane Lipid Peroxidation and Its Prevention, *J. Am. Oil Chem. Soc. 57,* 393–397.
36. Miyazawa, T., Yasuda, K., Fujimoto, K., and Kaneda, T. (1988) Presence of Phosphatidylcholine Hydroperoxide in Human Plasma, *J. Biochem. 103,* 744–746.
37. Crawford, D.L., Yu, T.C., and Sinnhuber, R.O. (1966) Reaction of Malonaldehyde with Glycine, *J. Agr. Food Chem. 14,* 182–184.
38. Chio, K.S., and Tappel, A.L. (1969) Synthesis and Characterization of the Fluorescent Products Derived from Malonaldehyde and Amino Acids, *Biochemistry 8,* 2821–2827.
39. Kikugawa, K., and Ido, Y. (1984) Studies on Peroxidized Lipid. V. Formation and Characterization of 1,4-Dihydropyridine-3,5-dicarbaldehydes as Model of Fluorescent Components in Lipofuscin, *Lipids 19,* 600–608.
40. Shimasaki, H., Hirai, N., and Ueta, N. (1988) Comparison of Fluorescence Characteristics of Products of Peroxidation of Membrane Phospholipids with Those of Products Derived from Reaction of Malonaldehyde with Glycine as a Model of Lipofuscin Fluorescent Substances, *J. Biochem 104,* 761–766.

[Received April 14, 1999, and in revised form January 14, 2000; revision accepted January 28, 2000]

Biophysical Studies and Intracellular Destabilization of pH-sensitive Liposomes

Françoise Van Bambeke[a,*], Anne Kerkhofs[a], André Schanck[b], Claude Remacle[c], Etienne Sonveaux[d], Paul M. Tulkens[a], and Marie-Paule Mingeot-Leclercq[a]

[a]Unité de Pharmacologie Cellulaire et Moléculaire, Brussels; [b]Unité de Chimie Physique Moléculaire et de Cristallographie, Louvain-La-Neuve; [c]Laboratoire de Biologie Cellulaire, Unité de Biologie Animale, Louvain-La-Neuve; and [d]Unité de Chimie Pharmaceutique et de Radiopharmacie, Brussels; Université Catholique de Louvain, Belgium

ABSTRACT: We examined changes in membrane properties upon acidification of dioleoylphosphatidylethanolamine/cholesterylhemisuccinate liposomes and evaluated their potential to deliver entrapped tracers in cultured macrophages. Membrane permeability was determined by the release of entrapped calcein or hydroxypyrene-1,3,6-trisulfonic acid (HPTS)-*p*-xylene-bis-pyridinium bromide (DPX); membrane fusion, by measuring the change in size of the liposomes and the dequenching of octadecylrhodamine-B fluorescence; and change in lipid organization, by ^{31}P nuclear magnetic resonance spectroscopy. Measurement of cell-associated fluorescence and confocal microscopy examination were made on cells incubated with liposomes loaded with HPTS or HPTS-DPX. The biophysical studies showed (i) a lipid reorganization from bilayer to hexagonal phase progressing from pH 8.0 to 5.0, (ii) a membrane permeabilization for pH <6.5, (iii) an increase in the mean diameter of liposomes for pH <6.0, and (iv) a mixing of liposome membranes for pH <5.7. The cellular studies showed (i) an uptake of the liposomes that were brought from pH 7.5–7.0 to 6.5–6.0 and (ii) a release of ~15% of the endocytosed marker associated with its partial release from the vesicles (diffuse localization). We conclude that the permeabilization and fusion of pH-sensitive liposomes occur as a consequence of a progressive lipid reorganization upon acidification. These changes may develop intracellularly after phagocytosis and allow for the release of the liposome content in endosomes associated with a redistribution in the cytosol.

Paper no. L8278 in *Lipids 35,* 213–223 (February 2000).

Delivery of macromolecules and other nonpermeant constituents into the cytosol of target cells is essential for the development of many new therapeutic approaches. Conventional liposomes are often ineffective in this context since they tend to bring their load to lysosomes (1). pH-sensitive liposomes (2) may represent a significant improvement for intracellular drug unloading thanks to their progressive, acid-driven destabilization along the endocytic pathway (3). These liposomes, indeed, not only are susceptible to releasing their content in acid vacuoles, such as late endosomes and lysosomes, but also are capable of promoting the transfer of encapsulated tracers to the cytosol (4). Accordingly, they have been assessed in a series of studies for potential therapeutic applications, including antitumor and antibacterial chemotherapy (5–6), and for the delivery of proteins, oligonucleotides, or even DNA (7–9).

In the present study, we examined a typical type of pH-sensitive liposomes made of dioleoylphosphatidylethanolamine and an anionic component, cholesterylhemisuccinate (DOPE/CHEMS). The small cross-sectional area of the headgroup of phosphatidylethanolamine, relative to that of the acyl chains, confers to this molecule a propensity to spontaneously form an inverted hexagonal phase H_{II} structure, a particular organization involved in membrane destabilization and fusion (10). At alkaline or neutral pH, however, the negatively charged CHEMS will reduce the intermolecular repulsions of phosphatidylethanolamine head groups and stabilize the structure in a bilayer organization. Yet, upon acidification, CHEMS will become less charged and will no longer hinder the reorganization of phosphatidylethanolamine in an H_{II} structure, ensuring the destabilization of the membrane structure (3). This mechanism has been documented concerning the increase in membrane permeability (11–16) and fusogenicity (2,12,14,17) of liposomes, and to a lesser extent, the cellular delivery of the vesicles' contents (1,4,18,19). Yet the changes in polymorphic organization of the lipids (20) remain largely undefined in this context. Moreover, most of these studies have used different types and compositions of liposomes, which make their conclusions difficult to generalize because lipid composition critically determines the pH sensitivity of acid-labile liposomes (4,11). In the present study, we have therefore undertaken to characterize, in a more systematic fashion, the biophysical phenomena (including changes in polymorphic organization) leading to an effective *in vitro* release of membrane-impermeant probes from one type of li-

*To whom correspondence should be addressed at UCL 73.70 avenue E. Mounier 73, 1200 Brussels; Belgium. E-mail: vanbambeke@facm.ucl.ac.be

Abbreviations: CHEMS, cholesterylhemisuccinate; DOPC, dioleoylphosphatidylcholine; DOPE, dioleoylphosphatidylethanolamine; DPX, *p*-xylene-

MATERIALS AND METHODS

Liposome preparation. Large unilamellar vesicles (LUV) were used throughout all experiments, but large multilamellar vesicles (MLV) were also included for ^{31}P nuclear magnetic resonance (NMR) studies. Both DOPE/CHEMS and DOPC/CHEMS liposomes were made at a phospholipid/CHEMS molar ratio of 7:3. Depending on the experiments and on the sensitivity of the method used, the volume of buffer varied between 1 and 5 mL, and the concentration of lipids, between 1 and 50 mg/mL. MLV were obtained by hydration of the dry lipid films for 1 h under nitrogen at 37°C in a 40 mM glycine-NaOH solution adjusted to pH 11 and containing the fluorescent probes (see below). They were thereafter submitted to five successive cycles of freezing (at –80°C) and thawing (at 37°C). LUV were obtained by extruding the resulting suspension 10 times through two superposed polycarbonate filters (pore size, 100 nm; Nucleopore Costar Corporation, Badhoevedorp, The Netherlands) under a nitrogen pressure of 17 bars, in a 10-mL Thermobarrel Extruder (Lipex Biomembranes, Vancouver, Canada) (21,22). The actual phospholipid concentration of each preparation was determined by phosphorus assay, as decribed previously (22), and adjusted to the desired value by dilution in the appropriate buffer just prior to each experiment. (All concentrations of liposomes are expressed by reference to their total lipid concentration, based on phospholipid determination and on a molar ratio of phospholipid/CHEMS of 7:3. In preliminary experiments, we checked that the phospholipid/cholesterol molar ratio was effectively very close to 7:3 after the hydration and extrusion procedures.) Liposomes were stored under nitrogen at 4°C until the beginning of the experiment, to minimize the risk of extensive lipid hydrolysis and oxidation (23), and were used within 24 h. The lack of chemical hydrolysis of phosphatidylethanolamine in our experimental conditions was checked by preparing DOPE/CHEMS liposomes with a trace amount of phosphatidylethanolamine 1-palmitoyl-2-(1-^{14}C)-linoleoyl (100 μCi/mmol of DOPE), and letting them age at 4°C for 24 h. Samples were then analyzed by thin-layer chromatography using $CHCl_3/CH_3OH/NH_3$ (25%)/H_2O 24:16:2:1 (by vol) as mobile phase. The radioactivity associated with free fatty acid and lysophosphatidylethanolamine was then measured and found to be less than 2% of the total amount of radioactivity recovered, whereas approximately 94% co-migrated with phosphatidylethanolamine.

Studies on liposomes. (i) Permeability studies. The release of calcein [entrapped at a self-quenching concentration (18,22,24)] and of HPTS [hydroxypyrene-1,3,6-trisulfonic acid (25)] coentrapped with and quenched by DPX (*p*-xylene-bis-pyridinium bromide (11)] from the liposomes was fol-

vanced Instruments, Needham Heights, MA). HPTS and DPX were dissolved in a 40 mM glycine-NaOH mixture adjusted to pH 11 (393 mOsm/kg) at a concentration of 31.8 and 35 mM, respectively (4,11). In preliminary experiments, we checked that DPX effectively quenched the fluorescence of HPTS for this concentration ratio. These solutions were then used for hydration of the lipid films as described above. After liposome preparation at a lipid concentration of 30 mM, the unencapsulated dye was removed by minicolumn centrifugation (22). Before each experiment, liposomes were adjusted to a total lipid concentration of 7.14 μM and 2.16 μM for calcein- and HPTS-release studies, respectively, using isoosmotic phosphate buffers of pH ranging from 8.0 to 5.0. Calcein fluorescence was measured at room temperature on a PerkinElmer 2000 Fluorescence Spectrophotometer [PerkinElmer, Beaconsfield, United Kingdom; λ_{exc}, 490 nm; λ_{em}, 516 nm (22)]; the inner effect was checked and found to be negligible. The fluorescence of free calcein in solution was found to be time- and pH-dependent, and our measurements were therefore systematically corrected for by appropriate factors. These factors were calculated by measuring the fluorescence of calcein solutions at all the pH values investigated as a function of the time and by comparing these values to that a calcein solution incubated for the same period of time and at pH 7.5. Fluorescence of HPTS was recorded at room temperature, using a λ_{em} of 520 nm and λ_{exc} of 390 and 450 nm (25), using a LS-30 Fluorescence Spectrophotometer (PerkinElmer). The percentage of dye release at any given time was defined as the ratio between the fluorescence measured at that time and that observed at the same time after disruption of the liposomes by exposure to 0.1% Triton X-100 in the same buffer. For each pH- and time-condition tested, the fluorescence values recorded were corrected for the influence of Triton X-100 by comparing the fluorescence value measured for a calcein solution in the absence of Triton to that measured in the presence of the detergent. A leakage efficiency factor, defined as the ratio between the percentage of marker released at a given pH to that measured at pH 7.5, was then used to assess the lability of the liposomes upon pH change.

(ii) Mixing of the liposome membranes: studies with octadecylrhodamine B (R18). Mixing of the liposome membranes was followed by measuring the fluorescence increase of R18, a lipid-soluble probe, upon dilution in the membrane occurring by fusion between labeled and unlabeled liposomes (26,27). Labeled liposomes were obtained by incorporating R18 in the dry lipid film at a concentration of 5.7% of the total lipids. Labeled and unlabeled liposomes, prepared at 2 mM, were mixed at a ratio of 1:4 and diluted to a final concentration of 5 μM by addition of appropriate buffers at the time of

posomes labeled by 1.16% of R18 (i.e., an identical total amount of marker diluted five times in membranes).

(iii) Size studies. The apparent size of the liposomes diluted to 50 μM in 40 mM cacodylate buffers of pH ranging from 8.0 to 5.0 was measured by quasi-elastic light scattering spectroscopy (28) using a Coulter Nano-sizer N4 MD particle Analyzer (Coulter Electronics Inc., Luton, England) at an angle of 90°, using both unimodal and size distribution analysis modes to determine the mean diameter and the full size distribution profile of each preparation, respectively.

(iv) Polymorphic behavior of the lipids as determined by ^{31}P NMR. The phase behavior of liposomes was determined as a function of pH and temperature. Classically, three types of phases can be distinguished on the basis of their ^{31}P NMR signals. The so-called bilayer signal is characterized by a high-field maximum and a low-field shoulder; the inverted hexagonal phase, by an inverse symmetry and a twofold reduced width; and the isotropic signal, by a sharp symmetric signal. In practice, MLV give a bilayer signal due to their organization in concentric bilayers, where rapid motion of phospholipid molecules along their long axis results in axial symmetry and partially averages the chemical shift anistropy (29). LUV give an isotropic signal, because the ^{31}P atoms are submitted to rapid isotropic motion owing to the rapid tumbling of the vesicles (30). As stated in the introduction, phosphatidylethanolamine has a propensity to organize itself in hexagonal phase (especially upon warming), in which the molecules project radially from the center of a cylinder of very small radius. The rapid rotation of the cylinders causes further averaging of chemical shift anistropy, explaining the reversed shape and the reduced width of the spectrum by comparison with the bilayer spectrum (29). To compare the appearance of this hexagonal phase starting from an isotropic or a bilayer phase, we performed NMR studies on both LUV and MLV. Liposome suspensions prepared at an initial lipid concentration of 75 mM were diluted in the appropriate buffers (Na carbonate from pH 10.0 to 9.2; Tris-HCl from pH 9.0 to 7.0; citric acid-NaOH from pH 6.2 to 5.2; and Na citrate-HCl from pH 5.0–3.0) and mixed with 0.2 mL D_2O (for locking on the deuterium signal) in 10 mm RMN tubes (final lipid concentration, 12.5 mM). The actual pH value of each suspension was measured with a minielectrode and a 691 Metrohm pH meter (Herisau, Switzerland), at both 30 and 70°C. All spectra were obtained at 101.3 MHz with a WM 250 Bruker instrument. Typical Fourier transform conditions were as follows: spectral width 20 kHz; 8 K data acquisition points; flip angle 60° (17 μs); 1 s repetition time. Five thousand free induction decays (FID) were accumulated with broad-band proton powergated decoupling. A line broadening of 50 Hz was applied to the FID before

with liposomes. J774 macrophages, a continuous reticulosarcoma cell line of murine origin (32), were grown as monolayers in 5% CO_2/95% air, at 37°C in an RPMI (Rosewell Park Memorial Institute) 1640 medium supplemented with 10% (vol/vol) fetal calf serum, 1.45% (wt/vol) $NaHCO_3$, and antibiotics (streptomycin 50 μg/mL, penicillin 50 IU/mL). Confluent cells were suspended by incubation with trypsin (0.5%)/EDTA (0.2%) in phosphate-buffered saline (PBS; 8 g/L NaCl, 0.2 g/L KCl, 1.15 g/L Na_2HPO_4, 0.2 g/L KH_2PO_4; pH 7.4), centrifuged, and plated in six-well plates for 3 d in RPMI medium supplemented with fetal calf serum, $NaHCO_3$, and antibiotics, as decribed above. At the time of the experiment, the cells were washed three times with PBS and reincubated during 15 min with 2 mL PBS containing liposomes (90 μM total lipid concentration) loaded with HPTS or HPTS-DPX. In preliminary experiments, the total fluorescence of the liposome preparations was determined after disruption by exposure to Triton X-100 (0.1%) and corrected for Triton X-100 influence as described above. These studies showed that the amount of HPTS or HPTS/DPX entrapped in DOPC/CHEMS was slightly larger than that entrapped in DOPE/CHEMS liposomes (30% in excess). After 15 min of uptake at 37°C, the cells were washed 10 times with ice-cold PBS and returned in growth medium at 37°C for different chase times.

(ii) Fluorescence assay. The cells were detached by trypsinization, pelleted by centrifugation, washed twice with ice-cold PBS, and gently resuspended in PBS. Viability and membrane integrity were checked by measuring the release of the cytosolic enzyme lactate dehydrogenase. HPTS fluorescence was recorded at a λ_{em} of 520 nm upon excitation at 363, 390, 450, or 488 nm and the signal expressed by reference to the protein cell content (33). The wavelengths of 390 and 450 nm correspond to the maximum in the excitation spectrum of HPTS at acidic and neutral pH, respectively (25), whereas those at 363 and 488 nm were the λ_{exc} used for confocal microscopy studies (see below). The 450/390 fluorescence ratio of HPTS was then used to evaluate the pH at which the probe was exposed in cells, based on calibration curves constructed by preparing the probe in phosphate buffers of known pH (between 5 and 8).

(iii) Confocal microscopy. Cells were treated as described above, except that they were cultivated in Lab-Tek Permanox culture chambers (Nunc, Roskilde, Denmark) allowing for the observation of living cells at high magnification under an inverted microscope. Images were recorded during incubation at 37°C using a Bio-Rad MRC 1024-UV laser scanning confocal microscope (Hemel Hempstead, United Kingdom) operated under control of the Lasersharp 2.10 software. Conditions of imaging were: filters E2 and UBHS, 63× oil-immersion ob-

screen and micrographs. Although the excitation wavelengths, which were imposed by the equipment, are not optimal, they nevertheless allowed for a clear-cut analysis of the pH differences in HPTS environment. The pH at which the fluorescence signals recorded upon excitation at 363 and 488 nm are equal was determined to be ~7.15, setting therefore the value for shifting the appearance of the tracer from green to red.

Materials. DOPE and DOPC were obtained from Avanti Polar Lipids, Inc. (Alabaster, AL), and radiolabeled phosphatidylethanolamine (specific radioactivity = 54 mCi/mmol), from Amersham International plc (Amersham, United Kingdom). Calcein and CHEMS were purchased from Sigma Chemical Co (St. Louis, MO). HPTS, DPX, and R18 came from Molecular Probes Inc. (Eugene, OR). Cell culture media and fetal calf serum were obtained from Gibco-Biocult (Peisley, Scotland). Other products were of analytical grade and obtained from E. Merck (Darmstadt, Germany).

RESULTS

Studies with liposomes. (i) Permeability studies. Figure 1A shows the release of calcein from LUV as a function of the time of incubation in buffers of different pH. DOPE/CHEMS liposomes released a large proportion (~ 60%) of calcein almost instantaneously when exposed to pH 5.0, with no further release after this first burst. The effect was highly dependent on pH since less than 10% release was observed at pH 7.5. DOPE/CHEMS liposomes exposed to pH 5.5 showed an intermediate behavior. In contrast, DOPC/CHEMS liposomes released a much lower proportion of calcein at pH 5.0, and this release proceeded slowly over the first 10 min of observation (Fig. 1B). Figure 1C shows the comparative release of calcein at 5 min over pH values from 8.0 to 5.0. The data confirm that acidity exerts a marked influence on calcein-release from DOPE/CHEMS liposomes, with a significant effect already observed at pH 6.0 ($P < 0.05$ by *t*-test). In contrast, DOPC/CHEMS liposomes appear considerably less sensitive to the decrease of pH. In parallel experiments, we measured the release of another marker (HPTS/DPX) from DOPE/CHEMS liposomes (Fig. 1C) with essentially similar results. HPTS/DPX did not significantly leak out from DOPC/CHEMS liposomes under the same conditions (data not shown).

(ii) Liposome membranes mixing studies. Figure 2A shows the fluorescence of R18 upon mixing of labeled and unlabeled LUV made of DOPE/CHEMS at different pH values. Liposomes exposed to pH 5.0 quickly (<5 min) showed a marked signal increase which amounted to approximately 10 times that recorded for the same liposomes exposed to pH 7.4. Liposomes exposed to pH 5.4 showed an intermediate behavior. (More time seems to be needed to reach a plateau value at pH

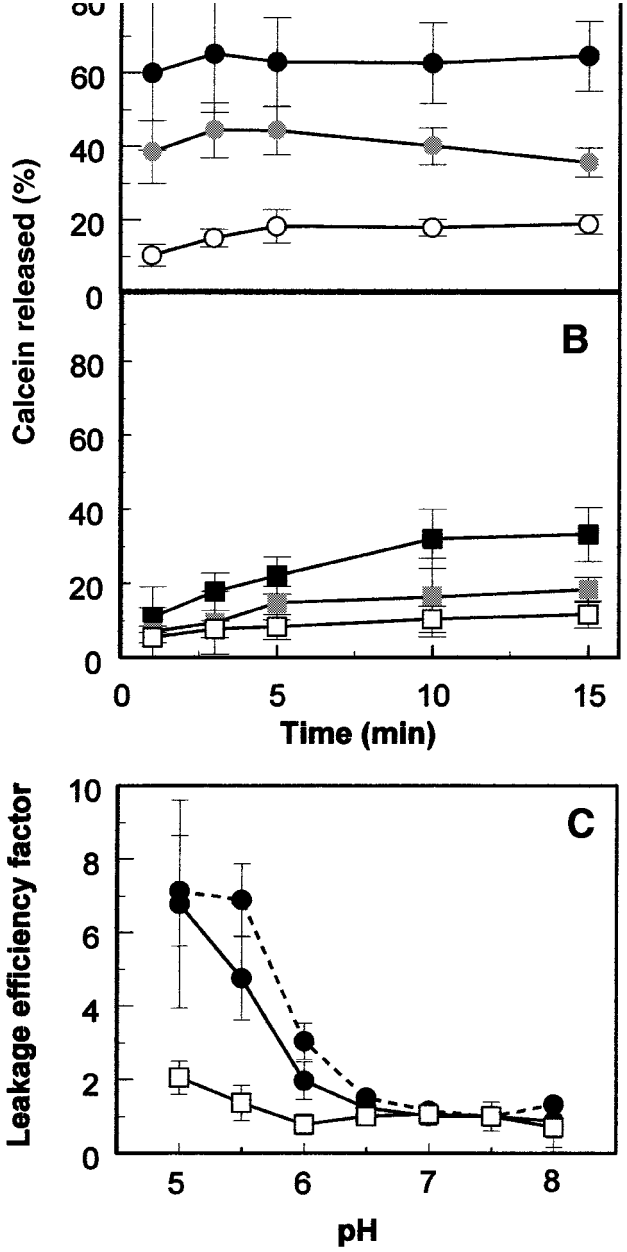

FIG. 1. Release of fluorescent tracers from large unilammelar vesicles (LUV) upon acidification. (A) Percentage of calcein released from dioleoyl phosphatidylethanolamine/cholesterylhemisuccinate (DOPE/CHEMS) or (B) dioleoylphosphatidylcholine/CHEMS (DOPC/CHEMS) liposomes after dilution and incubation at 37°C in isoosmotic phosphate buffers (closed symbols, pH 5.0; grey symbols, pH 5.5; open symbols, pH 7.5). Data shown are the mean values of three independent measurements in single liposome preparations. (C) Leakage efficiency factor (see Materials and Methods section) of DOPE/CHEMS (closed circles) and DOPC/CHEMS (open squares) liposomes loaded with calcein (——) or with hydroxy-

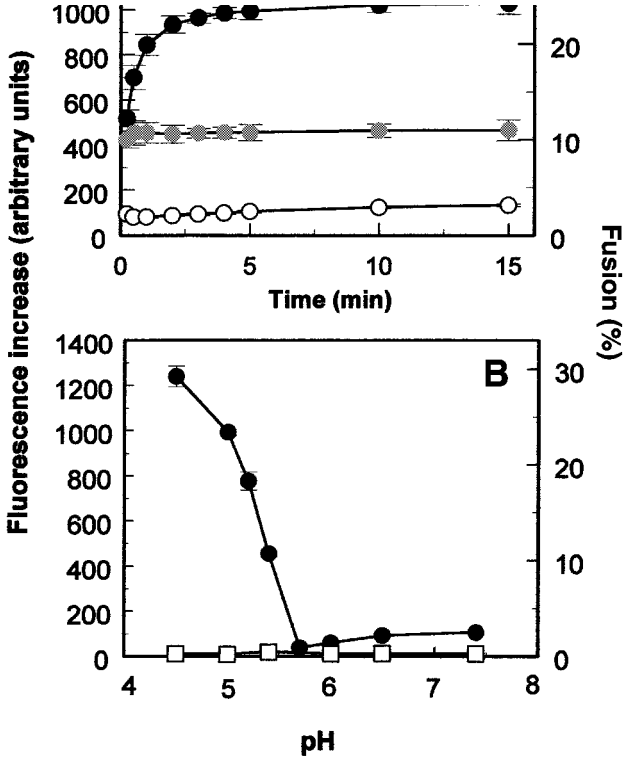

FIG. 2. Octadecylrhodamine B fluorescence dequenching in mixtures of labeled and unlabeled LUV upon acidification. (A) fluorescence recorded for DOPE/CHEMS liposomes after dilution and incubation of the mixed liposome population in 40 mM buffers (closed circles, pH 5.0; grey circles, pH 5.4; open circles, pH 7.4). Each curve is the mean of three independent determinations in single liposome preparations. (B) fluorescence recorded 5 min after dilution in 40 mM buffers for DOPE/CHEMS liposomes (closed circles) and DOPC/CHEMS liposomes (open squares). The right ordinate shows the percentage of fusion. Results are the mean ± SD of three independent measures on a single preparation of liposomes. For abbreviations see Figure 1.

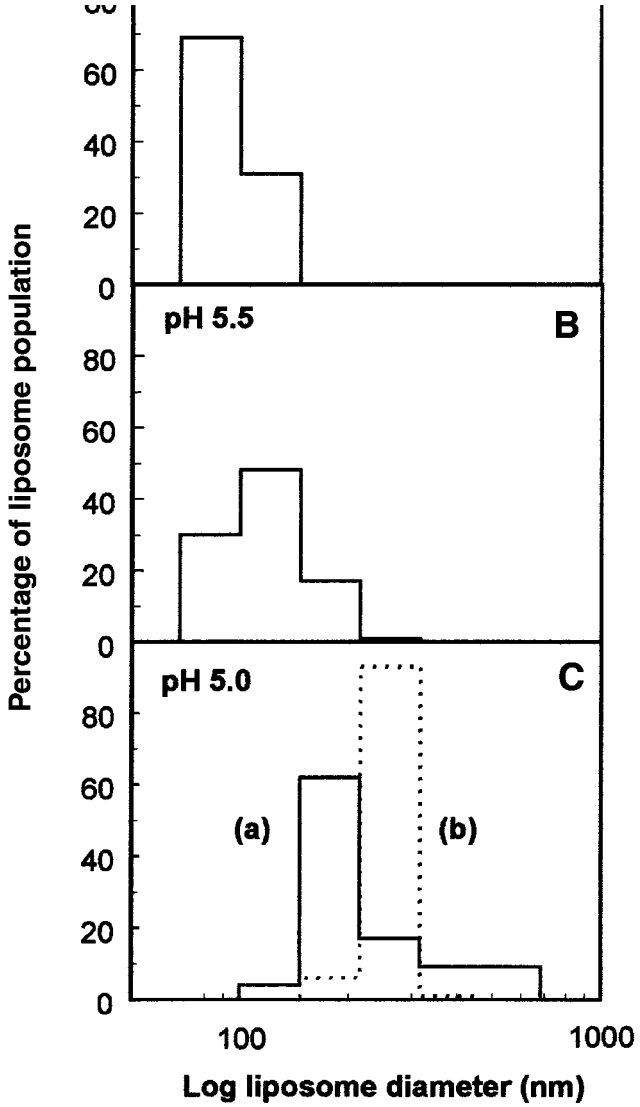

FIG. 3. Size distribution analysis of DOPE/CHEMS LUV determined by light-scattering spectroscopy 5 min after dilution and incubation at 37°C in buffers of different pH. For samples exposed to (C) pH 5.0, one reading was made after acidification [diagram in solid line (a)] and one additional reading was made after titration back to pH 7.5 [diagram in dotted line (b)]. For abbreviations see Figure 1.

slowly thereafter; thus time-dependence of the increase can only be assessed at pH 5.0.) These experiments were then repeated over a whole range of pH values, and DOPE/CHEMS liposomes were compared to DOPC/CHEMS liposomes. Figure 2B shows that the increase of the signal became significant at pH ≤ 5.4. DOPC/CHEMS liposomes did not show significant fluorescence increase throughout the whole range of pH values. The data of Figure 2 were also used to calculate the percentage of liposome fusion and this is shown on the right ordinate. Finally, similar experiments were also run in phosphate buffers (as used in permeability studies) to rule out any influence of the buffer system used. No difference were found when comparing data at the same pH with the phosphate and cacodylate buffer systems.

whereas the mean diameter of DOPC/CHEMS liposomes remained nearly constant at 100 nm in the same range of pH. The size distribution analysis of the DOPE/CHEMS liposomes illustrated in Figure 3 showed a narrowly distributed population at pH 7.5, but a progressive and marked shift toward large-diameter vesicles at acid pH. Titration back to pH 7.5 of liposomes exposed to pH 5.0 did not reverse this effect, and

obtained at other pH values is shown in the right panel of Figure 4. In alkaline medium and at 30°C, the spectrum was symmetric, with a half-height width of 3 ppm, and it can be considered as that of an isotropic-like phase. A decrease of pH caused the appearance of a spectrum characteristic of a hexagonal phase, showing a low-field peak and a high-field shoulder with a chemical shift anisotropy ($\Delta\sigma$) reduced by a factor of two compared to the $\Delta\sigma$ of a "bilayer" spectrum (10,29). Warming of the liposomes to 70°C caused a narrowing of the isotropic signal in alkaline medium and increased the proportion of hexagonal phase at intermediate pH values, but had no significant effect on the spectrum shapes of hexagonal phase at low pH values. By using the spectra obtained at 30°C for pH 3.7 and 9.3 as references for hexagonal and isotropic phases, respectively, the quantitative analysis showed that the

and 9.3 were taken as references for hexagonal and isotropic phases. The curves were very similar but slightly (approximately 0.4 pH units) displaced to less acidic values.

Similar studies were performed on MLV to better evidence the phase transitions. As shown in Figure 5 (left panel), these liposomes displayed a typical bilayer spectrum at 30°C and alkaline pH, with a high-field peak and a low-field shoulder. In contrast, the mixture was clearly organized in hexagonal phase at acidic pH. The phase transformation upon acidification was progressive and accompanied by the appearance of a low proportion of isotropic-type phase detected by a small peak at 0 ppm at pH 7.8. After warming to 70°C, the isotropic signal became detectable at pH 8.7 and was predominant at pH 7.8. After recooling to 30°C, the spectrum observed at pH

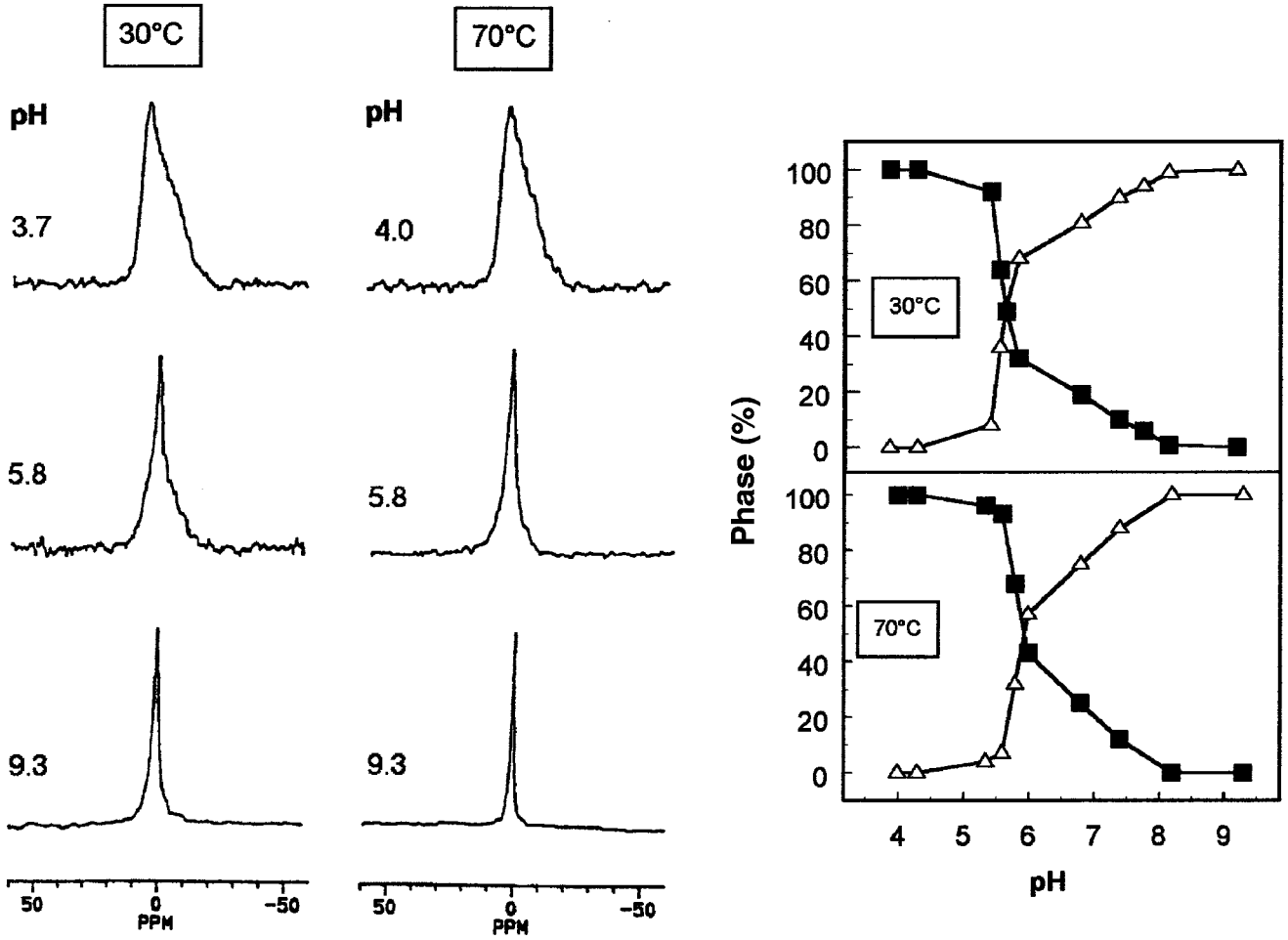

FIG. 4. ^{31}P nuclear magnetic resonance (NMR) spectroscopy of DOPE/CHEMS LUV. Left panel: typical spectra obtained at three different pH values at two temperatures. Right panel: phase behavior of the vesicles over the whole range of pH values investigated at both temperatures. Quanti-

reference to a bilayer phase, an isotropic phase, and an hexagonal phase, respectively. The results, presented in Figure 5 (right panel) show that 50% of the phospholipids adopt a hexagonal phase organization at a pH close to neutrality. This transformation from bilayer to hexagonal phase involved a passage through isotropic structures, the proportion of which drastically increased after one cycle of heating and cooling.

Studies with cultured cells. (i) Fate of entrapped HPTS. Figure 6 (upper panel) shows the accumulation and cellular fate of HPTS encapsulated in DOPE/CHEMS and DOPC/CHEMS LUV, in J774 macrophages during a first exposure to the vesicles for a 15-min period (uptake) followed

nal obtained by excitation at 450 nm declined while that obtained by excitation at 390 nm remained stable with a trend toward an increase. HPTS encapsulated in DOPC/CHEMS liposomes was accumulated to a considerably lesser extent, but its fate during the chase was qualitatively similar to that of HPTS encapsulated in DOPE/CHEMS liposomes. To get more insight on the intracellular fate of HPTS, we present in the panel B the ratio of the signals recorded upon excitation at 450 and 390 nm. This shows that a steady and significant shift of pH occurs in the environment of the probe, both with DOPE/CHEMS and DOPC/CHEMS liposomes from early uptake (pH 7.0–7.5) to late chase phase (pH 6.0–6.5); some

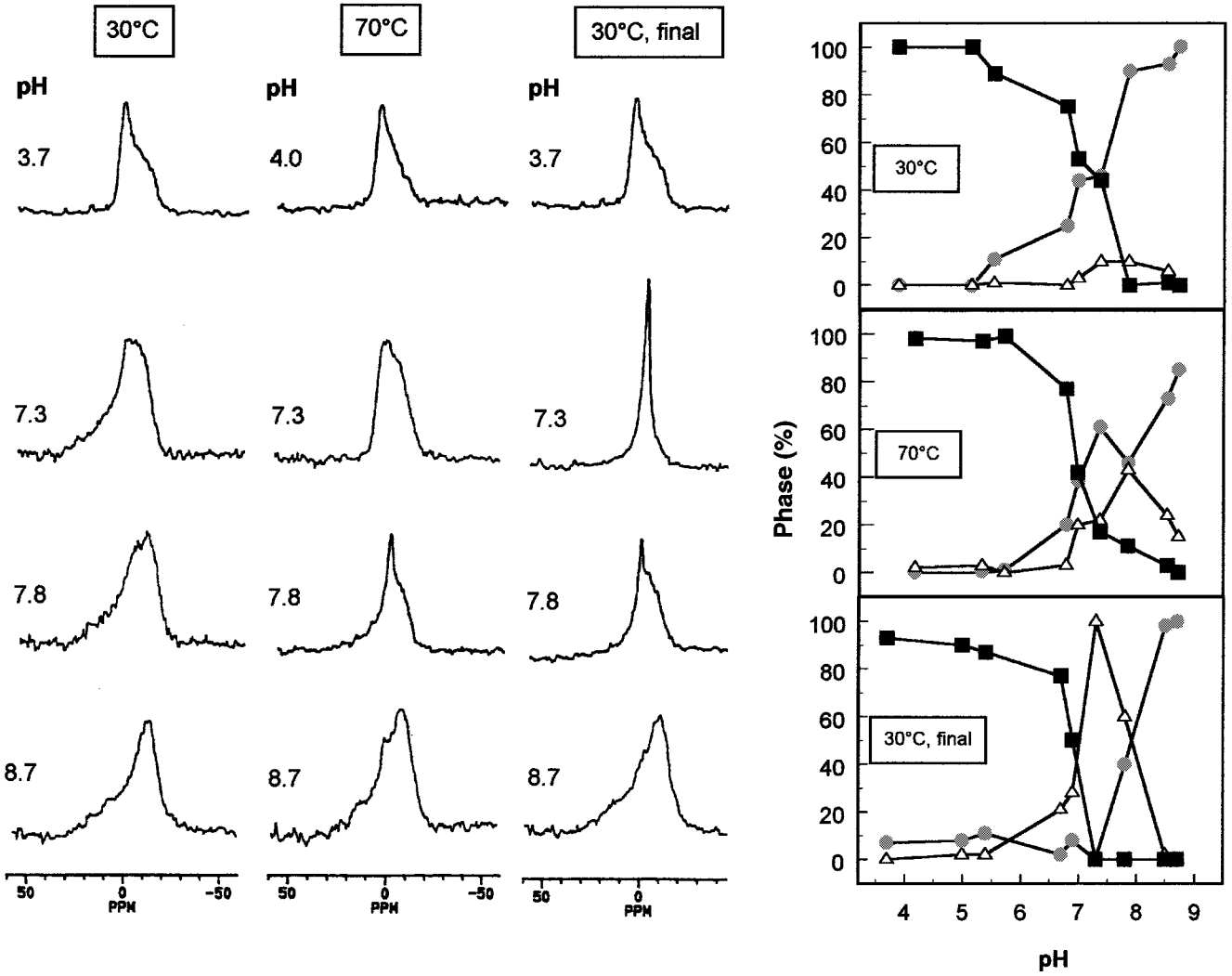

FIG. 5. ^{31}P NMR spectroscopy of DOPE/CHEMS large multilamellar vesicles (MLV). Left panel: typical spectra obtained at four different pH values

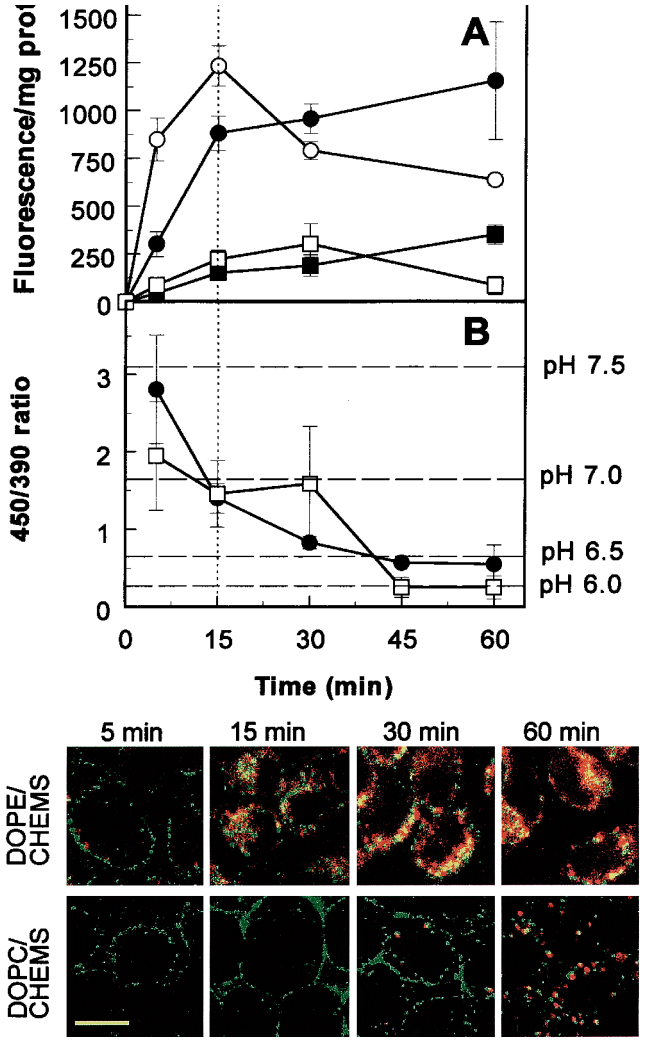

FIG. 6. Accumulation and distribution of fluorescence in J774 macrophages during incubation in the presence of HPTS-containing LUV (uptake) and subsequent transfer to liposome-free medium (chase). Circles, DOPE/CHEMS vesicles; squares, DOPC/CHEMS vesicles. (A) Readings obtained with suspensions of living cells upon excitation at 450 nm (open symbols) or 390 nm (closed symbols); (B), ratio of the recordings made upon excitation at these two wavelengths. Results are the mean of three independent experiments (±SD) (these ratios were used to calculate the mean pH to which HPTS is exposed, and the corresponding values are shown on the right ordinate). Bottom panel: confocal microscopy of cells treated as indicated in the upper panels. Cells were illuminated at 488 nm (green look-up table) and 363 nm (red look-up table). The yellow color results from the colocalization of green and red signals. Bar = 10 μm. For abbreviations see Figure 1.

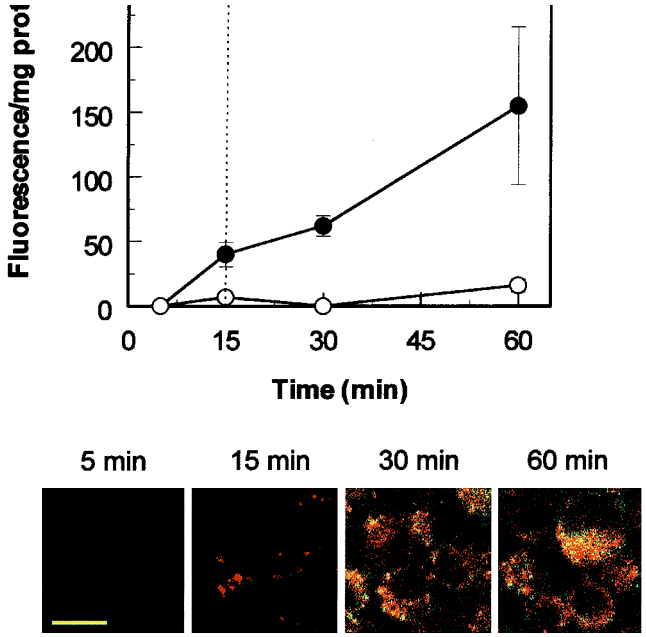

FIG 7. Accumulation and distribution of fluorescence in J774 macrophages incubated in the presence of DOPE/CHEMS LUV containing HPTS together with DPX. The protocol and the experimental conditions were similar to those of Figure 6. Upper panel: readings obtained with cell suspensions (open symbols, λ_{exc} 450 nm; closed symbols, λ_{exc} 390 nm). Lower panel: confocal microscopy observations. Bar = 10 μm. For abbreviations see Figure 1.

delay, however, was noted for DOPC/CHEMS liposomes (to make the link with the confocal microscopy studies, all measurements were also made at 488 and 363 nm, with essentially similar results). The confocal microscopic studies analysis (il-

entrapped in DOPC/CHEMS vesicles. With both types of liposomes, the tracer initially appeared as tiny dots located at the periphery of the cell (set to a green color). With DOPE/CHEMS liposomes, these structures became progressively enlarged and more centrally located in a perinuclear fashion, while also gradually emitting a larger proportion of the signal in the red channel, the yellow color resulting from the colocalization of green and red signals. Some of these structures were already visible at 5 min. After 45 min chase, most of the tracer was detected as large red/yellow patches, often with a diffuse appearance. With DOPC/CHEMS liposomes, the tracer still displayed a peripheral appearance after 30 min of incubation. It eventually, but slowly, became associated with larger structures, some of which appeared as red/yellow dots. Yet it was never present in a diffuse fashion.

(ii) Release of HPTS. Figure 7 (upper panel) shows that suspensions of cells incubated with DOPE/CHEMS LUV loaded with HPTS and DPX display almost no signal when excited at 450 nm. At the end of the uptake period, however, they showed a minor signal when excited at 390 nm, the value of which increased throughout the chase period. In confocal microscopy (lower panel), only a few red structures were seen

DISCUSSION

pH-sensitive liposomes have been developed for the purpose of enhancing the cytosolic delivery of drugs and other entrapped solutes through destabilization in the acid milieu of the endosomal/phagosomal apparatus (2–4). We selected DOPE/CHEMS liposomes since vesicles of this composition show a greater stability than liposomes made of DOPE and oleic acid (34), and also because CHEMS induces destabilization through transition to inverted hexagonal (H_{II}) phase (20) in a physiological pH range [7 to 5 (35)]. DOPC/CHEMS liposomes were used as controls since these vesicles cannot undergo reorganization to H_{II} phase, which is considered essential for membrane destabilization and fusion (10). As structural modifications could be the initiating factor of the destabilization of pH-sensitive liposomes upon acidification, we have focused our attention on the changes in lipid organization as well as their relation with membrane permeabilization and fusion.

A first observation in this respect is that change in polymorphic organization of the lipids occurs over a wide pH range and that the hexagonal-phase proportion increases from pH 8.0 down to ~6.0. At this pH value, it affects a large proportion of the lipids and probably reaches a critical threshold to cause alterations of other membrane properties. This threshold cannot, however, be more quantitatively defined in LUV. The broad component seen in the ^{31}P NMR spectra at acid pH, which is typical of a hexagonal phase (10), may indeed include a symmetrical broader component associated with fused liposomes of a still sufficiently small size (see below) to undergo motional averaging of $\Delta\sigma$ (30). The role of structures giving rise to an isotropic signal in the process of phase transition is further substantiated by the ^{31}P NMR studies made on MLV. The highly mobile structures responsible for the isotropic signal may also be involved in membrane fusion (36). However, a quantitative relationship between the proportion of these structures in the membrane and the fusion process cannot be established since MLV are too heterogeneous in size to be used in fusion assays. In addition, LUV, which were therefore used for fusion studies, reorganize in hexagonal phase at a lower pH than MLV. The endothermic character of the transition clearly appears for LUV, since it occurs at a higher pH at 70 than at 30°C. This effect of temperature is particularly dramatic for MLV, since a rise from 30 to 70°C increases the percentage of isotropic-type structures from ~10 to ~40%, and cooling down to 30°C causes a complete transformation of the spectrum in a narrow symmetrical signal. It therefore appears that heating and cooling induce the formation of isotropic-type structures in an irreversible manner. The nature of this structural change is difficritical membrane properties such as permeability and fusion capacity.

A second observation in this study is that DOPE/CHEMS liposomes require more membrane structure reorganization for fusion than for permeabilization, since there is a difference of approximately 0.5 pH units between the onset of each phenomenon (see data on calcein release on the one side and light-scattering spectroscopy and R18 dequenching on the other side). Our data therefore support and extend those obtained by Collins *et al.* (17), who also reported that leakage occurs at a less acidic pH than membrane fusion. Quite surprisingly, we found that a 100% leakage or fusion could not be achieved, at least in the range of pH investigated, suggesting that a part of the liposome population is resistant to acidification or that membrane perturbations are not sufficient to cause the complete release of the entrapped probe or the fusion of all the vesicles. Incomplete release of a tracer entrapped in DOPE/CHEMS liposomes containing higher proportions of CHEMS was also noted by other investigators (11). In the present study, the kinetic data unambiguously show that a plateau has been reached. It has been proposed (11) that destabilization of pH-sensitive liposomes is primarily mediated by bilayer contact. The degree of permeabilization may therefore be directly related to the lipid concentration. However, in these studies, the authors (11) did not specifically consider whether the aggregation process is followed by fusion of the liposomes. The mixing of lipid components we detected is actually highly suggestive of a true fusion process rather than a simple aggregation, since the increase in LUV size was moderate (only 2–3 times the diameter of control liposomes) and irreversible, and since R18 fluorescence increased very rapidly upon liposome mixing. The present data are therefore very similar to those we reported earlier for negatively charged liposomes incubated with typical fusogenic agents like melittin or (β-diethylaminoethylether)hexestrol (these agents cause a two to five times increase in liposome diameter and an immediate dequenching of R18 fluorescence). They are also in sharp contrast with what we found for aggregating agents like spermine and gentamicin, which induce an at least 10-fold increase in liposome diameter associated with a slow increase of R18 fluorescence (26,37). Altogether, the biophysical studies discussed so far strongly suggest that DOPE/CHEMS liposomes of the composition we selected may become destabilized and release their contents when pH falls from >7 to approximately 6. This range corresponds to that encountered along the endocytic pathway (38). The results of the cellular studies with HPTS-entrapped liposomes (in which the tracer is used to quantify the liposome uptake and to estimate the pH at which

represent an average value for a material that, as evidenced by confocal microscopy (Fig. 6, lower panel), is spread among vacuoles whose pH values range from neutrality to a low value. Our studies also show that cells handle DOPE/CHEMS and DOPC/CHEMS liposomes very differently. First, the fluorescence signal recorded in cells was markedly lower for DOPC/CHEMS liposomes than for DOPE/CHEMS liposomes. This cannot be attributed to a difference in the amount of probe entrapped (see Materials and Methods section) and must therefore be ascribed to a low endocytic rate of DOPC/CHEMS liposomes, as already observed in P388D1 macrophages (4). This clearly points to the importance of liposome composition for uptake, beyond a simple variation in charge (39). Second, the confocal microscopy studies show that HPTS entrapped in DOPC/CHEMS liposomes remains for about 30 min in the periphery of the cell and at neutral pH before being transferred to vesicles of lower pH. Because our calibration studies indicate that the shift from the green to the red signal should occur around pH 7.15, the data therefore suggest that DOPC/CHEMS liposomes remain associated with the cell surface, or with invaginations of the plasma membrane, for quite a time before being transferred to early endosomes and other acidic vacuoles. In contrast, HPTS entrapped in DOPE/CHEMS liposomes appears to move more quickly into the cell where it progressively shows a diffuse appearance in parallel with a marked shift from green to yellow and red. Again, taking into account the pH at which this shift is observed (~7.15), we interpret these images as indicating a rapid internalization into early endosomes followed by a partial release of the tracer in the cytosol, the pH of which appears to be precisely around this value in J774 macrophages (40). An effective release of the content of DOPE/CHEMS liposomes into the cytosol also is largely evidenced by the results of the experiments using vesicles containing both HPTS and its quenching agent DPX. Comparing the values of the fluorescence signal obtained with these liposomes (Fig. 7) to that obtained with vesicles without the quenching agent (Fig. 6), we suggest that approximately 15% of the HPTS has been made free within 45 min after endocytosis, a figure close to that found by Chu *et al.* (4) for DOPE/CHEMS (3:2) liposomes. This value may, however, be underestimated, since a significant increase in HPTS fluorescence will be only observed upon high dilution of the dye/quencher mixture (41).

In conclusion, our data confirm the potential usefulness of DOPE/CHEMS liposomes as pH-sensitive vehicles for the intracytosolic delivery of an entrapped tracer. This delivery seems to occur without grossly affecting cell viability, suggesting interesting applications for therapeutics. Our biologi-

Recherche Scientifique. Francine Renoird, Marie-Claire Cambier, and Christelle Flore provided expert technical assistance. This work was supported by the Belgian Fonds de la Recherche Scientifique Médicale (grants nos. 9.4541.95F, 3.4516.94 and 9.451492), the Fonds National de la Recherche Scientifique (grant no. 9.4546.94), the Actions de Recherches Concertées 94/99-172 of the Direction Générale de la Recherche Scientifique—Communauté Française de Belgique, Belgium.

REFERENCES

1. Straubinger, R.M., Hong, K., Friend, D., and Papahadjopoulos, D. (1983) Endocytosis of Liposomes and Intracellular Fate of Encapsulated Molecules: Encounter with a Low pH Compartment After Internalization in Coated Vesicles, *Cell 32*, 1069–1079.
2. Connor, J., Yatvin, M.B., and Huang, L. (1984) pH-Sensitive Liposomes: Acid-Induced Liposome Fusion, *Proc. Natl. Acad. Sci. USA 81,* 1715–1718.
3. Chu, C.J., and Szoka, F.C. (1994) pH-Sensitive Liposomes, *J. Liposome Res. 4,* 361–395.
4. Chu, C.J., Dijkstra, J., Lai, M.Z., Hong, K., and Szoka, F.C. (1990) Efficiency of Cytoplasmic Delivery by pH-Sensitive Liposomes to Cells in Culture, *Pharm. Res. 7,* 824–834.
5. Connor, J., and Huang, L. (1986) pH-Sensitive Immunoliposomes as an Efficient and Target-Specific Carrier for Antitumor Drugs, *Cancer Res. 46,* 3431–3435.
6. Lutwyche, P., Cordeiro, C., Wiserman, D.J., St. Louis, M., Uh, M., Hope, M.J., and Finlay, B.B. (1998) Intracellular Delivery and Intracellular Activity of Gentamicin Encapsulated in pH-Sensitive Liposomes, *Antimicrob. Agents Chemother. 42,* 2511–2520.
7. Couvreur, P., Fattal, E., Malvy, C., and Dubernet, C. (1997) pH-Sensitive Liposomes: an Intelligent System for the Delivery of Antisense Oligonucleotides, *J. Liposome Res. 7,* 1–18.
8. Nair, S., Zhou, F., Reddy, R., Huang, L., and Rouse, B.T. (1992) Soluble Proteins Delivered to Dendritic Cells *via* pH-Sensitive Liposomes Induce Primary Cytotoxic T Lymphocyte Responses *in vitro, J. Exp. Med. 175,* 609–612.
9. Wang, C.Y., and Huang, L. (1987) Plasmid DNA Adsorbed to pH-Sensitive Liposomes Efficiently Transforms the Target Cells, *Biochem. Biophys. Res. Commun. 147,* 980–985.
10. Seddon, J.M. (1990) Structure of the Inverted Hexagonal (H_{II}) Phase, and Nonlamellar Phase Transitions of Lipids, *Biochim. Biophys. Acta 1031,* 1–69.
11. Ellens, H., Bentz, J., and Szoka, F.C. (1984) pH-Induced Destabilization of Phosphatidylethanolamine-Containing Liposomes: Role of Bilayer Contact, *Biochemistry 23,* 1532–1538.
12. Düzgünes, N., Straubinger, R.M., Baldwin, P.A., Friend, D.S., and Papahadjopoulos, D. (1985) Proton-Induced Fusion of Oleic-Phosphatidylethanolamine Liposomes, *Biochemistry 24*, 3091–3098.
13. Liu, D., and Huang, L. (1989) Small, but Not Large, Unilamellar Liposomes Composed of Dioleoylphosphatidylethanolamine and Oleic Acid Can Be Stabilized by Human Plasma, *Biochemistry 28,* 7700–7707.

16. Tari, A.M., Fuller, N., Boni, L.T., Collins, D., Rand, P., and Huang, L. (1994) Interactions of Liposome Bilayers Composed of 1,2-Diacyl-3-succinylglycerol with Protons and Divalent Cations, *Biochim. Biophys. Acta 1192,* 253–262.
17. Collins, D., Maxfield, F., and Huang, L. (1989) Immunoliposomes with Different Acid Sensitivities as Probes for the Cellular Endocytic Pathway, *Biochim. Biophys. Acta 987*, 47–55.
18. Straubinger, R.M., Düzgünes, N., and Papahadjopoulos, D. (1985) pH-Sensitive Liposomes Mediate Cytoplasmic Delivery of Encapsulated Macromolecules, *FEBS Lett. 179,* 148–154.
19. Kono, K., Igawa, T., and Takagishi, T. (1997) Cytoplasmic Delivery of Calcein Mediated by Liposomes Modified with a pH-Sensitive Poly(ethylene Glycol) Derivative, *Biochim. Biophys. Acta 1325,* 143–154.
20. Lai, M.Z., Vail, W.J., and Szoka, F.C. (1985) Acid- and Calcium-Induced Structural Changes in Phosphatidylethanolamine Membranes Stabilized by Cholesterol Hemisuccinate, *Biochemistry 24,* 1654–1661.
21. Hope, M.J., Bally, M.B., Webb, G., and Cullis, P.R. (1985) Production of Large Unilamellar Vesicles by a Rapid Extrusion Procedure. Characterization of Size Distribution, Trapped Volume and Ability to Maintain a Membrane Potential, *Biochim. Biophys. Acta 812,* 55–65.
22. Van Bambeke, F., Mingeot-Leclercq, M.P., Schanck, A., Brasseur, R., and Tulkens, P.M. (1993) Alterations in Membrane Permeability Induced by Aminoglycoside Antibiotics: Studies on Liposomes and Cultured Cells, *Eur. J. Pharmacol. 247,* 155–168.
23. Grit, M., Zuidam, N.J., Underberg, W.J.M., and Crommelin, D.J.A. (1993) Hydrolysis of Partially Saturated Egg Phosphatidylcholine in Aqueous Liposome Dispersions and the Effect of Cholesterol Incorporation on Hydrolysis Kinetics, *J. Pharm. Pharmacol. 45,* 490–495.
24. Weinstein, J.N., Yoshikami, S., Henkart, P., Blumenthal, R., and Hagins, W.A., (1977) Liposome–Cell Interaction: Transfer and Intracellular Release of a Trapped Fluorescent Marker, *Science 195,* 489–491.
25. Straubinger, R.M., Papahadjopoulos, D., and Hong, K. (1990) Endocytosis and Intracellular Fate of Liposomes Using Pyranine as a Probe, *Biochemistry 29,* 4929–4939.
26. Van Bambeke, F., Tulkens, P.M., Brasseur, R., and Mingeot-Leclercq, M.P. (1995) Aminoglycoside Antibiotics Induce Aggregation but Not Fusion of Negatively-Charged Liposomes, *Eur. J. Pharmacol. 289,* 321–333.
27. Hoekstra, D., de Boer, T., Klappe, K., and Wilschut, J. (1984) Fluorescence Method for Measuring the Kinetics of Fusion Between Biological Membranes, *Biochemistry 23,* 5675–5681.
28. Mazer, N.A., Carey, M.C., Kwasnick, R.F., and Benedek, G.B. (1979) Quasi-elastic Light Scattering Studies of Aqueous Biliary Lipid Systems. Size, Shape and Thermodynamics of Bile Salt Micelles, *Biochemistry 18,* 3064–3075.
29. Tilcock, C.P.S., Bally, M.B., Farren, S.B., and Cullis, P.R. (1982) Influence of Cholesterol and Polyethylene Glycol Phosphatidylethanolamine on the Interbilayer Fusion of Dioleoylphosphatidylethanolamine Vesicles Induced by Ca^{2+}, *Biochemistry 21,* 4039–4042.
30. Tilcock, C.P.S., Bally, M.B., Farren, S.B., and Cullis, P.R. (1984) Lipid Polymorphism and Membrane Properties of Vesicles Composed of Phosphatidylethanolamine Modified with Polyethylene Glycol, *Biochemistry 23,* 2696–2703.
31. Tilcock, C.P.S., Bally, M.B., Farren, S.B., and Cullis, P.R. (1984) Influence of Cholesterol and Polyethylene Glycol Phosphatidylethanolamine on the Interbilayer Fusion of Dioleoylphosphatidylethanolamine Vesicles Induced by Ca^{2+}, *Biochemistry 21,* 4039–4042.
32. Tilcock, C.P.S., Bally, M.B., Farren, S.B., and Cullis, P.R. (1984) Lipid Polymorphism and Membrane Properties of Vesicles Composed of Phosphatidylethanolamine Modified with Polyethylene Glycol, *Biochemistry 23,* 2696–2703.
33. Tilcock, C.P.S., Bally, M.B., Farren, S.B., and Cullis, P.R. (1984) Influence of Cholesterol and Polyethylene Glycol Phosphatidylethanolamine on the Interbilayer Fusion of Dioleoylphosphatidylethanolamine Vesicles Induced by Ca^{2+}, *Biochemistry 21,* 4039–4042.
34. Tilcock, C.P.S., Bally, M.B., Farren, S.B., and Cullis, P.R. (1984) Lipid Polymorphism and Membrane Properties of Vesicles Composed of Phosphatidylethanolamine Modified with Polyethylene Glycol, *Biochemistry 23,* 2696–2703.
35. Tilcock, C.P.S., Bally, M.B., Farren, S.B., and Cullis, P.R. (1984) Influence of Cholesterol and Polyethylene Glycol Phosphatidylethanolamine on the Interbilayer Fusion of Dioleoylphosphatidylethanolamine Vesicles Induced by Ca^{2+}, *Biochemistry 21,* 4039–4042.
36. Tilcock, C.P.S., Bally, M.B., Farren, S.B., and Cullis, P.R. (1984) Lipid Polymorphism and Membrane Properties of Vesicles Composed of Phosphatidylethanolamine Modified with Polyethylene Glycol, *Biochemistry 23,* 2696–2703.
37. Tilcock, C.P.S., Bally, M.B., Farren, S.B., and Cullis, P.R. (1984) Influence of Cholesterol and Polyethylene Glycol Phosphatidylethanolamine on the Interbilayer Fusion of Dioleoylphosphatidylethanolamine Vesicles Induced by Ca^{2+}, *Biochemistry 21,* 4039–4042.
38. Tilcock, C.P.S., Bally, M.B., Farren, S.B., and Cullis, P.R. (1984) Lipid Polymorphism and Membrane Properties of Vesicles Composed of Phosphatidylethanolamine Modified with Polyethylene Glycol, *Biochemistry 23,* 2696–2703.
39. Tilcock, C.P.S., Bally, M.B., Farren, S.B., and Cullis, P.R. (1984) Influence of Cholesterol and Polyethylene Glycol Phosphatidylethanolamine on the Interbilayer Fusion of Dioleoylphosphatidylethanolamine Vesicles Induced by Ca^{2+}, *Biochemistry 21,* 4039–4042.
40. Tilcock, C.P.S., Bally, M.B., Farren, S.B., and Cullis, P.R. (1984) Lipid Polymorphism and Membrane Properties of Vesicles Composed of Phosphatidylethanolamine Modified with Polyethylene Glycol, *Biochemistry 23,* 2696–2703.
41. Tilcock, C.P.S., Bally, M.B., Farren, S.B., and Cullis, P.R. (1984) Influence of Cholesterol and Polyethylene Glycol Phosphatidylethanolamine on the Interbilayer Fusion of Dioleoylphosphatidylethanolamine Vesicles Induced by Ca^{2+}, *Biochemistry 21,* 4039–4042.

[Received June 9, 1999, and in revised form November 18, 1999; revision accepted January 4, 2000]

Qualitative and Quantitative Analysis of Lipoxygenase Products in Bovine Corneal Epithelium by Liquid Chromatography–Mass Spectrometry with an Ion Trap

Maria Liminga* and Ernst Oliw

Division of Biochemical Pharmacology, Department of Pharmaceutical Biosciences, Uppsala University, Uppsala Biomedical Center, SE-751 24 Uppsala, Sweden

ABSTRACT: Electrospray ionization ion trap mass spectra of 5-, 12-, and 15-hydroperoxyeicosatetraenoic (HPETE), hydroxyeicosatetraenoic (HETE), and ketoeicosatetraenoic (KETE) acids were recorded. The HPETE were partly dehydrated to the corresponding KETE in the heated capillary of the mass spectrometer. 12-HPETE and 15-HPETE were also converted to KETE by collision-induced dissociation (CID) in the ion trap, whereas CID of 5-HPETE yielded little formation of 5-KETE. Subcellular fractions of bovine corneal epithelium were incubated with arachidonic acid (AA) and the metabolites were analyzed. 15-HETE and 12-HETE were consistently formed, whereas significant accumulation of HPETE and KETE was not detected. Biosynthesis of 12- and 15-HETE was quantified with octadeuterated 12-HETE and 15-HETE as internal standards. The average biosynthesis of 15-HETE and 12-HETE from 30 μM AA by the cytosol was 38 ± 8 and below 3 ng/mg protein/30 min, respectively, which increased to 78 ± 21 and 10 ± 4 ng/mg protein/30 min in the presence of 1 mM free Ca^{2+}. The microsomal biosynthesis was unaffected by Ca^{2+}. The microsomes metabolized AA to 15-HETE as the main metabolite at a low protein concentration (0.3 mg/mL), whereas 12-HETE and 15-HETE were formed in a 2:1 ratio at a combined rate of 0.7 ± 0.2 μg/mg protein/30 min at a high protein concentration (1.8 mg/mL). The level of 12-HETE in corneal epithelial cells was 50 ± 13 pg/mg tissue, whereas the endogenous amount of 15-HETE was low or undetectable (<3 pg/mg tissue). Incubation of corneas for 20 min at 37°C before processing selectively increased the amounts of 12-HETE in the epithelium fourfold to ~0.2 ng/mg tissue. We conclude that 12-HETE is the main endogenously formed lipoxygenase product of bovine corneal epithelium.

Paper no. L8409 in *Lipids 35*, 225–232 (February 2000).

Lipoxygenases (LOX) are widely distributed in mammalian and plant tissues (1–5). They catalyze dioxygenation of polyunsaturated fatty acids and formation of 1-hydroperoxy-2*E*,4*Z*-pentadiene structures. LOX metabolites can often be analyzed and quantified with chromatography with ultraviolet (UV) detection. Alternatively, deuterated internal standards may be used to quantify LOX metabolites by gas chromatography–mass spectrometry (GC–MS) or by liquid chromatography–mass spectrometry (LC–MS) .

Quantification by GC–MS methods has superior sensitivity and selectivity, but has nevertheless many drawbacks. It requires derivatization, and it is not suitable for analysis of labile compounds like hydroperoxy fatty acids. LC–MS with electrospray ionization is a robust technique without many of these disadvantages (8). LC–MS has proved to be valuable for analysis of LOX metabolites of arachidonic acid (AA) and linoleic acid in many tissues and experimental systems, e.g., hydroxyeicosatetraenoic acids (HETE), hydroperoxyeicosatetraenoic acids (HPETE), hydroxyoctadecadienoic acids, and hydroperoxyoctadecadienoic acids (6,7,9–13).

The corneal epithelia of many species contain prominent 12- and 15-LOX activities (14–18). The bovine corneal epithelial tissue expresses at least three LOX, 12(*S*)-lipoxygenase (12-LOX) of the leukocyte (tracheal) type, 12-LOX of the platelet type, and 15-LOX type 2 (19). 15-LOX activity is mainly present in the cytosol, whereas both 15- and 12-LOX activities are found in the microsomal fraction (17,18). In addition, 5-LOX is present along with inflammatory cells following corneal lesions in the rabbit *in vivo* (20). Reverse transcription-polymerase chain reaction (RT-PCR) and Northern blot analysis suggest that mRNA of 5-LOX is present in bovine corneal epithelium (Liminga, M., and Oliw, E., unpublished observation). In addition to these LOX, cytochrome P450 occur in the corneal epithelium (21) and are reported by Schwartzman and colleagues to synthesize 12(*R*)-HETE (22,23).

The main objective of the present investigation was to use LC–MS for analysis of LOX products in bovine corneal epithelium and to study the fragmentation mechanism of HPETE. With an ion trap mass spectrometer, we first recorded the LC–MS mass spectra of 5-, 12-, and 15-HPETE, the corresponding HETE and KETE, and some octadeuterated HPETE and HETE. In the second part, we analyzed subcellular fractions of corneal epithelial cells for biosynthesis of LOX products. We quantified the rate of biosynthesis of 15-HETE and

*To whom correspondence should be addressed at Dept. of Pharmaceutical Biosciences, Uppsala Biomedical Center, Uppsala University, P.O. Box 591, SE-751 24 Uppsala, Sweden. E-mail: Maria.Liminga@farmbio.uu.se

Abbreviations: AA, arachidonic acid; CID, collision-induced dissociation; GC, gas chromatography; HETE, hydroxyeicosatetraenoic acid; HPETE, hydroperoxyeicosatetraenoic acid; HPLC, high-performance liquid chromatography; KETE, ketoeicosatetraenoic acid; LC, liquid chromatography; LOX, lipoxygenase; MS, mass spectrometry; PBS, phosphate buffered saline; RP, reversed phase; RT-PCR, reverse transcription-polymerase chain reaction; UV, ultraviolet.

12-HETE *in vitro* and the endogenous amounts of 15-HETE and 12-HETE in the epithelium.

MATERIALS AND METHODS

Materials. AA (99%) was from Sigma Chemical Co. (St. Louis, MO) and [5,6,8,9,11,12,14,15-$^2H_8$]-AA (d_8-AA) was a gift from Unilever Research Laboratory (Vlaardingen, The Netherlands). 5(*R,S*)-HETE, d_8-12(*S*)-HETE, 12(*S*)-HPETE, 12-KETE, and 8(*R,S*)-HETE were purchased from Cayman Chemical Co. (Ann Arbor, MI). 15(*S*)-HETE, 15(*S*)-HPETE, d_8-15(*S*)-HETE, and d_8-15(*S*)-HPETE were prepared by biosynthesis from AA and d_8-AA with soybean LOX (lipoxidase IV, Sigma), essentially as described elsewhere; (24) 5(*S*)-HETE, 5(*S*)-HPETE, d_8-5(*S*)-HETE, and d_8-5(*S*)-HPETE were prepared with partially purified potato tuber 5-LOX as described by Reddanna *et al*. (25). HPETE were reduced to HETE with $SnCl_2$ or $NaBH_4$ (24). 15-KETE and 5-KETE were prepared from 15-HETE and 5-HETE by dehydrogenation as described elsewhere (26). All synthetic products were purified by reversed-phase high-performance liquid chromatography (RP-HPLC) and characterized by UV analysis and by MS. A-23187 was from Calbiochem (La Jolla, CA). Solvents for RP-HPLC and other chemicals were from Merck (Darmstadt, Germany). Bovine eyes were put on ice at a local slaughterhouse and brought to the laboratory within 2 h.

Preparation of subcellular fractions of corneal epithelial cells. Subcellular fractions were prepared at +4°C, essentially as described by Liminga *et al*. (17). Bovine eyes were thoroughly washed with phosphate buffered saline (PBS; pH 7.4). The epithelial cells were scraped off the cornea and put into homogenization buffer (0.05 M Tris-HCl/1 mM EDTA/1 mM EGTA/ 0.5 mM dithiothreitol/0.1 mM phenylmethane-sulfonylfluoride; pH 7.4). The tissue was carefully homogenized with a glass–glass homogenizer. The homogenate was sonicated and usually centrifuged at 10,000 × *g* for 15 min. The low-speed supernatant was either stored at –80°C or centrifuged at 100,000 × *g* for 90 min. The high-speed pellet was designated the microsomal fraction and the high-speed supernatant was designated the cytosolic fraction. Protein concentration was estimated by the Bradford method (27).

Biosynthesis of LOX products in vitro. Low-speed supernatant (4 mg protein) and cytosolic (4–6 mg protein) and microsomal fractions (0.3, 0.6, or 1.8 mg protein) were incubated with 30 μM AA in 1 mL of the buffer above for 30 min at 37°C with constant shaking. In some experiments, 1 mM ATP and/or 1 mM Ca^{2+} were added to PBS, which is sufficient to stimulate 5-LOX activity (*cf.* Ref. 28). The incubations were terminated with 4 vol of ethanol, and 90 ng d_8-15-HETE and 100 ng d_8-12-HETE were added.

Endogenous 12- and 15-HETE. Epithelial cells from four corneas (~200 mg) were analyzed in five different experiments. The cells were put into 1.5 mL ethanol containing d_8-15-HETE (45 ng) and d_8-12-HETE (50 ng), weighed, and immediately homogenized as described above. The metabolites were extracted on SepPak/C_{18} as described (17), and analyzed by LC–MS. In additional experiments, multiples of four corneas were placed in PBS (pH 7.4) with (n = 4) or without (n = 4) 1 mM added calcium and incubated for 20 min at 37°C. In three experiments, the calcium ionophore A-23187 (10 μM) was also added. After incubation, the corneas were chilled and immediately processed for endogenous LOX products as above.

LC–MS analysis. LC–MS analysis was performed with equipment as described by Bylund *et al.* and Oliw *et al.* (12,13). The pump for HPLC was from ThermoQuest (P2000). The column contained octadecasilane silica (5 μm, 250 × 2 mm; Phenomenex, Torrance, CA) and was eluted with methanol/water/acetic acid, 80:20:0.01 (by vol), at 0.2 mL/min. The effluent was first analyzed by UV detection at 235 nm and then by electrospray ionization MS with an ion trap mass analyzer (LCQ; ThermoQuest, San Jose, CA). Negative ions were monitored and prostaglandin $F_{1\alpha}$ was infused (100 ng/min) for tuning. The targets for automatic gain control were set at 5×10^7 for full MS and at 1×10^7 for MS^n. The capillary temperature was 230°C, but reduced to 170°C for analysis of HPETE. The source voltage was 4.25 kV and source current 0.1 mA. The sheath and auxillary flow of N_2 were 80 and 20 units, respectively, and He was used as collision gas. Off-line nanoelectrospray was performed with 2–3 μL samples (~10 ng/μL) in disposable gold-coated capillary probes (Protana A/S, Odense, Denmark) with a spray voltage of 0.8 kV. The samples were dissolved in methanol/water, 1:1. The collision energy (in arbitrary units) was adjusted 25–30% for MS^2 analysis so that >90% of the parent ion fragmented. The mass range was usually set from 80 to 400. Standard curves were constructed from analysis of different amounts 12-HETE and 15-HETE with fixed amounts of d_8-15-HETE and d_8-12-HETE by selective ion monitoring at *m/z* 319 (carboxylate anion of HETE) and *m/z* 327 (carboxylate anion of d_8-HETE). The ratio of the peak areas of 12-HETE and d_8-12-HETE and the ratio of the peak areas of 15-HETE and d_8-15-HETE yielded linear standard curves. The slopes of the standard curves for 12-HETE/d_8-12-HETE and for 15-HETE/d_8-15-HETE were 0.59 and 0.67, respectively. The d_8-HETE contained less than 0.5% HETE.

RESULTS

LC–MS analysis of HPETE and KETE. LC–MS analysis of 5-, 12-, and 15-HPETE yielded two strong signals, *m/z* 335 and *m/z* 317 (Fig. 1). They corresponded to the carboxylate anion of the hydroperoxide ($[M - H]^-$) and the anion of its dehydration product ($[M - H - H_2O]^-$), respectively. The intensity of the latter was relatively low (about 5%) at heated capillary temperatures of 170°C and increased with temperature to ~30% at 230°C. The temperature effect was more pronounced during nanoelectrospray ionization. 5-, 12-, and 15-KETE separated from 5-, 12-, and 15-HPETE, respectively, on RP-HPLC. These KETE were therefore likely formed by dehydration of 5-, 12-, and 15-HPETE in the heated capillary. As discussed below, collision-induced dissociation (CID) in the ion trap of 15-HPETE and 12-HPETE yielded 15-KETE and 12-KETE as

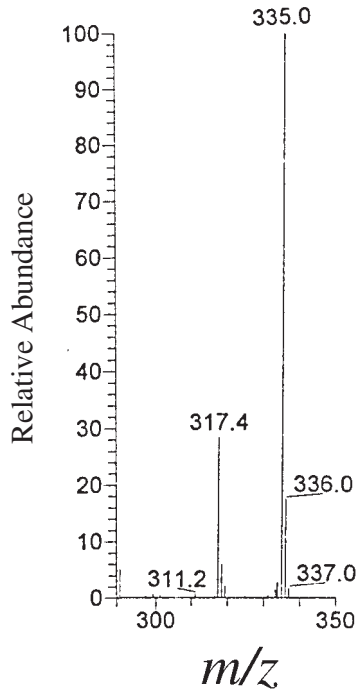

FIG. 1. A partial mass spectrum of 5-hydroperoxyeicosatetraenoic (HPETE) acid. The intensity of other ions than the carboxylate anion (*m/z* 335) and its dehydration product (*m/z* 317) was only a few percent.

major products, but 5-HPETE was not converted to 5-KETE in appreciable amounts.

5-HPETE and 5-KETE. LC–MS analysis of 5-HPETE showed that this compound eluted after 30 min (Fig. 2A, top panel). The mass spectrum yielded two strong signals at *m/z* 335 and 317 as discussed above. MS^2 analysis of the carboxylate anion of 5-HPETE (MS^2 335 → full scan) yielded virtually no daughter ions (Fig. 2A, middle panel), whereas analysis of the dehydration product (MS^2 317 → full scan) yielded many daughter ions (Fig. 2A, bottom panel).

Analysis of the facile dehydration product of 5-HPETE (MS^2 317 → full scan; *cf.* Fig. 2A, bottom trace) yielded an informative mass spectrum with many strong signals as shown in Figure 2B. Signals were noted at *m/z* 299 (317 – 18), 273 (317 – 44), and 255 (317 – 44 – 18). Other ions were noted at *m/z* 245, 239, 207, 203 (α-cleavage between C5 and C6), 181, 167, 153, 149 (167 – 18), 129, 123 (167 – 44), and 113. MS analysis of d_8-5-HPETE yielded signals corresponding to the carboxylate ions ($[M - H]^-$) at *m/z* 343 (100%, d_8-5-HPETE) and 342 (38%, d_7-5-HPETE) and the carboxylate ions of the dehydration product ($[M - H - H_2O]^-$) at *m/z* 325 (17%) and 324 (17%) (data not shown). The MS^2 analysis of the dehydration

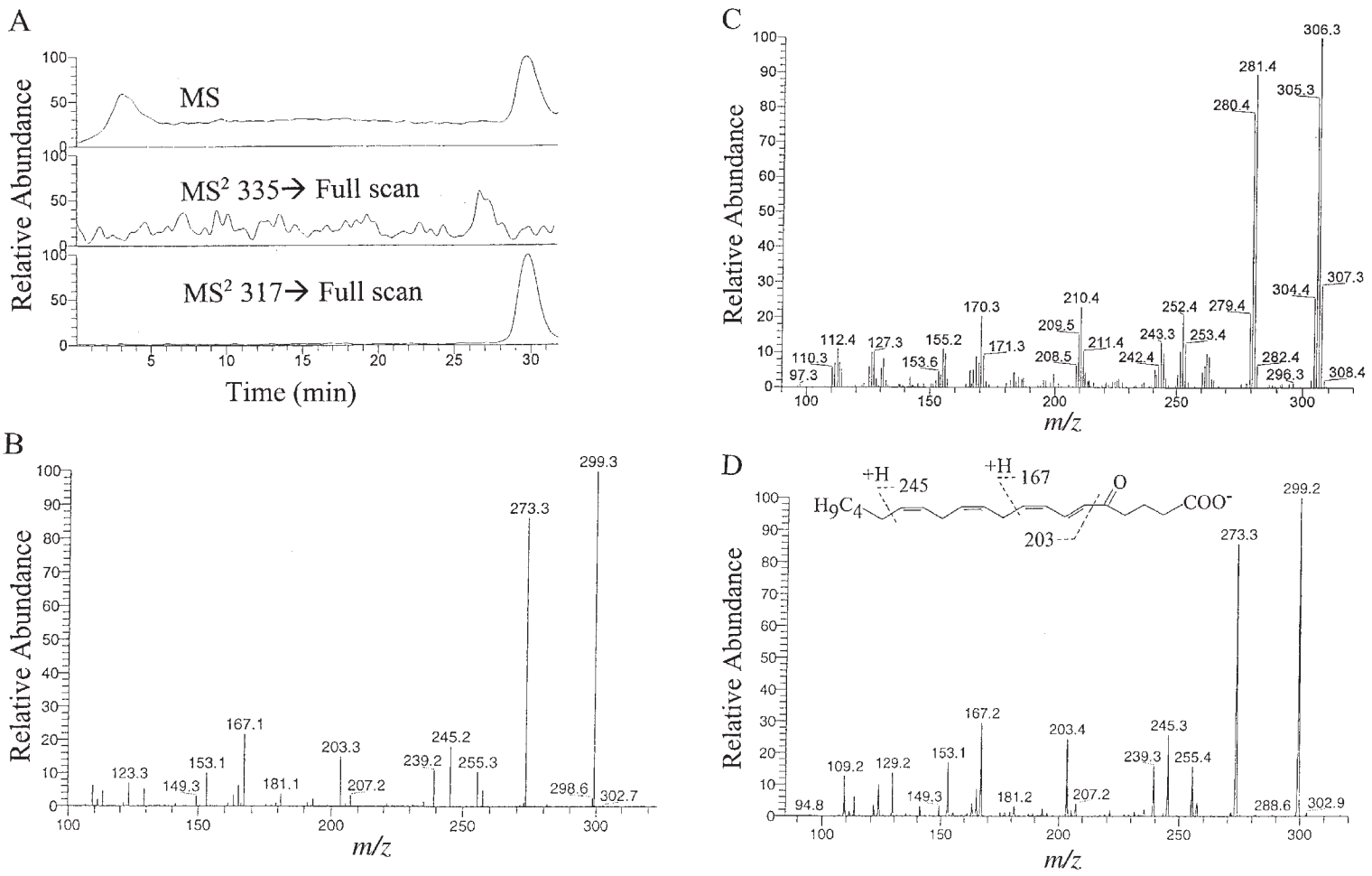

FIG. 2. Liquid chromatography–mass spectrometry (LC–MS) analysis of the carboxylate ions of 5-HPETE, its dehydration product, and 5-keto-eicosatetraenoic (KETE) acid. (A) Selected ion chromatograms from LC–MS analysis of 5-HPETE. Top trace, total ion intensity during full MS analysis; middle trace, total ion intensity of MS^2 analysis of *m/z* 335 (MS^2 335 → full scan); bottom trace, total ion intensity of MS^2 analysis of *m/z* 317 (MS^2 317 → full scan). (B) MS^2 analysis of the dehydration product of 5-HPETE formed in the heated capillary (MS^2 317 → full scan). (C) MS^2 analysis of the dehydration product of d_8-5-HPETE formed in the heated capillary (MS^2 325 → full scan). (D) MS^2 analysis of the carboxylate ion of KETE (MS^2 317 → full scan). The inset shows the structural formula of 5-KETE and the deduced fragmentation during collision-induced dissociation (CID) in the ion trap. See Figure 1 for other abbreviation.

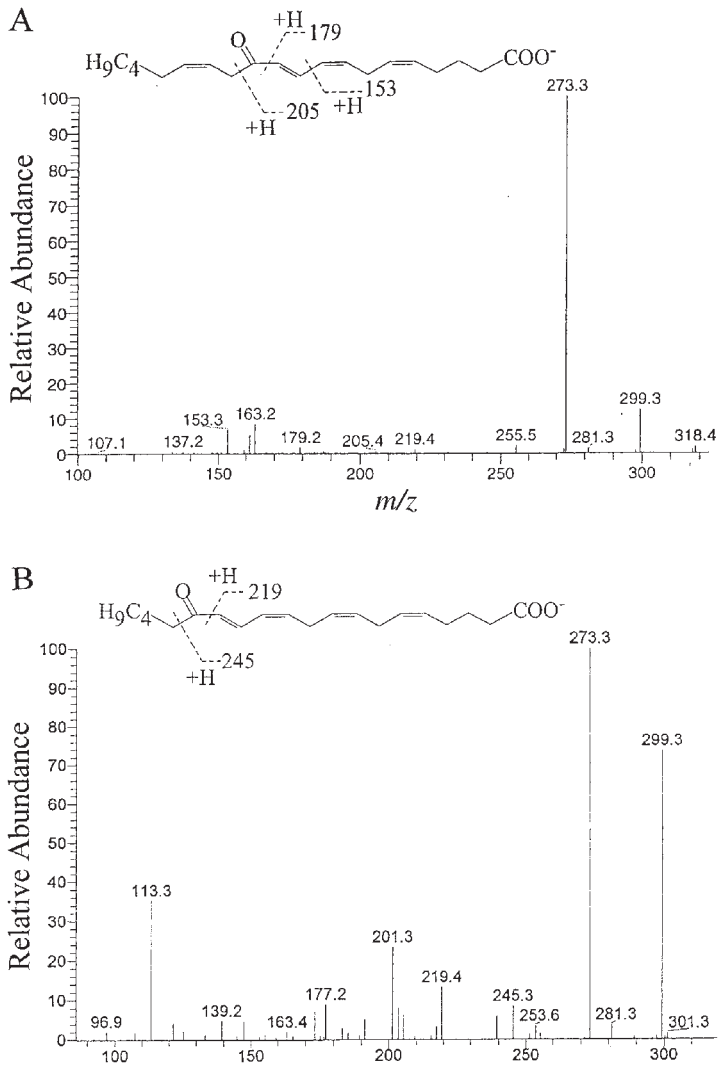

FIG. 3. LC–MS analysis of the carboxylate ions of the dehydration products of 12-HPETE and 15-HPETE. (A) Analysis of 12-HPETE (MS^2 317→ full scan). The inset shows 12-KETE and its CID in the ion trap, as MS^2 analysis of 12-KETE (MS^2 317→ full scan) yielded an identical mass spectrum [and so did MS^3 analysis of 12-HPETE (MS^3 335→ 317→ full scan)]. (B) MS analysis of 15-HPETE (MS^3 335→ 317→ full scan). MS^2 analysis of 15-KETE (MS^2 317→ full scan) yielded an identical mass spectrum. The inset shows 15-KETE and its fragmentation in the ion trap. See Figures 1 and 2 for abbreviations.

product of d_8-5-HPETE was helpful for interpretation of the fragmentation. A comparison between this mass spectrum (Fig. 2C) and that of 5-HPETE (Fig. 2B) indicated that the signals at *m/z* 306 and 305 in Figure 2C corresponded to *m/z* 299 in Figure 2B; *m/z* 281 and 280 corresponded to *m/z* 273; *m/z* 253, 252, and 251 corresponded to *m/z* 245*; m/z* 210 and 209 corresponded to *m/z* 203; and *m/z* 171 and 170 corresponded to *m/z* 167. MS analysis of 5-KETE (MS^2 317 → full scan; Fig. 2D) and MS analysis of the heated capillary dehydration product of 5-HPETE (MS^2 317 → full scan; Fig. 2B) yielded virtually identical mass spectra. Based on the mass spectra discussed above, the CID of 5-KETE was deduced as shown by the inset in Figure 2D. We conclude that 5-HPETE is partially dehydrated to 5-KETE in the heated capillary.

12-HPETE and 12-KETE. The carboxylate ion (*m/z* 335) and the facile dehydrated molecular ion (*m/z* 317) of 12-HPETE were subject to MS^2 analysis. MS^2 335 → full scan yielded mainly a prominent signal at *m/z* 317, whereas MS^2 317 → full scan gave rise to characteristic mass spectra with many informative fragments (Fig. 3A), which appeared to be almost identical to the MS^3 spectrum of 12-HPETE (MS^3 335 → 317 → full scan; data not shown) and the MS^2 spectrum of 12-KETE (MS^2 317 → full scan; data not shown). Signals were noted at *m/z* 299, 281, 273, 255, and 219, 205 (possibly α-cleavage between C11 and C12), 187 (205 – 18; weak), 179 (possibly α-cleavage between C12 and C13), 163, 161 (205 – 44) and 153. The major fragments could be formed as indicated by the inset in Figure 3A.

15-HPETE and 15-KETE. The MS^3 analysis of 15-HPETE [MS^3 335 → 317 → full scan (Fig. 3B)] showed signals at *m/z* 299 (317 – 18), 281 (299 – 18), 273 (317 – 44), 255 (317 – 44 – 18), 245 (317 – 72), 219 (317 – 98, possibly loss of $C_6H_{11}O$ with gain of a hydrogen), 203, 201 (245 – 44), 173, 139, and 113. The MS^2 analysis of the dehydration product (MS^2 317 → full scan) showed a similar mass spectrum, which also was identical to that of 15-KETE. The MS analysis of d_8-15-HPETE yielded signals at *m/z* 343 (335 + 8) and 342, and at *m/z* 325 (317 + 8) and 324. MS^2 analysis of *m/z* 325 (range *m/z* 327 – 323) showed strong signals at *m/z* 305 – 307, 279 – 281, and weaker signals at *m/z* 225 and 226, 207 and 208, 181, 152, 141 and 114. The MS^2 spectrum of 15-KETE (MS^2 317 → full scan) appeared to be virtually identical with the MS^2 and MS^3 spectra of 15-HPETE discussed above. The deduced fragmentation of 15-KETE is shown by the inset in Figure 3B.

We conclude that 5-HPETE, 12-HPETE, and 15-HPETE can be partially dehydrated to 5-KETE, 12-KETE, and 15-KETE, respectively, in the heated capillary of the mass spectrometer. 12-KETE and 15-KETE also can be formed by CID of the corresponding hydroperoxide anions in the ion trap. CID of 5-HPETE, however, indicated that 5-HPETE was mainly transformed to products outside the mass range of the ion trap with little formation of 5-KETE.

LC–MS analysis of HETE and d_8*-HETE.* MS^2 analysis of the carboxylate ions (*m/z* 319) of 15-HETE, 12-HETE, and 5-HETE yielded ion trap mass spectra which were similar to those previously reported with other MS/MS instruments (7,9,10). In addition to loss of 18 (water), 44 (CO_2), and 62 (water plus CO_2), MS^2 analysis of 15-HETE yielded signals at *m/z* 219 (α-cleavage between C14 and C15 with gain of H), 175, and 113, whereas12-HETE yielded characteristic signals at *m/z* 208 (α-cleavage C12-C13), 179 (α-cleavage C11-C12 with gain of H), and 163. 8-HETE showed a strong signal at *m/z* 155 (α-cleavage C8-C9 with loss of H), and weaker signals at 163 (α-cleavage, 319 – 156) and 127 (α-cleavage between C7-C8 with gain of H). 5-HETE showed a strong signal at *m/z* 115 (α-cleavage between C5-C6 with gain H), but the other fragment formed by α-cleavage (*m/z* 203) was very weak. d_8-15-HETE, d_8-12-HETE, and d_8-5-HETE fragmented as expected.

LOX activity of cell homogenates and subcellular fractions. Cell homogenates and low-speed supernatant of bovine corneal epithelium converted 30-μM AA to 15-HETE and 12-HETE, about 70% 15-HETE and 30% 12-HETE as judged from

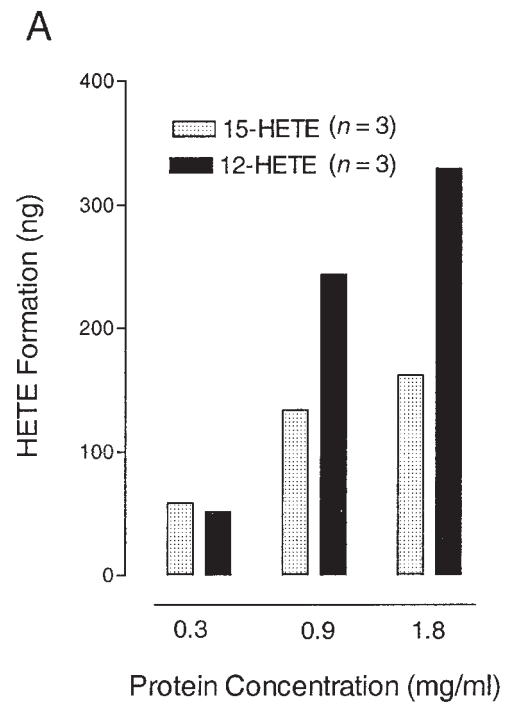

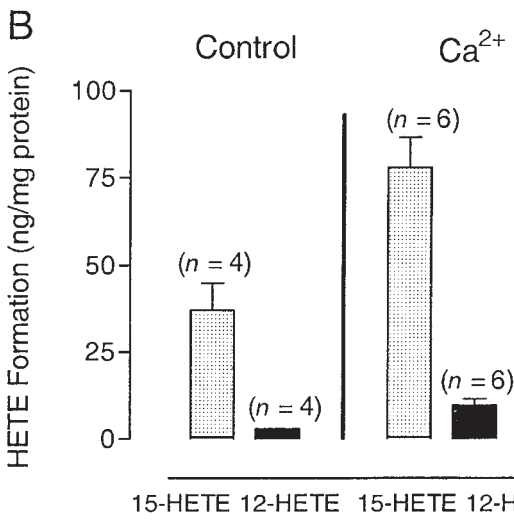

FIG. 4. Biosynthesis of 12-hydroxyeicosatetraenoic acid (HETE) and 15-HETE by subcellular fractions of bovine corneal epithelial cells. (A) Lipoxygenase activity at three different concentrations of microsomal protein. (B) Effect of 1 mM free Ca^{2+} on the biosynthesis of 12- and 15-HETE in the cytosolic fraction of bovine corneal epithelium. Left, control without calcium and, right, with calcium. Mean ± SD.

LC–MS analysis. The relative amounts of 15- and 12-HETE were unchanged with 3–100 μM AA. The microsomal fraction also metabolized AA to 15-HETE and 12-HETE as major products. The microsomal biosynthesis of 12-HETE increased with the amount of protein but the biosynthesis of 15-HETE did not increase to the same extent. The relative amounts of 12-HETE and 15-HETE thus changed. As shown in Figure 4A, 15-HETE was the main metabolite at low protein concentration (0.3 mg/mL), whereas 12-HETE was the most prominent metabolite at higher protein concentration (≥0.9 mg/mL). The total rate of biosynthesis of LOX products by the microsomes was high, ~0.7 ± 0.2 μg/mg protein/30 min (n = 6), equivalent to 0.07 ± 0.02 nmol/mg protein/min. 12-HPETE, 12-KETE, 15-HPETE, and 15-KETE could not be detected.

The high-speed supernatant formed 15-HETE as the main metabolite, but only small amounts of 12-HETE. The rate of biosynthesis of 15-HETE and 12-HETE was 38 ± 8 and below 3 ng/mg protein/30 min, respectively. As mRNA of 5-LOX is present in bovine corneal epithelium and biosynthesis of 5-HETE has been detected occasionally (Liminga, M., and Oliw, E., unpublished data), we investigated the effect of ~1 mM free Ca^{2+} and 1 mM ATP. There was no consistent 5-LOX activity, but the biosynthesis of 15-HETE and 12-HETE appeared to increase in the presence of added Ca^{2+} to 78 ± 21 and 10 ± 4 ng/mg protein/30 min (Fig. 4B), respectively. Addition of calcium had no apparent effect on microsomal LOX activity.

Endogenous 12-HETE and 15-HETE in corneal epithelial cells. The main endogenous LOX metabolite in bovine corneal epithelium was 12-HETE, whereas 15-HETE was found in much lower amounts (Fig. 5A). The amounts of 12- and 15-HETE were 50 ± 13 and 9 ± 6 pg/mg tissue, respectively (n = 5). In another set of experiments, the corneas were transferred from +4 to 37°C for 20 min [in PBS with (n = 4) and without 1 mM calcium (n = 4) and 10 μM A-23187 (n = 3)], and then processed. This procedure resulted in a fourfold increase in the biosynthesis of 12-HETE from endogenous AA to about 0.2 ng/mg tissue, while 15-HETE was undetectable in these experiments (Figs. 5B and 5C).

DISCUSSION

In the first part of this study, we looked at the mass spectra of 5-, 12-, and 15-HPETE, the corresponding HETE and KETE in an ion trap instrument. The carboxylate ions of 12-HPETE and 15-HPETE (m/z 335) were isolated in the trap and dehydrated to the corresponding KETE (m/z 317) by CID as indicated by the scheme below. 5-, 12-, and 15-KETE could also be formed from 5-, 12-, and 15-HPETE, respectively, by temperature-dependent dehydration in the heated capillary.

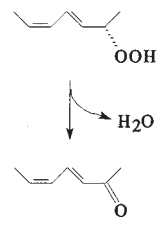

The present work demonstrates that the ion trap MS^2 spectra of these three dehydration products were indeed identical to the MS^2 spectra of the corresponding KETE compounds. Facile dehydration of fatty acid hydroperoxides to keto fatty acids by CID or the high temperature of the heated capillary is therefore a convenient way to analyze these compounds (6,7). 8- and 11-Hydroperoxylinoleic acids also appear to be dehydrated to 8- and 11-keto compounds by the same mechanisms (13).

By analogy, it seems likely that 5-HPETE also was dehydrated to 5-KETE by CID in the ion trap, but this daughter ion could hardly be detected. This finding was unexpected. MacMillan and Murphy (6) reported that tandem MS of the 5-HPETE (m/z 335) and 5-KETE (m/z 317) anions in a triple quadrupole mass spectrometer with argon as the collision gas

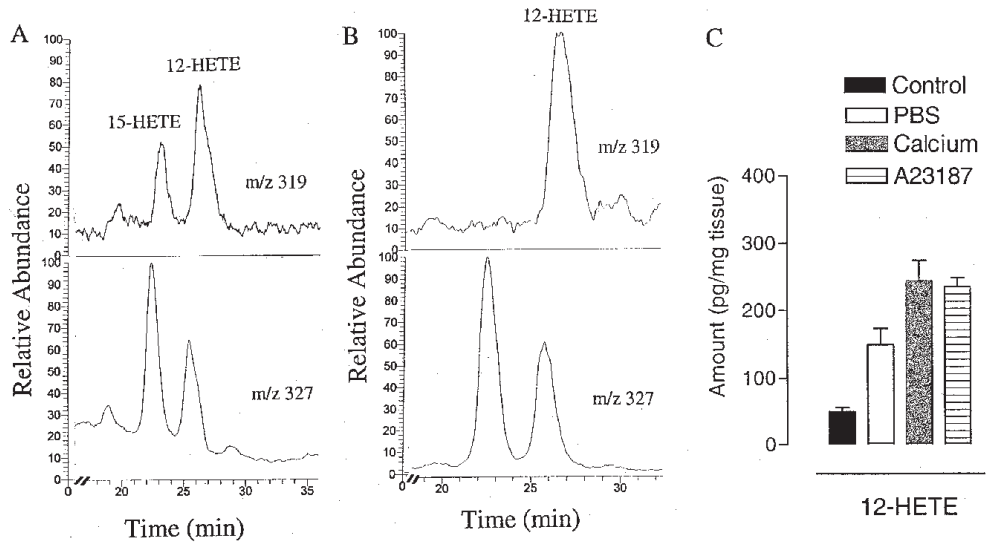

FIG. 5. LC–MS analysis of endogenous levels of 15-HETE and 12-HETE in bovine corneal epithelium. (A) The top trace shows the chromatogram of single ion monitoring of the carboxylate ions (*m/z* 319) of HETE in epithelial tissue from four corneas, whereas the bottom trace shows single ion monitoring of the carboxylate ions (*m/z* 327) of the internal standards, d_8-15-HETE and d_8-12-HETE. The deuterated standards elute ~1 min before the endogenous metabolites. (B) Analysis of HETE in epithelial cells from four bovine corneas, which were incubated in phosphate-buffered saline (PBS) for 20 min at 37°C before single ion monitoring as in A. (C) Amounts of 15-HETE and 12-HETE in epithelial cells from four corneas, which were placed in PBS for 20 min at 37°C in absence (n = 4) or presence of ~1 mM Ca^{2+} (n = 4) and 10 μM A-23187 (n = 3). Single ion monitoring as in (A). Data are presented as mean ± SD. See Figure 4 for abbreviations.

both yielded mass spectra with strong signals at *m/z* 317. The base peak of the 5-HPETE mass spectrum was *m/z* 59 ($H_2C{=}C(OH)O^-$, likely formed through a six-membered transition state from the dehydration product of 5-HPETE by cleavage between C-2 and C-3), whereas *m/z* 59 was much weaker in the 5-KETE mass spectrum (6). Although similar, the mass spectra of 5-HPETE and 5-KETE thus differed in a triple quadrupole instrument. A plausible explanation to the low intensity of the daughter ion at *m/z* 317 of 5-HPETE in the ion trap might be formation the daughter ion at *m/z* 59, which was below the mass range of the ion trap and could therefore not be detected.

In the second part, we measured and quantified the formation of LOX metabolites from exogenous AA in subcellular fractions of bovine corneal epithelial cells. 12-HPETE and 15-HPETE were not detected and were apparently efficiently reduced to 12-HETE and 15-HETE. Alternatively, 15-HPETE might be converted to 14,15-leukotrienes or related products (29). The biosynthesis of 12-HETE and 15-HETE by subcellular fractions appeared to be influenced by the calcium concentration in the cytosolic fraction and by the amount of protein in the microsomal assay. 15-HETE was the main product in the cytosol, and only small amounts of 12-HETE were formed. Addition of ~1 mM free Ca^{2+} augmented the biosynthesis of 15-HETE twofold. Effect of Ca^{2+} on LOX activity also has been reported in other broken cells (30–32). The microsomal fractions formed both 12-HETE and 15-HETE. 12-HETE was the main product at a high protein concentration, whereas 15-HETE was favored at low concentrations. These observations show that the experimental conditions must be standardized in order to assess pathological or physiological changes of LOX activity of broken cells. We used a fixed and relatively long incubation time. 15-LOX type 2 and 12-LOX of platelet type could be expected to be maintain a near linear rate for 30 min, whereas the rate 5-LOX and 12-LOX of the leukocyte type might decrease after a few minutes (33–35). There is also a marked intra-individual variation in LOX activity of bovine corneal epithelium (data not shown).

The endogenous levels of HETE were also determined in the epithelium. The rate-limiting step in LOX catalysis is likely release of AA from phospholipids (36). Phospholipases might be activated *post mortem* and the tissue levels we measured might not reflect the cellular levels of HETE under normal conditions. 12-HETE was the main LOX metabolite of endogenous AA. 15-HETE was undetectable or present in low amounts. This parallels findings in human leukocytes, where 15-LOX activity only could be detected following incubation with exogenous AA (37). 12-HETE increased 3–5 times after incubation of the cornea at 37°C, whereas 15-HETE now was undetectable. These findings were unexpected as 15-HETE was the main product from exogenous 3–100 μM AA by low-speed supernatant or cell homogenates. This suggests that incubation at 37°C makes AA available for 12-LOX. The concentration of endogenously released AA might be less than 3 μM. It is therefore conceivable that low concentrations of AA might be more efficiently oxidized by 12- rather than by 15-LOX. Indeed, 12-LOX of platelet type has a K_m of ~ 8 μM for AA (34), whereas the K_m of 15-LOX type 2 for AA is ~25 μM

(31). It will be of interest to determine whether the accumulation of 12-HETE can be explained by different kinetic properties of the bovine corneal LOX.

In summary, we have shown that the fragmentation of 5-HPETE differs from other HPETE during CID in the ion trap. 12-HETE is the main endogenous LOX product in bovine corneal epithelial cells, whereas 15-HETE is the main product from exogenous AA of crude cells homogenates. Our findings emphasize that corneal LOX of subcellular fractions should be studied under standardized conditions.

ACKNOWLEDGMENTS

Support by the Swedish Medical Research Council (03X-06523) and the Swedish Society for Medical Research is gratefully acknowledged.

REFERENCES

1. Kühn, H. (1999) Lipoxygenases, in *Prostaglandins, Leukotrienes and Other Eicosanoids* (Marks, F., and Fürstenberger, G., eds.), pp. 109–141, Wiley-VCH, Weinheim.
2. Brash, A.R. (1999) Lipoxygenases: Occurrence, Functions, Catalysis, and Acquisition of Substrate, *J. Biol. Chem. 274*, 23679–23682.
3. Funk, C.D. (1993) Molecular Biology in the Eicosanoid Field, *Prog. Nucleic Acid Res. Mol. Biol. 45*, 67–98.
4. Funk, C.D. (1996) The Molecular Biology of Mammalian Lipoxygenases and the Quest for Eicosanoid Functions Using Lipoxygenase-Deficient Mice, *Biochim. Biophys. Acta 1304*, 65–84.
5. Prigge, S.T., Boyington, J.C., Gaffney, B.J., and Amzell, L.M. (1996) Structure Conservation in Lipoxygenases: Structural Analysis of Soybean Lipoxygenase-1 and Modeling of Human Lipoxygenases, *Proteins 24*, 275–291.
6. MacMillan, D.K., and Murphy, R.C. (1995) Analysis of Lipid Hydroperoxides and Long-Chain Conjugated Keto Acids by Negative Ion Electrospray Mass Spectrometry, *J. Am. Soc. Mass Spectrom. 6*, 1190–1201.
7. Hall, L.M., and Murphy, R.C. (1998) Electrospray Mass Spectrometric Analysis of 5-Hydroperoxy and 5-Hydroxyeicosatetraenoic Acids Generated by Lipid Peroxidation of Red Blood Cell Ghost Phospholipids, *J. Am. Soc. Mass. Spectrom. 9*, 527–532.
8. Fenn, J.B., Mann, M., Meng, C.K., Wong, S.F., and Whitehouse, C.M. (1989) Electrospray Ionization for Mass Spectrometry of Large Biomolecules, *Science 246*, 64–71.
9. Deterding, L.J., Curtis, J.F., and Tomer, K.B. (1992) Tandem Mass Spectrometry Identification of Eicosanoids: Leukotrienes and Hydroxyeicosatetraenoic Acids, *Biol. Mass. Spectrom. 21*, 597–609.
10. Wheelan, P., Zirrolli, J.A., and Murphy, R.C. (1993) Low-Energy Fast Atom Bombardment Tandem Mass Spectrometry of Monohydroxy Substituted Unsaturated Fatty Acids, *Biol. Mass Spectrom. 22*, 465–473.
11. Schneider, C., Schreier, P., and Herderich, M. (1997) Analysis of Lipoxygenase-Derived Fatty Acid Hydroperoxides by Electrospray Ionization Tandem Mass Spectrometry, *Lipids 32*, 331–336.
12. Bylund, J., Ericsson, J., and Oliw, E.H. (1998) Analysis of Cytochrome P450 Metabolites of Arachidonic and Linoleic Acids by Liquid Chromatography–Mass Spectrometry with Ion Trap MS^2, *Anal. Biochem. 265*, 55–68.
13. Oliw, E.H., Su, C., Skogstrom, T., and Benthin, G. (1998) Analysis of Novel Hydroperoxides and Other Metabolites of Oleic, Linoleic, and Linolenic Acids by Liquid Chromatography–Mass Spectrometry with Ion Trap MS^n, *Lipids 33*, 843–852.
14. Williams, R.N., Delamere, N.A., and Paterson, C.A. (1985) Generation of Lipoxygenase Products in the Avascular Tissues of the Eye, *Exp. Eye Res. 41*, 733–738.
15. Hurst, J.S., Balazy, M., Bazan, H.E., and Bazan, N.G. (1991) The Epithelium, Endothelium, and Stroma of the Rabbit Cornea Generate 12(*S*)-Hydroxyeicosatetraenoic Acid as the Main Lipoxygenase Metabolite in Response to Injury, *J. Biol. Chem. 266*, 6726–6730.
16. Oliw, E.H. (1993) Biosynthesis of 12(*S*)-Hydroxyeicosatetraenoic Acid by Bovine Corneal Epithelium, *Acta Physiol. Scand. 147*, 117–121.
17. Liminga, M., Fagerholm, P., and Oliw, E.H. (1994) Lipoxygenases in Corneal Epithelia of Man and Cynomolgus Monkey, *Exp. Eye Res. 59*, 313–321.
18. Liminga, M., Hörnsten, L., Sprecher, H.W., and Oliw, E.H. (1994) Arachidonate 15-Lipoxygenase in Human Corneal Epithelium and 12- and 15-Lipoxygenases in Bovine Corneal Epithelium: Comparison with Other Bovine 12-Lipoxygenases, *Biochim. Biophys. Acta 1210*, 288–296.
19. Liminga, M., and Oliw, E.H. (1999) cDNA Cloning of 15-Lipoxygenase Type 2 and 12-Lipoxygenases of Bovine Corneal Epithelium, *Biochim. Biophys. Acta 1437*, 124–135.
20. Bazan, H.E., Birkle, D.L., Beuerman, R., and Bazan, N.G. (1985) Cryogenic Lesion Alters the Metabolism of Arachidonic Acid in Rabbit Cornea Layers, *Invest. Ophthamol. Vis. Sci. 26*, 474–480.
21. Offord, E.A., Sharif, N.A., Mace, K., Tromvoukis, Y., Spillare, E.A., Avanti, O., Howe, W.E., and Pfeifer, A.M. (1999) Immortalized Human Corneal Epithelial Cells for Ocular Toxicity and Inflammation Studies, *Invest. Ophthalmol. Vis. Sci. 40*, 1091–1101.
22. Conners, M.S., Stoltz, R.A., and Schwartzman, M.L. (1996) Chiral Analysis of 12-Hydroxyeicosatetraenoic Acid Formed by Calf Corneal Epithelial Microsomes, *J. Ocul. Pharm. Ther. 12*, 19–26.
23. Vafeas, C., Mieyal, P.A., Urbano, F., Falck, J.R., Chauhan, K., Berman, M., and Schwartzman, M.L. (1998) Hypoxia Stimulates the Synthesis of Cytochrome P450-Derived Inflammatory Eicosanoids in Rabbit Corneal Epithelium, *J. Pharmacol. Exp. Ther. 287*, 903–909.
24. Oliw, E.H., and Sprecher, H. (1989) Metabolism of Polyunsaturated Fatty Acids by an (n-6)-Lipoxygenase Associated with Human Ejaculates, *Biochim. Biophys. Acta 1002*, 283–291.
25. Reddanna, P., Whelan, J., Maddipati, K.R., and Reddy, C.C. (1990) Purification of Arachidonate 5-Lipoxygenase from Potato Tubers, *Methods Enzymol. 187*, 268–277.
26. Becker, H.-D., Björk, A., and Adler, E. (1980) Quinone Dehydrogenation. Oxidation of Benzylic Alcohols with 2,3-Dichloro-5,6-dicyanobenzoquinone, *J. Org. Chem. 45*, 1596–1600.
27. Bradford, M.M. (1976) A Rapid and Sensitive Method for the Quantitation of Microgram Quantities of Protein Utilizing the Principle of Protein–Dye Binding, *Anal. Biochem. 7*, 248–254.
28. Jakobsson, P.-J., Odlander, B., Steinhilber, D., Rosén, A., and Claesson, H.-E. (1991) Human B Lymphocytes Possess 5-Lipoxygenase Activity and Convert Arachidonic Acid to Leukotriene B_4. *Biochem. Biophys. Res. Commun. 178*, 302–308.
29. Maas, R.L., and Brash, A.R. (1983) Evidence for a Lipoxygenase Mechanism in the Biosynthesis of Epoxide and Dihydroxy Leukotrienes from 15(*S*)-Hydroperoxyeicosatetraenoic Acid by Human Platelets and Porcine Leukocytes. *Proc. Natl. Acad. Sci. USA 80,* 2484–2888.
30. Brinckmann, R., Schnurr, K., Heydeck, D., Roesenbach, T., Kolde, G., and Kühn, H. (1998) Membrane Translocation of 15-Lipoxygenase in Hematopoietic Cells Is Calcium-Dependent

and Activates the Oxygenase Activity of the Enzyme, *Blood 91*, 64–74.
31. Kilty, I., Logan, A., and Vickers, P.J. (1999) Differential Characteristics of Human 15-Lipoxygenase Isozymes and a Novel Splice Variant of 15*S*-Lipoxygenase, *Eur. J. Biochem. 266*, 83–93.
32. Oliw, E.H. (1990) Biosynthesis of 20-Hydroxyeicosatetraenoic Acid (20-HETE) and 12 (*S*)-HETE by Renal Cortical Microsomes of the Cynomolgus Monkey, *Eicosanoids 3*, 161–164.
33. Takahashi, Y., Ueda, N., and Yamamoto, S. (1988) Two Immunologically and Catalytically Distinct Arachidonate 12-Lipoxygenases of Bovine Platelets and Leukocytes, *Arch. Biochem. Biophys. 266*, 613–621.
34. Hada, T., Ueda, N., Takahashi, Y., and Yamamoto, S. (1991) Catalytic Properties of Human Platelet 12-Lipoxygenase as Compared with the Enzymes of Other Origins, *Biochim. Biophys. Acta 1083*, 89–93.
35. Qiao, N., Takahashi, Y., Takamatsu, H., and Yoshimoto, T. (1999) Leukotriene A Synthase Activity of Purified Mouse Skin Arachidonate 8-Lipoxygenase Expressed in *Escherichia coli, Biochim. Biophys. Acta 1438*, 131–139.
36. Dieter, P. (1999) The Generation of Free Arachidonic Acid, in *Prostaglandins, Leukotrines and Other Eicosanoids* (Marks, F., and Fürstenberger, G., eds.), pp. 47–59, Wiley-VCH, Weinheim.
37. Fruteau de Laclos, B., Braquet, P., and Borgeat, P. (1984) Characteristics of Leukotriene (LT) and Hydroxy Eicosatetraenoic Acid (HETE) Synthesis in Human Leukocytes *in vitro*: Effect of Arachidonic Acid Concentration, *Prostaglandins Leukotrienes Med. 13*, 47–52.

[Received December 6, 1999, and in revised form January 19, 2000; revision accepted January 27, 2000]

Determining Double-Bond Positions in Monoenoic 2-Hydroxy Fatty Acids of Glucosylceramides by Gas Chromatography–Mass Spectrometry

Hiroyuki Imai[a,*], Kohei Yamamoto[b], Akira Shibahara[c], Shuichi Miyatani[c], and Takao Nakayama[b]

[a]Department of Biology, Faculty of Science, Konan University, Kobe 658-8501, Japan, [b]General Testing Research Institute of Japan Oil Stuff Inspectors' Corporation, Kobe 658-0044, Japan, and [c]Department of Clinical Nutrition, Osaka Prefectural College of Health Sciences, Habikino 583-8555, Japan

ABSTRACT: We applied a gas chromatography–mass spectrometry (GC–MS) method using dimethyl disulfide (DMDS) adducts and were able to determine the double-bond positions in monounsaturated 2-hydroxy fatty acids (2-HFA). 2-HFA methyl esters, prepared from the hydrolysate of *Arabidopsis thaliana* leaf glucosylceramides, were acetylated and methylthiolated. GC–MS analysis of the resulting DMDS adducts showed simple mass spectra with recognizable molecular ions and a series of key fragment ions indicating the original double-bond positions in the aliphatic chain. Based on this GC–MS elucidation, we confirmed that *Arabidopsis* leaf glucosylceramides have C_{22}, C_{23}, C_{24}, C_{25}, and C_{26} chain length 2-HFA with monounsaturation, and all their double bonds are placed at the n-9 position. This procedure is simple, time efficient, and highly sensitive.

Paper no. L8338 in *Lipids 35,* 233–236 (February 2000).

Locating the double-bond positions in monounsaturated 2-hydroxy fatty acids (2-HFA) of plant glucosylceramides (1,2) has been accomplished by using methods that employ ozonolysis (1) or OsO_4 oxidation (2). These methods, however, are complex, time consuming, and tedious, which might explain why in-depth studies on the structure of double-bond positions in these acids have been scarce, and the metabolic sequence for the biosynthesis of these monoenoic 2-HFA still remains unknown. Our simple gas chromatography–mass spectrometry (GC–MS) method with dimethyl disulfide (DMDS) adducts makes it possible to easily verify the double-bond positions in monounsaturated 2-HFA and will facilitate further research in this field.

MATERIALS AND METHODS

Plant materials. Seeds of *Arabidopsis thaliana* (L.) Heynh. ecotype Columbia were germinated in a soil mixture (Soil for Saintpaulia, Tosho Co., Yaizu, Japan) and grown for 8 wk under a 8/16 h light/dark cycle of at 23°C. Rosette leaves were harvested.

Lipid extraction. Fifty grams of the rosette leaves were steamed with boiling water for 3 min and homogenized with 150 mL of chloroform/methanol (1:2, vol/vol) in a homogenizer (Physcotron NS-50; Niti-on Irikaki, Funabashi, Japan) and filtered by suction through a sheet of filter paper. The resultant residue on the filter paper was homogenized again with 50 mL of chloroform and filtered again, as above. The filtrates were combined, and 50 mL of 0.9% (wt/vol) KCl in water was added. Total lipids were recovered in the lower phase, dried under reduced pressure, and dissolved in 1 mL of chloroform/methanol (2:1, vol/vol).

Purifying the glucosylceramides. The total lipids were subjected to mild alkaline hydrolysis, which removed the glycerolipids. After incubating for 1 h at 37°C with 4 mL of 0.4 M KOH in methanol, an alkaline preparation was neutralized with 150 μL of HCl and mixed with 80 mL of chloroform, 76 mL of methanol, and 40 mL of water. The alkaline-stable lipid fraction, including glucosylceramides, was then recovered in the lower phase. The lower phase was evaporated to dryness, dissolved in 0.5 mL of chloroform/methanol (2:1, vol/vol), and subjected to thin-layer chromatography (TLC) on precoated silica gel plates (Wakogel B-10; Wako Pure Chemical Industries, Osaka, Japan) using chloroform/methanol/water (65:16:2, by vol) as a solvent system. Spots of glucosylceramides contaminated with a small amount of steryl glycoside were scraped off the plate and acetylated with acetic anhydride in pyridine at room temperature overnight (3). These acetylated lipids were then separated by silica gel TLC using chloroform/benzene/acetone (8:2:1, by vol) as a developing system, and the acetyl esters of the glucosylceramides were scraped off the plates. The glucosylceramides reached satisfactory purity as determined by silica gel TLC.

Analyzing the 2-HFA. The glucosylceramides were methanolyzed with 3% (wt/vol) HCl (gaseous) in dry methanol at 100°C for 3 h. After adding water, the resultant total fatty acid methyl esters were extracted with *n*-hexane, dried under nitrogen, and separated into the 2-hydroxy and the non-HFA

*To whom correspondence should be addressed.
E-mail: imai@base2.ipc.konan-u.ac.jp

Abbreviations: DMDS, dimethyl disulfide; GC–MS, gas chromatography–mass spectrometry; 2-HFA, 2-hydroxy fatty acid (Xh:Y, 2-hydroxy fatty acid containing X carbons with Y double bonds); TLC, thin-layer chromatography.

fractions by silica gel TLC using *n*-hexane/diethyl ether (17:3, vol/vol) as a mobile phase.

2-HFA methyl esters of the glucosylceramides were identified by GC–MS equipped with a mass data system (GCQ, Finnigan MAT Instruments, Austin, TX). The capillary column used was coated with dimethyl polysiloxane of 0.25 μm thickness (0.25 mm i.d. × 30 m; SPB-5, Supelco, Bellefonte, PA). The column temperature was programmed from 100°C (2 min hold) to 280°C at 10°C/min and maintained at 280°C for an additional 45 min. The mass spectra were measured under the following conditions: ion source temperature, 200°C; ionizing voltage, 70 eV; ionizing current, 250 μA; scanning rate, 1 s/cycle from 50 to 600 amu.

Preparing and analyzing DMDS adducts. An aliquot of the 2-HFA methyl esters of glucosylceramides was converted to *O*-acetyl derivatives as described by Renkonen (3). The *O*-acetylated methyl esters were subjected to I_2-catalyzed methylthiolation at 37°C for 30 min (4). After adding 1 mL of *n*-hexane/diethyl ether (1:1, vol/vol) with stirring, 10% (wt/vol) $Na_2S_2O_3$ of water solution was added with vigorous shaking until the color of I_2 disappeared. The mixture was allowed to stand for a few minutes, and the upper phase containing the resulting DMDS adducts was withdrawn, concentrated, and analyzed by GC–MS under the same conditions as mentioned in the preceding paragraph.

RESULTS AND DISCUSSION

Imai (5) had previously observed 13 kinds of 2-HFA in glucosylceramides from the leaves of *A. thaliana*. The 2-HFA profile is complex and clearly different from those of glucosylceramides from the leaves of Solanaceae (eggplant, tomato, etc.) and Leguminoseae (pea, white clover, etc.), which consist mostly of saturated 2-HFA (2). In that study (5), *Arabidopsis* 2-HFA had been identified using capillary GC, based on the coincidence of their retention times with those of the 2-HFA mixtures, which had been prepared from wheat leaf glucosylceramides (2), but we wanted more evidence to confirm the structure of *Arabidopsis* 2-HFA.

We once again prepared *Arabidopsis* 2-HFA methyl esters, and then, for this study, we analyzed them by GC–MS to ascertain the position of the hydroxyl group. Mass spectra taken at the mass chromatographic responses revealed characteristic fragment ions [$M^+ - 59$] resulting from the 1,2-cleavage and the loss of the methoxycarbonyl group (6). A typical mass spectrum of 2-HFA methyl ester from *Arabidopsis* leaf glucosylceramides is shown in Figure 1. The spectrum exhibits a molecular ion at *m/z* 368 and a characteristic peak at *m/z* 309 corresponding to the $M^+ - 59$ fragment. This indicates that the compound is a 2-hydroxy docosenoic acid methyl ester. By using a combination of capillary GC and GC–MS analysis, the other 12 kinds of the methyl esters were identified as saturated or monounsaturated 2-HFA.

To determine the double-bond positions in monounsaturated 2-HFA of *Arabidopsis* leaf glucosylceramides, a mixture of the 2-HFA methyl esters was *O*-acetylated and then methylthiolated. The resulting DMDS adducts were analyzed by GC–MS. Figure 2 shows the mass chromatogram in which five compounds (peaks 1 to 5) eluted.

Figure 3 shows the mass spectrum of the compound corresponding to peak 3 in Figure 2. A molecular ion at *m/z* 532 can be easily detected, identifying the adducts as methyl 2-*O*-acetyl bis(methylthio)tetracosanoate. Sets of fragment ions at *m/z* 173, 359, and 327 were produced from the cleavage be-

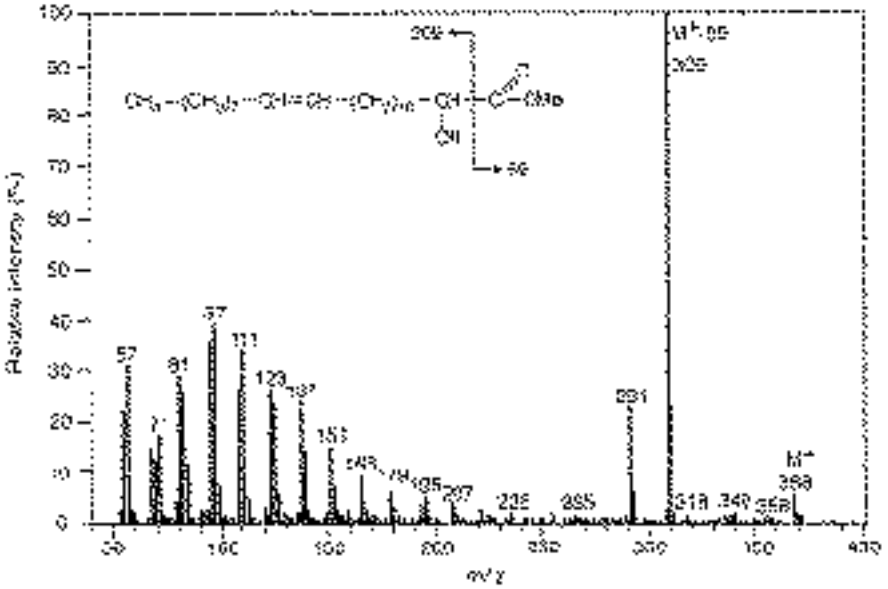

FIG. 1. Mass spectrum of one of 2-hydroxy fatty acid (2-HFA) methyl esters from *Arabidopsis* leaf glucosylceramides. The spectrum indicates the 2-hydroxy docosenoic acid (22h:1) methyl ester.

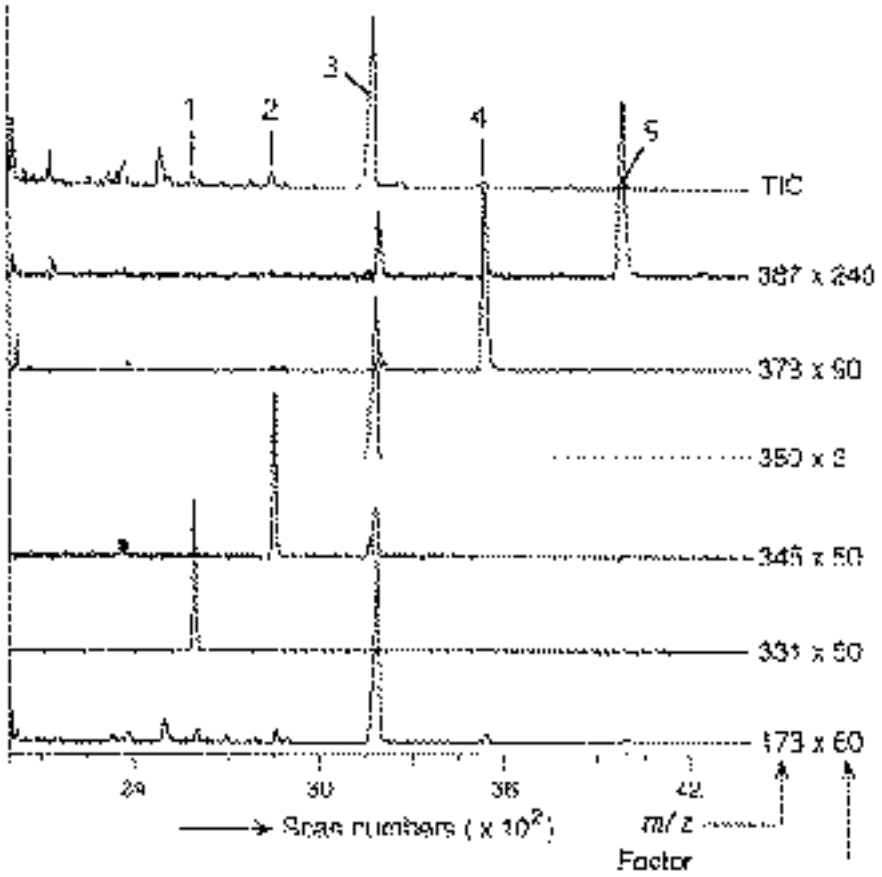

FIG. 2. Mass chromatogram of dimethyl disulfide adducts of 2-HFA *O*-acetyl methyl ester from *Arabidopsis* leaf glucosylceramides. (1) 22h:1; (2) 23h:1; (3) 24h:1; (4) 25h:1; (5) 26h:1. Gas chromatography–mass spectrometry conditions: ion source temperature, 200°C; ionizing voltage, 70 eV; ionizing current, 250 μA; scanning rate, 1 s/cycle from 50 to 600 amu. The other peaks not numbered in this figure are probably by-products from dimethyl disulfide adducts preparation. See Figure 1 for other abbreviation.

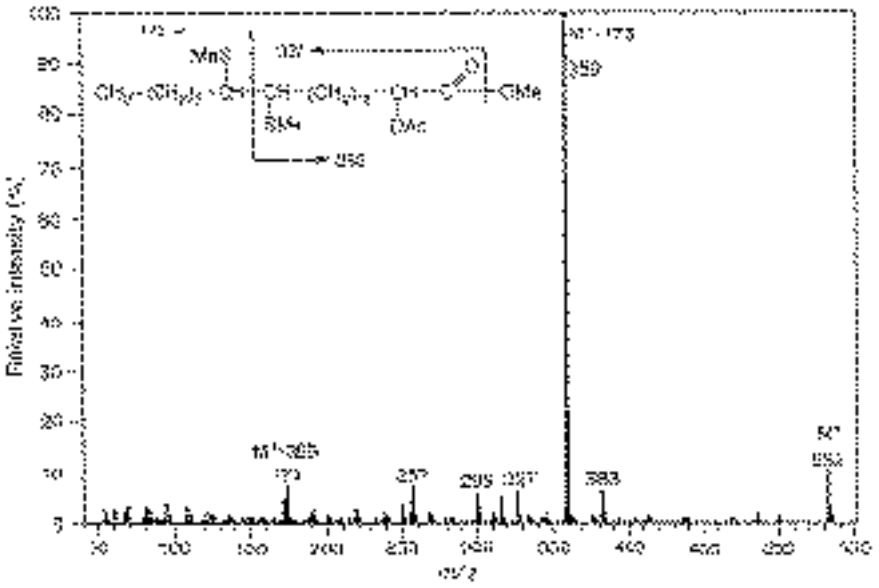

FIG. 3. Mass spectrum of dimethyl disulfide adducts of 2-HFA *O*-acetyl methyl ester from *Arabidopsis* leaf glucosylceramides. The spectrum is taken at peak 3 in Figure 2. The original acid is identified as 2-hydroxy-15-tetracosenoic acid (24h:1). See Figure 1 for abbreviation.

tween the methylthio-substituted carbons at C-15 and C-16. From these observations, the original acid was identified as 2-hydroxy-15-tetracosenoic acid.

The smaller peaks, 1, 2, 4, and 5 in Figure 2, also gave the key fragment ion at *m/z* 173 and the characteristic fragment ions [$M^+ - 173$] as the base peaks at *m/z* 331, 345, 373, and 387, respectively, indicating the presence of an n-9 series of monoenoates having C_{22}, C_{23}, C_{25}, and C_{26} chain lengths.

Based on this GC–MS elucidation, we confirmed that *Arabidopsis* leaf glucosylceramides have C_{22}, C_{23}, C_{24}, C_{25}, and C_{26} chain-length 2-HFA with monounsaturation, and all their double bonds are placed at the n-9 position.

We can easily prepare DMDS adducts of 2-HFA methyl esters. The yield of their adducts (over 90% of the original ester) is almost the same as that of the adducts of monoenoates without any hydroxyl groups (7). As a preliminary experiment, we analyzed the reaction products with DMDS and *O*-acetyl methyl ester of ricinoleic acid (12-hydroxy-9-octadecenoic acid), a major component in castor oil. The sets of ions resulting from the cleavage between the methylthio-substituted carbons, however, could not be identified. This may be due to steric hindrance; the distance between the double-bond position and the hydroxyl base may be important for the formation of the DMDS adducts of *O*-acetyl esters. Blocking the hydroxyl base (*O*-acetylated, in this study) is, however, necessary in electron impact ionization analysis of DMDS adducts.

Biosynthetic pathways for monounsaturated 2-HFA of plant glucosylceramides have not yet been verified. We speculate that the monounsaturated 2-HFA in glucosylceramides are formed either by elongation from an oleate moiety or by the action of an n-9 desaturase inserting a double bond relative to the methyl end of the acyl chain, because all the double bonds in monoenoic 2-HFA of *Arabidopsis* leaf glucosylceramides are at the n-9 position. Using a technique that combines three processes (stable isotopically labeled precursor preparation, DMDS adduct preparation, and GC–MS analysis), as Yamamoto *et al.* (4) discussed, will help in confirming the biosynthetic pathways for n-9 monounsaturated 2-HFA of plant glucosylceramides. Preliminary experiments are underway in our laboratories.

ACKNOWLEDGMENTS

We wish to thank Professor Masao Ohnishi (Obihiro University of Agriculture and Veterinary Medicine) for his helpful discussions. This work was supported, in part, by the Grant for Basic Science Research Project (970659) from The Sumitomo Foundation.

REFERENCES

1. Falsone, G., Budzikiewicz, H., and Wendisch, D. (1987) Constituents of *Euphorbiaceae*, 9 Comm. [1]. New Cerebrosides from *Euphorbia biglandulosa* Desf., *Z. Naturforsch. 42b*, 1476–1480.
2. Imai, H., Ohnishi, M., Kinoshita, M., Kojima, M., and Ito, S. (1995) Structure and Distribution of Cerebroside Containing Unsaturated Hydroxy Fatty Acids in Plant Leaves, *Biosci. Biotechnol. Biochem. 59*, 1309–1313.
3. Renkonen, O. (1966) Individual Molecular Species of Phospholipids III. Molecular Species of Ox-Brain Lecithins, *Biochim. Biophys. Acta 125*, 288–309.
4. Yamamoto, K., Shibahara, A., Nakayama, T., and Kajimoto, G. (1991) Determination of Double-Bond Positions in Methylene-Interrupted Dienoic Fatty Acids by GC–MS as Their Dimethyl Disulfide Adducts, *Chem. Phys. Lipids 60*, 39–50.
5. Imai, H. (1998) Glucocerebrosides Containing Unsaturated Hydroxy Fatty Acids in *Arabidopsis thaliana*, in *Advances in Plant Lipid Research* (Sánchez, J., Cerdá-Olmedo, E., and Martínez-Force, E., eds.), pp. 38–40, Universidad de Sevilla, Sevilla.
6. Ragnar, R., and Einar, S. (1960) Mass Spectrometric Studies VI. Methyl Esters of Normal Chain Oxo-, Hydroxy-, Methoxy- and Epoxy-acids, *Ark. Kemi 15*, 545–574.
7. Shibahara, A., Yamamoto, K., Nakayama, T., and Kajimoto, G. (1985) Rapid Determination of Double Bond Positions in Monounsaturated Fatty Acids by GC–MS and Its Application to Fatty Acid Analysis, *J. Jpn. Oil Chem. Soc. 34*, 618–625.

[Received August 24, 1999 and in revised form January 3, 2000; revison accepted January 5, 2000]

Chemistry, Biochemistry, and Function of Sterols

Presented at the 90th AOCS Annual Meeting & Expo in Orlando, Florida, May 1999

John D. Weete[a], Edward J. Parish[b], and W. David Nes[c]

Departments of [a]Biology, West Virginia University, Morgantown, West Virginia 28506, [b]Chemistry, Auburn University, Auburn, Alabama 36849, and [c]Chemistry and Biochemistry, Texas Tech University, Lubbock, Texas 79409

The first sterol symposium was held at the 1970 American Oil Chemists' Society Annual Meeting in New Orleans and was organized by Henry Kircher. Since that time, sterol symposia focusing on sterol structure, biosynthesis, chemistry, regulation, function, and other steroids and isoprenoids have been held regularly at AOCS annual meetings.

The 1999 Sterol Symposium, "Chemistry, Biochemistry, and Function of Sterols," held at the AOCS Annual Meeting in Orlando, Florida, was fittingly dedicated to Dr. George J. Schroepfer Jr. of Rice University in Houston, Texas. He was scheduled to be the keynote speaker, but unfortunately, Dr. Schroepfer passed away on December 11, 1998. Although this was to be his first sterol symposium, his contributions to the field of steroid chemistry and biochemistry have influenced many of the symposium participants as well as steroid researchers worldwide.

We would like to thank our corporate partners who gave generous financial support to help make the symposium a success: Steraloids, Inc., Pharmacia & Upjohn, and DuPont Pharmaceutical Co.

This symposium was sponsored by the biotechnology division of the AOCS. Speakers in the 1999 Sterol Symposium represented an international mix of senior and junior scientists, and students from six countries. We would like to express our appreciation to them for their cooperation during the planning process, and for their participation in the symposium. By all accounts, the symposium was a success, and we are looking forward to the next one.

Previous Sterol Symposia

Year	Title	Location	Organizers
1970	Sterol Biosynthesis	New Orleans	H. Kircher
1971	Role of Sterols in Fungi	Houston	J. Hendrix
1973	Phytosterols	New Orleans	J.L. Laseter
1974	Sterols—Biosynthesis, Metabolism	Philadelphia	H. Kircher
1978	Functions of Steroids and Other Isopentenoids	St. Louis	W.R. Nes, G. Heftman
1980	Sterol Analysis	New York	H. Kircher, G. Heftman
1981	Steroids: Biosynthesis, Plants and Insects Microbes, Functions	New Orleans	H. Kircher, W.R. Nes
1985	Chemistry, Biosynthesis, and Function of Sterols (Kircher Memorial)	Philadelphia	W.D. Nes, L.W. Parks
1986	Phytolipids	Honolulu	G.W. Patterson
1990	Plant and Fungal Sterols: Biosynthesis, Metabolism and Function	Baltimore	J.D. Weete, G.W. Patterson
1994	Regulation of Biosynthesis and Function of Isopentenoids	Atlanta	W.D. Nes, E. Parish
1996	Biochemistry of Sterols	Indianapolis	W.D. Nes, R. Norton
1997	Biochemistry, Chemistry, and Function of Sterols	Seattle	E. Parish, W.D. Nes
1999	Chemistry, Biochemistry, and Function of Sterols (Schroepfer Memorial)	Orlando	J.D. Weete, E. Parish, W.D. Nes

In Remembrance

George J. Schroepfer Jr.

June 15, 1932–December 11, 1998

George J. Schroepfer Jr. was to have been the keynote speaker at the Steroid Symposium held at the 90th Annual Meeting of the AOCS in Orlando. His unexpected death represents a great loss to the community of scientists working in the field of sterols and sphingolipids.

The son of a distinguished professor of civil engineering, George was born in the midst of the Great Depression. The economic uncertainties and the influence of his family instilled in him a healthy dose of conservatism and skepticism that pervaded his life and his approach to science. Growing up in Minneapolis, Minnesota, George received an excellent education, due in no small part to the constant encouragement of his family. His parents suffered through his adolescent preoccupation with sports—basketball, tennis, football, speed skating, and hockey—and were relieved when George confronted the bitter reality that his athletic talents were not sought at the University of Minnesota.

Accepted into medical school after his junior year at Minnesota, George greatly enjoyed his medical studies. He showed a special gift for biomedical research and was encouraged to pursue advanced studies with Ivan D. Frantz after finishing an internship in internal medicine. George met many eminent scientists through Dr. Frantz, a profound experience for a young physician. After completing a Ph.D. in biochemistry with a minor in organic chemistry, George worked as a postdoctoral fellow with Sir John Cornforth and the late George Popjak to carry out a series of ingenious deuterium- and tritium-labeling studies that elucidated the stereospecificity of hydrogen transfer in the biosynthesis of squalene. During a subsequent postdoctoral year with Konrad Bloch, Schroepfer applied similar methods to delineate the stereospecific conversion of stearic acid to oleic acid and on to 10-hydroxystearic acid.

George returned to the University of Minnesota as an assistant professor, but was immediately recruited by the University of Illinois. By 1968, he had become director of the School of Basic Medical Sciences, an august title for a 36-year-old scientist. In 1972, George accepted an invitation from Rice University to establish a new department of biochemistry. His 13-year reign as a strong and dynamic chairman resulted in a flourishing department with a vigorous research program. In later years, he turned his attention from administrative responsibilities to concentrate on his expanding research program.

Much of George's research dealt with the biosynthesis of cholesterol, including 14α-demethylation, olefin migration from Δ^{14} to Δ^{5}, and alternative pathways of this migration. Another focus of his research was the role of oxysterols in the regulation of cholesterol metabolism and related processes, the subject of a monumental review completed just prior to his death. George developed painstakingly thorough methods for measuring oxysterol levels in blood and tissues and was often baffled by the slipshod methodology and implausible claims of many groups working in this area. He also oversaw the chemical synthesis of well over 100 oxysterols for use as standards and for study of their effects on the regulation of cholesterol homeostasis.

Perhaps the most important of these oxysterols was 3β-hydroxy-5α-cholest-8(14)-en-15-one. This 15-ketosterol and its various analogs were subjected to intensive investigations of their metabolism and biological activities. The 15-ketosterol markedly lowered serum cholesterol levels in nonhuman primates and simultaneously raised high-density lipoprotein cholesterol, effects that are generally considered desirable for the treatment and prevention of atherosclerosis. Although pharmaceutical development of the 15-ketosterol was terminated after phase I clinical trials, George continued to study the many intriguing properties of 15-ketosterols and their analogs until his death.

His laboratory always maintained strong synthetic capabilities, which ultimately led to a vast and diverse collection of sterols and sphingolipids. George routinely insisted on thorough characterization of virtually every sample, and this requirement contributed to the development of uncommon chromatographic and spectroscopic expertise in his laboratory. The combination of synthetic and analytical strengths led to definitive manuscripts on the analysis of oxysterols and unsaturated C_{27} sterols by gas chromatography, high-performance liquid chromatography (HPLC), mass spectrometry, and nuclear magnetic resonance. George also pioneered the application of silver ion HPLC to sterols and isoprenoids, with spectacular results for many separations that would otherwise be extremely difficult.

George was an enthusiastic and inspiring mentor, with a sharp mind and personal charm. He was a hard worker and expected the same of others, but his laboratory bore the mark of his infectious enthusiasm. Scores of postdoctoral scientists and graduate students matured scientifically under his tutelage. The experience of working with George left an indelible mark on each person, and most inherited his high scientific standards, learning to design and implement definitive experiments and to describe the protocols in precise detail. George's untimely death has left us with a large body of sound scientific knowledge in the field of sterols and sphingolipids. But more profoundly, he has given us an ideal to strive toward.

William K. Wilson

Biochemical Modifications and Transcriptional Alterations Attendant to Sterol Feeding in *Phytophthora parasitica*

W. David Dotson, Shirley R. Tove, and Leo W. Parks*

Department of Microbiology, North Carolina State University, Raleigh, North Carolina 27695-7615

ABSTRACT: *Phytophthora* species are eukaryotic sterol auxotrophs that possess the ability to grow, albeit poorly, in the complete absence of sterols. Growth of *Phytophthora* is often improved substantially when an exogenous source of sterol is provided. Additionally, sterols may be required for sexual and asexual sporulation in *Phytophthora*. Our research has been focused on identifying and characterizing the immediate physiological effects following sterol addition to cultures of *P. parasitica*. Through gas chromatographic analysis of extracts from *P. parasitica* cultures that were fed various sterols, we have obtained evidence for sterol C5 desaturase and Δ^7 reductase activities in this organism. Zoo blots were probed with DNA sequences encoding these enzymes, from *Saccharomyces cerevisiae* and *Arabidopsis thaliana*. Hybridization of a *S. cerevisiae ERG3* probe to *P. parasitica* DNA was observed, implicating sequence similarity between the sterol C5 desaturase encoding genes. Differential display experiments, using RNA from *P. parasitica,* have demonstrated a pattern of altered gene expression between cultures grown in the presence and absence of sitosterol. Characterization of sterol-related metabolic effects and sterol functions in *Phytophthora* should lead to improved measures for control of this important group of plant pathogens.

Paper no. L8273 in *Lipids 35,* 243–247 (March 2000).

Phytophthora species are eukaryotic pseudofungi, well known for their aggressive nature as plant pathogens. The type species, *P. infestans*, has been studied intensively since the Irish potato famine of the 19th century. Nevertheless, understanding the genetics and physiology of this genus has progressed slowly. Although many eukaryotes exist in nature as sterol auxotrophs, most require an exogenous sterol source in order to survive. *Phytophthora* species are sterol auxotrophs, however, they have the rare capacity to survive and even grow in the complete absence of sterols (1). When sterols are available, from a culture medium or a plant host, growth of *Phytophthora* is often greatly improved. It has been widely held that sterols are required for both sexual and asexual sporulation, although one recent study has indicated otherwise (2). Nevertheless, sterol metabolism may be a critical determinant of the success of *Phytophthora* as a pathogen. A protein secreted by *P. cryptogea,* which triggers a plant defense response, has recently been characterized as a sterol carrier protein (3). Differential expression of genes encoding 3-hydroxy-3-methylglutaryl coenzyme A, which may result in reduced levels of available sterol, has been demonstrated in plants inoculated with incompatible races of *P. infestans* (4). Clearly sterols must have broad and complex roles in the metabolism as well as in the pathogenicity of *Phytophthora*.

Sterols relevant to this study are illustrated in Scheme 1. Sitosterol (stigmast-5-en-3β-ol) is the predominant sterol form found in plants; ergosterol (22*E*-ergosta-5,7,22-trien-3β-ol) is the predominant sterol among higher fungi. Lanosterol (lanosta-8,24-dien-3β-ol) and zymosterol (5α-cholesta-8,24-dien-3β-ol) are relatively early intermediates in ergos-

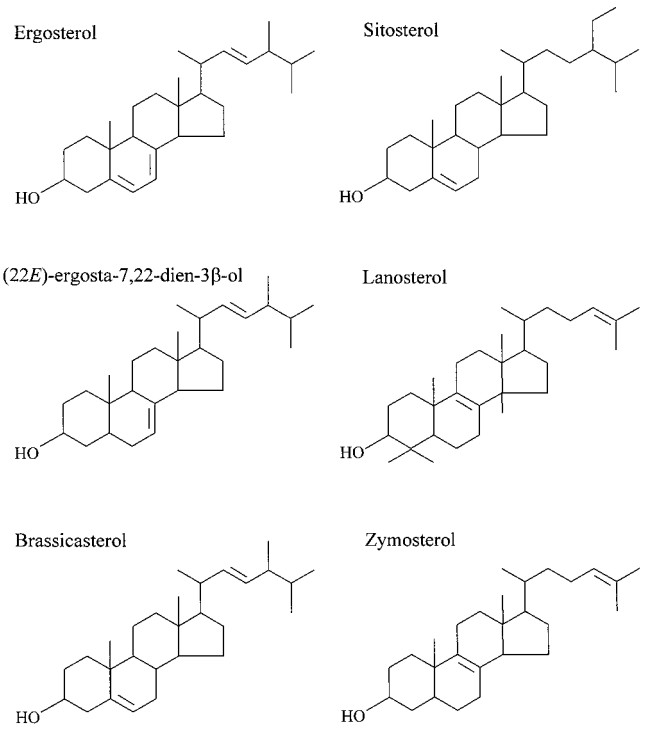

SCHEME 1

*To whom correspondence should be addressed.
E-mail: parks@mbio.ncsu.edu

Abbreviations: Brassicasterol, (22*E*)-ergosta-5,22-dien-3β-ol; DDRT-PCR, differential display reverse transcriptase polymerase chain reaction; ergosterol, (22*E*)-ergosta-5,7,22-trien-3β-ol; GC, gas chromatography; $HT_{11}VN$, modified oligo-dT anchored primers; lanosterol, lanosta-8,24-dien-3β-ol; PB, *Phytophthora* basal medium; RRT, relative retention time; sitosterol, stigmast-5-en-3β-ol; TLC, thin-layer chromatography; zymosterol, 5α-cholesta-8,24-dien-3β-ol.

terol biosynthesis, while (22*E*)-ergosta-7,22-dien-3β-ol is a later intermediate of the same pathway. Brassicasterol [(22*E*)-ergosta-5,22-dien-3β-ol] was recovered from *Phytophthora parasitica* cultures that were fed either ergosterol or (22*E*)-ergosta-7,22-dien-3β-ol.

In this study, we have used feeding experiments to investigate sterol metabolism in *P. parasitica*. Where enzymatic activities were found, DNA sequence similarities were sought in *Saccharomyces cerevisiae* and *Arabidopsis thaliana*. These model organisms are biochemically and genetically well characterized, and *S. cerevisiae* offers the further advantages of rapid growth and a completed genome sequence (5). Zoo blots, which are Southern blots done at reduced stringency to facilitate cross-species hybridization, were used as an indicator of possible sterol metabolic gene homologs. Finally, differential display reverse transcriptase polymerase chain reaction (DDRT-PCR) was used to investigate alterations in gene expression resulting from the addition of sterol to a culture. This technique employs sets of degenerate and arbitrary oligonucleotide primers, which allow amplification of sequence-specific subsets of an mRNA population (6,7). The gene expression profiles generated were compared for cultures that were treated identically except for the addition of sterol.

MATERIALS AND METHODS

Strains, media, and culture conditions. *Phytophthora parasitica* strain 5-3A was obtained as a gift from J.B. Ristaino (North Carolina State University, Raleigh, NC). Genotypes for the *S. cerevisiae* strains used were as follows: SY12A (**a** *erg3::LEU2 leu2 ura3-52 his4*) (8) and SY114 + pSN301 (**a** *LEU2 ura3-52 his3 trp1Δ1*; with p*ERG3-lacZ* fusion, integrated plasmid) (9). *Phytophthora* basal medium (PB) consisted of 1% sucrose and 0.67% yeast nitrogen base without amino acids, with 0.1% potassium phthalate (10) as a buffer (wt/vol). Sterols used in this study were obtained commercially (Sigma, St. Louis, MO). Exceptions were zymosterol and (22*E*)-5α-ergosta-7,22-dien-3β-ol, which were extracted from *S. cerevisiae* strains bearing *erg6* and *erg3* insertional inactivations, respectively, as indicated below. Sterols were dissolved in a solubilizing solution of Tergitol NP-40/ethanol (1:1, vol/vol) to give stock concentrations of 2.5 mg/mL. For supplemented cultures, the stock solutions were added to give a final sterol concentration of 10 mg/L. An equivalent volume of sterol-free solubilizing solution was added to nonsupplemented cultures, which were used as controls. Yeast strains were grown in YPD medium, which consisted of 2% D-glucose, 1% peptone, and 0.5% yeast extract (wt/vol). Both *P. parasitica* and *S. cerevisiae* were cultured in broth medium, with rotary shaking at 200 rpm. Incubation was at 24°C for *P. parasitica*, and at 30°C for *S. cerevisiae* cultures.

Sterol extraction and separation. Preparative and analytical sterol extractions were done by alkaline saponification (11). A Hewlett-Packard (Palo Alto, CA) model 5890 gas chromatograph was used for isothermal analysis of sterol extracts. The gas chromatograph was equipped with a 30 m × 0.32 mm i.d., 0.25 µm film thickness fused-silica capillary column (SPB-1; Supelco, Bellefonte, PA). Oven temperature was set at 235°C, injector and flame-ionization detector were at 280°C. Samples were dissolved in chloroform preceding injection, and cholesterol was added as an internal control. Identity and purity of preparative sterol extracts were further analyzed by thin-layer chromatography (TLC) on 20 × 20 cm silica gel plates ($60F_{254}$; EM Separation Labs, Gibbstown, NJ) in cyclohexane/ethyl acetate (85:15, vol/vol). Ultraviolet quenching of the fractions was ascertained before developing the chromatograms in a spray of 3% phosphomolybdic acid in ethanol (wt/vol) followed by heating.

Nucleic acid blotting and hybridization. Phenol/choroform (1:1, vol/vol) extraction followed by ethanol precipitation was used to prepare genomic DNA from *P. parasitica* (12) and *S. cerevisiae* cultures (13). Restriction enzymes, used in all DNA manipulations, were obtained commercially (New England Biolabs, Beverly, MA), and all digests were carried out under the conditions recommended by the manufacturer. Electrophoresis and immobilization of DNA onto nylon membranes (Genescreen; NEN, Boston, MA) were done according to accepted protocols (14). A radiolabeled DNA probe corresponding to the yeast *ERG3* gene was prepared by random priming (High Prime; Roche Molecular Biochemicals, Mannheim, Germany) a 2.2-kb *Hin*dIII fragment of pSN318 (8) with α^{32}P-dCTP (NEN). Another probe, corresponding to the yeast *ERG5* gene, was prepared as above except a 2-kb *Kpn*I-*Bam*HI fragment from pFLY105 (15) served as the template. A probe, corresponding to the *A. thaliana ST7R* (16) coding region, was obtained by standard PCR amplification (PE 2400 thermocycler; PerkinElmer, Norwalk, CT) of this sequence from a cDNA library (13). The ST7R product was subcloned into a pGEM-T vector (Promega, Madison, WI) and sequenced (DNA Sequencing Facility, Iowa State University, Ames, IA) to ensure PCR fidelity. A 0.8-kb *Pvu*I-*Spe*I fragment from the ST7R-pGEM-T construct was radiolabeled as described above. Membrane hybridizations were done under standard Southern blotting conditions (14), except the temperature was decreased incrementally within a 65–30°C range for different blots. Following hybridization, all blots were washed twice in a solution of 300 mM NaCl, 30 mM trisodium citrate (pH 7.0), and 0.1% (wt/vol) sodium dodecyl sulfate. Each wash was done for 30 min, at 25°C to reduce hybrid stringency. Autoradiograms were developed following 24-h exposure to X-ray film with no intensifying screens.

DDRT-PCR. *Phytophthora parasitica* cultures were grown in PB with no sterol supplementation. Each culture was subsequently divided equally by volume into two separate flasks, with sitosterol added to one flask and an equal volume of sterol-free solubilizing solution added to the other flask. After 2.5 h of further incubation, the cultures were harvested by vacuum filtration. Mycelia were then frozen under liquid nitrogen and ground thoroughly in sterilized mortars. Total RNA was extracted from each homogenate using hot acidic phenol (9). RNA quality and yield were assessed spectrophotometrically using ratios of A_{260}/A_{280}, and by agarose gel

electrophoresis. DDRT-PCR was done using enzymes and primers obtained commercially as a kit (RNAimage; GenHunter, Nashville, TN). Reverse transcription and PCR followed the protocol of the manufacturer. Briefly, first strand cDNA was synthesized from equal amounts of RNA using Maloney murine leukemia virus reverse transcriptase and modified oligo-dT anchored primers (designated $HT_{11}VN$ by the manufacturer). $HT_{11}VN$ primers consisted of 11 central dT residues, flanked by a 5′ terminal *Hin*dIII recognition sequence and two degenerate nucleotides at the 3′ terminus. Equal amounts of cDNA were used as template for PCR amplification and radiolabeling with α^{35}S-dATP. Arbitrary 16-mer primers (designated HAP by the manufacturer), which also included the 5′ terminal *Hin*dIII recognition sequence, were used along with the original $HT_{11}VN$ primer for PCR. Ten reactions were done, with different combinations of the arbitrary and $HT_{11}VN$ primers. Equal volumes of the PCR products were electrophoresed on a 6% polyacrylamide sequencing gel. After drying, the gel was placed on X-ray film for 48 h and an autoradiogram developed.

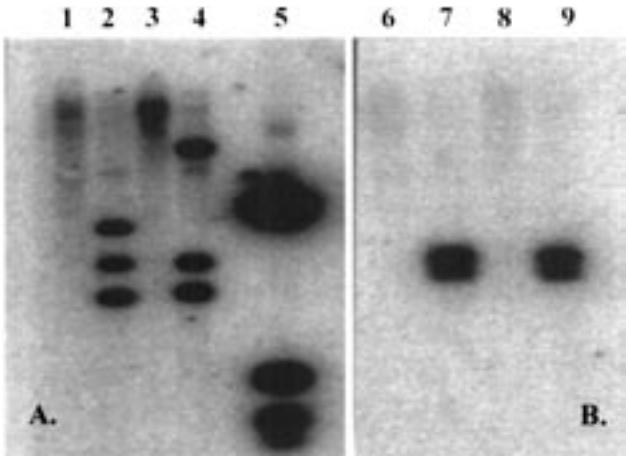

FIG. 1. Autoradiogram of Zoo blots hybridized at 45°C. (A) *ERG3* probe and (B) *ERG5* probe are shown. Lanes: (1) *Phytophthora parasitica* (*Eco*RI, *Bam*HI, *Hin*dIII), (2) *Saccharomyces cerevisiae* (*Eco*RI, *Bam*HI, *Hin*dIII), (3) *P. parasitica* (*Eco*RI, *Hin*dIII), (4) *S. cerevisiae* (*Eco*RI, *Hin*dIII), (5) Kb DNA ladder, (6) *P. parasitica* (*Eco*RI, *Bam*HI, *Hin*dIII), (7) *S. cerevisiae* (*Eco*RI, *Bam*HI, *Hin*dIII), (8) *P. parasitica* (*Eco*RI, *Hin*dIII), (9) *S. cerevisiae* (*Eco*RI, *Hin*dIII).

RESULTS AND DISCUSSION

In this study, we have sought to determine the immediate effects of sterol on the metabolism of *P. parasitica*. A field isolate of *P. parasitica* was used in this work. This strain was chosen based on the impressive magnitude of growth difference between cultures incubated in the presence and absence of sterols. Based on qualitative observations of the growth of this strain in PB medium, we estimate a two- to tenfold increase in mycelial mass following 1 wk of sterol supplementation. Feeding experiments involved the addition of individual sterols to cultures of *P. parasitica*. The cultures were then incubated for 8 d, harvested, and sterols were extracted. Extracts from each culture were analyzed by gas chromatography (GC). Transformation of the proffered sterol was determined based on retention time relative (RRT) to an internal cholesterol standard (Table 1). In extracts from cultures fed zymosterol, lanosterol, or sitosterol, the major GC peaks were observed at the same RRT as found for the respective pure sterols. The major peaks observed from cultures fed ergosterol and (22*E*)-5α-ergosta-7,22-dien-3β-ol occurred at an RRT of 1.11, which corresponded to neither of the pure sterols that were fed. Based on expected RRT values (17,18), we presume this compound to be brassicasterol. In order for these transformations to occur, *P. parasitica* must possess enzymes with sterol C5 desaturase and Δ^7 reductase activities. These results are consistent with activities demonstrated previously in *P. cactorum* (19).

We have sought to extend our biochemical evidence for these activities by investigating possible similarities between C5 desaturases in *S. cerevisiae* and *P. parasitica* at the DNA level. Following autoradiography of Zoo blots, bands were observed in *P. parasitica* genomic DNA lanes that had been probed with *ERG3* (Fig. 1). This binding of the *ERG3* probe was observed following separate hybridizations at 37 and 45°C, but not at 55 or 65°C (Table 2). The bands were present in similar positions for hybridizations at 37 and 45°C (data not shown).

Since no side-chain alterations were observed for any of the sterols fed to *P. parasitica*, we have used the yeast gene encoding a C22 desaturase (*ERG5*) as a control for stringency. No hybridization of the *ERG5* probe to *P. parasitica* DNA was observed over the same temperature range as used for *ERG3* above. Hybridization of the *ERG3* and *ERG5* probes to *S. cerevisiae* genomic DNA was observed at all temperatures tested.

TABLE 1
Sterol Feeding Results

Sterol proffered	Sterol recovered	Conversion
C_{30}, $\Delta^{8,24}$	C_{30}, $\Delta^{8,24}$	None
C_{27}, $\Delta^{8,24}$	C_{27}, $\Delta^{8,24}$	None
C_{28}, $\Delta^{5,7,22}$	C_{28}, $\Delta^{5,22}$	Δ^7 reduction
C_{28}, $\Delta^{7,22}$	C_{28}, $\Delta^{5,22}$	Δ^7 reduction C_5 desaturation
C_{29}, Δ^5	C_{29}, Δ^5	None

TABLE 2
Zoo Blot Results

		Hybridization temperature (°C)[a]			
Probe	DNA tested	65	55	45	37
ERG3	*Saccharomyces cerevisiae*	+	+	+	+
ERG3	*Phytophthora parasitica*	–	–	+	+
ERG5	*S. cerevisiae*	+	+	+	+
ERG5	*P. parasitica*	–	–	–	–

[a]+ indicates band observed following hybridization at the specified temperature; – indicates no band observed following hybridization at the specified temperature.

Repeated hybridizations of the *ERG3* probe to *P. parasitica* DNA under conditions where *ERG5* failed to hybridize indicated that the stringency levels used were sufficient for this experiment. When considered along with the feeding experiments, these data suggest that the gene encoding the *P. parasitica* C5 desaturase may have considerable sequence similarity with the *ERG3* gene of *S. cerevisiae*. Attempts to alter the gel mobility of the *P. parasitica* DNA fragment that bound the *ERG3* probe by varying the restriction enzymes used were not successful. However, this may simply be due to the lack of a *Bam*HI recognition sequence in the *Phytophthora* DNA fragment.

Since *S. cerevisiae* does not exhibit Δ^7 reductase activity, the *A. thaliana* gene encoding this enzyme was employed as a probe. The predicted protein sequence encoded by *ST7R* displays a high degree of similarity with lamin B receptors and sterol reductases found in other organisms, including the *ERG24* gene product of *S. cerevisiae* (14). Surprisingly, the *ST7R* cDNA probe showed no significant hybridization with either *P. parasitica* or *S. cerevisiae* genomic DNA (at 30, 37, and 45°C; data not shown). One possible explanation is that the *P. parasitica* gene encoding a Δ^7 reductase may be dissimilar to any of those characterized to date in other organisms. This would not be unprecedented, since even a gene as generally conserved as that encoding actin has been shown to be divergent in certain species of *Phytophthora* (15,16). The results of this study have allowed us to predict low similarity between the *P. parasitica* Δ^7 reductase gene and *A. thaliana ST7R*.

DDRT-PCR results indicate a number of genes are differentially regulated following addition of sitosterol to *P. parasitica* cultures. Ten experiments were performed using different combinations of the arbitrary and anchored primers. The results from two of these experiments are shown (Fig. 2). Electrophoresis was done with DDRT-PCR products from *P. parasitica* cultures with and without added sitosterol in adjacent gel lanes, to facilitate comparison. The majority of bands corresponding to cDNA species that co-migrated were found to be of similar intensities. However, for every primer pair tested, some co-migrating bands of different intensity were observed between the two culture conditions. Because the culture conditions were otherwise identical, it is reasonable to conclude that differential expression of these genes resulted from the brief period of sterol supplementation. Examples of enhanced, as well as reduced, gene expression were observed to result from sitosterol feeding. While differential accumulation of the displayed transcripts has not yet been confirmed by other methods, the expression profile generated will provide targets for selective characterization of genes involved in sterol related functions. The sterol mediated differential gene expression implied by these experiments supports predictions of broad ranging physiological roles for sterols in *Phytophthora*.

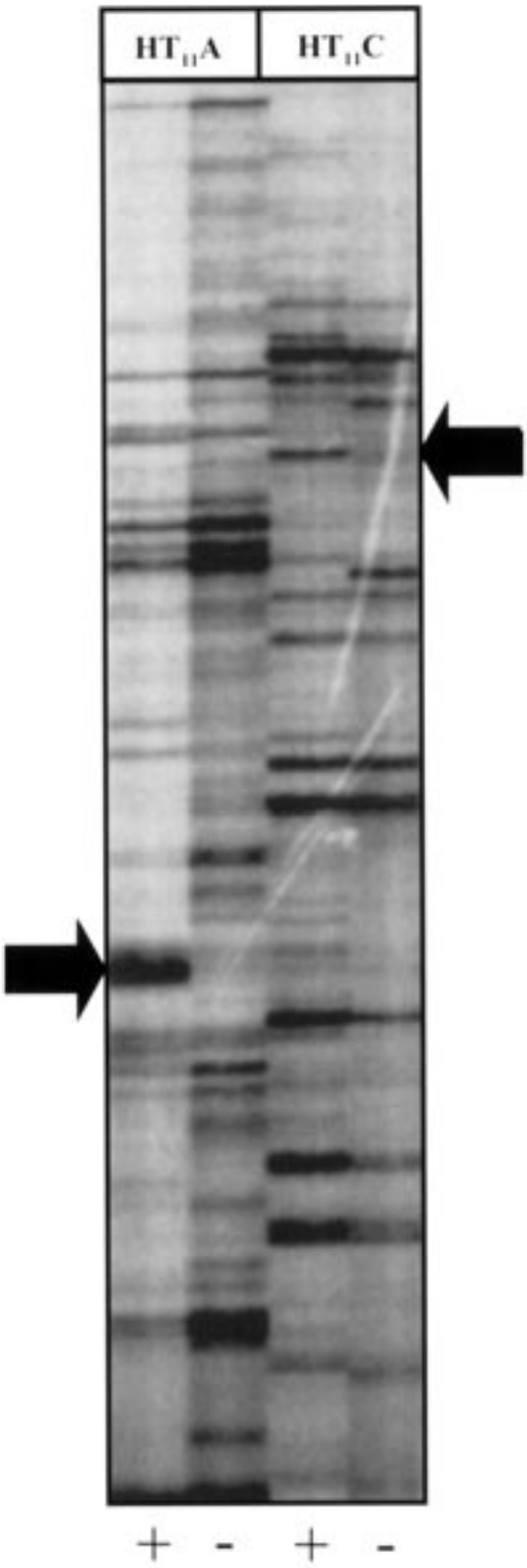

FIG. 2. Autoradiogram of a differential display reverse transcriptase polymerase chain reaction gel. Primers used for reverse transcription are shown above the lanes. Cultures supplemented with sitosterol (+) and nonsupplemented cultures (–) are indicated below the lanes. Arrows indicate bands where increased expression following sterol addition was observed.

ACKNOWLEDGMENTS

This research was supported by the North Carolina Agricultural Research Service, by a grant from the U.S. Army Research Office (DAAAH04-97-003), and an AASERTS award (DAAAH0494-

G0179). We thank Laura E. Braly and Kevin V. Shianna for critical evaluations of this manuscript, and Dr. Jean B. Ristaino for the *Phytophthora* strain used in these experiments and for helpful discussions. Material contained in this manuscript was presented in the "Symposium on Sterols Biochemistry," organized by J.D. Weete, E.J. Parish, and W.D. Nes, and held during the 90th AOCS Annual Meeting & Expo, Orlando, FL, May 11 and 12, 1999.

REFERENCES

1. Hendrix, J.W. (1970) Sterols in Growth and Reproduction of Fungi, *Annu. Rev. Phytopathol. 8*, 111–130.
2. Jee, H.J., Tang, C.S., and Ko, W.H. (1997) Stimulation of Sexual Reproduction in *Phytophthora cactorum* by Phospholipids Is Not Due to Sterol Contamination, *Microbiology 143*, 1631–1638.
3. Mikes, V., Milat, M.L., Ponchet, M., Ricci, P., and Blein, J.P. (1997) The Fungal Elicitor Cryptogein Is a Sterol Carrier Protein, *FEBS Lett. 416*, 190–192.
4. Choi, D., Ward, B.L., and Bostock, R.M. (1992) Differential Induction and Suppression of Potato 3-Hydroxy-3-methylglutaryl-coenzyme A Reductase Genes in Response to *Phytophthora infestans* and Its Elicitor Arachidonic Acid, *Plant Cell 4*, 1333–1344.
5. Goffeau, A., Barrell, B.G., Bussey, H., Davis, R.W., Dujon, B., Feldman, H., Galibert, F., Hoheisel, J.D., Jacq, C., Johnston, M., Louis, E.J., Mewes, H.W., Murakami, Y., Philippsen, P., Tettelin, H., and Oliver, S.G. (1996) Life with 6000 Genes, *Science 274*, 546–567.
6. Liang, P., and Pardee, A.B. (1992) Differential Display of Eukaryotic Messenger RNA by Means of the Polymerase Chain Reaction, *Science 257*, 967–971.
7. Liang, P., and Pardee, A.B. (1993) Distribution and Cloning of Eukaryotic mRNAs by Means of Differential Display: Refinements and Optimization, *Nucleic Acids Res. 21*, 3269–3275.
8. Smith, S.J., and Parks, L.W. (1993) The *ERG3* Gene in *Saccharomyces cerevisiae* Is Required for the Utilization of Respiratory Substrates and in Heme-Deficient Cells, *Yeast 9*, 1177–1187.
9. Smith, S.J., Crowley, J.H., and Parks, L.W. (1993) Transcriptional Regulation by Ergosterol in the Yeast *Saccharomyces cerevisiae*, *Mol. Cell. Biol. 16*, 5427–5432.
10. Gonzales, R.A. (1981) The Development of *Phytophthora cactorum* as a Model System for the Study of Sterol Metabolism, Ph.D. Thesis, Oregon State University, Corvallis, pp. 23–30.
11. Parks, L.W., Bottema, C.D.K., Rodriguez, R.J., and Lewis, T.A. (1985) Yeast Sterols: Yeast Mutants as Tools for the Study of Sterol Metabolism, *Methods Enzymol. 111*, 333–346.
12. Goodwin, S.B., Drenth, A., and Fry, W.E. (1992) Cloning and Genetic Analyses of Two Highly Polymorphic, Moderately Repetitive Nuclear DNAs from *Phytophthora infestans*, *Curr. Genet. 22*, 107–115.
13. Collart, M.A., and Oliviero, S. (1993) Preparation of Yeast RNA, *Curr. Protoc. Mol. Biol. 2*, 13.12.1–13.12.5.
14. Sambrook, J., Fritsch, E.R., and Maniatis, T. (1989) *Molecular Cloning: A Laboratory Manual*, 2nd edn., Cold Spring Harbor Laboratory Press, Cold Spring Harbor, New York, pp. 9.31–9.62.
15. Leak, F.W. (1997) The Phenotypic Diversity of the *upc2* Mutation in *Saccharomyces cerevisiae*, M.S. Thesis, North Carolina State University, Raleigh, pp. 33–34.
16. Lecain, E., Chenivesse, X., Spagnoli, R., and Pompon, D. (1996) Cloning by Metabolic Interference in Yeast and Enzymatic Characterization of *Arabidopsis thaliana* Sterol Delta 7-Reductase, *J. Biol. Chem. 271*, 10866–10873.
17. Goad, J.L., and Toshihira, A. (1997) Gas–Liquid Chromatography of Sterols, in *Analysis of Sterols*, pp. 123–131, Chapman and Hall, New York.
18. Lamparczyk, H. (1992) Sterols, in *Analysis and Characterization of Steroids*, pp. 119–137, CRC Press, Boca Raton.
19. Knights, B.A., and Elliot, C.G. (1976) Metabolism of Δ^7 and $\Delta^{5,7}$-Sterols by *Phytophthora cactorum*, *Biochim. Biophys. Acta 441*, 341–346.
20. Holmer, L., Pezhman, A., and Worman, H.J. (1998) The Human Lamin B Receptor/Sterol Reductase Multigene Family, *Genomics 15*, 469–476.
21. Dudler, R. (1990) The Single-Copy Actin Gene of *Phytophthora megasperma* Encodes a Protein Considerably Diverged from Any Other Known Actin, *Plant Mol. Biol. 14*, 415–422.
22. Unkles, S.E., Moon, R.P., Hawwkins, A.R., Duncan, J.M., and Kinghorn, J.R. (1991) Actin in the Oomycetous Fungus *Phytophthora infestans* Is the Product of Several Genes, *Gene 100*, 105–112.

[Received June 2, 1999; and in revised form and accepted January 20, 2000]

Cloning and Characterization of the *Dictyostelium discoideum* Cycloartenol Synthase cDNA

Sharotka M. Godzina[a,1,2], Martha A. Lovato[b,2,3], Michelle M. Meyer[a,b], Kimberly A. Foster[a], William K. Wilson[a], Wei Gu[a,4], Eugenio L. de Hostos[a,5], and Seiichi P. T. Matsuda[a,b,*]

Departments of [a]Biochemistry and Cell Biology and [b]Chemistry, Rice University, Houston, Texas

ABSTRACT: Cycloartenol synthase converts oxidosqualene to cycloartenol, the first carbocyclic intermediate en route to sterols in plants and many protists. Presented here is the first cycloartenol synthase gene identified from a protist, the cellular slime mold *Dictyostelium discoideum*. The cDNA encodes an 81-kDa predicted protein 50–52% identical to known higher plant cycloartenol synthases and 40–49% identical to known lanosterol synthases from fungi and mammals. The encoded protein expressed in transgenic *Saccharomyces cerevisiae* converted synthetic oxidosqualene to cycloartenol *in vitro*. This product was characterized by ^{1}H and ^{13}C nuclear magnetic resonance and gas chromatography–mass spectrometry. The predicted protein sequence diverges sufficiently from the known cycloartenol synthase sequences to dramatically reduce the number of residues that are candidates for the catalytic difference between cycloartenol and lanosterol formation.

Paper no. L8307 in *Lipids 35*, 249–255 (March 2000).

The oxidosqualene cyclases are a family of enzymes that convert 2,3-(*S*)-oxidosqualene to more than 80 different cyclic triterpenes (1–3). The best-studied oxidosqualene cyclases are lanosterol synthase (4), which forms the first carbocyclic sterol precursor in animals and fungi, and cycloartenol synthase (5), which forms an isomeric sterol precursor in plants and many protists (6). Both of these enzymes cyclize oxidosqualene to the protosteryl cation and then to the lanosteryl cation (Fig. 1). These enzymes differ by abstracting alternative protons from the common intermediate to make distinct products.

We are studying how oxidosqualene cyclases catalyze these cyclization, rearrangement, and deprotonation reactions. Of particular interest is determining how two different oxidosqualene cyclases direct the formation of distinct products. Mutating conserved residues is now a classical method for identifying catalytic motifs, and residues that are apparently important in protonating oxidosqualene have been identified by mutating residues conserved in all oxidosqualene cyclases (7). A similar approach could uncover residues that promote specific deprotonation, but residues conserved in all oxidosqualene cyclases would not be good candidates. Residues that function in deprotonation to lanosterol should be conserved in all lanosterol synthases, but not in cycloartenol synthases, and vice versa. The best candidate positions for mutagenesis are those where lanosterol synthases conserve one residue, but cycloartenol synthases conserve a different one. The known lanosterol synthases (8–16) represent a sufficiently diverse array from both the animal and fungal kingdoms that relatively few positions (187/721 or 26%) are conserved. The known cycloartenol synthases (17–20) are all from dicots and are closely related (544/756 residues or 72% are conserved). The similarity of the known cycloartenol synthases makes the positions that are differently conserved in lanosterol synthases and cycloartenol synthases too numerous to be efficiently investigated by site-directed mutagenesis. Obtaining one or more cycloartenol synthases from organisms far diverged from plants should significantly reduce the number of differently conserved residues, possibly to a number that would be reasonably addressed by site-directed mutagenesis.

We report the cloning of a cycloartenol synthase complementary DNA (cDNA) from the slime mold *Dictyostelium discoideum*. The encoded protein cyclized oxidosqualene to cycloartenol following heterologous expression and is only ~50% identical to the previously reported cycloartenol synthases from plants.

*To whom correspondence should be addressed at Department of Chemistry, Rice University, 6100 S. Main St., Houston, TX 77005.
E-mail: matsuda@rice.edu

[1]Current affiliation: Department of Biology, Massachusetts Institute of Technology, Cambridge, MA.
[2]Co-first authors.
[3]Current affiliation: Departments of Chemistry and Molecular Biology, The Scripps Research Institute, La Jolla, CA.
[4]Current affiliation: Tanox, Inc., Houston, TX.
[5]Current affiliation: Tropical Disease Research Unit, University of California, San Francisco, CA.

Abbreviations: A, alanine; C, cysteine; D, aspartate; E, glutamate; F, phenylalanine; G, glycine; H, histidine; I, isoleucine; K, lysine; L, leucine; M, methionine; N, asparagine; P, proline; Q, glutamine; R, arginine; S, serine; T, threonine; V, valine; W, tryptophan; Y, tyrosine; AaSHC, *Alicyclobacillus acidocaldarius* squalene-hopene cyclase; cDNA, complementary deoxyribonucleic acid; GC/MS, gas chromatography/mass spectrometry; HSQC, heteronuclear single quantum coherence; kbp, kilobase pair; NMR, nuclear magnetic resonance; PCR, polymerase chain reaction; PEG, polyethylene glycol; SC-UHET+gal, synthetic complete medium lacking uracil with 2% galactose, 13 mg/L heme, 20 mg/L ergosterol, 0.5% Tween 80; ScERG7, *Saccharomyces cerevisiae* lanosterol synthase; SC-UHET+glu, synthetic complete medium lacking uracil with 2% glucose, 13 mg/L heme, 20 mg/L ergosterol, 0.5% Tween 80; SHC, squalene-hopene cyclase; TLC, thin-layer chromatography; YPDHET, 1% yeast extract, 2% peptone, 2% glucose, 13 mg/L heme, 20 mg/L ergosterol, and 0.5% Tween 80.

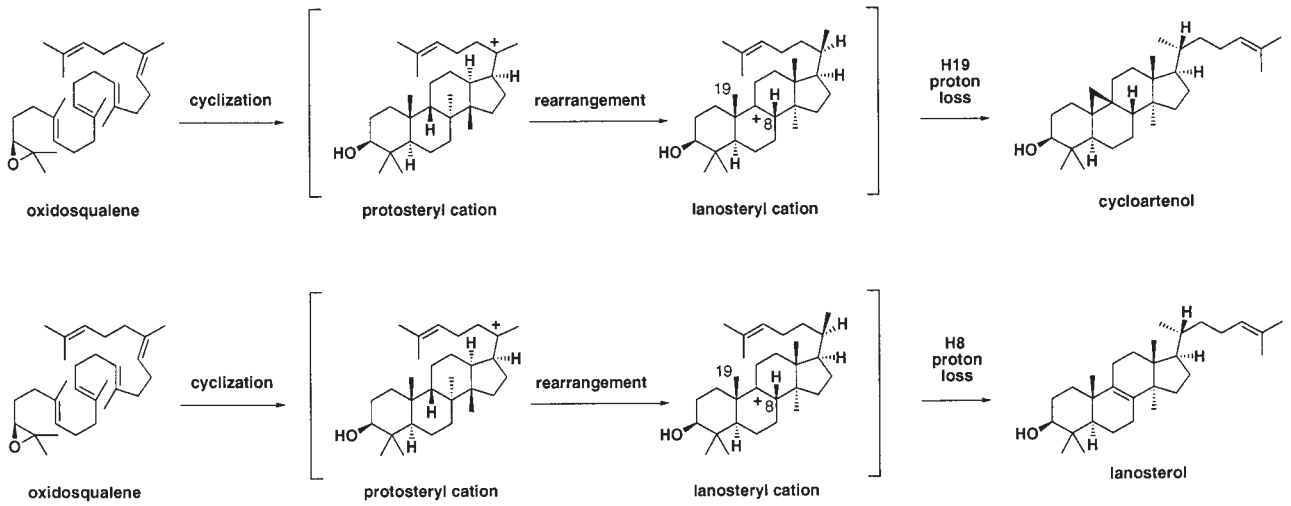

FIG. 1. Mechanism of cycloartenol synthase and lanosterol synthase. Cycloartenol synthase protonates oxidosqualene, cyclizes to the chair-boat-chair protosteryl cation, rearranges to the lanosteryl cation, and abstracts a proton from C19 to form cycloartenol. Lanosterol synthase catalyzes the same protonation, cyclization, and rearrangement, but abstracts a proton from C8 to form lanosterol.

EXPERIMENTAL PROCEDURES

Strains, media, molecular biological methods. Escherichia coli strain DH5α was the host for DNA manipulation, and transformants were maintained on Luria broth + 100 μg/mL ampicillin (21). The *D. discoideum* cycloartenol synthase was expressed in the *Saccharomyces cerevisiae* lanosterol synthase mutant SMY8 (*MAT***a** *erg7::HIS3 hem1::TRP1 ura3-52 trp1-Δ63 leu2-3,112 his3-Δ200 ade2* Gal^+) (16). Nontransformed yeast was grown in YPDHET (1% yeast extract, 2% peptone, 2% glucose, 13 mg/L heme, 20 mg/L ergosterol, and 0.5% Tween 80) (16), and yeast transformants were selected and grown in synthetic complete medium (21) lacking uracil and supplemented with 13 mg/L heme, 20 mg/L ergosterol, and 0.5% Tween 80 with 2% glucose for nonexpressing growth (SC-UHET + glu) or 2% galactose for expression (SC-UHET + gal). Restriction enzymes were purchased from New England Biolabs (Beverly, MA). Molecular biological manipulation followed established techniques (21).

Cloning a D. discoideum *oxidosqualene cyclase cDNA fragment.* A partial cDNA homologous to oxidosqualene cyclases was cloned serendipitously while screening for sequences encoding a cytoskeletal protein. The lambda Zap II cDNA library used (generously provided by Dr. Richard Firtel) was made from cells isolated between 8 and 12 h of development. The library was screened by hybridizing a radiolabeled probe at 65°C in phosphate buffer (250 mM NaH_2PO_4, 250 mM NaCl, 10% wt/vol polyethylene glycol (PEG) 8000, 1 mM EDTA, pH 7.2) as described (22). *In vivo* subcloning of the cDNA insert was performed according to the vector manufacturer's instructions (Stratagene). The plasmid was used to transform DH5α and sequenced using the Applied Biosystems International Automated Sequencer and the dye primer method. An alignment with other oxidosqualene cyclase sequences indicated that the cDNA encoded a nearly complete fragment of an oxidosqualene cyclase that was missing <100 bp from the 5′ end.

Obtaining the 5′ end of the D. discoideum *oxidosqualene cyclase cDNA.* A reverse primer (GGTACCTAAATCACATCCTTCTGGAC) complementary to the internal sequenced portion of the gene was designed. A polymerase chain reaction (PCR; 40 cycles of 30 s at 95°C, 30 s at 56°C, and 3 min at 72°C) using this primer and forward primer lac (from the library vector) amplified an appropriately sized DNA fragment. The nested reverse primer AATGTGTTCCTGGTTCTTTT (5′ of the original gene-specific primer) was designed and used with the lac forward primer to reamplify the DNA from the previous PCR reaction. The PCR product was polished (Perfectly Blunt Cloning Kit, Novagen), ligated to pBluescript II KS(+) linearized with *Eco*R V, and used to transform *E. coli.* The construct was sequenced and confirmed to contain the 5′ missing portion of the cDNA. This sequence was used to PCR-amplify the 5′ end with appropriate sites to reconstruct the full-length cDNA. Two gene-specific primers (TTCTCGAGAGCTCAATTTCACACAGGAAACAGG and GGGGATCCAATGTCTTCCTGGTTCTTTT) were used to PCR-amplify library DNA (using the same conditions as before) with the high-fidelity enzyme *Pfu*. The PCR product was subcloned as above to make pML3.9, which was sequenced with the original amplification primers. The amplified DNA had two base mutations, but neither altered the encoded amino acid sequence.

Reconstructing the D. discoideum *oxidosqualene cyclase cDNA.* The full-length *D. discoideum* oxidosqualene cyclase cDNA (GenBank accession number AF159949) was reconstructed using *Sca* I as follows. The *Kpn* I/*Sac* I fragment of the original cDNA was subcloned into pBluescript KS(+) cut with the same enzymes to give pML3.7. Both pML3.7 and pML3.9 contain *Sca* I sites in their oxidosqualene cyclase cDNA and

their β-lactamase gene, so both plasmids were bisected upon *Sca* I digestion. The 3.3 kilobase pair (kbp) band from the pML3.7 digest (containing the 2.2 kbp 3′ end of the cDNA and 1.1 kbp of the plasmid) and the 2 kbp band from the pML3.9 digest (containing the 200 bp 5′ end of the cDNA and 1.8 kbp of the plasmid) were ligated to one another and transformed into *E. coli*. Ampicillin-resistant transformants contained plasmids that assembled to reconstruct both the oxidosqualene cyclase cDNA and the β-lactamase gene in the plasmid. The resultant plasmid encodes the reconstructed *D. discoideum* oxidosqualene cyclase fused to the N-terminal peptide MNSSRFTR initiated by an ATG in the vector. A *Xho* I site 5 bp 3′ of the vector ATG was conveniently used to excise the false initiation site and allow translation initiation at an ATG within the *D. discoideum* sequence by subcloning a *Xho* I fragment into the *Sal* I site of the high-copy yeast expression plasmid pRS426GAL.

Yeast transformation, enzyme expression, and product characterization. A yeast expression subclone was created by ligating a 2.5 kbp *Sac* I/*Sal* I fragment containing the reconstructed fusion protein to pRS426GAL cut with the same two enzymes. The *erg7 hem1 S. cerevisiae* strain SMY8 (16) was transformed with plasmid DNA at 25°C overnight with 10 μg purified plasmid DNA, 500 μg single-stranded salmon sperm DNA, pelleted cells from a 5-mL SMY8 culture grown to saturation in sterile YPDHET, and 2 mL yeast transformation buffer (40% PEG 3350, 0.1 M lithium acetate, 10 mM Tris pH 7.5, 1 mM EDTA, 0.1 M dithiothreitol). Cells were allowed to recover at 25°C for 24 h in 2 mL YPDHET, and transformants were selected on (SC-UHET+glu) plates.

A 1-L culture grown to saturation in SC-UHET+glu was used to inoculate 5 L (SC-UHET+gal). After shaking for 48 h at 30°C, cells were pelleted, suspended as a 40% slurry in 0.1 M potassium phosphate buffer at pH 6.4, and lysed using a French press at 20,000 psi. After diluting the homogenate with 1 vol of the same buffer, racemic oxidosqualene was added to 0.2 mg/mL from a 20 mg/mL stock in 20% Triton X-100. The reaction continued for 24 h at 25°C, when thin-layer chromatography (TLC) with methylene chloride indicated that the cyclization had gone nearly to completion.

The reaction was quenched with 4 vol of ethanol and centrifuged to remove precipitated proteins. The supernatant was dried by rotary evaporation, and the resulting oil was dissolved in ethyl acetate. The solution was vacuum-filtered through a Celite-covered frit, dried with magnesium sulfate, and rotary evaporated. Ethyl ether and 230–400 mesh silica were added to the resulting oil. The slurry was passed through a dry silica plug, triterpenes were eluted with ethyl ether, and the combined extracts were rotary evaporated.

The triterpene alcohol (which comigrated with cycloartenol on TLC using methylene chloride) was purified by two silica columns. The first eluted with a gradient from 3 to 15% ethyl ether in hexane, and the second was run isocratically using 15% ether in hexane. The purified product was acetylated with excess triethylamine and acetic anhydride and catalytic dimethylaminopyridine, and the triterpene acetates were purified by two silica columns, the first using methylene chloride and the second 3% ether in hexane. The purified triterpenes were fully characterized by gas chromatography/mass spectrometry (GC/MS) and nuclear magnetic resonance (NMR; 500 MHz spectrometer; 25 mM solution in $CDCl_3$; 25°C). The clone lacking the fusion peptide was transformed and expressed similarly, and provided triterpenes that were examined by GC and GC/MS as the acetates.

RESULTS AND DISCUSSION

A search for cycloartenol synthases distantly related to dicot cycloartenol synthases should focus on the protists. Protists diverged early in the course of eukaryotic evolution, and many protists share with higher plants a cycloartenol-based sterol biosynthetic pathway. Protists that make sterol from cycloartenol include *Ochromonas malhamensis* (23), *Euglena gracilis* (24,25), *Acanthamoeba polyphaga* (26), *Naegleria lovaniensis* (27), *N. gruberi* (27), and *D. discoideum* (28). Finding cycloartenol biosynthesis in *N. lovaniensis*, *N. gruberi*, and *D. discoideum* was particularly interesting because it suggested that these amoebas are more closely related to plants than to fungi or animals.

It seemed advisable to pursue the gene from *D. discoideum* because it is a widely studied model organism, and both genetic information and libraries are available. While efforts were underway to clone the *D. discoideum* cycloartenol synthase by sequence homology, we serendipitously discovered a 3′ fragment of the corresponding cDNA during a search for an unrelated gene. The 5′ end was obtained by anchored PCR, and an appropriately sized cDNA fused to a short vector-derived sequence was reconstructed from the two fragments. This fusion was used for large-scale expression and NMR characterization. The derivative lacking the fusion peptide was later expressed, and was shown by GC and GC/MS to have equivalent catalytic properties. The *D. discoideum* sequence encoded a 81 kDa predicted protein 50–52% identical to known higher plant cycloartenol synthases and 40–49% identical to known lanosterol synthases from fungi and mammals (Fig. 2).

The reconstructed cDNA was subcloned into the yeast expression vector pRS426GAL (see Experimental Procedures section) and used to transform the yeast lanosterol synthase mutant SMY8 (16), which lacks oxidosqualene cyclase activity to complicate the analysis. A homogenate of SMY8 expressing the *D. discoideum* cDNA cyclized oxidosqualene to a compound that comigrated with cycloartenol on TLC. This triterpene alcohol was acetylated and was analyzed by GC–flame-ionization detection and GC/MS. Only two components have the appropriate mass for a triterpenyl acetate. The major component (99%) coeluted with cycloartenyl acetate at 36 min and displayed fragmentation patterns consistent with that compound. A minor component (1%) coeluted with parkeyl acetate at 35 min and has the appropriate mass for a triterpenyl acetate. Insufficient minor compound was available to separate and characterize as a pure sample. ^{1}H NMR of the acetylated product indicated a major (~90%) component with

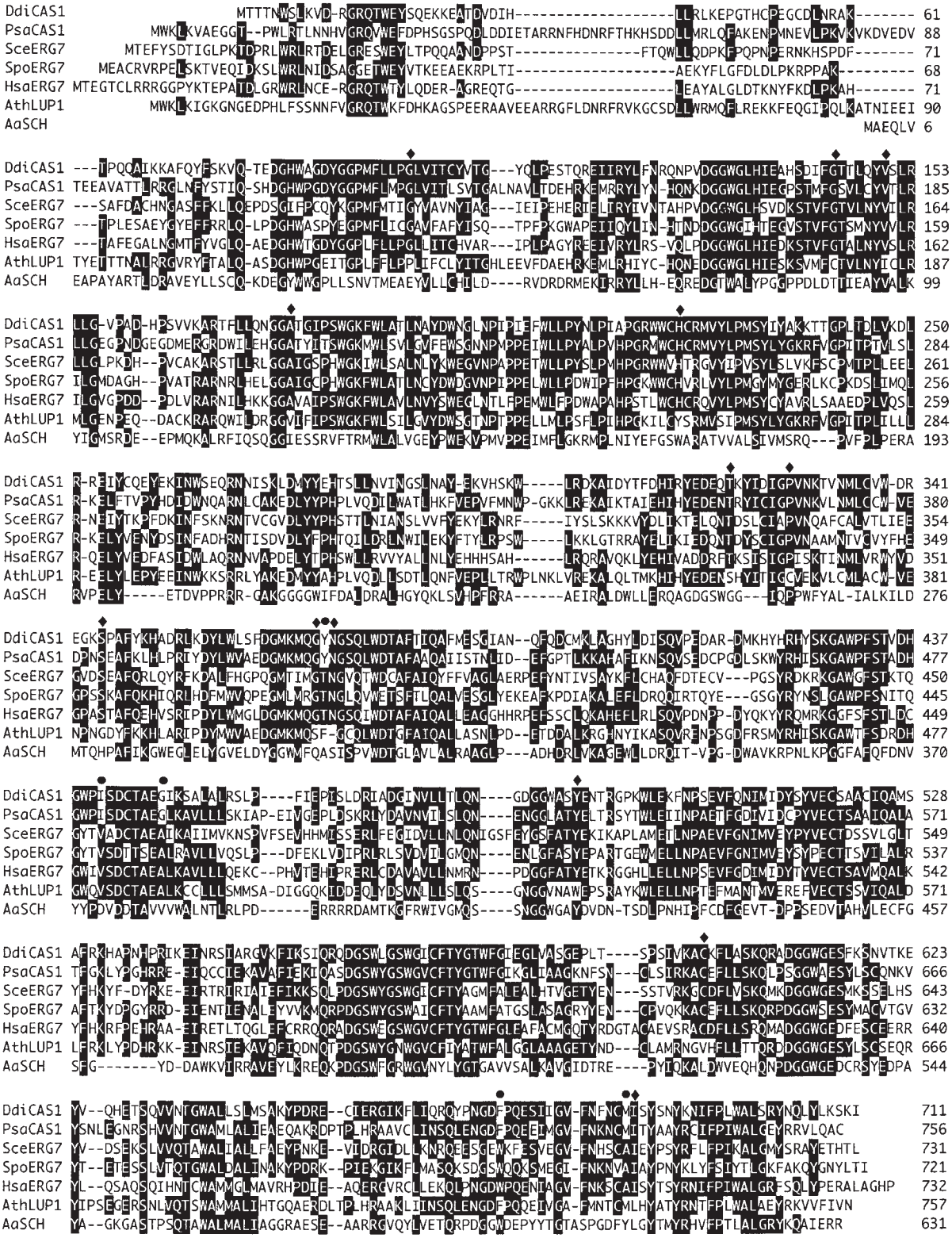

FIG. 2. Alignment of selected oxidosqualene cyclases with squalene-hopene cyclase. The *Dictyostelium discoideum* (DdiCAS1) and *Pisum sativum* (PsaCAS1) cycloartenol synthases (18), *Saccharomyces cerevisiae* (SceERG7), *Schizosaccharomyces pombe* (SpoERG7), and *Homo sapiens* (HsERG7) lanosterol synthases (10,11,14–16), *Arabidopsis thaliana* lupeol synthase (AthLUP1) (35), and *Alicyclobacillus acidocaldarius* squalene-hopene cyclase (AaSHC) (36) are aligned. Dashes indicate gaps introduced to maximize the alignment. Even using this restricted data set, only five residues (marked with a circle) are conserved as one residue in lanosterol synthases, but as a different residue in cycloartenol synthases. The 13 residues marked with a diamond are conserved as one residue in all enzymes with protosteryl intermediates (lanosterol synthase and cycloartenol synthase), and as a different residue in enzymes with dammarenyl intermediates (lupeol synthase and β-amyrin synthase).

signals essentially identical to those obtained from an authentic sample of cycloartenyl acetate: cyclopropyl δ_H 0.340 (*d*, 4.2 Hz), 0.576 (*d*, 4.2 Hz) and methyl δ_H 0.847 (*s*), 0.883 (*s*), 0.889 (*d*, 6 Hz), 0.894 (*s*), 0.960 (*s*), 1.606 (*dq*, 1.4, 0.6 Hz), 1.685 (*q*, 1.3 Hz). These signals agreed with literature values for the free alcohol (29). The ^{13}C NMR chemical shifts (δ_C 15.13, 17.63, 17.96, 18.22, 19.26, 20.12, 20.91, 21.33, 24.93, 25.41, 25.72, 25.80, 25.94, 26.48, 26.79, 28.12, 29.76, 31.59, 32.83, 35.52, 35.87, 36.33, 39.43, 45.26, 47.16, 47.81, 48.79, 52.24, 80.68, 125.24, 130.89, 171.00) were within 0.2 ppm of those reported for cycloartenyl acetate (30). ^1H NMR and heteronuclear single quantum coherence spectra of the acetylated product also revealed various minor 4α-methyl and $\Delta^{24(28)}$ sterols and a 1% component with resolved signals matching NMR data (±0.001 ppm for ^1H, ±0.1 ppm for ^{13}C) for a parkeyl acetate standard (31): δ_H 5.228 (*dt*, 6, 2 Hz, H-11), 4.484 (*dd*, 11.7, 4.2 Hz, H-3α), 1.068 (*s*, H-19; correlated to δ_C 22.3), 0.736 (*s*, 14α-Me; correlated to δ_C 18.5), 0.644 (*s*, H-18; correlated to δ_C 33.6). Despite the difficulty of identifying a trace component definitively, the GC and NMR data strongly suggest that this 1% component is parkeyl acetate. The 4α-methyl and $\Delta^{24(28)}$ sterols are structurally inconsistent with being direct oxidosqualene cyclization products and are probably metabolites of cycloartenol produced *in vivo.*

The origin of the parkeol is uncertain, but is probably not nonenzymatic degradation of cycloartenol during the reaction or workup. Cycloartenol can be isomerized to parkeol using acid (32), but the reaction requires extreme conditions (10% H_2SO_4 in isopropanol, 80°C, 24 h) and produces the by-products lanosterol and cucurbitadienol, neither of which appears in the enzymatic reaction. Yeast has been reported to metabolize cycloartenol to $\Delta^{9(11)}$ sterols (33), and some or all of the parkeol may result from the native yeast enzymes metabolizing the cycloartenol biosynthesized *in vitro*. Some may be a cycloartenol synthase by-product produced by inaccurate deprotonation. The contribution from each process will be most rigorously determined by purifying the enzyme to remove isomerase activity and for assaying parkeol synthase activity.

Comparing the *D. discoideum* cycloartenol synthase sequence with other oxidosqualene cyclases is informative. Analysis of oxidosqualene cyclase sequences has revealed shared features, including conserved aspartate and histidine residues shown to be catalytically essential (7), multiple QW motifs that may absorb thermal energy released upon cyclization (34,35), and an abundance of aromatic amino acids (8). Many of these amino acids are presumably conserved by chance, but some are probably catalytically essential. The conserved amino acid pool should include both the catalytic elements of the active site and components that maintain the correct structure of the active enzyme. Comparing oxidosqualene cyclases that are highly diverged from one another restricts the number of amino acids that are conserved due to chance.

Amino acids that are conserved among all oxidosqualene cyclases may perform a function common to these enzymes (maintaining the structure of the enzyme, protonating the epoxide, or forming the A-ring). When the *D. discoideum* cycloartenol synthase is aligned (Clustal W) with the known oxidosqualene cyclases (8–20,36), the number of conserved residues decreases to 95 (amino acid positions described here use the *S. cerevisiae* numbering system). These are G27, W31, Q88, G93, G101, P102, F104, E127, D140, G141, G142, W143, G144, H146, S151, F154, Y160, R164, L166, G167, G186, W194, G195, K196, W198, L199, L202, W207, G209, N211, E216, P221, P225, P228, R236, P241, Y244, R262, E264, Y288, H291, I338, F361, R367, D370, G378, M379, G386, Q388, W390, F394, Q397, Q425, R436, G441, F445, S446, G451, D456, E460, E511, E520, N523, P524, E526, E539, C540, F551, Q577, D580, G581, S582, W583, G585, W587, C590, Y593, F597, G606, F621, L622, G630, G631, W632, E634, Y644, W657, A658, L662, Q684, G688, G697, F699, Y707, and L719.

The likelihood that these residues are catalytic can be probed further by estimating their position within the protein. Some of them align with active-site residues in the 21–26% identical *Alicyclobacillus acidocaldarius* squalene-hopene cyclase (AaSHC) (37), which has been structurally characterized by X-ray diffraction (38,39). *Saccharomyces cerevisiae* lanosterol synthase (ScERG7) residues W194, W390, D456, W587, and Y593 clearly align with AaSHC residues F129, W312, D376, W489, and Y495, respectively. These SHC active-site residues are within 8 Å (measured using the Rasmol program) of the ligand in the 2 Å resolution *A. acidocaldarius* crystal structure. Mutagenic studies have already shown that ScERG7 residue D456 (7) and AaSHC residues W312 (40), D376 (41), and W489 (42) are catalytically important. A comprehensive list of conserved residues that map to the active site could not be compiled because the enzyme sequences did not align reliably.

The *D. discoideum* oxidosqualene cyclase sequence is particularly useful for identifying positions that contribute to the catalytic distinction between oxidosqualene cyclase classes. The early divergence of *D. discoideum* from plants makes its cycloartenol synthase only distantly related to the plant cycloartenol synthases. The plant cycloartenol synthases have 544 conserved residues, but including the *D. discoideum* sequence decreases the number to 312. The number of amino acid residues that have conservation patterns consistent with performing catalytic functions that differ between cycloartenol synthase and lanosterol synthase is reduced correspondingly. Positions where the identity of the residue correlates with product structure (such as where one residue is conserved in all cycloartenol synthases, but a different residue is conserved in all lanosterol synthases) may be active site components that control product structure. Twenty-three residues show this conservation pattern in the previously known cycloartenol and lanosterol synthases, but as shown in Figure 2, only five residues are similarly conserved when the *D. discoideum* cycloartenol synthase sequence is included (T384, V454, A461, W690, and A704 in the *S. cerevisiae* numbering system).

The first two residues are apparently closest to the active site and are consequently excellent candidates for the catalytic residues that cause the difference between cycloartenol synthase and lanosterol synthase. T384 aligns with either AaSHC

A306 or AaSHC S307, and V454 aligns with AaSHC D374. These SHC residues are within 5 Å (measured using the Rasmol program) of the ligand. A704 aligns with either AaSHC F605 or Y606, and both residues are <8 Å from the ligand. A461 aligns with AaSHC V381 (11 Å from the ligand), and W690 aligns with AaSHC W591 (20 Å from the ligand). These lanosterol synthase residues have conservation patterns consistent with a deprotonation-specific role, and several seem sufficiently near the ligand to participate in catalysis. It should be noted that residue conservation might result from coincidence rather than shared function. Furthermore, if either of two similar residues (e.g., aspartate or glutamate) can perform the same role, conservation may not be strict. Finally, this analysis will not reveal positions that have a catalytic role in one enzyme class but not in another.

Candidate residues for forming the intermediate protosteryl or dammarenyl cations can be identified similarly. Cycloartenol synthase and lanosterol synthase cyclize initially to the protosteryl cation, whereas lupeol synthase and β-amyrin cyclize to the dammarenyl cation (Fig. 3). The *D. discoideum* cycloartenol synthase is so far diverged from the plant cycloartenol synthases that the *A. thaliana* and *D. discoideum* cycloartenol synthases share fewer conserved residues (50%) than do the *A. thaliana* cycloartenol synthase and lupeol synthase (59%). This sequence divergence greatly decreases the pool of residues that are likely candidates for forming the protosteryl and dammarenyl cations. The 13 residues marked with a diamond in Figure 2 are conserved as one residue in both lanosterol synthase and cycloartenol synthase (which cyclize initially to the protosteryl cation), but are conserved as a different residue in β-amyrin synthase and lupeol synthase (which produce pentacyclic triterpenes *via* the dammarenyl cation). This conservation pattern is consistent with a role in forming the protosteryl or dammarenyl cations.

ScERG7 residues H234, T333, Y510, and I705 align with AaSHC residues W169, G259, Y420, and L607. ScERG7 G383 aligns with either AaSHC Q305 or A306, and ScERG7 N385 aligns with either residue AaSHC S307 or I308. All of these SHC residues map to within 8 Å of the ligand, making the corresponding oxidosqualene cyclase residues attractive candidates for directing dammarenyl or protosteryl cation formation. Mutating either ScERG7 H234 (7) or AaSHC Y420 (41) to alanine alters catalysis. Two differentially conserved ScERG7 residues seem too distant from the active site to participate directly in catalysis. ScERG7 residue V161 aligns unambiguously with AaSHC V96 (26 Å from the ligand), and A188 aligns with AaSHC I123 (18 Å from the ligand). Residues G108, G155, P340, S358, and C619 did not align reliably. Site-directed mutagenesis experiments are underway to determine whether the residues at these positions perform important functions in enzymatic oxidosqualene cyclization.

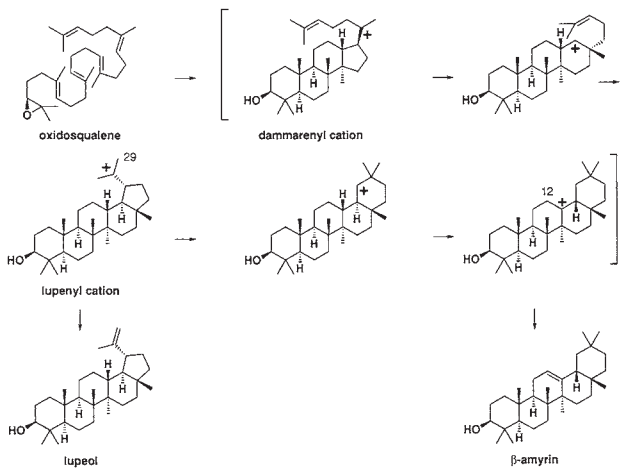

FIG. 3. Mechanisms of lupeol synthase and β-amyrin synthase. Lupeol synthase cyclizes oxidosqualene to the chair-chair-chair dammarenyl cation, catalyzes ring expansion and cyclization to the lupenyl cation, and deprotonates primarily at C29 to form lupeol. Substantial amounts of isomeric triterpenes (including β-amyrin) are also produced. β-Amyrin synthase promotes the same lupenyl cation formation, but terminates the reaction by ring expansion followed by deprotonation at C12.

ACKNOWLEDGMENTS

This research was supported by grants from the National Institutes of Health (AI41598) and the Robert A. Welch Foundation (C-1323). E.d.H and W.G. were supported by a Career Development Award from the American Heart Association and NSF grant MCB 9600923. M.M.M. was supported by an American Society of Pharmacognosy Undergraduate Fellowship, and K.A.F as an Undergraduate Trainee of the Keck Center for Computational Biology (NSF RTG grant BIR-94-13229).

REFERENCES

1. Nes, W.R., and McKean, M.L. (1977) *Biochemistry of Steroids and Other Isopentenoids*, p. 690, University Park Press, Baltimore.
2. Abe, I., Rohmer, M., and Prestwich, G.D. (1993) Enzymatic Cyclization of Squalene and Oxidosqualene to Sterols and Triterpenes, *Chem. Rev. 93*, 2189–2206.
3. Matsuda, S.P.T. (1998) On the Diversity of Oxidosqualene Cyclases, in *Biochemical Principles and Mechanisms of Biosynthesis and Biodegradation of Polymers* (Steinbüchel, A., ed.), pp. 300–307, Wiley-VCH, Weinheim.
4. Corey, E.J., and Ortiz de Montellano, P.R. (1967) Enzymic Synthesis of β-Amyrin from 2,3-Oxidosqualene, *J. Am. Chem. Soc. 89*, 3362–3363.
5. Rees, H.H., Goad, L.J., and Goodwin, T.W. (1968) Cyclization of 2,3-Oxidosqualene to Cycloartenol in a Cell-Free System from Higher Plants, *Tetrahedron Lett. 9*, 723–725.
6. Gibbons, G.F., Goad, L.J., Goodwin, T.W., and Nes, W.R. (1971) Concerning the Role of Lanosterol and Cycloartenol in Steroid Biosynthesis, *J. Biol. Chem. 246*, 3967–3976.
7. Corey, E.J., Cheng, H.M., Baker, C.H., Matsuda, S.P.T., Li, D., and Song, X.L. (1997) Studies on the Substrate Binding Segments and Catalytic Action of Lanosterol Synthase—Affinity Labeling with Carbocations Derived from Mechanism-based Analogs of 2,3-Oxidosqualene and Site-directed Mutagenesis Probes, *J. Am. Chem. Soc. 119*, 1289–1296.
8. Buntel, C.J., and Griffin, J.H. (1992) Nucleotide and Deduced Amino Acid Sequences of the Oxidosqualene Cyclase from *Candida albicans*, *J. Am. Chem. Soc. 114*, 9711–9713.
9. Roessner, C.A., Min, C., Hardin, S.H., Harris-Haller, L.W., Mc-

Collum, J.C., and Scott, A.I. (1993) Sequence of the *Candida albicans* erg7 Gene, *Gene 127*, 149–150.
10. Corey, E.J., Matsuda, S.P.T., and Bartel, B. (1994) Molecular Cloning, Characterization, and Overexpression of *ERG7*, the *Saccharomyces cerevisiae* Gene Encoding Lanosterol Synthase, *Proc. Natl. Acad. Sci. USA 91*, 2211–2215.
11. Shi, Z., Buntel, C.J., and Griffin, J.H. (1994) Isolation and Characterization of the Gene Encoding 2,3-Oxidosqualene-Lanosterol Cyclase from *Saccharomyces cerevisiae*, *Proc. Natl. Acad. Sci. USA 91*, 7370–7374.
12. Kusano, M., Shibuya, M., Sankawa, U., and Ebizuka, Y. (1995) Molecular Cloning of cDNA Encoding Rat 2,3-Oxidosqualene:Lanosterol Cyclase, *Biol. Pharm. Bull. 18*, 195–197.
13. Abe, I., and Prestwich, G.D. (1995) Molecular Cloning, Characterization, and Functional Expression of Rat Oxidosqualene Cyclase cDNA, *Proc. Natl. Acad. Sci. USA 92*, 9274–9278.
14. Baker, C.H., Matsuda, S.P.T., Liu, D.R., and Corey, E.J. (1995) Molecular Cloning of the Human Gene Encoding Lanosterol Synthase from a Liver cDNA Library, *Biochem. Biophys. Res. Commun. 213*, 154–160.
15. Sung, C.-K., Shibuya, M., Sankawa, U., and Ebizuka, Y. (1995) Molecular Cloning of cDNA Encoding Human Liver Lanosterol Synthase, *Biol. Pharm. Bull. 18*, 1459–1461.
16. Corey, E.J., Matsuda, S.P.T., Baker, C.H., Ting, A.Y., and Cheng, H. (1996) Molecular Cloning of a *Schizosaccharomyces pombe* cDNA Encoding Lanosterol Synthase and Investigation of Conserved Tryptophan Residues, *Biochem. Biophys. Res. Commun. 219*, 327–331.
17. Corey, E.J., Matsuda, S.P.T., and Bartel, B. (1993) Isolation of an *Arabidopsis thaliana* Gene Encoding Cycloartenol Synthase by Functional Expression in a Yeast Mutant Lacking Lanosterol Synthase by the Use of a Chromatographic Screen, *Proc. Natl. Acad. Sci. USA 90*, 11628–11632.
18. Morita, M., Shibuya, M., Lee, M.-S., Sankawa, U., and Ebizuka, Y. (1997) Molecular Cloning of Pea cDNA Encoding Cycloartenol Synthase and Its Functional Expression in Yeast, *Biol. Pharm. Bull. 20*, 770–775.
19. Kushiro, T., Shibuya, M., and Ebizuka, Y. (1998) β-Amyrin Synthase. Cloning of Oxidosqualene Cyclase That Catalyzes the Formation of the Most Popular Triterpene Among Higher Plants, *Eur. J. Biochem. 256*, 238–244.
20. Hayashi, H., Hiraoka, N., Ikeshiro, Y., Kushiro, T., Morita, M., Shibuya, M., and Ebizuka, Y. (1999) Molecular Cloning and Characterization of a cDNA for *Glycyrrhiza glabra* Cycloartenol Synthase, *GenBank* accession number AB025968.
21. Ausubel, F.M., Brent, R., Kingston, R.E., Moore, D.D., Seidman, J.G., Smith, J.A., and Struhl, K. (eds.) (1999) *Current Protocols in Molecular Biology*, Wiley-Interscience, New York, p. 13.1.2.
22. Amasino, R.M. (1986) Acceleration of Nucleic Acid Hybridization Rate by Polyethylene Glycol, *Anal. Biochem. 152*, 304–307.
23. Rees, H.H., Goad, L.J., and Goodwin, T.W. (1969) 2,3-Oxidosqualene Cycloartenol Cyclase from *Ochromonas malhamensis*, *Biochim. Biophys. Acta 176*, 892–894.
24. Brandt, R.D., Pryce, R.J., Anding, C., and Ourisson, G. (1970) Sterol Biosynthesis in *Euglena gracilis* Z., *Eur. J. Biochem. 17*, 344–349.
25. Anding, C., Brandt, R.D., and Ourisson, G. (1971) Sterol Biosynthesis in *Euglena gracilis* Z., *Eur. J. Biochem. 24*, 259–263.
26. Raederstorff, D., and Rohmer, M. (1987) The Action of the Systemic Fungicides Tridemorph and Fenpropimorph on Sterol Biosynthesis by the Soil Amoeba *Acanthamoeba polyphaga*, *Eur. J. Biochem. 164*, 421–426.
27. Raederstorff, D., and Rohmer, M. (1987) Sterol Biosynthesis *via* Cycloartenol and Other Biochemical Features Related to Photosynthetic Phyla in the Amoebae *Naegleria lovaniensis* and *Naegleria gruberi*, *Eur. J. Biochem. 164*, 427–434.
28. Nes, W.D., Norton, R.A., Crumley, F.G., Madigan, S.J., and Katz, E.R. (1990) Sterol Phylogenesis and Algal Evolution, *Proc. Natl. Acad. Sci. USA 87*, 7565–7569.
29. Nes, W.D., Koike, K., Jia, Z.H., Sakamoto, Y., Satou, T., Nikaido, T., and Griffin, J.F. (1998) 9β,19-Cyclosterol Analysis by ^{1}H and ^{13}C NMR, Crystallographic Observations, and Molecular Mechanics Calculations, *J. Am. Chem. Soc. 120*, 5970–5980.
30. Radics, L., Kajtar-Peredy, M., Corsano, S., and Standoli, L. (1975) Carbon-13 NMR Spectra of Some Polycyclic Triterpenoids, *Tetrahedron Lett. 48*, 4287–4290.
31. Shimizu, N., Itoh, T., Saito, M., and Matsumoto, T. (1984) Acid-Catalyzed Isomerization of Cycloartane Triterpene Alcohols. The Formation of Cucurbitane- and Lanostane-Isomers, *J. Org. Chem. 49*, 709–712.
32. Venkatramesh, M., and Nes, W.D. (1995) Novel Sterol Transformations Promoted by *Saccharomyces cerevisiae* Strain GL7—Evidence for 9-β,19-Cyclopropyl to 9(11) Isomerization and for 14-Demethylation to 8,14 Sterols, *Arch. Biochem. Biophys. 324*, 189–199.
33. Poralla, K. (1994) The Possible Role of a Repetitive Amino Acid Motif in Evolution of Triterpenoid Cyclases, *Bioorg. Med. Chem. Lett. 4*, 285–290.
34. Poralla, K., Hewelt, A., Prestwich, G.D., Abe, I., Reipen, I., and Sprenger, G. (1994) A Specific Amino Acid Repeat in Squalene and Oxidosqualene Cyclases, *Trends Biochem. Sci. 19*, 157–158.
35. Herrera, J.B.R., Bartel, B., Wilson, W.K., and Matsuda, S.P.T. (1998) Cloning and Characterization of the *Arabidopsis thaliana* Lupeol Synthase Gene, *Phytochemistry 49*, 1905–1911.
36. Ochs, D., Kaletta, C., Entian, K.-D., Beck-Sickinger, A., and Poralla, K. (1992) Cloning, Expression, and Sequencing of Squalene-Hopene Cyclase, a Key Enzyme in Triterpenoid Metabolism, *J. Bacteriol. 174*, 298–302.
37. Wendt, K.U., Poralla, K., and Schulz, G.E. (1997) Structure and Function of a Squalene Cyclase, *Science 277*, 1811–1815.
38. Wendt, K.U., Lenhart, A., and Schulz, G.E. (1999) The Structure of the Membrane Protein Squalene-Hopene Cyclase at 2.0 Angstrom Resolution, *J. Mol. Biol. 286*, 175–187.
39. Sato, T., Kanai, Y., and Hoshino, T. (1998) Overexpression of Squalene-Hopene Cyclase by the Pet Vector in *Escherichi coli* and First Identification of Tryptophan and Aspartic Acid Residues Inside the QW Motif as Active Sites, *Biosci. Biotechnol. Biochem. 62*, 407–411.
40. Feil, C., Sussmuth, R., Jung, G., and Poralla, K. (1996) Site-Directed Mutagenesis of Putative Active-Site Residues in Squalene-Hopene Cyclase, *Eur. J. Biochem. 242*, 51–55.
41. Merkofer, T., Pale-Grosdemange, C., Wendt, K.U., Rohmer, M., and Poralla, K. (1999) Altered Product Pattern of a Squalene-Hopene Cyclase by Mutagenesis of Active Site Residues, *Tetrahedron Lett. 40*, 2121–2124.

[Received July 7, 1999; and in revised form and accepted December 17, 1999]

Cloning and Sequencing of the *Candida albicans* C-4 Sterol Methyl Oxidase Gene (*ERG25*) and Expression of an *ERG25* Conditional Lethal Mutation in *Saccharomyces cerevisiae*

Matthew A. Kennedy[a], Theresa A. Johnson[a], N. Douglas Lees[a,]*, Robert Barbuch[b], James A. Eckstein[b], and Martin Bard[a]

[a]Department of Biology, Indiana University Purdue University Indianapolis, Indianapolis, Indiana 46202-5132, and [b]Department of Drug Disposition, Eli Lilly and Company, Lilly Corporate Center, Indianapolis, Indiana 46285

ABSTRACT: The *ERG25* gene encoding the *Candida albicans* C-4 sterol methyl oxidase was cloned and sequenced by complementing a *Saccharomyces cerevisiae erg25* mutant with a *C. albicans* genomic library. The Erg25p is comprised of 308 amino acids and shows 65 and 38% homology to the enzymes from *S. cerevisiae* and *Homo sapiens*, respectively. The protein contains three histidine clusters common to nonheme iron-binding enzymes and an endoplasmic reticulum retrieval signal as do the proteins from *S. cerevisiae* and humans. A temperature-sensitive (ts) conditional lethal mutation of the *C. albicans ERG25* was isolated and expressed in *S. cerevisiae*. Sequence analysis of the ts mutant indicated an amino acid substitution within the region of the protein encompassed by the histidine clusters involved in iron binding. Results indicate that plasmid-borne conditional lethal mutants of target genes have potential use in the rescue of *Candida* mutations in genes that are essential for viability.

Paper no. L8270 in *Lipids 35,* 257–262 (March 2000).

The ergosterol biosynthetic pathway in fungi remains the target of the major classes of antifungal compounds currently employed to treat human infections. The recent, dramatic increase in reports of resistance (1) to these compounds has mandated a continued search for new antifungal target sites against which novel compounds can be developed and employed. Of particular concern is the rapidly emerging resistance to the azole antifungals, which are now the most widely employed antifungals in systemic, life-threatening infections. Most of the basic research in defining the ergosterol biosynthetic pathway and in determining the types of sterol molecules that support fungal growth has been conducted in *Saccharomyces cerevisiae* (2,3). This organism is readily amenable to genetic analysis, and the availability of haploid strains has made the isolation and characterization of ergosterol biosynthetic genes possible. At this time, all the genes encoding sterol biosynthetic enzymes in this organism have been cloned and disrupted with the exception of one of the genes involved in the complex series of reactions responsible for removing the two methyl groups from the C-4 position of the sterol molecule. All genes prior to the sterol methyl transferase (*ERG6*) gene are essential for viability and thus represent possible new targets for the discovery of novel antifungal compounds.

The use of S. *cerevisiae* as a model system for gene isolation and the determination of essential pathway steps is a useful tool in making similar determinations in pathogenic fungi such as *Candida albicans*, where haploid strains and sexual reproduction are not found. The complementation of *S. cerevisiae* sterol mutants with a *C. albicans* genomic library to isolate sterol genes in *C. albicans* is a first step in verifying gene essentiality in this organism and the suitability of that step for seeking inhibitors that might serve as antifungal agents. This approach has recently been used to clone and disrupt the *ERG6* gene of *C. albicans* (4). Although the *ERG6* gene is not essential in *S. cerevisiae*, its disruption results in a cell that is severely compromised in several functions associated with membrane permeability (5,6). The disruption of both copies of the *ERG6* gene in *C. albicans* likewise does not render the cell inviable but does make it hypersusceptible to a number of antifungal compounds and cellular inhibitors (4).

The final step in fungal sterol biosynthesis to be explored at the molecular level in *S. cerevisiae* is the multicomponent reaction which sequentially removes the two methyl groups from the C-4 position. Three enzymes are required, and the genes of two of these, the C-4 methyl oxidase gene (*ERG25*) and the C-3 sterol dehydrogenase (C-4 decarboxylase) gene (*ERG26*), have been isolated and characterized (7,8). Disruptions of *ERG25* and *ERG26* have been found to be lethal (7,8). Here we report the cloning and sequencing of the C-4 sterol methyl oxidase gene from *C. albicans* achieved by the complementation of an *S. cerevisiae erg25* mutant with a *C. albicans* library. Disruption of both copies of an essential sterol gene in *C. albicans*, however, is problematic since this organism will not take up exogenous sterol to allow viability

*To whom correspondence should be addressed at Department of Biology, Indiana University Purdue University Indianapolis, 723 W. Michigan St., Indianapolis, IN 46202-5132. E-mail: nlees@iupui.edu

Abbreviations: *ERG25,* C-4 methyl oxidase gene; *ERG26,* C-3 sterol dehydrogenase; GC, gas chromatography; plasmid pCERG25, the original complementing clone of 4kb in the *Candida albicans* shuttle vector YPB1; SD, synthetic dropout; ts, temperature-sensitive.

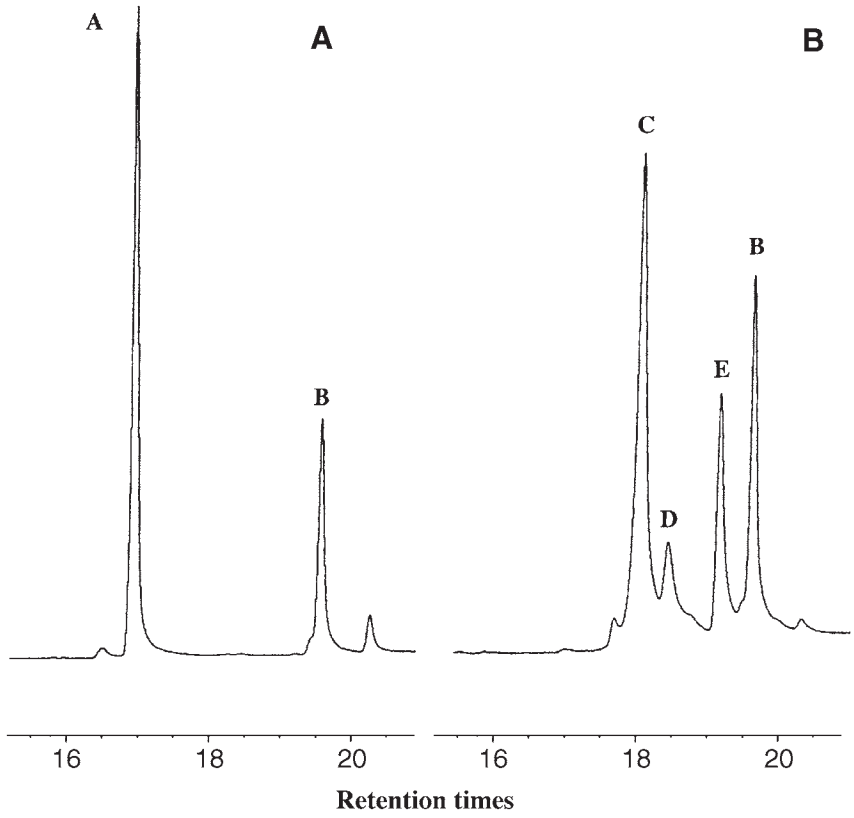

FIG. 1. Sterol profiles of *Saccharomyces cerevisiae* strain *erg25-25C* (A) and the same strain containing the *Candida albicans ERG25* on plasmid pIU873 (*erg25*/pCERG25) (B). Sterol extraction was carried out as described previously (Ref. 5). Peak A: cholesterol; peak B: 4,4-dimethyl zymosterol; peak C: ergosterol; peak D: fecosterol; peak E: 4-methyl fecosterol.

in order to verify that the double disruption has taken place. As a possible means to circumvent this situation, the *C. albicans ERG25* gene has been used to create a conditional lethal *ERG25* mutation which can be expressed on autonomous plasmids in *S. cerevisiae* to rescue *erg25* mutations under permissive conditions but not under nonpermissive conditions.

MATERIALS AND METHODS

Strains and plasmids. The *S. cerevisiae erg25* strain used in this study has been previously described (7). The *C. albicans* strain CAI8 (*ade2::hisG/ade2::hisG,* Δ*ura3::imm434/*Δ*ura3::imm434*) was a gift from William Fonzi, Georgetown University, and has been previously described (9). Plasmid pCERG25, the original complementing clone of 4 kb in the *C. albicans* shuttle vector YPB1, was isolated from a *C. albicans* genomic library obtained from Stew Scherer, University of Minnesota. The pIU870 contains the 2.5 kb *BglII-BamHI C. albicans ERG25* gene subcloned from pCERG25 into pRS316 at the *BamHI* site. The pIU908 is identical to pIU870 but with a temperature-sensitive (ts) conditional lethal mutation in *ERG25*. The pIU873 contains the 3.7 kb *XbaI-SalI C. albicans ERG25* gene subcloned from pCERG25 into pRS316 at the *XbaI-SalI* sites. *Escherichia coli* strain DH5α was used to manipulate and maintain all the plasmids used in this study.

Growth conditions. Sterol auxotrophs were grown anaerobically on complete medium supplemented with 1% ergosterol at 30°C. *Candida* strains were grown in complete or SD (synthetic dropout) media supplemented with 100 μg/mL uridine. Temperature shift growth conditions were as follows: duplicate cultures were grown to early log phase (OD_{660} = 0.4) at the permissive temperature in complete or SD media at which time one set of the cells was shifted to the nonpermissive temperature (38.5°C) and the second set remained at 30°C. Both sets were incubated for 24 h prior to sterol analysis.

Transformation. Saccharomyces cerevisiae transformations were carried out with the high-efficiency lithium acetate procedure previously described (10). *Escherichia coli* transformations were carried out by standard methods.

Mutagenesis. Conditional lethal mutations were isolated following mutagenesis of plasmid pIU870 carrying the *ERG25* gene. The pIU870 was transformed into *E. coli* strain XL1-Red (11), a strain that is deficient in three genes employed in DNA repair and has a mutation rate about 5,000 times higher than that in wild-type strains. Following 8 h of growth in XL1-Red, the plasmid DNA was isolated and transformed into *S. cerevisiae erg25*-25C. Transformants were plated at 30°C followed by replica plating on the same medium but incubated at 38.5°C. Colonies not growing at 38.5°C were screened to make certain that the ts mutation was

```
   1  ttttgattcattaattgttatatttcaacatatacatattcctttattccttgatccttttttaaagtattcaatttat
  80  tatttatttgtttgtttgaagtttata ATG TCT TCC ATT AGT AAT GTT TAT CAT GAC TAT TCG AGT
                                  M   S   S   I   S   N   V   Y   H   D   Y   S   S     13

 147  TTT CTG AAT GCA ACT ACT TTT TCC CAA GTT TAT CAA AAT TTC AAT CAA TTA GAT AAT TTA
      F   S   N   A   T   T   F   S   Q   V   Y   Q   N   F   N   Q   L   D   N   L     33

 207  AAT GTT TTT GAA AAA TTA TGG GGG TCA TAT TAT TAT TAT ATG GCC AAT GAT TTA TTT GCT
      N   V   F   E   K   L   W   G   S   Y   Y   Y   Y   M   A   N   D   L   F   A     53

 267  ACT GGA TTA TTA TTT TTT TTA ACT CAT GAA ATT TTT TAT TTT GGT AGA TGT TTA CCA TGG
      T   G   L   L   F   F   L   T   H   E   I   F   Y   F   G   R   C   L   P   W     73

 327  GCT ATA ATT GAT AGA ATT CCT TAT TTT AGA AAA TGG AAA ATT CAA GAT GAA AAA ATC CCT
      A   I   I   D   R   I   P   Y   F   R   K   W   K   I   Q   D   E   K   I   P     93

 387  AGT GAT AAA GAA CAA TGG GAA TGT CTT AAA TCA GTT TTA ACA TCT CAT TTC TTA GTT GAA
      S   D   K   E   Q   W   E   C   L   K   S   V   L   T   S   H   F   L   V   E    113

 447  GCT TTC CCA ATT TGG TTT TTC CAT CCA TTA TGT CAA AAA ATT GGT ATT AGT TAT CAA GTA
      A   F   P   I   W   F   F   H   P   L   C   Q   K   I   G   I   S   Y   Q   V    133

 507  CCA TTC CCT AAA ATT ACT GAT ATG TTG ATT CAA TGG GCA GTA TTT TTT GTT TTG GAA GAT
      P   F   P   K   I   T   D   M   L   I   Q   W   A   V   F   F   V   L   E   D    153

 567  ACT TGG CAT TAT TGG TTT CAT AGA GGA TTA CAT TAT GGG GTT TTC TAT AAA TAT ATT CAT
      T   W   H   Y   W   F   H   R   G   L   H   Y   G   V   F   Y   K   Y   I   H    173

 627  AAA CAA CAT CAT AGA TAT GCT GCT CCA TTT GGA TTG GCA GCA GAA TAT GCT CAT CCA GTT
      K   Q   H   H   R   Y   A   A   P   F   G   L   A   A   E   Y   A   H   P   V    193

 687  GAA GTT GCC TTA TTA GGA TTG GGT ACG GTT GGT ATT CCG ATT GTT TGG TGT CTT ATC ACT
      E   V   A   L   L   G   L   G   T   V   G   I   P   I   V   W   C   L   I   T    213

 747  GGT AAC TTG CAT CTT TTC ACA GTT TCC ATT TGG ATC ATT TTA AGA TTA TTC CAA GCC GTT
      G   N   L   H   L   F   T   V   S   I   W   I   I   L   R   L   F   Q   A   V    233

 807  GAT GCT CAT TCC GGT TAT GAA TTC CCT TGG TCT TTA CAT AAT TTC TTG CCA TTT TGG GCT
      D   A   H   S   G   Y   E   F   P   W   S   L   H   N   F   L   P   F   W   A    253

 867  GGT GCT GAT CAT CAT GAT GAA CAT CAT CAT TAT TTC ATT GGT GGA TAC TCT TCA TCT TTT
      G   A   D   H   H   D   E   H   H   H   Y   F   I   G   G   Y   S   S   S   F    273

 927  AGA TGG TGG GAT TTC ATT TTG GAT ACC GAA GCT GGT CCA AAA GCT AAA AAG GGT AGA GAA
      R   W   W   D   F   I   L   D   T   E   A   G   P   K   A   K   K   G   R   E    293

 987  GAC AAA GTC AAA CAA AAT GTT GAA AAA TTA CAA AAG AAG AAC TTA TAG agagagaaagagtat
      D   K   V   K   Q   N   V   E   K   L   Q   K   K   N   L                      308

1049  atgtgtacaacttctcaatgtttgtaccactttcaatattaatactgtttatttttggttttatttaatatatatatc
1126  atatctattcatagtgctacat
```

FIG. 2. The base and amino acid sequences of the *ERG25* gene from *Candida albicans*.

in the *ERG25* gene and not in the selectable *URA3* gene. The mutant strain carrying the plasmid with the ts *ERG25* (pIU908) was designated *erg25*-25C/pIU908 or ts. A control strain carrying a plasmid with the wild-type *ERG25* gene (pIU870) was designated *erg25*-25C/pIU870 or wild-type.

Sequencing. Sequencing was performed with the Sequenase 2.0 dideoxy-sequencing kit and [^{35}S-dATP] purchased from Amersham (Arlington Heights, IL).

Sterol analysis. Sterol extraction and preliminary gas chromatography (GC) sterol analyses were carried out as described previously (7). GC separation and mass spectral (MS) analyses were done with a 5890 Hewlett-Packard GC (Palo Alto, CA) coupled to a Hewlett-Packard 5972 mass selective detector. All data analyses were performed with the Hewlett-Packard Chemstation software. GC separations of sterols were obtained on a J&W Scientific DB-5MS column (20 m × 0.18 mm) (Folsom, CA) with a film thickness of 0.18 µm. Injections were programmed in the splitless mode with an inlet temperature of 280°C. Helium was used as the carrier gas with a linear velocity of 30 cm/s. The oven was programmed to hold the initial temperature of 100°C for 1 min and then increased to 300°C at 10°C per min. The oven temperature was held at 300°C for an additional 15 min. The interface temperature of 280°C resulted in a detector temperature of 180°C. Mass spectra were generated in the electron impact mode at an electron energy of 70 eV. The instrument was programmed to scan from 40 to 700 amu at 1-s intervals.

RESULTS AND DISCUSSION

The *ERG25* gene from *S. cerevisiae* has been cloned and characterized in our lab (7). The Erg25p is an essential enzyme that

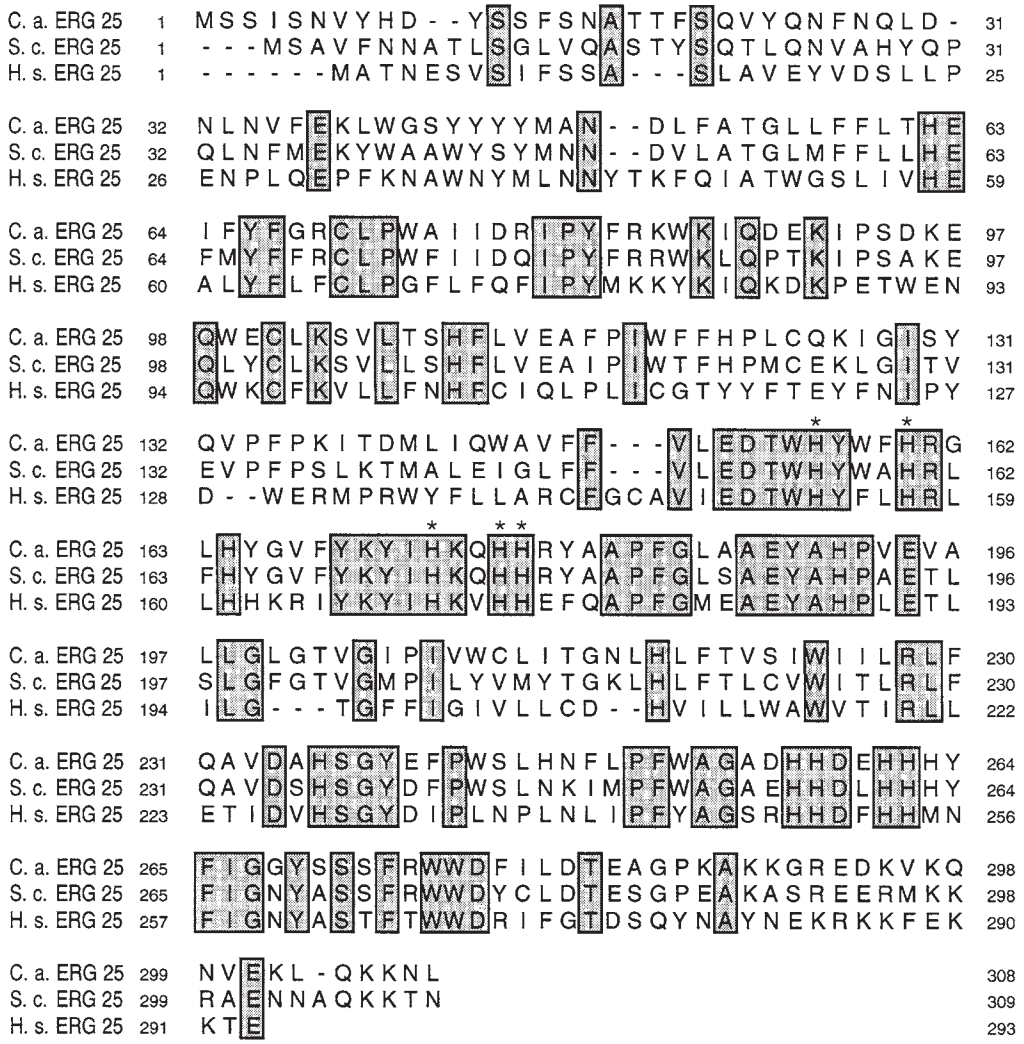

FIG. 3. The multiple sequence alignment for the *ERG25* genes from *Candida albicans* (C. a.), *Saccharomyces cerevisiae* (S. c.), and *Homo sapiens* (H. s.). Shaded boxes indicate regions of amino acid homology among all three species. Histidines in the three histidine clusters are designated by an asterisk at each position.

is responsible for the first of three reactions which sequentially remove the two methyl groups from the C-4 position of the sterol intermediate, 4,4-dimethylzymosterol. In this study *S. cerevisiae* strain *erg25*-25C was transformed with a *C. albicans* genomic library (12), and two clones (pCERG25) capable of growing without ergosterol supplementation were isolated. From these two clones, several subclones containing the *ERG25* gene were created. The two smallest complementing subclones, pIU870 (2.5 kb insert) and pIU873 (3.7 kb insert), were employed in this study. Restoration of ergosterol biosynthesis was used to confirm the cloning of the *ERG25* gene. Figure 1 shows the sterol profiles, as determined by GC, of the *S. cerevisiae erg25* mutant, grown on cholesterol to maintain viability, and a *C. albicans ERG25*-complemented transformant (*erg25*/pCERG25). The *erg25* strain accumulated 4,4-dimethylzymosterol and no ergosterol. The complemented strain accumulated both ergosterol and 4,4-dimethylzymosterol, indicating only partial complementation by the *C. albicans* gene.

DNA from several *ERG25* subclones was used to sequence the *C. albicans ERG25* gene. The nucleotide base and amino acid sequences (GenBank Accession Number AF051914) of the *C. albicans ERG25* are shown in Figure 2. The *ERG25* open-reading frame is comprised of 927 bases which encode a 308 amino acid protein. Figure 3 shows the multiple sequence alignment of the *ERG25* genes from *C. albicans*, *S. cerevisiae*, and *H. sapiens*. The shaded regions indicate where the sequences are identical among all three organisms. The CTG leucine codon at amino acid position 15 is translated as a serine in *C. albicans* (13). The *C. albicans* gene is 65% homologous at the amino acid level to the *S. cerevisiae* gene (7) and 38% homologous to the human gene (14). As in the case of the *S. cerevisiae* and human Erg25p, the *C. albicans* Erg25p contains three histidine-rich clusters comprising the eight histidine motif $HX_{3-4}H$, $HX_{2-3}HH$, and $HX_{2-3}HH$ starting at amino acid positions 156, 173, and 258, respectively. This motif is common to over 60 iron-binding, nonheme inte-

gral membrane desaturases, hydroxylases, and oxidases (15), including the *S. cerevisiae* C-5 sterol desaturase (16). The *C. albicans ERG25* gene also contained a C-terminal endoplasmic reticulum retrieval signal that is also present in the *S. cerevisiae* (7) and human (14) versions of the gene.

In the process of selecting new target sites in the ergosterol pathway for the identification of new antifungals, it would be advantageous to identify reactions that are essential for viability. This has been done extensively in *S. cerevisiae,* and several genes (7,8,17,18) have been identified by disruption techniques as providing sterol structural characteristics that are essential for cell viability. Repeating these determinations in *C. albicans* is more problematic due to its diploid nature, which requires two separate disruption events, and because of the inability of the organism to take-up exogenous sterol (19). Thus, the successful disruption of an essential gene would create an inviable cell with no obvious mechanism for rescue.

The isolation of conditional lethal mutations of the gene in question would provide a potential solution to this problem. The conditional lethal could be introduced into the cell on a complementing plasmid before the second allele is disrupted, and the absence of the wild-type gene product would occur only under nonpermissive conditions. This allows for the survival of the double disruptant and the opportunity for molecular confirmation of the disruption.

A ts conditional lethal of the *C. albicans ERG25* was isolated following mutagenesis in *E. coli* XL1-Red (11). Table 1 shows the sterol compositions of *S. cerevisiae* strains *erg25*-25C/pIU870 (wild-type *ERG25* allele) and *erg25*-25C/pIU908 (ts *ERG25* allele) grown under permissive (30°C) and nonpermissive (38.5°C) growth conditions on SD medium. Cells containing the wild-type allele show nearly identical sterol profiles at both temperatures. On the other hand, cells containing the ts allele produce significantly elevated levels of 4,4-dimethylzymosterol at the nonpermissive growth temperature. Growth of this strain at the permissive temperature results in some elevation of C-4 methyl sterol content, indicating that the ts mutation results in diminished enzyme efficiency even

TABLE 1
Accumulated Sterols[a] at Permissive and Nonpermissive Growth Temperatures of *Saccharomyces cerevisiae erg25* Mutants Carrying Wild-Type (pIU870) or Temperature-Sensitive (pIU908)[b] *Candida albicans ERG25* Alleles

	erg25-25C/pIU870		*erg25*-25C/pIU908	
Sterol	30°C	38.5°C	30°C	38.5°C
Squalene	5.9	2.4	31.9	15.2
Zymosterol	4.0	5.7	<1	<1
Ergosterol	61.9	63.6	32.6	16.2
Fecosterol	2.7	6.4	<1	<1
4-Methyl fecosterol	3.6	6.7	20.6	29.4
Lanosterol	1.7	2.2	<1	<1
4,4-Dimethyl zymosterol	6.6	8.0	14.9	34.8
4,4-Dimethyl fecosterol	—	—	—	4.4

[a]Sterols represented as percentage of total sterol.
[b]Cells containing the temperature-sensitive *ERG25* allele were pregrown at the permissive temperature (30°C) before being shifted to the nonpermissive temperature (38.5°C) and grown for 24 h.

```
WT    837   TCT TTA CAT AAT TTC TTG CCA   857
      244   S   L   H   N   F   L   P     250

T^S   837   TCT TTA CAT GAT TTC TTG CCA   857
      244   S   L   H   D   F   L   P     250
```

FIG. 4. Base and amino acid sequences of the region surrounding the temperature-sensitive mutation in the *Candida albicans ERG25* gene.

at 30°C. Identical results were obtained with cells grown on complete medium. The 38.5°C grown cells were pregrown at 30°C and shifted to 38.5°C for 24 h prior to sterol extraction. Thus, the ergosterol detected was produced during pregrowth at 30°C. The cells grew for 1–1.5 generations after the shift to 38.5°C. Cessation of growth is likely due to the increased ratio of C-4 methyl sterol to ergosterol that results from the absence of a functional *ERG25* allele.

In order to conclusively demonstrate that the ts phenotype of *erg25*-25C/pIU908 is due to a mutation in the *ERG25* gene and not defects in the plasmid created by passage through XL1-Red, the *ERG25* insert was removed from the plasmid and reinserted into an identical, but nonmutagenized, plasmid backbone. The reconstructed plasmid was then transformed into the *S. cerevisiae erg25*-25c and analyzed for sterol composition following growth at 30 and 38.5°C. The profiles that emerged were identical to those shown for *erg25*-25C/pIU908 shown in Table 1, indicating that a mutation in the *ERG25* gene is responsible for the ts phenotype of *erg25*-25C/pIU908.

Further evidence for the nature of the ts mutation was derived from sequencing of the open-reading frame of the ts allele. Figure 4 shows the *C. albicans* wild type *ERG25* allele and the ts *ERG25* allele from base positions 837 to 857. The base at position 846 in the wild-type allele has been changed from an A to a G, resulting in a change from asparagine to aspartic acid at amino acid position 247. The location of the change is between histidine clusters 2 and 3 (Fig. 3) and could involve the inability of the altered gene product to bind iron.

The data presented report that the cloning and sequencing of the *C. albicans ERG25* gene encoding the C-4 sterol methyl oxidase, a nonheme, iron-binding enzyme, are similar in sequence and other characteristics to the enzymes found in *S. cerevisiae* and humans. A ts conditional lethal mutation of the *C. albicans ERG25* can be expressed in *S. cerevisiae,* indicating that plasmid-borne *ERG25* conditional lethals can be employed to rescue double disruptions of essential genes in *C. albicans.*

ACKNOWLEDGMENT

This work was supported by a grant DAMD17-95-1-5067 to M.B. and N.D.L. from the Defense Women's Health Research Program of the U.S. Army.

REFERENCES

1. White, T.C., Marr, K.A., and Bowden, R.A. (1998) Clinical, Cellular, and Molecular Factors That Contribute to Antifungal Resistance, *Clin. Microbiol. Rev. 11*, 382–402.

2. Daum, G., Lees, N.D., Bard, M., and Dickson, R. (1998) Biochemistry, Cell Biology, and Molecular Biology of Lipids of *Saccharomyces cerevisiae*, *Yeast 14*, 1471–1510.
3. Lees, N.D., Bard, M., and Kirsch, D.R. (1997) Biochemistry and Molecular Biology of Sterol Synthesis in *Saccharomyces cerevisiae*, in *Biochemistry and Function of Sterols* (Parish, E.J., and Nes, W.D., eds.) pp. 85–99, CRC Press, Boca Raton.
4. Jensen-Pergakes, K.L., Kennedy, M.A., Lees, N.D., Barbuch, R., Koegel, C., and Bard, M. (1998) Sequencing, Disruption, and Characterization of the *Candida albicans* Sterol Methyltransferase (*ERG6*) Gene: Drug Susceptibility Studies in *erg6* Mutants, *Antimicrob. Agents Chemother. 42*, 1160–1167.
5. Gaber, R.F., Copple, D.M., Kennedy, B.K., Vidal, M., and Bard, M. (1989) The Yeast Gene *ERG6* Is Required for Normal Membrane Function but Is Not Essential for Biosynthesis of the Cell-Cycle Sparking Sterol, *Mol. Cell Biol. 9*, 3447–3456.
6. Lees, N.D., Lofton, S.L., Woods, R.A., and Bard, M. (1980) The Effects of Varied Energy Source and Detergent on the Growth of Sterol Mutants of *Saccharomyces cerevisiae*, *J. Gen. Microbiol. 118*, 209–214.
7. Bard, M., Bruner, D.A., Pierson, C.A., Lees, N.D., Biermann, B., Frye, L., Koegel, C., and Barbuch, R. (1996) Cloning and Characterization of *ERG25*, the *Saccharomyces cerevisiae* Gene Encoding the C-4 Sterol Methyl Transferase, *Proc. Natl. Acad. Sci. USA 93*, 186–190.
8. Gachotte, D., Barbuch, R., Gaylor, J., Nickel, E., and Bard, M. (1998) Characterization of the *Saccharomyces cerevisiae ERG26* Gene Encoding the C-3 Sterol Dehydrogenase (C-4 decarboxylase) Involved in Sterol Biosynthesis, *Proc. Natl. Acad. Sci. USA 95*, 13794–13799.
9. Fonzi, W.A., and Irwin, M.Y. (1993) Isogenic Strain Construction and Gene Mapping in *Candida albicans*, *Genetics 134*, 717–728.
10. Gietz, R.D., Schiestl, R.H., Willems, A.R., and Woods, R.A. (1995) Studies on the Transformation of Intact Yeast Cells by the LiAc/SS-DNA/PEG Procedure, *Yeast 11*, 355–360.
11. Greener, A., Callahan, M., and Jerpseth, B. (1996) An Efficient Random Mutagenesis Technique Using an *E. coli* Mutator Strain, *Methods Mol. Biol. 57*, 375–385.
12. Goshorn, A.K., Grindle, S.M., and Scherer, S. (1992) Gene Isolation by Complementation in *Candida albicans* and Applications to Physical and Genetic Mapping, *Infect. Immun. 60*, 876–884.
13. Santos, M.A.S., Perreau, V.M., and Tuite, M.F. (1996) Transfer RNA Structural Change Is a Key Element in the Reassignment of the CUG Codon in *Candida albicans*, *EMBO J. 15*, 5060–5068.
14. Li, L., and Kaplan, J. (1996) Characterization of Yeast Methyl Sterol Oxidase (*ERG25*) and Identification of a Human Homologue, *J. Biol. Chem. 271*, 16927–16933.
15. Shanklin, J., Achim, C., Schmidt, H., Fox, B.G., and Munck, E. (1997) Mossbauer Studies of Alkane ω-Hydroxylase: Evidence for a Diiron Cluster in an Integral-Membrane Protein, *Proc. Natl. Acad. Sci. USA 94*, 2981–2986.
16. Arthington, B.A., Bennett, L.G., Skatrud, P.L., Guynn, C.J., Barbuch, R.J., Ulbright, C.E., and Bard, M. (1991) Cloning, Disruption, and Sequence of the Gene Encoding Yeast C-5 Desaturase, *Gene 102*, 39–44.
17. Bard, M., Lees, N.D., Turi, T., Craft, D., Coffrin, L., Barbuch, R., Koegel, C., and Loper, J.C. (1993) Sterol Synthesis and Viability of *erg11* (cytochrome P-450 lanosterol demethylase) Mutations in *Saccharomyces cerevisiae* and *Candida albicans*, *Lipids 28*, 963–967.
18. Lorenz, R.T., and Parks, L.W. (1992) Cloning, Sequencing, and Disruption of the Gene Encoding the C-14 Reductase in *Saccharomyces cerevisiae*, *DNA Cell Biol. 11*, 685–692.
19. Kurtz, M.B., and Marrinan, J. (1989) Isolation of *hem3* Mutants from *Candida albicans* by Sequential Gene Disruptions, *Mol. Gen. Genet. 217*, 47–52.

[Received June 1, 1999, and in final revised form and accepted December 20, 1999]

Plant Sterol-C24-Methyl Transferases: Different Profiles of Tobacco Transformed with *SMT1* or *SMT2*[1]

Aurélie Schaeffer, Pierrette Bouvier-Navé, Pierre Benveniste, and Hubert Schaller*

Institut de Biologie Moléculaire des Plantes, Département Biosynthèse et Fonctions des Isoprenoïdes, Institut de Botanique, 67083 Strasbourg, France

ABSTRACT: Higher plant cells contain a mixture of 24-desmethyl, 24-methyl(ene), and 24-ethyl(idene) sterols in given proportions according to species but also to cell type. As a first step to investigate the function of such sterol compositions in the physiology of a plant, we have illustrated in the present work the coexistence of two distinct (*S*)-adenosyl-L-methionine sterol-C24-methyltransferases (SMT) in transgenic *Nicotiana tabacum* L. Indeed, modulation of the expression of the tobacco gene *SMT1-1*, which encodes a cycloartenol-C24-methyltransferase, results in variations of the proportion of cycloartenol and a concomitant effect on the proportion of 24-ethyl sterols. Overexpression in tobacco of the *Arabidopsis thaliana* (L.) Heynh. gene *SMT2-1* which encodes a 24-methylene lophenol-C24[1]-methyltransferase, results in a dramatic modification of the ratio of 24-methyl cholesterol to sitosterol associated with a reduced growth, a topic discussed in the present work.

Paper no. L8306 in *Lipids 35*, 263–269 (March 2000).

Molecular cloning of (*S*)-adenosyl-L-methionine sterol-C24-methyltransferases (SMT) was recently achieved in a number of higher plant species including *Glycine max* (1), *Arabidopsis thaliana* (2), *Nicotiana tabacum*, *Oryza sativa*, and *Ricinus communis* (3,4), and *Zea mays* (5). Comparison of the amino acid sequences deduced from all of these cDNA indicated that SMT are distributed into two gene families, *SMT1* and *SMT2* (3) (Fig. 1). Furthermore, functional characterization of the SMT using a yeast *erg6* expression system demonstrated unambiguously that an *SMT1* sequence encodes a cycloartenol-C24-methyltransferase (SMT1) and a *SMT2* sequence encodes a 24-methylene lophenol-C24[1]-methyltransferase (SMT2) in a given plant species (3,4). This demonstration fully validates previous conclusions supporting the fact that exocyclic C24 carbon atoms are added during the course of plant sterol biosynthesis *via* discrete enzymatic steps (6–12).

		At 2-1								
At	*SMT2-1*	100	*At* 2-2							
At	*SMT2-2*	81	100	*Nt* 2-1						
Nt	*SMT2-1*	83	80	100	*Nt* 2-2					
Nt	*SMT2-2*	78	75	86	100	*Os* 2-1				
Os	*SMT2-1*	70	68	73	72	100	*Nt* 1-1			
Nt	*SMT1-1*	43	40	44	44	40	100	*Nt* 1-2		
Nt	*SMT1-2*	42	39	43	44	39	91	100	*Rc* 1-1	
Rc	*SMT1-1*	39	38	41	41	38	78	75	100	*Os* 1-1
Os	*SMT1-1*	42	43	42	42	42	81	78	76	100

FIG. 1. Comparison of deduced amino acid sequences from *SMT* clones. Percent identity between two given clones was obtained from the alignment of *SMT* cDNA performed with the PILEUP program of the UGCG package run with the default parameters (3,4). *At*, *Arabidopsis thaliana*; *Nt*, *Nicotiana tabacum*; *Os*, *Oryza sativa*; *Rc*, *Ricinus communis*.

SMT in higher plant cells are responsible for their capability to produce a mixture of 24-methyl(ene) sterols and 24-ethyl(idene) sterols. The proportion of each of these sterols must be genetically defined since it is invariant with respect to species and, even more, organ. To understand the physiological significance of a given 24-alkylsterol composition in a plant material and the modality of its regulation throughout ontogeny, we have modified such a sterol composition in transgenic plants as a first step of this study.

Transgenic plants are a powerful tool to modulate the expression of a gene. In this article we report on transformation experiments of *N. tabacum* with *SMT1* (*Nt SMT1*) and comment on additional results to previous work on transformation of tobacco with *SMT2* (13) in order to demonstrate further the *in planta* coexisting SMT1 and SMT2 functions.

MATERIALS AND METHODS

Plasmid constructs. The cDNA *Nt SMT1-1* was isolated from a tobacco callus library as reported (3). A 1.4 kb BamHI-KpnI fragment comprising the open reading frame (ORF) of *SMT1-1* was excised from the pBluescript SK cloning vector (Strata-

[1]Based in part on a paper presented at the Steroid Symposium of the American Oil Chemists' Society Annual Meeting, Orlando, Florida, May 1999.

*To whom correspondence should be addressed at the CNRS/IBMP, Institut de Botanique, 28 rue Goethe, F-67083 Strasbourg Cedex, France. E-mail: Hubert.Schaller@ibmp-ulp.u-strasbg.fr

Abbreviations: *At*, *Arabidopsis thaliana* (L.) Heynh.; AdoMet, (*S*)-adenosyl-L-methionine; cDNA, complementary DNA; GC–MS, gas chromatography–mass spectrometry; kb, kilobase; lophenol, 3β,4α,5α-isomer of 4-methyl-cholest-7-en-3-ol; MS, Murashige and Skoog culture medium; *Nt*, *Nicotiana tabacum* L.; ORF, open reading frame; PCR, polymerase chain reaction; SMT, AdoMet-sterol-C24-methyltransferase; SMT1, AdoMet-cycloartenol-C24-methyltransferase; SMT2, AdoMet-24-methylene-lophenol-C24[1]-methyltransferase; T-DNA, transfer DNA; TLC, thin-layer chromatography.

gene, La Jolla, CA) and subcloned in the same sites of the plant expression vector pBD515.3 to generate a sense expression cassette of *Nt SMT1-1*. A 0.6 kb SacI-KpnI fragment of the cDNA *Nt SMT1-1* was excised from the pSK vector and subcloned into the KpnI-SacI sites of pBD515.3 to generate an antisense expression cassette of *Nt SMT1-1*. The plant promoter of pBD515.3 is the CaMV 35S promoter sequence with a duplicated enhancer region (14); therefore, the sense expression cassette is referred to as pD35S-*Nt SMT1-1* and the antisense expression cassette as pD35S-a-*Nt SMT1-1*. Standard cloning procedures are described in Reference 15. Recombinant pD35S derivatives and the corresponding void plasmid pD35S referred to as control were introduced into the *Agrobacterium tumefaciens* strain LBA4404 by triparental mating using pRK 2013 in *Escherichia coli* HB101 as a helper plasmid (16).

Plant material, transformation, culture conditions, and genetic analysis. Nicotiana tabacum L. var. *xanthi* was transformed with pD35S, pD35S-*Nt SMT1-1*, and pD35S-a-*Nt SMT1-1 via A. tumefaciens* using the leaf-disk co-cultivation method originally reported (17). Shoots were regenerated on Murashige and Skoog (MS) medium with supplements as described in Reference 13 and 100 mg/L kanamycin as the transgenic plant-selective agent. Primary transformants (generation T1) and their progenies obtained by selfing (generation T2) were grown *in vitro* on MS medium under a 16-h light period at 24°C and an 8-h dark period at 20°C. Eight-week-old *in vitro* plants were transferred to the greenhouse to set seeds. Integration of the transgene(s) into the plant genome was checked by polymerization chain reaction (PCR) on chromosomal DNA according to the method described in (18); detection of pD35S-*Nt SMT1-1* was achieved with primer AS1 (sense, 5′ CATTTGGAGAGAACACGG 3′) complementary to the pD35S sequence and with primer AS2 (antisense, 5′ GCCGGGTACCTTACTGAGAGTCTGAAATGGGC 3′) complementary to *Nt SMT1-1*; detection of pD35S-a-*Nt SMT1-1* was achieved with AS1 and AS3 (antisense, 5′ GGCCTCCCTGAGGTTAGATTG 3′) complementary to *Nt SMT1-1*. The number of transgenic loci per plant line was determined according to the Mendelian segregation of the kanamycin-resistant phenotype in T2 generations: seed samples were germinated on MS medium supplemented with 300 mg/L kanamycin.

Transgenic *N. tabacum* L. var. *xanthi* expressing an *A. thaliana* cDNA encoding a 24-methylene-lophenol-C24^1-methyltransferase (*At SMT2-1*) is described in Reference 13. Greenhouse-grown plants from the T3 generation were used in the present work.

DNA and RNA gel blot analysis. Genomic DNA was prepared according to Dellaporta *et al.* (19). DNA (20 μg) was restricted with EcoRI, HindIII, or SacI; restriction fragments were separated electrophoretically on a 0.7% agarose gel and blotted onto Hybond N^+ (Amersham, Buckinghamshire, United Kingdom) membranes. Hybridizations with ^{32}P-radiolabeled DNA probes obtained by random priming were carried out at high stringency according to the manufacturer's recommendations.

Total RNA from leaf material were extracted according to Goodall *et al.* (20). Northern analysis was done by separating 10 to 20 μg RNA samples on formaldehyde gels as described (15) and blotting them onto Hybond N^+. Hybridizations were done as for DNA blots. Pictures were prepared by scanning the autoradiographs with Adobe Photoshop 5.0 (San Jose, CA).

SMT enzymatic assay. Isolation of membranes from *in vitro*- grown tobacco was carried out as follows: 6 g of leaf tissue was ground in a 0.2 M KH_2PO_4 buffer (pH 7.5) containing 0.35 M sorbitol, 10 mM $Na_2EDTA{\cdot}2H_2O$, 5 mM $MgCl_2{\cdot}6H_2O$, 40 g/L polyvinylpyrrolidone, and 10 mM dithioerythritol. The supernatant fraction resulting from a 15-min centrifugation at 10,000 × *g* was centrifuged for 1 h at 100,000 × *g*. The membrane fraction was then resuspended in a 0.1 M Tris-HCl buffer (pH 7.5) containing 1 mM β-mercaptoethanol and 20% (vol/vol) glycerol. Microsomal proteins were quantified by the Bio-Rad (Richmond, CA) protein assay using bovine serum albumin as a standard. A radiochemical assay for SMT activities was carried out based on that reported (7). The standard assay consisted of 0.1 M Tris-HCl at pH 7.5, 1 mM β-mercaptoethanol, 20% glycerol (vol/vol), 0.1% Tween 80 (wt/vol), 30 μM 24-methylene lophenol or 100 μM cycloartenol, 100 μM [methyl-^{3}H]-AdoMet (475,000 cpm) and 0.8 mg/mL microsomal proteins. The mixture was incubated at 30°C for 45 min and the reaction was then stopped by adding 100 μL of 12% (wt/vol) ethanolic KOH. Sterol carriers were added before neutral lipids were extracted with *n*-hexane. Sterols were purified by thin-layer chromatography (TLC) (two runs of dichloromethane), and bands of interest (4,4-dimethylsterols or 4α-methylsterols) were scraped off and collected into scintillation vials together with 10 mL of Beckman's Ready Organic cocktail (Fullerton, CA). Radioactivity was determined in a liquid scintillation counter (Packard Instruments, Downers Grove, IL).

Sterol analysis. Lipids from 5 to 10 mg (small-scale qualitative analysis) or 100 to 500 mg (quantitative analysis) of ground dry material were extracted at 70°C in dichloromethane/methanol (2:1, vol/vol). The dried residue was saponified with 6% (wt/vol) KOH in methanol at 90°C for 1 h to release the sterol moiety of steryl esters. Sterols were then extracted with 3 vol of *n*-hexane, and an acetylation reaction was performed on the dried residue for 1 h at 60°C in toluene with a mixture of pyridine/acetic anhydride (1:1, vol/vol). Steryl acetates were resolved by TLC (Merck 60F254 precoated silica plates; Darmstadt, Germany) with one run of dichloromethane as a single band at R_f = 0.5. Purified steryl acetates were separated, identified, and quantified by gas chromatography (GC) using a Varian 8300 gas chromatograph with a flame-ionization detector, a glass capillary column (Wall-Coated Open Tubular, 30-m long, 0.25 mm i.d., coated with DB1; J&W Scientific, Folsom, CA), and H_2 as a carrier gas (2 mL/min). The temperature program included a fast increase from 60 to 220°C (30°C/min) and a slow increase from 220 to 280°C (2°C/min). Data from the detector were monitored with the Varian Star computer program. Sterol structures were confirmed by GC–mass spectrometry (MS) [Fison MD800 equipped with a glass capillary column (WCOT coated with DB5; J&W Scientific, Folsom, CA] according to Rahier and Benveniste (21).

RESULTS AND DISCUSSION

Expression of A. thaliana *SMT2-1 in* N. tabacum. We have generated transgenic tobacco overexpressing *At SMT2-1* cDNA under control of a strong constitutive promoter, namely, the CaMV 35S promoter, and have shown that the accumulation of *At SMT2-1* transcripts led to an increase of 24-methylene lophenol-C24[1]-methyltransferase activity in microsomes from leaf tissue (13). Consequently, the sterol biosynthetic flux was boosted toward the 24-ethyl sterol branch of the pathway (Fig. 2) and therefore a dramatic drop in the amount of 24-methyl cholesterol and a concomitant increase in that of sitosterol was observed. Indeed, the ratio of 24-methyl cholesterol to sitosterol, which was ~1 in wild-type leaf tissue, decreased to 0.03 in leaf tissue from the engineered plants. In succeeding generations, a low ratio of 24-methyl cholesterol to sitosterol was associated with reduced growth. Because the size of cells was almost unchanged in small transgenic tobacco when compared to the wild-type, we suggested that cell division rather than cell elongation was affected by such a novel sterol profile (13).

Cells that undergo divisions are located at the shoot or root apex. The sterol composition of such material is reported in Table 1. These data indicate that the ratio of 24-methyl cholesterol to sitosterol is equal to ~0.5 in shoot meristematic tissue from wild-type tobacco; this value is half the one calculated for leaf tissue taken from the same plants (13) as just reported above. This observation underlines the fact that to a given cell type at a given stage of development corresponds a given 24-alkyl sterols status as already illustrated, for instance, in the case of maize (22). In transgenic shoot meristematic tissues expressing *At SMT2-1*, the ratio of 24-methyl cholesterol to sitosterol dropped to 0.1 (Table 1). This further verifies that a consistent variation in the 24-alkylsterol status is associated with plant growth reduction. The mechanisms through which a decrease of 24-methyl cholesterol and/or an increase of sitosterol may be responsible for modifications in cell division and (or) cell elongation have now to be clarified. Although we have shown that overexpressing an *SMT2* sequence results in a unique and selective change in a sterol profile, namely, a variation of the ratio of 24-methyl cholesterol to sitosterol (13), it is interesting to note a reduction of the proportion of cholesterol in the sterol composition of *At SMT2-1* shoot meristematic tissues when compared to the wild-type. At this point of our

TABLE 1
Sterol Composition of Shoot Meristematic[a] Tissue from Greenhouse-Grown *Nicotiana tabacum* Expressing *At SMT2-1*

	Lines	
Sterol (%)	Wild-type	p35S-*At SMT2-1*
β-Amyrin	0.5	1
Cycloartenol	1	1
24-Methylene cycloartanol	0.5	0.5
Cycloeucalenol	Trace[b]	Trace
24-Ethylidene lophenol	0.5	1
Δ^7-Avenasterol	Trace	Trace
Δ^7-Sitostenol	0.5	1
Cholesterol	12	5
24-Methylene cholesterol	3	1
24-Methyl cholesterol	16	4.5
Isofucosterol	10	12
Sitosterol	31	47
Stigmasterol	25	26
Total sterol (mg/g dry weight)	2.2	2.1

[a]Meristematic tissue consists of the shoot meristem, *primordia*, and the first and second meristematic leaves dissected under the binocular.
[b]Trace, less than 0.1%. *At SMT2-1, Arabidopsis thaliana* cDNA which encodes a 24-methylene lophenol-C24[1]-methyltransferase.

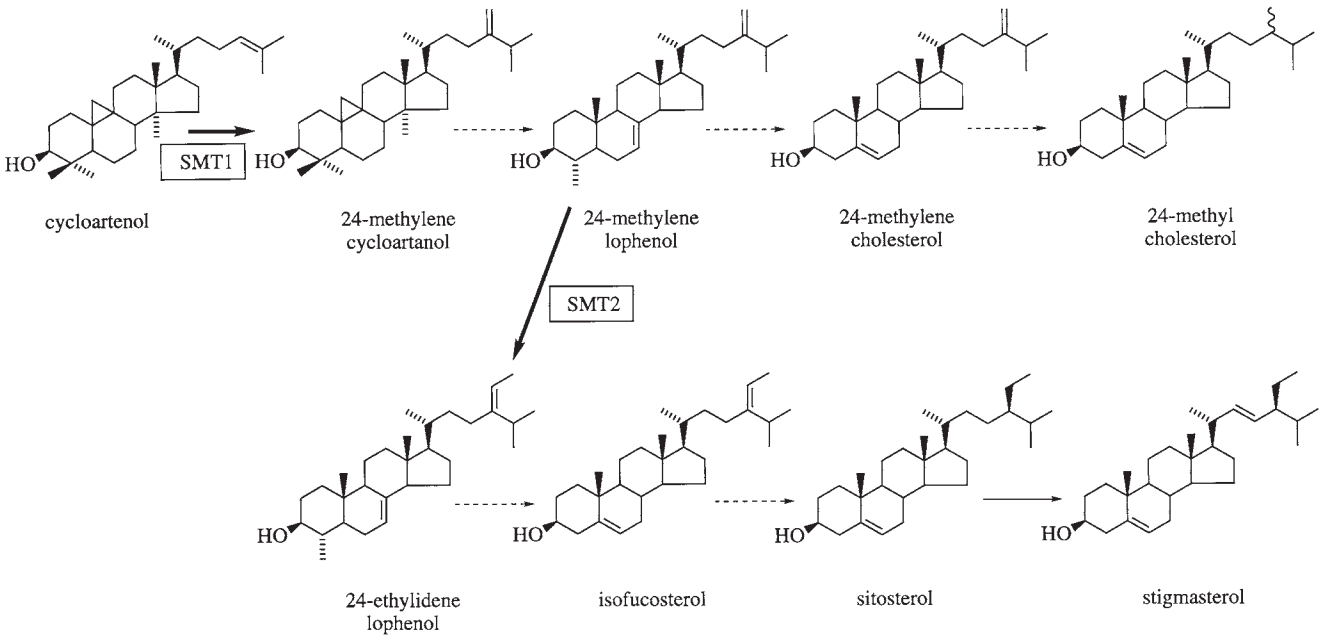

FIG. 2. Simplified post-squalene pathway of sterols in higher plants. The dashed arrows indicate more than one biosynthetic step not shown here.

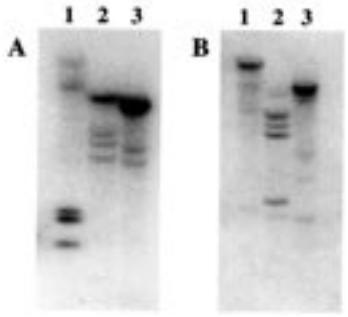

FIG. 3. Genomic DNA gel blot analysis. (A), 20 μg of tobacco chromosomal DNA was restricted with Sac I (lane 1), Hind III (lane 2), or EcoR I (lane 3). Hybridization was performed with a ^{32}P-random-labeled *Nt SMT1-1* cDNA as a probe. (B) The blot used in A was washed in 0.1% SDS at 80°C for 3 h and hybridized with a ^{32}P-random labeled *Nt SMT2-1* cDNA as a probe.

study, a possible role for cholesterol in the reported plant growth modifications cannot be excluded.

Ectopic expression of N. tabacum SMT1-1. Tobacco *SMT1* cDNA have been isolated from a callus library. One of these cDNA, called *Nt SMT1-1*, has been expressed in the yeast mutant *erg6*, which is deficient in zymosterol-C24-methyltransferase (23–25). Whereas *erg6* is devoid of 24-alkyl sterols, *erg6 Nt SMT1-1* contained a majority of 24-methylene sterols; furthermore, delipidated microsomes from *erg6 Nt SMT1-1* were shown to efficiently convert cycloartenol into 24-methylene cycloartanol but not 24-methylene lophenol into 24-ethylidene lophenol in the presence of S-AdoMet (3). Therefore, *Nt SMT1-1* and sequences highly similar to it encode a cycloartenol C24-methyltransferase. Two full-length cDNA encoding a SMT1 have been isolated so far from the tobacco callus library; the deduced amino acid sequences share 91% identity (Fig. 1) indicating that they are encoded by two distinct genes. The existence of at least two transcribed genes at the callus stage is consistent with the number of genes evaluated from the genomic DNA gel blot analysis (Fig. 3A). Indeed, hybridization carried out at high stringency revealed more than two bands in the case of Hind III or EcoR I restriction patterns using the cDNA *Nt SMT1-1* as a probe. Therefore, *SMT1* gene family in tobacco contains at least two members. Likewise, it is shown in the same hybridization experiment using the cDNA *Nt SMT2-1* (4) as a probe that *SMT2* gene family in tobacco also contains at least two members (Fig. 3B). Although genetic redundancy is known to occur in higher plants, it is not excluded that a given function may be encoded by different genes from the same family, each of the genes presenting a unique spatio-temporal expression pattern.

SMT1 is the first step of the enzymatic conversion of cycloartenol into Δ^5-sterols (Fig. 2). This step has been studied as a putative key regulatory point in the pathway (22). In order to challenge such a regulatory aspect of this enzyme and its influence on the sterol composition of the plant cell, we have transformed tobacco *via Agrobacterium* using a transfer DNA (T-DNA) vector carrying an *Nt SMT1-1* ORF driven by a double CaMV 35S promoter for sense transformation or a truncated 3′ end of the same ORF cloned in antisense orientation behind the duplicated p35S promoter in order to promote lowered expression of the endogenous gene. Twenty primary transformants were subjected to PCR analysis with a T-DNA specific primer and a gene specific primer; amplification of a single product in the case of both sense and antisense plantlets demonstrated the integration of the T-DNA into the target genome (data not shown). The analysis of the transgenic lines was carried out as follows: a qualitative sterol profile was determined on leaf material from *in vitro*-grown primary transformants; after selfing of these plants and germination of the second generation (T2), the expression of the transgene, the enzyme activities for SMT, and the total sterol content were determined for a representative set of *SMT1-1* lines, all containing a single transgenic locus (data not shown).

Most strikingly, a significant variation in the proportion of cycloartenol was found among the transgenic lines when compared to the control. Cycloartenol accounted for 12% of the total sterols in the control (Table 2). Sense transformants A, B, and C had a reduced content in cycloartenol indicating an in-

TABLE 2
Leaf Sterol Composition of 6-wk-old *in vitro Nicotiana tabacum* Primary Transformants Expressing a Sense or Antisense *SMT1-1* Construct[a]

	Lines									
		pD35S-*SMT1-1*						pD35S-a-*SMT1-1*		
Sterol (%)	Control	A	B	C	D	E	F	G	H	I
Cycloartenol	12	1.5	4	4	18	17	30	34	32	34
24-Methylene cycloartanol	4	2	10	1	4	3	1.5	4	1	3
24-Ethylidene lophenol	1	0.5	1	0	1	1	0.5	0	2	2
Δ^7-Avenasterol	3	1	2	1	2	2	0.5	2	2	2
Δ^7-Sitostenol	2.5	4	5	5	2	2	1	3	2	3
Δ^7-Cholestenol	1	0.5	0.5	0	1	1	0.5	1	2	2
Cholesterol	8	6	5	9	9	9	9	7	9	10
24-Methyl cholesterol	12.5	14	11	11	13	14	11	9	9	7
Isofucosterol	6	2.5	1	1	3	3	2	2	3	2
Sitosterol	18	24	24	23	13	13	11	10	10	8
Stigmasterol	32	44	36.5	45	34	35	33	28	28	27

[a]SMT1-1, cDNA which encodes a cycloartenol-C24-methyltransferase.

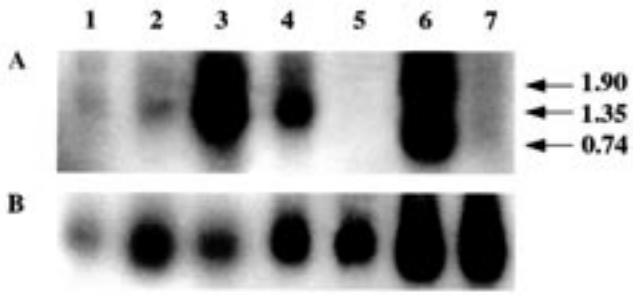

FIG. 4. Total leaf RNA gel blot analysis of transgenic *SMT1-1* tobacco. Lane 1, wild-type; lane 2, transgenic control; lanes 3 to 5, pD35S-*SMT1-1* plant lines A, B, and F, respectively; lanes 6 and 7, pD35S-a-*SMT1-1* plant lines G and I. (A) The blot was hybridized with a ^{32}P-labeled *Nt SMT1-1* cDNA probe. Sizes of bands are indicated in kb according to the standard RNA molecular markers. (B) The blot used in A was washed in 0.1% SDS at 80°C for 3 h and hybridized with a ^{32}P-random labeled 4.6 kb 18S rRNA probe as an internal standard.

creased metabolism of the latter *via* SMT1. Sense transformants D, E, and F and antisense transformants G, H, and I displayed an up to threefold increase in their cycloartenol content indicating a reduced rate of SMT1-mediated conversion of cycloartenol into 24-methylene cycloartanol. In the case of transformants D, E, and F the reduction of SMT1-mediated transformation of cycloartenol most probably results from cosuppression of *Nt SMT1-1* expression; in the case of transformants G, H, and I, the reduction in SMT1-mediated transformation of cycloartenol most probably results from antisense-mediated decrease of *Nt SMT1-1* messenger RNA (for literature on cosuppression and antisense gene expression see Ref. 26, 27).

In fact, these conclusions are fully validated by the pattern of *Nt SMT1-1* expression which was established for T2 *in vitro*-grown plants and is shown in Figure 4. The blot of leaf RNA was probed with *Nt SMT1-1* radiolabeled DNA fragments. A weak signal at ~1.35 kb was detected in the case of the wild-type and the transgenic control. A stronger signal of the same size was detected in the case of the sense transformants A and B; no signal was detected in the case of the sense transformant F. Such results demonstrating overexpression (lines A and B) and cosuppression (line F) of *Nt SMT1-1* are in agreement with an increase (lines A and B) and a decrease (line F) of SMT1-mediated metabolism of cycloartenol leading to a reduction and an increase, respectively, of the total percentage of 24-desmethyl sterols (Table 3). In the case of the antisense line G, the blot shows two distinct signals: the 1.9 kb signal might correspond to the unspliced transcript of *Nt SMT1-1* but this is at present still unclear; the 0.74 kb signal may indicate a significant expression of the antisense transgene. Interestingly, the key common point in the expression pattern of the antisense lines G and I and of the cosuppressed line F is the absence of a detectable signal at 1.35 kb corresponding to the *Nt SMT1-1* messenger RNA (Fig. 4). Consequently, antisense expression and cosuppression of *Nt SMT1-1* lead to the accumulation of 24-desmethyl sterols (Table 3) among which cycloartenol is predominant.

From the results in Table 2 one sees that the product of the SMT1 reaction, namely, 24-methylene cycloartanol, does not vary significantly. More generally, this is the case for all of the sterol intermediates leading to the end products of the pathway to 24-alkyl-Δ^5-sterols. This shows that a modified *SMT1-1* expression level and consequently an increase or a decrease in the proportion of cycloartenol does not have any apparent effect on enzymes beyond cycloartenol in the pathway. In addition, challenging the *SMT1-1* expression level in tobacco has a moderate effect on the total amount of sterols in the case of only some of the lines (Table 3).

Finally, a modification in the proportion of 24-methylsterols and of 24-ethylsterols is concomitant to the change in cycloartenol content (Tables 2 and 3). Essentially, an increase of sitosterol corresponds to a decrease of cycloartenol, and an increase of cycloartenol to a decrease of sitosterol (Table 2). Additionally, the proportion of stigmasterol [which results from the desaturation at C22 of sitosterol (6,28)] varies in the same sense as that of sitosterol does. This is intriguing because in the case of the overexpression of *At SMT2-1* in tobacco, a twofold increase in the amount of sitosterol is followed by only very moderate effects on the proportion of stigmasterol (Table 1; Ref. 13).

In order to explain the variations in the proportions of 24-ethylsterols (pathway end products) in transgenic *SMT1-1* to-

TABLE 3
Sterol Content and SMT Enzyme Assay of *in vitro* Transgenic *SMT1-1* Tobacco from the T2 Generation

	Lines					
		pD35S-*SMT1-1*			pD35S-a-*SMT1-1*	
Analysis	Control	A	B	F	G	I
Sterol (%)						
24-Desmethylsterols (C8-side chain)	13	9	7	32	39	24
24-Methyl(ene) sterols (C9-side chain)	18	19	20	15	12	18
24-Ethyl(idene) sterols (C10-side chain)	69	72	73	53	49	58
Total sterols (mg/g dry weight)	2.3	2.1	1.8	2.2	1.7	1.5
SMT enzyme activity[a] (substrate)						
SMT1 (cycloartenol)	0.31	0.29	0.50	0.06	0.24	0.17
SMT2 (24-methylene lophenol)	1.45	1.25	1.27	1.66	1.31	1.25

[a]nmol product/(mg protein)(h); SD never exceeded 30%. SMT, (*S*)-adenosyl-L-methionine-sterol-C24-methyltransferase. For other abbreviations see Tables 1 and 2.

bacco compared to the control, two hypotheses may be proposed; (i) SMT1 has a minor SMT2 activity *in planta*; this might be deduced from the SMT activities measured in microsomes from transgenic tobacco leaves (Table 3). However, variations of SMT2 activity do not follow the variations of SMT1 activity in the case of transgenic *Nt SMT1-1* lines B and F (Table 3). Moreover, variations of SMT2 never exceed 13% when compared to the control, whereas SMT1 activity increases up to 62% or decreases up to 80% of the control value among transgenic *Nt SMT1-1* lines (Table 3), confirming the substrate specificity of the *Nt SMT1-1* gene product as it was determined in the yeast mutant *erg6* (3). In contrast, leaf microsomes from tobacco transformed with the *A. thaliana SMT2-1* displayed similar increases of SMT2 and SMT1 activities as compared with the wild-type activities (Table 4) in agreement with the lower substrate specificity of SMT2 as it was determined in the yeast mutant *erg6* (4). Finally, if SMT1 or SMT2 ever display a SMT nonspecific *in planta* activity, this definitely has a limited impact on the sterol composition of the plant material based on the radically different sterol composition of transgenic tobacco transformed either with *SMT1* or with *SMT2*: in the first case, the proportion of cycloartenol varies with a concomitant effect on 24-ethylsterols (Table 2), whereas in the second case, the ratio of 24-methyl cholesterol to sitosterol is specifically modified (Table 1). Hence, SMT1 and SMT2 are indeed two different enzymatic proteins *in planta*. (ii) *SMT1* and *SMT2* gene expression may be co-regulated, and changing the transcription level of one of the genes therefore would affect the transcription of the other. Further experiments are required on the expression pattern of *SMT* in wild-type and transgenic plants to clarify this point.

CONCLUDING REMARKS

Sterol-C24-methyltransferases in higher plants are distributed into two gene families, *SMT1* and *SMT2*, according to sequence comparison and to heterologous functional expression of *SMT1* or *SMT2* cDNA originating from the same plant species (3). In the present work we further demonstrate the *in planta* coexistence of two enzymatic proteins, SMT1 and SMT2, owing to the distinct sterol composition of transgenic tobacco expressing ectopically an *SMT1-1* cDNA or an *A. thaliana SMT2-1* cDNA. It is clearly shown indeed that in the first case a modulation of the expression of *SMT1* (and consequently a modulation of the cycloartenol-C24-methyltransferase activity) results in a significant variation of the proportion of cycloartenol with additional effects on the proportion of 24-ethylsterols; in the second case, an increase of the expression of *SMT2* (and consequently an increase of the 24-methylene lophenol-C24[1]-methyltransferase) results in a dramatic drop of the ratio of 24-methyl cholesterol to sitosterol (13). In the case of both sets of transformation experiments reported here, it is worth noting that the total amount of sterols does not vary significantly, indicating that *SMT1* and *SMT2* expression levels have no major effects on the biosynthetic flux, at least within the limits of the sterol profile modifications reported here. This is in agreement with previous results showing that tobacco lines overaccumulating sterols by means of an enhanced 3-hydroxy-3-methylglutaryl-coenzyme A reductase gene expression level/enzyme activity also accumulate cycloartenol, because SMT1-mediated conversion of cycloartenol into 24-methylene cycloartanol is a slow step in plant sterol biosynthesis (29,30).

The presence of both 24-methyl sterols and 24-ethyl sterols in higher plant cell membranes raised the exciting question of the significance of their relative proportions with respect to plant physiology and growth. We have been able to show that a modulation of SMT2 in tobacco has a remarkable impact on the 24-alkyl sterol status and consequently on plant growth (13). On the contrary, we have not detected either in *in vitro* or in greenhouse-grown transgenic *SMT1-1* tobacco any clear-cut biological effect putatively linked to a modified cycloartenol or 24-alkyl sterol profile. Further experiments that challenge the expression level of *SMT1* in a given plant species are required to further assess the influence of *SMT1* on plant cell biochemistry and physiology.

TABLE 4
SMT Enzyme Assay of Greenhouse-Grown *N. tabacum* Expressing *At SMT2-1*

SMT enzyme activity[a] (substrate)	Lines		
		p35S-*At SMT2-1*	
	Wild-type	α	β
SMT1 (cycloartenol)	0.25	1.00	1.40
SMT2 (24-methylene lophenol)	0.86	3.55	5.36

[a]nmol product/mg protein·h-1; SD never exceeded 30%. For abbreviations see Tables 1–3.

ACKNOWLEDGMENTS

We thank Prof. John D. Weete and Prof. Ed J. Parish for the organization of the American Oil Chemists' Society Symposium on Steroids. We are much indebted to Bernadette Bastian for the preparation of the manuscript. We acknowledge Annie Hoeft for help in GC–MS analysis.

REFERENCES

1. Shi, J., Gonzales, R.A., and Bhattacharyya, M.K. (1996) Identification and Characterization of an *S*-Adenosyl-L-methionine: Δ^{24}-Sterol-C-methyltransferase cDNA from Soybean, *J. Biol. Chem. 271*, 9384–9389.
2. Husselstein, T., Gachotte, D., Desprez, T., Bard, M., and Benveniste, P. (1996) Transformation of *Saccharomyces cerevisiae* with a cDNA Encoding a Sterol *C*-Methyltransferase from *Arabidopsis thaliana* Results in the Synthesis of 24-Ethyl Sterols, *FEBS Lett. 381*, 87–92.
3. Bouvier-Navé, P., Husselstein, T., and Benveniste, P. (1998) Two Families of Sterol Methyltransferases Are Involved in the First and the Second Methylation Steps of Plant Sterol Biosynthesis, *Eur. J. Biochem. 256*, 88–96.
4. Bouvier-Navé, P., Husselstein, T., Desprez, T., and Benveniste, P. (1997) Identification of cDNAs Encoding Sterol Methyltransferases Involved in the Second Methylation Step of Plant Sterol Biosynthesis, *Eur. J. Biochem. 246*, 518–529.
5. Grebenok, R.J., Galbraith, D.W., and Penna, D.D. (1997) Characterization of *Zea mays* Endosperm C-24 Sterol Methyltrans-

ferase: One of Two Types of Sterol Methyltransferase in Higher Plants, *Plant Mol. Biol. 34*, 891–896.
6. Benveniste, P. (1986) Sterol Biosynthesis, *Annu. Rev. Plant Physiol. 37*, 275–308.
7. Fonteneau, P., Hartmann, M.A., and Benveniste, P. (1977) A 24-Methylene Lophenol C-28 Methyl Transferase from Suspension Cultures of Bramble Cells, *Plant Sci. Lett. 10*, 147–155.
8. Malhotra, H.C., and Nes, W.R. (1971) The Mechanism of Introduction of Alkyl Groups at C-24 of Sterols. IV—Inhibition by Triparanol, *J. Biol .Chem .246*, 4934–4937.
9. Nes, W.D., Janssen, G.G., and Bergenstrahle, A. (1991) Structural Requirements for Transformation of Substrates by the (*S*)-Adenosyl-L-Methionine: $\Delta^{24(25)}$-Sterol Methyltransferase, *J. Biol. Chem. 266*, 15202–15212.
10. Nes, W.R., and McKean, M.L. (1977) Occurrence, Physiology and Ecology of Sterols, in *Biochemistry of Steroids and Other Isopentenoids* pp. 411–533, University Park Press, Baltimore.
11. Rahier, A., Génot, J.C., Schuber, F., Benveniste, P., and Narula, A.S. (1984) Inhibition of (*S*)-Adenosyl-L-Methionine Sterol-C-24-Methyltransferase by Analogues of a Carbonium Ion High Energy Intermediate—Structure Activity Relationship for C-25 Heteroatoms (N,As,S) Substituted Triterpenoid Derivatives, *J. Biol. Chem. 259*, 15215–15223.
12. Wojciechowski, Z.A., Goad, L.J., and Goodwin, T.W. (1973) *S*-Adenosyl-L-methionine-cycloartenol Methyltransferase Activity in Cell-Free Systems from *Trebouxia* sp. and *Scenedesmus obliquus*, *Biochem. J. 136*, 405–412.
13. Schaller, H., Bouvier-Navé, P., and Benveniste, P. (1998) Overexpression of an *Arabidopsis thaliana* (L.) Heynh. cDNA Encoding a Sterol-C24[1]-methyltransferase in *Nicotiana tabacum* L. Modifies the Ratio of 24-Methyl Cholesterol to Sitosterol and Is Associated with Growth Reduction, *Plant Physiol. 118*, 461–469.
14. Husselstein, T., Schaller, H., Gachotte, D., and Benveniste, P. (1999) Δ7-Sterol-C5-desaturase Molecular Characterization and Functional Expression of Wild Type and Mutant Alleles, *Plant Mol. Biol. 39*, 891–906.
15. Sambrook, J., Fritsch, E.F., and Maniatis, T. (1989) *Molecular Cloning*, 2nd edn., Cold Spring Harbor Laboratory Press, Cold Spring Harbor.
16. Bevan, M. (1984) Binary *Agrobacterium* Vectors for Plant Transformation, *Nucl. Acids Res. 12*, 8711–8721.
17. Horsch, R.B., Fry, J.E., Hoffmann, N.L., Eichholtz, D., Rogers, S.G., and Fraley, R.T. (1985) A Simple and General Method for Transferring Genes into Plants, *Science 227*, 1229–1231.
18. Krysan, P.J., Young, J.C., Tax, F., and Sussman, M.R. (1996) Identification of Transferred DNA Insertions Within *Arabidopsis* Genes Involved in Signal Transduction and Ion Transport, *Proc. Natl. Acad. Sci. USA 93*, 8145–8150.
19. Dellaporta, S.L., Woods, J., and Hicks, J.B. (1983) A Plant DNA Mini Preparation: Version II, *Plant Mol. Biol. Rep. 1*, 19–21.
20. Goodall, G.J., Wiebauer, K., and Filipowicz, W. (1990) Analysis of Pre-mRNA Processing in Transfected Plant Protoplasts, *Methods Enzymol. 88*, 148–161.
21. Rahier, A., and Benveniste, P. (1989) Mass Spectral Identification of Phytosterols, in *Analysis of Sterols and Other Biologically Significant Steroids* (Nes, W.D., and Parish, E.J., eds.), pp. 223–250, Academic Press, San Diego.
22. Guo, D.A., Venkatramesh, M., and Nes, D.W. (1995) Developmental Regulation of Sterol Biosynthesis in *Zea mays*, *Lipids 30*, 203–219.
23. Gaber, R.F., Copple, D.M., Kennedy, B.K., Vidal, M., and Bard, M. (1989) The Yeast Gene *ERG 6* Is Required for Normal Membrane Functions but Is Not Essential for Biosynthesis of the Cell-Cycle-Sparking Sterol, *Mol. Cell. Biol. 9*, 3447–3456.
24. Hardwick, K.G., and Pelham, H.R.B. (1994) *SED6* Is Identical to *ERG6* and Encodes a Putative Methyl Transferase Required for Ergosterol Biosynthesis, *Yeast 10*, 265–269.
25. Venkatramesh, M., Guo, D.A., Harman, J.G., and Nes, W.D. (1996) Sterol Specificity of the *Saccharomyces cerevisiae ERG6* Gene Product Expressed in *Escherichia coli*, *Lipids 31*, 373–377.
26. Depicker, A., and Van Montagu, M. (1997) Post-Transcriptional Gene Silencing in Plants, *Curr. Opin. Cell Biol. 9*, 373–382.
27. Stam, M., Mol, J.N.M., and Kooter, J.M. (1997) The Silence of Genes in Transgenic Plants, *Ann. Bot. 79*, 3–12.
28. Grünwald, C. (1975) Plant Sterols, *Annu. Rev. Plant Physiol. 26*, 209–236.
29. Maillot-Vernier, P., Schaller, H., Benveniste, P., and Belliard, G. (1989) Biochemical Characterization of Sterol Mutant Plant Regenerated from a Tobacco Callus Resistant to a Triazole Cytochrome P-450-Obtusifoliol-14-demethylase Inhibitor, *Biochem. Biophys. Res. Commun. 165*, 125–130.
30. Schaller, H., Grausem, B., Benveniste, P., Chye, M.L., Tan, C.T., Song, Y.H., and Chua, N.H. (1995) Expression of the *Hevea brasiliensis* (H.B.K.) Müll. Arg. 3-Hydroxy-3-methylglutaryl-Coenzyme A Reductase 1 in Tobacco Results in Sterol Overproduction, *Plant Physiol. 109*, 761–770.

[Received July 6, 1999; accepted January 19, 2000]

Design and Synthesis of New Steroidal Inhibitors of Estrogen Synthase (aromatase)

Edward J. Parish*, Shengrong Li, and Zhigang Rao

Department of Chemistry, Auburn University, Alabama 36849-5312

ABSTRACT: The estrogen synthase (aromatase) enzyme system is responsible for the biosynthesis of estrogen hormones in human females. Estrogens are vital for normal growth and development, but will promote the growth of certain breast cancers. Approximately 30–50% of breast cancers are considered to be hormone-dependent. Consequently regulation of estrogen biosynthesis has advanced as a potential therapeutic strategy. This has led to the development of active-site inhibitors, which may have potential for the control of breast cancer. We have recently prepared a number of new steroidal inhibitors that have been evaluated as aromatase inhibitors. These include steroidal A/B-ring isoxazoles and a series of A/B-ring pyrazoles with alkyl- and aryl-substituted nitrogen. In addition, we have developed new chemical procedures for the synthesis of 6β-hydroxy steroids, which could be key intermediates in the preparation of C-19 inhibitors of aromatase activity.

Paper no. L8317 in *Lipids 35,* 271–277 (March 2000).

Aromatase is the enzyme responsible for catalyzing the conversion of androgens to estrogens in the last step of estrogen biosynthesis and is important in estrogen metabolic and reproductive processes. The inhibition of aromatase is an important and specific route for control of estrogen levels and estrogen-dependent diseases (1,2). The estrogen synthase (aromatase) enzyme system is responsible for the biosynthesis of estrogen hormones in women. Estrogens are vital for normal growth and development, but will promote the growth of certain breast cancers. Approximately 30–50% of breast cancers are considered to be hormone-dependent. Consequently, regulation of estrogen biosynthesis has advanced as a potential therapeutic strategy (3,4). This has led to the development of active-site inhibitors that may have potential for the control of breast cancer (5).

The estrogen elements of the biochemical pathway, which utilize aromatase in the biosynthesis of estrogens from androgens, is shown in Scheme 1. Aromatase was first isolated by Ryan in 1959 (6) from the microsomal fraction of fresh human placental tissue. Aromatase is a cytochrome P-450 enzyme. The region of greatest homology among all steroidogenic P-450 enzymes is the heme-binding region (7). The term "aromatase" usually refers either to Thompson's crude, insoluble preparation (8) or to Vickery's solubilized preparation (9) rather than to the unstable, purified enzymes (10). Aromatase is 55 kDa protein of 503 amino acids. An X-ray structure of cytochrome P-450 aromatase is not available due to the difficulty of purification and crystallization of this membrane-bound enzyme. However, modeling studies using a variety of computational programs to predict the three-dimensional structure of aromatase have given us insights into the enzyme structure and its action (11).

Because of the importance of estrogen in mammalian metabolism and reproductive processes, considerable progress has been made in understanding the structure, biochemical mechanism, and inhibition of aromatase. The inhibition of aromatase is a potentially important and specific route to control estrogen levels. Inhibitors of aromatase have found application in such estrogen-related processes as contraception, maintenance of pregnancy, and treating gynecomatsia, endometriosis, and estrogen-dependent breast cancer (12–15).

The biochemical mechanism of aromatase has been studied extensively, and considerable progress has been made in understanding the important reactions (Scheme 1) catalyzed by this enzyme. Aromatase converts androgens to estrogens by oxidizing the C-19 methyl group and aromatizing the steroid A-ring. It has been shown that three molecular oxygens and six reducing equivalents from NADH are consumed during estrogen formation. The mechanisms involved in this enzymatic process have recently been extensively reviewed (4,5).

AROMATASE INHIBITION

Steroidal aromatase inhibitors have been studied extensively. A variety of substrate analogs with other functional groups on C-19, C-1, C-2, C-4 and C-6 has been synthesized and shown to be good inhibitors of aromatase (16). Mechanistically, steroidal inhibitors can be classified as competitive and noncompetitive. Almost all of the noncompetitive inhibitors are mechanism-based inhibitors. Modification of the A-ring of the androstenedione molecule initially focused on substituents at C4. The steroids 4-hydroxy-4-androstene-3,17-dione (4-OHA) and 4-acetoxy-4-androstene-3,17-dione are

*To whom correspondence should be addressed.
E-mail: parisej@mail.auburn.edu

Abbreviations: Enz, enzyme; IC_{50}, concentration producing 50% inhibition; 4-OHA, 4-hydroxy-4-androstene-3,17-dione.

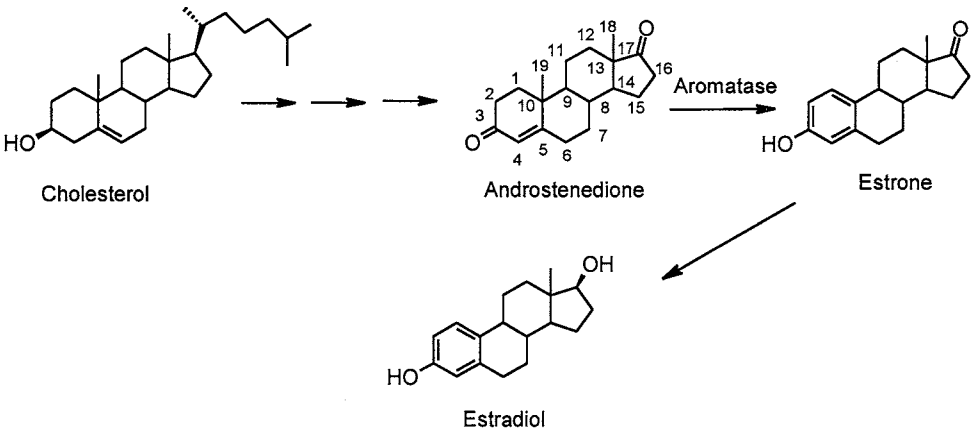

SCHEME 1

effective inhibitors *in vitro* with reported K_i values of 2 and 10 μM, respectively, and they produce enzyme-mediated inactivation (17,18). The mechanism possibly involves catalytic substrate conversion to a reactive intermediate, which then causes active-site inactivation. Covey and Hood (19) invoked enzyme-assisted addition–elimination at C-4 to explain the irreversible inhibition caused by 4-OHA and other 4-substituted androstenediones (Scheme 2). Lombardi (20) and collaborators have synthesized 4-aminoandrogens that are also mechanism-based irreversible inhibitors. Further modifications with extended conjugation through $\Delta^{1,4}$ or $\Delta^{4,6}$ double bonds enhance the inhibitory activity. In general, the spatial requirements of the A-ring for binding of the steroidal inhibitors to aromatase are rather restrictive and permit few structural modifications to be made. Incorporation of the polar hydroxy group at C-4 enhances inhibitory activity.

Effective aromatase inhibitors derived from B-ring modification are mainly C-6- and C-7α-substituted derivatives of 4-androstenedione. The 6-ketoxime derivatives of 4-androstenediones are potent aromatase inhibitors (21). Although the 6-keto derivative is one of the most common clinical inhibitors in use, it exhibits relatively poor affinity (19). Proposed mechanisms of inhibition have invoked delocalization of the charge toward the C-6 instead of the C-4 position. The nucleophile addition–elimination mechanism would explain the inhibition by androgens that bear leaving groups on C-6 (Scheme 3). Derivatives with 6-fluoro, chloro, hydroxy, or acetoxy groups showed good activity in the inhibition of human placental aromatase *in vitro* (22,23). In these proposed mechanisms, the nucleophile (Enz-X) shown in Schemes 2 and 3 is from the sulfhydryl group on the amino acid cysteine found in the active site of the enzyme (5,24,25).

Substituents at the C-7α position of the B-ring have provided a number of potent aromatase inhibitors (26,27). Brueggemeir has prepared a wide variety of these and has discovered the presence of a hydrophobic pocket at C-7α that is able to bond covalently to selective steroidal derivatives that are able to correctly extend into this lipophilic region of aromatase.

Combined with the results of site-directed mutagenesis studies and the structures of substrates and inhibitors, a number of attempts have been made to predict the structure of this

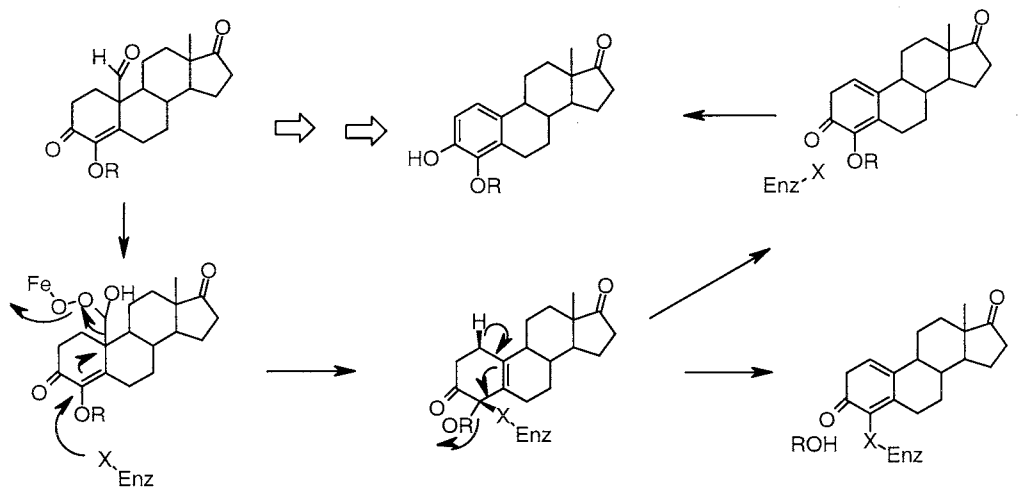

SCHEME 2

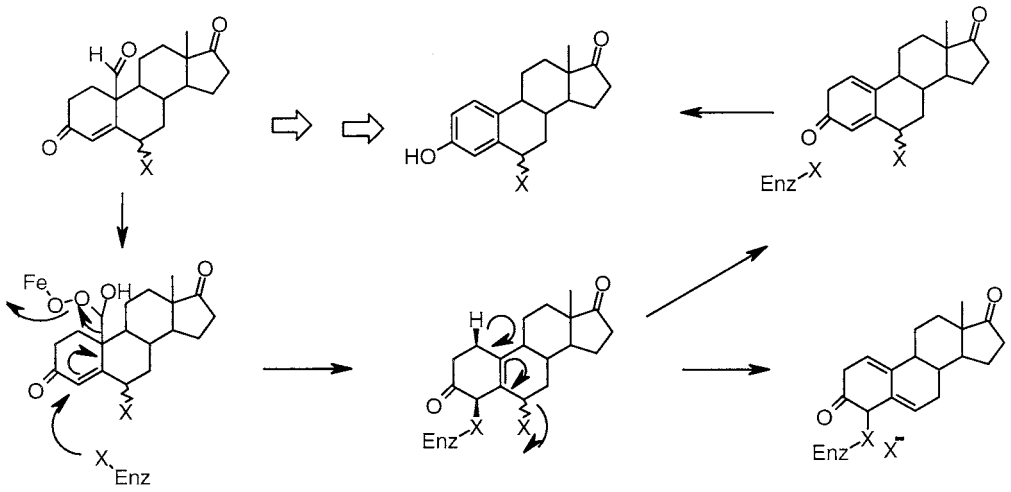

SCHEME 3

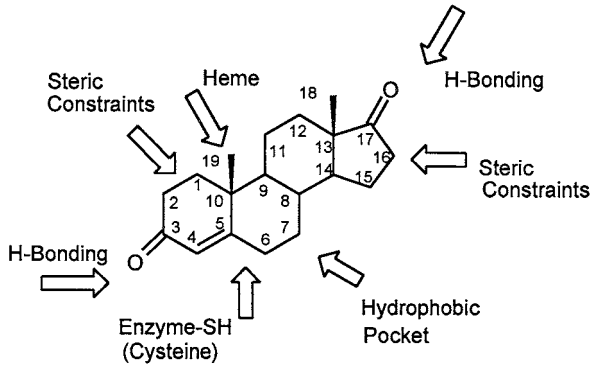

SCHEME 4

enzyme by a variety of computational programs (5). These predictions fit quite well with the required elements of the active-site structure of aromatase as deduced from the experimental data on substrates and inhibitors (Scheme 4).

NEW STEROIDAL INHIBITORS

Since the discovery that 4-OHA (**1**) is an effective aromatase inhibitor (17), many 4-substituted 4-OHA analogs have been synthesized and tested as aromatase inhibitors (18,20,28,29) (Scheme 5). Very recently, Di Salle *et al*. (30) reported that androst-3,17-dione-4-eno[4,5,6,*b*,*c*]pyrole (**3**) was effective as an aromatase inhibitor. The prevailing explanation for the inhibitory activity of these types of compounds is that the nearby nucleophile attacks at the C-4 position, and the following elimination of a C-4 leaving group results in permanent binding of the inhibitor to the enzyme (26). This hypothesis is based on the assumption that these inhibitors take the same orientation as the substrate in the active site of the enzyme. In addition, 6-hydroxyiminoandrost-4-en-3,17-dione (**2**) has shown a high affinity for human placental aromatase and functions as a competitive inhibitor of the enzyme (31). To take advantage of these structural features (Scheme 5), we

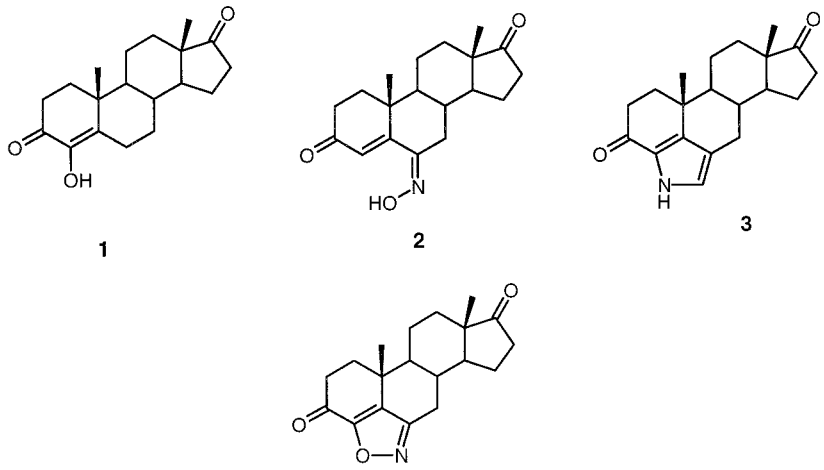

1 **2** **3** **4**

SCHEME 5

have recently prepared androst-3,17-dione-4-eno[6,5,4-*c,d*] isoxazole (**4**) and found it to be an effective inhibitor against aromatase (32).

The chemical synthesis of **4** and its companion A/B-ring isoxazoles **5** and **6** is outlined in Scheme 6. We have prepared these products using two independent approaches utilizing 3β,17β-diacetoxyandrost-4-en-6-one as a starting material (32). Aromatase assays were performed using established procedures (32) and the following concentrations producing 50% inhibition (IC_{50}) were obtained: **4**, 1.889 μM; **5**, 120.5 μM; **6**,18.57 μM. The structural requirements of C-19 steroids needed for a favorable interaction with the enzymatic site of aromatase have been determined (29). These include ketone functionality at C-3 and a 17-keto or 17β-hydroxyl substituent. Also, steroids with a linear configuration (e.g., 4-en-3-one) in the A and B ring are known to be effective inhibitors. The isoxazoles **7** and **9** exhibited the most potent inhibition and possessed structural features that were most consistent with those described for previous effective inhibitors. The model steroids **1** and **2** (Scheme 5) have been shown to possess greater inhibitory activity than the described isoxazoles **4** and **6**. However, this is the first report describing the inhibition of aromatase activity by steroidal A/B-ring isoxazoles.

In related studies, we have completed the chemical synthesis of a series of H-aryl androsterone pyrazoles (Scheme 7) (33). Using the steroidal pyrole **3** (Scheme 5) and the isoxazoles **4,5**, and **6** (Scheme 6) as structural models, we have completed the chemical synthesis of the androsterone pyrazole **7** and its N-substituted derivatives **8–13** (Scheme 7; MCPBA, *m*-chloroperoxy-benzoic acid). If these inhibitors take the same orientation as the substrate in the enzymatic site, the aryl groups on the C-6 nitrogen could project to the 7α-hydrophobic pocket and increase the affinity according to the molecular modeling observations (27). The comparison of the low-energy conformers, generated using the SPARTAN molecular modeling program using the MM2 (molecular mechanics 2) force field, of *N*-benzylandrost-3,17-dion-5-eno[4,5,6-*c,d*]1H-pyrazole **12** and 7α-(phenylthio)androst-4-ene-3,17-dione (a well-known inhibitor) indicated the phenyl groups on these two molecules could be partially overlapped (33). However, the increased inhibitory activity was not observed for these N-substituted compounds in comparison with

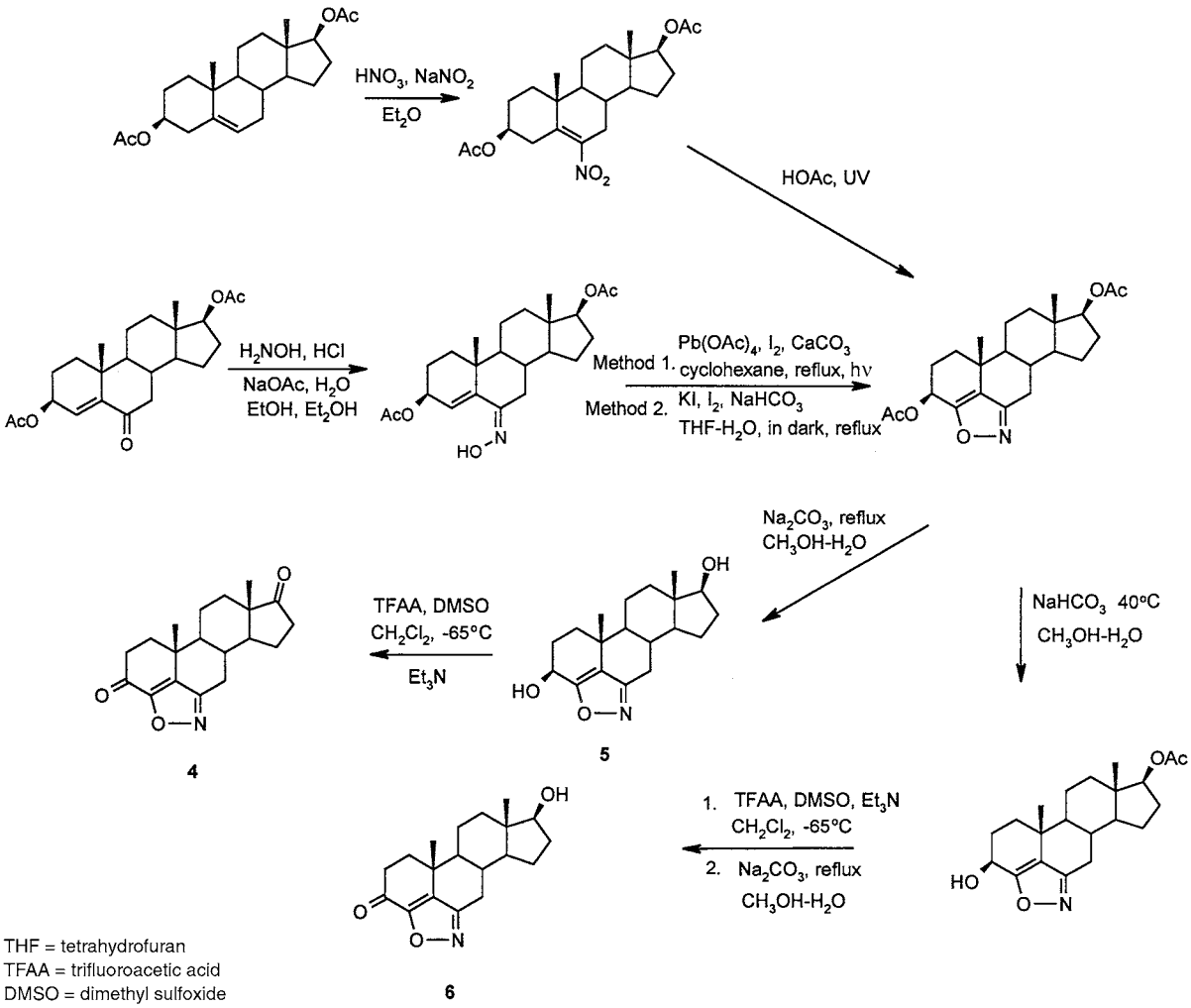

THF = tetrahydrofuran
TFAA = trifluoroacetic acid
DMSO = dimethyl sulfoxide

SCHEME 6

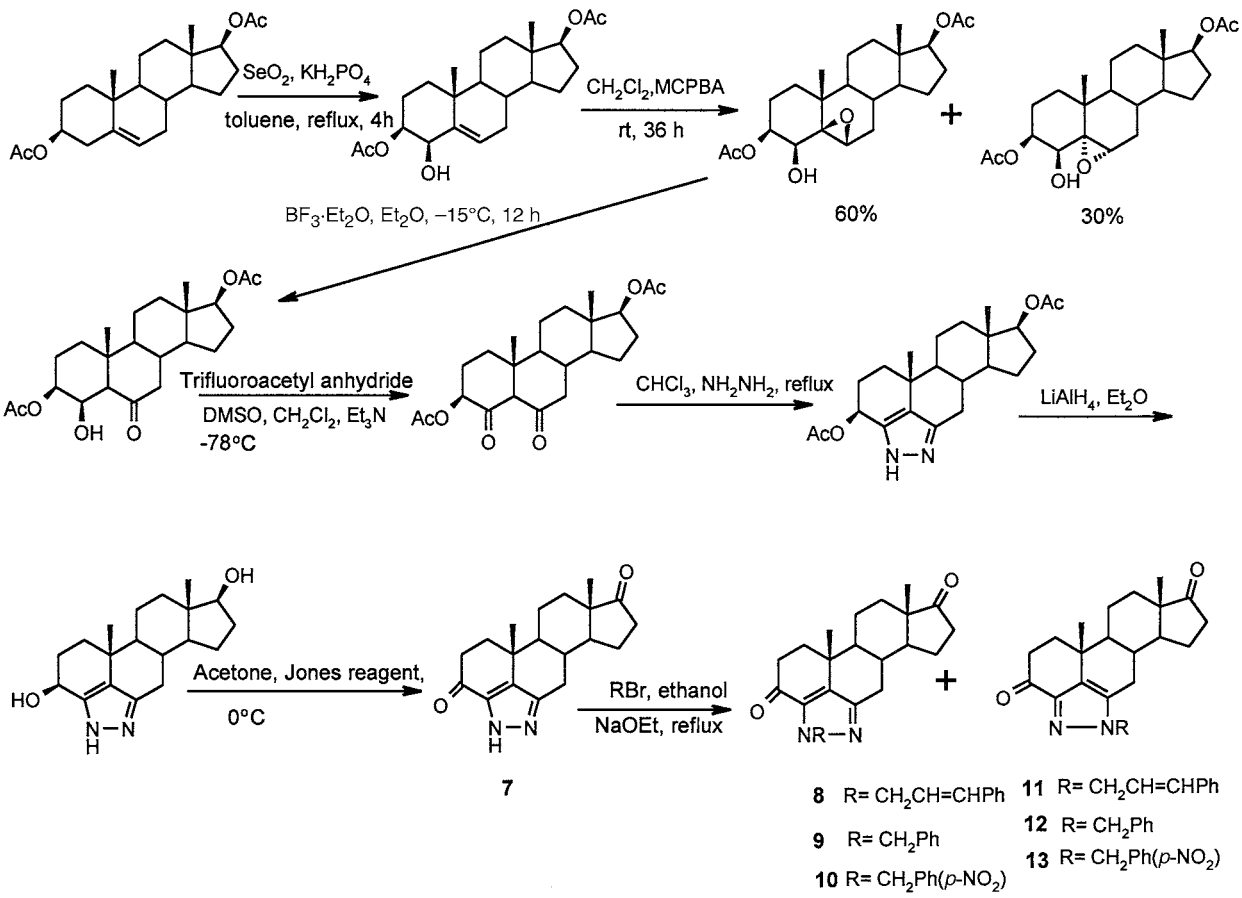

SCHEME 7

the unsubstituted parent compound androst-3,17-dione-5-eno[4,5,6-*c*,*d*]1H-pyrazole **7**. The results imply these inhibitors may not take the same orientation as the substrate in the enzyme active site. The C-4 heteroatom could orient toward the heme in the enzyme active site, which could result from the molecular rotation around an axis from C-3 to C-17, and therefore act as heme binders (Scheme 4).

The following are inhibitory results (IC_{50}, μM) obtained using human placental aromatase for compounds **7–13**: **7**, 0.236; **8**, 0.900; **9**, 0.342; **10**, 0.658; **11**, 0.950; **12**, 0.245; **13**, 0.490. The clinically used drug 4-OHA was tested in the same system for comparison. Androst-3,17-dione-4-eno[6,5,4-*c*,*d*]1H-pyrazole (**7**) and its *N*-benzyl derivatives (**9** and **12**) display relatively good inhibitory activity and appear to be about equiactive as 4-OHA. Interestingly, substitution of a 4′-nitro group in these compounds as in **10** and **13** appears to double the IC_{50} values (or decrease inhibitory activity by about 50%), suggesting that this substitution is detrimental toward activity. Replacing the *N*-benzyl substituents with a 3-phenylallyl moiety as in **8** and **11** appears to result in a further decrease in inhibitory activity.

In companion studies, we have made significant progress toward the synthesis of aromatase inhibitors at C-19 (the angular methyl group attached to C-10). Derivatives with heteroatoms at C-19 are obvious substrate analogs of aromatase, and many of them compete for the enzyme active site (Scheme 4). The heteroatom at C-19 could coordinate to the heme iron as the sixth ligand and compete with oxygen binding. Several of these types of inhibitors are modified as mechanism-based inhibitors, presumably undergoing enzyme-mediated oxidation at the C-19 carbon to form the alkylating group and in the process become potent enzyme-activated inhibitors of aromatase (4,5).

6β-Hydroxy steroids are key intermediates for the functionalization of the C-19 methyl group (34). Functionalization and subsequent modification at C-19 have previously yielded a large number and variety of potent inhibitors of aromatase (35,36). With these facts in mind, we have worked to develop a new and streamlined chemical synthesis of 6β-hydroxy steroids that could be easily converted to a C-19 functionalized derivative containing keto groups at C-3 and C-17. This type of intermediate can be prepared by "classical" synthesis using well-established chemical techniques (37,38). Unfortunately, this method requires a number of synthetic steps and is time-consuming (Scheme 8). The synthesis of the key intermediate **14** may be shortened by the use of our novel procedure to prepare the 6β-hydroxy intermediate **15** (Scheme 9) (38).

The intermediate **15** (Scheme 9; NBA, *N*-bromoacetamide) was prepared from a Δ^5-3β-hydroxy sterol using a mix-

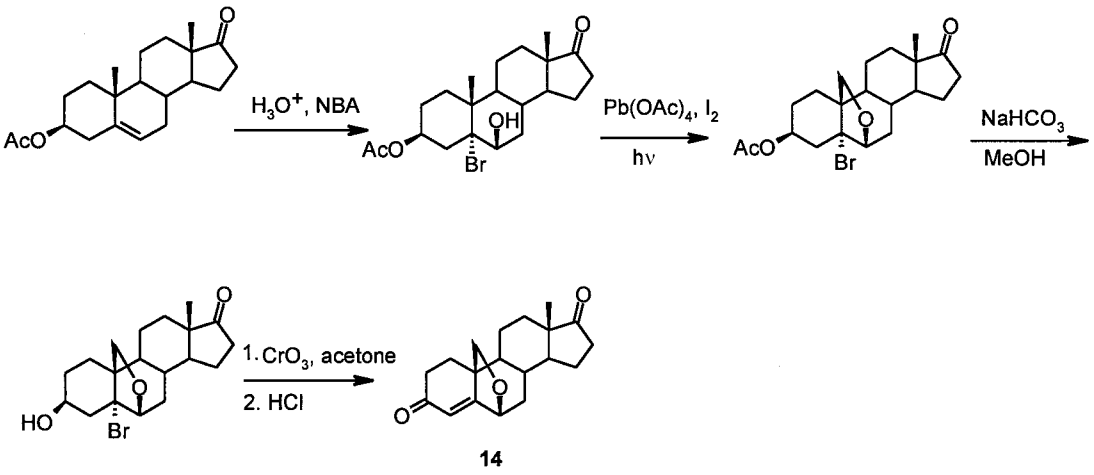

14

SCHEME 8

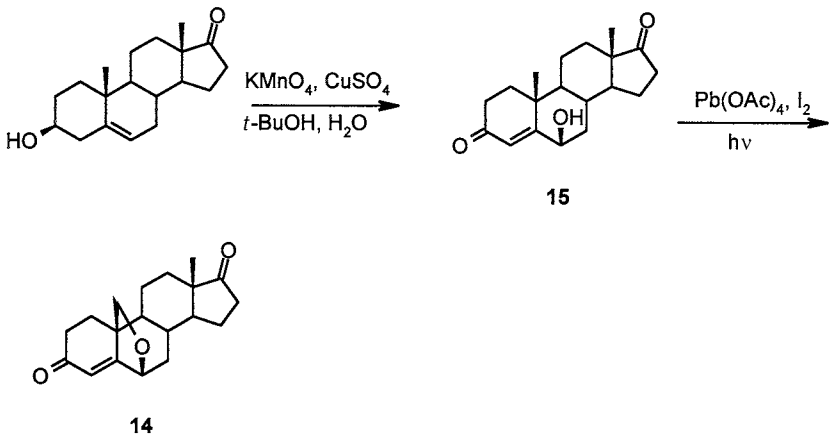

15

14

SCHEME 9

ture of $KMnO_4$, $CuSO_4$, *t*-butanol, and water in methylene chloride, an oxidizing system previously used to prepare steroidal β-epoxides in high yields (39,40). This oxidizing reagent system serves as a phase-transfer catalyst and is believed to function in the omega phase, which is formed by water and *tert*-butyl alcohol over the surface of the inorganic salt, in the epoxidation with $KMnO_4$–$CuSO_4$ in methylene chloride and in the presence of water and *tert*-butyl alcohol (39,40). In contrast to these results, more hydrophilic substrates produced α-diketones as a predominant product (38). To further explore this permanganate reagent system, we studied its reaction with Δ^5-3β-hydroxy sterol substrates and found that sterols with hydrophobic side chains (e.g., cholesterol) gave 5β,6β-epoxy sterols in high yields. Identical sterols containing polar or hydrophilic side chains gave 3-keto-Δ^4-6β-hydroxy products (38).

These results may suggest that the face selectivity of this oxidizing reagent system results from the initial copper ion (or other metal ions) coordination on the less hindered α-face of the double bond forming a π-complex between the double bond and copper ion or other metal ions. The following permanganate attack on the β-face results in the β-epoxide. The formation of a π-complex also weakens the double bond and makes the permanganate attack possible. Apparently, the main group metal ions and metal ions with coordinate anions cannot form a π-complex with the double bond, so the reaction will not proceed. Mechanistically, further rearrangement may occur *via* the concomitant β-epoxidation of the Δ^5 double bond and oxidation of the 3-hydroxy group, followed by epoxide ring opening and proton elimination at C-4 to yield the Δ^4-unsaturated ketone (38).

In conclusion, we feel the results presented herein provide useful information on the structure–activity relationships of steroidal substrates and their orientation into the active site of aromatase. In addition, we have explored new chemical techniques that we believe will be useful to other investigators studying steroidal inhibitors of aromatase and will be of general interest to scientists in the steroid field.

REFERENCES

1. Brodie, A.H.M. (1994) Aromatase Inhibitors in the Treatment of Breast Cancer, *J. Steroid Biochem. Molec. Biol. 49*, 281–287.
2. Schwarzel, W.C., Kruggel, W.G., and Brodie, H.J. (1973) Studies on the Mechanism of Estrogen Biosynthesis. VIII. The De-

velopment of Inhibitors of the Enzyme System in Human Placenta, *Endocrinology 92*, 866,873.
3. Insker, S., Yue, W., and Brodie, A.H.M. (1995), Studies on the Mechanism of Estrogen Biosynthesis, *J. Clin. Endocrinol. Metab. 80*, 1941–1949.
4. Johnston, J.O. (1997), Aromatase Inhibitors, in *Biochemistry and Function of Sterols* (Parish, E.J., and Nes, W.D., eds.), pp. 23–54, CRC Press, Boca Raton.
5. Li, S., and Parish, E.J. (1996) Design and Action of Steroidal Aromatase Inhibitors, *J. Am. Oil Chem. Soc. 73*, 1435–1451.
6. Ryan, K.J.J. (1959) Biological Aromatization of Steroids, *J. Biol. Chem. 234*, 268–272.
7. Corbin, C.J., Graham-Lorene, S., McPhaul, M., Mason, J.I., Mendelson, C.R., and Simpson, E.R. (1988) Isolation of a Full-Length cDNA Insert Encoding Human Aromatase System Cytochrome P-450 and Its Expression in Nonsteroidogenic Cells, *Proc. Natl. Acad. Sci. USA 85*, 8948–8953.
8. Thompson, E.A., and Siiteri, P.K. (1974) The Involvement of Human Placental Microsomal Cytochrome P-450 in Aromatization, *J. Biol. Chem. 249*, 5373–5382.
9. Kellis, J.T., and L.E. Vickery (1987) Purification and Characterization of Human Placental Aromatase Cytochrome P-450, *J. Biol. Chem. 262*, 4413–4420.
10. Osawa, Y., and Higanshiyama, T. (1980) Isolation of Human Placental Aromatase Cytochrome P-450 and Its Mechanism of Action of Androgen Aromatization in Microsomes, in *Drug Oxidation* (Estabrook, R.W.J., ed.), Vol. 1, pp. 115–248, Academic Press, Orlando.
11. Simpson, E.R., and Hendelson, C.R. (1993) Tissue-Specific Promotors Regulate Aromatase Cytochrome P-450 Expression, *J. Steroid Biochem. Mol. Biol. 44*, 4–6.
12. Koymans, L.M.H., Moereels, H., and Bossche, H.V.J. (1995) A Molecular Model for the Interaction Between Vorozole and Other Nonsteroidal Inhibitors and Human Cytochrome P-450 (P-450 aromatase), *J. Steroid Biochem. Mol. Biol. 53*, 191–197.
13. Brodie, A.M.H. (1983) Overview of Recent Development of Aromatase Inhibitors, *Cancer Res. (Suppl.) 42*, 3312s–3319s.
14. Brodie, A.M.H., Wing, L.Y., Goss, P., Dowsett, M., and Coombes, R.C. (1982) Aromatase Inhibitors and Their Potential Clinical Significance, *J. Steroid Biochem. 25*, 859–865.
15. Kuhnel.R., Delemarre, J.F.M., Rao, B.R., and Strolk, J.G. (1986) Correlation of Aromatase Activity and Steroid Receptors in Human Ovarian Carcinoma, *Anticancer Res. 6*, 889–892.
16. Santen, R.J. (1987) Potential Clinical Role of New Aromatase Inhibitors, *Steroids 50*, 1–65.
17. Marsh, D.A., Brodie, H.J., Garrett, W., Tsai-Morris, C.H., and Brodie, A.M.H. (1985) Aromatase Inhibitors—Synthesis and Biological Activity of Androsenedione Derivatives, *J. Med. Chem. 28*, 788–796.
18. Brodie, A.M.H., Garrett, N., and Hendrickson, J.R. (1981) Inactivation of Aromatase *in vitro*, *Steroids 38*, 693–897.
19. Covey, D.F., and Hood, W.F. (1981) Enzyme-Generated Intermediates Derived from 4-Androstene-3,6,17-trione and 1,4,6-Androstatriene-3,17-dione Cause a Time-Dependent Decrease in Human Placental Aromatase Activity, *Endocrinology 108*, 1597–1599.
20. Lombardi, P. (1986) Recent Studies on the Inhibition of Aromatase Using Steroidal Substrates, in *Proceedings of the Seventh Conference on Hormonal Steroids*, Barcelona, Spain, pp. 36–37, Plenum Press, New York.
21. Holland, H.L., Kumaresan, S., Tan, L., and Njar, V.C.O. (1992) Synthesis of 6-Hydroxyimino-3-oxo Steroids, a New Class of Aromatase Inhibitor, *J. Chem. Soc. Perkin Trans. 1*, 585–592.
22. Numazawa, N., Tsuji, M., and Osawa, Y. (1986) Synthesis and Evaluation of Bromo-acetoxy 4-Androsten-3-ones as Active Site-Directed Inhibitors of Human Placental Aromatase, *Steroids 48*, 347–359.
23. Mann, J., and Pietrzak, B. (1983) The Synthesis of 4-Hydroxyandrost-ene-3,17-dione and Other Aromatase Inhibitors, *J. Chem. Soc. Perkin Trans. 1*, 2681–2690.
24. Numazawa, M., Mutsumi, A., and Tachibana, M. (1996) Mechanism for Aromatase Inactivation by a Suicide Substrate, Androst-4-ene-3,6,17-trione, *Biochem. Pharmacol. 52*, 1253–1259.
25. Numazawa, M., Tsuji, M., and Osada, R. (1986) Studies Directed Toward a Mechanistic Evaluation of Aromatase Inhibition with Androst-4-ene-3,6,17-trione: Its Reactions with Thiols, *J. Chem. Res. (Synop.)*, 54–55, *(Miniprint)* 718–726.
26. Brueggemeier, R.W., and Li, P.K. (1993) Steroidal Inhibitors as Chemical Probes of the Active Site of Aromatase, *J. Steroid Biochem. Mol. Biol. 44*, 357–365.
27. Bruggemeier, R.W. (1995) New Inhibitiors of Aromatase, *J. Med. Chem. 38*, 378–384.
28. Abuj-Haij, Y.J. (1986) Synthesis and Evaluation of 4-(substituted thio)-4-Androstene-3,17-dione Derivatives as Potential Aromatase Inhibitors, *J. Med. Chem. 29*, 582–584.
29. Brueggemeier, R.W. (1990) Biochemical and Molecular Aspects of Aromatase, *J. Enzyme Inhib. 4*, 101–111.
30. Di Salle, E., Briatico, G., Giudici, D., Ornati, G., Zaccheo, T., Buzzeti, F., Nesi, M., and Panzeri, A. (1994) Novel Aromatase and 5α-Reductase Inhibitors, *J. Steroid Biochem. Mol. Biol. 49*, 289–294.
31. Holland, H. L., Kumunesan, S., Tank, K.L., and Njar, V.C.O. (1992) Synthesis of 6-Hydroxyimino-3-oxo. Steroids. A New Class of Aromatase Inhibitor, *J. Chem. Soc. Perkin Trans. 1*, 585–592.
32. Li, S., Parish, E.J., Valenzuela, C.R., and Brodie, A.M.H. (1998) Synthesis of New Steroidal Isoxazoles: Inhibitors of Estrogen Synthase, *Bioorganic Med. Chem. 6*, 1525–1529.
33. Li, S., Parish, E.J., Webb, T., and Brodie, A.M.H. (1997) The Synthesis of *N*-Aryl Androsterone Pyrazoles as Aromatase Inhibitiors, *Bioorg. Med. Chem. Lett. 7*, 403–408.
34. Fried, D.J., and Edward, J.A. (1972) *Organic Reactions in Steroid Chemistry*, Vol. 2, pp. 1–42, 237–287, Van Nostrand Reinhold, New York.
35. Wright, J.H., Van Leersum, P.T., Chamberlin, S.G., and Akhtar, M. (1989) Inhibition of Aromatase by Steroids Substituted at C-19 with Halogen Sulfur and Nitrogen, *J. Chem. Soc. Perkin I*, 1647.
36. Burkhart, J.D., Norton, P.P., Wright, C.L., and Johnston, J.D. (1991) New C-19 Inhibitors of Aromatase, *J. Med. Chem. 34*, 1748–1754.
37. Kalvoda, J., Hausler, K., Ueberwesser, H., Anner, G., and Wettstein, A. (1963) The Synthesis of C-19 Functionalized Steroids, *Helv. Chim. Acta 48*, 1361–1369.
38. Parish, E.J., and Li, S. (1996) A One-Step Synthesis of 6β-Hydroxy-Δ^4-3-ketones. Novel Oxidation of Homoallylic Alcohols with Permanganate Ion, *J. Org. Chem. 61*, 5665–5666.
39. Parish, E.J., and Li, S. (1996) The Study of Epoxidation of Steroidal Alkenes with Potassium Permanganate-Inorganic Salts, *J. Chem. Res. (Synop.)*, 288–289.
40. Parish, E.J., Li, H., and Li, S. (1995) Facile β-Epoxidation of Unsaturated Steroids with Permanganate Ion, *Synth. Commun. 25*, 927–940.

[Received july 26, 1999; and in revised form and accepted February 8, 2000]

Biosynthesis of Sterols and Ecdysteroids in *Ajuga* Hairy Roots

Yoshinori Fujimoto[a,*], Kiyoshi Ohyama[a], Keiko Nomura[a], Ryo Hyodo[a], Kyoko Takahashi[b], Junko Yamada[b], and Masuo Morisaki[b]

[a]Department of Chemistry and Materials Science, Tokyo Institute of Technology, Tokyo 152-8551, Japan, and [b]Kyoritsu College of Pharmacy, Shibakoen, Tokyo 105-8512, Japan

ABSTRACT: Hairy roots of *Ajuga reptans* var. *atropurpurea* produce clerosterol, 22-dehydroclerosterol, and cholesterol as sterol constituents, and 20-hydroxyecdysone, cyasterone, isocyasterone, and 29-norcyasterone as ecdysteroid constituents. To better understand the biosynthesis of these steroidal compounds, we carried out feeding studies of variously ^{2}H- and ^{13}C-labeled sterol substrates with *Ajuga* hairy roots. In this article, we review our studies in this field. Feeding of labeled desmosterols, 24-methylenecholesterol, and $^{13}C_2$-acetate established the mechanism of the biosynthesis of the two C_{29}-sterols and a newly accumulated codisterol, including the metabolic correlation of C-26 and C-27 methyl groups. In *Ajuga* hairy roots, 3α-, 4α-, and 4β-hydrogens of cholesterol were all retained at their original positions after conversion into 20-hydroxyecdysone, in contrast to the observations in a fern and an insect. Furthermore, the origin of 5β-H of 20-hydroxyecdysone was found to be C-6 hydrogen of cholesterol exclusively, which is inconsistent with the results in the fern and the insect. These data strongly support the intermediacy of 7-dehydrocholesterol 5α,6α-epoxide. Moreover, 7-dehydrocholesterol, 3β-hydroxy-5β-cholest-7-en-6-one (5β-ketol), and 3β,14α-dihydroxy-5β-cholest-7-en-6-one (5β-ketodiol) were converted into 20-hydroxyecdysone. Thus, the pathway cholesterol → 7-dehydrocholesterol → 7-dehydrocholesterol 5α,6α-epoxide → 5β-ketol → 5β-ketodiol is proposed for the early stages of 20-hydroxyecdysone biosynthesis. 3β-Hydroxy-5β-cholestan-6-one was also incorporated into 20-hydroxyecdysone, suggesting that the introduction of a 7-ene function is not necessarily next to cholesterol. C-25 Hydroxylation during 20-hydroxyecdysone biosynthesis was found to proceed with *ca*. 70% retention and 30% inversion. Finally, clerosterol was shown to be a precursor of cyasterone and isocyasterone.

Paper no. L8274 in *Lipids 35,* 279–288 (March 2000).

20-Hydroxyecdysone is a molting hormone of most arthropods. The structure of the steroidal hormone is characterized by polyhydroxyl groups, a 7-en-6-one conjugated system, and a *cis*-A/B-ring junction. It is well documented that cholesterol serves as a biosynthetic precursor of the hormone in insects. Studies on the biosynthetic pathway of 20-hydroxyecdysone from cholesterol, exclusively carried out in insect species, are summarized in Scheme 1. 7-Dehydrocholesterol and 3β,14α-dihydroxy-5β-cholest-7-en-6-one (5β-ketodiol) are generally accepted intermediates. However, the mechanism of the early stages in 20-hydroxyecdysone biosynthesis (i.e., the mechanism of the formation of the 5β-H-7-en-6-one structure) remains uncertain (1–3).

20-Hydroxyecdysone and related steroids also are distributed in the plant kingdom (4,5), and they are designated as phytoecdysteroids. Cholesterol also is converted to 20-hydroxyecdysone in plants (6–10), but biosynthetic studies focusing on the chemical structures of intermediates have been limited in plants (11,12).

Ajuga (Labiatae) is a plant genus well known for its ecdysteroids. More than 150 varieties and subspecies of *Ajuga* plants are distributed over the world (13). These are especially abundant in China, Korea, and Japan and also are widespread in Europe. They have been used in folk medicine in various cultures; in China some *Ajuga* plants have been used to treat inflammation (14). Ecdysteroid constituents of a dozen of *Ajuga* plants are summarized in a review (15), and 20-hydroxyecdysone and cyasterone are phytoecdysteroids typical of these species. It is reported that *A. reptans* var. *atropurpurea* contains 20-hydroxyecdysone, cyasterone, 29-norcyasterone, and isocyasterone (16) (Scheme 2).

A decade ago, researchers of Daicel Chemical Industry Co. Ltd. developed clones of *A. reptans* var. *atropurpurea* hairy roots by infecting *Agrobacterium rhizogenes*, and this transformant reportedly contains ecdysteroids at levels several times higher than the original roots (16). We anticipated that the hairy roots would be appropriate for biosynthetic studies of ecdysteroids. In fact, our preliminary feeding studies of [1-^{13}C]acetate and [26,27 $^{13}C_2$]cholesterol resulted in successful incorporation; feeding of the ^{13}C-cholesterol (100 mg) to a liquid medium (1,000 mL distributed in four flasks, each containing cultures arising from *ca*. 1 g of fresh hairy roots) yielded *ca*. 5 mg of 20-hydroxyecdysone after a 2-wk incubation (following the 2-wk preincubation prior to the addition of substrate) with *ca*. 0.5% incorporation (17).

Ajuga plants are also unique in their sterol compositions, i.e., Δ^{25}-24β-alkylsterols (18). Analysis of the sterol fraction

*To whom correspondence should be addressed at Department of Chemistry and Materials Science, Tokyo Institute of Technology, O-okayama, Meguro-ku, Tokyo 152-8551, Japan. E-mail: fujimoto@cms.titech.ac.jp

Abbreviations: cDNA, complementary deoxyribonucleic acid; HPLC, high-performance liquid chromatography; NMR, nuclear magnetic resonance; SAM, *S*-adenosyl-L-methionine.

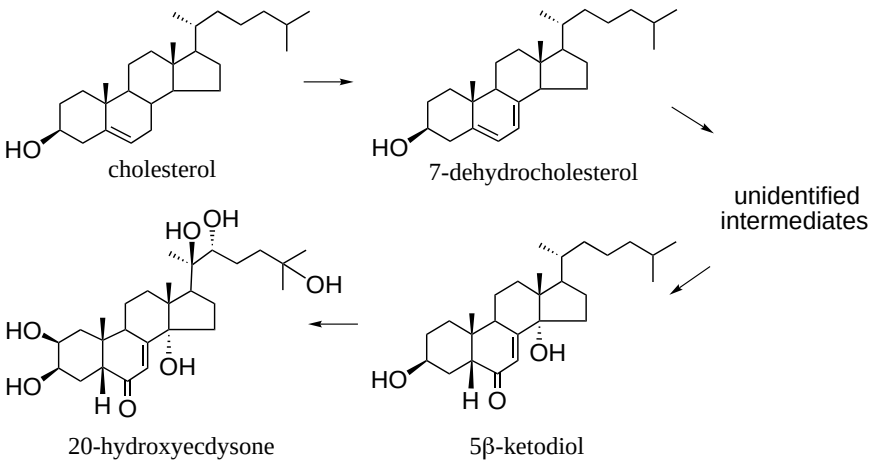

SCHEME 1

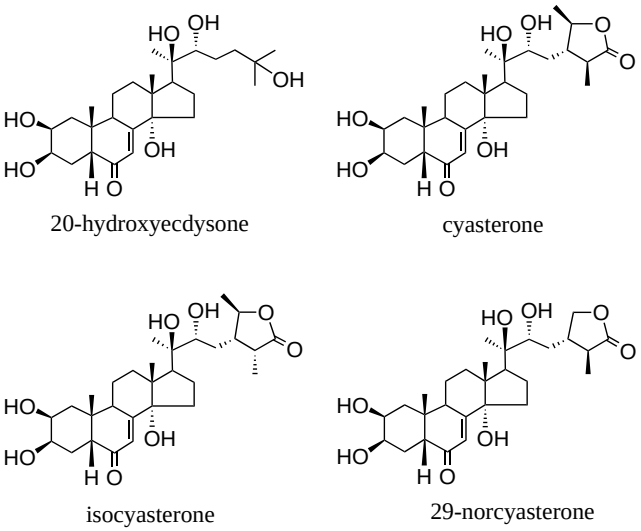

SCHEME 2

from the hairy roots of *A. reptans* var. *atropurpurea* revealed that clerosterol [(24*S*)-stigmasta-5,25-dien-3β-ol] and 22-dehydroclerosterol [(24*S*)-stigmasta-5,22,25-trien-3β-ol] were the two major sterol constituents, accompanied by a lesser amount of cholesterol (19) (Scheme 3). The two C_{29}-sterols are also identified in *A. nipponensis* (Fujimoto, Y., and Nomura, K., unpublished data).

We have undertaken studies of the mechanism of sterol and ecdysteroid biosynthesis with *Ajuga* hairy roots. Information on sterol biosynthesis is a prerequisite for better understanding of ecdysteroid biosynthesis. In this article, we review our work in this area.

STEROL BIOSYNTHESIS

The Δ^{24}-double bond of a steroid side chain, such as cycloartenol, is alkylated to give 24-alkylsterols or reduced to afford cholesterol after a concomitant transformation of steroid nucleus structure. To obtain a general picture on the capacity of alkylative and/or reductive modification of Δ^{24}-double bond in *Ajuga* hairy roots, we first carried out a feeding experiment with [26,27-$^{13}C_2$]desmosterol. ^{13}C nuclear magnetic resonance (NMR) analysis of the biosynthesized sterols, isolated by a reversed-phase high-performance liquid chromatgraphy (HPLC), revealed that desmosterol is efficiently converted into clerosterol. Interestingly, a small amount of ^{13}C-enriched codisterol [(24*S*)-ergosta-5,25-dien-3β-ol], which has not been found in the original hairy roots but can be postulated as a precursor of 29-norcyasterone, was identified. ^{13}C-Desmosterol was also incorporated into cholesterol, but less efficiently than clerosterol and codisterol. Conversion into 22-dehydroclerosterol was negligible (19).

We then fed [28-^{13}C]-24-methylenecholesterol, which was found to be converted into clerosterol and 22-dehydroclerosterol. In addition, a small amount of ^{13}C-labeled campesterol, not present in the original hairy roots, was identified. Moreover, feeding of [24-^{2}H]-desmosterol revealed that the resulting codisterol and clerosterol had deuterium atoms at their C-24 positions, as indicated by ^{2}H NMR spectroscopy (19).

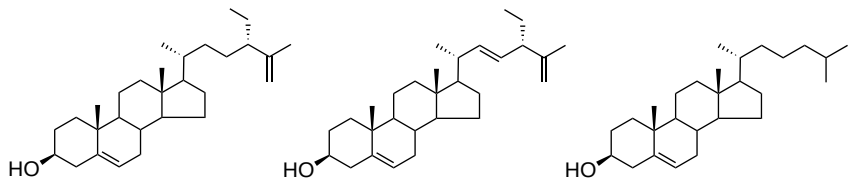

SCHEME 3

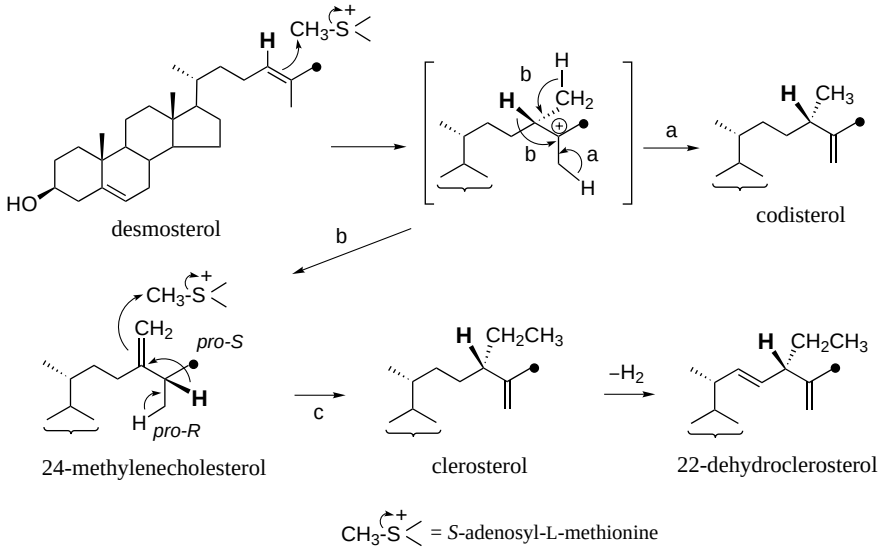

SCHEME 4

Metabolic correlation of C-26 and C-27 groups (Scheme 4; dots refer to a carbon correlated to C-2 of mevalonate) during these transformations was made possible by feeding desmosterol that was specifically ^{13}C-labeled at the isopropylidene (*E*)-methyl group. The resulting codisterol and clerosterol were ^{13}C-labeled at the methyl group, but not methylene, of the isopropenyl terminal (19). The relationships of C-26 and C-27 in these sterols was confirmed by experiments involving feeding [$^{13}C_2$]acetate. An intact ^{13}C-^{13}C bond connectivity was observed clearly between C-25 and exomethylene carbon of clerosterol and dehydroclerosterol, as evidenced by satellite doublet signals in ^{13}C NMR (Fujimoto, Y., and Nakagawa, T., unpublished data). Codisterol was not produced in this feeding condition.

On the basis of the data just described, the mechanism of Δ^{25}-24-alkyl sterol biosynthesis in *Ajuga* hairy roots is proposed as shown in Scheme 4 (19).The C-24 methylated cationic intermediate (in brackets in Scheme 4) generated by transfer of the methyl group of SAM from C-24 *Si*-face would be deprotonated by two pathways. Pathway "a" directly affords codisterol by deprotonation from the methyl group arising from (*Z*)-methyl group of desmosterol, i.e., C-6 of mevalonate. Pathway "b" leads to 24-methylenecholesterol *via* the migration of hydrogen at C-24 to C-25, followed by deprotonation from C-28. The second methylation from SAM at C-28 of $\Delta^{24(28)}$ double bond would produce the C-24 cationic intermediate, which affords clerosterol *via* the migration of hydrogen at C-25 to C-24, followed by deprotonation again from the methyl group arising from C-6 of mevalonate (Pathway "c").

Concerning the biosynthesis of cholesterol, puzzling data were obtained. Cholesterol obtained by feeding $^{13}C_2$-acetate showed satellite doublet signals for C-25 and C-27, whereas the C-26 signal appeared as a singlet, thus indicating that reduction of a Δ^{24}-sterol took place stereospecifically from the 25-*Si* face (20), in accordance with the observations with rats (21,22) and insects (23). In contrast, cholesterol derived from [(*E*)-methyl-^{13}C]desmosterol was enriched with ^{13}C both at *pro-R* (C-26) and *pro-S* (C-27) methyl groups, with the former being predominant. This partial scrambling of ^{13}C was further confirmed by complementary experiments using [(*Z*)-methyl-^{13}C]desmosterol (24). It appears that sterol Δ^{24}-reductase in the hairy roots works less efficiently than methyl transferase on desmosterol, since the conversion of desmosterol into cholesterol is rather poor. Feeding of the [exomethylene carbon-(C-27)-^{13}C]-Δ^{25}-cholesterol afforded cholesterol having ^{13}C label only at the *pro-S*-methyl group, thus establishing that hydrogen at C-25 was introduced stereospecifically from the 25-*Re* face (24). A similar stereospecific reduction of Δ^{25}-cholesterol was also observed with *Oryza sativa* cell cultures (24). On the basis of these findings, a double-bond isomerization pathway depicted in Scheme 5 [the carbons correlated to the (*E*)-methyl of desmosterol are indicated by

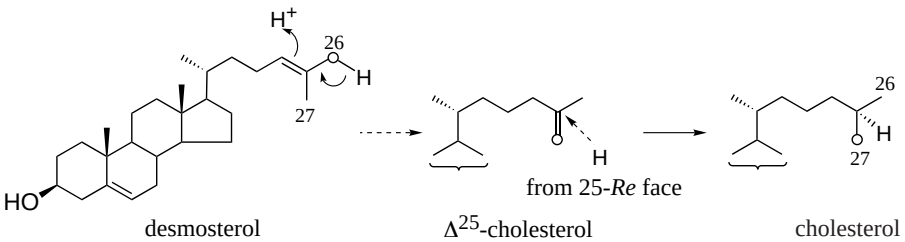

SCHEME 5

○], in addition to a straightforward reduction of desmosterol to cholesterol, would be proposed as an alternative route leading to cholesterol. A possible biological significance of Δ^{25}-cholesterol and a possible occurrence of sterol Δ^{25}-reductase distinct from Δ^{24}-reductase are open questions.

In an attempt to accumulate desmosterol or any 24,25-tetrasubstituted olefinic sterol, effects of addition of triparanol to the culture medium were examined. Triparanol is a well-known Δ^{24}-sterol reductase inhibitor in mammals (25), and various steps of sterol synthesis in yeast and/or algae also were reported to be inhibited by triparanol (26,27). However, its effects on sterol synthesis in higher plants have not fully been understood. Feeding of triparanol to *Ajuga* hairy roots did not lead to an accumulation of desmosterol, although the yields of cholesterol, clerosterol, and 22-dehydroclerosterol were decreased in a dose-dependent manner. Instead, two new sterols, (24ξ)-stigmasta-8,25-dien-3β-ol and (24ξ)-stigmasta-8,22,25-trien-3β-ol, appeared. Their structures were determined by spectral analysis of the isolated materials (Morisaki, M., and Takahashi, K., unpublished work). It seems that triparanol inhibited the isomerization of Δ^{8}- into Δ^{7}-olefin at some stage(s) of clerosterol and 22-dehydroclerosterol biosynthesis.

Effects of 25-azacholesterol, an inhibitor of sterol Δ^{24}-reductase and sterol Δ^{24}-methyl transferase (28), were also investigated. For example, addition (3 ppm) of 25-azacholesterol to the medium caused a reduction in growth of about one-half of the hairy roots; and accumulation of desmosterol (8% of total sterol), 24-methylenecholesterol (6%), and 24-methylcholesterol (2%) was observed (Fujimoto, Y., Nakagawa, T., and Ohyama, K., unpublished data). ^{13}C NMR analysis of desmosterol biosynthsized from [2-^{13}C]mevalonate in the presence of 25-azacholesterol revealed ^{13}C-label at the expected positions including the isopropylidene (*E*)-methyl group (Fujimoto, Y., and Ohyama, K., unpublished data). It appears that 25-azacholesterol is more potent in inhibiting Δ^{24}-sterol methyl transferase than triparanol in our hairy roots.

20-HYDROXYECDYSONE BIOSYNTHESIS

Once we knew that cholesterol was successfully converted into 20-hydroxyecdysone (17), we then investigated the fate of A-ring hydrogens during the conversion into 20-hydroxyecdysone. Our results obtained by feeding 3α-, 4α-, or 4β-^{2}H-labeled cholesterol followed by ^{2}H NMR analysis of the biosynthesized 20-hydroxyecdysone are summarized in Scheme 6 (29). Earlier data obtained by Goodwin's group using radioisotopes (^{3}H/^{14}C) in the fern *Polypodium vulgare* (30) and the insect *Schistocerca gregaria* (31) also are included in this scheme In *S. gregaria*, approximately 20% of 3α-hydrogen is reportedly retained at positions other than the C-3 of 20-hydroxyecdysone. In *Ajuga* hairy roots all three hydrogens remained at their original positions after conversion into 20-hydroxyecdysone (29). Very interestingly, comparison of the fates of A-ring hydrogens suggests that at least three distinct mechanisms are operating for the *cis*-A/B-ring formation. It was reported that in *Taxus baccatta* the 3α-hydrogen of cholesterol remains during the conversion into 20-hydroxyecdysone (32).

First, 7-dehydrocholesterol (in the form of 4-^{13}C) and 5β-ketodiol (in the form of 22,23,24,25-$^{3}H_4$) were fed to the hairy roots to compare the pathway established in insects. The two substrates were found to be incorporated into 20-hydroxyecdysone (Fujimoto, Y., Kushiro, T., Makka, T., and Sonobe, H., unpublished data). The results, combined with the observation that A-ring modification is not involved in *Ajuga* hairy roots, suggested that the Δ^{5}-double bond of 7-de-

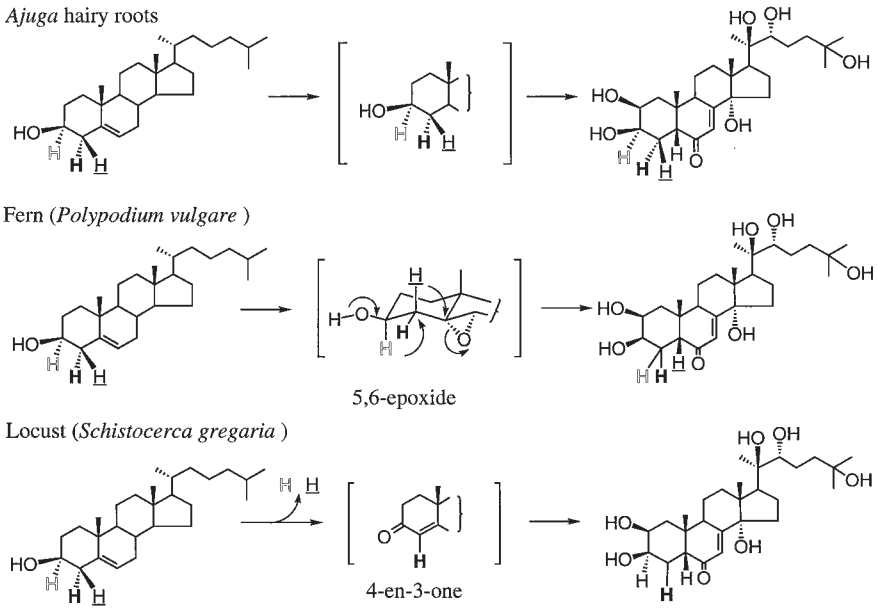

SCHEME 6

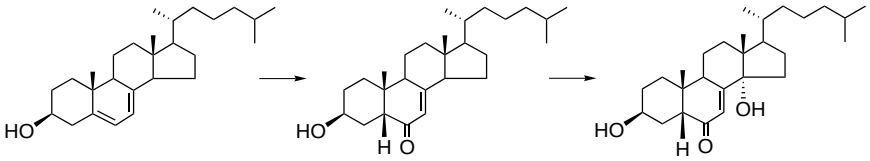

7-dehydrocholesterol 5β-ketol 5β-ketodiol

SCHEME 7

hydrocholesterol is transformed to 5β-H-6-one system *via* a rather simple, but as yet unidentified mechanism. This prompted us to examine a possible intermediary role of 3β-hydroxy-5β-cholest-7-en-6-one (5β-ketol), which is not regarded as an intermediate in insects (33–35). [3α-^{2}H]- and [5-^{2}H]-5β-Ketols were converted into 20-hydroxyecdysone when fed to the hairy roots (29). The corresponding [3α-^{2}H]-5α-ketol was not converted into 20-hydroxyecdysone at all. It is therefore reasonable to place 5β-ketol as an intermediate between 7-dehydrocholesterol and 5β-ketodiol (Scheme 7).

We then focused on the origin of 5β-hydrogen of 20-hydroxyecdysone. In theory, it can be derived from C-4 or C-6 hydrogen of the substrate sterol, water, or a reducing cofactor such as NADPH. In the fern *P. vulgare*, the 4β-H of cholesterol reportedly is the origin (30), whereas in *S. gregaria*, 4β-H is lost during the transformation (30) (Scheme 6). In *Locusta migratoria*, we reported that most (90%) of 6-H of cholesterol is lost during the conversion into 20-hydroxyecdysone (36). In *Ajuga* hairy roots, feeding of [6-^{2}H]cholesterol followed by ^{2}H NMR analysis of the biosynthesized 20-hydroxyecdysone led to a deuterium signal at δ 2.95 corresponding to 5β-hydrogen, indicating 1,2-hydrogen migration from C-6 to C-5. Feeding a mixture of [6-^{2}H]- and [4β-^{2}H]-cholesterol as well as of a mixture of [6-^{2}H]- and [4α-^{2}H]cholesterol confirmed the 1,2-migration. However, the signal intensity of 5β-deuterium appeared to be somewhat smaller than expected (37). To eliminate a possible deuterium isotope effect and to estimate the precise magnitude of the 1,2-hydrogen migration, [3α,6-$^2H_2$]cholesterol was synthesized and fed to the hairy roots. The ^{2}H NMR spectrum of the resulting 20-hydroxyecdysone is illustrated in Figure 1, which clearly indicates that 70% of the 5β-hydrogen of 20-hydroxyecdysone comes from 6-H of cholesterol and the remaining 30% from other source (37).

Grebenok and Adler (9) have demonstrated that lathosterol is incorporated into 20-hydroxyecdysone in spinach leaves, but without discussing the intermediary role of 7-dehydrocholesterol. We synthesized [3α,6β-$^2H_2$]- and [3α,6α-$^2H_2$]-lathosterols, and they were separately fed to *Ajuga* hairy roots. ^{2}H NMR analysis of the resulting 20-hydroxyecdysone unambigously established that 6β-^{2}H migrated to the C-5 position of 20-hydroxyecdysone, whereas 6α-^{2}H was lost during the conversion, probably due to the well-known *cis*-elimination in the formation of Δ^5-sterol from Δ^7-sterol in plants (38–40). Again, the behavior of 6β-^{2}H of lathosterol was nonstoichiometric (*ca*. 70% migration) (41). The observed 1,2-migration of 6β-hydrogen of lathosterol supports the obligatory intermediary role of

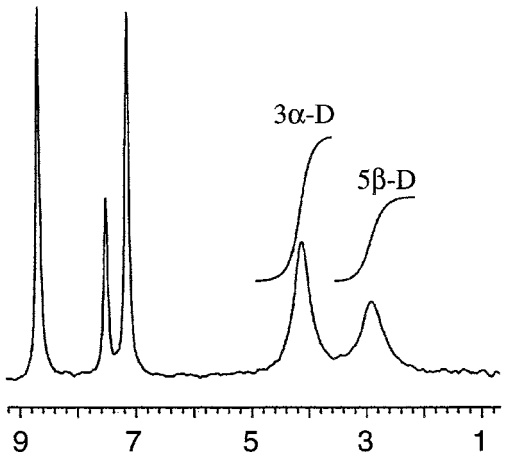

FIG. 1. ^{2}H Nuclear magnetic resonance (NMR) spectrum (pyridine, 77 MHz) of 20-hydroxyecdysone derived from [3α,6-$^2H_2$]cholesterol. The spectrum indicates that *ca*. 70% of the 6-hydrogen (compared to the 100% retention of the 3α-hydrogen) of cholesterol migrates to the C-5 position of 20-hydroxyecdysone.

7-dehydrocholesterol, ruling out a pathway involving a direct C-6 oxidation of lathosterol in *Ajuga* hairy roots.

The ^{2}H NMR spectrum of cholesterol, isolated from hairy roots upon feeding [3α,6β-$^2H_2$]lathosterol, showed two deuterium signals at δ 3.51 and 5.35 corresponding to 3α-H and 6-H, respectively, in an equal intensity. As expected, cholesterol derived from [3α,6α-$^2H_2$]lathosterol showed a single signal at δ 3.51. These data further supported the highly stereospecific elimination of 6α-hydrogen and, more importantly, evidenced no loss of 6β-hydrogen during the conversion of lathosterol into cholesterol *via* 7-dehydrocholesterol (41). Furthermore, we recently found that the C-5 hydrogen of 5β-ketol is retained completely during the subsequent conversion into 20-hydroxyecdysone (41). Thus, it is in the step of *cis*-A/B-ring formation, i.e., the conversion of a key oxidized intermediate into 5β-ketol, that *ca*. 30% of C-5 hydrogen of 20-hydroxyecdysone not derived from 6-H of cholesterol is introduced.

We (42) and others (30,43–45) postulated a possible involvement of 7-dehydrocholesterol 5α,6α-epoxide in ecdysteroid biosynthesis. Chemical stability of this epoxide and its 5β,6β-isomer has also been reported (46). Our present demonstration of 1,2-hydrogen migration from C-6 to C-5 position strongly suggests that the 5α,6α-epoxide would produce 5β-ketol *via* epoxy-carbonyl rearrangement as shown in path "a" of Scheme 8. Partial (30%) solvolytic hydrolysis of the same epoxide (path "b" in Scheme 8) yielding the 5,6-gly-

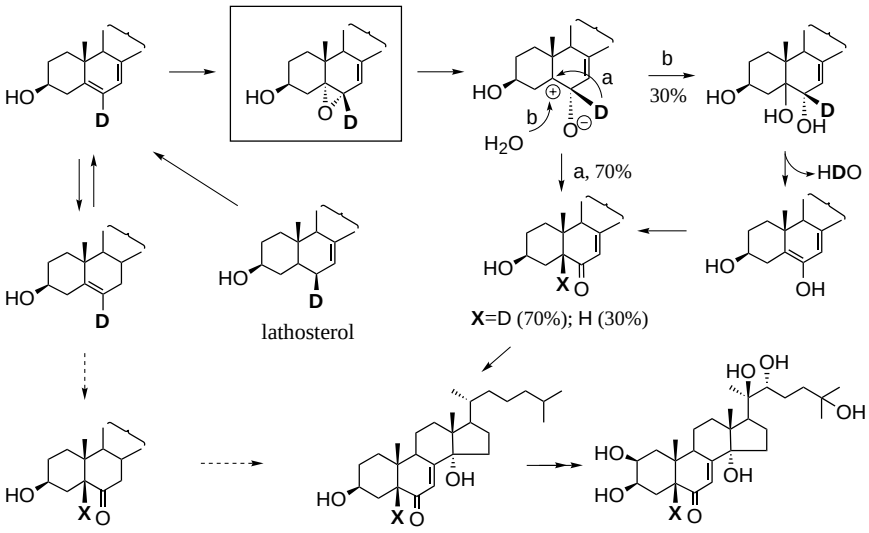

SCHEME 8

col, which is reminiscent of the structure of bombycosterol isolated from ovaries of the silkworm, *Bombyx mori* (42), and the subsequent dehydration would account for the formation of the nonlabeled 5β-ketol.

Quite recently we found that [3-^{2}H]-3β-hydroxy-5β-cholestan-6-one is incorporated into 20-hydroxyecdysone, whereas the corresponding 5α-congener is not incorporated at all (47). Further, the isolation and characterization of 7,8-dihydroecdysteroids are reported (48,49). These data may suggest that a Δ^7-double bond (or its absence) is not essential for the enzymatic formation of 5β-H-6-one structure. In other words, Δ^7-double bond can be introduced at a later stage. Our preliminary study of feeding of [3-^{2}H]cholesterol 5α,6α-epoxide resulted in negligible conversion into 20-hydroxyecdysone (47). Neither 5α,6α- nor 5β,6β-epoxides, possible intermediates in this pathway, are reportedly converted into 20-hydroxyecdysone in a plant (50).

STEREOCHEMICAL COURSE OF 25-HYDROXYLATION

The transformation in the later stages of 20-hydroxyecdysone involves a hydroxylation at the C-2, C-20, C-22, and C-25 positions. It was reported that C-20, C-22, and C-25 hydroxylations are catalyzed by P_{450} monooxygenase enzymes (51–54), whereas a different type monooxygenase (not inhibited by CO) is responsible for C-2 hydroxylation (55,56). Further, C-2 hydroxylation in *S. gregaria* (57) and *Ajuga* hairy roots (58) and C-22 hydroxylation in *S. gregaria* (59) were reported to proceed with retention of stereochemistry.

As described above, C-26 and C-27 of cholesterol are stereospecifically derived from C-2 and C-6 of mevalonate, respectively. Inspection of the ^{13}C NMR spectrum of 20-hydroxyecdysone derived from [$^{13}C_2$]acetate revealed that the signal of C-25 (δ 71.3) has a flanking doublet. In accord with this pattern, one of the methyl signals on C-25 (δ 29.7) was accompanied by a flanking doublet. The other methyl signal (δ 28.9) on C-25 is also accompanied by satellite peaks with a weak, but significant intensity. The incorporation of an acetate unit into both C-25–C-26 and C-25–C-27 of 20-hydroxyecdysone, combined with the above finding on cholesterol (no scrambling), suggested a possibility that C-25 hydroxylation during the formation of 20-hydroxyecdysone is not stereospecific.

To know metabolic relationships of the isopropyl *pro-R* and *pro-S* methyl groups of cholesterol and 20-hydroxyecdysone, one must be able to discriminate the two methyl groups on C-25 prochiral center. A ^{13}C labeling technique can be conveniently employed to trace the metabolic fates of the diastereotopic methyl groups, provided that the ^{13}C chemical shifts for the isopropyl *pro-R* and *pro-S* methyl groups of the substrate and product are unequivocally assigned. Thus, the ^{13}C chemical shifts of *pro-S* (C-27) (δ 28.9) and *pro-R* (C-26) (δ 29.7) of 20-hydroxyecdysone were first assigned by chemical synthesis of stereochemically defined model compounds having the same 20*R*,22*R*,25-trihydroxy side-chain structure as in 20-hydroxyecdysone, [26-^{2}H]-(20*R*,22*R*,25)-trihydroxycholesterol 3-methyl ether (one of the hydrogen atoms of the *pro-R*-methyl group is substituted by deuterium) and its [27-^{2}H]epimer (20).

Stereospecifically synthesized [*pro-R*-methyl-^{13}C]- and [*pro-S*-methyl-^{13}C]cholesterols were separately fed to *Ajuga* hairy roots. As shown in the ^{13}C NMR spectrum (Fig. 2), 20-hydroxyecdysone derived from the former isomer revealed that ^{13}C label was found in *pro-S*- (*ca.* 75%) and *pro-R*- (*ca.* 25%) methyl groups. Feeding of [*pro-S*-methyl-^{13}C]cholesterol afforded complementary results (20). Subsequently, six hydrogens at the C-26 and C-27 methyl groups were shown to be completely retained during this conversion (Fujimoto, Y., and Tatara, A., unpublished data). It is therefore concluded that C-25 hydroxylation in the biosynthesis of 20-hydroxyecdysone

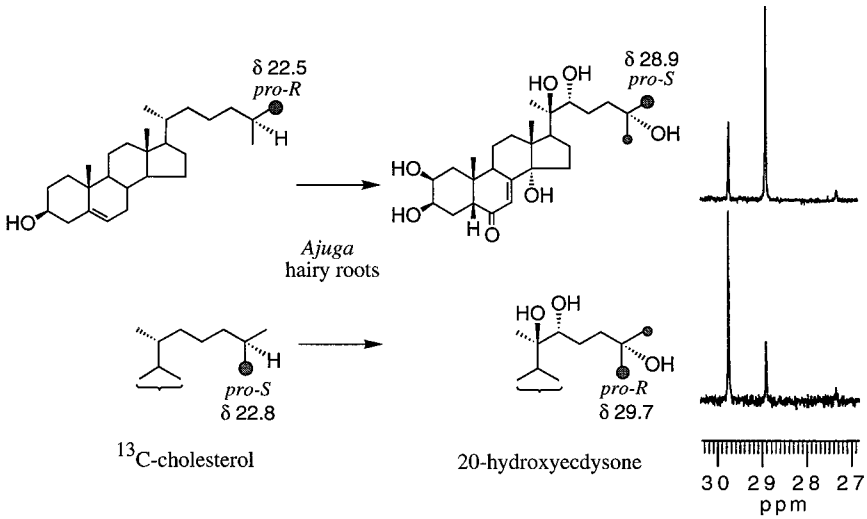

FIG. 2. Nonstereospecific C-25 hydroxylation (*ca*. 3:1 ratio retention/inversion) in 20-hydroxyecdysone biosynthesis in *Ajuga* hairy roots. The ^{13}C NMR spectra (in CD_3OD, 75 MHz) are those of 20-hydroxyecdysones derived from each ^{13}C-labeled cholesterol (>98% specifically labeled with ^{13}C at either C-26 or C-27). For abbreviation see Figure 1.

from cholesterol in *Ajuga* hairy roots is not stereospecific, but proceeds with a ratio of *ca*. 3:1 retention/inversion.

Another example of steroidal C-25 hydroxylation of vitamin D_3, mediated by the microorganism *Sphingomonas* sp. HD-1 (60), was revealed to be stereospecific with retention of configuration (Fujimoto, Y., and Tatara, A., unpublished data); C-25 hydroxylation in 20-hydroxyecdsone biosynthesis seems to be unique and studies in enzyme level are eagerly awaited. cDNA cloning of mouse and human cholesterol 25-hydroxylases has been reported recently (61).

BIOSYNTHESIS OF CYASTERONE AND ITS CONGENERS

In the feeding experiment with [26,27-$^{13}C_2$]cholesterol, which was converted into 20-hydroxyecdysone, neither cyasterone, isocyasterone, nor 29-norcyasterone was labeled with ^{13}C. On [1-^{13}C]- or $^{13}C_2$-acetate feeding, the C-24 substituents of these phytoecdysteroids were not labeled (17). These data imply that the biosynthetic route leading to these C_{29}- and C_{28}-ecdysteroids is branched at a stage before cholesterol. In fact, [26,27-$^{13}C_2$]cycloartenol was converted into cyasterone, isocyasterone, and 29-norcyasterone as well as 20-hydroxyecdysone (Morisaki, M., and Yamada, J., unpublished data). Cyasterone was first isolated from *Cyathula capitata* (62), whose major sterols appear to be [24α]-alkylsterols such as sitosterol and stigmasterol (63,64). Subsequently, a biosynthetic study was performed in this plant, resulting in negligible conversion of sitosterol and fucosterol into cyasterone (63,64). In contrast, Δ^{25}-24-ethylsterols and phytoecdysteroids of *Ajuga* hairy roots have the same 24β configuration. Thus, it is reasonable to assume that these sterols could serve as the precursors of C_{29}-phytoecdysteroids.

We previously found that a mixture of [26,27-$^{13}C_2$]clerosterol and its C-24 epimer was incorporated into cyasterone. More recently, several C_{29}-sterols including [27-^{13}C]clerosterol, its [27-^{13}C]-C-24-epimer, [26-^{13}C]-(25*RS*)-sitosterol, and [26-^{13}C]-(25*RS*)-clionasterol were fed to hairy roots, and only clerosterol was found to be incorporated into cyasterone and isocyasterone (Fujimoto, Y., Nomura, K., Takahashi, K., and Morisaki, M., unpublished data). This provides the first clear evidence for the structure of sterol precursor of the C_{29}-phytoecdysteroids. Similarly, codisterol is likely to be a precursor of 29-norcyasterone, although we only have the results obtained by feeding a mixture of ^{13}C-labeled codisterol and its C-24-epimer. It should be noted that the ^{13}C-label was found in lactone carbonyl both of cyasterone and isocyasterone biosynthesized from [27-^{13}C]clerosterol. Feeding experiments with $^{13}C_2$-acetate showed an intact ^{13}C-^{13}C connectivity between C-25 and methyl (C-26) group of cyasterone and isocyasterone as well as 29-norcyasterone. From these data it can be concluded that lactone carbonyl carbon of the three phytoecdysteroids is derived from C-2 of mevalonate while C-27 comes from C-6 of mevalonate (Scheme 9; dots refer to a carbon correlated to C-2 of mevalonate).

It was reported that co-occurrence of cyasterone and isocyasterone was caused by nonstereospecific hydroxylation of both methyl groups of the isopropyl terminal of side chain (65). Our observation above ruled out this possibility. Rather, the co-occurrence is due to a nonstereospecific hydrogenation at a certain stage in which exomethylene group is converted into methyl group. A biosynthetic pathway leading to cyasterone and isocyasterone is depicted as in Scheme 9, in which an intermediate structure with fully oxidized nuclei is adopted from several oxygenated steroids isolated from *C. capitata*, which also contains cyasterone (66).

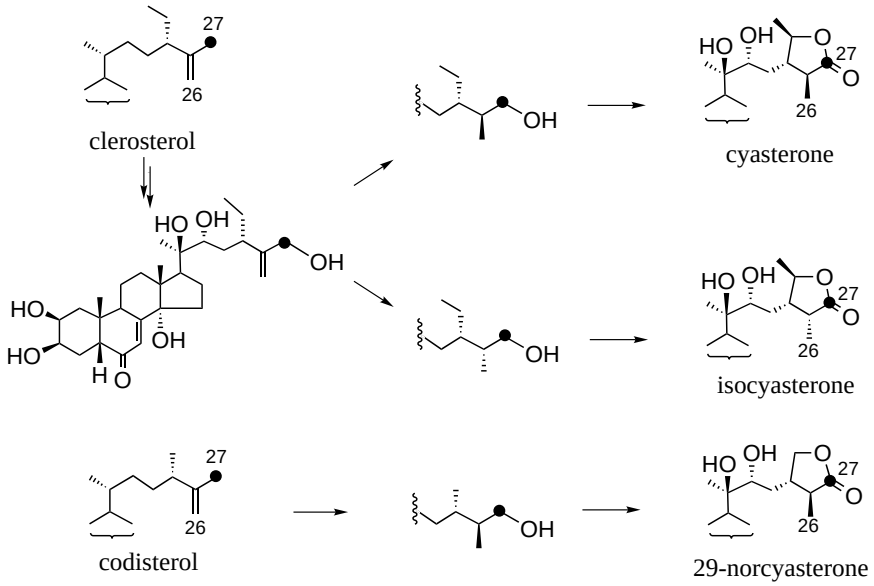

SCHEME 9

CONCLUSION

In *Ajuga* hairy roots, feeding studies of synthetic ^{13}C- or ^{2}H-labeled sterols and/or $^{13}C_2$-acetate have provided several lines of evidence that shed light on the biosynthesis of Δ^{25}-24-alkylsterols (clerosterol, 22-dehydroclerosterol, and codisterol) as well as 20-hydroxyecdysone, cyasterone, isocyasterone, and 29-norcyasterone. The origin of C-26 and C-27 of these steroidal compounds was correlated with each other, and further with C-2 and C-6 of mevalonate. As demonstrated with *Ajuga* hairy roots and *O. sativa* cell cultures, plants appear to have a capacity to reduce Δ^{25}-cholesterol, although its physiological importance is unclear at present.

As for the biosynthesis of 20-hydroxyecdysone, crucial evidence supporting the intermediacy of 7-dehydrocholesterol 5α,6α-epoxide has been obtained for the first time; the C-6 hydrogen of cholesterol mostly migrates to the C-5 position of 20-hydroxyecdysone. An epoxy-carbonyl rearrangement of this epoxide would afford 5β-ketol which also characterized as an intermediate in *Ajuga* hairy roots. It should be noted that the metabolic fate of A-ring hydrogens as well as the C-6 hydrogen of cholesterol is different between *Locusta*, *Polypodium*, and *Ajuga* hairy roots. This suggests three distinct mechanisms are operating in construction of a 5β-H-7-en-6-one structure of 20-hydroxyecdysone, depending on the species. It is important to examine the fate of C-6 hydrogen of cholesterol in insects and other plants.

Based on our recent finding that 3β-hydroxy-5β-choletan-6-one is converted into 20-hydroxyecdysone in *Ajuga* hairy roots, an alternate pathway, cholesterol → cholesterol 5α,6α-epoxide → 3β-hydroxy-5β-cholestan-6-one → 5β-ketol should be also considered, in addition to the previously proposed route: cholesterol → 7-dehydrocholesterol → 7-dehydrocholesterol 5α,6α-epoxide → 5β-ketol.

ACKNOWLEDGMENTS

We wish to express our thanks to Professor Emeritus Nobuo Ikekawa of Tokyo Intitute of Technology for his continued encouragement. We are grateful to Mitsuhiro Nagakari, Takayoshi Nakagawa, Akinori Tatara, Kinya Nakamura, Tomoko Yazaki-Yagi, and Dr. Tetsuo Kushiro for their partial contribution in the work. Part of this research was supported by a Grant-in-Aid for Scientific Research (No. 02640422) and a Grant-in-Aid for Scientific Research on Priority Areas (08276207) to Y.F. from the Ministry of Education, Science, Sports and Culture of Japan. Thanks are also due to Drs. Takeshi Matsumoto and Nobukazu Tanaka, Bioassay Laboratory, Research Center, Daicel Chemical Industries Ltd., for providing *Ajuga* hairy root cultures, and Dr. Akio Ozaki, Tokyo Research Laboratories, Kyowa Hakko Kogyo Co. Ltd., for providing the strain of *Sphingomonas* sp.

REFERENCES

1. Hoffmann, J.A. (1986) Ten Years of Ecdysone Workshops, *Insect Biochem. 16*, 1–10.
2. Koolman, J. (1990) Ecdysteroids, *Zool. Sci. 7*, 563–580.
3. Warren, J.T., and Hetru, C. (1990) Ecdysone Biosynthesis: Pathways, Enzymes, and the Early Steps Problem, *Invertebr. Reprod. Develop. 18*, 91–99.
4. Lafont, R., and Horn, D.H.S. (1989) Phytoecdysteroids: Structures and Occurrence, in *Ecdysone* (Koolman, J., ed.), pp. 39–64, Thieme Medical Publishers, New York.
5. Camps, F. (1991) *Ecological Chemistry and Biochemistry of Plant Terpenoids* (Harbone, J.B., and Tomas-Barberán, F.A., eds.), pp. 331–376, Clarendon Press, Oxford.
6. Heftmann, E., Sauer, H.H., and Bennet, R.D. (1968) Biosynthesis of Ecdysterone from Cholesterol by a Plant, *Naturwissenschaften 55*, 37–38.
7. Hikino, H., Kohama, T., and Takemoto, T. (1970) Biosynthesis of Ponasterone A and Ecdysterone from Cholesterol in *Podocarpus macrophyllus*, *Phytochemistry 9*, 367–369.
8. De Souza, N.J., Ghisalberti, E.L., Rees H.H., and Goodwin, T.W. (1970) Studies on Insect Moulting Hormones: Biosynthe-

sis of Ecdysone, Ecdysterone and 5β-Hydroxyecdysterone in *Polypodium vulgare*, *Phytochemistry 9*, 1247–1252.
9. Grebenok, R.J., and Adler, J.H. (1993) Ecdysteroid Biosynthesis During the Ontogeny of Spinach Leaves, *Phytochemistry 33*, 341–347.
10. Devarenne, T.P., Sen-Michael, B., and Adler, J.H. (1995) Biosynthesis of Ecdysteroids in *Zea mays*, *Phytochemistry 40*, 1125–1131.
11. Tomita, Y., and Sakurai, E. (1974) Biosynthesis of Phytoecdysone: Incorporation of 2β,3β,14α-Trihydroxy-5β-cholest-7-en-6-one into β-Ecdysone and Inokosterone in *Achyranthes fauriei*, *J. Chem. Soc. Chem. Commun*., 434–435.
12. Adler, J.H., and Grebenok, R.J. (1995) Biosynthesis and Distribution of Insect-Molting Hormones in Plants—A Review, *Lipids 30*, 257–262.
13. Darvas, B. (1991) Phytoecdysteroids of *Ajuga* spp., as Insect Growth Regulator-Type Botanical Insecticides, *Novenyvedelem Budapest 27*, 481–489.
14. Shimomura, H., Sashida, Y., and Ogawa, K. (1989) Neo-clerodane Diterpenes from *Ajuga ciliata* var. *villosior*, *Chem. Pharm. Bull. 37*, 988–992.
15. Camps, F., and Coll, J. (1993) Insect Allelochemicals from *Ajuga* Plants, *Phytochemistry 32*, 1361–1370.
16. Matsumoto, T., and Tanaka, N. (1991) Production of Phytoecdysteroids by Hairy Root Cultures of *Ajuga reptans* var. *atropurpurea*, *Agric. Biol. Chem. 55*, 1019–1025.
17. Nagakari, M., Kushiro, T., Matsumoto, T., Tanaka, N., Kakinuma, K., and Fujimoto, Y. (1994) Incorporation of Acetate and Cholesterol into 20-Hydroxyecdysone by Hairy Root Clone of *Ajuga reptans* var. *atropurpurea*, *Phytochemistry 36*, 907–910.
18. Camps, F., Coll, J., and Cortel, A. (1983) Sterols from *Ajuga reptans* (Labiatae), *Ann. Quim. Ser. C. 79*, 228–229.
19. Yagi, T., Morisaki, M., Kushiro, T., Yoshida, H., and Fujimoto, Y. (1996) Biosynthesis of 24β-Alkyl-Δ^{25}-sterols in Hairy Roots of *Ajuga reptans* var. *atropurpurea*, *Phytochemistry 41*, 1057–1064.
20. Nakagawa, T., Hara, N., and Fujimoto, Y. (1997) Biosynthesis of 20-Hydroxyecdysone in *Ajuga* Hairy Roots: Stereochemistry of C-25 Hydroxylation, *Tetrahedron Lett. 38*, 2701–2704.
21. Kienle, M.G., Varma, R.K., Mulheirn, L.J., and Yagen, B. (1973) Reduction of Δ^{24} of Lanosterol in the Biosynthesis of Cholesterol by Rat Liver Enzymes. II. Stereochemistry of Addition of the C-25 Proton, *J. Am. Chem. Soc. 95*, 1996–2001.
22. Yagi, T., Kobayashi, N., Morisaki, M., Hara, N., and Fujimoto, Y. (1994) Stereochemistry of Hydrogen Addition to C-25 of Desmosterol by Sterol-Δ^{24}-reductase of Rat Liver Homogenate, *Chem. Pharm. Bull. 42*, 680–682.
23. Fujimoto, Y., Nagakari, N., Ikuina, Y., Ikekawa, N., and Kakinuma, K. (1991) Stereochemistry of the Hydrogen Addition to C-25 of Desmosterol by Sterol-Δ^{24}-reductase of the Silkworm, *Bombyx mori*, *J. Chem. Soc. Chem. Commun*., 688–689.
24. Nagano, M., Yamada, J., Yazaki-Yagi, T., Morisaki, M., Nakagawa, T., and Fujimoto, Y. (1997) Stereochemistry of Hydrogen Introduction at C-25 during Cholesterol Biosynthesis in Higher Plants, *Chem. Pharm. Bull. 45*, 944–946.
25. Steinberg, D., and Avigan, J. (1960) Studies on Cholesterol Biosynthesis, *J. Biol. Chem. 235*, 3127–3129.
26. Campagnoni, C., Holmlund, C.E., and Whittaker, N. (1977) The Effect of Triparanol on the Composition of Free and Esterified Sterols of *Saccharomyces cerevisiae*, *Arch. Biochem. Biophys. 184*, 555–560.
27. Chan, J.T., Patterson, G.W., Dutky, S.R., and Cohen, C.F. (1974) Inhibition of Sterol Biosynthesis in *Chlorella sorokiniana* by Triparanol, *Plant Physiol. 53*, 244–249.
28. Svoboda, J.A., and Robbins, W.E. (1971) The Inhibitive Effects of Azasterols on Sterol Metabolism and Growth and Development in Insects with Special Reference to the Tobacco Hornworm, *Lipids 6*, 113–119.
29. Nagakari, M., Kushiro, T., Yagi, T., Tanaka, N., Matsumoto, T., Kakinuma, K., and Fujimoto, Y. (1994) 3β-Hydroxy-5β-cholest-7-en-6-one as an Intermediate of 20-Hydroxyecdysone Biosynthesis in a Hairy Root Culture of *Ajuga reptans* var. *atropurpurea*, *J. Chem. Soc. Chem. Commun.*, 1761–1762.
30. Davies, T.G., Lockley, W.J.S., Boid, R., Rees, H.H., and Goodwin, T.W. (1980) Mechanism of Formation of the A/B *Cis* Ring Junction of Ecdysteroids in *Polypodium vulgare*, *Biochem. J. 190*, 537–544.
31. Davies, T.G., Dinan, L.N., Lockley, W.J.S., Rees, H.H., and Goodwin, T.W. (1981) Formation of the A/B *Cis* Ring Junction of Ecdysteroids in the Locust, *Schistocerca gregaria*, *Biochem. J. 94*, 53–62.
32. Lloyd-Jones, J.G., Rees, H.H., and Goodwin, T.W. (1973) Biosynthesis of Ecdysterone from Cholesterol in *Taxus baccatta*, *Phytochemistry 12*, 569–572.
33. Boileubacter, W.E., Galbraith, M.N., Gilbert, I.L., and Horn, D.H. (1977) *In vitro* Metabolism of 3β-Hydroxy- and 3β,14α-Dihydroxy (3α-^{3}H)-5β-cholest-7-en-6-one by the Prothoracic Glands of *Manduca sexta*, *Steroids 29*, 47–63.
34. Faux, A.F., Horn, D.H.S., Kinnear, J.F., Martin, M.D., Wilkie, J.S., and Willing, R.I. (1979) Evaluation of 3β-Hydroxy-5β-cholest-7-en-6-one and Related Steroids as Precursors of Ecdysteroids in *Calliphora stygia*, *Insect Biochem. 9*, 101–105.
35. Haag, T., Meister, M.-F., Hetru, C., Kappler, C., Nakatani, Y., Beaucourt, J.P., Rousseau, B., and Luu, B. (1987) Synthesis of a Labelled Putative Precursor of Ecdysone—II, *Insect Biochem. 17*, 291–301.
36. Fujimoto, Y., Hiramoto, M., Kakinuma, K., and Ikekawa, N. (1989) Elimination of C-6 Hydrogen During the Formation of Ecdysteroids from Cholesterol in *Locusta migratoria* Ovaries, *Steroids 53*, 477–485.
37. Fujimoto, Y., Kushiro, T., and Nakamura, K. (1997) Biosynthesis of 20-Hydroxyecdysone in *Ajuga* Hairy Roots: Hydrogen Migration from C-6 to C-5 During *cis*-A/B Ring Formation, *Tetrahedron Lett. 38*, 2697–2700.
38. Goad, L.J., Gibbons, G.F., Bolger, L.M., Rees, H.H., and Goodwin, T.W. (1969) Incorporation of (5*R*)-Mevalonic-2-^{14}C-5-^{3}H Acid into Cholesterol by a Rat Liver Homogenate and into β-Sitosterol and 28-Isofucosterol by *Larix decidua* Leaves, *Biochem. J. 114*, 885–892.
39. Goad, L.J. and Goodwin, T.W. (1972), The Biosynthesis of Plant Sterols, in *Progress in Phytochemistry* (Reinhold, L., and Liwschitz, Y., eds.), Vol. 3, pp. 113–198, Interscience, London.
40. Sliwowski, S., and Kasprzyk, A. (1974) Stereospecificity of Sterol Biosynthesis in *Calendula officinalis* Flowers, *Phytochemistry 13*, 1451–1457.
41. Ohyama, K., Kushiro, T., Nakamura, K., and Fujimoto, Y. (1999) Biosynthesis of 20-Hydroxyecdysone in *Ajuga* Hairy Roots: Metabolic Fate of 6α- and 6β-Hydrogens of Lathosterol, *Bioorg. Med. Chem. 7*, 2925–2930.
42. Fujimoto, Y., Miyasaka, S., Ikeda, T., Ikekawa, N., Ohnishi, E., Mizuno, T., and Watanabe, K. (1985) An Unusual Ecdysteroid, (20*S*)-Cholesta-7,14-diene-3β,5α,6α,20,25-pentaol (bombycosterol) from the Ovaries of the Silkworm, *Bombyx mori*, *J. Chem. Soc. Chem. Commun*., 10–12.
43. Rees, H.H. (1985) Biosynthesis of Ecdysone, in *Comprehensive Insect Physiology, Biochemistry and Pharmacology* (Kerkut, G.A., and Gilbert, L.I., eds.), Vol. 7, pp. 249–269, Pergamon Press, Oxford.
44. Grieneisen, M.L., Warren, J.T., Sakurai, S., and Gilbert, L.I. (1991) A Putative Route to Ecdysteroids: Metabolism of Cholesterol *in Vitro* by Mildly Disrupted Prothoracic Glands of *Manduca sexta*, *Insect Biochem. 21*, 41–51.
45. Grieneisen, M.L. (1994) Recent Advances in Our Knowledge

of Ecdysteroid Biosynthesis in Insects and Crustaceans, *Insect Biochem. Molec. Biol. 24*, 115–132.
46. Michaud, D.P., Nashed, N.T., and Jerina, D.M. (1985) Stereoselective Synthesis and Solvolytic Behavior of the Isomeric 7-Dehydrocholesterol 5,6-Oxides, *J. Org. Chem. 50*, 1835–1840.
47. Hyodo, R., and Fujimoto, Y. (2000) Biosynthesis of 20-Hydroxyecdysone in *Ajuga* Hairy Roots: The Possibility of 7-Ene Introduction at a Later Stage, *Phytochemistry 53*, 733–737.
48. Faux, A., Galbraith, M.N., Horn, D.H.S., Middleton, E.J., and Thomson, J.A. (1970) The Structures of Two Ecdysone Analogue, Cheilanthones A and B, from the Fern *Cheilanthes tenuifolia*, *Chem. Commun*., 243–244.
49. Pomilio, A.B., Gonzále, M.D., and Eceizabarrena, C.C. (1996) 7,8-Dihydroajugasterone C, Norhygrine and Other Constituents of *Nierembergia hippomanica*, *Phytochemistry 41*, 1393–1398
50. Joly, R.A., Svahn, C.M., Bennett, R.D., and Heftmann, E. (1969) Investigation of Intermediate Steps in the Biosynthesis of Ecdysterone from Cholesterol in *Podocarpus elata*, *Phytochemistry 8*, 1917–1920.
51. Kappler, C., Kabbouh, M., Hetru, C., Durst, F., and Hoffmann, J.A. (1988) Characterization of Three Hydroxylases Involved in the Final Steps of Biosynthesis of the Steroid Hormone Ecdysone in *Locusta migratoria* (Insecta, Orthoptera), *J. Steroid Biochem. 31*, 891–898.
52. Feyereisen, R., and Durst, F. (1978) Ecdysterone Biosynthesis: A Microsomal Cytochrome-p-450-linked Ecdysone 20-Monooxygenase from Tissues of the African Migratory Locust, *Eur. J. Biochem. 88*, 37–47.
53. Smith, S.L., Bollenbacher, W.E., Cooper, D.Y., Schleyer, H., Wieigus, J.J., and Gilbert, L.I. (1979) Ecdysone 20-Hydroxylase: Characterization of an Insect Cytochrome p-450 Dependent Steroid Hydroxylase, *Mol. Cell. Endocrinol. 15*, 111–133.
54. Grebenok, R.J., Galbraith, D.W., Benveniste, I., and Feyereisen, R. (1996) Ecdysone 20-Monooxygenase, a Cytochrome P450 Enzyme from Spinach, *Spinacia oleracea*, *Phytochemistry 42*, 927–933.
55. Kappler, C., Kabbouh, M., Durst, F., and Hoffmann, J.A. (1986) Studies on the C-2 Hydroxylation of 2-Deoxyecdysone in *Locusta migratoria*, *Insect Biochem. 16*, 25–32.
56. Kabbouh, M., Kappler, C., Hetru, C., and Durst, F. (1987) Further Characterization of the 2-Deoxyecdysone C-2 Hydroxylase from *Locusta migratoria*, *Insect. Biochem. 17*, 1155–1161
57. Greenwood, D.R., Dinan, L.N., and Rees, H.H. (1984) Mechanism of Hydroxylation at C-2 During the Biosynthesis of Ecdysone in Ovaries of Locust *Schistocerca gregaria*, *Biochem. J. 217*, 783–789.
58. Nomura, K., and Fujimoto, Y. (2000) Biosynthesis of 20-Hydroxyecdysone in *Ajuga* Hairy Roots: Stereochemistry of the C-2 Hydroxylation, *Chem. Pharm. Bull. 48*, 400–405.
59. Greenwood, D.R., and Rees, H.H. (1982) Mechanism of Hydroxylation at C-22 During the Biosynthesis of Ecdysteroids in the Locust *Schistocerica gregaria*, *Biochem. J. 208*, 857–864.
60. Ozaki, A., Takano, H., Ando, K., and Ochiai, K. (1995) 25-Hydroxyvitamin D Manufacture with *Sphingomonas*, Japan Patent 241,197.
61. Lund, E.G., Kerr, T.A., Sakai, J., Li, W.-P., and Russell, D.W. (1998) cDNA Cloning of Mouse and Human Cholesterol 25-Hydroxylases, Polytopic Membrane Proteins That Synthesize a Potent Oxysterol Regulator of Lipid Metabolism, *J. Biol. Chem. 273*, 34316–34327.
62. Takemoto, T., Hikino, Y., Nomoto, K., and Hikino, H. (1967) Structure of Cyasterone, A Novel C_{29} Insect-Moulting Substance from *Cyathula capitata*, *Tetrahedron Lett. 8*, 3191–3194.
63. Boid, R., Rees, H. H., and Goodwin, T.W. (1974) Biosynthesis of the Insect-Moulting Hormone Cyasterone in the Plant *Cyathula capitata*, *Biochem. Soc. Trans. 2*, 1066–1070.
64. Boid, R., Rees, H.H., and Goodwin, T.W. (1975) Studies in Insect-Moulting Hormone Biosynthesis Biosynthesis of Cyasterone in the Plant, *Cyathula capitata*, *Biochem. Physiol. Pflanz. 168*, 27–40.
65. Hikino, H., Nomoto, K., and Takemoto, T. (1971) Structure of Isocyasterone and Epicyasterone, Novel C_{29} Insect-Moulting Subtances from *Cyathula capitata*, *Chem. Pharm. Bull. 19*, 433–435.
66. Takemoto, T., Nomoto, K., Hikino, Y., and Hikino, H. (1968) Structure of Capitasterone, a Novel C_{29} Insect-Moulting Substance from *Cyathula capitata*, *Tetrahedron Lett. 9*, 4929–4932.

[Received June 3, 1999; accepted February 2, 2000]

Cholesterol Synthesis in the Vertebrate Retina: Effects of U18666A on Rat Retinal Structure, Photoreceptor Membrane Assembly, and Sterol Metabolism and Composition

S.J. Fliesler[a,*], M.J. Richards[a], C.-Y. Miller[a], and R.J. Cenedella[b]

[a]Saint Louis University Eye Institute and Program in Cell and Molecular Biology, Saint Louis University School of Medicine, St. Louis, Missouri, and [b]Department of Biochemistry, Kirksville College of Osteopathic Medicine, Kirksville, Missouri

ABSTRACT: Treatment of neonatal rats with U18666A, an inhibitor of desmosterol Δ^{24}-reductase, results in accumulation of desmosterol ($\Delta^{5,24}$) and depletion of cholesterol (Δ^{5}) in various bodily tissues and also causes cataracts. We evaluated the effects of U18666A on the sterol composition, *de novo* sterol synthesis, and histological structure of the retina. Neonatal Sprague-Dawley rats were injected subcutaneously with U18666A (15 mg/kg, in olive oil) every other day from birth through 3 wk of age; in parallel, control rats received olive oil alone. At 21 d, treated and control groups each were subdivided into two groups: one group of each was injected intravitreally with [^{3}H]acetate; retinas were removed 20 h later and nonsaponifiable lipids (NSL) were analyzed by radio-high-performance liquid chromatography. The other group was injected intravitreally with [^{3}H]leucine; 4 d later, one eye of each animal was evaluated by light and electron microscopy and light microscopic autoradiography, while contralateral retinas and rod outer segment (ROS) membranes prepared therefrom were analyzed by sodium dodecyl sulfate-polyacrylamide gel electrophoresis/fluorography. In the treated group, the $\Delta^5/\Delta^{5,24}$ mole ratio of retinas was *ca.* 1.0, and >88% of the NSL radioactivity was in $\Delta^{5,24}$; in contrast, control retinas had $\Delta^5/\Delta^{5,24}$ >170, with >80% of the NSL radioactivity in Δ^5. Retinal histology, ultrastructure, ROS renewal rates, and rhodopsin synthesis and intracellular trafficking were comparable in both treated and control animals. These results suggest that desmosterol can either substitute functionally for cholesterol in the retina or it can complement subthreshold levels of cholesterol by sterol synergism.

Paper no. L8271 in *Lipids 35*, 289–296 (March 2000).

One focus of our research over the past two decades has been the elucidation of the biological roles of sterols (e.g., cholesterol) and other isoprenoids in the vertebrate retina, with emphasis on their involvement in the biogenesis and renewal of retinal rod outer segment (ROS) membranes (reviewed in Ref. 1). To address this problem, we took two different general approaches. In the first, we attempted to deplete the retina of its endogenous cholesterol by intravitreal administration of lovastatin (mevinolin; Mevacor®, Merck & Co., Rahway, NJ), a global inhibitor of *de novo* isoprenoid biosynthesis (2), and then we examined the effects of this treatment on retinal lipid metabolism, histology, and ultrastructure. While this strategy proved effective in blocking *de novo* cholesterol synthesis in adult rat retinas (3,4) and caused a profound and irreversible retinal degeneration (4,5), we were unable to reduce appreciably the steady-state cholesterol content of the retina by this method. This latter finding likely is due to a combination of two factors: (i) lovastatin treatment does not prevent delivery and uptake of blood-borne cholesterol to the retina (e.g., *via* the low density lipoprotein pathway), and (ii) the endogenous cholesterol in the retina has a very slow turnover rate and also apparently is "recycled" within the retina (for a detailed discussion, see Ref. 1). The degenerative effects of intravitreal lovastatin are thought to be a consequence of the inhibition of protein prenylation, rather than due to effects on *de novo* sterol biosynthesis (4). Hence, we sought to use a different approach, this time attempting to replace the endogenous cholesterol in the retina with other, biogenically related sterols, using selective, late-stage inhibitors of the sterol pathway that cause reduction of endogenous cholesterol and concomitant accumulation of cholesterol precursors. One such late-stage inhibitor is 3-β(2-diethylaminoethoxy)androst-5-en-17-one hydrochloride (U18666A), which blocks desmosterol Δ^{24}-reductase and also (at much higher concentrations) can inhibit oxidosqualene cyclase (6,7) (Fig. 1). Previously, it was shown that systemic treatment of neonatal rats with U18666A leads to cataract formation (8). In the present study, we evaluated the effects of U18666A treatment on retinal sterol composition and metabolism, as well as its effects on retinal histology, ultrastructure, and ROS membrane assembly in neonatal rats.

*To whom correspondence should be addressed at Saint Louis University Eye Institute, 1755 S. Grand Blvd., St. Louis, MO 63104-1540.
E-mail: Fliesler@slu.edu.

Abbreviations: EM, electron microscopy; HPLC, high-performance liquid chromatography; LM, light microscopy; LMARG, light microscopic autoradiography; NSL, nonsaponifiable lipids; RIS, rod inner segment; ROS, rod outer segment; SDS, sodium dodecyl sulfate; SDS-PAGE, SDS-polyacrylamide gel electrophoresis; SLO, Smith-Lemli-Opitz syndrome; U18666A, 3-β(2-diethylaminoethoxy) androst-5-en-17-one hydrochloride; Δ^5, cholesterol (cholest-5-en-3β-ol); $\Delta^{5,24}$, desmosterol (cholesta-5,24-dien-3β-ol).

EXPERIMENTAL PROCEDURES

Materials. Unless otherwise stated, all reagents and lipid standards were of analytical reagent grade or higher and were used as purchased from Sigma Chemical Co. (St. Louis, MO).

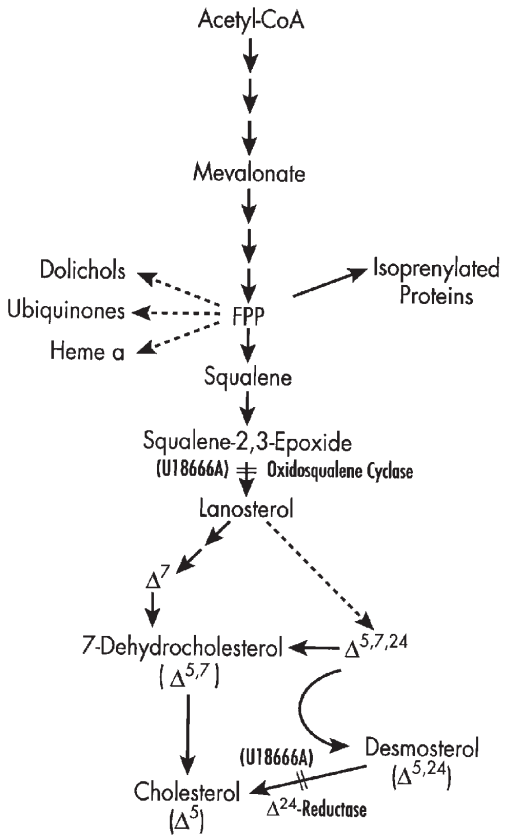

FIG. 1. Schematic diagram of the isoprenoid pathway, illustrating inhibition of the pathway by 3-β(2-diethylaminoethoxy)androst-5-en-17-one hydrochloride (U18666A). The primary site of enzymatic inhibition is at the level of desmosterol reductase (Δ^{24}-reductase); a secondary site of inhibition (at high concentrations of U18666A) is at the level of oxidosqualene cyclase. FPP, farnesyl pyrophosphate.

U18666A was a generous gift from Upjohn Co. (Kalamazoo, MI). [^{3}H]Acetate (Na salt; 15 Ci/mmol) and L-[3,4,5-^{3}H]leucine (120 Ci/mmol) were used as purchased from American Radiolabeled Chemicals (St. Louis, MO). All organic solvents were high-performance liquid chromatography (HPLC) grade (Burdick & Jackson, McGraw Park, IL). Microscopy supplies were obtained from Electron Microscopy Sciences (Fort Washington, PA) and from Polysciences, Inc. (Warrington, PA). Gel electrophoresis reagents and supplies and protein molecular weight markers were from Bio-Rad Laboratories (Richmond, CA).

Animals. All procedures performed on animals were in compliance with the *NIH Guide for the Care and Use of Laboratory Animals* and with the *ARVO Resolution on the Use of Animals in Research*. Female Sprague-Dawley rats (200–250 g; Hilltop Lab Animals, Scottdale, PA, or Harlan Sprague-Dawley, Inc., Indianapolis, IN) and their litters (8–11 pups each) were maintained under cyclic lighting (12 h light, 12 h dark; standard fluorescent room illumination) at 70–75°C ambient temperature, with *ad libitum* access to water and standard rodent chow (LM-485; Tek Lad, Indianapolis, IN). Animals were euthanized by exposure to carbon dioxide vapors.

U18666A treatment protocol. Using the protocol essentially as described by Cenedella and Bierkamper (8), litters of rat pups were injected every other day with U18666A (15 mg/kg, in U.S.P. olive oil suspension. *s.c.*), starting on postnatal day 1 (P1) and continuing through 3 wk (P21). Control pups received olive oil vehicle injections alone. In this series, at least 80% of the treated animals developed cataracts by P21, whereas cataracts were not observed in any of the control animals.

Lipid analysis. Retinas and lenses from P21 animals were harvested in pairs, pooling the tissues from both eyes of a given animal. Intracardiac blood was drawn and allowed to clot, and serum was obtained by centrifugation. Livers were removed, rinsed briefly with phosphate-buffered saline, blotted dry, and weighed prior to saponification. Conditions for saponification, extraction of nonsaponifiable lipids, and analysis of the nonsaponifiable lipids by HPLC and radio-HPLC were as described previously (9). For these analyses, we employed a Brownlee Spheri-5 C18 reversed-phase column (100 × 4.6 mm; PerkinElmer, Norwalk, CT) with a NewGuard® RP-18 guard column (PerkinElmer), using MeOH as the mobile phase (flow rate, 1 mL/min), with detection at 205 nm. Using this system, desmosterol (cholesta-5,24-dien-3β-ol) ($\Delta^{5,24}$) had a relative retention time of 0.82 [relative to that of cholesterol (cholest-5-en-3β-ol) (Δ^5), 1.00] and a relative molar response factor of 2.53 (relative to cholesterol, 1.00). Squalene had a relative retention time of 1.43 and a relative molar response factor of 12.89. By comparison, squalene-2,3-epoxide (a gift from Dr. Thomas Spencer, Department of Chemistry, Dartmouth College) had a relative retention time of 0.74. HPLC peak assignments were made in comparison with these reference standards, and each sterol was quantified by integrated peak area analysis in comparison with the empirically determined response factor (integration units per nmol) for the given standard compound.

Assessing de novo *lipid synthesis.* To evaluate the effect of U18666A on *de novo* synthesis of retinal sterols, 3-wk-old rat pups (four treated, four control) were injected in each eye with [^{3}H]acetate (0.43 mCi/eye), by methods described in detail previously (3). After allowing 20 h for metabolism of the radiolabeled precursor, the animals were euthanized, and retinas were harvested in pairs and subjected to subcellular fractionation to obtain purified ROS membranes and a "residual retina" membrane fraction (see below). Those tissue fractions were then saponified, extracted, and the nonsaponifiable lipids were analyzed by radio-HPLC.

Subcellular fractionation. Purified ROS membranes and a "residual retina" membrane fraction (ROS-depleted retinal membranes) were prepared from pairs of pooled rat retinas by discontinuous sucrose gradient ultracentrifugation, using a minor modification of a procedure originally designed for frog retina, as described in detail elsewhere (10). In this case, density gradient solutions of 36, 32, and 26% sucrose (by weight) were employed, and ROS membranes were harvested from the 26%/32% sucrose solution interface.

Microscopy and autoradiography. In order to evaluate the effect of U18666A on the rate of ROS membrane assembly, as

well as to assess the effects on retinal histology and ultrastructure, another group of 3-wk-old rat pups (four treated, four control) was injected in each eye with [^{3}H]leucine (0.164 mCi/eye). Four days later (P25), the animals were euthanized; one eye from each animal was subjected to fixation in mixed aldehydes, processed for embedment in plastic resin, and subsequently analyzed by light and electron microscopy (LM, EM), as well as by light microscopic autoradiography (LMARG), as previously described (4,11). LM and LMARG sections were viewed and photographed with an Olympus BH-2 photomicroscope, using a 20× DPlanApo lens. The displacement of "bands" of silver grains from the base of ROS in LMARG autoradiograms from treated and control retinas was measured using an ocular micrometer reticule and a 63× oil immersion lens, making five independent measurements from three retinal sections per animal and three animals per group (treated vs. controls). EM sections were viewed and photographed with a JEOL 1200EX electron microscope (Tokyo, Japan).

Gel electrophoresis of retinal proteins. Companion retinas from contalateral eyes of animals injected intravitreally with [^{3}H]leucine were harvested, and ROS and residual retina membranes were prepared therefrom (see above). The tissue fractions were solubilized in sodium dodecyl sulfate (SDS) "sample buffer" (12), subjected to SDS-polyacrylamide gel electrophoresis (SDS-PAGE) on 10% polyacrylamide gels and then processed for fluorography as previously described (10,11) to visualize the radiolabeled retinal proteins. Total retinal protein (~50 μg) and ROS protein (5 μg) were loaded per lane from treated and control animal specimens. Apparent molecular weights of proteins were determined in comparison with authentic protein molecular weight standards.

RESULTS

The reversed-phase HPLC profiles for nonsaponifiable lipids obtained from the serum and livers of U18666A-treated and control rats at P21 are shown in Figure 2. In control tissues (Figs. 2C and 2D), cholesterol (Δ^5) was virtually the only sterol detected in appreciable amounts. However, in the corresponding tissues from U18666A-treated rats (Figs. 2A and 2B), the major identifiable sterol was desmosterol ($\Delta^{5,24}$), while cholesterol represented a comparatively minor component. Appreciable squalene mass also was observed in livers, but not serum, of both control and treated animals. Since the molar absorbance for desmosterol at 205 nm is 2.53 times that of cholesterol (due to the additional double bond), one cannot compare the peak heights directly by visual inspection to ascertain the relative proportion of each sterol. The corresponding quantitative data, taking the molar absorbance values for each sterol into account, for serum and liver sterols are given in Table 1. Total serum sterol levels were reduced by about one-third in treated animals, relative to controls. While serum cholesterol levels in treated rats were only about 17% of control values, desmosterol levels were nearly 280 times higher than in controls. Consequently, whereas the cholesterol/desmosterol molar ratio in control serum was ~480, this ratio was only 0.33 in the serum

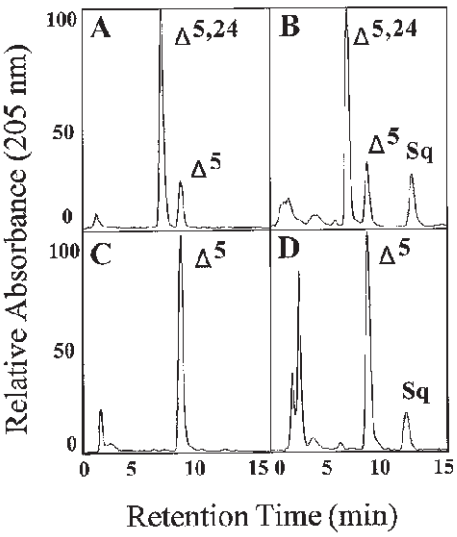

FIG. 2. Reversed-phase high-performance liquid chromatography (HPLC) chromatograms of nonsaponfiable lipids from serum (A,C) and liver (B,D) obtained from U18666A-treated (upper panels) and control (lower panels) rats. The elution positions corresponding to cholesterol (cholest-5-en-3β-ol) (Δ^5), desmosterol (cholesta-5,24-dien-3β-ol) ($\Delta^{5,24}$), and squalene (Sq) are indicated. Detector response (absorbance at 205 nm) is normalized to full-scale response for the predominant component. See Figure 1 for other abbreviation.

of treated animals (i.e., 0.07% of the control ratio). Similarly, total sterol levels in livers from treated animals were only about 84% of control levels, and cholesterol levels were only about 36% of control levels. However, desmosterol values from livers of treated animals were about 350 times the control levels; hence, the cholesterol/desmosterol molar ratio in livers of treated animals was only about 0.1% that of control livers.

A similar trend was found in the pattern of sterols obtained from "residual retina" and purified ROS membranes, as determined by HPLC (Fig. 3). Again, in control tissue fractions (Figs. 3C and 3D), cholesterol was the predominant sterol; a small peak corresponding to desmosterol also was observed. However, in retinas and ROS membranes from U18666A-treated animals (Figs. 3A and 3B), desmosterol was the major sterol, while cholesterol represented only a minor component. [The material eluting as broad, unresolved peaks prior to 5 min by reverse-phase HPLC represents variable, unidentified, polar components.] In good agreement with prior studies (3,9), rat retinas did not contain appreciable amounts of squalene. Quantitative sterol data for ROS membranes and residual retina are presented in Table 1. In control P21 rats, cholesterol accounted for >99 mol% of the total sterol mass in residual retina and ROS membranes, and the cholesterol/desmosterol molar ratios were ~171 and 149, respectively. In contrast, cholesterol represented only about one-half the total sterol mass in residual retina and ROS membranes (49.0 and 52.6%, respectively) of U18666A-treated P21 rats, so the cholesterol/desmosterol molar ratio in each was about one (0.98 and 1.11, respectively).

These data demonstrate that systemic treatment of neonatal rats with U18666A, using the given treatment protocol, re-

TABLE 1
Sterol Composition of Tissues from P21 Control and U18666A-Treated Rats[a]

	Total sterol	Cholesterol	Desmosterol	$\Delta^5/\Delta^{5,24}$ Molar ratio
Serum (μmol/mL)				
Control	2.79 ± 0.08	2.78 ± 0.09	0.005 ± 0.003	480 ± 110
U18666A	1.87 ± 0.14	0.47 ± 0.07	1.40 ± 0.09	0.33 ± 0.04
Liver (μmol/g wet wt)				
Control	2.18 ± 0.28	2.18 ± 0.28	0.003 ± 0.001	757 ± 235
U18666A	1.83 ± 0.17	0.78 ± 0.10	1.05 ± 0.09	0.73 ± 0.10
Residual retina (nmol/retina)				
Control	33.4 ± 2.1[b]	33.2 ± 2.1	0.20 ± 0.01	171 ± 21
U18666A	32.4 ± 1.2[b]	15.9 ± 0.04	16.5 ± 1.2	0.98 ± 0.09
ROS membranes (nmol/retina)				
Control	4.8 ± 0.6[b]	4.8 ± 0.6	0.03 ± 0.01	149 ± 26
U18666A	3.8 ± 0.9[b]	2.0 ± 0.9	1.8 ± 0.7	1.11 ± 0.09

[a]Values expressed as means ± SEM. $n = 4$ for control rats; $n = 3$ for U18666A rats. Unless otherwise indicated, all values are statistically significant (Student's *t*-test) at the $P < 0.001$ level, comparing a given sterol in treated vs. control tissue. U18666A, 3-β(2-diethylaminoethoxy)androst-5-en-17-one hyhdrochloride; Δ^5, cholesterol (cholest-5-en-3β-ol); $\Delta^{5,24}$, desmosterol (cholesta-5,24-dien-3β-ol).
[b]Not significant at the $P < 0.05$ confidence level.

sulted in abnormal and marked accumulation of desmosterol and substantial reduction of cholesterol in serum, liver, retina, and ROS membranes, with desmosterol accounting for the predominant sterol in all tissues examined. In addition, the lack of reduction in total sterols plus the absence of a component exhibiting the chromatographic properties of squalene-2,3-epoxide (which would have eluted just prior to desmosterol on the HPLC system employed) in the residual retina and ROS membrane fractions suggests that, under these conditions, the enzymatic inhibition was restricted to desmosterol reductase and did not compromise oxidosqualene cyclase (*cf.* Ref. 7 and Fig. 1). Although squalene-2,3-epoxide was not detected in the liver or serum of U18666A-treated rats, the apparent reduction of total sterols in these fractions (Table 1) suggests that inhibition occurred at an earlier enzymatic site in the cholesterol pathway, in addition to desmosterol reductase.

The data presented above represent the steady-state composition of the tissues examined. In the case of retina and ROS membranes, the marked increase in desmosterol could arise by two different mechanisms: either desmosterol synthesized in the liver and transported *via* the blood was taken up by the retina or the systemically administered U18666A was able to cross the blood-retina barrier and affect "local" (endogenous) retinal sterol metabolism. To distinguish between these two possibilities, control and U18666A-treated rats were injected intravitreally with [^{3}H]acetate, and the resulting radiolabeled nonsaponifiable lipid products from the retinas were analyzed by reversed-phase, radio-HPLC. The chromatographic profiles are shown in Figure 4. As before, cholesterol represented virtually all of the sterol mass in the control profile (Fig. 4A, upper panel), ~80% of the total recovered radioactivity was coincident with the cholesterol mass peak by radio-HPLC (Fig. 4A, lower panel). About 15% of the total radioactivity exhibited the chromatographic properties of desmosterol. In contrast, almost the reverse pattern of incorporation was observed in retinas from U18666A-treated animals (Fig. 4B). Of the total recovered nonsaponifiable radioactivity, ~88% was coincident with the major mass peak, which corresponded to desmosterol; only about 11% of the radioactivity exhibited the chromatographic properties of cholesterol, coincident with the minor sterol mass peak. These data demonstrate that U18666A, administered subcutaneously, was able to enter the retina (i.e., by crossing the blood-retina barrier) and alter endogenous retinal sterol metabolism, such that *de novo* cholesterol biosynthesis was effectively blocked and desmosterol levels were increased.

Having documented that treatment of neonatal rats for 3 wk with U18666A caused a dramatic change in the sterol composition and metabolism of the retina, we then examined the his-

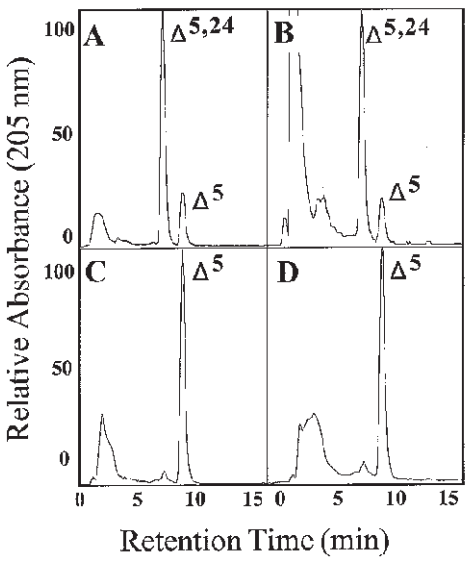

FIG. 3. Reversed-phase HPLC chromatograms of nonsaponfiable lipids from "residual retina" (A,C) and rod outer segment (ROS) layer membranes (B,D) obtained from U18666A-treated (upper panels) and control (lower panels) rats. The elution positions corresponding to Δ^5 and $\Delta^{5,24}$ are indicated. Detector response (absorbance at 205 nm) is normalized to full-scale response for the predominant component. See Figures 1 and 2 for abbreviations.

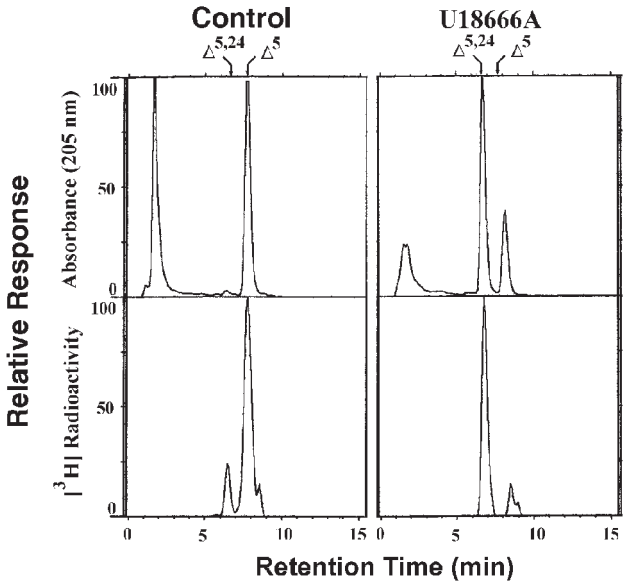

FIG. 4. Reversed-phase, radio-HPLC chromatograms of nonsaponifiable lipids obtained from control (left panels) and U18666A-treated rat retinas (right panels), 20 h after intravitreal injection with [3H]acetate. The elution positions for Δ^5 and $\Delta^{5,24}$ are indicated. Upper panels, absorbance at 205 nm, normalized to full-scale response for predominant component; lower panels, radioactivity, normalized to full-scale response for predominant component. See Figures 1 and 2 for abbreviations.

tological and ultrastructural consequences of these alterations. Initially, we evaluated retinas of control and U18666A-treated rats by light microscopy. As shown in Figure 5, there were no apparent alterations in retinal histology of the treated animals (Fig. 5B), compared with controls (Fig. 5A). Retinas exhibited normal histological organization, without evidence of dysplasia, unusual incidence of cell death, or other cytopathological features. Cell layer thickness and nuclear counts (e.g., vertical rows of nuclei in the outer nuclear layer) were qualitatively comparable between control and treated specimens, and the photoreceptors exhibited normal outer segment length and appearance. At the EM level (Fig. 6), the ultrastructural features of U18666A-treated retinas (Figs. 6B and 6D) also were comparable to those of control retinas (Figs. 6A and 6C). Cells of the retinal pigment epithelium exhibited the normal, polarized distribution of intracellular organelles: mitochondria were localized in close apposition to the basal infoldings of the plasma membrane, the cytoplasm did not contain unusual or excessive inclusions, the apical microvilli were extended normally, and the cells did not exhibit hypertrophy, pyknosis, or other evidence of cytopathology. ROS exhibited comparable ultrastructure in treated and control specimens, although the membranes in both were somewhat disorganized, most likely as a consequence of the immersion fixation employed. Rod inner segments (RIS), which contain the cell's metabolic machinery (endoplasmic reticulum, Golgi apparatus, mitochondria, lysosomes, etc.), appeared normal, and there were no obvious defects in the connecting cilium or other cytological elements. Hence, despite the marked alteration of sterol composition and metabolism in the retina caused by U18666A treatment, there were no obvious concomitant histological or ultrastructural changes in the retina.

In order to evaluate the possibility that ROS membrane as-

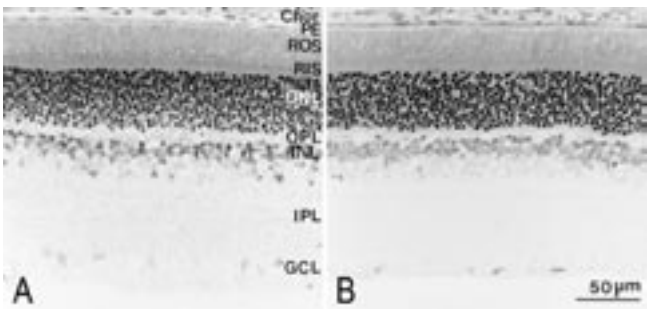

FIG. 5. Light microscopy of rat retinas from a control (A) and a U18666A-treated animal (B). Abbreviations (from top to bottom): Chor, choroid; PE, retinal pigment epithelium; RIS, rod inner segment layer; ONL, outer nuclear layer; OPL, outer plexiform layer; INL, inner nuclear layer; IPL, inner plexiform layer; GCL, ganglion cell layer. See Figures 1 and 3 for other abbreviations. Scale bar (both panels), 50 μm.

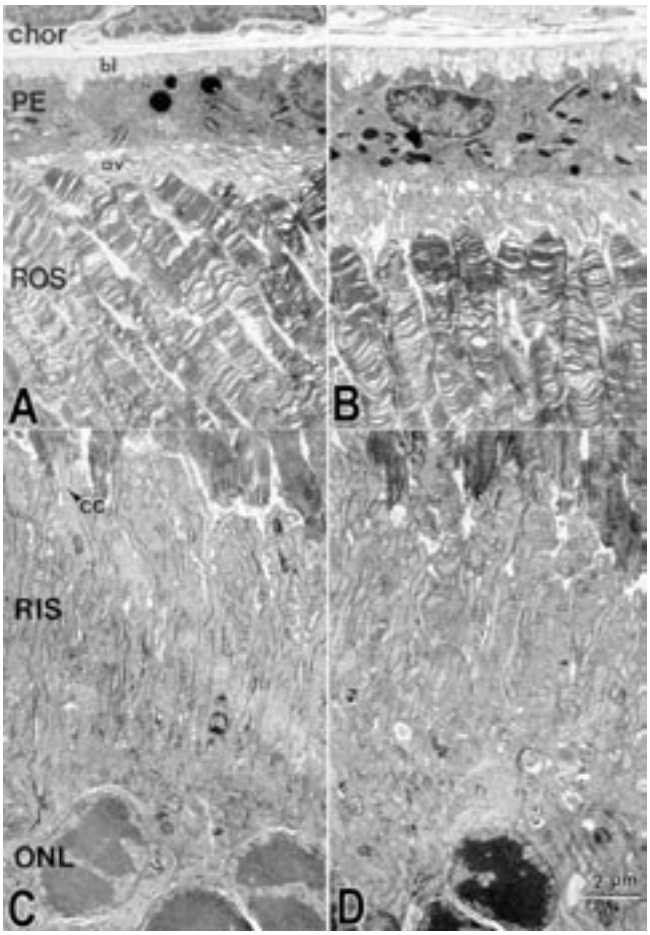

FIG. 6. Electron micrographs of the outer retinal layer from a control (A,C) and a U18666A-treated rat (B,D). Upper panels: PE and ROS; lower panels: RIS and ONL. Scale bar (all panels), 2 μm. See Figures 1,3, and 5 for abbreviations.

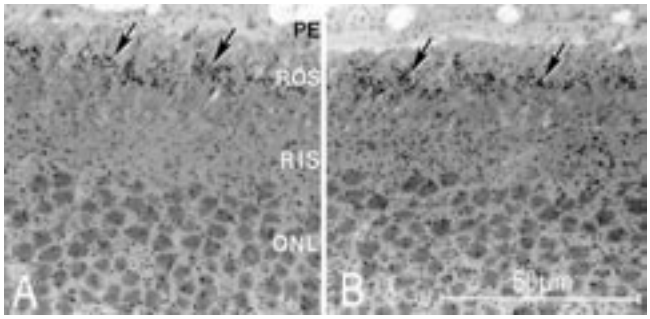

FIG. 7. Light microscopic autoradiograms of retinas from a control (A) and a U18666A-treated rat (B), 4 d after intravitreal injection with [^{3}H]leucine. "Bands" of silver grains (arrows), denoting the presence of newly synthesized proteins, are seen approximately half-way up the length of the ROS, while the other retinal layers exhibit a lighter, diffuse distribution of silver grains. See Figures 1, 3, and 5 for abbreviations. Scale bar (both panels), 50 μm.

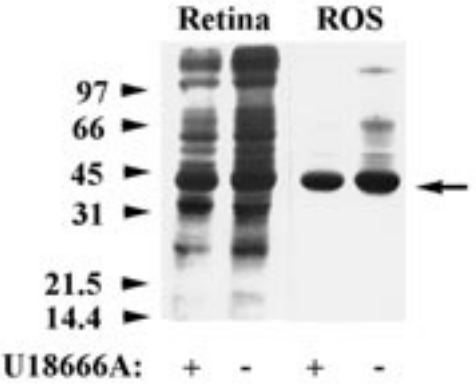

FIG. 8. Sodium dodecyl sulfate-polyacrylamide gel electrophoresis fluorogram of proteins obtained from control (–) and U18666A-treated (+) rat retinas and ROS membranes, 4 d after intravitreal injection of [^{3}H]leucine. Arrow denotes the migration position of opsin, the visual pigment apoprotein. Migration position of authentic protein molecular weight markers is indicated (values in kilodaltons). See Figures 1 and 3 for abbreviations.

sembly and turnover rates might be affected by the changes in retinal sterol composition and metabolism, we examined the retinas of control and U18666A-treated animals 4 d after intravitreal injection of [^{3}H]leucine, using LMARG. The autoradiograms obtained are shown in Figure 7. While the majority of the retinal tissue exhibited a diffuse "peppering" with silver grains (indicative of active protein synthesis in all cell types), the ROS exhibited a distinct, focal concentration of silver grains (so-called "bands"; arrows, Fig. 5), corresponding to the assembly of newly synthesized proteins into ROS disc membranes and their subsequent displacement from the base of the ROS toward the distal tip of the cell, due to membrane renewal (13,14). ROS length at P25 in the region of the retina chosen for analysis (superior, midperipheral retina, along the vertical meridian) was ~23.0 ± 2.1 μm , in good agreement with previous authors (15). Since the ROS renewal rate in rats is about 3 μm/d (16), a 4-d renewal period should yield a linear displacement of the band of silver grains ~12 μm from the base of the ROS, or about half-way up the length of the ROS, in good agreement with our experimental results (12.5 ± 2.5 m). No differences in band displacement between treated and control rats were observed; hence, there was no detectable difference in ROS membrane renewal rates as a function of U18666A treatment, despite the marked difference in retinal sterol composition and metabolism. These results also are consistent with the finding that ROS lengths were comparable in treated and control animals.

We also evaluated the effect of U18666A treatment on the *de novo* synthesis of total retinal proteins as well as the biosynthesis and incorporation of opsin (the "bleached," apoprotein form of rhodopsin) into ROS membranes, analyzing companion retinas and ROS membranes prepared therefrom by SDS-PAGE and fluorography from animals that had been injected intravitreally with [^{3}H]leucine and used for LMARG analysis (see above). The fluorograms are shown in Figure 8. The lanes containing proteins from whole retinas exhibited numerous radiolabeled protein bands, with the band corresponding to opsin (Fig. 8, arrow; $M_r \approx 38$ kDa), representing a dominant radiolabeled component. Qualitatively, while the overall intensity of the lane corresponding to proteins from the control retinas was slightly greater than that corresponding to proteins from the U18666A-treated retinas [likely due to variations in the intravitreal isotope injection efficiency (17)], there was a one-to-one correspondence between radiolabeled protein bands between the two lanes. This indicates that overall retinal protein synthesis was not adversely affected by U18666A treatment. In addition, both lanes corresponding to ROS proteins exhibited an intensely labeled band of approximately equal intensity, corresponding to opsin, which accounted for the overwhelming majority of the label on each lane by qualitative inspection. Hence, these results demonstrate that U18666A treatment did not perturb either opsin synthesis or its intracellular trafficking and subsequent incorporation into ROS membranes.

DISCUSSION

Previously, it was shown that systemic treatment of neonatal rats over a 3-wk period with U18666A results in cataract formation, which represents a significant change compared to normal lens structure and optical properties (8). In striking contrast, the present study demonstrates that, despite profound alterations in retinal sterol composition and metabolism under similar treatment conditions, there are no apparent histological or ultrastructural consequences to the retina. Furthermore, ROS membrane assembly and the biosynthesis, intracellular trafficking, and integration of rhodopsin into ROS membranes are not compromised by U18666A treatment.

One interpretation of these findings is that desmosterol, which accumulates in the retina and other tissues of U18666A-treated animals with concomitant reduction in the normal levels of cholesterol in those tissues, can effectively replace cholesterol functionally in the retina. If true, this is surprising, in view of previous studies that have examined the structural requirements for various sterols to support membrane enzymatic or other functions and structural integrity in defined lipid-pro-

tein systems and in living cells (reviewed in Refs. 18–20). In general, those studies have shown that sterols other than cholesterol (including desmosterol) typically do not support these biological activities or functions as well as does cholesterol. For example, in one study comparing the effects of various sterols on the activity of muscle membrane ion transporters in reconstituted proteoliposomes (21), it was found that desmosterol and 7-dehydrocholesterol were only 16.5 and 27% as effective, respectively, as cholesterol in supporting Na^+/Ca^{2+} exchanger activity, whereas those same sterols were 11.6 and 83.2% as effective, respectively, as cholesterol in supporting Na^+/K^+-ATPase activity. However, it is important to realize that in most studies of this kind, cholesterol was replaced quantitatively with an alternate sterol. The *in vivo* treatment protocol employed in the present study was only effective in replacing about half of the cholesterol in the retina or ROS membranes with desmosterol. Hence, it may be that there was still sufficient amounts of endogenous cholesterol remaining to support its biological functions in the retina.

Another possible explanation for the findings in this study may be "sterol synergism"—the ability of a nonphysiological sterol to supplement or act in concert with subthreshold levels of the endogenous sterol normally present in a cell or tissue, thereby supporting normal biological structure and function. Sterol synergism has been demonstrated with broad phylogenetic diversity (22–26). In the present study, possibly the unusually high levels of desmosterol (the "nonphysiological" sterol) that form and accumulate in the retina in response to U18666A treatment can somehow compensate for the diminished levels of cholesterol (the endogenous, physiological sterol), and the two act together to fulfill the sterol requirements of retinal cells. In the vertebrate retina, cholesterol accounts for only about 10 mol% of the total lipid in the retina and ROS membranes (27), which is considerably lower than the level of cholesterol in most other vertebrate tissues and plasma membranes (18–20). Hence, this level of cholesterol may be close to the threshold level necessary to support sterol-dependent biological functions in retinal cells.

Very little is known about the exact functions of cholesterol in the retina. In a series of elegant studies, Albert and coworkers (28–30) have provided evidence for a specific requirement for cholesterol in modulating rod photoreceptor signal transduction, *via* rhodopsin–cholesterol interactions, stabilization of rhodopsin and early photopigment "bleaching" intermediates, and possible membrane structure stabilization. It remains to be demonstrated whether or not sterols such as desmosterol can mimic or replace cholesterol in these functions.

It should be noted that a lethal, human, autosomal recessive disease has been described recently (31), for which the biochemical hallmarks are diminished cholesterol levels and profoundly elevated desmosterol levels in all tissues examined. This disease has been termed "desmosterolosis," and the findings are consistent with a genetic defect in 3β-hydroxysterol-Δ^{24}-reductase. Multiple congenital malformations are associated with this disease, including macrocephaly, ambiguous genitalia, osteosclerosis, craniofacial abnormalities, and short limbs. In the single case report of this disease, there was no description of the gross ocular anatomy or histology; hence, it is not known whether there are any ocular abnormalities (e.g., cataracts, retinal dystrophy, etc.) associated with this disease. This general presentation is reminiscent, in some respects, of the first multiple congenital anomalies syndrome described in the literature, namely Smith-Lemli-Opitz syndrome (SLO) (32), an autosomal recessive, frequently lethal disease that involves a defect in 3β-hydroxysterol-Δ^7-reductase, another late-stage enzyme in the cholesterol pathway (reviewed in Refs. 33,34). In that syndrome, patients accumulate massively abnormal levels of 7-dehydrocholesterol ($\Delta^{5,7}$) in their tissues and exhibit moderately to severely diminished cholesterol levels. Interestingly, the one documented report of retinal histopathology in an SLO patient (35) described relatively normal retinal morphogenesis, including normal stratification of retinal cell layers and differentiated morphology of the rod and cone photoreceptors. Hence, there is the possibility that sterols other than cholesterol can be accommodated in the normal development and maturation of the visual system, particularly the retina. In support of this, we have shown recently (36) that rats treated with AY9944, a selective inhibitor of 3β-hydroxysterol-Δ^7-reductase, exhibit normal ocular development, without cataracts or retinal dysplasia, as well as normal retinal electrophysiology, despite the fact that their retinas, ROS membranes, and all other tissues examined contain markedly elevated 7-dehydrocholesterol levels and profoundly diminished levels of cholesterol. Currently, we are performing similar studies to develop an animal model of desmosterolosis, using U18666A in place of AY9944, in order to further examine the effects of desmosterol accumulation and cholesterol synthesis inhibition on ocular development, with particular regard to the histological and ultrastructural maturation and electrophysiological function of the retina.

ACKNOWLEDGMENTS

The authors dedicate this article to the memory of Prof. George J. Schroepfer Jr. (d. Dec. 11, 1998), whose rigorous professional standards and numerous contributions have significantly advanced the field of sterol biochemistry and have influenced the careers of many scientists worldwide. These studies were supported by U.S.P.H.S. grants EY07361 (S.J.F.) and EY02568 (R.J.C.).

REFERRENCES

1. Fliesler, S.J., and Keller, R.K. (1997) Isoprenoid Metabolism in the Vertebrate Retina, *Int. J. Biochem. Cell Biol. 29*, 877–894.
2. Alberts, A.W., Chen, J., Kuron, G., Hunt, V., Hoffman, C., Rothrock, J., Lopez, M., Joshua, H., Harris, E., Patchett, A., Monaghan, R., Currie, S., Stapley, E., Albers-Schonberg, G., Hensens, O., Hirshfield, J., Hoogsteen, K., Liesch, J., and Springer, J. (1980) Mevinolin: A Highly Potent Competitive Inhibitor of Hydroxymethylglutaryl-coenzyme A Reductase and a Cholesterol-Lowering Agent, *Proc. Natl. Acad. Sci. USA 77*, 3957–3961.
3. Fliesler, S.J., Florman, R., Rapp, L.M., Pittler, S.J., and Keller, R.K. (1993) *In Vivo* Biosynthesis of Cholesterol in the Rat Retina, *FEBS Lett. 335*, 234–238.

4. Pittler, S.J., Fliesler, S.J., Fisher, P.L., Keller, R.K., and Rapp, L.M. (1995) *In Vivo* Requirement of Protein Prenylation for Maintenance of Retinal Cytoarchitecture and Photoreceptor Structure, *J. Cell Biol. 130*, 431–439.
5. Pittler, S.J., Fliesler, S.J., and Rapp, L.M. (1992) Novel Morphological Changes in Rat Retinas Induced by Intravitreal Lovastatin, *Exp. Eye Res. 54*, 149–152.
6. Phillips, W.A., and Avigan, J. (1963) Inhibition of Cholesterol Biosynthesis in the Rat by 3β-(2-diethylaminoethoxy) Androst-5-en-3-one Hydrochloride, *Proc. Soc. Exp. Biol. Med. 112*, 233–236.
7. Cenedella, R.J. (1980) Concentration-Dependent Effects of AY9944 and U18666A on Sterol Synthesis in the Brain, *Biochem. Pharmacol. 29*, 2751–2754.
8. Cenedella, R.J., and Bierkamper, G.G. (1979) Mechanism of Cataract Production by 3-β(2-diethylaminoethoxy) Androst-5-en-17-one Hydrochloride, U18666A: An Inhibitor of Cholesterol Biosynthesis, *Exp. Eye Res. 28*, 673–688.
9. Fliesler, S.J., and Keller, R.K. (1995) Metabolism of [^{3}H]Farnesol to Cholesterol and Cholesterogenic Intermediates in the Living Rat Eye, *Biochem. Biophys. Res. Commun. 210*, 695–702.
10. Fliesler, S.J., Florman, R., and Keller, R.K. (1995) Isoprenoid Lipid Metabolism in the Retina: Dynamics of Squalene and Cholesterol Incorporation and Turnover in Frog Rod Outer Segment Membranes, *Exp. Eye Res. 60*, 57–69.
11. Fliesler, S.J., and Basinger, S.F. (1985) Tunicamycin Blocks the Incorporation of Opsin into Retinal Rod Outer Segment Membranes, *Proc. Natl. Acad. Sci. U.S.A. 82*, 1116–1120.
12. Laemmli, U.K. (1970) Cleavage of Structural Proteins During the Assembly of the Head of Bacteriophage T4, *Nature 227*, 680–685.
13. Droz, B. (1963) Dynamic Conditions of Proteins in the Visual Cells of Rats and Mice as Shown by Radioautography with Labeled Amino Acids, *Anat. Rec. 145*, 157–168.
14. Young, R.W. (1976) Visual Cells and the Concept of Renewal, *Invest. Ophthalmol. 15*, 700–725.
15. Dowling, J.E., and Sidman, R.L. (1962) Inherited Retinal Dystrophy in the Rat, *J. Cell Biol. 14*, 73–109.
16. Rapp, L.M., Tolman, B.L., Koutz, C.A., and Thum, L.A. (1990) Predisposing Factors to Light-Induced Photoreceptor Cell Damage: Retinal Changes in Maturing Rats, *Exp. Eye Res. 51*, 177–184.
17. O'Brien, P.J. (1993) *In vivo* Labeling of Retinal Components by Intraocular Injection, in *Methods in Neurosciences* (Hargrave, P.A., ed.), Vol. 15, pp. 75–85, Academic Press, San Diego.
18. Bloch, K. (1983) Sterol Structure and Membrane Function, *Crit. Rev. Biochem. 14*, 47–92.
19. Yeagle, P.L. (1988) Cholesterol and the Cell Membrane, in *Biology of Cholesterol* (Yeagle, P.L., ed.), pp. 121–145, CRC Press, Boca Raton.
20. Dahl, C., and Dahl, J. (1988) Cholesterol and Cell Function, in *Biology of Cholesterol* (Yeagle, P.L., ed.), pp. 148–171, CRC Press, Boca Raton.
21. Vemuri, R., and Philipson, K.D. (1989) Influence of Sterols and Phospholipids on Sacrolemmal and Sarcoplasmic Reticular Cation Transporters, *J. Biol. Chem. 264*, 8680–8685.
22. Dahl, J.S., Dahl, C.E., and Block, K. (1981) Effect of Cholesterol on Macromolecular Synthesis and Fatty Acid Uptake by *Mycoplasma capricolum*, *J. Biol. Chem. 256*, 87–91.
23. Ramgopal, M., and Block, K. (1983) Sterol Synergism in Yeast, *Proc. Natl. Acad. Sci. U.S.A. 80*, 712–715.
24. Parks, L.W., and Casey, W.M. (1995) Physiological Implications of Sterol Biosynthesis in Yeast, *Ann. Rev. Microbiol. 49*, 95–116.
25. Whitaker, B.D., and Nelson, D.L. (1988) Sterol Synergism in *Paramecium tetraurelia*, *J. Gen. Microbiol. 134*, 1441–1447.
26. Rujanavech, C., and Silbert, D.F. (1986) LM Cell Growth and Membrane Lipid Adaptation to Sterol Structure, *J. Biol. Chem. 261*, 7196–7203.
27. Fliesler, S.J., and Anderson, R.E. (1983) Chemistry and Metabolism of Lipids in the Vertebrate Retina, *Progr. Lipid Res. 22*, 79–131.
28. Boesze-Battaglia, K., and Albert, A.D. (1990) Cholesterol Modulation of Photoreceptor Function in Bovine Retinal Outer Segments, *J. Biol. Chem. 265*, 20727–20730.
29. Albert, A.D., Young, J.E., and Yeagle, P.L. (1996) Rhodopsin–Cholesterol Interactions in Bovine Rod Outer Segment Disk Membranes, *Biochim. Biophys. Acta. 1285*, 47–55.
30. Albert, A.D., Boesze-Battaglia, K., Paw, A., Watts, A., and Epand, R.M. (1996) Effect of Cholesterol on Rhodopsin Stability in Disk Membranes, *Biochim. Biophys. Acta. 1297*, 77–82.
31. FitzPatrick, D.R., Keeling, J.W., Evans, M.J., Kan, A.E., Bell, J.E., Porteous, M.E.M., Mills, K., Winter, R.M., and Clayton, P.T. (1998) Clinical Phenotype of Desmosterolosis, *Am. J. Med. Genet. 75*, 145–152.
32. Smith, D.W., Lemli, L., and Opitz, J.M. (1964) A Newly Recognized Syndrome of Multiple Congenital Anomalies, *J. Pediatr. 64*, 210–217.
33. Opitz, J.M., and de la Cruz, F. (1994) Cholesterol Metabolism in the RSH/Smith-Lemli-Opitz Syndrome: Summary of an NICHD Conference, *Am. J. Med. Genet. 50*, 326–338.
34. Tint, G.S., Batta, A.K., Xu, G., Shefer, S., Honda, A., Irons, M., Elias, E.R., and Salen, G. (1997) The Smith-Lemli-Opitz Syndrome: A Potentially Fatal Birth Defect Caused by a Block in the Last Enzymatic Step in Cholesterol Biosynthesis, in *Subcellular Biochemistry* (Bittman, R., ed.), Vol. 28, pp. 117–144, Plenum, New York.
35. Kretzer, F.L., Hittner, H.M., and Mehta, R.S. (1981) Ocular Manifestations of the Smith-Lemli-Opitz Syndrome, *Arch. Ophthalmol. 99*, 2000–2006.
36. Fliesler, S.J., Richards, M.J., Miller, C.-Y., and Peachey, N.S. (1999) Marked Alteration of Sterol Metabolism and Composition Without Compromising Retinal Development or Function, *Invest. Ophthalmol. Vis. Sci., 40*, 1792–1801..

[Received June 1, 1999, and in final revised form and accepted December 20, 1999]

Rationally Designed Inhibitors as Tools for Comparing the Mechanism of Squalene-Hopene Cyclase with Oxidosqualene Cyclase

Franca Viola[a], Maurizio Ceruti[a], Luigi Cattel[a], Paola Milla[a], Karl Poralla[b], and Gianni Balliano[a,*]

[a]Dipartimento di Scienza e Tecnologia del Farmaco, Università di Torino, 10125 Torino, Italy, and [b]Biologisches Institut, Mikrobiologie/Biotechnologie, Universität Tübingen, D-72076 Tübingen, Germany

ABSTRACT: The inhibition of squalene-hopene cyclase (SHC) (E.C. 5.4.99.-), an enzyme of bacterial membranes catalyzing the formation of pentacyclic sterol-like triterpenes, was studied by using different classes of compounds originally developed as inhibitors of oxidosqualene cyclase (OSC) (E.C. 5.4.99.7), the enzyme of eukaryotes responsible for the formation of tetracyclic precursors of sterols. The mechanism of cyclization of squalene by SHC, beginning with a protonation of the 2,3 double bond by an acidic residue of the enzyme, followed by a series of electrophilic additions of the carbocationic intermediates to the double bonds, is similar to the mechanism of cyclization of 2,3-oxidosqualene by OSC. The inhibitors studied included: (i) analogs of the carbocationic intermediates formed during cyclization, such as aza-analogs of squalene and 2,3-oxidosqualene; (ii) affinity-labeling inhibitors bearing a methylidene reactive group; and (iii) vinyldioxidosqualenes and vinylsulfide derivatives of the substrates. Comparison of the results obtained with the two enzymes, SHC and OSC, showed that many of the most effective inhibitors of OSC were also able to inhibit SHC, while some derivatives acted as specific inhibitors. Differences could be easily explained on the basis of the different substrate specificity of the two enzymes.

Paper no. L8276 in *Lipids 35,* 297–303 (March 2000).

Squalene-hopene cyclase (SHC) (E.C. 5.4.99.-) catalyzes a crucial step in the formation of hopene and hopanoids, a class of pentacyclic, sterol-like triterpenes present in many bacterial membranes. These molecules seem to be able to modulate membrane fluidity, similarly to the sterols in the membranes of eukaryotes (1). Squalene is cyclized by SHC with a mechanism sharing many important mechanistic similarities with the cyclization of 2,3-oxidosqualene by 2,3-oxidosqualene cyclase (OSC) (Scheme 1). During the complex cyclization reaction, the substrate squalene or 2,3-oxidosqualene, bound to the enzyme, is prefolded in a definite conformation, then protonated by a suitable aminoacidic residue of the active site, giving a series of carbocationic intermediates, which are stabilized by negative points of charge in the active site of the enzyme. The reaction is terminated by a final deprotonation which, in the case of OSC, follows a sequence of 1-2 hydride and methyl shifts (2).

Squalene-hopene cyclase from *Alicyclobacillus acidocaldarius* has been recently overexpressed in *Escherichia coli*, purified and crystallized (3,4). In comparing the sequence of SHC with sequences of eukaryotic OSC cloned from different animals, plants, and yeasts (5), a 17–27% identity between the two enzymes was found. Both enzymes have a molecular weight of 70–85 KDa and contain several repeats of a highly conserved motif rich in aromatic amino acids, the QW motif (6). Site-directed mutagenesis studies have shown that the two aspartate residues 376 and 377 in SHC and the corresponding aspartate residue 456 in yeast OSC are essential for enzymatic activity (7,8). These essential aspartic acid residues are located in a DCTAEA sequence, completely conserved in eukaryotic OSC, and in the corresponding sequence DDTA of SHC, similar to the known consensus DDXXD sequence of other terpene cyclases (9). Furthermore, the crystallization of SHC in the presence of the competitive inhibitor *N,N*-dimethyldodecylamine *N*-oxide has shown that the active site of the enzyme is a central cavity lined with aromatic amino acids, supporting a cyclization mechanism that starts with the protonation of the 2,3 double bond of squalene by the aspartate residue 376, situated on the top of the cavity and assisted by a near histidine residue (4).

Since no OSC have yet been crystallized, all information available about oxidosqualene cyclization mechanism is inferred from mutagenesis experiments and inhibition studies. The DCTAEA sequence has been shown to play a part in the active site of mammalian OSC by the irreversible inactivation and affinity labeling of the enzyme by the inhibitor 29-MOS, a methylidene derivative of the substrate (10) and a mechanistic hypothesis has been formulated by Corey *et al.* (11) on the basis of the results obtained with different sub-

*To whom correspondence should be addressed at: Dipartimento di Scienza e Tecnologia del Farmaco, Università di Torino, Via Pietro Giuria, 9, 10125, Torino, Italy. E-mail: balliano@pharm.unito.it

Abbreviations: CIMS, chemical ion mass spectrometry; EIMS, electron ion mass spectrometry; HRMS, high-resolution mass spectrometry; IC_{50}, inhibitor concentration reducing enzymatic conversion by 50%; IR, infrared; 29-MOS, 29-methylidene-2,3-oxidosqualene; NMR, nuclear magnetic resonance; OSC, 2,3-oxidosqualene-lanosterol cyclase; SHC, squalene-hopene cyclase; THF, tetrahydrofuran; TLC, thin-layer chromatography.

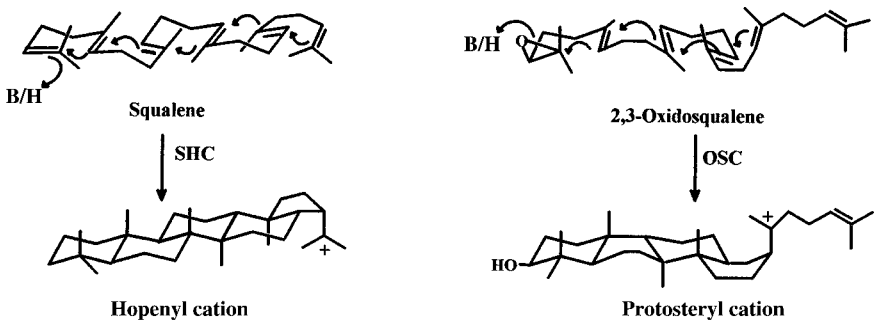

SCHEME 1

strate-modified inhibitors. So far, inhibition studies are the most important way to obtain insight into the mechanism of cyclization by OSC and have also given results consistent with crystallographic data on the active site structure of SHC.

Several inhibitors of OSC are known, but only few have also been studied as SHC inhibitors (12). Here we describe the effects on SHC of different classes of compounds previously studied by us only as OSC inhibitors. Our aim is to gather new information about similarities and differences in the mechanism of cyclization of the two enzymes, which could integrate the structural studies on SHC.

Basically three types of inhibitors were studied: (i) analogs of the carbocationic intermediates formed during cyclization, such as aza-analogs of squalene and 2,3-oxidosqualene (compounds **1–6**) (13), (ii) oxidosqualene derivatives bearing a conjugated methylidene group, designed as affinity-labeling inhibitors (compounds **7–13**) (14), and (iii) diepoxymethylidene and β-hydroxysulfide derivatives of the substrate, bearing the reactive groups at positions 15 or 19 (compounds **14–18**) (15,16).

MATERIALS AND METHODS

Chemicals. The ^{1}H nuclear magnetic resonance (NMR) spectra were recorded either on a JEOL EX 400 (JEOL, Inc., Peabody, MA) or a Bruker AC 200 instrument (Karlsruhe, Germany) in $CDCl_3$ solution at room temperature, with $SiMe_4$ as internal standard. Mass spectra were obtained on a Finnigan MAT TSQ 700 spectrometer (San Jose, CA). Infrared (IR) spectra were recorded on a PE 781 spectrophotometer (PerkinElmer, Palo Alto, CA). Microanalyses were performed on an elemental analyzer 1106 (Carlo Erba Strumentazione, Milano, Italy). The reactions were monitored by thin-layer chromatography (TLC) on F_{254} silica gel precoated sheets; after development, the sheets were exposed to iodine vapor. Flash-column chromatography was performed on 230–400 mesh silica gel. Tetrahydrofuran (THF) was dried over sodium benzophenone ketyl. All solvents were distilled prior to flash chromatography.

Nonradiolabeled and [3-^{3}H] squalene epoxide and [3-^{3}H] squalene were synthesized as previously described (17). Squalene, lanosterol, Triton X-100, and Na taurodeoxycholate were obtained from Sigma Chemical Co. (St. Louis, MO).

C_{27} squalene aldehyde **19** (Scheme 2) was obtained as previously reported (18). 2–Aza-2,3-dihydrosqualene **1** and its *N*-oxide **2** were synthesized and purified as previously reported (18). (6*E*)- **3** and (6*Z*)-10-azasqualene-2,3-epoxide **4** were obtained as described (19). 19-Azasqualene **5** and 19-azasqualene-2,3-epoxide **6**, respectively, were obtained as reported (13,20). The syntheses of (18*Z*)- **7**, (18*E*)-29-methylidene-2,3-oxidosqualene **8**, (18*E*)- **9,** and (18*Z*)-29-methylidene-2,3-oxidohexanorsqualene **10** were as reported (14). Vinyloxidosqualenes **13–15** and β-hydroxysulfide derivatives **16–18** were obtained as reported (21).

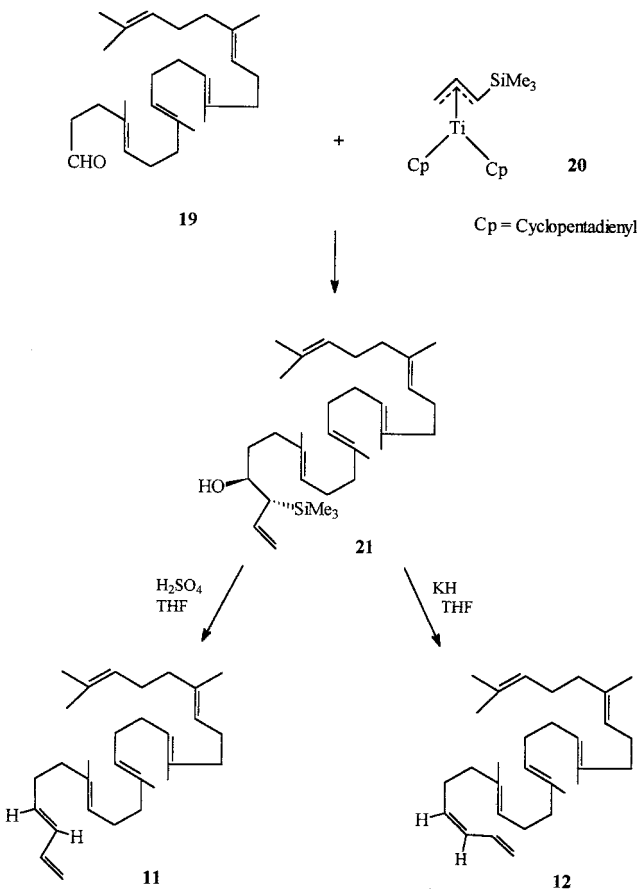

SCHEME 2

*(3*R**,4*S**,7*E*,11*E*,15*E*,19*E*)-7,11,16,20,24-Pentamethyl-3-(trimethylsilyl)-1,7,11,15,19,23-pentacosahexaen-4-ol (21, Scheme 2). (i) Reaction 1.* The allyl trimethylsilane (1.20 equiv., 174 mg, 1.52 mmol) was dissolved in anhydrous THF (5 mL) in a two-necked flask equipped with a perforable cap and stirred under a flux of dry argon. The reaction mixture was cooled to –60°C, and only a faint light was allowed in the laboratory. *n*-Butyllithium (1.6 M solution in hexane, 1.30 equiv., 1 mL, 1.65 mmol) was then added; during this time, the solution remained colorless. Hexamethylphosphoramide (0.4 mL) was added after 10 min, and the color turned orange. The mixture was then stirred for 1 h at –60°C.

(ii) Reaction 2. In another two-necked flask equipped with a perforable cap, dicyclopentadienyltitanium(II) dichloride $[(\eta^5C_5H_5)_2TiCl_2]$ (1.30 equiv., 411 mg, 1.65 mmol) was rapidly added, dissolved in anhydrous THF (5 mL), and stirred at room temperature under a flux of dry argon. Isobutylmagnesium chloride (2.0 M solution in diethyl ether, 1.30 equiv., 0.83 mL, 1.65 mmol) was added to the orange suspension. During the addition, effervescence occurred and the color turned to dark olive green. The flask was stirred in an oil bath at +40°C for 30 min.

(iii) Reaction 3. Both the flasks containing reaction 1 and reaction 2 were cooled to –90°C, and reaction 1 was transferred into reaction 2 using a cold glass syringe. The color turned immediately to dark purple, indicating the formation of the intermediate allyltrimethylsilyl dicyclopentadienyl titanium **20**; if the color turns brown, a sufficient amount of this intermediate has not formed. The reaction mixture was stirred for 30 min at –90°C.

(iv) Reaction 4. The C_{27} squalene aldehyde **19** (1 equiv., 488 mg, 1.27 mmol) dissolved in anhydrous THF (1 mL) was slowly added, with vigorous stirring at –90°C, slowly allowed to reach room temperature within 2 h in the acetone bath, and maintained for 30 min at room temperature. During this time the color turned to dark brown.

(v) Reaction 5. The 4 N HCl (5 mL) was slowly added at 0°C, while the reaction mixture turned orange, and was left for 30 min at this temperature, forming stereospecifically (3*R**,4*S**) trimethylsilyl alcohol **21**.

(vi) Reaction 6. The reaction mixture was transferred into an Erlenmeyer flask; water (50 mL) and diethyl ether (50 mL) were added, followed by oxidation with bubbling compressed air for 15 min. The mixture was extracted with diethyl ether (2 × 50 mL) after addition of brine (50 mL). The combined extracts were washed with brine (1 × 50 mL), dried with anhydrous sodium sulfate, and evaporated *in vacuo*. The crude orange oil was purified by flash chromatography with petroleum ether/diethyl ether, 99:1, to give 507 mg (80% yield from **19**) of (±)-(*R**,*S**) isomer **21** as a colorless oil. ^{1}H NMR ($CDCl_3$) δ 0.06 [*s*, 9 H, Si(C*H*$_3$)$_3$], 1.53–1.70 (*m*, 20 H, allylic CH_3 and C*H*$_2$CHOH), 1.98–2.20 (*m*, 19 H, allylic CH_2 and C*H*Si), 3.80 (*m*, 1 H, C*H*OH), 4.87–5.06 (*m*, 2 H, C*H*$_2$=CH), 5.00–5.25 (*m*, 5 H, vinylic CH), 5.82 (*m*, 1 H, CH_2=C*H*); IR (liquid film) 3620–3560, 2960, 2930, 2860, 1535, 1450 cm^{-1}; electron ion mass spectrometry (EIMS) *m/z* 498 (0.1), 481 (0.2), 411 (0.1), 365 (0.1), 343 (0.2), 310 (0.3), 203 (5), 134 (20), 93 (35), 81 (70), 73 (100); chemical ion mass spectrometry (CIMS) (isobutane) *m/z* 499 (0.5), 482 (40), 466 (33), 410 (100); high resolution mass spectrometry (HRMS) *m/z* 498.4261 (calc. for $C_{33}H_{58}OSi$ 498.4257). Anal. ($C_{33}H_{58}OSi$) C, H, O, Si.

(2E)-1-Methylidenenorsqualene: (3E,7E,11E,15E,19E)-7,11,16,20,24-pentamethyl-1,3,7,11,15,19,23-pentacosaheptaene (11, Scheme 2). Silyl alcohol **21** (150 mg, 0.30 mmol) was dissolved in THF (10 mL) and stirred under dry nitrogen. Two drops of concentrated H_2SO_4 were added, and it was allowed to react at room temperature for 24 h with stirring. The reaction mixture was poured in a separation funnel containing 10% nonradiolabeled $NaHCO_3$/diethyl ether, 1:1 (20 mL) and extracted with diethyl ether (3 × 30 mL). The combined extracts were washed with saturated brine (2 × 30 mL), dried with anhydrous sodium sulfate, and evaporated *in vacuo*. The resulting oil was purified by flash chromatography with petroleum ether to give 86 mg (70% yield from **21**) of compound **11** as a colorless oil. ^{1}H NMR ($CDCl_3$) δ 1.53–1.68 (*m*, 18 H, allylic CH_3), 2.00–2.20 (*m*, 20 H, allylic CH_2), 4.92–5.10 (*m*, 2 H, C*H*$_2$CH), 5.05–5.20 (*m*, 5 H, trisubstituted double-bond vinylic CH), 5.67 (*m*, 1 H, CH_2C*H*=CH), 6.03 (*m*, 1 H, CH_2CH=C*H*), 6.30 (*m*, 1 H, CH_2=C*H*); IR (liquid film) 2970, 2930, 2860, 1440, 1380 cm^{-1}; EIMS *m/z* 408 (1), 365 (0.5), 339 (1), 271 (2), 229 (4), 203 (5), 161 (8), 147 (12), 134 (40), 69 (100); CIMS (isobutane) *m/z* 409; HRMS *m/z* 408.3755 (calc. for $C_{30}H_{48}$ 408.3756). Anal. ($C_{30}H_{48}$) C, H.

(2Z)-1-Methylidenenorsqualene: (3Z,7E,11E,15E,19E)-7,11,16,20,24-pentamethyl-1,3,7,11,15,19,23-pentacosaheptaene (12, Scheme 2). KH (35% suspension in oil) was washed with pentane and rapidly dried. Pure KH (3 equiv., 36 mg, 0.90 mmol) was added in a two-necked flask, anhydrous THF (5 mL) was added, and the reaction mixture was stirred under dry nitrogen. Silyl alcohol **21** (150 mg, 0.30 mmol) was added at +10°C and allowed to react for 15 min. The mixture was then poured into nonradiolabeled 10% NH_4Cl/diethyl ether (1:1, 50 mL) and extracted with diethyl ether (3 × 30 mL). The combined extracts were washed with saturated brine (1 × 30 mL), dried with anhydrous sodium sulfate, and evaporated *in vacuo*. The resulting oil was purified by flash chromatography with petroleum ether, to give 105 mg (86% yield from **21**) of compound **12**, as a colorless oil. ^{1}H NMR ($CDCl_3$) δ 1.55–1.70 (*m*, 18 H, allylic CH_3), 1.98–2.20 (*m*, 18 H, allylic CH_2), 2.30 (*q*, 2 H, C*H*$_2$CH=CH), 5.02–5.24 (*m*, 7 H, trisubstituted double-bond vinylic CH and C*H*$_2$=CH), 5.45 (*m*, 1 H, CH_2C*H*=CH), 6.00 (*m*, 1 H, CH_2CH=C*H*), 6.63 (*m*, 1 H, CH_2=C*H*); IR (liquid film) 2970, 2930, 2860, 1440, 1380 cm^{-1}; EIMS *m/z* 408 (1), 365 (0.5), 339 (1), 271 (2), 229 (4), 203 (5), 161 (8), 147 (12), 134 (40), 69 (100); CIMS (isobutane) *m/z* 409; HRMS *m/z* 408.3759 (calc. for $C_{30}H_{48}$ 408.3756). Anal. ($C_{30}H_{48}$) C, H.

Enzymatic assays. Solubilized and partially purified pig liver and yeast oxidosqualene cyclase were obtained and the enzymatic activity determined as previously described (13,14). Recombinant squalene hopene cyclase was obtained as previously described (22).

For enzymatic activity determination, 10 μM squalene and 15,000 cpm of [3-^{3}H]squalene were dissolved in ethanol in the presence of Triton X-100 (final concentration 0.05%) in test tubes. Solvent was evaporated under nitrogen, and the enzyme (3 μg) in 1 mL of citrate buffer, 0.1 M, pH 6.0, containing 0.2% Na-taurodeoxycholate, was added to test tubes and incubated for 15 min at 60°C. The reaction was stopped by cooling the tubes in ice. After extracting with 2 mL of a mixture of *n*-hexane–isopropanol 3:2 (vol/vol), the solvent was evaporated. The extracts were redissolved in a small amount of CH_2Cl_2 and spotted on TLC plates developed twice, first 5 cm in CH_2Cl_2, then 15 cm in *n*-hexane. The conversion of squalene to labeled hopene and diplopterol was analyzed by radio-TLC scanner (Packard System 2000 Imaging Scanner; Hewlett-Packard, Palo Alto, CA), and percentage of transformation was calculated by integration. Alternatively, bands corresponding to squalene and hopene were scraped off and counted with a liquid scintillator (Beckman LS500 TD; Beckman Instruments, Fullerton, CA).

IC_{50} values (the concentration of inhibitor that reduced by 50% the enzymatic conversion) were determined by adding the inhibitors, as ethanolic solution, to the mixture of nonradiolabeled and labeled substrates and by incubating with SHC, as described.

The assay of cyclization of inhibitors **11** and **12** was carried out as follows: inhibitor (100 μM) was dissolved in ethanol in the presence of Triton X-100 (final concentration 0.05%) in test tubes. Ethanol was removed under nitrogen, and the enzyme (3 μg) in 1 mL of citrate buffer, 0.1 M, pH 6.0, containing 0.2% Na-taurodeoxycholate, was added to test tubes and incubated 1 h at 60°C. Reaction was stopped by cooling, and the mixture was worked up as described for substrate transformation except for the treatment of developed TLC plates, which were visualized by exposure to iodine or sulfuric acid.

RESULTS AND DISCUSSION

Several aza-derivatives of squalene and 2,3-oxidosqualene have already been studied as inhibitors of OSC. The most effective inhibitors were compounds such as 2–aza-2,3-dihydrosqualene **1** and its *N*-oxide **2** or 10- and 19-azasqualene-2,3-epoxide **3** and **6**. All of these compounds are supposed to be active because of their similarity to the carbocations formed in positions C-2, C-8, and C-20 during the cyclization of 2,3-oxidosqualene.

In Table 1, the IC_{50} inhibition values of SHC with these aza derivatives are compared with those found in pig liver and yeast OSC (13). It is evident that the aza derivatives **1** and **2** are inhibitors of SHC; our IC_{50} values are about the same as those obtained previously by Flesch and Rohmer (23). These compounds are analogs of the carbocation formed after the initial step of cyclization, i.e., the protonation of the 2,3 double bond in squalene cyclization, or the protonation of the 2,3-epoxide in the oxidosqualene cyclization.

The 6*E*-10-azasqualene-2,3-epoxide **3** was a very effective inhibitor, much more effective than the 6*Z*-10-aza-derivative **4**: a correct configuration of the analog, corresponding to the configuration of the substrate, is able to improve the inhibition of SHC as previously seen with OSC, indicating that the formation of the C-8 carbocation is an important step during the enzymatic cyclization of squalene and oxidosqualene.

The 19-azasqualene **5** and 19-azasqualene-2,3-epoxide **6**, differing only in the presence of the epoxidic function, were both active inhibitors of SHC: this result is not surprising,

TABLE 1
Inhibition Values (IC_{50}, μM) of Squalene-Hopene Cyclase (SHC) and Oxidosqualene Cyclase (OSC) by Azasqualene Derivatives

Compound		IC_{50} (μM)[a] SHC	OSC (pig liver)	OSC (yeast)
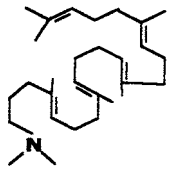	**1**	1.25	0.15	10
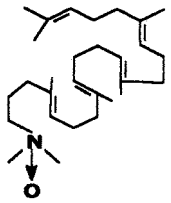	**2**	3.5	3.3	16
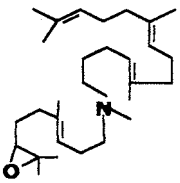	**3**	0.5	2.4	5
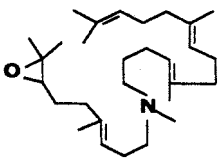	**4**	4	44	>100
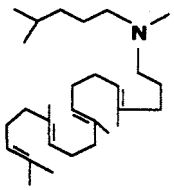	**5**	0.6	70	>100
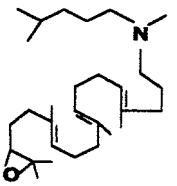	**6**	1	1.7	35

[a]IC_{50}, inhibitor concentration reducing enzymatic conversion by 50%.

since SHC is able to cyclize very efficiently, *in vitro*, not only squalene, the natural substrate, but 2,3-oxidosqualene, as well (16). The OSC, that cyclizes only (3*S*)-2,3-oxidosqualene, was differently inhibited by compounds **5** and **6**, the latter bearing the epoxidic function and being the only active inhibitor. The 19-azasqualene-2,3-epoxide **6** was a time-dependent, irreversible inhibitor of mammalian OSC (13). The SHC by contrast was not labeled after 1 h of incubation with [^{3}H]-19-azasqualene-2,3-epoxide: fluorography of the enzyme after the incubation in the presence of the labeled inhibitor showed no spots after 1 wk of exposure. Different inhibitory properties of **6** toward SHC (reversibly inhibited) and OSC (irreversibly inhibited) probably result from the different prefolding of inhibitor within the active site of the two enzymes and the different interaction between the nitrogen atom of the inhibitor and critical amino acidic residues in the active site.

The inhibitors listed in Table 2 are derivatives of different length, bearing a vinylic function at position C-19 or C-2. The (18*Z*)-29-MOS **7** (10,14) and the (18*E*)-hexanor-29-MOS **9** (14), were effective time-dependent inhibitors of pig liver and yeast OSC. Abe and Prestwich (9), using [^{3}H]-(18*Z*)-29-MOS **7**, have been able to label rat OSC, and Corey *et al*. (11), using a mixture of the two *E* and *Z* isomers **9** and **10** succeeded in labeling yeast OSC. Compound **7** has been found by Abe *et al.* (24) to label SHC 10 times less efficiently than OSC. A polycyclic C-31 dammarene derivative was obtained as cyclization product (24). Our results showed that SHC is inhibited at the same extent by the *Z* **7** and *E* **8** isomers of 29-MOS. Mammalian OSC by contrast was 10 times less sensitive to *E*-29-MOS **8,** which was also a poor time-dependent inhibitor (14).

SHC showed the same insensitivity for steric configuration, also with respect to *E* and *Z* isomers of hexanor derivatives **9** and **10**, which were both 5–15 times more efficient than *Z*-29-MOS **7** as inhibitors of SHC. The selective response to the configuration of the inhibitors bearing a vinyl function at C-19 seems to be a peculiar characteristic of OSC. This could be a consequence of mechanistic differences between the eukaryotic oxidosqualene and the bacterial squalene cyclases, which require a less elaborate system of directing the cyclization reaction, since the folding of the squalene in the active site of SHC is all prechair, a conformation less stressed than the prechair-preboat-prechair-preboat conformation of oxidosqualene in the active site of OSC. The rather free fitting of squalene-like molecules in the active site cavity of SHC is also demonstrated by the ability of SHC to cyclize not only (3*S*)-oxidosqualene but also the (3*R*)-isomer (2). The introduction of a vinylic group at C-19 in the oxidosqualene or hexanoroxidosqualene skeleton, such as in compounds **7**, **8**, **9**, **10**, made these compounds inhibitors of both OSC and SHC: conversely the introduction of the vinylic function at the C-2 of squalene, such as in compounds **11** and **12**, did not give any inhibitory properties either on OSC or SHC. Since a C-2 vinyl-derivative of oxidosqualene is both a poor inhibitor and a good substrate of OSC (25), compounds **11** and **12** could be expected to be cyclized by SHC: no metabolites or cyclization products, even in trace amounts, were instead detected after 1 h of incubation with SHC under conditions commonly adopted to obtain an effective transformation of the substrate to hopene. Surprisingly, *trans*-2-vinyl-2,3-oxido-1,1′-bisnorsqualene **13**, was selectively recognized by SHC and OSC, being a highly effective inhibitor of the prokaryotic enzyme and almost ineffective on the eukaryotic

TABLE 2
IC_{50} (μM) of SHC and OSC by Methylidene Derivatives of Squalene and Oxidosqualene[a]

Compound		IC_{50} (μM) SHC	OSC (pig liver)	OSC (yeast)
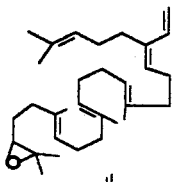	**7**	3	0.4	1
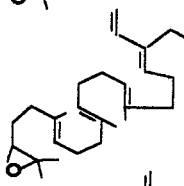	**8**	3	4	5
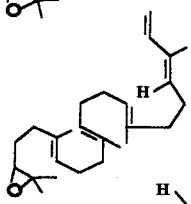	**9**	0.2	3.5	1.5
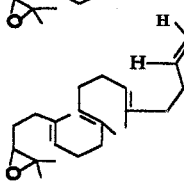	**10**	0.6	20	15
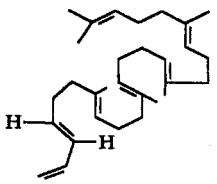	**11**	100	>100	>100
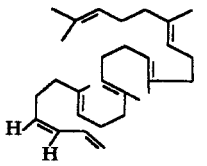	**12**	>100	>100	>100
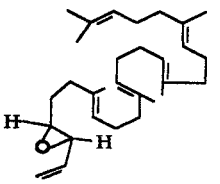	**13**	0.8	100	50

[a]See Table 1 for abbreviations.

TABLE 3
IC_{50} (μM) of SHC and OSC by Vinyldioxidosqualenes and Vinylsulfide Derivatives[a]

Compound		IC_{50} (μM) SHC	OSC (pig liver)	OSC (yeast)
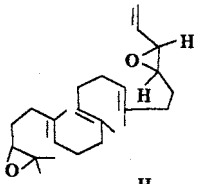	**14**	2.3	2.5	1.5
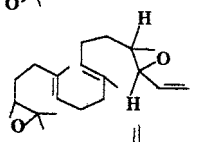	**15**	4.5	0.4	1.7
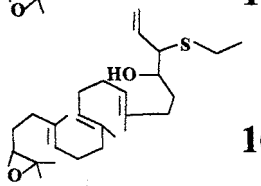	**16**	4.7	1.1	2.5
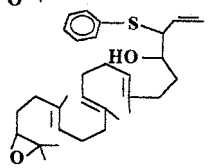	**17**	10	27	5
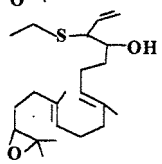	**18**	5	12	25

[a]See Table 1 for abbreviations.

cyclase. This result is difficult to explain, but we could tentatively hypothesize that this compound can be recognized by the enzymatic active site of SHC in both orientations: with the vinylepoxide in position 2,3 or in 22,23. In the second orientation it could interact with the cyclization of the fifth ring, only catalyzed by SHC. Experiments are in progress to check the time-dependent inhibition of **9** and **10** on SHC.

In Table 3, the inhibition values of some vinyldioxidosqualenes and β-hydroxysulfide derivatives are shown. The vinyldioxidosqualenes **14** and **15** were also inhibitors of SHC but with a lower extent than compounds **9** and **10**. The vinyl-β-hydroxysulfide derivatives **16**, **17,** and **18** are characterized by the presence of a sulfur atom at, or adjacent to, the critical positions of carbocationic intermediates formed by both OSC and SHC during the cyclization of substrate. All the compounds showed a good inhibition of SHC, while only **16** was very effective on pig liver OSC.

Work is in progress to crystallize SHC in the presence of some of the more active inhibitors.

ACKNOWLEDGMENTS

This work was supported by grants from the Ministero della Università e della Ricerca Scientifica e Tecnologica (MURST) and from Università degli Studi di Torino.

REFERENCES

1. Prince, R.C. (1987) Hopanoids: The World's Most Abundant Biomolecules? *Trends Biochem. Sci. 20*, 455–456.
2. Abe, I., Rohmer, M., and Prestwich, G.D. (1993) Enzymatic Cyclization of Squalene and Oxidosqualene to Sterols and Triterpenes, *Chem. Rev. 93*, 2189–2206.
3. Ochs, D., Kaletta, C., Entian, K.-D., Beck-Sickinger, A., and Poralla, K. (1992) Cloning, Expression, and Sequencing of Squalene-Hopene Cyclase, A Key Enzyme in Triterpenoid Metabolism, *J. Bacteriol. 174*, 298–302.
4. Wendt, K.U., Poralla, K., and Schulz, G.E. (1997) Structure and Function of a Squalene Cyclase, *Science 277*, 1811–1815.
5. Abe, I., Liu, W., Oehlschlager, A.C., and Prestwich, G.D. (1996) Mechanism-Based Active Site Modification of Oxidosqualene Cyclase by Tritium-Labeled 18-Thia-2,3-oxidosqualene, *J. Am. Chem. Soc. 118*, 9180–9181.
6. Poralla, K. (1994) The Possible Role of a Repetitive Amino Acid Motif in Evolution of Triterpenoid Cyclases, *Bioorg. Med. Chem. Lett. 4*, 285–290.
7. Feil, C., Sussmuth, R., Jung, G., and Poralla, K. (1996) Site-Directed Mutagenesis of Putative Active-Site Residues in Squalene-Hopene Cyclase, *Eur. J. Biochem. 242*, 51–55.
8. Corey, E.J., Cheng, H., Baker, C.H., Matsuda, S.P.T., Li, D., and Song, X. (1997) Methodology for the Preparation of Pure Recombinant *S. cerevisiae* Lanosterol Synthase Using a Baculovirus Expression System. Evidence That Oxirane Cleavage and A-Ring Formation Are Concerted in the Biosynthesis of Lanosterol from 2,3–Oxidosqualene, *J. Am. Chem. Soc. 119*, 1277–1288.
9. Abe, I., and Prestwich, G.D. (1995) Identification of the Active Site of Vertebrate Oxidosqualene Cyclase, *Lipids 30*, 231–234.
10. Xiao, X., and Prestwich, G.D. (1991) 29-Methylidene-2,3-oxidosqualene: A Potent Mechanism-Based Inactivator of Oxidosqualene Cyclase, *J. Am. Chem. Soc. 113*, 9673–9674.
11. Corey, E.J., Cheng, H., Baker, C.H , Matsuda, S.P.T., Li, D., and Song, X. (1997) Studies of the Substrate Binding Segments and Catalytic Action of Lanosterol Synthase. Affinity Labeling with Carbocations Derived from Mechanism-Based Analogs of 2,3-Oxidosqualene and Site-Directed Mutagenesis Probes, *J. Am. Chem. Soc. 119*, 1289–1296.
12. Ochs, D., Tappe, C.H., Gartner, P., Kellner, R., and Poralla, K (1990) Properties of Purified Squalene-Hopene Cyclase from *Bacillus acidocaldarius*, *Eur. J. Biochem. 194*, 75–80.
13. Viola, F., Brusa, P., Balliano, G., Ceruti, M., Boutaud, O., Schuber, F., and Cattel, L. (1995) Inhibition of 2,3-Oxidosqualene Cyclase and Sterol Biosynthesis by 10- and 19-Azasqualene Derivatives, *Biochem. Pharmacol. 50*, 786–796.
14. Ceruti, M., Rocco, F., Viola, F., Balliano, G., Milla, P., Arpicco, S., and Cattel, L. (1998) 29-Methylidene-2,3-oxidosqualene Derivatives as Stereospecific Mechanism-Based Inhibitors of Liver and Yeast Oxidosqualene Cyclase, *J. Med. Chem. 41*, 540–554.
15. Abad, J., Guardiola, M., Casas, J., Sanchez-Baeza, F., and Messeguer, A. (1996) 2,3;18,19-Dioxidosqualene Stereoisomers: Characterization and Activity as Inhibitors of Purified Pig Liver 2,3-Oxidosqualene-Lanosterol Cyclase, *J. Org. Chem. 61*, 7603–7607.
16. Rohmer, M., Bouvier, P., and Ourisson, G. (1980) Nonspecific Lanosterol and Hopanoid Biosynthesis by a Cell-Free System from the Bacterium *Methylococcus capsulatus*, *Eur. J. Biochem. 112*, 557–560.
17. Ceruti, M., Grosa, G., Rocco, F., Dosio, F., and Cattel, L. (1994) A Convenient Synthesis of [3-^{3}H]Squalene and [3-^{3}H]-2,3-Oxidosqualene, *J. Labelled Comp. Radiopharm. 34*, 577–585.

18. Ceruti, M., Balliano, G., Viola, F., Cattel, L., Gerst, N., and Schuber, F. (1987) Synthesis and Biological Activity of Azasqualenes, Bis-azasqualenes and Derivatives, *Eur. J. Med. Chem. 22*, 199–208.
19. Ceruti, M., Balliano, G., Viola, F., Grosa, G., Rocco, F., and Cattel, L. (1992) 2,3–Epoxy-10-aza-10,11-dihydrosqualene, A High-Energy Intermediate Analogue Inhibitor of 2,3-Oxidosqualene Cyclase, *J. Med. Chem. 35*, 3050–3058.
20. Ceruti, M., Rocco, F., Viola, F., Balliano, G., Grosa, G., Dosio, F., and Cattel, L. (1993) Synthesis and Biological Activity of 19-Azasqualene 2,3-Epoxide as Inhibitor of 2,3-Oxidosqualene Cyclase, *Eur. J. Med. Chem. 28*, 675–682.
21. Ceruti, M., Rocco, F., and Cattel, L., New Time-Dependent Inhibitors of 2,3–Oxidosqualene Cyclase with Hypocholesterolemic and Antifungal Activity, XIII Convegno Nazionale della Divisione di Chimica Farmaceutica, Paestum, 23–27 September, 1996, p. 50.
22. Wendt, K.U., Feil, C., Lenhart, A., Poralla, K., and Schulz, G. (1997) Crystallization and Preliminary X-ray Crystallographic Analysis of Squalene-Hopene Cyclase from *Alicyclobacillus acidocaldarius*, *Protein Sci. 6*, 722–724.
23. Flesch, G., and Rohmer, M. (1987) Growth Inhibition of Hopanoid Synthesizing Bacteria by Squalene Cyclase Inhibitors, *Arch. Microbiol. 147*, 100–104.
24. Abe, I., Dang, T., Zheng, Y.F., Madden, B.A., Fei, C., Poralla, K., and Prestwich, G.D. (1997) Cyclization of (3*S*)-29-Methylidene-2,3-oxidosqualene by Bacterial Squalene-Hopene Cyclase: Irreversible Inactivation and Isolation of an Unnatural Dammarenoid, *J. Am. Chem. Soc. 119*, 11333–11334.
25. Xiao, X., Sen, S.E., and Prestwich, G.D. (1990) Vinyl Oxirane Analog of (3*S*)-2,3-Epoxysqualene: A Substrate for Oxidosqualene Cyclase from Yeast and from Hog Liver, *Tetrahedron Lett. 31*, 2097–2100.

[Received June 8, 1999, and in final revised form and accepted December 17, 1999]

Structure-Apoptotic Potency Evaluations of Novel Sterols Using Human Leukemic Cells

Betty H. Johnson[a], Michael J. Russell[a], Alexander S. Krylov[b], Rheem D. Medh[a], Sylvette Ayala-Torres[a], Justin Lee Regner[a], and E. Brad Thompson[a,*]

[a]Department of Human Biological Chemistry and Genetics, The University of Texas Medical Branch, Galveston, Texas 77555-0645, and [b]Cardiology Research Center, Russian Academy of Medical Sciences, 121552 Moscow, Russia

ABSTRACT: Three oxidized analogs of cholesterol have been characterized for their ability to cause apoptotic cell death in CEM-C7-14 human leukemic cells. In addition to testing 15-ketocholestenol (K15), 15-ketocholestenol hydroxyethyl ether (CK15), and 7-ketocholesterol hydroxyethyl ether (CK7), an oxysterol of known apoptotic response, 25-hydroxycholesterol (25OHC), served as a standard for comparison. Growth studies based on dye exclusion by viable cells while using a sublethal concentration of oxysterols ranked their potency for cell kill as 25OHC > K15 > CK15 > CK7. Both the TUNEL assay (terminal deoxynucleotidyl transferase-mediated dUTP-X nick end labeling), which quantifies the amount of DNA nicks caused by a toxic agent, and the MTT assay, which measures cell metabolism and thus reflects cell viability, substantiated the same rank order. An ELISA assay for evaluating release of DNA fragments into the cytosol after treatment gave a similar potency order. The oncogene c-*myc* mRNA was suppressed by all three oxysterols, with 25OHC and K15 being the most potent suppressors. Hoechst and Annexin V staining documented that these oxysterols kill cells by an apoptotic pathway as evidenced by condensation of nuclear chromatin and plasma membrane inversion, respectively. From these *in vitro* studies, we believe that 25OHC, K15, and possibly CK15 have the potential to be chemotherapeutic agents.

Paper no. L8259 in *Lipids 35,* 305–315 (March 2000).

Both glucocorticoids and oxysterols can cause apoptosis of certain cells. For this action, glucocorticoids require a specific cytosolic protein, the glucocorticoid receptor (GR). No oxysterol receptor has been unequivocally identified, although two cellular proteins do specifically bind oxysterols: the oxysterol binding protein (OBP) and LXR, a member of the nuclear receptor family of proteins. As yet it is not certain that either protein is required for oxysterols' apoptotic actions. In our test system, the human leukemic cell line CEM, analysis of the events following addition of either class of steroid shows similarities at several points. These include a delay of about 1 d before the activation of caspases and nucleases, which occurs around the time of overt apoptosis. During this initial phase of cell death when the steroidal effects can be reversed, both types of steroids cause profound suppression of the oncogene product, cMyc (1,2). Because of their apoptotic action, glucocorticoids are used widely as antileukemic drugs. The similarity of effects of oxysterols suggests that they also might have therapeutic usefulness, alone, or in conjunction with glucocorticoids.

Oxysterols are able to elicit changes in cholesterol synthesis, cell growth, and membrane composition, and can cause immunosuppression (3–8). These activities have led to many studies of oxysterols, usually as toxins in the environment and foods (9,10), or as implicated in atherosclerosis (11–14). The relatively greater sensitivity of certain malignant, as opposed to normal, cells offers an opportunity to use oxysterols as chemotherapeutic drugs. A few investigators have recognized their potential as therapeutic agents (15–18).

Two oxysterols that are known to cause apoptosis have been well studied: one with high potency, 3β-hydroxycholest-5-en-25-diol (25-hydroxycholesterol, 25OHC) and the weaker 3β-hydroxycholest-5-en-7-one (7-ketocholesterol, K7) (19–23). Here we present tests of three oxysterols: 3β-hydroxy-5α-cholest-8(14)-en-15-one (15-ketocholestenol, K15), 3β-hydroxy-5α-cholest-8(14)-en-15-one 3β-2′-hydroxyethyl ether (15-ketocholestenol hydroxyethyl ether, CK15), and 3β-hydroxycholest-5-en-7-one 3β-2′-hydroxyethyl ether (7-ketocholesterol hydroxyethyl ether, CK7), comparing their apoptotoic effects and potencies to those caused by the known compound, 25OHC. The structures of these five oxysterols, as well as their parent compound, cholesterol, are shown in Scheme 1.

Two of the oxysterols under investigation were synthesized with bulky substitutions in the 3 position with the original intent of studying the importance of that position for binding to OBP. The third experimental oxysterol tests the effect of a keto substitution at position 15. C15 oxysterols have been evaluated for their synthetic paths, metabolism, occurrence, and effects on 3-hydroxy-3-methylglutaryl coenzyme A (HMGCoA) reductase; they are quite potent inhibitors of

*To whom correspondence should be addressed.
E-mail: bthompso@utmb.edu

Abbreviations: 7-ADD, 7-amino-actinomycin D; BSA, bovine serum albumin; CK7, 7-ketocholesterol hydroxyethyl ether; CK15, 15-ketocholestenol hydroxyethyl ether; HPLC, high-performance liquid chromatography; K7, 7-ketocholesterol; K15, 15-ketocholestenol; 25OHC, 25-hydroxycholesterol; DFBS, delipidated fetal bovine serum; FBS, fetal bovine serum; FITC, fluorescein isothiocyanate; GR, glucocorticoid receptor; HMGCoA, 3-hydroxy-3-methylglutaryl coenzyme A; LDL, low density lipoprotein; MTT, dimethyl tetrazolium salt; OBP, oxysterol binding protein; PS, phosphatidylserine; TUNEL, terminal deoxynucleotidyl transferase-mediated dUTP-X nick end labeling.

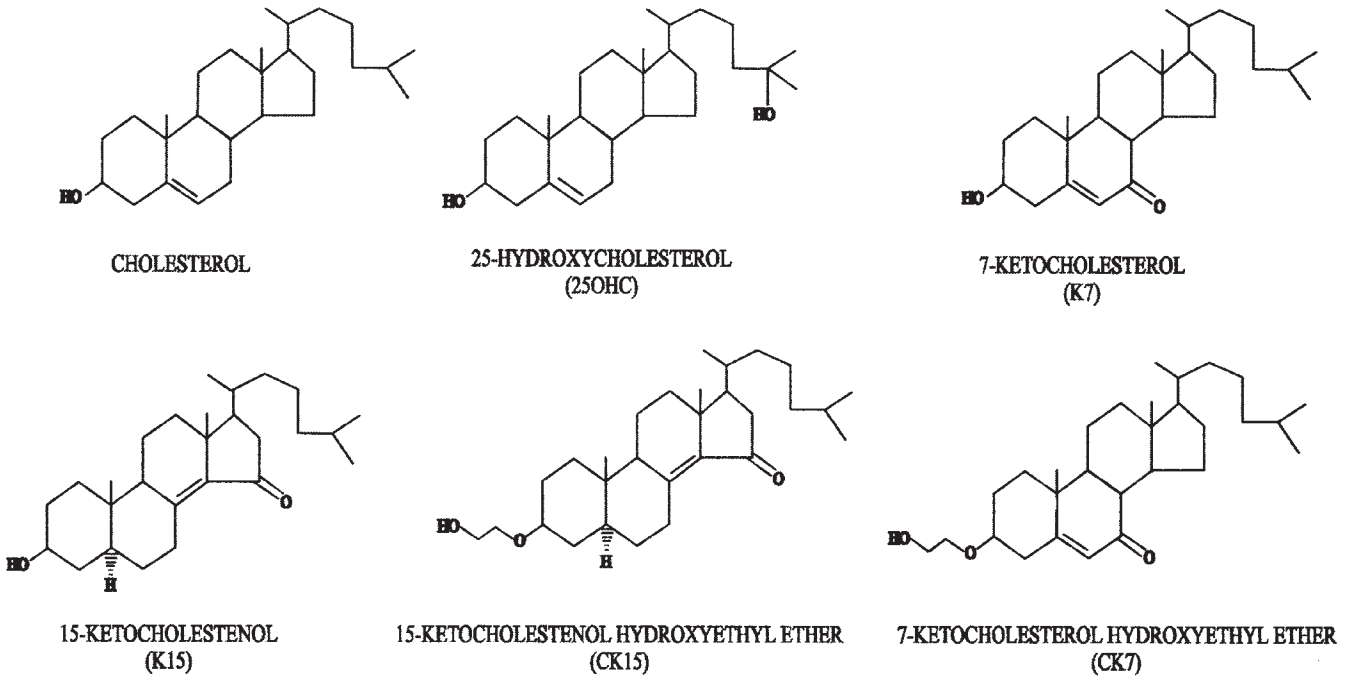

SCHEME 1

HMGCoA receptor expression and bind well to OBP (15). However, they have not been tested for their antileukemic effects. Clearly, it is important to determine the structural basis for other oxysterols' potency as apoptotic agents.

These agents were examined in the well-characterized human $CD4^+$ acute lymphoblastic leukemic clone CEM-C7, which was cloned without selective pressure from the original CEM line (24). CEM-C7 and cells of a recently obtained subclone CEM-C7-14 are both sensitive to glucocorticoids and oxysterols, but through independent pathways (20).

MATERIALS AND METHODS

Materials. K15, CK7, and CK15 were synthesized in the Cardiology Research Center (Moscow, Russia). 25OHC and K7 were purchased from Steraloids (Wilton, NH). All oxysterols were dissolved in ethanol and stored at a concentration of 10^{-2} M at –20°C in glass, protected from light. Prior to use each oxysterol was assayed by high-performance liquid chromatography (HPLC) to ascertain purity. RPMI 1640 medium was obtained from Fisher Scientific (Houston, TX), fetal bovine serum (FBS) from Atlanta Biologicals (Norcross, GA), and trypan blue dye from Gibco/BRL (Grand Island, NY). Delipidated FBS (DFBS), Dulbecco's phosphate-buffered saline (PBS), pH 7.4, propidium iodide, Hoechst 3342 stain, bovine serum albumin (BSA), growth supplements (insulin, transferrin, selenium), and the tetrazolium salt 3-[4,5-dimethyl(thiazol-2-yl)-3,5-diphenyl] tetrazolium bromide (MTT) were obtained from Sigma Chemical Co. (St. Louis, MO). All the reagents used for RNA extraction were molecular biology grade. Formamide and TRIzol reagent were purchased from Gibco/BRL, formaldehyde from J.T. Baker Chemical (Phillipsburg, NJ), and electrophoresis-grade agarose from FMS Products (Rockland, ME). The blotting membrane was from Schleicher & Schuell (Keene, NH). Radionuclides were purchased from ICN Radiochemicals (Cleveland, OH). The human c-*myc* exon 3 cDNA was obtained from Oncor (Gaithersburg, MD). The TUNEL and Cell Death Detection ELISA^{Plus} kits were purchased from Boehringer Mannheim (Mannheim, Germany). Ribonuclease A was obtained from Worthington Biochemical (Freehold, NJ). The Annexin V/FITC kit was from PharMingen (San Diego, CA).

Cell culture/growth inhibition. CEM-C7-14 cells were cultured in RPMI 1640 medium with 5% heat-inactivated whole FBS at 37°C, maintaining logarithmic growth in a humidified atmosphere of 95% air and 5% CO_2. To avoid any effects from the sterols in whole serum prior to oxysterol addition, cells were acutely transferred to 3% DFBS with 1% growth supplements in medium and incubated overnight. Oxysterols were then added as an ethanolic solution in 1% BSA in PBS; controls received ethanol only plus BSA; ethanol never exceeded 1% of culture volume. The number of viable cells at every time point was determined by using a hemacytometer and the trypan blue vital dye exclusion method (25). Control cells were fully viable for at least 4 d in medium containing delipidated serum and supplements.

MTT. An *in vitro* MTT assay for sensitivity to oxysterols was performed with the following modifications (26). For each concentration of oxysterol, triplicate 80 µL samples containing 2×10^5 cells/mL were plated in a 96-well tissue culture plate. Each well then received 20 µL oxysterol from stock solutions or dilutions thereof; final concentrations were 0.3, 0.5, 0.7, and 1 µM. Controls consisted of CEM-C7-14 cells in medium without oxysterol and medium without cells. After incubation at 37°C in 5% CO_2 for 48 h, 25 µL of MTT stock

solution was added. Following a 4 h incubation, 150 µL lysis buffer (20% sodium dodecyl sulfate, 20% dimethylformaldehyde, 2.5% 1 N HCl, 2.5% 80% acetic acid) was added to each well. After overnight incubation at 37°C, the samples were analyzed colorimetrically on a Biotek plate reader at 600 nm which was zeroed by assay blanks containing no cells.

DNA fragmentation. DNA fragmentation was followed by two methods. The first was a photometric enzyme immunoassay using the Cell Death Detection ELISA^{Plus} according to the protocol of the supplier (Boehringer Mannheim). CEM-C7-14 cells adapted to culture in supplemented medium with delipidated serum were treated with 1 µM oxysterol for 48 h. Triplicate samples (5×10^4 cells) were centrifuged 200 × *g* for 10 min at room temperature, and the supernatant was carefully removed. Two positive controls (DNA-histone complex) and two background samples (incubation buffer) were included. Color intensity was evaluated on a Packard microplate reader at 405 nm against the substrate solution as a blank.

The second DNA fragmentation method employed the terminal deoxynucleotidyl transferase-mediated dUTP-X nick end labeling (TUNEL) assay performed according to the protocol provided by the manufacturer (Boehringer Mannheim) with some modifications. Before fixation, 3×10^6 cells were washed twice with PBS containing 1% BSA. Cells were then fixed with freshly prepared 4% paraformaldehyde in PBS and incubated at room temperature for 30–60 min. Each assay contained one negative control (no transferase enzyme) and one positive control (cells treated with DNase I + transferase enzyme). After washing, all samples were stained with propidium iodide according to a method described by Van Houten and Budd (27) and incubated overnight in the dark. Samples (2×10^4 cells) were analyzed for DNA content and DNA breaks by flow cytometry using a FACScan (Fluorescence Activated Cell Sorter; Becton Dickinson, Bedford, MA) with Cell Quest 3.1 software (Becton Dickinson). Analysis was done with an argon-ion laser with excitation at 488 nm. Doublets and cells aggregates were excluded, and only the singlet cell population was analyzed. Red (propidium iodide) and green (fluorescein-dUTP) fluorescences were detected using 530- and 548-nm filters, respectively.

Northern blots. Total RNA was isolated using the TRIzol reagent according to the method provided by the manufacturer, Gibco/BRL. Total RNA was subjected to electrophoresis under denaturing conditions using a 1% agarose/6% formaldehyde gel and electroblotted on Nytran Plus nylon membranes. Hybridization was carried out for 18 h at 60°C with a ^{32}P-labeled random-primed c-*myc* cDNA fragment with specific activities of 1 to 8×10^9 dpm/µg of DNA. Normalization was accomplished by using the ethidium bromide stained ribosomal RNA that was transferred to the filter. The membranes were exposed for 24 h in a PhosphorImager cassette and analyzed using a PhosphorImager 425 (Molecular Dynamics, Sunnyvale, CA). The densities of the mRNA bands obtained from the PhosphorImager screen were quantified using the MD ImageQuant software (version 3.3) from Molecular Dynamics. The relative amounts of c-*myc* mRNA on the filters were compared by normalizing the quantified values to 18S ribosomal RNA bands on the same filters. At the exposure time selected for quantification, RNA signals were linear.

Flow cytometry. The staining for the flow cytometric evaluation of apoptotic changes was performed with the AnnexinV-FITC-7-AAD kit from Boehringer Mannheim. After CEM-C7-14 cells had been treated with 1 µM oxysterol for 4, 6, 24, 30, or 52 h, 2×10^5 cells were treated with Annexin V and 7-amino-actinomycin D (7-AAD) according to the supplier's protocol. CEM-C7-14 cells treated with 1 µM dexamethasone for 48 h were used as a positive control. Cells (2×10^4) were analyzed for Annexin V- and 7-AAD-positive cells by flow cytometry using a 488-nm excitation and a 515-nm bandpass filter for fluorescein detection and a filter >600 nm for 7-AAD detection on a FACScan (Becton-Dickinson). For photographs of stained cells, 3×10^5 CEM-C7-14 cells ± 1

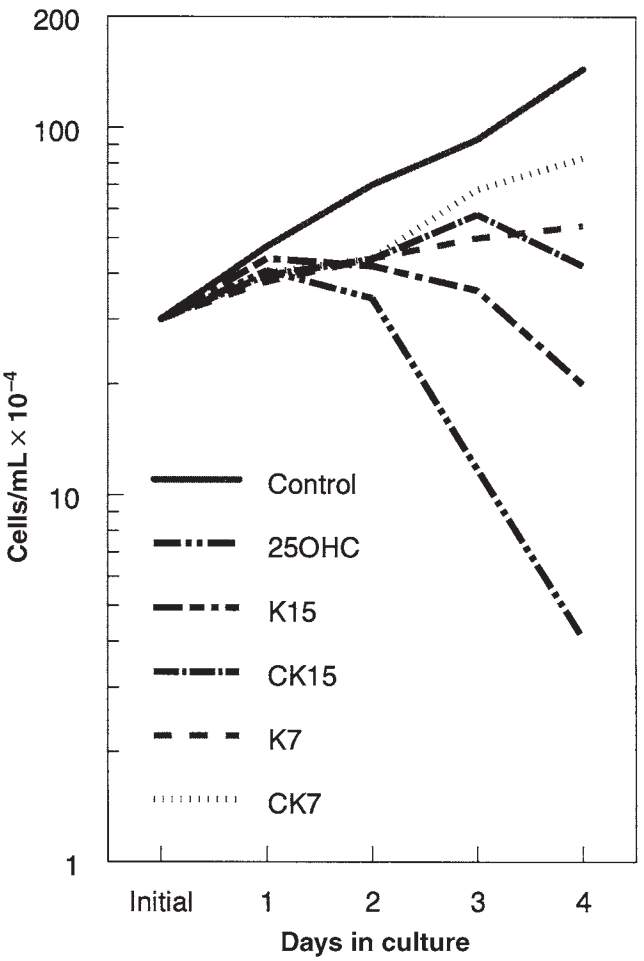

FIG. 1. Effect of 300 nM oxysterols on the growth and viability of CEM-C7-14 cells. Cells in logarithmic growth were exposed to 300 nM of each oxysterol, as described in the Materials and Methods section. Viable cells were counted daily for 4 d. The legend identifying each oxysterol is located to the left of the graph. Each time point represents the mean of 3–5 independent experiments; error bars were omitted for clarity of presentation, but the SD of each data point was less than or equal to 5%. 25OHC, 25-hydroxycholesterol; K15, 15-ketocholestenol; CK15, 15-ketocholestenol hydroxyethyl ether; K7, 7-ketocholesterol; CK7, 7-ketocholestenol hydroxyethyl ether.

μM oxysterols were treated with Annexin V/7-AAD as above and fixed with 4% fresh paraformaldehyde solution in PBS. Cells pellets were washed twice in cold PBS/BSA and resuspended in 100 μL permeabilization buffer (0.1% Triton-X 100 in 0.1% sodium citrate), washed twice in cold PBS/BSA, and resuspended in 800 μL PBS/BSA. Microscope slides that had been precoated with poly-L-lysine solution and dried were loaded with 2×10^4 cells and cytospun at 600 rpm for 5 min. The slides were stained for 10 min Hoechst 3342 stain (0.1 mg/mL water). Slides were mounted with Crystal Mount (Biomeda, Foster City, CA) and stored in the dark at 4°C. Photographs of the cytospun, stained cells were taken on a Nikon Eclipse E600 microscope (Melville, NY) with a Nikon FDX-35 camera at 100× magnification with illumination by white polarized light, 360/500-nm filter for the Hoechst stain and 488/515-nm for the Annexin V/7AAD stain.

RESULTS

Potency of oxysterol as judged by growth inhibition. The growth responses of cells from the freshly isolated CEM-C7-14 clone to the three experimental oxysterols were compared to those caused by the reaction of these cells to the standards 25OHC and K7. Sublethal concentrations of each oxysterol (300 nM) were added to cultures growing logarithmically in supplemented, delipidated RPMI 1640 medium. Total viable cells were counted initially and every 24 h for 4 d. Figure 1 shows the results of such a study with little to no cell death occurring in any oxysterol treatment during the first 24 h, though all slowed cell growth. Even by 48 h, there was little difference in the effect caused by these agents. However, beyond 72 h, 25OHC exhibited the greatest cell kill, followed by K15, K7 and CK15 continued to retard growth, and CK7 had the least effect. All of the treated cultures did contain trypan blue-positive cells, indicating that some cell death had occurred.

Extent of apoptosis as judged by MTT, cytosolic DNA fragmentation, and TUNEL assays. Although there are numerous assays available to evaluate cell death, we selected three diverse methods to quantify an apoptotic process: the MTT, cytosolic DNA fragmentation, and TUNEL assays. The MTT assay evaluates mitochondrial reduction of the yellow MTT tetrazolium salt dye to a highly colored blue formazan prod-

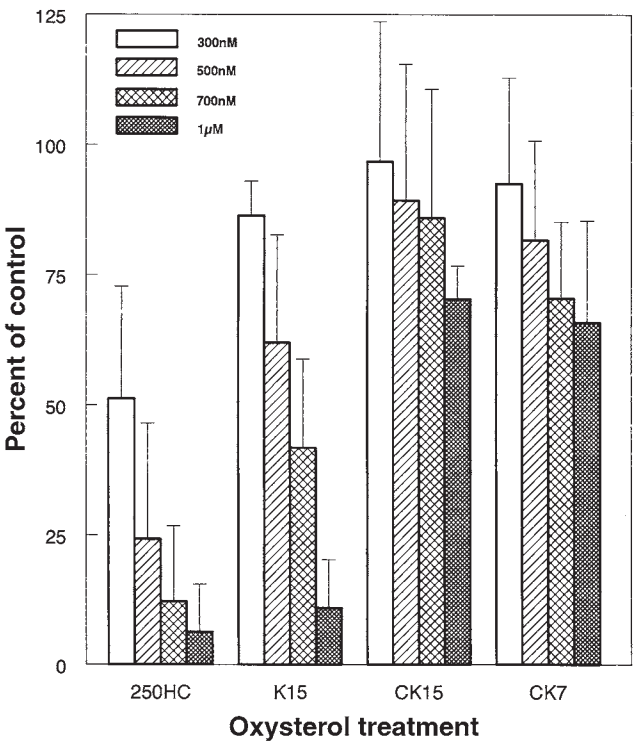

FIG. 2. Effects of varying concentrations (300 nM, 500 nM, 700 nM, and 1 μM) of oxysterols on the mitochrondrial reductive capacities of CEM-C7-14 cells. Growth conditions and delivery of oxysterols were the same as in Figure 1. After 48 h of incubation, the dimethyl tetrazolium salt MTT reagent was added, and cells were cultured for an additional 4 h before being lysed and then analyzed on a Biotek plate reader at 600 nm. The results were an average percentage of absorbance values by oxysterol-treated wells vs. the average of control wells and expressed as percentage of control. Each bar represents the mean from five independent experiments; error bars = 1 SD. See Figure 1 for abbreviations.

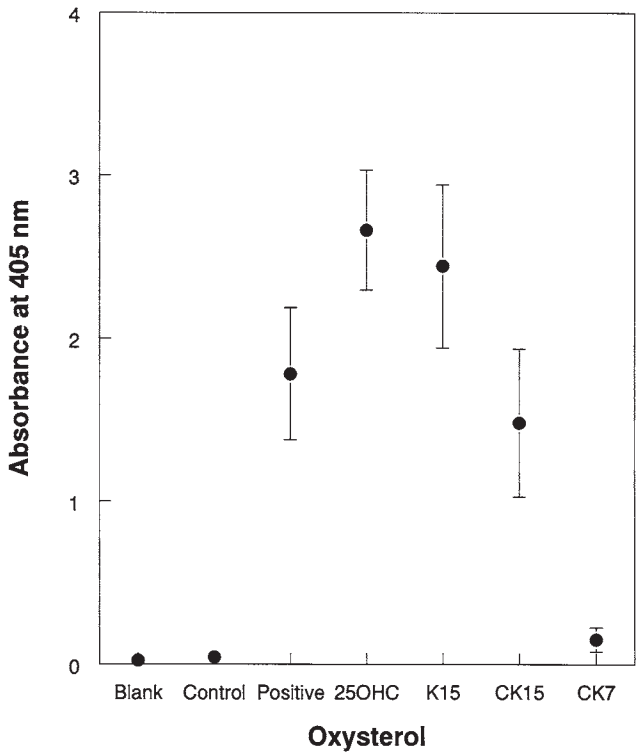

FIG. 3. Effect of 1 μM oxysterols treatment on internucleosomal DNA fragmentation in CEM-C7-14 cells. Growth conditions and delivery of oxysterols were the same as in Figure 1. After 48 h of treatment with each oxysterol, cells were collected, lysed, and the cytosolic fraction was prepared. Of this, triplicate samples were complexed with biotin-labeled antihistone and peroxidase-conjugated anti-DNA antibodies. The absorbance was read on a microplate reader at 405 nm against the substrate solution as blank. The blank averaged 25 mU, CEM-C7-14 control 44 mU, and the positive control (DNA histone complex) 1759 mU. Each dot with its error bar represents the mean ± 1 SD from three independent experiments. See Figure 1 for abbreviations.

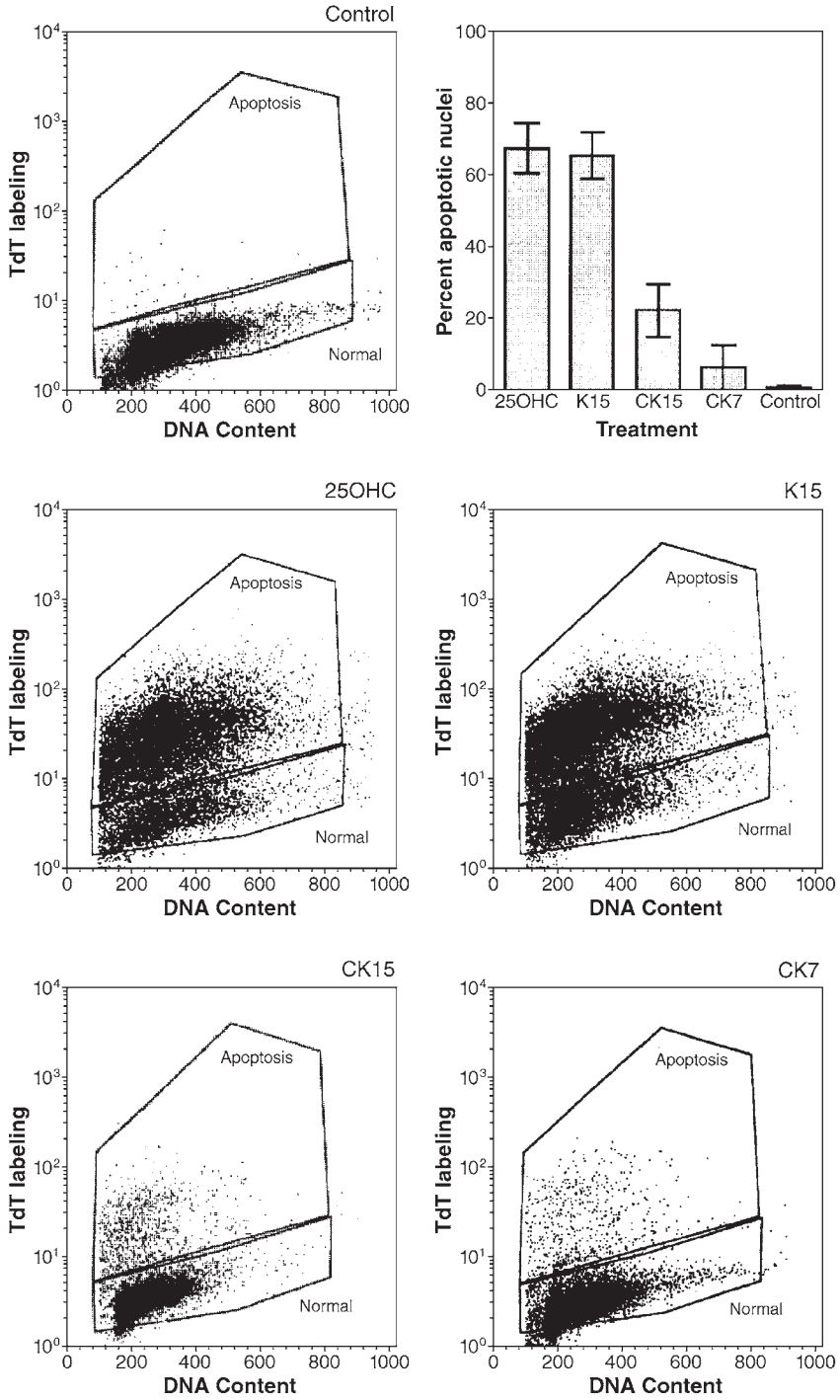

FIG. 4. Terminal deoxynucleotidyl transferase (TdT)-mediated dUTP nick end labeling (TUNEL) evaluation of single-stranded nicks and double-stranded breaks in DNA caused by the treatment of CEM-C7-14 cells with 1 μM oxysterols for 48 h. Growth conditions and delivery of oxysterols were the same as in Figure 1. Vehicle-treated control cells were used to establish the gates for normal and apoptotic cells. Twenty thousand cells were counted for controls and each oxysterol treatment, and the data were expressed as "percent apoptotic nuclei," i.e., percentage TUNEL-positive nuclei. The upper right-hand graph shows the mean values from four separate experiments with standard deviations. The remaining five panels are typical data obtained by FACS (Fluorescence Activated Cell Sorter; Becton Dickinson, Bedford, MA) analyses. See Figure 1 for abbreviations.

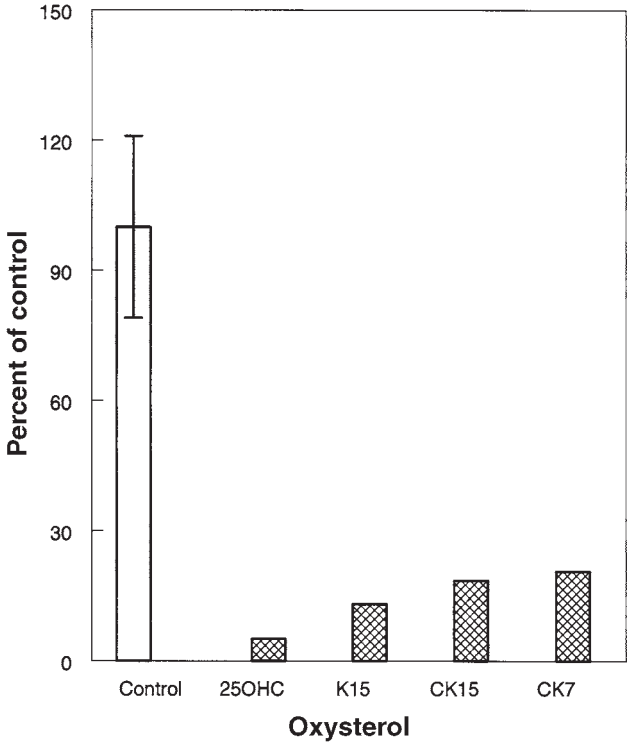

FIG. 5. Effect of 1 µM oxysterols on the level of c-myc mRNA in CEM-C7-14. Growth conditions and delivery of oxysterols were the same as in Figure 1. After 48 h in oxysterol, total RNA was extracted from the cells and 20 µg was electrophoresed, transferred to Nytran Plus® nylon membrane, and hybridized with a human c-myc exon 3 cDNA. Ethidium bromide-stained 18S ribosomal RNA was transferred to the same membrane to estimate the efficiency of RNA loading and transfer. Each oxysterol treatment included an individual control of vehicle-treated CEM-C7-14 cells. The error bar indicates the mean ± SD for the four control samples of constitutive c-myc mRNA levels. See Figure 1 for abbreviations.

uct. This assay has shown a high correlation with cell viability (28). Figure 2 demonstrates that at each of four sterol concentrations K15 was slightly less potent than 25OHC. At 1 µM, the two were not statistically different. Both CK15 and CK7 were much less able to suppress cell reductive capacity.

The "cytosolic" DNA fragmentation assay evaluates internucleosomal DNA cleavage, assayed by measuring the accumulation of mono- and oligonucleosomes in the cytoplasm of apoptotic cells, which occurs before plasma membrane breakdown. In Figure 3, a pattern of potency similar to that seen in Figures 1 and 2 for the four oxysterols is observed: 25OHC and K15 were the most potent apoptotic agents with almost the same ability to cause extensive appearance of DNA/histones in the cytoplasm. In this assay, CK15 clearly caused some DNA cleavage in CEM-C7-14 cells and CK7 showed little effect.

A flow cytometric TUNEL assay combined with a secondary stain for total DNA was used to detect both single-stranded nicks and double-stranded breaks in DNA. In Figure 4 (upper right-hand panel) the percentage of TUNEL-positive "apoptotic nuclei" in CEM-C7-14 cells after 48 h of treatment with 1 µM oxysterol showed the potency pattern: 25OHC ≥ K15 > CK15 > CK7 ≥ control cells. The remaining panels in Figure 4 present the data as directly obtained by FACS analyses. In each panel, the lower gated area reflects the normally cycling cells, while the upper gated area shows the TUNEL-positive cells.

Suppression of c-myc *mRNA by oxysterols.* In 1993, the suppression of the c-*myc* protooncogene, which plays an important role in the control of normal cell growth and differentiation, was shown to be a critical step in the glucocorticoid-induced lysis of CEM-C7 cells (1). More recently, Ayala-Torres *et al.* found that c-*myc* also is suppressed by 25OHC in apoptotic CEM-C7 cells (2). Figure 5 documents that in CEM-C7-14 cells treated with 1 µM 25OHC or K15 for 48 h, c-*myc* mRNA levels were also suppressed to 5 and 13%, respectively, of constitutive levels. The 1 µM concentrations of the CK15 and CK7 also depressed c-*myc* mRNA significantly (19% of control for CK15 and 21% for CK7). Thus, the rank order of potency for c-*myc* suppression is 25OHC > K15 > CK15 > CK7, although all oxysterols depressed c-*myc* significantly.

Documentation of apoptosis by phosphatidylserine (PS) and DNA staining. One of the earliest features of cells undergoing apopotsis is the translocation of the phospholipid PS from the inner to the outer side of the plasma membrane. This externalization of PS precedes the nuclear changes associated with apoptosis. The phospholipid-binding protein Annexin V, when conjugated to a fluorochrome, such as fluorescein isothiocyanate (FITC), can be used to identify cells that have translocated their PS to the outer plasma membrane. The nucleic acid dye 7-AAD enters and binds to DNA in dead cells. We followed its entry with FITC-labeled monoclonal antibodies. Two-color analysis, with minimal spectral overlap between the 7-AAD and FITC fluorescence emissions, allowed simultaneous assay of the two reactions. Chromatin condensation, another hallmark of apoptosis, was followed by staining the same cells with Hoechst 33342 dye.

Figure 6 presents the density plots from a two-color FACS analysis of CEM-C7-14 cells treated for 52 h and stained with Annexin V and 7-ADD. The upper panel shows the reactivity of control cells and defines the areas containing cells with specific fluorochrome reactions. The lower panels illustrate the effects of treatment with the various oxysterols. Note the dense numbers of dead cells after 25OHC and K15 treatment (quadrant 3). Virtually no cells reacted with 7-AAD unless they were also positive for Annexin V binding, but some cells were Annexin V positive without being 7-ADD positive (quadrant 2). Table 1 provides the percentages of cells for these five conditions over the time course of 4, 6, 24, 30, and 52 h. The increase in apoptotic cells in the 1 µM 25OHC is seen by 24 h, in K15 by 6 h, in CK15 by 52 h, and little increase is seen in CK7 treated cells at any time of treatment. By 52 h, both 1 µM 25OHC and K15 had killed >90% of the CEM-C7-14 cells.

The upper photographs in Figure 7 were taken at 30 h for control CEM-C7-14 cells and 1 µM 25OHC- and K15-treated cells, while the lower two sets of photographs were taken at 52 h for 1 µM CK15- and CK7-treated cells. The photographs using polarized white light clearly identify the field of cells. Hoechst dye staining of the same cells reveals the onset of nu-

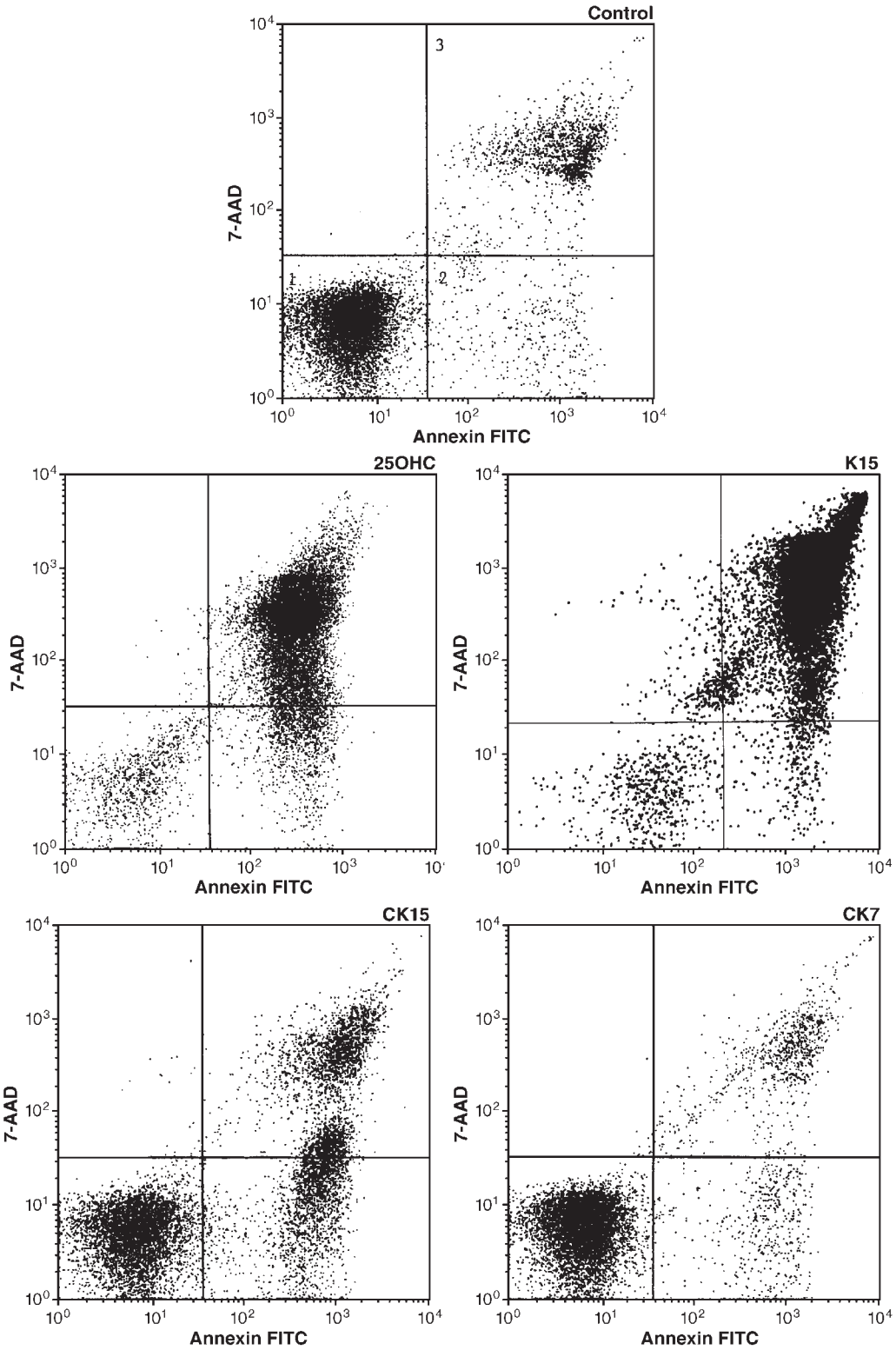

FIG. 6. Two-color FACS analysis of cells reacted with Annexin V for evidence of externalized membrane phosphatidylserine (PS) and 7-amino-actinomycin D (7-AAD) for DNA staining due to loss of membrane integrity. CEM-C7-14 cells were treated with 1 μM of each oxysterol for 52 h. Growth conditions and delivery of oxysterols were the same as in Figure 1. The five panels represent FACS analyses of CEM-C7-14 cells treated with oxysterol or vehicle. Upper panel: vehicle-treated control cells were used to establish the gates for unstained, viable cells in the lower left quadrant [1]; Annexin V positive/7-AAD negative, apoptotic cells in the lower right quadrant [2]; and Annexin V/7-AAD positive, dead cells in the upper right quadrant [3]. Other panels: cells that had been exposed to the indicated sterol. FITC, fluorescein isothiocyanate; for other abbreviations see Figure 1.

TABLE 1
Apoptotic Response of CEM-C7-14 Cells (control and 1 μM oxysterol-treated)

	Time (h)				
Treatment	4	6	24	30	52
Control					
Annexin V positive (%)	5.6	5.6	4.4	5.6	5.8[b]
+ 7-AAD positive (%)	10.0	7.1	11.1	13.6	8.1[c]
25OHC					
Annexin V positive (%)	4.7	5.9	5.4	26.5	7.9
+ 7-AAD positive (%)	10.6	8.7	9.0	48.8	86.5
K15					
Annexin V positive (%)	6.1	6.7	12.9	15.0	1.7
+ 7-AAD positive (%)	10.8	11.9	18.8	17.6	93.2
CK15					
Annexin V positive (%)	5.2	5.6	4.1	6.1	19.3
+ 7-AAD positive (%)	8.1	11.6	9.5	4.5	24.6
CK7					
Annexin V positive (%)	5.1	5.9	5.3	7.0	7.1
+ 7-AAD positive (%)	7.9	5.9	7.9	11.4	8.5

[a]25OHC, 25-hydroxycholesterol; K15, 15-ketocholestenol; CK15, 15-ketocholestenol hydroxyethyl ether; CK7, 7-ketocholesterol hydroxyethyl ether; 7-AAD, 7-amino-actinomycin D.
[b]Mean for controls = 5.4 ± 0.6.
[c]Mean for controls = 10.0 ± 2.5.

clear condensation and fragmentation as seen in the second panel. The intensity of the fluorescent dyes is sometimes faint, making it difficult to identify every cell in the second and third panels. In viewing the same field, the third panel shows the progressive stages of apoptosis as monitored by Annexin V/7-AAD. Those cells in the early stage of apoptosis contain only the green stain of Annexin V-FITC. The strong yellow to orange signal is due to the movement of 7-AAD across the plasma membrane, which becomes increasingly permeable during the later stages of apoptosis. In order to demonstrate apoptosing cells in the CK15 and CK7 cultures, it was necessary to photograph increased times (52 h), whereas late-stage apoptotic cells could be seen in 30-h cultures of 25OHC- and K15-treated cells.

DISCUSSION

The focus of this study has been threefold: (i) to examine three oxysterols for their ability to kill human leukemic cells; (ii) to determine if the pathway of death was an apoptotic one; and (iii) to assess their relative cell-kill potency. We designed and implemented a battery of tests that were useful in the evaluation of such agents for their apoptotic potential, which could lead to future drug discovery and development. In each of the assays utilized, 25OHC served as a standard for comparison of cell-kill potency because there have been several studies of oxysterol-dependent apoptosis that have used this agent.

To avoid the confounding effects of sterols in whole serum, we carried out this study on cells cultured in medium supplemented with DFBS. We also added BSA as an oxysterol carrier to prevent the loss of drug because of adhesion to the culture flask wall. The *in vivo* environment may be quite different. Human cells express cell-surface receptors for low density lipoprotein (LDL) (29). Since LDL is the major cholesterol-carrying lipoprotein in human plasma, oxysterols may enter cells through this mechanism as well as directly. Previous *in vitro* studies have shown that LDL receptor activity can be enhanced by incubating cells in a lipoprotein-deficient medium (30). However, for this systematic evaluation of the effects of oxysterols on these leukemic cells, a defined culture medium was deemed desirable.

The compounds studied here examined the effects of a keto group on C15 and the addition of a 3β-2′-hydroxyethyl ether on C15 or C7. The initial growth studies demonstrated that all three test oxysterols did inhibit cell growth in treated cultures as compared to control cells under conditions in which the untreated cells maintained logarithmic growth. The most potent agent of the experimental oxysterols to diminish proliferating cells was K15, which was nearly as potent as 25OHC. Adding the 3β-2′-hydroxyethyl ether group reduced the potency of both K15 and K7; in fact, the already weak K7 was rendered nearly nonapoptotic.

Having established that all three test oxysterols could decrease the number of leukemic cells in culture relative to controls, the remainder of our study evaluated the nature of this reduction. Were the cells killed or merely slowed in growth? By examining the reductive metabolism of the treated cells' mitochrondria in the MTT assay, it was demonstrated that these three oxysterols did diminish CEM-C7-14 cells' ability to reduce the MTT dye, with K15 again being the most potent. CK15 and CK7, at the highest concentration tested, only reduced this mitochrondrial function by ~25%.

The Hoechst chromatin staining, TUNEL, and cytosolic DNA fragmentation assays all indicated that the test sterols did cause apoptotic cell death, as determined by DNA condensation, nicks, and fragmentation. Again, K15 created far more DNA damage than CK15 or CK7. Finally, this apoptotic cell death was associated with the classic alterations of the cellular plasma membrane as well as the suppression of an important growth controlling gene, c-*myc*. Fluorescence staining using Annexin V and 7-AAD demonstrated that in K15-treated CEM-C7-14 cells, the plasma membrane's integrity was compromised earlier than with CK15 or CK7.

Northern blot analyses showed a decrease in the level of c-*myc* mRNA for all four oxysterols tested. CK15 and CK7 were much more effective in reducing c-*myc* mRNA than they were in causing apoptosis. This may account for their ability to slow cell growth (Fig. 1) since progression through the cell cycle demands an adequate level of cMyc. Our studies so far have only examined c-*myc* mRNA levels after treatment with the test sterols. Since cMyc protein can be regulated independently from its mRNA, it will be necessary to determine the levels of the protein before drawing further conclusions.

In sum, oxysterols continue to show potential as chemotherapeutic agents. Some reports have even suggested that oxysterols could increase the sensitivity of tumor cells to other cancer drugs (31,32). The ability of oxysterols to kill cells could result from the simple regulation of sterol *de novo* synthesis or from the inhibition of the many biologically impor-

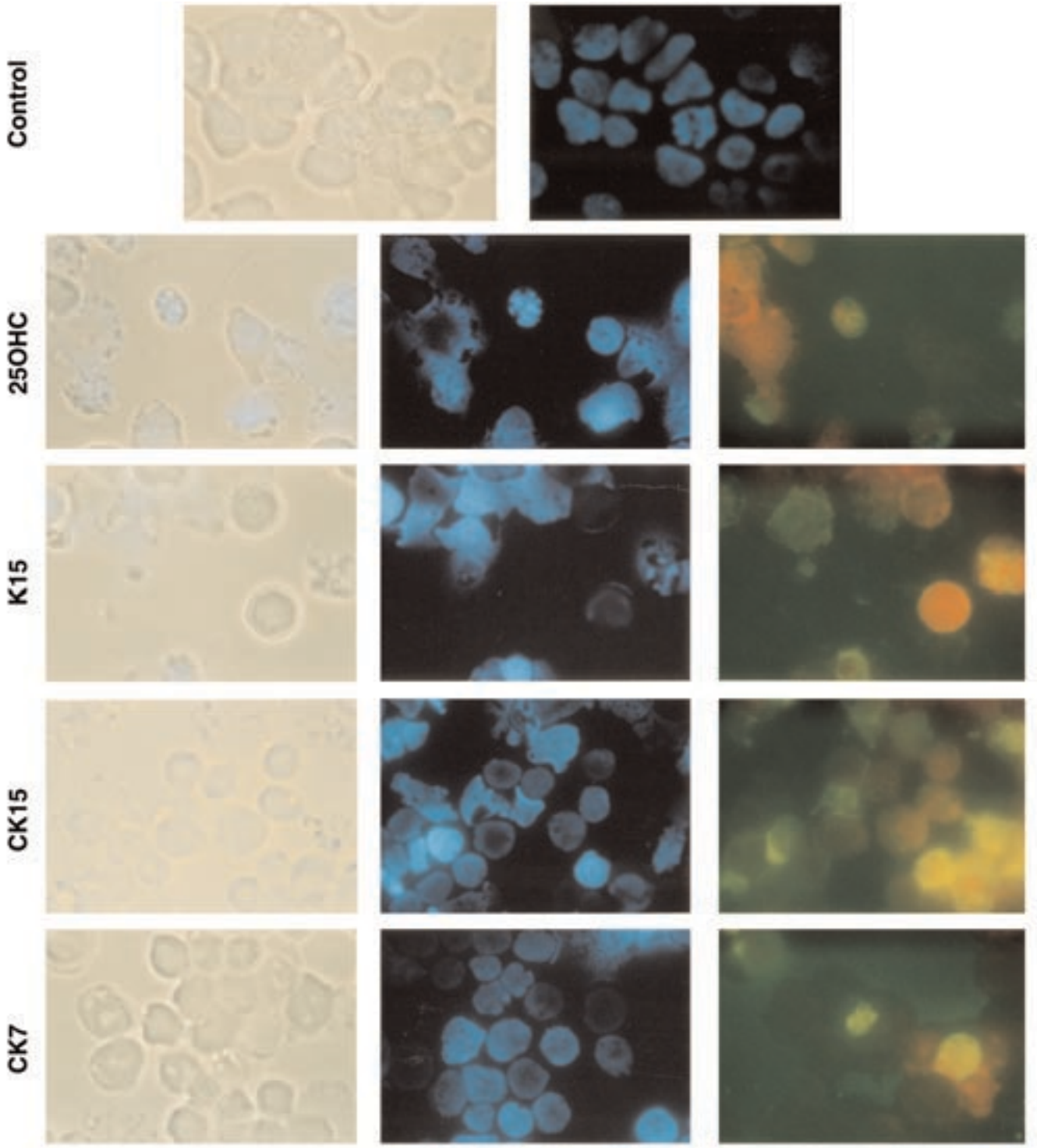

FIG. 7. Fluorescent microscopy of apoptotic events in CEM-C7-14 cells treated ± 1 μM oxysterol. Growth conditions and delivery of oxysterols were the same as in Figure 1. CEM-C7-14 cells were stained with Hoechst 33342, Annexin V, and 7-AAD at the various time points, 30 h for 25OHC and K15; 52 h for CK15 and CK7. Photographs of stained cells were taken on a Nikon Eclipse E600 microscope with a Nikon FDX-35 camera at 100× magnification: first, viewed with polarized light to demonstrate all the cells in the field, second viewed at 488 and at 515 nm to detect the initial loss of membrane integrity (Annexin V, green/yellow) followed by the death of the cell (7-AAD, red); and third, at 355 and at 460 nm to reveal condensed chromatin found in apoptotic cells. See Figures 1 and 6 for abbreviations.

tant mevalonate-derived products such as dolichol, ubiquinones, or isopentyl/farnesyl moieties or some other unidentified pathway. Some years ago it was shown that the relative binding affinity of many oxysterols to OBP correlated with their ability to suppress the rate-limiting step in *de novo* cholesterol synthesis, which is essential for cell homeostasis and

proliferation (33). Taylor and Kandutsch (34) reported that the 3β-hydroxy position of an oxysterol was essential for high OBP binding affinity and that substitution of a hydroxyl or keto function at positions C15, 20, 25, or 26 of the parent cholesterol molecule also produced high OBP affinity ligands. In 1993, our laboratory reported that oxysterol-induced cell death correlated with OBP occupancy with 25OHC demonstrating ~30 nM and K7 ~450 nM OBP-binding affinity in serum-free medium (20). Of the test oxysterols, K15 was the strongest ligand for OBP and in one competition assay was a slightly better competitor than 25OHC for OBP; 50% competition of 25OHC by 8.8 pM for K15, whereas unlabeled 25OHC required 12.5 pM. CK15 required 40 pM for 50% competition and CK7 competed only 10% at 40 pM (Alexander S. Krylov, unpublished data). While there have been studies evaluating the effects of different oxysterols on cholesterol biosynthesis (35), Sinensky *et al*. have challenged the correlation between the regulation of HMG-CoA reductase and the effectiveness of those agents as anticancer drugs (36).

The effectiveness of oxysterols *in vivo* might be diminished by the availability of cholesterol from LDL. For cells in the circulation, this could be protective. In tissues or malignant cells outside the vascular compartment, LDL-cholesterol is not as available. Certainly, higher concentrations of 25OHC are required to kill CEM cells when serum is present. Even so, the protection is not absolute, and no amount of added cholesterol can protect if sufficient 25OHC is present (20). Therefore, the question will be whether *in vivo* oxysterols can be administered to levels sufficient to overcome whatever protection LDL-cholesterol gives.

As to structure–function relations, Zhang *et al*. have reported that 7α-hydroxylation and 3-dehydrogenation abolish the ability of 25OHC and 27-hydroxycholesterol to induce apoptosis in thymocytes (37). For the present study we find that the sterols tested can cause apoptosis. We conclude that a keto group at position 15 produces an oxysterol with high apoptotic potency. The 3β-2′-hydroethyl ethers greatly reduce potency. Our data show the usefulness of applying a battery of tests for cell changes correlated with apoptosis, and they add to the body of relevant structure–function knowledge.

ACKNOWLEDGMENTS

The authors wish to acknowledge the work of summer student Jacquelyn Payne, as well as the technical assistance in the MTT assays of David Chilton and the use of the fluorescence microscope in the laboratory of Dr. Tensheng Chan in the Microbiology Department of the University of Texas Medical Branch. The evaluation of the purity of the oxysterols was performed by Drs. Jon Teng and Stefan Serabyn of the HPLC Core facility of the Sealy Center for Molecular Science at this institution. The authors also would like to express their appreciation for the privilege to preview the late Dr. George J. Schroepfer Jr.'s review in *Physiological Reviews* titled "Oxysterols: Modulators of Cholesterol Metabolism and Other Processes." Dr. Leland L. Smith, professor emeritus in this department, provided invaluable advice in the preparation of this manuscript. This work was supported in part by National Institutes of Cancer grant CA 41407 and The Walls Medical Research Foundation.

REFERENCES

1. Thulasi, R., Harbour, D.V., and Thompson, E.B. (1993) Suppression of c-*myc* Is a Critical Step in Glucocorticoid-Induced Human Leukemic Cell Lysis, *J. Biol. Chem. 268*, 18306–18312.
2. Ayala-Torres, S., Zhou, F., and Thompson, E.B. (1999) Apoptosis Induced by Oxysterol in CEM Cells Is Associated with Negative Regulation of c-*myc*, *Exper. Cell Res. 246*, 193–202.
3. Smith, L.L., and Johnson, B.H. (1989) Biological Activities of Oxysterols, *Free Radical Biol. Med. 7*, 285–332.
4. Luu, B., and Moog, C. (1991) Biological Activities and Physicochemical Studies, *Biochimie 73*, 1317–1320.
5. Guardiola, F., Codony, R., Addis, P.B., Rafecas, M., and Boatella, J. (1996) Biological Effects of Oxysterols: Current Status, *Food Chem. Toxicol. 34*, 193–211.
6. Parish, E.J., Parish, S.C., and Li, S. (1995) Side-Chain Oxysterol Regulation of 3-Hydroxy-3-methylglutaryl Coenzyme A Reductase Activity, *Lipids 30*, 247–251.
7. Dushkin, M., Schwartz, Y., Volsky, N., Musatov, M., Vereschagin, E., Ragino, J., Perminova, O., and Kozlov, V. (1998) Effects of Oxysterols upon Macrophage and Lymphocyte Functions *in Vitro*, *Prostaglandins Other Lipid Mediat. 55*, 219–236.
8. Lehmann, J.M., Kliewer, S.A., Moore, L.B., Smith-Oliver, T.A., Oliver, B.B., Su, J.L., Sundseth, S.S., Winegar, D.A., Blanchard, D.E., Spencer, T.A., and Willson, T.M. (1997) Activation of the Nuclear Receptor LXR by Oxysterols Defines a New Hormone Response Pathway, *J. Biol. Chem. 272*, 3137–3140.
9. Hwang, P.L. (1991) Biological Activities of Oxygenated Sterols: Physiological and Pathological Implications, *BioEssays 13*, 583–589.
10. Smith, L.L. (1996) Review of Progress in Sterol Oxidations: 1987–1995, *Lipids 31*, 453–487.
11. Stehbens, W.E. (1990) Basic Precepts and the Lipid Hypothesis of Atherogenesis, *Med. Hypotheses 31*, 105–113.
12. Seifert, P.S., and Kazatchkine, M.D. (1988) The Complement System in Atherosclerosis, *Atherosclerosis 73*, 91–104.
13. Brown, A.J., Leong, S.L., Dean, R.T., and Jessup, W. (1997) 7-Hydroperoxycholesterol and Its Products in Oxidized Low Density Lipoprotein and Human Atherosclerotic Plaque, *J. Lipid Res. 38*, 1730–1745.
14. Hajjar, D.P., and Haberland, M.D. (1997) Lipoprotein Trafficking in Vascular Cells: Molecular Trojan Horses and Cellular Saboteurs, *J. Biol. Chem. 272*, 22975–22978.
15. Schroepfer, G.J., Jr. (1999) Oxysterols: Modulators of Cholesterol Metabolism and Other Processes—Oxysterols as Potential Cancer Chemotherapeutic Agents, *Physiol. Rev. 80*, 361–554.
16. Moog, C., Frank, N., Luu, B., and Bertram, B. (1993) Metabolism of New Anticancer Oxysterol Derivatives in Rats, *Anticancer Res. 13*, 953–958.
17. Luu, B. (1995) From Cholesterol to Oxysterols: Current Data, *C.R. Seances Soc. Biol. Fil. 189*, 827–837.
18. Hyun, J.W., Weltin, D., Holl, V., Marchal, J., Dufour, P., Luu, B., and Bischoff, P. (1997) Cytotoxic Properties of a Phosphoglycoconjugated Derivative of 7-beta-Hydroxycholesterol upon Normal and Tumor Cells in Culture, *Anticancer Res. 17*, 2621–2626.
19. Ayala-Torres, S., Moller, P.C., Johnson, B.H., and Thompson, E.B. (1997) Characteristics of 25-Hydroxycholesterol-Induced Apoptosis in the Human Leukemic Cell Line CEM, *Exper. Cell Res. 235*, 35–47.
20. Bakos, J.T., Johnson, B.H., and Thompson, E.B. (1993) Oxysterol-Induced Cell Death in Human Leukemic T-Cells Correlates with Oxysterol Binding Protein Occupancy and Is Independent of Glucocorticoid-Induced Apoptosis, *J. Steroid Biochem. Molec. Biol. 46*, 415–426.
21. Nishio, E., and Watanabe, Y. (1996) Oxysterols Induced Apoptosis in Cultured Smooth Muscle Cells Through CPP32 Protease

Activation and Bcl-2 Protein Downregulation, *Biochem. Biophys. Res. Com. 226*, 928–934.
22. Harada, K., Ishibashi, S., Miyashita, T., Osuga, J., Yagyu, H., Ohashi, K., Yazaki, Y., and Yamada, N. (1997) Bcl-2 Protein Inhibits Oxysterol-Induced Apoptosis Through Suppressing CPP32-Mediated Pathway, *FEBS Lett. 411*, 63–66.
23. Lizard, G., Lemaire, S., Monier, S., Gueldry, S., Neel, D., and Gambert, P. (1997) Induction of Apoptosis and of Interleukin-1 beta Secretion by 7 beta-Hydroxycholesterol and 7-Ketocholesterol: Partial Inhibition by Bcl-2 Over-expression, *FEBS Lett. 419*, 276–280.
24. Norman, M.R., and Thompson, E.B. (1977) Characterization of a Glucocorticoid-sensitive Human Lymphoid Cell Line, *Cancer Res. 37*, 3785–3791.
25. Philips, H.J. (1973) Dye Exclusion Tests for Cell Viability, in *Tissue Culture: Methods and Applications* (Kruse, M.K., Jr., and Patterson, P.F., Jr., eds.), pp. 406–408, Academic Press, New York.
26. Pieters, R., Loonen, A.H., Huismans, D.R., Broekema, G.J., Dirven, M.W.J., Heyenbrok, M.E., Hahlen, K., and Veerman, A.J.P. (1990) *In Vitro* Sensitivity of Cells from Children with Leukemia Using the MTT Assay with Improved Culture Conditions, *Blood 76*, 2327–2336.
27. Van Houten, N., and Budd, R.C. (1992) Accelerated Programmed Cell Death of MRL-lpr/lpr T lymphocytes, *J. Immunol. 149*, 2513–2517.
28. Bellamy, W.T. (1992) Prediction of Response to Drug Therapy of Cancer: A Review of *In Vitro* Assays, *Drugs 44*, 690–708.
29. Vitols, S., Gahrton, F., Ost, A., and Peterson, C. (1984) Elevated Low Density Lipoprotein Receptor Activity in Leukemic Cells with Monocytic Differentiation, *Blood 63*, 1186–1193.
30. Vitols, S., Gahrton G., and Peterson, C. (1984) Significance of the Low-Density Lipoprotein (LDL) Receptor Pathway for the *in vitro* Accumulation of AD-32 Incorporated into LDL in Normal and Leukemic White Blood Cells, *Cancer Treat. Rep. 68*, 515–520.
31. Lenz, M., Miehe, W.-P., Vahrenwald, F., Bruchehelt, G., Schweizer, T.P., and Girgert, R. (1997) Cholesterol Based Antineoplastic Strategies, *Anticancer Res. 17*, 1143–1146.
32. Gaffney, D.K., Feix, J.B., Schwarz, H.P., Stuve, M.F., and Sieber, F. (1991) Cholesterol Content but Not Plasma Membrane Fluidity Influences the Susceptibility of L1210 Leukemic Cells to Merocyanine 540-Sensitized Irradiation, *Photochem. Photobiol. 54*, 717–723.
33. Taylor, F.R., Saucier, S.E., Shown, E.P., Parish, E.J., and Kandutsch, A.A. (1984) Correlation Between Oxysterol Binding to a Cytosolic Binding Protein and Potency in the Repression of Hydroxymethylglutaryl Coenzyme A Reductase, *J. Biol. Chem. 259*, 12382–12387.
34. Taylor, F.R., and Kandutsch, A.A. (1985) Oxysterol Binding Protein, *Chem. Phys. Lipids 38*, 187–194.
35. Lund, E., and Bjorkhem, I. (1995) Role of Oxysterols in the Regulation of Cholesterol Homeostasis: A Critical Evaluation, *Accounts Chem. Res. 28*, 241–249.
36. Sinensky, M., Beck, L.A., Leonard, S., and Evans, R. (1990) Differential Inhibitory Effects of Lovastatin on Protein Isoprenylation and Sterol Synthesis, *J. Biol. Chem. 265*, 19937–19941.
37. Zhang, J., Xue, Y., Jondal, M., and Sjovall, J. (1997) 7 Alpha-hydroxylation and 3-Dehydrogenation Abolish the Ability of 25-Hydroxycholesterol and 27-Hydroxycholesterol to Induce Apoptosis in Thymocytes, *Eur. J. Biochem. 247*, 129–135.

[Received May 17, 1999; and in revised form and accepted February 7, 2000]

C_{27} to C_{32} Sterols Found in *Pneumocystis*, an Opportunistic Pathogen of Immunocompromised Mammals

Edna S. Kaneshiro* and Michael A. Wyder

Department of Biological Sciences, University of Cincinnati, Cincinnati, Ohio 45221-0006

ABSTRACT: *Pneumocystis carinii* is the paradigm of opportunistic infections in immunocompromised mammals. Prior to the acquired immunodeficiency syndrome (AIDS) pandemic and the use of immunosuppressive therapy in organ transplant and cancer patients, *P. carinii* was regarded as a curiosity, rarely observed clinically. Interest in this organism exploded when it was identified as the agent of *P. carinii* pneumonia (PcP), the direct cause of death among many AIDS patients. Aggressive prophylaxis has decreased the number of acute PcP cases, but it remains among the most prevalent opportunistic infections found within this patient population. The taxonomic assignment of *P. carinii* has long been argued; molecular genetics data now demonstrate that it is a fungus. Several antimycotic drugs are targeted against ergosterol or its biosynthesis, but these are not as effective against PcP as they are against other fungal infections. This can now be explained in part by the identification of the sterols of *P. carinii*. The organism lacks ergosterol but contains distinct C_{28} and C_{29} Δ^7 24-alkylsterols. Also, 24-methylenelanost-8-en-3β-ol (C_{31}) and pneumocysterol, (24*Z*)-ethylidenelanost-8-en-3β-ol (C_{32}) were recently identified in organisms infecting humans. Together, the Δ^7 24-alkylsterols and pneumocysterol are regarded as signature lipids of the pathogen that can be useful for the diagnosis of PcP, since no other lung pathogen is known to contain them. Cholesterol (C_{27}), the dominant sterol component in *P. carinii*, is probably totally scavenged from the host. *De novo* synthesis of sterols has been demonstrated by the presence of lovastatin-sensitive 3-hydroxy-3-methylglutaryl-CoA reductase activity, the incorporation of radiolabeled mevalonate and squalene into *P. carinii* sterols, and the reduction in cellular ATP in cells treated with inhibitors of enzymes in sterol biosynthesis.

Paper no. L8325 in *Lipids 35,* 317–324 (March 2000).

Pneumocystis carinii pneumonia (PcP) remains among the most prevalent opportunistic infections in acquired immunodeficiency syndrome (AIDS) patients (1,2). It is now evident that the high incidence of PcP is not limited to AIDS patients in the United States of America and Europe, but is true globally. The combination of trimethoprim and sulfamethoxazole (TMP/SMX) and other agents (e.g., atovaquone) used for prophylaxis and for clearing *P. carinii* infection has successfully reduced the number of deaths directly attributed to PcP (1,2). However, about 80% of AIDS patients still develop PcP at least once, and many patients experience recurrent episodes due to their long-term immunodeficient status. Also, some individuals cannot tolerate certain drugs and some develop undesirable side effects, and the development of drug-resistant pathogen populations is of serious concern. Thus, there is a need to develop a larger armamentarium of diverse drugs to handle these problems. The most effective and widely prescribed antimycotics are targeted against ergosterol in the pathogen's membranes (e.g., amphotericin B), or against its synthesis (e.g., azoles, morpholines, thiocarbamates, allylamines) (3,4). Antiergosterol agents have proved to be particularly useful for deeply invasive or systemic mycosis, but at clinical doses, amphotericin B does not clear PcP. Unlike other fungal pathogens of humans, *P. carinii* does not contain ergosterol (6,7). In this article, we describe what is currently known about the sterols in this unique and unusual organism.

THE *PNEUMOCYSTIS* COMPLEX

Since its discovery almost a century ago, the taxonomic status of *Pneumocystis* has been actively debated (8–11). Investigators have given particularly good arguments for placing it among the protozoa or fungi. Within the last two decades, molecular genetic analyses have provided strong evidence for placing it within the fungi, but there is yet insufficient evidence for solidly placing it among the ascomycetes, basidiomycetes, or on a branch independent of the major fungal groups (1).

It is widely accepted that *P. carinii* is host species-specific; experimental introduction of *P. carinii* isolated from one host species into another host species does not result in fulminant infections (12,13), but transient colonization probably occurs (14–20). Although subtle phenotypic differences have been reported between isolates from different host species (21–26), nucleotide sequences of a number of regions of DNA indicate that *P. carinii* populations isolated from different hosts have highly divergent genetic backgrounds: sequences can vary from 15–50% at selected gene loci (2,9,10,27–29). Genetic populations exhibiting different chromosomal patterns (kary-

*To whom correspondence should be addressed.
E-mail: Edna.Kaneshiro@uc.edu

Abbreviations: AIDS, acquired immunodeficiency syndrome; BALF, bronchoalveolar lavage fluid; GLC, gas–liquid chromatography; HIV, human immunodeficiency virus; HMG-CoA, 3-hydroxy-3-methylglutaryl coenzyme A; MS, mass spectrometry; PC, phosphatidylcholine; PcP, *Pneumocystis carinii* pneumonia; SAM:SMT, *S*-adenosylmethionine:sterol methyltransferase; SP-A, surfactant protein A; TLC, thin-layer chromatography; TMP/SMX, trimethoprim and sulfamethoxazole.

otypes) have also been detected in organisms within a single host species (2,9,10,29–34). The distinct populations in rats have been designated "prototype" (*P. carinii carinii*) and "variant" (*P. carinii ratti)* (31,32,34). Investigators working on *Pneumocystis* have yet to agree on designating separate species, but use an interim trinomial nomenclature indicating the mammalian host species; e.g., *P. carinii hominis* for organisms proliferating in humans (2,9,10).

PNEUMOCYSTIS ORGANISM PREPARATIONS FOR LIPID ANALYSIS

One of the most serious hindrances to advancing *P. carinii* research has been the lack of continuous cultivation procedures for this organism (35). Until now, most *in vitro* studies have been performed on short-term primary cultures of *P. carinii* freshly isolated from infected animal lungs, and on monoxenous cultures with freshly isolated organisms placed in tissue cultures with mammalian cell lines. These primary cultures begin to die out after about 2 wk.

Recently, Merali *et al.* (36) have succeeded in making a major breakthrough by achieving continuous axenic cultivation of rat-derived *P. carinii* and *P. carinii hominis* placed in transwell plates. The present culture conditions allow for only very slow organism proliferation and have not yet been modified to produce mass amounts of organisms to perform most types of direct biochemical analyses.

Analysis of organisms in continuous axenic cultures may identify compounds synthesized by the organism. On the other hand, microbes can take up nutrients such as lipids from the culture medium similar to that by which parasites scavenge nutrients from their hosts. Analysis of infectious agents freshly isolated from their host provides insight into the biochemical nature of the organisms as they are actually growing in the host. Metabolic processes in parasites grown in culture very likely differ from those proliferating in the host.

To study *P. carinii* isolated from mammalian lungs, it was imperative that the purity of the organisms prepared from a given protocol be rigorously characterized, thus enabling credible interpretion of data obtained from such preparations. The alveolar lining in which *P. carinii* proliferates is bathed in lung surfactant, 88% of which is lipid with smaller amounts of protein and carbohydrate (37). Lung surfactant lipids are characterized by the predominance (75%) of phosphatidylcholine (PC), especially dipalmitoyl PC. Cholesterol constitutes approximately 3–10% of surfactant total lipids. Lung surfactant lipids and proteins bind avidly to the surfaces of *P. carinii* and are not completely removed by washing with ordinary buffered salt solutions. Treatment with reagents, such as the divalent cation chelator EDTA, is required to remove surfactant components (e.g., surfactant protein A, SP-A) (38).

During the initial phase of our studies on *P. carinii*, we developed a protocol for the isolation and purification of organisms from the lungs of corticosteroid-immunosuppressed rats (39). Included in the protocol is the mucolytic agent glutathione, which detaches organisms from each other and from type I pneumocytes of the lung epithelium, presumably by breaking disulfide linkages. Hence, alveolar type I cells to which *P. carinii* are adherent (40–43) and the elaborate tubular extensions of the surface membrane of trophic forms (44) remain intact.

The critical aspect of developing a contaminant-free preparation is the documentation that it is free of host cell fragments and molecules. Thus, the purity of our preparations was demonstrated by multiple criteria, including light and electron microscopy, biochemical, and immunochemical (SP-A) analyses. The lowest (not average) values obtained by at least four separate criteria were >95–100% purity of the organism preparations (39). The final pure preparations contain mixed life-cycle stages (trophic and cystic forms plus intermediate stages and other forms whose placement within the pulmonary life cycle is not yet understood) (44).

Using (i) a dual fluorescence staining live/dead assay (44), (ii) quantitation of cellular ATP (46), and (iii) the incorporation of radiolabeled precursors into *P. carinii*-specific compounds (47–50) also shows that these preparations contain metabolically active organisms.

STEROLS IN *PNEUMOCYSTIS* ISOLATED FROM RAT AND HUMAN PcP LUNGS

In considering the difficulties faced in studying *P. carinii* by direct analytical biochemistry, significant advances have been made with respect to its lipids within the last decade (47–60). Over 20 sterol components have been detected in rat-derived *P. carinii carinii* (5–7,53,58) and human-derived *P. carinii hominis* (6–8,60) (Table 1). The structural identities of most major sterols have been determined by relative retention times and cochromatography with authentic standards using gas–liquid chromatography (GLC) and high-resolution mass spectrometry (MS). In a few cases, nuclear magnetic resonance spectroscopy has been performed on isolated and purified sterol components, providing unequivocal structural identifications (60). The structural assignments for some minor sterol components and those with several double bonds are considered tentative.

Campesterol and β-sitosterol were identified in both rat and human-derived organisms (5–9), but these were also found in the sterols of their respective lung controls without *P. carinii* infection. Thus, it is very likely that these plant sterols are scavenged by *P. carinii* from the host, and the presence of these components in the host lung lipids results from plant material in the hosts' diets.

It is interesting that Δ^7 24-alkylsterols are the dominant sterols present in representatives of the rust fungi (61,62). It is unclear whether this observation has any phylogenetic or environmental implications (e.g., lateral gene transfer) for the apparent commonality between the sterols of *P. carinii* and the rust fungi (basidiomycetes).

Distinct C_{31} and C_{32} Δ^8 sterols were also found in *P. carinii hominis* samples. Pneumocysterol [(24*Z*)-ethylidenelanost-8-en-3β-ol] was found in some, but not all *P. carinii hominis* preparations. The only other reported occurrence of pneumocysterol is in the plant *Neolitsea sericea* (63). This sterol is not

TABLE 1
Sterols of Isolated Organism Preparations of *Pneumocystis carinii carinii* from Rats and *P. carinii hominis* from Humans

	P. carinii carinii		*P. carinii hominis*	
Steroid component	Weight % of total sterols	Weight % of signature sterols	Weight % of total sterols	Weight % of signature sterols
Cholest-5-en-3β-ol (cholesterol)	78.4		83.8	
Unidentified	Trace		3.8	
Cholest-7-en-3β-ol (lathosterol)	0.6		0.5	
Unidentified	0.1		0.2	
Cholesta-5,24(25)-dien-3β-ol (desmosterol)	0.2		0.5	
Unidentified	Trace		Trace	
24-Methylcholesta-5,24(25)-dien-3β-ol	0.6		0.2	
24-Methylcholest-5-en-3β-ol (campesterol)	3.7		3.5	
24-Methylenecholesta-7,24(28)-dien-3β-ol	0.2		0.1	
Cholest-5-en-3-one	1.5		0.2	
Unidentified	Trace		Trace	
24-Methylcholestadiene-3β-ol	1.2		ND[a]	
24-Methylcholest-7-en-3β-ol (fungisterol)	4.5	40.9	0.9	20.5
Unidentified	0.1		Trace	
24-Ethylcholest-5-en-3β-ol (β-sitosterol)	2.1		0.7	
24-Ethylcholestadiene-3β-ol	1.2	10.9	1.2	27.3
Lanosta-8,24(25)dien-3β-ol (lanosterol)	0.1		0.1	
24-Ethylcholest-7-en-3β-ol	1.8	16.4	0.2	4.5
24-Ethylidenecholesta-7,24(28)-dien-3β-ol	3.5	31.8	0.3	6.8
Unidentified	0.1		0.1	
Unidentified	0.1		Trace	
24-Methylenelanost-8,24(28)-dien-3β-ol	ND[a]		Trace	
24-Ethylidenelanost-8,24(28)-dien-3β-ol (pneumocysterol)	Trace	Trace	1.8	40.9

[a]ND, not detected.

found in any organism known to infect mammalian lungs and hence is another distinct signature sterol of *P. carinii*. The proportions of pneumocysterol can vary widely from sample to sample, from only undetectable or trace amounts up to 50% of the *P. carinii*-specific sterols (i.e., excluding cholesterol) (8,60,67; Amit, Z., Baughman, R.P. and Kaneshiro, E.S., unpublished results) (Fig. 1). The occurrence and accumulation of pneumocysterol is not correlated with coinfection with human immunodeficiency virus (HIV).

Among several possible explanations for the wide range of pneumocysterol concentrations in human-derived *P. carinii hominis* is the highly divergent nature of organisms within the *Pneumocystis* complex (2,9,10,29). It is now well accepted that an individual host can harbor single or mixed populations of *P. carinii* with highly divergent genetic backgrounds equivalent to distances separating at least species of fungi and metazoa. If organisms within the *P. carinii* complex are that different, the synthesis and accumulation of different compounds such as sterols would not be extraordinary. Thus, the population of organisms used for sterol analyses may represent single or mixed populations of *P. carinii hominis*. If one species/strain synthesizes pneumocysterol and another does not, the full range of pneumocysterol proportions actually observed could result from single populations represented by these two species/strains with intermediate values representing different percentages of the two species/strain (which differ in their sterol composition) in a simultaneous infection. More samples from humans as well as from mammalian species other than humans and rats need to be examined for a better understanding of sterol profile diversity in the *P. carinii* complex.

Because pneumocysterol and 24-methylenelanost-8-en-3β-ol (found in substantial amounts in samples with high pneumocysterol; Giner, J., Parish, E.J., Jayasimhulu, K., and Kaneshiro, E.S., unpublished data) are 24-alkylated lanosterol molecules, this indicates that *P. carinii S*-adenosylmethionine:sterol methyltransferase (SAM:SMT) can readily use lanosterol as a substrate and suggests that sterol C-24 alkylation activity in this organism is high. Consistent with this suggestion is that the gene for SAM:SMT was among the first identified in an expressed sequence tag analysis in an ongoing *P. carinii* genome project (Cushion, M.T., personal communication). The message for this gene could have been detected as a random event, or because it is there in several copies. Nonetheless, it appears that the gene encoding SAM:SMT is expressed in *P. carinii*.

PNEUMOCYSTIS SIGNATURE STEROLS IN NON-PcP HUMAN SUBJECTS

The Δ^7 24-alkylsterols found in *P. carinii* are not common among fungi (61,62), and are not found in any other pathogen known to infect mammalian lungs. These are distinct signatures of *P. carinii carinii* and *P. carinii hominis* and are therefore useful marker compounds of the pathogen.

The identification and detection of signature lipids is a powerful approach employed by microbial ecologists. The assem-

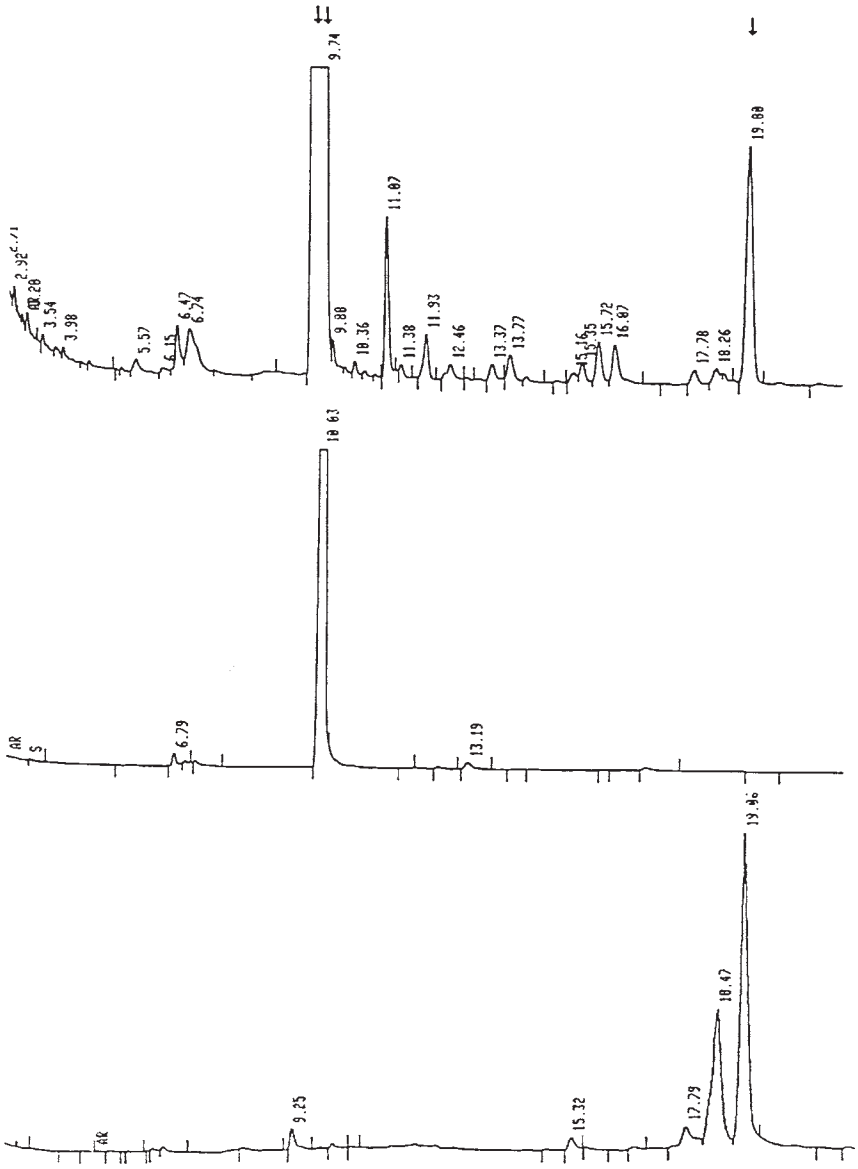

FIG. 1. Gas–liquid chromatography (GLC) tracing of the sterols of a human lung infected with *Pneumocystis carinii hominis*. This sample was prepared from a formalin-fixed lung taken from a patient who died from *Pneumocystis carinii* pneumonia with no known history of treatment for the infection. Thin-layer chromatographically purified free sterols were analyzed using a DB-5 or SPB-5 capillary column (Supelco, Bellefonte, PA) in a Hewlett-Packard gas–liquid chromatograph (Palo Alto, CA) with He as the carrier gas (1 mL/min; split ratio was 50:1). Isothermal (280°C) analysis was performed with injection and flame-ionization detector temperatures set at 300 and 290°C, respectively. Top tracing, sterols from lungs of *P. carinii*-infected patient. Cholesterol (double arrow; retention time, 9.74 min) from the host lung and scavenged by the organism was the dominant component. Pneumocysterol (single arrow; retention time, 19.00 min) was the major *P. carinii*-specific sterol in this sample. Middle tracing, authentic standard of cholesterol (retention time, 10.03 min). Bottom tracing, authentic (24*Z*)-ethylidenelanost-8-en-3β-ol (chemically synthesized by E.J. Parish; retention time, 19.06 min). The smaller peak eluting at 18.47 min is the 24*E* isomer. GLC tracings were kindly provided by D.H. Beach.

blages of different soil, aquatic, and other microbiota are characterized by detecting markers for specific bacterial species, and their signature lipids are among the most utilized for that purpose (64–66). In a similar fashion, the relatively rare, distinct *P. carinii* signature sterols could be used to detect the organism in human samples and may prove useful for diagnosis of infection or transient colonization by the pathogen.

In a recent study of bronchoalveolar lavage fluid (BALF) from HIV patients with PcP, the *P. carinii* signature sterols were detected by GLC analysis in samples containing suffi-

cient levels of sterols (67). It was also found that the BALF of PcP patients had dramatically reduced levels of total sterols, only about 20% of normal. A reduction in total lipids and phospholipids in BALF obtained from PcP patients was previously reported (68). Thus, for this patient group, a 1-mL BALF sample did not contain sufficient levels of total and *P. carinii* signature sterols for identification by routine GLC procedures (67).

The analyses of sterols in human BALF from normal, healthy volunteers and from different groups of patients, including those with pulmonary disease other than PcP (Amit, Z., Baughman, R.P., and Kaneshiro, E.S., unpublished observations) provided some additional interesting and potentially important observations with respect to *P. carinii* epidemiology. In every patient group examined, as well as in at least one normal healthy individual, the *P. carinii* signature sterols were present even though the organism was not detected by light microscopic analysis of the samples. One patient group consisted of sarcoidosis patients (pulmonary disorder of unknown cause characterized by granulomatous tubercles of the skin, lymph nodes, lungs, eyes, and other tissues and organs). The *P. carinii* signature sterols were detected in about 78% of the samples from these patients, suggesting that BALF sterol analysis may be a good alternative method complementing light microscopy for the detection of this pathogen. Furthermore, the detection of *P. carinii* signature sterols in some samples from HIV-positive patients cleared of PcP suggests that even though the patients' lungs had been cleared of live organisms, these signature lipids persist in the host lung, i.e., *P. carinii* sterols are retained in the host lung after the organisms are no longer identifiable by light microscopy or DNA amplification by polymerase chain reaction (PCR). The sterols may be recycled in the lung surfactant and alveolar type II epithelial cells that synthesize and secrete lung surfactant. Alveolar type II epithelial cells have been shown to take up lung surfactant components as well as secrete them (69).

The detection of *P. carinii* signature sterols in normal, healthy individuals is consistent with reports that asymptomatic animals, including those trapped from the wild, have *P. carinii* (15–19). These organisms have been detected by employing DNA amplification techniques; light microscopic examinations usually do not provide sufficient sensitivity. Hence, signature sterols by routine GLC techniques may be a sensitive procedure for detecting low-level infections. The detection of the signature sterols in healthy individuals is also consistent with the proposal that, although *P. carinii* organisms are host species-specific, they could transiently colonize and persist for some time in other closely related species (14,70). Thus, colonization in those with intact immune systems and by organisms that can cause fulminant infections in other host species may be detectable by the sterol profiles of BALF.

DE NOVO BIOSYNTHESIS OF STEROLS

De novo sterol biosynthesis in *P. carinii carinii* was initially demonstrated by the incorporation *in vitro* of radiolabeled mevalonate and squalene into the organism's sterols as determined by radioactivity in the sterol TLC fraction (47,49). The individual sterol components that became radioactive have yet to be identified.

Preliminary results demonstrate 3-hydroxy-3-methylglutaryl (HMG)-CoA reductase activity in *P. carinii* organisms incubated with radiolabeled mevalonate and a detergent to permeabilize the cells (47). In the absence of detergent, no activity was observed. Under normal conditions, the gene for this enzyme is not expressed in mammalian lungs. In the *P. carinii* studies, only low HMG-CoA reductase activity was detected in the lungs of normal and corticosteroid-treated uninfected rats, which verified that the activity detected was in the organism. Under these experimental conditions, the activity in the purified *P. carinii* preparations was approximately 100 pmol/mg protein/min at 37°C. Lovastatin inhibited the activity at an IC_{50} concentration of 4 nM (49).

Lanosterol, but not cycloartenol, was detected by GLC/MS among the *P. carinii* sterols (Jayasimhulu, K., and Kaneshiro, E.S., unpublished results). Thus, lanosterol is the key intermediate leading to the synthesis of a variety of sterols found in this organism.

Responses to inhibitors targeted against sterol biosynthesis further demonstrate that *P. carinii* synthesizes some of the sterols found in the organism. In earlier studies (71), antisterol drugs appeared to have no effect on this pathogen. For example, six imidazole drugs, presumably targeted against lanosterol demethylation (3,72,73) were tested against PcP in rats; none was effective in clearing the infection (71). Five of the six had no effect on isolated organism proliferation *in vitro* at the highest concentration tested (10 μg/mL), and miconazole had only a slight effect. On the other hand, terbinafine, an inhibitor of squalene epoxidase, reduced the cellular ATP content of *P. carinii* primary axenic cultures (74), suppressed *P. carinii* proliferation *in vitro* (75), and cleared experimental PcP in immunosuppressed rats (75). Recently, several inhibitors of squalene synthase, squalene epoxide:lanosterol cyclase, lanosterol demethylase, and Δ^8-to-Δ^7 isomerase were tested for their effects on *P. carinii* viability. All were found effective in reducing ATP when organisms were treated *in vitro* with 100 μg/mL of these drugs; several were effective at lower concentrations at shorter incubation times (74). Together, these observations demonstrate that *P. carinii de novo* synthesizes sterols, particularly those that are unique to the organism and that are not found in mammalian lungs or in other infectious agents.

Organisms with parasitic life styles commonly scavenge host sterols to synthesize new membranes and to participate in other cellular functions. An organism must maintain the precise three-dimensional conformation of its specific membrane components involved in vital functions (e.g., pumps). Thus, if the array of available host sterols does not include molecules that fulfill the precise stereochemical requirements for proper functioning of the parasite's membrane components, the organism must synthesize those distinct sterols to survive and proliferate. These parasite-synthesized sterols,

distinct from those available from the host and which are essential for the organism, have been described as "metabolic" sterols (76). The *P. carinii* Δ^7 24-alkylsterols appear to be required for viability and proliferation of the pathogen; blocking their syntheses inhibited cell proliferation (58). Since mammals lack SAM:SMT, the reactions involved in sterol C-24 alkylation in *P. carinii* represent attractive targets for the development of chemotherapeutic approaches against this opportunistic pathogen. Drugs that inhibit the formation of 24-alkylsterols are likely to have less toxicity in humans than drugs that inhibit the synthesis of compounds made by both humans and pathogens.

SUMMARY

Pneumocystis, the agent that can cause a life-threatening pneumonia in AIDS and other immunocompromised or immunodeficient patients, actually includes organisms of broad genetic backgrounds. Different genetic populations most likely represent different species. The sterols of this exotic fungus have been analyzed by direct biochemical analysis on organism preparations isolated from the lungs of rats and humans. The sterol profiles of these preparations include sterols scavenged from its environment in the lungs of mammalian hosts, dominated by cholesterol (C_{27}). Several C_{28} and C_{29} Δ^7 24-alkylsterols are also present, which are either synthesized *de novo* by *P. carinii* or formed by metabolism of sterols scavenged from the host. In some, but not all, organism preparations obtained from humans, C_{31} and C_{32} Δ^8 24-alkyllanosterol compounds have been identified. The distinct *P. carinii*-specific sterols, which include some very rare compounds, appear useful as signatures or markers of the organism, since no other organisms known to infect mammalian lungs have been reported to synthesize these sterols. Thus, these signature sterols may be useful for detecting the organism in samples obtained from patients suspected of having the infection. Since mammals lack SAM:SMT activity, the reactions in the pathogen involved in sterol C-24 alkylation are an excellent target for the development of drugs designed to clear PcP.

ACKNOWLEDGMENTS

Supported in part by NIH grants RO1 AI38758 and RO1 AI29316.

REFERENCES

1. Walzer, P.D. (1994) Pneumocystis carinii *Pneumonia*, 2nd edn., Marcel Dekker, Inc., New York.
2. Cushion, M.T. (1998) *Pneumocystis carinii*, in *Topley and Wilson's Microbiology and Microbial Infections, Medical Mycology* (Collier, L.A., and Sussman, M., eds.), 9th edn., Vol. 4, pp. 645–683, Arnold Publishers, Oxford University Press, New York.
3. Mercer, E.I. (1991) Sterol Synthesis Inhibitors: Their Current Status and Modes of Action, *Lipids 26*, 584–597.
4. Guo, D., Mangla, A.T., Zhou, W., Lopez, M., Jia, Z., Nichols, S.D, and Nes, W.D. (1997) Antifungal Sterol Biosynthesis Inhibitors, in *Cholesterol: Its Functions, and Metabolism in Biology and Medicine* (Bittman, R., ed.), *Subcell. Biochem. 28*, 91–116.
5. Kaneshiro, E.S., Ellis, J.E., Jayasimhulu, K., and Beach, D.H. (1994) Evidence for the Presence of "Metabolic Sterols" in *Pneumocystis*: Identification and Initial Characterization of *Pneumocystis carinii* Sterols, *J. Eukaryot. Microbiol. 41*, 78–85.
6. Kaneshiro, E.S. (1998) The Lipids of *Pneumocystis carinii*, *Clin. Microbiol. Rev. 11*, 27–41.
7. Kaneshiro, E.S. (1998) Lipid Metabolism of *Pneumocystis*: Toward the Definition of New Molecular Targets, in *Pneumocystis & Pneumocystosis: Advances in Pneumocystis Research (*Dei-Cas, E., and Cailliez , J.-C., eds.), *FEMS Immunol. Med. Microbiol. 22*, 135–144.
8. Kaneshiro, E.S., Amit, Z., Chandra, J., Baughman, R.P., Contini, C., and Lundgren, B. (1999) The Sterol Composition of *Pneumocystis carinii hominis* Organisms Isolated from Human Lungs, *Clin. Diag. Lab. Immunol. 6*, 970–976.
9. Stringer, J.R. (1993) The Identity of *Pneumocystis carinii*: Not a Single Protozoan but a Diverse Group of Exotic Fungi, *Infect. Agents Dis. 2*, 109–117.
10. Stringer, J.R. (1996) *Pneumocystis carinii*: What Is It Exactly? *Clin. Microbiol. Rev*. 9, 489–498.
11. Alexopoulous, C.J., Mims, C.W., and Blackwell, M. (1996) *Introductory Mycology*, pp. 258–271, John Wiley & Sons, New York.
12. Yoshida, Y., Yamada, M., Shiota, T., Ikai, T., Takeuchi, S., and Ogina, K. (1981) Provocation Experiment: *Pneumocystis carinii* in Several Kinds of Animals, *Zentral. Bakteriol. Mikrobiol. Hyg. 250*, 206–212.
13. Gigliotti, F., Harmsen, A.G., Haidaris, C.G., and Haidaris, P.J. (1993) *Pneumocystis carinii* Is Not Universally Transmissible Between Mammalian Species, *Infect. Immun. 61*, 2886–2890.
14. Walzer, P.D., Schnelle, V., Armstrong, D., and Rosen, P.D. (1977) Nude Mouse: A New Experimental Model for *Pneumocystis carinii* Infection, *Science 197*, 177–179.
15. Pifer, L.L., Hughes, W.T., Stagno, S., and Woods, D. (1978) *Pneumocystis carinii* Infection: Evidence for High Prevalence in Normal and Immunosuppressed Children, *Pediatrics 61*, 35–41.
16. Shimizu, A., Kimura, F., and Kimura, S. (1985) Occurrence of *Pneumocystis carinii* in Animals in Japan, *Jpn. J. Vet. Sci. 47*, 309–311.
17. Shiota, T., Kurimoto, H., and Yoshida, Y. (1986) Prevalence of *Pneumocystis carinii* in Wild Rodents in Japan, *Zentral. Bakteriol. Mikrobiol. Hyg. 261*, 381–389.
18. Wakefield, A.E., Stewart, T.J., Moxon, E.R., Marsh, K., and Hopkin, J.M. (1990) Infection with *Pneumocystis carinii* Is Prevalent in Healthy Gambian Children, *Trans. Royal Soc. Trop. Med. Hyg. 84*, 800–802.
19. Laakkonen, J. (1998) *Pneumocystis carinii* in Wildlife, *Int. J. Parasitol*. 28, 241–252.
20. Nevez, G., Jounieaux, V., Linas, M.D., Guyot, K., Leophonte, P., Massip, P., Schmit, J.-L., Seguela, J.-P., Camus, D., Dei-Cas, E., Raccurt, C., and Mazars, E. (1997) High Frequency of *Pneumocystis carinii* sp. f. *hominis* Colonization in HIV-Negative Patients, *J. Eukaryot. Microbiol. 44*, 36S.
21. Gigliotti, F., (1992) Host Species-Specific Antigenic Variation of a Mannosylated Surface Glycoprotein of *Pneumocystis carinii*, *J. Infect. Dis. 165*, 329–336.
22. Bauer, N.L., Paulsrud, J.R., Bartlett, M.S., Smith, J.W., and Ilde, C.E., III (1993) *Pneumocystis carinii* Organisms from Rats, Ferrets, and Mice Are Antigenically Different, *Infect. Immun. 61*, 1315–1319.
23. Latouche, S., Roux, P., Poirot, J.L., Lavrard, I., Hermelin, B., and Bertand, V. (1994) Preliminary Results of *Pneumocystis carinii* Strains Differentiation by Using Molecular Biology, *J. Clin. Microbiol. 32*, 3052–3053.

24. Christensen, C.B.V., Settnes, O.P., Bille-Hansen, V., Henriksen, S.E., and Lundgren, B. (1996) *Pneumocystis carinii* from Pigs and Humans Are Antigenically Distinct. *J. Med. Vet. Mycol*. 34, 431–433.
25. Laakkonen, J., and Sukura, A. (1997) *Pneumocystis carinii* of the Common Shrew, *Sorex araneus*, Shows a Discrete Phenotype, *J. Eukaryot. Microbiol. 44*, 117–121.
26. Mazars, E., Guyot, K., Durand, I., Dei-Cas, E., Boucher, S., Abderrazak, S.B., Banuls, A.L., Tibayrenc, M., and Camus, D. (1997) Isoenzyme Diversity in *Pneumocystis carinii* from Rats, Mice, and Rabbits, *J. Infect. Dis. 175*, 655–660.
27. Weinberg, G.A., and Durant, P.J. (1994) Genetic Diversity of *Pneumocystis carinii* Derived from Infected Rats, Mice, Ferrets, and Cell Cultures, *J. Eukaryot. Microbiol. 41*, 223–228.
28. Peters, S.E., Wakefield, A.E., Whitwell, K.E., and Hopkin, J.M. (1994) *Pneumocystis carinii* Pneumonia in Thoroughbred Foals: Identification of a Genetically Distinct Organism by DNA Amplification, *J. Clin. Microbiol. 32*, 213–216.
29. Stringer, J.R., and Walzer, P.D. (1996) Molecular Biology and Epidemiology of *Pneumocystis carinii* Infection in AIDS, *AIDS 10*, 561–571.
30. Hong, S.T., Steele, P.E., Cushion, M.T., Walzer, P.D., Stringer, S.L., and Stringer, J.R. (1990) *Pneumocystis carinii* Karyotypes, *J. Clin. Microbiol. 28*, 1785–1795.
31. Cushion, M.T., Zhang, J., Kaselis, M., Giuntoli, D., Stringer, S.L., and Stringer, J.R. (1993) Evidence for Two Genetic Variants of *Pneumocystis carinii* Coinfecting Laboratory Rats, *J. Clin. Microbiol. 31*, 1217–1223.
32. Cushion, M.T., Kaselis, M., Stringer, S.L., and Stringer, J.R. (1993) Genetic Stability and Diversity of *Pneumocystis carinii* Infecting Rat Colonies, *Infect. Immun. 61*, 4801–4813.
33. Keely, S., Stringer, J.R., Baughman, R.P., Linke, M.J., Walzer, P.D., and Smulian, A.G. (1995) Genetic Variation Among *Pneumocystis carinii hominis* Isolates in Recurrent Pneumocystosis, *J. Infect. Dis. 172*, 595–598,
34. Cushion, M.T. (1998) Genetic Heterogeneity of Rat-Derived *Pneumocystis*, *FEMS Immunol. Med. Microbiol. 22*, 51–58.
35. Sloand, E., Laughon, B., Armstrong, M., Bartlett, M.S., Blumenfield, W., Cushion, M., Kalica, A., Kovacs, J.A., Martin, W., Pitt, E., Pesanti, E.L., Richards, F., Rose, R., and Walzer, P.D. (1993) The Challenge of *Pneumocystis carinii* Culture, *J. Eukaryot. Microbiol. 40*, 188–195.
36. Merali, S., Frevert, U., Williams, J.H., Chin, K., Bryan, R., and Clarkson, A.B., Jr. (1999) Continuous Axenic Cultivation of *Pneumocystis carinii*, *Proc. Natl. Acad. Sci. USA 96*, 2402–2407.
37. Harwood, J.L. (1987) Lung Surfactant, *Prog. Lipid Res*. 26, 211–256.
38. Zimmerman, P.E., Voelker, D.R., McCormack, F.X., and Martin, W.J. (1992) 120 kDa Surface Glycoprotein of *Pneumocystis carinii* Is a Ligand for Surfactant Protein A, *J. Clin. Invest. 89*, 143–149.
39. Kaneshiro, E.S., Wyder, M.A., Zhou, L.H., Ellis, J.E., Voelker, D.R., and Langreth, S.G. (1993) Characterization of *Pneumocystis carinii* Preparations Developed for Lipid Analysis, *J. Eukaryot. Microbiol. 40*, 805–815.
40. Yoneda, K., and Walzer, P.D. (1983) Attachment of *Pneumocystis carinii* to Type I Alveolar Cells Studied by Freeze-Fracture Electron Microscopy, *Infect. Immun. 40*, 812–815.
41. Limper, A.H., and Martin, W.J. (1990) *Pneumocystis carinii*: Inhibition of Lung Cell Growth Mediated by Parasite Attachment, *J. Clin. Invest. 85*, 391–397.
42. Pottratz, S.T. (1998) *Pneumocystis carinii* Interactions with Respiratory Epithelium, *Semin. Respir. Infect. 13*, 323–329.
43. O'Riordan, D.M., Standing, J.E., Kwon, K.Y., Chang, D., Crouch, E.C., and Limper, A.H. (1995) Surfactant Protein D Interacts with *Pneumocystis carinii* and Mediates Organism Adherence to Alveolar Macrophages, *J. Clin. Invest. 95*, 2699–2710.
44. Yoshida, Y. (1989) Ultrastructural Studies of *Pneumocystis carinii*, *J. Protozool. 36*, 53–60.
45. Kaneshiro, E.S., Wu, Y-P., and Cushion, M.T. (1991) Assays for Testing *Pneumocystis carinii* Viability, *J. Protozool. 38*, 85S–87S.
46. Chen, F., and Cushion, M.T. (1994) Use of an ATP Bioluminescent Assay to Evaluate Viability of *Pneumocystis carinii* from Rats, *J. Clin. Microbiol. 32*, 2791–2800.
47. Kaneshiro, E.S., Ellis, J.E., Zhou, L.H., Rudney, H., Gupta, A., Jayasimhulu, K., Setchell, K.D.R., and Beach, D.H. (1994) Isoprenoid Metabolism in *Pneumocystis carinii*, *J. Eukaryot. Microbiol. 41*, 93S.
48. Florin-Christensen, M., Florin-Christensen, J., and Kaneshiro, E.S. (1995) Uptake and Metabolism of L-Serine by *Pneumocystis carinii carinii*, *J. Eukaryot. Microbiol. 42*, 669–675.
49. Ellis, J.E., Wyder, M.A., Zhou, L., Gupta, A., Rudney, H., and Kaneshiro, E.S. (1996) Composition of *Pneumocystis* Neutral Lipids and Identification of Coenzyme Q_{10} as the Major Ubiquinone Homolog in *P. carinii carinii*, *J. Eukaryot. Microbiol. 43*, 165–170.
50. Sul, D., and Kaneshiro, E.S. (1997) Ubiquinone Synthesis by *Pneumocystis carinii*: Incorporation of Radiolabeled Polyprenyl Chain and Benzoquinone Ring Precursors, *J. Eukaryot. Microbiol. 44*, 60S.
51. Paulsrud, J.R., Queener, S.F., Bartlett, M.S., and Smith, J.W. (1991) Total Cellular Fatty Acid Composition of Cultured *Pneumocystis carinii*, *J. Clin. Microbiol. 31*, 1899–1902.
52. Sorice, M., Lenti, L., Misasi, R., Contini, C., Cignarella, L., Griggi, T., Vullo, V., and Masala, C. (1992) Evidence for the Existence of Ganglioside Molecules on *Pneumocystis carinii* from Human Lungs, *Parasitology 105*, 1–6.
53. Furlong, S.T., Samia, J.A., Rose, R.M., and Fishman, J.A. (1994) Phytosterols Are Present in *Pneumocystis carinii*, *Antimicrob. Agents Chemother. 38*, 2534–2540.
54. Paulsrud, J.R., and Queener, S.F. (1994) Metabolism of Fatty Acids and Amino Acids by Cultured *Pneumocystis carinii*, *J. Eukaryot. Microbiol. 41*, 633–638.
55. Guo, Z., and Kaneshiro, E.S. (1995) Phospholipid Composition of *Pneumocystis carinii carinii* and the Effects of Methylprednisolone Immunosuppression on Rat Lung Lipids, *Infect. Immun. 63*, 1286-1290.
56. Guo, Z., Beach, D.H., and Kaneshiro, E.S. (1996) Fatty Acid Composition of the Major Phospholipids of *Pneumocystis carinii carinii*: Comparison with Those in the Lungs of Normal and Methylprednisolone-Immununosuppressed Rats, *Infect. Immun. 64*, 1407–1412.
57. Kaneshiro, E.S., Ellis, J.E., Guo, Z., Jayasimhulu, K., Maiorano, J.N., and Kallam, K.A. (1996) Characterizations of Neutral Lipid Fatty Acids and *cis*-9,10-Epoxy Octadecanoic Acid in *Pneumocystis carinii carinii*, *Infect. Immun. 64*, 4105–4114.
58. Urbina, J.A., Visbal, G.,. Contreras, L.M., McLaughlin, G., and Docampo, R. (1997) Inhibitors of $\Delta^{24(25)}$ Sterol Methyltransferase Block Sterol Synthesis and Cell Proliferation in *Pneumocystis carinii*, *Antimicrob. Agents Chemother. 41*, 1428–1432.
59. Kaneshiro, E.S., Guo, Z., Sul, D., Kallam, K., Jayasimhulu, K., and Beach, D.H. (1998) Characterizations of *Pneumocystis carinii* and Rat Lung Lipids: Glyceryl Ethers and Fatty Alcohols, *J. Lipid Res. 39*, 1907–1917.
60. Kaneshiro, E.S., Amit, Z., Swonger, M.M., Kreishman, G.P., Brooks, E.E., Kreishman, M., Jayasimhulu, K., Parish, E.J., Sun, H., Kizito, S.A., and Beach, D.H. (1999) Pneumocysterol [(24*Z*)-ethylidenelanost-8-en-3β-ol], a Rare Sterol Detected in the Opportunistic Pathogen *Pneumocystis carinii* f. sp. *hominis*: Structural Identity and Chemical Synthesis, *Proc. Natl. Acad. Sci. USA 96*, 97–102.

61. Weete, J.D. (1980) *Lipid Biochemistry of Fungi and Other Organisms*, Plenum Press, New York.
62. Weete, J.D. (1989) Structure and Function of Sterols in Fungi, *Adv. Lipid Res. 23*, 484–491.
63. Sharma, M.C., Ohira, T., and Yatagai, M. (1994) Lanostane Triterpenes from the Bark of *Neolitsea sericea*, *Phytochemistry 37*, 201–203.
64. Nichols, P.D., Leeming, R., Rayner, M.S., Latham, V., Ashbolt, N.J., and Turner, C. (1993) Comparison of the Abundance of the Fecal Sterol Coprostanol and Fecal Bacterial Groups in Inner-Shelf Waters and Sediments near Sydney, Australia, *J. Chromatogr. 643*, 189–195.
65. Zelles, L. (1997) Phospholipid Fatty Acid Profiles in Selected Members of Soil Microbial Communities, *Chemosphere 35*, 275–294.
66. Shi, Y., Odt, C.L., and Weimer, P.J. (1997) Competition for Cellulose Among Three Predominant Ruminal Cellulolytic Bacteria Under Substrate-Excess and Substrate-Limited Conditions, *Appl. Environ. Microbiol. 63*, 734–742.
67. Chandra, J., Amit, Z., Baughman, R.P., Kleykamp, B., and Kaneshiro, E.S. (1999) *Pneumocystis* Infection Is Correlated with a Reduction in the Total Sterol Content of Human Bronchoalveolar Lavage Fluid, *J. Eukaryot. Microbiol. 46*, 146S–148S.
68. Hoffman, A.G., Lawrence, M.G., Ognibene, F.P., Suffredini, A.F., Lipschik, G.Y., Kovacs, J.A., Masur, H., and Shelhamer, J.H. (1992) Reduction in Pulmonary Surfactant in Patients with Human Immunodeficiency Virus Infection and *Pneumocystis carinii* Pneumonia, *Chest 102*, 1730–1736.
69. Ryan, R.M., Morris, R.E., Rice, W.R., Ciraolo, G., and Whitsett, J.A. (1989) Binding and Uptake of Pulmonary Surfactant Protein (SP-A) by Pulmonary Type II Epithelial Cells, *J. Histochem. Cytochem. 37*, 429–440.
70. Beard, C.B., Jennings, V.M., Teague, W.G., Carter, J.L., Mabry, J., Moura, H., Visvesvara, G.S., Collins, W.E., and Navin, T.R. (1999) Experimental Inoculation of Immunosuppressed Owl Monkeys with *Pneumocystis carinii* f. sp. *hominis*, *J. Eukaryot. Microbiol. 46*, 113S–115S.
71. Bartlett, M.S., Queener, S.F., Shaw, M.M., Richardson, J.D., and Smith, J.W. (1994) *Pneumocystis carinii* Is Resistant to Imidazole Antifungal Agents, *Antimicrob. Agents Chemother. 38*, 1859–1861.
72. Marriott, M.S., Pye, G.W., Richardson, K., and Troke, P.F. (1986) The Activity of Fluconazole (UK-49,858), a Novel bis-Triazole Antifungal and Ketoconazole Against Fungal and Mammalian Sterol C14 Demethylases, in In Vitro *and* In Vivo *Evaluation of Antifungal Agents* (Iwata, K., and Vanden Bossche, H., eds.), pp. 143–149, Elsevier, Amsterdam.
73. Mercer, E.I. (1984) The Biosynthesis of Ergosterol, *Pesticide Sci. 15*, 133–135.
74. Kaneshiro, E.S., Collins, M., and Cushion, M.T. (1999) The Effects of Sterol Biosynthesis Inhibitors on the ATP Content of *Pneumocystis carinii*, *J. Eukaryot. Microbiol. 46*, 142S–143S.
75. Contini, C., Colombo, D., Cultrera, R., Prini, E., Sechi, T., Angelici, E., and Canipari, R. (1996) Employment of Terbinafine Against *Pneumocystis carinii* Infection in Rat Models, *Br. J. Dermatol. 134*, 30–32.
76. Haughan, P.A., and Goad, L.J. (1991) Lipid Biochemistry of Trypanosomatids, in *Biochemical Protozoology* (Coombs, G.H., and North, M. D., eds.), pp. 312–328, Taylor & Frances, London.

[Received July 30, 1999, and in revised form and accepted January 21, 2000]

The Effects of Dehydroepiandrosterone on Carcinogenesis, Obesity, the Immune System, and Aging

John R. Williams*

Department of Chemistry, Temple University, Philadelphia, Pennsylvania 19122

ABSTRACT: With the passage of the U.S. Dietary Supplement Health and Education Act of 1994, dehydroepiandrosterone (DHEA , 5-androsten-3β-ol-17-one) has become widely available, and a large and growing market has developed for this "fountain of youth." DHEA has been shown to have significant beneficial effects in animals, which may lead to clinical uses in man. Historically, the U.S. Food and Drug Administration removed DHEA from the over-the-counter market in 1985 because there was no support for the health claims that were made for this product. Almost all of the biological data was on animals and there was a lack of demonstrated efficacy in humans. Recently there have been a number of small clinical trials in humans but the results have not been as positive as in the animal tests. This review will be restricted to the effects of DHEA on carcinogenesis, obesity, the immune system, and aging. Four hypotheses have been proposed to explain the underlying biochemical mechanism(s) by which DHEA exerts its beneficial properties. The first is based on the inhibitory effect of DHEA on mammalian glucose-6-phosphate dehydrogenase. This mechanism can explain the antiinitiation and antipromotion steps in some cases of carcinogenesis. The second biochemical mechanism involves the induction of peroxisomes and peroxisome-associated enzymes. The third explanation is that DHEA works in a similar fashion to the known anticarcinogenic action of food restriction. An antiglucocorticoid mechanism has also been suggested. A hypothesis for the increase followed by the decrease in the levels of DHEA with age is proposed. A number of new synthetic DHEA analogs have been synthesized and tested. They offer the best hope for the development of a clinically useful drug based on the properties of DHEA.

Paper no. L8319 in *Lipids 35*, 325–331 (March 2000).

There is increasing evidence that dehydroepiandrosterone (DHEA, 5-androsten-3β-ol-17-one) **1a** may have a number of significant clinical uses (1–3). With the passage of the U.S. Dietary Supplement Health and Education Act of 1994, DHEA has become widely available, and a large and growing market has developed for this "fountain of youth." DHEA has become a topic for talk shows and reports in the print and broadcast media. It has been claimed to be a "super hormone" that can help with obesity; build muscle mass; prevent cancer, heart disease, and noninsulin dependent diabetes; slow aging, prevent or slow the progression of Alzheimer's and Parkinson's diseases; boost libido; strengthen the immune system; and help in the treatment of systemic lupus erythematosis. Unfortunately most of the work done so far has been on animals, and there is still no large randomized clinical trial on the long-term effects of DHEA in humans.

Historically, the U.S. Food and Drug Administration removed DHEA from the over-the-counter market in 1985 because there was no support for the health claims that were made for this product. Almost all of the biological data was on animals, and there was a lack of demonstrated efficacy in humans. One major problem in much of the extrapolation of data obtained from the administration of DHEA to subprimate species is that primates synthesize adrenal androgens to a greater degree than do many other mammals, and the metabolism and effects of these compounds are known to be different in, for instance, rodents and primates. Thus, many of the metabolic and immune effects that this compound might have in laboratory animals have not been found in humans. Since so many people are now taking DHEA, what are the risks and what are the benefits to them? Owing to the large number of beneficial effects attributed to DHEA, I have chosen to restrict this review to carcinogenesis, obesity, immune system, and aging. Other topics are covered in a number of excellent reviews (1–3).

DHEA **1a** is formed from DHEA sulfate (DHEAS) **1b** by sulfatases in peripheral tissue (4,5). DHEAS is the major circulating steroid in blood plasma and arises primarily by secretion from the adrenal cortex (5). The ratio of DHEAS to DHEA in plasma is approximately 200:1 (5). The levels of DHEAS rise through puberty, reaching maxima at age 20–24 yr in men and 15–19 yr in women (6). Levels then decline steadily with age with males having approximately 40% more DHEAS than women of the same age (5).

Metabolism of cholesterol **2** proceeds *via* pregnenolone **3** to yield DHEA **1** as outlined in Scheme 1. Further metabolism of DHEA by oxidation at C-3 yields the androstendione **4**, which is isomerized to the conjugated androstendione **5** ("andro," the steroid taken by Mark McGwire, the 1998 baseball star), testosterone **6**, androsterone **7a**, etiocholanolone **7b**, and estradiol **8**, many of which are biologically active (7).

Carcinogenesis. In 1971 Bulbrook *et al.* (8) presented re-

*E-mail: jwilli07@nimbus.ocis.temple.edu

Abbreviations: BMI, body mass index; DHEA, dehydroepiandrosterone (5-androsten-3β-ol-17-one); DHEAS, DHEA sulfate; DMBA, dimethylbenz[a]anthracene; G6PDH, glucose-6-phosphate dehydrogenase; TPA, 12-O-tetradecanoylphorbol-13-acetate.

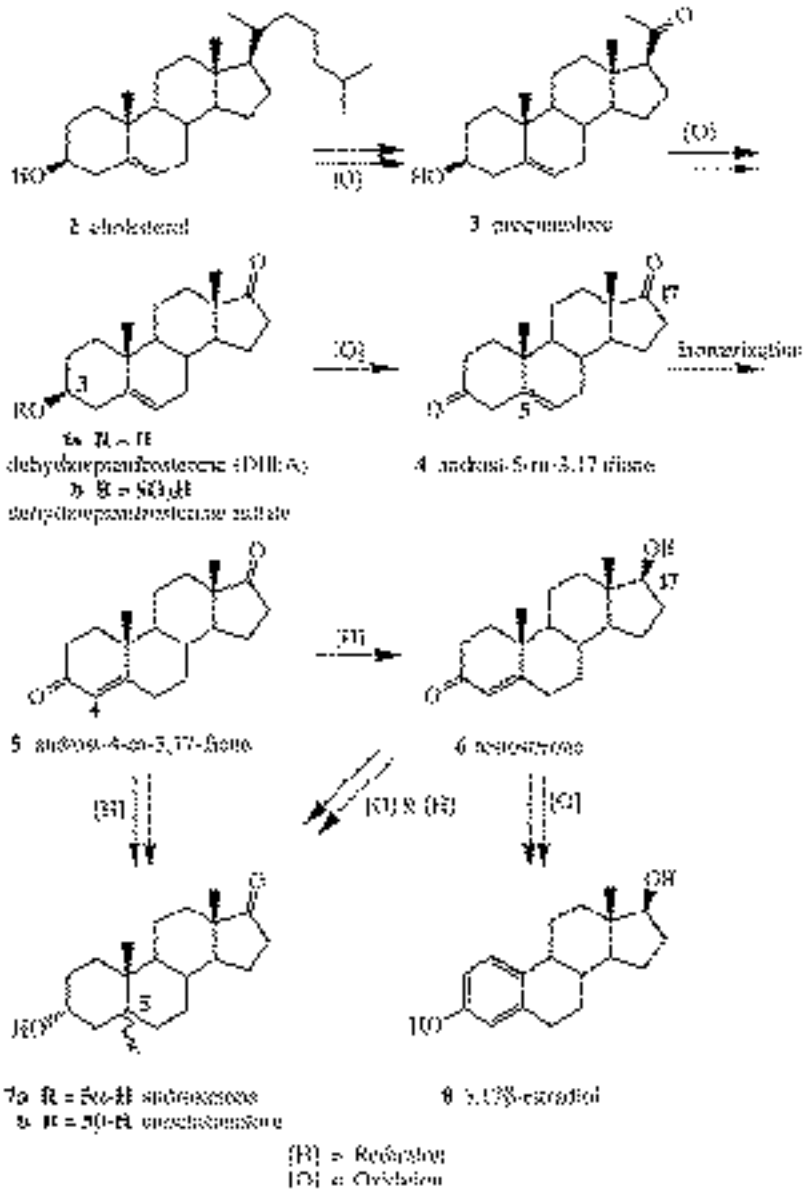

SCHEME 1

sults regarding 5,000 premenopausal women who had been studied for up to 9 yr and reported that the excretion of the DHEA metabolites androsterone **7a** and etiocholanolone **7b** was subnormal in 27 women who subsequently developed breast cancer. This result assumes there is a correlation between the endogenous level of a steroid and the level of a metabolite when it is excreted. To avoid diurnal fluctuation in steroid levels, Zumoff *et al.* (9) measured the 24-h mean plasma concentrations of DHEA and DHEAS on pooled blood samples obtained every 20-min from 11 women with primary operable breast cancer. When matched with 37 normal women those premenopausal women with breast cancer were found to have subnormal levels of DHEA and DHEAS (9). Similarly, in a study of 20,300 women, the 15 who developed premenopausal breast cancer were compared to 29 matched controls. The mean serum level of DHEA among cases was 10% lower than among controls. No correlation between DHEAS level and premenopausal breast cancer was observed (10). It is uncertain whether the lower levels of DHEA precede or are a consequence of breast cancer.

Since the 1970s Schwartz *et al.* (11) and others have been studying the metabolic effects of DHEA on mice and rats. DHEA shows an amazingly wide range of beneficial and therapeutic effects in rodents, including prevention of cancer, use in antiautoimmune diseases, antiatherogenic effects as well as antiobesity and antidiabetic activities (11). However, the effect of DHEA on any of these diseases is only now being studied in humans.

In 1975 Schwartz and Perantoni (12) demonstrated that DHEA protected rat liver epithelial-like cells and hamster em-

bryonic fibroblasts against aflatoxin B_1 and 7,12-dimethylbenz[a]anthracene (DMBA)-induced cytotoxicity and transformation. The rate of metabolism of [^{3}H]DMBA to water-soluble products by cultured fibroblasts was also inhibited by DHEA. Schwartz and coworkers also showed that long-term administration of DHEA inhibited the development of spontaneous breast cancer in C3H-*A^{vy}/A* (obese) (13) and C3H-*A/A* mice (14) and of DMBA- and urethane-induced lung tumors in A/J mice (15).

Topical DHEA treatment inhibits papilloma formation when applied 1 h before 12-*O*-tetradecanoylphorbol-13-acetate (TPA) treatment, a result indicating that the steroid also blocks tumor promotion. A single intraperitoneal injection of DHEA into CD-1 mice immediately before TPA application also abolishes the TPA stimulation in epidermal [^{3}H]thymidine incorporation (16,17). Tumor promoters such as TPA produce diverse effects on mammalian cells, and the mechanism by which they enhance skin papilloma formation is not fully understood.

Some evidence exists that justifies concern about the safety of DHEA supplements. Large doses of DHEA can be converted to potent androgens such as testosterone, which can masculinize women, resulting in increased hair growth on the face and body. Furthermore in a nested, case control prospective study of serum samples from 20,000 women, a higher risk of ovarian cancer was associated with increased levels of DHEA and DHEAS (18). However, these results are contradicted by other workers who found the circulating levels of DHEAS are lower in those women who have ovarian cancer (19). In another study a woman was given a 150-mg dose of DHEA and developed transient jaundice and hepatic dysfunction 1 wk later (20).

A number of hypotheses have been proposed to explain the underlying biochemical mechanism(s) by which DHEA exerts its beneficial properties. The first hypothesis is based on the inhibitory effect of DHEA on mammalian glucose-6-phosphate dehydrogenase (G6PDH).

G6PDH DEHYDROGENASE INHIBITION

Although DHEAS is the main precursor of placental estrogen and may be converted into DHEA and then into biologically active androgens, there is no obvious role for DHEAS or DHEA in the normal individual. DHEA is a potent uncompetitive inhibitor of mammalian G6PDH (21-23). G6PDH is the rate-controlling enzyme in the pentose-phosphate cycle, a pathway that is a major source of ribose-5-phosphate and extramitochondrial NADPH. Two moles of NADPH are generated in the conversion of glucose-6-phosphate into ribose-5-phosphate (Eq. 1). Thus, as one ages and the level of DHEA decreases, the availability of ribose-5-phosphate and extramitochondrial NADPH should increase.

$$\begin{matrix}\text{Glucose 6 - phosphate} + \\ 2\,\text{NADP}^+ + \text{H}_2\text{O}\end{matrix} \xrightarrow{\text{G6PDH}} \begin{matrix}\text{ribose 5 – phosphate} + \\ 2\,\text{NADPH} + 2\,\text{H}^+ + \text{CO}_2\end{matrix} \quad [1]$$

Agents that damage DNA or interfere with its replication or repair cause most cancers. Three processes that contribute to tumor development are the following: (i) tumor initiation by covalent binding of an active species (usually a hard electrophile) to DNA. The active species can be generated by metabolic activation of a carcinogen through the action of cytochrome P-450 (24); (ii) tumor promotion by cell stimulation to produce activated forms of oxygen, including superoxide anion radicals (0_2^-) and peroxides, agents that are free radicals or generators of free radicals (25); and (iii) tumor promoter stimulation of cell proliferation *via* agents such as TPA (26).

In the first process, cytochrome P-450 oxidizes polyaromatic hydrocarbons such as benz[a]pyrene **9** twice to yield a highly electrophilic and highly carcinogenic polyaromatic epoxy diol, **10** (Scheme 2). This epoxy diol **10** has been shown to bind covalently with native DNA to yield an adduct, from which a polyaromatic-deoxyguanosine adduct **11** has been obtained (24). Since cytochrome P-450 is an NADPH-dependent enzyme, lowering the amount of NADPH should decrease the

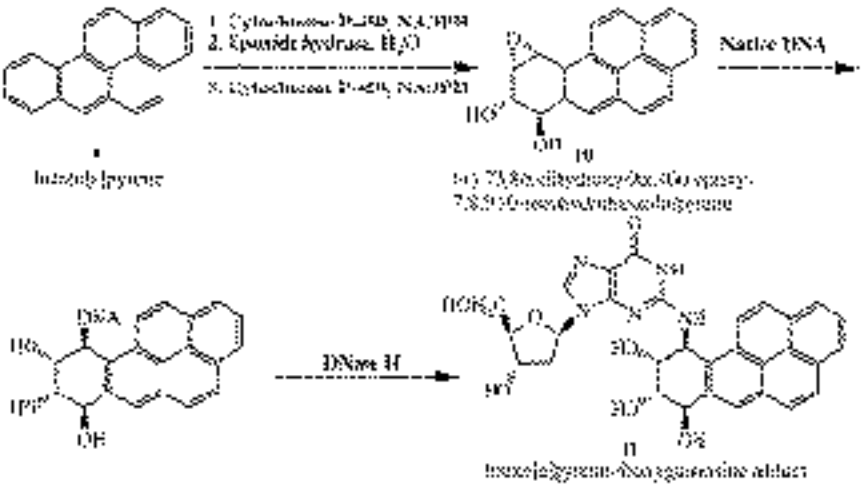

SCHEME 2

amount of metabolic activation resulting in a decrease in the initiation of cancer. In the second process, tumor promoters stimulate the generation of activated forms of oxygen by mixed function oxidases (25). Here again the generation of activated forms of oxygen by mixed function oxidases is also an NADPH-dependent process. Lowering the amount of NADPH should decrease the amount of metabolic activation resulting in a decrease in the initiation of cancer.

In the third process, there is a good correlation between a steroid's ability to inhibit G6PDH and its inhibition of cell proliferation by the tumor promoter TPA (26). Treatment of CD-1 mice with DHEA immediately before the application of TPA stops the TPA stimulation in epidermal [H]thymidine incorporation (27). 16α-Bromoepiandrosterone **12** (Scheme 3) is 30 to 50 times more potent as an inhibitor of mammalian G6PDH and is similarly much more active as an inhibitor of TPA stimulation (27). Conversely, various sex steroids that do not inhibit G6PDH also failed to inhibit TPA stimulation.

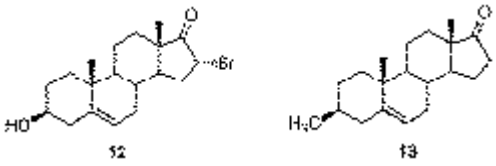

12 13

SCHEME 3

Furthermore cancer cells undergo excessive proliferation when compared to normal cells, thereby increasing the demand for cellular components. By inhibiting the pentose-phosphate pathway, DHEA inhibits the formation of ribose-5-phosphate, an important component in cancer cell growth.

A second biochemical mechanism that may explain the effect of DHEA on the livers of mice and rats is the induction of peroxisomes and peroxisome-associated enzymes, which would lead to an increase in fatty acid β-oxidation (28). Whether the beneficial and therapeutic effects that result from the administration of DHEA are associated with changes in the liver remains to be established (29).

A third explanation is that DHEA works in a similar fashion to the known anticarcinogenic action of food restriction (30). Dietary restriction also significantly extends the life of rodents *via* an anti-aging mechanism (31). The anti-aging effect is now felt to be due to the lowering of the body temperature during sleep, and there is evidence suggesting that this temperature fall enhances the DNA reparative action *via* DNA polmerases (31) and decreases the expression of protooncogenes (32). Do DHEA or its metabolites effect the efficiency of DNA repair to mutagenesis or radiation? DHEA has been shown to stimulate mutagenic repair mechanisms *via* promotion of sister chromosomal exchange (33). Furthermore, Sonka *et al.* reported that, depending on timing of DHEA administration to whole body radiation, it has radiation-protective and/or -enhancing action (34).

In other experiments, DHEA has been shown to oppose the anti-inflammatory action of glucocorticoids by an unknown mechanism (35).

In conclusion, there does not appear to be a unifying biochemical mechanism to the anticarcinogenic action of DHEA. There may be no single answer as to its anticarcinogenic effects.

OBESITY

Administration of DHEA to metabolically obese mice bearing the A^{vy}/a mutation, significantly inhibited their weight gain (36). Measurements of food consumption showed that treated and untreated mice consumed equivalent amounts of food but that the DHEA-treated mice weighed less. Thus, DHEA is exerting its antiobesity effect by altering the metabolism of the mice in decreasing the efficiency of their food utilization rather than as a result of appetite suppression (37). DHEA inhibits G6PDH thereby decreasing the formation of NADPH, which is an essential cofactor with one mole needed for every methylene unit in the biosynthesis of a fatty acid. Thus, this anabolic pathway may be reduced under conditions of reduced NADPH availability. The stoichiometry of the synthesis of hexadecanoic acid (palmitic) is:

$$8\ \text{Acetyl CoA} + 7\ \text{ATP} + 14\ \text{NADPH} \rightarrow \text{CH}_3(\text{CH}_2)_{14}\text{COOH} + 14\ \text{NADP}^+ + 8\ \text{CoA} + 6\ \text{H}_2\text{O} + 7\ \text{ADP} + 7\ \text{Pi} \quad [2]$$

It appears unlikely that the antiobesity action of DHEA is completely due to G6PDH inhibition. 16α-Bromoepiandrosterone **12** failed to produce an antiweight effect or lower blood sugar in genetically diabetic (*db/db)* C57BL/KsJ mice when fed in the diet at 0.4%, even though the bromosteroid **12** is a much more potent inhibitor of G6PDH than DHEA (38). In contrast, DHEA had a dramatic effect on the control of diabetes in genetically diabetic (*db/db)* C57BL/KsJ mice and in regulating weight in similar mutant strains.

In a study of weight gain in lean and obese mice it was found that obese mice ate less food but this resulted in a decrease in body weight which was greatest for those DHEA-fed obese mice (39). These changes in body weight were also accompanied by less body fat and lower fat cell size and number in the DHEA- treated rats. Fat-free mass and organ growth was preserved in DHEA-treated rats. This is a different response from that found in food-restricted obese rats which preserve body fat at the expense of lean tissue. Recently Cleary (39,40) showed that when obese rats were food-restricted to the degree necessary to weight-match them to DHEA-treated obese rats, fat pad weights of the weight-matched rats were substantially greater than those of the DHEA-treated rats. The fat pad weights of the weight-matched rats were similar to those of *ad libitum* fed rats. Thus, the results of both pair-feeding and weight-matching studies indicate that DHEA treatment is mediated through a different mechanism than that for caloric intake (40).

DHEA has been shown to increase liver weight in rats as well as other effects including enhanced ATP synthesis (41). The activity of the enzyme, long-chain fatty acyl-coenzyme A hydrolase, was found to be elevated, resulting in an increase in

a futile cycle of deacylation/reacylation. These mechanisms could explain DHEA's antiobesity effects (42).

In humans there is conflicting data. Some studies indicate there is a relationship between body mass index (BMI) and DHEA and/or DHEAS (43–46). Other studies conclude there is no relationship between DHEA and BMI (47–50). The administration of DHEA to volunteers in controlled trials to assess whether DHEA can affect body fat has been studied by a number of groups (51–53). The results of these studies show that exogenous DHEA does not have any significant effect on human obesity or fat-store distribution. The most obvious reason for this lack of activity is that the dosage is too low. Animal studies require at least 60–75 mg/kg/d, but such levels in humans would be intolerable owing to androgenic side effects.

IMMUNE FUNCTION

There is also conflicting clinical data concerning the immunoaugmentory effects of DHEA replacement in the elderly. A dose of 50/mg/d of DHEAS, given twice a day at the time as a vaccination, was found to increase influenza (but not tetanus) titer response over that seen with a placebo (54). On the other hand in a different study in which elderly volunteers were given 50 mg of DHEA for four consecutive days starting 2 d before immunization, DHEA treatment did not enhance established immunity (55). A significant decrease in attainment of protective antibody titer against A/Texas in subjects with nonprotective baseline antibody titer was recorded following DHEA treatment compared to placebo (52 vs. 84%, $P < 0.05$) (55).

NEW SYNTHETIC DHEA ANALOGS

The studies reported in this review have demonstrated that oral treatment of mice and rats with DHEA protects against the development of a broad range of tumors and has antiobesity activity. Although long-term treatment of mice and rats is without apparent side effect, DHEA is convertible into testosterone and estrone. DHEA is uterotrophic at therapeutic doses in the sexually immature rat, and conversion into sex steroids should limit the usefulness of DHEA as a cancer chemopreventive drug. The synthetic steroid 3β-methylandrost-5-en-17-one **13**, (Scheme 3) in which the 3β-hydroxyl group of DHEA is replaced by a 3β-methyl group, was specifically designed to prevent metabolism of **1** into androstenedione, **4**, an intermediate on the pathway to testosterone **6** and estradiol **8** (16,17). 3β-Methylandrost-5-en-17-one **10** was without activity in the rat uterotrophic test at doses at which DHEA was highly active. On oral administration the steroid **10** is about three times as active as DHEA as an antiobesity and antidiabetic agent in the mouse.

Two other synthetic steroids, 16α-fluoroandrost-5-en-17-one, **14**, and 16α-fluoro-5-androstan-17-one, **15**, which also lack the uterotrophic and seminal vesicle-enlarging effects of DHEA, have shown 15 times greater potency than DHEA when given orally in blocking both [^{3}H]DMBA binding to skin DNA and TPA stimulation in epidermal [^{3}H]thymidine incorporation (56). The lack of estrogenic and androgenic activity of **14** and **15** along with their greater potency suggests that these analogs may find application as cancer chemopreventive drugs in humans.

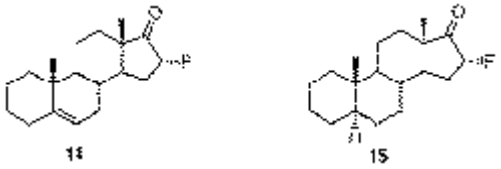

SCHEME 4

AGING

The aging process is accompanied by the development of obesity and glucose intolerance. Hyperinsulinemia has been shown to lead to low levels of DHEAS and DHEA. The mechanism whereby insulin decreases DHEAS production without affecting adrenal production of glucocorticoids or mineralocorticoids is unknown. DHEA administration had no effect on tissue sensitivity to insulin, unlike androgen therapy, which results in decreased tissue sensitivity to insulin (57).

Why should DHEA levels vary with age? A possible explanation of why mankind has evolved with varying levels of DHEA upon aging is because it aided in our survival as a species. The rise in DHEAS and DHEA levels that maximize in the late teens and early twenties corresponds with mankind's optimal time for reproduction. The increased levels of sex hormones should result in the increased physical strength, increased libido, and procreation. Then why should DHEA decrease with aging? Lower levels of DHEA result in higher levels of NADPH, leading to more fat formation, i.e., more efficient metabolism. It has only been in recent centuries that mankind has not been constantly faced with starvation. People survived who could get by on less, i.e. those with the most efficient metabolisms. As we get older we need less food to maintain the same weight.

Conversely, many of today's problems associated with aging may be the result of lower levels of DHEA resulting in a higher NADPH cellular pool. The ready availability of food in unlimited quantities has resulted in the increase in cancer, obesity, and heart disease. It is well known that reducing the weight gain of laboratory mice and rats through food restriction is a very effective method for cancer prevention (30). Spontaneous, chemically induced, and radiation-induced tumors in many different organs are all reduced in frequency in food-restricted rodents. Not only does underfeeding inhibit tumor development but also it retards the rate of appearance of autoimmune disease processes as well as many age-related pathological changes, and it is believed to slow the rate of aging (58). The biochemical mechanism by which underfeeding protects against cancer and autoimmune disease is obscure. As we grow older we get "the middle aged spread." The decrease in DHEA and androgenic metabolites could explain the resulting decrease in muscle mass as we age and our increase in flabby tis-

sue. In males, higher levels of NADPH may lead to more dihydrotestosterone resulting in increased hair loss, benign prostate hyperthropy, and increased prostate cancer.

In conclusion, the new synthetic analogs of DHEA should be more active and have fewer side effects than DHEA. It is hoped that one of these new molecules will be approved clinically for some or all of the beneficial properties attributed to DHEA.

ACKNOWLEDGMENTS

This work was supported in part by grants from the National Institutes of Health, Temple University Research Incentive Fund, Howard Hughes Medical Institute, Pharmacia & Upjohn, SmithKline Beecham, Wyeth-Ayerst, Merck, and DuPont Pharmaceuticals.

REFERENCES

1. Kalimi, M., and Regelson, W. (1990) *The Biologic Role of Dehydroepiandrosterone (DHEA)*, Walter de Gruyter, New York.
2. Bellino, F.L., Daynes, R.A., Hornsby, P.J., Lavrin, D.H., and Nestler, J.E., eds. (1995) Dehydroepiandrosterone (DHEA) and Aging, *Ann. NY Acad. Sci. 774*.
3. Nieuwenhuyse, H., and Thijssen, J.H.H. (1999) *DHEA: A Comprehensive Review*, Parthenon, New York.
4. Zumoff, B., and Bradlow, H.L. (1980) Sex Difference in the Metabolism of Dehydroisoandrosterone Sulfate, *J. Clin. Endocrinol. Metab. 51*, 334–336.
5. Parker, L.N. (1989) *Adrenal Androgens in Clinical Medicine*, 615 pp., Academic Press, New York.
6. Orentreich, N., Brind, J.L., Rizer, R.L., and Vogelman, J.H. (1984) Age Changes and Sex Differences in Serum Dehydroepiandrosterone Sulfate Concentrations Throughout Adulthood, *J. Clin. Endocrinol. Metab. 59*, 551–555.
7. Coleman, D.L., Leiter, E.H., and Applezweig, N. (1984) Therapeutic Effects of Dehydroepiandrosterone Metabolites in Diabetes Mutant Mice (C57BL/K_sJ-db/db), *Endocrinology 115*, 239–243.
8. Bulbrook, R.D., Hayward, J.L., and Spicer, C.C. (1971) Relation Between Urinary Androgen and Corticoid Excretion and Subsequent Breast Cancer, *Lancet*, 395–398.
9. Zumoff, B., Levin, J., Rosenfeld, R.S., Markham, M., Strain, G.W., and Fukushima, D., (1981) Abnormal 24-Hr Mean Plasma Concentrations of Dehydroepiandrosterone and Dehydroepiandrosterone Sulfate in Women with Primary Operable Breast Cancer, *Cancer Res. 41*, 3360–3363.
10. Helzlsouer, K.J., Gordon, G.B., Alberg, A.J., Bush, T.L., and Comstock, G.W. (1992) Relationship of Prediagnostic Serum Levels of Dehydroepiandrosterone and Dehydroepiandrosterone Sulfate in Women with Primary Operable Breast Cancer, *Cancer Res. 52*, 1–4.
11. Schwartz, A.G., Whitcomb, J.M., Nyce, J.W., Lewbart, M.L., and Pashko, L.L. (1988) Dehydroepiandrosterone and Structural Analogs: A New Class of Cancer Chemopreventive Agents, *Adv. Cancer Res. 51*, 391–424.
12. Schwartz, A.G., and Perantoni, A. (1975) Protective Effect of Dehydroepiandrosterone Against Aflatoxin B_1 and 7,12-Dimethylbenz[a]anthracene-induced Cytotoxicity and Transformation in Cultured Cells, *Cancer Res. 35*, 2482–2487
13. Schwartz, A.G. (1979) Inhibition of Spontaneous Breast Cancer Formation in Female C3H (A^{vy}/a) Mice by Long-Term Treatment with Dehydroepiandrosterone, *Cancer Res. 39*, 1129–1132.
14. Schwartz, A.G., Hard, G.C., Pashko, L.L., Abou-Gharbia, M., and Swern, D. (1981) Dehydroepiandrosterone: An Antiobesity and Anti-Carcinogenic Agent, *Nutr. Cancer 3*, 46–53.
15. Schwartz, A.G., and Tannen, R.H. (1981) Inhibition of 7,12-Dimethylbenz[a]anthracene and Urethane Induced Lung Tumor Formation in A/J Mice by Long-Term Treatment with Dehydroepiandrosterone, *Carcinogenesis 2*, 1335–1337.
16. Pashko, L.L., Rovito, R.J., Williams, J.R., Sobel, E.L., and Schwartz, A.G. (1984) Dehydroepiandrosterone (DHEA) and 3β-Methylandrost-5-en-17-one: Inhibitors of 7,12-Dimethylbenz[a]anthracene (DMBA)-Initiated and 12-*O*-Tetradecanoylphorbol-13-acetate (TPA) Promoted Skin Papilloma Formation in Mice, *Carcinogenesis 5*, 463–466.
17. Pashko, L.L., Hard, G.C., Rovito, R.J., Williams, J.R., Sobel, E.L., and Schwartz, A.G. (1985) Inhibition of 7,12-Dimethylbenz[a]anthracene-Induced Skin Papillomas and Carcinomas by Dehydroepiandrosterone and 3β-Methylandrost-5-en-17-one, *Cancer Res. 45*, 164–166.
18. Helzlsouer, K.J., Alberg, A.J., Gordon, G.B., Longcope, C., and Bush, T.L. (1995) Serum Gonadotropins and Steroid Hormones and the Development of Ovarian Cancer, *JAMA 274*, 1926–1930.
19. Heinonen, P.K., Koivlila, T., and Pystynen, P. (1987) Decreased Serum Level of Dehydroepiandrosterone Sulfate in Postmenopausal Women with Ovarian Cancer, *Gynecol. Obstet. Invest. 23*, 271–274.
20. Buster, J.E., Casson, P.R., and Straughn, A.B. (1992) Postmenopausal Steroid Replacement with Micronized Dehydroepiandrosterone: Preliminary Oral Bioavailability and Dose Proportionality Studies, *Am. J. Obstet. Gynecol. 166*, 1163–1170.
21. Marks, P.A., and Banks, J. (1960) Inhibition of Mammalian Glucose-6-Phosphate Dehydrogenase by Steroids, *Proc. Natl. Acad. Sci. USA 46*, 447–452.
22. Raineri, R., and Levy, H.R. (1970) On the Specificity of Steroid Interaction with Mammary Glucose-6-phosphate Dehydrogenase, *Biochemistry 9*, 2233–2243.
23. Oertel, G.W., and Benes, P. (1972) The Effects of Steroids on Glucose-6-phosphate Dehydrogenase, *J. Steroid Biochem. 3*, 493–496.
24. Levin, W., Wood, A.W., Wislock, P.G., Chang, R.L., Kapitulnik, J., Mah, H.D., Yagi, H., Jerina, D.M., and Conney, A.H. (1978) Mutagenicity and Carcinogenicity of Benzo[a]pyrene Derivatives, in *Polycyclic Hydrocarbons and Cancer: Environment, Chemistry, and Metabolism* (Gelboin, H.V., and Ts'o, P.O.P., eds.) Vol. 1, pp. 189–202, Academic Press, New York.
25. Emerit, I., and Cerutti, P. (1983) Clastogenic Action of Tumor Promoter Phorbol 12-Myristate-13-acetate in Mixed Human Leukocyte Cultures, *Carcinogenesis 4*, 1313–1316.
26. Kinzel, V., Loerke, H., Goerttler, K., Furstenberger, G., and Marks, F. (1984) Suppression of the First Stage of Phorbol 12-Tetradecanoate-13-acetate Effected Tumor Promotion in Mouse Skin by Nontoxic Inhibition of DNA Synthesis, *Proc. Natl. Acad. Sci. USA 81*, 5858–5862.
27. Pashko, L.L., Schwartz, A.G., Abou-Gharbia, M., and Swern, D. (1981) Inhibition of DNA Synthesis in Mouse Epidermis and Breast Epithelium by Dehydroepiandrosterone and Related Steroids, *Carcinogenesis 2*, 717–721.
28. Wu, H.Q., Masset-Brown, J., Tweedie, D.J., Milewich, L., Frenkel, R.A., Martin-Wixtrom, C., Estabrook, R.W., and Prough, R.A. (1989) Induction of Microsomal NADPH-Cytochrome P-450 Reductase and Cytochrome P-450IVAI ($P\text{-}450_{LA\omega}$) by Dehydropiandrosterone in Rats: a Possible Peroxisomal Proliferator, *Cancer Res. 49*, 2337–2343.
29. Moore, M.A., Weber, E., Thornton, M., and Bannasch, P. (1988) Sex Dependent, Tissue-Specific Opposing Effects of Dehydroepiandrosterone on Initiation and Modulation Stages of Liver

and Lung Carcinogenesis Induced by Dihydroxy-di-*n*-propylnitrosamine in F344 rats, *Carcinogenesis 9*, 1507–1509.
30. Tannenbaum, A., and Silverstone, H. (1953) Nutrition in Relation to Cancer, *Adv. Cancer Res. 1*, 451–501.
31. Lipman, J.M., Turturro, A., and Hart, R.W. (1989) The Influence in Dietary Restriction on DNA Repair in Rodents: a Preliminary Study, *Mech. Ageing Dev. 48*, 135–143.
32. Nakamura, K.D., Duffy, P.H., and Cu, M.H. (1989) The Effect of Dietary Restriction on myc Protooncogene Expression in Mice: A Preliminary Study, *Mech. Ageing Dev. 48*, 199–205.
33. Reff, M.E., and Schneider, E.L. (1980) *Biological Markers in Aging*, National Institutes of Health, Bethesda, Pub. #82-2221.
34. Sonka, J. (1976) Dehydroepiandrosterone. Metabolic Effects, *Acta Univ. Carol. Med., Monogr. 71*, 1–137, 146–171.
35. Bradlow, H.L., Murphy, J., and Byrne, J.J. (1999) Immunological Properties of Dehydroepiandrosterone, Its Conjugates and Metabolites, *Ann. NY Acad. Sci. 876*, 91–101.
36. Yen, T.T., Allan, J.A., Pearson, D.V., and Acton, J.M. (1977) Control of Obesity in A^{vy}/a Mice by 5α-Androstan-17-one, *Lipids 12*, 409–413.
37. Pashko, L.L., Fairman, D.K., and Schwartz, A.G. (1986) Inhibition of Proteinuria Development in Aging Sprague-Dawley Rats and C57BL/6 Mice by Long-term Treatment with Dehydroepiandrosterone, *J. Gerontol. 41*, 433–438.
38. Coleman, D.L., Schwizer, R.W., and Leiter, E.H. (1984) Effect of Genetic Background on the Therapeutic Effect of DHEA in Diabetes-Obesity Mutants and in Aged Normal Mice, *Diabetes 33*, 26–32.
39. Cleary, M.P., Shepherd, A., and Jenks, B. (1984) Effect of DHEA on Growth in Lean and Obese Zucker Rats, *J. Nutr. 114*, 1242–1251.
40. Cleary, M.P., Fox, N., Lazin, B., and Billheimer, J.T. (1985) A Comparison of the Effects of DHEA Treatment to *ad libitum* and Pair Feeding in the Obese Zucker Rat, *Nutr. Res. 5*, 1247–1257.
41. Kritchevsky, D., Tepper, S.A., Klurfeld, D.M., and Schwartz, A.G. (1983) Influence of DHEA on Cholesterol Metabolism in Rats, *Pharmacol. Res. Commun. 15*, 797–803.
42. Mohan, P.F., and Cleary, M.P. (1988) Effect of Short-term DHEA Administration on Liver Metabolism of Lean and Obese Rats, *Am. J. Physiol. 255*, E1–E8.
43. Tchernof, A., Despres, J.P., Belanger, A., Dupont, A., Prud'homme, D., Moorjani, S., Lupien, P.J., and Labrie, F. (1995) Reduced Testosterone and Adrenal C_{19} Steroid Levels in Obese Men, *Metabolism 44*, 513–519.
44. Tchernof, A., Labrie, F., Belanger, A., and Despres, J.P. (1996) Obesity and Metabolic Complications: Contribution of Dehydroepiandrosterone and Other Steroid Hormones, *J. Endocrinol. 150*, S155–S164.
45. Mantzoros, C.S., and Georgiadis, E.I. (1995) Body Mass and Physical Activity Are Important Predictors of Serum Androgen Concentrations in Healthy Young Men, *Epidemiology 6*, 432–435.
46. De Pergola, G., Zamboni, M., and Sciaraffia, M. (1996) Body Fat Accumulation Is Possibly Responsible for Lower Dehydroepiandrosterone Circulating Levels in Premenopausal Obese Women, *Int. J. Obes. Relat. Metab. Dis. 20*, 1105–1110.
47. Votiagtzi, M.G., Boeck, M.A., and Vlachopapadopoulou, E. (1996) Dehydroepiandrosterone in Morbidly Obese Adolescents: Effects on Weight, Body Composition, Lipids, and Insulin Resistance, *Metabolism 45*, 1011–1015.
48. Haffner, S.M., Valdez, R.A., and Stern, M.P. (1993) Obesity Body Fat Distribution and Sex Hormones in Men, *Int. J. Obes. Relat. Metab. Dis. 17*, 643–649.
49. Vermeulen, A., Kaufman, J.M., and Giagulli, V.A. (1996) Influence of Some Biological Indexes on Sex Hormone Binding Globulin and Androgen Levels in Aging or Obese Males, *J. Clin. Endocrinol. Metab. 81*, 1821–1826.
50. Leenen, R., van der Kooy, K., and Seidell, J.C. (1994) Visceral Fat Accumulation in Relation to Sex Hormones in Obese Men and Women Undergoing Weight Loss Therapy, *J. Clin. Endocrinol. Metab. 78*, 1515–1520.
51. Nestler, J.E., Barlascini, C.O., and Clore, J.N. (1988) Dehydroepiandrosterone Reduces Serum Low Density Lipoprotein Levels and Body Fat but Does Not Alter Insulin Sensitivity in Normal Men, *J. Clin. Endocrinol. Metab. 66*, 57–61.
52. Usiskin, K.S., Butterworth, S., and Clore, J.N. (1990) Lack of Effect of Dehydroepiandrosterone in Obese Men, *Int. J. Obes. 14*, 457–463.
53. Welle, S., Jozefowicz, R., and Statt, M. (1990) Failure of Dehydroepiandrosterone to Influence Energy and Protein Metabolism in Humans, *J. Clin. Endocrinol. Metab. 71*, 1259–1264.
54. Araneo, B.A., Dowell, T., and Woods, M.A. (1995) DHEAS as an Effective Vaccine Adjuvant in Elderly Humans, in *Dehydroepiandrosterone (DHEA) and Aging* (Bellino, F.L., Daynes, R.A., Hornsby, P.J., Lavrin, D.H., and Nestler, J.E., eds.) *Ann. NY Acad. Sci. 774*, 16–28.
55. Ben-Yehuda, A., Danenberg, H.D., Zakay-Rones, Z., Gross, D.J., and Friedman, G. (1998) The Influence of Sequential Annual Vaccination and of DHEA Administration on the Efficacy of the Immune Response to Influenza Vaccine in the Elderly, *Mech. Ageing Dev. 102*, 299–306.
56. Schwartz, A.G., Fairman, D.K., Polansky, M., Lewbart, M.L., and Pashko, L.L. (1989) Inhibition of 7,12-Dimethylbenz[a]anthracene-Initiated and 12-*O*-Tetradecanoylphorbol-13-acetate-Promoted Skin Papilloma Formation in Mice by Dehydroepiandrosterone and Two Synthetic Analogs, *Carcinogenesis 10*, 1809–1813.
57. Mooradian, A.D., Morley, J.E., and Korenman, S.G. (1987) Biological Actions of Androgens, *Endocr. Rev. 8*, 1–28.
58. Fernades, G., and Good, R.A. (1984) Inhibition by Restricted-Calorie Diet of Lymphoproliferative Disease and Renal Damage in MRL/lpr Mice, *Proc. Natl. Acad. Sci. USA 81*, 6144–6148.

[Received July 27, 1999; and in revised form and accepted March 6, 2000]

ARTICLE

Plasma Oxysterols and Tocopherol in Patients with Diabetes Mellitus and Hyperlipidemia

Hiroshi Murakami[a], Naoki Tamasawa[a,*], Jun Matsui[a], Minoru Yasujima[b], and Toshihiro Suda[a]

[a]Third Department of Internal Medicine and [b]Department of Laboratory Medicine, Hirosaki University School of Medicine, Hirosaki, 036-8562, Japan

ABSTRACT: The plasma levels of free oxysterols (7-ketocholesterol; 7α-hydroxy-,7β-hydroxy-, 25-hydroxy-, and 27-hydroxycholesterol; and 5α,6α-epoxycholestanol) in patients with diabetes mellitus and hypercholesterolemia were determined using gas chromatography–mass spectrometry with selective ion monitoring. We studied 39 patients with diabetes mellitus, 20 nondiabetic patients with hypercholesterolemia, and 37 normal controls. Plasma cholesterol levels in diabetic and hypercholesterolemic patients showed no statistical difference. Plasma 7-ketocholesterol was significantly higher in patients with diabetes (31.6 ± 2.8 ng/mL) or hypercholesterolemia (52.3 ± 5.9) than in the control group (22.4 ± 1.2). The increased plasma cholesterol can be regarded as an oxidation substrate for the oxidant stress and the higher absolute levels of oxysterols in hypercholesterolemic plasma compared with the control plasma. This difference disappeared when 7-ketocholesterol was expressed in proportion to total cholesterol. The oxidizability of plasma cholesterol was evaluated by comparing the increased ratio of 7-ketocholesterol after $CuSO_4$ oxidation to the ratio before. We demonstrated that the patients with diabetes showed increased oxidizability (77.5%) compared with the control (36.6%) or hyperlipemic group (45.3%), which is likely due to the lower amounts of α-tocopherol in the diabetics. Measurement of oxysterols may serve as a marker for *in vivo* oxidized lipoproteins in diabetes and hyperlipemia.

Paper no. L8081 in *Lipids 35*, 333–338 (March 2000).

Oxidation of lipoproteins is believed to play an important role in atherosclerosis in patients with diabetes mellitus (DM) and hypercholesterolemia (HL) (1). When low density lipoprotein (LDL) undergoes oxidation *in vitro*, various changes in lipid composition occur, including a substantial loss of free and esterified cholesterol and the concomitant generation of oxidation products of cholesterol (oxysterols) (2,3). In fact, oxidatively modified lipoproteins in the circulating plasma are reported to contain an oxysterol-enriched subfraction (4,5), and oxysterols are considered to be the important lipid component in oxidized lipoproteins. Oxysterols have potent biological effects, some of which suggest a role in the initiation and/or progression of atherosclerosis (1,6). Further support for an atherogenic role for oxysterols comes from an epidemiological study of Indian migrants who were exposed to oxysterols in their diet: they had higher than expected morbidity and mortality from atherosclerosis but did not show the usual risk factors for this disorder (7).

In this study, we measured plasma free oxysterols in patients with DM, using gas chromatography–mass spectrometry (GC–MS) with selective ion monitoring (SIM). We also compared the oxidizability of plasma cholesterol among the patients on the basis of increased 7-ketocholesterol in response to *in vitro* incubation with $CuSO_4$ (8,9).

MATERIALS AND METHODS

Subjects. Subjects included 39 patients with DM, 20 non-diabetic patients with HL, and 37 normal controls. We defined HL as a total cholesterol level more than 220 mg/dL. Blood was collected in blood collection tubes containing heparin after overnight fasting. One microgram of butylated hydroxytoluene was added per milliliter of plasma, and samples were stored at –20°C until analysis.

Table 1 summarizes the clinical characteristics, including age, sex, body mass index, plasma lipid levels, and glycosylated hemoglobin (HbA1c), for each group of subjects. In the DM group, 18 patients were treated by dietary management, 11 with oral hypoglycemic agents (glibenclamide 1.25–7.5 mg/d), and 10 with insulin. Diabetic complications included nephropathy in 28 patients (microalbuminuria in 18 patients and macroalbuminuria in 10 patients), neuropathy in 10 patients, and retinopathy in 25 patients. The frequencies of diabetic complications were not affected by the presence or absence of hypercholesterolemia. None of the subjects was taking supplementary antioxidants such as probucol or α-tocopherol.

*To whom correspondence should be addressed at Third Department of Internal Medicine, Hirosaki University School of Medicine, Zaifu-cho, Hirosaki, 036-8562, Japan. E-mail: tmsw@cc.hirosaki-u.ac.jp

Abbreviations: Cholestane-3β,6α-diol, 5α-cholestane-3β,6α-diol; cholesterol, cholest-5-en-3β-ol; CV, coefficient of variation; DM, diabetes mellitus; 5α,6α-epoxycholestanol, 5,6α-epoxy-5α-cholestan-3β-ol; GC–MS, gas chromatography–mass spectrometry; HbA1c, glycosylated hemoglobin; HL, hypercholesterolemia; 7α-hydroxycholesterol, cholest-5-ene-3β,7α-diol; 7β-hydroxycholesterol, cholest-5-ene-3β,7β-diol; 25-hydroxycholesterol, cholest-5-ene-3β,25-diol; 27-hydroxycholesterol, cholest-5-ene-3β,27-diol; 7-ketocholesterol, 3β-hydroxycholest-5-en-7-one; LDL, low density lipoprotein; SIM, selective ion monitoring; TC, total cholesterol; TG, triglyceride; TMS, ether, trimethylsilyl ether.

TABLE 1
Clinical Characteristics of Study Subjects[a]

	n	Age (yr)	Male/female ·	BMI (kg/m^2)	HbA1c (%)
Control	37	56.7 ± 3.1	17/20	22.3 ± 1.1	4.9 ± 0.03
DM	39	63.1 ± 1.5	14/25	22.9 ± 0.7	6.7 ± 0.25[b]
HL	20	53.2 ± 2.7	5/15	24.0 ± 0.7	5.2 ± 0.12

[a]Results are expressed as mean ± S.E.
[b]$P < 0.05$ vs. control. Abbreviations: BMI, body mass index; HbA1c, glycosylated hemoglobin; DM, diabetes mellitus; HL, hypercholesterolemia.

Measurement of plasma free oxysterols. Cholestane-3β,6α-diol dissolved in ethanol (22 ng/5 mL) was added to 2 mL of plasma as an internal standard. Plasma lipids were extracted with 20 vol of chloroform/methanol (2:1,vol/vol), and the separation of oxysterols from cholesterol was carried out in an early step in the procedure because it is important to prevent cholesterol autoxidation during sampling. The dried material was dissolved in 4 mL of hexane/dichloromethane(4:1, vol/vol) solution and applied to a packed silica column (800 mg; 0.8 cm i.d., Gasukuro Kogyo Inc., Tokyo, Japan). The column was washed out with 8 mL of hexane/dichloromethane (4:1, vol/vol) solution and 10 mL of dichloromethane, and the free oxysterols were then eluted with 8 mL of ethyl acetate. This fraction was dried and dissolved in 10 mL of chloroform and passed through another silica column (400 mg, 0.8 cm i.d.) to remove cholesterol completely. Then the oxysterols were eluted with 6 mL of ethyl acetate.

The average recovery rate of 7α- and 7β-hydroxycholesterol, 7-ketocholesterol, cholestane-3β,6α-diol, and 25- and 27-hydroxycholesterol were 87.5 ± 2.8, 97.3 ± 8.7, 85.3 ± 9.3, 82.7 ± 9.3, 68.3 ± 8.9, and 82.7 ± 6.3%, respectively.

Analysis by GC–MS. Extracted oxysterols were derivatized to their trimethyl (TMS) ether derivatives by treatment with 350 mL pyridine/hexamethyldisilazane/trimethyl-chlorosilane (3:2:1, by vol) at 60°C for 30 min. After evaporation of the solvent under a nitrogen stream, the residue was dissolved in 10 mL hexane and analyzed by GC–MS, using a Shimadzu gas chromatograph (model GC-17A; Kyoto, Japan) equipped with a high-resolution capillary column, DB-1 (30 m × 0.25 mm i.d., J&W Scientific, CA), and a QP-5000 mass spectrometer with a Shimadzu Chemical Laboratory Analysis System & Software CLASS-5000. The oven temperature program was as follows: 150°C for 2 min, 20°C/min to 280°C, and then 5°C/min to 300°C and held for 10.0 min. Helium was used as the carrier gas at a flow rate of 0.8 mL He/min. The injector was operated in the splitless mode and was kept at 270°C, while the detector transfer line was heated at 280°C. The separator and ion source temperatures were 300°C, and the ionization energy was 70 eV.

7-Ketocholesterol and 7β-hydroxycholesterol were purchased from Sigma Chemical Co. (St. Louis, MO), and 7α-hydroxycholesterol, 5α,6α-epoxycholestanol, 25-hydroxy- and 27-hydroxycholesterol, and cholestane-3β,6α-diol were obtained from Steraloids Inc. (Wilton, NH).

The selected ions used for analysis (*m/z*) and the retention times (min) of the compounds were as follows: 7α-hydroxycholesterol, 456 (M – 90), 14.78; 7β-hydroxycholesterol, 456 (M – 90), 16.19; 5α,6α-epoxycholestanol, 384, 16.64; cholesterol-3β,6α-diol, 458, 16.78; 7-ketocholesterol, 472 (M), 18.74; 25-hydroxycholesterol 131, 18.85; and 27-hydroxycholesterol, 456 (M – 90), 19.82.

Figure 1 presents the total ion chromatogram and mass chromatogram for each of the authentic compounds. Each of the oxysterols and the internal standard (cholestane-3β,6α-diol) were separated and quantified with adequate sensitivity. The detection limit for every oxysterol was under 0.02 ng/mL. In triplicate experiments, the within-day variation (coefficient of variation, CV) for 7α-hydroxy, 7β-hydroxy-, and 7-ketocholesterol was 16.2%, and the day-to-day variation (CV%) within one week was 11.9%.

In a preliminary study, we monitored the formation of oxysterols by $CuSO_4$-catalyzed oxidation of plasma. $CuSO_4$ was added to 2 mL of plasma at a final concentration of either 0.5 or 1.0 mM. Incubation was carried out for 24 h at 37°C. The oxidized plasma samples were subjected to polyacrylamide gel electrophoresis (LipoPhor kit, Jyoko, Tokyo, Japan), and the oxysterols were extracted and measured as described above. As shown in Figure 2, the LDL fraction was dispersed and then it migrated depending on the negative charge. Figure 3 presents the gas chromatograms of oxysterols in the same plasma. The C-7 position of the cholesterol ring was predominantly oxidized, and 7-keto-, 7α-hydroxy-, and 7β-hydroxycholesterol increased as a result of $CuSO_4$ induced oxidation in a dose-dependent fashion. Other oxysterols also increased, however, those increases were not so large as those for the C-7 oxidized products. This finding demonstrated that increases in electrophoretic mobility and in yields of oxysterol products are equally useful as indicators of oxidative modification of lipoproteins.

Next, the oxidizability of the plasma cholesterol was evaluated in response to incubation with $CuSO_4$. Plasma samples were selected randomly from each group (DM, $n = 16$; HL, $n = 8$; control, $n = 10$). After incubation of plasma samples with 100 μM $CuSO_4$ for 24 h at 37°C, oxysterols were measured as described above. The oxidizability of plasma cholesterol was expressed in terms of the ratio (%) of the amount of 7-ketocholesterol after the oxidation to the level before.

Statistical analysis. The values in the text and tables are given as means ± SE. Statistical analysis was performed using analysis of variance and the least significant difference to compare differences among three groups. $P < 0.05$ was considered to represent statistical significance.

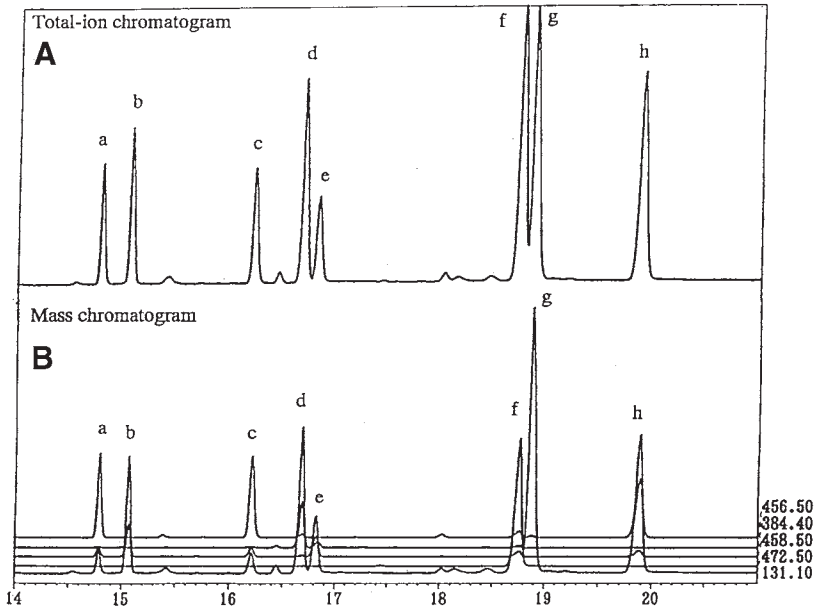

FIG. 1. Gas chromatography–mass spectrometry chromatograms of each oxysterol. Total-ion chromatogram (A) and mass chromatogram (B) are illustrated. The selective ion (*m/z*) of each oxysterol was as follows: 131, 25-hydroxycholesterol (g); 384, 5α,6α-epoxycholesterol (d); 456, 7α-hydroxycholesterol (a), 7β-hydroxycholesterol (c) and 27-hydroxycholesterol (h); 458, cholestane-3β,6α-diol (internal standard) (e); 472, 7-ketocholesterol (f); (b), cholesterol.

RESULTS

Table 2 presents the data on the oxysterol concentrations in each group. Total cholesterol (TC) levels in patients in the DM group showed no difference from those in the HL group (Table 3). There was no difference in oxysterol levels among the subgroups with age or body weight (data not shown). In the DM group, significantly higher absolute levels of 7-keto-, 25-hydroxy- and 27-hydroxycholesterol were observed compared with the control group. In the HL group, all oxysterols except 7α-hydroxycholesterol were significantly increased. 7-Ketocholesterol, the major autoxidation product of cholesterol, was highest in the HL group, and lowest in the control group. However, this difference disappeared when oxysterols were expressed in proportion to TC (Table 3). In the DM group, there was no significant correlation between the oxysterol levels and glycemic control. However, patients with long duration of diabetes showed a tendency to have high plasma oxysterol.

We compared the susceptibility of the plasma cholesterol of each group to oxidation by $CuSO_4$. Based on the results of the preliminary study, as described in Materials and Methods section, we focused on 7-ketocholesterol as the marker of cholesterol autoxidation. 7-Ketocholesterol level before and after the $CuSO_4$-oxidation in each group is indicated in Table 4. The mean increased rate of 7-ketocholesterol from before to after $CuSO_4$ oxidation was 77.5% (23.42 to 41.56 ng/mL) in DM, 45.3% (42.57 to 61.86 ng/mL) in HL, and 36.0% (23.31 to 31.70 ng/mL in the control group. α-Tocopherol levels relative to plasma triglyceride (TG) were also compared, and the value was lowest in the diabetic group as shown in Table 4.

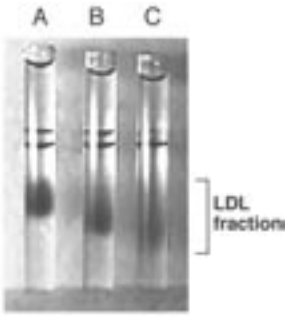

FIG. 2. $CuSO_4$ oxidation of plasma lipoproteins. $CuSO_4$ was added to plasma to a final concentration to 0 (A), 0.5 (B), or 1.0 (C) mM. Incubation was carried out for 24 h at 37°C. Then the oxidized plasma was analyzed by polyacrylamide gel electrophoresis.

DISCUSSION

Oxidation of cholesterol gives rise to a large number of oxidation products (oxysterols) (10). Oxysterols such as 7α-hydroxycholesterol (11) and 27-hydroxycholesterol largely are formed enzymatically and may be involved in elimination of cholesterol from macrophages and endothelial cells (12). On the other hand, a free radical-mediated process (autoxidation) can lead to the formation of a variety of oxysterols, e.g., epoxy, keto-, and hydroxy-derivatives of cholesterol (10). These oxys-

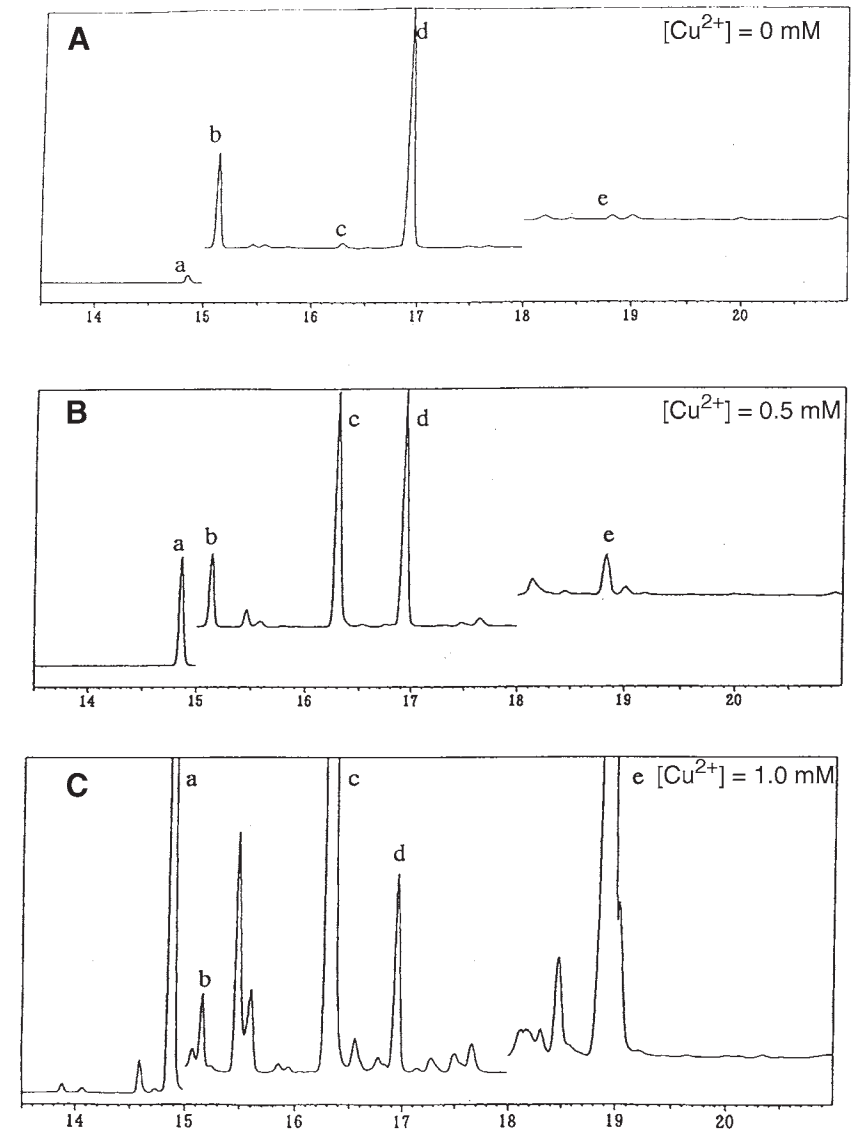

FIG. 3. $CuSO_4$ oxidation of plasma cholesterol. Total-ion chromatograms of plasma oxysterols before and after oxidation with 0, 0.5, or 1.0 mM $CuSO_4$. (a) 7α-Hydroxycholesterol; (b) cholesterol; (c) 7β-hydroxycholesterol; (d) cholestane-3β,6α-diol (internal standard); (e) 7-ketocholesterol.

terols have various biological activities (13), including cytotoxicity (8,10), inhibition of DNA synthesis (14), inhibition of cholesterol synthesis (15), and effects on cell membrane structure and function (16).

Analysis of oxysterols in biological materials is not easy because of the presence of various compounds having structures closely related to cholesterol and because of great differences between their concentrations and the concentration of cholesterol. At present, most analytical methods for oxysterols are based on GC–MS with SIM (17). A substantial portion of the oxysterols in plasma is present as fatty acyl esters like cholesterol (10). Most oxysterols with an established enzymatic origin are esterified to a great extent, whereas other oxysterols are less esterified (17). In order to determine the total or esterified oxysterols by GC, a hydrolysis step is necessary (18). However, the reaction conditions have to be chosen carefully, otherwise, cholesterol autoxidation products induced artifactually could completely mask the endogenous oxysterol levels (19). In our method, plasma free oxysterols were separated from free and esterified cholesterol, and the analytical procedures were practical and highly reliable. Each molecular species was analyzed using a GC-quadrupole mass spectrometer with SIM, and sufficient sensitivity for plasma oxysterols was demonstrated.

The oxidation of LDL may possibly take place during its circulation in the blood. Actually, the lipoprotein particles enriched in oxidatively modified lipids and proteins are proposed

TABLE 2
Plasma Levels of Free Oxysterols (ng/mL) in Study Groups[a]

	n	7α-Hydroxy-cholesterol	7β-Hydroxy-cholesterol	5α,6α-Epoxy-cholestanol	7-Keto-cholesterol	25-Hydroxy-cholesterol	27-Hydroxy-cholesterol
Control	37	36.53 ± 3.52	2.85 ± 0.16	5.85 ± 1.11	22.42 ± 1.20	0.07 ± 0.01	4.77 ± 0.50
DM	39	33.51 ± 2.60	2.84 ± 0.19	8.84 ± 1.15	31.59 ± 2.78[a]	0.20 ± 0.01[a]	8.30 ± 0.50[a]
HL	20	41.93 ± 5.59	3.56 ± 0.24[a,b]	12.72 ± 2.03[a]	52.33 ± 5.85[a,b]	0.19 ± 0.02[a]	10.05 ± 0.80[a,b]

[a]Results are expressed as mean ± SE. [a]$P < 0.05$ vs. control; [b]$P < 0.05$ vs. DM; for abbreviations see Table 1.

TABLE 3
Plasma Lipids and α-Tocopherol of Study Groups[a]

Group	No.	TC (mg/dL)	7KC (ng/ML)	T.OXY (ng/mL)	7KC/TC (× 10^{-4})	T.OXY/TC (× 10^{-4})	TG (mg/dL)	αToc (μg/mL)	αToc/TG (μg/mg TG%)
Control	37	168.5 ± 6.0	22.42 ± 1.2	72.58 ± 4.3	0.15 ± 0.011	0.46 ± 0.03	85.0 ± 4.1	19.2 ± 1.8	0.23 ± 0.03
DM	39	226.5 ± 10.0[a]	31.59 ± 2.8[a]	85.27 ± 5.1	0.15 ± 0.019	0.41 ± 0.04	121.1 ± 16.6[a]	28.1 ± 1.8[a]	0.32 ± 0.03
HL	20	244.9 ± 10.7[a]	52.33 ± 5.9[a]	120.78 ± 9.5[a,b]	0.19 ± 0.028	0.45 ± 0.05	101.9 ± 9.9	34.5 ± 3.6[a]	0.34 ± 0.03

[a]Results are expressed as means ± SE. [a]$P < 0.05$ vs. control; [b]$P < 0.05$ vs. DM. Abbreviations: 7KC, 7-ketocholesterol; T.OXY, total oxysterol (which includes 7α-, 7β-, 25-, 27-hydroxy-, 5α,6α-epoxy-, and 7keto-cholesterol); αToc, α-tocopherol. For other abbreviations see Table 1.

TABLE 4
Plasma Oxysterols After $CuSO_4$-Oxidation[a]

			Before oxidation		After oxidation				
Group	No.	TC (mg/dL)	7KC-n (ng/mL)	7KC-n/TC (× 10^{-4})	7KC-a (ng/mL)	7KC-a/TC (× 10^{-4})	αToc (μg/mL)	TG (mg/dL)	αToc/TG (μg/mg TG%)
Control	10	178.1 ± 10.5	23.31 ± 1.58	0.13 ± 0.01	31.70 ± 3.06	0.18 ± 0.02	25.0 ± 2.9	77.5 ± 6.0	0.34 ± 0.05
DM	16	244.3 ± 7.9[a]	23.42 ± 2.24	0.10 ± 0.01	41.56 ± 5.03	0.18 ± 0.02	29.7 ± 1.9	144.5 ± 25.2[a]	0.27 ± 0.04
HL	8	270.9 ± 17.8[a]	42.57 ± 8.00[a,b]	0.17 ± 0.03[b]	61.86 ± 7.47[a,b]	0.24 ± 0.04	42.2 ± 7.9[a,b]	134.1 ± 21.5	0.35 ± 0.06

[a]Results are expressed as means ± SE. [a]$P < 0.05$ vs. control; [b]$P < 0.05$ vs. DM. Abbreviations: 7KC, 7-ketocholesterol; T.OXY, total oxysterol (which includes 7α-, 7β-, 25-, 27-hydroxy-, 5α,6α-epoxy-, and 7keto-cholesterol); αToc, α-tocopherol. For other abbreviations see Table 1.

to exist in the plasma on the basis of measurements of small amounts of plasma cholesterol oxides (4), fragmented apolipoprotein B (20), and thiobarbituric acid-reactive substances (21). Hodis *et al.* (4) reported that circulating oxidatively modified lipoproteins in the monkey contain an oxysterol-enriched subfraction (53% of cholesterol as oxysterols), and oxysterols are important lipid components of oxidized LDL (22,23).

We evaluated the extent of cholesterol oxidation by assessing the plasma free oxysterol levels. In our study, the plasma free 7-ketocholesterol levels in patients with DM and HL were significantly higher than those in normal subjects. However, there was no difference between the groups when expressed in proportion to total cholesterol level (Table 3). The increased plasma levels of cholesterol can be regarded as an oxidation substrate to oxidation stress, by endothelial cells and activated monocytes (24). This may explain the higher absolute levels of oxysterols in hypercholesterolemic plasma compared with the control plasma.

DM has been proposed to be a state of increased free radical activity and high oxidant stress (25,26). This may include increased nonenzymatic glycosylation, which can also be associated with generation of oxygen free radicals (27,28). Although the factors determining the susceptibility of LDL to oxidation are not thoroughly understood (29), $CuSO_4$ oxidation of lipoproteins has been widely used to examine LDL oxidation (8,11). As demonstrated in the present study, free oxysterols, particularly C-7 oxidized oxysterols, are major products of $CuSO_4$ oxidation of plasma lipids. In this study, we compared plasma levels of 7-ketocholesterol and 7-ketocholesterol/TC after $CuSO_4$ oxidation (100 μM) with the basal level (Table 4). We found that the rate of 7-ketocholesterol/TC in the DM group was higher than that in other groups, likely owing to the lowest amounts of α-tocopherol in expression per plasma TG (Table 4). The small number of data from these groups did not allow statistical difference to be identified, however, our results may indicate one reason for the susceptibility of plasma cholesterol to $CuSO_4$ oxidation in diabetics in our study. However, reports on the levels of antioxidants as defense mechanisms (i.e., superoxide dismutase, vitamin E, or C, etc.) in diabetic patients are still contradictory: both increases and decreases of antioxidant activity are reported (30). Oxidizability has also been postulated to increase in small, dense LDL, which is commonly found in diabetic patients with hypertriglyceridemia (29). The patient's age, sex, type of treatment, and diabetic complications had no correlation with plasma oxysterol levels (data not shown).

In conclusion, plasma free oxysterol levels were measured using a GC–MS SIM method. Plasma oxysterol levels were high in patients with DM and HL. Our study suggests the possibility that oxysterols may serve as a marker for *in vivo* lipoprotein oxidative modification (31).

REFERENCES

1. Steinberg, D., Parthasarathy, S., Carew, T.E., Khoo, J.C., and Witztum, J.L. (1989) Beyond Cholesterol. Modifications of Low-Density Lipoprotein That Increase Its Atherogenicity, *N. Engl. J. Med. 320*, 915–924.
2. Bhadra, S., Arshad, M.A.Q., Rymaszewski, Z., Norman, E., Wherley, R., and Subbiah, M.T.R. (1991) Oxidation of Cholesterol Moiety of Low Density Lipoprotein in the Presence of Human Endothelial Cells or $CuSO_4$ (II) Ions: Identification of Major Products and Their Effects, *Biochem. Biophys. Res. Commun. 176*, 431–440.
3. Carpenter, K.L., Wilkins, G.M., Fussell, B., Ballantine, J.A., Taylor, S.E., Mitchinson, M.J., and Leak D.S. (1994) Production of Oxidized Lipids During Modification of Low-Density Lipoproteins, *Biochem. J. 304*, 625–633.
4. Hodis, H.N., Crawford, D.W., and Sevanian, A. (1991) Cholesterol Feeding Increases Plasma and Aortic Tissue Cholesterol Oxide Levels in Parallel: Further Evidence for the Role of Cholesterol Oxidation in Atherosclerosis, *Atherosclerosis 89*, 117–126.
5. Hessler, J.R., Morel, D.W., Lewis, L.J., and Chisolm, G.M. (1983) Lipoprotein Oxidation and Lipoprotein-Induced Cytotoxicity, *Atherosclerosis 3*, 215–222
6. Brown, M.S., and Goldstein, J.L. (1983) Beyond Cholesterol. Modification of Low-Density Lipoprotein That Increases Its Atherogenicity, *Annu. Rev. Biochem. 52*, 223–261.
7. Jacobson, M.S. (1987) Cholesterol Oxides in Indian Ghee: Possible Cause of Unexpected High Risk of Atherosclerosis in Indian Immigrant Populations, *Lancet 2*, 656–658.
8. Esterbauer, H., and Jurgens, G. (1993) Mechanistic and Genetic Aspects of Susceptibility of LDL to Oxidation, *Curr. Opin. Lipidol. 4*,114–124.
9. Esterbauer, H., Striegl, G., Puhl, H., and Rotheneder, M. (1989) Continuous Monitoring of *in vitro* Oxidation of Human Low-Density Lipoprotein, *Free Radical Res .Commun. 6*, 67–75.
10. Smith, L.L. (1981) Distribution of Autoxidation Products, in *Cholesterol Autoxidation* (Smith, L.L., ed.), pp. 49–124, Plenum Press, New York.
11. Bjorkhem, I. (1985) Mechanism of Bile Acid Biosynthesis in Mammalian Liver, in *Sterols and Bile Acids* (Danielsson, H., and Sjovall, J., eds.) pp. 231–278, Elsevier, Amsterdam.
12. Bjorkhem, I., Andersson, O., Diczfalusy, U., Sevastik, B., Xiu, R.J., and Lund, E. (1994) Atherosclerosis and Sterol 27-Hydroxylase: Evidence for a Role of This Enzyme in Elimination of Cholesterol from Human Macrophages, *Proc. Natl. Acad. Sci. USA 91*, 8592–8596.
13. Smith, L.L., and Johnson, B.H. (1989) Biological Activities of Oxysterols, *Free Radical Biol. Med. 7*, 285–332.
14. Kosugi, K., Morel, D.W., Dicorleto, P.E., and Chisolm, G.M. (1987) Toxicity of Oxidized Low-Density Lipoprotein to Cultured Fibroblasts is Selective for S Phase of the Cell Cycle, *J. Cell Physiol. 130*, 311–320.
15. Chen, H.W., Kandutsch, A.A., and Waymouth, C. (1974) Inhibition of Cell Growth by Oxygenated Derivatives of Cholesterol, *Nature 251*, 419–421.
16. Richert, L., Castagna, M., Beck, J.P., Rong, S., Luu, B., and Ourisson, G. (1984) Growth Rate-Related and Hydroxysterol-Induced Changes in Membrane Fluidity of Cultured Hepatoma Cells: Correlation with 3-Hydroxy-3-methyl-glutaryl CoA Reductase Activity, *Biochem. Biophys. Res. Commun. 120*, 192–198.
17. Dzeletovic, S., Breuer, O., Lund, E., and Diczfalusy, U. (1995) Determinant of Cholesterol Oxidation Products in Human Plasma by Isotope Dilution-Mass Spectrometry, *Anal. Biochem. 225*, 73–80.
18. Van Lier, J.E., and Smith, L.L. (1967) Sterol Metabolism. I. 26-Hydroxycholesterol in the Human Aorta, *Biochemistry 6*, 3269–3278.
19. Maerker, G., and Unruh, J. (1986) Cholesterol Oxides. 1. Isolation and Determination of Some Cholesterol Oxidation Products, *J. Am. Oil Chem. Soc. 63*, 767–771.
20. Schuh, J., Fairclough, G.F., and Haschemeyer, R.H. (1978) Oxygen-Mediated Heterogeneity of Apo-low-density Lipoprotein, *Proc. Natl. Acad. Sci. USA 75*, 3173–3177.
21. Yagi, K. (1987) Lipid Peroxides and Human Diseases, *Chem. Phys. Lipids 45*, 337–351.
22. Hodis, H.N., Kramsch, D.M., Avogaro, P., Bittolo-Bon, G., Hwang, J., Peterson, H., and Sevanian, A. (1994) Biochemical and Cytotoxic Characteristics of an *in vivo* Circulating Oxidized Low Density Lipoprotein (LDL), *J. Lipid Res. 35*, 669–677.
23. Sevanian, A., Bittolo-Bon, G., Cazzolato, G., Hodis, H., Hwang, J., Zamburlini, A., Mariorino, M., and Ursin, F. (1997) LDL Is a Lipid Hydroperoxide-Enriched Circulating Lipoprotein, *J. Lipid Res. 38*, 419–428.
24. Henriksen, T., Mahoney, E.M., and Steinberg, D. (1981) Enhanced Macrophage Degradation of Low-Density Lipoprotein Previously Incubated with Cultured Endothelial Cells: Recognition by Receptors for Acetylated Low-Density Lipoproteins, *Proc. Natl. Acad. Sci. USA 78*, 6499–6503.
25. Mullarkey, C.J., Edelstein, D., and Brownlee, M. (1990) Free Radical Generation by Early Glycation Products: A Mechanism for Accelerated Atherogenesis in Diabetes, *Biochem. Biophys. Res. Commun. 173*, 932–939.
26. Hunt, J.V., Smith, C.C., and Wolff, S.P. (1990) Autoxidative Glycosylation and Possible Involvement of Peroxides and Free Radicals in LDL Modification by Glucose, *Diabetes 39*, 1420–1424.
27. Griesmacher, A., Kindhauser, M., Andert, S.E., Schreiner, W., Toma, C., Knobl, P., Pietschmann, P., Prager, R., Schnack, C., and Schernthaner, G. (1995) Enhanced Serum Levels of Thiobarbituric-Acid-Reactive Substances in Diabetes Mellitus, *Am. J. Med. 98*, 469–475.
28. Mol, M.J., Rijke, Y.B., Demacker, P.N., and Stalenhoef, A.F. (1997) Plasma Levels of Lipid and Cholesterol Oxidation Products and Cytokines in Diabetes Mellitus and Cigarette Smoking: Effects of Vitamin E Treatment, *Atherosclerosis 129*, 169–176.
29. Austin, M.A., and Edwards, K.L. (1996) Small, Dense Low Density Lipoproteins, the Insulin Resistance Syndrome and Noninsulin-Dependent Diabetes, *Curr. Opin. Lipidol. 7*, 167–171.
30. Matkovics, B., Varga, S.I., Szabo, L., and Witas, H. (1982) The Effect of Diabetes on the Activities of the Peroxide Metabolism Enzymes, *Horm. Metab. Res. 14*:77–79.
31. Jialal, I., Freeman, D.A., and Grundy, S.M. (1991) Varying Susceptibility of Different Low Density Lipoproteins to Oxidative Modification, *Arterioscler. Thromb. 11*, 482–488.

[Received December 3, 1998; and in final revised form and accepted February 13, 2000]

Use of a ^{13}C Tracer to Quantify the Plasma Appearance of a Physiological Dose of Lutein in Humans

Lihang Yao[a], Yuexia Liang[b], Walter S. Trahanovsky[c], Robert E. Serfass[a], and Wendy S. White[a,*]

[a]Department of Food Science and Human Nutrition, [b]Center for Designing Foods to Improve Nutrition, and [c]Department of Chemistry, Iowa State University, Ames, Iowa 50011

ABSTRACT: Increased intake of lutein from vegetables promotes increased density of the macular pigment and therefore may protect against age-related macular degeneration. Our objective was to use a ^{13}C tracer and high-precision gas chromatography–combustion interfaced–isotope ratio mass spectrometry (GC–C–IRMS) to investigate metabolism of a lutein dose equivalent to that absorbed from vegetables. Biosynthetic per-labeled (>99% ^{13}C) lutein was purified from a commercially available extract of algal biomass. Subjects (n = 4) ingested 3 mg of [^{13}C]lutein with a standardized low-carotenoid breakfast. Blood samples were collected at baseline and then hourly for 12 h; additional blood samples were drawn at 16, 24, 48, 72, 96, 192, 360, and 528 h. To produce perhydro-β-carotene suitable for analysis by GC–C–IRMS, the plasma lutein fraction was hydrogenated on palladium-on-carbon catalyst with acid-catalyzed hydrogenolysis. The stable carbon isotope ($^{13}C/^{12}C$) ratio measured by GC–C–IRMS was used to calculate the plasma concentration of [^{13}C]lutein. There was a rapid increase in [^{13}C]lutein in plasma until peak enrichment at 16 h followed by a decline to the next measurement at 24 h. At 528 h, small changes in ^{13}C enrichment from baseline could still be measured in plasma lutein. High-precision GC–C–IRMS enables complete definition of the appearance and disappearance of [^{13}C]lutein in plasma after ingestion of a dose similar to that absorbed from foods.

Paper no. L8328 in *Lipids 35,* 339–348 (March 2000).

Gas chromatography–combustion interfaced–isotope ratio mass spectrometry (GC–C–IRMS) combines the resolving capacity of gas–liquid chromatography and the high precision of IRMS. To be separated by a gas–liquid chromatograph, carotenoids such as β-carotene and lutein (β,ε-carotene-3,3′-diol) (Fig. 1) must be converted to derivatives that are thermally stable, chemically inert, and volatile at temperatures below *ca.* 300°C (1). Due to the thermal instability of the conjugated polyene chain of β-carotene, stable carbon isotope ratio analysis using GC–C–IRMS requires hydrogenation to the perhydro analog (2,3). We showed that stable carbon isotope ratio analysis of the dihydroxy carotenoid lutein using GC–C–IRMS requires alcohol hydrogenolysis and hydrogenation to enhance volatility and provide thermal stability (4). The major derivatization product of both β-carotene and lutein was identified by using GC–MS as perhydro-β-carotene which is suitable for GC–C–IRMS analysis (4,5).

GC–C–IRMS and a biosynthetically labeled [^{13}C]β-carotene tracer have been successfully applied to investigate metabolism of β-carotene in humans (2,3,6). A major advantage is the ability to use small tracer doses that model those typically derived from the major dietary sources, fruits and vegetables (7). Knowledge of the metabolism of such small doses is important for preventive medicine. People who ingest the highest dietary amounts of carotenoids such as β-carotene and lutein have reduced risks of epithelial cancers (8,9) and of coronary heart disease (10,11). High dietary intakes of lutein and an isomeric dihydroxy carotenoid zeaxanthin (β,β-carotene-3,3′-diol) may protect against age-related macular degeneration (12), the leading cause of new cases of legal blindness in the United States (13). Of the individual

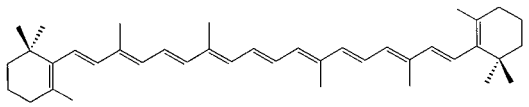

β-Carotene

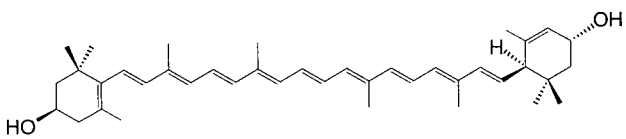

Lutein

FIG. 1. Lutein is a nonprovitamin A dihydroxy structural analog of β-carotene.

*To whom correspondence should be addressed at Department of Food Science and Human Nutrition, 1111 Human Nutritional Sciences Building, Iowa State University Ames, IA 50011-1120. E-mail: wswhite@iastate.edu

Abbreviations: AMD, age-related macular degeneration; APE, atom percent excess; AUC, area under the concentration vs. time curve; C_{max}, maximum plasma concentration; EA–IRMS, elemental analyzer–isotope ratio mass spectrometry; GC–C–IRMS, gas chromatography–combustion interfaced–isotope ratio mass spectrometry; GC–MS, gas chromatography–mass spectrometry; HPLC, high-performance liquid chromatography; IRMS, isotope ratio mass spectrometry; LDL, low density lipoproteins; MTBE, methyl *tert*-butyl ether; PDB, Pee Dee Belemnite; t_{max}, time to maximum plasma concentration; VLDL, very low density lipoproteins.

carotenoids circulating in the blood, lutein and zeaxanthin are selectively deposited in the retina and accumulate to form an area of dense pigmentation known as the macular pigment (14). The macular pigment is thought to protect the light-sensitive portions of the photoreceptor cells from damage mediated by blue visible light (15). Increased consumption of lutein and zeaxanthin in the form of corn and spinach increases the density of the macular pigment (16), which in turn is thought to provide greater protection against photooxidative damage to the retina and retinal pigment epithelium. Estimated mean intakes of lutein among adults in the United States stratified by gender and by race are 1.65–3.64 mg/d (17). Because of the potential public health importance, there is a need to investigate the metabolism of lutein in amounts that simulate such dietary exposures.

Our objective was to modify the ^{13}C tracer approach using GC–C–IRMS developed by Parker *et al.* (2,3) for human metabolic studies of β-carotene to enable similar studies of the plasma appearance and metabolism of lutein. Due to the scarcity of carotenoids labeled with stable isotopes, no tracer studies in humans using labeled carotenoids other than β-carotene appear in the literature.

EXPERIMENTAL PROCEDURES

Subjects. Healthy women (n = 4), aged 25–38 yr, were selected based on interview, physical examination, and complete blood count and blood biochemistry profile. Criteria for exclusion were current or recent cigarette smoking, chronic disease, lipid malabsorption or gastrointestinal disorder, lactose intolerance, vegetarianism, hyperlipidemia confirmed by blood lipid profile, history of anemia or excessive bleeding, pregnancy, use of oral contraceptive agents or contraceptive implants, use of medications that may affect lipid absorption or transport (including antibiotics), use of vitamin or mineral supplements, and frequent consumption of alcoholic beverages (>1 drink per day). Informed consent was obtained from all subjects, and the study protocol was approved by the Human Subjects Review Committee of Iowa State University.

Diets. Subjects were provided a list of foods to exclude and were instructed to avoid consumption of carotenoid-rich fruits and vegetables for 4 d before the beginning of the study period. During the study period, subjects consumed a controlled low-carotenoid diet of conventional foods for 2 d before and 4 d after dosing. A single daily menu of weighed food portions was provided. The meals were prepared and consumed in the Human Nutrition Metabolic Unit of the Center for Designing Foods to Improve Nutrition at Iowa State University, except for the carry-out lunches and evening snacks on weekdays. Adherence to the experimental diet was monitored by written self-report and by analysis of fasting plasma carotenoid concentrations using high-performance liquid chromatography (HPLC). Duplicate aliquots of 24-h diet composites from each of the two study periods were analyzed for carotenoid content. The extraction of the carotenoids followed the protocol described previously (18). On average, across two study periods, the daily diet provided (means ± SD): 123.3 ± 5.2 μg lutein, 46.0 ± 0.7 μg β-carotene, 7.4 ± 0.7 μg zeaxanthin, and no detectable α-carotene, β-cryptoxanthin, or lycopene. The macronutrient composition of the diet was estimated using Nutritionist V software (N-Squared Computing Inc., Salem, OR). The daily diet of 8.8 MJ was distributed as 14% of total energy from protein, 59% of total energy from carbohydrate, and 27% of total energy from fat.

Preparation of a biosynthetic ^{13}C-labeled tracer. Autotrophic algae grown with $^{13}CO_2$ as sole carbon source were previously used to economically produce per-labeled (>98% ^{13}C) β-carotene for use as a stable tracer (2,3). In the current study, we applied the same biotechnology and a different algal strain to produce tracer doses of per-labeled [^{13}C]lutein. Solvent partitioning was used to purify per-labeled [^{13}C]-lutein from the nonsaponifiable fraction of a crude lipid extract of *Chlorella* sp. generously donated by Martek, Inc. (Columbia, MD). The nonsaponifiable fraction (50 mg) was mixed with 5 mL of HPLC-grade water and extracted repeatedly with 15 mL of a mixture of hexane and ethyl ether (2:1, vol/vol) until the residue was almost colorless. The combined hexane/ethyl ether layers were evaporated to dryness *in vacuo.* Hexane (2 mL) was added to the residue to dissolve β-carotene and other hydrocarbon carotenes but to sparingly dissolve lutein (19), which was then isolated by filtration. Lutein was further purified from the yellow residue by crystallization. The yellow residue was dissolved in 4 mL of warm (40°C) methanol/water (90:10, vol/vol) solution and stored under argon overnight at –20°C to allow crystallization of lutein. The lutein crystals in methanol/water solution were then filtered and washed with hexane (50 mL). The purity of the lutein was estimated to be 93% on the basis of peak area using HPLC analysis with photodiode array detection; the contaminants were 2% β-carotene and 5% zeaxanthin. The ^{13}C enrichment was >99% as determined by using serial dilution with unlabeled lutein (Kemin Industries, Des Moines, IA) and stable carbon isotope-ratio analysis by GC–C–IRMS. A confirmatory mass spectrum of the purified [^{13}C]lutein was obtained using a Finnigan (currently Thermoquest, San Jose, CA) TSQ 700 triple quadrupole mass spectrometer in electron ionization mode (70 eV). The sample was introduced into the ion source by direct insertion probe at 200°C. Mass spectra were acquired over the range m/z 100–800 in 0.75 s.

A tracer dose of 3 mg (5.3 μmol) of [^{13}C]lutein was ingested with 28.0 g of high-oleic acid safflower oil (Neobee 18; Stepan Co, Maywood, NJ), 30 g of banana, and 120 mL of nonvitamin-fortified nonfat milk (generously donated by Anderson Erickson Dairy Co., Des Moines, IA). Specifically, the lutein was solubilized in 18.7 g of high-oleic acid safflower oil and emulsified using a hand-held mixer with a puree of 30 g of banana and 70 mL of nonvitamin-fortified nonfat milk (3). An additional 9.3 g of safflower oil was used to rinse the original vial that contained the tracer dose and the rinse was added to the emulsion while blending. The original vial and the hand-held mixer were then rinsed with 30 mL of

nonvitamin-fortified nonfat milk, which was added to the emulsion. After drinking the emulsion, the subjects were instructed to rinse the container with 20 mL of nonvitamin-fortified nonfat milk and to consume the rinse.

Study protocol. On the morning of the third day on the low-carotenoid diet, subjects arrived at the metabolic unit after an overnight (12-h) fast, and a baseline blood sample (14 mL) was drawn *via* a catheter placed in a forearm vein by a registered nurse. After ingestion of the [^{13}C]lutein, blood samples (14 mL) were drawn at hourly intervals for 12 h *via* the intravenous catheter into a syringe and transferred to tubes containing heparin as anticoagulant. The patency of the catheter was maintained by flushing with sterile physiological saline, as described previously (20). During the period of hourly blood collection, subjects continued the low-carotenoid experimental diet, including a breakfast ingested with the [^{13}C]lutein tracer dose, a lunch ingested immediately after the 5-h blood draw, and an evening meal ingested immediately after the 10-h blood draw. Additional blood samples were drawn from the antecubital vein *via* venipuncture at 16 h and after an overnight fast at 24, 48, 72, 96, 192, 360, and 528 h. Blood samples were immediately placed on ice and protected from light. Plasma was separated by centrifugation (1380 × *g*, 4°C, 20 min) and stored at –80°C in the dark until analyzed.

Purification of the plasma lutein fraction. Lutein was purified from individual plasma samples in amounts needed to produce sufficient perhydro-β-carotene (major derivatization product of alcohol hydrogenolysis and hydrogenation of lutein) to enable stable carbon isotope ratio measurement by using GC–C–IRMS. Plasma samples (4.0 mL) were divided into four 1.0-mL aliquots to ensure efficient extraction of lutein, deproteinized with 1 vol of ethanol, and extracted twice with 8 vol of hexane containing 0.1 g/L of butylated hydroxytoluene. The combined hexane layers were evaporated to dryness under vacuum. A saponification step was needed to remove lipid that would otherwise interfere with the gas–liquid chromatographic separation of the major product of lutein derivatization, perhydro-β-carotene, before elution into the combustion interface of the GC–C–IRMS. The dried hexane extract was dissolved in 0.5 mL of ethanol containing 0.1 g/L of butylated hydroxytoluene in a 3-mL screw-capped vial. Another 0.5 mL of ethanol containing 5.5 mM pyrogallol was added to the vial followed by 1.0 mL of 5.3 M aqueous potassium hydroxide. The contents of the vial were mixed and saponified at 65°C for 60 min in the dark under an atmosphere of argon. After cooling, the contents were transferred to a glass culture tube (16 × 100 mm) and extracted twice with 8.0 mL of hexane containing 0.1 g/L of butylated hydroxytoluene. The combined hexane extracts were washed twice with 5.0 mL of water and dried under vacuum in preparation for isolation of the lutein fraction by HPLC.

The dried residue was dissolved in 50 μL of ethyl ether and 150 μL of methanol, and 195 μL was injected into the HPLC system. The components of the HPLC system were manufactured by Waters Chromatography (Milford, MA) and consisted of the 717Plus autosampler with temperature control set at 5°C, two 510 solvent delivery systems, and the 996 photodiode array detector. The system operated with Millennium 2010 Chromatography Manager software. Solvents were HPLC grade; methanol, methyl *tert*-butyl ether (MTBE), and ammonium acetate were purchased from Fisher Scientific (Chicago, IL). The mobile phase was filtered (nylon-66 filter, 0.2 μm; Rainin Instruments Co., Woburn, MA) and degassed before use. A 5-μm C_{30} carotenoid column (YMC, Inc., Wilmington, NC) (4.6 × 250 mm) protected by a precolumn packed with the same stationary phase was used to achieve baseline resolution of lutein and the constitutional isomer, zeaxanthin. Carotenoids were eluted by using a linear mobile phase gradient from 100% methanol (1g/L ammonium acetate) to 100% MTBE over 35 min, as modified from Sander *et al.* (21). The flow rate was 1.0 mL/min. Elution of plasma carotenoids was monitored at 453 nm. The lutein fraction was collected, dried under vacuum, and repurified by using the same reversed-phase HPLC conditions in order to reduce residual sample matrix and prevent contamination by the close-eluting constitutional isomer, zeaxanthin. The lutein fraction was again collected, dried under vacuum, and redissolved in 50 μL of ethyl ether and 150 μL of isooctane/ethanol (95:5, vol/vol).

The lutein fraction was then subjected to further purification to remove contaminating lipids by using normal-phase HPLC (3). A 195-μL aliquot was injected into a Betasil Cyano analytical column (Keystone Scientific, Bellefonte, PA) (4.6 × 150 mm) and eluted by using an isocratic mobile phase of isooctane/ethanol (95:5, vol/vol). The flow rate was 1.0 mL/min. The lutein fraction was collected and dried under vacuum in preparation for derivatization for stable carbon isotope ratio analysis using GC–C–IRMS. Procedures were performed under yellow light.

Derivatization of lutein for GC–C–IRMS analysis. The conjugated polyene system of carotenoids is thermally labile so that alcohol hydrogenolysis and hydrogenation of lutein to produce a thermally stable analog, perhydro-β-carotene, was necessary prior to stable carbon isotope analysis by using GC–C–IRMS. We compared catalytic activities on platinum and palladium catalysts for hydrogenation of β-carotene and for alcohol hydrogenolysis and hydrogenation of lutein to produce perhydro-β-carotene. Lutein (Reagent grade, 95% purity; Kemin Industries, Des Moines, IA) and β-carotene (>97% purity; Fluka Chemical, Milwaukee, WI) were used as the reactants. The platinum oxide catalyst and the platinum and palladium catalysts supported on carbon (5 wt%) were supplied by Alfa Aesar (Ward Hill, MA). The catalyst (1 mg of platinum oxide or 10 mg of platinum-on-carbon or 10 mg of palladium-on-carbon) was suspended in 0.5 mL of HPLC-grade cyclohexane and 0.5 mL of glacial acetic acid containing 0.02 M *p*-toluenesulfonic acid monohydrate (Aldrich, Milwaukee, WI), and reduced by hydrogen gas prior to addition of 1.0 μg of β-carotene or lutein in 250 μL of cyclohexane; the reaction proceeded at 60°C and 10 psi hydrogen

pressure for 16 h. The reaction products were washed with 2 mL of HPLC-grade water and extracted twice with 3 mL of hexane. The combined hexane layers were washed twice with 2 mL of HPLC-grade water, dried under vacuum, and stored at –20°C until analyzed by using GC–C–IRMS. The yield of the perhydro-β-carotene product was quantified by using gas–liquid chromatography after addition of squalane (Aldrich) as an internal standard. Calibration curves were generated from the ratio of the peak height of the perhydro-β-carotene standard to that of the squalane internal standard plotted against the injected amount of perhydro-β-carotene standard. The perhydro-β-carotene standard was prepared by two sequential hydrogenations of β-carotene using platinum oxide as catalyst, and the purity was determined to be 100% by using gas–liquid chromatography. Because catalytic hydrogenation on palladium-on-carbon was determined to result in the highest yield of perhydro-β-carotene and the lowest production of side reaction products, this catalyst was used for derivatization of the plasma lutein fraction for analysis by using GC–C–IRMS.

A confirmatory mass spectrum of the perhydro-β-carotene reaction product was obtained using a Fisons (currently Thermoquest, San Jose, CA) GC 8000 gas chromatograph interfaced to a Fisons Trio 1000 quadrupole mass spectrometer in electron ionization mode (70 eV). A 15 m × 0.25 mm i.d. (0.25-μm film thickness) DB™-1 (J&W Scientific, Folsom, CA) fused-silica capillary column with on-column injector was used with ultrapure helium as carrier gas at a flow rate of 40 cm/s. The temperature program proceeded from 50°C followed by a gradient of 30°C/min to 150°C followed by a gradient of 15°C/min to 310°C, and a 10-min hold at 310°C. The interface temperature was 310°C, and the ion source temperature was 150°C. Mass spectra were acquired over the range *m/z* 50–600 in 0.90 s.

To determine whether derivatization resulted in isotopic alteration of the sample (isotopic fractionation), the isotopic composition of commercial lutein standard (reagent grade, 95% purity; Kemin Industries) was determined before derivatization and compared with that of the major derivatization product, perhydro-β-carotene. The $^{13}C/^{12}C$ ratio of lutein was analyzed without hydrogenation by using a NA1500 elemental analyzer (EA) (CE Elantech, Lakewood, NJ) interfaced to the Optima isotope ratio mass spectrometer. Lutein was quantitatively combusted to CO_2 and H_2O; H_2O vapor was removed by a chemical trap, and the CO_2 was further purified by GC on a Poropak QS column (2 m × 4 mm i.d.) and admitted into the Fisons/VG Isotech Optima IRMS (currently Micromass UK, Manchester, United Kingdom). The stable carbon isotope ratio (expressed as $\delta^{13}C$ vs. the international standard, Pee Dee Belemnite, in per mil units, denoted ‰) of lutein measured without derivatization by using EA–IRMS was compared with that of the perhydro-β-carotene product of lutein derivatization measured by using GC–C–IRMS.

GC–C–IRMS analysis. The stable carbon isotope ratio of the perhydro-β-carotene product of lutein derivatization was determined using a 5890A Hewlett-Packard (Wilmington, DE) GC fitted with a Fisons/VG Isotech Isochrom GC-combustion interface to the Fisons/VG Isotech Optima IRMS. A 10 m × 0.25 mm i.d. (0.25 μm film thickness) DB-1 (J&W Scientific) fused-silica capillary column with on-column injector was used with ultrapure helium as carrier gas at a flow rate of 40 cm/s. The temperature program proceeded from 50°C followed by a gradient of 30°C/min to 150°C followed by a gradient of 15°C/min to 325°C and a 20-min hold at 325°C. The computer-generated stable carbon isotope ratio measurements, expressed in delta (δ), per mil (part per thousand, ‰) units, were used to calculate the atom percent ^{13}C in each plasma lutein sample according to the following formula:

$$\text{atom\% } ^{13}\text{C} = \frac{(100 \times R_{PDB}) \times \left(\delta^{13}\text{C}/1000 + 1\right)}{1 + (R_{PDB}) \times \left(\delta^{13}\text{C}/1000 + 1\right)} \quad [1]$$

in which R_{PDB} represents the $^{13}C/^{12}C$ ratio for the international standard for carbon, Pee Dee Belemnite (PDB), with an accepted value $R_{PDB} = 0.0112372$ (7). For each subject, the atom percent excess (APE) ^{13}C in plasma lutein at each time point was calculated by subtraction of the atom percent ^{13}C in plasma lutein at baseline from that in plasma lutein after ingestion of the [^{13}C]lutein tracer. The APE reflects the percentage of plasma lutein that is present as the ^{13}C-enriched isotopomer after ingestion of the tracer and controls for natural abundance ^{13}C (3).

Calculation of [^{13}C]lutein in plasma. The plasma concentration of [^{13}C]lutein was calculated from the total (labeled plus unlabeled) plasma lutein concentration determined by using HPLC and the APE ^{13}C in the plasma lutein fraction determined by using GC–C–IRMS. In order to measure the total plasma lutein concentration, duplicate 200-μL aliquots of plasma were denatured by addition of an equal volume of absolute ethanol containing 0.1g/L butylated hydroxytoluene and echinenone (generously donated by Roche Vitamins, Parsippany, NJ) as internal standard. Samples were then extracted twice with 2 mL hexane containing 0.1 g/L butylated hydroxytoluene, and the combined hexane layers were evaporated to dryness under vacuum. The residues were reconstituted with ethyl ether and methanol (1:3, vol/vol), and 50-μL aliquots were injected into the HPLC system. The HPLC conditions were as previously described for purification of the plasma lutein fraction by reversed-phase HPLC. Calibration curves were generated from the ratio of the peak area of the lutein standard (reagent-grade lutein, 95% purity; Kemin Industries) to that of the echinenone internal standard plotted against the injected amount of the lutein standard. Analyses were performed under yellow light. The plasma concentration of [^{13}C]lutein was calculated as the product of the total plasma lutein concentration determined by using HPLC and the atom fraction excess ^{13}C (F), where F = APE/100. The areas under the plasma [^{13}C]lutein concentration vs. time curves (AUC) were calculated by using trapezoidal approximation (22).

RESULTS

The retention time and ultraviolet/visible absorbance spectrum of the biosynthetic [^{13}C]lutein tracer (Fig. 2) measured by using HPLC with photodiode array detection were identical to those of a commercial lutein standard (reagent-grade lutein, 95% purity, Kemin Industries). The electron ionization (70 eV) mass spectrum showed fragmentation of perlabeled [^{13}C]lutein to form a molecular ion of *m/z* 608.4 (Fig. 3). The molecular mass of unlabeled lutein, a C_{40} carotenoid, is 568.4. The tracer was therefore identified as lutein in which all carbon atoms were uniformly labeled with ^{13}C.

Hydrogenation of the hydrocarbon β-carotene with platinum as catalyst is complete and produces a single product, perhydro-β-carotene (3). Catalytic hydrogenation of the dihydroxycarotenoid, lutein, produces perhydro-β-carotene and secondary products, which likely result from the favored acid-catalyzed dehydration of the allylic hydroxyl group (4). In order to optimize the yield of the perhydro-β-carotene product, we compared catalytic activities on platinum and palladium catalysts for hydrogenation of β-carotene and for alcohol hydrogenolysis and hydrogenation of lutein (Fig. 4). Perhydro-β-carotene was quantified by using GC. For the respective catalysts, respective recoveries of perhydro-β-carotene (mol% ± SD; $n = 3$) from β-carotene and lutein were: platinum oxide, 102.8 ± 0.5 and 21.7 ± 3.9; platinum-on-carbon, 101.9 ± 3.0 and trace; palladium-on-carbon, 45.9 ± 1.0 and 55.3 ± 4.8. The identity of the major product of lutein derivatization was determined to be perhydro-β-carotene based on comparison of retention time during GC analysis with that of perhydro-β-carotene produced by hydrogenation of synthetic β-carotene (>97% purity; Fluka), and was further confirmed by using GC–MS (Fig. 5). Catalytic activity for hydrogenation of β-carotene was optimal on platinum, whereas catalytic activity for alcohol hydrogenolysis and hydrogenation of lutein was optimal on palladium; palladium is known to be the best catalyst for most hydrogenolysis reactions (23). There was good-to-excellent yield of the perhydro-β-carotene product which enabled reliable GC–C–IRMS analysis of nanomolar quantities of derivatized lutein. Thus our approach was sufficiently sensitive to measure the stable carbon isotope ratio of perhydro-β-carotene produced from lutein isolated from small volumes of human plasma; such sensitivity is a requisite for stable isotope tracer methods.

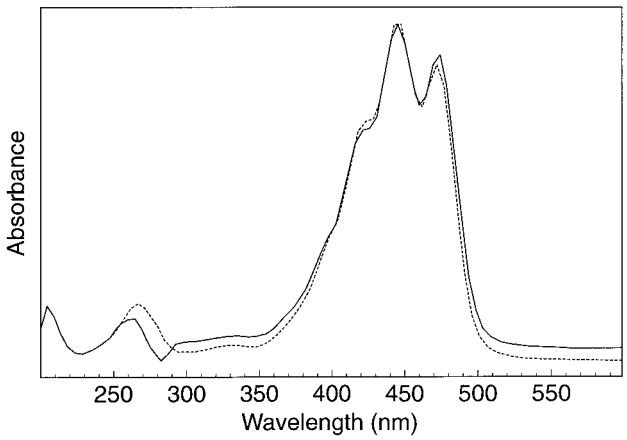

FIG. 2. Near identical ultraviolet/visible absorbance spectra of commercial lutein standard (reagent-grade lutein, 95% purity; Kemin Industries, Des Moines, IA) (----) and of biosynthetic [^{13}C]lutein (—) isolated from a commercially available extract of algal biomass (Martek Bioscience, Columbia, MD).

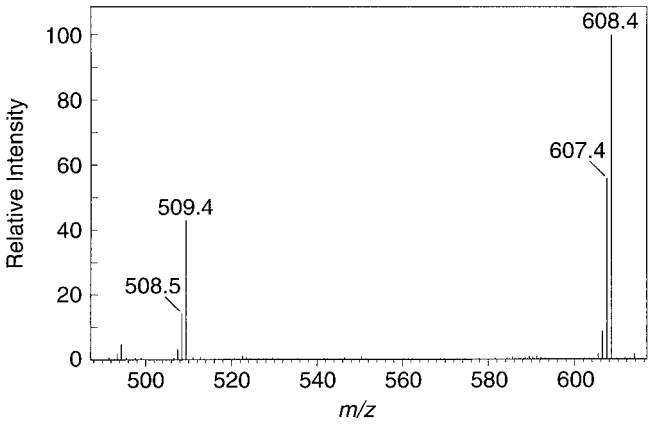

FIG. 3. Electron ionization (70 eV) mass spectrum showing fragmentation of per-labeled [^{13}C]lutein to form a molecular ion of *m/z* 608.4. The molecular mass of unlabeled lutein, a C_{40} carotenoid, is 568.4. This confirms the identity of the biosynthetically-labeled [^{13}C]lutein tracer.

The incomplete yield of the perhydro-β-carotene product of lutein derivatization indicates a potential for isotopic fractionation during derivatization of the plasma lutein fraction for GC–C–IRMS analysis. The stable carbon isotope ratio (expressed as δ^{13}C vs. the international standard, PDB, in per mil units, denoted ‰) of lutein measured without derivatization by using EA–IRMS was determined to be −30.82 ± 0.10‰ (mean ± SD; $n = 4$); the stable carbon isotope ratio of the perhydro-β-carotene product of lutein hydrogenation on palladium measured by using GC–C–IRMS was determined to be −30.97 ± 0.27‰ (means ± SD; $n = 7$). Thus our protocol for derivatization of lutein did not result in carbon isotopic fractionation; such isotopic alteration would preclude accurate determination of ^{13}C enrichment in lutein isolated from human plasma.

A representative GC–C–IRMS chromatogram of derivatized plasma lutein with the *m/z* 44 ($^{12}CO_2$) signal trace and corresponding upper 45 ($^{13}CO_2$ + $^{12}C^{17}O^{16}O$)/44 isotope ratio signal trace is shown in Figure 6. The chromatogram at *m/z* 44 is almost identical to that from a flame-ionization detector, since both arise from the detection of carbon (24). The 45/44 isotope ratio trace is indicative of the shift of isotope ratio from background to that of enriched plasma lutein. The derivatization products and coeluting components or contaminants are simultaneously combusted to CO_2 and detected in the mass spectrometer. Therefore, accurate and precise measurement of the stable carbon isotope ratio requires high-resolution GC separation of the analyte, perhydro-β-carotene. Despite extensive purification of the plasma lutein fraction,

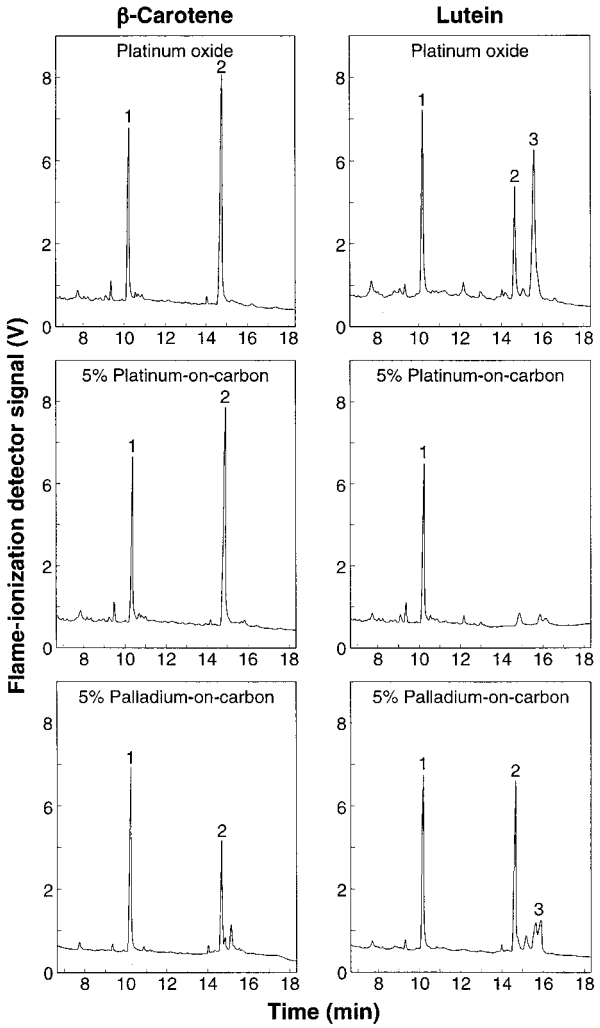

FIG. 4. Gas chromatograms of hydrogenated commercial standards of β-carotene (>97% purity; Fluka Chemical, Milwaukee, WI) and lutein (reagent-grade lutein, 95% purity; Kemin Industries, Des Moines, IA). Catalytic activities for hydrogenation of β-carotene and for alcohol hydrogenolysis and hydrogenation of lutein were compared on palladium and platinum catalysts. Peak identity: 1, squalane internal standard (Aldrich Chemical, Milwaukee, WI); 2, perhydro-β-carotene; 3, unidentified side reaction product(s).

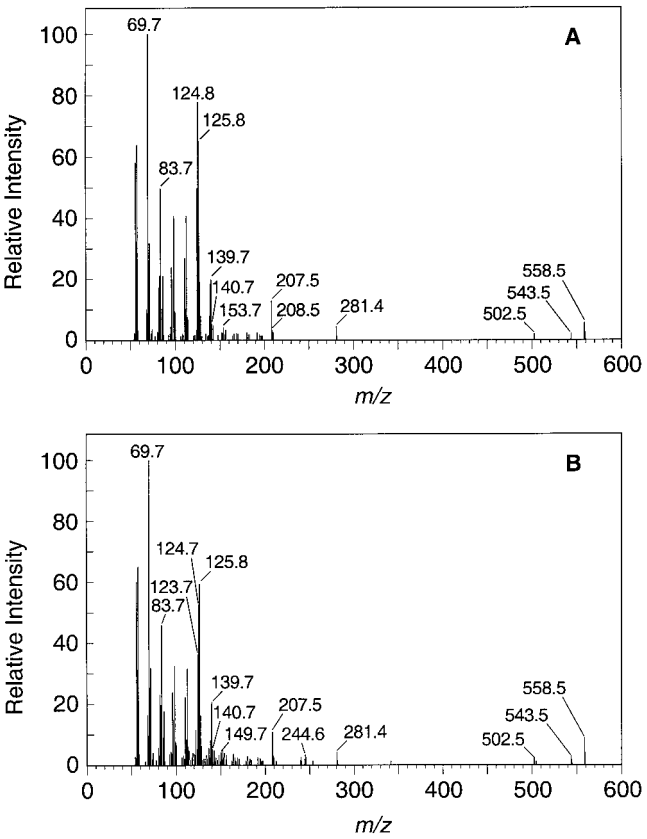

FIG. 5. Electron ionization (70 eV) mass spectra showing similar fragmentation of the product of β-carotene hydrogenation (A) and of the major product of alcohol hydrogenolysis and hydrogenation of lutein (B). Both produced the perhydro-β-carotene molecular ion at *m/z* 558.5.

the presence of sample matrix is apparent in the baseline of the GC–C–IRMS chromatogram. The 45/44 isotope ratio measurement was corrected by automated data processing for this contribution to background. However, sensitivity would be enhanced by elimination of sample matrix which would reduce ^{12}C dilution of measured ^{13}C enrichment. Our approach was still sufficiently sensitive to enable measurement of the stable carbon isotope ratio of lutein isolated from small volumes of plasma after ingestion of only 3 mg of [^{13}C]lutein.

The plasma concentration vs. time curve for [^{13}C]lutein after subjects ingested a 3-mg (5.3-μmol) dose of per-labeled [^{13}C]lutein is shown in Figure 7. The relatively rapid increase to a peak at 11–16 h was followed by a moderate and then slow decline to the final measurement at 528 h. At 528 h, ^{13}C enrichment was still detected in the plasma lutein pool. Thus,

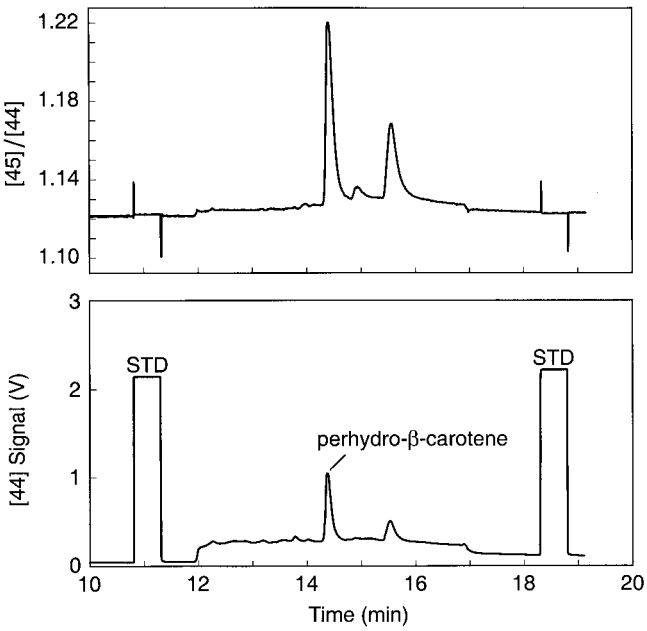

FIG. 6. Gas chromatography–combustion interfaced–isotope ratio mass spectrometry plot of the hydrogenated lutein fraction isolated from the plasma of a subject who ingested 3.0 mg of per-labeled [^{13}C]lutein. Shown are the *m/z* 44 ($^{12}CO_2$) signal trace and corresponding upper 45 ($^{13}CO_2$ + $^{12}C^{17}O^{16}O$)/44 isotope ratio signal trace.

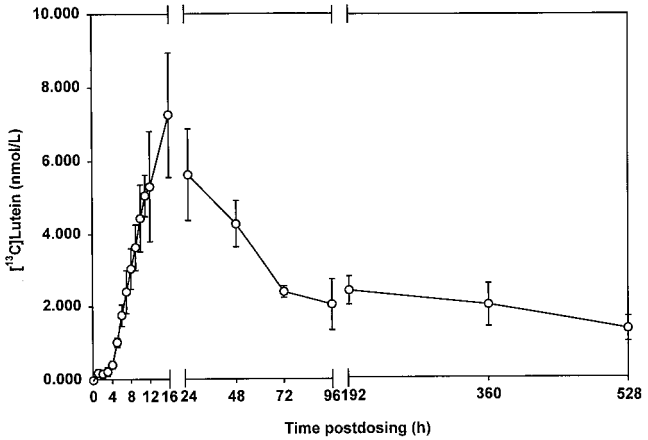

FIG. 7. The appearance and disappearance of [^{13}C]lutein in the plasma of subjects who each ingested a 3-mg oral dose of per-labeled [^{13}C]lutein. $\bar{x}$ ± SEM; n = 4.

TABLE 1
Maximal Plasma Concentrations (C_{max}), Corresponding Times (t_{max}), and Areas Under the Plasma [^{13}C]Lutein Concentration vs. Time Curves (AUC) for 0–528 h After Subjects Ingested 3.0 mg of Per-Labeled [^{13}C]Lutein[a]

Subject	C_{max} (nmol/L)	t_{max} (h)	$AUC_{(0–528\ h)}$ (nmol·h/L)
1	5.22	11	1123.4
2	5.45	16	414.0
3	5.74	16	780.5
4	11.82	16	1401.2
Means	7.06	14.8	929.8
SD	3.18	2.5	427.4
CV%	45.0	16.9	46.0

[a]CV, coefficient of variation.

the ^{13}C tracer approach using GC–C–IRMS is able to measure small changes in stable carbon isotope ratio in lutein over a prolonged period of time. Such sensitivity and precision are needed in order to characterize the kinetics of elimination of carotenoids which are transported in lipoproteins with slow turnover rates, such as low density lipoprotein (LDL) and high density lipoprotein (7). The maximal plasma concentrations (C_{max}), corresponding times (t_{max}), and areas under the concentration vs. time curve (AUC) for the four subjects are shown in Table 1. The peak plasma concentration of [^{13}C]lutein for individual subjects ranged from 5.22–11.82 nmol/L. For three of four subjects, the highest measured plasma concentration of [^{13}C]lutein occurred at 16 h; for the remaining subject, the highest concentration occurred at 11 h after ingestion of the dose. Bioavailability is proportional to the AUC (22). The AUC data in Table 1 indicate that there was a threefold variation among subjects in the bioavailability of the [^{13}C]lutein tracer dose.

DISCUSSION

We successfully adapted the ^{13}C tracer approach developed by Parker *et al.* (2,3) and previously used in human studies of the metabolism of β-carotene (6) for use in study of the metabolism of another prominent dietary carotenoid, lutein. Of the 14 major dietary carotenoids absorbed in the small intestine and incorporated into plasma (25), lutein and zeaxanthin are selectively deposited in the macular pigment of the human retina (26). The macular pigment is thought to function to attenuate transmission of blue visible light and resultant photoxidative damage to photoreceptor cells (15). The amount of macular pigment was recently shown to be modifiable by the amount of lutein ingested in vegetables (16). Consumption of lutein-rich vegetables is negatively correlated with deterioration of the retina in the form of age-related macular degeneration (AMD) (12). Thus there is a need for experimental approaches to identify factors that modulate the intestinal absorption and plasma appearance of lutein when ingested in physiologically relevant amounts by humans. The advantage of a tracer approach using GC–C–IRMS is the sensitivity and selectivity to quantify the appearance of ^{13}C in the plasma lutein pool after ingestion of 3 mg or less of [^{13}C]lutein.

The basis for the current application is a metabolic tracer technique using highly enriched substrates uniformly labeled with ^{13}C and analysis by high-precision GC–C–IRMS (27). Isotope-ratio monitoring differs from conventional GC–MS in that organic samples are combusted on line in order to quantitatively produce analytes (CO_2, N_2, and potentially other fixed gases) amenable to high-precision isotope ratio analysis (28). In our application, the carbon atoms of the major derivatization product of lutein, perhydro-β-carotene, are combusted to CO_2, which is admitted to the mass spectrometer. Ion currents at *m/z* 44 ($^{12}C^{16}O_2$), 45 ($^{13}C^{16}O_2$ + $^{12}C^{17}O^{16}O$), and 46 ($^{12}C^{18}O^{16}O$) are continuously monitored using three Faraday cup detectors. To control for instrumental effects, the isotope ratio of CO_2 derived from the analyte is compared with that of a CO_2 standard admitted to the ion source. The CO_2 standard is isotopically calibrated relative to PDB, the accepted primary standard for carbon isotopic abundances. Results are expressed in δ notation defined as

$$\delta(‰) = \left(\frac{R_{sample} - R_{standard}}{R_{standard}} \right) \times 10^3 \quad [2]$$

where R is the $^{13}C/^{12}C$ isotope ratio. The computer-generated δ value is used to calculate the atom percent ^{13}C in the analyte, as previously described (see the Experimental Procedures section).

A major advantage of this approach for metabolic tracer studies is the low detection limits and high-precision isotope-ratio monitoring that enable use of physiological amounts of tracer. GC–MS in selected ion-monitoring mode is widely used to measure stable isotope abundance in nanomole samples, but is limited by relatively poor precision (0.1–0.5 mol%) (29). Conventional IRMS offers high precision (<0.0001 mol%) but requires micromoles of sample. Isotope-ratio monitoring using GC–C–IRMS combines the small sample amount of GC–MS and the high precision of conventional

IRMS. We have adapted this approach for use with a highly enriched [^{13}C]lutein tracer that is readily purified from a commercially available extract of algal biomass.

Most studies of the intestinal absorption of carotenoids have focused on β-carotene. However, the majority of carotenoids are oxycarotenoids, also referred to as xanthophylls, that are distinguished from the hydrocarbon carotenes by one or more oxygen functions (30). Lutein is the predominant oxycarotenoid in human plasma, which reflects its wide dietary distribution in green vegetables, in corn, and, to a lesser extent, in fruits such as mango and papaya. Although internationally lutein is more consistently detected than β-carotene in human plasma (31), the metabolism of β-carotene has been comparatively well studied. The comparative interest in β-carotene reflects its role as the major dietary source of provitamin A, whereas lutein lacks provitamin A activity. Of the components of green and yellow vegetables and fruits, carotenoids are most strongly correlated with decreased risk of cancer (32). Investigations of the phytoprotective component(s) in these foods focused initially on β-carotene because of its established nutritional importance as a provitamin A carotenoid and the known importance of retinoids in cancer prevention (33). After the disappointing results of the β-carotene supplementation trials (34–36), interest has shifted to other major dietary carotenoids such as lutein and to physiological ingestion of carotenoids in the form of fruits and vegetables rather than pharmacological ingestion in the form of supplements.

In the current study, the high precision of GC–C–IRMS was used to quantify the plasma appearance and disappearance of a physiological 3-mg dose of [^{13}C]lutein in healthy women. The bioavailability of lutein in spinach products was recently shown to be 45–55% relative to that of crystalline lutein suspended in vegetable oil when ingested by humans (37). Thus the bioavailability of 3 mg of [^{13}C]lutein tracer would be roughly equivalent to that of 6 mg of lutein ingested in the form of spinach, which, in turn, would equate to *ca.* 0.50 cup (90 g) of cooked or 1.0 cup (56 g) of raw spinach (38). By using a per-labeled [^{13}C] tracer and the high-precision of GC–C–IRMS, we were able to completely define the plasma appearance and disappearance of lutein after a dose equivalent to that absorbed from a single vegetable serving.

The mean plasma concentration of [^{13}C]lutein showed a single peak at 16 h, which is consistent with the plasma appearance observed in healthy adults who ingested a single pharmacological dose (0.5 μmol/kg body weight) of unlabeled lutein (39). The data provide additional evidence of the metabolic heterogeneity of dietary carotenoids (40). The monophasic plasma appearance of [^{13}C]lutein is distinct from the biphasic plasma appearance of a physiological (1-mg) dose of [^{13}C]β-carotene (6). The plasma concentration vs. time curve for [^{13}C]β-carotene is characterized by a peak enrichment at 5 h and a second broader peak between 24 and 48 h. These two peaks reflect the dynamics of incorporation of [^{13}C]β-carotene into plasma lipoproteins involved in the transport and disposition of β-carotene (7). Our previous studies (20,41) and those of others (42,43) using large, unlabeled doses of β-carotene showed that the initial plasma peak coincides with appearance of β-carotene in postprandial triacylglycerol-rich lipoproteins [chylomicrons and large very low density lipoproteins (VLDL)] and the second peak with delayed appearance of β-carotene in LDL. The interval that separates the two peaks is presumed to reflect uptake of β-carotene in chylomicron remnants by the liver, incorporation of β-carotene into nascent VLDL secreted by the liver, and subsequent metabolism of VLDL to LDL.

Like that of [^{13}C]β-carotene, the plasma appearance of [^{13}C]lutein would be expected to reflect movement into and out of plasma lipoproteins involved in absorption and distribution. The plasma appearance of [^{13}C]lutein resembles that of another oxycarotenoid, canthaxanthin (β,β-carotene-4,4′-dione) (18). Previously, we showed that the monophasic plasma appearance of canthaxanthin is the result of coincident increments in triacylglycerol-rich lipoproteins and in LDL (20). In contrast, the accumulation of β-carotene in LDL is delayed. In the present study, we showed that the plasma appearance, and most likely the plasma lipoprotein transport, of lutein is distinct from that of β-carotene, which was studied previously (2,6). Because of the physiological tracer doses used, our findings are extrapolatable to the metabolism of lutein and β-carotene absorbed from dietary fruits and vegetables.

ACKNOWLEDGMENTS

Supported by USDA grant 94-34115-2835 to the Center for Designing Foods to Improve Nutrition, Iowa State University; journal paper no. J-18546 of the Iowa Agriculture and Home Economics Experiment Station, Ames, IA; project no. 3171; and supported by Hatch Act and State of Iowa funds.

REFERENCES

1. Wolfe, R.R. (1992) Gas Chromatography–Mass Spectrometry: Instrumentation, in *Radioactive and Stable Isotope Tracers in Biomedicine*, p. 37, Wiley-Liss, New York.
2. Parker, R.S., Swanson, J.E., Marmor, B., Goodman, K.J., Spielman, A.B., Brenna, J.T., Viereck, S.M., and Canfield, W.K. (1993) Study of β-Carotene Metabolism in Humans Using ^{13}C-β-Carotene and High Precision Isotope Ratio Mass Spectrometry, *Ann. N.Y. Acad. Sci. 691*, 86–95.
3. Parker, R.S., Brenna, J.T., Swanson, J.E., Goodman, K.J., and Marmor, B. (1997) Assessing Metabolism of β-[^{13}C]Carotene Using High-Precision Isotope Ratio Mass Spectrometry, *Methods Enzymol. 282*, 130–140.
4. Liang, Y., White, W.S., Yao, L., and Serfass, R.E. (1998) Use of High-Precision Gas Isotope Ratio Mass Spectrometry to Determine Natural Abundance ^{13}C in Lutein Isolated from C_3 and C_4 Plant Sources, *J. Chromatogr. A 800*, 51–58.
5. Yao, L., Trahanovsky, W.S., Liang, Y., Serfass, R.E., and White, W.S. (1998) Stable Carbon Isotope Analysis of Lutein, *FASEB J. 12*, A543.
6. You, C.-S., Parker, R.S., Goodman, K.J., Swanson, J.E., and Corso, T.N. (1996) Evidence of *Cis-Trans* Isomerization of 9-*Cis*-β-Carotene During Absorption in Humans, *Am. J. Clin. Nutr. 64*, 177–183.
7. Swanson, J.E., Wang, Y.-Y., Goodman, K.J., and Parker,

R.S. (1996) Experimental Approaches to the Study of β-Carotene Metabolism: Potential of a ^{13}C Tracer Approach to Modeling β-Carotene Kinetics in Humans, *Adv. Food Nutr. Res. 40*, 55–79.
8. Le Marchand, L., Hankin, J.H., Bach, F., Kolonel, L.N., Wilkens, L.R., Stacewicz-Sapuntzakis, M., Bowen, P.E., Beecher, G.R., Laudon, F., Baque, P., *et al.* (1995) An Ecological Study of Diet and Lung Cancer in the South Pacific, *Int. J. Cancer 63*, 18–23.
9. Comstock, G.W., Alberg, A.J., Huang, H.Y., Wu, K., Burke, A.E., Hoffman, S.C., Norkus, E.P., Gross, M., Cutler, R.G., Morris, J.S., Spate, V.L., and Helzlsouer, K.J. (1997) The Risk of Developing Lung Cancer Associated with Antioxidants in the Blood: Ascorbic Acid, Carotenoids, Alpha-Tocopherol, Selenium, and Total Peroxyl Radical Absorbing Capacity, *Cancer Epidemiol. Biomarkers Prev. 6*, 907–916.
10. Street, D.A., Comstock, G.W., Salkeld, R.M., Schuep, W., and Klag, M.J. (1994) Serum Antioxidants and Myocardial Infarction. Are Low Levels of Carotenoids and Alpha-Tocopherol Risk Factors for Myocardial Infarction? *Circulation 90*, 1154–1161.
11. Howard, A.N., Williams, N.R., Palmer, C.R., Cambou, J.P., Evans, A.E., Foote, J.W., Marques-Vidal, P., McCrum, E.E., Ruidavets, J.B., Nigdikar, S.V., Rajput-Williams, J., and Thurnham, D.I. (1996) Do Hydroxy-Carotenoids Prevent Coronary Heart Disease? A Comparison Between Belfast and Toulouse, *Int. J. Vitam. Nutr. Res. 66*, 113–118.
12. Seddon, J.M., Ajani, U.A., Sperduto, R.D., Hiller, R., Blair, N., Burton, T.C., Farber, M.D., Gragoudas, E.S., Haller, J., Miller, D.T., Yannuzzi, L.A., and Willett, W. (1994) Dietary Carotenoids, Vitamins A, C, and E, and Advanced Age-Related Macular Degeneration, *JAMA 272*, 1413–1420.
13. Hampton, G.R., and Nelsen, P.T. (1992*) Age Related Macular Degeneration. Principles and Practice*, pp. 1–300, Raven Press, New York.
14. Bone, R.A., and Landrum, J.T. (1992) Distribution of Macular Pigment Components, Zeaxanthin and Lutein, in Human Retina, *Methods Enzymol. 213*, 360–366.
15. Marshall, J. (1985) Radiation and the Ageing Eye, *Ophthal. Physiol. Opt. 5*, 241–263.
16. Hammond, B.R., Jr., Johnson, E.J., Russell, R.M., Krinsky, N.I., Yeum, K.J., Edwards, R.B., and Snodderly, D.M. (1997) Dietary Modification of Human Macular Pigment Density, *Invest. Ophthalmol. Vis. Sci. 38*, 1795–1801.
17. Nebeling, L.C., Forman, M.R., Graubard, B.I., and Snyder, R.A. (1997) Changes in Carotenoid Intake in the United States: The 1987 and 1992 National Health Interview Surveys, *J. Am. Diet. Assoc. 97*, 991–996.
18. White, W.S., Stacewicz-Sapuntzakis, M., Erdman, J.W., Jr., and Bowen, P.E. (1994) Pharmacokinetics of β-Carotene and Canthaxanthin After Ingestion of Individual and Combined Doses by Human Subjects, *J. Am. Coll. Nutr. 13*, 665–671.
19. Craft, N.E., and Soares, J.H., Jr. (1992) Relative Solubility, Stability, and Absorptivity of Lutein and β-Carotene in Organic Solvents, *J. Agric. Food Chem. 40*, 431–434.
20. Paetau, I., Chen, H., Goh, N.M.-Y., and White, W.S. (1997) Interactions in the Postprandial Appearance of β-Carotene and Canthaxanthin in Plasma Triacylglycerol-Rich Lipoproteins in Humans, *Am. J. Clin. Nutr. 66*, 1133–1143.
21. Sander, L.C., Sharpless, K.E., Craft, N.E., and Wise, S.A. (1994) Development of Engineered Stationary Phases for the Separation of Carotenoid Isomers, *Anal. Chem. 66*, 1667–1674.
22. Rowland, M., and Tozer, T.N. (1995) Extravascular Dose, in *Clinical Pharmacokinetics: Concepts and Applications*, 3rd edn., p. 37, Williams & Wilkins, Baltimore.
23. Augustine, R.L. (1965) *Catalytic Hydrogenation*, p. 36, Marcel Dekker, New York.
24. Brenna, J.T. (1994) High-Precision Gas Isotope Ratio Mass Spectrometry: Recent Advances in Instrumentation and Biomedical Applications, *Acc. Chem. Res. 27*, 340–346.
25. Khachik, F., Spangler, C.J., Smith, J.C., Jr., Canfield, L.M., Pfander, H., and Steck, A. (1997) Identification, Quantification, and Relative Concentration of Carotenoids and Their Metabolites in Human Milk and Serum, *Anal. Chem. 69*, 1873–1881.
26. Bone, R.A., Landrum, J.T., Hime, G.W., Cains, A., and Zamor, J. (1993) Stereochemistry of the Human Macular Carotenoids, *Invest. Ophthalmol. Vis. Sci. 34*, 2033–2040.
27. Goodman, K.J., and Brenna, J.T. (1992) High Sensitivity Tracer Detection Using High-Precision Gas Chromatography–Combustion Isotope Ratio Mass Spectrometry and Highly Enriched [U-^{13}C]-Labeled Precursors, *Anal. Chem. 64*, 1088–1095.
28. Ricci, M.P., Merritt, D.A., Freeman, K.H., and Hayes, J.M. (1994) Acquisition and Processing of Data for Isotope-Ratio-Monitoring Mass Spectrometry, *Org. Geochem. 21*, 561–571.
29. Tetens, V., Kristensen, N.B., and Calder, A.G. (1995) Measurement of ^{13}C Enrichment of Plasma Lactate by Gas Chromatography/Isotope Ratio Mass Spectrometry, *Anal. Chem. 67*, 858–862.
30. Weedon, B.C.L., and Moss, G.P. (1995) Structure and Nomenclature, in *Carotenoids* (Britton, G., Liaaen-Jensen, S., and Pfander, H., eds.), Vol. 1 A, p. 31, Birkhäuser Verlag, Basel.
31. Thurnham, D.I., Northrop-Clewes, C.A., Paracha, P.I., and McLoone, U.J. (1997) The Possible Significance of Parallel Changes in Plasma Lutein and Retinol in Pakistani Infants During the Summer Season, *Br. J. Nutr. 78*, 775–784.
32. Bertram, J.S., Kolonel, L.N., and Meyskens, F.L., Jr. (1987) Rationale and Strategies for Chemoprevention of Cancer in Humans, *Cancer Res. 47*, 3012–3031.
33. King, T.J., Khachik, F., Bortkiewicz, H., Fukushima, L.H., Morioka, S., and Bertram, J.S. (1997) Metabolites of Dietary Carotenoids as Potential Cancer Preventive Agents, *Pure Appl. Chem. 69*, 2135–2140.
34. The Alpha-Tocopherol, Beta Carotene Cancer Prevention Study Group (1994) The Effect of Vitamin E and Beta Carotene on the Incidence of Lung Cancer and Other Cancers in Male Smokers, *N. Engl. J. Med. 330*, 1029–1035.
35. Omenn, G.S., Goodman, G.E., Thornquist, M.D., Balmes, J., Cullen, M.R., Glass, A., Keogh, J.P., Meyskens, F.L., Jr., Valanis, B., Williams, J.H., Jr., Barnhart, S., and Hammar, S. (1996) Effects of a Combination of Beta Carotene and Vitamin A on Lung Cancer and Cardiovascular Disease, *N. Engl. J. Med. 334*, 1150–1155.
36. Hennekens, C.H., Buring, J.E., Manson, J.E., Stampfer, M., Rosner, B., Cook, N.R., Belanger, C., LaMotte, F., Gaziano, J.M., Ridker, P.M., Willett, W., and Peto, R. (1996) Lack of Effect of Long-Term Supplementation with Beta Carotene on the Incidence of Malignant Neoplasms and Cardiovascular Disease, *N. Engl. J. Med. 334*, 1145–1149.
37. Castenmiller, J.J.M., West, C.E., Linssen, J.P.H., van het Hof, K.H., and Voragen, A.G.J. (1999) The Food Matrix of Spinach Is a Limiting Factor in Determining the Bioavailability of β-Carotene and to a Lesser Extent of Lutein in Humans, *J. Nutr. 129*, 349–355.
38. U.S. Department of Agriculture and the Nutrition Coordinating Center of the University of Minnesota (1998) *USDA-NCC Carotenoid Database for U.S. Foods—1998*. Online at http://www.nal.usda.gov/fnic/foodcomp/Data/car98/car98.html.
39. Kostic, D., White, W.S., and Olson, J.A. (1995) Intestinal Absorption, Serum Clearance, and Interactions Between Lutein and β-Carotene When Administered to Human Adults in Separate or Combined Oral Doses, *Am. J. Clin. Nutr. 62*, 604–610.
40. White, W.S., and Paetau, I. (1998) Carotenoid–Carotenoid Interactions, in *Phytochemicals—A New Paradigm* (Bidlack,

W.R., Omaye, S.T., Meskin, M.S., and Jahner, D., eds.), pp. 97–112, Technomic, Lancaster, PA.
41. Hu, X., Jandacek, R.J., and White, W.S. Intestinal Absorption of β-Carotene Ingested with a Meal Rich in Sunflower Oil or Beef Tallow: Postprandial Appearance in Triacylglycerol-Rich Lipoproteins in Women. *Am. J. Clin. Nutr.*, in press.
42. Cornwell, D.G., Kruger, F.A., and Robinson, H.B. (1962) Studies on the Absorption of Beta-Carotene and the Distribution of Total Carotenoid in Human Serum Lipoproteins After Oral Administration, *J. Lipid Res. 3*, 65–70.
43. Johnson, E.J., and Russell, R.M. (1992) Distribution of Orally Administered β-Carotene Among Lipoproteins in Healthy Men, *Am. J. Clin. Nutr. 56*, 128–135.

[Received August 3, 1999, and in final revised form and accepted February 2, 2000]

ARTICLE

New Cyclopentenone Fatty Acids Formed from Linoleic and Linolenic Acids in Potato

Mats Hamberg*

Department of Medical Biochemistry and Biophysics, Division of Physiological Chemistry II, Karolinska Institutet, S-171 77 Stockholm, Sweden

ABSTRACT: [1-^{14}C]Linoleic acid was incubated with a whole homogenate preparation from potato stolons. The reaction product contained four major labeled compounds, i.e., the α-ketol 9-hydroxy-10-oxo-12(*Z*)-octadecenoic acid (59%), the epoxy alcohol 10(*S*),11(*S*)-epoxy-9(*S*)-hydroxy-12(*Z*)-octadecenoic acid (19%), the divinyl ether colneleic acid (3%), and a new cyclopentenone (13%). The structure of the last-mentioned compound was determined by chemical and spectral methods to be 2-oxo-5-pentyl-3-cyclopentene-1-octanoic acid (trivial name, 10-oxo-11-phytoenoic acid). Steric analysis demonstrated that the relative configuration of the two side chains attached to the five-membered ring was *cis,* and that the compound was a racemate comprising equal parts of the 9(*R*),13(*R*) and 9(*S*),13(*S*) enantiomers. Experiments in which specific trapping products of the two intermediates 9(*S*)-hydroperoxy-10(*E*),12(*Z*)-octadecadienoic acid and 9(*S*),10-epoxy-10,12(*Z*)-octadecadienoic acid were isolated and characterized demonstrated the presence of 9-lipoxygenase and allene oxide synthase activities in the tissue preparation used. The allene oxide generated from linoleic acid by action of these enzymes was further converted into the cyclopentenone and α-ketol products by cyclization and hydrolysis, respectively. Incubation of [1-^{14}C]linolenic acid with the preparation of potato stolons afforded 2-oxo-5-[2′(*Z*)-pentenyl]-3-cyclopentene-1-octanoic acid (trivial name, 10-oxo-11,15(*Z*)-phytodienoic acid), i.e., an isomer of the jasmonate precursor 12-oxo-10,15(*Z*)-phytodienoic acid. Quantitative determination of 10-oxo-11-phytoenoic acid in linoleic acid-supplied homogenates of different parts of the potato plant showed high levels in roots and stolons, lower levels in developing tubers, and no detectable levels in leaves.

Paper no. L8431 in *Lipids 35,* 353–363 (April 2000).

*E-mail: Mats.Hamberg@mbb.ki.se

Abbreviations and trivial names: 9-H(P)OD, 9-hydro(pero)xy-10(*E*),12(*Z*)-octadecadienoic acid; 9-H(P)OT, 9-hydro(pero)xy-10(*E*),12(*Z*),15(*Z*)-octadecatrienoic acid; 12-oxo-PDA, 12-oxo-10,15(*Z*)-phytodienoic acid {4-oxo-5-[2′(*Z*)-pentenyl]-2-cyclopentene-1-octanoic acid}; 12-oxo-PEA, 12-oxo-10-phytoenoic acid [4-oxo-5-pentyl-2-cyclopentene-1-octanoic acid]; 13-H(P)OD, 13-hydro(pero)xy-9(*Z*),11(*E*)-octadecadienoic acid; 13-H(P)OT, 13-hydro(pero)xy-9(*Z*),11(*E*),15(*Z*)-octadecatrienoic acid; AOS, allene oxide synthase; colneleic acid, 9-[1′(*E*),3′(*Z*)-nonadienyloxy]-8(*E*)-nonenoic acid; colnelenic acid, 9-[1′(*E*),3′(*Z*),6′(*Z*)-nonatrienyloxy]-8(*E*)-nonenoic acid; CP-HPLC, chiral-phase high-performance liquid chromatography; FTIR, Fourier transform infrared; GC–MS, gas chromatography–mass spectrometry; GLC, gas–liquid chromatography; GSH, reduced glutathione; GSH-px, glutathione peroxidase; MC, (–)-menthoxycarbonyl; NMR, nuclear magnetic resonance; RP-HPLC, reversed-phase high-performance liquid chromatography; SP-HPLC, straight-phase high-performance liquid chromatography; UV, ultraviolet.

Jasmonates constitute a group of biologically important compounds in plants. Members of the jasmonate family have been implicated in defense reactions against insects and other pathogens, in mechanical responses such as tendril coiling, and in pollen development (1). Jasmonic acid is biosynthesized from the cyclopentenone 12-oxo-10,15(*Z*)-phytodienoic acid (12-oxo-PDA) by action of reductase and β-oxidation enzymes (2). 12-Oxo-PDA is formed by a pathway involving 13-lipoxygenase, allene oxide synthase, and allene oxide cyclase (3,4). The last-mentioned enzyme is specific for allene oxides in which the epoxide group is located in the n-6,7 position and in which there is also a double bond in the n-3 position (5). In agreement with these structural requirements, cyclopentenone fatty acids hitherto isolated from higher plants originate in linolenic acid (1,4) or 7(*Z*),10(*Z*),13(*Z*)-hexadecatrienoic acid (6). The present paper is concerned with the oxidative metabolism of linoleic and linolenic acids in preparations of stolons of potato. An alternative route to cyclopentenone fatty acids initiated by a 9-lipoxygenase is described.

EXPERIMENTAL PROCEDURES

Plant materials. Tubers of potato (*Solanum tuberosum* L., var. Bintje) were stored in the dark at 18°C. Stolons of 0.5–5 cm length were used for the incubations.

Fatty acids. Linoleic and linolenic acids were purchased from Nu-Chek-Prep (Elysian, MN). [1-^{14}C]Linoleic and [1-^{14}C]linolenic acids (DuPont NEN, Boston, MA) were mixed with the corresponding unlabeled acids and purified by SiO_2 chromatography to afford specimens having specific radioactivities of 5.4 and 9.1 kBq/μmol, respectively. [1-^{14}C]9(*S*)-Hydroperoxy-10(*E*),12(*Z*)-octadecadienoic acid [9(*S*)-HPOD] and [1-^{14}C]9(*S*)-hydroperoxy-10(*E*),12(*Z*),15(*Z*)-octadecatrienoic acid [9(*S*)-HPOT] were prepared in 30–50% yield by incubation of labeled linoleic acid and linolenic acid, respectively, with tomato lipoxygenase (7) under an atmosphere of oxygen gas. The α-ketol 9-hydroxy-10-oxo-12(*Z*)-octadecenoic acid and the γ-ketol 13-hydroxy-10-oxo-11(*E*)-octadecenoic acid were prepared by incubation of 9(*S*)-HPOD with allene oxide synthase (AOS) from corn seeds (8,9) followed by isolation by reversed-phase high-performance liquid chromatography (RP-HPLC). 9-Methoxy-10-oxo-12(*Z*)-octadecenoic acid was prepared from 9(*S*)-HPOD in brief incu-

bations with corn seed AOS interrupted by addition of 20 vol of methanol (8,9). The macrolactones 10-oxo-12(*Z*)-octadecen-9-olide and 10-oxo-12(*Z*)-octadecen-11-olide were obtained in a similar way in incubations interrupted by addition of 20 vol of acetonitrile (9,10). Incubation of 13(*S*)-hydroperoxy-9(*Z*),11(*E*),15(*Z*)-octadecatrienoic acid [13(*S*)-HPOT] with corn seed AOS in the presence of corn allene oxide cyclase afforded natural 9(*S*),13(*S*)-12-oxo-10,15(*Z*)-phytodienoic acid [9(*S*),13(*S*)-12-oxo-PDA] (11), whereas 12-oxo-10-phytoenoic acid [12-oxo-PEA (side-chain *trans* form)] was obtained by brief incubation of 13(*S*)-hydroperoxy-9(*Z*),11(*E*)-octadecadienoic acid [13(*S*)-HPOD] with corn seed AOS followed by addition of bovine serum albumin (12). The methyl ester of the epoxy alcohol 10(*S*),11(*S*)-epoxy-9(*S*)-hydroxy-12(*Z*)-octadecenoic acid was obtained by incubation of 9(*S*)-HPOD with a homogenate of potato leaves (13), whereas the divinyl ethers colneleic acid and colnelenic acid were prepared by incubation of 9(*S*)-HPOD and 9(*S*)-HPOT, respectively, with a preparation from potato tubers (14).

Enzyme preparations. Stolons of potato were minced and homogenized at 0°C in 0.1 M potassium phosphate buffer pH 7.4 (1:10, wt/vol) with an Ultra-Turrax. The homogenate was filtered through gauze, and the filtrate (protein, 1.3 mg/mL) was used as enzyme source in preparative incubations carried out to generate products for structural analysis. Centrifugation at 9300 × *g* for 15 min afforded a low-speed sediment and a supernatant. Further centrifugation of the latter at 105,000 × *g* for 60 min provided a high-speed particle fraction and a particle-free supernatant (protein, 0.9 mg/mL). The former was resuspended in buffer to give a suspension (protein, 0.8 mg/mL), which was used as enzyme source in experiments carried out to study conditions affecting formation of cyclopentenones. A particle fraction containing AOS from corn seeds was prepared as described (15). Glutathione peroxidase (GSH-px) and reduced glutathione (GSH) were purchased from Sigma Chemical Co. (St. Louis, MO).

Incubations and treatments. Incubations of [1-^{14}C]linoleic acid, [1-^{14}C]linolenic acid, 9(*S*)-HPOD and 9(*S*)-HPOT (63–245 μM as indicated) were carried out by stirring the substrate at 23°C for times indicated with the whole homogenate preparation of potato stolons. The mixtures were extracted with 2 vol of diethyl ether at pH 5, and the products were methyl-esterified and subjected to straight-phase high-performance liquid chromatography (SP-HPLC) [solvent system, 2-propanol/hexane (1:99, vol/vol)]. Cyclopentenone formation under various conditions was studied by stirring [1-^{14}C]9(*S*)-HPOD at 23°C with a suspension of the 105,000 × *g* particle fraction of potato stolons (2 mL, pre-warmed at 23°C for 5 min). This incubation was modified as indicated with respect to temperature, pH, and substrate concentration.

*Preparation of **3a***. For large-scale preparation of cyclopentenone **3a** (see Scheme 1 for numbered key to all struc-

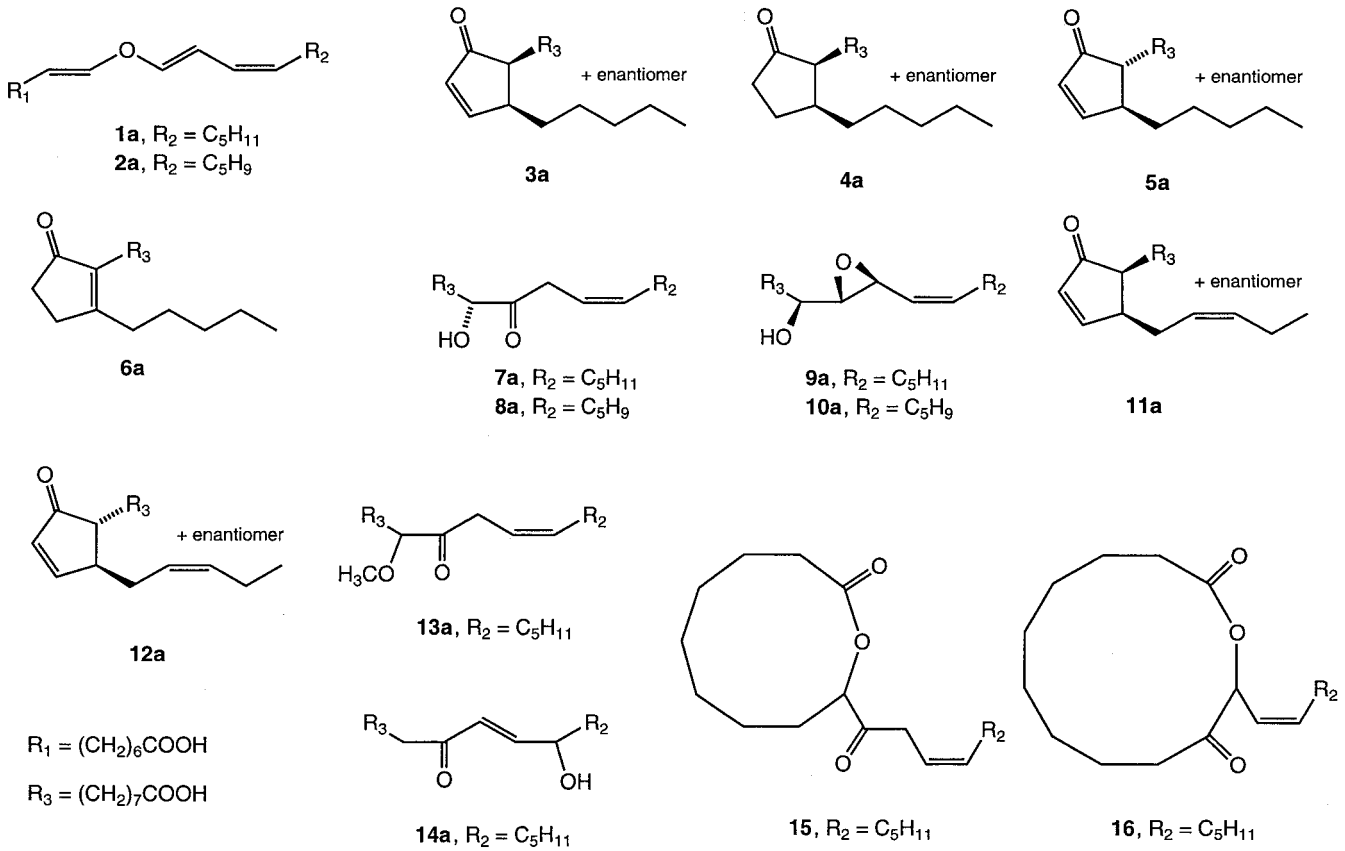

SCHEME 1

tures; free carboxylic acids are designated by **a** and methyl esters by **b**), batches of 13 g of potato stolons were minced and homogenized in 130 mL of 0.1 M potassium phosphate buffer pH 7.4 at 0°C. The homogenate was filtered through gauze, and 110 mL of the filtrate was diluted with 400 mL of potassium phosphate buffer and warmed at 26°C for 5 min. Linoleic acid (245 μM) was added, and the mixture was stirred at 26°C for 30 min. The material obtained by extraction with diethyl ether was subjected to RP-HPLC using a column of Nucleosil C_{18} 100-7 (250 × 10 mm) purchased from Macherey-Nagel (Düren, Germany) and a solvent system consisting of acetonitrile/water/2 M hydrochloric acid (55:45:0.013, by vol; 4 mL/min). The material collected was subjected to SP-HPLC using a column of Nucleosil 50-7 (250 × 10 mm) and a solvent system of 2-propanol/hexane/acetic acid (1.5:98.5:0.01, by vol; 4 mL/min). This procedure afforded **3a** as a colorless oil in 2–4% overall yield.

*Quantitative determination of **3a** in potato plant homogenates supplied with linoleic acid*. Different tissue types (2 g) from the potato plant were placed in ice-cold potassium phosphate buffer pH 7.4 (20 mL) and homogenized with an Ultra-Turrax. The homogenate was filtered through gauze, and an aliquot of the filtrate (5 mL) was prewarmed at 23°C for 5 min. Linoleic acid or 9(*S*)-HPOD (both 200 μM) was added, and the mixture was stirred for 10 min at 23°C. Ethanol (15 mL) containing 12-oxostearic acid (51.5 μg) was added, and the mixture was extracted with diethyl ether. Aliquots of the methyl-esterified material were directly subjected to gas chromatography–mass spectrometry (GC–MS) operated in the selected ion monitoring mode. The ions *m/z* 95 and 152 (typical for **3b**) and *m/z* 242 and 281 (typical for methyl 12-oxostearate) were used. The amounts of **3a** were calculated from the ratio of intensities of ions (*m/z* 95 + 152)/(*m/z* 242 + 281) and a standard curve constructed by analyzing mixtures of **3a** and 12-oxostearic acid in known proportions.

Chemical methods. Catalytic hydrogenation, oxidation with potassium permanganate, oxidative ozonolysis, and derivative preparation for GC–MS were performed as described earlier (13,16). Preparation of diastereomeric derivatives of cyclopentenones and steric analysis of these by gas–liquid chromatography (GLC) were carried out using a published procedure (15). Methyl-esterification was performed by brief (*ca.* 10 s) treatment with ethereal diazomethane.

Chromatographic and instrumental methods. The equipment and conditions used for RP-HPLC, SP-HPLC, GLC, GC–MS, ultraviolet (UV), and Fourier transform infrared (FTIR) spectrometry have been described in detail (13,16). Chiral phase HPLC (CP-HPLC) was carried out with a Chiralcel OB-H column (250 × 4.6 mm) purchased from Daicel Chemical Industries (Osaka, Japan) using mixtures of 2-propanol/hexane as the solvent and a flow rate of 0.5 mL/min. Nuclear magnetic resonance (NMR) spectra were recorded with a JEOL JNM-EX270 instrument. Deuteriochloroform containing 0.03% tetramethylsilane was used as the solvent.

RESULTS

Isolation and structure determination of oxidation products. (i) Incubation of linoleic acid. [1-^{14}C]Linoleic acid (200 μM) was stirred at 23°C for 10 min with whole homogenate of potato stolons, and the methyl-esterified product was subjected to SP-radio-HPLC. As seen in Figure 1A, four major radioactive compounds appeared, i.e., **1b** (3% of the recovered radioactivity; effluent volume, 2.5 mL), **3b** (13%; 6.3 mL), **7b** (59%; 7.5 mL), and **9b** (19%; 9.7 mL).

*(ii) Identification of compound **1b***. The UV spectrum of **1b** showed an absorption band with λ_{max} = 250 nm, suggesting a fatty acid divinyl ether derivative (14,16). The C-value (*cf.* Ref. 13), i.e., 19.41, and the mass spectrum were identical to those of methyl colneleate, a lipoxygenase product formed in tubers of potato (14). Results of catalytic hydrogenation and oxidative ozonolysis performed on compound **1b** (*cf.* Refs. 14,16) conclusively established its identity to methyl colneleate.

*(iii) Identification of compound **7b***. The UV spectrum of **7b** was featureless, whereas the FTIR spectrum showed strong absorption bands at 3480 (OH), 1739 (ester C=O), and 1716 cm^{-1} (ketone C=O). No significant absorption band was observed in the region 900–1000 cm^{-1}, thus excluding the presence of a *trans* double bond. The Me_3Si derivative of **7b** gave a C-value of 20.93 on GLC analysis, and the mass spectrum showed prominent ions at *m/z* 383 (3%; $M^+ - 15$; loss of $\cdot CH_3$), 259 [100; $Me_3SiO^+{=}CH{-}(CH_2)_7{-}COOCH_3$], 155 [37; $OHC{-}(CH_2)_7{-}C{\equiv}O^+$], 129 (9; $Me_3SiO^+{=}CH{-}CH{=}CH_2$), 109 (19), and 73 (47; Me_3Si^+). Identical results were obtained upon analysis of the methyl ester/Me_3Si derivative of 9-hydroxy-10-oxo-12(*Z*)-octadecenoic acid, an α-ketol fatty acid which is formed as the major product upon incubation of 9(*S*)-HPOD with corn seed AOS (9). An aliquot of **7b** (0.5 mg) was treated with sodium borohydride in methanol and subsequently subjected to catalytic hydrogenation. The product was identified by GLC and GC–MS as methyl 9,10-dihydroxystearate (mixture of *erythro*- and *threo*-isomers; authentic reference compounds were prepared by *cis*- and *trans*-hydroxylation, respectively, of methyl oleate). In another experiment, compound **7b** (1 mg) was derivatized with (−)-menthoxycarbonyl (MC) chloride, and the resulting MC derivative was subjected to $KMnO_4$ oxidation. The methyl-esterified product consisted of a main chiral fragment, i.e., the MC derivative of dimethyl 2-hydroxy-1,10-decanedioate. Steric analysis by GLC revealed that 92% of the sample was due to the 2(*R*)-hydroxy derivative and 8% 2(*S*)-hydroxy derivative. Steric analysis of compound **7b** also could be effected by resolution by CP-HPLC [solvent system, 2-propanol/hexane (6:94, vol/vol)]. Peaks due to the *R* (effluent volume, 10.0 mL) and *S* (9.0 mL) enantiomers in a 92:8 ratio were observed. Accordingly, **7b** was a mixture containing 92% methyl 9(*R*)-hydroxy-10-oxo-12(*Z*)-octadecenoate and 8% methyl 9(*S*)-hydroxy-10-oxo-12(*Z*)-octadecenoate.

*(iv) Identification of compound **9b***. Analysis of the Me_3Si derivative of **9b** by GC–MS showed a C-value (20.86) and a mass spectrum identical to those of the corresponding deriva-

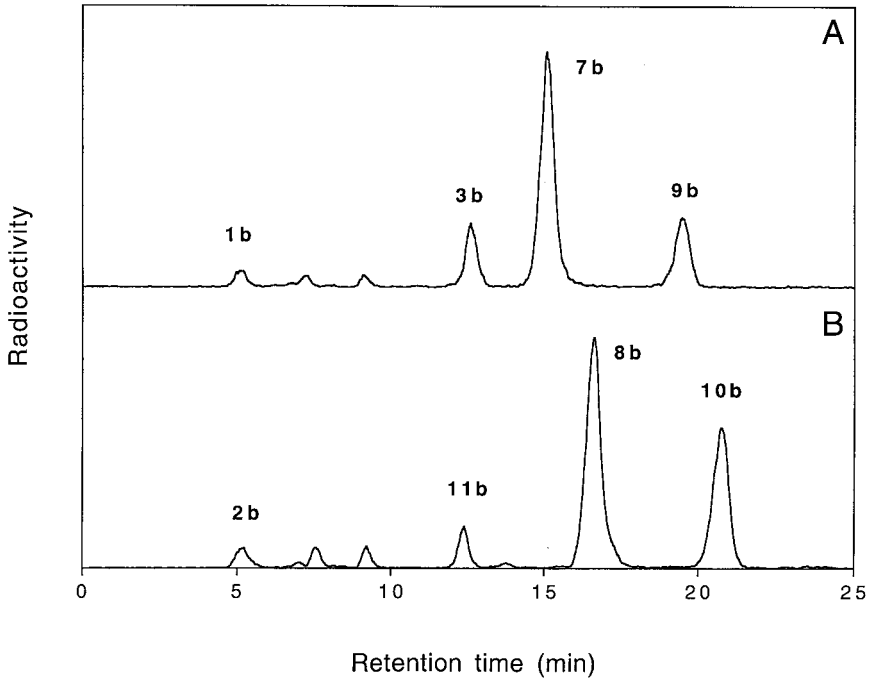

FIG. 1. Analysis by straight-phase radio high-performance liquid chromatography of methyl-esterified reaction products obtained following incubations of [1-^{14}C]linoleic acid (200 μM; panel A) and [1-^{14}C]linolenic acid (200 μM; panel B) at 23°C for 10 min with whole homogenate of stolons of potato. The column was eluted at a flow rate of 0.5 mL/min with 2-propanol/hexane (1:99, vol/vol). The structures of the compounds indicated are given in Scheme 1.

tive of methyl 10(*S*),11(*S*)-epoxy-9(*S*)-hydroxy-12(*Z*)-octadecenoate, an epoxy alcohol recently isolated following incubation of linoleic acid with a preparation of potato leaves (13). Further support for the identity of **9b** with this epoxy alcohol was provided by catalytic hydrogenation, which afforded methyl *erythro*-9,10-dihydroxystearate, and by results of mild acid-catalyzed hydrolysis, which afforded methyl 9(*S*),10(*R*),13(*R*)-trihydroxy-11(*E*)-octadecenoate and methyl 9(*S*),10(*R*),13(*S*)-trihydroxy-11(*E*)-octadecenoate as the main products (13).

*(v) Structure of compound **3b***. The UV spectrum of **3b** showed a strong absorption band with λ_{max} = 220 nm (solvent, ethanol) (Table 1), and the FTIR spectrum showed carbonyl absorption bands at 1739 (ester C=O) and 1709 cm^{-1} (ring ketone C=O) (Fig. 2). The mass spectrum showed ions at *m/z* 308 (3%; M^+), 277 (9; $M^+ - 31$; loss of $\cdot OCH_3$), 237 [2; M^+ - 71; loss of $\cdot(CH_2)_4CH_3$], 233 (3), 192 (5), 152 [93; $M^+ - 156$; cleavage β to ring carbonyl and elimination of CH_2=CH–$(CH_2)_5COOCH_3$], 123 (11), 109 (20), 95 [100; C_6H_7O; tentatively ascribed to loss of $\cdot(CH_2)_3CH_3$ from *m/z* 152], and 82 [34; C_5H_6O; loss of CH_2=CH–$(CH_2)_2CH_3$ from *m/z* 152]. These spectral data suggested that **3b** was built up by a cyclopentenone ring carrying two side chains, i.e., C_5H_{11} and C_7H_{14}–$COOCH_3$. Signals observed in the NMR spectrum of **3b** are given in Table 2. Protons belonging to a pentyl side chain (H14 to H18; 11 protons) and to a carboxylic ester side chain (H2 to H8; 14 protons) were readily discerned. Olefinic protons that were part of a cyclopentenone structure (H11 and H12; 2 protons) appeared at 6.15 and 7.71 ppm, whereas the protons at the side chain bearing carbons (H9 and H13; 2 protons) gave rise to signals at 2.32 and 2.96 ppm. The chemical shifts of the two last-mentioned signals were similar to those previously recorded for the H13 and H9 protons, respectively, of the methyl ester of natural 12-oxo-PDA (17), thus indicating a *cis* relationship between the two side chains in **3b**. Conclusive evidence for the *cis* relative configuration was provided by the alkali-promoted conversion of **3b** into the side-

TABLE 1
Ultraviolet and Gas Chromatographic Data of Cyclopentenones

Compound	λ_{max}[a] (nm)	C-value[b]
3b	220	20.17
4b	—	19.87
5b	221	19.77
6b	237	20.37
11b	217	20.11
12b	217	19.75

[a]Ultraviolet spectra were recorded on compounds dissolved in 99.5% ethanol.
[b]Gas–liquid chromatography was performed using a methylsilicone capillary column (25 m) operated at 230°C. Abbreviations: **3b**, 2-oxo-5-pentyl-3-cyclopentene-1-octanoic acid (1,5-*cis* isomer, methyl ester); **4b**, 2-oxo-5-pentylcyclopentane-1-octanoic acid (1,5-*cis* isomer, methyl ester); **5b**, 2-oxo-5-pentyl-3-cyclopentene-1-octanoic acid (1,5-*trans*-isomer, methyl ester); **6b**, 2-oxo-5-pentyl-1(5)-cyclopentene-1-octanoic acid (methyl ester); **11b**, 2-oxo-5-[2′(*Z*)-pentenyl]-3-cyclopentene-1-octanoic acid (1,5-*cis* isomer; methyl ester); **12b**, 2-oxo-5-[2′(*Z*)-pentenyl]-3-cyclopentene-1-octanoic acid (1,5-*trans* isomer; methyl ester).

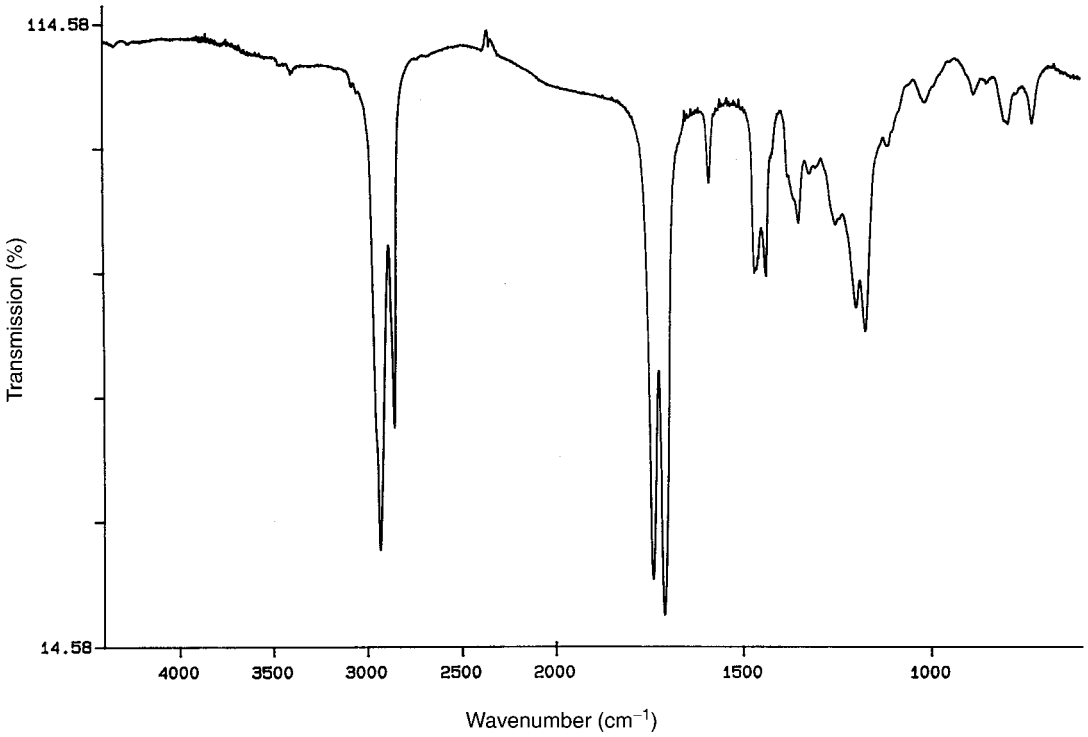

FIG. 2. Fourier transform infrared spectrum (film) of compound **3b**, (±)-2-oxo-5-pentyl-3-cyclopentene-1-octanoic acid, methyl ester.

chain *trans* isomer **5b**, and the NMR spectrum of this compound (see below).

Independent support for the structure of **3b** was provided by an experiment in which a sample (0.5 mg) was subjected to oxidative ozonolysis. The methyl-esterified product was analyzed by GC–MS and found to be due to a major fragment identified as trimethyl tetradecane-1,8,9-tricarboxylate by its mass spectrum, i.e., *m/z* 341 (63%; $M^+ - 31$; loss of $\cdot OCH_3$), 308 (12; $M^+ - 2 \times 32$), 270 [26; $M^+ - (70 + 32)$; loss of $CH_2{=}CH{-}(CH_2)_2CH_3$ plus CH_3OH], 216 [22; $M^+ - 156$; loss of $CH_2{=}CH{-}(CH_2)_5COOCH_3$], 184 (37; *m/z* 216 – 32), 152 (46; *m/z* 216

TABLE 2
Proton Nuclear Magnetic Resonance Data for Compounds 3b and 5b[a]

	Compound **3b**			Compound **5b**		
Carbon #	δ (ppm)	Multiplicity	*J* (Hz)	δ (ppm)	Multiplicity	*J* (Hz)
2	2.31	*t*	7.4	2.30	*t*	7.4
3	1.63	*m*		1.62	*m*	
4	1.28–1.36	*m*		1.27–1.35	*m*	
5	1.28–1.36	*m*		1.27–1.35	*m*	
6	1.28–1.36	*m*		1.27–1.35	*m*	
7	1.28–1.36	*m*		1.27–1.35	*m*	
8	1.38–1.48	*m*		—[b]		
9	2.32	*m*		1.94	*m*	
11	6.15	*dd*	5.9, 1.8	6.10	*dd*	5.7,1.8
12	7.71	*dd*	5.9, 2.7	7.60	*dd*	5.7, 2.5
13	2.96	*m*		2.58	*m*	
14	≈1.15, ≈1.70	*m*		—[b]		
15	1.28–1.36	*m*		1.27–1.35	*m*	
16	1.28–1.36	*m*		1.27–1.35	*m*	
17	1.28–1.36	*m*		1.27–1.35	*m*	
18	0.90	*t*	6.6	0.90	*t*	6.7
OCH_3	3.67	*s*		3.66	*s*	

[a]Proton nuclear magnetic resonance spectra were recorded at 270 MHz in $CDCl_3$ with tetramethylsilane as internal chemical shift reference.
[b]The absorptions due to H-8 and H-14 were hidden in other absorption bands and could not be adequately resolved. For abbreviations see Table 1.

– 2 × 32), and 55 (100). Formation of this product involved cleavage of the double bond of the five-membered ring followed by oxidative decarboxylation of the resulting 2-oxoacid.

The absolute stereochemistry of **3b** was studied in two ways. In one set of experiments, previously developed methodology for steric analysis of 12-oxo-PDA (11,15) and 12-oxo-PEA (12) involving reduction into epimeric cyclopentanols and derivatization of these with MC chloride was applied to a sample of **3b**. Analysis of the diastereomeric MC derivatives showed two peaks in a ratio of 50:50 corresponding to the 9(*R*),13(*R*) and 9(*S*),13(*S*) enantiomers of **3b**. In another experiment, **3b** was subjected to CP-HPLC using a solvent system of 2-propanol/hexane (1:9, vol/vol). Two peaks (8.6 and 10.6 mL effluent) appeared in a ratio of 50:50 (49:51 – 51:49 in different runs). On the basis of these results, compound **3a** was assigned the structure (±)-2-oxo-5-pentyl-3-cyclopentene-1-octanoic acid. The trivial name of **3a** will be 10-oxo-11-phytoenoic acid using the phytonoic acid (18) stem.

*(vi) Preparation and analysis of **5b***. Compound **3b** (4 mg) was treated with 0.1 M NaOH in 90% aqueous methanol at 23°C for 30 min. The reesterified product was purified by SP-HPLC to yield compound **5b**. Analysis of this material by UV spectroscopy showed an absorption band with λ_{max} (EtOH) = 221 nm. The FTIR spectrum showed carbonyl absorption bands at 1739 (ester C=O) and 1708 cm^{-1} (ring ketone C=O), and the mass spectrum was similar to that of **3b**. As seen in Table 1, the C-value of **5b** (19.77) was significantly lower than that of **3b** (20.17), suggesting that **5b** was a side-chain *trans* isomer (*cf.* Refs. 12,19). Conclusive evidence for the notion that alkali-treatment of **3b** resulted in reversible enolization at C-9 and formation of the thermodynamically more stable *trans* isomer **5b** was provided by the NMR spectrum of **5b** (Table 2). As seen, the protons attached to C-9 and C-13 gave rise to signals (1.94 and 2.58 ppm, respectively) that were shifted upfield compared to the corresponding signals of **3b** (2.32 and 2.96 ppm, respectively). Such an upfield shift is expected for a vicinal dialkylcyclopentane derivative in which the carbon chains are oriented *syn* with respect to the vicinal ring juncture proton (20), and therefore demonstrated that in the pair **3b** and **5b** the latter is the *trans* and the former is the *cis* side-chain stereoisomer. The NMR spectra of **3b** and **5b** were analogous to those earlier recorded on the *cis*- and *trans*-forms, respectively, of the methyl ester of 12-oxo-PDA (17).

*(vii) Preparation and analysis of **6b***. Compound **3b** (1 mg) was treated with 0.5 M NaOH in 50% aqueous methanol at 70°C for 1 h. The product was methyl-esterified and purified by SP-HPLC to afford **6b**. The UV spectrum of this compound showed a strong absorption band with λ_{max} (EtOH) = 237 nm, and the FTIR spectrum showed carbonyl absorption bands at 1739 (ester C=O) and 1699 cm^{-1} (ring ketone C=O) as well as an olefinic absorption band at 1640 cm^{-1} (C=C stretching of tetrasubstituted double bond conjugated to ring ketone). Analysis by GC–MS revealed a C-value of 20.37 and a mass spectrum showing prominent ions at *m/z* 308 (50%; M^+), 276 (37; M^+ – 32; loss of CH_3OH), 237 [59; M^+ – 71; loss of $\cdot(CH_2)_4CH_3$], 233 [100; M^+ – (43 + 32); loss of $\cdot(CH_2)_2CH_3$ plus CH_3OH], 205 (38; *m/z* 237 – 32), 123 (79), and 110 (93).

Oxidative ozonolysis performed on cyclopentenone **6b** followed by methyl-esterification afforded comparable amounts of dimethyl 1,9-nonanedioate and methyl 4-oxononanoate. The latter compound was identified by its mass spectrum, which showed prominent ions at *m/z* 155 (20%; M^+ – 31; loss of $\cdot OCH_3$), 130 (59; M^+ – 56; β-cleavage with loss of CH_2=CH–CH_2CH_3), 115 [67; M^+ – 71; α-cleavage with loss of $\cdot(CH_2)_4CH_3$], 98 (100; *m/z* 130 – 32), 71 (57), and 55 (75). The ozonolysis fragments were likely formed from **6b** by initial cleavage of the tetrasubstituted double bond followed by oxidative cleavage of the resulting α-dioxo structure.

*(viii) Preparation and analysis of **4b***. Compound **3b** (0.5 mg) was hydrogenated using platinum catalyst to provide dihydro derivative **4b** (C-value, 19.87) as well as a smaller amount of the corresponding side-chain *trans* derivative (C-value, 19.60). The mass spectra recorded on these compounds were similar and showed a molecular ion at *m/z* 310 (1%), as well as prominent ions at *m/z* 154 [18; M^+ – 156; β-cleavage with loss of CH_2=CH–$(CH_2)_5COOCH_3$], and 83 [100; C_5H_7O; loss of $\cdot(CH_2)_4CH_3$ from *m/z* 154].

(ix) Incubation of 9(S)-HPOD. Stirring 9(*S*)-HPOD (200 μM) at 23°C for 10 min with the whole homogenate preparation from potato stolons afforded compounds **1a**, **3a**, **7a**, and **9a** in a proportion closely similar to that observed following incubation of linoleic acid. The enzymes catalyzing hydroperoxide metabolism were mainly located in the particle fraction sedimenting at 105,000 × *g* as shown by experiments in which 9(*S*)-HPOD incubated with this fraction was converted into a mixture of **1a**, **3a**, **7a**, and **9a**. It seemed likely that an AOS was involved in the conversion of 9(*S*)-HPOD into α-ketol **7a** and cyclopentenone **3a**, and it was therefore of interest to study the metabolism of 9(*S*)-HPOD by another AOS. To this end, a suspension of the 105,000 × *g* particle fraction of corn seed homogenate was stirred with 9(*S*)-HPOD, and the methyl-esterified reaction product was analyzed by HPLC. As seen in Figure 3, the preparation of corn seed AOS produced a high yield of **7a** (analyzed as its methyl ester **7b**) but only a very small amount of cyclopentenone **3a** (analyzed as **3b**; ratio **3a**/**7a**, 0.005). The corresponding ratio observed with the AOS from potato stolons was 0.11 (Fig. 3).

(x) Incubation of linolenic acid and 9(S)-HPOT. As seen in Figure 1, linolenic acid (200 μM) was converted by the whole homogenate preparation of potato stolons in a way analogous to that of linoleic acid. In the methyl-esterified product, divinyl ether **2b** (4% of the product) and α-ketol **8b** (50%) were identified using the authentic reference compounds, whereas the structure of epoxy alcohol **10b** (31%) was tentatively assigned as methyl 10(*S*),11(*S*)-epoxy-9(*S*)-hydroxy-12(*Z*),15(*Z*)-octadecadienoate on the basis of analysis by GC–MS and on experiments in which isomeric trihydroxyesters (13) were isolated and characterized following mild acid-catalyzed conversion of **10b**. Compound **11b** (6%)

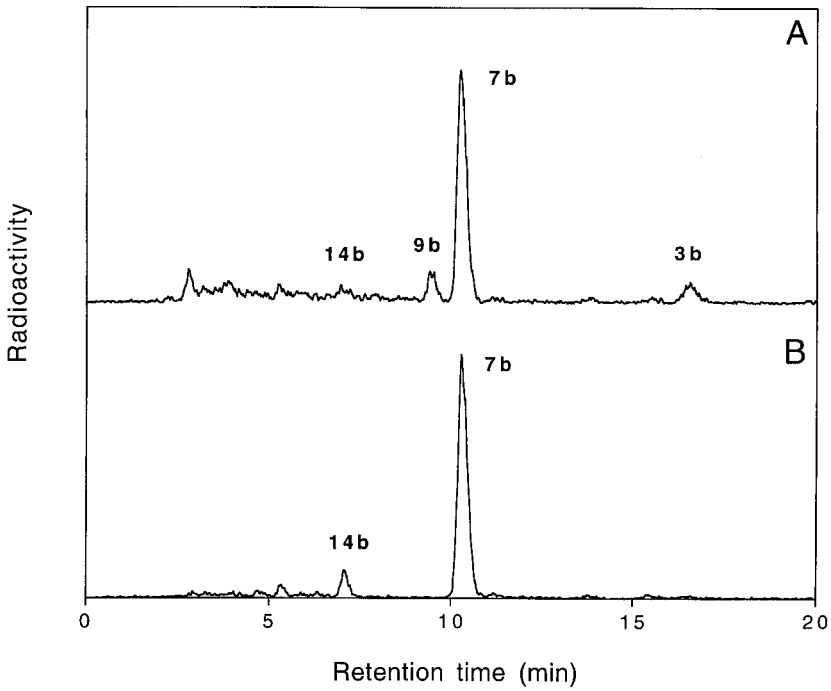

FIG. 3. Analysis by reversed-phase radio high-performance liquid chromatography of methyl-esterified reaction products obtained following incubations of [1-^{14}C]9(*S*)-hydroperoxy-10(*E*),12(*Z*)-octadecadienoic acid (100 μM) at 23°C for 2 min with the 105,000 × *g* particle fraction of homogenate of potato stolons (panel A) or with the corresponding fraction of homogenate of corn seed (panel B). The column was eluted at a flow rate of 1.5 mL/min with acetonitrile/water (65:35, vol/vol). The structures of the compounds indicated are given in Scheme 1. Compound **1b** was not eluted from the column during the time period used, and under the conditions used, compound **9b** suffered partial hydrolysis into more polar trihydroxy derivatives.

was a new cyclopentenone and was characterized as described below. A similar pattern of products was observed following incubation of 9(*S*)-HPOT.

*(xi) Structure of compound **11b***. The UV spectrum of **11b** showed a λ_{max} (EtOH) = 217 nm due to the cyclopentenone chromophore. Analysis by GC–MS showed a C-value of 20.11 and a mass spectrum exhibiting prominent ions at *m/z* 306 (1%; M^+), 275 (3; $M^+ - 31$; loss of $\cdot OCH_3$), 238 (4; $M^+ - 68$; loss of C_5H_8), 150 [9; $M^+ - 156$; β-cleavage with loss of $CH_2{=}CH{-}(CH_2)_5COOCH_3$], 121 (15), and 82 (100; C_5H_6O; loss of C_5H_8 from *m/z* 150). Treatment of **11b** with 0.1 M sodium hydroxide resulted in epimerization at C-9 and, following reesterification, to the formation of the side-chain *trans* derivative **12b**. As would be expected (12,19), the mass spectrum of **12b** was very similar to that of **11b**, but the C-value was lower (Table 1). Catalytic hydrogenation of **11b** afforded a tetrahydro derivative that was identical in all respects to **4b** prepared by hydrogenation of **3b**. The double bond in the pentenyl side chain of **11b** was localized by oxidative ozonolysis, which afforded tetramethyl decane-1,8,9,10-tetracarboxylate as the predominant product. Prominent ions in the mass spectrum of this compound were observed at *m/z* 343 (100%; $M^+ - 31$; loss of $\cdot OCH_3$), 310 (48; $M^+ - 2 \times 32$); 229 [32; $M^+ - 145$; cleavage at C-8/C-9 and elimination of $\cdot CH(COOCH_3){-}CH_2COOCH_3$], 218 [38; $M^+ - 156$; β-cleavage with loss of $CH_2{=}CH{-}(CH_2)_5COOCH_3$], 186 (70; *m/z* 218 – 32), 146 {39; cleavage at C-8/C-9 and charge retention in the fragment $[CH_3OOC{-}CH_2{-}CH{=}COH(OCH_3)]^+$}, 114 (43; *m/z* 146 – 32), and 55 (64).

Analysis of **11b** by CP-HPLC [solvent system, 2-propanol/hexane (2:8, vol/vol)] showed two peaks in a 1:1 ratio (7.5 and 10.0 mL), thus demonstrating that **11b** was a racemate due to equal parts of the 9(*R*),13(*R*) and 9(*S*),13(*S*) enantiomers. Based on the results mentioned, **11a** was assigned the structure (±)-2-oxo-5-[2′(*Z*)-pentenyl]-3-cyclopentene-1-octanoic acid.

Trapping experiments. (i) Incubations in the presence of GSH-px. Linoleic acid (200 μM) was stirred with a suspension of the 105,000 × *g* particle fraction of homogenate of potato stolons in the presence of GSH-px (2 U/mL) and GSH (2 mM). Analysis of the methyl-esterified product by SP-HPLC showed a major peak accounting for 90% of the total radioactivity. This material cochromatographed with the methyl ester of 9-HOD and was conclusively identified as this compound by analysis of the Me_3Si derivative by GC–MS. Only trace amounts (<1%) of the regioisomeric 13-HOD methyl ester could be detected. Analysis of the 9-HOD methyl ester by CP-HPLC revealed it to be the natural *S* enantiomer.

(ii) Trapping of an allene oxide with methanol. 9(*S*)-HPOD (63 μM) was stirred at 0°C for 30 s with 2 mL of a suspen-

sion of the 105,000 × *g* particle fraction of homogenate of potato stolons. Methanol (40 mL) was added, and the mixture was kept at 23°C for 1 h. Analysis of the reaction product by SP-HPLC [solvent system, 2-propanol/hexane/acetic acid (1:99:0.01, by vol)] revealed the presence of compound **13a** (16% of the total radioactivity; 9.2 mL effluent)) in addition to α-ketol **7a** (51%; 24.8 mL) and other minor compounds. Formation of **13a** successively decreased when longer times of incubations were used and was not noticeable at 5 min of incubation. Its identity with 9-methoxy-10-oxo-12(*Z*)-octadecenoic acid was ascertained using GC–MS analysis of the methyl ester with the authentic compound as reference. The mass spectrum of **13b** showed prominent ions at *m/z* 340 (2%; M^+), 309 (5; $M^+ - 31$; loss of $\cdot OCH_3$), 201 [100; $CH_3O^+{=}CH{-}(CH_2)_7COOCH_3$], 169 (24; *m/z* 201 – 32), 137 (44; *m/z* 201-2 × 32), and 71 (35). Analysis of **13b** by CP-HPLC [solvent system, 2-propanol/hexane (4:96, vol/vol)] showed separation into two enantiomers, tentatively assigned as methyl 9(*R*)-methoxy-10-oxo-12(*Z*)-octadecenoate (76%; 7.5 mL effluent) and methyl 9(*S*)-methoxy-10-oxo-12(*Z*)-octadecenoate (24%; 6.5 mL). Steric analysis of **13b** obtained as a trapping product in the corn seed AOS-catalyzed reaction gave a similar enantiomeric composition, i.e., 73:27.

As shown in previous work, α-methoxy ketones are formed as trapping products of unstable allene oxides (8,9), and the transient appearance of **13a** indicated the formation of 9(*S*),10-epoxy-10,12(*Z*)-octadecadienoic acid from 9(*S*)-HPOD catalyzed by potato stolon AOS. The half-life of the allene oxide estimated from the rate of disappearance of **13a** was 44 s (0°C; pH 7.4). The half-life of the corresponding allene oxide generated in the corn seed AOS system was 33 s, a value almost identical to that (34 s) previously published (9).

(iii) Intramolecular trapping of an allene oxide—formation of macrolactones. 9(*S*)-HPOD (100 μM) was stirred at 0°C for 30 s with 11 mL of a suspension of the 105,000 × *g* particle fraction of homogenate of potato stolons. Ice-cold acetonitrile (220 mL) was added, and the mixture was kept at 0°C for 1 h. The mixture was extracted with hexane (no acidification), and the product was subjected to SP-HPLC using a solvent system of 2-propanol/hexane (0.2:99.8, vol/vol). Two peaks of nonpolar radioactive materials appeared, i.e., **16** (3.9 mL effluent; 25%) and **15** (6.2 mL; 75%). The mass spectrum of **16** showed prominent ions at *m/z* 294 (13%; M^+), 223 [4; $M^+ - 71$; loss of $\cdot(CH_2)_4CH_3$], 169 (13), 98 (100), and 55 (63), whereas the mass spectrum of **15** exhibited ions at *m/z* 294 (2%; M^+), 183 [10; $M^+ - 111$; loss of $\cdot CH_2{-}CH{=}CH{-}(CH_2)_4CH_3$], 155 [100; $M^+ - 139$; loss of $\cdot CO{-}CH_2{-}CH{=}CH{-}(CH_2)_4CH_3$], 109 (38), and 55 (39). Authentic macrolactones **15** and **16**, which were prepared by short-time incubation of 9(*S*)-HPOD with corn seed AOS (9), gave identical analytical results. Interestingly, a significant difference between the proportions of **15**/**16** was noted, i.e., 75:25 using the potato stolon AOS and 89:11 using the corn seed AOS.

*Formation of **3a** and **14a** under various conditions*. *(i) Effect of pH, temperature, and substrate concentration*. In a series of incubations, 9(*S*)-HPOD was stirred with the 105,000 × *g* particle fraction from homogenate of potato stolons or with the corresponding fraction from corn seed homogenate. The compositions of the reaction products were determined by SP-radio-HPLC. As seen in Table 3, formation of **3a** (relative to **7a**) was temperature- and pH-dependent. On the other hand, diluting the enzyme preparation 10-fold, or changing the substrate concentration in the range 30–300 μM, did not alter the ratio **3a**/**7a**.

γ-Ketols are significant products in incubations with corn seed AOS (8,15). Although the γ-ketol **14a** accounted for only 2% of the recovered radioactivity in the potato stolon incubations, it appeared to be of interest to include this AOS product in the analyses and to study the pH-dependency of its formation. γ-Ketols can give a by-product when methyl-esterified by diazomethane (21), and the radio-HPLC analysis was accordingly carried out on the nonesterified incubation products. As seen in Table 3, formation of **14a** showed a pH-dependency in agreement with its postulated formation from the protonated allene oxide (22). The reason for the lower ratio

TABLE 3
Formation of Allene Oxide Synthase Products Under Various Conditions

	Parameter changed[a]						**3a**	**7a**
Tissue	Concentration	Temperature	pH	Time	**3a/7a**	**14a/7a**	Enantiomers, *S/R*	
Potato	—	—	—	—	0.11	0.04	50:50	9:91
Potato	—	0°C	—	5 min	0.03	—	50:50	6:94
Potato	—	37°C	—	—	0.19	—	49:51	11:89
Potato	—	—	6.7	—	0.08	0.08	—	—
Potato	—	—	8.0	—	0.14	0.02	—	—
Potato	30 μM	—	—	—	0.11	—	49:51	9:91
Potato	300 μM	—	—	—	0.11	—	50:50	10:90
Potato, 1:10	—	—	—	—	0.11	—	50:50	10:90
Corn	—	—	—	—	0.005	0.11	—	34:66
Corn	—	0°C	—	5 min	<0.005	—	—	26:74

[a]Standard conditions: 9(*S*)-Hydroperoxy-10(*E*),12(*Z*)-octadecadienoic acid (100 μM) was stirred for 2 min at 23°C with a suspension of the 105,000 × *g* particle fraction of homogenate of potato stolons, pH 7.4. Abbreviations: **3a**, 2-oxo-5-pentyl-3-cyclopentene-1-octanoic acid (1,5-*cis* isomer); **7a**, 9-hydroxy-10-oxo-12(*Z*)-octadecenoic acid; **14a**, 13-hydroxy-10-oxo-11(*E*)-octadecenoic acid .

TABLE 4
Formation of Compound 3a in Homogenates of Tissues from the Potato Plant[a]

Tissue	Compound **3a** (nmol/g)	
	Linoleic acid incubation	9(*S*)-HPOD incubation
Stolons	79.4 ± 9.5	84.3 ± 6.4
Tubers, 5–10 mm diam.	20.7 ± 7.1	24.7 ± 4.3
Tubers, 30–40 mm diam.	7.4 ± 2.8	7.7 ± 2.8
Leaves	<1.5	<1.5
Roots	159.0 ± 21.8	172.8 ± 15.5

[a]For determination of **3a**, 2 g of tissue was minced and homogenized in 20 mL of 0.1 M potassium phosphate buffer pH 7.4. Five milliliters of the filtrate were prewarmed at 23°C and subsequently stirred with 200 μM linoleic acid or 200 μM 9(*S*)-HPOD for 10 min. The amounts of **3a** were determined by gas chromatography–mass spectrometry using 12-oxostearic acid as internal standard. For abbreviation see Table 3.

14a/**7a** in the potato stolon incubation compared to the corn seed incubation is unknown.

(*ii) Stereochemical compositions of **3a** and **7a***. Compounds **3b** and **7b** obtained from the various incubations shown in Table 3 were subjected to steric analysis using CP-HPLC. As seen in Table 3, cyclopentenone **3a** was consistently formed as a racemate, whereas the α-ketol **7a** was enriched with respect to the *R* enantiomer. The latter result was in agreement with its mode of formation from the allene oxide partly by S_N2 type of hydrolysis at C-9 (8,9,22,23). Interestingly, **7a** generated in the potato stolon system had an enantiomeric purity that was significantly higher than that of **7a** produced in the corn seed system (Table 3).

*(iii) Formation of **3a** in different parts of the potato plant*. Whole homogenate preparations (1:10, wt/vol; 5 mL) of different parts of the potato plant were stirred with linoleic acid or 9(*S*)-HPOD (200 μM), and the amounts of **3a** were determined by GC–MS. As seen in Table 4, the highest levels were obtained with homogenates of roots and stolons. Homogenate of potato tubers gave smaller amounts, and leaves produced no detectable levels of **3a**. The fact that multiple enzymes metabolizing 9(*S*)-HPOD were present in the homogenates used meant that the amounts of **3a** did not necessarily reflect the capacity of formation of **3a**. Rather, the values indicated the partitioning of 9(*S*)-HPOD between different hydroperoxide-degrading enzymes present in the tissue preparations.

DISCUSSION

The present study is mainly concerned with the metabolism of linoleic acid by an enzyme preparation from potato stolons. The initial reaction was catalyzed by a 9-lipoxygenase (9-LOX) and resulted in the formation of 9(*S*)-HPOD. Three enzymes, i.e., divinyl ether synthase, epoxy alcohol synthase and AOS, catalyzed the further metabolism of 9(*S*)-HPOD to afford colneleic acid (**1a**), the epoxy alcohol 10(*S*),11(*S*)-epoxy-9(*S*)-hydroxy-12(*Z*)-octadecenoic acid (**9a**), and the allene oxide 9(*S*),10-epoxy-10,12(*Z*)-octadecadienoic acid, respectively (Scheme 2). Of these compounds, colneleic acid was originally obtained following incubation of linoleic acid with a preparation of potato tubers (14), and the epoxy alcohol was recently isolated as one of the major products of linoleic acid metabolism in homogenate of potato leaves (13). The allene oxide, like allene oxides derived from the 13-hydroperoxides of linoleic and linolenic acids (8,23), was highly unstable and had an estimated half-life at 0°C of 44 s. No attempts at its isolation were made; however, its presence was proved by trapping experiments with methanol, which afforded 9-methoxy-10-oxo-12(*Z*)-octadecenoic acid. Furthermore, when brief incubations of 9(*S*)-HPOD were carried out at 0°C and interrupted by the addition of 20 vol of the nonhydroxylic solvent acetonitrile, the two macrolactones **15** and **16** were formed. These compounds had been encountered in an earlier study as products formed by intramolecular trapping of the allene oxide structure (9). Under normal conditions for incubation, further conversion of the allene oxide resulted in the formation of compounds **7a** and **3a** (Scheme 2). α-Ketol **7a** was originally isolated and characterized in a study of linoleic acid metabolism in corn seed homogenate (24) and was later shown to be a product formed by hydrolysis of an allene oxide generated by corn seed AOS (9). Cyclopentenone **3a**, a new oxylipin, was fully characterized by chemical and spectral methods. Steric analysis by NMR spectroscopy, CP-HPLC, and GLC demonstrated that the two appendages of the five-membered ring had the *cis* relative configuration and that the compound was a racemate consisting of equal parts of the 9(*R*),13(*R*) and 9(*S*),13(*S*) enantiomers. Compounds related to **3a** had been encountered previously in studies of the formation of cyclopentenones employing the hydroperoxides 9(*S*)-hydroperoxy-6(*Z*),10(*E*),12(*Z*)-octadecatrienoic acid (5,25) and 9(*R*,*S*)-hydroperoxy-10(*E*),12(*E*)-octadecadienoic acid (26), i.e., two hydroperoxides which are not typical constituents of plant tissue. In the present study, natural linoleic acid 9-hydroperoxide served as the precursor of cyclopentenone, and this result was extended to linolenic acid and its 9-hydroperoxide, which were metabolized to cyclopentenone **11a**. This compound [10-oxo-11,15(*Z*)-phytodienoic acid] was a regioisomer of the jasmonate precursor 12-oxo-10,15(*Z*)-phytodienoic acid, differing from this compound with respect to the positions of the keto group and the double bond in the five-membered ring.

Studies of the mode of formation of cyclopentenone **3a** and α-ketol **7a** were carried out by performing incubations of 9(*S*)-HPOD with the 105,000 × *g* particle fraction of homogenate of potato stolons. As seen in Table 3, formation of **3a**, as monitored by the ratio **3a**/**7a**, was temperature- and pH-dependent. Interestingly, when different concentrations of 9(*S*)-HPOD (30–300 μM) were used, thus providing varying concentrations of the corresponding allene oxide, the ratio **3a**/**7a** remained unchanged. Likewise, diluting the enzyme preparation 10-fold did not affect the ratio. These results, and the fact that **3a** was isolated as a racemate, suggested that **3a** (and **11a**) were formed from their allene oxide precursors by way of nonenzymatic cyclization. This conclusion was unexpected in view of the fact that earlier reported cases of nonen-

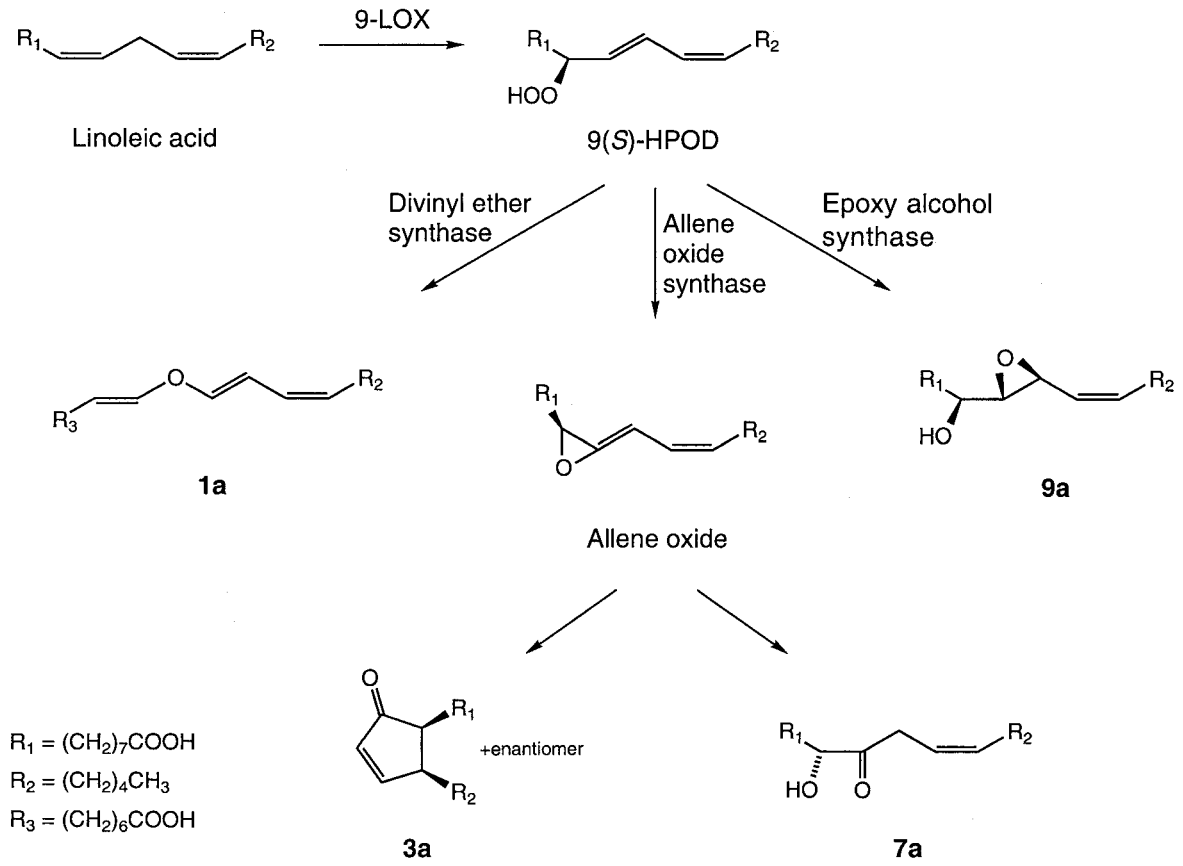

SCHEME 2

zymatic cyclization of fatty acid allene oxides had been restricted to allene oxides possessing a double bond in the β,γ-position relative to the epoxide group (5,15,23,27). In agreement with this notion, it was confirmed in the present study that the allene oxide generated from 9(*S*)-HPOD using the previously studied AOS from corn seeds (8,9,15) was a very poor precursor of cyclopentenone (Table 3, Fig. 3). Interestingly, the potato stolon and corn seed AOS-catalyzed reactions differed also in another way, i.e., with respect to the enantiomeric composition of the α-ketol product (Table 3). The large proportion of the *R* enantiomer in **7a** produced by the potato stolon AOS indicated that this α-ketol was formed from its allene oxide precursor largely by an S_N2-type of hydrolysis (*cf.* Refs. 8,23). A third difference between the potato stolon and corn seed AOS preparations was the different extent of formation of the γ-ketol **14a** (Table 3). Further studies are needed in order to explain these results. It can only be speculated that a configurational or conformational property in the allene oxide generated by the potato stolon AOS exists, or is induced, which has consequences for the further conversion of the allene oxide.

It seems likely that the cyclopentenones **3a** and **11a** can be further converted in plant tissue in the same way as 12-oxo-PDA, i.e., by reduction of the ring double bond and β-oxidation. Such transformations as well as the biological properties of the new cyclopentenones are being studied (Kod, Y., and Hambeg, M., unpublished data).

ACKNOWLEDGMENTS

Gunvor Hamberg is thanked for expert technical assistance. The author is indebted to Prof. Per-Erik Jansson and Reine Eserstam (Clinical Research Center, Huddinge University Hospital, Stockholm) for their help with the NMR analyses and to Dr. A.N. Grechkin (Institute of Biochemistry and Biophysics, Russian Academy of Sciences, Kazan, Russia) and Prof. B.A. Hess (Department of Chemistry, Vanderbilt University, Nashville, TN) for discussion of possible mechanisms of allene oxide cyclization into cyclopentenones. This work was supported by the Swedish Medical Research Council (Proj. No. 03X-5170) and by Vesical Co. (Stockholm).

REFERENCES

1. Creelman, R.A., and Mullet, J.E. (1997) Biosynthesis and Action of Jasmonates in Plants, *Annu. Rev. Plant Physiol. Plant Mol. Biol. 48*, 355–381.
2. Vick, B.A., and Zimmerman, D.C. (1983) The Biosynthesis of Jasmonic Acid: A Physiological Role for Plant Lipoxygenase, *Biochem. Biophys. Res. Commun. 111*, 470–477.
3. Mueller, M.J. (1997) Enzymes Involved in Jasmonic Acid Biosynthesis, *Physiol. Plant. 100*, 653–663.
4. Grechkin, A. (1998) Recent Developments in Biochemistry of the Plant Lipoxygenase Pathway, *Prog. Lipid Res. 37*, 317–352.

5. Ziegler, J., Wasternack, C., and Hamberg, M. (1999) On the Specificity of Allene Oxide Cyclase, *Lipids 34*, 1005–1015.
6. Weber, H., Vick, B.A., and Farmer, E.E. (1997) Dinor-oxo-phytodienoic Acid: A New Hexadecanoid Signal in the Jasmonate Family. *Proc. Natl. Acad. Sci. USA 94*, 10473–10478.
7. Matthew, J.A., Chan, H.W.-S., and Galliard, T. (1977) A Simple Method for the Preparation of Pure 9-D-Hydroperoxide of Linoleic Acid and Methyl Linoleate Based on the Positional Specificity of Lipoxygenase in Tomato Fruit, *Lipids 12*, 324–326.
8. Hamberg, M. (1987) Mechanism of Corn Hydroperoxide Isomerase: Detection of 12,13(*S*)-Oxido-9(*Z*),11-octadecadienoic Acid, *Biochim. Biophys. Acta 920*, 76–84.
9. Hamberg, M., and Hughes, M.A. (1988) Biosynthesis and Conversions of Fatty Acid Allene Oxides, in *Advances in Prostaglandin, Thromboxane, and Leukotriene Research* (Samuelsson, B., Wong, P.Y.-K., and Sun, F.F., eds.), Vol. 19, pp. 64–69, Raven Press, New York.
10. Hamberg, M. (1988) Fatty Acid Allene Oxides II. Formation of Two Macrolactones from 12,13(*S*)-Epoxy-9(*Z*),11-octadecadienoic Acid, *Chem. Phys. Lipids 46*, 235–243.
11. Hamberg, M., Miersch, O., and Sembdner, G. (1988) Absolute Configuration of 12-Oxo-10,15(*Z*)-phytodienoic Acid, *Lipids 23*, 521–524.
12. Hamberg, M., and Hughes, M.A. (1988) Fatty Acid Allene Oxides. III. Albumin-Induced Cyclization of 12,13(*S*)-Epoxy-9(*Z*),11-octadecadienoic Acid, *Lipids 23*, 469–475.
13. Hamberg, M. (1999) An Epoxy Alcohol Synthase Pathway in Higher Plants: Biosynthesis of Antifungal Trihydroxy Oxylipins in Leaves of Potato, *Lipids 34*, 1131–1142.
14. Galliard, T., and Phillips, D.R. (1972) The Enzymic Conversion of Linoleic Acid into 9-(nona-1′,3′-dienoxy)Non-8-enoic Acid, a Novel Unsaturated Ether Derivative Isolated from Homogenates of *Solanum tuberosum* Tubers, *Biochem. J. 129*, 743–753.
15. Hamberg, M., and Fahlstadius, P. (1990) Allene Oxide Cyclase: A New Enzyme in Plant Lipid Metabolism, *Arch. Biochem. Biophys. 276*, 518–526.
16. Hamberg, M. (1998) A Pathway for Biosynthesis of Divinyl Ether Fatty Acids in Green Leaves, *Lipids 33*, 1061–1071.
17. Baertschi, S.W., Ingram, C.D., Harris, T.M., and Brash, A.R. (1988) Absolute Configuration of *cis*-12-Oxophytodienoic Acid of Flaxseed: Implications for the Mechanism of Biosynthesis from the 13(*S*)-Hydroperoxide of Linolenic Acid, *Biochemistry 27*, 18–24.
18. Zimmerman, D.C., and Feng, P. (1978) Characterization of a Prostaglandin-Like Metabolite of Linolenic Acid Produced by a Flaxseed Extract, *Lipids 13*, 313–316.
19. Vick, B.A., Zimmerman, D.C., and Weisleder, D. (1979) Thermal Alteration of a Cyclic Fatty Acid Produced by a Flaxseed Extract, *Lipids 14*, 734–740.
20. Anteunis, M., and Danneels, D. (1975) Stereochemical Aspects of Proton Chemical Shifts III. Configurational Assignments in Pentacyclic Systems Without Recourse to a Karplus Equation, *Org. Magn. Reson. 7*, 345–348.
21. Abian, J., Gelpi, E., and Pages, M. (1991) Effect of Abscisic Acid on the Linoleic Acid Metabolism in Developing Maize Embryos, *Plant Physiol. 95*, 1277–1283.
22. Grechkin, A.N., Kuramshin, R.A., Safonova, E.Y., Latypov, S.K., and Ilyasov, A.V. (1991) Formation of Ketols from Linolenic Acid 13-Hydroperoxide *via* Allene Oxide. Evidence for Two Distinct Mechanisms of Allene Oxide Hydrolysis, *Biochim. Biophys. Acta 1086*, 317–325.
23. Brash, A.R., Baertschi, S.W., Ingram, C.D., and Harris, T.M. (1988) Isolation and Characterization of Natural Allene Oxides: Unstable Intermediates in the Metabolism of Lipid Hydroperoxides, *Proc. Natl. Acad. Sci. USA 85*, 3382–3386.
24. Gardner, H.W. (1970) Sequential Enzymes of Linoleic Acid Oxidation in Corn Germ: Lipoxygenase and Linoleate Hydroperoxide Isomerase, *J. Lipid Res. 11*, 311–321.
25. Vick, B.A., Feng, P., and Zimmerman, D.C. (1980) Formation of 12-[^{18}O]Oxo-*cis*-10,*cis*-15-Phytodienoic Acid from 13-[^{18}O]-Hydroperoxylinolenic Acid by Hydroperoxide Cyclase, *Lipids 15*, 468–471.
26. Grechkin, A.N., and Hamberg, M. (1999) Formation of Cyclopentenones from All-(*E*) Hydroperoxides of Linoleic Acid *via* Allene Oxides. New Insight into the Mechanism of Cyclization, *FEBS Lett. 466*, 63–66.
27. Grechkin, A.N. (1994) Cyclization of Natural Allene Oxide Fatty Acids. The Anchimeric Assistance of β,γ-Double Bond Beside the Oxirane and the Reaction Mechanism, *Biochim. Biophys. Acta 1213*, 199–206.

[Received January 6, 2000, and in revised form February 18, 2000; revision accepted March 1, 2000]

Fatty Acid-Specific, Regiospecific, and Stereospecific Hydroxylation by Cytochrome P450 (CYP152B1) from *Sphingomonas paucimobilis*: Substrate Structure Required for α-Hydroxylation

Isamu Matsunaga[a,*], Tatsuo Sumimoto[a,b], Atsuo Ueda[a], Emi Kusunose[a], and Kosuke Ichihara[a]

[a]Department of Molecular Regulation, Osaka City University Medical School, Osaka 545-8585, Japan, and [b]Osaka Prefectural Institute of Public Health, Osaka 537-0025, Japan

ABSTRACT: Fatty acid α-hydroxylase from *Sphingomonas paucimobilis* is an unusual cytochrome P450 enzyme that hydroxylates the α-carbon of fatty acids in the presence of H_2O_2. Herein, we describe our investigation concerning the utilization of various substrates and the optical configuration of the α-hydroxyl product using a recombinant form of this enzyme. This enzyme can metabolize saturated fatty acids with carbon chain lengths of more than 10. The K_m value for pentadecanoic acid (C_{15}) was the smallest among the saturated fatty acids tested (C_{10}–C_{18}) and that for myristic acid (C_{14}) showed similar enzyme kinetics to those seen for C_{15}. As shorter or longer carbon chain lengths were used, K_m values increased. The turnover numbers for fatty acids with carbon chain lengths of more than 11 were of the same order of magnitude (10^3 min^{-1}), but the turnover number for undecanoic acid (C_{11}) was less. Dicarboxylic fatty acids and methyl myristate were not metabolized, but monomethyl hexadecanedioate and ω-hydroxypalmitic acid were metabolized, though with lower turnover values. Arachidonic acid was a good substrate, comparable to C_{14} or C_{15}. The metabolite of arachidonic acid was only α-hydroxyarachidonic acid. Alkanes, fatty alcohols, and fatty aldehydes were not utilized as substrates. Analysis of the optical configurations of the α-hydroxylated products demonstrated that the products were *S*-enantiomers (more than 98% enantiomerically pure). These results suggested that this P450 enzyme is strictly responsible for fatty acids and catalyzes highly stereo- and regioselective hydroxylation, where structure of ω-carbon and carboxyl carbon as well as carbon chain length of fatty acids are important for substrate–enzyme interaction.

Paper no. L8370 in *Lipids 35*, 365–371 (April 2000).

α-Hydroxy fatty acids are found in the sphingolipids of a wide variety of organisms. *Sphingomonas paucimobilis* is a bacterium having a large amount of sphingolipids, most of which contain α-hydroxymyristic acid as an acyl moiety (1). To clarify biosynthesis of α-hydroxy fatty acids, we have used *S. paucimobilis* as a source of fatty acid α-hydroxylase and identified this enzyme and its gene (2). Sequence analysis of the fatty acid α-hydroxylase gene and spectral analysis of the recombinant enzyme revealed that this enzyme is a member of cytochrome P450 (P450) superfamily. Interestingly, this P450 enzyme [designated $P450_{SP\alpha}$ here; tentatively given systematic name of CYP 152B1 by Dr. David Nelson, University of Tennessee Medical Center (personal communication)] oxidizes fatty acids with high turnover rates in the presence of H_2O_2, where an oxygen atom from H_2O_2 is introduced into the α-carbon of fatty acids to form the corresponding α-hydroxy fatty acids (3). Moreover, we demonstrated that $P450_{SP\alpha}$ specifically required H_2O_2, but not other hydroperoxides such as cumene hydroperoxide (4).

Many P450 enzymes have been isolated from various organisms, including both prokaryotes and eukaryotes, and then characterized. P450 enzymes constitute a superfamily, members of which catalyze hydroxylation of a variety of endogenous substances (e.g., fatty acids) and xenobiotics (e.g., drugs and other hydrocarbon derivatives in the environment). In terms of the hydroxylation of fatty acids by P450 enzymes, ω-hydroxylation has been well studied. From these studies, researchers have determined that some fatty acid-hydroxylating P450 can, to some extent, metabolize hydrocarbon substrates other than fatty acids, i.e., the substrate specificity may not be specifically limited. In fact, some members of the CYP 4 and CYP 52 families are able to ω-hydroxylate alkanes, fatty alcohols, and fatty aldehydes, as well as fatty acids. CYP 4A1, which ω-hydroxylates fatty acids such as lauric acid, is also able to metabolize lauroyl alcohol but not dodecane (5). CYP 4B1, which is most commonly recognized as a xenobiotics-metabolizing P450 enzyme, hydroxylates *n*-alkanes as well as fatty acids (6). CYP 52A3, isolated from an alkane-assimilating yeast, is able to metabolize hexadecane, 1-hexadecanol, hexadecanal, hexadecanoic acid, and 16-hydroxyhexadecanoic acid (7).

Regioselectivity of the hydroxylated carbon of fatty acids appears to be loosely restricted. For example, CYP102A, which is a bacterial P450 enzyme metabolizing fatty acids, attacks not only the n-1, n-2, or n-3 carbon of fatty acids to produce hydroxy fatty acids but also double bonds of polyunsaturated fatty acids to produce epoxy fatty acids (8). In contrast to

*To whom correspondence should be addressed at Department of Molecular Regulation. Osaka City University Medical School, 1-4-3 Asahi-machi, Abeno-ku, Osaka 545-8585, Japan. E-mail: matsunagai@med.osaka-cu.ac.jp

Abbreviations: *ADAM*, 9-anthryldiazomethane; GC–MS, gas chromatography–mass spectrometry; HPLC, high-performance liquid chromatography; P450, cytochrome P450; $P450_{SP\alpha}$, fatty acid α-hydroxylating P450 enzyme from *Sphingomonas paucimobilis*; TMS, trimethylsilyl.

regioselectivity, ω-hydroxylation of fatty acid by P450 is enantiomerically restricted. In the case of CYP102A, highly stereoselective oxidation of polyunsaturated fatty acids such as arachidonic acid has been reported (8).

In a previous study (4), we observed that $P450_{SP\alpha}$ metabolizes several saturated and monounsaturated fatty acids. However, it remained to be elucidated whether $P450_{SP\alpha}$ was able to metabolize other hydrocarbon derivatives such as long-chain alkanes, fatty alcohols, fatty aldehydes, and xenobiotics, and whether stereospecific hydroxylation occurred. In this study, we investigated whether various hydrocarbon derivatives were utilized as substrates of $P450_{SP\alpha}$. Additionally, we performed kinetic studies to elucidate the affinity of the substrate for the enzyme and, moreover, investigated the optical configurations of the α-hydroxyl products by the reaction of $P450_{SP\alpha}$. Based on the results obtained, we discuss what $P450_{SP\alpha}$ requires structurally of its substrates.

MATERIALS AND METHODS

Materials. 1,14-Tetradecanedioic acid, 1,16-hexadecanedioic acid, monomethyl hexadecanedioate, and 9-anthryldiazomethane (ADAM) were purchased from Funakoshi Co., Ltd. (Tokyo, Japan). Other fatty acids, 7-ethoxycoumarin, and 7-ethoxyresorufin were purchased from Sigma-Aldrich Japan (Tokyo, Japan). Diazomethane was synthesized from *N*-nitroso-*N*-methylurea (Sigma-Aldrich Japan). *n*-Tetradecane and cholic acid were purchased from Nacarai Tesque (Kyoto, Japan). Benzphetamine was provided as a gift from Upjohn (Kalamazoo, MI). [1-^{14}C]Myristic acid was obtained from Daiichi Pure Chemicals Co. Ltd. (Tokyo, Japan). Other reagents were purchased from Wako Pure Chemical Industries, Ltd. (Osaka, Japan).

Preparation of the recombinant $P450_{SP\alpha}$ and enzyme assay. Expression and purification of the recombinant $P450_{SP\alpha}$ was described previously (9). The recombinant enzyme was almost pure, as manifested by sodium dodecyl sulfate-polyacrylamide gel electrophoresis. The purified enzyme was then dissolved in 0.1 M sodium phosphate buffer (pH 7.0), 30% ethylene glycol, 0.4% cholate, and 1mM dithiothreitol. The standard reaction mixture contained 0.1 M Tris-HCl (pH 8.0), 0.2 mM H_2O_2, 80 μM substrate, and 1 pmol of $P450_{SP\alpha}$ in a total volume of 0.2 mL. All of the substrates were added to the reaction mixture as an ethanol solution. When fatty acids were used as the substrates, α-hydroxylation activity was determined as described previously (4). Briefly, the reaction was carried out at 37°C for 2 min and then stopped by the addition of HCl. The fatty acid substrate and the product were extracted with ethyl acetate. After washing the extract with distilled water, the organic layer was collected. The extract was evaporated and then the residue was treated with ADAM. ADAM-derivatized fatty acids were analyzed by high-performance liquid chromatography (HPLC) according to a minor modification of the method described by Sawamura *et al.* (10). Kinetic studies for fatty acid substrates were carried out within the substrate concentration of 0 to 120 μM.

For determination of the metabolites by the reaction of $P450_{SP\alpha}$ by gas chromatography–mass spectrometry (GC–MS), the product and the substrate were extracted by ethyl acetate, and the extract was washed with distilled water and evaporated. The residue was treated with diazomethane and then with *N*,*O*-bis(trimethylsilyl)trifluoroacetamide. The methyl, trimethylsilyl (TMS) product and substrate were dissolved in hexane and subjected to GC–MS analysis described previously (9).

When methyl myristate, *n*-tetradecane, 1-tetradecanol, or tetradecanal was used as the substrate, the hydrocarbon derivatives were extracted by chloroform/methanol (2:1, vol/vol) after the reaction of $P450_{SP\alpha}$ and α-hydroxylation activity was determined by analysis of gas chromatography (9). In turn, H_2O_2 consumption in this reaction was determined by using the method of Bos *et al*. (11) to confirm whether $P450_{SP\alpha}$ utilized these compounds as the substrates. Competition experiments of myristic acid α-hydroxylation by these hydrocarbon derivatives were performed by the assay method using [1-^{14}C]myristic acid and thin-layer chromatography as described previously (3). Briefly, the assay condition was the same as described above except the reaction mixture contained 80 μM [1-^{14}C]myristic acid (231 Bq/nmol) as a substrate and 800 μM myristic acid analog as a competitor. After the reaction, nonradiolabeled myristic acid and α-hydroxymyristic acid were added as carriers into the reaction mixture, the reaction mixture was extracted with ethyl acetate, and the extract was evaporated. The residue was dissolved in a small amount of ethanol, applied to a thin-layer plate of silica gel G (Analtech Inc., Newark, DE), and developed with hexane/diethylether/acetic acid (70:30:3, vol/vol/vol). The lipid spots corresponding to myristic acid and α-hydroxymyristic acid were detected by spraying distilled water; they were scraped from the plate, and the radioactivities were determined by liquid scintillation counting.

N-Demethylation activities for benzphetamine were determined by measuring formaldehyde production (12). O-Deethylation activities for 7-ethoxycoumarin and 7-ethoxyresorufin were determined by the method of Greenlee and Poland (13) and the method of McDanell and McLean (14), respectively.

Analysis of optical configuration of α-hydroxy fatty acids. The optical configuration of the α-hydroxyl products was determined by HPLC with an OA-3100 column (Sumika, Osaka, Japan) according to the method of Nakagawa *et al*. (15). For the analysis of optical configuration, the enzyme preparation was dialyzed against 0.1 M Tris-HCl (pH 7.5), 30% ethylene glycol, and 1 mM dithiothreitol in order to remove cholate. After the reaction by $P450_{SP\alpha}$ the α-hydroxyl fatty acids were treated with 3,5-dinitrophenyl isocyanate (SUMIKA, Osaka, Japan) in the presence of a small amount of dry pyridine at room temperature overnight. Solvents used for analysis of the products included methanol containing 50mM ammonium acetate and 10% distilled water. The flow rate was 0.5 mL/min.

RESULTS

Substrate specificity. We investigated the utilization of various substrates by $P450_{SP\alpha}$. $P450_{SP\alpha}$ was able to metabolize saturated fatty acids with carbon chain lengths of 11 to 18 (Table

TABLE 1
Substrate Specificity of $P450_{SP\alpha}$

Substrates	K_m (μM)	Turnover rate[a] (× 10^3 nmol/min/nmol P450)
Nonhydroxy saturated fatty acids[b]		
Capric acid	—	—
Undecanoic acid	220	0.49
Lauric acid	140	3.0
Tridecanoic acid	65	3.6
Myristic acid	41	3.8
Pentadecanoic acid	36	3.4
Palmitic acid	57	4.7
Heptadecanoic acid	260	4.0
Stearic acid	460	2.5
Arachidonic acid[b]	34	4.4
16-Hydroxypalmitic acid[b]	110	0.63
1,14-Tetradecanedioic acid[b]	—	—
1,16-Hexadecanedioic acid[b]	—	—
Monomethyl hexadecanedionate[b]	360	0.55
Methyl myristatec	—	—
n-Tetradecane[c]	—	—
1-Tetradecanolc	—	—
Tetradecanal[c]		

[a]Kinetic study was performed within the substrate concentration range of 0 to 120 μM. The highest activity is shown.
[b]The activity was determined by high-performance liquid chromatographic analysis (see Material and Methods section).
[c]The activity was determined by gas chromatography and H_2O_2 consumption (see Material and Methods section). —, Catalytic activity not detected.

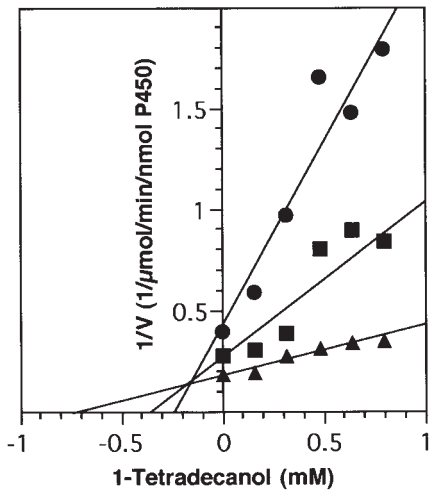

FIG. 1. Inhibition of myristic acid α-hydroxylation by 1-tetradecanol. Dixon plot of α-hydroxylation activity in the presence of 30 μM (●), 60 μM (■), and 120 μM (▲) of myristic acid. The K_i value was 145 μM.

1). No activity was detected when capric acid was used as a substrate. 1,14-Tetradecanedioic acid and 1,16-hexadecanedioic acid were not metabolized by $P450_{SP\alpha}$, whereas 16-hydroxypalmitic acid and monomethyl hexadecanedionate were α-hydroxylated. Methyl myristate was not metabolized. Interestingly, though, $P450_{SP\alpha}$ can metabolize arachidonic acid with a high turnover rate. Among fatty acid analogs, no hydroxylated products of *n*-tetradecane, 1-tetradecanol, and tetradecanal were detected by gas chromatography. Moreover, when 1,14-tetradecanedioic acid, methyl myristate, *n*-tetradecane, 1-tetradecanol, or tetradecanal were used as substrates, no H_2O_2 consumption was detected in the same assay conditions where myristic acid substrate was completely α-hydroxylated (data not shown). To further confirm that these hydrocarbon derivatives were not metabolized by $P450_{SP\alpha}$, the inhibition of myristic acid α-hydroxylation by these same hydrocarbon derivatives was investigated. In the absence of competitor, the reactive rate was 2.3 ± 0.2 μmol product formed/min/nmol of $P450_{SP\alpha}$, where values are means ± SD, calculated from triplicate experiment. In the presence of the following competitors [added at a concentration 10-fold that of myristic acid (80 μM)], the reaction rates are given as μmol product formed/min/nmol of $P450_{SP\alpha}$: methyl myristate, 27 ± 0.3; 1,14-tetradecanedioic acid, 2.2 ± 0.1; *n*-tetradecane, 3.3 ± 0.1; 1-tetradecanol, 1.2 ± 0.03; tetradecanal, 2.3 ± 0.1. That is, no inhibition was observed when 1,14-tetradecanedioic acid, methyl myristate, tetradecanal, or *n*-tetradecane were added as competitors, while the α-hydroxylation activity was, to some extent, increased by the addition of *n*-tetradecane. These results suggested that at least 1,14-tetradecanedioic acid, methyl myristate, tetradecanal, or *n*-tetradecane did not bind to the catalytic pocket of $P450_{SP\alpha}$. Unexpectedly, the addition of 1-tetradecanol significantly inhibited myristic acid α-hydroxylation. This inhibition seemed to be competitive in nature toward myristic acid (Fig. 1). N-Demethylation of benzphetamine and O-deethylation of 7-ethoxycoumarin or 7-ethoxyresorufin were not detected even when excess amounts of $P450_{SP\alpha}$ were used (data not shown).

Determination of metabolite by GC–MS. In order to determine the metabolite of arachidonic acid following the reaction with $P450_{SP\alpha}$, we analyzed a methyl, trimethyl (TMS) derivative of the product by GC–MS. The total ion chromatogram showed that only one product was found at the retention time of 22.1 min (Fig. 2A). The fragmentation pattern of this product corresponded to that of the methyl, TMS derivative of α-hydroxyarachidonic acid (Fig. 2B). The ion of *m/z* 391 (M – 15) is formed by cleavage between CH_3 and Si of the TMS moiety. The ion of *m/z* 347 (M – 59) is the characteristic fragment ion of a 2-hydroxy fatty acid that has lost the carboxylmethyl group of *m/z* 406 (M). Cleavage of the C_2–C_3 bond and the McLafferty rearrangement yield *m/z* 162. No peaks derived from auto-oxidation products were detected. Therefore, we concluded that the metabolite of arachidonic acid was only α-hydroxyarachidonic acid. Furthermore, we determined the metabolites of 16-hydroxypalmitic acid and monomethyl hexadecanedioate by GC–MS. In the mass spectra of methyl, TMS-derivatives of the metabolites that we obtained, peaks of (M – 15) ion and (M – 59) ion were found (data not shown). Thus, these metabolites were α-hydroxyl derivatives of 16-hydroxypalmitic acid and monomethyl hexadecanedioate, respectively.

Kinetic study for various fatty acid substrates. We attempted to determine the affinity of substrate for $P450_{SP\alpha}$ by spectral analysis, but failed because $P450_{SP\alpha}$ did not show significant substrate-binding spectra. Thus, we performed kinetic studies for various fatty acid substrates in order to estimate the affinity

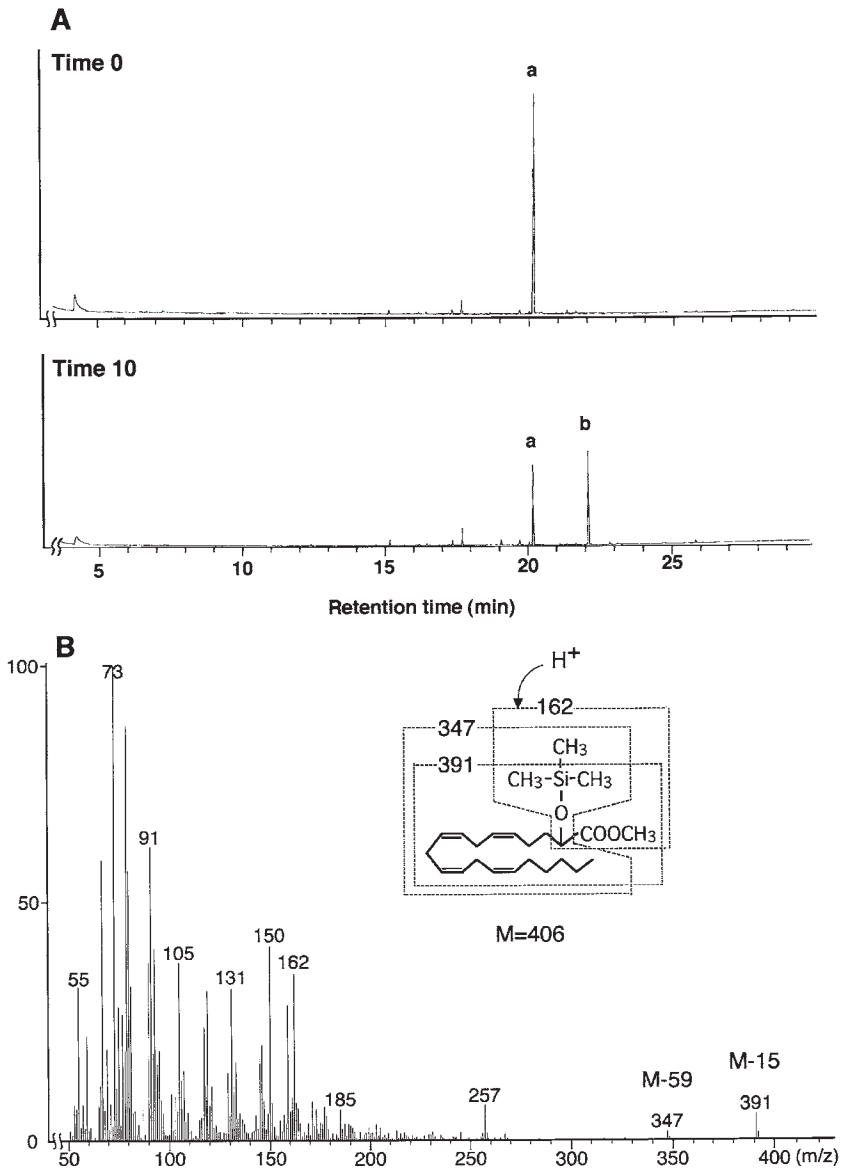

FIG. 2. Gas chromatography–mass spectrometric analysis of arachidonic acid metabolite from the reaction with $P450_{SP\alpha}$. (A) Total ion chromatograms at time 0 and after a 10 min incubation of $P450_{SP\alpha}$. Peaks of arachidonic acid and its metabolite are indicated as **a** and **b**, respectively. (B) Mass spectrum of the methyl, trimethylsilyl metabolite of arachidonic acid from the reaction with $P450_{SP\alpha}$.

of substrate for the enzyme by their apparent K_m values. When saturated fatty acids were used as the substrates, pentadecanoic acid showed the smallest K_m value (Table 1). The K_m value for myristic acid was comparable to that of pentadecanoic acid. As shorter or longer carbon chain lengths were tested for the fatty acids, the K_m values increased. The turnover rates for the fatty acids with carbon chain lengths of more than 11 were similar, but that for undecanoic acid was about eightfold smaller than that for myristic acid. The K_m value and turnover rate for ω-hydroxypalmitic acid were approximately twofold greater and sevenfold smaller than those of palmitic acid, respectively. The K_m value for monomethyl hexadecanedioate was threefold greater than that for ω-hydroxypalmitic acid. The K_m value and the turnover rate for arachidonic acid were comparable to those for myristic acid or pentadecanoic acid.

Configuration of α-hydroxyl products. We investigated the optical configuration of the α-hydroxyl product when myristic acid was used as a substrate. By HPLC analysis of the 3,5-dinitrophenyl isocyanate derivative of hydroxymyristic acid, a peak and a second very small peak, newly produced after the α-hydroxylation reaction, were detected at the retention times of 23.5 and 18.9 min, respectively (Fig. 3A). The retention times of these peaks corresponded to those of *S*-α-hydroxymyristic acid and *R*-α-hydroxymyristic acid, respectively. α-

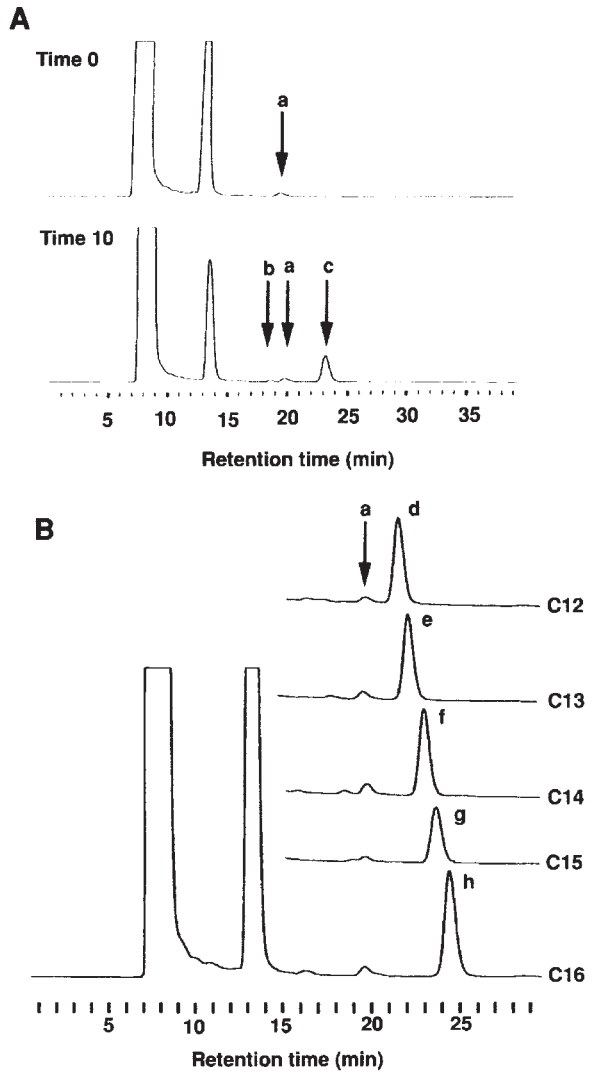

FIG. 3. Stereospecific α-hydroxylation of fatty acids by $P450_{SP\alpha}$. (A) High-performance liquid chromatographic (HPLC) analysis of optical configuration of the myristic acid metabolite at time 0 and after a 10 min incubation with $P450_{SP\alpha}$. Arrows show the retention times of authentic *R*-enantiomer (**b**, 18.9 min), *S*-enantiomer (**c**, 23.5 min), and cholic acid (**a**, 20.1 min). (B) HPLC analysis of optical configuration of the products when lauric acid (C_{12}), tridecanoic acid (C_{13}), myristic acid (C_{14}), pentadecanoic acid (C_{15}), and palmitic acid (C_{16}) were used as the substrates. The retention times of major peaks (**d**–**h**) correspond to those of *R*-α-hydroxy fatty acids.

Hydroxy fatty acids produced during reactions with $P450_{SP\alpha}$ were nearly enantiomerically pure (more than 98%). Next, we investigated the effect of carbon chain length of fatty acids for enantiomerically restricted hydroxylations. As shown in Figure 3B, any dominant products obtained from these reactions were *S*-enantiomers (L-form) when fatty acids with carbon chain lengths of 12 to 16 were used as the substrates. The amounts of derived *R*-α-hydroxy fatty acids were, if any, very small.

DISCUSSION

$P450_{SP\alpha}$ was strictly responsible for fatty acids and did not act upon any of the additional substrates known to exist for the other fatty acid-hydroxylating P450. This specificity of the enzyme was different from other members of fatty acid-hydroxylating P450 family such as CYP 4 and CYP 52. The observation that $P450_{SP\alpha}$ utilized fatty acids but not long-chain alkanes, fatty alcohols, and fatty aldehydes suggests that the negative charge of the carboxyl moiety of fatty acid substrates is crucial for appropriate substrate–enzyme interaction. In fact, methylation of the carboxyl moiety of myristic acid appeared to prevent substrate binding, as judged from competition analysis. Alterman *et al.* (5) proposed a model of the CYP 4A1 active site and described its key feature as a recognition site for a carboxyl or polar end group located approximately the length of an extended 12-carbon chain from the heme iron. Presumably owing to the relatively loose selectivity of this recognition site, CYP 4A1 utilized lauryl alcohol, methyl laurate, and lauric acid as substrates. In the case of $P450_{SP\alpha}$, selectivity of such recognition sites, if it does exist as the data suggest, appears to be more strict. This selective recognition site may be located near the heme iron, given that $P450_{SP\alpha}$ attacks α-carbon of fatty acids. Fatty alcohol appears to bind to the catalytic pocket of $P450_{SP\alpha}$ with low affinity, but is not metabolized by $P450_{SP\alpha}$. Although this reason remains unclear, fatty alcohol may not be able to bind in the catalytic pocket in an appropriate position to permit its metabolism.

The structures of the ω-end of fatty acid substrates also affect utilization of substrate by $P450_{SP\alpha}$. ω-Hydroxy fatty acid was metabolized with a higher K_m value and a lower turnover rate than the corresponding nonhydroxy fatty acid. The hydroxyl group of the ω-carbon of a fatty acid appeared to prevent substrate affinity and metabolism by $P450_{SPa}$. Moreover, dicarboxylic fatty acids with carbon chain lengths of 14 and 16 were not metabolized, whereas monomethyl derivatives of 1,16-hexadecanedioic acid were metabolized, although with higher K_m values and lower turnover rates. Because the fatty acid methylated on one hand of two carboxyl moieties was able to bind $P450_{SP\alpha}$ and was metabolized, the negative charge of the carboxyl moiety of dicarboxylic fatty acid appear to prevent substrate binding to the catalytic pocket of $P450_{SP\alpha}$. Interestingly, such substrate specificity has been observed on *Pisum sativum* α-oxidase which does not metabolize dicarboxylic acid but is able to metabolize monomethyl ester of the dicarboxylic acid, albeit at a significant diminished reaction rate (16).

Fatty acid substrates with carbon chain lengths of more than 11 were metabolized with high turnover rates. However, the turnover rate was dramatically decreased when undecanoic acid was used as a substrate, and capric acid was not metabolized at all by $P450_{SP\alpha}$. These results indicated that a carbon chain length of at least 12 was required for effective metabolism by $P450_{SP\alpha}$. As described in the Results Section, we were not able to determine the binding affinities of substrates for this

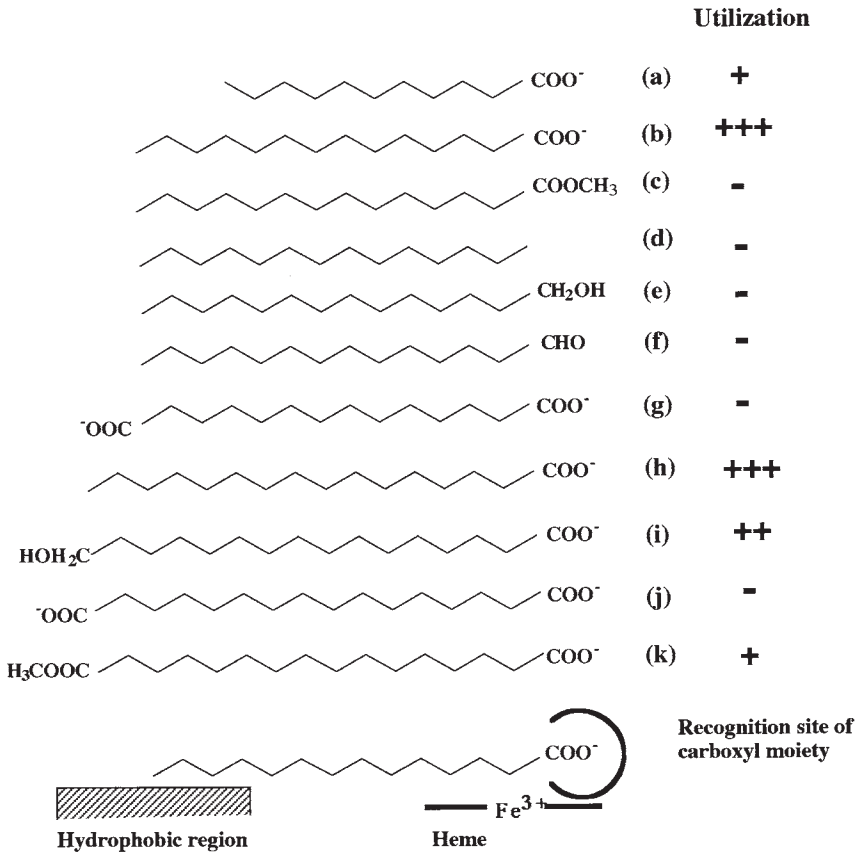

FIG. 4. Utilization of substrates by $P450_{SP\alpha}$ and schematic representation of a presumed model of catalytic pocket of $P450_{SP\alpha}$. Degree of efficiency of each substrate utilization by $P450_{SP\alpha}$ was represented with 3+ (highly utilized), 2+ (moderately utilized), 1+ (slightly utilized), or minus (–, not utilized). (a) Undecanoic acid; (b) myristic acid; (c) methyl myristate; (d) -tetradecane; (e) 1-tetradecanol; (f) tetradecanal; (g) 1,14-tetradecanedioic acid; (h) palmitic acid; (i) 16-hydroxypalmitic acid; (j) 1,16-hexadecanedioic acid; (k) monomethyl hexadecanedioic acid.

enzyme by spectral analysis. Instead, we estimated the binding affinity of a given substrate from its apparent K_m value obtained by kinetic study. Among those for the saturated fatty acids tested, the K_m values for myristic acid or pentadecanoic acid were smallest, suggesting that fatty acids with 14 or 15 carbon atoms can bind to the enzyme most efficiently. In known ω-hydroxylating P450, a hydrophobic region interacting with the methylene unit of the substrate was theorized (6). In $P450_{SP\alpha}$, such a hydrophobic interaction between the enzyme and the fatty acid substrate could restrict substrate specificity.

Analysis of the optical configuration of a-hydroxy fatty acids produced by $P450_{SP\alpha}$ demonstrated that the product was nearly enantiomerically pure *S*-isomer. This result can be considered informative with respect to the biosynthesis of α-hydroxy fatty acid. For instance, Nakagawa *et al.* (15) clearly demonstrated that α-hydroxymyristic acid in sphingolipid of *S. paucimobilis* is the *S*-enantiomer (L-form). This observation was consistent with our result obtained from the optical configuration analysis of the α-hydroxyl product from $P450_{SP\alpha}$ supporting the idea that the α-hydroxymyristic acid in this bacterium is produced by $P450_{SP\alpha}$.

Capdevila *et al.* (8) demonstrated that arachidonic acid is a good substrate for CYP102A. Specifically, CYP102A metabolizes arachidonic acid to produce 18(*R*)-hydroxyeicosatetraenoic acid and 14(*S*),15(*R*)-epoxyeicosatrienoic acid in a highly stereoselective manner, and moreover, metabolizes eicosatrienoic acid to produce 17-, 18-, and 19-hydroxyeicosatrienoic acid. In the case of $P450_{SP\alpha}$, not only the stereoselectivity but also the regioselectivity of this enzyme were very strict. That is, $P450_{SP\alpha}$ strictly attacks the α-carbon of polyunsaturated fatty acids such as arachidonic acid as well as saturated fatty acids with different carbon chain lengths. Unlike CYP 102A, $P450_{SP\alpha}$ did not attack the double bond of arachidonic acid to produce epoxy fatty acid. Thus, it is possible that the α-carbons of fatty acids are "fixed", presumably near the heme group within the catalytic pocket of this enzyme.

In this study, we investigated the relationship between the structure of substrates and their utilization by $P450_{SP\alpha}$. The appropriate substrate for $P450_{SP\alpha}$ has a carboxyl moiety, a methyl

group in the ω-end, and a carbon chain length of more than 11. Here, we propose a presumed model of the catalytic pocket of $P450_{SP\alpha}$ (Fig. 4). In this model, the carboxyl moiety of the substrate is "recognized" by the site located near the heme group and the α-carbon of the substrate located at the position where the carbon most closely interacts with the heme iron. At the opposite site, the methylene group of the ω-terminus of the substrate loosely binds to the hydrophobic region in the catalytic pocket. The substrate is, thus, "fixed" by the recognition site and the hydrophobic region. To confirm whether this model is correct, analysis of crystal structure of $P450_{SP\alpha}$ is now required. Regardless, it is encouraging that progress is being made in characterizing this important enzyme. A molecule which is classified within the P450 group should provide important information about sphingolipid metabolism not only in this bacterium but also in other organisms, and the mechanism of P450 reactions in general.

ACKNOWLEDGMENT

We thank Dr. Yoshio Imai, Hagoromo Gakuen Junior College, for many valuable discussions.

REFERENCES

1. Yabuuchi, E., Yano, I., Oyaizu, H., Hashimoto, Y., Ezaki, T., and Yamamoto, H. (1990) Proposals of *Sphingomonas paucimobilis* gen. nov. and comb. nov., *Sphingomonas parapaucimobilis* sp. nov., *Sphingomonas yanoikuyae* sp. nov., *Sphingomonas adhaesiva* sp. nov., *Sphingomonas capsulata* comb. nov., and Two Genospecies of the Genus *Sphingomonas*, *Microbiol. Immunol. 34*, 99–119.
2. Matsunaga, I., Yokotani, N., Gotoh, O., Kusunose, E., Yamada, M., and Ichihara, K. (1997) Molecular Cloning and Expression of Fatty Acid α-Hydroxylase from *Sphingomonas paucimobilis*, *J. Biol. Chem. 272*, 23592–23596.
3. Matsunaga, I., Yamada, M., Kusunose, E., Nishiuchi, Y., Yano, I., and Ichihara, K. (1996) Direct Involvement of Hydrogen Peroxide in Bacterial α-Hydroxylation of Fatty Acid, *FEBS Lett. 386*, 252–254.
4. Matsunaga, I., Yamada, M., Kusunose, E., Miki, T., and Ichihara, K. (1998) Further Characterization of Hydrogen Peroxide-Dependent Fatty Acid α-Hydroxylase from *Sphingomonas paucimobilis*, *J. Biochem. 124*, 105–110.
5. Alterman, M.A., Chaurasia, C. S., Lu, P., Hardwick, J.P., and Hanzlik, R.P. (1995) Fatty Acid Discrimination and ω-Hydroxylation by Cytochrome P450 4A1 and a Cytochrome P4504A1/NADPH-P450 Reductase Fusion Protein, *Arch. Biochem. Biophys. 320*, 289–296.
6. Fisher, M.B., Zheng, Y.-M., and Rettie, A.E. (1998) Positional Specificity of Rabbit CYP4B1 for ω-Hydroxylation of Short–Medium Chain Fatty Acid and Hydrocarbons, *Biochem. Biophys. Res. Commun. 248*, 352–355.
7. Scheller, U., Zimmer, T., Becher, D., Schauer, F., and Schunck, W.-H. (1998) Oxygenation Cascade in Conversion of *n*-Alkane to α,ω-Dioic Acids Catalyzed by Cytochrome P450 52A3, *J. Biol. Chem. 273*, 32528–32534.
8. Capdevila, J.H., Wei, S., Helvig, C., Falck, J.R., Belosludtsev, Y., Truan, G., Graham-Lorence, S.E., and Peterson, J.A. (1996) The Highly Stereoselective Oxidation of Polyunsaturated Fatty Acids by Cytochrome P450BM-3, *J. Biol. Chem. 271*, 22663–22671.
9. Matsunaga, I., Sumimoto, T., Kusunose, E., and Ichihara, K. (1998) Phytanic Acid α-Hydroxylation by Bacterial Cytochrome P450, *Lipids 33*, 1213–1216.
10. Sawamura, A., Kusunose, E., Satouchi, K., and Kusunose, M. (1993) Catalytic Properties of Rabbit Kidney Fatty Acid ω-Hydroxylase Cytochrome P-450ka2 (CYP4A7), *Biochim. Biophys. Acta 1168*, 30–36.
11. Bos, E.S., van der Doelen, A.A., van Rooy, N., and Schuurs, A. H.W.M. (1981) 3,3′,5,5′-Tetramethylbenzidine as an Ames Test Negative Chromogen for Horseradish Peroxidase in Enzyme-Immunoassay, *J. Immunoassay 2*, 187–204.
12. Nash, T. (1953) The Colorimetric Estimation of Formaldehyde by Means of the Hantzsch Reaction, *Biochem. J. 55*, 416–421.
13. Greenlee, W.F., and Poland, A. (1978) An Improved Assay of 7-Ethoxycoumarin O-Deethylase Activity: Induction of Hepatic Enzyme Activity in C57BL/6J and DBA/2J Mice by Phenobarbital, 3-Methylcholanthrene and 2,3,7,8-Tetrachlorodibenzo-*p*-dioxin, *J. Pharmcol. Exp. Ther. 205*, 596–605.
14. McDanell, R.E., and McLean, A.E.M. (1984) Differences Between Small and Large Intestine and Liver in the Inducibility of Microsomal Enzymes in Response to Stimulation by Phenobarbitone and Betanaphthoflavone in the Diet, *Biochem. Pharmacol. 33*, 1977–1980.
15. Nakagawa, Y., Kishida, K., Kodani, Y., and Matsuyama, T. (1997) Optical Configuration Analysis of Hydroxy Fatty Acids in Bacterial Lipids by Chiral Column High-Performance Liquid Chromatography, *Microbiol. Immunol. 41*, 27–32.
16. Adam, W., Boland, W., Hartmann-Schreier, J., Humpf, H.-U., Lazarus, M., Saffert, A., Saha-Möller, C.R., and Schreier, P. (1998) α Hydroxylation of Carboxylic Acids with Molecular Oxygen Catalyzed by the α Oxidase of Peas (*Pisum sativum*): A Novel Biocatalytic Synthesis of Enantiomerically Pure (*R*)-2-Hydroxy Acids, *J. Am. Chem. Soc. 120*, 11044–11048.

[Received October 18, 1999, and in revised form January 20, 2000; revision accepted January 30, 2000]

Biased Distribution of the Branched-Chain Fatty Acids in Ceramides of Vernix Caseosa

Hirosuke Oku[a,*], Kunio Mimura[b], Yumi Tokitsu[b], Kyoko Onaga[a], Hironori Iwasaki[a], and Isao Chinen[a]

[a]Laboratory of Applied Biochemistry, Faculty of Agriculture, University of the Ryukyus, Okinawa-Ken 903-0213, Japan, and [b]Kanebo Ltd., Cosmetic Laboratory, Kanagawa-Ken 250-0002, Japan

ABSTRACT: The compositions of ester- and amide-linked fatty acids from ceramides of human vernix caseosa were described with emphasis on the distribution of the branched-chain fatty acid (BCFA). Two novel ceramides were isolated from vernix caseosa in the course of this study: the acylated type of esterified α-OH-hydroxyacid/sphingosine ceramide (Cer[EAS]) and nonacylated type of non-OH fatty acid/hydroxysphingosine ceramide (Cer[NH]). Their chemical structures were identified by nuclear magnetic resonance and chemical procedure. The Cer[EAS] was an acylceramide and consisted of the highest concentrations of ester- and amide-linked BCFA (62 and 67%, respectively). The iso- or anteiso-branching structures of the aliphatic chains were confirmed by the mass spectra of their picolinyl or pyrrolidide derivatives. As a whole, amide-linked fatty acids of ceramides 1-7 and Cer[NH] were normal types of straight-chain fatty acids with or without α- or ω-hydroxylation. The BCFA concentrations of amide-linked fatty acids in these ceramides (ceramides 1–7 and Cer[NH]) were low and less than 10%. The BCFA thus occurred exclusively in a novel acylceramide of Cer[EAS] in the vernix caseosa.

Paper no. L8401 in *Lipids 35,* 373–381 (April 2000).

Vernix caseosa is a mixture of lipids covering the skin surface of a fetus, and is believed to be a protective substance against undesirable influences from the environment (1). A number of studies therefore have been devoted to understanding the chemical nature of vernix caseosa (2–5). These studies, however, mainly focused on the chemical structures of the neutral lipids, and few studies were conducted to characterize the polar lipid of vernix caseosa. Our preliminary (Tokitsu, Y., unpublished data) and subsequent studies (6) have suggested that the polar lipid constituted a significant proportion of vernix caseosa, and the ceramides are the largest component of the polar lipids from human vernix caseosa.

The present study thus describes the amide- or ester-linked fatty acid compositions of ceramides from human vernix caseosa. Since our interest has been on the biosynthesis of the branched-chain fatty acids (BCFA) in mammalian skin tissues, a special emphasis was placed on the distribution of the BCFA among the ceramide subclasses. As a result, the present study is the first to demonstrate the presence of BCFA with or without α-hydroxy groups in the ceramides of human vernix caseosa, and also reveals a higher concentration of BCFA in acylceramides compared with the case for nonacylated-type of ceramides.

*To whom correspondence should be addressed at Laboratory of Applied Biochemistry, Faculty of Agriculture, University of the Ryukyus, Nishihara-Cho, Okinawa-Ken 903-0213, Japan. E-mail: b986101@agr.u-ryukyu.ac.jp

Abbreviations: BCFA, branched-chain fatty acid; Cer[EAS], esterified α-OH-hydroxyacid/sphingosine ceramide; Cer[NH], non-OH fatty acid/hydroxysphingosine ceramide; GC–MS, gas chromatography–mass spectrometry; HPTLC, high-performance thin-layer chromatography; NMR, nuclear magnetic resonance; TLC, thin-layer chromatography.

MATERIALS AND METHODS

Vernix caseosa. Samples of vernix caseosa were collected from 22 male and 24 female newborn babies immediately after birth at the hospital of St. Marianna University School of Medicine. The vernix caseosa collected with a gauze was dissolved and stored in chloroform/methanol (2:1, vol/vol).

Purification of ceramides. The ceramides of human vernix caseosa were purified by a combination of column and thin-layer chromatography (TLC). Figure 1 shows the purification protocol of ceramides from human vernix caseosa. Vernix caseosa (4.1 g) was dissolved in a minimal volume of chloroform/methanol (39:1, vol/vol) and loaded to 450 g of Iatrobeads (6RS-8060, Iatron Laboratory, Tokyo, Japan) packed in a glass column (50 mm i.d. × 500 mm length). The column was then washed with 700 mL of chloroform/methanol (39:1, vol/vol) and eluted with the mixture of chloroform/methanol as shown in Figure 1. The eluant fractions in a volume of 200–300 mL were concentrated to dryness by flushing with a N_2 stream. The lipid concentrations of 11 successive fractions are shown in Figure 1. The ceramides in these Iatrobeads column fractions were further resolved by two developments of TLC (20 × 20 cm, 2-mm thickness; Merck, Tokyo, Japan). Development solvents used were chloroform/methanol (49:1, 39:1, or 29:1, vol/vol) for ceramides Cer[EAS], 1 and 2; chloroform/methanol (19:1, vol/vol) for ceramides 3, 4, 5, and Cer[NH]; and chloroform/methanol (15:1 or 9:1, vol/vol) for ceramides 6 and 7. (See the Results section for discussion of ceramide nomenclature.) The chromatogram was visualized by spraying 0.01% primuline, and the ceramide bands localized were extracted with chloroform/methanol (2:1, vol/vol). The identical ceramides were combined and further purified by TLC for homogeneity. Reso-

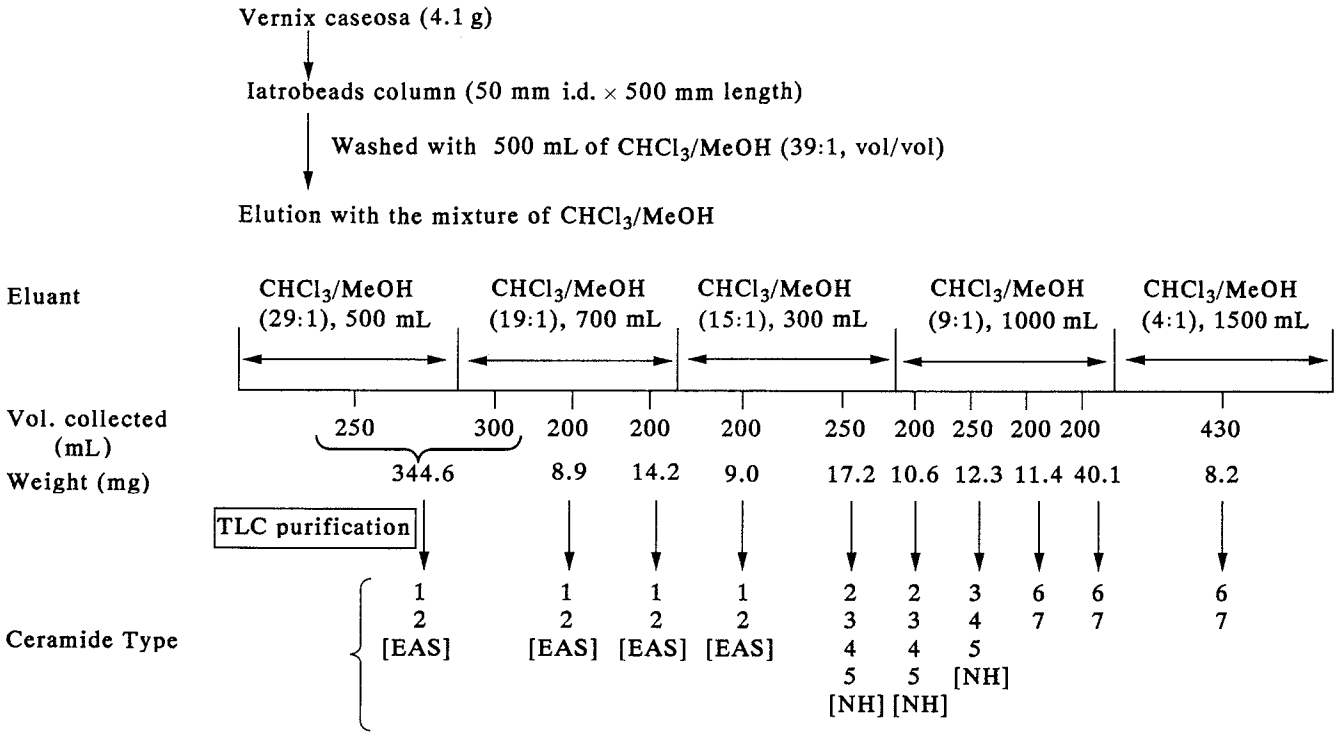

FIG. 1. Purification protocol of human vernix caseosa ceramides.

lution by TLC was repeated at least three times to give a single band on TLC analysis. The purified ceramides dissolved in chloroform/methanol (9:1, vol/vol) were passed through an Iatrobeads column packed in a cotton-plugged Pasteur pipette and concentrated to dryness for later analysis by high-performance thin-layer chromatography (HPTLC).

Chemical structure of ceramides. The chemical structure of ceramides was determined by proton nuclear magnetic resonance (NMR) spectra and by chemical procedure. Ceramides dissolved in $CDCl_3/CD_3OD$ (4:1, vol/vol) were used to obtain proton NMR spectra in a 400-MHz spectrometer (JMN-LA400; JEOL, Tokyo, Japan).

Fatty acid composition. The ester-linked fatty acids were liberated by alkaline hydrolysis and converted into methyl ester as follows. The acylceramide (1 mg) was reacted with 1 mL of 1 N NaOH in 95% methanol at 45°C for 60 min. The reactions were acidified to pH 2–3 with 2 N HCl, and mixed with 1.9 mL of chloroform and 0.72 mL of H_2O. The fatty acids extracted into chloroform were then redissolved in chloroform/methanol (19:1, vol/vol) and purified by passing through an Iatrobeads column packed in a Pasteur pipette.

The amide-linked fatty acids were directly transmethylated with methanolic hydrogen chloride. Briefly, ceramides (1 mg) dissolved in 1 N methanolic hydrogen chloride were heated at 75°C for 18 h in glass-stoppered tubes. Prepared fatty acid methyl esters were extracted into hexane and concentrated on a rotary evaporator. This transmethylation procedure also was applied for the preparation of the methyl esters from ester-linked fatty acids isolated as described above. In the case of amide-linked fatty acids, the methyl esters were further trimethylsilylated by heating them with (trimethylsilyl)trifluoroacetamide at 60°C for 10 min (7).

The fatty acid derivatives (3 μg) were analyzed by a gas chromatograph (GC 14A; Shimadzu, Kyoto, Japan) equipped with a flame-ionization detector. A fused-silica capillary column (CBP1-M50-025, 0.2 mm i.d. × 50 m length; Shimadzu) was used with nitrogen as the carrier gas at a flow rate of 0.35 mL/min. The column temperature was programmed from 50°C for 1 min, to 100°C at a rate of 10°C/min, and then raised to the final temperature of 300°C at a rate of 5°C/min. The final temperature for analysis of trimethylsilyl derivatives of α- or ω-hydroxy fatty acids was 320°C.

Chain structure of fatty acid. The identification of the chemical structure of fatty acids was made by interpretation of the mass spectrum. The amide- or ester-linked ceramide fatty acids were converted into picolinyl esters or pyrrolidides as described previously (7,8). The authors first attempted to prepare the picolinyl derivatives from both ester- and amide-linked fatty acids. Preparation of picolinyl esters from amide-linked fatty acids was, however, unsuccessful for unknown reasons. We therefore prepared pyrrolidides of amide-linked fatty acids, and analyzed them by gas chromatography–mass spectrometry (GC–MS). The mass spectrometer used was a Shimadzu GC/MS-QP1000EX. The column used was the same as described above, and operated with helium as the carrier gas at a flow rate of 0.38 mL/min. The column temperature was programmed from 50°C for 1 min to 100°C at a rate of 10°C/min, and then raised to the final temperature of 320°C at a rate of 5°C/min. Ionization of samples was by electron impact at 70 eV.

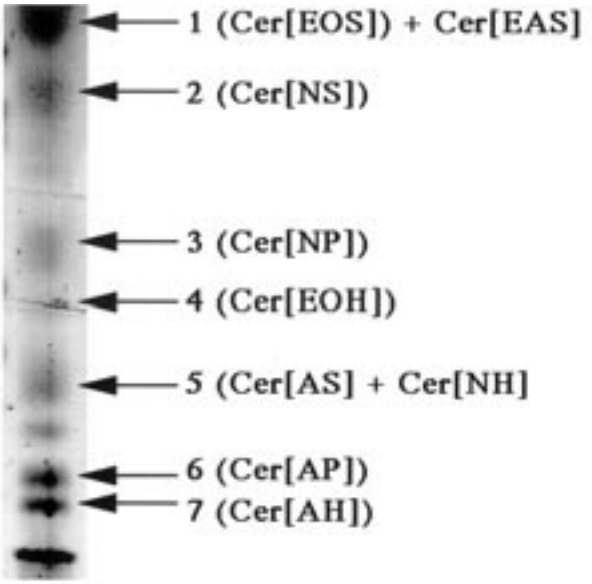

FIG. 2. High-performance thin-layer chromatogram of human vernix caseosa ceramides. Human vernix caseosa (100 μg) was spotted onto high-performance thin-layer chromatography plates, and developed first with benzene, followed by two developments with chloroform/methanol/acetic anhydride (180:10:1, by vol). The chromatogram was sprayed with 10% copper sulfate in 8% phosphoric acid, and charred at 180°C for 10 min. The authors adopted the nomenclature system of Motta *et al*. (9) for the new ceramides of Cer[EAS] and Cer[NH].

RESULTS

Figure 2 shows the HPTLC chromatogram of human vernix caseosa ceramides. The authors adopted the nomenclature system of Motta *et al*. (9) for the new ceramides based on grouping ceramides carrying structural similarities under common codes. The combination of Iatrobead column chromatography and TLC isolated two new types of ceramides, Cer[EAS] and Cer[NH], from human vernix caseosa besides the free types of ceramide 1–7. [While this paper was in preparation, Stewart and Downing (10) reported the presence of a new 6-hydroxy-4-sphingenine-containing ceramide identical to our Cer[NH] in human skin.] The identification of the chemical structure of new ceramides was mainly by interpretation of proton NMR spectra, and will be described in detail in a forthcoming paper. A densitometric analysis of the chromatogram revealed that the vernix caseosa had a higher concentration of ceramide 6 and a lower concentration of ceramide 5 compared with the data for adult epidermal lipid (11) (data not shown). In addition to new free ceramides, two unidentified ceramides also were seen between ceramides 2 and 3, and between ceramides 5 and 6 (see Fig. 2). The chemical structure for these novel ceramides should be determined in a coming study.

Cer[EAS] was resolved from ceramide 1 by TLC by two developments with chloroform/methanol (49:1, vol/vol), and migrated slightly faster than ceramide 1. The proton NMR spectrum showed that Cer[EAS] was an acylceramide, and the sphingoid base for this ceramide was dihydrosphingosine (sphinganine).

Figure 3 shows the gas chromatogram of the methyl ester of ester-linked fatty acids from Cer[EAS]. Inspection of the mass spectrum of fatty acid methyl ester found that the ester-linked fatty acids from Cer[EAS] consisted largely of saturated fatty acid. Furthermore, a major proportion of fatty acids was eluted slightly faster than the corresponding straight-chain fatty acid counterpart on gas chromatography, suggesting the presence of methyl branching in the aliphatic carbon chain of these fatty acids. The mass spectrum of the methyl esters gives little information on aliphatic chain structures. The fragmentation pattern of picolinyl ester, however, had been shown to be useful for the structural identification of the fatty acid carbon chain. The authors therefore prepared the picolinyl derivative from ester-linked fatty acids of Cer[EAS]. The gas chromatogram of picolinyl ester was similar to that of methyl ester with increased elution temperature.

Figures 4 and 5 depict the mass spectra for iso-24:0 and

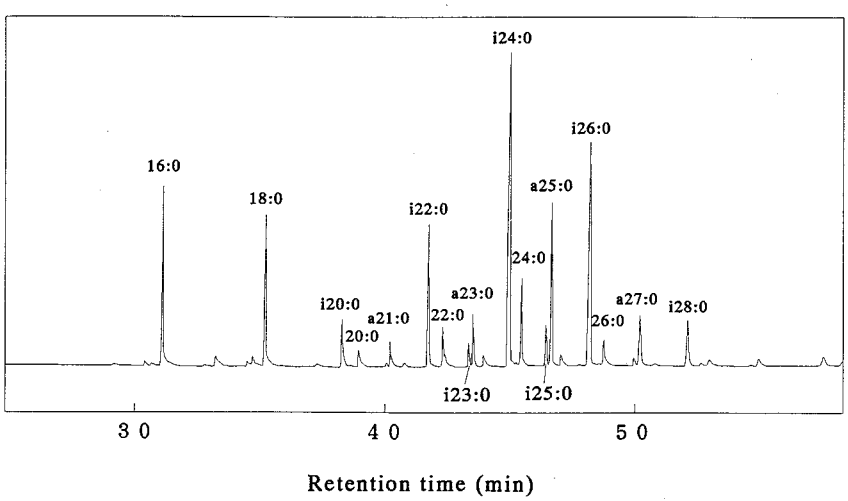

FIG. 3. Gas chromatogram of methyl ester of Cer[EAS] ester-linked fatty acid. The identifications for major fatty acid components are given. Abbreviations: i, iso; a, anteiso.

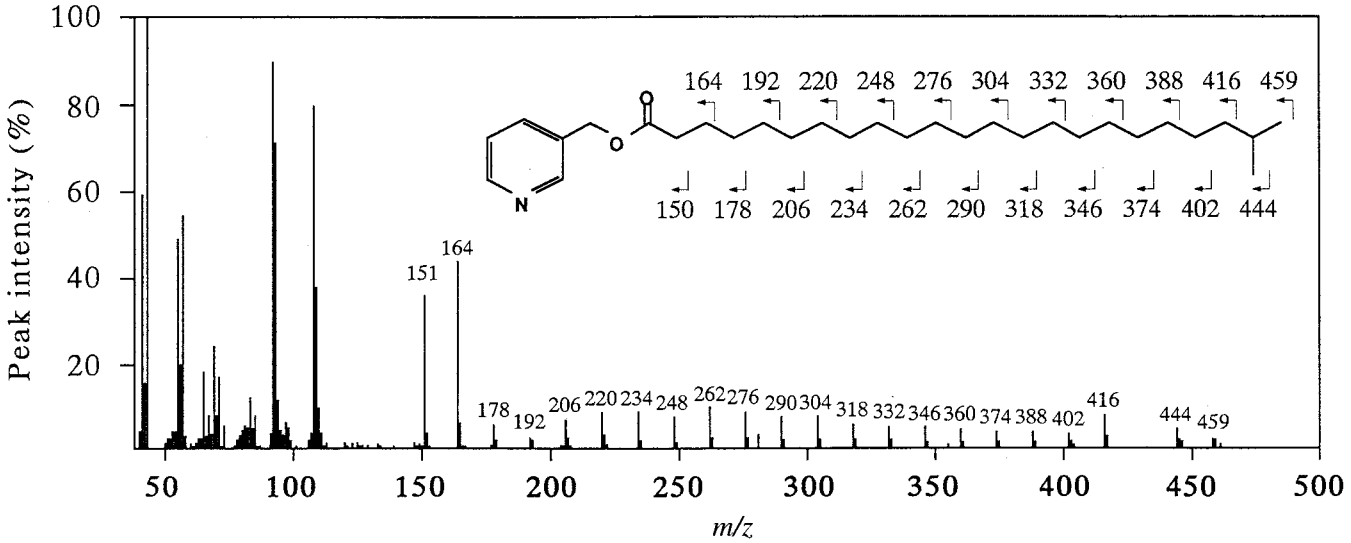

FIG. 4. Mass spectrum of picolinyl ester of iso-tetracosanoic acid (iso-24:0) from Cer[EAS] ester-linked fatty acids. The figure inset shows the formation of fragments.

anteiso-25:0 fatty acids esterified to Cer[EAS], respectively. As has already been demonstrated, the fragmentation pattern of the picolinyl ester was sensitive to the structure of the fatty acid aliphatic chain. The presence of a methyl substitution on one of the aliphatic carbons caused a 28-mass-unit gap in the series of fragments separated by 14 mass units. This series of ions can clearly be seen in the spectra of the picolinyl ester of the iso-24:0 and anteiso-25:0 fatty acids isolated from Cer[EAS]. The mass spectra for iso- and anteiso-fatty acids therefore lack M – 29 and M – 43 ions, respectively (see Figs. 4 and 5). Thus, we herein first demonstrate the presence of the BCFA in ceramides of human vernix caseosa. Inspection of the mass spectra found no evidence of the presence of other types of methyl-substituted fatty acids in this new ceramide.

Table 1 lists the composition of ester-linked fatty acids of Cer[EAS] from human vernix caseosa. The ester-linked fatty acids consisted of a large spectrum of fatty acids C_{16} to C_{28}. The largest component consisted of iso-24:0 fatty acids. The sum of the BCFA, iso- and anteiso-series, amounted to 62.6%, while the sum of the straight-chain fatty acids was 33.8%.

Figure 6 is the gas chromatogram of amide-linked fatty acids from Cer[EAS]. With respect to amide-linked fatty acids of Cer[EAS], there were a limited number of fatty acid components compared with ester-linked fatty acids. The mass spectrum of methyl ester showed that large parts of amide-linked fatty acids had the characteristic fragmentation profile of α-hydroxy fatty acids: the intense molecular ion, *m/z*

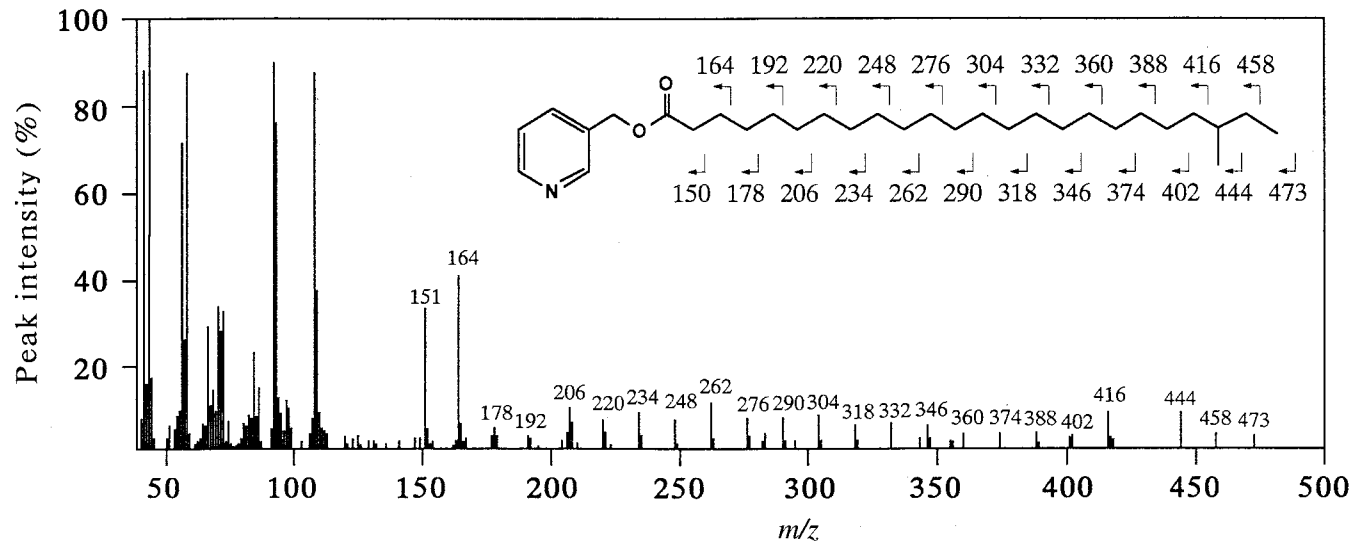

FIG. 5. Mass spectrum of picolinyl ester of anteiso-pentacosanoic acid (anteiso-25:0) from Cer[EAS] ester-linked fatty acids. The figure inset shows the formation of fragments.

TABLE 1
Composition of Ester-Linked Fatty Acids from Cer[EAS][a]

	Straight chain		Branched chain	
Carbon no.	Normal	Monoene	Iso	Anteiso
16	8.2	0.3	0.3	
17	1.2			
18	6.9	0.7	0.4	
19	0.3			
20	1.4		2.7	
21	0.4			1.1
22	1.9		6.3	
23	0.9		0.9	2.6
24	4.3		20.3	
25	0.9		1.8	8.1
26	2.0		14.7	
27	3.4			
28	1.0		3.4	
Sum	32.8	1.0	50.8	11.8

[a]Data are means of duplicate analyses. Sum of other fatty acid components was 3.6%. Ceramide nomenclature based on Reference 9.

TABLE 2
Composition of Amide-Linked Fatty Acid from Cer[EAS][a]

	Straight chain		Branched chain α-hydroxy	
Carbon no.	Normal	α-Hydroxy	Iso	Anteiso
20		1.2		
22		8.8	5.7	
23		3.8	2.9	3.3
24		8.6	55.9	
25		2.4		
Sum	0.0	24.8	64.5	3.3

[a]Data are means of duplicate analyses. Sum of other fatty acid components was 7.4%. Ceramide nomenclature based on Reference 9.

M – 59 generated by loss of $COOCH_3$, M – 32, 90, 57, and 55 fragments (data not shown). The elution volumes in gas chromatography also were slightly earlier than those expected for straight-chain α-hydroxy fatty acids, suggesting the presence of branched-aliphatic chain structure in these fatty acids. As stated in the Materials and Methods section, the authors first tried to prepare the picolinyl derivatives of these fatty acids to elucidate their chain structure. However, the preparation of picolinyl esters from the amide-linked fatty acids was unsuccessful for unknown reasons. We therefore prepared the pyrrolidides of these fatty acids for the structural identification of aliphatic chain.

In the case of pyrrolidides, the intensities of the diagnostic ions at high mass range appeared to be less abundant than in the case of picolinyl ester. These derivatives were, however, useful for the identification of the aliphatic chain structure. Fragmentation of pyrrolidides involves the same type of radical-induced cleavage as observed with the picolinyl ester (data not shown). A series of ions of carbon atoms separated by 14 mass units were demonstrated with α-hydroxy hexadecanoic acids as shown in Figure 7. The rationale for the generation of these ions was also shown in the inset of Figure 7.

Figure 8 thus shows the mass spectrum for pyrrolidides of amide-linked α-hydroxy iso-24:0 fatty acid in Cer[EAS]. The fragment of *m/z* 408 for the straight-chain structure was missing, and the 28-mass-unit gap occurred between *m/z* 394 and 422 ions, showing clearly the iso-branching chain structure at methyl terminus. This elucidation of the chain structure herein first allows us to demonstrate the presence of α-hydroxy BCFA in the amide-linked fatty acids of Cer[EAS].

Table 2 lists the fatty acid composition of amide-linked fatty acids from Cer[EAS]. As was the case for ester-linked fatty acid composition, BCFA constituted the major proportion of amide-linked fatty acid, accounting for 67.8% of total fatty acid.

Tables 3 and 4, respectively, show the fatty acid compositions for ester- and amide-linked fatty acids of ceramide 1. In both cases, BCFA with or without α-hydroxy group were present. The sum of BCFA was 21.4% for the ester-linked and

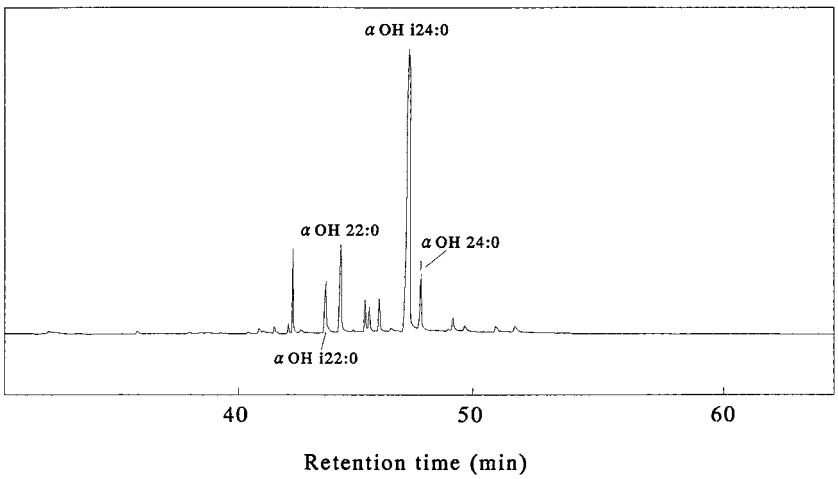

FIG. 6. Gas chromatogram of methyl ester of Cer[EAS] amide-linked fatty acid. The identifications for major fatty acid components are given. Abbreviations: α-OH, α-hydroxy; i, iso.

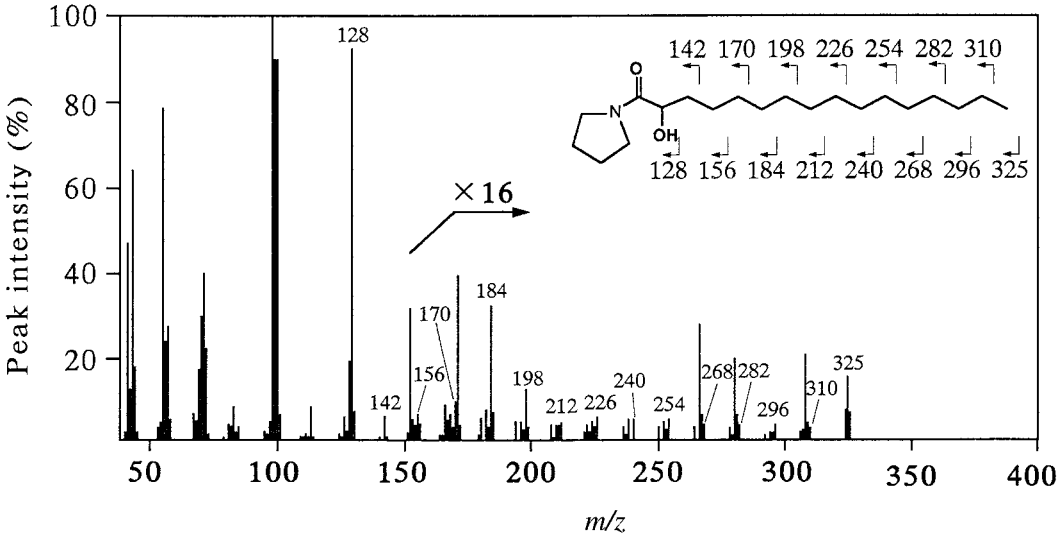

FIG. 7. Mass spectrum of pyrrolidide derivatives of authentic α-hydroxy hexadecanoic acid. The fragments of *m/z* greater than 150 were magnified 16 times (note the arrow). The figure inset shows the formation of fragments.

10.9% for the amide-linked fatty acids. The BCFA concentrations of both ester- and amide-linked fatty acids for ceramide 1 were lower than those for Cer[EAS]. The largest fatty acid constituent was predictably linoleic acid (18:2), and the predominant fatty acid for ceramide 1 was therefore a straight-chain fatty acid.

Table 5 shows the composition of amide-linked fatty acids from ceramide 2. The length of the aliphatic chain of the fatty acids ranged from C16 to C30 with the largest being C24. The lower concentration (13.6%) of the BCFA compared to Cer[EAS] was noted with this ceramide as well as for ceramide 1. Table 6 lists the fatty acid composition of ceramide 3. The profile was largely similar to that of ceramide 2 with a much lower concentration (8.1%) of BCFA.

Table 7 shows the fatty acid composition of ceramide 5. In this case, α-hydroxy straight-chain fatty acids were the major amide-linked fatty acids, which accounted for 49.8% of total fatty acids. The sum of BCFA was 7.5%.

Table 8 shows the fatty acid composition of Cer[NH]. An analysis of the proton NMR spectrum revealed that the sphingoid base of this ceramide was 6-hydroxy-4-sphingenine, and was identical with that of ceramide 7. The chemical structure of this ceramide was as follows: the amide-linked α-hydroxy fatty acid of ceramide 7 was substituted by normal-type fatty acids. Thus, this ceramide was less polar than ceramide 7 and co-migrated with ceramide 5 on development of the thin-layer chromatogram with chloroform/methanol/acetic anhydride (180:10:1, by vol) as shown in Figure 2. The Cer[NH] was, however, resolved from ceramide 5 by a thin-layer chromatogram developed with chloroform/methanol/acetic anhydride

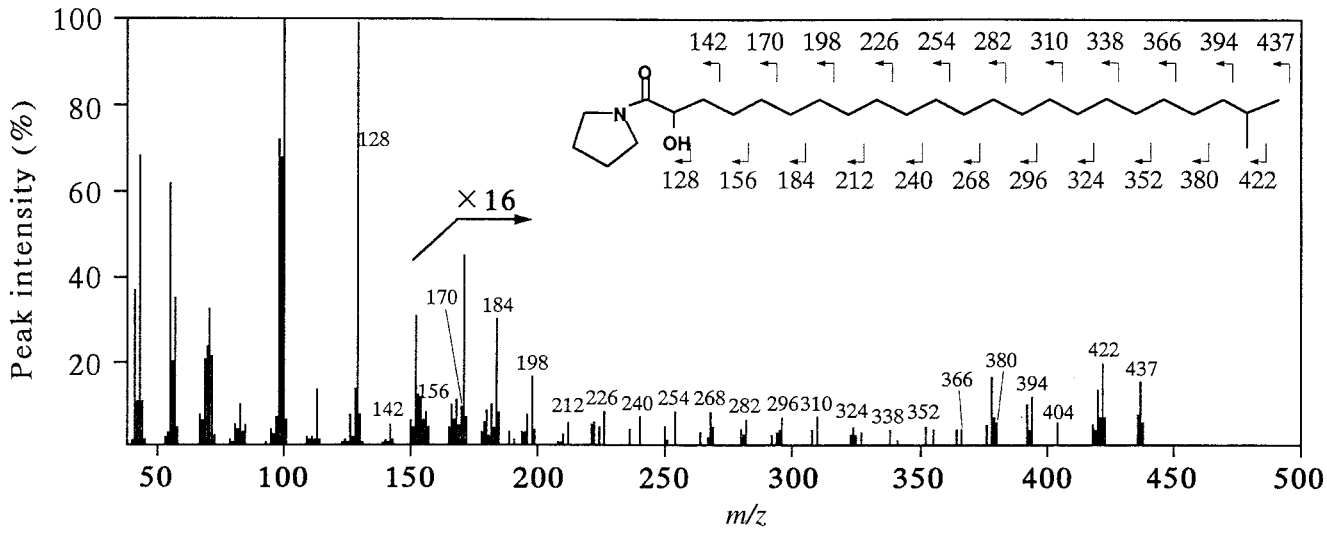

FIG. 8. Mass spectrum of pyrrolidide derivatives of α-hydroxy iso-tetracosanoic acid (α-hydroxy iso-24:0) from Cer[EAS] amide-linked fatty acids. The fragments of *m/z* greater than 150 were magnified 16 times (note the arrow). The figure inset shows the formation of fragments.

TABLE 3
Composition (%) of Ester-Linked Fatty Acid from Ceramide 1[a]

	Straight chain			Branched chain	
Carbon no.	Normal	Monoene	Diene	Iso	Anteiso
14	0.9				
15	0.6				
16	7.8	0.7		0.7	
17	1.1				0.4
18	5.6	5.0	36.5		
19	0.9				
20	3.2			2.3	
21	0.9			0.2	0.8
22	3.7			3.0	
23	1.2			0.4	1.1
24	4.5			5.9	
25	0.9			0.5	2.1
26	1.7			3.3	
27	0.7			0.0	
28	0.9			0.7	
Sum	34.6	5.7	36.5	17.0	4.4

[a]Data are means of duplicate analyses. Sum of other fatty acid components was 1.8%.

TABLE 5
Composition (%) of Fatty Acids from Ceramide 2[a]

	Straight chain	Branched chain	
Carbon no.	Normal	Iso	Anteiso
16	2.1		
17	0.4		
18	4.0		
19	0.7		
20	3.4	0.4	
21	0.9		
22	8.2	0.8	
23	4.8		0.4
24	23.7	4.4	
25	6.7	1.4	0.5
26	18.1	3.8	
27	3.3		0.9
28	8.9	0.9	
29	1.0		
30	0.6		
Sum	86.8	11.7	1.8

[a]Data are means of duplicate analyses.

(250:10:2, by vol). Table 8 shows that the predominant amide-linked fatty acids were straight-chain fatty acids, and supported the identification described above. The sum of the BCFA was 4.3% in this ceramide. The largest amide-linked fatty acid constituent of Cer[NH] was hexacosanoic acid (26:0), and this appeared to be a characteristic of this ceramide because the largest one for ceramides 2, 3, 5, 6, and 7 was tetracosanoic acid (24:0).

Tables 9 and 10 show the amide-linked fatty acid composition of ceramides 6 and 7, respectively. In both cases, α-hydroxy fatty acids were predictably the major amide-linked fatty acid component. The concentration of BCFA was 3.3% for ceramide 6 and 5.3% for ceramide 7.

TABLE 4
Composition (%) of Amide-Linked Fatty Acids from Ceramide 1[a]

	Straight chain		Branched chain α-hydroxy	
Carbon no.	α-Hydroxy	ω-Hydroxy	Iso	Anteiso
16	1.3			
18				
19				
20				
21				
22				
23	0.7			
24	1.9		6.0	
25	1.9			
26	2.6		4.9	
27				
28		9.0		
29		11.1		
30		49.5		
31		6.1		
32		5.9		
Sum	8.3	81.6	10.9	0.0

[a]Data are means of duplicate analyses.

DISCUSSION

The present study describes the fatty acid composition of human vernix caseosa ceramides for the first time. Two new free ceramides, Cer[EAS] and Cer[NH], were isolated by a combination of column chromatography and TLC. Cer[EAS] is an acylceramide and consists of ester- and amide-linked fatty acids and the sphingoid base of dihydrosphingosine. The amide-linked fatty acid of Cer[EAS] was found to be an α-hydroxy branched-chain fatty acid in this study. There were

TABLE 6
Composition (%) of Fatty Acids from Ceramide 3[a]

	Straight chain	Branched chain	
Carbon no.	Normal	Iso	Anteiso
16	1.2		
17	0.1		
18	1.2		
19	0.2		
20	1.5	0.3	
21	0.5		
22	9.1	0.4	
23	5.8		
24	28.3	3.2	
25	10.1	0.5	1.0
26	21.4	1.8	
27	3.9	0.1	0.4
28	6.9	0.4	
Sum	90.2	6.7	1.4

[a]Data are means of duplicate analyses. Sum of other fatty acid components was 1.8%.

TABLE 7
Composition of Fatty Acids from Ceramide 5[a]

Carbon no.	Straight chain		Branched chain α-hydroxy	
	Normal	α-Hydroxy	Iso	Anteiso
16	0.4	0.9		
18		1.6		
19		0.3		
20		1.8		
21		0.3		
22	0.8	2.8	0.8	
23	1.0	3.0		
24	5.4	19.9	6.7	
25		6.5		
26	8.7	11.6		
27	3.5	0.9		
28	9.2	0.2		
29	1.6			
30	1.3			
Sum	31.9	49.8	7.5	0

[a]Data are means of duplicate analyses. Sum of other fatty acid components was 10.8%.

therefore three hydroxy groups for the esterification: two on dihydrosphingosine base and one on α-hydroxy acyl moiety. The site for the ester linkage is under investigation, and will be described in a forthcoming paper.

Even though there was some uncertainty as to the chemical structure of Cer[EAS], analysis of amide-linked fatty acids in this study gave additional evidence for the structural identification of Cer[EAS]. Cer[EAS] was thus apparently different from ceramide 1 in that the amide-linked fatty acid for this ceramide was an α-hydroxy fatty acid, while that for ceramide 1 was an ω-hydroxy fatty acid.

In this study, the authors employed GC–MS of the picolinyl ester for the elucidation of the fatty acid chain structure. The

TABLE 8
Composition of Fatty Acids from Cer[NH][a]

Carbon no.	Straight chain		Branched chain	
	Normal	α-Hydroxy	Iso	Anteiso
16	0.6	6.2		
17		0.9		
18	0.8	3.3		
19		0.4		
20	0.7	1.2		
21	0.5			
22	2.9	1.0		
23	2.7	0.9		
24	17.8	2.8	1.0	
25	8.1	0.4	0.4	0.5
26	23.4	0.5	1.4	
27	5.3		0.2	0.4
28	12.2		0.4	
29	1.1			
Sum	76.1	17.6	3.4	0.9

[a]Data are means of duplicate analyses. Sum of other fatty acid components was 2.0%.

TABLE 9
Composition of Fatty Acids from Ceramide 6[a]

Carbon no.	Straight chain	Branched chain α-hydroxy	
	α-Hydroxy	Iso	Anteiso
20	2.0		
22	9.8		
23	7.7		
24	43.1	3.3	
25	10.2		
26	16.5		
Sum	89.3	3.3	0

[a]Data are mean of duplicate analysis. Sum of other fatty acid components was 7.4%.

equivalent chain length on isothermal analysis is a good index, but not decisive for the identification of the chain structure of fatty acid. As mentioned in the Results section, the mass spectrum of picolinyl ester was sensitive to the location of methyl substitution in the aliphatic chain. In the case of straight-chain fatty acid, the radical-induced fission of every carbon–carbon bond gives a series of fragments separated by 14 mass units. The presence of methyl substitution in the aliphatic chain, however, interrupts the generation of this series of ions, and gives a 28-mass-unit gap at the site of methyl branching. Thus the mass spectra of iso- and anteiso-fatty acids, respectively, lack M – 29 and M – 43 fragments, as shown in Figures 4 and 5, and this feature enables us to distinguish easily the iso- and anteiso-branching structure. The radical-induced cleavage of pyrrolidides has essentially the same mass spectrometric characteristics as picolinyl derivatives.

A single class of ceramide cannot have two types of amide-linked fatty acid. Analysis in the current study, however, found two types of amide-linked fatty acids in a single ceramide subclass. This may largely be due to insufficient purification of the ceramides. Even though the ceramide subclasses gave a single band on the HPTLC chromatogram, this

TABLE 10
Composition of Fatty Acids from Ceramide 7[a]

Carbon no.	Straight chain		Branched chain α-hydroxy	
	Normal	α-Hydroxy	Iso	Anteiso
16	0.6	0.9		
18	0.9	1.2		
19		0.3		
20	0.5	0.9		
22	2.6	2.1		
23		3.2		
24	2.5	32.5	2.7	
25		12.2		
26	1.7	23.3	2.6	
27		1.3		
Sum	8.8	77.9	5.3	0.0

[a]Data are means of duplicate analyses. Sum of other fatty acid components was 8.0%.

may not necessarily guarantee the purity of the specimen. The removal of any impurities may be essential for the detection of the single type of amide-linked fatty acid for the single ceramide subclass.

The uniqueness of Cer[EAS] manifested itself in that the greater proportion of ester- or amide-linked fatty acids of this ceramide consisted of the BCFA of the iso or anteiso series. The physiological significance of BCFA in skin surface lipids is still an open question. A postulate for the physiological role is that the BCFA resist bacterial flora, and consequently prevent the possible outgrowth of bacteria on the skin surface. This explanation appears to be true in the case of triacylglycerols of BCFA (12,13). The lower digestibility of BCFA therefore may contribute to some extent to minimize the undesirable growth of bacteria on the skin surface of a newborn baby.

Another point to note is that the melting point of BCFA is much lower than that of its straight-chain counterpart (14). This property also may be beneficial to keep the skin surface moist at the relatively low temperature of the skin surface. The BCFA concentration of vernix caseosa has been shown to be much higher than that for the skin surface lipid of adults (15,16). The pseudo skin surface lipid of a newborn baby showed a higher water-holding and -retaining capacity than that of an adult and superior aqueous vapor permeability (17).

The skin surface lipid of an adult is a mixture of cutaneous and sebaceous contributions, and the sebum production appears to be a determinant of the BCFA concentration of the skin surface lipid (18,19). An exclusively high concentration of BCFA in Cer[EAS] thus could be related to the contribution of this lipid by the sebaceous gland. The sebaceous gland of a fetus has been shown to be active after 110 gestational days (6).

ACKNOWLEDGMENTS

The authors thank Dr. Mark Dadebo for the correction of the grammatical errors of the manuscript. This study was supported in part by a Program for Promotion of Basic Research Activities or Innovative Bioscience from the Bio-Oriented Technology Research Advanced Institute (BRAIN) of Japan.

REFERENCES

1. Okah, F.A., Wickett, R.R., Pompa, K., and Hoath, S.B. (1994) Human Newborn Skin: The Effect of Isopropanol on Skin Surface Hydrophobicity, *Pediatr. Res. 35*, 443–446.
2. Fu, H.C., and Nicolaides, N. (1969) The Structure of Alkane Diols of Diesters in Vernix Caseosa, *Lipids 4*, 170–175.
3. Ansari, M.N.A., Fu, H.C., and Nicolaides, N. (1970) Fatty Acids of the Alkane Diol Diester of Vernix Caseosa, *Lipids 5*, 279–282.
4. Nicolaides, N. (1971) The Structure of the Branched Fatty Acids in the Wax Esters of Vernix Caseosa, *Lipids 6*, 901–905.
5. Nicolaides, N., Fu, H.C., Ansari, M.N.A., and Rice, G.R. (1972) The Fatty Acids of Wax Esters and Sterol Esters from Vernix Caseosa and from Human Surface Lipid, *Lipids 7*, 506–517.
6. Williams, M.L., Hincenbergs, M., and Holbrook, K.A. (1988) Skin Lipid Content During Early Fetal Development, *J. Invest. Dermatol. 91*, 263–268.
7. Harvey, D.J. (1992) Mass Spectrometry of Picolinyl and Other Nitrogen-Containing Derivatives of Lipids, in *Advances in Lipid Methodology* (Christie, W.W. eds.), The Oily Press, Ayr, Vol. 2, pp. 20–80.
8. Anderson, B.Å., and Halman, R.T. (1973) Pyrrolidides for Mass Spectrometric Determination of the Position of the Double Bond in Monounsaturated Fatty Acids, *Lipids 9*, 185–190.
9. Motta, S., Monti, M., Sesana, S., Caputo, R., Carelli, S., and Ghidoni, R. (1993) Ceramide Composition of the Psoriatic Scale, *Biochim. Biophys. Acta 1182*, 147–151.
10. Stewart, M.E., and Downing, D.T. (1999) A New 6-Hydroxy-4-sphingenine-Containing Ceramide in Human Skin, *J. Lipid Res. 40*, 1434–1439.
11. Robson, K., Stewart, M.E., Michelsen, S., Lazo, N.D., and Downing, D.T. (1994) 6-Hydroxy-4-sphingenine in Human Epidermal Ceramides, *J. Lipid Res. 35*, 2060–2068.
12. Tagiri, M., Endo, Y., Fujimoto, K., and Suzuki, T. (1992) Hydrolysis of Triglycerides of Branched-Chain Fatty Acids and Castor Oil Derivatives by Pancreatic Lipase, *Biosci. Biotechnol. Biochem. 56*, 1490–1491.
13. Tagiri, M., Endo, Y., Fujimoto, K., and Suzuki, T. (1994) Hydrolysis of Branched-Chain Triacylglycerols and Their Effects on Plasma and Hepatic Lipid Levels in the Rat, *Biosci. Biotechnol. Biochem. 58*, 1093–1096.
14. Weitkamp, W. (1945) The Acidic Constituents of Degras. A New Method of Structure Elucidation, *J. Am. Chem. Soc. 67*, 447–454.
15. Nazzaro-Porro, M., Passi, S., Boniforti, L., and Belsito, F. (1979) Effect of Aging on Fatty Acids in Skin Surface Lipids, *J. Invest. Dermatol. 73*, 112–117.
16. Yamamoto, A., Serizawa, S., Ito, M., and Sato, Y. (1987) Effect of Aging on Sebaceous Gland Activity and on the Fatty Acid Composition of Wax Ester, *J. Invest. Dermatol. 89*, 507–512.
17. Yakumaru, M., Tokitsu, Y., Sumida, Y., and Mimura, K. (1997) A Study on the Skin Surface of Newborn Baby and Its Application to Cosmetics, *Fragrance J. 1997-10*, 105–110 (in Japanese).
18. Stewart, M.E., Quinn, M.A., and Downing, D.T. (1982) Variability in the Fatty Acid Composition of Wax Esters from Vernix Caseosa and Its Possible Relation to Sebaceous Gland Activity, *J. Invest. Dermatol. 78*, 291–295.
19. Stewart, M.E., and Downing, D.T. (1985) Proportions of Various Straight and Branched Fatty Acid Chain Types in the Sebaceous Wax Esters of Young Children, *J. Invest. Dermatol. 84*, 501–503.

[Received November 29, 1999, and in revised form January 26, 2000; accepted February 3, 2000]

Utilization of Docosahexaenoic Acid from Intravenous Egg Yolk Phospholipid

Scott Morris, Karen Simmer, and Robert Gibson*

Faculty of Health Sciences, Flinders University of South Australia, and the Department of Pediatrics and Child Health, Flinders Medical Centre, Bedford Park, South Australia, 5042, Australia

ABSTRACT: Docosahexaenoic acid (DHA, 22:6n-3) is provided directly to human premature infants during parenteral nutrition from the egg yolk fraction of an intravenous fat emulsion. This study aimed to determine whether the high egg yolk phospholipid content of Intralipid 10% (IL 10%, Pharmacia, Uppsala, Sweden) relative to the standard emulsion Intralipid 20% (IL 20%, Pharmacia) could be a strategy to increase the delivery of DHA to the developing brain. Male, Large White piglets were randomly selected from sows 3 d after birth. Piglets were assigned to receive a 9-d continuous intravenous infusion commencing 5 d after birth of either Intralipid (IL) 10%, IL 20%, or Lipofundin S 20% (LFS; B. Braun, Melsungen, Germany). There were four piglets in each treatment group. IL 10% provides twice as much DHA as IL 20%, while LFS provides no DHA. Protein and other nutrients were provided enterally using a low-fat milk formula. After 9 d, animals were killed, and the fatty acid compositions of blood, liver, and cerebral cortex were analyzed. IL 10% infusion approximately doubled the amount of plasma phospholipid DHA (μg/mL of plasma) in comparison to IL 20%. However, red blood cells, liver, and cerebral cortex phospholipid DHA levels were indistinguishable between these two groups. LFS was associated with reduced levels of DHA in plasma, red blood cell and liver phospholipids in comparison to IL 20%. We conclude that infusion of additional phospholipid is an ineffective strategy for increasing DHA delivery to piglet tissues. This may be due to the formation of inert phospholipid particles in plasma. The data do not support the concept of using IL 10% as a means of providing additional DHA to premature human infants.

Paper no. L8224 in *Lipids 35*, 383–388 (April 2000).

A dietary source of docosahexaenoic acid (DHA, 22:6n-3) is potentially important for normal functional development of the human premature infant's brain (1,2). This hypothesis raises concerns regarding DHA provision to very immature infants, in whom significant quantities of milk feeds are often precluded and for whom a reliance is placed on parenteral nutrition (3). The only external source of DHA and precursor fatty acids during parenteral nutrition is an intravenous fat emulsion. The standard fat emulsion utilized in most neonatal units worldwide is Intralipid 20% (IL 20%, Pharmacia, Uppsala, Sweden), which is composed of soybean triglyceride emulsified with egg yolk phospholipid. DHA is contained within the egg yolk phospholipid fraction.

The quantity of DHA provided by the maximal infusion rate of IL 20% recommended by the American Academy of Pediatrics (3g/kg/d of triglyceride) is approximately 13 mg/d for a 1,500-g preterm infant (based on our laboratory measurement of 2.94 mg DHA/g of triglyceride) (4). This quantity of DHA is approximately 40% of that provided by 200 mL/kg/d of breast milk, assuming a fat content of 3.5 g/100 mL with DHA constituting 0.3% of total fatty acid. Limited data also indicate that DHA levels in liver of preterm infants that received parenteral nutrition with IL 20% are reduced in comparison to infants nourished *in utero* (5). These observations suggest that even maximal recommended quantities of IL 20% may be inadequate to support normal fetal accretion of DHA during parenteral nutrition. Infants receiving less than recommended quantities of IL 20% would be expected to be at greater risk of abnormally low tissue DHA levels.

Our aim was to determine whether the infusion of a commercially available intravenous fat emulsion with a high egg yolk phospholipid content (and therefore a relatively high DHA content) could increase the level of DHA in cerebral cortex above that induced by IL 20%. A newborn piglet model of the human infant was utilized because the perinatal timing of the brain growth spurt in the piglet provides an opportunity to study the effect of intravenous fat infusion on the immature brain (6).

EXPERIMENTAL PROCEDURES

All study methods were approved by the Animal Ethics Committee at Flinders Medical Centre.

Treatment groups. Male, pure-bred Large White piglets were randomly selected from litters after 72 h of suckling and assigned to receive one of three intravenous fat emulsions: IL 20% (Pharmacia, Sweden), IL 10% (Pharmacia), or Lipofundin S 20% (LFS; B. Braun, Melsungen, Germany). The fatty acid composition of these three emulsions is shown in Table 1. Soybean triglyceride is the predominant fat in all three emulsions, and the fatty acid composition of this fraction was similar in each case. The rationale was to maintain a constant triglyceride fatty acid intake, and therefore a constant supply of essential

*To whom correspondence should be addressed at Child Nutrition Research Centre, Child Health Research Institute, Flinders Medical Center, South Australia, 5042. E-mail: rgibson@flinders.edu.au

Abbreviations: DHA, docosahexaenoic acid, 22:6n-3; IL 20%, Intralipid 20%; IL 10%, Intralipid 10%; LA, linoleic acid; LFS, Lipofundin S; LP-X, lipoprotein X.

TABLE 1
Composition of IL 20%, IL 10%, and LFS 20%[a]

	Total lipid			Triglyceride			Phospholipid		
Fatty acid	IL 20%	IL 10%	LFS	IL 20%	IL 10%	LFS	IL 20%	IL 10%	LFS
Total sat.	16.6 ± 0.0	17.9 ± 0.0	15.5 ± 0.0	15.6 ± 0.2	15.9 ± 0.1	15.4 ± 0.1	44.6 ± 0.1	42.3 ± 0.2	18.5 ± 0.2
18:1n-9	21.4 ± 0.0	21.5 ± 0.0	21.8 ± 0.1	21.2 ± 0.2	21.2 ± 0.0	22.5 ± 0.1	26.9 ± 0.2	24.2 ± 0.2	12.6 ± 0.1
Total mono.	23.1 ± 0.0	23.2 ± 0.1	23.5 ± 0.1	22.9 ± 0.2	22.9 ± 0.0	24.4 ± 0.2	29.3 ± 0.1	26.5 ± 0.2	14.3 ± 0.1
18:2n-6	52.7 ± 0.0	50.8 ± 0.0	53.2 ± 0.1	53.8 ± 0.2	53.7 ± 0.1	52.6 ± 0.1	13.8 ± 0.1	14.3 ± 0.2	60.7 ± 0.1
18:3n-6	—	—	—	—	—	—	—	0.1 ± 0.0	—
20:3n-6	—	—	—	—	—	—	0.2 ± 0.1	0.3 ± 0.0	—
20:4n-6	0.2 ± 0.0	0.5 ± 0.0	—	—	—	—	5.2 ± 0.0	5.7 ± 0.1	—
22:4n-6	—	—	—	—	—	—	0.3 ± 0.0	0.5 ± 0.0	—
22:5n-6	—	—	—	—	—	—	0.6 ± 0.0	0.7 ± 0.0	—
18:3n-3	7.2 ± 0.0	6.7 ± 0.0	7.2 ± 0.1	7.3 ± 0.1	7.2 ± 0.0	7.2 ± 0.1	—	0.2 ± 0.0	5.2 ± 0.0
20:5n-3	—	—	—	—	—	—	—	0.3 ± 0.0	—
22:5n-3	—	—	—	—	—	—	0.3 ± 0.0	0.4 ± 0.0	—
22:6n-3	0.2 ± 0.0	0.4 ± 0.0	—	—	—	—	4.9 ± 0.0	5.1 ± 0.0	—

[a]All values are the mean ± SD of three analyses, expressed as percentages of total fatty acid. Where no value is entered, the fatty acid constituted <0.05% of the total. The amount of phospholipid provided per gram of triglyceride is 60 mg for IL 20%, 120 mg for IL 10%, and 75 mg for LFS. Intravenous fat emulsions: IL 20% (Pharmacia, Uppsala, Sweden), IL 10% (Pharmacia), and LFS (Lipofundin S 20%; B. Braun, Melsungen, Germany). Abbreviations: Total sat., total saturated fatty acids; total mono; total monounsaturated fatty acids.

precursor fatty acids for long-chain polyunsaturated fatty acid synthesis. The isolated effect of infused phospholipid on tissue fatty acid composition could then be assessed. DHA is contained in the egg yolk phospholipid fraction of both IL 20% and IL 10%. IL 10% provides double the amount of phospholipid and hence DHA for a given quantity of triglyceride in comparison to IL 20%. LFS contains soybean phospholipid and is therefore devoid of DHA.

Calculations of sample size were based on cerebral cortex fatty acid data derived from milk-fed piglets (7). To detect a difference in cortex DHA of 0.6% (percentage of total phospholipid fatty acid) with a study power of 80%, four piglets per group were required (7). All piglets within each treatment group were from separate litters.

Nutrition. A model was established whereby fat was delivered intravenously, while other nutrients were provided *via* the enteral route using a low-fat milk formula. The details of the development of this model have been published previously, and information regarding milk composition and macronutrient and energy intake in the experimental piglets is referenced (8). Briefly, piglets were first trained over a 36-h period to accept a low-fat milk formula devoid of DHA (Wombaroo Foods, Glen Osmond, Australia). The milk contained 0.4 g fat, 6.1 g protein, 4.8 g carbohydrate, and 198 kJ total energy per 100 mL of milk. The fatty acid composition of the milk fat (percentage of total fatty acid expressed as the mean ± SD of three analyses) was 61.7 ± 0.1% saturates, 31.8 ± 0.1% monounsaturates, 2.8 ± 0.2% 18:2n-6, 0.2 ± 0.0% 20:3n-6, 0.3 ± 0.0% 20:4n-6, 1.3 ± 0.0% 18:3n-3, 0.3 ± 0.0% 20:5n-3, and 0.5 ± 0.1% 22:5n-3. The milk was made daily by reconstituting dry milk powder with water. Piglets were required to suck the milk *via* a straw from a graduated container positioned below the teat, to minimize milk losses. Piglets were housed individually in clean pens with a plastic grill floor, to avoid the animals eating feces, urine, or bedding. A constant thermoneutral environment (30°C) was maintained.

On experimental day 1 (day 5 of life), a central venous catheter was inserted, and a continuous intravenous infusion of fat emulsion commenced at 3.0 g/kg/d of the triglyceride component within 2–3 h of surgery. The infusion rate was increased to 6.0 g/kg/d on experimental day 2 and to 10 g/kg/d from experimental d 3 to 9. At the peak rate of triglyceride infusion, IL 20% and IL 10% provide 29 and 61 mg/kg/d of DHA from egg yolk phospholipid, respectively, while LFS provides no DHA. A limit of 10 g/kg/d of fat infusion had been determined from pilot studies, as higher infusion rates had been associated with lung injury (8).

Piglets were weighed daily, and nutrient intake (dose of intravenous fat and mass of dry milk powder) was determined for the subsequent 24 h based on a predicted daily weight gain of 150 g. If the daily lipid dose was not delivered due to line occlusion or pump failure, then the deficit was given over the following 24 h. As the rate of lipid infusion (and therefore intravenous fluid) increased, the milk concentration was increased (enteral fluid intake reduced) to ensure piglets consumed a constant mass of protein and other nutrients each day before satiation.

By using this method, approximately 90% of total fat was delivered intravenously, with the quantity of enteral fat consumed kept constant between the groups (8). During the period of maximal intravenous lipid infusion (10 g/kg/d), the total energy provided *via* the combined intravenous and enteral routes was approximately 978 kJ/kg/d, with intravenous fat providing approximately 38% of total energy. Enteral fat intake was approximately 1.1 g/kg/d (4.3% of total energy), protein 18.8 g/kg/d (32% of total energy), and carbohydrate 14.7 g/kg/d (25% total energy).

The rationale for a 9-d period of lipid infusion was based on validation studies showing that the newborn piglet model could be reliably maintained for this period, but not beyond (8). Large changes in DHA levels in cerebral cortex and other tissues are also inducible by diet over a 14-d time period (7). Hence a 9-d period was considered likely to be adequate to detect an effect of differing parenteral DHA intakes.

Collection of tissue samples. On experimental day 10 (9 full days after surgery), the lipid infusion was turned off and the central venous catheter clamped. The piglets were then immediately anesthetized by intravenous injection of pentobarbitone sodium (30 mg/kg) *via* the catheter, and 1 mL of blood was collected by cardiac puncture into lithium heparin tubes. Piglets were then killed with intracardiac pentobarbitone sodium (110 mg/kg). Body weight was then recorded, and the liver and brain were removed and weighed. Blood and tissue samples were transported to the laboratory on ice and unfrozen. Fatty acids were extracted from red blood cells within 2 h of collection. Plasma and tissue samples were frozen within the same time period.

Fatty acid analysis of red blood cells. A 400-μL aliquot of blood was centrifuged at 13,000 rpm for 2 min, and the plasma removed and frozen at –20°C for batch analysis. Red blood cells were washed three times with isotonic saline and transferred to a glass tube for immediate analysis.

Total lipids from red blood cells were extracted according to the method of Broekhuyse (9). The volume of packed red blood cells after centrifugation was made up to 1.5 mL with isotonic saline, and isopropanol and chloroform (2 mL/4 mL) added. Following centrifugation (3,000 rpm for 10 min), the bottom layer was transferred to an evaporation flask and the solvents were evaporated under nitrogen. The evaporation flasks were rinsed twice with 9:1 chloroform/methanol to transfer the lipid extract to glass vials.

The solvent–lipid extract was then evaporated to dryness under nitrogen, 150 μL of chloroform/methanol 9:1 added, the solution spotted onto a silica gel-coated thin-layer chromatography plate (Merck Silica Gel spread on 10 × 20 or 20 × 20 cm glass plates, 0.30-mm thick, activated at 100°C for 30 min), and the plate run in a solvent solution of petroleum spirit/acetone 3:1. The phospholipid band was scraped into glass vials containing 1% sulfuric acid in methanol, and heated for 3 h at 70°C. After cooling, 0.25 mL of distilled water and 0.5 mL of heptane were added to each vial, the solution was mixed, and the top layer transferred into gas chromatography vials containing anhydrous sodium sulfate.

Gas chromatographic analysis of fatty acid methyl esters was performed with a Hewlett-Packard 5880 gas chromatograph. Separation utilized a 50-m capillary column, 0.33 mm i.d. coated with 0.25 μm BPX-70 (SGE Pty. Ltd., Victoria, Australia). The injector temperature was set at 250°C, and the initial oven temperature was 140°C and programmed to rise to 220°C at 5°C/min. Helium was used as the carrier gas at a velocity of 35 cm/s. The flame-ionization detector temperature was set at 300°C. Fatty acid methyl esters were identified based on the retention time of authentic lipid standards (Nu-Chek-Prep Inc., Elysian, MN). Fatty acid peaks were integrated using Hewlett-Packard Chemstation software and expressed as a percentage of total phospholipid fatty acid.

Fatty acid analysis of plasma. Plasma samples were defrosted by standing, and allowed to come to room temperature (22°C). Lipid extraction from plasma followed the method of Bligh and Dyer (10), with the exception of the addition of diheptodecanoyl glycero-3-phosphocholine and triheptadecanoic acid internal standards (10). The volume of each plasma sample was determined by weighing into a tared glass tube to an accuracy of five decimal places. Isotonic saline was added to make the volume to 1.5 mL, followed by 2 mL of methanol. The internal standards were added at this step, and chloroform (4 mL) was then added. Data validating this method of fatty acid quantitation have been presented elsewhere by the authors (11).

The subsequent treatment of plasma lipids was identical to that described for red blood cells with the exception of separation of plasma phospholipids and triglycerides by thin-layer chromatography using petroleum spirit/diethylether/glacial acetic acid 90:15:1. Individual fatty acids were expressed both as a percentage of total phospholipid or triglyceride fatty acid and as μg/mL of plasma. Microgram per milliliter values were utilized to reflect the quantity of infused fatty acids, whereas percentages of total fatty acid were considered more reflective of plasma composition.

Fatty acid analysis of cerebral cortex and liver. The whole left cerebral hemisphere and a constant portion of the left lobe of the liver from each piglet were frozen at –20°C for later batch analysis. Each cerebral hemisphere was defrosted by standing at room temperature. The frontal area of the hemisphere was sliced in a coronal plane, and the gray and white matter were separated by manual dissection without magnification. A sample of gray matter approximately 50 μg in weight was extracted with 2.45 mL of saline, 3 mL of methanol, and 6 mL of chloroform and subsequently analyzed as for red blood cell phospholipid fatty acids. Fatty acids were expressed as a percentage of total phospholipid fatty acid. Validation of this methodology in our laboratory has shown the coefficient of variance for fatty acids in the frontal cortex contributing >5% of the total to range between 0.4–7.2%, and for fatty acids contributing 0.5–5.0% of the total to range between 0.3 and 14.5%. The lipid extraction and fatty acid analysis of liver samples followed the same method as cerebral cortex.

Statistical methods. Data were analyzed by one-way analysis of variance, with *post-hoc* analysis using the Tukey Honestly Significant Difference test, and using SPPS for Windows 6.1.3 (SPSS Inc., Berkeley, CA, 1995).

RESULTS

Nutrient intake and growth. Nutrient intake and growth of piglets was detailed in a previous methodological paper (8). There were no detectable differences in the measured amounts of intravenous triglyceride, enteral carbohydrate, protein, or fat received over the experimental period between the treatment groups.

There were no detectable differences in the initial and final body weights, and final brain weights between the groups. The final body weight (mean ± SD) of the 12 experimental piglets was 2,950 ± 241 g. Final body weight was less than that observed in age-matched sow-fed piglets (95% confidence intervals of four sow-fed piglets, 3,570–3,958 g). The final brain

TABLE 2
Plasma Triglyceride Fatty Acids[a]

Fatty acid	IL 20% (*n* = 4)	IL 10% (*n* = 4)	LFS (*n* = 4)
Total sat.	29.1 ± 15.3	43.0 ± 23.2	32.9 ± 8.9
	(19.3 ± 1.3)	(19.6 ± 0.9)	(17.4 ± 1.3)
18:1n-9	29.2 ± 16.9	42.5 ± 24.2	41.3 ± 12.9
	(18.9 ± 0.8)^{a}	(19.0 ± 1.0)^{a}	(21.6 ± 1.0)^{b}
Total	33.4 ± 19.4	48.0 ± 27.5	47.4 ± 15.0
mono.	(21.5 ± 0.7)	(21.4 ± 1.0)	(24.7 ± 0.8)
18:2n-6	63.5 ± 38.2	94.3 ± 56.1	78.7 ± 26.6
	(40.0 ± 3.2)	(41.6 ± 2.5)	(40.8 ± 1.0)
18:3n-6	5.2 ± 3.7	5.5 ± 4.2	3.9 ± 2.3
	(3.1 ± 0.8)	(2.3 ± 0.6)	(1.9 ± 0.5)
20:3n-6	0.3 ± 0.1	0.4 ± 0.2	0.5 ± 0.2
	(0.2 ± 0.1)	(0.2 ± 0.0)	(0.3 ± 0.0)
20:4n-6	5.6 ± 2.8	7.0 ± 3.6	10.4 ± 5.3
	(3.8 ± 0.8)^{a,b}	(3.3 ± 0.9)^{a}	(5.2 ± 1.0)^{b}
22:4n-6	0.3 ± 0.1	0.4 ± 0.2	0.8 ± 0.4
	(0.3 ± 0.1)^{a,b}	(0.20 ± 0.0)^{a}	(0.4 ± 0.1)^{b}
22:5n-6	0.2 ± 0.1	0.2 ± 0.1	0.2 ± 0.1
	(0.1 ± 0.1)	(0.1 ± 0.0)	(0.1 ± 0.0)
18:3n-3	6.6 ± 4.0	10.7 ± 6.6	6.2 ± 2.1
	(4.1 ± 0.7)^{a,b}	(4.6 ± 0.5)^{a}	(3.2 ± 0.2)^{b}
20:5n-3	2.4 ± 1.2	3.1 ± 1.5	3.3 ± 2.2
	(1.6 ± 0.1)	(1.5 ± 0.5)	(1.6 ± 0.5)
22:5n-3	1.3 ± 0.6	1.6 ± 0.9	2.0 ± 1.3
	(0.9 ± 0.2)	(0.7 ± 0.2)	(1.0 ± 0.4)
22:6n-3	2.4 ± 1.3	3.4 ± 1.5	2.2 ± 1.3
	(1.6 ± 0.3)	(1.7 ± 0.4)	(1.1 ± 0.3)
Total	155.0 ± 88.5	222.9 ± 126.4	193.1 ± 65.6

[a]Data are presented as μg/mL of plasma on the first line of each row, with percentages of total fatty acid in parentheses on the second line. All data are means ± SD. Unlike superscripted letters indicate statistical difference, $P < 0.05$. For abbreviations and manufacturers see Table 1.

TABLE 3
Plasma Phospholipid Fatty Acids[a]

Fatty acid	IL 20% (*n* = 4)	IL 10% (*n* = 4)	LFS (*n* = 4)
Total sat.	346.8 ± 54.1^{a}	892.2 ± 123.4^{b}	336.6 ± 48.7^{a}
	(42.8 ± 0.7)^{a}	(44.0 ± 0.4)^{a}	(36.7 ± 1.0)^{b}
18:1n-9	126.7 ± 22.9^{a}	444.8 ± 71.8^{b}	89.5 ± 12.3^{a}
	(15.6 ± 0.8)^{a}	(21.9 ± 0.9)^{b}	(9.8 ± 0.4)^{c}
Total	147.2 ± 26.4^{a}	492.4 ± 79.0^{b}	114.2 ± 14.7^{a}
mono.	(18.1 ± 0.9)^{a}	(24.3 ± 1.0)^{b}	(12.5 ± 0.4)^{c}
18:2n-6	133.9 ± 25.2^{a}	308.4 ± 41.3^{b}	286.8 ± 36.8^{b}
	(16.4 ± 1.0)^{a}	(15.2 ± 0.2)^{a}	(31.4 ± 1.0)^{b}
18:3n-6	1.4 ± 0.7^{a}	2.7 ± 0.7^{b}	1.5 ± 0.4^{a}
	(0.2 ± 0.1)	(0.1 ± 0.0)	(0.2 ± 0.0)
20:3n-6	4.9 ± 0.6^{a}	8.9 ± 0.9^{b}	4.5 ± 0.9^{a}
	(0.6 ± 0.1)^{a}	(0.4 ± 0.0)^{b}	(0.5 ± 0.0)^{a,b}
20:4n-6	96.6 ± 18.4^{a}	173.2 ± 19.4^{b}	96.8 ± 23.0^{a}
	(11.9 ± 0.4)^{a}	(8.6 ± 0.4)^{b}	(10.5 ± 1.3)^{a}
22:4n-6	4.2 ± 0.6^{a}	9.5 ± 0.9^{b}	3.0 ± 0.7^{a}
	(0.5 ± 0.0)^{a}	(0.5 ± 0.0)^{a}	(0.3 ± 0.1)^{b}
22:5n-6	3.5 ± 0.8^{a}	11.6 ± 0.9^{b}	0.6 ± 0.1^{c}
	(0.4 ± 0.0)^{a}	(0.6 ± 0.0)^{b}	(0.1 ± 0.0)^{c}
18:3n-3	3.4 ± 0.7^{a}	5.4 ± 1.1^{a}	12.9 ± 1.3^{b}
	(0.4 ± 0.0)^{a}	(0.3 ± 0.0)^{b}	(1.4 ± 0.1)^{c}
20:5n-3	3.4 ± 0.7^{a,b}	5.1 ± 1.4^{a}	2.8 ± 0.5^{b}
	(0.4 ± 0.0)^{a}	(0.3 ± 0.0)^{b}	(0.3 ± 0.0)^{b}
22:5n-3	8.6 ± 0.9	12.1 ± 2.4	11.5 ± 4.1
	(1.1 ± 0.2)^{a,b}	(0.6 ± 0.1)^{a}	(1.3 ± 0.5)^{b}
22:6n-3	46.9 ± 2.4^{a}	89.7 ± 13.4^{b}	32.7 ± 5.5^{a}
	(5.7 ± 0.9)^{a}	(4.4 ± 0.2)^{b}	(3.6 ± 0.2)^{b}
Total	812.7 ± 137.1^{a}	2026.2 ± 279.7^{b}	916.3 ± 128.9^{a}

[a]Data are presented as μg/mL of plasma on the first line of each row, with percentages of total fatty acid in parentheses on the second line. All data are means ± SD. Unlike superscripted letters indicate statistical difference, $P < 0.05$. For abbreviations and manufacturers see Table 1.

weight of the experimental piglets was 30.1 ± 2.2 g, comparable to that of sow-fed piglets (95% confidence intervals of four sow-fed piglets 30.7–31.5). The energy intake of the experimental piglets was limited to 978 ± 23 kJ/kg/d, in comparison to estimates of 1,410 kJ/kg/d in sow-fed piglets, due to limitations in the quantity of intravenous fat able to be safely infused (8).

Plasma triglyceride fatty acids. Plasma triglyceride fatty acid data are shown Table 2. Plasma triglyceride composition and total fatty acid levels showed only minor differences between the treatment groups, reflecting the constancy of intravenous triglyceride input between the groups.

Plasma phospholipid fatty acids. Plasma phospholipid data are presented in Table 3. When expressed as μg/mL amounts, plasma phospholipid DHA levels were higher during IL 10% in comparison to IL 20% infusion. A similar pattern was seen with other plasma phospholipid fatty acids. When expressed as a percentage of total phospholipid fatty acid, phospholipid fatty acids during IL 10% infusion were similar to or reduced in comparison to IL 20% infusion. LFS infusion resulted in trends to lower DHA levels expressed as μg/mL, and to lower DHA levels as a percentage of total phospholipid fatty acids. The enrichment of the soybean phospholipid of LFS with 18:2n-6 and 18:3n-3 was reflected in the higher levels of these fatty acids in comparison to IL 20%.

Red blood cell phospholipid fatty acids. Red blood cell phospholipid fatty acids were indistinguishable in piglets receiving IL 20% or IL 10% (Table 4). Trends to higher levels of linoleic acid (LA) and a statistically significant reduction in red blood cell DHA were induced by LFS in comparison to IL 20%.

Liver and cerebral cortex phospholipids. In liver and cerebral cortex phospholipids, IL 20% and IL 10% had a similar effect on fatty acid composition (Table 5). LFS induced statistically significant elevations in LA in comparison to the other emulsions in both tissues, although this increase was quantitatively minor in the brain. LFS also induced a statistically significant reduction in DHA and a trend to lower arachidonic acid levels in liver in comparison to the other emulsions, but these changes were not apparent in the brain.

DISCUSSION

Increasing the intravenous delivery of phospholipid DHA is one potential strategy to provide additional DHA to developing tissues during parenteral nutrition. This strategy was tested by comparing the effect of IL 10% (high phospholipid content) with IL 20% (low phospholipid content) on tissue DHA composition. IL 10% induced high μg/mL amounts of plasma phospholipid DHA relative to IL 20%, indicating a greater influx of phospholipid DHA from the emulsion. However, there was no detectable difference in the DHA composition of red blood

TABLE 4
Red Blood Cell Phospholipid Fatty Acids[a]

Fatty acid	IL 20% (n = 4)	IL 10% (n = 4)	LFS (n = 4)
Total sat.	35.9 ± 0.8	36.5 ± 1.2	35.1 ± 0.6
18:1n-9	29.2 ± 2.7	30.3 ± 2.0	28.1 ± 2.6
Total mono.	34.4 ± 2.7	35.2 ± 1.8	33.5 ± 2.3
18:2n-6	17.5 ± 1.4	17.3 ± 0.6	20.6 ± 2.5
18:3n-6	0.1 ± 0.0	0.1 ± 0.0	0.1 ± 0.1
20:3n-6	0.4 ± 0.0	0.3 ± 0.1	0.3 ± 0.1
20:4n-6	4.8 ± 0.7	4.6 ± 0.7	4.3 ± 1.1
22:4n-6	0.6 ± 0.1	0.6 ± 0.1	0.5 ± 0.2
22:5n-6	0.4 ± 0.2	0.4 ± 0.1	0.4 ± 0.2
18:3n-3	0.7 ± 0.1[a]	0.6 ± 0.1[b]	0.9 ± 0.0[a]
20:5n-3	0.2 ± 0.0	0.2 ± 0.0	0.2 ± 0.1
22:5n-3	1.0 ± 0.1	0.8 ± 0.1	0.9 ± 0.2
22:6n-3	2.8 ± 0.3[a]	2.6 ± 0.4[a,b]	2.1 ± 0.3[b]

[a]Data are presented as percentages of total phospholipid fatty acid. All data are means ± SD. Unlike superscripted letters indicate statistical difference, $P < 0.05$. For abbreviations and manufacturers see Table 1.

cells, liver, and cerebral cortex of piglets receiving either IL 10% or IL 20%.

One explanation for this result is the accumulation of DHA in an inert plasma phospholipid pool. The majority of phospholipid in IL 10% is not associated with the surface of triglyceride particles, but rather exists as liposomal phospholipid (12–14). The quantity of liposomal material infused with IL 10% is approximately fourfold in comparison to IL 20% (14). High rates of liposome infusion exceed the capacity for clearance and lead to the formation of circulating phospholipid particles, termed lipoprotein X (LP-X), which are enriched in free cholesterol (13). LP-X particles have a half-life of up to 6 d in human studies (14). This indicates stability in plasma and poor interaction of the particle phospholipid with cell membranes and other circulating lipoprotein particles (14). Observations in parenterally fed rats suggest that egg yolk phospholipid infused with IL 10% accumulates in plasma, partially replacing endogenous phospholipids (15). Data derived from the rat model also show a discordance in plasma and tissue fatty acid composition, consistent with poor bioavailability of the infused phospholipid (15).

Alternative explanations for the inability of the additional phospholipid DHA from IL 10% to increase tissue DHA levels may be a confounding influence of early sow milk feeding, or an inadequate study length. It is unlikely that the early intake of sow milk would influence later treatment effects, because the duration of sow milk feeding was short (3 d) and sow milk from our experimental herd contains very low (0.06% of total fatty acid) DHA levels. While it is possible that the study duration of 9 d was too short to see a change in cerebral cortex, an adequate time frame for change in red blood cells and liver is confirmed by reduced DHA in these tissues in the LFS group compared to the IL 20% group. This is consistent with other observations of a rapid response in newborn piglet tissue fatty acid composition following enteral DHA supplementation, where an increase in DHA content to saturation levels has been achieved in liver and cerebral cortex after 14 d (7).

Other possible explanations for our results are that the additional amount of DHA was too small to induce a detectable change in tissues, or that membranes have reached saturation with DHA. The additional quantity of DHA provided by IL 10% (IL 20% provides 29 mg/kg/d of DHA, and IL 10% provides 61 mg/kg/d when 10 g/kg/d of triglyceride is infused) would be expected to induce a detectable change in liver and cerebral cortex based on the liver and synaptic membrane DHA response to incremental increases in enteral DHA provision over a similar dose range in newborn piglets fed milk for 15 d (16). Membrane saturation is unlikely as the DHA levels in liver and frontal cortex observed in this study are well below the saturation levels of corresponding piglet tissues achieved after 2 wk of enteral DHA supplementation (approximately 19 and 15–16% of total phospholipid fatty acid in liver and frontal cortex, respectively) (7). Furthermore, the plasma–tissue disparity is also apparent with fatty acids other than DHA.

Although the μg/mL quantity of DHA was higher in plasma during IL 10% infusion in comparison to IL 20%, when expressed as a percentage of total phospholipid fatty acid, DHA was lower during IL 10% compared to IL 20%. It is possible that tissue DHA levels could remain unchanged by IL 10%

TABLE 5
Liver and Frontal Cortex Phospholipid Fatty Acids[a]

	Liver			Frontal cortex		
Fatty acid	IL 20% (n = 4)	IL 10% (n = 4)	LFS (n = 4)	IL 20% (n = 4)	IL 10% (n = 4)	LFS (n = 4)
Total sat.	39.1 ± 0.2	40.1 ± 0.3	40.5 ± 2.1	47.5 ± 0.1	47.8 ± 0.6	47.7 ± 0.3
18:1n-9	8.1 ± 0.7	8.7 ± 0.6	7.8 ± 0.3	11.0 ± 0.5	10.8 ± 0.4	10.4 ± 0.4
Total mono.	10.7 ± 0.8	10.9 ± 0.7	10.6 ± 0.4	18.4 ± 0.5[a]	17.4 ± 0.6[a,b]	17.1 ± 0.5[b]
18:2n-6	18.7 ± 1.3[a]	17.9 ± 0.2[a]	22.9 ± 1.5[b]	1.2 ± 0.1[a]	1.3 ± 0.1[a]	1.8 ± 0.2[b]
18:3n-6	0.4 ± 0.1	0.4 ± 0.1	0.3 ± 0.1	0.1 ± 0.1	0.1 ± 0.0	0.1 ± 0.0
20:3n-6	0.7 ± 0.1	0.6 ± 0.1	0.6 ± 0.0	0.7 ± 0.0[a]	0.7 ± 0.0[a]	0.8 ± 0.1[b]
20:4n-6	16.6 ± 0.8	16.6 ± 0.9	14.3 ± 1.7	10.6 ± 0.5	10.8 ± 0.4	10.8 ± 0.4
22:4n-6	0.6 ± 0.1	0.5 ± 0.0	0.5 ± 0.1	4.3 ± 0.5	4.4 ± 0.4	4.5 ± 0.4
22:5n-6	0.3 ± 0.0[a]	0.5 ± 0.0[b]	0.2 ± 0.0[c]	2.8 ± 0.3	3.0 ± 0.1	3.0 ± 0.2
18:3n-3	0.6 ± 0.1	0.5 ± 0.0	0.6 ± 0.2	—	—	—
20:5n-3	0.6 ± 0.1[a]	0.6 ± 0.1[a]	0.3 ± 0.0[b]	—	—	—
22:5n-3	1.4 ± 0.2	1.2 ± 0.2	1.5 ± 0.4	0.4 ± 0.0[a,b]	0.4 ± 0.0[a]	0.5 ± 0.0[b]
22:6n-3	8.8 ± 1.3[a]	8.9 ± 1.1[a]	6.3 ± 1.0[b]	12.9 ± 0.8	12.9 ± 0.8	12.7 ± 0.6

[a]Data are presented as percentages of total phospholipid fatty acid. All data are means ± SD. Unlike superscripts indicate statistical difference, $P < 0.05$. Where no value is entered, the fatty acid constituted <0.05% of the total. For abbreviations see Table 1.

owing to an increase in the total amount of phospholipid, were the phospholipid composition to reflect that of the plasma. We did not measure total phospholipid in tissues, although the total phospholipid content of rat liver (mg/g wet weight) has been shown to remain stable during IL 10% infusion, suggesting this to be an unlikely explanation (15). However, an increase in red blood cell phospholipid (mg/g protein) has been noted under the same conditions in the rat (17).

The effect of IL 10% infusion on levels of plasma lipoproteins, and the distribution of DHA between lipoprotein subfractions, were not investigated in this experiment. Therefore, the ultimate fate of the infused liposomal DHA cannot be determined. Liposomal phospholipid is cleared from the circulation by facilitated transfer and direct fusion with plasma lipoproteins, in particular high density lipoprotein, and with cell membranes (14). LP-X particles are predominantly cleared by reticuloendothelial and hepatic phagocytosis (14). It may be speculated that DHA in LP-X particles becomes sequestered in a reticuloendothelial pool. The subsequent availability of DHA to developing tissues is unknown and requires further study.

One limitation of the piglet as a model of the human premature infant is the large quantity of intravenous fat required to maintain adequate health and growth, in comparison to the human infant where maximal rates of 3 g/kg/d of triglyceride are recommended (4,8). However, an accumulation of liposomal phospholipid has also been shown in human premature infants receiving IL 10% at standard infusion rates of the triglyceride fraction (2 g/kg/d), indicating that this phenomenon is not restricted to the piglet nor purely related to the high rate of fat infusion used in our experiment (18,19). The accumulation of LP-X during the infusion of IL 10% in human infants is associated with impaired triglyceride clearance, due to inhibition of lipoprotein lipase and the hepatic clearance of remnant triglyceride particles, placing an important clinical limitation on the use of this emulsion (14,18,19).

We conclude that the use of IL 10% for the specific purpose of providing additional DHA cannot be justified in human premature infants based on this data, as the capacity of tissues to assimilate the phospholipid from this emulsion appears limited. If the hypothesis of an inadequate supply of DHA to the human preterm infant during parenteral nutrition is accepted, then alternative strategies to provide DHA are required.

ACKNOWLEDGMENTS

This study was funded by a National Health and Medical Research Council Medical Postgraduate Scholarship. The assistance of the Pharmacy Department of Flinders Medical Centre is gratefully acknowledged. The assistance of Dani Dixon and Mark Neumann is also acknowledged. LFS was given to the study by B. Braun (Melsungen, Germany). Financial assistance was provided by the MS McLeod Research Fund.

REFERENCES

1. Birch, E.E., Birch, D.G., Hoffman, D.R., and Uauy, R. (1992) Dietary Essential Fatty Acid Supply and Visual Acuity Development, *Invest. Ophthalmol. Vis. Sci. 32*, 3242–3253.
2. Carlson, S.E., Werkman, S.H., Rhodes, P.G., And Tolley, E.A. (1993) Visual Acuity Development in Healthy Preterm Infants: Effect of Marine-Oil Supplementation, *Am. J. Clin. Nutr. 58*, 35–42.
3. Simmer, K., Metcalf, R., and Daniels, L. (1997) The Use of Breastmilk in a Neonatal Unit and Its Relationship to Protein and Energy Intake and Growth, *J. Paediatr. Child Health 33*, 55–60.
4. American Academy of Pediatrics Committee on Nutrition (1985) Nutritional Needs of Low-Birth-Weight Infants, *Pediatrics 75*, 976–986.
5. Martinez, M. (1992) Tissue Levels of Polyunsaturated Fatty Acids During Early Human Development, *J. Pediatr. 120*, S129–S138.
6. Dobbing, J., and Sands, J. (1979) Comparative Aspects of the Brain Growth Spurt, *Early Hum. Dev. 3*, 79–83
7. Morris, S.A., Simmer, K., and Gibson, R. (1999) Developmental Sensitivity of the Piglet Brain to Docosahexaenoic Acid, *Pediatr. Res. 46*, 401–405.
8. Morris, S., Simmer, K., van Barneveld, R., and Gibson, R.A. (1998) A Simplified Method to Study the Effect of Intravenous Fat Infusion in Neonatal Piglets, in *Lipids in Infant Nutrition*, (Huang, Y.-S., and Sinclair, A.J., eds.) AOCS Press, Champaign, pp. 100–110.
9. Broekhuyse, R.M. (1974) Improved Lipid Extraction of Erythrocytes, *Clin. Chim. Acta 51*, 341–343.
10. Bligh, E.G., and Dyer, W.J. (1959) A Rapid Method of Total Lipid Extraction and Purification, *Can. J. Biochem. Physiol. 37*, 911–917.
11. Morris, S., Simmer, K., and Gibson, R. (1998) Characterisation of Fatty Acid Clearance in Premature Neonates During Intralipid Infusion, *Pediatr. Res. 43*, 245–249.
12. Lutz, O., Meraihi, Z., Ferezou, J., Frey, A., Lutton, C., and Bach, A. (1990) The Mesophase of Parenteral Fat Emulsion Is Both Substrate and Inhibitor of Lipoprotein Lipase and Hepatic Lipase, *Metabolism 39*, 1225–1231.
13. Hajri, T., Ferezou, J., and Lutton, C. (1990) Effects of Intravenous Infusions of Commercial Fat Emulsions (Intralipid 10 or 20%) on Rat Plasma Lipoproteins: Phospholipids in Excess Are the Main Precursors of Lipoprotein-X-Like Particles, *Biochim. Biophys. Acta 1047*, 121–130.
14. Bach, A.C., Férezou, J., and Frey, A. (1996) Phospholipid-Rich Particles in Commercial Parenteral Fat Emulsions, an Overview, *Prog. Lipid Res. 35*, 133–153.
15. Innis, S.M. (1986) Effect of Total Parenteral Nutrition With Linoleic Acid-Rich Emulsions on Tissue ω6 and ω3 Fatty Acids in the Rat, *Lipids 21*, 132–138.
16. Arbuckle, L.D., Rioux, F.M., Mackinnon, M.J., Hrboticky, N., and Innis, S.M. (1991) Response of (n-3) and (n-6) Fatty Acids in Piglet Brain, Liver and Plasma to Increasing, but Low, Fish Oil Supplementation of Formula, *J. Nutr. 121*, 1536–1547.
17. Innis, S. (1989) Alteration of Erythrocyte Lipid Composition Following Total Parenteral Nutrition in the Rat, *JPEN 13*, 47–50.
18. Haumont, D., Deckelbaum, R.J., Richelle, M., Dahlan, W., Coussaert, E., Bihain, B.E., and Carpentier, Y.A. (1989) Plasma Lipid and Plasma Lipoprotein Concentrations in Low Birth Weight Infants Given Parenteral Nutrition with 10 or 20 Percent Lipid Emulsion, *J. Pediatr. 115*, 787–793.
19. Haumont, D., Richelle, M., Deckelbaum, R.J., Coussaert, E., and Carpentier, Y.A. (1992) Effect of Liposomal Content of Lipid Emulsions on Plasma Lipid Concentrations in Low Birth Weight Infants Receiving Parenteral Nutrition, *J. Pediatr. 121*, 759–763.

[Received April 5, 1999; accepted February 1, 2000]

High Dietary 18:3n-3 Increases the 18:3n-3 but Not the 22:6n-3 Content in the Whole Body, Brain, Skin, Epididymal Fat Pads, and Muscles of Suckling Rat Pups

Raffick A.R. Bowen[a] and Michael T. Clandinin[a,b,*]

Nutrition and Metabolism Research Group, Departments of [a]Agricultural, Food and Nutritional Science and [b]Medicine, University of Alberta, Edmonton, Alberta, T6G 2P5, Canada

ABSTRACT: The objective of this study was to test the hypothesis that increasing maternal dietary 18:3n-3 by decreasing the 18:2n-6/18:3n-3 ratio will increase the 18:3n-3 and 22:6n-3 content of the whole body, liver, skin (epidermis, dermis, and subcutaneous tissue), epididymal fat pads, and muscles (arms and legs) of 2-wk-old rat pups. Sprague-Dawley dams at parturition were fed semipurified diets containing either a low (18:2n-6 to 18:3n-3 ratio of 24.7:1) or a high (18:2n-6 to18:3n-3 ratio of 1.0:1) 18:3n-3 fatty acid content. During the first 2 wk of life, rat pups received only their dams' milk. Fatty acid composition of the pups' stomach contents (dams' milk), whole body, brain, liver, skin, epididymal fat pads, and muscles was determined. The stomach fatty acid composition of 18:3n-3 reflected the dams' diet. The content of 18:3n-3 in whole body, brain, liver, skin, epididymal fat pads, and muscles was significantly ($P < 0.05$) greater in rat pups fed the high compared with the low 18:3n-3 fatty acid diet. The 22:6n-3 content of the whole body, brain, skin, epididymal fat pads, and muscles was not quantitatively different in rat pups fed either the low or high 18:3n-3 fatty acid diet. The 20:5n-3 and 22:5n-3 content of the whole body, skin, and epididymal fat pads was significantly increased in rat pups fed the high compared with the low 18:3n-3 fatty acid diet. High content of 18:3n-3 was found in the skin of rat pups fed either a low or high 18:3n-3 fatty acid diet. These findings demonstrate that high maternal dietary 18:3n-3 significantly increases the 18:3n-3 but not the 22:6n-3 content of the whole body, brain, skin, epididymal fat pads, and muscles with approximately 39 and 41% of the whole body 18:3n-3 content being deposited in the skin of suckling rat pups fed either the low or high 18:3n-3 diet, respectively.

Paper no. L8298 in *Lipids 35*, 389–394 (April 2000).

Research in infant nutrition has demonstrated that during the last trimester of gestation the fetal brain accrues fatty acids of the n-6 and n-3 types (1). These fatty acids may be derived from the placenta *in utero* (1–3). The hepatic and adipose reserves cannot meet whole body needs for essential fatty acids and total fat if fetal development is interrupted by premature birth early in the third trimester (3). Mothers' milk provides 20:4n-6 and 22:6n-3, approximating the predicted requirements at day 16 of life at oral intake (3). Long-chain essential fatty acids are synthesized from 18:2n-6 or 18:3n-3; however, the amounts produced *in vivo* may be inadequate to support the accretion rates attained in breast-fed infants (4–8). Deficiencies of dietary 22:6n-3 during perinatal development results in poor 22:6n-3 accretion in brain and retina, subsequently leading to altered neurological and visual function in animals (9,10). Thus, it seems prudent to feed the preterm infant human milk or formulas with a fatty acid balance similar to human milk containing long-chain polyenoic homologs of 18:2n-6 and 18:3n-3 (11).

Current infant formulas in North America contain 18:2n-6 and 18:3n-3 but are devoid of 20:4n-6 and 22:6n-3 (12,13). Infants fed these formulas must rely on *in vivo* elongation and desaturation of 18:2n-6 and 18:3n-3 to support a similar rate of accretion of 20:4n-6 and 22:6n-3 to that attained in breast-fed infants. Addition of 20:4n-6 and 22:6n-3 to preterm infant formulas to optimize brain development has been recommended (3,11,14–17). Infant formulas supplemented with 20:4n-6 and 22:6n-3 produce a clear dose response in the content of 20:4n-6 and 22:6n-3 in erythrocyte total plasma membrane phospholipids with 0.6% 20:4n-6 and 0.4% 22:6n-3 in the formula fat providing sufficient amounts of these fatty acids to achieve a fatty acid composition of 20:4n-6 and 22:6n-3 similar to that of infants fed human milk (18). Thus, in the United Kingdom, Europe, South America, Australia, and the Middle East, 20:4n-6 and 22:6n-3 have been added to infant formulas.

The question of whether preformed 22:6n-3 is needed or if providing more 18:3n-3 can enable synthesis of 22:6n-3 persists. In human adults, it is more effective to supply a dietary source of preformed 22:6n-3 from fish oil to increase the 22:6n-3 content in plasma phospholipids than 18:3n-3 from flaxseed oil (19). Increasing maternal dietary 18:3n-3 by decreasing the diet 18:2n-6/18:3n-3 from 7.3:1 to 4:1 was not as effective as preformed 22:6n-3 at raising the 22:6n-3 content of neuronal cell phospholipids of weanling rats (20,21). Increasing maternal dietary 18:3n-3 content does not significantly increase the 22:6n-3 content in phosphatidylcholine, phosphatidylethanolamine, or

*To whom correspondence should be addressed at Nutrition and Metabolism Research Group, Department of Agricultural, Food and Nutritional Science, 4-10 Agriculture/Forestry Center, University of Alberta, Edmonton, Alberta, T6G 2P5, Canada. E-mail: tclandin@gpu.srv.ualberta.ca

Abbreviations: ANOVA, analysis of variance; PUFA, polyunsaturated fatty acid.

phosphatidylserine of neuronal cell phospholipids of rat pups at 2 wk of age (22). These observations beg the question: If 18:3n-3 does not give rise to significant quantities of 22:6n-3, then what is the metabolic fate of high intakes of 18:3n-3?

The purpose of this study was to determine if the dietary 18:3n-3 consumed could increase the 18:3n-3 and 22:6n-3 content of other whole body tissue lipids. It is hypothesized that increasing maternal dietary 18:3n-3 by decreasing the 18:2n-6/18:3n-3 ratio will increase the 18:3n-3 and 22:6n-3 content in the whole body, liver, skin (epidermis, dermis, and subcutaneous tissue), epididymal fat pads, and muscles (arms and legs) in 2-wk-old rat pups.

EXPERIMENTAL PROCEDURES

Animals and diets. The University of Alberta Animal Ethics Committee approved all animal procedures. Sprague-Dawley rats were obtained from the University of Alberta vivarium. During breeding, three females and one male were housed together for a 2-wk mating period. Females were then moved to individual cages in a room maintained at 21°C with a 12-h light/dark cycle. Water and food were supplied *ad libitum*. Laboratory rodent diet, 5001 (PMI Feeds, Inc., St. Louis, MO) was fed to the rats when not receiving experimental diets. Rats were switched to experimental diets on the day of parturition. All litters were culled to 12 pups within 24 h of parturition. Pups received only maternal milk. Pups were sacrificed at 2 wk of age.

One entire litter of rat pups fed the same experimental diet was sexed and weighed prior to decapitation. Rat pups randomly chosen for whole body lipid analysis were frozen in liquid nitrogen. The brains, livers, skin (epidermis, dermis, and subcutaneous tissue), epididymal fat pads, and muscles (arms and legs) were quickly removed and rinsed with ice-cold physiological saline, blotted dry, weighed, and frozen in liquid nitrogen. Stomach contents of three rats from each litter were also removed and analyzed for fatty acid composition to reflect the composition of maternal milk. All tissue samples were stored under nitrogen and kept in a –80°C freezer until analysis. Analysis of whole organs was performed on at least three individual rat pups from each of three different litters per diet treatment. Three litters per diet treatment were used.

The basal diet fed to the dams contained 20% (w/w) fat varying in 18:2n-6 and 18:3n-3 fat composition. Two experimental diets were formulated by addition of various triglycerides from vegetable oils to alter the fatty acid 18:2n-6/18:3n-3 ratio (Table 1). An 18:2n-6 to 18:3n-3 fatty acid ratio of 24.7 to 1 (low 18:3n-3) was obtained by addition of corn oil to the diet fat blend. The 18:2n-6 to 18:3n-3 fatty acid ratio of 1 to 1 (high 18:3n-3) was obtained by the addition of flaxseed oil. The low and high 18:3n-3 fatty acid diet was nutritionally adequate, providing for all known essential nutrient requirements as described earlier (23). To minimize any changes in sample composition due to fatty acid oxidation, the diets were sealed under nitrogen and stored in a freezer at –30°C in darkness. Every day, the required amount of diet was taken out, mixed, and placed in individual feed cups.

Lipid extraction and fatty acid analysis. Total lipids were extracted from aliquots of tissue homogenate (24). The extracted lipids were evaporated under nitrogen and weighed to determine the total fat content of the tissues. The tissue lipids were saponified by a 0.5 N KOH in 95% methanol solution and heated at 100°C for 1 h. Fatty acid methyl esters were prepared using BF_3/methanol reagent (25).

Fatty acid methyl esters were separated by automated gas–liquid chromatography (Varian model 6000 GLC equipped with a Vista 654 data system and a Vista 8000 autosampler; Varian Instruments, Georgetown, Ontario, Canada) using a bonded fused-silica BP20 capillary column (25 × 0.25 mm i.d.)

TABLE 1
Fatty Acid Composition of Experimental Diets Fed to Lactating Dams and Stomach Contents of Rat Pups of 2 wk of Age[a]

	Diet[b]		Stomach contents[b]	
Fatty acid (wt%)	Low 18:3n-3	High 18:3n-3	Low 18:3n-3	High 18:3n-3
12:0	15.3	7.90	0.2 ± 0.0[a]	0.1 ± 0.02[a]
14:0	6.8	3.1	20.2 ± 1.5[a]	16.11 ± 1.4[a]
16:0	13.1	9.0	21.1 ± 0.3[a]	18.5 ± 0.8[b]
18:0	4.7	3.7	4.0 ± 0.2[a]	3.3 ± 0.2[b]
18:1n-7 + n-9	26.4	27.2	26.7 ± 0.9[a]	26.2 ± 0.7[a]
18:2n-6	27.2	20.4	25.4 ± 0.4[a]	19.3 ± 0.4[b]
18:3n-3	1.1	20.1	1.1 ± 0.2[b]	14.9 ± 1.1[a]
20:4n-6	ND	ND	0.7 ± 0.1[a]	0.4 ± 0.1[a]
22:6n-3	ND	ND	0.04 ± 0.01[a]	0.12 ± 0.0[a]
ΣSat	43.4	30.3	46.1 ± 1.3[a]	38.7 ± 2.1[b]
ΣMono	28.2	29.2	26.7 ± 0.9[a]	26.2 ± 0.7[a]
Σn-6	27.2	20.4	26.1 ± 0.5[a]	19.7 ± 0.4[b]
Σn-3	1.3	20.1	1.2 ± 0.2[b]	15.4 ± 1.2[a]
18:2n-6 to 18:3n-3 ratio	24.7:1	1.0:1	23.1:1	1.3:1

[a]ND = not detected. ΣSat, sum of saturated fatty acids; ΣMono, sum of monounsaturated fatty acids; Σn-6, sum of n-6 fatty acids; and Σn-3, sum of n-3 fatty acids.
[b]Values represent mean ± SEM for $n = 9$ rat pups for each experimental diet. Values without a common roman letter superscript are significantly different at $P < 0.05$.

and quantitated using a flame-ionization detector as described earlier (20,21). These conditions are capable of separating methyl esters of saturated, *cis*-monounsaturated, and polyunsaturated fatty acids from 12 to 24 carbons in chain length. Quantitation and identification of peaks were based on relative retention times compared with known standards [polyunsaturated fatty acids (PUFA) 1 and 2, bacterial methyl ester mix-14; Supelco Canada, Mississauga, Ontario, Canada] (26).

Statistical analysis. The effects of diet treatment and sex of rat pups on the lipid content and fatty acid composition of whole body and tissues lipids were assessed by one-way analysis of variance (ANOVA) procedures using the SAS package, version 6.11 (27). Significant differences between diet treatments and sex were determined by a Duncan's multiple range test at a significance level of $P < 0.05$ after a significant ANOVA (28). Values are expressed as mean ± SEM for $n = 9$.

RESULTS

Fatty acid composition of stomach contents. The stomach content of rat pups was analyzed for the fatty acid composition. These analyses reflected dams' milk composition (20,21,29–32). The increase in dietary 18:3n-3 fed to the dams increased the 18:3n-3 in the stomach contents of the rat pups (Table 1) indicating that the range of dietary fat composition fed in the present experiment produced similar changes in the fat composition of the dams' milk.

Whole body and tissue weights and lipid content. Whole body and tissue weights, lipid content, and fatty acid composition of the tissues were not significantly different for male ($n = 5$) and female ($n = 4$) rat pups (data not shown), hence in statistical analyses to test subsequent effects of diet, treatments were combined for both sexes. The whole body and tissue weights were not significantly different between the two experimental diet treatments (Table 2), indicating that the body and tissue growth in the 2-wk-old rat pups is not different between low and high 18:3n-3 fatty acid diets. The lipid content of whole body and tissues was not significantly different in rat pups fed either the low or high 18:3n-3 fatty acid diet (Table 2).

Brain. The brain of 2-wk-old rat pups contained small amounts of 18:3n-3 and 18:2n-6. The 18:3n-3 content of brain was significantly increased in rat pups fed the high compared with the low 18:3n-3 fatty acid diets. The 18:2n-6 content of brain was significantly increased in animals fed the low compared with a high 18:3n-3 fatty acid diet. The predominant n-3 and n-6 fatty acids in brain of rat pups fed low or high 18:3n-3 fatty acid diet were 22:6n-3 and 20:4n-6, respectively. The 22:6n-3 content of brain was not significantly different in the animals fed the high compared with the low 18:3n-3 fatty acid diets. The 20:5n-3 content of brain was not significantly different between rat pups fed low vs. high 18:3n-3 fatty acid diet. However, the 22:5n-3 content of brain was significantly different between rat pups fed low vs. high 18:3n-3 fatty acid diet. The 20:4n-6 content of brain was significantly increased in rat pups fed the low vs. high 18:3n-3 fatty acid diet.

Liver. The partial fatty acid composition of liver from 2-wk-old rat pups is shown (Table 3). The 18:3n-3 and 22:6n-3 content of liver was considerably lower than the 18:2n-6 and 20:4n-6 content for animals fed either the low or high 18:3n-3 diets. High content of 18:2n-6 and 20:4n-6 was observed in the liver of rat pups fed either a low or high 18:3n-3 fatty acid diet. The content of 18:3n-3 in liver was approximately 3% in animals fed the high 18:3n-3 fatty acid diet and was significantly different when compared with animals fed the low 18:3n-3 fatty acid diet. Significant differences were observed in the 18:2n-6 content of liver between rat pups fed low vs. high 18:3n-3 fatty acid diet. The 22:6n-3 content of liver was significantly increased in animals fed high vs. low 18:3n-3 fatty acid diets (Table 3). The 20:5n-3 and 22:5n-3 content of liver was significantly different between rat pups fed low vs. high 18:3n-3 fatty acid diet. The 20:4n-6 content of liver did not differ between rat pups fed low vs. high 18:3n-3 fatty acid diet.

Skin (epidermis, dermis, and subcutaneous tissue). The fatty acid composition of skin (epidermis, dermis, and subcutaneous tissue; Table 3) shows that 18:3n-3 content of skin was significantly increased by high maternal dietary 18:3n-3 content. The 22:6n-3 content of skin, however, was not statistically different in animals fed either the low or high 18:3n-3 diet. The 20:5n-3 and 22:5n-3 content of skin was significantly different between rat pups fed low vs. high 18:3n-3 fatty acid diet. The 18:2n-6 plus 20:4n-6 were major fatty acids of skin constituting approximately 23 and 17% for animals fed the low and high 18:3n-3 fatty acid diet, respectively. The 18:2n-6 content in skin was significantly higher in rat pups fed a low compared with a high 18:3n-3 fatty acid diet. However, there was no significant difference in 20:4n-6 content of skin between the two diet groups.

TABLE 2
Whole Body and Tissue Weights and Lipid Content of Rat Pups at 2 wk of Age[a]

	Weight (g)		Lipid (%)	
	Low 18:3n-3	High 18:3n-3	Low 18:3n-3	High 18:3n-3
Whole body	31.8 ± 1.0[a]	32.0 ± 1.2[a]	13.6 ± 1.0[a]	13.4 ± 0.8[a]
Brain	1.15 ± 0.0[a]	1.12 ± 0.1[a]	4.40 ± 0.4[a]	4.20 ± 0.3[a]
Liver	0.66 ± 0.1[a]	0.67 ± 0.1[a]	6.90 ± 0.7[a]	6.90 ± 0.8[a]
Skin	9.00 ± 1.0[a]	8.95 ± 1.0[a]	24.0 ± 1.3[a]	25.0 ± 1.1[a]
Epididymal fat pads	0.05 ± 0.0[a]	0.05 ± 0.0[a]	ND	ND
Muscles	1.00 ± 0.0[a]	0.91 ± 0.1[a]	1.70 ± 0.0[a]	1.60 ± 0.0[a]

[a]Values represent mean ± SEM for $n = 9$ rat pups for each experimental diet. Values without a common roman superscript are significantly different at $P < 0.05$.

TABLE 3
Effect of Low and High 18:3n-3 Diet on the Essential Fatty Acid Composition of Whole Body and Tissue Lipids[a]

Diet 18:3n-3 content	Whole body		Brain		Liver		Skin		Epididymal fat pad		Muscles	
	Low	High	Low	High	Low	High	Low	High	Low	High	Low	High
Fatty acid (% w/w)												
18:2n-6	$24.5^{a} \pm 0.4$	$19.3^{b} \pm 0.3$	$2.8^{a} \pm 0.5$	$1.7^{b} \pm 0.0$	$16.3^{a} \pm 0.2$	$13.0^{b} \pm 0.4$	$21.6^{a} \pm 1.1$	$15.5^{b} \pm 0.5$	$19.9^{a} \pm 0.6$	$18.8^{a} \pm 0.6$	$20.8^{a} \pm 1.8$	$15.9^{b} \pm 0.7$
18:3n-3	$0.9^{b} \pm 0.0$	$14.7^{a} \pm 0.4$	$0.1^{b} \pm 0.0$	$0.5^{a} \pm 0.0$	$0.2^{b} \pm 0.1$	$3.3^{a} \pm 0.3$	$0.7^{b} \pm 0.1$	$11.6^{a} \pm 0.4$	$1.8^{b} \pm 0.7$	$13.3^{a} \pm 0.7$	$1.6^{b} \pm 1.0$	$10.7^{b} \pm 0.3$
20:4n-6	$1.7^{a} \pm 0.1$	$1.0^{b} \pm 0.1$	$12.0^{a} \pm 0.3$	$10.0^{b} \pm 0.2$	$15.0^{a} \pm 2.1$	$12.4^{a} \pm 1.0$	$0.8^{a} \pm 0.2$	$0.6^{a} \pm 0.1$	$1.1^{a} \pm 0.1$	$0.9^{a} \pm 0.1$	$1.7^{a} \pm 0.3$	$0.9^{b} \pm 0.3$
20:5n-3	$0.0^{b} \pm 0.0$	$0.7^{a} \pm 0.0$	$0.0^{a} \pm 0.0$	$0.1^{a} \pm 0.0$	$0.1^{b} \pm 0.0$	$1.5^{a} \pm 0.1$	$0.0^{b} \pm 0.0$	$0.5^{a} \pm 0.0$	$0.1^{b} \pm 0.0$	$0.4^{a} \pm 0.1$	$0.1^{b} \pm 0.1$	$0.6^{a} \pm 0.1$
22:5n-3	$0.1^{b} \pm 0.0$	$0.7^{a} \pm 0.0$	$0.1^{b} \pm 0.0$	$0.5^{a} \pm 0.0$	$0.4^{b} \pm 1.3$	$1.3^{a} \pm 0.1$	$0.0^{b} \pm 0.0$	$0.4^{a} \pm 0.0$	$0.1^{b} \pm 0.0$	$0.3^{a} \pm 0.1$	$0.0^{a} \pm 0.0$	$0.2^{a} \pm 0.1$
22:6n-3	$0.3^{a} \pm 0.1$	$0.5^{a} \pm 0.1$	$6.5^{a} \pm 0.3$	$7.1^{a} \pm 0.6$	$3.5^{b} \pm 0.8$	$6.1^{a} \pm 0.6$	$0.2^{a} \pm 0.1$	$0.4^{a} \pm 0.0$	$0.2^{a} \pm 0.1$	$0.4^{a} \pm 0.1$	$0.2^{a} \pm 0.1$	$0.3^{a} \pm 0.1$

[a]Values represent mean ± SEM for $n = 9$ rat pups for each experimental diet. Values without a common roman superscript for each fatty acid are significantly different at $P < 0.05$.

Epididymal fat pads. The 18:3n-3 content of this tissue was significantly increased by the dietary 18:3n-3 content (Table 3). The content of 18:3n-3 in epididymal fat pads was approximately 1.8 and 13.3% for animals fed either low or high 18:3n-3 fatty acid diet, respectively. The 18:2n-6 content of epididymal fat pads from rat pups was high, approximately 19–20% of the total fatty acids. The 18:2n-6 content in epididymal fat pads was not significantly affected by the two dietary fat treatments. However, unlike 18:2n-6, 22:6n-3 and 20:4n-6 content in epididymal fat pads was not significantly different between animals fed the two diet groups. The 20:5n-3 and 22:5n-3 content of epididymal fat pads was significantly different between rat pups fed low vs. high 18:3n-3 fatty acid diet.

Muscle (arms and legs). The fatty acid composition of muscle (arms and legs) from 2-wk-old rat pups is shown (Table 3). The 18:3n-3 content of muscles was significantly different between rat pups fed low vs. high 18:3n-3 fatty acid diet (1.6 vs. 10.7%, respectively). The 18:2n-6 content in muscles was significantly different between rat pups fed low vs. high 18:3n-3 fatty acid diet. The 18:2n-6 content in muscles of rat pups fed low or high 18:3n-3 fatty acid diet was approximately 21 and 16%, respectively. No significant differences were observed in the 22:6n-3 content of muscles in the two diet groups. The 20:5n-3 but not the 22:5n-3 content of muscles was significantly different between rat pups fed low vs. high 18:3n-3 fatty acid diet. The 20:4n-6 content in muscles of rat pups was significantly higher in the low compared with the high 18:3n-3 fatty acid diet (1.7 vs. 0.9%, respectively).

Tissue 18:3n-3 content (i) Whole body. Raising the 18:3n-3 content from a low to a high 18:3n-3 fatty acid diet significantly increased the 18:3n-3 content of whole body lipids (Table 3). Feeding a low 18:3n-3 fatty acid diet to the dams significantly increased the 18:2n-6 content of whole body lipids of the rat pups compared with the high 18:3n-3 fatty acid diet. The 22:6n-3 content of whole body lipids was not significantly different between rat pups fed the low vs. high 18:3n-3 fatty acid diet. The 20:5n-3 and 22:5n-3 content of whole body was significantly different between rat pups fed low vs. high 18:3n-3 fatty acid diet. However, the 20:4n-6 content of whole body lipids was significantly different. Based on the lipid content and 18:3n-3, 20:5n-3, 22:5n-3, and 22:6n-3 content, as well as the weight of the tissues examined in the present study, the 18:3n-3, 20:5n-3, 22:5n-3, and 22:6n-3 content in whole body of rat pups fed either low or high 18:3n-3 fatty acid diet was calculated to be approximately 39 and 630 mg, 0 and 30 mg, 4.3 and 30 mg, and 12.9 and 21.4 mg, respectively (data not shown). The other tissues examined in this study including brain, liver, epididymal fat pads, and muscles (arms and legs) from 2-wk-old rat pups fed either low or high 18:3n-3 fatty acid diet contained small amounts of 18:3n-3, 20:5n-3, and 22:5n-3 (data not shown). Interestingly, the skin (epidermis, dermis, and subcutaneous tissue) of rat pups fed either low or high 18:3n-3 fatty acid diet contained a significant amount of 18:3n-3. The total 18:3n-3 content in skin for the low and high 18:3n-3 fatty acid diet was approximately 15 and 260 mg, respectively (data not shown).

DISCUSSION

The results from the present study demonstrate that increasing maternal dietary 18:3n-3 significantly increases the 18:3n-3 but not the 22:6n-3 content of the whole body, brain, skin (epidermis, dermis, and subcutaneous tissue), epididymal fat pads, and muscles (arms and legs) in 2-wk-old rat pups. The 2-wk-old rat pups in the present study were used because at this age very active brain growth occurs with rapid accretion of PUFA, especially 22:6n-3, for brain membrane synthesis (33,34). Therefore, the demand for 22:6n-3 in 2-wk-old rat pups for postnatal brain growth and development is high and must be provided by the maternal diet.

It is well known that the fatty acid composition of tissues can be readily modified by dietary fat [reviewed by Clandinin *et al.* (35,36)]. The significant differences observed in whole body and tissue 18:2n-6 and 18:3n-3 content between rat pups fed low vs. high 18:3n-3 fatty acid diet were largely a reflection of the dietary fatty acid composition (37–39).

The content of 22:6n-3 was not significantly increased in whole body, brain, skin (epidermis, dermis, and subcutaneous tissue), epididymal fat pads, and muscles (arms and legs) when rat pups were fed the high 18:3n-3 diet. This could be due to the fact that desaturase activity is age-related and that at 2 wk of age desaturase activity may be limited. In this regard, Bourre *et al.* (40) demonstrated in rats that Δ-6 desaturase activity, a rate-limiting step in 20:4n-6 and 22:6n-3 synthesis, varies during the first 21 d following gestation. Therefore, if Δ-6 desaturase activity is low at 2 wk of age, the amount of 18:3n-3 added in the diet would not have any significant effect on increasing the 22:6n-3 content of these tissues. The significant increase in 20:5n-3 (except for brain) and 22:5n-3 (except for muscles) but not 22:6n-3 content of tissues examined in this study when rat pups were fed the high compared with low 18:3n-3 diet shows that 18:3n-3 is metabolized to long-chain n-3 metabolites but that there is a limit on the conversion of 20:5n-3 and 22:5n-3 to 22:6n-3.

The milk (stomach contents) provided to the rat pups by the dam during the 2-wk feeding period provides some preformed 22:6n-3 (Table 1). It is possible that the preformed 22:6n-3 (0.1%) present in the milk of dams fed the high 18:3n-3 fatty acid diet (Table 1) is sufficient to significantly increase the content of 22:6n-3 observed in liver of rat pups fed the high 18:3n-3 fatty acid diet (Table 3) without the need for additional synthesis of 22:6n-3 from dietary 18:3n-3. With the exception of the brain, increasing dietary 18:3n-3 by reducing the 18:2n-6/18:3n-3 ratio from 24.7:1 to 1.0:1 did not show any competitive effect of reduced 20:4n-6 and increased 22:6n-3 incorporation into whole body or tissue lipids. This would suggest that either desaturase activity is low or that a lower 18:2n-6/18:3n-3 ratio than that used in the present study may be required to reduce the 20:4n-6 and increase the 22:6n-3 content in the tissues examined (20).

Quantitative analysis of the 18:3n-3 content in rat pup tissues examined in the present study showed that a significant amount of 18:3n-3 was incorporated into whole body lipids. The 18:3n-3 content of rat pup whole body lipids was significantly greater in rat pups fed the high compared with the low 18:3n-3 diet (approximately 630 vs. 39 mg, respectively). The skin of rat pups fed low or high 18:3n-3 fatty acid diet contained significant quantities of 18:3n-3 (approximately 39 and 41% of the total 18:3n-3 content in whole body, respectively). The high amounts of 18:3n-3 found in the skin were stored as part of the fatty acid component of triglycerides in the subcutaneous fat (data not shown).

Thus, it appears that the skin, including epidermis, dermis and subcutaneous tissue, is a major deposition site for 18:3n-3 in 2-wk-old rat pups.

The saturated fatty acid content in whole body, skin, and epididymal fat pads was significantly decreased ($P < 0.05$) when the pups were fed maternal milk from the dams fed the high 18:3n-3 diet (data not shown). This decrease in the saturated fatty acid content of tissues was due to the substantial increase in the content of 18:3n-3 in these tissues by the high 18:3n-3 diet.

In conclusion, the results from the present study demonstrate that increasing maternal dietary 18:3n-3 content from 1.1 to 20.1% of the total dietary fatty acids significantly increases the 18:3n-3 but not the 22:6n-3 content in most tissues. If the present findings from this study are extrapolated to neonates, it appears that increasing the dietary 18:3n-3 content of the neonate's feed will significantly increase the 18:3n-3 but not the 22:6n-3 content of neonatal tissues.

ACKNOWLEDGMENTS

This research was supported by the Natural Sciences and Engineering Research Council of Canada, and Wyeth Nutritionals International.

REFERENCES

1. Clandinin, M.T., Chappell, J.E., Leong, S., Heim, T., Swyer, P.R., and Chance, G.W. (1980) Intrauterine Fatty Acid Accretion Rates in Human Brain: Implications for Fatty Acid Requirements, *Early Human Dev. 4*, 121–129.
2. Clandinin, M.T., Chappell, J.E., Leong, S., Heim, T., Swyer, P.R., and Chance, G.W. (1980) Extrauterine Fatty Acid Accretion in Infant Brain: Implications for Fatty Acid Requirements, *Early Human Dev. 4*, 131–138.
3. Clandinin, M.T., Chappell, J.E., Heim, T., Swyer, P.R., and Chance, G.W. (1981) Fatty Acid Utilization in Perinatal *de novo* Synthesis of Tissues, *Early Human Dev. 5*, 355–366.
4. Demmelmair, H., Rinke, U., Behrendt, E., Sauerwald, T., and Koletzko, B. (1995) Estimation of Arachidonic Synthesis in Fullterm Neonates Using Natural Variation of ^{13}C-Abundance, *J. Pediatr. Gastroenterol. Nutr. 21*, 31–36.
5. Salem, N., Jr., Wegher, B., Mena, P., and Uauy, R. (1996) Arachidonic and Docosahexaenoic Acids Are Biosynthesized from Their 18-Carbon Precursors in Human Infants, *Proc. Natl. Acad. Sci. USA 93*, 49–54.
6. Sauerwald, T.U., Hachey, D.L., Jensen, C.L., Chen, H.M., Anderson, R.E., and Heird, W.C. (1996) Effect of Dietary α-Linolenic Acid Intake on Incorporation of Docosahexaenoic and Arachidonic Acids into Plasma Phospholipids of Term Infants, *Lipids 31*, S131–S135.

7. Sauerwald, T.U., Hachey, D.L., Jensen, C.L., Chen, H.M., Anderson, R.E., and Heird, W.C. (1997) Intermediates in Endogenous Synthesis of C22:6ω-3 and C20:4ω-6 by Term and Preterm Infants, *Pediatr. Res. 41*, 183–187.
8. Carnielli, V.P., Wattimena, J.L.D., Luijendijk, I.H.T., Boerlage, A., Degenhart, H.J., and Sauer P.J.J. (1996) The Very Low Birth Weight Premature Infant Is Capable of Synthesizing Arachidonic and Docosahexaenoic Acids from Linoleic and Linolenic Acids, *Pediatr. Res. 40*, 169–174.
9. Bourre, J.M., Francis, M., Youyou, A., Dumont, O., Piciotti, M., Pascal, G., and Durand, G. (1989) The Effects of Dietary α-Linolenic Acid on the Composition of Nerve Membranes, Enzymatic Activity, Amplitude of Electrophysiological Parameters, Resistance to Poisons and Performance of Learning Tasks in Rats, *J. Nutr. 119*, 1880–1892.
10. Connor, W.E., Neuringer, M., and Lin, D.S. (1990) Dietary Effects on Brain Fatty Acid Composition: the Reversibility of n-3 Fatty Acid Deficiency and Turnover of Docosahexaenoic Acid in the Brain, Erythrocytes, and Plasma of Rhesus Monkeys, *J. Lipid Res. 31*, 237–247.
11. Clandinin, M.T., Chappell, J.E., and Heim, T. (1982) Do Low Birth Weight Infants Require Nutrition with Chain Elongation-Desaturation Products of Essential Fatty Acids? *Prog. Lipid Res. 20*, 901–904.
12. Clandinin, M.T., Garg, M.L., Parrott, A., Van Aerde, J., Hervada, A., and Lien, E. (1992) Addition of Long-Chain Polyunsaturated Fatty Acids to Formula for Very Low Birth Weight Infants, *Lipids 27*, 896–900.
13. Clandinin, M.T., Parrot, A., Van Aerde, J.E., Hervada, A.R., and Lien, E. (1992) Feeding Preterm Infants a Formula Containing C20 and C22 Fatty Acids Simulates Plasma Phospholipid Fatty Acid Composition of Infants Fed Human Milk, *Early Human Dev. 31*, 41–51.
14. European Society of Paediatric Gastroenterology and Nutrition: Committee on Nutrition (1991) Comment on the Content and Composition of Lipids in Infant Formula, *Acta Paediatr. Scand. 80*, 887–896.
15. British Nutrition Foundation (1992) *The Report of the British Nutrition Foundation's Task Force, Recommendations for Intakes of Unsaturated Fatty Acids*, pp. 156–163, Chapman and Hall, London.
16. International Society for the Study of Fatty Acids and Lipids (1994) Recommendations for the Essential Fatty Acid Requirements of Infant Formula, *ISSFAL Newsletter 1*, 4.
17. FAO/WHO (1994) *Fats and Oils in Human Nutrition*, *Report of a Joint Expert Consultation,* pp. 49–55, Rome.
18. Clandinin, M.T., Van Aerde, J.E., Parrott, A., Field, C.J., Euler, A.R., and Lien, E. (1997) Assessment of the Efficacious Dose of Arachidonic and Docosahexaenoic Acids in Preterm Infant Formulas: Fatty Acid Composition of Erythrocyte Membrane Lipids, *Pediatr. Res. 42*, 819–825.
19. Layne, K.S., Goh, Y.K., Jumpsen, J.A., Ryan, E.A., Chow, P., and Clandinin, M.T. (1996) Normal Subjects Consuming Physiological Levels of 18:3(n-3) and 20:5(n-3) from Flaxseed or Fish Oils Have Characteristic Differences in Plasma Lipid and Lipoprotein Fatty Acid Levels, *J. Nutr. 126*, 2130–2140.
20. Jumpsen, J.A., Lien, E., Goh, Y.K., and Clandinin, M.T. (1997) Diets Varying in n-3 and n-6 Fatty Acid Content Produce Differences in Phosphatidylethanolamine and Phosphatidylcholine Fatty Acid Composition During Development of Neuronal and Glial Cells in Rats, *J. Nutr. 127*, 724–731.
21. Jumpsen, J.A., Lien, E., Goh, Y.K., and Clandinin, M.T. (1997) During Neuronal and Glial Cell Development Diet n-6 to n-3 Fatty Acid Ratio Alters the Fatty Acid Composition of Phosphatidylinositol and Phosphatidylserine, *Biochim. Biophys. Acta 1347*, 40–50.
22. Bowen, R.A.R., Wierzbicki, A.A., and Clandinin, M.T. (1999) Does Increasing Dietary Linolenic Acid Content Increase the Docosahexaenoic Acid Content of Phospholipids in Neuronal Cells of Neonatal Rats? *Pediatr. Res. 45*, 815–819.
23. Clandinin, M.T., and Yamashiro, S. (1980) Effects of Basal Diet Composition on the Incidence of Dietary Fat Induced Myocardial Lesions, *J. Nutr. 110*, 1197–1203.
24. Folch, J., Lee, M., and Sloane Stanley, G.H. (1957) A Simple Method for the Isolation and Purification of Total Lipids from Animal Tissues, *J. Biol. Chem. 226*, 497–506.
25. Morrison, W.R., and Smith, L.M. (1964) Preparation of Fatty Acid Methyl Esters and Dimethyl-Acetals from Lipids with Boron Fluoride-Methanol, *J. Lipid Res. 5*, 600–608.
26. Hargreaves, K.M., and Clandinin, M.T. (1987) Phosphatidylethanolamine Methyltransferase: Evidence for Influence of Diet Fat on Selectivity of Substrate for Methylation in Rat Brain Synaptic Plasma Membrane, *Biochim. Biophys. Acta 918*, 97–105.
27. SAS Institute Inc. (1988) *SAS/STAT User's Guide*, Release 6.11 Edition, SAS Institute Inc., Cary.
28. Steel, R.G.D., and Torrie, J.H. (1960) *Principles and Procedures of Statistics*, 2nd edn., McGraw-Hill, New York.
29. Wainwright, P.E., Xing, H.C., Mutsaers, L., McCutcheon, D., and Kyle, D. (1997) Arachidonic Acid Offsets the Effects on Mouse Brain and Behavior of a Diet with a Low (n-6):(n-3) Ratio and Very High Levels of Docosahexaenoic Acid, *J. Nutr. 127*,184–193.
30. Lien E.L., Boyle, F.G., Yuhas, R.J., and Kuhlman, C.F. (1994) Effect of Maternal Dietary Arachidonic or Linoleic Acid on Rat Pup Fatty Acid Profiles, *Lipids 29*, 53–59.
31. Yonekubo, A., Honda, S., Okano, M., Takahashi, K., and Yamamoto, Y. (1993) Dietary Fish Oil Alters Rat Milk Composition and Liver and Brain Fatty Acid Composition of Fetal and Neonatal Rats, *J. Nutr. 123*, 1703–1708.
32. Nouvelot, A., Bourre, J.M., Sezille, G., Dewailly, P., and Jaillard, J. (1983) Changes in the Fatty Acid Patterns of Brain Phospholipids During Development of Rats Fed Peanut or Rapeseed Oil, Taking into Account Differences Between Milk and Maternal Food, *Ann. Nutr. Metab. 27*, 173–181.
33. Sinclair, A.J., and Crawford, M.A. (1972) The Accumulation of Arachidonate and Docosahexaenote in the Developing Rat Brain, *J. Neurochem. 19*, 1753–1758.
34. Dobbing, J., and Sands, J. (1979) Comparative Aspects of the Brain Growth Spurt, *Early Human Dev. 3*, 79–83.
35. Clandinin, M.T., Field, C.J., Hargreaves, K., Morson, L.A., and Zsigmond, E. (1985) Role of Diet Fat in Subcellular Structure and Function, *Can. J. Physiol. Pharmacol. 63*, 546–556.
36. Clandinin, M.T., Cheema, S., Field, C.J., Garg, M.L., Venkatraman, J., and Clandinin, T.T. (1991) Dietary Fat: Exogenous Determination of Membrane Structure and Cell Function, *FASEB J. 5*, 2761–2769.
37. Srinivasarao, P., Narayanareddy, K., Vajreswari, A., Rupalatha, M., Prakash, P.S., and Rao, P. (1997) Influence of Dietary Fat on the Activities of Subcellular Membrane-Bound Enzymes from Different Regions of Rat Brain, *Neurochem. Int. 31*, 789–794.
38. Lin, D.S., and Connor, W.W. (1990) Are the n-3 Fatty Acids from Dietary Fish Oil Deposited in the Triglyceride Stores of Adipose Tissue? *Am. J. Clin. Nutr. 51*, 535–539.
39. Field, C.J., Angel, A., and Clandinin, M.T. (1985) Relationship of Diet to the Fatty Acid Composition of Human Adipose Tissue Structure and Stored Lipids, *Am. J. Clin. Nutr. 42*, 1206–1220.
40. Bourre, J.M., Piciotti, M., and Dumont, O. (1990) Δ6-Desaturase in Brain and Liver During Development and Aging, *Lipids 25*, 354–356.

[Received June 29, 1999; and in revised form and accepted January 26, 2000]

Increased α-Linolenic Acid Intake Increases Tissue α-Linolenic Acid Content and Apparent Oxidation with Little Effect on Tissue Docosahexaenoic Acid in the Guinea Pig

Zhong Fu and Andrew J. Sinclair*

Department of Food Science, RMIT University, Melbourne, Victoria, 3001, Australia

ABSTRACT: The essential fatty acids do not have identical roles in nutrition. Linoleic acid (LA) accumulates throughout the body of most mammals, whereas α-linolenic acid (ALA) is rarely found in tissue lipids to the same extent as LA. It has been argued that this is the result of metabolism of ALA to docosahexaenoic acid (DHA) or that ALA is rapidly β-oxidized to acetyl CoA and CO_2. In this study, we consider the effect of high and low ALA levels on the tissue distribution of ALA and other n-3 polyunsaturated fatty acids (PUFA) in all tissues. Guinea pigs were fed one of two defined diets for 3 wk from weaning with both diets containing 1.8% (by weight) of LA and either 1.7% ALA or 0.03% ALA. The high ALA diet was associated with significantly increased ALA levels in all tissues except the brain and significantly increased levels of long-chain n-3 PUFA in all tissues except intestines, brain, carcass, and skin. The long-chain n-3 PUFA content of the whole body was less than 5% of that of the ALA content in both diet groups, and the major long-chain n-3 PUFA (>66% of total) in the body was 22:5n-3. The brain was the only tissue where the DHA content exceeded that of 22:5n-3. On the low ALA diet, there appeared to be conservation of ALA based on a comparison of the ratio of LA to ALA in the tissues compared with that in the diet. On the high ALA diet there was a loss of ALA relative to LA in the tissues compared with the diet. These studies suggest that the low levels of tissue ALA in the guinea pig are likely the result of β-oxidation or excretion *via* the skin and fur rather than metabolism to DHA.

Paper no. L8412 in *Lipids 35,* 395–400 (April 2000).

Since the discovery of the essential fatty acids (EFA), linoleic (LA) and α-linolenic acid (ALA) in 1930 (1), there has been much emphasis on the importance of LA in nutrition in different species such as man and domestic animals (2). It is acknowledged that LA is the more important EFA in reversing the classical symptoms of EFA deficiency such as scaly skin, dry hair, and membrane dysfunction, although recent studies have raised important questions about the role of LA in EFA deficiency (3). It is recognized that LA prevents water loss through the skin (4), while arachidonic acid (AA) is the precursor of all the main eicosanoids and related compounds. In the last 20 yr the importance of the ALA family has been recognized in different terrestrial species (5,6), with eicosapentaenoic acid (EPA) and docosahexaenoic acid (DHA) being effective in reducing plasma triacylglycerol levels (7) while DHA plays an important role in membrane structure and function in excitable tissues such as the brain, retina, and heart (8–11).

For many years, scientists have remarked on apparent differences in deposition of LA and ALA in the tissues of different species. This is exemplified by the extent to which LA accumulates in tissue lipids in a wide variety of species compared with ALA (5,11), which does not appear in high concentrations even in circumstances where equal amounts of LA and ALA are fed (12,13). Often the only evidence of the presence of the ALA family is in tissues like retina and brain where its metabolite, DHA, is found in relative abundance and there is almost no ALA. There are several explanations offered for this, including (i) that ALA is rapidly converted to EPA, docosapentaenoic acid (DPA), and DHA (14), (ii) that ALA is even more rapidly metabolized to saturated and monounsaturated fatty acids and cholesterol in neural tissue (14,15), and (iii) that ALA is rapidly β-oxidized by comparison with LA, a suggestion which has support from direct measurements of LA and ALA β-oxidation in the rat *in vivo* and *in vitro* (16–18). It is interesting that the extent of ALA β-oxidation may depend on the LA intake, based on data in the rat showing increased ALA β-oxidation with increasing levels of LA in the diet (18). Humans also show differences in LA and ALA accumulation. For example, in a recent study in vegetarian males, Li *et al.* (13) showed that equal amounts of LA and ALA fed for 4 wk raised the levels of ALA in platelets and plasma lipids, but the amount of ALA in these fractions was substantially less than that of LA. In that study there were only minor increases in long-chain n-3 polyunsaturated fatty acids (PUFA) in plasma and platelets.

Many studies on tissue distributions of ALA in animals and man have investigated only a few tissue compartments, such as liver, muscle and brain, which may limit the ability to interpret the events in the whole body. The aim of this study was to examine the distribution of ALA throughout the body

*To whom correspondence should be addressed.
E-mail: sinclair@rmit.edu.au

Abbreviations: AA, arachidonic acid; ALA, α-linolenic acid; DHA, docosahexaenoic acid; DPA, docosapentaenoic acid; EFA, essential fatty acids; EPA, eicosapentaenoic acid; LA, linoleic acid; PUFA, polyunsaturated fatty acid; TLC, thin-layer chromatography.

in young guinea pigs raised on diets with either a high or low ALA intake in an attempt to determine why ALA does not accumulate in tissue lipids.

MATERIALS AND METHODS

Eight 4-wk-old male pigmented guinea pigs were purchased from Monash University (Melbourne, Australia). After having been fed on a guinea pig chow diet for 10 d, they were randomly divided into two groups, fed with one of two semisynthetic diets (Glen Forrest Stockfeeders, Glen Forrest, Western Australia) mixed with normal chow for 1 wk, and then fed with the semisynthetic diet only for the next 3 wk. The major ingredients including the vitamin and mineral composition have been reported previously in similar studies by our group using guinea pigs (19). The fat (vegetable oils), protein (casein), and carbohydrate (sucrose, glucose and starch) contents of the diets were 10, 30, and 47%, respectively. The fatty acid compositions of these two different diets are shown in Table 1; the 18:2n-6 content of each diet was 18% of the total fatty acids, while 18:3n-3 was 17.3% in the high ALA diet and 0.3% in the low ALA diet. The oils used in the diets consisted of mixtures of coconut, linseed, palm stearin, safflower, sunola, and canola oils in order to provide a constant LA and variable ALA contents. At the conclusion of the study, the guinea pigs were asphyxiated in CO_2 gas, the head was severed from the body, and then the skin and fur removed from the skull and carcass of the body, respectively. The other tissues were collected, washed free from blood in ice-cold normal saline, and dried with blotting paper; the total weight of the organs was recorded and then the tissues were stored at –20°C. The stomach and intestines were opened and washed free of digesta/feces and stored as above. Prior to lipid extraction, all tissues were finely cut up using a scalpel and were thoroughly mixed, except in the case of the carcass (muscle plus bone) which was minced using an industrial mincer prior to being diced as above. Lipids were extracted from approximately 2 g of each tissue (2 × 2 g for the carcass) using chloroform/methanol as described by Nelson (20); a precise amount of internal standard fatty acid (23:0; Nu-Chek-Prep, Elysian, MN) was added to each tissue at the start of the lipid extraction. One aliquot of each tissue lipid was converted to fatty acid methyl esters for determination of the tissue fatty acid content by capillary GLC using on a BPX-70 column (SGE, Melbourne, Australia) (21). The fatty acids were identified by comparison with standard mixtures of fatty acid methyl esters, and the results were calculated using response factors derived from chromatographing standards of known composition which contained 23:0.

TABLE 1
Fatty Acid Composition of the Two Diets

	Fatty acid composition (%)	
Fatty acid	High ALA diet[a]	Low ALA diet[a]
12:0 + 14:0	10.9	11.4
16:0	13.7	31.7
18:0	4.3	4.1
18:1	35.3	34.5
18:2n-6	18.2	17.5
18:3n-3	17.3	0.3
18:2/18:3	1.05	58

[a]Twenty- and 22-carbon polyunsaturated fatty acids were below the level of 0.01% of total fatty acids. ALA, α-linoleic acid.

RESULTS

The weights of the animals at the conclusion of the feeding study were 587 ± 55 and 570 ± 55 g in the high- and low-ALA diet groups, respectively. The animals in each group appeared healthy.

The distribution of PUFA in the different tissues is shown in Table 2. LA was the major PUFA in the whole body (>20 g), followed by ALA (2–9 g), AA (≈1 g), and relatively small amounts of long-chain n-3 PUFA (0.3 g). The adipose tissue, skin, and carcass (muscle plus bone) were the main sites of LA, ALA, AA, and EPA deposition. The main sites for DHA deposition were carcass and brain. This table also shows that the high ALA diet resulted in a significant accumulation of ALA in every tissue except the brain, with the greatest difference between the two diets being in the adipose tissue, and the highest proportional rise in liver and digestive tract. The high ALA diet significantly increased the EPA, DPA, and DHA levels in most tissues although the increases were not large by comparison with the increases in the ALA in different tissues. Although the intake of LA was constant in the two diet groups, the LA content was significantly increased in most of the tissues in the high ALA diet group, except for liver, kidney, and brain. AA was significantly increased in heart, stomach, and intestines, and significantly decreased in adipose, carcass, and skin in the high ALA group. The whole body content of ALA and EPA showed significant increases in animals with high ALA diet.

The complete tissue fatty acid compositions are presented in Table 3. With high ALA intake, the ALA proportion was increased in all tissues except brain. The EPA, 22:5n-3, and DHA proportions were significantly increased in all tissues except skin. The high ALA diet was associated with some significant changes in saturated fatty acids in most tissues. In all tissues except brain, there were significant decreases in the proportions of palmitic acid on the high ALA diet which had less than half the palmitic acid content of the low ALA diet. On the high ALA diet, the proportion of stearic acid rose in heart, lung, and spleen. On the high ALA diet, the proportion of LA increased significantly in heart, lung and spleen, skin, and carcass.

DISCUSSION

The aim of this study was to examine the distribution of ALA throughout the body in young guinea pigs on diets with either a high or low ALA intake in an attempt to determine why ALA does not accumulate in tissue lipids.

TABLE 2
Tissue n-6 and n-3 Fatty Acid Contents in Guinea Pigs Fed a Diet High or Low in ALA[a] (mg/tissue)

Fatty acids	Diet LA/ALA[b]	Heart	Stomach and intestines	Liver	Brain	Lung and spleen	Kidney and adrenal	Adipose	Skin	Carcass	Total[c]
18:2n-6	1.05	31 ± 4[a]	554 ± 67[a]	354 ± 27	5 ± 0.4	37 ± 3[a]	85 ± 5	12,149 ± 1,226[a]	3,428 ± 181	9,780 ± 53[a]	26.4 ± 1.8[a]
	58	18 ± 1	385 ± 52	336 ± 73	5 ± 1	25 ± 4	86 ± 6	8,409 ± 945	3,759 ± 315	8,457 ± 227	20.1 ± 2.0
20:4n-6	1.05	20 ± 3[a]	82 ± 6[a]	58 ± 4	35 ± 1	13 ± 2	29 ± 7	147 ± 12[a]	115 ± 12[a]	446 ± 18[a]	0.9 ± 0.0[a]
	58	12 ± 2	40 ± 3	47 ± 6	32 ± 6	11 ± 3	36 ± 4	26 ± 16	156 ± 21	703 ± 55	1.1 ± 0.2
22:4n-6	1.05	1 ± 0.1	9 ± 3	4 ± 0.4	14 ± 0.4	2 ± 0.3	2 ± 1	50 ± 6[a]	24 ± 3[a]	66 ± 1[a]	0.2 ± 0.0[a]
	58	1 ± 0.03	8 ± 3	5 ± 1	14 ± 3	3 ± 1	2 ± 0.4	67 ± 8	41 ± 4	112 ± 12	0.3 ± 0.0
22:5n-6	1.05	1 ± 0.1	4 ± 1	3 ± 0.3	18 ± 3	0.4 ± 0.1[a]	1 ± 0.1	21 ± 3[a]	33 ± 1[a]	55 ± 3[a]	0.1 ± 0.0[a]
	58	1 ± 0.1	4 ± 1	4 ± 1	20 ± 4	1 ± 0.2	1 ± 0.1	28 ± 4	51 ± 4	82 ± 6	0.2 ± 0.0
18:3n-3	1.05	5 ± 1[a]	189 ± 19[a]	105 ± 11[a]	0.4 ± 0.0	9 ± 2[a]	24 ± 4[a]	4,765 ± 260[a]	745 ± 53[a]	2,921 ± 13[a]	8.8 ± 0.4[a]
	58	1 ± 0.3	22 ± 3	11 ± 3	0.3 ± 0.1	3 ± 1	6 ± 2	785 ± 41	393 ± 52	1,070 ± 155	2.3 ± 0.3
20:5n-3	1.05	1 ± 0.1[a]	ND	3 ± 1	1 ± 0.1[a]	1 ± 0.1	2 ± 0.3[a]	13 ± 0.3[a]	10 ± 2	24 ± 3	0.06 ± 0.0[a]
	58	ND	ND	ND	0.3 ± 0.1	ND	1 ± 0.1	ND	10 ± 2	ND	0.01 ± 0.00
22:5n-3	1.05	3 ± 1[a]	23 ± 5[a]	10 ± 1[a]	3 ± 0.4[a]	3 ± 0.3[a]	2 ± 1[a]	46 ± 6[a]	40 ± 6	109 ± 18	0.2 ± 0.01
	58	1 ± 0.2	4 ± 2	4 ± 1	1 ± 0.2	1 ± 0.2	1 ± 0.1	25 ± 2	43 ± 9	101 ± 16	0.2 ± 0.03
22:6n-3	1.05	1 ± 0.0[a]	2 ± 1	5 ± 1[a]	23 ± 4	0.2 ± 0.0	1 ± 0.1[a]	9 ± 1[a]	7 ± 1	43 ± 1	0.09 ± 0.01
	58	0.3 ± 0.1	ND	2 ± 1	17 ± 3	ND	0.4 ± 0.1	ND	8 ± 1	47 ± 3	0.08 ± 0.01

[a]Means ± SD. n = 4 animals in each group. ND, not detectable; LA, linoleic acid; for other abbreviation see Table 1. For each fatty acid, in each tissue, means followed by the superscript roman letter "a" are significantly different between diets, $P < 0.05$.
[b]High ALA diet has LA/ALA of 1.05:1, low ALA diet has LA/ALA of 58:1.
[c]g/100 g.

TABLE 3
Fatty Acid Composition (%) in Tissues from Guinea Pigs Fed Diets Either High or Low in ALA[a]

Fatty acids	Diet LA/ALA[b]	Heart	Stomach and intestines	Liver	Brain	Lung and spleen	Kidney	Adipose	Skin	Carcass
14:0	1.05	0.9 ± 0.2[a]	1.7 ± 0.2	0.9 ± 0.1	0.4 ± 0.0	2.9 ± 0.1	1.7 ± 0.1	2.5 ± 0.0	2.5 ± 0.2	2.1 ± 0.6[a]
	58	1.5 ± 0.4	2.2 ± 0.2	0.7 ± 0.1	0.4 ± 0.1	3.3 ± 0.1	1.9 ± 0.4	2.8 ± 0.3	2.6 ± 0.1	2.7 ± 0.1
16:0	1.05	15.4 ± 1.4[a]	19.4 ± 1.8[a]	13.8 ± 2.0[a]	21.3 ± 0.9	30.5 ± 1.2[a]	18.4 ± 1.3[a]	22.2 ± 1.6[a]	23.8 ± 2.2[a]	22.2 ± 1.4[a]
	58	22.2 ± 2.8	25.8 ± 2.2	18.7 ± 0.7	22.2 ± 0.9	35.0 ± 1.1	22.8 ± 2.7	28.1 ± 0.3	27. 6 ± 1.1	27.9 ± 0.4
16:1	1.05	0.4 ± 0.1	0.9 ± 0.2	0.2 ± 0.1	0.5 ± 0.1	1.4 ± 0.1	1.0 ± 0.2	1.3 ± 0.3	1.9 ± 0.5	1.6 ± 0.2
	58	0.7 ± 0.4	1.5 ± 0.7	0.2 ± 0.1	0.5 ± 0.0	1.6 ± 0.4	1.1 ± 0.1	1.7 ± 0.1	2.2 ± 0.4	1.8 ± 0.2
18:0	1.05	15.2 ± 0.5[a]	8.9 ± 1.1	21.0 ± 2.4	20.8 ± 0.3	9.6 ± 0.5[a]	10.9 ± 1.0	4.0 ± 0.3	4.3 ± 0.6	4.8 ± 0.7
	58	13.0 ± 1.4	9.3 ± 1.3	20.1 ± 1.7	21.3 ± 0.1	8.7 ± 1.4	11.2 ± 2.7	4.5 ± 0.6	4.4 ± 0.2	5.7 ± 0.6
18:1	1.05	19.3 ± 2.3	28.3 ± 1.7	17.5 ± 1.4	21.1 ± 1.4	25.6 ± 1.3	27.2 ± 1.4	33.0 ± 0.6	31.2 ± 0.8	32.4 ± 0.5
	58	20.5 ± 1.5	31.0 ± 2.0	17.5 ± 1.0	21.4 ± 1.9	29.7 ± 2.0	24.8 ± 0.9	32.4 ± 1.2	31.0 ± 0.4	34.5 ± 0.6
18:2n-6	1.05	23.0 ± 0.7[a]	24.2 ± 3.4	28.8 ± 1.3	1.6 ± 0.1	16.9 ± 0.6[a]	21.3 ± 0.5	22.6 ± 0.8	28.1 ± 0.3[a]	25.6 ± 0.3[a]
	58	21.8 ± 0.4	24.6 ± 3.4	32.4 ± 0.6	1.7 ± 0.1	11.6 ± 0.9	21.3 ± 1.0	22.4 ± 0.5	21.8 ± 0.7	17.6 ± 0.4
20:4n-6	1.05	14.8 ± 0.2	3.6 ± 0.3	4.7 ± 0.7	11.4 ± 0.3	5.8 ± 0.7	7.2 ± 1.6	0.3 ± 0.0[a]	0.7 ± 0.1	1.2 ± 0.1
	58	14.0 ± 2.7	2.5 ± 0.3	4.5 ± 0.3	11.6 ± 0.3	5.3 ± 1.7	9.0 ± 1.1	0.6 ± 0.0	0.8 ± 0.1	1.5 ± 0.3
22:4n-6	1.05	0.4 ± 0.0	0.4 ± 0.1	0.3 ± 0.0	4.4 ± 0.3[a]	0.9 ± 0.1	0.4 ± 0.1	0.1 ± 0.0	0.1 ± 0.0	0.2 ± 0.0
	58	0.6 ± 0.0	0.5 ± 0.1	0.5 ± 0.0	5.1 ± 0.0	1.3 ± 0.3	0.5 ± 0.2	0.2 ± 0.0	0.2 ± 0.0	0.2 ± 0.0
22:5n-6	1.05	0.5 ± 0.1	0.2 ± 0.0	0.3 ± 0.0	5.9 ± 1.2[a]	0.2 ± 0.0	0.1 ± 0.0	ND	0.2 ± 0.0	0.1 ± 0.0
	58	0.8 ± 0.1	0.2 ± 0.1	0.4 ± 0.0	7.2 ± 1.1	0.3 ± 0.1	0.2 ± 0.1	0.1 ± 0.0	0.3 ± 0.0	0.2 ± 0.0
18:3n-3	1.05	3.7 ± 0.4[a]	8.2 ± 0.4[a]	8.5 ± 0.5[a]	0.1 ± 0.0	4.3 ± 0.8[a]	6.1 ± 1.0[a]	8.9 ± 1.1[a]	6.0 ± 0.7[a]	7.7 ± 0.4[a]
	58	0.9 ± 0.3	1.4 ± 0.1	0.9 ± 0.3	0.1 ± 0.0	1.1 ± 0.2	1.4 ± 0.2	2.1 ± 0.1	2.3 ± 0.3	2.2 ± 0.2
20:5n-3	1.05	0.4 ± 0.1	ND	0.3 ± 0.1	0.2 ± 0.0	0.4 ± 0.1	0.5 ± 0.1[a]	<0.1	0.1 ± 0.0	0.1 ± 0.0
	58	ND	ND	ND	0.1 ± 0.0	ND	0.1 ± 0.0	ND	0.1 ± 0.0	ND
22:5n-3	1.05	2.2 ± 0.4[a]	1.0 ± 0.2[a]	0.8 ± 0.1[a]	0.9 ± 0.1[a]	1.5 ± 0.1[a]	0.6 ± 0.1[a]	0.1 ± 0.0	0.3 ± 0.1	0.3 ± 0.1
	58	1.0 ± 0.2	0.3 ± 0.1	0.3 ± 0.1	0.4 ± 0.0	0.4 ± 0.1	0.2 ± 0.0	0.1 ± 0.0	0.2 ± 0.1	0.2 ± 0.0
22:6n-3	1.05	0.6 ± 0.1	0.1 ± 0.0	0.4 ± 0.1[a]	7.4 ± 0.9[a]	0.1 ± 0.0	0.2 ± 0.0	<0.1	<0.1	0.1 ± 0.0
	58	0.4 ± 0.1	ND	0.2 ± 0.0	6.4 ± 1.4	ND	0.1 ± 0.0	ND	<0.1	0.1 ± 0.0

[a]Means ± SD. n = 4 animals in each group. With each tissue, for each fatty acid, means followed by the superscript roman letter "a" are significantly different between diets, $P < 0.05$. For abbreviations see Tables 1 and 2.

Where did ALA accumulate in the body? The major sites for ALA accumulation were adipose, carcass, and skin, these tissues accounting for approximately 90% of the whole body distribution of ALA. In this study, skin would include epidermis, dermis, and perhaps some subcutaneous fat. Skin has not been reported as a major site of ALA deposition previously, in this species. LA was also mainly found in the same tissues (adipose, carcass, and skin). The carcass, as sampled in this study, includes muscle and bone; however, it is assumed that the majority of the lipids originated from muscle. Few other studies have examined all tissues as sites for deposition of PUFA. Becker *et al*. (22) showed that in the rat, the major sites in the body for the deposition of radiolabeled ALA were liver, brown fat, and adrenal cortex. It is presumed that the skin was removed prior to autoradiography in that particular study. Cunnane and Anderson (23) examined all major tissues in young rats fed equal amounts of LA and ALA and found that adipose, carcass, and skin were the main sites for both LA and ALA accumulation. In the present study, the major sites of EPA and DPA deposition were adipose, skin, and carcass, while DHA deposition occurred in the carcass, brain, skin, and adipose tissue. Since the carcass contained 47–62% of the whole body DHA, it is possible that this tissue could act as a reservoir of long-chain n-3 PUFA such as DHA for vital times such as pregnancy and lactation, even on diets low in ALA.

Did the high ALA diet result in more DHA in the whole body and other tissues? This is an important issue since there is evidence that in the brain ALA is rapidly metabolized to DHA (14,15), while in the infant formula area there has been much discussion recently about the effectiveness of ALA as a DHA precursor (24–27). Increasing the ALA content of the diet substantially increased the tissue stores of ALA; however, there were only modest increases in the long-chain n-3 PUFA; these increases occurred in all tissues except skin and carcass in the guinea pig. While the whole body ALA content increased 3.8× on the high-ALA diet, the EPA content increased 6×, the DPA content did not change, and the DHA content increased only 1.1×. On a mass basis, the high ALA diet led to a 5.5 g increase in the whole body ALA level, compared with an increase of 0.06 g of long-chain n-3 PUFA. In this species therefore, conversion of ALA to DHA does not appear to be a major metabolic route for ALA metabolism unless there is a very high turnover of DHA. Several groups have reported that in the brain β-oxidation of ALA and carbon recycling into saturated and monounsaturated fatty acids and cholesterol are quantitatively more important than conversion of ALA to DHA (15,28).

If ALA is not being converted to DHA, what happens to it? The proportion of LA in all tissues, except brain, lung and spleen, was high, where it ranged from 18–32% of the total

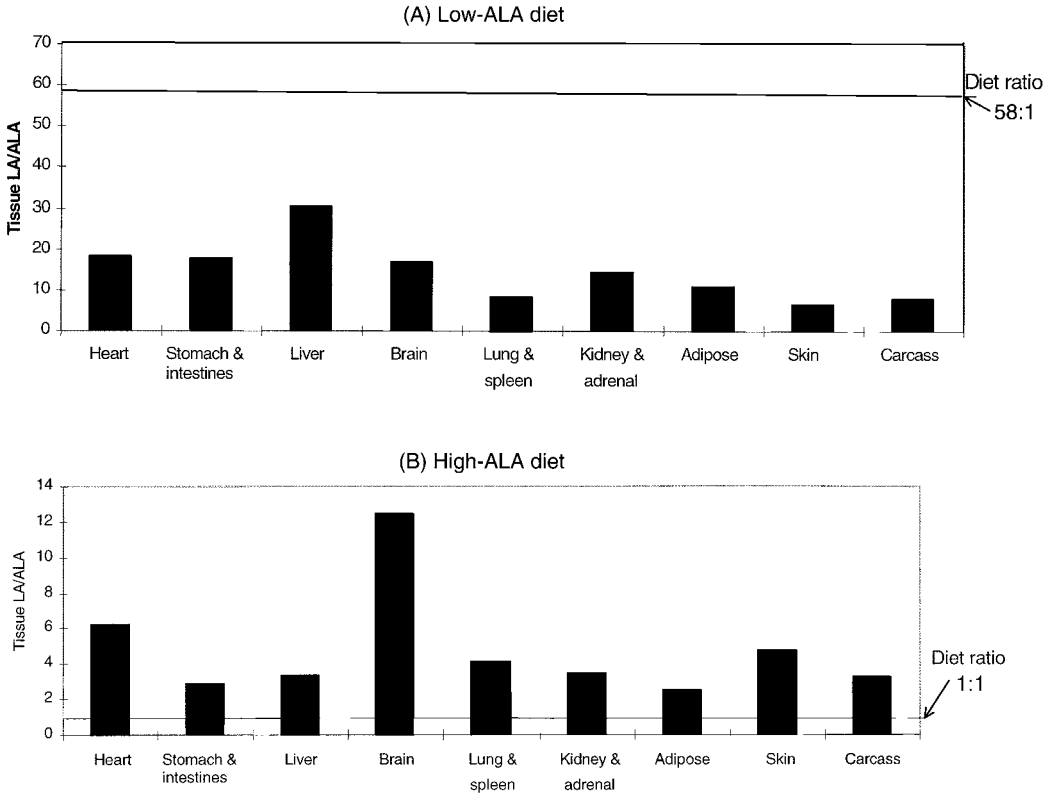

FIG. 1. The effect of high- and low-α-linolenic acid (ALA) diets on the proportions of ALA in body tissues in guinea pigs. The data are shown as the ratio of linoleic acid (LA) to ALA in each tissue compared with the LA to ALA ratio in the diet. (A) On the low-ALA diet, all tissue LA/ALA ratios were less than that in the diet, indicating conservation of ALA relative to LA; (B) on the high-ALA diet, all tissue LA/ALA ratios were higher than that in the diet indicating a relative loss of ALA compared with LA.

tissue fatty acids. In comparison, the ALA levels in these tissues varied from 4–9% on the high ALA diet and 1–2% on the low ALA diet. Cunnane and colleagues (29) have used a modification of a balance method to determine the apparent oxidation of fatty acids in the rat based on the disappearance of fatty acids (intake – [accumulation + losses from excretion]). We did not determine food intake or excretion of fatty acids; however, since the LA and ALA are essential, it is possible to arrive at an expression of fatty acid losses based on a comparison of the ratios of LA to ALA in the tissues compared with the same ratio in the diet. On the diet low in ALA, the LA/ALA value in all tissues was substantially less than that of the diet. For example in the diet the LA/ALA was 58:1, while in the whole body it was 9:1 and in the individual tissues it ranged from 2:1 to 18:1 (Fig. 1A). This suggests that there was a conservation of ALA in the body relative to LA on the diet with the very low ALA intake (0.03 g/100 g diet). This is consistent with data in rats from Becker *et al.* (30,31) who showed that less LA was β-oxidized in rats on a low-EFA diet compared with a high-EFA diet. In contrast, on the high-ALA diet, there appeared to be a loss of ALA relative to LA. That is, on the high-ALA diet with a LA/ALA value of 1.05:1 the whole body ratio was 3:1, and in individual tissues it ranged from 3 to 10:1 (Fig. 1B). These data suggest that in the circumstances of a high-ALA intake there is increased loss of this fatty acid. Others have reported that ALA is preferentially β-oxidized *in vivo* and *in vitro* (16–18), while the long-chain n-3 PUFA induce a marked stimulation of brown adipose tissue thermogenic activity (32). The effect of these two dietary regimes on ALA can be summarized as follows: first, the low-ALA diet was associated with a conservation of tissue ALA while on the diet rich in ALA there was a preferential loss of ALA, possibly through β-oxidation or other routes of excretion such as that *via* the skin and fur as reported recently in the guinea pig (33). On the high-ALA diet, there was a 30% increase in tissue LA content. This observation is hard to explain, however, since those tissues which showed increased proportions of LA also showed decreases in the proportions of palmitic acid; it may be related to the lower palmitic acid level of this high ALA diet. An alternative explanation could be that there was a relative conservation of LA due to the apparent increase in β-oxidation of ALA.

In conclusion, these data show that (i) high intakes of dietary ALA (1.7% ALA in diet) in the guinea pig led to very little increase in the whole body content of long-chain n-3 PUFA compared with a diet with a low ALA level (0.03% ALA in diet), (ii) the high-ALA diet resulted in an increased tissue ALA level and decreased palmitic acid level in all tissues except the brain, (iii) no one tissue mirrors the whole body distribution of n-3 or n-6 PUFA, (iv) ALA retention in the body varied according to intake, with low ALA intakes being associated with a higher retention of ALA in the body than on diets rich in ALA. These data suggest the low tissue levels of tissue ALA in the guinea pig are likely to be the result of β-oxidation of ALA to CO_2 or excretion *via* skin and fur, rather than metabolism to DHA.

ACKNOWLEDGMENTS

The support of the Grains & Research Development Corporation and Meadow Lea Foods Australia is gratefully acknowledged.

REFERENCES

1. Burr, G.C., and Burr, M.M. (1930) On the Nature and Role of the Fatty Acids Essential in Nutrition, *J. Biol. Chem. 86*, 587–621.
2. Holman, R.T. (1968) Essential Fatty Acid Deficiency, A Long Scaly Tale, *Prog. Chem. Fats & Other Lipids 9*, 275–348.
3. Cunnane, S.C. (1999) The Long History of Essential Fatty Acids But Belated Knowledge About Linoleate Deficiency *Per Se*: A Paradox, *J. Nutr. 129*, 446.
4. Hansen, H.S., and Jensen, B. (1985) Essential Function of Linoleic Acid Esterified in Acylglucosylceramide and Acylceramide in Maintaining the Epidermal Water Permeability Barrier. Evidence from Feeding Studies with Oleate, Linoleate, Arachidonate, Columbinate, and α-Linolenate, *Biochim. Biophys. Acta 834*, 357–363.
5. Crawford, M.A., Casperd, N.M., and Sinclair, A.J. (1976) The Long-Chain Metabolites of Linoleic and Linolenic Acids in Liver and Brain in Herbivores and Carnivores, *Comp. Biochem. Physiol. 54B*, 395–401.
6. Salem, N., and Ward, G.R. (1993) Are Omega-3 Fatty Acids Essential Nutrients for Animals? *World Rev. Nutr. Dietet. 72*, 128–147.
7. Grimsgaard, S., Bonaa, K.H., Hansen, J.-B., and Nordoy, A. (1997) Highly Purified Eicosapentaenoic Acid and Docosahexaenoic Acid in Humans Have Similar Triacylglycerol-Lowering Effects but Divergent Effects on Serum Fatty Acids, *Am. J. Clin. Nutr. 66*, 649–659.
8. Neuringer, M., Connor, W.E., Lin, D.S., Barstad, L., and Luck, S.J. (1986) Biochemical and Functional Effects of Prenatal and Postnatal Omega-3 Fatty Acid Deficiency on Retina and Brain in Rhesus Monkeys, *Proc. Natl. Acad. Sci. USA 83*, 4021–4025.
9. Billman, G.E., Kang, J.X., and Leaf, A. (1997) Prevention of Ischemia-Induced Cardiac Sudden Death by n-3 Polyunsaturated Fatty Acids in Dogs, *Lipids 32*, 1161–1168.
10. Litman, B.J., and Mitchell, D.C. (1996) A Role for Phospholipids in Modulating Membrane Protein Function, *Lipids 31*, S193–S198.
11. Horrobin, D.F., Huang, Y.S., Cunnane, S.C., and Manku, M.S. (1984) Essential Fatty Acids in Plasma, Red Blood Cells and Liver Phospholipids in Common Laboratory Animals as Compared to Humans, *Lipids 19*, 806–811.
12. Mantzioris, E., James, M.J., Gibson, R.A., and Cleland, L.G. (1994) Dietary Substitution with an α-Linolenic Acid-Rich Vegetable Oil Increases Eicosapentaenoic Acid Concentrations in Tissue, *Am. J. Clin. Nutr. 59*, 1304–1309.
13. Li, D., Sinclair, A.J., Wilson, A., Nakkote, S., Kelly, F., Abedin, L., Mann, N.J., and Turner, A.T. (1999) Effect of Dietary α-Linolenic Acid on Thrombotic Risk Factors in Vegetarian Men, *Am. J. Clin. Nutr. 69*, 872–882.
14. Sinclair, A.J. (1975) Incorporation of Radioactive Polyunsaturated Fatty Acids into Liver and Brain of the Developing Rat, *Lipids 10*, 175–184.
15. Sheaff Greiner, R.C., Zhang, Q., Goodman, K.J., Guissani, D.A., Nathanielsz, P.W., and Brenna, J.T. (1996) Linoleate, α-Linolenate and Docosahexaenoate Recycling into Saturated and Monounsaturated Fatty Acids Is a Major Pathway in Pregnant and Lactating Adults or Infant Rhesus Monkeys, *J. Lipid Res. 37*, 2675–2686.
16. Leyton, J., Drury, P.J., and Crawford, M.A. (1987) Differential Oxidation of Saturated and Unsaturated Fatty Acids *in Vivo* in the Rat, *Br. J. Nutr. 57*, 383–393.

17. Ide, T., Murata, M., and Sugano, M. (1996) Stimulation of the Activities of Hepatic Fatty Acid Oxidation Enzymes by Dietary Fat Rich in α-Linolenic Acid in Rats, *J. Lipid Res. 37*, 448–463.
18. Pan, D.A., and Storlien, L.H. (1993) Dietary Lipid Profile Is a Determinant of Tissue Phospholipid Fatty Acid Composition and Rate of Weight Gain in Rats, *J. Nutr. 123*, 512–519.
19. Weisinger, H.S., Vingrys, A.J., Bui, B.V., and Sinclair, A.J. (1999) Effects of Dietary n-3 Fatty Acid Deficiency and Repletion in the Guinea Pig, *Invest. Ophthalmol. Vis. Sci. 40*, 327–338.
20. Nelson, G.J. (1993) Isolation and Purification of Lipids from Biological Matrices, in *Analysis of Fats, Oil and Derivatives*, *(*Perkins, E.G., ed.), pp. 20–59, AOCS Press, Champaign.
21. Li, D., Ng, A., Mann, N.J., and Sinclair, A.J. (1998) Contribution of Meat Fat to Dietary Arachidonic Acid, *Lipids 33*, 437–440.
22. Becker, W., Mohammed, A., and Slanina, P. (1985) Uptake of Radiolabelled α-Linolenic, Arachidonic and Oleic Acid in Tissues of Normal and Essential Fatty Acid-Deficient Rats—An Autoradiographic Study, *Ann. Nutr. Metab. 29*, 65–75.
23. Cunnane, S.C., and Anderson, M.J. (1997) The Majority of Dietary Linoleate in Growing Rats Is β-Oxidized or Stored in Visceral Fat, *J. Nutr. 127*, 146–152.
24. Innis, S.M., Sprecher, H., Hachey, D., Edmond, J., and Anderson, R.E. (1999) Neonatal Fatty Acid Metabolism, *Lipids 34*, 139–150.
25. Salem, N., Wegher, B., Mena, P., and Uauy, R. (1996) Arachidonic and Docosahexaenoic Acids Are Biosynthesized from Their 18-Carbon Precursors in Human Infants, *Proc. Natl. Acad. Sci. USA 93*, 49–54.
26. Gerster, H. (1998) Can Adults Adequately Convert α-Linolenic Acid to Eicosapentaenoic Acid and Docosahexaenoic Acid*?* *Internat. J. Vit. Nutr. Res. 68*, 159–173.
27. Abedin, L., Lien, E.L., Vingrys, A.J., and Sinclair, A.J. (1999) The Effects of Dietary α-Linolenic Acid Compared with Docosahexaenoic Acid on Brain, Retina, Liver, and Heart in the Guinea Pig, *Lipids 34*, 475–482.
28. Menard, C.R., Goodman, K.J., Corso, T.N., Brenna, J.T., and Cunnane, S.C. (1998) Recycling of Carbon into Lipids Synthesized *de novo* Is a Quantitatively Important Pathway of α-[U-^{13}C]Linolenate Utilization in the Developing Rat Brain, *J. Neurochem. 71*, 2151–2158.
29. Cunnane, S.C., Yang, J., and Chen, Z.-Y. (1993) Low Zinc Intake Increases Apparent Oxidation of Linoleic and α-Linolenic Acids in the Pregnant Rat, *Can. J. Physiol. Pharmacol. 71*, 205–210.
30. Becker, W., and Bruce, A. (1986). Retention of Linoleic Acid in Carcass Lipids of Rats Fed Different Levels of Essential Fatty Acids, *Lipids 21*, 121–126.
31. Becker, W. (1984) Distribution of C14 After Oral Administration of 1-^{14}C-Linoleic Acid in Rats Fed Different Levels of Essential Fatty Acids, *J. Nutr. 114*, 1690–1696.
32. Oudart, H., Groscolas, R., Calgari, C., Nibbelink, M., Leray, C., Maho, Y.L., and Malan, A. (1997) Brown Fat Thermogenesis in Rats Fed High Fat Diets Enriched with n-3 Polyunsaturated Fatty Acids, *Int. J. Obesity 21*, 955–962.
33. Fu, Z., and Sinclair, A.J. (2000) Novel Pathway of Metabolism of α-Linolenic Acid in the Guinea Pig, *Paediatr. Res. 47*, 414–417.

[Received December 7, 1999, and in revised form March 8, 2000; revision accepted March 22, 2000]

Effect of n-3 Polyunsaturated Fatty Acid Supplementation on Lipid Peroxidation of Rat Organs

Ken Ando[a], Kunihide Nagata[a], Rie Yoshida[a], Kiyomi Kikugawa[a,*], and Masao Suzuki[b]

[a]School of Pharmacy, Tokyo University of Pharmacy and Life Science, Hachioji, Tokyo 192-0392, Japan, and [b]Advanced Science and Technology Research Center, Kyushu University, Kasuga, Fukuoka 816-8580, Japan

ABSTRACT: The present study was undertaken in order to re-examine the effect of n-3 polyunsaturated fatty acid (PUFA)-rich diet supplementation on lipid peroxidation and vitamin E status of rat organs. Male Wistar rats were fed a diet containing safflower or fish oil at 50 g/kg diet and an equal amount of vitamin E at 59 mg/kg diet (1.18 g/kg oil; and 1.5 g/kg PUFA in safflower oil diet, and 4.3 g/kg PUFA in fish oil diet) for 6 wk. Fatty acid composition of total lipids of brain, liver, heart, and lung of rats fed fish oil was rich in n-3 PUFA, whereas that of each organ of rats fed safflower oil was rich in n-6 PUFA. The vitamin E levels in liver, stomach, and testis of the fish oil diet group were slightly lower than those of the safflower oil diet group, but the levels in brain, heart, lung, kidney, and spleen were not different between the two diet groups. The levels of phospholipid hydroperoxides were determined by the high-performance liquid chromatography–chemiluminescence method and the levels of thiobarbituric acid-reactive substances (TBARS) were determined at pH 3.5 in the presence of butylated hydroxytoluene with or without EDTA. Levels of phospholipid hydroperoxides and TBARS in the brain, liver, heart, lung, kidney, spleen, stomach and testis of the fish oil diet group were similar to those of the safflower oil diet group. The results indicate that high fish oil intake does not induce increased levels of phospholipid hydroperoxides and TBARS in rat organs.

Paper no. L8346 in *Lipids 35*, 401–407 (April 2000).

Epidemiological studies have shown apparent beneficial effects of fish oil containing high n-3 polyunsaturated fatty acids (PUFA), eicosapentaenoate (20:5n-3) and docosahexaenoate (22:6n-3), on mortality from heart disease and cancer (1,2). On the other hand, undesirable effects of high fish oil intake have been a concern because n-3 PUFA whose unsaturation index (UI) and peroxidizability index (PI) are higher than those of n-6 PUFA and n-9 monounsaturated fatty acids are more readily oxidized under aerobic conditions (3). Lipid peroxidation occurring in the human body has been considered to cause various disorders including atherosclerosis, diabetes, burn injury, and retinopathy (4).

Many earlier studies suggested that intake of a diet high in fish oil results in high n-3 PUFA content in membrane lipids and enhances lipid peroxidation in organs, blood and urine of experimental animals and humans (5–16). Low doses of fish oils do not significantly affect lipid peroxidation *in vivo* (17–22). Decreased tissue levels of vitamin E following an increase in the intake of fish oil have been demonstrated (7,9,23–31). Most of these studies, however, have employed traditional thiobarbituric acid (TBA) assay without incorporation of an antioxidant for estimation of lipid peroxidation of the samples. Artificial TBA-reactive substances (TBARS) generated during the assay in the absence of an antioxidant may have been measured.

The present study was undertaken to reexamine the effect of supplementation of safflower or fish oil on vitamin E status and lipid peroxidation of rat organs. Two different classes of lipid peroxidation products, phospholipid hydroperoxides (32,33) and TBARS in the presence of butylated hydroxytoluene (BHT) as an antioxidant (34–38), were measured.

MATERIALS AND METHODS

Materials. Phosphatidylcholine (egg yolk) (PC) and phosphatidylethanolamine (egg yolk) (PE) were obtained from Nippon Fats and Oil Liposome Company (Tokyo, Japan). PC hydroperoxide (PCOOH) and PE hydroperoxide (PEOOH) were prepared just before use according to a method described elsewhere (32). Briefly, PC and PE were photooxidized at 10°C for 10 h in the presence of methylene blue, and methylene blue was removed by passing through a column of florisil. Peroxide values of PCOOH and PEOOH were estimated to be 1380–1680 and 770–840 neq/mg, respectively. Cytochrome c and luminol were purchased from Sigma Chemical Co. (St. Louis, MO) and Wako Pure Chemical Industries (Osaka, Japan), respectively. TBA was obtained from Merck (Darmstadt, Germany).

Animals and diets. The protocol of animal preparations for the present experiment was approved by the Ethics Committee of our institute. Twenty-four 4-wk-old male Wistar rats weighing 50–70 g were supplied by Japan Laboratory Animals Corp. (Tokyo, Japan). Rats were divided into two groups of six animals each, and each group was fed a diet with safflower or fish oil at 50 g/kg diet for 6 wk as described previously (39). Saf-

*To whom correspondence should be addressed at School of Pharmacy, Tokyo University of Pharmacy and Life Science, 432-1 Horinouchi, Hachioji, Tokyo 192-0392, Japan. E-mail: kikugawa@ps.toyaku.ac.jp

Abbreviations: BHT, butylated hydroxytoluene; HPLC, high-performance liquid chromatography; PC, phosphatidylcholine; PCOOH, PC hydroperoxide; PE, phosphatidylethanolamine; PEOOH, PE hydroperoxide; PI, peroxidizability index; PUFA, polyunsaturated fatty acids; TBA, thiobarbituric acid; TBARS, TBA-reactive substances; UI, unsaturation index.

flower oil was rich in n-6 fatty acids (n-6 total: 78.0%, and n-3 total: 0.3%), and fish oil was rich in n-3 fatty acids (n-6 total: 1.3%, and n-3 total: 26.5%) (39). While UI, as expressed by the sum of percentages of individual fatty acids × number of double bonds, of fish oil [168] was equal to that of safflower oil, PI, as expressed by the sum of percentages of individual fatty acids × number of active methylene groups (40), of fish oil [114] was higher than that of safflower oil [78], indicating that fish oil can be more readily peroxidized under aerobic conditions. Peroxide and acid values of safflower oil were 1.1 and 0.2, respectively, and those of fish oil were 1.2 and 0.2, respectively. The overall content of vitamin E in both the diets was equal at 59 mg/kg dried solid diet (1.18 g/kg oil; and 1.5 g/kg PUFA in safflower oil diet, and 4.3 g/kg PUFA in fish oil diet).

Rat organ sampling. At the end of the feeding period, six rats of each diet group were sacrified by bleeding. Brain, liver, heart, lung, kidney, spleen, stomach, and testis were quickly isolated and washed with physiological saline. Each organ was homogenized in about tenfold amount of 10 mM potassium phosphate buffer containing 30 mM KCl (pH 7.8) (wt/vol) with a ice-cooled Potter-type Teflon homogenizer. The homogenate was stored at –80°C under nitrogen atmosphere before use. The amount of protein in the homogenate was determined by the Lowry *et al.* method (41) using bovine serum albumin as a reference standard.

Fatty acid composition of total lipids of rat organs. Total lipids of rat brain, liver, heart, and lung were extracted according to the method of Bligh and Dyer (42). Thus, 1–10 mL of each homogenate containing 0.3–10 g wet isolated organ was mixed with sixfold volumes of $CHCl_3$/MeOH (2:4, vol/vol), and the mixture was centrifuged at 800 × *g* at 4°C for 30 min. Supernatant and pellet were separated. The pellet was mixed with threefold volumes of the organic solvent mixture and 0.8-fold volume of water, and the mixture was centrifuged to obtain supernatant. The supernatants were combined and mixed with threefold volumes of $CHCl_3$ and threefold volumes of water, and the mixture was centrifuged. The lower organic phase was dried by purging with nitrogen gas, and redissolved into 2 mL of $CHCl_3$. The solution was stored at –20°C before analysis. Fatty acid composition was determined by gas chromatography after methylation with HCl/methanol by Special Reference Laboratory Inc. (Tokyo, Japan).

Determination of vitamin E levels in the homogenates of rat organs. Vitamin E levels of rat organs were determined according to the method previously described (43). To 0.1–1.0 mL of the organ homogenate, 1.0 mL of 6% pyrogallol solution in ethanol and 1.0 mL of ethanol were added. After heating the mixture at 70°C for 2 min, 0.2 mL of 60% KOH solution was added, and the mixture was heated at 70°C for 30 min. Vitamin E was extracted by addition of 2.5 mL of water and 5.0 mL of *n*-hexane, and subsequent centrifugation at 1,500 × *g* for 5 min. The upper phase (4.0 mL) was collected and evaporated to dryness to be redissolved into 0.2 mL of methanol. High-performance liquid chromatography (HPLC) was carried out by using an Hitachi 655 liquid chromatograph (Tokyo, Japan) equipped with an Inertsil ODS-2 column (4.6 mm i.d. × 250 mm; GL Sciences Incorporated, Tokyo, Japan) by injection of 10 μL of the sample solution in methanol, and the column was eluted with a mobile phase composed of methanol/water (98:2, vol/vol) at a flow rate of 1.4 mL/min. A fluorescent peak was detected at 292/335 nm with a Shimadzu RF-535 fluorescence spectromonitor (Osaka, Japan). The peak due to vitamin E appeared at a retention time of 17–19 min. The amount of vitamin E in the sample was estimated by comparing the peak area with those of the calibration curve of the standard DL-α-tocopherol. Vitamin E level in each organ was expressed per milligram protein.

HPLC–chemiluminescence determination of PEOOH and PCOOH in total lipids of rat organs. Levels of PCOOH and PEOOH in the total lipid fractions of rat organ homogenates were determined by HPLC–chemiluminescence method (32,33). The lipid fraction was obtained from 0.5–3 mL of each organ homogenate containing 0.1–0.7 g wet organ according to the method of Bligh and Dyer (42), as described. The lower organic phase was dried by purging nitrogen gas, and redissolved into 2.5 mL of a mixture of $CHCl_3$/MeOH (2:1, vol/vol) and 0.5 mL of 0.05 M KCl. The mixture was centrifuged to obtain 1.6 mL of lower phase, which was evaporated to dryness and redissoved into 100 μL of $CHCl_3$. A 10-μL portion of this extract was subjected to HPLC using a column of YMC A-012 S-5 120 A SIL (4.6 mm i.d. × 250 mm) (Yamamura Chemical Laboratories, Kyoto, Japan) and a mobile phase composed of chloroform/methanol (1:9, vol/vol) at a flow rate of 1.0 mL/min. A solution composed of 10 μg/mL cytochrome c and 1 μg/mL luminol in 50 mM borate buffer (pH 9.3) was mixed with the eluate at a flow rate of 0.9 mL/min and chemiluminescence generated was detected using a JASCO 825-CL Intelligent CL detector (Tokyo, Japan). The chemiluminescent peaks due to PEOOH and PCOOH exhibited retention times of 4 and 8 min, respectively. The amounts (neq) of PCOOH and PEOOH were determined by comparing their peak areas with a calibration curve of the peak areas of the standard solutions of PCOOH and PEOOH (0–100 neq).

TBARS in the homogenates of rat organs. TBARS in the homogenates of rat organs were determined according to the method previously described (34–38). The homogenate of each rat organ (200 μL); 650 μL of a mixture consisting of 0.20 mL of 5.2% sodium dodecyl sulfate in water, 50 μL of 0.8% BHT solution in glacial acetic acid, 1.50 mL of 0.8% TBA solution in water, and 1.70 mL of water with or without EDTA at a final concentration of 2 mM; and 150 μL of 20% acetate buffer (pH 3.5) were placed in this order (total volume: 1.0 mL). The mixture was kept at 5°C for 60 min and then heated at 100°C for 60 min. The mixture was extracted with 1.0 mL of a mixture of 1-butanol/pyridine (15:1, vol/vol). Absorbance at 532 nm of the extract was measured. The amount of red pigment reflecting TBARS was calculated using a molecular extinction coefficient of pigment:156,000 M^{-1} cm^{-1}.

Statistical analysis. Data were analyzed by Student's *t*-test.

RESULTS

Two groups of male Wistar rats (n = 6) were fed a diet containing safflower oil or fish oil with an equal amount of vitamin E.

TABLE 1
Fatty Acid Composition of Total Lipids of Brain, Liver, Heart, and Lung of Rats Fed a Diet Containing Safflower Oil (S) or Fish Oil (F)[a]

	Brain		Liver		Heart		Lung	
Fatty acid	S	F	S	F	S	F	S	F
14:0							1.9 ± 0.2	2.8 ± 0.3*
16:0	19.1 ± 0.3	19.3 ± 0.4	21.5 ± 2.1	28.6 ± 1.8*	11.8 ± 0.8	16.1 ± 1.9*	31.6 ± 0.4	35.8 ± 0.7*
16:1n-7			1.5 ± 0.5	4.6 ± 0.9*	0.7 ± 0.2	3.3 ± 0.4*	4.5 ± 1.6	7.1 ± 1.0
18:0	22.3 ± 0.2	21.5 ± 0.3*	18.4 ± 1.6	13.4 ± 1.1*	22.4 ± 0.9	25.5 ± 2.6	9.6 ± 1.2	9.3 ± 0.4
18:1n-9	21.1 ± 0.4	22.7 ± 0.1*	7.1 ± 1.7	18.1 ± 4.3*	5.7 ± 0.8	10.9 ± 0.9*	17.6 ± 2.6	20.5 ± 1.2
18:2n-6			14.1 ± 1.2	3.0 ± 0.4*	26.4 ± 1.7	8.6 ± 0.8*	16.3 ± 1.7	2.5 ± 0.6*
20:1n-9	2.5 ± 0.1	2.4 ± 0.2						
20:4n-6	9.6 ± 0.1	7.3 ± 0.1*	30.6 ± 2.6	9.5 ± 0.8*	25.9 ± 1.0	13.1 ± 1.8*	10.1 ± 1.4	3.9 ± 0.3*
20:5n-3			0.0 ± 0.0	7.2 ± 0.9*	0.0 ± 0.0	3.6 ± 0.9*	0.1 ± 0.0	4.3 ± 0.2*
22:4n-6	3.5 ± 0.1	2.1 ± 0.0*	1.1 ± 0.1	0.1 ± 0.0*	1.9 ± 0.2	0.1 ± 0.0*	3.6 ± 0.7	0.3 ± 0.0*
22:5n-3			0.2 ± 0.0	1.9 ± 0.2*	0.3 ± 0.0	2.3 ± 0.3*	0.1 ± 0.0	4.2 ± 0.5*
22:6n-3	11.7 ± 0.3	14.6 ± 0.1*	3.1 ± 0.3	11.2 ± 4.2*	2.7 ± 0.6	13.7 ± 3.6*	0.3 ± 0.1	4.2 ± 0.4*
24:0	2.1 ± 0.2	2.1 ± 0.1					0.9 ± 0.2	1.1 ± 0.0
24:1n-9	3.5 ± 0.2	3.2 ± 0.2					0.8 ± 0.2	1.3 ± 0.1*
n-3 Fatty acids	11.9 ± 0.3	15.6 ± 0.2*	3.4 ± 0.3	20.5 ± 5.0*	3.1 ± 0.6	19.6 ± 4.7*	0.5 ± 0.1	12.9 ± 1.0*
n-6 Fatty acids	14.4 ± 0.2	10.2 ± 0.2*	46.5 ± 2.3	13.2 ± 1.3*	54.6 ± 0.8	22.5 ± 1.2*	30.9 ± 3.0	7.2 ± 1.0*
UI[b]	154 ± 1.9	162 ± 0.2*	186 ± 9.2	183 ± 27.6	190 ± 4.3	198 ± 31.5	116 ± 6.0	121 ± 5.7
PI[c]	100 ± 2.0	107 ± 0.5*	127 ± 8.8	126 ± 26.3	125 ± 4.8	142 ± 27.0	61 ± 7.2	71 ± 5.9

[a]Expressed as percentages (w/w) of total fatty acids present. Values are means ± SD for three rats. *Significantly different from S as measured by Student's *t*-test at $P < 0.05$.
[b]UI: Unsaturation index (sum of percentages of individual fatty acids × number of double bond).
[c]PI: Peroxidizability index (sum of percentages of individual fatty acids × number of active methylenes).

Fatty acid compositions of total lipids of brain, liver, heart, and lung of three rats of each rat group were determined (Table 1). Each organ of the rats fed fish oil showed significantly higher n-3 PUFA content than the organs from rats fed safflower oil. Likewise, each organ of the rats fed safflower oil showed significantly higher n-6 PUFA content than those fed fish oil. In total lipids of these organs, the amounts of linoleate (18:2n-6) and arachidonate (20:4n-6) were decreased, and the amounts of eicosapentaenoate (20:5n-3) and docosahexaenoate (22:6n-3) were increased in the fish oil diet group. UI and PI of the total lipids of these organs from the fish oil diet group were slightly higher than or similar to those of the corresponding organs from the safflower oil diet group.

Vitamin E levels in brain, liver, heart, lung, kidney, spleen, stomach, and testis from six rats were compared between two diet groups (Table 2). The levels in liver and testis of the fish oil diet group were slightly lower than those of the safflower oil diet group, but the levels in other organs were not different between two diet groups.

Levels of phospholipid hydroperoxides, PCOOH and PEOOH, in rat organs of two diet groups were determined by HPLC–chemiluminescence method (32,33). A representative HPLC chromatogram from rat brain is shown in Figure 1. PEOOH levels were always higher than PCOOH levels in each organ. The mean values of the levels of these phospholipid hydroperoxides of six rats were compared between two diet groups (Table 3). There were large variations in the levels of the hydroperoxides in some organs, which may be due to the instability of the hydroperoxides converting into more stable TBARS. The PCOOH and the PEOOH levels of organs of both the diet groups were lower than 3 nmol/mg protein, and there were no differences in the levels between two diet groups.

TBARS levels in rat organs of two diet groups were determined. TBA assay of the Ohkawa's procedure at pH 3.5 was employed by incorporating BHT into the assay medium (36–38). Representative absorption spectra of the TBA assay mixtures with and without EDTA of rat brain are shown in Figure 2. Absorption spectra of the assay mixtures of brain, heart, and kidney were very similar to the spectrum of the pure red pigment with a maximal absorption at 532 nm, but the spectra of other organs indicated contamination with yellow or orange pigments with maximal absorptions at the lower wavelengths. When the mean values of TBARS of organs of six rats of two diet groups as assessed by the assay with and without EDTA were compared (Table 4), no significant differences between the two diet groups were observed. While TBARS level of each organ obtained in the presence of EDTA was slightly lower than that obtained in the absence of EDTA, TBARS of each organ may be derived mainly from malonaldehyde derivatives. TBARS levels of brain of both the diet groups were the highest among those of eight organs, and estimated to be 6 nmol/mg protein in the absence of EDTA and 4 nmol/mg protein in the presence of EDTA.

DISCUSSION

Many earlier data have suggested undesirable effects of dietary fish oil or n-3 PUFA intake on the lipid peroxidation of organs, blood, and urine in animal and human subjects (5–31). In the studies of rats, the TBARS levels of plasma and liver of the rats

TABLE 2
Vitamin E Contents of Organs of Rats Fed a Diet Containing Safflower Oil (S) or Fish Oil (F)[a]

Organs	Vitamin E (μg/mg tissue protein)	
	S	F
Brain	0.11 ± 0.02	0.10 ± 0.01
Liver	0.14 ± 0.02	0.09 ± 0.02*
Heart	0.20 ± 0.02	0.22 ± 0.02
Lung	0.24 ± 0.09	0.22 ± 0.07
Kidney	0.13 ± 0.03	0.12 ± 0.01
Spleen	0.24 ± 0.06	0.23 ± 0.03
Stomach	0.42 ± 0.09	0.31 ± 0.01
Testis	0.21 ± 0.03	0.15 ± 0.01*

[a]Results are expressed as means ± SD for 3 rats. *Significantly different from S as measured by Student's *t*-test at $P < 0.05$.

TABLE 3
Level of PCOOH and PEOOH in the Lipid Fraction of Organs of Rats Fed a Diet Containing Safflower Oil (S) or Fish Oil (F)[a]

Organs	Hydroperoxides (nmol/mg tissue protein)			
	S		F	
	PCOOH	PEOOH	PCOOH	PEOOH
Brain	0.23 ± 0.12	0.73 ± 0.29	0.15 ± 0.10	0.97 ± 0.65
Liver	0.64 ± 0.51	0.49 ± 0.24	0.35 ± 0.47	0.45 ± 0.44
Heart	0.19 ± 0.27	1.60 ± 1.25	1.03 ± 0.85	4.25 ± 3.19
Lung	0.32 ± 0.41	0.24 ± 0.32	0.41 ± 0.32	2.22 ± 2.99
Kidney	0.13 ± 0.22	0.53 ± 0.13	0.40 ± 0.27	0.68 ± 0.16
Spleen	0.37 ± 0.53	0.55 ± 0.74	0.14 ± 0.37	0.68 ± 0.78
Stomach	0.57 ± 0.89	1.83 ± 3.40	ND	0.99 ± 0.87
Testis	0.39 ± 0.55	0.47 ± 0.57	0.56 ± 0.97	0.74 ± 1.05

[a]Results are expressed as means ± SD for 6 rats. ND, not detected; PCOOH, phosphatidylcholine hydroperoxides; PEOOH, phosphatidylethanolamine hydroperoxides.

fed fish oil with the higher vitamin E content were lower than those of rats fed fish oil with the low vitamin E content (9). The TBARS levels of liver microsomal fraction of the rats fed fish oil were decreased by increased vitamin E levels (23). Fish oil intake reduces vitamin E content in rat liver (25). Vitamin E levels in the heart of rats fed n-3 PUFA were lowered (26). Urinary TBARS were higher in the rats fed n-3 PUFA compared with those in rats fed n-6 PUFA (27). In human subjects, higher doses of fish oil have been shown to increase plasma (10,11), low density lipoprotein (14), and urinary TBARS levels (12,13), although some authors (12) have suggested that the increase in urine is caused by the lipid peroxidation products formed in food before its consumption.

Most of these studies employed the traditional TBA assay for estimation of degree of lipid peroxidation. It is now known that the TBA assay should be conducted in the presence of an antioxidant, such as BHT, in order to avoid artificial lipid peroxidation during the assay (35). In the heated acidic medium of the TBA assay under aerobic conditions, biological samples with higher n-3 PUFA would be more susceptible to artificial oxidation. Recent studies by Kubo *et al.* (44) have shown that isolated organs of the rats fed high dietary n-3 PUFA do not contain TBARS to the levels expected from PI of the total organ lipids by the TBA assay with an antioxidant (BHT) indicating that incorporation of BHT in the TBA assay system is important to avoid artificial lipid peroxidation during the assay.

It is claimed that TBARS obtained at pH 3.5 in the presence of EDTA reflect exclusively malonaldehyde derivatives that liberate malonaldehyde under the assay conditions, and TBARS obtained at pH 3.5 in the absence of EDTA reflects not only malonaldehyde but alkadienals/alkenal derivatives that liberate malonaldehyde and alkadienals/alkenals, respectively, under the assay conditions (36–38). Moreover, plasma and urine may not be good samples for TBARS. Hackett *et al.* (45) have strongly argued that the TBA asssay of plasma is not reliable, and the present authors (46) have shown that TBARS in serum or plasma are usually very low and cannot be identified. Human urinary TBARS levels vary from time to time and from day to day (47).

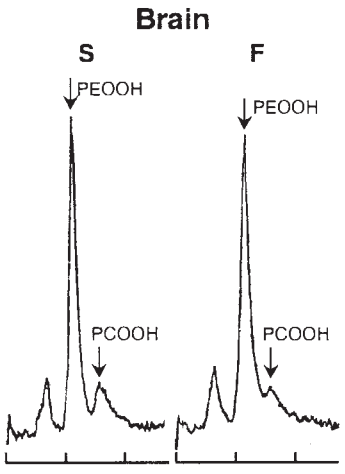

FIG. 1. Representative chromatogram of the high-performance liquid chromatography-chemiluminescence assay of phosphatidylcholine hydroperoxides (PCOOH) and phosphatidylethanolamine hydroperoxides (PEOOH) in the lipid fraction of brain of rats fed a diet containing safflower oil (S) or fish oil (F).

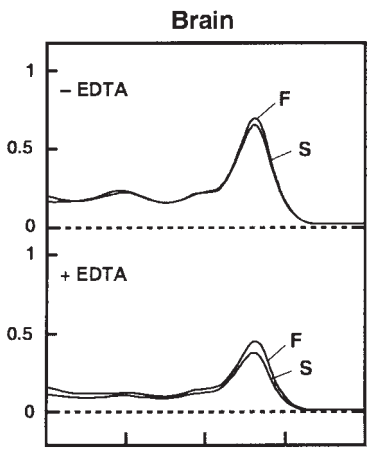

FIG. 2. Representative absorption spectra of the thiobarbituric acid (TBA) reaction mixtures with and without EDTA of brain of rats fed a diet containing safflower oil (S) or fish oil (F).

TABLE 4
Levels of TBARS Obtained With and Without EDTA in Organs of Rats Fed a Diet Containing Safflower Oil (S) or Fish Oil (F)[a]

	Aldehydes (nmol/mg tissue protein)			
	S		F	
Organs	–EDTA	+EDTA	–EDTA	+EDTA
Brain	6.64 ± 0.89	3.72 ± 0.56	6.61 ± 0.38	4.12 ± 0.31
Liver	1.05 ± 0.11	0.88 ± 0.11	1.09 ± 0.09	0.87 ± 0.06
Heart	2.21 ± 0.54	1.18 ± 0.25	2.41 ± 0.35	1.32 ± 0.17
Lung	2.29 ± 0.47	2.08 ± 0.56	2.35 ± 0.76	1.83 ± 0.45
Kidney	2.27 ± 0.22	1.89 ± 0.17	2.91 ± 0.26	2.19 ± 0.13
Spleen	3.20 ± 0.33	3.05 ± 0.22	3.57 ± 0.56	3.43 ± 0.72
Stomach	1.78 ± 0.52	1.60 ± 0.45	1.51 ± 0.18	1.24 ± 0.26
Testis	0.98 ± 0.24	0.73 ± 0.10	0.96 ± 0.12	0.72 ± 0.06

[a]Results are expressed as means ± SD for six rats. TBARS, thiobarbituric acid reactive substances. For other abbreviations see Table 3.

Another important reason for the estimation of lipid peroxidation of biological samples is to employ more than two assay methods based on different principles. The present authors employed two assay methods for *in vivo* lipid peroxidation studies of the organs of rats fed fish oil: HPLC–chemiluminescence assay for phospholipid hydroperoxides developed by Miyazawa *et al*. (32,33) and the TBA assay at pH 3.5, originally developed by Ohkawa *et al.*, in the presence of BHT with and without EDTA (36–38).

In the present study, the oil content in the rat diet was 50 g/kg diet, which was lower than those (100–300 g/kg diet) in the earlier studies (9,23,25–27). However, the oil content in the present study was enough to affect the fatty acid composition of rat organs. Vitamin E content in the diet was regulated at 59 mg/kg diet and 1.2 g/kg oil, which was in the ranges used in the earlier studies (45–210 mg/kg diet and 0.03–2.1 g/kg oil) (9,23,25–27). Vitamin E contents against PUFA were 1.5 g/kg PUFA (for safflower oil diet) and 4.3 g/kg PUFA (for fish oil diet), whereas those were between 0.7 and 5 g/kg PUFA in the earlier studies (9,23,26). The vitamin E content against PUFA in the fish oil diet was threefold higher than those in the safflower oil diet.

We have previously demonstrated the effect of the fish oil feeding on lipid peroxidation of rat erythrocyte membranes (39). Phospholipids of erythrocyte membranes of the safflower oil diet group are rich in n-6 PUFA and those of the fish oil diet group are rich in n-3 PUFA. UI and PI of the membrane phospholipids of the fish oil diet group are higher than those of the safflower oil diet group, and the vitamin E level of the membranes of the fish oil diet group is slightly lower than that of the membranes of the safflower oil diet group. Both the phospholipid hydroperoxide levels and the TBARS levels estimated in the presence of BHT with and without EDTA are not different between the two diet groups.

In the present study, we showed the effect of feeding fish oil on lipid peroxidation of total lipids of rat brain, liver, heart, lung, kidney, spleen, stomach, and testis. n-3 PUFA contents of brain, liver, heart, and lung of the fish oil diet group were higher than those of the safflower oil diet group. UI and PI of total lipids of the organs of the fish oil diet group were higher than or similar to those of the corresponding organs of the safflower oil diet group. The vitamin E levels in liver and testis of the fish oil diet group were slightly lower than those of the safflower oil diet group, but the levels in other organs were not different between the diet groups. Both the phospholipid hydroperoxide and TBARS levels in each organ of the fish oil diet group were similar to those of the safflower oil diet group. The present results indicate that high fish oil intake does not induce increased levels of phospholipid hydroperoxides and TBARS in rat organs.

The discrepancy between the observations in the earlier *in vivo* rat studies (9,23,25–27) and those in our present and previous (39) studies may be due to the difference of the assay methods for TBARS. In the earlier studies, the TBARS levels obtained in the assay without an antioxidant may have reflected the susceptibility of the samples to *in vitro* lipid peroxidation during the assay. In our present and previous (39) studies, the phospholipid hydroperoxide and TBARS levels may little reflect the *in vitro* susceptibility of the samples to the oxidation. In the previous study (39), we showed that both the phospholipid hydroperoxide and TBARS levels of the erythrocyte membranes of the rats of the fish oil diet group become remarkably higher than those of the membranes of the safflower oil diet group when the *in vitro* oxidation is induced. Although the susceptibility of the isolated organs of the rats of the fish oil diet group to the *in vitro* oxidation may be increased when compared to that of the safflower oil diet group, the levels of lipid peroxidation products *in vivo* may not be different.

In conclusion, n-3 PUFA supplementation did not increase lipid peroxidation in rat organs *in vivo* as well as erythrocyte membranes. It is likely that when a sufficient amount of vitamin E is supplied, n-3 PUFA supplementation does not induce undesirable effects in relation to lipid peroxidation.

ACKNOWLEDGMENT

This work was supported in part by a grant provided by the Ministry of Education, Science, Sports and Culture.

REFERENCES

1. Lands, W.W.M. (1986) *Fish and Human Health*, Academic Press, Orlando.
2. Kromhout, D., Bosschieter, E.B., and De Lezenne Coulander, C. (1985) The Inverse Relation Between Fish Consumption and 20-Year Mortality from Coronary Heart Disease, *N. Engl. J. Med. 312*, 1205–1209.
3. Fritsche, K.I., and Johnston, P.V. (1988) Rapid Autooxidation of Fish Oil in Diets Without Added Antioxidants, *J. Nutr. 118*, 425–426.
4. Yagi, K. (1982) Assay for Serum Lipid Peroxide Level and Its Clinical Significance, in *Lipid Peroxides in Biology and Medicine* (Yagi, K., ed.), pp. 223–242, Academic Press, Orlando.
5. Mouri, K., Ikesu, H., Esaka, T., and Igarashi, O. (1984) The Influence of Marine Oil Intake Upon Levels of Lipids, Alpha-Tocopherol and Lipid Peroxidation in Serum and Liver of Rats, *J. Nutr. Sci. Vitaminol. 30*, 307–318.
6. Garrido, A., Garrido, F., Guerra, R., and Valenzuela, A. (1989) Ingestion of High Doses Fish Oil Increases the Susceptibility of

Cellular Membranes to the Induction of Oxidative Stress, *Lipids 24*, 833–835.
7. Van Den Berg, J.J.M., De Fouw, N.J., Kuypers. F.A., Roelofsen, B., Houstmuller, U.M.T., and Op Den Kamp, J.A.F. (1991) Increased n-3 Polyunsaturated Fatty Acids Content of Red Blood Cells from Fish Oil-Fed Rabbits Increases *in Vitro* Lipid Peroxidation, but Decreases Hemolysis, *Free Radical Biol. Med. 11*, 393–399.
8. Kaasgaard, S.G., Holmer, G., Hoy, C.E., Beherens, W.A., and Beare-Rogers, J.L. (1992) Effects of Dietary Linseed Oil and Marine Oil on Lipid Peroxidation in Monkey Liver *in Vivo* and *in Vitro*, *Lipids 27*, 740–745.
9. Cho, S.H., and Cho, Y.S. (1994) Lipid Peroxidation and Antioxidant Status Is Affected by Different Vitamin E Levels When Feeding Fish Oil, *Lipids 29*, 47–52.
10. Brown, J.E., and Wahle, K.W.J. (1990) Effect of Fish-Oil and Vitamin E Supplementation on Lipid Peroxidation and Whole-Blood Aggregation in Man, *Clin. Chim. Acta 193*, 147–156.
11. Meydani, M., Natiello, F., Goldin, B., Free, N., Woods, M., Schaefer, E., Blumberg, J.B., and Gorbach, S.L. (1991) Effect of Long-Term Fish-Oil Supplementation on Vitamin E Status and Lipid Peroxidation in Women, *J. Nutr. 121*, 489–491.
12. Piche, L.A., Draper, H.H., and Cole, P.D. (1988) Malondialdehyde Excretion by Subjects Consuming Cod Liver Oil vs. a Concentrate of n-3 Fatty Acids, *Lipids 23*, 370–371.
13. Nelson, G.E., Morris, V.C., Schmidt, P.C., and Levander, O. (1993) Urinary Excretion of Thiobarbuturic Acid Reactive Substances and Malonaldehyde by Normal Adult Males After Consuming a Diet Containing Salmon, *Lipids 28*, 757–781.
14. Harats, D., Dabach, Y., Hollander, G., Ben-Naim, M., Schwarz, R., Berry, E.M., Stein, O., and Stein, Y. (1991) Fish-Oil Ingestion in Smokers and Nonsmokers Enhances Peroxidation of Plasma Lipoproteins, *Atherosclerosis 90*, 127–139.
15. Haglund, O., Luostarinen, R., Wallin, R., Wibell, L., and Saldeen, T. (1991) The Effects of Fish Oil on Triglycerides, Cholesterol, Fibrinogen and Malonaldehyde in Humans Supplemented with Vitamin E, *J. Nutr. 121*, 165–169.
16. Allard, J.P., Kurian, R., Aghdassi, E., Muggli, R., and Royall, D. (1997) Lipid Peroxidation During n-3 Fatty Acid and Vitamin E Supplementation in Humans, *Lipids 32*, 535–541.
17. Berlin, E., Bhathena, S.J., Judd, J.T., Mair, P.P., Peters, R.C., Bhagavan, H.N., Barlard-Barbbash, R., and Taylor, P.R. (1992) Effects of Omega-3 Fatty Acid and Vitamin E Supplementation on Erythrocyte Membrane Fluidity, Tocopherols, Insulin Binding and Lipid Composition in Adult Men, *J. Nutr. Biochem. 3*, 392–400.
18. Palozza, P., Sgarlata, E., Luberto, C., Piccioni, E., Anti, M., Marra, G., Armelao, F., Franceschelli, P., and Bartoli, G.M. (1996) n-3 Fatty Acids Induce Oxidative Modifications in Human Erythrocytes Depending on Dose and Duration of Dietary Supplementation, *Am. J. Clin. Nutr. 64*, 297–304.
19. Calviello, G., Palozza, P., Franceschelli, P., and Bartoli, G.M. (1997) Low-Dose Eicosapentaenoic or Docosahexaenoic Acid Administration Modifies Fatty Acid Composition and Does Not Affect Susceptibility to Oxidative Stress in Rat Erythrocytes and Tissues, *Lipids 32*, 1075–1083.
20. Vaagenes, H., Muna, Z.A., Madsen, L., and Berge, R.K. (1998) Low Dose of Eicosapentaenoic Acid, Docosahexaenoic Acid, and Hypolipidemic Eicosapentaenoic Acid Derivatives Have No Effect on Lipid Peroxidation in Plasma, *Lipids 33*, 1131–1137.
21. Turley, E., Wallace, J.M.W., Gilmore, W.S., and Strain, J.-J. (1998) Fish Oil Supplementation With and Without Added Vitamin E Differentially Modulates Plasma Antioxidant Concentration in Healthy Women, *Lipids 33*, 1163–1167.
22. Hansen, J.-B., Berge, R.K., Nordøy, A., and Bønaa, K.H. (1998) Lipid Peroxidation of Isolated Chylomicrons and Oxidative Status in Plasma After Intake of Highly Purified Eicosapentaenoic or Docosahexaenoic Acid, *Lipids. 33*, 1123–1129.
23. Hammer, C.T., and Wills, E.D. (1978) The Role of Lipid Components of the Diet in the Regulation of the Fatty Acid Composition of the Rat Liver Endoplasmic Reticulum and Lipid Peroxidation, *Biochem. J. 174*, 585–593.
24. Meydani, S.N., Shapiro, A.C., Meydani, M., Macauley, J.B., and Blumberg, J.B. (1987) Effect of Age and Dietary Fat (fish, corn and coconut oils) on Tocopherol Status of C57BL/6Nia Mice, *Lipids 22*, 345–350.
25. Chautan, M., Calaf, R., Leonard, J., Charbonnier, M., Andre, M., Portugal, H., Pauli, A.-M., Lafont, H., and Nalbone, G. (1990) Inverse Modifications of Heart and Liver-Tocopherol Status by Various Dietary n-6/n-3 Polyunsaturated Fatty Acid Ratios, *J. Lipid Res. 31*, 2201–2208.
26. Javouhey-Donzel, A., Guenot, L., Maupoil, V., Rochette, L., and Roequelin, G. (1993) Rat Vitamin E Status and Heart Lipid Peroxidation: Effect of Dietary Alpha-Linolenic Acid and Marine n-3 Fatty Acids, *Lipids 28*, 651–655.
27. L'Abbe, M.R., Trick, K.D., and Beare-Rogers, J.L. (1991) Dietary (n-3) Fatty Acids Affect Rat Heart, Liver and Aorta Protective Enzyme Activities and Lipid Peroxidation, *J. Nutr. 121*, 1331–1340.
28. Mendani, M. (1992) Vitamin E Requirement in Relation to Dietary Fish Oil and Oxidative Stress in Elderly, *Free Radicals Aging Degener. Dis. 102*, 411–418.
29. Leibovitz, B.E., Hu, M.-L., and Tappel, A.L. (1990) Lipid Peroxidation in Rat Tissue Slice: Effect of Dietary Vitamin E, Corn Oil, Lard and Menhaden Oil, *Lipids 25*, 125–129.
30. Saito, M., and Nakatsugawa, K. (1994) Increased Susceptibility of Liver to Lipid Peroxidation After Ingestion of a High Fish Oil Diet, *Internat. J. Vit. Nutr. Res. 64*, 144–151.
31. Farwer, S.R. (1994) The Vitamin E Nutritional Status of Rats Fed on Diets High in Fish Oil, *Br. J. Nutr. 72*, 127–145.
32. Miyazawa, T., Yasuda, K., and Fujimoto, K. (1987) Chemiluminescence-High-Performance Liquid Chromatography of Phosphatidylcholine Hydroperoxide, *Anal. Lett. 20*, 915–925.
33. Miyazawa, T., Yasuda, K., Fujimoto, K., and Kaneda, T. (1988) Presence of Phosphatidylcholine Hydroperoxide in Human Plasma, *J. Biochem. 103*, 744–766.
34. Kosugi, H., and Kikugawa, K. (1989) Potential Thiobarbituric Acid-Reactive Substances in Peroxidized Lipids, *Free Radical Biol. Med. 7*, 205–207.
35. Kikugawa, K. (1997) Use and Limitation of Thiobarbituric Acid (TBA) Test for Lipid Peroxidation, *Recent Res. Dev. Lipid Res. 1*, 73–96.
36. Kosugi, H., Kato, T., and Kikugawa, K. (1988) Formation of Red Pigment by a Two-Step 2-Thiobarbituric Acid Reaction of Alka-2,4-dienals. Potential Products of Lipid Oxidation, *Lipids 23*, 1024–1031.
37. Kosugi, H., Kojima, T., Yamaki, S., and Kikugawa, K. (1992) Interpretation of the Thiobarbituric Acid Reactivity of Rat Liver and Brain Homogenates in the Presence of Ferric Ion and Ethylenediamine-tetraacetic Acid, *Anal. Biochem. 202*, 249–255.
38. Kosugi, H., Kojima, T., and Kikugawa, K. (1991) Characteristics of the Thiobarbituric Acid Reactivity of Oxidized Fats and Oils. *J. Am. Oil Chem. Soc. 68*, 51–55.
39. Ando, K., Nagata, K., Beppu, M., Kikugawa, K., Kawabata, T., Hasegawa, K., and Suzuki, M. (1998) Effect of n-3 Fatty Acid Supplementation on Lipid Peroxidation and Protein Aggregation in Rat Erythrocyte Membranes, *Lipids 33*, 505–512.
40. Hu, M.L., Frankel, E.N., Leibovitz, B.E., and Tappel, A.L. (1989) Effect of Dietary Lipids and Vitamin E on *in vitro* Lipid Peroxidation in Rat Liver and Kidney Homogenates, *J. Nutr. 119*, 1574–1582.
41. Lowry, O.H., Rosebrough, N.J., Farr, A.L., and Randall, R.J. (1951) Protein Measurement with the Folin Phenol Reagent, *J. Biol. Chem. 193*, 265–275.

42. Bligh, E.G., and Dyer, W.J. (1959) A Rapid Method of Total Lipid Extraction and Purification, *Can. J. Biochem. Physiol. 37*, 911–917.
43. Lehmann, J., and Martin, H.L. (1982) Improved Direct Determination of Alpha- and Gamma-Tocopherols in Plasma and Platelets by Liquid Chromatography with Fluorescence Detection, *Clin. Chem. 28*, 1784–1787.
44. Kubo, K., Saito, M., Tadahiro, T., and Maekawa, A. (1998) Dietary Docosahexaenoic Acid Does Not Promote Lipid Peroxidation in Rat Tissue to the Extent Expected from Peroxidizability Index of the Lipids, *Biosci. Biotechnol. Biochem. 62*, 1698–1706.
45. Hackett, C., Linley-Adams, M., Lloyd, B., and Walker, V. (1988) Plasma Malondialdehyde: A Poor Measure of *in vivo* Lipid Peroxidation, *Clin. Chem. 34*, 208.
46. Kojima, T., Kikugawa, K., and Kosugi, H. (1990) Is the Thiobarbituric Acid-Reactivity of Blood Plasma Specific to Lipid Peroxidation? *Chem. Pharm. Bull. 38*, 3414–3418.
47. Kosugi, H., Enomoto, H., Ishizuka, Y., and Kikugawa, K. (1994) Variations in the Level of Urinary Thiobarbituric Acid Reactant in Healthy Humans Under Different Physiological Conditions, *Biol. Pharm. Bull. 17*, 1645–1650.

[Received September 1, 1999; and in final revised form January 18, 2000; revision accepted January 28, 2000]

Influence of Sources of Dietary Oils on the Life Span of Stroke-Prone Spontaneously Hypertensive Rats

W.M.N. Ratnayake[a,]*, L. Plouffe[a], R. Hollywood[a], M.R. L'Abbé[a], N. Hidiroglou[a], G. Sarwar[a], and R. Mueller[b]

[a]Nutrition Research Division, and [b]Toxicology Research Division, Food Directorate, Health Protection Branch, Health Canada, Ottawa, Ontario, Canada K1A OL2

ABSTRACT: In recent studies, the life span of stroke-prone spontaneously hypertensive (SHRSP) rats was altered by a variety of dietary fats. It was relatively shorter in rats fed canola oil as the sole source of fat. The present study was performed to find out whether the fatty acid profile and the high content of sulfur compounds in canola oil could modulate the life span of SHRSP rats. SHRSP rats (47 d old, n = 23/group) were matched by body weight and systolic blood pressure and fed semipurified diets containing 10% canola oil, high-palmitic canola oil, low-sulfur canola oil, soybean oil, high-oleic safflower oil, a fat blend that mimicked the fatty acid composition of canola oil, or a fat blend high in saturated fatty acids. A 1% sodium chloride solution was used as drinking water to induce hypertension. After consuming the diets for 37 d, five rats from each dietary group were killed for collection of blood and tissue samples for biochemical analysis. The 18 remaining animals from each group were used for determining their life span. The mean survival time of SHRSP rats fed canola oil (87.4 ± 4.0 d) was not significantly different (P > 0.05) from those fed low-sulfur canola oil (89.7 ± 8.5 d), suggesting that content of sulfur in canola oil has no effect on the life span of SHRSP rats. The SHRSP rats fed the noncanola oil-based diets lived longer (mean survival time difference was 6–13 d, P < 0.05) than those fed canola and low-sulfur canola oils. No marked differences in the survival times were observed among the noncanola oil-based groups. The fatty acid composition of the dietary oils and of red blood cells and liver of SHRSP rats killed after 37 d of treatment showed no relationship with the survival times. These results suggest that the fatty acid profile of vegetable oils plays no important role on the life span of SHRSP rat. However, phytosterols in the dietary oils and in liver and brain were inversely correlated with the mean survival times,indicating that the differential effects of vegetable oils might be ascribed, at least partly, to their different phytosterol contents.

Paper no. L8311 in *Lipids 35,* 409–420 (April 2000).

Canola oil (CO) is generally considered to provide positive cardiovascular benefits (1,2) because of its favorable fatty acid profile. It has a low content of saturated fatty acids (SFA) (6–7%) and high content of oleic acid (55–60%). In addition it is a good source of α-linolenic acid (7–10%) and provides a low ratio of linoleic to linolenic acids (2:1). Nevertheless, a series of recent studies reported that CO was one of the oils that had a life-shortening effect on stroke-prone spontaneously hypertensive (SHRSP) rats (3–6). CO shortened the survival time by about 15–50% under 1% NaCl loading compared to soybean oil (SBO) and perilla oil. The life-shortening activity, however, is not specific to CO. A few other common vegetable oils, including high-oleic sunflower, olive and evening primrose oils, also shortened the life span compared to SBO. Although many experiments were performed using various fat blends and subfractions prepared from CO, the life-shortening factor and the mechanism by which CO and other vegetable oils shorten the life span of SHRSP rats are yet to be resolved (5,6).

This study was therefore undertaken to determine whether the fatty acid profile *per se* in CO might account for the shortening of life span of SHRSP rats associated with CO treatment. In order to exclude an effect of the high sulfur content in CO, a special canola variety low in sulfur compounds was used, in addition to regular CO. CO contains slightly higher levels of sulfur compounds than other common edible vegetable oils (7), and historically nothing is known about the health effects of sulfur compounds in CO.

In this report, survival data are presented for SHRSP rats fed diets containing CO, high-palmitic CO (HPCO), low-sulfur CO (LSCO), SBO, high-oleic safflower oil (HOSFO), a fat blend that mimicked the fatty acid composition of CO (MIMIC), another fat blend that provided a large proportion of SFA (HSFAB), and laboratory rat chow (CHOW). The systolic blood pressure (SBP), hematological indices, serum cho-

*To whom correspondence should be addressed at Nutrition Research Division, Food Directorate, Health Protection Branch, Health Canada, Banting Building, Postal Locator 2203C, Ottawa, Ontario, Canada K1A OL2.
E-mail: nimal_ratnayake@hc-sc.gc.ca

Abbreviations: AAS, flame atomic absorption spectroscopy, AES, atomic emission spectroscopy; BUN, blood urea nitrogen; CO, canola oil; CHOW, rat chow; CNO, coconut oil; FO, flaxseed oil; HDL, high density lipoprotein; HOSFO, high-oleic safflower oil; HPCO, high-palmitic canola oil; HSFAB, a fat blend high in saturated fat; LC-PUFA, long-chain (C20 + C22) polyunsaturated fatty acids; LSCO, low-sulfur canola oil; MIMIC, a fat blend which mimicked the fatty acid composition of canola oil; MUFA, monounsaturated fatty acids; PO, palm oil; PUFA, polyunsaturated fatty acids; RBC, red blood cells; SBO, soybean oil; SBP, systolic blood pressure; SD, pooled standard deviation; SFA, saturated fatty acids; SHRSP, stroke-prone spontaneously hypertensive rats, TBARS, thiobarbituric acid-reacting substances.

lesterol, fatty acid profiles, sterols, vitamin E and trace elements of some selected tissues are compared in order to assess whether these parameters are correlated with the mean survival time of SHRSP rats.

EXPERIMENTAL PROCEDURES

Dietary oils. The oils used in these studies, alone or in blends, included CO (Loblaws, Ottawa, Canada), SBO (Loblaws), coconut oil (CNO) (CanAmera Foods Inc., Toronto, Canada), palm oil (PO) (CanAmera Foods Inc.), HPCO (CanAmera Foods Inc.), LSCO (TR4 turnip rapeseed oil, extracted and refined by POS Pilot Plant Corp., Saskatoon, Canada), HOSFO (Damingo Inc., Mississauga, Canada), and flaxseed oil (FO) (Canola Industries Canada Inc., Nisku, Canada). It may be noted here that HPCO and LSCO are oils derived from new varieties of canola, and their physical and chemical characteristics are different from those of CO. Two fat blends were prepared. MIMIC (major fatty acids only) was prepared by mixing HOSFO (75 parts), FO (15 parts), and SBO (10 parts). The second blend, HSFAB, was prepared by mixing HOSFO (55 parts), PO (31 parts), CNO (10 parts), and FO (4 parts).

Experimental diets. Seven semipurified diets were prepared using CO, SBO, HOSFO, MIMIC, HSFAB, HPCO, and LSCO as test oils. The diets contained 20.0% casein, 49.95% cornstarch, 10% granulated sugar, 5% alphacel, 3.5% AIN-93G mineral mix, 1% AIN-93VX vitamin mixture (8), 0.3% L-cysteine, 0.25% choline bitartarate, 10% test oil, and 0.0014% *tertiary*-butylhydroquinone as antioxidant. The diets were prepared weekly and stored at –4°C. Laboratory Rodent Diet 5001 (rat chow) (PMI Feeds, Inc., St. Louis, MO) was used as the control diet. According to the specifications provided by the supplier, this commercial diet contained 23% protein, 4.5% fat, not more than 6% fiber, not more than 8% ash, and not more than 2.5% added minerals. Table 1 shows the relative proportions of the fatty acids in the eight diets. The sulfur content of CO and LSCO oils (analyzed by POS Pilot Plant Corporation, Saskatoon, Canada, using inductively coupled plasma) is also shown in Table 1.

Animals and feeding phase. One hundred eighty four SHRSP rats obtained from Seac Yoshitomi Ltd. (Yoshitomi-Cho, Chikujyo-gun, Fukuoka-ken, Japan) at 28 d of age were acclimatized to the environment for 19 d. During this period they were fed the control diet (rat chow) and normal drinking water. After the acclimation period, animals were placed in 8 dietary groups of 23 rats per group in a randomized block according to body weight and SBP. The rats were housed individually in metal cages in a climate-controlled room maintained at 22 ± 1°C and 60% relative humidity with 12-h day/12-h night cycle. Drinking water contained 1% NaCl to induce earlier hypertension. The rats had free access to one of the eight diets and the 1% NaCl solution. SBP was measured once every 2 wk by trained technicians by the tail cuff method (Rat Tail Blood Pressure Systems, Harvard Instruments).

TABLE 1
Fatty Acid Composition (% total fatty acids) of Dietary Oils and Total Sulfur Content of Canola and Low-Sulfur Canola Oils

Fatty acid	CO	SBO	HOSFO	MIMIC	HSFAB	HPCO	LSCO	CHOW[a]
12:0	0.0	0.0	0.0	0.0	3.3	0.0	0.0	0.1
14:0	0.1	0.1	0.1	0.1	2.1	0.1	0.1	2.1
16:0	3.9	10.0	4.7	5.3	18.6	10.6	3.3	19.4
18:0	1.9	4.1	1.8	2.2	3.1	1.7	1.6	8.8
20:0	0.6	0.3	0.4	0.4	0.4	0.6	0.5	0.3
22:0	0.3	0.4	0.4	0.4	0.3	0.3	0.3	0.3
∑SFA[b]	7.0	15.2	7.6	8.5	27.9	13.5	6.1	31.6
16:1n-7	0.2	0.1	0.1	0.1	0.1	2.4	0.3	2.8
18:1n-9	57.4	23.2	77.7	63.1	56.5	45.2	56.3	26.1
18:1n-7	3.4	1.5	0.9	1.0	0.8	6.5	4.0	1.8
20:1n-9	2.3	0.6	0.3	0.3	0.2	0.9	2.7	0.0
22:1n-9	0.5	0.0	0.0	0.0	0.0	0.0	0.0	0.1
24:1	0.2	0.1	0.2	0.2	0.0	0.2	0.3	0.0
∑MUFA[b]	64.2	25.7	79.4	64.7	57.5	55.2	63.7	30.7
18:2n-6	19.9	50.3	12.6	17.8	11.5	19.3	21.4	29.8
18:3n-3	7.6	8.0	0.1	9.1	2.5	11.2	6.0	3.3
∑PUFA[b]	27.8	58.5	12.9	26.3	14.0	30.8	27.6	36.4
t-18:2	0.3	0.3	0.2	0.1	0.2	0.1	0.8	0.2
t-18:3	0.8	0.3	0.0	0.4	0.3	0.4	1.8	1.0
S (ppm)	7.5	ND	ND	ND	ND	ND	0.5	ND

[a]In addition to the fatty acids listed, rat chow contained 0.2% 20:4n-6, 1.4% 20:5n-3, 0.3% 22:5n-3, 0.9% 22:6n-3, and 0.4% other minor n-6 and n-3 long-chain (>C20) polyunsaturated fatty acids (LC-PUFA).

[b]The sums for SFA (total saturated fatty acids), MUFA (total monounsaturated fatty acids), and PUFA (total polyunsaturated fatty acids) may include some minor fatty acids not listed in the table. Dietary oil abbreviations: CO, canola oil; SBO, soybean oil; HOSFO, high-oleic safflower oil; MIMIC, canola oil mimic; HSFAB, a fat blend high in saturated fatty acids; HPCO, high-palmitic canola oil; LSCO, low-sulfur canola oil; CHOW, rat chow. S (ppm), total sulfur content in parts per million; ND, not determined.

At 37 d on the diet, five animals from each group were randomly selected and placed in metabolic cages; fasting urine samples were collected overnight. Immediately after the urine collection, these rats were euthanized by complete exsanguinations under isofluorene anesthesia, and blood from aorta and tissues was collected for biochemical analyzes. The tissue samples intended for lipid analyzes were immediately frozen in liquid nitrogen and stored at –80°C.

The 18 remaining animals from each group were used for the life span study. When an animal was found to suffer from severe stroke, paralysis, to be in pain, or was judged to be unable to survive overnight, euthanasia was performed. The study protocol was approved by the Animal Care Committee of Health Canada.

Blood lipid and clinical measurements. About 3 mL of fasting blood was centrifuged in a vacutainer serum separation tube at 1300 × *g* for 20 min and serum separated. Triglyceride and total cholesterol were determined using an Abbott-VP Bichromatic Analyzer, with the A-Gent Triglyceride test and A-Gent Cholesterol test enzymatic kits (Abbott Laboratories, Mississauga, Canada). High density lipoprotein (HDL) cholesterol was isolated by selectively precipitating the non-HDL cholesterol with A-Gent HDL Reagent (Abbott Laboratories).

Urine and serum creatinine, and serum urea nitrogen (BUN) were determined on an Abbott-VP autoanalyzer using A-Gent reagents, kits and standards (Abbott Laboratories).

Hematological measurements. For hematological analysis 0.5 mL of blood was taken into a tube containing EDTA as anticoagulant. Complete blood cell count was measured using a Coulter Counter S-PLUS IV system (Coulter Electronic Inc., Hialeah, FL).

Fatty acid analysis. For analysis of fatty acids in diets, lipids were extracted using 25 vol of chloroform/methanol (1:2, vol/vol). For analysis of fatty acids in red blood cells (RBC), about 3 mL of blood was placed in tubes containing silicone and centrifuged at 2500 × *g* for 20 min. Serum was drawn and RBC were collected. After tissue homogenization (Polytron, Brinkmann, Rexdale, Canada) total lipids in RBC, liver and brain were extracted using chloroform/methanol/water as outlined by Brooks *et al*. (9). The extracted lipids were converted to methyl esters using 14% BF_3/methanol and analyzed by gas–liquid chromatography using an SP-2560 flexible fused-silica capillary column (100 m × 0.25 mm i.d.; Supelco Inc., Bellefonte, PA).

Analysis of sterols in diets and tissues. Tissues (200–400 mg) and fat (20 mg) extracted from the diets were mixed with 25 mg betulinol (internal standard), and the mixture was saponified (0.5 g KOH, 0.4 mL water, 5 mL ethanol). The nonsaponifiable matter was recovered by extraction with hexane/methylene chloride (85:15) and purified by successive washing with water and water/ethanol (80:20, vol/vol). After drying with anhydrous sodium sulfate, the nonsaponifiable matter was treated with 100 μL of 1-methyl imidazole/*N*-methyl-*N*-(trimethylsilyl)-heptafluorobutyramide (1:20, vol/vol) for converting the sterols to trimethylsilyl ethers. The content and composition of the silylated sterols were determined in relation to the internal standard by gas–liquid chromatography using a DB-1 flexible fused-silica capillary column (30 m × 0.25 mm i.d.; J&W Scientific, Folsom, CA).

Analysis of vitamin E. α- and γ-Tocopherols in tissues were determined by the high-performance liquid chromatography method of Thompson and Hatina (10).

Analysis of minerals and thiobarbituric acid-reacting substances (TBARS). Drinking water and urine samples were acidified with 1% nitric acid and sodium was determined by flame atomic emission spectroscopy (AES). Liver samples were dry-ashed, dissolved in 1 N HCl, and minerals (Fe, Cu, Zn) were determined by flame atomic absorption spectroscopy (AAS). Na and K were determined by flame AES and Ca and Mg determined by AAS in the presence of 0.5% lanthanum in 1 N HCl. Urinary TBARS were determined as described previously (11).

Statistics. Survival data were analyzed using Wilcoxon's nonparametric test for comparing survival curves to provide tests for the effects of diet (12). The effects of diet on mean survival time and various biochemical parameters were examined by analysis of variance using the STATISCA system for personal computers (Release 5, 1997 Edition, Statsoft, Inc., Tulsa, OK). *Post-hoc* comparisons of means were performed using Tukey Honest Significant Difference Test. Differences were considered significant when $P < 0.05$. All data in tables are reported as means and pooled standard deviations (SD). Correlations between mean survival times and the various variables of the diets (fatty acid, vitamin E, and sterol contents) or the tissue biochemical parameters (fatty acid, vitamin E, mineral, and sterol contents) were examined by linear regression analysis using mean values for each dietary group.

RESULTS

The fatty acid composition of the eight diets is shown in Table 1. The total content of SFA varied between 6.1 and 32.5% in all diets. CO, LSCO, HOSFO, and MIMIC diets containing very low levels of SFA (<8.5%), while the high-SFA diet and rat chow contained the highest levels of SFA. CO, LSCO, and MIMIC contained almost similar amounts of total SFA, total monounsaturated fatty acids (MUFA), linoleic acid, and α-linolenic acid. The HPCO displayed a slightly different fatty acid profile from the other two CO; in particular, HPCO contained higher levels of 16:0, 16:1, 18:1n-7, 18:3n-3, and lower levels of 18:1n-9, 20:1n-9 than the other two CO. The fat derived from rat chow contained minor amounts of arachidonic (20:4n-6), eicosapentaenoic (20:5n-3), docosahexaenoic (22:6n-3), and other C20 and C22 n-6 and n-3 fatty acids, which may indicate the use of fish meal and some animal products in the preparation of the commercial rat chow used in this study.

The survival curves of the rats in the life span study are shown in Figures 1 and 2. One rat in the CHOW group died

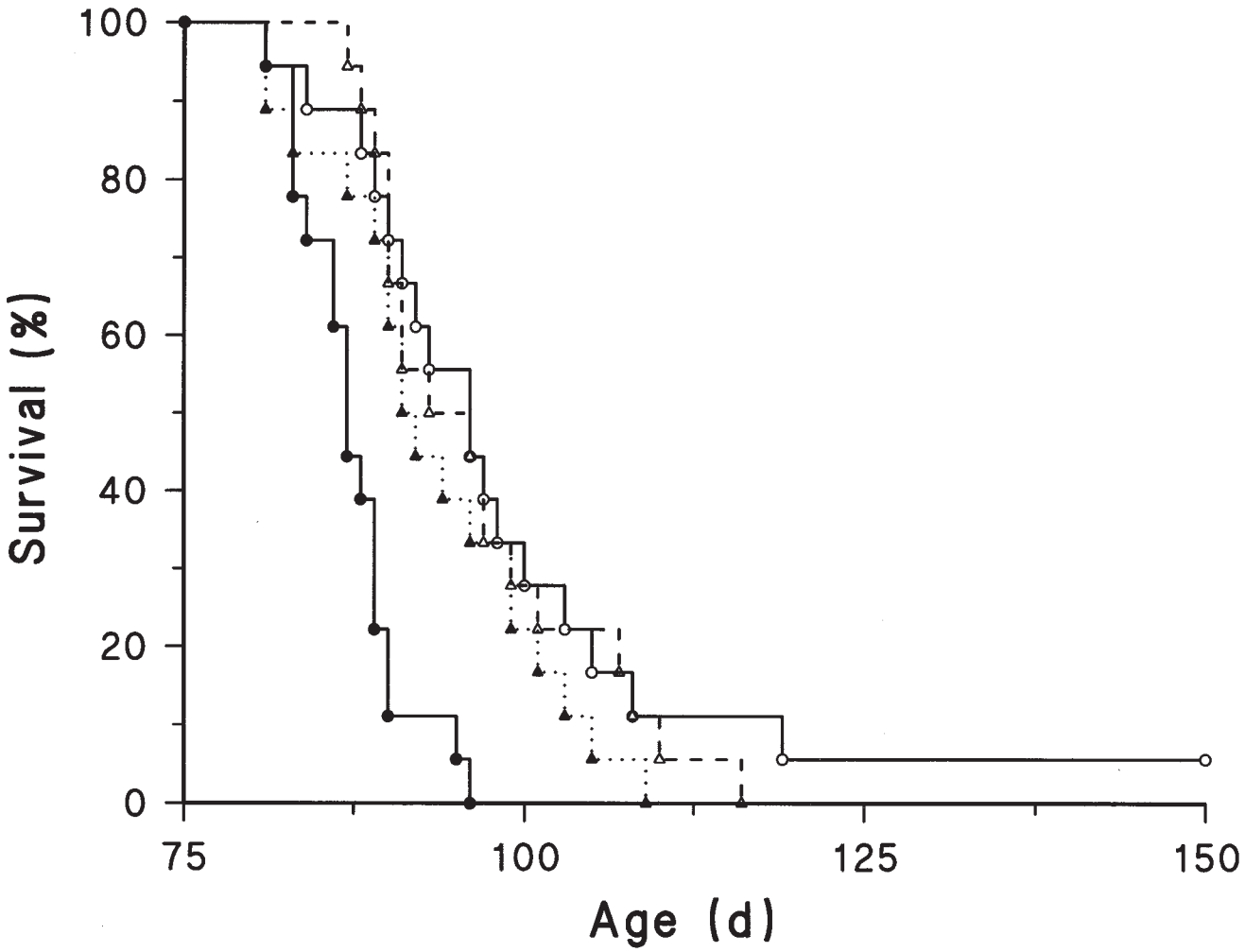

FIG. 1. Survival curves of stroke-prone spontaneously hypertensive rats (SHRSP) fed diets containing canola oil (CO, ●), soybean oil (SBO, ○), high-oleic safflower oil (HOSFO, ▲), and canola oil mimic (MIMIC, △). n = 18 per group. Survival rate for CO group significantly different from that of all the other dietary groups (Wilcoxon test $P < 0.0001$). No significant differences were found in the survival rates between SBO, HOSFO, and MIMIC groups (Wilcoxon test $P > 0.05$).

early, 8 d on diet, of dehydration (kidney failure) and was not included in the analysis of the survival data. One animal in the SBO group had an unusually longer life span (207 d) than all the other animals in this study and therefore, this animal was also not included in the analysis of the survival data. There was a highly significant effect ($P \leq 0.0001$) of diet on the survival rates. This was largely due to lower survival rates for CO and LSCO groups. There was no evidence ($P = 0.58$) that the survival rates for these two groups were different from each other. The HPCO group exhibited a lower survival than the non-CO diets after 95 d, but there was no evidence ($P = 0.17$) of a diet effect among these groups.

Analysis of the mean survival times also showed significant ($P < 0.05$) life-shortening activity associated with CO and LSCO groups compared to non-CO groups (Table 2). The mean survival time of the HPCO group was slightly higher than the other two CO groups and slightly lower than non-CO groups, but the differences were not significant ($P > 0.05$). There were no significant differences in the mean survival times among the non-CO groups ($P > 0.05$).

During the course of the study, SBP was measured five times, at 2-wk intervals. The SBP readings (160–210 mm Hg) were highly variable but confirmed the hypertensive-prone

TABLE 2
Mean Survival Times of SHRSP Rats Fed Various Dietary Oils[a]

Dietary oil	Mean survival time ± SD (d)
CO	87.4 ± 4.0[a]
SBO[b]	95.9 ± 9.3[b]
HOSFO	93.4 ± 8.0[b]
MIMIC	96.7 ± 8.6[b]
HSFAB	100.2 ± 9.2[b]
HPCO	92.2 ± 6.5[a,b]
LSCO	89.7 ± 8.5[a]
CHOW[b]	98.6 ± 11.6[b]

[a]For abbreviations see Table 1. SD, standard deviation.
[b]n = 17 in SBO and CHOW; n = 18 in all other groups. Mean survival times with different superscripts are significantly different ($P < 0.05$).

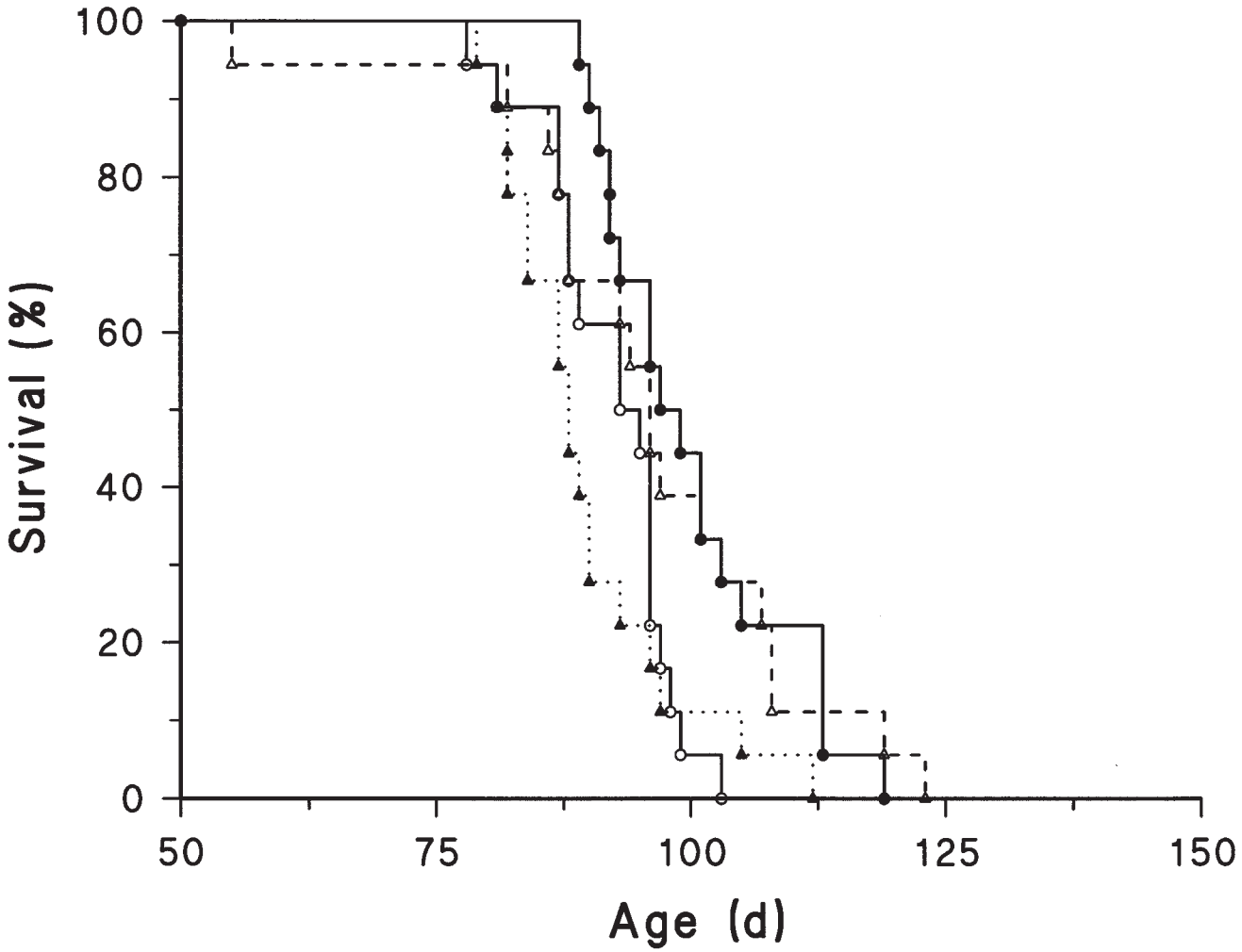

FIG. 2. Survival curves of SHRSP fed diets containing a fat blend high in saturated fatty acids (HSFAB, ●), high-palmitic canola oil (HPCO, ○), low-sulfur canola oil (LSCO, ▲), and rat chow (CHOW, △). n = 18 per group. Survival rate for LSCO significantly different from that for HSFAB and CHOW groups (Wilcoxon test $P < 0.0001$). Survival rate for HPCO not significantly different from that of LSCO, HSFAB, and CHOW (Wilcoxon test $P > 0.05$). There was no significant difference between HSFAB and CHOW (Wilcoxon test $P > 0.05$).

nature of the SHRSP rats. No significant differences were noted in the SBP among the dietary groups (data not shown). The hematological indices (mean platelet volume, platelet count, white blood cell, RBC, hemoglobin, mean corpuscular volume, mean corpuscular hemoglobin, and red cell distribution width) of the animals killed at 37 d on diet were not significantly influenced by the type of dietary oil (data not shown). Similarly, no significant changes related to the diet were observed in the levels of serum total cholesterol (68–82 mg/dL), HDL cholesterol (30–41 mg/dL), and triglycerides (58–106 mg/dL) of the animals killed at 37 d on diet (data for each group are not shown).

The content of α-tocopherol in the semipurified diets was substantially higher than that in CHOW (Table 3). This is to be expected because the semipurified diets were supplemented with a 1% vitamin mixture containing vitamin E and in addition, the test oils themselves contributed important amounts of α-tocopherol and other vitamin E congeners to the diet. The dietary vitamin E levels in various tissues reflected the levels in the corresponding diets (γ-tocopherol values are not shown). The tissues from the CHOW group contained significantly lower levels of α-tocopherol compared to all the other groups, whereas tissues of rats fed HOSFO, MIMIC, and HSFAB displayed higher levels. The α-tocopherol level of animals fed CO was almost identical to that of animals fed SBO-diet. The γ-tocopherol content in the all the diets was low (0–17 μg/g diet), except in SBO-diet (39 μg/g diet) and consequently, all the tissues (heart 0–0.2, kidney 0–0.7, liver 0–0.6, and plasma 0–0.6 μg/g) , except adipose tissue (1.0–5.4 μg/g) had only trace levels of this vitamin E congener. There was no correlation between tissue mean levels of α- and γ-tocopherol of the animals killed after 37 d with the mean survival times of the animals in the life span study (Table 4; correlation data for γ-tocopherol are not shown).

Fatty acid composition of RBC, liver, and brain were analyzed and used for diet comparisons. The different diets virtually had no influence on the fatty acid profile of the brain (data not shown). Generally, the fatty acid profiles of RBC

TABLE 3
α-Tocopherol Content in Diets and Tissues of Animals Killed After 37 d on Different Dietary Oils

Dietary oil[a]	Diet (μg/g)	Tissue (μg/g wet weight)				
		Heart	Kidney	Liver	Adipose	Plasma
CO	66.1	33.3 ± 3.0[b]	19.9 ± 1.7[b,c]	37.4 ± 2.7[d,c]	39.9 ± 1.7[b]	7.1 ± 0.7[b]
SBO	66.8	31.9 ± 0.9[b]	17.7 ± 2.7[b]	31.1 ± 4.7[b,c]	38.6 ± 2.2[b]	5.5 ± 1.2[a,b]
HOSFO	90.1	35.9 ± 4.3[b]	22.9 ± 0.6[c]	42.7 ± 9.2[d]	56.8 ± 5.2[c]	8.0 ± 1.1[b]
MIMIC	80.1	34.8 ± 2.0[b]	23.2 ± 3.0[c]	31.6 ± 3.3[b,c]	53.4 ± 5.2[c]	8.5 ± 2.9[b]
HSFAB	72.7	42.1 ± 3.2[c]	20.8 ± 1.6[c]	35.3 ± 1.9[d,c]	34.0 ± 3.6[b]	6.7 ± 0.6[a,b]
HPCO	61.2	31.1 ± 3.7[b]	22.6 ± 2.3[c]	32.5 ± 3.5[b,c]	38.8 ± 1.9[b]	9.1 ± 2.6[b]
LSCO	61.7	28.8 ± 2.6[b]	20.0 ± 1.9[b,c]	27.2 ± 1.4[b]	39.2 ± 3.7[b]	7.1 ± 0.4[b]
CHOW	38.8	17.5 ± 2.0[a]	11.0 ± 2.1[a]	11.9 ± 1.2[a]	24.3 ± 2.4[a]	4.0 ± 3.4[a]

[a]For abbreviations see Table 1. $n = 5$ in all dietary groups. Means in a column with different roman superscript letters are significantly different ($P < 0.05$).

(Table 5) and liver lipids (Table 6) of animals fed CO, SBO, MIMIC, HPCO, LSCO, and HSFAB were not different from each other. The most notable changes in the fatty acid profiles of RBC and liver were generally associated with the animals fed HOSFO and CHOW. The HOSFO diet contained the highest amount of oleic acid and the lowest amount of α-linolenic acid (Table 1). Consequently, the RBC and liver of the animals of this group contained the highest proportion of oleic acid and the lowest proportion of the n-3 long chain (C20 + C22) polyunsaturated fatty acid (LC-PUFA) metabolites (mainly 22:6n-3) of α-linolenic acid. The animals fed CHOW, which received appreciable amounts of pre-formed 20:5n-3, 22:5n-3, and 22:6n-3 from CHOW diet, showed higher abundance of these n-3 LC-PUFA in the liver and RBC. However, none of the fatty acids in brain, liver, and RBC showed a correlation with the mean survival time of SHRSP rats in the life span study (Table 7). The dietary total SFA content was significantly correlated ($R = 0.78$, $P = 0.0219$) with the mean survival time. However, RBC or liver total SFA content was not significantly correlated with mean survival time ($P > 0.24$).

The diets prepared with CO, HPCO, and LSCO contained higher contents of campesterol, β-sitosterol, and brassicasterol (Table 8). The CO and HPCO diets contained more brassicasterol than the LSCO diet. Among the non-CO diets, CHOW contained the largest content of phytosterols. In addition, this diet contained a considerable amount of cholesterol, whereas all the other diets contained very little cholesterol. The amount of phytosterols in liver (Table 9) and brain (Table 10), of the animals killed after 37 d on diet, reflected the levels in the corresponding diets. Animals fed the CO-based diets (CO, HPCO, and LPCO) showed significantly higher amounts of campesterol, β-sitosterol and total phytosterols compared to those animals fed non-CO-based diets. In all the dietary groups, campesterol was the major phytosterol followed by β-sitosterol (Tables 9 and 10). In addition to the common phytosterols, trace levels (<1 mg/100 g tissue) of brassicasterol were detected in tissues of rats fed the three CO-based diets. These data on the relative amounts of phytosterols in brain and liver are consistent with the previous studies on the absorption rates for phytosterols in animal studies, where higher intestinal absorption rates are reported for campesterol than for sitosterol and stigmasterol is absorbed minimally (13). The content of cholesterol in liver and brain was not significantly different among the dietary groups (Tables 9 and 10).

The campesterol, sitosterol, and total phytosterol contents in the diets as well as those of liver and brain of the SHRSP rats killed after 37 d on the diets displayed significant and strong inverse correlations ($R > 0.69$) with the mean survival times of the SHRSP rats in the life span study group (Table 11). Regression analysis to examine whether brassicasterol, which is the characteristic sterol of CO, is associated with the mean survival time was not performed, because only two diets (CO and HPCO) had reasonable levels of this sterol. Furthermore, as mentioned previously, even with CO and HPCO dietary groups, only very little brassicasterol was found in liver or brain.

The urinary creatinine levels were highest in the CO and LSCO groups and lowest in the CHOW and MIMIC groups; levels in the other dietary groups were in between (Table 12). These levels showed an inverse correlation with mean survival times of the rats in the life span study group ($R = –0.70$, $P = 0.0517$) (Table 13). Urinary sodium levels were higher only in the CHOW fed group as were BUN levels (Table 12). These parameters showed no significant relationship with mean survival times (Table 13). No significant differences

TABLE 4
Correlation Coefficients (*R*) Between the Mean Survival Time of SHRSP Rats in the Life Span Study Group[a] and α-Tocopherol Content of Diets and Various Tissues of SHRSP Rats Killed After 37 d

Parameter	*R*	*P*
Diet	–0.07	0.8614
Liver	+0.34	0.4084
Heart	+0.03	0.9318
Kidney	+0.30	0.4643
Adipose	+0.25	0.5223
Plasma	+0.39	0.3362

[a]Correlation coefficients obtained from linear regression analysis of mean survival time vs. α-tocopherol content (mean values for tissues). $n = 17$ or 18 per dietary group in life span study and $n = 5$ per group in rats killed after 37 d. For abbreviations see Table 2.

TABLE 5
Fatty Acid Composition[a] (% total fatty acids) of Total Lipids from Red Blood Cells of SHRSP Rats Fed Different Dietary Oils for 37 d

	Dietary oil fed								
Fatty acid	CO	SBO	HOSFO	MIMIC	HSFAB	HPCO	LSCO	CHOW	SD
16:0	26.1	25.6	24.1	25.8	25.3	25.9	25.6	24.7	1.5
18:0	13.3	14.1	13.0	13.2	12.9	11.9	12.4	14.9	1.7
∑SFA	41.8	42.8	39.9	41.7	41.5	39.7	40.2	43.1	3.0
16:1n-7	0.7	0.6	0.8	1.0	1.0	1.0	0.9	0.7	0.3
18:1n-9	16.4^{c}	10.2^{a,b}	17.0^{c}	15.2^{b,c}	15.8^{c}	16.7^{c}	15.2^{c}	9.3^{a}	3.8
18:1n-7	3.5^{a,b}	2.8^{a,b}	3.1^{a,b}	3.0^{a,b}	2.6^{a}	3.8^{b}	3.7^{b}	2.7^{a}	0.7
∑MUFA	22.3^{b}	15.0^{a}	23.0^{b}	20.5^{a,b}	21.2^{a,b}	23.1^{b}	21.4^{b}	14.4^{a}	4.7
18:2n-6	8.8^{a,b}	10.0^{b}	7.2^{a}	7.2^{a}	7.6^{a,b}	7.4^{a}	8.4^{a,b}	9.3^{a,b}	1.5
20:3n-6	0.4	0.3	0.3	0.3	0.4	0.4	0.3	0.4	0.1
20:4n-6	21.2	23.0	22.7	21.7	21.3	20.6	21.5	23.1	1.9
22:4n-6	0.9^{a}	1.4^{b}	1.5^{b}	0.9^{a}	1.2^{a}	1.0^{a}	0.9^{a}	1.3^{a}	0.4
22:5n-6	0.2^{a}	0.3^{a}	0.6^{b}	0.2^{a}	0.3^{a}	0.3^{a}	0.2^{a}	0.3^{a}	0.2
∑n-6LC-PUFA	22.6	25.0	25.2	23.2	23.2	22.3	23.0	25.1	2.3
18:3n-3	0.5^{a,b}	0.4^{a,b}	0.5^{a,b}	0.4^{a,b}	0.4^{a,b}	0.5^{a,b}	0.7^{b}	0.2^{a}	0.2
20:5n-3	1.3	1.3	0.8	1.1	1.4	1.6	1.0	1.3	0.6
22:5n-3	2.3^{b}	2.2^{b}	1.4^{a}	2.4^{b}	1.6^{a,b}	2.2^{b}	2.1^{b}	2.3^{b}	0.6
22:6n-3	3.1^{b}	2.9^{b}	2.1^{a}	3.2^{b}	2.8^{a,b}	2.8^{a,b}	3.1^{b}	4.1^{c}	0.6
∑n-3LC-PUFA	6.7^{b}	6.3^{b}	4.0^{a}	6.7^{b}	5.9^{a,b}	6.7^{b}	6.2^{b}	7.6^{b}	1.5

[a]For abbreviations see Tables 1 and 2. SD, pooled standard deviation. Minor SFA, MUFA and LC-PUFA are included in the totals of these groups of fatty acids. Means across a row with different roman superscript letters are significantly different ($P < 0.05$) and those rows without a superscript are not significantly different ($P > 0.05$). $n = 5$ per group.

were seen in liver mineral levels (Table 12); although liver iron levels were different between the different groups, the differences were not related to the mean survival time of the different groups (Table 13).

DISCUSSION

The present study confirms the recent observation of Okuyama's research group (3–6) of the life-shortening activity of several vegetable oils, including CO compared to SBO in salt-loaded SHRSP rats. Although the rats fed CO died earlier than those fed SBO, the difference in the mean survival time was only 8.5 d (or 8.9%). In contrast, differences ranging from 53 to 121 d were reported in the earlier reports of Okuyama's research group (2,3). Also, all the animals in their study, including those fed CO lived longer (mean survival time ranged from 122 to 146 d vs. 87 d in the present study) than those in the present study. The source of animals in our study was different from that of Okuyama's earlier studies, and this might be the reason for the large difference in the

TABLE 6
Fatty Acid Composition[a] (% total fatty acids) of Liver Total Lipids of SHRSP Rats Fed Different Dietary Oils for 37 d

	Dietary oil fed								
Fatty acid	CO	SBO	HOSFO	MIMIC	HSFAB	HPCO	LSCO	CHOW	SD
16:0	17.9^{a}	18.9^{a,b}	18.2^{a,b}	18.7^{a,b}	19.9^{b}	19.0^{a,b}	17.9^{a}	18.6^{a,b}	1
18:0	13.9	14.2	13.2	14.7	12.7	13.8	14.1	16.6	3.2
∑SFA	33.8	34.7	32.5	34.9	34.1	34.8	33.9	37.6	3.2
16:1n-7	1.2	1.2	1.6	1.3	1.5	1.6	1.1	1.2	0.6
18:1n-9	21.8^{a,b}	17.2^{a}	31.2^{b}	24.2^{a,b}	23.3^{a,b}	20.0^{a,b}	20.9^{a,b}	13.4^{a}	8.2
18:1n-7	2.9^{b}	2.2^{a}	2.5^{a,b}	2.1^{a}	2.5^{a,b}	3.9^{c}	3.0^{a,b}	2.3^{a}	0.6
∑MUFA	27.8	22.0	36.0	29.3	28.5	28.1	26.6	17.9	8.8
18:2n-6	13.8^{a,b}	19.3^{b}	7.9^{a}	12.1^{a,b}	13.6^{a,b}	13.6^{a,b}	14.3^{a,b}	16.3^{a,b}	5.1
20:4n-6	15.9	16.1	17.2	15.0	15.6	14.9	16.0	17.7	3.0
∑n-6LC-PUFA	16.5	18.8	19.1	15.2	16.4	14.6	16.6	18.4	3.7
18:3n-3	0.1^{b}	0.1^{b}	0.1^{b}	0.1^{b}	0.1^{b}	0.1^{b}	0.1^{b}	0.0^{a}	0.0
20:5n-3	0.1	0.2	0.1	0.2	0.1	0.2	0.2	0.2	0.1
22:6n-3	5.9^{a,b}	4.5^{a,b}	3.4^{a}	6.1^{a,b}	5.4^{a,b}	5.8^{a,b}	6.2^{a,b}	7.7^{b}	2.0
∑n-3LC-PUFA	7.2^{a,b}	5.7^{a,b}	3.8^{a}	7.6^{a,b}	6.6^{a,b}	7.4^{a,b}	7.7^{a,b}	9.0^{b}	2.3

[a]For abbreviations see Tables 1 and 2. SD, pooled standard deviation. Means across a row with different roman superscript letters are significantly different ($P < 0.05$) and those rows without a superscript are not significantly different ($P > 0.05$). $n = 5$ per group.

TABLE 7
Correlation Coefficients[a] (*R*) Between the Mean Survival Time of SHRSP Rats in the Life Span Study Group and Levels of SFA, MUFA, n-6 PUFA, and n-3 PUFA in Diets, Red Blood Cells, and Livers of SHRSP Rats Killed After 37 d

Parameter	*R*	*P*
Diet		
Total SFA	+0.78	0.0219
Total MUFA	–0.34	0.4041
Total n-6 PUFA	+0.10	0.8134
Total n-3 PUFA	+0.33	0.4205
Red blood cells		
Total SFA	+0.47	0.2447
Total MUFA	–0.52	0.1879
Total n-6 PUFA	+0.27	0.5216
Total n-3 PUFA	0.00	0.9935
Liver		
Total SFA	+0.47	0.2426
Total MUFA	+0.29	0.4929
Total n-6 PUFA	–0.24	0.5744
Total n-3 PUFA	+0.05	0.8987

[a]Correlation coefficients obtained from linear regression analysis of mean survival time vs. total SFA, MUFA , n-6 and n-3 PUFA (mean values for tissues). n = 17 or 18 per dietary group in life span study and n = 5 per group in rats killed after 37 d. For abbreviations see Tables 1 and 2.

mean survival time between the two laboratories. Consistent with this suggestion, the difference between CO and SBO was shown to be much smaller (16–24 d) in the subsequent experiments of Okuyama (3–6) performed using animals purchased from the same source as in our experiments.

In the present study we observed a positive association between dietary SFA content and the mean survival times. However, when all the dietary and tissue fatty acid data are taken into consideration, it would appear that the lower SFA content or the fatty acid profile might not be the life-shortening factor associated with CO. This is primarily because the CO mimic of this study, which closely resembled the fatty acid profile of CO, and HOSFO, which also contained a lower level of SFA (8%), prolonged the life span of SHRSP rats by 9.6 and 6.4%, respectively, compared to those fed CO. Furthermore, although the HSFAB of this study, which mimicked the ideal fatty composition for the optimal growth of normal rats in studies by Hopkins *et al.* (14), displayed the best survival results, the mean survival time (100 ± 9 d) was not significantly different from the dietary groups fed other non-CO. These data further suggest that the life span of SHRSP rats is not modulated by the dietary fatty acid composition. Similarly Huang *et al.* (4) postulated that high oleic acid content in CO, high-oleic sunflower oil, HOSFO, and olive oil could not be the life-shortening factor associated with these oils, because feeding lard and a microbial oil containing approximately 35% oleic acid prolonged the life span of SHRSP rats whereas evening primrose oil, containing only 13% oleic acid, shortened the life span in a manner similar to that found with CO.

Fish oils, however, could be exceptional dietary fats. Previous studies have shown that fish oils, relative to olive oil, CO and safflower oil, are more effective in controlling blood pressure and stroke (15,16), and in prolonging the life span of SHRSP rats (3). Fish oil also prevents the development of proteinurea, which is a marker of renal damage in SHRSP rats (16). The efficacy of fish oil has been attributed to increased incorporation of 20:5n-3 and 22:6n-3 in the kidney. In the present study the different diets contained variable levels of α-linolenic acid (ranging from 0 to 11% of total fatty acids), with CO, SBO, MIMIC, and HPCO diets providing the highest levels. In addition, the rat chow contained about 2% preformed n-3 LC-PUFA metabolites of α-linolenic acid. These different amounts and types of n-3 LC-PUFA in the diets, however, showed no association with the life span of SHRSP rats. The tissue (RBC and liver) levels of 22:6n-3 and other n-3 LC-PUFA metabolites of α-linolenic acid also showed no relationship with the life span. The SBP and BUN content also were not correlated with the life span. These results therefore suggest that α-linolenic acid in vegetable oils and the minor amounts of dietary n-3 LC-PUFA cannot alter the life span, SBP or development of proteinuria in SHRSP rats. A similar suggestion was made by Hobbs *et al.* (16) regarding CO and they concluded that, although CO is a rich source of α-linolenic acid, it may not be possible to derive sufficient 22:6n-3 from consumption of vegetable oils to alter blood pressure and renal function significantly. This suggestion could be equally applicable to SBO, which also contains the same proportion of α-linolenic acid as does CO. Perilla oil on the other hand is an exceptional vegetable oil. In experiments performed by Huang *et al.* (3,4), this oil consistently prolonged the life span of SHRSP rats to a very great extent

TABLE 8
Cholesterol and Phytosterol Contents of Different Diets[a] (mg per 100 g diet)

Sterol	CO	SBO	HOSFO	MIMIC	HSFAB	HPCO	LSCO	CHOW
Cholesterol	0.3	0.2	0.3	0.3	0.1	0.5	0.4	24.8
Brassicasterol	10.5	0.1	0.1	0.2	0.2	9.5	0.7	0.1
24-Methylenecholesterol	1.2	0.5	0.2	0.3	0.2	2.3	0.9	1.0
Campesterol	29.5	11.4	3.4	5.0	2.8	42.7	34.4	10.3
Stigmasterol	0.8	7.3	1.7	2.0	1.3	0.5	0.3	4.4
β-Sitosterol	47.8	24.1	14.0	14.7	9.5	54.5	39.3	32.8
Δ5-Avenasterol	3.2	2.1	1.7	2.2	0.9	1.7	2.4	3.0
Total phytosterols	96.8	48.5	24.6	32.5	18.2	116.5	80.3	53.9

[a]For abbreviations see Table 1. Minor phytosterols (<0.1 mg/100 g diet) are not shown in the table but are included in the total phytosterols.

TABLE 9
Cholesterol and Phytosterol Concentrations in Liver of SHRSP Rats Fed Different Dietary Oils[a] for 37 d

	Concentrations (mg sterols per 100 g liver)								
Sterol	CO	SBO	HOSFO	MIMIC	HSFAB	HPCO	LSCO	CHOW	SD
Cholesterol	252	170	244	167	167	189	213	160	63
Brassicasterol	0.7^{b}	0.0^{a}	0.0^{a}	0.0^{a}	0.0^{a}	0.6^{b}	0.1^{a}	0	0
24-Methylenecholesterol	1.0^{b}	0.5^{a}	0.8^{a,b}	0.8^{a,b}	0.5^{a}	0.5^{a}	0.5^{a}	0.8^{a,b}	0
Campesterol	24.1^{b}	8.0^{a}	7.1^{a}	7.2^{a}	6.2^{a}	38.9^{c}	25.1^{b}	10.0^{a}	13
Stigmasterol	0.7	1.7	1.6	1.3	1.6	1.3	1.0	0.7	1
β-Sitosterol	15.9^{c}	7.9^{a,b}	8.9^{a,b}	7.8^{a,b}	4.8^{a}	22.3^{d}	13.0^{b,c}	8.2^{a,b}	6
Δ5-Avenasterol	1.7^{b}	1.1^{a,b}	0.9^{a,b}	1.5^{a,b}	1.0^{a,b}	1.7^{a,b}	1.3^{a,b}	0.9^{a}	0
Total sterol	296^{b}	189^{a}	263^{a,b}	186^{a}	181^{a}	255^{a,b}	254^{a,b}	180^{a}	74
Total phytosterol	44.2^{b}	19.1^{a}	20.2^{a}	17.8^{a}	13.8^{a}	65.1^{c}	41.3^{b}	20.0^{a}	20
Phytosterol/cholesterol	0.19^{b}	0.11^{a}	0.08^{a}	0.11^{a}	0.09^{a}	0.34^{c}	0.2^{b}	0.13^{a}	0

[a]For abbreviations see Tables 1 and 2. SD, pooled standard deviation. Minor phytosterols (<0.1 mg/100 g liver) are not shown in the table but are included in the total phytosterols. Means across a row with different roman superscript letters are significantly different ($P < 0.05$) and those rows without a superscript are not significantly different ($P > 0.05$). $n = 5$ per group.

compared to CO and SBO. Perilla oil is a rich source of α-linolenic acid (55 vs. 7–8% in CO or SBO) and therefore may support the view of Hobbs *et al*. (16) regarding the beneficial effects of n-3 fatty acids. But unfortunately, Huang *et al*. (3,4) did not report the levels of n-3 LC-PUFA in tissues of SHRSP rats, and therefore whether the life-prolonging activity of perilla oil is due to its high α-linolenic acid content or some other component in the oil is unknown.

The present study also indicated that the amount of sulfur in CO has no influence on the life span of the SHRSP rat, because the mean survival time of rats fed LSCO, despite its lower sulfur content (0.5 vs. 7.5 ppm in CO), was not significantly different from that of CO.

This study also showed that the high sodium load, although known to accelerate the development of hypertension in this animal model (17), is not reflected in abnormalities in tissue levels of sodium or other minerals. The high urinary excretion of Na in the chow-fed group likely reflects the very high Na content of this diet (4,000 ppm, manufacturer's specification). In addition, there is no biochemical evidence of impairment of kidney function, which can be related to the differences in survival between the different groups, nor of increased lipid peroxidation and SBP. Thus, it might be suggested that the mechanism by which vegetable oils alter the life span of SHRSP rats is not related to any of the above biochemical parameters. The significant correlation seen in the present study between urinary creatinine and mean survival is not surprising, because very sick animals, such as the SHRSP rat, would be expected to excrete high amounts of creatinine, indicative of increased muscle wasting (18).

Recently it was reported that there is significantly higher vitamin E requirement when neonatal pigs are fed milk replacers containing CO as the sole fat source (19). In contrast, piglets fed SBO showed no evidence of vitamin E deficiency. The factor present in CO which increases vitamin E requirements of newborn piglets has not been identified yet. In the present study, however, canola-fed SHRSP rats, compared to other test oils, showed no signs of vitamin E deficiency, which indicates that a factor other than vitamin E antagonistic factor may be responsible for the shorter life span of SHRSP rats fed CO.

In contrast with the other parameters examined in this study, inverse associations were observed between life span and levels of phytosterols, specifically campesterol and β-sitosterol, of rat tissues and diets. This was mainly due to the high content of phytosterols in the three CO varieties. Certainly, further studies are required to determine whether the life-shortening activity of CO could be attributed to their high

TABLE 10
Cholesterol and Phytosterol Concentrations in Brain of SHRSP Rats Fed Different Dietary Oils for 37 d

	Concentrations (mg sterols per 100 g liver)								
Sterol	CO	SBO	HOSFO	MIMIC	HSFAB	HPCO	LSCO	CHOW	SD
Cholesterol	1840	1916	1710	1770	1867	1646	1752	1860	220
Brassicasterol	0.7^{b}	0.0^{a}	0.0^{a}	0.0^{a}	0.0^{a}	0.5^{b}	0.2^{a}	0.0^{a}	0.2
Campesterol	6.8b^{c}	4.5^{a,b,c}	3.2^{a,b}	3.2^{a,b}	2.7^{a}	8.1^{c}	6.9^{b,c}	3.5^{a,b}	2.7
Stigmasterol	0.5	0.6	0.4	0.6	0.4	0.3	0.4	0.6	0.5
β-Sitosterol	4.2^{c}	3.2^{a,b,c}	3.0^{a,b,c}	2.6^{a,b}	2.3^{a}	4.2^{c}	3.6^{b,c}	2.8^{a,b}	0.9
Δ5-Avenasterol	0.7	0.6	0.7	0.6	0.7	0.5	0.7	0.7	0.2
Total phytosterols	12.9^{b,c}	8.9^{a,b}	7.3^{a,b}	7.0^{a,b}	6.1^{a}	13.6^{c}	11.8^{b,c}	7.6^{a,b}	4.5

[a]For abbreviations see Tables 1 and 2. SD, pooled standard deviation. Minor phytosterols (<0.1 mg/100 g brain) are not shown in the table but are included in the total phytosterols. Means across a row with different roman superscript letters are significantly different ($P < 0.05$) and those rows without a superscript are not significantly different ($P > 0.05$). $n = 5$ per group.

TABLE 11
Correlation Coefficients (*R*) Between the Mean Survival Time of SHRSP Rats in the Life Span Study Group and Sterol Content of Diet, Liver, and Brain of SHRSP Rats Killed After 37 d

Parameter	*R*	*P*
Diet		
Cholesterol	+0.39	0.3397
Campesterol	–0.74	0.0355
β-Sitosterol	–0.69	0.0557
Total phytosterols	–0.72	0.0433
Liver		
Cholesterol	+0.82	0.0121
Campesterol	–0.69	0.0608
β-Sitosterol	–0.71	0.0440
Total phytosterols	–0.72	0.0447
Brain		
Cholesterol	+0.40	0.3294
Campesterol	–0.80	0.0182
β-Sitosterol	–0.88	0.0044
Total phytosterols	–0.84	0.0091

[a]Correlation coefficients obtained from linear regression analysis of mean survival time and sterol concentrations (mean values for tissues). n = 17 or 18 per dietary group in life span study and n = 5 per group in rats killed after 37 d.

content of phytosterols, and these are currently ongoing in our laboratory. Meanwhile, it is interesting to note that phytosterols have been shown to replace the cholesterol complement in cell membranes and consequently increase the osmotic fragility of human erythrocytes in *in vitro* experiments (20) and rigidity of liver microsomes in Wistar rats fed a diet supplemented with 3% β-sitosterol + 2% campesterol (21). Such changes in cell membrane characteristics might exert adverse physiological consequences for SHRSP rats, because these animals have defective and abnormal cell membranes (17). The abnormalities include high membrane rigidity and low fluidity, and they are considered to be the key factors related to pathogenesis of hypertension and hemorrhagic stroke (22–25). Moreover, the abnormalities of cell membrane in essential hypertension appear to be related to its low content of cholesterol (26–28). Studies have shown that dietary cholesterol is beneficial in delaying the onset of hemorrhagic stroke and prolonging the life span of SHRSP rats (29). Considering these reports, it is reasonable to propose that replacement of cholesterol in tissues by phytosterols from the diet may further weaken the functionality of cell membranes, which could be detrimental to SHRSP rats.

On the basis of the phytosterol hypothesis, HPCO with the largest phytosterol content of the three canola oils tested would be expected to produce the most adverse effects on SHRSP rats. However, the survival rates of SHRSP rats fed this oil were not different from those of the other two CO varieties. This might be explained by the high content of palmitoleic acid (16:1n-7, 2.4% of total fatty acids) in HPCO. A significant reduction in the incidence of stroke and marked increase in the life span (mean survival time increased by 64 d) of SHRSP rats were observed following supplementation of basal diet with 1% palmitoleic acid, whereas supplementation with 1% palmitic, oleic, linoleic, or linolenic acids produced no changes in the life span (30). The preventive mechanism of palmitoleic acid was ascribed to its rapid incorporation into the vascular wall and efficient utilization in improving the impaired metabolism of vascular muscle cells exposed to hypertension (31). Thus it might be suggested that in HPCO, the adverse effect of phytosterols would have been counteracted by palmitoleic acid. In the other two CO varieties such a counteraction was not possible because they contained very little palmitoleic acid (0.1–0.3%).

TABLE 12
Urinary Creatinine, TBARS, and Sodium; Blood Urea Nitrogen; and Liver Mineral Levels of SHRSP Rats Fed Different Dietary Oils for 37 d

	CO	SBO	HOSFO	MIMIC	HSFAB	HPCO	LSCO	CHOW	SD
Urinary creatinine (mg/100 mL urine)	12.3[b]	8.4[a,b]	6.2[a,b]	5.8[a]	8.4[a,b]	11.4[a,b]	9.5[a,b]	5.2[a]	4.7
Urinary TBARS (μmol/mmol creatinine)	8.5	12.7	15.5	11.1	9.8	14.2	10.9	19.5	10.0
Urinary Na (mg/mg creatinine)	9.5[a]	8.4[a]	14.9[a]	14.9[a]	13.9[a]	11.7[a]	10.2[a]	23.6[b]	7.6
Blood urea nitrogen (mg/100 mL serum)	16.3[a,b]	14.9[a]	14.7[a]	17.1[a,b]	13.6[a]	18.1[a,b]	19.5[b,c]	22.7[c]	4.2
Liver minerals (μg/g dry wt)									
Na	47.8	78.9	50.1	43.8	57.6	54.3	68.5	68.1	30.0
K	285	449	264	230	298	301	410	377	178
Ca	2.5	4.0	2.8	2.2	2.7	3.8	3.6	3.3	1.9
Mg	23.0	36.4	21.3	18.4	23.3	23.9	32.7	29.7	14.0
Fe	13.4[a]	22.9[a,b]	10.7[a]	13.4[a]	12.2[a]	14.0[a]	26.2[b]	18.3[a,b]	10.0
Cu	0.4	0.6	0.4	0.3	0.4	0.4	0.5	0.5	0.3
Zn	2.8	4.1	2.4	2.2	2.6	3.0	4.0	3.7	1.7

[a]TBARS, thiobarbituric acid-reactive substances; for other abbreviations see Tables 1 and 2. SD, pooled standard deviation. Means across a row with different roman superscript letters are significantly different (P < 0.05) and those rows without a superscript are not significantly different (P > 0.05). n = 5 per group.

TABLE 13
Correlation Coefficients[a] (*R*) Between the Mean Survival Time of SHRSP Rats in the Life Span Study Group and Urinary Creatinine, TBARS, Sodium, Blood Urea Nitrogen, and Liver Mineral Levels of SHRSP Rats Killed After 37 d

Parameter	*R*	*P*
Urinary creatinine	–0.70	0.0517
Urinary TBARS	+0.37	0.3740
Urinary Na	+0.59	0.1303
Blood urea nitrogen	–0.06	0.8265
Liver minerals		
Na	+0.21	0.6214
K	–0.01	0.9797
Ca	+0.08	0.8543
Mg	+0.01	0.9697
Fe	+0.16	0.7024
Cu	–0.02	0.9593
Zn	+0.06	0.8265

[a]Correlation coefficients obtained from linear regression analysis of mean survival time vs. urinary, blood, and tissue parameters (mean values). $n = 17$ or 18 per dietary group in life span study and $n = 5$ per group in rats killed after 37 d. For abbreviations see Tables 2 and 12.

Data reported in other SHRSP rat studies may not appear to be consistent with the proposed life-shortening effect of phytosterols. In efforts to identify the life-shortening factor in CO, Huang *et al*. (4) prepared several fractions from CO using different techniques and then mixed these fractions with SBO, fed them to SHRSP rats, and determined survival times. The various canola fractions, however, did not exhibit any life-shortening activity. The fractions tested included CO nonsaponifable matter prepared by a conventional procedure, components soluble in polar organic solvents (acetone, ethanol, and methanol), and a hexane/diethyl ether soluble fraction isolated after treating a hexane solution of CO with silicic acid. Unfortunately, the report provided no information on the purity, composition, and levels of phytosterols of the CO fractions. Therefore, the results of the Huang *et al*. (4) study are difficult to interpret, particularly with regard to antinutrient effects of phytosterols. Information on phytosterols was also lacking in another SHRSP rat study that examined the effects of lipase-treated CO and other vegetable oils (6).

It has been noted that olive oil, high-oleic sunflower oil, HOSFO, and evening primrose oil have life-shortening activities comparable to that seen with CO (4). The life-shortening activity of these oils may not be solely attributable to their phytosterol contents, because these oils contain much lower levels of phytosterols than do CO. In addition to phytosterols, these oils may contain some other component(s) that significantly affect the life span of SHRSP rats. Results from the present study and other studies (4–6) suggest that this unknown component might not be associated with fatty acids. More research would be required to fully elucidate the different factors in various common vegetable oils that would affect the life span of SHRSP rat.

In conclusion, we have demonstrated that neither the high level of sulfur nor the fatty acid profile of canola are the factors responsible for the observed life-shortening effects of CO on SHRSP rats. Our results appear to indicate that a high content of phytosterols may be a possible antinutritional factor in CO for SHRSP rats. This hypothesis is being currently examined in our laboratory.

ACKNOWLEDGMENTS

Partial funding was provided by the Canola Council of Canada. We are grateful to the members of the Scientific Subcommittee of the Canola Council of Canada for their oversight and helpful input: Bruce McDonald (University of Manitoba, Winnipeg), Sheila Innis (University of British Columbia, Vancouver), and Peter Fischer (Health Canada, Ottawa). The staff of the Animal Resources Division, Health Canada is acknowledged for care of the animals. Stephen Hayward is thanked for statistical analysis of the survival data and Keith Trick, René Madère, and Judy Edgar for technical assistance.

REFERENCES

1. McLennan, P.L., and Dallimore, J.A. (1995) Dietary Canola Oil Modifies Myocardial Fatty Acids and Inhibits Cardiac Arrhythmias in Rats, *J. Nutr. 125*, 1009–1013.
2. Siebert, B.D., McLennan, P.L., Woodhouse, J.A., and Charnock, J.S. (1993) Cardiac Arrhythmia in Rats in Response to Dietary n-3 Fatty Acids from Red Meat, Fish Oil and Canola Oil, *Nutr. Res.13*, 1407–1418.
3. Huang, M.Z., Naito, Y., Watanabe, S., Kobayashi, T., Kanai, H., Nagai, H., and Okuyama, H. (1996) Effect of Rapeseed and Dietary Oils on the Mean Survival Time of Stroke-Prone Spontaneously Hypertensive Rats, *Biol. Pharm. Bull. 19*, 554–557.
4. Huang, M.Z., Watanabe, S., Kobayashi, T., Nagatsu, A., Sakakibara, J., and Okuyama, H. (1997) Unusual Effects of Some Vegetable Oils on the Survival Time of Stroke-Prone Spontaneously Hypertensive Rats, *Lipids 32*, 745–751.
5. Miyazaki, M., Huang, M.Z., Watanabe, S., Kobayashi, T., and Okuyama, H. (1998) Early Mortality Effect of Partially Hydrogenated Vegetable Oils in Stroke Prone Spontaneously Hypertensive (SHRSP) Rats, *Nutr. Res. 18*, 1049–1056.
6. Miyazaki, M., Huang, M.-Z., Takemura, N., Watanabe, S., and Okuyama, H. (1998) Free Fatty Acid Fractions from Some Vegetable Oils Exhibit Reduced Survival Time-Shortening Activity in Stroke-Prone Spontaneously Hypertensive Rats, *Lipids 33*, 655– 661.
7. Ackman, R.G. (1983) Chemical Composition of Rapeseed Oil, in *High and Low Erucic Acid Rapeseed Oils* (Kramer, J.K.G., Sauer, F.D., and Pigden, W.J., eds.), pp. 85–129, Academic Press, New York.
8. Reeves, P.G., Nielsen, F.H., and Fahey, G.C., Jr. (1993) AIN-93 Purified Diets for Laboratory Rodents: Final Report of the American Institute of Nutrition Ad Hoc Writing Committee on the Reformulation of the AIN-76A Rodent Diet, *J. Nutr. 123*, 1939–1951.
9. Brooks, S.P.J., Ratnayake, W.M.N., Lampi, B.J., and Hollywood, R. (1998) Measuring Total Lipid Content in Rat Carcasses: A Comparison of Commonly Employed Extraction Methods, *J. Agric. Food Chem. 46*, 4214–4217.
10. Thompson, J.N., and Hatina, G. (1979) Determination of Tocopherols and Tocotrienols in Foods and Tissues by High-Pressure Liquid Chromatography, *J. Liquid Chromatogr. 2*, 327–344.
11. L'Abbé, M.R., Trick, K.D., and Beare-Rogers, J.L. (1991) Dietary (n-3) Fatty Acids Affect Rat Heart, Liver and Aorta Protective Enzyme Activities and Lipid Peroxidation, *J. Nutr. 121*, 1331–1340.

12. Lawless, J.F. (1982) *Statistical Models and Methods for Lifetime Data*, John Wiley, New York.
13. Ling, W.H., and Jones, P.J.H. (1995) Minireview Dietary Phytosterols: A Review of Metabolism, Benefits and Side Effects, *Life Sci. 57*, 195–206.
14. Hopkins, C.Y., Murray,T.K., and Campbell, J.A. (1955) Optimum Ratio of Saturated to Unsaturated Fatty Acids, *Can. J. Biochem. Physiol. 33*, 1047–1054.
15. Howe, P.R.C., Head, R.J., and Smith, R.M. (1989) High Dietary Sodium Intake Counteracts the Antihypertensive Effect of Fish Oil in Spontaneously Hypertensive Rats, *Proc. Nutr. Soc. Aust. 14*, 148.
16. Hobbs, L.M., Rayner, T.E., and Howe, P.R.C. (1996) Dietary Fish Oil Prevents the Development of Renal Damage in Salt-Loaded Stroke-Prone Spontaneously Hypertensive Rats, *Clin. Expt. Pharmacol. Physiol. 23*, 508–513.
17. Yamori, Y. (1989) Predictive and Preventive Pathology of Cardiovascular Diseases, *Acta Pathol. Jpn. 39*, 683–705.
18. Loeb, W.F., and Quimby, F.W. (1999) *The Clinical Chemistry of Laboratory Animals*, 2nd edn., Edward Brothers, Ann Arbor.
19. Sauer, F.D., Farnworth, E.R., Bélanger, J.M.R., Kramer, J.K.G., Miller, R.B., and Yamashiro, S. (1997) Additional Vitamin E Required in Milk Replacer Diets That Contain Canola Oil, *Nutr. Res. 17*, 259–269.
20. Bruckdorfer, K.R., Demel, R.A., De Gier, J., and Van Deenen, L.L.M. (1969) The Effect of Partial Replacements of Membrane Cholesterol by Other Steroids on the Osmotic Fragility and Glycerol Permeability of Erythrocytes, *Biochim. Biophys. Acta 183*, 334– 345.
21. Leiken, A.L., and Brenner, R. (1989) Fatty Acid Desaturase Activities Are Modulated by Phytosterol Incorporation in Microsomes, *Biochim. Biophys. Acta 1005*, 187–191.
22. Yamori, Y., Nara, Y., Horie, R., and Ooshima, A. (1980) Abnormal Membrane Characteristics of Erythrocytes in Rat Models and Men with Predisposition to Stroke, *Clin. Exp. Hypertens. 2*, 1009–1021.
23. De Mendonca, M., Grichois, M.L., Garay, R.P., Sassard, J., Benlshay, D., and Meyer, P. (1980) Abnormal Net Na^+ and K^+ Fluxes in Erythrocytes of Three Varieties of Genetically Hypertensive Rats, *Proc. Natl. Acad. Sci. USA 77*, 4283–4286.
24. Canessa, M., Adragna, N., Connolly, T., Solomon, H., and Tosteson, D.C. (1980) Na-Li Countertransport Is Increased in Red Cells of Hypertensive Patients, *N. Engl. J. Med. 302*, 772–776.
25. Tsuda, K., Ueno, Y., Nishio, I., and Masuyama, Y. (1992) Membrane Fluidity as a Genetic Marker of Hypertension, *Clin. Exp. Pharmacol. Physiol. 19* (Suppl. 20), 11–16.
26. Ooneda, G., Yoshida, Y., Suzuki, K., Kobori, K., Takayama, Y., and Sekiguchi, M. (1978) Smooth Muscle Cells in the Development of Plasmatic Arterionecrosis, Arteriosclerosis, and Arterial Contraction, *Blood Vessels 15*, 148–156.
27. Yamori, Y., Horie, R., Ohtaka, M., Nara, Y., and Fukase, M. (1977) Effect of Hypercholesterolaemic Diet on the Incidence of Cerebrovascular and Myocardial Lesions in Spontaneously Hypertensive Rats (SHR), *Clin. Exp. Pharmacol. Physiol. (Suppl.) 3*, 205–208.
28. Kroes, J., and Ostwald, R. (1971) Erythrocyte Membranes—Effect of Increased Cholesterol Content on Permeability, *Biochim. Biophys. Acta 249*, 647–650.
29. Hamano, M., Mashiko, S., Onda, T., Tomita, I., and Tomita, T. (1995) Effects of Cholesterol-Diet on the Incidence of Stroke and Life-Span in Malignant Stroke Prone Spontaneously Hypertensive Rats, *Jpn. Heart J. 36*, 511.
30. Yamori,Y., Nara, Y., Tsubouchi, T., Sogawa, Y., Ikeda, K., and Horie, R. (1986) Dietary Prevention of Stroke and Its Mechanisms in Stroke-Prone Spontaneously Hypertensive Rats—Preventive Effect of Dietary Fibre and Palmitoleic Acid, *J. Hypertens. 4* (Suppl. 3), S449–S452.
31. Yamori, Y., Nara, Y., Ikeda, K., Tsuchikura, S., Eguchi, T., Mano, M., Horie, R., and Sugahara, T. (1989) Recent Advances in Experimental Studies on Dietary Prevention of Cardiovascular Diseases, in *New Horizons in Preventing Cardiovascular Diseases* (Yamori, Y., and Strasser, T., eds.), pp. 1–11, Elsevier Science Publishers, Amsterdam.

[Received July 15, 1999, and in final revised form January 31, 2000; revision accepted February 18, 2000]

Dietary Fat-Induced Suppression of Lipogenic Enzymes in B/B Rats During the Development of Diabetes

S.K. Cheema[a] and M. Thomas Clandinin[a,b,*]

Departments of [a]Agricultural, Food and Nutritional Science and [b]Medicine, University of Alberta, Nutrition and Metabolism Research Group, Edmonton, Alberta, T6G 2P5, Canada

ABSTRACT: This study was designed to determine the level of inhibition of gene transcription by the reduction in insulin levels upon the onset of diabetes in spontaneously diabetic B/B rats and if reducing the level of polyunsaturated fatty acids (PUFA) in the diet will increase lipogenic enzyme activity. Control (eight animals per group) and spontaneously diabetic B/B male weanling rats (25 animals per group) were fed semipurified diets containing 20% (w/w) fat of either low (0.25) or high (1.0) polyunsaturated to saturated (P/S) fatty acid ratio. Rats were killed at the onset of diabetes [blood glucose level of ≅100 mg/dL (5.55 mM)] and as they became highly diabetic [blood glucose level of ≅400 mg/dL (22.22 mM)]. Total RNA was extracted from liver, and the relative amount of mRNA coding for fatty acid synthase (FAS), acetyl-CoA carboxylase, malic enzyme, pyruvate kinase, and phosphoenolpyruvate carboxykinase was determined. Liver enzyme activities were also measured. The mRNA levels for FAS, acetyl-CoA carboxylase, and malic enzyme decreased compared to control animals. The mRNA level for pyruvate kinase decreased at the onset of diabetes as compared to control animals. Feeding animals the low P/S diet treatment elevated the level of mRNA and lipogenic enzyme activity compared to animals fed the high P/S diet treatment, suggesting that the effect of PUFA on lipogenic enzymes is through a direct effect on gene expression.

Paper no. L8389 in *Lipids 35,* 421–425 (April 2000).

Lipogenic enzymes are affected by dietary nutrients and hormones (1–4). Fatty acids are known to potentiate glucose-induced insulin release *in vitro*, whereas *in vivo* fatty acids increase plasma insulin levels in various species, including humans (5). The mechanism by which fatty acids may modulate β-cell function has not been characterized. The composition of dietary fat is a key determinant of membrane fatty acid composition, membrane-bound enzyme activity, glucose transport, insulin binding, and signal transduction mechanisms (6–8). Essential fatty acids govern the transcription of specific genes (9–12). Polyunsaturated fatty acids (PUFA) inhibit transcription of genes coding for lipogenic enzymes and enzymes for glucose metabolism (13).

The spontaneously diabetic B/B rat is a unique model exhibiting human type I diabetes mellitus (14). Diabetes in B/B rats results from an autoimmune disease where insulin-producing β-cells of the pancreas are destroyed (15). Once B/B rats become diabetic, immunoreactive insulin declines to almost zero. Thus, gene transcription should be suppressed in spontaneously diabetic B/B rats for genes normally stimulated by insulin. The objective of this study was to assess the amount of effect of dietary fatty type on expression of lipogenic genes as insulin becomes limiting *in vivo*.

MATERIALS AND METHODS

Animals and diets. B/B rats were obtained from BioBreeding Laboratories of Canada Ltd. (Ottawa, Canada). The incidence of diabetes in these B/B rats in our facility is 40–70%. The onset of diabetes occurs 60–120 d of age. Control (eight animals per group) and spontaneously diabetic B/B male weanling rats (25 animals per group) were randomly assigned a semipurified diet containing 20% (w/w) fat of either low (0.25) or high (1.0) polyunsaturated to saturated (P/S) fatty acid ratio (Table 1; 8). The dietary fat treatments were similar in fatty acid composition to the range of fat intakes typical of that consumed by much of the North American population. Animals were housed in individual wire-bottom cages in a well-ventilated room maintained at 22 ± 2°C on a 12:12 h

TABLE 1
Fatty Acid Composition of Diet Fats[a]

Fatty acid	P/S = 1.0	P/S = 0.25
14:0	1.3	3.7
16:0	16.1	23.0
16:1	0.2	0.3
18:0	27.5	47.11
18:2n-6	44.0	17.6
18:3n-3	0.9	0.9
∑ Polyunsaturated	44.9	19.1
∑ Saturated	44.9	71.8
∑ Monounsaturated	8.2	4.5
P/S ratio	1.0	0.25

[a]P/S, polyunsaturated to saturated fatty acid ratio.

*To whom correspondence should be addressed at Nutrition and Metabolism Research Group, University of Alberta, Department of Agricultural, Food, and Nutritional Science and Department of Medicine 4-10 Agriculture/Forestry Centre, Edmonton, Alberta, T6G 2P5 Canada.
E-mail: tclandin@gpu.srv.ualberta.ca

Abbreviations: ACC, acetyl-CoA carboxylase; FAS, fatty acid synthase; ME, malic enzyme; PEPCK, phosphoenolpyruvate carboxykinase; PUFA, polyunsaturated fatty acid; P/S, ratio of polyunsaturated to saturated fatty acid; SSC, a solution containing 0.3 M NaCl + 0.03 M sodium citrate at pH 7.0; SDS, sodium dodecyl sulfate.

light/dark cycle. Animals were fed *ad libitum* and weighed twice weekly. Blood glucose level was checked daily, and diabetes was diagnosed on the basis of a plasma glucose level in excess of 250 mg/dL (13.89 mM), polyuria, and failure to gain weight. Animals with a blood glucose level of 350–500 mg/dL (19–28 mM) were characterized as highly diabetic. Serum insulin level was determined by radioimmune assay (Insulin RIA 100 kit; Pharmacia Co., Uppsala, Sweden) against a rat insulin standard. Rats were killed at the onset of diabetes [blood glucose level of ~100 mg/dL (5.55 mM)] and when they became highly diabetic [blood glucose level of ~400 mg/dL (22.22 mM)]. Livers were collected immediately and frozen at –70°C.

Quantitation of mRNA. Total RNA was extracted from liver samples using a guanidinium-isothiocyanate method (16). RNA concentrations were measured spectrophotometrically. A known amount of total RNA was applied to nitrocellulose paper, and the relative amount of mRNA coding for fatty acid synthase (EC 2.3.1.85), acetyl-CoA carboxylase (EC 6.4.1.2), malic enzyme (ME) (EC 1.1.1.40), pyruvate kinase (EC 2.7.1.40), and phosphoenolpyruvate carboxykinase (PEPCK) (EC 4.1.1.32) was determined by slot-blot hybridization with specific ^{32}P-labeled cDNA probes. The probes, generously donated by Dr. D.W. Back of Queen's University, Kingston, Ontario, Canada, were labeled by the random primer method (Prime-A-Gene Labeling System; Promega, Madison, WI). Hybridization was carried out in a shaking water bath for 36 h at 42°C. After hybridization, the membranes were washed in 2 × SSC (a solution containing 0.3 M NaCl and 0.03 M sodium citrate, pH 7.0), 0.1% SDS (sodium dodecyl sulfate); 1 × SSC, 0.1% SDS at room temperature; and 0.1 × SSC, 0.1% SDS at 50°C for 30 min. Membranes were air-dried and slots were cut out and counted in a scintillation counter, or membranes were used for autoradiophy. Nonspecific binding was evaluated using pBR322.

Enzyme assays. Fatty acid synthase (FAS) activity was measured. A unit of enzyme activity represents the synthesis of 1 nmol of palmitic acid/min/mg of protein (17). ME was using the rate of NADPH (18). For determination of acetyl-CoA carboxylase (ACC) (19) and pyruvate kinase (20), one unit of enzyme was defined as the amount catalyzing the formation of 1 µmol of product/min/mg of protein. PEPCK was measured as nmol of NADH oxidized/min/mg protein (21).

Statistical analysis. The effect of diet and diabetes on enzyme activities and mRNA levels was determined by analysis of variance procedures. Values are group means ± SE, n = 8. Treatments without a common superscript are significantly different ($P > 0.05$).

RESULTS

Spontaneously diabetic rats weighed less and exhibited a lower serum insulin level compared to control animals (Table 2). The serum insulin level decreased further in spontaneously diabetic rats with the increase in blood glucose level. Dietary fat did not alter the insulin or glucose level in control or spontaneously diabetic rats (Table 2) or the time of onset of diabetes.

Effect of diet fat and diabetes on lipogenic enzymes. FAS is a multifunctional polypeptide which, using acetyl-CoA as a primer, catalyzes formation of long-chain saturated fatty acids from malonyl-CoA and NADPH. ACC is an important rate-controlling enzyme both in the synthesis of fatty acids and in generating intracellular malonyl-CoA, whereas ME catalyzes the oxidative decarboxylation of malate to pyruvate and CO_2, simultaneously generating NADPH from NADP. The effect of diet and diabetes on activity and mRNA level of these lipogenic enzymes revealed that enzyme activity of FAS, ACC, and ME decreased at the onset of diabetes compared to control animals (Fig. 1). As the animals became highly diabetic, the enzyme activity decreased further compared to animals at the onset of diabetes (Fig. 1). The mRNA levels for FAS, ACC, and ME also decreased compared to control animals (Fig. 1). As the animals became highly diabetic, the mRNA level decreased below that observed for animals at the onset of diabetes. Feeding the higher polyunsaturated fat diet reduced the level of lipogenic enzymes in both control and diabetic animals.

TABLE 2
Effect of Diet and Diabetes on the Body Weight, Liver Weight, and Serum Insulin of Control and Spontaneously Diabetic B/B Rats[a]

Group	Diet	Blood glucose (mg/dL)	Final body weight (g)	Final liver weight (g)	Serum insulin (mU/L)
Control	P/S = 1.0	84	404 ± 12.0[a]	14.2 ± 0.7[a]	82.0 ± 8.0[a]
	P/S = 0.25	84	384 ± 11.0[a]	14.0 ± 1.2[a]	75.0 ± 6.0[a]
Spontaneously diabetic	P/S = 1.0	100	303 ± 7.3[b]	11.1 ± 0.2[b]	76.0 ± 9.4[a]
	P/S = 0.25	100	311 ± 12.0[b]	11.0 ± 0.6[b]	68.0 ± 8.5[a]
Spontaneously diabetic	P/S = 1.0	400	311 ± 14.0[b]	9.1 ± 0.4[b]	26.0 ± 6.5[b]
	P/S = 0.25	400	300 ± 12.0[b]	10.5 ± 1.4[b]	30.0 ± 3.4[b]

[a]Weanling rats were fed a semipurified diet either high or low in polyunsaturated fatty acids as explained in the Materials and Methods section. At 50 d postpartum, blood glucose level was checked on alternate days. Values are group means ± SE, n = 10. Treatments without a common superscript are significantly different ($P < 0.05$). See Table 1 for abbreviation.

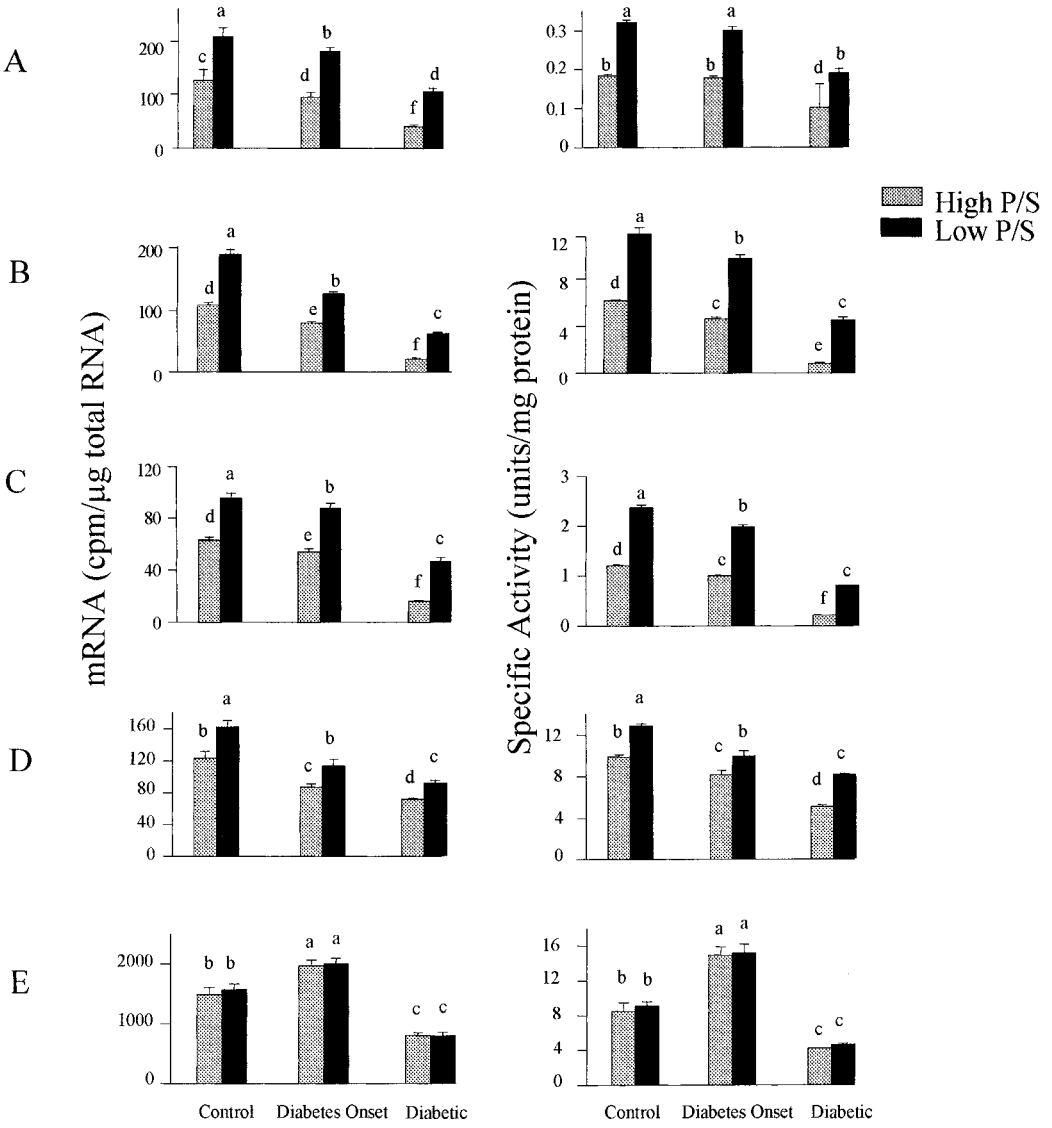

FIG. 1. Effect of diet and diabetes in B/B rats on the mRNA level and specific activity of: (A) acetyl-CoA carboxylase; (B) fatty acid synthase; (C) malic enzyme; (D) pyruvate kinase; (E) phosphoenolpyruvate carboxykinase. P/S, polyunsaturated to saturated ratio. Treatments without a common superscript are significantly different ($P > 0.05$).

Effect of diet and diabetes on enzymes of glucose metabolism. L-type pyruvate kinase catalyzes conversion of phosphoenolpyruvate to pyruvate, whereas PEPCK is part of a potentially futile cycle involved in interconversion of pyruvate and phosphoenolpyruvate, playing a central role in the regulation of glucose synthesis. The mRNA level for pyruvate kinase decreased at the onset of diabetes compared to control animals. A further decrease in specific activity occurred as animals became highly diabetic compared to animals at the onset of diabetes (Fig. 1). PEPCK mRNA level and enzyme specific activity also decreased as the animals became highly diabetic compared to control animals (Fig. 1). However, the mRNA level and specific activity were significantly higher at the onset of diabetes compared to control animals. Feeding the high polyunsaturated fat diet reduced the level of pyruvate kinase but not phosphoenol carboxykinase in both control and diabetic animals.

DISCUSSION

Diverse physiological conditions that modify rates of FAS are accompanied by corresponding changes in other lipogenic enzymes. In uncontrolled, treated diabetes, fatty acids reach extremely high levels and may play a role in causing an insulin-resistant state. Our results with B/B rats agree with previous observations, suggesting that lack of insulin reduces ACC, FAS, and ME mRNA and activity (2,4). Witters and Kemp (22) proposed an insulin-modulated cascade of action initiated through inhibition of 5′-AMP activated protein kinase, leading to activation of ACC. For FAS, insulin primarily stimulates transcription of the FAS gene as the effect of insulin on mRNA level is abolished by treatment with cycloheximide (2). For pyruvate kinase activity, mRNA level decreased with onset of diabetes, suggesting that change in con-

centration of L-type pyruvate kinase protein is due to changes in the rate of mRNA synthesis.

The increase in rate of transcription caused by insulin is by a mechanism requiring ongoing protein synthesis. Noguchi *et al.* (23) showed that 5′-flanking region up to 3 kb of the L-type pyruvate kinase gene contained all *cis*-acting elements necessary for tissue-specific expression of L-type pyruvate kinase and its stimulation by diet and insulin. These elements alone were not sufficient for dietary and hormonal regulation of L-type pyruvate kinase (24).

In the present investigation, PEPCK activity and mRNA level increased significantly at the onset of diabetes, and then decreased as the animals became highly diabetic. The reason for this observation is not apparent.

Feeding a diet containing a higher PUFA content suppressed gene expression of the lipogenic enzymes studied. Dietary polyunsaturated fats are known to be potent inhibitors of hepatic fatty acid and triglyceride synthesis. For protein S14, which behaves like FAS, Jump *et al.* (12) showed that feeding a menhaden oil diet to rats rapidly attenuates hepatic S14 gene transcription. Deletion analysis of transfected S14 CAT fusion gene indicates that *cis*-linked PUFA response elements were localized to a region within the S14 proximal promoter (at –80 to –220 Lp). Blake and Clarke (9) also showed that ingestion of a diet containing fats rich in n-6 and n-3 fatty acids results in a very low level of FAS mRNA; however, the inhibitory action of dietary PUFA did not extend to PEPCK genes as observed in the present investigation. Inability of dietary PUFA to influence PEPCK expression is not consistent with the notion that dietary PUFA may enhance gluconeogenesis. The PEPCK gene contains a cAMP response element that is very sensitive to changes in intracellular cAMP concentrations (24). The failure of PUFA to influence PEPCK gene expression perhaps suggests that suppression of FAS, ME, ACC, and PK gene transcription is not mediated by cAMP. Specific nuclear proteins involved in regulating genes coding for lipogenic enzymes may bind PUFA or their metabolites, and such lipid-binding may directly govern the rate of gene transcription (11). Recently we showed that physiological levels of insulin at the nucleus causes phosphorylation of a nuclear protein to enhance its binding to the promoter region of the ME to simulate gene expression (25). The interaction of this binding with PUFA remains to be determined.

Dietary fatty acids also may be rapidly incorporated into nuclear fatty acid pools and thus may be involved in nuclear regulation of induction of the lipogenic enzyme. In the present study, we observed suppression of enzymes for lipogenesis and glucose metabolism by PUFA, suggesting that the effect of PUFA is through a direct effect at the level of gene expression. The notion that a more saturated dietary fat will tend to normalize the changes in lipogenic capacity that occurs with the development of diabetes is clearly worthy of further research.

ACKNOWLEDGMENT

The authors are grateful for the financial support of the Natural Sciences and Engineering Research Council of Canada.

REFERENCES

1. Back, D.W., Wilson, S.B., Morris, S.M, and Goodridge, A.G. (1986) Hormonal Regulation of Lipogenic Enzymes in Chick Embryo Hepatocytes in Culture, *J. Biol. Chem. 261*, 12555–12561.
2. Katsurada, A., Iritani, N., Fakuda, H., Matsurada, Y., Nishimoto, N., Noguchi, T., and Tanaka, T. (1990) Effects of Nutrients and Hormones on Transcriptional and Post Transcriptional Regulation of Acetyl CoA Carboxylase in Rat Liver, *Eur. J. Biochem. 190*, 435–441.
3. McHugh, K.M., and Drake, R.L. (1989) Insulin-Mediated Regulation of Epididymal Fat Pad Malic Enzyme, *Mol. Cell. Endocrinol. 62*, 227–233.
4. Pape, M.E., Lopez-Casillas, F., and Kim, K.H. (1988) Physiological Regulation of Acetyl CoA Carboxylase Gene Expression: Effects of Diet, Diabetes, and Lactation on Acetyl CoA Carboxylase mRNA, *Arch. Biochem. Biophys. 267*, 104–109.
5. Warnotte, C., Gilon, P., Nenquin, M., and Henquin, J. (1994) Mechanisms of the Stimulation of Insulin Release by Saturated Fatty Acids. A Study of Palmitate Effects in Mouse β-Cells, *Diabetes 43*, 703–711.
6. Clandinin, M.T., Cheema, S., Field, C.J., Garg, M.L., Venkatraman, J., and Clandinin, T.R. (1991) Dietary Fat: Exogenous Determination of Membrane Structure and Cell Function, *FASEB J. 5*, 2761–2769.
7. Clandinin, M.T., Jumpsen, J., and Suh, M. (1994) Relationship Between Fatty Acid Accretion, Membrane Composition and Biologic Functions (rev.), *J. Pediatrics 125*, S25–S32.
8. Field, C.J., Ryan, E.A., Thomson, A.B.R., and Clandinin, M.T. (1988) Dietary Fat and the Diabetic State Alter Insulin Binding and the Fatty Acyl Composition of the Adipocyte Plasma Membrane, *Biochem. J. 253*, 417–424.
9. Blake, W.L., and Clarke, S.D. (1990) Suppression of Rat Hepatic Fatty Acid Synthase and S14 Gene Transcription by Dietary Polyunsaturated Fat, *J. Nutr. 120*, 1727–1729.
10. Clarke, S.D., Armstrong, M.K., and Jump, D.B. (1990) Dietary Polyunsaturated Fats Uniquely Suppress Rat Liver Fatty Acid Synthase and S14 mRNA Content, *J. Nutr. 120*, 225–231.
11. Clarke, S.D., and Jump, D.B. (1993) Regulation of Gene Transcription by Polyunsaturated Fatty Acids, *Prog. Lipid Res. 32*, 139–149.
12. Jump, D.B., Clarke, S.D., MacDougald, O., and Thelen, A. (1993) Polyunsaturated Fatty Acids Inhibit S14 Gene Transcription in Rat Liver and Cultured Hepatocytes, *Proc. Natl. Acad. Sci. USA 90*, 8454–8458.
13. Clarke, S.D., Armstrong, M.K., and Jump, D.B. (1990) Nutritional Control of Rat Liver Fatty Acid Synthase and S14 mRNA Abundance, *J. Nutr. 120*, 218–224.
14. Marliss, E.B., Nakhooda, A.F., Poussier, P., and Sima, A.A.F (1982) The Diabetic Syndrome of the "BB" Wistar Rat: Possible Relevance to Type 1 (insulin-dependent) Diabetes in Man, *Diabetologia 22*, 225–232.
15. Like, A.A., Appel, M.C., and Rossini, A.A. (1982) Autoantibodies in the BB/W Rat, *Diabetes 31*, 816–820.
16. Chomczynski, P., and Sacchi, N. (1987) Single-Step Method of RNA Isolation by Acid Guanidinium Thiocyanate–Phenol–Chloroform Extraction, *Anal. Biochem. 162*, 156–159.
17. Nepokroeff, C.M., Lakshman, M.R., and Porter, J.W. (1975) Fatty Acid Synthase from Rat Liver, *Methods Enzymol. 35*, 37–44.
18. Hsu, R.Y., and Lardy, H.A. (1969) L-Malate:NADP Oxidoreductase (decarboxylating), *Methods Enzymol. 13*, 230–235.
19. Inoue, H., and Lowenstein, J.M. (1975) Acetyl Coenzyme A

Carboxylase from Rat Liver, EC 6.4.1.2 Acetyl-CoA: Carbon Dioxide Ligase (ADP), *Methods Enzymol. 35*, 3–11.
20. Imamura, K., and Tanaka, T. (1982) Pyruvate Kinase Isozymes from Rat, *Methods Enzymol. 90*, 150–165.
21. Petrescu, I., Brojan, O., Saied, M., Barzu, O., Schmidt, F., and Kuhnle, H.F. (1979) Determination of Phosphoenol Pyruvate Carboxykinase Activity with Deoxyguanosine 5′-Diphosphate as Nucleotide Substrate, *Anal. Biochem. 96*, 279–281.
22. Witters, L.A., and Kemp, B.E. (1992) Insulin Activation of Acetyl CoA Carboxylase Accompanied by Inhibition of the 5′-AMP-Activated Protein Kinase, *J. Biol. Chem. 267*, 2864–2867.
23. Noguchi, T., Inoue, H., and Tanaka, T. (1985) The MI and M2 Type Isozymes of Rat Pyruvate Kinase Are Produced from the Same Gene by Alternative RNA Splicing, *J. Biol. Chem. 260*, 14393–14397.
24. Lamers, W.H., Hanson, R.W., and Meisner, H.M. (1982) cAMP Stimulates Transcription of the Gene for Cytosolic Phosphoenolpyruvate Carboxykinase in Rat Liver Nuclei, *Proc. Natl. Acad. Sci. USA 79*, 5137–5141.
25. Gletsu, N., Dixon, W., and Clandinin, M.T. (1999) Insulin Receptor at the Nucleus Following a Glucose Meal Induces Dephosphorylation of a 30 KDa Transcription Factor and a Concomitant Increase in Malic Enzyme Gene Expression, *J. Nutr. 129*, 2154–2161.

[Received November 17, 1999, and in final revised form February 14, 2000; revision accepted March 20, 2000]

Effects of Dietary Phenolic Compounds on Tocopherol, Cholesterol, and Fatty Acids in Rats

Afaf Kamal-Eldin[a,*], Jan Frank[a], Alexander Razdan[a], Siv Tengblad[b], Samar Basu[b], and Bengt Vessby[b]

[a]Department of Food Science, Swedish University of Agricultural Sciences, S-750 07 Uppsala, Sweden, and [b]Department of Public Health and Caring Sciences/Geriatrics, University of Uppsala, 751 25 Uppsala, Sweden

ABSTRACT: The effects of the phenolic compounds butylated hydroxytoluene (BHT), sesamin (S), curcumin (CU), and ferulic acid (FA) on plasma, liver, and lung concentrations of α- and γ-tocopherols (T), on plasma and liver cholesterol, and on the fatty acid composition of liver lipids were studied in male Sprague-Dawley rats. Test compounds were given to rats *ad libitum* for 4 wk at 4 g/kg diet, in a diet low but adequate in vitamin E (36 mg/kg of γ-T and 25 mg/kg of α-T) and containing 2 g/kg of cholesterol. BHT significantly reduced feed intake ($P < 0.05$) and body weight and increased feed conversion ratio; S and BHT caused a significant enlargement of the liver ($P < 0.001$), whereas CU and FA did not affect any of these parameters. The amount of liver lipids was significantly lowered by BHT ($P < 0.01$) while the other substances reduced liver lipid concentrations but not significantly. Regarding effects on tocopherol levels, (i) feeding of BHT resulted in a significant elevation ($P < 0.001$) of α-T in plasma, liver, and lung, while γ-T values remained unchanged; (ii) rats provided with the S diet had substantially higher γ-T levels ($P < 0.001$) in plasma, liver, and lung, whereas α-T levels were not affected; (iii) administration of CU raised the concentration of α-T in the lung ($P < 0.01$) but did not affect the plasma or liver values of any of the tocopherols; and (iv) FA had no effect on the levels of either homolog in the plasma, liver, or lung. The level of an unknown substance in the liver was significantly reduced by dietary BHT ($P < 0.001$). BHT was the only compound that tended to increase total cholesterol (TC) in plasma, due to an elevation of cholesterol in the very low density lipoprotein + low density lipoprotein (VLDL + LDL) fraction. S and FA tended to lower plasma total and VLDL + LDL cholesterol concentrations, but the effect for CU was statistically significant ($P < 0.05$). FA increased plasma high density lipoprotein cholesterol while the other compounds reduced it numerically, but not significantly. BHT, CU, and S reduced cholesterol levels in the liver TC ($P < 0.001$) and percentages of TC in liver lipids ($P < 0.05$). With regard to the fatty acid composition of liver lipids, S increased the n-6/n-3 and the 18:3/20:5 polyunsaturated fatty acids (PUFA) ratios, and BHT lowered total monounsaturated fatty acids and increased total PUFA (n-6 + n-3). The effects of CU and FA on fatty acids were not highly significant. These results suggest some *in vivo* interactions between these phenolic compounds and tocopherols that may increase the bioavailability of vitamin E and decrease cholesterol in rats.

Paper no. L8310 in *Lipids 35*, 427–435 (April 2000).

Currently, much research interest is focused on the beneficial effects of bioactive phytochemicals present at a micro level in our daily diet, especially the heterogeneous group of phenolic antioxidants. Phenolic compounds are common constituents of our diet and are abundant in grains, vegetables, fruits, seeds, nuts, and processed foods thereof (1,2). As early as the 1930s, the Nobel Laureate Szent-Györgyi and co-workers reported that a number of bioactive compounds from fruits and vegetables could heal scorbutic pigs and gave a vitamin P (for permeability) status for flavonoids (3,4). Phenolic compounds in red wine were suggested as one factor responsible for the "French paradox," the phenomenon of a lower incidence of cardiovascular diseases in France compared to matching European populations with similar exposure to risk factors (5,6). Besides cardiovascular diseases (7,8), phenolic compounds are believed to contribute positively to prevention of other degenerative malfunctions such as aging (9) and cancer (1,10,11). The mechanisms behind the different beneficial effects of dietary phenolic compounds are not fully elucidated, but these compounds are known to act as antioxidants (12,13), hypocholesterolemic (14,15) and enzyme-modulating agents (16–18) as well as phytohormones (19).

Research strongly indicates that protection against degenerative diseases cannot be attributed to a single dietary factor, such as vitamin E (e.g., 20,21), but that a wide range of environmental, dietary, and life-style factors determine our resistance or vulnerability to such diseases. On the dietary level, protection seems to require the right balance of a multitude of phytoprotectants including essential n-6 and n-3 fatty acids, vitamins, antioxidants, folates, and dietary fiber components (e.g., 22–24). Studies on interactive mechanisms of protection are therefore highly warranted. For example, synergistic

To whom correspondence should be addressed at Department of Food Science, SLU, Box 7051, 750 07 Uppsala, Sweden.
E-mail: Afaf.Kamal-Eldin@lmv.slu.se

Abbreviations: BHT, butylated hydroxytoluene; CU, curcumin; FA, ferulic acid; GLM, general linear model; HDL, high density lipoprotein; HPLC, high-performance liquid chromatography; LDL, low density lipoprotein; PUFA, polyunsaturated fatty acid; S, sesamin; T, tocopherol; TC, total cholesterol; TMS, trimethylsilyl; TTP, tocopherol transfer protein; VLDL, very low density lipoprotein.

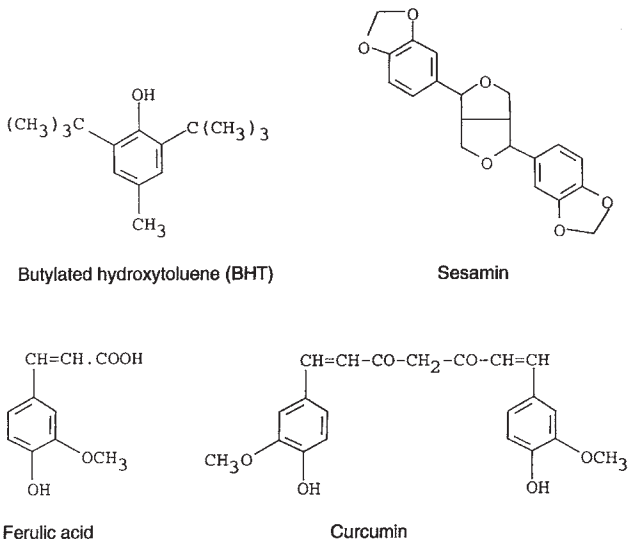

SCHEME 1

TABLE 1
Composition of the Basal Diet[a]

Ingredient	g/kg
Maize starch	528
Casein (vitamin-free)	200
Rapeseed oil[b]	100
Sucrose	80
Cellulose powder	40
Mineral and trace element premix[c]	40
Vitamin premix (vitamin E-free)[c]	10
Cholesterol[d]	2

[a]Antioxidants were added to the experimental diets at a concentration of 4 g/kg.
[b]All vitamin E in the diet originated from the rapeseed oil. Tocopherol and tocotrienol concentrations were determined according to IUPAC 2.432 and were as follows: α-tocopherol 252 ppm, γ-tocopherol 361 ppm, δ-tocopherol 9 ppm; α-, γ-, and δ-tocotrienol were present at concentrations less than 5 ppm. The fatty acid composition of the rapeseed oil, determined according to IUPAC 2.302, was 16:0 (4.3%), 16:1 (0.1%), 17:1 (0.2%), 18:0 (1.6%), 18:1 (60.2%), 18:2 (20.1%), 18:3 (10.2%), 20:0 (0.6%), 20:1 (1.5%), 20:2 (0.1%), 22:0 (0.4%), 22:1 (0.5%), 24:0 (0.1%), and 24:1 (0.2%).
[c]The mineral and trace element premix and the vitamin premix were formulated to meet the nutritional requirements of laboratory rats with the exception of vitamin E and were purchased from Lactam (Lidköpingh, Sweden).
[d]The cholesterol was dissolved in ethanol and sprayed onto the diet.

interactions between tocopherols (T) and dietary phenolic antioxidants, such as sesamin (S) and caffeic acid, have been shown to lead to an increase in the biological activity of T and whole-body resistance to oxidation (25–28).

Within the concept of interactive antioxidant mechanisms, this work aimed to test the effect of selected phenolic compounds , *viz.*, butylated hydroxytoluene (BHT), S, curcumin (CU) and ferulic acid (FA) (Scheme 1), on T and cholesterol levels in rat plasma and tissues. The effects of these compounds on the fatty acid composition of the liver lipids were also studied.

MATERIALS AND METHODS

Experimental animals and diets. The animals used in this study were 50 male, 21-d old Sprague-Dawley rats with a mean body weight of 57 g purchased from B&K Universal AB (Sollentuna, Sweden). They were housed individually in Macrolon IV cages with mesh bottoms (Ehret GmbH & Co., Emmendingen, Germany) in a conditioned room at 25°C and 60% relative humidity with a cycle of 12 h light (0700 to 1900) and 12 h darkness. Each cage was equipped with a water bottle with metal lid, a cup for feed administration attached to a stainless steel plate to avoid overthrowing and spillage, a black plastic tube which the rats used for resting and hiding in, and a table-tennis ball to play with. This experiment was carried out according to the guidelines of and approved by the Ethical Committee for Animal Experiments in the Uppsala region.

The composition of the basal diet is shown in Table 1. Rapeseed oil was provided by Karlshamns AB (Karlshamn, Sweden), and cholesterol was purchased from Sigma Chemical Co. (St. Louis, MO). The phenolics, added to the basal diet at concentrations of 4 g/kg, were obtained from the following sources: S (a mixture of equal amounts of sesamin and episesamin, <0.1 μg/g γ-tocopherol by high-performance liquid chromatography (HPLC) was a gift from Takemoto Oil & Fat Co. Ltd. (Gamagori Aichi, Japan), BHT and FA were purchased from Sigma Chemical Co. while curcumin (CU) was purchased from E. Merck (Darmstadt, Germany). The rats had free access to water and feed throughout the whole experiment.

Study design and sample collection. The 50 animals were divided into five groups of 10 rats of about the same average body weight and fed the experimental diets *ad libitum* for 4 wk. Feed intakes were monitored every day during feeding, and body weights were determined weekly. After the feeding period, the animals were fasted for 12 h before intraperitoneal injection of an overdose of sodium pentobarbital and killed by exsanguination. Blood samples were taken from the *vena cava* and collected in test tubes containing EDTA. After centrifugation (3000 rpm, 10 min), blood plasma was transferred to a test tube with screw cap and stored at –20°C until analyzed. Liver and lung tissues were excised, weighed, and stored in isopropanol at –80°C.

Extraction of tissue lipids. For the extraction of plasma T, blood plasma (500 μL) was mixed with ethanol containing 0.005% BHT (500 μL) and extracted with hexane (2 mL) after manually shaking for 3 min. Liver and lung lipids were extracted according to the method developed by Hara and Radin (29). The tissues, which were collected in isopropanol, were homogenized in 100 mL hexane/isopropanol after adjusting the ratio of these solvents to 3:2 (vol/vol) employing a Diax 600 homogenizer (Heidolph Elektro GmbH & Co. Kelheim, Germany), centrifuged (5000 rpm, 10 min, 0°C), and the lipid extract was collected. The extraction was repeated twice and the extracts were pooled and mixed with 150 mL aqueous sodium sulfate. After 30 min the lower layer was discarded, and the upper layer was filtered after drying with anhydrous sodium sulfate. The solvent was evaporated on a ro-

tary vacuum evaporator at 30°C and the lipids were dissolved in 10 mL chloroform and stored at –20°C until analyzed.

Tocopherol analyses. Plasma T were analyzed by HPLC using a Merck-Hitachi system (pump L-6000, autosampler AS-4000, detector D-2500). The separation of plasma T was performed on a LiChrospher 100 NH_2 column (250 × 4 mm, E. Merck) using isooctane/methyl *tert*-butylether/methanol (75:25:0.035, by vol) as the mobile phase. Because the chromatograms of liver T analyzed by this method contained an unknown substance that interfered with the determination of γ-T, liver and lung T were analyzed on a LiChrosorb Diol 5 μm column (250 × 4 mm, E. Merck) using hexane/1,4-dioxane (96:4, vol/vol) as mobile phase, in an HPLC system consisting of an LKB 2157 autosampler, LKB 2248 pump (Pharmacia LKB Biotechnology AB, Bromma, Sweden) and a Fluor LC 304 fluorescence detector (Linear Instruments, Reno, NV). In both cases the detectors were set to excitation wavelengths of 294 nm and emission wavelengths of 326 nm. Peaks were recorded and integrated using the chromatography software JCL 6000 (Jones Chromatography, Mid-Glamorgan, United Kingdom). The concentrations of α- and γ-T were quantified using authentic T as external standards (T standards, Art. No. 15496 from E. Merck).

Cholesterol analyses. Cholesterol was quantified in the plasma and in the isolated lipoprotein fractions according to the IL test cholesterol Trinder's method 181618-80 and IL test enzymatic-colorimetric method 181709-00 employing a Monarch apparatus (Instrumentation Laboratories, Lexington, MA). Serum high density lipoproteins (HDL) were separated and quantified as reported by Seigler and Wu (30) using sodium phosphotungstate and magnesium chloride with the modification of leaving the sample to precipitate at 4°C for 20 min. Very low density lipoprotein (VLDL) + low density lipoprotein (LDL) cholesterol levels were calculated by subtraction of HDL-cholesterol values from those for total cholesterol (TC).

For cholesterol analyses in the liver and lung tissues, cholestane (Sigma) was added as an internal standard to a part of the lipid extracts in a glass-stoppered test tube, and solvents were removed under nitrogen gas. KOH in ethanol (1 mL, 2 M) was added for saponification in a boiling waterbath with intermittent shaking for 10 min. After cooling to room temperature, water (1 mL) and hexane (2 mL) were added and the test tubes were shaken and allowed to stand until the two layers separated. The hexane layer was transferred to another glass tube and dried under a stream of nitrogen. Trimethylsilyl (TMS) ether derivatives of cholesterol were prepared by incubation at 60°C for 45 min with Tri-Sil reagent (Reagent No. 48999 from Pierce Chemical Co., Rockford, IL). Thereafter, the solvent was evaporated under nitrogen, and the TMS ether derivatives were dissolved in hexane, shaken and centrifuged at 3000 rpm for 3 min. TMS ether derivatives of cholesterol were analyzed on a Varian 3700 gas chromatograph (Varian, Walnut Creek, CA) equipped with a nonpolar fused-silica BP5 column (25 m × 0.33 mm i.d., 0.25 μm film, SGE Scientific Pty. Ltd., Ringwood, Victoria, Australia). Helium was used as carrier gas at an inlet pressure of 16 psi and a flow rate of 25 mL/min. The injector temperature was set to 250°C, the oven temperature to 280°C, and the detector temperature to 300°C.

Fatty acid analyses. The fatty acid composition of the liver lipids was determined by gas chromatography after methylation with acidic methanol (85°C, 2 h). The relative percentages of fatty acid methyl esters from 14:0 to 22:6 were determined after separation on a 25-m NB-351 capillary column (0.32 mm i.d., 0.2 μm film thickness, Nordion, Ltd., Helsinki, Finland) by using flame ionization for detection and quantification.

Statistical analyses. Statistical analysis of the registered variables was performed by an analysis of variance procedure, the general linear model (GLM) supported by the Statistical Analysis System (31). Least significant differences from the *t*-test function of the SAS GLM procedure were used to make statistical comparisons.

RESULTS

Table shows parameters related to animal performance during the experimental time and the body and liver weights at sacrifice. Feed intake and body weights were similar in all groups except for the BHT group where both parameters were significantly reduced ($P < 0.05$). The conversion of feed into body weight, expressed as feed conversion ratio (feed intake/weight gain), was not affected by S, CU, or FA intake but was significantly impaired in rats fed BHT ($P < 0.001$). Total liver weight

TABLE 2
Animal Performance and Body and Liver Weights[a]

Diet	Control (n = 10)	Sesamin (n = 10)	BHT (n = 10)	Curcumin (n = 10)	Ferulic acid (n = 10)	P less than
Feed intake (g/4 wk)	337 ± 3.4[a]	335 ± 5.8[a]	325 ± 1.8[b]	342 ± 1.7[a]	340 ± 2.1[a]	0.05
Feed conversion ratio[b]	1.8 ± 0.04[a]	1.8 ± 0.03[a]	2.0 ± 0.01[b]	1.8 ± 0.03[a]	1.8 ± 0.02[a]	0.001
Body weight (g)	248.5 ± 3.68[a]	246.0 ± 5.88[a]	220.0 ± 1.34[b]	252.7 ± 3.49[a]	251.4 ± 2.44[a]	0.001
Liver weight (g)	12.4 ± 0.40[a,b]	15.3 ± 0.54[c]	13.5 ± 0.29[b]	12.2 ± 0.37[a,*]	12.4 ± 0.26[a,b]	0.05
Relative liver weight (g/100 g BW)	4.94 ± 0.13[a]	6.03 ± 0.08[b]	5.96 ± 0.10[b]	4.70 ± 0.11[a,*]	4.77 ± 0.10[a]	0.001

[a]Values represent means ± SEM. Values within each row not sharing a common superscript roman letter are statistically different at P. *n = 9, because of one missing value for liver weight.
[b]Feed conversion ratio = feed intake/weight gain. Abbreviations: BHT, butylated hydroxy toluene; BW, body weight.

TABLE 3
Effect of Phenolic Compounds on Tocopherol Concentrations in Rat Plasma, Liver, and Lungs[a]

Diet	Control	Sesamin	BHT	Curcumin	Ferulic acid	*P* less than
Plasma (μg/mL)	*n* = 10	*n* = 10	*n* = 10	*n* = 10	*n* = 10	
α-T	1.5 ± 0.25[a]	1.3 ± 0.08[a]	3.8 ± 0.35[b]	1.7 ± 0.09[a]	1.2 ± 0.07[a]	0.001
γ-T	0.2 ± 0.03[a]	2.0 ± 0.15[b]	0.1 ± 0.03[a]	0.2 ± 0.03[a]	0.1 ± 0.01[a]	0.001
α-T + γ-T	1.7 ± 0.25[a]	3.3 ± 0.19[b]	3.9 ± 0.36[b]	1.9 ± 0.12[a]	1.3 ± 0.08[a]	0.001
γ-T/α-T	0.12 ± 0.02[a]	1.58 ± 0.11[b]	0.03 ± 0.01[a]	0.10 ± 0.02[a]	0.07 ± 0.01[a]	0.001
Liver (μg/g)	*n* = 9	*n* = 9	*n* = 8	*n* = 8	*n* = 9	
α-T	3.1 ± 0.50[a]	3.1 ± 0.37[a]	6.8 ± 1.21[b]	3.8 ± 0.49[a]	3.2 ± 0.31[a]	0.001
γ-T	0.6 ± 0.10[a]	8.7 ± 1.05[b]	0.5 ± 0.05[a]	0.6 ± 0.11[a]	0.4 ± 0.04[a]	0.001
α-T + γ-T	3.7 ± 0.58[a]	11.8 ± 1.39[b]	7.3 ± 1.21[c]	4.4 ± 0.56[a]	3.6 ± 0.34[a]	0.001
γ-T/α-T	0.19 ± 0.03[a]	2.82 ± 0.16[b]	0.09 ± 0.01[a]	0.17 ± 0.03[a]	0.13 ± 0.01[a]	0.001
US[b]	14.2 ± 2.30a	12.3 ± 1.86[a]	1.5 ± 0.41[b]	17.6 ± 2.94a	12.9 ± 1.89a	0.001
Lung (μg/g)	*n* = 8	*n* = 6	*n* = 7	*n* = 7	*n* = 5	
α-T	6.2 ± 0.50[a]	8.1 ± 0.58[a,b]	22.8 ± 1.09[c]	9.2 ± 0.47[b]	6.0 ± 0.59[a]	0.01
γ-T	1.6 ± 0.20[a]	26.5 ± 1.29[b]	1.8 ± 0.22[a]	2.7 ± 0.36[a]	1.2 ± 0.17[a]	0.001
α-T + γ-T	7.8 ± 0.66[a]	34.6 ± 1.67[b]	24.6 ± 1.29[c]	11.9 ± 0.78[d]	7.2 ± 0.75[a]	0.001
γ-T/α-T	0.25 ± 0.02[a,b]	3.30 ± 0.18[c]	0.08 ± 0.01[a]	0.29 ± 0.03[b]	0.20 ± 0.01[a,b]	0.05

[a]*n* = number of observations; values represent means ± SEM. Values within each row not sharing a common superscript roman letter are statistically different at *P*.
[b]The level of this unknown substance (US) was calculated as relative peak area to that of α-tocopherol (α-T), i.e., using the same response factor as α-T, γ-tocopherol; for other abbreviation see Table 2.

was increased significantly only by S ($P < 0.001$). When corrected for body weight, BHT-feeding also resulted in a significant enlargement of the liver ($P < 0.001$). The liver lipid content was significantly lower in rats receiving the BHT diet ($P < 0.01$) and slightly lower in all other groups.

Table 3 shows the effects of the four phenolic compounds on the absolute and relative levels of α-T and γ-T in rat plasma, liver and lung. Results showed that S-feeding did not alter the α-T level but caused more than a 10-fold increase in γ-T levels in plasma, liver, and lungs ($P < 0.001$). The γ-T/α-T-ratio, normally about 0.1, ranged from 1.6 in the plasma to 3.3 in the lung of the S-fed rats. Feeding of BHT to rats led to more than a twofold increase in α-T concentrations in plasma, liver, and lung ($P < 0.001$) but changed neither the level of γ-T nor the γ-T/α-T ratio. CU feeding affected neither plasma and liver α-T nor γ-T, but significantly elevated α-T ($P < 0.01$) levels in the lung. No effects on α-T and γ-T levels or on γ-T/α-T ratios were observed in plasma, liver, and lung of rats fed FA.

During the determination of T in the liver lipids, an unknown substance (US; not present in plasma and lung) eluted immediately before γ-T (Fig. 2). This US was not fully separated from γ-T on the amino column used for the analysis of plasma T and, therefore, a diol column was employed for the analysis of T in liver and lung (see Materials and Methods section). The level of this unknown substance expressed as a relative value of the peak area of α-T (Table 3) in the liver

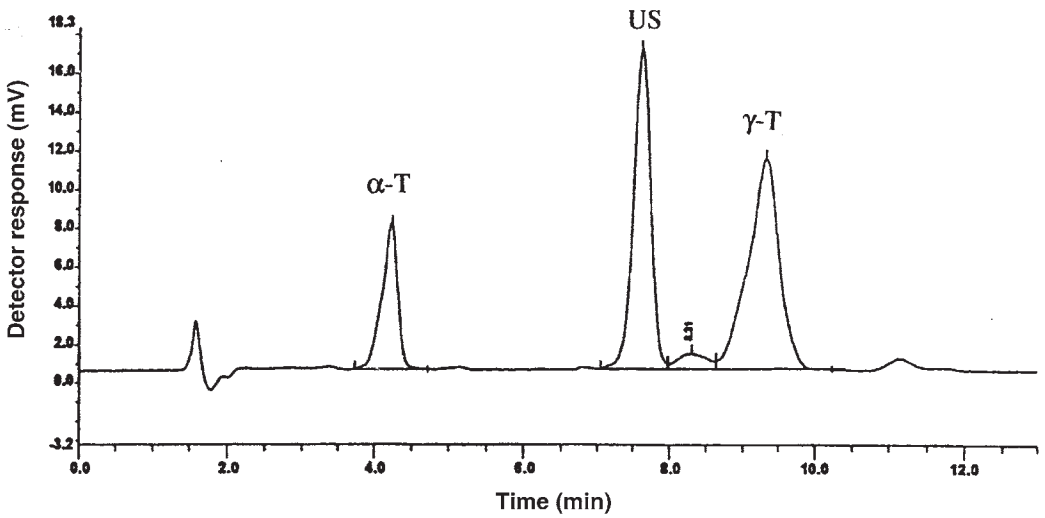

FIG. 1. Chromatogram from high-performance liquid chromatographic-analyses of a liver lipid extract, employing a diol silica column to separate the unknown substance (US) from γ-tocopherol (γ-T) and α-tocopherol (α-T).

TABLE 4
Effect of Phenolic Compounds on Plasma Cholesterol (mg/dL) and Liver Cholesterol and Total Lipids (mg/g fresh weight)[a]

Diet	Control	Sesamin	BHT	Curcumin	Ferulic acid	*P* less than
Plasma concentrations of cholesterol (mg/dL)						
	n = 10	*n* = 10	*n* = 10	*n* = 10	*n* = 10	
Total cholesterol (TC)	64.52 ± 4.77^{a,c}	55.40 ± 3.04^{b,c}	69.67 ± 4.44^{a}	51.61 ± 2.47^{b}	59.50 ± 3.31^{a,b}	0.05
HDL	38.12 ± 4.14^{a,b}	30.08 ± 2.08^{a}	35.76 ± 2.87^{a,b}	32.90 ± 2.32^{a,b}	39.94 ± 3.09^{b}	0.05
VLDL + LDL	26.41 ± 4.25^{a,b}	25.32 ± 2.74^{b}	33.91 ± 3.63^{a}	18.71 ± 1.16^{b}	19.56 ± 1.81^{b}	0.05
HDL/TC	0.59 ± 0.05^{a,b,c}	0.55 ± 0.03^{a,b}	0.52 ± 0.03^{a}	0.63 ± 0.03^{b,c}	0.67 ± 0.03^{c}	0.05
Liver concentrations of cholesterol and lipids (mg/g fresh weight)						
	n = 8	*n* = 8	*n* = 9	*n* = 6	*n* = 9	
TC	42.20 ± 4.42^{a}	25.76 ± 4.09^{b}	16.25 ± 2.02^{b}	26.75 ± 1.83^{b}	40.86 ± 4.20^{a}	0.001
Liver lipids	119.6 ± 8.03^{a}	108.9 ± 9.34^{a}	77.1 ± 4.53^{b}	114.9 ± 8.11^{a}	109.1 ± 6.74^{a}	0.01
%TC in liver lipids	36.9 ± 5.72^{a}	24.6 ± 4.22^{b}	21.1 ± 2.50^{b}	24.2 ± 2.83^{b}	38.3 ± 4.04^{a}	0.05

[a]Values within each row not sharing a common roman superscript letter are statistically different at indicated *P*-values. Abbreviations: HDL, high density lipoprotein; VLDL, very low density lipoprotein; LDL, low density lipoprotein; for other abbreviation see Table 2.

was not affected by S, FA, or CU but was significantly reduced by BHT ($P < 0.001$).

The results on the effect of phenolic compounds on the cholesterol levels in the plasma and liver are shown in Table 4. BHT numerically elevated plasma TC and VLDL + LDL cholesterols and lowered HDL but significantly lowered liver TC ($P < 0.001$), liver lipids ($P < 0.01$), and the percentage of TC in liver lipids ($P < 0.05$). S did not induce significant effects on plasma cholesterols but significantly lowered liver TC ($P < 0.01$) and percent TC in liver lipids ($P < 0.05$). CU significantly lowered plasma TC ($P < 0.05$) and hepatic TC ($P < 0.001$) and percent TC in liver lipids ($P < 0.05$) while only slightly lowering the values for HDL and VLDL + LDL cholesterol. FA did not cause significant effects on cholesterol levels in the blood or in the liver although it slightly lowered liver lipids, plasma TC, and VLDL + LDL concentrations and slightly elevated HDL cholesterol.

Table 5 shows results on the fatty acid composition of liver lipids. Generally CU and FA did not show significant effects but S and BHT did. S significantly increased the percentages of 18:3n-6, 20:3n-6, 20:4n-6 ($P < 0.001$). BHT, on the other hand, significantly decreased the percentage of 16:0 and the monounsaturated fatty acids ($P = 0.001$) and increased the percentages of 18:0 ($P < 0.001$) and of the polyunsaturated

TABLE 5
Effect of Phenolic Compounds on the Fatty Acid Composition of Liver Lipids[a]

Fatty acids	Control (*n* = 10)	Sesamin (*n* = 10)	BHT (*n* = 10)	Curcumin (*n* = 10)	Ferulic acid (*n* = 10)	*P* less than
Relative fatty acids (%)						
14:0	0.836^{a}	0.624^{b}	0.705^{b,c}	0.768^{a,c}	0.771^{a,c}	0.01
15:0	0.166^{a}	0.142^{b,c}	0.135^{b}	0.131^{b}	0.161^{a,c}	0.005
16:0	21.33^{a}	20.81^{a}	18.91^{b}	21.56^{a}	21.35^{a}	0.001
17:0	0.126^{a}	0.114^{b}	0.122^{a,b}	0.109^{b}	0.133^{a}	0.05
18:0	4.99^{a}	5.59^{a}	6.75^{b}	5.34^{a}	5.68^{a}	0.001
Total saturated	27.46^{a,b}	27.29^{a,b}	26.63^{b}	27.91^{a,b}	28.09^{a}	0.001
16:1n-9	0.876^{a}	1.67^{b}	1.31^{c}	0.863^{a}	0.811^{a}	0.001
16:1n-7	4.47^{a}	2.39^{b}	2.21^{b}	3.75^{c}	2.64^{a,c}	0.001
18:1	44.08^{a}	43.58^{a}	37.83^{b}	43.46^{a}	42.76^{a}	0.001
Total monounsaturated	49.31^{a}	47.64^{a}	41.35^{b}	48.08^{a}	47.82^{a}	0.001
18:2	11.59^{a}	12.37^{a}	14.94^{b}	11.99^{a}	11.39^{a}	0.001
18:3	0.163^{a}	0.275^{b}	0.32^{c}	0.179^{a}	0.178^{a}	0.001
20:3	0.379^{a}	0.545^{b}	0.527^{b}	0.322^{a}	0.398^{a}	0.001
20:4	4.68^{a}	5.97^{b}	6.73^{b}	5.09^{a}	5.55^{a}	0.001
Total n-6	16.82^{a}	19.16^{b,c}	22.52^{c}	17.58^{a,b}	17.51^{a,b}	0.001
18:3	2.23^{a}	1.89^{a}	2.75^{b}	2.27^{a}	1.99^{a}	0.005
20:5	0.840^{a,b}	0.612^{a}	1.11^{c}	0.726^{a,b}	0.858^{b}	0.005
22:5	0.702^{a}	0.773^{a}	1.41^{b}	0.678^{a}	0.727^{a}	0.001
22:6 (+ trace of 24:0)	2.63^{a}	2.63^{a}	4.23^{b}	2.76^{a}	3.00^{a}	0.001
Total n-3	3.78^{a}	3.28^{a}	5.27^{b}	3.67^{a}	3.58^{a}	0.001
Ratios of selected fatty acids						
n-6/n-3	4.58^{a}	6.09^{b}	4.52^{a}	4.95^{a}	4.99^{a}	0.005
20:3/20:4n-6	0.082^{a,b}	0.093^{a,c}	0.081^{b,c}	0.063^{b}	0.072^{b}	0.05
18:3/20:5n-3	2.66^{a,d}	3.55^{b,c}	2.66^{a,d}	3.26^{a,b}	2.42^{d}	0.05

[a]Values within each row not sharing a common superscript roman letter are statistically different at indicated *P*-values.

fatty acids (PUFA) 18:2, 18:3n-6, 20:3n-6, 20:4n-6 ($P < 0.001$) and 18:3n-3, 20:5n-3, and 22:5n-3 ($P < 0.005$). In addition to its effect on the fatty acid percentages, S also significantly increased the ratios of n-6/n-3 ($P < 0.005$) and 18:3n-3/20:5n-3 ($P < 0.05$).

DISCUSSION

This experiment was designed to investigate the effects of BHT, CU, FA, and S on T and cholesterol levels in rat plasma and tissues and on the fatty acid composition of the liver lipids. In order to attribute these effects to the different test compounds, the compounds were added at supra-physiological levels as compared to their expected daily intake. For example, Srinivasan and Satyanarayana (32) estimated an average daily intake of CU for Indian citizens in the range of 0.4–1.5 mg/kg body weight. For the synthetic phenolic antioxidant BHT, the average human daily consumption in Canada and the United States of America was estimated to be approximately 0.1–0.4 mg/kg body weight (33). Throughout this experiment, the average daily intake of these compounds was from 480–850 mg/kg body weight. To be able to compare their effects, we established the phenolic compounds as the only variables in the experimental diets.

Effect of phenolic compounds on rat performance and body and liver weights. Results from the study of the effect of the phenolic compounds on animal performance (Table 2) showed that only BHT led to a decrease in body weight. Both BHT and S induced a significant increase in liver weight relative to body weight in agreement with previous studies carried out with rats (15,27,33–39). Our results are, however, in contrast with Simán and Eriksson (39) who reported an accumulation of lipids in livers of rats fed a BHT diet. Liver enlargement in BHT-fed rats was previously attributed to an induction of detoxifying enzymes (33,34), an effect thought to play an important role in the anticarcinogenic action of phenolic antioxidants (33). Liver enlargement in rats fed S was previously reported but was not attributed to hypertrophy and was found not to disturb the "normal" function of the liver (15,35,36). In the present study, the liver lipid content was significantly lower in rats receiving the BHT diet ($P < 0.01$), in general agreement with previously published data (15,32,34,37,38,40,41).

Effect of phenolic compounds on α-T and γ-T levels. Results from this study showed that S-feeding caused a 10-fold increase in γ-T levels while BHT-feeding caused a two-fold increase in α-T levels in plasma, liver, and lungs (Table 3). The increase in γ-T levels in plasma, liver, and lungs of rats fed Sesamin is in general agreement with our previous results (26) and with those of Yamashita *et al.* (25,27) while the results with BHT are in contradiction with those of Simán and Eriksson (39) who found BHT to lower α-T levels in rat liver but to increase it in the adipose tissue of rats. Despite the fact that γ-T is the major T in the human diet (42,43), α-T is the predominant form of vitamin E in animal plasma and tissues, and its biological activity was estimated to be 10 times that of γ-T (44–46). A Tocopherol transfer protein (TTP) in the hepatocytic cytosol with a specific affinity for α-T (47–49) is considered responsible for the discrimination between the different E-homologs by a selective incorporation of α-T into nascent VLDL (50). γ-T and other forms of vitamin E which are discriminated during this process as well as excess α-T are metabolized and excreted *via* the bile (46,51) and urine (52–55). At the time a transfer-mechanism was saturated, excess α-T was found in the bile to the same extent as the other vitamers (46,50). The fact that the total T levels in plasma were increased by some phenolic compounds, represented by BHT and S, suggests that discrimination by the TTP may not be the only reason for the elimination of T and that other mechanisms might also be involved in vitamin E metabolism and retention.

Although a hypothesis implying that S-feeding in a diet low in α-T might improve the binding capacity of γ-T to the TTP was proposed (27), other possibilities cannot be excluded. Possible mechanisms may involve: (i) stimulatory or inhibitory effects on enzymes involved in the production of free radicals that consume T in the body, (ii) antioxidant interactions of dietary phenols and/or their metabolites with these free radicals, and/or (iii) stimulatory or inhibitory effects on the TTP.

Simán and Eriksson (39) attributed the α-T-decreasing effect to a cytochrome P_{450}-catalyzed formation of prooxidative compounds from BHT that lead to oxidative depletion of hepatic α-T stores. Lignans possessing the methylenedioxyphenyl function, such as S, are known to inhibit mixed function oxidases (56), suggesting that S might spare T by protecting them from radicals produced by the metabolism of lipids and other xenobiotics. Piperonyl butoxide, a synthetic methylenedioxy-phenyl compound, was shown to decrease the hepatic level and to increase the biliary output of α-T in the rat (57). These results, dissimilar to our findings with S, were attributed to increased integrity of the biliary microtubule system, which is disrupted by chemicals such as colchine and vinblastine (58). The reasons for variation in effects of S (this study), BHT (39), and piperonyl butoxide (57,58) on Tocopherol cannot be explained and require more knowledge about coupled metabolism of T and these phenolics. These anomalous effects coupled with the facts that CU did not affect plasma or liver concentrations of α-T or γ-T but significantly elevated α-T levels in the lungs, and that FA lacked effect on α-T and γ-T levels in plasma, liver, and lung show that different phenolic compounds behave differently as regards their effects on body T. It is also worth mentioning that caffeic acid was found to elevate α-T concentrations in plasma and plasma lipoproteins and to improve the antioxidant defense system in the rat (28). Further studies involving a multivariate design based on dose-dependent interactions between these phenolics and T are necessary for further insights into the mechanism of interaction.

Effect of phenolic compounds on cholesterol levels. In the present study (Table 4), BHT had no effect on plasma cholesterol but significantly lowered TC ($P < 0.001$), total lipids (*P*

< 0.01), and percentage of TC in lipids ($P < 0.05$) in the liver. Different results were reported by previous workers who had used very high doses of cholesterol; e.g. Yamamoto *et al.* (38) reported reduced plasma TC and elevated HDL but no changes in liver TC after feeding BHT to rats at a concentration of 0.2% for 4 wk and Takahashi and Hiraga (34) reported that BHT increased liver weight and liver TC and lowered the amount of liver lipids when fed to rats for 1 wk at a 1.2% level. The amount of BHT used in the latter experiment was approximately 150% of the oral LD_{50} reported for rats (59). Our results are comparable to those obtained using the rabbit as a model animal, which showed an increase in plasma TC, triacylglycerols, LDL, and VLDL as well as lower levels of cholesterol oxidation products and a reduced area of atherosclerotic lesions after BHT intake (60). A similar study using butylated hydroxyanisole also revealed an increase in serum TC accompanied by a decrease in liver cholesterol (61). BHT was also shown to lower the activity of lecithin-cholesterol-acyltransferase (62), the enzyme located in HDL that catalyzes the conversion of cholesterol to cholesterol esters, and which is essential for the formation of HDL. An impaired incorporation of cholesterol esters into nascent HDL and thus a lower rate of HDL formation may explain the reduced plasma HDL and elevated TC and VLDL + LDL concentrations observed in the present work. A decrease in the activity of acyl-CoA cholesterol acyltransferase in liver microsomes coupled with impaired reverse cholesterol transport from the peripheral tissues may explain the decrease in liver TC content (61). The elevation of VLDL + LDL and the reduction of HDL concentrations in blood plasma, caused by the oral intake of BHT, may not be true for the concentrations in which BHT is actually taken up by humans; the daily intake of BHT per kg body weight in humans appears to be about 1:1000 to 1:2500 of the concentrations administered to the rats throughout this experiment.

In this study, S lowered plasma values of TC and HDL and liver TC and percent cholesterol in liver lipids but did not affect VLDL + LDL, in agreement with previous results (15,35–37,63). Hirose *et al.* (15) showed that S feeding reduces both cholesterol absorption and synthesis due to a reduced activity of hydroxy methylglutaryl-CoA reductase in liver microsomes. In addition, the total activity of cholesterol 7α-hydroxylase was higher in S-fed rats, suggesting an enhanced cholesterol catabolism and, thereby, reduced liver cholesterol concentrations (15,36). Nakabayashi *et al.* (37) also showed that increasing α-T concentrations enhanced these hypocholesterolemic effects of S. Hirata *et al.* (63) showed that S reduces plasma concentrations of TC and LDL cholesterol in humans although less significantly.

CU significantly lowered both plasma and hepatic TC in conformity with previous publications (40,64). Furthermore, these studies showed an increase in fecal excretion of bile acids and free cholesterol when CU was included in the diet, suggesting that an enhanced requirement of cholesterol for synthesis of biliary juices and a reduced uptake of cholesterol from the intestines, due to a lower concentration of bile acids, causes the reduction in blood and tissue cholesterol levels.

FA feeding did not induce significant effects on cholesterol levels in the blood or in the liver. Feeding of rats with 75 mg% of FA in a 1% cholesterol diet for 7 wk was reported to cause a significant decrease in serum TC and VLDL + LDL and an increase in HDL cholesterol, but no effect on liver TC (65). These results show that phenolic compounds have different effects on cholesterol levels in the rat and that these effects vary with the type and the concentration of the phenolic compound in question.

Effect of phenolic compounds on fatty acid composition of liver lipids. Apart from their effects on T and cholesterol levels (*vide supra*), BHT and S also significantly influenced the fatty acid composition of the total liver lipids. In agreement with previous results (66), S increased the n-6/n-3 PUFA ratio by significantly elevating the percentages of the n-6 acids without affecting the n-3 acids. On the other hand, BHT did not affect the n-6/n-3 PUFA ratio since it increased the percentages of both n-6 and n-3 at the expense of the monounsaturated acids. S elevated the 20:3/20:4n-6 ratio slightly and the 18:3/20:5n-3 ratio significantly, supporting the previous findings on its specific inhibition of Δ^5-desaturase (67). The effect of S on the fatty acid composition of different tissues was found to differ slightly depending on the type of dietary fatty acids.

With increased interest in dietary phenolic compounds in cereals, fruits, and vegetables as protective agents against coronary heart disease and cancer (23,68–70), results obtained in the present investigation show that different phenolic compounds may employ various mechanisms to induce variable effects on different lipid parameters. In this study, S, BHT, and CU increased T bioavailability and lowered cholesterol in plasma and/or tissues (liver and lungs). Further studies aiming to screen various phenolic compounds for their effects on rat lipids and to elucidate their mechanisms of action are underway in our laboratories.

ACKNOWLEDGMENTS

Our research on the antioxidant and cholesterol-lowering properties of dietary phenolic compounds is financed by the Swedish Council for Forestry and Agricultural Research (SJFR, grant No. 50.0496/98) and partially by Kalsec Inc. (Kalamazoo, MI). We thank Karlshamns AB (Sweden) for supplying rapeseed oil, and Takemoto Oil & Fat Co. Ltd. (Gamagori Aichi, Japan) for the kind gift of sesamin/episesamin and Charlotta Wall, from this Department, for kind help with rat sacrifice.

REFERENCES

1. Huang, M.T., and Ferraro, T. (1992) Phenolic Compounds in Food and Cancer Prevention, in *Phenolic Compounds in Food and their Effects on Health (II)*, pp. 8–34, American Chemical Society, Washington, DC.
2. Henn, T., and Stehle, P. (1998) [Total Phenolics and Antioxidant Activity of Commercial Wines, Teas and Fruit Juices], *Ernährungs-Umschau 45*, 308–313.
3. Bentsath, A., Rusznyak, S., and Szent-Györgi, A. (1936) Vitamin Nature of Flavones, *Nature 138*, 798.

4. Bentsath, A., Rusznyak, S., and Szent-Györgi, A. (1937) Vitamin P, *Nature 139*, 326–327.
5. Anonymous (1993) Inhibition of LDL Oxidation by Phenolic Substances in Red Wine: A Clue to the French Paradox? *Nutr. Rev. 51*, 185–187.
6. Staley, L.L., and Mazier, M.J.P. (1999) Potential Explanation for the French Paradox, *Nutr. Res. 19*, 3–15.
7. Hoffman, R.M., and Garewal, H.S. (1995) Antioxidants and the Prevention of Coronary Heart Disease, *Arch. Intern. Med. 155*, 241–246.
8. Pace-Asciak, C.R., Hahn, R.S., Diamandis, E.P., Soleas, G., and Goldberg, D.M. (1995) The Red Wine Phenolics *trans*-Resveratrol and Quercetin Block Human Platelet Aggregation and Eicosanoid Synthesis: Implications for Protection Against Coronary Heart Disease, *Clin. Chim. Acta 235*, 207–219.
9. Harman, D. (1992) Free Radical Theory of Aging, *Mutat. Res. 275*, 257–266.
10. Guyton, K.Z., and Kensler, T.W. (1993) Oxidative Mechanisms in Carcinogenesis, *Br. Med. Bull. 49*, 523–544.
11. Bartsch, H., Ohshima, H., and Pignatelli, B. (1988) Inhibitors of Endogenous Nitrosation: Mechanisms and Implications in Human Cancer Prevention, *Mutat. Res. 202*, 307–324.
12. Shahidi, F., Janitha, P.K., and Wanasundara, P.D. (1992) Phenolic Antioxidants, *Crit. Rev. Food Sci. Nutr. 32*, 67–103.
13. Steinberg, D., Parthasarathy, S., Carew, T.E., Khoo, J.C., and Witztum, J.L. (1989) Beyond Cholesterol, Modifications of Low-density Lipoprotein That Increase Its Atherogenity, *New Engl. J. Med. 320*, 915–924.
14. Ikeda, I., Imasato, Y., Sasaki, E., Nakayama, M., Nagao, H., Takeo, T., Yayabe, F., and Sugano, M. (1992) Tea Catechins Decrease Micellar Solubility and Intestinal Absorption of Cholesterol in Rats, *Biochem. Biophys. Acta 1127*, 141–146.
15. Hirose, N., Inoue, T., Nishihara, K., Sugano, M., Akimoto, K., Shimizu, S., and Yamada, H. (1991) Inhibition of Cholesterol Absorption and Synthesis in Rats by Sesamin, *J. Lipid Res. 32*, 629–638.
16. Agarwal, R., Wang, Z.Y., Bik, D.P., and Mukhtar, H. (1991) Nordihydro-Guaiaretic Acid, an Inhibitor of Lipoxygenase, Also Inhibits Cytochrome P-450-Mediated Mono-Oxygenase Activity in Rat Epidermal and Hepatic Microsomes, *Drug. Metab. Dispos. 19*, 620–624.
17. Alanko, J., Riutta, A., Mucha, T., Vapaatalo, H., and Metsa-Ketela, T. (1993) Modulation of Arachidonic Acid Metabolism by Phenols: Relation to Positions of Hydroxyl Groups and Peroxyl Radical Scavenging Properties, *Free Radical-Biol. Med. 14*, 19–25.
18. Laughton, M.J., Evans, P.J., Moroney, M.A., Hoult, J.R., and Halliwell, B. (1991) Inhibition of Mammalian 5-Lipoxygenase and Cyclo-Oxygenase by Flavonoids and Phenolic Dietary Additives. Relationship to Antioxidant Activity and to Iron Ion-Reducing Ability, *Biochem. Pharmacol. 42*, 1673–1681.
19. Mazur, W., and Adlercreutz, H. (1998) Natural and Anthropogenic Environmental Oestrogens: The Scientific Basis for Risk Assessment, *Pure Appl. Chem. 70*, 1759–1776.
20. The ATBC Cancer Prevention Study Group (1994) The Effect of Vitamin E and β-Carotene on the Incidence of Lung Cancer and Other Cancers in Male Smokers, *New Engl. J. Med. 330*, 1029–1035.
21. Chan, A.C. (1998) Vitamin E and Atherosclerosis, *J. Nutr. 128*, 1593–1596.
22. Takahata, K., Monobe, K., Tada, M., and Weber, P.C. (1998) The Benefits and Risks of n-3 Polyunsaturated Fatty Acids, *Biosci. Biotechnol. Biochem. 62*, 2079–2085.
23. Willett, W.C. (1998) The Dietary Pyramid: Does the Foundation Need Repair? *Am. J. Clin. Nutr. 68*, 218–219.
24. Pietinen, P., Rimm, E.B., Korhonen, P., Hartman, A.M., Willett, W.C., Albanes, D., and Virtamo, T.J. (1996) Intake of Dietary Fiber and Risk of Coronary Heart Disease in a Cohort of Finnish Men: The α-Tocopherol, β-Carotene Cancer Prevention Study, *Circulation 94*, 2720–2727.
25. Yamashita, K., Nohara, Y., Katayama, K., and Namiki, M. (1992) Sesame Seed Lignans and α-Tocopherol Act Synergistically to Produce Vitamin E Activity in Rats, *J. Nutr. 122*, 2440–2446.
26. Kamal-Eldin, A., Pettersson, D., and Appelqvist, L.Å. (1995) Sesamin (a compound from sesame oil) Increases Tocopherol Levels in Rats Fed *ad libitum*, *Lipids 30*, 499–505.
27. Yamashita, K., Iizuka, Y., Imai, T., and Namiki, M. (1995) Sesame Seed and Its Lignans Produce Marked Enhancement of Vitamin E Activity in Rats Fed a Low α-Tocopherol Diet, *Lipids 30*, 1019–1028.
28. Nardini, M., Natella, F., Gentili, V., Di Felice, M., and Scaccini, C. (1997) Effect of Caffeic Acid Dietary Supplementation on the Antioxidant Defense System in Rat: An *in vivo* Study, *Arch. Biochem. Biophys. 342*, 157–160.
29. Hara, A., and Radin, N.S. (1978) Lipid Extraction of Tissues with a Low-Toxicity Solvent, *Anal. Biochem. 90*, 420–426.
30. Seigler, L., and Wu, W.T. (1981) Separation of Serum High-Density Lipoprotein for Cholesterol Determination: Ultracentrifugation vs. Precipitation with Sodium Phosphotungstate and Magnesium Chloride, *Clin. Chem. 27*, 838–841.
31. SAS® (1988) *User's Guide: Statistics*, version 6.03 Edition, SAS Institute, Inc., Cary, NC.
32. Srinivasan, M.R., and Satyanarayana, M.N. (1988) Influence of Capsaicin, Eugenol, Curcumin and Ferulic Acid on Sucrose-Induced Hypertriglyceridemia in Rats, *Nutr. Reports Intern. 38*, 571–581.
33. Kahl, R., and Kappus, H. (1992) [Toxicology of the Synthetic Antioxidants BHA and BHT in Comparison with the Natural Antioxidant Vitamin-E], *Z. Lebensm. Unters. Forsch. 196*, 329–338.
34. Takahashi, O., and Hiraga, K. (1981) Effect of Butylated Hydroxytoluene on the Lipid Composition of Rat Liver, *Toxicology 22*, 161–170.
35. Sugano, M., Inoue, T., Koba, K., Yoshida, K., Hirose, N., Shinmen, Y., Akimoto, K., and Amachi, T. (1990) Influence of Sesame Lignans on Various Lipid Parameters in Rats, *Agric. Biol. Chem. 54*, 2669–2673.
36. Sugano, M., and Akimoto, K. (1993) Sesamin: A Multifunctional Gift from Nature, *J. Chinese Nutr. Soc. 18*, 1–11.
37. Nakabayashi, A., Kitagawa, Y., Suwa, Y., Akimoto, K., Asami, S., Shimizu, S., Hirose, N., Sugano, M., and Yamada, H. (1995) α-Tocopherol Enhances the Hypocholesterolemic Action of Sesamin in Rats, *Int. J. Vit. Nutr. Res. 65*, 162–168.
38. Yamamoto, K., Fukuda, N., Shiroi, S., Yoshida, K., Hirose, N., Shinmen, Y., Akimoto, K., and Amachi, T. (1995) Effect of Dietary Antioxidants on the Susceptibility to Hepatic Microsomal Lipid Pperoxidation in the Rat, *Ann. Nutr. Metabol. 39*, 99–106.
39. Simán, C.M., and Eriksson, U.J. (1996) Effect of Butylated Hydroxytoluene on α-Tocopherol Content in Liver and Adipose Tissue of Rats, *Toxicol. Lett. 87*, 103–108.
40. Subba Rao, D., Chandra Sekhara, N., Satyanarayana, N., and Srinivasan, M. (1970) Effect of Curcumin on Serum and Liver Cholesterol Levels in the Rat, *J. Nutr. 100*, 1307–1316.
41. Satchithanandam, S., Chanderbhan, R., Kharroubi, A.T., Calvert, R.J., Klurfeld, D., Tepper, S.A., and Kritchevsky, D. (1996) Effect of Sesame Oil on Serum and Liver Lipid Profiles in the Rat, *Int. J. Vit. Nutr. Res. 66*, 386–392.
42. Bieri, J.G., and Evarts, R.P. (1974) Vitamin E Activity of α-Tocopherol in the Rat, Chick and Hamster. *J. Nutr. 104*, 850–857.
43. Bieri, J.G., and Evarts, R.P. (1974) Gamma Tocopherol: Metabolism, Biological Activity and Significance in Human Vitamin E Nutrition, *Am. J. Clin. Nutr. 27*, 980–986.
44. Leth, T., and Søndergaard, H. (1977) Biological Activity of Vitamin E Compounds and Natural Materials by the

Resorption–Gestation Test, and Chemical Determination of the Vitamin E Activity in Foods and Feeds, *J. Nutr. 107*, 2236–2243.
45. Tran, K., and Chan, A.C. (1992) Comparative Uptake of α- and γ-Tocopherol by Human Endothelial Cells, *Lipids 27*, 38–41.
46. Kayden, H.J., and Traber, M.G. (1993) Absorption, Lipoprotein Transport, and Regulation of Plasma Concentrations of Vitamin E in Humans, *J. Lipid Res. 34*, 343–358.
47. Sato, Y., Hagiwara, K., Arai, H., and Inoue, K. (1991) Purification and Characterization of the α-Tocopherol Transfer Protein from Rat Liver, *FEBS Lett. 288*, 41–45.
48. Arita, M., Nomura, K., Arai., H, and Inoue, K. (1997) α-Tocopherol Transfer Protein Stimulates the Secretion of α-Tocopherol from a Cultured Liver Cell Line Through a Brefeldin A-Insensitive Pathway, *Proc. Natl. Acad. Sci. USA 94*, 12437–12441.
49. Hosomi, A., Arita, M., Sato, Y., Kiyose, C., Ueda, T., Igarashi, O., Arai, H., and Inoue, K. (1997) Affinity for α-Tocopherol Transfer Protein as a Determinant of the Biological Activities of Vitamin E Analogs, *FEBS Lett. 409*, 105–108.
50. Traber, M.G., and Kayden, H.J. (1989) Preferential Incorporation of α-Tocopherol vs. γ-Tocopherol in Human Lipoproteins, *Am. J. Clin. Nutr. 49*, 517–526.
51. Bjorneboe, A., Bjorneboe, G.E., and Drevon, C.A. (1987) Serum Half-Life, Distribution, Hepatic Uptake and Biliary Excretion of α-Tocopherol in Rats, *Biochim. Biophys. Acta 921*, 175–181.
52. Chiku, S., Hamamura, K., and Nakamura, T. (1984) Novel Urinary Metabolite of d-δ-Tocopherol in Rats, *J. Lipid Res. 25*, 40–48.
53. Schonfeld, A., Schultz, M., Petrzika, M., and Gassmann, B. (1993) A Novel Metabolite of *RRR*-α-Tocopherol in Human Urine, *Nahrung 37*, 498–500.
54. Schultz, M., Leist, M., Petrzida, M., Gassmann, B., and Brigelius-Flohe, R. (1995) A Novel Urinary Metabolite of α-Tocopherol: 2,5,7,8-Tetramethyl-2(2′-carboxyethyl)-6-hydroxychroman (α-CEHC) as an Indicator of an Adequate Vitamin E Supply?, *Am. J. Clin. Nutr. 62 (Suppl)*, 1527S–1543S.
55. Swanson, J.E., Ben, R.N., Burton, G.W., and Parker, R.S. (1999) Urinary Excretion of 2,7,8-Trimethyl-2-(β-carboxyethyl)-6-hydroxychroman Is a Major Route of Elimination of γ-Tocopherol in Humans, *J. Lipid Res. 40*, 665–671.
56. Casida, J.E. (1970) Mixed Function Oxidase Involvement in the Biochemistry of Insecticidal Synergists, *J. Agric. Food Chem. 18*, 753–772.
57. Mustacich, D.J., Shields, J., Horton, R.A., Brown, M.K., and Reed, D.J. (1998) Biliary Secretion of α-Tocopherol and the Role of the mdr2 P-Glycoprotein in Rats and Mice, *Arch. Biochem. Biophys. 350*, 183–192.
58. Mustacich, D.J., Brown, M.K., and Reed, D.J. (1996) Colchicine and Vinblastine Prevent the Piperonyl Butoxide-Induced Increase in Rat Biliary Output of α-Tocopherol, *Toxicol. Applied Pharmacol. 139*, 411–417.
59. Joint Industrial Safety Council (1997) *Chemical Substances*, CD-ROM ISBN 91-7522-551-4, Joint Industrial Safety Council, Stockholm.
60. Björkhem, I., Henriksson-Freyschuss, A., Breuer, O., Diczfalusy, U., Berglund, L., and Henriksson, P. (1991) The Antioxidant Butylated Hydroxytoluene Protects Against Atherosclerosis, *Atheroscler. Thromb. 11*, 15–22.
61. Leblanc, G., and Gillette, I.S. (1993) Elevation of Serum Cholesterol Levels in Mice by the Antioxidant Butylated Hydroxyanisole, *Biochem. Pharmacol. 45*, 513–515.
62. Tamizhselvi, R., Samikkannu, T., and Niranjali, S. (1995) Pulmonary Phospholipid Changes Induced by Butylated Hydroxy Toluene, an Antioxidant, in Rats, *Ind. J. Exper. Biol. 33*, 796–797.
63. Hirata, F., Fujita, K., Ishikura, Y., Hosoda, K., Ishikawa, T., and Nakamura, H. (1995) Hypocholesteremic Effect of Sesame Lignan in Humans, *Atherosclerosis 122*, 135–136.
64. Patil, T.N., and Srinivasan, M. (1971) Hypocholesteremic Effect of Curcumin in Induced Hypercholesterolemic Rats, *Ind. J. Exper. Biol. 9*, 167–169.
65. Seetharamaiah, G.S., and Chandrasekhara, N. (1990) Effect of Oryzanol on Cholesterol Absorption and Biliary and Fecal Bile Acids in Rats, *Ind. J. Med. Res. [B] 92*, 471–475.
66. Igarashi, O., Umeda-Sawada, R., and Fujiyama-Fujiwara, Y. (1995) Effect of Dietary Factors on the Metabolism of Essential Fatty Acids: Focusing on the Components of Spices, in *Nutrition, Lipids, Health and Disease* (Ong, A.S.H., Niki, E. and Packer, L., eds.), pp. 59–66, AOCS Press, Champaign.
67. Shimizu, S., Akimoto, K., Shinmen, Y., Kawashima, H., Sugano, M., and Yamada, H. (1991) Sesamin Is a Potent and Specific Inhibitor of Δ5 Desaturase in Polyunsaturated Fatty Acid Biosynthesis, *Lipids 26*, 512–516.
68. Dwyer, J.T. (1988) Health Aspects of Vegetarian Diets, *Am. J. Clin. Nutr. 48(suppl.)*, 712–738.
69. Steinmetz, K.A., and Potter, J.D. (1991) Vegetables, Fruits and Cancer. II. Mechanisms, *Cancer Causes Control 1*, 427–442.
70. Block, G., Patterson, B., and Subar, A. (1992) Fruit, Vegetables and Cancer Prevention: A Review of the Epidemiological Evidence, *Nutr. Cancer 18*, 1–29.

[Received July 12, 1999, and in revised form January 24, 2000; revision accepted February 23, 2000]

Cholesterol-Lowering Effects of Guar Gum: Changes in Bile Acid Pools and Intestinal Reabsorption

Stéphanie Moriceau, Catherine Besson, Marie-Anne Levrat, Corinne Moundras, Christian Rémésy, Christine Morand, and Christian Demigné*

Unité Maladies Métaboliques & Micronutriments, INRA de Theix, 63122 St-Genès-Champanelle, France

ABSTRACT: Soluble fibers such as guar gum (GG) may exert cholesterol-lowering effects. It is generally accepted that bile acid (BA) reabsorption in portal blood is reduced, thus limiting the capacity of BA to down-regulate liver cholesterol 7α-hydroxylase, the rate-limiting enzyme of BA synthesis. In the present work, rats were adapted to fiber-free (FF) or 5% GG diets (supplemented or not with 0.25% cholesterol), to investigate various aspects of enterohepatic BA cycling. GG in the diet at a level of 5% elicited a significant lowering of plasma cholesterol during the absorptive period, in cholesterol-free (–13%) or 0.25% cholesterol (–20%) diet conditions. In rats adapted to the GG diets, the small intestinal and cecal BA pools and the ileal vein-artery difference for BA were markedly enhanced; reabsorption in the cecal vein was also enhanced in these rats. [^{14}C]Taurocholate absorption, determined in perfused ileal segments, was not significantly different in rats adapted to the FF or GG diet, suggesting that a greater flux of BA in the ileum might support a greater ileal BA reabsorption in rats adapted to the GG diet. In contrast, capacities for [^{14}C]cholate absorption from the cecum at pH 6.5 were higher in rats adapted to the GG diet than to the FF diet. Acidification of the bulk medium in isolated cecum (from pH 7.1 down to pH 6.5 or 5.8) or addition of 100 mM volatile fatty acids was also found to stimulate cecal [^{14}C]cholate absorption. These factors could contribute to accelerated cecal BA absorption in rats fed the GG diet. The effects of GG on steroid fecal excretion thus appear to accompany a greater intestinal BA absorption and portal flux to the liver. These results suggest that some mechanisms invoked to explain cholesterol-lowering effect of fibers should be reconsidered.

Paper no. L8087 in *Lipids 35,* 437–444 (April 2000).

A large part of the adult population in Western countries have elevated cholesterol values (>5 mmol/L) and may be in need of treatment. Pharmacological treatment should be reserved to cases of hypercholesterolemia not responding satisfactorily to dietary changes, because of cost and persistent doubts on the long-term safety of cholesterol-lowering drugs. A treatment program for hypercholesterolemia usually consists of dietary changes toward low-fat/low-cholesterol diets that should also be rich in complex carbohydrates, especially fiber. Evidence for a cholesterol-lowering effect of fiber in animals models and man has accumulated in recent years, especially with viscous fibers such as guar gum (1–5). The effect varies depending on the amount and properties of the gums and the cholesterol level of the diet.

The mechanism by which guar gum (GG) lowers serum cholesterol is still unclear on some points. The enterohepatic cycling of steroids, especially bile acids (BA), is a process susceptible to the interfering effects of BA sequestrants or of high-viscosity compounds such as GG (6): a reduced BA reabsorption is likely to reduce the body's pool of cholesterol. Furthermore, cholesterol absorption itself could also be depressed by soluble fibers, compared to fiber-free conditions (2,7,8), resulting in a greater excretion of neutral sterols (chiefly bacterial metabolites of cholesterol). The prevailing concepts of the effect of fibers on BA cycling in the splanchnic area have probably been influenced by studies carried out with cholestyramine or other types of sequestrants such as β-cyclodextrin, which are potent inhibitors of BA reabsorption in the small intestine (6). It is generally accepted that unconjugated BA, which constitute a small fraction of the luminal BA, are reabsorbed by passive diffusion along the entire small intestine. Active transport systems in the distal ileum account for the bulk of conjugated BA reabsorption, especially when BA are conjugated with taurine (9). Finally, BA escaping absorption in the terminal ileum are deconjugated and partially 7α-dehydroxylated by colonic bacteria; these luminal BA may be reabsorbed by passive diffusion across colonic mucosa (9). The first step of active transport of BA from the distal intestinal lumen is performed by the apical sodium-dependent bile acid transporter (ASBT). This brush border membrane glycoprotein, which co-transports Na^+ and BA into ileocytes, has been cloned and characterized (10,11). After internalization, BA bind to specific cytosolic proteins and subsequently exit the ileocyte by an anion exchanger located in the basolateral membrane. It is conceivable that viscous fibers exert effects on the physical characteristics of the ileal bulk phase (enhanced viscosity, accumulation of endogenous materials) that may alter BA access to the transporter units and thus impair their reabsorption. Little is known of a possi-

*To whom correspondence should be addressed.
E-mail: demigne@clermont.inra.fr

Abbreviations : ANOVA, analysis of variance; ASBT, active sodium-dependent bile acid transporter; BA, bile acid; C, cholate; FF, fiber-free; GG, guar gum; Iv-A, arteriovenous difference; PBS, phosphate-buffered saline; SCFA, short-chain fatty acid; TC, taurocholate. Convention: steroid = sterols + bile acids (in digestive or fecal samples).

ble effect of fiber on the BA-transporting capacity of the ileum; however, investigations in rats fed resistant starch showed a doubling of [^{14}C]taurocholate (TC) transport (12). Up-regulation of ASBT has been reported in rodents when there is a spillover of the BA pool (13) or, alternatively, in cholic-acid fed rats (14). Attempts to quantify the reabsorption flux in the portal vein have not provided data that clearly show an impaired recycling of BA to the liver when the diet contains sequestrants (15) or GG (4,16). This point is particularly important because a lowering of portal BA is likely to be (i) the result of intestinal BA spillover and (ii) a stimulatory factor for hepatic BA synthesis, *via* cholesterol 7α-hydroxylase induction (17,18).

Thus, to further investigate the mechanisms of cholesterol-lowering effects of GG in rats, experiments were carried out to measure the effects of this gum on plasma cholesterol and on the digestive BA pools, as well as on ileal BA and cecal reabsorption (*in vivo* or on perfused segments).

MATERIALS AND METHODS

Animals and diets. Male Wistar rats (IFFA-CREDO, l'Arbresle, France) weighting approximately 150 g, were fed semi-purified diets distributed as a moistened powder for 21 d. The experimental diets were: fiber-free (FF) control, 5% GG, 0.25% cholesterol, or 5% GG/0.25% cholesterol (Table 1). GG or cholesterol was included at the expense of wheat starch.

Animals were housed two per cage and maintained in temperature-controlled rooms (22°C), with the dark period from 2000 to 0800. Rats were maintained and handled according to the recommandations of the Institutional Ethics Committee (Clermont-Ferrand University). The body weights of rats were recorded every 48 h during the experimental period; food intake and fecal excretion were recorded over two 3-d periods during the last 10 d.

TABLE 1
Composition of the Diets

Diet group	Fiber-free	Guar gum	Fiber-free/ cholesterol	Guar gum/ cholesterol
Wheat starch[a]	727.5	677.5	725.0	675.0
Casein[a]	150	150	150	150
Corn oil[b]	50	50	50	50
Cholesterol	0	0	2.5	2.5
Guar gum[b]	0	50	0	50
Mineral mix[c]	60	60	60	60
Vitamin mix[c]	10	10	10	10

[a]Louis François, Paris, France.
[b]Sigma, St. Quentin, France.
[c]Minerals supplied, per kg of diet: $CaHPO_4$, 15 g; KCl, 6 g; NaCl, 6 g; $MgCl_2{\cdot}6H_2O$, 6.8 g; Fe_2O_3, 2.5 mg; $MnSO_4$, 125 mg; $CuSO_4{\cdot}7H_2O$, 0.2 mg; $ZnSO_4{\cdot}7H_2O$, 100 mg; KI, 0.4 mg. Vitamins supplied, per kg of diet: thiamin, 20 mg; riboflavin, 15 mg; pyridoxin, 10 mg; nicotinamide, 100 mg; calcium pantothenate, 70 mg; folic acid, 5 mg; biotin, 0.3 mg; cyanocobalamin, 0.05 mg; retinyl palmitate, 1.5 mg; DL-α-tocopheryl acetate, 125 mg; cholecalciferol, 0.15 mg; menadione, 1.5 mg; ascorbic acid, 50 mg; *myo*-inositol, 100 mg; choline, 1.36 g. Both mixes were purchased from UAR (Villemoisson, Epinay-sur-Orge, France).

Sampling procedures. Rats were killed at the end of dark period, namely, at a time when cecal fermentations are still very active. They were anesthetized with sodium pentobarbital (40 mg/kg) and maintained at 37°C. An abdominal incision was made and blood was withdrawn from the ileal branch of the mesenteric artery (after clamping a lower afferent branch that drains the cecum and the proximal colon) and from the abdominal aorta (two 1-mL samples taken). The blood of each animal was placed in a plastic tube containing heparin and centrifuged at 10,000 × *g* for 5 min. After centrifugation, plasma was removed and kept at +4°C for lipid and BA analysis.

After blood sampling, the cecum with contents was removed and weighed, and two aliquot samples of cecal content were transferred into microfuge tubes and immediately frozen at –20°C. The small intestine was clamped at the pylorus and the ileal-cecal junction, removed, stripped of mesentery and fat, and weighed. After injection of 5 mL saline, the contents were drained into a tube by gentle finger stripping, then frozen at –20°C (total small intestine pool). In a separate experiment on two groups of rats (adapted to the FF/control diet or to the GG diet), jejunal and ileal segments were treated separately: after collection of the contents as described above, the intestine segments were opened longitudinally and fixed on a support with pins; then the mucosa was recovered by scraping and frozen at –20°C.

In situ *absorption studies*. In separate series of anesthetized rats, the appearance of radiolabeled BA in bile was used to monitor absorption from intestinal segments (ileum or cecum). A mid-line laparotomy was performed and the bile duct exposed and ligated distally. The bile duct was then catheterized with a PE10 polyethylene catheter (Biotrol, Paris, France), and bile was allowed to drain into preweighed vials cooled on ice.

(i) Ileum. Ileal segments (extending proximally from the ileocecal junction, measured with a 15-cm length of string) were isolated, care being taken to protect the mesenteric vasculature. An opening was made at the distal end of the segment and this last was gently flushed with 20 mL of phosphate-buffered saline (PBS; pH 7) at 37°C. Then, a cannula (external diameter 4 mm, internal diameter 2.5 mm) was inserted at each extremity of the segment and secured. Determination of [^{14}C]TC absorption was performed by two procedures: (i) kinetic determination of [^{14}C]TC absorption from segments filled with 2 mL of a medium containing 1 mM [^{14}C]TC and either 0, 0.5, or 1% GG (this procedure is suitable to study a viscous medium), or (ii) determination of transport by continuous infusion (1 mL/min) of a medium containing 1 mM [^{14}C]TC (to minimize influence of unstirred layer and to achieve steady-state conditions). The composition of the medium was: NaCl 75 mM, KCl 50 mM, $NaHCO_3$ 5 mM, $MgCl_2$ 2 mM, $CaCl_2$ 2 mM, glucose 10 mM, mannitol 40 mM, and potassium phosphate buffer (pH 7.0) 10 mM. Bile was collected sequentially either every 2 or 3 min (procedure 1) or every 5 min (procedure 2) for 30–40 min.

(ii) Cecum. A cannula was introduced in the cecum *via* the ileocecal valve and secured, then an opening was effected at

the appendix extremity and the cecum was flushed by 20 mL of PBS by gentle finger stripping, drained, and this extremity was tied. The cecum was then filled with 2 mL (FF-adapted rats) or 3 mL (fiber-fed rats) of a solution containing 100 mM major anions [sodium salts of short-chain fatty acids (SCFA) or sodium isothionate], 20 mM KCl, 2 mM $MgCl_2$, 2 mM $CaCl_2$, 25 mM potassium phosphate buffer, and 1 mM [^{14}C]-cholate (C) (the pH was adjusted to the required value, namely, 7.1, 6.5, or 5.8). Bile was collected every 5 min during 30 min; because of the relatively low rate of BA absorption and the size of the BA cecal pool, steady-state conditions were maintained over more than 15 min (generally from 5 to 25 min).

Analytical procedures. BA were quantified using the reaction catalyzed by the 3α-hydroxysteroid dehydrogenase (EC 1.1.1.50; Sigma). The enzymatic determination was effected either directly on undiluted plasma, or on digestive samples (small intestine or cecal contents, intestinal mucosa) extracted by a two-step procedure. For this purpose, 1 vol sample was first dispersed in 10 vol ethanolic KOH (0.5 M) using a Polytron disintegrator (Lucerne, Switzerland) and extracted at 70°C for 2 h, then 1 vol of this suspension (typically 2.5 mL) was redispersed in 4 vol of ethanolic KOH and re-extracted at 70°C for 2 h. Triglycerides and total cholesterol were determined in plasma by enzymatic procedures (Biotrol, Paris, France, and Biomerieux, Charbonnières-les-bains, France, respectively).

Calculations and data analysis. Values are given as the means ± SEM. Statistics were examined using a statistical software package (Statview/SuperANOVA; Abacus, Berkeley, CA) on an Apple Macintosh. Data were analyzed either by two-way analysis of variance (ANOVA) to examine the main effect of GG, cholesterol, and their interaction, or one-way ANOVA for other experiments. Least significance difference was used for mean comparison when significant treatment differences existed. Some experiments were analyzed using by Student's *t*-test. Significant differences among means were determined at $P < 0.05$.

RESULTS

As shown in Table 2, the plasma cholesterol concentration was markedly enhanced by 0.25% cholesterol in the diet in rats adapted to FF diet. In rats fed cholesterol-free diets, GG had a slight but significant cholesterol-lowering effect (–13%); this effect was more potent (–20%) in rats fed diets enriched in cholesterol. Plasma triglycerides were not significantly affected by dietary GG or cholesterol in the present experiment.

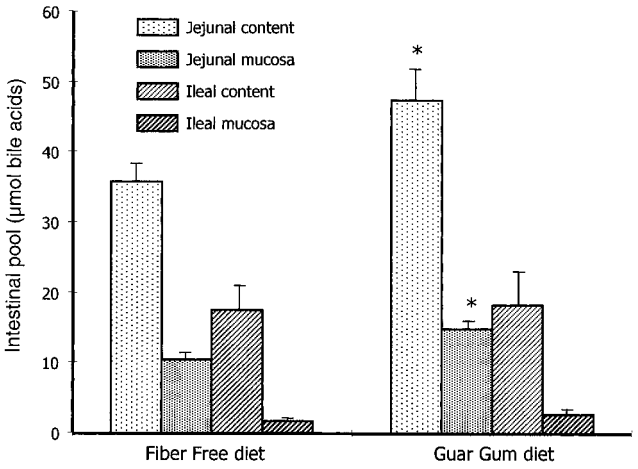

FIG. 1. Comparison of the bile acid pools in the small intestine of rats adapted to a fiber-free or a 5% guar gum diet. Values are means ± SEM (n = 8/group); *$P < 0.05$ vs. fiber-free by Student's *t*-test.

Effects of GG and cholesterol on the BA digestive pools and reabsorption. In rats fed FF diets, the BA pool in the small intestine was about 45 µmol, and the presence of GG in the diet caused a marked enlargement of this pool (Table 3). Cholesterol feeding was also very effective in raising the small intestinal pool, and the maximal value (up to 73 µmol) was found in rats fed the GG/cholesterol diet. The cecal BA pool (about 10 µmol in rats fed an FF diet) was much lower than the small intestine pool. It was enhanced by either dietary GG or cholesterol, and there was a synergistic effect between these two factors. In a separate experiment on rats adapted to FF or GG diets, the intestinal luminal and mucosal bile acids were measured (Fig. 1). It appeared that the rise of the intestinal pool observed in rats fed GG was chiefly due to an enlargement of the jejunal pool. In this segment, a noticeable mucosal pool was measured, corresponding to about 30–35% of the luminal pool. In contrast, the ileal mucosal pool was relatively low, representing about 10% of the luminal pool.

In Figure 2 are presented concentrations of BA in the arterial and ileal venous (mesenteric branch draining the ileum)

TABLE 2
Effect of the Diets on Plasma Cholesterol and Triglyceride Concentrations[a]

	Dietary groups			
	Fiber-free	Guar gum	Fiber-free/cholesterol	Guar gum/cholesterol
Plasma cholesterol (mmol/L)	1.59 ± 0.05[c]	1.37 ± 0.04[b]	2.09 ± 0.07[d]	1.68 ± 0.0[c]
Plasma triglyceride (mmol/L)	1.33 ± 0.12	1.13 ± 0.08	1.38 ± 0.11	1.41 ± 0.18

[a]Values are means ± SEM (n = 8/group); means not sharing a common superscript are significantly different at $P < 0.05$ by two-way analysis of variance (ANOVA) and least squares difference (LSD) comparison.

TABLE 3
Effect of the Diets on the Intestinal Pools and Reabsorption of Bile Acids[a]

	Dietary groups			
	Fiber-free	Guar gum	Fiber-free/cholesterol	Guar gum/cholesterol
Small intestinal pool (μmol/organ)	45.1 ± 3.1[b]	59.2 ± 5.4[c]	64.5 ± 3.4[c]	73.8 ± 5.2[d]
Cecal pool (μmol/organ)	9.7 ± 1.4[b]	15.8 ± 1.2[c]	19.7 ± 3.0[b]	38.6 ± 9.6[d]
Portal vein flux (μmol/min)	37.0 ± 8.0[b]	60.2 ± 7.3[c]	45.6 ± 5.6[b]	68.0 ± 9.7[c]
Cecal vein flux (μmol/min)	7.3 ± 0.8[b]	9.0 ± 1.8[b,c]	11.2 ± 2.0[c]	19.4 ± 2.5[d]

[a]Values are means ± SEM (n = 8/group); means not sharing a common superscript are significantly different at $P < 0.05$ by two-way ANOVA and LSD comparison. For abbreviations see Table 2.

plasma. No significant differences in the arterial BA concentrations were observed (ranging from 0.05 to 0.08 mmol/L). In all diet conditions, much higher concentrations were found in the ileal vein, some exceeding 0.30 mmol/L in rats adapted to the GG/cholesterol diet. When the diet contained GG or was supplemented with cholesterol, the ileal vein concentrations were significantly higher than in FF controls. The calculated arteriovenous difference (Iv-A) was +0.12 mmol/L in FF controls, and this difference was not substantially enhanced in rats fed the FF/cholesterol diet (+0.15 mmol/L). In contrast, a striking rise in the Iv-A arteriovenous difference (practically doubled) was found in rats adapted to GG diets, and the highest arteriovenous difference was observed in the GG/cholesterol diet group.

Effect of GG on [^{14}C]TC absorption rate in ileal segments. The time course recording of [^{14}C]TC appearance in bile indicates a very rapid absorption from the ileal loop; the maximal level of ^{14}C BA was achieved within 5–8 min after introduction of the experimental TC solution in the loop (Fig. 3). The plot of the cumulative [^{14}C]TC as a function of time offers a possibility to estimate the kinetic characteristic of TC absorption. In control conditions, the maximal slope corresponded to a rate of 2.8 nmol/min/cm. When GG was present in the experimental medium, the lowest concentration (0.5%) was apparently ineffective in modifying the rate of TC absorption whereas the 1% concentration exerted a marked inhibition on TC absorption (–52%).

By using the procedure of isolated ileal loop perfusion, steady-state conditions of [^{14}C]TC appearance in bile were found to be attained readily, within about 5 min. Sequential collection of bile was effected over 20 min. In this model, the rate of [^{14}C]TC absorption from the ileum (in nmol/min/cm

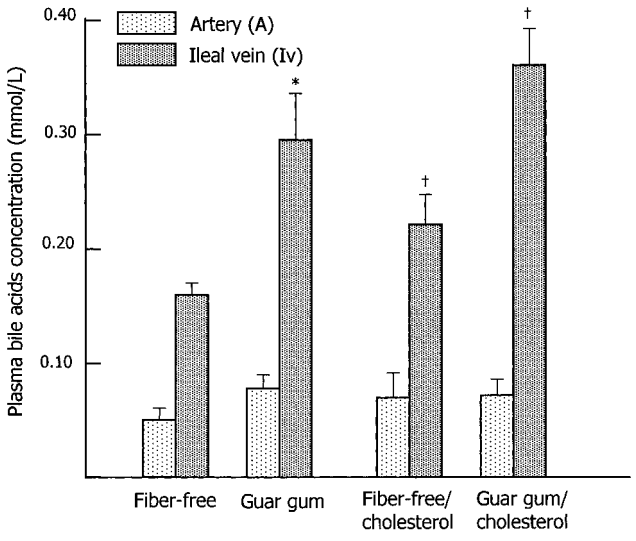

FIG. 2. Ileal vein and artery concentrations of bile acids in rats adapted to dietary guar gum; the experimental diets were either cholesterol-free or contained 0.2% cholesterol. Values are means ± SEM (n = 8/group); means not sharing a common superscript are significantly different at $P < 0.05$ by two-way analysis of variance and least squares difference comparison.

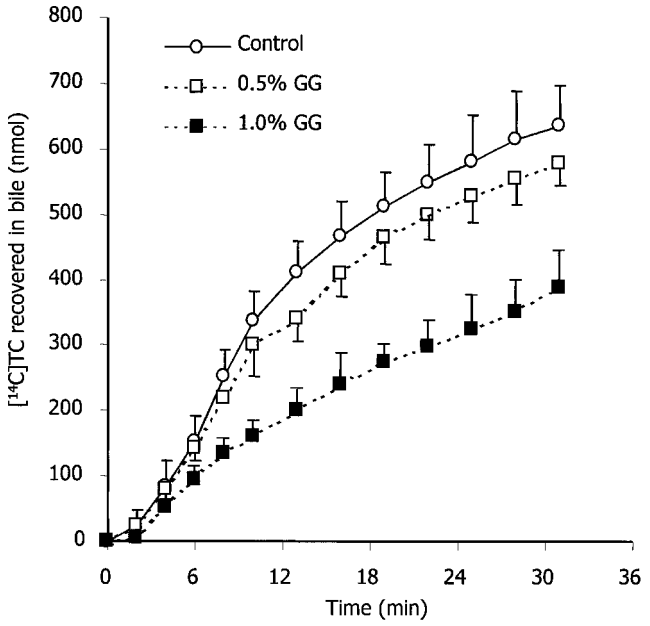

FIG. 3. Taurocholate absorption from ileal segments filled with 1 mmol/L [^{14}C]taurocholate medium, and 0, 0.5, or 1.0% guar gum. Appearance in bile of radiolabeled bile acids was used to monitor absorption from the ileum. Values are means ± SEM (n = 6/group).

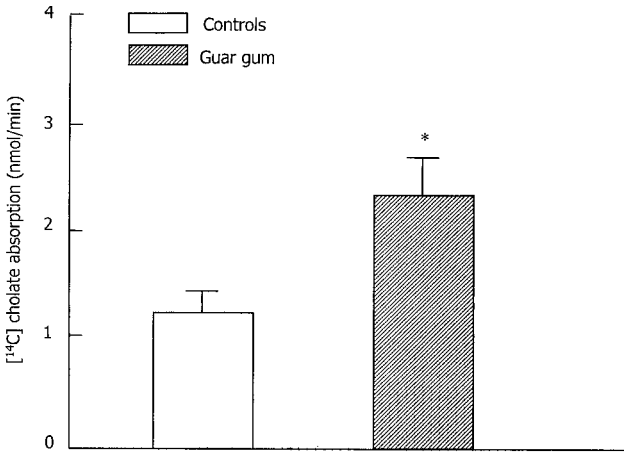

FIG. 4. Effect of adaptation to a fiber-free control or a 5% guar gum diet on cholate absorption from the cecum. The cecum was flushed with saline, then the experimental solutions containing 1 mmol/L [^{14}C]-cholate were injected. Appearance of radiolabeled bile acids was used to monitor absorption from the cecum. The medium contained 100 mM short-chain fatty acid salts pH 6.5. Values are means ± SEM (n = 6/group). *P < 0.05 vs. control by Student's t-test.

intestine) of rats adapted to a 5% GG diet (6.37 ± 0.69) was not significantly modified, compared to FF controls (5.05 ± 0.69).

Effects of pH, short-chain fatty acids (SCFA), and adaptation to a GG diet on the capacity for [^{14}C]cholate (C) absorption in the cecum. The rate of [^{14}C]C absorption from the cecum was affected by the bulk pH and the major anions present in the experimental solution. Substitution of 100 mmol/L SCFA Na salts (a realistic concentration in the caecum), as 60 mmol acetate + 25 mmol propionate + 15 mmol butyrate, by equimolar Na isothionate elicited a 31% lower absorption of [^{14}C]C (1.64 ± 0.23 vs. 2.41 ± 0.30 nmol [^{14}C]cholate absorbed/min/cecum; n = 6; P < 0.05).

In another experiment the luminal pH was modified in the presence of 100 mmol/L SCFA, within a physiological range, namely from 7.5 to 5.8 with an intermediate value at 6.5. The results indicated that the cecal [^{14}C]C absorption was slightly accelerated in acidic pH conditions, but the highest absorption rate was found at pH 6.5 [at pH 7.1, 1.56 ± 0.24 nmol [^{14}C]cholate absorbed vs. 2.32 ± 0.26 at pH 5.8, n = 7, P < 0.05; absorption at pH 6.5 was 2.61 ± 0.31, n = 7; absorption at pH 7.1 was significantly different from pH 6.5 (P < 0.5), but absorption at pH 6.5 and 5.8 were not significantly different].

The cecum was enlarged and its wall heavier in rats fed GG than in controls (0.97 vs. 0.59 g, respectively). As shown in Figure 4, the rate of [^{14}C]C absorption from the cecum was significantly greater in the cecum of rats adapted to the GG diet than in controls (+87%). Taking into account the differences in volume of test solution between the two groups, it appears that cecal [^{14}C]C absorption was only 26% greater in rats fed the GG diet than in those fed the control FF diet.

DISCUSSION

The present work confirms, in agreement with other investigations (4,19,20), that GG is liable to lower plasma cholesterol, this effect being more potent when the diet contains a significant percentage (0.25%) of cholesterol. Effects of GG, which should be related to modifications of luminal viscosity, have been ascribed to disturbances of micelle formation, slowing of cholesterol transfer across the unstirred layer, and inhibition of bile acid reabsorption (1,6,19). This last mechanism has been frequently invoked for steroid sequestrants, such as resins or cyclodextrins, or gel-forming compounds, such as pectin, psyllium or gums (6,21). The present experiments indicate that GG, in the isolated ileal loop model, may be very effective in inhibiting TC reabsorption in the distal part of the small intestine. Nevertheless, the fact that the 0.5% concentration was ineffective, whereas the 1% concentration was markedly inhibitory, suggests that there is a threshold effect in the inhibition of TC absorption by GG. This could be connected to differences in medium viscosity, which could impair TC diffusion to the ileal brush border membrane, as suggested by examining the kinetics of ^{14}C appearance in the bile.

Previous work showed that fecal excretion of bile acids is raised by GG (4) but, with moderate levels of dietary GG (5% or less) this rise is rather limited. In fact, enhanced fecal steroid excretion is represented chiefly by neutral sterols rather than bile acids (22). In parallel, biliary BA secretion may be accelerated by GG, as shown also for other fibers (23,24). In the rat, the BA pool is almost entirely found in the digestive tract, especially in the small intestine. The present work, in keeping with previous data (4,25), indicates that the small intestine pool is markedly enhanced by GG and to a lesser extent by cholesterol,and both factors are apparently cumulative. A more detailed study of the small intestinal pools in rats adapted to the FF or GG diet indicated that most of BA were present in the duodenal/jejunal part, and this pool was the most affected by GG. The ileal pool was found to be smaller than the jejunal pool and was not markedly enlarged by GG. A substantial mucosal BA pool (about 30% of the luminal pool) was found in the jejunum but it represented less than 10% in the ileum, as previously reported (26). The significance of a large capacity for BA accumulation in the jejunal mucosa is still unclear, but it tended to increase in rats adapted to a GG diet. This could represent a storage compartment for a portion of the BA in rats since this species is devoid of a gall bladder, or it could be involved in BA absorption since the proximal small bowel may take a significant part in this process (27). Capacities for passive BA reabsorption have been identified in both the upper and lower part of the small intestine, as well as in the large intestine (9). In the small intestine, this passive process should essentially transfer glyco-conjugates whereas, in the large intestine, it represents the unique possibility of unconjugated BA reabsorption. Besides the passive component, ASBT exhibiting a high affinity for tauro-conjugated BA is located in the ileum. Neg-

ative feedback regulation by conjugated BA has been reported in rats and guinea pigs, together with an upregulation of ileal transport by cholestyramine (13). Enhanced capacities of ileal BA reabsorption have been reported by Riottot and Sacquet (12) in rats adapted to a resistant starch diet. Upregulation of ileal ASBT has been described in the presence of excess cholic acid or after glucocorticoid treatment (14,28). However, Arrese *et al*. (29) have recently questioned the view that a reduction in presentation of bile salts to the apical surface of the ileum would modulate the expression of the genes involved in their transport. In the present case, no significant change in TC absorption capacity could be found in rats adapted to the GG diet, at least under conditions in which an unstirred layer plays practically no role. The IvA differences across the ileum were markedly elevated in rats adapted to a GG diet. Because local blood flow is not available, these IvA differences cannot be interpreted in terms of fluxes. Nevertheless, blood flow in the ileum of rats fed GG diets was probably as great as in controls (or even somewhat greater) since (i) GG elicits trophic effects on the ileal intestinal wall (30) and (ii) digesta in the ileum are bulkier than in FF controls. Gel-forming fibers are effective in slowing digestive transit in the upper part of the digestive tract (31) but, owing to the bulking effect of GG (31,32), the flux of materials (hence of BA) might be higher in rats fed GG than in controls. The dietary load of cholesterol may cause an inhibition of BA absorption in the ileum (33), but this is not particularly clear in the present experiment with a relatively limited cholesterol supplementation.

Soluble fiber has been reported to alter BA conjugation by increasing the percentage of glyco-conjugated at the expense of tauro-conjugated BA(34). It is still unclear whether ileal reabsorption of glyco-conjugated BA is really different from that of the tauro-conjugates, especially *in vivo* in the presence of complex mixtures of both glyco- and tauro-conjugates. As reported recently (11), ileal ASBT mediates the uptake of TC as well as that of unconjugated C, or of glycine conjugates of deoxycholate, chenodeoxycholate, or ursodeoxycholate (with a low K_m for these last). A shift of BA conjugation from tauro- to glyco-conjugation could thus improve BA reabsorption because glyco-conjugated compounds are subjected to active transport by ASBT as well as to passive diffusion in the jejunum and the ileum. In this last segment, diffusion could be higher through a less fluid membrane (high cholesterol/phospholipid ratio) than in the jejunum (35). It must be noted that dietary factors, including cholesterol, are likely to affect ileal transport through membrane lipid compositional changes (36), a domain still poorly known.

Possibilities of passive BA diffusion across the large intestine wall are reflected by the presence of secondary BA in the body's pool (9,37) and by absorption measurements (4). This reabsorption was found to be greater in rats adapted to GG than in controls, and it was also greater when cholesterol was present in the diet, in parallel to an enlargement of the BA cecal pool. The solubility of bile acids in the large intestine lumen is governed by complex factors: luminal pH, CaPi concentration, bacterial proliferation (38,39). Expression of ASBT in the cecal wall is uncertain (10,11), but in rats fed GG diets the larger surface area of exchange and local blood flow are likely to accelerate the diffusion flux. Furthermore, parameters related to the presence of active fermentations in the cecal lumen may promote BA reabsorption, that is, moderately acidic pH conditions and the presence of high SCFA concentrations. The mechanisms are still unclear, and they could be related to the general effects of SCFA on mineral and water fluxes. *In vivo*, the cecal BA flux may represent less than 10% of the portal flux (FF diet) but nearly 25% under favorable conditions (GG/cholesterol diet) (16). The contribution of the cecum is probably enhanced when the small intestine pool is enlarged and when ileal absorption fails to match a very large flux of BA.

The existence of a higher portal BA concentration in rats adapted to GG or GG/cholesterol diets, compared to FF controls (16), probably resulted in a larger hepatic uptake since the systemic BA concentration was not substantially enhanced by the various diet treatments. Furthermore, the overall BA synthesis might be increased by GG, in keeping with previous observations showing a larger fecal BA excretion and an induction of cholesterol 7α-hydroxylase with GG diets (2,22) compared to FF conditions. Classical concepts on the lipid-lowering effects of soluble fiber postulate that portal BA should be depressed which, in turn, up-regulates the hepatic cholesterol 7α-hydroxylase. In fact, some experimental reports do not verify this view: Cronholm and Sjövall (40), for example, and Fukushima *et al*. (15) did not find any significant decrease of portal BA in rats fed a sequestrant. Pandak *et al*. (41) have proposed that the effects of BA on cholesterol 7α-hydroxylase may be indirect and involve intestinal factors secreted (or absorbed) under the influence of BA in the intestine lumen. Negative control of cholesterol 7α-hydroxylase expression by BA has been extensively investigated, and secondary (hydrophobic) BA are considered as the most effective (42). This action may involve the protein kinase C (PKC) signaling pathway; it has be shown that the α isoform of Ca-dependent PKC is translocated to the plasma membrane in response to application of physiological concentrations of BA (43). At a molecular scale, regulation of cholesterol 7α-hydroxylase expression is particularly complex: several elements have been identified that confer to the gene responsiveness to BA (BA response elements) and to stimuli such as insulin, cAMP, and phorbol esters (44). This point suggests that the metabolic and endocrine status is liable to modulate the activity of cholesterol 7α-hydroxylase (18). In this view, a high-fiber diet may blunt postprandial hyperinsulinemia and alter the profile of the nutrients absorbed in the portal vein, especially the glucose/SCFA ratio (45,46). Furthermore, it must be kept in mind that part of BA synthesis is dependent on a sterol 27 hydroxylase pathway, the nutritional regulation of which is still poorly known, although it is generally considered less inducible than cholesterol 7α-hydroxylase (18,47).

In conclusion, GG elicits marked changes in the intestinal pools of BA and, since secretion and fecal excretion fluxes

may be raised in such diet conditions (4,16), it seems conceivable that enterohepatic cycling of BA is accelerated by GG. Nevertheless, cholesterol oxidation could remain relatively active in the presence of high concentrations of BA in hepatic afferent blood, supporting the view that the control of cholesterol 7α-hydroxylase activity is particularly complex. Compositional changes of portal BA or other metabolic factors (subtrates, hormones) could play a critical role in this control.

REFERENCES

1. Glore, S.R., Van Treeck, D., Knehaus, A.W., and Guild, M. (1994) Soluble Fiber and Serum Lipids: A Literature Review, *J. Am. Diet. Assoc. 94*, 425–436.
2. Fernandez, M.L., Sun, D.M., Tosca, M., and McNamara, D.J. (1995) Guar Gum Effects on Plasma Low-Density Lipoprotein and Hepatic Cholesterol Metabolism in Guinea Pigs Fed Low- and High-Cholesterol Diets: A Dose-Dependent Study, *Am. J. Clin. Nutr. 61*, 127–134.
3. Truswell, A.S. (1995) Dietary Fibre and Blood Lipids, *Curr. Opin. Lipidol. 6*, 14–19.
4. Moundras, C., Behr, S.R., Rémésy, C., and Demigné, C. (1997) Fecal Losses of Sterols and Bile Acids Induced by Feeding Rats Guar Gum Are Due to a Greater Pool Size and Liver Bile Acids Secretion, *J. Nutr. 127*, 1068–1076.
5. Trautwein, E.A., Kunath-Rau, A., and Erbersdobler, E. (1998) Effect of Different Varieties of Pectin and Guar Gum on Plasma, Hepatic and Biliary Lipids and Cholesterol Gallstone Formation in Hamsters Fed on High-Cholesterol Diets, *Br. J. Nutr. 79*, 463–471.
6. Stedronsky, E.R. (1994) Interaction of Bile Acids and Cholesterol with Non-systemic Agents Having Hypocholesterolemic Properties, *Biochim. Biophys. Acta 1210*, 255–287.
7. Gee, J.M., Blackburn, N.A., and Johnson, I.T. (1983) The Influence of Guar Gum on Intestinal Cholesterol Transport in the Rat, *Br. J. Nutr. 50*, 215–224.
8. Phillips, D.R. (1986) The Effect of Guar Gum in Solution on Diffusion of Cholesterol Mixed Micelles, *J. Sci. Food Agric. 37*, 548.
9. Hofmann, A.F. (1994) in *Physiology of the Gastrointestinal Tract* (Johnson, L.R., ed.) 3rd edn., pp. 1845–1865, Raven Press, New York.
10. Schneider, B.L., Dawson, P.A., Christie, D-M., Hardikar, W., Wong, M.H., and Suchy, F.J. (1995) Cloning and Molecular Characterization of the Ontogeny of Rat Ileal Sodium-Dependent Bile Acid Transporter, *J. Clin. Invest. 95*, 745–754.
11. Craddock, A.L., Love, M.W., Daniel, R.W., Kirby, L.C. Walters, H.C., Wong, M.H., and Dawson, P.A. (1998) Expression and Transport Properties of the Human Ileal and Renal Sodium-Dependent Bile Acid Transporter, *Am. J. Physiol. 274*, G157–G169.
12. Riottot, M., and Sacquet, E. (1985) Increase in the Ileal Absorption Rate of Sodium Taurocholate in Germ-free or Conventional Rats Given an Amylomaize-Starch Diet, *Br. J. Nutr. 53*, 307–310.
13. Lillienau, J., Crombie, D.L., Munoz, J., Longmire-Cook, S.J., Hagey, L.R., and Hofmann, A.F. (1993) Negative Feedback Regulation of the Ileal Bile Transport System in Rodents, *Gastroenterology 104*, 38–46.
14. Stravitz, R.T., Sanya, A.J., Pandak, W.M., Vlahcevic, Z.R., Beets, J.W., and Dawson, P.A. (1997) Induction of Sodium-Dependent Bile Acid Transporter Messenger RNA, Protein, and Activity in Rat Ileum by Cholic Acid, *Gastroenterology 113*, 1599–1608.
15. Fukushima, K., Ichimiya, H., Higashijima, H., Yamashita, H., Kuroki, S., Chijiwa, K., and Tanaka, M. (1995) Regulation of Bile Acid Synthesis in the Rat: Relationship Between Hepatic Cholesterol 7α-Hydroxylase Activity and Portal Bile Acids, *J. Lipid Res. 36*, 315–321.
16. Demigné, C., Levrat, M.-A., Behr, S., Moundras, C., and Rémésy, C. (1998) Cholesterol-Lowering Action of Guar Gum in the Rat: Changes in Bile Acids and Sterols Excretion and in Enterohepatic Cycling of Bile Acids, *Nutr. Res. 18*, 1215–1225.
17. Danielsson, H., Einarsson, K., and Johansson, G. (1967) Effect of Biliary Drainage on Individual Reactions in the Conversion of Cholesterol to Taurocholic Acid, *Eur. J. Biochem. 2*, 44–49.
18. Princen, H.M.G., Post, S.M., and Twisk, J. (1997) Regulation of Bile Acid Biosynthesis, *Current Pharmaceut. Design 3*, 59–84.
19. Todd, P.A., Benfield, P., and Goa, K.L. (1990) Guar Gum. A Review of Its Pharmacological Properties, and Use as a Dietary Adjunct in Hypercholesterolemia, *Drugs 39*, 917–928.
20. Anderson, J.W., Jones, A.E., and Riddell-Mason, S. (1994) Ten Different Dietary Fibers Have Significant Different Effects on Serum and Liver Lipids on Cholesterol-Fed Rats, *J. Nutr. 124*, 78–83.
21. Vahouny, G.V., Tombes, R., Cassidy, M.M., Kritchevsky, D., and Gallo, L.L (1980) Dietary Fibers: V. Binding of Bile Salts, Phospholipids and Cholesterol from Mixed Micelles by Bile Acid Sequestrants and Dietary Fibers, *Lipids 15*, 1012–1018.
22. Favier, M.-L., Bost, P-E., Guittard, C., Demigné, C., and Rémésy, C. (1997) The Cholesterol-Lowering Effect of Guar Gum Is Not the Result of a Simple Diversion of Bile Acids Toward Fecal Excretion, *Lipids 32*, 953–959.
23. Ikegami, S., Tsuchihashi, F., Harada, H., Tsuchihashi, N., Nishide, E., and Innani, S. (1990) Effect of Viscous Indigestible Polysaccharide on Pancreatic-Biliary Secretion and Digestive Organs in Rats, *J. Nutr. 120*, 353–360.
24. Ide, T., Moruichi, H., and Nihimoto, K. (1991) Hypolipidemic Effects of Guar Gum and Its Enzyme Hydrolysate in Rats Fed Highly Saturated Fat Diets, *Ann. Nutr. Metab. 35*, 34–44.
25. Ide, T., and Horii, M. (1987) A Simple Method for Extraction and Determination of Non-conjugated and Conjugated Luminal Bile Acids in Rats, *Agric. Biol. Chem. 51*, 3155–3157.
26. Lewis, M.C., and Root, C. (1990) *In vivo* Transport Kinetics and Distribution of Taurocholate by Rat Ileum and Jejunum, *Am. J. Physiol. 259*, G233–G238.
27. Juste, C., Legrand-Defretin, V., Corring, T., and Rerat, A. (1988) Intestinal Absorption of Bile Acids in the Pig. Role of Distal Bowel, *Dig. Dis. Sci. 33*, 67–73.
28. Nowicki, M.J., Shneider, B.L., Paul, J.M., and Heubi, J.E. (1997) Glucocorticoids Upregulate Taurocholate Transport by Ileal Brush-border Membrane, *Am. J. Physiol. 273*, G197–G203.
29. Arrese, M., Trauner, M., Sacchiero, R.J., Crossman, M.W., and Schneider, B.L. (1998) Neither Intestinal Sequestration of Bile Acids Nor Common Bile Duct Ligation Modulate the Expression and Function of the Rat Ileal Bile Acid Transporter, *Hepatology 28*, 1081–1087.
30. Stark, A., Nyska, A., and Madar, Z. (1996) Metabolic and Morphometric Changes in Small and Large Intestine in Rats Fed High-Fiber Diets, *Toxicol. Pathol. 24*, 166–171.
31. Brown, N.J., Worlding, J., Rumsey, R.D.E., and Read, N.W. (1988) The Effect of Guar Gum on the Distribution of a Radiolabelled Meal in the Gastrointestinal Tract of the Rat, *Br. J. Nutr. 59*, 223–231.
32. Cherbut, C., Albina, E., Champ, M., Doublier, J.L., and Lecannu, G. (1990) Action of Guar Gums on the Viscosity of Digestive Contents and on the Gastrointestinal Motor Function in Pigs, *Digestion 46*, 205–213.
33. Björkhem, I., Eggerston, G., and Andersson, U. (1991) On the Mechanism of Stimulation of Cholesterol 7α-Hydroxylase by Dietary Cholesterol, *Biochim. Biophys. Acta 1085*, 329–335.

34. Ide, T., Horii, M., Yamamoto, T., and Kawashima, K. (1990) Contrasting Effects of Water-Soluble and Water-Insoluble Dietary Fibers on Bile Acid Conjugation and Taurine Metabolism in the Rat, *Lipids 25,* 335–340.
35. Aldini, R., Montagnani, M., Roda, A., Hrelia, S., Biagi, P.L., and Roda, E. (1996) Intestinal Absorption of Bile Acids in the Rabbit: Different Transport Rates in Jejunum and Ileum, *Gastroenterology 110,* 459–468.
36. Dumaswala, R., Berkowitz, D., Setchell, K.D., and Heubi, J.E. (1994) Effects of Fasting on the Enterohepatic Circulation of Bile Acids in Rats, *Am. J. Physiol. 267,* G836–G842.
37. Walker, S., Stiehl, A., Raedsch, R., Kloters, P., and Kommerell, B. (1985) Absorption of Urso- and Chenodeoxycholic Acid and Their Taurine and Glycine Conjugates in Rat Jejunum, Ileum, and Colon, *Digestion 32,* 47–52
38. Rémésy, C., Levrat, M-A., Gamet, L., and Demigné, C. (1993) Cecal Fermentations in Rats Fed Oligosaccharides (inulin) Are Modulated by Dietary Calcium Level, *Am. J. Physiol. 264,* G855–G862.
39. Gelissen, I., and Eastwood, M.A. (1995) Taurocholic Adsorption During Non-starch Polysaccharide Fermentation: An *in vitro* Study, *Br. J. Nutr. 74,* 221–228.
40. Cronholm, T., and Sjövall, J. (1967) Bile Acids in Portal Blood of Rats Fed Different Diets and Cholestyramine, *Eur. J. Biochem. 2,* 375–383.
41. Pandak, W.M., Heuman, D.M., Hylemon, P.B., Chiang, J.Y.L., and Vlahcevic, Z.R. (1995) Failure of Intravenous Infusion of Taurocholate to Down-regulate Cholesterol 7α-Hydroxylase in Rats with Biliary Fistula, *Gastroenterology 108,* 533–544.
42. Stange, E.F., Scheibner, J., and Ditschuneit, H. (1989) Role of Primary and Secondary Bile Acids as Feedback Inhibitors of Bile Acid Synthesis in the Rat *in vivo, J. Clin. Invest. 84,* 173–180.
43. Stravitz, R.T., Vlahcevic, Z.R., Gurley, E.C., and Hylemon, P.B. (1995) Repression of Cholesterol 7α-Hydroxylase Transcription by Bile Acids Is Mediated Through Protein Kinase C in Primary Cultures of Rat Hepatocytes, *J. Lipid Res. 36,* 1359–1369.
44. Stroup, D., Crestani, M., Chiang, J.Y.L. (1997) Identification of a Bile Acids Response Element in the Cholesterol 7α-Hydroxylase Gene CYP7A, *Am. J. Physiol. 273,* G508–G517.
45. Jenkins, D.J.A., Leeds, A.R., Gassull, M.A., Cochet, B., and Alberti, K.G.M.M. (1977) Decrease in Postprandial Insulin and Glucose Concentrations by Guar and Pectin, *Ann. Intern. Med. 86,* 20–23.
46. Morand, C., Levrat, M., Besson, C., Demigné, C., and Rémésy C. (1994) Effect of a Diet Rich in Resistant Starch on Hepatic Lipid Metabolism in the Rat, *J. Nutr. Biochem. 5,* 138–144.
47. Vlahcevic, Z.R., Stravitz, R.T., Heuman, D.M., Hylemon, P.B., and Pandak, W.M. (1997) Quantitative Estimations of the Contribution of Different Bile Acid Pathways to the Total Bile Acid Synthesis in the Rat, *Gastroenterology 113,* 1949–1957.

[Received December 15, 1998; and in final revised form September 23, 1999; revision accepted February 21, 2000]

Changes in Liver Fatty Acid Unsaturation After Partial Hepatectomy in the Rat

Tomonori Kishino[a,*], Munehiko Tanno[b], Hideo Yamada[b], Shozo Saito[a], and Shigenobu Matsumoto[c]

[a]The Third Department of Internal Medicine, Kyorin University School of Medicine, Tokyo, 181-8611, Japan,
[b]Department of Radiology, Tokyo Metropolitan Geriatric Hospital, Tokyo, 173-0015, Japan, and
[c]Department of Biochemistry and Isotopes, Tokyo Metropolitan Institute of Gerontology, Tokyo, 173-0015, Japan

ABSTRACT: The purpose of this study was to assess changes in the degree of fatty acid unsaturation in rat liver after partial hepatectomy. This is the first study in which liver fatty acid unsaturation has been analyzed over a long period of regeneration until day 28 after operation. The relationship between changes in unsaturation and fatty acid composition in the regenerating liver were also investigated in this study. Proton nuclear magnetic resonance spectroscopy revealed significantly elevated levels of unsaturation with a maximum on day 5 after partial hepatectomy, compared with untreated controls (11.72 ± 0.55 vs. 11.05 ± 0.26%, $P < 0.05$). No significant changes in unsaturation were found in day 1 regenerating liver, which is rich in absolute amounts of fatty acids. Based on gas–liquid chromatography, the relative amounts of oleic acid (18:1n-9) and linoleic acid (LA; 18:2n-6) were increased, while polyunsaturated fatty acids such as arachidonic acid (20:4n-6) and docosahexaenoic acid (DHA; 22:6n-3) were decreased on day 1. On the other hand, on day 5 of regeneration, while most fatty acids were returning to their preoperative control levels, only DHA was higher than the control value (7.69 ± 0.58 vs. 5.57 ± 0.37%, $P < 0.001$). The high levels of unsaturation on day 5 were found to be partly due to the increase in DHA. The findings suggest that some significant signals are transmitted during the regeneration process owing to alterations in the membrane structure by the high levels of fatty acid unsaturation and the increase in DHA levels on day 5 after partial hepatectomy.

Paper no. L7992 in *Lipids 35*, 445–452 (April 2000).

Much remains unknown concerning the mechanisms of liver regeneration. Regenerating rat liver is an ideal model system in which to study the mechanisms that control cell proliferation. It is now well established that some of the biochemical changes that occur during liver regeneration also occur during tumor growth. Therefore, observations about liver regeneration also will lead to a better understanding of the mechanisms of neoplastic and some liver diseases.

Fatty acids form one category of cell constituents, and among them, unsaturated fatty acids are related to membrane permeability (1–6), signal transduction (7–9), and cell proliferation (10,11). It has been reported that the composition of liver fatty acids changes during regeneration (12–16). However, there have been few studies concerning fatty acid unsaturation in the regenerating liver. Bruscalupi *et al.* (16) analyzed changes in the degree of unsaturation for up to 24 h after partial hepatectomy by gas–liquid chromatography. Many investigators have focused on the time around day 1 after hepatectomy when DNA synthesis reaches its peak and is followed by the mitotic peak (17–19). Details concerning unsaturation have not yet been fully investigated over long periods of liver regeneration.

In this study, we extended the analysis of changes in fatty acid unsaturation to day 28 after hepatectomy, at which time regeneration is essentially complete. Proton nuclear magnetic resonance (^{1}H NMR) spectroscopy shows that the degree of unsaturation of the liver fatty acids appears to increase to a maximum on day 5 after hepatectomy. In addition, gas–liquid chromatography reveals some contribution of docosahexaenoic acid (DHA; 22:6n-3) to the high degree of unsaturation at this time.

MATERIALS AND METHODS

Experiment 1 (changes in fatty acid unsaturation in the liver after partial hepatectomy). (i) Animal model. Male Wistar rats were obtained from Japan Slc Co. (Shizuoka, Japan) at the age of 12 wk and raised to 30–35 wk for experiments. All animals received humane care according to the Guideline for Animal Experimentation published by the Japanese Association for Laboratory Animal Science. Rats were housed in a windowless room with 12 h light/12 h dark and allowed free access to a standard laboratory diet and water preoperatively and postoperatively. Standard laboratory chow was obtained from Oriental Yeast Co. (Osaka, Japan). The fatty acid composition of the liver had been stabilized by the diet at the time of operation. Three groups of rats were studied. (i) Rats in group 1 were controls and underwent no treatment ($n = 6$); (ii) rats in group 2 were subjected to partial hepatectomy and sacrificed after operation on day 1, 2, 3, 5, 7, 10, 14, 21, or 28 ($n = 6$ at each time); and (iii) rats in group 3 were subjected to simple laparotomy, a so-called sham operation, and sacrificed after operation on day 1, 2, 3, 5, 7, 10, 14, 21, or 28 ($n =$

*To whom correspondence should be addressed at The Third Department of Internal Medicine, Kyorin University School of Medicine, 6-20-2 Shinkawa, Mitaka-shi, Tokyo, 181-8611, Japan. Fax: 81-422-40-1662.

Abbreviations: AA, arachidonic acid; ANOVA, analysis of variance; DHA, docosahexaenoic acid; ^{1}H NMR, proton nuclear magnetic resonance; LA, linoleic acid; OA, oleic acid; PUFA, polyunsaturated fatty acids.

6 at each time). It is well known that surgical stress alone causes changes in the fatty acid composition of the liver (12–16). All groups of rats were given same diet both before and after surgery. The mean body weight of the rats was 390 g at the time of surgery.

(ii) Surgery. Partial (70%) hepatectomies were performed between 1200 and 1300 under light diethylether anesthesia by the method of Higgins and Anderson (20). Sham operations were carried out during the same period.

(iii) Lipid extraction. Rats were killed at various times after surgery described above. Liver samples were taken at random from one of the regenerating lobes. Minor liver lobes, corresponding to the remaining liver lobes in the hepatectomized rats, were taken from the control and sham-operated rats.

Five samples of 0.5 g tissue were taken for analysis from each rat liver, and the average of the five samples was regarded as the value from one rat by ^{1}H NMR spectroscopy analysis. A total of six animals were used from each group at each time after operation, so 30 samples were analyzed at each time.

Lipids were extracted by the method of Kwee *et al.* (21) [modified Folch *et al.* (22) method] as described below. Chloroform/methanol (4.5 mL; 2:1, vol/vol) was added to each 0.5 g piece of liver, and the lipids were extracted for 1 d under nitrogen. The solution was washed with 0.15 mL of 6 N HCl for 2 h, vortexed with 7 mL of chloroform for 2 min, then vortexed again for 2 min after the addition of 1.5 mL of 0.05 N KCl. The solution was allowed to stand for 2 h, the bottom layer was removed, and the upper phase was washed again with 3 mL chloroform. The combined organic solution was evaporated under a stream of nitrogen to prevent the oxidation of unsaturated fatty acids. This lipid sample contained the total fatty acids from all kinds of lipids (triacylglycerol, phospholipid, glycolipid, and cholesterol ester). Samples were stored under nitrogen at –40°C until ^{1}H NMR spectroscopy measurement on the following day.

(iv) ^{1}H NMR spectroscopy. The lipid extracts were redissolved in 0.7 mL of deuterochloroform and placed in 5-mm NMR tubes for ^{1}H NMR spectroscopic analysis. Spectra were taken on a VXR-400S Varian Spectrometer (Varian NMR Instruments, Palo Alto, CA) operating at a proton frequency of 399.952 MHz. All spectra were obtained using an 18° pulse, a spectral width of 6000 Hz, a repetition time of 3.7 s, 44 K data points, and a sample spinning rate of 16 Hz. Thirty-two to sixty-four acquisitions were required to attain an adequate signal. Chemical shifts are expressed with respect to residual $CHCl_3$ at 7.24 ppm. During data processing, line broadening of 0.3 Hz was applied as a noise filter. Peaks were assigned by comparison with literature data (21,23–26). Each proton on the fatty acyl chain has its own chemical shift determined by its binding character, and its assignment is shown on the spectrum in Figure 1. Peak intensity is related to the number of protons. Peak intensities were determined by computerized integration after careful baseline correction.

Values were calculated using arithmetic functions of integrated peak intensities. The degree of unsaturation was analyzed by obtaining the ratio between the double-bond peak and the sum of all peaks. Changes in unsaturation were evaluated over the time course of liver regeneration.

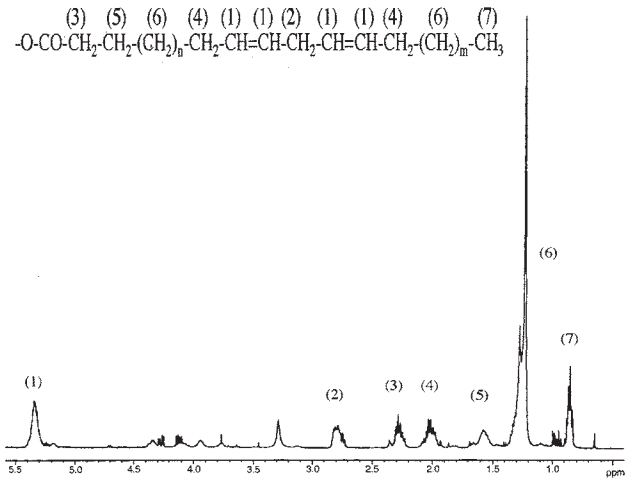

FIG. 1. Representative ^{1}H nuclear magnetic resonance (NMR) spectrum of a rat liver lipid extract. The major peaks assignable to protons in different positions on the fatty acids are indicated by numbers on the spectrum. Peak (1) represents the protons of double bonds in fatty acyl chains. Minor peaks on the spectrum from 3.0 to 4.5 ppm correspond to the remaining polar heads of phospholipids.

Experiment 2 (changes in fatty acid composition of regenerating livers). After Experiment 1, the unsaturation of the liver fatty acids after partial hepatectomy was shown to reach a maximum on day 5. The fatty acid composition was then analyzed by gas–liquid chromatography.

(i) Animal model. Male Wistar rats, age 30–35 wk, were used and surgery was performed under the same conditions as for Experiment 1. Samples from the following groups were subjected to gas–liquid chromatographic analysis: (i) untreated controls (n = 10); (ii) partial hepatectomy (n = 10 for days 1 and 5; n = 5 for days 2, 3, 7, 10, 14, 21, and 28).

(ii) Gas–liquid chromatography. Fatty acid methyl esters for gas chromatographic analysis were prepared from hepatic lipids as follows. Lipids were extracted in chloroform/methanol (2:1, vol/vol) as described for Experiment 1; the lipid sample obtained was again a mixture of all kinds of lipids. Lipid extracts were evaporated to dryness under a stream of nitrogen and then redissolved in 1 mL of dichloromethane, 2 mL of 4.5% HCl/methanol, and 0.5 mL of 1,2,3-trihydroxybenzene (pyrogallol; Sigma, St. Louis, MO). The mixtures were heated at 80°C for 1 h. After cooling, the lipids were extracted three times with hexane (5 mL × 3). The hexane extracts were combined, and 4 mL of 2% $KHCO_3$ was added. The hexane layers were separated, dried over sodium sulfate, filtered, and evaporated to dryness under nitrogen. The resulting residue was redissolved in 500 μL of hexane; then 1 μL of pentadecanoic acid methyl ester was added as an internal standard to obtain the absolute amount, and 1 μL of the total aliquot was subjected to gas–liquid chromatographic analysis.

The fatty acid methyl esters were separated in an HP5890 Series II Gas Chromatograph (Hewlett-Packard GmbH, Waldbronn, Germany) with an Omegawax 250 capillary col-

umn (Supelco Inc., Bellefonte, PA) using a flame-ionization detector. The injector, column, and detector temperatures were maintained at 250, 205, and 260°C, respectively. Helium was employed as the carrier gas at a linear velocity of 30 cm/s. The amount of each fatty acid was quantitated by automatic calculation of the peak area by an HP3396 Series II integrator (Hewlett-Packard GmbH). For identification of fatty acids, retention times were compared to a standard mixture of known composition. Fatty acid compositions are expressed in terms of mole percentages of total fatty acids and absolute amounts. Fatty acid unsaturation was also analyzed from the results of gas–liquid chromatography. The method of calculation is shown in Table 1. However, the evaluation is different from that by ^{1}H NMR spectroscopy. On the one hand, the ^{1}H NMR spectroscopy in Experiment 1 deals with the degree of unsaturation as the ratio between protons on double bonds and total protons on fatty acids, but gas–liquid chromatography deals with the unsaturation as the mean number of double bonds per one fatty acid molecule.

The percentage was then calculated for the ratio of double bonds in each major unsaturated fatty acid to total double bonds in all fatty acids in the liver. (See legend to Fig. 4.)

Statistical analysis. For Experiment 1 with ^{1}H NMR spectroscopy, two-factor factorial analysis of variance (ANOVA) was used to analyze the effects of treatment (partial hepatectomy vs. sham operation) and time after operation. The significance of differences was assessed by *post hoc* tests.

For Experiment 2 with gas–liquid chromatography, *post*

TABLE 1
Fatty Acid Composition of Untreated Control and Day 1 and Day 5 Regenerating Livers[a]

Fatty acid	Control	Day 1	Day 5	P1	P2	P3
14:0	0.80 ± 0.05	0.56 ± 0.06	0.31 ± 0.05	<0.001	<0.001	<0.001
	(0.23 ± 0.03)	(0.32 ± 0.11)	(0.11 ± 0.03)	0.022	<0.001	<0.001
16:0	27.86 ± 0.83	23.33 ± 1.23	23.20 ± 1.41	<0.001	<0.001	NS
	(8.95 ± 1.08)	(14.64 ± 4.00)	(8.70 ± 2.02)	<0.001	NS	<0.001
16:1n-7	2.80 ± 0.50	1.17 ± 0.20	0.58 ± 0.10	<0.001	<0.001	<0.001
	(0.91 ± 0.20)	(0.75 ± 0.31)	(0.22 ± 0.06)	NS	<0.001	<0.001
17:0	0.44 ± 0.06	0.34 ± 0.05	0.38 ± 0.05	<0.001	0.025	NS
	(0.15 ± 0.01)	(0.22 ± 0.05)	(0.15 ± 0.02)	<0.001	NS	<0.001
18:0	10.97 ± 1.07	8.11 ± 1.66	12.03 ± 1.85	<0.001	NS	<0.001
	(3.81 ± 0.42)	(5.40 ± 0.88)	(4.90 ± 0.99)	<0.001	0.005	NS
18:1n-9	9.78 ± 1.14	12.27 ± 1.51	10.23 ± 1.33	<0.001	NS	0.004
	(3.53 ± 0.67)	(8.77 ± 3.33)	(4.22 ± 1.13)	<0.001	NS	<0.001
18:1n-7	4.05 ± 0.20	2.52 ± 0.25	3.08 ± 0.41	<0.001	<0.001	0.002
	(1.43 ± 0.17)	(1.73 ± 0.50)	(1.24 ± 0.23)	NS	NS	0.011
18:2n-6	19.11 ± 1.27	32.05 ± 3.29	25.70 ± 2.35	<0.001	<0.001	<0.001
	(6.71 ± 1.01)	(22.53 ± 7.79)	(10.64 ± 3.08)	<0.001	0.001	<0.001
18:3n-6	0.22 ± 0.02	0.19 ± 0.04	0.22 ± 0.05	0.040	NS	NS
	(0.08 ± 0.02)	(0.14 ± 0.06)	(0.09 ± 0.02)	0.008	NS	0.022
18:3n-3	0.59 ± 0.08	1.56 ± 0.30	0.49 ± 0.14	<0.001	NS	<0.001
	(0.21 ± 0.04)	(1.11 ± 0.41)	(0.21 ± 0.09)	<0.001	NS	<0.001
20:1n-9	0.20 ± 0.05	0.18 ± 0.03	0.27 ± 0.08	NS	0.030	0.003
	(0.08 ± 0.02)	(0.14 ± 0.06)	(0.12 ± 0.04)	0.008	0.011	NS
20:2n-6	0.46 ± 0.08	0.36 ± 0.02	0.54 ± 0.15	0.001	NS	0.001
	(0.18 ± 0.04)	(0.27 ± 0.08)	(0.24 ± 0.07)	0.005	0.030	NS
20:3n-6	0.71 ± 0.12	0.40 ± 0.07	0.60 ± 0.18	<0.001	NS	0.004
	(0.27 ± 0.06)	(0.30 ± 0.12)	(0.26 ± 0.07)	NS	NS	NS
20:4n-6	13.51 ± 0.95	9.48 ± 1.78	11.75 ± 1.93	<0.001	0.019	0.014
	(5.01 ± 0.45)	(6.78 ± 1.29)	(5.08 ± 0.96)	<0.001	NS	0.004
20:5n-3	0.75 ± 0.12	0.99 ± 0.14	0.48 ± 0.10	<0.001	<0.001	<0.001
	(0.28 ± 0.05)	(0.76 ± 0.31)	(0.22 ± 0.09)	<0.001	NS	<0.001
22:4n-6	0.48 ± 0.09	0.53 ± 0.05	0.71 ± 0.12	NS	<0.001	<0.001
	(0.20 ± 0.05)	(0.43 ± 0.15)	(0.34 ± 0.10)	<0.001	<0.001	NS
22:5n-3	1.62 ± 0.25	1.35 ± 0.11	1.64 ± 0.27	0.006	NS	0.006
	(0.66 ± 0.12)	(1.10 ± 0.38)	(0.81 ± 0.28)	0.003	NS	NS
22:6n-3	5.57 ± 0.37	4.51 ± 0.91	7.69 ± 0.58	0.003	<0.001	<0.001
	(2.24 ± 0.27)	(3.55 ± 1.07)	(3.67 ± 0.93)	0.001	<0.001	NS
Unsaturation	1.61 ± 0.05	1.66 ± 0.04	1.77 ± 0.03	0.020	<0.001	<0.001

[a]Values are expressed as relative percentages of the molar amount of each fatty acid. Values in parentheses are the absolute amounts of fatty acids expressed as μg/g tissue. Mole percentages of various fatty acids were calculated on the basis of the actual amounts of fatty acids determined from the integrated peak areas on the chromatogram and the molecular weights of the respective fatty acid methyl esters. Fatty acids are designated as number of carbon atoms:number of double bonds. Unsaturation is presented as the mean number of double bonds per fatty acid molecule at the bottom. Values were calculated using the following formula: Σ (x × each fatty acid mol%/100), where x represents the number of double bonds in the fatty acid (0–6). Each number represents the mean ± SD of 10 values from 10 rats. P1: comparison of untreated control vs. day 1; P2: comparison of untreated control vs. day 5; P3: comparison of day 1 vs. day 5. NS: not significant.

hoc tests were used to analyze the significance of differences among the untreated controls and rats on days 1 and 5 after partial hepatectomy. For changes in the amounts of total fatty acids and DHA (day 0 through day 28), one-factor ANOVA and *post hoc* tests were used to analyze the effect of time after partial hepatectomy.

RESULTS

A representative ^{1}H NMR spectrum of lipid extracts from rat liver is shown in Figure 1.

Figure 2 shows changes in the degree of unsaturation after partial hepatectomy. The rat liver fatty acids after partial hepatectomy were highly unsaturated during regeneration. Unsaturation reached a maximum on day 5 after hepatectomy and then decreased gradually to control levels. As compared with the control level (11.05 ± 0.26%), unsaturation was significantly increased on day 5 and day 7 at 11.72 ± 0.55 and 11.67 ± 0.53%, respectively (vs. control, $P < 0.05$). No significant difference was observed between control and sham-operated rats at any time after operation. The degree of unsaturation after partial hepatectomy was significantly higher than that after sham operation on day 5 and day 7 ($P < 0.05$). On day 1 following partial hepatectomy, a small decrease in the level of unsaturation (10.81 ± 0.44%) was noted, but this was not statistically significant.

The fatty acid composition of livers after partial hepatectomy was analyzed by gas–liquid chromatography. As shown in Figure 3, the absolute amount of total fatty acids was increased during the early phase of regeneration from day 1 to day 3 ($P < 0.0001$), and peaked on day 2 (96.7 ± 13.5 μg/g tissue). The amount of each fatty acid reached a maximum on day 2 (data not shown).

Values from untreated control and regenerating livers on day 1 and day 5 are shown in Table 1.

The absolute amounts of most fatty acids were greatly increased during the early phase of regeneration and were returning to the preoperative control level on day 5. However, as far as the relative amounts were concerned, the individual fatty acids demonstrated different interesting characteristics. The percentages of mono- and dienoic unsaturated fatty acids such as oleic acid (OA; 18:1n-9) and linoleic acid (LA; 18:2n-6) rose to 12.27 ± 1.51 and 32.05 ± 3.29%, respectively, on day 1 (vs. control, $P < 0.001$) and then were returning to the preoperative level on day 5. This change was the same as the change in their absolute amounts. On the other hand, the relative amounts of the major polyunsaturated fatty acids (PUFA) were decreased on day 1, in contrast to their absolute amounts. Arachidonic acid (AA; 20:4n-6) decreased to 9.48 ± 1.78% on day 1 (vs. control, $P < 0.001$), then recovered but failed to reach the preoperative value by day 5. DHA, another PUFA, demonstrated a more interesting behavior. DHA decreased to 4.51 ± 0.91% on day 1 (vs. control, $P < 0.01$), like AA, but it recovered from the decrease and had increased over the preoperative control level on day 5 (7.69 ± 0.58 vs. 5.57 ± 0.37%, $P < 0.001$). Moreover, the absolute amount of

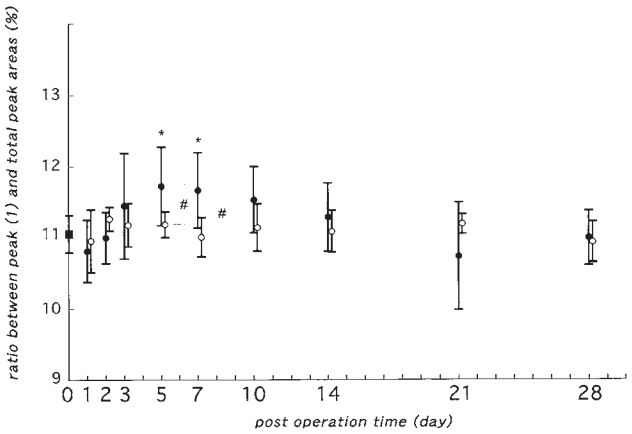

FIG. 2. Changes in the degree of unsaturation of hepatic lipids after partial hepatectomy as determined by ^{1}H NMR spectroscopy. Unsaturation is determined as the ratio between peak (1) and the total peak area (peaks are identified in Fig. 1). Values were calculated from the ratio between the integrals of peak (1) and the sum of peaks [(1) + (2) + (3) + (4) + (5) + (6) + (7)]. ■: control (n = 6), ●: partial hepatectomy (n = 6/each time after operation, day 1, 2, 3, 5, 7, 10, 14, 21, 28), ○: sham operation (n = 6/each time after operation, day 1, 2, 3, 5, 7, 10, 14, 21, 28). An average of five pieces from one liver was regarded as the value for one rat. Thirty pieces were used for analysis at each time. Each point represents the mean ± SD of 6 values from 6 rats. *$P < 0.05$, compared with the untreated control value; #$P < 0.05$ for comparisons between partial hepatectomy and sham operation. For abbreviation see Figure 1.

DHA was significantly increased on day 5, compared with the preoperative control level (3.67 ± 0.93 vs. 2.24 ± 0.27 μg/g tissue, $P < 0.001$). This is different from the change in the absolute amounts of the other fatty acids described above.

Fatty acid unsaturation was also evaluated based on the calculated values from gas–liquid chromatography. The mean number of double bonds per fatty acid molecule is also shown in Table 1. The number in day 5 regenerating liver was 1.77 ±

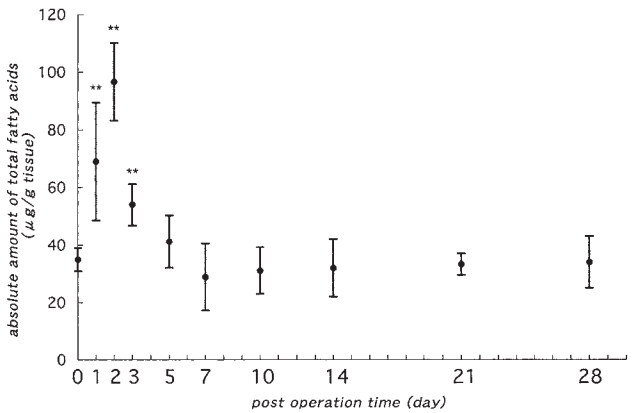

FIG. 3. Changes in the absolute amount of total fatty acids in regenerating liver plotted against time after partial hepatectomy. Each point represents the mean ± SD of 10 or 5 values from 10 or 5 rats. (n = 10 for untreated control, day 1, 5 after partial hepatectomy and n = 5 for day 2, 3, 7, 10, 14, 21, 28 after partial hepatectomy). **$P < 0.0001$, compared with the untreated control value.

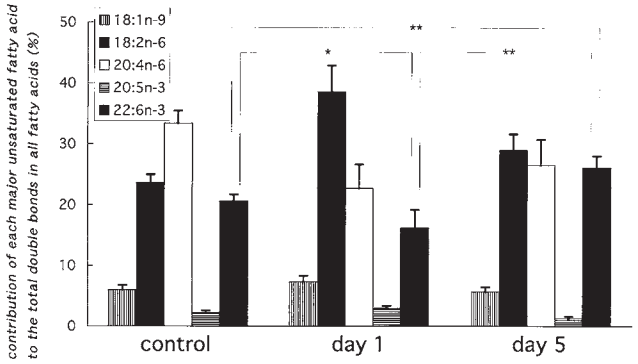

FIG. 4. Contribution of each major unsaturated fatty acid to the total double bonds in all fatty acids. Bars represent the mean ± SD of 10 values from 10 rats, calculated on the basis of the actual amounts of fatty acids determined from the integrated peak areas on the chromatogram, the respective molecular weights of the fatty acid methyl esters, and the number of double bonds in each fatty acid. Fatty acids are designated as number of carbon atoms:number of double bonds. Values were calculated from the following formula: [y × each fatty acid mol/Σ (x × each fatty acid mol)] × 100 where x represents the number of double bonds in the fatty acid (0, 1, 2, 3, 4, 5, or 6) and y represents (1, 2, 4, 5, or 6). *P < 0.001, **P < 0.0001, for comparisons of DHA among untreated control, day 1, and day 5 after partial hepatectomy.

0.03/fatty acid, higher than that in control or day 1 regenerating liver (P < 0.001). In contrast to unsaturation determined by ^{1}H NMR spectroscopy, the mean number of double bonds on day 1 was slightly higher than the control level, but no significance was found between them.

The ratio of double bonds in each major unsaturated fatty acid that contribute to the total double bonds in all fatty acids is shown in Figure 4. The value of LA was increased on day 1, then decreased on day 5 but was still higher than the control level. The decreased value of AA on day 1 compared with control was returning to but had not yet reached the preoperative level by day 5. On the other hand, the value of DHA was decreased on day 1 as in the case of AA, then increased and was higher on day 5 than the preoperative level (26.00 ± 1.96 vs. 20.58 ± 1.09%, P < 0.0001). This is different from the change in the level of AA.

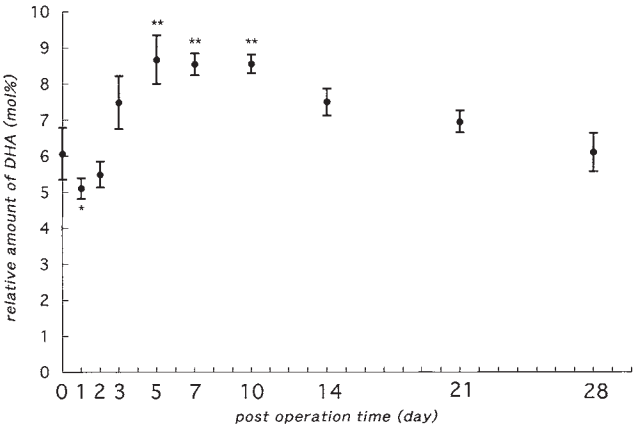

FIG. 5. Changes in the relative amount of docosahexaenoic acid (DHA) in regenerating liver plotted against various times after partial hepatectomy. Each point represents the mean ± SD of 10 or 5 values from 10 or 5 rats (n = 10 for untreated control, day 1, 5 after partial hepatectomy and n = 5 for day 2, 3, 7, 10, 14, 21, 28 after partial hepatectomy). *P < 0.001; **P < 0.0001.

The high degree of unsaturation on day 5 after partial hepatectomy was due to changes in the composition of fatty acids and found to be partly related to the increase in DHA.

Changes in the relative amount of DHA in regenerating liver are shown in Figure 5. The pattern seems to be the same as for the changes in the degree of unsaturation as analyzed by ^{1}H NMR spectroscopy (Fig. 2). The value was found to reach its highest level of 8.67 ± 0.67 mol% on day 5 (vs. control, P < 0.0001) and then remained high for several days.

DISCUSSION

One major advantage of ^{1}H NMR spectroscopy is its ability to analyze directly the protons associated with double bonds. This provides information concerning the relative ratio of fatty acyl double bonds, and thus differs from other methods such as gas–liquid chromatography. In Experiment 1, we demonstrated changes in the degree of fatty acid unsaturation, which increased during liver regeneration with a maximum on day 5 after partial hepatectomy (Fig. 2). We also evaluated fatty acid unsaturation by extrapolation from the results of gas–liquid chromatography in Experiment 2. There is a difference in the evaluation of unsaturation between the two methods as described above. Also, the definition of unsaturation is somewhat different by the two analytical methods. In any case, gas–liquid chromatography also indicates more unsaturation in day 5 than in untreated control or day 1 regenerating liver (Table 1).

Most investigators have focused their attention on the early phase of regeneration around day 1 when DNA synthesis reaches its peak and is followed by the mitotic peak (17–19). It has been reported that the total lipid content of the liver reaches a maximum around day 1 after partial hepatectomy (12–14,27–29). Total fatty acids in the liver were also greatly increased during the early phase of regeneration as shown in Figure 3. Fatty acid oxidation is the main energy source for the remnant liver when it undergoes its burst of mitotic activity around day 1 (30). Most studies have shown changes in the fatty acid composition up to day 3 after partial hepatectomy at the longest (13–15). Furthermore, there are no reports that evaluate the ratio of double bonds. Bruscalupi *et al.* (16) have shown changes in the unsaturation of membrane phospholipids of the regenerating liver by gas–liquid chromatography. However, their data extend only until 24 h after surgery, and DHA was not included in their analyses. As shown in this study, DHA has some effect on the overall degree of unsaturation (Fig. 4). Thus DHA must be included when changes in unsaturation are evaluated.

In Experiment 2, we showed changes in the hepatic fatty acid composition. These changes might be caused by changes

in the amount of food intake after surgery. Chow intake is influenced by partial hepatectomy (31–35), being depressed after operation, but restored by 3 or 4 d post-surgery. No significant difference in food intake is found on day 5 between partially hepatectomized and sham-operated animals (31). This transient decrease in the amount of chow eaten would contribute somewhat to the difference in fatty acid composition between the two populations during the early phase of regeneration. Next, hepatic fatty acid composition is influenced by the great accumulation of lipids in the liver around day 1 after partial hepatectomy caused by synthesis in the liver (29,36) and mobilization from peripheral adipose tissue (12,28).

Because of the increased amounts of hepatic lipids during the early phase of regeneration, the absolute amounts of most fatty acids are increased to maximum around day 1 (data not shown). But the relative amounts of fatty acids show very interesting differences. We show relative increases in mono- and dienoic unsaturated fatty acids such as OA and LA with decreases in PUFA such as AA and DHA on day 1 after partial hepatectomy (Table 1). The same results have been reported previously for day 1 regenerating livers (13–15,37). Ishihara *et al.* (15) have also concluded that the significant increase in OA in 28-h regenerating liver nuclei occurs at the expense of AA and DHA in the phospholipids. Carreau *et al.* (38) have demonstrated that the Δ^9-desaturase (stearyl-CoA desaturase) activity increased with a maximum on day 1 after partial hepatectomy; Δ^9-desaturase is the enzyme that transforms stearic acid (18:0) into OA. They also reported that the activities of Δ^6- and Δ^5-desaturases are least decreased on day 1; these are the enzymes related to the sequential reactions involved in the synthesis of PUFA from LA or α-linolenic acid (18:3n-3), which form C_6-C_7 and C_5-C_6 double bonds, respectively, and synthesize AA from LA or DHA from α-linolenic acid (39). These enzymes could be partly related to the relative changes in fatty acid composition (Table 1).

An increase in monoenoic fatty acids, such as OA, and a concomitant decrease in PUFA such as AA and DHA are also characteristic of membrane phospholipids in hepatomas, another model containing actively growing cells (15,40–42). Tumor cells that lack OA fail to grow because they cannot initiate chromosome DNA replication, and it has been reported that an increase in OA is essential for cell proliferation (10,15). Thus, a high level of OA accompanied by low levels of AA and DHA is suggested to be essential for the most active cell growth on day 1 after partial hepatectomy in the rat.

On the other hand, in day 5 regenerating livers, when unsaturation was at a maximum (Fig. 2), an interesting phenomenon was observed. OA and LA, whose levels were increased, and AA, whose level was decreased on day 1, were returning to their preoperative control levels at that time. But the relative amount of DHA was higher in day 5 regenerating liver than in control or day 1 regenerating liver. In addition to the fact that Δ^6- and Δ^5-desaturases are least decreased on day 1 as described above, Carreau *et al.* (39) have also reported that the Δ^6-desaturase activity increases to a maximum on day 3, and Δ^5-desaturase activity increases to its maximum level on day 4. On the other hand, the Δ^9-desaturase activity decreases gradually to a minimum on day 7 following an initial increase on day 1 (38). These enzymes might be somewhat associated with the changes in the fatty acid composition on day 5 (Table 1). As shown in Figure 4, the high degree of unsaturation in day 5 regenerating liver is partly related to an increase in DHA.

One possibility is that some significant signals might be sent to the regenerating liver owing to its high degree of unsaturation on day 5 after partial hepatectomy, since it has been suggested that changes in fatty acid unsaturation affect membrane fluidity (1–3), lipid–protein interactions, and subsequent receptor functions (4–6), and biological information is transmitted through cell membranes.

Another possibility is that DHA might have its own biological effects, for example, an inhibitory effect on liver regeneration. Regenerating liver must stop growing when it reaches its preoperative size. That is different from tumor growth which is another cell growth model that shows unlimited proliferation. There must be some complex mechanisms inhibiting liver regeneration. Day 5 is much later than the peak time in the regeneration process that occurs around day 1 when DNA synthesis reaches a maximum (17–19). In fact, Kikuchi *et al.* (43) have reported that liver mitochondrial respiratory control and ATP synthetic activity increase to maximal levels on day 1, then decrease to minimal levels on day 5 after partial hepatectomy, after which the levels return to their preoperative values.

Moreover, numerous investigations have confirmed the inhibitory effects of n-3 PUFA, including DHA, on cell proliferation (44–46). Prostaglandins, synthesized from AA, have been reported to be involved in tumor growth, and n-3 PUFA, like DHA, have inhibitory effects on prostaglandin synthesis (47–49). Prostaglandins are also associated with regenerating cell growth after partial hepatectomy (50–52).

Thus, the data suggest that some significant signals might be transmitted through the high levels of unsaturation of liver fatty acids on day 5 by altering the structure of the membrane lipid bilayer. Thus, day 5 after partial hepatectomy could be related to the inhibitory mechanism of the liver regeneration process.

In conclusion, we have demonstrated changes in the degree of unsaturation of liver fatty acids over a long period of regeneration after partial hepatectomy in the rat. Unsaturation appears to increase during the regeneration process, reaching a maximum on day 5. The high degree of unsaturation at that time is partly due to the relative increase in DHA. However, how the increased unsaturation is involved in the mechanism of liver regeneration remains poorly understood. Some significant signals, for example, inhibitory information, might be transmitted through the high levels of unsaturation and the relative increase in DHA on day 5 after partial hepatectomy. Further investigations are required concerning these possibilities.

ACKNOWLEDGMENT

Special thanks go to Dr. Margaret Dooley Ohto for her comments and suggestions concerning the manuscript.

REFERENCES

1. Jaiswal, R.K., Rama Sastry, B.V., and Landon, E.J. (1982) Changes in Microsomal Membrane Microviscosity and Phospholipid Methyltransferases During Rat Liver Regeneration, *Pharmacology 24*, 355–365.
2. Burns, C.P., Luttenegger, D.G., Dudley, D.T., Buettner, G.R., and Spector, A.A. (1979) Effect of Modification of Plasma Membrane Fatty Acid Composition on Fluidity and Methotrexate Transport in L1210 Murine Leukemia Cells, *Cancer Res. 39*, 1726–1732.
3. Treen, M., Uauy, R.D., Jameson, D.M., Thomas, V.L., and Hoffman, D.R. (1992) Effect of Docosahexaenoic Acid on Membrane Fluidity and Function in Intact Cultured Y-79 Retinoblastoma Cells, *Arch. Biochem. Biophys. 294*, 564–570.
4. Ginsberg, B.H., Brown, T.J., Simon, I., and Spector, A.A. (1981) Effect of the Membrane Lipid Environment on the Properties of Insulin Receptors, *Diabetes 30*, 773–780.
5. Litman, B.J., and Mitchell, D.C. (1996) A Role for Phospholipid Polyunsaturation in Modulating Membrane Protein Function, *Lipids 31*, S-193–S-197.
6. Stillwell, W., Ehringer, W., and Jenski, L.J. (1993) Docosahexaenoic Acid Increases Permeability of Lipid Vesicles and Tumor Cells, *Lipids 28*, 103–108.
7. Nishizuka, Y. (1992) Intracellular Signaling by Hydrolysis of Phospholipids and Activation of Protein Kinase C, *Science 258*, 607–614.
8. Shinomura, T., Asaoka, Y., Oka, M., Yoshida, K., and Nishizuka, Y. (1991) Synergistic Action of Diacylglycerol and Unsaturated Fatty Acid for Protein Kinase C Activation: Its Possible Implications, *Proc. Natl. Acad. Sci. USA 88*, 5149–5153.
9. Craven, P.A., and DeRubertis, F.R. (1988) Role of Activation of Protein Kinase C in the Stimulation of Colonic Epithelial Proliferation by Unsaturated Fatty Acids, *Gastroenterology 95*, 676–685.
10. Yung, B.Y-M., and Kornberg, A. (1988) Membrane Attachment Activates DNA A Protein, the Initiation Protein of Chromosome Replication in *Escherichia coli*, *Proc. Natl. Acad. Sci. USA 85*, 7202–7205.
11. Sakaguchi, M., Hiramatsu, Y., Takada, H., Yamamura, M., Hioki, K., Saito, K., and Yamamoto, M. (1984) Effect of Dietary Unsaturated and Saturated Fats on Azoxymethane-induced Colon Carcinogenesis in Rats, *Cancer Res. 44*, 1472–1477.
12. Gove, C.D., and Hems, D.A. (1978) Fatty Acid Synthesis in the Regenerating Liver of the Rat, *Biochem. J. 170*, 1–8.
13. Glende, E.A., Jr., and Morgan, W.S. (1968) Alteration in Liver Lipid and Lipid Fatty Acid Composition After Partial Hepatectomy in the Rat, *Exp. Mol. Pathol. 8*, 190–200.
14. Slater, T.F., Cheeseman, K.H., Benedetto, C., Collins, M., Emery, S., Maddix, S.P., Nodes, J.T., Proudfoot, K., Burton, G.W., and Ingold, K.U. (1990) Studies on the Hyperplasia ("regeneration") of the Rat Liver Following Partial Hepatectomy, *Biochem. J. 265*, 51–59.
15. Ishihara, H., Tamiya-Koizumi, K., Kuriki, H., Yoshida, S., and Kojima, K. (1991) Growth-Associated Changes in Fatty Acid Compositions of Nuclear Phospholipids of Liver Cells, *Biochim. Biophys. Acta 1084*, 53–59.
16. Bruscalupi, G., Curatola, G., Lenaz, G., Leoni, S., Mangiantini, M.T., Mazzanti, L., Spagnuolo, S., and Trentalance, A. (1980) Plasma Membrane Changes Associated with Rat Liver Regeneration, *Biochim. Biophys. Acta 597*, 263–273.
17. McGowan, J.A., and Fausto, N. (1978) Ornithine Decarboxylase Activity and the Onset of Deoxyribonucleic Acid Synthesis in Regenerating Liver, *Biochem. J. 170*, 123–127.
18. Smith, H.C., and Berezney, R. (1982) Nuclear Matrix-Bound Deoxyribonucleic Acid Synthesis: An *in Vitro* System, *Biochemistry 21*, 6751–6761.
19. Okamoto, Y., Nishimura, K., Nakayama, M., Nakagawa, M., and Nakano, H. (1988) Protein Kinase C in the Regenerating Rat Liver, *Biochem. Biophys. Res. Commun. 151*, 1144–1149.
20. Higgins, G.M., and Anderson, R.M. (1931) Experimental Pathology of the Liver. I. Restoration of the Liver of the White Rat Following Partial Surgical Removal, *Arch. Pathol. 12*, 186–202.
21. Kwee, I.L., Nakada, T., and Ellis, W.G. (1991) Elevation in Relative Levels of Brain Membrane Unsaturated Fatty Acids in Alzheimer's Disease: High Resolution Proton Spectroscopic Studies of Membrane Lipid Extracts, *Magn. Reson. Med. 21*, 49–54.
22. Folch, J., Lees, M., and Sloane Stanley, G.H. (1957) A Simple Method for the Isolation and Purification of Total Lipides from Animal Tissues, *J. Biol. Chem. 226*, 497–509.
23. Sze, D.Y., and Jardetzky, O. (1990) Characterization of Lipid Composition in Stimulated Human Lymphocytes by ^{1}H-NMR, *Biochim. Biophys. Acta 1054*, 198–206.
24. Pollesello, P., Eriksson, O., Kvam, B.J., Paoletti, S., and Saris, N-E.L. (1991) ^{1}H-NMR Studies of Lipid Extracts of Rat Liver Mitochondria, *Biochem. Biophys. Res. Commun. 179*, 904–911.
25. Miccheli, A., Tomassini, A., Ricciolini, R., Di Cocco, M.E., Piccolella, E., Manetti, C., and Conti, F. (1994) Dexamethasone-Dependent Modulation of Cholesterol Levels in Human Lymphoblastoid B Cell Line Through Sphingosine Production, *Biochim. Biophys. Acta 1221*, 171–177.
26. Ling, M., and Brauer, M. (1992) Ethanol-Induced Fatty Liver in the Rat Examined by *in Vivo* ^{1}H Chemical Shift Selective Magnetic Resonance Imaging and Localized Spectroscopic Methods, *Magn. Reson. Imaging 10*, 663–677.
27. Ludewig, S., Minor, G.R., and Hortenstine, J.C. (1939) Lipid Distribution in Rat Liver After Partial Hepatectomy, *Proc. Soc. Exp. Biol. Med. 42*, 158–161.
28. Girard, A., Roheim, P.S., and Eder, H.A. (1971) Lipoprotein Synthesis and Fatty Acid Mobilization in Rats After Partial Hepatectomy, *Biochim. Biophys. Acta 248*, 105–113.
29. Tijburg, L.B.M., Nyathi, C.B., Meijer, G.W., and Geelen, M.J.H. (1991) Biosynthesis and Secretion of Triacylglycerol in Rat Liver After Partial Hepatectomy, *Biochem. J. 277*, 723–728.
30. Nakatani, T., Ozawa, K., Asano, M., Ukikusa, M., Kamiyama, Y., and Tobe, T. (1981) Differences in Predominant Energy Substrate in Relation to the Resected Hepatic Mass in the Phase Immediately After Hepatectomy, *J. Lab. Clin. Med. 97*, 887–898.
31. Unterman, T.G., and Phillips, L.S. (1986) Circulating Somatomedin Activity During Hepatic Regeneration, *Endocrinology 119*, 185–192.
32. Kallenbach, M., Roome, N.O., and Schulte-Hermann, R. (1983) Kinetics of DNA Synthesis in Feeding-Dependent and Independent Hepatocyte Populations of Rats After Partial Hepatectomy, *Cell Tissue Kinet. 16*, 321–332.
33. Ohtake, M., Sakaguchi, T., Yoshida, K., and Muto, T. (1993) Hepatic Branch Vagotomy Can Suppress Liver Regeneration in Partially Hepatectomized Rats, *HPB Surg. 6*, 277–286.
34. Tanaka, K., Ohkawa, S., Nishino, T., Niijima, A., and Inoue, S. (1987) Role of the Hepatic Branch of the Vagus Nerve in Liver Regeneration in Rats, *Am. J. Physiol. 253*, G439–G444.
35. Chan, Y-C., Maekawa, T., Maeuchihara, K., Yokota, A., Korin, T., Ohshiro, Y., Shimada, K., and Yamamoto, S. (1993) Comparative Effect of Proteins, Peptides, and Amino Acid Mixtures on Recovery from 70% Hepatectomy in Rats, *J. Nutr. Sci. Vitaminol. 39*, 527–536.
36. Stein, T.A., Burns, G.P., Tropp, B.E., and Wise, L. (1985) Hepatic Fat Accumulation During Liver Regeneration, *J. Surg. Res. 39*, 338–343.
37. Imai, T., Nishimaki, K., Shiga, T., Kawasaki, S., and Makuuchi, M. (1996) Lipid Peroxidation and Antioxidant Activities in Regenerating Liver After Partial Hepatectomy in Splenectomized Rats, *Res. Exp. Med. 196*, 1–7.

38. Carreau, J.-P., Mazliak, P., and Frommel, D. (1981) Stearyl-CoA Desaturation Capacity of the Rat Liver During Regeneration After Partial Hepatectomy, *Int. J. Biochem. 13*, 765–767.
39. Carreau, J.-P., Mazliak, P., and Frommel, D. (1981) Δ^6-, Δ^5-Fatty Acyl-CoA Desaturases and γ-Linolenyl-CoA Elongase in Regenerating Rat Liver, *Int. J. Biochem. 13*, 831–836.
40. Hartz, J.W., Morton, R.E., Waite, M.M., and Morris, H.P. (1982) Correlation of Fatty Acyl Composition of Mitochondrial and Microsomal Phospholipid with Growth Rate of Rat Hepatomas, *Lab. Invest. 46*, 73–78.
41. Satouchi, K., Mizuno, T., Samejima, Y., and Saito, K. (1984) Molecular Species of Phospholipid in Rat Hepatomas and in Fetal, Regenerating, and Adult Rat Livers, *Cancer Res. 44*, 1460–1464.
42. Mowri, H., Nojima, S., and Inoue, K. (1988) Lack of Protein-mediated α-Tocopherol Transfer Between Membranes in the Cytoplasm of Ascites Hepatomas, *Lipids 23*, 459–464.
43. Kikuchi, J., Ouchi, K., and Matsuno, S. (1991) Effects of Mitochondrial Lipoperoxidation on Liver Regeneration After Partial Hepatectomy of the Cirrhotic Rat Liver, *Nippon Geka Gakkai Zasshi 92*, 167–174.
44. Simopoulos, A.P. (1989) Summary of the NATO Advanced Research Workshop on Dietary ω3 and ω6 Fatty Acids: Biological Effects and Nutritional Essentiality, *J. Nutr. 119*, 521–528.
45. Shiina, T., Terano, T., Saito, J., Tamura, Y., and Yoshida, S. (1993) Eicosapentaenoic Acid and Docosahexaenoic Acid Suppress the Proliferation of Vascular Smooth Muscle Cells, *Atherosclerosis 104*, 95–103.
46. Sauer, L.A., and Dauchy, R.T. (1992) The Effect of Omega-6 and Omega-3 Fatty Acids on ^{3}H-Thymidine Incorporation in Hepatoma 7288CTC Perfused *in Situ*, *Br. J. Cancer 66*, 297–303.
47. Cave, W.T., Jr. (1991) Dietary n-3 (ω-3) Polyunsaturated Fatty Acid Effects on Animal Tumorigenesis, *FASEB J. 5*, 2160–2166.
48. de Bravo, M.G., Antueno, R.J., Toledo, J., De Tomás, M.E., Mercuri, O.F., and Quintans, C. (1991) Effects of an Eicosapentaenoic and Docosahexaenoic Acid Concentrate on a Human Lung Carcinoma Grown in Nude Mice, *Lipids 26*, 866–870.
49. Karmali, R.A., Doshi, R.U., Adams, L., and Choi, K. (1987) Effect of n-3 Fatty Acids on Mammary Tumorigenesis, *Adv. Prostaglandin Thromboxane Leukot. Res. 17*, 886–889.
50. Tsujii, H., Okamoto, Y., Kikuchi, E., Matsumoto, M., and Nakano, H. (1993) Prostaglandin E_2 and Rat Liver Regeneration, *Gastroenterology 105*, 495–499.
51. McNeil, G.E., Chen, T.S., and Leevy, C.M. (1985) Reversal of Ethanol and Indomethacin-Induced Suppression of Hepatic DNA Synthesis by 16,16-Dimethyl Prostaglandin E_2, *Hepatology 5*, 43–46.
52. Callery, M.P., Mangino, M.J., and Flye, M.W. (1991) Kupffer Cell Prostaglandin-E_2 Production Is Amplified During Hepatic Regeneration, *Hepatology 14*, 368–372.

[Received July 27, 1998, and in final revised form December 14, 1999; revision accepted March 9, 2000]

Lipid Composition of Erythrocytes and Thrombocytes of a Subantarctic Seabird, the King Penguin

Christine Fayolle[a], Claude Leray[a], Philippe Ohlmann[a], Geneviève Gutbier[a], Jean-Pierre Cazenave[a], Christian Gachet[a,*], and René Groscolas[b]

[a]INSERM U.311, Etablissement Français du Sang-Alsace, 67065 Strasbourg Cédex, France, and [b]Centre d'Ecologie et Physiologie Energétiques, UPR 9010, CNRS, 67087 Strasbourg, France

ABSTRACT: Phospholipid (PL) compositions and fatty acid (FA) patterns of PL were determined in the erythrocytes and blood thrombocytes of a seabird, the king penguin, living in the subantarctic area and feeding on prey rich in n-3 polyunsaturated FA. Results were compared between birds in three different physiological states (breeding and molting adults, chicks) to those reported for other birds. In erythrocytes, the ratios of cholesterol to PL and of sphingomyelin to phosphatidylcholine (PC) were lower than in other birds. The PL distribution was similar to those previously reported in the hen and pigeon. In contrast to other birds, cardiolipin levels were unexpectedly high (4%). Very long chain n-3 FA were abundant (13–27%) in phosphatidylethanolamine (PE), phosphatidylserine and PC, probably in relation to the natural diet of these birds. Among n-3 FA, 22:6n-3 was the most abundant in all PL (2–20%), whereas the highest levels of arachidonic acid were observed in PE (14%). In thrombocytes, the PL distribution and FA composition of the main PL (PC, PE) differed from those of erythrocytes, and in particular, levels of n-3 FA (9–12%) were 1.5–2 times lower. The highest levels of arachidonic acid were found in phosphatidylinositol (24%). The lipid profile of penguin erythrocytes could contribute to the efficiency of blood circulation and oxygen delivery in microvascular beds, thus favoring diving capacity of these animals. Our observations do not support the hypothesis of a common origin of avian thrombocytes and erythrocytes.

Paper no. L8305 in *Lipids 35*, 453–459 (April 2000).

Knowledge of the hemostasis of birds is unfortunately limited (1–3) even in species reared for human consumption. Avian red blood cells (RBC) have aroused some interest, mainly in connection with the presence of a nucleus (4,5), but no recent publication in this field would appear to be available. The other blood cell type involved in hemostasis, the thrombocyte, performs a role similar to that of the mammalian platelet and offers a specific feature since the thrombocytes of birds are nucleated (5,6). In addition to hemostasis, these cells have been reported to play an active role in phagocytosis (7,8) but are not a component of the lymphocyte system (9). Finally, avian thrombocytes and erythrocytes share many similarities, and the two cell types are thought to be derived from a common progenitor cell line (10).

Only a few biochemical studies of avian blood cells exist, and lipids have been explored in erythrocytes but not in thrombocytes and only in hens (4,11,12) and pigeons (13). In mammalian species, studies of the lipid composition of blood cells are of great interest since there is strong evidence to suggest that diets rich in n-3 polyunsaturated fatty acids (PUFA) of marine origin are associated with a reduction in the risk of thrombosis (14,15). Thus, it was found that the incorporation of n-3 PUFA into the phospholipids (PL) of mammalian erythrocytes and platelets improved their functional properties, at the levels of peripheral blood circulation (16,17), and platelet reactivity (18,19).

The main objective of this study was to explore the lipid composition of erythrocytes and thrombocytes in a seabird, the king penguin (*Aptenodytes patagonicus)*, which has been extensively investigated on account of its unique life cycle (20,21) and its diet naturally rich in n-3 fatty acid (FA) (22). This species was also chosen for its high diving capacity (animals dive to depths of up to 300 m and for as long as 7.5 min) (23,24), which probably requires efficient protection against thrombotic risks. The physiological cycle of the king penguin is characterized by periods of fasting ashore and feeding at sea. In spring, after a fattening phase of about 4 wk at sea, the adults arrive ashore to molt, from September for early breeders to late December. During molt, the birds fast for about 1 mon and renew their whole plumage. Since feather materials (amino acids) must be drawn from tissues, this process involves high protein catabolism (25,26) and the animals lose about 40% of their body weight. On completion of the molt phase, the birds return to sea and feed heavily again for about 1 mon, before they go back to shore in the early summer for breeding. The courtship period (approximately 10 d) is followed by incubation (53 d) during which time the two mates alternate in caring for the egg, spending alternately 2 wk fasting and 2 wk feeding. Chick brooding is very long (13 mon) and is characterized by successive spells of feeding and fasting of the parents, until early autumn. If the chicks are fed

*To whom correspondence should be addressed at INSERM U.311, Etablissement Français du Sang-Alsace, 10 rue Spielmann, BP 36, 67065 Strasbourg Cédex, France. E-mail: christian.gachet@etss.u-strasbg.fr

Abbreviations: CHOL, cholesterol; CL, cardiolipin; FA, fatty acid; MUFA, monounsaturated fatty acid; PC, phosphatidylcholine; PE, phosphatidylethanolamine; PI, phosphatidylinositol; PL, phospholipid; PS, phosphatidylserine; PUFA, polyunsaturated fatty acids; RBC, red blood cell; SAT, saturated FA; SM, sphingomyelin; TLC, thin-layer chromatography.

regularly by their parents during the first 3 mon, they are fed only episodically over the next 4 mon and thus undergo a long winter fast while losing 30 to 50% of their body weight. Thereafter, they are again regularly fed until they depart to sea and feed on their own, in late spring. The breeding and brooding fasts of the adults and the winter fast of the chicks correspond to long periods of protein sparing and are associated with use of lipids as the main metabolic fuel (26).

In the present work, we analyzed the lipid constituents of the erythrocytes and thrombocytes of the king penguin at three stages of its life cycle in the Crozet Islands: in adults during the courtship fast (breeding adults), in adults during molt, and in chicks during their winter fast. The resulting information, together with further functional studies, should contribute to a better knowledge of the relation between hemostasis, diet, and life cycle in birds.

MATERIALS AND METHODS

Animals. A total of 18 animals was selected in 1997 at Possession Island (46°26′ S and 51°52′ E) of the Crozet Archipelago, in the austral Indian Ocean. These animals were divided into three groups. The first group consisted of eight breeding, fasting adult males weighing 10–14 kg each, sampled in January during courting and after a 3–5 d fast. All were used for RBC studies and three also for thrombocyte analyses. In the second group of nine adults weighing 14–15 kg each, sampled during molt and after a 5–10 d fast, four birds were used for erythrocyte and five for thrombocyte studies. These molting birds could not be sexed, but there is no evidence for physiological, metabolic, or endocrine differences between sexes at this stage of the life cycle (25). The third group constituted five chicks weighing 3–9 kg each, sampled in September toward the end of their natural winter fast, two of which were used for erythrocyte and the other three for thrombocyte analyzes. The study was approved by the Ethical Committee of the "Institut Français pour la Recherche et la Technologie Polaires" and conformed to the Agreed Measures for the Conservation of Antarctic and Subantarctic Fauna.

Blood collection and cell preparation. Blood was drawn from a brachial vein of conscious birds into plastic syringes containing acid–citrate–dextrose anticoagulant (1:7 volume ratio) and processed within 1 h of sampling in a field station. Erythrocytes were counted and measured with a hemacytometer after a 1:200 dilution. Hematocrits were determined by centrifugation in glass capillary tubes. The mean cell volumes (μm^3) were calculated from hematocrits and red cell counts. As thrombocytes are difficult to count due to their low numbers and tendency to clump, thrombocyte counts and sizes were estimated by microscopic observation of blood smears according to Campbell (5). RBC and thrombocytes were separated by brief low-speed centrifugation (1300 × *g*, 37°C, 5 s). RBC were washed twice in physiological saline, and thrombocytes were further processed according to Cazenave *et al*. (27) with slight modifications. Thrombocyte-rich plasma was centrifuged (1000 × *g*, 37°C, 8 min), and the thrombocyte pellet was washed in Tyrode's buffer containing human serum albumin prior to lipid analyses. None of the sampled birds was in a hyperlipidemic state since plasmas were clear and yellowish but never lactescent.

Lipid analyses. Total lipids were extracted immediately from washed RBC or thrombocytes as previously described (28) and dissolved in 1 mL chloroform/methanol (2:1, vol/vol). One extract was prepared from each sample. The erythrocyte nuclear and plasma membranes were not separated because the required methodology was unavailable in the field station where blood treatment and lipid extraction were carried out. After addition of 0.3 mg/mL ethyl gallate as an antioxidant, the extracts were stored at –20°C for about 6 mon until laboratory processing in France. Cholesterol (CHOL) and PL were separated by thin-layer chromatography (TLC) using boric acid-impregnated silica gel plates with chloroform/ethanol/water/triethylamine (30:35:7:35, by vol) as eluant (29). Total PL were quantified by phosphorus estimation (30), and CHOL was measured by colorimetry (31). The FA compositions of individual PL were determined by transmethylation with BF_3/methanol reagent and gas–liquid chromatography, after addition of a known amount of heptadecanoic acid as an internal standard (29). Plasmalogens were estimated by gas–liquid chromatography from the amounts of dimethyl acetals obtained during the transmethylation process. The cardiolipin (CL) fraction was determined by running PL samples in two other eluent systems, chloroform/methanol/conc. ammonia (65:20:4, by vol) and chloroform/methanol/water (40:10:1, by vol), and by mass spectrometry using a Micromass Autospec instrument in the liquid secondary ion mass spectrometry mode. Samples were dissolved in a small quantity of chloroform/methanol (2:1, vol/vol) and mixed with 3-nitrobenzyl alcohol as a matrix.

Statistical analyses. Results are expressed as the means ± SEM of individual values. The means were examined by one-way analysis of variance, and significant differences between groups were determined by the Bonferroni post-test. When indicated, a nonparametric test (Mann-Whitney) was used.

RESULTS

Erythrocytes. Hematocrits and PL and CHOL contents of RBC in adults and chicks are given in Table 1. The mean erythrocyte count for all animals was estimated to be 2×10^6 cells/μL in whole blood, and the mean cell volume was 209 ± 17 μm^3, with dimensions of 14.7 ± 0.1 (length) and 9.2 ± 0.1 μm (width). Hematocrit ranged from 43 to 48% and did not vary significantly between the different groups. The PL content, close to 1.65 mg/mL RBC (0.46 μmol/10^9 RBC), was likewise not different between groups. The CHOL content, about 0.4 mg/mL RBC (0.23 μmol/10^9 RBC), was similar in the three groups but tended to be lower in breeding adults. Hence, the CHOL/PL ratio was lower in breeding adults, and this difference was marginally significant as compared to the other groups.

The distribution of erythrocyte PL is shown in Table 2. In all groups, phosphatidylcholine (PC, 43%) and phosphatidyl-

TABLE 1
Hematocrit (Ht), Total Phospholipid (PL), and Cholesterol (CHOL) Content of Erythrocytes of King Penguins in Different Physiological States[a]

	Breeding adults (n = 8)	Molting adults (n = 3)	Fasting chicks (n = 3)
Ht (%)	46.3 ± 2.0	48.2 ± 1.4	43.2 ± 1.0
PL (mg/mL RBC)	1.69 ± 0.13	1.61 ± 0.19	1.64 ± 0.18
CHOL (mg/mL RBC)	0.34 ± 0.02	0.41 ± 0.04	0.42 ± 0.04
CHOL/PL (mol/mol)	0.41 ± 0.03	0.51 ± 0.02	0.51 ± 0.04

[a]Values are the means ± SEM. RBC, red blood cells.

TABLE 2
PL Composition of Erythrocytes of King Penguins in Different Physiological States[a]

	Breeding adults (n = 8)	Molting adults (n = 4)	Fasting chicks (n = 2)
Phosphatidylcholine (PC)	43.4 ± 1.0	43.0 ± 0.7	43.7 ± 2.1
Phosphatidylethanolamine (PE)	24.1 ± 1.7	25.5 ± 1.5	29.0 ± 1.0
Phosphatidylserine (PS)	6.0 ± 0.7	6.0 ± 1.3	4.9 ± 0.7
Phosphatidylinositol (PI)	4.4 ± 0.4	3.4 ± 0.4	2.7 ± 0.5
Sphingomyelin (SM)	17.8 ± 2.5	16.1 ± 0.5	14.8 ± 0.3
Cardiolipin (CL)	4.2 ± 0.9	5.9 ± 1.3	5.0 ± 2.1

[a]Values are the means ± SEM of the molar percentage of each PL class. See Table 1 for abbreviation.

inositol (PI, 3–4%) were the most and least abundant PL, respectively. There was no significant difference between groups in the distribution of the various PL and the sphingomyelin to phosphatidylcholine (SM/PC) ratio was comparable in all three groups (close to 0.4). CL was noticeably present (4.2–5.9%) in lipid extracts from erythrocytes. Its identity was confirmed by the fact that the phosphorus-containing spot displayed chromatographic properties similar to those of a CL standard from bovine heart (Sigma-Aldrich Chimie, Saint Quentin Fallavier, France) in three TLC systems. Furthermore, mass spectrometric analysis in the LSIMS mode of the purified compound revealed four predominant groups of species, with two minor peaks at ion masses of *m/z* 1422 and 1500 and two major peaks at masses of *m/z* 1450 and 1478. These molecular weights are in accordance with the expected structures of the CL molecules present in king penguin erythrocytes as deduced from the FA composition (Table 3).

Figure 1 shows the FA composition of the total PL pool in erythrocytes, the data being restricted for clarity to the major n-3 and n-6 FA and FA classes. Monounsaturated FA (MUFA) and saturated FA (SAT) were the predominant classes, accounting for about 39 and 35% of the total FA, respectively. MUFA mainly consisted of 18:1n-9 (19.4%), 22:1n-9 (5.4%), and to a lesser extent 20:1n-9 (1.4%). Overall, the patterns did not vary greatly between the three groups, although there was a lower n-3 FA content in chicks as compared to breeding adults, the value in molting birds being intermediate. This difference was observed for both 22:6n-3 and 20:5n-3.

TABLE 3
Fatty Acid Composition of PL in the Erythrocytes of Breeding Adult King Penguins[a]

	PE	PC	PS	CL	PI	SM
14:0	1.1 ± 0.4	1.2 ± 0.2	2.5 ± 0.6	2.6 ± 0.6	4.6 ± 0.8	1.6 ± 0.2
16:0	6.9 ± 1.1	26.6 ± 2.3	9.5 ± 1.7	18.1 ± 3.6	14.8 ± 1.3	15.6 ± 3.1
18:0	9.1 ± 1.4	5.7 ± 0.4	21.2 ± 0.5	23.4 ± 4.0	20.3 ± 1.3	7.4 ± 0.3
20:0	—	—	0.5 ± 0.0	—	—	3.7 ± 0.6
22:0	—	—	—	—	—	6.8 ± 1.1
22:1n-11	2.2 ± 0.1	0.8 ± 0.2	1.8 ± 0.2	1.0 ± 0.2	1.2 ± 0.1	1.4 ± 0.2
16:1n-9	0.8 ± 0.2	0.7 ± 0.1	1.6 ± 0.3	1.5 ± 0.3	1.8 ± 0.3	1.5 ± 0.2
18:1n-9	13.5 ± 0.6	30.0 ± 0.7	9.2 ± 0.6	11.9 ± 1.4	13.6 ± 0.6	6.4 ± 1.3
20:1n-9	2.1 ± 0.1	0.8 ± 0.1	1.8 ± 0.1	1.6 ± 0.3	2.0 ± 0.1	1.1 ± 1.1
20:2n-9	0.7 ± 0.2	0.5 ± 0.1	1.8 ± 0.4	1.5 ± 0.4	3.1 ± 0.4	1.3 ± 1.2
22:1n-9	3.0 ± 0.2	1.4 ± 0.2	12.6 ± 1.9	6.8 ± 1.5	12.1 ± 1.3	17.5 ± 2.4
24:1n-9	—	—	—	—	—	22.5 ± 2.5
16:1n-7	1.1 ± 0.2	3.6 ± 0.6	—	1.5 ± 0.2	1.2 ± 0.1	1.1 ± 0.2
18:1n-7	2.6 ± 0.3	4.7 ± 0.2	3.6 ± 0.5	5.4 ± 0.7	7.0 ± 0.5	1.3 ± 0.2
22:1n-7	—	—	—	—	—	1.0 ± 0.1
18:2n-6	3.3 ± 0.2	3.2 ± 0.2	1.9 ± 0.2	4.0 ± 0.6	1.3 ± 0.2	0.9 ± 0.2
18:3n-6	—	—	1.7 ± 0.2	0.8 ± 0.1	1.7 ± 0.1	2.4 ± 0.2
20:3n-6	0.8 ± 0.0	1.1 ± 0.1	1.2 ± 0.2	0.8 ± 0.2	—	—
20:4n-6	14.4 ± 0.9	4.8 ± 0.5	5.5 ± 0.9	6.1 ± 0.9	5.0 ± 0.7	1.0 ± 0.2
22:4n-6	0.7 ± 0.1	—	0.5 ± 0.1	—	—	—
20:5n-3	2.9 ± 0.3	3.1 ± 0.2	0.7 ± 0.1	1.2 ± 0.2	—	—
22:5n-3	3.5 ± 0.2	1.3 ± 0.2	2.4 ± 0.3	1.5 ± 0.2	1.8 ± 0.2	—
22:6n-3	20.3 ± 1.6	9.0 ± 1.1	17.1 ± 2.9	7.9 ± 1.5	5.2 ± 0.6	1.6 ± 0.4
DMA	8.9 ± 1.1	—	—	—	—	—
DBI	258 ± 13	160 ± 10	195 ± 20	135 ± 19	122 ± 5	89 ± 4
UNSAT/SAT	3.5 ± 0.3	2.3 ± 0.3	2.0 ± 0.2	1.8 ± 0.6	1.5 ± 0.1	2.0 ± 0.3
n-3/n-6	1.3 ± 0.1	1.4 ± 0.1	1.7 ± 0.2	0.9 ± 0.1	0.9 ± 0.1	0.7 ± 0.2

[a]Values are the means ± SEM of the molar percentage for eight birds. —, fatty acids amounting to less than 0.5% of the total; DMA, dimethyl acetal derivatives formed from plasmalogens; DBI, double-bond index, mean number of double bonds per 100 mol fatty acids; UNSAT/SAT, unsaturated to saturated fatty acids ratio. See Tables 1 and 2 for other abbreviations.

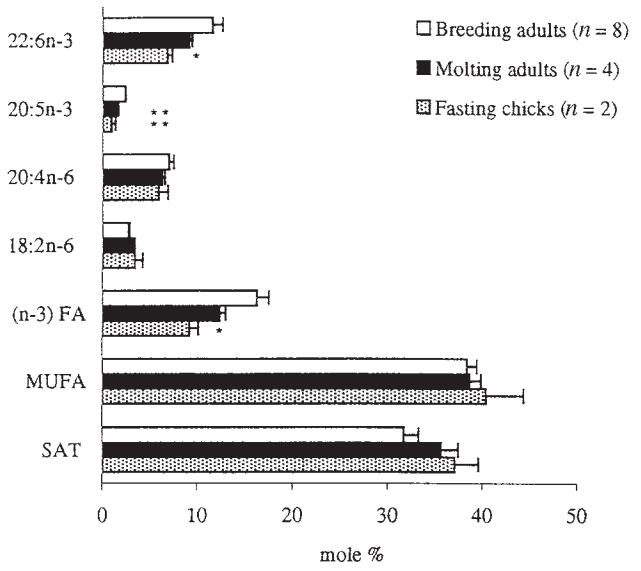

FIG. 1. Fatty acid (FA) composition of phospholipids in the erythocytes of king penguin. Values are the means ± SEM of the molar percentage of each FA. MUFA, monounsaturated FA; SAT, saturated FA. Molting adults and fasting chicks were compared to breeding adults using the Mann-Whitney test. *$P < 0.05$, **$P < 0.01$. For a FA or a FA class, asterisks indicate significant differences when compared to breeding adults. Other means were not significantly different.

Table 3 gives the FA composition of PL isolated from the erythrocytes of breeding adults, taken as a reference profile. Phosphatidylethanolamine (PE), including diacyl and plasmalogen subclasses, was the most strongly unsaturated PL having the highest levels of n-3 and n-6 FA, respectively, about 27 and 20%. The three major glycerophospholipids [PC, PE, and phosphatidylserine (PS)] had greater n-3 FA than n-6 FA contents, the n-3/n-6 ratio ranging from 1.3 to 1.7. Among n-6 FA, levels of 20:4n-6 were the highest in PE (14.4%), which represented approximately 56% of the total erythrocyte arachidonic acid, the other glycerophospholipids containing only low levels (about 5%). Among n-3 FA, 22:6n-3 was the most abundant in all PL, 3 and 24 times more abundant than 20:5n-3 in PC and PS, respectively. Among n-9 FA, the content of 22:1n-9 was remarkably high (12–17%) in PS, PI, and SM. The FA profile of CL, comparable to that of PI, displayed no dominant component, whereas SM was characterized by high proportions of molecular species containing 16:0, 22:1, or 24:1n-9.

In molting birds, the FA profiles of PL were not very different from those of breeding adults except for some significant differences in PC, PE, and PS (data not shown). Thus, PC contained less 20:5n-3, PE more plasmalogens, and PS more SAT in molting than in breeding birds ($P < 0.05$).

Fasting chicks displayed a general trend to higher PL saturation as compared to breeding adults, and this was accompanied by lower levels of n-3 FA (data not shown). The individual MUFA contents of the different PL were similar in breeding and molting adults and in chicks (data not shown).

TABLE 4
Total PL and CHOL Content of the Thrombocytes of King Penguins in Different Physiological States[a]

	Breeding adults ($n = 3$)	Molting adults ($n = 3$)	Fasting chicks ($n = 3$)
PL (mg/10^9 cells)	1.50 ± 0.41	0.83 ± 0.10	1.14 ± 0.48
CHOL (mg/10^9 cells)	1.18 ± 0.13	0.39 ± 0.16*	0.91 ± 0.20
CHOL/PL (mol/mol)	1.76 ± 0.25	0.76 ± 0.32	1.31 ± 0.35

[a]Values are the means ± SEM. Molting adults and fasting chicks were compared to breeding adults. *$P < 0.05$. For abbreviations see Table 1.

Thrombocytes. The mean thrombocyte count of king penguins was estimated to be about 18,000 cells/μL in all groups, and the cell dimensions were 7.1 ± 0.1 μm (length) and 5.9 ± 0.2 μm (width). As shown in Table 4, the PL content of thrombocytes was comparable between groups, whereas the CHOL content was lower in molting than in breeding adults ($P < 0.05$). Nevertheless, owing to a large dispersion of the results, all groups displayed a similar CHOL/PL ratio.

Table 5 gives the PL distribution of thrombocyte membranes, which was similar in the three groups. PC was the major constituent (about 31 to 41%), as in erythrocytes, while the remaining PL each contributed from 11 to 20%, in contrast to the erythrocyte profile where PI and PS did not exceed 6%.

The FA composition of the total PL pool in thrombocytes (Fig. 2) revealed some differences between groups in the distribution of the various FA classes. Unlike in erythrocytes, SAT formed the most prominent class in thrombocytes of breeding adults (46%) or chicks (39%), while MUFA amounted to only 25–30% in all three groups. It is noteworthy that n-3 FA were about two times less abundant in thrombocytes (7%) than in erythrocytes ($P < 0.001$). This was mainly due to markedly lower levels of 22:6n-3 in thrombocytes (1.5%) than in erythrocytes (11.5%) ($P < 0.001$), whereas the 20:5n-3 content was about 60% higher in thrombocytes ($P < 0.001$). The FA composition of thrombocytes was also characterized by 50% higher levels of SAT ($P < 0.001$) and by greater amounts of 20:4n-6 (about twofold, $P < 0.01$), as compared to erythrocytes. The global n-3 FA content of thrombocytes was significantly lower in molting than in breeding adults ($P < 0.01$).

Table 6 shows the FA compositions of the five PL isolated from the thrombocytes of breeding adults, which were taken

TABLE 5
PL Composition of the Thrombocytes of King Penguins in Different Physiological States[a]

	Breeding adults ($n = 3$)	Molting adults ($n = 3$)	Fasting chicks ($n = 3$)
Phosphatidylcholine	40.6 ± 0.6	36.3 ± 3.7	31.4 ± 2.7
Phosphatidylethanolamine	16.0 ± 1.7	20.1 ± 2.0	20.5 ± 2.5
Phosphatidylserine	10.6 ± 1.0	12.7 ± 1.0	15.1 ± 2.4
Phosphatidylinositol	13.5 ± 0.5	11.1 ± 0.9	15.4 ± 3.3
Sphingomyelin	17.8 ± 2.5	19.8 ± 5.2	17.6 ± 5.3

[a]Values are the mean ± SEM of the molar percentage of each PL class. See Table 1 for abbreviation.

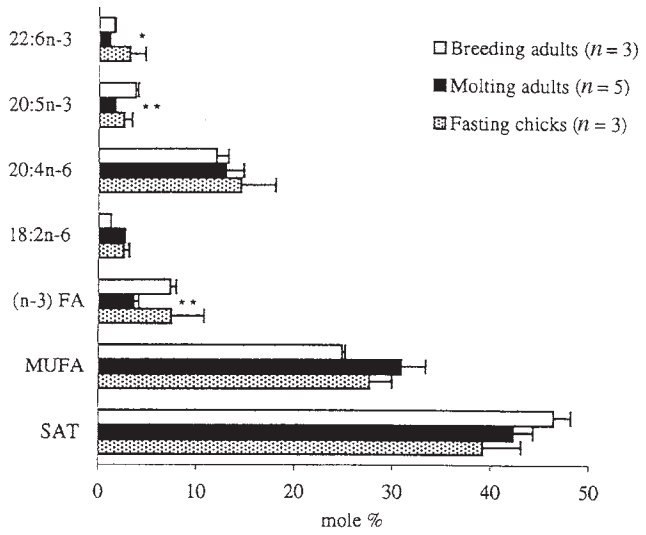

FIG. 2. Fatty acid compositions of phospholipids in the thrombocytes of king penguin. Values are the means ± SEM of the molar percentage of each fatty acid. Molting adults and fasting chicks were compared to breeding adults using the Mann-Whitney test. *$P < 0.05$, **$P < 0.01$. For a FA or a FA class, asterisks indicate significant differences when compared to breeding adults. Other means were not significantly different. For abbreviations see Figure 1.

as reference profiles. These FA compositions displayed the same general characteristics as in erythrocytes but with some specific features. Thus, PE, PS, and SM were more saturated in thrombocytes than in erythrocytes ($P < 0.05$). In all glycerophospholipids, levels of 22:6n-3 were lower (4–13 times, $P < 0.05$) and levels of 20:5n-3 higher (1.5–6 times, $P < 0.01$) in thrombocytes. The levels of 22:1n-9 in PS, PI, and SM of thrombocytes were 4.5–6 times lower than in erythrocytes ($P < 0.01$). Unexpectedly and in contrast to erythrocytes, about half the arachidonic acid pool of thrombocytes was present in PC instead of PE, another 26% being acylated in PI. Except in SM, the n-3/n-6 ratio was two to four times lower ($P < 0.01$) in thrombocytes than in erythrocytes. Thrombocyte SM exhibited a specific profile with large amounts of 16:0 (about 40%) and a long-chain FA content (22- and 24-carbon chains) several times lower than in erythrocytes.

Significant differences were observed between molting and breeding birds in the levels of PC, PI, and SM (data not shown). Thus, PC contained less 20:5n-3 ($P < 0.05$) and more 18:2n-6 ($P < 0.05$) in molting birds, and the ratio of n-3 to n-6 FA was lower in these animals. In PI, although 20:4n-6 levels were similar in both groups, 20:5n-3 levels were lower in molting than in breeding adults ($P < 0.05$). The degree of unsaturation of SM was higher in molting than in breeding birds, in relation to variations in the MUFA content ($P < 0.05$). Lastly, the FA profiles of fasting chicks and breeding adults displayed no significant differences (data not shown).

DISCUSSION

The low erythrocyte count and large cell size observed in the king penguin are in accordance with those reported for numerous bird species (32). Nevertheless, the king penguin ap-

TABLE 6
Fatty Acid Composition of PL in the Thrombocytes of Breeding Adult King Penguins[a]

	PE	PC	PS	PI	SM
14:0	3.0 ± 0.6	1.2 ± 0.3	3.9 ± 0.4	2.3 ± 0.4	7.6 ± 0.7
16:0	14.1 ± 3.0	27.1 ± 3.6	14.9 ± 2.0	10.8 ± 2.4	40.2 ± 1.8
18:0	16.9 ± 1.4	14.3 ± 0.7	29.1 ± 0.8	29.2 ± 1.5	11.4 ± 0.6
20:0	—	—	—	—	0.5 ± 0.1
22:1n-11	0.5 ± 0.1	—	1.8 ± 0.2	—	—
16:1n-9	2.2 ± 0.9	1.3 ± 0.5	2.6 ± 1.1	2.1 ± 0.6	4.2 ± 0.7
18:1n-9	8.8 ± 0.8	17.1 ± 1.1	19.0 ± 2.1	7.8 ± 0.4	6.8 ± 1.0
20:1n-9	0.8 ± 0.0	1.2 ± 0.2	0.8 ± 0.1	0.7 ± 0.1	—
20:2n-9	3.7 ± 0.6	1.4 ± 0.5	4.7 ± 1.0	3.3 ± 0.3	5.2 ± 0.5
22:1n-9	1.5 ± 0.5	0.9 ± 0.3	2.8 ± 0.9	2.2 ± 0.7	2.9 ± 0.5
24:1n-9	—	—	—	—	5.6 ± 1.1
16:1n-7	1.0 ± 0.1	1.4 ± 0.2	1.0 ± 0.1	0.7 ± 0.1	1.3 ± 0.2
18:1n-7	3.0 ± 0.6	5.1 ± 0.2	3.1 ± 0.2	2.5 ± 0.3	2.0 ± 0.2
22:1n-7	—	—	—	—	0.8 ± 0.3
18:2n-6	0.8 ± 0.1	1.6 ± 0.1	0.9 ± 0.1	0.9 ± 0.1	1.3 ± 0.2
18:3n-6	2.2 ± 0.5	1.8 ± 0.4	3.6 ± 1.0	2.8 ± 0.8	5.0 ± 1.1
20:3n-6	—	0.7 ± 0.0	—	1.6 ± 0.7	—
20:4n-6	16.5 ± 3.6	13.7 ± 1.4	2.8 ± 0.3	24.0 ± 2.4	1.6 ± 0.2
22:4n-6	1.5 ± 3.3	0.6 ± 0.1	0.8 ± 0.0	—	—
22:5n-6	—	—	1.9 ± 1.0	1.2 ± 0.5	—
20:5n-3	5.9 ± 1.1	5.3 ± 0.8	1.0 ± 0.3	3.0 ± 0.1	0.6 ± 0.1
22:5n-3	3.1 ± 0.7	1.8 ± 0.3	1.7 ± 0.1	2.1 ± 0.3	—
22:6n-3	3.2 ± 0.3	2.0 ± 0.4	1.6 ± 0.2	—	—
DMA	9.1 ± 0.6	—	—	—	—
DBI	176 ± 22	148 ± 14	104 ± 9	171 ± 7	68 ± 2
UNSAT/SAT	1.4 ± 0.2	1.4 ± 0.2	1.1 ± 0.1	1.3 ± 0.1	0.7 ± 0.0
n-3/n-6	0.6 ± 0.0	0.5 ± 0.0	0.4 ± 0.1	0.2 ± 0.0	0.2 ± 0.0

[a]Values are the means ± SEM of three birds. For abbreviations see Tables 2 and 3.

pears to lie at the lower end of the range for cell count and at the higher end for cell size. These features also have been described in other diving seabirds, the cormorant and little penguin, in contrast to flying birds, which have higher erythrocyte counts and lower cell volumes (33,34). In the king penguin, thrombocytes were less abundant but similar in size when compared with the only reliable values reported in a bird, those for the hen (18,000 vs. 30,000 cells/μL) (35).

Comparison of our data with previously published results for the lipid composition of avian blood cells proved more difficult, as we could find only four reports, all concerning erythrocyte lipids, three in the hen (4,11,12) and one in the pigeon (13). The CHOL to PL ratio of penguin erythrocytes (0.5) was lower than those reported in other birds (0.7–0.8). As the nucleus to cell ratio in king penguin erythrocytes was similar (data not shown) to that of other avian erythrocytes (35), the nuclei could not contribute more than one-tenth of the total cell lipids (36). Thus, it may be hypothesized that the comparatively low ratios of CHO to PL and of SM to PC and likewise the high unsaturation largely characterize the plasma membrane and could confer a high deformability on king penguin erythrocytes. Despite the size of the red cells, 50% larger than those of the hen, these properties probably improve the oxygen delivery in the microvascular bed, as is required in the cooled peripheral tissues of diving penguins (24). A better knowledge of the erythrocyte plasma membrane, cell deformability, and microvascular system in penguins, as in other diving birds, is necessary before formulating a more general hypothesis.

The PL composition of penguin erythrocytes corresponded to that of pigeon erythrocytes (13), except for a higher ratio of PC to PE, and to that of hen erythrocytes (4,11), although in these studies PI and PS were not separated. The higher level of PI in penguin erythrocytes as compared to mammals (37) raises the question of the role of inositol PL in the signal transduction of these nucleated cells. Although the synthetic pathways of inositol phosphates in avian erythrocytes remain unknown (38), their well-known role in the regulation of hemoglobin function (39) would justify further investigation of the involvement of the erythrocyte inositol PL in avian respiratory function. CL, a unique phosphoglyceride known to be concentrated in mitochondria, was previously reported to be present at low levels in hen red cells (11) and chicken erythrocyte nuclei (36). Since we extracted lipids from whole RBC, our study gives no information concerning the CL distribution. Furthermore, in contrast to mammalian (40) or pigeon (41) CL, which contain large amounts of linoleic acid, no specific fatty acid pattern could be assigned to this compound, which displayed a composition similar to that of PI. This feature could be related to the scarcity of linoleic acid and the abundance of n-3 FA in king penguin prey (22). A comparison of the relative concentrations of the major FA in the erythrocytes of the king penguin and the hen, the only other bird in which FA profiles have been studied (11), shows marked differences, and these may be partly ascribed to dietary influences. In contrast to seed-based diets, marine diets are very rich in very long-chain n-3 PUFA and poor in linoleic (18:2n-6) and α-linolenic (18:3n-3) acids (42). Thus, the identical diet of adults and chicks of king penguins (myctophid fishes) contains on the average 6% 20:5n-3 and 10% 22:6n-3, but only 1% 18:2n-6 and 0.3% 18:3n-3 (22). The erythrocytes of king penguins similarly contain large amounts of very long chain n-3 PUFA but small amounts of linoleic and α-linolenic acids. On the other hand, penguin erythrocytes have a higher arachidonic acid content than hen erythocytes, which could be due to taxonomic rather than dietary differences. Hence, an assessment of the value of erythrocyte analyses to determine the nutritional status of such birds sampled in their natural environment would require further experiments, in particular in animals soon after they arrive ashore and later during their natural fast.

Although not accurately documented, the degree of unsaturation of PL acyl chains has been related to prothrombin activation in experimental models (43,44). Thus, it is possible that the higher degree of unsaturation of PS in penguin as compared to hen erythrocytes plays a definite role in the procoagulant activity of these cells in circulating blood. It would be of interest to carry out further investigations on the influence of PL unsaturation on the generation of thrombin in birds. Contrary to erythrocytes, the absence of previous studies of the lipid composition of thrombocytes in birds precludes any comparison of our findings with data for other avian species. Although thrombocytes and erythrocytes have been suggested to be genealogically closely related in birds (10), our results do not support this hypothesis since each cell type has its own PL distribution and FA composition. Although the possibility of late biochemical differentiation in the circulating blood cannot be excluded, it would seem unlikely that avian erythrocytes and thrombocytes derive from closely related cells. The recent demonstration of an aggregatory function of penguin thrombocytes (Fayolle, C., Ohlmann, P., Groscolas, R., Leray, C., and Gachet, C., unpublished data) is consistent with this conclusion.

ACKNOWLEDGMENTS

This work was supported by INSERM and the Institut Français pour la Recherche et la Technologie Polaires (Programme 119), and it received logistic support from the Terres Australes et Antarctiques Françaises. The authors would like to thank Dr. Alain Van Dorsselaer (Service de Spectrométrie de Masse, Université Louis Pasteur, URA 31, Strasbourg) for the mass spectrometric analyses and Juliette Mulvihill for revising the English of the manuscript.

REFERENCES

1. Wartelle, O. (1957) Mécanisme de la Coagulation chez la Poule. I. Etude des Eléments du "Complexe Prothrombique" et de la Thromboplastino-formation, *Rev. Hematol. 12*, 351–387.
2. Johnson, G.S., Turrentine, M.A., and Swayne, D.E. (1985) Coagulation of Plasma from the Chicken (*Gallus domesticus*): Phospholipids Influence Clotting Rates Induced by Components from Russel's Viper Venom, *Comp. Biochem. Physiol. 82B*, 647–653.
3. Fernandez, A., Verde, M.T., Gomez, J., Gascon, M., and Ramos, J.J. (1995) Changes in the Prothrombin Time, Haematology and Serum Proteins During Experimental Aflatoxicosis in Hens and Broiler Chickens, *Res. Vet. Sci. 58*, 119–122.

4. Kleinig, H., Zentgraf, H., Comes, P., and Stadler, J. (1971) Nuclear Membranes and Plasma Membranes from Hen Erythrocytes. II. Lipid Composition, *J. Biol. Chem. 246*, 2996–3000.
5. Campbell, T.W. (1988) *Avian Hematology and Cytology*, pp. 3–17, Iowa State University Press, Ames.
6. Grant, R.A., and Zucker, M.B. (1973) Avian Thrombocyte Aggregation and Shape Change *in vitro*, *Am. J. Physiol. 225*, 340–343.
7. Carlson, H.C., Sweeny, P.R., and Tokaryk, J.M. (1968) Demonstration of Phagocytic and Trephocytic Activities of Chicken Thrombocytes by Microscopy and Vital Staining Techniques, *Avian Dis. 12*, 700–715.
8. Taffarel, M., and Oliveira, M.P. (1993) Cytochemical Analysis of the Content of Chicken Thrombocytes Vacuoles, *Cell Biol. Int. 17*, 993–999.
9. Ries, S., Käufer, I., Reinacher, M., and Weiss, E. (1984) Immunomorphologic Characterization of Chicken Thrombocytes, *Cell Tissue Res. 236*, 1–3.
10. Krajewska, W., and Klyszejko-Stefanowicz, L. (1980) Comparative Studies on Chromatin Proteins from Chicken Thrombocytes and Erythrocytes, *Biochim. Biophys. Acta 624*, 522–530.
11. Soula, G. (1972) Etude Analytique des Phospholipides des Globules Rouges de Poulet, *Biochimie 54*, 1483–1486.
12. Kester, M., and Privitera, C.A. (1984) Phospholipid Composition of Dystrophic Chicken Erythrocyte Plasmalemmae. I. Isolation of a Unique Lipid in Dystrophic Erythrocyte Membranes, *Biochim. Biophys. Acta 778*, 112–120.
13. Watts, C., and Wheeler, K.P. (1978) Protein and Lipid Components of the Pigeon Erythrocyte Membrane, *Biochem J. 173*, 899–907.
14. Leaf, A., and Weber, P.C. (1988) Cardiovascular Effects of n-3 Fatty Acids, *N. Engl. J. Med. 318*, 549–557.
15. Connor, W.E., DeFrancesco, C.A., and Connor, S.L. (1993) n-3 Fatty Acids from Fish Oil. Effects on Plasma Lipoproteins and Hypertriglyceridemic Patients, *Ann. N.Y. Acad. Sci. 683*, 16–34.
16. Cooper, R.A. (1977) Abnormalities of Cell-membrane Fluidity in the Pathogenesis of Disease, *N. Engl. J. Med. 297*, 371–377.
17. Pöschl, J.M.B., Leray, C., Groscolas, R., Ruef, P., and Linderkamp, O. (1996) Dietary Docosahexaenoic Acid Improves Red Blood Cell Deformability in Rats, *Thromb. Res. 81*, 283–288.
18. Croset, M., Bayon, Y., and Lagarde, M. (1992) Incorporation and Turnover of Eicosapentaenoic and Docosahexaenoic Acids in Human Blood Platelets *in vitro*, *Biochem. J. 281*, 309–316.
19. Marangoni, F., Angeli, M.T., Colli, S., Eligini, S., Tremoli, E., Sirtori, C.R., and Galli, C. (1993) Changes of n-3 and n-6 Fatty Acids in Plasma and Circulating Cells of Normal Subjects, After Prolonged Administration of 20:5 (EPA) and 22:6 (DHA) Ethyl Esters and Prolonged Washout, *Biochim. Biophys. Acta 1210*, 55–62.
20. Stonehouse, B. (1960) The King Penguin *Aptenodytes patagonica* of South Georgia. I. Breeding Behaviour and Development, *Falk. Isl. Dep. Survey Scient. Rep. 23*, 1–81.
21. Weimerskirch, H., Stahl, J.C., and Jouventin, P. (1992) The Breeding Biology and Population Dynamics of King Penguins *Aptenodytes patagonica* on the Crozet Islands, *Ibis 134*, 107–117.
22. Raclot, T., Groscolas, R., and Cherel, Y. (1998) Fatty Acid Evidence for the Importance of Myctophid Fish in the Diet of King Penguins, *Aptenodytes patagonicus*, *Marine Biol. 132*, 523–533.
23. Butler, P.J., and Jones, D.R. (1997) Physiology of Diving of Birds and Mammals, *Physiol. Rev. 77*, 837–899.
24. Handrich, Y., Bevan, R.M., Charrassin, J.B., Butler, P.J., Pütz, K., Woakes, A.J., Lage, J., and Le Maho, Y. (1997) Hypothermia in Foraging King Penguins, *Nature 388*, 64–67.
25. Cherel, Y., Leloup, J., and Le Maho, Y. (1988) Fasting in King Penguin. II. Hormonal and Metabolic Changes During Molt, *Am. J. Physiol. 254*, R178–R184.
26. Groscolas, R. (1990) Metabolic Adaptations to Fasting in Emperor and King Penguins, in *Penguin Biology* (Davis, L.S., and Darby, J.T., eds.) pp. 269–296, Academic Press, New York.
27. Cazenave, J.P., Hemmendinger, S., Beretz, A., Sutter-Bay, A., and Launay, J. (1983) L'Agrégation Plaquettaire: Outil d'Investigation Clinique et d'Etude Pharmacologique. Méthodologie, *Ann. Biol. Clin. 41*, 167–179.
28. Leray, C., Andriamampandry, M., Gutbier, G., Cavadenti, J., Klein-Soyer, C., Gachet, C., and Cazenave, J.P. (1997) Quantitative Analysis of Vitamin E, Cholesterol and Phospholipid Fatty Acids in a Single Aliquot of Human Platelets and Cultured Endothelial Cells, *J. Chromatogr. 696*, 33–42.
29. Leray, C., Pelletier, X., Hemmendinger, S., and Cazenave, J.P. (1987) Thin-Layer Chromatography of Human Platelet Phospholipids with Fatty Acid Analysis, *J. Chromatogr. 420*, 411–416.
30. Rouser, G., Fleicher, S., and Yamamoto, A. (1970) Two Dimensional Thin-Layer Chromatographic Separation of Polar Lipids and Determination of Phosphorus Analysis of Spots, *Lipids 5*, 494–496.
31. Rudel, L.L., and Morris, M.D. (1973) Determination of Cholesterol Using *o*-Phthalaldehyde, *J. Lipid Res. 14*, 364–366.
32. Hawkey, C.M., Bennet, P.M., Gascoyne, S.C., Hart, M.G., and Kirkwood, J.K. (1991) Erythrocyte Size, Number and Haemoglobin Content in Vertebrates, *Br. J. Haematol. 77*, 392–397.
33. Nicol, S.C., Melrose, W., and Stahel, C.D. (1988) Haematology and Metabolism of the Blood of the Little Penguin, *Eudyptula minor*, *Comp. Biochem. Physiol. 89A*, 383–386.
34. Melrose, W.D., and Nicol, S.C. (1992) Haematology, Red Cell Metabolism and Blood Chemistry of the Black-Faced Cormorant *Leucocarbo fuvescens*, *Comp. Biochem. Physiol. A 102*, 67–70.
35. Lucas, A.M., and Jamroz, C. (1961) *Atlas of Avian Hematology*, pp. 211–219, Agriculture Monograph 25, United States Department of Agriculture, Washington, DC.
36. Souillard, C., and Soula, G. (1976) Les Noyaux de Globules Rouges de Poussin: Composition et Analyse des Phospholipides, *Biochimie 58*, 1263–1271.
37. White, D.A. (1973) The Phospholipid Composition of Mammalian Tissues, in *Form and Function of Phospholipids* (Ansell, G.B., Hawthorne, J.N., and Dawson, R.M.C., eds.) Vol. 3, pp. 441–482, Elsevier, Amsterdam.
38. Isaacks, R.E., Kim, C.Y., Johnson, A.E., Jr., Goldman, P.H., and Harkness, D.R. (1982) Studies on Avian Erythrocyte Metabolism. XII. The Synthesis and Degradation of Inositol Pentakis (dihydrogen phosphate), *Poult. Sci. 61*, 2271–2281.
39. Coates, M.L. (1975) Hemoglobin Function in the Vertebrates: An Evolutionary Model, *J. Mol. Evol. 6*, 285–307.
40. Ioannou, P.V., and Golding, B.T. (1979) Cardiolipins: Their Chemistry and Biochemistry, *Prog. Lipid Res. 17*, 279–318.
41. Desmeth, M., and Vandeputte, P.J. (1981) Phospholipids and Component Fatty Acids of the Pigeon Liver, *Lipids 16*, 700–702.
42. Clarke, A. (1989) Seabirds, in *Marine Biogenic Lipids, Fats and Oils* (Ackman, R.G., ed.) pp. 383–398, CRC Press, Boca Raton.
43. Hecht, E.R. (1965) *Lipids in Blood Clotting*, pp. 28–122, Charles C. Thomas, Springfield.
44. Govers-Riemslag, J.W.P., Janssen, M.P., Zwaal, R.F.A., and Rosing, J. (1992) Effect of Membrane Fluidity and Fatty Acid Composition on the Prothrombin-Converting Activity of Phospholipid Vesicles, *Biochemistry 31*, 10000–10008.

[Received July 6, 1999, and in revised form March 6, 2000; revision accepted March 14, 2000]

METHOD

Esterification of Polyunsaturated Fatty Acids by Various Forms of Immobilized Lipase from *Rhizomucor miehei*

Yoshitsugu Kosugi*, Prodyut Kumar Roy[1], Qinglong Chang[2], Cao Shu-gui[3], Makoto Fukatsu[4], Kenji Kanazawa, and Hiroshi Nakanishi

National Institute of Bioscience and Human-Technology, Agency of Industrial Science and Technology, Tsukuba 305-8566, Japan

ABSTRACT: Ethyl esterification specificity of a lipase from *Rhizomucor miehei* for polyunsaturated fatty acids (PUFA) was compared at 1 and 100 mM to study molecular recognition of PUFA. The chemical shift of methylene adjacent to carboxyl groups in the nuclear magnetic resonance spectrum of docosahexaenoic acid (DHA) in ethanol moved to a lower magnetic field as the concentration of DHA increased, suggesting that the degree of dissociation of DHA decreased. Specificity constants or apparent second-order rate constants (V_{max}/K_m or catalytic power) for 1 mM esterification by immobilized lipases were higher than the native lipase. Immobilized hydrophobic carrier of low mass transfer resistance for the esterification substrate may improve maximal velocity and affinity for the substrate. Higher specificity constants for 1 mM substrates were observed using immobilized lipases fixed on an anion exchange resin with glutaraldehyde and on a cation exchange carrier with carbodiimide. Activity yields measured with 1 mM PUFA substrate were high. For the substrates at a concentration of 100 mM, higher specific constants with these bifunctional reagents were not observed but higher activity yields were found.

Paper no. L7917 in *Lipids 35,* 461–466 (April 2000).

Lipase attacks the ester bond that binds hydrophobic and hydrophilic residues. In an aqueous solution esters are heterogeneous with respect to charge distribution. Porcine pancreatic lipase activity is greatly increased at the water/lipid interface, suggesting interfacial activation (1). The catalytic triad (Ser-144, His-203, Asp-257) of *Rhizomucor miehei* lipase is buried completely beneath a short helical segment (residue 82-96), or lid (2). X-ray crystallographic analysis of the lipase–inhibitor complex revealed that interfacial activation is achieved by the displacement of the lid structure, which exposes the catalytic groups and creates a hydrophobic surface that stabilizes the contact between the lipase and the lipid interface (3). We previously reported that higher hydrolysis rates for 1 mM substrates were observed using immobilized lipases (on anion exchange resin with glutaraldehyde and on cation exchange carrier with carbodiimide) than for native lipase or for lipase adsorbed on weak anion exchange resin, indicating some modification of the environment of basic amino acids related to the lid of *R. miehei* lipase. Activations with these bifunctional reagents were not observed for substrates at the concentration of 100 mM, indicating that interfacial activation always occurred by formation of the aggregates of substrates at high concentrations (4).

Polyunsaturated fatty acids (PUFA) are important because of their many biological functions and utility in low-temperature adaptation of biological membranes. Amphipathic PUFA have an alkyl group in combination with a polar and/or ionizing carboxyl group, displaying an extensive range of molecular clustering patterns depending on chemical structure, concentration, and temperature (5). In a previous paper (4) we reported that at concentrations below the critical micelle concentration (CMC) of docosahexaenoic acid (DHA), 0.35 mM, the DHA sodium salt in water exists in a monomeric state. When the DHA sodium salt concentration is near the CMC, DHA salts exist in an equilibrium between the monomeric and aggregate states, where the exchange rate between a monomer and aggregate is slow. At concentrations above the CMC, DHA sodium salt exists in micelles or an aggregate state. When fatty acids are dissolved in ethanol, however, there is no interface in the homogeneous substrate at concentrations of 1 to 100 mM.

A competitive factor α is proposed for lipase specificity toward fatty acids in organic solvents (6). A specific constant $1/\alpha$ is proposed for the lipase specificity with respect to degree of unsaturation. In the earlier study, the specificity con-

*To whom correspondence should be addressed at National Institute of Bioscience and Human-Technology, 1-1 Higashi Tsukuba, 305-8566, Japan. E-mail: kosugi@nibh.go.jp

[1]Present address: Central Drug Research Institute, Chattar Manzil, Lucknow-226001, India.

[2]Present address: Soil and Plant Analysis Lab, University of Wisconsin, Madison, WI 53705.

[3]Present address: National Laboratory of Enzyme Engineering, Jilin University, Changchun, 130023, China.

[4]Present address: College of Science and Technology, Nihon University, 1-8 Kanda Surugadai, 101-8308, Japan.

Abbreviations: CMC, critical micelle concentration; DHA, docosahexaenoic acid; K_m or K_{Ac1X}, K_{Ac2X}, Michaelis constant; NMR, nuclear magnetic resonance; PUFA, polyunsaturated fatty acid; V_{max}, V_{Ac2X},V_{Ac1X}, maximal velocity.

stants were compared over a rather narrow range of substrate concentrations, i.e., 0.1 vs. 0.2 M and 1 vs. 2 M (7). The specificity constant of esterification has been studied for PUFA and less common fatty acids catalyzed by lipases from different sources (8,9). The present study describes polyunsaturated fatty acyl donor specificities in ethyl esterification by lipase from *R. miehei* using substrates in 1 and 100 mM concentration.

MATERIALS AND METHODS

Materials. Lipase (Lipozyme 10,000 L) from *R. miehei* was provided by Novo Nordisk (Chiba, Japan) as a liquid containing 10,000 LU/g specified by the maker. DHA was a product of Nu-Chek-Prep, Inc. (Elysian, MN). Eicosapentaenoic acid was obtained from Funakoshi Co. (Tokyo, Japan). Arachidonic, linolenic, and linoleic acids were products of Serdary Research Laboratories Inc. (London, Ontario, Canada). Sperisil C, a weakly acidic cation exchange carrier with carboxylic acid groups, was provided by Rhône-Poulenc Industry (Paris, France). Water-soluble carbodiimide of 1-ethyl-3-(3-dimethyl-aminopropyl)-carbodiimide HCl was obtained from Sigma Chemical Co. (St. Louis, MO). Dowex MWA-1, a macroporous weakly basic anion exchange resin with tertiary amine groups, was obtained from The Dow Chemical Co. (Midland, MI).

Immobilization of lipase. Lipase from *R. miehei* used in this study was prepared as previously reported (4). The flexible lipase was prepared as follows. One gram of Spherosil C was activated with the water-soluble carbodiimide as described previously (10). The activated Spherosil C and 2 g of Lipozyme 10,000L were combined with 1 mL of 0.067 M McIlvaine buffer at pH 5 (9.7:10.3, vol/vol mixture of 0.067 M citric acid and 0.133 M Na_2HPO_4), and the resultant mixture was shaken overnight at 4°C. The lipase immobilized on the cation exchange carrier was washed with water, and excess liquid was removed by suction. The adsorbed lipase was prepared as follows. One gram of Dowex MWA-1 was washed with water and mixed with 2 g of Lipozyme 10,000L and 1 mL of 0.067 M McIlvaine buffer at pH 5. The mixture was shaken at 4°C overnight and dried as described above. The rigid lipase was prepared from the above adsorbed lipase by treatment with glutaraldehyde as previously described (11).

Esterification reaction. The reaction mixture containing 1 mM fatty acid was composed of 50.0 mL ethanol, 1 mM (10–18 mg) fatty acid, and 30 mg immobilized lipase or 75 mg of Lipozyme 10,000L. The reaction mixture containing 100 mM fatty acid was composed of 1 mL of ethanol, 100 mM (20–30 mg) fatty acid, and 30 mg immobilized lipase or 75 mg of Lipozyme 10,000L. The reaction mixture was put in a round-bottomed tube saturated with nitrogen and agitated with a small magnetic stirrer at 45°C for 1–3 h. During the reaction, nitrogen was continuously blown over the surface of the reaction mixture. Three separate batches of reaction with each fatty acid were carried out under identical conditions. The standard deviation of reaction with each fatty acid was calculated and used as experimental errors.

Assay methods for esterification product. The esterification product was extracted with hexane, and the upper phase was collected after adding a small amount of water to promote the separation of two phases. The solvent was evaporated under a gentle stream of nitrogen. The esterification product was redissolved in acetone. The concentrated hydrolysate was analyzed by high-performance liquid chromatography (GL Science, Tokyo, Japan) using a refractive index detector (RI model 504; GL Science) and a chromatointegrator (D-2500; Hitachi, Tokyo, Japan). The fixed-phase column was a Superspher RP-18 (4 × 25 mm; Merck, Darmstadt, Germany), and the mobile phase was a mixture of acetone and acetonitrile (1:1, vol/vol, at a flow rate of 0.8 mL/min and pressure of 120 kg/cm^2).

Kinetic studies. The esterification rate or initial velocity was calculated from the composition of the reaction products and is expressed as the amount of ester (μmol) produced/g/min. The competitive factor α was obtained as follows. In the competitive reaction of two substrates (Ac1X and Ac2X with the same leaving group × and two different acyl groups, Ac1 and Ac2) at the same catalytically active site of the enzyme molecule, the ratio of the esterification rates for each substrate (v_1 and v_2) is given (12) by

$$v_1/v_2 = \left[\left(V_{Ac1X}/K_{Ac1X}\right)/\left(V_{Ac2X}/K_{Ac2X}\right)\right](Ac1X)/(Ac2X) \quad [1]$$

where (Ac1X) and (Ac2X) are the concentrations of the two acyl donors (two fatty acyl ethyl esters), (V_{Ac1X}) and (V_{Ac2X}) are the maximal velocities, and (K_{Ac1X}) and (K_{Ac2X}) are the Michaelis constants for each substrate. The competitive factor α is then defined as the ratio of the catalytic powers according to the following equation (6,7):

$$\left(V_{Ac1X}/K_{Ac1X}\right)/\left(V_{Ac2X}/K_{Ac2X}\right) = \alpha \quad [2]$$

The competitive factor α is calculated from the integral form of Equation 1:

$$\log\left([Ac1X]_0/[Ac1X]\right) = \alpha \log\left([Ac2X]_0/[Ac2X]\right) \quad [3]$$

From Equations 2 and 3, the specificity constant 1/α (7) can then be expressed as Equation 4

$$\left(V_{Ac2X}/K_{Ac2X}\right)/\left(V_{Ac1X}/K_{Ac1X}\right) = \log\left([Ac2X]_0/[Ac2X]\right)/\log\left([Ac1X]_0/[Ac1X]\right) \quad [4]$$

The specificity constant 1/α is an apparent second-order catalytic constant or catalytic power as log(V_{Ac2X}/K_{Ac2X}) based on the log(V_{Ac1X}/K_{Ac1X}) being equal to 1. In this paper the Ac1X is lauric acid.

Nuclear magnetic resonance (NMR) measurement. ^{1}H NMR was measured at room temperature (25°C) with 0.1–10 mM of PUFA in deuterium-labeled ethanol (C_2D_5OD) using a JEOL α-500 NMR spectrometer (499.45 Mhz; Tokyo,

Japan). The PUFA sample was poured into an NMR cell under an argon atmosphere. The standard compound was tetramethylsilane used in a C_2D_5OD capillary system.

RESULTS AND DISCUSSION

PUFA substrates. Figure 1 shows the ^1H NMR spectra of the methylene regions of DHA. The positions of methylene resonance signals (*b*, *d*, and *e* in Fig. 1) remained almost unchanged as the DHA concentration increased. However, the signal (*c* in Fig. 1) of the methylene (2-CH_2) group adjacent to the carboxylic group (–COOH) was remarkably shifted to a lower magnetic field as the concentration of DHA increased from 0.1 to 10 mM. On the other hand, as the concentration of DHA changed, all signals from DHA in chloroform solution showed neither a downfield nor an upfield shift (data not shown). This result shows that DHA does not form reversed micelles in chloroform, owing to the fact that DHA is highly soluble in chloroform. Since DHA dissolves well in ethanol too, it can scarcely form reversed micelles in ethanol. These results suggest that DHA should dissociate into ions in ethanol solution because DHA is an acid and ethanol is a polar solvent. On the other hand chloroform is nonpolar, and DHA dissociates only slightly into ions in chloroform. As the DHA concentration in ethanol increases, the degree of the dissociation decreases, which can cause the change in chemical shift of the signal of methylene group adjacent to the carboxylic one.

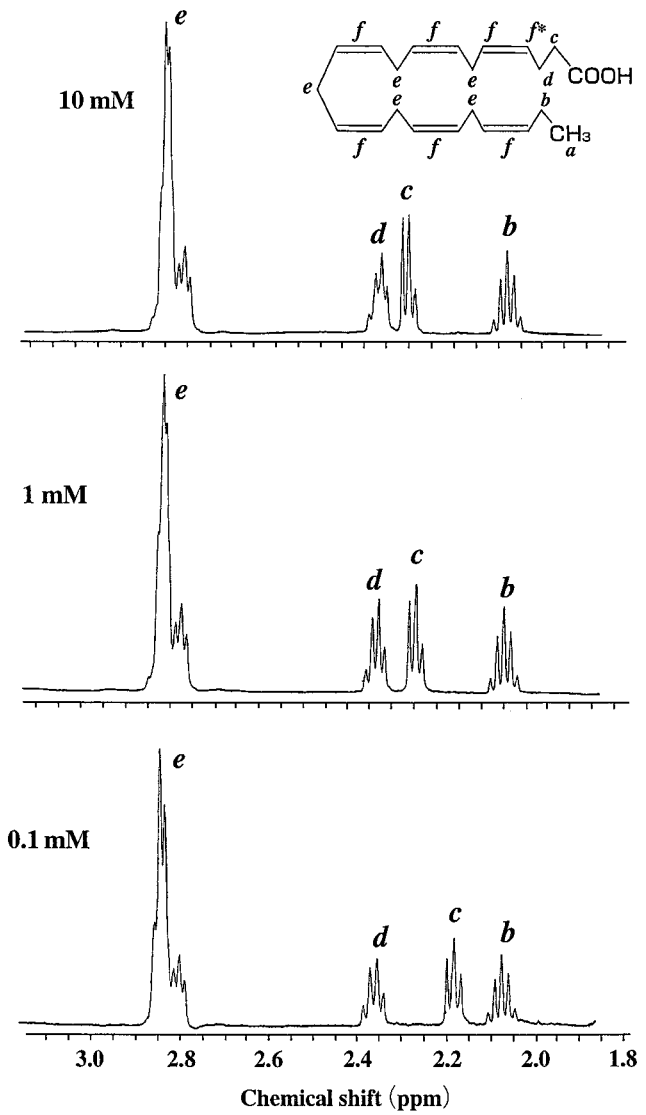

FIG. 1. ^1H Nuclear magnetic resonance spectra of the methylene regions of three concentrations of docosahexaenoic acid in C_2D_5OD. The labeled peaks (*b, c, d,* and *e*) correspond to the functional groups indicated in the structure of docosahexaenoic acid.

Immobilization of lipase. Lipase from *R. miehei,* with an isoelectric point of 4.3 (according to the manufacturer), generally does not adsorb onto a cation exchange carrier through electrostatic repulsion but rather is fixed on the carrier by covalent bonding and is called flexible lipase. The lipase also can be attached to an anion exchange resin through ionic and hydrophobic bonding and is then called adsorbed lipase. Adsorbed lipase treated with glutaraldehyde can be fixed onto an anion exchange resin through covalent bonding, ionic bonding, and hydrophobic bonding and is called rigid lipase. Native lipase and flexible lipase can easily undergo structural change, but rigid lipase undergoes little structural change despite changes in the physical conditions.

Specificity spectrum for PUFA. Lipase specificity was markedly influenced by the type of immobilization used, as shown in Figures 2–5. Esterification rates decreased with increasing substrate unsaturation as shown in Figures 2 and 4, although several exceptions existed. Higher specificity constants for 1 mM substrates were observed for flexible lipase on cation exchange carrier with carbodiimide and for rigid lipase fixed on anion exchange resin with glutaraldehyde as shown in Figure 5. Carbodiimide and glutaraldehyde attack basic amino acids such as arginine, histidine, and lysine. The enhanced activity with these bifunctional reagents was not observed using 100 mM substrates (Fig. 3). As reported previously (4), some modification may be introduced in the basic amino acids related to the lid, and some activation of esterification of the 1 mM substrate was observed. The Arg 86 in the lid of *R. miehei* lipase is exposed on the surface of molecule in the interfacial activation state (3), and the residue may be modified with these bifunctional reagents.

The substrate fatty acids used in these experiments were dissolved in ethanol. Chemical shifts of 1 and 100 mM DHA in ethanol were different, and the difference may be derived from the degree of dissociation as mentioned previously. That the lipase from *R. miehei* recognized these differences was reflected in the specific constant $1/\alpha$. The recognition is different from interfacial activation because ethyl esterification was carried out in homogeneous reactants. In our previous paper on hydrolysis, the specificity constant between 1 and 100 mM substrate was not significantly different, but differences were seen in hydrolysis rates (4). It was reported that in organic solvents, the formation and the solvolysis of the acyl enzyme occur in two independent steps. The use of competitive factor

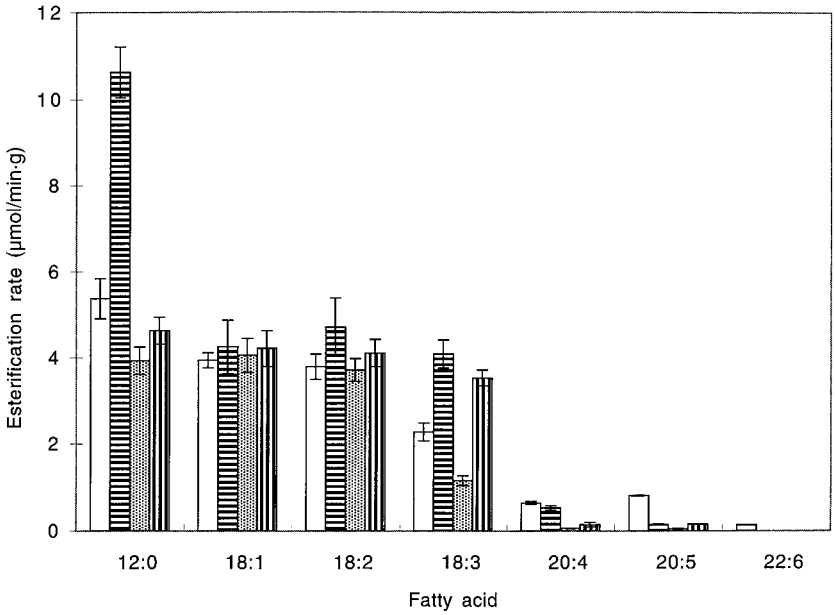

FIG. 2. Reaction rates for the esterification of 100 mM fatty acid. The columns show the data for native lipase (open bar), flexible lipase (horizontally striped bars), adsorbed lipase (stippled bars), and rigid lipase (vertically striped bars) from *Rhizomucor miehei*. The error bars represent the standard deviations obtained by more than three reaction batches.

α is not appropriate in a biphasic system where the kinetics are usually much more complex than in a organic system (6).

Higher esterification rates for 100 mM fatty acid were observed using flexible lipase and the highest esterification rate for 100 mM lauric acid as shown in Figure 2. Lower specific constants for PUFA substrates at 1 mM were observed using native lipase as shown in Figure 5. In hydrolysis, the native lipase showed a higher specific constant for PUFA substrates at 1 mM fatty acyl ester, and the highest hydrolysis rate for 100 mM linolenic acyl ethyl ester was observed using the adsorbed lipase (4). These observations show the changes occurring in the specificities of the different forms of lipase from *R. miehei* in esterification and hydrolysis.

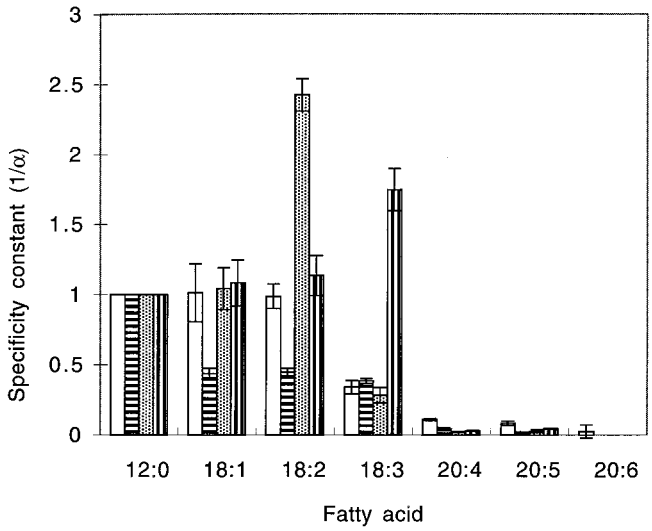

FIG. 3. Specificity constants (1/α) for the esterification of 100 mM fatty acid. For keys, error bars, and organism see Figure 2.

We observed various changes in the fatty acid specificities and competitive factors in 1 and 100 mM fatty acids as described above. However, it was reported that competition factors are not influenced by changes in the physical conditions of the reaction (water content, substrate concentration, nature of nucleophiles, etc.) (7). One simple explanation for these contradictory phenomena is that the assembling structures of the fatty acyl ethyl ester are very different between 1 and 100 mM substrate, and therefore these substrates behave as different entities. The V_{max}/K_m for fatty acid esterification of the lipase from *Candida rugosa* also changed at different concentrations of fatty acids (14).

The activity yields (immobilized lipase activity divided by used lipase activity for the nonimmobilized preparation used) using 1 mM oleic acid, linolenic acids, arachidonic acid, and eicosapentaenoic acid were extraordinarily high, as much as 150–480%. Although both 1 and 100 mM PUFA were well dissolved in ethanol, the substrate at 1 mM may be more dissociated and better suited to undergo mass transfer. Reaction rates of immobilized lipases with 1 mM PUFA were higher than that of the native lipase as shown in Figure 4 and previously observed in the hydrolysis reaction (4). The high activity yields show that immobilization results in a suitable conformation and microenvironment (13) for *R. miehei* lipase to esterify the substrates. Figure 5 shows that specificity constant 1/α of immobilized lipases was higher than that of the native lipase. Immobilized hydrophobic carriers of low mass

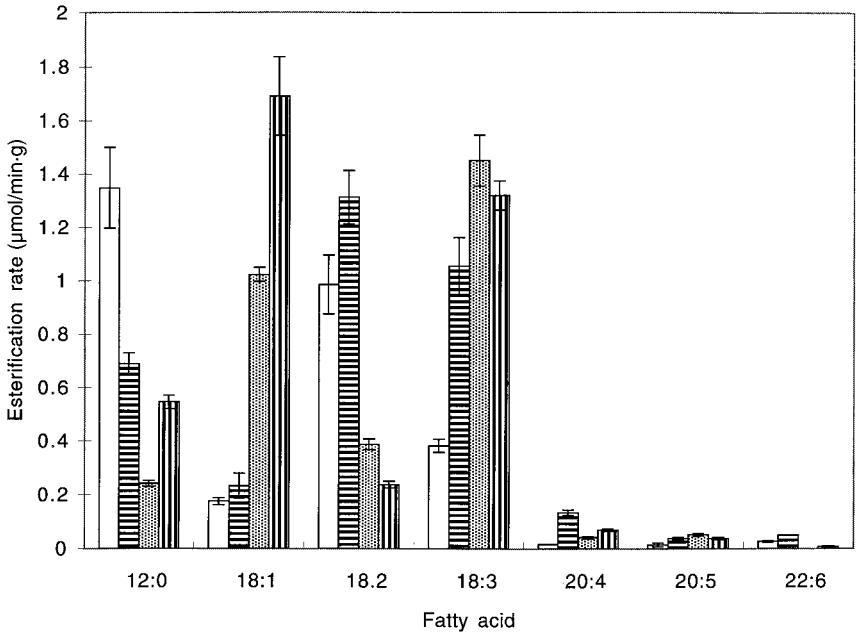

FIG. 4. Reaction rates for the esterification of 1 mM fatty acid. For keys, error bars, and organism see Figure 2.

transfer resistance for the esterification substrate improved the affinity for the substrate (Fig. 5) as well as overall rate of esterification (Fig. 4). However, the native lipase showed a higher specificity constant for the hydrolysis of 1 mM PUFA esters (4). Activity yields measured with 100 mM PUFA substrate were not extraordinary high. For the substrates at a concentration of 100 mM, higher specific constants with these bifunctional reagents were not observed but higher activity yields were found.

The "Induced Fit" theory of enzyme action says that the substrate induces conformational changes in the protein and stabilizes a new substrate–protein structure because of the new hydrophobic, hydrophilic, and electrostatic interactions formed in the binding process. The conformational flexibility

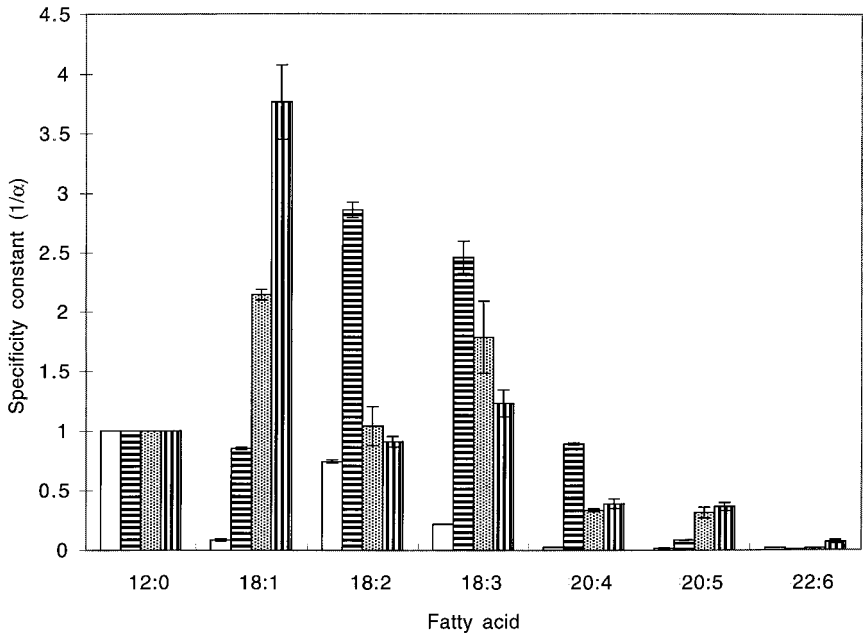

FIG. 5. Specificity constants ($1/\alpha$) for the esterification of 1 mM fatty acid. For keys, error bars, and organism see Figure 2.

of proteins appears to be a universal property that enables these molecules to be adapted to their widespread functions in the living system (15). Our conclusion is that lipase from *R. miehei* recognizes the molecular conformation of lipids even in organic solvents and that changes occur in the esterification for fatty acids under these conditions.

ACKNOWLEDGMENT

We thank Dr. Alain Roussel of AFMB-CNRS (Marseille, France) for providing the structure model of lipases.

REFERENCES

1. Sarda, L., and Desnuelle, P. (1958) Action de la lipase pancreatique sur les esters en emulsion, *Biochim. Biophys. Acta 30*, 513–521.
2. Brandy, L., Brzozowski, A.M., Derewenda, Z.S., Dodson, E., Dodson, G., Tolley, S., Turkenburg, J.P., Christiansen, L., Huge-Jensen, B., Norskov, L., Thim, L., and Menge, U. (1990) A Serine Protease Triad Forms the Catalytic Centre of a Triacylglycerol Lipase, *Nature 343*, 767–770.
3. Brzozowski, A.M., Derewenda, U., Derewenda, Z.S., Godson, G.G., Lawson, D.M., Turkenburg, J.P., Bjorkling, F., Huge-Jensen, B., Patkar, S.A., and Thim, L. (1991) A Model for Interfacial Activation in Lipases from the Structure of a Fungal Lipase–Inhibitor Complex, *Nature 351*, 491–494.
4. Kosugi, Y., Qinglong, C., Kanazawa, K., and Nakanishi, H. (1997) Changes in Hydrolysis Specificities of Lipase from *Rhizomucor miehei* to Polyunsaturated Fatty Acyl Esters in Different Aggregation States, *J. Am. Oil Chem. Soc. 74*, 1395–1399.
5. Jones, M.N., and Chapman, D. (1995) The Chemistry and Role of Amphipathic Molecules, in *Micelles, Monolayers, and Biomembranes*, pp. 1–23, Wiley-Liss, New York.
6. Deleuze, H., Langand, G., Millet, H., Baratti, J., Buono, G., and Triantaphylides, C. (1987) Lipase-Catalyzed Reactions in Organic Media: Competition and Applications, *Biochim. Biophys. Acta 911*, 117–120.
7. Rangheard, M.-S., Langland, G., Triantaphylides, C., and Baratti, J. (1989) Multi-Competitive Enzymatic Reactions in Organic Media: A Simple Test for the Determination of Lipase Fatty Acid Specificity, *Biochim. Biophys. Acta 1004*, 20–28.
8. Mukherjee, K.D., Kiewitt, I., and Hills, J. (1993) Substrate Specificities of Lipases in View of Kinetic Resolution of Unsaturated Fatty Acids, *Appl. Microbiol. Biotechnol. 40*, 489–493.
9. Jachmanian, I., Schulte, E., and Mukherjee, K.D. (1996) Substrate Selectivity in Esterification of Less Common Fatty Acids Catalyzed by Lipases from Different Sources, *Appl. Microbiol. Biotechnol. 44*, 563–567.
10. Kosugi, Y., and Suzuki, H. (1992) Functional Immobilization of Lipase Eliminating Lipolysis Product Inhibition, *Biotechnol. Bioeng. 40*, 369–374.
11. Kosugi, Y., Igusa, H., and Tomizuka, N. (1987) Glyceride Production from High Free Fatty Acid Rice Bran Oil Using Immobilized Lipase, *J. Jpn. Oil Chem. Soc. 36*, 769–776.
12. Foster, R.J., and Niemann, C. (1951) The Kinetics of the α-Chymotrypsin-Catalyzed Competitive Hydrolysis of Acetyl-L-tryptophanamide and Acetyl-L-tyrosineamide in Aqueous Solutions at 25°C and pH 7.9, *J. Am. Chem. Soc. 73*, 1552–1554.
13. Katchalski, E., Silman, I., and Goldman, R. (1971) Effect of the Microenvironment on the Mode of Action of Immobilized Enzymes, *Adv. Enzymol. 34*, 445–536.
14. Janssen, A.E.M., Vaidya, A.M., and Halling, P.J. (1996) Substrate Specificity and Kinetics of *Candida rugosa* Lipase in Organic Media, *Enzyme Microb. Technol. 18*, 340–346.
15. Koshland, D.E., Jr., and Neet, K.E. (1968) The Catalytic and Regulatory Properties of Enzymes, *Annu. Rev. Biochem. 37*, 359–410.

[Received April 28, 1998; and in final revised form March 6, 2000; revision accepted March 8, 2000]

ARTICLE

Changes in Fatty Acid Composition in Plant Tissues Expressing a Mammalian Δ9 Desaturase

Hangsik Moon[a,1], Jan Hazebroek[b], and David F. Hildebrand[a,*]

[a]Department of Agronomy, University of Kentucky, Lexington, Kentucky 40546-0091 and [b]Pioneer Hi-Bred International, Inc., Johnston, Iowa 50131-1004

ABSTRACT: Plant tissues expressing a mammalian stearoyl-CoA Δ9 desaturase were reported to accumulate Δ9 hexadecenoic acid (16:1), normally very minor in most plant tissues. The transgenic plants were thoroughly analyzed for alterations of individual lipids in different subcellular sites. Western blot analysis indicated that the animal desaturase was targeted to the microsomes. The Δ9 16:1 was incorporated into both the *sn*-1 and *sn*-2 positions of all the major membrane lipids tested, indicating that the endoplasmic reticulum acyltransferases do not exclude unsaturated C_{16} fatty acids from the *sn*-2 position. In addition to increases in monounsaturated and decreases in saturated fatty acids, accumulation of 16:1 was accompanied by a reduction in 18:3 in all the lipids tested except phosphatidylglycerol, and increases in 18:2 in phospholipids. Total C_{16} fatty acid content in the galactolipids of the transgenics was significantly higher than that in the control, but those in the phospholipids were unchanged. In transgenics, Δ11 18:1 was detected in the *sn*-1 position of the lipids tested except phosphatidylinositol and phosphatidylserine. Introduction of the animal desaturase, controlled by a seed-specific phaseolin promoter, into soybean somatic embryo resulted in a significant reduction in saturated fatty acids. Such effects were greater in cotyledons than hypocotyl-radicles. This study demonstrated that the animal desaturase can be used to decrease the levels of saturated fatty acids in a crop plant.

Paper no. L8357 in *Lipids 35,* 471–479 (May 2000).

Membrane and reserve lipids of plants contain fatty acids with different degrees of unsaturation which in part is controlled by different desaturase enzymes. The first double bond is introduced into 18:0 acyl carrier protein (ACP) by a stromal Δ9-stearoyl-ACP desaturase. The additional double bonds of polyunsaturated fatty acids are introduced into acyl chains linked to the glycerol backbone of membrane lipids (1). There are two sets of membrane-bound desaturases that catalyze the introduction of a second Δ12 and a third Δ15 double bond, resulting in linoleic (18:2) and linolenic acids (18:3), respectively. One set is located in the chloroplasts and uses ferredoxin as the electron donor (2), whereas the other set is located in microsomal membranes and receives electrons from cytochrome b_5 (3,4).

The acyl composition of lipids is determined by three factors: the substrate specificity of the acyltransferase, the pool of acyl donors available, and modifications, such as desaturation, made to the acyl group after esterification to the glycerol moiety (5). Because of the acyl-group specificity of the acyltransferases in the various organelles, lipids synthesized in the plastid have a C_{16} fatty acid on the *sn*-2 position (6), whereas lipids synthesized in the ER have a C_{18} fatty acid (7) or an unsaturated C_{16} fatty acid [when available in transgenic plants (8)] on the *sn*-2 position; the main extraplastidial C_{16} fatty acid normally present, 16:0, is confined to the *sn*-1 position (9). The fact that plant membranes are not fully unsaturated suggests a complex regulation of membrane lipid composition. The level of unsaturation may be limited by the amount of the various desaturases, or the enzymes may be subject to some form of feedback regulation. The entire system of fatty acid and glycerolipid synthesis is regulated to meet the demand for particular lipid molecular structures for optimal membrane function (5).

Many properties of fats and oils are determined by their fatty acid composition. Because of the commercial importance of seed oils both for food and industrial use, considerable attention has been given to the genetic engineering of oilseed crops. Soybean is the most important source of edible oil in the world, and also is one of the largest sources of calories in the U.S. diet. Soybean oil is relatively high in saturated fatty acids (>10% total), most of which is palmitic acid (16:0) (10). Numerous studies indicate that it is beneficial to reduce human dietary consumption of saturated fatty acids, which are undesirably abundant in many edible oils (11). Owing to the fairly well-developed understanding of lipid biosynthesis in plants, it has been possible to alter fatty acid composition in oil seeds by recombinant DNA technology. One of the many objectives for genetically engineering plant oil composition is the reduction of saturated fatty acid levels in edible oils.

[1]Present address: University of British Columbia, Dept. of Botany, 6270 University Blvd., Vancouver, BC V6T 174, Canada.

*To whom correspondence should be addressed at N-103 Agricultural Science Center-North, Department of Agronomy, University of Kentucky, Lexington, KY 40546-0091. E-mail: dhild@pop.uky.edu

Abbreviations: ACP, acyl carrier protein; BHT, butylated hydroxytoluene; C_n fatty acid(s), fatty acid(s) with *n* carbon atoms; DGD, digalactosyldiacylglycerol; ER, endoplasmic reticulum; GC, gas chromatography; KAS, 3-ketoacyl-ACP synthase; LPAAT, lysophosphatidic acid acyltransferase; MGD, monogalactosyldiacylglycerol; MS, mass spectrometry; PA, phosphatidic acid; PC, phosphatidylcholine; PE, phosphatidylethanolamine; PG, phosphatidylglycerol; PI, phosphatidylinositol; PS, phosphatidylserine; RDS, rat liver stearoyl-CoA Δ9 desaturase; SDS, sodium dodecyl sulfate; X/Y, a fatty acyl group containing X carbon atoms and Y *cis* double bonds; UV, ultraviolet.

As previously reported (12), a rat liver stearoyl-CoA Δ9 desaturase (RDS) gene has been shown to be functioning in transgenic tobacco tissues, reducing the levels of saturated fatty acids. Tissues from the RDS-transgenic plants showed an accumulation of *cis* Δ9 16:1, which is normally a very minor constituent in tobacco tissues. Thus, these transgenic tissues can be useful to study plant fatty acid desaturation and glycerolipid biosynthesis. Subsequently, the RDS gene was introduced into soybean somatic embryos with a seed-specific phaseolin promoter (13). The transgenic soybean somatic embryos also showed significant conversions of saturated to monounsaturated fatty acids. Here we report the detailed investigation of the effects of the mammalian Δ9 desaturase on specific membrane lipids and reserve lipids in the transgenic plant tissues.

MATERIALS AND METHODS

Plant materials. Tobacco plants (*Nicotiana tabacum* cv. Xanthi) used in these studies were transformed with a gene encoding RDS (12). These plants were allowed to self-pollinate. Individuals with a significant amount of palmitoleic acid (*cis* Δ9 16:1) were selected from the segregating population. Plants were selected that were homozygous for palmitoleic acid accumulation. Progeny plants with the highest accumulation of 16:1 were allowed to self-pollinate again. Among the progeny, a plant with the highest level of 16:1 was selected for use in the experiments. Here we designated RDS-transgenic and control plants as plants transformed with an RDS gene under the control of the constitutive 35S promoter and those transformed with the vector only, respectively. Plants were grown in commercial potting mix in greenhouse under a 16-h photoperiod at 26 ± 2°C except as noted in the text. Leaf tissues were used for the analyses of the fatty acid composition of individual lipids, the positional analyses, and subcellular localization of RDS protein.

For soybean transformation, soybean (*Glycine max* Merill. cv. J103) somatic embryos were prepared as described by Liu *et al*. (14) and bombarded with pDGN (35*S* promoter-driven GUS::NPTII and phaseolin promoter-driven RDS) for the mammalian Δ9 desaturase expressor or pBI426 (35*S* promoter-driven GUS::NPTII only) for a control as described by Liu *et al*. (13).

Fatty acid and lipid analysis. The overall fatty acid composition of leaves and other tissues was analyzed by modifications of the procedure of Dahmer *et al*. (15). About 1–10 mg tissue samples were placed into 2 mL of 2% (vol/vol) H_2SO_4 in methanol and ground finely. The samples were then heated at 80°C until the volume was reduced to approximately 0.5 mL. One and one-half milliliters of hexane containing 0.01% (wt/vol) butylated hydroxytoluene (BHT) was added, and the mixture was vortexed vigorously. The fatty acid methyl esters in the hexane layer were separated by gas chromatography on a Hewlett-Packard (Palo Alto, CA) 0.25 mm i.d. × 0.33 μm × 10 m FFAP column and quantified using a flame-ionization detector. A Hewlett-Packard 5890A gas chromatograph was programmed for an initial temperature of 120°C for 1 min followed by increases of 12°C/min to 210°C and 50°C/min to 235°C. The final temperature was maintained for 8 min. The injector and detector temperatures were 220 and 250°C, respectively. Helium was used as the carrier gas with a flow rate of 10 mL/min.

Total lipids were extracted from leaf tissue as described by Miquel and Browse (16). Individual lipids were separated by one-dimensional thin-layer chromatography on $(NH_4)_2SO_4$-impregnated silica gel by the method of Khan and Williams (17). The $(NH_4)_2SO_4$-impregnated plates were prepared by dipping the plates (silica layer 250 μm thick; J.T. Baker Inc., Phillipsburg, NJ) in 0.15 M $(NH_4)_2SO_4$ and drying them at room temperature followed by activation for 90 min at 110°C prior to use (16). Lipids were located by spraying the plates with solution of 0.0046% primulin in 80% (vol/vol) acetone, followed by visualization under ultraviolet (UV) light. In order to determine the fatty acid composition of individual lipids, the silica gel from each lipid band was transferred to a tube containing 2 mL of 2% (vol/vol) H_2SO_4 in methanol, and fatty acid methyl esters were prepared and analyzed as described above.

Determination of position of unsaturation by gas chromatography (GC)–mass spectrometry (MS). Lipids were saponified directly, and the fatty acids were methylated by heating in 2 mL of 2% H_2SO_4 in methanol as described above. To determine double-bond positions, fatty acid methyl esters were derivatized with dimethyl disulfide (Aldrich, Milwaukee, WI) as described (18), except that the derivatization was done overnight. The dimethyl disulfide derivatives were separated by GC on a Hewlett-Packard 0.25 mm i.d. × 0.25 μm × 30 m HP-5MS column. Injections (1 μL) were made in the splitless mode with a Hewlett-Packard 7673 autosampler. A Hewlett-Packard 5890 Series II Plus gas chromatograph was programmed for an initial temperature of 50°C for 2 min, increased to 190°C at 20°C/min where it was held for 5 min, then increased to 250°C at 10°C/min where it was held for 5 min. The injector and detector temperatures were 250 and 280°C, respectively. Helium was used as the carrier gas with a constant flow rate of 1 mL/min maintained by electronic pressure control. The structure of each fatty acid was determined by an on-line Hewlett-Packard 5972 MSD mass spectrometer. A mass range of *m/z* 50–550 was scanned at a sampling rate of 1.5 scans/s. Identification of monounsaturated fatty acids was based on comparing both retention times and mass spectra of their dimethyl disulfide derivatives with those of standards.

Positional analysis. After thin layer-chromatography, silica containing each lipid band was transferred to a Pasteur pipette fitted with a glass wool filter. Lipids were extracted with 2 mL of chloroform/methanol (2:1, vol/vol) containing 0.01% BHT. Fatty acid composition at the *sn*-1 and *sn*-2 positions of individual lipids was determined using a lipase from *Rhizopus arrhizus* (Sigma) as described by Fischer *et al*. (19), except that 50 mM H_3BO_3 was added to the buffer used for lipase digestion to minimize intramolecular acyl transfer on

the lyso-lipids produced during the course of the reaction (16).

Subcellular fractionation. To examine intracellular distribution of RDS protein in the transgenic tissues, subcellular fractions were prepared by stepwise sucrose density gradients (20). This method yielded enough material to analyze fatty acid composition of the chloroplast lipids, but not the microsomal lipids. In order to study fatty acid composition of individual lipids from the microsomes, washed microsomal fractions were prepared by differential centrifugation as described by Roughan *et al*. (21). The purity of each fraction was estimated by measuring the activities of marker enzymes (22) and the chlorophyll content (23). Western immunoblotting was performed using standard procedures. For this, proteins were separated on a 10% sodium dodecyl sulfate (SDS)-polyacrylamide gel and electrophoretically transferred into a nitrocellulose membrane. The proteins in the membrane were probed with rat liver Δ9 stearoyl-CoA desaturase-specific rabbit polyclonal antibodies (24) and visualized using alkaline phosphatase-conjugated goat anti-rabbit second antibodies.

RESULTS

Fatty acid composition of different tissues of transgenic tobacco. Previously Grayburn *et al*. (12) showed that introduction of an RDS gene into tobacco resulted in altered fatty acid composition characterized by large increase in 16:1, which is normally a very minor constituent in tobacco tissues. In order to study further the effect of this animal enzyme on plant lipid biosynthesis, the RDS-transgenic tobacco plants were thoroughly analyzed. Different plant tissues showed striking differences in fatty acid composition (Table 1). Large increases in total monounsaturated fatty acid level, especially 16:1, were observed in leaves, stem, and root tissues, with corresponding decreases in 16:0 and 18:0, and 18:3 levels. However, petal and seed showed little change in fatty acid composition. Since similar low standard error values were observed for the fatty acid compositions reported in the other tables, only mean values are reported in the other tables to avoid excessive complication.

During our analysis of the fatty acid composition of the RDS-transgenic tissues, we observed a unique peak that eluted as a shoulder after Δ9 18:1. This peak was obtained from the RDS-transgenic tissues, but not from the control tissues. In order to identify its structure, dimethyl disulfide fatty acid derivatives were synthesized. Analysis of the derivatives by GC–MS demonstrated that the unknown compound was *cis* Δ11 18:1 (data not shown). The highest level of *cis* Δ11 18:1 was observed in the stem tissue (3.6% of total fatty acid), which showed the highest level of *cis* Δ9 16:1 (20.1%) as well. The *cis* Δ11 18:1 was not detected in the petals or seeds, where the levels of 16:1 were also very low.

Expression of the animal desaturase in soybean somatic embryos. In an attempt to decrease the level of saturated fatty acids in soybean seed storage lipid, the RDS gene was introduced into soybean somatic embryos with a seed-specific phaseolin promoter by particle bombardment (13). As in the case of the transgenic tobacco, RDS-transgenic soybean somatic embryos contained significantly reduced levels of saturated palmitic (16:0) and stearic (18:0) acids (Table 2). The decreased levels of saturated fatty acids were accompanied by increases in monounsaturated fatty acids including palmitoleic acid (16:1, Δ9), which does not normally accumulate in soybean seeds as well. However, the levels of polyunsaturated fatty acids, 18:2 and 18:3, were not significantly changed.

Use of the seed-specific phaseolin promoter resulted in higher accumulation of monounsaturated fatty acids and more reduction in saturated fatty acids in cotyledons than in hypocotyl-radicles (Table 2). For example, cotyledons exhibited significant reductions in 16:0 and 18:0 levels from 17.4 and 11.0% in the controls to 6.1% and undetectable level in the RDS-transgenics, respectively, whereas in hypocotyl-radicles those were from 21.7 and 7.9% to 15.4 and 4.3% of total fatty acid, respectively. The greater conversion of saturated to monounsaturated fatty acids in cotyledons than hypocotyl-radicles is apparently a consequence of the higher expression

TABLE 1
Fatty Acid Composition[a] of Vector-Transformed and RDS-Transformed Tobacco Tissues

Plant[b]/organ	16:0	16:1*c*[c]	16:1*t*[d]	16:3	18:0	18:1	Δ11 18:1[e]	18:2	18:3
CK leaves	13.9 ± 0.25	ND[f]	4.5 ± 0.30	8.7 ± 0.31	2.7 ± 0.17	1.7 ± 0.22	ND	10.8 ± 0.78	57.6 ± 0.64
RDS leaves	10.9 ± 0.35	9.0 ± 0.44	4.3 ± 0.36	7.7 ± 0.42	1.9 ± 0.15	2.1 ± 0.13	2.0 ± 0.19	15.6 ± 1.32	46.5 ± 1.49
CK stem	20.6 ± 0.58	ND	ND	8.2 ± 1.04	6.6 ± 0.23	3.3 ± 0.73	ND	27.8 ± 1.81	33.6 ± 2.06
RDS stem	16.2 ± 0.31	20.1 ± 1.57	ND	3.5 ± 0.93	1.6 ± 0.19	4.3 ± 0.21	3.6 ± 0.17	29.8 ± 1.17	21.0 ± 1.21
CK root	23.7 ± 0.62	ND	ND	ND	4.3 ± 0.33	3.0 ± 0.64	ND	50.1 ± 0.79	18.9 ± 0.60
RDS root	15.1 ± 1.95	14.2 ± 0.42	ND	ND	1.7 ± 0.26	5.8 ± 0.65	2.2 ± 0.18	46.9 ± 2.10	14.1 ± 1.03
CK petal	15.8 ± 0.98	ND	ND	3.1 ± 0.31	9.9 ± 0.45	16.7 ± 3.24	ND	36.0 ± 2.50	18.5 ± 1.17
RDS petal	14.4 ± 0.94	1.4 ± 0.09	ND	5.5 ± 0.64	5.2 ± 0.64	20.0 ± 2.91	ND	37.8 ± 1.69	15.6 ± 0.53
CK seed	9.4 ± 0.04	ND	ND	ND	2.7 ± 0.06	12.0 ± 0.20	ND	74.0 ± 0.21	1.8 ± 0.09
RDS seed	8.9 ± 0.08	0.3 ± 0.01	ND	ND	2.6 ± 0.04	11.9 ± 0.17	ND	74.6 ± 0.24	1.7 ± 0.02

[a]Values (% of total fatty acid) are means ± standard errors obtained from at least three replications.
[b]CK, plants transformed with the vector only; RDS, plants transformed with the rat liver Δ9 desaturase.
[c]16:1*c*, 16:1 (*cis* Δ7 and *cis* Δ9).
[d]16:1*t*, 16:1 (*trans* Δ3).
[e]Δ11 18:1, 18:1 (*cis* Δ11).
[f]ND, not detected (<0.1% of total fatty acid).

TABLE 2
Fatty Acid Composition[a] of the Control- and RDS-Transgenic Soybean Somatic Embryos

	Control-transgenics		RDS-transgenics	
Fatty acid	Cotyledon	H/R[b]	Cotyledon	H/R
16:0	17.4	21.7	6.1	15.4
16:1	ND	ND	11.9	6.9
18:0	11.0	7.9	ND	4.3
18:1	7.6	6.5	18.3	7.4
18:2	50.9	47.4	52.6	53.3
18:3	13.1	16.5	11.1	12.7

[a]Values (% of total fatty acid) are means obtained from two replications.
[b]H/R, the hypocotyl and radicle part of somatic embryos. For other abbreviations see Table 1.

of the RDS protein under control of the phaseolin promoter in cotyledons (Fig. 1).

Localization of mammalian Δ9 desaturase in plant tissue. Western blot analysis of subcellular fractions prepared by stepwise sucrose density gradients using transgenic soybean somatic embryos showed that the RDS protein was mainly found in the microsomal fraction (Fig. 2). From transgenic tobacco leaf tissues, the RDS protein was found to be associated mainly with microsomes as well (data not shown). These results strongly suggest an association of the RDS with the endoplasmic reticulum (ER) of the transgenic tissue, which is consistent with the enzyme's original location in the mammalian liver (25).

Fatty acid composition of individual leaf lipids. Analysis of leaf polar lipids indicated that *cis* Δ9 16:1 produced by RDS was incorporated into all the major membrane lipids, including the chloroplast lipids, monogalactosyldiacylglycerol (MGD) and digalactosyldiacylglycerol (DGD), apparently due to metabolic fluxes of fatty acids between the eukaryotic and prokaryotic pathways (Table 3). The highest level of the 16:1 was found in phosphatidylcholine (PC) (13.6%). In all the lipids examined except phosphatidylglycerol (PG), accumulation of 16:1 was accompanied by a reduction in 18:3

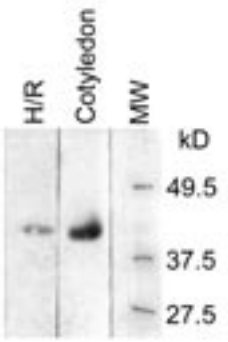

FIG. 1. Differential expression of rat Δ9 desaturase gene (RDS) in cotyledon and hypocotyl-radicle tissue of transgenic soybean somatic embryos. Each lane was loaded with an equal amount of protein (5.5 μg). Proteins were probed with the antibody against a rat liver Δ9 desaturase. MW, Molecular weight marker; H/R, hypocotyl and radicle part of somatic embryos.

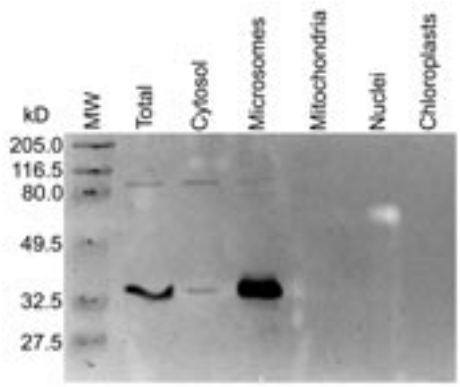

B

	Cyt	Mic	Mit	Nuc	Chl
NADH-cytochrome c	24	100	3	0	7
Cytochrome c oxidase	4	8	100	0	10
Chlorophyll	0	11	18	0	100

FIG. 2. Subcellular localization of the RDS protein in the transgenic soybean somatic embryos. (A) Western blot analysis of subcellular fractions from differential centrifugation of the transgenic soybean somatic embryos. Each lane was loaded with an equal amount of protein (10 μg). Proteins were probed with the antibody against a rat liver Δ9 desaturase. Total, unfractionated crude embryo extract. (B) Relative marker enzyme activities and chlorophyll concentrations. The organelles' purity is presented as a percentage of the highest values (100%). Cyt, cytosol; Mic, microsomes; Mit, mitochondria; Nuc, nuclei; Chl, chloroplasts. See Figure 1 for other abbreviation.

level, in addition to increases in the monounsaturated fatty acids, 16:1 and 18:1, and decreases in the saturated fatty acids, 16:0 and 18:0, as expected. For example, MGD, a galactolipid, and PC, a phospholipid, exhibited reductions in 18:3 levels from 84.3 to 70.9% and 37.2 to 19.7%, respectively. An increase in the 18:2 level in the phospholipids was another change.

Total C_{16} fatty acid contents in galactolipids of the RDS-transgenic leaves were significantly higher than those in the control tissues, although those in phospholipids were unchanged. In case of MGD, C_{16} fatty acids constituted 24.7% in the RDS-transgenics, compared to only 12.3% in the control plants. However, C_{16} fatty acids in PC of the RDS-transgenic and control plants were 27.9 and 25.5%, respectively.

Positional analysis. Positional analysis using the lipase from *R. arrhizus* that is specific for the *sn*-1 position of the glycerol moiety (19) indicated that the overproduced 16:1 was incorporated into both the *sn*-1 and *sn*-2 of all the lipids tested (Tables 4,5). These results are in contrast to the data obtained by Polashock *et al.* (8), in which the majority of the 16:1 overproduced by a yeast Δ9 desaturase was incorporated into the *sn*-2 position of the lipids. However, incorporation of *cis* Δ9 16:1 into the *sn*-2 position is consistent with their data in that the ER acyltransferases involved in the production of PA in the

TABLE 3
Fatty Acid Composition[a] of Individual Lipids from Tobacco Leaf Extracts

	Glycerolipids									
	MGD		DGD		PG		PE		PC	
Fatty acid[b]	CK[c]	RDS[d]	CK	RDS	CK	RDS	CK	RDS	CK	RDS
16:0	2.4	1.9	15.8	12.8	27.5	22.5	28.6	18.1	24.9	14.3
16:1*c*	0.4	7.6	0.4	9.7	0.6	1.0	0.8	6.3	0.6	13.6
16:1*t*	ND[e]	ND	ND	ND	27.7	29.0	ND	ND	ND	ND
16:3	9.5	15.2	0.6	1.3	ND	ND	ND	ND	ND	ND
18:0	0.3	0.2	2.6	1.2	3.1	1.8	4.3	1.9	5.7	2.2
18:1	0.4	0.8	0.6	1.5	4.7	9.3	2.2	3.8	4.0	11.7
Δ11 18:1	ND	0.7	ND	1.4	ND	0.4	ND	2.7	ND	1.1
18:2	2.7	2.7	3.1	3.3	13.7	12.5	30.3	46.7	27.6	37.3
18:3	84.3	70.9	76.9	68.8	22.7	23.5	33.7	20.5	37.2	19.7
Number of double bonds per lipid molecule	2.9	2.7	2.4	2.3	1.3	1.4	1.6	1.7	1.7	1.6

[a]Values (% of total fatty acid) are means obtained from at least three replications.
[b]16:1c, 16:1 (*cis* Δ7 and *cis* Δ9); 16:1*t*, 16:1 (*trans* Δ3); Δ11 18:1, 18:1 (*cis* Δ11).
[c]Plants transformed with the vector only.
[d]Plant transformed with the rat liver Δ9 desaturase.
[e]ND, Not detected (<0.1% of total fatty acid). MGD, monogalactosyldiacylglycerol; DGD, digalactosyldiacylglycerol; PG, phosphatidylglycerol; PE, phosphatidylethanolamine; PC, phosphatidylchoine.

eukaryotic pathway do not exclude 16-carbon fatty acid at the *sn*-2 position when it is unsaturated (8). The distribution of 16:1 was dependent upon individual lipids: in MGD and PC, the 16:1 was evenly distributed, while DGD contained more 16:1 in the *sn*-2 position and phosphatidylethanolamine (PE) had the majority of 16:1 in the *sn*-1 position. In both galactolipids and phospholipids except for PG, the majority of the saturated fatty acids (16:0 and 18:0) were incorporated into the *sn*-1 position.

Cis Δ11 18:1, found only in the RDS-transgenics, was detected exclusively in the *sn*-1 position of MGD, DGD, PG, PE, and PC.

Lipids of the chloroplasts and microsomes. Since fatty acid biosynthesis occurs almost exclusively in the chloroplast and the RDS enzyme appeared to be localized in the ER (Fig. 2), we determined the fatty acid compositions of lipids from the isolated chloroplasts and microsomes to examine the distribution of the *cis* Δ9 16:1 overproduced by the mammalian stearoyl-CoA desaturase and the metabolic fluxes between the eukaryotic and prokaryotic pathways.

In the lipids of the microsomal fraction, the site of RDS, the ratios of 18:1/18:0 were much higher than the ratios of 16:1/16:0, even though the levels of 16:0 were considerably higher than the levels of 18:0 (Table 6). In contrast, in the chloroplast lipids except for PG, which is known to be derived exclusively from the prokaryotic pathway (26,27), cytoplasmically produced *cis* Δ9 16:1 accumulated in large quantities while the levels of 18:1 in the RDS-transgenics were the same as in the control plants (Table 7). These results suggest that the mammalian Δ9 desaturase functioning in the ER of the transgenic plants converted 18:0 to 18:1 more efficiently than 16:0 to 16:1, and that 16:1-containing lipids were preferentially reimported into the chloroplasts. The reduction in 18:3 levels in all the microsomal and chloroplast lipids except for PG was consistent with the results from the total leaf lipids (Tables 3,6,7). Another interesting observation was that in the microsomal lipids and the chloroplast PC fraction, accumulation of monounsaturated fatty acids was accompanied by an increase in 18:2 levels, whereas most of the C_{18} fatty acids in MGD and DGD of the chloroplast were fully desaturated up to 18:3. All

TABLE 4
Positional Analysis of Major Chloroplast Lipids from Tobacco Leaves[a]

	MGD				DGD				PG			
	CK[c]		RDS[d]		CK		RDS		CK		RDS	
Fatty acid[b]	*sn*-1	*sn*-2	*sn*-1	*sn*-2	*sn*-1	*sn*-2	*sn*-1	*sn*-2	*sn*-1	*sn*-2	*sn*-1	*sn*-2
16:0	3.7	1.0	1.8	1.7	23.1	6.4	30.4	13.1	27.6	30.2	17.1	34.1
16:1*c*	0.2	0.5	7.1	7.7	0.3	0.1	5.4	10.4	0.3	0.3	1.8	0.8
16:1*t*	ND[e]	ND	ND	ND	ND	ND	ND	ND	5.6	67.0	1.7	62.1
16:3	1.6	28.6	2.6	36.1	0.1	1.3	ND	1.8	ND	ND	ND	ND
18:0	0.4	0.1	0.2	0.1	4.3	0.2	7.7	0.3	5.1	0.3	4.1	0.4
18:1	0.9	0.3	1.5	0.5	1.0	0.7	1.2	1.5	12.2	0.3	15.7	0.5
Δ11 18:1	ND	ND	1.2	ND	ND	ND	2.0	ND	ND	ND	3.0	ND
18:2	3.1	2.3	5.0	2.1	3.8	2.6	3.7	3.09	19.4	0.7	17.1	0.6
18:3	90.0	67.2	80.5	51.8	67.4	88.7	49.5	69.9	29.8	1.2	39.5	1.4

[a]For footnotes see Table 3.

TABLE 5
Positional Analysis of Major Phospholipids from Tobacco Leaves[a]

	PE				PC			
	CK[c]		RDS[d]		CK		RDS	
Fatty acid[b]	*sn*-1	*sn*-2	*sn*-1	*sn*-2	*sn*-1	*sn*-2	*sn*-1	*sn*-2
16:0	51.7	0.7	29.8	2.2	50.2	1.0	24.6	1.7
16:1*c*	0.4	0.2	17.9	2.9	0.7	0.4	12.5	15.3
18:0	7.7	0.2	2.4	0.3	10.0	0.3	2.7	0.3
18:1	3.8	2.8	6.3	11.6	5.5	12.4	17.0	29.3
Δ11 18:1	ND[e]	ND	4.6	ND	ND	ND	3.5	ND
18:2	20.7	50.6	25.1	58.7	20.0	37.5	25.7	30.0
18:3	15.7	45.5	13.9	24.2	13.6	48.4	13.9	23.3

[a]For footnotes see Table 3.

TABLE 6
Fatty Acid Composition[a] of Lipids from Isolated Microsomes of Tobacco Leaves

	PE		PI		PS		PC	
Fatty acid[b]	CK[c]	RDS[d]	CK	RDS	CK	RDS	CK	RDS
16:0	25.5	19.7	54.0	48.9	17.7	18.5	26.4	18.9
16:1*c*	0.3	6.5	0.5	5.8	1.0	4.7	0.3	10.5
18:0	6.5	2.8	1.5	2.3	16.5	6.0	7.1	2.9
18:1	3.2	7.1	1.7	5.6	3.7	11.0	5.0	12.8
Δ11 18:1	ND[e]	3.0	ND	ND	ND	ND	ND	2.8
18:2	30.8	35.3	12.3	17.0	20.6	29.6	22.2	26.4
18:3	33.5	25.6	29.9	20.4	21.1	16.2	39.0	25.6
Unknown	ND	ND	ND	ND	19.	14.0	ND	ND

[a]Values (% of total fatty acid) are means obtained from three replications.
[b]16:1*c*, 16:1 (*cis* Δ9); Δ11 18:1, 18:1 (*cis* Δ11).
[c]Plants transformed with the vector only.
[d]Plant transformed with the rat liver Δ9 desaturase. See Table 3 for abbreviations.

TABLE 7
Fatty Acid Composition of Lipids from Isolated Chloroplasts of Tobacco Leaves[a]

	MGD		DGD		PG		PC	
Fatty acid[b]	CK[c]	RDS[d]	CK	RDS	CK	RDS	CK	RDS
16:0	2.8	1.6	9.9	7.0	31.9	22.3	20.6	7.3
16:1*c*	0.4	9.8	0.3	8.1	0.3	1.4	n.d.	17.3
16:1t	n.d.[e]	n.d.	n.d.	n.d.	29.9	30.7	n.d.	n.d.
16:3	16.9	16.5	3.1	4.7	n.d.	n.d.	n.d.	n.d.
18:0	0.4	0.2	1.7	0.6	2.9	2.4	7.7	2.6
18:1	0.3	0.3	0.3	0.4	2.2	3.7	3.9	4.1
Δ11 18:1	n.d.	1.2	n.d.	1.3	n.d.	2.4	n.d.	0.9
18:2	3.3	2.9	2.6	2.5	10.4	11.8	20.4	27.4
18:3	75.9	67.5	82.0	75.4	22.4	25.2	47.4	40.4

[a]For footnotes see Table 3.

these observations point to the complex and fine regulation of individual desaturases in the ER and the chloroplast.

Cis Δ11 18:1, detected in all the RDS-transgenic chloroplast lipids tested, was not found in either PI or PS of the microsomal fraction (Table 6).

DISCUSSION

The acyl-CoA desaturases are one of three groups of desaturases classified according to their specificities toward fatty acid substrates (28). The rat liver microsomal stearoyl-CoA desaturation system requires three protein components for activity: NADH-cytochrome b_5 reductase, cytochrome b_5, and the terminal desaturase (25,29). Unlike most common acyl-lipid desaturases in plants that are specific to fatty acids esterified to glycerolipids, the mammalian desaturase (RDS) *in vitro* uses acyl-CoA derivatives with chain lengths of 12 to 19 carbons (29). Introduction of the RDS into plant tissues resulted in large increase in 16:1 and 18:1 levels. Western blot analysis of the transgenic plant tissues indicates that this en-

zyme functions in the microsomes. Thus, it appears that the RDS uses both 16:0-CoA and 18:0-CoA as substrates that are exported from the chloroplast prior to their acylation into phospholipids, and that the enzyme utilizes the plant microsomal electron transport system involving cytochrome b_5 and cytochrome b_5 reductase.

Almost all the lipids examined from control tissues contained low levels of *cis* Δ9 16:1. This is not surprising because Δ9 16:1 is produced in the chloroplasts by the low activity of the soluble stearoyl-ACP desaturase toward 16:0-ACP (30). However, because the *cis* Δ9 16:1 is a very minor component in most plant tissues including tobacco, the increased level of *cis* Δ9 16:1 is a good *in vivo* measure of the mammalian desaturase activity. Furthermore, since *cis* Δ9 16:1 overproduction by RDS apparently occurs in the microsomes, the distribution of the 16:1 should be a good indicator of the metabolic flux between the eukaryotic and prokaryotic pathways.

Analysis of the lipids from the isolated microsomes showed that the conversion of 18:0 to 18:1 was greater than that of 16:0 to 16:1. These results suggest that the mammalian desaturase in the microsomes of the transgenic plant cells showed higher activity toward 18:0-CoA, as it appeared to function *in vivo* primarily as a stearoyl-CoA desaturase in rat liver (29). In contrast to the microsomal lipids, the chloroplast lipids of the transgenic plants contained higher levels of Δ9 16:1. For example, chloroplast PC contained 17.3% of *cis* Δ9 16:1 and 4.1% of Δ9 18:1, whereas the microsomal PC had 10.5% of Δ9 16:1 and 12.8% of Δ9 18:1. These data suggest that the 16:1-containing lipids are preferentially transported into the chloroplasts over 18:1-containing lipids, supporting the idea that the metabolic fluxes between the eukaryotic and prokaryotic pathways occur in a highly regulated manner (5).

Another example of fine-controlled regulation is evident from the level of desaturation. In all the lipids examined, there was no significant difference in the average number of double bonds per glycerolipid molecule between the control and the RDS-transgenic plants, in spite of increase in mono-unsaturated fatty acids and decrease in saturated fatty acids. In all the glycerolipids examined except PG, decreases in saturated fatty acids and increases in monounsaturated fatty acid were accompanied by reductions in the level of 18:3. In case of the microsomal lipids, concomitant increases in 18:2 were observed as well. The reduction in 18:3 level was also seen by Polashock *et al*. (8) in tobacco transformed with a yeast Δ9 desaturase gene. However, it is not clear how this effect is related to the increase in the ratio of monounsaturated to saturated fatty acids in the transgenic plants. A possible explanation for these results is that there might be a very fine mechanism to sense the degree of desaturation in plant cell membranes. Thus, the decreases in 18:3 level in the RDS-transgenic plant can be interpreted as a compensatory mechanism in response to the increase in the level of monounsaturated fatty acids.

The expression of a mammalian Δ9 desaturase under the control of the 35*S* promoter resulted in little change in the fatty acid composition of mature tobacco seeds. However, when the transgenic seeds were analyzed at the early stage of development, a significant amount of 16:1 was detected (data not shown). The accumulation of 16:1 appeared positively related to the level of the RDS protein as the Western blot analysis showed a significant amount of the RDS protein in the transgenic tobacco seeds at the early stage of seed development (Fig. 3). The RDS protein disappeared as seeds developed to maturity and as a result, the level of 16:1 dramatically decreased. Williamson *et al*. (31) reported that the transcript of the maize storage protein (zein) gene, when expressed under the control of 35*S* promoter in transgenic tobacco, was greatly reduced as seeds of the transgenic tobacco matured. The reduction started 15 d after pollination, and no transcript of the zein gene was detectable 25 d after pollination.

The biosynthetic pathway of *cis* Δ11 18:1 (*cis*-vaccenic acid) is not clear. Since Δ9 16:1-ACP is formed at a low level by the action of the plastid stearoyl-ACP desaturase toward 16:0-ACP (30), we cannot rule out the possibility that Δ11 18:1 could be produced from Δ9 16:1-ACP by the condensing enzyme, 3-ketoacyl-ACP synthase (KAS II), in the chloroplast. In this case, Δ11 18:1 should be detected in control plants as well. The absence of *cis*-vaccenic acid in detectable amounts in the control tissues indicates that the activities of the plastid stearoyl-ACP desaturase for 16:0-ACP and KAS II for Δ9 16:1-ACP are too low and/or that the size of 16:1 pool is too small to be available for those enzymes to produce detectable amounts of *cis*-vaccenic acid. Shibahara *et al*. (32) proposed chain elongation from palmitoleic acid and reversible enzymatic double-bond shifting of Δ9 18:1 (33) as pathways for *cis*-vaccenic acid biosynthesis based on a labeling experiment of Chinese persimmon or kaki (*Diospyros kaki* L.) pulp with deuterated fatty acids. The rat liver Δ9 desaturase in the ER of the transgenic tissue converted 16:0-CoA and 18:0-CoA to 16:1-CoA and 18:1-CoA, respectively. Accumulation of the monounsaturated fatty acyl-CoA may provide a larger size of the substrate pool for the elongase and/or isomerase to give rise to *cis* Δ11 18:1.

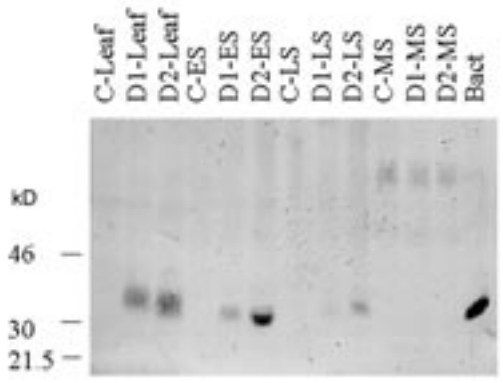

FIG. 3. Expression of RDS in *Nicotiana tabacum* seeds during development. C, control plant; D1, D2, RDS-transgenic plants; ES, seeds at early developmental stage (~10 d after pollination, DAP); LS, seeds at late developmental stage (~20 DAP); MS, mature seeds; Bact, *Escherichia coli* expressing the Δ9 desaturase.

The *cis* Δ11 18:1, which was found only in the RDS-transgenic plants, was detected exclusively in the *sn*-1 position of all the lipids tested except for PI and PS. These findings suggest that the *cis* Δ9 16:1 overproduced by the activity of the RDS was elongated to Δ11 18:1 by an ER elongase and incorporated exclusively into the *sn*-1 position of certain lipids by a specific acyltransferase. However, we cannot rule out the possibility that *cis* Δ11 18:1 is excluded from the *sn*-2 position of tobacco lipids because *cis*-vaccenic acid might be a poor substrate for lysophosphatidic acid acyltransferase (LPAAT) in tobacco leaf as Ichihara *et al*. (34) showed for the acyl-CoA specificity of the LPAAT in maturing safflower seeds.

Even though the tobacco tissues expressing RDS under the control of 35*S* promoter showed a significant reduction in the total saturated fatty acid content, very little change in seed triacylglycerol fatty acid composition was seen. Since fatty acid biosynthesis is an essential metabolic pathway in all the tissues, modification of seed oil composition may require seed-specific expression. When the rat desaturase was expressed, under the control of seed-specific phaseolin promoter, transgenic soybean somatic embryos showed significantly reduced levels of saturated fatty acids. Since the mammalian Δ9 desaturase utilizes both 16:0-CoA and 18:0-CoA as a substrate, in transgenic soybean somatic embryos, these cytoplasmic CoA, which are the main saturated fatty acyl-CoA pool for the triacylglycerol in soybean oil, were desaturated to Δ9 16:1-CoA and 18:1-CoA before being incorporated into glycerol backbones. As the seed-specific phaseolin promoter led the animal desaturase to be expressed more strongly in cotyledons than in hypocotyl-radicles, such effects on lipids of somatic embryos are expected in seeds of regenerated plants.

In conclusion, we demonstrated that a mammalian Δ9 desaturase functioned in the microsomes of plant cells, apparently using the plant's electron transport system involving cytochrome b_5 and cytochrome b_5 reductase, and reduced the levels of saturated and increased the levels of monounsaturated fatty acids in the transgenic plant tissues. The finding of *cis* Δ11 18:1 only in the *sn*-1 position of certain lipids could imply the existence of an acyltransferase with a previously undescribed function. A significant amount of the cytoplasmically produced 16:1 reenters plastids. Incorporation of *cis* Δ9 16:1, overproduced by the RDS in the microsomes of the transgenic plants, into both the *sn*-1 and *sn*-2 positions strongly indicates that the acyl-CoA-specific acyltransferases of the ER involved in production of the eukaryotic lipids do not exclude 16-carbon fatty acids at the *sn*-2 position when they are desaturated. Finally, the seed-specific expression of the RDS in soybean somatic embryos showed that the mammalian stearoyl-CoA Δ9 desaturase significantly lowered the levels of saturated fatty acids, especially in cotyledons.

ACKNOWLEDGMENTS

This work was supported by Pioneer Hi-Bred International, the United Soybean Board, the Kentucky Soybean Promotion Board, and the Kentucky Agricultural Experiment Station. Rebecca Torisky and Sergei Avdiushko provided very helpful technical support.

REFERENCES

1. Somerville, S., and Browse, J. (1991) Plant Lipids: Metabolism, Mutants, and Membranes, *Science 252*, 80–87.
2. Schmidt, H., and Heinz, E. (1990) Involvement of Ferredoxin in Desaturation of Lipid-Bound Oleate in Chloroplasts, *Plant Physiol. 94*, 214–220.
3. Smith, M.A., Cross, A.R., Jones, O.T.G., Griffiths, W.T., Stymne, S., and Stobart, K. (1990) Electron-Transport Components of the 1-Acyl-2-oleoyl-*sn*-glycero-3-phosphocholine Δ^{12}-Desaturase (Δ^{12}-desaturase) in Microsomal Preparations from Developing Safflower (*Carthamus tinctorius* L.) Cotyledons, *Biochem. J. 272*, 23–29.
4. Kearns, E.V., Hugly, S., and Somerville, C. (1991) The Role of Cytochrome b_5 in Δ12 Desaturation of Oleic Acid by Microsomes of Safflower (*Carthamus tinctorius* L.), *Arch. Biochem. Biophys. 284*, 431–436.
5. Browse, J., and Somerville, C. (1991) Glycerolipid Synthesis: Biochemistry and Regulation, *Annu. Rev. Plant. Physiol. 42*, 467–506.
6. Frentzen, M., Heinz, E., Mckeon, T.A., and Stumpf, P.K. (1983) Specificities and Selectivities of Glycerol-3-phosphate Acyltransferase and Monoacylglycerol-3-phosphate Acyltransferase from Pea and Spinach Chloroplasts, *Eur. J. Biochem. 129*, 629–636.
7. Frentzen, M. (1993) Acyltransferases and Triacylglycerols, in *Lipid Metabolism in Plants* (Moore, T.S., Jr., ed.) pp. 195–231, CRC Press, Boca Raton.
8. Polashock, J.J., Chin, C.-K., and Martin, C.E. (1992) Expression of the Yeast Δ-9 Fatty Acid Desaturase in *Nicotiana tabacum*, *Plant Physiol. 100*, 894–901.
9. Ohlrogge, J., and Browse, J. (1995) Lipid Biosynthesis, *Plant Cell 7*, 957–970.
10. Schnebly, S.R., and Fehr, W.R. (1993) Effect of Years and Planting Dates on Fatty Acid Composition of Soybean Genotypes, *Crop Sci. 33*, 716–719.
11. Sizer, F., and Whitney, E. (1994) *Nutrition Concepts and Controversies*, 6th edn., West Publishing Co., St. Paul, MN.
12. Grayburn, W.S., Collins, G.B., and Hildebrand, D.F. (1992) Fatty Acid Alteration by a Δ9 Desaturase in Transgenic Tobacco Tissue, *Biotechnology 10*, 675–678.
13. Liu, W., Torisky, R.S., McAllister, K.P., Avdiushko, S., Hildebrand, D., and Collins, G.B. (1996) Somatic Embryo Cycling: Evaluation of a Novel Transformation and Assay System for Seed-Specific Gene Expression in Soybean, *Plant Cell Tissue Organ Cult. 47*, 33–42.
14. Liu, W., Moore, P.J., and Collins, G.B. (1992) Somatic Embryogenesis in Soybean *via* Somatic Embryo Cycling, *In Vitro Cell Dev. Biol. 28P*, 153–160.
15. Dahmer, M.L., Fleming, P.D., Collins, G.B., and Hildebrand, D.F. (1989) A Rapid Screening Technique for Determining the Lipid Composition of Soybean Seeds, *J. Am. Oil Chem. Soc. 66*, 543–548.
16. Miquel, M., and Browse, J. (1992) *Arabidopsis* Mutants Deficient in Polyunsaturated Fatty Acid Synthesis: Biochemical and Genetic Characterization of a Plant Oleoyl-Phosphatidylcholine Desaturase, *J. Biol. Chem. 267*, 1502–1509.
17. Khan, M.-U., and Williams, J.P. (1977) Improved Thin-Layer Chromatographic Method for the Separation of Major Phospholipids and Glycerolipids from Plant Lipid Extracts and Phosphatidylglycerol and bis (monoacylglyceryl) Phosphate from Animal Lipid Extracts, *J. Chromatogr. 140*, 179–185.
18. Yamamoto, K., Shibahara, A., Nakayama, T., and Kajimoto, G.

(1991) Determination of Double-Bond Position in Methylene-Interrupted Dienoic Fatty Acids by GC–MS as Their Dimethyl Disulfide Adducts, *Chem. Phys. Lipids 60*, 39–50.
19. Fischer, W., Heinz, E., and Zeus, M. (1973) The Suitability of Lipase from *Rhizopus arrhizus delemar* for Analysis of Fatty Acid Distribution in Dihexosyl Diglycerides, Phospholipids and Plant Sulfolipids, *Hoppe-Seyler's Z. Physiol. Chem. 354*, 1115–1123.
20. Lord, J.M., Kagawa, T., and Beevers, H. (1972) Intracellular Distribution of Enzymes of the Cytidine Diphosphate Choline Pathway in Castor Bean Endosperm, *Proc. Natl. Acad. Sci. USA 69*, 2429–2432.
21. Roughan, P.G., Holland, R., and Slack, C.R. (1980) The Role of Chloroplasts and Microsomal Fractions in Polar-Lipid Synthesis from [1-^{14}C]Acetate by Cell-Free Preparations from Spinach (*Spinacia oleracea*) Leaves, *Biochem. J. 188*, 17–24.
22. Tolbert, N.E. (1974) Isolation of Subcellular Organelles of Metabolism on Isopycnic Sucrose Gradients, *Methods Enzymol. 31*, 734–746.
23. Arnon, D.I. (1947) Copper Enzymes in Isolated Chloroplasts: Polyphenoloxidase in *Beta vulgaris*, *Plant Physiol. 24*, 1–15.
24. Grayburn, W.S., and Hildebrand, D.F. (1995) Progeny Analysis of Tobacco That Express a Mammalian Δ9 Desaturase, *J. Am. Oil Chem. Soc. 72*, 317–321.
25. Holloway, P.W. (1983) Fatty Acid Desaturation, in *The Enzymes* (Boyer, P.D., ed.) Vol. 16, pp. 63–83, Academic, New York.
26. Browse, J., Warwick, N., Somerville, C.R., and Slack, C.R. (1986) Fluxes Through the Prokaryotic and Eukaryotic Pathways of Lipid Synthesis in the "16:3" Plant *Arabidopsis thaliana*, *Biochem. J. 235*, 25–31.
27. Roughan, P.G., and Slack, C.R. (1982) Cellular Organization of Glycerolipid Metabolism, *Annu. Rev. Plant Physiol. 33*, 97–132.
28. Nishida, I., and Murata, N. (1996) Chilling Sensitivity in Plants and Cyanobacteria: The Crucial Contribution of Membrane Lipids, *Annu. Rev. Plant Physiol. 47*, 541–546.
29. Enoch, H.G., Catala, A., and Strittmatter, P. (1976) Mechanism of Rat Liver Microsomal Stearyl-CoA Desaturase: Studies of the Substrate Specificity, Enzyme-Substrate Interactions, and the Function of Lipid, *J. Biol. Chem. 251*, 5095–5103.
30. Mckeon, T.A., and Stumpf, P.K. (1982) Purification and Characterization of the Stearoyl-Acyl Carrier Protein Desaturase and the Acyl-Acyl Carrier Protein Thioesterase from Maturing Seeds of Safflower, *J. Biol. Chem. 257*, 12141–12147.
31. Williamson, J.D., Hirsch-Wyncott, M.E., Larkins, B.A., and Gelvin, S.B. (1989) Differential Accumulation of a Transcript Driven by the CaMV 35*S* Promoter in Transgenic Tobacco, *Plant Physiol. 90*, 1570–1576.
32. Shibahara, A., Yamamoto, K., Takeoka, M., Kinoshita, A., Kajimoto, G., Nakayama, T., and Noda, M. (1989) Application of a GC–MS Method Using Deuterated Fatty Acids for Tracing *cis*-Vaccenic Acid Biosynthesis in Kaki Pulp, *Lipids 24*, 488–493.
33. Shibahara, A., Yamamoto, K., Takeoka, M., Kinoshita, A., Kajimoto, G., Nakayama, T., and Noda, M. (1990) Novel Pathways of Oleic and *cis*-Vaccenic Acid Biosynthesis by an Enzymatic Double-Bond Shifting Reaction in Higher Plants, *FEBS Lett. 264*, 228–230.
34. Ichihara, K., Asahi, T., and Fujii, S. (1987) 1-Acyl-*sn*-glycerol-3-phosπphate Acyltransferase in Maturing Safflower Seeds and Its Contribution to the Non-Random Fatty Acid Distribution of Triacylglycerol, *Eur. J. Biochem. 167*, 339–347.

[Received September 21, 1999, and in final revised form December 29, 1999; revision accepted January 16, 2000]

Metabolism of 1-Acyl-2-oleoyl-*sn*-glycero-3-phosphoethanolamine in Castor Oil Biosynthesis

Jiann-Tsyh Lin[a,*], Karen M. Lew[a], Jennifer M. Chen[a], Yugo Iwasaki[b], and Thomas A. McKeon[a]

[a]U.S. Department of Agriculture, Agricultural Research Service, Western Regional Research Center, Albany, California 94710, and [b]Department of Biological Mechanisms and Functions, Nagoya University, Nagoya 464-8601, Japan

ABSTRACT: We have examined the role of 2-oleoyl-PE (phosphatidylethanolamine) in the biosynthesis of triacylglycerols (TAG) by castor microsomes. In castor microsomal incubation, the label from ^{14}C-oleate of 1-palmitoyl-2-[1-^{14}C]oleoyl-*sn*-glycero-3-phosphoethanolamine is incorporated into TAG containing ricinoleate. The enzyme characteristics, such as optimal pH, and the effect of incubation components of the oleoyl-12-hydroxylase using 2-oleoyl-PE as incubation substrate are similar to those for 2-oleoyl-PC (phosphatidylcholine). However, compared to 2-oleoyl-PC, 2-oleoyl-PE is a less efficient incubation substrate of oleoyl-12-hydroxylase in castor microsomes. Unlike 2-oleoyl-PC, 2-oleoyl-PE is not hydroxylated to 2-ricinoleoyl-PE by oleoyl-12-hydroxylase and is not desaturated to 2-linoleoyl-PE by oleoyl-12-desaturase. We have demonstrated the conversion of 2-oleoyl-PE to 2-oleoyl-PC and vice versa. The incorporation of label from 2-[^{14}C]oleoyl-PE into TAG occurs after its conversion to 2-oleoyl-PC, which can then be hydroxylated or desaturated. We detected neither PE-*N*-monomethyl nor PE-*N*,*N*-dimethyl, the intermediates from PE to PC by *N*-methylation. The conversion of 2-oleoyl-PE to 2-oleoyl-PC likely occurs *via* hydrolysis to 1,2-diacyl-*sn*- glycerol by phospholipase C and then by cholinephosphotransferase. This conversion does not appear to play a key role in driving ricinoleate into TAG.

Paper no. L8396 in *Lipids 35*, 481–486 (May 2000).

The presence of the hydroxy group on ricinoleate imparts physical and chemical properties that underlie many industrial uses such as the production of aviation lubricants, coatings, and specialty plastics. Castor (*Ricinus communis* L.) bean, the only commercial source of ricinoleate, contains the toxin ricin and potent allergens, making it hazardous to grow, harvest, and process. It is desirable to produce ricinoleate in an oilseed of a transgenic plant lacking these components.

The cDNA for oleoyl-12-hydroxylase, the key enzyme in the biosynthesis of castor oil [triacylglycerols (TAG) containing ricinoleate], has been cloned in castor and expressed in tobacco, resulting in accumulation of low levels of ricinoleate in seed lipids (1). Later, the expression of this enzyme in transgenic *Arabidopsis thaliana* plants was improved but also resulted in low levels of hydroxy fatty acids (FA; 2) compared to castor (20 vs. 90% ricinoleate in castor oil). For the purpose of developing a transgenic plant that produces castor oil, it is important to know the biosynthetic pathway and to identify the key enzymatic steps that drive ricinoleate into TAG in castor bean. We have previously used 1-palmitoyl-2-[1-^{14}C]oleoyl-*sn*-glycero-3-phosphocholine (2-[^{14}C]oleoyl-PC) as the substrate in castor microsomal incubation to prove that 2-oleoyl-PC is the immediate substrate of oleoyl-12-hydroxylase and to identify oleoyl-12-hydroxylase, phospholipase A_2, and 1,2-diacyl-*sn*-glycerol acyltransferase in the biosynthetic pathway as the key enzymatic steps that drive ricinoleate into TAG (3). Since phosphatidylethanolamine (PE) is endogenous in castor bean and is similar to phosphatidylcholine (PC) structurally, we examine here the role of 1-acyl-2-oleoyl-*sn*-glycero-3-phosphoethanolamine (2-oleoyl-PE) in the biosynthesis of TAG containing ricinoleate in castor microsomes.

EXPERIMENTAL PROCEDURES

Preparation of the substrate. 1-Palmitoyl-2-[1-^{14}C]oleoyl-*sn*-glycero-3-phosphoethanolamine was prepared similarly to the method of Paltauf and Hermetter (4). 1-Palmitoyl-2-[1-^{14}C]oleoyl-*sn*-glycero-3-phosphocholine (6 μCi; NEN Life Science Products, Boston, MA) was dissolved in 1 mL diethyl ether. To this solution 3 mL buffer (0.2 M sodium acetate, 0.1 M calcium chloride, 20% ethanolamine, adjusted to pH 5.6 with 6 N HCl) containing phospholipase D (1 mg) was added. The mixture was vigorously stirred with a magnetic stirrer for 10 h at 40°C in a capped tube. The diethyl ether was evaporated by nitrogen flow. The aqueous phase and residue were then extracted three times with 2 mL of chloroform/methanol (2:1, vol/vol). The chloroform phase was dried and PE was purified by silica high-performance liquid chromatography (HPLC) as shown below. All commercially available phospholipase D proved unsuitable for the preparation of radioactive PE due to contamination with other lipase activities. We

*To whom correspondence should be addressed at U.S. Department of Agriculture, 800 Buchanan St., Albany, CA 94710. E-mail: jtlin@pw.usda.gov

Abbreviations: DAG, diacylglycerol; FA, fatty acid; FAME, fatty acid methyl ester; FFA, free fatty acid; HPLC, high-performance liquid chromatography; 2-linoleoyl-PC, 1-acyl-2-linoleoyl-*sn*-glycero-3-phosphocholine; 2-oleoyl-PC, 1-acyl-2-oleoyl-*sn*-glycero-3- phosphocholine; 2-oleoyl-PE, 1-acyl-2-oleoyl-*sn*-glycero-3-phosphoethanolamine; PC, phosphatidylcholine; PE, phosphatidylethanolamine; 2-ricinoleoyl-PC, 1-acyl-2-ricinoleoyl-*sn*-glycero-3-phosphocholine; 2-ricinoleoyl-PE, 1-acyl-2-ricinoleoyl-*sn*-glycero-3- phosphoethanolamine; TAG, triacylglycerol.

used the phospholipase D of *Streptomyces antibioticus* prepared from recombinant *Escherichia coli* (5). This method was also used to prepare the nonradioactive standards, 1-palmitoyl-2-oleoyl-*sn*-glycero-3-phosphoethanolamine-*N*-monomethyl and 1-palmitoyl-2-oleoyl-*sn*-glycero-3-phosphoethanol-amine-*N*,*N*-dimethyl, using buffers containing 2-(methyl-amino)ethanol and 2-(dimethylamino)ethanol instead of ethanolamine.

Microsomal incubation. Microsomes from castor bean were prepared as described previously (3,6). The microsomal incubation mixture in a total volume of 1 mL included: sodium phosphate buffer (0.1 M, pH 6.3), NADH (0.5 mol), ATP (0.5 mol), $MgCl_2$ (0.5 μmol), catalase (1000 units), and the microsomal fraction of endosperm from immature castor bean (15 μL, 138 μg of protein). The radioactive substrate prepared here, 2-[^{14}C]oleoyl-PE (0.125 μCi, 2.16 nmol, 58.0 Ci/mol), in 20 μL ethanol was added last into a screw-capped tube followed by immediate mixing. The mixture was then incubated in a shaking water bath for 30 min at 22°C. The incubation was stopped by adding 3.75 mL of chloroform/methanol (1:2, vol/vol) to form a suspension. The mixture was again mixed with 0.63 mL of chloroform and 0.63 mL of water. The lower chloroform layer containing the lipid extract was dried and fractionated on a silica HPLC system for the separation of lipid classes described below. To identify the FA constituents of various lipids, lipid extracts or HPLC fractions together with NADH (0.5 μmol) as antioxidant were transmethylated in 5% HCl/methanol (1 mL) at 80°C for 1 h. The fatty acid methyl esters (FAME) formed were extracted with 2 × 1 mL of hexane. Tocopherol and butylated hydroxytoluene (also called 2,6-di-*tert*-butyl-4-methylphenol) were also used as antioxidants, but lower yields resulted.

HPLC. HPLC was carried out on a liquid chromatograph (Waters Associates, Milford, MA), using a photodiode array detector (Waters 996) detecting at 205 nm. Radioactive lipids were separated by HPLC and identified by cochromatography with lipid standards matching the retention times from ultraviolet absorbance at 205 nm and the radioactivity detector. The flow rates of eluants of different HPLC systems were 1 mL/min. The flow rate of liquid scintillation fluid (Ultima Flo M, Packard Instrument Co., Downers Grove, IL) of the radioactivity flow detector (150TR; Packard Instrument Co.) was 3 mL/min.

(i) Separation of lipid classes. Lipid classes were separated according to Singleton and Stikeleather (7) on a silica column [25 × 0.46 cm, 5 μm, Luna, silica (2); Phenomenex, Torrance, CA] with a linear gradient starting at isopropanol/hexane (4:3, vol/vol) to isopropanol/hexane/water (4:3:0.75, by vol) in 20 min, then isocratically for 20 min. A prepacked silica saturator column (3 × 0.46 cm, 15–25 μm; Phenomenex) was installed between the pump and injector to saturate the mobile phase with silica before it reached the analytical column.

(ii) Separation of molecular species of PC and PE. Molecular species of PC were separated as we reported previously (8) using a C_8 column (25 × 0.46 cm, 5 μm, Luna C8; Phenomenex) with a linear gradient of 90–100% methanol (containing 0.1% of conc. NH_4OH as silanol-suppressing agent) in 40 min. Molecular species of PE were separated with a linear gradient of 88–100% (containing 0.1% of conc. NH_4OH as silanol-suppressing agent) in 40 min.

(iii) Separation of molecular species of TAG. Molecular species of TAG were separated as we reported previously (9,10) using a C_{18} column (25 × 0.46 cm, 5 μm, Luna C18; Phenomenex) with a linear gradient starting at 100% methanol to 100% isopropanol in 40 min.

(iv) Separation of free fatty acids (FFA). FFA were separated as we previously reported (11) using a C_{18} column (25 × 0.46 cm, 5 μm, Luna C18; Phenomenex) with a linear gradient of 85–100% methanol (containing 0.05% HOAc as ion-suppressing agent) in 40 min.

(v) Separation of FAME. FAME were separated on a C_{18} column (25 × 0.46 cm, 5 m, Luna C18; Phenomenex) with a linear gradient of 90–100% methanol in 40 min (11). More rapid analyses used a short C_{18} column [5 × 0.46 cm, 3 μm, Luna C18(2); Phenomenex] with a linear gradient of 90–100% methanol in 15 min for a 10-min run (6).

RESULTS AND DISCUSSION

In the biosynthesis of TAG containing ricinoleate using 2-[^{14}C]oleoyl-PC as incubation substrate in castor microsomal incubation, we identified [^{14}C]PE as one of the metabolites (3). Given its metabolic relation and similar structure to 2-oleoyl-PC, we wanted to determine the role of 2-oleoyl-PE in the biosynthesis of TAG containing ricinoleate in castor bean. In a preliminary study we showed the conversion of oleate from 2-[^{14}C]oleoyl-PE to ricinoleate in the total lipid extract. To compare the enzyme characteristics of oleoyl-12-hydroxylase using 2-oleoyl-PE as incubation substrate to those using 2-oleoyl-PC in our earlier report (6), we examined the activities of oleoyl-12-hydroxylase as a function of pH and various incubation components that affect hydroxylase activity when oleoyl-CoA was used as incubation substrate (12–14). The total lipid extracts from the incubation mixtures at various pH values were transmethylated. The profiles of labeled FAME were similar to those we reported previously when 2-[^{14}C]oleoyl-PC was used as incubation substrate (6). The HPLC radiochromatograms showed the presence of radioactive methyl esters of oleate and its metabolites, ricinoleate and linoleate. The activities of oleoyl-12-hydroxylase using 2-[^{14}C]oleoyl-PE as incubation substrate at various pH values are shown as Figure 1. The optimal pH value is 6.3, which is the same as that of the incubations using 2-[^{14}C]oleoyl-PC as incubation substrate (6). The effects of some incubation components on the activity of oleoyl-12-hydroxylase using 2-oleoyl-PE as incubation substrate in castor microsomal incubations (30 min) were as follows: 140 pmol/30 min of [^{14}C]ricinoleate methyl ester, average of two determinations; + bovine serum albumin, 75; –catalase, 174; +CoA, 178; –ATP, 89; –NADH, +NADPH, 70; –$MgCl_2$, 95; PC incubation (the control incubations used 2-[^{14}C]oleoyl-PC as incubation substrate instead of 2-[^{14}C]oleoyl-PE), 211.

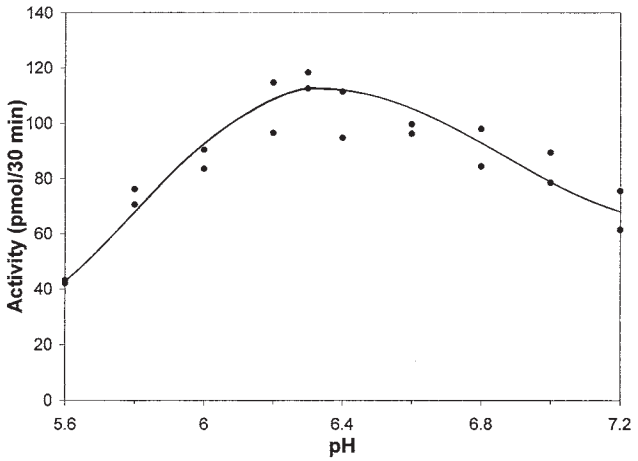

FIG. 1. Effect of pH (0.1 M sodium phosphate buffer) on the activity of oleoyl-12-hydroxylase using 1-acyl-2-[^{14}C]oleoyl-*sn*-glycero-3-phosphoethanolamine (2-[^{14}C]oleoyl-PE) as incubation substrate in castor microsomal incubations (30 min). Activity is the amount of the methyl ester of [^{14}C]ricinoleate formed after the transmethylation of the total lipid. The paired dots represent the data from two determinations.

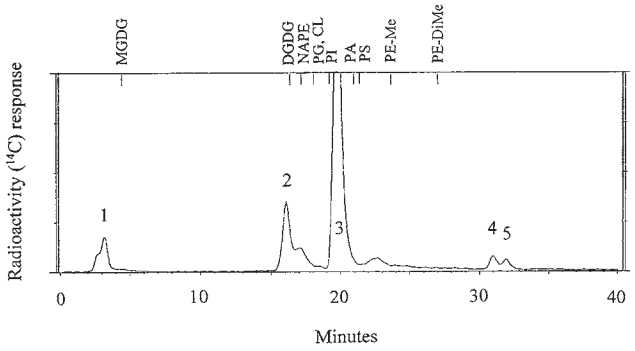

FIG. 2. Separation of lipid classes of total lipid extract from the castor microsomal incubation (60 min) with 2-[^{14}C]oleoyl-PE using a silica high-performance liquid chromatography (HPLC) system (see the Experimental Procedures section, HPLC, (i). The radioactive peaks were: (1) acylglycerols and free fatty acids (FFA) (retention time, 3.2 min); (2) the unknown (16.1 min); (3) phosphatidylethanolamine (PE) (19.8 min); (4) 1-acyl-2-oleoyl-*sn*-glycero-3-phosphocholine (2-oleoyl-PC) (30.9 min); (5) 1-acyl-2-ricinoleoyl-*sn*-glycero-3-phosphocholine (2-ricinoleoyl-PC) (31.9 min). Retention times of other lipid classes in this HPLC system are also shown in the figure. MGDG, monogalactosyl diacylglycerol; DGDG, digalactosyl diacylglycerol; NAPE, *N*-acyl-phosphatidylethanolamine; PG, phosphatidylglycerol; CL, cardiolipin; PI, phosphatidylinositol; PA, phosphatidic acid; PS, phosphatidylserine; PE-Me, PE-*N*-monomethyl; PE-DiMe, PE-*N*,*N*-dimethyl; for other abbreviation see Figure 1.

The inclusion of bovine serum albumin (1 mg) decreases the activity. The microsomal fraction was suspended in buffer containing catalase, and the further addition of catalase in the incubation did not increase the activity. The inclusion of CoA (0.5 μmol) does not significantly enhance the activity using 2-oleoyl-PE as incubation substrate. There is no effect of added CoA on the activity with 2-oleoyl-PC as incubation substrate (6). ATP (0.5 μmol) and $MgCl_2$ (0.5 μmol) enhance the activity as shown earlier using 2-oleoyl-PC as incubation substrate (6). The cofactor NADH could be replaced with NADPH but resulted in less activity than with NADH, as previously reported using 2-oleoyl-PC as incubation substrate (6). The similarity of the enzyme characteristics of oleoyl-12-hydroxylase using 2-oleoyl-PC and 2-oleoyl-PE as incubation substrates indicates the action of a single enzyme. However, 2-oleoyl-PC is a more efficient incubation substrate for oleoyl-12-hydroxylase than 2-oleoyl-PE.

Radioactive 2-oleoyl-PE was incubated with castor microsomes for various times. The total lipid extracts from the incubation mixtures were separated on a silica HPLC column for the separation of lipid classes as shown in Figure 2. The radiochromatograms (e.g., Fig. 2) showed the radioactive lipid classes of acylglycerols and FFA, the unknown, 2-oleoyl-PE (substrate), 2-oleoyl-PC, and 2-ricinoleoyl-PC (1-acyl-2-ricinoleoyl-*sn*-glycero-3-phosphocholine), which were the same lipid classes as those we reported (3) using 2-[^{14}C]oleoyl-PC as incubation substrate. The amounts of each lipid classes formed at various times are shown in Figure 3. The maximal amount of 2-ricinoleoyl-PC formed from 2-oleoyl-PE is 40 pmol, compared with 120 pmol from 2-oleoyl-PC (3), and it takes 60 vs. 30 min from the PC substrate (3). This suggests that the oleate from 2-oleoyl-PE is converted to ricinoleate after 2-oleoyl-PE is converted to 2-oleoyl-PC. The amounts of the lipid classes including acylglycerols and FFA, an unknown, and 2-oleoyl-PC increase with time at least up to 90 min. The dip at 60 min for the amount of 2-oleoyl-PC formed corresponds to the time of maximal amount of 2-ricinoleoyl-PC formed, suggesting the conversion of 2-oleoyl-PC to 2-ricinoleoyl-PC instead of the conversion of 2-ricinoleoyl-PE (1-acyl-2-ricinoleoyl-*sn*-glycero-3-phosphoethanolamine) to 2-ricinoleoyl-PC. The continuously smooth increase of the amount of unknown with time suggests that the formation of the unknown (peak 2, Fig. 3) from 2-oleoyl-PE is not on the pathway to TAG.

Figure 4 shows the HPLC separation of the molecular species of acylglycerols and FFA (peak 1, Fig. 2) from the castor microsomal incubation of radioactive 2-oleoyl-PE for 60 min. This radiochromatogram shows the presence of the same TAG and FFA as those obtained previously when the microsomes were incubated with radioactive 2-oleoyl-PC and ricinoleate (3). Oleate from 2-oleoyl-PE is incorporated into TAG containing ricinoleate by castor microsomes as shown in Figure 4. Similar to 2-oleoyl-PC, 2-oleoyl-PE is also hydrolyzed by phospholipase C in castor microsomes whereby 1-acyl-2-oleoyl-*sn*-glycerol accumulates (peak 5, Fig. 4). As shown earlier (3), the conversion of 1-acyl-2-oleoyl-*sn*-glycerol to TAG by diacylglycerol (DAG) acyltransferase is blocked when the DAG contains no ricinoleate.

We collected and transmethylated the unknown (peak 2, Fig. 2). We separated the FAME formed by a C_{18} HPLC and detected only the radioactive methyl ester of oleate. The ratio of the radioactivities of the methyl esters of oleate, linoleate, and ricinoleate was 100:0:0 in the incubation of 2-oleoyl-PE, whereas the ratio from the unknown in the incubation of 2-

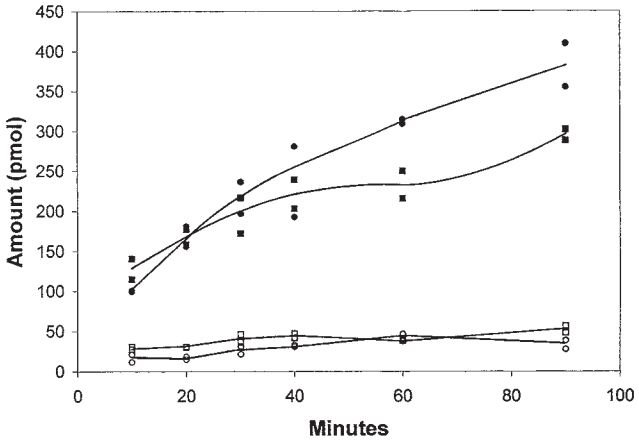

FIG. 3. Amounts of lipid classes shown in Figure 2 formed at various times of castor microsomal incubations with 2-[^{14}C]oleoyl-PE. Units for y axes are pmol of labeled fatty acids in each lipid class derived from [^{14}C]oleate of the substrate. (■), acylglycerols and FFA (including triricinolein); (●), unknown; □, 2-oleoyl-PC; (○), 2-ricinoleoyl-PC. The paired symbols represent the data from two determinations. For abbreviations see Figures 1 and 2.

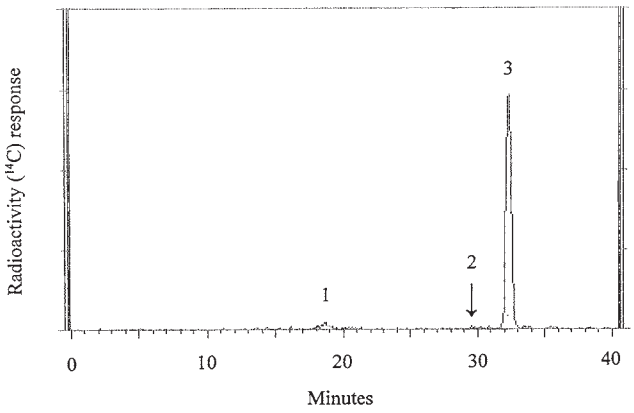

FIG. 5. HPLC radiochromatogram of phosphatidylethanolamine fraction (peak 3, Fig. 2) from the castor microsomal incubation (60 min) with 2-[^{14}C]oleoyl-PE using a reversed-phase C_8 HPLC system for the separation of molecular species of PE [see the Experimental Procedures section, HPLC, (ii)]. Peak 1, unknown (retention time, 18.6 min which is very close to that of 1-palmitoyl-2-ricinoleoyl-*sn*-glycero-3-phosphoethanolamine); arrow 2, 1-palmitoyl-2-linoleoyl-sn-glycero-3- phosphoethanolamine (retention time, 29.7 min); peak 3, 2-oleoyl-PE (32.4 min). For abbreviations see Figures 1 and 2.

oleoyl-PC was 90:4:6 which is very close to the ratio of 2-oleoyl-PC/2-linoleoyl-PC(1-palmitoyl-2-linoleoyl-*sn*-glycero-3-phosphocholine)/2-ricinoleoyl-PC, 91:3:6, in the same incubation (3). The results indicate that the unknown contains the DAG derived from the incubation substrate PE or PC, and 2-oleoyl-PE is not hydroxylated and desaturated, whereas 2-oleoyl-PC is. We are in the process of identifying this unknown lipid, which appears to be derived from PE or PC after hydrolysis by phospholipase C or D.

Figure 2 and the silica HPLC chromatogram from the incubation of 2-[^{14}C]oleoyl-PC reported earlier (3) show the presence of 2-[^{14}C]ricinoleoyl-PC, whereas 2-[^{14}C]ricinoleoyl-PE (retention time about 1 min after peak 3) is not seen in Figure 2. We hydrolyzed the PE fraction (peak 3, Fig. 2) from the microsomal incubation of radioactive 2-[^{14}C]oleoyl-PE with phospholipase A_2 (from *Naja mocambique mocambique*; Sigma P-4034, St. Louis, MO), and the FFA obtained were cochromatographed with the potential products, oleate, linoleate and ricinoleate on C_{18} HPLC [see the Experimental Procedures section, HPLC, (iv)]. The radioactive oleate (incubation substrate, 31.3 min) was present in the radiochromatogram, but radioactive ricinoleate (12.1 min) and linoleate (26.7 min) were not. We chromatographed the same PE fraction (peak 3, Fig. 2) on C_8 HPLC as shown in Figure 5 to separate the intact molecular species of PE. There are two radioactive peaks shown in Figure 5, and peak 3 (32.4 min) represents the incubation substrate 2-[^{14}C]oleoyl-PE. We hydrolyzed material in peak 1 (18.6 min) in Figure 5 with phospholipase A_2 and cochromatographed the FFA obtained with oleate, linoleate, and ricinoleate standards on C_{18} HPLC. We detected only radioactive oleate, and no radioactive ricinoleate and linoleate. 1-Palmitoyl-2-linoleoyl-*sn*-glycero-3-phosphoethanolamine should elute at 29.7 min in Figure 5 (arrow 2) according to the HPLC run of the standard. We do not have 1-palmitoyl-2-ricinoleoyl-*sn*-glycero-3-phosphoethanolamine available as a standard; however, based on the HPLC of PC we reported recently (8), we can predict its retention time to be about 18.3 min. We have proved that peak 1 of Figure 5 is not 2-ricinoleoyl-PE. The conversions of 2-[^{14}C]oleoyl-PE to 2-[^{14}C]ricinoleoyl-PE and 1-acyl-2-linoleoyl-*sn*-glycero-3-phosphoethanolamine (2-[^{14}C]linoleoyl-PE) appear completely blocked. We have shown earlier the intact 2-[^{14}C]ricinoleoyl-PC and 2-[^{14}C]linoleoyl-PC on a C_8 HPLC radiochromatogram when the castor microsomes were incubated with 2-[^{14}C]oleoyl-PC (3). Thus, both oleoyl-

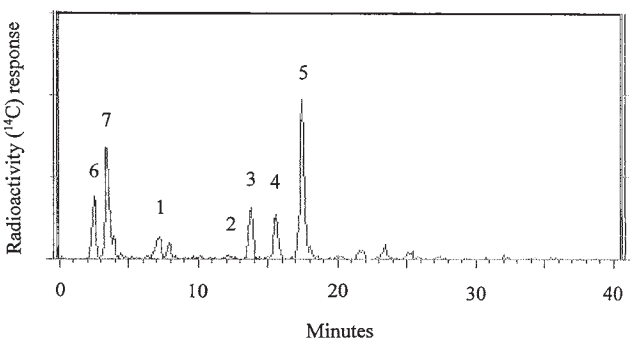

FIG. 4. HPLC identification of radioactive acylglycerols in the fraction of acylglycerols and FFA (peak 1, Fig. 3) from the castor microsomal incubation (60 min) of 2-[^{14}C]oleoyl-PE, using a C_{18} HPLC system [see the Experimental Procedures section, HPLC, (iii)]. Peak 1, triricinolein (retention time, 7.2 min); peak 2, diricinoleoyl-linolenoyl-glycerol (12.1 min); peak 3, diricinoleoyl-linoleoyl-glycerol (13.8 min); peak 4, diricinoleoyl-oleoyl-glycerol (15.6 min); peak 5, 1-palmitoyl-2-oleoyl-*sn*-glycerol (17.5 min); peak 6, ricinoleate (2.5 min); peak 7, may be 1,2-diricinoleoyl-*sn*-glycerol (3.4 min). For abbreviations see Figure 2.

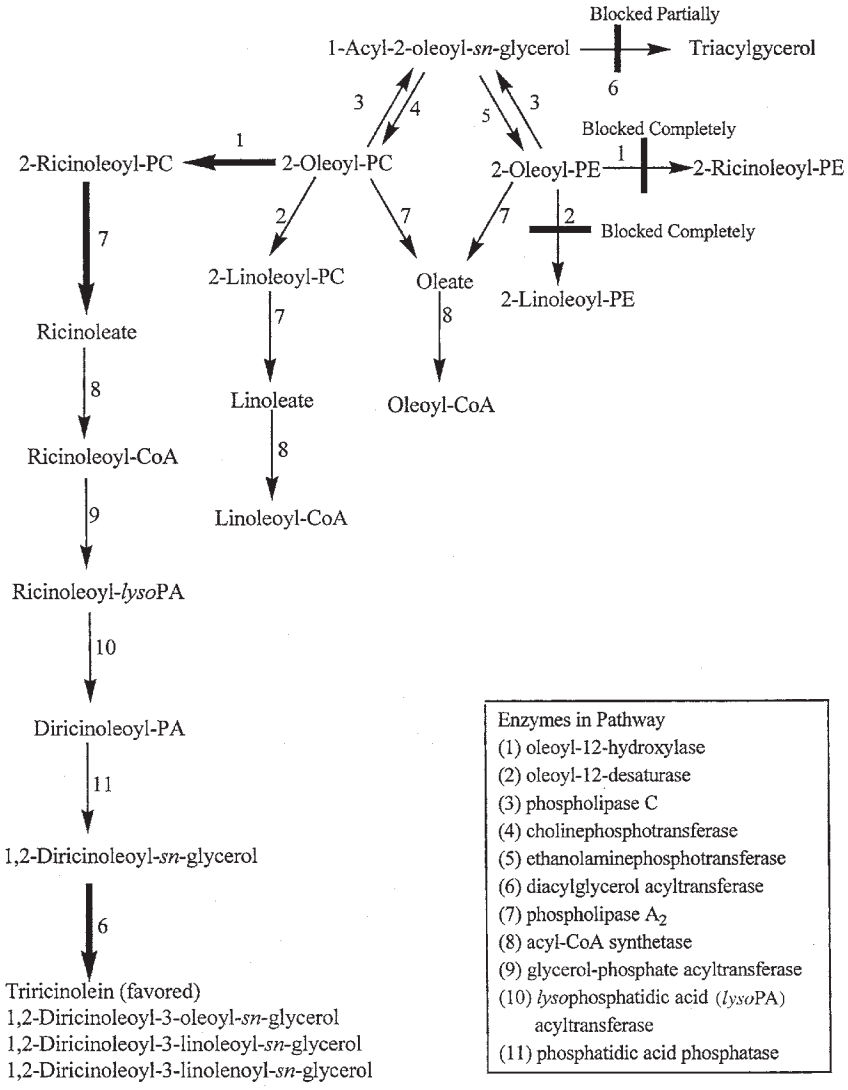

SCHEME 1

12-hydroxylase and oleoyl-12-desaturase in castor microsomes are specific for the PC head group. Since the structure of PE among the major lipid classes is similar to that of PC, and PE cannot be used as the immediate substrate of either enzyme, it is likely that 2-oleoyl-PC is the only substrate of these two enzymes.

We have synthesized 1-palmitoyl-2-oleoyl-*sn*-glycero-3-phosphoethanolamine-*N*-monomethyl and 1-palmitoyl-2-oleoyl-*sn*-glycero-3-phosphoethanolamine-*N,N*-dimethyl, the intermediate metabolites of PE to PC by N-methylation (15). Their retention times are shown in Figure 2 in a silica HPLC for the separation of lipid classes. Neither of these two compounds is detected as ^{14}C-labeled as shown in Figure 2. Even using 22-fold higher levels of labeled materials, we were unable to detect the intermediates from conversion of PE to PC by N-methylation either by silica HPLC or C_8 HPLC using the standards we synthesized.

Scheme 1 shows the biosynthetic pathway of TAG containing ricinoleate using 2-oleoyl-PE and 2-oleoyl-PC (3) as the incubation substrates in castor microsomal incubations. Enzyme 1: Oleoyl-12-hydroxylase, with cytochrome b_5, NADH, O_2, ATP (16). It is blocked completely when the substrate is 2-oleoyl-PE. Enzyme 2: Oleoyl-12-desaturase, with cytochrome b_5, NADH, O_2, ATP (16). It is blocked completely when the substrate is 2-oleoyl-PE. Enzyme 3: Phospholipase C. It is likely that 2-oleoyl-PE itself as well as 2-oleoyl-PC is hydrolyzed by phospholipase C in castor microsomes. A large amount of 1-acyl-2-oleoyl-*sn*-glycerol accumulated when 2-oleoyl-PE was incubated in castor microsomes as shown in Figure 4, and we have shown that 2-oleoyl-PE can be hydrolyzed by phospholipase C (from *Bacillus cereus*). Enzyme 4: CDP-choline:1,2-DAG cholinephosphotransferase (15). It is likely that most of the conversion of PE to PC goes *via* enzymes 3 and 4 as shown in Scheme 1, because DAG is a major metabolite of PE (Fig. 4), and it has been shown that DAG (both 1,2-diricinoleoyl-*sn*-

glycerol and 1,2-dioleoyl-*sn*-glycerol) can be efficiently converted to PC (17). There are three other possible pathways from PE to PC: (i) *S*-adenosyl-L-methionine:PE *N*-methyltransferase (15); in this study, the intermediates of the conversion from PE to PC by N-methylation were not detected; (ii) a base group exchange reaction, transfer of the phosphatidyl unit to free choline, requires Ca^{2+} (18); and (iii) conversion of 2-oleoyl-PE to lysoPE by phospholipase A_2 (enzyme step 7), conversion of the released ^{14}C-oleate to oleoyl-CoA (enzyme step 8), followed by acylation of lysoPC (13) because ATP, CoA, and Mg seem to stimulate the formation of ricinoleate from PE (see above). Enzyme 5: CDP-ethanolamine:1,2-DAG ethanolaminephosphotransferase (19). PE also could be formed from PC by a base group exchange reaction (18), transfer of the phosphatidyl unit to ethanolamine, which requires Ca^{2+}. Enzyme 6, DAG acyltransferase, with acyl CoA, is partially blocked when the DAG contain no ricinoleate (17). Because of the block, 1-acyl-2-oleoyl-*sn*-glycerol accumulated. Enzyme 7: phospholipase A_2. It is likely that 2-oleoyl-PE itself is hydrolyzed by phospholipase A_2 in castor microsomes. We have shown that 2-oleoyl-PE can be hydrolyzed by phospholipase A_2 (from *N. mocambique mocambique*). Enzyme 8: acyl-CoA synthetase, with ATP, CoA. Enzyme 9: glycerol-phosphate acyltransferase, with acyl CoA. Enzyme 10: lysophosphatidic acid acyltransferase. Enzyme 11: phosphatidic acid phosphatase.

In conclusion, the incorporation of the label from 2-[^{14}C]oleoyl-PE into TAG containing ricinoleate passes through 2-oleoyl-PC, which is then hydroxylated and desaturated. The conversion of 2-oleoyl-PE to 2-oleoyl-PC does not appear to be a key enzymatic step for driving ricinoleate into TAG, because our results indicate that 2-oleoyl-PE is not an effective incubation substrate for hydroxylation, but a precursor of 2-oleoyl-PC. In addition, the enzyme characteristics of oleoyl-12-hydroxylase using 2-oleoyl-PE as incubation substrate were shown to be the same as those using 2-oleoyl-PC, the immediate substrate (6).

REFERENCES

1. van de Loo, F.J., Broun, P., Turner, S., and Somerville, C. (1995) An Oleate 12-Hydroxylase from *Ricinus communis* L. Is a Fatty Acyl Desaturase Homolog, *Proc. Natl. Acad. Sci. USA 92*, 6743–6747.
2. Broun, P., and Somerville, C. (1997) Accumulation of Ricinoleic, Lesquerolic, and Densipolic Acids in Seeds of Transgenic *Arabidopsis* Plants That Express a Fatty Acyl Hydroxylase cDNA from Castor Bean, *Plant Physiol. 113*, 933–942.
3. Lin, J.T., Woodruff, C.L., Lagouche, O.J., McKeon, T.A., Stafford, A.E., Goodrich-Tanrikulu, M., Singleton, J.A., and Haney, C.A. (1998) Biosynthesis of Triacylglycerols Containing Ricinoleate in Castor Microsomes Using 1-Acyl-2-oleoyl-*sn*-glycero-3-phosphocholine as the Substrate of Oleoyl-12-hydroxylase, *Lipids 33*, 59–69.
4. Paltauf, F., and Hermetter, A. (1991) Preparation of Alkyl Ether and Vinyl Ether Substrates for Phospholipases, *Methods Enzymol. 197*, 134–149.
5. Mishima, N., Mizumoto, K., Iwasaki, Y., Nakano, H., and Yamane, T. (1997) Insertion of Stabilizing Loci in Vectors of T7 RNA Polymerase-Mediated *Escherichia coli* Expression Systems: A Case Study on the Plasmids Involving Foreign Phospholipase D Gene, *Biotechnol. Prog. 13*, 864–868.
6. Lin, J.T., McKeon, T.A., Tanrikulu, M.G., and Stafford, A.E. (1996) Characterization of Oleoyl-12-hydroxylase in Castor Microsomes Using the Putative Substrate, 1-Acyl-2-oleoyl-*sn*-glycero-phosphocholine, *Lipids 31*, 571–577.
7. Singleton, J.A., and Stikeleather, L.F. (1995) High-Performance Liquid Chromatography Analysis of Peanut Phospholipids. II. Effect of Postharvest Stress on Phospholipid Composition, *J. Am. Oil Chem. Soc. 72*, 485–488.
8. Lin, J.T., McKeon, T.A., Woodruff, C.L., and Singleton, J.A. (1998) Separation of Synthetic Phosphatidylcholine Molecular Species by High-Performance Liquid Chromatography on a C_8 Column, *J. Chromatogr. A 824*, 169–174.
9. Lin, J.T., Woodruff, C.L., and McKeon, T.A. (1997) Non-Aqueous Reversed-Phase High-Performance Liquid Chromatography of Synthetic Triacylglycerols and Diacylglycerols, *J. Chromatogr. A 782*, 41–48.
10. Lin, J.T., Snyder, L.R., and McKeon, T.A. (1998) Prediction of Relative Retention Times of Triacylglycerols in Non-Aqueous Reversed-Phase High-Performance Liquid Chromatography, *J. Chromatogr. A 808*, 43–49.
11. Lin, J.T., McKeon, T.A., and Stafford, A.E. (1995) Gradient Reversed-Phase High-Performance Liquid Chromatography of Saturated, Unsaturated and Oxygenated Free Fatty Acids and Their Methyl Esters, *J. Chromatogr. A 699*, 85–91.
12. Galliard, T., and Stumpf, P.K. (1966) Fat Metabolism in Higher Plants XXX. Enzymatic Synthesis of Ricinoleic Acid by a Microsomal Preparation from Developing *Ricinus communis* Seeds, *J. Biol. Chem. 241*, 5806–5812.
13. Bafor, M., Smith, M.A., Jonsson, L., Stobart, K., and Stymne, S. (1991) Ricinoleic Acid Biosynthesis and Triacylglycerol Assembly in Microsomal Preparations from Developing Castor Bean (*Ricinus communis*) Endosperm, *Biochem. J. 280*, 507–514.
14. Moreau, R.A., and Stumpf, P.K. (1981) Recent Studies of the Enzyme Synthesis of Ricinoleic Acid by Developing Castor Beans, *Plant Physiol. 67*, 672–676.
15. Moore, T.S. (1976) Phosphatidylcholine Synthesis in Castor Bean Endosperm, *Plant Physiol. 57*, 383–386.
16. Smith, M.A., Jonsson, L., Stymne, S., and Stobart, K. (1992) Evidence for Cytochrome b_5 as an Electron Donor in Ricinoleic Acid Biosynthesis in Microsomal Preparations from Developing Castor Bean (*Ricinus communis* L.), *Biochem. J. 287*, 141–144.
17. Vogel, G., and Browse, J. (1996) Cholinephosphotransferase and Diacylglycerol Acyltransferase, Substrate Specificities at a Key Branch Point in Seed Lipid Metabolism, *Plant Physiol. 110*, 923–931.
18. Shin, S., and Moore, T.S. (1990) Phosphatidylethanolamine Synthesis by Castor Bean Endosperm, a Base Exchange Reaction, *Plant Physiol. 93*, 148–153.
19. Sparace, S.A., Wagner, L.K., and Moore, T.S. (1981) Phosphatidylethanolamine Synthesis in Castor Bean Endosperm, *Plant Physiol. 67*, 922–925.

[Received November 23, 1999, and in revised form February 21, 2000; revision accepted March 14, 2000]

Purification of the Acyl-CoA Elongase Complex from Developing Rapeseed and Characterization of the 3-Ketoacyl-CoA Synthase and the 3-Hydroxyacyl-CoA Dehydratase

Frédéric Domergue[a], Sylvette Chevalier[b], Anne Créach[c], C. Cassagne[b], and René Lessire[b,*]

[a]Institute für Allgemeine Botanik, Universität Hamburg, 22609 Hamburg, Germany, [b]Laboratoire de Biogenèse Membranaire, Université Victor Segalen Bordeaux 2 (CNRS-UMR 5544), 33076 Bordeaux Cédex, France, and [c]USTL, UPRES-A CNRS 8013 "ELICO," 59655 Villeneuve d'Ascq Cédex, France

ABSTRACT: Oleoyl-CoA elongase catalyzes four successive reactions: condensation of malonyl-CoA to oleoyl-CoA, reduction, dehydration, and another reduction. Evidence supporting this mechanism and the multienzymatic nature of the elongation complex are reported. A particulate membrane fraction from rapeseed is able to elongate intermediates (*R,S*) 3-hydroxy-20:0-CoA and (*E*) 2,3-20:1-CoA to very long chain fatty acids in the presence of malonyl-CoA. Studies of the 3-ketoacyl-CoA synthase activities showed that maximal activity could be measured by using 15 to 30 µM 18:1-CoA and 30 µM malonyl-CoA, and that 18:0-CoA and 18:1-CoA were the best substrates. Comparison of the condensation and the overall elongation activities indicated that condensation is the rate-limiting step of the elongation process. The 3-hydroxyacyl-CoA dehydratase activity was maximal in the presence of 75 µM Triton X-100 and 25 µg of proteins. Finally, the acyl-CoA elongase complex was solubilized and purified. During the purification process, the 3-hydroxyacyl-CoA dehydratase copurified with the elongase complex, strongly suggesting that this enzyme belongs to the elongase complex. The apparent molecular mass of 700 kDa determined for the elongase complex, and the fact that four different polypeptide bands were detected after sodium dodecyl sulfate-polyacrylamide gel electrophoretic analysis of the purified fraction, further suggest that the acyl-CoA elongase is a multienzymatic complex.

Paper no. L8414 in *Lipids 35,* 487–494 (May 2000).

Erucic acid (22:1) and its derivatives offer so many industrial applications that if an oil with about 90% 22:1 could be obtained, it would replace many petrochemical alternatives (1). Erucic acid is highly enriched in several oleaginous plants. It represents up to 60% of the total fatty acids in some varieties of rapeseed called high erucic acid rapeseed (HEAR). Higher percentages of 22:1 cannot be obtained because rapeseed lysophosphatidic acid acyl transferase cannot esterify 22:1 in the *sn*-2 position of the triacylglycerols (TAG). Recently, Lassner *et al.* (2) transformed HEAR lines with the gene of the lysophosphatidic acid acyl transferase from *Limnanthes alba,* an enzyme capable of inserting 22:1 in the *sn*-2 position of TAG. Analysis of transgenic plants showed that the total erucic acid oil content was unchanged although 22:1 was present in the *sn*-2 position of TAG. In fact, it was demonstrated that 22:1 was less abundant in the *sn*-1 and *sn*-3 positions when compared to the original HEAR lines. These results strongly suggest that the erucoyl-CoA pool is limiting, and therefore that the very long chain fatty acid (VLCFA) synthesis pathway needs to be enhanced in order to increase the total erucic acid oilseed content.

In higher plants, VLCFA are synthesized from long-chain acyl-CoA and malonyl-CoAs by membrane-bound enzymes called acyl-CoA elongases (3). From the identification of the intermediates of the elongation process (4), it has been hypothesized that four intermediate reactions occur during acyl-CoA elongation: firstly, malonyl-CoA and a long-chain acyl-CoA are condensed by a ketoacyl-CoA synthase or condensing enzyme; the resulting 3-ketoacyl-CoA is then reduced by the action of a 3-ketoacyl-CoA reductase, resulting in the synthesis of a 3-hydroxyacyl-CoA; the latter is transformed during a third step into an enoyl-CoA by a 3-hydroxyacyl-CoA dehydratase; finally, a second reduction catalyzed by (*E*) 2,3-enoyl-CoA reductase yields the elongated acyl-CoA. This scheme has recently been demonstrated in leaves using chemically synthesized intermediates (5).

Whereas the mechanism of elongation is now well characterized, the structure of the acyl-CoA elongases remains poorly understood because their membrane-bound nature has so far hindered most purification attempts. Nevertheless, several studies have provided important information. By using Triton X-100, acyl-CoA elongase complexes were successfully solubilized from various seeds (6–8). Moreover, zwitterionic detergents resulted in the solubilization of the sole condensing enzyme, indicating that the different activities may be catalyzed by independent proteins (9). Similarly, attempts to purify elongases from *Lunaria annua* seeds resulted in the

*To whom correspondence should be addressed at Laboratoire de Biogenèse Membranaire, Université Victor Segalen Bordeaux 2 (CNRS-UMR 5544), 146 rue Léo Saignat, 33076 Bordeaux Cédex, France.
E-mail: rene.lessire@biomemb.u-bordeaux2.fr

Abbreviations: ACP, acyl carrier protein; DTT, dithiothreitol; HEAR, high erucic acid rapeseed; HPTLC, high-performance thin-layer chromatography; SDS-PAGE, sodium dodecyl sulfate-polyacrylamide gel electrophoresis; TAG, triacylglycerols; VLCFA, very long chain fatty acid.

partial purification of only the first two enzyme activities (6). Finally, Créach *et al*. (10), in a preliminary work, reported the partial purification of the entire 18:1-CoA elongase from *Brassica napus* seeds.

Here we report biochemical studies of two intermediate reactions of the elongation process, i.e., those catalyzed by the 3-ketoacyl-CoA synthase and 3-hydroxyacyl-CoA dehydratase. We demonstrate that the 18:1-CoA elongase is a multienzymatic complex and that dehydratase is one of its components.

EXPERIMENTAL PROCEDURES

Plant material. HEAR plants (*B. napus* L.) were grown outdoors at INRA (Le Rheu, France). Seeds were collected 6 to 8 wk after flowering and stored at –80°C.

Chemicals. [2-^{14}C]Malonyl-CoA (2.1 GBq/mmol) was purchased from New England Nuclear (Boston, MA). (*R,S*) 3-Hydroxy-20:0-CoA, (*E*) 2,3 20:1-CoA, and (*R/S*) [1-^{14}C] 3-hydroxy-20:0-CoA (52 Ci/mol) were chemically synthesized as already described (11). All other chemicals were from Sigma Chemical Co. (St. Louis, MO).

3-Ketoacyl-CoA synthase (condensing enzyme) activity. Routinely 50 µg samples of proteins were incubated for 30 min at 30°C in the presence of 1 mM $MgCl_2$, 2 mM dithiothreitol (DTT), 9 µM [2-^{14}C]malonyl-CoA, and 30 µM acyl-CoAs in a final volume of 100 µL 0.08 M HEPES (pH 7.2). The reaction was stopped by addition of 0.8 mL of reductant buffer containing 5% (wt/vol) $NaBH_4$, 0.1 M K_2HPO_4, 0.4 M KCl, and 30% (vol/vol) tetrahydrofuran. The samples were vigorously shaken for 45 min at 37°C, the condensing products were extracted by 0.8 mL hexane, and the radioactivity was determined as reported previously (12).

Alternatively, 3-ketoacyl-CoA synthase activity was measured using the elongase assay in the absence of NADH and NADPH.

3-Hydroxyacyl-CoA dehydratase assay. Routinely, 50 µg samples of proteins were incubated for 1 h at 30°C in the presence of 1 mM $MgCl_2$, 2 mM DTT, and 11.5 µM (*R/S*) [1-^{14}C] 3-hydroxy-20:0-CoA (52 Ci/mol) in a final volume of 100 µL 0.08 M HEPES (pH 7.2). The reaction was stopped by addition of 100µL 5 N KOH in H_2O/CH_3OH (9:1,vol/vol), and saponified at 80°C for 1 h. After acidification with 100 µL 10 N H_2SO_4 containing 10% (wt/vol) malonic acid, the fatty acids were extracted and analyzed by high-performance thin-layer chromatography (HPTLC) on Merck silica gel 60F 254 plates (10 × 10 cm) eluted with hexane/diethyl ether/acetic acid (75:25:1, by vol). Under these conditions, the R_f of 3-OH fatty acids, straight-chain fatty acids (saturated or unsaturated), and methyl ketones were, respectively, 0.15, 0.7, and 0.9.

After autoradiography of the plates using DuPont NEF-485 films, the fatty acid bands corresponding to 3-hydroxy-20:0-CoAs and (*E*) 2,3-20:1-CoAs were scraped into vials, 100 µL water was added, and the radioactivity was measured using a Packard Tri Carb 2000CA liquid scintillation spectrometer. Activities were calculated as the difference between the percentage of conversion of [1-^{14}C] 3-hydroxy-20:0-CoA into (*E*) 2,3-20:1-CoA in the assay and the control (incubation time = 0) and were expressed as nmol (*E*) 2,3-20:1-CoA synthesized.

Acyl-CoA elongase assay. Routinely, 50 µg samples of proteins were incubated for 1 h at 30°C in the presence of 9 µM [2-^{14}C] malonyl-CoA, 0.5 mM NADH, 0.5 mM NADPH, 1 mM $MgCl_2$, 2 mM DTT, and 30 µM oleoyl-CoA in a final volume of 100 µL 0.08 M HEPES (pH 7.2) containing 0.02% (wt/vol) Triton X-100.

The reaction was stopped by addition of 100 µL 5 N KOH in H_2O/CH_3OH (9:1, vol/vol). The reaction mixture was saponified for 1 h at 80°C and then acidified with 100 µL 10 N H_2SO_4 containing 10% (wt/vol) malonic acid. The fatty acids were extracted with 2 mL of $CHCl_3$, washed with water (3 × 2 mL), and the radioactivity was determined. The acyl-CoA elongation was estimated as the radioactivity present in the total fatty acids.

Analysis of the reaction products. The fatty acids extracted from the elongase assay were alternatively analyzed by HPTLC using the same plates and solvent separation as in the dehydratase assay. After autoradiography of the plates using DuPont NEF-485 films, the different bands were scraped into vials, 100 µL water was added to each and the radioactivity was measured.

Preparation of the F15 fraction. The preparation of the F15 fraction was derived from the protocol published by Agrawal and Stumpf (13). Developing rapeseeds were ground with a mortar in a 0.08 M HEPES (pH 7.2) buffer containing 0.32 M sucrose, 10 mM β-mercaptoethanol, and 5% (wt/vol) polyvinylpyrrolidone. The homogenate was filtered through two layers of Miracloth and centrifuged successively at 300 × *g* (5 min) and 15,000 × *g* (25 min). The pellet from the latter centrifugation was resuspended in a 0.08 M HEPES (pH 7.2) buffer containing 10 mM β-mercaptoethanol and centrifuged again at 15,000 × *g* (25 min). The resulting pellet was resuspended in a 0.08 M HEPES (pH 7.2) buffer containing 0.32 M sucrose and 10 mM β-mercaptoethanol. This particulate fraction (F15) contained membranes from different cellular compartments and was used to characterize the condensing and dehydratase enzymes and to solubilize and purify the elongation complex.

Protein contents were determined using Bradford's method (14) with bovine serum albumin as standard.

Acyl-CoA elongase purification. Typically, 150 g of developing seeds were used per purification. The proteins of the F15 fraction (150 mg) were incubated at 4°C for 2 h with a Triton X-100 to protein ratio of 2.5 (w/w) (8). The mixture was centrifuged for 1 h at 100,000 × *g*, and after removal of the oil body-floating layer, the solubilized proteins contained in the supernatant were collected (fraction FS). FS was carefully loaded onto a palmitoyl-CoA agarose (Sigma) column (1.6 × 2 cm) which was previously equilibrated with buffer A [0.08 M HEPES (pH 7.0), Triton X-100 (0.02%, vol/vol), β-mercaptoethanol (10 mM), and ethyleneglycol (10%, vol/vol)]. After washing with the same buffer, the retained proteins were eluted with a 0–2 M NaCl gradient in buffer A. Fractions presenting the highest elongation activities were

pooled (fraction N16) and loaded on a Sephacryl S300 (Pharmacia, Uppsala, Sweden) column (1.6 × 63 cm) pre-equilibrated with buffer A. Elution was performed using a 0.25 mL/min flow rate; the fractions with the highest elongation activity were pooled (fraction S300) and loaded on a Q-Sepharose (Pharmacia) column (1.6 × 0.5 cm) previously equilibrated with buffer A. The column was washed and eluted with 1 M NaCl in the same buffer. The fractions having the highest activities were pooled and considered as the partially purified fraction (fraction Q-Seph).

Lipid stimulation. Fractions unretained on the palmitoyl-CoA agarose column (0–30 mL) were pooled and their lipids were extracted with chloroform/methanol (2:1, vol/vol). The solvent was evaporated, and the lipids were resuspended in 0.08 M HEPES (pH 7.0). Lipid analysis revealed that the major components were phospholipids, TAG, and Triton X-100 (data not shown). Usually, the proteins obtained from the different chromatographic steps were mixed with these lipids before the elongase reaction mixture was added.

Sodium dodecyl sulfate-polyacrylamide gel electrophoresis (SDS-PAGE) analysis. Protein samples were delipidated and precipitated with frozen acetone as already described by Bessoule *et al.* (15). The proteins were separated on 10% acrylamide gel using a vertical gel unit (model SE 440) from Hoefer Scientific Instrument. Fixation, staining, and destaining of the gels were carried out according to Laemmli (16).

Lipid analysis. Lipids were extracted with chloroform/methanol (2:1, vol/vol) and resolved by thin-layer chromatography. Neutral and polar lipids were separated using hexane/diethyl ether/acetic acid (90:15:2, by vol) and methyl acetate/*n*-propanol/$CHCl_3$/CH_3OH/0.1 M KCl (25:25:28:10:7, by vol), respectively. The different classes of lipids were visualized according to Macala *et al.* (17) and quantified by densitometry.

RESULTS AND DISCUSSION

Characterization of the 3-ketoacyl-CoA synthase. The specificity of the 3-ketoacyl-CoA synthase was assayed using the F15 fraction as enzyme source and different acyl-CoAs (Fig. 1A). In the presence of acyl-CoAs with 14 carbon atoms or fewer, no activity significantly different from the control (in the absence of exogenously added acyl-CoAs) was observed. Both 16:0-CoA and 16:1-CoA led to very low activities, and the highest 3-ketoacyl-CoA synthase activities were obtained in the presence of saturated and monounsaturated 18- or 20-acyl-CoAs. Surprisingly, the highest activities were measured using 18:0-CoA as the substrate, whereas the corresponding elongated product (20:0) is found only in traces in most *B. napus* seed oils. This apparent discrepancy can be explained by the fact that in plant cells, most of the 18:0-acyl carrier protein (ACP) is desaturated in the chloroplast to 18:1-ACP, which is then transformed into 18:1-CoA when entering the cytosol compartment. Owing to this *in vivo* compartmentalization, 18:0 is not accessible to the cytosolic membrane-bound elongases. Interestingly, 18:2-acyl-CoAs was a poor substrate of the condensing enzyme. These results suggest that acyl-CoA chain length seems to be the major factor, with unsaturation a secondary determinant in the specificity of 3-ketoacyl-CoA synthase. Similar results were reported for the condensing enzyme purified from jojoba (9). Finally, these results confirmed that the condensing enzyme determines the specificity of the acyl-CoA elongase demonstrated by Millar and Kunst (18).

3-Ketoacyl-CoA synthase and total elongation activities were studied as a function of time and substrate concentrations (Fig. 1B–D). The 3-ketoacyl-CoA synthesis was maximal after 15 min and remained stable or slightly decreased afterward, suggesting that condensation activity had stopped by 15 min (Fig. 1B). This may indicate that the accumulation of the reaction product of the condensing enzyme, i.e., 3-keto 20:1-CoA exerts a feedback inhibition on the enzyme. However, when NADPH and NADH were added, thereby allowing full elongation cycles to proceed, the label in fatty acids increased up to 90 min. 3-Ketoacyl-CoA synthase activity increased up to 30 µM malonyl-CoA and then plateaued, whereas the elongation increased up to 50 µM in the presence of the reducing coenzymes (Fig. 1C). The effects of oleoyl-CoA concentration on the condensation and elongation reaction were similar (Fig. 1D). Both reached maximal activity at 15–30 µM 18:1-CoA, and decreased at higher concentrations. This result could reflect an inhibition due to (i) an excess of substrate, (ii) the detergent effect of acyl-CoAs, or, most probably, (iii) the presence of enzymatic activities using the same substrate in the vicinity of the elongase as already described for leek epidermis elongases (19). Although it appeared that 3-ketoacyl-CoAs and VLCFA syntheses occurred at the same rate, the amount of 3-ketoacyl-CoAs neosynthesized was repeatedly lower than that of the VLCFA obtained after complete elongation cycles. This may indicate that the accumulation of the reaction products of the condensing enzyme, i.e., 3-ketoacyl-CoAs, exerts a feedback inhibition on this enzyme. Such an inhibition is not seen in the presence of reducing agents, thus allowing full elongation cycles to proceed. This situation has been described in *Cuphea lanceolata* where the accumulation of 3-ketoacyl-ACP retroinhibits 3-ketoacyl ACP synthase I (KAS I) (20). Fehling and Muhkerjee (4) have shown in *L. annua* that the kinetics of formation of very long chain 3-ketoacyl-CoAs and saturated acyl-CoAs are similar, therefore supporting the rate-limiting role of 3-ketoacyl-CoA synthase. Similarly, Millar and Kunst (18) showed that the accumulation and the nature of VLCFA are controlled by the 3-ketoacyl-CoA synthase. In conclusion, our data indicated that the condensing enzyme could be the rate-limiting step of the elongating process and that that 3-ketoacyl-CoAs could act as retroinhibitors.

Elongation of acyl-CoA intermediates. Elongation of (*R,S*) 3-OH-20:0-CoA and (*E*) 2,3-20:1-CoA was measured in standard conditions by incubation of 50 µg of proteins of F15 for 1 h at 30°C in the presence of 9 µM [2-^{14}C]malonyl-CoA, 1 mM $MgCl_2$, 2 mM DTT, and 30 µM of the different acyl-CoAs in a final volume of 100 µL 0.08 M HEPES (pH 7.2); the reaction stopped and activity estimated as reported in the Experimental Procedures section using the F15 fraction as the

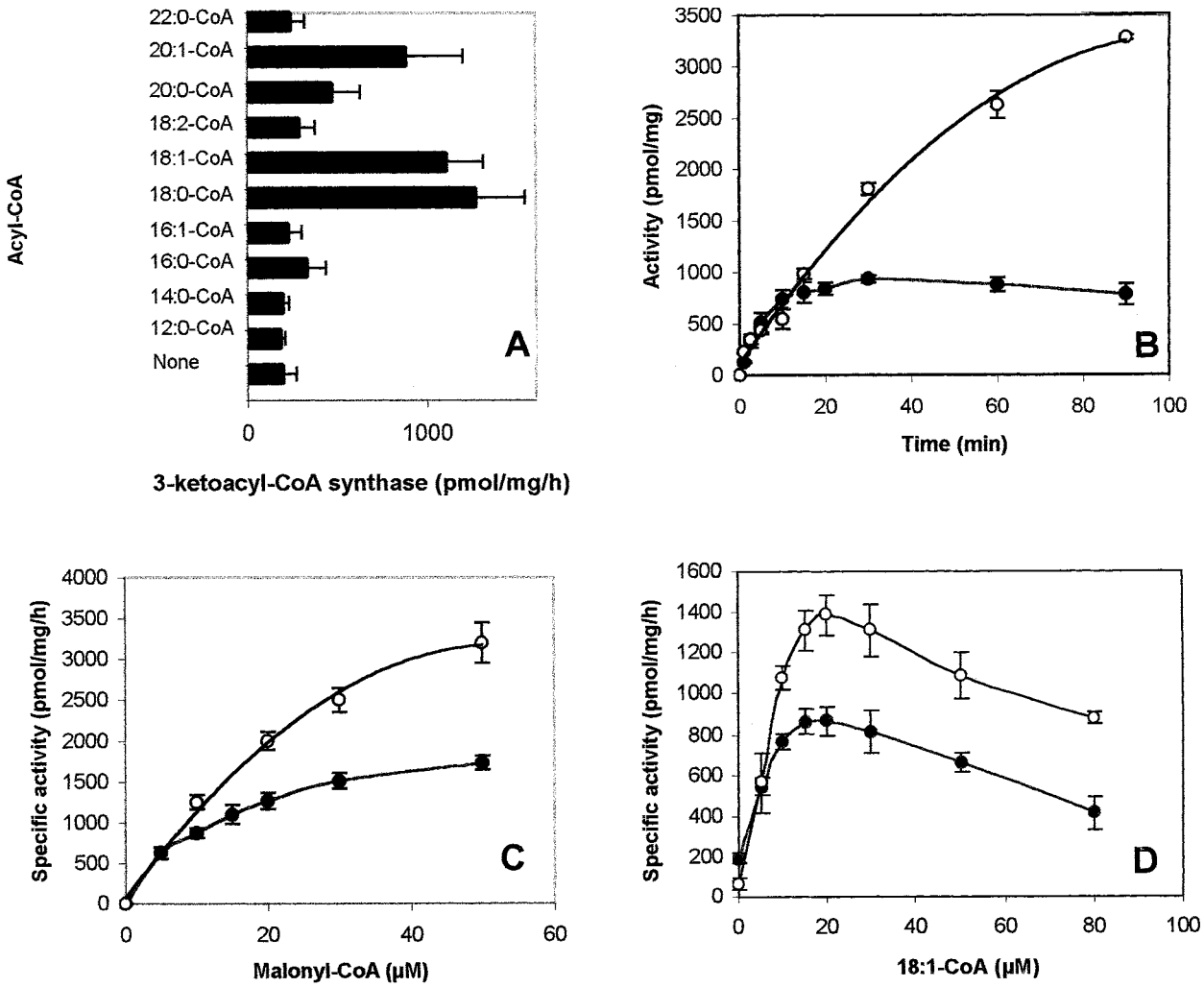

FIG. 1. Kinetic studies and specificity of condensing enzyme. (A) Condensation was measured by incubating 50 µg of proteins from fraction F15 for 30 min at 30°C in the presence 9 µM [2-^{14}C]malonyl-CoA, 1 mM $MgCl_2$, 2 mM dithiothreitol (DTT), and 30 µM acyl-CoA in a final volume of 100 µL 0.08 M HEPES (pH 7.2). The reaction was stopped and the condensing enzyme activity estimated as reported in the Experimental Procedures section. All results in this figure are expressed as mean values ± SD of three duplicate experiments. (B) Condensation (●) was measured by incubating at 30°C for various times 50 µg of proteins from F15 in the presence of 9 µM [2-^{14}C]malonyl-CoA, 1 mM $MgCl_2$, 2 mM DTT, and 30 µM oleoyl-CoA in a final volume of 100 µL 0.08 M HEPES (pH 7.2). Elongation (○) medium contained in addition 0.5 mM NADH and 0.5 mM NADPH. The reactions were stopped and the activities estimated as reported in the Experimental Procedures section. These results are expressed as mean value ± SD of three different experiments. (C) Condensation (●) and elongation (○) were measured as described in B but with an incubation time of 30 min and in the presence of increasing concentrations of [2-^{14}C] malonyl-CoA. These results are expressed as mean values ± SD of three duplicate experiments. (D) Condensation (●) and elongation (○) were measured as described in B but with an incubation time of 30 min and in the presence of increasing concentrations of oleoyl-CoA. These results are expressed as mean values ± SD of four duplicate experiments.

enzyme source. The control activity was determined using 20:0-CoA as substrate. VLCFA synthesis from 3-OH-20:0-CoA and (*E*) 2,3-20:1-CoA were 0.35 ± 0.07 and 0.37 ± 0.04 nmol/mg/h, respectively, and represented, respectively, 85 and 90% of that using 20:0-CoA as substrate (0.41± 0.03 nmol/mg/h; all results expresed as mean value ± SD of three duplicate experiments). Analysis of the reaction products showed that, irrespective of the nature of the substrate used, the label was exclusively associated with very long chain acyl-CoAs (data not shown). The absence of accumulation of intermediate products indicated that 3-OH-20:0-CoA and (*E*) 2,3-20:1-CoA entered the elongation cycle at their enzymatic sites, the dehydratase and second reductase, respectively. These intermediates were subsequently dehydrated and/or reduced during a first elongation before being condensed with [2-^{14}C]malonyl-CoA during a complete second elongation cycle (5). In good agreement with rapeseed oil composition and Figure 1A, 18:1-CoA led to the highest elongation activity (1.48 ± 0.18 nmol/mg/h).

Characterization of the 3-hydroxyacyl-CoA dehydratase. Since it was demonstrated in leek that the 3-hydroxy eicosanoyl-CoA dehydratase had a marked preference for the (*R*) 3-OH-20:0-CoA and that the inactive isomer was not inhibitory (11), dehydratase activity present in the F15 fraction was measured using the chemically synthesized [1-^{14}C] (*R,S*) 3-hydroxy-20:0-CoA. Dehydration activity was studied as a

function of the amount of protein from F15 (Fig. 2A). In the presence of 75 µM Triton, dehydration was maximal with 25 µg protein, whereas in the absence of detergent, no plateau was reached even in the presence of 90 µg protein. Time-course experiments showed that dehydration increased linearly for 15 min with a velocity of 0.45 nmol/mg/min in the presence of 75 µM Triton X-100. In the absence of detergent, dehydration velocity was only 0.05 nmol/mg/min (Fig. 2B). Altogether, these results showed that the presence of detergent induced a ninefold increase in the dehydratase activity, and it is required for maximal activity. As the dehydratase was shown to be deeply embedded within the membrane (21), it was hypothesized that Triton-X100 could improve the access of the substrate to the catalytic site.

Purification of the acyl-CoA elongase. The solubilization step allowed the recovery of 50% of the membrane proteins, while the 18:1-CoA elongation specific activity was nearly doubled and the dehydratase activity in FS was about one-fifth that in F15 (Table 1). Whereas untreated membrane synthesized mainly straight-chain acyl-CoAs, FS was unable to complete elongating cycles, and intermediates normally absent from the reaction mixture accumulated (about 80% of the total label, Table 2). In FS, 3-hydroxyacyl-CoAs were the major products of the reaction (Table 2), an observation that is in good agreement with the low dehydratase activity (Table 1).

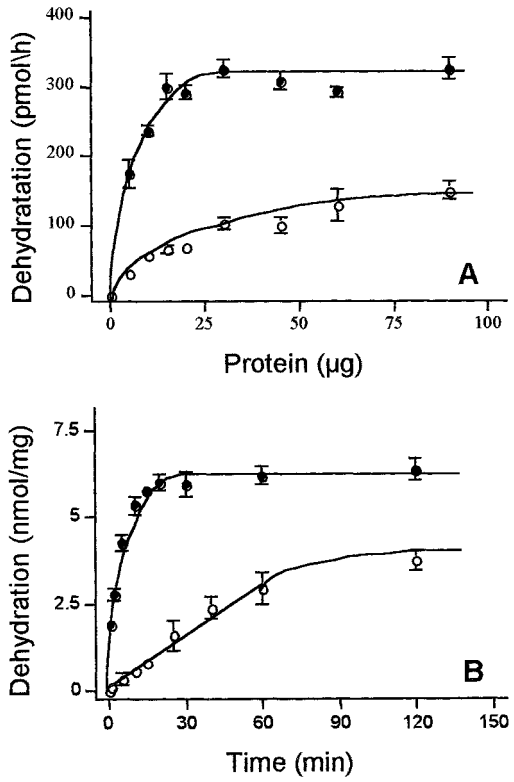

FIG. 2. Effect of Triton X-100 on dehydratase activity. (A) Dehydratase activity was measured by incubating at 30°C for 1 h different amounts of proteins from fraction F15 in the presence of 11.5 µM (*R/S*) [1-^{14}C] 3-hydroxyeicosanoyl-CoA (52 Ci/mol), 1 mM $MgCl_2$, and 2 mM DTT in a final volume of 100 µL 0.08 M HEPES (pH 7.2) buffer containing (●) or not containing (○) 75 µM Triton X-100. The fatty acids were extracted and dehydration was estimated as reported in the Experimental Procedures section. (B) Dehydratase activity was measured as in panel A but in the presence of 50 µg of proteins from F15 and over various incubation times in the presence (●) or absence (○) of 75 µM Triton X-100. Results in A and B are expressed as mean values ± SD of three duplicate experiments.

The best purification yields were obtained using the three successive chromatographic steps reported in Figure 3. FS was first subjected to affinity chromatography using a palmitoyl-CoA agarose column (Fig. 3A). Nonretained fractions contained high amounts of lipids and Triton X-100, but no elongation activity. Although some dehydratase activity was recovered in the nonretained fractions, 60% of the total activity was associated with the proteins bound to the palmitoyl-CoA agarose. These retained proteins were eluted as a single peak using a 0–1 M NaCl gradient. As shown in Figure 3A, the fractions constituting this peak contained both dehydratase and elongase activities, and they were accordingly pooled (fraction C16). Further analysis showed that this fraction contained a low lipid amount, as the lipid-to-protein ratio was four times lower in C16 than in FS (Table 2). 3-Hydroxyacyl-CoA dehydratase activity was increased threefold. This stimulation was probably due to the elimination of the excess of Triton X-100 present in FS. On the other hand, the elongase activity of N16 was one-tenth that of FS. In the presence of additional lipids, acyl-CoA elongation was stimulated threefold (Table 1), thereby demonstrating the importance of the lipid environment for these membrane-bound enzymes. Whereas straight chain acyl-CoA represented only 20% of the products synthesized in FS, they accounted for 96% in N16, in good agreement with the dehydratase activity being four times higher in N16 than in FS (Tables 1 and 2).

Figure 3B shows the elution profile obtained when N16 was loaded on a Sephacryl S300 column. The elongation and dehydration activities coeluted just after the void volume (fraction S300), indicating that the acyl-CoA elongase complex had an apparent molecular mass of 700 kDa in the presence of 0.02% (wt/vol) Triton X-100. This estimation is in good agreement with the presence of the entire elongating complex but should be taken with care, since the presence of Triton X-100 could introduce mis-estimations of molecular masses using gel filtration chromatography (22). This chromatographic step eliminated more than 90% of the proteins of N16 and lowered the lipid content. The lipid per protein ratio was one-third that of F15 (Table 2). The elongation (in the presence of lipids) and dehydration activities were increased respectively, by 12 and 3 times (Table 1). Surprisingly, 3-hydroxyacyl-CoAs accumulated although the 3-hydroxyacyl-CoA dehydratase activity was high.

The last step was a anion exchange chromatography (Fig. 3C). By using a 1 M NaCl concentration step, both activities eluted in a single peak, corresponding to the partially purified acyl-CoA elongase (fraction Q-Seph). When Q-Seph was analyzed for its lipid content, no lipid was detected (Table 2). Assuming that we were able to detect a minimum of 0.1 µg of lipid (23) and that the phospholipids-to-protein ratio was

TABLE 1
Purification of Acyl-CoA Elongase[a]

Fraction	Proteins (mg)	3-Hydroxy-acyl-CoA dehydratase (nmol/mg/h)	18:1-CoA elongase (nmol/mg/h)		Purification factor
			Control	+ Lipids (% stimulation)	
F15	142	5.01	0.46	0.67 (145)	1.0
FS	72	1.07	1.04	1.50 (144)	2.2
C16	13.9	4.25	0.09	0.26 (284)	0.4
S300	0.75	12.48	0.51	3.24 (635)	4.8
Q-Seph	0.35	3.19	0.38	3.39 (893)	5.0

[a]Protein contents were estimated using Bradford's method (Ref. 14) with bovine serum albumin as standard. The enzymatic activities were measured using 50 µL of each fraction as described in the Experimental Procedures section. The purification factor was calculated using the 18:1-CoA elongase activity in the presence of lipids.

0.27 in F15, the lipid-to-partially purified enzyme ratio could be estimated to be 0.0017. This value is at least 160-fold lower than that measured in the native membranes. Whereas neutral lipids were predominant in the F15, the phospholipid content increased during the purification process (Table 2). These results suggest that only the phospholipids strongly associated with the proteins remained after the final step. When compared to F15, the Q-Seph fraction contained 0.25% of the proteins, its elongation activity was five times higher, and its dehydratase activity was about 37% lower (Table 1). 3-Hydroxyacyl-CoAs were the major reaction products of the Q-Seph fraction, but the presence of 9% straight-chain acyl-CoAs [saturated acyl-CoAs and (*E*) 2,3-acyl-CoAs, Table 2] indicated that the partially purified fraction was able to catalyze at least the first three intermediate reactions of 18:1-CoA elongation. During each chromatographic step involved in the purification process, both elongase (condensing enzyme) and dehydratase activities co-eluted, suggesting that the 3-hydroxy dehydratase is one of the components of the partially purified oleoyl-CoA elongase.

SDS-PAGE analysis. Figure 4 shows the evolution of the protein composition of the different fractions during the purification procedure. The first chromatographic step eliminated the storage proteins (cruciferins and napins) which were present in F15 and FS (Fig. 4). The next ones led to an enrichment in four major polypeptide bands, whose apparent molecular masses were 56, 59, 61, and 63 kDa. Similar results were obtained in previous studies (6,15), and these results are compatible with the estimated molecular masses of the dehydratase (24) and of the 3-ketoacyl-CoA synthases (9,25,26). As a 700 kDa molecular mass was estimated for the entire elongating complex by filtration chromatography, it seems reasonable to suggest that the oleoyl-CoA from rapeseed is a multienzymatic complex composed of four different proteins. Each of the four polypeptide bands visualized after SDS-PAGE could correspond to one of the four enzyme activities that participate in the elongating process.

By assuming the latter hypothesis, SDS-PAGE analysis shows a higher purification factor as reported in Table 1. This discrepancy could be related to the presence of 91% 3-hydroxyacyl-CoA in the products synthesized by the purified fraction (Table 2). These products would inhibit the condensing enzyme and enable the elongase to complete its full cycle.

In summary, we have demonstrated that the acyl-CoA elongase from rapeseed is a multienzymatic complex and have characterized two of its constituents, the 3-ketoacyl-CoA synthase and the 3-hydroxyacyl-CoA dehydratase.

TABLE 2
Lipid Content and Elongation Products of Different Fractions Obtained During Purification Procedure[a]

Fractions	Lipid-to-protein ratio (a.u.)	Phospholipid content (%)	Elongation products		
			Straight-chain acyl-CoAs	3-Hydroxy-acyl-CoAs	3-Keto-acyl-CoAs
F15	1.00	19 ± 7	82	12	4
FS	1.77	25 ± 8	20	45	35
C16	0.42	33 ± 9	96	0	4
S300	0.32	55 ± 9	22	48	30
Q-Seph	ND	ND	9	91	0

[a]Lipids were extracted and analyzed as reported in the Experimental Procedures section. The lipid-to-protein ratio of F15 was normalized to 1. Elongation activities were assayed using 50 µL of each fraction, and the products were separated by thin-layer chromatography according to the Experimental Procedures section. ND, not detected; a.u., arbitrary units.

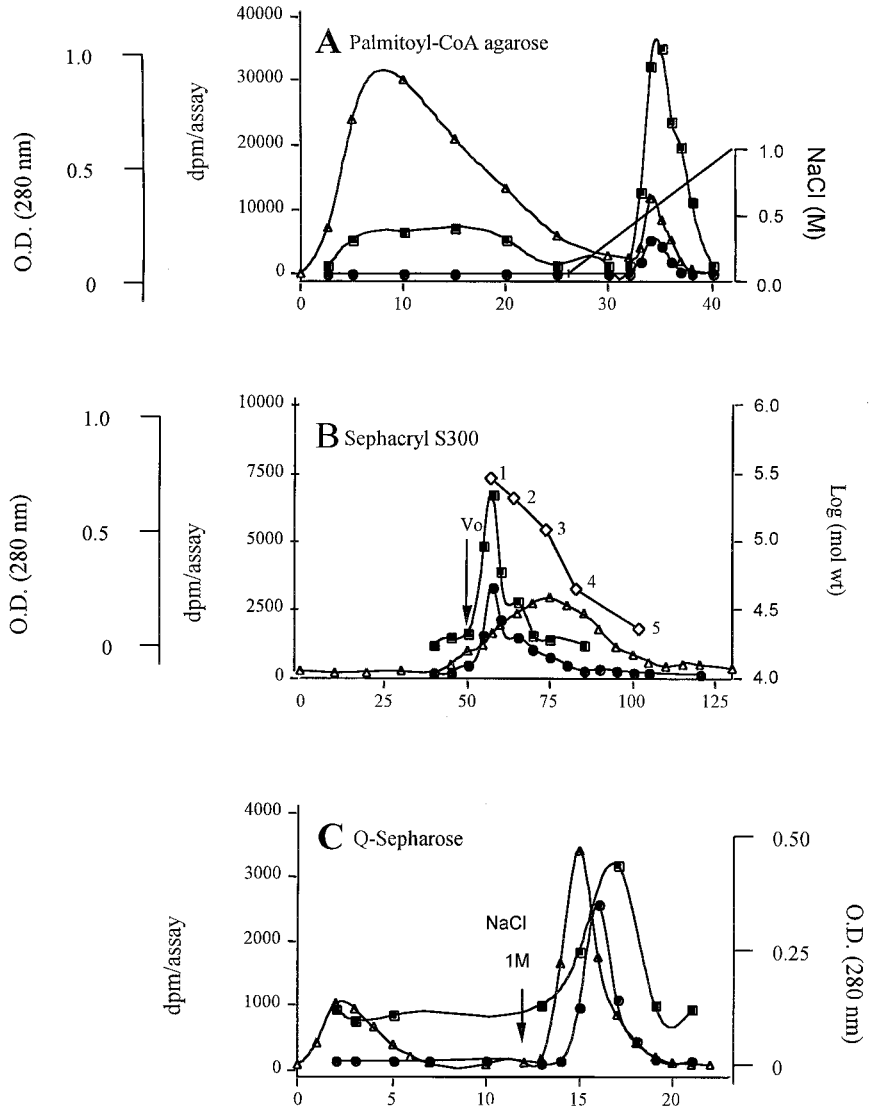

FIG. 3. Purification of acyl-CoA elongase. Symbols: (△) optical density (O.D.) (280nm), (●) elongation (dpm/assay), (■) dehydration (dpm/assay). (A) Palmitoyl-CoA agarose chromatography: Solubilized proteins (fraction FS) were applied on a palmitoyl-CoA agarose column previously equilibrated with a 0.08 M HEPES (pH 7.0) buffer containing Triton X-100 (0.02%, vol/vol), β-mercaptoethanol (10 mM), and ethylenglycol (10%, vol/vol). After washing with equilibration buffer, the elongation activity was eluted with a 0–2 M NaCl gradient in the same buffer. (B) Sephacryl S300 chromatography: Fractions eluted from the first column presenting the highest elongating activities were pooled (C16) and applied to a Sephacryl S300 column preequilibrated with the same buffer and using a 0.25 mL/min flow rate. Diamonds (◇) represent the molecular mass standards (mol wt): 1, thyroglobulin (670 kD); 2, ferritin (440 kD); 3, catalase (232 kD); 4, bovine serum albumin (66 kD); 5, α-chymotrypsinogen (28 kD). V_0 = void volume. (C) Q-Sepharose chromatography. Fractions eluted from the Sephacryl S300 column presenting the highest elongation activities were pooled (S300) and applied to a Q-Sepharose column that had been equilibrated with the same buffer. The column was washed and the activity eluted with a 1 M NaCl concentration step in the same buffer. The fractions having the highest activities were pooled and considered as the partially purified fraction (Q-Seph). Usually, elongation and dehydration activities were assayed using 50 µL of each fraction and according to the conditions described in the Experimental Procedures section.

ACKNOWLEDGMENTS

This work was conducted within the ECODEV-CNRS program and was supported by MESR, ONIDOL, RUSTICA, and SERASEM. The help of the Conseil Régional d'Aquitaine is gratefully acknowledged.

REFERENCES

1. Ohlrogge J.B. (1994) Design of New Plant Products: Engineering of Fatty Acid Metabolism, *Plant Physiol. 104*, 821–826.
2. Lassner M.W., Levering, C.K., Davies, M., and Knutzon, D.S. (1995) Lysophosphatidic Acid Acyltransferase from Meadow-

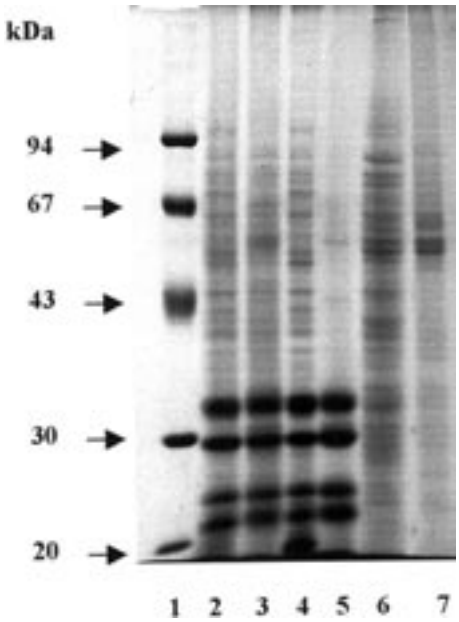

FIG. 4. Sodium dodecyl sulfate-polyacrylamide gel electrophoretic analysis of the different fractions obtained during the purification protocol. Proteins were resolved on a 10% gel and stained with Coomassie blue. Lane 1, molecular weight markers; lane 2, F15; lane 3, FS; lane 4, oil body fraction; lane 5, unretained proteins on C_{16}-CoA agarose column; lane 6, N16; lane 7, Q-Seph (partially purified acyl-CoA elongase).

foam Mediates Insertion of Erucic Acid at the *sn*-2 Position of Triacylglycerol in Transgenic Rapeseed Oil, *Plant Physiol. 109*, 1389–1394 .
3. Cassagne C., Lessire, R., Bessoule, J.J., Moreau, P., Créach, A., Schneider, F., and Sturbois, B. (1994) Biosynthesis of Very Long Chain Fatty Acids in Higher Plants, *Prog. Lipid Res. 33*, 55–69.
4. Fehling, G., and Mukherjee, K.D. (1991) Acyl-CoA Elongase from Higher Plant (*Lunaria annua*). Metabolic Intermediates of Very Long Chain Acyl-CoA Products and Substrate Specificity, *Biochim. Biophys. Acta 1082*, 239–247.
5. Lessire, R., Domergue, F., Spinner, C., Lucet-Levannier, K., Lellouche, J.P., Mioskowski, C., and Cassagne, C. (1998) Dehydration of 3-Hydroxy Icosanoyl-CoA and Reduction of (*E*) 2,3 Icosenoyl-CoA Are Required for Elongation by Leek Microsomal Elongase(s), *Plant. Physiol. Biochem. (Paris) 36*, 205–211.
6. Fehling E., Lessire, R., Cassagne, C., and Mukherjee, K.D. (1992) Solubilization and Partial Purification of Constituents of Acyl-CoA Elongase from *Lunaria annua*, *Biochim. Biophys. Acta 1126*, 88–94.
7. Lardans A., and Trémolière, A. (1992) Fatty Acid Elongation Activities in Subcellular Fractions of Developing Seeds of *Limnanthes alba*, *Phytochemistry 31*, 121–127.
8. Créach, A., and Lessire, R. (1993) Solubilization of Acyl-CoA Elongases from Developing Rapeseed (*Brassica napus* L.), *J. Am. Oil. Chem. Soc. 70*, 1129–1133.
9. Lassner, M.W., Lardizabal, K., and Metz, J.G. (1996) A Jojoba β-Ketoacyl-CoA Synthase cDNA Complements the Canola Fatty Acid Elongation Mutation in Transgenic Plants, *Plant Cell 8*, 281–292.
10. Créach A., Domergue, F., and Lessire, R. (1995) Study of the Partially Purified C18:1-CoA Elongase from Developing Rapeseeds (*Brassica napus* L.), in *Plant Lipid Metabolism*, (Kader, J.-C., and Mazliak, P., eds.), Kluwer Academic Publishers, pp. 121–123, Dordrecht, The Netherlands.
11. Lessire, R., Chevalier, S., Lucet-Levannier, K., Lellouche, J.P., Mioskowski, C., and Cassagne, C. (1999) Study of 3-Hydroxy Eicosanoyl-coenzyme A Dehydratase and (*E*)-2,3 Enoyl-coenzyme A Reductase in Acyl-Coenzyme A Elongation in Etiolated Leek Seedlings, *Plant Physiol. 119*, 1009–1015.
12. Schneider F., Lessire, R., Bessoule, J.J., Juguelin, H., and Cassagne, C. (1993) Effect of Cerulenin on the Synthesis of Very Long Chain Fatty Acids in Microsomes from Leek Seedlings, *Biochim. Biophys. Acta 1152*, 243–252.
13. Agrawal, V.P., and Stumpf, P.K. (1985) Elongation Systems Involved in the Biosynthesis of Erucic Acid from Oleic Acid in Developing *Brassica juncea* Seeds, *Lipids 20*, 361–366.
14. Bradford, M.M. (1976) A Rapid Sensitive Method for the Quantitation of Microgram Quantities of Protein Utilizing the Principle of Protein–Dye Binding, *Analytical Biochem. 72*, 248–254.
15. Bessoule, J.J., Lessire, R., and Cassagne, C. (1989) Partial Purification of the Acyl-CoA Elongase of *Allium porrum* Leaves, *Arch. Biochem. Biophys. 268*, 475–484.
16. Laemmli, U.K. (1970) Cleavage of Structural Proteins During the Assembly of the Head of Bacteriophage T4, *Nature 227*, 680–685 .
17. Macala, L.J., Yu, R.K., and Ando, S. (1983) Analysis of Brain Lipids by High-Performance Thin-Layer Chromatography and Densitometry, *J. Lipids Res. 24*, 1243–1250.
18. Millar, A.A., and Kunst, L. (1997) Very Long Chain Fatty Acid Biosynthesis Is Controlled Through the Expression and Specificity of the Condensing Enzyme, *Plant J. 12*, 121–131.
19. Bessoule, J.J., Lessire, R., and Cassagne, C. (1989) Theoretical Analysis of the Activity of Membrane-Bound Enzymes Using Amphiphilic or Hydrophobic Substrates. Application to the Acyl-CoA Elongases from *Allium porrum* Cells and to Their Purification, *Biochim. Biophys. Acta 983*, 35–41.
20. Winter, E., Brummel, M., Schuch, R., and Spener, F. (1997) Decarboxylation of Malonyl-(acyl carrier protein) by 3-Oxoacyl-(acyl carrier protein) Synthases in Plant Fatty Acid Biosynthesis, *Biochem. J. 321*, 313–318.
21. Osei, P., Suneja, S.K., Laguna, J.C., Nagi, M.N., Cook, L., Prasad, M.R., and Cinti, D.L. (1989) Topography of Rat Hepatic Microsomal Enzymatic Components of the Fatty Acid Chain Elongation System, *J. Biol. Chem. 264*, 6844–6849.
22. Laue, T.M., and Rhodes, D.G. (1990) Determination of Size, Molecular Weight, and Presence of Subunits, *Methods Enzymol. 182*, 566–587.
23. Heape, A.N., Juguelin, H., Boiron, F., and Cassagne, C. (1985) Improved One-Dimensional Thin-Layer Chromatographic Technique for Polar Lipids, *J. Chromatogr. 322*, 391–395.
24. Lessire, R., Bessoule, J.J., Cook, L., Cinti, D.L., and Cassagne, C. (1993) Occurrence and Characterization of a Dehydratase Enzyme in the Leek Icosanoyl-CoA Synthase Complex, *Biochim. Biophy. Acta 1169*, 243–249.
25. James, D.W., Lim, E., Keller, J., Plooy, I., Ralston, E., and Donner, H.K. (1995) Directed Tagging of the *Arabidopsis* Fatty Acid Elongation (FAE1) Gene with the Maize Transposon Activator, *Plant Cell 7*, 309–319.
26. Barret, P., Delourme, R., Renard, M., Domergue, F., Lessire, R., Delseny, M., and Roscoe, T.J. (1997) The Rapeseed *FAE1* Gene Is Linked to the E1 Locus Associated with Variation in the Content of Erucic Acid, *Theor. Appl. Genet. 96*, 177–186.

[Received December 9, 1999, and in revised form March 27, 2000; revision accepted April 6, 2000]

Purification and Biochemical Characterization of a Novel Thermostable Lipase from *Aspergillus niger*

Variketta M. Haridasan Namboodiri[1] and Rajagopal Chattopadhyaya*

Department of Biochemistry, Bose Institute, Calcutta 700054, India

ABSTRACT: An extracellular 1,3-specific lipase with molecular weight of 35.5 kDa and an isoelectric point of 4.4 from *Aspergillus niger* has been purified 50-fold by pH precipitation followed by a series of chromatographic steps with an overall yield of 10%. The enzyme was homogeneous as judged by denaturing polyacrylamide gel electrophoresis and size-exclusion fast-performance liquid chromatography. It contained 2.8% sugar which was completely removed by endoglycosidase F treatment, and the deglycosylated enzyme retained full activity. The native lipase showed optimal activity between temperatures 35 and 55°C and pH 5.0 and 6.0. The amino acid composition and the N-terminal sequence were found to be different from lipases previously purified from *A. niger*. The enzyme was resistant to trypsin, chymotrypsin, endoprotease Glu-C, thrombin, and papain under native conditions but was susceptible to cleavage by the same proteases when heat-denatured.

Paper no. L8402 in *Lipids 35*, 495–502 (May 2000).

Lipases or triacylglycerol acylhydrolases (EC 3.1.1.3) are hydrolytic enzymes that catalyze reversibly the cleavage of ester bonds of triglycerides. Lipases are unique serine esterases whose catalytic activity is greatly enhanced at the lipid–water interface, a phenomenon known as "interfacial activation" (1–3). Lipases are widely distributed in animals, plants, and microorganisms (4,5). In particular, extracellular microbial lipases are regarded as important because of their potential use in biotechnology (6). Microbial lipases have been isolated, purified, and biochemically characterized from a variety of sources (5). The enzymes differ in their molecular weights, pH optima, pH and thermal stability, isoelectric points, and other biochemical properties (4,5,7).

Previous studies on the purification and biochemical characterization of fungal lipases showed one enzyme per organism (8–11). However, it was shown later that the same microbial species can secrete more than one lipase having different properties (5).

*To whom correspondence should be addressed at Department of Biochemistry, Bose Institute, P-1/12 CIT Scheme VII M, Calcutta 700054, India. E-mail: raja@boseinst.ernet.in.

[1]Present address: Department of Biophysics, Boston University School of Medicine, 700 Albany St., Boston, MA 02118-2526.

Abbreviations: BSA, bovine serum albumin; DMSO, dimethylsulfoxide; FPLC, fast-performance liquid chromatography; HPLC, high-performance liquid chromatography; PAS, periodate Schiff's stain; PITC, phenylisothiocyanate; PMSF, phenylmethylsulfonylfluoride; SDS-PAGE, polyacrylamide gel electrophoresis in sodium dodecyl sulfate; TCA, trichloroacetic acid; TLC, thin-layer chromatography.

The structures of many triacylglycerol lipases were determined by X-ray crystallography (12). All of them were found to have a similar molecular architecture with a central β-sheet and a catalytic triad consisting of serine, histidine, and a carboxylate group reminiscent of serine proteases (13).

As early as 1963, Fukumoto *et al.* reported the purification and partial characterization of a lipase from *Aspergillus niger* (9). However, its molecular weight was not reported. Tombs and Blake (14) published the purification of another lipase from a crude *Aspergillus* media concentrate obtained from commercial sources. Its molecular weight was found to be 47.8 kDa which on boiling fell to 33.8 kDa. Höfelmann (15) reported the purification of two lipases from *A. niger* with molecular weights of 31 and 19 kDa, respectively. Sugihara *et al.* (16) later reported in brief the purification of the same enzyme from the same source with a molecular weight of 35 kDa. Another acid-resistant *A. niger* lipase was reported (17) from a crude commercial preparation and was shown to be similar in biochemical properties to Sugihara's lipase.

Aspergillus niger lipase is being successfully used in traditional areas of food industry (6). Lipases with more stability and requiring improved reaction conditions for various chemical processes are required (6). Here we report the purification and characterization of a thermostable lipase from *A. niger* which was compared with previously reported lipases from the same fungus and was found to be different from them.

MATERIALS AND METHODS

Materials. The *A. niger* strain was a kind gift from Hindustan Lever Research Centre (Bombay, India). Phenyl agarose, Sephadex G75, Sephacryl HR100, corn steep liquor, protein markers, dialysis tubing, *N*, *N*, *N*′, N′-tetramethylene diamine, β-mercaptoethanol, phenylmethylsulfonylfluoride (PMSF), Coomassie brilliant blue G250, proteases, agar, ammonium persulfate, phenylisothiocyanate (PITC), triolein, 1,3-diglyceride, diolein (85% 1,3-isomer and 15% 1,2-isomer), monoolein, and sodium metabisulfite were obtained from Sigma Chemical Company (St. Louis, MO). Isoelectric focusing markers were obtained from Beckman (Fullerton, CA). The plates for thin-layer chromatography (TLC) (Kieselgel 60 WF_{254}s) were obtained from E. Merck (Darmstadt, Germany). Silver nitrate, gum acacia, isooctane, rho-

damine B, cupric acetate, calcium chloride, disodium hydrogen phosphate, magnesium sulfate, glycine, sodium dodecyl sulfate, ammonium sulfate, basic fuchsin, periodic acid, trifluoroacetic acid, trichloroacetic acid (TCA), dimethylsulfoxide (DMSO), EDTA, petroleum ether, diethyl ether, acetic acid, and 1,10-phenanthroline monohydrate were obtained from E. Merck (Calcutta, India) Ltd. Tris base, acrylamide, *N,N*-methylenebisacrylamide were obtained from Spectrochem Pvt. Ltd., (Bombay, India). Olive oil was purchased from commercial sources. Hydroxyapatite was prepared in the laboratory as described in Reference 18.

Isolation and purification. The *A. niger* strain was grown in a medium containing 0.1% $CaCl_2$, 0.1% Na_2HPO_4, 0.1% $MgSO_4$, 0.3% $NaNO_3$, 0.5% corn steep liquor, 3.0% olive oil, and 1.0% gum acacia. The pH of the medium was adjusted to 6.5 and the culture grown at 37°C for 48 h on a rotary shaker. The oil was homogenized by sonication at 300 W for 3 min. A 40-mL preculture grown for 24 h at 37°C was used to inoculate a 400-mL culture. Two liters of the media were distributed into five 1-L flasks and the cultures grown on a rotary shaker. After 48 h the cells were separated by cheesecloth filtration and the supernatant raised to pH 7.5 with 1 M NaOH. It was centrifuged at 18,000 × *g* for 20 min at 4°C and the precipitate discarded. The salt concentration of the resulting supernatant was raised to 2 M with solid $(NH_4)_2SO_4$ and charged into a phenyl agarose column (1.0 × 12.0 cm) equilibrated with 2 M $(NH_4)_2SO_4$ containing 5 mM phosphate buffer (pH 6.0). After washing the column with 300 mL of the same buffer, the bound proteins were eluted with 60 mL each of 1.9, 1.8, 1.7, 1.6, 1.5, 1.4, and 1.3 M $(NH_4)_2SO_4$. Finally, the column was eluted with 500 mL of 5 mM phosphate buffer. The final fraction was dialyzed overnight against 1 mM phosphate buffer (pH 6.0) and then loaded onto a hydroxyapatite column (1.0 × 9.0 cm) equilibrated with 1 mM phosphate buffer (pH 6.0). After washing with the same buffer, the bound proteins were eluted with 400 mL of 60 mM phosphate buffer. The eluant was concentrated roughly 50-fold in a rotary evaporator, dialyzed against water, then further concentrated to 2 mL and subsequently loaded on a Sephadex G75 column (45.0 × 1.5 cm) equilibrated with 25 mM acetate buffer (pH 5.6) at a flow rate of 12 mL/h. Active lipase fractions were pooled, concentrated, and loaded into a Sephacryl HR100 column (45.0 × 2.5 cm) equilibrated with 5 mM acetate buffer (pH 5.6) at a flow rate of 30 mL/h to get the pure lipase. All steps were performed in a 4°C cold room.

Measurement of lipase activity. Lipase activity was measured following two different assays. (i) Spectrophotometric assay: Lipase activity was measured spectrophotometrically by observing the color developed due to the liberated free fatty acids using copper acetate pyridine as the color-developing reagent (19). One unit of enzyme activity was defined as 1 μM of fatty acid liberated per minute. All assays were done by incubating the enzyme substrate mixture at 37°C for 30 min. Olive oil was used as the substrate, and the quantitation was done with a standard oleic acid curve. (ii) Plate assay: Qualitative assay to detect lipase during purification was done with rhodamine B agar diffusion assay with olive oil as the substrate (20) using 0.1% $CaCl_2$ instead of NaCl. Wells were filled with aliquots from fractions examined and incubated at 37°C. Orange fluorescence could be observed in lipase-containing fractions within 30 to 60 min under ultraviolet light.

Protein estimation. The dye-binding method of Bradford (21) was used to estimate the protein concentration. Bovine serum albumin (BSA) was used as the standard.

Polyacrylamide gel electrophoresis in sodium dodecyl sulfate (SDS-PAGE). All PAGE was performed with a Sigma mini gel apparatus (80 × 100 mm). A 12% SDS-PAGE (1.0 mm thickness) was performed as described by Laemmli (22). The molecular weight of the lipase was determined from the mobilities of known protein markers (Dalton Mark VII-L; Sigma). Nondenaturing electrophoresis was carried out with 12% gels with Tris-glycine buffer (pH 7.5). All the gels were silver-stained (23).

Isoelectric focusing. Isoelectric focusing was carried out on slab gels (80 × 100 mm) at 4°C with 5% polyacrylamide containing 2% Biolyte (3/10 ampholytes) according to the manufacturer's instructions (Bio-Rad Laboratories, Hercules, CA). RNase (pI 9.65), carbonic anhydrase (pI 5.90), and α-lactoglobulin (pI 5.10) were used as standards. Before loading the samples, prefocusing was done at 100 V for 30 min. The sample (25 μg) in each of two lanes and the standards were loaded in different lanes of the gel. Focusing was then carried out in a stepped fashion (200 V for 1 h, 300 V for 1 h, and then finally 400 V for 16 h). The portion of the gel excepting one extreme sample lane was washed with 20% TCA and then silver-stained. To check whether the band was that of lipase, the remaining gel portion was excised at the position corresponding to the lipase in the stained gel and placed on rhodamine B plates overnight for orange fluorescence.

Amino acid analysis. The purified lipase was extensively dialyzed against water before amino acid analysis. Of the sample, 25 μg was hydrolyzed with 6 N HCl for 24 h at 110°C in a nitrogen atmosphere followed by derivatization with PITC and run through a Pico-Tag high-performance liquid chromatography (HPLC) column (amino acid analysis system; Millipore Corporation, Waters Chromatographic Division, Bedford, MA) according to the manufacturer's instructions. Peaks were identified by comparing the retention times with those of known standards obtained from Sigma Chemicals.

N-Terminal sequence analysis. Of the purified lipase, 88 pmol was loaded on a biobrene-equilibrated glass fiber disk and N-terminal sequence analysis performed by automated Edman degradation using instrumentation, reagents, and protocols from Perkin Elmer (Rotkreuz, Switzerland). A model 476A gas phase sequencer equipped with an online 120A PTH analyzer and a 610A control/data analysis module was employed.

Molecular weight and Stokes' radius by size-exclusion fast-performance liquid chromatography (FPLC). The molecular weight and Stokes' radius of the native enzyme were determined by size-exclusion FPLC using a Superose 12 col-

umn (30.0 × 1.0 cm) obtained from Pharmacia Biotech (Uppsala, Sweden). The elution was carried out with 25 mM acetate buffer (pH 5.6) at a flow rate of 60 mL/h. BSA (66 kDa), egg ovalbumin (42.7 kDa), β-lactoglobulin (36.8 kDa), carbonic anhydrase (29 kDa), and bovine α-lactalbumin (14 kDa) were used as standards. Blue dextran and tryptophan were used to determine V_o, the void volume, and V_t, the total volume, respectively. The distribution coefficient K_d was calculated for each protein and was plotted against logarithm of molecular weight. From the plot, the molecular weight of the unknown lipase was determined. The Stokes' radius was also determined with the help of a calibration plot of $1000/V_e$ against the Stokes' radius of the standards (BSA: 33.9 Å, ovalbumin: 28.7 Å, carbonic anhydrase: 24.4 Å, and bovine α-lactalbumin: 20.4 Å), V_e being the measured elution volume for each protein.

Temperature and pH effects on lipase activity. The optimal temperature for activity was determined quantitatively after incubating the enzyme substrate mixture at temperatures ranging from 20 to 75°C for 30 min. Residual activity was calculated by taking the activity at 37°C as 100%. In a second set of experiments, the temperature stability was determined by preincubating the enzyme for 60 min at temperatures ranging between 20 and 75°C and then measuring the remaining activity at 37°C after adding the substrate. Residual activity was calculated by taking the activity at 37°C as 100%.

The optimal pH for enzyme activity was measured by incubating the enzyme substrate mixture at pH values ranging from 3.0 to 9.5 for 30 min at 37°C. Residual activity at various pH was calculated by taking the activity at pH 6.0 at 37°C as 100%. In another set of experiments, the pH stability was determined by incubating the enzyme in buffers from pH 3.0 to 10.0 for 60 min at 37°C. Residual activity was expressed by taking the activity at pH 6.0 as 100%. The different buffers used were citrate (pH 3.0), acetate (pH 3.5 to 5.5), phosphate (pH 6.0 to 8.0), Tris (pH 8.5 to 9.0), and glycine-NaOH (pH 9.5 to 10.0).

Effect of various chemicals on lipase activity. The effect of various salts at concentrations ranging from 10 mM to 1.0 M on the enzyme activity was checked. The reaction mixture was incubated at 37°C for 30 min and the residual activity determined quantitatively with respect to a control.

Sugar content analysis. The sugar content was determined by quantification on an SDS gel stained with periodate Schiff's stain (PAS) (24) using a gel documentation system (Gel Doc 1000; Bio-Rad Laboratories). Schiff's reagent was prepared as described in (25). Egg ovalbumin was used as the standard. As an alternative, the purified lipase was treated with endoglycosidase F (*Flavobacterium meningosepticum)* for 24 and 48 h, and the shift in mobility was observed by SDS-PAGE relative to the untreated lipase. The extent of carbohydrate removed was also checked by staining the gel with periodic acid Schiff's reagent.

Positional specificity. To determine the positional specificity of the *A. niger* lipase, the products were analyzed by TLC (26). The substrates, lipid standard [mono-, di-(85% 1,3-isomer and 15% 1,2- isomer) and triglyceride], 1,3-diglyceride (1,3-diolein), diolein (85% 1,3-isomer and 15% 1,2-isomer) and monoolein (1 monooleoyl-*rac*-glycerol) were emulsified by sonication in 0.2 M phosphate buffer (pH 6.0) containing 1% (wt/vol) gum acacia. The enzyme (10 μL of 1.2 mg/mL stock diluted to 50 μL) was added to each substrate emulsion in buffer (450 μL of emulsion prepared at the following concentrations: lipid standard mixture at 100 mg/mL; 1,3-diacylglycerol at 5 mg/mL; diolein at 50 mg/mL; or monoolein at 25 mg/mL) and incubated at 37°C for 30 min. Water was substituted for the enzyme in the respective blanks. All the mixtures were spotted on TLC plates (Kieselgel 60 WF_{254}s; E. Merck) and developed in two solvents, one after the other: solvent 1, petroleum ether/diethyl ether/acetic acid (70:30:1, by vol), and solvent 2: petroleum ether/diethyl ether (95:5, vol/vol). Plates were stained by iodine vapors.

Protease digestion. The action of typsin, chymotrypsin, and endoproteinase Glu-C, type XVII (*Staphylococcus aureus,* strain VB) on the native lipase was checked. The protein was initially dialyzed against 10 mM $NaHCO_3$ buffer (pH 8.7) and then evaporated to dryness. It was redissolved in 0.4 M $NaHCO_3$ (pH 8.7) to a final concentration of 1.6 mg/mL for trypsin and chymotrypsin digestions and 0.4 M acetate (pH 4.7) for endoproteinase Glu-C in an enzyme to substrate ratio of 1:40. The substrate was incubated with the proteases for 4, 8, 16, and 24 h at 37°C. The reaction was stopped by the addition of 30 mM PMSF in DMSO and immediately subjected to 20% SDS-PAGE. Also, the lipase was heat-denatured by boiling for 60 min, cooled, and separately treated with trypsin, chymotrypsin, papain, and thrombin for 24 h at 37°C. The conditions for reaction with papain and thrombin were similar to those for trypsin and chymotrypsin. The papain digest was stopped by adding Koshland reagent [(2-bromoacetamido)-4-nitrobenzene] to a final concentration of 4 mM while the thrombin reaction was terminated by adding PMSF to a final concentration of 3 mM. Fragments were checked on a 15% SDS-PAGE. In yet another experiment, the heat-denatured lipase was separately treated with trypsin, chymotrypsin, papain, thrombin, and endoproteinase Glu-C for 6 h at 37°C, and the fragments were purified on a preparative scale by reverse-phase HPLC on an Econosphere C18 5U column (250 × 4.6 mm; Alltech Associates Inc, Deerfield, IL). The fragments were eluted with solvent A (0.1% TFA in water) and solvent B [acetonitrile/water, 60:40 (vol/vol)] at a flow rate of 0.5 mL/min using the following gradient: 0–5 min: 0% B, 100% A; 5–45 min: 0–45% B; 45–100 min: 45–55% B; 100–145 min: 55–100% B; 145–150 min: 100% B; 150–155 min: 0% B.

RESULTS

Lipase purification. Similar activity was obtained when the fermentation was carried out at 30°C for 72 h or at 37°C for 48 h. Olive oil was used not only as an inducer but also as the major carbon source. No lipase was produced without the oil. The results of the purification protocol are shown in Table 1.

TABLE 1
Purification Table of Lipase

Step	Total activity (units)	Total protein (mg)	Specific activity (units/mg)	Yield (%)	Purification factor
Crude extract	1,200	286	4.2	100	1
pH Precipitation	1,200	156	7.7	100	1.8
Phenyl agarose	700	19.3	36.3	58.3	8.6
Hydroxyapatite	794	14.7	54	66.1	12.8
Sephadex G-75	322	2.17	148.4	26.8	35.3
Sephacryl HR 100	122	0.586	208.2	10.1	49.5

As seen from the table, the first pH precipitation step not only resulted in the removal of about 45% protein but also helped in cleaning up the medium of free fatty acids which formed the corresponding soap with NaOH. The active lipase fraction was eluted from the phenyl agarose column with a 5 mM phosphate buffer (pH 6.0) hold to speed up the elution. For the same reason elution from the hydroxyapatite column was performed with a 60 mM phosphate buffer (pH 6.0) hold instead of a gradient. The activity was found to be stable after the hydroxyapatite step. The final purified protein after Sephacryl HR 100 chromatography was homogeneous, and the elution pattern is shown in Figure 1. The purification process at different stages is shown in Figure 2. A single band was also obtained by gel electrophoresis under nondenaturing conditions (results not shown). The scheme resulted in a 50-fold purification and an overall yield of 10%. The purified lipase gave a band corresponding to 35.5 kDa in SDS-PAGE. Isoelectric focusing gave a pI of 4.4 (Fig. 3). An adjacent lane band when cut and placed on the rhodamine B plate gave an orange fluorescence, confirming that the purified protein is the lipase (results not shown).

Amino acid analysis and N-terminal sequence. The results of the amino acid analysis are shown in Table 2. The acidic amino acids (Asx and Glx) accounted for 27.1% of the total residues, while the hydrophobic residues constituted 29.1%.

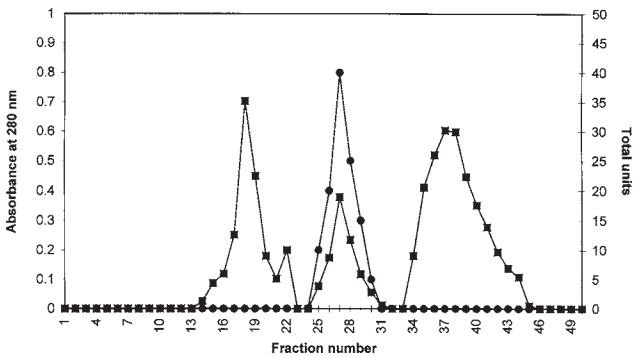

FIG. 1. Elution profile from Sephacryl HR 100. Fractions were assayed for protein content (-■-) and for lipase activity (-●-). Fractions were initially checked for lipase activity by the rhodamine B plate assay. Fractions showing orange fluorescence were then quantitated for lipase activity by the copper acetate pyridine method. Two-milliliter fractions were collected. The void volume was found to be 75 ml.

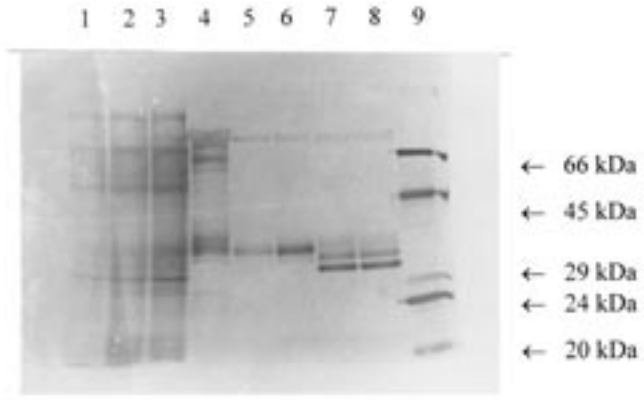

FIG. 2. Sodium dodecylsulfate-polyacrylamide gel electrophoresis (SDS-PAGE) at different stages of purification. The purification at each step was monitored by SDS-PAGE (12.5%) with silver staining. Lane 1: supernatant after pH precipitation, Lane 2: fraction after phenyl agarose chromatography, Lane 3: fraction after hydroxyapatite chromatography, Lane 4: pooled fraction after Sephadex G75 chromatography, Lane 5: purified lipase after Sephacryl HR 100 chromatography, Lane 6: purified lipase (unboiled), Lane 7: purified lipase after glycosidase treatment (24 h), Lane 8: purified lipase after glycosidase treatment (48 h), Lane 9: molecular weight standards.

Glycine residue was also abundant (10.08%). The high percentage of acidic amino acids (Asp and Glu) gives the molecule a net negative charge in conformation with the pI value and is estimated to be greater than 13.59%, the total for the positively charged residues (Arg, Lys, and His). The N-terminal amino acid sequence is given below:

NH_2-Ala-Val-Leu-Asp-Phe-Trp-Leu-Asp-Asn-Leu-
Gln-Leu-Phe-Ala-Gln-Trp-Ala-Ile-Leu-Ala-

Molecular weight and Stokes' radius. The molecular weight of the native lipase by size-exclusion FPLC was calculated to be 35.5 kDa. The Stokes' radius was calculated to be 27 Å.

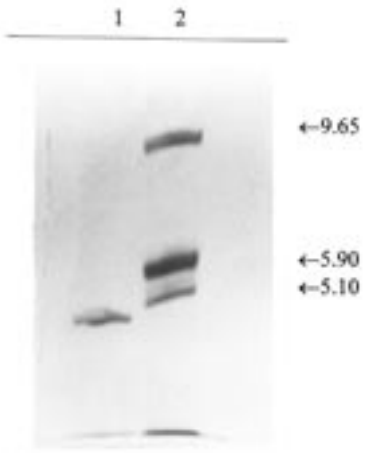

FIG. 3. Isoelectric focusing. Isoelectric focusing was carried out with 5% polyacrylamide containing 2% ampholyte (pH 3.0 to 10.0). The gel was washed with 20% trichloroacetic acid and then silver-stained. Lane 1: purified lipase, Lane 2: pI standards.

TABLE 2
Amino Acid Composition of Lipase

Amino acid	Mole percentage
Asx	8.27
Glx	18.84
Ser	8.00
Gly	10.08
His	2.86
Arg	7.26
Thr	9.00
Ala	3.00
Pro	6.57
Tyr	2.39
Val	5.35
Met	1.96
Cys	0.70
Ile	2.50
Leu	6.16
Phe	3.47
Lys	3.47

*Optimal activity and thermal stability***.** As seen from Figure 4A**,** the optimal activity for lipase was found to be in the temperature range 35 to 55°C. As seen in Figure 4B, the enzyme was stable for 60 min till 50°C beyond which the activity started falling. At 60°C it retained about 50% of the original activity (Fig. 4B).

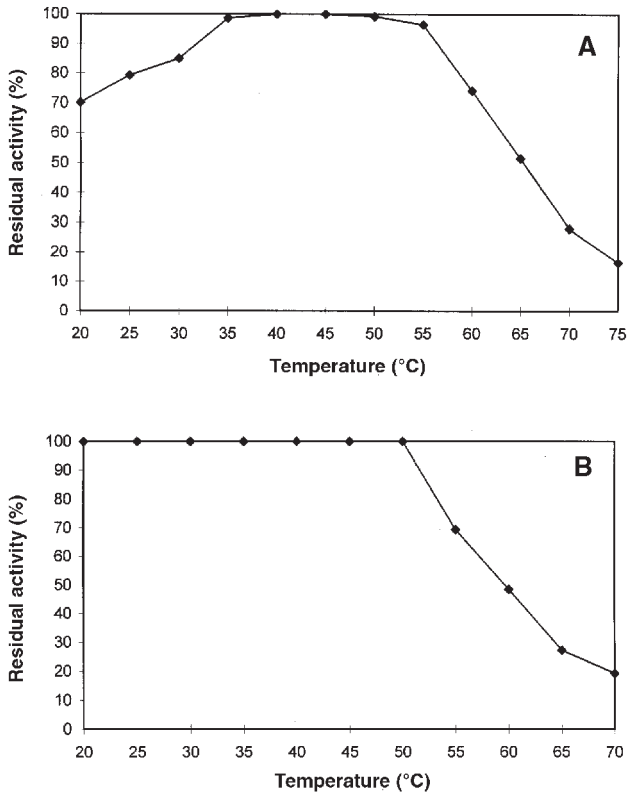

FIG. 4. Thermal activity of purified lipase. The optimal thermal activity and thermal stability of the purified lipase were quantitatively determined. (A) The optimal temperature for activity was measured quantitatively after incubating the enzyme substrate mixture at various temperatures. (B) The thermal stability was determined by incubating the enzyme alone for 60 min at a given temperature and then measuring the residual activity at 37°C. In both the cases the residual activity was calculated by taking the activity at 37°C as 100%.

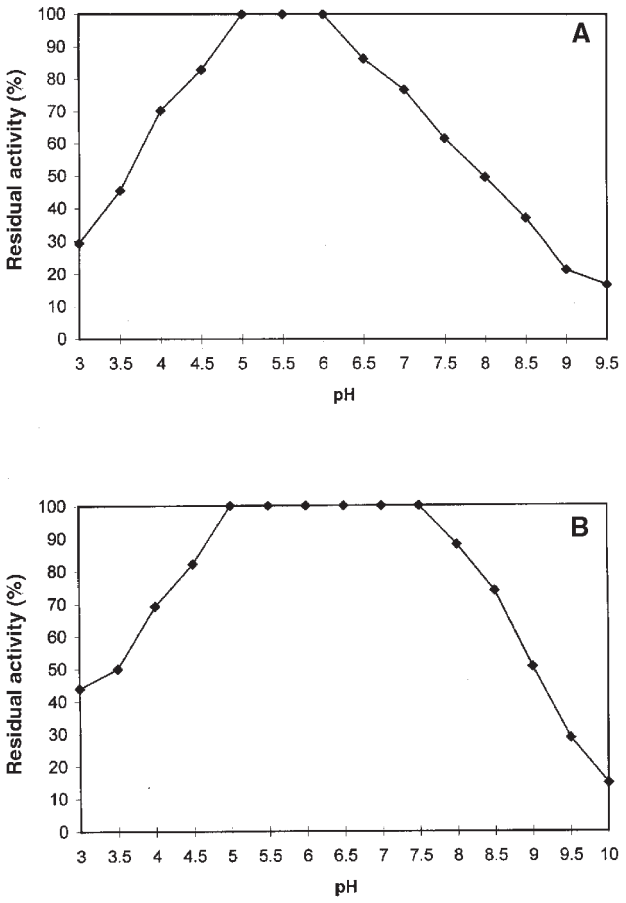

FIG. 5. pH effects of purified lipase. The optimal pH for lipase activity and the pH stability of the purified lipase were determined quantitatively. (A) The optimal pH for enzyme activity was measured by incubating the enzyme substrate mixture at pH ranging from 3.0 to 9.0 for 30 min at 37°C. (B) The pH stability was determined by incubating the enzyme alone in buffers (pH 3.0 to 10.0) for 60 min at 37°C and then by measuring the residual activity. The residual activity were calculated by taking the activity at pH 6.0 as 100%.

Optimal pH and pH stability. The optimal pH for lipase activity was found to be in the range 5.0 to 6.0 in phosphate buffer (Fig. 5A). As seen from Figure 5B, the enzyme was active in the pH range 5.0 to 7.5. Below pH 5.0 and above pH 7.5, there was a gradual loss in activity. (Fig. 5B).

Effect of various salts. Lipase activity was not found to be affected by Mg^{2+}, K^{+}, Na^{+}, Ca^{2+}, Mn^{2+}, NH_4^{+}, and Zn^{2+} up to 1.0 M, whereas strong inhibition was observed for Fe^{2+} (30% residual activity), Fe^{3+} (25% residual), and Cu^{2+} (40% residual) at 50 mM concentrations.

Carbohydrate content. The sugar content of the lipase was found to be 2.8% by densitometric scanning of the PAS-stained gel. After the protein was treated with endoglycosidase F, there was a small shift in the molecular weight as analyzed by gel electrophoresis (Fig. 2, lanes 7, 8). Their molecular weights correspond to about 34 and 32 kDa, respectively.

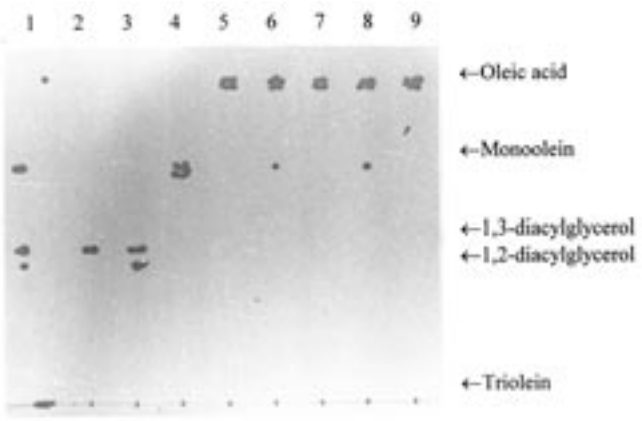

FIG. 6. Thin-layer chromatography (TLC) to determine the positional specificity of lipase. The substrates lipid standard (mixture of triolein, diolein, and monoolein), 1,3-diacylglycerol, diolein (85% 1,3-isomer and 15% 1,2-isomer), and 1-monooleoyl-*rac*-glycerol were emulsified by sonication in 0.2 M phosphate buffer (pH 6.0). Purified lipase was added to each of them separately and allowed to react at 37°C for 30 min. The products were analyzed by spotting 5–20 μL on TLC plates and developed in a solvent containing petroleum ether/diethyl ether/acetic acid (70:30:1, by vol), followed by another solvent containing petroleum ether/diethyl ether (95:5, vol/vol). The spots were identified after staining with iodine vapors. Lane 1: lipid standard, Lane 2: 1,3-diglyceride, Lane 3: diolein, Lane 4: monoolein, Lane 5: oleic acid, Lanes 6–9: reaction products after treating lipase with lipid standard, 1,3-diacylglycerol, diolein and 1-monooleoyl-*rac*-glycerol, respectively. That 2-monoolein derived from the 1,2-diolein is resistant to this lipase is evident from the 2-monoolein spots in lanes 6 and 8.

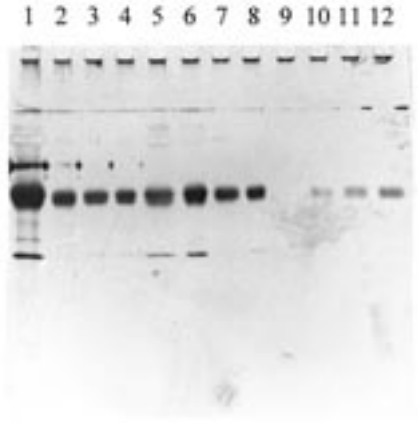

FIG. 7. SDS-PAGE of native lipase treated with proteases. The purified lipase was treated with trypsin, chymotrypsin, and endoproteinase Glu-C for 4, 8, 16, and 24 h. The samples were then analyzed in a 20% SDS-PAGE and the fragments detected by silver staining. Lane 1: untreated lipase, Lanes 2–5: lipase treated with trypsin for 4, 8, 16, and 24 h, respectively, Lanes 6–9: Lipase treated with chymotrypsin for 4, 8, 16, and 24 h, respectively, Lanes 10–12: lipase treated with Glu-C for 4, 8, 16 h, respectively. See Figure 2 for abbreviation.

We believe that the higher molecular weight species is the intact lipase without the sugar while the lower molecular weight species is a proteolytically cleaved fragment of the lipase, as it is reported that the purest forms of commercially available endoglycosidases have a metalloprotease as an impurity (29). We tried to inhibit this metalloprotease activity by adding EDTA and 1,10-phenanthroline to the digestion mixture. While 1 and 50 mM EDTA were ineffective in inhibiting the protease action, phenanthroline at 10 and 30 mM concentration was able to inhibit the protease activity to a large extent as the intensity of the lower molecular weight species was greatly reduced at the corresponding position. There was no change in the mobility of the 24 and 48 h glycosidase-treated sample, indicating complete removal of the carbohydrate moiety within 24 h (Fig. 2, lanes 7, 8). Moreover, when the glycosidase-treated samples were PAS-stained, no band was visible either for the 24 or the 48 h sample, indicating complete removal of the sugar after 24 h (results not shown). We obtained similar results when the enzyme was incubated with the glycosidase for just 2 h (results not shown).

Positional specificity. The stained TLC plate indicated that this lipase conventionally cleaves the ester bonds at the 1- and 3-positions of the triacylglycerol molecule (Fig. 6).

Protease digestion. Figure 7 shows the native lipase when treated with different proteases for different time intervals. It is evident that the tested proteases had no effect on native lipase. When the enzyme was heat-denatured by boiling at 100°C and then protease-treated for 24 h, no fragments could be detected by gel electrophoresis (results not shown). However, when the reactions were terminated after 6 h, there was restricted digestion, and the various fragments could be purified by reverse-phase HPLC (not shown).

DISCUSSION

We successfully purified a new extracellular lipase from *A. niger* involving various chromatographic steps to obtain a 50-fold purification. The molecular weight of this lipase was 35.5 kDa by SDS-PAGE and size-exclusion FPLC. There was no change in the electrophoretic mobility on boiling the pure lipase (Fig. 2, lane 5) as observed by Tombs and Blake (14). The isoelectric point was 4.4, whereas Sugihara *et al.* (16) and Torossian and Bell (17) reported a pI of 4.1 and 4.0, respectively. The purified lipase was stable for at least 8 wk when stored in 50 mM acetate buffer (pH 5.6) at 4°C.

The amino acid composition of our lipase shows a high percentage of Glx, Gly, Thr, Asx, and Ser with Thr in excess over Ser residues. In contrast the lipase of Torossian and Bell (17) and Tombs and Blake (14) contains Ser in far excess over Thr residues. As seen for other lipases there is no high hydrophobic residue content although the natural substrates of the enzyme are hydrophobic. The N-terminal amino acid sequence of our lipase is completely different from those determined by Sugihara *et al*. (16) and Torossian and Bell (17). This suggests that our lipase is novel.

The optimal thermal activity of this lipase was within the temperature range 35 to 55°C at pH 6.0, while Sugihara's enzyme had a temperature optimum of 30°C at pH 5.0 (16). The lipase purified by Tombs and Blake, was stable up to 55°C (14) while Sugihara's lipase was stable up to 65°C for 30 min

though further details were not given (16). The thermal stability profile of this lipase is given in Figure 4B.

This lipase had a pH optimum between pH 5.0 and 6.0 (Fig. 5A). Sugihara's lipase was stated to be stable between pH range 3.0 to 10.5 without further details (16). This enzyme was stable until pH 7.5. At pH 10.0, about 20% of the original activity remained (Fig. 5B).

Salt effects on activity were previously reported for *Geotrichum candidum* (7), *Penicillium simplicissimum* (26), and *Rhizopus delemar* (27) lipases as well as with another *Aspergillus* lipase (16). While these studies were conducted with millimolar salt concentrations, the present lipase was examined up to 1 M for various salts. Unlike the *R. delemar* lipase, which was inhibited by monovalent salts (27), the present lipase was not inhibited. Like the lipase of Sugihara *et al.* (16), the present lipase was inhibited by Fe^{2+} though not by Zn^{2+}. Some divalent cations like Mg^{2+}, Ca^{2+}, and Mn^{2+} also did not affect activity of the present lipase.

The carbohydrate content of fungal lipases varies from as low as 0.5% (27) to as high as 10% (28). *Aspergillus niger* lipase has been shown to contain about 7% sugar (16). In contrast, our lipase had only 2.8% oligosaccharide. The endoglycosidase F-treated enzyme resulted in the removal of all the sugar. Hence, it can be concluded that the sugars attached to the protein are exclusively Asn-linked (29). Moreover, there was no loss of enzyme activity after sugar removal.

The structure of our lipase seems to be quite compact in the native form as evident from the protease digestion experiments (Fig. 7). Another *A. niger* lipase was also shown to be trypsin- and chymotrypsin-resistant (14). Once heat-denatured, our lipase was susceptible to protease cleavage: a 24-h incubation led to complete digestion, and restricted digestion for 6 h did yield fragments detectable by HPLC.

The commercial exploitation of lipases in particular has traditionally been hampered by their inadequate stability and the limitations imposed by reaction conditions (neutral buffers, moderate temperature and pH stability, and so on) (6). However, the recent developments in biocatalysis in unconventional media, especially organic solvents (30), transformed the industrial perception of enzymes as very delicate catalysts, generally unsuitable for large-scale chemical synthesis. Most of the commercially available detergents have proteases as additives (31). The resistance of our enzyme toward proteases is another property which may be of industrial importance as there is a growing interest to engineer lipases to be protease-resistant for use in detergents. (31). The lipase purified by us may be suitable for some of the above biotransformations.

ACKNOWLEDGMENTS

This work was funded by the Council of Scientific and Industrial Research (CSIR), Government of India, Scheme No: 37(0870)/94/EMR-II. We thank Hindustan Lever Research Centre, Bombay for the *A. niger* strain, V.M.H.N. acknowledges a research fellowship from the Bose Institute and the Department of Microbiology for use of their various facilities.

REFERENCES

1. Sarda, L., and Desnuelle, P. (1958) Action de la Lipase Pancreatique sur les Esters en Emulsion. *Biochim. Biophys. Acta 30*, 513–520.
2. Derewanda, Z.S., and Sharp, A.M. (1993) News from the Interface: the Molecular Structures of Triglyceride Lipases, *TIBS 18*, 20–25.
3. Derewanda, Z.S. (1995) A Twist in the Tale of Lipolytic Enzymes, *Nat. Struct. Biol. 2*, 347–349.
4. Desnuelle, P. (1972) The Lipases, in *The Enzymes* (Boyer, P.D., ed.), pp. 575–616, Academic Press, New York.
5. Aires-Barros, M.R., Angela Taipa, M., and Cabral, J.M.S. (1994) Isolation and Purification of Lipases, in *Lipases, Their Structure, Biochemistry, and Application* (Woolley, P., and Peterson, S.B., eds.), pp. 243–270, Cambridge University Press, Cambridge.
6. Vulfson, E.N. (1994) Industrial Applications of Lipases, in *Lipases, Their Structure, Biochemistry and Application* (Woolley, P., and Peterson, S.B., eds.), pp. 271–288, Cambridge University Press, Cambridge.
7. Veeraragavan, K., Colpitts, T., and Gibbs, B.F. (1990) Purification and Characterization of Two Distinct Lipases from *Geotrichum candidum*, *Biochim. Biophys. Acta 1044*, 26–33.
8. Nagaoka, K., and Yamada, Y. (1973) Purification of *Mucor* Lipases and Their Properties, *Agric. Biol. Chem. 37*, 2791–2796.
9. Fukumoto, J., Iwai, M., and Tsujisaka, Y. (1964) Purification and Crystallization of a Lipase Secreted by *Aspergillus niger*, *J. Gen. Appl. Microbiol. 10*, 257.
10. Tsujisaka, Y., Iwai, M., and Tominaga, Y. (1973) Purification, Crystallization, and Some Properties of Lipases from *Geotrichum candidum*, *Agric. Biol. Chem. 37*, 1457–1464.
11. Tomizuka, N., Ota, Y., and Yamada, K. (1966) Studies on Lipase from *Candida cylindracea*. Part 1 Purification and Properties, *Agric. Biol. Chem. 30*, 576–584.
12. Rubin, B. (1994) Grease Pit Chemistry Exposed, *Nat. Struct. Biol. 1*, 568–572.
13. Derewanda, U., Swenson, L., Green, R., Wei, Y., Dodson, G.G., Yamaguchi, S., Haas, M.J., and Derewanda, Z.S. (1994) An Unusual Buried Polar Cluster in a Family of Fungal Lipases, *Nat. Struct. Biol. 1*, 36–47.
14. Tombs, M.P., and Blake, G.G. (1982) Stability and Inhibition of *Aspergillus* and *Rhizopus* Lipases, *Biochim. Biophys. Acta 700*, 81–89.
15. Höfelmann, M. (1985) Isolation, Purification, and Characterization of Lipase Isozymes from a Technical *Aspergillus niger* Enzyme, *J. Food Sci. 50*, 1721–1725.
16. Sugihara, A., Shimada, Y., and Tominaga, Y. (1988) Purification and Characterization of *Aspergillus niger* Lipase, *Agric. Biol. Chem. 52*, 1591–1592.
17. Torossian, K., and Bell, A.W. (1991) Purification and Characterization of an Acid-Resistant Lipase from *Aspergillus niger*, *Biotechnol. Appl. Biochem. 13*, 205–211.
18. Bernardi, G. (1971) Chromatography of Proteins on Hydroxyapatite, *Methods Enzymol. 22*, 325–339.
19. Kwon, D.Y., and Rhee, J.S. (1986) A Simple and Rapid Colorimetric Method for Determination of Free Fatty Acids for Lipase Assay, *J. Am. Oil Chem. Soc. 63*, 89–92.
20. Kouker. G., and Jaeger, K. (1987) Specific and Sensitive Plate Assay for Bacterial Lipase, *Appl. Environ. Microbiol. 53*, 211–213.
21. Bradford, M.M. (1976) A Rapid and Sensitive Method for the Quantitation of Microgram Quantities of Protein Utilizing the Principle of Protein-Dye Binding, *Anal. Biochem. 72*, 248–254.
22. Laemmli, U.K. (1970) Cleavage of Structural Proteins During the Assembly of the Head of Bacteriophage T4, *Nature 227*, 680–685.

23. Butcher, L.A., and Tomkins, J.K. (1986) A Comparison of Silver Staining Methods for Detecting Proteins in Ultrathin Gels on Support Films After Isoelectric Focussing, *Anal. Biochem. 148*, 384–388.
24. Konat, G., Offner, H., and Mellah, J. (1984) Improved Sensitivity for Detection and Quantitation of Glycoproteins on Polyacrylamide Gels, *Experientia 40*, 303.
25. Thornton, D.J., Carlstedt, I., and Sheehan, J.K. (1994) Identification of Glycoproteins on Nitrocellulose Membranes and Gels, in *Basic Protein and Peptide Protocols* (Walker, J.M., ed.) pp. 119–128, Humana Press, New Jersey.
26. Sztajer, H., Lunsdorf, H., Erdmann, H., Menge, U., and Schmid, R.D. (1992) Purification and Properties of Lipase from *Penicillium simplissimum, Biochim. Biophys. Acta 1124*, 253–261.
27. Haas, M.J., Cichowicz, D.J., and Bailey, D.G. (1992) Purification and Characterization of an Extracellular Lipase from *Rhizopus delemar, Lipids 27*, 571–576.
28. Boel, E., Huge-Jensen, B., Christensen, M., Thim, L., and Fiil, N.P. (1988) *Rhizomucor miehei* Triglyceride Lipase Is Synthesized as a Precursor, *Lipids 23*, 701–706.
29. Maley, F., Trimble, R.B., Tarentino, A.L., and Plummer, T.H., Jr. (1989) Characterization of Glycoproteins and Their Associated Oligosaccharides Through the Use of endoglycosidases, *Anal. Biochem. 180*, 195–204.
30. Klibanov, A.M. (1989) Enzymatic Catalysis in Anhydrous Organic Solvents, *Trends. Biochem. Sci. 14*, 141–144.
31. Bott, R., Shield, J.W., and Poulose, A.J. (1994) Protein Engineering of Lipases, in *Lipases, Their Structure, Biochemistry and Application* (Woolley, P., and Peterson. S.B., eds.), pp. 337–354, Cambridge University Press, Cambridge.

[Received November 30, 1999, and in final revised form February 21, 2000; revision accepted March 1, 2000]

Effects of Passive Smoking on the Regulation of Rat Aortic Cholesteryl Ester Hydrolases by Signal Transduction

Fusako Maehira*, Fusako Zaha, Ikuko Miyagi, Asami Tanahara, and Ayano Noho

Laboratory of Biochemistry, Department of Health Technology, School of Health Sciences, Faculty of Medicine, University of the Ryukyus, Okinawa 903-0215, Japan

ABSTRACT: The effects of exogenous oxidative stress due to passive smoking on cholesteryl ester (CE)-metabolizing enzymes and their regulatory kinases were examined by exposing rats to cigarette smoke (CS) for a 1-h period twice a day for 8, 12, or 20 wk. An oxidatively modified low density lipoprotein (Ox-LDL) with a high lipid peroxide was identified in three CS groups after all three exposure periods. The rat aortic acid and neutral CE hydrolases (ACEH and NCEH) were activated to similar extents by both cAMP-dependent protein kinase (PKA) and protein kinase C (PKC) in the presence of their respective cofactors. The aortic PKC activity in the three CS groups exhibited significant reductions of 72, 84, and 75% as compared with the respective controls, which coincided with the reductions in the ACEH activities (86, 71, and 80%, respectively), whereas the PKA activities increased to 121, 197, and 252% in the three CS groups, respectively. Reflecting the increase of the PKA activity, the NCEH activity exhibited increases of 112% at 8 wk and 140% until 12 wk of exposure and decreased by 50% of the control value at 20 wk of exposure, suggesting inactivation of NCEH itself. The activation of acyl-CoA:cholesterol *O*-acyltransferase activity was associated with an increase of free cholesterol in aorta. The vitamin E diet prevented the formation of Ox-LDL and the oxidative inactivation of most enzymes, especially PKC, until 12 wk, but was less effective by 20 wk. The oxidative inactivation of PKC, particularly its activated form that translocated to the membrane fraction, was confirmed in the *in vitro* exposure to active oxygen generators at an optimal concentration; this inactivation was prevented by catalase and superoxide dismutase. These results suggested that the formation of Ox-LDL and alterations in CE-metabolizing enzymes caused by passive smoking could contribute to a twofold increase in the aortic CE content, thereby contributing to one of the mechanisms for atherosclerosis associated with smoking.

Paper no. L8351 in *Lipids 35,* 503–511 (May 2000).

Accumulation of cholesteryl esters (CE) in atherosclerotic lesions could result from a variety of metabolic disturbances, including an increased influx of low density lipoprotein (LDL) cholesterol into the cells *via* the formation of oxidized LDL (Ox-LDL), imbalances between cholesterol esterification and hydrolysis, or imbalances between synthesis of cholesterol and its efflux from the cells, perhaps mediated by reduced concentrations of high density lipoprotein. The key enzymes in cholesterol metabolism as well as their regulatory enzymes in the signal transduction system may play important roles in the accumulation of CE in the arterial wall. The short-term regulation of cholesteryl ester hydrolases (CEH; EC 3.1.1.13) by reversible phosphorylation in the coordinated control of other key enzymes in cholesterol metabolism, such as 3-hydroxy-3-methylglutaryl-CoA (EC 1.1.1.34), cholesterol 7α-hydroxylase (EC 1.14.13.7) and acyl-CoA:cholesterol *O*-acyltransferase (ACAT; EC 2.3.1.26), has been well-characterized in many cell types including adipose tissue (1), macrophages (2), aorta (3,4), liver (5,6), adrenal cortex (7), and testis (8). Most studies have described the activation of CEH by cAMP-dependent protein kinase A (PKA; EC 2.7.1.37; ATP:protein phosphotransferase), followed by the initial report of neutral CEH (NCEH) activation by protein kinase C (PKC) in the rat liver (6). We recently reported the activations of rat aortic acid CEH (ACEH) and NCEH by both PKA and PKC to a similar extent in the presence of respective cofactors using selective inhibitors of two kinases (9). A cholesterol-esterifying enzyme, ACAT, is an integral membrane protein located in the endoplasmic reticulum, and evidence currently available for the involvement of phosphorylation in regulating ACAT is controversial; the dependence of ACAT activity on cholesterol availability has been documented in several studies (10,11): some evidence suggests the activation of ACAT by phosphorylation (12,13), whereas other evidence against the regulation of ACAT by phosphorylation has been presented (14,15).

We previously reported age-related decreases of the activities of lipolytic enzymes such as ACEH (16) and lipoprotein lipase (EC 3.1.1.34) (17) in mononuclear leukocytes from 214 and 158 human subjects, respectively. Inverse relations were observed between the ACEH activity and both serum cholesterol and lipid peroxide (LPO) as well as between the lipoprotein lipase activity and serum triglyceride (TG) levels.

*To whom correspondence should be addressed.
E-mail: fmaehira@med.u-ryukyu.ac.jp

Abbreviations: ACAT, acyl-CoA:cholesterol *O*-acyltransferase; ACEH, acid cholesteryl ester hydrolase; AO, active oxygen; BHT, butylated hydroxytoluene; CE, cholesteryl ester; CEH, cholesteryl ester hydrolase; CS, cigarette smoke; CSE, rats exposed to cigarette smoke and dietary vitamin E; CSC, control rats not exposed to cigarette smoke; G/GO, glucose/glucose oxidase; LDL, low density lipoprotein; LHPO, linoleate hydroperoxide; LPO, lipid peroxide; NCEH, neutral cholesteryl ester hydrolase; Ox-LDL, oxidized LDL; PKA, protein kinase A; PKC, protein kinase C; PP, protein phosphatase; SOD, Cu, Zn-superoxide dismutase; TBARS, thiobarbituric acid-reactive substance; TG, triglyceride; X/XO, xanthine/xanthine oxidase.

Both *in vivo* and *in vitro* inactivation of CEH in the aorta and liver was also observed in air-oxidized linoleate hydroperoxide (LHPO)-fed rats (18) and in an enzyme assay system with the addition of LHPO or LDL isolated from LHPO-fed rats (18,19), respectively. These studies suggest that oxidative inactivations of lipolytic enzymes may contribute to the extra- or intracellular increases of lipids.

Cigarette smoke (CS) contains reactive peroxy radicals that can increase lipid peroxidation (20), and the incidence of atherosclerosis in the abdominal aorta is approximately eight times higher in smokers than in nonsmokers (21). One of the mechanisms of atherosclerosis associated with smoking involves oxidative inactivation of intracellular CEH by free radicals in Ox-LDL (22). Recently, we also reported that the age-related decline of rat aortic ACEH and NCEH activities, together with their regulatory enzymes involving PKA and PKC, may be caused by long-term exposure to low levels of active oxygens such as those generated endogenously by metabolism (9). The aim of the present study was to investigate whether an exogenous oxidant burden due to passive smoking during different exposure periods generates oxidative inactivation of the aortic CEH and/or their regulatory enzymes in the signal transduction system, as had been previously observed in aging-related physiological changes that eventually led to increases of the aortic lipid content (9).

MATERIALS AND METHODS

Materials. The reagents used and their commercial sources were as follows: cholesteryl [1-^{14}C]oleate (57.0 mCi/mmol) from DuPont NEN (Boston, MA); [1-^{14}C]oleoyl-CoA (52.2 mCi/mmol) and [γ-^{32}P]ATP (25 Ci/mmol) from Amersham (Tokyo, Japan); Triton WR-1339, cholesteryl oleate, butylated hydroxytoluene (BHT), histone type III-S, ATP disodium salt, adenosine 3′,5′-cyclic monophosphate (sodium salt), diolein (18:1, *cis*-9), L-α-phosphatidyl-L-serine, xanthine oxidase (1.2 units/mg protein), glucose oxidase (178 units/mg), superoxide dismutase (4200 units/mg), and catalase (2000 units/mg) from Sigma (St. Louis, MO). Other chemicals were of analytical grade or higher. Prepacked LiChrolut RP-18 200-mg columns and the vacuum column holder unit were purchased from Merck KGaA (Darmstadt, Germany).

Animal experiments. This experiment was approved by the Animal Experiment Ethics Committee of the University of the Ryukyus. Eight-week-old male Wistar rats were housed in a room maintained on 12-h light/12-h dark cycles and a constant temperature of 20–23°C. Rats were exposed to sidestream smoke (CS) from cigarettes in an ashtray placed 10 cm below the rat cage in an exposure box (50 L × 40 W × 50 H, in cm) made of polypropylene, which was placed in a laboratory draft chamber (22). The cover of the exposure box was half opened, so that the smoke was drawn from the bottom by a fan of the draft chamber. Six groups of rats were exposed to CS for a 1-h period twice a day, once in the morning and once in the afternoon, for 8, 12, or 20 wk (two groups each). Three of these six groups, i.e., one of the two CS-exposed groups at each of the exposure periods, were given a chow supplemented with 5.1 mg DL-α-tocopherol per 100 g diet (CSE groups) and the other groups were not (CS groups). Three additional groups, control (CSC) groups for each of the exposure periods, were exposed in the same manner to atmospheric air. Both the CSC and CSE groups were given the same amount of diet intake as the CS group since the appetite of the CS groups was reduced by the nicotine in the CS (23,24). All groups consisted of 8 rats each, except that there were 10 rats in the three groups that received 12 wk of exposure. The animal experiments were started for each exposure period according to a schedule in which all rats were bled to death under anesthesia at the same time after overnight fasting.

Preparation of samples. Heparinized blood was obtained from each rat by heart-puncture under Nembutal anesthesia. Aliquots (2 mL) of plasma from each rat were pooled for each group, and LDL was fractionated from the pooled plasma in the presence of 0.002% (wt/vol) BHT and 0.01% (wt/vol) EDTA by discontinuous gradient ultracentrifugation at 4°C, 250,000 × *g* for 48 h (18). The thoracic-to-abdominal aortae (from which other tissues were removed) were kept at –80°C until assayed. Homogenates of the aorta (10%, wt/vol) were prepared in cold 0.02 M Tris-HCl buffer, pH 7.4, containing 0.25 M sucrose, 1 mM EDTA, 5 mM EGTA, 1 mM phenylmethyl sulfonyl fluoride, and 40 nM pepstatin, using a high-speed homogenizer at 25,000 rpm for 1 min. After centrifugation at 700 × *g*, 4°C for 10 min, 10-μL aliquots of the post-nuclear supernatants were used as samples in duplicate for the enzyme assays of CEH, ACAT, protein kinases, and protein determinations. The remaining part of the aortic preparation was immediately extracted twice with chloroform/methanol (2:1, vol/vol) containing 0.002% BHT. The solvent of the extract was evaporated *in vacuo*, and the residues were dissolved in an aliquot of the solvent and kept under N_2 at –20°C until analyses of lipids and LPO as thiobarbituric acid-reactive substances (TBARS). To study the effect of free radicals on the aortic PKC activity of the homogenate, cytosol, and membrane fractions, the cytosolic fraction was prepared by centrifuging the 10% aortic homogenate at 100,000 rpm (436,000 × *g*), 4°C for 15 min using a preparative micro-ultracentrifuge (HIMAC model CS120; Hitachi, Tokyo, Japan). The resulting pellet was homogenized after resuspending it in the original volume of homogenizing buffer containing 0.025% (wt/vol) Triton X-100 to make a homogeneous suspension and used for the membrane fraction. All measurements were made at least in duplicate. Statistical analyses were conducted by comparing the mean values and tested by the two-tailed *t*-test. The level of significance was set at $P < 0.05$.

Measurements of CE-metabolizing enzymes. The ACEH and NCEH activities were assayed on micellar substrates of 2.5 mM cholesteryl [1-^{14}C]oleate and 5 mM lecithin at pH 4.5 containing 1 mM β-mercaptoethanol and at pH 7.4 containing 0.15 M NaCl, respectively (9), in the absence (basal activity, Base) or the presence of the activating cofactors of 1 mM $MgCl_2$, 5 mM ATP, and 100 μM cAMP for PKA (total

activity, CoA-T) or 1 mM $MgCl_2$, 5 mM ATP, 1 mM $CaCl_2$, 20 µg/mL phosphatidylserine, and 4 µg/mL diolein for PKC (total activity, CoC-T) as described by Ghosh and Grogan (6). The difference between the basal and total activities was taken as the PKA- or PKC-activated CEH activity. After 10 µL of enzyme source was preincubated with 10 µL of cofactors, the reaction was started by adding 30 µL of the substrate, and the mixture was incubated at 37°C for 90 min as described previously (9). The enzyme activity was defined as the amount of enzyme catalyzing the release of 1 nmol oleic acid/h/mg protein. The ACAT activity was assayed as described by Billheimer (25), except that the isolation of the cholesteryl [1-^{14}C]oleate product was carried out using a prepacked reversed-phase minicolumn, LiChrolut RP-18 200 mg, according to the method of Kaluzny *et al.* (26). The recovery of cholesteryl [1-^{14}C]oleate product from the [1-^{14}C]oleate substrate was determined separately by adding authentic cholesteryl [1-^{14}C]oleate to the cold substrate in triplicate separations at every run of the ACAT assay. The recovery was usually around 60% due to the presence of Triton WR-1339, and for which the correction was made.

Assays of PKA and PKC. For the measurement of PKA activity (27), the final reaction mixture contained 50 mM Tris-HCl at pH 7, 10 mM $MgCl_2$, 20 µM [γ-^{32}P]ATP, 10 µM cAMP (cofactor for PKA, CoA), 200 µg/mL histone III-S, 0.25 mg/mL bovine serum albumin, 10 mM NaF, and 2 mM theophylline in a final volume of 50 µL. For the assay of PKC (28), the final reaction mixture consisted of 20 mM Tris-HCl at pH 7.4, 5 mM $MgCl_2$, 10 µM [γ-^{32}P]ATP, 200 µg/mL histone III-S, 0.1 mM $CaCl_2$ 25 µg/mL phosphatidylserine, 5 µg/mL diolein, and 0.3% (wt/vol) Triton X-100 in a final volume of 50 µL. The PKA and PKC reactions were started by the addition of 10 µL of the enzyme sources, containing less than 20 µg of protein, to the other components. After 5 min at 30°C, the reactions were stopped by the addition of 10 µL of 0.45 M H_3PO_4. Aliquots (45 µL) of the reaction mixture were transferred to phosphocellulose paper-P81 (dia. 2.3 cm; Whatman, Tokyo, Japan) which was placed in a vial, and the [γ-^{32}P]ATP was removed by washing three times with 10 mL of 75 mM H_3PO_4 (27). After drying for 5 min at 100°C, the scintillator was added, and the radioactivity was measured using a scintillation counter. The enzyme activity is expressed as the transfer of 1 pmol of ^{32}P to histone per min per mg of protein. Basal activity (Base) was measured in the presence of 0.5 mM EGTA and the absence of cofactors for PKC (CoC), i.e., $CaCl_2$, phosphatidylserine, and diolein. Base was subtracted from the CoC- or CoA-stimulated activity, and the difference was taken as the PKC or PKA activity. To investigate the effect of free radicals on the aortic PKC activity of the homogenate, cytosol, and membrane fractions, 10-µL aliquots of active oxygen (AO) generators, i.e., superoxide anions produced by xanthine/xanthine oxidase (X/XO) and H_2O_2 produced by glucose/glucose oxidase (G/GO), were preincubated with 10 mL of the enzyme source and 10 µL of the cofactors of protein kinases for 5 min at 30°C, and then the reaction was initiated by adding 30 µL of the substrate. Antioxidative enzymes such as Cu, Zn-superoxide dismutase (SOD) and catalase, and hydroxyl radical scavengers such as desferal and dimethylsulfoxide were first preincubated with the enzyme sources for 10 min at 30°C, followed by exposure to AO-producing systems.

Other measurements. LPO was measured fluorometrically (29) for LDL and colorimetrically (30) for the solvent extract from the aortic homogenate as TBARS after butanol extraction. Agarose gel electrophoresis was performed according to the instructions provided by the manufacturer (Ciba Corning, Palo Alto, CA), and the pattern was visualized by staining with Fat Red 7B. Lipids were measured manually using commercial clinical laboratory analysis kits (Wako, Tokyo, Japan). The CE contents were obtained by subtracting free cholesterol from total cholesterol. The amounts of proteins in the LDL and in the enzyme sources were measured by the method of Lowry *et al.* (31).

RESULTS

In vivo *formation of oxidized LDL and aortic lipid contents.* LPO expressed as TBARS values increased significantly in LDL isolated from the plasma pool of each CS group, to 143% at 8 wk, 137% at 12 wk, and 151% at 20 wk, compared to the respective control values (Table 1). The vitamin E diet prevented these increases until 12 wk of exposure, but thereafter the TBARS value in the CSE group increased to 136% relative to the control value by 20 wk. Electrophoretic exami-

TABLE 1
The Contents of Lipid Peroxides in LDL Isolated from Rats Exposed to Cigarette Smoke for 8, 12, and 20 wk[a]

	8-wk exposure		12-wk exposure		20-wk exposure	
Groups (*n*)	(µmol/g)	(%)	(µmol/g)	(%)	(µmol/g)	(%)
CSC (8)	3.80 ± 0.69	100	2.97 ± 0.55	100	2.90 ± 0.60	100
CS (10)	5.45 ± 0.72*	142.9	3.82 ± 0.62	137.0	4.38 ± 0.64*	151.0
CSE (8)	3.38 ± 0.65	88.9	2.63 ± 0.51	94.3	3.93 ± 0.70	135.5

[a]Values shown are the mean of triplicates ± SD. Aliquots (2 mL) of plasma from each rat were pooled for each group, and low density lipoprotein (LDL) was fractionated as described in the Materials and Methods section. Units are expressed per gram of protein. *P < 0.05 vs. the CSC group. Abbreviations: CSC, control group, no cigarette smoke (CS) exposure; CS, exposed to cigarette smoke; CSE, exposed to CS + dietary vitamin E.

nation of LDL fractions on agarose gels revealed a typical Ox-LDL with an increase in the net negative charges in the three CS groups, as indicated by small arrows in Figure 1. Slight increases of TBARS levels were observed in the aorta of the CS groups after all three exposure periods (Table 2). The aortic CE contents of the CS groups were elevated to 236, 258, and 209% compared to the control values after 8, 12, and 20 wk exposure periods, respectively, while the increases in the CSE groups were 114, 200, and 255% for the three exposure periods, respectively. A reduction of the aortic TG content in the CS groups was observed, probably due to increased TG turnover by transient epinephrine secretion in response to the nicotine in CS (23,24,32,33).

Activations of aortic CEH by protein kinases. The aortic CEH of the control rats (CSC groups in Fig. 2) were activated to similar extents by both PKA and PKC in the presence of their respective cofactors. However, ACEH activation by PKC (224% of the basal activity) tended to be greater than that by PKA (197%), whereas the NCEH activation by PKA (169%) tended to be greater than that by PKC (142%). A similar observation in the CEH activations by two kinases was previously reported as a result of using the selective inhibitors H-7 and HA1004 of PKC and PKA, respectively (9). CS exposure significantly reduced the PKC-activated fraction of ACEH to 36% in the CS group, but the vitamin E feeding stimulated it to 218%, as compared with the value of the control CSC group. The PKA-activated fraction decreased to about 75% in two CS-exposed groups (Fig. 2A). The PKA- and PKC-acti-

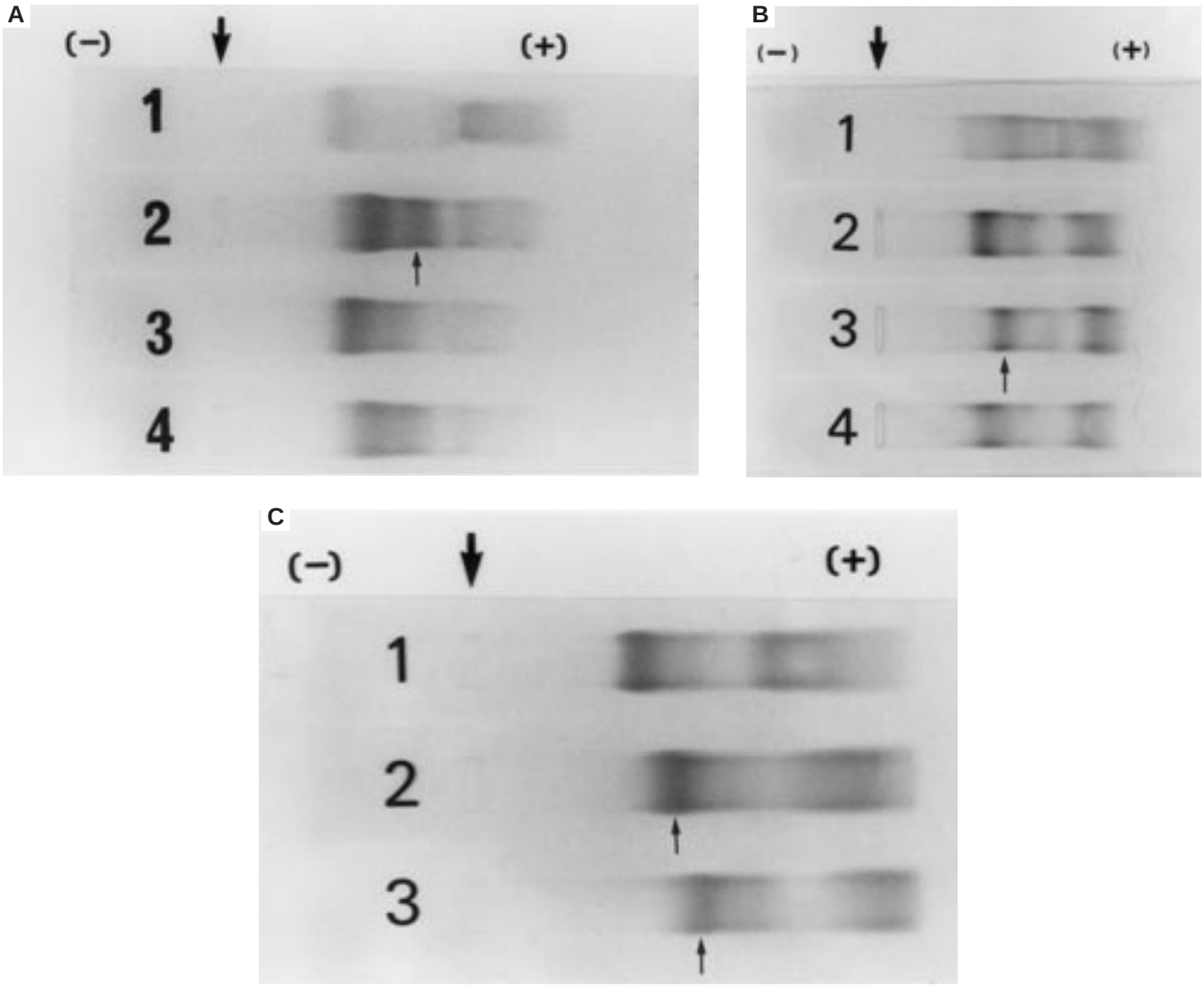

FIG. 1. Agarose gel electrophoresis of low density lipoprotein (LDL) isolated from rats exposed to cigarette smoke (CS) for 8, 12, and 20 wk. (A) 8-wk exposure. Lane 1, plasma from the CSC group (control: no CS); lanes 2, 3, and 4, LDL from the CS, CSE (CS rats fed dietary vitamin E), and CSC groups, respectively. (B) 12-wk exposure. Lane 1, plasma from the CSC group; lanes 2, 3, and 4, LDL from the CSC, CS, and CSE groups, respectively. (C) 20-wk exposure. Lanes, 1, 2, and 3, LDL from the CSC, CSE, and CS groups, respectively. The large arrow indicates the origin and the small arrow indicates the *in vivo*-modified LDL with increased net negative charges.

TABLE 2
Aortic Contents of TBARS and Lipids in Rats Exposed to CS for 8, 12, and 20 wk[a]

	TBARS		Total cholesterol		Free cholesterol		Cholesterol esters		Triglycerides	
Groups	(nmol/g)[b]	(%)	(mg/g)	(%)	(mg/g)	(%)	(mg/g)	(%)	(mg/g)	(%)
8-wk exposure (8 rats/group)										
CSC	19.8 ± 2.4	100	2.09 ± 0.17	100	1.87 ± 0.11	100	0.22 ± 0.03	100	4.43 ± 0.14	100
CS	22.0 ± 4.3	111.1	2.28 ± 0.44*	108.8	1.77 ± 0.13	78.1	0.52 ± 0.05**	236.4	3.80 ± 0.19**	85.8
CSE	15.9 ± 2.0**	80.3	2.14 ± 0.14	102.4	1.89 ± 0.14	101.1	0.25 ± 0.09	113.6	5.78 ± 0.52**	130.5
12-wk exposure (10 rats/group)										
CSC	16.4 ± 2.2	100	1.15 ± 0.10	100	0.89 ± 0.04	100	0.26 ± 0.03	100	6.60 ± 0.24	100
CS	19.3 ± 3.0*	118.0	1.70 ± 0.06**	147.8	1.03 ± 0.09**	115.7	0.67 ± 0.09**	257.7	3.97 ± 0.13**	60.2
CSE	17.7 ± 2.4	108.0	1.49 ± 1.00**	129.6	0.97 ± 0.07*	109.0	0.52 ± 0.06**	200.0	7.34 ± 0.40**	111.2
20-wk exposure (8 rats/group)										
CSC	17.9 ± 2.2	100	1.24 ± 0.04	100	1.02 ± 0.66	100	0.22 ± 0.03	100	5.31 ± 0.24	100
CS	20.3 ± 3.1	113.0	1.56 ± 0.10**	125.8	1.10 ± 0.08	107.8	0.46 ± 0.04**	209.1	4.57 ± 0.15**	86.1
CSE	19.0 ± 2.1	105.0	1.76 ± 0.14**	141.9	1.20 ± 0.07**	117.6	0.56 ± 0.07**	254.5	5.89 ± 0.47*	110.9

[a]Values shown are the means ± SD for 8–10 animals.
[b]Units are expressed per gram wet weight of tissues. *$P < 0.05$ and **$P < 0.005$ vs. the CSC control group. TBARS, thiobarbituric acid-reactive substances; for other abbreviations see Table 1.

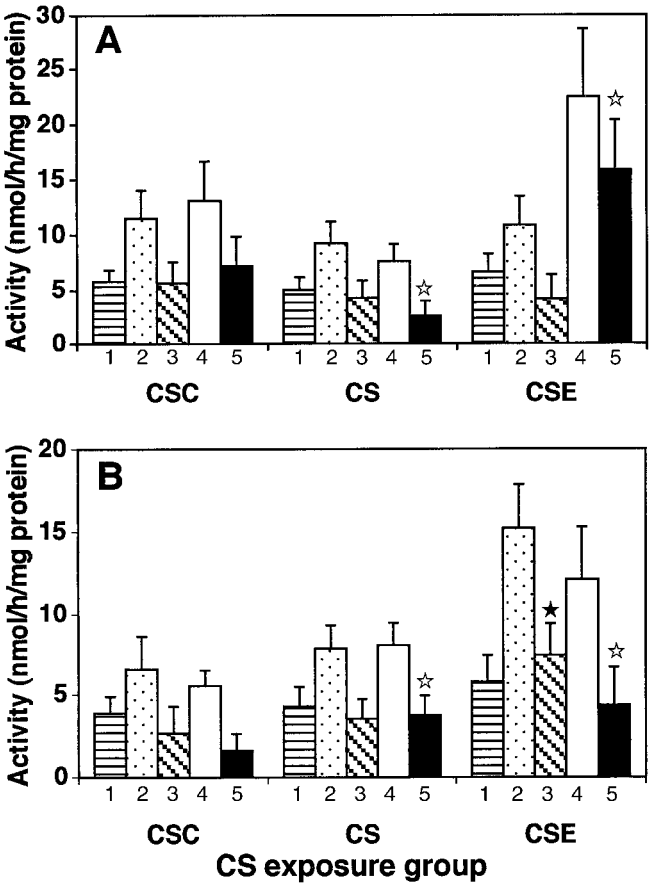

FIG. 2. The activities of aortic cholesteryl ester hydrolases (CEH) and their activations by protein kinases in rats exposed to CS for 8 wk. The activities of acid (panel A) and neutral (panel B) cholesteryl ester hydrolases were measured in the absence (Bar no. 1) and the presence of activating cofactors for protein kinase A (PKA) (CoA-T, no. 2) or protein kinase C (PKC) (CoC-T, no. 4) as described in the Materials and Methods section. The difference between the basal and the total activity was taken as the PKA (no. 3)- or PKC (no. 5)-activated CEH activity. Open stars, $P < 0.05$; solid stars, $P < 0.005$ vs. the CSC group. Values are means ± SD. For other abbreviations see Figure 1.

vated fractions of NCEH increased to 133 and 352% in the CS group and 229 and 264% in the CSE group, respectively, as compared with the values of each respective CSC group (Fig. 2B). The PKC and PKA activities were also examined on the same aortic samples of rats exposed to CS for 8 wk (Fig. 3). The two aortic kinase activities (Fig. 3) showed changes similar to those of the CS exposure-associated alterations in the CEH activities (Fig. 2): the PKC activities were significantly reduced to 72% in the CS group and increased to 118% in the CSE group compared with the activity of the CSC group (Fig. 3A), whereas the PKA activities increased in the two CS-exposed groups as follows: 121% for the CS group and 168% for the CSE group (Fig. 3B). The PKC activities in the CSC, CS, and CSE groups seem to be related to the PKC-activated fractions of ACEH (Fig. 2A), whereas the PKA activities in the three groups appear to be related to both PKA- and PKC-activated fractions of NCEH (Fig. 2B).

Activities of aortic CE-metabolizing enzymes and protein kinases in three CS-exposure periods. The CS exposure period-associated changes in the activities of CE-metabolizing enzymes and protein kinases in the rat aorta are summarized in Figure 4. The basal activities of ACEH and NCEH in Figure 2 and the PKC and PKA activities in Figure 3 are presented in Figure 4A for comparison with the other two exposure periods. The activity of aortic PKC, the regulatory enzyme of CEH, was significantly reduced to 72, 84, and 75% of the respective control values after 8, 12, and 20 wk exposure periods, respectively, while the PKA activity increased progressively to 121, 197, and 252% for the three exposure periods, respectively. The elevation of the PKA activity is probably related to a transient epinephrine secretion in response to the nicotine in CS (23,24). The ACEH activity of the CS groups remained significantly depressed, showing values of 86, 71, and 82% compared to the controls after the three exposure periods. The low ACEH activities after the three exposure periods probably reflected reduced PKC activities along with an inactivation of ACEH itself, since ACEH

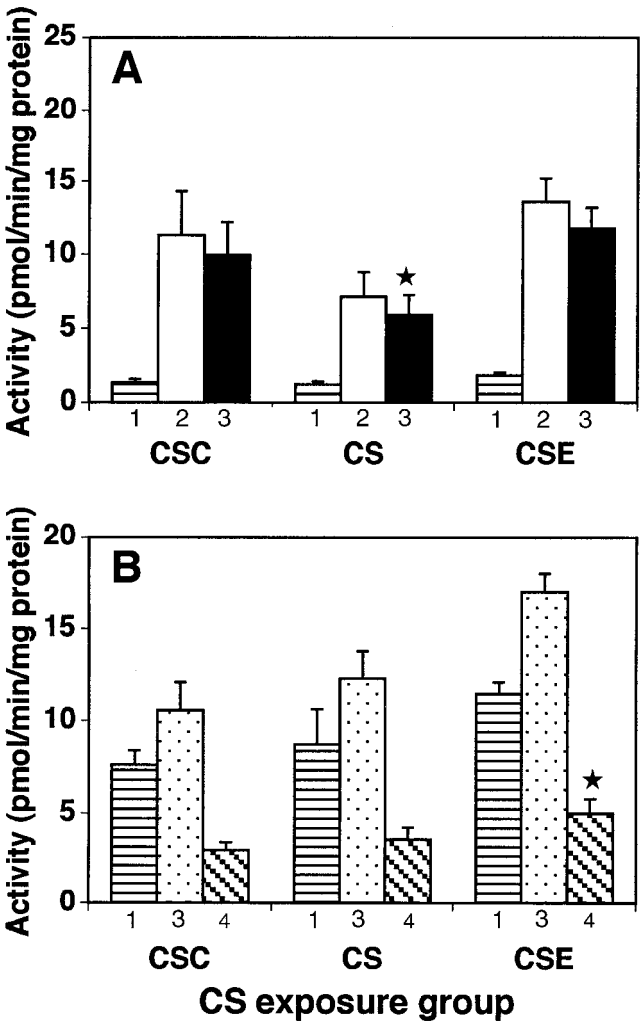

FIG. 3. The PKC and PKA activities of the aorta from rats exposed to CS for 8 wk. The difference between the activities in the absence (bar no. 1) and the presence (bar no. 2, PKC; bar no. 4, PKA) of the activating cofactors for each of the two protein kinases represents the activity of PKC (bar no. 3 in panel A) or PKA (bar no. 4 in panel B). For symbols denoting significance and other abbreviations see Figures 1 and 2. Values are means ± SD.

is activated by both types of kinases (Fig. 2; Ref. 9), and the PKA activities increased from 121 to 252 over the three exposure periods. Owing to marked elevations in the PKA activities of the CS groups, the NCEH activity continued to increase to 111% at 8 wk and 140% at 12 wk of exposure, and then decreased by 50% at 20 wk of exposure, suggesting inactivation of NCEH itself with long-term exposure to CS. The activity of cholesterol-esterifying enzyme, ACAT, exhibited significant elevations of 138% in the CS group at 12 wk and 130% in the CSE group at the 20-wk exposure; these activities were associated with increases in the aortic free cholesterol content of 116% in the CS group at 12 wk and 118% in the CSE group at 20 wk (Table 2) rather than the kinase activities. The aortic ACAT activations obtained here were roughly compatible with the hepatic microsomal ACAT reported (10), in that 25% increases of free cholesterol in microsomes increased the enzyme activity about sixfold.

Effects of antioxidants on active oxygen-mediated inhibitions of aortic PKC. The inactivation of aortic PKC by AO and its protections by antioxidants were examined. The effects of various antioxidants on the X/XO- and G/GO-mediated inhibitions of aortic PKC in the homogenate, cytosol, and membrane fractions are summarized in Table 3. The 5-min *in vitro* exposure of aortic PKC in the presence of activating cofactors to superoxide anion or hydrogen peroxide generated by X/XO or G/GO systems caused oxidative inactivation of PKC, particularly the activated form of PKC, which was translocated to the membrane as follows: 73% residual activity for the homogenate, 48% for the cytosolic fraction, and 24% for the membrane fraction, relative to the respective control PKC activities without AO exposure. Moreover, the observed inactivation of PKC in the membrane fraction was most effectively protected by catalase, and partially protected by SOD and desferal (Table 3).

DISCUSSION

The measurement of the TBARS content of LDL isolated from the plasma pool of each group showed approximately

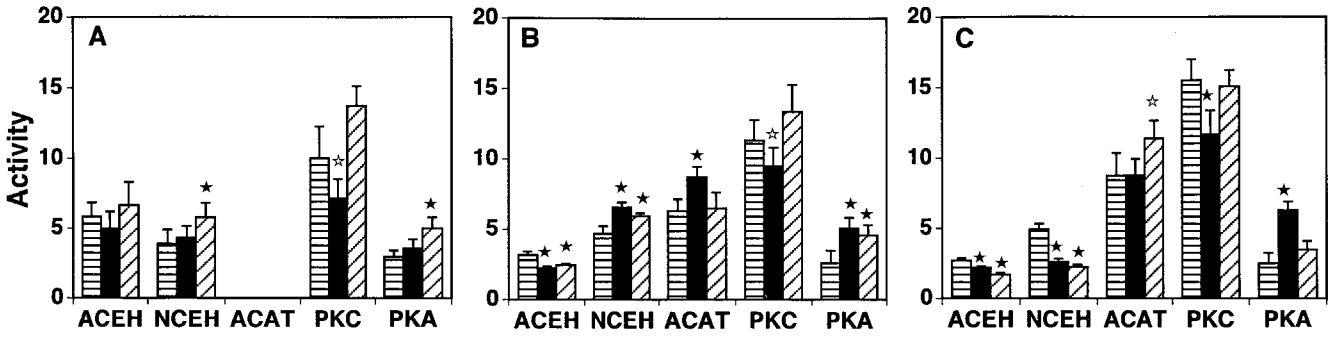

FIG. 4. Activities of cholesteryl ester-metabolizing enzymes and protein kinases in the aorta of rats exposed to CS for 8 (panel A), 12 (panel B), and 20 (panel C) wk. The height of the bars represents the specific activity in units (nmol/h for ACEH, NCEH, and ACAT; pmol/min for PKC and PKA) per mg protein for the CSC groups (horizontally striped bars), for the CS groups (solid bars), and for the CSE groups (diagonally striped bars). For symbols denoting significance, see Figure 2. Values are means ± SD. ACEH, acid cholesteryl ester hydrolase; ACAT, acyl-CoA:cholesterol *O*-acyltransferase; NCEH, neutral cholesteryl ester hydrolase; for other abbreviations see Figures 1–3.

TABLE 3
Effects of Antioxidants on the Xanthine/Xanthine Oxidase- and Glucose/Glucose Oxidase-Mediated Alterations of Protein Kinase C in the Rat Aorta[a]

	Homogenate			Cytosolic fraction			Membrane fraction		
	(units[b]/mg)	(%)	(%)	(units[b]/mg)	(%)	(%)	(units[b]/mg)	(%)	(%)
Base (+ none)	31.5 ± 1.0			29.9 ± 1.4			24.9 ± 1.3		
Control (+ CoC)	45.5 ± 2.1	100		54.1 ± 2.7	100		51.2 ± 2.9	100	
X/XO (25 µg/mL)/(2.5 µg/mL)									
Control + PBS	33.3 ± 1.2	73.2**	100	26.1 ± 1.5	48.2**	100	12.4 ± 0.5	24.2**	100
+ SOD 250 U/mL	37.1 ± 1.9	81.5*	111.4*	34.3 ± 2.2	63.4**	131.4*	25.9 ± 0.5	50.6**	208.9**
+ CAT 250 U/mL	42.6 ± 2.2	93.6	127.9**	45.2 ± 1.5	85.3*	173.2**	52.7 ± 2.0	102.9	425.0**
G/GO (5.0 mg/mL)/(5.0 µg/mL)									
Control + PBS	39.5 ± 2.2	86.8*	100	37.2 ± 1.8	68.8**	100	15.9 ± 0.5	63.9**	100
+ CAT 250 U/mL	46.3 ± 2.3	101.8	117.2*	46.7 ± 1.2	86.3*	125.5**	44.3 ± 1.5	86.5*	278.6**
+ DES 100 mM	36.4 ± 1.9	80.0*	92.2	46.3 ± 1.1	85.6*	124.5**	35.8 ± 2.3	69.9**	225.2**
+ DMSO 100 mM	33.2 ± 1.7	73.0**	84.1*	30.0 ± 1.0	55.5**	80.6**	27.3 ± 1.1	53.3**	171.7**

[a]Values shown are the mean of triplicates ± SD. *$P < 0.05$ and **$P < 0.005$ vs. 100% activity. CoC, cofactor for PKC, i.e., phosphatidylserine at 25 µg/mL in the presence of 5 µg/mL diolein, 5 mM Mg^{2+}, 0.5 mM Ca^{2+}; PBS, phosphate-buffered saline; SOD, superoxide dismutase; CAT, catalase; DES, desferal; DMSO, dimethylsulfoxide.
[b]pmol/min.

150% elevation in all three CS groups (three exposure periods), indicating systemic exposure to free radicals introduced by passive smoking (Table 1). Electrophoresis of LDL revealed a typical Ox-LDL with an increase in the net negative charge in the CS groups for all three CS-exposure periods (Fig. 1). This finding suggests that AO introduced by passive smoking into the blood is incorporated into cells through Ox-LDL which then inhibits the intracellular CEH (18,19) and their activating enzymes (9), thereby resulting in an increased cellular content of CE.

In the two-compartment model of CE metabolism in macrophages (34), Ox-LDL in the circulation is taken up rapidly by specific "scavenger receptors" on macrophages and vascular smooth muscle cells (35). There are three functional enzymes in this scheme: lysosomal ACEH, which degrades blood-derived exogenous CE to cholesterol; ACAT, which esterifies cholesterol to endogenous CE as a storage form by stimulation due to an increase in the intracellular cholesterol pool; and microsomal NCEH, which hydrolyzes endogenous CE. Although we have demonstrated the loss of ACEH and NCEH activity as a result of their exposure to oxidants both *in vivo* and *in vitro* (9,18,19,22), cloning of human ACEH has revealed the presence of cysteine within the mature protein (36), and the involvement of cysteine residues in the catalytic activity of ACEH has been recently clarified (37). On the other hand, evidence currently available for the presence of cysteine residues in NCEH is scant and controversial, in that the rat hepatic NCEH has been cloned and found to be a 66 kDa protein with no cysteine residues showing great overall homology with liver carboxyesterases (38,39), while the rat hepatic microsomal NCEH has been highly purified and found to be a 106 kDa protein with 30 cysteine groups exhibiting inactivation by the free sulfhydryl-reacting reagents (40). Chemical modification studies have identified histidyl and sulfhydryl residues necessary for ACAT activity; two types of sulfhydryl groups were involved, one at the active site and the other at the regulatory site (41). The presence of histidyl and sulfhydryl residues in ACAT has also been confirmed by molecular cloning of ACAT in rat (42) as well as in other species. From evidence, CE-metabolizing enzymes seemed to be sensitive to an oxidative inactivation. In our results (discussed below), NCEH was relatively resistant to an oxidative inactivation brought about during CS-exposure periods when compared to ACEH.

We previously reported that the activities of ACEH and NCEH and their regulatory enzymes, PKC and PKA, may be modulated by the dual effects of endogenous AO: activation of CEH at low doses and inactivation at high doses; or by long-term exposure to a low level of endogenous AO, which contributes to the age-related accumulation of CE in the arterial wall (9). The present study demonstrated that a continuous burden of exogenous oxidative stress due to passive smoking can also inactivate both CEH and their regulatory enzymes (Fig. 4), thereby contributing to increases in the aortic CE content (Table 2). The aortic CEH were activated by PKA and PKC, as shown in Figure 2 and also in a previous study (9). At the short-term exposure to CS (8 wk), 28% reduction in the PKC activity of the CS group (Fig. 3A) caused 64% reduction in the PKC-activated fraction of ACEH (Fig. 2A), whereas the PKA-activated fraction of ACEH of the two CS-exposed groups showed 25% reductions (Fig. 2A) despite the 20–68% elevations in the PKA activities of the two CS groups (Fig. 3B). This indicated that both ACEH and PKC were inactivated by CS, with more damage in lysosomal ACEH which was exposed to blood-derived Ox-LDL with a high LPO content (Fig. 1, Table 1). On the other hand, the activation of NCEH by the two kinases was not much affected by the 8-wk exposure to CS (Fig. 2B), and it was consistent with the elevation in the PKA activity (Fig. 3B). By 12 wk of exposure (Fig. 4B), the longer exposure to Ox-LDL brought a significant inactivation in the ACEH activity along with a significant elevation in the ACAT activity, which was in accord with the increased substrate-cholesterol availability (10,11) in the aorta (Table 2), whereas the NCEH activity was

significantly elevated, in parallel with an increase in PKA activity which was probably related to a transient epinephrine secretion in response to nicotine in CS (4,23). After long-term exposure (20 wk), two CE-hydrolyzing enzymes were more severely inactivated than CE-esterifying enzyme, and the antioxidant effect of vitamin E did not act efficiently as protection against AO-induced inactivation of CEH, whereas it did protect the PKC activity effectively from the inactivation that occurred in the CS groups through all exposure periods. The latter finding suggested that the inactivation of PKC was caused by AO in CS. In a previous study (9), AO-mediated activation of CEH was observed in the CEH activation system by PKC at the optimal low concentration of AO. The AO-induced inactivation of PKC at the high AO concentrations and its prevention by catalase were notable for the activated form of PKC which translocated to the membrane (Table 3). This evidence suggested that the inactivation of PKC in the aortic cells may be mediated by Ca^{2+}-dependent proteases (43) *via* an elevation of intracellular Ca^{2+} (44) through calcium mobilization from the intracellular calcium store, which was caused by AO (45). The free radical species responsible for the PKC inactivation were likely hydroxyl radicals, since the PKC inactivation due to AO exposure was efficiently eliminated by antioxidative enzymes and hydroxyl radical scavengers. An intracellular increase of Ca^{2+} may also activate Ca^{2+}/calmodulin-dependent protein phosphatase (PP)2B and PP1 which inactivate PKA by at least three mechanisms (46): (i) the dephosphorylation of the regulatory subunit R II of PKA; (ii) the reduction of the cAMP levels through the activation of cAMP phosphodiesterase by dephosphorylation; and (iii) the dephosphorylation of the substrate of PKA as well as other protein kinases like PKC *via* the activation of PP1 through the dephosphorylation of inhibitor-1 by PP2B. Alterations of activities of CE-metabolizing enzymes by phosphorylation/dephosphorylation depend on the relative activities of protein kinases and PP. The alteration of the latter enzymes by passive smoking remains to be clarified, and work along this line is currently under way.

In conclusion, the present results regarding long-term exposure (20 wk) to CS demonstrated that: nicotine in CS caused elevation of the PKA activity that modulates aortic CEH, while AO in CS produced an Ox-LDL with a high LPO content that was incorporated into aortic cells, consequently inhibiting ACEH, NCEH, and PKC that regulate aortic CEH. These alterations in CE-metabolizing enzymes by passive smoking could contribute to the twofold increase in aortic CE accumulation, thereby contributing to one of the mechanisms for atherosclerosis associated with smoking.

ACKNOWLEDGMENT

This study was supported in part by a grant-in-aid from Mitsui Life Welfare Foundation.

REFERENCES

1. Pittman, R.C., Khoo, J.C., and Steinberg, D. (1975) Cholesterol Esterase in Rat Adipose Tissue and Its Activation by Cyclic Adenosine 3′:5′-Monophosphate-Dependent Protein Kinase, *J. Biol. Chem. 250*, 4505–4511.
2. Khoo, J.C., Mahoney, E.M., and Steinberg, D. (1981) Neutral Cholesterol Esterase Activity in Macrophages and Its Enhancement by cAMP-Dependent Protein Kinase, *J. Biol. Chem. 256*, 12659–12661.
3. Hajjar, D.P., Weksler, B.B., Falcone, D.J., Hefton, J.M., Tack-Goldman, K., and Minick, C.R. (1982) Prostacyclin Modulates Cholesteryl Ester Hydrolytic Activity by Its Effect on Cyclic Adenosine Monophosphate in Rabbit Aortic Smooth Muscle Cells, *J. Clin. Invest. 70*, 479–488.
4. Hajjar, D.P., Minick, C.R., and Fowler, S. (1983) Arterial Neutral Cholesterol Esterase. A Hormone-Sensitive Enzyme Distinct from Lysosomal Cholesterol Esterase, *J. Biol. Chem. 258*, 192–198.
5. Beg, Z.H., Stonik, J.A., and Brewer, H.B., Jr. (1987) Modulation of the Enzymatic Activity of 3-Hydroxy-3-methylglutaryl Coenzyme A Reductase by Multiple Kinase Systems Involving Reversible Phosphorylation: A Review, *Metabolism 36*, 900–917.
6. Ghosh, S., and Grogan, W.M. (1989) Activation of Liver Cholesterol Ester Hydrolase by cAMP-Dependent Protein Kinase and Protein Kinase C, *Lipids 24*, 733–736.
7. Beckett, G.J., and Boyd, G.S. (1977) Purification and Control of Bovine Adrenal Cortical Cholesterol Ester Hydrolase and Evidence for the Activation of the Enzyme by a Phosphorylation, *Eur. J. Biochem. 72*, 223–233.
8. Bailey, M.L., and Grogan, W.M. (1986) Protein Kinase-Mediated Activation of Temperature-Labile and Temperature-Stable Cholesteryl Ester Hydrolases in the Rat Testis, *J. Biol. Chem. 261*, 7717–7722.
9. Maehira, F., Harada, K., Shimoji, J., Miyagi, I., and Nakano, M. (1998) Age-Related Changes in the Activation of Aortic Cholesteryl Ester Hydrolases by Protein Kinases in Rats, *Biochim. Biophys. Acta 1389*, 197–205.
10. Einarsson, K., Benthin, L., Ewerth, S., Hellers, G., Ståhlberg, D., and Angelin, B. (1989) Studies on Acyl-Coenzyme A:Cholesterol Acyltransferase Activity in Human Liver Microsomes, *J. Lipid Res. 30*, 739–746.
11. Cheng, D., Chang, C.C.Y., Qu, X., and Chang, T.Y. (1995) Activation of Acyl-Coenzyme A:Cholesterol Acyltransferase by Cholesterol or by Oxycholesterol in a Cell-Free System, *J. Biol. Chem. 270*, 685–695.
12. Suckling, K.E., Stange, E.F., and Dietschy, J.M. (1983) *In vivo* Modulation of Rat Liver Acyl-CoA:Cholesterol Acyltransferase Activity by Phosphorylation and Substrate Supply, *FEBS Lett. 158*, 29–32.
13. Gavey, K.L., Trujillo, D.L., and Scallen, T.J. (1983) Evidence for Phosphorylation/Dephosphorylation of Rat Liver Acyl-CoA:Cholesterol Acyltransferase, *Proc. Natl. Acad. Sci. USA 80*, 2171–2174.
14. Corton, J.M., and Hardie, D.G. (1992) Evidence Against a Role for Phosphorylation/Dephosphorylation in the Regulation of Acyl-CoA:Cholesterol Acyltransferase, *Eur. J. Biochem. 204*, 203–208.
15. Hernández, M.L., Martínez, M.J., Heredia, M.L., and Ochoa, B. (1997) Protein Phosphatase 1 and 2A Inhibitors Activate Acyl-CoA:Cholesterol Acyltransferase and Cholesterol Ester Formation in Isolated Rat Hepatocytes, *Biochim. Biophys. Acta 1349*, 233–241.
16. Maehira, F., Miyagi, I., Kohno, S., and Nakada, F. (1991) Possible Inhibitory Effect of Lipid Peroxides on Acid Lipase Activity *via* Low-Density Lipoprotein in Human Mononuclear Leukocytes, *J. Clin. Biochem. Nutr. 11*, 129–138.
17. Maehira, F., Miyagi, I., and Eguchi, Y. (1990) Sex- and Age-Related Variations in the *in vitro* Heparin-Releasable Lipopro-

tein Lipase from Mononuclear Leukocytes in Blood, *Biochim. Biophys. Acta 1042*, 344–351.
18. Maehira, F., Yonaha, M., Nakazono, N., Miyagi, I., and Shinjoh, S. (1994) *In vivo* Formation of Oxidatively Modified Low-Density Lipoprotein and Its Inhibitory Effects on Cholesteryl Ester Hydrolases in the Rat, *J. Clin. Biochem. Nutr. 16*, 37–50.
19. Maehira, F. (1994) Inhibitory Effect of Lipid Hydroperoxide on Cholesteryl Esterases, *Biochem. Mol. Biol. Inter. 32*, 221–231.
20. Pryor, W.A., Tamura, M., Dooley, M.M., Premovic, P., Hales, B.J., and Church, D.F. (1983) Reactive Oxy-Radicals from Cigarette Smoke and Their Physiological Effects, in *Oxy Radicals and Their Scavenger Systems. Vol. II, Cellular and Medical Aspects* (Greenwald, R.A., and Cohen, G., eds.), pp. 185–192, Elsevier, Amsterdam.
21. Auerbach, O., and Garfinkel, L. (1980) Atherosclerosis and Aneurysm of Aorta in Relation to Smoking Habits and Age, *Chest 78*, 805–809.
22. Maehira, F., Miyagi, I., Kawano, N., Kawano, M., and Shinjoh, S. (1995) Tobacco Smoke Exposure Alters Cholesteryl Esterase Activities and Causes Accumulation of Cholesteryl Esters in the Rat Aorta, *J. Clin. Biochem. Nutr. 18*, 145–155.
23. Westfall, T.C., and Watts, D.T. (1963) Effect of Cigarette Smoke on Epinephrine Secretion in the Dog, *Proc. Soc. Exp. Biol. Med. 112*, 843–847.
24. Winders, S.E., and Grunberg, N.E. (1989) Nicotine, Tobacco Smoke, and Body Weight: A Review of the Animal Literature, *Ann. Behav. Med. 11*, 125–133.
25. Billheimer, J.T. (1985) Cholesterol Acyltransferase, *Methods Enzymol. 111*, 286–296.
26. Kaluzny, M.A., Duncan, L.A., Merritt, M.W., and Epps, D.E. (1985) Rapid Separation of Lipid Classes in High Yield and Purity Using Bonded Phase Columns, *J. Lipid Res. 26*, 135–140.
27. Roskoski, R., Jr. (1983) Assay of Protein Kinase, *Methods Enzymol. 99*, 3–6.
28. Bell, R.M., Hannun, Y., and Loomis, C. (1986) Mixed Micelle Assay of Protein Kinase C, *Methods Enzymol. 124*, 353–359.
29. Yagi, K. (1976) A Simple Fluorometric Assay for Lipidperoxide in Blood Plasma, *Biochem. Med. 15*, 212–216.
30. Ohkawa, H., Ohishi, N., and Yagi, K. (1979) Assay for Lipid Peroxides in Animal Tissues by Thiobarbituric Acid Reaction, *Anal. Biochem. 95*, 351–358.
31. Lowry, O.H., Rosebrough, N.J., Farr, A.L., and Randall, R.J. (1951) Protein Measurement with Folin Phenol Reagent, *J. Biol. Chem. 183*, 265–275.
32. Brunzell, D.J., Goldberg, A.P., and Schwartz, R.S. (1980) Cigarette Smoking and Adipose Tissue Lipoprotein Lipase, *Int. J. Obes. 4*, 101–103.
33. Lafontan, M., Barbe, P., Galitzky, J., Tavernier, G., Langin, D., Carpene, C., Bousquet-Melou, A., and Berlan, M. (1997) Adrenergic Regulation of Adipocyte Metabolism, *Hum. Reprod. 12 Suppl. 1*, 6–20.
34. Brown, M.S., and Goldstein, J.L. (1983) Lipoprotein Metabolism in Macrophage: Implications for Cholesterol Deposition in Atherosclerosis, *Annu. Rev. Biochem. 52*, 223–261.
35. Inaba, T., Gotoda, T., Shimano, H., Shimada, M., Harada, K., Kozaki, K., Watanabe, Y., Hoh, E., Motoyoshi, K., Yazaki, Y., and Yamada, N. (1992) Platelet-Derived Growth Factor Induces c-flms and Scavenger Receptor Genes in Vascular Smooth Muscle Cells, *J. Biol. Chem. 267*, 13107–13112.
36. Anderson, R.A., and Sando, G.N. (1991) Cloning and Expression of cDNA Encoding Human Lysosomal Acid Lipase/Cholesteryl Ester Hydrolase, *J. Biol. Chem. 266*, 22479–22484.
37. Lohse, P., Lohse, P., Chahrokh-Zadeh, S., and Seidel, D. (1997) Human Lysosomal Acid Lipase/Cholesteryl Ester Hydrolase and Human Gastric Lipase: Site-Directed Mutagenesis of Cys_{227} and Cys_{236} Results in Substrate-Dependent Reduction of Enzymatic Activity, *J. Lipid. Res. 38*, 1896–1905.
38. Ghosh, S., Mallonee, D.H., Hylemon, P.B., and Grogan, W.M. (1995) Molecular Cloning and Expression of Rat Hepatic Neutral Cholesteryl Ester Hydrolase, *Biochim. Biophys. Acta 1259*, 305–312.
39. Natarajan, R., Ghosh, S., and Grogan, W.M. (1996) Catalytic Properties of the Purified Rat Hepatic Cytosolic Cholesteryl Ester Hydrolase, *Biochem. Biophys. Res. Commun. 225*, 413–419.
40. Cristobal, S., Ochoa, B., and Fresnedo, O. (1999) Purification and Properties of a Cholesteryl Ester Hydrolase from Rat Liver Microsomes, *J. Lipid Res. 40*, 715–725.
41. Kinnunen, P.M., Spilberg, C.A., and Lange, L.G. (1988) Chemical Modification of Acyl-CoA:Cholesterol *O*-Acyltransferase. 2. Identification of a Coenzyme A Regulatory Site by *p*-Mercuribenzoate Modification, *Biochemistry 27*, 7351–7356.
42. Matsuda, H., Hakamata, H., Kawasaki, T., Sakashita, N., Miyazaki, A., Takahashi, K., Shichiri, M., and Horiuchi, S. (1998) Molecular Cloning, Functional Expression and Tissue Distribution of Rat Acyl-Coenzyme A:Cholesterol Acyltransferase, *Biochim. Biophys. Acta 1391*, 193–203.
43. Kishimoto, A., Mikawa, K., Hashimoto, K., Yasuda, I., Tanaka, S., Tomonaga, M., Kuroda, T., and Nishizuka, Y. (1989) Limited Proteolysis of Protein Kinase C Subspecies by Calcium-Dependent Neutral Protease (Calpain), *J. Biol. Chem. 264*, 4088–4092.
44. Nicotera, P., Hartzell, P., Baldi, C., Svensson, S.A., Bellomo, G., and Orrenius, S. (1986) Cystamine Induces Toxicity in Hepatocytes Through the Elevation of Cytosolic Ca^{2+} and the Stimulation of a Nonlysosomal Proteolytic System, *J. Biol. Chem. 261*, 14628–14635.
45. Jones, D.P., Thor, M., Smith, M.T., Jewell, S.A., and Orrenius, S. (1983) Inhibition of ATP-Dependent Microsomal Ca^{2+} Sequestration During Oxidative Stress and Its Prevention by Glutathione, *J. Biol. Chem. 258*, 6390–6393.
46. Cohen, P. (1989) The Structure and Regulation of Protein Phosphatases, *Annu. Rev. Biochem. 58*, 435–508.

[Received September 3, 1999, and in final revised form February 21, 2000; revision accepted March 22, 2000]

Aggregation and Fusion of Vesicles Composed of *N*-Palmitoyl Derivatives of Membrane Phospholipids

Margarita Mora, Ferran Mir, M. Africa de Madariaga, and M. Luisa Sagristá*

Department of Biochemistry and Molecular Biology, Faculty of Chemistry, University of Barcelona, 08028-Barcelona, Spain

ABSTRACT: *N*-Acylphosphatidylethanolamines and *N*-acylphosphatidylserines have been isolated from mammalian cells and have been associated with some tissue degenerative changes, although the relationship between their synthesis and the uncontrolled sequence of events that ends in irreversible tissue damage is not completely established. Our results show that monovalent and divalent cations induce aggregation and fusion of liposomes constituted by *N*-palmitoylphosphatidylethanolamine (NPPE) and *N*-palmitoylphosphatidylserine (NPPS). The effectiveness of cations to induce the aggregation of NPPE and NPPS liposomes is $Ca^{2+} > Mg^{2+} \gg Na^{+}$. NPPS liposomes aggregate at lower concentrations of divalent cations than NPPE liposomes, but with sodium NPPE liposomes aggregate to a higher extent than NPPS liposomes. The reaction order for the aggregation processes depends on the lipid and the cation nature and range from 1.04 to 1.64. Dynamic light scattering shows an irreversible increase of the size of the aggregates in the presence of all cations tested. The irreversibility of the aggregation process and the intermixing of bilayer lipids, as studied by resonance energy transfer assay, suggest that fusion, rather than aggregation, occurs. The existence of a real fusion was demonstrated by the coalescence of the aqueous contents of both NPPS and NPPE liposomes in the presence of either monovalent or divalent cations. The different binding sensitivity of Ca^{2+} to NPPS and NPPE liposomes, determined by ζ potential measurements, agrees with the results obtained in the aggregation and fusion assays. Our results suggest that the synthesis *in vivo* of N-acylated phospholipids can introduce important changes in membrane-mediated processes.

Paper no. L8222 in *Lipids 35,* 513–524 (May 2000).

N-Acylaminophospholipids are a widespread family of membrane phospholipids in animal and plant tissues (1,2). *N*-Acyl derivatives of phosphatidylethanolamine (*N*-acylPE) have been found in cell membranes under some pathological conditions, such as the disruption of the sarcolemma, which follows myocardial infarct and ischemia, and in cells with a high catabolic activity (3,4). *N*-Acyl derivatives of phosphatidylserine have also been identified in sheep erythrocytes (5), in the central nervous system of freshwater fish (6), and in ischemic bovine brain (7). *N*-AcylPE are synthesized by N-acylation reactions carried out by a transacylase system that catalyzes the transfer of fatty acids from the *sn*-1 position of various 1,2-diacyl glycerophospholipids to the amino group of aminophospholipids. In dog heart the reaction is calcium-dependent and utilizes phosphatidylcholine, PE, and cardiolipin as main acyl donors (8). In contrast, Chapman and More (9) established that higher plants *in vivo*, under normal physiological growth conditions, and cottonseed microsomes *in vitro* synthesize *N*-acylPE by direct enzymatically catalyzed acylation of PE, without a requirement for divalent cations.

Recently, there has been a renewed interest in the study of *N*-acylPE. Their metabolism gives *N*-acylethanolamines, some of which, as the *N*-arachidonylethanolamine (anandamide), are physiologically important. For example, the latter has a role as endogenous ligand for the cannabinoid receptor in mammalian brain (10–12).

Despite the role of *N*-acylPE as putative cannabinoid precursors (13), the ability of the amides of fatty acids to act as lipid bioregulators (14), and the numerous studies carried out to ascertain completely the metabolic role of the *N*-acyl derivatives of membrane aminophospholipids, the physiological meaning of the N-acylation reactions is not yet totally established. However, the special structural characteristics of such molecules and the physicochemical properties of their aqueous dispersions show that instead of being merely the products of a high lipid catabolism, and so physiologically useless, they can be functionally useful lipids to cellular membranes. They can protect biomembranes from the high activity of some phospholipases, which easily hydrolyze PE but not their N-acyl derivatives (15). They can modulate the activity of membrane enzymes because of the decrease in the bilayer fluidity and the increase in the negative surface charge by means of their incorporation into the bilayer (16). They protect biomembranes from dehydration processes because of the increase of the hydration degree of the polar head (17). They are metabolic intermediates in the catabolism of PE, and their degradation gives *N*-acylethanolamines, which can pro-

*To whom correspondence should be addressed at the Department of Biochemistry and Molecular Biology, Faculty of Chemistry, University of Barcelona, Martí i Franquès, 1-11, 08028-Barcelona. Spain.
E-mail: sagrista@sun.bq.ub.es

Abbreviations: *N*-acylPE, *N*-acyl derivative of phosphatidylethanolamine; DPA, dipicolinic acid; IR, infrared; LUV, large unilamellar vesicles; MLV, multilamellar vesicle; NBD-PE, *N*-(7-nitrobenz-2-oxa-1,3-diazol-4-yl)-phosphatidylethanolamine; NMPE, *N*-myristoylphosphatidylethanolamine; NMR, nuclear magnetic resonance; NPPE, *N*-palmitoylphosphatidylethanolamine; NPPS, *N*-palmitoylphosphatidylserine; NTA, nitrilotriacetic acid; PCS, photon correlation spectroscopy; PE, phosphatidylethanolamine; PS, phosphatidylserine; RET, resonance energy transfer; Rh-PE, *N*-(lissamine Rhodamine B sulfonyl)-phosphatidylethanolamine; SUV, small unilamellar vesicle; TLC, thin-layer chromatography; TPE, transphosphatidylated phosphatidylethanolamine.

tect biomembrane integrity from ischemia since they inhibit calcium release, decrease the levels of lyso-PE, and inhibit phospholipase A_2 by acting as agonist (1,18). They affect the permeability and fluidity of the membrane bilayers. In this way, previous studies in our laboratory have shown (i) that the incorporation of *N*-acylPE decreases the permeability of lipid bilayers because of the rigidifying effect of the N-acylation of PE (19) and (ii) that liposomal formulations containing *N*-acyl derivatives of PE are very stable in biological media (20). Besides these considerations, their biosynthesis could have a stabilizing effect on biological membranes by reducing the effective concentration of free fatty acids, by producing a bilayer phospholipid able to form closed and stable vesicle structures by itself, and by reducing the concentration of the nonbilayer PE in membranes (9,21–23).

It has been suggested that acidic phospholipids, like phosphatidic acid and phosphatidylserine (PS), and nonbilayer lipids, like PE, contribute actively in the membrane fusion processes induced by Ca^{2+} and specific membrane proteins (24–26). In this way, Verkleij and Post (27) have shown the ability of calcium to induce a lateral phase separation of the negatively charged phospholipids, mainly located in the inner monolayer of the sarcolemma, which leads to the destabilization of the bilayer and to uncontrolled fusion events. This hypothesis could suggest a relationship between the synthesis of the negatively charged N-acylated phospholipids and the processes that lead to the degeneration of membranes.

We have previously reported the irreversible mono- and divalent cation-induced aggregation of liposomes prepared from a methylated analog of *N*-acylPE (28) and the divalent cation-induced fusion of *N*-stearoyl-PS liposomes (29). Our results have shown that the divalent cation concentrations necessary to induce the aggregation and fusion of liposomes containing *N*-acylaminophospholipids would be of physiological relevance in those pathological states in which the transient opening of calcium channels lead to an abrupt increase of calcium levels. A membrane protective role for the synthesis of *N*-acyl derivatives of PE (17,19) and PS (29) in the first stages of tissue damage has been postulated since N-acylation converts the nonbilayer unsaturated PE into a bilayer lipid and decreases the sensitivity of PS to calcium- and magnesium-induced fusion. Nevertheless, if calcium levels did not return to basal levels the degenerative changes would be favored by *N*-acyl derivatives of PE and PS.

Liposomes (phospholipid vesicles) have been used as relatively simple membrane models to investigate the molecular requirements for membrane fusion (30–33). In general, they are stable structures that do not normally fuse spontaneously. Nevertheless, a great number of references in the literature show that monovalent cations induce aggregation of liposomes containing acidic phospholipids or negative charges at the bilayer surface (34–36), whereas divalent cations are able to induce fusion processes (37–39).

All these considerations, as well as our previous results (28,29), have led us to carry out a more exhaustive study of monovalent and divalent cation-induced aggregation, lipid exchange, and aqueous content mixing of sonicated unilamellar liposomes made from *N*-palmitoylphosphatidylethanolamine (NPPE) and *N*-palmitoylphosphatidylserine (NPPS) so as to demonstrate that fusion occurs. The influence of the polar head of both lipid species on the fusogenic properties of liposomes are also considered. The electrostatic properties of NPPE and NPPS bilayers, in the absence and in the presence of calcium ions, are determined as well in order to establish the importance of electrostatic forces in the formation of stable aggregates required for vesicle fusion. The results obtained regarding the ability to fuse liposomes constituted by *N*-acyl derivatives of PE and PS can be helpful in designing drug delivery vesicles with long-circulating and fusogenic properties.

MATERIALS AND METHODS

Chemicals. Egg transphosphatidylated phosphatidylethanolamine (TPE) and the fluorophore-labeled phospholipids, *N*-(7-nitrobenz-2-oxa-1,3-diazol-4-yl)-phosphatidylethanolamine (NBD-PE) and *N*-(lissamine Rhodamine B sulfonyl)-phosphatidylethanolamine (Rh-PE) were obtained from Avanti Polar Lipids (Birmingham, AL). Bovine brain PS (80–85%) was a product from Sigma Chemical Co. (St. Louis, MO) and was purified by thin-layer chromatography (TLC) before use (29). Palmitoyl chloride for synthesis was from Merck (Schuchardt, Germany), and cation salts for aggregation or fusion studies were from Merck (Darmstadt, Germany). All other reagents were of analytical grade. Water was twice-distilled (Millipore Systems, Molsheim, France), and all organic solvents were redistilled before use.

Analytical TLC was performed on layers of silica gel G (Sil G-25) purchased from Macherey-Nagel (Düren, Germany). Chromatographic material for purification processes (Kieselgel 60H, 15 μm for TLC, and Kieselgel 60G and 0.1–0.2 mm for column chromatography) was obtained from Merck (Darmstadt). Samples were made visible with iodine, by spraying with ninhydrin or with ammonium molybdate in H_2SO_4, or by charring.

Synthesis of N-*acyl phospholipids*. NPPE was synthesized by condensing palmitoyl chloride with egg TPE as described previously (28). NPPS was obtained from PS, previously purified from a bovine brain extract, by means of an acylation reaction with palmitoyl chloride (29). Silicic acid column chromatography and preparative TLC-purified NPPE and NPPS were assayed for purity by TLC using two solvent systems and were identified by ^1H nuclear magnetic resonance (NMR) and infrared (IR) spectroscopy. The formation of the amide bonds was checked by means of the observation of amide I and amide II bands in the IR spectra and by ^1H NMR spectroscopy. The analysis, after chemical degradation of both products, by gas–liquid chromatography of the fatty acid methyl esters showed the incorporation of the third palmitoyl chain. Lipid concentration was determined by phosphorus analysis (40).

Preparation of liposomes. Unilamellar liposomes were prepared by using the sonication method. NPPS or NPPE was

dissolved in trichloromethane, and the organic solvent was evaporated by a stream of nitrogen gas to deposit a lipid film on the wall of a glass test tube. Final traces of residual solvent were removed under vacuum for 18 h. Multilamellar vesicles (MLV) were prepared by suspending the dried lipid film at a concentration of 0.5 mg lipid/mL of 20 mM Tris-HCl buffer (pH 7.4), containing 100 mM NaCl and 100 μM EDTA, and by vortexing for 10 min. Small unilamellar vesicles (SUV) were obtained by sonication of the MLV in a Braun Labsonics 2000 probe sonifier, equipped with a 9.5-mm titanium probe, for 15 min operating at 48 W. During sonication, the lipid suspension was kept at 45°C under a nitrogen stream. Titanium particles (arising from the progressive disintegration of the sonifier probe) and possible undispersed lipids were removed by centrifugation. It was verified by TLC that the lipids did not suffer degradation due to the sonication process. Before use, the liposome dispersion was filtered through a 0.45 μm filter.

Multilamellar liposomes for surface potential measurements were prepared by shaking the lipid film in the electrolyte for 10 min, followed by a 30-min period of sonication in a bath sonicator. The final lipid concentration in the aqueous sample was 0.5 mg/mL.

Vesicle aggregation assay. Vesicle aggregation was monitored by continuous measurements of the turbidity of SUV suspensions as a function of the monovalent (Na^+) and divalent (Ca^{2+} and Mg^{2+}) cation concentrations. The optical density changes were followed at 400 nm during 2 min, using a UV/VIS Beckman DU-70 spectrophotometer equipped with a Peltier temperature control cell and continuous stirring. The wavelength in the visible range at which our sonicated unilamellar vesicles caused maximal light scattering was found to be approximately 400 nm. For the aggregation assays, NPPE and NPPS liposomes were suspended at 0.05 mg phospholipid/mL in the same buffered salt solution used to prepare the liposomes. Measurements were performed at 20°C before and after the addition of small aliquots of the concentrated cation salt solutions to the liposome suspensions. In order to omit the initial bubbling problems or the formation of large vesicles, the results shown represent the increments of absorbance obtained 20 s after the cation addition. The threshold concentrations (c_t) for the aggregation process were calculated as the cation concentrations corresponding to the maximal increase in the rate of absorbance changes (36).

Vesicle size analysis. The aggregation of NPPE and NPPS liposomes induced by monovalent and divalent ions can also be followed by measuring the changes in size and size distribution of unilamellar phospholipid vesicles when adding the cations (32). The analysis was carried out by dynamic light scattering using a PCS41 particle sizer (Malvern Autosizer IIc) and a 5 mW He-Ne laser (Spectra Physics), at an excitation wavelength of 633 nm. The data were collected with a Malvern 7032N 72 data channel correlator, and the mean hydrodynamic diameter was calculated from a cumulant analysis of the intensity autocorrelation function. The possible reversibility of the monovalent and divalent cation-induced aggregation reaction was verified by measuring vesicle size 2 min after dilution of the aggregated vesicles up to 200 mM sodium concentration or after the addition of EDTA at six times the concentration of divalent ions to the aggregated vesicles.

Vesicle fusion assay. The fusion of NPPE and NPPS liposomes induced by monovalent and divalent cations was measured by monitoring the exchange of the bilayer lipids and the mixing of the internal aqueous contents, using fluorescent probes. Fusion of the liposomal membranes was followed by measuring lipid mixing using a modification of the fluorescence resonance energy transfer assay (RET) described by Struck *et al*. (41). SUV constituted by NPPE or NPPS were prepared without and with NBD-PE and Rh-PE at 1 and 0.5 mol%, respectively, with respect to the total lipid content (0.5 mg/mL). The fluorescent-labeled liposomes and a ninefold excess of unlabeled vesicles were mixed at 20°C to monitor the dilution of the fluorescent lipids by following continuously the decrease in energy transfer from NBD-PE to Rh-PE, using a Kontron SFM 25 spectrofluorimeter at excitation and emission wavelengths of 440 and 536 nm, respectively, using a 530-nm cut-off filter to eliminate the contribution of light scattering. The maximal fusion was determined using reference liposomes containing 0.1% NBD-PE and 0.05% Rh-PE. Light-scattering controls were performed using unlabeled vesicles. The percentage of fusion was expressed as the percentage of maximal fluorescence,

$$\%\ \text{maximal fluorescence} = \frac{\left(F_t - S_t\right)/\left(F_T - S_T\right) - \left(F_0 - S_0\right)/\left(F_T - S_T\right)}{\left(R_t - S_t\right)/\left(R_T - S_T\right) - \left(F_0 - S_0\right)/\left(F_T - S_T\right)} \times 100 \quad [1]$$

where F_t = fluorescence intensity at time t; F_0 = fluorescence intensity at time zero; F_T = fluorescence intensity in the presence of 0.7% Triton X-100. R and S represent the same measurements for reference liposomes and light-scattering controls, respectively (42). However, Equation 1 can be simplified by assuming that light-scattering values can be neglected in our experimental conditions. Thus, taking into account this consideration, we calculate the percentage of maximal fluorescence as

$$\%\ \text{maximal fluorescence} = \frac{F_t - F_0}{R_t \dfrac{F_T}{R_T} - F_0} \times 100 \quad [2]$$

A modification of the method of Nir *et al*. (43) was used for the assay of the mixing of the aqueous contents of lipid vesicles. Three populations of unilamellar vesicles (0.5 mg lipid/mL) were prepared in the following solutions: (i) 10 mM $TbCl_3 \cdot 6H_2O$/100 mM nitrilotriacetic acid (NTA)/20 mM Tris-HCl buffer (pH 7.4), (ii) 100 mM dipicolinic acid (DPA)/20 mM NaCl/20 mM Tris-HCl buffer (pH 7.4) and (iii) 5 mM $TbCl_3 \cdot 6H_2O$/50 mM NTA/50 mM DPA/10 mM NaCl/20 mM Tris-HCl buffer (pH 7.4). After vesicle preparation, the nonentrapped material was separated by gel filtration of 0.4 mL of the liposomal suspension on a Sephadex G-50 (Pharmacia Biotech, Uppsala, Sweden) column (200 × 10 mm), previously

equilibrated with 100 mM NaCl/0.75 mM EDTA/20 mM Tris-HCl buffer (pH 7.4). Liposomes were eluted by the solution used in the equilibration process; and 1.6 mL of liposomes free of nonentrapped material, containing 99% of the applied lipid, was collected. $TbCl_3$ and DPA vesicles were mixed in a 1:1 molar ratio at a final lipid concentration of 0.05 mg/mL for the fusion assay in a 100 mM NaCl/20 mM Tris-HCl buffer (pH 7.4). Fluorescence measures were performed at 20°C for 2 min after the addition of small aliquots of concentrated NaCl, $CaCl_2$, or $MgCl_2$ solutions to the liposome suspensions, in a Kontron SFM 25 spectrofluorimeter at an excitation wavelength of 276 nm. The emission fluorescence was measured at 545 nm using a 530-nm cut-off filter to eliminate the contribution of light scattering. The value for 100% fusion was determined using the reference liposomes (*R*) prepared with solution (*C*). Light scattering controls were performed using unlabeled vesicles. The percentage of fusion was calculated in the same way as for the lipid-mixing assay.

Zeta potential measurement. The zeta potential of the liposomes was measured by the commercial device ZetaSizer 4 of Malvern Instruments (Malvern, Worchestershire, United Kingdom), based on the method of photon correlation spectroscopy (PCS) (44,45). The method uses the autocorrelation function of the light scattered in a colloid solution measured by a photon counting system. The particles move in an electric field of known strength in the interference pattern of two laser beams and produce scattered light, which oscillates in time in a way that depends on the speed of the particles. The light scattered by the particles is collected by the photomultiplier and the measured autocorrelation function is first converted, using a Fourier transform, into a frequency spectrum. The frequencies are then converted successively to velocities, electrophoretic mobility and, finally, zeta potentials. The zeta potential of the liposomes is calculated by means of the Henry correction of Smoluchowski's equation (44),

$$\mu = \frac{2\varepsilon\zeta}{3\eta} f(\kappa a) \qquad [3]$$

where μ is the particle electrophoretic mobility, ε the dielectric constant, ζ the zeta potential, η the aqueous solution viscosity, and $f(\kappa a)$ is the Henry coefficient (46). The Malvern ZetaSizer 4 has an optic unit containing a 5 mW helium-neon laser; a ZET5104 electrophoresis cell, which uses a 4-mm diameter quartz capillary; a sample handling unit; and a multi-8 bit correlator with 72 data channels and 7 monitor channels with variable time expansion. The measurements of the zeta potential were performed at a fixed electrolyte concentration (50 mM NaCl in 10 mM Tris-HCl buffer of pH 7.4) and 25°C, with liposomes prepared from NPPE or NPPS, as described above. The method of liposome preparation used here gave particles with z-average diameters ranging from 300 to 400 nm. In order to check the Malvern device, a carboxy-modified polystyrene latex sample, with a zeta potential of –55 mV at 25°C, was used before each set of determinations.

Surface pressure measurements: compression isotherms. The compression isotherms were measured on a Langmuir film balance equipped with a Wilhelmy platinum plate, similar to that described by Verger and De Haas (47). The output of the pressure pick-up (Beckman LM 600 microbalance) was calibrated by recording the well-known isotherms of stearic acid and dipalmitoylphosphatidylcholine. The Teflon trough (surface area 495 cm^2, volume 330 mL) was regularly cleaned with hot chromic acid; moreover, before each experiment, it was washed with ethanol and rinsed with double-distilled water. Before each run, the platinum plate was cleaned with chromic acid and rinsed with double-distilled water. The films were spread on the aqueous surface using a Hamilton microsyringe, and at least 10 min was allowed for solvent evaporation. Films were compressed at a rate of 4.2 cm/min. Changes in the compression rate did not alter the shape of the isotherms. All the isotherms were run at least three times in the direction of increasing pressure with freshly prepared films. The accuracy of the system under the conditions in which the bulk of the reported measurements were made was ±0.5 mN/m for surface pressure.

RESULTS

Vesicle aggregation. Cation-dependent NPPE and NPPS liposome aggregation was followed by measuring the turbidity changes of lipid vesicle suspensions. Turbidities of small unilamellar NPPE and NPPS liposomes with respect to various Ca^{2+} and Mg^{2+} concentrations are shown in Figure 1A. The sharp increase in turbidity of NPPS liposomes was observed from about 1 mM Ca^{2+} and 2 mM Mg^{2+}. However, when NPPE liposome aggregation was determined, the significant increases in turbidity were observed at higher concentrations, from about 4 mM and above for both Ca^{2+} and Mg^{2+}. In this case, the slopes of the plots obtained for both divalent cations were much less steep, and thus the extent of the aggregation, measured at a given time, was smaller than that corresponding to the NPPS liposomes. The aggregation of NPPS and NPPE liposomes as a function of the lipid concentration is given in Figure 1B. A clear difference between NPPS and NPPE liposomes with regard to the sensitivity toward the aggregation processes was observed when increases in absorbance of the liposome suspensions were plotted vs. the concentration of both aminophospholipid derivatives. As in Figure 1A, the slopes of the Ca^{2+}- and Mg^{2+}-induced aggregation of NPPS liposomes as a function of the lipid concentration were considerably steeper than those obtained for NPPE liposomes. Besides this, the extent of the Mg^{2+}-induced aggregation is higher than that obtained in the presence of Ca^{2+} for either NPPS or NPPE.

In Figure 2, the sodium-induced aggregation of NPPS and NPPE liposomes is plotted vs. cation concentration (A) and vs. lipid concentration (B). The shapes of the curves corresponding to the turbidity values obtained at different Na^+ concentrations are quite different, being more sigmoidal than those obtained for NPPS. Besides this, at the lowest Na^+ concentrations, the aggregation of NPPS liposomes is delayed compared to NPPE liposomes. When turbidities were plotted

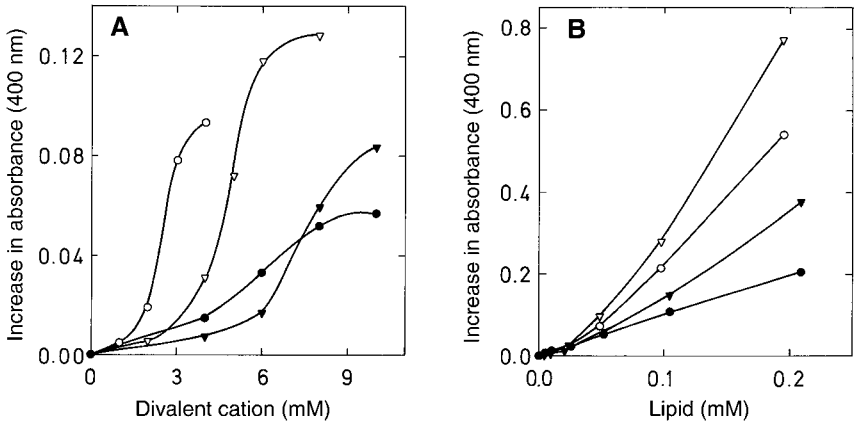

FIG. 1. Divalent cation-induced aggregation of *N*-palmitoylphosphatidylethanolamine (NPPE) and *N*-palmitoylphosphatidylserine (NPPS) unilamellar liposomes as a function of cation (A) and phospholipid (B) concentrations. (A) Influence of calcium (○,●) and magnesium (▽,▼) concentrations in the aggregation of NPPS (○, ▽) and NPPE (●,▼) liposomes. Phospholipid concentration was 0.05 mg/mL in a solution that contained 20 mM Tris-HCl buffer (pH 7.4), and 0.1 mM EDTA. (B) The dependence of the aggregation process on the phospholipid concentration was followed in 20 mM Tris-HCl buffer (pH 7.4), 0.1 mM EDTA, using $CaCl_2$ 3 mM for NPPS (○) and 8 mM for NPPE (●) or $MgCl_2$ 5.5 mM for NPPS (▽) and 8 mM for NPPE (▼). The values in the plots correspond to the average of four independent experiments. Variation coefficients ranged from 1.8 to 3.4.

vs. lipid concentrations (Fig. 2B), at a fixed Na^+ concentration of 0.5 M, great differences between both lipid species were observed. The slope corresponding to the aggregation of NPPE liposomes is very much steeper in comparison to that for NPPS liposomes. These results show a greater influence of lipid concentration in the monovalent cation-induced aggregation of NPPE liposomes in contrast with the results obtained for divalent cations, where the steeper plots were those corresponding to NPPS liposomes (Fig. 1B).

The threshold concentrations were calculated as the cation concentration corresponding to the maximal increase in the rate of absorbance change from the experimental data in Figures 1A and 2A. The calcium, magnesium, and sodium threshold concentrations were, respectively, 6.2, 7.0, and 440 mM for the aggregation of NPPE and 1.9, 4.4, and 720 mM for the aggregation of NPPS unilamellar liposomes. The results obtained show that the order of effectiveness of the cations to induce the initial spontaneous NPPE and NPPS liposomes aggregation is $Ca^{2+} > Mg^{2+} > Na^+$, although at cation concentrations above the corresponding threshold values the extent of the process is greater with Mg^{2+} ions. When comparing the threshold concentrations of divalent cations,

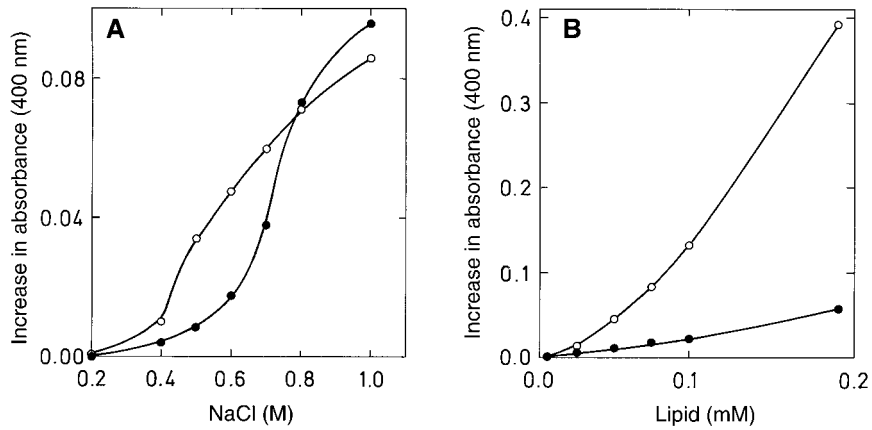

FIG. 2. Turbidity changes of NPPE and NPPS liposome suspensions measured at different sodium (A) and phospholipid (B) concentrations. Phospholipid concentration was 0.05 mg/mL in a solution that contained 20 mM Tris-HCl buffer (pH 7.4), and 0.1 mM EDTA, when the influence of the sodium concentration was studied. The dependence of the aggregation process on the phospholipid concentration was followed in 20 mM Tris-HCl buffer (pH 7.4), 0.1 mM EDTA, using NaCl 0.5 M. (○): NPPE; (●): NPPS. The values in the plots correspond to the average of four independent experiments. For abbreviations see Figure 1. Variation coefficients ranged from 2.1 to 3.8.

we observed that NPPS is more sensitive to aggregation than NPPE but, when Na^+ threshold values were considered, the sensitivity of both lipids to aggregation was reversed.

In Figure 3, the log of the initial rate of aggregation increase at a fixed cation concentration is plotted against the log of the lipid concentration for NPPS and NPPE liposomes. The data yield reasonably linear plots in the range of lipid concentrations from 25 to 200 µM. The slopes, ranging from 1.04 to 1.62, indicate the order of the aggregation reaction and show again the different behavior of NPPS and NPPE liposomes toward the aggregation processes.

Vesicle size changes. The state of aggregation of unilamellar NPPS and NPPE liposomes induced by divalent and monovalent cations was also followed by PCS. Figure 4 shows the changes in the vesicle diameter distribution of NPPS and NPPE liposomes in the presence of divalent (Ca^{2+} and Mg^{2+}) and monovalent (Na^+) cations with respect to their size without added cations. The analysis of the data shows that NPPS and NPPE liposomes, prepared by sonication in 10 mM Tris-HCl buffer media, have an average diameter of 37.8 ± 9.1 and 43.8 ± 9.3 nm, respectively, but the particle size increases in the presence of both divalent and monovalent cations. Table 1 shows the changes in vesicle size resulting from the aggregation processes. It can be seen that, when Ca^{2+} or Mg^{2+} was added to NPPE liposomes to a final concentration slightly lower than the corresponding threshold concentrations, two different-sized vesicle populations were observed. Their mean diameters were 4 and 10 times higher than those observed when the cations were not present. However, only one population of vesicles was obtained when divalent cations were added to NPPS liposomes, the mean di-

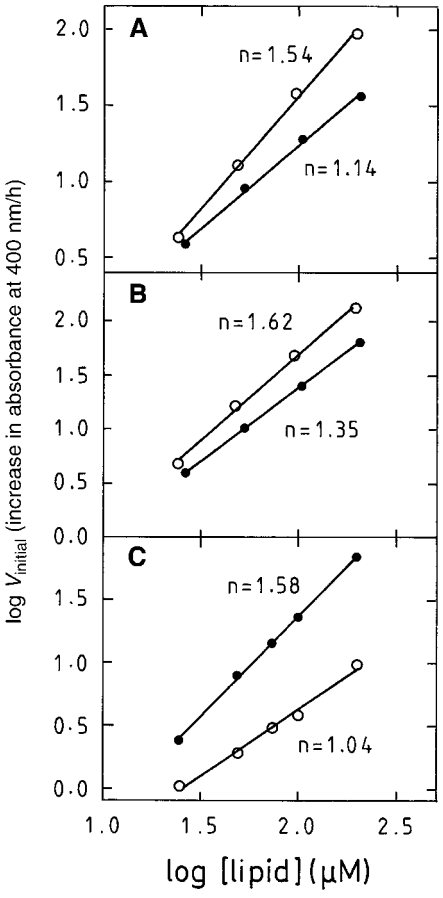

FIG. 3. Dependence of aggregation of small unilamellar liposomes on lipid concentration. Initial rates of aggregation (increase in absorbance units per hour) were plotted in a double-logarithmic manner against NPPS (○) and NPPE (●) concentrations. The aggregation was initiated by addition of: (A) $CaCl_2$ 3 mM for NPPS and 8 mM for NPPE, (B) $MgCl_2$ 5.5 mM for NPPS and 8 mM for NPPE, and (C) NaCl 500 mM for NPPS and NPPE, to liposomes at various lipid concentrations. Initial rates of aggregation have been obtained from the experimental data in Figures 1 and 2. For abbreviations see Figure 1.

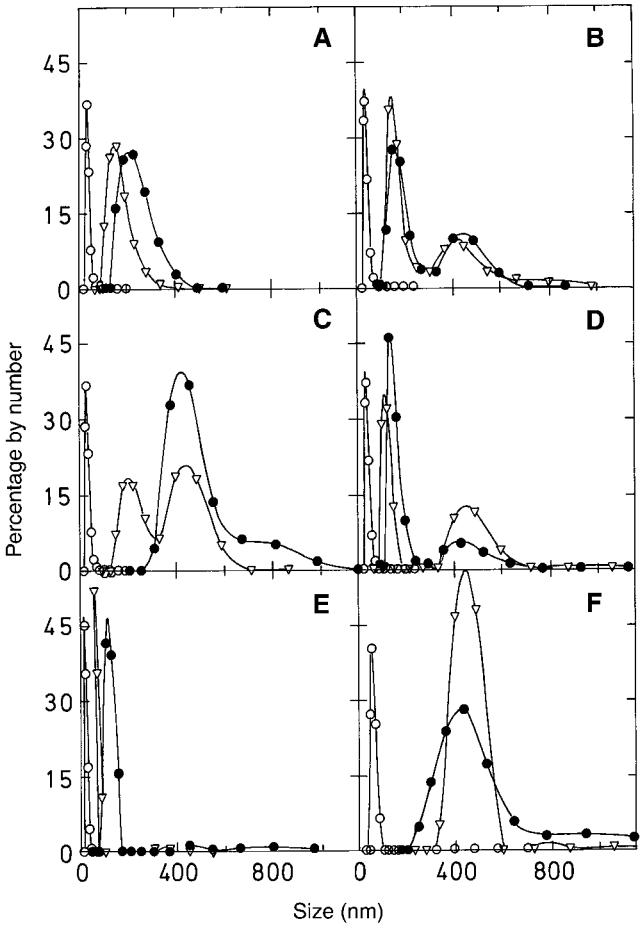

FIG. 4. Light scattering particle size analysis of NPPS (A,C,E) and NPPE (B,D,F) liposomes in the presence of calcium (A,B), magnesium (C,D), and sodium (E,F) ions. The vesicle diameter was measured before (○) and after (●) addition of the three ions. The reversibility of divalent and monovalent cation-induced aggregation was tested measuring vesicle size after EDTA addition (▽) at six times the concentration of divalent cation to the aggregated vesicles or after dilution of the aggregated vesicles up to 200 mM sodium concentration (▽). For this study, NPPS and NPPE concentrations were in all cases 0.1 mg/mL. The $CaCl_2$ concentration was 1.5 mM for NPPS and 5 mM for NPPE. The $MgCl_2$ concentration was 3.5 mM for NPPS and 5 mM for NPPE. The NaCl concentration was 480 mM for NPPS and NPPE. The values in the plots correspond to the average of three independent experiments. For abbreviations see Figure 1. Variation coefficients ranged from 4.3 to 6.2.

TABLE 1
Change in the Number-Size Distribution of NPPE and NPPS Vesicles in the Presence of Different Cations, Measured by Photon Correlation Spectroscopy[a]

Treatment	Average diameter in nm (%)			
	NPPE		NPPS	
None	43.8 ± 9.3 (100)	—	37.8 ± 9.1 (100)	—
+ $CaCl_2$	176.9 ± 36.2 (76)	449.1 ± 73.8 (24)	230 ± 59.8 (100)	—
+ $CaCl_2$ + EDTA	168.7 ± 30.0 (76)	451.7 ± 121.4 (24)	164.8 ± 48.2 (100)	—
+ $MgCl_2$	154.1 ± 25.4 (87)	435.5 ± 89.5 (13)	475.8 ± 132.8 (100)	—
+ $MgCl_2$ + EDTA	124.3 ± 17.5 (73)	474. 9 ± 77.5 (26)	212.5 ± 39.5 (52)	444.3 ± 73.7 (48)
NaCl	453.9 ± 169.9 (100)	—	123.9 ± 17.8 (97)	635.2 ± 172.7 (3)
NaCl + dilution	441.9 ± 50.5 (99)	1168.3 ± 111.8 (1)	68.1 ± 9.4 (98)	358.9 ± 114.8 (2)

[a]For conditions of the assay see Figure 4. The data are the mean diameter values calculated from the number-size distribution for each population ± SD obtained in the measure. The percentage of each vesicle population is indicated in parentheses. NPPE, *N*-palmitoylphosphatidylethanolamine; NPPS, *N*-palmitoylphosphatidylserine.

ameter after Mg^{2+} addition being twice that obtained with Ca^{2+}. After addition of 480 mM Na^+, NPPE liposomes increased their mean size up to 453.9 nm, whereas the increase in size of NPPS liposomes was less significant (mean diameter 123.9 nm).

After addition of EDTA to the divalent cation-aggregated vesicles or after dilution of the sodium-aggregated ones, only a partial reversibility of the aggregation processes occurred, since the size of liposomes did not return to the initial value in any case. These results indicate that divalent and monovalent ions would induce the formation of irreversible aggregates and suggest that vesicle fusion may occur in the presence of both cations.

NPPS and NPPE liposomes fusion. Mixing analysis for both lipid and internal aqueous contents (Figs. 5 and 6), shows that fusion rather than aggregation of NPPS and NPPE liposomes occurs in the presence of both divalent and monovalent ions, as suggested by the irreversibility of the aggregation processes. Figure 5 shows the percentage of fusion of NPPS (A–C) and NPPE (D–F) liposomes, measured as the transfer of resonance energy between NBD-PE and Rh-PE, after the addition of various concentrations of Ca^{2+} (Fig. 5A,D), Mg^{2+} (Fig. 5B,E) and Na^+ (Fig. 5C,F). The percentage of fusion depends on the nature and on the concentration of the cation and increases with time after cation addition. Lipid exchange between NPPS liposomes happened to a similar extent when Ca^{2+} (Fig. 5A) and Mg^{2+} (Fig. 5B) were added at the same concentrations, ranging from 2 to 4 mM, but the extent of this process was much less in the presence of Na^+ (Fig. 5C). In this case the concentrations needed to reach the same percentage of fusion were two orders of magnitude higher. NPPE liposomes also fuse in the presence of divalent (Fig. 5D,E) and monovalent (Fig. 5F) ions, although there are significant differences with regard to the results obtained for NPPS liposomes. Thus, the effectiveness of the divalent cations in inducing lipid mixing was higher for opposed bilayers of NPPS than for NPPE. However, NPPE liposomes were more sensitive than NPPS liposomes to sodium-induced lipid mixing, the most marked differences occurring between the two for additions of 400 and 600 mM sodium. The data obtained from the lipid exchange assays agree with the results of the aggregation studies. In order to show (i) the differences observed between NPPS and NPPE liposomes with regard to their sensitivity to aggregation and fusion in the presence of the cations and (ii) the agreement between the aggregation and fusion behavior of both lipid species, the initial velocity values of the aggregation and fusion processes at a fixed cation concentration have been compared and the ratios between the values obtained for NPPS and NPPE liposomes have been calculated (Table 2).

The data obtained when the mixing of the internal aqueous contents was monitored by the increase in the fluorescence of the Tb^{3+}-DPA complex are shown in Figure 6. Aqueous mixing was studied for both NPPS (Fig. 6 A,B,C) and NPPE (Fig. 6 D,E,F) as a function of Ca^{2+} (Fig. 6A,D), Mg^{2+} (Fig. 6B,E), and Na^+ (Fig. 6C,F). The results obtained show the coalescence of the aqueous contents of both NPPS and NPPE liposomes in the presence of either monovalent and divalent ions and demonstrate the existence of a real fusion, which has already been suggested by the irreversibility of the aggregation processes and the lipid mixing between opposed bilayers of different liposome populations. The effectiveness of divalent and monovalent cations in inducing the mixing of the aqueous contents for both types of liposomes correlates

TABLE 2
Relative Kinetics of Different Cation-Induced Aggregation and Fusion for NPPE and NPPS Small Unilamellar Liposomes[a]

Cation concentration (mM)	Initial rate of increase			
	Absorbance at 400 nm (unit increase/min)		Fluorescence (max/min, %)	
	NPPE	NPPS	NPPE	NPPS
Ca^{2+}: 4	0.044	0.281(6.39)	60	420(7)
Mg^{2+}: 4	0.020	0.093(4.65)	63	330(5.22)
Na^+: 600	0.143	0.053(0.37)	183	66(0.36)

[a]Aggregation and fusion were initiated by addition of the different cations at the concentration indicated at the table. The total lipid concentration was 0.05 mg/mL. Fusion data correspond to lipid exchange measured by the RET assay. Values in parentheses indicate the ratio of initial rates of NPPS aggregation over NPPE aggregation (column three) or the ratio of initial rates of NPPS fusion over NPPE fusion (column five). For abbreviations see Table 1.

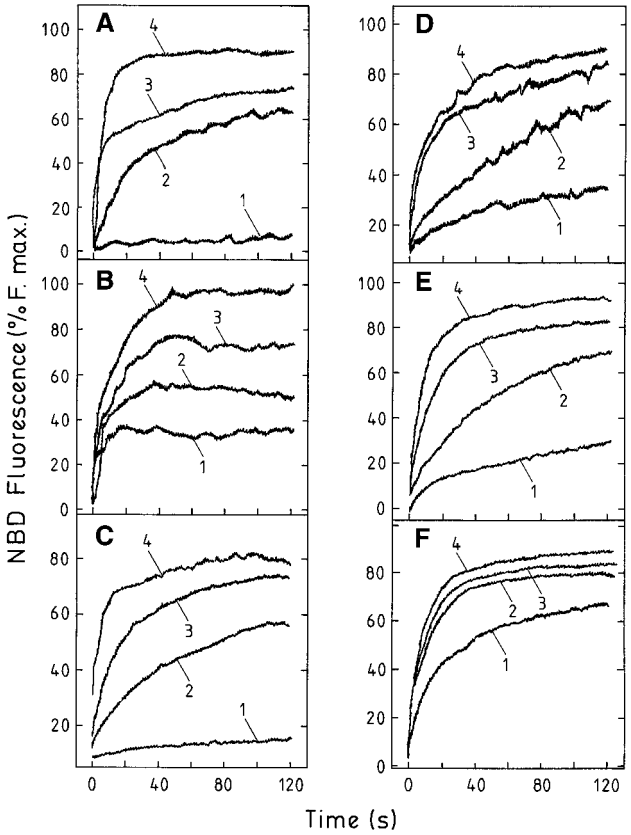

FIG. 5. Lipid mixing by the probe dilution assay of NPPS (A–C) and NPPE (D–F) liposomes, containing 0.5% Rh-PE and 1% NBD-PE, after cation addition. Percent maximal fluorescence changes were plotted vs. time at 20°C after the addition (numbered lines, 1, 2, 3 and 4, in increasing order of concentration) of $CaCl_2$ 1, 2, 3, and 4 mM (A) or 4, 6, 8, and 10 mM (D); $MgCl_2$ 1, 2, 3, and 4 mM (B) or 4, 6, 8, and 10 mM (E); and NaCl 400, 600, 750, and 1000 mM (C,F). The phospholipid concentration was 0.05 mg/mL in a solution that contained 20 mM Tris-HCl buffer (pH 7.4), and 0.1 mM EDTA, 100 mM NaCl. The values in the plots correspond to the average of four independent experiments. Variation coefficients ranged from 3.2 to 5.3. Rh-PE, *N*-(lissamine Rhodamine B sulfonyl)-phosphatidylethanolamine; NBD-PE, *N*-(7-nitrobenz-2-oxa-1,3-diazol-4-yl)-phosphatidylethanolamine; for other abbreviations see Figure 1.

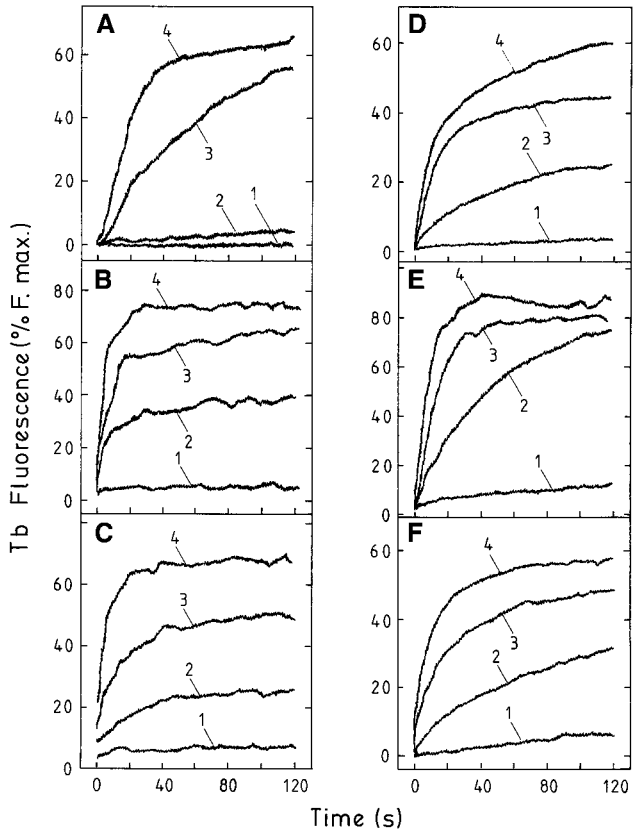

FIG. 6. Aqueous contents mixing of NPPS (A–C) and NPPE (D–F) liposomes, containing 10 mM $TbCl_3$ and 100 mM dipicolinic acid, after cation addition. Percent maximal fluorescence changes were plotted vs. time at 20°C after the addition (numbered lines, 1, 2, 3, and 4, in increasing order of concentration) of $CaCl_2$ 1, 2, 3, and 4 mM (A) or 4, 6, 8, and 10 mM (D); $MgCl_2$ 1, 2, 3, and 4 mM (B) or 4, 6, 8 and 10 mM (E); and NaCl 400, 600, 750 and 1000 mM (C,F). The phospholipid concentration was 0.05 mg/mL of 20 mM Tris buffer solution (pH 7.4). The values in the plots correspond to the average of three independent experiments. Variation coefficients ranged from 3.6 to 6.1. For abbreviations see Figure 1.

well with their effectiveness shown by the RET assay. Nevertheless, despite the fact that the extent of lipid mixing was similar using the same amounts of calcium and magnesium for both NPPS and NPPE liposomes, magnesium was more effective than calcium in inducing aqueous contents mixing. Moreover, regardless of the cation and the lipid used, at a given cation concentration, the extent of the fusion process expressed as mixing of aqueous contents was always lower than the value calculated from the lipid exchange assays.

Modification of liposome surface potential. The zeta potential changes of multilamellar NPPE and NPPS liposomes with respect to Ca^{2+} concentration are plotted in Figure 7. The results show that NPPS liposomes are slightly more negative than NPPE liposomes and that the effect of calcium in increasing the zeta potential values is more marked for NPPS liposomes. These results are in agreement with those obtained in the aggregation and fusion assays.

Compression isotherms. The molecular areas of NPPS and NPPE were estimated from studies of monolayer surface pressure. Compression isotherms were obtained after spreading 25 µL of 1 mg/mL $CHCl_3$ solutions of both lipid species on an aqueous buffered surface (pH 7.4) containing 20 mM Tris-HCl, 100 mM NaCl, and 0.1 mM EDTA. The molecular area values were calculated assuming that, in normal bilayers, the surface pressure is about 32–35 mN/m (48). The area/molecule values obtained from the plots of the compression isotherms were 99 $Å^2$ for NPPE and 106 $Å^2$ for NPPS. This result shows the similarity between the molecular areas of both *N*-acyl derivatives. On the other hand, the significant change in the molecular areas of the *N*-acyl derivatives with respect to their precursors PE and PS points out the influence of the incorporation of the third saturated (palmitic) fatty acid. The molecular areas of both aminophospholipids (PE and PS) reported in the literature range from 65 to 75 $Å^2$ (49,50).

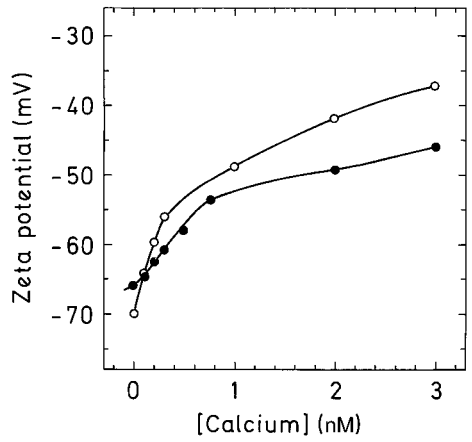

FIG. 7. Modification of the surface charge of multilamellar NPPS (○) and NPPE (●) liposomes by calcium ions at 25°C. Zeta potential variations are plotted as a function of calcium concentration. The total lipid concentration in the measurement cell was 0.5 mg/mL. Experiments were carried out in triplicate. Variation coefficients ranged from 4.4 to 6.5. For abbreviations see Figure 1.

DISCUSSION

These results show the ability of monovalent and divalent cations to induce aggregation and fusion of liposomes constituted by NPPE and NPPS and the differences that existed with regard to the nature of the cation and the nature of the lipid. The threshold concentrations for the aggregation of NPPE and NPPS unilamellar liposomes show that the order of effectiveness of the cations to induce the spontaneous aggregation of NPPE and NPPS liposomes is $Ca^{2+} > Mg^{2+} > Na^{+}$. The data also show that NPPS liposomes aggregate at lower concentrations of divalent cations than NPPE liposomes do and that the greater extent of aggregation at a given concentration of Na^{+} is obtained with NPPE liposomes. The almost linear dependence of the absorbance increases with regard to lipid concentration for NPPE liposomes in the presence of calcium and for NPPS liposomes in the presence of sodium and the exponential curves obtained with magnesium and sodium for NPPE liposomes and with calcium and magnesium for NPPS liposomes show that the reaction order for the aggregation processes depends on the lipid and the cation. The logarithmic secondary plots of the initial aggregation rates vs. lipid concentrations (Fig. 3) give the order of the aggregation reactions, which ranges from 1.04 to 1.64. An order of reaction of about 1 denotes that there is a direct relationship between the aggregation rate and the lipid concentration and that the extent of the process depends on the frequency of the collisions, which in turn depends on the concentration of vesicles. On the other hand, the initial rate of vesicle aggregation can be expected to be second order with respect to vesicle concentration if the existence of a bivesicular step in aggregation is considered (39,51). The order of the aggregation reactions near 1.5, determined in this work, could be justified by assuming that the formation of stable dimers does not occur for all the collisions between two vesicles. A reaction order of 1.5 also has been predicted for the fusion process of the dimyristoylphosphatidylcholine-myristic acid system, in which the rate-limiting step is the activation of a vesicle that remains active for several fusions with either nonactivated (without free fatty acid) or other activated (with free fatty acid) vesicles (52).

The irreversibility of the aggregation process and the intermixing of bilayer components, proved by the probe dilution assay of the RET method, suggest that vesicle fusion rather than mere aggregation occurs with both mono- and divalent cations. Cation concentrations that cause massive aggregation are those that initiate bilayer lipid mixing. Compared to NPPE liposomes, the greater tendency of NPPS liposomes to aggregate or to show lipid mixing in the presence of calcium correlates well with the higher negative surface charge of NPPS vesicles. The zeta potential values obtained by laser Doppler anemometry show the greater affinity of calcium to bind to NPPS bilayers and agree with the higher effectiveness of this cation to induce aggregation and lipid mixing of NPPS liposomes.

The zeta potential values have been calculated from the Henry correction of the Smoluchowski equation, which implies that the mobility of a phospholipid vesicle should be essentially independent of its size and shape for all charge densities. However, electrophoretic mobility depends on the size of vesicles (46) and on the salt concentration (53). In this way, O'Brien and White (54) reported that zeta potentials obtained from the application of classical electrokinetic theory might be seriously underestimated, especially at low electrolyte concentrations. The results of Egorova *et al.* (55), showing that the zeta potential as a function of the ionic strength deviates significantly from the predictions of the double-layer theory in the 1–50 mM range, and the analysis of the electrophoretic mobility by Wiersema *et al.* (56), indicating that for all experimentally accessible charge densities the mobility of a phospholipid vesicle in a 0.114 M monovalent salt solution should be independent of its size, show that in our experimental conditions (ionic strength > 60 mM) the zeta potentials obtained should not differ significantly from the theoretical values. All these considerations point out that the difference in behavior reported in this paper for the two kind of liposomes, in the presence of calcium and under conditions of equal ionic strength, is due to the different nature of their lipid constituents, which determines the different affinities to bind calcium.

The facts that the initial sizes of NPPS and NPPE small liposomes are alike and the molecular areas of both lipid species also are alike point out that the number of lipid molecules per vesicle is similar. However, the higher negative charge of the NPPS molecule, due to its carboxyl group, at physiological pH conditions would account for the differences in the zeta potential values obtained for NPPS and NPPE large liposomes, either in the absence or in the presence of calcium.

The results of the aggregation and lipid exchange studies and the above considerations suggest that the observed differences in the threshold concentrations of monovalent and di-

valent cations that induce massive aggregation and lipid mixing of NPPS and NPPE liposomes are related to the different chemical structures of the polar group of both lipid species and to differences in the negative surface charge of the bilayers.

To prove that sodium, calcium, and magnesium ions induce the fusion of liposomes constituted by NPPE and NPPS, we studied the mixing of the internal aqueous compartments of the vesicles. The assay, which relies on the formation of the fluorescent Tb/DPA complex upon mixing of the vesicle contents and allows continuous monitoring of fusion processes, meets a rigorous criterion for vesicle–vesicle fusion (39,57). Our results demonstrate the coalescence of the aqueous contents of both NPPS and NPPE liposomes in the presence of both monovalent and divalent cations and, thus, the existence of real fusion. However, in spite of the similar effectiveness of monovalent and divalent cations in inducing the mixing of the aqueous contents of NPPE and NPPS liposomes and the exchange of the lipid components of the NPPE and NPPS bilayers, the extent of the mixing of the aqueous contents was always lower than the intermixing of lipid components.

The lower extent of mixing of the internal aqueous contents can be explained in two ways. First, in lipid-mixing measurements there may be a contribution of fusion (mixing of membrane components and coalescence of aqueous contents) and hemifusion processes (merging of the contacting monolayers of opposing membranes, such that only half of each membrane's lipids can mix) (58–60); in this case the hemifusion would give structures stable enough not to develop the initial fusion pores to yield fusion. On the other hand, the lower extent of mixing of internal aqueous contents observed can be explained by a loss of fluorescence due to the leakage of the encapsulated Tb/DPA complex into the EDTA-containing medium or to the entry of EDTA. A more exhaustive study to establish the real extent and the mechanisms of the fusion processes, which includes the consideration of the possible leakage of the fluorescent complex from fused vesicles, is now in progress. On the other hand, the study of aggregation, fusion, and bilayer destabilization carried out in our laboratory with a different *N*-acylaminophospholipid (*N*-myristoylphosphatidylethanolamine, NMPE) has shown a significant Mg^{2+}- and Na^{+}-induced release either of the Tb/DPA complex or carboxyfluorescein, suggesting a vesicle destabilization after fusion; nevertheless, this event does not occur in the presence of Ca^{2+} (Mora, M., Rosell, F., and de Madariaga, M.A., unpublished results). All the same, the curves corresponding to the time course of the mixing of NMPE vesicles content were fairly different from those obtained for NPPS and NPPE with respect to the lesser extent of mixing of internal aqueous contents toward the extent of lipid exchange between the bilayers and the decrease in the fluorescence of the Tb/DPA complex 20 s after cation addition, attributable to Tb/DPA leakage (Mg^{2+}- and Na^{+}-induced fusion) or to the entry of Ca^{2+} or EDTA (Ca^{2+}-induced fusion). Despite the absence of leakage curves, the results of the Tb/DPA assays presented here show the ability of monovalent and divalent ions to induce a real fusion of NPPS and NPPE liposomes, although the percentages of fusion reported could be slightly underestimated with regard to those obtained from the RET assays in the case of a leakage of the Tb/DPA complex or an entry of EDTA happened as the result of membrane destabilization induced by monovalent and divalent cations (Mora, M., Rosell, F., and de Madariaga, M.A., unpublished results).

The differences between the abilities of Ca^{2+} and Mg^{2+} to induce NPPS and NPPE liposome fusion must be related to the effect of ions on the stabilizing hydration layer at the lipid–water interface and to the nature of the membrane surface, which will in turn be related to the conformation of the polar group of the lipid. Wilschut *et al*. (39) reported differences in the fusion of large unilamellar vesicles (LUV) and SUV, composed of pure bovine brain PS, induced by Ca^{2+} and Mg^{2+}. They showed (i) that magnesium does not induce the fusion of LUV but does induce the fusion of SUV, although the extent of this process is limited to a small increase in vesicle size, and (ii) that calcium induces rapid and extensive fusion of LUV and SUV. By contrast, our results showed the ability of Mg^{2+} to induce an extensive fusion of SUV constituted by NPPE or NPPS, that fusion is accompanied by a remarkable increase in vesicle size, and that the effect of magnesium on the NPPS liposome fusion, as measured by size increases, is greater than that of calcium. The different sensitivity of NPPS and NPPE liposomes to Ca^{2+}- and Mg^{2+}-induced fusion with regard to the data reported for PS liposomes could by justified on the basis of the structural modifications due to the N-acylation reaction. The fusion observed in the presence of the monovalent sodium ion underlines the different physical and chemical properties of the *N*-acyl derivatives of membrane aminophospholipids with regard to their precursors. To date, the ability of monovalent cations to induce fusion of liposomal membranes had been reported only by Eklund (61), who showed that sonicated vesicles consisting of acidic phospholipids with fully saturated fatty acids fuse in the presence of monovalent cations, whereas those containing unsaturated fatty acids do not. However, NPPS and NPPE synthesized in this work from natural bovine brain PS and egg TPE contain unsaturated fatty acids at the *sn*-2 position and fuse in the presence of sodium.

The results presented in this paper, together with the cited references (1,11,12,16,19–22,28,29), emphasize the fact that synthesis *in vivo* of N-acylated phospholipids can introduce important changes in membrane-mediated processes. The establishment of the real physiological meaning of the N-acylation reactions, which affect some membrane phospholipids, and the elucidation of the mechanisms by which the N-acylated constituents influence or modify the structure or dynamics of biological membranes are aims of our research. Our results to date seem to point out a protective role of *N*-acylaminophospholipids against membrane damage, as the N-acylation changes the nonbilayer PE into a bilayer lipid, with the resulting stabilization of the lipid bilayer. On the other hand, the incorporation of *N*-acyl derivatives into cell mem-

branes increases their negative charge, because of the formation of an amide bond, and makes them more sensitive to cation-induced fusion. Moreover, the facts (i) that NPPS-containing liposomes fuse to a lesser extent than PS-containing liposomes do, and (ii) that one of the suggested mechanisms for vesicle–vesicle fusion involves the formation of micellar intermediates from the nonbilayer PE, the synthesis of NPPS or NPPE from PS and PE and the resultant decrease in the bilayer levels of both aminophospholipids, would also account for the stabilizing effect of cell membranes against the sudden increases in cation concentrations that occur in some pathological situations. However, the experimental data reported here do not allow us to extrapolate to physiological conditions because the vesicles used were composed of only NPPE or NPPS. The present aggregation and fusion studies, together with our previous publications about permeability properties (19,62), bilayer fluidity (19), and polymorphic behavior (21,63,64) of *N*-acylPE-containing liposomes, have led us to consider the fusogenic characteristics of different mixed liposomes. Moreover, the fusogenic behavior of liposomes containing *N*-acyl derivatives of PE and PS could be helpful in developing drug delivery systems.

ACKNOWLEDGMENTS

This work was supported by grant no. PB94-0911-A from D.G.I.C.Y.T. (Spain).

REFERENCES

1. Schmid, H.H.O., Schmid, P.C., and Natarajan, V. (1990) *N*-Acylated Glycerophospholipids and Their Derivatives, *Prog. Lipid Res. 29*, 1–43.
2. Chapman, K.D., and Moore, T.S., Jr. (1993) *N*-Acylphosphatidylethanolamine Synthesis in Plants: Occurrence, Molecular Composition and Phospholipid Origin, *Arch. Biochem. Biophys. 301*, 21–33.
3. Epps, D.E., Natarajan, V., Schmid, P.C., and Schmid, H.H.O. (1980) Accumulation of *N*-Acylethanolamine Glycerophospholipids in Infarcted Myocardium, *Biochim. Biophys. Acta 618*, 420–430.
4. Natarajan, V., Schmid, P.C., and Schmid, H.H.O. (1986) *N*-Acylethanolamine Phospholipid Metabolism in Normal and Ischaemic Rat Brain, *Biochim. Biophys. Acta 878*, 32–41.
5. Nelson, G.J. (1970) Studies on the Lipids of Sheep Red Blood Cells. IV. The Identification of a New Phospholipid, *N*-Acylphosphatidylserine, *Biochem. Biophys. Res. Commun. 38*, 261–265.
6. Natarajan, V., Schmid, P.C., Reddy, P.V., Zuzarte-Augustin, M.L., and Schmid, H.H.O. (1985) Occurrence of *N*-Acylethanolamine Phospholipids in Fish Brain and Spinal Cord, *Biochim. Biophys. Acta 835*, 426–433.
7. Schmid, P.C., Natarajan, V., Weis, B.K., and Schmid, H.H.O. (1986) Hydrolysis of *N*-Acylated Glycerophospholipids by Phospholipases A_2 and D: A Method of Identification and Analysis, *Chem. Phys. Lipids 41*, 195–207.
8. Reddy, P.V., Natarajan, V., Schmid, P.C., and Schmid, H.H.O. (1983) *N*-Acylation of Dog Heart Ethanolamine Phospholipids by Transacylase Activity, *Biochim. Biophys. Acta 750*, 472–480.
9. Chapman, K.D., and Moore, T.S., Jr. (1993) Catalytic Properties of a Newly Discovered Acyltransferase That Synthesizes *N*-Acylphosphatidylethanolamine in Cottonseed (*Gossypium hirsutum* L.) Microsomes, *Plant Physiol. 102*, 761–769.
10. Devane, W.A., Hanus, L., Breuer, A., Pertwee, R.G., Stevenson, L., Griffin, G., Gibson, D., Mandelbaum, A., Etinger, A., and Mechoulam, R. (1992) Isolation and Structure of a Brain Constituent That Binds to the Cannabinoid Receptor, *Science 258*, 1946–949.
11. Schmid, H.H.O., Schmid, P.C., and Natarajan, V. (1996) The N-Acylation–Phosphodiesterase Pathway and Cell Signaling, *Chem. Phys. Lipids 80*, 133–142.
12. Chapman, K.D., Tripathy, S., Venables, B., and Desouza, A.D. (1998) *N*-Acylethanolamines: Formation and Molecular Composition of a New Class of Plant Lipids, *Plant Physiol. 116*, 1163–1168.
13. Cadas, H., Schinelli, S., and Piomelli, D. (1996) Membrane Localization of *N*-Acylphosphatidylethanolamine in Central Neurons—Studies with Exogenous Phospholipases, *J. Lipid Mediators Cell Signal. 14*, 63–70.
14. Bezuglov, V.V., Bobrov, M.Y., and Archakov, A.V. (1998) Bioactive Amides of Fatty Acids, *Biokhimiya (Moscow) 63*, 22–30.
15. Ellingson, J.S., and Dischinger H.C. (1985) Concurrent Disappearance of *N*-Acylethanolamine Glycerophospholipids and Phagolysosomes Enriched in *N*-Acylethanolamine Glycerophospholipids as *Dictyostelium discoideum* Aggregate, *Biochim. Biophys. Acta 812*, 255–260.
16. Basu, A., Prence, E., Garret, K., and Ellingson, J.S. (1985) Comparison of *N*-Acylphosphatidylethanolamines with Different *N*-Acyl Groups as Activators of Glucocerebrosidase in Various Forms of Gaucher's Disease, *Arch. Biochem. Biophys. 243*, 28–34.
17. LaFrance, D., Marion, D., and Pezolet, M. (1990) Study of Structure of *N*-Acyldipalmitoylphosphatidylethanolamines in Aqueous Dispersions by Infrared and Raman Spectroscopy, *Biochemistry 29*, 4592–4599.
18. Hansen, H.S., Lauritzen, L., Strand, A.M., Vinggaard, A.M., Frandsen, A., and Schousboe, A. (1997) Characterization of Glutamate-Induced Formation of *N*-Acylphosphatidylethanolamine and *N*-Acylethanolamine in Cultured Neocortical Neurons, *J. Neurochem. 69*, 753–761.
19. Domingo, J.C., Mora, M., and De Madariaga, M.A. (1993) Incorporation of *N*-Acylethanolamine Phospholipids Into Egg Phosphatidylcholine Vesicles: Characterization and Permeability Properties of the Binary Systems, *Biochim. Biophys. Acta 1148*, 308–316.
20. Mercadal, M., Domingo, J.C., Bermudez, M., Mora, M., and De Madariaga, M.A. (1995) *N*-Palmitoylphosphatidylethanolamine Stabilizes Liposomes in the Presence of Human Serum. Effect of Lipid Composition, *Biochim. Biophys. Acta 1235*, 281–288.
21. García, A.M., Rosell, F., Sagristá, M.L., Mora, M., and De Madariaga, M.A. (1996) Structural Organization of *N*-Acyl Derivatives of PE into Bilayers: Polymorphic and Thermotropic Studies, *Colloids Surf. 115*, 73–82.
22. Newman, J., Stiers, D., Anderson, W., and Schmid, H.H.O. (1986) Phase Behavior of Synthetic *N*-Acylethanolamine Phospholipids, *Chem. Phys. Lipids 42*, 249–260.
23. Sandoval, J.A., Huang, Z., Garrett, D.C., Gage, D.A., and Chapman, K.D. (1995) *N*-Acylphosphatidylethanolamine in Dry and Imbibing Cottonseeds. Amounts, Molecular Species and Enzymatic Synthesis, *Plant Physiol. 109*, 269–275.
24. Wilschut, J. (1991) Membrane Fusion in Lipid Vesicle Systems. An Overview, in *Membrane Fusion* (Wilschut, J., and Hoekstra, D., eds.), pp. 89–126, Marcel Dekker Inc., New York.
25. Burger, K.N.J., and Verkleij, A.J. (1990) Membrane Fusion, *Experientia 46*, 631–644.
26. Chernomordik, L., Kozlov, M.M., and Zimmerberg, J. (1995) Lipids in Biological Membrane Fusion, *J. Membrane Biol. 146*, 1–14.
27. Verkleij, A.J., and Post, J.A. (1987) Physico-chemical Proper-

ties and Organization of Lipids in Membranes: Their Possible Role in Myocardial Injury, *Basic Res. Cardiol. 82*, 85–92.
28. Ortiz, J., Rosell, F., Mora M., and De Madariaga, M.A. (1992) Cation-Induced Aggregation and Fusion of *N*-Acyl-*N*-methylphosphatidylethanolamine Vesicles, *Chem. Phys. Lipids 61*, 185–191.
29. Morillo, M., Sagristá, M.L., and De Madariaga, M.A. (1989) *N*-Stearoylphosphatidylserine: Synthesis and Role in Divalent-Cation-Induced Aggregation and Fusion, *Lipids 33*, 607–616.
30. Ohki, S., and Arnold, K. (1990) Surface Dielectric Constant, Surface Hydrophobicity and Membrane Fusion, *J. Membrane Biol. 114*, 195–203.
31. Bailey, A.L., and Cullis, P.R. (1997) Liposome Fusion, in *Lipid Polymorphism and Membrane Properties* (Epand, R.M., ed.) Vol. 44, pp. 359–373, Academic Press Inc., San Diego.
32. Komatsu, H., and Okada, S. (1995) Ethanol-Induced Aggregation and Fusion of Small Phosphatidylcholine Liposomes: Participation of Interdigitated Membrane Formation in Their Processes, *Biochim. Biophys. Acta 1235*, 270–280.
33. Terletskaya, Y.T., Trikasha, I.O., Serdyuk, E.S., and Andreev, S.M. (1995) Fusion of Negatively Charged Liposomes Induced by Peptides of the N-Terminal Fragment Of HIV-1 Transmembrane Protein, *Biokhimiya (Moscow) 60*, 1309–1314.
34. Eklund, K.K., Takkunen, J.E., and Kinnunen, P.K.J. (1991) Cation-Induced Aggregation of Acidic Phospholipid Vesicles: The Role of Fatty Acid Unsaturation and Cholesterol, *Chem. Phys. Lipids 97*, 59–66.
35. Ohki, S., Roy, S., Ohshima, H., and Leonards, K. (1984) Monovalent Cation-Induced Phospholipid Vesicles Aggregation: Effect of Ion Binding, *Biochemistry 23*, 6126–6132.
36. Ohki, S., Düzgünes, N., and Leonards, K. (1982) Phospholipid Vesicles Aggregation: Effect of Monovalent and Divalent Ions, *Biochemistry 21*, 2127–2133.
37. Bental, M., Wilschut, J., Scholma, J., and Nir, S. (1987) Ca^{2+}-Induced Fusion of Large Unilamellar Phosphatidylserine/Cholesterol Vesicles, *Biochim. Biophys. Acta 898*, 239–247.
38. Ohki, S., and Duax, J. (1986) Effect of Cations and Polyamines on the Aggregation and Fusion of Phosphatidylserine Membranes, *Biochim. Biophys. Acta 861*, 177–186.
39. Wilschut, J., Düzgünes, N., and Papahadjopoulos, D. (1981) Calcium/Magnesium Specificity in Membrane Fusion: Kinetics of Aggregation and Fusion of Phosphatidylserine Vesicles and the Role of Bilayer Curvature, *Biochemistry 20*, 3126–3133.
40. Rouser, G., Siakotos, A.N., and Fleisher, S. (1966) Quantitative Analysis of Phospholipids by Thin-Layer Chromatography and Phosphorus Analysis of Spots, *Lipids 1*, 85–86.
41. Struck, D.K., Hoekstra, D., and Pagano, R.E. (1981) Use of Resonance Energy Transfer to Monitor Membrane Fusion, *Biochemistry 20*, 4093–4099.
42. Holland, J.V., Hui, C., Cullis, P.R., and Madden, T.D. (1996) Poly(ethylene glycol)–Lipid Conjugates Regulate the Calcium-induced Fusion of Liposomes Composed of Phosphatidylethanolamine and Phosphatidylserine, *Biochemistry 35*, 2618–2624.
43. Nir, S., Düzgünes, N., and Bentz, J. (1983) Binding of Monovalent Cations to Phosphatidylserine and Modulation of Ca^{2+}- and Mg^{2+}-Induced Vesicle Fusion, *Biochim. Biophys. Acta 735*, 160–172.
44. Hunter, R.J. (1988) *Zeta Potential in Colloid Science*, Academic Press, London.
45. Ware, B.R. (1983) The Application of Laser Light Scattering to the Study of Biological Motion, *NATO ASI Ser.* A *59*, 89–122.
46. Roy, M.T., Gallardo, M., and Estelrich, J. (1988) Influence of Size on Electrokinetic Behavior of Phosphatidylserine and Phosphatidylethanolamine Lipid Vesicles, *J. Colloid Interface Sci. 206*, 512–517.
47. Verger, R., and De Haas, G.H. (1973) Enzyme Reactions in a Membrane Model. I. New Technique to Study Enzyme Reactions in Monolayers, *Chem. Phys. Lipids 10*, 127–136.
48. Cevc, G., and Marsh, D. (1987) Bilayer Elasticity, in *Phospholipid Bilayers: Physical Principles and Methods* (Bittar, E.E., ed.), pp. 347–368, John Wiley & Sons, New York.
49. Marsh, D. (1990) *Handbook of Lipid Bilayers*, CRC Press, Inc., Boca Raton.
50. McIntosh, T.J., and Magid, A.D. (1993) Phospholipid Hydration, in *Phospholipids Handbook* (Cevc, G., ed.), pp. 553–577, Marcel Dekker, Inc., New York.
51. Liao, M., and Prestegard, J.H. (1980) Fusion Kinetics of Phosphatidylcholine–Phosphatidic Acid Mixed Lipid Vesicles. A Proton Nuclear Magnetic Resonance Study, *Biochim. Biophys. Acta 599*, 81–94.
52. Kantor, H.L., and Prestegard, J.H. (1975) Fusion of Fatty Acid Containing Lecithin Vesicles, *Biochemistry 14*, 1790–1795.
53. Eisenberg, M., Gresalfi, T., Riccio, T., and McLaughlin, S. (1979) Adsorption of Monovalent Cations to Bilayer Membranes Containing Negative Phospholipids, *Biochemistry 18*, 5213–5223.
54. O'Brien, R.W., and White, L.R. (1978) Electrophoretic Mobility of a Spherical Colloidal Particle, *J. Chem. Soc. Faraday Trans. 2 74*, 1607–1626.
55. Egorova, E.M., Dukhin, A.S., and Svetlova, I.E. (1992) Some Problems of Zeta Potential Determinations in Electrophoretic Measurements on Lipid Membranes, *Biochim. Biophys. Acta 1104*, 102–110.
56. Wiersema, P.H., Loeb, A.L., and Overbeek, J.T.G. (1966) Calculation of the Electrophoretic Mobility of a Spherical Colloid Particle, *J. Colloid Interface Sci. 22*, 78–99.
57. Wilschut, J., Düzgünes, N., Fraley, R., and Papahadjopoulos, D. (1980) Studies on the Mechanism of Membrane Fusion of Phosphatidylserine Vesicles Followed by a New Assay for Mixing of Aqueous Vesicle Contents, *Biochemistry 19*, 6011–6021.
58. Song, L.Y., Ahkong, Q.F., Georgescauld, D., and Lucy, J.A. (1991) Membrane Fusion Without Cytoplasmic Fusion (hemifusion) in Erythrocytes That Are Subjected to Electrical Breakdown, *Biochim. Biophys. Acta 1065*, 54–62.
59. Chernomordik, L.V., Chantoriya, A., Green, J., and Zimmemberg, J. (1995) The Hemifusion Intermediate and Its Conversion to Complete Fusion: Regulation by Membrane Composition, *Biophys. J. 69*, 922–92.
60. Zimmemberg, J., and Chernomordik, L.V. (1999) Membrane Fusion. *Adv. Drug Delivery Rev. 38*, 197–205.
61. Eklund, K.K. (1990) Monovalent Cation-Induced Fusion of Acidic Phospholipid Vesicles, *Chem. Phys. Lipids 52*, 199–206.
62. Sagrista, M.L., Mora, M., and De Madariaga, M.A. (1997) Permeability Studies of Liposomes of PC and *N*-(oleoyl/linoleoyl)-Phosphatidylethanolamines: Modification of the Head Group, in *Spectroscopy of Biological Molecules: Modern Trends* (Carmona, P., Navarro, R., and Hernanz, A., eds.), pp. 317–318, Kluwer Acad. Pub., Dordrecht, The Netherlands.
63. Domingo, J.C., Mora, M., and De Madariaga, M.A., (1994) Role of Head Group Structure in the Phase Behavior of *N*-Acylethanolamine Phospholipids: Hydrogen-Bonding Ability and Head Group Size, *Chem. Phys. Lipids 69*, 229–240.
64. Domingo, J.C., Mora, M., and De Madariaga, M.A., (1995) The Influence of *N*-Acyl Chain Length on the Phase Behavior of Natural and Synthetic *N*-Acylethanolamine Phospholipids, *Chem. Phys. Lipids 75*, 15–25.

[Received April 15, 1999, and in revised form February 7, 2000; revision accepted April 3, 2000]

Characterization of Inositol Phospholipids and Identification of a Mastoparan-Induced Polyphosphoinositide Response in *Tetrahymena pyriformis*

George Leondaritis and Dia Galanopoulou*

Department of Chemistry, University of Athens, 15771 Athens, Greece

ABSTRACT: The unicellular eukaryote *Tetrahymena* is a popular model for the study of lipid metabolism. Less attention, however, has been given to the inositol phospholipids of the cell, although it is known that this class of lipids plays an important role in eukaryotic cell signaling. *Tetrahymena pyriformis* phosphatidylinositol was isolated, purified, and characterized by proton nuclear magnetic resonance analysis and [2-^{3}H]myo-inositol labeling. Labeling was also used for polyphosphoinositide (phosphatidylinositol phosphate and phosphatidylinositol bisphosphate) identification. *Tetrahymena* inositol phospholipids were found to belong to the diacylglycerol group, although major *Tetrahymena* phospholipids, phosphatidylcholine and aminoethylphosphonoglycerides, have been found to be mainly alkylacylglyceroderivatives. Further characterization of *Tetrahymena* phosphatidylinositol by gas chromatographic analysis indicated that 80% of fatty acids were myristic acid and palmitic acid. This is also in contrast to the fatty acid profile of *Tetrahymena* phosphatidylcholine and phosphatidylethanolamine, with respect both to the fatty acid length and degree of unsaturation, and may indicate that specific diacylglycerol species are connected with the phosphatidylinositol metabolism in this cell. Treatment of [^{3}H]inositol-labeled *Tetrahymena* cells with mastoparan, a G-protein-activating peptide, induced changes in the polyphosphoinositide levels, suggesting that inositol phospholipids may form in *Tetrahymena* a functional signaling system similar to that of higher eukaryotes. Addition of 10 μM mastoparan resulted in a rapid and transient increase in [^{3}H]phosphatidylinositol phosphate followed by a decrease in [^{3}H]phosphatidylinositol bisphosphate. Similar changes in lipids have been reported when phosphoinositide-phospholipase C pathway is activated in both animal and plant cells.

Paper no. L8411 in *Lipids 35,* 525–532 (May 2000).

Tetrahymena is a popular model for the study of various aspects of cell biology including membrane function and lipid metabolism (1). Phospholipid studies have focused on the major glycerophospholipids as well as on their ether and phosphonate derivatives (2). Less attention, however, has been given to some minor constituents like phosphatidylinositol (PI) and its phosphorylated derivatives, although these lipids are known to play a variety of specific roles in cell signaling, protein trafficking, cytoskeletal protein regulation, and secretion, at least in animal cells (3). PI has been described in several *Tetrahymena* species as a component of glycosylphosphatidylinositol (GPI)-anchored proteins which can serve as surface immobilization antigens or participate in cell differentiation (4,5). Interestingly, in *T. mimbres*, the lipid moiety of GPI-anchored proteins has been identified as an inositolphosphorylceramide (6). PI was not detected by proton nuclear magnetic resonance (NMR) analysis of lipids of *T. thermophila* (7). In contrast, using [^{32}P]phosphate labeling, PI and putative phosphatidylinositol phosphate (PIP) and phosphatidylinositol bisphosphate (PIP_2) were purported to be present in *T. pyriformis* and to change in response to hormonal (insulin) imprinting; however, a complete characterization of the [^{32}P]phosphate-labeled lipids was not done (8). In a recent report, stomatin, which induces cytodifferentiation in *T. vorax*, was found to change polyphosphoinositide levels as an early response (9).

In the present report we have isolated, purified, and characterized PI from *T. pyriformis* W cultures; we have established the presence of polyphosphoinositides by [^{3}H]inositol labeling, and we show that treatment of cells with mastoparan, a G-protein-activating peptide, induces changes in the intracellular levels of polyphosphoinositides, suggesting that these lipids may form a functional signaling pathway, as described for higher organisms. Finally, we draw attention to the potential benefits of using *Tetrahymena* as a model cell system for the study of other polyphosphoinositide-regulated cellular functions like regulated exocytosis, a pathway known to exist in *Tetrahymena*.

EXPERIMENTAL PROCEDURES

Materials. Yeast extract, phospholipid standards, PI, phosphoinositides, boron trifluoride/methanol, and mastoparan were obtained from Sigma (Steinheim, Germany, or St. Louis,

*To whom correspondence should be addressed at Department of Chemistry, University of Athens, Zografou, 15771 Athens, Greece.
E-mail: galanopoulou@chem.uoa.gr

Abbreviations: AEPL, aminoethylphosphonoglyceride; 1-D, one-dimensional; 2-D, two-dimensional; DAG, diacylglycerol; GC, gas chromatography; GPI, glycosylphosphatidylinositol; GroPI, glycerophosphoinositol; GroPIP, glycerophosphoinositol phosphate; $GroPIP_2$, glycerophosphoinositol bisphosphate; NMR, nuclear magnetic resonance; PC, phosphatidylcholine; PE, phosphatidylethanolamine; PI, phosphatidylinositol; PIP, phosphatidylinositol 4-phosphate; PIP_2 phosphatidylinositol 4,5-bisphosphate; PLC, phospholipase C; PTX, pertussis toxin; TLC, thin-layer chromatography.

MO). Silica gel 60H and 60G and proteose peptone were purchased from Merck (Darmstadt, Germany). LK5D silica gel plates were from Whatman (Clifton, NJ) and Dowex AG 1-x8 Poly-Prep columns, formate form, from Bio-Rad (Hercules, CA). D-Myo [2-^{3}H]inositol (specific activity 21.0 Ci/mmol) was purchased from ICN (Irvine, CA) and phosphatidyl[2-^{3}H]inositol 4,5-bisphosphate (specific activity 1–5 Ci/mmol) from Amersham (Buckinghamshire, United Kingdom). Fatty acid methyl ester standards were obtained from Chem Service (West Chester, PA). All other chemicals and solvents were of analytical grade.

Cell cultures and labeling. Tetrahymena pyriformis, strain W was cultured at 25°C under constant shaking in an enriched proteose peptone medium consisting of 2% proteose peptone, 0.5% glucose, and 0.2% yeast extract. For the study of incorporation of [^{3}H]inositol into *Tetrahymena* lipids and for mastoparan experiments, cultures were supplemented with Fe^{2+}/EDTA 9 mM, pH 5.5 (2%, vol/vol) (10). For isolation and characterization of PI and [^{3}H]inositol phospholipid characterization, cultures grown at a slower rate were used. These cultures were generated using stock cultures of the same enriched growth medium and had a late log phase at around 70 h. [^{3}H]Inositol was added to 42-h-old cultures (25 mL, 0.4–0.6 × 10^6 cells/mL) at a final concentration of 1 μCi/mL. Cells were labeled for 24 h and then harvested by centrifugation for lipid extraction.

Lipid extraction and thin-layer chromatography (TLC). For quantitative recovery of inositol phospholipids from aliquots of cell suspensions, cells were harvested by centrifugation (1,000 × *g* for 5 min), and lipids were extracted according to Schacht (11). Briefly, 1.5 mL of ice-cold chloroform/methanol (1:2, vol/vol) was added to the cell pellet (4 × 10^6 cells or less), and after 30 min on ice and frequent vortexing, EDTA 0.1 M, HCl 2.4 N, and chloroform (0.5 mL each) were added sequentially with vortexing at room temperature. The mixture was centrifuged at 2,500 × *g* for 6 min, the lower phase was removed, and the upper phase was reextracted twice with 0.5 mL chloroform. The combined chloroform phases were washed with an equal amount of methanol/HCl 1 N (1:1, vol/vol). Lipid extraction from a whole 25-mL culture was accomplished by adding 12 mL of chloroform/methanol (1:2, vol/vol) to the cell pellet. For small lipid samples, lipids were separated by one-dimensional (1-D) TLC on oxalate-impregnated heat-activated LK5D plates (12) or, for lipid purification, on silica gel H plates, prepared my mixing silica gel H and 2.1% potassium oxalate at a ratio of 1:2.6 (wt/vol). For inositol phospholipid separation, a chloroform/methanol/ammonium hydroxide/water (86:76:6:16, by vol) solvent system was used (12). Two-dimensional (2-D) TLC was performed on silica gel G plates according to Kates (13). In this case, lipids were identified by running authentic standards on a different plate. Lipids separated by TLC were detected by exposure to iodine vapor. For the quantification of [^{3}H]inositol-labeled lipids, the silica gel was scraped off the 1-D plate in 0.3–1 cm fractions or, alternatively, bands corresponding to inositol phospholipid internal standards were scraped off. All samples were assayed for radioactivity by liquid scintillation counting using 5–10 mL of a toluene-based scintillation fluid in a Pharmacia, model 1209 RackBeta counter (Turku, Finland). For further analysis of inositol phospholipids, lipids were extracted from the silica gel according to Schacht (11) by addition of 2.4–12 mL chloroform/methanol (1:2, vol/vol) depending on the amount of silica gel. The volumes of EDTA 0.1 M, HCl 2.4 N, and chloroform were also adjusted. Lipid phosphorus determination was performed as described by Marinetti (14).

Alkaline hydrolysis of lipids and Dowex chromatography. Mild alkaline hydrolysis of 2-D TLC-purified [^{3}H]inositol-labeled PI and 1-D TLC-purified [^{3}H]inositol-labeled PIP and PIP_2 was performed according to Dittmer and Wells (15). Samples were resuspended in 0.5 mL chloroform/methanol (1:4, vol/vol) and, after addition of 0.050 mL of NaOH 1 N in methanol/water 1:1 (vol/vol), the lipids were hydrolyzed at 37°C for 10 min. Isobutanol, which was included in the subsequent partitioning, enhances the recovery of lysophospholipids in the organic phase. The resulting water-soluble products were chromatographed on Dowex AG 1-x8 columns, formate form. The aqueous phase of the hydrolysis was diluted with water (1:1), loaded onto Dowex columns, and the products were eluted batchwise with increasing concentrations of ammonium formate in formic acid (16). Glycerophosphoinositol (GroPI) was eluted with 60 mM ammonium formate/5 mM sodium borate, and the glycero-derivatives of PIP and PIP_2 were eluted with 12–14 mL of 0.4 M ammonium formate/0.1 M formic acid and 10–12 mL of 1 M ammonium formate/0.1 M formic acid, respectively. Deacylated standard phosphatidyl[2-^{3}H]-inositol 4,5-bisphosphate was used for the calibration of the columns. Total [^{3}H]inositol-labeled *Tetrahymena* lipids were deacylated with methanolic NaOH as described by Downes and Michell (16), and the water-soluble products were analyzed as above. In all cases, 2-mL fractions were collected, and the radioctivity was assayed by liquid scintillation counting using a dioxane/naphthalene/water scintillation fluid.

Proton NMR analysis. Tetrahymena PI or standard PI (approx. 15 μg of lipid phosphorus) was dissolved in 0.8 mL methanol-d_4/chloroform-d_1 (2:1, vol/vol) and transferred to 5-mm NMR tubes. Proton NMR spectra were recorded using Bruker DRX400 and AM 500 NMR spectrometers at 20°C in the Fourier transform (FT) mode with 32K data points, using a 45° detection pulse and 4.0-s acquisition time. Chemical shifts were referenced to the residual methanol resonance at 3.3 ppm.

Fatty acid analysis. Fatty acid composition of PI, phosphatidylcholine (PC), and phosphatidylethanolamine (PE) was estimated by gas chromatography (GC) of the methyl ester derivatives. The lipids were methylated by heating the samples at 70°C for 30 min in boron trifluoride/methanol (14% wt/vol), and the fatty acid methyl esters were extracted two times with diethyl ether which was then dried with sodium sulfate (17). GC was performed using a Hewlett-Packard GC (flame-ionization detector) on a BPX70-coated fused-silica capillary column (25.0 m × 0.32 mm i.d., 0.2 μm film thickness) (SGE, Ringwood, Australia), under pro-

grammed conditions from 100°C at 4°C/min to 200°C (3 min) and a post run at 250°C for 2 min. Carrier gas was He at a flow rate of 1 mL/min. Commercially obtained fatty acid methyl esters were used as standards.

Cell treatment with mastoparan. Tetrahymena cultures (25 mL) were incubated at 25°C for 48 h with [^{3}H]inositol (1.2 μCi/mL, added at the time the cells were transferred into fresh medium), and the cells were harvested by centrifugation and resuspended at 0.7×10^6 cells/mL in 0.25 M sucrose adjusted to pH 7.0. After 40 min, 1-mL aliquots were removed, placed in Eppendorf tubes and treated with 10 μM (final concentration) mastoparan or water (control samples) for the indicated times. Cells were then harvested by a 10-s centrifugation in a microfuge. After the medium was discarded, the lipids were extracted as described above and analyzed by TLC. Microscopic examination of cells revealed no visible changes in cell morphology or motility after mastoparan treatment.

RESULTS

Tetrahymena *PI isolation and identification by ^{1}H NMR spectroscopy.* Lipids of logarithmic phase *T. pyriformis* cells were extracted and separated by 1-D TLC. The spot with R_f identical to that of authentic PI was scraped off the plate and, after elution from the silica gel, lipids were subjected to a 2-D TLC separation as shown in Figure 1. In two separate experiments, isolated PI, after extraction from the silica gel and phosphorus determination, was found to account for 3.9 ± 0.3% of total lipid phosphorus.

Proton NMR analysis of 2-D TLC-purified *Tetrahymena* PI revealed the presence of an inositol moiety; the ^{1}H NMR spectrum of *Tetrahymena* PI was identical to that of standard PI (not shown), however, minor differences did occur and were attributed to structural differences of the two molecules, e.g., fatty acids esterified on the glycerol moiety. Characteristic chemical shifts corresponding to the six protons of the inositol ring (18) were observed at about 3.6 (H-4), 3.8 (H-6, a triplet), 4.0 (H-1), and 4.2 ppm (H-2) (Fig. 2) and at 3.2 and 3.4 ppm (H-5 and H-3 respectively, triplets which are not shown in the expanded version of the spectrum in Fig. 2). Peaks at 4–4.2 ppm were partially overlapped by the glycerol C-1 and C-3 proton multiplets. The signal at about 4.4 ppm (double doublets) is assigned to the glycerol C-1 proton downfield resonance (7,18). No indication of other possible contaminating lipids such as choline or ethanolamine phospholipids (singlets at 3.2 ppm or a triplet at 3.1 ppm, respectively) (7,18) was obtained from the NMR data.

Characterization of PI by [^{3}H]inositol labeling and alkaline hydrolysis. Mid-log *T. pyriformis* cells were incubated with [^{3}H]inositol, and the radioactive lipid extract was chromatographed on 1-D and 2-D TLC as described above. Under these conditions, PI was found to be labeled at a specific radioactivity of 4,500 cpm/nmol. The 2-D TLC-purified [^{3}H]inositol-labeled PI was further characterized by mild alkaline hydrolysis. By using the conditions of Dittmer and Wells (15), 98.9 ± 0.1% (n = 2) of the radioactivity was released in the aqueous phase, while the remaining chloroform-soluble radioactivity was found to consist exclusively of nonhy-

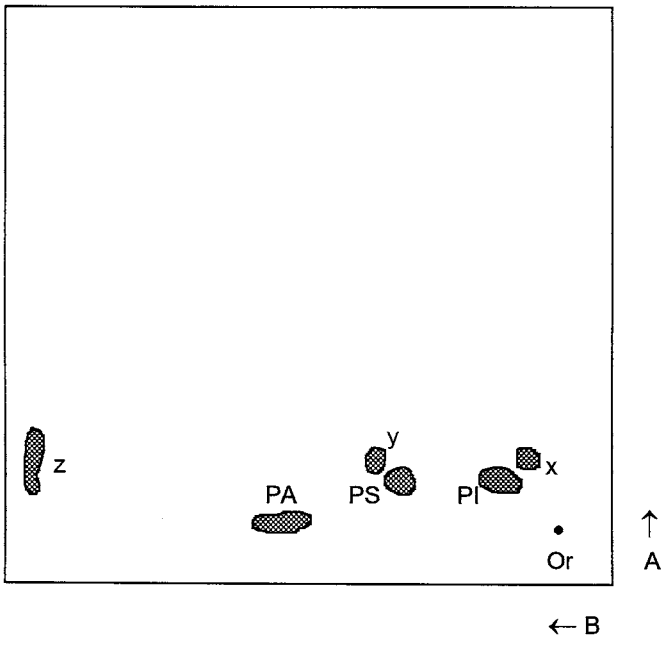

FIG. 1. Two-dimensional (2-D) thin-layer chromatography (TLC) analysis of *Tetrahymena* lipids co-chromatographed with phosphatidylinositol (PI) on 1-D TLC. Solvent systems: (A) chloroform/methanol/ammonium hydroxide (65:35:5, by vol) and (B) chloroform/acetone/methanol/acetic acid/water (14:4:2:2:1, by vol). *x, y* and *z,* unidentified lipids. PA, phosphatidic acid; PS, phosphatidylserine; Or, origin.

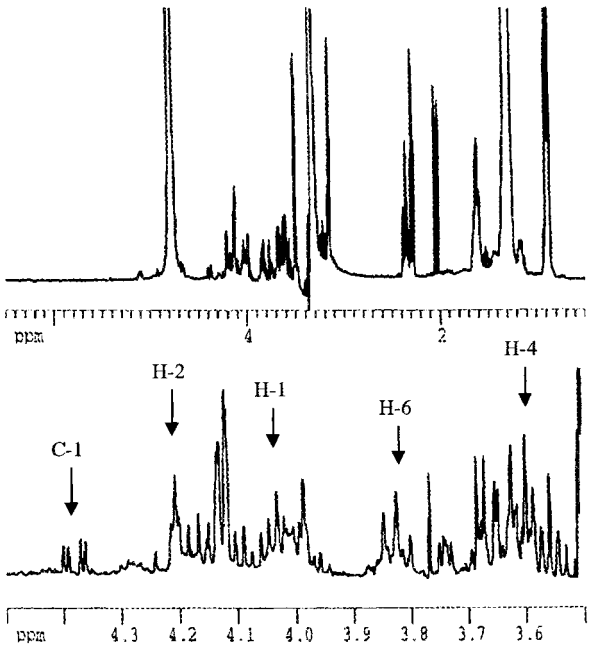

FIG. 2. Proton nuclear magnetic resonance spectrum of 2-D TLC-purified *Tetrahymena* PI. An expanded version (3.5–4.5 ppm) is shown at the lower half of the figure. C-1 and H-1, H-2, H-4, H-6 refer to glycerol and inositol ring protons, respectively. For abbreviations see Figure 1.

drolyzed PI when chromatographed on TLC. No [^{3}H]inositol-labeled lyso-PI, indicative of an alkylacyl inositol phospholipid, was detected. Furthermore, as inositolphosphorylceramide is not hydrolyzable under these conditions, its presence can be excluded as well.

The water-soluble product(s) of alkaline hydrolysis were studied by anion-exchange Dowex chromatography. As shown in Figure 3, the major product was GroPI (95%), while some inositol (3%) and inositol monophosphate (1.5%) were also detected. These results show that PI is almost exclusively a diacyl phospholipid, in contrast to other *Tetrahymena* phospholipids like PC and aminoethylphosphonoglyceride (AEPL) (19,20).

Fatty acid analysis of Tetrahymena *PI.* As the fatty acid profile of PI (and PIP and PIP_2) can give an indication of the diacyglycerol (DAG) species connected to the metabolism of these phospholipids, *Tetrahymena* PI, isolated as described above, was subjected to fatty acid analysis after preparation of the fatty acid methyl esters. PI fatty acid composition is shown in Table 1, together with the fatty acid content of the main *Tetrahymena* phospholipids, PC and PE. PC and PE were isolated from the same cell extract, by separation on silica gel G plates with a chloroform/methanol/water (65:25:4, by vol) solvent system. As shown in Table 1, the fatty acid profile of *Tetrahymena* PI was significantly different compared to that of PC and PE with respect to the fatty acid chain length and degree of unsaturation. Myristic acid (14:0) was the predominant PI fatty acid (48.1%). Myristic acid and palmitic acid (16:0) together represent about 82% of total fatty acid content of PI. Pentadecanoic acid (15:0), another saturated fatty acid, also was detected; however, stearic acid (18:0) was present only in trace amounts. Although C18 fatty acids were absent from PI, they accounted for more than 50% of PE and PC fatty acids. The fatty acid profile of PC and PE was comparable with previously published data (19,20), except that oleic acid (18:1), and not linolenic acid (18:3), was found to be the predominant C18 fatty acid. This could be attributed to the different culture growth conditions, but it also could be due to the different isolation procedure used. The absence of unsaturation in the fatty acids of *T. pyriformis* PI was confirmed by the NMR data, since no characteristic double-bond proton resonances at 5.3–5.4 and 2.8 ppm (7) were obtained (Fig. 2). Fatty acid analysis of PIP and PIP_2 was not performed due to the low content of these phospholipids.

TABLE 1
Fatty Acid Composition (wt% of total fatty acids) of *Tetrahymena* PI, PC, and PE[a]

Fatty acid	PI	PC	PE
12:0	—	1.9	6.0
14:0	48.1	5.0	6.3
15:0	5.0	1.5	1.5
(R_T 6.85)	3.5	0.4	0.5
(R_T 7.65)	2.7	1.1	0.8
16:0	33.5	10.5	10.9
16:1	—	7.0	8.8
(R_T 9.20)	2.6	1.6	1.5
18:0	0.6	2.1	1.9
18:1	0.2	38.6	32.8
18:2	—	4.8	7.1
γ-18:3	—	9.0	9.8
20:1	—	1.0	4.1

[a]Values represent means of four determinations from two different cell cultures. PI, phosphatidylinositol; PC, phosphatidylcholine; PE, phosphatidylethanolamine. Fatty acids in parentheses are unidentified and have the retention times (R_T) given.

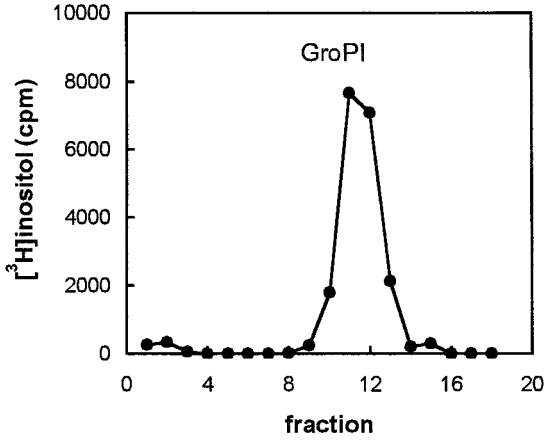

FIG. 3. Analysis of water-soluble deacylation products of [^{3}H]inositol-labeled 2-D TLC-purified *Tetrahymena* PI on Dowex AG 1-x8 columns. Deacylation was performed with methanolic NaOH as described in the Experimental Procedures section. Fractions 1–7 were eluted with water, fractions 8–14 with ammonium formate 60 mM/sodium tetraborate 5 mM, and fractions 15–18 with ammonium formate 0.2 M/formic acid 0.1 M. GroPI, glycerophosphoinositol; for other abbreviations see Figure 1.

Tetrahymena *polyphosphoinositide analysis.* Since *Tetrahymena* can readily incorporate exogenous [^{3}H]inositol into PI, we employed the same strategy to examine both the presence of polyphosphoinositides and their possible implication in cell signaling. When logarithmic phase *Tetrahymena* cells were incubated with [^{3}H]inositol, the radioactivity was incorporated not only into PI but also into PIP and PIP_2. Figure 4 shows a typical TLC separation of [^{3}H]inositol-labeled lipids of *T. pyriformis* on Whatman LK5D plates. Cells were labeled for 24 h with [^{3}H]inositol (1 μCi/mL) and extracted according to Schacht (11). The polyphosphoinositides were identified by the addition of unlabeled standard PIP and PIP_2 to the lipid extract prior to TLC. The PI/PIP/PIP_2 ratio, based on the incorporation of radioactivity, was 85:4.4:1. In fact, the PIP/PIP_2 ratio ranged between experiments from 4.4:1 to 1.3:1, depending on the labeling time. The rate of incorporation of [^{3}H]inositol into the phosphoinositides was examined using logarithmic cells labeled for 1, 4, and 18 h. Incorporation of [^{3}H]inositol into PI and PIP reached saturation after 4 h. In contrast, [^{3}H]inositol incorporation into PIP_2 had not reached saturation even after 18 h (data not shown).

In order to verify the data obtained from TLC analysis with respect to the identity of polyphosphoinositides, 1-D TLC-purified [^{3}H]inositol-labeled PIP and PIP_2 or total [^{3}H]inositol-labeled lipids were subjected to alkaline hydrolysis. The

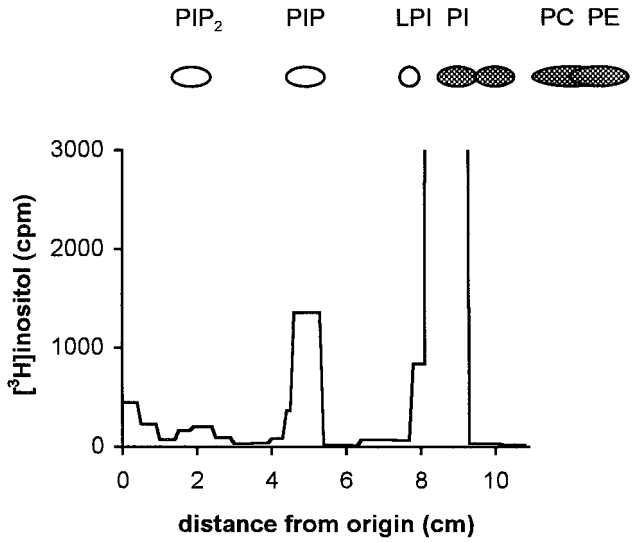

FIG. 4. TLC analysis of *Tetrahymena* [^{3}H]inositol-labeled inositol phospholipids on oxalate-impregnated Whatman LK5D plates. Solvent system: chloroform/methanol/ammonium hydroxide/water (86:76:6:16, by vol). Silica gel was scraped off the plate in 0.3–1 cm fractions and assayed for radioactivity. Unshaded spots represent inositol phospholipid internal standards and shaded spots *Tetrahymena* lipids detected by iodine vapor. PIP, phosphatidylinositol phosphate; PIP_2, phosphatidylinositol bisphosphate; LPI, lysophosphatidylinositol; PC, phosphatidylcholine; PE, phosphatidylethanolamine; for other abbreviation see Figure 1.

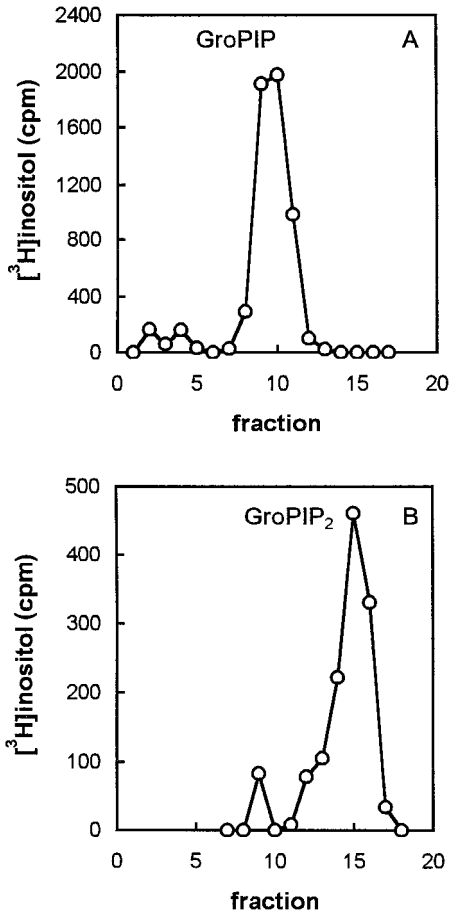

FIG. 5. Analysis of water-soluble deacylation products of [^{3}H]inositol-labeled 1-D TLC-purified *Tetrahymena* PIP (A) and PIP_2 (B) on Dowex AG 1-x8 columns. In (A), fractions 1–6 were eluted with ammonium formate 0.2 M/formic acid 0.1 M, fractions 7–13 with ammonium formate 0.4 M/formic acid 0.1 M, and fractions 13–17 with ammonium formate 1 M/formic acid 0.1 M. In (B), fractions 7–11 were eluted with ammonium formate 0.4 M/formic acid 0.1 M and fractions 12–18 with ammonium formate 1 M/formic acid 0.1 M. GroPIP, glycerophosphoinositol phosphate; $GroPIP_2$, glycerophosphoinositol bisphosphate. For other abbreviations see Figures 1 and 4.

deacylated phospholipid products were then analyzed by Dowex chromatography. Figure 5 shows the deacylation products of PIP (glycerophosphoinositol monophosphate, GroPIP; 93%) and PIP_2 (glycerophosphoinositol bisphosphate, $GroPIP_2$; 87%), eluted with 0.4 and 1 M ammonium formate/0.1 M formic acid, respectively. When total [^{3}H]inositol-labeled *Tetrahymena* lipids were deacylated, the ratio of GroPI to GroPIP to $GroPIP_2$ was very similar to that of the parent lipids (Table 2).

In order to investigate whether *Tetrahymena* PIP is the 4- and/or 3-isomer, 1-D TLC-purified [^{3}H]inositol-labeled PIP was chromatographed using the borate-based TLC system of Walsh *et al.* (21). The silica gel was scraped off the plate in 0.2–0.3 cm fractions, and the radioactivity was counted. All the [^{3}H]inositol label was found to constitute one peak with an R_f value of 0.46 corresponding to phosphatidylinositol 4-phosphate; no evidence for the presence of phosphatidylinositol 3-phosphate (expected R_f value 0.51) was obtained. We cannot, however, exclude at this point the presence of phosphatidylinositol 3-phosphate, since this isomer might be present in substantially lower amounts than phosphatidylinositol 4-phosphate. Different labeling or growth conditions may well reveal the 3-isomer.

Stimulation of polyphosphoinositide metabolism by mastoparan. As polyphosphoinositides are known to be involved in animal cell signaling, we carried out experiments to test for

TABLE 2
Percentage Distribution of [^{3}H]Inositol-Labeled *Tetrahymena* PI, PIP and PIP_2 and Their Corresponding Water-Soluble Products After Lipid Deacylation[a]

	% of total [^{3}H]inositol
TLC	
PI	93.5
PIP	5.6
PIP_2	0.87
Dowex	
GroPI	94.7
GroPIP	4.7
$GroPIP_2$	0.69

[a]The same lipid extract was analyzed by thin-layer chromatography (TLC) and by Dowex chromatography after deacylation. PIP, phosphatidylinositol-4-phosphate; PIP_2, phosphatidylinositol bisphosphate; GroPI, glycerophosphoinositol; GroPIP, glycerophosphoinositol phosphate; $GroPIP_2$, glycerophosphoinositol bisphosphate. For other abbreviation see Table 1.

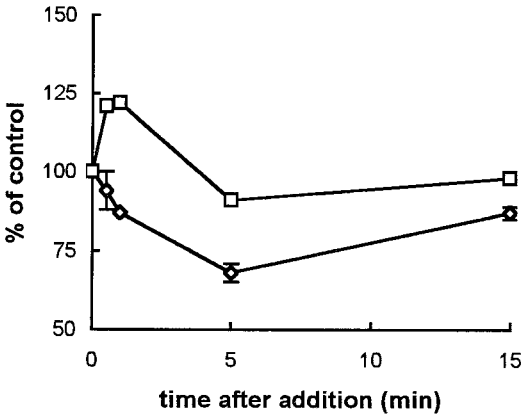

FIG. 6. Effect of 10 μM mastoparan on [^{3}H]inositol-labeled PIP (□) and PIP_2 (◇). Each value is the mean of duplicate determinations from a representative of three independent experiments. Results are expressed as percentages of their corresponding controls. In these experiments, PIP and PIP_2 accounted for 3.0–3.4 and 0.5–0.7%, respectively, of total radioactivity present in control samples (33,000–38,000 dpm). For abbreviations see Figure 4.

a similar role in *T. pyriformis*. [^{3}H]Inositol-labeled *T. pyriformis* cells were treated with 10 μM mastoparan, an effective phospholipase C (PLC) stimulator in several cell systems (22–25). Figure 6 shows mastoparan effects on both PIP and PIP_2 levels. Mastoparan increased [^{3}H]inositol-labeled PIP (20% in 0.5–1 min), which then returned to basal levels. [^{3}H]PIP_2 was decreased by 30% after a 5-min treatment. The decrease of PIP_2 was followed by a slower recovery toward control values at 15 and 30 min. In one experiment, a PIP_2 increase similar to that of PIP was observed immediately after treatment (not shown). This was followed by the PIP_2 decrease shown in Figure 6. These observations could reflect an enhanced PIP and probably PIP_2 synthesis prior to or concurrently with PIP_2 breakdown, as suggested in the case of platelet response to thrombin stimulation (26), mastoparan-treated *Chlamydomonas* cells (25), and osmostimulated *Galdieria sulphuraria* cells (27).

DISCUSSION

There are a number of reports on the utilization of PI by the unicellular *Tetrahymena* for cell surface protein anchoring (4–6), but less attention has been given to free PI which has never been convincingly shown to exist in this organism. In this report, we present for the first time structural characterization of *T. pyriformis* PI, and we also study the presence of polyphosphoinositides and their possible implication in *Tetrahymena* cell signaling.

PI was identified by ^{1}H NMR analysis, and it was found to account for about 4% of *Tetrahymena* phospholipids. In a study employing [^{32}P]phosphate labeling of *T. pyriformis* phospholipids, Kovacs and Csaba (28) reported a value of 12% for PI, but this result could be attributed to an overestimation of the PI content in the TLC or, to possible nonequilibrium labeling conditions. When we incubated *Tetrahymena* cells with [^{3}H]inositol, PI presence was confirmed. The incubation resulted in the incorporation of radioactivity not only into PI but also into PIP and PIP_2. These polyphosphoinositides were identified by co-migration with standards on TLC plates and by anion-exchange chromatography of their glyceroderivatives on Dowex columns after alkaline hydrolysis. In animal cells polyphosphoinositides are usually present in equal amounts; however, in *Tetrahymena* the PIP/PIP_2 ratio is close to that found in other unicellular organisms like the protozoa *Trypanosoma* and *Paramecium* (29,30).

Studies of the main phospholipids of *Tetrahymena* have revealed the presence of alkyl moieties in PC and AEPL (60% of the corresponding lipid) (19,20). Therefore, the presence of alkylacylphospholipids tends to be one of the cell structural characteristics. We carried out experiments to test for a possible alkylacyl content of PI isolated from *Tetrahymena* extracts, for the additional reason that other protozoa have been found to contain similar lipids (31). We found that PI is exclusively a diacylphospholipid, since mild alkaline hydrolysis resulted in a water-soluble product identified as GroPI.

Fatty acid analysis of *Tetrahymena* PI resulted in a profile that contradicts what is known for mammalian cells and other unicellular eukaryotes. For example, mammalian cell PI is rich in arachidonoyl-oleoyl-species (32), and in *Paramecium*, PI has been found to contain mainly unsaturated C18 acids and palmitic acid (30). The most striking finding, however, was the significantly different PI fatty acid profile when compared with that of PC and PE, with the high percentage of myristic acid, the absence of C18 fatty acids, and the absence of any unsaturation as the main differences. A quite similar pattern concerning these differences has been reported for *Saccharomyces cerevisiae* in which saturated fatty acids predominate in PI, whereas they are present in low amounts in PC and PE (33). The similarity in the fatty acid content of PC and PE (Table 1) can be attributed to the common biosynthetic pathways of the two lipids, as PC in *Tetrahymena* is synthesized mainly by methylation of PE (2). A possible explanation for the different PI fatty acid profile is the use of a distinct phosphatidic acid pool for the generation of CDP-DAG available for PI biosynthesis. However the existence of a fatty acid remodeling pathway after PI biosynthesis (32) cannot be excluded, since recently we have found in *Tetrahymena* an active deacylation pathway *via* phospholipase A and lysophospholipase leading from PI to GroPI (Leondaritis, G., Kapetaniou, V., and Galanopoulou, D., unpublished data). The fatty acid profiles of PI and PC/PE may well indicate the specific DAG species with which the turnover of these lipids is connected. Thus, a specific PLC activity against PI (and possibly PIP and PIP_2, since these three lipids are expected to share a common fatty acid content) would lead to the formation of DAG species with relatively short and saturated fatty acids in contrast to what is expected when a PC–PLC is considered. It is likely therefore that such DAG species may have distinct roles in the cell.

In animal cells, signaling by PIP_2 hydrolysis to DAG and water-soluble inositol 1,4,5-trisphosphate is a central path-

way in cell control mechanisms, and it often proceeds through the activation of G-proteins (34). To test for the involvement of *Tetrahymena* polyphosphoinositides in cell signaling, we investigated mastoparan effects on *T. pyriformis* PIP and PIP_2 levels. Mastoparan is a G-protein-activating peptide, and it is more potent against members of the pertussis toxin (PTX)-sensitive Gi/o family (35). The choice of mastoparan for our experiments was supported by indications for the involvement of PTX-sensitive G-proteins in the regulation of phagocytosis in *Tetrahymena* (36) and the effective use of an antibody specific for the preserved GTP-binding site of the G-protein α-subunits in the same organism (37). It is important to add, however, that, in some systems, mastoparan can increase cytosolic calcium *via* different pathways, and therefore its effects on phosphoinositide metabolism could be attributed to a calcium-regulated pathway. Results shown in Figure 6 suggest that a PLC-based signaling pathway may exist in *Tetrahymena* cells. Although the kinetics of stimulated PIP_2 depletion was slower compared to that obtained from studies in animal cells (22,38), this response could be partially explained by the observed upregulation of PIP levels, which could initially mask the breakdown of PIP_2. This kind of stimulated polyphosphoinositide metabolism has been suggested to take place in several cases of agonist or stress-induced activation of the PI cycle in animal or plant cells (25–27). However, conclusive evidence for the existence of a "PI cycle" in this lower eukaryote needs further studies aimed at elucidating different aspects of the pathway, such as the presence of inositol 1,4,5-trisphosphate and of PIP_2-specific PLC(s). Work from our laboratory and others has already shown that such components are present in *Tetrahymena* cells (39,40). Recently, Ryals *et al*. (9) have provided evidence for the activation of the PI cycle by stomatin during cytodifferentiation of *T. vorax*. It is interesting that they have observed the same early upregulation of polyphosphoinositide levels prior to the observed decrease as we had in this report (Fig. 6). They also tested the effect of mastoparan on differentiation and observed minimal stimulation. However, the concentrations of mastoparan and cells, which are important factors concerning the effectiveness of stimulation by this peptide (25), are not given and furthermore, the effects of mastoparan on phosphoinositide levels were not examined.

Among animal cell functions, in the regulation of which polyphosphoinositides play an essential, though not yet fully understood role, are regulated exocytosis and membrane trafficking events. It has been suggested that phosphorylation–dephosphorylation of the polar heads of phosphoinositides in specific intacellular compartments can regulate the function of proteins essential for these transport events (41). We find very interesting the fact that *Tetrahymena* possesses at least two different, well-characterized secretory pathways: a rather constitutive release of hydrolytic enzymes possibly of lysosomal origin (42) and a regulated exocytosis of dense core vesicles known as mucocysts, which are docked permanently at the plasma membrane (43). Therefore, it would be intriguing to examine whether polyphosphoinositides are implicated in the regulation of these secretory pathways, particularly the latter, since regulated exocytosis in *Tetrahymena* shares many common characteristics to regulated exocytosis in mammalian cells (43,44). The availability of *Tetrahymena* mutants with defects in several stages of this pathway (45) and the recent advances in genetic manipulation of *Tetrahymena* (46) will probably provide us with a simple model for the study of polyphosphoinositide involvement in the secretory pathways of animal cells.

ACKNOWLEDGMENTS

We wish to thank Dr. Emmanuel Mikros, University of Athens and Dr. Anastasios Troganis, University of Ioannina, Greece, for the NMR analysis and very helpful discussions. We also thank Dr. Cleanthis Froussios for his comments on NMR spectra. This work was partially supported by a grant (70/4/2507) from the University of Athens.

REFERENCES

1. Thompson, G.A., and Nozawa, Y. (1977) *Tetrahymena*: A System for Studying Dynamic Membrane Alterations Within the Eukaryotic Cell, *Biochim. Biophys. Acta 472*, 55–92.
2. Smith, J.D. (1993) Phospholipid Biosynthesis in Protozoa, *Prog. Lipid Res. 32*, 47–60.
3. Michell, R.H. (1997) The Multiplying Roles of Inositol Lipids and Phosphates in Cell Control Processes, *Essays Biochem. 32*, 31–47.
4. Ryals, P.E., Pak, Y., and Thompson, G.A. (1991) Phosphatidylinositol-Linked Glycans and Phosphatidylinositol-Anchored Proteins of *Tetrahymena mimbres*, *J. Biol. Chem. 266*, 15048–15053.
5. Yang, X., and Ryals, P.E. (1994) Cytodifferentiation in *Tetrahymena vorax* Is Linked to Glycosyl-Phosphatidylinositol-Anchored Protein Assembly, *Biochem. J. 298*, 697–703.
6. Ko, Y.-G., Hung C.-Y., and Thompson, G.A. (1995) Temperature Regulation of the *Tetrahymena mimbres* Glycosylphosphatidylinositol-Anchored Protein Lipid Composition, *Biochem. J. 307*, 115–121.
7. Adosraku, R.K., Smith, J.D., Nicolaou, A., and Gibbons, W.A. (1996) *Tetrahymena thermophila*: Analysis of Phospholipids and Phosphonolipids by High-Field ^{1}H-NMR, *Biochim. Biophys. Acta 1299*, 167–174.
8. Kovacs, P., and Csaba, G. (1990) Involvement of the Phosphoinositol (PI) System in the Mechanism of Hormonal Imprinting, *Biochem. Biophys. Res. Commun. 170*, 119–126.
9. Ryals, P.E., Bae, S., and Patterson, C.E. (1999) Evidence for Early Signalling Events in Stomatin-Induced Differentiation of *Tetrahymena vorax*, *J. Euk. Microbiol. 46*, 77–83.
10. Conner, R.L., and Cline, S.G. (1964) Iron Deficiency and the Metabolism of *Tetrahymena pyriformis*, *J. Protozool. 11*, 491–497.
11. Schacht, J. (1981) Extraction and Purification of Polyphosphoinositides, *Methods Enzymol. 72*, 626–631.
12. Cho, M.H., Chen, Q., Okpodu, C.M., and Boss, W.F. (1992) Separation and Quantitation of [^{3}H]Inositol Phospholipids Using Thin-Layer Chromatography and a Computerized ^{3}H Imaging Scanner, *LC-GC 10*, 464–468.
13. Kates, M. (1990) Glycolipids of Higher Plants, Algae, Yeasts and Fungi, in *Glycolipids, Phosphoglycolipids, and Sulfoglycolipids* (Kates, M., ed.) *Handbook of Lipid Research*, Vol. 6, pp. 235–320, Plenum Press, New York.
14. Marinetti, G.V. (1962) Chromatographic Separation, Identification, and Analysis of Phosphatides, *J. Lipid Res. 3*, 1–20.

15. Dittmer, J.C., and Wells, M.A. (1969) Quantitative and Qualitative Analysis of Lipids and Lipid Components, *Methods Enzymol. 14*, 482–530.
16. Downes, C.P., and Michell, R.H. (1981) The Polyphosphoinositide Phosphodiesterase of Erythrocyte Membranes, *Biochem. J. 198*, 133–140.
17. Sen, A., Williams, W.P., and Quinn, P.J. (1981) The Structure and Thermotropic Properties of Pure 1,2-Diacylgalactosylglycerols in Aqueous Systems, *Biochim. Biophys. Acta 663*, 380–389.
18. Casu, M., Anderson, G.T., Choi, G., and Gibbons, W.A. (1991) NMR Lipid Profiles of Cells, Tissues and Body Fluids. I—1D and 2D Proton NMR of Lipids from Rat Liver, *Magn. Reson. Chem. 29*, 594–602.
19. Pieringer, J., and Conner, R.L. (1979) Positional Distribution of Fatty Acids in the Glycerophospholipids of *Tetrahymena pyriformis*, *J. Lipid Res. 20*, 363–370.
20. Watanabe, T., Fukushima, H., Kasai, R., and Nozawa, Y. (1981) Studies on Thermal Adaptation in *Tetrahymena* Membrane Lipids. Changes in Positional Distribution of Fatty Acids in Diacyl-Phospholipids and Alkyl-Acyl-Phospholipids During Temperature Acclimation, *Biochim. Biophys. Acta 665*, 66–73.
21. Walsh, J.P., Caldwell, K.K., and Majerus, P.W. (1991) Formation of Phosphatidylinositol 3-Phosphate by Isomerization from Phosphatidylinositol 4-Phosphate, *Proc. Natl. Acad. Sci. USA 88*, 9184–9187.
22. Okano, Y., Takagi, H., Tohmatsu, T., Nakashima, S., Kuroda, Y., Saito, K., and Nozawa, Y. (1985) A Wasp Venom Mastoparan-Induced Polyphosphoinositide Breakdown in Rat Peritoneal Mast Cells, *FEBS Lett. 188*, 363–366.
23. Quarmby, L.M., Yueh, Y.G., Cheshire, J.L., Keller, L.R., Snell, W.J., and Crain, R.C. (1992) Inositol Phospholipid Metabolism May Trigger Flagellar Excision in *Chlamydomonas reinhardtii*, *J. Cell Biol. 116*, 737–744.
24. Cho, M.H., Tan, Z., Erneux, C., Shears, S.B., and Boss, W.F. (1995) The Effects of Mastoparan on the Carrot Cell Plasma Membrane Polyphosphoinositide Phospholipase C, *Plant Physiol. 107*, 845–856.
25. Munnik, T., van Himbergen, J.A.J., ter Riet, B., Braun, F.-J., Irvine, R.F., van den Ende, H., and Musgrave, A. (1998) Detailed Analysis of the Turnover of Polyphosphoinositides and Phosphatidic Acid upon Activation of Phospholipases C and D in *Chlamydomonas* Cells Treated with Nonpermeabilizing Concentrations of Mastoparan, *Planta 207*, 133–145.
26. Lassing, I., and Lindberg, U. (1990) Polyphosphoinositide Synthesis in Platelets Stimulated with Low Concentrations of Thrombin Is Enhanced Before the Activation of Phospholipase C, *FEBS Lett. 262*, 231–233.
27. Heilmann, I., Perera, I.Y., Gross, W., and Boss, W.F. (1999) Changes in Phosphoinositide Metabolism with Days in Culture Affect Signal Transduction Pathways in *Galdieria sulphuraria*, *Plant Physiol. 119*, 1331–1339.
28. Kovacs, P., and Csaba, G. (1997) Indomethacin Alters Phospholipid and Arachidonate Metabolism in *Tetrahymena pyriformis*, *Comp. Biochem. Physiol. 117C*, 311–315.
29. Docampo, R., and Pignataro, O.P. (1991) The Inositol Phosphate/Diacylglycerol Signalling Pathway in *Trypanosoma cruzi*, *Biochem. J. 275*, 407–411.
30. Suchard, S.J., Rhoads, D.E., and Kaneshiro, E.S. (1989) The Inositol Lipids of *Paramecium tetraurelia* and Preliminary Characterizations of Phosphoinositide Kinase Activity in the Ciliary Membrane, *J. Protozool. 36*, 185–190.
31. Uhrig, M.L., Couto, A.S., Colli, W., and de Lederkremer, R.M. (1996) Characterization of Inositol Phospholipids in *Trypanosoma cruzi* Trypomastigote Forms, *Biochim. Biophys. Acta 1300*, 233–239.
32. Augert, G., Blackmore, P.F., and Exton, J.H. (1989) Changes in Concentration and Fatty Acid Composition of Phosphoinositides Induced by Hormones in Hepatocytes, *J. Biol. Chem. 264*, 2574–2580.
33. Wagner, S., and Paltauf, F. (1994) Generation of Glycerophospholipid Molecular Species in the Yeast *Saccharomyces cerevisiae* Fatty Acid Turnover at *sn*-1 and *sn*-2 Positions, *Yeast 10*, 1429–1437.
34. Berridge, M.J. (1993) Inositol Trisphosphate and Calcium Signalling, *Nature 361*, 315–325.
35. Higashijima, T., Uzu, S., Nakajima, T., and Ross, E.M. (1988) Mastoparan, a Peptide Toxin from Wasp Venom, Mimics Receptors by Activating GTP-Binding Regulatory Proteins (G-Proteins), *J. Biol. Chem. 263*, 6491–6494.
36. Renaud, F.L., Chiesa, R., de Jesus, J.M., Lopez, A., Miranda, J., and Tomassini, N. (1991) Hormones and Signal Transduction in Protozoa, *Comp. Biochem. Physiol. 100A*, 41–45.
37. Renaud, F.L., Colon, I., Lebron, J., Ortiz, N., Rodriguez, F., and Cadilla, C. (1995) A Novel Opioid Mechanism Seems to Modulate Phagocytosis in *Tetrahymena*, *J. Euk. Microbiol. 42*, 205–207.
38. Creba, J.A., Downes, C.P., Hawkins, P.T., Brewster, G., Michell, R.H., and Kirk, C.J. (1983) Rapid Breakdown of Phosphatidylinositol 4-Phosphate and Phosphatidylinositol 4,5-Bisphosphate in Rat Hepatocytes Stimulated by Vasopressin and Other Ca^{2+} Mobilizing Hormones, *Biochem. J. 212*, 733–747.
39. Kovacs, P., and Csaba, G. (1997) PLA_2 Activity in *Tetrahymena pyriformis*. Effects of Inhibitors and Stimulators, *J. Lipid Med. Cell Signall. 15*, 233–247.
40. Leondaritis, G., and Galanopoulou, D. (1997) Phospholipase C Activity in *Tetrahymena pyriformis*, *Chem. Phys. Lipids 88*, 150.
41. de Camilli, P., Emr, S.D., McPherson, P.S., and Novick, P. (1996) Phosphoinositides as Regulators in Membrane Traffic, *Science 271*, 1533–1539.
42. Kiy, T., Vosskuhler, C., Rasmussen, L., and Tiedke A. (1993) Three Pools of Lysosomal Enzymes in *Tetrahymena thermophila*, *Exp. Cell Res. 205*, 286–292.
43. Haddad, A., and Turkewitz, A.P. (1997) Analysis of Exocytosis Mutants Indicates Close Coupling Between Regulated Secretion and Transcription Activation in *Tetrahymena*, *Proc. Natl. Acad. Sci. USA 94*, 10675–10680.
44. Hutton, J.C. (1997) *Tetrahymena*: The Key to the Genetic Analysis of the Regulated Pathway of Polypeptide Secretion? *Proc. Natl. Acad. Sci. USA 94*, 10490–10492.
45. Melia, S.M., Cole, E.S., and Turkewitz, A.P. (1998) Mutational Analysis of Regulated Exocytosis in *Tetrahymena*, *J. Cell Sci. 111*, 131–140.
46. Hai, B., and Gorovsky, M.A. (1997) Germ-Line Knockout Heterokaryons of an Essential α-Tubulin Gene Enable High-Frequency Gene Replacement and a Test of Gene Transfer from Somatic to Germ-Line Nuclei in *Tetrahymena thermophila*, *Proc. Natl. Acad. Sci. USA 94*, 1310–1315.

[Received December 6, 1999; and in final revised form March 20, 2000; revision accepted March 23, 2000]

Molecular Analysis of Intact Preen Waxes of *Calidris canutus* (Aves: Scolopacidae) by Gas Chromatography/Mass Spectrometry

Marlèn H.A. Dekker[a], Theunis Piersma[b,c], and Jaap S. Sinninghe Damsté[a,*]

Departments of [a]Marine Biogeochemistry and Toxicology and [b]Marine Ecology, Netherlands Institute for Sea Research (NIOZ), Texel, The Netherlands, and [c]Centre for Ecological and Evolutionary Studies, University of Groningen, Groningen, The Netherlands

ABSTRACT: The intact preen wax esters of the red knot *Calidris canutus* were studied with gas chromatography/mass spectrometry (GC/MS) and GC/MS/MS. In this latter technique, transitions from the molecular ion to fragment ions representing the fatty acid moiety of the wax esters were measured, providing additional resolution to the analysis of wax esters. The C_{21}–C_{32} wax esters are composed of complex mixtures of hundreds of individual isomers. The odd carbon-numbered wax esters are predominantly composed of even carbon-numbered *n*-alcohols (C_{14}, C_{16}, and C_{18}) esterified predominantly with odd carbon-numbered 2-methyl fatty acids (C_7, C_9, C_{11}, and C_{13}), resulting in relatively simple distributions. The even carbon-numbered wax esters show a far more complex distribution due to a number of factors: (i) Their *n*-alcohol moieties are not dominated by even carbon-numbered *n*-alcohols esterified with odd carbon-numbered 2-methyl fatty acids, but odd and even carbon-numbered *n*-alcohols participate in approximately equal amounts; (ii) odd carbon-numbered methyl-branched alcohols participate abundantly in these wax ester clusters; and (iii) with increasing molecular weight, various isomers of the 2,6-, 2,8-, and 2,10-dimethyl branched fatty acids also participate in the even carbon-numbered wax esters. The data demonstrate that there is a clear biosynthetic control on the wax ester composition although the reasons for the complex chemistry of the waxes are not yet understood.

Paper no. L8441 in *Lipids 35,* 533–541 (May 2000).

The survival of marine birds depends on an intact and waterproof plumage kept in good shape. A key component in the maintenance systems of the feather coat of birds is the preen (or uropygial) gland, located near the tail, which produces a variety of waxes (1). Yet, we understand very little of the preen gland waxes, but they may fulfill several crucial functions: keeping feathers flexible, protecting against wetting, reducing damage (including ultraviolet protection), playing a role as antiparasitic agents, and acting as pheromones (2; and references cited therein). Preen gland secretions consist predominantly of monoester waxes (3), which are composed of a fatty acid esterified to an alcohol moiety. These moieties may possess straight-chain, monomethyl alkyl, polymethyl alkyl, or even more complex carbon skeletons. Usually a mixture of fatty acids and alcohols with varying chain lengths and degree and location of branching is used, resulting in a complex mixture composed of hundreds of individual wax esters. The pattern of the lipid constituents has been found to be quite characteristic for a species and differs markedly between various bird taxa (1,4).

The very complex wax composition is usually determined by the analysis of fatty acids and alcohols released after hydrolysis of the monoester preen waxes (2,5). This leads to a loss of information concerning the molecular distribution, which determines the physical properties of the preen wax. In this paper the preen gland wax composition of a long-distance migrating shore bird, the red knot (*Calidris canutus),* was studied in detail using an approach by which the intact waxes were analyzed by capillary gas chromatography/mass spectrometry (GC/MS) and gas chromatography/mass spectrometry/mass spectrometry (GC/MS/MS). Recent studies of the preen waxes of male and female *C. canutus* revealed significant changes over the annual cycle in the chemical composition of the preen waxes (6,7) from monoester preen waxes to diester waxes. This warranted a detailed chemical and ecological study of the structure and role of preen waxes in *C. canutus*. Here we focus on the analytical characterization of the complex monoester wax of *C. canutus*.

EXPERIMENTAL PROCEDURES

Birds. Preen wax samples were taken from the red knot, *C. canutus*, subspecies *islandica,* kept in outdoor cages at north-temperate latitudes over several annual cycles. The composition of the preen wax of *C. canutus* has been shown to vary strongly over the annual cycle (6). Here we describe the detailed chemical composition of the preen wax pattern observed in the July–March period. Knot #283 was used for this purpose. To compare the wax patterns of different species, three other species (*Limosa lapponica* 1374068, *Tringa nebularia* 1374069, and *C. alba* H227028) were captured with

*To whom correspondence should be addressed at NIOZ, P.O. Box 59, 1790 AB Den Burg, Texel, The Netherlands. E-mail: damste@nioz.nl

Abbreviations: GC/MS, gas chromatography/mass spectrometry; GC/MS/MS, gas chromatography/mass spectrometry/mass spectrometry; RIC, reconstructed ion current; TLC, thin-layer chromatography.

mistnets on Augusts 2, 1998, on the intertidal flats near Vlieland, an island in the Dutch Wadden Sea.

Sample processing. Wax samples were taken from the living birds by softly squeezing the gland area (4). The cotton-wool was extracted with 1 mL ethyl acetate and filtered by column chromatography using Na_2SO_4 and ethyl acetate as eluent. The dried extract was analyzed directly by GC, GC/MS, and GC/MS/MS. To study the fatty acid and alcohol composition of the monoesters, wax samples of Knots #294, #382, and #389 were combined for preparative thin-layer chromatography (TLC) analysis (8). TLC bands were scraped off the TLC plate and extracted with ethyl acetate and analyzed by GC and GC/MS. The monoester fraction (representing the largest TLC fraction) was saponified (1 M KOH in 96% methanol), and the fatty acids and alcohols released from the monoesters were derivatized with diazomethane and bis(trimethylsilyl)trifluoroacetamide to their corresponding methyl esters and trimethylsilyl ether derivatives and analyzed by GC/MS.

GC. GC was performed with a Hewlett-Packard 6890 Series II instrument (Palo Alto, CA), using an on-column injector. Detection was accomplished using a flame-ionization detector. Helium was used as the carrier gas. Separation was achieved using a fused-silica capillary column (25 m × 0.32 mm i.d.) coated with CP-Sil 5CB (film thickness 0.12 µm). The samples, dissolved in ethyl acetate, were injected at 70°C, and subsequently the oven was programmed to 130°C at 20°C/min and then 4°C/min to 320°C, where it was held for 30 min. Saponified extracts were injected at 40°C, programmed to 200°C at 4°C/min, 10°C/min to 300°C where it was held for 15 min.

GC/MS. GC/MS was performed on a Hewlett-Packard 5890 Series II gas chromatograph interfaced to a VG Autospec Ultima Q mass spectrometer. GC conditions were identical as described above. Electron impact spectra were obtained at 70 eV using the following conditions: mass range *m/z* 800–50; cycle time 1.6 s; resolution 1000. For GC/MS/MS, dissociation of the parent ions was induced by collision with argon (collision energy 20 eV). The parent ion to daughter ion transitions were analyzed with 20 ms settling and 75 ms sampling periods resulting in a 1.33 s total cycle time. Separation was achieved using the same capillary column and temperature program as described for GC analyses.

RESULTS AND DISCUSSION

Analysis of intact preen waxes. Figure 1 shows the gas chromatograms of the preen gland lipids of four different species, *L. lapponica, T. nebularia, C. alba,* and *C. canutus islandica* to illustrate the complex distribution of the intact wax lipids. The preen lipids of the four species investigated are dominated by monoester waxes. The *L. lapponica* preen lipids are dominated by C_{22}–C_{38} monoester waxes, those of *T. nebularia* consist mainly of C_{23}–C_{34} monoester waxes, C_{22}–C_{33} monoester waxes for *C. alba,* and C_{21}–C_{32} monoester waxes are dominant in the preen lipids of *C. canutus*. The molecular weight, fatty acid, and alcohol moiety of the wax esters were established by GC/MS. For example, Figure 2 shows mass spectra of two C_{24} wax esters composed of a C_8 fatty acid esterified with a C_{16} alcohol and a C_{10} fatty acid esterified with a C_{14} alcohol. The base peaks result from loss of the fatty acid substituents with concomitant transfer of two hydrogen atoms (9). Together with the molecular ion, this leads to identification of the wax ester, although no specific information on the carbon skeleton of the fatty acid and alcohol is obtained.

Detailed mass spectrometric analysis. Captive *C. canutus* were used to examine the intact preen gland lipids in detail by GC/MS and GC/MS/MS analysis. Mass chromatography of the molecular ions is a useful tool to analyze individual clusters of wax esters with the same molecular weight in the preen wax. Figure 3 has been constructed on this basis and shows the mass chromatograms of C_{21}–C_{32} wax esters (*m/z* 326 + n × 14). Each individual cluster of wax esters with the same molecular weight has been normalized to the most abundant isomer present. Figure 3 shows that with increasing molecular weight the distribution of wax esters becomes increasingly complex.

To obtain information on the building blocks of the wax esters, a monoester fraction was isolated from the preen wax, hydrolyzed, and the fatty acids and alcohols formed were identified after derivatization. Fatty acids and alcohols were identified based on MS data reported in the literature (4) and the recognition of (pseudo) homologous series through linear Kovats plots (Table 1; Ref. 9). Figure 4 shows the total ion current of the hydrolyzed waxes and summed mass chromatograms of *m/z* 88 + 101 and *m/z* 199 + 213 + 227 + 241 + 255 to show the distributions of the dominant fatty acids and alcohols, respectively. Straight-chain fatty acids are present only in trace quantities and occur in the range C_{16}–C_{28} with even carbon-numbered components predominating. The abundant fatty acids are 2-methyl branched fatty acids with characteristic *m/z* 88 and 101 fragment ions (resulting from McLafferty rearrangements) in their mass spectra. They comprise C_6–C_{15} 2-methyl fatty acids and 2,6-, 2,8-, and 2,10-dimethyl fatty acids (Fig. 4B). The distribution of the C_{14}–C_{18} alcohols is exemplified by a mass chromatogram of M – 15 (Fig. 4C). The even carbon-numbered alcohols show a simple distribution composed of only the straight-chain alcohol isomers. The odd carbon-numbered alcohols have, however, a very different distribution pattern characterized by the straight-chain alcohol and ω-2-, ω-4- and ω-6-methyl and 2-methyl alcohols. These results are in general agreement with those reported by Jacob and Poltz (5), although these authors also reported 4-methyl fatty acids and 4-methyl alcohols, which were not encountered as abundant compounds in this study.

The intact C_{21} wax ester (i.e., the one peak in the mass chromatogram of *m/z* 340, Fig. 3) possesses an *m/z* 131 fragment ion in its mass spectrum, indicating that it contains a C_7 fatty acid moiety. With this information it can be identified as tetradecyl 2-methylhexanoate on the basis of the distribution of the alcohols and fatty acids formed upon hydrolysis

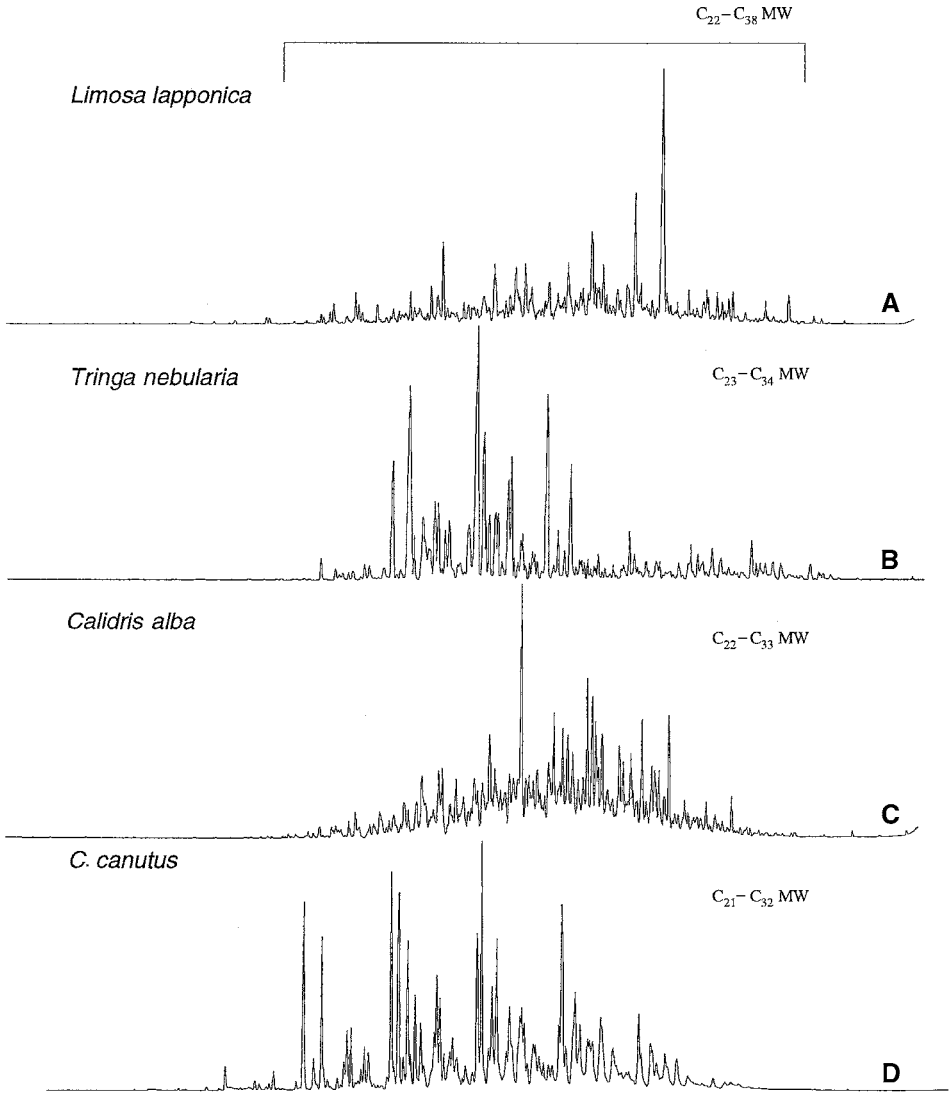

FIG. 1. Partial gas chromatography–flame-ionization detection chromatograms of the intact preen gland wax samples of several species: (A) bar-tailed godwit *Limosa lapponica*; (B) greenshank *Tringa nebularia*; (C) sanderling *Calidris alba*; (D) red knot *C. canutus*.

TABLE 1
Retention Data of Branched Fatty Acids and Alcohols

		RI[b]			
	Homologous series[a]	*a*	*b*	r^2	Range
Fatty acid	2-Methylalkanoic acid	100	0	n.a.	C_6–C_{16}
	2,6-Dimethylalkanoic acid	96	1	0.9999	C_8–C_{14}
	2,8-Dimethylalkanoic acid	93.5	44.5	0.9998	C_{10}–C_{14}
	2,10-Dimethylalkanoic acid	90.4	103.7	0.9998	C_{12}–C_{14}
Alcohol	*n*-Alkanols	100	0	n.a.	C_{12}–C_{19}
	2-Methylalkanols	99.5	–58.3	1	C_{12}–C_{19}
	2-Ethylalkanols	100	–96.2	1	C_{14}–C_{18}
	ω-2-Methylalkanols	100	–30	1	C_{15}–C_{17}
	ω-4-Methylalkanols	100.4	–55.9	0.9997	C_{14}–C_{19}
	ω-6-methylalkanols	99.5	–48.3	1	C_{15}–C_{17}

[a]Analyzed as their methyl esters or trimethylsilyl ethers.
[b]Retention index (RI) measured on CP-Sil 5CB, 130 to 320°C at 4°C/min, with the homologous series of 2-methylalkanoic acid and *n*-alcohols, respectively, as calibration standards, resulting in Kovats' plots $y = a \cdot x + b$ with correlation coefficient r^2. $RI = 100 \cdot z + 100 \cdot \{t(x) - t(z)\}/\{t(z + 1) - t(z)\}$ where $t(x)$ is retention time of compound for which RI is to be determined, $t(z)$ and $t(z + 1)$ are the retention times of the homologous which bracket the compound, and z is the number of carbon atoms. n.a., not applicable.

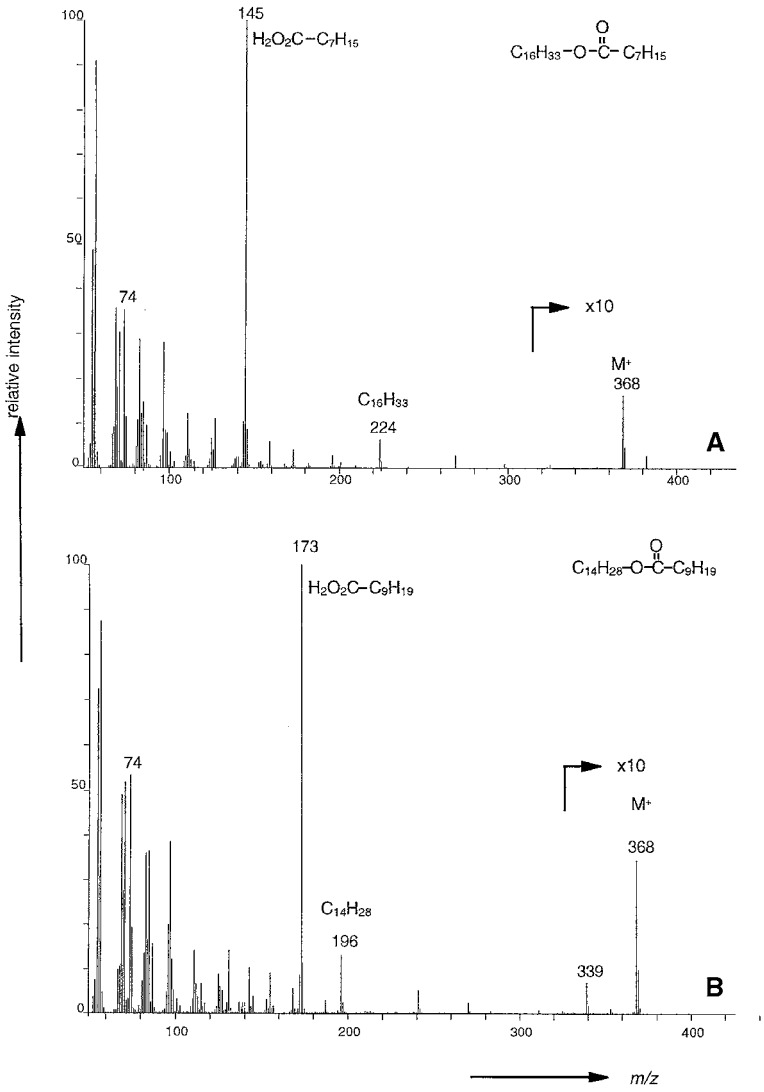

FIG. 2. Mass spectra (corrected for background) of two C_{23} wax esters: (A) hexadecyl 2-methylheptanoate (peak number 22 listed in Table 2); (B) tetradecyl 2,6-dimethyloctanoate (peak number 17 listed in Table 2).

(Fig. 4) since this represents the only possible combination of a C_7 fatty acid and C_{14} alcohol moiety to build a C_{21} wax ester. Due to the increasing complexity of the wax ester distribution pattern with increasing molecular weight (Fig. 3), these lines of argument become increasingly difficult to apply. The increasingly complex distribution with increasing molecular weight is due to: (i) the increasing number of possible combinations of fatty acids and alcohols to form a wax ester with a specific total number of carbon atoms and (ii) the increasing number of positional isomers for especially the fatty acids with increasing molecular weight (Fig. 4).

These problems in identifying intact wax esters can be partially overcome by using mass chromatograms of the characteristic fragment ion formed from the fatty acid moiety of the wax ester (i.e., *m/z* 131 + n·14) in combination with mass chromatograms of the molecular ions. However, since the clusters of wax esters with the same molecular weight partially overlap (Fig. 3), the coupling of molecular weight and specific fatty acid fragment ion becomes unreliable.

GC/MS/MS analysis. One way to overcome this problem in the identification of the intact wax esters is the application of GC/MS/MS. In this technique an ion with a specific mass (parent) is selected by the first mass spectrometer, led into the collision cell of the second mass spectrometer, and selected daughter ions, formed by collision-induced fragmentation, are collected on the second mass detector. Using this GC/MS/MS technique, it is possible to get detailed information on the composition of the preen wax. The major wax esters identified in this way are listed in Table 2.

As an example, the GC/MS/MS results for C_{24} wax esters are shown in Figure 5. These results are based on selection of the molecular ion (*m/z* 368) in the first mass spectrometer and detection of daughter ions representing the fatty acid part of the wax ester (Fig. 2) in the second mass spectrometer. Fig-

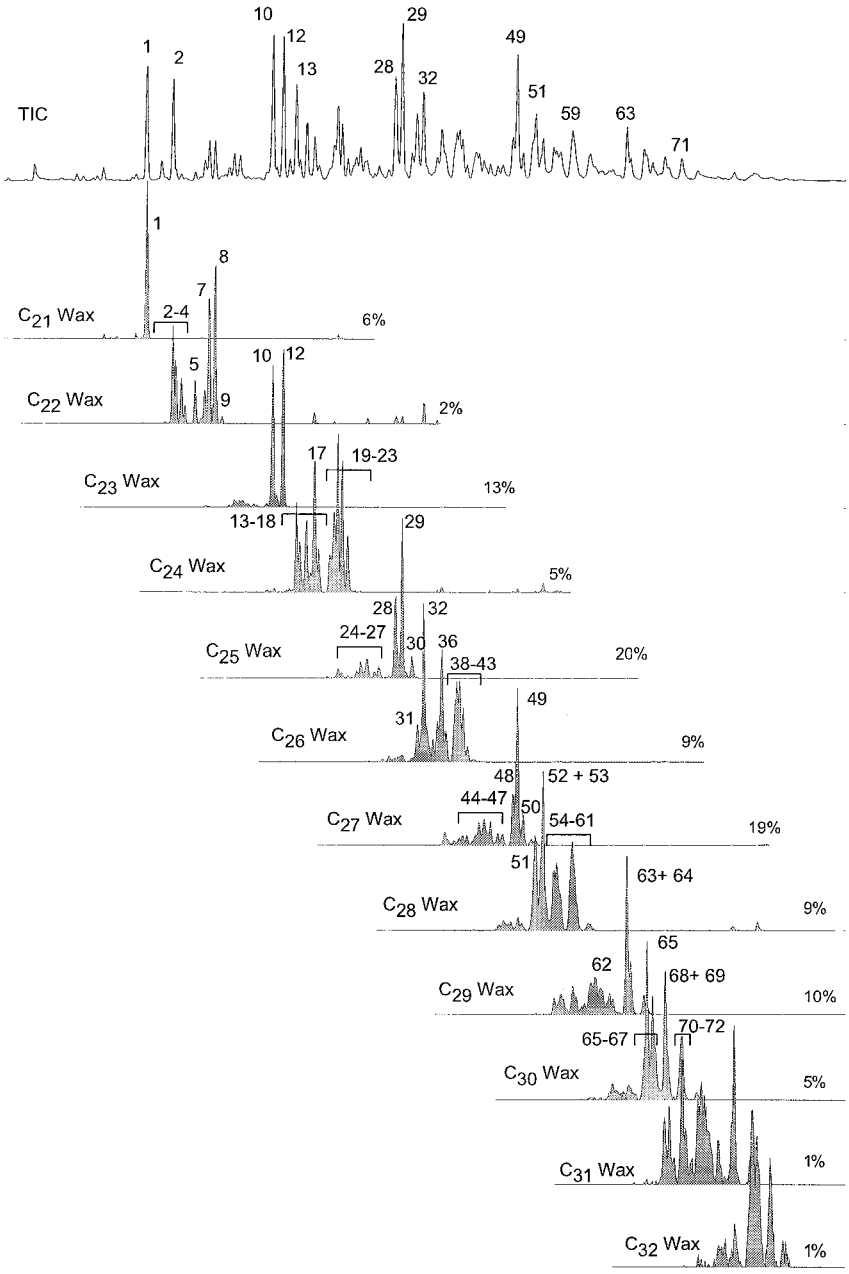

FIG. 3. Partial and mass chromatograms of the molecular ions of the C_{21}–C_{32} wax esters (*m/z* 340, 354, 368, 382, 396, 410, 424, 438, 452, 466, 480, 494) present in the nonsaponified preen wax of *C. canutus* #283. Numbers refer to specific wax ester listed in Table 2. Numbers at the end of the traces (in %) indicate the abundance based on peak height of the most abundance peak of the cluster (total set to 100%). TIC, total ion current; see Figure 1 for other abbreviation.

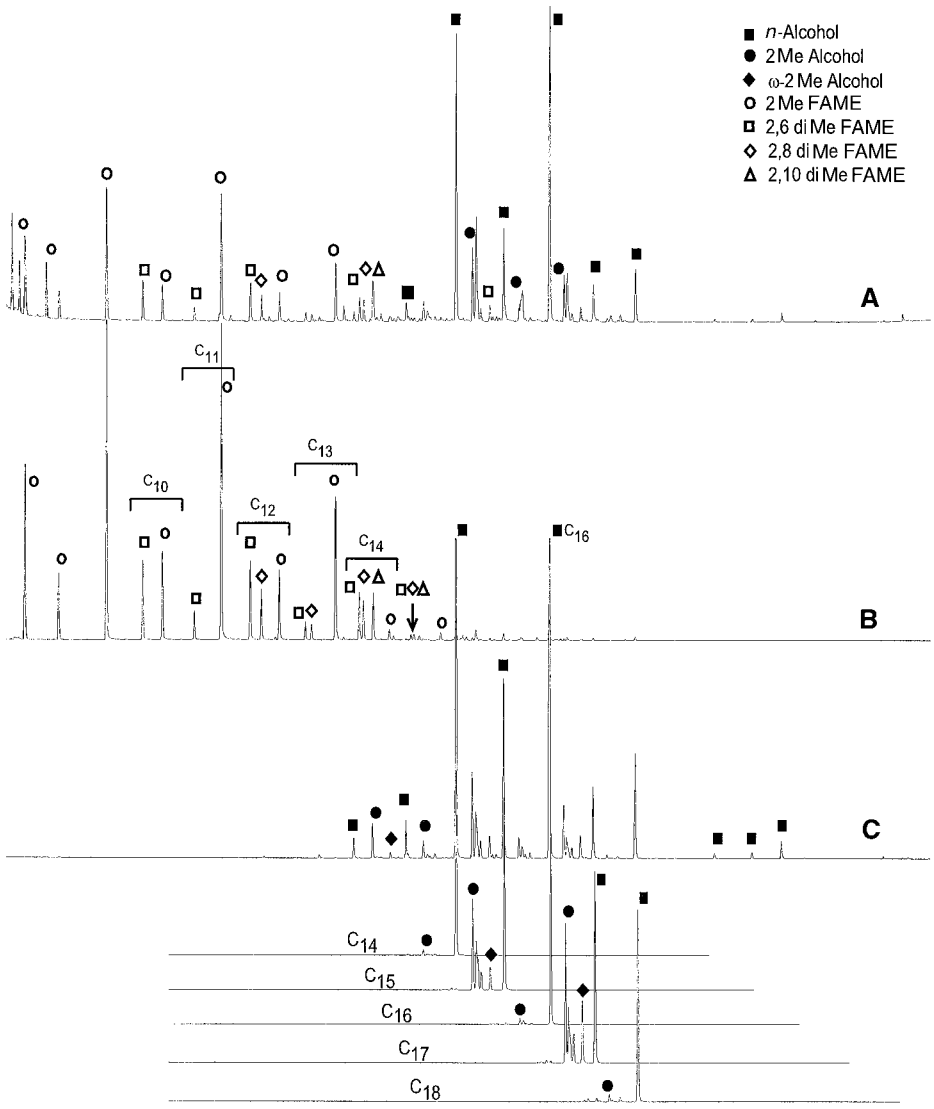

FIG. 4. Partial TIC (A) and (summed) mass chromatograms of *m/z* 88 + 101 (B) and 199 + 213 + 227 + 241 + 255 (C), showing homologous series of 2-methyl and dimethyl fatty acids and linear and methyl alcohols in the saponified monoester fraction of the preen wax of *C. canutus*. Numbers indicate the total number of carbon atoms. FAME, fatty acid methyl esters. See Figures 1 and 3 for other abbreviation.

ure 5D shows the *m/z* 368 → *m/z* 131 transition, representing C_{24} wax esters, containing a C_7 fatty acid moiety and, consequently, a C_{17} alcohol moiety. Hydrolysis has demonstrated that there is only one C_7 fatty acid (i.e., 2-methylhexanoic acid) but at least five structural isomers of the C_{17} alcohol (i.e., heptadecan-1-ol and various methyl-branched C_{17} alcohols) (Fig. 4). In fact, the distribution of peaks in the *m/z* 368 → *m/z* 131 transition is quite similar to the distribution of C_{17} alcohols in the hydrolyzed preen wax (Fig. 3). This is due to the presence of wax esters composed of 2-methylhexanoic acid esterified with all C_{17} alcohol isomers (Table 2). Due to the additivity principle (10), the retention behavior of these wax esters is similar to that of the alcohols. In this way all transitions can be analyzed. The *m/z* 368 → *m/z* 159 transition (Fig. 5F) is rather similar and shows the wax esters of 2-methyloctanoic acid with various C_{15} alcohols. In contrast, the *m/z* 368 → *m/z* 145 transition (Fig. 5E), revealing the C_{24} wax esters comprised of combinations of C_8 fatty acids and C_{16} alcohols, is dominated by one component (hexadecyl 2-methylheptanoate), in agreement with the relatively simple distribution of the C_{16} alcohols (Fig. 4). The *m/z* 368 → *m/z* 173 transition (Fig. 5G), revealing the C_{10}/C_{14} (FA/Alc.) wax esters, is comparatively simple, although in addition to tetradecyl 2-methylnonanoate another earlier-eluting wax ester is present. This is because dimethyl branched fatty acids are present in the hydrolyzed preen wax from C_{10} onward (Fig. 3). The earlier-eluting C_{10}/C_{14} wax ester was therefore identified as tetradecyl 2,6-dimethyloctanoate. The *m/z* 368 → *m/z* 187 and *m/z* 368 → *m/z* 201 transitions (Fig. 5H and 5I) revealed trace amounts of C_{11}/C_{13} and C_{12}/C_{12} wax

TABLE 2
Major Components of the Preen Gland Wax Esters from *Calidris canutus*

Peak number	MW[a]	Compound	Peak number	MW	Compound
1	326	Tetradecyl 2-methylhexanoate	35	396	Tetradecyl 2,8-dimethyldecanoate
2	340	2-Methyltetradecyl 2-methylhexanoate	36	396	Hexadecyl 2,6-dimethyloctanoate
3	340	8-Methyltetradecyl 2-methylhexanoate	37	396	14-Methylhexadecyl 2-methyloctanoate
4	340	10-Methyltetradecyl 2-methylhexanoate	38	396	Tridecyl 2-methyldodecanoate
5	340	12-Methyltetradecyl 2-methylhexanoate	39	396	Tetradecyl 2-methylundecanoate
6	340	Tridecyl 2-methyloctanoate	40	396	Pentadecyl 2-methyldecanoate
7	340	Tetradecyl 2-methylheptanoate	41	396	Hexadecyl 2-methylnonanoate
8	340	Pentadecyl 2-methylhexanoate	42	396	Heptadecyl 2-methyloctanoate
9	340	Hexadecyl 2-methylpentanoate	43	396	Octadecyl 2-methylheptanoate
10	354	Tetradecyl 2-methyloctanoate	44	410	Tetradecyl 2,6-dimethylundecanoate
11	354	Pentadecyl 2-methylheptanoate	45	410	Tetradecyl 2,8-dimethylundecanoate
12	354	Hexadecyl 2-methylhexanoate	46	410	Hexadecyl 2,6-dimethylnonanoate
13	368	2-Methyltetradecyl 2-methyloctanoate	47	410	Heptadecyl 2,6-dimethyloctanoate
14	368	8-Methyltetradecyl 2-methyloctanoate		410	14-Methylhexanoate 2-methylnonanoate
15	368	10-Methyltetradecyl 2-methyloctanoate	48	410	Tetradecyl 2-methyldodecanoate
16	368	10-Methylhexadecyl 2-methylhexanoate	49	410	Hexadecyl 2-methyldecanoate
17	368	Tetradecyl 2,6-dimethyloctanoate	50	410	Octadecyl 2-methyloctanoate
	368	12-Methylhexadecyl 2-methylhexanoate	51	424	Tetradecyl 2,6-dimethyldodecanoate
18	368	12-Methyltetradecyl 2-methyloctanoate	52	424	Tetradecyl 2,8-dimethyldodecanoate
19	368	Tridecyl 2-methyldecanoate	53	424	Hexadecyl 2,6-dimethyldecanoate
	368	14-Methylhexadecyl 2-methylhexanoate	54	424	Tetradecyl 2,10-dimethyldodecanoate
20	368	Tetradecyl 2-methylnonanoate	55	424	Hexadecyl 2,8-dimethyldecanoate
21	368	Pentadecyl 2-methyloctanoate	56	424	14-Methylhexadecyl 2-methyldecanoate
22	368	Hexadecyl 2-methylheptanoate	57	424	Octadecyl 2,6-dimethyloctanoate
23	368	Heptadecyl 2-methylhexanoate	58	424	Pentadecyl 2-methyldodecanoate
24	382	Tridecyl 2,6-dimethyldecanoate	59	424	Hexadecyl 2-methylundecanoate
	382	8-Methyltetradecyl 2-methylnonanoate	60	424	Heptadecyl 2-methyldecanoate
	382	12-Methyltetradecyl 2,6-dimethyloctanoate	61	424	Octadecyl 2-methylnonanoate
25	382	Tetradecyl 2,6-dimethylnonanoate	62	438	Hexadecyl 2,6-dimethylundecanoate
26	382	Tridecyl 2,8-dimethyldecanoate	63	438	Hexadecyl 2-methyldodecanoate
	382	12-Methylhexadecyl 2-methylheptanoate	64	438	Octadecyl 2-methyldecanoate
27	382	Pentadecyl 2,6-dimethyloctanoate	65	452	Hexadecyl 2,6-dimethyldodecanoate
	382	12-Methyltetradecyl 2-methylnonanoate	66	452	Hexadecyl 2,8-dimethyldodecanoate
28	382	Tetradecyl 2-methyldecanoate	67	452	Octadecyl 2,10-dimethyldecanoate
29	382	Hexadecyl 2-methyloctanoate	68	452	Hexadecyl 2,10-dimethyldodecanoate
30	382	Octadecyl 2-methylhexanoate	69	452	Octadecyl 2,8-dimethyldecanoate
31	396	2-Methyltetradecyl 2-methyldecanoate	70	452	Hexadecyl 2-methyltridecanoate
32	396	Tetradecyl 2,6-dimethyldecanoate	71	452	Heptadecyl 2-methyldodecanoate
33	396	10-Methylhexadecyl 2-methyloctanoate	72	452	Octadecyl 2-methylundecanoate
34	396	12-Methylhexadecyl 2-methyloctanoate			

[a]Molecular weight.

esters. The reconstructed ion current (RIC) from these seven transitions (Fig. 5B) is remarkably similar to the mass chromatogram of *m/z* 368 in the full scan mode (Fig. 5A), indicating that the GC/MS/MS technique can be used not only for qualitative but also for distributional purposes.

For the C_{25} wax esters, a quite different distribution pattern is observed by the GC/MS/MS technique (Fig. 6); components comprised of even carbon-numbered straight-chain alcohols (C_{14}, C_{16}, and C_{18}) esterified with odd 2-methyl fatty acids dominate this cluster. The transitions *m/z* 382 → *m/z* 145 and *m/z* 382 → *m/z* 173 transitions (Fig. 6D and 6F) reveal minor quantities of wax esters containing odd carbon-numbered alcohols, again comprised of various structural isomers. The distribution revealed by the latter transition is especially complex since wax esters composed of straight-chain and methyl branched C_{15} alcohols with both 2-methylnonanoic acid and 2,6-dimethyloctanoic acid occur. The RIC (Fig. 6B) shows again a good match with the mass chromatogram of *m/z* 382 in the full scan mode (Fig. 6A).

General observations. These examples are indicative of the composition of all clusters of wax esters with the same molecular weight. The odd carbon-numbered wax esters are predominantly composed of even carbon-numbered *n*-alcohols (C_{14}, C_{16}, and C_{18}) esterified predominantly with odd carbon-numbered 2-methyl fatty acids (C_7, C_9 C_{11}, and C_{13}), resulting in relatively simple distributions (Fig. 3). This is in good overall agreement with the results from the hydrolysis (Fig. 4). They show specifically that the distributions of odd carbon-numbered fatty acids and even carbon-numbered alcohols are relatively simple. The even carbon-numbered wax

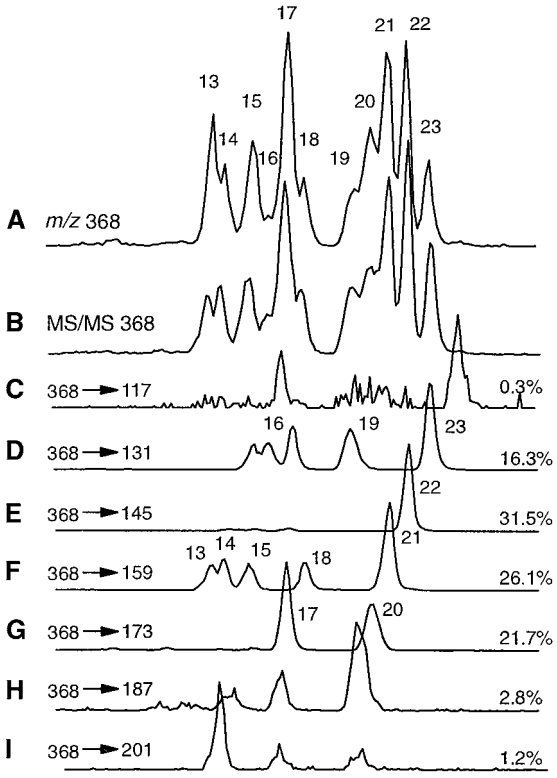

FIG. 5. Gas chromatography/mass spectrometry/mass spectrometry (GC/MS/MS) transitions (C–I) for C_{24} wax esters in the intact preen wax of *C. canutus* #283. The data were acquired by collision-induced decomposition GC/MSMS. Each trace is identified with the masses of the molecular ion (*m/z* 368) and daughter ions (i.e., C_6 fatty acid *m/z* 117, C_7 fatty acid *m/z* 131, C_8 fatty acid *m/z* 145, C_9 fatty acid *m/z* 159, C_{10} fatty acid *m/z* 173, C_{11} fatty acid *m/z* 187, C_{12} fatty acid *m/z* 201). Trace B shows the reconstructed ion current (RIC) from the measured transitions. The upper trace (A) shows a mass chromatogram of *m/z* 368 (*cf*. Fig. 3) of the GC/MS analysis in full scan mode for comparison. Numbers refer to specific wax esters listed in Table 2. Numbers at the end of the traces (in %) indicate the abundance based on peak height of the most abundance peak of the cluster (total set to 100%). See Figure 1 for other abbreviation.

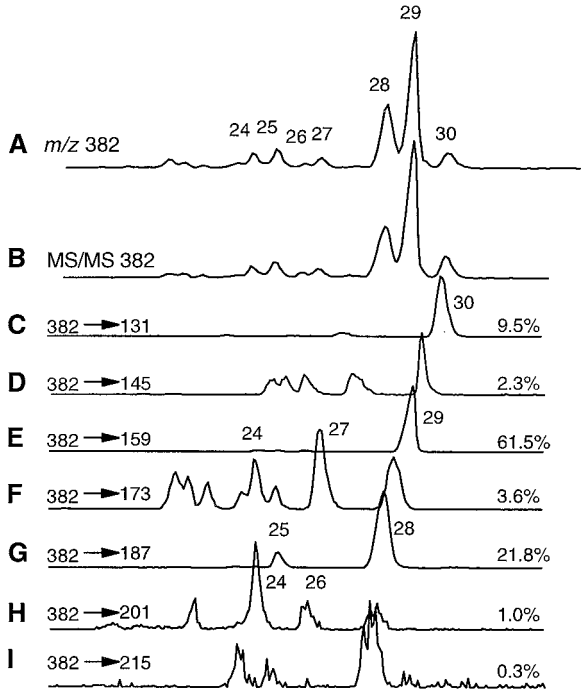

FIG. 6. GC/MS/MS transitions (C–I) for C_{25} wax esters in the intact preen wax of *C. canutus* #283. The data were acquired by collision-induced decomposition GC/MS/MS. Each trace is identified with the masses of the molecular ion (*m/z* 382) and daughter ions (i.e., C_7 fatty acid *m/z* 131, C_8 fatty acid *m/z* 145, C_9 fatty acid *m/z* 159, C_{10} fatty acid *m/z* 173, C_{11} fatty acid *m/z* 187, C_{12} fatty acid *m/z* 201, C_{12} fatty acid *m/z* 215). Trace B shows the RIC from the measured transitions. The upper trace (A) shows a mass chromatogram of *m/z* 382 (*cf*. Fig. 3) of the GC/MS analysis in full scan mode for comparison. Numbers refer to specific wax esters listed in Table 2. Numbers at the end of the traces (in %) indicate the abundance based on peak height of the most abundance peak of the cluster (total set to 100%). See Figures 1 and 5 for abbreviations.

esters show a far more complex distribution. This is due to a number of factors. First of all, the wax esters containing *n*-alcohol moieties are not dominated by even carbon-numbered *n*-alcohols esterified with odd carbon-numbered 2-methyl fatty acids, but odd and even carbon-numbered *n*-alcohols participate in approximately equal amounts. Second, odd carbon-numbered methyl-branched alcohols participate abundantly in these wax ester clusters (e.g., Fig. 5), leading to many more structural isomers. Third, with increasing molecular weight, the various isomers of the dimethyl branched fatty acids also participate in the even carbon-numbered wax esters. These fatty acid isomers are especially abundant in the clusters of even carbon-numbered fatty acids (Fig. 3), explaining why they are not so abundant in the odd carbon-numbered wax esters, which contain predominantly odd carbon-numbered fatty acid moieties. In the higher molecular weight, even carbon-numbered wax esters containing these dimethyl branched fatty acid moieties predominate as indicated by Figure 7, showing the important transitions for the C_{28} wax ester cluster. This example also reveals that even with such a powerful technique as GC/MS/MS full resolution of all structural isomers in this cluster is not obtained.

This is the first time that full structural identification of intact wax esters in complex preen waxes is achieved. In contrast to conventional techniques, which identify fatty acids and alcohols after hydrolysis, our method allows the determination of the structure of the components as they occur in the biological system. This is important if we want to understand the physiological role preen waxes play in birds, and their biosynthesis. In view of the rapid changes of the chemical composition of preen waxes in *C. canutus* over the annual cycle (6), this is most relevant, also from an ecological point of view. Our data already demonstrate that the biosynthesis of preen waxes is complex since the distribution of intact wax esters indicates that it is certainly not a random combination of available fatty acids and alcohols. It seems likely that this will influence the physical properties of the preen wax, but presently the reasons for the complex chemistry of the preen waxes are not at all understood.

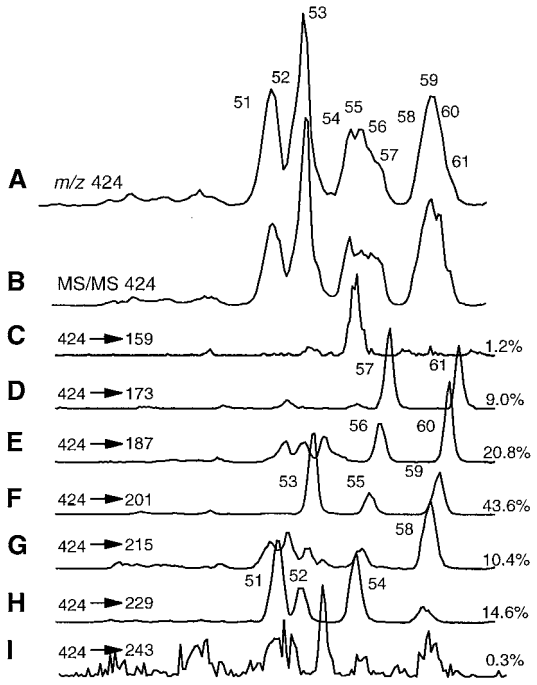

FIG. 7. GC/MS/MS transitions (C–I) for C_{28} wax esters in the intact preen wax of *C. canutus* #283. The data were acquired by collision-induced decomposition GC/MS/MS. Each trace is identified with the masses of the molecular ion (*m/z* 424) and daughter ions (i.e., C_9 fatty acid *m/z* 159, C_{10} fatty acid *m/z* 173, C_{11} fatty acid *m/z* 187, C_{12} fatty acid *m/z* 201, C_{13} fatty acid *m/z* 215, C_{14} fatty acid *m/z* 229, C_{15} fatty acid *m/z* 243). Trace B shows the RIC from the measured transitions. The upper trace (A) shows a mass chromatogram of *m/z* 424 (*cf*. Fig. 3) of the GC/MS analysis in full scan mode for comparison. Numbers refer to specific wax esters listed in Table 2. Numbers at the end of the traces (in %) indicate the abundance based on peak height of the most abundance peak of the cluster (total set to 100%). See Figures 1 and 5 for abbreviations.

ACKNOWLEDGMENTS

We thank Bernard Spaans, Anita Koolhaas, and Anne Dekinga for help in the field and with the captive birds. This work was partly supported by a PIONIER-grant to TP from The Netherlands Organization for Scientific Research (NWO). This is NIOZ-publication 3448.

REFERENCES

1. Jacob, J., and Ziswiler, V. (1982) The Uropygial Gland, *Avian Biol. 6*, 199–324.
2. Jacob, J., Eigener, U., and Hoppe, U. (1997) The Structure of Preen Gland Waxes from Pelecaniform Birds Containing 3,7-Dimethyloctan-1-ol: An Active Ingredient Against Dermatophytes, *Z. Naturforsch. 52c*, 114–123.
3. Stevens, L. (1996) *Avian Biochemistry and Molecular Biology*, Cambridge University Press, Cambridge.
4. Jacob, J. (1976) Bird Waxes, in *Chemistry and Biochemistry of Natural Waxes* (Kolattukudy, P.E., ed.), pp. 93–146, Elsevier, Amsterdam.
5. Jacob, J., and Poltz, J. (1973) Chemotaxonomische Untersuchungen an Limikolen. Die Zusammensetzung des Bürzeldrüsen Sekretes von Austernfischer, Rotschenkel, Knutt and Alpenstrandläufer, *Biochem. Syst. Ecol. 1*, 169–172.
6. Piersma, T., Dekker, M.H.A., and Sinninghe Damsté, J.S. (1999) An Avian Equivalent for Make-up? *Ecol. Lett. 2*, 201–203.
7. Sinninghe Damsté, J.S., Dekker, M., van Dongen, B., Schouten, S., and Piersma, T. (2000) Structural Identification of the Diester Preen Gland Wax in the Red Knot (*Calidris canutus*), *J. Nat. Prod. 63*, 381–384.
8. Skipski, V.P., Smolowne, A.F., Sullivan, R.C., and Barclay, M. (1965) Separation of Lipid Classes by Thin-Layer Chromatography, *Biochim. Biophys. Acta 106*, 386–396.
9. Aasen, A.J., Hofstetter, H.H., Ivengar, B.T.R., and Holman, R.T. (1971) Identification and Analysis of Wax Esters by Mass Spectrometry, *Lipids 6*, 502–507.
10. Kissin, Y.V., Feulmer, G.P., and Payne, W.B. (1986) Gas Chromatographic Analysis of Polymethyl-Substituted Alkanes, *J. Chromatogr. Sci. 24*, 164–182.

[Received January 14, 2000, and in revised form March 27, 2000; revision accepted March 29, 2000]

Polyunsaturated Monoglycerides and a Pregnadiene in Defensive Glands of the Water Beetle *Agabus affinis*

Otmar Schaaf and Konrad Dettner*

University of Bayreuth, Department of Animal Ecology II, D-95440 Bayreuth, Germany

ABSTRACT: In addition to the C_{21} steroid 15α-hydroxypregna-4,6-dien-3,20-dione, four 1- or 2-acylated polyunsaturated monoglycerides, 1- or 2-(*cis*-5,8,11,14-eicosatetraenoyl)-glycerol and 1- or 2-(*cis*-5,8,11,14,17-eicosapentaenoyl)glycerol were identified as constituents of the prothoracic defensive gland secretion of the dytiscid beetle *Agabus affinis* by gas chromatography–mass spectrometry of trimethylsilylated gland extracts. In a feeding assay with minnows, synthetic samples of the two 2-acylated monoglycerides showed only a weak activity as a feeding deterrent. For that reason, other possible functions of the monoglycerides are discussed, such as roles as emulsifiers of cannabimimetics.

Paper no. L8304 in *Lipids 35,* 543–550 (May 2000).

Most adult dytiscid beetles (Coleoptera: Dytiscidae) contain two complex gland systems. The pygidial glands on the hindmost abdominal segment contain substantial quantities of low molecular weight aromatic substances like benzoic acid, phenylacetic acid, and *p*-hydroxybenzaldehyde (1). The beetles distribute the pygidial secretion on their surfaces using their hind legs. In addition to their antimicrobial activity, the pygidial compounds result in an increased wettability of the integument, which facilitates reentry into the water, for example after a flight (1).

Members of the dytiscid subfamilies Dytiscinae, Colymbetinae, Hydroporinae, and Laccophilinae possess an additional pair of exocrine glands located underneath the pronotum. These glands are designated as prothoracic defensive glands in order to differentiate them from the endocrine prothoracic glands of insects. When the beetles are irritated mechanically or seized by a predator, a white or yellowish milky fluid usually emerges from the anterior margin of the pronotum.

Schildknecht (2–6) was the first to show that the prothoracic defensive glands of dytiscids predominantly contain steroids of the vertebrate hormone type as active agents. In a few species, sesquiterpenes (6,7), a nucleoproteid (8), or an alkaloid (4,5) were identified as major or minor constituents of the secretion.

The constitution of the prothoracic defensive secretion of many dytiscids remains largely unknown. The present paper deals with the gas chromatography–mass spectroscopy analysis of the prothoracic defensive secretion of *Agabus affinis* (Payk.), a stenoecious (i.e., dependent on certain habitats and environmental conditions) member of the subfamily Colymbetinae. Some Colymbetinae and Dytiscinae species have already been studied (mostly common and abundant European species; reviewed in Refs. 9,10). However, knowing the defensive gland chemistry of many other rather uncommon species could contribute much to our understanding of biosynthesis of the defensive compounds or even phylogenetic correlations. *Agabus affinis* occurs exclusively in acid peat bogs in northern, eastern, and central Europe and is regularly associated with *Sphagnum* mosses. The feeding deterrence of two novel gland constituents of *A. affinis* was tested in a bioassay with minnows.

EXPERIMENTAL PROCEDURES

Beetles. Adult males and females of *A. affinis* were captured in peat bogs in the Oberpfalz and Oberfranken regions (northern Bavaria, Germany). The beetles were frozen immediately by cooling with dry ice and stored at –40°C until used.

Sample preparation. Beetles were dissected by separating the thorax from head and abdomen and by removing legs and wings with dissecting needles. The glands were freed from surrounding tissues. Gland reservoirs were detached from the pronotum with a fine needle and transferred to 40 µL ethyl acetate in a glass reacti-vial. For each sample, the reservoirs of five beetles were pooled and sonicated for 15 min. Solid residues were removed by centrifugation (2800 × *g*, 15 min). Subsequently, 30 µL of the ethyl acetate extract was transferred to a new vial. The solvent was removed, and the residue was dissolved in 30 µL pyridine/tetrahydrofuran (1:1, vol/vol). Prior to gas chromatography–mass spectrometry (GC–MS) analysis, the samples were trimethylsilylated with 30 µL *N*-mehyl-*N*-trimethylsilyltrifluoroacetamide (Fluka, Buchs, Switzerland) by heating to 40°C for 16 h; 1 µL per sample of this solution was injected into the GC–MS system.

As a control, small samples of fat body and prothoracic

*To whom correspondence should be addressed at Universität Bayreuth, Lehrstuhl Tierökologie II, Universitätsstrasse 30, D-95440 Bayreuth, Germany. E-mail: k.dettner@uni-bayreuth.de

Abbreviations. 1- or 2-ara-gl, 1- or 2-(*cis*-5,8,11,14-eicosatetraenoyl)glycerol (1- or 2-arachidonoylglycerol); 1- or 2-epa-gl, 1- or 2-(*cis*-5,8,11,14,17-eicosapentaenoyl)glycerol; GC–MS, gas chromatography–mass spectrometry; TMS, trimethylsilyl; TMSO, trimethylsilyloxy-.

muscular tissue were taken with fine tweezers from the dorsally opened abdomen and thorax, respectively, prior to dissection of the glands and treated and analyzed accordingly.

GC–MS analysis. Analyses were performed, and 70 eV electron ionization mass spectra were recorded with a Finnigan MAT GCQ™ GC–MS system equipped with an SGE 25QC2/HT5 capillary column; 25 m × 0.22 mm i.d., film = 0.1 µm. Samples were injected in splitless mode (1 min). Carrier gas was helium (40 cm/s; automatic flow control). Further experimental conditions: electron multiplier voltage: 1125 V, high mass adjust: 100%, injector temperature: 230°C, transfer line temperature: 275°C, ion source temperature: 150°C. The column oven temperature program consisted of an initial temperature of 60°C, a 10°C/min increase to 240°C, 3°C/min increase to 320°C, where the temperature was maintained for 5 min. Relative retention times were calculated compared to 5α-cholestane. Compounds were identified by comparing retention times and mass spectra with those of authentic standards. If no reference compounds were available, structures were proposed to comply with mass spectrometric fragmentation behavior.

Reference compounds. 15α-Hydroxypregna-4,6-dien-3,20-dione was prepared from 15α-hydroxypregn-4-en-3,20-dione (15α-hydroxyprogesterone) by selective dehydrogenation at C_6 with *p*-chloranil (11). 15α-Hydroxyprogesterone and 15β-hydroxypregna-4,6-dien-3,20-dione were gifts of Schering AG (Berlin, Germany). 2-(*Cis*-5,8,11,14-eicosatetraenoyl)-glycerol (2-arachidonoylglycerol; 2-ara-gl) and 2-(*cis*-5,8,11,14,17-eicosapentaenoyl-)glycerol (2-epa-gl) were purchased from Deva Biotech (Hatboro, PA).

Feeding assay. Agar pellets containing definite amounts of the compounds to be tested were produced similar to the method of Gerhart *et al*. (12). First, stock solutions (1.8×10^{-1} M) of the test substances in methanol were prepared. Agar (1.5%, wt/vol) was dissolved at 120°C; after the solution was cooled to 45°C, calculated amounts of agar and stock solutions were mixed, and pulverized commercial fish food (TetraMin Flockenfutter, Melle, Germany; 10 mg per mL agar solution) was added as a flavoring agent. Pellets were produced by pipetting 25 µL of the mixture per cavity in the inner surface of 96-well microplate covers and subsequent cooling to room temperature. Control pellets without addition of the test compounds were prepared similarly.

The initial amounts of the test substances per pellet (100 µg) were estimated by comparison of the GC–MS peak areas of the prothoracic gland constituents of *A. affinis* to that of authentic standards. For the second test series, a threefold amount (300 µg/pellet) compared to the natural abundance in the glands was used.

Six adult minnows (*Phoxinus phoxinus* L.) were kept in an aquarium of 60 × 30 × 30 cm at 20°C (photoperiod 8:00 a.m.–7:00 p.m). Inside the aquarium, a test area was separated by a longitudinal pane of glass and a rectangular metal grid held by a Plexiglas frame (Fig. 1). The fish were starved for 3 d before the test started. All assays were performed at 2:00 p.m. to exclude an influence of changing feeding motivation depending on the time of day. In order to minimize a susceptibility of test results to learning behavior, only one randomly selected fish per day was tested. The fish was transferred to the test area 1 h before the test started. In each test, four pellets were dropped into the test area in the same sequence in intervals of 1 min: control pellet C1 → test pellet T1 → test pellet T2 → control pellet C2; by that means, an influence to the feeding behavior by experience could have been registered through the acceptance rates of T_2 and C_2. Reactions were recorded as acceptance (pellet swallowed) or rejection (pellet spat out). Pellets that were not noticed by the fish were not scored. After each test, the fish was left in the test area until the next day in order to record possible behavioral changes due to narcotic or toxic effects. Afterward the fish was removed, and a new fish was used for the next test until every minnow was tested once; subsequently, random selection started again. The number of test repetitions ($n = 10$) was limited by the available amount of the test substances 2-ara-gl and 2-epa-gl.

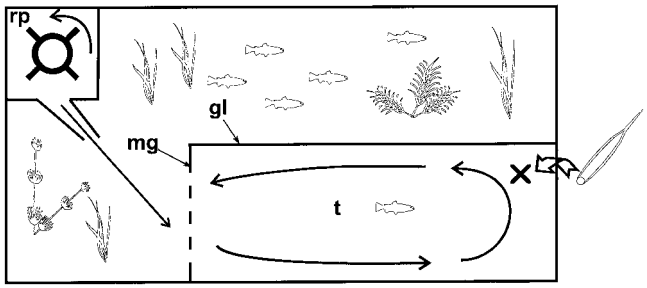

FIG. 1. Schematic drawing of experimental apparatus (view from above) for feeding assay with minnows: t = separate testing area, rp = aquarium filter with rotatory pump, gl = plane of glass, mg = Plexiglas frame with metal grid, × = insertion place for pellets. Arrows indicate the direction of water flow.

Statistics. Acceptance rates of test and control pellets were examined for significant differences employing the G-test of independence in combination with Yates' correction (13). G was calculated and compared to critical χ^2 values using statistical tables (14).

RESULTS AND DISCUSSION

Identification of prothoracic defensive gland constituents of A. affinis. During GC–MS analysis of the trimethylsilylated gland extract, the total ion current chromatogram showed five component peaks (Fig. 2). Compounds 1 and 2 as well as 3 and 4 eluted as doublet peaks with only slightly different retention times, whereas compound 5 eluted with a considerably higher retention time. Because cholesterol (C) is a ubiquitous constituent of animal cell membranes, the small amounts of it found in the ethyl acetate extracts are therefore not regarded as an original active compound of the glands but rather as a contaminant of surrounding tissues, since it was also found in comparable amounts in control extracts of fat body and prothoracic tissue.

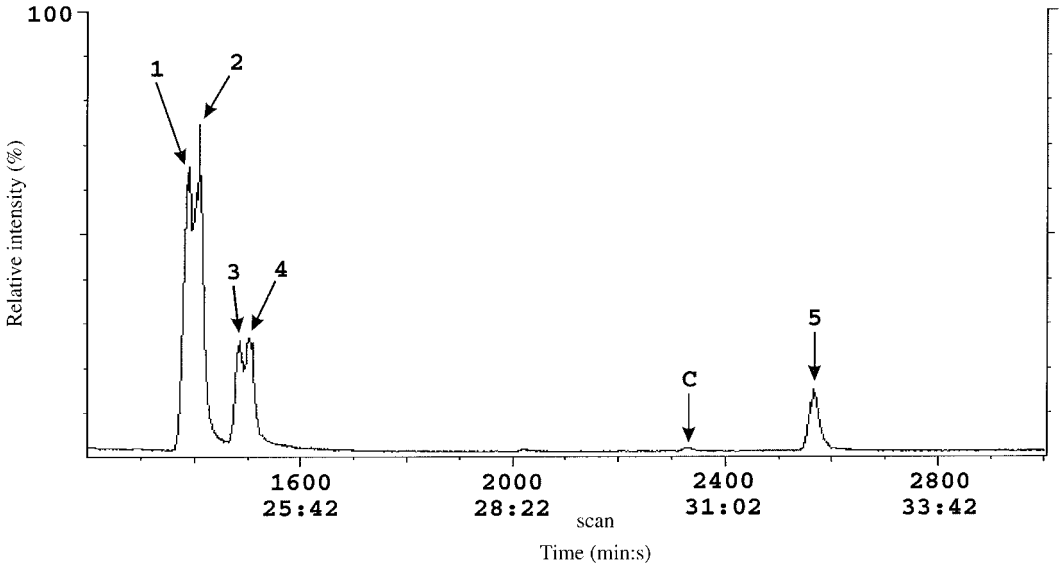

FIG. 2. Section of total ion current chromatogram of a trimethylsilylated extract of prothoracic defensive glands of *Agabus affinis* (five specimens): 1 = 2-(*cis*-5,8,11,14-eicosatetraenoyl)glycerol-bis-TMS (2-ara-gl-bis-TMS; RT = 0.94); 2 = 2-(*cis*-5,8,11,14,17-eicosapentaenoyl)glycerol-bis-TMS (2-epa-gl-bis-TMS, RT = 0.95); 3 = 1-(*cis*-5,8,11,14-eicosatetraenoyl)glycerol-bis-TMS (1-ara-gl-bis-TMS; RT = 0.97); 4 = 1-(*cis*-5,8,11,14,17-eicosapentaenoyl)glycerol-bis-TMS (1-epa-gl-bis-TMS, RT = 0.97); 5 = 15α-hydroxypregna-4,6-dien-3,20-dione-TMS (RT = 1.32); C = cholesterol-TMS. TMS = trimethylsilyl ether; RT = relative retention time (5α-cholestane = 1.00); for experimental conditions see text.

The mass spectra of compounds 1, 2, 3, and 4 showed the characteristic appearance of trimethylsilylated monoglycerides (15–17). The molecular ions of compounds 1 and 2 as well as of 3 and 4 were only of weak abundance and differed from each other in only two mass units (M^+ 520/522; see Figs. 3, 4).

The *m/z* 203 ion is formed in monoglycerides by elimination of the acyloxy radical R–COO· (+1H) from the [M – 15] fragment (*m/z* 505 or 507). The corresponding cleavage from the molecular ion, resulting in the formation of an ion at *m/z* 218, is of pronounced intensity in the mass spectra of 2-acylated monoglycerides only. In contrast, a [M – 103] fragment, which is missing in 2-acyl glycerides, is characteristic for the spectra of 1-acylated monoglycerides (16). Accordingly, compounds 1 and 2 were presumed to be 2-acylated and compounds 3 and 4 1-acylated monoglycerides (*cf*. Figs. 3, 4).

Acyl fragment $[R–CO]^+$ (–1H) at *m/z* 286 (compounds 1 and 3) and *m/z* 284 (compounds 2 and 4) indicated the acyl chain length and the number of double bonds of the acyl moiety. By comparison with authentic compounds, the structures of 1 and 2 were determined as 2-ara-gl and 2-epa-gl, respectively. Although compounds 3 and 4 were not available as authentic substances, their mass spectrometric fragmentation patterns showed high evidence for the corresponding 1-acylated monoglycerides, 1-(*cis*-5,8,11,14-eicosatetraenoyl)glycerol (1-ara-gl) and 1-(*cis*-5,8,11,14,17-eicosapentaenoyl)glycerol (1-epa-gl). Although 1- and 2-ara-gl were extracted from canine gut tissue and identified by comparison with authentic compounds in derivatized and underivatized form (18), the spectra of the trimethylsilylated monoglycerides were not published.

Only one steroid (compound 5) was found in the prothoracic defensive glands of *A. affinis*; this showed the same retention time and mass spectrum as the trimethylsilyl (TMS) ether of 15α-hydroxypregna-4,6-dien-3,20-dione. The mass spectrum of compound 5 exhibited a distinct molecular ion (M^+ 400, Fig. 5). The presence of a trimethylsilyloxy (TMSO) group was indicated by the [M – 90] ion at *m/z* 310. The base peak at *m/z* 267 = [310 – 43] is formed by subsequent elimination of the side chain (C_{20} + C_{21}). The ion at *m/z* 172, which comprises C_{15}–C_{17}, C_{20} and C_{21} together with the 15-TMSO group, is derived from D-ring cleavage and represents an important key fragment for steroids containing a 15- or 16-TMSO-20-one structure (19,20). A corresponding [M – 172] ion was also observed (*m/z* 228). The fragment at *m/z* 157 = [172 – 15] results from additional elimination of a methyl radical. The presence of a 16-TMSO group can be excluded by the absence of pronounced ions at *m/z* 109, 159, and 186 and the occurrence of an [M – 71] fragment at *m/z* 329, which is formed by C_{16}–C_{21} and promoted by a TMSO group at C_{15}. Authentic 15β-hydroxypregna-4,6-dien-3,20-dione was also analyzed by GC–MS and showed a similar fragmentation pattern, but widely differing peak intensities and a divergent retention time.

$\Delta^{4,6}$-Unsaturated C_{21} steroids were also detected in the prothoracic defensive secretion of several dytiscid species from the subfamilies Dytiscinae and Colymbetinae (9,10). The 15α-hydroxypregna-4,6-dien-3,20-dione was identified in *A. sturmi* (Gyll.) in underivatized form along with steroid isobutyric esters (21), which are obviously missing in *A. affinis*.

In contrast, the presence of considerable amounts of polyun-

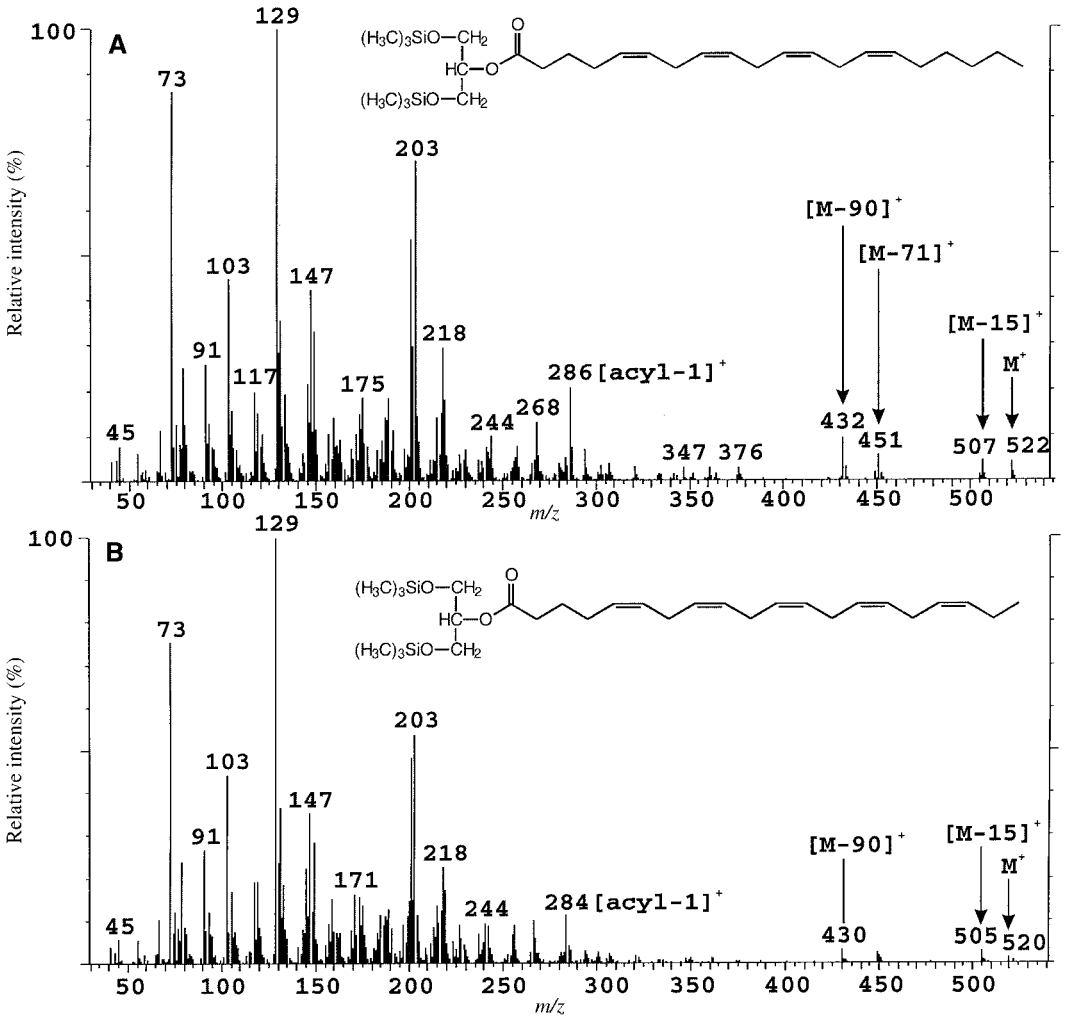

FIG. 3. Mass spectra of (A) 2-(*cis*-5,8,11,14-eicosatetraenoyl)glycerol (2-ara-gl) and (B**)** 2-(*cis*-5,8,11,14,17-eicosapentaenoyl)glycerol (2-epa-gl), derivatized as bis-trimethylsilyl ethers (compounds 1 and 2 of prothoracic defensive glands of *Agabus affinis*; *cf*. Fig. 2).

saturated monoacylglycerols as main components of the prothoracic defensive glands in *A. affinis* was a surprising result, since it was the first time that such compounds have been found to be accumulated and stored in exocrine glands, not only in water beetles but also in other insects or arthropods.

Feeding assay. Monoglycerides are common and widespread intermediates of lipid metabolism in animals and plants. In the food and cosmetics industries, they are utilized as emulsifiers. Therefore, a biological function of monoglycerides as deterring or toxic agents once appeared improbable. However, during investigation of endogenous ligands of cannabinoid receptors, Mechoulam *et al.* (18) isolated 2-ara-gl from canine gut tissues. Interestingly, 2-ara-gl not only bound to cannabinoid receptors in mouse tissue cultures but also caused the same four suppressive effects (antinociception, immobility, decrease in spontaneous activity, lowering of body temperature) induced by Δ^9-tetrahydrocannabinol. Recent studies showed that 2-ara-gl plays an important role in Ca^{2+} regulation in the central nervous system of mammals (22,23) and possibly serves as a vasomodulator in human blood vessels (24). Cannabinoid receptors (which might be 2-ara-gl receptors primarily) were detected not only in mammals but also in birds (chicken, pigeon), frogs (*Rana pipiens*), and fish (*Salmo gairdnerii*) (25); accordingly, they seem to be widespread in vertebrates. The cannabimimetic potential of 2-ara-gl in mice (16) resembles in many respects the anesthetic effects of many steroids in vertebrates.

These cannabimimetic effects have been observed thus far only upon intravenous administration of 2-ara-gl. For our purposes, an oral application of the test compounds seemed appropriate in order to match natural conditions as closely as possible. The 1-acylated monoglycerides could not be tested because of lack of the authentic compounds.

With an amount of 100 µg 2-ara-gl and 2-epa-gl each per pellet, 3 of 9 (33%) of the test pellets T1 and T2 were swallowed, whereas higher acceptance rates of the control pellets C1 (70%) and C2 (63%) were observed (Fig. 6). Thus, the pellets containing monoglycerides were consumed less fre-

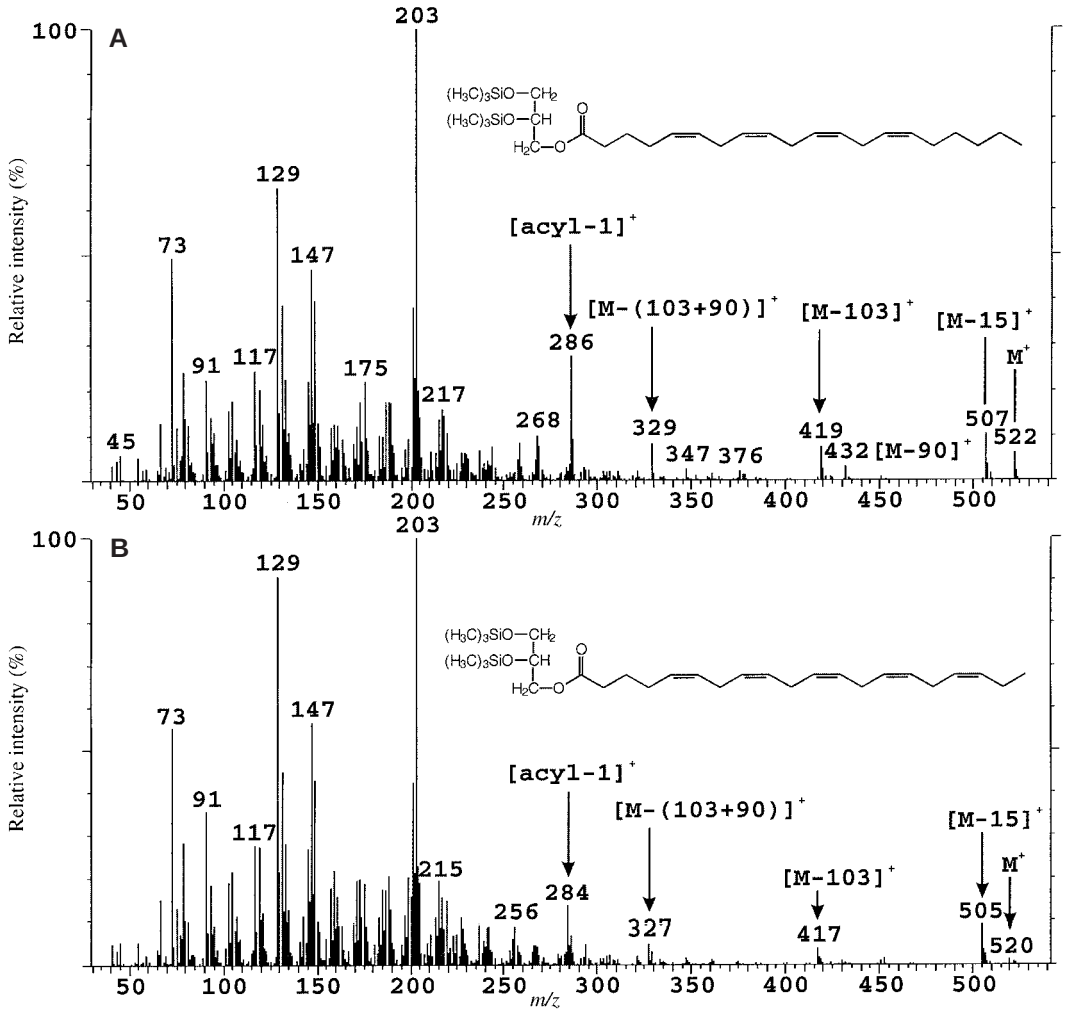

FIG. 4. Mass spectra of (A) 1-(*cis*-5,8,11,14-eicosatetraenoyl)glycerol (1-ara-gl) and (B**)** 1-(*cis*-5,8,11,14,17-eicosapentaenoyl)glycerol (1-epa-gl), derivatized as bis-trimethylsilyl ethers (compounds 3 and 4 of prothoracic defensive glands of *Agabus affinis*; *cf*. Fig. 2).

quently than the control pellets; however, statistical evaluation showed no significant differences, either between single pellet categories or upon pooling control pellets (C1 + C2) and test pellets (T1 + T2).

The threefold increase of the monoglyceride amounts per pellet (300 µg 2-ara-gl and 2-epa-gl each) led to an enhanced deterring effect (Fig. 6): the acceptance rates of the monoglyceride pellets declined to 13 (T1) and 29% (T2). In contrast, 80 (C1) and 86% (C2) of the control pellets were accepted. Upon addition of the results of T1/T2 and C1/C2, respectively, at a significance level of $\alpha = 0.01$, a significant difference between T1 + T2 and C1 + C2 as well as between T1 and C1 + C2 was calculated. T2 and C1 + C2 also differed significantly ($\alpha = 0.05$), just as T1 and C1, while the acceptance of T2 was not significantly reduced compared to C2. No significant differences were found between the first and second test and control pellets (T1 and T2, C1 and C2).

The fish bioassays showed that the monoglycerides obviously can be perceived by the fish. A deterring effect was observed; however, statistical significance occurred only after administration of amounts markedly higher than those naturally occurring in the glands of the beetles. Changes in behavior, pointing to cannabimimetic activity of the monoglycerides, were not noticed. It cannot be excluded that such effects would take place upon application of even higher amounts. On the other hand, the monoglycerides might be inactivated in the gut by lipid metabolism enzymes (lipases, acyltransferases) upon oral application.

Therefore, other functions of the monoglycerides should be considered. Analogous to the pygidial gland components of dytiscids, an improvement in the wettability of the integument is conceivable, as well as antimicrobial activity (1). Another possible role of the monoglycerides might be related to their emulsifying properties, since the prothoracic steroid of *A. affinis* is highly water-insoluble. Accordingly, the monoglycerides might serve as an emulsifier or enhance the efficacy of the steroid by influencing membrane transfer or uptake rate.

The anesthetic or toxic properties of some steroids against

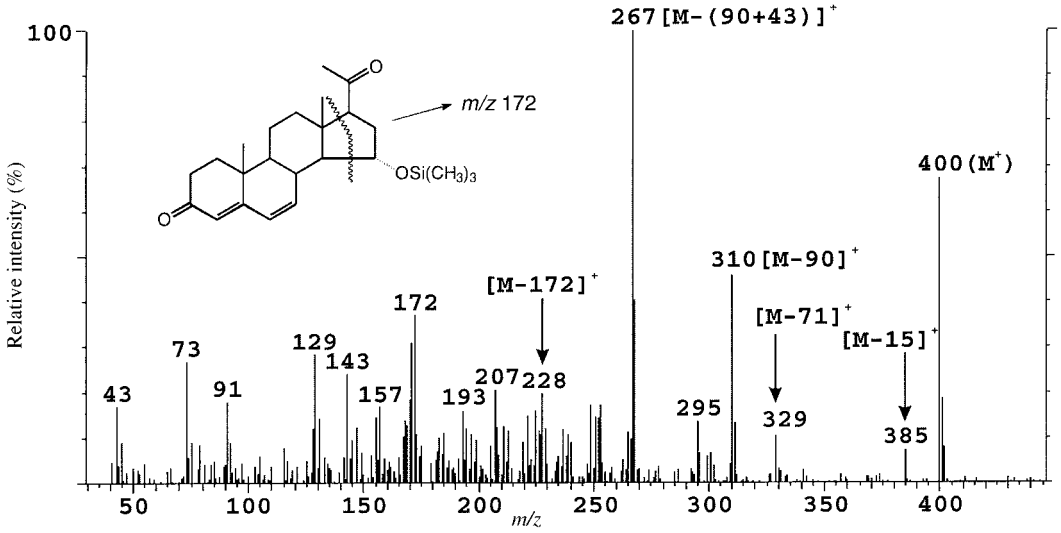

FIG. 5. Mass spectrum of 15α-hydroxypregna-4,6-dien-3,20-dione, derivatized as trimethylsilyl ether (compound 5 of prothoracic defensive glands of *Agabus affinis*, *cf.* Fig. 2).

mammals are well known; the effects depend on dose and structure of the steroid (26–29). An anesthetic effect of dytiscid steroids on fish was demonstrated, causing reversible loss of balance and mobility at lower doses, but being irreversible and lethal at high doses (30–33). In contrast to the anesthetic and toxic effects against predators observed with percutaneous administration, a deterring effect of steroids was found by feeding to the sunfish *Lepomis macrochirus* agar pellets that contained dytiscid defensive steroids leading to a significant decrease of pellet acceptance rates (10). These results have been confirmed recently in a bioassay with the European minnow *P. phoxinus* (34).

An intriguing question exists about the possible synergistic effect of the prothoracic defensive steroid of *A. affinis*, 15α-hydroxypregna-4,6-dien-3,20-dione, and the polyunsaturated monoglycerides. Unfortunately, this effect could not

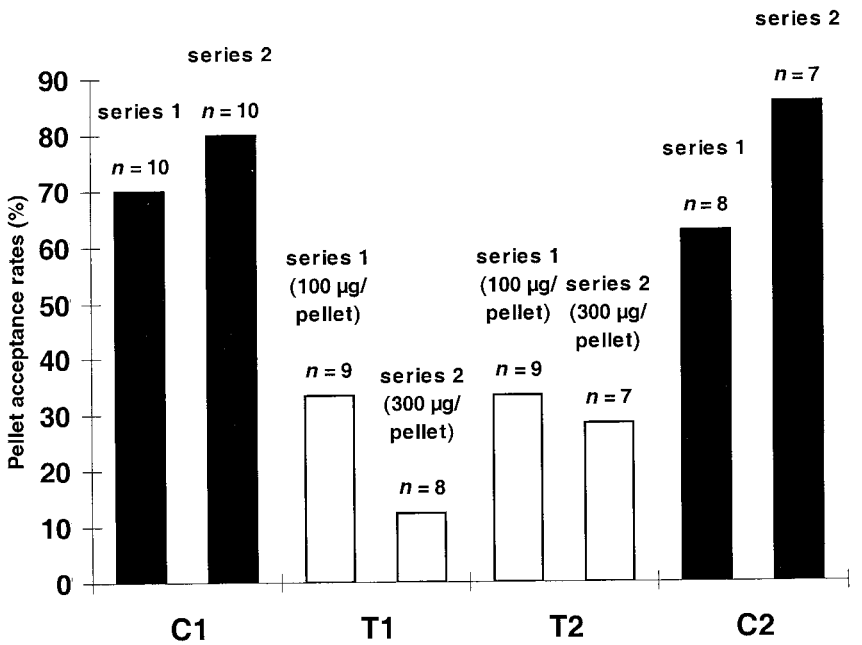

FIG. 6. Results of feeding assays with six minnows (*Phoxinus phoxinus*); 100 µg 2-arachidonoylglycerol + 100 µg 2-(*cis*-5,8,11,14,17-eicosapentaenoyl)glycerol per pellet or 300 µg 2-ara-gl + 300 µg 2-epa-gl per pellet as active agents; C1 = C2 = control pellet 1 and 2, T1 = T2 = test pellet 1 and 2; *n* = number of pellets that were noticed by the minnows, total number of test repetitions = 10; statistical evaluation, see text. Open bars (□), test pellets; solids bars (■), control pellets.

be examined because sufficient amounts of the authentic steroid were not available for testing. Additionally, it would be highly desirable to test the activity of the natural secretion, which also has not been possible so far owing to the small-sized prothoracic defensive glands and the low abundance of *A. affinis* (which cannot yet be kept under laboratory conditions) in its natural habitats.

ACKNOWLEDGMENTS

The authors express their thanks to Dr. Werner Boidol and Schering AG, Berlin, for supplying reference steroids and personal support, to Prof. Raphael Mechoulam and Dr. Shimon Ben-Shabat (Hebrew University Jerusalem), Dr. Thomas Paululat (Hans-Knöll-Institut für Naturstoff-Forschung, Jena), and Prof. Karlheinz Seifert (Universität Bayreuth) for help and assistance in identifying 2-ara-gl and 2-epa-gl, and to BASF AG, Ludwigshafen, and the Bundesministerium für Bildung, Wissenschaft, Forschung und Technologie (BMBF; reference no. 0310722) for financial support.

REFERENCES

1. Dettner, K. (1985) Ecological and Phylogenetic Significance of Defensive Compounds from Pygidial Glands of *Hydradephaga* (Coleoptera), *Proc. Acad. Nat. Sci. Phil. 137*, 156–171.
2. Schildknecht, H. (1968) Das Arsenal der Schwimmkäfer: Sexualhormone und "Antibiotica," *Nachr. Chem. Techn. 16*, 311–312.
3. Schildknecht, H. (1970) The Defensive Chemistry of Land and Water Beetles, *Angew. Chem. Internat. Edit. 9*, 1–9.
4. Schildknecht, H. (1971) Evolutionsspitzen der Insekten-Wehrchemie, *Endeavour 30*, 136–141.
5. Schildknecht, H. (1976) Chemische Ökologie—ein Kapitel moderner Naturstoffchemie, *Angew. Chem. 88*, 235–243.
6. Schildknecht, H. (1977) Protective Substances of Arthropods and Plants, *Pont. Acad. Sci. Scripta Varia 41*, 59–107.
7. Weber, B. (1979) Über Inhaltsstoffe in den Wehrdrüsen von *Ilybius fenestratus*, *Dytiscus marginalis* und *Laccophilus minutus*, Ph.D. Thesis, University of Heidelberg, Germany.
8. Schildknecht, H., and Tacheci, H. (1971) Colymbetin, a New Defensive Substance of the Water Beetle, *Colymbetes fuscus*, That Lowers Blood Pressure–LII, *J. Insect Physiol. 17*, 1889–1896.
9. Blum, M.S. (1981) *Chemical Defenses of Arthropods*, Academic Press, New York.
10. Scrimshaw, S., and Kerfoot, W.C. (1987) Chemical Defenses of Freshwater Organisms: Beetles and Bugs, in *Predation—Direct and Indirect Impacts on Aquatic Communities* (Kerfoot, W.C., and Sih, A., eds.), pp. 240–262, University Press of New England, Hanover.
11. Agnello, E.J., and Laubach, G.D. (1960) The Dehydrogenation of Corticosteroids with Chloranil, *J. Am. Chem. Soc. 82*, 4293–4299.
12. Gerhart, D.J., Bondura, M.E., and Commito, J.A. (1991) Inhibition of Sunfish Feeding by Defensive Steroids from Aquatic Beetles: Structure–Activity Relationships, *J. Chem. Ecol. 17*, 1363–1370.
13. Sokal, R.R., and Rohlf, F.J. (1981) *Biometry*, W.H. Freeman and Company, New York.
14. Rohlf, F.J., and Sokal, R.R. (1981) *Statistical Tables*, W.H. Freeman and Company, New York.
15. Myher, J.J. (1979) Separation and Determination of the Structure of Acylglycerols and Their Analogues, in *Handbook of Lipid Research 1—Fatty Acids and Glycerides* (Kuksis, A., ed.), pp. 123–196, Plenum Press, New York.
16. Wood, G. (1980) Complex Lipids, in *Biochemical Applications of Mass Spectrometry* (Waller, G.R., and Dermer, O.C., eds.) 1st Suppl. Vol., pp. 173–209, John Wiley & Sons, New York.
17. Weintraub, S.T. (1990) Mass Spectrometry of Lipids, in *Mass Spectrometry of Biological Materials* (McEwen, C.N., and Larsen, B.S., eds.), pp. 257–286, Marcel Dekker, Inc., New York.
18. Mechoulam, R., Ben-Shabat, S., Hanus, L., Ligumsky, M., Kaminski, N.E., Schatz, A.R., Gopher, A., Almog, S., Martin, B.R., Compton, D.R., Pertwee, R.G., Griffin, G., Bayewitch, M., Barg, J., and Vogel, Z. (1995) Identification of an Endogenous 2-Monoglyceride, Present in Canine Gut, That Binds to Cannabinoid Receptors, *Biochem. Pharmacol. 50*, 83–90.
19. Gustafsson, J.-Å., and Sjövall, J. (1968) Steroids in Germfree and Conventional Rats—6. Identification of 15α- and 21-Hydroxylated C_{21} Steroids in Faeces from Germfree Rats, *Eur. J. Biochem 6*, 236–247.
20. Eriksson, H., Gustafsson, J.-Å., and Sjövall, J. (1971) Studies on the Structure, Biosynthesis, and Bacterial Metabolism of 15-Hydroxylated Steroids in the Female Rat, *Eur. J. Biochem. 19*, 433–441.
21. Schildknecht, H., and Hotz, D. (1970) Naturally Occurring Steroid-Isobutyrates, *Exc. Med. Int. Congr. Ser. 219*, 158–166.
22. Sugiura, T., Kodaka, T., Kondo, S., Tonegawa, T., Nakane, S., Kishimoto, S., Yamashita, A., and Waku, K. (1996) 2-Arachidonoylglycerol, a Putative Endogenous Cannabinoid Receptor Ligand, Induces Rapid, Transient Elevation of Intracellular Free Ca^{2+} in Neuroblastoma × Glioma Hybrid NG108-15 Cells, *Biochem. Biophys. Res. Comm. 229*, 58–64.
23. Sugiura, T., Kodaka, T., Kondo, S., Tonegawa, T., Nakane, S., Kishimoto, S., Yamashita, A., and Waku, K. (1997) Inhibition by 2-Arachidonoylglycerol, a Novel Type of Possible Neuromodulator, of the Depolarization-Induced Increase in Intracellular Free Calcium in Neuroblastoma Glioma Hybrid NG108-15 Cells, *Biochem. Biophys. Res. Comm. 233*, 207–210.
24. Sugiura, T., Kodaka, T., Nakane, S., Kishimoto, S., Kondo, S., and Waku, K. (1998) Detection of an Endogenous Cannabimimetic Molecule, 2-Arachidonoylglycerol, and Cannabinoid CB1 Receptor mRNA in Human Vascular Cells: Is 2-Arachidonoylglycerol a Possible Vasomodulator? *Biochem. Biophys. Res. Comm. 243*, 838–843.
25. Howlett, A.C., Bidaut-Russell, M., Devane, W.A., Melvin, L.S., Johnson, M.R., and Herkenham, M. (1990) The Cannabinoid Receptor: Biochemical, Anatomical, and Behavioral Characterization, *Trends Neurosci. 13*, 420–423.
26. Selye, H. (1942) Correlations Between the Chemical Structure and the Pharmacological Actions of the Steroids, *Endocrinology 30*, 437–453.
27. Phillipps, G.H. (1975) Structure–Activity Relationships in Steroidal Anaesthetics, *J. Steroid Biochem. 6*, 607–613.
28. Harrison, N.L., Majewska, M.D., Harrington, J.W., and Barker, J.L. (1987) Structure–Activity Relationships for Steroid Interaction with the γ-Aminobutyric $Acid_A$ Receptor Complex, *J. Pharmacol. Exp. Ther. 241*, 346–353.
29. Ueda, I., Tatara, T., Chiou, J.-S., Krishna, P.D., and Kayama, H. (1994), Structure-Selective Anesthetic Action of Steroids: Anesthetic Potency and Effects on Lipid and Protein, *Anesth. Analg. 78*, 718–725.
30. Schildknecht, H., Siewerdt, R., and Maschwitz, U. (1966) Ein Wirbeltierhormon als Wehrstoff des Gelbrandkäfers (*Dytiscus marginalis*), *Angew. Chem. 78*, 392.
31. Schildknecht, H., Birringer, H., and Maschwitz, U. (1967) Testosteron als Abwehrstoff des Schlammschwimmers *Ilybius*, *Angew. Chem. 79*, 579–580.
32. Schildknecht, H., Hotz, D., and Maschwitz, U. (1967) Über Arthropoden-Abwehrstoffe XXVII—Die C_{21}-Steroide der Prothorakalwehrdrüsen von *Acilius sulcatus*, *Z. Naturf. 22 b*, 938–944.

33. Miller, J.R., and Mumma, R.O. (1976) Physiological Activity of Water Beetle Defensive Agents. I. Toxicity and Anesthetic Activity of Steroids and Norsesquiterpenes Administered in Solution to the Minnow *Pimephales promelas* Raf., *J. Chem. Ecol. 2*, 115–130.
34. Schaaf, O., Baumgarten, J., and Dettner, K. (2000) Identification and Function of Prothoracic Exocrine Gland Steroids of the Dytiscid Beetles *Graphoderus cinereus* (L.) and *Laccophilus minutus* (L.), *J. Chem. Ecol.*, in press.

[Received July 6, 1999, and in final revised form March 20, 2000; revision accepted April 12, 2000]

Lipids of Gelatinous Antarctic Zooplankton: Cnidaria and Ctenophora

Matthew M. Nelson[a,b,*], Charles F. Phleger[a], Ben D. Mooney[c], and Peter D. Nichols[c,d]

[a]Department of Biology, San Diego State University, San Diego, California 92182 and [b]Department of Zoology, University of Tasmania, Hobart, Tasmania 7001, Australia, [c]CSIRO Marine Research, Hobart, Tasmania 7001, Australia, and [d]Antarctic CRC, Hobart, Tasmania 7001, Australia

ABSTRACT: Antarctic gelatinous zooplankton, including Cnidaria (*Calycopsis borchgrevinki, Diphyes antarctica, Stygiomedusa gigantea, Atolla wyvillei, Dimophyes arctica*) and Ctenophora (*Beroe cucumis, B. forskalii, Pleurobrachia pileus, Bolinopsis infundibulum*) were collected near Elephant Island, South Shetland Islands, during January and February 1997 and 1998. Total lipid was low in all zooplankton (0.1–5 mg g^{-1} wet mass) and included primarily polar lipids (59–96% of total lipid). Triacylglycerols were 0–26% of total lipids, and wax esters were 0–11% in all species. Cholesterol was the major sterol in all Cnidaria (50–63% of total sterols) whereas in most ctenophores it was lower at 26–45%. These cholesterol levels are consistent with a combined carnivorous and phytoplanktivorous diet in the ctenophores, with the carnivorous diet more dominant in the Cnidaria. Other sterols included primarily *trans*-dehydrocholesterol, desmosterol, 24-methylcholest-5,22*E*-dien-3β-ol, 24-nordehydrocholesterol, and 24-methylenecholesterol. Total stanols were 0–6% in all zooplankton. Eicosapentaenoic acid and docosahexaenoic acid were the major polyunsaturated fatty acids (PUFA) in all samples (7–25% of total fatty acids) except for *A. wyvillei* in which docosapentaenoic acid was 10% of total fatty acids. The PUFA 18:5n-3 was not detected in 1997 samples, but constituted 0.2–0.8% in most 1998 samples. Monounsaturated fatty acids included primarily 18:1n-9*c*, 16:1n-7*c*, and 18:1n-7*c*. The principal saturated fatty acids in all samples were 16:0, 18:0, and 14:0. These data are the first for many of these zooplankton species and the first sterol data for most species. The use of the signature lipid approach has enabled examination of aspects of trophodynamics not obtainable by conventional techniques.

Paper no. L8387 in *Lipids 35*, 551–559 (May 2000).

The Southern Ocean has a complex food web including planktivorous herbivores (krill, salps, copepods) fed upon by birds, fish, squid, seals, and baleen whales (1). Gelatinous organism, such as salps, ctenophores, and medusae are often neglected in studies of energy flow through marine pelagic ecosystems. Their importance has only recently been recognized (2,3). They are major zooplankton constituents in the ocean and are important regulators of biogeochemical flux (4).

Lipid class, fatty acid, and sterol compositional profiles can be used to understand and identify food web interactions (5,6). There are limited lipid studies of Antarctic gelatinous zooplankton in the literature. Low lipid values are characteristic of most species, such as *Calycopsis borchgrevinki* and *Diphyes antarctica* (7), with an average lipid content of approximately 3% for Antarctic gelatinous zooplankton (8). Polar lipid (PL) is typically the major lipid class, as in *C. borchgrevinki* and *D. antarctica* (7,9). High cholesterol was reported in *Bolinopsis infundibulum* from a Scottish sea loch (10). Fatty acid composition of the scyphomedusan *Atolla wyvillei* was provided by Reinhardt and Van Vleet (1) who first noted high docosapentaenoic acid (DPA, 22:5n-3) in this species. High DPA was also reported in another Antarctic scyphomedusan, *Periphylla periphylla*, and sterol and fatty acid compositions were given for the Antarctic cnidarian *C. borchgrevinki* and *Arctopodema ampla* (11). Lipids of gelatinous salps (*Salpa thompsoni*) have been observed to be reflected in their commensal hyperiid amphipods (12). Lipid and fatty acid compositions of a number of non-Antarctic Cnidaria have been reviewed by Joseph (13).

The purpose of this study, conducted with animals collected in Elephant Island waters, is to examine lipid classes, specific sterols, and fatty acid biomarkers of the Antarctic Cnidaria *C. borchgrevinki, D. antarctica*, *Stygiomedusa gigantea*, *A. wyvillei*, and *Dimophyes arctica*, and the Ctenophora *Beroe cucumis, B. forskalii*, *Pleurobrachia pileus*, and *Bolinopsis infundibulum*. The data, to our knowledge, are the first reports for some of these species. The use of signature lipids in food chain studies offers potential to gain additional information not available with conventional procedures. The lipid profiles obtained will help to clarify trophodynamics of the oceanographic region near Elephant Island. This area, intensively surveyed for zooplankton by the United States Antarctic Marine Living Resources (U.S. AMLR) Program, is noted for high biological productivity and rich krill populations (14).

*To whom correspondence should be addressed at Department of Zoology, University of Tasmania, GPO Box 252-05, Hobart, Tasmania 7001, Australia. E-mail: mmnelson@postoffice.utas.edu.au

Abbreviations: AMLR, Antarctic Marine Living Resources; BSTFA, *N,O*-bis-(trimethylsilyl)trifluoroacetamide; DHA, docosahexaenoic acid; DMDS, dimethyl disulfide; DPA, docosapentaenoic acid; EPA, eicosapentaenoic acid; FFA, free fatty acids; FID, flame-ionization detector; GC, gas chromatography; MS, mass spectrometry; MUFA, monounsaturated fatty acids; PL, polar lipids; PUFA, polyunsaturated fatty acids; SFA, saturated fatty acids; ST, sterols; TAG, triacylglycerols; TLC, thin-layer chromatography; TMSi, trimethylsilyl; VLC-PUFA, very long chain PUFA; WE, wax esters.

MATERIALS AND METHODS

Sample description. Cnidarians and ctenophores were collected from the R/V *Yuzhmorgeologiya* by Isaacs-Kidd midwater trawl fitted with a 505-μm mesh plankton net during January and February, 1997 and 1998. The samples were obtained as part of the AMLR Field Study conducted annually in the Elephant Island region of the Antarctic Peninsula (14–16). The AMLR study area is located between 60–62.5°S and 53–59°W. The net was obliquely towed to 170 m depth for 30 min at a speed of 2 knots, or to 10 m above the bottom in shallower waters. Samples were identified with the assistance of V. Loeb and V. Siegel. Samples were frozen in liquid nitrogen directly after identification and sorting on board ship. Samples were then transported frozen (dry ice) by air to CSIRO Marine Research, in Hobart, Tasmania, where they were maintained at –70°C prior to analysis. Fresh masses of zooplankton extracted for lipid analysis were as follows: *A. wyvillei*, 2.4–5.6 g; *D. antarctica*, 3.5 g (which included 18 pooled individuals for 1997; for 1998 2 or 3 individuals were pooled for each sample, 0.2–0.5 g); *C. borchgrevinki*, 0.6 g; *S. gigantea*, 2.1 g (oral arm tissue only); *Dimophyes arctica*, 0.1 g (3 pooled individuals); *B. forskalii*, 0.9–8.8 g; *B. cucumis*, 2.9 g; *Pleurobrachia pileus*, 0.1 g; and *Bolinopsis infundibulum*, 0.7–1.2 g.

Lipid extraction. Samples were quantitatively extracted using a modified Bligh and Dyer (17) one-phase methanol/chloroform/water extraction (2:1:0.8, by vol); the sample was extracted overnight and the phases were separated the following day by the addition of chloroform and water (final solvent ratio, 1:1:0.9, by vol, methanol/chloroform/water). The total solvent extract was concentrated (i.e., solvents removed *in vacuo*) using rotary evaporation at 30°C. Lipid class analyses were conducted immediately; samples were stored for no more than 3 d in a known volume of chloroform.

Lipids. An aliquot of the total solvent extract was analyzed using an Iatroscan MK V TH10 thin-layer chromatography–flame-ionization detector (TLC–FID) anlyzer (Tokyo, Japan) to determine the abundance of individual lipid classes (18). Samples were applied in duplicate or triplicate to silica gel SIII chromarods (5 μm particle size) using 1 μL disposable micropipettes. Chromarods were developed in a glass tank lined with pre-extracted filter paper. The solvent system used for the lipid separation was hexane/diethyl ether/acetic acid (60:17:0.2, by vol), a mobile phase that resolves nonpolar compounds such as wax esters (WE), triacylglycerols (TAG), free fatty acids (FFA) and sterols (ST). A second nonpolar solvent system of hexane/diethyl ether (96:4, vol/vol) was also used to separate hydrocarbons from WE and TAG. After development, the chromarods were oven-dried and analyzed immediately to minimize adsorption of atmospheric contaminants. The FID was calibrated for each compound class (phosphatidylcholine, cholesterol, cholesteryl ester, oleic acid, squalene, triolein, and diacylglyceryl ether purified from shark liver oil; 0.1–10 μg range). A laboratory standard of WE (derived from orange roughy oil) was used for peak identification, and steryl ester was used for quantification of WE. WE and steryl esters coelute in the systems used. Based on the TLC–FID analyses and subsequent analysis of component fatty acids and alcohols by gas chromatography (GC), steryl esters were either absent or present only as trace components. Peaks were quantified on an IBM-compatible computer using DAPA software (Kalamunda, Western Australia). Iatroscan results are generally reproducible to ±5% (Nichols, P., unpublished data).

Fatty acids. Samples of the solvent extract were treated with potassium hydroxide/methanol (5% wt/vol) under N_2 for 3 h at 80°C. Nonsaponifiable neutral lipids (e.g., 1-*O*-alkyl glycerols, fatty alcohols, and hydrocarbons) were then extracted into hexane/chloroform (4:1, vol/vol, 3 × 1.5 mL) and transferred to sample vials. Following acidification of the remaining aqueous layer using hydrochloric acid (pH = 2), fatty acids were extracted and methylated to produce their corresponding fatty acid methyl esters using methanol/hydrochloric acid/chloroform (10:1:1, by vol; 80°C, 2 h). Products were then extracted into hexane/chloroform (4:1, vol/vol, 3 × 1.5 ml) and stored at –20°C. The nonsaponifiable neutral lipid fractions were treated with *N*,*O*-bis-(trimethylsilyl)-trifluoroacetamide (BSTFA, 50 μL, 60°C, 1 h) to convert alcohols and ST to their corresponding TMSi (trimethylsilyl) ethers.

GC analyses of ST-containing nonsaponifiable neutral lipids and methyl esters of fatty acids were performed with a Hewlett-Packard 5890A gas chromatograph (Avondale, PA) equipped with an HP-1 cross-linked methyl silicone fused-silica capillary column (50 m × 0.32 mm, i.d.), an FID, a split/splitless injector, and an HP 7673A auto sampler. H_2 was the carrier gas. Following addition of methyl tricosanoate internal standard, samples were injected in splitless mode at an oven temperature of 50°C. After 1 min, the oven temperature was raised to 150°C at 30°C min^{-1} then to 250°C at 2°C min^{-1}, and finally to 300°C at 5°C min^{-1}. Peaks were quantified with either DAPA Scientific or Waters Millenium software. Individual components were identified using mass spectral data and by comparing retention time data with those obtained for authentic and laboratory standards. GC results are subject to an error of ±5% of individual component abundance.

GC–mass spectrometry (GC–MS) analyses were performed on a Fisons MD 800 GC–mass spectrometer (Manchester, United Kingdom) fitted with an on-column injector. The gas chromatograph was fitted with a capillary column similar to that described above.

Determination of double-bond configuration in fatty acids. Dimethyl disulfide (DMDS) adducts of monounsaturated fatty acids (MUFA) were formed for selected samples by treating the total fatty acid methyl esters with DMDS (19,20). Adducts were then extracted using hexane/chloroform (4:1, vol/vol) and treated with BSTFA to form TMSi derivatives prior to GC–MS analysis.

RESULTS

Lipid content and class composition. Lipid content was low in all gelatinous zooplankton from both years (0.1–5 mg g^{-1}

TABLE 1
Lipid Class Composition (% of total lipids) in 1997 and 1998 Gelatinous Antarctic Zooplankton

	Wax esters	TAG[a]	Free fatty acids	Sterols	Polar lipids	Lipid (mg g^{-1} wet mass)	Lipid (% dry mass[d])
1997							
Cnidaria							
Calycopsis borchgrevinki	11	15	5	4	65	1.5	3.1
Diphyes antarctica[b]	1	10	2	6	81	0.6	1.2
Stygiomedusa gigantea	trace	26	3	13	59	5.1	10.2
Ctenophora							
Beroe cucumis	—	—	2	16	83	1.4	2.9
Beroe forskalii	—	1	3	16	80	3.4	6.8
Pleurobrachia pileus	—	—	10	15	75	3.6	7.1
1998							
Cnidaria							
Atolla wyvillei (*n* = 2)	7 ± 10	4 ± 5	2 ± 3	7 ± 6	80 ± 12	0.1 ± 0.1	0.3 ± 0.2
Diphyes antarctica (*n* = 2)	—	—	—	4 ± 3	96 ± 3	0.7 ± 0.2	1.3 ± 0.3
Dimophyes arctica[c]	—	6	3	4	87	2.9	5.8
Ctenophora							
Beroe forskalii (*n* = 3)	—	—	1 ± 1	10 ± 1	90 ± 1	1.1 ± 0.2	2.2 ± 0.4
Bolinopsis infundibulum (*n* = 2)	—	—	—	8 ± 7	92 ± 3	0.9 ± 1	1.9 ± 1.9

[a]TAG, triacylglycerols.
[b]18 pooled samples.
[c]3 pooled samples.
[d]Calculated assuming 95% water data presented as mean ± SD; trace (<0.5%).

wet mass). PL were the major lipid class in all Antarctic gelatinous zooplankton (59–96%, Table 1). TAG were the second-most abundant lipid class in *C. borchgrevinki*, *D. antarctica*, *S. gigantea*, and *Dimophyes arctica* (6–26% of total lipids). WE constituted 11% of the total lipid in *C. borchgrevinki*, 7% in *A. wyvellei*, and 0.1% in *D. antarctica*; only trace amounts were detected in *S. gigantea* (Table 1). FFA were 1–5% of total lipid in all samples and ST 4–16% in all samples. ST were the second-most abundant lipid class in ctenophore species (8–16% of total lipids).

Sterols. Cholesterol was the major ST in all Cnidaria, and constituted 50–63% of total ST (Table 2). In most ctenophores, cholesterol was less than half of the total ST (26–43%). The ctenophore *B. forskalii* (1998) was an exception; cholesterol constituted 82% of total ST (Table 2). A number of other ST were present in all gelatinous zooplankton. *trans*-Dehydrocholesterol was 14–26% of total ST in zooplankton, except for lower levels in *A. wyvillei* (8%), *S. gigantea* (4%), and *B. forskalii* (2%). There were low levels of all ST (0.0–3%) in *B. forskalii*, except for cholesterol. Levels of desmosterol in Cnidaria were 0–8% and Ctenophora 3–21% (Table 2). Desmosterol was not detected in *A. wyvillei* and *D. arctica*. 24-Methylcholest-5,22*E*-dien-3β-ol was 0–15% of total ST in all zooplankton; it was not detected in *D. antarctica*, and levels were highest in the ctenophore *Bolinopsis infundibulum* (15%). 24-Nordehydrocholesterol was 3–12% in all zooplankton; it was not detected in *B. forskalii*. Levels of 24-methylenecholesterol were 2–9% of total ST in all zooplankton, except for lower levels in *A. wyvillei* (1%), *Bolinopsis infundibulum* (1%), and *B. forskalii* (0.1%) (Table 2). Total stanols were 0–6% in all zooplankton, with 6% stanols in *A. wyvillei*. Low levels of 24-nordehydrocholestanol were present in seven of the zooplankton species (<1%, Table 2). Cholestanol was detected in all but one species (1998; *D. antarctica*) at 0.3–3.5%. Dehydrocholestanol was also present at low levels (0–1%) in most organisms.

Fatty acids. Eicosapentaenoic acid (EPA, 20:5n-3) and docosahexaenoic acid (DHA, 22:6n-3) were the two major polyunsaturated fatty acids (PUFA) in all samples (7–23% and 4–25% of total fatty acids, respectively), except 1998 *A. wyvillei* (Table 3). In 1998 *A. wyvillei*, DPA (22:5n-3) was 10% of total fatty acids vs. 4% for DHA. In 1997 DPA in *A. wyvillei*, *C. borchgrevinki*, and *S. gigantea* constituted 2% of total fatty acids, whereas in all other organisms DPA was 0–0.4% (not detected in *Bolinopsis infundibulum*). The PUFA 18:5n-3, included as "other" in Table 3, was not detected in 1997 samples. However, 18:5n-3 made up 0.2–0.8% of total fatty acids in all 1998 samples of Cnidaria and *B. forskalii*; 18:5n-3 was not detected in *Bolinopsis infundibulum*. The PUFA 18:4n-3 comprised 0.1–5% in all samples, except *P. pileus* and *B. infundibulum*, where none was detected. Total PUFA ranged from 31–52% in all samples except *C. borchgrevinki* (24% PUFA), *Pleurobrachia pileus* (21% PUFA), and *Dimophyes arctica* (20% PUFA) (Table 3).

Total MUFA ranged from 21–47% in all samples, with highest total MUFA in *C. borchgrevinki* (47%), *S. gigantea* (41%), and *Dimophyes arctica* (41%) (Table 3). The MUFA included primarily 18:1n-9*c* (5–26%), 16:1n-7*c* (1–15%), and 18:1n-7*c* (2–11%). Total saturated fatty acids (SFA) ranged from 21–39% in all samples except *Pleurobrachia pileus* where SFA made up 53% of total fatty acids. The principal SFA in all samples were 16:0 (12–26%), 18:0 (2–20%), and 14:0 (2–8%) (Table 3).

TABLE 2
Sterol Composition (% of total sterols) of 1997 and 1998 Gelatinous Antarctic Zooplankton

	1997						1998				
	Cnidaria			Ctenophora			Cnidaria			Ctenophora	
Sterol	*Atolla wyvillei*	*Calycopsis borchgrevinki*	*Diphyes antarctica*[a]	*Stygiomedusa gigantea*	*Beroe cucumis*	*Beroe forskalii*	*Pleurobrachia pileus*	*Atolla wyvillei* ($n = 2$)	*Diphyes antarctica* ($n = 3$)	*Dimophyes arctica*[b]	*Beroe forskalii* ($n = 3$)	*Bolinopsis infundibulum* ($n = 2$)
24-Nordehydrocholesterol	4.2	3	6.7	3.4	6.8	7.9	8.5	4.5 ± 1.3	9.8 ± 11.1	12.4	—	5.4 ± 7.7
24-Nordehydrocholestanol	0.8	—	0.5	0.6	0.3	0.8	0.4	0.3 ± 0.4	—	—	—	—
cis-Dehydrocholesterol/27-nor-24-methylcholest-5,22*E*-dien-3β-ol	2.1	4.8	2.1	1.8	1.6	2.8	14.8	3.2 ± 2.7	—	1.8	1.8 ± 2	0.8 ± 1.1
trans-Dehydrocholesterol	8.2	24.2	18.9	3.8	21.5	21.8	14	14.6 ± 4.3	26.3 ± 11.7	19.7	1.9 ± 0.1	18.7 ± 2.6
Dehydrocholestanol	1.4	—	0.8	0.5	0.3	1.1	0.4	1.1 ± 1.5	—	—	—	0.4± 0.6
Cholesterol	57.4	57.5	58.9	62.8	38.1	28.6	26.2	55.1 ± 6.0	55.6 ± 23.8	49.5	81.7 ± 1.7	43.4 ± 9.9
Cholestanol	1.7	1	2.8	1	0.3	0.8	1.7	1.9 ± 2.6	—	3.5	0.6 ± 0.1	0.4 ± 0.6
Desmosterol	9	5.5	3.7	3.7	21	16.4	15.2	—	6.2 ± 5.9	—	2.7 ± 1.9	2.9 ± 0.4
24-Methylcholest-5,22*E*-dien-3β-ol	9.1	2.1	3.1	6.4	3.1	7.8	8.2	8 ± 0.1	—	2.7	1.8 ± 1.6	15.1 ± 3
24-Methyl-5a-cholest-22*E*-en-3β-ol	1.1	0	0.5	1.4	0.2	1.2	—	1 ± 1.4	—	—	0.2 ± 0.3	0.5 ± 0.8
24 Methylenecholesterol	4	1.8	1.6	7	5.4	8.5	7.7	0.8 ± 1.1	2.2 ± 3.8	5.3	0.1 ± 0.2	1± 1.4
24 Methylenecholestanol	1	Trace	—	0.7	0.4	0.9	—	—	—	—	—	—
24-Ethylcholest-5,22*E*-dien-3β-ol	—	—	—	0.7	—	—	—	—	—	—	—	—
24 Ethylcholesterol	—	—	0.4	2.3	0.6	0.7	Trace	3.4 ± 1.8	—	—	0.3 ± 0.5	0.7 ± 0.9
Isofucosterol	—	—	—	—	—	—	—	0.8 ± 1.1	—	—	—	—
Isofucostanol	—	—	—	2.5	0.3	0.6	2.9	—	—	—	—	—
4-Methyl-24-ethyl-cholesta-5,24(28)-dien-3β-ol	—	—	—	0.8	0.1	0.3	—	—	—	—	—	—
Other	—	—	—	0.6	—	—	—	5.4	—	5.1	9.0	10.6
Phytoplankton-derived sterols[c]	21.5	34.1	31.2	18.5	33.7	41	48.4	34.5	36	36.6	5.7	40.6

[a]18 pooled samples.
[b]3 pooled samples; Trace; below integration; data presented as mean ± SD.
[c]Phytoplankton-derived sterols include: 24-nordehydrocholesterol, dehydrocholesterol, 24-methylcholest-5,22*E*-dien-3β-ol, 24-ethylcholest-5,22*E*-dien-3β-ol, 24-ethylcholesterol, isofucosterol.

DISCUSSION

Lipid content and class composition. Lipid values for most gelatinous zooplankton in this study ranged from 0.1–5 mg g^{-1} wet mass. To facilitate comparison, lipid as percentage dry mass was calculated (assuming 95% water) (21) with a range from 0.3–6.8%. *Stygiomedusa gigantea* had 10.2 mg lipid g^{-1} dry mass. *Stygiomedusa gigantea* has oral arms up to 10 m long and a medusa up to 50 cm in diameter (22). These massive oral arms capture and digest prey, which may cause the high observed lipid values. According to Larson and Harbison (8) the average lipid content of Antarctic gelatinous zooplankton is approximately 3% (0.4–6% range), whereas Arctic gelatinous zooplankton have on average 8% lipid as a percent dry mass (1.5–22% range). Lower lipid levels in Antarctic gelatinous predators probably reflect lower lipid in their prey, such as the pteropod *Limacina helicina* (23).

Visible stored lipid in the lumen of the gastrovascular system was less abundant in Antarctic than in Arctic Cnidaria and Ctenophora (8). *Beroe cucumis* from Bute Inlet, Canada, had 13% lipid as percent dry mass (24), which was greater than calculated values for *B. cucumis and B. forskalii* (2.9 and 2.2–6.8% lipid, as percent dry mass) in this study. Another ctenophore, *Bathocyroe fosteri*, from the Cape Hatteras, NC, area, had very low lipid (0.01%, as percent wet mass) (4). The ctenophores *Bolinopsis infundibulum* and *B. cucumis* from the Arctic had 4.7 and 0.6 mg lipid per g fresh mass (25). These latter values are similar to those in this study (Table 1). Lipid values for *C. borchgrevinki* and *D. antarctica* from Southern Ocean waters were 2.7 and 2.3% dry mass, respectively (7), similar to our lipid values for those species (3.1 and 1.2–1.3% lipid, as percent dry mass, respectively).

PL, the major lipid class in both 1997 and 1998 Antarctic gelatinous zooplankton (Table 1), is primarily a structural membrane component. *Beroe* sp., *D. antarctica*, and *Sibogita* (*Calycopsis*) *borchgrevinki*, from the Southern Ocean around South Georgia Island, were also characterized by high values for structural lipid classes (PL and ST) (9). PL are also important in nematocysts, which are stinging organelles on tentacles of Cnidaria. PL were constituted primarily of phosphatidylcholine and phosphatidylethanolamine in the scyphomedusan *Pelagia noctiluca* (26). Nemotocyst toxin in another scyphomedusan *Physalia physalis* was high in lipid, according to Stillway (27), who proposed that nematocyst lipids have important roles in stability and pharmacology of the toxin. PL or proteins could also possibly be used as an energy reserve during starvation. *Bolinopsis infundibulum*, from a sea loch in Scotland, shrank to less than two thirds of its length after 4 wk of starvation (10). Low FFA (0–5%, Table 1) and no detectable diacylglycerols are evidence for almost no sample degradation during frozen storage and analysis. The levels of WE present in *C. borchgrevinki* (11%, as percent of total lipids) and *A. wyvillei* (7%) may reflect feeding on WE-rich copepods or their larvae. The low level of WE, and the absence of it in other 1998 samples, suggest that this dietary contribution is only minor.

Cholesterol and phytosterols. The cholesterol level in all

TABLE 3
Fatty Acid Composition (% of total fatty acids) in 1997 and 1998 Gelatinous Antarctic Zooplankton

	1997							1998				
	Cnidaria				Ctenophora			Cnidaria			Ctenophora	
Fatty acid	*Atolla wyvillei*	*Calycopsis borchgrevinki*	*Diphyes antarctica*[a]	*Stygiomedusa gigantea*	*Beroe cucumis*	*Beroe forskalii*	*Pleurobrachia pileus*	*Atolla wyvillei* (*n* = 2)	*Diphyes antarctica* (*n* = 3)	*Dimophyes arctica*[b]	*Beroe forskalii* (*n* = 3)	*Bolinopsis infundibulum* (*n* = 2)
12:0	0.6	0.5	0.8	Trace	0.1	0.3	0.5	—	—	—	2.7 ± 0.7	—
14:0	6.1	2.5	5.7	6.6	4.4	4.5	5.4	2.0 ± 1.0	7.6 ± 0.8	3.9	5.0 ± 0.7	6.5 ± 0.7
15:0	0.6	0.3	1.0	0.6	0.7	0.7	0.8	0.5 ± 0.1	1.1 ± 0.3	0.8	0.4 ± 0.1	1.0 ± 0.1
16:0	20.8	16.6	20.1	12.1	19.9	23.4	25.8	16.0 ± 2.2	18.0 ± 2.7	18.9	17.4 ± 1.6	14.3 ± 9.2
18:0	2.8	4.8	7.6	4.9	4.6	9.9	20.0	11.9 ± 9.4	8.8 ± 3.7	9.3	2.3 ± 0.1	10.5 ± 1.6
16:1n-7*c*	5.3	9.2	3.8	10.2	1.8	2.3	1.4	2.6 ± 1.4	4.0 ± 2.8	15.3	2.2 ± 0.2	0.7 ± 0.0
18:1n-9*c*	11.8	26.4	7.3	18.6	6.0	8.8	10.2	9.0 ± 4.2	8.7 ± 4.8	17.2	6.4 ± 2.6	4.9 ± 0.5
18:1n-7*c*	7.2	3.7	4.1	5.8	2.1	3.2	10.7	4.1 ± 2.3	2.0 ± 1.8	4.1	4.9 ± 0.7	2.2 ± 0.3
18:1n-5	0.8	1.9	1.0	0.5	0.3	0.5	—	1.1 ± 0.2	0.9 ± 0.1	0.4	0.7 ± 0.1	0.4 ± 0.1
19:1	0.5	0.6	—	—	1.2	0.8	—	1.3 ± 1.4	Trace	0.2	0.5 ± 0.1	1.9 ± 0.3
20:1n-9*c*	3.2	2.5	1.7	2.6	2.8	2.2	2.7	4.2 ± 5.1	1.2 ± 1.3	1.1	1.3 ± 0.8	2.5 ± 0.5
20:1n-7*c*	1.4	2.8	0.6	3.0	4.2	1.7	—	3.1 ± 1.0	3.6 ± 5.1	1.0	4.2 ± 1.4	2.6 ± 0.5
22:1n-11*c*	0.2	—	—	0.1	—	—	—	—	0.2 ± 0.4	—	0.3 ± 0.5	3.7 ± 5.2
22:1n-9*c*	Trace	—	—	0.3	2.1	1.3	—	0.5 ± 0.2	0.1 ± 0.1	1.3	1.1 ± 1.0	3.0 ± 3.5
22:1n-7*c*	0.2	—	0.3	0.2	0.2	0.4	—	—	0.3 ± 0.5	—	0.3 ± 0.2	1.2 ± 1.7
18:4n-3	5.0	0.1	0.6	1.3	0.3	0.7	—	0.9 ± 1.2	2.1 ± 2.9	0.2	2.3 ± 0.1	—
18:2n-6	2.5	1.5	1.9	1.0	1.4	1.3	0.9	1.4 ± 0.4	2.2 ± 0.3	1.0	1.7 ± 0.3	0.7 ± 0.1
18:3n-3	1.0	0.2	0.2	0.3	0.2	Trace	—	0.5 ± 0.5	0.3 ± 0.3	0.1	1.2 ± 0.3	—
20:4n-6	—	1.4	1.2	Trace	2.0	1.5	2.6	4.2 ± 6.0	1.4 ± 0.2	—	—	0.5 ± 0.7
20:5n-3	16.6	9.6	19.1	20.8	17.4	14.6	7.2	15 ± 6.2	16.5 ± 1.3	8.2	21.3 ± 2.9	17.1 ± 3.4
20:2n-6	0.3	0.6	0.4	0.8	0.6	0.6	1.3	0.4 ± 0.5	0.1 ± 0.1	—	1.0 ± 0.0	0.5 ± 0.1
C_{21}-PUFA	0.5	0.7	1.0	—	0.4	0.2	—	2.2 ± 3.1	—	—	0.3 ± 0.3	—
22:6n-3	5.6	7.0	17.6	4.2	24.8	18.0	9.1	3.9 ± 0.6	16.9 ± 5.3	10.4	16.8 ± 0.5	22.7 ± 3.9
22:4n-6	0.3	0.9	—	0.7	—	—	—	1.3 ± 0.9	—	—	0.1 ± 0.1	—
22:5n-3	2.4	2.1	0.3	1.9	0.2	0.2	—	9.7 ± 8.7	0.2 ± 0.2	0.1	0.4 ± 0.1	—
Sum saturates	30.9	24.7	35.2	24.2	29.7	38.8	52.5	30.4 ± 12.7	35.5 ± 7.5	32.9	27.8 ± 3.2	32.3 ± 11.6
Sum MUFA	30.6	47.1	18.8	41.3	20.7	21.2	25.0	25.9 ± 15.8	21.0 ± 16.9	40.6	21.9 ± 7.6	23.1 ± 12.6
Sum PUFA	34.2	24.1	42.3	31.0	47.3	37.1	21.1	39.5 ± 28.1	39.7 ± 10.6	20.0	45.1 ± 4.6	41.5 ± 8.1
Other	4.3	4.1	3.7	3.5	2.3	2.9	1.4	4.2	3.8	6.5	5.2	3.1
EPA/DHA	3.0	1.4	1.1	4.9	0.7	0.8	0.8	3.8	1.0	0.8	1.3	0.8
16:1/16:0	0.3	0.6	0.2	0.9	0.1	0.1	0.1	0.2	0.2	0.8	0.1	0.1
18:1n-7/n-9	0.6	0.1	0.6	0.3	0.3	0.4	1.1	0.5	0.2	0.2	0.8	0.5

[a]18 pooled samples.

[b]3 pooled samples; Trace = below integration; data presented as mean ± SD; other includes all fatty acids present at <1% of total fatty acids: i.e., 10:0, 17:0, 20:0, i14:0, i15:0, a15:0, i16:0, i17:0, a17:0, i19:0, 4,8,12-trimethyltridecanoic acid, 14:1n-7*c*, 14:1n-5, 15:1, 16:1n-9*c*, 16:1n-7*t*, 16:1n-5*c*, 17:1, 18:1, 18:1n-7*t*, 20:1n-11/13, C_{16} PUFA, 18:5n-3, C_{19} PUFA, 20:3n-6, 20:4n-3, 22:2, C_{24} PUFA; EPA, eicosapentaenoic acid (20:5n-6); DHA, docosahexaenoic acid (22:6n-3).

these scyphozoan Cnidaria (50–63%, as percent of total ST, Table 2) is consistent with a largely carnivorous diet. It is uncertain if Cnidaria can synthesize cholesterol; it may be a slow process inhibited by dietary ST (28). Attempts to demonstrate [1-^{14}C]acetate incorporation into ST failed in the jellyfish *Rhizostoma* (29). The hydrozoan jellyfish species *Spirocodon saltatrix*, *Aurelia aurita*, and *Stomolophus* sp. were characterized by even higher cholesterol levels (72–89%) (30).

The ST profiles of the 1997 Ctenophora and 1998 *Bolinopsis infudibulum* were characterized by less cholesterol (26–43%, as percent of total ST, Table 2). The 1998 *B. forskalii* specimens, in contrast, contained higher levels of cholesterol. Higher levels of the phytoplankton-derived ST were present in animals with lower cholesterol, although several ST, such as *trans*-dehydrocholesterol and 24-nordehydrocholesterol, may also be either intermediates in cholesterol biosynthesis or from animal sources, respectively. *trans*-Dehydrocholesterol was the major ST in the Antarctic ice diatom *Nitzschia cylindrus* (31), and interestingly the structurally similar 27-nor-24-methylcholest-5,22*E*-dien-3β-ol has also been recently found as a major ST in an Antarctic dinoflagellate (Thompson, P., unpublished data). Care is needed, through examination of other signature lipids or other procedures, before the precise algal source of this ST can be determined. Further research is also needed examining the lipid composition of Southern Ocean dinoflagellates and other phytoplankton. The ST of these Ctenophora (except *B. forskalii*) were relatively enhanced in *trans*-dehydrocholesterol (14–22%) and desmosterol (15–21%; except *Bolinopsis infundibulum* with 15% 24-methylcholest-5,22*E*-dien-3β-ol and 3% desmosterol). With the exception of the 1998 *B. forskalii*, the ST composition of the ctenophores is less consistent with a carnivorous diet than the Cnidaria. This may reflect the fact that their foods (such as *Limacina helicina*) are herbivorous. Cholesterol is generally not a major phytoplankton ST, although it was present in 6 of 14 diatoms species analyzed by Barrett *et al*. (32) and in the Antarctic sea-ice diatom *N. cylindrus* (31).

The ST composition of Cnidaria and Ctenophora is usually quite diverse. *Bolinopsis infundibulum*, from a sea loch in Scotland, had a complex range of C_{26}–C_{29} ST (including 67% cholesterol) that was deemed to reflect a diet of surface calanoid copepods (10). *trans*-Dehydrocholesterol, the second-most common ST in most species (Table 2), is, as noted above, an intermediate in cholesterol synthesis. Similar levels of *trans*-dehydrocholesterol were reported in the Cnidaria *C. borchgrevinki*, *Arctopodema ampla*, and *P. periphylla* from Antarctic waters as well as the Antarctic ctenophore *B. cucumis* (23).

The greater amount of desmosterol in 1997 gelatinous zooplankton than in 1998 may reflect a different phytoplankton diet in their prey. Desmosterol is produced as an intermediate from phytosterol dealkylation and is also found in marine microalgae *N. closterium* (100% demosterol) and *Rhizoselenia setigeria* (94% desmosterol) (32). 24-Methylcholest-5,22*E*-dien-3β-ol (2–15% of total ST, Table 2) may have originated from dietary prymnesiophytes such as *Phaeocystis* and diatoms, where brassicasterol is a major ST (33,34). Levels of 24-nordehydrocholesterol observed in these gelatinous zooplankton are similar to levels reported for 1996 Cnidaria from the same study area (23). 24-Methylenecholesterol is the main ST in the diatom *Chaetoceros* (34). Levels of 24-methylenecholesterol, which were higher in 1997 jellies (1.6–8.5% of total ST, Table 2) than in 1998 (0.1–5.3%) may reflect differences in herbivore diatom diet between these years.

Stanols, which reflect diet, were generally low in all gelatinous zooplankton (Table 2). Cholestanol was 24% of total ST in the marine dinoflagellate *Scrippsiella* sp. (35), and a *Gymnodinium* species from Australian waters had 24% dinosterol (6). Dinosterol, a biomarker for dinoflagellates, was not detected in the gelatinous zooplankton analyzed in this study, nor was dinosterol detected in salps and their hyperiid amphipods from the same study area during the same years (11). This suggests that either dinoflagellates are absent from the diet, or, if members of this algal group are present, they are species that lack dinosterol.

Fatty acids: trophic relationships. All Cnidaria and Ctenophora were characterized by moderate to high levels of PUFA (20–47%, Table 3) with the exception of *Pleurobrachia pileus*. An inverse relationship between n-3 PUFA and MUFA was apparent (Fig. 1). A similar relationship has been noted for fish (36). MUFA content of fish has been observed to increase with increasing lipid content (37), however, MUFA content of the gelatinous Antarctic zooplankton was not related to lipid content. MUFA levels were in the range 20–25% for most species analyzed, with three species containing 40–47% MUFA (*S. gigantea*, 1998 *D. arctica*, *C. borchgrevinki*, Table 3). EPA and DHA levels observed in this study are in agreement with values for *B. cucumis*, *C. borchgrevinki*, and *Arctopodema ampla* collected from the same AMLR study area in 1996 (23). Somewhat lower values for *B. cucumis* from Bute Inlet, British Columbia (3–16% 22:6 and 20:5), were observed by Lee (24). High EPA and DHA were also observed in the pink jellyfish *Cyanea capillata* (38) and the Portuguese man-of-war *Physalia physalis* from tropical waters (39).

The ratio EPA/DHA was higher (≥3) in *A. wyvellei* (both years) and *S. gigantea*, but in all other animals the ratio was between 0.7–1.4 (Table 3). The differences observed may be due to variations in metabolic rates of the two PUFA. However, it may also reflect differences in the diatom vs. dinoflagellate diet; EPA is typically found in higher proportions in diatoms whereas dinoflagellates contain higher DHA relative to EPA. Of the two species showing a high EPA/DHA ratio, only *S. gigantea* also exhibited a high 16:1/16:0 ratio (Table 3). The latter is a characteristic feature of diatom fatty acid profiles, particularly in combination with elevated proportions of EPA.

The level of DPA (22:5n-3) in 1998 *A. wyvillei* (10% of total fatty acids, Table 3) is higher than DHA (4%), and higher than DPA levels in 1997 *A. wyvillei* (2.4%) and all other species of gelatinous zooplankton in this study (Table 3). High DPA was also observed in *A. wyvillei* (18.4%) collected in the Croker Passage off the Antarctic Peninsula in 1983 (5). Levels of 12–19% DPA were reported in another

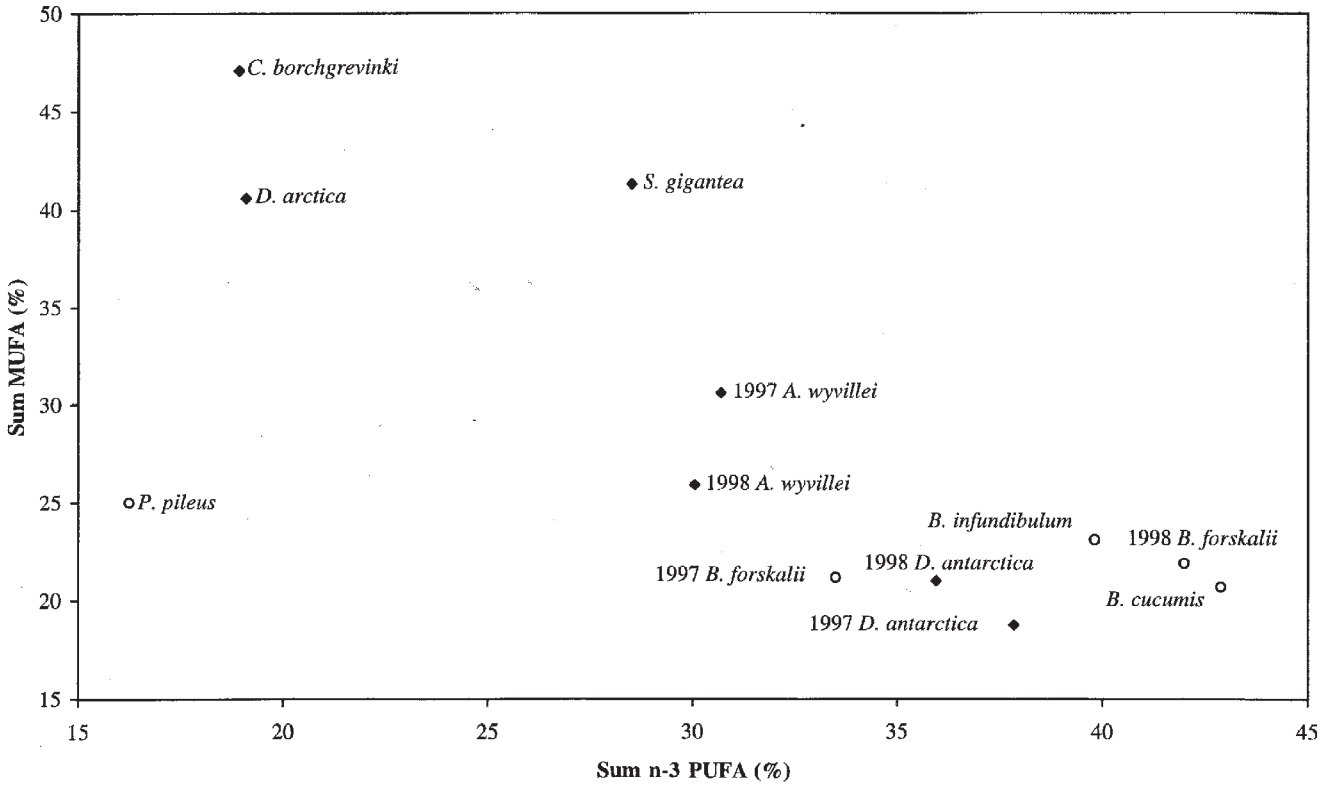

FIG. 1. Sum of monounsaturated fatty acids (MUFA) vs. sum n-3 polyunsaturated fatty acids (PUFA) in 1997 and 1998 gelatinous Antarctic zooplankton. ◆ = Cnidaria; ○ = Ctenophora. Species: *Calycopsis borchgrevinki, Atolla wyvillei, Diphyes antarctica, Dimophyes arctica, Stygiomedusa gigantea, Beroe cucumis, Beroe forskalii, Pleurobrachia pileus, Bolinopsis infundibulum.*

large Antarctic scyphomedusan, *P. periphylla*, collected in the AMLR study area in 1996 (23). There are few animals that contain appreciable levels of DPA. Of the lower members of the food chain, a high level of DPA has recently been reported in the California green abalone, *Haliotis fulgens* (up to 12% in the foot muscle) (40). DPA levels of 11–15% were found in the foot muscle of the Australian abalone *H. laevigata* and *H. rubra* (41). DPA levels in *H. laevigata* and *H. rubra* were associated with the occurrence of C_{22} PUFA in their diet. However, in *H. fulgens*, DPA was suggested to be a desaturation product of DHA (22:6n-3), since there was no correlation with the levels of C_{22} PUFA in their macroalgal diet (40). Presently, we have no explanation for the high DPA in *A. wyvillei* observed in this study, since its diet is unknown.

The unusual octapentadecaenoic acid (18:5n-3) is synthesized by certain species of dinoflagellates from 20:5n-3 (42). It is found as a major fatty acid in dinoflagellates (6) and coccolithophorids (43), and was first reported in marine zooplankton (chaetognaths and copepods) by Mayzaud *et al.* (44), who recognized its usefulness as a biomarker. We did not detect 18:5n-3 in zooplankton samples from 1997 (Table 3) nor 1996 (23). We detected 18:5n-3 in the 1998 samples reported here (up to 0.8%, Table 3) and in 1998 pteropods (*Spongiobranchaea australis*) and amphipods (*Hyperiella dilatata*) (11). Its presence in these 1998 samples, albeit at low relative abundance, points to a greater contribution from dinoflagellates and possibly other algal groups, such as coccolithophorids, in the AMLR study area during 1998. Very long chain PUFA (C_{24}, C_{26}, and C_{28} VLC-PUFA) were detected in the samples analyzed in this study. Novel VLC-PUFA were detected in 1998 salps and their commensal amphipods from the same AMLR study area (12). VLC-PUFA have been reported from dinoflagellates (35), and VLC-MUFA were present in sea ice diatoms (31). The lack of VLC-PUFA in the gelatinous zooplankton analyzed in this study indicates different dietary sources compared to salps and their commensal amphipods.

Oleic acid varied from 4.9–26.4% (Table 3). In a range of Antarctic zooplankton, higher levels of oleic acid have been proposed as consistent with a carnivorous diet (23). With a phytoplankton diet, 16:1n-7*c* is converted to 18:1n-7*c*. These observations have been exploited with the use of the ratio 18:1n-7*c*/18:1n-9 (Table 3) In animals with a carnivorous diet, the ratio is less than 0.5, and it is greater than 0.5 in animals with a phytoplankton diet. The long-chain MUFA (20:1 and 22:1, several isomers of each) were present in all animals (2.5–13%; Table 3). The long-chain MUFA are present in large amounts in calanoid copepods and are reported as the major site for their formation in the marine food web (45). Their presence in the Cnidaria and Ctenophora is further supporting evidence for the carnivorous/omnivorous nature of the diet of these animals.

A range of Antarctic gelatinous zooplankton have shown

broadly similar lipid profiles. These profiles are consistent with a largely carnivorous diet for most animals. Specific differences observed are due to dietary and other influences. Only single samples were available for some species analyzed here; these, however, are the first data for many species and the first ST data for most species. While comparisons are made, we recognize the need for further detailed sampling and analysis. The use of the signature lipid approach has enabled examination of aspects of trophodynamics not obtainable by conventional techniques.

ACKNOWLEDGMENTS

This work was supported in part by FRDC. We thank Jane Martin, Valerie Loeb, Roger Hewitt, and Rennie Holt for the AMLR Expeditions to the Elephant Island study area. Volker Siegel, Valerie Loeb, Dawn Outram, Wesley Armstrong, Ellie Linen, Rachel Johnson, Jackie Popp, David Demer, and Michael Force gave invaluable help in collection and identification of samples. Danny Holdsworth managed the CSIRO GC–MS and Kendrea Snyder assisted in preparation of the manuscript. Our appreciation is extended to the captain and crew of the R/V *Yuzhmorgeologiya*. Charles F. Phleger was a recipient of a 1997–98 CSU award for Research, Scholarship, and Creative Activity.

REFERENCES

1. Quetin, L.B., and Ross, R.M. (1991) Behavioral and Physiological Characteristics of the Antarctic Krill, *Euphausia superba*, *Am. Zool. 31*, 49–63.
2. Longhurst, A.R. (1985) The Structure and Evolution of Plankton Communities, *Progr. Oceanogr. 15*, 1–35.
3. Thuesen, E.V., and Childress, J.J. (1994) Oxygen Consumption Rates and Metabolic Activities of Oceanic California Medusae in Relation to Body Size and Habitat Depth, *Biol. Bull. 187*, 84–98.
4. Bailey, T.G., Youngbluth, M.J., and Owen, G.P. (1995) Chemical Composition and Metabolic Rates of Gelatinous Zooplankton from Midwater and Benthic Boundary Layer Environments off Cape Hatteras, North Carolina, USA, *Mar. Ecol. Progr. Ser. 122*, 121–134.
5. Reinhardt, S.B., and Van Vleet, E.S. (1986) Lipid Composition of Twenty-Two Species of Antarctic Midwater Zooplankton and Fish, *Mar. Biol. 91*, 149–159.
6. Nichols, P.D., Jones, G.J., deLeeuw, J.W., and Johns, R.B. (1984) Lipid Composition of the Marine Dinoflagellates *Gymnodinium* sp. and *Prorocentrum* sp.: Sterols and Fatty Acids, *Phytochemistry 23*, 1043–1047.
7. Hagen, W. (1988) On the Significance of Lipids in Antarctic Zooplankton, *Ber. Polarforsch. 49*, 1–117.
8. Larson, R.J., and Harbison, G.R. (1989) Source and Fate of Lipids in Polar Gelatinous Zooplankton, *Arctic 42*, 339–346.
9. Clarke, A. (1984) The Lipid Content and Composition of Some Antarctic Macrozooplankton, *Br. Antarct. Surv. Bull. 63*, 57–70.
10. Morris, R.J., McCartney, M.J., and Schulze-Röbbecke, A. (1983) *Bolinopsis infundibulum* (O.F. Müller): Biochemical Composition in Relation to Diet, *J. Exp. Mar. Biol. Ecol. 67*, 149–157.
11. Phleger, C.F., Nelson, M.M., Mooney, B., and Nichols, P.D. (1999) Lipids of Abducted Antarctic Pteropods, *Spongiobranchaea australis*, and Their Hyperiid Amphipod Host., *Comp. Biochem. Physiol. 124B*, 295–307.
12. Phleger, C.F., Nelson, M.M., Mooney, B., and Nichols, P.D. (2000) Lipids of Antarctic Salps and Their Commensal Hyperiid Amphipods, *Polar Biol. 23*, 329–337.
13. Joseph, J.D. (1979) Lipid Composition of Marine and Estuarine Invertebrates: Porifera and Cnidaria, *Progr. Lipid Res. 18*, 1–30.
14. Loeb, V., Siegel, V., Holm-Hansen, O., Hewitt, R., Fraser, W., Trivelpiece, W., and Trivelpiece, S. (1997) Effects of Sea-Ice Extent and Krill or Salp Dominance on the Antarctic Food Web, *Nature 387*, 897–900.
15. Martin, J. (1997) AMLR 1996/97 Field Season Report LJ-97-09, Southwest Fisheries Science Center, Antarctic Ecosystem Research Group, La Jolla, 118 pp.
16. Martin, J. (1998) AMLR 1997/98 Field Season Report LJ-97-07, Southwest Fisheries Science Center, Antarctic Ecosystem Research Group, La Jolla, 161 pp.
17. Bligh, E.G., and Dyer, W. (1959) A Rapid Method of Total Lipid Extraction and Purification, *Can. J. Biochem. Physiol. 37*, 911–917.
18. Volkman, J.K., and Nichols, P.D. (1991) Applications of Thin Layer Chromatography–Flame Ionization Detection to the Analysis of Lipids and Pollutants in Marine Environmental Samples, *J. Planar Chromatogr. 4*, 19–26.
19. Dunkelblum, E., Tan, S.H., and Silk, R.J. (1985) Double-Bond Location in Monounsaturated Fatty Acids by Dimethyl Disulphide Derivitization and Mass Spectrometry, *J. Chem. Ecol. 11*, 265–277.
20. Nichols, P.D., Guckert, J.B., and White, D.C. (1986) Determination of Monounsaturated Fatty Acid Double-Bond Position and Geometry for Microbial Monocultures and Complex Consortia by Capillary GC–MS of Their Dimethyl Disulphide Adducts, *J. Microbiol. Methods 5*, 49–55.
21. Clarke, A., Holmes, L.J., and Gore, D.J. (1992) Proximate and Elemental Composition of Gelatinous Zooplankton from the Southern Ocean, *J. Exp. Mar. Biol. Ecol. 155*, 55–68.
22. Larson, R.J. (1986) Pelagic Scyphomedusae (Scyphozoa: Coronatae and Semaeostomeae) of the Southern Ocean, *Biology of the Antarctic Seas XVI, Antarctic Research Series 41(3)*, 59–165.
23. Phleger, C.F., Nichols, P.D., and Virtue, P. (1998) Lipids and Trophodynamics of Antarctic Zooplankton, *Comp. Biochem. Physiol. 120B*, 311–323.
24. Lee, R.F. (1974) Lipids of Zooplankton from Bute Inlet, British Columbia, *J. Fish. Res. Board Can. 31*, 1577–1582.
25. Clarke, A., Holmes, L.J., and Hopkins, C.C.E. (1987) Lipid in an Arctic Food Chain: *Calanus, Bolinopsis, Beroe, Sarsia 72*, 41–48.
26. Nakhel, I.C., Mastronicolis, S.K., and Miniadis-Meimaroglon (1988) Phospho- and Phosphonolipids of the Aegean Pelagic Scyphomedusa *Pelagia noctiluca*, *Biochim. Biophys. Acta 958*, 300–307.
27. Stillway, L.W. (1976) Fatty Acids of the Portuguese Man-of-War, *Physalia physalis., Comp. Biochem. Physiol. 53B*, 535–537.
28. Goad, L.J. (1978) The Sterols of Marine Invertebrates: Composition, Biosynthesis, and Metabolites, in *Marine Natural Products: Chemical and Biological Perspectives* (Scheuer, P.J., ed.), Academic Press, New York. pp. 45–47.
29. Van Aarem, H.E., Vonk, H.J., and Zander, D.I. (1964) Lipid Metabolism in *Rhizostoma*, *Arch. Int. Physiol. Biochim. 72*, 606–614.
30. Yasuda, S. (1974) Sterol Compositions of Jelly Fish (medusae), *Comp. Biochem. Physiol. 48B*, 225–230.
31. Nichols, P.D., Palmisano, A.C., Smith, G.A., and White, D.C. (1986) Lipids of the Antarctic Sea Ice Diatom *Nitzschia cylindrus*, *Phytochemistry 25*, 1649–1653.
32. Barrett, S.M., Volkman, J.K., and Dunstan, G.A. (1995) Sterols of 14 Species of Marine Diatoms (Bacillariophyta), *J. Phycol. 31*, 360–369.
33. Nichols, P.D., Skerratt, J.H., Davidson, A., McMeekin, T.A.,

and Burton, H. (1991) The Lipid Composition of Cultured *Phaeocystis pouchetti*: Signatures for Food-web, Biogeochemical and Environmental Studies in Antarctica and the Southern Ocean, *Phytochemistry 30*, 3209–3214.
34. Tsitsa-Tzardis, E., Patterson, G.W., Wikfors, G.H., Gladu, P.K., and Harrison, D. (1995) Sterols of *Chaetoceros* and *Skeletonema*, *Lipids 28*, 465–467.
35. Mansour, M.P., Volkman, J.K., and Holdsworth, D.G. (1999) Very-Long Chain C_{28} Highly Unsaturated Fatty Acids in Marine Dinoflagellates. *Phytochemistry 50*, 541–548.
36. Ratkowsky, D.A., Olley, J., Jayasinghe, J.A.G., and Wijesundara, R.C. (1996) A Consistent Correlation Between Monousaturated and n-3 Polyunsaturated Fatty Acids in Flesh of Fish Caught at Different Latitudes, *ASEAN Food J. 11*, 43–47.
37. Brown, A.J., Roberts, D.C.K., and Truswell, A.S. (1989) Fatty Acid Composition of Australian Marine Finfish: A Review, *Food Australia 41*, 655–666.
38. Sipos, J.C., and Ackman, R.G. (1968) Jellyfish (*Cyanea capillata*) Lipids: Fatty Acid Composition, *J. Fish. Res. Board Can. 25*, 1561–1569.
39. Stillway, L.W. (1974) Nematocyst Lipids of the Portuguese Man-of-War *Physalia physalis*, *Comp. Biochem. Physiol. 48B*, 35–38.
40. Nelson, M.M. (1999) Influences of Dietary Lipid in Macroalgae on the Somatic and Gonadal Growth in the Green Abalone, *Haliotis fulgens* Philippi, M.S. Thesis, San Diego State University, San Diego, 140 pp.
41. Dunstan, G.A., Baillie, H.J., Barrett, S.M., and Volkman, J.K. (1996) Effect of Diet on the Lipid Composition of Wild and Cultured Abalone, *Aquaculture 140*, 115–127.
42. Joseph, J.D. (1975) Identification of 3,6,9,12,15-Octadecapentaenoic Acid in Laboratory-Cultured Photosynthetic Dinoflagellates, *Lipids 10*, 395–403.
43. Volkman, J.K., Smith, D.J., Eglinton, G., Forsberg, T.E.V., and Corner, E.D.S. (1981) Sterol and Fatty Acid Composition of Four Marine Haptophycean Algae, *J. Mar. Biol. Ass. UK 61*, 509–528.
44. Mayzaud, P., Eaton, C.A., and Ackman, R.G. (1976) The Occurrence and Distribution of Octadecapentaenoic Acid in a Natural Plankton Population. A Possible Food Chain Index, *Lipids 11*, 858–862.
45. Sargent, J.R., and Whittle, J.J. (1981) Lipids and Hydrocarbons in the Marine Food Web, in *Analysis of Marine Ecosystems* (Longhurst, A.R., ed.) pp. 491–453, Academic Press, London.

[Received November 12, 1999; and in revised version March 24, 2000; revision accepted April 12, 2000]

Trans Fatty Acids in Adipose Tissue of French Women in Relation to Their Dietary Sources

C. Boué[a], N. Combe[b,*], C. Billeaud[c], C. Mignerot[b], B. Entressangles[a], G. Thery[d], H. Geoffrion[d], J.L. Brun[d], D. Dallay[d], and J.J. Leng[d]

[a]Laboratoire de Lipochimie Alimentaire, Université Bordeaux I, F-33405 Talence Cedex, [b]ITERG, Laboratoire de Lipochimie Alimentaire, Université Bordeaux I, [c]Service de Néonatologie, and [d]Maternités Pellegrin, CHU Bordeaux, F-33000 Bordeaux, France

ABSTRACT: This study reports the fatty acid composition of subcutaneous adipose tissue in French women with special emphasis on the content of *trans* fatty acids originating from two main dietary sources, ruminant fats and partially hydrogenated vegetable oils (PHVO). Adipose tissue *trans* fatty acid levels from 71 women, recruited between 1997 and 1998, were determined using a combination of capillary gas chromatography and silver nitrate thin-layer chromatography. Results indicate that on average *cis* monounsaturates accounted for 47.9% of total fatty acids, saturates for 32.2%, and linoleic acid for 14.4%. *Cis* n-3 polyunsaturates represented only 0.7%. Total content of *trans* fatty acids was 2.32 ± 0.50%, consisting of *trans* 18:1 (1.97 ± 0.49%), *trans* 18:2 (0.28 ± 0.08%), and *trans* 16:1 (0.06 ± 0.03%). *Trans* 18:3 isomers were not detectable. The level of *trans* fatty acids found in adipose tissue of French women was lower than those reported for Canada, the United States, and Northern European countries but higher than that determined in Spain. Therefore, *trans* fatty acid consumption in France appears to be intermediate between that of the United States or North Europe and that of Spain. Based on the equation of Enig *et al.*, we estimated the mean daily *trans* 18:1 acid intake of French women at 1.9 g per person. The major *trans* 18:1 isomer in adipose tissue was Δ11*trans*, as in ruminant fats. Estimates of relative contribution of *trans* fatty acid intake were 55% from ruminant fats and 45% from PHVO. This pattern contrasts sharply with those established for Canada and the United States where PHVO is reported to be the major dietary source of *trans* fatty acids.

Paper no. L8376 in *Lipids 35,* 561–566 (May 2000).

At the beginning of the 1990s, epidemiological and clinical studies (1–8) suggested that dietary *trans* fatty acids might represent a risk for coronary heart disease. Clinical studies showed that *trans* fatty acids cause, in a dose-dependent manner (2), an increase of plasma low density lipoprotein cholesterol, and in some cases a decrease of plasma high density lipoprotein cholesterol (1–5,7). Occurrence of *trans* fatty acids in human tissues depends on their availability in the diet, because humans do not synthesize these fatty acid isomers. It is now well known that *trans* fatty acids are provided by three different dietary sources: the ruminant fats (milk and dairy products, beef, mutton, tallow) (9), the partially hydrogenated vegetable oils (PHVO) (some margarines, shortenings, baked goods, and chips) (10), and to a lesser extent, the refined vegetable oils (11). In France, the *trans* fatty acid content of most table margarines, both soft and hard, and low-fat spreads has decreased since 1995. At present, most of these products contain less than 1% total *trans* fatty acids (12) except for a few products which may contain up to 15% total *trans* fatty acids. In addition, products such as biscuits, crackers and French-fried potatoes that are marketed in France still contain 10–20% total *trans* fatty acids.

Estimates of *trans* fatty acids intake in France are 2.8 g/d capita from fat disappearance data (9) or 2.3 g from food consumption survey data (13). There are limitations in determining the *trans* fatty acids intake from nutrient databases, and therefore another approach should be considered. The *trans* fatty acid composition of adipose tissue is a reliable biochemical indicator of the consumption of "exogenous" fatty acids (14,15). The turnover rate of fatty acids in adipose tissue was shown to be approximately 3 yr (16), and therefore, its fatty acid composition would reflect dietary fats over that period.

The main objectives of this study were to determine the level of the different *trans* isomers (16:1*t*, 18:1*t*, 18:2*t*, and 18:3*t*) in adipose tissue of French adults, to assess their availability in the diet, and to determine their dietary origin (animal or processing) using the distribution of selected positional *trans* 18:1 isomers present in adipose tissue. In addition, the total fatty acid composition of adipose tissue of these French adults is reported, since such data are not available to date.

EXPERIMENTAL PROCEDURES

Subjects and sample collection. The study protocol was approved by the local ethical review committee, and informed consent was obtained from 71 participating women (age, 37 ± 10 yr; body mass index, 22 ± 3). They were recruited be-

*To whom correspondence should be addressed at the Unité de Biochimie-Nutrition ITERG, Laboratoire de Lipochimie Alimentaire, Université Bordeaux I, Ave. des Facultés, 33405 Talence Cedex, France.
E-mail: n.combe@istab.u-bordeaux.fr

Abbreviations: FAME, fatty acid methyl ester; GC, gas chromatography; PHVO, partially hydrogenated vegetable oils; PUFA, polyunsaturated fatty acids; TLC, thin-layer chromatography.

tween 1997 and 1998. The selected participants were free of cancer and diabetes, and their lifestyles had not changed in the past 5 yr. Those who reported making major changes in their diet in the previous 5 yr were excluded. About 0.5–1 g abdominal subcutaneous adipose tissue was removed during abdominal surgery (hysterectomy, ovary cyst removal, etc.). The adipose tissue samples were immediately rinsed with an isotonic saline solution (0.9% NaCl) and then frozen and stored at –20°C until analyzed.

Sampling of foods containing PHVO. Fifteen brands of margarines and bakery products (biscuits, brioches, puff pastry, etc.) were purchased in local supermarkets in 1996 and 1997.

Lipid extraction. Thawed adipose tissue and food samples were ground in a mixture of chloroform/methanol (2:1, vol/vol). Total lipids were then extracted according to the method of Folch *et al.* (17). Solvents were evaporated to dryness under a stream of nitrogen. Lipids were taken up in an appropriate volume of chloroform/methanol (2:1, vol/vol) and stored in glass tubes at –20°C under nitrogen.

Fatty acid analysis. Fatty acid methyl esters (FAME) of total lipids were prepared using 14% boron trifluoride in methanol according to Morrison and Smith (18) and stored in hexane at –20°C under nitrogen. Analyses of total FAME were carried out on a gas chromatograph (Carlo Erba 5160, Milano, Italy) equipped with a flame-ionization detector and a split injector. A fused-silica capillary column (BPX 70, 60 m × 0.25 mm i.d., 0.25 μm film; SGE, France) was used with H_2 as a carrier gas (inlet pressure: 90 kPa). The split ratio was 1:70. The column temperature was programmed from 150 to 200°C at 1.5°C/min, then to 230°C at 2.5°C/min and held at 230°C until completion of the analysis (30 min). The injection port and the detector were maintained at 250°C. The gas chromatography (GC) peaks were integrated using an SP 4400 integrator (Spectra Physics, San Jose, CA). The different *trans* isomers of 18:2 and 18:3 were identified by comparing the GC retention times with authentic standards (Sigma, Saint Quentin Fallavier, France) or with well-characterized FAME mixtures prepared in our laboratory (11,19). In using these chromatographic conditions, all positional *trans* 18:1 isomers (6*t*-18:1 to 16*t*-18:1) could not be measured because of the overlap of five isomers (12*t*-18:1 to 16*t*-18:1) with *cis* 18:1 isomers. To measure the levels of all these isomers, the total *trans* 18:1 isomers were separated from *cis* 18:1 isomers by an additional step using $AgNO_3$ thin-layer chromatography (TLC) according to Wolff (19), with one minor modification. The developing solvent used for FAME separation was a mixture of hexane/diethylether (90:10, vol/vol). Analysis of the *trans* fraction was performed using a fused-silica capillary column (CP Sil 88, 100 m × 0.25 mm i.d., 0.20 μm film; Chrompack, Middelburg, The Netherlands) operated isothermally at 160°C, and using H_2 as the carrier gas (inlet pressure: 130 kPa) (19). Individual positional isomers of *trans* 18:1 were identified by comparison with synthetic isomers purchased from Sigma and with literature values (20). The total *trans* 18:1 content was calculated according to Ratnayake and Pelletier (21) by comparing the *trans* monoene fraction with the total FAME prior to $AgNO_3$ TLC fractionation. The *trans* 18:1 isomers, 6*t*-18:1 to 11*t*-18:1, well-separated on the total FAME chromatogram were therefore used as internal standard.

All the results are expressed as weight percentages of fatty acids using the factor (F'_t) described by Wolff *et al.* (22). This factor is linked to the theoretical response factor (F_t) by: $F'_t = F_t \times$ (fatty acid molecular weight/FAME molecular weight).

RESULTS

Fatty acid composition of abdominal adipose tissue. The detailed fatty acid compositions of women's adipose tissue (mean, standard deviation, and range) are presented in Table 1. *Cis* monounsaturated fatty acids accounted for about half (47.9% of total fatty acids), the major being oleic acid (9*c*-18:1) with 39.7%. The mean content of saturated fatty acids was 32.2%; palmitic acid (16:0) was the most prevalent with 22.2%. *Cis* n-6 polyunsaturated fatty acids (PUFA) ranged from 9.0 to 22.9% of total fatty acids (mean 15.3%), the main component being linoleic acid (9*c*,12*c*-18:2). *Cis* n-3 PUFA were present at very low levels (0.7% of total fatty acids).

The mean content of all *trans* fatty acids combined in adipose tissue in the 71 women examined was 2.32 ± 0.50% of total fatty acids, with a range of 1.41 to 3.96%. The *trans* fatty acids comprised isomers of 16:1, 18:1, and 18:2 acids (Table 2). The most prevalent *trans* isomers in adipose tissue were *trans* 18:1 acids, which were also the most abundant in foods. They represented 85% of the *trans* content and 1.97 ± 0.49% of adipose total fatty acids. There were several *trans*-18:1 isomers that ranged from Δ6 to Δ16. Accurate determination of the positional *trans* 18:1 isomers was obtained by a combination of $AgNO_3$-TLC and GC methods described above. The 18:1 isomers of the *trans* monounsaturated fatty acid band isolated from adipose tissue total FAME by $AgNO_3$-TLC were separated by GC into six individual FAME and two groups of FAME. The first group comprised 6*t*-, 7*t*-, and 8*t*-18:1, and the second the 13*t*- and 14*t*-18:1. Individual *trans* 18:1 isomers were 9*t*-, 10*t*-, 11*t*-, 12*t*-, 15*t*-, and 16*t*-18:1. Mean and range of their respective levels in all samples are shown in Table 2. The 11*t*-18:1 isomer was the most prevalent (0.65 ± 0.19%) in adipose total fatty acids. The only *trans* 16:1 fatty acid found in adipose tissue was 9*t*-16:1 which was well-separated from the iso and anteiso branched chain 17:0 fatty acids present in adipose tissue. The average content of 9*t*-16:1 was 0.06% of adipose tissue total fatty acids.

Total *trans* 18:2 isomer content was 0.28% of total fatty acids. The main 18:2 *trans* isomer was 9*c*,12*t*-18:2 at 0.13%, followed by 9*t*,12*c*-18:2 (0.06%). It is worth noticing that in our GC conditions, we could not exclude the possibility that the peak identified as the 9*t*,12*c*-18:2 also contained the 11*t*,15*c* isomer which has been found in bovine milk fat (23). The 9*t*,12*t*-18:2 was partially separated from 9*c*,13*t*-18:2. This isomer was identified in hydrogenated oils (21) and in bovine milk fat (23). Based on the partial overlap of these two

TABLE 1
Fatty Acid Composition of Total Lipids of Adipose Tissue from 71 Women (wt% total fatty acids)

Fatty acids[a]	Means ± SD	Range Min	Range Max
∑ SFA	32.23 ± 3.03	25.50	39.48
12:0	0.50 ± 0.22	ND[b]	0.97
14:0	3.43 ± 0.67	1.82	5.09
15:0	0.37 ± 0.09	0.20	0.73
16:0 iso	0.10 ± 0.03	ND	0.16
16:0	22.15 ± 1.80	17.51	26.01
17:0 iso	0.15 ± 0.06	ND	0.46
17:0	0.29 ± 0.06	0.18	0.47
18:0 iso	0.02 ± 0.06	ND	0.29
18:0	4.92 ± 1.20	2.43	7.79
20:0	0.23 ± 0.09	ND	0.47
22:0	0.04 ± 0.04	ND	0.17
24:0	0.01 ± 0.02	ND	0.06
∑ *cis*-MUFA	47.87 ± 3.00	40.39	57.52
14:1n-5	0.36 ± 0.14	0.08	0.76
16:1n-9	0.56 ± 0.13	0.4	1.44
16:1n-7	4.23 ± 1.08	2.00	7.09
17:1	0.27 ± 0.09	ND	0.45
18:1n-9	39.69 ± 2.55	32.28	49.75
18:1n-7	1.83 ± 0.48	ND	3.19
20:1n-9	0.7 ± 0.22	0.31	1.48
20:1n-7	0.18 ± 0.09	ND	0.4
22:1n-9	0.04 ± 0.03	ND	0.18
24:1n-9	0.00 ± 0.01	ND	0.03
∑ *cis* n-6 PUFA	15.34 ± 3.03	9.05	22.95
18:2n-6	14.35 ± 3.03	5.64	21.80
18:3n-6	0.05 ± 0.04	ND	0.15
20:2n-6	0.26 ± 0.09	0.1	0.55
20:3n-6	0.18 ± 0.08	0.08	0.55
20:4n-6	0.37 ± 0.42	0.15	3.72
22:4n-6	0.12 ± 0.08	ND	0.52
22:5n-6	0.01 ± 0.02	ND	0.09
∑ *cis* n-3 PUFA	0.74 ± 0.26	ND	1.4
18:3n-3	0.43 ± 0.17	ND	0.8
20:5n-3	0.03 ± 0.03	ND	0.12
22:5n-3	0.14 ± 0.07	ND	0.34
22:6n-3	0.14 ± 0.08	ND	0.43
Other *cis*-PUFA			
20:2n-9	0.17 ± 0.11	ND	0.71
20:3n-9	0.01 ± 0.03	ND	0.22
∑ TFA	2.32 ± 0.50	1.41	3.96

[a]SFA, saturated fatty acid; MUFA, monounsaturated fatty acid; PUFA, polyunsaturated fatty acid; TFA, *trans* fatty acid; ND, not detected (detection limit: 0.01%).

TABLE 2
***Trans* Fatty Acid Composition of Total Lipids of Adipose Tissue from 71 Women (wt% total fatty acids)**

Fatty acids	Means ± SD	Range Min	Range Max
∑ TFA	2.32 ± 0.50	1.41	3.96
9*t*-16:1	0.06 ± 0.03	0.01	0.21
∑ *trans* 18:1	1.97 ± 0.49	1.06	3.50
6*t* to 8*t*-18:1	0.09 ± 0.06	0.02	0.25
9*t*-18:1	0.27 ± 0.11	0.07	0.65
10*t*-18:1	0.29 ± 0.10	0.10	0.57
11*t*-18:1	0.65 ± 0.19	0.26	1.09
12*t*-18:1	0.24 ± 0.09	0.09	0.62
13*t* + 14*t*-18:1	0.27 ± 0.11	0.06	0.55
15*t*-18:1	0.07 ± 0.03	0.02	0.13
16*t*-18:1	0.09 ± 0.05	0.00	0.24
∑ *trans* 18:2	0.28 ± 0.08	0.16	0.52
9*t*,12*t* + 9*c*,13*t*-18:2	0.09 ± 0.04	0.03	0.19
9*c*,12*t*-18:2	0.13 ± 0.04	0.05	0.24
9*t*,12*c*-18:2[a]	0.06 ± 0.02	0.03	0.13
∑ *trans* 18:3	ND	ND	ND

[a]9*t*,12*c*-18:2; this peak might correspond to the sum of 9*t*,12*c* + 11*t*,15*c*. See Table 1 for abbreviations.

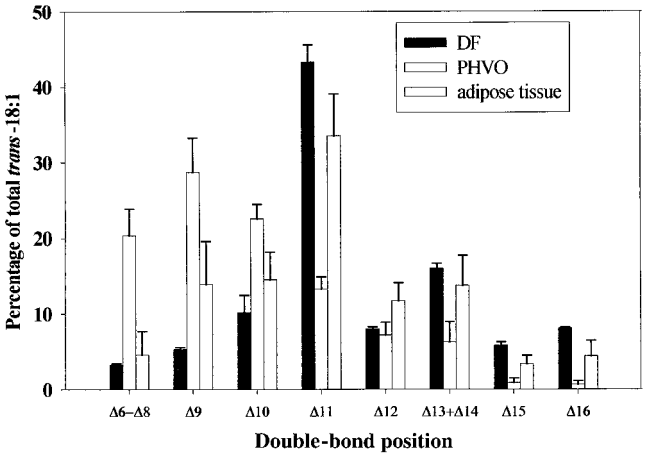

FIG. 1. Comparison of *trans* 18:1 positional isomer profiles in women's adipose tissue (n = 71), in dairy fat (DF; n = 10), and in partially hydrogenated vegetable oils (PHVO; n = 15). Positional isomers were analyzed using a combination of gas chromatography and silver nitrate thin-layer chromatography of fatty acid methyl esters. Values for each positional isomer are expressed as percentage of total positional isomers. Error bars represent standard deviation.

18:2 isomers, we estimated that 9*t*,12*t*-18:2, on average, represented about 20% of the complex peak (9*t*,12*t* plus 9*c*,13*t*), or 1% of the *trans* content and 0.02% of total fatty acids in adipose tissue. Therefore, 9*t*,12*t*-18:2 was the least common isomer of *trans*-18:2 found.

Profile of positional trans*-18:1 isomers in abdominal adipose tissue.* Figure 1 illustrates the mean distribution of positional *trans*-18:1 isomers in abdominal adipose tissue found in the 71 participating women; values were compared to those found in ruminant fats (average of 10 dairy products) and in PHVO (average of 15 selected *trans*-containing food products in France). The average distribution of *trans*-18:1 isomers in adipose tissue showed a greater similarity to ruminant fats than to PHVO *trans* fatty acids (Fig. 1). Vaccenic acid (11*t*-18:1) was the most prevalent both in adipose tissue fat (33% of total *trans* 18:1 acids) and in ruminant fats (43%).

DISCUSSION

Adipose tissue is regarded as a good reflection of long-term intake of fatty acids, some of which cannot be synthesized by humans, like linoleic, α-linolenic, and *trans* fatty acids

(15,24). Consequently, adipose tissue measurements may provide independent information on dietary habits. There are few data on the fatty acid composition of adipose tissue in European adults, and to our knowledge, none in France. Therefore, besides *trans* fatty acids, we report here the whole fatty acid composition of adipose tissue for 71 French women in 1997–1998. The content of *cis* PUFA (16%), consisting mainly of linoleic acid, was similar to that observed in 1985 in 59 Dutch women (17%) (24) or in 1986 in 76 U.S. males (16%) (25). However, it was lower than that reported in 1986 in 115 post-menopausal U.S. women (19.7%) (15) or in 1986 in 140 U.S. women (20.8%) (26). The contents of saturated (32.2%) and *cis* monounsaturated (47.9%) fatty acids found in this study were similar only to those reported in U.S. males (25). Because saturated and monounsaturated fatty acids are endogenously synthesized, their adipose content may not reflect their dietary intake.

Conversely, some studies have observed a correlation of *trans* fatty acid content between adipose tissue and the diet (14,15,27). The *trans* content in our French adipose tissue samples was 2.32% of total fatty acids, present as 16:1, 18:1, and 18:2 in all samples. On the other hand, *trans* fatty acids with 14 and 20–22 carbon atoms, and *trans* 18:3 isomers were below detection limits (0.01%) by GC. We noted that the 9*t*-16:1 level (0.06%), without contamination by branched-chain 17:0 fatty acids, was often lower than previously reported (15,25,27–29). The origin of this isomer is ruminant fats (30) and partially hydrogenated fish oils (31). Because *trans* 16:1 isomers sometimes have been associated with an increased risk of coronary artery disease (32), accurate chromatographic analysis is mandatory to avoid the overestimation due to closely coeluting branched-chain 17:0 fatty acids that are present. *Trans* polyunsaturates in adipose tissue of these French women contained less *trans* 18:2 acids (0.28%) than those observed in the American studies (0.9–1.3%). Data reported for Germany and the United Kingdom were similar to ours (0.34–0.59%) (29,33). These *trans* isomers were provided by PHVO (<2%) and by ruminant fats (about 1%). Differences of *trans* polyunsaturate adipose content between American and European populations reflect differences of their dietary fats. The *trans*-18:2 acids in decreasing order were: 9*c*,12*t* (0.13%) > 9*c*,13*t* (0.07%) > 9*t*,12*c* (0.06%) > 9*t*,12*t* (0.02%). *Trans* isomers of long-chain n-6 PUFA could be endogenously synthesized from mono-*trans*-18:2, and they are potential precursors of *trans* eicosanoid isomers (34). However, no *trans* isomers of long-chain n-6 PUFA were detected in adipose tissue. The di-*trans* isomer (9*t*,12*t*-18:2), which is known to alter the activity of Δ6-desaturase toward linoleic acid (9*c*,12*c*-18:2) (35), was found at <0.09%.

The bulk of *trans* fatty acids present in adipose tissue was *trans*-18:1 isomers. Their content ranged from 1.06 to 3.50% of total fatty acids of adipose tissue, with a mean value of 1.97%. These results are directly comparable to those determined in Canada (28), since the same combination $AgNO_3$-TLC and GC was used. *Trans*-18:1 content of adipose tissue from French women was lower than that of Canadians (4.8%), while the U.S. study (2.7 to 3.9%) was probably underestimated by omitting the 12*t*-18:1 to 16*t*-18:1 isomers (15,24–26). This suggests that *trans* fatty acid intake of these French women was lower than that of the Canadian and U.S. adults. The European data on *trans*-18:1 content of adipose tissue show that it varied from 0.43 to 2.43% among the eight countries participating in the Euramic Study (36). These values did not take into account the 12*t*-18:1 to 16*t*-18:1 isomers. As shown in Figure 1, these isomers constituted an average of 33% of total *trans*-18:1 isomers present in adipose tissue of the French women. Based on this estimate, we recalculated the published European data for comparison and observed that the *trans* content of French adipose tissue (1.97 ± 0.49%) was lower than those of North Europe countries (3.2–3.6%), but higher than that of Spain (0.6%). That would suggest that *trans*-18:1 acid intake in France was intermediate between countries of North and South Europe, which is in agreement with fat consumption data (9,37). Furthermore, our results on adipose tissue *trans*-18:1 acid content were similar to those obtained in France on *trans*-18:1 acid level in human milk (30,38), a biochemical indicator of *trans* fatty acid consumption of the previous day (39). Values of 1.8 ± 0.9% and 2.0 ± 0.6% (relative to total fatty acids) were found in milk of French women in 1995 by Combe *et al.* (38) in the Bordeaux region, and by Chardigny *et al.* (40) in the Dijon region, respectively.

The percentage value of *trans*-18:1 in adipose tissue of the 71 French women was applied to the equation of Enig *et al.* (14):

$$y = 0.97 + 0.44\,x \qquad [1]$$

which describes the relationship of *trans*-18:1 percentages between adipose tissue (y) and dietary fat (x). The estimated average of *trans*-18:1 in dietary fat was 2.27%, using this equation (Table 3). The mean total fat intake of our French women was 85 g/d/person, or 42% of energy based on dietary records (Boué, C., and Combe, N., unpublished data). We calculated that the consumption per capita of *trans*-18:1 acid might vary from 0.12 to 4.10 g/d, with an average value of 1.9 g/d (Table 3).

If we assume that there are no metabolic differences in turnover between the several positional *trans*-18:1 isomers in adipose tissue, then the respective proportions of these isomers in adipose tissue would depend on the availability in the diet. As shown in Figure 1, the pattern of *trans*-18:1 acids in adipose tissue was the result of contributions from both ruminant fats and PHVO. These results contrast widely with those reported by Chen *et al.* (28) for Canada and Ohlrogge *et al.* (41) for the United States. In these countries, the distributions of *trans*-18:1 isomers in adipose tissue were similar to those of dietary PHVO, indicating that they were the major dietary sources of *trans*-18:1 acids.

We assessed the relative contribution of both dietary origins to adipose storage of *trans*-18:1 isomers, using an equation proposed by Wolff (30) for human milk, which is based on the absence of 16*t*-18:1 in PHVO and its presence in ruminant fats. In Equations 2 and 3,

TABLE 3
Estimates of Human Consumption of Dietary *trans* Fatty Acids Based on Percentage of *trans* 18:1 in Adipose Tissue of 71 Women

		Range	
	Means	Min	Max
% *Trans* 18:1 in adipose tissue = *y* (wt% total fatty acids)	1.97	1.06	3.50
Equation of Enig *et al.* (Ref. 14)		$y = 0.97 + 0.44\,x$	
Estimate % *trans* 18:1 in women dietary fat = *x* (wt% total fatty acids)	2.27	0.33	5.34
Daily per capita total fat intake (g/d/person)	84.70	31.10	136.00
Estimate daily per capita intake of *trans* 18:1 (g/d/person)	1.93	0.12	4.10

$$8.1X + 0.5Y = Z \quad [2]$$

$$X + Y = 1 \quad [3]$$

X represents the intake of milk fat and *Y* the intake of margarines. *Z* is the percentage of 16*t*-18:1 relative to total *trans*-18:1 isomers in human milk. The author considered cow milk as the primary dominant source of ruminant fats for lactating French women and therefore used the value 8.1 as the mean proportion of the 16*t*-18:1 isomer in cow milk fat (30). However, this value was found to be 4.9% of the total *trans*-18:1 isomers in ruminant meat (30). Based on our dietary questionnaire, we found that ruminant fats were derived from 85% dairy products and 15% ruminant meat (Boué, C., and Combe, N., unpublished data). By using these values, the average percentage of 16*t*-18:1 in ruminant fats was 7.6%, which was applied to the above equations: $7.6X + 0.5Y = 4.4$ and $X + Y = 1$. *Z*, the mean 16*t*-18:1 proportion in adipose tissue, was 4.4% (Table 2). The relative contributions to *trans* fatty acid in the diet were estimated at 55% from ruminant fats and 45% from PHVO. These values were very similar to those deduced (58 and 42%, respectively) from the 16*t*-18:1 proportion in French human milk (30). These results suggest that lactating women consume little more dairy products than nonlactating women.

Ascherio *et al.* (42) recently reported clinical studies utilizing diets containing 3.3–10% of energy from *trans* fatty acids (elaidic acid: 9*t*-18:1). They showed that an increase of 2% in the intake of *trans* fatty acids raised the ratio of low density lipoprotein cholesterol to high density lipoprotein cholesterol by 0.1 unit when compared to a diet with isocaloric amounts of oleic acid. For the diet of the French women of our study, the percentage of energy from *trans*-18:1 acid was about 1%, with extreme values of 0.1 and 2.2% of total energy. These data were determined from the percentage of *trans*-18:1 acid in dietary fats (2.3%; range: 0.3–5.3%) and from total energy as fats (42%) in the diet of these subjects. The cholesterol levels of serum lipoproteins in these French women in relation to their total *trans* fatty acid intake and from either dietary source will be the subject of a further report.

ACKNOWLEDGMENTS

The authors gratefully acknowledge the expert technical assistance of Laurence Fonseca and Pascale Nonatel. The work was supported by grants from CSM (Chambre Syndicale de la Margarinerie), ONIDOL (Organisation Nationale Interprofessionnelle des Oléagineux), SIDO (Société Interprofessionnelle des Oléagineux), and SGFHTF (Syndicat Général des Fabricants d'Huile et de Tourteaux de France). Carole Boué received a joint grant from the Ministère de la Recherche et de la Technologie and the Société Astra-Calvé (CIFRE, n°: 538/96).

REFERENCES

1. Mensink, R.P., and Katan, M.B. (1990) Effect of Dietary *Trans* Fatty Acids on High Density Lipoprotein Cholesterol Levels in Healthy Subjects, *N. Engl. J. Med. 23,* 439–445.
2. Zock, P.L., and Katan, M.B. (1992) Hydrogenation Alternatives: Effects of *trans* Fatty Acids and Stearic Acid versus Linoleic Acid on Serum Lipids and Lipoproteins in Human, *J. Lipid Res. 33,* 399–410.
3. Troisi, R., Willett, W.C., and Weiss, S.T. (1992) *Trans* Fatty Acid Intake in Relation to Serum Lipid Concentrations in Adult Men, *Am. J. Clin. Nutr. 56,* 1019–1024.
4. Mensink, R.P., Zock, P.L., Katan, M.B., and Hornstra, G. (1992) Effect of Dietary *cis* and *trans* Fatty Acids on Serum Lipoprotein[a] Levels in Humans, *J. Lipid Res. 33,* 1493–1501.
5. Nestel, P., Noakes, M., Belling, B., McArthur, R., Clifton, P., Janus, E., and Abbey, M. (1992) Plasma Lipoprotein Lipid and Lp[a] Changes with Substitution of Elaidic Acid for Oleic Acid in the Diet, *J. Lipid Res. 33,* 1029–1036.
6. Willett, W.C., Stampfer, M.J., Manson, J.E., Colditz, G.A., Speizer, F.E., Rosner, B.A., Sampson, L.A., and Hennekens, C.H. (1993) Intake of *trans* Fatty Acids and Risk of Coronary Heart Disease Among Women, *Lancet 341,* 581–585.
7. Judd, J.T., Clevidence, B.A., Muesing, R.A., Wittes, J., Sunkin, M.E., and Podczasy, J.J. (1994) Dietary *trans* Fatty Acid: Effects on Plasma and Lipoproteins of Healthy Men and Women, *Am. J. Clin. Nutr. 59,* 861–868.
8. Ascherio, A., Hennekens, C.H., Buring, J.E., Master, C., Stampfer, M.J., and Willett, W.C. (1994) *Trans* Fatty Acids Intake and Risk of Myocardial Infarction, *Circulation 89,* 94–101.
9. Wolff, R.L., Precht, D., and Molkentin, J. (1998) Occurrence and Distribution Profile of *trans*-18:1 Acids in Edible Fats of Natural Origin, in Trans *Fatty Acids in Human Nutrition* (Sébédio, J.L., and Christie, W.W., eds.), pp. 1–33, Oily Press, Ayr, Scotland.
10. Craig-Schmidt, M.C. (1992) Fatty Acid Isomers in Foods, in

Fatty Acids in Foods and Their Health Implications (Chow, C.K., ed.), pp. 365–398, Marcel Dekker, Inc., New York.
11. Wolff, R.L. (1993) Heat-Induced Geometrical Isomerization of α-Linolenic Acid: Effect of Temperature and Heating Time on the Appearance of Individual Isomers, *J. Am. Oil Chem. Soc. 70,* 425–430.
12. Aro, A., Van Amelsvoort, J., Becker, W., Van Erp-Baart, M.A., Kafatos, A., Leth, T., and Van Poppel, G. (1998) *Trans* Fatty Acids in Dietary Fats and Oils from 14 European Countries: the TRANSFAIR Study, *J. Food Compos. Anal. 11,* 137–149.
13. Van Poppel, G.V. (1998) Intake of *trans* Fatty Acids in Western Europe: the TRANSFAIR Study, *Lancet 351,* 1099.
14. Enig, M.G., Atal, S., Keeney, M., and Sampugna, J. (1990) Isomeric *trans* Fatty Acids in the U.S. Diet, *J. Am. Coll. Nutr. 9,* 471–486.
15. London, S.J., Sacks, F.M., Caesar, J., Stampfer, M.J., Siguel, E., and Willett, W.C. (1991) Fatty Acid Composition of Subcutaneous Adipose Tissue and Diet in Postmenopausal U.S. Women, *Am. J. Clin. Nutr. 54,* 340–345.
16. Beynen, A.C., Hermus, R.J.J., and Hautvast, J.G.A.J. (1980) A Mathematical Relationship Between Fatty Acid Composition of the Diet and That of Adipose Tissue in Man, *Am. J. Clin. Nutr. 33,* 81–85.
17. Folch, J., Lees, M., and Sloane Stanley, G.H. (1957) A Simple Method for the Isolation and Purification of Total Lipids from Animal Tissues, *J. Biol. Chem. 226,* 497–509.
18. Morrison, W.R., and Smith, L.M. (1964) Preparation of Fatty Acid Methyl Esters and Dimethylacetals with Boron Fluoride Methanol, *J. Lipid Res. 5,* 600–608.
19. Wolff, R.L. (1991) Geometrical Isomers of Linolenic Acid in Low-Calorie Spreads Marketed in France, *J. Am. Oil Chem. Soc. 68,* 719–725.
20. Wolff, R.L., and Bayard, C.C. (1995) Improvement in the Resolution of Individual *trans*-18:1 Isomers by Capillary Gas Liquid Chromatography: Use of a 100-m CP-Sil 88 Column, *J. Am. Oil Chem. Soc. 72,* 1197–1201.
21. Ratnayake, W.M.N., and Pelletier, G. (1992) Positional and Geometrical isomers of Linoleic Acid in Partially Hydrogenated Oils, *J. Am. Oil Chem. Soc. 69,* 95–105.
22. Wolff, R.L., Bayard, C.C., and Fabien, R.J. (1995) Evaluation of Sequential Methods for the Determination of Butterfat Fatty Acid Composition with Emphasis on *trans*-18:1 Acids. Application to the Study of Seasonal Variations in French Butters, *J. Am. Oil Chem. Soc. 72,* 1471–1483.
23. Ulberth, F., and Henninger, M. (1994) Quantitation of *Trans* Fatty Acids in Milk Fat Using Spectroscopic and Chromatographic Methods, *J. Dairy Res. 61,* 517–527.
24. Van Staveren, D.A.F., Deurenberg, P., Katan, M.B., Burema, J., De Groot, L.C.P.G.M., and Hoffmans, D.A.F. (1986) Validity of the Fatty Acid Composition of Subcutaneous Fat Tissue Microbiopsies as an Estimate of the Long-Term Average Fatty Acid Composition of the Diet of Separate Individuals, *Am. J. Epidemiol. 123,* 455–463.
25. Hudgins, L.C., Hirsch, J., and Emken, E.A. (1991) Correlation of Isomeric Fatty Acids in Human Adipose Tissue with Clinical Risk Factors for Cardiovascular Disease, *Am. J. Clin. Nutr. 53,* 474–482.
26. Garland, M., Sacks, F.M., Colditz, G.A., Rimm, E.B., Sampson, L.A., Willett, W.C., and Hunter, D.J. (1998) The Relation Between Dietary Intake and Adipose Tissue Composition of Selected Fatty Acids in U.S. Women, *Am. J. Clin. Nutr. 67,* 25–30.
27. Lemaitre, R.N., King, I.B., Patterson, R.E., Psaty, B.M., Kestin, M., and Heckbert, S.R. (1998) Assessment of *trans* Fatty Acid Intake with a Food Frequency Questionnaire and Validation with Adipose Tissue Levels of *trans* Fatty Acids, *Am. J. Epidemiol. 148,* 1085–1093.
28. Chen, Z.Y., Ratnayake, W.M.N., Foetier, L., Ross, R., and Cunnanne, S.C. (1995) Similar Distribution of *trans* Fatty Acids Isomers in HPVO and Adipose Tissue of Canadians, *Can. J. Physiol. Pharmacol. 73,* 718–723.
29. Fritsche, J., Steinhart, H., Kardalinos, V., and Klose, G. (1998) Contents of *trans* Fatty Acids in Human Substernal Adipose Tissue and Plasma Lipids: Relation to Angiographically Documented Coronary Heart Disease, *Eur. J. Med. Res. 3,* 401–406.
30. Wolff, R.L. (1995) Content and Distribution of *trans*-18:1 Acids in Ruminant Milk and Meat Fats. Their Importance in European Diets and Their Effect on Human Milk, *J. Am. Oil Chem. Soc. 72,* 259–272.
31. Molkentin, J., and Precht, D. (1997) Occurrence of *trans*-C16:1 Acids in Bovine Milk Fats and Partially Hydrogenated Edible Fats, *Mischwissenschaft 52,* 380–385.
32. Siguel, E.N., and Lerman, R.H. (1993) *Trans* Fatty Acid Patterns in Patients with Angiographically Documented Coronary Artery Disease, *Am. J. Cardiol. 71,* 916–920.
33. Roberts, T.L., Wood, D.A., Riemersma, R.A., Gallagher, P.J., and Lampe, F.C. (1995) *Trans* Isomers of Oleic and Linoleic Acids in Adipose Tissue and Sudden Cardiac death, *Lancet 345,* 278–282.
34. Berdeaux, O., Blond, J.P., Bretillon, L., Chardigny, J.M., Mairot, T., Vatele, J.M., Poullain, D., and Sébédio, J.L. (1998) *In Vitro* Desaturation or Elongation of Mono *trans* Isomers of Linoleic Acid by Rat Liver Microsomes, *Mol. Cell. Biochem. 185,* 17–25.
35. Anderson, R.L., Fullmer, C.S.J., and Hollenback, E.J. (1975) Effects of the *trans* Isomers of Linoleic Acid on the Metabolism of Linoleic Acid in Rats, *J. Nutr. 105,* 393–400.
36. Aro, A., and Kardinaal, A.F.M. (1995) Adipose Tissue Isomeric *trans* Fatty Acids and Risk of Myocardial Infarction in 9 Countries—The EURAMIC Study, *Lancet 345,* 273–278.
37. Hulshof, K.F.A.M., Van Erp-Baart, M.A., Anttolainen, M., Becker, W., Church, S.M., Couet, C., Hermann-Kunz, E., Kesteloot, H., Leth, T., Martins, I., *et al.* (1999) Intake of Fatty Acids in Western Europe with Emphasis on *trans* Fatty Acids: The TRANSFAIR Study, *Eur. J. Clin. Nutr. 53,* 143–157.
38. Combe, N., Billeaud, C., Mazette, S., Entressangles, B., and Sandler, B. (1995) *Trans* Fatty Acids (TFA) in Human Milk Reflect Animal or Vegetable TFA Consumption in France, *Pediatric Res. 37,* 304A.
39. Craig-Schimdt, M.C., Weete, J.D., Faircloth, S.A., Wickwire, M.A., and Livant, E.J. (1984) The Effect of Hydrogenated Fat in the Diet of Nursing Mothers on Lipid Composition and Prostaglandin Content of Human Milk, *Am. J. Clin. Nutr. 39,* 778–786.
40. Chardigny, J.M., Wolff, R.L., Mager, E., Sébédio, J.L., Martine, L., and Juaneda, P. (1995) *Trans* Mono- and Polyunsaturated Fatty Acids in Human Milk, *Eur. J. Clin. Nutr. 49,* 523–531.
41. Ohlrogge, J.B., Gulley, R.M., and Emken, E.A. (1982) Occurrence of Octadecenoic Fatty Acid Isomers from Hydrogenated Fats in Human Tissue Lipid Classes, *Lipids 17,* 551–557.
42. Ascherio, A., Katan, M.B., Zock, P.L., Stampfer, M.J., and Willett, W.C. (1999) *Trans* Fatty Acids and Coronary Heart Disease, *N. Engl. J. Med. 340,* 1994–1998.

[Received October 26, 1999, and in final revised form March 15, 2000; revision accepted March 21, 2000]

Blood Fatty Acid Composition of Pregnant and Nonpregnant Korean Women: Red Cells May Act as a Reservoir of Arachidonic Acid and Docosahexaenoic Acid for Utilization by the Developing Fetus

K. Ghebremeskel[a,]*, Y. Min[a], M.A. Crawford[a], Joo-Hyun Nam[b], Ahm Kim[b], Ja-Nam Koo[b], and Hiramitsu Suzuki[c]

[a]Institute of Brain Chemistry and Human Nutrition, The University of North London, London N7 8DB, United Kingdom, [b]Asan Medical Centre, Department of Obstetrics and Gynaecology, College of Medicine, University of Ulsan, Seoul, South Korea, and [c]National Food Research Institute, Konnondai, Tsukuba, Ibaraki 305-8642, Japan

ABSTRACT: Relative fatty acid composition of plasma and red blood cell (RBC) choline phosphoglycerides (CPG), and RBC ethanolamine phosphoglycerides (EPG) of pregnant (n = 40) and nonpregnant, nonlactating (n = 40), healthy Korean women was compared. The two groups were of the same ethnic origin and comparable in age and parity. Levels of arachidonic (AA) and docosahexaenoic (DHA) acids were lower ($P < 0.05$) and palmitic and oleic acids higher ($P < 0.0001$) in plasma CPG of the pregnant women. Similarly, the RBC CPG and EPG of the pregnant women had lower AA and DHA ($P < 0.05$) and higher palmitic and oleic acids ($P < 0.01$). The reduction in DHA and total n-3 fatty acids in plasma CPG of the pregnant women was paralleled by an increase in docosatetraenoic (DTA) and docosapentaenoic (DPA) acids of the n-6 series and in DPA/DTA ratio. In the RBC phospholipids (CPG and EPG) of the pregnant women, DTA and DPA acids of the n-6 series and DPA/DTA ratio did not increase with the decrease of the n-3 metabolites (eicosapentaenoic acid, DPA, and DHA) and total n-3. Since pregnancy was the main identifiable variable between the two groups, the lower levels of AA and DHA in RBC CPG and EPG of the pregnant women suggest that the mothers were mobilizing membrane AA and DHA to meet the high fetal requirement for these nutrients. It may also suggest that RBC play a role as a potential store of AA and DHA and as a vehicle for the transport of these fatty acids from maternal circulation to the placenta to be utilized by the developing fetus.

Paper no. L8318 in *Lipids 35*, 567–574 (May 2000).

The fetus and neonate require arachidonic acid (AA) and docosahexaenoic acid (DHA) for the development of all vital cellular and subcellular membranes (1). The demand for these essential nutrients is at its highest in the later part of pregnancy and in early infancy, when priority is given to brain growth. In the human cerebrum and cerebellum, over a threefold increase in AA and DHA occurs, during the third trimester and another threefold increase between birth and postnatal week 12 (2–4). AA and DHA are selectively transferred to the fetus by the placenta from maternal circulation *in utero* and supplied in maternal milk postnatally (5).

In longitudinal studies, a decrease in the relative amounts of plasma AA and DHA has been reported in plasma total phospholipids of British, Dutch, Hungarian, and Ecuadorian (6) and Dutch (7) pregnant women. Differences in plasma phospholipid DHA levels between lactating and nonlactating mothers and a decline in plasma DHA with lactation have been observed (8). Al *et al.* (9) have found that the DHA content of maternal plasma phospholipids is significantly lower in multigravidae and neonates compared with primagravidae and their babies. Similarly, Prentice *et al.* (10) have reported a marked reduction in the proportions of endogenous fatty acids in breast milk of Gambian mothers of very high parity. These studies indicate that pregnancy, parity, and lactation deplete maternal AA and DHA stores.

There are no comprehensive data that compare the essential fatty acid status of pregnant and nonpregnant, nonlactating women. Hence, the extent of metabolic adjustment and the consequential changes in blood AA and DHA levels that may occur during the transition from nonpregnancy to pregnancy are not apparent. We have studied plasma and red blood cell (RBC) fatty acid composition of pregnant, and nonpregnant, nonlactating women from Seoul, South Korea. The aims of the study were to (i) establish if there is a difference in blood fatty acid composition between pregnant and nonpregnant women who are ethnically homogenous and (ii) explore whether the fatty acid composition of plasma and RBC phospholipids, and RBC phospholipid classes are differentially influenced by pregnancy.

MATERIALS AND METHODS

Subjects and sample collection. Healthy women with a singleton pregnancy were recruited during the third trimester from the Asan Medical Centre, Seoul, South Korea. Their age range was 23–38 yr and parity 0–2. All the mothers delivered at term and had no health complication during delivery. Nonpregnant, nonlactating healthy women aged 23 to 39 and par-

*To whom correspondence should be addressed at Institute of Brain Chemistry and Human Nutrition, University of North London, 166-222 Holloway Road, London N7 8DB, UK. E-mail: keb@kebgm.demon.co.uk

Abbreviations: AA, arachidonic acid; ALA, α-linolenic acid; BHT, butylated hydroxytoluene; CPG, choline phosphoglyceride; EPA, eicosapentaenoic acid; EPG, ethanolamine phosphoglyceride; DHA, docosahexaenoic acid; DHGLA, dihomo-γ-linolenic acid; DPA, docosapentaenoic acid; DTA, docosatetraenoic acid; FAME, fatty acid methyl ester; LA, linoleic acid; PUFA, polyunsaturated fatty acid; RBC, red blood cell.

TABLE 1
Demographic Data of the Population Groups

	Pregnant Women			Non-pregnant Women		
	n	Mean	Range	*n*	Mean	Range
Age (yr)		29.1	23–38		34.3	23–39
Height (cm)		161.3	150–173			
Pre-pregnancy wt (kg)		52.7	41–70			
BMI[a]		20.1	16.2–28			
Parity						
0	25			10		
1	13			3		
2	2			23		
3				4		
Gestational age (wk)		39.2	37–42			
Birthweight (g)		3179	2390–3965			
Length (cm)		50.3	46.5–54.0			
Head circumference (cm)		33.7	31.5–36.0			
Sex						
Male	23					
Female	17					

[a]BMI, body mass index.

ity 0–3 were also enrolled from the Medical Centre. Demographic data of the population groups are given in Table 1.

Blood samples were collected in EDTA from the pregnant women between pregnancy week 36 and 42, and from the nonpregnant women at recruitment. Plasma and RBC were separated by cold centrifugation at 1000 × *g* for 15 min. After washing the RBC twice with an equal volume of saline (0.85% NaCl), both blood fractions were flushed with nitrogen and stored at –70°C and subsequently transported in dry ice to London for analysis. Ethical approval for the protocol was granted by the Ethics Committee of the Asan Medical Centre, and informed consent was obtained from the participating women. The samples were processed within 2 mon of collection.

Fatty acid analysis. Total plasma and RBC lipid was extracted by the method of Folch *et al.* (11) by homogenizing the samples in chloroform and methanol (2:1 vol/vol) containing 0.01% butylated hydroxytoluene (BHT) as an antioxidant under N_2. Phosphoglyceride classes were separated by thin-layer chromatography on silica gel plates by the use of the developing solvents: chloroform/methanol/water (60:30:4, by vol) containing 0.01% BHT. Bands were detected by spraying with a methanolic solution of 2,7-dichlorofluorescein (0.01% wt/vol) and identified by the use of standards.

Fatty acid methyl esters (FAME) were prepared by heating the lipid fractions with 4 mL of 15% acetyl chloride in methanol in a sealed vial at 70°C for 3 h under N_2. FAME were separated using a gas–liquid chromatograph (HRGC MEGA 2 Series; Fisons Instruments, Milan, Italy) fitted with a BP20 capillary column (25 m × 0.32 mm i.d., 0.25 μm film). Hydrogen was used as a carrier gas; and the injector, oven, and detector temperatures were 250, 200, and 280°C, respectively. The FAME were identified by comparison of retention times with authentic standards and calculation of equivalent chain-length values. Peak areas were quantified by a computer chromatography data system (EZChrom Chromatography Data System; Scientific Software, Inc., San Ramon, CA).

Data analyses. Data are expressed as means ± SD. Unpaired *t*-test was use to compare the difference in plasma and RBC fatty acid composition between the pregnant and nonpregnant women. A statistical package, SPSS for Windows (Release 7; SPSS (UK) Ltd., Woking, Surrey, United Kingdom) was used to analyze the data.

RESULTS

Plasma and RBC choline phosphoglycerides (CPG) and RBC ethanolamine phosphoglycerides (EPG) were analyzed from 40 pregnant and an equal number of nonpregnant, nonlactating women. CPG is the major phospholipid in plasma. CPG and EPG are major phospholipid fractions in RBC membranes, representing the outer and inner leaflet, respectively.

Plasma CPG fatty acid composition. Percentage fatty acid data of plasma CPG are shown in Table 2. Palmitic, palmitoleic, oleic acids, Σsaturates, and Σmonoenes were higher ($P < 0.0001$), and stearate was lower ($P < 0.0001$) in the pregnant compared with the nonpregnant women. Of the n-6 fatty acids, AA was lower ($P = 0.005$), and eicosadienoic (20:2n-6), dihomo-γ-linolenic (DHGLA; 20:3n-6), docosatetraenoic (DTA; 22:4n-6) and docosapentaenoic (DPA; 22:5n-6) acids were higher in the pregnant women ($P < 0.0001$). There was no difference in the mean proportion of linoleic acid (LA) between the two groups ($P > 0.05$). Eicosapentaenoic (EPA; 20:5n-3), DPA (22:5n-3), docosahexaenoic (DHA; 22:6n-3) acids and Σn-3 were lower ($P < 0.0001$), and α-linolenic acid (ALA) was higher ($P = 0.002$) in the pregnant as compared to the nonpregnant women. The level of Mead acid (20:3n-9) was significantly elevated in the pregnant women ($P = 0.004$).

RBC CPG fatty acid composition. Mean fatty acid composition of RBC CPG is given in Table 3. Similar to the plasma CPG, the percentage levels of palmitic, palmitoleic, oleic acids, and Σ monoenes were higher, and stearic acid was

TABLE 2
Mean Percentage Fatty Acid Composition of Plasma Choline Phosphoglycerides of Pregnant and Nonpregnant Korean Women[a]

Fatty acids	Pregnant (n = 40)	Nonpregnant (n = 40)	P value
16:0	33.96 ± 1.7	28.12 ± 1.3	<0.0001
18:0	10.44 ± 1.43	13.79 ± 1.1	<0.0001
20:0	0.04 ± 0.01	0.06 ± 0.01	<0.0001
22:0	Trace	Trace	—
24:0	Trace	Trace	—
Σ Saturates	44.45 ± 1.41	41.98 ± 1.04	<0.0001
16:1n-7	1.37 ± 0.44	0.68 ± 0.2	<0.0001
18:1n-9	10.39 ± 1.3	9.17 ± 0.81	<0.0001
20:1n-9	0.12 ± 0.04	0.13 ± 0.05	NS
22:1n-9	Trace	Trace	—
24:1n-9	0.04 ± 0.02	Trace	—
Σ Monenes	11.96 ± 1.61	9.97 ± 0.92	<0.0001
18:2n-6	20.15 ± 4.14	21.16 ± 2.51	NS
20:2n-6	0.48 ± 0.07	0.37 ± 0.09	<0.0001
20:3n-6	3.70 ± 0.96	2.73 ± 0.60	<0.0001
20:4n-6	7.98 ± 2.2	9.20 ± 1.40	=0.005
22:4n-6	0.31 ± 0.10	0.22 ± 0.07	<0.0001
22:5n-6	0.73 ± 0.41	0.18 ± 0.07	<0.0001
Σ n-6	33.30 ± 2.28	33.87 ± 2.37	NS
18:3n-3	0.32 ± 0.14	0.22 ± 0.13	=0.002
20:5n-3	0.73 ± 0.30	2.20 ± 1.10	<0.0001
22:5n-3	0.65 ± 0.20	1.16 ± 0.26	<0.0001
22:6n-3	5.34 ± 0.98	7.48 ± 1.11	<0.0001
Σ n-3	7.02 ± 1.23	10.98 ± 2.20	<0.0001
20:3n-9	0.15 ± 0.13	0.07 ± 0.05	=0.004

[a]NS, not significant.

TABLE 3
Mean Percentage Fatty Acid Composition of Red Blood Cell Choline Phosphoglycerides of Pregnant and Nonpregnant Korean Women[a]

Fatty acids	Pregnant (n = 40)	Nonpregnant (n = 40)	P value
16:0	31.07 ± 5.34	27.81 ± 2.21	=0.001
18:0	17.00 ± 2.21	19.97 ± 1.02	<0.0001
20:0	0.12 ± 0.03	0.11 ± 0.01	NS
22:0	0.23 ± 0.11	0.17 ± 0.10	=0.032
24:0	0.72 ± 0.34	0.49 ± 0.31	=0.003
Σ Saturates	49.70 ± 4.01	48.85 ± 2.01	NS
16:1n-7	1.11 ± 0.53	0.53 ± 0.12	<0.0001
18:1n-9	13.76 ± 2.47	12.33 ± 1.12	=0.002
20:1n-9	0.25 ± 0.12	0.25 ± 0.12	NS
22:1n-9	Trace	Trace	—
24:1n-9	0.50 ± 0.20	0.33 ± 0.20	=0.001
Σ Monenes	15.59 ± 3.09	13.36 ± 1.30	<0.0001
18:2n-6	14.34 ± 2.58	14.07 ± 1.43	NS
20:2n-6	0.46 ± 0.09	0.38 ± 0.05	<0.0001
20:3n-6	2.07 ± 0.59	1.49 ± 0.28	<0.0001
20:4n-6	8.06 ± 2.11	9.11 ± 1.41	<0.05
22:4n-6	0.73 ± 0.37	0.66 ± 0.18	NS
22:5n-6	0.47 ± 0.25	0.96 ± 0.54	<0.0001
Σ n-6	26.14 ± 5.10	26.74 ± 1.94	NS
18:3n-3	0.20 ± 0.07	0.13 ± 0.06	<0.0001
20:5n-3	0.40 ± 0.18	0.91 ± 0.44	<0.0001
22:5n-3	0.92 ± 0.34	1.17 ± 0.27	=0.001
22:6n-3	4.79 ± 2.12	5.97 ± 1.49	=0.006
Σ n-3	6.22 ± 2.68	8.19 ± 2.01	=0.001
20:3n-9	0.07 ± 0.05	0.06 ± 0.03	NS

[a]NS, not significant.

lower ($P < 0.01$) in the RBC CPG of the pregnant women compared with that of the nonpregnant group. The proportions of eicosadienoic acid (20:2n-6) and DHGLA were higher ($P < 0.0001$), AA ($P < 0.05$), and DPA (22:5n-6) lower ($P < 0.0001$) in the RBC CPG of the pregnant women. In contrast to the plasma CPG, there was no difference in the level of DTA (22:4n-6) in RBC CPG of the two groups. Total n-3 fatty acids, EPA, DPA (22:5n-3), and DHA were reduced ($P < 0.01$) and ALA increased ($P < 0.0001$) in the RBC CPG of the pregnant women compared with the nonpregnant group. There was no difference in the level of Mead acid between the two groups ($P > 0.05$).

RBC EPG fatty acid composition. Consistent with the pattern in the plasma and RBC CPG, the RBC EPG of the pregnant women had elevated levels of palmitic and palmitoleic acids, total saturates and monoenes ($P < 0.0001$) in comparison with the RBC EPG of the nonpregnant, nonlactating women. In contrast to saturates and monoenes, the proportions of AA, DTA (22:4n-6), DPA (22:5n-6), total n-6 fatty acids, EPA, DPA (22:5n-3), DHA and total n-3 fatty acids were higher ($P < 0.05$) in the nonpregnant group. The parent n-6 and n-3 fatty acids, LA ($P = 0.002$) and ALA ($P = 0.001$) were higher in the pregnant women. Compared to the pregnant women, the nonpregnant group had higher levels of Mead acid ($P < 0.0001$). Data of the fatty acid composition of RBC EPG are shown in Table 4.

DISCUSSION

The present plasma and RBC fatty acid data of pregnant and nonpregnant women of the same ethnic origin and comparable age and parity provided comprehensive information on the changes in fatty acid metabolism which may occur as a consequence of pregnancy.

The results demonstrate a striking difference in the relative composition of blood fatty acids between the pregnant and the nonpregnant, nonlactating women. The pregnant women did not report a change in dietary habits as a result of their pregnancy. Their response was consistent with the classical longitudinal study covering 20 yr (12) which demonstrated that women change diets very little on becoming pregnant. Hence, the observed difference in fatty acid status, as assessed by a relative percentage, between the two groups of women appears to be primarily a reflection of a shift in metabolism in response to the demands of pregnancy.

There were contrasting levels of saturated, monounsaturated, n-6 and n-3 fatty acids in the phospholipid classes in the pregnant and nonpregnant women. Palmitic, palmitoleic, stearic, oleic acids, total saturates and monoenes followed a similar trend in the plasma and RBC CPG during the transition from nonpregnancy to pregnancy. The RBC EPG differed from plasma and red cell RBC in that the level of stearic acid was lower in the pregnant compared with the nonpregnant

TABLE 4
Mean Percentage Fatty Acid Composition of Red Cell Ethanolamine Phosphoglycerides of Pregnant and Nonpregnant Korean Women[a]

Fatty acids	Pregnant (n = 40)	Nonpregnant (n = 40)	P value
16:0	21.50 ± 4.63	16.80 ± 4.63	<0.0001
18:0	7.77 ± 2.60	7.26 ± 1.16	NS
20:0	0.10 ± 0.07	0.07 ± 0.07	NS
22:0	0.08 ± 0.06	0.09 ± 0.08	NS
24:0	0.22 ± 0.24	0.14 ± 0.06	NS
Σ Saturates	29.83 ± 7.09	24.45 ± 3.39	<0.0001
16:1n-7	0.66 ± 0.23	0.35 ± 0.07	<0.0001
18:1n-9	18.01 ± 3.95	14.17 ± 1.82	<0.0001
20:1n-9	0.31 ± 0.14	0.40 ± 0.98	NS
22:1n-9	0.09 ± 0.03	0.02 ± 0.01	NS
24:1n-9	0.28 ± 0.21	0.10 ± 0.05	<0.0001
Σ Monenes	19.14 ± 2.0	14.92 ± 3.28	<0.0001
18:2n-6	5.23 ± 0.89	4.63 ± 0.75	=0.002
20:2n-6	0.38 ± 0.14	0.36 ± 0.06	NS
20:3n-6	0.95 ± 0.28	0.88 ± 0.20	NS
20:4n-6	12.47 ± 3.47	17.14 ± 2.13	<0.0001
22:4n-6	3.22 ± 1.0	3.82 ± 0.85	=0.022
22:5n-6	0.64 ± 0.34	1.52 ± 1.11	<0.0001
Σ n-6	22.90 ± 5.06	28.36 ± 2.76	<0.0001
18:3n-3	0.26 ± 0.09	0.18 ± 0.09	=0.001
20:5n-3	0.88 ± 0.39	2.03 ± 0.77	<0.0001
22:5n-3	2.27 ± 1.0	3.23 ± 0.65	<0.0001
22:6n-3	8.27 ± 2.92	9.42 ± 1.85	<0.05
Σ n-3	11.68 ± 4.12	14.85 ± 3.03	<0.0001
20:3n-9	0.13 ± 0.13	0.59 ± 0.16	<0.0001

[a]NS, not significant.

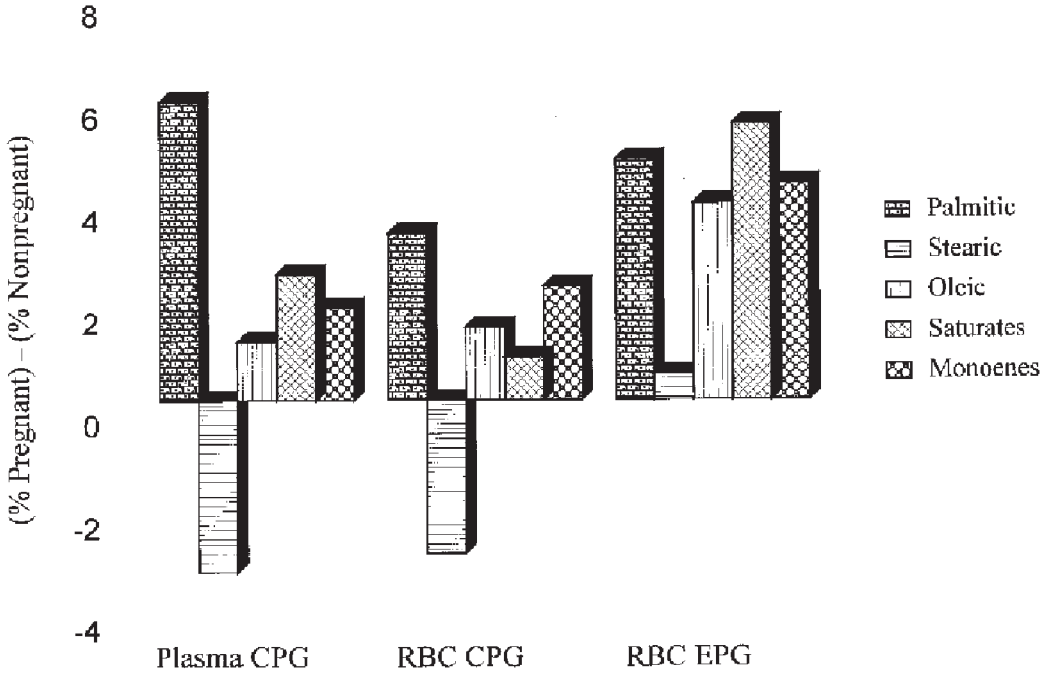

FIG. 1. Percentage difference in saturated and monounsaturated fatty acids of pregnant compared to nonpregnant women. CPG, choline phosphoglyceride; RBC, red blood cell; EPG, ethanolamine phosphoglyceride.

women (Fig. 1). In contrast, pregnancy was characterized by a decrease in the relative amounts of the major n-3 fatty acids with the exception of ALA in plasma CPG, and RBC CPG and EPG (Fig. 2). The pregnant women had lower levels of AA in plasma CPG and RBC CPG and EPG, and total n-6 in RBC EPG; however, they had higher DHGLA in plasma and RBC CPG and LA in RBC EPG (Fig. 3). A decline in the n-3 fatty acids in plasma CPG of the pregnant women was marked by a

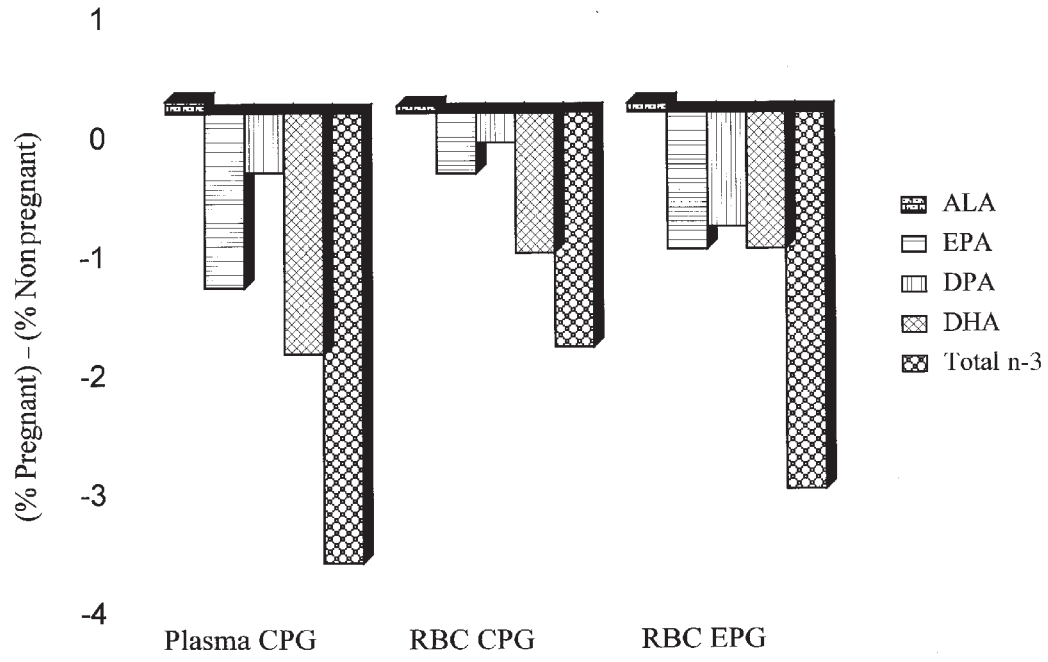

FIG. 2. Percentage difference in α-linolenic (ALA), eicosapentaenoic (EPA), docosapentaenoic (DPA), docosahexaenoic (DHA), and total n-3 fatty acids of pregnant compared to nonpregnant women. For other abbreviations see Figure 1.

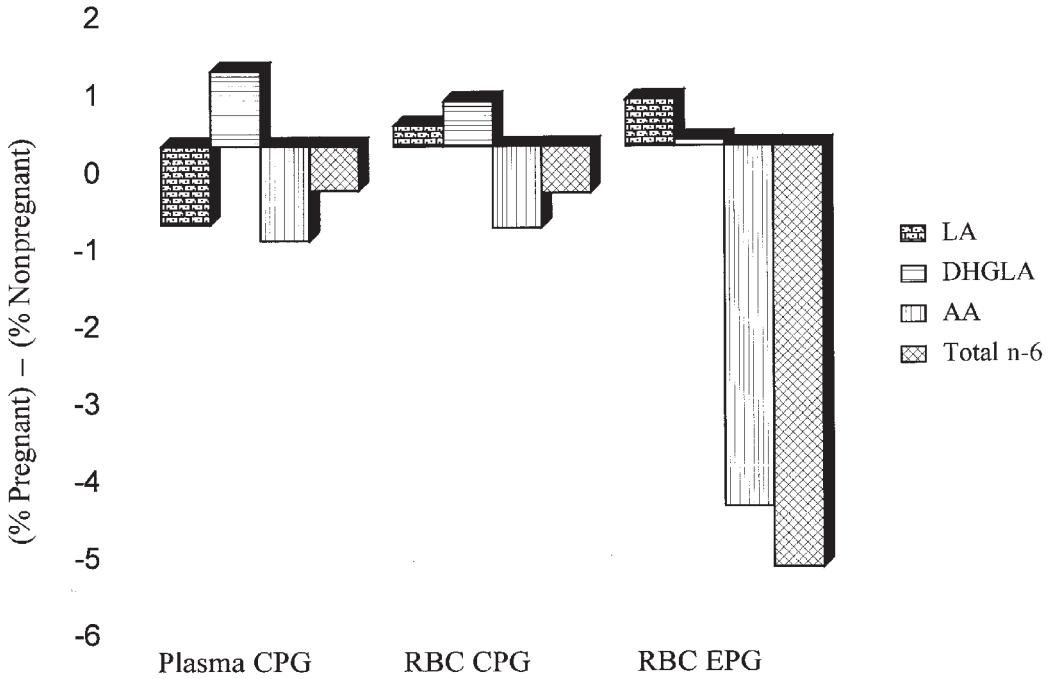

FIG. 3. Percentage difference in linoleic (LA), dihomo-γ-linolenic (DHGLA), arachidonic (AA), and total n-6 fatty acids of pregnant compared to nonpregnant women. For other abbreviations see Figure 1.

corresponding increase in the incorporation of DTA and DPA of the n-6 series. DPA/DTA ratio, a biochemical indicator of DHA deficiency (13), was also significantly higher in plasma CPG of the pregnant women (2.4 vs. 0.82, $P < 0.0001$). Surprisingly, in spite of the significant reduction in total n-3 fatty acids, DHA, DPA (22:5n-3), and EPA in RBC of the pregnant women, there was no concomitant increase in the incorporation of DPA of the n-6 series or DPA/DTA ratio. Indeed, the DPA/DTA ratio was higher in RBC CPG (1.5 vs. 0.62, $P < 0.0001$) and EPG (0.41 vs. 0.19, $P < 0.0001$) of the nonpregnant women. This may have been due to the transfer of maternal RBC DPA (22:5n-6) to the fetus to meet the enhanced fetal requirement for DHA. There is some indication to support this conceivable explanation. In the small number (six cases) of cord blood collected from the group, the level of DPA was three times higher in the RBC of the neonates compared to the mothers.

Predictably, in response to the lower levels of AA, DHA, and total n-3 fatty acids, there was a higher proportion of Mead acid in plasma CPG of the pregnant women (Table 2). A similar pattern was not apparent in RBC CPG and EPG (Tables 3 and 4). This incongruity suggests the two blood components (plasma and RBC) respond differently to an "insufficiency" of AA and DHA during pregnancy. As is the case with AA and DHA, there may be a decline in the proportion of Mead acid in RBC of pregnant women. This could be due to reduced incorporation or to mobilization and transfer to the fetus. Indeed, the presence of an appreciable proportion of Mead acid in cord blood (Ghebremeskel, K., and Crawford, M.A., unpublished data) indicates that it may be transferred from the mother to the fetus to compensate for the shortage of n-6 and n-3 long-chain polyunsaturated fatty acids (PUFA). In contrast to our results, Holman *et al.* (14) did not find an increase in Mead acid in plasma total phospholipids during pregnancy. The authors suggested that deficiency of n-6 and n-3 PUFA in pregnancy is distinct from a simple nutritional deficiency of essential fatty acids and may not lead to an increase in the level of Mead acid.

Al *et al.* (7) have shown an initial increase and subsequent decline in plasma phospholipid DHA during pregnancy. Similarly, Otto *et al.* (6) have reported a decline in relative amounts of plasma phospholipid AA and DHA in pregnancy. Sanjurjo *et al.* (15) have found notable difference in the levels of some fatty acids in plasma total lipids of pregnant and nonpregnant women. Our plasma CPG data are consistent with the above findings. Significantly, the results also show that RBC of the pregnant women have reduced levels of these two vital nutrients. Since AA and DHA are not oxidized in preference to either palmitic acid, LA, α-ALA, or monounsaturates (16), it is not clear why the percentage levels of AA and DHA in RBC CPG and EPG were lower in the pregnant women. There is a suggestion that RBC may be involved in the transfer of glucose (17) and amino acids (18). Moreover, it has been postulated (19) that fetal erythrocytes play an important role in the transport of essential fatty acids to the developing tissue. If this is the case, maternal erythrocyte may play a role as a potential store of the long-chain PUFA, AA and DHA and as a vehicle for the transport of these nutrients to the placenta.

To our knowledge, there are no published studies that have investigated the role of maternal RBC as a source of PUFA to

the fetus. RBC have particular advantages as a potential store and delivery vehicle for AA and DHA. Primarily, they are relatively rich in AA and DHA and can enrich themselves through dynamic interaction with the plasma environment. Secondarily, RBC will be able to transport PUFA to the placenta without the involvement of mediators. In contrast, plasma fatty acid transport is a complex process of modeling and remodeling, which involves transport proteins and several enzymes.

Is the lower relative amount of AA and DHA in plasma CPG and RBC CPG and EPG of the pregnant women a physiological response to pregnancy or a reflection of the depletion of maternal AA and DHA stores due to the demand for these nutrients by the developing fetus? If it is the latter, it should be possible to forestall the depletion by raising maternal status before or during pregnancy. Indeed, studies demonstrate that maternal and neonatal DHA status can be enhanced by administration of fish oil (20) and sardines and fish oil (21) sources of DHA, during pregnancy.

It has been claimed that a low level of AA in cord plasma and umbilical artery is associated with low birth weight (22–24); and cord plasma levels of both AA and DHA are positively correlated with head circumference (24,25). Biochemical signs of essential fatty acid deficiency have been reported in the endothelium and umbilical arteries of low birthweight babies with reduced synthesis of prostacyclin by the umbilical endothelium (26). These studies suggest that an imbalance between maternal supply and fetal demand for AA and DHA during the prenatal period may impair development.

Healthy women may have some restricted ability of mobilizing AA and DHA in order to meet the high demand of pregnancy for these fatty acids. However, regardless of this ability of mobilization, the requirement for AA and DHA is unlikely to be met if the mothers had low status prior to their pregnancy, and/or impairment of PUFA metabolism. Women from some developing countries where the first pregnancy occurs at a very young age followed by successive pregnancies at short intervals also may not be able to provide AA and DHA required for optimal fetal development.

ACKNOWLEDGMENTS

The financial support of The Royal Society, Mother and Child Foundation, and The Christopher H.R. Reeves Charitable Trust is gratefully acknowledged. We thank all the women who participated in the study.

REFERENCES

1. Connor, W.E., and Neuringer, M. (1987) Importance of Dietary Omega-3 Fatty Acids in Retinal Function and Brain Chemistry, in *Nutritional Modulation of Neural Function* (Morley, J.E., Walsh, J.H., and Sterman, M.B., eds.), UCLA Forum in Medical Sciences series, Number 28, pp. 191–201, Academic Press, New York.
2. Clandinin, M.T., Chappell, J.E., Leong, S., Heim, T., Swyer, P.R., and Chance, G.W. (1980) Intrauterine Fatty Acid Accretion Rates in Human Brain: Implications for Fatty Acid Requirements, *Early Hum. Dev. 4*, 121–129.
3. Clandinin, M.T., Chappell, J.E., Leong, S., Heim, T., Swyer, P.R., and Chance, G.W. (1980) Extrauterine Fatty Acid Accretion in Infant Brain: Implications for Fatty Acid Requirements, *Early Hum. Dev. 4*, 131–138.
4. Martinez, M., Conde, C., and Ballabriga, A. (1974) Some Chemical Aspects of Human Brain Development. II. Phosphoglyceride Fatty Acids, *Pediatr. Res. 8*, 93–102.
5. Crawford, M.A., Hall, B., Laurance, B.M., and Nunhambo, A. (1976) Milk Lipids and Their Variability, *Curr. Med. Res. Opin. 4* (Suppl. 1), 33–43.
6. Otto, S.J., Houwelingen, A.C. van, Antal, M., Manninen, A., Godfrey, K., López-Jaramillo, P., and Hornstra, G. (1997) Maternal and Neonatal Essential Fatty Acid Status in Phospholipids: An International Comparative Study, *Eur. J. Clin. Nutr. 51*, 232–242.
7. Al, M.D.M., Houwelingen, A.C. van, Kester, A.D.M., Hasaart, T.H.M., Jong, A.E.P. de., and Hornstra, G. (1995) Maternal Essential Fatty Acid Pattern During Normal Pregnancy and Their Relationship to Neonatal Essential Fatty Acid Status, *Br. J. Nutr. 74*, 55–68.
8. Otto, S.J., Houwelingen, A.C. van, Badart-Smook, A., and Hornstra, G. (1998) The Postpartum Docosahexaenoic Acid Status of Lactating and Nonlactating Mothers, *Lipids 34* (Suppl), S227 (1999).
9. Al, M.D.M., Houwelingen, A.C. van, and Hornstra, G. (1997) Relation Between Birth Order and the Maternal and Neonatal Docosahexaenoic Acid Status, *Eur. J. Clin. Nutr. 51*, 548–553.
10. Prentice, A., Landing, M.A.J., Patrick, J.D., Odile, D., and Crawford, M.A. (1989) Breast-Milk Fatty Acids of Rural Gambian Mothers: Effects of Diet and Maternal Parity, *J. Pediatr. Gastroenterol Nutr. 8*, 486–490.
11. Folch, J., Lees, M., and Sloane-Stanley, G.H. (1957) A Simple Method for the Isolation and Purification of Total Lipids from Animal Tissue, *J. Biol. Chem. 226*, 497–507.
12. Beal, V.A. (1970) Nutritional Studies During Pregnancy, *J. Am. Diet. Assoc. 58*, 312–320.
13. Holman, R.T. (1986) Control of Polyunsaturated Fatty Acids in Tissue of Lipids, *J. Coll. Nutr. 5*, 183–211.
14. Holman, R.T., Johnson, S.B., and Ogburn, P.L (1991) Deficiency of Essential Fatty Acids and Membrane Fluidity During Pregnancy and Lactation, *Proc. Natl. Acad. Sci. USA 88*, 4835–4839.
15. Sanjurjo, P., Matorras, R., Ingunza, N., Alonso, M., Rodriguez-Alarcon, J., and Peteagudo, L. (1993) Cross-Sectional Study of Percentual Changes in Total Plasmatic Fatty Acids During Pregnancy, *Horm. Metab. Res. 25*, 590–593.
16. Leyton, J., Drury, P.J., and Crawford, M.A. (1987) Differential Oxidation of Saturated and Unsaturated Fatty Acids *in vivo* in the Rat, *Br. J. Nutr. 57*, 383–393.
17. Jacquez, J.A. (1984) Red Blood Cell Membrane as Glucose Carrier: Significance for Placental and Cerebral Glucose, *Am. J. Physiol. 246*, R289–R298.
18. Tunnicliff, G. (1994) Amino Acid Transport by Human Erythrocyte Membranes, *Comp. Biochem. Physiol. 108*, 471–478.
19. Ruyle, M., Connor, W.E., Anderson, G.J., and Lowensohn, R.I. (1990) Placental Transfer of Essential Fatty Acids in Humans. Venous-Arterial Difference for Docosahexaenoic Acid in Fetal Umbilical Erythrocytes, *Proc. Natl. Acad. Sci. USA 87*, 7902–7906.
20. Houwelingen, A.C. van, Sørensen, J.D., Hornstra, G., Simonis, M.M.G., Boris, J., Olsen, S.F., and Secher, N.J. (1995) Essential Fatty Acid Status in Neonates After Fish-Oil Supplementation During Late Pregnancy, *Br. J. Nutr. 74*, 723–731.
21. Connor, W.E., Lowensohn, R., and Hatcher, L. (1996) Increased Docosahexaenoic Acid Levels in Human Newborn Infants by Administration of Sardines and Fish Oils During Pregnancy, *Lipids 31*, S183–S187.

22. Crawford, M.A., Doyle, W., Drury, P.J., Lennon, A., Costeloe, K., and Leighfield, M.J. (1989) n-6 and n-3 Fatty Acids During Early Human Development, *J. Intern. Med. 225* (Suppl. 1), 159–169.
23. Crawford, M.A., Costeloe, K., Doyle, W., Leighfield, M.J., Lennon, A., and Meadows, N.A. (1990) Potential Diagnostic Value of the Umbilical Artery as a Definition of Neural Fatty Acid Status During Its Growth, *Biochem. Soc. Trans. 18*, 761–766.
24. Leaf, A., Leighfield, M.J., Costeloe, K., and Crawford, M.A. (1992) Factors Affecting Long-Chain Polyunsaturated Fatty Acid Composition of Plasma Choline Phosphoglycerides in Preterm Infants, *J. Pediatr. Gastroenterol. Nutr. 14*, 300–308.
25. Leaf, A., Leighfield, M.J., Costeloe, K., and Crawford, M.A. (1992) Long-Chain Polyunsaturated Fatty Acids and Fetal Growth, *Early Hum. Dev. 30*, 183–191.
26. Ongari, M.A., Ritter, J.M., Orchard, M.A., Waddell, K.A., Blair, L.A., and Lewis, P.J. (1984) Correlation of Prostacyclin Synthesis by Human Umbilical Artery with Status of Essential Fatty Acid, *Am. J. Obstet. Gynecol. 149*, 455–460.

[Received July 27, 1999, and in final revised form April 10, 2000; revision accepted April 17, 2000]

Simultaneous Derivatization of Acyl and *S*-Alkyl Moieties of Acyl Thioesters by Using Trimethylsulfonium Hydroxide for Gas Chromatographic Analysis

Erika Klein and Nikolaus Weber*

Institut für Biochemie und Technologie der Fette, Bundesanstalt für Getreide-, Kartoffel- und Fettforschung, 48147 Münster, Germany

ABSTRACT: The reaction of long-chain acyl thioesters, *viz.* lauric acid dodecyl thioester, 1,8-di-*S*-palmitoyl octanedithiol, and tristearoyl α-monothioglycerol, with trimethylsulfonium hydroxide in the presence of methanol leads to simultaneous derivatization of acyl moieties and *S*-alkyl moieties of acyl thioesters to the corresponding fatty acid methyl esters and methyl alkylsulfides, respectively. These derivatized products were analyzed by gas chromatographic technique.

Paper no. L8374 in *Lipids 35*, 575–577 (May 2000).

The preparation of methylthio derivatives by the treatment of thiol groups of compounds with trimethylsulfonium hydroxide (TMSH) in the presence of methanol is well known (1). Very recently we demonstrated that TMSH is also useful for derivatization of thiol compounds to the corresponding methyl alkylsulfides for gas chromatography (GC) analysis (2).

Base-catalyzed transesterification of *O*-acyl lipids with methanol in the presence of TMSH is a convenient method for the preparation of fatty acid methyl esters for GC analyses (3–5). So far, this method has not been applied to the transesterification of *S*-acyl lipids (lipid thioesters), which are common constituents of microorganisms, plants, and animals (6).

In this paper, we describe the analysis of acyl and *S*-alkyl moieties of long-chain acyl thioesters by GC after derivatization with TMSH reagent. This method allowed simultaneous derivatization of both acyl and *S*-alkyl moieties of acyl thioesters. In contrast, acid- and alkali-catalyzed transmethylations, which are commonly used for the derivatization of acyl thioesters (6), yield fatty acid methyl esters and alkane thiols. The latter easily form thiyl radicals which are able to attack >C=C< double bonds, finally leading to *cis/trans*-isomerization of, e.g., unsaturated fatty acids (7,8).

EXPERIMENTAL PROCEDURES

Chemicals. 1-Dodecanethiol, 1,8-octanedithiol, and α-monothioglycerol (3-mercapto-1,2-propanediol) as well as lauric acid were purchased from Sigma-Aldrich-Fluka (Deisenhofen, Germany). Palmitoyl and stearoyl chlorides were purchased from Nu-Chek-Prep (Elysian, MN). TMSH reagent (0.2 M TMSH in methanol) was a product of Macherey-Nagel (Düren, Germany).

Preparation of standards. Methyl sulfide derivatives were prepared by the reaction of thiol compounds with TMSH (1,2) or diazomethane (2). Lauric acid was thioesterified with 1-dodecanethiol in the presence of immobilized lipase Novozym 435® (Novo Nordisk, Bagsvaerd, Denmark); the lauric acid dodecyl thioester was separated from the reaction mixture as described recently (9,10). 1,8-Di-*S*-palmitoyl octanedithiol was synthesized by the reaction of palmitoyl chloride with 1,8-octadecanedithiol in pyridine (11). Similarly, tristearoyl α-monothioglycerol was prepared by reacting α-monothioglycerol with stearoyl chloride. After stirring for 24 h at room temperature, water was added to the reaction mixture and thioester compounds were extracted with isohexane. The extract was washed with water, dried, and concentrated. Lauric acid dodecyl thioester was finally purified by preparative thin-layer chromatography (TLC) on 0.5-mm layers of Silica Gel H (E. Merck, Darmstadt, Germany) using isohexane/diethyl ether (99:1, vol/vol) as the developing solvent. In the case of 1,8-di-*S*-palmitoyl octanedithiol and tristearoyl α-monothioglycerol isohexane/diethyl ether (80:20, vol/vol) was used as the solvent system. Bands were located by slight iodine staining, scraped off the plates; and acyl thioesters were eluted from the adsorbent with water-saturated diethyl ether. Purity of the isolated compounds was checked by GC (9,10) and/or TLC.

Derivatization for GC. Under standard conditions, 20 μL TMSH reagent was added to 1 μmol thioester compound (molar ratio TMSH/thioester equivalent = around 4:1) in 40 μL methyl *t*-butyl ether. The derivatization mixtures were concentrated in a stream of nitrogen at 40°C to 20–40 μL and then reacted in closed screw-capped Teflon-lined 1-mL autosampler vials at 120°C in a heating block for 3 min. The reaction mixtures were cooled to room temperature, and dimethylsulfide was removed under a stream of nitrogen. The samples were dissolved in 20 μL methyl *t*-butyl ether and 1–2 μL of these solutions were injected into the gas chromatograph.

*To whom correspondence should be addressed at the Institut für Biochemie und Technologie der Fette, Bundesanstalt für Getreide-, Kartoffel- und Fettforschung, Piusallee 68, 48147 Münster, Germany.
E-mail: ibtfett@uni-muenster.de

Abbreviations: GC, gas chromatography; TLC, thin-layer chromatography; TMSH, trimethylsulfonium hydroxide.

GC. These derivatized products of long-chain acyl thioesters, i.e., fatty acid methyl esters as well as methyl dodecylsulfide or 1,8-di-*S*-methyl octanedithiol or 1-*S*-methyl α-monothioglycerol were analyzed by GC on a Hewlett-Packard (Böblingen, Germany) HP-5890 Series II instrument equipped with a flame-ionization detector. Separations were carried out on a 0.2-μm DB-23 fused-silica capillary column (J&W Scientific, Folsom, CA), 40 m × 0.18 mm i.d., using hydrogen as the carrier gas (column pressure 140 kPa; linear velocity 31 cm · s^{-1}) initially at 160°C for 2 min, followed by linear programming from 160 to 180°C at 2°C · min^{-1}. The final temperature was kept constant for 10 min. The split ratio was 1:10, the injector as well as flame-ionization detector temperature was 250°C. Peaks in gas chromatograms were identified by comparison of their retention times with those of authentic standards (2,9). Peak areas and percentages were calculated using Hewlett-Packard GC ChemStation software.

RESULTS AND DISCUSSION

Base-catalyzed transesterification of *O*-acyl lipids using TMSH in the presence of methanol is a convenient method for the preparation of fatty acid methyl esters for GC analyses (3–5). *S*-Acyl lipids such as long-chain acyl thioesters are generally derivatized by acid- or alkali-catalyzed transmethylation leading to fatty acid methyl esters and alkanethiols (6). We have studied the reaction of a 0.2 M TMSH solution in methanol (TMSH reagent) for its use as derivatization reagent for very different long-chain acyl thioester compounds.

Figure 1 shows the gas chromatogram of lauric acid dodecyl thioester after derivatization with TMSH reagent. The peaks in Figure 1 match the retention times of known standards, showing that this thioester compound was converted to methyl laurate and methyl dodecylsulfide according to Scheme 1.

Figure 2 shows the GC separation of the products of the reaction of 1,8-di-*S*-palmitoyl-octanedithiol with TMSH reagent (Scheme 1). As expected the derivatization products, i.e., methyl palmitate and 1,8-di-*S*-methyl octanedithiol, were in a ratio of about 2:1.

GC separation of the derivatization products of tristearoyl

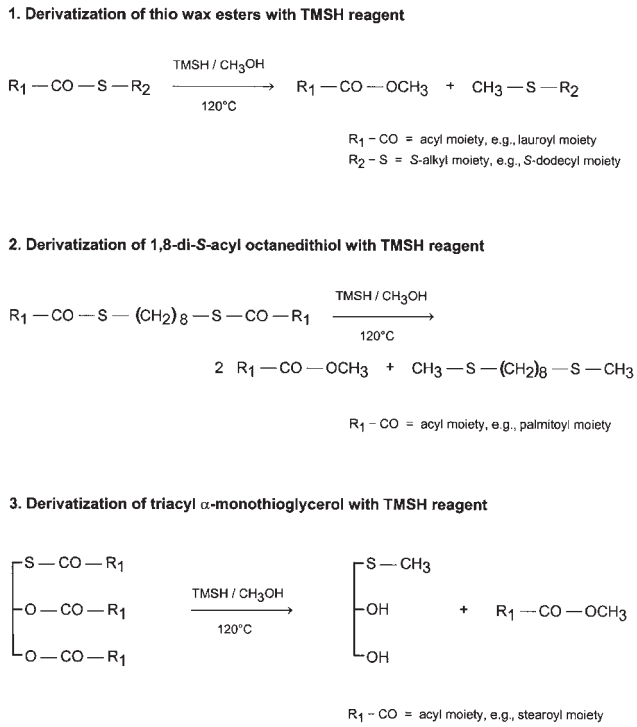

SCHEME 1

α-monothioglycerol with TMSH reagent is shown in Figure 3. The reaction products were identified as methyl stearate and *S*-methyl α-monothioglycerol (Scheme 1).

Triradyl sulfonium compounds such as TMSH are involved in very different types of chemical reactions (1,3,12–14). The first is base-catalyzed transesterification of acyl lipids using methanolic TMSH solutions, which transmethylate acyl lipids to the corresponding fatty acid methyl esters (3–5). The second type is a nucleophilic substitution reaction of TMSH leading to the methylation of nucleophiles including thiol compounds (1,2,14). In addition, pyrolytic methylation reactions of TMSH or similar thermally assisted methylation reactions, which have been described for tetramethylammonium hydroxide, may also be involved in *S*-methylation of thiol compounds (12,15). Both transesterifica-

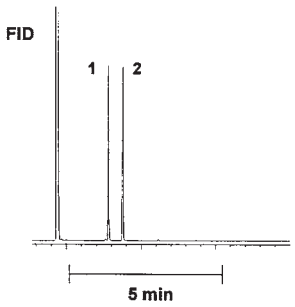

FIG. 1. Gas chromatographic separation of the products of the reaction of lauric acid dodecyl thioester with trimethylsulfonium hydroxide reagent (1, methyl dodecylsulfide; 2, methyl laurate).

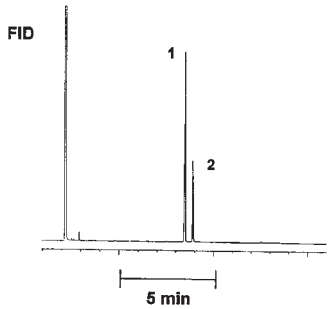

FIG. 2. Gas chromatographic separation of the products of the reaction of 1,8-di-*S*-palmitoyl octanedithiol with trimethylsulfonium hydroxide reagent (1, methyl palmitate; 2, 1,8-di-*S*-methyl octanedithiol).

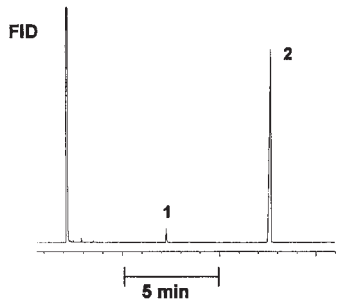

FIG. 3. Gas chromatographic separation of the products of the reaction of tristearoyl α-monothioglycerol with trimethylsulfonium hydroxide reagent (1, S-methyl α-monothioglycerol; 2, methyl stearate).

tion and nucleophilic substitution reactions may be involved in the derivatization of acyl thioesters by TMSH reagent leading to simultaneous derivatization of both acyl moieties and *S*-alkyl (alkylthio) moieties of long-chain acyl thioesters to the corresponding fatty acid methyl esters and methyl alkyl-sulfides, respectively. Thus, derivatization of acyl thioesters using TMSH reagent is advantageous over the usual acid- or alkali-catalyzed transmethylation of acyl thioesters for the analysis by GC.

REFERENCES

1. Yamauchi, K., Tanabe, T., and Kinoshita, M. (1979) Trimethylsulfonium Hydroxide: A New Methylation Agent, *J. Org. Chem. 44*, 638–639.
2. Vosmann, K., Klein, E., and Weber, N. (1998) S-Methyl Derivatives from Thiol Compounds by the Pyrolytic Reaction with Trimethylsulfonium Hydroxide, *Lipids 33*, 1037–1041.
3. Butte, W. (1983) Rapid Method for the Determination of Fatty Acid Profiles from Fats and Oils Using Trialkyl Sulphonium Hydroxide for Transesterification, *J. Chromatogr. 261*, 142–145.
4. Schulte, E. (1993) Gas Chromatography of Acylglycerols and Fatty Acids with Capillary Columns, in *CRC Handbook of Chromatography: Analysis of Lipids* (Mukherjee, K.D., and Weber, N., eds.), pp. 139–148, CRC Press, Boca Raton.
5. El-Hamdy, A.H., and Christie, W.W. (1993) Preparation of Methyl Esters of Fatty Acids with Trimethylsulphonium Hydroxide—an Appraisal, *J. Chromatogr. 630*, 438–441.
6. Taylor, D.C., and Weber, N. (1993) Acyl Coenzyme A Thioesters, in *CRC Handbook of Chromatography: Analysis of Lipids* (Mukherjee, K.D., and Weber, N., eds.) pp. 285–320, CRC Press, Boca Raton.
7. Kircher, H.W. (1964) The Elaidinization of Methyl Oleate with Mercaptans. *J. Am. Oil Chem. Soc. 41*, 351–354.
8. Weber, N., Klein, E., Vosmann, K., and Mukherjee, K.D. (2000) Antioxidants Eliminate Stereomutation and Thioether Formation During Lipase-Catalyzed Thioesterification and Transthioesterification for the Preparation of Uniform *cis*- and *trans*-Unsaturated Thioesters, *Chem. Phys. Lipids 105*, 215–223.
9. Weber, N., Klein, E., and Mukherjee, K.D (1999) Long-Chain Acyl Thioesters by Solvent-free Thioesterification and Transthioesterification Catalysed by Microbial Lipases, *Appl. Microbiol. Biotechnol. 47*, 401–404.
10. Weber, N., Klein, E., and Mukherjee, K.D. (1999) Solvent-free Lipase-Catalyzed Thioesterification and Transthioesterification of Fatty Acids and Fatty Acid Esters with Alkanethiols *in Vacuo*, *J. Am. Oil Chem. Soc. 76*, 1297–1300.
11. Ward, J.P. (1988) Synthesis of Hydroxy Thiol Esters from Glycidol Esters, *Chem. Phys. Lipids 47*, 217–224.
12. Butte, W., Eilers, J., and Kirsch, M. (1982) Trialkylsulfonium and Trialkylselenonium Hydroxides for the Pyrolytic Alkylation of Acidic Compounds, *Anal. Lett. 15A*, 841–850.
13. Buckley, N., Maltby, D., Burlingame, A.L., and Oppenheimer, N.J. (1996) Reactions of Charged Substrates. 4. The Gas-Phase Dissociation of (4-substituted benzyl) Dimethylsulfoniums and -pyridiniums, *J. Org. Chem. 61*, 2753–2762.
14. Yamauchi, K., Nakagima, T., and Kinoshita, M. (1986) Selective 2′-*O*-Methylation of Pyrimidine-Ribonucleosides by Trimethylsulfonium Hydroxide in the Presence of Mg^{2+} and Ca^{2+} Ions, *Bull. Chem. Soc. Jpn. 59*, 2947–2949.
15. Asperger, A., Engewald, W., and Fabian, G. (1999) Advances in the Analysis of Natural Waxes Provided by Thermally Assisted Hydrolysis and Methylation (THM) in Combination with GC/MS, *J. Anal. Appl. Pyrolysis 52*, 51–63.

[Received October 25, 1999, and in revised form March 9, 2000; revision accepted April 17, 2000]

COMMUNICATION

Reinvestigation of Positional Distribution of Fatty Acids in Docosahexaenoic Acid-Rich Fish Oil Triacyl-*sn*-glycerols

Yasuhiro Ando*, Motoi Satake, and Youichi Takahashi

Department of Marine Bioresources Chemistry, Faculty of Fisheries, Hokkaido University, Hakodate 041-8611, Japan

ABSTRACT: Positional distribution of fatty acids in triacyl-*sn*-glycerols of docosahexaenoic acid (DHA)-rich tuna orbital and bonito head oils has been reanalyzed by a method based on chromatographic separation of isomeric and enantiomeric monoacyl-*sn*-glycerol (MAG) derivatives. When boric acid thin-layer chromatography (TLC) was used for separation of 1(3)- and 2-MAG analytical intermediates, the stereospecific analysis showed the preferential association of DHA to the *sn*-2 position followed by the *sn*-3 position. This distribution pattern differed from that obtained by silicic acid TLC of their bis-3,5-dinitrophenylurethane (DNPU) derivatives. Reversed-phase high-performance liquid chromatography elution profiles of 1(3)- and 2-MAG intermediates revealed that 1(3)- and 2-MAG made up of both short- and long-chain lengths cannot be clearly resolved by TLC after preparation of the DNPU derivatives. The 1(3)- and 2-MAG must be resolved by boric acid TLC prior to derivatization.

Paper no. L8390 in *Lipids 35,* 579–582 (May 2000).

A method for stereospecific analysis of triacyl-*sn*-glycerols (TAG) involves chiral high-performance liquid chromatography (HPLC) of 1(3)-monoacyl-*sn*-glycerol (MAG) derivatives formed from TAG (1,2). For preliminary separation of isomeric 1(3)- and 2-MAG analytical intermediates, two procedures of thin-layer chromatography (TLC) were used, i.e., boric acid TLC of free form MAG prior to preparation of bis-3,5-dinitrophenylurethane (DNPU) derivatives (1) and silicic acid TLC after preparation of the derivatives (2). When the latter procedure was used in the analysis of docosahexaenoic acid (DHA)-rich tuna orbital and bonito head oil TAG, a high proportion of DHA was observed in the *sn*-3 position followed by the *sn*-1 position (3). However, many data obtained by other methodologies, such as chiral HPLC of diacyl-*sn*-glycerol derivatives (4), lipase hydrolysis (5,6), and ^{13}C nuclear magnetic resonance spectroscopy (7), showed preferential association of this acid to the *sn*-2 position. The present paper reports that the difference in distribution pattern is attributable to unsuitable TLC separation in the stereospecific analysis. Positional distribution of fatty acids in the same fish oil TAG was reanalyzed by the boric acid TLC procedure. Reversed-phase HPLC profiles of 1(3)- and 2-MAG intermediates were compared between the boric acid and silicic acid TLC separations to clarify which is applicable to analysis of DHA-rich fish oil TAG.

*To whom correspondence should be addressed.
E-mail: ando@pop.fish.hokudai.ac.jp

Abbreviations: DHA, docosahexaenoic acid; DNPU, dinitrophenylurethane; GLC, gas–liquid chromatography; HPLC, high-performance liquid chromatography; MAG, monoacyl-*sn*-glycerols; TAG, triacyl-*sn*-glycerols; TLC, thin-layer chromatography.

EXPERIMENTAL PROCEDURES

Materials. Tuna orbital and bonito head oils had been kept frozen at –30°C for 4 yr under nitrogen atmosphere. TAG were isolated from the other lipids by column chromatography on Silica gel 60 (Merck, Darmstadt, Germany) with *n*-hexane/diethyl ether for elution.

Stereospecific analysis of TAG. The method for stereospecific analysis of fish TAG (1,8) was used without essential modifications as follows. TAG (100 mg), mixed with trinonadecanoylglycerol (5 mg), were dissolved in 3 mL of dry diethyl ether, and ethyl magnesium bromide in dry diethyl ether (0.33 mL of 3 M solution) was added. The mixture was shaken for 1 min, and then 0.1 mL of glacial acetic acid followed by water (3 mL) was added to stop the reaction. The products were extracted with diethyl ether. The ether extract was washed six to seven times with 2% aqueous sodium bicarbonate, then washed with water, and dried over anhydrous sodium sulfate. After removal of the solvent at ambient temperature, resulting 1(3)- and 2-MAG were isolated by preparative TLC on a boric acid-impregnated silica gel plate (20 cm × 20 cm, 0.5 mm thickness, boric acid 10 wt% to Silica gel 60G) developed in chloroform/methanol (98:2, vol/vol) containing 0.002% of butylhydroxytoluene.

About a half of the 1(3)-MAG obtained was dissolved in dry toluene (0.5 mL) and reacted overnight at room temperature with 3,5-dinitrophenylisocyanate (15 mg) in the presence of dry pyridine (50 µL). Resulting bis-3,5-DNPU derivatives of 1(3)-MAG were purified by preparative TLC on a Silica gel 60G plate (0.5 mm thickness) with chloroform/acetone (96:4, vol/vol) for development. The 1(3)-MAG derivatives were resolved into *sn*-1- and *sn*-3-MAG fractions by HPLC with a Hitachi L-6200 pump (Hitachi Co., Tokyo, Japan), a Hitachi L-4200 ultraviolet spectrophotometric detector, and a Shimadzu C-R6A integrator (Shimadzu Co., Kyoto, Japan). Two columns of Sumichiral OA-4100 (25 cm × 4 mm i.d., 5 µm particles; Sumitomo Chemical Co., Osaka, Japan) in se-

ries were used with *n*-hexane/1,2-dichloroethane/ethanol (40:12:3, by vol) as mobile phase at a flow rate of 0.5 mL/min at –10°C. Detection was 254 nm.

Fatty acid methyl esters were prepared by reacting intact TAG, 1(3)-, 2-, *sn*-1-, and *sn*-3-MAG in a mixture of 1,2-dichloroethane (0.6 mL), methyl acetate (25 µL), and 1 M sodium methoxide–methanol solution (25 µL) at room temperature overnight. After adding acetic acid (6 µL) and removing the solvents, the products were taken up in *n*-hexane. Gas–liquid chromatography (GLC) of the methyl esters was performed on a Shimadzu GC-14A gas chromatograph equipped with a flame-ionization detector and an open-tubular column, Omegawax 320 (30 m × 0.32 mm i.d., 0.25 µm film thickness; Supelco Inc., Bellefonte, PA). The column temperature was 200°C, and injector and detector temperatures were 250 and 260°C, respectively. Helium was the carrier gas. Peak area percentages were measured with a Shimadzu C-R6A integrator. Assignments of each fatty acid to the *sn*-1-, *sn*-2-, and *sn*-3-positions of TAG were obtained from the peak area ratio of each fatty acid to 19:0 formed from the trinonadecanoylglycerol internal standard, and the fatty acid composition of each position was calculated on the basis of the assignments.

Reversed-phase HPLC of MAG derivatives. Chromatographic behaviors of the MAG intermediates on boric acid and silicic acid TLC plates were compared by reversed-phase HPLC of their bis-3,5-DNPU derivatives. HPLC was done by the same pump and detection systems described above. A column of Capcellpak C18 UG120-5 (25 cm × 4.6 mm i.d.; Shiseido Co., Tokyo, Japan) was used with acetonitrile and water as mobile phase at a flow rate of 1.0 mL/min. A linear gradient of 70% acetonitrile/30% water (held at this for 5 min) to 100% acetonitrile was generated over 185 min. Column oven temperatures were held at 10°C for 80 min and then immediately changed to 30°C. Samples were injected in 3 µL of 2-propanol.

RESULTS AND DISCUSSION

Table 1 shows the positional distribution of fatty acids in the DHA-rich fish oil TAG examined. In all of the fish oils, DHA was preferentially esterified in the *sn*-2 position, followed by the *sn*-3 position. DHA was low in the *sn*-1 position. When proportional distributions were calculated from the data, 50–52 and 42–43% of DHA were located in the *sn*-2 and *sn*-3 positions, respectively, whereas less than 8% of this acid was

TABLE 1
Positional Distribution of Fatty Acids in Triacyl-*sn*-glycerols of Tuna Orbital and Bonito Head Oils (mol%)

	Tuna orbital oil				Bonito head oil				Bonito head oil			
Fatty acid	Total	*sn*-1	*sn*-2	*sn*-3	Total	*sn*-1	*sn*-2	*sn*-3	Total	*sn*-1	*sn*-2	*sn*-3
14:0	4.1	3.5 ± 0.3[a]	5.8 ± 0.6	2.7 ± 0.4	5.0	4.5 ± 0.5	7.3 ± 0.3	3.0 ± 0.3	3.2	3.8 ± 0.2	3.8 ± 0.3	1.8 ± 0.1
15:0	1.1	1.3 ± 0.0	1.2 ± 0.1	0.6 ± 0.1	1.2	1.6 ± 0.1	1.4 ± 0.1	0.7 ± 0.0	0.8	1.1 ± 0.1	0.8 ± 0.1	0.3 ± 0.0
16:0	21.4	34.2 ± 0.9	18.1 ± 1.5	11.8 ± 1.1	20.6	34.0 ± 0.3	16.1 ± 0.6	10.7 ± 0.4	12.3	22.4 ± 0.3	9.4 ± 0.5	4.6 ± 0.2
16:1n-7	6.4	8.0 ± 0.2	6.1 ± 0.3	5.0 ± 0.4	7.3	9.5 ± 0.4	6.7 ± 0.4	5.6 ± 0.3	7.2	11.0 ± 0.2	5.9 ± 0.4	4.6 ± 0.2
16:1n-5	0.3	0.3 ± 0.0	0.3 ± 0.0	0.2 ± 0.0	0.2	0.3 ± 0.0	0.2 ± 0.0	0.1 ± 0.0	0.2	0.4 ± 0.0	0.2 ± 0.0	0.1 ± 0.0
iso-17:0	0.4	0.4 ± 0.2	0.3 ± 0.0	0.4 ± 0.3	0.3	0.5 ± 0.0	0.3 ± 0.1	0.2 ± 0.1	0.3	0.6 ± 0.1	0.2 ± 0.1	0.1 ± 0.0
16:2n-4	1.9	0.9 ± 0.1	3.1 ± 0.2	1.8 ± 0.1	1.9	0.9 ± 0.1	3.0 ± 0.1	1.9 ± 0.2	1.9	1.2 ± 0.1	2.8 ± 0.1	1.7 ± 0.1
17:0	1.1	2.1 ± 0.0	0.5 ± 0.0	0.6 ± 0.0	1.1	2.1 ± 0.0	0.5 ± 0.1	0.7 ± 0.0	0.5	1.1 ± 0.0	0.2 ± 0.0	0.2 ± 0.0
16:3n-4	0.9	1.1 ± 0.1	0.6 ± 0.0	0.9 ± 0.1	1.0	1.3 ± 0.0	0.7 ± 0.1	0.9 ± 0.0	1.0	1.7 ± 0.1	0.7 ± 0.1	0.8 ± 0.0
18:0	4.4	9.5 ± 0.2	1.2 ± 0.2	2.7 ± 0.1	4.2	8.6 ± 0.3	1.2 ± 0.1	2.4 ± 0.1	1.8	3.8 ± 0.1	0.6 ± 0.2	0.8 ± 0.1
18:1n-9	15.0	19.2 ± 0.5	7.3 ± 0.3	18.8 ± 0.3	13.3	17.4 ± 0.4	6.5 ± 0.4	16.1 ± 0.2	15.8	23.3 ± 0.6	7.0 ± 0.8	16.5 ± 0.3
18:1n-7	2.7	4.3 ± 0.1	1.5 ± 0.0	2.2 ± 0.1	2.5	4.0 ± 0.1	1.3 ± 0.1	2.0 ± 0.1	2.8	5.3 ± 0.3	1.3 ± 0.2	1.7 ± 0.0
18:1n-5	0.2	0.3 ± 0.0	0.2 ± 0.1	0.1 ± 0.0	—[b]	—	—	—	—	—	—	—
18:2n-6	2.3	2.1 ± 0.0	2.4 ± 0.1	2.5 ± 0.1	1.5	1.6 ± 0.1	1.2 ± 0.1	1.8 ± 0.1	2.4	2.6 ± 0.1	2.3 ± 0.2	2.4 ± 0.1
18:2n-4	0.6	0.1 ± 0.2	1.5 ± 0.3	0.1 ± 0.2	0.4	0.1 ± 0.1	1.2 ± 0.2	0.1 ± 0.1	0.3	0.1 ± 0.2	0.7 ± 0.2	0.1 ± 0.1
18:3n-3	0.6	0.5 ± 0.0	0.6 ± 0.0	0.6 ± 0.1	0.6	0.6 ± 0.0	0.6 ± 0.0	0.7 ± 0.0	0.7	0.8 ± 0.0	0.6 ± 0.0	0.7 ± 0.0
18:4n-3	0.8	0.4 ± 0.0	1.2 ± 0.1	0.8 ± 0.0	0.9	0.6 ± 0.0	1.4 ± 0.0	0.8 ± 0.0	1.1	0.8 ± 0.0	1.6 ± 0.1	1.0 ± 0.0
20:1n-11,n-13	0.5	0.4 ± 0.0	0.3 ± 0.0	0.8 ± 0.0	0.3	0.3 ± 0.0	0.2 ± 0.0	0.6 ± 0.0	0.5	0.5 ± 0.2	0.2 ± 0.0	0.6 ± 0.2
20:1n-9	1.0	1.0 ± 0.0	0.4 ± 0.0	1.6 ± 0.1	0.9	0.9 ± 0.1	0.4 ± 0.0	1.4 ± 0.1	1.0	1.2 ± 0.0	0.4 ± 0.1	1.4 ± 0.1
20:2n-6	0.2	0.2 ± 0.0	0.1 ± 0.0	0.3 ± 0.0	0.2	0.2 ± 0.0	0.1 ± 0.0	0.4 ± 0.0	0.2	0.2 ± 0.1	0.2 ± 0.1	0.3 ± 0.1
20:4n-6	1.6	0.6 ± 0.0	2.0 ± 0.1	2.2 ± 0.1	1.9	0.8 ± 0.0	2.3 ± 0.0	2.8 ± 0.1	2.1	1.2 ± 0.1	2.5 ± 0.1	2.8 ± 0.1
20:4n-3	0.4	0.5 ± 0.0	0.2 ± 0.0	0.5 ± 0.0	0.4	0.5 ± 0.0	0.2 ± 0.0	0.6 ± 0.0	0.6	0.8 ± 0.0	0.3 ± 0.1	0.6 ± 0.0
20:5n-3	5.4	2.4 ± 0.1	6.0 ± 0.1	8.1 ± 0.3	6.4	3.1 ± 0.1	6.8 ± 0.1	9.8 ± 0.3	8.1	5.0 ± 0.1	8.0 ± 0.1	11.6 ± 0.1
22:1n-11,n-13	0.6	0.4 ± 0.0	0.2 ± 0.0	1.1 ± 0.1	0.4	0.3 ± 0.0	0.2 ± 0.0	0.8 ± 0.1	0.5	0.4 ± 0.0	0.2 ± 0.1	0.9 ± 0.1
21:5n-3	—	—	—	—	—	—	—	—	0.3	0.0 ± 0.1	0.3 ± 0.0	0.5 ± 0.1
22:4n-6	—	—	—	—	0.2	0.0 ± 0.0	0.2 ± 0.0	0.5 ± 0.0	0.2	0.0 ± 0.0	0.2 ± 0.0	0.5 ± 0.1
22:5n-6	1.4	0.2 ± 0.2	1.8 ± 0.1	2.2 ± 0.2	1.5	0.3 ± 0.0	2.0 ± 0.1	2.3 ± 0.1	1.6	0.3 ± 0.0	2.1 ± 0.2	2.4 ± 0.1
22:5n-3	1.0	0.2 ± 0.2	1.3 ± 0.1	1.6 ± 0.2	1.2	0.3 ± 0.0	1.5 ± 0.1	1.8 ± 0.1	1.5	0.6 ± 0.1	1.7 ± 0.1	2.2 ± 0.0
22:6n-3	21.4	3.9 ± 0.5	33.5 ± 1.7	26.6 ± 1.7	22.1	3.9 ± 0.5	34.4 ± 1.7	28.9 ± 0.8	29.3	6.9 ± 1.0	44.5 ± 1.8	37.2 ± 0.7
24:1n-9	0.5	0.4 ± 0.1	0.3 ± 0.2	0.6 ± 0.1	0.3	0.2 ± 0.0	0.2 ± 0.0	0.4 ± 0.1	—	—	—	—
Others	2.1	1.6	2.1	2.6	2.1	1.9	2.0	2.2	2.0	3.0	1.7	1.7

[a]Means value ± standard deviation of triplicate analyses.
[b]Less than 0.2%.

esterified in the *sn*-1 position. This distribution pattern resembles that observed for tuna oil TAG in the report of Myher *et al.* (4). In contrast, our previous paper (3) reported 24–39, 8–26, and 50–59% of DHA were located in the *sn*-1, *sn*-2, and *sn*-3 positions, respectively. An opposite distribution pattern was obtained in the present study.

The analytical method used in our studies is based on chromatographic separation of isomeric and enantiomeric MAG formed from TAG (1,2). The method involves partial hydrolysis of TAG to MAG, isolation of 1(3)- and 2-MAG from the hydrolysis products, preparation of bis-3,5-DNPU derivatives of 1(3)-MAG, resolution of them by chiral HPLC, and GLC analysis of their fatty acids. In our previous study (3), the hydrolysis mixture of TAG was converted directly to the bis-3,5-DNPU derivatives, and then 1(3)- and 2-MAG derivatives were isolated by TLC on silicic acid with chloroform/acetone (96:4, vol/vol) as developing solvent. Presently, 1(3)- and 2-MAG generated by Grignard hydrolysis of TAG were resolved by boric acid TLC prior to the derivatization.

Figure 1 shows the reversed-phase HPLC elution profiles of the 1(3)- and 2-MAG intermediates formed from bonito head oil TAG. Under the HPLC conditions, peaks of 1(3)- and 2-docosahexaenoyl glycerols, prepared by Grignard hydrolysis of tridocosahexaenoyl glycerol, were partially separated from each other as their bis-3,5-DNPU derivatives. Figures 1A and 1B show the chromatograms of 1(3)- and 2-MAG isolated by boric acid TLC and then converted to the bis-3,5-DNPU derivatives, respectively. Essentially no cross-contamination of isomeric 1(3)-docosahexaenoylglycerol (peak I) and 2-docosahexaenoylglycerol (peak II) was observed in the chromatograms. A mixture of the bis-3,5-DNPU derivatives of 1(3)- and 2-MAG were subjected to preparative silicic acid TLC under the conditions previously used (see above). Figures 1C and 1D show 1(3)- and 2-MAG fractions resolved by silicic acid TLC as their bis-3,5-DNPU derivatives, respectively. The 1(3)-MAG fraction showed an apparent peak of 2-docosahexaenoylglycerol (Fig. 1C, peak II). In the 2-MAG fraction (Fig. 1D), this peak was much smaller than that observed in Figure 1B. Under the silicic acid TLC conditions used, 1(3)-MAG species migrate ahead of corresponding isomeric 2-MAG species. Although bis-3,5-DNPU derivatives of MAG formed from the fish oil TAG were split up into two bands, tentatively named as 1(3)- and 2-MAG bands, reversed-phase HPLC profiles of them (Figs. 1C and 1D) indicate that 2-docosahexaenoylglycerol species overlapped with the 1(3)-MAG band. Therefore, silicic acid TLC of bis-3,5-DNPU derivatives is unsuitable for separation of 1(3)- and 2-MAG prepared from DHA-rich fish oil TAG, and cannot be used in the stereospecific analysis without any modifications. In contrast, 1(3)- and 2-MAG could be clearly resolved into lower and upper bands on the boric acid-impregnated silicic acid plate, respectively.

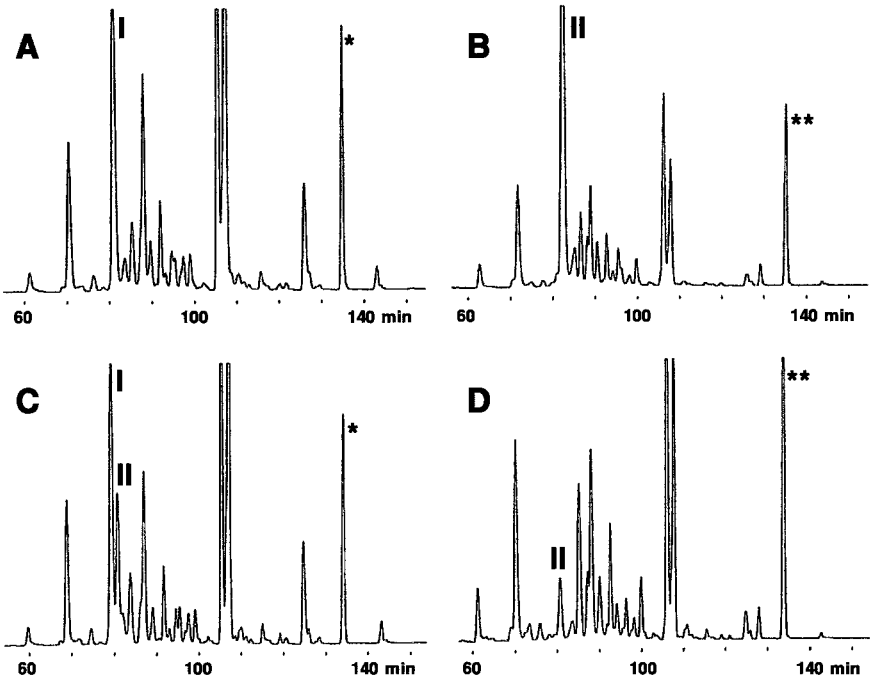

FIG. 1. Reversed-phase high-performance liquid chromatography (HPLC) profiles of bis-3,5-dinitrophenylurethanes (DNPU) of 1(3)- and 2-monoacyl-*sn*-glycerols (MAG) derived from bonito head oil triacyl-*sn*-glycerols. (A) and (B), 1(3)- and 2-MAG fractions separated by boric acid-impregnated silicic acid thin-layer chromatography (TLC) as free form of MAG, respectively; (C) and (D), 1(3)- and 2-MAG fractions separated by silicic acid TLC as bis-3,5-DNPU derivatives of MAG, respectively. I and II, 1(3)- and 2-docosahexaenoyl-*sn*-glycerols, respectively. *1(3)- and **2-Nonadecanoyl-*sn*-glycerols derived from trinonadecanoylglycerol internal standard. HPLC conditions are as given in the text.

The high content of DHA in the *sn*-1 and *sn*-3 positions observed in our previous analysis (3) is found to result from unsuitable TLC separation of 1(3)- and 2-MAG intermediates. Positional distributions obtained in the present study were similar in high content of DHA in the *sn*-2 position to those obtained by other stereospecific (4) or regiospecific (5–7) analyses. In conclusion, the 1(3)- and 2-MAG made up of both short- and long-chain lengths cannot be clearly resolved by TLC after preparation of the bis-3,5-DNPU derivatives. The 1(3)- and 2-MAG must be resolved by boric acid TLC prior to derivatization.

REFERENCES

1. Takagi, T., and Ando, Y. (1991) Stereospecific Analysis of Triacyl-*sn*-glycerols by Chiral High-Performance Liquid Chromatography, *Lipids 26*, 542–547.
2. Ando, Y., and Takagi, T. (1993) Micro Method for Stereospecific Analysis of Triacyl-*sn*-glycerols by Chiral-Phase High-Performance Liquid Chromatography, *J. Am. Oil Chem. Soc. 70*, 1047–1049.
3. Ando, Y., Ota, T., Matsuhira, Y., and Yazawa, K. (1996) Stereospecific Analysis of Triacyl-*sn*-glycerols in Docosahexaenoic Acid-Rich Fish Oils, *J. Am. Oil Chem. Soc. 73*, 483–487.
4. Myher, J.J., Kuksis, A., Geher, K., Park, P.W., and Diersen-Schade, D.A. (1996) Stereospecific Analysis of Triacylglycerols Rich in Long-Chain Polyunsaturated Fatty Acids, *Lipids 31*, 207–215.
5. Amate, L., Ramirez, M., and Gil, A. (1999) Positional Analysis of Triglycerides and Phospholipids Rich in Long-Chain Polyunsaturated Fatty Acids, *Lipids 34*, 865–871.
6. Sawada, T., Takahashi, K., and Hatano, M. (1993) Triglyceride Composition of Tuna and Bonito Orbital Fats, *Nippon Suisan Gakkaishi 59*, 285–290.
7. Sacchi, R., Medina, I., Aubourg, S.P., Giudicianni, I., Paolillo, L., and Addeo, F. (1993) Quantitative High-Resolution ^{13}C NMR Analysis of Lipids Extracted from the White Muscle of Atlantic Tuna (*Thunnus alalunga*), *J. Agric. Food Chem. 41*, 1247–1253.
8. Ando, Y., Nishimura, K., Aoyanagi, N., and Takagi, T. (1992) Stereospecific Analysis of Fish Oil Triacyl-*sn*-glycerols, *J. Am. Oil Chem. Soc. 69*, 417–424.

[Received November 19, 1999, and in final revised form March 20, 2000; revision accepted March 27, 2000]

Alterations in 3-Hydroxy-3-methylglutaryl-CoA Reductase mRNA Concentration in Cultured Chick Aortic Smooth Muscle Cells

Angel Carazo, Mª José Alejandre, Mª Dolores Suarez, and Ana Linares*

Department of Biochemistry and Molecular Biology, Faculty of Sciences, University of Granada, 18071 Granada, Spain

ABSTRACT: We observed and compared alterations in 3-hydroxy-3-methylglutaryl (HMG)-CoA reductase at the transcriptional level in unsynchronized, three-passage cultures of smooth-muscle cells from the aorta of chicks fed on a control diet (C-SMC) and those of chicks fed on a similar diet plus cholesterol (Ch-SMC). Alterations in reductase mRNA concentrations in senescent cultures were much lower. We used a modification of the competitive (c) reverse transcription polymerase chain reaction method, using a *Thermus thermophilus* DNA polymerase (Tth pol) to quantify the very scarce species of HMG-CoA reductase mRNA in samples of cytoplasmic SMC mRNA. We cloned and sequenced a 199 bp cDNA fragment of chicken HMG-CoA reductase, which encoded a region of 66 amino acids belonging to the catalytic domain of the enzyme. HMG-CoA reductase mRNA concentrations from young C-SMC cultures rose 3.89-fold 4 h after the change of medium and returned to base levels between 8 to 12 h afterward. Concentrations in Ch-SMC cultures increased less (2.36-fold) 8 h after the change to fresh medium. Increases in reductase mRNA in senescent cultures of Ch-SMC and C-SMC measured under similar conditions were only 1.28- and 1.39-fold, respectively.

Paper no. L8379 in *Lipids 35,* 587–593 (June 2000).

3-Hydroxy-3-methylglutaryl-CoA (HMG-CoA) reductase (EC 1.1.1.34) is an endoplasmic-reticulum-membrane enzyme that catalyzes the conversion of HMG-CoA to mevalonate, the rate-limiting step in cholesterol and polyisoprenoid biosynthesis (1). Several different mechanisms have been reported for regulating reductase activity in animal cells, including: (i) long-term control by changes in HMG-CoA reductase concentration through transcriptional, posttranscriptional, and posttranslational control levels as well as by enzyme degradation (2–4); (ii) the modulation of reductase activity or degradation by altering the lipid composition of the endoplasmic reticulum (5–7); and (iii) regulation by a bicyclic cascade system involving reversible phosphorylation of both HMG-CoA reductase and reductase kinase (8,9). The multivalent feedback regulation of HMG-CoA reductase involves cholesterol and one or more of the other products synthesized from mevalonate (10,11). In cell cultures, the addition of exogenous sources of cholesterol or mevalonate at the time of the change of medium blocks the rise found in reductase activity associated with feeding the cells (12).

Furthermore, HMG-CoA reductase activity is involved in cell division, showing a marked rise just before the S phase of the cell cycle (13,14). Parallel changes in HMG-CoA reductase activity are, however, observed to vary widely in both synchronized and unsynchronized cells under normal culture conditions [with fresh medium supplemented with fetal bovine serum (FBS)]. This variation is associated with feeding the cells (12), and thus other factors besides the cell cycle alone also may play a role. We report here on the variations in HMG-CoA reductase mRNA in cultures of aortic smooth-muscle cells isolated in our laboratory from cholesterol-fed chicks (Ch-SMC) and from control-fed chicks (C-SMC). The main characteristics of these two culture lines are: (i) The proliferation rate of Ch-SMC under identical culture conditions is superior compared to C-SMC; thus, DNA synthesis in Ch-SMC during the S phase (at 8 h) is fourfold higher, and (ii) with identical maintenance, the intracellular cholesterol content is the same in both cell lines for the first 14 d of culture but subsequently increases in Ch-SMC, rising to more than double the C-SMC value (15). To quantify the very scarce species of HMG-CoA reductase mRNA in samples of cytoplasmic SMC RNA, we used a modification of competitive reverse transcription-polymerase chain reaction [(c) RT-PCR], involving same-tube co-amplification of the gene and a synthetic internal standard fragment (16). Because the chick HMG-CoA reductase gene sequence is unknown, we designed and synthesized a fragment of reductase cDNA. We observed alterations in HMG-CoA reductase mRNA concentration in unsynchronized, three-passage C-SMC and Ch-SMC cultures associated with the feeding of the cells. These alterations are much lower in senescent cultures.

MATERIALS AND METHODS

Chicks. Newly hatched, male, White Leghorn chicks (*Gallus domesticus*) were bought from a commercial hatchery and fed

*To whom correspondence should be addressed at Department of Biochemistry and Molecular Biology, Faculty of Sciences, Fuentenueva sn, University of Granada, 18071 Granada, Spain. E-mail: analinar@goliat.ugr.es

Abbreviations: (c) RT-PCR, competitive reverse transcription-polymerase chain reaction; DMEM, Dulbecco's modification of Eagle's medium; dNTP, deoxy nucleotide 5′-triphosphate; FBS, fetal bovine serum; HMG-CoA, 3-hydroxy-3-methylglutaryl-CoA; PBS, phosphate-buffered saline; SMC, smooth muscle cell; UV, ultraviolet.

ad libitum in a chamber with a light cycle from 0900 to 2100 and a controlled temperature of 29–31°C.

Two groups of 10-d-old chicks were used; a control group was kept on a standard diet (Sanders A-00) while a treated group was fed on the same diet supplemented with 5% w/w powdered cholesterol mixed homogeneously (Panreac Reagent Barcelona, pure grade; Montplet & Esteban S.A., Barcelona, Spain). The diets were begun at hatching and continued until the chicks were killed 10 d afterward. Water was constantly available. None of the chicks died a natural death nor developed any illness during the treatment.

SMC cultures. SMC were isolated from the aortic arch of the chicks as described elsewhere (17,18) with slight modifications (15) and cultured in Dulbecco's modification of Eagle's medium (DMEM) supplemented with D-glucose (4.5 g/L), L-glutamate (0.584 g/mL) (Flow), an antibiotic cocktail composed of penicillin (100 µg/mL) and amphotericin (0.25 µg/mL) (Sigma, St. Louis, MO) and 10% (vol/vol) FBS. The medium was buffered with bicarbonate, and the cultures were kept at 37°C in a humidified atmosphere of 95% air and 5% CO_2. The medium was renewed three times a week. Secondary cultures were initiated after either low or high passages using 0.05%/0.02% trypsin-EDTA solution (Flow Laboratories Ltd., Irvine Ayrshire, Scotland).

All experiments were conducted using 3 or 13 passages. The cells were seeded at approximately 2×10^4 cells per dish (60 mm) containing 4 mL fresh medium. They were determined to be vascular smooth-muscle by their hill-and-valley configuration at confluence (18) and positive fluorescence staining for smooth-muscle actin and myosin (19). Trypan blue (Sigma) was added to the cells with the help of a hemacytometer, and the flasks were examined with an inverted light microscope (Olympus Opticals Co. Ltd., Tokyo, Japan) to count live and dead cells. Cell viability in our cultures was 90%.

Flow cytometry. Cell fixation was carried out as described elsewhere (20). They were harvested and washed with phosphate-buffered saline (PBS) containing 10% FBS. Cell pellets were resuspended in 250 µL PBS, followed by 250 µL PBS containing 2% paraformaldehyde. After incubation for 15 min at 4°C, the cells were washed, resuspended in 5 mL of ice-cold 70% ethanol, and incubated overnight at –20°C. They were then processed for DNA content and the cell-cycle distribution of SMC populations. Fixed cells were resuspended in PBS containing 200 µg/mL ribonuclease and 5 µg/mL propidium iodide and incubated for 30 min at room temperature. They were analyzed for red fluorescence (propidium iodide, allowing DNA quantification) using a FACS Vantage dual laser for flow cytometry (Becton Dickinson Immunocytometry System, San Jose, CA) with a Coherent Enterprise laser [160 mW, 488 nm; and 60 mW, ultraviolet (UV)]. The laser was set at 488 nm and 15 mW with the sample in the FL_2 detector regulated to 495 nm (linear), with a 585/42 BP filter; 5000 cells were analyzed (300 cells/s), and the data were processed on a CellFiT (v 2.01.2 Becton Dickinson).

Bacterial strain, growth conditions, plasmid, and primers. Cloning was carried out in *Escherichia coli* strain JM101 (F *tra*D36 *pro*A+ *pro*B+ *lac*I *lac*ZΔM15/*sup*E *thi* Δ(lac-*pro*AB) using the pGEM-T vector system I (Promega). *Escherichia coli* was cultured in Luria-Bertani broth containing the appropriate antibiotic (ampicillin, 50 µg/mL).

Oligonucleotide primers were synthesized with Gibco BRL (Barcelona, Spain) custom primers.

Isolation of total cytoplasmic RNA. Total cytoplasmic RNA from both the C-SMC and Ch-SMC lines was isolated by the acid guanidinium isothiocyanate method as described elsewhere (21) with the slight modifications described below.

The adherent cultured cells were harvested with a cell scraper, transferred to an autoclaved 1.5-mL microcentrifuge tube (10^6–10^8), and washed once with cold PBS. They were then centrifuged at room temperature at 12,000 rpm for 5 s (N.B. To avoid cell death, they should never be centrifuged for longer than 20 s.) The supernatant was removed and the cell pellet kept on ice; 100 µL ice-cold lysis buffer A [10 mM Tris-Cl pH 7, 0.15 M NaCl, 0.65% Nonidet P-40 (NP-40)] was added. The cells were then vortexed and incubated on ice for 5 min and subsequently centrifuged for 5 min to pellet the nuclei. The RNA contained in the supernatant was extracted by adding 400 µL guanidinium thiocyanate solution (4 M guanidinium thiocyanate, 25 mM sodium citrate, pH 7, 0.5% *N*-lauroylsarcosine, 0.1 M 2-mercaptoethanol) and precipitated as described elsewhere (22). The final RNA concentration was determined by absorbance using a spectrophotometer. This method yields about 30 µg of cytoplasmic RNA per 25 cm^3 plaques at 60% confluency.

Construction and sequencing of a chick HMG-CoA reductase c-DNA fragment. We designed two pairs of heterologous primers corresponding to *Xenopus laevis* HMG-CoA reductase using the primer sense 5′-AGCCAGCTGCTATTAACTGGAT-3′ (anneals with the 2023–2044 region of *X. laevis* cDNA) and antisense: 5′-ACCTGTTGTGGACCATGTGACT-3′ (annealing to the 2692–2713 region of *X. laevis* cDNA), giving a single band of 243 pb of cDNA of chicken HMG-CoA reductase detected by RT-PCR. The 243 pb fragment obtained was cloned into a pGEM-T plasmid, the result being referred to as pRC-243 (3246 pb). This gave a fragment without primers (22 pb) of 199 pb, which was gel-purified and both strands sequenced by the chain-termination DNA sequencing method of Sanger *et al.* (23) using AmpliTaq® FS and deoxy nucleotide 5′-triphosphates (dNTP) (ABI PRISM™ fluorescence labeled) in a Dye Terminator Cycle Sequencing Ready Reaction (Perkin-Elmer/Applied Biosystems Division, Foster City, CA). Nucleotide sequences were analyzed with the Clustad X, Macaw, and TreeView program (National Center for Biotechnology Information, Bethesda, MD).

Competitive RT-PCR. RT-PCR was carried out in a single reaction tube using Tth polymerase (Gene Craft, Münster, Germany), a thermostable DNA polymerase that shows RT activity, by using Mn^{2+} (24,25). All RT and PCR reactions took place in a DNA Thermal Cycler 480 (Techne, Cambridge, United Kingdom). The RT reaction was set up in 20 µL containing the appropriate amount of total cytoplasmic RNA, 10× RT buffer [670 mM Tris-HCl, pH 8.8, 166 mM

$(NH_4)_2SO_4$, 0.1% Tween-20], 1 mM $MnCl_2$, 0.25 mM dNTP, 1.25 pmol/μL downstream primer, and 0.12 units/μL of Tth polymerase, and incubated at 72°C for 30 min. Competitor DNA, as indicated above, was added before amplification. For the amplification reaction, 30 μL of a mix containing 5× PCR buffer [33.5 mM Tris-HCl, pH 8.8, 83 mM $(NH_4)_2SO_4$, 3.75 mM EGTA, 25% glycerol, 0.196 Tween-20], 1.5 mM $MgCl_2$, 0.2 mM dNTP, 0.5 pmol/μL of both primers (upstream and downstream) and 0.05 units/μL Tth polymerase were added per reaction. Routinely performed were 30 cycles with 1 min denaturation at 95°C, 1 min annealing at 52ºC, and 1 min per cycle of PCR at 72ºC.

Separation and quantification of PCR products. PCR products were loaded directly onto a 2% agarose gel and electrophoresed at 5 V/cm for 1.5 or 2 h. DNA was visualized and photographed under UV light (320 nm) after ethidium bromide staining (25). The picture was digitalized and analyzed using the Quantyscan Program (Biosoft, Ferguson, MO). This DNA quantitation system is very sensitive and is able to detect nanogram amounts of DNA. Reactions containing the different mass of DNA were performed in triplicate. All the ethidium bromide colorimetric data included fall into the range where the DNA quantity ratio was linear. A plot of the log of the ratio of target to competitor product against the log of the competitor concentration should give a straight line with a slope of −1 (26). The amount of competitor used at which the ratio of target to competitor PCR products is equal to unity (log ratio = 0; the equivalence point) can be used to calculate the initial number of molecules of the target sequence.

RESULTS

To establish the experimental design, we prepared unsynchronized C-SMC cultures of different numbers of passages; early-passage, or young cultures (3 passages) and late-passage, or senescent cultures (13 passages). Flow cytometry was used to analyze the cell cycles by cell DNA content. Figure 1A shows the cell cycle of young cultures with 30.4% of the cells in the S phase and Figure 1B the cell cycle of senescent cultures with 15.5% of the cells in the S phase. We chose

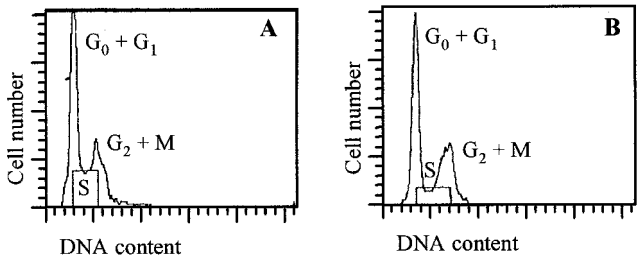

FIG. 1. DNA content histogram of chick smooth muscle cells. Cells were fixed in ethanol and stained with propidium iodide prior to analysis by flow cytometry, as described in the Materials and Methods section. (A) Third passage cultures, the percentages of cells in G_0/G_1, S, and G_2/M phases, respectively, are: 46.6, 30.4, and 23%. (B) Thirteenth passage cultures, the percentages of cells in G_0/G_1, S, and G_2/M phases, respectively, are: 56, 15.5, and 28.5%.

2 to 12 h after the change of medium to measure the HMG-CoA reductase mRNA concentration because the S phase occurs in chick Ch-SMC and C-SMC cultures at about 8 h.

HMG-CoA mRNA in chick aorta SMC was quantified after the change of medium. Unsynchronized Ch-SMC and C-SMC of 3 and 13 passage cultures were used to carry out competitive RT of mRNA from the cytoplasm of these cells, followed by PCR. Because the chick HMG-CoA reductase sequence is unknown, the design and construction of a cDNA were our first necessity. We sequenced a 199 bp fragment of chick HMG-CoA reductase cDNA from the pRC-243 plasmid and obtained a sense sequence of: 5′-AGAGGGAA-GAGGGAAGTCTGTTGTCTGTGAAGCAGTCATTC-CAGCCAAGGTTGTTAAAGAAGTACTGAAGACAAC-TACGGAAGATATAGTTGAAGTGAATATAAACAAAAA-TCTGGTGGGTTCTGCTATGGCTGGTAGCATAGGTG-GCTACAACGCGCATGCTGCAAACATTGTTACAGC-TATCTACATTGCCTGTGGT-3′. This sequence was analyzed using the Clustad X program to check that it did in fact correspond to a fragment of HMG-CoA reductase gene. By aligning the 199 nucleotides of *Gallus domesticus* reductase with other species, it could be seen that the reading frame started on the second nucleotide, and we deduced a sequence of 66 amino acids belonging to the soluble carboxy terminal. The similarity index found with the published sequences from other species is shown in Figure 2.

As the quantification of mRNA by (c) RT-PCR includes a standard RNA molecule to coamplify with the mRNA problem, we synthesized homologous primers. From the 199 pb cDNA fragment of chick HMG-CoA reductase, we designed the primers referred to as Sen-G sense: 5′-GAAGTCTGT-TGTCTGTGAAGCA-3′ (13–34 position of 199 pb fragment) and Ant-G antisense: 5′-CACAGGCAATGTAGATAGCT-GT-3′ (176–197 position of 199 pb fragment). Using the Sen-G and Ant-G primers, RT-PCR with cytoplasmic RNA from chick SMC cultures showed the amplification of only one molecule (185 bp).

To construct a chick HMG-CoA reductase mRNA standard (competitive template), we designed composite primers. Figure 3 is a scheme for the construction of a competitive template and PCR quantification.

One primer contained the upstream primer Sen G, resulting in the composite primer sense, referred to as Sen-L: 5′-GAAGTCTGTTGTCTGTGAAGCACCATAGTTGCCT-GACTCC-3′ (the Sen-G sequence is 40 nucleotides: upstream of 22 nucleotides and the rest is the upstream position 1378–1395 of pGEM).

The other composite primer contained the downstream primer Ant G, resulting in the antisense, referred to as Ant-L: 5′-CACAGGCAATGTAGATAGCTGTATGCCAA-CAACGTTGCGC-3′ (the Ant-G sequence is represented by 40 nucleotides: downstream of 22 nucleotides and the rest to the downstream position 1616–1633 of pGEM-T). Using the composite primers Sen-L and Ant-L and the plasmid pGEM, we synthesized a DNA 300 pb by PCR (annealing to the primers SenG and AntG). The 300 bp PCR product was

G. domesticus	KVVKEGRGKSVVCEAVIPAEVLKTTTEDIVEVNINKNLVGSAMAGSIGGYNAHAANIVTAIYIACG
X. laevis	EGRGKTVVCEAIIPARVVREVLKSSTEALIDVNINKNFIGSAMAGSIGGYNAHAANIVTAIYIACG
M. auratus	EGRGKSVVCEAVIPARVVREVLKTTTEAMIDVNINKNLVGSAMAGSIGGYNAHAANIVTAIYIACG
B. germanica	EGRGKSVVCEAIVPADIIKSVLKTSVGALMDVNITKNLIGSAVAGSIGGFNAHAANIVTAIFIATG
S. cerevesiae	EGRGKSVVAEATIPGDVVKSVLKSDVSALVELNISKNLVGSAMAGSVGGFNAHAANLVTALFLALG

	Position	Similarity (%)
Xenopus laevis	695–760	87.9
Mesocricetus auratus	699–764	89.4
Blattella germanica	668–733	69.7
Saccharomyces cerevesiae	852–917	69.7

FIG. 2. Comparison of the deduced amino acid sequence from 199 bp cDNA fragment of chick 3-hydroxy-3-methylglutaryl-CoA (HMG-CoA) reductase and homology with other species.

constructed by cloning into pGEM-T, and the result was a recombinant plasmid, referred to as pST-300 (3.303 pb). This plasmid linearized with EcoRI was used as a standard in c-RT-PCR.

This RNA fragment was subsequently purified, quantified, and used in cRT-PCR to measure HMG-CoA reductase mRNA. The concentration of mRNA was determined by UV absorption spectrometry. Four experiments were made with the amount of standard ranging between 10,000 and 740,000 copies.

Competitive RT-PCR analysis involves titrating the standard with a constant amount of sample SMC cytoplasmic RNA per reaction tube (25 ng from young cells and 50 ng from senescent cells). The amount of competitor used at which the ratio of target to competitor PCR products is equal to unity (log ratio = 0; the equivalence point) can be employed to calculate the initial number of molecules in the target sequence. A plot of the log of the ratio of the densitometric values for reductase products against the log of the number of copies of reductase RNA added was linear, with a slope of 1 (Fig. 4).

The quantification of HMG-CoA reductase mRNA in young SMC cultures is shown in Figure 5A; the number of molecules from C-SMC cultures shows a rise of 3.89-fold 4 h after changing the medium and thence returns to base values between 8 and 12 h. Figure 5A also shows the rise in the number of HMG-CoA reductase mRNA molecules in Ch-SMC, albeit with a lower increase (2.36-fold) in reductase mRNA 8 h after changing the medium in Ch-SMC. Figure 5B shows a comparison between the increase in reductase mRNA in both C-SMC and Ch-SMC senescent cultures (1.39 and 1.28, respectively), which represents the smallest changes and the smallest numbers of mRNA molecules.

DISCUSSION

Quantitative measurements of gene expression at transcriptional level are hampered by generally low quantities of HMG-CoA reductase mRNA. To combat this, we used the competitive (c) RT-PCR method to quantify the very scarce species of HMG-CoA reductase mRNA in cytoplasmic SMC mRNA.

We report the development and validation of a simple, nonradioactive, and highly reproducible technique (RT-PCR) to determine the relative HMG-CoA reductase gene expression in different SMC cultures. This technique exploits the tremendous sensitivity of competitive RT-PCR (17,19) and the advantages of RT at elevated temperature using Tth DNA

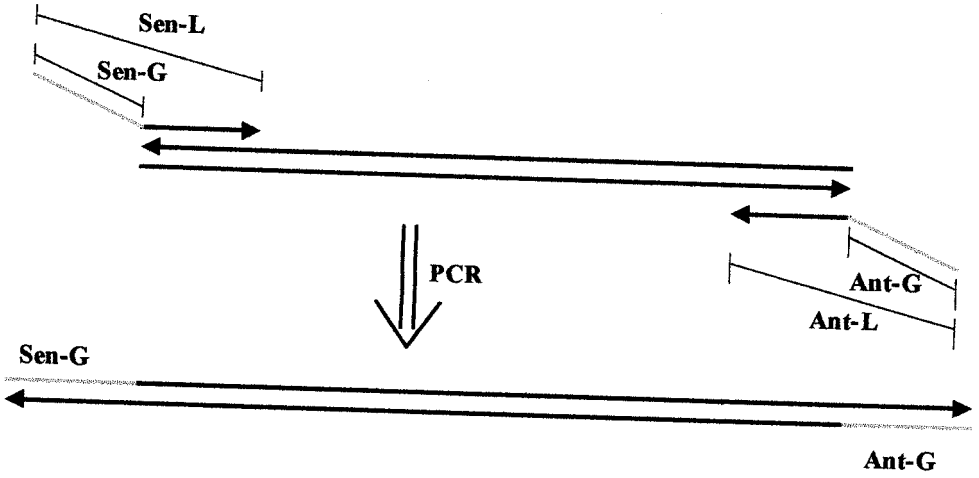

FIG. 3. A scheme for the construction of a competitive template and polymerase chain reaction (PC) quantification.

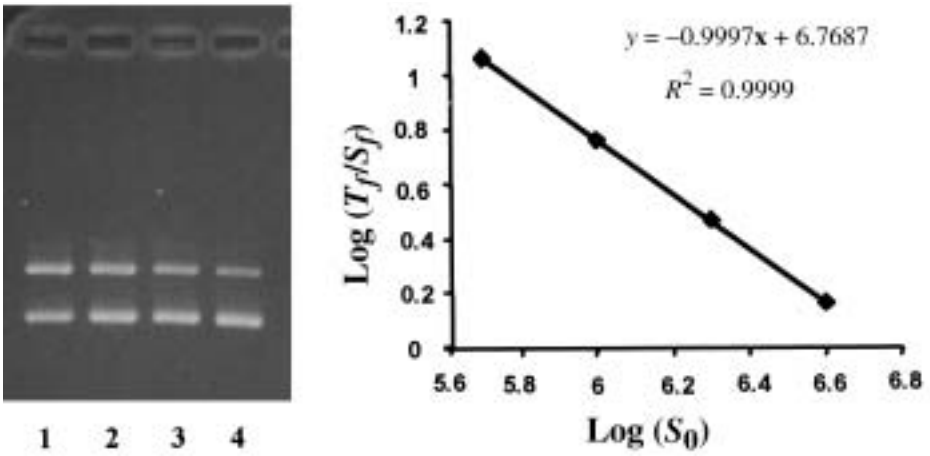

FIG. 4. Competitive reverse transcriptase-polymerase chain reaction (RT-PCR). In the left-hand panel, the four RT-PCT products were run in gel electrophoresis and stained with ethidium bromide. The DNA product was 243 bp (final target) and 300 bp (final standard) in length. In the right-hand panel, the densitometric results were plotted. T_f final target amount, S_f, final standard amount and S_0, initial standard amount. Each sample was assayed in triplicate. The ± SEM do not exceed 5%.

polymerase (a thermostable enzyme that also has RT activity) (16,18). The DNA quantitation system used by ethidium bromide staining is really sensitive; we performed the assay in the linear range of total DNA added per reaction. Only the assays made in the linear range of DNA gave an $R^2 > 0.98$.

As this method includes an mRNA standard and the chick HMG-CoA reductase gene sequence is unknown, we sequenced and cloned a 199 bp cDNA fragment, which encodes a region of 66 amino acids (Fig. 2) belonging to the soluble (catalytic) domain of the enzyme (28,29). From the alignment of this sequence, we made a cladogram (not shown), where the sequence of *G. domesticus* is located between amphibians and mammals. The 199 bp cDNA fragment and the composite primers designed to construct a chick HMG-CoA reductase mRNA standard (competitive template) will be essentials to quantify the mRNA and study in the future the regulation of this enzyme in chick aorta SMC at transcriptional levels.

In this paper we present an application to validate this method by measure of the fluctuations of HMG-CoA reductase mRNA concentration after media change in SMC cultures. It is well-established that marked changes in HMG-CoA reductase activity occur under normal cell-culture conditions; early experiments by Brown *et al.* (27), for example, demonstrated a small increase in HMG-CoA reductase activity in cultured fibroblasts 19 h after changing the medium to a fresh one supplemented with FBS, and a large increase (fivefold) with lipoprotein-deficient serum. The increase in activity has been put down to an induction of reductase after a change in the medium. Other previous studies into reductase activity, using

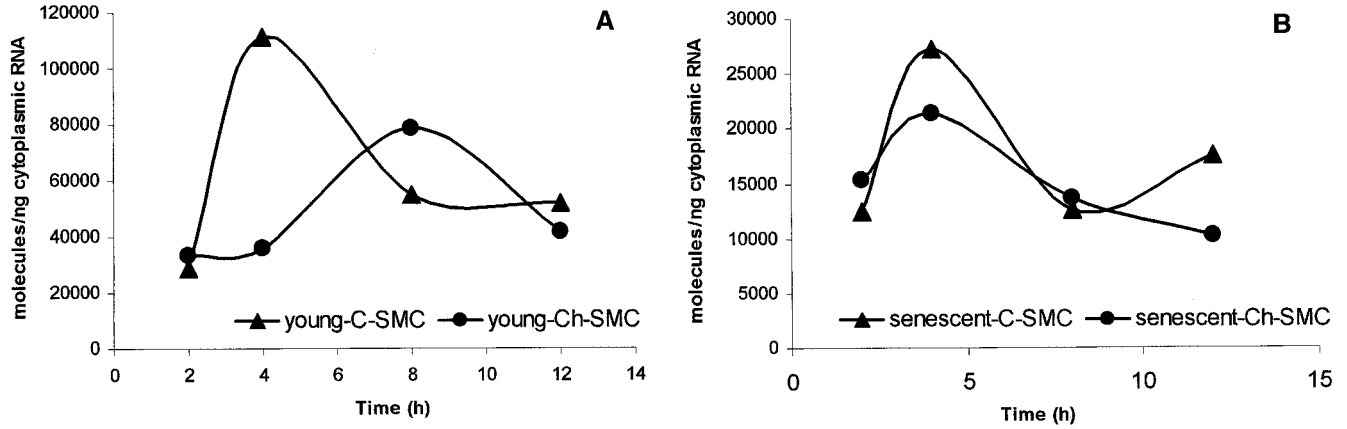

FIG. 5. Alterations to HMG-CoA reductase mRNA in smooth muscle cell (SMC) cultures after changing the medium. At $T = 0$, monolayer third-passage cultures (A) and 13-passage cultures (B) that presented a 60–70% confluency were washed with phosphate buffered saline and then fed a fresh medium. Cells were harvested at each point of time and the HMG-CoA reductase mRNA was quantified by (c)RT-PCR as described in the Materials and Methods section. Aortic SMC cultures were obtained from both control chick (SMC-C) and hypercholesterolemic chick (SMC-Ch). Each sample was assayed in triplicate. The ± SEM do not exceed 10%. See Figures 2 and 4 for abbreviations.

the murine macrophage as cell line J774 (12), suggested that HMG-CoA reductase activity varies widely under normal culture conditions with FBS and that these variations are associated with feeding the cells. Nevertheless, few reports have been published concerning changes in reductase mRNA concentrations after changing the medium.

Our results indicate that after a change of medium alterations in HMG-CoA reductase mRNA occur at transcriptional level both in C-SMC and Ch-SMC cultures (Fig. 5A,B). The exposure of cultured C-SMC to a fresh medium containing FBS caused a rapid increase in HMG-CoA reductase mRNA molecules as soon as 4 h after feeding the cells. Although some of the media supplements contained lipoprotein cholesterol sources (FBS), the amounts added to the media were insufficient to block the increase seen in HMG-CoA reductase mRNA. The intracellular cholesterol level in C-SMC and Ch-SMC remained the same during the first 12 h of culture, although subsequently it increased in Ch-SMC to double the levels found in C-SMC (15). In identical medium and culture conditions, the increase in reductase mRNA concentration in CH-SMC was almost 50% lower after feeding the cells for 8 h, although both C-SMC and Ch-SMC reductase mRNA returned to base values by 12 h. Senescent cultures of both C-SMC and CH-SMC had low concentrations of reductase mRNA and showed small changes after changing the medium, which agrees with Figure 1, where it can be seen that senescent cultures contain only half as many cells in the S phase (i.e., less rapidly dividing cells) as do the young cultures. We obtained similar results with HMG-CoA reductase activity, with a greater increase in young C-SMC cultures compared to Ch-SMC cultures and very low activity in senescent cultures (data not shown). It is known that HMG-CoA reductase activity is high in rapidly dividing cells and decreases as they reach confluency (30–32). The C-SMC and Ch-SMC cultures used in our work were unsynchronized (Fig. 1A,B), and the sustained increase in reductase mRNA concentration did not depend upon the cell cycle, although both lines did contain rapidly dividing cells (60–70% confluency), which might explain the increase in reductase mRNA. Nevertheless, further studies will be necessary to explain the differences between the increases in mRNA reductase in the two lines of SMC culture.

ACKNOWLEDGMENTS

This work was supported partly by a grant from DGICYT (PB93-1160) and also from the Research grant from Junta de Andalucía (Group code 3229). Flow cytometry was done at the Centro de Instrumentación científica at the University of Granada. We thank J. Trout for revising the English text.

REFERENCES

1. Rodwell, V.W., Nordstrom, J.L., and Mitschelen, J.J. (1976) Regulation of HMG-CoA Reductase, *Adv. Lipid Res. 14*, 1–74.
2. Chin, D.J., Gil, G., Faust, J.R., Goldstein, J.L., Browun, M.S., and Luskey, K.L. (1985) Sterols Accelerate Degradation of Hamster 3-Hydroxy-3-methylglutaryl-Coenzyme A Reductase Encoded by Constitutively Expressed cDNA, *Mol. Cell Biol. 5,* 634–641.
3. Choi, J.W., and Peffley, D.M. (1995) 3′-Untranslated Sequences Mediate Post-transcriptional Regulation of 3-Hydroxy-3-methylglutaryl-CoA Reductase mRNA by 25-Hydroxycholesterol, *Biochem. J. 307,* 233–238.
4. Simonet, W.S., and Ness, G.C. (1989) Post-transcriptional Regulation of 3-Hydroxy-3-methylglutaryl-Coenzyme A Reductase mRNA in Rat Liver, *J. Biol. Chem. 264,* 569–573.
5. Mitropoulos, K.A. (1983) Molecular Control of HMG-CoA Reductase: The Role of Nonesterified Cholesterol, in *3-Hydroxy-3-methylglutaryl CoA Reductase* (Sabine, J.R., ed.) pp. 107–127, CRC Press, Boca Raton.
6. García-Gonzalez, M., Segovia, J.L., and Alejandre, M.J. (1992) Homeostatic Restoration of Microsomal Lipids and Cholesterol Acyltransferase in Chick Liver, *Mol. Cell. Biochem. 115,* 173–178.
7. Kumagai, H., Chun, M.T., and Simoni, R.D. (1995) Molecular Disection of the Role of the Membrane Domain in the Regulated Degradation of 3-Hydroxy-3-methylglutary Coenzyme A Reductase, *J. Biol. Chem. 270,* 19107–19113.
8. Beg, Z., and Brewer, H.B. (1981) Regulation of Liver 3-Hydroxy-3-methylglutaryl-CoA Reductase, *Curr. Top. Cell Regul. 20,* 139–184.
9. Clarke, P.R., and Hardie, D.G. (1990) Regulation of HMG-CoA Reductase: Identification of the Site Phosphorylated by the AMP-Activated Protein Kinase *in vitro* and in Intact Rat Liver, *EMBO J. 9*, 2439–2446.
10. Goldstein, J.L., and Brown, M.S. (1990) Regulation of Mevalonate Pathway, *Nature 343*, 425–430.
11. Vallet, S.M., Sanchez, H.B., Rosenfeld, J.M., and Osborne, T.F. (1996) A Direct Role for Sterol Regulatory Element Binding Protein in Activation of 3-Hydroxy-3-methylglutaryl Coenzyme A Reductase Gene, *J. Biol. Chem. 271*, 12247–12253.
12. Tavangar, K., and Kraemer, F.B. (1988) The Regulation of Hydroxymethylglutaryl-CoA Reductase in Cultured Cells, *Biochim. Biophys. Acta 970,* 251–261.
13. Quesney-Huneeus, V., Wiley, M.H., and Siperstein, M.D. (1979) Essential Role for Mevalonate Synthesis in DNA Replication, *Proc. Natl. Acad. Sci. USA 76,* 5056–5060.
14. Quesney-Huneeus, V., Galick, H.A., Siperstein, M.D., Erickson, S.K., Spencer, T.A., and Nelson, J.A. (1983) The Dual Role of Mevalonate in the Cell Cycle, *J. Biol. Chem. 258,* 378–385.
15. Carazo, A., Alejandre, M.J., Diaz, R., Rios, A., Castillo, M., and Linares, A. (1998) Changes in Cultured Arterial Smooth Muscle Cells Isolated from Chicks Upon Cholesterol Feeding, *Lipids 33*, 181–190.
16. Bolton, M.C., Dudhja, J., and Bayliss, M.T. (1996) Quantification of Aggrecan and Link-Protein mRNA in Human Articular Cartilage of Different Ages by Competitve Reverse Transcriptase-PCR, *Biochem. J. 319,* 489–498.
17. Habenicht, A.J.R., Glonset, J.A., and Ross, R. (1980) Relation of Cholesterol and Mevalonic Acid to the Cell Cycle in Smooth Muscle and Swiss 3T3 Cells Stimulated to Divide by Platelet-derived Growth Factor, *J. Biol. Chem. 255,* 5134–5140.
18. Ross, R. (1971) The Smooth Muscle Cell II. Growth of Smooth Muscle in Culture and Formation of Elastic Fibers, *J. Cell Biol. 50,* 172–186.
19. Chamley-Campbell, J.H., Campbell, G.R., and Ross, R. (1979) The Smooth Muscle Cell in Culture, *Physiol. Rev. 58*, 1–61.
20. Hanon, E., Vanderplasschen, A., and Pastoret, P.P. (1996) The Use of Flow Cytometry for Concomitant Detection of Apoptosis and Cycle Analysis, *Biochem. 2*, 25–27.
21. Chomczinski, P., and Sacchi, N. (1987) Single-Step Methods of RNA Isolation by Acid Guanidinium Thiocyanate-Phenol-Chloroform Extraction, *Anal. Biochem. 162,* 156–159.

22. Jiang, Y.H., Davidson, L.A., Lupton, J.R., and Chapkin, R.S. (1996) Rapid Competitive PCR Determination of Relative Gene Expression in Limiting Tissue Samples, *Clin. Chem. 42,* 227–231.
23. Sanger, F., Nicklen, S., and Couldson, A.R. (1977) DNA Sequencing with Chain-Terminating Inhibitors, *Proc. Natl. Acad. Sci. USA 74*, 5463–5467.
24. Myers, T.W., and Geldfand, D.H. (1991) Reverse Transcription and DNA Amplification by a *Thermus thermophilus* DNA Polymerase, *Biochemistry 30*, 7661–7666.
25. Gebhardt, A., Peters, A., Gerding, D., and Niendorf, A. (1994) Rapid Quantitation of mRNA Species in Ethidium Bromide-stained Gels of Competitive RT-PCR Products, *J. Lipid Res. 35,* 977–981.
26. Raeymaekers, L. (1993) Quantitative PCR: Theoretical Considerations with Practical Implications, *Anal. Biochem. 214,* 582–585.
27. Brown, M.S., Dana, S.E., and Goldstein, J.L. (1973) Regulation of 3-Hydroxy-3-methyl-glutaryl Coenzyme A Reductase Activity in Human Fibroblasts by Lipoproteins, *Proc. Natl. Acad. Sci. USA 70*, 2162–2166.
28. Chin, D.J., Gil, G., Russell, D.W., Liscum, L., Luskey, K.L., Basu, S.K., Okayama, H., Berg, P., Golstein, J.L., and Brown, M.S. (1984) Nucleotide Sequence of 3-Hydroxy-3-methylglutaryl Coenzyme A Reductase, A Glycoprotein of Endoplasmic Reticulum, *Nature 308*, 613–617.
29. Liscum L., Cummings, C., Anderson, R.G.W., DeMartino, G.N., Goldstein, J.L., and Brown, M.S. (1983) 3-Hydroxy-3-methylglutary Coenzyme A Reductase: A Transmembrane Glycoprotein of the Endoplasmic Reticulum with N-linked "High-mannose" Oligosaccharides, *Proc. Natl. Acad. Sci. USA 80*, 7165–7169.
30. Cohen, D.C., Massoglia, S.L., and Gospodarowicz, D. (1982) Correlation Between Two Effects of High Density Lipoproteins on Vascular Endothelial Cells. The Induction of 3-Hydroxy-3-methylglutaryl Coenzyme A Reductase Activity and the Support of Cellular Proliferation*, J. Biol. Chem. 257*, 9429–9437.
31. Chen, H.W. (1981) The Activity of 3-Hydroxy-3-methylglutaryl Coenzyme A Reductase and the Rate of Sterol Synthesis Diminish in Cultures with High Cell Density*, J. Cell Physiol. 108*, 91–97.
32. Harwood, H.J., Jr., Schneider, M., and Stacpoole, P.W. (1984) Measurement of Human Leukocyte Microsomal HMG-CoA Reductase Activity, *J. Lipid Res. 25*, 967–978.

[Received October 28, 1999, and in final revised form March 14, 2000; revision accepted March 20, 2000]

Membrane Physical Properties Do Not Explain Increased Cyclic AMP Production in Hepatocytes from Rats Fed Menhaden Oil

Michael E. Bizeau* and Jeffrey R. Hazel

Department of Biology, Arizona State University, Tempe, Arizona 85287

ABSTRACT: To study the effect of altering plasma membrane fatty acid composition on the glucagon signal transduction pathway, cAMP accumulation was measured in hepatocytes from rats fed diets containing either menhaden oil (MO) or coconut oil (CO). Hepatocytes from MO-fed animals produced significantly more cAMP in response to glucagon and forskolin compared to CO-fed animals. Glucagon receptor number and affinity were similar in MO- and CO-fed rats. Liver plasma membranes from MO-fed animals were enriched in long-chain n-3 fatty acids and contained significantly lower amounts of saturated C_{10}–C_{16} and 18:1n-9 than CO-fed animals. Membrane physical properties were examined using both Fourier transform infrared spectroscopy (FTIR) and the fluorescent probe 1,6-diphenyl-1,3,5-hexatriene (DPH). FTIR analysis revealed that below 34°C, CO membranes were more ordered than MO membranes. However, as assay temperature approached 37°C, MO and CO membranes became similarly ordered. DPH polarization values indicated no differences in membrane order at 37°C, whereas membrane order was decreased in CO-fed animals at 25°C. These data indicate the importance of assay temperature in assessing the influence of membrane physical properties on the activity of signal transduction pathways. Whereas increased signal transduction activity has been correlated to reduced membrane order in MO-fed animals, these data indicate that at physiological temperatures membrane order did not vary between groups. Enhanced cAMP accumulation in response to forskolin indicates that adenylate cyclase activity or content may be elevated in MO- vs. CO-fed rats. Enhanced adenylate cyclase activity may result, in part, from changes in specific fatty acids in hepatocyte plasma membranes without demonstrable changes in membrane physical properties.

Paper no. L8297 in *Lipids 35,* 595–600 (June 2000).

Signal transduction is a membrane-dependent process and is regulated, in part, by the fatty acid composition of the plasma membrane (1). In the liver, the glucagon-signaling pathway (GSP) is a principal regulator of hepatic glucose output (2). The GSP pathway comprises three distinct components that are all either embedded in or associated with the plasma membrane (3). These are the glucagon receptor, the G-protein complex, and the enzyme adenylate cyclase. Alterations in plasma membrane lipid composition can alter signal transduction at any of these steps in the cascade by altering the physical or chemical properties of the membrane (1).

In mammals, a primary determinant of membrane fatty acid composition is the fatty acid composition of the diet (4). In general, changes in plasma membrane fatty acid composition mimic changes in dietary fatty acid composition. An increase in the percentage of polyunsaturated fatty acids in plasma membranes increases the binding of insulin to the insulin receptor in adipose tissue, skeletal muscle and liver (5–7), increases cAMP production in liver and heart (8,9), and increases catecholamine binding in heart and adipose tissue (9–11).

Although dietary fatty acids have the potential to alter the transcription of components involved in signal transduction pathways (12), the activation of adenylate cyclase is remarkably sensitive to alterations in plasma membrane lipid composition (1,8,9,13–15). Changes in membrane fatty acid composition most likely alter adenylate cyclase activation by altering the bulk physical properties of the membrane or the specific chemical environment surrounding the signal transduction components. Studies relating signal transduction activity to membrane physical properties have produced contradictory results: in some cases lipid-induced changes in adenylate cyclase activity have been attributed to changes in membrane physical properties (16,17), whereas other studies suggest that changes in membrane fatty acid composition do not elicit significant changes in membrane physical properties (9,18). This disparity may, in part, reflect the condition and methods used to assess membrane physical state. While some studies have determined membrane order at 37°C (18), others have assessed order at 25°C (11) or assumed that changes in fatty acid composition must result in altered membrane physical properties (16,17).

In an attempt to resolve these disparities, we characterized membrane order over a broad temperature range using Fourier transform infrared (FTIR) spectroscopy in plasma membranes in which membrane fatty acid composition was altered by feeding diets enriched in menhaden oil (MO) or coconut oil (CO). Infrared spectroscopy has the advantage of permitting the estimation of membrane physical properties

*To whom correspondence should be addressed at PEBE, Arizona State University, Tempe, AZ 85287-0404. E-mail: Bizeau@asu.edu

Abbreviations: BSA, bovine serum albumin; CO, coconut oil; DPH, 1,6-diphenyl-1,3,5-hexatriene; FTIR, Fourier transform infrared; GSP, glucagon-signaling pathway; MO, menhaden oil; TLC, thin-layer chromatography.

from stretching vibrations of native membrane constituents without the introduction of potentially perturbing membrane probes (19). Additionally, we have assessed the efficacy of glucagon signaling in functionally intact hepatocytes and have related these measurements to FTIR measurements of membrane order.

METHODS

Animals and feeding. Male Sprague-Dawley rats were obtained from an institutional breeding stock at 35–40 d of age, weighed, and divided into two groups. Each group received a nutritionally complete semipurified diet containing, in g/kg: casein (239), corn starch (179), sucrose (247), cellulose (60), AIN-76 vitamin mix (12), AIN-76 mineral mix (41), DL-α-tocopherol (4), DL-methionine (4), choline bitartrate (2), corn oil (12), treatment oil (205). Fatty acid composition of the diets was determined by gas chromatography (Table 1). Diets were prepared fresh weekly, gassed with nitrogen, and stored at –20°C until used. Animals had free access to food and water and were housed in wire-bottomed cages in a room that was maintained at 25°C on a 12 h light/dark cycle. Animals consumed the experimental diet for 4 wk. Food consumption was monitored daily, and animal weight was recorded weekly. All procedures for animal use were approved by the Institutional Animal Care and Use Committee at Arizona State University.

Hepatocyte isolation. Hepatocytes were obtained by collagenase perfusion of the liver as described by Berry and Friend (20) and modified by Blackmore and Exton (21). Cells were suspended at 100 mg/mL wet weight and kept on ice until used in experiments. The initial quality of the cell preparation was assessed by trypan blue exclusion (0.2% final concentration) and measurement of cellular ATP content (22).

Measurement of cyclic AMP. Before being used to assess rates of cAMP production, hepatocytes were gassed with 95% O_2/5% CO_2 for 20 min at 37°C. Cells (50 mg/mL) were then incubated for 10 min in Krebs-Ringer's bicarbonate buffer (pH 7.4) containing either no addition (basal), glucagon (1 nM), forskolin (1 μM), or a combination of glucagon and insulin (1 nM glucagon + 10 nM insulin). After 10 min, incubations were stopped using ice-cold ethanol (final concentration 66% vol/vol) and cAMP was assayed using a radioimunoassy (Amersham, Arlington Heights, IL).

Liver plasma membrane isolation. Liver plasma membranes were isolated using a combination of differential and density gradient centrifugation according to a modification of the methods of Armstrong and Newman (23). Membrane preparations were enriched in the plasma membrane markers Na^+/K^+ ATPase and 5′-nucleotidase activity (~9- and ~8-fold, respectively) and essentially devoid of cytochrome-C-reductase (<0.2-fold), acid phosphatase (<0.5-fold), and NADPH cytochrome-C-reductase (<0.9-fold) activity.

Glucagon receptor assay. Glucagon receptor binding characteristics were assayed using the method of Rojas and Birnbaumer (24). Briefly, liver plasma membranes were incubated (in duplicate) at a final protein concentration in the assay of ~0.025 mg/mL in a final volume of 100 μL of reaction medium containing 20 mM HEPES, 0.1% bovine serum albumin (BSA), 1.0 mM EDTA, and various concentrations of ^{125}I-glucagon (cat.# NEX-207; New England Nuclear, Boston MA) pH 7.6. Nonspecific binding was determined in the presence of 1 μM (final concentration) unlabeled glucagon. Samples were incubated at 32.5°C for 20 min. Incubations were terminated by adding 4 mL of wash buffer (20 mM HEPES, 0.2% BSA pH 7.6) and vacuum-filtered onto presoaked (10% BSA overnight) cellulose acetate filters. The tubes were rinsed and vacuum-filtered twice with an additional 4 mL of rinse buffer. Radioactivity of the filters was quantified using a gamma counter, and the amount of specifically bound ^{125}I-glucagon was calculated as the difference in the mean (duplicate determinations) of total and nonspecific binding. Binding data were analyzed with Graph Pad Prism software (GraphPad Software, San Diego, CA) using nonlinear regression with a single binding site model. Binding affinity and receptor number are expressed as the K_D (nM) and the B_{max} (pmol/mg protein), respectively.

FTIR measurements. Plasma membrane samples were placed between two CaF_2 windows separated by a 50.8 μm Teflon spacer. Sample temperature was controlled to within 0.1°C by a combination of circulating coolant and microprocessor-controlled heating elements in a custom-designed (CIC Photonics) cell. Data were collected under continuous nitrogen gas purge with a PerkinElmer Spectrum 2000 FTIR spectrophotometer. Seventy-five spectra were averaged at each temperature and Fourier-transformed employing a strong apodization function to yield data every 1 cm^{-1}. Peak frequencies were determined, without baseline correction, from second-derivative spectra following subtraction of a background scan (collected under nitrogen purge) using spectrum 2000 software. From the FTIR data, the midpont temperature (point of inflection) of the gel–fluid transition was determined by first-derivative analysis of the temperature de-

TABLE 1
Fatty Acid Composition of the Diets[a]

Fatty acid	MO	CO
8:0	ND	2.12
10:0	ND	6.0
12:0	ND	45.09
14:0	7.41	19.23
16:0	19.09	10.72
16:1n-7	9.21	ND
18:0	3.97	10.82
18:1n-9	12.9	ND
18:2n-6	4.6	6.32
20:2n-6	1.87	ND
18:3n-3	1.59	ND
20:5n-3	16.05	ND
22:6n-3	15.79	ND

[a]Results are presented as percentage of total fatty acids. Fatty acids present at less than 1% are not shown (ND). Data are the average of three separate determinations. MO, menhaden oil; CO, coconut oil; ND, none detected.

pendence of the methylene asymmetric stretching frequencies employing the TableCurve-2D software package (SPSS Inc., Chicago, IL).

1,6-Diphenyl-1,3,5-hexatriene (DPH) polarization. Plasma membrane was suspended in a 20 mM potassium phosphate buffer (pH 7.4) to give a final protein concentration of 200 μg/mL. The fluorescent probe DPH (4 mM) in tetrahydrofuran was added to the membrane suspension in a ratio of 3 μL of probe solution to 5 mL of membrane suspension and incubated for 1 h at 25°C. Steady-state polarization measurements were performed using a PerkinElmer (Norwalk, CT) LS 50B luminescence spectrophotometer fitted with a constant-temperature cuvette holder. Excitation and emission monochromators were set at 358 and 430 nm, respectively. Polarization was calculated from the fluorescence intensities according to Equation 1:

$$P = (IV_V - GIV_H)/(IV_V + GIV_H) \quad [1]$$

where P = polarization, IV_V = emission intensity of vertically polarized light parallel to the plane of excitation, IV_H = emission intensity of horizontally polarized light perpendicular to the plane of excitation, and G is a configuration-specific correction factor. Measurements were performed at 25 and 37°C.

Membrane lipid extraction and analysis. Membrane lipid was extracted by the method of Bligh and Dyer (25). Neutral lipids were separated from phospholipids by thin-layer chromatography (TLC) using a solvent mixture composed of hexane/ether/acetic acid (90:10:1, by vol). Lipid spots were visualized in iodine vapors. The phospholipid and neutral lipid spots were scraped from the TLC plate and lipids extracted by washing with chloroform/methanol (2:1, vol/vol) three times, dried under a stream of nitrogen, and stored at –20°C until used for fatty acid analysis.

Fatty acid analysis. Phospholipids were prepared for fatty acid analysis by acid-catalyzed transesterification to their respective methyl esters (26). Fatty acid analysis was performed on a Hewlett-Packard 2850A gas chromatograph at 190°C equipped with an Omegawax™ 320 capillary column, 30 m × 0.32 mm × 0.25 μm film thickness (Supelco, Bellefonte, PA). Identification of fatty acids was accomplished by running multiple sets of standards (Matreya, Inc., Pleasant Gap, PA) and matching their retention times to those of the samples.

Statistical analysis. A two-way analysis of variance was used to examine differences between groups. If the overall F test was significant, comparisons between means were made using a student Newman-Kuels test. Statistical significance was set at $P < 0.5$ for all comparisons

RESULTS

Animal and cell characteristics. After 4 wk on the experimental diets there were no differences in body or liver weights between diet groups (Table 2). Food consumption averaged 15.5 ± 1.5 g/d and 15.2 ± 1.5 g/d for MO- and CO-fed groups, respectively, over the entire dietary treatment period with no differences between diet groups. Isolated hepatocytes from both groups displayed >90% trypan blue exclusion and normal cellular ATP content (Table 2), indicating a high quality cell preparation.

TABLE 2
Animal and Cell Characteristics[a]

	MO	CO
Animal weight (g)	297 ± 5.4	301 ± 3.4
Liver weight (g)	18.8 ± 1.2	19.7 ± 1.4
Dye exclusion (g)	94.5 ± 0.5	93.7 ± 0.4
Cell ATP (nmol/mg)	2.75 ± 0.05	2.68 ± 0.04

[a]Data are mean ± SE for $n = 6$ per diet group. Dye exclusion is the percentage of cells excluding trypan blue immediately prior to the start of incubations. For abbreviations see Table 1.

cAMP accumulation in isolated hepatocytes. Rates of cAMP accumulation (pmol/10 min) were measured in the absence (basal) and presence of several hormone and agonist combinations (Fig. 1). Basal cAMP accumulation was not different between the MO- and CO-fed groups. When glucagon (1 nM) was added to the incubation, hepatocytes from MO-fed rats accumulated significantly greater (~2-fold) amounts of cAMP than those from CO-fed animals. To examine if there had been a direct effect of MO feeding on adenylate cyclase, we employed forskolin (1 μM). Forskolin directly stimulates adenylate cyclase (27), bypassing the glucagon receptor and G-protein coupling steps in the GSP. In the presence of forskolin, significantly greater (~1.25-fold) cAMP accumulation occurred in hepatocytes from MO- vs. CO-fed rats. Insulin (10 nM), which stimulates cAMP degradation, was also added in combination with 1 nM glucagon to assess the

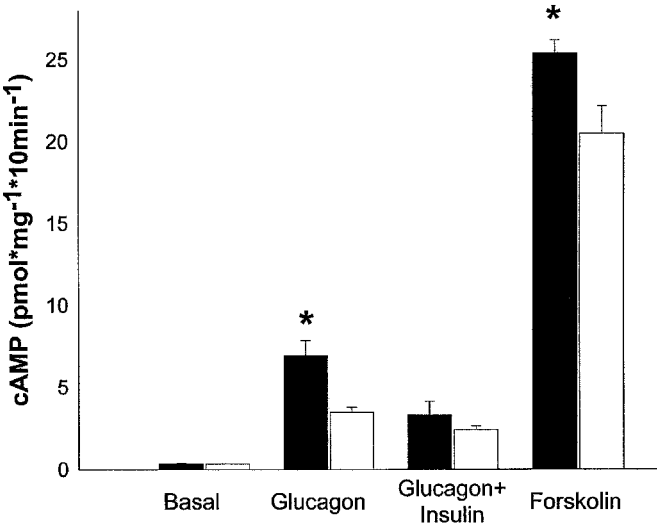

FIG.1. cAMP accumulation measured in hepatocytes from menhaden oil (MO; ■)- and coconut oil (CO; □)-fed animals. Cells were incubated in assay buffer containing no hormone (basal), 1 nM glucagon, 1 nM glucagon + 10 nM insulin, and 1 μM forskolin for 10 min and cAMP was measured. Data are the average ± SE for hepatocytes prepared for 6 animals from each diet group. *Significantly different ($P < .05$) from the other diet group for a given incubation condition.

ability of insulin to suppress cAMP production. cAMP accumulation in the presence of insulin did not differ between MO- and CO-fed groups although the relative magnitude of the reduction, compared to maximal glucagon stimulation, was greater ($P < .05$) in the MO-fed (45 ± 2.4 vs. 30 ± 3.2%) compared to the CO diet group.

Glucagon receptor binding characteristics. There were no differences in glucagon receptor B_{max} or K_D between the MO and CO groups. B_{max} for the MO-fed group was 5.02 ± 0.29 pmol/mg protein, and for the CO group it was 4.72 ± 0.43 pmol/mg protein. K_D values were 1.54 ± 0.45 nM and 1.71 ± 0.73 nM for MO- and CO-fed animals, respectively.

Membrane lipid composition. Plasma membrane fatty acid composition, in general, reflected the composition of the respective dietary fatty acids provided (Table 3). Plasma membranes from CO-fed animals were enriched in 14:0, 16:0, and 18:1n-9 and essentially depleted of 18:2n-6 and the long-chain n-3 fatty acids 20:5 and 22:6 compared to MO-fed animals.

FTIR and DPH. Measurements of membrane physical properties at different temperatures were performed using the fluorescent membrane probe DPH and by FTIR spectroscopy. DPH measurements indicated that at 37°C membranes from CO- and MO-fed animals exhibit similar degrees of acyl chain order, whereas at 25°C membranes from CO-fed animals are significantly more ordered compared to MO-fed membranes (Table 4). Higher frequencies of CH_2 stretching vibration in the FTIR spectra are associated with a less-ordered membrane. At temperatures below 34°C, membranes from CO-fed animals were more ordered than those from MO fed animals (Fig. 2). The gel–fluid transition midpoint temperature was significantly reduced in MO vs. CO, being 11.3 vs. 19.8°C in MO and CO, respectively. However, as assay temperature is increased to the animal's body temperature, MO and CO fed membranes exhibit similar CH_2 vibrational motion, indicating similar degrees of order in the acyl chain region.

TABLE 3
Fatty Acid Composition[a] of Liver Plasma Membranes Isolated from Animals Fed MO or CO for 4 wk

Fatty acid	MO	CO
14:0	3.4 ± 0.26*	7.18 ± 1.6
16:0	23.6 ± 0.33*	31.51 ± 1.7
16:1n-7	7.4 ± 1.1	5.56 ± 1.5
18:0	15.9 ± 0.72	17.5 ± 2.2
18:1n-7	2.9 ± 0.65	1.9 ± 0.54
18:1n-9	9.9 ± 1.1*	16.1 ± 0.57
18:2n-6	7.3 ± 1.9*	2.68 ± 0.61
20:0	1.8 ± 0.28	1.7 ± 0.48
20:4n-6	5.1 ± 1.0	4.64 ± 0.40
20:5n-3	3.2 ± 0.53*	ND
22:6n-3	10.64 ± 1.2*	3.28 ± 0.82

[a]Results are presented as percentage of total fatty acids. Fatty acids present at less than 1% are not shown. Data are the mean ± SE from 6 membrane preparations per diet group. *Significantly different ($P < .05$) from other diet group. For abbreviations see Table 1.

TABLE 4
DPH Polarization Values[a] of Plasma Membranes Isolated from MO- and CO-Fed Animals Measured at 37 and 25°C

	Diet group	
Temperature (°C)	MO	CO
25	0.248 ± 0.011	0.278 ± 0.012*
37	0.246 ± 0.011	0.245 ± 0.013

[a]Values presented are the mean ± SE for measurements obtained from four separate membrane preparations per diet group. *Significantly different ($P < .05$) from all other groups. DPH, 1,6-diphenyl-1,3,5-hexatriene; for other abbreviations see Table 1.

DISCUSSION

Dietary-induced alterations in GSP function may result from changes in binding properties of the glucagon receptor, the number of glucagon receptors, altered functioning of the G-protein complex, or increases in the activity or amount of the terminal component in the pathway, adenylate cyclase. Additionally, changes in membrane fatty acid composition may result in altered coupling efficiency (29) between these components, which may, in turn, alter cAMP production. It has been

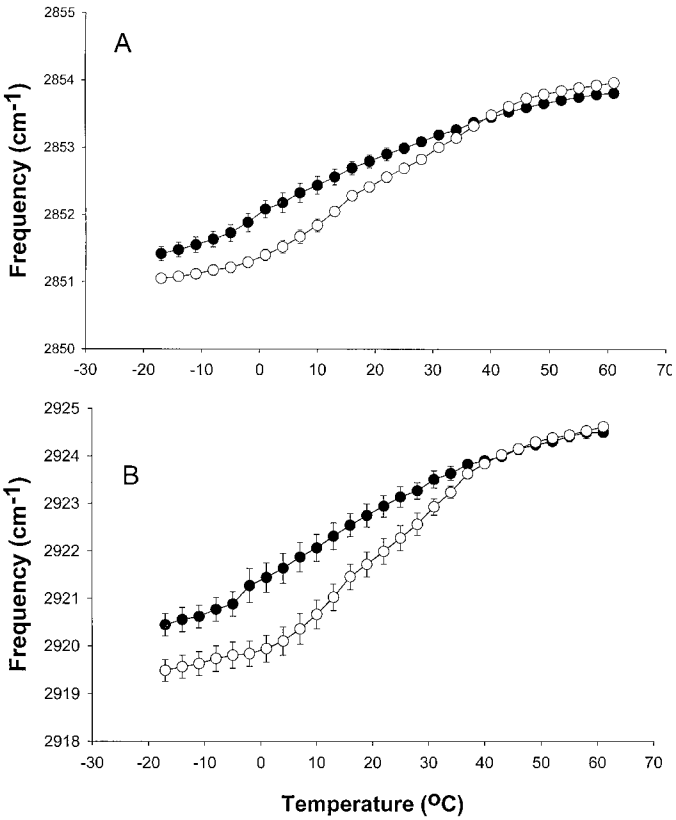

FIG. 2. Temperature dependence of CH_2 symmetric (panel A) and asymmetric (panel B) stretching vibrations in plasma membranes obtained from animals fed either MO (●) or CO (○). Data are average ± SE for plasma membranes obtained from 4 separate membrane preparations per diet group. Values are significantly different ($P < .05$) from the other diet group at all temperatures below 34°C. Above 34°C values are not significantly different. For abbreviations see Figure 1.

shown previously that the capacity to produce cAMP is higher in plasma membranes isolated from animals fed a MO diet vs. diets containing either butter or corn oil as the fat source (8). By using functionally intact hepatocytes, the results of the present study confirm that feeding MO increases glucagon-stimulated cAMP accumulation in whole cells. In order to determine the locus of the altered glucagon signaling, cAMP production was stimulated with forskolin. Forskolin stimulates cAMP production by directly and maximally stimulating adenylate cyclase at the catalytic subunit (28). Forskolin-stimulated cAMP production was 1.25-fold greater in hepatocytes fed a MO compared to a CO diet. This result suggests that a proportion of the increased glucagon-stimulated cAMP production may be due to changes in activity of adenylate cyclase, which may be attributed to the observed changes in membrane lipid composition. Although it cannot be ruled out that diet influenced the amount of enzyme in the membrane by regulating transcription, there were no differences in glucagon receptor numbers or binding characteristics between the two groups, a result similar to previous studies (8). These results suggest that the additional contributions to the twofold rise in glucagon-stimulated cAMP production may be attributed to alterations in membrane fatty acid composition, which could alter the coupling between components in this signal transduction pathway.

Altered functioning of signal transduction pathways in response to feeding different dietary fats has been most frequently explained by alterations in membrane "fluidity." In these studies we used FTIR to measure the CH_2 vibrational frequency in the acyl chains of isolated plasma membrane from animals fed MO or CO diets. Additionally, these measurements were conducted over a wide temperature range (–20 to 58°C) which enabled us to examine the possible involvement of the gel-to-liquid crystalline phase transition temperature in altered GSP functioning. FTIR measurements of CH_2 symmetric and asymmetric stretching vibrations indicate that when assayed at body temperature the vibrational motion of methylene stretching (i.e., membrane order) is similar between the two diet groups. When assay temperature is reduced, membranes from CO-fed animals have lower CH_2 vibrational motion and are more ordered than MO-fed animals. Previous reports have been equivocal as to whether dietary fat alters hepatocyte membrane "fluidity" (8,16). The results of the FTIR measurements conducted in this study clearly demonstrate that although membrane order is decreased at temperatures below the physiological range in CO-fed membranes, a compensatory mechanism exists to preserve membrane order at body temperature. This mechanism is most likely the inclusion of greater amounts of the monounsaturated fatty acid 18:1n-9 in the membranes of CO-fed animals. The addition of 18:1n-9 has been demonstrated to be highly effective at reducing membrane order (29). One important result revealed by the FTIR measurements is the importance of assay temperature in interpreting the results of studies in which membrane lipid composition is thought to influence signal transduction pathways. It is clear from both the symmetric and asymmetric stretching vibrations of the CH_2 moieties that motion in the CO-fed membranes is restricted relative to MO-fed membranes below 34°C. If measurements of cAMP production, receptor binding, or other hormonally stimulated events that are dependent on membrane physical properties are to be meaningful, they must all be conducted at the same, and ideally, the physiological temperature. This is exemplified by examining FTIR measurements of CH_2 vibrational stretching at 32 vs. 37°C. Many measurements of hormone binding are conducted at temperatures from 32 down to 25°C. The FTIR spectra demonstrate that membrane order is indeed increased in the CO-fed animals at these temperatures. Given this observation, hormone binding to receptors could therefore be influenced at lower assay temperatures by membrane physical properties. Whereas if the receptor-binding measurements are made at 37°C, where membrane physical properties are similar, differences in hormone binding may not exist. Additionally, if the results of assays conducted at temperatures below 37°C are correlated to those made below 37°C, this may lead to false interpretation of the role the membrane is playing in regulation signal transduction pathways.

Alterations in plasma membrane fatty acid composition have been associated with the development of many disease processes. In diabetes, glucagon-stimulated cAMP production is decreased along with insulin inhibition of cAMP production (30–32). The relative lack of cAMP production in response to glucagon in CO-fed animals resembles the alteration in glucagon signaling that is present in diabetes. Thus, diets high in CO may lead to alteration in glucagon signal transduction that can directly affect the regulation of hepatic glucose metabolism *via* multiple mechanisms. First, the capacity to produce glucose from glycogen may be compromised. Since a major regulator of hepatic glycogenolysis is cAMP, the decreased accumulation of cAMP in CO-fed rats suggests this process could be impaired. Second, and of major importance, decreased levels of cAMP may lead to changes in the expression of the enzymes that regulate the flow/production of glucose into and out of the liver. This lack of glucagon signaling may contribute to the enzymatic profile that is present in non-insulin dependent diabetes mellitus. Thus, modifications in dietary fatty acid composition could be directly involved in the etiology /prevention of diabetes by altering glucagon signaling in the liver.

In summary, the results of these experiments demonstrate that in intact hepatocytes, cAMP accumulation with either glucagon or forskolin stimulation is markedly elevated in animals where plasma membrane fatty acid composition was enriched in n-3 fatty acids *via* MO feeding compared to a diet high in saturated fats. This effect is not the result of changes in membrane physical properties induced by dietary fat, although dietary fat type did significantly influence membrane fatty acid composition. The results of this study, when taken together with those of Lee and Hamm (8), strongly suggest that the specific fatty acids present in MO such as 20:5n-3 or 22:6n-3 may directly modulate adenylate cyclase activity in the liver. The

exact mechanism by which MO increases adenylate cyclase activity in liver is unknown. It is quite possible that MO feeding results in the formation of specific lipid microdomains in the membrane which directly influence adenylate cyclase activity and is an area which has yet to examined in detail.

ACKNOWLEDGMENTS

This work was supported by NSF grant IBN 981643 to J.R.H. and an ASU Graduate Student Research Support Organization Award to M.E.B.

REFERENCES

1. Murphy, M.G. (1990) Dietary Fatty Acids and Membrane Protein Function, *J. Nutr. Biochem. 1,* 68–79.
2. Pagliassotti, M.J., Davis, S.N., and Cherrington, A.D. (1994) *The Role of the Liver in Maintaining Glucose Homeostasis,* R.G. Landes, Austin, TX.
3. Rodbell, M., Lad, P.M., Nielsen, T.B., Cooper, D.M.F., Schlegel, W., Presten, M.S., Londos, C., and Kempner, E.S. (1981) The Structure of Adenylate Cyclase Systems, *Adv. Cyclic Nucleotide Res. 14,* 3–14.
4. Clandinin, M.T., Field, C.J., Hargreaves, K., Morson, L., and Zsigmond, E. (1985) Role of Diet in Subcellular Structure and Function, *Can. J. Physiol. Pharmacol. 63,* 546–556.
5. Field, C.J., Ryan, E.A., Thomson, A.B.R., and Clandinin, M.T. (1990) Diet Fat Composition Alters Membrane Phospholipid Composition, Insulin Binding, and Glucose Metabolism in Adipocytes from Control and Diabetic Animals, *J. Biol. Chem. 265,* 11143–11150.
6. Lui, S., Baracos, V.E., Quinney, A.H., and Clandinin, M.T. (1994) Dietary ω-3 and Polyunsaturated Fatty Acids Modify Fatty Acyl Composition and Insulin Binding in Skeletal-Muscle Sarcolemma, *Biochem. J. 299,* 831–837.
7. Pan, J.S., and Berdanier, C.D. (1991) Dietary Fat Saturation Affects Hepatocyte Insulin Binding and Glucose Metabolism in BHE Rats, *J. Nutr. 121,* 1820–1826.
8. Lee, C.R., and Hamm, M.W. (1989) Effect of Dietary Fat and Cholesterol Supplements on Glucagon Receptor Binding and Adenylate Cyclase Activity of Rat Liver Plasma Membrane, *J. Nutr. 119,* 539–546.
9. Alam, S.Q., Alam, B.S., and Ren, Y.F. (1987) Adenylate Cyclase Activity, Membrane Fluidity and Fatty Acid Composition of Rat Heart in Essential Fatty Acid Deficiency, *J. Mol. Cell Cardiol. 19,* 465–475.
10. McMurchie, E.J., Patten, G.S., Charnock, J.S., and Mclennan, P.L. (1987) The Interaction of Dietary Fatty Acid and Cholesterol on Catecholamine-Stimulated Adenylate Cyclase Activity in the Rat Heart, *Biochim. Biophys. Acta 898,* 137–153.
11. Matsuo, T., Sumida, H., and Suzuki, M. (1995) Beef Tallow Diet Decreases β-Adrenergic Receptor Binding and Lipolytic Activities in Different Adipose Tissues of Rat, *Metabolism 44,* 1271–1277.
12. Clarke, S.D., and Jump, D.B. (1993) Regulation of Gene Transcription by Polyunsaturated Fatty Acids, *Prog. Lipid Res. 32,* 139–149.
13. Pohl, S.L., Krans, H.M., Kozyreff, V., Birnbaumer, L., and Rodbell, M. (1971) The Glucagon-Sensitive Adenyl Cyclase System in Plasma Membranes of Rat Liver VI. Evidence for a Role of Membrane Lipids, *J. Biol. Chem. 246,* 4447–4454.
14. Dipple, I., and Houslay, M.D. (1978) The Activity of Glucagon-Stimulated Adenylate Cyclase from Rat Liver Plasma Membranes Is Modulated by the Fluidity of Its Lipid Environment, *Biochem J. 174,* 179–190.
15. Sinensky, M., Minneman, K.P., and Molinoff, P.B. (1978) Increased Membrane Acyl Chain Ordering Activates Adenylate Cyclase, *J. Biol. Chem. 254,* 9135–9141.
16. Neelands, P.J., and Clandinin, M.T. (1983) Diet Fat Influences Liver Plasma-Membrane Lipid Composition and Glucagon-Stimulated Adenylate Cyclase Activity, *Biochem. J. 212,* 573–583.
17. Morson, L.A., and Clandinin, M.T. (1986) Diets Varying in Linoleic and Linolenic Acid Content Alter Liver Plasma Membrane Lipid Composition and Glucagon-Stimulated Adenylate Cyclase Activity, *J. Nutr. 116,* 2355–2362.
18. Lee, C.R., Beattie, O.P., and Hamm, M.W. (1989) Saturated, n-6, or n-3 Fatty Acids and Cholesterol Supplementation: Differential Effects on Liver and Heart Lipid Composition, *Nutr. Res. 9,* 293–305.
19. Mantsch, H.H., and McElhaney, R.N. (1991) Phospholipid Phase Transitions in Model and Biological Membranes as Studied by Infrared Spectroscopy, *Chem. Phys. Lipids 57,* 231–226.
20. Berry, M.N., and Friend, D.S. (1969) High-Yield Preparation of Isolated Rat Liver Parenchymal Cells. A Biochemical and Fine Structural Study, *J. Cell Biol. 43,* 506–519.
21. Blackmore, P.F., and Exton, J.H. (1985) Assessment of Effects of Vasopressin, Angiotensin II, and Glucagon on Ca^{++} Fluxes and Phosphorylase Activity in Liver, *Methods Enzymol. 109,* 550–558.
22. Trautschold, I., Lamprecht, W., and Scheitzer, G. (1985) Adenosine 5′-Triphosphate: UV Method with Hexokinase and Glucose-6-phosphate Dehydrogenase, in *Methods of Enzymatic Analysis* (Bergmeyer, H.U., ed.), pp. 346–357, Academic Press, New York.
23. Armstrong, J.M., and Newman, J.D. (1985) A Simple, Rapid Method for the Preparation of Plasma Membranes from Liver, *Arch. Biochem. Biophys. 238,* 619–628.
24. Rojas, F.J., and Birnbaumer, L. (1985) Assays for Glucagon Receptor Binding, *Methods Enzymol. 109,* 3–12.
25. Bligh, E.G., and Dyer, W.J. (1959) A Rapid Method of Total Lipid Extraction and Purification, *Can. J. Biochem. Physiol. 37,* 911–923.
26. Christie, W.W. (1982) Lipid Analysis, 2nd edn., Pergamon Press, Oxford, England.
27. Wong, S.K.-F., and Martin, B.R. (1983) The Role of a Guanine Nucleotide-Binding Protein in the Activation of Rat Liver Plasma-Membrane Adenylate Cyclase by Forskolin, *Biochem. J. 216,* 753–759.
28. Orly, J., and Schramm, M. (1975) Fatty Acids as Modulators of Membrane Functions: Catecholamine-Activated Adenylate Cyclase of the Turkey Erythrocyte, *Proc. Natl. Acad. Sci. USA 72,* 3433–3437.
29. Quinn, P.J., Joo, F., and Vigh, L. (1989) The Role of Unsaturated Lipids in Membrane Structure and Function, *Prog. Biophys. Molec. Biol. 53,* 71–103.
30. Brucelin, R., Katz, E.B., and Charron, M.J. (1996) Molecular and Cellular Aspects of the Glucagon Receptor: Role in Diabetes and Metabolism, *Diabetes Metab. Rev. 22*, 373–396.
31. Dighe, R.R., Rojas, F.J., Birnbaumer, L., and Garber, A.J. (1984) Glucagon-Stimulable Adenylyl Cyclase in the Rat Liver. The Impact of Streptozotocin-Induced Diabetes Mellitus, *J. Clin. Invest. 73,* 1013–1023.
32. Bhathena, S.J., Voyles, N.R., Smith, S., and Recant, L. (1978) Decreased Glucagon Receptors in Diabetic Rat Hepatocytes. Evidence for Regulation of Glucagon Receptors by Hyperglucagonemia, *J. Clin. Invest. 61,* 1488–1497.

[Received June 29, 1999, and in revised form March 3, 2000; revision accepted April 30, 2000]

Dietary Cod Liver Oil Decreases Arachidonic Acid in Rat Gastric Mucosa and Increases Stress-Induced Gastric Erosions

Sigurdur Oli Olafsson[a], Jonas Hallgrimsson[b], and Sigmundur Gudbjarnason[a,*]

[a]Science Institute and [b]Department of Pathology, University of Iceland, IS-107 Reykjavík, Iceland

ABSTRACT: The purpose of this study was to examine the influence of long-term feeding of dietary fat rich in either n-3 or n-6 fatty acids on the availability of arachidonic acid (20:4n-6) in major phospholipids of gastric mucosa in rats. Three groups of male Wistar rats were fed either a standard diet, a cod liver oil-enriched diet (10% by weight), or a corn oil-enriched diet (10% by weight) for 8 mon. Dietary cod liver oil significantly reduced the level of 20:4n-6 in phosphatidylcholine (PC) and in phosphatidylethanolamine (PE) of gastric mucosa. The loss of 20:4n-6 was compensated for by eicosapentaenoic acid (20:5n-3) in PC, whereas the decrease in 20:4n-6 in PE corresponded to the increase in three n-3 fatty acids: 20:5n-3, docosapentaenoic acid (22:5n-3), and docosahexaenoic acid (22:6n-3). The level of 20:5n-3 was higher than the level of 22:6n-3 both in PC and PE of mucosa in rats fed cod liver oil. Diets supplemented with corn oil increased the level of 18:2n-6 but decreased the monoene fatty acids 16:1 and 18:1n-7 in PC but not in PE of gastric mucosa. The 20:4n-6 levels of both PC and PE were markedly reduced by dietary cod liver oil, to about one-third of control levels. Similar changes were also observed in the stomach wall. Gastric erosions were observed in all rats exposed to restriction stress, but this form of stress induced twice the number of erosions in rats fed fish oil compared to control rats or rats fed corn oil. We conclude that a diet rich in fish oil altered the balance between n-6 and n-3 fatty acids in major gastric mucosal phospholipids, markedly reduced the availability of 20:4n-6, and increased the incidence of gastric erosions induced by restriction or emotional stress.

Paper no. L8358 in *Lipids 35*, 601–605 (June 2000).

The fatty acid composition of membrane phospholipids plays an important role in the stomach. On the luminal surface of the stomach is a layer of surface-active phospholipids that render the mucosal surface hydrophobic and resistant to damage induced by luminal acid (1,2). Ulcerogenic substances cause a dissipation of this layer, leading to back-diffusion of acid and mucosal necrosis (3).

Infection with *Helicobacter pylori* has been shown to be associated with peptic ulcer disease (1). *Helicobacter pylori* release phospholipases and ammonia, which have the capacity to reduce the phospholipid-dependent hydrophobic lining of the stomach and reduce mucosal defenses. The majority of people infected with this bacterium do not, however, develop ulcers, suggesting that individual differences in mucosal response to infection determine whether an ulcer develops (4).

The availability of arachidonic acid in gastric phospholipids plays an important role in the stomach because the ability of gastric mucosa to resist injury induced by luminal irritants is influenced by eicosanoids derived from arachidonic acid. The influence of specific n-6 fatty acids, such as linoleic acid (18:2n-6) and arachidonic acid (20:4n-6), on gastric mucosal resistance to injury in rats has been studied extensively (5–8). Dietary deficiency of linoleic acid was shown to predispose rats to increased gastric mucosal injury, whereas chronic dietary supplementation with linoleic acid increased the concentration of prostaglandin E_2 (PGE-$_2$) in the gastric lumen and decreased cold restraint injury. Reduced availability of arachidonic acid and impaired conversion of arachidonic acid to gastric prostaglandins diminish the ability of gastric mucosa to resist injury (8).

Diets enriched in fish oils protect duodenal (9) and gastric mucosae (10) against ethanol injury. The polyunsaturated fatty acids present in fish oils are eicosapentaenoic acid (EPA, 20:5n-3) and docosahexaenoic acid (DHA, 22:6n-3), and EPA has reportedly been converted to a family of trienoic eicosanoids with reduced inflammatory potential (11). The n-3 fatty acids are readily incorporated into gastric phospholipids, displacing arachidonic acid and potentially affecting both the cyclooxygenase and lipoxygenase pathway. The result is a likely decrease of prostaglandin PGE_2 and thromboxane A_2 synthesis and an increase in that of PGE_3 and leukotriene B_5 which may be less biologically active in inflammation. Furthermore, in some *in vitro* studies, dietary fish oil reduces leukotriene B_4, free radicals, and platelet-activating factor, all of which are considered significant mediators of mucosa damage.

The type and degree of stomach pathology depend on age and the nature of stress (12). The fatty acid composition of dietary fat also has significant effects on development of stomach pathology, either decreasing or increasing the susceptibility to mucosal damage depending on the nature of the injury. Dietary fish oil has thus been shown to protect the mucosa against ethanol-induced damage of gastric or duodenal mucosa in rats and humans (9,10,13). The damaging effects

*To whom correspondence should be addressed at Science Institute, University of Iceland, Vatnsmyrarvegur 16, IS-107 Reykjavík, Iceland.
E-mail: sigmgudb@raunvis.hi.is

Abbreviations: DHA, docosahexaenoic acid (22:6n-3); EPA, eicosapentaenoic acid (20:5n-3); PC, phosphatidylcholine; PE, phosphatidylethanolamine; PGE_2, prostaglandin E_2.

of aspirin on the gastric mucosa, however, are not influenced by dietary fish oil (14).

The purpose of this study was to examine the long-term influence of dietary cod liver oil and corn oil upon the balance between the n-3 and n-6 fatty acids in major phospholipids of gastric mucosa in middle-aged rats and upon the resistance to mucosal erosions induced by restriction or emotional stress. The results indicate that consumption of dietary cod liver oil can enhance the development of gastric erosions during emotional stress.

MATERIALS AND METHODS

Animals. Male Wistar rats at the age of 2 mon were randomly assigned to three groups. One group was fed a diet enriched with 10% cod liver oil containing 14.2% 18:2n-6, 15.8% 18:1n-9, 7.2% 20:5n-3, 6.7% 22:6n-3, and 11.2% of 20:1 + 22:1, for 8 mon. Another group was fed a diet enriched with 10% corn oil containing 50.9% 18:2n-6 and 28.2% 18:1n-9 for the same length of time. The diet enriched with fat was prepared once a week by mixing 90 g of regular diet (rat and mouse maintenance diet no. 1, Special Diets Services Ltd., Essex, United Kingdom) with 10 g of the dietary oil, followed by storage in the dark at 4°C. The antioxidant nutrient status of the diets is comparable: the corn oil contained 71.4 μg vitamin E/g oil, whereas the cod liver oil contained 65 μg vitamin E, 302 μg vitamin A and 130 IU vitamin D/g. The total sterol content of the cod liver oil was 0.6%.

A third group was fed a standard diet containing 18.1% 16:0, 13.9% 18:n-9, 56.5% 18:2n-6, and 6.5% 18:3n-3, with a fat content of 2% in the diet. The rats were housed in cages, three or four rats per cage, and maintained on 12 h/12 h light/dark cycle with free access to water and food. At the age of 10 mon the rats from each of these three groups were separated into a treatment group and a control group, with 15 rats in each group. Those in the treatment groups were placed in a narrow plastic cage where the rats were unable to move about or turn around (restriction stress) (15). All rats were fasted during the 18 h period of restraint and at the end they were anesthetized with CO_2 and killed by decapitation. The control rats were unrestrained and fasted for 18 h but had free access to water before decapitation. The stomachs were removed, opened along the greater curvature, and thoroughly washed with saline and inspected for gastric erosions following pinning on a board. The number of erosions was recorded by macroscopical examination. For further confirmation of the nature of the lesions eight stomachs were examined histologically (16).

Lipid extraction and analyses. Gastric mucosa from three stomachs were pooled for each experiment to reduce the effect of individual variations within each group. The lower glandular part was gently scraped, and the mucosal scrapings were immediately suspended in a mixture of chloroform/methanol (2:1, vol/vol). Each mucosal fraction was extracted in chloroform/methanol (2:1, vol/vol) for 8 h at room temperature as described previously (17).

Parts from mucosally denuded stomachs were used for each analysis. The upper part of the stomach, the forestomach, was cut from the glandular part along the limiting ridge and each part was analyzed separately, cut into small pieces in 76 mL of methanol/chloroform/water [2:1:0.8, by vol (15)] and homogenized in a Polytron model PTA. After filtration a biphasic system was produced by dilution with 1 vol of chloroform and 0.73% NaCl solution. The lower layer was withdrawn and evaporated in a rotary evaporator.

The lipid extracts from mucosa and the two mucosally denuded stomach parts were dissolved in a small volume of chloroform and separated on silicic acid columns. The phospholipids were separated by thin-layer chromatography as described previously (17).

The statistical tests used in the analyses of data were one-way analyses of variance. Data are expressed as mean ± SE for five preparations where mucosa from three rat stomachs were pooled per preparation.

RESULTS

There were some differences in the weight gain of rats fed the fat-supplemented diets during the 8-mon feeding period, final body weights being: standard diet, 450 ± 11 g; corn oil, 462 ± 8 g; and cod liver oil, 488 ± 14 g. The weight gain of rats fed cod liver oil was 8.4% greater than observed for rats fed the standard diet ($P < 0.01$) whereas the weight gain of rats fed the corn oil was not significantly different from the rats fed the standard diet.

Effect of dietary fat upon the fatty acid composition of phosphatidylcholine (PC) and phosphatidylethanolamine (PE) in the mucosa. The effects of dietary fat upon the fatty acid composition of PC and PE in the gastric mucosa are shown in Tables 1 and 2. In rats fed cod liver oil there was a significant decrease in 20:4n-6 in PC, to one-third of control

TABLE 1
Fatty Acid Composition of Phosphatidylcholine (PC) of Stomach Mucosa in Animals Fed Different Dietary Fat[a]

Fatty acid	Standard diet	10% Cod liver oil	10% Corn oil
16:0	28.09 ± 0.46	27.99 ± 0.22	28.17 ± 0.51
16:1	2.87 ± 0.18	2.25 ± 0.04	0.48 ± 0.23[b]
18:0	6.10 ± 0.27	6.26 ± 0.25	6.96 ± 0.24
18:1n-9	18.24 ± 0.89	18.79 ± 0.35	16.97 ± 0.59
18:1n-7	4.25 ± 0.16	4.21 ± 0.06[c]	2.78 ± 0.08[b]
18:2n-6	24.32 ± 0.77	26.23 ± 0.53	29.01 ± 0.57[b]
20:1	0.10 ± 0.10	0.74 ± 0.02[b,c]	0.13 ± 0.13
20:4n-6	11.76 ± 0.53	3.91 ± 0.24[b,c]	10.86 ± 0.38
20:5n-3	—[d]	4.66 ± 0.34	—[d]
22:0	0.27 ± 0.27	0.28 ± 0.17	0.50 ± 0.25
22:6n-3	0.31 ± 0.31	1.05 ± 0.06[c]	0.06 ± 0.06
Others	3.69 ± 1.04	3.63 ± 0.51	4.08 ± 1.16

[a]Values are % area means ± SE of five preparations. Three stomachs were pooled per preparation.
[b]$P < 0.05$ vs. standard diet group.
[c]$P < 0.05$ vs. corn oil group.
[d]Not detected.

TABLE 2
Fatty Acid Composition of Phosphatidylethanolamine (PE) of Stomach Mucosa in Animals Fed Different Dietary Fat[a]

Fatty acid	Standard diet	10% Cod liver oil	10% Corn oil
16[b]	6.23 ± 0.41	6.23 ± 0.06	6.03 ± 0.58
16:0	7.75 ± 0.45	7.15 ± 0.18	7.04 ± 0.25
16:1	—[e]	1.38 ± 0.13	—[e]
18[b]	8.69 ± 1.02	10.33 ± 1.06	10.19 ± 0.53
18:0	8.07 ± 0.44	8.12 ± 0.72	8.50 ± 0.67
18:1n-9	20.02 ± 0.42	21.75 ± 0.62	20.26 ± 0.57
18:1n-7	1.88 ± 0.11	1.80 ± 0.06	1.92 ± 0.09
18:2n-6	11.90 ± 0.67	11.51 ± 0.79	14.48 ± 0.50
20:4n-6	29.15 ± 0.92	10.67 ± 0.60[c,d]	26.84 ± 0.85
20:5n-3	0.42 ± 0.19	11.91 ± 1.51[c,d]	0.09 ± 0.09
22:0	0.22 ± 0.14	0.20 ± 0.12	0.76 ± 0.27
22:5n-3	0.07 ± 0.07	0.47 ± 0.12[c]	—[e]
22:6n-3	1.17 ± 0.08	4.10 ± 0.25[c,d]	0.67 ± 0.17
Others	3.69 ± 1.04	3.63 ± 0.51	4.08 ± 1.16

[a]Values are % area means ± SE of five preparations. Three stomachs were pooled per preparation.
[b]Plasmalogens.
[c]$P < 0.05$ vs. standard diet group.
[d]$P < 0.05$ vs. corn oil group.
[e]Not detected.

levels (Table 1). The loss of 20:4n-6 was compensated in part by a marked increase in EPA (20:5n-3), whereas DHA (22:6n-3) did not increase significantly. In rats fed corn oil there was an increase in 18:2n-6 and a corresponding decrease in 16:1 and 18:1n-7 in PC. The n-6/n-3 ratio of PC was 116 for rats fed the control diet, 5.3 for rats fed the cod liver oil, and 665 for rats fed corn oil.

In mucosal PE dietary cod liver oil also induced a marked decrease in 20:4n-6, to about one-third of control levels (Table 2). The decrease in 20:4n-6 was met by a corresponding increase in 20:5n-3, EPA, and DHA, with the greatest increase in 20:5n-3. Diets supplemented with corn oil did not influence the fatty acid composition of PE, compared to rats fed the standard diet. The n-6/n-3 ratio of PE was 25 for rats fed the control diet, 1.4 for rats fed cod liver oil, and 54 for rats fed corn oil.

Effect of dietary fat upon PC and PE in the denuded glandular parts and forestomach. The effects of dietary fat upon the fatty acid composition of PC and PE in the glandular parts and forestomach are shown in Tables 3 and 4. Dietary cod liver oil decreased the level of 20:4n-6 in PC by two-thirds in the glandular parts, the same as in mucosa, whereas the decrease in the forestomach was about 50%, compared to rats fed the regular diet. The loss of 20:4n-6 in PC was compensated for by an increase in several fatty acids, primarily 18:2n-6, EPA, and DHA. Dietary corn oil induced a small increase in 18:2n-6 and 20:4n-6 and a corresponding decrease in 16:1 and 18:1n-7 (Table 3).

Dietary cod liver oil reduced the level of 20:4n-6 in PE by about 50% in the glandular parts and by 36% in the forestomach. This decrease in 20:4n-6 was largely compensated for by the n-3 fatty acids, 20:5n-3, 22:5n-3 and DHA (Table 4). Dietary corn oil had only a minor influence on the fatty acid profile of PE in the stomach wall.

Restriction stress and pathological changes in gastric mucosa. Restriction stress caused gastric erosions that appeared as hemorrhagic spots measuring 1–2 mm in diameter in the glandular acid-bearing portion of the stomach. To confirm the nature of these lesions eight stomachs were examined microscopically. The lesions were acute and consisted of necrotic areas confined to the mucosa, i.e., in the category of erosions. The squamous epithelium of the forestomach was erosion-free in all rats.

The results are summarized as follows: Of the 15 rats in each group, two control rats fed standard diet and one control rat fed corn oil had erosions, whereas six control rats fed cod liver oil-enriched diet had gastric erosions. Erosions were observed in all rats exposed to restriction stress. The number of stress erosions was significantly greater in rats fed cod liver oil, with 17.14 ± 0.89 erosions per rat stomach, than in rats fed the

TABLE 3
Fatty Acid Composition of PC of Stomach Tissue in Animals Fed Different Dietary Fat[a]

Fatty acid	Standard diet		10% Cod liver oil		10% Corn oil	
	Glandular part	Forestomach	Glandular part	Forestomach	Glandular part	Forestomach
14:0	0.70 ± 0.18	0.65 ± 0.16	0.16 ± 0.16	—	—	—
16:0	42.45 ± 0.18	35.40 ± 0.50	40.03 ± 0.37[b]	34.15 ± 0.33	45.84 ± 0.64	36.56 ± 0.42
16:1	1.80 ± 0.07	1.99 ± 0.04	1.56 ± 0.19	2.66 ± 0.16[c]	—	1.08 ± 0.20[c]
18:0	10.06 ± 0.67	12.05 ± 0.29	13.92 ± 0.33[b]	11.09 ± 0.17[c]	10.44 ± 0.20	14.81 ± 0.15[c]
18:1n-9	8.57 ± 0.13	9.65 ± 0.12	10.71 ± 0.17[b]	12.59 ± 0.14[c]	8.34 ± 0.08	9.85 ± 0.11
18:1n-7	6.36 ± 0.06	4.66 ± 0.07	5.12 ± 0.04[b]	3.79 ± 0.03[c]	3.77 ± 0.20[b]	3.03 ± 0.08[c]
18:2n-6	8.45 ± 0.41	9.69 ± 0.25	12.53 ± 0.46[b]	16.50 ± 0.43[c]	11.90 ± 0.43[b]	11.04 ± 0.26[c]
20:1	—[d]	—[d]	1.44 ± 0.33	0.56 ± 0.56	—	—
20:4n-6	15.39 ± 0.45	20.82 ± 0.39	5.49 ± 0.27[b]	10.15 ± 0.36[c]	17.97 ± 0.16[b]	19.77 ± 0.64
20:5n-3	—	—	2.82 ± 0.14	3.24 ± 0.17	—	—
22:0	1.15 ± 0.18	0.71 ± 0.18	0.69 ± 0.18	—	—	0.90 ± 0.03
22:6n-3	0.52 ± 0.14	0.52 ± 0.21	1.98 ± 0.06[b]	2.82 ± 0.23[c]	—	—
Others	4.55 ± 0.69	3.86 ± 0.64	3.55 ± 0.40	2.45 ± 0.60	1.74 ± 0.55	2.96 ± 0.63

[a]Values are the % area mean ± SE of five preparations. Three stomachs were pooled per preparation.
[b]$P < 0.05$ vs. standard diet, glandular part.
[c]$P < 0.05$ vs. standard diet, forestomach. For abbreviation see Table 1.
[d]Not detected.

TABLE 4
Fatty Acid Composition of PE of Stomach Tissue in Animals Fed Different Dietary Fat[a]

Fatty	Standard diet		10% Cod liver oil		10% Corn oil	
acid	Glandular part	Forestomach	Glandular part	Forestomach	Glandular part	Forestomach
16[b]	12.59 ± 0.47	13.57 ± 0.17	10.87 ± 0.24[c]	11.17 ± 0.47[d]	11.18 ± 0.24[b]	11.39 ± 0.28[d]
16:0	7.06 ± 0.13	4.57 ± 0.07	6.72 ± 0.10	4.87 ± 0.06[d]	7.74 ± 0.27	4.36 ± 0.02[d]
16:1	0.95 ± 0.09	0.16 ± 0.16	0.96 ± 0.11	0.83 ± 0.21	0.66 ± 0.29	0.63 ± 0.16
18[b]	13.03 ± 0.78	10.98 ± 0.20	11.36 ± 0.25	9.65 ± 0.24[d]	10.26 ± 1.60	11.99 ± 0.11[d]
18:0	11.20 ± 0.50	12.08 ± 0.35	12.32 ± 0.45	13.42 ± 0.42[d]	11.51 ± 0.75	13.43 ± 0.12[d]
18:1n-9	5.04 ± 0.08	5.43 ± 0.07	7.44 ± 0.09[c]	9.49 ± 0.31[d]	5.88 ± 0.27[c]	5.66 ± 0.09
18:1n-7	1.96 ± 0.07	1.51 ± 0.04	2.02 ± 0.08	1.91 ± 0.05[d]	0.96 ± 0.39[c]	1.68 ± 0.05
18:2n-6	5.32 ± 0.63	5.07 ± 0.13	6.33 ± 0.97	6.58 ± 0.11[d]	5.82 ± 1.07	4.90 ± 0.12
20:4n-6	29.19 ± 0.38	31.63 ± 0.53	15.00 ± 0.71[c]	18.56 ± 0.60[d]	33.32 ± 1.44[c]	30.49 ± 0.36
20:5n-3	—	—	6.14 ± 0.18	4.27 ± 0.07	—	—
22:5n-3	1.67 ± 0.16	2.17 ± 0.27	4.39 ± 0.39[c]	4.75 ± 0.19[d]	0.32 ± 0.32[c]	1.38 ± 0.05[d]
22:6n-3	2.98 ± 0.20	3.76 ± 0.14	9.18 ± 0.31[c]	8.53 ± 0.14[d]	3.82 ± 0.39	2.35 ± 0.15[d]
Others	9.01 ± 0.79	9.07 ± 0.81	7.27 ± 0.51	5.97 ± 0.36	8.53 ± 0.67	11.74 ± 0.57

[a]Values are the % area mean ± SE of five preparations. Three stomachs were pooled per preparation.
[b]Plasmalogens.
[c]$P < 0.05$ vs. standard diet, glandular part.
[d]$P < 0.05$ vs. standard diet, forestomach. For abbreviation see Table 2.

standard diet, with 9.50 ± 0.64 erosions per stomach ($P < 0.01$), or corn oil-enriched diet, with 7.69 ± 0.60 erosions per stomach. The difference in number of gastric erosions between corn oil-fed rats and rats fed the standard diet was not significant.

DISCUSSION

In a previous study we showed that the functionally most active part of the stomach, the gastric mucosa, has the lowest level of 20:4n-6 in PC (17), reflecting the high turnover and utilization of 20:4n-6 in mucosa. The dietary modification of fatty acid composition of gastric phospholipids observed in this study was primarily seen in rats fed a cod liver oil-enriched diet. The most noticeable effect was a 63–67% decrease in 20:4n-6 in PE and PC, respectively. The loss of 20:4n-6 was mostly compensated for by the n-3 fatty acids derived from the fish oil. The cod liver oil-induced decrease in gastric arachidonic acid levels extended also to the stomach wall, with the greater loss in PC of the glandular part, underlying the mucosa (65% decrease) and somewhat less in the forestomach (50% decrease).

The corn oil-enriched diet had only a minor effect on the fatty acid composition of PC and no significant effect on PE. This is not surprising since the fatty acid profiles of the standard diet and the corn oil-enriched diet were similar. The fat content of the diet did not seem to influence the fatty acid profile of PC and PE since the fat content of the corn oil-enriched diet was much greater than in the standard diet.

Reduced availability of arachidonic acid and impaired conversion of arachidonic acid to gastric prostaglandins have been shown to diminish the ability of gastric mucosa to resist injury caused by aspirin (8). It is curious, however, that dietary fish oil had little effect on aspirin-induced gastric erosions in human volunteers (14). The ability of gastric mucosa to resist injury induced by luminal irritants is influenced by prostaglandins. Prostaglandin and nitric oxide influence the various components of mucosal defenses: they inhibit acid secretion, stimulate mucus and bicarbonate secretion, elevate mucosal blood flow, and accelerate the healing of ulcers (18). Among the eicosanoids are also lipid mediators of inflammation, such as leukotrienes and thromboxane, which may contribute to the pathogenesis of gastric ulcers.

The n-3 fatty acid EPA present in fish oils has been demonstrated to be metabolized to trienoic eicosanoids, and in some models these have exhibited less inflammatory potential than the arachidonate-derived analogs. The n-3 fatty acids are readily incorporated into gastric phospholipids, displacing arachidonic acid as described above and potentially affecting both the cyclooxygenase and lipoxygenase pathways. It has been shown that gastric prostaglandin synthesis can be adversely affected by ingestion of fish oil (13).

In this study we have shown that long-term and large intakes of fish oil leads to a very marked reduction of 20:4n-6 in mucosa. The results show furthermore that dietary fish oil, accompanied by restriction stress, enhanced the development of gastric erosions in rats. Dietary fish oil influences the susceptibility of gastric mucosa to injury differently, depending on the nature of the injury. Fish oil reduces ethanol-induced mucosal injury (9), whereas it increased the development of gastric erosions induced by emotional stress, as shown in this study. The injury may be caused by elevated levels of stress hormones (19) and persistent stimulation of the adrenergic system accompanied by increased activity of phospholipases. Rats fed the cod liver oil-supplemented diet developed twice the number of gastric erosions, induced by restriction stress, compared to control rats or rats fed the corn oil-supplemented diet. Our data support the view that arachidonic acid and prostaglandins play an important role in protection of gastric mucosa during emotional stress.

ACKNOWLEDGMENT

This work was supported by the Research Fund of the University of Iceland and the Science Fund of the Icelandic Research Council.

REFERENCES

1. Wallace, J.L., and Granger, D.N. (1996) The Cellular and Molecular Basis of Gastric Mucosal Defense, *FASEB J. 10*, 731–740.
2. Hills, B.A., Butler, B.D., and Lichtenberger, L.M. (1983) Gastric Mucosal Barrier: Hydrophobic Lining to the Lumen of the Stomach, *Am. J. Physiol. 244*, G561–G568.
3. Goddard, P.J., Hills, B.A., and Lichtenberger, L.M. (1987) Does Aspirin Damage Canine Gastric Mucosa by Reducing Its Surface Hydrophobicity? *Am. J. Physiol. 252*, G421–G430.
4. Walsh, J.H., and Peterson, W.L. (1995) The Treatment of *Helicobacter pylori* Infection in the Management of Peptic Ulcer Disease, *New Engl. J. Med. 333*, 984–991.
5. Schepp, W., Steffen, B., Ruoff, H.J., Schusdziarra, V., and Classen, M. (1988) Modulation of Rat Gastric Mucosal Prostaglandin E_2 Release by Dietary Linoleic Acid: Effects on Gastric Acid Secretion and Stress-Induced Mucosal Damage, *Gastroenterology 95*: 18–25.
6. Hollander, D., and Tarnawski, A. (1991) Is There a Role for Dietary Essential Fatty Acids in Gastroduodenal Mucosal Protection? *J. Clin. Gastroenterol. 13*, S72–S74.
7. Hollander, D., Tarnawski, A., Ivey, K.J., Wilson, N.H, and Misiwic, J.J. (1982) Arachidonic Acid Protection of Rat Gastric Mucosa Against Ethanol Injury, *J. Lab. Clin. Med. 100*, 296–308.
8. Tarnawski, A., Hollander, D., Stachura, J., Krause, W.J., and Gergly, H. (1989) Protection of the Rat Gastric Mucosa Against Aspirin Injury by Arachidonic Acid: A Dietary Prostaglandin Precursor Fatty Acid, *Eur. J. Clin. Invest. 19*, 278–290.
9. Schepp, W., Peskar, B.M., Trautmann, M., Stolte, M., Hagenhuller, F., Schusdziarra, V., and Classen, M. (1991) Fish Oil Reduces Ethanol-Induced Damage of the Duodenal Mucosa in Humans, *Eur. J. Clin. Invest. 21*:230–237.
10. Leung, F.W. (1992) Fish Oil Protection Against Ethanol-Induced Gastric Mucosal Injury in Rats, *Dig. Dis. Sci. 37*:636.
11. Simopoulos, A.P. (1991) Omega-3 Fatty Acids in Health and Disease and in Growth and Development, *Am. J. Clin. Nutr. 54*: 438–463.
12. Wideman, C.H., and Murphy, H.M. (1985) Effects of Vasopressin Deficiency, Age and Stress on Stomach Ulcer Induction in Rats, *Peptides 6*, 63–67.
13. Faust, T.W., Redfern, J.S., Lee, E., and Feldman, M. (1989) Effects of Fish Oil on Gastric Mucosal 6-Keto-$PGF_{1\alpha}$ Synthesis and Ethanol Induced Injury, *Am. J. Physiol. Gastrointest. Liver Physiol. 257*, G9–G13.
14. Faust, T.W., Redfern, J.S., Podolsky, I., Lee, E., Grundy, S.M., and Feldman, M. (1990) Effects of Aspirin on Gastric Mucosal Prostaglandin E_2 and $F_{2\alpha}$ Content and on Gastric Mucosal Injury in Humans Receiving Fish Oil or Olive Oil, *Gastroenterology 98*, 586–591.
15. Mikhail, A.A., and Holland, H.C. (1966) A Simplified Method of Inducing Stomach Ulcers, *J. Psychosomatic Res. 9*, 343–347.
16. Mikhail, A.A., and Holland, H.C. (1966) Evaluating and Photographing Experimentally Induced Stomach Ulcers, *J. Psychosomatic Res. 9*, 349–353.
17. Olafson, S.O., and Gudbjarnason, S. (1996) Availability of Arachidonic Acid in Major Phospholipids of Mucosa and the Stomach Wall of Rats, *Lipids 31*, 1323–1325.
18. Whittle, B.J.R., Lopez-Belmonte, J., and Moncada, S. (1990) Regulation of Gastric Mucosal Integrity by Endogenous Nitric Oxide: Interaction with Prostanoids and Sensory Neuropeptides in the Rat, *Br. J. Pharmacol. 99*, 607–611.
19. Kvetnansky, K., Sun, C.L., Lake, C.R., Thoa, N., Torda, T., and Kopin, I.J. (1978). Effect of Handling and Forced Immobilization on Rat Plasma Levels of Epinephrine, Norepinephrine, and Dopamine-β-Hydroxylase, *Endocrinology 103*, 1868–1874.

[Received September 21, 1999, and in final revised form April 25, 2000; revision accepted May 4, 2000]

Low Erucic Acid Canola Oil Does Not Induce Heart Triglyceride Accumulation in Neonatal Pigs Fed Formula

Timothy J. Green and Sheila M. Innis*

Department of Paediatrics, University of British Columbia, Vancouver, British Columbia, Canada V5Z 4H4

ABSTRACT: Canola oil is not approved for use in infant formula largely because of concerns over possible accumulation of triglyceride in heart as a result of the small amounts of erucic acid (22:1n-9) in the oil. Therefore, the concentration and composition of heart triglyceride were determined in piglets fed from birth for 10 (n = 4–6) or 18 (n = 6) d with formula containing about 50% energy fat as 100% canola oil (0.5% 22:1n-9) or 100% soybean oil, or 26% canola oil or soy oil (blend) with palm, high-oleic sunflower and coconut oil, providing amounts of 16:0 and 18:1 closer to milk, or a mix of soy, high-oleic sunflower and flaxseed oils with C_{16} and C_{18} fatty acids similar to canola oil but without 22:1. Biochemical analysis found no differences in heart triglyceride concentrations among the groups at 10 or 18 d. Assessment of heart triglycerides using Oil Red O staining in select treatments confirmed no differences between 10-d-old piglets fed formula with 100% canola oil (n = 4), 100% soy oil (n = 4), or the soy oil blend (n = 2). Levels of 22:1n-9 in heart triglyceride and phospholipid, however, were higher (P<0.01) in piglets fed 100% canola oil or the canola oil blend, with higher levels found in triglycerides compared with phospholipids. The modest accumulation of 22:1n-9 associated with feeding canola oil was not associated with biochemical evidence of heart triglyceride accumulation at 10 and 18 d.

Paper no. L8232 in *Lipids 35*, 607–612 (June 2000).

Diets containing rapeseed oils with greater than 10% erucic acid (22:1n-9) result in accumulation of 22:1n-9 in tissue lipids, reduced growth and rates of fatty acid oxidation, and myocardial lipidosis and necrosis in rats. The maximal safe intake of 22:1n-9 that does not lead to lipidosis in rat heart has been estimated to be 2 to 10% dietary fatty acids (1–8). The U.S. Food and Drug Administration currently permits dietary oils containing no more than 2% fatty acids as 22:1n-9 in foods for adults and children, but does not permit use of canola oils in infant formulas (9). Canola, a low 22:1n-9 hybrid derived from rapeseed, is widely used to prepare cooking and salad oils, table spreads, and in the preparation of bakery and fast foods in many countries. Canola oils are generally considered favorable dietary oils because of the relatively high proportion of 18:1 (about 50–60% fatty acids) and α-linolenic acid (18:3n-3), modest levels of linoleic acid (18:2n-6), and low levels of saturated fatty acids (10–15).

The restriction relating to the use of canola oil in infant formula is based, in part, on concerns that infants fed formula may consume higher amounts of 22:1n-9 than would be consumed through usual diets that contain a variety of foods, and the absence of experimental evidence demonstrating the safety of feeding formulas with canola oils to infants. In contrast to usual diets, infant formulas provide about 40–50% energy from fat, and formulas represent the major source of dietary fat for bottle-fed infants for the first 6 mon. Transient lipidosis has been noted in 5-d-old piglets fed sow's milk or a milk replacer with canola oil (0.8% 22:1n-9) (16). Definite lipidosis was observed in the heart of piglets fed oils containing between 7 and 42.9% 22:1n-9, values that generally paralleled the percentage of 22:1n-9 in heart triglyceride (16). Infant formulas usually provide a mixture of oils to provide levels of saturated and unsaturated fatty acids resembling human milk. Although some studies have reported that replacing a portion of the rapeseed oil with a saturated fat resulted in a lower incidence and/or severity of myocardial necrosis (17–19), a more recent study found that addition of saturated fat to the diet along with rapeseed oil (with 2.5 or 9% 22:1n-9) did not alter myocardial lipidosis, heart triglyceride, or 22:1n-9 in rats (20).

The present study was undertaken to determine whether the small amount of 22:1n-9 in canola oil resulted in increased heart triglyceride or 22:1 accumulation in formula-fed piglets, when canola oil was used as the sole source of fat or was blended with saturated fat to resemble more closely the fatty acid composition of pig and human milk and of infant formula. To address the possibility that the small amount of 22:1 or some other unusual feature of canola oil, such as the sterol components or triglyceride fatty acid distribution, is responsible for the adverse effects on heart lipids we designed an oil mix to mimic the levels of C_{16} and C_{18} carbon chain fatty acids of canola oil without 22:1 or the sterols components. Piglets were used for these studies because the proportion and composition of fat in pig milk resembles human milk, and lipid metabolism in pigs is similar to humans (21).

*To whom correspondence should be addressed at Department of Paediatrics, University of British Columbia, B.C. Research Institute for Children's & Women's Health, 950 W. 28th Ave., Vancouver, B.C., Canada V5Z 4H4. E-mail: sinnis@unixg.ubc.ca

Abbreviations: ANOVA, analysis of variance; Canola blend, 26% canola, 42% palm, 4% high-oleic sunflower, 16% sunflower, 12% coconut oil; Canola mimic, 29% soybean, 59% high-oleic sunflower, 12% flax oil; OCT, tissue embedding compound; Soy blend, 26% soybean, 48% palm, 14% high-oleic sunflower, 12% coconut oil.

METHODS

Animals and formulas. The formulas were prepared as liquid ready-to-feed formulas using procedures identical to those used in the manufacture of infant formula by Ross Laboratories, (Columbus, OH). The formulas contained identical amounts of carbohydrate, protein, fat, vitamins, and minerals and differed only in the source and composition of the fat (Table 1). Five fat blends, each providing about 50% of the dietary energy, were prepared: 100% canola oil (Canola); 100% soybean oil (Soy); 26% canola, 42% palm, 4% high- oleic sunflower, 16% sunflower, and 12% coconut oil (Canola blend); 26% soybean, 48% palm, 14% high-oleic sunflower, and 12% coconut oil (Soy blend); or 29% soybean, 59% high-oleic sunflower, and 12% flax oil (Canola mimic) (Table 1). The Canola mimic was designed to give as similar a composition of 16:0, 18:1, 18:2n-6, and 18:3n-3 to that in canola oil as practically possible, without the inclusion of 20:1n-9, 22:1n-9, or the sterol components of canola oil. The formulas with 26% canola or soybean oil (Canola blend and Soy blend, respectively) were designed to resemble formula for feeding healthy term gestation infants that include 16:0 and 18:1 at levels similar to those in human milk.

Male piglets of birth weight >1 kg were obtained from Kintail Meats (Langley, British Columbia, Canada). The piglets were randomly assigned to one of the five formulas, 10–12 piglets each, and bottle-fed from the first day of life until day 10 (n = 4–6/group) or 18 (n = 6/group) after birth (22). The piglets were housed in groups of three in a temperature-, humidity-, and light-controlled animal unit. The formula-fed piglets were bottle-fed the formula by hand every 1 1/2 to 2 h for the first 5 d, then every 3 h from 0600 to 2400 h. Passive immunity was provided to the formula-fed piglets by inclusion of colostrum-derived immunoglobulins (La Belle Assoc. Inc. Bellingham, WA) in the formula, 15 g/L for the first 72 h after birth, then 7.5 g/L for the next 72 h, and 2.5 g/L for the following 72 h. A group of piglets fed sow's milk (n = 10) by their natural mothers was studied for reference at a similar age and time after the last feed. All of the formula-fed and sow milk-fed piglets were given iron dextran, 10% (MTC Pharmaceutical, Cambridge, Ontario, Canada) on day 5 after birth. The Animal Care Committee of the University of British Columbia approved all procedures.

Pathology. The piglets were killed at 10 or 18 d of age, 3–4 h after the last feed by intracardiac injection of sodium pentabarbitol (1 mL) and decapitated. The heart was immediately excised and five sections, each 5-mm thick, were cut laterally from the heart starting at the apex (sections A, B, C, D, E). The fifth section (E) was cut just below the atria and was composed of tissue from both ventricle and the intraventricular septum. Sections F and G (5-mm in thickness) were cut from the left and right atria and an additional section of atria (H) was removed. Sections A, C, E, F, and G were cut into four small (5-mm) sections and used for histology. Sections B, D, and H were used for biochemical analysis and were frozen in liquid N_2 and stored at –80°C until analyzed. Two of the four sections from samples A, C, E, F, and G were placed into OCT compound (Tissue-Tek, Sakura Finetek, U.S.A. Inc., Torrance, CA), frozen in liquid N_2, and stored at –80°C.

TABLE 1
Fat Blend and Fatty Acid Composition of Formulas[a]

	Formula oil				
	Canola	Soy	Canola mimic	Canola blend	Soy blend
Oil (% total)					
Canola	100			26	
Soybean		100	29		26
High oleic sunflower			59	4	14
Flax			12		
Palm				42	48
Sunflower				16	
Coconut				12	12
Fatty acids (g/100 g)					
≤14:0	0.1	0.1	<0.0	8.7	8.8
16:0	4.7	10.3	5.9	20.1	23.3
18:0	2.0	3.4	4.7	3.6	4.2
18:1	56.6	23.7	56.8	39.6	38.6
18:2n-6	23.1	48.4	22.7	22.0	20.7
18:3n-3	9.7	7.7	9.1	2.7	2.0
20:0	0.7	0.3	0.3	0.5	0.4
20:1n-9	1.6	0.3	<0.1	0.5	0.1
22:0	0.3	0.3	0.2	0.2	0.1
22:1n-9	0.5	0.0	0.0	0.1	0.0

[a]The formulas were made to contain (per liter) 58 g total fat, 60 g protein from nonfat milk, 62 g carbohydrate with 240 μg vitamin A as retinyl palmitate, 4.4 μg cholecalciferol, 6.4 μg d-α-tocopherol equivalents, 60 μg phylloquinone, 150 mg vitamin C, 1.2 mg thiamin, 225 μg folic acid, 2.0 mg riboflavin, 13 mg niacin, 0.75 mg pyridoxine, 8.0 μg vitamin B_{12}, 7 mg pantothenic acid, 300 mg choline, 50 μg biotin, 56 mg inositol, 85 mg taurine, 2.3 g calcium, 1.76 g phosphorus, 175 mg magnesium, 800 mg sodium, 1.75 g potassium, 900 mg chloride, 25 mg iron, 25 mg zinc, 1.5 mg copper, 0.42 mg iodine, 0.8 mg manganese, 34 μg selenium.

Biochemistry. A portion (0.5–1.0 g) of each heart section (B, D, H) was homogenized, total lipids were extracted (23), and the concentrations of triglycerides and total cholesterol were analyzed using enzymatic methods (22,24). Phospholipid phosphorus was assayed after digestion with 70% perchloric acid according to Chen *et al.* (25). Triglycerides and phospholipids were separated from the total lipids by thin-layer chromatography (22), the fatty acid components converted to their respective methyl esters, and separated and quantitated by gas–liquid chromatography (26). The fatty acid composition of the formulas was determined following direct methylation of fatty acids (27), as in previous studies (26).

Histology. Heart histology was performed on 10-d-old piglets from select treatments only to confirm and extend the biochemical analysis of triglyceride concentrations. The hearts of piglets fed 100% Canola or 100% Soy oil (n = 4 each) were compared because these formulas contained 100% oil as either canola or soy, thus any effect of canola oil on cardiac lipid accumulation should be apparent by comparison of these treatments. The hearts of piglets fed the Soy blend (n = 2) were also analyzed because this formula is similar to some current commercial infant formulas. Sections (A, C, E, F, G), 8–10 μm thick, were cut from the tissues in OCT longitudinally on a cryostat at –16°C, stained with Oil Red O, and examined at a 400-fold magnification for the presence of myocardial lipid. Forty consecutive fields were examined and the number of cells that showed lipid accumulation counted. Because most of the myocardial lipid was extracellular, the number of individual streaks of lipid within each field was also determined. The pathologist was blinded with respect to formula and oils fed.

Statistical analysis. The results concerning growth, formula intake, heart lipid concentrations and fatty acids were analyzed by one-way analysis of variance (ANOVA) for piglets fed the Canola, Soy, Canola blend, or Soy blend formula for 10 or 18 d. The results for piglets fed the formula with Canola or the Canola mimic were also analyzed using ANOVA (secondary hypothesis). The natural log was used to obtain homogeneity of variance (Levene's Statistic) across treatment groups where appropriate. Two-way ANOVA found no significant differences ($P > 0.05$) in the concentration or composition of lipids in different regions of the heart within piglets. Therefore, values for different regions were averaged for each piglet for subsequent analysis of treatment effects. Results were compared between the groups of formula-fed piglets using one-way ANOVA and Fisher's Exact Test.

Preplanned comparisons (contrasts) were used to determine how the effect of feeding the formula with canola oil (Canola) compared with feeding soy oil (Soy) and how the effect of feeding 100% canola or soy oil compared with feeding a blend containing 26% canola (Canola blend) or soy oil (Soy blend) with other oils, respectively. The latter analysis considered the effect of replacing a portion of canola or soy oil with saturated fat. Finally, the effect of feeding 100% canola oil (Canola) compared to the effect of an oil blend with a similar fatty acid profile but with no 22:1n-9 or 20:1n-9 (Canola mimic) was considered. All calculations were performed with SPSS, release 7.5.1, for Windows 95. Results for a group fed sow's milk are included with the tables for reference but were not considered in the statistical analysis because of the many differences, in addition to lipids, between milk and formula, and in the housing and feeding environment of sow-fed and bottle-fed piglets.

RESULTS

There were no significant differences in formula intake, body weight, weight gain, liver weight or kidney weight among the groups at either 10 or 18 d of age (data not shown). The mean heart weight of piglets fed the Canola formula was higher than for those fed the Canola mimic, but was not different from that of piglets fed the other formulas at 18 d of age (mean ± SEM, 37.9 ± 1.5, 35.8 ± 2.5, 33.4 ± 0.9, 34.1 ± 1.1, 33.7 ± 1.2 g) for piglets fed the Canola, Soy, Canola blend, Soy blend and Canola mimic formula, respectively). There were no differences in heart weight at 10d, or in the heart per kg body weight, among the groups at 10 or 18 d.

The analysis of the heart triglyceride, phospholipid, and cholesterol concentrations found no significant difference among the groups at 10 or 18 d of age (Table 2). Histological evaluations using Oil Red O found trace to moderate amounts

TABLE 2
Heart Triglyceride, Phospholipid, and Cholesterol Concentration[a]

Formula Group	Age (d) 10	18
	(nmol/g)	
Triglyceride		
Canola	0.91 ± 0.28	0.81 ± 0.22
Soy	0.80 ± 0.17	0.60 ± 0.06
Canola blend	0.57 ± 0.08	0.51 ± 0.04
Soy blend	0.90 ± 0.27	0.74 ± 0.13
Canola mimic	0.97 ± 0.38	1.09 ± 0.28
Sow reference	0.71 ± 0.09	0.73 ± 0.13
Phospholipid		
Canola	1.81 ± 0.20	2.03 ± 0.17
Soy	1.86 ± 0.32	1.78 ± 0.17
Canola blend	2.05 ± 0.12	1.96 ± 0.15
Soy blend	2.10 ± 0.11	1.82 ± 0.21
Canola mimic	2.13 ± 0.22	1.94 ± 0.14
Sow reference	1.59 ± 0.09	2.42 ± 0.08
Cholesterol		
Canola	3.49 ± 0.23	3.74 ± 0.08
Soy	3.60 ± 0.35	3.44 ± 0.17
Canola blend	3.40 ± 0.19	3.05 ± 0.15
Soy blend	4.20 ± 0.27	3.63 ± 0.18
Canola mimic	3.35 ± 0.33	3.46 ± 0.18
Sow reference	3.90 ± 0.51	3.58 ± 0.22

[a]Data reported as mean ± SEM, n = 4–6/group at 10 d, and n = 6/group at 18 d. There were no statistically significant differences between the groups at 10 or 18 d for piglets fed formula with Canola compared to Soy oil, the Canola blend compared to Soy blend, Canola compared to the Canola Blend, or Canola compared to the Canola mimic. Definitions: Canola, 100% canola oil; Soy, 100% soybean oil; Canola blend, 26% canola, 42% palm, 4% high-oleic sunflower, 16% sunflower, and 12% coconut oil; Soy blend, 26% soybean, 48% palm, 18% high-oleic sunflower, and 12% coconut oil; Canola mimic, 29% soybean, 59% high-oleic sunflower, 12% flax oil.

TABLE 3
Cardiac Triglyceride Accumulation[a] in 10-d-old Pigs for Select Treatments[b]

	Formula oil		
	Canola	Soy	Soy blend
Intracellular lipid[c]	0.66 ± 0.23	0.69 ± 0.08	0.66 ± 0.16
Extracellular lipid[d]	9.33 ± 2.42	9.13 ± 1.73	6.39 ± 3.06
Total	10.00 ± 2.61	9.83 ± 1.65	7.06 ± 2.94

[a]Sections were stained with Oil Red O and were examined at a 400-fold magnification. Forty consecutive fields were counted
[b]Data are presented as means ± SEM for each of Canola and Soy and for Soy blend (n = 4).
[c]Number of cells that showed lipid accumulation was counted.
[d]Number of individual streaks of lipid located extracellularly. For formula compositions see Table 2.

of lipid in the hearts of almost all the 10-d-old piglets, irrespective of whether the formula contained canola oil, soy oil, or the blended oils (Table 3). Consistent with the biochemical analysis, there were no significant differences in the number of cells containing intercellular lipid, that is, 0.66 ± 0.23, 0.69 ± 0.08, 0.66 ± 0.16 cells with lipid for piglets fed the 100% Canola, 100% Soy, or the Soy oil blend, respectively. Similarly, there was no statistically significant difference among the groups in the number of extracellular lipid streaks at 10 d of age (9.33 ± 2.42, 9.13 ± 1.73, 6.39 ± 3.06, respectively).

The fatty acid composition of the heart triglycerides is shown in Table 4. The differences in the fatty acid composition of the heart triglycerides among the groups reflected the differences in fatty acid composition of the formulas fed. The results concerning the levels of 22:1, the fatty acid of concern in canola oil, are discussed in detail. The results for the n-3 fatty acids, particularly docosahexaenoic acid (22:6n-3) are also discussed because canola oil is high in 18:3n-3, while providing modest amounts of linoleic acid (18:2n-6). The statistical analysis to show treatment effects on other major fatty acids are shown in Table 4. At 18 d of age the heart triglyceride 20:1n-9 and 22:1n-9 of piglets fed the Canola formula were significantly higher than of piglets fed the Soy or the Canola mimic formulas. There were no significant differences in the heart triglyceride 22:1n-9 between piglets fed the Canola and Canola blend formulas, despite the difference in 22:1n-9 in the formulas (0.5 and 0.1%, respectively, Table 1). The heart triglyceride 20:1n-9, however, was significantly higher in piglets fed the Canola than Canola blend formula at 18 d. The concentrations of 24:1n-9 were not increased in the heart triglycerides of piglets fed either Canola or the Canola blend when compared to Soy or the Soy blend, or the Canola mimic. The concentrations of 20:1n-9 and 22:1n-9 in the heart phospholipid were much lower than in the triglycerides and did not exceed 0.5 and 0.2% fatty acids, respectively (data not

TABLE 4
Major Fatty Acids in Heart Triglycerides of Piglets Fed Formula with Different Oil Sources to 10 or 18 d of Age[a]

	Formula					Sow
	Canola	Soy	Canola blend	Soy blend	Canola mimic	milk
10 d						
16:0	18.5 ± 2.7	14.4 ± 3.2	23.2 ± 7.2	25.2 ± 0.7[d]	12.5 ± 1.5	21.1 ± 1.7
18:0	13.5 ± 2.2	9.9 ± 4.7	14.3 ± 3.2	14.2 ± 1.6	11.9 ± 2.9	19.6 ± 7.5
18:1n-9	29.2 ± 4.6	21.6 ± 3.4	28.8 ± 3.0	31.3 ± 3.3	37.2 ± 6.0	24.5 ± 4.4
20:1n-9	1.1 ± 0.2	0.5 ± 0.1[b]	0.8 ± 0.3	0.4 ± 0.1	0.7 ± 0.2	0.6 ± 0.1
22:1n-9	1.2 ± 0.4	0.5 ± 0.2	1.6 ± 0.9	0.4 ± 0.1[d]	0.2 ± 0.1[f]	2.0 ± 0.7
24:1n-9	0.1 ± 0.0	0.1 ± 0.0	0.2 ± 0.1	0.5 ± 0.2[d,e]	0.1 ± 0.1	0.1 ± 0.1
18:2n-6	15.2 ± 1.7	39.4 ± 3.3[b]	15.1 ± 1.6	15.2 ± 1.3[d]	18.1 ± 0.3	12.4 ± 2.3
20:4n-6	0.5 ± 0.1	0.9 ± 0.4	0.6 ± 0.1	0.9 ± 0.2	1.5 ± 0.8	2.9 ± 1.4
18:3n-3	3.1 ± 0.5	4.6 ± 0.5	1.8 ± 0.4	1.6 ± 0.4[d]	4.0 ± 0.7	1.2 ± 0.1
20:5n-3	0.2 ± 0.1	0.1 ± 0.0	0.2 ± 0.1	0.0 ± 0.0	0.2 ± 0.1	0.2 ± 0.1
22:6n-3	0.5 ± 0.3	0.1 ± 0.0	0.2 ± 0.0	0.2 ± 0.1	0.3 ± 0.1	0.4 ± 0.2
18 d						
16:0	11.0 ± 1.2	13.1 ± 3.6	19.0 ± 1.2[c]	26.2 ± 1.8[d,e]	10.2 ± 0.9	25.9 ± 0.8
18:0	13.5 ± 2.5	18.3 ± 1.2[b]	17.1 ± 3.0	17.1 ± 3.0	11.5 ± 2.1	16.4 ± 1.4
18:1n-9	40.1 ± 3.5	20.2 ± 1.4[b]	28.3 ± 1.1	25.2 ± 4.6	37.6 ± 4.8	24.4 ± 1.4
20:1n-9	1.4 ± 0.1	0.6 ± 0.1[b]	0.9 ± 0.2[c]	0.5 ± 0.1	0.6 ± 0.2[f]	0.9 ± 0.3
22:1n-9[g]	1.9 ± 0.3	0.6 ± 0.2[b]	3.7 ± 1.4	0.5 ± 0.1[e]	0.3 ± 0.1[f]	2.1 ± 0.6
24:1n-9	0.2 ± 0.1	0.1 ± 0.1	0.3 ± 0.1	0.2 ± 0.1	0.2 ± 0.1	0.1 ± 0.0
18:2n-6	17.0 ± 1.6	32.1 ± 1.6[b]	16.0 ± 1.0	17.1 ± 1.6[d]	19.7 ± 0.8	10.9 ± 0.5
20:4n-6	0.6 ± 0.1	1.2 ± 0.1[b]	1.1 ± 0.1[c]	1.0 ± 0.3	0.9 ± 0.3	1.7 ± 0.8
18:3n-3	4.6 ± 0.6	2.8 ± 0.2[b]	1.3 ± 0.1[c]	1.3 ± 0.3[d]	5.0 ± 0.4	0.9 ± 0.2
20:5n-3	0.1 ± 0.0	0.1 ± 0.0	0.1 ± 0.0	0.1 ± 0.0	0.1 ± 0.0	0.1 ± 0.0
22:6n-3	0.2 ± 0.0	0.1 ± 0.0	0.2 ± 0.0	0.3 ± 0.1	0.2 ± 0.0	0.8 ± 0.3

[a]Results shown are % total fatty acid methyl ester as means ± SEM, n = 4–6/group at 10 d and n = 6/group at 18 d.
[b]Canola compared to Soy oil, $P < 0.05$.
[c]Canola compared to Canola blend, $P < 0.05$.
[d]Soy compared to Soy blend, $P < 0.05$.
[e]Canola blend compared to Soy blend, $P < 0.05$.
[f]Canola mimic compared to Canola blend, $P < 0.05$.
[g]There is a statistically significant higher 22:1 in heart triglyceride at 18 d compared to 10 d of age in analysis of variance considering the effect of age for all animals.

shown). The concentrations of 20:1n-9, 22:1n-9, and 24:1n-9, however, were significantly higher in the heart phospholipids of piglets fed the Canola oil formula at 10 d (0.3 ± 0.1, 0.2 ± 0.1, 0.4 ± 0.1%, respectively) and 18 d (0.5 ± 0.0, 0.2 ± 0.0, 0.4 ± 0.0, respectively) than in piglets fed the Soy oil formula at 10 d (0.1 ± 0.0, 0.1 ± 0.0, 0.2 ± 0.0, respectively) or 18 d (0.1 ± 0.0, 0.1 ± 0.0, 0.1 ± 0.0, respectively). The levels of 22:1n-9 and 24:1n-9 at 10 d, and 20:1n-9, 22:1, and 24:1n-9 at 18 d were also significantly higher in piglets fed the Canola blend compared to Soy blend formula, although again the levels were very low and did not exceed 0.4% fatty acids. The physiological significance, if any, of these differences is not known.

Canola oil, like soy oil, has relatively high amounts of 18:3n-3, which can be desaturated and elongated to 22:6n-3. There were no significant differences in the concentration of 20:5n-3 or 22:6n-3 in the heart triglycerides at either 10 or 18 d. The concentrations of 18:3n-3 were higher in the heart triglyceride at 18 d in piglets fed Canola compared with Soy, or the Canola blend, but not the Canola mimic formula. The heart phospholipid concentrations of 18:3n-3 and 20:5n-3 were also higher in piglets fed the Canola compared with Soy or the Canola blend formula at both 10 and 18 d of age (data not shown). There were, however, no significant differences in 22:6n-3, with the exception of higher 22:6n-3 in the heart phospholipid of the 10-d-old piglets fed the Canola compared with Soy formula.

DISCUSSION

The studies described here show that the fat composition of formulas fed to rapidly growing young piglets had no significant effect on body weight, weight gain, or organ weight with the exception of a higher heart weight (by about 12%), but not heart/body weight in 18-d-old piglets fed the formula with 100% Canola oil compared with the Canola mimic. The heart weight, however, was not different between piglets fed the Canola and Soy formulas, or the Canola and Canola blend formulas, suggesting that the differences between piglets fed Canola and the Canola mimic are best explained as a lower heart weight in piglets fed the canola oil mimic.

The biochemical and histological analyses found no evidence of increased heart lipid in piglets fed formula with canola oil, containing 0.5% of fatty acids as 22:1n-9 and representing about 0.25% dietary energy, when compared to piglets fed formula with soy oil. Newborn piglets show a transient myocardial lipidosis that resolves by 7 d (16), possibly reflecting the rapid increase in capacity for fatty acid oxidation in the first week of life (28). Thus, histological analysis was done at 10 d, and biochemical analysis was done at 10 and 18 d of age to assess potential lipid accumulation due to feeding Canola oil. Our studies confirm the work of Kramer *et al.* (16), who showed no increased incidence of myocardial lipidosis either in piglets fed a sow milk replacer with canola oil (0.8% 22:1n-9) when compared to sow-fed animals, or in 10-d-old piglets fed a milk replacer with rapeseed oil (4.7% 22:1n-9) when compared to soybean oil. Definite myocardial lipidosis that correlated with dietary 22:1n-9, however, was found in piglets fed a milk replacer with 7 to 43% 22:1n-9 (16). Most of the 10-d-old piglet hearts that we examined showed the presence of lipid droplets. These droplets were unevenly distributed, with the majority located extracellularly and subjacent to the epicardium.

These findings were not unexpected because several studies have noted trace to moderate lipidosis in rats and piglets fed oils without 22:1n-9 (1,7,8,16,20), and the neonate is known to have an immature capacity for fatty acid oxidation (28). The biochemical analysis did not find lower heart triglyceride concentrations in piglets fed the Canola mimic (which provided similar amounts of C_{16} and C_{18} fatty acids without 22:1n-9 or the sterols of canola oil) or the formula with soybean oil than in piglets fed the formulas with canola oil. The weight of evidence therefore suggests that formula with canola oil providing ≤0.5% 22:1n-9 in total fatty acids has no adverse effect on neonatal heart lipid accumulation. The reason for the lower heart triglyceride at 10 ($P = 0.37$) and 18 d ($P = 0.22$) in piglets fed the canola oil blend (0.57 ± 0.08 and 0.51 ± nmol/g protein, respectively) than in piglets fed 100% canola oil (0.91 ± 0.28 and 0.81 ± 0.22, respectively) is not known, and may warrant further investigation.

Our studies show higher 22:1n-9 levels in heart triglyceride and phospholipid of piglets fed formulas with canola oil, either as the single oil or when blended with other oils. The amounts of 22:1n-9 in heart triglyceride and phospholipid of the piglets fed canola oil were less than 2.0 and 0.25% total fatty acids, respectively. Despite the much lower amount of 22:1n-9 in the Canola blend, piglets fed the Canola blend with 26% canola oil did not have lower 22:1n-9 in heart lipids than those fed the Canola formula with 100% canola oil. Whether this is explained by the relatively low levels of 22:1n-9 in all the treatment groups or by selective oxidation of fatty acids other than 22:1n-9 resulting in 22:1n-9 accumulation is not known. The small amounts of 22:1n-9 in the heart triglycerides and phospholipids of piglets fed the soy and canola mimic formulas and in the reference group of sow milk-fed piglets probably reflects exposure to 22:1n-9 from canola oil in the maternal diet. Canola oil is used as a fat source in pig feeds in British Columbia.

In conclusion, these studies show that formulas with canola oils providing 0.5% fatty acids as 22:1n-9, representing about 0.25% total dietary energy, have no adverse effects on growth, feed intake, or organ weight. The modest accumulation of 22:1n-9, predominantly in triglycerides, associated with feeding canola oil was not associated with biochemical evidence of heart triglyceride accumulation at 10 and 18 d, or histological evidence of heart lipid accumulation at 10 d of life.

ACKNOWLEDGMENT

This research was supported by a grant from the Canola Council of Canada, Saskatoon, Canada.

REFERENCES

1. Abdellatif, A.M., and Vles, R.O. (1973) Short-Term and Long-Term Pathological Effects of Glyceryl Trierucate and of Increasing Levels of Dietary Rapeseed Oil in Rats, *Nutr. Metab. 15*, 219–231.
2. Beare-Rogers, J.L., Nera, E.A., and Craig, B.M. (1972) Cardiac Lipids in Rats and Gerbils Fed Oils Containing C 22 Fatty Acids, *Lipids 7*, 548–552.
3. Christophersen, B.O., Norseth, J., Thomassen, M.S., Christiansen, E.N., Norum, K.R., Osmundsen, H., and Bremer, J. (1982) Metabolism and Metabolic Effects of C22:1 Fatty Acids With Special Reference to Cardiac Lipidosis, in *Nutritional Evaluation of Long-Chain Fatty Acids in Fish Oil* (Barlow, S.M., and Stansby, M.E., eds.), pp. 89–139, Academic Press, New York.
4. Darnerud, P.O., Olsen, M., and Wahlstrom, B. (1978) Effects of Cold Stress on Rats Fed Different Levels of Docosenoic Acids, *Lipids 13*, 459–463.
5. Kramer, J.K. (1973) Changes in Liver Lipid Composition of Male Rats Fed Rapeseed Oil Diets, *Lipids 8*, 641–648.
6. Kramer, J.K., Hulan, H.W., Trenholm, H.L., and Corner, A.H. (1979) Growth, Lipid Metabolism and Pathology of Two Strains of Rats Fed High Fat Diets, *J. Nutr. 109*, 202–213.
7. McCutcheon, J.S., Umemura, T., Bhatnagar, M.K., and Walker, B.L. (1976) Cardiopathogenicity of Rapeseed Oils and Oil Blends Differing in Erucic, Linoleic and Linolenic Acid Content, *Lipids 11*, 545–552.
8. Rose, S.P., Bell, J.M., Wilkie, I.W., and Schiefer, H.B. (1981) Influence of Weed Seed Oil Contamination on the Nutritional Quality of Diets Containing Low Erucic Acid Rapeseed (*Brassica napus*, Tower cultivar) Oil When Fed to Rats, *J. Nutr. 111*, 355–364.
9. Federal Register (1985) Direct Food Substances Affirmed as Generally Recognized as Safe; Low Erucic Acid Rapeseed, *Fed. Reg. 50*, 3745–3755.
10. Dreon, D.M., Vranizan, K.M., Krauss, R.M., Austin, M.A., and Wood, P.D. (1990) The Effects of Polyunsaturated Fat vs. Monounsaturated Fat on Plasma Lipoproteins, *JAMA 263*, 2462–2466.
11. Chan, J.K., McDonald, B.E., Gerrard, J.M., Bruce, V.M., Weaver, B.J., and Holub, B.J. (1993) Effect of Dietary α-Linolenic Acid and Its Ratio to Linoleic Acid on Platelet and Plasma Fatty Acids and Thrombogenesis, *Lipids 28*, 811–817.
12. Gustafsson, I.B., Vessby, B., Ohrvall, M., and Nydahl, M. (1994) A Diet Rich in Monounsaturated Rapeseed Oil Reduces the Lipoprotein Cholesterol Concentration and Increases the Relative Content of n-3 Fatty Acids in Serum in Hyperlipidemic Subjects, *Am. J. Clin. Nutr. 59*, 667–674.
13. Keys, A., Menotti, A., Karvonen, M.J., Aravanis, C., Blackburn, H., Buzina, R., Djordjevic, B.S., Dontas, A.S., Fidanza, F., Keys, M.H., *et al.* (1986) The Diet and 15-Year Death Rate in the Seven Countries Study, *Am. J. Epidemiol. 124*, 903–915.
14. Mensink, R.P., and Katan, M.B. (1989) Effect of a Diet Enriched with Monounsaturated or Polyunsaturated Fatty Acids on Levels of Low-Density and High-Density Lipoprotein Cholesterol in Healthy Women and Men, *N. Engl. J. Med. 321*, 436–441.
15. Sirtori, C.R., Tremoli, E., Gatti, E., Montanari, G., Sirtori, M., Colli, S., Gianfranceschi, G., Maderna, P., Dentone, C.Z., Testolin, G., *et al.* (1986) Controlled Evaluation of Fat Intake in the Mediterranean Diet: Comparative Activities of Olive Oil and Corn Oil on Plasma Lipids and Platelets in High-Risk Patients, *Am. J. Clin. Nutr. 44*, 635–642.
16. Kramer, J.K., Farnworth, E.R., Johnston, K.M., Wolynetz, M.S., Modler, H.W., and Sauer, F.D. (1990) Myocardial Changes in Newborn Piglets Fed Sow Milk or Milk Replacer Diets Containing Different Levels of Erucic Acid, *Lipids 25*, 729–737.
17. Beare, J.L., Campbell, J.A., Youngs, C.G., and Craig, B.M. (1963) Effects of Saturated Fats in Rats Fed Rapeseed Oils, *Can. J. Biochem. Physiol. 41*, 605–612.
18. Farnworth, E.R., Kramer, J.K., Thompson, B.K., and Corner, A.H. (1982) Role of Dietary Saturated Fatty Acids on Lowering the Incidence of Heart Lesions in Male Rats, *J. Nutr. 112*, 231–240.
19. Clandinin, M.T., and Yamashiro, S. (1983) Effect of Dietary Supplementation with Stearic Acid on the Severity of Myocardial Lesions, *Res. Vet. Sci. 3*, 306–309.
20. Kramer, J.K., Sauer, F.D., Wolynetz, M.S., Farnworth, E.R., and Johnston, K.M. (1992) Effects of Dietary Saturated Fat on Erucic Acid Induced Myocardial Lipidosis in Rats, *Lipids 27*, 619–623.
21. Innis, S.M. (1993) The Colostrum-Deprived Piglet as a Model for Study of Infant Lipid Nutrition, *J. Nutr. 123*, 386–390.
22. Hrboticky, N., MacKinnon, M.J., and Innis, S.M. (1990) Effect of a Vegetable Oil Formula Rich in Linoleic Acid on Tissue Fatty Acid Accretion in the Brain, Liver, Plasma, and Erythrocytes of Infant Piglets, *Am. J. Clin. Nutr. 51*, 173–182.
23. Folch, J., Lees, M., and Sloane-Stanley, G. (1957) A Simple Method for the Isolation and Purification of Total Lipids from Animal Tissues, *J. Biol. Chem. 226*, 497–509.
24. Rioux, F.M., and Innis, S.M. (1993) Cholesterol and Fatty Acid Metabolism in Piglets Fed Sow Milk or Infant Formula With or Without Addition of Cholesterol, *Metabolism 42*, 1552–1559.
25. Chen, P.S., Toribara, T.Y., and Warner, H. (1956) Microdetermination of Phosphorus, *Anal. Chem. 28*, 1756–1758.
26. Innis, S.M., Dyer, R., and Nelson, C.M. (1994) Evidence That Palmitic Acid Is Absorbed as *sn*-2 Monoacylglycerol from Human Milk by Breast-Fed Infants. *Lipids 29*, 541–545.
27. Lepage, G., and Roy, C.C. (1988) Specific Methylation of Plasma Nonesterified Fatty Acids in a One-Step Reaction, *J. Lipid Res. 29*, 227–235.
28. Werner, J.C., Whitman, V., Vary, T.C., Fripp, R.R., Musselman, J., and Schuler, H.G. (1983) Fatty Acid and Glucose Utilization in Isolated, Working Newborn Pig Hearts, *Am. J. Physiol. 244*, E19–E23.

[Received April 12, 1999; and in revised form March 23, 2000; revision accepted May 4, 2000]

Dehydroepiandrosterone Alters Lipid Profiles in Zucker Rats

Jude M. Abadie[a,*], Gray T. Malcom[a], Johnny R. Porter[b], and Frank Svec[c]

Departments of [a]Pathology, [b]Physiology, and [c]Medicine, Louisiana State University Medical Center, New Orleans, Louisiana 70112

ABSTRACT: High free fatty acid (FFA) levels are common in obesity and in diseases such as diabetes that are associated with the obese state. Dehydroepiandrosterone (DHEA) decreases dietary fat consumption, body fat content, and insulin levels in the obese Zucker rat (ZR), a genetic model of human youth-onset obesity and type 2 diabetes mellitus. This study was conducted to investigate the effects of DHEA on lean and obese ZR serum, adipose, and hepatic tissue fatty acid (FA) profiles and serum FFA levels. Because DHEA is known to decrease fat consumption and body fat, we postulate that DHEA may also alter FA profiles and FFA levels of the obese ZR such that they more closely resemble the profiles and levels of their lean siblings. In this study there was a DHEA and a pair-fed (PF) group ($n = 6$) for 12 lean and 12 obese ZR. The diet of the treatment groups was supplemented with 0.6% DHEA, and PF groups were given the same average calories consumed by their corresponding DHEA group for 30 d. Fasted animals were sacrificed, and FA profiles and FFA levels were measured. Serum FFA levels were higher in obese (~1 mmol/L) compared to lean rats (~0.6 mmol/L). After 30 d of DHEA treatment, FFA levels were lower ($P < 0.05$) in both lean and obese groups. Although several significant differences in FA profile of serum, hepatic, and adipose lipid components were observed between lean and obese ZR, DHEA-related changes were only observed in the serum phospholipid (PL) and liver PL and triglyceride fractions. The slight but significant decrease in serum FFA levels may be reflected by changes in serum PL FA profiles. Specific hepatic FA profile alterations may be related to DHEA's known effects in inducing hepatic peroxisomes. We speculate that such FA changes may give insight into a mechanism for the action of DHEA.

Paper no. L8340 in *Lipids 35,* 613–620 (June 2000).

The fa/fa obese Zucker rat (ZR) is a genetic model of human youth-onset obesity and diseases associated with the obese state. Specifically, compared to their lean siblings, obese ZR demonstrate higher serum free fatty acid (FFA) levels, hyperphagia, hyperinsulinemia, hypertriglyceridemia, hypercorticosteronemia, hyperleptinemia, increased lipogenesis, adipoctye hypertrophy, and hyperplasia (1–6), and they become hyperglycemic with advancing age (7).

Excess adipose tissue, a fatty liver, and increased hepatic lipid synthesis alter fatty acid (FA) flux (8). It is often suggested that this "lipotoxicity" may be responsible for the increased serum FFA levels associated with obesity-related diseases (9–11). Although the liver is the first site for insulin resistance (IR) development in obese ZR, adipose is the most insulin sensitive tissue (8). Many investigators implicate FA as a major mediator of IR development in hepatic and adipose tissue (12–20), and specific FA in serum highly correlate with the development of IR and diabetes in humans (21). Mechanisms by which FA alterations may lead to IR are poorly understood.

Altered adipose FA flux may be an important metabolic alteration central to the pathophysiology of the obese ZR (9,10). However, control mechanisms governing FA flux have not been determined. Moreover, such mechanisms may be quite difficult to establish. After all, FA are critical energy substrates, building blocks for cell membrane components, precursors of cell mediators such as prostaglandins, and important intracellular mediators of gene expression (22). Such diverse roles suggest complex and specific regulatory factors governing FA flux.

This study investigates possible lipid-altering effects of dehydroepiandrosterone (DHEA), the most abundantly produced human adrenal steroid. In the past we and others have shown that DHEA treatment in the obese ZR acts as an anti-obesity agent in that it decreases body weight, fat intake (2–4), size of specific adipose depots and their cellularity, and liver adiposity (2–4,24). Additionally, we have shown that DHEA alters the total lipid (TL) FA compositions of skeletal and cardiac muscle in the obese ZR such that they resemble more closely the profile of their lean siblings (Abadie, J.M., Malcom, G.T., Porter, J.R., and Svec, F., unpublished data).

Because of the specific anti-obesity effects of DHEA on adipose mass, fat intake, and liver fat content, as well as alterations in muscle TL FA profiles and serum FFA levels, we hypothesize that these DHEA alterations may correlate with changes in FA profiles in serum, adipose, and hepatic tissue.

This study was conducted to determine the effect of DHEA on (i) adipose tissue TL FA profiles (mammary, retroperi-

*To whom correspondence should be addressed at Madigan Army Medical Center, Department of Pathology, Ft. Lewis, WA 98431.
E-mail: judeabadie@medscape.com

Abbreviations: BW, body weight; CE, cholesteryl ester; CI, caloric intake; DHA, docosahexaenoic acid; DHEA, dehydroepiandrosterone; FA, fatty acid; FFA, free fatty acid; IR, insulin resistance; LDHEA, lean DHEA; LPF, lean pair-fed; MAT, mammary adipose tissue; MU, monounsaturated; ODHEA, obese DHEA; OPF, obese pair-fed; PF, pair-fed; PL, phospholipid; PU, polyunsaturated; RPAT, retroperitoneal adipose tissue; SFA, saturated fatty acid; SQAT, subcutaneous adipose tissue; TG, triglyceride; TL, total lipid; ZR, Zucker rat.

toneal, and subcutaneous depots), (ii) liver phospholipid (PL), FFA, and TG FA lipid profiles, and (iii) serum FFA levels and PL, FFA, triglyceride (TG), and cholesteryl ester (CE) FA lipid profiles.

EXPERIMENTAL PROCEDURES

Animals. Twenty-four female ZR 12 to 16 wk of age were obtained from our colony in the Department of Physiology at the Louisiana State University Medical Center in New Orleans, LA; the study was approved by the IRB and IACUC boards from the Louisiana State University Medical Center in New Orleans. Twelve lean (Fa/fa) and 12 obese ZR (fa/fa) were used for the experiment. Animals were maintained on a 12-h light-dark cycle (lights on at 0600) in a room whose temperature was maintained at 22 ± 1°C. Prior to the experiment, all animals were maintained on Purina Rodent Laboratory Chow #5001 whose physiologic fuel value, as reported by the manufacturer, is 3.30 kcal/g. The proportions of energy as carbohydrate, protein, and fat are 63.7, 30.4, and 5.9%, respectively. Both food and water were available *ad libitum*. Animals were housed individually in wire mesh cages.

Specialized diet. A specialized macronutrient diet as previously described (24) was combined so that the proportions of energy as carbohydrate, protein, and fat were 30, 20, and 50%, respectively. This "high fat" single-bowl diet was given to each animal for the duration of the experiment. The energy density of the diet was 5.256 kcal/g. The diet of the group designated DHEA was supplemented with 0.6% DHEA.

Study design. On day 1, 24 female ZR 9 to 12 wk old were weight/age matched and divided into four groups ($n = 6$). For both lean and obese rats there was a DHEA and a pair-fed (PF) group. For days 1 through 7, each animal had *ad libitum* access to their dish containing the DHEA-free diet. For the subsequent 30 d (days 8 through 37), the diet of the two DHEA groups (lean and obese) was supplemented with 0.6% DHEA. The PF groups were pair-fed to the intakes of their corresponding DHEA-treated group. Because DHEA decreases caloric intake, each animal in each PF group was given the average number of calories consumed by their corresponding DHEA group during the previous day. On the first day of pair-feeding, PF groups were given half the amount that they had consumed during the previous day (day 7). After 30 d of DHEA treatment or pair-feeding, animals were fasted for 14 h and sacrificed by rapid decapitation. Serum, livers, mammary adipose tissue (MAT), retroperitoneal adipose tissue (RPAT), and a 500-mg piece of subcutaneous adipose tissue (SQAT) were frozen in liquid nitrogen and stored at –80°C until lipid analysis.

All FA profiles were determined by gas–liquid chromatography. Adipose depots and livers were homogenized in a chloroform/methanol solution (2:1, vol/vol), and TL was extracted, evaporated to dryness, and redissolved in 10 mL of chloroform as described earlier (25).

The 10 mL of chloroform containing the TL extracts was dried down under a nitrogen stream, and 150 μL of petroleum ether (BP 35–50°C) was added to the TL extract, spotted on glass plates coated with Silica Gel-G (E. Merck, Darmstadt, Germany), and separated into PL, FFA, TG, and CE (for serum) fractions. The thin-layer chromatography solvent mobile phase used was petroleum ether/ethyl ether/glacial acetic acid (90:10:1, by vol).

A standard mixture of lipids was spotted adjacent to the samples to ensure correct class identification at the end of a migration period of approximately 45 min. Plates containing the partitioned lipid classes were visualized under ultraviolet light after spraying with 2,7-dichlorofluorescein in methanol. The band of silica gel containing each lipid class was scraped off of the glass plate, and transmethylation was performed with 2 mL of 6% (vo/vol) sulfuric acid in anhydrous methanol in Teflon-lined screw-cap tubes at 75°C for 15 h. The mixture containing FA methyl esters was washed with water and extracted with hexane. The hexane was stored under nitrogen prior to injection directly onto the column of a gas chromatograph as previously described (25).

A standard mixture of FA methyl esters (Applied Science Labs, College Station, PA) was run daily for standardization and proper identification of each FA. The proportions of individual FA were calculated and expressed as a weight percentage of the TL FA present in the sample.

Statistical analysis. Variations in experimental measurements were examined by one-way analysis of variance (ANOVA) on a Power Macintosh 7600/120 Superanova program (®Abacus Concepts from Macintosh). Significance for $P < 0.05$ was measured using Fisher's Projected least squares difference, giving the exact P-value for each comparison.

RESULTS

For all tables, values are presented as means ± SEM. Rows not sharing the same letter are significantly different ($P \leq 0.05$). Significant differences occurring when comparing measurements from PF control vs. the corresponding DHEA group are presented in **bold** type. Values in columns are not statistically compared. The abbreviations for the groups are: obese pair-fed (OPF), obese DHEA (ODHEA), lean pair-fed (LPF), and lean DHEA (LDHEA).

Body weights (BW) in grams on days 7, 14, 21, and 36 and caloric intakes (CI) in kcal on days 5, 6, 8, 14, 21, 28, and 36 are recorded in Table 1. On day 7, BW were not different within phenotype groups; however, on days 14, 21, and 36, both lean and obese DHEA groups weighed significantly less than their PF controls. CI decreased by the first day of DHEA treatment (day 8) for both lean and obese rats. This decrease remained lowered in the obese; however, by day 14, the CI of the LDHEA group returned to their pretreatment consumption.

The TL liver content, weights of right MAT and RPAT, and liver weights are recorded in Table 2. For each of these measurements, values for obese controls (OPF) are significantly higher than lean controls (LPF). The liver weights of both DHEA groups were significantly greater compared to their corresponding control group. For every other measurement in

TABLE 1
Body Weights (BW) and Caloric Intakes (CI)[a]

Measurement	OPF	ODHEA	LPF	LDHEA
BW day 7	321 ± 8 a	323 ± 9 a	264 ± 7 b	270 ± 5 b
BW day 14	336 ± 8 a	319 ± 6 b	275 ± 5 c	256 ± 4 d
BW day 21	363 ± 7 a	322 ± 5 b	280 ± 6 c	249 ± 4 d
BW day 36	366 ± 8 a	318 ± 5 b	282 ± 7 c	245 ± 6 d
CI day 5	100.6 ± 4.1 a	104.3 ± 4.6 a	69.3 ± 4.0 b	69.9 ± 5.3 b
CI day 6	102.9 ± 3.8 a	103.7 ± 3.6 a	65.3 ± 2.6 b	68.1 ± 4.3 b
CI day 8		39.8 ± 5.3 a		47.1 ± 3.8 b
CI day 14		59.3 ± 2.5 a		73.1 ± 1.8 b
CI day 21		61.7 ± 2.2 a		71.1 ± 1.4 b
CI day 28		65.0 ± 3.5 a		70.2 ± 2.9 b
CI day 36		64.6 ± 4.1 a		62.8 ± 2.6 a

[a]BW (g) and CI (kcal) are recorded on the indicated study days as mean ± SEM for each group (n = 6): obese pair-fed (OPF), obese dehydroepiandrosterone (ODHEA), lean pair-fed (LPF), and lean DHEA (LDHEA). Values in rows that do not share the same letter are significantly different ($P \leq 0.05$).

Table 2, the values of both DHEA groups were significantly less compared to their corresponding PF control group.

Figure 1 represents the serum FFA levels for each group. The FFA levels of the OPF group were almost twice as high compared to the LPF group ($P \leq 0.0001$). The FFA levels of both DHEA groups were significantly lower ($P \leq 0.05$) compared to their corresponding control group.

Serum PL FA profiles are recorded in Table 3. The proportions of linoleic acid (18:2n-6) and adrenic acid (22:4n-6) are significantly greater in lean compared to obese control rats. After 30 d of DHEA treatment, there were greater proportions of palmitic acid (16:0) in both lean and obese DHEA groups. Serum PL FA proportions of stearic acid (18:0) and docosahexaenoic acid (DHA) (22:6n-6) are significantly lower in both lean and obese DHEA groups.

Serum FFA profiles are recorded in Table 4. The proportions of palmitic acid, palmitoleic acid (16:1), DHA, and saturated fatty acids (SFA) are significantly lower in lean compared to obese control rats, and proportions of linoleic acid and polyunsaturated (PU) FA are significantly greater in lean compared to obese control rats. There are no DHEA treatment effects observed in serum FFA profiles.

Serum TG FA profiles are recorded in Table 5. The proportions of palmitic acid, palmitoleic acid, DHA, SFA, and

TABLE 2
Weights of Right Mammary Adipose Tissue (MAT) Depots, Right Retroperitoneal Adipose Tissue (RPAT) Depots, Whole Livers, and Total Lipid Liver Content[a]

Measurement	OPF	ODHEA	LPF	LDHEA
MAT (g)	14.2 ± 1.3 a	9.9 ± 0.9 b	1.3 ± 0.3 c	0.7 ± 0.1 d
RPAT (g)	12.6 ± 1.1 a	8.2 ± 0.8 b	1.5 ± 0.3 c	0.7 ± 0.2 d
Liver (g)	13.0 ± 1.0 a	18.2 ± 0.9 b	7.8 ± 0.7 c	11.9 ± 1.3 a
Liver lipid content (mg/g)	92.5 ± 5.3 a	75.7 ± 3.8 b	60.9 ± 2.5 c	51.7 ± 2.0 d

[a]Values are recorded as mean ± SEM for each group (n = 6). Values in rows that do not share the same letter are significantly different ($P \leq 0.05$). For other abbreviations see Table 1.

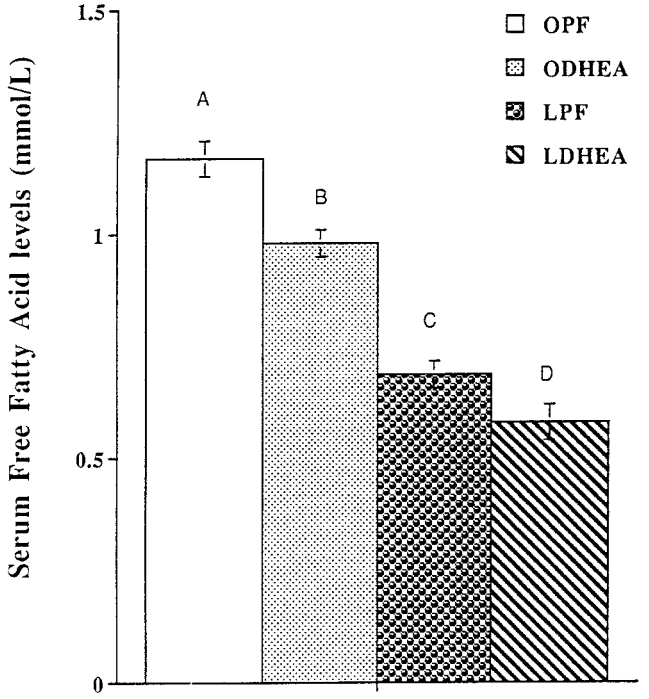

FIG. 1. Serum free fatty acid levels. n = 6 for obese pair-fed (OPF), obese DHEA (ODHEA), lean pair-fed (LPF), and lean DHEA (LDHEA). Groups not sharing the same letter are significantly different ($P < 0.05$). Bars represent SEM. DHEA, dehydroepiandrosterone.

TABLE 3
Serum Phospholipid Fatty Acid Profiles[a]

Fatty acid	OPF	ODHEA	LPF	LDHEA
12:0	0.0	0.0	0.0	0.0
14:0	0.2 a	0.2 a	0.2 a	0.2 a
14:1	0.1 a	0.1 a	0.1 a	0.1 a
16:0	**10.2 ± 0.8 a**	**17.5 ± 1.2 b**	**10.4 ± 1.1 a**	**16.9 ± 1.3 b**
16:1	0.3 a	0.3 a	0.3 a	0.3 a
18:0	**28.2 ± 0.9 a**	**23.5 ± 1.0 b**	**26.7 ± 1.4 a**	**22.4 ± 1.1 b**
18:1	5.1 ± 0.4 a	5.9 ± 0.5 a	5.8 ± 0.3 a	6.0 ± 0.7 a
18:2	4.6 ± 0.5 a	4.5 ± 0.4 a	6.3 ± 0.5 b	6.9 ± 0.5 b
20:0	0.1 a	0.1 a	0.1 a	0.1 a
18:3	0.1 a	0.1 a	0.1 a	0.1 a
20:1	0.2 a	0.2 a	0.2 a	0.2 a
20:2	0.2 a	0.2 a	0.2 a	0.2 a
20:3	0.9 ± 0.1 a	0.8 ± 0.2 a	0.8 ± 0.2 a	0.8 ± 0.2 a
22:0	0.4 a	0.4 a	0.4 a	0.4 a
20:4	31.0 ± 1.9 a	31.5 ± 1.8 a	28.7 ± 1.6 a	30.8 ± 1.7 a
22:1	0.0	0.0	0.0	0.0
20:5	0.0	0.0	0.0	0.0
22:4	1.2 ± 0.2 a	1.5 ± 0.2 a	2.5 ± 0.2 b	2.7 ± 0.3 b
24:1	0.5 a	0.5 a	0.5 a	0.5 a
22:5	0.5 a	0.5 a	0.5 a	0.5 a
22:6	**12.7 ± 0.7 a**	**8.9 ± 0.5 b**	**12.2 ± 0.9 a**	**8.9 ± 0.7 b**
SFA	39.3 ± 2.0 a	41.7 ± 2.1 a	37.9 ± 1.8 a	39.8 ± 2.3 a
MUFA	6.2 ± 0.8 a	6.9 ± 0.5 a	6.9 ± 0.7 a	7.0 ± 0.7a
PUFA	51.3 ± 3.1 a	48.0 ± 2.8 a	51.3 ± 2.7 a	51.1 ± 2.3 a

[a]Values are recorded as mean ± SEM for each group (n = 6). Values in rows that do not share the same letter are significantly different ($P \leq 0.05$). DHEA effects are typed in **bold**. SFA, saturated fatty acids; MUFA, monounsaturated fatty acids; PUFA, polyunsaturated fatty acids; for other abbreviations see Table 1.

TABLE 4
Serum Free Fatty Acid Profiles[a]

Fatty acid	OPF	ODHEA	LPF	LDHEA
12:0	0.1 a	0.1 a	0.1 a	0.1 a
14:0	0.7 ± 0.1 a	0.8 ± 0.2 a	0.7 ± 0.1 a	0.6 ± 0.1 a
14:1	0.2 a	0.2 a	0.2 a	0.2 a
16:0	23.8 ± 1.3 a	23.5 ± 1.5 a	17.7 ± 0.8 b	17.7 ± 1.1 b
16:1	3.5 ± 0.4 a	3.5 ± 0.5 a	1.4 ± 0.2 b	1.5 ± 0.1 b
18:0	9.6 ± 1.3 a	9.4 ± 1.4 a	7.9 ± 1.6 a	8.1 ± 1.0 a
18:1	22.9 ± 1.8 a	23.0 ± 2.3 a	25.0 ± 1.6 a	24.0 ± 1.7 a
18:2	11.6 ± 0.9 a	11.6 ± 1.1 a	23.8 ± 2.0 b	22.5 ± 2.2 b
20:0	0.0	0.0	0.0	0.0
18:3	0.4 a	0.4 a	0.4 a	0.4 a
20:1	0.3 a	0.3 a	0.3 a	0.3 a
20:2	0.9 ± 0.2 a	1.0 ± 0.2 a	1.1 ± 0.2 a	1.0 ± 0.2 a
20:3	0.4 a	0.4 a	0.4 a	0.4 a
22:0	0.3 a	0.3 a	0.3 a	0.3 a
20:4	11.4 ± 1.5a	11.9 ± 1.6a	11.7 ± 1.7a	12.9 ± 1.8 a
22:1	0.0	0.0	0.0	0.0
20:5	0.4 a	0.4 a	0.4 a	0.4 a
22:4	0.5 a	0.5 a	0.5 a	0.5 a
24:1	0.5 a	0.5 a	0.5 a	0.5 a
22:5	1.2 ± 0.2 a	1.2 ± 0.2 a	1.4 ± 0.3 a	0.9 ± 0.2 a
22:6	6.3 ± 0.4 a	6.2 ± 0.6 a	3.4 ± 0.5 b	3.6 ± 0.3 b
SFA	35.0 ± 2.8 a	34.1 ± 2.3 a	27.0 ± 1.6 b	27.0 ± 1.9 b
MUFA	27.4 ± 1.7 a	27.6 ± 1.8 a	27.4 ± 1.9 a	26.6 ± 1.7 a
PUFA	32.9 ± 2.4 a	33.6 ± 2.6 a	42.9 ± 3.0 b	41.9 ± 3.2 b

[a]Values are recorded as mean ± SEM for each group (n = 6). Values in rows that do not share the same letter are significantly different ($P \leq 0.05$). For abbreviations see Tables 1 and 3.

monounsaturated (MU) FA are significantly lower in lean compared to obese control rats. Proportions of linoleic acid, lignoceric acid, and PU FA are significantly greater in lean compared to obese controls. There are no DHEA treatment effects observed in serum TG FA profiles.

Serum CE FA profiles are recorded in Table 6. The proportions of palmitic acid, palmitoleic acid, stearic acid, and oleic acid (18:1) are significantly lower in lean compared to obese control rats. Proportions of adrenic acid, nervonic acid (24:1) and eicosapentaenoic acid (22:5n-3) are significantly greater in lean compared to obese controls. There are no DHEA treatment effects observed in serum CE FA profiles.

Liver PL FA profiles are recorded in Table 7. The proportions of stearic acid are significantly greater in lean compared to obese controls. After 30 d of DHEA treatment, there were greater proportions of palmitic acid in both lean and obese DHEA groups. Serum CE FA proportions of DHA are significantly lower in both lean and obese DHEA groups.

Liver FFA profiles are not reported in this study. First, for many of these samples, FFA yield was not great enough to generate readable peaks from our gas chromatography. Second, readable chromatograms containing strong peaks were highly variable from sample to sample due to the highly variable flux of this lipid component.

Liver TG FA profiles are recorded in Table 8. This is the only FA profile measured in this study where phenotypic differences were not observed; however, it is the fraction where the greatest DHEA-related alterations were observed. After 30 d of DHEA

TABLE 5
Serum Triglyceride Fatty Acid Profiles[a]

Fatty acid	OPF	ODHEA	LPF	LDHEA
12:0	0.1 a	0.1 a	0.1 a	0.1 a
14:0	0.1 a	0.1 a	0.1 a	0.1 a
14:1	0.2 a	0.2 a	0.2 a	0.2 a
16:0	24.9 ± 1.1 a	24.9 ± 0.9 a	18.9 ± 1.2 b	19.6 ± 1.0 b
16:1	2.8 ± 0.3 a	2.7 ± 0.2 a	0.9 ± 0.1 b	0.9 ± 0.1 b
18:0	4.9 ± 0.4 a	5.1 ± 0.6 a	4.3 ± .05 a	4.1 ± 0.5 a
18:1	29.8 ± 1.8 a	29.5 ± 1.4 a	27.7 ± 1.6 a	26.6 ± 1.9 a
18:2	13.9 ± 0.9 a	12.8 ± 0.6 a	19.8 ± 1.7 b	20.3 ± 1.6 b
20:0	0.2 a	0.2 a	0.2 a	0.2 a
18:3	0.2 a	0.2 a	0.2 a	0.2 a
20:1	0.2 a	0.2 a	0.2 a	0.2 a
20:2	1.1 ± 0.1 a	1.0 ± 0.2 a	0.9 ± 0.1 a	1.2 ± 0.2 a
20:3	0.7 ± 0.1 a	0.8 ± 0.1 a	0.8 ± 0.2 a	0.9 ± 0.2 a
22:0	0.2 a	0.2 a	0.2 a	0.2 a
20:4	6.4 ± 1.0 a	7.8 ± 1.1 a	14.7 ± 1.5 b	12.5 ± 1.4 b
22:1	0.0	0.0	0.0	0.0
20:5	0.4 a	0.4 a	0.4 a	0.4 a
22:4	0.2 a	0.2 a	0.2 a	0.2 a
24:1	0.8 ± 0.2 a	0.8 ± 0.1 a	0.8 ± 0.1 a	0.9 ± 0.2 a
22:5	1.5 ± 0.2 a	1.4 ± 0.2 a	1.1 ± 0.2 a	1.0 ± 0.2a
22:6	6.4 ± 0.4 a	5.8 ± 0.5 a	3.9 ± 0.2 b	4.3 ± 0.6 b
SFA	30.6 ± 3.1 a	30.9 ± 2.6 a	24.0 ± 2.1 b	24.7 ± 1.9 b
MUFA	33.9 ± 2.7 a	33.4 ± 2.4 a	29.8 ± 2.7 a	30.8 ± 2.4 a
PUFA	30.8 ± 2.7 a	31.0 ± 2.5 a	41.8 ± 2.9 b	40.8 ± 3.2 b

[a]Values are recorded as mean ± SEM for each group (n = 6). Values in rows that do not share the same letter are significantly different ($P \leq 0.05$). For abbreviations see Tables 1 and 3.

TABLE 6
Serum Cholesteryl Ester Fatty Acid Profiles[a]

Fatty acid	OPF	ODHEA	LPF	LDHEA
12:0	0.1 a	0.1 a	0.1 a	0.1 a
14:0	0.3 a	0.3 a	0.3 a	0.3 a
14:1	0.1 a	0.1 a	0.1 a	0.1 a
16:0	4.7 ± 0.3 a	5.3 ± 0.8 a	3.5 ± 0.3 b	3.5 ± 0.3 b
16:1	0.9 ± 0.5 a	1.0 ± 0.2 a	0.3 ± 0.1 b	0.4 ± 0.1 b
18:0	2.1 ± 0.4 a	2.7 ± 1.0 a	0.7 ± 0.1 b	0.6 ± 0.1 b
18:1	3.6 ± 0.6 a	4.2 ± 0.6 a	2.6 ± 0.3 b	2.9 ± 0.2 b
18:2	5.4 ± 0.4 a	6.2 ± 0.8 a	5.8 ± 0.7 a	5.7 ± 0.6 a
20:0	0.3 a	0.3 a	0.3 a	0.3 a
18:3	0.1 a	0.1 a	0.1 a	0.1 a
20:1	0.0	0.0	0.0	0.0
20:2	0.0	0.0	0.0	0.0
20:3	0.4 ± 0.1 a	0.6 ± 0.2 a	0.5 ± 0.3 a	0.6 ± 0.2 a
22:0	0.0	0.0	0.0	0.0
20:4	66.1 ± 2.5a	60.6 ± 2.6 a	63.2 ± 2.6 a	62.5 ± 2.7 a
22:1	0.0	0.0	0.0	0.0
20:5	0.3 a	0.3 a	0.3 a	0.3 a
22:4	0.7 ± 0.2 a	0.8 ± 0.2 a	4.6 ± 1.1 b	4.8 ± 0.9 b
24:1	1.2 ± 0.1 a	1.3 ± 0.2 a	3.8 ± 1.2 b	4.1 ± 0.8 b
22:5	3.1 ± 0.1 a	3.0 ± 0.4 a	6.5 ± 0.7 b	5.4 ± 0.5 b
22:6	5.9 ± 0.9 a	5.5 ± 0.8 a	4.8 ± 1.0 a	4.8 ± 0.7 a
SFA	7.4 ± 1.2 a	8.8 ± 1.7 a	4.6 ± 0.9 b	4.6 ± 0.9 b
MUFA	6.5 ± 0.6 a	6.5 ± 0.9 a	6.7 ± 0.8 a	7.0 ± 0.8 a
PUFA	81.9 ± 1.6 a	80.6 ± 2.0 a	85.1 ± 1.8 b	84.7 ± 2.4 b

[a]Values are recorded as mean ± SEM for each group (n = 6). Values in rows that do not share the same letter are significantly different ($P \leq 0.05$). For abbreviations see Tables 1 and 3.

TABLE 7
Liver Phospholipid Fatty Acid Profiles[a]

Fatty acid	OPF	ODHEA	LPF	LDHEA
12:0	0.1 a	0.1 a	0.1 a	0.1 a
14:0	0.2 a	0.2 a	0.2 a	0.2 a
14:1	1.5 ± 0.2 a	1.6 ± 0.2 a	1.4 ± 0.2 a	1.5 ± 0.2 a
16:0	**11.1 ± 0.7 a**	**15.3 ± 0.8 b**	**11.7 ± 0.8 a**	**14.1 ± 0.9 b**
16:1	0.3 ± 0.1 a	0.4 ± 0.1 a	0.3 ± 0.1 a	0.3 ± 0.1 a
18:0	26.9 ± 2.3 a	26.4 ± 1.8 a	23.7 ± 1.2 b	23.1 ± 1.0 b
18:1	6.5 ± 0.5 a	6.4 ± 0.4a	6.7 ± 0.3 a	6.7 ± 0.4 a
18:2	5.5 ± 0.8 a	6.0 ± 0.6 a	6.3 ± 0.6 a	6.9 ± 0.6 a
20:0	0.1 a	0.1 a	0.1 a	0.1 a
18:3	0.1 a	0.1 a	0.1 a	0.1 a
20:1	0.1 a	0.1 a	0.1 a	0.1 a
20:2	0.3 a	0.3 a	0.3 a	0.3 a
20:3	0.7 ± 0.1 a	1.0 ± 0.2 a	0.8 ± 0.2 a	1.0 ± 0.2 a
22:0	0.5 ± 0.1 a	0.4 ± 0.1 a	0.5 ± 0.1 a	0.4 ± 0.1a
20:4	27.9 ± 1.2 a	28.1 ± 1.1a	26.7 ± 1.2 a	28.5 ± 1.2 a
22:1	0.0	0.0	0.0	0.0
20:5	0.2 a	0.2 a	0.2 a	0.2 a
22:4	1.0 ± 0.1 a	1.2 ± 0.1 a	1.1 ± 0.1 a	1.1 ± 0.1 a
24:1	0.5 ± 0.1 a	0.6 ± 0.1 a	0.5 ± 0.1 a	0.5 ± 0.1 a
22:5	0.9 ± 0.2 a	0.8 ± 0.1 a	0.8 ± 0.1 a	0.7 ± 0.2a
22:6	**15.0 ± 1.1 a**	**11.1 ± 0.9 b**	**16.9 ± 1.2 a**	**12.6 ± 1.0 b**
SFA	39.1 ± 1.6 a	41.6 ± 1.1 a	37.3 ± 1.3 a	40.1 ± 0.8 a
MUFA	8.9 ± 0.6 a	9.1 ± 0.7 a	9.0 ± 0.5 a	9.1 ± 0.8 a
PUFA	50.6 ± 1.4 a	49.8 ± 1.3 a	52.1 ± 1.4 a	51.8 ± 1.1 a

[a]Values are recorded as mean ± SEM for each group (n = 6). Values in rows that do not share the same letter are significantly different ($P \leq 0.05$). DHEA effects are typed in **bold**. For abbreviations see Tables 1 and 3.

TABLE 8
Liver Triglyceride Fatty Acid Profiles[a]

Fatty acid	OPF	ODHEA	LPF	LDHEA
12:0	0.1 a	0.1 a	0.1 a	0.1 a
14:0	0.5 ± 0.1 a	0.7 ± 0.2 a	0.6 ± 0.1 a	0.5 ± 0.1 a
14:1	0.1 a	0.1 a	0.1 a	0.1 a
16:0	21.3 ± 0.7 a	22.7 ± 0.5 a	22.4 ± 1.0 a	23.9 ± 0.7 a
16:1	1.3 ± 0.4 a	1.3 ± 0.4 a	1.1 ± 0.2 a	1.1 ± 0.1 a
18:0	**3.9 ± 0.2 a**	**5.6 ± 0.4 b**	**3.7 ± 0.3 a**	**5.7 ± 0.3 b**
18:1	**27.4 ± 1.4 a**	**34.2 ± 1.3 b**	**26.5 ± 1.3 a**	**32.0 ± 1.7 b**
18:2	**26.8 ± 1.2 a**	**17.9 ± 0.9 b**	**29.0 ± 1.7 a**	**19.5 ± 1.1 b**
20:0	0.3 a	0.3 a	0.3 a	0.3 a
18:3	0.9 ± 0.2 a	0.6 ± 0.3 a	1.0 ± 0.4 a	0.8 ± 02 a
20:1	0.4 ± 0.2 a	0.2 ± 0.1 a	0.2 ± 0.1 a	0.5 ± 0.2 a
20:2	1.1 ± 0.2 a	1.2 ± 0.2 a	1.1 ± 0.4 a	1.1 ± 0.3 a
20:3	1.1 ± 0.2 a	1.0 ± 0.1 a	1.0 ± 0.2 a	1.1 ± 0.2 a
22:0	0.0	0.0	0.0	0.0
20:4	6.0 ± 0.5a	5.3 ± 0.6a	5.7 ± 0.7a	5.8 ± 0.5 a
22:1	0.1 a	0.1 a	0.1 a	0.1 a
20:5	0.3 a	0.3 a	0.3 a	0.3 a
22:4	0.3 a	0.3 a	0.3 a	0.3 a
24:1	0.0	0.0	0.0	0.0
22:5	1.4 ± 0.2 a	1.0 ± 0.2 a	1.0 ± 0.3 a	0.9 ± 0.2 a
22:6	**2.9 ± 0.3 a**	**4.0 ± 0.4 b**	**2.2 ± 0.2 a**	**3.7 ± 0.3 b**
SFA	**26.4 ± 0.8 a**	**29.9 ± 0.7 b**	**26.0 ± 0.7 a**	**30.8 ± 1.0 b**
MUFA	**30.0 ± 0.9 a**	**35.9 ± 1.1 b**	**28.1 ± 0.8 a**	**33.8 ± 0.8 b**
PUFA	**41.3 ± 1.3 a**	**31.3 ± 0.8 b**	**41.4 ± 1.3 a**	**32.6 ± 0.9 b**

[a]Values are recorded as mean ± SEM for each group (n = 6). Values in rows that do not share the same letter are significantly different ($P \leq 0.05$). DHEA effects are typed in **bold**. For abbreviations see Tables 1 and 3.

TABLE 9
MAT Fatty Acid Profiles[a]

Fatty acid	OPF	ODHEA	LPF	LDHEA
12:0	0.1 a	0.1 a	0.1 a	0.1 a
14:0	1.4 ± 0.2 a	1.4 ± 0.2 a	1.0 ± 0.2 a	1.0 ± 0.2 a
14:1	0.3 a	0.3 a	0.3 a	0.3 a
16:0	23.6 ± 0.8 a	23.4 ± 0.7 a	18.8 ± 0.4 b	18.8 ± 0.6 b
16:1	7.2 ± 0.4 a	6.8 ± 0.4 a	1.5 ± 0.3 b	1.5 ± 0.3 b
18:0	3.2 ± 0.2 a	3.1 ± 0.3 a	2.9 ± 0.2 a	3.2 ± 0.4 a
18:1	41.1 ± 0.5 a	41.7 ± 0.4a	40.2 ± 0.5 a	40.4 ± 0.8 a
18:2	16.8 ± 0.9 a	17.0 ± 0.8 a	28.9 ± 1.5 b	27.3 ± 1.6 b
20:0	0.2 a	0.2 a	0.2 a	0.2 a
18:3	1.0 ± 0.1 a	0.9 ± 0.1 a	1.0 ± 0.1 a	0.9 ± 0.2 a
20:1	0.0	0.0	0.0	0.0
20:2	0.5 ± 0.1 a	0.4 ± 0.1 a	0.5 ± 0.1 a	0.6 ± 0.1 a
20:3	0.2 a	0.2 a	0.2 a	0.2 a
22:0	0.0	0.0	0.0	0.0
20:4	0.8 ± 0.2 a	0.8 ± 0.2 a	0.9 ± 0.2 a	1.2 ± 0.4 a
22:1	0.0	0.0	0.0	0.0
20:5	0.1 a	0.1 a	0.1 a	0.1 a
22:4	0.1 a	0.1 a	0.1 a	0.1 a
24:1	0.0	0.0	0.0	0.0
22:5	0.3 a	0.3 a	0.3 a	0.3 a
22:6	0.6 ± 0.1 a	0.7 ± 0.2 a	0.5 ± 0.1 a	0.7 ± 0.2 a
SFA	26.9 ± 0.9 a	27.2 ± 1.0 a	23.0 ± 1.0 b	23.2 ± 0.7 b
MUFA	49.0 ± 0.6 a	49.2 ± 0.7 a	42.2 ± 0.5 b	42.6 ± 0.7 b
PUFA	20.4 ± 0.6 a	20.7 ± 0.7 a	32.2 ± 1.0 b	31.3 ± 1.2 b

[a]Values are recorded as mean ± SEM for each group (n = 6). Values in rows that do not share the same letter are significantly different ($P \leq 0.05$). For abbreviations see Tables 1–3.

treatment, there are greater proportions of stearic acid, oleic acid, DHA, SFA, and MU FA in both lean and obese DHEA groups. Liver PL FA proportions of acid and PU FA are significantly lower in both lean and obese DHEA groups.

In each instance where DHEA-related alterations in FA profiles were observed in this study, the same changes were observed for both phenotypes.

The TL FA profiles for MAT, RPAT, and SQAT are recorded in Tables 9, 10, and 11, respectively. For each of these adipose tissue depots, the proportions of palmitic acid and palmitoleic acid are significantly lower in lean compared to obese control rats, and proportions of linoleic acid are significantly greater in lean compared to obese controls. For FA totals, MU FA are proportionally lower and PU FA are proportionally greater in the lean compared to obese rats for both MAT and SQAT. For RPAT, the proportions of SFA are lower and proportions of PU FA were greater in the lean compared to obese rats. After 30 d of DHEA treatment, there were no FA profile alterations in any of these three adipose depots.

DISCUSSION

Perhaps the lipid profile differences between lean and obese ZR observed in this study better distinguish these two phenotypes than do the combined differences in FFA levels, liver lipid content, and degree of adiposity. ZR treated with DHEA have altered tissue FA profiles such that the obese become more like the lean with respect to FA composition.

TABLE 10
Retroperitoneal Fatty Acid Profiles[a]

Fatty acid	OPF	ODHEA	LPF	LDHEA
12:0	0.1 a	0.1 a	0.1 a	0.1 a
14:0	0.1 a	0.1 a	0.1 a	0.1 a
14:1	0.3 a	0.3 a	0.3 a	0.3 a
16:0	25.0 ± 0.3 a	25.4 ± 0.2 a	18.3 ± 0.3 b	18.5 ± 0.5 b
16:1	4.7 ± 0.2 a	4.6 ± 0.1 a	1.4 ± 0.2 b	1.3 ± 0.2 b
18:0	4.5 ± 0.7 a	4.9 ± 0.1 a	4.7 ± 0.2 a	4.8 ± 0.2 a
18:1	41.3 ± 0.8 a	40.3 ± 0.9a	41.1 ± 1.0 a	41.4 ± 1.1 a
18:2	17.6 ± 0.3 a	17.5 ± 0.2 a	27.2 ± 1.2 b	27.4 ± 0.3 b
20:0	0.1 a	0.1 a	0.1 a	0.1 a
18:3	0.9 ± 0.1 a	0.9 ± 0.1 a	1.0 ± 0.1 a	1.0 ± 0.1 a
20:1	0.3 a	0.3 a	0.3 a	0.3 a
20:2	0.4 ± 0.1 a	0.4 ± 0.1 a	0.5 ± 0.1 a	0.4 ± 0.1 a
20:3	0.2 a	0.2 a	0.2 a	0.2 a
22:0	0.0	0.0	0.0	0.0
20:4	0.3 a	0.3 a	0.3 a	0.3 a
22:1	0.0	0.0	0.0	0.0
20:5	0.0	0.0	0.0	0.0
22:4	0.1 a	0.1 a	0.1 a	0.1 a
24:1	0.0 a	0.0 a	0.0 a	0.0 a
22:5	0.1a	0.1a	0.1a	0.1 a
22:6	0.3 a	0.3 a	0.3 a	0.3 a
SFA	31.1 ± 0.4 a	31.9 ± 0.3 a	23.9 ± 0.2 b	24.3 ± 0.5 b
MUFA	46.6 ± 0.8 a	45.5 ± 0.9 a	44.0 ± 1.1 a	43.3 ± 1.8 a
PUFA	19.6 ± 0.6 a	19.8 ± 0.7a	30.3 ± 1.3 b	29.4 ± 0.4 b

[a]Values are recorded as mean ± SEM for each group ($n = 6$). Values in rows that do not share the same letter are significantly different ($P \leq 0.05$). For abbreviations see Tables 1 and 3.

TABLE 11
Subcuteanous Adipose Tissue Fatty Acid Profiles[a]

Fatty acid	OPF	ODHEA	LPF	LDHEA
12:0	0.2 a	0.2 a	0.2 a	0.2 a
14:0	1.3 ± 0.2 a	1.2 ± 0.2 a	1.1 ± 0.2 a	1.0 ± 0.2 a
14:1	0.3 a	0.3 a	0.3 a	0.3 a
16:0	22.0 ± 0.5 a	21.9 ± 0.4 a	18.8 ± 0.8 b	19.6 ± 0.9 b
16:1	7.1 ± 0.6 a	6.6 ± 0.4 a	1.5 ± 0.3 b	1.3 ± 0.4 b
18:0	4.3 ± 0.3 a	4.4 ± 0.2 a	4.9 ± 0.6 a	4.8 ± 0.5 a
18:1	41.2 ± 0.9 a	41.6 ± 0.8 a	39.1 ± 1.1 a	39.7 ± 1.2 a
18:2	16.8 ± 0.3 a	17.8 ± 0.2 a	26.1 ± 0.8 b	24.4 ± 0.9 b
20:0	0.1 a	0.1 a	0.1 a	0.1 a
18:3	0.9 ± 0.1 a	1.0 ± 0.1 a	1.0 ± 0.1 a	1.1 ± 0.2 a
20:1	0.3 a	0.3 a	0.3 a	0.3 a
20:2	0.5 ± 0.1 a	0.6 ± 0.1 a	0.8 ± 0.2 a	0.7 ± 0.1 a
20:3	0.2 a	0.2 a	0.2 a	0.2 a
22:0	0.0	0.0	0.0	0.0
20:4	0.4 a	0.4 a	0.4 a	0.4 a
22:1	0.0	0.0	0.0	0.0
20:5	0.1 a	0.1 a	0.1 a	0.1 a
22:4	0.1 a	0.1 a	0.1 a	0.1 a
24:1	0.1 a	0.1 a	0.1 a	0.1 a
22:5	0.1a	0.1a	0.1a	0.1 a
22:6	0.5 a	0.5 a	0.5 a	0.5 a
SFA	28.0 ± 1.1 a	27.8 ± 1.3 a	25.2 ± 1.2 a	25.9 ± 0.8 a
MUFA	49.0 ± 0.9 a	48.9 ± 1.5 a	41.3 ± 1.6 b	43.3 ± 1.8 b
PUFA	19.5 ± 0.6 a	20.7 ± 0.7a	29.2 ± 1.3 b	27.5 ± 0.9 b

[a]Values are recorded as mean ± SEM for each group ($n = 6$). Values in rows that do not share the same letter are significantly different ($P \leq 0.05$). For abbreviations see Tables 1 and 3.

This study investigates DHEA's lipid-altering effects on liver, specific fat depots, and serum. Defining these areas in terms of lipid and FA profiles seemed to be the next logical step in our investigation of DHEA's effects on lipid profiles. Elevated serum FFA levels are common in obesity (7,21) and IR (26). Several studies show that high FFA levels decrease hepatocyte insulin sensitivity (27–31). This study shows a significant decrease in FFA levels in both lean and obese ZR after 30 d of DHEA treatment. This decrease is slight; however, it may reflect the specific alterations that we observed in serum PL FA profiles.

DHEA-related alterations in serum PL FA profiles may be a reflection of specific tissue changes. This study shows significant phenotypic FA profile differences in each of the four serum lipid fractions measured. Some of the DHEA-induced changes may be reflected as accumulation of elongation end products. For example, adrenic acid is an end product of arachidonic acid. Subsequently, when serum proportions of arachidonic acid increase, there is a proportional increase in adrenic acid.

As mentioned earlier, FA profiles and levels can be related to diseases associated with the obese state. For example, several investigators have shown that palmitic acid potentiates glucose-induced insulin release (32–34). Our study shows that palmitic acid is proportionally greater in the serum FFA, TG FA, and CE FA lipid fractions of obese compared to lean ZR. Other studies suggest that increased CE oleic acid strongly correlates with high FFA levels and possibly IR development (21,35). CE was the only serum lipid fraction whose proportion of oleic acid was significantly greater in obese compared to lean ZR.

Although the significance of these FA alterations in the development of IR is not known, corresponding FA alterations in insulin-sensitive tissue may reflect a mechanism by which IR is decreased with DHEA treatment. This study does not measure IR. Therefore, any discussion of a DHEA effect on IR is only speculative.

In our study, liver TL content is much greater in obese compared to lean ZR. Table 2 shows that TL liver content significantly decreases after 30 d of DHEA treatment in both lean and obese rats. Moreover, several DHEA-related changes are noted in the liver PL and TG FA fractions. These changes may be related to DHEA-induced changes in hepatic stearoyl-CoA desaturase reported by Imani *et al*. (36). This would explain the selective proportional elevation that we observed in liver TG oleic acid (18:1).

DHEA is a known peroxisome proliferator in hepatic tissue (37). Hepatic peroxisomal proliferation is accompanied by hepatomegaly, resulting from hyperplasia and hypertrophy (38). This may explain the increased liver weights observed in lean and obese rats after 30 d of DHEA treatment (Table 2). Because FA, specifically arachidonic acid (20:4), also have been shown to induce peroxisome proliferation (38), perhaps the DHEA-induced FA alterations observed in this study favor increased peroxisomal proliferation.

Our study suggests that adipose tissue FA profiles are phenotype specific and, within each phenotype, are nearly identi-

cal for MAT, RPAT, and SQAT. If the speculation is true that DHEA alters peroxisomal activation indirectly by increasing proportions of 20:4, then the same speculation for adipose tissue is not likely. First, adipose tissue contains very few FA greater than 18 carbons long. Second, because DHEA did not proportionately alter any adipose tissue FA, a corresponding mechanism utilizing different FA to activate adipose peroxisomes is not likely. Furthermore, the rate of adipose FA turnover is not as rapid as in other tissue. Therefore, 30 d of DHEA treatment may not be long enough to demonstrate FA profile alterations in adipose tissue. Such changes occurring within 30 d of DHEA treatment seem to be better observed in serum and in hepatic tissue than in adipose tissue.

The results of this study show that there are marked FA profile differences between lean and obese ZR and that DHEA has multiple effects on FA profiles of several tissues. These FA profile alterations are changed consistently in both phenotypes. If FA profiles are phenotypically specific between lean and obese ZR, then DHEA's ability to alter FA profiles needs further investigation. Further studies may provide a better understanding and elucidate a mechanism to link DHEA-induced FA profile alterations to metabolic differences between lean and obese ZR.

REFERENCES

1. Cleary, M.P. (1991) Minireview: The Antiobesity Effect of Dehydroepiandrosterone in Rats, *Proc. Soc. Exp. Biol. Med. 196*, 8–16.
2. Cleary, M.P., Zabel, T., and Sartin, J.L. (1988) Effects of Short-Term Dehydroepiandrosterone Treatment on Serum and Pancreatic Insulin in Zucker Rats, *J. Nutr. 118,* 382–387.
3. Tagliaferro, A.R., Ronam, A.M., Payne, J., Meeker, L.D., and Tse, S. (1995) Increased Lipolysis to β-Adrenergic Stimulation After Dehydroepiandrosterone Treatment in Rats, *Am. J. Physiol. 268,* R1374–R1380.
4. Svec, F., Abadie, J., Browne, E.S., and Porter, J.R. (1995) Dehydroepiandrosterone and Macronutrient Selection by Obese Zucker Rats *(fa/fa)*, *Appetite 25*, 143–154.
5. Peret, J., Foustock, S., and Chanez, M. (1981) Hepatic Metabolites and Amino Acid Levels During Adaptation of Rats to a High-Protein, Carbohydrate-Free Diet, *J. Nutr. 111*, 1704–1710.
6. Peret, J., Foustock, S., and Chanez, M. (1981) Plasma Glucagon and Insulin Concentrations and Hepatic Phosphoenolpyruvate Carboxykinase and Pyruvate Kinase Activities During and Upon Adaptation of Rats to a High Protein Diet, *J. Nutr. 111*, 1173–1184.
7. Kalopissis, A.-D., Griffaton, G., and Fau, D. (1995) Inhibition of Hepatic Very-Low-Density Lipoprotein Secretion in Obese Zucker Rats Adapted to a High-Protein Diet, *Metabolism 44*, 19–29.
8. Fontbonne, A. (1991) Relationship Between Diabetic Dyslipoproteinemia and Coronary Heart Disease Risk in Subjects with Non-Insulin-Dependent Diabetes, *Diabetes/Metab. Rev. 7*, 179–189.
9. Schwieterman, W., Sorrentino, D., Potter, B.J., Rand, J.,Kiang, C.-L., and Berk, P.D. (1988) Uptake of Oleate by Isolated Rat Adipocytes Is Mediated by a 40-kDa Plasma Membrane Fatty Acid Binding Protein Closely Related to That in Liver and Gut, *Proc. Natl. Acad. Sci. USA 85*, 359–363.
10. Sorrentino, D., Stump, D., Potter, B.J., Robinson, R.B.,White, R., Kiang, C.-L., and Berk, P.D. (1988) Oleate Uptake by Cardiac Myocytes Is Carrier Mediated and Involves a 40-kD Plasma Membrane Fatty Acid Binding Protein Similar to That in Liver, Adipose Tissue and Gut, *J. Clin. Invest. 82*, 928–935.
11. Stump, D.D., Nunes, R.M., Sorrentino, D., and Berk, P.D. (1992) Characteristics of Oleate Binding to Liver Plasma Membrane and Its Uptake by Isolated Hepatocytes, *J. Hepatol. 16*, 304–315.
12. Berk, P.D., Zhou, S.-L., Bradbury, M., Stump, D., Kiang, C.-L., and Isola, L.M. (1997) Regulated Membrane Transport of Free Fatty Acids in Adipocytes, Role in Obesity and Non-insulin Dependent Diabetes Mellitus, *Trans. Am. Clin. Climatol. Assoc. 108*, 26–47.
13. Eisenstein, A.B., Strack, I., and Steiner, A. (1974) Glucagon Stimulation of Hepatic Gluconeogenesis in Rats Fed a High-Protein, Carbohydrate-Free Diet, *Metabolism 23*, 15–23.
14. Cadorniga-Valino, C., Grummer, R.R., Armentano, L.E., Donkin, S.S., and Bertics, S.J. (1997) Effects of Fatty Acids and Hormones on Fatty Acid Metabolism and Gluconeogenesis in Bovine Hepatocytes, *J. Dairy Sci. 80*, 646–656.
15. Martin, R.J. (1974) *In vivo* Lipogenesis and Enzyme Levels in Fat and Liver from Obese and Lean Rats, *Life Sci. 14*, 1447–1453.
16. Bevilacqua, S., Bonadonna, R., Buzzigoli, G., Boni, C., Ciociaro, D., Maccari, F., Giorico, M.A., and Ferrannini, E. (1987) Acute Elevation of Fatty Acid Levels Leads to Hepatic Insulin Resistance in Obese Subjects, *Metabolism 36*, 502–506.
17. Frederick, R.C.J., Kahn, B.B., Peach, M.J., and Flier J.S. (1992) Tissue-Specific Nutritional Regulation of Angiotensinogen and Adipose Tissue, *Hypertension 19*, 339–344.
18. Hotamisligil, G.S., Budavari, A., Murray, D., and Spiegelman, B.M. (1994) Reduced Tyrosine Kinase Activity of the Insulin Receptor in Obesity-Diabetes, Central Role of Tumor Necrosis Factor-a, *J. Clin. Invest. 93*, 1543–1549.
19. Zhang, Y., Proenca, R., Maffel, M., Barone, M., Leopold, L., and Friedman, J.M. (1994) Positional Cloning of the Mouse *Obese* Gene and Its Human Homologue, *Nature 372*, 425–431.
20. Pelleymounter, M.A., Cullen, M.J., Baker, M.B., Hecht, R., Winters, D., Boone, T., and Collins, F. (1995) Effects of the Obese Gene Product on Body Weight Regulation on ob/ob Mice, *Science 269,* 540–543.
21. Vessby, B., Antti, A., Skarfors, E., Berglund, L., Salminen, I., and Lithell, H. (1994) The Risk to Develop NIDDM Is Related to the Fatty Acid Composition of Serum Cholesterol Esters, *Diabetes 43,* 1353–1357.
22. Abumrand, N.A., Perkins, R.C., Park, J.H., and Park, C.R. (1981) Mechanism of Long Chain Fatty Acid Permeation in the Isolated Adipocyte, *J. Biol. Chem. 256*, 9183–9191.
23. Eich, D.M., Nestler, J.E., Johnson, D.E., Dworkin, G.H., Ko, D., Wechsler, A.S., and Hess, M.L. (1993) Inhibition of Accelerated Coronary Atherosclerosis with Dehydroepiandrosterone in the Heterotopic Rabbit Model of Cardiac Transplantation, *Circulation 87*, 261–269.
24. Abadie, J., Mathew, M., Happel, M., Kumar, S., Prasad, A., delaHoussaye, A., and Prasad, C. (1993) Regulation of Dietary Fat Preference, Establishing a Reproducible Profile of Dietary Fat Preference in Rats, *Life Sci. 53*, 131–139.
25. Malcolm, G.T., Bhattacharyya, A.K., Velez-Duran, M., Guzman, M.A., Oalmann, M.C., and Strong, J.P. (1989) Fatty Acid Composition of Adipose Tissue in Humans, Differences Between Subcutaneous Sites, *Am. J. Clin. Nutr. 50*, 288–291.
26. Wiesenthal, S.R., Sandhu, H., McCall, R.H., Tchipashvili, V., Yoshii, H., Polonsky, K., Shi, Z.Q., Lewis, G.F., Mari, A., and Giacca, A. (1999) Free Fatty Acids Impair Hepatic Insulin Extraction *in vivo, Diabetes 48*, 766–774.
27. Gorden, E.S. (1960) Non-esterfied Fatty Acids in Blood of Obese and Lean Subjects, *Am. J. Clin. Nutr. 8*, 740–747.
28. Reaven, G. (1995) Pathophysiology of Insulin Resistance in Human Disease, *Physiol. Rev. 75*, 473–486.

29. Reaven, G.M., Hollenbeck, C., Jeng, C.-Y., Wu, M.S., and Chen, Y.-D. (1988) Measurement of Plasma Glucose, Free Fatty Acid, Lactate and Insulin for 24 h in Patients with NIDDM, *Diabetes 37*, 1020–1024.
30. Svedberg, J., Bjorntorp, P., Smith, L., and Lonnroth, P. (1990) Free Fatty Acid Inhibition of Insulin Binding, Degradation, and Action in Isolated Rat Hepatocytes, *Diabetes 39*, 570–574.
31. Hennes, M.M.I., Shrago, E., and Kissebah, A.H. (1990) Receptor and Postreceptor Effects of Free Fatty Acids (FFA) on Hepatocyte Insulin Dynamics, *Int. J. Obesity 14*, 831–841.
32. Svedberg, J., Stromblad, G., Wirth, A., Smith, U., and Bjorntorp, P. (1991) Fatty Acids in the Portal Vein of the Rat Regulate Hepatic Insulin Clearance, *J. Clin. Invest. 88*, 2054–2068.
33. Warnotte, C., Patrick, G., Nenquin, M., and Henquin, J. (1994) Mechanisms of the Stimulation of Insulin Release by Saturated Fatty Acids, *Diabetes 43*, 703–711.
34. Prentki, M., Vischer, S., Glennon, C., Regazzi, R., Deeney, J., and Corkey, B. (1992) Malonyl-CoA and Long Chain Acyl-CoA Esters as Metabolic Coupling Factors in Nutrient-Induced Insulin Secretion, *J. Biol. Chem. 267*, 5802–5810.
35. Deeney J., Tornheim, K., Korchak, H., Prentki, M., and Corkey, B. (1992) Acyl-CoA Esters Modulate Intracellular Calcium Handling by Permeabilized Clonal Pancreatic B-Cells, *J. Biol. Chem. 267*, 19840–19845.
36. Imani, K., Koyama, M., Kudo, N., Shirahata, A., and Kawashima, Y. (1999) Increases in Hepatic Content of Oleic Acid Induced by Dehydroepiandrosterone in the Rat, *Biochem. Pharmacol. 58,* 925–933.
37. Bevilacqua, S. (1987) Acute Elevation of Free Fatty Acid Levels Lead to Hepatic Resistance in Obese Subjects, *Metab. Clin. Exp. 36*, 502–506.
38. Keller, H., Dreyer, C., Medin, J., Mahfoundi, A., Ozato, K., and Wahli, W. (1993) Fatty Acids and Retinoids Control Lipid Metabolism Through Activation of PPAR/RXR Heterodimers, *Proc. Natl. Acad. Sci. USA 90*, 2160–2164.

[Received August 16, 1999, and in final revised form and accepted May 3, 2000]

Cholesterol Vehicle in Experimental Atherosclerosis. 23. Effects of Specific Synthetic Triglycerides

David Kritchevsky[a,*], Shirley A. Tepper[a], Shirley C. Chen[b], Gert W. Meijer[c,1], and Ronald M. Krauss[d]

[a]The Wistar Institute, Philadelphia, Pennsylvania 19104, [b]Lipton, Baltimore, Maryland 21229 , [c]Unilever Research, Vlaardingen, The Netherlands, and [d]E.O. Lawrence Berkeley National Laboratory, Berkeley, California 94720

ABSTRACT: Earlier work has shown that increasing concentration of palmitic acid at the *sn*-2 position of a fat enhances the atherogenic properties of that fat. This effect has been observed with lard, tallow, cottonseed oil, and palm oil. In the experiment reported here, we have studied the atherogenic effects of four synthetic fats fed to rabbits as 58% (w/w) of the total fat (15%) (w/w) of a semipurified diet containing 0.05% cholesterol. The fats being tested were: 1,3-stearoyl-2-oleoylglycerol (SOS); 1,2-stearoyl-3-oleoylglycerol (SSO); 1,3-palmitoyl-2-oleoylglycerol (POP); and 1,2-palmitoyl-3-oleoylglycerol (PPO). After 20 wk on diet there were no differences among the groups in weight gain, liver weight, serum, or liver lipids. These data are consistent with our previous findings. There were significant differences in atherosclerosis. The most severe atherosclerosis was observed in group PPO and the least in groups SSO and POP. Severity of atherosclerosis was graded visually on a 0–4 scale. The average atherosclerosis [(aortic arch and thoracic aorta) ÷ 2] was: SOS—1.35; SSO—0.97; POP—0.83; and PPO—1.80. Fecal fat excretion (an indicator of fat absorption) was higher in the two groups fed the stearic acid-rich fats and lower in groups fed the palmitic acid-rich fats. There were no differences in low density lipoprotein particle size. The results confirm previous findings concerning the increased atherogenicity of fats bearing palmitic acid at the *sn*-2 position. The mechanism underlying these observations is moot but may, in part, reflect greater absorption of the atherogenic fat.

Paper no. L8422 in *Lipids 35,* 621–625 (June 2000).

We have observed in the course of studies of atherogenesis in rabbits that the atherogenicity of fats appears to be, in part, a function of the level of palmitic acid (16:0) present at the *sn*-2 position. Thus, lard, which contains 21.4% 16:0 of which 98% is at *sn*-2, is 51% more atherogenic than randomized lard, which contains 21.4% 16:0 only 7.6% of which is at *sn*-2 (1); tallow, which contains 24.8% 16:0 of which 3.8% is at *sn*-2, is 9% less atherogenic than randomized tallow, which contains 24.8% 16:0 of which 8.5% is at *sn*-2 (1); cottonseed oil, which contains 25% 16:0 of which 1.7% is at *sn*-2, is 66% less atherogenic than randomized cottonseed oil (9.9% at *sn*-2) (2); and palm oil, which contains 41.2% 16:0 of which 2.6% is at *sn*-2, is 24% less atherogenic than randomized palm oil (13.6% 16:0 at *sn*-2) (3). The atherogenic, semipurified diets used in the studies cited here contained between 0.1 and 0.4% cholesterol.

The present study involves the use of synthetic triglycerides, namely, 1,3-stearoyl-2-oleoylglycerol (SOS), 1,2-distearoyl-3-oleoylglycerol (SSO), 1,3-dipalmitoyl-2-oleoylglycerol (POP), and 1,2-dipalmitoyl-3-oleoylglycerol (PPO). Comparison of the atherogenic effects of these four fats when fed as part of an atherogenic, semisynthetic diet is the subject of this report.

MATERIALS AND METHODS

Male New Zealand White rabbits were used. The rabbits were housed individually in stainless steel cages in an air-conditioned, humidified room maintained on a 12-h on–off light schedule. Rabbits were allowed free access to water and food. The rabbits were obtained as weanlings and placed on an adaptation diet (Tables 1 and 2). The purpose of the adaptation diet was to ensure that the starting serum cholesterol lev-

TABLE 1
Adaptation Diet

Ingredient	%	% Calories
Casein	24.00	24.5
DL-Methionine	0.30	
Sucrose	40.40	41.2
Safflower oil	2.70	6.2
High-oleic sunflower[a]	2.85	6.5
Palm oil	1.35	3.1
Cocoa butter	8.10	18.6
Cellulose	15.00	
Salt mix	4.00	
Vitamin mix	1.00	
Choline bitartrate	0.25	
Cholesterol	0.05	
Total	100.0	100.1, or 392.6 Kcal/100 g

[a]85% oleic acid.

*To whom correspondence should be addressed at The Wistar Institute, 3601 Spruce St., Philadelphia, PA 19104. E-mail: kritchevsky@wistar.upenn.edu

[1]Present address: Lipton, Englewood Cliffs, NJ 07632.

Abbreviations: ANOVA, analysis of variance; HDL, high density lipoprotein; LDL, low density lipoprotein; POP, 1,3-palmitoyl-2-oleoylglycerol; PPO, 1,2-palmitoyl-3-oleoylglycerol; SOS, 1,3-stearoyl-2-oleoylglycerol; SSO, 1,2-stearoyl-3-oleoylglycerol.

TABLE 2
Adaptation Diet—Fatty Acid Composition

Fatty acid	%
12:0	0.1
14:0	0.2
16:0	20.5
16:1	0.2
17:0	0.2
18:0	21.2
18:1	39.0
18:2	17.3
18:3	0.1
20:0	0.7
20:1	0.2
22:0	0.3
24:0	0.1

TABLE 3
Atherogenic Diet

Ingredient	%	% Calories
Casein	24.0	24.4
Sucrose	40.7	41.3
Safflower oil	2.7	6.2
Sunflower oil	3.6	8.2
Test fat	8.7	19.9
Cellulose	15.0	
Cholesterol	0.05	
Mineral mix	4.0	
Vitamin mix	1.0	
Choline bitartrate	0.25	
	100	100, or 393.8 Kcal/100 g

els of all the rabbits would be in the same range. The diet was intended to cull out hyper- or hyporesponders. After 2 wk the rabbits were randomized into four groups of 10 animals each. Each group had the same average serum cholesterol level. The rabbits were then placed on semipurified diets (Table 3) containing 0.05% cholesterol and 15% fat of which 58% was one of the special test fats, 24% was sunflower oil, and 18% was oleic acid-rich safflower oil. SOS was fractionated from the stearate fraction of shea nut oil. SSO was obtained by enzymatic rearrangement (interesterification) of fully hydrogenated sunflower seed oil with high-oleic sunflower seed oil fatty acids. POP was obtained from regular palm oil midfraction, and PPO was obtained by fractionation of the product obtained after enzymic rearrangement of a palm oil stearate fraction with high-oleic sunflower seed oil fatty acids. The fatty acid composition of the test diets is given in Table 4. Diets were prepared to our specifications and pelletted by Dyets, Inc. (Bethlehem, PA). The rabbits were maintained on the special diets for 20 wk and were weighed and their serum cholesterols were determined every 5 wk. After 20 wk, rabbits were bled under light barbiturate anesthesia and killed by exsanguination. Serum total cholesterol, high density lipoprotein (HDL) cholesterol, and triglycerides were determined using appropriate kits (Sigma, St. Louis, MO).

Livers were weighed, washed and aliquots were extracted with chloroform/methanol 2:1 (4). The lipid extract was analyzed for free and total cholesterol (5) and triglycerides (6). Aortas were cleaned of adhering tissue, opened longitudinally, and severity of atherosclerosis was graded visually on a 0–4 scale (7). The molecular diameters of the low density lipoproteins (LDL) were carried out using the method of Krauss and Burke (8). Briefly, nondenaturing polyacrylamide gradient gel electrophoresis of whole plasma was performed at 10°C by using 2–16% polyacrylamide gradient gels for 24 h at 125 V in Tris (0.09 M)/boric acid (0.08 M)/Na_2EDTA (0.003 M) buffer (pH 8.3). Gels were fixed and stained for lipids in a solution containing oil red 0 in 60% ethanol at 55°C. Gels were scanned at 530 nm with a transidyne densitometer. Migration distance for each absorbance peak was determined, and the molecular diameter corresponding to each

TABLE 4
Fatty Acid (FA) Composition Test Diets[a]

SOS			SSO		POP			PPO	
FA	% Total	% at *sn*-2	% Total	% at *sn*-2	FA	%	% at *sn*-2	%	% at *sn*-2
12:0	0.0	0.0	0.0	0.0	12:0	0	0	0.1	0.1
14:0	0.1	0.0	0.1	0.0	14:0	0.4	0.2	0.3	0.3
16:0	6.3	1.4	5.3	1.1	16:0	21.9	4.4	22.3	29.3
16:1	0.1	0.0	0.1	0.0	16:1	0.1	0	0.1	0.0
17:0	0.1	0.0	0.1	0.0	17:0	0.1	0	0.1	0.0
18:0	20.3	2.4	21.2	27.8	18:0	4.8	0.6	4.3	1.6
18:1	29.4	46.4	29.1	23.8	18:1	29.9	46.2	29.4	23.6
18:2	42.0	49.5	42.3	46.7	18:2	41.6	48.4	41.5	44.9
18:3	0.2	0.2	0.2	0.2	18:3	0.2	0.2	0.6	0.2
20:0	0.8	0.0	0.7	0.4	20:0	0.4	0.0	0.4	0.1
20:1	0.2	0.2	0.2	0.1	20:1	0.2	0.2	0.2	0.1
22:0	0.4	0.0	0.6	0.1	22:0	0.4	0.0	0.5	0.0
24:0	0.2	0.0	0.2	0.0	24:0	0.1	0.0	0.2	0.0

[a]SOS = 1,3-distearoyl-2-oleoylglycerol; SSO = 1,2-distearoyl-3-oleoylglycerol; POP = 1,3-dipalmitoyl-2-oleoylglycerol; PPO = 1,2-dipalmitoyl-3-oleoylglycerol. Boxed values represent predominant fatty acids in the particular fats.

peak was calculated from a calibration curve generated from the migration distance of protein standards of known diameter, which included carboxylated latex beads (Duke Scientific, Palo Alto, CA), thyroglobulin, and apoferritin (HMW Std; Pharmacia, Piscataway, NJ) with molecular diameters of 380, 170, and 122 Å, respectively, and lipoprotein calibrators of previously determined particle size. The precise methodology, including staining for proteins, has been described by Nichols *et al*. (9). For extraction of fecal fat, feces were collected for 3 d after the rabbits had been on the diets for 10 wk. The feces were dried in an oven at 100°C and pulverized. Aliquots (1 g) of the dry fecal powder were slurried with 10 mL water containing 1 mL of concentrated HCl. Each slurry was extracted with 20 mL of chloroform/methanol 1:1 by vigorous stirring on a magnetic stirrer for 6 h. The chloroform layer was separated, washed with saline, dried over anhydrous Na_2SO_4, and an aliquot was taken to dryness under N_2 and weighed.

All experimental procedures were approved by the Wistar Institutional Animal Care and Use Committee.

RESULTS

Forty weanling male New Zealand White rabbits were fed an adaptation diet containing 0.05% cholesterol for 2 wk (Table 1). At 2 wk the average weight (±SE) of all the rabbits was 842 ± 65 g. The average serum cholesterol level was 4.93 ± 0.01 mmol/L, and the average triglyceride level was 1.24 ± 0.08 mmol/L. The rabbits were randomized to four groups of 10 each of approximately similar weight and serum cholesterol. They were then placed on the four test diets (Table 2) containing 15% fat. The test fats represented 58% of the total fat or 8.7% of the diet. The rabbits were weighed and bled under light anesthesia every 5 wk (weeks 5, 10, 15 in Table 5). All four groups gained weight—1.42 kg for group SOS, 1.30 kg for group SSO, 1.23 kg for group POP, and 1.14 kg for group PPO. Serum cholesterol levels rose significantly in all four groups in the first 5 wk; at 10 wk serum cholesterol levels had plateaued and they fell at week 15, but not significantly. The drop in serum cholesterol levels between weeks 10 and 15 was 30% in group SOS, 21% in group SSO, 22% in group POP, and 32% in group PPO. Between week 0 and 15, triglyceride levels fell in group SOS (by 32%), were unchanged in group SSO, and rose by 32 and 61%, respectively, in groups POP and PPO; none of the changes was statistically significant. After 20 wk on the diet the rabbits were weighed, bled, and exsanguinated under heavy anesthesia. The results are summarized in Table 6. At week 20 there were no differences in weight gain or in actual or relative liver weight. All the rabbits had lost weight in the last 5 wk of the experiment. Serum cholesterol levels had risen between weeks 15 and 20, and while none of the changes were significant, the percentage increase was 44.5% in group SOS, 21.6% in group SSO, 3.2% in group POP, and 32.0% in group PPO. There were no significant differences between the serum cholesterol levels in the four groups. The percentage of HDL cholesterol was also similar for all groups. Serum triglyceride levels were all lower than they had been at week 15, but there were no differences among the groups. Liver total cholesterol, percentage esterified cholesterol, and triglycerides were virtually identical among the groups. Average total liver cholesterol was 3.03 ± 0.01 mmol/100 g, esterified cholesterol was 63.8 ± 0.8%, and liver triglyceride was 0.86 ± 0.01 mmol/100 g.

LDL particle size (angstroms) was the same in all four groups, namely: SOS, 283.3 ± 3.23; SSO, 285.2 ± 3.37; POP, 283.4 ± 2.89; and PPO, 279.8 ± 1.88. Fecal fat, determined after 10 wk of feeding, was: SOS, 47 ± 4 mg/g feces; SSO, 38 ± 3 mg/g feces; POP, 28 ± 3 mg/g feces; and PPO, 23 ± 2 mg/g feces.

Severity of atherosclerosis was not significantly different

TABLE 5
Serum Lipids and Weights of Rabbits Maintained on Diets Containing Special Fats[a]

	Weeks			
	0	5	10	15
SOS				
Weight (g)	842 ± 41	1446 ± 90	1917 ± 20	2262 ± 201
Cholesterol (mMol/L)	4.94 ± 0.34	8.59 ± 1.03	8.33 ± 1.68	5.87 ± 1.42
Triglycerides (mMol/L)	1.45 ± 0.26	1.36 ± 0.23	1.12 ± 0.20	0.99 ± 0.08
SSO				
Weight (g)	843 ± 39	1540 ± 54	1868 ± 93	2140 ± 100
Cholesterol (mMol/L)	4.91 ± 0.31	10.01 ± 1.11	9.78 ± 1.32	7.68 ± 1.84
Triglycerides (mMol/L)	1.28 ± 0.12	1.25 ± 0.21	1.04 ± 0.11	1.17 ± 0.33
POP				
Weight (g)	841 ± 29	1432 ± 75	1540 ± 101	2070 ± 185
Cholesterol (mMol/L)	4.97 ± 0.39	10.29 ± 1.58	9.93 ± 1.09	7.71 ± 1.63
Triglycerides (mMol/L)	1.10 ± 0.11	1.26 ± 0.19	151 ± 0.26	1.46 ± 0.40
PPO				
Weight (g)	840 ± 37	1419 ± 89	1722 ± 102	1982 ± 117
Cholesterol (mMol/L)	4.91 ± 0.39	9.13 ± 1.76	11.97 ± 2.02	8.12 ± 2.28
Triglycerides (mMol/L)	1.14 ± 0.02	1.64 ± 0.53	2.37 ± 0.77	1.83 ± 0.87

[a]Values ± SE. See Table 4 for abbreviations.

TABLE 6
Necropsy Data. Rabbits Fed Atherogenic Diets Containing Special Fats for 20 wk[a]

	Group			
	SOS	SSO	POP	PPO
Number	5	7	7	6
Weight gain, g	1366 ± 199	1355 ± 125	1033 ± 165	1157 ± 143
Liver wt, g	49 ± 4	45 ± 6	42 ± 4	41 ± 5
Liver as % base weight	2.14 ± 0.18	2.00 ± 0.18	2.29 ± 0.23	2.04 ± 0.19
Serum (mMol/L)				
Total cholesterol	8.48 ± 2.09	7.03 ± 1.42	7.96 ± 1.42	10.73 ± 2.66
% HDL-cholesterol	7.14 ± 1.87	9.34 ± 3.03	8.27 ± 3.02	7.93 ± 3.14
Triglycerides	0.77 ± 0.09	0.94 ± 0.11	1.06 ± 0.18	0.91 ± 0.28
Liver (mMol/100 g)				
Total cholesterol	3.00 ± 0.36	3.00 ± 0.26	3.02 ± 0.36	3.10 ± 0.54
% Ester	66.0 ± 6.94	63.9 ± 5.58	62.8 ± 2.72	62.5 ± 6.44
Triglycerides	0.80 ± 0.06	0.89 ± 0.03	0.87 ± 0.09	0.89 ± 0.08
Atherosclerosis				
Aortic arch	1.60 ± 0.10	1.36 ± 0.34	1.36 ± 0.26	2.42 ± 0.51[b,c]
Thoracic aorta	1.10 ± 0.33	0.57 ± 0.28	0.29 ± 0.18	1.17 ± 0.21[b]

[a]Values ± SE. HDL, high density lipoprotein; see Table 4 for other abbreviations.
[b]Significantly different from POP ($P < 0.005$).
[c]Significantly different from all groups by ANOVA ($P < 0.017$).

between the two groups fed the stearic acid-rich triglycerides. In the rabbits fed the palmitic acid-rich triglycerides, the severity of atherosclerosis in the group fed PPO was significantly greater in both the aortic arch and thoracic aorta [both $P < 0.05$ by analysis of variance (ANOVA)]. Of all four groups, severity of atherosclerosis was greatest in the PPO group. Comparison by ANOVA of aortic atherosclerosis in group PPO vs. the other groups showed it to be significantly higher ($P < 0.017$). The same test for the thoracic aorta was not significant.

DISCUSSION

In this study we tested the atherogenic effects of specific fatty acids present at the *sn*-2 position of a dietary triglyceride. Comparison of SOS and SSO showed no significant difference in atherogenicity. Comparison of the palmitic acid-containing fats showed PPO to be significantly more atherogenic than POP ($P < 0.05$). This comparison confirms results obtained with lard and tallow (1), cottonseed oil (2), and palm oil (3) and shows that increasing the proportion of palmitic acid present at *sn*-2 of a triglyceride enhances the atherogenicity of that triglyceride. The mechanism underlying these observations remains moot, but there are several possibilities. Serum cholesterol levels are unaffected in rabbits fed native or randomized fats. Studies in rats have shown that serum lipids are unaffected when the animals are fed native or randomized peanut oil (10), fish oil (10), or palm oil (11). In human subjects Zock *et al*. (12) also found no difference in cholesterol levels between probands fed native or randomized fat. Nelson and Innis (13) compared cholesterol levels in human infants fed a standard formula containing 27.2% palmitic acid (5.0% at *sn*-2), a formula containing a synthetic triglyceride (24.8% palmitic acid, 29.1% at *sn*-2), or breast milk (23.1% palmitic acid, 56.4% at *sn*-2). Breast milk-fed infants had significantly higher cholesterol levels after 30 or 120 d, but cholesterol levels in the groups fed either standard or special formulas were the same. In our study of native and randomized cottonseed oil (2), we hypothesized that the LDL derived from the two fats might be of different sizes; this was found not to be the case. In this present study LDL particle size was also the same in all four dietary groups.

Studies in human infants (14–16) and rats (17,18) have indicated that fats containing palmitic acid at the *sn*-2 position are absorbed more completely than other fats. Increased absorption was indicated by decreased fecal excretion of fat. After the rabbits in this study had been on the various diets for 10 wk, we determined the level of fat excretion by group. Fat excretion was higher in the two groups fed the stearic acid-rich fats than in those fed the palmitic acid-rich fats. The rabbits fed the 2-oleoyl glycerides excreted more fat than their counterparts whose diets contained 16:0 or 18:0 in that position.

Redgrave *et al*. (19) reported that the structure of a triglyceride affected its removal from the circulation of rats, that rate being slower when saturated fatty acids were present at the *sn*-2 position. However, a more recent study (20) showed no clear pattern of lipolysis as a function of triglyceride structure. Generally, the authors concluded that a saturated fatty acid at *sn*-2 does not affect lipolysis, but rather the specific arrangement of acyl chains is important. Still, in their hands SOS was lipolyzed more rapidly than SSO, whereas the reverse was true with POP and PPO. A mechanism to explain the consistent observations relating to the atherogenic effects of 2-palmitoyltriglycerides cannot be based on either plasma or liver lipids or on LDL size since they do not differ. Martins *et al*. (21) have studied the effects of particle size and number on plasma clearance of chylomicrons and lipoprotein remnants and conclude that particle number is more important than particle size. Clearance was significantly decreased

when there were increased numbers of particles. The more efficient absorption of triglycerides bearing palmitic acid at *sn*-2 may reduce clearance time, thus increasing contact between lipid-bearing lipoproteins and the vessel wall. The increased absorption of the triglycerides in question suggests a mass effect, i.e., the tissues are exposed to greater concentrations of the fat over a given time. Differences in catabolic rate or tissue uptake may also have an effect, but there are no data relating to such effects in rabbits.

The study described above confirms again the increased atherogenicity of fats bearing palmitic acid at the *sn*-2 position.

ACKNOWLEDGMENTS

This study was supported, in part, by a Research Career Award (HL00734) from the National Institutes of Health and by funds from Unilever Research Laboratories, Vlaardingen, The Netherlands. We are indebted to Pat Blanche, Laura Holl, and Joseph Orr for the gradient gel electrophoresis analyses which were supported by the National Institutes of Health Program Project Grant HL18574 from the National Heart, Lung, and Blood Institute, a grant from the National Dairy Promotion and Research Board and were conducted at the Ernest Orlando Lawrence Berkeley National Laboratory through the U.S. Department of Energy under Contract No. DE-AC03-76SF00098.

REFERENCES

1. Kritchevsky, D., Tepper, S.A., Kuksis, A., Eghtedary, K., and Klurfeld, D.M. (1998) Cholesterol Vehicle in Experimental Atherosclerosis. 21. Native and Randomized Lard and Tallow, *J. Nutr. Biochem. 9*, 582–585.
2. Kritchevsky, D., Tepper, S.A., Wright, S., Kuksis, A., and Hughes, T.A. (1998) Cholesterol Vehicle in Experimental Atherosclerosis. 20. Cottonseed Oil and Randomized Cottonseed Oil, *Nutr. Res. 18*, 259–264.
3. Kritchevsky, D., Tepper, S.A., and Kuksis, A. (1999) Effects of Palm Oil, Randomized Palm Oil, and Red Palm Oil on Experimental Atherosclerosis, *FASEB J. 13*, A213.
4. Folch, J., Lees, M., and Sloane-Stanley, G.H. (1957) A Simple Method for the Isolation and Purification of Total Lipids from Animal Tissue, *J. Biol. Chem. 226*, 497–509.
5. Sperry, W.M., and Webb, M. (1950) A Revision of the Schoenhemer-Sperry Method for Cholesterol Determination, *J. Biol. Chem. 187*, 97–106.
6. Levy, A.I., and Keyloun, C. (1972) Measurement of Triglycerides Using Nonane Extraction and Colorimetry, *Autom. Anal. 1*, 487–502.
7. Duff, G.L., and McMillan, G.C. (1949) The Effect of Alloxan Diabetes on Experimental Cholesterol Atherosclerosis in the Rabbit, *J. Exp. Med. 89*, 611–630.
8. Krauss, R.M., and Burke, J. (1982) Identification of Multiple Classes of Plasma Low Density Lipoproteins in Humans, *J. Lipid Res. 23*, 97–104.
9. Nichols, A.V., Krauss, R.M., and Musliner, T.A. (1986) Nondenaturing Polyacrylamide Gradient Gel Electrophoresis, in *Methods in Enzymology, Vol. 128, Plasma Lipoproteins* (Segrest, J.P., and Albers, J.J., eds.), pp. 417–431, Academic Press, New York.
10. De Schrijver, R., Vermeulen, D., and Viaene, E. (1991) Lipid Metabolism Responses in Rats Fed Beef Tallow, Native or Randomized Fish Oil and Native or Randomized Peanut Oil, *J. Nutr. 121*, 948–955.
11. Sugano, M., Ikeda, I., Imasoto, Y., Nakayama, M., and Yoshida, K. (1990) Is Triglyceride Structure of Palm Oil Responsible for Its Characteristic Effect on Lipid Metabolism, *Lipid Res. (Life Sci. Adv.) 9*, 21–25.
12. Zock, P.L., deVries, J.H.M., deFouw, N.J., and Katan, M.B. (1995) Positional Distribution of Fatty Acids in Dietary Triglycerides: Effects on Fasting Blood Lipoprotein Concentrations in Humans, *Am. J. Clin. Nutr. 61*, 48–55.
13. Nelson, C.M., and Innis, S.M. (1999) Plasma Lipoprotein Fatty Acids Are Altered by the Positional Distribution of Fatty Acids in Infant Formula Triacylglycerols and Human Milk, *Am. J. Clin. Nutr. 70*, 62–69.
14. Tomarelli, R.M., Meyer, B.J., Weaber, J.R., and Bernhart, F.W. (1968) Effect of Positional Distribution on the Absorption of Fatty Acids of Human Milk and Infant Formulas, *J. Nutr. 95*, 583–590.
15. Filer, L.J., Jr., Mattson, F.H., and Fomon, S.J. (1969) Triglyceride Configuration and Fat Absorption by the Human Infant, *J. Nutr. 99*, 293–298.
16. Lien, E. (1994) The Role of Fatty Acid Composition and Positional Distribution in Fat Absorption in Infants, *J. Pediatr. 125*, S62–S68.
17. Renaud, S.G., Ruf, J.C., and Petithory, D. (1995) The Positional Distribution of Fatty Acids in Palm Oil and Lard Influences Their Biologic Effects in Rats, *J. Nutr. 125*, 229–237.
18. Lien, E.L., Boyle, F.G., Yuhas, R., Tomarelli, R.M., and Quinlan, P. (1997) The Effect of Triglyceride Positional Distribution on Fatty Acid Absorption in Rats, *J. Ped. Gastroenterol. Nutr. 25*, 167–174.
19. Redgrave, T.G., Kodali, D.R., and Small, D.M. (1988) The Effect of Triacyl-*sn*-glycerol Structure on the Metabolism of Chylomicrons and Triglyceride-Rich Emulsions in the Rat, *J. Biol. Chem. 263*, 5118–5123.
20. Mortimer, B.-C., Holthouse, D.J., Martins, I.J., Stick, R.V., and Redgrave, T.G. (1994) Effects of Triacylglycerol-Saturated Acyl Chains on the Clearance of Chylomicron-Like Emulsions from the Plasma of the Rat, *Biochim. Biophys. Acta 1211*, 171–180.
21. Martins, I.J., Mortimer, B.-C., Miller, J., and Redgrave, T.G. (1996) Effects of Particle Size and Number on the Plasma Clearance of Chylomicrons and Remnants, *J. Lipid Res. 37*, 2696–2705.

[Received December 17, 1999, and in final revised form April 20, 2000; revision accepted April 24, 2000]

L-Carnitine Effects on Chemical Composition of Plasma Lipoproteins of Rabbits Fed with Normal and High Cholesterol Diets

Maritza Diaz[a,b,c], Flor Lopez[b], Frank Hernandez[a], and Julio A. Urbina[a,c,*]

[a]Centro de Investigaciones del Ozono, Centro Nacional de Investigaciones Científicas, Havana, Cuba, [b]Laboratorio de Trombosis Experimental and [c]Laboratorio de Química Biológica, Centro de Biofísica y Bioquímica, Instituto Venezolano de Investigaciones Científicas, Caracas 1020A, Venezuela

ABSTRACT: L-Carnitine plays an important role in the mitochondrial uptake of long-chain fatty acids in mammals. It has recently been shown that this compound has a marked hypo-cholesterolemic effect when used in conjunction with lipid-rich diets. The aim of this study was to investigate the effects of L-carnitine on the fatty acid composition of plasma lipoproteins in rabbits fed with different diets. Four different groups were investigated: group I (standard diet), group II (standard diet supplemented with L-carnitine at 80 mg/kg), group III (standard diet supplemented with 0.5% cholesterol), and group IV (standard diet supplemented with 0.5% cholesterol plus L-carnitine at 80 mg/kg). The feeding period was 126 d. Total plasma cholesterol was indistinguishable in groups I and II, but increased nearly 40-fold in group III. This increment was reduced by 50% in group IV. Correspondingly, total cholesterol content in lipoprotein fractions [very low density lipoprotein (VLDL), low density lipoprotein (LDL), high density lipoprotein (HDL) separated by agarose gel chromatography was the same for groups I and II, while for animals fed a cholesterol-rich diet (III) total cholesterol in VLDL + LDL increased nearly 100-fold when compared with groups I and II but, again, the increment was reduced by 50% in group IV. In contrast, total cholesterol in HDL increased only fivefold for both groups III and IV when compared with groups I and II, indicating no effects of L-carnitine on this parameter. The reduction of total cholesterol in VLDL + LDL particles in animals fed a cholesterol-rich diet plus L-carnitine was associated with a marked decrease in the ratio of cholesteryl ester to free cholesterol and a dramatic increase in their phospholipid content; opposite effects were observed for HDL. L-Carnitine induced a marked decrease in the saturated to unsaturated $C_{16} + C_{18}$ fatty acid ratio in cholesteryl esters associated with VLDL and LDL from animals fed with both normal and cholesterol-rich diets. The opposite effect (a large increase in the saturated to unsaturated fatty acid ratio) was observed for both cholesteryl esters and phospholipids associated with HDL in animals fed with both diets. The results suggested that the hypocholesterolemic effects of L-carnitine could be associated with increased systemic breakdown of cholesteryl esters, a probable increase in reverse cholesterol transport, and the stabilization of a phospholipid-based structure of VLDL + LDL particles.

Paper no. L8292 in *Lipids 35*, 627–632 (June 2000).

L-Carnitine (β-hydroxy-γ-trimethylamino butyrate) is a conditionally essential nutrient for humans (1) and animals (2). Among other cellular functions, this compound has been associated with the uptake of long-chain fatty acids by mitochondria, where they are utilized in energy-yielding processes, and with the removal of short- and medium-chain fatty acids that accumulate as a result of normal and abnormal metabolism (3–5). Additionally, L-carnitine has been reported as a hypolipidemic drug, capable of reducing the circulating levels of cholesterol, triglycerides, free fatty acids, phospholipids, and very low density lipoproteins (VLDL) and increasing the levels of high, intermediate, and low density lipoproteins (HDL, IDL, LDL, respectively; refs. 6–9). However, other reports indicated that this compound was unable to modify plasmatic levels of total cholesterol and LDL and that the levels of HDL were only reduced after cessation of therapy (6,10,11). Mondola *et al.* (12) reported that L-carnitine was able to restore normal plasma levels of cholesterol and patterns of lipoproteins in rats nourished with a high cholesterol diet. Further, Bell *et al.* (13) reported that administration of L-carnitine modified the chemical composition of lipoproteins, both *in vitro* and *in vivo*, and also modulated hepatic lipogenesis from oleate and mevalonate.

On the other hand, it has been found that nutritional or pharmacological intervention with L-carnitine or its esters may be beneficial for infants and children with various clinical conditions associated with low circulating L-carnitine levels and in some chronic diseases associated with aging such as cardiovascular disease and Alzheimer's disease.

The plasma lipid-lowering effects of L-carnitine have been associated with several possible processes, including increase in whole body cholesterol turnover due to increased biliary excretion, increased conversion of cholesterol to bile acids, or repartitioning of whole body cholesterol (13); however, very little is known on the molecular basis of such processes. The purpose of the present study was to examine the compo-

*To whom correspondence should be addressed.
E-mail: jaurbina@cbb.ivic.ve

Abbreviations: ACAT, acyl-CoA cholesterol acyltransferase; CE, cholesterol ester; FC, free cholesterol; GLC, gas-liquid chromatography; HDL, high density lipoprotein; LCAT, lecithin-cholesterol acyltransferase; LDL, low density lipoprotein; TLC, thin-layer chromatography; VLDL, very low density lipoprotein.

sitional changes induced by L-carnitine treatment in plasma lipoproteins of rabbits subject to both normal and cholesterol-rich diets.

MATERIALS AND METHODS

Male New Zealand rabbits (2.5–3 kg) were used in all experiments. Animals were fed with 100 g of basic rabbit chow per day (Alimentos Protinal, Valencia, Venezuela) and water *ad libitum*. The cholesterol-rich diet consisted of the basal diet supplemented with 0.5% (wt/wt) cholesterol (Sigma-Aldrich Chemical Company, St. Louis, MO; >95% purity) dissolved at 5% (wt/vol) in corn oil, which contained 15% saturated fatty acids and 85% unsaturated acids (Mazeite, Refinadora de Maiz Venezolana, Aragua, Venezuela). L-Carnitine (Laboratorios Elmor, S.A., Caracas, Venezuela, >95%) was given by gavage, using a stainless steel cannula. The experimental protocols used in the present study conformed to accepted standards, defined by the Bioethics Commission of the Institute Venezolano de Investigaciones Científicas.

After an initial adaptation period, rabbits were randomized and separated into four groups: group I (normal diet), 6 animals; group II (normal diet supplemented with L-carnitine at 80 mg/kg), 6 animals; group III (cholesterol-rich diet), 6 animals; and group IV (cholesterol-rich diet supplemented with L-carnitine at 80 mg/kg). Feeding was carried out for 126 d.

Blood samples were taken at day 0 from marginal ear veins and at day 126 by cardiac puncture; EDTA was used as anticoagulant, at a final concentration of 4 mM. Blood cells were removed by centrifugation at 2000 × *g* for 20 min and plasma from the six rabbits of each group was pooled for subsequent analysis. Lipoprotein fractions were isolated sequentially by centrifugation through KBr gradients as described by Camejo *et al.* (14); solid KBr was used to obtain the desired densities. The isolated fractions were dialyzed exhaustively against phosphate buffer (0.2 M monobasic sodium phosphate, 0.2 M dibasic sodium phosphate, 0.16 M sodium chloride, pH 7.4) and stored at 2ºC until further use. Final purification was achieved by agarose gel electrophoresis (14).

Analysis of lipid components of lipoprotein fractions was carried out using the following methods: Bowman and Wolf (15) for the determination of cholesterol and its esters, after separation by thin-layer chromatography (TLC); Biggs *et al.* (16) for the determination of tryglycerides; Beveridge and Johnson (17) for phospholipids; and Schacterle and Pollack (18) for proteins.

For gas–liquid chromatographic (CLC) analysis of fatty acids esterified to different components, methyl ester derivatives were first prepared by transesterification as described (19), after separation of phospholipids and cholesteryl esters by TLC (20). Methyl esters were separated in a 180-cm fused-silica column (2 mm i.d.), packed with 10% Silar 10C, coated with 30–200 mesh Diatoport S. The analyses were carried out in a Varian 3700 gas chromatograph, equipped with a flame-ionization detector and a digital PerkinElmer integrator. Helium was used as carrier gas (1.9 mL/min) and nitrogen as makeup gas. The temperature was programmed from 145 to 245ºC at 4ºC/min. External fatty acid standards (Sigma-Aldrich Chemical Company) were used to identify components.

All data are expressed as means ± standard deviations; when applicable Wilcoxon or Mann-Whitney tests were used to determine statistical significance.

RESULTS AND DICUSSION

Figure 1 shows the effect of L-carnitine administration (80 mg/kg) on total plasma levels of cholesterol in normal and cholesterol-fed rabbits (126 d of feeding). L-Carnitine had no significant effects on plasma cholesterol levels of animals that received normal diet (groups I and II). Animals fed with the atherogenic diet alone (group III) responded with marked (>40-fold) increase in plasma cholesterol levels, but this increment was reduced by 50% in group IV ($P = 0.0065$). The total cholesterol levels in lipoprotein fractions, separated by agarose gel electrophoresis, for the different experimental groups are presented in Table 1. In agreement with the results from total serum cholesterol, the cholesterol load in VLDL, LDL, and HDL from animals fed with normal diets was not altered by L-carnitine supplementation. In cholesterol-fed animals (group III), VLDL and LDL appeared as a single fraction, as reported before (14), and there was a great (>100-fold) increase in their cholesterol content after 126 d of feeding, when compared with groups I and II. For group IV (cholesterol-fed supplemented with L-carnitine) the increase in cholesterol levels was about 50% of that observed in group III ($P = 0.0065$). In contrast, the cholesterol load in HDL increased only five fold in both groups III and IV, when compared with I and II, indicating no effect of L-carnitine supplementation in this parameter. The dose of L-carnitine used in the present study (80 mg/kg·d) has been employed previously

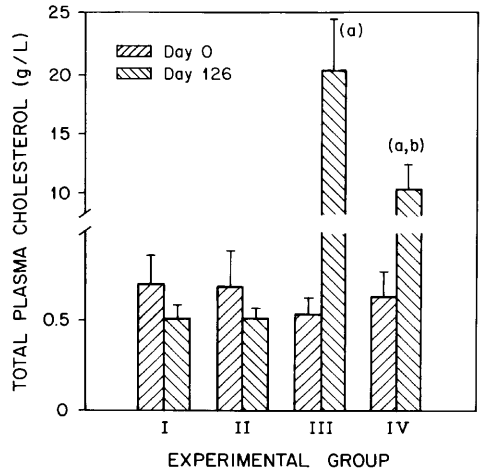

FIG. 1. Effects of L-carnitine on total plasma cholesterol levels in rabbits fed with normal and high cholesterol diets. (I) Normal diet, (II) Normal diet plus 80 mg/kg·d L-carnitine, (III) high cholesterol diet, (IV) high cholesterol diet plus 80 mg/kg·d L-carnitine. Values are means ± SD for six animals in each experimental group. (a) $P < 0.05$ when compared with day 0, (b) $P < 0.05$ when compared with group III at 126 d.

TABLE 1
Effects of L-Carnitine Supplementation on Cholesterol Load of Lipoproteins[a]

Diet (group no.)	Day 0	Day 126
	VLDL	
Normal (I)	0.23 ± 0.06	0.17 ± 0.02
Normal plus L-carnitine (II)	0.21 ± 0.09	0.18 ± 0.02
	LDL	
Normal (I)	0.28 ± 0.08	0.20 ± 0.04
Normal plus L-carnitine (II)	0.25 ± 0.08	0.20 ± 0.06
	HDL	
Normal (I)	0.20 ± 0.04	0.18 ± 0.04
Normal plus L-carnitine (II)	0.24 ± 0.10	0.18 ± 0.02
	VLDL	
Cholesterol-fed (III)	0.13 ± 0.02	
Cholesterol-fed plus L-carnitine (IV)	0.18 ± 0.10	
	VLDL + LDL	
		19.83 ± 4.42[b]
		9.39 ± 1.95[b,c]
	LDL	
Cholesterol-fed (III)	0.21 ± 0.06	
Cholesterol-fed plus L-carnitine (IV)	0.25 ± 0.08	
	HDL	
Cholesterol-fed (III)	0.20 ± 0.05	1.14 ± 0.24
Cholesterol-fed plus L-carnitine (IV)	0.21 ± 0.03	1.00 ± 0.13

[a]Obtained by agarose electrophoresis from normal and hypercholesterolemic rabbits. Values are means ± SD (g/L) of data from six rabbits per group.
[b]In these groups there was a single VLDL + LDL fraction.
[c]$P < 0.05$ compared to cholesterol-fed group. The results were obtained in a pool of sera from six experimental animals. Abbreviations VLDL, very low density lipoprotein; LDL, low density lipoprotein; HDL, high density lipoprotein.

in humans, without adverse effects, for the treatment of different primary or secondary disturbances of the levels of this important metabolic component (21). Additionally, L-carnitine at the same level has been reported as a cholesterol- and triglyceride-lowering agent in both humans and experimental animals (11,12,22,23), although its mechanism of action was not established. On the other hand, dietary supplementation with L-carnitine at 40 mg/kg led to rapid elevation of plasma and hepatic carnitine levels, without effects on total serum cholesterol levels (13). In our studies we confirmed that L-carnitine at the high dose level (80 mg/kg) leads to a marked and statistically significant reduction in total plasma cholesterol and the cholesterol load of all serum lipoproteins in hypercholesterolemic animals but has no significant effects on total plasma cholesterol in animals that receive normal diets and have normal cholesterol levels.

Detailed chemical analyses of isolated lipoprotein fractions from the different experimental groups were carried out from a pool of sera for each group and are presented as absolute concentration and percent composition in Tables 2 and 3. Only minor differences in the percent composition were observed as a result of L-carnitine supplementation in animals fed with a normal diet (Table 2), except for a probably significant (*ca.* threefold) reduction of the level of triglycerides associated with HDL, with a concomitant increase in phospholipids. In hypercholesterolemic animals (group III, Table 3) both the absolute and percent cholesterol content increased markedly in VLDL + LDL particles when compared with groups I and II (see Table 2), but there was a marked reduction of this parameter as consequence of L-carnitine supplementation (group IV, Table III). These differences are most probably significant, as they correspond to the statistically significant effects observed in total serum cholesterol level and lipoprotein cholesterol load (Fig. 1 and Table 1). The reduction in cholesterol content of VLDL + LDL as a consequence of L-carnitine supplementation was also associated with a three fold reduction in the percentage of esterified cholesterol and a concomitant increase in free cholesterol (FC; see Table 3). Although the relative content of triglycerides in VLDL + LDL particles of cholesterol-fed animals decreased, its absolute value increased *ca.* threefold (probably associated with the corn oil carrier), but this increment was again reduced by half as consequence of L-carnitine supplementation (Table 3). There was also a remarkable (>50-fold) increase in the relative phospholipid content of VLDL + LDL particles associated with L-carnitine supplementation, which suggested important structural modifications in these lipoproteic particles. Finally, the relative cholesterol content of HDL

TABLE 2
Composition (g/L) and Percentage of Plasma Lipoproteins Obtained by Differential Ultracentrifugation from Normocholesterolemic Rabbits[a]

Diet (group no.)	Total cholesterol	Free cholesterol	Esterified cholesterol	Triglyceride	Phospholipids	Protein
			VLDL			
Normal (I)	0.22 (11.7)	0.13 (6.9)	0.09 (4.8)	0.80 (42.7)	0.39 (20.8)	0.46 (24.7)
Normal plus L-carnitine (II)	0.24 (13.6)	0.14 (8.0)	0.10 (5.6)	0.73 (41.4)	0.62 (35.1)	0.17 (9.9)
			LDL			
Normal (I)	0.27 (26.4)	0.13 (13.0)	0.14 (13.4)	0.27 (26.0)	0.23 (22.1)	0.26 (25.4)
Normal plus L-carnitine (II)	0.26 (26.4)	0.15 (15.5)	0.11 (10.9)	0.33 (33.3)	0.21 (21.4)	0.18 (18.2)
			HDL			
Normal (I)	0.20 (10.4)	0.17 (8.7)	0.03 (1.7)	0.46 (23.7)	0.60 (31.0)	0.67 (34.9)
Normal plus L-carnitine (II)	0.22 (8.6)	0.13 (5.0)	0.09 (3.6)	0.21 (8.2)	1.35 (52.7)	0.78 (30.4)

[a]The results were obtained from a pool of sera (six animals in each experimental group) and are expressed as g/L; values in parentheses are percentages of the total weight of each particle. For abbreviations see Table 1.

TABLE 3
Percentage Composition of Plasma Lipoproteins Obtained by Differential Ultracentrifugation from Hypercholesterolemic Rabbits[a]

Diet (group no.)	Total cholesterol	Free cholesterol	Esterified cholesterol	Triglyceride	Phospholipids	Protein
			VLDL + LDL			
Cholesterol-fed (III)	19.6 (73.4)	3.15 (11.8)	16.35 (61.2)	2.30 (8.6)	0.11 (0.4)	4.81 (18.0)
Cholesterol-fed plus L-carnitine (IV)	9.2 (52.0)	5.40 (30.6)	3.80 (21.4)	1.28 (7.2)	4.28 (24.2)	2.92 (16.5)
			HDL			
Cholesterol-fed (III)	1.12 (37.4)	0.51 (17.1)	0.61 (20.3)	0.006 (0.2)	0.41 (13.6)	1.46 (48.8)
Cholesterol-fed plus L-carnitine (IV)	1.09 (27.8)	0.14 (3.6)	0.95 (24.2)	0.06 (1.5)	0.27 (6.9)	2.50 (63.8)

[a]The results were obtained from a pool of sera (six animals in each experimental group) and are expressed as g/L; values in parentheses are percentage of the total weight of each particle. For abbreviations see Table 1.

TABLE 4
Fatty Acid[a] Composition[b] of Cholesteryl Esters in HDL from Normo- and Hypercholesterolemic Rabbits

Diet (group no.)	16:0	18:0	18:1	18:2	Saturated/unsaturated
Normocholesterolemic					
Normal (I)	ND	11.0 ± 0.6	48.0 ± 0.6	41.3 ± 0.4	0.1
Normal plus L-carnitine (II)	44.9 ± 0.2	24.7 ± 0.6	8.1 ± 0.5	22.9 ± 0.2	2.2
Hypercholesterolemic					
Cholesterol-fed (III)	87.0 ± 0.2	2.0 ± 0.1	11.0 ± 0.2	ND	8.1
Cholesterol-fed plus L-carnitine (IV)	85.1 ± 0.4	8.1 ± 0.2	7.0 ± 0.2	ND	13.3

[a]Number of carbon atoms:number of double bonds. ND, not detectable; for other abbreviation see Table 1.
[b]The results were obtained in a pool of sera from (six experimental animals for each experimental group) and are expressed as percentages.

particles also increased in cholesterol-fed animals, and L-carnitine supplementation led to a reduction of this parameter, mostly associated with a drop in both the absolute and relative content of FC.

These concerted compositional changes could be explained by an increased peripheral and hepatic breakdown of cholesterol esters (CE) from VLDL + LDL as a consequence of L-carnitine-induced catabolism of fatty acids (3,21), combined with transfer of CE from VLDL + LDL to HDL, probably mediated by cholesteryl ester transfer protein (see Refs. 24,25), leading to increased cholesterol reverse transport and excretion (26,27). The compositional changes of HDL in hypercholesterolemic animals treated with L-carnitine could also suggest activation of lecithin-cholesterol acyl transferase (LCAT). An increase in the activity of hepatic acyl-CoA cholesterol acyl transferase (ACAT) has been observed in rabbits given a hyperlipidemic diet along with L-carnitine (9). It has been postulated that ACAT must first be stimulated by exogenous cholesterol before a stimulatory effect by L-carnitine can take place (13,28); a similar effect on LCAT could explain the differential effects of L-carnitine supplementation on HDL composition of normo- and hypercholesterolemic animals (Tables 2 and 3).

The $C_{16} + C_{18}$ fatty acid composition of cholesteryl esters associated with lipoproteins in different experimental groups is presented in Tables 4–6. These fatty acids constituted >70% of total fatty acids, the rest being a variable mixture of long-chain polyunsaturated acids. In both normal and cholesterol-fed animals L-carnitine supplementation led to a large increase in the saturated ($C_{16} + C_{18}$) to unsaturated ($C_{18:1} + C_{18:2}$) fatty acid ratio in association with cholesteryl esters (Table 4) and, to a lesser extent, with phospholipids (Table 5) associated with HDL. In contrast, L-carnitine supplementation was associated with a marked reduction in the ratio of saturated to unsaturated fatty acids of cholesteryl esters pres-

TABLE 5
Fatty Acid[a] Composition[b] of Cholesteryl Esters in HDL from Normo- and Hypercholesterolemic Rabbits

Diet (group no.)	16:0	18:0	18:1	18:2	Saturated/ Unsaturated
Cholesterol-fed (III)	ND	75.3 ± 0.2	ND	25.1 ± 0.4	3.0
Cholesterol-fed plus L-carnitine (IV)	41.4 ± 0.1	42.2 ± 0.3	17.1 ± 0.4	ND	4.9

[a]Number of carbon atoms:number of double bonds.
[b]The results were obtained for a pool of sera from (six animals for each experimental group) and are expressed as percentages. For abbreviations see Tables 1 and 4.

TABLE 6
Fatty Acid[a] Composition[b] in Cholesteryl Esters of LDL and VLDL + LDL from Normo- and Hypercholesterolemic Rabbits

Diet (group no.)	16:0	18:0	18:1	18:2	Saturated/unsaturated
Normal (I)	27.9 ± 0.6	43.0 ± 0.8	6.0 ± 0.5	23.0 ± 0.6	2.4
Normal plus L-carnitine (II)	27.0 ± 0.4	19.0 ± 0.6	3.2 ± 0.5	41.0 ± 0.5	0.9
Cholesterol-fed (III)	23.9 ± 0.2	11.9 ± 0.3	31.0 ± 0.2	31.0 ± 0.2	0.6
Cholesterol-fed plus L-carnitine (IV)	7.1 ± 0.3	12.1 ± 0.3	56.0 ± 0.2	56.0 ± 0.2	0.2

[a]Number of carbon atoms:number of double bonds.
[b]The results were obtained in a pool of sera from (six experimental animals for each experimental group) and are expressed at percentages of total fatty acids. For abbreviations see Tables 1 and 4.

ent in VLDL and LDL in both normal and cholesterol-fed animals (Table 6). These fatty acid compositional changes could be associated with a preferential stimulation by L-carnitine of saturated fatty acid breakdown in peripheral tissues due to the specificity of the transesterifying enzymes of mitochondrial outer membranes (3). Although these effects were seen in both normo- and hypercholesterolemic rabbits they could be significant in terms of the reduction of the atherogenic potential of VLDL + LDL particles due to their increased unsaturated fatty acid and phospholipid content (29).

ACKNOWLEDGMENTS

This work was supported by the Instituto Venezolano de Investigaciones Cientificas (IVIC). M.D.G. was a United Nations University fellow. We thank Gonzalo Visbal for technical assistance.

REFERENCES

1. Mitchell, E.M. (1978) Carnitine Metabolism in Human Subjects. I. Normal Metabolism, *Am. J. Clin. Nutr. 31*, 293–306.
2. Rebouche, C.J. (1982) Sites and Regulation of Carnitine Biosynthesis in Mammals, *Fed. Proc. 41*, 2848–2852.
3. Rebouche, C.J. (1992) Carnitine Function and Requirements During the Life Cycle, *FASEB J. 6*, 3379–3386.
4. Rebouche, C.J., and Paulson, D.J. (1986) Carnitine Metabolism and Function in Humans, *Annu. Rev. Biochem. 6*, 41–66.
5. Borum, P.R. (1986) Carnitine Function, in *Clinical Aspects of Human Carnitine Deficiency* (Borum, P.R. ed.), pp. 16–27, Pergamon, New York.
6. Bell, F.P., Raymon, T.L., and Painode, C.L. (1987) The Influence of Diet and Carnitine Supplementation on Plasma Carnitine, Cholesterol and Triglycerides in WHHL (Watanabe-heritable hyperlipidemic) Netherland Dwarf and New Zealand Rabbits (*Oryctolagus cuniculus*), *Comp. Biochem. Physiol. 87B*, 587–591.
7. Brady, L.J., Knowber, C.M., Hoppel, C.L., Leathers, C.W., Mcfarland, D., and Brady, P.S. (1986) Pharmacologic Action of L-Carnitine in Hypertriglyceridemia in Obese Zucker Rats, *Metabolism 35*, 555–562.
8. Maccari, F., Arseni, A., Chiodi, P., Ramacci, M.T., Angelucci, L., and Hulsmann, W.C. (1987) L-Carnitine Effect on Plasma Lipoproteins of Hyperlipidemic Fat-Loaded Rats, *Lipids 22*, 1005–1008.
9. Seccombe, D.W., James, L., Hann, P., and Jones, E. (1987) L-Carnitine Treatment in the Hyperlipidemic Rabbit, *Metabolism 36*, 1192–1196.
10. Maebachim, M., Kawamura, N., Sato, M., Imamura, A., and Yoshinaga, K. (1978) Lipid-Lowering Effect of Carnitine in Patients with Type IV Hyperliproproteinemia, *Lancet 2*, 805–807.
11. Raymond, T.L., Reynolds, S.A., Swanson, J.A., Patnode, C.A., and Bell, F.P. (1987) The Effect of Oral L-Carnitine on Lipoprotein Composition in the Watanabe Heritable Hyperlipidemic Rabbit (*Oryctolagus cuniculus*), *Comp. Biochem. Physiol. 88A*, 503–506.
12. Mondola, P., Belfiore, A., Santangelo, F., and Santillo, M. (1989) The Effect of L-Carnitine on the Apolipoprotein Pattern on Rats Fed a Cholesterol-Rich Diet, *Comp. Biochem. Physiol. 100B*, 69–73.
13. Bell, F.P., Vidmar, T.J., and Raymond, T.L. (1992) L-Carnitine Administration and Withdrawal Affect Plasma and Hepatic Carnitine Concentrations, Plasma Lipid and Lipoprotein Composition, and *in vitro* Hepatic Lipogenesis from Labeled Mevalonate and Oleate in Normal Rabbits, *J. Nutr. 122*, 959–966.
14. Camejo, G., Bosch, V., Arreaza, C., and Mendez, H.C. (1973) Early Changes in Plasma Lipoprotein Structure and Biosynthesis in Cholesterol-Fed Rabbits, *J. Lipid Res. 14*, 61–68.
15. Bowman, R.E., and Wolf, R.C. (1962) A Rapid and Specific Ultramicro Method for Total Serum Cholesterol, *Clin. Chem. 8*, 302–309.
16. Biggs, H.G., Erikson, J.M. and Moorehead, W.R.A. (1975) A Manual Colorimetric Assay of Triglycerides in Serum, *Clin. Chem. 21*, 437–441.
17. Beveridge, J.M., and Johnson, S.E. (1949). The Determination of Phospholipid Phosphorus, *Can. J. Res. 27*, 159–163.
18. Schacterle, G.R., and Pollack, R.L. (1973) A Simplified Method for the Quantitative Assay of Small Amounts of Protein in Biologic Material, *Anal. Biochem. 51*, 654–655.
19. Lepage, G., and Roy, C.C. (1986) Direct Transesterification of All Classes of Lipids in a One-Step Reaction, *J. Lipid Res. 27*, 114–120.
20. Bitman, J.D., Wood, L., and Ruth, J.M. (1981) Two-Stage, One-Dimensional Thin-Layer Chromatographic Method for Separation of Lipid Classes, *J. Liq. Chromatogr. 4*, 1007–1021.
21. Goa, K.L., and Brogden, R.N. (1987). L-Carnitine. A Review of Its Characteristics and Therapeutic Use in Cardiac Ischemy and in Primary and Secondary Deficits of Carnitine, Associated to Fatty Acid Metabolism, *Drugs 34*, 1–10.
22. Vacha, G.M., Giocelli, G., Siliprandi, N., and Corsi, M. (1983) Favorable Effects of L-Carnitine Treatment on Hypertriglyceridemia in Hemodialysis Patients: Decisive Role of Low Levels of High-Density Lipoprotein-Cholesterol, *Am. J. Clin. Nutr. 38*, 532–540.
23. Guarnieri, G.F., Ranieri, F., Toigo, G., Vasile, A., Climan, M., Rizzoli, V., Moracchielo, M., and Campanacci, L. (1980) Lipid-Lowering Effect of Carnitine in Chronically Uremic Patients Treatment with Maintenance Hemodialysis, *Am. J. Clin. Nutr. 33*, 1489–1492.
24. Tall, A.R. (1993) Plasma Cholesteryl Ester Protein, *J. Lipid Res. 34*, 1255–1274.

25. Bruce, C., Chauinord, R.A., Jr. and Tall, A.R. (1998) Plasma Lipid Transfer Proteins, High Density Lipoproteins and Reverse Cholesterol Transport. *Annu. Rev. Nutr. 18*, 297–330.
26. Reichl, D., and Miller, N.E. (1986) The Anatomy and Physiology of Reverse Cholesterol Transport, *Clin. Sci. 70*, 221–231.
27. Fielding, C.J., and Fielding, P.E. (1995) Molecular Physiology of Reverse Cholesterol Transport, *J. Lipid Res. 36*, 211–228.
28. Bell, F.P. (1986) Arterial Cholesterol Esterification by AcylCoA Cholesterol Acyltransferase: Its Possible Significance in Atherogenesis and Its Inhibition by Drugs, in *Pharmacology Control of Hyperlipidemia* (Fears, R., Levy, R.L., Shepherd, C.J., Packard, J.R., and Miller, N.E., eds.), pp. 409–422, Pro Science Publishers, Barcelona.
29. Hurt-Camejo, E., and Camejo G., (1999) Mecanismos Aterogénicos de las Lipoproteínas, in *Hiperlipidemias, Clínica y Tratamiento* (Carmena, R., and Ordovas, J.M., eds.), pp. 63–84, Ediciones Dayma, S.A., Barcelona.

[Received June 25, 1999, and in revised form March 22, 2000; revision accepted April 3, 2000]

Protective Effect of Olive Oil and Its Phenolic Compounds Against Low Density Lipoprotein Oxidation

Montserrat Fitó[a], María Isabel Covas[a,b,*], Rosa M. Lamuela-Raventós[c], Joan Vila[a], Jaume Torrents[a,b], Carmen de la Torre[c], and Jaume Marrugat[a]

[a]Unitat de Lípids i Epidemiologia Cardiovascular, Institut Municipal d'Investigació Médica (IMIM), 08003 Barcelona, Spain, [b]Laboratori de Referència de Catalunya, 08907 L'Hospitalet, Barcelona, Spain, and [c]Departament de Bromatologia i Nutrició, Facultat de Farmacia, Universitat de Barcelona, 08029 Barcelona, Spain

ABSTRACT: The protective effect of phenolic compounds from an olive oil extract, and of olive oils with (extra-virgin) and without (refined) phenolic components, on low density lipoprotein (LDL) oxidation was investigated. When added to isolated LDL, phenolics [0.025–0.3 mg/L caffeic acid equivalents (CAE)] increased the lag time of conjugated diene formation after copper-mediated LDL oxidation in a concentration-dependent manner. Concentrations of phenolics greater than 20 mg/L inhibited formation of thiobarbituric-acid reactive substances after AAPH-initiated LDL oxidation. LDL isolated from plasma after preincubation with phenolics (25–160 mg/L CAE) showed a concentration-dependent increase in the lag time of conjugated diene formation after copper-mediated LDL oxidation. Refined olive oil (0 mg/L CAE) and extra-virgin olive oil (0.1 and 0.3 mg/L CAE) added to isolated LDL caused an increase in the lag time of conjugated diene formation after copper-mediated LDL oxidation that was related to olive oil phenolic content. Multiple regression analysis showed that phenolics were significantly associated with the increase in lag time after adjustment for effects of other antioxidants; α-tocopherol also achieved a statistically significant effect. These results indicate that olive oil phenolic compounds protect LDL against peroxyl radical-dependent and metal-induced oxidation *in vitro* and could associate with LDL after their incubation with plasma. Both types of olive oil protect LDL from oxidation. Olive oil containing phenolics, however, shows more antioxidant effect on LDL oxidation than refined olive oil.

Paper no. L8314 in *Lipids 35,* 633–638 (June 2000).

Coronary heart disease (CHD) is the main cause of mortality in industrialized countries, with the Mediterranean area having the lowest CHD mortality rate (1). A Mediterranean diet has been shown to be effective in secondary prevention of CHD endpoints such as death and reinfarction (2). The lower incidence of CHD in Mediterranean countries has been attributed to a diet rich in fruits, vegetables, legumes, and grains, the major fat component of which is olive oil. These foods contain natural antioxidants that can prevent low density lipoprotein (LDL) oxidation (3).

There is evidence that oxidation of LDL by free radicals plays a significant role in the development of atherosclerosis (4). In some human and animal dietary studies, oleic acid-rich diets have been shown to reduce LDL susceptibility to oxidation (5–7). Studies on olive oil as a protective factor against atherosclerosis have focused mainly on the role of oleic acid. However, the nonsaponifiable fraction of extra-virgin olive oil, which is obtained from the first pressing of the olive fruit, is rich in phenolic compounds that have strong antioxidant properties (8,9). Phenolic compounds isolated from olive oil such as phenolic acids (10), resveratrol (11), and hydroxytyrosol (12) have antioxidant properties *in vitro*. Some flavonoids (13,14) and catechins (15) also have antioxidant properties *in vivo*. Olive oil contains other antioxidant compounds such as α-tocopherol and, in small amounts, β-carotene.

Phenolic compounds are removed in the olive oil refining processes. However, unlike other oils, extra-virgin olive oil of high quality is consumed directly without further refining. In this study we examined antioxidant activity of different olive oils against *in vitro* LDL oxidation to determine whether a protective effect correlates with their phenolic content. Our study also investigated whether phenolic compounds extracted from olive oil could be incorporated into lipophilic LDL particles after their incubation with plasma.

MATERIALS AND METHODS

Materials and chemicals. The fatty acid compositions of refined and extra-virgin olive oils were determined by gas chromatography, and α-tocopherol and β-carotene contents in olive oils were determined by high-performance liquid chromatography (HPLC) as previously described (16–18). Total phenolic content of olive oils was measured by the Folin-Ciocalteau method (19). Measurement of phenolic compounds of

*To whom correspondence should be addressed at Unitat de Lípids i Epidemiologia Cardiovascular, Institut Municipal d'Investigació Mèdica (IMIM), Carrer Doctor Aiguader, 80, 08003 Barcelona, Spain.
E-mail: mcovas@imim.es

Abbreviations: AAPH, 2,2′-azobis(2-amidinopropane) dihydrochloride; ANOVA, analysis of variance; CAE, caffeic acid equivalents; CHD, coronary heart disease; HPLC, high-performance liquid chromatography; IC, inhibitory concentration; LDL, low density lipoprotein; MDA, malondialdehyde; MUFA, monounsaturated fatty acids; PBS, phosphate-buffered saline; PUFA, polyunsaturated fatty acids; SFA, saturated fatty acids; TBARS, thiobarbituric acid-reactive substances.

extra-virgin olive oil was also performed by HPLC as previously described (20). Phenolics were extracted from extra-virgin olive oil by liquid–liquid extraction with 80% ethanol (21). Cupric sulfate, 2,2′-azobis(2-amidinopropane) dihydrochloride (AAPH), and 2-thiobarbituric acid were purchased from Sigma Chemical Co. (St. Louis, MO). All chemicals and organic solvents were of analytical grade.

LDL preparation and isolation. Blood from healthy volunteers was collected after an overnight fast in tubes containing 1 g/L EDTA. Plasma was separated by centrifugation at 1000 × *g* at 4ºC for 15 min. LDL isolation was performed by sequential flotation ultracentrifugation (22). Native LDL was dialyzed by molecular size exclusion chromatography in a G-25 Sephadex column (Pharmacia, Uppsala, Sweden), with 2.7 mL phosphate-buffered saline (PBS), 0.01 M, pH 7.4, under gravity feed at 4ºC. Protein content was determined by the red pyrogallol method (Sigma).

Copper-mediated LDL oxidation. To initiate oxidation, dialyzed LDL (0.05 g protein/L) was incubated with cupric sulfate (5 μM) in PBS at a final volume of 1 mL. Absorbance at 234 nm was continually monitored at 2-min intervals for 5 h at 35ºC (23) by using a spectrophotometer (Hewlett-Packard, Palo Alto, CA) fitted with a heater and equipped with a 7-position automatic sample changer.

AAPH-initiated LDL oxidation. To initiate oxidation, dialyzed LDL (0.10 g protein/L) was incubated with 10 mM AAPH in PBS plus 1 mM EDTA at 35ºC for 8 h at a final volume of 1 mL. Oxidation of LDL, quantified as the generation of malondialdehyde (MDA) equivalents, was measured by the thiobarbituric acid-reactive substances (TBARS) method as previously described for isolated LDL (24). TBARS formation was measured at intervals of 2 h.

Assays for antioxidant activity of phenolic compounds on LDL oxidation. Copper-mediated LDL oxidation was performed as just described in two separate experiments: (i) after addition to the isolated LDL of phenolic extracts containing from 0.025 to 0.3 mg/L (final concentration) caffeic acid equivalents (CAE). (ii) After plasma incubation with phenolic extracts containing from 25 to 160 mg CAE/L (0.09 to 0.58 mg CAE/mg LDL protein) (final concentration) for 3 h at 35ºC, followed by LDL isolation. The incubation of plasma with phenolics was performed with rotatory incubation in the dark to avoid antioxidant photodegradation.

AAPH-initiated oxidation was performed as described above with addition of phenolic extracts containing from 5 to 25 mg CAE/L (final concentration) to isolated LDL.

Assay for antioxidant activity of olive oils on LDL oxidation. Extra-virgin olive oil was diluted (1:10) with refined olive oil. Carefully weighed aliquots of refined (40 mg) and diluted extra-virgin olive oil (11 and 40 mg) were added to isolated LDL to produce phenolic concentrations of 0 mg CAE/L (refined) and 0.1 and 0.3 mg CAE/L (extra-virgin). LDL oxidation was performed as decribed above.

Statistical analysis. Linear and quadratic regression analyses were used to assess the relationship between continuous variables. One-way analysis of variance (ANOVA) followed by Dunnett's *t*-test was used for simultaneous, multiple comparisons between groups. Spearman's correlation test was employed to assess the association between two continuous variables. Multiple linear regression analysis was performed, with data of six experiments, to estimate the increase of lag time of conjugated diene formation associated with a 0.1 mg CAE/L concentration increase in olive oil. An adjustment by the concentrations of other antioxidants added to isolated LDL with the olive oils was performed. A criterion of $P < 0.1$ in simple associations was used to include variables in the model. $P < 0.05$ was considered statistically significant. These statistical analyses were performed using the SPSS statistical package (SPSS Inc. Co., Chicago, IL).

RESULTS

Olive oil analysis. The percentages of monounsaturated (MUFA), polyunsaturated (PUFA), and saturated fatty acids (SFA) were 73, 10, and 17% for extra-virgin and 74, 11, and 15% for refined olive oil, respectively. α-Tocopherol and β-carotene concentrations of each oil were 214 and 5.05 mg/kg for extra-virgin and 174 and <0.01 mg/kg for refined olive oil, respectively. The concentrations of phenolic compounds were 139 and 0 mg CAE/kg for extra-virgin and refined olive oil, respectively. Figure 1 is a chromatogram of the phenolic compounds present in the extra-virgin oil used in the assay. The percentages of phenolic compounds were as follows: Peak 1 (hydroxytyrosol), 1.7; Peak 2 (protocatechuic acid), 2.8; Peak 3 (tyrosol), 1.5; Peak 4 (vanillic acid), 0.5; Peaks 5, 6, and 7 (unidentified), 0.8, 2.6, and 0.8, respectively; Peak 8 (*m*-coumaric acid), 6.7; Peak 9 (oleuropeine), 0.7; Peak 10 (oleuropeine aglycone), 41.6; Peaks 11, 12, and 13 (unidentified), 14.7, 4.0, and 16.4 , respectively.

Effects of olive oil phenolic compounds on LDL oxidation. (i) Addition of phenolic extracts to isolated LDL. In copper-mediated LDL oxidation the addition of olive oil phenolics at concentrations ranging from 0.025 to 0.3 mg CAE/L increased ($P < 0.001$) the lag time before the formation of conjugated dienes in a concentration-dependent manner ($r^2 = 0.994$, $P < 0.0001$, linear regression) (Fig. 2). From extrapolation of the dose–response plot of percentage increase in lag phase, the concentrations of phenolic compounds required to cause 50 (IC_{50}) and 100% (IC_{100}) inhibition of the lag phase were established at 0.115 and 0.235 mg CAE/L, respectively. The generation of TBARS during AAPH-initiated LDL oxidation is shown in Figure 3. In control LDL, a significant increase in MDA equivalents ($P < 0.001$) was observed from 0 to 8 h. The same occurred with concentrations of 5 ($P < 0.01$) and 10 mg CAE/L ($P < 0.01$). The increase was maximal following 8 h of oxidation. When 15 mg CAE/L phenolic extract was added to isolated LDL, the increase in TBARS formation was significant ($P < 0.01$) only after more than 6 h of incubation. Concentrations of phenolics greater than or equal to 20 mg CAE/L inhibited TBARS formation in AAPH-initiated LDL oxidation ($P < 0.01$).

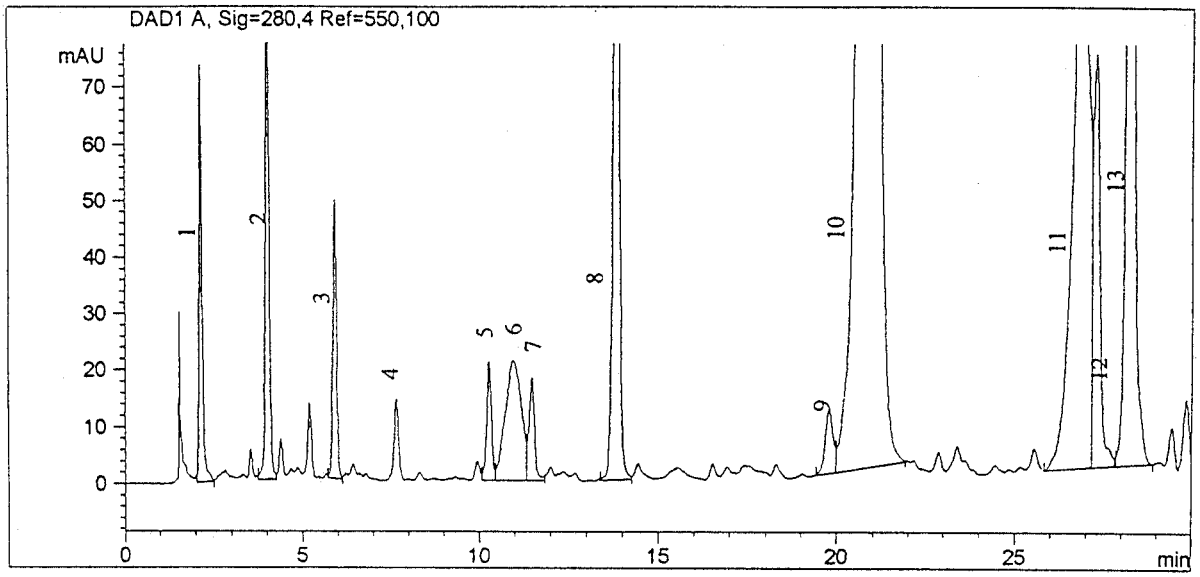

FIG. 1. High-performance liquid chromatogram showing the phenolic profile of extra-virgin olive oil. Peak numbers: (1) hydroxytyrosol; (2) protocatechuic acid; (3) tyrosol; (4) vanillic acid; (8) *m*-coumaric acid; (9) oleuropeine; (10) oleuropeine aglycone; (5–7) and (10–13) unidentified phenols.

(ii) Preincubation of phenolic extracts with plasma and subsequent LDL isolation. When copper-mediated oxidation of LDL that had been isolated from plasma following preincubation with olive oil phenolics (25 to 160 mg CAE/L; 0.09 to 0.58 mg CAE/mg LDL protein) was carried out, the lag time before conjugated diene formation increased ($P < 0.001$, ANOVA) in a phenol concentration-dependent manner ($r^2 = 0.995$, $P < 0.0001$, quadratic regression) (Fig. 2). From extrapolation of the dose–response plot of percentage increase in lag phase, IC_{50} and IC_{100} were established at 98.5 and 148 mg CAE/L, respectively.

Effect of olive oil on LDL oxidation. As shown in Figure 4 all olive oils increased the lag time of diene formation in comparison with the control in a phenol concentration-dependent manner ($P < 0.001$, ANOVA). When simple associations were performed, a positive correlation was obtained between lag time of conjugated diene formation and the concentrations of phenolics ($P = 0.001$), α-tocopherol ($P = 0.05$), and β-carotene ($P = 0.01$) added to isolated LDL. No associations between lag time and MUFA, PUFA, or SFA added to LDL were found. Results of multiple linear regression analysis (Table 1) showed that phenolics concentration was significantly ($P < 0.001$) associated with the increase in lag time of conjugated diene formation. The effects of α-tocopherol concentrations were of borderline significance ($P = 0.064$). The increase in lag time associated with an increase of 0.1 mg/L in phenolics concentration, adjusted for α-tocopherol and β-carotene, was 108 min (88–129 min, 95% confidence interval).

TABLE 1
Multiple Linear Regression Analysis of the Increase in the Lag Time of LDL Oxidation and of Antioxidant Compounds in Olive Oil[a]

Antioxidant	B (SE)	*P*
Phenolics	108 (9.8)	<0.001
α-Tocopherol	6.54 (3.0)	0.064
β-Carotene	—	—

[a]LDL, low density lipoprotein; B, regression coefficient; SE, standard error.

DISCUSSION

Growing epidemiological evidence indicates that a Mediterranean diet has beneficial effects on diseases associated with oxidative damage such as CHD and cancer, and on aging (2,3,25). Olive oil (and its constituent antioxidant compounds) is one of the main components of the Mediterranean diet. Olive oil consumption has been associated with a lower coronary risk profile (26) and with a reduced breast-cancer risk (27). Besides antioxidant olive oil components, dietary MUFA are associated with lower risk of CHD (28). Also, the results of some large prospective studies have indicated that a high vitamin E intake is associated with lower CHD risk (29). Intake of flavonoids has been associated with a reduction in cardiovascular mortality in some epidemiological prospective studies (30). The effects of olive oil and its antioxidant compounds warrant evaluation since their presence in food may explain at least part of the benefits of the Mediterranean diet. Our experiments were designed to examine the effect of olive oils, with and without phenolic compounds, as well as the antioxidant activity of the entire phenolic content of an extra-virgin olive oil. The present study has confirmed *in vitro* the antioxidant activity of extra-virgin olive oil phenolic compounds in inhibiting LDL oxidation by copper- and AAPH-initiated systems.

The copper-catalyzed oxidation of LDL, isolated from plasma preincubated with olive oil phenolics, was also significantly inhibited. In this situation, only phenols that are on the surface of or within LDL particles can be responsible for

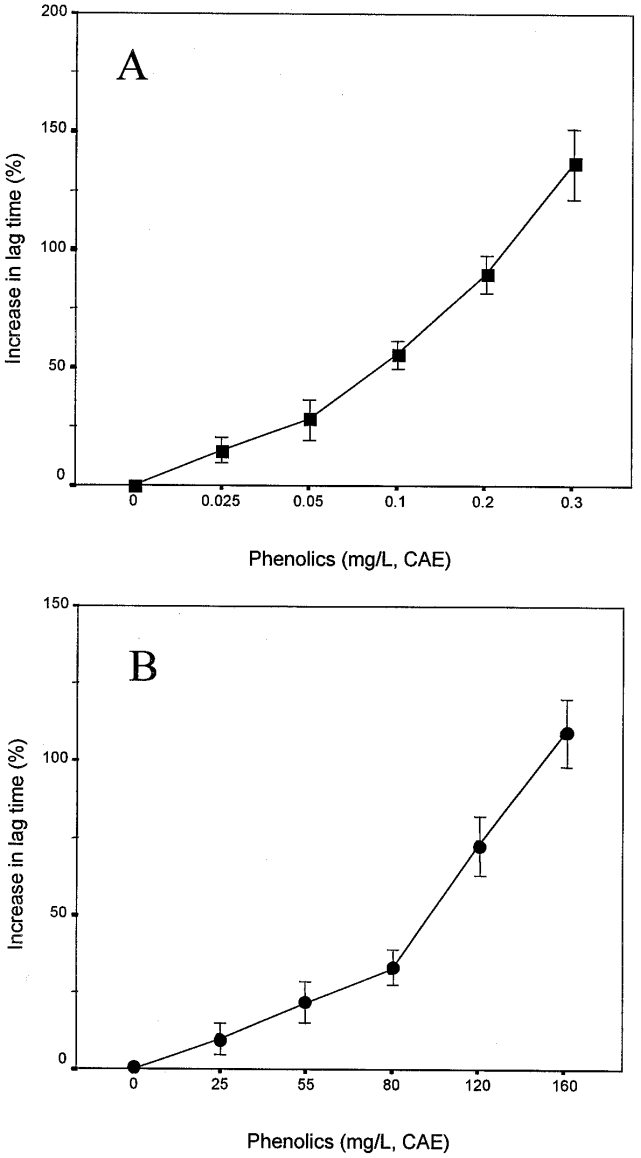

FIG. 2. Effect of the extra-virgin olive oil phenolics on the lag time of copper-mediated low density lipoprotein (LDL) oxidation. (A) Isolated LDL (0.05 g protein/L) was oxidized with 5 μM copper in the presence of indicated amounts of phenolic compounds (CAE, caffeic acid equivalents). (B) Plasma was incubated at 35°C for 3 h with indicated amounts of phenolic compounds; LDL was isolated from plasma and oxidation was performed. Each point represents the mean ± standard deviation of three experiments. For both experiments there was a significant ($P < 0.001$) relationship between the amount of phenolics added and the lag time of conjugated diene formation.

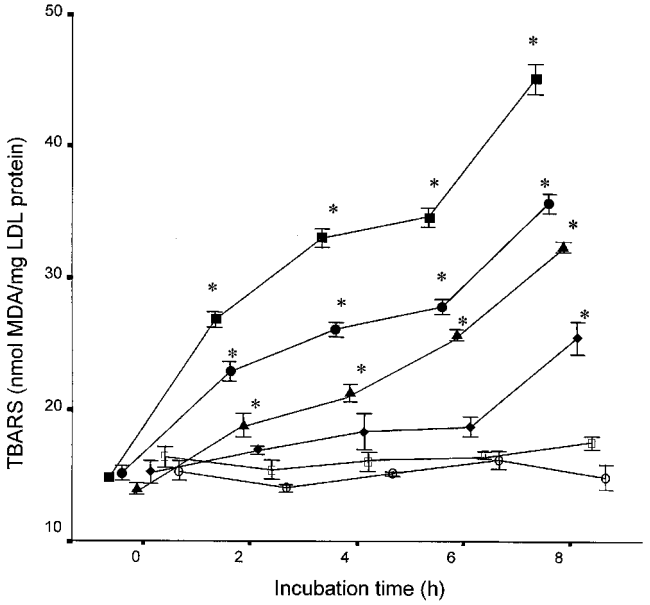

FIG. 3. Effect of extra-virgin olive oil phenolics on thiobarbituric acid-reactive substances (TBARS) generation following AAPH-initiated LDL oxidation. LD (0.10 g protein/L) was incubated with azo-compound (10 mM) at 35°C for up to 8 h in the presence of the indicated amounts of phenolic compounds expressed as CAE: (■) 0 mg/L (control); (●) 5 mg/L; (▲) 10 mg/L; (◆) 15 mg/L; (□) 20 mg/L; (○) 25 mg/L. TBARS formation was measured at intervals of 2 h. Each point represents the mean ± standard deviation of three experiments. *$P < 0.01$ compared with 0 h. MDA, malondialdehyde; for other abbreviations see Figure 2.

the inhibition of LDL oxidation. Preincubation of plasma with different doses of phenolic extract led to antioxidant activity against LDL oxidation that exhibited an exponential relationship to phenol concentration. This type of effect could relate to direct suppression by the phenolic compounds of the autocatalytic chain reaction of fatty acid peroxidation or to preservation of other chain-breaking antioxidants such as α-tocopherol (12).

The concentration of olive oil phenolics required to inhibit copper-mediated LDL oxidation when added directly to LDL *in vitro* (IC_{50} = 0.115 mg CAE/L; IC_{100}= 0.235 mg CAE/L) or following their preincubation with plasma (IC_{50} = 98.5 mg CAE/L; IC_{100}= 148 mg CAE/L) differs considerably. We es-

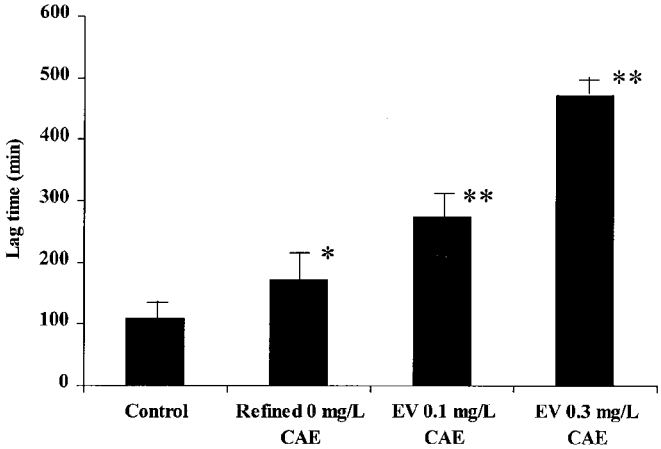

FIG. 4. Effect of olive oil on the lag time of copper-mediated LDL oxidation *in vitro.* LDL (0.05 g protein/L) was oxidized with 5 μM copper in the presence of refined olive oil and extra-virgin (EV) olive oil with indicated amounts of phenolic compounds, expressed as CAE. Bars represent the mean ± standard deviation of six experiments. There was a significant ($P < 0.001$) relationship between the amount of phenolics added and the lag time of conjugated diene formation. Asterisks indicate significant differences from control. *$P < 0.05$; **$P < 0.001$. For abbreviations see Figure 2.

timate in this last case that an 850- and a 650-fold greater concentration of olive oil phenols is required to cause a 50 and a 100% inhibition, respectively, in the lag time of conjugated diene formation. These results suggest that only a small fraction of the phenolic compounds in extra-virgin olive oil binds to LDL *in vitro*, as has been reported for other phenolic compounds. Ishikawa *et al*. (15) and Kerry and Abbey (31) recently published the results of experiments involving the preincubation of tea flavonoids (15) or red wine (31) with plasma. Concentrations of 93 mg/L of epigallocatechin gallate and 70 mg/L of red wine were required to achieve an inhibition of 50 and 60 % in conjugated diene formation, respectively.

The results from the preincubation of plasma with olive oil phenolic compounds indicated they could be incorporated into the LDL particles. The addition of olive oil phenolics to isolated LDL could be representative of the situation in plasma where phenolic compounds inhibit oxidation both in the aqueous medium and from within the lipoprotein. Plasma preincubation with olive oil phenolics after LDL isolation may be more like the situation in arterial intima, where lipoprotein oxidation appears to occur predominantly in microdomains sequestered from antioxidants present in plasma (4). Thus, olive oil phenols, in accordance with their amphipathic nature, may act both within the LDL particle and in the extraparticle environment of LDL.

Beside phenolic compounds, olive oil contains other compounds with antioxidant capacity. We examined the antioxidant capacity of olive oils with and without phenolic content. Although both olive oils protected LDL from oxidation, an increase in the antioxidant activity was observed with increasing concentration of phenolics. Refined olive oil, without detectable phenols, delayed the lag phase of diene formation by 52%. Thus, this delay in LDL oxidation could be attributed to the presence other, nonphenolic compounds with antioxidant capacity. When refined olived oil was added to isolated LDL the final concentration of α-tocopherol was 4.38 mg/L. At similar α-tocopherol concentrations Frankel *et al*. (11) reported delays up to 42% in the lag phase of conjugated diene formation on copper-induced LDL oxidation. We found that lag-time delay with refined olive oil was lower than that obtained when extra-virgin olive oil was added to the incubation. Thus, olive oil phenolics showed more antioxidant activity against LDL oxidation in the present experiment than did α-tocopherol. These results agree with those obtained by others (11,15), in which antioxidant activity of other phenolic compounds such as resveratrol, epicatechin, or quercetin was higher than the α-tocopherol antioxidant activity as studied by *in vitro* LDL oxidation.

The concentrations of phenolics, α-tocopherol and β-carotene, added to LDL with the olive oils, correlated with the lag time of LDL oxidation. Thus, to estimate the effect on LDL oxidation that was attributable to each antioxidant component, a multiple regression analysis was performed with these variables. Only the phenolic content, present in extra-virgin olive oil, was significantly correlated; the α-tocopherol content showed a weak association as well. On the other hand, the concentrations of β-carotene present in the incubation mixture were smaller than those commonly tested for their ability to inhibit conjugated diene formation (32). These results indicate that, although all antioxidant components of olive oil could be involved in protection against LDL oxidation, phenols showed the greatest antioxidant activity. These results support the hypothesis that consumption of olive oil and particularly of extra-virgin olive oil with high phenolic content, may have a protective effect on atherosclerotic processes.

In summary, phenolic compounds of extra-virgin olive oil protected LDL from peroxyl radical-dependent and copper-induced oxidation *in vitro*. Extra-virgin olive oil phenols could be incorporated into LDL particles following their incubation with plasma and exert their antioxidant activity. The amounts of extra-virgin olive oil phenols required to achieve this effect are comparatively high, and further studies investigating the bioavailability and the subsequent antioxidant activity of olive oils phenols *in vivo* need to be undertaken. Although olive oils both with and without phenolic content protected LDL from oxidation, an increase in antioxidant activity that was dependent on the concentration of phenolics in the olive oil was observed.

ACKNOWLEDGMENTS

This work was supported by grants ALI97-1607-CO2-01 from CICYT, 98/9562 FPI from FIS, and by Federació de Cooperatives Agraries de Catalunya .

REFERENCES

1. Pérez, G., Pena, A., Sala, J., Roset, P., Masiá, R., and Marrugat, J. (1998) Acute Myocardial Infarction Case Fatality, Incidence and Mortality Rates in a Population Registry in Gerona, Spain, 1990–1992, *Int. J. Epidemiol. 27,* 599–604.
2. De Lorgeril, M., Salen, P., Martin, J.L., Monjaud, I., Delaye, J., and Mamelle, N. (1999) Mediterranean Diet, Traditional Risk Factors, and the Rate of Cardiovascular Complications After Myocardial Infarction. Final Report of the Lyon Diet Heart Study, *Circulation 99,* 779–785.
3. Renaud, S., de Lorgeril, M., Delaye, M., Guidollet, J., Jacquard, F., Mamelle, N., Martin, J.L., Monjaud, I., Salen, P., and Toubol, P. (1995) Cretan Mediterranean Diet for Prevention of Coronary Hearth Disease, *Am. J. Clin. Nutr. 61,* 1360–1365.
4. Witzum, J.L. (1994) The Oxidation Hypothesis of Atherosclerosis, *Lancet 344,* 793–795.
5. Mata, P., Alonso, R., López-Farré, A., Ordovas, J.M., Lahoz, C., Garces, C., Caramelo, C., Codoceo, R., Blazquez, E., and de Oya, M. (1996) Effect of Dietary Fat Saturation on LDL Oxidation and Monocyte Adhesion to Human Endothelial Cells *in vitro*, *Arterioscler. Thromb. Vasc. Biol. 16,* 1347–1355.
6. Wiseman, S., Mathot, J.N., de Fouw, N.J., and Tijburg, L.B. (1996) Dietary Non-tocopherol Antioxidants Present in Extra-Virgin Olive Oil Increase the Resistance of Low Density Lipoproteins to Oxidation in Rabbits, *Atherosclerosis 120,* 15–23.
7. Parthasaraty, S., Khoo, J.C., Miller, E., Barnett, J., Witzum, J.L., and Steinberg, D. (1990) Low-Density Lipoprotein Rich in Oleic Acid Is Protected Against Oxidative Modification: Impli-

cations for Dietary Prevention of Atherosclerosis, *Proc. Natl. Acad. Sci. USA 87,* 3894–3898.
8. Papadopoulos, G., and Boskou, D. (1991) Antioxidant Effect of Natural Phenols on Olive Oil, *J. Am. Oil Chem. Soc. 68,* 669–671.
9. Perrin, J.L. (1992) Les Composés Mineurs et les Antioxygènes Naturels de l´Olive et de son Huile, *Rev. Fr. Corps Gras 39,* 25–32.
10. Vinson, J.A., Jang, J., Dabbagh, Y.A., Serry, M.M., and Cai, S. (1995) Plant Polyphenols Exhibit Lipoprotein-Bound Antioxidant Activity Using an *in vitro* Oxidation Model for Heart Disease, *J. Agric. Food Chem. 43,* 2798–2799.
11. Frankel, E.N., Waterhouse, A.L., and Kinsella, J.E. (1993) Inhibition of Human LDL Oxidation by Resveratrol, *Lancet 341,* 1103–1104.
12. Visioli, F., Bellomo, G., Montedoro, G., and Galli, C. (1995) Low Density Lipoprotein Oxidation Is Inhibited *in vitro* by Olive Oil Constituents, *Atherosclerosis 117,* 25–32.
13. Miyake, Y., Yamamoto, K., Tsujihara, N., and Osawa, T. (1998) Protective Effects of Lemon Flavonoids on Oxidative Stress in Diabetic Rats, *Lipids 33,* 689–695.
14. Hollman, P.C.H., and Katan, M.B. (1997) Absorption, Metabolism and Health Effects of Dietary Flavonoids in Men, *Biomed. Pharmacother. 51,* 305–310.
15. Ishikawa, T., Suzukawa, M., Ito, T., Yoshida, H., Ayaori, M., Nishiwaki, M., Yonemura, A., Hara, Y., and Nakamara, H. (1997) Effect of Tea Flavonoid Supplementation on the Susceptibility of Low Density Lipoprotein to Oxidative Modification, *Am. J. Clin. Nutr. 66,* 261–266.
16. Bondia, E.M., Castellote, A.I., López, M.C., and Rivero, M. (1994) Determination of Plasma Fatty Acid Composition in Neonates by Gas Chromatography, *J. Chromatogr. 658,* 369–374.
17. López-Sabater, M.C., Satué, T., Gónzalez, M., and Agramont, A. (1995) α-Tocopherol Content in Trout Oil, *Food Chem. 53,* 67–70.
18. Manzi, P., Panfili, G., Esti, M., and Pizzoferrato, L. (1998) Natural Antioxidants in the Unsaponifiable Fraction of Virgin Olive Oils from Different Cultivars, *J. Sci. Food Agric. 77,* 115–120.
19. Singleton, V.L., and Ross, J.A. (1965) Colorimetry of Total Phenolics with Phosphomolybdic-Phosphotungstic Acid Reagent, *Am. J. Enol. Vitic. 16,* 144–158.
20. Betés-Saura, C., Andrés-Lacueva, C., and Lamuela Raventós, R.M. (1996) Phenolic in White Free Run Juices and Wines: Changes During Vinification, *J. Agric. Food Chem. 44,* 3040–3060.
21. Tsimidou, M., Papadopoulos, G., and Boskou D. (1992) Determination of Phenolic Compounds in Virgin Olive Oil by Reversed-Phase HPLC with Emphasis on UV Detection, *Food Chem. 44,* 53–60.
22. Havel, R.J., Eder, H.A., and Bragdon, J.H. (1955) The Distribution and Chemical Composition of Ultracentrifugally Separated Lipoproteins in Human Serum, *J. Clin. Invest. 34,* 1345–1349.
23. Esterbauer, H., Striegl, G., Puhl H., and Rotheneder, M. (1989) Continuous Monitoring of *in vitro* Oxidation of Human Low Density Lipoprotein, *Free Radical Res. Commun. 6,* 67–75.
24. Nourooz-Zadeh, J., Tajaddini-Sarmadi, J., Ling, K.L.E, and Wolff, S.P. (1996) Low-Density Lipoprotein Is the Major Carrier of Lipid Hydroperoxides in Plasma, *Biochem. J. 313,* 781–786.
25. De Lorgeril, M., Salen, P., Martin, J.L., Monjaud, I., Boucher, P., and Mammelle, N. (1998) Mediterranean Dietary Pattern in a Randomized Trial: Prolonged Survival and Possible Reduced Cancer Rate, *Arch. Intern. Med. 158,* 1181–1187.
26. Trevisan, M., Krogh, V., Freudenheim, J., Blake, A., Muti, P., Panico, S., Farinaro, E., Mancini, M., Menotti, A., and Ricci, G. (1990) Consumption of Olive Oil, Butter and Vegetable Oils and Coronary Heart Disease Risk Factors, *JAMA 263,* 688–692.
27. Trichopoulou, A., Katsouyanni, K., Stuver, S., Tzala, L., Gnardellis, C., Rimm, E., and Trichopoulos, D. (1995) Consumption of Olive Oil and Specific Food Groups in Relation to Breast Cancer Risk in Greece, *J. Natl. Cancer Inst. 87,* 110–116.
28. Kris-Etherthon, P.M. (1999) Monounsaturated Fatty Acids and Risk of Cardiovascular Disease, *Circulation 100,* 1253–1258.
29. Price, J.F., and Fowkes, F.G.R. (1997) Antioxidant Vitamins in the Prevention of Cardiovascular Disease, *Eur. Heart J. 18,* 719–727.
30. Hollman, P.C.H., and Katan, M.B. (1997) Absorption, Metabolism and Health Effects of Dietary Flavonoids in Man, *Biomed. Pharmacother. 51,* 305–310.
31. Kerry, N.L., and Abbey, M. (1997) Red Wine and Fractionated Phenolic Compounds Prepared from Red Wine Inhibit Low Density Lipoprotein Oxidation *in vitro, Atherosclerosis 135,* 93–102.
32. Jialal, I., Norkus, E.P., Cristol, L., and Grundy, S.M. (1991) Beta-Carotene Inhibits the Oxidative Modification of Low-Density Lipoprotein, *Biochim. Biophys. Acta 1086,* 134–138.

[Received July 19, 1999, and in revised form October 13, 1999; revision accepted October 26, 1999]

Composition of Cecal Bile Acids in Ex-germfree Mice Inoculated with Human Intestinal Bacteria

Seiko Narushima[a], Kikuji Itoh[a,*], Kazuo Kuruma[b], and Kiyohisa Uchida[c]

[a]Laboratory of Veterinary Public Health, Graduate School of Agriculture and Life Science, The University of Tokyo, Bunkyo, Tokyo 113-8657, [b]Shionogi Research Laboratories, Toyonaka, Osaka 561-0825, and [c]The Cell Research Foundation, Osaka 541-0045, Japan

ABSTRACT: Germfree (GF) mice were orally inoculated with human fecal suspension or various components of human fecal microbiota. Three weeks after the inoculation, cecal bile acid composition of these mice was examined. More than 80% of total bile acids was deconjugated in the cecal contents of ex-GF mice associated with human fecal dilutions of 10^{-2} or 10^{-6}, or anaerobic growth from a dilution of 10^{-6}. In these ex-GF mice, deoxycholic acid accounted for about 20% of total bile acids. In the cecal contents of ex-GF mice associated only with clostridia, unconjugated bile acids made up less than 40% of total bile acids, about half of those in other ex-GF groups. However, the percentage of deoxycholic acid in these mice was the same as that in the other groups. These results indicate that dominant anaerobic bacterial combination is efficient for deconjugation of primary bile acids, and that clostridia in the human feces may play an important role in 7α-dehydroxylation of unconjugated primary bile acids in the intestine.

Paper no. L8347 in *Lipids 35,* 639–644 (June 2000).

In humans and animals, intestinal flora are indispensable for bile acid transformation. Many experimental reports imply the correlation between colorectal cancer and secondary bile acids, deoxycholic acid and lithocholic acid, which are the 7 α-dehydroxylated forms of cholic acid and chenodeoxycholic acid, respectively (1–3). Deconjugating activity of conjugated bile acids is widely observed in many kinds of intestinal bacteria (4–7), and 7 α-dehydroxylating activity has also been reported in certain groups of intestinal bacteria (8). However, for some of the species, the results of investigators are contradictory (9–16), and only certain strains belonging to *Eubacterium* and *Clostridium* have been reported specifically (17–21). Many reports indicated that the difficulties of isolating 7 α-dehydroxylating intestinal bacteria arise from the small populations of these bacteria in the intestine (15,22). However, most of the primary bile acids in the intestine are deconjugated and transformed into secondary bile acids, and the precise mechanism of transformation of bile acids by intestinal bacteria in the intestine is still unknown.

Previously, we inoculated human intestinal bacteria that had the ability to transform bile acids *in vitro* into germfree (GF) mice; however, only a little amount of secondary bile acids was found in their cecal contents, indicating that bacterial transforming ability of bile acids *in vitro* is not necessarily reflected *in vivo* (23,24). In this study, we produced various groups of ex-GF mice associated with human fecal dilution, or with anaerobic growth from a dilution of 10^{-6}, or with only human fecal clostridia. The aim of this study is to clarify which bacterial groups harbored in the human intestine are responsible for bile acid transformation in the intestine.

MATERIALS AND METHODS

Animals. GF ICR female mice (15 wks old) were purchased from Japan SLC Co. (Hamamatsu, Japan). Each group of five female GF mice was kept in an autoclavable stainless steel isolator (25) and given pelleted commercial diet (CMF; Oriental Yeast Co., Tokyo, Japan) sterilized with γ-irradiation at 50 kGy and autoclaved water *ad libitum*. Specific pathogen-free (SPF) ICR mice of the same age were also purchased from Japan SLC Co. The study was approved by the Laboratory Animal Use and Care Committee of Faculty of Agriculture, the University of Tokyo.

Production of ex-GF and gnotobiotic (GB) mice. Human fecal samples were obtained from a 47-yr-old healthy male donor. Of the bile acids in the fecal sample 99.6% were deconjugated, and 96% of the unconjugated bile acids were transformed to secondary bile acids. Preparation of the fecal dilution and bacterial suspension is summarized in Scheme 1.

(i) Groups A to E. One gram of fresh feces was immediately placed in 9 mL of an anaerobic diluent (26) under oxygen-free CO_2 gas. A portion was transferred into an anaerobic chamber and serially diluted with anaerobic Trypticase soy (TS) broth supplemented with 0.084% Na_2CO_3, 0.05% agar, and 0.05% cysteine hydrochloride monohydrate. The 10^{-2} and 10^{-6} diluted fecal suspensions were prepared for inoculation into GF mice to produce ex-GF mice of group A

*To whom correspondence should be addressed at Laboratory of Veterinary Public Health, Graduate School of Agriculture and Life Science, The University of Tokyo, 1-1-1 Yayoi, Bunkyo-ku, Tokyo 113-8657, Japan. E-mail: akikuji@mail.ecc.u-tokyo.ac.jp

Abbreviations: EG, Eggerth Gagnon; GB, gnotobiotic; GF, germfree; PHP-LH-20, piperidinohydroxypropyl Sephadex-LH-20; SPF, specific pathogen-free; TS, Trypticase soy.

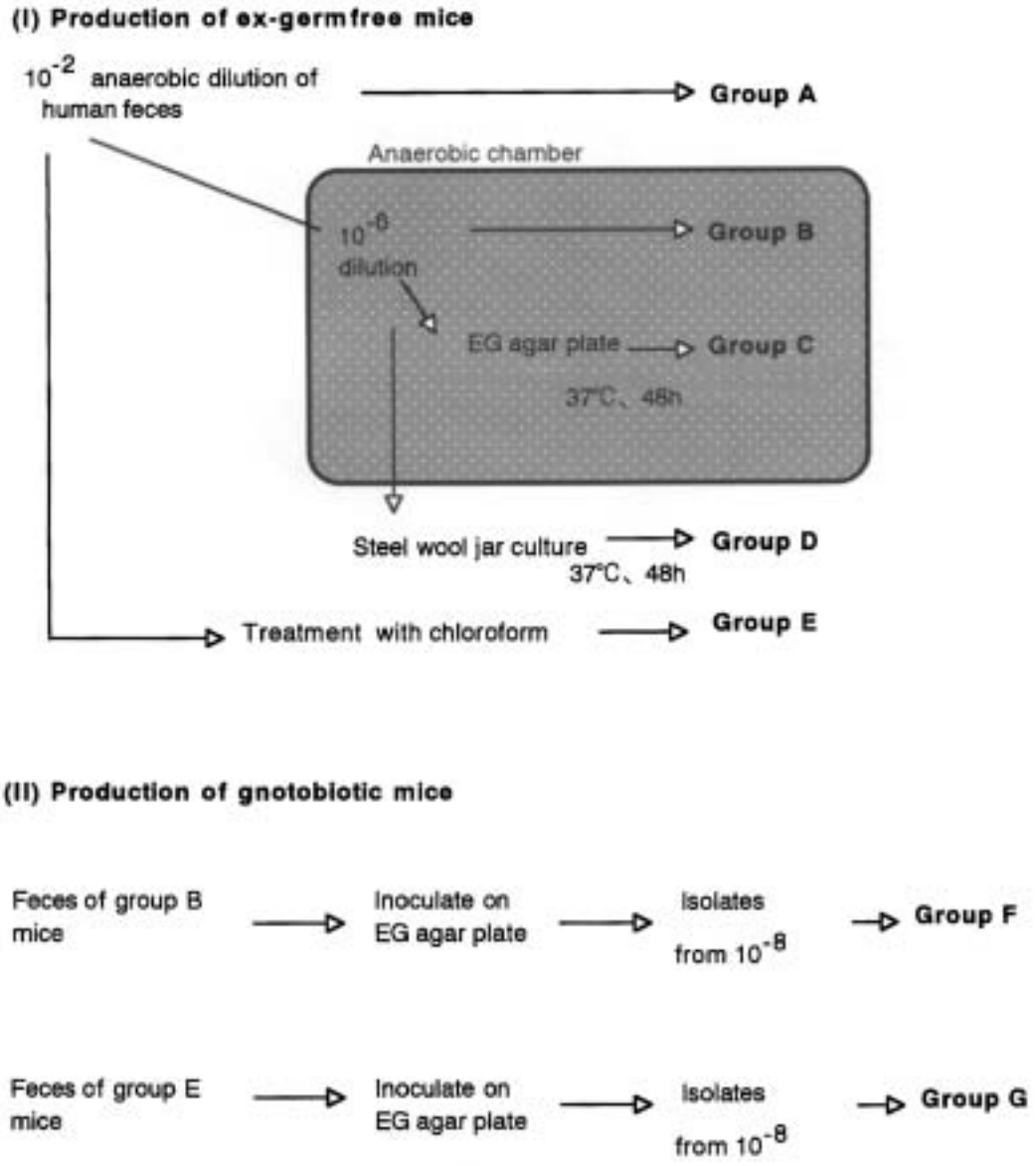

SCHEME 1

and group B, respectively. Another 0.1 mL of 10^{-6} diluted solution was inoculated on Eggerth Gagnon (EG) agar plates (26) in an anaerobic chamber with 5% CO_2, 10% H_2 and 85% N_2, and incubated at 37°C for 48 h. Another 0.1 mL of 10^{-6} solution was inoculated on modified EG agar (Nissui Pharmaceutical Co. Ltd., Tokyo, Japan) plates and incubated in an anaerobic steel wool jar filled with 100% CO_2 at 37°C for 48 h. From all colonies which developed on each plate, cells were scratched and suspended in anaerobic TS broth for group C and group D, respectively. The remaining portion of the 10^{-1} dilution of human feces was further diluted to 10^{-2} and treated with chloroform as described below for group E.

(ii) Groups F and G. Two weeks after the inoculation, fecal bile acid composition in ex-GF mice of groups A to E was examined. From the feces of ex-GF mice of groups B and E in which deoxycholic acid was detected, we prepared two groups of bacterial combinations. Feces of group B mice was diluted to 10^{-8} in anaerobic TS broth, inoculated on EG agar plates, and incubated in an anaerobic chamber at 37°C for 48 h. Each of the developed colonies was isolated from the agar plates, purified, and subcultured. Each bacterial growth was then suspended in an anaerobic TS broth, and this predominant bacterial suspension was inoculated into GF mice for group F. From the feces of ex-GF mice of group E, we also obtained the predominant bacterial suspension for group G. Both groups F and G were gnotobiotic (GB) mice.

Each fecal dilution and bacterial suspension (0.5 mL) was orally inoculated into the stomach of GF mice with a stainless steel catheter.

Treatment of feces with chloroform. Chloroform-treated

feces of humans and mice were prepared according to the method of Itoh and Mitsuoka (27). A fecal suspension was added for a final concentration of 3% chloroform, was shaken vigorously for about 30 s, and was subsequently incubated for 1 h at 37°C. After the incubation chloroform was eliminated from the suspensions by percolating with O_2-free N_2 gas. Only bacterial spores survived this treatment.

Cecal bile acid determination. Three weeks after the inoculation, cecal contents from each mouse were collected, freeze-dried, and pulverized. A portion of 50 mg dry cecal contents was extracted three times with 10 mL of absolute ethanol at 90°C for 1 h and filtered. The extracts were mixed, dried, and purified through a Bond Elute LRC cartridge (Varian, Palo Alto, CA). A purified solution in 90% ethanol was subjected to piperidinohydroxypropyl Sephadex-LH-20 (PHP-LH-20) column chromatography (Shimadzu Co., Kyoto, Japan) to obtain free, glycine-conjugated, and taurine-conjugated fractions (28).

Bile acids were analyzed using the LC module-1 high-performance liquid chromatography system (Waters, MA) with a Symmetry C18 separation column (150 × 4.6 mm i.d. Waters). Bile acids were then detected by the post-column fluorescent method with a 3 α-hydroxysteroid dehydrogenase (HSD) immobilized column (E-3 α-HSD, 20 × 4.0 mm i.d., Sekisui Chemical Co. Ltd., Osaka, Japan), and β-NAD solution by an A-60-S pump (Eldex Laboratories Inc., Napa, CA) and a 474 scanning fluorescence detector (Waters) at an excitation wavelength of 340 nm and an emission wavelength of 460 nm (28,29). Each bile acid was identified by its relative retention time compared with that of standard bile acids, and peak heights were calculated automatically on a Waters 805 data station.

Analysis of intestinal flora. Cultivation of fecal bacteria was carried out according to the methods of Mitsuoka *et al.* (26,30) and Itoh and Mitsuoka (27), except that an anaerobic chamber was employed instead of the "plate-in-bottle" method. Three weeks after inoculation, feces from two mice of each group were collected, immediately weighed, and transferred into an anaerobic chamber. They were homogenized with a 50-fold volume (vol/wt) of anaerobic TS broth, serially diluted, and plated on 5 nonselective and 11 selective agar media (26,27,30). Isolated bacteria were identified on the basis of Gram staining, colony morphology, cell morphology, and aerobic growth. The bacterial numbers were expressed as $\log_{10}$ counts of viable bacteria per gram wet weight of feces.

Statistical analysis. A statistical analysis was performed by analysis of variance followed by Bonferroni's *t*-test, and a *P* value less than 0.05 was considered to be significant.

RESULTS

Table 1 shows the bacterial counts in feces of ex-GF and GB mice 3 wk after the inoculation of fecal suspensions. Among the ex-GF mice in groups A, B, C, and D, bacteroidaceae were detected at the highest levels, and eubacteria and clostridia were also detected in high numbers. Among aerobic bacteria, enterobacteriaceae and streptococci were detected in the feces of the four ex-GF groups, but staphylococci were detected only in the feces of group A mice. Bacilli, yeasts, bifidobacteria, veillonellaceae, and lactobacilli, which were detected in the original human donor feces, were lower than the minimum detectable level of 10^3 CFU per g in feces of inoculated mice. In feces of group E mice, which were inoculated with chloroform-treated fecal suspension, only clostridia were observed. In group F mice inoculated with 15 strains of predominant bacteria isolated from feces of a group B mouse, 10 strains colonized at a level of 10^9 CFU per g feces. In group G mice associated with 15 strains of predominant clostridia isolated from feces of a group E mouse, the total fecal bacterial count was 6.0×10^{10} CFU per g feces, and 10 out of 15 strains showed more than 10^9 CFU per g feces.

TABLE 1
Composition of Fecal Bacteria in Ex-germfree (GF) and Gnotobiotic (GB) Mice

	Original	Groups of ex-GF and GB mice[a]													
	human	A		B		C		D		E		F		G	
Bacteria	fecal sample	A1[b]	A2	B1	B2	C1	C2	D1	D2	E1	E2	F1	F2	G1	G2
Total bacteria	10.9[c]	11.0	11.5	11.5	11.5	11.4	11.2	11.2	11.1	10.8	11.1	11.4	11.3	10.8	10.8
Bacteroidaceae	10.7	10.7	11.1	11.3	11.2	11.2	10.9	11.0	10.9	—[d]	—	11.3	11.1	—	—
Eubacteria	10.4	10.4	10.8	10.3	10.4	10.6	10.2	10.5	10.4	—	—	—	—	—	—
Clostridia	10.0	10.5	10.9	11.0	10.7	10.8	10.7	10.3	10.5	10.8	11.1	10.9	10.8	10.8	10.8
Bifidobacteria	9.3	—	—	—	—	—	—	—	—	—	—	—	—	—	—
Veillonellaceae	3.4	—	—	—	—	—	—	—	—	—	—	—	—	—	—
Lactobacilli	3.8	—	—	—	—	—	—	—	—	—	—	—	—	—	—
Enterobacteriaceae	8.8	7.3	7.6	7.8	7.8	6.2	6.2	5.9	6.3	—	—	—	—	—	—
Streptococci	7.8	7.5	6.6	6.2	8.0	9.0	9.3	7.7	7.9	—	—	—	—	—	—
Staphylococci	2.9	8.0	6.7	—	—	—	—	—	—	—	—	—	—	—	—
Bacilli	8.7	—	—	—	—	—	—	—	—	—	—	—	—	—	—
Yeasts	2.8	—	—	—	—	—	—	—	—	—	—	—	—	—	—

[a]Explanations for A–G appear in Scheme 1.
[b]Mouse number.
[c]Log_{10}/g of feces.
[d]Not detected.

TABLE 2
Cecal Bile Acid Composition Ex-GF and GB Mice

		Groups of ex-GF mice					Groups of GB mice	
	SPF mice	A	B	C	D	E	F	G
	(n = 5)	(n = 5)	(n = 4)	(n = 5)	(n = 5)	(n = 4)	(n = 5)	(n = 5)
Total bile acids[a]	431 ± 361[a]	677 ± 211	452 ± 138	387 ± 143	375 ± 125	316 ± 101	877 ± 376[b]	266 ± 153
% of each bile acid[c]								
Un-cholic acid[d]	0.8 ± 0.6	13.9 ± 4.7	11.6 ± 5.7	11.6 ± 5.4	11.3 ± 3.5	4.0 ± 1.7	0.8 ± 0.6	8.2 ± 1.7
Tc-cholic acid	2.2 ± 0.9	5.6 ± 2.8	2.6 ± 1.1	4.2 ± 2.6	3.9 ± 0.9	15.5 ± 5.4	28.5 ± 6.2	17.7 ± 3.9
Un-deoxycholic acid	17.3 ± 4.1	18.7 ± 9.9	25.7 ± 4.7	22.8 ± 8.1	17.4 ± 5.4	18.0 ± 9.3	ND[e]	ND
Tc-deoxycholic acid	Trace[f]	Trace	ND	Trace	Trace	Trace	ND	ND
Un-7-Oxo-deoxycholic acid	Trace	1.9 ± 0.9	2.8 ± 0.9	2.5 ± 0.8	2.0 ± 0.5	0.5 ± 0.4	Trace	Trace
Un-chenodeoxycholic acid	0.5 ± 0.1	0.5 ± 0.2	0.6 ± 0.2	0.8 ± 0.3	0.7 ± 0.2	0.5 ± 0.1	Trace	0.5 ± 0.1
Tc-chenodeoxycholic acid	Trace	Trace	Trace	Trace	Trace	Trace	Trace	Trace
Tc-lithocholic acid	3.2 ± 0.9	0.8 ± 0.7	0.9 ± 0.2	1.0 ± 0.5	0.8 ± 0.3	1.0 ± 0.4	ND	ND
Tc-lithocholic acid	ND	ND	ND	ND	ND	ND	ND	ND
Un-α-muricholic acid	2.4 ± 0.6	2.3 ± 0.4	2.7 ± 0.6	3.3 ± 1.2	3.1 ± 1.1	0.8 ± 0.2	1.4 ± 0.5	Trace
Tc-α-muricholic acid	0.5 ± 0.5	Trace	Trace	Trace	Trace	2.3 ± 0.1	1.1 ± 0.5	2.5 ± 0.8
Un-β-muricholic acid	33.0 ± 7.9	40.1 ± 8.1	48.3 ± 8.6	46.7 ± 6.4	53.2 ± 3.3	13.1 ± 1.5	31.5 ± 9.6	6.3 ± 1.6
Tc-β-muricholic acid	4.8 ± 2.5	5.7 ± 3.0	2.8 ± 1.2	4.9 ± 2.4	5.6 ± 1.2	42.9 ± 9.1	33.5 ± 14.7	63.7 ± 3.3
Un-ω-muricholic acid	28.1 ± 8.5	ND	ND	ND	ND	ND	ND	ND
Tc-ω-muricholic acid	ND	ND	ND	ND	ND	ND	ND	ND
Un-hyodeoxycholic acid	1.1 ± 0.5	ND	ND	ND	Trace	ND	ND	ND
Tc-hyodeoxycholic acid	ND	ND	ND	ND	ND	ND	ND	ND
Others	1.2 ± 0.5	0.9 ± 0.3	1.3 ± 0.1	1.2 ± 0.5	1.0 ± 0.2	0.7 ± 0.1	0.7 ± 0.1	0.7 ± 0.3

[a]Mean ± SD nmol/g wet cecal contents.
[b]Significantly higher than SPF, C, D, E, and G ($P < 0.05$).
[c]% of total bile acids.
[d]Un, unconjugated; Tc, taurine conjugated.
[e]ND, not detected.
[f]Trace, amounts less than 0.5%. SPF, specific pathogen free; for other abbreviations see Table 1.

Table 2 shows the bile acid composition in the cecal contents of ex-GF and GB mice 3 wk after inoculation. All conjugated bile acids in ex-GF mice were taurine-conjugated, and no glycine-conjugates were detected. ω-Muricholic acid was detected in the cecal contents of SPF mice as a major bile acid, but was not detected in any of the ex-GF mice associated with human intestinal bacteria. Deoxycholic acid, a secondary bile acid transformed from cholic acid, was observed in the cecal contents of ex-GF mice in groups of A–E. The percentage of deoxycholic acid in total bile acids was about 20%, and no significant difference was detected among the five groups. However, deoxycholic acid was not formed in the cecal contents of GB mice in groups F and G.

Figure 1 shows the percentage of unconjugated bile acids in the cecal contents of ex-GF mice. In groups A to D, the deconjugating ratio was 80–90% of total bile acids. However, in group E, in which intestinal bacteria consisted of only clostridia, the percentage of unconjugated bile acids was significantly lower than those in groups A to D ($P < 0.05$). In group F, about 30% of total bile acids were unconjugated, but the percentage of unconjugated bile acids in groups G was remarkably low.

Figure 2 shows the conversion ratio from unconjugated primary bile acids to secondary bile acids. In the cecal contents of SPF mice, 44.1% of muricholic acid was transformed into ω-muricholic acid, but transformation to ω-muricholic acid did not occur in the cecal contents of any group of ex-GF or GB mice associated with human fecal bacteria. The conversion ratio from cholic acid to deoxycholic acid and from chenodeoxycholic acid to lithocholic acid was significantly higher in SPF mice than that in ex-GF mice. Although the difference was not statistically significant, the cecal contents of ex-GF mice in group E showed a tendency toward a slightly higher conversion ratio from cholic acid to deoxycholic acid than those in groups in A, B, C, and D.

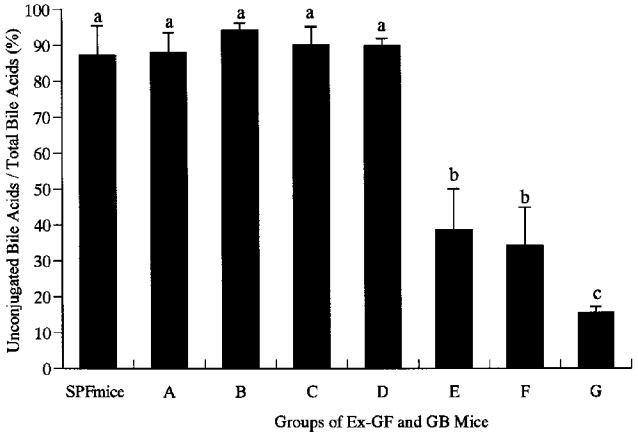

FIG. 1. Deconjugation ratio of total bile acids in the cecal contents of ex-germfree (GF) and gnotobiotic (GB) mice. Bars marked with different letters are significantly different ($P < 0.05$). SPF, specific pathogen free.

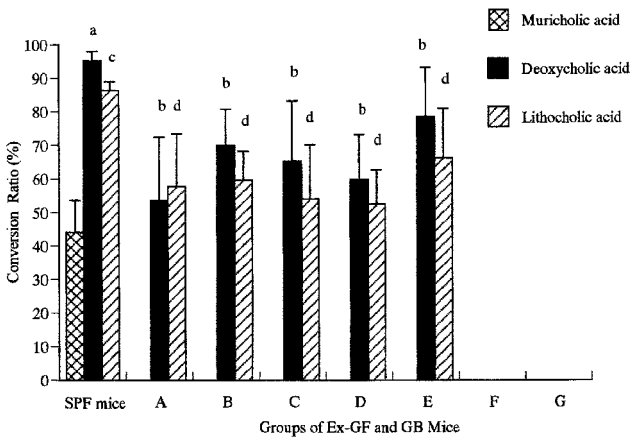

FIG. 2. Conversion ratio (primary to secondary) of unconjugated bile acids in the cecal contents of ex-GF and GB mice. Values in the same coded bars with different letters are significantly different ($P < 0.05$). For abbreviations see Figure 1.

DISCUSSION

The present data show that a 10^{-6} fecal dilution of human feces can transform bile acids to the secondary form in the intestines of mice. In the human intestine, the bacterial count reaches the order of 10^{11} CFU per gram. According to our results, it was suggested that the count of 7 α-dehydroxylating bacteria in the human feces of this sample may be at least 10^6 CFU per g feces. This number is a little higher than those in previous reports (19,31). Takamine and Imamura reported (22) that 7 α-dehydroxylation was detected in dilutions of human feces below 10^{-5}.

Total bile acid concentration in GB mice group F was significantly higher than that in SPF, C, D, E, and G mice. However, we have no speculation or data to explain this difference.

In the ex-GF A, B, C, and D groups, with fecal bacteria consisting mainly anaerobic bacteria, including bacteroidaceae, eubacteria and clostridia, about 90% of the cecal bile acids were deconjugated. In contrast, in the cecal contents of ex-GF mice of group E, only 40% of total bile acids was deconjugated. These results indicate that deconjugation of cecal bile acid mainly depends on bacteria belonging to bacteroidaceae or eubacteria, as reported in *in vitro* experiments (4,5,32,33). It was also suggested that bile acid-transforming bacteria are culturable on EG agar plates and do not require extreme anaerobic conditions, since there was no significant difference in the cecal bile acid composition between ex-GF groups C (including extremely oxygen sensitive bacteria) and D (not including strict anaerobic bacteria).

ω-Muricholic acid was not detected in any group of ex-GF mice. This result is consistent with that of Sacquet *et al.* (34), indicating that human intestinal bacteria have no activity to transform α- or β-muricholic acid to ω-muricholic acid. It is suggested that human intestinal bacteria react differently, especially to chenodeoxycholic acid group, from murine intestinal bacteria.

In mice and rats, clostridia (fusiform-shaped bacteria) are one of the key groups for the normalization of GF animals (35,36). Recently, Uchida *et al.* (37) reported that clostridia isolated from rat cecum play an important role in the formation of secondary bile acids in rats. Although it is not yet clear what intestinal bacterial groups in humans correspond to fusiform-shaped bacteria in mice and rats, it is suspected from the results of this study that clostridia also exert an effect on the formation of secondary bile acids in human intestines. In the cecal contents of ex-GF mice associated with chloroform-treated human fecal suspension, deoxycholic acid was detected at a level equivalent to that of SPF mice, even though the deconjugating ratio was significantly lower than those in other ex-GF mice. It is assumed that clostridia transformed almost all unconjugated cholic acid to the secondary form.

No deoxycholic acid was detected in the cecal contents of GB mice in group F or G. They were inoculated with predominant bacteria isolated from ex-GF mice in group B or E, respectively, in which a considerable amount of deoxycholic acid was detected in the cecal contents. There may be some reasons for the absence of deoxycholic acid in group F or G. One possibility is that 7 α-dehydroxylating bacteria are not present in large numbers in the intestine of group B or E, and bacterial combinations isolated from a 10^{-8} fecal dilution of a group B or E mouse may not have 7 α-dehydroxylating activity. Another reason for the absence of deoxycholic acid in the cecal contents of these mice may be the lower percentage of deconjugated bile acids in group F or G. Batta *et al.* (38) reported that previous deconjugation of bile acids is required for further bacterial 7 α-dehydroxylation *in vitro*. Bacteroidaceae harbored in group F might be able to deconjugate muricholates, not cholic acid.

ACKNOWLEDGMENT

This study was supported in part by a grant from the Programme for Promotion of Basic Research Activities for Innovative Bio-science (PROBRAIN).

REFERENCES

1. Narisawa, T., Magadia, N.E., Weisburger, J.H., and Wynder, E.L. (1974) Promoting Effect of Bile Acids on Colon Carcinogenesis After Intrarectal Instillation of *N*-Methyl-*N*′-nitro-*N*-nitrosoguanidine in Rats, *J. Natl. Cancer Inst. 53*, 1093–1097.
2. Reddy, B.S., Watanabe, K., Weisburger, J.H., and Wynder, E.L. (1977) Promoting Effect of Bile Acids in Colon Carcinogenesis in Germ-free and Conventional F344 Rats, *Cancer Res. 37*, 3238–3242.
3. Morotomi, M., Guillen, J.G., Legerfo, P., and Weinstein, I.B. (1990) Production of Diacylglycerol, an Activator of Protein Kinase C by Human Intestinal Microflora, *Cancer Res. 50*, 3595–3599.
4. Stellwag, E.J., and Hylemon, P.B. (1976) Purification and Characterization of Bile Salt Hydrolase from *Bacteroides fragilis* subsp. *fragilis, Biochim. Biophys. Acta 452*, 165–176.
5. Masuda, N. (1980) Deconjugation of Bile Salts by *Bacteroides* and *Clostridium*, *Microbiol. Immunol. 25*, 1–11.

6. Archer, R.H., Chong, R., and Maddox, I.S. (1982) Hydrolysis of Bile Acid Conjugates by *Clostridium bifermentans, Eur. J. Appl. Microbiol. Biotechnol. 14*, 41–45.
7. Grill, J-P., Schneider, F., Crociani, J., and Ballongue, J. (1995) Purification and Characterization of Conjugated Bile Salt Hydrolase from *Bifidobacterium longum* BB536, *Appl. Environ. Microbiol. 61*, 2577–2582.
8. Bortolini, O., Medici, A., and Poli, S. (1997) Biotransformations on Steroid Nucleus of Bile Acids, *Steroids 62*, 564–577.
9. Gustafsson, B.E., Midtvedt, T., and Norman, A. (1966) Isolated Fecal Microorganisms Capable of 7 α-Dehydroxylating Bile Acids, *J. Exp. Med. 123*, 413–432.
10. Midtvedt, T. (1967) Properties of Anaerobic Gram-positive Rods Capable of 7 α-Dehydroxylating Bile Acids, *Acta Path. Microbiol. Scand. 71*, 147–160.
11. Aries, V., and Hill, M.J. (1970) Degradation of Steroids by Intestinal Bacteria. II. Enzymes Catalyzing the Oxidoreduction of the 3 α-, 7 α-, and 12 α-Hydroxyl Group in Cholic Acid, and the Dehydroxylation of the 7 α-Hydroxyl Group. *Biochim. Biophys. Acta 202*, 535–543.
12. Dickinson, A.B., Gustafsson, B.E., and Norman, A. (1971) Determination of Bile Acid Conversion Potencies of Intestinal Bacteria by Screening *in Vitro* and Subsequent Establishment in Germfree Rats, *Acta Path. Microbiol. Scand. Sect. B 79*, 691–698.
13. Stellwag, E.J., and Hylemon, P.B. (1978) Characterization of 7 α-Dehydroxylase in *Clostridium leptum, Am. J. Clin. Nutr. 31*, 243–247.
14. Ferrari, A., Pacini, N., and Canzi, E. (1980) A Note on Bile Acids Transformations by Strains of *Bifidobacterium, J. Appl. Bacteriol. 49*, 193–197.
15. Hirano, S., Nakamura, R., Tamaki, M., Masuda, N., and Oda, H. (1981) Isolation and Characterization of Thirteen Intestinal Microorganisms Capable of 7 α-Dehydroxylating Bile Acid, *Appl. Environ. Microbiol. 41*, 737–745.
16. Takahashi, T., and Morotomi, M. (1994) Absence of Cholic Acid 7 α-Dehydroxylase Activity in the Strains of *Lactobacillus* and *Bifidobacterium*, *J. Dairy Sci. 77*, 3275–3286.
17. Hayakawa, S., and Hattori, T. (1970) 7 α-Dehydroxylation of Cholic Acid by *Clostridium bifermentans* Strain ATCC 9714 and *Clostridium sordellii* Strain NCIB 6929, *FEBS Lett. 6*, 131–133.
18. Ferrari, A., and Beretta, L. (1977) Activity on Bile Acids of a *Clostridium bifermentans* Cell-free Extract, *FEBS Lett. 75*, 163–165.
19. Stellwag, E.J., and Hylemon, P.B. (1979) 7 α-Dehydroxylation of Cholic Acid and Chenodeoxycholic Acid by *Clostridium leptum*, *J. Lipid Res. 20*, 325–333.
20. Hylemon, P.B., Cacciapuoti, A.F., White, B.A., Whitehead, T.R., and Fricke, R.J. (1980) 7 α-Dehydroxylation of Cholic Acid by Cell Extracts of *Eubacterium* Species V.P.I. 12708, *Am. J. Clin. Nutr. 33*, 2507–2510.
21. Archer, R.H., Maddox, I.S., and Chong, R. (1981) 7 α-Dehydroxylation of Cholic Acid by *Clostridium bifermentans, Eur. J. Appl. Microbiol. Biotechnol. 12*, 46–52.
22. Takamine, F., and Imamura, T. (1995) Isolation and Characterization of Bile Acid 7-Dehydroxylating Bacteria from Human Feces, *Microbiol. Immumol. 39*, 11–18.
23. Narushima, S., Itoh, K., Kuruma, K., and Uchida, K. (1999) Cecal Bile Acid Compositions in Gnotobiotic Mice Associated with Human Intestinal Bacteria with the Ability to Transform Bile Acids *in Vitro, Microb. Ecol. Health Dis. 11*, 55–60.
24. Narushima, S., Itoh, K., Takamine, F., and Uchida K. (1999) Absence of Cecal Secondary Bile Acids in Gnotobiotic Mice Associated with Two Human Intestinal Bacteria with the Ability to Dehydroxylate Bile Acids *in Vitro, Microbiol. Immunol. 43*, 893–897.
25. Itoh, K., Ozaki, A., and Yamamoto, T. (1978) An Autoclavable Stainless Steel Isolator for Small Scale Gnotobiotic Experiments, *Exp. Anim. 27*, 13–16.
26. Mitsuoka, T., Sega, T., and Yamamoto, S. (1965) Eine Verbesserte Methodik der Qualitativen und Quantativen Analyse der Darmflora von Menschen und Tieren, *Zentralbl. Bacteriol. Parasitenkd. Infektionskrankh. Hyg. I. Orig. A 195*, 455–469.
27. Itoh, K., and Mitsuoka, T. (1980) Production of Gnotobiotic Mice with Normal Physiological Functions. I. Selection of Useful Bacteria from Faeces of Conventional Mice, *Z. Versuchstierkd. 22*, 173–178.
28. Goto, J., Hasegawa, M., Kato, H., and Nambara, T. (1978) A New Method for Simultaneous Determination of Bile Acids in Human Bile Without Hydrolysis, *Clin. Chim. Acta. 87*, 141–147.
29. Okuyama, S., Kokubun, N., Higashidate, S., Uemura, D., and Hirata, Y. (1979) A New Analytical Method of Individual Bile Acids Using High Performance Liquid Chromatography and Immobilized 3 α-Hydroxysteroid Dehydrogenase in Column Form, *Chem. Lett*, 1443–1446.
30. Mitsuoka, T., Ohno, K., Benno, Y., Suzuki, K., and Namba, K. (1976) Die Faekal-flora bei Menschen. IV. Mitteilung: Vergleich des Neuentwickelten Verfahrens mit dem Bisheringen Üblichen Verfahren zur Darmfloraanalyse, *Zentralbl. Bacteriol. Parasitenkd. Infektionskrankh. Hyg. I. Orig. A 234*, 219–233.
31. Ferrari, A., Padini, N., Canzi, E., and Bruno, F. (1980) Prevalence of Oxygen-Intolerant Microorganisms in Primary Bile Acid 7 α-Dehydroxylating Mouse Intestinal Microflora, *Current Microbiol. 4*, 257–260.
32. Chikai, T., Nakao, H., and Uchida, K. (1987) Deconjugation of Bile Acids by Human Intestinal Bacteria Implanted in Germfree Rats, *Lipids 22*, 669–671.
33. Kawamoto, K., Horibe, I., and Uchida, K. (1989) Purification and Characterization of New Hydrolase for Conjugated Bile Acids, Chenodeoxycholyltaurine Hydrolase, from *Bacteroides vulgatus, J. Biochem. 106*, 1049–1053.
34. Sacquet, E.C., Gadelle, D.P., Riottot, M.J., and Raibaud, P.M. (1984) Absence of Transformation of β-Muricholic Acid by Human Microflora Implanted in the Digestive Tracts of Germfree Male Rats, *Appl. Environ. Microbiol. 47*, 1167–1168.
35. Itoh, K., Urano, T., and Mitsuoka, T. (1986) Colonization Resistance Against *Pseudomonas aeruginosa* in Gnotobiotic Mice, *Lab. Anim. 20*, 197–201.
36. Koopman, J.P., and Janssen, F.G.J. (1975) The Suitability for Rats of an Intestinal Microflora of Mice Tested Under Practical Circumstances, *Z. Versuchstierkd. 17*, 208–211.
37. Uchida, K., Satoh, T., Narushima, S., Itoh, K., Takase, H., Kuruma, K., Nakao, H., Yamaga, N., and Yamada, K. (1999) Transformation of Bile Acid and Sterols by Clostridia (fusiform bacteria) in Wistar Rats, *Lipids 34*, 269–273.
38. Batta, A.K., Salen, G., Arora, R., Shefer, S., Batta, M., and Person, A. (1990) Side Chain Conjugation Prevents Bacterial 7-Dehydroxylation of Bile Acids, *J. Biol. Chem. 256*, 10925–10928.

[Received September 3, 1999, and in final revised form February 24,

Lipid and Fatty Acid Composition and Energy Partitioning During Embryo Development in the Shrimp *Macrobrachium borellii*

Horacio Heras*, M.R. Gonzalez-Baró, and Ricardo J. Pollero

Instituto de Investigaciones Bioquímicas de La Plata (INIBIOLP), CONICET-UNLP, (1900) La Plata, Argentina

ABSTRACT: Energy partitioning, composition of lipids and fatty acids, and their utilization by embryos were determined in the lecithotrophic shrimp *Macrobrachium borellii* during seven development stages. The biochemical composition at stage I is represented by lipids, proteins, and carbohydrates, with 29.3, 28.7, and 0.2% dry weight, respectively. The former two were identified as the major energy-providing components, contributing 131 and 60 cal/100 mg egg, dry weight, respectively. The overall conversion efficiency (CE) was 45.0% (calculated as percentage of vitelline energy transformed into embryonic tissues). Lipids were the most important energy reserve (CE 39.3%), followed by proteins (CE 57.1%), both being simultaneously utilized during development while carbohydrates were synthesized *de novo* (CE 587.5%). Variation in the lipid class composition of embryos and vitellus showed an accumulation of triacylglycerols (TAG) and phospholipids (PL) up to stage IV, a more active accumulation and selective utilization phase (stages V and VI), and a consumption and *de novo* synthesis period until hatching. Structural lipids (PL and cholesterol) and pigment astaxanthin were selectively conserved in embryos, but TAG, hydrocarbons, and esterified sterols were preferentially depleted. Monounsaturated fatty acids (FA) were the major group in TAG, whereas polyunsaturated FA (PUFA) were the major group in PL after organogenesis. Certain PUFA such as 22:6n-3 and 20:5n-3 were selectively accumulated in PL.

Paper no. L8410 in *Lipids 35,* 645–651 (June 2000).

Physiological energetics encompasses the study of gains and losses of energy and the efficiency of its transformation from the standpoint of the whole organism. Studies on the energetics during embryogenesis in invertebrates are difficult to compare because of the different methodologies employed and also because of the varied life histories of invertebrate species (1–5).

Conversion efficiency (CE) gives a rough estimate of the amount of each constituent used for growth and formation of energy reserves in the embryo and of the amount used for metabolism. In most cases CE is significantly higher for proteins than for lipids, a fact that is consistent with the assumption that during development amino acids are conserved to build up the structure of embryos, while lipids would serve as fuel for active cell division and differentiation (2).

In many aquatic invertebrates such as crustaceans, bivalves, cephalopods, and sea urchins, the amount of proteins and lipids in the egg is higher than carbohydrate, clearly showing that carbohydrate is not the major energy reserve for egg development (2,6–8).

Crustacean oviposited eggs have two compartments, the ooplasm and the vitellus or yolk, which are enclosed by an egg membrane, the chorion. The ooplasm contains mitochondria, cortical granules (glycoproteins), and lipid globules. The yolk is surounded by the vitelline sac which contains water, lipids, proteins, and also minor amounts of carotenoid pigments, carbohydrates, and free amino acids (9,10). Most crustacean eggs store some of the nutrients in the yolk in the form of a complex lipoprotein called lipovitelin or as lipid droplets scattered throughout the cytoplasm. Most studies made on crustacean eggs refer to whole egg composition and show that lipid is the major energy reserve, although there is no mention of species such as *Macrobrachium borellii, in* which the egg has an abbreviated development and hatches into a postlarval stage. There are also no available data on the transfer of yolk into decapod embryos from the biochemical point of view. For our study we selected the decapod *M. borellii,* which is an endemic South American lecithotrophic freshwater shrimp in Argentina, Paraguay, and Uruguay (approximately from 22 to 37°S and 53 to 60°W) (11). Females brood large, yolky eggs during late spring and summer in turbid, temperature water streams (November to February). The small clutches (50–60 eggs) are kept by females attached to the pleopods. Eggs take about 50 d to hatch at 25°C (11). Hatchlings are 5–6 mm long, translucent postlarvae of benthic habits and are omnivorous scavengers.

In the present work, we studied the energy partitioning and the lipid and fatty acid (FA) composition in *M. borellii* eggs from fertilization until hatching in order to identify the nutrient sources of eggs, and how they are utilized by embryos during development.

*To whom correspondence should be addressed at INIBIOLP, Fac. Medicina, Universidad Nacional de La Plata, Calles 60 y 120, (1900) La Plata, Argentina. E-mail: h-heras@atlas.med.unlp.edu.ar

Abbreviations: BSA, bovine serum albumin; CE, conversion efficiency; DHA, docosahexaenoic acid; EPA, eicosapentaenoic acid; FA, fatty acid; HP-TLC, high-performance thin-layer chromatography; PL, polar lipid; PUFA, polyunsaturated fatty acid; SM, sphingomyelin; TAG, triacylglycerol; TLC, thin-layer chromatography.

EXPERIMENTAL PROCEDURES

Sample collection. Eggs from *M. borellii* were sampled from ovigerous females collected during spring and summer (October to February) in the Zapata Stream (20 km southwest of La Plata, Argentina), which has turbid waters with temperatures ranging from 22 to 26°C. The females were taken to the laboratory and kept in dechlorinated tap water at room temperature until the eggs were removed for the experiments. Embryo size and development stages were checked in each egg brood using a stereoscopic microscope (Nikon SMZ-10, Tokyo, Japan). Seven developmental stages were therefore identified using major development events.

Stage I constitutes embryos from four-cell morula to gastrula with a highly viscous vitellus that takes up about 90% of the egg; in Stage II (10–18 d) vitellus fills up to 80% of the egg volume; in Stage III (18–26 d), embryos have incipient eyes visible and the vitellus fills up to 70%. At stage IV (26–35 d) the vitellus mass is divided into four lobules; in Stage V (36–40 d) the cuticle pigmentation becomes evident and embryo is under active organogenesis. At stage VI (40–46 d) blue from hemocyanin becomes visible and the vitellus has almost internalized into the embryo and represents about 20% of the egg volume; organisms in Stage VII (46–50 d) are 4–5 mm long with all the characteristics of postlarvae ready to hatch. In general, vitellus decreases its viscosity along with development.

Wet weight and moisture were obtained from egg masses of each developing stage and analyzed following a method from the International Association of Fish Meal Manufacturers (12). Samples were analyzed in triplicate and each replicate was composed of pools including eggs from 3 or 4 clutches.

Isolation of embryos and vitellus. Eggs were weighed; then egg shells, vitellus, and embryos were separated from each other. Embryos from stage I were virtually impossible to isolate free from vitellus due to its high viscosity and the size of the morula. Therefore, at this stage we studied the whole egg homogenate without the egg shells, which were separated by gentle centrifugation.

Stages II to IV: Embryos were first manually isolated from vitellus by breaking the vitelline sac under a stereoscopic microscope followed by the separation of embryo, egg shell, and vitellus using a Percoll® discontinuous density gradient (Pharmacia LKB, Uppsala, Sweden) with solutions of 100, 50, and 25% Percoll diluted with 75 mM NaCl. Samples were loaded onto the gradient and then centrifuged at 400 × *g* for 10 min (13). Thus, a shell-containing pellet was formed while the embryos were located in the interphase of the two Percoll solutions, and the yolk floated on top of the gradient.

Stage V and VI: Embryos were manually isolated from vitellus under a stereoscopic microscope and washed repeatedly with a solution of 75 mM NaCl. Stage VII embryos have already internalized the vitelline sac and therefore were analyzed as a whole egg homogenate.

Embryos were homogenized in a Potter-type homogenizer (Thomas Scientific, Swedesboro, NJ) using 0.02 M, pH 7.5 Tris-HCl buffer containing 2 mg/mL aprotinin (Trasylol, Mobay Chemical Co., New York). The ratio buffer/sample was kept at 3:1, vol/vol. All samples obtained were frozen at –70°C until analysis.

Protein, lipid, and carbohydrate determination. Proteins were determined by the method of Markwell *et al*. (14) using bovine serum albumin (BSA) as a standard. Samples and BSA were first digested with 1 N NaOH, 5:1 vol/vol, vortexed, and incubated overnight at 37°C.

Lipids were extracted with a chloroform/methanol mixture following the method of Bligh and Dyer (15), and total lipid concentrations were determined gravimetrically. Carbohydrates were determined following the spectrophotometric procedure of van Handel (16).

Lipid analysis. Eighty percent of each sample was employed for lipid analysis. Lipid class analysis was performed by thin-layer chromatography (TLC) on silica gel Chromarods (type S-III) with quantitation by flame-ionization detection using an Iatroscan TH-10, Mark III (Iatron Laboratories Inc., Tokyo, Japan) as described by Parrish and Ackman (17). The separation was conducted with a sequence of three different solvent systems according to Ackman and Heras (18). The first development was carried out for 45 min in hexane/ethyl acetate/diethyl ether/formic acid (91:6:3:1, by vol). Chromarods were dried, partially scanned to determine neutral lipids, and then developed in acetone for 15 min to quantify the carotenoid (astaxanthin) peak. Finally, the Chromarods were developed in chloroform/methanol/formic acid/water (50:30:4:2, by vol) for 60 min and completely scanned to reveal the different phospholipids. Tetracosanol was used as an internal standard, and quantitation was performed with calibration curves of authentic standards run under the same conditions. Lipids were also identified on HP-TLC plates (Merck, Darmstadt, Germany) developed with hexane/diethyl ether/acetic acid (80:20:1.5, by vol) for neutral lipids and chloroform/methanol/acetic acid/water (65:25:4:4, by vol) for polar lipids (PL). Esterified sterols and hydrocarbons coeluted using the first developing solvent system, although a qualitative separation performed on HP-TLC showed that esterified sterols were the major component of the unresolved peak. Standard lipids, iodine vapor, and specific reagents were used to identify lipid classes. Preparative HP-TLC of neutral lipids, as described above, was used to isolate PL and neutral lipids for fatty acid analysis and to isolate an egg carotenoid pigment, which was then employed as a standard for Chromarod calibration.

FA analysis. FA methyl esters from total lipids, triacylglycerols (TAG), and PL, were prepared with BF_3/MeOH according to the method of Morrison and Smith (19). The analyses were performed by gas chromatography using a Shimadzu 9A gas chromatograph (Tokyo, Japan) fitted with an Omegawax 250 fused-silica column, 30 m × 0.25 mm, with 0.25 µm phase (Supelco, Bellefonte, PA). Peaks were identified by comparing the retention times with those from a mixture of standard methyl esters.

Energy conversion factors. We employed the energy conversion factors described by Beningher (3) calculated for aquatic invertebrates: carbohydrates, 4.1 kcal/g or 17.2 kJ/g; proteins, 4.3 kcal/g or 17.9 kJ/g; and lipids, 7.9 kcal/g or 33.0 kJ/g.

Statistical analyses. Data collected from all experiments were analyzed by analysis of variance using Instat v.2.0 (GraphPad Software, San Diego, CA). Whenever significant differences among samples were found, a *post-hoc* Tukey's test was performed to identify the differing means. Results were considered significant at the 5% level.

RESULTS

Dry weight variations. The optimized methodology, employing Percoll gradients, allowed us to separate the vitellus from embryos and egg shells of *M. borellii*. Dry weight of whole eggs showed a steady decrease during development from 0.98 ± 0.05 mg/egg to 0.81 ± 0.08 mg/egg ($P < 0.05$). Morphological changes under the stereoscopic microscope were also evident in the 1.7–2.0 mm eggs, the vitellus being more condensed and reduced in size as the embryo developed, finally occupying about 20% of the egg volume at the last stage.

Energetic changes during development. Analysis of the composition of just-layed-egg vitellus showed that the major nutrients were lipids (29.3% dry weight) followed by proteins (28.7% dry weight) and carbohydrates (0.2% dry weight) (Fig. 1). From the biochemical composition of the developing eggs it was possible to calculate the equivalent calories depicted in Figure 2. The overall CE calculated as the percentage of vitellus total energy transformed into embryonic tissue energy was 45.5%. All reserves displayed significant changes from stages IV to V (Fig. 1), evidencing a net fall in the vitellus and an increase in the embryo content. The CE for lipids was 39.3, 57.1 for proteins, and 587.5% for carbohydrates.

Changes in lipid and FA composition along development. In order to determine the role of lipids during development, each lipid class was studied separately in embryos and in yolk. PL and TAG were the most important lipids in vitelline fluid, representing more than 89% w/w at stage I (Table 1). TAG evidenced significant changes between stages IV and V ($P < 0.01$), decreasing to 33% of the whole lipids, a reduction of more than 30% compared to the percentage in the original vitellus total lipid (Table 1). On the other hand, sphingomyelin (SM) increased in the embryos ready to hatch. Phosphatidylcholine was the second-most important lipid during the whole development, changing its relative amount from 14 to 25% by weight but without any defined pattern. Phosphatidylethanolamine also showed significant changes in vitellus between stages IV and V. Therefore, at the end of development, the composition of the vitellus remaining in the hatched postlarvae is particularly enriched in esterified sterols, astaxanthin pigments, and SM at the expense of TAG. The changes observed at stage V yolk were accompanied by an increase of PL in embryos, followed by a significant increase in embryo cholesterol at stage VI (Table 2). The astaxanthin pigment was also taken up by embryos at stages VI and VII, mainly at the end of embryogenesis, accounting for 11% of the total lipids in embryos ready to hatch as postlarvae. Free FA were always found in small amounts in the vitellus as well as in embryos, except in the yolk at stage V where it was 3.3% w/w. Esterified sterols, which cochromatographed with hydrocarbons, did not show any changes in embryos, although they were selectively conserved in vitellus, particularly at the end of development ($P < 0.01$). Nevertheless, they were always minor components.

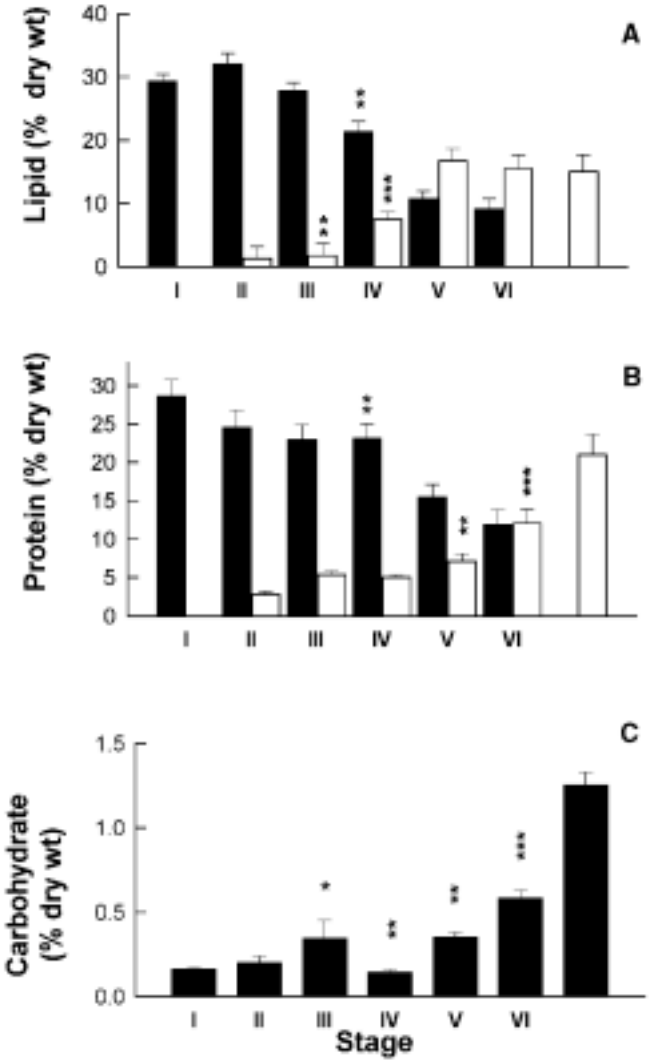

FIG. 1. Changes in (A) lipid, (B) protein, and (C) carbohydrate content in embryos (□) and vitellus (■) during development. Values are expressed as % dry weight of whole egg. Bars with different characters on top are significantly different from the next bar. $*P < 0.05$; $**P < 0.01$; $***P < 0.001$.

Regardless of variations according to lipid class or development stage analyzed, the major FA were 16:0, 18:0, 16:1n-7 18:1n-9, 18:1n-7, 18:2n-6 18:3n-3, 20:4n-6, and 20:5n-3 (Table 3). Monounsaturated FA were the major group in the TAG fraction at all stages. Polyunsaturated fatty acids

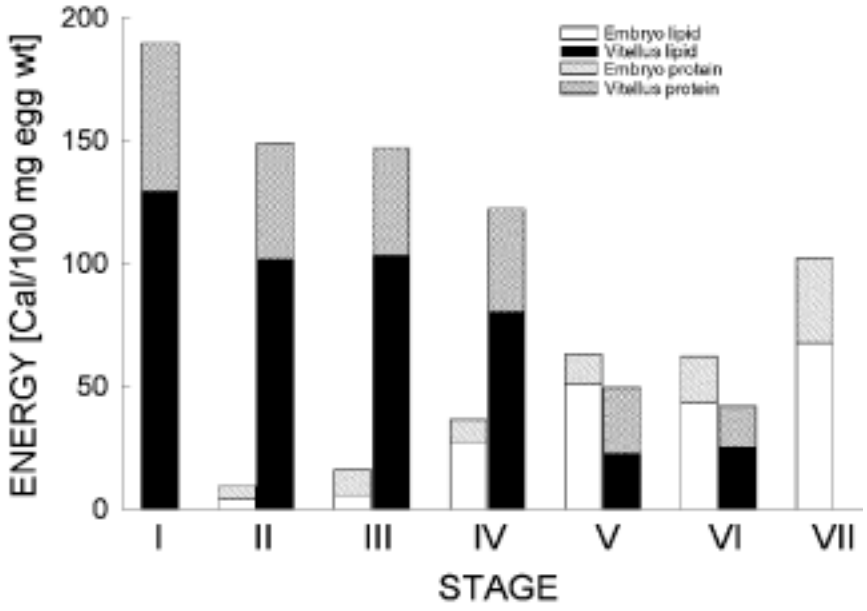

FIG. 2. Total caloric changes in embryos and vitellus during development. Values are expressed as total cal/100 mg egg (wet weight) for each stage, and they were calculated by adding protein and lipid calories. Carbohydrates represented less than 1.5% of the calories, and they were omitted for calculations.

(PUFA), on the other hand, were the main FA group in PL after embryos reached stage V; this increase was paralleled by a decrease in PL saturated and monounsaturated FA. The PUFA increment in PL fraction continued until hatching, reaching a value of 43.6% of total FA. Moreover, some PUFA such as 22:6n-3 (docosahexaenoic acid; DHA) and 20:5n-3 (eicosapentaenoic acid; EPA) were selectively accumulated in PL during development while 18:0 and 16:3 showed a clear association with PL throughout development.

Changes in protein and carbohydrate composition along development. Protein reserves in *M. borellii* yolk represent about 29% dry weight at stage I. Lipid and proteins were catabolized in equal proportion for energy until stage VII, where a much greater proportion of energy appears to have been derived from the catabolism of lipids and a greater proportion of the protein retained for converting into body components (Figs. 1 and 2). Therefore, yolk protein values fell, reaching a minimum of 14% at stage VII. The protein uptake by embryos was rather constant from stage II on, and did not increase until the end of embryogenesis. Embryo protein reached a maximum of 24% dry weight before hatching.

Compared to protein and lipid, the total carbohydrate content was low throughout development and increased strikingly at the end of embryogenesis, but it never exceeded 1.2% dry weight (Fig. 1).

DISCUSSION

Eggs in decapod carideans are surrounded by a chitin membrane that confers impermeability. However, it was interesting to note that *M. borellii* eggs increased their water content with development, probably due to a variation in inside os-

TABLE 1
Lipid Class Composition[a] of Vitellus During *Macrobrachium borellii* Development

Class[b]	Stage I	Stage II	Stage III	Stage IV	Stage V	Stage VI
SM	6.10 ± 0.42	5.05 ± 0.56	4.03 ± 0.25	3.40 ± 0.27	6.23 ± 0.13*	9.09 ± 0.48*
PC	14.72 ± 0.77	25.00 ± 1.14*	24.94 ± 0.89	21.01 ± 0.53	24.84 ± 1.07*	16.48 ± 0.84*
PE	13.28 ± 1.06	9.90 ± 3.63	13.69 ± 1.00	16.98 ± 0.70	14.13 ± 0.31*	13.59 ± 0.82
ASX	6.42 ± 0.21	6.86 ± 0.65	6.21 ± 0.12	5.72 ± 0.54	11.15 ± 0.23*	12.44 ± 3.95
Cho	4.05 ± 0.23	4.49 ± 0.26	3.65 ± 0.20	3.16 ± 0.07	5.61 ± 0.33*	8.51 ± 0.29*
FFA	Trace	Trace	Trace	0.53 ± 0.18	3.30 ± 0.06*	1.44 ± 0.12
TAG	55.40 ± 2.05	48.63 ± 1.59	47.43 ± 1.18	48.99 ± 1.95	32.95 ± 2.26*	37.38 ± 1.86
HC+ SS	Trace	Trace	Trace	0.21 ± 0.05	1.78 ± 1.41*	1.06 ± 0.45

[a]Values (mg lipid/g egg wet weight) are the mean of triplicate analyses ± SD. *Significant changes compared with the preceding stage ($P < 0.05$).
[b]HC + SS, hydrocarbons + esterified sterols; TAG, triacylglycerols; FFA, free fatty acids; ST, free sterols; ASX, astaxanthin; PE, phosphatidylethanolamine; PC, phosphatidylcholine; SM, sphingomyelin; Cho, cholesterol.

TABLE 2
Changes in Lipid Class Composition[a] of *M. borellii* Embryos During Development

	Stage II	Stage III	Stage IV	Stage V	Stage VI	Stage VII
SM	2.65 ± 0.12	3.23 ± 0.06	2.95 ± 0.23	2.39 ± 0.12	3.77 ± 0.40	6.34 ± 0.87*
PC	11.92 ± 1.21	9.04 ± 0.52	8.07 ± 0.45	15.61 ± 1.21*	14.62 ± 1.07	18.12 ± 2.59
PE	9.78 ± 0.52	6.97 ± 0.67	7.70 ± 0.14	12.50 ± 1.52*	11.63 ± 0.66	11.00 ± 1.63
ASX	3.91 ± 0.52	3.38 ± 0.27	4.19 ± 0.72	4.33 ± 0.34	5.73 ± 0.59	11.24 ± 2.86*
Cho	3.53 ±0.25	3.21 ± 0.25	3.38 ± 0.24	3.33 ± 0.24	5.29 ± 0.12*	5.93 ± 0.21
FFA	0.75 ± 0.25	0.66 ± 0.07	0.73 ± 0.13	0.36 ± 0.10	0.54 ± 0.04	0.78 ± 0.33
TAG	66.32 ± 1.25*	72.25 ± 1.21	71.68 ± 1.10	60.39 ± 1.54*	56.09 ± 1.50	45.53 ± 1.17*
HC + SS	1.13 ± 0.15	1.26 ± 0.21	1.30 ± 0.10	1.10 ± 0.10	2.32 ± 0.03*	1.06 ± 0.13

[a]Values (mg lipid/g egg wet weight) are the mean of triplicate analyses ± SD. *Significant changes compared with the preceding stage ($P < 0.05$). For abbreviations see Table 1.

molarity that favored the exchange of water and some other compound responsible for keeping the embryos under optimal conditions. Nevertheless, *M. borellii* is a lecithotrophic shrimp, and therefore once fertilized, the yolk content of each egg wholly supports the development of the embryo and the first postlarval stage until the postlarva starts feeding. This strategy implies that maternal diet modifies the biochemical composition of eggs because there is, to a variable extent, a direct dietary input to oocyte lipid accumulation (20). Therefore, the composition of *M. borellii* eggs was always analyzed using wild gravid females. Yolk composition of just-layed eggs (stage I) showed that the major component was lipid (34.8% dry weight) followed by proteins (33.0%), but only a small amount of carbohydrates was detected (1.5%). High lipid levels are a common feature of other crustacean eggs. Holland (2) reviewed the biochemical composition of several invertebrate eggs, reporting that crustaceans showed a heterogeneous picture, with protein prevailing in some cases whereas lipids were the most important reserves in the majority of crustaceans, with carbohydrates always being a minor component. It is worth pointing out that comparisons among decapod eggs should be made taking into account the different life histories of the group. For example, the prawn *M. idella* has an egg composition in which proteins constitute more than 80% of dry weight (2) and a life cycle that includes very small eggs and feeding larvae. On the other hand, Sarojini *et al.* (21) reported the composition of eggs of *M. kistnensis,* showing that lipids were the most important reserve. Although the three species belong to the genus *Macrobrachium*, their life histories and type of eggs are different. Anger (22) reviewed the importance of lecithotrophy, as compared to feeding, on early larval development.

Regarding the use of the energy sources, we found that lipids, followed by proteins, are the major source of energy available in vitellus for embryogenesis. On the other hand, there was a net carbohydrate synthesis as the mass in the em-

TABLE 3
Major Fatty Acids of Triacylglycerols and Polar Lipids of Whole Eggs During *M. borellii* Embryogenesis[a]

	Stage													
	I		II		III		IV		V		VI		VII	
Fatty acid	TAG	PL	TAG	PL	TAG	PL	TAG	PL	TAG	PL	TAG	PL	TAG	PL
14:0	2.56	2.75	2.54	2.03	2.28	0.97	2.95	1.89	2.35	1.34	2.80	0.84	2.88	0.77
16:0	18.15	19.09	20.80	18.06	19.89	18.57	19.79	18.30	19.32	15.40	18.87	14.07	18.93	14.26
18:0	3.66	4.43	4.03	6.08	3.87	6.07	3.43	5.64	3.46	6.58	3.98	8.19	3.98	9.60
16:1n-7	13.23	13.12	12.72	8.82	12.99	8.80	13.42	11.36	14.09	9.21	11.99	6.68	12.84	7.06
18:1n-9	15.94	15.01	16.22	15.67	15.66	15.47	15.51	15.70	15.28	14.08	15.52	15.12	14.08	10.21
18:1n-7	9.20	6.11	6.34	6.40	7.84	7.06	6.21	5.52	6.43	6.82	7.50	7.47	7.13	7.77
18:2n-6	5.40	5.12	6.15	4.74	6.11	4.12	6.92	4.06	6.33	4.24	6.56	4.74	6.30	4.79
16:3[b]	1.80	5.68	1.55	5.05	1.41	4.80	1.12	4.54	1.33	5.67	1.24	5.82	1.81	5.24
18:3n-3	4.98	6.83	4.44	7.19	6.35	6.53	7.83	5.54	9.84	5.15	10.87	7.38	9.59	7.12
20:4n-6	4.58	4.04	5.08	5.15	4.22	5.16	4.04	5.40	3.96	4.82	3.73	5.23	3.21	5.96
20:5n-3	10.10	8.19	10.35	8.26	9.76	8.98	9.19	10.25	8.37	11.48	8.35	11.80	7.66	11.93
22:6n-3	1.62	1.39	1.56	1.53	1.36	1.62	1.39	1.57	1.50	2.46	1.14	2.07	1.20	2.61
∑ Saturates	26.43	28.51	29.45	27.85	28.24	27.44	29.61	28.44	27.29	25.12	27.64	24.27	28.06	26.85
∑ Monounsaturates	40.36	36.20	37.17	36.10	38.47	36.60	37.10	35.80	37.51	35.45	37.25	32.72	36.25	29.66
∑ Polyunsaturates	33.22	35.27	33.41	36.05	33.24	35.96	33.51	35.81	35.18	39.46	35.16	43.01	35.68	43.58

[a]Values are the mean of duplicate analyses as % w/w. SD have been omitted for clarity but never exceeded 10% of the mean. PL, Phospholipid; for other abbreviations see Table 1.
[b]Identity not established.

bryos exceeds the mass incorporated from the vitellus. Approximately 78% of the vitellus lipid was absorbed by the embryos during development, particularly during organogenesis (stages IV and V), and about 22% was left in hatchlings, suggesting lipids were actively catabolized by embryos for their growth and maintenance. There was a delay in the utilization of vitellus lipids until stage V, which is coincident with observations in a related work where we found at this stage the highest activity of several enzymes involved in the lipid metabolism. In particular, we found higher β-oxidation and TAG-lipase and palmitoyl-CoA ligase activities at stage V (23).

Protein levels showed significant changes along development. Embryos took up 90% of vitellus proteins, which decreased sharply between stages IV and V, similarly to the case for lipids. Subramoniam (24) also found that proteins were used for the growth of *Emerita asiatica* during embryogenesis, and Claybrook (25) reported that during embryonic development of *Palaemon serratus*, yolk proteins were apparently oxidized for energy as well as reincorporated into tissues of the embryo, indicated by a 25% decrease in total protein content of the whole egg.

Interestingly, there was no net increase in embryo protein content until stage VII, just before hatching, suggesting that most proteins incorporated at stages IV and V must have been consumed as energy sources or were converted into other body components. The embryo protein level also showed a trend of increasing between stages III and IV. The major vitellus protein in decapods is vitellin, whose site of biosynthesis has aroused great controversy. A combination of autosynthesis as well as heterosynthesis occurring sequentially in ovaries along with vitellogenesis is the most probable picture (26–29). The ratio of energy supplied by lipids and proteins throughout development was quite constant at around 2, indicating a simultaneous utilization of both.

The calculated protein CE was 57%, comparable to CE values of 50 to 80% that have been observed in other crustaceans that use proteins as the major energy source (2). The protein at stage VII would be all newly synthesized protein and represents 57% of the total protein available in the egg provided from maternal sources.

Stage VII embryos increased their carbohydrate content fivefold compared with stage I. The energy CE was 587%, suggesting an active carbohydrate synthesis throughout development, probably associated with the active shell synthesis that takes place in the late stages of embryogenesis.

We could therefore suggest that absorption of nutrients from vitellus should be divided into two phases. The first one shows a mild uptake up to stage IV, followed by very active uptake and consumption phase from stage V until hatching where carbohydrates, lipids and proteins would be used for organogenesis. At the same time embryos would consume the previously accumulated nutrients, particularly after stage V, together with a *de novo* synthesis of molecules. This is merely a simplification of the real picture, because we are only considering interconversions from the different reserves, but as postlarvae hatch, they become an open system. On the whole, vitellus seems to provide the embryo with both an adequate environment throughout development and a nourishing medium, particularly for late embryogenesis. Proteins provide structural precursors during embryogenesis, and they also contribute to the embryo energetics, mainly supplied by lipids, especially TAG.

FA of PL and neutral lipids presented a similar pattern throughout development, regardless of variation either in lipid class or development stage. Some n-3 PUFA such as DHA and EPA were selectively accumulated in PL during development, while 18:0 and 16:3 showed a clear association with PL. Teshima *et al*. (30), using a double tracer experiment in *Penaeus japonicus,* reported that n-3 FA were partitioned primarily into PL whereas palmitic acid was partitioned into TAG. We have shown that in this direct-development species, PUFA are only preferentially conserved in PL at the end of development, whereas at the begining PUFA are equally distributed in TAG and PL. In the lobster *Homarus americanus*, Sasaki *et al.* (31) found that reserves of egg yolk, especially essential FA, may be depleted during embryogenesis and thus are insufficient to support larval development.

The amount of EPA and DHA is somewhat higher than that expected for a freshwater species and for other invertebrates living in the same area (32) where the n-3/n-6 ratio is below one. Nevertheless, values are similar to those observed in adult *M. borellii* (33). This composition may probably be linked to the fact that the genus *Macrobrachium* has recently colonized the freshwater environment and came from a marine environment where n-3 fatty acids prevail over the n-6 family.

Lipids have the highest energetic yield of all molecules and represent a compact and concentrated form of energy storage. Most aquatic invertebrates have taken advantage of this property, and a high lipid content is a common feature in many marine species (34). This is a common situation for females that need a compact energy store since egg volume imposes body space restrictions. Thus, the use of lipid catabolism as an energy source during embryogenesis may endow the species with some advantages in the unpredictable freshwater environment. Ongoing research in our laboratory has revealed a very active lipid metabolism in these shrimp embryos (23). This is also coincident with the general observation on the life history of marine species that conquered freshwater environments; they frequently present a series of adaptations to this environment, including a tendency to brood protection, low fecundity, large egg size, unusually high lipid content in eggs and larvae, abbreviated larval development, and lecithotrophy (35,36). All of these characteristics were found in *M. borellii* eggs compared to other members of the genus, making this species well-adapted to the nonmarine environment.

ACKNOWLEDGMENTS

This work was partially supported by grants from CONICET, CIC, ANPCyT, and Fundación Antorchas (Argentina), and the International Foundation for Science (Sweden). RJP is member of Carrera del Investigador, CIC (Bs. As.), Argentina. HH and MGB are members of CONICET, Argentina.

REFERENCES

1. Gabbott, P.A. (1975) Storage Cycles in Marine Bivalve Molluscs: A Hypothesis Concerning the Relationship Between Glycogen Metabolism and Gametogenesis, in *Proceedings of the Ninth European Marine Biology Symposium* (Barnes, H., ed.), pp. 191–211, Aberdeen University Press, Aberdeen.
2. Holland, D.L. (1978) Lipid Reserves and Energy Metabolism in the Larvae of Benthic Marine Invertebrates, in *Biochemical and Biophysical Perspectives in Marine Biology* (Mallins, D.C., and Sargent, J.R., eds.), Vol. 4, pp. 85–123, Academic Press, London.
3. Beningher, P.G. (1984) Seasonal Variations of the Major Lipid Classes in Relation to the Reproductive Activity of Two Species of Clams Raised in a Common Habitat: *Tapes decussatus* L. (Jeffreys) and *Tapes philippinarum* (Adams & Reeve), *J. Exp. Mar. Biol. Ecol. 79*, 79–90.
4. Beningher, P.G., and Lucas, A. (1984) Seasonal Variations in Condition, Reproductive Activity, and Gross Biochemical Composition of Two Species of Adult Clam Reared in a Common Habitat: *Tapes decussatus* L. (Jeffreys) and *Tapes philippinarum* (Adams & Reeve), *J. Exp. Mar. Biol. Ecol. 79*, 19–37.
5. McEdward, L.R., Carson, S.F., and Chia, F. (1988) Energetic Content of Eggs, Larvae and Juveniles of *Florometria serratissima* and the Implications for the Evolution of Crinoid Life Histories, *Int. J. Inv. Reprod. Devel. 13*, 9–22.
6. Pandian, T.J. (1969) Yolk Utilization in the Gastropod *Crepidula fornicata, Mar. Biol. 3*, 117–121.
7. Heras, H. (1990) Mecanismo de Transporte Hemolinfático de Lípidos en *Octopus tehuelchus* d'Orb. 1835, Ph.D. Thesis, University of La Plata, La Plata, Argentina, 206 pp.
8. Whyte, J.N.C., Bourne, N., Ginther, N.G., and Hodgson, C.A. (1992) Compositional Changes in the Larva to Juvenile Development of the Scallop *Crassadoma gigantea* (Gray), *J. Exp. Mar. Biol. Ecol. 163*, 13–29.
9. Wallace, R.A., Walker, S.L., and Hauschka, P.V. (1967) Crustacean Lipovitellin: Isolation and Characterization of the Major High-Density Lipoprotein from Eggs of Decapods, *Biochemistry 6*, 1582–1590.
10. Adiyodi, R.G., and Subramoniam, T. (1983) Arthropoda-Crustacea, in *Reproductive Biology of Invertebrates* (Adiyodi, K.G., and Adiyodi, R.G., eds.) Vol. 1*, Oogenesis, Oviposition and Oosorption,* pp. 443–495, John Wiley & Sons Ltd., New York.
11. Boschi, E.E. (1981) Decapoda: Natantia, in *Fauna Argentina de Agua Dulce* (Boschi, E.E., ed.) Vol. 26, pp. 19–61, FECIC, Buenos Aires, Argentina.
12. IAFMM (1979) Recommended Method of Analysis for Determination of Moisture in Fish Meal, No. 9, in *International Association of Fish Meal Manufacturers*, Technical Bulletin.
13. Heras, H., Garin, C., and Pollero, R.J. (1998) Biochemical Composition and Energy Sources During Embryo Development and in Early Juveniles of the Snail *Pomacea canaliculata* (Mollusca: Gastropoda), *J. Exp. Zool. 280*, 375–393.
14. Markwell, M.A.K., Haas, S.M., Bieber, L.L., and Tolbert, N.E. (1978) A Modification of the Lowry Procedure to Simplify Protein Determination in Membrane and Lipoprotein Samples, *Anal. Biochem. 87*, 206–210.
15. Bligh, E.G., and Dyer, W.J. (1959) A Rapid Method of Total Lipid Extraction and Purification, *Can. J. Biochem. Physiol. 37*, 911–917.
16. van Handel, E. (1965) Estimation of Glycogen in Small Amounts of Tissue, *Anal. Biochem. 11*, 256–265.
17. Parrish, C.C., and Ackman, R.G. (1985) Calibration of the Iatroscan-Chromarod System for Marine Lipid Class Analyses, *Lipids 20*, 521–530.
18. Ackman, R.G., and Heras, H. (1997) Recent Applications of Iatroscan TLC–FID Methodology, in *New Techniques and Applications in Lipid Analysis* (McDonald, R.E., and Mossoba, M.M., eds.) pp. 325–340, AOCS Press, Champaign.
19. Morrison, W.R., and Smith, L.M. (1964) Preparation of Fatty Acid Methyl Esters and Dimethylacetals from Lipid with Boron Fluoride-Methanol, *J. Lipid Res. 5*, 600–608.
20. Harrison, K.E. (1990) The Role of Nutrition in Maturation, Reproduction and Embryonic Development of Decapod Crustaceans: A Review, *J. Shellfish Res. 9*, 1–28.
21. Sarojini, R., Mirajkar, M.S., and Nagabhushanam, R. (1985) Reproduction and Associated Biochemical Changes in the Freshwater Prawn *Macrobrachium kistnensis* (Tiwari), *J. Anim. Morphol. Physiol. 32*, 23–32.
22. Anger, K. (1996) Physiological and Biochemical Changes During Lecithotrophic Larval Development and Early Juvenile Growth in the Northern Stone Crab, *Lithodes maja* (Decapoda, Anomura), *Mar. Biol. 126*, 283–296.
23. Gonzalez-Baró, M.R., Heras, H., and Pollero, R.J. (2000) Enzyme Activities Involved in Lipid Metabolism During Embryonic Development of *Macrobrachium borellii, J. Exp. Zool. 286,* 231–237.
24. Subramoniam, T. (1991) Yolk Utilization and Esterase Activity in the Mole Crab *Emerita asiatica* (Milne Edwards*),* in *Crustacean Issues* (Wenner, A., and Kuris, A., eds.) Vol. 7, *Crustacean Egg Production,* pp. 19–30, Balkena, Rotterdam.
25. Claybrook, D.L. (1983) Nitrogen Metabolism*,* in *The Biology of Crustacea* (Mantel, L.H., ed.), pp. 163–213, Academic Press, New York.
26. Quackenbush, L.S. (1986) Crustacean Endocrinology: A Review, *Can. J. Fish. Aquat. Sci. 43*, 2271–2282.
27. Quackenbush, L.S. (1989) Vitellogenesis in the Shrimp, *Penaeus vannamei*: *in vitro* Studies of the Isolated Hepatopancreas and Ovary, *Comp. Biochem. Physiol. 94*, 253–261.
28. Mohamed, K.S., and Diwan, A.D. (1992) Biochemical Changes in Different Tissues During Yolk Synthesis in Marine Prawn *Penaeus indicus,* H. Milne Edwards, *Indian J. Mar. Sci. 21*, 30–34.
29. Charniaux-Cotton, H. (1985) Vitellogenesis and Its Control in Malacostracan Crustacea, *Am. Zool. 25*, 197–206.
30. Teshima, S., Kanzawa, A., Horinouchi, K., and Koshio, S. (1988) Lipid Metabolism in Destalked Prawn *Penaeus japonicus*: Induced Maturation and Transfer of Lipid Reserves to the Ovaries, *Nippon Suisan Gakkaishi 54*, 123–129.
31. Sasaki, G.C., Capuzzo, J.M., and Biesiot, P.M. (1986) Nutritional and Bioenergetic Consideration in the Development of the American Lobster *Homarus americanus*, *Can. J. Fish. Aquat. Sci. 43*, 2311–2319.
32. Pollero, R.J., and Brenner, R.R. (1981) Effect of Environment and Fasting on the Lipid and Fatty Acid Composition of *Diplodon delodontus, Lipids 16*, 685–690.
33. Gonzalez-Baró, M.R., and Pollero, R.J. (1988) Lipid Characterization and Distribution Among Tissues of the Freshwater Crustacean *Macrobrachium borellii* During an Annual Cycle, *Comp. Biochem. Physiol. 91*, 711–715.
34. Joseph, J.D. (1989) Distribution and Composition of Lipids in Marine Invertebrates, in *Marine Biogenic Lipids, Fats and Oils* (Ackman, R.G., ed.), Vol. 1, pp. 49–143, CRC Press, Boca Raton.
35. Anger, K., Storch, V., Capuzzo, J.M., and Anger, V. (1985) Effects of Starvation on Moult Cycle and Hepatopancreas of Stage I Lobster (*Homarus americanus*) Larvae, *Helgol. Meeresunters. 39*, 107–116.
36. Anger, K. (1996) The Conquest of Freshwater and Land by Marine Crabs. Adaptations in Life-History Patterns and Larval Bioenergetics, *J. Exp. Mar. Biol. Ecol. 193*, 119–245.

[Received December 6, 1999, and in revised form March 13, 2000; revision accepted April 1, 2000]

Lipid Metabolism and Tissue Composition in Atlantic Salmon (*Salmo salar* L.)—Effects of Capelin Oil, Palm Oil, and Oleic Acid-Enriched Sunflower Oil as Dietary Lipid Sources

Bente E. Torstensen*, Øyvind Lie, and Livar Frøyland

Institute of Nutrition, Directorate of Fisheries, N-5804 Bergen, Norway

ABSTRACT: Triplicate groups of Atlantic salmon *(Salmo salar* L.*)* were fed four diets containing different oils as the sole lipid source, i.e., capelin oil, oleic acid-enriched sunflower oil, a 1:1 (w/w) mixture of capelin oil and oleic acid-enriched sunflower oil, and palm oil (PO). The β-oxidation capacity, protein utilization, digestibility of dietary fatty acids and fatty acid composition of lipoproteins, plasma, liver, belly flap, red and white muscle were measured. Further, the lipid class and protein levels in the lipoproteins were analyzed. The different dietary fatty acid compositions did not significantly affect protein utilization or β-oxidation capacity in red muscle. The levels of total cholesterol, triacylglycerols, and protein in very low density lipoprotein (VLDL), low density lipoprotein (LDL), high density lipoprotein (HDL), and plasma were not significantly affected by the dietary fatty acids. VLDL, LDL, and HDL fatty acid compositions were decreasingly affected by dietary fatty acid composition. Dietary fatty acid composition significantly affected both the relative fatty acid composition and the amount of fatty acids (mg fatty acid per g tissue, wet weight) in belly flap, liver, red and white muscle. Apparent digestibility of the fatty acids, measured by adding yttrium oxide as inert marker, was significantly lower in fish fed the PO diet compared to the other three diets.

Paper no. L8415 in *Lipids 35,* 653–664 (June 2000).

Farmed Atlantic salmon (*Salmo salar* L.) are traditionally fed high-lipid diets with ingredients of marine origin containing high levels of n-3 fatty acids, resulting in a salmon fillet high in n-3 fatty acids. Lipids of marine origin are recommended in human health care as beneficial in protection against heart disease, autoimmune disease, and other disorders because of their high levels of n-3 fatty acids (1). However, the recent decreasing worldwide supplies of marine oils and fish meal have forced the industry to investigate alternative lipid sources for use in Atlantic salmon diets. Plant oils do not contain n-3 fatty acids with a chain length exceeding 18 carbon atoms and more than three double bonds. Instead, plant oils contain higher levels of saturated, monoene, and n-6 fatty acids, and their fatty acid compositions are different from marine oils. Little information is available on how these dietary fatty acids influence the uptake, transport, and utilization of fatty acids in Atlantic salmon.

Lipids are a major part of the Atlantic salmon diet, constituting more than 30% of the diet, and are an important source of energy. Atlantic salmon posses a high capacity to utilize fat as energy source (2–4). *In vitro* studies done on mitochondrial β-oxidation in fish suggest that substrate preferences exist for saturated and monounsaturated fatty acids over polyunsaturated fatty acids (PUFA). Especially 16:0, 16:1, 18:1n-9, and 18:2n-6 seem to be preferentially mobilized during starvation whereas 22:6n-3 is oxidized at low rates (5) [reviewed by Henderson (6)]. Further, 22:1n-11 and 16:0 serve equally well as substrates for mitochondrial β-oxidation in trout liver (7). However, in developing yolk-sac larvae of Atlantic halibut (*Hippoglossus hippoglossus* L.) 22:6n-3 is reported to be the quantitatively most important fatty acid in energy metabolism (8). Certain vegetable oils contain a great surplus of fatty acids such as 16:0 and 18:1n-9, which are possibly preferred for β-oxidation. This surplus might increase β-oxidation capacity and thus spare dietary protein for muscle growth. Results obtained after the onset of the current study indicate that, when measuring β-oxidation capacity, acyl-carnitines are β-oxidized at significantly higher rates compared to acyl-CoA by Atlantic salmon mitochondria in several tissues (4,9). Carnitine palmitoyl transferase-I (CPT-I) is considered to be the key enzyme for β-oxidation regulation, thus by using acyl-CoA as substrate in the assay for β-oxidation, measurement might be more physiologically relevant.

The transport of fatty acids and other lipid-soluble components to peripheral tissues is predominantly mediated by lipoproteins (10). Both the amount and fatty acid composition of dietary lipids are reported to affect plasma lipoprotein composition and metabolism in different species of rodents (11–14), in humans (15,16), and in Atlantic salmon (17; Torstensen, B.E., Lie, Ø., and Hamre, K., unpublished data).

The digestibility of monoene and saturated fatty acids by fish is generally lower compared to PUFA (18–20). The ab-

*To whom correspondence should be addressed at Institute of Nutrition, Directorate of Fisheries, P.O. Box 185 Sentrum, N-5804 Bergen, Norway. E-mail: bente.torstensen@nutr.fiskeridir.no

Abbreviations: AD, apparent digestibility; BW, body weight; CO, capelin oil; COSF, mix (1:1) of oleic acid-enriched sunflower oil and capelin oil; CPT-I, carnitine palmitoyl transferase-I; FCR, feed conversion ratio; HDL, high density lipoprotein; LDL, low density lipoprotein; NFE, nitrogen-free extract; PCA, principal component analysis; PL, phospholipid; PO, palm oil; PPV, productive protein value; PUFA, polyunsaturated fatty acid; SF, oleic acid-enriched sunflower oil; SGR, specific growth rate; TAG, triacylglycerol; VLDL, very low density lipoprotein.

sorption of fatty acids in fish is reported to decrease with increasing saturation of the acid and increasing chain length (19–21). This is probably due either to the melting point of the individual fatty acids or to the fact that fatty acids form insoluble soaps especially with long-chain saturated and monoene fatty acids with divalent cations in the intestine (19–21).

The aim of this study was (i) to investigate whether the dietary fatty acid composition, based on marine and different vegetable oil sources, influences the β-oxidation capacity of fatty acids in adult Atlantic salmon tissues, and (ii) to examine possible effects on plasma, lipoprotein, and tissue lipid composition and on the digestibility of fatty acids.

MATERIALS AND METHODS

Fish and diets. The feeding experiment was performed with four diets containing three lipid sources fed to four triplicate groups of Atlantic salmon. The following oils were used: capelin oil (CO) (Norsildmel, Norway), palm oil (PO) (Karlshamns Sweden AB, Karlshamn, Sweden), oleic acid-enriched sunflower oil (SF) (Loders Croklaan Inc., USA), and a 1:1 (w/w) mixture of SF and CO (COSF). The feeding experiment was carried out at NorAqua Innovation A/S Research Station, Dirdal, Norway, from March to August 1998 (total: 21 wk). Adult Atlantic salmon (*S. salar,* L.) (1.5 ± 0.6 kg) were stocked at 40 fish/tank in 12 indoor tanks of 2.8 m^3. Four different diets were produced by NorAqua Innovation A/S; Table 1 summarizes the fatty acid contents of the diets. The main components of the diets were 296 g kg^{-1} oil (CO, COSF, SF, or PO), 20 g kg^{-1} binder, 114.5 g kg^{-1} wheat flour, 549 g kg^{-1} low-temperature (LT) fish meal, and 20.5 g kg^{-1} vitamin and mineral mix. The four diets were formulated to contain 400 g kg^{-1} protein, 350 g kg^{-1} lipid, 63 g kg^{-1} water, 72 g kg^{-1} ash, and 92 g kg^{-1} nitrogen-free extract (predominantly carbohydrates). The diets were fed in excess by automatic feeders. Yttrium oxide was added to the experimental diets as inert marker (90 ± 5 mg kg^{-1}) for calculations of apparent digestibility of fatty acids. Feces were collected by stripping. Mortalities were recorded and dead fish removed daily. Biomass and average weight were determined by bulk weighing and counting of all fish in each tank at every sampling. The mean temperature, O_2 level, and salinity during the experimental period were 8.0 ± 0.4°C, 12.5 ± 0.6 mg/L, and 30.5 ± 1.0 g/L, respectively. The fish were exposed to continuous light. The protocol was approved by the Norwegian State Board of Biological Experiments with Living Animals.

TABLE 1
Dietary Fatty Acid Composition of the Four Experimental Diets[a]

	Capelin		Capelin/sunflower		Sunflower		Palm oil	
	%	mg/g	%	mg/g	%	mg/g	%	mg/g
14:0	5.3	14.3	3.1	9.3	1.1	3.2	1.7	4.5
16:0	13.3	36.1	9.7	29.3	6.5	19.3	37.8	99.7
18:0	1.3	3.5	2.5	7.6	3.6	10.8	5.1	13.6
Sum saturated	20.8	56.5	16.4	49.7	12.5	37.2	45.3	119.5
16:1n-7	7.1	19.2	4.1	12.3	1.3	3.9	1.2	3.2
16:1n-9	—	—	—	—	—	—	—	—
18:1n-7	3.1	8.4	2.1	6.3	0.6	1.8	1.0	2.6
18:1n-9	10.9	29.5	40.8	123.6	68.5	203.8	35.9	94.6
18:1n-11	0.2	0.6	—	—	—	—	—	—
20:1n-9	12.2	33.2	6.7	20.4	1.7	5.2	1.5	4.0
20:1n-11	0.3	0.7	0.3	0.8	—	—	—	—
22:1n-9	1.9	5.2	1.1	3.3	0.2	0.7	—	—
22:1n-11	14.5	39.5	7.9	24.0	1.8	5.3	1.7	4.4
24:1n-9	—	—	0.3	0.9	—	—	—	—
Sum monoene	51.0	138.4	63.6	192.8	74.2	220.7	41.2	108.8
18:2n-6	2.1	5.7	4.7	14.3	7.2	21.4	8.1	21.3
20:4n-6	0.3	0.9	0.2	0.7	—	—	—	—
Sum n-6	2.6	7.1	5.0	15.1	7.2	21.4	8.1	21.3
18:3n-3	0.6	1.7	0.4	1.2	0.2	0.6	0.3	0.8
18:4n-3	3.5	9.5	1.9	5.8	0.4	1.3	0.4	1.0
20:4n-3	0.5	1.2	0.3	0.8	—	—	—	—
20:5n-3	9.3	25.2	5.7	17.2	2.4	7.2	2.1	5.4
22:5n-3	0.6	1.6	0.4	1.2	0.2	0.6	—	—
22:6n-3	7.0	19.1	4.8	14.6	2.8	8.2	2.5	6.5
Sum n-3	22.5	61.0	13.9	42.2	6.0	17.9	5.2	13.7
n-3/n-6	8.6	8.6	2.8	2.8	0.8	0.8	0.6	0.6
Sum total FA	97.5	271.5	99.3	303.2	100.0	297.3	99.8	263.8
Rest FA	2.5	6.7	0.7	2.1	0.0	0.0	0.2	0.6

[a]Data reported as weight % and mg fatty acid g^{-1} tissue (wet weight). Data are presented as mean (n = 3). Values <0.1 are represented by an em dash (—).

Sampling procedure. Samples were taken from all diets and stored at –20°C. Fish were sampled at the start, after 12 wk, and at the end of the feeding trial, i.e., after 21 wk. The fish were fasted for 24 h prior to sampling. Five randomly sampled fish from each tank were anesthetized with methomidate (7 g/L). Blood was collected from caudal vein using EDTA vacutainers, and the fish was killed by a blow to the head followed by dissection of liver, belly flap, red muscle, and white muscle. Plasma was separated from the blood samples by low-speed centrifugation, the five plasma samples from each tank were pooled, and the 12 plasma samples were stored on ice until lipoprotein fractionation. The liver, belly flap, red muscle, and white muscle samples from the same five fish from each tank were homogenized. These samples as well as an aliquot of the pooled plasma were immediately frozen on dry ice and stored at –80°C until further analyses.

Mitochondrial β-oxidation. Liver, red and white muscle were weighed and homogenized to 20% (wt/vol) in ice-cold sucrose solution containing 0.25 M sucrose in 10 mM *N*-2-hydroxyethylpiperazine-*N*′-2-ethanesulfonic acid (HEPES) buffer and 1 mM EDTA, pH 7.4. The resulting total homogenates were then stored on ice during transport before being centrifuged (1,880 × *g* for 10 min at 2°C). The resulting postnuclear fractions were collected, and portions were used immediately to determine mitochondrial β-oxidation. The mitochondrial β-oxidation was determined in postnuclear fractions as acid-soluble products using radiolabeled [1-^{14}C]-palmitoyl-CoA as a substrate as described previously (22). [1-^{14}C]Palmitoyl-CoA was purchased from New England Nuclear (Boston, MA). Palmitoyl-CoA and other cofactors were purchased from Sigma Chemical Co. (St. Louis, MO).

Separation of lipoproteins. Very low density lipoprotein (VLDL), low density lipoprotein (LDL), and high density lipoprotein (HDL) in pooled plasma samples of five fish from each tank were obtained by sequential centrifugal flotation (23,24) as described by Lie *et al*. (25) using a Pegasus 65 ultracentrifuge equipped with a 70-Ti fixed-angle rotor. The centrifugation was done at 107,500 × *g* and 4°C. The density intervals were obtained by addition of solid KBr (26). Run times for separation of the lipoproteins were: VLDL, $d <$ 1.015 g mL^{-1} for 20 h; LDL, 1.015 < d < 1.085 g mL^{-1} for 20 h; HDL, 1.085 < d < 1.21 g mL^{-1} for 44 h. The fractions were stored at –80°C until further analyses.

Analytical procedures. Fatty acid composition was analyzed in the diets, feces, liver, white muscle, red muscle, belly flap, plasma, and lipoproteins. Lipids from the pooled samples were extracted by adding chloroform/methanol (2:1, vol/vol), and 19:0 was added as internal standard. The samples were filtered, saponified, and methylated using 12% BF_3 in methanol. Fatty acid composition of total lipids was analyzed using methods described by Lie and Lambertsen (27) where the methyl esters were separated using a Carlo Erba gas chromatograph ("cold on column" injection, 69°C for 20 s, increase at 25°C/min to 160°C, hold at 160°C for 28 min, increase at 25°C/min to 190°C, hold at 190°C for 17 min, increase at 25°C/min to 220°C, hold at 220°C for 9 min), equipped with a 50-m CP-Sil 88 (Chrompack, Middelburg, The Netherlands) fused-silica capillary column (i.d. 0.32 mm). The fatty acids were identified by retention time using standard mixtures of methyl esters (Nu-Chek-Prep, Elysian, MN), and the fatty acid composition (wt%) was calculated using an integrator (Turbochrom Navigator, Version 4.0, PerkinElmer Corp.), connected to the gas–liquid chromatograph. The amount of fatty acid per gram of tissue was calculated using 19:0 as internal standard. Total protein, triacylglycerol, and total cholesterol in lipoproteins and plasma were analyzed on a Technicon RA-1000 clinical analyzer system (Bayer) according to standard Technicon methods, also described by Sandnes *et al*. (28). Total lipid in feces was measured gravimetically after acidification to dissolve fatty acids bound to cations and extraction with ethyl acetate.

Statistics. The relative fatty acid composition data of the tissues and lipoproteins were analyzed using SIRIUS for Windows (Version 6.0) (Pattern Recognition Systems) (Fig. 1). Principal component analysis (PCA) (29) of the relative fatty acid compositions was performed in each data matrix. The purpose of PCA is to express the main information in the variables by a lower number of variables, the so-called principal components (PC1, PC2, …). A high positive or negative loading reveals a significant variable in the actual PCA model. Score plots from the PCA explore the main trends in the data, and their respective loadings reveal fatty acids with a significant loading. The samples with similar relative fatty acid composition are located in the same area in the score plot. These classes are indicated in Figures 1A and 1C by circles drawn on freehand. Since samples with the same relative fatty acid composition will be located on top of each other, to ease interpretation the samples the classes contain are written beside the circle.

Significant differences in amount of fatty acid (mg g^{-1}, wet weight) between the dietary treatments in the final sampling, lipid class and protein content in the lipoproteins and plasma, and β-oxidation in red muscle were analyzed by breakdown and one-way analysis of variance followed by Tukey's honest significant difference (HSD) test, using CSS:Statistica (version 4.5) (Statsoft Inc. 1993). The β-oxidation data and lipoprotein composition data were analyzed by using the same statistical methods. The following fatty acids were tested: 14:0, 16:0, 18:0, 16:1n-7, 18:1n-9, 22:1n-11, 18:2n-6, 20:4n-3, 20:5n-3, 22:5n-3, 22:6n-3, sum n-6, sum n-3, sum saturated, sum total fatty acids, and n-3/n-6. The significance level was set to $P \leq 0.05$, and data are presented as mean ± SEM. The apparent digestibility (AD) of dietary fatty acids (d.w.), related to yttrium oxide (Y_2O_3) (d.w.) as inert marker, was calculated as follows:

$$\text{AD (\%)} = 100 - [100 \cdot (\text{conc. of } Y_2O_3 \text{ in feed/conc. of } Y_2O_3 \text{ in feces}) \cdot (\text{conc. FA in feces/conc. of FA in feed})] \quad [1]$$

For calculation of the fatty acid AD percentage, the amount of fatty acids in feces was calculated based on the relative fatty acid composition and total lipid in feces.

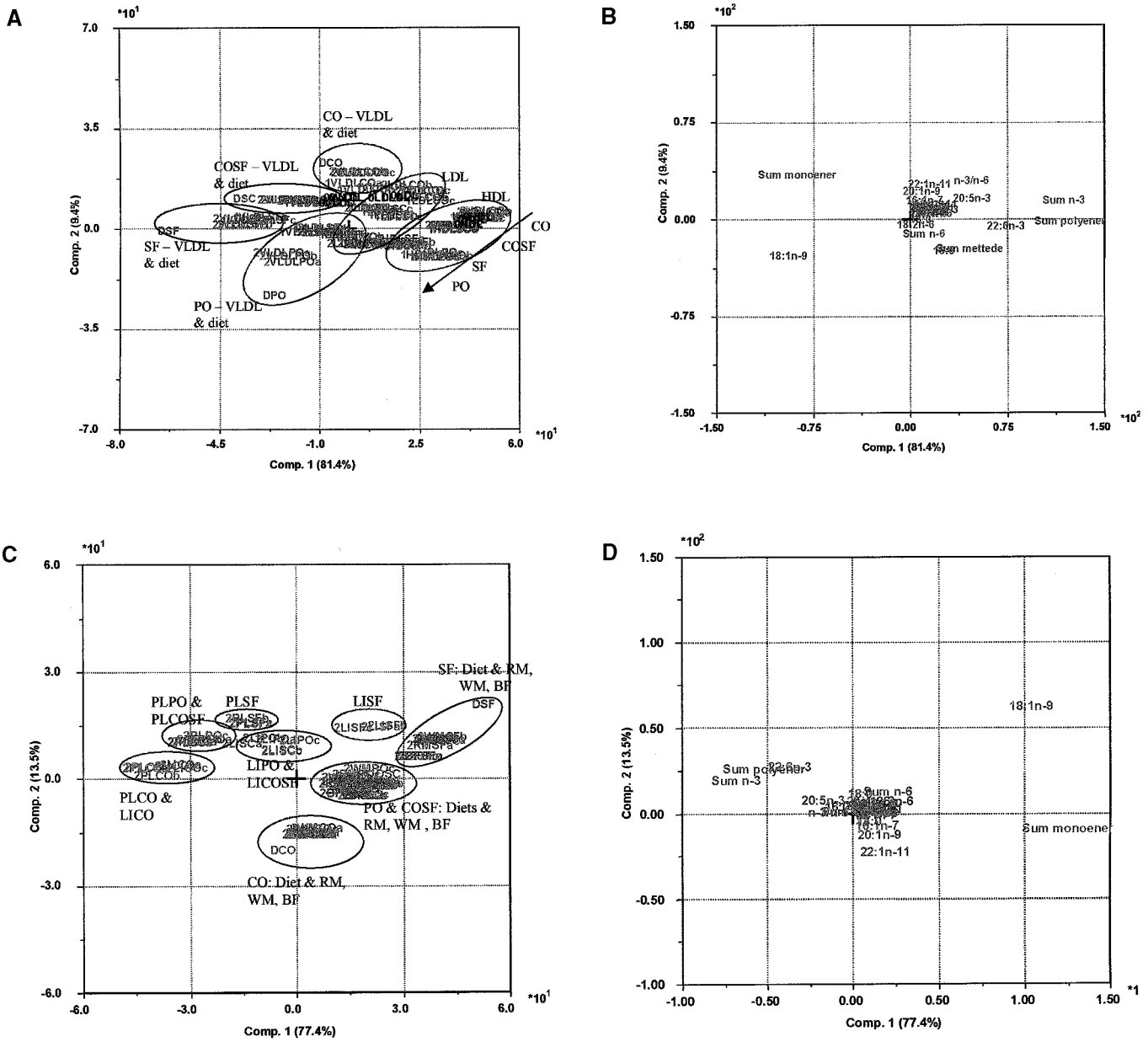

FIG. 1. Score plots (A and C) and load plots (B and D) revealed from principal component analysis of fatty acid composition data. (A and B) Score and load plots of the fatty acid composition data of very low density lipoprotein (VLDL), low density lipoprotein (LDL), and high density lipoprotein (HDL) from Atlantic salmon fed the experimental diets for 21 wk and dietary fatty acid composition data. (C and D) Score and load plots of the fatty acid composition data of plasma (PL), red muscle (RM), white muscle (WM), belly flap (BF), and liver (LI) from Atlantic salmon fed the experimental diets for 21 wk and dietary fatty acid composition data. The arrow in Figure 1A indicates the orientation of the different dietary groups within HDL and LDL. The diets are coded according to dietary oil source; CO, capelin oil; COSF, capelin oil and oleic acid-enriched sunflower oil; SF, oleic acid-enriched sunflower oil; and PO, palm oil.

RESULTS

Triplicate groups of Atlantic salmon were fed four diets containing different oils, i.e., CO, SF, PO, and COSF. The four diets had characteristic fatty acid compositions: CO, high levels of long-chain monoenes and n-3 PUFA; SF, high levels of 18:1n-9 and low levels of n-3 PUFA; COSF, intermediate levels of the characteristic fatty acids of CO and SF; and PO, high levels of 16:0 and 18:1n-9 and low levels of n-3 PUFA. Fish weights increased 2.4 times during the experimental period, and growth was not significantly affected by dietary lipid source. Although the PO group had the lowest [0.55 ± 0.08% body weight (BW) d^{-1}] and the SF group the highest (0.67 ± 0.01% BW d^{-1}) growth, the differences were not statistically significant. The fish weight (mean ± SD) at the end of the experiment was 3.6 ± 0.2 kg in the CO group, 3.7 ± 0.4 kg in the COSF group, 3.8 ± 0.2 kg in the SF group, and 3.2 ± 0.2 kg in the PO group. The feed conversion factor (feed/weight gain) was affected by dietary lipid source, however, not statistically significant. The PO group had a higher

feed conversion factor (1.04) compared to the other three dietary groups (0.91–0.95). Mortality was negligible throughout the experimental period with no more than two dead fish per dietary group. Calculated for the whole experimental period, the productive protein value (PPV) ranged from 0.43 ± 0.01 in the PO group to 0.47 ± 0.05 in the CO group, and there were no significant differences in PPV between the dietary groups. The lipid utilization [(biomass lipid final sampling) – (biomass lipid initial sampling)/(amount of lipid intake)], however, was significantly lower in the PO group (0.51 ± 0.03) compared to the other three dietary groups (CO: 0.78 ± 0.04, COSF: 0.78 ± 0.04; SF: 0.83 ± 0.04).

Total β-oxidation. The red muscle was the only tissue with significant β-oxidation of [1-^{14}C]palmitoyl-CoA in all samplings (Fig. 2). The β-oxidation capacity was not significantly affected by the dietary treatments in any of the samplings. However, there was a trend toward higher β-oxidation capacity in the SF group compared to the other dietary treatments in the intermediate sampling. The β-oxidation capacity in white muscle and liver was low at the initial sampling with 4.9 and 0.7 pmol/min/mg protein, respectively. At the two following samplings, no β-oxidation was detected in liver or white muscle using the [1-^{14}C]palmitoyl-CoA assay.

Plasma and lipoprotein lipid composition. Protein, total cholesterol, and triacylglycerol (TAG) were analyzed in total plasma, VLDL, LDL, and HDL at the intermediate and final sampling (Table 2). The levels of all the analyzed components increased significantly from the intermediate to the final sampling in plasma, VLDL, and LDL. HDL composition was, however, unchanged from intermediate to final sampling. There were no significant differences between the four dietary treatments regarding levels of protein, total cholesterol, or TAG in any of the lipoproteins or plasma. However, the SF group in the final sampling tended to have higher levels of protein, cholesterol, and TAG in the HDL fraction compared to the other three dietary groups. Further, the PO group had lower levels of protein and total cholesterol in the HDL fraction in both samplings. The recoveries of cholesterol and TAG ranged from 77 to 97% and from 80 to 98%, respectively.

Fatty acid composition of VLDL, LDL, and HDL was affected decreasingly by dietary fatty acid composition (Figs. 1A and 1B). The LDL and HDL fractions contained higher levels of polyenes and n-3 fatty acids compared to the diets and VLDL. HDL was the lipoprotein fraction with the highest relative levels of polyene and n-3 fatty acids. Sum monoene, 22:1n-11, n-3/n-6, and sum n-3 had high positive loadings along principal component 2 (PC2), whereas 16:0, sum n-6, and 18:1n-9 had high negative loadings along PC2 (Fig. 1B). Therefore, the samples from the dietary groups have gradually decreasing scores along PC2: CO > COSF > SF > PO (indicated by an arrow in Fig. 1A).

Tissue lipid composition. Relative fatty acid composition of white muscle, red muscle, and belly flap almost directly reflected the dietary fatty acid composition in the four dietary groups (Figs. 1C and 1D). Further, PCA of the relative fatty acid composition of plasma, liver, white and red muscle, and belly flap revealed that the plasma and liver fatty acid compositions were differently affected in the four dietary groups. Especially in the dietary SF group, plasma and liver had distinctly different relative fatty acid compositions. The variables 22:6n-3, sum n-3, and polyenes had high negative loadings, and monoenes and 18:1n-9 had high positive loadings along PC1 (Fig. 1D). Consequently, the plasma and liver samples containing higher levels of n-3, 22:6n-3, and polyene fatty acids had high scores along PC1 whereas the diets, white- and red muscle, and belly flap samples containing high levels of 18:1n-9 and monoenes had low scores along PC1

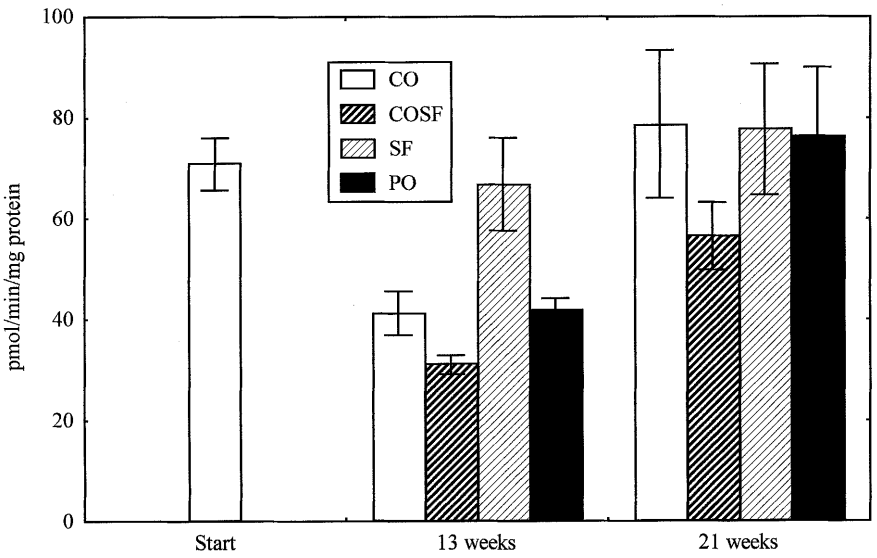

FIG. 2. Mitochondrial β-oxidation of [1-^{14}C]palmitoyl-CoA in red muscle from Atlantic salmon fed the experimental diets for 21 wk. Data are presented as mean ± SEM (n = 3). For abbreviations see Figure 1.

TABLE 2
Total Protein, Total Cholesterol, and Triacylglycerol in VLDL, LDL and HDL Expressed as Concentration in Lipoproteins of Total Plasma[a,b]

	Protein	Chol	TAG	Protein	Chol	TAG
Plasma						
Initial sampling	44.4 ± 1.1	7.3 ± 0.2	2.1 ± —			
	Intermediate sampling			Final sampling		
Plasma						
Capelin	58.1 ± 0.6	10.8 ± 0.1[a]	3.1 ± 0.2[a]	67.7 ± 2.6	14.5 ± 0.6[b]	6.7 ± 0.5[b]
Capelin/sunflower	59.2 ± 1.7	11.2 ± 0.3	2.8 ± 0.1[a]	62.4 ± 0.6	12.6 ± 0.1	5.5 ± 0.2[b]
Sunflower	55.9 ± 1.1	10.8 ± 0.1[a]	3.1 ± 0.1[a]	62.9 ± 2.0	13.6 ± 0.3[b]	5.7 ± 0.1[b]
Palm oil	49.3 ± 2.1	9.1 ± 0.6	2.8 ± 0.2[a]	56.3 ± 1.3	11.7 ± 0.1	5.5 ± 0.2[b]
VLDL						
Capelin	0.1 ± —[a]	0.2 ± —[a]	0.4 ± 0.1[a]	1.3 ± 0.1[b]	0.6 ± —[b]	2.3 ± 0.2[b]
Capelin/sunflower	0.1 ± —	0.1 ± —[a]	0.3 ± —	3.5 ± 1.1	0.6 ± 0.1[b]	3.6 ± 0.9
Sunflower	0.1 ± —[a]	1.0 ± 0.4	0.6 ± 0.1[a]	1.9 ± 0.2[b]	0.4 ± —	1.9 ± 0.1[b]
Palm oil	0.1 ± —[a]	0.2 ± —	0.3 ± —[a]	1.9 ± 0.2[b]	0.4 ± 0.1	1.9 ± 0.1[b]
LDL						
Capelin	0.6 ± 0.1	1.2 ± 0.1[a]	0.5 ± 0.1[a]	1.1 ± 0.1	2.1 ± 0.1[b]	1.0 ± 0.1[b]
Capelin/sunflower	0.7 ± —	1.3 ± 0.1	0.5 ± —[a]	0.9 ± —	1.7 ± 0.1	0.9 ± 0.1[b]
Sunflower	0.6 ± —	1.2 ± 0.2[a]	0.4 ± —[a]	0.8 ± —	1.8 ± 0.1[b]	0.8 ± —[b]
Palm oil	0.7 ± 0.1	1.5 ± 0.1	0.6 ± —[a]	1.0 ± 0.1	1.9 ± 0.1	1.1 ± 0.1[b]
HDL						
Capelin	10.9 ± 0.1	7.6 ± 0.1	1.9 ± —	11.2 ± 0.1	7.8 ± 0.1	1.7 ± —
Capelin/sunflower	10.7 ± 0.5	7.8 ± 0.4	1.6 ± —	11.8 ± 0.2	8.7 ± —	1.7 ± 0.1
Sunflower	10.4 ± 0.3	7.8 ± 0.3	1.6 ± 0.1	13.8 ± 1.0	9.8 ± 0.8	2.0 ± 0.2
Palm oil	7.7 ± 0.6	5.8 ± 0.4	1.5 ± 0.1	10.3 ± 0.1	7.6 ± 0.1	1.7 ± 0.1
Recovery						
Capelin		90 ± 1	98 ± 1		77 ± 1	80 ± 1
Capelin/sunflower		88 ± 1	96 ± 2		93 ± 2	89 ± 1
Sunflower		97 ± 6	95 ± 1		93 ± 7	88 ± 3
Palm oil		89 ± 1	97 ± 1		93 ± 2	91 ± 2

[a]Protein, g/L; Chol (cholesterol), mM; TAG (triacylglycerol), mM; VLDL, very low density lipoprotein; LDL, low density lipoprotein; HDL, high density lipoprotein. Lipoproteins and plasma were sampled from fish prior to feeding the experimental diets and from salmon fed the experimental diets for 12 wk and for 23 wk. Data are presented as mean ± SEM, $n = 3$. Values <0.1 are represented by an em dash (—).
[b]Superscript roman letters indicate significant differences ($P \leq 0.05$) between the intermediate and final sampling for each analyzed parameter. Where no letters are present, no significant differences were observed.

(Fig. 1C). The acid 18:1n-9 had a high positive loading whereas 22:1n-11 had a high negative loading along PC2 (Fig. 1D). This resulted in samples from the SF group having high positive scores and samples from the CO group having high negative scores along PC2 in the score plot (Fig. 1C).

The amount of fatty acids (mg g^{-1} tissue, wet weight) of belly flap, liver (Table 3), red and white muscle (Table 4) shows that the different dietary treatments produced significantly different fatty acid contents and composition in the tissues analyzed. The dietary PO and SF groups generally had the lowest and highest levels of total fatty acids, respectively, in the tissues analyzed. However, this was statistically significant only in red muscle and liver in the groups fed PO and SF, respectively. When comparing the levels of 16:0, 18:1n-9, 18:2n-6, and sum n-3 fatty acids of the dietary CO group with the other three dietary treatments, the large differences seen in the diets were rather modified in the various tissues. The SF diets, characterized by high 18:1n-9 levels, had significantly higher 18:1n-9 levels in all tissues analyzed. The PO diet contained 5.2 and 2.7 times more 16:0 than the SF and CO diet, respectively. When studying the tissue 16:0 levels, the PO groups contained significantly more 16:0 only in belly flap. The 16:0 levels in belly flap were 1.7 and 1.3 times higher in the PO groups compared to SF and CO groups, respectively. The SF and PO diets both contained 3.7 times more 18:2n-6 compared to the CO diet. In all tissues analyzed, the CO groups contained significantly less 18:2n-6 than the SF and PO groups. CO is characterized by high levels of 22:1n-11, thus in all tissues analyzed the dietary CO group contained the significantly highest tissue levels of 22:1n-11. The dietary COSF group contained intermediate tissue levels of 22:1n-11, whereas the dietary SF and PO groups had significantly the lowest tissue levels of 22:1n-11. The diets that supplied oils of plant origin typically contained low levels of long-chain n-3 fatty acids. This was reflected in belly flap, liver, plasma, red and white muscle where the CO groups contained the significantly highest levels of 20:5n-3, 22:6n-3, and sum n-3. The dietary groups fed a mixture of capelin and sunflower oil (1:1, w/w) (COSF) contained intermediate levels of n-3 fatty acids in the tissues analyzed, often

TABLE 3
Belly Flap and Liver Fatty Acid Composition from the Initial Sampling and from Fish Fed the Experimental Diets for 21 wk[a,b]

	Belly flap (n = 3)					Liver (n = 3)				
	Initial	Capelin	Capelin/ sunflower	Sunflower	Palm oil	Initial	Capelin	Capelin/ sunflower	Sunflower	Palm oil
14:0	15.1 ± 0.1	31.1 ± 1.4[a]	25.3 ± 0.8[a,b]	18.3 ± 0.2[b]	23.1 ± 1.2[b]	0.6 ± —	0.7 ± —[a]	0.6 ± —[a,b]	0.6 ± —[a,b]	0.4 ± —[b]
16:0	41.6 ± 0.2	92.4 ± 4.2[a]	82.9 ± 1.5[a]	72.4 ± 1.2[a]	122.1 ± 3.3[b]	4.2 ± 0.1	5.7 ± 0.1[a,b]	5.1 ± 0.3[a]	6.2 ± 0.1[a,b]	6.8 ± —[b]
18:0	8.8 ± —	18.1 ± 0.9[a]	22.5 ± 0.3[a,c]	26.9 ± 0.3[b,c]	27.4 ± 0.6[b]	1.2 ± —	2.2 ± —[a]	2.3 ± 0.2[b]	3.2 ± 0.1[b]	3.0 ± —[a,b]
Sum saturated	67.4 ± 0.3	145.5 ± 6.8[a,b]	136.4 ± 2.7[a]	123.0 ± 1.7[a]	176.4 ± 5.4[b]	6.2 ± 0.1	8.9 ± 0.1	8.2 ± 0.6	10.0 ± 0.2	10.3 ± 0.1
16:1n-7	19.3 ± 0.1	43.9 ± 2.1[a]	33.0 ± 1.0[a,b]	23.0 ± 0.5[b]	30.6 ± 1.6[b]	0.6 ± —	1.2 ± —	1.1 ± 0.1	1.2 ± —	1.3 ± 0.1
16:1n-9	1.0 ± —	1.9 ± 0.1	1.9 ± 0.1	2.1 ± —	2.3 ± 0.1	0.1 ± —	0.1 ± —	0.1 ± —	0.3 ± —	0.2 ± —
18:1n-7	10.4 ± 0.1	22.7 ± 1.1	19.1 ± 0.5	14.0 ± 0.2	16.9 ± 0.8	0.7 ± —	1.0 ± —	0.9 ± 0.1	0.9 ± —	0.7 ± —
18:1n-9	45.3 ± 0.2	108.5 ± 5.2[a]	220.0 ± 4.1[b]	345.6 ± 2.8[c]	210.2 ± 4.3[b]	2.0 ± —	4.6 ± 0.2[a]	11.0 ± 1.0[a,c]	27.1 ± 1.5[b]	12.2 ± 0.5[c]
18:1n-11	5.4 ± 0.1	9.7 ± 0.9	5.3 ± —	1.7 ± 0.1	3.4 ± 0.2	0.4 ± —	0.8 ± —	0.5 ± —	0.2 ± —	0.2 ± —
20:1n-9	30.4 ± 0.2	74.1 ± 3.1	57.7 ± 1.6	47.2 ± 0.2	45.7 ± 2.3	0.8 ± —	2.1 ± 0.1	2.2 ± 0.2	3.3 ± 0.2	1.2 ± —
20:1n-11	4.0 ± 0.1	6.9 ± 0.5	5.8 ± 0.2	4.0 ± 0.1	5.1 ± 0.3	0.1 ± —	0.4 ± —	0.2 ± —	0.1 ± —	0.1 ± —
22:1n-9	3.8 ± —	10.3 ± 0.5	7.6 ± 0.2	5.1 ± —	5.4 ± 0.3	—	0.2 ± —	0.2 ± —	0.1 ± —	0.1 ± —
22:1n-11	32.2 ± 0.1	78.2 ± 3.4[a]	55.3 ± 1.5[b]	32.2 ± 0.2[c]	40.5 ± 2.5[b,c]	0.4 ± —	1.0 ± —[a]	0.7 ± 0.1[a]	0.3 ± —[b]	0.2 ± —[b]
24:1n-9	2.2 ± —	4.5 ± 0.2	3.7 ± 0.1	3.0 ± 0.1	3.3 ± 0.1	—	—	—	—	—
Sum monoenes	155.4 ± 0.8	364.8 ± 17.1	412.3 ± 9.2	479.5 ± 3.6	365.3 ± 12.1	5.0 ± 0.1	11.5 ± 0.4	17.1 ± 1.6	33.6 ± 1.8	16.1 ± 0.6
18:2n-6	9.3 ± —	19.7 ± 0.9[a]	27.3 ± 0.8[b]	36.5 ± 0.4[c]	41.7 ± 0.6[c]	0.6 ± —	0.3 ± —[a]	0.9 ± 0.1[b]	2.1 ± 0.1[c]	1.6 ± —[c]
20:4n-6	1.3 ± —	1.8 ± 0.1	1.7 ± 0.1	1.6 ± —	1.9 ± 0.1	0.3 ± —	0.5 ± —	0.4 ± —	0.6 ± —	0.6 ± —
Sum n-6	11.8 ± —	24.2 ± 1.1[a]	32.8 ± 0.8[b]	45.2 ± 0.4[c]	51.1 ± 0.8[c]	1.0 ± —	1.1 ± —[a]	1.7 ± 0.1[a]	3.7 ± 0.1[b]	3.0 ± —[b]
18:3n-3	2.7 ± —	5.0 ± 0.2	4.0 ± 0.2	3.4 ± —	4.4 ± 0.2	0.1 ± —	—	—	—	—
18:4n-3	4.9 ± —	12.3 ± 0.5	7.9 ± 0.2	5.0 ± —	6.4 ± 0.4	0.1 ± —	0.1 ± —	—	—	—
20:4n-3	4.6 ± —	10.3 ± 0.5[a]	8.2 ± 0.2[a,c]	4.9 ± 0.1[b]	6.2 ± 0.3[b,c]	0.3 ± —	0.4 ± —[a]	0.3 ± —[a]	0.1 ± —[b]	0.1 ± —[b]
20:5n-3	21.1 ± 0.1	44.1 ± 1.8[a]	34.2 ± 1.1[a,b]	23.4 ± 0.3[b]	29.4 ± 1.9[b]	2.4 ± 0.1	4.5 ± 0.1[a]	3.3 ± 0.2[b]	2.3 ± —[c]	2.4 ± —[c]
22:5n-3	10.2 ± —	15.9 ± 0.7[a]	13.8 ± 0.5[a,b]	9.9 ± 0.1[b]	12.3 ± 0.7[a,b]	0.9 ± —	1.1 ± —[a]	0.9 ± 0.1[a,b]	0.7 ± —[b]	0.7 ± —[b]
22:6n-3	36.1 ± 0.1	50.8 ± 2.3[a]	43.1 ± 1.6[a,b]	35.2 ± 0.6[b]	42.1 ± 1.9[a,b]	7.2 ± —	8.4 ± 0.1[a]	7.0 ± 0.3[a,b]	7.1 ± 0.1[a,b]	6.9 ± 0.1[b]
Sum n-3	81.4 ± 0.3	141.0 ± 6.2[a]	113.3 ± 3.9[a,b]	83.5 ± 1.1[b]	103.1 ± 5.6[b]	11.0 ± 0.1	14.6 ± 0.2[a]	11.7 ± 0.6[b]	10.2 ± 0.1[b]	10.1 ± 0.2[b]
Sum polyene	94.6 ± 0.3	168.0 ± 7.4	148.2 ± 4.8	130.3 ± 1.5	156.0 ± 6.4	12.0 ± 0.1	15.7 ± 0.2	13.3 ± 0.7	14.0 ± 0.2	13.1 ± 0.1
n-3/n-6	6.9 ± —	5.8 ± —[a]	3.5 ± —[b]	1.8 ± —[c]	2.0 ± 0.1[c]	11.0 ± 0.2	13.6 ± 0.1[a]	7.1 ± 0.1[b]	2.8 ± 0.1[c]	3.3 ± 0.1[c]
Sum total FA	324.5 ± 1.5	698.1 ± 32.2	710.4 ± 17.5	738.4 ± 6.7	707.1 ± 24.3	23.3 ± 0.2	36.7 ± 0.8[a]	39.1 ± 2.8[a]	57.8 ± 2.2[b]	39.7 ± 0.6[a]
Rest FA	7.1 ± —	19.9 ± 0.9	13.4 ± 0.8	5.6 ± —	9.4 ± 0.5	0.6 ± —	0.6 ± —	0.5 ± —	0.3 ± —	0.3 ± —

[a]Compositions given in mg fatty acid g^{-1} sample, wet weight. Data are shown as mean ± SEM. Values <0.1 are represented by an em dash (—).
[b]Superscript roman letters indicate significant differences ($P \leq 0.05$) between the dietary groups for individual fatty acids. Where no letters are present, no significant differences were observed. (Fatty acids tested for significant differences are listed in the Materials and Methods section).

not significantly different from the CO groups. Furthermore, in HDL the levels of n-3 fatty acids in the four dietary groups were not significantly different. The HDL 18:2n-6 levels, however, were six and seven times higher in PO and SF groups compared to the CO group. Thus, the n-3/n-6 ratios were significantly different between the dietary groups. The n-3/n-6 ratio in all tissues analyzed was significantly highest in the CO groups, followed by the COSF; and finally, the SF and PO groups had the lowest n-3/n-6 ratio. The 20:5n-3/22:6n-3 ratios were reversed in all tissues analyzed in all dietary groups, except the PO group, compared to the ratio in the diets.

AD of dietary fatty acids. The AD% was analyzed at the end of the experimental period (Table 5) using yttrium oxide as inert marker (0.01% inclusion level). The general trend was to decreasing AD% with increasing fatty acid chain length and to increasing AD% with increasing desaturation of the fatty acids. However, the dietary SF and PO groups had significantly lower AD% of monoene and n-3 fatty acids. The PO groups had significantly lower AD% of the saturated fatty acids, and especially 16:0 and 18:0 with, respectively, only 15.7 and 22.5 AD%. The dietary CO and COSF groups generally had the same AD% for all fatty acids, whereas the dietary groups with plant oils as dietary oil source, and especially the PO groups, had significantly lower AD% for a large number of fatty acids.

DISCUSSION

Total β-oxidation. The Atlantic salmon tissues were measured for total β-oxidation. However, in both Atlantic salmon (9) and mammals (30) peroxisomal β-oxidation is reported to account for less than 10% of the total β-oxidation. Thus, the β-oxidation measured is predominantly mitochondrial. Lipid catabolism has been shown to provide energy for sustained slow swimming, which is employed by the red muscle fibers. Red muscle was the only tissue in the adult Atlantic salmon with significant β-oxidation capacity, whereas liver and white muscle had negligible or undetectable β-oxidation capacities using the current assay with palmitoyl-CoA as substrate. Red muscle, liver, and heart, but not white muscle, are generally regarded as the most important tissues of fatty acid oxidation

TABLE 4
Red and White Muscle Fatty Acid Composition from the Initial Sampling and from Fish Fed the Experimental Diets for 21 wk[a,b]

	Red muscle (n = 3)					White muscle (n = 3)				
	Initial	Capelin	Capelin/ sunflower	Sunflower	Palm oil	Initial	Capelin	Capelin/ sunflower	Sunflower	Palm oil
14:0	10.2 ± 0.4	11.3 ± 0.1[a]	8.3 ± 0.2[b]	5.3 ± 0.2[c]	5.6 ± 0.3[c]	0.8 ± —	3.4 ± 0.1[a]	2.4 ± 0.1[a,b]	1.4 ± —[b]	1.4 ± 0.1[b]
16:0	28.1 ± 1.1	33.8 ± 0.5[a,c]	28.7 ± 0.8[a,b]	24.5 ± 0.6[b]	38.0 ± 1.5[c]	2.5 ± 0.1	11.0 ± 0.4	9.3 ± 0.6	7.5 ± 0.1	11.4 ± 0.6
18:0	5.6 ± 0.3	6.3 ± 0.2[a]	7.8 ± 0.2[a,c]	9.9 ± 0.2[b]	8.1 ± 0.3[c]	0.5 ± —	2.0 ± 0.1	2.6 ± 0.2	2.9 ± 0.1	2.4 ± 0.1
Sum saturated	45.3 ± 1.8	52.5 ± 0.8[a]	46.5 ± 1.3[a,b]	41.4 ± 1.0[b]	52.3 ± 2.0[a]	3.9 ± 0.2	16.8 ± 0.6[a]	14.8 ± 0.9[b]	12.3 ± 0.2[c]	15.3 ± 0.8[a,b]
16:1n-7	13.1 ± 0.5	16.8 ± 0.2[a]	11.5 ± 0.3[b]	6.7 ± 0.3[c]	7.5 ± 0.4[c]	1.0 ± —	4.8 ± 0.2	3.2 ± 0.2	1.7 ± —	1.9 ± 0.1
16:1n-9	0.6 ± —	0.6 ± —	0.6 ± —	0.7 ± —	0.6 ± —	0.1 ± —	0.2 ± —	0.2 ± —	0.2 ± —	0.2 ± —
18:1n-7	6.8 ± 0.3	8.7 ± 0.2	6.9 ± 0.2	4.6 ± 0.2	4.7 ± 0.2	0.5 ± —	3.0 ± 0.1	2.7 ± 0.2	2.3 ± —	1.8 ± 0.1
18:1n-9	29.3 ± 1.3	40.9 ± 1.3[a]	89.0 ± 2.5[b]	140.3 ± 3.0[c]	65.6 ± 1.8[d]	2.3 ± 0.1	12.0 ± 0.7[a]	26.2 ± 1.8[b]	39.6 ± 1.1[c]	18.3 ± 1.1[a,b]
18:1n-11	3.3 ± 0.1	4.2 ± 0.2	1.6 ± 0.1	—	1.2 ± 0.1	0.2 ± —	0.9 ± —	—	—	—
20:1n-9	20.5 ± 0.8	28.0 ± 0.3	20.0 ± 0.5	15.4 ± 0.8	11.9 ± 0.5	1.5 ± 0.1	8.0 ± 0.3	5.7 ± 0.3	3.9 ± —	2.7 ± 0.2
20:1n-11	2.6 ± 0.1	2.8 ± —	2.0 ± —	1.3 ± 0.1	1.4 ± 0.1	0.2 ± —	0.7 ± —	0.5 ± —	0.2 ± —	0.2 ± —
22:1n-9	2.6 ± 0.1	4.1 ± —	2.7 ± 0.1	1.7 ± 0.1	1.5 ± 0.1	0.2 ± —	1.3 ± 0.1	0.9 ± 0.1	0.4 ± —	0.3 ± —
22:1n-11	22.0 ± 1.0	30.7 ± 0.4[a]	19.0 ± 0.5[b]	9.5 ± 0.6[c]	10.1 ± 0.5[c]	1.5 ± 0.1	8.0 ± 0.3[a]	4.9 ± 0.3[b]	2.0 ± —[c]	2.0 ± 0.1[c]
24:1n-9	1.4 ± 0.1	1.7 ± —	1.5 ± —	1.1 ± —	1.0 ± 0.1	0.1 ± —	0.4 ± —	0.3 ± —	0.2 ± —	0.2 ± —
Sum monoenes	103.3 ± 4.3	140.2 ± 2.5	156.0 ± 4.2	181.6 ± 5.0	106.1 ± 3.3	7.6 ± 0.4	39.7 ± 1.6[a,b]	44.9 ± 2.9[a]	50.8 ± 1.2[a]	27.7 ± 1.7[b]
18:2n-6	6.0 ± 0.2	8.2 ± 0.1[a]	11.9 ± 0.3[b]	16.1 ± 0.4[c]	14.6 ± 0.4[b,c]	0.4 ± —	2.1 ± 0.1[a]	3.0 ± 0.2[a,b]	4.0 ± 0.1[b]	3.7 ± 0.2[b]
20:4n-6	0.9 ± —	0.7 ± —	0.6 ± —	0.6 ± —	0.6 ± —	0.1 ± —	0.3 ± —	0.2 ± —	0.2 ± —	0.2 ± —
Sum n-6	7.7 ± 0.3	9.8 ± 0.2[a]	13.7 ± 0.3[b]	19.5 ± 0.5[c]	17.5 ± 0.5[c]	0.6 ± —	2.6 ± 0.1[a]	3.6 ± 0.2[a,b]	5.0 ± 0.1[b]	4.6 ± 0.2[b]
18:3n-3	1.8 ± 0.1	2.1 ± —	1.5 ± —	1.2 ± 0.1	1.3 ± 0.1	0.1 ± —	0.5 ± —	0.3 ± —	0.2 ± —	0.3 ± —
18:4n-3	3.5 ± 0.1	5.0 ± —	2.9 ± 0.1	1.4 ± 0.1	1.6 ± 0.1	0.3 ± —	1.4 ± —	0.7 ± —	0.3 ± —	0.3 ± —
20:4n-3	3.0 ± 0.1	3.9 ± —[a]	2.9 ± 0.1[b]	1.5 ± 0.1[c]	1.6 ± 0.1[c]	0.2 ± —	1.1 ± —	0.8 ± 0.1	0.3 ± —	0.3 ± —
20:5n-3	14.9 ± 0.5	16.2 ± 0.1[a]	11.4 ± 0.3[b]	7.1 ± 0.3[c]	7.5 ± 0.4[c]	1.3 ± 0.1	4.6 ± 0.1[a]	3.2 ± 0.2[b]	1.7 ± —[c]	1.7 ± 0.1[c]
22:5n-3	6.3 ± 0.2	6.0 ± 0.1[a]	4.9 ± 0.1[b]	3.3 ± 0.2[c]	3.5 ± 0.2[c]	0.5 ± —	1.6 ± —[a]	1.3 ± 0.1[a]	0.7 ± —[b]	0.7 ± —[b]
22:6n-3	22.6 ± 0.7	21.6 ± 0.2[a]	17.6 ± 0.4[b]	14.4 ± 0.6[b]	14.8 ± 0.6[b]	2.0 ± 0.1	6.1 ± 0.2[a]	5.2 ± 0.2[a]	3.7 ± —[b]	3.7 ± 0.2[b]
Sum n-3	53.4 ± 1.8	55.8 ± 0.4[a]	41.8 ± 1.1[b]	28.9 ± 1.2[c]	30.4 ± 1.4[c]	4.5 ± 0.3	15.5 ± 0.5[a]	11.8 ± 0.6[b]	7.1 ± 0.1[c]	7.0 ± 0.4[c]
Sum polyene	62.0 ± 2.1	66.7 ± 0.6[a]	56.3 ± 1.4[a,b]	48.3 ± 1.7[b]	48.2 ± 1.9[b]	5.2 ± 0.3	18.4 ± 0.6[a]	15.6 ± 0.8[a,b]	12.1 ± 0.1[b]	11.6 ± 0.6[b]
n-3/n-6	7.0 ± —	5.7 ± 0.1[a]	3.1 ± —[b]	1.5 ± —[c]	1.7 ± 0.1[c]	7.9 ± 0.1	5.9 ± 0.1[a]	3.3 ± —[b]	1.4 ± 0.1[c]	1.5 ± 0.1[c]
Sum total FA	215.7 ± 8.3	266.4 ± 3.9[a]	262.2 ± 7.0[a]	272.0 ± 7.8[a]	208.7 ± 7.2[b]	17.2 ± 0.9	74.9 ± 2.8	75.3 ± 4.7	75.2 ± 1.5	54.6 ± 3.1
Rest FA	5.1 ± 0.1	7.0 ± 0.1	3.5 ± 0.2	0.7 ± 0.1	2.1 ± 0.1	0.4 ± —	1.8 ± 0.1	1.0 ± 0.1	0.2 ± —	0.3 ± —

[a]Compositions given in mg fatty acid g^{-1} sample, wet weight. Data are shown as mean ± SEM. Values <0.1 are represented by an em dash (—).
[b]Superscript roman letters indicate significant differences ($P \leq 0.05$) between the dietary groups for individual fatty acids. Where no letters are present, no significant differences were observed (fatty acids tested for significant differences are listed in the Materials and Methods section).

in fish (31). However, when analyzing β-oxidation capacity using palmitoyl-L-carnitine and expressing it as activity per tissue, the white muscle is reported to contribute significantly to the overall β-oxidation of fatty acids in adult and post-smolt Atlantic salmon (4). Recent experiments by Frøyland *et al.* (4,9) on β-oxidation in various tissues in adult Atlantic salmon, done after starting the current fish experiment, demonstrated that the substrate used in the assay was significant to the obtained results. When β-oxidation capacities in Atlantic salmon tissues were measured using palmitoyl-L-carnitine as substrate, the results were approximately 2.5-fold higher in red muscle compared to experiments using palmitoyl-CoA as substrate. The measured β-oxidation capacities in liver and white muscle were 5- to 20-fold higher when measured using palmitoyl-L-carnitine compared to palmitoyl-CoA as substrate (4,9). Atlantic salmon post-smolt (weight approximately 400 g) are also reported to have higher β-oxidation capacities in red muscle (twofold), liver (twofold), and white muscle (10-fold) than adult Atlantic salmon (weight approximately 4 kg) (9). Consequently, the use of palmitoyl-CoA as substrate in the current experiment, as well as the high fish weights might explain the relatively low β-oxidation activity in red muscle and the lack of β-oxidation detectability in liver and white muscle. CPT-I in the outer mitochondria membrane converts acyl-CoA to acyl-carnitine (32). This step is essential since acyl-CoA cannot penetrate the inner mitochondrial membrane. By adding palmitoyl-L-carnitine as substrate in the β-oxidation assay, the CPT-I step is avoided, thus this substrate is more readily available for β-oxidation. Since palmitoyl-L-carnitine as substrate results in higher β-oxidation capacity compared to palmitoyl-CoA, this indicates that either the CPT-I activity or the availability of carnitine is rate-limiting for β-oxidation in Atlantic salmon tissues. It can therefore be argued that using palmitoyl-CoA as substrate when measuring mitochondrial β-oxidation gives a more physiologically accurate picture since the probable key point of regulation is included in contrast to using palmitoyl-carnitine as substrate.

Saturated and monoene fatty acids are reported to be preferred substrates, whereas PUFA are reported to be poor sub-

TABLE 5
Apparent Digestibility (%) of Fatty Acids Measured at the End of the Experimental Period[a,b]

	Capelin	Capelin/sunflower	Sunflower	Palm oil
14:0	89.8 ± 0.2[a]	92.2 ± 0.2[a]	83.4 ± 0.9[a]	52.9 ± 2.7[b]
16:0	84.8 ± 0.1[a]	85.0 ± 0.8[a]	76.5 ± 1.3[a]	15.7 ± 4.7[b]
18:0	81.7 ± 0.2[a]	85.8 ± 0.9[a]	72.3 ± 2.1[a]	22.5 ± 4.6[b]
Sum saturated	86.0 ± 0.1[a]	86.3 ± 0.7[a]	74.0 ± 1.4[a]	18.3 ± 4.6[b]
16:1n-7	95.1 ± 0.2[a]	96.6 ± 0.1[a]	89.3 ± 1.0[b]	84.5 ± 0.7[c]
18:1n-7	93.1 ± 0.3[a]	93.7 ± 0.2[a]	73.2 ± 2.4[b]	69.7 ± 2.0[b]
18:1n-9	93.7 ± 0.3[a]	97.1 ± 0.1[a]	94.9 ± 0.6[a]	60.5 ± 1.5[b]
20:1n-9	93.0 ± 0.2[a]	94.5 ± 0.2[a]	84.6 ± 1.2[b]	80.3 ± 1.0[b]
22:1n-11	91.4 ± 0.2[a]	92.9 ± 0.2[a]	88.6 ± 3.4[b]	79.6 ± 1.0[b]
Sum monoenes	92.7 ± 0.2[a]	96.0 ± 0.1[a]	94.2 ± 0.7[a]	62.9 ± 1.4[b]
18:2n-6	89.4 ± 0.3[b]	94.3 ± 0.1[c]	93.6 ± 0.4[b,c]	77.3 ± 1.0[a]
20:4n-6	92.2 ± 0.3	90.9 ± 0.4	—	—
Sum n-6	90.5 ± 0.3[a]	94.1 ± 0.1[a]	93.1 ± 0.4[a]	77.3 ± 1.0[b]
18:3n-3	94.2 ± 0.2[a]	93.8 ± —[a]	84.5 ± 0.9[b]	—
20:5n-3	94.7 ± 0.2[a]	95.0 ± 0.2[a]	84.5 ± 1.2[b]	84.1 ± 0.9[b]
22:5n-3	92.2 ± 0.4[a]	89.9 ± 0.7[a]	70.6 ± 3.3[b]	—
22:6n-3	90.6 ± 0.5[a]	88.2 ± 0.8[a]	68.4 ± 2.4[b]	75.0 ± 1.1[b]
Sum n-3	93.9 ± 0.3[a]	93.2 ± 0.4[a]	77.6 ± 1.7[b]	81.7 ± 0.9[b]
Sum polyene	93.6 ± 0.3[a]	93.6 ± 0.3[a]	86.0 ± 1.0[b]	79.0 ± 0.9[c]
Sum total FA	91.4 ± 0.2[a]	93.7 ± 0.2[a]	90.2 ± 0.5[a]	45.0 ± 2.8[b]

[a]Apparent digestibility calculated accordng to Equation 1. Data are shown as mean ± SEM (n = 3). Values <0.1 are represented by an em dash (—).
[b]Superscript roman letters indicate significant differences ($P \leq 0.05$) between the dietary groups for individual fatty acids. Where no letters are present, no significant differences were observed (fatty acids tested for significant differences are listed in the Materials and Methods section).

strates for mitochondrial β-oxidation in fish red muscle (5,6). The SF diet contained high levels of oleic acid (68.5%), and one could expect that this fatty acid would be selectively β-oxidized *in vivo* since 18:1n-9 are oxidized by mitochondria at relatively high rates *in vitro* (7 and 44% higher than, respectively, 16:0 and 22:6n-3) (6). The β-oxidation capacity in red muscle at the intermediate sampling was higher in the SF groups than in the other dietary treatments, however, not significantly. To increase the total β-oxidation capacity in a tissue, the number of mitochondria, peroxisomes, and enzymes, and/or the enzyme activity has to be increased (33). Certain fatty acids, such as 20:5n-3, have been found to act as a mitochondrial proliferator, thus increasing β-oxidation capacity, whereas prolonged feeding of 22:6n-3 increased peroxisomal β-oxidation capacity in rats (34). This effect of 20:5n-3 and 22:6n-3 was not detected in the groups fed the CO or COSF diets, which contained significantly higher dietary levels of these n-3 fatty acids. The fatty acid 16:0 is considered to be a good substrate for β-oxidation in mammals and fish. The PO group fed high levels of 16:0 (37.8%) and high levels of 18:1n-9 (35.9%) showed no tendency of induced mitochondrial β-oxidation in red muscle. However, when considering the low digestibility of 16:0 in the PO diet (15.7%), the actual amount of 16:0 absorbed by the fish was only 15.5 mg 16:0 per g feed, a lower 16:0 level than in both the CO and COSF diets. Studies done with acyl-carnitine as substrate suggest that 22:1n-11 is selectively utilized as an energy source by fish (7,35) and that 22:1 and 16:0 fatty acids serve equally well as substrates for β-oxidation (36). The CO and COSF diets contain, respectively, high and intermediate levels of 22:1n-11; thus, these diets are thought to contain fatty acids that are preferred substrates for β-oxidation. To detect possible significant differences in tissue β-oxidation capacities between dietary treatments, a diet containing fatty acids that are poor substrates for β-oxidation should be included. Further, high levels of dietary lipids increase fish growth, spare dietary protein, and increase feed efficiency. A dietary fatty acid composition that induces β-oxidation would further increase the protein utilization by selectively providing energy through lipid oxidation, sparing protein for muscle growth. The growth, feed efficiency, and protein utilization were not significantly affected by dietary fatty acid composition during the experimental period. The observed trends, however, indicate that the experimental diets, fed over longer time periods and in life stages with higher growth rates, would probably result in significant differences. Further, when already operating at dietary lipid levels exceeding 30%, the possible effects on β-oxidation capacity of adding dietary fatty acids preferred as substrates for β-oxidation might be masked by high dietary lipid levels. To fully study *in vivo* induction of β-oxidation by dietary fatty acids, factors such as digestibility, transport and absorption of fatty acids into cells have to be taken into account. To achieve conclusive results regarding which fatty acids possibly induce β-oxidation in fish, further *in vitro* experiments would be valuable.

Plasma and lipoprotein composition. It is well established

through studies on mammals that dietary fatty acid composition is important in determining plasma lipoprotein cholesterol concentrations. Saturated fatty acids especially are reported to increase plasma cholesterol levels (37). In this experiment the amount of dietary saturated fatty acids varied from 12.5% in the SF diet to 45.3% in the PO diet. These differences in dietary fatty acid composition did not affect plasma or lipoprotein cholesterol levels in the Atlantic salmon. However, when taking the digestibility of the fatty acids into account (Table 5), the actual amount of 16:0 absorbed from the PO diet is close to the SF dietary 16:0 level. Thus, unaffected salmon plasma cholesterol levels might be due to the low digestibility of the saturated fatty acids especially in the PO groups.

Generally the amounts of cholesterol, protein, and TAG in plasma, VLDL, and LDL increased (not always significantly) from the intermediate to the final sampling, whereas the HDL levels remained unchanged. The fish were unfed 24 h prior to sampling, which probably was too short a time for the fish to totally empty its intestine at the final sampling. Thus, the salmon were not in a postabsorptive phase in the final sampling, giving the higher levels of plasma VLDL and LDL. Plasma HDL levels, however, seem to be unaffected by the feeding status of the fish.

Although the fatty acid composition of the lipoproteins were affected by dietary fatty acid composition, it seems that HDL is especially high in n-3 fatty acids and that this level is independent of dietary fatty acid composition. This is in accordance with previously reported (17) and submitted (Torstensen, B.E., Lie, Ø., and Hamre, K., unpublished data). results on lipoprotein fatty acid composition in Atlantic salmon. These differences in dietary fatty acid response might be related to the different metabolism and site of synthesis of the different lipoproteins (17). HDL is the dominant lipoprotein in Atlantic salmon (17; Torstensen, B.E., Lie, Ø., and Hamre, K., unpublished data), and the plasma fatty acid composition mirrored the HDL fatty acid composition in all dietary groups.

Tissue lipid composition. It is well known that tissues of Atlantic salmon, as well as other fish species, are markedly influenced by dietary fatty acid composition (38–40). However, different Atlantic salmon tissues are affected by dietary fatty acid composition in varying degree (40). Especially belly flap, red and white muscle were affected by dietary fatty acid composition (Figs. 1C and 1D; Tables 3 and 4). Histological studies have shown that belly flaps, the subcutaneous fat layer, and myosepta are the main sites for adipocytes in Atlantic salmon, whereas lipid droplets are found in the endomysium around red muscle fibers (41). Adipocytes and lipid droplets contain considerable amounts of TAG, which have been shown to be more influenced by dietary fatty acid composition than phospholipids (PL) (42). This observation, in addition to some influence on PL fatty acid composition, might to some extent explain the great influence of dietary fatty acids on belly flap, red and white muscle fatty acid compositions. The Atlantic salmon liver was relatively low in lipids (approximately 4%), and the fatty acid composition was less affected by dietary fatty acid composition than muscle and belly flap. A significantly increased liver lipid level (6% lipid) was observed in the SF group (Table 3). A pale-lipid enriched liver in Atlantic salmon is an indication of essential fatty acid deficiency (43). Thus, the minor accumulation of liver lipids in the SF group might be an indication of lipid metabolism imbalance in this dietary group.

AD of fatty acids. To fully evaluate the effects of adding alternative oil sources to salmon feeds it is important also to investigate the effects of different dietary fatty acid compositions on the digestibility of lipids and other feed ingredients. AD% indicates fractional net absorption of the fatty acids from the experimental diets, and it does not account for any variation in dietary intake of lipids ($\mu g\ g^{-1}$ BW d^{-1}) (44). Yttrium oxide is increasingly used as an inert nonabsorbable marker as a preferred alternative over chromium oxide for evaluation of AD (44). AD% of the fatty acids in the groups fed CO, COSF, and SF diets was in the same range as previously reported fatty acid digestibility in Atlantic salmon (19), with CO and COSF groups having somewhat higher AD%. In the groups fed the experimental PO diets, however, the AD was significantly lower for all fatty acids investigated except the n-3 fatty acids. The saturated and n-6 fatty acids especially had low AD in the PO groups. Concomitantly, lipid utilization was significantly lower in the PO group compared to the other dietary groups, probably owing to the significantly lower digestibility of lipids in the PO group. This affected the specific growth rate (SGR) and feed conversion ratio (FCR), however not statistically significantly. This might be due to the short experimental time period and to the fact that the high dietary lipid level (above 30%) allows large variations in lipid digestibility before significant effects are seen in SGR and FCR. Saturated and long-chain monounsaturated fatty acids have lower digestibility in Atlantic salmon (19), cod *(Gadus morhua)* (18), and Arctic charr *(Salvelinus alpinus)* (20). The fatty acid compositions of the PO and SF diet were drastically different from fish oil-based diets. However, the Atlantic salmon managed to digest the SF lipids more efficiently than the high saturated fatty acid PO diet. Ringø (45) found that 18:2n-6 supplementation to formulated feed reduced growth and the lipid and proein digestibility by Arctic charr, possibly by affecting the intestinal bacterial flora (46). The dietary levels of 18:2n-6 were higher in both the SF (7%) and PO (8%) groups compared to the COSF (4%) and CO (2%) groups. However, since the digestibility of 16:0 was particularly low in the PO group, a high load of 16:0 may disturb the overall lipid digestibility in this group, in addition to a negative effect of 18:2n-6 on digestibility in both the SF and PO groups. To fully understand the mechanisms of the effects of dietary fatty acid composition on fatty acid AD in Atlantic salmon, further studies need to be performed.

In conclusion, the different dietary oil sources—CO, SF, COSF, and PO—resulted in diets with significantly different fatty acid compositions. The dietary fatty acid compositions were gradually less reflected by the belly flap, red muscle,

white muscle, VLDL, LDL, liver, plasma and HDL concomitantly with increased liver lipid level in the fish fed the SF diet. Mitochondrial β-oxidation capacity in red muscle was not significantly induced by any of the dietary fatty acid compositions. The fatty acids in the diet based on PO as dietary oil source were poorly digested. Further, the mixture of CO and COSF resulted in a salmon with n-3 white muscle levels similar to the CO group; no negative effects were observed using this oil mixture in the adult Atlantic salmon diet.

ACKNOWLEDGMENTS

This study was supported by NorAqua Innovation AS and the Norwegian Research Council, project number 112317/120. Thu Thao Nguen, Kari Elin Langeland Rød, and Kjersti Ask are acknowledged for technical assistance.

REFERENCES

1. Drevon, C.A. (1992) Marine Oils and Their Effects, *Nutr. Rev. 50,* 38–45.
2. Bilinski, E. (1963) Utilization of Lipids by Fish. I. Fatty Acid Oxidation by Tissue Slices from Dark and White Muscle of Rainbow Trout *(Salmo gairdnerii), Can. J. Biochem. Physiol. 41,* 107–112.
3. Bilinski, E., and Jonas, E.E. (1970) Effects of Coenzyme A and Carnitine on Fatty Acid Oxidation by Rainbow Trout Mitochondria *(Salmo gairdnerii), J. Fish. Res. Bd. Can. 27,* 857–864.
4. Frøyland, L., Madsen, L., Eckhoff, K.M., Lie, Ø., and Berge, R. (1998) Carnitine Palmitoyltransferase I, Carnitine Palmitoyl Transferase II, and Acyl-CoA Oxidase Activities in Atlantic Salmon *(Salmo salar), Lipids 33,* 923–930.
5. Kiessling, K.-H., and Kiessling, A. (1993) Selective Utilization of Fatty Acids in Rainbow Trout (*Onchorhychus mykiss* Walbaum) Red Muscle Mitochondria, *Can. J. Zool. 71,* 248–251.
6. Henderson, R.J. (1996) Fatty Acid Metabolism in Freshwater Fish with Particular Reference to Polyunsaturated Fatty Acids, *Arch. Anim. Nutr. 49,* 5–22.
7. Henderson, R.J., and Sargent, J.R. (1985) Chain Length Specificities of Mitochondrial and Peroxisomal β-Oxidation of Fatty Acids in Livers of Rainbow Trout *(Salmo gairdneri), Comp. Biochem. Biophys. 82B,* 79–85.
8. Rønnestad, I., Finn, R.N., Lein, I., and Lie, Ø. (1995) Compartmental Changes in the Contents of Total Lipid, Lipid Classes and Their Associated Fatty Acids in Developing Yolk-sac Larvae of Atlantic Halibut, *Hippoglossus hippoglossus* (L.), *Aquacult. Nutr. 1,* 119–130.
9. Frøyland, L., Berge, R., and Lie, Ø. (1999) Mitochondrial and Peroxisomal β-Oxidation Capacities in Various Tissues from Atlantic Salmon *(Salmo salar), Aquacult. Nutr.,* in press.
10. Babin, P.J., and Vernier, J.-M. (1989) Plasma Lipoproteins in Fish, *J. Lipid Res. 30,* 467–489.
11. Fernandez, M.J., Soscia, A.E., Sun, G.S., Tosca, M., and McNamara, D.J. (1996) Olive Oil and Rapeseed Oil Differ in Their Effect on Plasma Low-Density Lipoprotein Metabolism in the Guinea-Pig, *Br. J. Nutr. 76,* 869–880.
12. Fernandez, M.L., Vergara-Jimenez, M., Conde, K., and Abdel-Fattah, G. (1996) Dietary Carbohydrate Type and Fat Amount Alter VLDL and LDL Metabolism in Guinea Pigs, *J. Nutr. 126,* 2494–2504.
13. Salter, A.M., Mangiapane, E.H., Bennett, A.J., Bruce, J.S., Billett, M.A., Anderson, K.L., Marenah, C.B., Lawson, N., and White, D.A. (1998) The Effect of Different Dietary Fatty Acids on Lipoprotein Metabolism: Concentration-Dependent Effects of Diets Enriched in Oleic, Myristic, Palmitic and Stearic Acids, *Br. J. Nutr. 79,* 195–202.
14. Asset, G., Staels, B., Wolff, R.L., Baugé, E., Madj, Z., Fruchart, J.C., and Dallongeville, J. (1999) Effects of *Pinus pinaster* and *Pinus koraiensis* Seed Oil Supplementation on Lipoprotein Metabolism in the Rat, *Lipids 34,* 39–44.
15. Temme, E.H.M., Mensink, R.P., and Hornstra, G. (1997) Effects of Medium Chain Fatty Acids (MCFA), Myristic Acid, and Oleic Acid on Serum Lipoproteins in Healthy Subjects, *J. Lipid Res. 38,* 1746–1754.
16. Truswell, A.S., and Choudhury, N. (1998) Monounsaturated Oils Do Not All Have the Same Effect on Plasma Cholesterol, *Eur. J. Clin. Nutr. 52,* 312–315.
17. Lie, Ø., Sandvin, A., and Waagbø, R. (1993) Influence of Dietary Fatty Acids on the Lipid Composition of Lipoproteins in Farmed Atlantic Salmon *(Salmo salar), Fish Physiol. Biochem. 12,* 249–260.
18. Lie, Ø., Lied, E., and Lambertsen, G. (1987) Lipid Digestion in Cod *(Gadus morhua), Comp. Biochem. Physiol. 88B,* 697–700.
19. Sigurgisladottir, S., Lall, S.P., Parrish, C.C., and Ackman, R.G. (1992) Cholestane as a Digestibility Marker in the Absorption of Polyunsaturated Fatty Acid Ethyl Esters in Atlantic Salmon, *Lipids 27,* 418–424.
20. Olsen, R.E., Henderson, R.J., and Ringø, E. (1998) The Digestion and Selective Absorption of Dietary Fatty Acids in Arctic Charr, *Salvelinus alpinus, Aquacult. Nutr. 4,* 13–21.
21. Lied, E., and Lambertsen, G. (1982) Apparent Availability of Fat and Individual Fatty Acids in Atlantic Cod *(Gadus morhua), Fisk. Dir. Skrifter, Ser. Ernæring II,* 63–75.
22. Frøyland, L., Asiedu, D.K., Vaagenes, H., Garras, A., Lie, Ø., Totland, G.K., and Berge, R.K. (1995) Tetradecylthioacetic Acid Incorporated into Very Low Density Lipoprotein: Changes in the Fatty Acid Composition and Reduced Plasma Lipids in Cholesterol-Fed Hamsters, *J. Lipid Res. 36,* 2529–2540.
23. Havel, R.J., Eder, H.A., and Havel, R.J. (1955) The Distribution and Chemical Composition of Ultra-Centrifugally Separated Lipoproteins in Human Sera, *J. Clin. Invest. 34,* 1345–1353.
24. Aviram, A. (1983) Plasma Lipoprotein Separation by Discontinuous Density Gradient Ultracentrifugation in Hyperlipo-proteinemic Patients, *Biochem. Med. 30,* 111–118.
25. Lie, Ø., Sandvin, A., and Waagbø, R. (1994) Transport of α-Tocopherol in Atlantic Salmon *(Salmo salar)* During Vitellogenesis, *Fish Physiol. Biochem. 13,* 241–247.
26. Warnick, G.R., Cheung, M.C., and Albers, J.J. (1979) Comparison of Current Methods for High-Density Lipoprotein Cholesterol Quantitation, *Clin. Chem. 25,* 596–604.
27. Lie, Ø., and Lambertsen, G. (1991) Fatty Acid Composition of Glycerophospholipids in Seven Tissues of Cod *(Gadus morhua),* Determined by Combined High-Performance Liquid Chromatography and Gas Chromatography, *J. Chromatogr. 565,* 119–129.
28. Sandnes, K., Lie, Ø., and Waagbø, R. (1988) Normal Ranges of Some Blood Chemistry Parameters in Adult Farmed Atlantic Salmon, *Salmo salar, J. Fish Biol. 32,* 129–136.
29. Wold, S., Esbensen, K., and Geladi, P. (1987) Principal Component Analysis, *Chemom. Intell. Lab. Syst. 2,* 37–52.
30. Mannaerts, G.P., and Van Veldhoven, P.P. (1993) Metabolic Role of Mammalian Peroxisomes, in *Peroxisomes. Biology and Importance in Toxicology and Medicine* (Gibson, G., and Lake, B., eds.), pp. 19–62, Taylor & Francis, London.
31. Henderson, R.J. and Tocher, D.R. (1987) The Lipid Composition and Biochemistry of Freshwater Fish, *Prog. Lipid Res. 26,* 281–347.
32. Bremer, J. (1997) The Role of Carnitine in Cell Metabolism, in *Carnitine Today* (De Simone, C., and Famularo, G., eds.), pp. 1–38, Landes Bioscience, Austin.
33. Schoonjans, K., Staels, B. and Auwerx, J. (1996) The Peroxi-

some Proliferator Activated Receptors (PPARs) and Their Effects on Lipid Metabolism and Adipocyte Differentiation, *Biochim. Biophys. Acta 1302,* 92–109.
34. Frøyland, L., Madsen, L., Vaagenes, H., Totland, G.K., Auwerx, J., Kryvi, H., Staels, B. and Berge, R.K. (1997) Mitochondrion Is the Principal Target for Nutritional and Pharmacological Control of Triglyceride Metabolism, *J. Lipid. Res. 38,* 1851–1858.
35. Henderson, R.J. and Sargent, J.R. (1982) Peroxisomal Oxidation of Fatty Acids in Livers of Rainbow Trout *(Salmo gairdneri)* Fed Diets of Marine Zooplankton, *Comp. Biochem. Biophys. 73B,* 565–570.
36. Henderson, R.J. and Sargent, J.R. (1985) Fatty Acid Metabolism in Fish, in *Nutrition and Feeding in Fish* (Cowey, C.B., Mackie, A.M., and Bell, J.G., eds.), pp. 349–364, Academic Press, London.
37. Grundy, S.M. and Denke, M.A. (1990) Dietary Influences on Serum Lipids, *J. Lipid. Res. 31,* 1149–1172.
38. Lie, Ø., Waagbø, R. and Sandnes, K. (1988) Growth and Chemical Composition of Adult Atlantic Salmon *(Salmo salar)* Fed Dry Silage Based Diets, *Aquaculture 69,* 343–353.
39. Waagbø, R., Sandnes, K., Sandvin, A. and Lie, Ø. (1991) Feeding Three Levels of n-3 Polyunsaturated Fatty Acids at Two Levels of Vitamin E to Atlantic Salmon *(Salmo salar)*. Growth and Chemical Composition, *Fisk. Dir. Skr., Ser. Ernaering 4,* 51–63.
40. Brodtkorb, B.T., Rosenlund, G. and Lie, Ø. (1997) Effects of 20:5n-3 and 22:6n-3 on Tissue Lipid Composition in Juvenile Atlantic Salmon, *Salmo salar,* with Emphasis on Brain and Eye, *Aquacult. Nutr. 3,* 175–187.
41. Zhou, S., Ackman, R.G. and Morrison, C. (1996) Adipocytes and Lipid Distribution in the Muscle of Atlantic Salmon *(Salmo salar), Can. J. Fish. Aquat. Sci. 53,* 326–332.
42. Olsen, R.E. and Henderson, R.J. (1997) Muscle Fatty Acid Composition and Oxidative Stress Indices of Arctic Charr, *Salvelinus alpinus* (L.), in Relation to Dietary Polyunsaturated Fatty Acid Levels and Temperature, *Aquacult. Nutr. 3,* 227–238.
43. Watanabe, T. (1982) Lipid Nutrition in Fish, *Comp. Biochem. Physiol. 73B,* 3–15.
44. Sugiura, S.H., Dong, F.M., Rathbone, C.K. and Hardy, R.W. (1998) Apparent Protein Digestibility and Mineral Availability in Various Feed Ingredients for Salmonid Feeds, *Aquaculture 159,* 177–202.
45. Ringø, E. (1989) The Effect of Linoleic Acid (18:2n-6) on Lipid and Protein Digestibility and Growth in Arctic charr, *Salvelinus alpinus* (L.), *Physiol. Ecol. Jpn. Spec. 1,* 473–482.
46. Ringø, E. (1993) Does Dietary Linoleic Acid Affect Intestinal Microflora in Arctic Charr, *Salvelinus alpinus* (L.)? *Aquacult. Fish. Manage. 24,* 133–135.

[Received December 9, 1999, and in final revised form April 28, 2000; revision accepted May 3, 2000]

Evidence for the Presence of 1,2-Cyclic Acetal Type *sn*-Glycero-3-phosphoethanolamines in the Sea Anemone, *Actiniogeton* sp.

Ryuichiro Tanaka, Hiroaki Ishizaki, Takahiro Morita, Kazumoto Miyahara, and Naoki Noda*

Faculty of Pharmaceutical Sciences, Setsunan University, Osaka 573-0101, Japan

ABSTRACT: Five 1,2-cyclic acetal-type *sn*-glycero-3-phosphoethanolamines (CGPE) were isolated in a pure state from the sea anemone, *Actiniogeton* sp. (Coelenterata). Their structures, including the absolute configurations, have been determined on the basis of chemical and spectral data to be so-called Feulgen's acetalphosphatides, which have been regarded as artifacts derived from original plasmalogens. We examined whether these CGPE are intact constituents in the animal tissues and obtained reliable confirmation that CGPE are normally present in the sea anemone.

Paper no. L8395 in *Lipids 35,* 665–671 (June 2000).

In 1939, 1,2-cyclic acetal-type glycerophospholipids were first obtained from bovine muscle by Feulgen and Bersin (1). During the structural elucidation of naturally occurring plasmalogens, these compounds have usually been called Feulgen's acetalphosphatide, and they are generally believed to be artifacts derived from the native plasmalogens in the course of isolation procedures, which involves alkaline treatment of a tissue (2,3).

In 1958, Bergmann and Landowne obtained analogous compounds from the sea anemone, *Anthopleura elegantissima* (4) by the use of neutral solvents, and they suggested that at least two types of plasmalogens occur in nature. They did not prove, however, that the compound was naturally present in the sea anemone.

In our systematic survey of the lipid compositions of invertebrates (5–8), we examined a phospholipid fraction from the sea anemone, *Actiniogeton* sp., and isolated five glycerophospholipids in a homogeneous state. Unlike the known constituents of sea anemones, such as phospho-, phosphonosphingolipids (9–11) and cerebrosides (12,13), all five have 1,2-cyclic acetal structures corresponding to the so-called Feulgen's acetalphosphatide.

In this study, we determined the structures of five 1,2-cyclic acetal-type glycerophosphoethanolamines (CGPE), including the absolute configurations, using homogeneous samples. We have made detailed nuclear magnetic resonance (NMR) spectral analyses of the phospholipid fraction, together with a histochemical assay of the tissue (14), and concluded that the CGPE are not artifacts but are natural constituents of the sea anemone.

MATERIALS AND METHODS

Isolation of 1,2-cyclic acetal-type sn*-glycero-3-phosphoethanolamines,* ***1–5***. Whole bodies of the sea anemone, *Actiniogeton* sp. (50 kg), which were collected from the Ariake Sea (Japan) in 1997, were soaked in 10 L of ethanol, then 8 L of chloroform/methanol (1:1, vol/vol), each stage being 7 d at room temperature. The extracts were combined and concentrated *in vacuo* to give a crude extract (570 g). This was shaken with 900 mL of chloroform/methanol/water (1:1:1, by vol). The lower phase gave, on evaporation, a fraction (35 g), which was placed on a silica gel column (Kieselgel 60; Merck, Darmstadt, Germany) and eluted successively with the following solvent systems: chloroform/methanol (20:1 → 10:1 → 8:2, vol/vol) → chloroform/methanol/water (7:3:0.5 → 6:4:1 → 1:2:0.5, by vol) . The eluates were monitored by silica gel thin-layer chromatography (TLC) (Silica gel 60 F_{254}; Merck) using as mobile phase chloroform/methanol/water (6:4:1, by vol). Those eluates showing a positive tailing band on spraying with Dittmer-Lester's reagent (15) were combined and concentrated *in vacuo* to give two phospholipid fractions, fr-a (7 g) and fr-b (4 g). The former was passed through a Sephadex LH-20 column (Pharmacia, Uppsala, Sweden) using chloroform/methanol (3:7, vol/vol) to give three fractions, fr-1 (0.6 g), fr-2 (3.0 g), and fr-3 (3.2 g). Fraction 3 was treated with ether, and the ether layer was subjected to preparative high-performance liquid chromatography (HPLC) on a reversed-phase octadecylsilylated column (ODS; Chemicals Inspection and Testing Institute, Tokyo, Japan; size, 10 mm i.d. × 250 mm × 2 columns) using chloro-

*To whom correspondence should be addressed at Faculty of Pharmaceutical Sciences, Setsunan University, 45-1, Nagaotoge-cho, Hirakata, Osaka 573-0101, Japan. E-mail: noda@pharm.setsunan.ac.jp

Abbreviations: CGPE, cyclic glycerophosphoethanolamine; EI MS, electron impact mass spectrometry; FAB MS, fast atom bombardment mass spectrometry; HMBC, two-dimensional heteronuclear multiple bond connectivity spectroscopy; HPLC, high performance liquid chromatography; NMR, nuclear magnetic resonance; NOESY, two-dimensional nuclear Overhauser effect spectroscopy; ODS, octadecylsilylated; TLC, thin-layer chromatography; TMS, tetramethylsilane.

form/methanol/water (1:9:0.5, by vol) to give a crude CGPE fraction (fr. I, 2.8 g), together with compound **1**. A part of fr. I (0.4 g) was separated by HPLC using chloroform/methanol/water (1:10:1.1, by vol). Fractions corresponding to peaks (I-a–I-d) were collected and were further subjected to HPLC in a recycling mode using chloroform/methanol/water (1:10:1.1, by vol) to furnish five compounds, **1–5**. **1** (80 mg, $[\alpha]_D$ +15.1° at a concentration *c* of 1.5 g/100 mL solvent in chloroform/methanol, 1:1 by vol. Negative ion fast atom bombardment mass spectrometry (FAB MS), *m/z* = 464 $[M - H]^-$). **2** (12 mg, $[\alpha]_D$ +14.2° at *c* of 0.8 g/100 mL in chloroform/methanol, 1:1 by vol. *m/z* = 450 $[M - H]^-$). **3** (20 mg, $[\alpha]_D$ +16.1° at *c* of 0.6 g/100 mL in chloroform/methanol, 1:1 by vol. *m/z* = 436 $[M - H]^-$). **4** (4 mg, $[\alpha]_D$ +2.7° at *c* of 0.1 g/100 mL in chloroform/methanol, 1:1 by vol. *m/z* = 462 $[M - H]^-$). **5** (2 mg, $[\alpha]_D$ +2.7° at *c* of 0.1 g/100 mL in chloroform/methanol, 1:1 by vol. *m/z* = 450 $[M - H]^-$).

A commercial plasmalogen (Sigma Chemical Co., St. Louis, MO) α-L-phosphatidylethanolamine-type plasmalogen) was placed on silica gel and treated with the same separation procedures described above.

NMR spectroscopy. The NMR spectra were recorded at 600 MHz (^{1}H) and 150 MHz (^{13}C) (Omega 600, Fremont, CA) and at 400 MHz (JMN GSX 400, JEOL Ltd., Tokyo, Japan) with tetramethylsilane (TMS) as the internal standard, at a probe temperature of 35°C. The two-dimensional nuclear Overhauser effect (NOESY) spectrum was obtained using a mixing time of 300 ms. The two-dimensional heteronuclear multiple bond connectivity (HMBC) spectrum was recorded at 600 MHz with 32 scans ($^{2,3}J_{CH}$ = 7.0 Hz).

Mass spectrometer. The mass spectra were taken on a JMS DX-300 spectrometer equipped with a JMA 3500 data system (JEOL Ltd.) [FAB MS: accelerating voltage, 3 kV; matrix, triethylene glycol and triethylamine; collision gas, Xe; electron impact mass spectrometry (EI MS): ionization voltage, 30 eV; accelerating voltage, 3 kV].

*Preparation of the dimethyl disulfide derivative of **4***. According to the method reported by Vincenti *et al*. (16), carbon disulfide (0.2 mL) and iodine (1 mg) were added to **4** (1 mg) in dimethyl disulfide (0.2 mL). The mixture was kept at 60°C for 60 h, quenched with a 5% aqueous solution of sodium thiosulfate, and then shaken with chloroform/methanol (1:1, vol/vol, 3 mL). The lower phase was evaporated under a nitrogen stream, and the residue was subjected to analysis by EI MS spectrometry.

*Syntheses of four stereoisomers, **6–9***. Stearyl aldehyde (3.5 g) was dissolved in benzene (100 mL). (*R*)-3-Chloro-1,2-propanediol acetonide (6 mL, Azmax Co. Ltd. Kisarazu, Japan) and *p*-toluenesulfonic acid (100 mg) were added to the solution and heated at 55°C for 2.5 h. The reaction mixture was poured into ice water and shaken. The benzene layer was collected and concentrated *in vacuo* to give a fraction that was subjected to column chromatography on silica gel to give a mixture of two stereoisomers (3.2 g). They were separated by preparative HPLC (ODS; GL Science Inc., Tokyo, Japan; 20 mm i.d. × 25 cm, methanol) to give two 2*R*-derivatives, **6** and **7**. (*S*)-3-Chloro-1,2-propanediol acetonide was treated in the same manner as described above to yield two 2*S*-derivatives, **8** and **9**. **6** (2*R*, 1′*R* form, m.p. 43.2–45.0°C. $[\alpha]_D$ +17.0° at a *c* of 2.0 g/100 mL in chloroform. EI MS *m/z* = 360 $[M]^{\cdot+}$). **7** (2*R*, 1′*S* form, m.p. 38.0–40.2°C. $[\alpha]_D$ +21.9° at a *c* of 2.0 g/100 mL in chloroform. *m/z* = 360 $[M]^{\cdot+}$). **8** (2*S*, 1′*R* form, m.p. 43.5–44.3°C. $[\alpha]_D$ −20.7° at a *c* of 2.0 g/100 mL in chloroform). **9** (2*S*, 1′*S* form, m.p. 46.2–46.5°C. $[\alpha]_D$ −19.9° at a *c* of 2.0 g/100 mL in chloroform).

*Preparation of **10***. Compound **6** was dissolved in 1% KOH in methanol/water (4:1, vol/vol, 10 mL) and refluxed for 10 h to give 3-OCH_3 derivative (**10**). **10** $[\alpha]_D$ +9.8° at a *c* of 0.8 g/100 mL in chloroform. *m/z* = 356 $[M]^{\cdot+}$.

*Preparation of **10** from **1***. Compound **1** (42 mg) was dissolved in 1.5% $Ba(OH)_2$ in *n*-hexane/methanol/water (1:1:1, by vol, 4.5 mL), and the mixture was refluxed for 3 h. After removal of the *n*-hexane layer, *n*-hexane (1.5 mL) was added to the remaining solution, and it was refluxed again for 3 h. The *n*-hexane layers were combined and the solvent evaporated under a nitrogen stream to give a dephosphorylated product (25.4 mg). This product was methylated by the Hakomori method (17), and the product was subjected to silica gel column chromatography with *n*-hexane/ethyl acetate (20:1, vol/vol) to give **10** (9.2 mg, $[\alpha]_D$ +10.2° at a *c* of 0.9 g/100 mL in chloroform).

Histochemical assay. Frozen sea anemone tissues were sectioned at 5–8 μm and were treated according to the modified Feulgen-Voit method reported by Hayes (18).

RESULTS AND DISCUSSION

Isolation of five 1,2-cyclic acetal-type sn*-glycero-3-phosphoethanolamines, **1–5***. The total sea anemone lipid fraction obtained by the method of Folch *et al*. (19) was subjected to a combination of Sephadex LH-20 and silica gel column chromatographies with various solvent systems to give a crude phospholipid fraction (Fig. 1). The final purification was achieved by mean of preparative HPLC under a recycling mode to give five CGPE **1–5** (Scheme 1). Each exhibited a single $[M - H]^-$ ion peak in its negative ion FAB MS spectra, and no other $[M - H]^-$ ion peak due to analogous compounds. These observations showed that all were homogeneous compounds.

^{1}H and ^{13}C NMR spectroscopy. The ^{1}H NMR spectrum of **1** showed signals due to a saturated carbon chain and a phosphoethanolamine group, together with signals, 1-H_2 (*dd*, δ 3.68 and 4.13) and 2-H (*m*, δ 3.92), of a glycerol moiety. In addition, a characteristic double doublet signal ascribable to an acetal proton was observed at δ 4.98. In the ^{13}C NMR spectrum, the signals of 1-C, 2-C, and 3-C due to the glycerol unit as well as two methylene carbon signals of the ethanolamine group appeared as doublets owing to coupling with ^{31}P (7). Furthermore, the signal of the acetal carbon was observed at δ 105.0. Its HMBC spectrum showed long-range correlation peaks between the acetal proton (1′-H) and two carbons (1-C and 2-C of the glycerol unit). From the information obtained above, compound **1** was defined as 1,2-cyclic

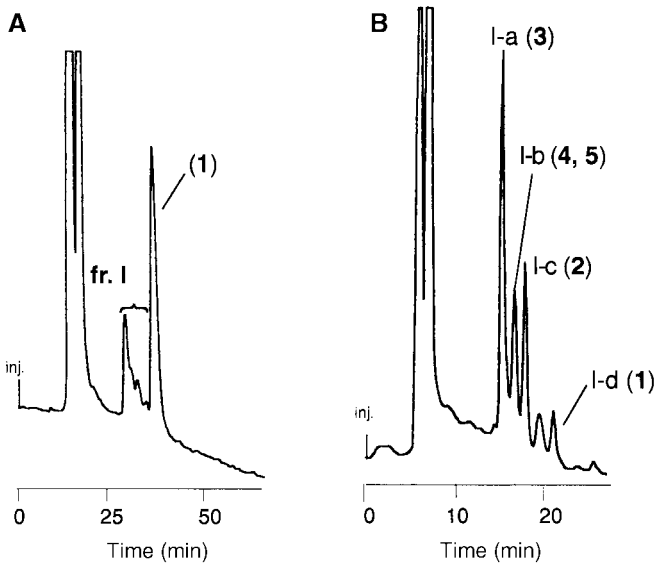

FIG. 1. High-performance liquid chromatography of cyclic glycerophosphoethanolamine. For description of fraction nomenclature see the Materials and Methods section, first paragraph. Column: L-column (10 × 250 mm) × 2; refractive index detector. (A) Solvent: $CHCl_3$/MeOH/H_2O, 1:9:0.5 by vol, 2.0 mL/min. (B) Solvent: $CHCl_3$/MeOH/H_2O, 1:10:1.1, by vol, 2.5 mL/min.

acetal glycero-3-phosphoethanolamine with a C_{18} straight carbon chain.

Determination of the absolute configuration. Compound **1** showed specific rotation, $[\alpha]_D$ + 15.1°. The NOESY spectrum of **1** exhibited a clear NOE correlation between 1′-H and 2-H, suggesting that the stereochemistry between 1′-H and 2-H is *cis*, namely, 2*R*,1′*R* or 2*S*,1′*S* configuration. From this finding, in conjunction with the fact that 2-C of the glycerol moiety of natural glycerophospholipid commonly has the *R* configuration, 1′-C was considered to be *R* configuration.

For confirmation of the above hypothesis, four stereoisomers, **6**–**9**, were synthesized using the starting materials, (*R*)- and (*S*)-3-chloro-1,2-propanediol acetonides (Scheme 2).

The ^{1}H NMR spectrum of **6** (2*R*,1′*R*) showed, when compared with that of **1**, quite similar chemical shifts and coupling patterns attributable to 1′-H and 2-H of **6** to those of **1** (Table 1). In the NOESY spectrum of **6**, a NOE correlation between 1′-H and 2-H similar to that of **1** was observed (Scheme 3). In contrast, compound **7** (2*R*,1′*S*) gave no correlation peak between 1′-H and 2-H in its NOESY spectrum. These facts exclude the possibilities of 2*R*,1′*S* or 2*S*,1′*R* structures, and therefore **1** was concluded to have 2*R*,1′*R* or 2*S*,1′*S* configuration. The final discrimination between 2*R*,1′*R* and 2*S*,1′*S* was achieved by comparing the specific rotation value.

Treatment of **6** with 1% KOH in methanol/water (4:1, vol/vol) for 10 h yielded **10** ($[\alpha]_D$ +9.8°). In addition, when **1** was refluxed with 1.5% $Ba(OH)_2$ in 50% methanol/*n*-hexane (2:1, vol/vol), and the lyso product formed methylated according to the Hakomori method to give a 3-OCH_3 derivative, it showed almost the same specific rotation ($[\alpha]_D$ +10.2°) as that of **10** (Scheme 2). On the basis of the results described above, the stereochemistry of **1** was concluded to be 2*R*,1′*R*.

*Structures of **2**–**5***. The structures of **2**–**5** were elucidated in the same manner as described for **1**, and their spectral data revealed that they have the same 1,2-cyclic acetal structures as **1**, and that they differ only in the long carbon-chain structure. Among these, compound **4** has a double bond in the carbon chain. The position of the double bond was determined according to the method of Vincenti *et al*. (16) with compound **4** converted into a dimethyl disulfide derivative. Its EI MS spectrum gave a diagnostically important fragment ion peak at *m/z* = 174 ($C_{10}H_{22}S$), which was regarded as due to the fragment ion peak produced by cleavage between the 9′-C and 10′-C sulfided carbons. The geometry of the double bond was assigned as *cis,* based on the coupling constants of 9′-H and 10′-H, together with the chemical shifts of the allylic carbons, 8′-C and 11′-C (δ 27.6, 27.8) (Table 2) (20). Taking account of the fact that the signals of 2-H and 1′-H showed almost the same chemical shifts and coupling patterns as those of **1**, and the same specific rotation signs, all were considered to have 2*R*,1′*R* configurations.

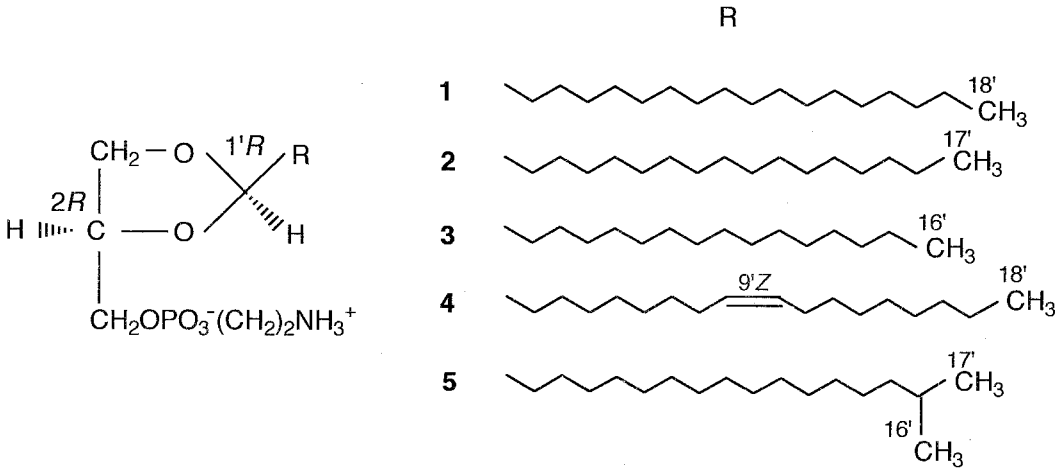

SCHEME 1

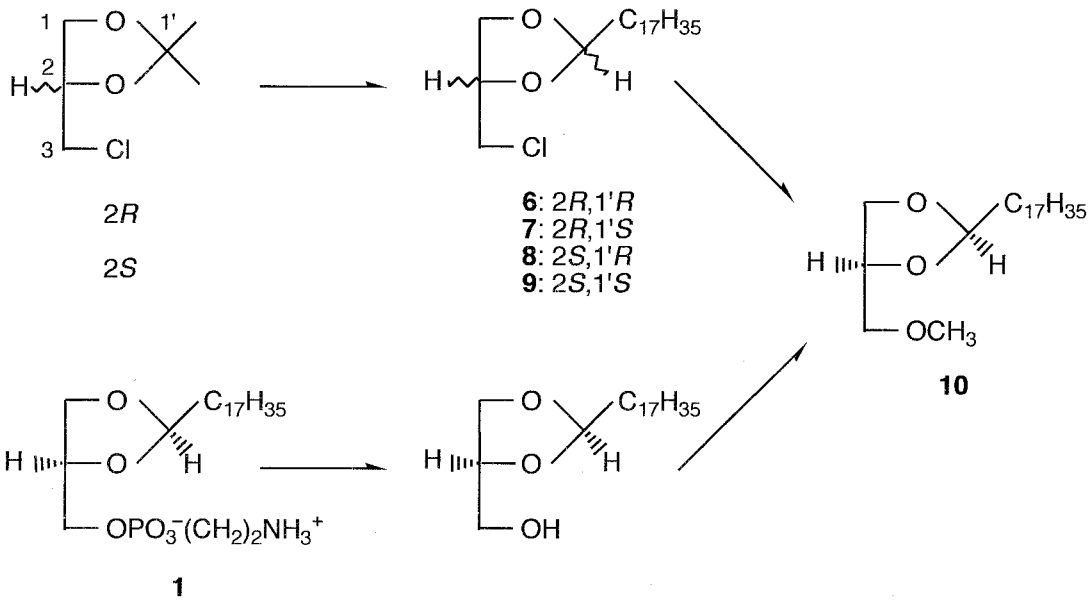

SCHEME 2

^{1}H NMR examination of the total lipid fraction obtained from fresh tissue. Live sea anemone materials were freeze-dried and then soaked in chloroform/methanol (1:1, vol/vol) at –5°C for 1 d. The solvent was added to water and shaken. A lower phase was collected and shaken with *n*-hexane. The lower phase was then concentrated to give a crude phospholipid fraction. This fraction showed no spot corresponding to that of the commercial plasmalogen on TLC. Moreover, its ^{1}H NMR spectrum showed the characteristic double doublet signal due to the acetal proton at δ 4.99, but no diagnostically important signal (*ca.* δ 5.9) ascribable to the vinyl proton of the native plasmalogen appeared (Fig. 2).

Formation of 1,2-cyclic acetal. The commercial plasmalogen was placed on silica gel and treated with the same isola-

TABLE 1
^{1}H Nuclear Magnetic Resonance (NMR) Chemical Shifts[a] of 1–10

	1	**2**	**3**	**4**	**5**
1-H_a	3.68 (*dd, J* = 6.5, 9.0)	3.71 (*dd, J* = 6.5, 9.0)	3.71 (*dd, J* = 6.5, 9.0)	3.72 (*dd, J* = 6.5, 9.0)	3.72 (*dd, J* = 6.5, 9.0)
1-H_b	4.13 (*dd, J* = 6.5, 9.0)	4.15 (*dd, J* = 6.5, 9.0)	4.14 (*dd, J* = 6.5, 9.0)	4.18 (*dd, J* = 6.5, 9.0)	4.18 (*dd, J* = 6.5, 9.0)
2-H	4.28 (*m*)	4.29 (*m*)	4.29 (*m*)	4.29 (*m*)	4.27 (*m*)
3-H_2	3.92 (*m*)	3.93 (*m*)	3.92 (*m*)	3.93 (*m*)	3.93 (*m*)
1′-H	4.98 (*dd, J* = 5.0, 5.0)	4.99 (*dd, J* = 5.0, 5.0)	4.99 (*dd, J* = 5.0, 5.0)	4.99 (*dd, J* = 5.0, 5.0)	4.98 (*dd, J* = 5.0, 5.0)
2′-H_2	1.61 (*m*)	1.60 (*m*)	1.60 (*m*)	1.62 (*m*)	1.61 (*m*)
9′-, 10′-H	NA	NA	NA	5.39 (*m*)	NA
8′-, 11′-H_2	NA	NA	NA	1.99 (*m*)	NA
15′-H	NA	NA	NA	NA	1.46 (*m*)
CH_3	0.88 (*t, J* = 7.0)	0.89 (*t, J* = 7.0)	0.89 (*t, J* = 7.0)	0.89 (*t, J* = 7.0)	0.89 (*d, J* = 7.0)
1″-H_2	4.09 (*m*)	4.07 (*m*)	4.07 (*m*)	4.07 (*m*)	4.07 (*m*)
2″-H_2	3.15 (*m*)	3.14 (*m*)	3.13 (*m*)	3.13 (*m*)	3.13 (*m*)

	6, 9	**7, 8**	**10**
1-H_a	3.72 (*dd, J* = 6.0, 9.0)	3.95 (*m*)	3.63 (*dd, J* = 6.0, 9.0)
1-H_b	4.20 (*dd, J* = 6.0, 9.0)	3.95 (*m*)	4.12 (*dd, J* = 6.0, 9.0)
2-H	4.30 (*m*)	4.25 (*m*)	4.25 (*m*)
3-H_a	3.50 (*dd, J* = 7.5, 11.0)	3.42 (*dd, J* = 7.5, 11.0)	3.42 (*dd, J* = 7.5, 11.0)
3-H_b	3.63 (*dd, J* = 4.5, 11.0)	3.55 (*dd, J* = 4.5, 11.0)	3.49 (*dd, J* = 4.5, 11.0)
1′-H	5.02 (*dd, J* = 5.0, 5.0)	4.91 (*dd, J* = 5.0, 5.0)	4.98 (*dd, J* = 5.0, 5.0)
2′-H_2	1.62 (*m*)	1.62 (*m*)	1.62 (*m*)
18′-CH_3	0.88 (*t, J* = 7.0)	0.88 (*t, J* = 7.0)	0.88 (*t, J* = 7.0)
OCH_3			3.39 (*s*)

[a]δ in ppm from tetramethylsilane (TMS) (splitting patterns and coupling constants, *J*, in Hz). **1–5** were dissolved in $CDCl_3/CD_3OD$ (1:1, vol/vol) and **6–10** were dissolved in $CDCl_3$. NA, not assignable due to overlapping. See Schemes 1 and 2 for chemical structures of **1–10**.

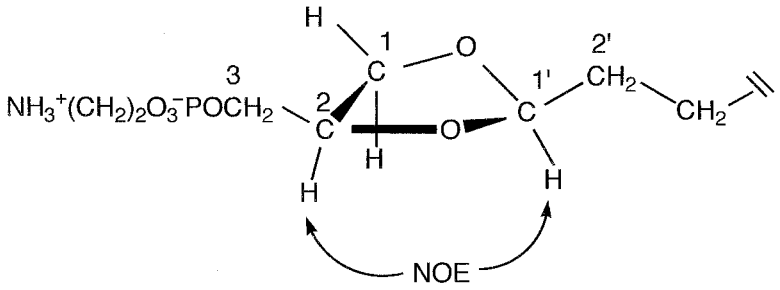

SCHEME 3

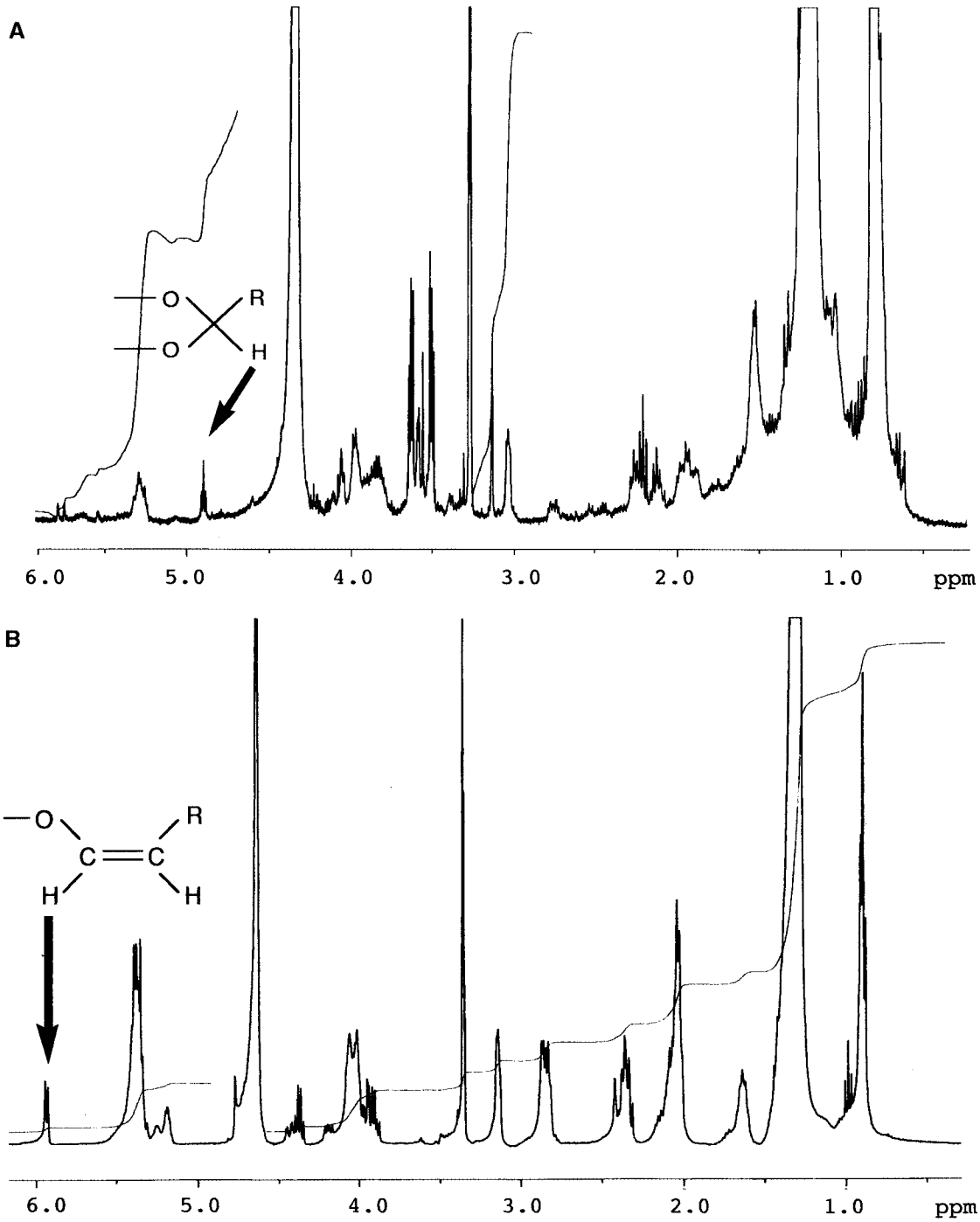

FIG. 2. ^{1}H nuclear magnetic resonance spectra of the phospholipid fraction obtained from *Actiniogeton* sp. (A) and commercial plasmalogen (B).

TABLE 2
^{13}C NMR Chemical Shifts[a] of 1–9

Carbon no.	1	2	3	4	5	6, 9	7, 8
1	67.2	67.4	67.5	67.6	67.6	68.8	68.2
2	74.7	75.0	75.1	75.2	75.2	75.0	75.4
3	66.0	66.0	66.1	66.2	66.1	44.3	44.5
1′	105.0	105.2	105.0	105.2	105.2	105.5	105.9
2′	34.2	34.4	34.4	34.4	34.4	34.0	34.1
9′, 10′	NA	NA	NA	130.1, 131.0	NA	NA	NA
8′, 11′	NA	NA	NA	27.6, 27.8	NA	NA	NA
1″	61.9	61.9	62.0	62.2	62.1		
2″	40.7	40.9	41.1	41.2	41.1		
CH_3	14.1	14.2	14.2	14.2	14.2	14.1	14.1

[a]δ in ppm from TMS. **1–5** were dissolved in $CDCl_3/CD_3OD$ (1:1, vol/vol) and **6–9** were dissolved in $CDCl_3$. For abbreviations see Table 1. For structures of **1–9** see Schemes 1 and 2.

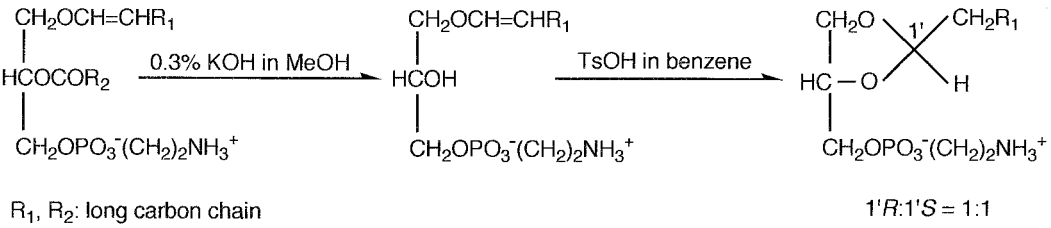

SCHEME 4

tion procedures to give a product. The ^{1}H NMR spectrum of the product was identical with that of the starting material. Then, it was refluxed with 0.3% KOH in methanol for 3 h to afford a lyso product which was refluxed with benzene for 30 min in the presence of *p*-toluenesulfonic acid to give a product that showed two characteristic signals in the ^{1}H NMR spectrum attributable to the acetal protons at δ 4.8 and 5.0 (ratio of the peak intensity, *ca.* 1:1). Table 1 shows that the acetal proton signal of the 2*R*,1′*S* form appears at a higher field than that of 2*R*,1′*R* form. It was concluded that this product was the mixture of 2*R*,1′*S* and 2*R*,1′*R* forms in the ratio of 1:1 (Scheme 4). This finding demonstrated that a lyso plasmalogen having an *sn*-2 free hydroxyl group is required as an intermediate for conversion of a plasmalogen into a 1,2-cyclic acetal compound.

Histochemical assay with the plasmal reagent. Fresh tissues prepared from bovine brain could be stained with an appropriate histochemical reagent (18); in contrast, the sliced tissues of the sea anemone, as well as compound **1**, did not stain on treatment under the same conditions. This observation showed that **1** released no fatty aldehyde on treatment with mercuric chloride.

In conclusion, five CGPE were obtained from the sea anemone, *Actiniogeton* sp. The structures of all were assigned to the 2*R*,1′*R* cyclic acetal type *sn*-glycero-3-phosphoethanolamines based on the NMR spectral analyses and chemical synthesis.

Currently there is a general conception that 1,2-cyclic acetal-type glycerophospholipids are formed during the course of isolation procedures, and hence that they are artifacts derived from native ethanolamine or choline plasmalogens. Contrary to the above conception, we have concluded from our results that the CGPE are actually present in the live sea anemone.

ACKNOWLEDGMENTS

The authors thank Dr. Hiroomi Uchida of the Laboratory of Sabiura Marine Garden, Wakayama, for identification of the sea anemone. Thanks are also due to Dr. Masatoshi Nishi and Mr. Shoji Yamaguchi of this university for the measurements of NMR and MS spectra. We are indebted to Dr. Kiyokazu Ozaki and Dr. Toshiyuki Takagi of this university for their valuable discussion. This work was financially supported by a Grant-in-Aid for Scientific Research (No. 10672013) from the Ministry of Education, Science, Sports and Culture.

REFERENCES

1. Feulgen, R., and Bersin, T. (1939) Zur Kenntnis des Plasmalogens. IV. Eine neuartige Gruppe von Phosphatiden (acetal Phosphatide), *Z. Physiol. Chem. 260,* 217–245.
2. Debuch, H., and Seng, P. (1972) The History of Ether-Linked Lipids Through 1960, in *Ether Lipids* (Snyder, F., ed.) pp. 1–13, Academic Press, New York.
3. Papport, M.M. (1984) The Discovery of Plasmalogen Structure, *J. Lipid Res. 25,* 1522–1527.
4. Bergmann, W., and Landowne, R.A. (1985) Contributions to the Study of Marine Products. XLVI. Phospholipids of a Sea Anemone, *J. Org. Chem. 23,* 1241–1245.

5. Noda, N., Tsunefuka S., Tanaka, R., and Miyahara K. (1992) Isolation and Characterization of Eight 1-*O*-Alkyl-*sn*-glycero-3-phosphocholines from the Crude Drug "Jiryu," the Earthworm, *Pheretima asiatica*, *Chem. Pharm. Bull. 40,* 2756–2758.
6. Noda, N., Tanaka, R., Miyahara, K., and Kawasaki, T. (1992) Two Novel Galactosylceramides from *Marphysa sanguinea*, *Tetrahedron Lett. 33,* 7527–7530.
7. Noda, N., Tanaka, R., Miyahara, K., and Kawasaki, T. (1993) Isolation and Characterization of a Novel Type of Glycosphingolipid from *Neanthes diversicolor*, *Biochim. Biophys. Acta 1169,* 30–38.
8. Noda, N., Tanaka, R., Miyahara, K., and Sukamoto. T. (1996) Six Trigalactosylceramides from the Leech (*Hirudo nipponica*), *Chem. Pharm. Bull. 44,* 895–899.
9. Simon, G., and Rouser, G. (1966) Phospholipids of the Sea Anemone. Quantitative Distribution; Absence of Carbon-Phosphorus Linkages in Glycerol Phospholipids. Structural Elucidation of Ceramide Aminoethylphosphonate, *Lipids 2,* 55–59.
10. Mason, W.T. (1972) Isolation and Characterization of the Lipids of the Sea Anemone, *Metridum senile*, *Biochim. Biophys. Acta 280,* 538–544.
11. Karlsson, K.A., and Samuelsson, B.E. (1974) The Structure of Ceramide Aminoethylphosphonate from the Sea Anemone, Metridium Senile, *Biochim. Biophys. Acta 337,* 204–213.
12. Karlsson, K.A., Leffler, H., and Samuelsson, BO.E. (1979) Characterization of Cerebroside (monoglycosylceramide) from the Sea Anemone, *Metridium senile*. Identification of the Major Long-chain Base as an Unusual Dienic Base with a Methyl Branch at a Double Bond, *Biochim. Biophys. Acta 574,* 79–93.
13. Sugita, M., Aoki, K., Sakata, A., and Hori, T. (1994) Glycosphingolipids in Coelenterata: Characterization of Cerebrosides from the Sea Anemone, *Actiniogeton* sp., *Memoirs of the Faculty of Education Shiga University, Natural Science and Pedagogic Science 44,* 25–30.
14. Feulgen, R., and Voit, K. (1924) Über einen weitverbreiteten festen Aldehyd. Seine Entstehung aus einer Vorstufe, sein mikrochemisher und mikroskopisch-chemischer Nachweis und die Wege zu seiner präparativen Darstellung, *Pflügers Arch. Gesamte Physiol. 206,* 26–47.
15. Dittmer, J.C., and Lester, R.L. (1964) Specific Spray for the Detection of Phospholipids on Thin-layer Chromatograms, *J. Lipid Res. 5,* 126–127.
16. Vincenti, M., Guglielmetti, G., Cassani, G., and Tonini, C. (1987) Determination of Double Bond Position in Diunsaturated Compounds by Mass Spectrometry of Dimethyl Disulfide Derivatives, *Anal. Chem. 59,* 694–699.
17. Hakomori, S. (1964) A Rapid Permethylation of Glycolipid, and Polysaccharide Catalyzed by Methylsulfinyl Carbanion in Dimethyl Sulfoxide, *J. Biochem. (Tokyo) 55,* 205–208.
18. Hayes, R.E. (1949) A Rigorous Re-definition of the Plasmal Reaction, *Stain Technology 24,* 19–23.
19. Folch, B.J., Lees, M., and Sloane Stanley, G.H. (1957) A Simple Method for the Isolation and Purification of Total Lipids from Animal Tissues, *J. Biol. Chem. 226,* 497–501.
20. Fusetani, N., Yasumuro, K., and Matsunaga, S. (1989) Haliclamines A and B, Cytotoxic Macrocyclic Alkaloids from a Sponge of the Genus *Haliclona*, *Tetrahedron Lett. 30,* 6891–6894.

[Received November 22, 1999, and in revised form February 14, 2000; revision accepted March 17, 2000]

Preparation of Functional Liposomes with Peptide Ligands and Their Binding to Cell Membranes

Nobuhiro Yagi[a,b], Yoshikatsu Ogawa[a], Masato Kodaka[a,*], Tomoko Okada[a], Takenori Tomohiro[a], Takeo Konakahara[b], and Hiroaki Okuno[a]

[a]Biomolecules Department, National Institute of Bioscience and Human-Technology, Ibaraki 305-8566, Japan, and [b]Faculty of Industrial Science and Technology, Science University of Tokyo, Chiba 278–8510, Japan

ABSTRACT: Two novel lipopeptides, which have the peptide ligands [α-melanocyte stimulating hormone (α-MSH)] sequence and repeated [Gly-Arg-Gly-Asp-Se (GRGDS) sequence], are designed, synthesized by the solid-phase method, and introduced into liposome membranes by the freeze–thaw method. These liposomes bearing the peptide ligands on their surface are expected to bind to cell membranes. We have confirmed that the lipopeptides are introduced into liposome membranes almost quantitatively, while such a high degree of incorporation has not been accomplished in conventional methods. In this respect, the present method is superior to prepare surface-modified liposomes that are applicable to drug carriers and so on. We have also confirmed by using immunoelectron microscopy that the peptide ligands are actually located in an aqueous phase. It has been shown by flow cytometry that the liposome bearing α-MSH peptide ligand binds to B16 cells and the liposome bearing the repeated GRGDS sequence binds to NIH3T3 cells.

Paper no. L8373 in *Lipids 35,* 673–679 (June 2000).

Though liposomes have been extensively studied as promising carriers of drugs (1), proteins (2), and DNA (3–5) for drug delivery systems (DDS), one of the major problems in using liposomes for DDS is their nonspecificity of delivery, which is the result of the entrapment of liposome by reticuloendothelial systems (6). Another type of drug carrier is a virus, which is used as a vector in the field of gene therapy (7). In spite of their prominent function as a drug carrier, problems endangering vital functions have not been fully solved yet, and therefore their clinical usage is restricted. In contrast to viruses, liposomes have superior points in safety and reproducibility if their specificity can be improved. Many studies have been undertaken to provide liposome with the binding specificity to cells. There are examples in which the liposome surface has been equipped with a glycolipid (8), transferrin (9), or an antibody (10,11) as a binding anchor to cells. Peptides seem to be the most suitable among various ligand candidates (12–14), because information about amino acid sequences of ligands and corresponding receptors can be easily obtained and synthetic methods have been well investigated (15). In usual methods like the "succinimide method" (10), peptides are reacted with lipids already incorporated into a liposome membrane. With these techniques, however, it is very difficult to modify the surface of liposomes at high density because the reaction is inhibited by steric repulsion between liposome surface and peptide parts. To solve this problem, we have developed a new method to modify the liposome surface efficiently and quantitatively using peptide ligands (16). Lipopeptide composed of peptide and lipid parts is chemically synthesized in advance and then is incorporated into liposome bilayer membrane at the same time that liposome is prepared. A notable feature of this method is the synthesis of lipopeptide by a solid-phase method. Namely, peptide ligands bound to resin are prepared first, then coupled with a lipid portion in the solid state; finally, the resultant lipopeptides are removed from the resin simultaneously with deprotecting reactions of the side chains. In the present study, two types of peptide sequences, α-melanocyte-stimulating hormone (α-MSH) (17) and cell adhesion sequence of fibronectin [*viz.*, [Gly-Arg-Gly-Asp-Se (GRGDS) sequence] (18), are used; their structures and properties are well known as ligands to receptors of cell membrane.

*To whom correspondence should be addressed at Biomolecules Department, National Institute of Bioscience and Human-Technology, 1-1 Higashi, Tsukuba, Ibaraki 305-8566, Japan.
E-mail: kodaka@nibh.go.jp

Abbreviations: BSA, bovine serum albumin; Ch, cholesterol; CMF, calcium magesium free; DDS, drug delivery system; DIPCI, *N,N′*-diisopropylcarbodiimide; DMAP, 4-dimethylaminopyridine; DMEM, Dulbecco's modified Eagle's medium; DMF, *N,N*-dimethylformamide; EDT, 1,2-ethanedithiol; EPC, egg phosphatidylcholine; FITC-PE, *N*-fluorescein-5-thiocarbamoyl-1,2-dihexadecanoyl-*sn*-glycerol-3-phosphoethanolamine; Fmoc, 9-fluorenylmethyloxycarbonyl; GRGDS sequence, cell adhesion sequence of fibromectin; HOBt, 1-hydroxybenzotriazole; HPLC, high-performance liquid chromatography; HRP, horseradish peroxidase; KLH, keyhole limpet, hemocyanin; MALDI-TOFMS, matrix-assisted laser desorption/ionization time of flight mass spectrum; α-MSH, α-melanocyte-stimulating hormone; NMP, NMP, *N*-methylpyrrolidone; NMR, nuclear magnetic resonance; PBS, phosphate-buffered saline; TFA, trifluoroacetic acid; WSCD, 1-ethyl-3-(3-dimethylaminopropyl)-carbodiimide hydrochloride.

EXPERIMENTAL PROCEDURES

Chemicals. Fmoc (9-fluorenylmethyloxycarbonyl) amino acids and trifluoroacetic acid (TFA) were purchased from Watanabe Chemical Ind. (Hiroshima, Japan). TGR-resin for peptide synthesis was commercially available from Calbiochem Novabiochem Corp (La Jolla, CA). Egg phosphatidylcholine (EPC) was purchased from Avanti Polar Lipids (Birmingham, AL). All other reagents were of the highest grade commercially available.

Instruments. Proton nuclear magnetic resonance (NMR) spectra were recorded at 270 MHz on a JEOL JNM EX-270 FT spectrometer (Tokyo, Japan). Matrix assisted laser desorption/ionization time of flight mass spectra (MALDI-TOFMS) were acquired on a Kratos Analytical Kompact Maldi III spectrometer (Kyoto, Japan), and fast atom bombardment mass spectra were measured on a JEOL JMS-SX102A mass spectrometer. Peptides were prepared with a PerSeptive Pioneer peptide synthesizer (Foster, CA). Fluorescence emitted from cells was analyzed by a Coulter Epics Elite flow cytometer (Hialeah, FL). Morphology of the liposomes was observed under a Hitachi H-7000 electron microscope operated at 75 kV (Tokyo, Japan).

Syntheses. (i) W5GRGDS. The peptide on TGR-resin was synthesized by the Fmoc solid-phase method (19). To obtain free peptide W5GRGDS (Fig. 1), the peptide-resin (0.1 mmol) was treated with a mixture of TFA (5.0 mL), 1,2-ethanedithiol (EDT) (125 μL), thioanisole (125 μL), and water (250 μL). After the mixture had reacted at room temperature for 5 h, it was filtered and cold diethyl ether (volume of more than 50 times) was added to the filtrate to obtain white precipitates. After the precipitate was isolated by centrifugation (3000 rpm, 30 min) and dried *in vacuo*, it was purified by high-performance liquid chromatography (HPLC) and the isolated fraction was lyophilized. Yield: 90 mg (37.8%, 37.8 μmol). Retention time in HPLC [YMC-Pack ODS-AM (YMC Co., Ltd., Kyoto, Japan), ϕ: 4.6 × 250 mm, TFA (0.08% in water)/acetonitrile from 100:0 to 70:30 over 25 min, flow rate: 0.8 mL/min]: 18.3 min. ^{1}H NMR (D_2O) δ 7.62 (*d*, 2H, Trp, J = 7.9 Hz), 7.49 (*d*, 2H, Trp, J = 7.9 Hz), 7.19 (*s*, 1H, Trp), 7.23 (*m*, 1H, Trp), 7.14 (*m*, 1H, Trp), 4.78 (*m*, 6H, CH), 4.24–4.46 (*m*, 10H, CH), 3.80–4.06 (*m*, 30H, Ser-CH_2, Gly-CH_2), 3.21 (*m*, 10H, Arg-$CH_2CH_2CH_2N$), 2.74–3.02 (*m*, 10H, Asp-CH_2), 1.54–2.00 (*m*, 20H, Arg-$CH_2CH_2CH_2N$), MALDI-TOFMS Calc'd: 2565 (MH^+), found: 2566.

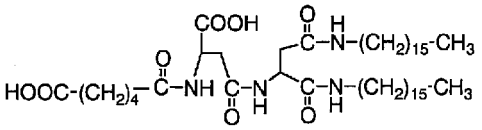

(C4)

H-Ser-Tyr-Ser-Met-Glu-His-Phe-Arg-Trp-Gly-Lys-Pro-Val-NH_2

(α-MSH; N-terminal free form)

H-Trp-(Gly-Arg-Gly-Asp-Ser)$_5$-NH_2

(W5GRGDS)

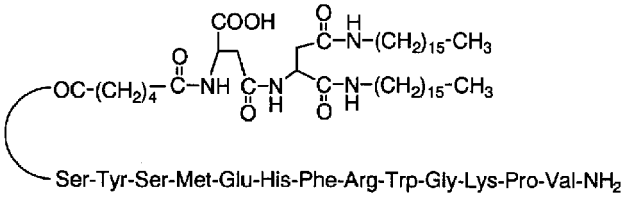

(MSH-C4A2)

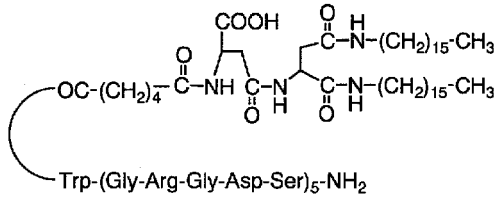

(RGD-C4A2)

FIG. 1. Structures of synthetic lipid, peptides, and lipopeptides. MSH, melanocyte-stimulating hormone; GRGDS, cell adhesion sequence of fibronectin.

(ii) RGD-C4A2 (Fig. 1). Lipid C4 (Fig. 1) (100 mg, 114 μmol) and 1-hydroxybenzotriazole (HOBt) (34.8 mg, 227 μmol) were dissolved in 5.0 mL of chloroform at 50°C, which was then added to the peptide-resin (363.2 mg, 38 μmol) suspended in 10.0 mL of *N,N*-dimethylformamide (DMF). 4-Dimethylaminopyridine (DMAP) (27.8 mg, 227 μmol) and 1-ethyl-3-(3-dimethylaminopropyl)-carbodiimide hydrochloride (WSCD·HCl) (43.6 mg, 227 μmol) dissolved in chloroform (1.0 mL) were added to the above suspension and stirred for 12 h at 50°C. Following separation of the resultant lipopeptide-resin by filtration, it was washed with DMF, chloroform, and methanol (2.0 mL × 10 times each), and dried *in vacuo*. This lipopeptide-resin was then added to a solution of TFA (2.5 mL), thioanisole (62.5 μL), EDT (62.5 μL), triisopropylsilane (62.5 μL), and water (125 μL) at 0°C. The suspension was shaken for 5 h at room temperature, the resin was removed by filtration, and a large excess of cold ethyl ether (*ca.* 50 mL) was added to the filtrate. The resultant white precipitate was separated by centrifugation (3000 rpm, 30 min) and dried *in vacuo*. The product was purified by HPLC and lyophilized. Yield: 10.1 mg, (7.9%, 3 μmol). Retention time in HPLC [YMC-Pack ODS-AM, ϕ: 4.6 × 250 mm, eluant: TFA (0.08% in water)/acetonitrile from 100:0 to 50:50 over 30 min, flow rate: 0.8 mL/min]: 17.4 min. ^{1}H NMR (D_2O); δ 7.34–7.60 (*m*, 2H, Trp), 7.19 (*s*, 1H, Trp), 6.98–7.14 (*m*, 2H, Trp), 4.68–4.82 (*m*, 6H, CH), 4.28–4.50 (*m*, 10H, CH), 3.75–4.12 (*m*, 30H, Ser-CH_2, Gly-CH_2), 3.21 (*m*, 10H, Arg-$CH_2CH_2CH_2N$), 2.74–2.94 (*m*, 10H, Asp-CH_2), 2.04–2.34 (*m*, 4H, $COCH_2$), 1.54–1.98 (*m*, 20H, Arg-$CH_2CH_2CH_2N$), 1.36–1.54 (*m*, 4H, $NHCH_2CH_2$), 1.27 (*s br*, 52H, $2(CH_2)_{13}CH_3$), 0.88 (*t*, 6H, $2CH_2CH_3$, J = 6.6 Hz). MALDI-TOFMS Calc'd: 3369.8 (MH^+), found: 3370.

Incorporation of lipopeptides to liposome membranes. Lipopeptide-containing liposomes were prepared according to the following method. The lipopeptide was dissolved in 10 μL of 20% acetic acid, and 100 μL of EPC/chloroform solution (5.0 mmol dm^{-3}) was added. These two separated phases

became homogeneous by adding a few drops of methanol. After evaporating the solvent under reduced pressure, a thin lipid film was formed on the wall of a test tube. To thoroughly remove the solvent, the lipid film was left *in vacuo* for at least 12 h. After adding 1.0 mL of Hank's buffer solution (pH 7.2) to the thin lipid film, this was vortexed for 5 min at room temperature, and freezing (–196°C) and thawing (70°C) procedures were repeated seven times (20). The resultant mixture was then extruded five times through a polycarbonate membrane with 0.1 μm pore size.

To confirm incorporation of the lipopeptides into liposome membranes, the liposome solution was eluted through a Sephacryl S-500HR column (Pharmacia Biotech AB, Uppsala, Sweden) immediately after the final extrusion (21). The chromatogram was obtained by measuring the fluorescence at 340 nm (λ_{ex} = 280 nm) of the indole groups in the tryptophan residues. A chromatogram of the control liposome without the lipopeptide was also obtained by measuring the light scattering of liposome at 340 nm. To confirm the existence of the inner aqueous phase, liposomes containing 1.0 mmol dm^{-3} calcein in this phase were prepared and subjected to gel filtration. The chromatograms were measured by monitoring the fluorescence of calcein (λ_{ex} = 490 nm, λ_{em} = 520 nm). The amount of lipopeptide incorporated in the liposome membranes was estimated as follows. The liposome suspension was first filtered through a polycarbonate membrane, and the amount of the lipopeptide entrapped on the membranes was determined by measuring the fluorescence intensity (λ_{ex} = 280 nm, λ_{em} = 340 nm) after the entrapped lipopeptides were dissolved in 1.0 mL of 20% acetic acid. The amount of incorporated lipopeptide was thus calculated by subtracting the entrapped amount from the total amount.

Electron microscopy. That the peptide parts are located in the aqueous phase was actually confirmed by immunoelectron microscopy (22,23). For this purpose, an antibody against CW5GRGDS, in which one cysteine residue was added to the N terminal of W5GRGDS, was prepared by the following method. A female New Zealand white rabbit (3 kg) (Japan Clea) was immunized by subcutaneous injection (in the footpads or back) of 100 mg KLH (keyhole limpet, hemocyanin)-CW5GRGDS mixed with complete Freund's adjuvant (2.0 mL). The rabbit had earlier been anesthetized with ketamine (Sankyo Co., Tokyo, Japan) and selectin (2.1 mg/kg) (Bayer Japan Co., Tokyo, Japan). Five booster injections of the same amount of KLH-CW5GRGDS were given subcutaneously at intervals of 2 wk, and 5.0 mL of blood was obtained each time from the ears. The serum was purified by affinity chromatography prepared from CNBr-activated Sepharose 4B column (Pharmacia Biotech AB) and CW5GRGDS. Production of antibody (the heavy chain) was detected by sodium dodecylsulfate-polyacrylamide gel electrophoresis (24) and Western blotting using horseradish peroxidase (HRP) antirabbit IgG (Wako Pure Chem. Ind., Ltd., Osaka, Japan) as a 50 kDa band. Antibody specificity was confirmed by Western blotting of a fibronectin fragment digested by α-chymotrypsin using the serum fraction as the first antibody and HRP-antirabbit IgG as the second antibody. Five μL of lipopeptide-containing liposome was put on collodion-coated copper mesh grids for 10 min, and the remaining fluid was drained off with filter paper. For labeling with immunogold, the grids were floated on droplets containing the primary antibodies at room temperature, where rabbit anti-α-MSH IgG (Biogenesis Inc., Poole, England) and the rabbit anti-RGD IgG were diluted 100 times and two times by 1% bovine serum albumin (BSA) in phosphate-buffered saline (PBS)(–) (i.e., PBS without calcium and magnesium), respectively. The labeling times were 1.5 h for the anti-α-MSH IgG and overnight for the anti-RGD IgG. After the labeling by the primary antibodies, both of the grids were washed by 1% BSA in PBS(–) 10 times. The grids were then floated on the droplets of secondary antibody, goat antirabbit IgG (E-Y Laboratories Inc., San Mateo, CA), at room temperature, which was diluted (1:50) by 1% BSA in PBS(–). After the labeling by the secondary antibody for 1 h, both of the grids were washed by 1% BSA in PBS(–) 10 times. The samples on the grids were negatively stained with droplets of 1% uranyl acetate for 15 min, stabilized by perpendicular carbon evaporation, and observed under a transmission electron microscope.

Binding of lipopeptide-containing liposome to cell. Two kinds of liposomes containing the lipopeptides RGD-C4A2 and MSH-C4A2 were prepared, and their binding ability toward two kinds of cell lines, NIH3T3 (25) and B16 (26), was estimated. The fluorescence emitted from the cells was measured on a flow cytometer. Table 1 summarizes the conditions

TABLE 1
Composition of Samples Used in Binding Experiment Toward NIH3T3 and B16 (2×10^6 cells/350 μL)

Peptide liposome type	Peptide liposome[a] (μL)	Control liposome[b] (μL)	CMF-Hank's buffer (μL)	DMEM (μL)	Peptide[c] (μL)
RGD liposome	0	0	700	300	0
	0	500	200	300	0
	500	0	200	300	0
	500	0	0	300	200
Melanocyte-stimulating	0	0	700	300	0
hormone liposome	0	500	200	300	0
	500	0	200	300	0

[a]Liposome composed of lipopeptide/cholesterol/*N*-(fluorescein-5-thiocarbamoyl)-1,2-dihexadecanoyl-*sn*-glycero-3-phosphoethanolamine/egg phosphatidylcholine (Ch/FITC-PE/EPC) (details are described in the text).
[b]Liposome composed of Ch/FITC-PE/EPC (details are described in the text).
[c]W5GRGDS (5×10^{-3} mol dm^{-3}); DMEM, Dulbecco's modified Eagle's medium.

of the binding experiment between the liposomes and the cells. As cholesterol (Ch) (30 mol%) increases the stability of liposomes bearing MSH-C4A2 (27), we added Ch to the liposome membranes in the binding experiment. The liposomes were prepared as follows. Into the lipopeptide (0.1 μmol) dissolved in 20% acetic acid (10 μL) was added chloroform solution containing EPC (1.6 μmol), Ch (0.4 μmol), and *N*-(fluorescein-5-thiocarbamoyl)-1,2-dihexadecanoyl-*sn*-glycero-3-phosphoethanolamine (FITC-PE) (0.02 μmol). A few drops of methanol were added to make the solution homogeneous. The lipopeptide-liposome was then prepared in a similar manner as described above. In the binding experiment between RGD liposome and the cells, the sample was incubated at 37°C for 30 min. The cells were washed by centrifugation (1000 rpm, 3 min) at 37°C, twice with Dulbecco's modified Eagle's medium (DMEM) and once with calcium magnesium free PBS (DMF-PBS). The cells were suspended in 1.0 mL of CMF-PBS containing BSA (0.1%) and sodium azide (0.1%), and the fluorescence emitted from the cells was measured on the flow cytometer. In the binding experiment between the MSH liposome and the cells, the sample was incubated at 0°C for 1 h; the cells were isolated by centrifugation (1000 rpm, 3 min), washed, and the fluorescence was measured in a similar manner as for RGD liposome.

RESULTS

Synthesis of lipopeptide. The following items are important in the design of the lipid portion: (i) it should contain two long alkyl chains; (ii) a polar group should be situated between a binding anchor (peptide ligand) and the two long alkyl chains to prevent the peptide part from migrating into the bilayer membrane; (iii) suitable distance is necessary between the peptide ligand and the lipid part situated in the bilayer membrane to lower the steric hindrance between cell receptors and liposome membrane; (iv) the lipid part should have a carboxyl group for binding to the peptides on the TGR-resin; and (v) the lipid part should be stable against TFA used to cut the lipopeptide from resin and to remove the protecting groups. In view of these necessary factors, the finally designed structure of the lipid is C4 in Figure 1, whose synthetic method has already been reported (27). It has two long alkyl chains (C16) and a terminal COOH group for binding to the terminal amino groups of the peptides. More hydrophobic lipids having the same skeleton as C4 were found to induce pH-controlled liposome fusion (28). For peptide sequences, we have chosen α-MSH and W5GRGDS as shown in Figure 1. Peptide α-MSH is a melanocyte-stimulating hormone of 13 amino acid residues (17), and the GRGDS sequence is observed on fibronectin and has the ability to recognize integrin (29). As repetition of RGD sequence can improve the binding ability to cells (30), GRGDS is repeated five times in W5GRGDS. Here, one tryptophan residue (W) is included at the N terminal of the peptide as a fluorescence probe for detecting the lipopeptide in gel chromatography. Figure 1 also shows the structures of lipopeptides MSH-C4A2 and RGD-C4A2; the synthetic method for MSH-C4A2 was reported earlier (27).

The peptide W5GRGDS was synthesized by the solid-phase Fmoc method. We used TGR-resin, since it has the advantage that the C terminal of a free peptide becomes an amide form under the deprotection condition with TFA. The observed ^{1}H NMR and MALDI-TOFMS were highly compatible with the structure of W5GRGDS, though the yield was not high (37.8%). The coupling between the peptide on the TGR-resin and W5GRGDS was performed using various reagent systems. The optimized system was HOBt/WSCD/DMAP, in which the coupling yield of RDG-C4A2 was 7.9%.

Incorporation of lipopeptide to liposome membrane. We first investigated which method was suitable for preparing liposomes. Both the ultrasonic method and the freeze-thaw method were tried, but the lipopeptides were efficiently incorporated into liposome membrane only by the latter method. Figures 2 and 3, respectively, show the elution patterns of the MSH liposome and the RGD liposome, which were monitored by fluorescence emitted at 340 nm. Liposomes composed of only EPC (control liposome) exhibited a small peak around 10 mL elution, which was attributed to the light scattering by liposomes. The MSH liposomes and the RGD liposomes gave peaks at almost the same elution volume with much higher fluorescence intensity emitted from the tryptophan residues, which unambiguously indicates that the lipopeptides exist in the liposome bilayer membranes. In Figures 2 and 3, some degree of trail-off was observed after the main peaks of the liposomes, probably due to the formation of small aggregates such as micelles.

To confirm that the peptide liposomes surely had the inner aqueous phase, calcein was introduced into the inner phase and the gel filtration pattern was observed at 340 and 520 nm, respectively, corresponding to tryptophan and calcein. If calcein exists in the inner phase, these two curves should give the peaks at the same elution volume. Figures 4 and 5 show the chromatograms of the MSH liposome and the RGD liposome, respectively, where two chromatograms measured at different wavelengths gave similar patterns. It is obvious therefore that both the MSH liposome and the RGD liposome have the inner aqueous phase and that they both hold the lipopeptides in the

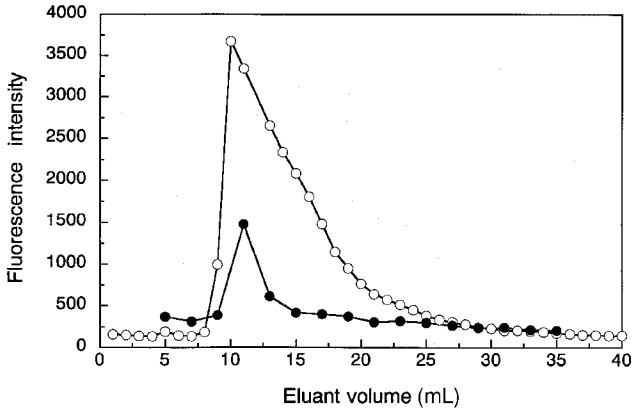

FIG. 2. Chromatograms of MSH liposome (○) and control liposome (●) See Figure 1 for abbreviation.

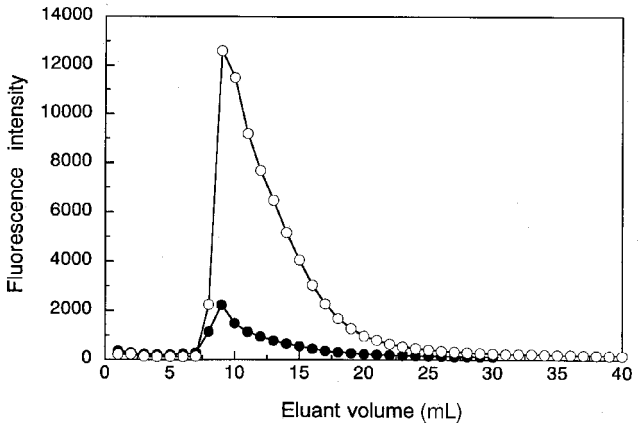

FIG. 3. Chromatograms of RGD liposome (○) and control liposome (●) See Figure 1 for abbreviation.

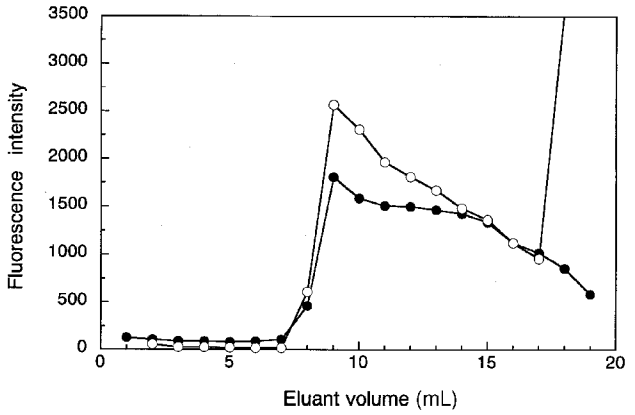

FIG. 5. Chromatograms of RGD liposome detected at 520 (○) and 340 nm (●). See Figure 1 for abbreviation.

bilayer membranes. It is also important to determine the amount of lipopeptides incorporated into liposome membranes. The results are summarized in Table 2, where the yields of incorporation are very high in both liposomes: 94–99% for RGD liposomes and 85–98% for MSH liposomes.

Electron microscopy. The peptide chain situated in the aqueous phase is believed to bind specifically to antipeptide antibody. Therefore the exposure of the peptide chains can be confirmed by detecting antipeptide antibody using a secondary antibody, which was labeled with colloidal gold. The gold colloidal particles attached on liposomes were detected by electron microscopy. The electron micrographs of the MSH liposomes and the RGD liposomes are shown in Figures 6 and 7, respectively, where we can clearly discriminate the liposomes with and without the lipopeptides. When the peptides were anchored to the liposomes, gold colloidal particles were observed (Figs. 6A and 7A), while the colloidal particles were hardly seen in the liposome without the peptides (Figs. 6B and 7B). These findings definitely show that the peptide ligands are located in the aqueous phase.

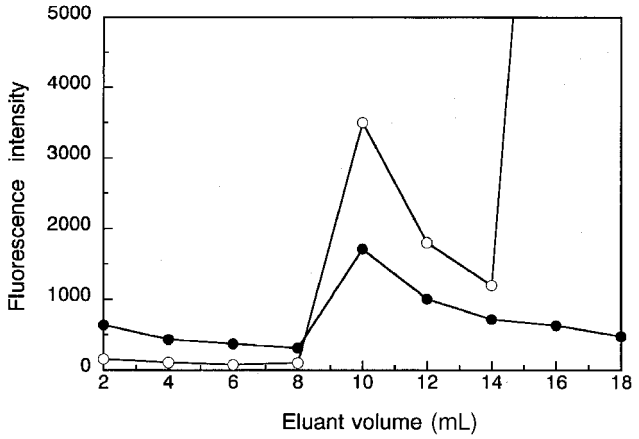

FIG. 4. Chromatograms of MSH liposome detected at 520 (○) and 340 nm (●). See Figure 1 for abbreviation.

Binding of liposome to cell. We applied the flow cytometry method to evaluate the binding ability of the liposomes to two cell lines, NIH3T3 and B16. Compositions of samples used are summarized in Table 1. NIH3T3 is established from mouse fibroblast, has normal cell-like properties, and is thought to have fibronectin receptors and to bind to the RGD liposomes. The result of flow cytometry is shown in Figure 8. It is worth noting that the RGD liposome/NIH3T3 (#2) gave higher fluorescence intensity than either the NIH3T3 alone (#0) or the EPC control-liposome/NIH3T3 (#1). We did an inhibition experiment to confirm that the peptide chain of the RGD liposome actually participates in the binding to the receptor of NIH3T3 cell. The fluorescence intensity was reduced by 34.8% by addition of the corresponding free RGD peptide (#3), which proves that the binding between the RGD liposome and NIH3T3 cells occurs through the RGD peptide ligand. The results of binding between the MSH liposomes and B16 cells are also shown in Figure 9. The fluorescence intensity was greatly increased on addition of the MSH liposomes to B16 cells, while the EPC liposomes did not enhance. This also demonstrates that the MSH liposomes bind to B16 cells through the MSH ligands.

DISCUSSION

The lipopeptide RGD-C4A2 was synthesized by the solid-phase method, but the final yields were not high owing to the low coupling yield between the lipid parts and the peptide ligands bound to the TGR-resin. It is thought that the solid-phase reaction between these large molecules is difficult owing to their steric repulsion and poor solubility of the lipid component. The coupling yields were actually 12.6% for MSH-C4A2 (27) and 7.9% for RDG-C4A2. We investigated various combinations of solvents, temperature, and coupling reagents to find the best reaction conditions. Lipid C4 was scarcely dissolved in DMF and *N*-methylpyrrolidone (NMP) up to about 60°C. As this condensation reaction was undertaken in a solid phase, it was essential that C4 should be completely dissolved

TABLE 2
Incorporation Efficiency of Lipopeptides to Liposome Membranes

Lipopeptide	Total amount (mol)[a]	Trapped amount (mol)[b]	Incorporation efficiency (%)[c]
RGD-C4A2 (5 mol%)[d]	2.5×10^{-8}	1.54×10^{-9}	93.8
RGD-C4A2 (10 mol%)	1.0×10^{-7}	2.95×10^{-9}	97.1
RGD-C4A2 (20 mol%)	2.5×10^{-7}	3.73×10^{-9}	98.5
MSH-C4A2 (2.5 mol%)	1.25×10^{-8}	1.87×10^{-9}	85.1
MSH-C4A2 (10 mol%)	5.0×10^{-8}	1.79×10^{-9}	96.4
MSH-C4A2 (20 mol%)	1.0×10^{-7}	1.92×10^{-9}	98.1

[a]Total amount of lipopeptide used to prepare liposome.
[b]Amount of lipopeptide trapped by a polycarbonate membrane.
[c]Incorporation efficiency = [(total amount – trapped amount)/total amount] × 100.
[d]Content of lipopeptide. See Table 1 for abbreviations.

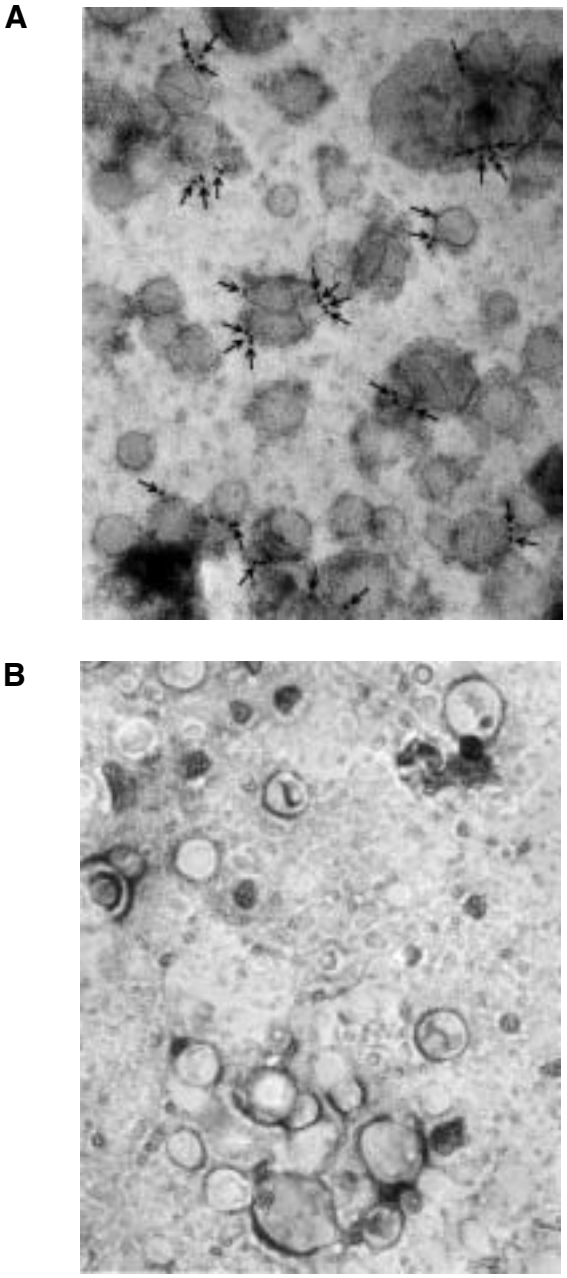

FIG. 6. Electron micrographs of MSH liposome (A) and control liposome (B). Arrows indicate position of gold colloidal particles on liposome surface. See Figure 1 for abbreviation.

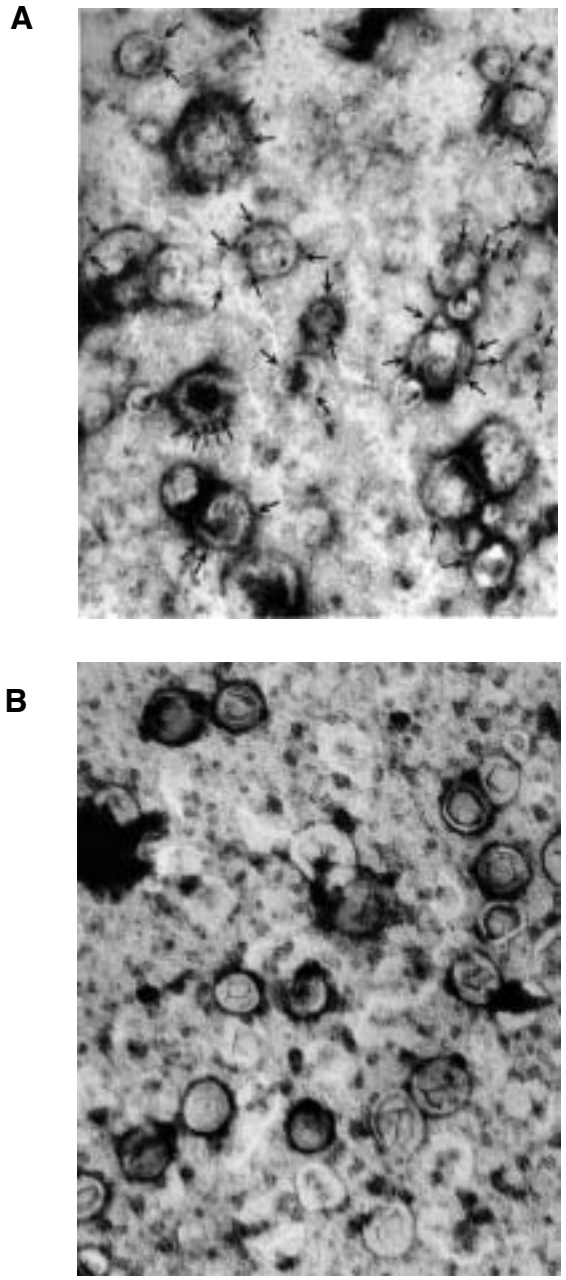

FIG. 7. Electron micrographs of RGD liposome (A) and control liposome (B). See Figure 1 for abbreviation and Figure 6 for meaning of arrows.

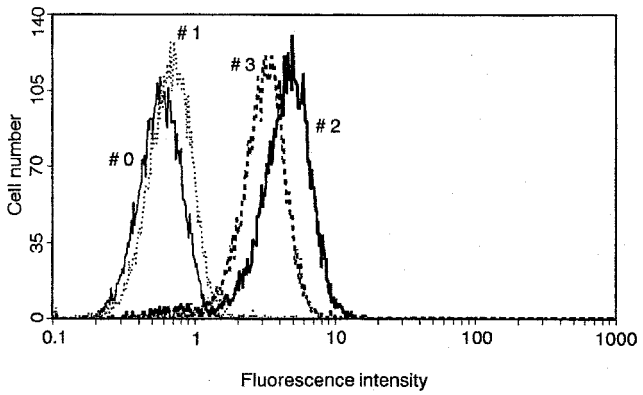

FIG. 8. Flow cytometry of RGD liposome/NIH3T3 cell; (#0) NIH3T3 only, (#1) NIH3T3 + control liposome, (#2) NIH3T3 + RGD liposome, (#3) NIH3T3 + RGD liposome + W5GRGDS. See Figure 1 for abbreviations.

in a solvent. To increase the solubility, we tried various solvents (38% chloroform/DMF, NMP, hexamethylphosphoramide, DMF, 20% dimethylsulfoxide/DMF), but the yields were not significantly enhanced. Another important property of the solvent is the ability to swell the resin to allow the reagents to approach each other easily. The solvents finally selected were NMP for MSH-C4A2 (27) and 38% chloroform/DMF for RGD-C4A2. We then tried three coupling reagents of active-ester type [HOBt; 2-(1H-benzotriazol-1-yl)-1,1,3,3-tetramethyluronium tetrafluoroborate; *O*-(7-azobenzotriazol-1-yl)-1,1,3,3-tetramethyluronium hexafluorophosphate], two coupling reagents of carbodiimide type [*N,N′*-diisopropylcarbodiimide (DIPCI), WSCD], and two bases (DMAP, *N,N′*-diisopropylethylamine). From these candidates, we chose DIPCI/HOBt in NMP for MSH-C4A2 (27) and WSCD/HOBt/DMAP in chloroform/DMF for RGD-C4A2. Since both DIPCI and WSCD were carbodiimide-type coupling reagents, HOBt was thought to increase the yields by depressing racemization and side reactions.

The GRGDS sequence is an integrin-recognition site on fibronectin, and the adhesion between cells takes place through this sequence (18). Polypeptides composed of repeated RGD sequences bind to the fibronectin receptor on B16 cell membrane and inhibit the adhesion between B16 and fibronectin-coated plates (30), where the high binding ability of these repeated RGD sequences might be induced by the conformational properties such as β-turn. It is also known that α-MSH is capable of binding to melanocyte (17). It was anticipated therefore that liposome could gain the ability to bind to cells by providing the liposome surface with these peptide ligands. Based on the above knowledge, we designed and synthesized the peptide with the repeated RGD sequences (RGD-C4A2) (16) and the peptide with α-MSH sequence (MSH-C4A2) (27). Actually it was confirmed by the increment of fluorescence using flow cytometry analysis that the liposomes bearing the lipopeptides bind to the cells while those without the lipopeptides do not. The RGD and the MSH liposomes are thought to bind to the NIH3T3 and B16 cells, respectively, through the peptide ligands on their surface. There is a possibility that side effects might be induced by the present liposomes, since the ligand peptides can bind to the membrane receptor and thus may act as agonists or antagonists affecting the signal response of the cells. This influence might be decreased, however, if the pinocytosis proceeds smoothly and thus the time of binding to the receptors is short.

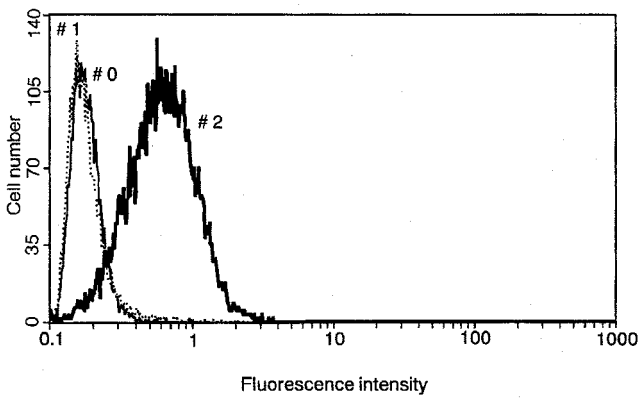

FIG. 9. Flow cytometry of MSH liposome/B16 cell; (#0) B16 only, (#1) B16 + control liposome, (#2) B16 + MSH liposome. See Figure 1 for abbreviation.

The liposomes which we have developed have the following three characteristics. The most notable feature is that the lipopeptide molecules (RGD-C4A2 and MSH-C4A2) can be incorporated into liposome membrane in a very high degree, *viz.*, more than 93% for the RGD liposome and more than 85% for the MSH liposome (Table 2); this is attributable to the adequate hydrophobicity of the two long alkyl chains in these lipopeptides. A conventional method using succinimide (10), in which ligands are added after preparing liposome, normally does not result in such a high degree of modification on the liposome surface. Another important property which the present liposomes should have is that the peptide ligands are located in an aqueous phase. This was actually confirmed by the immunogold labeling method with electron microscopy. The present method is consequently superior to the conventional ones and thus would be applicable for the preparation of various modified functional liposomes. The liposomes developed in the present study seem to be applicable to a DDS. Generally there are some characteristics in using liposomes as DDS. There is no need to modify drugs to accomplish targeting toward cells; namely, already-known drugs can be used, which makes the application to DDS easier. Instead, targeting becomes possible, for example, by modifying the surface of liposomes with ligands capable of binding to cell membrane receptors. There is a possibility that the present liposomes are incorporated into cells by pinocytosis. Though it is a preliminary experiment, it was actually observed by using a fluorescence microscope (data not shown) that FITC-PE (a fluorescence-probe lipid) included in the liposome membranes was introduced into both B16 and NIH3T3 under the conditions of the binding experiment. To confirm the pinocytosis, however, we should proceed with a further experiment carefully. A study along this line is now in progress.

In conclusion, we have succeeded in preparing new functional liposomes having α-MSH or repeated GRGDS sequence on the surface, which can bind to NIH3T3 or B16. These liposomes might be applied to DDS as specific drug carriers.

ACKNOWLEDGMENTS

We thank Dr. Kazunori Kawasaki, Dr. Toku Kanaseki, and Rena Kawai of National Institute of Bioscience and Human-Technology for assisting with the electron microscopy.

REFERENCES

1. Connor, J., and Huang, L. (1986) pH-Sensitive Immunoliposomes as an Efficient and Target-Specific Carrier for Antitumor Drugs, *Cancer Res. 46*, 3431–3435.
2. Briscoe, P., Caniggia, I., Graves, A., Benson, B., Huang, L., Tanswell, A.K., and Freeman, B.A. (1995) Delivery of Superoxide Dismutase to Pulmonary Epithelium *via* pH-Sensitive Liposomes, *Am. J. Physiol. 268*, L374–L380.
3. Ropert, C., Malvy, C., and Couvreur, P. (1993) Inhibition of the Friend Retrovirus by Antisense Oligonucleotides Encapsulated in Liposomes: Mechanism of Action, *Pharm. Res. 10*, 1427–1433.
4. Holmberg, E.G., Reuer, Q.R., Geisert, E.E., and Owens, J.L. (1994) Delivery of Plasmid DNA to Glial Cells Using pH-Sensitive Immunoliposomes, *Biochem. Biophys. Res. Commun. 201*, 888–893.
5. Lasic, D.D., Strey, H., Stuart, M.C.A., Podgornik, R., and Frederik, P.M. (1997) The Structure of DNA-Liposome Complexes, *J. Am. Chem. Soc. 119*, 832–833.
6. Higashi, N., and Sunamoto, J. (1995) Endocytosis of Poly(ethylene oxide)-Modified Liposome by Human Lymphoblastoid Cells, *Biochim. Biophys. Acta 1243*, 386–392.
7. Cooper, M.J., Lippa, M., Payne, J.M., Hatzivassiliou, G., Reifenberg, E., Fayazi, B., Perales, J.C., Morrison, L.J., Templeton, D., Piekarz, R.L., and Tan, J. (1997) Safety-Modified Episomal Vectors for Human Gene Therapy, *Proc. Natl. Acad. Sci. USA. 94*, 6450–6455.
8. Eggens, I., Fenderson, B., Toyokuni, T., Dean, B., Stroud, M., and Hakomori, S. (1989) Specific Interaction Between LeX and LeX Determinants, *J. Biol. Chem. 264*, 9476–9484.
9. Afzelius, P., Demant, E.J.F., Hansen, G.H., and Jensen, P.B. (1989) Covalent Modification of Serum Transferrin with Phospholipid and Incorporation into Liposomal Membranes, *Biochim. Biophys. Acta 979*, 231–238.
10. Martin, F.J., and Papahadjopoulos, D. (1982) Irreversible Coupling of Immunoglobulin Fragments to Preformed Vesicles, *J. Biol. Chem. 257*, 286–288.
11. Martin, F.J., Hubbell, W.L., and Papahadjopoulos, D. (1981) Immunospecific Targeting of Liposomes to Cells: A Novel and Efficient Method for Covalent Attachment of Fab' Fragments *via* Disulfide Bonds, *Biochemistry 20*, 4229–4238.
12. Romato, R., Dufresne, M., Prost, M.-C., Bali, J.-P., Bayerl, T.M., and Moroder, L. (1993) Peptide Hormone-Membrane Interactions. Intervesicular Transfer of Lipophilic Gastrin Derivatives to Artificial Membranes and Their Bioactivities, *Biochim. Biophys. Acta 1145*, 235–242.
13. Romato, R., Bayerl, T.M., and Moroder, L. (1993) Lipophilic Derivatization and Its Effect on the Interaction of Cholecystokinin (CCK) Nonapeptide with Phospholipids, *Biochim. Biophys. Acta 1151*, 111–119.
14. Jürgen, L., Romano-Götsch, R., Escrieut, C., Fourmy, D., Mathä, B., Müller, G., Kessler, H., and Moroder, L. (1997) Mapping of Ligand Binding Sites of the Cholecystokinin-B/Gastrin Receptor with Lipo-Gastorin Peptides and Molecular Modeling, *Biopolymers 41*, 799–817.
15. Merrifield, R.B. (1963) Solid-Phase Peptide Synthesis. I. The Synthesis of a Tetrapeptide, *J. Am. Chem. Soc. 85*, 2149–2154.
16. Yagi, N., Ogawa, Y., Kodaka, M., Okada, T., Tomohiro, T., Konakahara, T., and Okuno, H. (1999) A Surface-Modified Functional Liposome Capable of Binding to Cell Membranes, *Chem. Commun.*, 1687–1688.
17. Varga, J.M., Asato, N., Lande, S., and Lerner, A.B. (1977) Melanotropin-Daunomycin Conjugate Shows Receptor-Mediated Cytotoxicity in Cultured Murine Melanoma Cells, *Nature 267*, 56–58.
18. Pierschbacher, M.D., and Ruoslahti, E. (1984) Cell Attachment Activity of Fibronectin Can Be Duplicated by Small Synthetic Fragments of the Molecule, *Nature 309*, 30–33.
19. Fields, G.B., and Noble, R.L. (1990) Solid-Phase Peptide Synthesis Utilizing 9-Fluorenylmethoxycarbonyl Amino Acids, *Int. J. Peptide Protein Res. 35*, 161–214.
20. Pick, U. (1981) Liposomes with a Large Trapping Capacity Prepared by Freezing and Thawing of Sonicated Phospholipid Mixtures, *Arch. Biochem. Biophys. 212*, 186–194.
21. Zhao, J., Kimura, S., and Imanishi, Y. (1996) Receptor Affinity of Neurotensin Message Segment Immobilized on Lipozome, *Biochim. Biophys. Acta 1282*, 249–256.
22. Hülser, D.F., Rehkopf, B., and Traub, O. (1997) Dispersed and Aggregated Gap Junction Channels Identified by Immunogold Labeling of Freeze-Fractured Membranes, *Exp. Cell Res. 233*, 240–251.
23. Kamasawa, N., Naito, N., Kurihara, T., Kamada, Y., Ueda, M., Tanaka, A., and Osumi, M. (1992) Immunoelectron Microscopic Localization of Thiolases, β-Oxidation Enzymes of an *n*-Alkane-Utilizable Yeast, *Candida tropicalis*, *Cell Struct. Func. 17*, 203–207.
24. Laemmli, U.K. (1970) Cleavage of Structural Proteins During the Assembly of the Head of Bacteriophage T4, *Nature 227*, 680–685.
25. Fasano, O., Birnbaum, D., Edlund, L., Fogh, J., and Wigler, M. (1984) New Human Transforming Genes Detected by a Tumorigenicity Assay, *Mol. Cell. Biol. 4*, 1695–1705.
26. Silagi, S. (1969) Control of Pigment Production in Mouse Melanoma Cells *in vitro*, *J. Cell Biol. 43*, 263–274.
27. Ogawa, Y., Kawahara, H., Yagi, N., Kodaka, M., Tomohiro, T., Okada, T., Konakahara, T., and Okuno, H. (1999) Synthesis of a Novel Lipopeptide with α-Melanocyte-Stimulating Hormone Peptide Ligand and Its Effect on Liposome Stability, *Lipids 34*, 387–394.
28. Ogawa, Y., Tomohiro, T., Yamazaki, Y., Kodaka, M., and Okuno, H. (1999) Non-Peptidic Liposome-Fusion Compounds at Acidic pH, *Chem. Commun*., 823–824.
29. Akiyama, S.K., Hasegawa, E., Hasegawa, T., and Yamada, K.M. (1985) The Interaction of Fibronectin Fragments with Fibroblastic Cells, *J. Biol. Chem. 260*, 13256–13260.
30. Murata, J., Saiki, I., Ogawa, R., Nishi, N., Tokura, S., and Azuma, I. (1991) Molecular Properties of Poly(RGD) and Its Binding Capacities to Metastatic Melanoma Cells, *Int. J. Peptide Protein Res. 38*, 212–217.

[Received October 19, 1999, and in final revised form February 24, 2000; revision accepted April 25, 2000]

Quantitative Analysis of Long-Chain *trans*-Monoenes Originating from Hydrogenated Marine Oil

Robert Wilson[a,*], Karin Lyall[a], J. Anne Payne[a], and Rudolph A. Riemersma[a,b]

[a]Cardiovascular Research Unit, University of Edinburgh, Edinburgh, Scotland, and
[b]Department of Medical Physiology, University of Tromsø, Tromsø, Norway

ABSTRACT: Gas chromatography (GC) is used for the analysis of *trans*-fatty acids in partially hydrogenated vegetable oils. Although *trans*-isomers of C_{18} carbon length predominate in partially hydrogenated vegetable oils, *trans*-isomers of C_{20} and C_{22} carbon length occur in partially hydrogenated fish oil. We report a simple silver ion chromatographic combined with capillary GC technique for quantitative analysis of *trans*-monoenes derived from partially hydrogenated fish oil. Silver nitrate thin-layer chromatographic (TLC) plates are developed in toluene/hexane (50:50, vol/vol). Fatty acid methyl esters are separated into saturates (R_f 0.79), *trans*-monoenes (R_f 0.49), *cis*-monoenes (R_f 0.27), dienes (R_f 0.10), and polyunsaturated fatty acids with three or more double bonds remaining at the origin. The isolated *trans*-monoenes are quantitatively analyzed by capillary GC. The technique of argentation TLC with GC analysis of isolated methyl esters is highly reproducible with 4.8% variation (i.e., coefficient of variation , CV%) in R_f values and 4.3 and 6.9% CV% in quantification within batch and between batch, respectively. Furthermore, the combined technique revealed that direct GC analysis underestimated the *trans*-content of margarines by at least 30%. In this study, C_{20} and C_{22} *trans*-monoenes were found in relatively large quantities; 13.9% (range 10.3–19.6%) and 7.5% (range 5.3–11.5%), respectively, in margarine purchased in 1995, but these C_{20} and C_{22} *trans*-monoenes were much reduced (0.1%) in a fresh selection of margarine purchased in 1998. Compositional data from labels underestimated the *trans*-content of margarines, especially those derived from hydrogenated marine oil. Low levels of C_{20} *trans*-monoenes (range 0.1–0.3%) and C_{22} *trans*-monoenes (range 0.0–0.1%) were identified in adipose tissue obtained from healthy volunteers in 1995, presumably indicating consumption of partially hydrogenated fish oil.

Paper no. L8388 in *Lipids 35*, 681–687 (June 2000).

Trans-fatty acids are produced by the process of microbial biohydrogenation in the intestinal tract of ruminants and consequently are present in the milk, butterfat, and the meat of these animals (1). The process of partial catalytic hydrogenation of vegetable or marine oil, used by the food industry to produce stable and semisolid edible fats, increases the *trans*-fatty acid content of these foods (2,3). Butter, margarine, and shortenings (cakes, biscuits, etc.) are therefore major dietary sources of *trans*-fatty acids (1–7).

Partially hydrogenated vegetable oil has a complex fatty acid profile with 18:1 *trans*-isomers predominating. Gas chromatography (GC) has been used for the quantitative analysis of *trans*-fatty acids derived from vegetable oils (4–12). However, even when using a specialized 100-m column, overlap between C_{18} *cis*- and *trans*-monoenes can still occur (8,9), leading to the underestimation of some of these *trans*-fatty acids. Partially hydrogenated fish oil is much more complex in fatty acid composition than are hydrogenated vegetable oils. This material also contains many *trans*-isomers derived from C_{20} and C_{22} polyunsaturated fatty acids (PUFA) including *trans*-monoenes, *trans*-dienes, and *trans*-trienes (4,13). Techniques have been developed to determine *trans*-fatty acids in partially hydrogenated fish oil or other marine oils or in margarines derived from these oils (4,8,13). However, many *trans*-isomers are present in small concentrations, and the lack of authentic reference standards often confounds the analysis of *trans*-fatty acids.

The interest in *trans*-fatty acids originates from their association with coronary heart disease. Dietary intake of 18:1 *trans* increases the low density lipoprotein/high density lipoprotein (LDL/HDL) cholesterol ratio (14) and is therefore expected to augment the risk of coronary heart disease (15,16). There appears to be a discrepancy between studies using semiquantitative food frequency questionnaires and those using fatty acid analysis of adipose tissue, in estimation of dietary intakes of *trans*-fatty acids (15). Consumption of hydrogenated fish oil may lead to coronary heart disease (17), but in that case-control study *trans*-fatty acids were analyzed using a 40-foot packed column (17), now considered inadequate for this task. Thus, the issue of whether hydrogenated fish oil leads to coronary heart disease in humans will remain a question, unless better analytical methods are available.

In this paper we report a simple and efficient silver-ion thin-layer chromatographic (TLC) technique that permits the isolation and subsequent quantitative analysis by GC of *trans*-monoenes derived from partially hydrogenated fish oil in adi-

*To whom correspondence should be addressed at the Cardiovascular Research Unit, University of Edinburgh, George Square, Edinburgh EH8 9 XF. E-mail: R.Wilson@ed.ac.uk

Abbreviations: BHT, butylated hydroxytoluene; CV, coefficient of variation; FAME, fatty acid methyl ester; GC, gas chromatography; HDL, high density lipoprotein; LDL, low density lipoprotein; MS, mass spectrometry; MUFA, monounsaturated fatty acids; PUFA, polyunsaturated fatty acids; R_f, distance migrated by compound divided by the distance of solvent mobility; SPE, solid phase extraction; TLC, thin-layer chromatography.

pose tissue samples. The method therefore has the potential to resolve the controversy about whether hydrogenated fish or other oils do or do not lead to coronary heart disease.

MATERIALS AND METHODS

Materials. Butylated hydroxytoluene (BHT) was obtained from Sigma Chemical Co. (Poole, Dorset, United Kingdom). *Trans*-monoenoic and *trans*-dienoic fatty acid methyl esters (FAME) were obtained from Sigma Chemical Co. and Nu-Chek-Prep (Blast of Copenhagen, Denmark). Silver nitrate was obtained from Johnson Matthey (Royston, United Kingdom). Silica gel 60 TLC plates (Merck 5721, 20 cm × 20 cm × 0.25 mm; Darmstadt, Germany) and platinum (IV) oxide were purchased from BDH (Poole, Dorset, United Kingdom) A CP-Sil 88 fused-silica capillary column (50 m × 0.25 mm i.d. and 0.2 μm film thickness) was obtained from Chrompack (Middelburg, the Netherlands). Aminopropyl solid phase extraction (SPE) columns (500 mg) were purchased from IST (Hengoed, United Kingdom). High-performance liquid chromatography-grade solvents were purchased from Rathburn Chemicals (Walkerburn, Peebleshire, United Kingdom).

Margarine. Margarines were selected at random from a list provided by the Margarine and Shortening Manufacturers Association and were purchased from local supermarkets during 1995 (n = 22) and 1998 (n = 5). They included branded and nonbranded margarines. There was limited compositional data for margarine purchased in 1995. All margarines listed total fat, and the majority listed the saturated fat content. Only three margarines from 1995 listed the *trans*-content (less than 1%). Typical compositional data of margarines from 1995 were: hard [77% fat, 37% saturates, 23% monounsaturated fatty acids (MUFA), 14% PUFA], soft (82% fat, 23% saturates, 40% MUFA, 16% PUFA), spreads (71% fat, 27% saturates, 23% MUFA, 20% PUFA), low-fat spreads (40% fat, 12% saturates, 4% MUFA, 14% PUFA), and unsaturated spreads (73% fat, 15% saturates, 24% MUFA, 31% PUFA). Soft margarines purchased in 1998 gave more compositional data and indicated that margarines were being produced using various hydrogenated/nonhydrogenated vegetable oils. There was on average 79 ± 3% fat, 22 ± 2% saturates, 32 ± 7% MUFA, 20 ± 6% PUFA with the *trans*-content given as 1% in one margarine and 9% in another.

Preparation of FAME. A 25-mg sample of margarine was added to a screw-cap tube. To the sample was added 3 mg 17:0 and 0.28 mg Δ10-*trans*-17:1 (both as the methyl ester) as internal standards (in toluene). Δ10-*trans*-19:1 (0.56 mg) was used as an internal standard for recovery experiments. The sample was treated with sodium hydroxide (1 M), and FAME were prepared from the recovered fatty acids using etheral diazomethane (18). FAME were purified using 500 mg aminopropyl SPE columns (19) and then redissolved in hexane. Adipose tissue (15–20 mg) was cut up and treated as above using one-third of the amount of internal standards described above.

Separation of trans*-monoenes by argentation TLC.* Silver nitrate plates were prepared by dipping silica gel 60 TLC plates in acetonitrile containing 10% silver nitrate (wt/vol). Plates were air-dried in subdued light, heated at 110°C for 30 min to activate, and used within 1 h (20). FAME were applied to the impregnated TLC plates over 2–3 cm at a loading of 1.0 mg/cm. A solution containing Δ9-*trans*-22:1 and Δ9-*cis*-22:1 was streaked over 0.3 cm and used to identify the upper and lower limit of migration of the *trans*-monoenes (Fig. 1). The plates were developed at room temperature with toluene/hexane (50:50, vol/vol) to 1 cm from the top in a standard TLC chamber. The plates were dried, then lightly sprayed with 0.1% dichlorofluorescein and bands visualized under ultraviolet light. The areas corresponding to *trans*-monoenes were located, scraped from the plates, and eluted from the silica using 20 mL chloroform/methanol (2:1, vol/vol) containing 0.005% butylated hydroxytoluene (BHT); 5 mL 0.88% aqueous KCl was added and the solutions mixed (20). After separation, the chloroform layer was removed and the solvent removed under argon. Samples were redissolved in hexane containing 0.005% BHT and washed with 20% NaCl to precipitate any remaining silver (20). The hexane layer was removed, and FAME were purified on 500 mg aminopropyl SPE columns (19). Appropriate dilutions were made and samples analyzed by GC as described below.

FAME analysis. FAME were analyzed using a Fisons GC8000 gas chromatograph equipped with flame-ionization

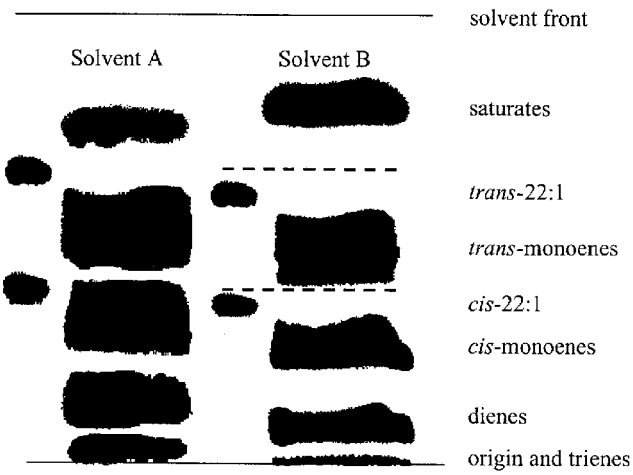

FIG. 1. Separation of *trans*-monoenes by silver-ion thin-layer chromatography (TLC). Methyl esters were separated by silver-ion TLC using hexane/ether (90:10, vol/vol); solvent A or toluene/hexane (50:50, vol/vol); solvent B. Bands were visualized by charring. The solvent system as described in the Materials and Methods section (solvent B) separated fatty acid methyl esters (FAME) into four distinct bands of saturates (R_f 0.79), *trans*-monoenes (R_f 0.49), *cis*-monoenes (R_f 0.27), dienes (R_f 0.10), and polyunsaturated fatty acids with three or more double bonds remaining at the origin. (R_f = distance migrated by compound divided by the distance migrated by solvent). The dotted lines show the upper and lower limits of the migration of *trans*-monoenes defined by the elution of *trans*-22:1 and *cis*-22:1. The area between the dotted lines is scraped from the plate and used for the analysis of *trans*-monoenes by capillary gas chromatography (GC). There is an improvement in resolution over that of solvent A; this method has been cited in the literature (18) as a method for separating *trans*-monoenes.

detector (FID) and autosampler (Fisons, Manchester, United Kingdom). For analysis 0.5 μL volumes were injected using an on-column injector. FAME were analyzed on a CP-Sil 88 capillary column (50 m × 0.25 mm i.d. and 0.2 μm film thickness) using an optimized temperature program: 1 min at 80°C, 25°C/min to 165°C, 12 min at 165°C, 2°C/min to 220°C, and 6 min at 220°C. Helium was carrier gas at a constant flow of 1.1 mL/ min, and the analysis time was 35 min. Under the chromatographic conditions just described there was optimal but not complete resolution between C_{18} *cis*- and *trans*-monoenes.

In the absence of authentic C_{20} and C_{22} *trans*-monoenes reference standards, the position of the carbon-carbon double bond was not identified. Hydrogenation to the corresponding saturated fatty acid confirmed that isolated *trans*-monoene fractions contained fatty acids of C_{16}, C_{18}, C_{20}, and C_{22} chain length. Analysis by GC/mass spectrometry (MS) and by GC of a few samples of margarine derived from fish oil confirmed that the isolated fraction contained only *trans*-monoenes. Notably, the position of the double bond can be assigned by GC/MS of dimethyloxazoline-derivatized monoenoic fatty acids (21). C_{18} *trans*-dienes were identified using authentic standards, whereas C_{18} *trans*-trienes were identified by reference to a *trans*-triene fraction isolated using silver nitrate TLC as described in the Materials and Methods section but using toluene as development solvent. Isolated *trans*-triene (or isolated *trans*-diene) fractions contained fatty acids of C_{20} and C_{22} chain length also.

Data were recorded and analyzed using Turbochrom software (PerkinElmer, Beaconsfield, United Kingdom). Δ10-*trans*-17:1 was used to quantify isolated *trans*-monoenes and to cross-reference between *trans*-analysis and total FAME analysis. Percentage composition was obtained after combining the weights of *trans*-fatty acids with the weights of other individual fatty acids from total FAME analysis.

Adipose tissue from healthy volunteers. Adipose tissue was obtained under local anesthetic from the abdominal wall from 16 men in 1995 and stored under liquid nitrogen until used. These apparently healthy volunteers (aged 25 to 55 yr) were selected at random from the Lothian Health Board Register, Edinburgh, United Kingdom. All men gave written informed consent.

RESULTS

Separation of *cis*- and *trans*-monoenes using a typical solvent system (Solvent A, hexane/ether, 90:10, vol/vol) as cited in the literature (18) is shown in Figure 1. We examined several other solvent systems for improved separation of *trans*-monoenes. Development of silver nitrate TLC plates in toluene (not shown) permitted separation of *trans*-dienes (R_f 0.38) and *trans*-trienes (R_f 0.10) from the corresponding *cis*-isomer, 18:2n-6 (R_f 0.25) and 18:3n-3 (R_f 0.03). However, there was overlap between C_{18}, C_{20}, and C_{22} *cis*-monoenes (R_f 0.53) with C_{18}, C_{20}, and C_{22} *trans*-monoenes (R_f 0.77) and that of saturates (R_f 0.91). Optimal separation of C_{18}, C_{20}, and C_{22} *cis*-monoenes from C_{18}, C_{20}, and C_{22} *trans*-monoenes was obtained using a mixture of toluene with hexane (50:50, vol/vol), and this solvent was used routinely when analyzing *trans*-monoenes (Solvent B; Fig. 1). FAME are resolved into four distinct bands of saturates (R_f 0.79), *trans*-monoenes (R_f 0.49), *cis*-monoenes (R_f 0.27), and dienes (R_f 0.10). PUFA containing more than three double bonds remain at the origin. The improved separation of *cis*- and *trans*-monoenes is illustrated.

TABLE 1
Comparison of Direct GC Analysis with Combined Argentation TLC Gas Chromatography Analysis for Measuring C18 *trans*-Isomers[a]

	C18 *trans*-isomers	
	Direct analysis	Combined analysis
Margarine 1	0.5 ± 0.1	0.7 ± 0.1
Margarine 2	1.7 ± 0.2	2.8 ± 0.2
Margarine 3	4.5 ± 0.1	6.9 ± 0.2
Margarine 4	10.2 ± 0.3	15.4 ± 0.7

[a]Values are gram fatty acid per 100 gram total fatty acid and represent means ± SD for triplicate analysis and have been rounded to one decimal place. The direct analysis as described in the Materials and Methods section underestimated C18 *trans*-monoenes by at least 30%.GC, gas chromatography; TLC, thin-layer chromatography.

The technique is highly reproducible with 4.8% variation (coefficient of variation %, CV%) in R_f values being recorded over repeated analysis (n = 6). For quantification of *trans*-monoenes, the within-batch CV% was 4.3% and between-batch CV% was 6.9% based on the recovery and quantification of Δ10-*trans*-17:1 using Δ10-*trans*-19:1 as the internal standard (n = 12). A comparison of the combined silver nitrate GC analysis with direct GC analysis is given in Table 1. Four margarines with increasing levels of *trans*-fatty acids were analyzed for C_{18} *trans*-isomers. Under optimal analysis conditions, as described in the Materials and Methods section, direct GC analysis underestimated C_{18} *trans*-isomers by 30% and failed to identify C_{20} and C_{22} *trans*-monoenes accurately.

We applied our method to the analysis of margarine (Table 2). There was on average 7.2% (range 4.2 to 18.1%) of C_{18} *trans*-monoenes in margarine purchased in 1995 (n = 17). However, many of the brands of margarine analyzed also contained *trans*-monoenes of 20- and 22-carbon chain length. The level of C20 and C22 *trans*-monoenes was of similar order of magnitude as that of *trans*-dienes and *trans*-trienes.

It was surprising that five brands of margarine purchased in 1995 contained on average 14 and 8% C20 and C22 *trans*-monoenes and 4.0% C18 *trans*-monoenes (Table 3). *Trans*-dienoic and *trans*-trienoic fatty acids of 20- and 22-carbon chain length were also present in some of these margarines but at a substantially reduced concentration (not shown). Analysis of a fresh selection of the same brand of margarine purchased in 1998 revealed substantially reduced amounts of C_{20} and C_{22} *trans*-monoenes (Table 3). The lowest level of C_{18} *trans*-monoenes (0.5%) was found in a recently purchased margarine, but relatively high levels of C_{18} *trans*-monoenes were found in recently purchased margarine (Table

TABLE 2
Fatty Acid Composition in a Random Selection of Margarine Determined by Combined Argentation TLC GC Analysis[a]

Fatty acid	Means (n = 17)	Range
14:0	2.8	0.2–8.7
15:0	0.1	0.0–0.5
16:0	15.2	7.6–24.5
18:0	6.1	5.0–7.2
20:0	0.5	0.0–1.6
22:0	0.2	0.0–0.6
cis-16:1	1.6	0.1–5.8
cis-18:1	31.2	24.0–50.8
cis-20:1	0.6	0.0–1.9
18:2n-6	28.4	4.8–50.8
18:3n-3	2.4	0.2–4.8
trans-16:1	1.8	0.0–7.9
trans-18:1	7.2	4.2–18.1
trans-20:1	0.3	0.0–1.3
trans-22:1	0.6	0.2–1.4
trans-18:2[b]	0.8	0.2–1.5
trans-18:3[c]	0.2	0.0–0.7

[a]Values are grams of fatty acid per 100 grams of total fatty acid and represent means and range and have been rounded to one decimal place. Brands of margarine were purchased in 1995. Data represent combined GC analysis of silver nitrate isolated TLC *trans*-monoenes and total FAME as described in the Materials and Methods section.
[b]*trans*-18:2 included all identifiable isomers using authentic reference standards.
[c]*trans*-18:3 included all identifiable isomers using silver nitrate isolated *trans*-triene standards. See Table 1 for abbreviations.

TABLE 3
Fatty Acid Composition of Five Identical, but Randomly Selected Brands of Soft Margarine, Purchased in 1995 and in 1998, Determined by Combined Argentation TLC and GC Analysis[a]

	Date of purchase			
	1995		1998	
Fatty acid	Means	Range	Means	Range
14:0	5.0	2.7–7.0	0.7	0.3–1.7
15:0	0.3	0.2–0.4	<0.1	0.0–0.1
16:0	14.6	10.9–17.8	16.9	11.9–22.8
18:0	4.3	2.9–5.0	5.9	5.1–6.9
20:0	1.2	0.8–1.6	0.7	0.5–0.9
22:0	0.5	0.3–0.7	—	—
cis-16:1	4.5	0.7–6.6	0.2	0.0–0.3
cis-18:1	23.4	18.0–28.7	35.9	25.9–49.4
cis-20:1	1.7[b]	1.4–1.9	0.5	0.1–1.1
cis-22:1	0.5[c]	0.3–0.9	—	—
18:2n-6	10.5	3.5–31.0	27.7	18.4–34.9
18:3n-3	4.6[b]	4.5–5.1	4.9	3.3–8.4
trans-16:1	2.7	1.4–3.9	<0.1	0.0–0.1
trans-18:1	4.0	2.7–5.4	5.9	0.6–13.9
trans-20:1	13.9	10.3–19.6	0.1	0–0.3
trans-22:1	7.5	5.3–11.5	0.1	0–0.2
trans-18:2[d]	0.8	0.6–1.1	0.3	0.1–0.5
trans-18:3[e]	[f]	[f]	0.2	0.1–0.3

[a]Values expressed as grams of fatty acid per 100 grams of total fatty acids and represent means and range and have been rounded to one decimal place. Data represent combined GC analysis of silver nitrate isolated TLC *trans* monoenes and total FAME as described in the Materials and Methods section.
[b]Including some 20:1 *trans*-monoene isomers.
[c]Including some 22:1 *trans*-monoene isomers)
[d]*trans*-18:2 included all identifiable isomers using authentic reference standards.
[e]*trans*-18:3 included all identifiable isomers using silver nitrate isolated *trans*-triene standards.
[f]Not analyzed in these samples. See Table 1 for abbreviations.

3). The fatty acid profile of margarine containing C_{20} and C_{22} *trans*-monoenes and the isolated *trans*-monoene fraction is shown in Figure 2.

Adipose tissue (n = 16) was analyzed for *trans*-monoenes. Direct GC analysis failed to quantify C_{20} and C_{22} *trans*-monoenes in adipose tissue and underestimated C_{18} *trans*-monoenes by 30% (1.6 vs. 2.6% of fatty acids) when compared to the combined silver nitrate GC method. It was also found that hydrogenation improved the quantification of C_{20} and C_{22} *trans*-monoenes because a single distinct peak corresponding to the saturated fatty acid was integrated, whereas normally numerous small amorphous unidentifiable peaks are integrated in the nonhydrogenated sample. The combined silver nitrate GC analysis revealed that C_{18} *trans*-monoenes were 2.6% of the total fatty acids, with C_{20} and C_{22} *trans*-monoenes accounting for 0.2 and 0.1% of total fatty acids, respectively (Table 4). The concentrations of C_{20} and C_{22} *trans*-monoenes are of a similar order of magnitude to that of most of the PUFA identified in adipose tissue.

DISCUSSION

Quantification of *trans*-fatty acids in edible fats has been performed using a number of different techniques, and these were recently and comprehensively reviewed (8). Traditionally, infrared spectroscopy has been used for quantification of *trans*-fatty acids, and the development of Fourier-transform infrared spectroscopy has greatly improved the accuracy of the technique especially for samples with *trans* content less than 5% (8). However, the technique can not give information about the chain length or the double-bond position of the *trans*-fatty acids present in the foods or tissues and has largely been used to analyze the *trans* content of partially hydrogenated vegetable oil (8).

GC, using highly polar capillary columns, has also been used routinely to analyze *trans*-fatty acids in partially hydrogenated vegetable oil (4–12), and overlap between C_{18} *cis*- and *trans*-monoenes still occurs when using a specialized 100-m column with optimized column temperature program (8,9). Also notably, highly polar columns as used in the analysis of *trans*-monoenes can degrade in efficiency, and resolution between C_{18} *cis*- and *trans*-monoenes can be further compromised. Several studies have isolated *trans*-fatty acids mainly of 18 carbon atoms together with saturated fatty acids using silver-ion chromatography prior to analysis by GC (4,6). These studies, as in this study, demonstrated that C_{18} *trans*-monoene content is underestimated using GC alone. It appears that current methods are unable to provide sufficient data on the complex composition of partially hydrogenated fish or marine oil. It was concluded in a recent review of available techniques that precise *trans*-fatty acid data and detailed isomer profiles could be obtained only by combining silver-ion chromatography with GC analysis (8).

It should be noted that there was limited compositional data on margarine purchased in 1995. Only three margarines purchased in 1995 gave the *trans* content as less than 1%,

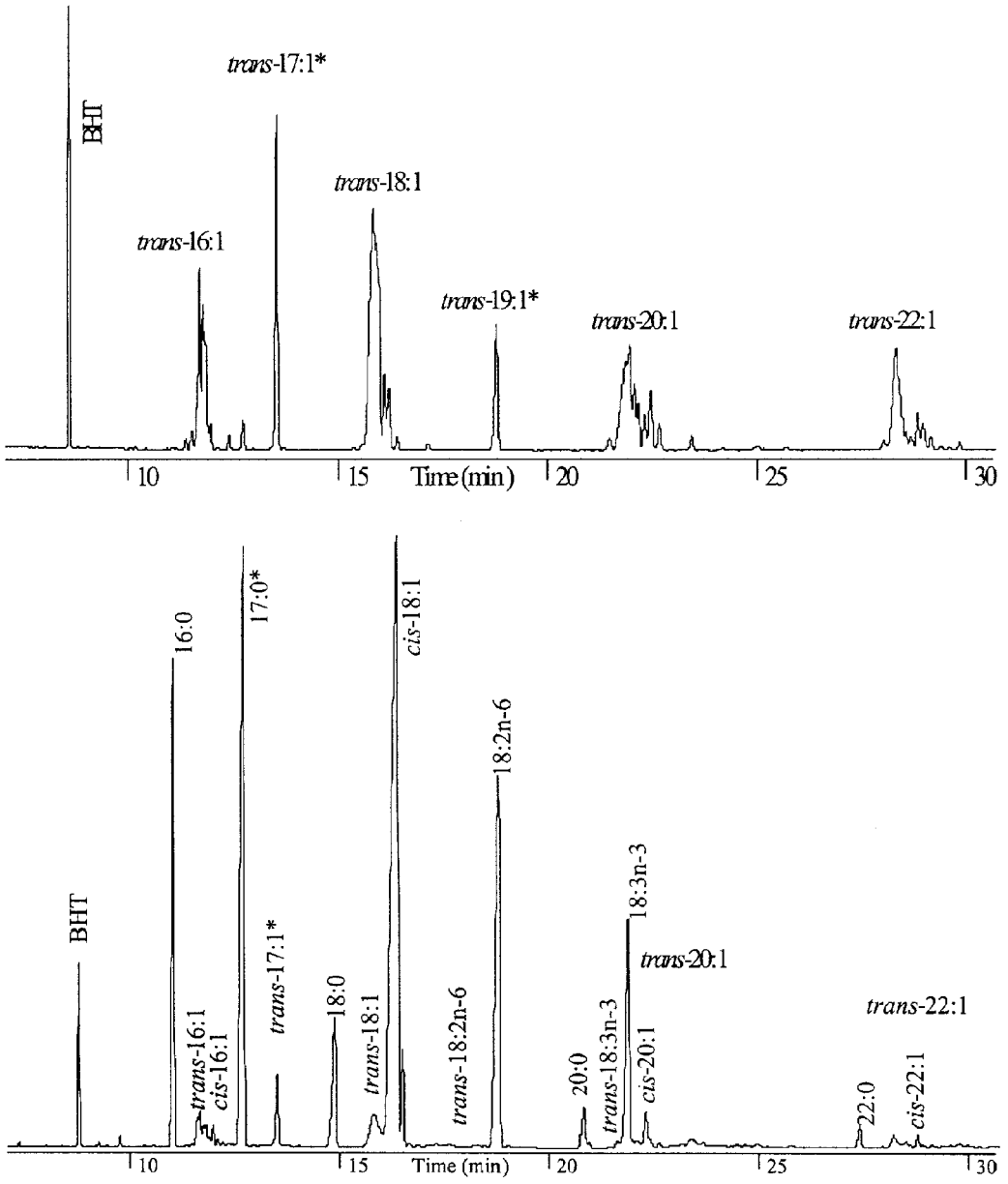

FIG. 2. Chromatogram showing C_{20} and C_{22} *trans*-monoenes in a margarine. Gas chromatogram of total FAME (lower trace) and isolated *trans*-isomers (upper trace) from a margarine made from hydrogenated fish oil. Sample preparation as described in the Materials and Methods section. The upper chromatogram of argentation TLC isolated *trans*-FAME demonstrates the complexity of the *trans*-isomer profile and shows the two internal standards, *trans*-17:1 and *trans*-19:1. The C_{18} *trans*-monoene content of this margine was 3.3% by direct GC analysis while the combined analysis gave 4.3% C_{18} *trans*-monoene, 3.8% C_{20} *trans*-monoene, and 2.9% C22 *trans*-monoene. *Trans*-18:2 was 0.1% of total fatty acids. BHT, butylated hydroxytoluene. See Figure 1 for other abbreviations. Asterisk indicates internal standards.

whereas in 1998 one brand of margarine gave the *trans* content as less than 1% and another gave the *trans* content as 9%. Our analysis revealed that the *trans* content of margarines was underestimated or not reported. Comparing margarine as a whole, then, there was a reduction in C_{18} *trans*-monoenes between 1995 and 1998. A reduction in C_{18} *trans*-monoenes has also been reported for German margarines over a similar period of time (5). Soft margarines purchased in 1995 contained relatively high levels of C_{20} and C_{22} *trans*-monoenes. However, recently purchased margarine had little C_{20} and C_{22} *trans*-monoenes, indicating that hydrogenated fish oil was no longer used in the production of these margarines. Nevertheless, hydrogenated fish or other oils are used in the production of margarine and shortenings in Northern Europe (1–4). Only brassica oils, such as rapeseed or low erucic acid rapeseed oil, are large-volume sources of 20:1 and 22:1 fatty acids.

Epidemiological and nutritional studies linking consumption of *trans*-fatty acids and coronary heart disease renewed

TABLE 4
Fatty Acid Composition of Adipose Tissue of 16 Healthy Men Determined by Combined Argentation TLC and GC Analysis[a]

Fatty acid	Mean	Range
14:0	3.0	2.3–4.6
15:0	0.3	0.2–0.5
16:0	25.0	20.8–28.5
18:0	5.4	3.9–8.0
20:0	0.2	0.1–0.3
cis-16.1	4.7	2.9–8.5
cis-18:1	42.9	39.8–46.6
cis-20:1	1.4	1.2–1.8
18:2n-6	11.3	8.6–17.1
20:2n-6	0.2	0.1–0.3
20:3n-9	<0.1	0.0–0.2
20:3n-6	0.2	0.0–0.4
20:4n-6	0.4	0.3–0.5
22:4n-6	0.1	0.1–0.2
18:3n-3	0.7	0.1–0.4
20:5n-3	0.1	0.1–0.5
22:5n-3	0.2	0.1–0.4
22:6n-3	0.3	0.1–0.5
trans-16:1	0.2	0.1–0.4
trans-18:1	2.5	1.1–3.6
trans-20:1	0.2	0.1–0.3
trans-22:1	0.1	0.0–0.1
trans-18:2[b]	0.5	0.0–0.7

[a]Values are percentage of total fatty acids and represent means and range. Data represent combined GC analysis of silver nitrate TLC-isolated *trans* monoenes and total FAME as described in the Materials and Methods section.
[b]*trans*-18:2 included all identifiable isomers using authentic reference standards. See Table 1 for abbreviations.

the interest in the possible detrimental health effects of *trans*-fatty acids (14–16). It should be noted that studies linking ischemic heart disease to the consumption of partially hydrogenated fish oil were founded on adipose tissue levels of C_{16} *trans*-monoenes (17), using inadequate analytical methodology. However, dietary *trans*-monoenoic fatty acids (22), including those from partially hydrogenated fish oil (23), raise serum LDL cholesterol or lower HDL lipoprotein cholesterol (22,23). The debate will therefore remain unless we have better methodology for the analysis of partially hydrogenated fish oil fatty acids in human tissues.

Fatty acids from the diet are incorporated into body tissues, and in humans adipose tissue fatty acid composition is used in many studies as a surrogate measure for long-term dietary intake of essential PUFA and 18:1 *trans*-fatty acids (24). The relative amount of C_{20} *trans*-monoenes in adipose tissue is related to the dietary intake of these *trans*-fatty acids in animals (25,26). In those studies (25,26) this relationship was not examined for C_{22} *trans*-monoenes because of overlapping peaks. It was interesting that for a given amount of *trans*-fatty acid in the diet, less C_{20} *trans*-monoenes than C_{18} *trans*-monoenes were deposited in adipose tissue (25,26). This could be attributed to increased oxidation of the longer-chain *trans*-monoenes or a conversion of C_{20} *trans*-monoenes to C_{18} *trans*-monoenes (27). Nevertheless, adipose tissue fatty acid composition is adequate to characterize a dietary intake of C_{18}, C_{20}, or C_{22} *trans*-monoenes in animals (25,26) and humans (24).

Our analysis of adipose tissue revealed that, on average, 2.6 and 0.5% of total fatty acids were C_{18} *trans*-monoenes and C_{18} *trans*-dienes. These levels are similar to those observed previously in British men (28). In that study it was not possible to quantify C_{20} and C_{22} *trans*-monoenes (28). C_{20} and C_{22} *trans*-monoenes were present in adipose tissue in apparently healthy Edinburgh men. Thus our analysis demonstrated that these Scottish subjects consumed C_{20} and C_{22} *trans*-monoenes. However, it is difficult from the small number of subjects analyzed at this time to estimate how much C_{20} and C_{22} *trans*-monoenes are consumed either in absolute terms or in relation to C_{18} *trans*-monoenes or total *trans*-monoenes.

In conclusion, we describe a simple and efficient silver-ion TLC technique for the isolation and subsequent quantitative analysis of the *trans*-isomer content of margarine and adipose tissue samples. The chromatographic separation of *cis*- and *trans*-monoenoic fatty acids and that of saturated fatty acids is improved when compared to existing techniques. The use of odd-chain *trans*-fatty acids as internal standards allows the quantitative analysis of the various *trans*-monoenoic fatty acids. The isolation of *trans*-monoenes without interference of saturated fatty acids permits hydrogenation of samples. Hydrogenation was only important in analyzing adipose tissue because of the limited sample size and the low concentrations of C_{20} and C_{22} *trans*-monoenes in adipose tissue. Hydrogenation improved the quantification of C_{20} and C_{22} *trans*-monoenes because a single distinct peak was quantified. The accurate measurement of C_{20} and C_{22} *trans*-monoenes in adipose tissue, which may be valuable as a biomarker of long-term consumption of hydrogenated fish oils, has implications in epidemiological and clinical studies. The method therefore has the potential to resolve the controversy as to whether hydrogenated fish or other oils lead to coronary heart disease.

ACKNOWLEDGMENTS

This study was supported by a LINK Agro Food Programme grant AFQ112. We wish to thank MAFF and the members of the Link management group (Nestlé UK Ltd., Roche Products Ltd., and Van den Bergh Foods Ltd.) for their support. We thank the nurses of the Cardiovascular Research Unit, University of Edinburgh, for collecting adipose fat biopsies and Jouni Niemelä of Räisio Margarinii, Räisio, Finland, for a sample of margarine prepared from hydrogenated fish oil.

REFERENCES

1. Aro, A., Antoine, J.M., Pizzoferrato, L., Reykdal, O., and van Poppel, G. (1998) *Trans*-Fatty Acids in Dairy And Meat Products From 14 European Countries: The Transfair Study, *J. Food Comp. Anal. 11*, 150–160.
2. Aro, A., Van Amelsvoort, J., Becker, W., Van Erp-Baart, M.A., Kafatos, A., Leth, T., and van Poppel, G. (1998) *Trans*-Fatty Acids in Dietary Fats and Oils from 14 European Countries: The Transfair Study, *J. Food Comp. Anal. 11*, 137–149.

3. van Erp-Baart, M.-A., Cout, C., Caudrado, C., Kafatos, A., Stanley, J., and van Poppel, G. (1998) *Trans*-Fatty Acids in Bakery Products from 14 European Countries: The Transfair Study, *J. Food Comp. Anal. 11*, 161–169.
4. Ovesen, L., Leth, T., and Hansen, K. (1998) Fatty Acid Composition and Contents of *trans* Monounsaturated Fatty Acids in Frying Fats and in Margarine and Shortenings Marketed in Denmark, *J. Am. Oil Chem. Soc. 75*, 1079–1083.
5. Fritche, J., and Steinhart, H. (1997) *Trans*-Fatty Acid Content in German Margarines, *Fett-Lipids 99*, 214–217.
6. Wolff, R.L. (1994) Contribution of *Trans*-18:1 Acids from Dairy Fat to European Diets, *J. Am. Oil Chem. Soc. 71*, 277–283.
7. Ratnayake, W.M.N., Pelletier, G., Hollywood, R., Bacler, S., and Leyte, D. (1998) *Trans*-Fatty Acids in Canadian Margarine: Recent Trends, *J. Am. Oil Chem. Soc. 75*, 1587–1594.
8. Ratnayake, W.M.N. (1998) Analysis of *Trans*-Fatty Acids, in Trans-*Fatty Acids in Human Nutrition*, (Sébédio, J.L., and Christie, W.W., eds.), pp. 115–162, Oily Press, Dundee.
9. Wolff, R.L., and Bayard, C.C. (1995) Improvement in the Resolution of Individual *Trans*-18:1 Isomers by Capillary Gas–Liquid Chromatography Use of a 100-M CP-Sil-88 Column, *J. Am. Oil Chem. Soc. 72*, 1197–1201.
10. van Bruggen, P.C., Duchateau, G.E., Mooren, M.W., and van Oosten, H.J. (1998) Precision of Low *Trans*-Fatty Acid Level Determination in Refined Oils. Results of a Collaborative Capillary Gas–Liquid Chromatography Study, *J. Am. Oil Chem. Soc. 75*, 483–488.
11. Chen, Z.Y., Ratnayake, W.M.N., Fortier, L., Ross, R., and Cunnane, S.C. (1995) Similar Distribution of *Trans*-Fatty Acid Isomers in Partially Hydrogenated Vegetable Oils and Adipose Tissue of Canadians, *Can. J. Physiol. Pharmacol. 73*, 718–723.
12. Duchateau, G.E., van Oosten, H.J., and Vasconcellos, M.A. (1996) Analysis of *Cis*- and *Trans*-Fatty Acid Isomers in Hydrogenated and Refined Vegetable Oils by Capillary Gas–Liquid Chromatography, *J. Am. Oil Chem. Soc. 73*, 275–282.
13. Sebedio, J.-L., and Ackman, R.G. (1983) Hydrogenation of a Menhaden Oil: I. Fatty Acid and C_{20} Monoethylenic Compositions as a Function of the Degree of Hydrogenation, *J. Am. Oil Chem. Soc. 60*, 1986–1991.
14. Mensink, R.P., and Katan, M.B. (1990) Effects of Dietary *trans*-Fatty Acids on High Density and Low Density Lipoprotein Cholesterol Levels in Healthy Subjects, *N. Engl. J. Med. 323*, 439–445.
15. Aro, A. (1998) Epidemiological of *Trans*-Fatty Acids and Coronary Heart Disease, in Trans-*Fatty Acids in Human Nutrition* (Sébédio, J.L., and Christie, W.W., eds.), pp. 235-260, Oily Press, Dundee.
16. Expert Panel on *Trans*-Fatty Acids and Coronary Heart Disease (1995) *Trans*-Fatty Acids and Coronary Heart Disease Risk, *Am. J. Clin. Nutr. 62*, 655S–708S.
17. Thomas, L.H., Jones, P.R., Winter, J.A., and Smith, H. (1981) Hydrogenated Oils and Fats: The Presence of Chemically Modified Fatty Acids in Human Adipose Tissue, *Am. J. Clin. Nutr. 34*, 877–886.
18. Christie, W.W. (1989) Preparation of Methyl Esters and Other Derivatives, in *Gas Chromatography and Lipids* (Christie, W.W., ed.), pp. 64–84, The Oily Press, Ayr.
19. Wilson, R., Henderson, R.J., Burrow, I.C., and Sargent, J.R. (1993) The Enrichment of n-3 Polyunsaturated Fatty Acids Using Aminopropyl Solid-Phase Extraction Columns, *Lipids 28*, 51–54.
20. Wilson, R., and Sargent, J.R. (1992) High-Resolution Separation of Polyunsaturated Fatty Acids by Argentation Thin-Layer Chromatography, *J. Chromatogr. 623*, 403–407.
21. Spitzer, V., Marx, F., and Pfeilsticker, K. (1994) Electron-Impact Mass-Spectra of the Oxazoline Derivatives of Some Conjugated Diene and Triene C-18 Fatty Acids, *J. Am. Oil Chem. Soc. 71*, 873–876.
22. Nestel, P., Noakes, M., Belling, B., McArthur, R., Clifton, P., Janus, E., and Abbey, M. (1992) Plasma Lipoprotein and Lp(A) Changes with Substitution of Elaidic Acid for Oleic Acid in the Diet, *J. Lipid Res. 32*, 1029–1036.
23. Almendingen, K., Jordal, O., Kierulf, P., Sandstad, B., and Pedersen, J.I. (1995) Effects of Partially Hydrogenated Fish Oil, Partially Hydrogenated Soybean Oil, and Butter on Serum-Lipoproteins and Lp[A] in Men, *J. Lipid Res. 36*, 1370–1384.
24. Garland, M., Sacks, F.M., Colditz, G.A., Rimm, E.B., Sampson, L.A., Willett, W.C., and Hunter, D.J. (1998) The Relation Between Dietary Intake and Adipose Tissue Composition of Selected Fatty Acids in U.S. Women, *Am. J. Clin. Nutr. 67*, 25–30.
25. Pettersen, J., and Opstvedt, J. (1992) *Trans*-Fatty Acids. 5. Fatty Acid Composition of Lipids of the Brain and Other Organs in Suckling Pigs, *Lipids 27*, 761–769.
26. Høy, C.-E., and Hølmer, G. (1988) Dietary Linoleic Acid and the Fatty Acid Profiles in Rats Fed Partially Hydrogenated Marine Oils, *Lipids 23*, 973–980.
27. Hølmer, G. (1998). Biochemistry of *Trans*-Monoenoic Fatty Acids, in Trans-*Fatty Acids in Human Nutrition* (Sébédio, J.L., and Christie, W.W., eds.), pp. 163–189, The Oily Press, Dundee.
28. Roberts, T.L., Wood, D.A., Riemersma, R.A., Gallagher, P.J. and Lampe, F.C. (1995) *Trans* Isomers of Oleic Acid and Linoleic Acids in Adipose Tissue and Sudden Cardiac Death, *Lancet 345*, 278–282

[Received November 12, 1999, and in final revised form April 18, 2000; revision accepted May 4, 2000]

Lipid Analog with 2-Nitrophenol Trigger Designed for Liposome Fusion at Physiological pH

S.N. Shah[1], Takenori Tomohiro, Yoshikatsu Ogawa, Masato Kodaka*, and Hiroaki Okuno

Biomolecules Department, National Institute of Bioscience and Human-Technology, Tsukuba, Ibaraki 305-8566, Japan

ABSTRACT: A novel lipid analog with two long alkyl (C_{16}) chains, an aspartate skeleton, a connecting alkyl (C_8) chain, and 2-nitrophenol trigger group is synthesized by an efficient synthetic route, which can induce liposome fusion at physiological pH.

Paper no. L8428 in *Lipids 35*, 689–691 (2000).

For the last decade, liposomes have been exploited predominantly for potent carriers of various polar materials into cells (1–6). In the present study we design and synthesize a novel functional lipid analog which accelerates the fusion between liposomes under physiological pH conditions. The lipid analog **8** (Scheme 1) designed for this purpose is composed of four parts: (A) two long hydrophobic alkyl chains (C_{16}) bound to an aspartate residue, which can be anchored to lipid bilayer, (B) a polar moiety (an aspartate residue) containing a free carboxyl group in the middle part, (C) an alkyl chain (C_8) connecting the aspartate skeleton and a terminal trigger part, and (D) a terminal trigger (2-nitrophenol group). The polar moiety (B) is thought to be necessary for **8** to exist stably in the lipid bilayer of a liposome. The terminal trigger of **8** is expected to be anchored into the lipid bilayer of another liposome before initiating membrane fusion. Here the 2-nitrophenol group is used as the trigger to induce liposome fusion at the physiological pH, since it is relatively hydrophobic and its pK_a value is normally around 7. Although there have been several studies on liposome fusion using carboxyl groups as triggers, the starting point of the fusion is in the acidic region since the pK_a values of the carboxyl group are less than 5 (7–9).

EXPERIMENTAL PROCEDURES

Lipid analog **8** was synthesized according to Scheme 1 in a manner similar to that previously reported (10) (yield 87%). Anal. Calc. for $C_{56}H_{97}N_6O_{10}$: C, 66.33; H, 9.57; N, 8.29. Found: C, 66.34; H, 9.72; N, 8.06. ^{1}H nuclear magnetic resonance (NMR) (270 MHz, $CDCl_3$ + CD_3OD, 50°C) δ 0.88 (*t*, 6 H, CH_3, *J* = 6.6 Hz), 1.26 (*bs*, 60H, CH_2), 1.40–1.54 (*m*, 4 H, $NHCH_2C\underline{H}_2$), 1.56–1.76 (*m*, 4 H, $COCH_2C\underline{H}_2$), 2.22 (*t*, 2 H, $COC\underline{H}_2$, *J* = 7.6 Hz), 2.34 (*t*, 2 H, $COC\underline{H}_2$, *J* = 7.6 Hz), 2.49 (*dd*, 1 H, $NHCHC\underline{H}_2CO$, *J* = 6.7, 14.9 Hz), 2.67 (*dd*, 1 H, $NHCHC\underline{H}_2CO$, *J* = 5.1, 14.9 Hz), 2.77 (*dd*, 1 H, $NHCHC\underline{H}_2CO$, *J* = 5.6, 15.1 Hz), 2.78 (*dd*, 1 H, $NHCHC\underline{H}_2CO$, *J* = 5.6, 15.1 Hz), 3.17–3.22 (*m*, 4 H, $NHC\underline{H}_2$), 4.63 (*dd*, 1 H, $NHC\underline{H}CH_2CO$, *J* = 5.1, 6.7 Hz), 4.76 (*t*, 1 H, $NHC\underline{H}CH_2CO$, *J* = 5.6 Hz), 7.10 (*d*, 1 H, arom., *J* = 9.0 Hz), 7.84 (*dd*, 1 H, arom., *J* = 9.0, 2.5 Hz), 8.32 (*d*, 1 H, arom., *J* = 2.5 Hz). ^{13}C NMR (270 MHz, $CDCl_3$ + CD_3OD, 50°C) δ 13.8 (*q*), 22.5 (*t*), 25.1 (*t*), 25.2 (*t*), 26.76 (*t*), 26.79 (*t*), 28.6 (*t*), 28.7 (*t*), 29.1 (*t*), 29.5 (*t*), 31.7 (*t*), 36.0 (*t*), 36.8 (*t*), 37.7 (*t*), 39.6 (*t*), 39.7 (*t*), 49.2 (*d*), 50.3 (*d*), 115.2 (*d*), 119.7 (*d*), 130.2 (*d*), 131.4 (*s*), 133.0 (*s*), 151.1 (*s*), 170.4 (*s*), 170.6 (*s*), 170.7 (*s*), 172.6 (*s*), 172.7 (*s*), 174.0 (*s*). Infrared (KBr) 3284 (–OH), 2920 (C-H asym.), 2851 (C-H sym.), 1717 (C=O), 1647 (C=O), 1542 cm^{-1} (Ar-NO_2, N=O asym.).

Liposome (PC-**8** liposome) composed of PC (egg yolk phosphatidylcholine) and **8** was prepared by the method described elsewhere (9). The fusion efficiency (%) was determined from the decrease in the efficiency of fluorescence resonance energy transfer between NBD-PE [*N*-(7-nitro-benza-2-oxa-1,3-diazol-4-yl) phosphatidylethanolamine], λ_{ex} = 460 nm, λ_{em} = 534 nm and Rh-PE (lissamine rhodamine B-sulfonyl phosphatidylethanolamine, λ_{ex} = 550 nm, λ_{em} = 590 nm) (9).

RESULTS AND DISCUSSION

Figure 1 exhibits the pH dependence of the fusion efficiency (%) at various reaction times. The three lines denote different measurement times: 5, 10, and 15 min. Liposome fusion is facilitated when pH is lowered and the 2-nitrophenolate group is protonated to form the more hydrophobic neutral form, though the starting pH point is somewhat shifted toward basic region. In order to interpret this pH-dependency, we estimated pK_a values of compound **8** located in a lipid bilayer of liposome. It was found unexpectedly that the pK_a value of **8** was shifted to basic side (pK_a = *ca*. 9.5) compared to ordinary 2-nitrophenol derivatives such as **10** (Scheme 1), whose pK_a is

[1]Present address: Polymer Science Research Center, The University of Southern Mississippi, P.O. Box 10076, Hattiesburg, MS 39406.

*To whom correspondence should be addressed at Biomolecules Department, National Institute of Bioscience and Human-Technology, 1-1 Higashi, Tsukuba, Ibaraki 305-8566, Japan.
E-mail: kodaka@nibh.go.jp

Abbreviations: DMAP, 4-dimethylaminopyridine; Fmoc, *N*-9-fluorenylmethoxy carbonyl; HOBt, *N*-hydroxybenzotriazole hydrate; NMR, nuclear magnetic resonance; PC, phosphatidylcholine; PE, phosphatidylethanolamine; TBTU, 2-(1H-benzotriazole-1-yl)-1,1,3,3-tetramethyluronium hexafluoroborate; TFA, trifluoroacetic acid; WSC, water soluble carbodiimide HCl.

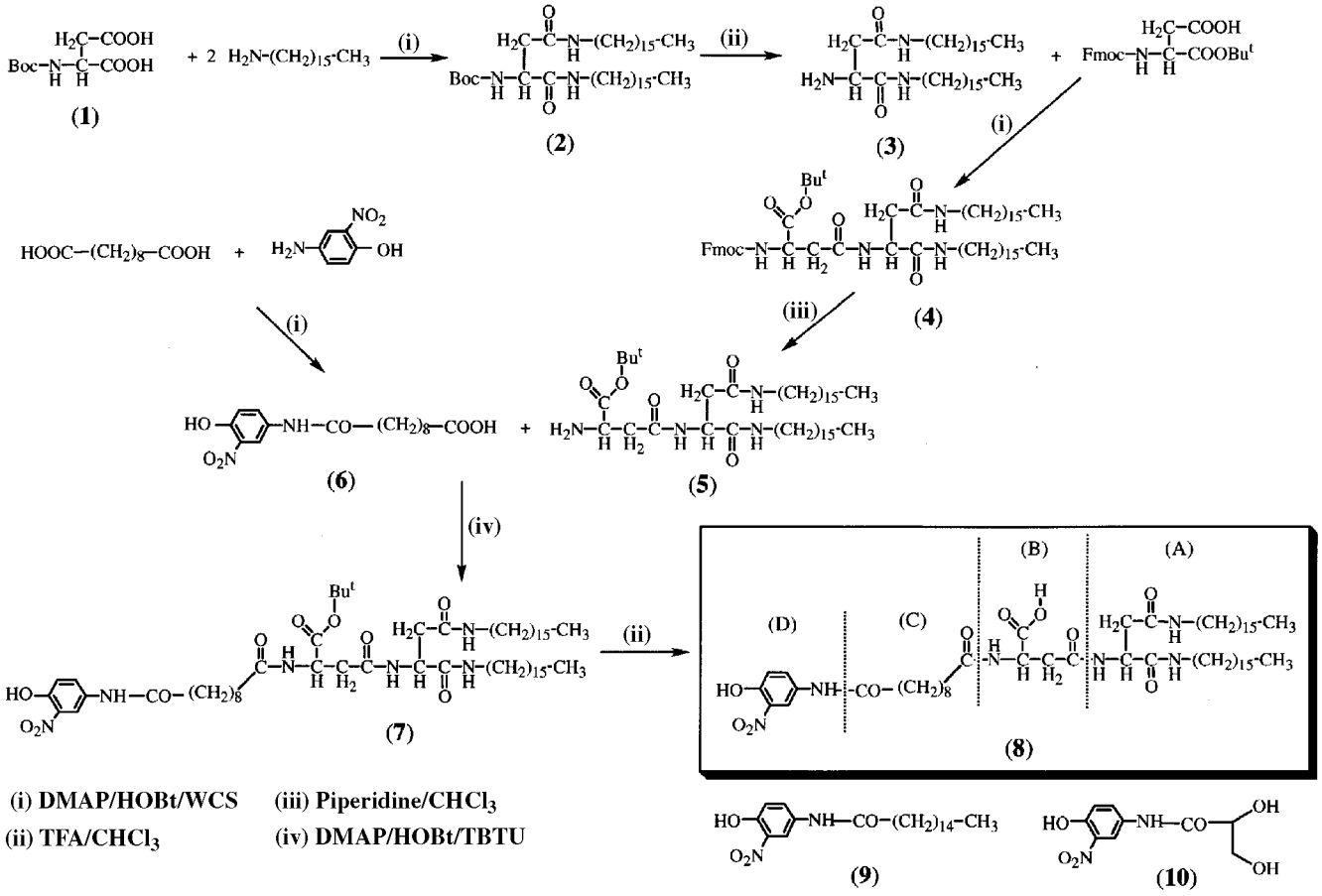

SCHEME 1

6.8 in aqueous solution. A similar shift of pK_a was observed for **9** (Scheme 1), whose pK_a is 8.7 in a lipid bilayer. These phenomena appear quite reasonable, if the 2-nitrophenol groups are assumed to be situated in hydrophobic environments such as the vicinity of liposome surface or inside the bilayer membrane, since the electrostatic interaction between the 2-nitrophenolate anion and a proton should be stronger in hydrophobic environments than in water. This is also supported by the absorption maxima (λ_{max}) of **8**, **9,** and **10** shown in Table 1, where λ_{max} in an aqueous solution is as a whole shorter than those in organic solvents such as chloroform and methanol. It is generally recognized that the blue shift in polar solvents is characteristic of n→π* transitions (11). In view of the pK_a values of **8** in liposome, it is concluded that the 2-nitrophenol group of **8** should be located in hydrophobic envi-

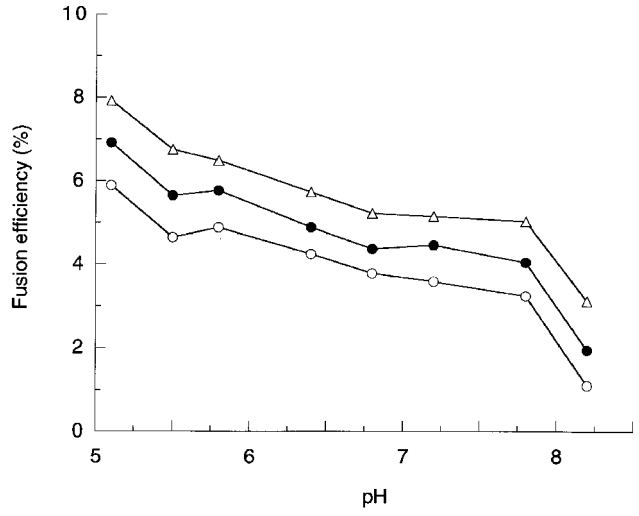

FIG. 1. Relation between fusion efficiency (%) and pH. Concentration of **8** is 5 mol%; Times: 5 min (○), 10 min (●), 15 min (△). Structure of **8** is presented in Scheme 1.

TABLE 1
Ultraviolet-Visible Absorption Maxima (nm) of Compounds 8–10 in Neutral and Anionic Forms[a]

	8		9		10	
	Neutral	Anionic	Neutral	Anionic	Neutral	Anionic
Liposome	374	448	379	448		
$CHCl_3$			390	446		
$CHCl_3$/MeOH (45:55)	384	433				
MeOH			383	433	379	430
H_2O					367	427

[a]Structures of **8–10** are illustrated in Scheme 1.

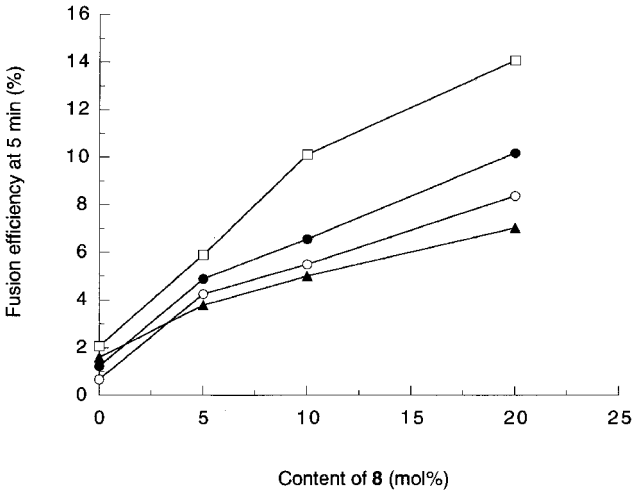

FIG. 2. Relation between fusion efficiency at 5 min (%) and content of **8** (mol%). pH: 5.1 (□), 5.8 (●), 6.4 (○), 6.8 (▲).

ronments. This is further suggested by the conformational analysis of **8** by molecular mechanics and dynamics calculation using MM3 parameters, from which two types of conformation with similar energies were obtained, *viz.*, stretched ones and folded ones. MM3 is the improved version of MM2 molecular mechanics method, which is used to determine molecular geometries using equations from classical Newtonian physics. In the folded conformations, the 2-nitrophenol group inevitably should be oriented toward the liposome surface. Figure 2 shows the relation between the fusion efficiency (%) and the content of **8** (mol%) included in the lipid bilayer of a liposome. The four lines denote different pH values of the solution: 5.1, 5.8, 6.4, and 6.8. The result, that the fusion efficiency increases monotonously with the amount of **8,** is compatible with our conclusion that lipid **8** is the key trigger compound to start the liposome fusion. Though the fusion occurred to a small extent in the absence of **8**, the fusion efficiency was considerably enhanced in the presence of **8**. In fact, it was increased about seven times when 20 mol% of **8** was included in the liposome membrane at pH 5.1. We are now preparing analogous lipids with 2-nitrophenol groups to explore in more detail the mechanism of liposome fusion.

ACKNOWLEDGMENTS

We thank Agency of Industrial Science and Technology (AIST) for providing AIST fellowship to Dr. S.N. Shah and also the M.S. University of Baroda in India for granting leave to Dr. S.N. Shah to pursue the research at NIBH.

REFERENCES

1. Wang, C.-Y., and Huang, L. (1987) pH-Sensitive Immunoliposomes Mediate Target-Cell-Specific Delivery and Controlled Expression of a Foreign Gene in Mouse, *Proc. Natl. Acad. Sci. USA 84*, 7851–7855.
2. Wang, C.-Y., and Huang, L. (1989) Highly Efficient DNA Delivery Mediated by pH-Sensitive Immunoliposomes, *Biochemistry 28*, 9508–9514.
3. Antonsson, B., Conti, F., Ciavatta, A.M., Montessuit, S., Lewis, S., Martinou, I., Bernasconi, L., Bernard, A., Mermod, J.-J., Mazzei, G., Maundrell, K., Gambale, F., Sadoul, R., and Martinou, J.-C. (1997) Inhibition of Bax Channel-Forming Activity by Bcl-2, *Science 277*, 370–372.
4. Ropert, C., Lavignon, M., Dubernet, C., Couvreur, P., and Malvy, C. (1992) Oligonucleotides Encapsulated in pH-Sensitive Liposomes Are Efficient Toward Friend Retrovirus, *Biochem. Biophys. Res. Commun. 183*, 879–885.
5. Yagi, N., Ogawa, Y., Kodaka, M., Okada, T., Tomohiro, T., Konakahara, T., and Okuno, H. (1999) A Surface-Modified Functional Liposome Capable of Binding to Cell Membranes, *Chem. Commun.,* 1687–1688.
6. Yagi, N., Ogawa, Y., Kodaka, M., Okada, T., Tomohiro, T., Konakahara, T., and Okuno, H. Preparation of Functional Liposomes with Peptide Ligands and Their Binding to Cell Membranes (*Lipids* in press).
7. Kono, K., Kimura, S., and Imanishi, Y. (1990) pH-Dependent Interaction of Amphiphilic Polypeptide Poly(Lys-Aib-Leu-Aib) with Lipid Bilayer Membrane, *Biochemistry 29*, 3631–3637.
8. Kono, K., Nishii, H., and Takagishi, T. (1993) Fusion Activity of an Amphiphilic Polypeptide Having Acidic Amino Acid Residues: Generation of Fusion Activity by α-Helix Formation and Charge Neutralization, *Biochim. Biophys. Acta 1164*, 81–90.
9. Ogawa, Y., Tomohiro, T., Yamazaki, Y., Kodaka, M., and Okuno, H. (1999) Non-Peptidic Liposome-Fusion Compounds at Acidic pH, *Chem. Commun*., 823–824.
10. Ogawa, Y., Kawahara, H., Yagi, N., Kodaka, M., Tomohiro, T., Okada, T., Konakahara, T., and Okuno, H. (1999) Synthesis of a Novel Lipopeptide with α-Melanocyte-Stimulating Hormone Peptide Ligand and Its Effect on Liposome Stability, *Lipids 34*, 387–394 [Erratum in *Lipids 34*, 643 (1999)].
11. McConnell, H. (1952) Effect of Polar Solvents on the Absorption Frequency of n→π Electronic Transitions, *J. Chem. Phys.*, 20, 700–704.

[Received January 3, 2000 and in final revised form and accepted May 4, 2000]

Evaluation of Brain Long-Chain Acylcarnitines During Cerebral Ischemia

J. Deutsch[a,*], B. Kalderon[b], A.D. Purdon[c], and S.I. Rapoport[c]

Departments of [a]Medicinal Chemistry and [b]Human Nutrition and Metabolism, Faculty of Medicine, The Hebrew University of Jerusalem, Jerusalem, Israel, and [c]Section on Brain Physiology and Metabolism, National Institute on Aging, National Institutes of Health, Bethesda, Maryland, 20892

ABSTRACT: Concentration and distribution of long-chain acylcarnitines in control microwaved and ischemic (decapitated) rat brain were measured by electrospray ionization tandem mass spectrometry. The total acylcarnitine concentration from control rat brains equaled 7–8 nmol/g wet weight brain, about one-fourth the total concentration of long-chain acyl-CoA, indicating a small role in buffering the total acyl-CoA pool concentration. Furthermore, acylcarnitine did not differ between ischemic and control rat brain with regard to total concentration or concentrations of molecular species of acylcarnitine. Therefore, the size of the acylcarnitine pool in brain is not affected by the dramatic increase in unesterified fatty acids (~4×) that occurs in ischemia.

Paper no. L8231 in *Lipids 35,* 693–696 (June 2000).

Acyl-CoA and acylcarnitine (acyl-Cn) are two fatty acid metabolic intermediates involved in the incorporation of fatty acids into phospholipids and neutral lipids (1) and in β-oxidation of fatty acids (2), respectively. Carnitine (Cn) palmitoyltransferase (CPT-1) (EC 2.3.1.21) catalyzes the reversible transfer of long-chain fatty acids from acyl-Cn to acyl-CoA (Eq. 1) (3):

$$\text{acyl-CoA} + \text{Cn} \xrightarrow{\text{CPT}} \text{acyl-Cn} + \text{CoA} \xrightarrow{\text{CPT}} \text{acyl-CoA} + \text{Cn} \quad [1]$$

Fatty acids entering the brain from plasma, or synthesized *de novo*, can be incorporated into lysolipids after being activated to acyl-CoA by acyl-CoA synthetase (EC 6.2.1.3) in the endoplasmic reticulum of the cell (1,4,5). Additionally, in the mitochondrial membrane cytosolic acyl-CoA can be converted by CPT-1 to acylcarnitine, which in turn is converted to acyl-CoA in the mitochondrial interior, which is further metabolized by β-oxidation (2,3).

Arduini *et al*. have proposed an additional role for acyl-Cn and CPT (6–8) based on their location in nonmitochondrial compartments [the endoplasmic reticulum, peroxisomes (9), and plasma membrane of red blood cells (6)] such that a cytosolic pool of acyl-Cn is maintained (9). Cytosolic, nonmitochondrial acyl-Cn is a potential reservoir of activated fatty acid for either mitochondrial or nonmitochondrial acyl-CoA and can buffer acyl-CoA and CoA concentrations at set levels (9).

In cerebral ischemia or trauma, there is a dramatic, well-documented increase (4–5 times) in the size of the brain unesterified fatty acid pool (10–12). However, in rat brain after decapitation (10), and in gerbil brain after ischemia (12), the total concentration of brain acyl-CoA is not altered, although there is a redistribution in the concentrations of individual molecular species of acyl-CoA (arachidonoyl-CoA increases at the expense of other molecular species). Cardiac ischemia also results in increased concentrations of unacylated fatty acids, but acyl-CoA (13) and acyl-Cn are both elevated (14).

We previously reported the concentrations of fatty acid and acyl-CoA molecular species in ischemic compared to control rat brain (10). In those studies, however, concentrations of acyl-Cn species were not measured, due to the lack of suitable analytical methodology. With recent advances in electrospray ionization tandem mass spectrometry (ESI/MS/MS) technology, quantifications of acyl-Cn in heart (ischemic and control) (14), and subsequently plasma have been reported (15–17).

In this study we measured the concentrations of long-chain acyl-Cn in ischemic (decapitation model) and microwaved (control) rat brain. Our aim was to determine baseline concentrations and monitor the effect of ischemia.

MATERIALS AND METHODS

Acyl-Cn standards were obtained from Deva Biotech (Hatboro, PA). *n*-Butanol and acetylchloride were purchased from Aldrich (Milwaukee, WI). Male rats, 200–250 g (Sprague-Dawley, Charles Rivers Laboratories, Wilmington, MA) were anesthetized with pentobarbital (50 mg/kg i.p.) and their heads subjected to microwave irradiation (Cober Electronics, Norwalk, CT), or they were decapitated (ischemic brain, 10 min). Brain (100–200 mg) was rapidly removed and then was mixed with methanol (2.0 mL), spiked with tetradecanoyl-d_3-Cn and heptadecanoyl-d_3-Cn (100 ng) as internal standards, and sonicated (Misonix, Farmingdale, NY) for 20 s. In the assay not all the molecular species have the same recovery. A

*To whom correspondence should be addressed at Dept. of Medicinal Chemistry, School of Pharmacy, The Hebrew University of Jerusalem, Jerusalem 91120, Israel. E-mail: odj@cc.huji.ac.il

Abbreviations: acyl-Cn, acylcarnitine; Cn, carnitine; CPT-1, carnitine palmitoyltransferase; ESI/MS/MS, electrospray ionization tandem mass spectrometry.

recovery of 72–75% was obtained for heptadecanoyl-Cn and 95–98% for tetradecanoyl-Cn. To overcome this difference, we used two internal standards: trideuterated tetradecanoyl-Cn for estimation of dodecanoyl-Cn and tetradecanoyl-Cn and heptadecanoyl-d_3-Cn for hexadecanoyl-Cn and stearoyl-Cn. After centrifugation, the extract was concentrated under nitrogen to 0.5 mL and the supernatant filtered and dried. We found that both the reproducibility and recovery decrease significantly if the proteins from the methanolic extract are not completely removed by filtration.

The dry extract was treated with a freshly prepared solution (0.5 mL) of *n*-butanol/acetylchloride (9:1) at 0°C for derivatization. The mixture was allowed to stand at room temperature for 10 min, concentrated under nitrogen at 40°C to 0.1 mL, and heated to 80°C for 20 min. The product was dried and the residue redissolved in 150 µL 60% acetonitrile. Ten microliters of solution was injected into a mass spectrometer. ESI/MS/MS was performed with a VG QUATTRO II instrument (Micromass, Altrincham, United Kingdom).

RESULTS

Extracts from nondecapitated, control brains and decapitated brains were analyzed for acyl-Cn molecular species. A tentative molecular species hydrocarbon profile from 14–22 carbon atoms long was anticipated based on previous analysis of brain acyl-CoA (10). Qualitative profiles of the acyl-Cn *n*-butyl esters were obtained by monitoring precursor-ion scans of the common fragment at *m/z* 85 of *n*-butylcarnitine derivatives (Scheme 1).

Mass spectral patterns are illustrated in Figure 1 and include long-chain acyl-Cn 20:4, 18:0, 18:1, 16:0, 16:1, 14:0, 14:1, and 12:0 from control rat brains and brains after decapitation (Table 1).

Results for acyl-Cn molecular species (n = 3) and total acyl-Cn (n = 3) in control brains and ischemic brains are presented in Table 1 and were compared by a standard t-test. Significance was assumed if $P > 0.05$. Control brains had a total acyl-Cn concentration of 7.24 ± 0.60 nmol/g while the concentration of total acyl-Cn in ischemic brains was 9.14 ± 0.83 nmol/g (average ± SEM), and these values were not significantly different. Although the concentrations of individual molecular species in ischemic brains were all numerically higher than those in control brains the numerical difference in each case was not significant.

TABLE 1
Distribution of Molecular Species of Acylcarnitines in Ischemic and Microwaved (control) Rat Brain

Molecular species acylcarnitine	Ischemic	Microwaved
	Concentration (nmol/g brain)[a]	
12:0	0.41 ± 0.58	0.38 ± 0.08
14:1	0.38 ± 0.10	0.22 ± 0.01
14:0	0.81 ± 0.10	0.67 ± 0.01
16:1	0.98 ± 0.26	0.80 ± 0.11
16:0	2.84 ± 0.39	2.46 ± 0.54
18:1	1.99 ± 0.26	1.75 ± 0.21
18:0	0.97 ± 0.14	0.82 ± 0.02
20:4	0.43 ± 0.12	0.14 ± 0.01
Total	9.14 ± 0.83	7.24 ± 0.60

[a]Mean ± SEM (n = 3). No statistical difference was found between individual molecular species of acylcarnitine in control vs. ischemic brains ($P > 0.05$).

DISCUSSION

The average total acyl-Cn concentration in this study was 7 nmol/g brain, which is considerably lower and only 25% of the 30 nmol/g brain for acyl-CoA (10). In the ischemic decapitated brain, four- to fivefold elevations of total unesterified fatty acids have been reported for this decapitated rat brain model (10,11), and in other ischemic brain models (11,12). The increases in unesterified fatty acids following ischemia in rat brain are clearly established. Unesterified arachidonic acid increases up to 50 times, whereas relative increases in the concentration of other fatty acids are of lesser magnitude (10,11). However, the net brain concentration of acyl-CoA is not altered, but arachidonoyl-CoA is elevated

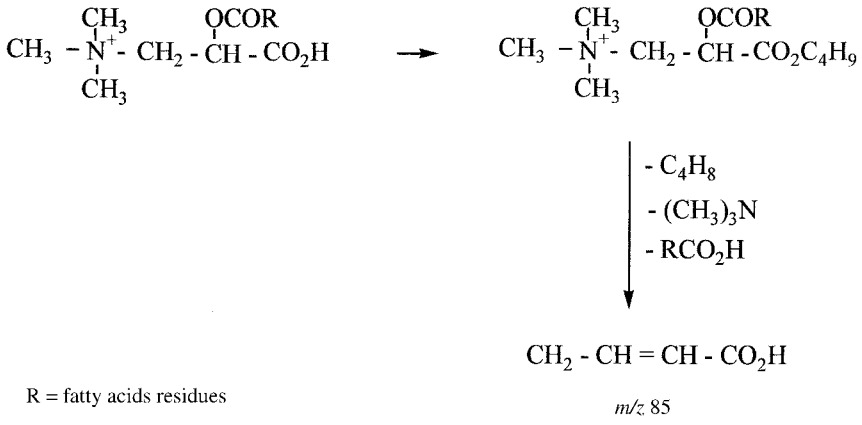

SCHEME 1

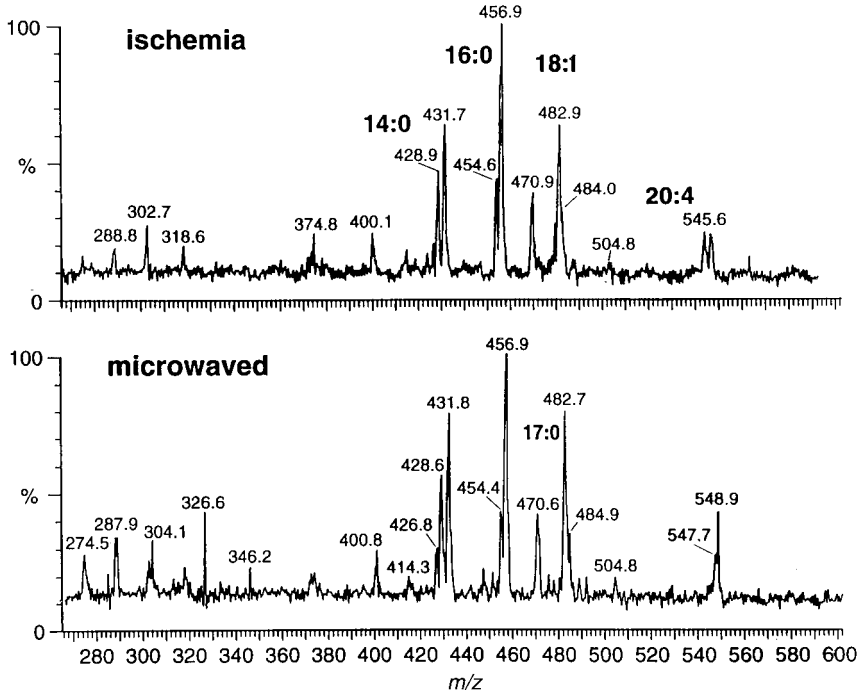

FIG. 1. Electrospray ionization tandem mass spectrometry of molecular species of acylcarnitines from rat brain spiked with tetradecanoyl-d_3-carnitine and heptadecanoyl-d_3-carnitine as internal standards (ischemia vs. microwaved).

fivefold, at the expense of changes in concentrations of palmitoyl-, stearoyl-, and docosahexaenoyl-CoA (10–12,18). In the present study, we found that the acyl-Cn pool also was not altered in the ischemic brain, and, furthermore, there was no redistribution involving arachidonoyl-Cn or other molecular species. Interestingly, we found an increase in the concentration of arachidonoyl-Cn in traumatized rat brain (15). In this work a trend toward an increase in arachidonoyl-Cn is evident ($P < 0.12$) compared to other molecular species, but no significant difference between ischemic and control brains was found.

In ischemic heart, there is evidence for an elevation of acyl-Cn in sarcolemmal membranes (13,14). In contrast, our work indicates that such elevations do not occur in ischemic brain, at least following the complete ischemia of decapitation. Therefore, membrane-destabilizing effects of increased levels of acyl-Cn on the membrane bilayer are not a concern in ischemic brain. This indicates a profound difference in the processing of fatty acids by brain and heart. It may be that the trend toward an increase in levels of acyl-Cn molecular species seen in our data (Table 1) may substantially increase with time during reperfusion *in vivo* such that significant differences would be observed. A thorough investigation of the time course of acyl-Cn concentration during reperfusion after different lengths of ischemia will investigate such metabolism.

The relatively low concentration of acyl-Cn compared to acyl-CoA (~7 nmol/g vs. ~30 nmol/g, respectively) in control brain could provide only a modest buffering capacity for maintaining the acyl-CoA/CoA ratio. The transit time of palmitic acid through the palmitoyl-CoA pool is approximately 6 s in rat brain (5). Obviously, an isolated pool of palmitoyl-Cn (2.4 nmol/g) could maintain a constant level of palmitoyl-CoA for only a few seconds. Similar considerations can be applied to other molecular species of these metabolic intermediates. However, we cannot deny a kinetic role for acyl-Cn in the incorporation of fatty acids into phospholipids or in helping to maintain the acyl-CoA/CoA ratio. Arduini *et al.* have demonstrated involvement of acyl-Cn in the acylation of lysophospholipids and diglyceride (6,9). There are 117 nmol Cn/g in control brain (18) which, with the 7 nmol/g acyl-Cn, indicates a considerable reserve of Cn for acylation and maintenance of acyl-Cn levels. Therefore, any decrease in acyl-CoA could be met by rapid transfer of fatty acid from acyl-Cn to acyl-CoA, and reacylation of carnitine could maintain acyl-Cn concentration. Of course, any increase in either acyl-CoA or acyl-Cn could be modulated through the reversible equilibration shown in Equation 1 and the equilibration between acyl-CoA and the unesterified fatty acid pool.

Studies of the entry of radiolabeled fatty acids into the acyl-Cn pool in brain could provide information on acyl-Cn turnover (5,11). During reperfusion in gerbil brain following 5 min of ischemia, we demonstrated accelerated reincorporation of arachidonic acid into brain phospholipids and a normal rate of incorporation of palmitic acid, in the face of very high concentrations of these fatty acids in brain (19). Maintenance of the total acyl-CoA and total acyl-Cn pools at control levels during reperfusion following ischemia may be crucial to the reacylation of lysolipids.

REFERENCES

1. Waku, K. (1992) Origin and Fates of Fatty Acyl-CoA Esters, *Biochim. Biophys. Acta 1124*, 101–111.
2. Eaton, S., Bartlett, R., and Pourfarzam, M. (1996) Mammalian Mitochondrial Beta-Oxidation, *Biochem. J. 320*, 345–357.
3. Bremer, J. (1983) Carnitine—Metabolism and Functions, *Physiol. Rev. 63*, 1420–1480.
4. Washizaki, K., Smith, Q.R., Rapoport, S.I., and Purdon, A.D. (1994) Brain Arachidonic Acid Incorporation and Precursor Pool Specific Activity During Intravenous Infusion of Unesterified [^{3}H]Arachidonate in the Anesthetized Rat, *J. Neurochem. 63,* 727–736.
5. Grange, E., Deutsch, J., Smith, Q.R., Chang, M., Rapoport, S.I., and Purdon, A.D. (1995) Brain Palmitic Acid Incorporation in the Conscious Rat: Relationship Between Specific Activity of [^{3}H]Palmitic Acid in Plasma and Brain Precursor Pools, *J. Neurochem. 65*, 2290–2298.
6. Arduini, A., Mancinelli, G., Radatti, G.L., Dottori, S., Molanjoni, F., and Ramsay, R.R. (1992) Role of Carnitine and Carnitine Palmitoyltransferase as Integral Components of the Pathway for Membrane Phospholipid Fatty Acid Turnover in Intact Human Erythrocytes, *J. Biol. Chem. 267*, 12673–12681.
7. Arduini, A., Mancinelli, G., and Ramsay, R.R. (1990) Palmitoyl-L-carnitine, a Metabolic Intermediate of the Fatty Acid Incorporation Pathway in Erythrocyte Membrane Phospholipids, *Biochem. Biophys. Res. Commun. 173*, 212–217.
8. Ramsay, R.R., Mancinelli, G., and Arduini, A. (1991) Carnitine Palmitoyltransferase in Human Erythrocyte Membranes. Properties and Malonoyl-CoA Sensitivity, *Biochem. J. 275*, 685–688.
9. Ramsey R.R., and Arduini, A. (1993) The Carnitine Acyltransferases and Their Role in Modulating Acyl-CoA Pools, *Arch. Biochem. Biophys. 302,* 307–314.
10. Deutsch, J., Rapoport, S.I., and Purdon, A.D. (1997) Relation Between Free Fatty Acid and Acyl-CoA Concentrations in Rat Brain Following Decapitation, *Neurochem. Res. 22*, 759–765.
11. Bazan, N.G. (1970) Effects of Ischemia and Electroconvulsive Shock on Free Fatty Acid Pool in the Brain, *Biochim. Biophys. Acta* 218, 1–10.
12. Rabin, O., Deutsch, J., Grange E., Pettigrew, K.D., Chang, M.C.J., Rapoport, S.I., and Purdon, A.D. (1997) Changes in Cerebral Acyl-CoA Concentrations Following Ischemia-Reperfusion in Awake Gerbils, *J. Neurochem. 68,* 2111–2118.
13. van der Vusse, G.J., and Stam, H. (1987) Lipid and Carbohydrate Metabolism in the Ischaemic Heart, *Basic Res. Cardiol. 82* (Suppl. 1), 149–153.
14. Ford, D.A., Han, X., Horner, C.C., and Gross, R.W. (1996) Accumulation of Unsaturated Acylcarnitine Molecular Species During Acute Myocardial Ischemia: Metabolic Compartmentalization of Products of Fatty Acyl Chain Elongation in the Acylcarnitine Pool, *Biochemistry 35*, 7903–7909
15. Deutsch, J., Heller, H., Kalderon, B., Shohami, E., Rapoport, S.I., and Purdon, D. (1997) Mass Spectral Evaluation of Long Chain Carnitines in Rat Brain During Cerebral Ischemia and Cerebral Trauma by Elecrospray Ionization, *Book of Abstracts, International Mass Spectrometry Conference,* p. 112, University of Tampera, Tampera, Finland.
16. Delome, F., Vianey-Saban, C., Guffon, N., Favre-Bonvin, J., Guiland, P., Beecki, M., Mathieu, M., and Divry, P. (1997). Diagnosis of Inborn Errors of Metabolism by Acylcarnitine Profiling in Blood Using Tandem Mass Spectrometry, *Arch. Pediatr. 4*, 819–826.
17. Moder, M., Loster, H., Herzschuh, R., and Popp, P. (1997) Determination of Urinary Acylcarnitines by ESI–MS Coupled with Solid-Phase Microextraction, *J. Mass Spectros. 32,* 1195–1204.
18. Brooks, D.E., and McIntosh, J.E.A. (1975) Turnover of Carnitine by Rat Tissues, *Biochem. J. 148,* 439–445.
19. Rabin, O., Chang, M.C.J., Grange, E., Bell, J., Rapoport, S.I., Deutsch, J., and Purdon, A.D. (1998) Selective Acceleration of Arachidonic Acid Reincorporation into Brain Phospholipid Following Transient Ischemia-Reperfusion in Awake Gerbils, *J. Neurochem. 70,* 325–334.

[Received April 12, 1999, and in final revised form March 1, 2000; revision accepted April 18, 2000]

Diversity of Mouse Lipoxygenases: Identification of a Subfamily of Epidermal Isozymes Exhibiting a Differentiation-Dependent mRNA Expression Pattern

Markus Heidt, Gerhard Fürstenberger, Sonja Vogel, Friedrich Marks, and Peter Krieg*

Research Program on Tumor Cell Regulation, Deutsches Krebsforschungszentrum, 69120 Heidelberg, Germany

ABSTRACT: By using reverse transcription-polymerase chain reaction technology (RT-PCR) and Northern blot analysis, the tissue-specific mRNA expression patterns of seven mouse lipoxygenases (LOX)—including 5S-, 8S-, three isoforms of 12S-, 12R-LOX, and a LOX of an as-of-yet unknown specificity, epidermis-type LOX-3 (*e*-LOX-3)—were investigated in NMRI mice. Among the various tissues tested epidermis and forestomach were found to express the broadest spectrum of LOX. With the exception of 5S- and platelet-type 12S-LOX (*p*12S-LOX) the remaining LOX showed a preference to exclusive expression in stratifying epithelia of the mouse, in particular the integumental epidermis. The expression of the individual LOX in mouse epidermis was found to depend on the state of terminal differentiation of the keratinocytes. mRNA of epidermis-type 12S-LOX (*e*12S-LOX) was detected in all layers of neonatal and adult NMRI mouse skin, whereas expression of *p*12S-LOX, 12R-LOX, and *e*-LOX-3 was restricted to suprabasal epidermal layers of neonatal and adult mice. 8S-LOX mRNA showed a body-site-dependent expression in that it was detected in stratifying epithelia of footsole and forestomach but not in back skin epidermis. In the latter, 8S-LOX mRNA was strongly induced upon treatment with phorbol esters. With the exception of *e*12S-LOX and *p*12S-LOX, the isozymes that are preferentially expressed in stratifying epithelia are structurally related and may be grouped together into a distinct subgroup of epidermis-type LOX.

Paper no. L8451 in *Lipids 35,* 701–707 (June 2000).

Lipoxygenases (LOX) are a family of dioxygenases that catalyze the stereo- and regiospecific oxygenation of polyunsaturated fatty acids with 1-*cis*,4-*cis*-pentadiene moieties. Mammalian LOX metabolize arachidonic acid into a series of bioactive compounds, such as leukotrienes, lipoxins, hydroxyeicosatetraenoic acids and hepoxilins (1). LOX metabolites play important roles in inflammatory processes, blood clotting, leukocyte chemotaxis (2,3), in distinct inflammatory skin diseases like psoriasis (4,5), atherosclerosis (6,7), and cancer (8,9).

Mammalian LOX are categorized according to the positional specificity of oxygen insertion into arachidonic acid. Four positional LOX isoforms have been identified in mammalian tissues, including the 5-, 8-, 12-, and 15-LOX, which insert oxygen to yield as primary products the corresponding S-enantiomeric hydroperoxyeicosatetraenoic acids. A further increase of LOX diversity was found to be due to the existence of isozymes with identical positional specificity such as the leukocyte-type (*l*), platelet-type (*p*), and epidermis-type (*e*) 12S-LOX. An additional complexity is introduced by the identification of a new mammalian LOX generating products with *R*-chirality.

We and others have cloned seven different LOX isoenzymes from mouse tissues, six of which were isolated from normal, phorbol ester-treated, and neoplastic epidermis including *l*-, *p*-, and *e*12S-LOX (9–13), an inducible 8S-LOX (14,15), a 12R-LOX (16), and another LOX of an as-of-yet unknown enzymatic specificity termed *e*-LOX-3 (17). In addition, a mouse 5S-LOX cDNA was cloned from mouse peritoneal macrophages (18). In this paper we analyzed the mRNA expression pattern of these LOX in mouse tissues and, in particular, in stratifying epithelia. According to the predominant expression in epidermis and the structural relationship of the proteins, 8S-, 12R-LOX, and *e*-LOX-3 are grouped together in a distinct LOX subfamily, i.e., the epidermis-type LOX, whereas *p*- and *e*12S-LOX belong to a distant subfamily.

EXPERIMENTAL PROCEDURES

Animals; treatment with phorbol ester. All tissues were obtained from 7-wk-old female NMRI mice (BRL, Füllinsdorf, Switzerland). Three days before treatment the back skin of the mice was shaved with electrical clippers. For topical application, 10 nmol of 12-*O*-tetradecanoylphorbol-13-acetate (TPA) was dissolved in 0.1 mL of acetone and applied onto the shaved back skin. After various time points (0.5, 1, 2, 4, 6, 24, 48 h) the animals were killed by cervical dislocation. After dissection of the back skin total RNA was extracted from epidermis. The animal experiments have been per-

*To whom correspondence should be addressed at Research Program on Tumor Cell Regulation, Deutsches Krebsforschungszentrum, Im Neuenheimer Feld 280, 69120 Heidelberg, Germany.
E-mail: p.krieg@dkfz-heidelberg.de

Abbreviations: dNTP, deoxynucleotide triphosphate mixture; *e*, epidermis-type; *l*, leukocyte-type; LOX, lipoxygenase; *p*, platelet-type; PCR, polymerase chain reaction; RT-PCR, reverse transcription-polymerase chain reaction; SDS, sodium dodecyl sulfate; TPA, 12-*O*-tetradecanoylphorbol-13-acetate.

formed according to the guidelines and with permission of the German animal protection committee.

Fractionation of keratinocytes from neonatal and adult epidermis. After decapitation (neonatal mice, 2 d old)/or cervical dislocation (adult mice) the back skin of the mice was dissected as described in detail (19,20). Epidermal cells were obtained from skin by trypsinization. The keratinocyte suspension was then centrifuged on a discontinous Percoll density gradient, obtaining a separation into four fractions. Fraction I on top of the gradient consisted mainly of squamous and large granular cells. With increasing density of the gradient fraction II consisted of early granular and spinous cells, and fractions III and IV contained basal keratinocytes. The individual fractions have previously been characterized thoroughly by monitoring expression of differentiation-specific keratin and lectin markers (19).

Preparation of RNA. Cells were washed with phosphate-buffered saline and scraped directly in guanidinium thiocyanate solution (RNA-Clean, AGS, Heidelberg, Germany). Various tissues frozen at –80°C were first homogenized in a dismembrator and then in guanidinium thiocyanate solution (RNA-Clean, AGS). Total RNA was extracted according to the manufacturer's instructions. RNA concentration was quantified by ultraviolet absorption at 260 nm.

Reverse transcription-polymerase chain reaction (RT-PCR) analysis. RNA samples were treated with DNAse I, and first strand cDNA synthesis was carried out with 1 μg of total RNA in 20 μL reaction mixtures using the RT-PCR kit (PerkinElmer, Foster City, CA) with oligo(dT) primer according to the manufacturer's specifications. The reverse transcription mixture contained 1 mM of deoxynucleotide triphosphate mixture (dNTP), 2 μL 10 × PCR buffer (500 mM KCL, 100 mM Tris-HCl, pH 8.3), 4 μL $MgCl_2$ (25 mM), 1 μL oligo(dT) primer (50 μM), 1 μL RNase inhibitor (20 units/μL), and 1 μL MuLV (Murine Leukemia Virus) reverse transcriptase (50 units/μL). This mixture was incubated for 10 min at room temperature and 15 min at 42°C, and heated to 99°C for 5 min.

Isoenzyme-specific primers (primer set "a") were selected from 3′-untranslated regions using "Oligo" primer analysis software (National Biosciences, Plymouth, MA). Second primer sets (set "b") spanning conserved intron positions were designed to discriminate amplification products originating from contaminating genomic DNA. Sequences of the PCR primers and the length of the the PCR products are listed in Tables 1 and 2. Amplification of β-actin (429 bp) was also performed as an internal control using the forward primer 5′-AAACTGGAACGGTGAAGGC-3′ and the reverse primer 5′-GCTGCCTCAACACCTCAAC-3′. The PCR reactions were primed with 3 μL of 10^{-1} dilutions of the cDNA reactions using 20 pmol of primers in 10 mM Tris/HCl, pH 9.0, 50 mM KCl, 1.5 mM $MgCl_2$, 0.1% Triton X100, 0.2 mg/mL bovine serum albumin with 0.2 mM of each dNTP, and 2.5 units Taq polymerase (Appligene Oncor, Illkirch, France) in 50 μL reactions. The PCR was programmed in a PTC-200 DNA Engine (MJ Research, Watertown, CA) as follows: 94°C, 5 min for one cycle; 94°C for 90 s, 51.8–60°C (see Table 2) for 4 min, and 72°C for 2 min 30 s for 30 cycles; 72°C for 10 min for one cycle. Then, the block temperature was held at 4°C. Aliquots (10 μL) of the reaction products were analyzed by electrophoresis on 2% agarose gels. The identity of the PCR products was confirmed either by restriction enzyme analysis or sequence determination.

Cloning of PCR products and DNA sequencing. The PCR-amplified bands were cloned into the vector pCRII-TOPO (Invitrogen, San Diego, CA). Sequences of the inserts were determined using the ABI Big Dye Terminator Cycle Sequencing Ready Reaction kit (PerkinElmer/Applied Biosystems, Foster City, CA), and the products were resolved on an ABI prism 310 Genetic analyzer (PerkinElmer/Applied

TABLE 1
Polymerase Chain Reaction (PCR) Primers and Expected Fragment Size for PCR Amplification and Detection of Mouse Lipoxygenase Isoenzymes[a]

Enzyme	Forward primer	Reverse primer
5S-LOX	a. 5′-AGCACGGAAGACATGCCCTTCT-3′ b. 5′-TGGTGATCTTCACGGCCTCTGC-3′	a. 5′-GTCAGGTACTCGGACAGCTTCT-3′ b. 5′-GCCTCCAGGTTCTTGCGGAATC-3′
8S-LOX	a. 5′-GGTGGCTCACAACCATCTGTAA-3′ b. 5′-GGGTGAGGGAGATCTTCTCTGAGG-3′	a. 5′-ACCCCAACCAAACCAAACCAAA-3′ b. 5′-GAACTGACAGCTGCATGCTTGG-3′
*p*12S-LOX	a. 5′-TACCTCAAGCCCAGCCGCATAG-3′ b. 5′-TCCGCCCACCAGCAAGGACGAC-3′	a. 5′-CAAGACATTTAGTGCCCTGTAG-3′ b. 5′-CCTCAGATGGTGATACTGTTCT-3′
*l*12S-LOX	a. 5′-TTCCAAGAGCCCGCTTTCCATA-3′ b. 5′-CATTGTGTCCCCCTGATGACTT-3′	a. 5′-TCTATCACTAGCCCAAAACATC-3′ b. 5′-CAAGATGGATGGAAGAGTGCTG-3′
*e*12S-LOX	a. 5′-TGCCCATCTCAGCCCCAGAGGA-3′ b. 5′-ATCAACACCCTGGCACGGAATA-3′	a. 5′-AGAAGTGGGTACTAGGGATTCA-3′ b. 5′-GGGCTCCAAGCAGTCCAACCTC-3′
12R-LOX	a. 5′-ACCGATGCAGACCAAGGGGCTAAC-3′ b. 5′-TCTGAGTGGGACTGGCTGTTGG-3′	a. 5′-CAGTGTATGGAGGGGAGGGCAGAA-3′ b. 5′-AGAGACCTCCCTTGTTGAGAAG-3′
e-LOX-3	a. 5′-GAAGTTACAACTAAGGGGAAGG-3′ b. 5′-CAGACCAAGGGCGACACGACAA-3′	a. 5′-CTGGGCTCAAAGACAGACAATA-3′ b. 5′-CTGGGCTCAAAGACAGACAATA-3′

[a]Abbreviations: LOX, lipoxygenase; *e,* epidermis type*; l,* leukocyte-type; *p,* platelet-type.

TABLE 2
Annealing Temperatures and Length of the Expected Products[a]

Target cDNA	Annealing a (°C)	Product size a (BP)	Annealing b (°C)	Product size b (bp)
5S-LOX	56.9	239	60.0	307
8S-LOX	53.8	335	56.0	143
p12S-LOX	54.0	197	55.0	301
l12S-LOX	51.8	259	57.5	318
e12S-LOX	55.0	200	58.0	337
12R-LOX	54.0	333	57.0	235
e-LOX-3	54.5	313	55.0	635

[a]For abbreviations see Table 1.

Biosystems, Foster City, CA). The sequences were analyzed using the Heidelberg Unix Sequence Analysis Resources (HUSAR, Heidelberg, Germany) software programs.

Northern blot analysis. Northern gels loaded with 10 μg of RNA were electrophoresed, and RNA was transferred to Hybond-N^+ membranes (Amersham Pharmacia Biotec, Freiburg, Germany) by established procedures (9). Labeling was performed using the Random Primed DNA labeling kit (AGS) with electroeluted and purified cDNA fragments. The filters were washed with a final stringency of 0.1 × standard saline citrate and 0.5% sodium dodecyl sulfate (SDS) for 20 min and exposed using intensifying screens at −80°C. Rehybridization of the blots with a second 18S-rRNA-specific probe was performed by washing off the filters with 0.1% SDS, 20 mM Tris-HCl, pH 7.0 three times for 20 min each time at 60°C and hybridizing under the same conditions as described above.

RESULTS

LOX mRNA expression in mouse tissues. The mRNA expression of seven LOX was investigated in 15 different tissues of NMRI mice by RT-PCR and Northern blot analysis. Two primer sets were used for each sample and isozyme in order to ensure specificity. The PCR products were further characterized by restriction enzyme analysis or by sequence determination. Expression of 5S-LOX mRNA was evident in epidermis of back skin and footsole, forestomach epithelium, colon, and small intestine by PCR amplification of two specific amplicons of 239 and 307 bp. PCR reactions using primer set b for the amplification of 5S-LOX specific sequences were in general more efficient. By using this primer set, 5S-LOX-specific amplification products of 307 bp were also identified in brain, platelets, kidney, and testis (Fig. 1A). An 8S-LOX-specific product of 143 bp was found in footsole epidermis and less abundantly in forestomach epithelium, but not in epidermis of back skin. In addition, 8S-LOX-specific signals were observed in lung, colon, and brain (Fig. 1A). After epicutaneous administration of the phorbol ester TPA to mouse back skin, 8S-LOX expression was found to be induced, reaching a maximum 6 h after treatment (Fig. 1B).

*l*12S-LOX-specific PCR products could not be demonstrated in any of the tissues analyzed in this study. On the other hand, *p*12S-LOX-specific bands were found in every tissue tested, with the strongest signal intensities localized in back skin and footsole epidermis, tongue, forestomach, and above all in platelets (Fig. 2).

Specific signals for *e*12S-LOX (200 and 337 bp) were found exclusively in back skin and footsole epidermis and in platelets (Fig. 2). 12R-LOX-specific fragments (333 and 235 bp) were identified preferentially in epidermis, tongue, forestomach, and trachea, and with lower abundance in lung, liver, and kidney (Fig. 3). No 12R-LOX signal was found in

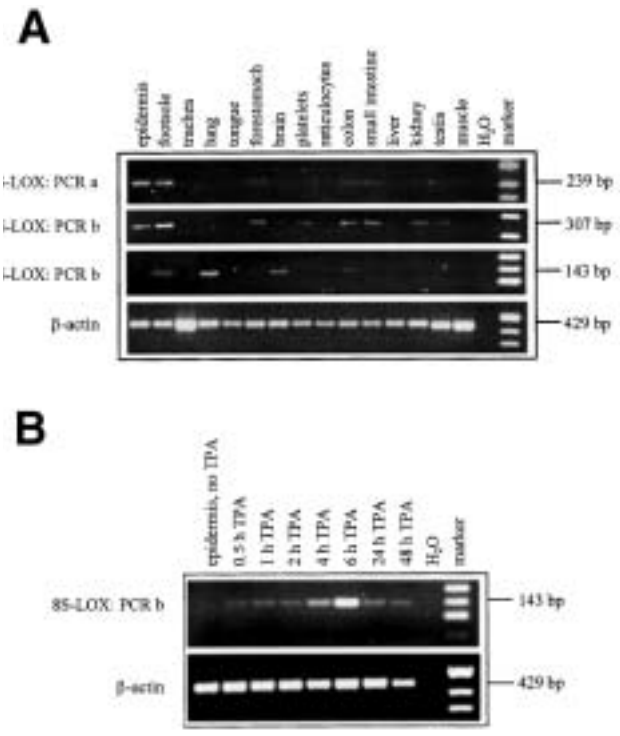

FIG. 1. Reverse transcription-polymerase chain reaction (RT-PCR) of 5S-lipoxygenase (LOX) and 8S-LOX mRNA in various mouse tissues (A) RNA from samples as indicated were reverse-transcribed to cDNA, and PCR were run with primer sets for 5S-LOX and for 8S-LOX and with a primer set for β-actin as an internal control as described in the Experimental Procedures section. H_2O indicates no cDNA template and was used as negative control. (B) Induction of 8S-LOX mRNA in mouse skin after 12-*O*-tetradecanoylphorbol-13-acetate (TPA) treatment. After topical application of 10 nmol TPA, total RNA was extracted from epidermis at the times indicated and reverse-transcribed to cDNA. PCR were run with 8S-LOX-specific primer set b and with a primer set for β-actin as internal control. H_2O indicates no cDNA template and was used as negative control.

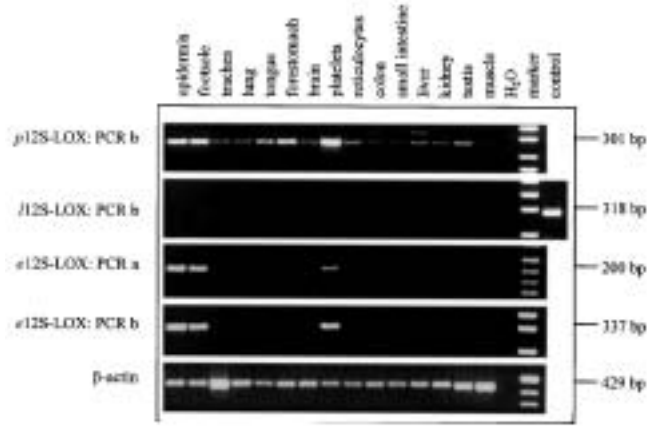

FIG. 2. RT-PCR of *p*12S-, *l*12S-, and *e*12S-LOX mRNA in various mouse tissues. RNA from samples as indicated were reverse-transcribed to cDNA, and PCR were run with primer sets for *p*12S-LOX, *l*12S-LOX and for *e*12S-LOX and with a primer set for β-actin as internal control as described in the Experimental Procedures section. H_2O indicates no cDNA template and was used as negative control. Control; cDNA template derived from HEK 293 cells transfected with a *l*12S-LOX expression construct. Abbreviations: *c*, epidermis-type; *l*, leukocyte-type; *p*, platelet type. For other abbreviation see Figure 1.

platelets. The most recent member of mouse LOX, *e*-LOX-3, showed a similar but not identical expression pattern as compared with that of 12R-LOX (Fig. 3). Strong specific signals of 313 bp were characteristic for epithelia, brain, and testis. Liver, colon, and kidney showed only weak signals, whereas no mRNA expression was found in platelets, reticulocytes, small intestine, and muscle (Fig. 3).

mRNA expression of LOX in keratinocyte layers of neonatal and adult mouse skin. As described above, preferential mRNA expression in stratifying epithelia was a consistent

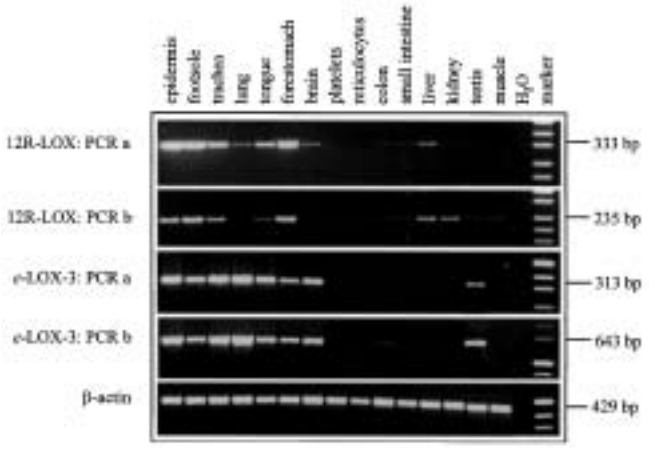

FIG. 3. RT-PCR of 12R-LOX and *e*-LOX-3 mRNA in various mouse tissues. RNA from samples as indicated were reverse-transcribed to cDNA, and PCR were run with primer sets for 12R-LOX and *e*-LOX-3 and with a primer set for β-actin as internal control as described in the Experimental Procedures section. H_2O indicates no cDNA template and was used as negative control. For abbreviations see Figures 1 and 2.

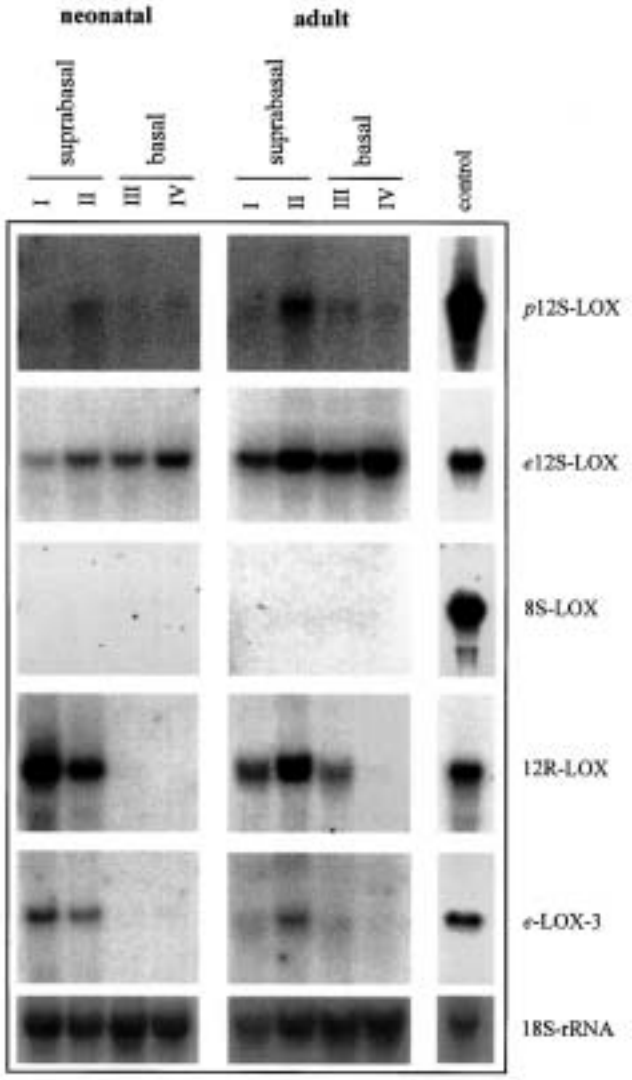

FIG. 4. Quantitation of mouse LOX mRNA in cellular subfractions of neonatal and adult mouse epidermis by Northern blot analysis. Single cell suspensions from neonatal and adult mouse epidermis were fractionated on Percoll gradients into basal (fractions III and IV) and differentiated cells (fractions I and II). Total RNA was isolated, separated on Northern gels , blotted and probed with ^{32}P-labeled isoenzyme-specific cDNA fragments as indicated on the left and then with a 18S rRNA-specific probe (lower panel). Control, RNA isolated from HEK 293 cells transiently transfected with the corresponding LOX-isoenzyme expression construct. For abbreviations see Figures 1 and 2.

feature for 8S-LOX (in particular upon induction by phorbol esters), *p*- and *e*12S- and 12R-LOX and *e*-LOX-3 as well. A more detailed Northern blot analysis of these LOX species indicated a differentiation-dependent expression pattern in skin epidermis. By centrifugation using a discontinuous Percoll density gradient, keratinocytes obtained from mouse epidermis can be subfractionated according to their stage of terminal differentiation (19,20). In using this approach, *e*12S-LOX mRNA was found to be associated with basal (fractions III and IV) and suprabasal (fractions I and II) cell layers of

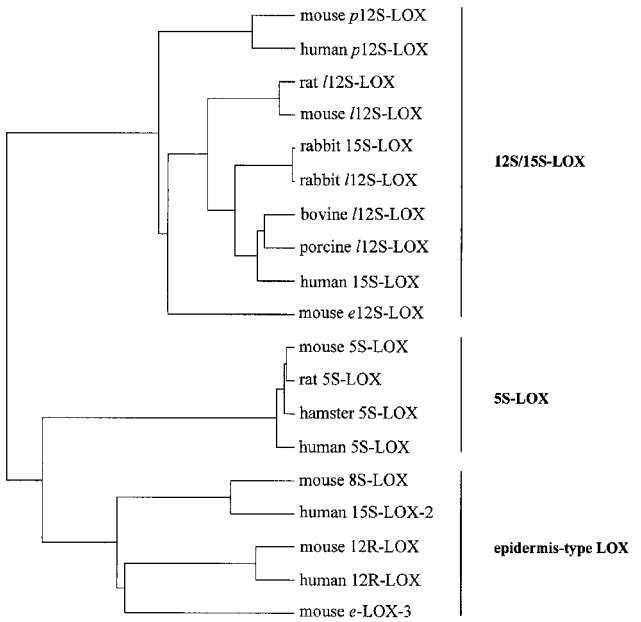

FIG. 5. Evolutionary tree of mammalian LOX. Multiple sequence alignments were performed using PileUp programs, and a phylogenetic tree was created from a distance matrix using the GrowTree program of the Heidelberg Unix Sequence Analysis Resources (HUSAR) software programs. Abbreviations and sources are as follows: *p*12S-LOX, platelet-type 12S-lipoxygenase (9,30); *l*12S-LOX, leukocyte-type 12S-lipoxygenase (9,31–34); 15S-LOX, 15S-lipoxygenase (35,36); *e*12S-LOX, epidermis-type 12S-lipoxygenase (12); 5S-LOX, 5S-lipoxygenase (18,37–39); 8S-LOX, 8S-lipoxygenase (15); 15S-LOX-2, 15S-lipoxygenase-2 (40); 12R-LOX, 12R-lipoxygenase (15,41); *e*-LOX-3, mouse epidermis-type lipoxygenase-3 (17).

neonatal epidermis, whereas12R-LOX and *e*-LOX-3 were predominantly expressed suprabasally with the strongest signals in fraction I (Fig. 4). *p*12S-LOX was predominantly expressed in fraction II consisting of spinous and early granular keratinocytes. A slightly different distribution of the mRNA for 12R-LOX and *e*-LOX-3 was found in adult epidermis in that the expression of the latter was restricted to fraction II whereas 12R-LOX mRNA could also be detected in basal keratinocytes of fraction III. All cell fractions obtained from untreated neonatal or adult mouse skin were negative for 8S-LOX (Fig. 4), 5S-LOX and *l*12S-LOX mRNA (data not shown).

Epidermis-type LOX. According to their preferential expression in epidermis and their phylogenetic relationship 8S-, 12R-LOX, and *e*-LOX-3 can be grouped together into a separate LOX subfamily. This subfamily of epidermis-type LOX also comprises the human ortholog of the mouse 12R-LOX as well as 15S-LOX-2, the human homolog of mouse 8S-LOX (Fig. 5). A remarkable feature of epidermis-type LOX isozymes is the diversity of the positional specificity and chirality of the LOX reaction of the individual members of this subfamily. *e*12S-LOX and *p*12S-LOX, being approximately equally expressed in epidermis and platelets, belong to a distant subfamily containing 12S- and 15S-LOX (Fig. 5).

DISCUSSION

The mRNA expression patterns of seven mouse LOX were analyzed in various tissues of NMRI mice. Stratifying epithelia such as back skin and footsole epidermis, forestomach, and tongue showed the most abundant mRNA content, both with respect to the spectrum of individual LOX isozymes and the relative strength of expression. The LOX species found in these stratifying epithelia included the more ubiquitously expressed *p*12S-LOX and the more specifically expressed 8S-, *e*12S-, 12R-LOX, and *e*-LOX-3, while expression of mouse *l*12S-LOX, representing the analog of the human and rabbit 15S-LOX (1), could not be detected in all tissues tested. A constitutive expression of *p*12S-LOX was previously demonstrated both in mouse and human epidermis (9,10). One might argue that the rather weak expression of *p*12S-LOX in all other tissues tested is attributable to platelet contamination. However, *e*12S-LOX, which also is strongly expressed in platelets, was not detected. Although not expressed in normal back skin epidermis (15,21) significant amounts of 8S-LOX mRNA were found in footsole epidermis and forestomach of NMRI mice. Lower amounts were also observed in lung and brain, confirming previously published data obtained using another mouse strain (14). Unique among all LOX is the strong inducibility of 8S-LOX upon TPA treatment of back skin, which leads to skin inflammation and a regenerative epidermal hyperproliferation (14,15,21,22). This response as well as the level of constitutive expression, has been shown to be strongly mouse strain-dependent (14). In general, 8S-LOX expression appears to be restricted to epithelial sites that are exposed either to permanent mechanical stress such as pressure (footsole) or stretching (forestomach) or to chemical irritation. *e*12S-LOX mRNA (11–13) showed the most selective expression in that it was found only in back skin and footsole epidermis as well as, unlike all other epidermis-type LOX, in platelets. A preferential expression in stratifying epithelia was also observed for 12R-LOX and *e*-LOX-3, which exhibited only weak signals in all other tissues. The strong constitutive mRNA expression of these LOX species suggests housekeeping functions in stratifying epithelia. Furthermore, the discrete expression on day 16.5 of fetal life indicates a critical function of 12R-LOX during embryonic development of skin (23).

5S-LOX mRNA was clearly detectable in back skin and footsole epidermis. Since a concomitant expression of the *l*12S-LOX was not detected, occurrence of 5S-LOX may not be attributed to contamination of the tissue with inflammatory cells. Furthermore, we were able to identify 5S-LOX mRNA in mouse skin-derived keratinocyte lines (data not shown), indicating that skin keratinocytes are a cellular source of this mRNA species. Accordingly, it was previously shown that human epidermis expressed 5S-LOX mRNA in both keratinocytes and Langerhans cells resident in epidermis (24,25).

The mRNA expression of LOX isozymes exhibited a complex differentiation-dependent pattern in mouse epidermis.

*e*12S-LOX was detected both in proliferating basal keratinocytes and—albeit less intensively—in terminally differentiating keratinocytes. Our observations differ from that of Funk *et al.* (11), which showed a strong expression of *e*12S-LOX restricted to newly differentiating keratinocytes by using *in situ* hybridization. Since they used C57BL/6x129 Sv mice, this difference may be explained by a strain-specific expression pattern.

For all other enzymes a characteristic compartmentalization was observed, indicating that mRNA for 12R-LOX and *e*-LOX-3 were predominantly to exclusively expressed in suprabasal keratinocytes of neonatal and adult mouse epidermis, i.e., these genes are expressed late in terminal differentiation. mRNA of *p*12S-LOX was predominantly found in spinous and granular keratinocytes. In contrast, the human enzyme has been identified in the basal cell compartment of epidermis by using immunohistochemistry (26).

Provided that the distinct expression pattern of mRNA for epidermal LOX reflects the distribution at the level of proteins and activity, it may be concluded that the constitutively expressed isozymes exhibit distinct functions for the structural and functional integrity of stratifying epithelia. Thus, the exclusive expression of 12R-LOX and *e*-LOX-3 in late granular and squamous keratinocytes points to a critical function of these isozymes in advanced stages of terminal differentiation such as the establishment of the epidermal lipid barrier. It has indeed been shown that suppression of LOX activity in skin leads to a disturbance of lipid barrier function (27). A recent report on changes of barrier function in *p*12S-LOX gene-knock-out mice is in line with this observation (28).

The strong expression of the *e*12S-LOX in basal keratinocytes indicates an association of this isozyme with cell proliferation. Accordingly, induction of cell proliferation in mouse epidermis was found to be accompanied by an induction *e*12S-LOX. In human skin a similar function may be attributed to the *p*12S-LOX, in that chronically proliferating psoriatic skin was shown to overexpress the human isozyme in the germinative compartment of epidermis (26). Interestingly, the human ortholog of the mouse *e*12S-LOX gene has been shown to be a functionally inactive pseudogene (29). As detailed above, the expression of 8S-LOX also seems to correlate with a distinct functional state of skin caused by chemical or mechanical stress. The delineation of the functional specificity of the epidermis-type LOX will require additional experimental efforts including the generation of transgenic mouse lines with a targeted expression or knock-out of the individual genes.

Most of these LOX isozymes expressed in stratifying epithelia are structurally related, as shown by sequence alignment. 12R-LOX, 8S-LOX, 15S-LOX-2, and *e*-LOX-3 share a higher overall amino acid similarity between each other than to all other mammalian LOX and thus can be grouped together into a novel subfamily within the LOX multigene family. Nevertheless, these enzymes exhibit a heterogeneous regio- and stereospecificity that is not easily explained on the basis of the available structural data. *p*- and *e*12S-LOX, which were found to be strongly expressed in epidermis and platelets, can be assigned with a distinct subgroup containing 12S- and 15S-LOX.

In summary, our findings demonstrate that among all tissues tested stratifying epithelia express the most diverse spectrum of LOX. In epidermis, the expression of individual LOX can be localized to different compartments, indicating that their expression and activity may be involved in processes of terminal differentiation. Our results may initiate further investigations into the functions of LOX in stratifying epithelia. Further efforts will critically depend on appropriate models as well as on further characterization of the enzymatic properties.

ACKNOWLEDGMENTS

The excellent assistance of Ina Kutschera, Brigitte Steinbauer, and Ingeborg Vogt is gratefully acknowledged. This work was supported by a grant from Deutsche Krebshilfe, Bonn, Germany.

REFERENCES

1. Yamamoto, S. (1992) Mammalian Lipoxygenases: Molecular Structures and Functions, *Biochim. Biophys. Acta 1128*, 117–131.
2. Funk, C.D. (1996) The Molecular Biology of Mammalian Lipoxygenases and the Quest for Eicosanoid Functions Using Lipoxygenase-Deficient Mice, *Biochim. Biophys. Acta 1304*, 65–84.
3. Spector, A.A., Gordon, J.A., and Moore, S.A. (1988) Hydroxyeicosatetraenoic Acids (HETES), *Prog. Lipid Res. 27*, 271–323.
4. Ruzicka, T., and Printz, M.P. (1984) Arachidonic Acid Metabolism in Skin: A Review, *Rev. Physiol. Biochem. Pharmacol. 100*, 121–160.
5. Fogh, K., Kiil, J., Herlin, T., Ternowitz, T., and Kragballe, K. (1987) Heterogeneous Distribution of Lipoxygenase Products in Psoriatic Skin Lesions, *Arch. Dermatol. Res. 279*, 504–511.
6. Kühn, H., Belkner, J., Zaiss, S., Fahrenklemper, T., and Wohlfeil, S. (1994) Involvement of 15-Lipoxygenase in Early Stages of Atherogenesis, *J. Exp. Med. 179*, 1903–1911.
7. Feinmark, S.J., and Cornicelli, J.A. (1997) Is There a Role for 15 Lipoxygenase in Atherogenesis? *Biochem. Pharmacol. 54*, 953–959.
8. Honn, K.V., Tang, D.G., Gao, X., Butovich, I.A., Liu, B., Timar, J., and Hagmann, W. (1994) 12-Lipoxygenases and 12(S)-HETE: Role in Cancer Metastasis, *Cancer Metastasis Rev. 13*, 365–396.
9. Krieg, P., Kinzig, A., Ress-Löschke, M., Vogel, S., Vanlandingham, B., Stephan, M., Lehmann, W.-D., Marks, F., and Fürstenberger, G. (1995) 12 Lipoxygenase Isoenzymes in Mouse Skin Tumor Development, *Mol. Carcinogen. 14*, 118–129.
10. Chen, X.-S., Kurre, U., Jenkins, N.A., Copeland, N.G., and Funk, C.D. (1994) cDNA Cloning, Expression, Mutagenesis of C-Terminal Isoleucine, Genomic Structure, and Chromosomal Localizations of Murine 12-Lipoxygenases, *J. Biol. Chem. 269*, 13979–13987.
11. Funk, C.D., Keeney, D.S., Oliw, E.H., Boeglin, W.E., and Brash, A.R. (1996) Functional Expression and Cellular Localization of a Mouse Epidermal Lipoxygenase, *J. Biol. Chem. 271*, 23338–23344.
12. Kinzig, A., Fürstenberger, G., Bürger, F., Vogel, S., Müller-Decker, K., Mincheva, A., Lichter, P., Marks, F., and Krieg, P. (1997) Murine Epidermal Lipoxygenase (Aloxe) Encodes a 12-Lipoxygenase Isoform, *FEBS Lett. 402*, 162–166.

13. van Dijk, K.W., Steketee, K., Havekes, L., Frants, R., and Hofker, M. (1995) Genomic and cDNA Cloning of a Novel Mouse Lipoxygenase Gene, *Biochim. Biophys. Acta 1259*, 4–8.
14. Jisaka, M., Kim, R.B., Boeglin, W.E., Nanney, L.B., and Brash, A.R. (1997) Molecular Cloning and Functional Expression of a Phorbol Ester-Inducible 8S-Lipoxygenase from Mouse Skin, *J. Biol. Chem. 272*, 24410–24416.
15. Krieg, P., Kinzig, A., Heidt, M., Marks, F., and Fürstenberger, G. (1998) cDNA Cloning of a 8-Lipoxygenase and a Novel Epidermis-Type Lipoxygenase from Phorbol Ester-Treated Mouse Skin, *Biochim. Biophys. Acta 1391*, 7–12.
16. Krieg, P., Siebert, M., Kinzig, A., Bettenhausen, R., Marks, F., and Fürstenberger, G. (1999) Murine 12(R)-Lipoxygenase: Functional Expression, Genomic Structure And Chromosomal Localization, *FEBS Lett. 446*, 142–148.
17. Kinzig, A., Heidt, M., Fürstenberger, G., Marks, F., and Krieg, P. (1999) cDNA Cloning, Genomic Structure and Chromosomal Localization of a Novel Murine Epidermis-Type Lipoxygenase, *Genomics 58*, 158–164.
18. Chen, X.S., Naumann, T.A., Kurre, U., Jenkins, N.A., Copeland, N.G., and Funk, C.D. (1995) cDNA Cloning, Expression, Mutagenesis, Intracellular Localization, and Gene Chromosomal Assignment of Mouse 5-Lipoxygenase, *J. Biol. Chem. 270*, 17993–17999.
19. Fürstenberger, G., Gross, M., Schweizer, J., Vogt, I., and Marks, F. (1986) Isolation, Characterization and *in vitro* Cultivation of Subfractions of Neonatal Mouse Keratinocytes: Effects of Phorbol Esters, *Carcinogenesis 7*, 1745–1753.
20. Gross, M., Fürstenberger, G., and Marks, F. (1987) Isolation, Characterization, and *in vitro* Cultivation of Keratinocyte Subfractions from Adult NMRI Mouse Epidermis: Epidermal Target Cells for Phorbol Esters, *Exp. Cell Res. 171*, 460–474.
21. Fürstenberger, G., Hagedorn, H., Jacobi, T., Besemfelder, E., Stephan, M., Lehmann, W.D., and Marks, F. (1991) Characterization of an 8-Lipoxygenase Activity Induced by the Phorbol Ester Tumor Promoter 12-*O*-Tetradecanoyl 13-acetate in Mouse Skin *in vivo, J. Biol. Chem. 266*, 15738–15745.
22. Bürger, F., Krieg, P., Kinzig, A., Schurich, B., Marks, F., and Fürstenberger, G. (1999) Constitutive expression of 8-Lipoxygenase in Papillomas and Clastogenic Effects of Lipoxygenase-Derived Arachidonic Acid Metabolites in Keratinocytes, *Mol. Carcinogen. 24*, 108–117.
23. Sun, D., Mcdonnell, M., Chen, X.-S., Lakkis, M.M., Li, H., Isaacs, S.N., Elsea, S.H., Patel, P.I., and Funk, C.D. (1998) Human 12(R)-Lipoxygenase and the Mouse Ortholog: Molecular Cloning, Expression, and Gene Chromosomal Assignment, *J. Biol. Chem. 50*, 33540–33547.
24. Janssen-Timmen, U., Vickers, P.J., Wittig, U., Lehmann, W.D., Stark, H. J., Fusenig, N.E., Rosenbach, T., Rådmark, O., Samuelsson, B., and Habenicht, A.J.R. (1995) Expression of 5-Lipoxygenase in Differentiating Human Skin Keratinocytes, *Proc. Natl. Acad. Sci. USA 92*, 6966–6970.
25. Spanbroek, R., Stark, H.J., Janssen Timmen, U., Kraft, S., Hildner, M., Andl, T., Bosch, F.X., Fusenig, N.E., Bieber, T., Radmark, O., Samuelsson, B., and Habenicht, A.J. (1998) 5-Lipoxygenase Expression in Langerhans Cells of Normal Human Epidermis, *Proc. Natl. Acad. Sci. USA 95*, 663–668.
26. Hussain, H., Shornick, L.P., Shannon, V.R., Wilson, J.D., Funk, C.D., Pentland, A.P., and Holtzman, M.J. (1994) Epidermis Contains Platelet-Type 12-Lipoxygenase that is Overexpressed in Germinal Layer Keratinocytes in Psoriasis, *Am. J. Physiol. 266*, C243–C253.
27. Nugteren, D.H., Christ Hazelhof, E., Van Der Beek, A., and Houtsmuller, U.M. (1985) Metabolism of Linoleic Acid and Other Essential Fatty Acids in the Epidermis of the Rat, *Biochim. Biophys. Acta 834*, 429–436.
28. Johnson, E.N., Nanney, L.B., Virmani, J., Lawson, J.A., and Funk, C.D. (1999) Basal Transepidermal Water Loss Is Increased in Platetel-Type 12 Lipoxygenase Deficient Mice, *J. Invest. Dermatol. 112*, 861–865.
29. Sun, D., Elsea, S.H., Patel, P.I. and Funk, C.D. (1998) Cloning of a Human "Epidermal-Type" 12-Lipoxygenase-Related Gene and Chromosomal Localization to 17p13, *Cytogenet. Cell Genet. 81*, 79–82.
30. Funk, C.D., Furci, L., and Fitzgerald, G.A. (1990) Molecular Cloning, Primary Structure, and Expression of the Human Platelet/Erythroleukemia Cell 12-Lipoxygenase, *Proc. Natl. Acad. Sci. USA 87*, 5638–5642.
31. Yoshimoto, T., Suzuki, H., Yamamoto, S., Takai, T., Yokoyama, C., and Tanabe, T. (1990) Cloning and Sequence Analysis of the cDNA for Arachidonate 12-Lipoxygenase of Porcine Leukocytes, *Proc. Natl. Acad. Sci. USA 87*, 2142–2146.
32. De Marzo, N., Sloane, D.L., Dicharry, S., Highland, E., and Sigal, E. (1992) Cloning and Expression of an Airway Epithelial 12-Lipoxygenase, *Am. J. Physiol. 262*, L198–L207.
33. Watanabe, T., Medina, J.F., Haeggström, J.Z., Rådmark, O., and Samuelsson, B. (1993) Molecular Cloning of a 12-Lipoxygenase cDNA from Rat Brain, *Eur. J. Biochem. 212*, 605–612.
34. Berger, M., Schwarz, K., Thiele, H., Reimann, I., Huth, A., Borngraber, S., Kühn, H., and Thiele, B.J. (1998) Simultaneous Expression of Leukocyte-Type 12-Lipoxygenase and Reticulocyte-Type 15-Lipoxygenase in Rabbits, *J. Mol. Biol. 278*, 935–948.
35. Thiele, B.J., Fleming, J., Kasturi, K., O'Prey, J., Black, E., Chester, J., Rapoport, S.M., and Harrison, P.R. (1987) Cloning of Rabbit Erythroid-Cell-Specific Lipoxygenase mRNA, *Gene 57*, 111–119.
36. Sigal, E., Craik, C.S., Highland, E., Grunberger, D., Costello, L.L., Dixon, R.A.F., and Nadel, J.A. (1988) Molecular Cloning and Primary Structure of Human 15-Lipoxygenase, *Biochem. Biophys. Res. Commun. 157*, 457–464.
37. Dixon, R.A.F., Jones, R.E., Diehl, R.E., Bennet, C.D., Kargman, S., and Rouzer, C.A. (1988) Cloning of the cDNA for Human 5-Lipoxygenase, *Proc. Natl. Acad. Sci. USA 85*, 416–420.
38. Balcarek, J.M., Theisen, T.W., Cook, M.N., Varrichio, A., Hwang, S.-M., Strohsacker, M.W., and Crooke, S.T. (1988) Isolation and Characterization of a cDNA Clone Encoding Rat 5-Lipoxygenase, *J. Biol. Chem. 263*, 13937–13941.
39. Kitzler, J.W., and Eling, T.E. (1996) Cloning, Sequencing and Expression of a 5-Lipoxygenase from Syrian Hamster Embryo Fibroblasts, *Prostaglandins Leukotrienes Essent. Fatty Acids 55*, 269–277.
40. Brash, A.R., Boeglin, W.E., and Chang, M.S. (1997) Discovery of a Second 15S-Lipoxygenase in Humans, *Proc. Natl. Acad. Sci. USA 94*, 6148–6152.
41. Boeglin, W.E., Kim, R.B., and Brash, A.R. (1998) A 12R-Lipoxygenase in Human Skin: Mechanistic Evidence, Molecular Cloning, and Expression, *Proc. Natl. Acad. Sci. USA 95*, 6744–6749.

[Received January 24, 2000, and in revised form April 14, 2000; revision accepted April 16, 2000]

Purification, Molecular Cloning, and Expression of the Gene Encoding Fatty Acid 13-Hydroperoxide Lyase from Guava Fruit *(Psidium guajava)*

Nathalie Tijet[a,1], Urs Wäspi[b], Duncan J.H. Gaskin[c], Peter Hunziker[d], Bernard L. Muller[e], Evgeny N. Vulfson[c,2], Alan Slusarenko[b,3], Alan R. Brash[a,*], and Ian M. Whitehead[e,4]

[a]Department of Pharmacology, Vanderbilt University, Nashville, Tennessee 37232, [b]Department of Plant Biology, University of Zürich, CH-8008, Switzerland, [c]Institute of Food Research, Department of Macromolecular Sciences, Reading RG6 6BZ, Berkshire, England, [d]Department of Biochemistry, University of Zürich, CH-8057, Switzerland, and [e]Firmenich S.A., Geneva 8, CH-1211, Switzerland

ABSTRACT: Guava fruit was identified as a particularly rich source of 13-hydroperoxide lyase activity. The enzyme proved stable to chromatographic procedures and was purified to homogeneity. Based on gel filtration and gel electrophoresis, the native enzyme appears to be a homotetramer with subunits of 55 kD. Starting with primers based on the peptide sequence, the enzyme was cloned by polymerase chain reaction with 3′ and 5′ rapid amplification of cDNA ends. The sequence shows approximately 60–70% identity to known 13-hydroperoxide lyases and is classified in cytochrome P450 74B subfamily as CYP74B5. The cDNA was expressed in *Escherichia coli* (BL21 cells), with optimal enzyme activity obtained in the absence of isopropyl-β-D-thiogalactopyranoside and δ-aminolevulinic acid. The expressed enzyme metabolized 13(*S*)-hydroperoxylinolenic acid over 10-fold faster than 13(*S*)-hydroperoxylinoleic acid and the 9-hydroperoxides of linoleic and linolenic acids. 13(*S*)-Hydroperoxylinolenic acid was converted to 12-oxododec-9(*Z*)-enoic acid and 3(*Z*)-hexenal, as identified by gas chromatography–mass spectrometry. The turnover number with this substrate, with enzyme concentration estimated from the Soret absorbance, was ≈2000/s, comparable to values reported for the related allene oxide synthases. Distinctive features of the guava 13-hydroperoxide lyase and related cytochrome P450 are discussed.

Paper no. L8473 in *Lipids 35,* 709–720 (July 2000).

[1]Present address: Department of Entomology, Forbes 410, University of Arizona, P.O. Box 210036, Tucson, AZ 85721-0036.

[2]Present address: Institute of Food Research, Norwich Research Park, Colney, Norwich NR4 7UA, England.

[3]Present address: RWTH Aachen, Institut für Biologie III (Plant Physiology), Worringerweg, D-52074, Aachen, Germany.

[4]Present address: Firmenich Asia Pte. Ltd, 10 Tuas West Road, Singapore 638377.

*To whom correspondence should be addressed at Dept. of Pharmacology, Vanderbilt University, 23rd Ave. at Pierce, Nashville, TN 37232-6602. E-mail: alan.brash@mcmail.vanderbilt.edu

Abbreviations: δ-ALA, δ-Aminolevulinic acid; AOS, allene oxide synthase; GC–MS, gas chromatography–mass spectrometry; GPC, gel permeation chromatography; HIC, hydrophobic interaction chromatography; HPL, hydroperoxide lyase; HPLC, high-pressure liquid chromatography; IFC, isoelectric focusing chromatography; IPTG, isopropyl-β-D-thiogalactopyranoside; LOX, lipoxygenase; NTA, nitrilotriacetic acid; PAGE, polyacrylamide gel electrophoresis; PCR, polymerase chain reaction; RACE, rapid amplification of cDNA ends; RP–HPLC, reversed-phase–high pressure liquid chromatography; SDS, sodium dodecyl sulfate; TFA, trifluoroacetic acid; UV, ultraviolet.

The metabolism of fatty acid hydroperoxides [lipoxygenase (LOX) products] involves conversion to epoxides, aldehydes, alcohols, and other derivatives, and these reactions are often catalyzed by cytochrome P450 enzymes. In green plant tissue, the fatty acid hydroperoxide lyase (HPL), an enzyme in the LOX pathway, catalyzes the cleavage of 13- and 9-hydroperoxides of linoleic and linolenic acid into volatile C_6- or C_9-aldehydes and C_{12}- or C_9-oxoacids, respectively (1,2). The C_6 and C_9 volatile compounds have a commercial value in the production of "natural" flavor in the food industry, and are potentially important in plant defense against pathogens (3) and pests (4).

The green notes [hexanal, hexan-1-ol, 2(*E*)-hexenal, 3(*Z*)-hexenal, 2(*E*)-hexen-1-ol, and 3(*Z*)-hexen-1-ol (also known as pipol)] are used widely in flavors (particularly fruit) to impart a fresh green character. The synthesis of these compounds starts from free polyunsaturated fatty acids such as linoleic [9(*Z*),12(*Z*)-octadecadienoic] and linolenic acids [9(*Z*),12(*Z*),15(*Z*)-octadecatrienoic]. In nature, these acids are released from cell membranes by lipolytic enzymes after cell damage. Fatty acid 13-hydroperoxides are formed by the action of a specific lipoxygenase (13-LOX), and these are subsequently cleaved by a 13-hydroperoxide lyase (13-HPL) into a C_6-aldehyde and a C_{12}-ω-oxoacid moiety. The aldehydes can subsequently undergo thermal isomerization and/or be reduced by dehydrogenase enzymes to give the other C_6 products mentioned above (2,5).

13-HPL was demonstrated for the first time in banana fruits (6) and subsequently characterized in a number of different plant materials (7–10). The enzyme has been purified to apparent homogeneity from tea leaves (11) and more recently green bell pepper fruits (12) and sunflower (13).

Cloning of the pepper 13-HPL cDNA confirmed that the enzyme is a member of the cytochrome P450 family of hemoproteins (14). The P450 family is designated as CYP74B. Subsequently, the 13-HPL of *Arabidopsis* was cloned from published expressed sequence tag sequences and identified as a related cytochrome P450 (15).

We began the present work with a survey of HPL activities in various commercial fruits and vegetables, and on this basis selected guava fruit as the starting material for further characterization. The 13-HPL activity in guava is substantially higher than in several other well-characterized sources such as bean and pepper. Guava is available on an almost year-round basis, making it an attractive source for the commercial production of fatty acid aldehydes. In the present paper, we describe purification of the 13-HPL from guava fruit, molecular cloning of the cDNA, and expression of the active protein in *Escherichia coli*.

EXPERIMENTAL PROCEDURES

Materials. For protein purification, fruits of *Psidium guajava* from Thailand (bought at a local market in Zürich) were frozen and stored at −20°C. For the molecular cloning, immature guava (≈3 cm in diameter) were collected in Brazil, frozen on dry ice on the same day, and subsequently stored at −80°C.

Measurement of 13-HPL activity in fruits and vegetables. The lyase reactions were performed in a four-necked glass vessel equipped with a mechanical stirrer, a dropping funnel topped with a nitrogen bubbler, a thermometer, and a pH electrode. Guava fruit homogenate (20 g) prepared in a Waring blender was stirred vigorously under nitrogen at the selected temperature and pH. An aqueous solution of hydroperoxyoctadecadienoic acid or hydroperoxyoctadecatrienoic acid, 20 g, containing 35 g/kg hydroperoxide as determined by iodometric titration, was then added. This solution of hydroperoxides consisted of either saponified sunflower oil (serving predominantly as a source of linoleic acid) or saponified linseed oil (linolenic acid) that had been treated with soybean flour (LOX) to form the corresponding 13-hydroperoxides. The formation of hexanal or 3(*Z*)- and 2(*E*)-hexenal was monitored by gas chromatography (GC) every 5 min for the first 15 min, and subsequently every 30 min. The C_6-aldehydes were quantified by direct injection of the filtered crude reaction samples onto a 3-m column of Carbowax 10% on Chromosorb W HP 80/100 mesh (Supelco, Bellefonte, PA) operated isothermally at 100°C in a PerkinElmer 2900 gas chromatograph equipped with a flame-ionization detector. The concentrations of hexanal or 3(*Z*) and 2(*E*)-hexenal were determined by comparison with an external standard solution of 500 mg/L hexanal or 2(*E*)-hexenal in 0.5% EtOH/99.5% water solution.

Purification of the 13-HPL from guava fruit. (i) Preparation of the crude extract. Guava fruits were peeled and the pericarp tissues chopped into small pieces. Two volumes of extraction buffer (50 mM sodium phosphate, 0.1% Triton X-100R, 5 mM sodium ascorbate, pH 7.0) were added to 500 g of chopped pericarp and homogenized for 2 min in a Sorvall mixer at 4°C. All of the following steps were carried out at room temperature.

(ii) Enzyme solubilization. The crude extract containing the 13-HPL activity was solubilized with 1% (vol/vol) of Triton X-100R with stirring for 30 min. After centrifugation at 16,000 × *g* for 15 min, 0.02% Pectinex Ultra SP-L solution from Novo Nordisk Ferment (Bagsvaerd, Denmark) was added to degrade pectin.

(iii) Ammonium sulfate precipitation. Solid $(NH_4)_2SO_4$ was added in small portions to the crude extract under stirring until 30% saturation was achieved. After stirring for 30 min, the mixture was centrifuged at 20,000 × *g* for 15 min and the resulting pellet discarded. The supernatant was brought to 60% saturation with more solid $(NH_4)_2SO_4$ added in portions. After stirring for 30 min, the pellet was collected by centrifugation as above.

(iv) Gel permeation chromatography (GPC). The $(NH_4)_2SO_4$ pellet was dissolved in 45 mL of extraction buffer and chromatographed on a Superdex 200 HL 26/60 column (Pharmacia, Uppsala, Sweden) with 50 mM sodium phosphate, 0.1% Triton X-100R pH 7.0 as running buffer at a flow rate of 2 mL/min. After GPC, samples were run on anion exchange chromatography or hydrophobic interaction chromatography (HIC) columns.

(v) Anion exchange chromatography. The sample from GPC was applied to a Q-Sepharose column (Pharmacia) with a loading buffer of 20 mM Tris-HCl pH 8.5 containing 0.1% Triton X-100R. 13-HPL activity was eluted with a gradient of NaCl in eluting buffer (0–100% 1 M NaCl in 133 min at a flow rate of 3 mL/min).

(vi) HIC. The fractions containing the 13-HPL activity from the GPC were brought to 30% $(NH_4)_2SO_4$ saturation before loading onto a Phenyl-Sepharose HR 26/10 column (Pharmacia) with loading buffer [50 mM sodium phosphate, 1 M $(NH_4)_2SO_4$, pH 7.0]. The proteins were eluted with a decreasing salt gradient (100–0% 1 M ammonium sulfate over 70 min) in 50 mM sodium phosphate pH 7.0 containing 1% Triton X-100R at a flow rate of 8 mL/min. Fractions containing the 13-HPL activity were concentrated by dialysis against polyethylene glycol 20,000 and desalted on a PD-10 column (Pharmacia) against the loading buffer for hydroxylapatite chromatography (10 mM sodium phosphate, 0.1% Triton X-100R, pH 6.8).

(vii) Hydroxylapatite chromatography. After HIC, the sample was applied to an Econo-Pac HTP column (BioRad, Cambridge, MA) in 10 mM sodium phosphate, 0.1% Triton X-100R, pH 6.8. The proteins were eluted with a gradient to 200 mM sodium phosphate buffer pH 6.8, containing 0.1% Triton X-100R over 30 min using a flow rate of 1 mL/min. Fractions with 13-HPL activity were concentrated by dialysis against polyethylene glycol 20,000 and desalted against the isoelectric focusing chromatography (IFC) loading buffer (75 mM Tris-acetic acid, pH 9.3).

(viii) IFC. The prepared sample from hydroxylapatite chromatography was applied to a Mono P HR 5/20 column (Phar-

macia). The proteins were eluted with 10% Polybuffer 96 (Pharmacia)/acetic acid, pH 6.0, at a flow rate of 0.5 mL/min.

Tryptic digest and amino acid sequence determination. Fractions of purified 13-HPL were concentrated and separated on a 6.5% sodium dodecyl sulfate-polyacrylamide gel (SDS-PAGE). The proteins were electrotransferred (0.8 mA cm^{-2} for 75 min) to an Immobilon CD membrane (Millipore, Bedford, MA) using 10 mM 3-[cyclohexylamino]-1-propanesulfonic acid containing 10% (vol/vol) methanol pH 11.0 as transfer buffer. Proteins were detected by staining using Quick-Stain (Zoion Research Inc., Newton, MA).

Direct sequencing of the purified 13-HPL by Edman degradation was not possible as the N-terminus was blocked. The 13-HPL purified protein was therefore cut out separately and incubated in 10 µL of 0.1 M Tris pH 8.2 containing 1 M NaCl, 10% (vol/vol) acetonitrile, 2 mM $CaCl_2$, and 0.1 µg trypsin at 37°C for 15 h. After acidification with 1 µL of 10% trifluoroacetic acid (TFA), the solution was injected directly into the high-pressure liquid chromatography (HPLC) system equipped with a Brownlee Aquapore RP-300 C8 column (PE Applied Biosystems, Foster City, CA). Chromatography solvents were 0.05% TFA and 2% acetonitrile in water (solvent A) and 0.045% TFA and 80% acetonitrile in water (solvent B). The gradient and flow rates used were as follows: 0–5 min, 80 µL/min at 2% solvent B; 5–65 min 50 µL/min at 2–65% solvent B; and 65–70 min 50 µL/min at 65–100% B. Absorbance at 214 nm was measured in a 200 nL flow cell with a path length of 2 mm. Peptides resolved by HPLC were collected manually for sequence analysis and applied to precycled polyprene-treated glass fiber discs. Automated sequencing used a model 477A pulsed-liquid phase sequencer (Applied Biosystems) equipped with a model 120A analyzer.

RNA isolation. Total RNA was extracted using the method of Wan and Wilkins (16). Immature guava fruit (1 g) was crushed to a fine powder in liquid nitrogen in a precooled pestle and mortar. The powder was added to 5 mL at 80°C of lysis buffer [200 mM borax, 30 mM EGTA, 10 mM dithiothreitol, 1% wt/vol SDS, 1% wt/vol sodium deoxycholate, 2% PVP 40,000 (Sigma Chemical Co., St. Louis, MO), 0.5% vol/vol NP-40 (Sigma)] and the mixture homogenized. Proteinase K (2.5 mg, Sigma) was added, and this mixture was incubated at 42°C for 90 min with shaking sufficient for mixing without excessive foaming. One milliliter of 1 M KCl was added. After mixing, the tubes were incubated on ice for 1 h and then centrifuged at 10,000 × *g* for 10 min. Three milliliters of 4 M LiCl was added, and the tubes were incubated at 4°C overnight. After 10 min of centrifugation at 10,000 × *g*, the supernatant was discarded, and the pellet washed with 2 M LiCl and centrifuged as before. The supernatant was discarded and the pellet resuspended in Tris/EDTA buffer (10 mM Tris, pH 8, 1 mM EDTA) or in H_2O.

For the purification of mRNA from total RNA, the mRNA purification kit from Pharmacia was used. This kit is based on the use of spun columns for the affinity purification of polyadenylated RNA on oligo(dT)-cellulose. The RNA was quantified by ultraviolet (UV) spectrophotometry. The yield was approximately 1 mg of total RNA and 20 µg of mRNA.

Cloning. (i) cDNA synthesis. Total RNA (20 µg) or 1 µg of mRNA was used in 50-µL reactions for the first strand cDNA synthesis using an oligo(dT)-adaptor primer (17). Aliquots of 1 µL cDNA were used directly in polymerase chain reactions (PCR).

(ii) PCR cloning. The PCR were primed with 1 µL cDNA (from a 50-µL cDNA synthesis using 20 µg total RNA), and using 10 mM Tris, pH 8.3, 50 mM KCl, 3 mM $MgCl_2$ with 0.2 mM each of dNTPs and 0.25 µL (1.25 units) of AmpliTaq DNA polymerase (PerkinElmer) in a PerkinElmer 480 thermocycler. After the addition of the cDNA at 80°C (hot start), the PCR reactions conditions were: 94°C, 2 min for 1 cycle; 50–55°C for 1 min, 72°C for 1 min, and 94°C for 1 min for 30 cycles; 72°C for 10 min for 1 cycle; and the block temperature was held at 4°C.

3′-Rapid amplification of cDNA ends (RACE) and 5′-RACE: The 3′-sequence was obtained using gene-specific upstream primers: $^{5'}$CCT CAA CAC GCT CAG GTG AAG$^{3'}$, $^{5'}$CTC CAA AAG TTC CTC TTC AAC TTC$^{3'}$, or $^{5'}$CCA GCT CCT CCC CAC CAT CAA$^{3'}$ against a downstream primer based on the adaptor-linked oligo(dT) primer used for cDNA synthesis (17). The 5′RACE was accomplished using a kit from GibcoBRL (Grand Island, NY), according to the manufacturer's instructions. The gene-specific downstream primers were: $^{5'}$GTC AGC GCC GAA GAT GGA CTT$^{3'}$ or $^{5'}$GTG TTG AGG CTC GGA AGT GTC$^{3'}$.

Full-length clones obtained by PCR. Four gene-specific primers were synthesized corresponding to the putative start sites of the coding sequence (at the four different methionines) and one primer corresponding to the stop codon. *Bam*HI and *Eco*RI restrictions sites were incorporated at the 5′ and 3′ ends, respectively, to facilitate subcloning. The four upstream primers were: $^{5'}$TAG GAT CCG ATC ATG GCG AGG GTC GTG$^{3'}$, $^{5'}$GCG GAT CCG GCC ATG AGC AAC ATG TCG$^{3'}$, $^{5'}$GCG GAT CCG GCC ATG TCG CCG GCC AT$^{3'}$, and $^{5'}$GCG GAT CCG GCC ATG TCG TCC ACC TAC$^{3'}$; and the downstream primer was: $^{5'}$GCG AAT TCT CAG TTG GCC TTT TCA ACG GCT GT$^{3'}$. These primers were purified by HPLC as the dimethoxytrityl derivative (17). After deprotection, they were used in PCR reactions (at 20 pmol/50 µL final concentration) with a proof-reading mixture of *Taq/Pwo* DNA polymerase (Expand High Fidelity, Boehringer-Mannheim, Indianapolis, IN) according to the manufacturer's instructions. The reactions conditions were 94°C, 2 min for 1 cycle; 60°C for 1 min, 72°C for 1 min, and 94°C for 1 min for 30 cycles; 72°C for 10 min for 1 cycle; and the block temperature was held at 4°C.

DNA sequencing. cDNA were sequenced using the Thermo Sequenase radiolabeled terminator cycle sequencing kit (Amersham Life Science, Inc., Arlington Heights, IL).

Bacterial expression. (i) Preparation of constructs. The four cDNAs encoding the 13-HPL-Met 1, 6, 9, and 13 in pCR2.1 were cut with *Bam*HI and *Eco*RI and subcloned into the expression vector plasmid pET30b (Novagen) digested

also with *Bam*HI and *Eco*RI. The 13-HPL-Met 1, 6, 9, and 13 constructs were transformed into *E. coli* strain XLI-Blue. The plasmid DNA was then used for transformation of *E. coli* strain BL21(DE3) to express the 13-HPL.

(ii) Preparation of bacterial cultures. The four different constructs described above were expressed in BL21(DE3) (Novagen, Madison, WI) cells using a modified expression methodology (18). A typical preparation of 50-mL culture was carried out as follows: A single bacterial colony from a complex agar plate containing 30 μg/mL of kanamycin was grown in 1 mL of LB medium containing 50 μg/mL of kanamycin at 37°C and 250 rpm for 3 h. An aliquot (200 μL) of this culture was used to inoculate 10 mL of TB medium containing 50 μg/mL of kanamycin and the culture was again grown at 37°C. After 3 h, this culture was diluted with 40 mL of TB containing 30 μg/mL of kanamycin and grown at 28°C, 250 rpm for 24 h. The bacterial cells were centrifuged at 4°C for 15 min at 5,000 rpm (3,500 × *g*) in a Jouan CR422 centrifuge, washed by resuspension in 10 mL of Tris-HCl buffer 50 mM pH 7.9, and centrifuged as before. The resulting pellet of cells was resuspended in 10 mL of Tris-acetate buffer 100 mM pH 7.6 containing 500 mM of sucrose, 0.5 mM of EDTA, and 1 mg/mL of lysozyme. After 30 min on ice, the cells were centrifuged as before to obtain a pellet of spheroplasts which were resuspended in 10 mL of potassium phosphate buffer (100 mM, pH 7.6). After at least 10 min at –80°C, a protease inhibitor (phenylmethylsulfonyl fluoride, 1 mM) was added, the cells were allowed to thaw for 10 min, and then they were sonicated twice for 30 s using a Virsonic 100 at a setting of 5. The resulting membranes were spun down at 100,000 × *g* for 90 min at 4°C. The 13-HPL activity was recovered in the 100,000 × *g* pellet. After solubilization using 1% Emulphogen BC-700™ (polyoxyethylene 10 tridecyl ether, Sigma) at 4°C overnight and centrifugation as before, the 13-HPL activity was recovered in the supernatant.

Purification of His-tagged proteins. The histidine-tagged 13-HPL was purified following the protocol described by Imai *et al*. (19). After solubilization, the 100,000 × *g* supernatant was loaded on a Ni-nitrilotriacetic acid (NTA) column (0.5 mL bed volume, Qiagen, Valencia, CA) equilibrated with potassium phosphate buffer 50 mM pH 7.6 containing 100 mM NaCl and 0.1% Emulphogene BC-720 detergent (buffer A) at 0.5 mL/min. The column was washed with the buffer A containing 50 mM glycine. The His-13-HPL was then eluted with the buffer A containing 40 mM L-histidine. Fractions of 1 mL were collected and assayed for the 13-HPL activity. Fractions containing the 13-HPL activity were dialyzed overnight against potassium phosphate 100 mM, pH 7.6 using a microdialyzer (Pierce, Rockford, IL).

Enzyme assays. (i) UV assay. 13-Hydroperoxides from linolenic and linoleic acids were produced with soybean lipoxygenase L1 (type V, Sigma) according to the methods of Vick (20) or Brash and Song (21). 13-HPL activity was measured by following the decrease in absorbance at 234 nm, representing disruption of the conjugated diene system in the fatty acid hydroperoxide substrate. The assay contained 5–10 μg of fatty acid 13-hydroperoxide in 0.5 mL of 100 mM potassium phosphate buffer at pH 7.

For the HPLC assay, 50 or 100 μM of a mixture of unlabeled and [1-^{14}C]-13(*S*)-hydroperoxylinole(n)ic acid (200,000 cpm) was used in 100 mM potassium phosphate buffer at pH 7. The reactions were stopped with 100 μL potassium dihydrogen phosphate (1 M) and the products extracted twice with 0.5 mL ethyl acetate. The combined organic phases were washed with water and dried under a stream of nitrogen. The extracts were dissolved in 50 μL methanol and stored at –20°C under argon prior to analysis. The compounds were analyzed using a Beckman Ultrasphere ODS column (5 μm, 25 × 0.46 cm) using MeOH/H_2O/glacial acetic acid (77.5:22.5:0.01, by vol) as solvent at a flow rate of 1.1 mL/min. Products were detected online using a Hewlett-Packard 1040A diode array detector and a Packard Flo-One radioactive monitor. The main ^{14}C-labeled enzymatic product from [1-^{14}C]13(*S*)-hydroperoxylinolenic acid on reversed-phase (RP)-HPLC (12-oxo-dodecenoic acid) was resolved into the main 9*Z* isomer and the 10*E* isomer formed during sample workup by normal-phase HPLC on a Beckman 5 μm silica column (25 × 0.46 cm) with a solvent of hexane/isopropanol/glacial acetic acid (100:1:0.01, by vol). The 9*Z* isomer chromatographed as a broad symmetrical peak (retention volume 17–22 mL), and the 10*E* isomer as a typically shaped peak at 24 mL. The two compounds were converted to the methoxime derivative (which eliminated further isomerization of the 9*Z* double bond) and methyl ester derivative and analyzed by GC–mass spectrometry (MS).

GC–MS. GC–MS analyses were carried out in the electron impact mode (70 eV) using a Finnigan Incos 50 mass spectrometer (for 3*Z*-hexenal analysis) or a Hewlett-Packard 5889A mass spectrometer (for 12-oxo-dodecenoate analysis), each coupled to a Hewlett-Packard 5890 gas chromatograph equipped with a SPB-1 fused-silica capillary column (15 or 30 m × 0.25 mm internal diameter). Samples were injected at 60°C, and the temperature was subsequently programmed to 300°C at 10 or 20°/min.

RESULTS

13-HPL in fruits and vegetables. The fruits of a number of commonly available plants were screened for the ability to convert 13-hydroperoxylinoleic acid (Table 1) and 13-hydroperoxylinolenic acid (Table 1) to the corresponding C_6 HPL products. On the basis of these results, initially bean was selected as a readily available and relatively inexpensive material for the purification of the enzyme. However, in pilot experiments the bean lyase proved to be unstable to freeze–thawing, and this compromised our ability to purify the enzyme. Accordingly, guava was chosen as an even more promising candidate on the basis of activity. It was soon established that this enzyme survived freezing and that its robust properties permitted its purification through multiple chromatographic steps.

Purification of the guava 13-HPL. Preliminary work confirmed literature reports that 13-HPL is a membrane-bound

TABLE 1
Screening of Plants for 13-Hydroperoxide Lyase Activity

Screening for 13-HPOD lyase activity			
Vegetable	Hexanal[a]	Fruit	Hexanal[a]
Alfalfa	1.36	Apple	0.38
Bean (green)	0.82	Banana	0.31
Bean (white)	0.78	Cashew fruit	<0.1
Celery leaf	0.16	Grape	0.33
Fennel	0.12	Kiwi	0.27
Parsley	0.20	Orange	0.61
Pea	0.25	Papaya	0.73
Pepper (green)	0.89	Pear	0.33
Radish leaf	0.23	Pineapple	0.19
Soya (sprout)	0.25	Raspberry	0.37
Tomato	0.51	Strawberry	0.40
Turnip	0.20	Guava[b]	2.20
Screening for 13-HPOT lyase activity			
Vegetable	(*Z*)-3 + (*E*)-2-Hexenal[a]	Fruit	(*Z*)-3 + (*E*)-2-Hexenal[a]
Alfalfa	0.21	Apple	0.22
Celery	<0.1	Banana	0.13
Cucumber	0.28	Apricot	0.23
Lettuce	<0.1	Cherry	<0.1
Pea	<0.1	Kiwi	0.24
Pepper (green)	0.37	Orange	0.23
Radish leaf	0.10	Papaya	0.11
Soya (sprout)	<0.1	Melon (water)	<0.1
Tomato	<0.1	Raspberry	<0.1
Sorrel	<0.1	Strawberry	<0.1
		Guava[b]	1.18

[a]g/kg reaction.
[b]With guava, optimized yields using higher substrate concentrations (80 g/kg hydroperoxide) were 5.07 g/kg hexanal and 1.43 g/kg hexenals. Abbreviations: HPOD, hydroperoxyoctadecadienoic acid; HPOT, hydroperoxyoctadecatrienoic acid.

enzyme and that detergents are necessary to solubilize the enzyme (11). The guava tissue was homogenized with a sodium phosphate buffer pH 7.0 containing 5 mM sodium ascorbate to prevent oxidation and 0.1% Triton X-100R. When the concentration of Triton X-100R was increased to 1% (vol/vol) and the homogenate was stirred for 30 min, the yield of soluble and active 13-HPL was doubled (data not shown).

A typical purification of 13-HPL from guava fruit is shown in Table 2. The crude extract was concentrated by $(NH_4)_2SO_4$ precipitation followed by a subsequent GPC step on a Superdex 200 column (Pharmacia). The fractions containing 13-HPL activity were pooled and chromatographed on an HIC column. After concentration and desalting, the pooled active fractions were chromatographed on a hydroxylapatite column. The eluted 13-HPL activity was again concentrated, desalted, and loaded onto an IFC column. Each purification step resulted in a considerable loss of 13-HPL activity, which was probably not due to proteolysis, and only 0.2% of the initial 13-HPL activity was recovered (Table 2). Analysis of the preparation by SDS-PAGE showed that the purified sample contained only one, apparently homogenous band with an apparent molecular weight of 48 kD. Because of the high losses of 13-HPL activity, an

TABLE 2
Purification of 13-Hydroperoxide Lyase from Guava Fruit[a]

Purification step	Total protein (mg)	Total 13-HPL activity (nkat)	Recovered activity (%)	Specific 13-HPL activity (nkat mg^{-1})	Purification factor
Crude extract	1,111	172,050	100.0	155	—
30–60% $(NH_4)_2SO_4$ pellet	762	62,300	36.2	82	—
GPC	39	32,640	19.0	837	5.4
HIC	16	15,160	8.8	947	6.1
Hydroxylapatite	1.6	6,500	3.8	4,062	26.2
IFC	0.03	317	0.2	10,566	68.2

[a]HPL, hydroperoxide lyase; GPC, gel permeation chromatography; HIC, hydrophobic interaction chromatography; IFC, isoelectric focusing chromatography.

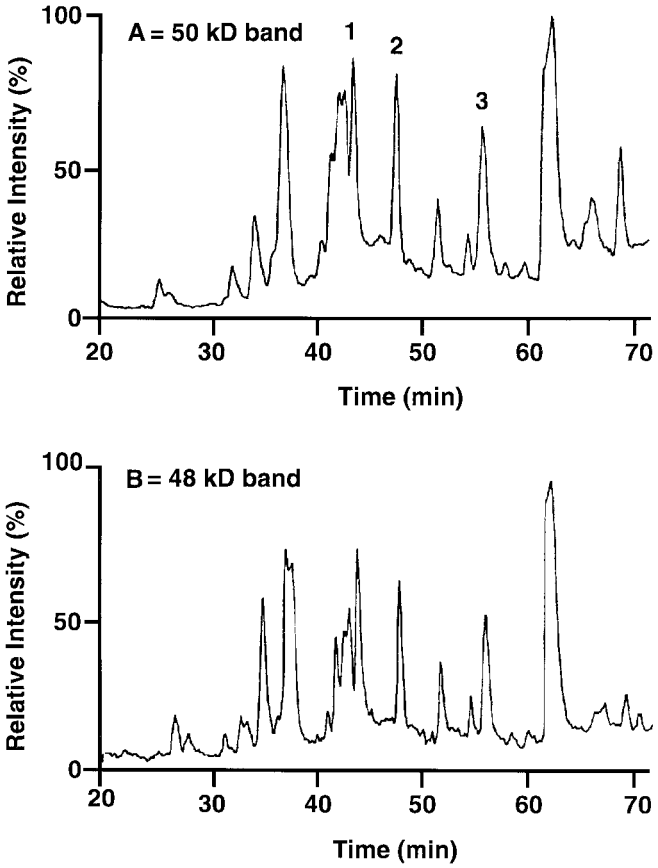

FIG. 1. High-pressure liquid chromatography (HPLC) analysis of purified guava 13-hydroperoxide lyase (13-HPL) digested with trypsin: comparison of the peptide maps of the 50 and 48 kD protein bands.

anion exchange chromatography step was used in place of HIC. In this case, analysis of the purified enzyme by SDS-PAGE showed two bands of 48 and 50 kD. The 13-HPL purified from guava fruit tissue had maximal activity around pH 6.0 and a pI of 6.8 determined by chromatofocusing.

The HPLC peptide maps of the trypsin cleavage products from the two protein bands are very similar (Fig. 1), indicating that there are only minor differences in amino acid composition and/or posttranslational modification. Three peptides of the 50 kD band were sequenced (Table 3).

A computer-aided search of the Swissprot and genEMBL databases found that five amino acids of peptide 3 (Phe Asn Phe Leu Ser, Table 3) are identical to amino acids 236 to 240 of flaxseed allene oxide synthase (AOS) (22). At this stage there was no obvious homology between the peptide sequences and the 13-HPL from green bell pepper fruit (14).

Cloning. Sense and antisense degenerate oligonucleotides (Table 4) deduced from the peptides sequences (Table 3) were synthesized. PCR reactions were performed using the different pairs of oligonucleotides with or without cDNA as template. One main product of 160 bp was subcloned and sequenced, and this was found to contain the three peptides, which were thus from the same peptide chain (see later). Moreover, a multiple alignment of this sequence with the AOS from flax (22), the AOS from guayule (23), the 13-HPL from green pepper (14), and the 13-HPL from *Arabidopsis* (15) showed the highest homology with the 13-HPL enzymes.

The remainder of the cDNA from guava fruit was cloned using 3′- and 5′-RACE (see Experimental Procedures section). cDNA corresponding to the open reading frame was prepared by PCR using a proof-reading mixture of *Taq/Pwo* as DNA polymerase. An amplification product was obtained, subcloned, and sequenced. The complete cDNA (1467 bp) and deduced amino acid sequence are shown in Figure 2. The open reading frame encodes a total of 489 amino acids corresponding to a protein with a molecular weight of 54,817 Daltons. The isoelectric point of the protein is estimated to be 7.29. Previously, the molecular weight of the native protein was estimated by SDS-PAGE as 50 kD, and we found a pI of 6.8 using chromatofocusing. The derived amino acid sequence has an identity of 65% with the pepper 13-HPL (14). The guava cDNA encodes four possible start sites within the first 13 amino acids (methionines 1, 6, 9, and 13) whereas the pepper gene has only two methionines, corresponding to guava-Met9 and guava-Met13.

Expression. Four different cDNA clones of the 13-HPL (13-HPL-Met1, -Met6, -Met9, -Met13) were inserted into the *E. coli* expression plasmids pET30b (see Experimental Procedures section) and transformed into *E. coli* strain BL21(DE3). The expression level was examined at different induction temperatures, with or without addition of isopropyl-β-D-thiogalactopyranoside (IPTG) and the heme precursor, δ-aminolevulinic acid (δ-ALA). The best activities were obtained at 28°C with both δ-ALA and IPTG omitted. Thus, in the system used here, with the pET30 plasmid, its T7 RNA

TABLE 3
Peptide Sequences Obtained from HPLC-Purified Tryptic Fragments

Peptide[a]	Sequence[b]
1	Asp Gly Asn Ala Ser Val Ile Phe Pro Leu Gln (Lys)
2	Asn Phe Ala Met Asp Ile Leu (Lys)
3	Phe Leu Phe Asn Phe Leu Ser (Lys)

[a]These numbers correspond to the peak number obtained during purification by high-performance liquid chromatography (HPLC).
[b]As trypsin cleaves specifically on the carbonyl side of lys-arg linkages, the residues in parentheses are predicted.

TABLE 4
Oligonucleotides Designed from Peptide Sequence for PCR Cloning Experiments

Oligonucleotide name	Sequence[a] (5′-3′ orientation)
12Sa	GAYGGNAAYGCNTCNGTNATHTTYCCNYT
12Sb	GAYGGNAAYGCNAGYGTNATHTTYCCNYT
12Aa	CTRCCNTTRCGNAGNCANTADAARGGNRA
12Ab	CTRCCNTTRCGNTCRCANTADAARGGNRA
13S	AAYTTYGCNATGGAYATHYT
13A	TTRAARCGNTACCTRTADRA
15S	TTYCTNTTYAAYTTYYT
15A	AARGANAARTTRAARRA

[a]Codes used here for the mixed bases are: D = G, A, T; H = A, T, C; R = A, G; Y = C, T. PCR, polymerase chain reaction.

```
ATG GCG AGG GTC GTG ATG AGC AAC ATG TCG CCG GCC ATG TCG TCC ACC TAC CCC CCG TCT CTG TCC
 M   A   R   V   V   M   S   N   M   S   P   A   M   S   S   T   Y   P   P   S   L   S
CCG CCG TCG TCG CCG CGG CCG ACC ACC CTC CCG GTG CGG ACG ATC CCG GGC AGC TAC GGG TGG CCC
 P   P   S   S   P   R   P   T   T   L   P   V   R   T   I   P   G   S   Y   G   W   P
CTC CTC GGC CCG ATA TCG GAC CGC CTG GAC TAC TTC TGG TTC CAA GGC CCG GAG ACG TTC TTC AGG
 L   L   G   P   I   S   D   R   L   D   Y   F   W   F   Q   G   P   E   T   F   F   R
AAG AGG ATC GAG AAG TAC AAG AGC ACC GTG TTC CGC GCG AAC GTG CCT CCG TGC TTC CCC TTC TTC
 K   R   I   E   K   Y   K   S   T   V   F   R   A   N   V   P   P   C   F   P   F   F
TCG AAC GTG AAC CCT AAC GTC GTG GTC GTC CTC GAT TGC GAG TCC TTC GCT CAC TTG TTC GAC ATG
 S   N   V   N   P   N   V   V   V   V   L   D   C   E   S   F   A   H   L   F   D   M
GAG ATC GTG GAG AAG AGC AAC GTC CTC GTC GGC GAC TTC ATG CCG AGC GTG AAG TAC ACC GGG AAC
 E   I   V   E   K   S   N   V   L   V   G   D   F   M   P   S   V   K   Y   T   G   N
ATC CGG GTC TGC GCT TAC CTC GAC ACT TCC GAG CCT CAA CAC GCT CAG GTG AAG AAC TTT GCG ATG
 I   R   V   C   A   Y   L   D   T   S   E   P   Q   H   A   Q   V   K   N   F   A   M
GAC ATA CTG AAG AGG AGC TCC AAA GTG TGG GAG AGC GAA GTG ATC TCG AAC TTG GAC ACC ATG TGG
 D   I   L   K   R   S   S   K   V   W   E   S   E   V   I   S   N   L   D   T   M   W
GAC ACC ATC GAG TCC AGC CTC GCC AAG GAC GGC AAC GCC AGC GTC ATC TTC CCT CTC CAA AAG TTC
 D   T   I   E   S   S   L   A   K   D   G   N   A   S   V   I   F   P   L   Q   K   F
CTC TTC AAC TTC CTC TCC AAG TCC ATC ATC GGC GCT GAC CCG GCC GCC TCG CCG CAG GTG GCC AAG
 L   F   N   F   L   S   K   S   I   I   G   A   D   P   A   A   S   P   Q   V   A   K
TCC GGC TAC GCC ATG CTT GAC CGG TGG CTC GCT CTC CAG CTC CTC CCC ACC ATC AAC ATT GGC GTA
 S   G   Y   A   M   L   D   R   W   L   A   L   Q   L   L   P   T   I   N   I   G   V
CTG CAG CCT CTA GTG GAG ATT TTT CTG CAT TCT TGG GCA TAC CCT TTT GCG CTG GTG AGC GGG GAC
 L   Q   P   L   V   E   I   F   L   H   S   W   A   Y   P   F   A   L   V   S   G   D
TAC AAC AAG CTC TAC CAG TTC ATC GAG AAG GAA GGC CGA GAA GCG GTC GAA AGG GCG AAG GCC GAG
 Y   N   K   L   Y   Q   F   I   E   K   E   G   R   E   A   V   E   R   A   K   A   E
TTC GGA TTG ACA CAC CAG GAG GCC ATC CAC AAC TTG CTG TTC ATC CTC GGC TTC AAC GCG TTC GGC
 F   G   L   T   H   Q   E   A   I   H   N   L   L   F   I   L   G   F   N   A   F   G
GGC TTC TCG ATC TTC CTC CCC ACG TTG CTG AGC AAC ATA CTT AGC GAC ACA ACC GGA CTG CAG GAC
 G   F   S   I   F   L   P   T   L   L   S   N   I   L   S   D   T   T   G   L   Q   D
CGG CTG AGG AAG GAG GTC CGG GCA AAG GGA GGG CCG GCG TTG AGC TTC GCC TCG GTG AAG GAG ATG
 R   L   R   K   E   V   R   A   K   G   G   P   A   L   S   F   A   S   V   K   E   M
GAA CTC GTG AAG TCG GTC GTG TAC GAG ACG CTG CGG CTC AAC CCG CCC GTC CCG TTC CAA TAC GCT
 E   L   V   K   S   V   V   Y   E   T   L   R   L   N   P   P   V   P   F   Q   Y   A
CGA GCC CGG AAG GAC TTC CAG CTC AAG TCC CAC GAC TCT GTC TTT GAT GTC AAG AAA GGC GAG CTG
 R   A   R   K   D   F   Q   L   K   S   H   D   S   V   F   D   V   K   K   G   E   L
CTA TGC GGG TAT CAG AAG GTG GTG ATG ACA GAC CCG AAA GTG TTC GAC GAA CCG GAG AGC TTC AAC
 L   C   G   Y   Q   K   V   V   M   T   D   P   K   V   F   D   E   P   E   S   F   N
TCG GAC CGG TTC GTC CAA AAC AGC GAG CTA CTG GAT TAC CTG TAC TGG TCC AAC GGG CCG CAG ACC
 S   D   R   F   V   Q   N   S   E   L   L   D   Y   L   Y   W   S   N   G   P   Q   T
GGA ACG CCG ACC GAG TCG AAC AAG CAG TGC GCG GCT AAG GAC TAC GTC ACC CTC ACC GCT TGT CTC
 G   T   P   T   E   S   N   K   Q   C   A   A   K   D   Y   V   T   L   T   A   C   L
TTC GTT GCC TAC ATG TTT CGA CGG TAC AAT TCC GTC ACA GGA AGC TCG AGC TCG ATC ACA GCC GTT
 F   V   A   Y   M   F   R   R   Y   N   S   V   T   G   S   S   S   S   I   T   A   V
GAA AAG GCC AAC TGA GTT TGA CGC GTG TTT ATG TTG TAC GGG CCA TTT GGG CTT TGT TGG GCT TGA
 E   K   A   N   .
GGC CCA GCC CAT TAT CCA TAC AGT GCG ATG GCC TCT TCA TAA GCG GTT CTC AAT CTC AAG TCC ACA
CCC TGA TGT ATG GTG GAG GCA ATA AGT CAT CCT TGA AAT GAT TTA AAG TAT GAA CAG CCG TTC AAT
CCA AAA AAA AAA AAA
```

FIG. 2. Nucleotide and deduced amino acid sequence of the guava 13-HPL. The four N-terminal methionines are boxed. The location of three peptides of known amino acid sequence are shown in bold. The enzyme is classified as CYP74B5, and the GenBank accession number is AF239670. For abbreviation see Figure 1.

polymerase promoter, and with the cells grown in a rich medium (TB), addition of heme precursor or IPTG inducer did not help with expression of active lyase.

Proteins from the transformed and induced cells were analyzed by SDS-PAGE (Fig. 3). High levels of protein with the expected molecular weight were expressed under all culture conditions (Fig. 3; lanes 2, 3, and 4). These levels appear to account for about half of the cellular protein. We obtained

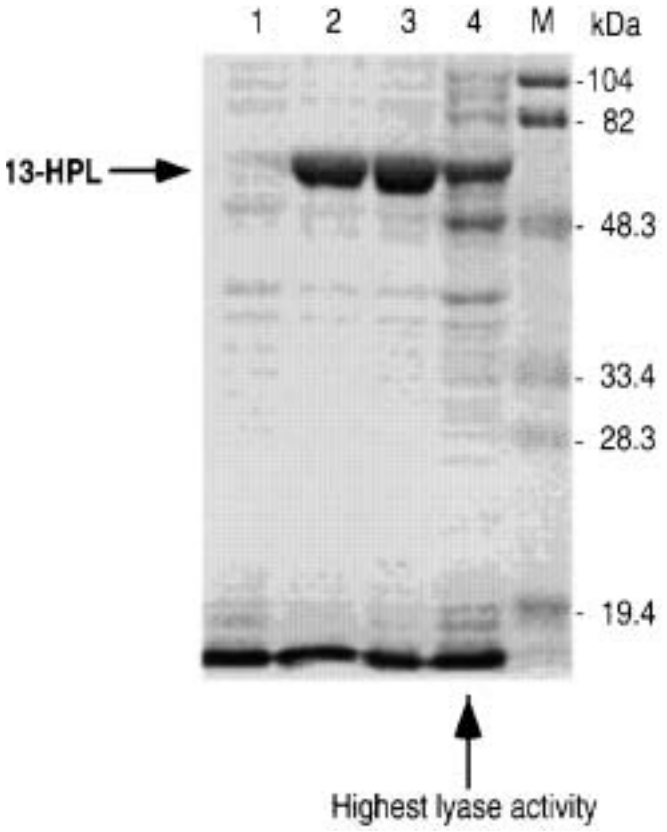

FIG. 3. Sodium dodecyl sulfate-polyacrylamide gel electrophoresis analysis of guava 13-HPL expressed in *Escherichia coli* (BL21 cells). Lane 1: cells were transformed with pET30 vector alone. In the other lanes, cells were transformed with pET30:13-HPL (containing all four N-terminal methionines) cultured with δ-ALA and IPTG (lane 2), with IPTG only (lane 3), and without δ-ALA and IPTG (lane 4). Molecular weight markers (M) are in the right-hand lane. δ-ALA, δ-aminolevulinic acid; IPTG, isopropyl-β-D-thiogalactopyranoside; for other abbreviation, see Figure 1.

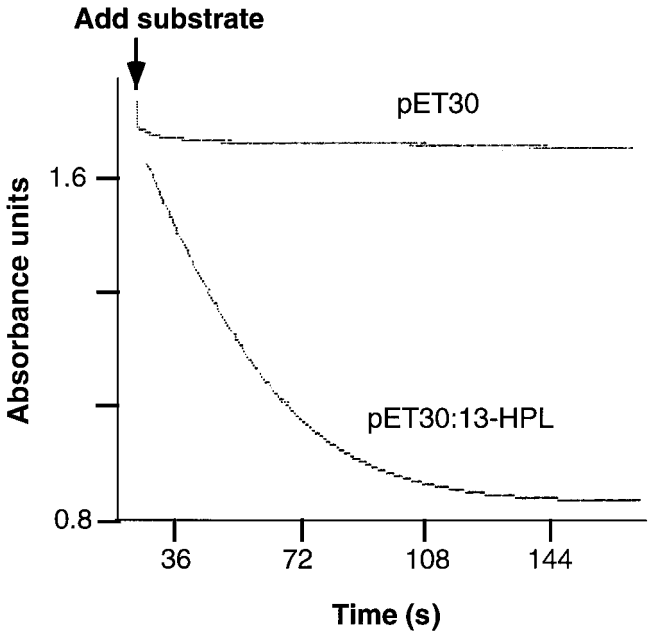

FIG. 4. Spectrophotometric assay of the guava 13-HPL expressed in *E. coli*. Absorbance changes were monitored at 235 nm in potassium phosphate buffer, pH 7.6. Comparison of activity of 1 µL aliquots of bacterial lysates transformed with pET30 vector alone and with pET30:13-HPL. For abbreviations, see Figures 1 and 3.

lower levels of protein but the highest lyase activity when the cells were grown in the absence of δ-ALA and IPTG (Fig. 3, lane 4). By using Emulphogen or cholate detergents, most of the expressed 13-HPL protein failed to solubilize, and the insoluble material was catalytically inactive. This likely reflects the fact that there is a very high basal induction in this system, and the cells are barely capable of handling the expressed protein. Examination of the cells under the microscope revealed many inclusion bodies, with the highest number in cells grown with IPTG. This supports the concept that the bacteria cannot handle the level of expressed protein and the main part of the translated lyase is deposited in inclusion bodies. Using IPTG as a further stimulus results in even lower recovery of correctly folded protein with catalytic activity.

Lyase activity. The four different guava 13-HPL constructs (-Met1, -Met6, -Met9, and -Met13) did not differ markedly in their catalytic activities in the UV assay. Figure 4 illustrates an example with pET30Met1, and also shows the lack of significant activity in the negative control in comparison to the reaction with 13-hydroperoxylinolenic acid. Approximately 10-fold lower rates of reaction were obtained with 13(*S*)-hydroperoxylinoleic acid, 9(*S*)-hydroperoxylinoleic acid, and 15(*S*)-hydroperoxyeicosatetraenoic acid.

For HPLC analysis of the nonvolatile products, an aliquot of the sonicated protein preparation containing the 13-HPL was incubated with [1-^{14}C]13(*S*)-hydroperoxylinolenic acid for 1 min as described in the Experimental Procedures section. Essentially all the substrate was metabolized in the 1 min of incubation, and the 1-^{14}C label was recovered in a major polar product (Fig. 5) with a retention time expected of the

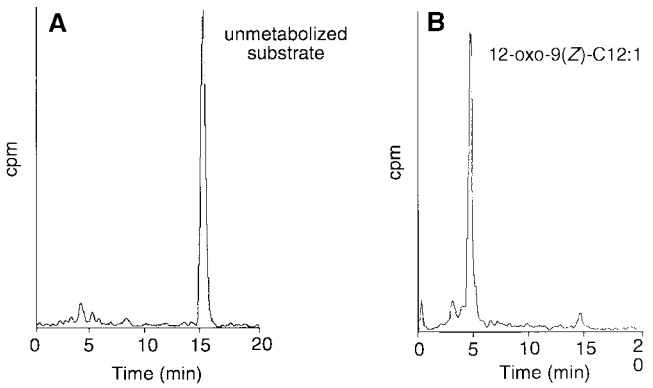

FIG. 5. HPLC analysis of catalytic activity of guava 13-HPL expressed in *E. coli*. Extracts were incubated with [1-^{14}C]13(*S*)-hydroperoxylinolenic acid, extracted, and aliquots injected on a Beckman Ultrasphere ODS column (25 × 0.46 cm) and eluted with a solvent system of methanol/water/glacial acetic acid (77.5:22.5:0.01, by vol) at a flow rate of 1.1 mL/min. (A) Incubation of extracts of BL21 cells expressing vector pET30 only. (B) Incubation of extracts of BL21 cells expressing pET30:13-HPL. Radioactivity was detected on-line using a Packard Flo-One scintillation detector. For abbreviations, see Figures 1 and 3.

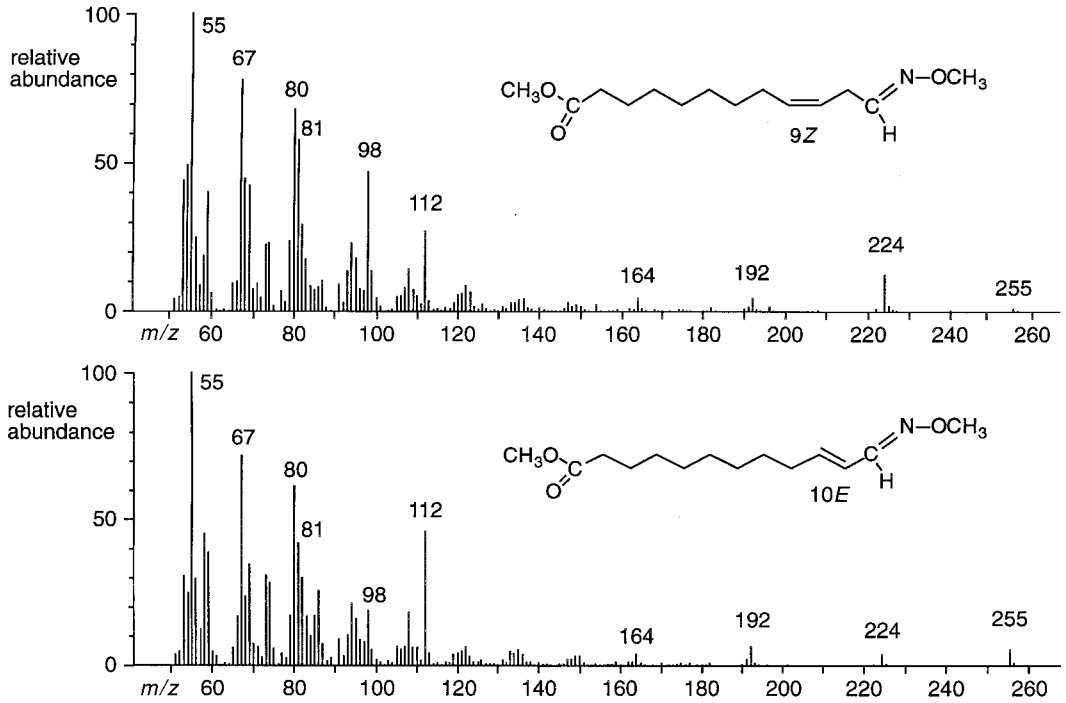

FIG. 6. Electron impact mass spectra of (9*Z*)-12-oxo-dodecenoic acid formed by reaction of the guava lyase with 13(*S*)-hydroperoxylinolenic acid and its 10*E* isomer. The two isomers were resolved by normal-phase HPLC and analyzed as the methyl ester methoxime derivative (top spectrum, 9*Z*; bottom, 10*E*). For abbreviation, see Figure 1.

13-HPL-derived aldehyde, 12-oxo-9(*Z*)-dodecenoic acid. This product, which partly isomerized to the 10*E* isomer during sample workup, was resolved into the 9*Z* and 10*E* isomers by normal-phase HPLC (as described in the Experimental Procedures section). The two isomers were converted to the methoxime methyl ester derivatives and identified by GC–MS analysis (Fig. 6). The methyl (9*Z*)-12-oxo-dodecenoate methoxime eluted from the GC as a single peak at the retention time approximately of a saturated C_{16} fatty acid methyl ester; the 10*E* analog eluted 0.6 min later as a double peak of *syn* and *anti* methoxime isomers. The 9*Z* isomer (assigned based on its featureless UV spectrum, recorded before and after methoxime formation) gave a mass spectrum that was particularly close in appearance to the first reported spectrum of methyl 12-oxo-dodecenoate methoxime (24). The similarity in the mass spectra was noticeable particularly in terms of the pattern of abundances of the higher mass ions [M^+ 255 (1% abundance), M – 31 at *m/z* 224 (14%), and *m/z* 192 (4%)], and the relative abundance of certain prominent lower mass ions such as *m/z* 98 (47%) and *m/z* 81 (54%). In retrospect, the original spectrum may have been predominantly the 9*Z* isomer. We assigned the 10*E* isomer as such on the basis of the characteristics of its UV spectrum: it displayed the expected enone chromophore with λ_{max} 225 nm in MeOH/H_2O (75:25, vol/vol) and extended conjugation after methoxime formation, producing a broad chromophore with λ_{max} 239 nm in MeOH. The mass spectrum of the 10*E* derivative contained the same ions as in the 9*Z*, but there were different patterns of ion abundances (Fig. 6). For example, M^+ (5% relative abundance) was slightly more prominent than *m/z* 224 (3%), whereas *m/z* 98 (20%) and *m/z* 81 (39%) were less prominent than in the 9*Z* isomer. This mass spectrum was a good match with another reported spectrum of the 10*E* isomer (25).

To detect the more volatile aldehyde product, we utilized direct GC–MS analysis of diethyl ether extracts of the reaction of 13-hydroperoxylinolenic acid with the expressed guava enzyme. The GC profile and mass spectrum identified the volatile product formed as 3(*Z*)-hexenal (Fig. 7).

DISCUSSION

An initial screening of the levels of 13-HPL in fruits and vegetables pointed to guava as a rich source of this activity. From the subsequent isolation of the protein we found that approximately a 70-fold purification was sufficient to give a homogeneous preparation of the enzyme. Seventyfold enrichment implies a level of about 1–2% of the protein in the original extract, consistent with guava as an abundant source of 13-HPL. The two bands isolated in the purification process are almost certainly an indication of partial proteolysis or deglycosylation of the higher molecular weight protein. The difference in molecular weight (2 kD) between the two forms could be explained if the heavier form is glycosylated by as few as the equivalent of 10 glucose residues. The purification of the 13-HPL from tea leaves (11) showed that the enzyme was separated with hydroxylapatite chromatography into two fractions, HPLI and HPLII with molecular weights of 53 and 55 kD. For the 13-HPL from green bell pepper fruits, Shibata *et al.* (12)

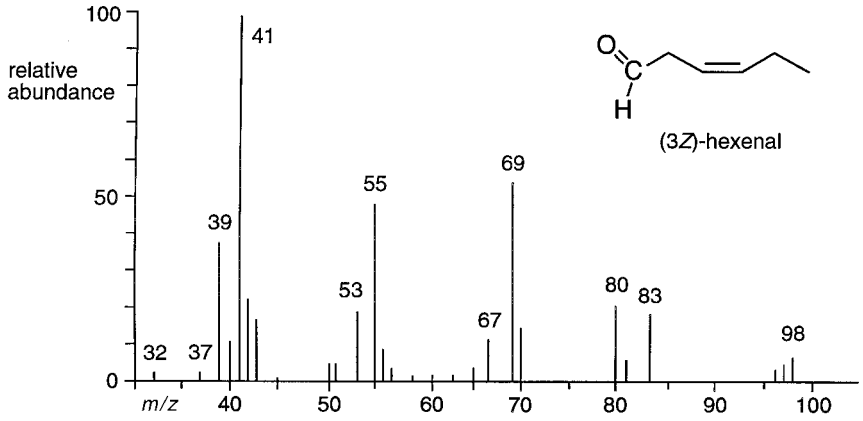

FIG. 7. Electron impact mass spectrum of the volatile C_6 product formed by reaction of the guava lyase with 13(*S*)-hydroperoxylinolenic acid. The spectrum matches a reference of (3*Z*)-hexenal (Chemical Abstract Service No. 006789-80-6) in the NIST (National Institute of Science and Technology) 75K database on a Hewlett-Packard 5989A mass spectrometer/DOS Chemstation software, entry number 1285 (1992).

showed also that 13-HPL could be resolved into two isoforms by hydroxylapatite chromatography; in this case, both isoforms had molecular masses of 55 kD (12). Similar to the lyases of sunflower (13), the apparent molecular weight of the guava 13-HPL as determined by gel filtration is in the order of 200,000 kD, implying a tetrameric structure for the native enzyme. This is in agreement with Olias *et al.* (10) who reported that 13-HPL from soybean seedlings had a native molecular mass of 240–260 kD and a subunit size of 62 kD. However, Shibata *et al.* (12) proposed that the 13-HPL from green bell pepper fruits is a trimer based on their measurements of the native molecular mass (170 kD) and subunit size (55 kD).

The 13-HPL of guava has a substrate specificity similar to several other reported 13-HPL enzymes. The preferred substrate is 13*S*-hydroperoxylinolenic acid. The corresponding linoleic acid 13*S*-hydroperoxide shows about one-tenth the rate of reaction, and the 9-hydroperoxides also are poor substrates. These results apparently contrast with the original data of lyase activity in guava fruit which indicated excellent recovery of the C_6-aldehydes of linoleic and linolenic acids (Table 1). However, a number of factors could account for this difference that relate more to differences in assay conditions. The activity values in fruit comprise recovered products whereas rates of reaction were measured with the expressed enzyme. As the hexenals derived from linolenate are considerably less stable than the saturated product of linoleate, this gives a bias favoring recovery of hexanal. Similarly, changes in enzyme activity due to the different substrate and product concentrations and the different reaction times (<1 min, vs. 1 h) in the two assays could further influence the results. It is also possible that other isoforms of hydroperoxide lyase might exist in guava. Of the two hydroperoxide lyases purified by Itoh and Vick (13) from sunflower hypocotyl, one resembled the guava and pepper enzymes and a second showed equal reactivity with the C18:2 analog, 13-hydroperoxylinoleic acid.

The guava cDNA sequence has about 60% amino acid identity to the 13-HPL of bell pepper and *Arabidopsis,* placing it in the same subfamily of cytochrome P450, CYP74B. The enzymes share about 35–40% identity with the plant AOS, which comprise the CYP74A subfamily. Within the majority of cytochrome P450 families there is a conserved sequence next to the cysteine that forms the proximal ligand to the heme (e.g., Ref. 26). In the CYP74 family, there are some unusual and distinctive sequences around this cysteine (Fig. 8). All reported 13-HPL and AOS enzymes have the sequence Asn-Lys-Gln (NKQ) immediately before the cysteine.

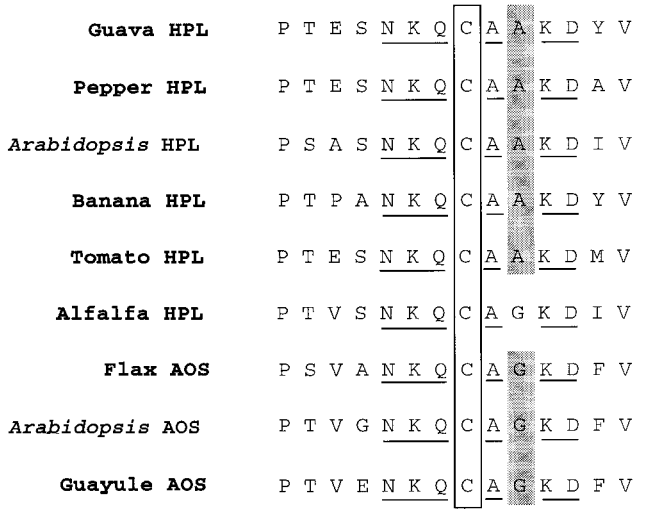

FIG. 8. Alignment of amino acid sequences around the proximal heme ligand. The cysteinyl heme ligand is boxed. The absolutely conserved sequence NKQCA is underlined. The shaded position is usually Ala in 13-HPL, whereas in AOS enzymes the residue is the more typical P450 consensus Gly. The GenBank accession numbers of the sequences, given in parentheses, are for guava HPL (AF239670), bell pepper HPL (U51674), *Arabidopsis* HPL (AF087932), banana HPL (A65873, the subject of U.S. patent 6,008,034, and patent EP0801133 assigned to Givaudan-Roure International S.A.), alfalfa HPL (AJ249247), flax AOS (U00428), *Arabidopsis* AOS (AF172727), and guayule AOS (X78166). AOS, allene oxide synthase; for other abbreviation, see Figure 1.

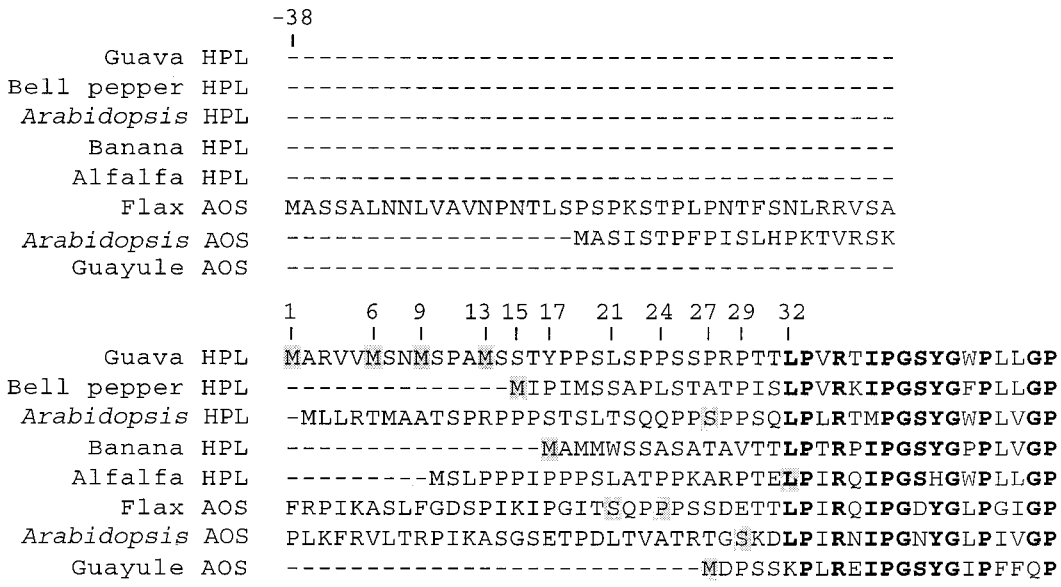

FIG. 9. N-terminal sequence comparison of 13-HPL and AOS enzymes. Comparison of the guava 13-HPL with other CYP74 members. The different enzyme sequences are presented with the conserved residues aligned and shown in bold. The shaded residues indicate the N-terminal start site for the four guava constructs described here and the reported constructs of other enzymes that expressed with catalytic activity (14,15,22,23,27, 31). GenBank accession numbers are given in the legend to Figure 8. For abbreviations, see Figures 1 and 8.

Following the cysteine, the AOS (CYP74A) enzymes have the commonly occurring sequence Ala-Gly (Gly in this position is the P450 consensus sequence), giving the overall sequence NKQCAG. On the other hand, the lyases are distinguished by having the sequence Ala-Ala after the Cys. The second alanine, conserved in the lyases, occurs among less than 5% of all reported cytochromes P450. It is possible that the CAA sequence gives a structurally significant tilt to the supporting polypeptide under the heme group. Mutation of this second alanine residue would be of interest for future experiments. Figure 8 also illustrates the absolutely conserved Val in the last position of this alignment. This is a very unusual residue in this position, which is normally represented by Gly or Ala in over 95% of all families of cytochrome P450.

There are remarkable differences in the sequences of the CYP74 family at the N-termini of the proteins (Fig. 9). Certain of the AOS, exemplified in Figure 9 by the flax and *Arabidopsis* enzymes, have a long presequence that includes a chloroplast transit peptide. In the flaxseed AOS, as deduced by Laudert *et al.* (27), this includes 21 amino acids that are cleaved to give the mature protein. By contrast, the AOS of guayule has a short N-terminus, more similar to the 13-HPL enzymes. The N-terminal sequence of the guava 13-HPL has some unusual features compared to the HPL of bell pepper and *Arabidopsis*. There are four methionines in the first 13 amino acids. We tested the effect of deleting these sequences (albeit with an additional N-terminal sequence from the pET vector still present in each of the expressed proteins). Active lyase was obtained when either the full-length cDNA was expressed, or in the shortened cDNAs with one, two, or three methionines removed. The *Arabidopsis* 13-HPL could be expressed as catalytically active enzyme after deletion of the first 28 amino acids. The shaded residues in Figure 9 indicate the most N-terminal amino acid in constructs that have been successfully expressed with catalytically active enzyme. For the guayule AOS, the CYP74 family member with the shortest known N-terminus, the clear homology to the other enzymes (bold characters in Fig. 9) begins only six amino acids after the initiating methionine. For the CYP74 family, it has yet to be determined what is the shortest possible N-terminus that remains compatible with expression of catalytically active enzyme.

One of the outstanding properties of the AOS enzymes is their very high initial rate of reaction, in the order of 1000 turnovers per second. This contrasts with turnover numbers as low as 1/min for sluggish P450 reactions (28,29), and ≈3200/min for the fastest P450-hydroxylations as catalyzed, for example, by the heme domain of $P450_{BM3}$ (30). The turnover number for HPL has not been reported. We were able to determine a value for the guava 13-HPL following its expression in *E. coli*. After partial purification of the His-tagged enzyme on a nickel affinity column, we obtained a weak UV-visible spectrum that permitted only an approximate quantitation of the enzyme based on the main Soret band at ≈400 nm. Nonetheless, the value obtained was sufficient to permit calculation of the turnover number. The initial reaction rates indicate a turnover number for the 13-HPL of approximately 2000/s, a value comparable to the AOS counterparts in the subfamily CYP74A.

ACKNOWLEDGMENTS

This work was supported by Firmenich S.A., Geneva, Switzerland, and the Kanton of Zürich (KWF Projekt Nr. 2544.1). We thank Dr.

Fredi Bruhlmann for helpful comments. Use of guava fruit in the commercial production of aliphatic aldehydes and alcohols from natural fatty acid precursors is covered by U.S. Patent number 5,464,761 assigned to Firmenich S.A.

REFERENCES

1. Kim, I.S., and Grosch, W. (1981) Partial-Purification and Properties of a Hydroperoxide Lyase from Fruits of Pear, *J. Agric. Food. Chem. 29,* 1220–1225.
2. Hatanaka, A., Kajiwara, T., and Sekija, J. (1987) Biosynthetic Pathway for C6-Aldehydes Formation from Linolenic Acid in Green Leaves, *Chem. Phys. Lipids 44,* 341–361.
3. Croft, K.P.C., Jüttner, F., and Slusarenko, A.J. (1993) Volatile Products of the Lipoxygenase Pathway Evolved from *Phaseolus vulgaris* (L.) Leaves Inoculated with *Pseudomonas syringae* pv. *phaseolicola, Plant Physiol. 101,* 13–24.
4. Dickens, J.C., Billings, R.F., and Payne, T.L. (1992) Green Leaf Volatiles Interrupt Aggregation Pheromone Response in Bark Beetles Infesting Southern Pines, *Experientia 48,* 523–524.
5. Hatanaka, A. (1993) The Biogeneration of Green Odor by Green Leaves, *Phytochemistry 34,* 1201–1218.
6. Tressl, R., and Drawert, F. (1973) Biogenesis of Banana Volatiles, *J. Agric. Food Chem. 21,* 560–565.
7. Vick, B.A., and Zimmerman, D.C. (1976) Lipoxygenase and Hydroperoxide Lyase in Germinating Watermelon Seedlings, *Plant Physiol. 57,* 780–788.
8. Schreier, P., and Lorenz, G. (1982) Separation, Partial Purification and Characterisation of a Fatty Acid Hydroperoxide Cleaving Enzyme from Apple and Tomato Fruits, *Z. Naturforsch. C 37,* 165–173.
9. Matsui, K., Shibata, Y., Kajiwara, T., and Hatanaka, A. (1989) Separation of 13-Hydroperoxide and 9-Hydroperoxide Lyase Activities in Cotyledons of Cucumber Seedlings, *Z. Naturforsch. C 44,* 883–885.
10. Olias, J.M., Rios, J.J., Valle, M., Zamora, R., Sanz, L.C., and Axelrod, B. (1990) Fatty Acid Hydroperoxide Lyase in Germinating Soybean Seedlings, *J. Agric. Food Chem. 38,* 624–630.
11. Matsui, K., Toyota, H., Kajiwara, T., Kakuno, T., and Hatanaka, A. (1991) Fatty Acid Hydroperoxide Cleaving Enzyme, Hydroperoxide Lyase, from Tea Leaves, *Phytochemistry 30,* 2109–2113.
12. Shibata, Y., Matsui, K., Kajiwara, T., and Hatanaka, A. (1995) Purification and Properties of Fatty Acid Hydroperoxide Lyase from Green Bell Pepper Fruits, *Plant Cell Physiol. 36,* 147–156.
13. Itoh, A., and Vick, B.A. (1999) The Purification and Characterization of Fatty Acid Hydroperoxide Lyase in Sunflower, *Biochim. Biophys. Acta 1436,* 531–540.
14. Matsui, K., Shibutani, M., Hase, T., and Kajiwara, T. (1996) Bell Pepper Fruit Fatty Acid Hydroperoxide Lyase Is a Cytochrome P450 (CYP74B), *FEBS Lett. 394,* 21–24.
15. Bate, N., Sivasankar, S., Moxon, C., Riley, J.M., Thompson, J.E., and Rothstein, S.J. (1998) Molecular Characterization of an *Arabidopsis* Gene Encoding Hydroperoxide Lyase, a Cytochrome P-450 That Is Wound Inducible, *Plant Physiol. 117,* 1393–1400.
16. Wan, C.Y., and Wilkins, T.A. (1994) A Modified Hot Borate Method Significantly Enhances the Yield of High-Quality RNA from Cotton (*Gossypium hirsutum* L.), *Anal. Biochem. 223,* 7–12.
17. Brash, A.R., Boeglin, W.E., Chang, M.S., and Shieh, B.-H. (1996) Purification and Molecular Cloning of an 8*R*-Lipoxygenase from the Coral *Plexaura homomalla* Reveal the Related Primary Structures of *R*- and *S*-Lipoxygenases, *J. Biol. Chem. 271,* 20949–20957.
18. Hoffman, B.J., Broadwater, J.A., Johnson, P., Harper, J., Fox, B.G., and Kenealy, W.R. (1995) Lactose Fed-Batch Overexpression of Recombinant Metalloproteins in *Escherichia coli* BL21 (DE3): Process Control Yielding High Levels of Metal-Incorporated Soluble Protein, *Prot. Express. Purific. 6,* 646–654.
19. Imai, T., Globerman, H., Gertner, J.M., Kagawa, N., and Waterman, M.R. (1993) Expression and Purification of Functional Human 17 Alpha-Hydroxylase/17,20-lyase (P450c17) in *Escherichia coli*. Use of This System for Study of a Novel Form of Combined 17 Alpha-Hydroxylase/17,20-Lyase Deficiency, *J. Biol. Chem. 26,* 19681–19689.
20. Vick, B.A. (1991) A Spectrophotometric Assay for Hydroperoxide Lyase, *Lipids 26,* 315–320.
21. Brash, A.R., and Song, W.-C. (1996) Detection, Assay, and Isolation of Allene Oxide Synthase, *Methods Enzymol. 272,* 250–259.
22. Song, W.-C., Funk, C.D., and Brash, A.R. (1993) Molecular Cloning of an Allene Oxide Synthase: A Cytochrome P450 Specialized for the Metabolism of Fatty Acid Hydroperoxides, *Proc. Natl. Acad. Sci. USA 90,* 8519–8523.
23. Pan, Z.Q., Durst, F., Werk-Reichhart, D., Gardner, H.W., Camara, B., Cornish, K., and Backhaus, R.A. (1995) The Major Protein of Guayule Rubber Particles Is a Cytochrome P450, *J. Biol. Chem. 270,* 8487–8494.
24. Zimmerman, D.C., and Coudron, C.A. (1979) Identification of Traumatin, a Wound Hormone, as 12-Oxo-*trans*-10-dodecenoic Acid, *Plant Physiol. 63,* 536–541.
25. Hatanaka, A., Kajiwara, T., Sekiya, J., and Fukumoto, T. (1982) Oxygen-Isotope Effect in Enzymatic Cleavage Reaction of 13-L-Hydroperoxylinoleic acid to Hexanal and 11-Formyl-*cis*-9-undecenoic Acid, *Z. Naturforsch. 37C,* 752–757.
26. Brash, A.R., and Song, W.-C. (1995) Structure–Function Features of Flaxseed Allene Oxide Synthase, *J. Lipid Mediat. Cell Signal. 12,* 275–282.
27. Laudert, D., Pfannschmidt, U., Lottspeich, F., Hollander Czytko, H., and Weiler, E.W. (1996) Cloning, Molecular and Functional Characterization of *Arabidopsis thaliana* Allene Oxide Synthase (CYP74), the First Enzyme of the Octadecanoid Pathway to Jasmonates, *Plant Mol. Biol. 31,* 323–335.
28. Guo, Z., Gillam, E.M.J., Ohmori, S., Tukey, R.H., and Guengerich, F.P. (1994) Expression of Modified Human Cytochrome P450 1A1 in *Escherichia coli*: Effects of 5′ Substitution, Stabilization, Purification, Spectral Characterization, and Catalytic Properties, *Arch. Biochem. Biophys. 312,* 436–446.
29. Gillam, E.M.J., Guo, Z., Ueng, Y.-F., Yamasaki, H., Cock, I., Reilly, P.E.B., Hooper, W.D., and Guengerich, F.P. (1995) Expression of Cytochrome P450 3A5 in *Escherichia coli*: Effects of 5′ Modification, Purification, Spectral Characterization, Reconstitution Conditions, and Catalytic Activities, *Arch. Biochem. Biophys. 317,* 374–384.
30. Capdevila, J.H., Wei, S., Helvig, C., Falck, J.R., Belosludtsev, Y., Truan, G., Graham-Lorence, S.E., and Peterson, J.A. (1996) The Highly Stereoselective Oxidation of Polyunsaturated Fatty Acids by Cytochrome P450BM-3, *J. Biol Chem. 271,* 22663–22671.
31. Noordermeer, M.A., van Dijken, A.J.H., Smeekens, S.C.M., Veldink, G.A., and Vliegenthart, J.F.G. (2000) Characterization of Three Cloned and Expressed 13-Hydroperoxide Lyase Isoenzymes from Alfalfa with Unusual N-Terminal Sequences and Different Enzyme Kinetics, *Eur. J. Biochem. 267,* 2473–2482.

[Received February 25, 2000, and in revised form and accepted April 25, 2000]

Gastroprotection of DNA with a Synthetic Cholic Acid Analog

Edmund J. Niedzinski[a], Michael J. Bennett[b], David C. Olson[b], and Michael H. Nantz[a,*]

[a]Department of Chemistry, University of California-Davis, Davis, California 95616, and [b]Genteric, Inc., Alameda, California 94501

ABSTRACT: The oral delivery of functional DNA to the gastrointestinal system would constitute a desirable, noninvasive method for potentially treating a variety of diseases. The digestive process, however, remains a formidable barrier. This dilemma may be addressed by using targeted liposomes both to protect the polynucleotide and to deliver the therapeutic DNA with high tissue specificity. The present study represents the initial steps toward developing a novel gene delivery system designed to interact with the enterohepatic receptors of the small intestine. Two cholic acid esters were synthetically modified at position C(3) to incorporate a DNA-binding domain. These novel compounds were evaluated for their ability to protect DNA from the nucleases found in gastrointestinal segments. Additionally, the compounds were screened as a component of a gene delivery vector. Formulations containing the new bile salt derivatives protected DNA from degradation for more than 2 h and were capable of transfecting cultured NIH 3T3 cells.

Paper no. L8456 in *Lipids 35,* 721–727 (July 2000).

Delivery of polynucleotides to the gastrointestinal system *via* oral administration potentially would provide an opportunity to treat a variety of disorders in a noninvasive manner (1). Even though challenging, the oral administration of a gene pharmaceutical also would constitute a more convenient route of administration than current methods. Although gene therapy clinical trials have proceeded using intranasal (2,3), intramuscular (4), or intravenous administration (5), gastrointestinal (GI) gene therapy remains to be clinically developed. To develop this route of administration, we have begun to address the barriers of GI gene delivery. Previous attempts to deliver DNA to the GI tract have utilized both viral and nonviral delivery vectors (6–9). While results from these studies are promising, we anticipate that thorough evaluation of the physical and biochemical obstacles in combination with the development of tissue specific vectors will lead to more effective GI transfection. We report herein the synthesis of novel cholic acid derivatives that have been designed to protect DNA from gastric digestion and to effectively promote DNA uptake by the enterohepatic receptors in the ileum. Using a series of stability studies and transfection assays, we present our analysis of these compounds as a potential GI delivery system.

Oral gene delivery must overcome a number of barriers to effectively present a polynucleotide to the intestinal lumen. These barriers include low gastric pH, high concentrations of digestive enzymes, detergents, and the mucosa that limits access to the gut epithelium. Since the selection of delivery vector ultimately will dictate how these obstacles are addressed, careful consideration must be given to the choice between viral or lipid-based delivery systems. Viral vectors have shown much promise in gene delivery; however, their use in clinical studies continues to be problematic (10). Low titer production, immunogenicity, and limitations on plasmid DNA size plague the use of viral vectors. Cationic lipid vectors do not suffer from these specific limitations. There have been many improvements in the use of cationic lipids as transfection agents since the prototype agent *N*-[2,3-(dioleyloxy)propyl]-*N,N,N*-trimethylammonium chloride (11) was reported (12,13). Furthermore, lipids may be chemically modified to interact with specific molecular receptors. This targeting aspect makes the use of cationic lipids an attractive choice for GI gene therapy.

To increase the interaction of a lipid-DNA complex (lipoplex) (14) with the terminal ileum, we prepared novel transfection lipids from cholic acid (Scheme 1) where the conditions for "a" include $(imid)_2CO$ (1.5 eq.), Et_3N, CH_2Cl_2, 0°C–room temperature; the conditions for "b" include $(CH_3)_2NCH_2$-CH_2NH_2 (1.5 eq), Et_3N, CH_2Cl_2, room temperature. We envisioned that these compounds would localize lipoplexes to the epithelium of the terminal ileum by taking advantage of the bile acid specificity for enterohepatic receptors. The enterohepatic receptors in the ileum are responsible for circulating between 12–30 g of bile salts in a day, and the

*To whom correspondence should be addressed.
E-mail: mhnantz@ucdavis. edu

Abbreviations: CMV, cytomegalovirus; DMDHP, *N,N*-bis(2-hydroxyethyl)-*N*-[2,3-(dimyristoyloxy)propyl]-*N*-methylammonium chloride; DMEM, Dulbecco's modified Eagle's medium; DOPE, 1,2-dioleoyl-*sn*-3-phosphoethanolamine; DOTAP, *N*-[2,3-(dioleoyloxy)propyl]-*N,N,N*-trimethylammonium chloride; DOTMA, *N*-[2,3-(dioleyloxy)propyl]-*N,N,N*-trimethylammonium chloride; GI, gastrointestinal; HMPA, hexamethylphosphoric triamide; HRMS, high-resolution mass spectroscopy; IR, infrared; NMR; nuclear magnetic resonance; PBS, phosphate-buffered saline; TAE, tris/acetic acid; TLC, thin-layer chromatography.

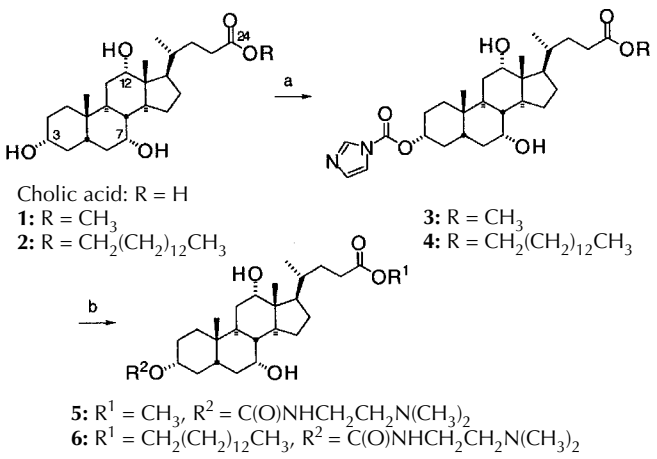

SCHEME 1

bile salts are reabsorbed in the terminal ileum with recovery efficiencies of up to 95% (15). C(3)-functionalized cholic acid derivatives have shown the ability to interact with molecular receptors in the ileum, aiding the delivery of molecules through the intestinal wall (16,17). Thus, we reasoned that a cholic acid derivative fitted with a DNA-binding domain might condense DNA and promote the intracellular delivery of DNA in a similar manner. Walker *et al.* (18) reported a series of cholic acid derivatives that were speculated to act as facial amphiphiles and were successfully used to facilitate DNA transfection. This work provides good precedent for the use of cholic acid derivatives in transfection experiments. We prepared novel cholate derivatives by straightforward chemical modifications of positions C(3) and C(24). Previous investigations showed that these positions may be functionalized for conjugation without compromising recognition by the bile acid transport system (19). The new cholate amphiphiles were evaluated for the ability to complex and protect DNA in the gastric environment. We also screened the novel lipids as lipoplex components to determine their compatibility with transfection agents. Results of these studies are presented herein.

MATERIALS AND METHODS

General. All chemical reactions were carried out under an atmosphere of nitrogen. CH_2Cl_2 was distilled from calcium hydride immediately prior to use. Methanol was distilled from magnesium and stored over 4 Å molecular sieves. All amine reagents were distilled from CaH_2. Dioleoylphosphatidylethanolamine (DOPE) was purchased from Avanti Polar Lipids, Inc. (Alabaster, AL), and *N*-[2,3-(dioleyloxy)propyl]-*N,N,N*-trimethylammonium chloride (DOTAP) was prepared using a literature procedure (20). Column chromatography was carried out using 230–400 mesh silica gel, slurry packed in glass columns, eluting with the solvents indicated. Thin-layer chromatography (TLC) was performed on Kieselgel 60 F_{254} plates, staining with a 3% w/w phosphomolybdic acid/ethanol solution. ^{1}H nuclear magnetic resonance (NMR) (300 MHz) and ^{13}C NMR (75 MHz) were recorded in $CDCl_3$. ^{13}C NMR assignments noted by an asterisk (*) are interchangeable for the carbons indicated. High-resolution mass spectrometry (HRMS) was performed by Mass Spectrometry Service Labs of the University of California, Riverside, and the University of Minnesota. Infrared (IR) data were obtained on Matteson Galaxy FTIR 3000 infrared spectrometer (Madison, WI), and melting point determination was obtained using a Thomas-Hoover (Swedesboro, NJ) capillary melting point apparatus and are uncorrected.

*Tetradecyl 3α,7α,12α-trihydroxy-5β-cholanate **(2)**.* Potassium carbonate (0.92 g, 6.0 mmol) was added to a suspension of cholic acid (2.72 g, 6.6 mmol) in hexamethylphosphoric triamide (HMPA) (10 mL). To the suspension was added tetradecyl iodide (1.8 g, 5.5 mmol), and the resultant mixture was heated to 130°C for 48 h. The reaction was cooled and diluted by addition of Et_2O and water. The layers were separated, and the organic layer was washed with water (5×) and dried with Na_2SO_4. The solvent was removed by rotary evaporation to afford the crude product. Purification by column chromatography, eluting with a gradient of MeOH in $CHCl_3$ (0 to 4%), yielded 1.32 g (39%) of **2** as a white foam; m.p., 69.4–70.0°C, R_f = 0.47 (MeOH/CH_2Cl_2 1:9); IR (neat) 3393, 2922, 2853, 1738 cm^{-1}; ^{1}H NMR ($CDCl_3$) δ 4.02 [*t*, *J* = 6.9 Hz, 2H, –C(O)CH_2–], 3.93 (*m*, 1H, C3-H), 3.81 (*m*, 1H, C7-H), 3.41 (*m*, 1H, C12-H), 2.19–0.70 (*m*, 59H), 0.64 (*s*, 3H); ^{13}C NMR ($CDCl_3$) δ 174.4 (C24), 73.0 (C3), 71.9 (C7/C12*), 68.4 (C7/C12*), 64.4 [–C(O)O$\underline{C}H_2$–], 47.1, 46.4, 41.6, 41.5, 39.5, 35.2, 34.8, 34.7, 31.9, 31.4, 30.9, 30.4, 29.6 (2), 29.5, 29.3, 29.2, 28.7, 28.2, 27.5, 26.4, 25.9, 23.2, 22.6, 22.4, 17.3, 14.1, 12.4; HRMS, $C_{38}H_{68}O_5$ calc'd 604.5067, found 622.5386 (M + NH_4^+).

*Methyl 3α-(*N*-imidazolecarbamoyl)-7α,12α-dihydroxy-5β-cholanate **(3)**.* Triethylamine (35 μL, 0.55 mmol) was added to a solution of **1** (150 mg, 0.37 mmol) in CH_2Cl_2 (10 mL). The solution was cooled to 0°C, and carbonyldiimidazole (90 mg, 0.55 mmol) was added. The reaction was allowed to warm to room temperature, and after 18 h the reaction was diluted with CH_2Cl_2. The organic layer was washed with a saturated solution of $NaHCO_3$, followed by brine, and finally water. The organic layer was separated and dried with Na_2SO_4. Purification by column chromatography eluting with a gradient of MeOH in CH_2Cl_2 (0 to 5%), yielded pure **3** (190 mg, 77%) as a white solid; m.p., 173.6–174°C; TLC, R_f = 0.64 (MeOH/CH_2Cl_2 1:19); IR (neat) 3416, 2964, 2870, 1759, 1739 cm^{-1}; ^{1}H NMR ($CDCl_3$) δ 8.06 (*s*, 1H), 7.35 (*d*, *J* = 1.2 Hz, 1H), 7.00 (*d*, *J* = 1.2 Hz, 1H), 4.73 (*m*, 1H, C3-H), 3.96 (*m*, 1H, C7-H), 3.82 (*m*, 1H, C12-H), 3.62 (*s*, 3H, –OCH_3), 2.31–0.87 (*m*, 34H), 0.66 (*s*, 3H); ^{13}C NMR ($CDCl_3$) δ 174.1 (C24), 147.7, 136.6, 129.8, 116.6, 78.9 (C3), 72.4 (C7/C12*), 67.6 (C7/C12*), 50.9 [–C(O)O$\underline{C}H_3$], 46.8, 45.9, 40.9, 40.2, 39.1, 34.4, 34.2, 30.6, 28.0, 26.9, 26.1, 22.7, 21.9, 16.9, 12.1; HRMS, $C_{29}H_{44}N_2O_6$ calc'd 516.3199, found 516.3199.

*Tetradecyl 3α-(*N*-imidazolecarbamoyl)-7α,12α-dihydroxy-5β-cholanate **(4)**.* Triethylamine (40 μL, 0.24 mmol) was added to a solution of **2** (93 mg, 0.16 mmol) in CH_2Cl_2 (3 mL). The solution was cooled to 0°C, and carbonyldiimidazole (40

mg, 0.24 mmol) was added. The reaction was warmed to room temperature and stirred for 18 h, after which the reaction was diluted with CH_2Cl_2. The organic layer was washed sequentially with saturated aqueous $NaHCO_3$, brine, and water. The organic layer was separated and dried (Na_2SO_4). Evaporation of the solvents afforded **4** (84 mg, 78%), and this material was used without further purification; TLC, R_f = 0.22 (MeOH/ CH_2Cl_2 1:19); ^{1}H NMR ($CDCl_3$) δ 8.10 (*s*, 1H), 7.38 (*d*, *J* = 1.5 Hz, 1H), 7.03 (*d*, *J* = 1.5 Hz, 1H), 4.77 (*m*, 1H, C3-H), 4.03 [*t*, *J* = 6.9 Hz, 2H, –C(O)CH_2–], 4.00 (*m*, 1H, C7-H), 3.86 (*m*, 1H, C12-H), 2.58–0.80 (*m*, 59H), 0.69 (*s*, 3H); ^{13}C NMR ($CDCl_3$) δ 174.3 (C24), 148.2, 137.0, 130.3, 117.1, 79.3 (C3), 72.9 (C7/C12*), 68.1 (C7/C12*), 64.4 [–C(O)-O$\underline{C}H_2$–], 47.3, 46.5, 42.0, 41.2, 39.5, 35.1, 34.8, 34.6, 34.3, 31.9, 31.3, 30.8, 29.6, 29.2, 28.6, 27.4, 26.7, 26.5, 25.9, 23.1, 22.6, 22.3, 17.3, 14.1, 12.5; HRMS, $C_{42}H_{70}N_2O_6$ calc'd 698.5234, found 699.5310 (M + H^+).

Methyl 3α [N-(N,N-*dimethylaminoethane)-carbamoyl*]-*7α,12α-dihydroxy-5β-cholanate* ***(5)***. To a solution of **3** (21 mg, 0.04 mmol) in CH_2Cl_2 (1 mL) at room temperature was added *N,N*-dimethylethylenediamine (10 μL, 0.06 mmol). After 16 h, the reaction was diluted with CH_2Cl_2 and washed sequentially with saturated aqueous $NaHCO_3$, brine, and water. The organic layer was separated and dried (Na_2SO_4). Purification by column chromatography, eluting with a gradient of MeOH in CH_2Cl_2 (0 to 15%), yielded 20.4 mg (95%) of **5** as a white solid; m.p., 116.6–120.7°C; TLC, R_f = 0.17 (MeOH/ $CHCl_3$ 1:7); IR (neat) 3425, 2939, 2870 cm^{-1}; ^{1}H NMR ($CDCl_3$) δ 5.53 (*m*, 1H, NH), 4.41 (*m*, 1H, C3-H), 3.93 (*m*, 1H, C7-H), 3.80 (*m*, 1H, C12-H), 3.63 (*s*, 3H, –OCH_3), 3.22 [*m*, 2H, –OC(O)NHC$\underline{H}_2$–], 2.41 [*t,* *J* = 5.1 Hz, 2H, $(CH_3)_2NC\underline{H}_2$–], 2.45–0.76 (*m*, 38H), 0.65 (*s*, 3H); ^{13}C NMR ($CDCl_3$) δ 174.7 (C24), 156.5 [–NH$\underline{C}$(O)O–], 74.5 (C3), 72.8 (C7/C12*), 68.1 (C7/C12*), 58.3 [–$\underline{C}H_2$NHC(O)O–], 51.4 [–C(O)O$\underline{C}H_3$], 47.0, 46.4, 45.0, 41.8, 41.2, 39.4, 38.0, 35.6, 35.1, 34.9, 34.6, 34.4, 31.0, 30.82, 28.29, 27.4, 26.9, 26.5, 23.1, 22.4, 22.2, 17.2, 12.4; HRMS, $C_{30}H_{52}N_2O_6$ calc'd 536.3825, found 537.3901 (M + H^+).

Tetradecyl-3α [N-(N,N-*dimethylaminoethane)-carbamoyl*]-*7α,12α-dihydroxy-5β-cholanate* ***(6)***. To a solution of **4** (84 mg, 0.12 mmol) in CH_2Cl_2 (2.5 mL) at room temperature was added *N,N*-dimethylethylenediamine (30 μL, 0.28 mmol). After 16 h, the reaction was diluted with CH_2Cl_2 and washed sequentially with saturated aqueous $NaHCO_3$, brine, and water. The organic layer was separated and dried (Na_2SO_4). Purification by column chromatography, eluting with a gradient of MeOH in CH_2Cl_2 (4 to 20%), yielded 46 mg (53%) of **6** as a white solid; m.p., 77.7–78.9°C; TLC, R_f = 0.40 (MeOH/ $CHCl_3$ 1:7); IR (neat) 3428, 2925, 2855, 1721, 1692, cm^{-1}; ^{1}H NMR ($CDCl_3$) δ 5.36 (*m*, 1H, NH), 4.43 (*m*, 1H, C7-H), 4.02 [*t,* *J* = 6.9 Hz, 2H, –C(O)OCH_2–], 3.95 (*m*, 1H, C7-H), 3.81 (*m*, 1H, C12-H), 3.21 [*m*, 2H, –C$\underline{H}_2$NHC(O)O–], 2.42–0.76 (*m*, 64H), 0.66 (*s*, 3H); ^{13}C NMR ($CDCl_3$) δ 174.5 (C24), 156.6 [–NH$\underline{C}$(O)O–], 74.6 (C3), 72.8 (C7/C12*), 68.2 (C7/C12*), 64.5 [–C(O)O$\underline{C}H_2$–], 58.2 [–$\underline{C}H_2$NHC(O)O–], 47.1, 46.5, 45.1, 41.9, 41.0, 39.4, 38.2, 35.5, 35.0, 34.6, 31.9 (2), 31.3, 29.6 (2), 29.5 (2), 29.2, 28.6, 25.9, 23.0, 22.6, 22.5, 17.3, 14.1, 12.36; HRMS, $C_{43}H_{78}N_2O_6$ calc'd 718.5860, found 719.5904 (M + H^+).

Formulations. All lipids were dissolved in chloroform to give 10 mg/mL solutions and then aliquoted into vials to give the desired amounts. The solvent was removed either by rotary evaporation or by passing a stream of nitrogen over the vial. Trace solvent was removed by placing the sample vial under vacuum for 30 min prior to use. Lipid films were hydrated in water, followed by vortex mixing and sonication to obtain homogeneous opaque solutions.

Plasmid DNA. Vector pFGH.cytomegalovirus (CMV) contains the genomic human growth hormone DNA sequence under transcriptional control of the immediate early promoter of human CMV (21). This vector yields high level expression in rodent cells. A similar plasmid, pCMV.FOX.Luc-2, yields high level expression of firefly luciferase (generously provided by Genteric, Inc., Alameda, CA). All vectors were prepared as endotoxin-reduced, supercoiled plasmids using anion exchange resins (Qiagen, Santa Clarita, CA).

Intestinal extracts. Fasted (24 h) female Balb-C mice (15–18 g) from Simonsen laboratories were sacrificed using CO_2 asphyxiation. One-inch sections were taken from the stomach and ileum. A syringe was fixed to the proximal end of each segment, and 1 mL of deionized water was flushed through each intestinal segment. The extracts were collected and stored at –20°C. The samples were thawed, vortexed and centrifuged at 4,000 rpm for 1 min prior to use. All studies involving animals were conducted at Genteric, Inc. in accordance with protocols approved by the Institutional Animal Care and Use Committee.

Intestinal stability. Hydrated lipid suspensions were diluted with water to obtain the desired concentration, vortex mixed, and an appropriate quantity of DNA was then added to form the lipoplex (typically 3 μg DNA/15 μL). For the control experiments, DNA was diluted with either an EDTA solution (10 mmol) or water. The lipoplex and control solutions were then incubated with 7.5 μL of the intestinal washes. The reactions were quenched at the appropriate time by adding 7.5 μL of a 10 mmol EDTA/20% sodium dodecyl sulfate solution. A 10 μL aliquot of quenched reaction (*ca.* 1 μg of DNA) was loaded onto a 0.7% agarose gel in tris/acetic acid/EDTA (TAE) buffer that was treated with ethidium bromide. The agarose gels were electrophoresed at 120 V and visualized under ultraviolet light.

Cell culture. NIH 3T3 cells were obtained from the American Type Culture Collection (Rockville, MD) and grown in Dulbecco's modified Eagle's medium (DMEM) with 10% fetal calf serum in a humidified 10% CO_2 atmosphere at 37°C. The cells were plated on 24-well tissue culture plates 72 h before transfection. Cells were used at 80–90% confluency. Hydrated lipid solutions were diluted with DMEM-serum free media to obtain the desired concentration, vortexed, and mixed with an appropriate volume of DNA. The growth medium was aspirated, and the cells were washed with 0.5 mL of phosphate-buffered saline (PBS). After re-

moval of the PBS, the lipid/DNA solution was added to the cells (200 μL, 1 μg DNA). After 4 h of exposure, the transfection solution was removed and replaced with growth medium (500 μL). Cells were lysed 48 h after lipid/ DNA administration by adding lysis buffer from the Enhanced Luciferase Assay Kit (Pharmingen, San Diego, CA).

Luciferase assays. Luciferase activity was assayed using the Enhanced Luciferase Assay Kit and a Moonlight 2010 luminometer. Luciferase activity was measured from 25-μL aliquots of the cell lysate over a 10-s period. The activity was expressed as relative light units, which is a function of assay conditions, luciferase concentration, instrument sensitivity, and background.

RESULTS AND DISCUSSION

The methyl ester of cholic acid was prepared using a literature procedure (22). Preparation of the tetradecyl ester **2** was achieved by reaction of potassium cholate with tetradecyliodide in HMPA. Cholate esters **1** and **2** were selectively functionalized at C(3) by reaction with carbonyl diimidazole to obtain the *N*-acyl-imidazole derivatives **3** and **4** in 77 and 78% yield, respectively. We were gratified with the regioselectivity of these reactions in that previous attempts to selectively functionalize the C(3)-hydroxyl group employed laborious protection-deprotection schemes (23,24). At this stage, attachment of a DNA-binding domain was accomplished by reaction of the C(3) activated carbamate with excess *N,N*-dimethylethylenediamine to obtain amphiphiles **5** and **6**. These compounds incorporate the DNA-binding domain of the transfection agent DC-cholesterol (Fig. 1) (25). This choice was motivated by the successful application of DC-cholesterol in many transfection studies (26). The robust nature of the C(3)-*N*-acyl imidazole should make this synthetic strategy adaptable to the synthesis of a variety of C(3) bile acid conjugates.

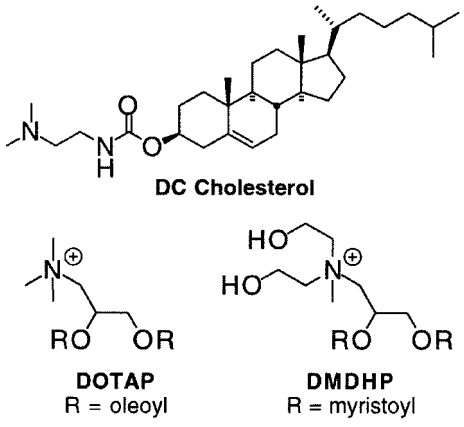

FIG. 1. Common transfection lipids. DC cholesterol, 3-β-[*N*-(*N′,N′*-dimethylaminoethane)carbamoyl]cholesterol; DOTAP, *N*-[2,3-(dioleoyloxy)propyl]-*N,N,N*-trimethylammonium chloride; DMDHP, *N,N*-bis(2-hydroxyethyl)-*N*-[2,3-(dimyristoyloxy)propyl]-*N*-methylammonium chloride.

The stability of lipoplex preparations containing amphiphiles **5** and **6** was examined by incubation with extracts obtained from the stomach and ileum of Balb-C mice. Solutions from the stomach and ileum were obtained by flushing water through freshly dissected segments. The integrity of DNA (pFGH.CMV) (27) was measured using electrophoresis (0.7% agarose in TAE buffer) after exposure of the plasmid to the GI extracts (Fig. 2). Uncomplexed DNA was incubated with extracts from the stomach and ileum (lanes 1 and 2). Comparison to the control experiment (lane 5) revealed that these extracts severely degraded the plasmid. An equivalent volume of an EDTA solution was added to the intestinal extracts to neutralize enzymatic activity (28). Subsequent incubation of DNA with the EDTA-intestinal extracts (lanes 3 and 4) revealed that the level of plasmid digestion was significantly reduced. This result supports a view that DNA digestion in the stomach and ileum is due to nuclease activity.

Next, we investigated the stability of DNA in the GI extracts by prior complexation of the plasmid with a cationic lipid. Gershon *et al.* (29) have shown that DNA within a lipoplex is resistant to nuclease activity. However, the GI tract contains other factors that might contribute to degradation of a lipoplex and its DNA. To establish lipid-based gastroprotective parameters, preliminary experiments were conducted using the transfection lipid DOTAP (30) (Fig. 1). Lipoplexes were prepared using a 1:1 formulation of DOTAP and DOPE as previously reported (31). Our preliminary work suggested that the cationic lipid/DNA phosphate molar ratio should be at least 2.5:1 to achieve plasmid protection. Thus, lipoplexes were formulated at a 3:1 charge ratio. After incubating the complexed DNA with the intestinal extracts for varying times (Table 1), the extent of degradation was analyzed by agarose

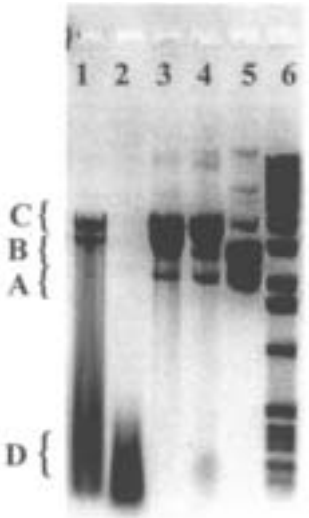

FIG. 2. Effect of gastrointestinal (GI) extracts on DNA. 0.7% Agarose in Tris/acetic acid/ethylenediaminetetraacetic acid (EDTA) buffer; lanes 1, 2: DNA after incubation (10 min at 37°C) with GI washes taken from the stomach and ileum, respectively; lanes 3, 4: DNA after incubation with EDTA-treated GI washes taken from the stomach and ileum, respectively; lane 5: DNA (control); lane 6: 1 kb ladder. Forms of DNA: A, supercoiled; B, linear; C, nicked circular; and D, digested.

TABLE 1
Incubation Conditions Using Extracts from Mouse Stomach and Ileum

Lane	Experiment (extract, DNA form)	Time (min)	Lane	Condition (extract, DNA form)	Time (min)
3	Stomach, free DNA	10	11	Stomach, free DNA	60
4	Ileum, free DNA	10	12	Ileum, free DNA	60
5	Stomach, lipoplex	10	13	Stomach, lipoplex	60
6	Ileum, lipoplex	10	14	Ileum, lipoplex	60
7	Stomach, free DNA	30	15	Stomach, free DNA	120
8	Ileum, free DNA	30	16	Ileum, free DNA	120
9	Stomach, lipoplex	30	17	Stomach, lipoplex	120
10	Ileum, lipoplex	30	18	Ileum, lipoplex	120

gel electrophoresis (Fig. 3). To dissociate the DNA from the cationic lipids and facilitate analysis by electrophoresis, the lipoplexes were treated with 10% SDS solution immediately following incubation (32). The results clearly show that DNA was protected from the GI extracts for up to 2 h only when complexed to the cationic lipid (lanes 17 and 18). Uncomplexed DNA was completely digested within 1 h (lanes 11 and 12). Based on the typical transit time in the GI (33), 2 h of gastroprotection may be a suitable time frame for achieving *in vivo* GI transfection.

Having noted that a lipoplex preparation survives the GI extracts, we examined whether addition of the cholate amphiphiles **5** and **6** would interfere with the gastroprotection. Cholates **5** and **6** were evaluated by formulation with DNA in varying ratios with DOTAP and DOPE (Table 2), incubated with the ileum extract, and then analyzed by agarose gel electrophoresis (Fig. 4). Once again, uncomplexed "free" DNA was degraded by the ileum extract without the protection afforded by lipid complexation (lane 3). However, DNA encapsulated as a lipoplex containing a cholate amphiphile (lanes 4–9) survived the incubation period. Thus, addition of the cholate lipids does not appear to compromise the gastroprotection afforded by lipoplex formulation of DNA.

Cholates **5** and **6** were formulated with DOPE and *N,N*-bis(2-hydroxyethyl)-*N*-[2,3-(dimyristoyloxy)propyl]-*N*-methyl-ammonium chloride (DMDHP) (31) and screened in NIH 3T3 cells using the luciferase assay. DMDHP was selected for the transfection experiments based on the superior transfection activity exhibited by DMDHP (34). Additionally, this provides the opportunity to determine whether adding a cholic acid amphiphile to a commercially available transfection system would impart a beneficial or detrimental effect on overall transfection activity. Cholate **5** was more active than cholate **6** as a transfection additive in the lipid formulations examined (Fig. 5). The inverse relationship between the molar ratio of **6** and the level of luciferase expression suggests that cholate **6** inhibits the activity of DMDHP as a transfection agent. In contrast, the formulations containing 20 and 30% of cholate **5** exhibited a two- to threefold increase in transfection activity relative to the 1:1 DMDHP/DOPE formulation. This result indicates that cholate **5** may be suitable for addition to a therapeutic lipoplex preparation without compro-

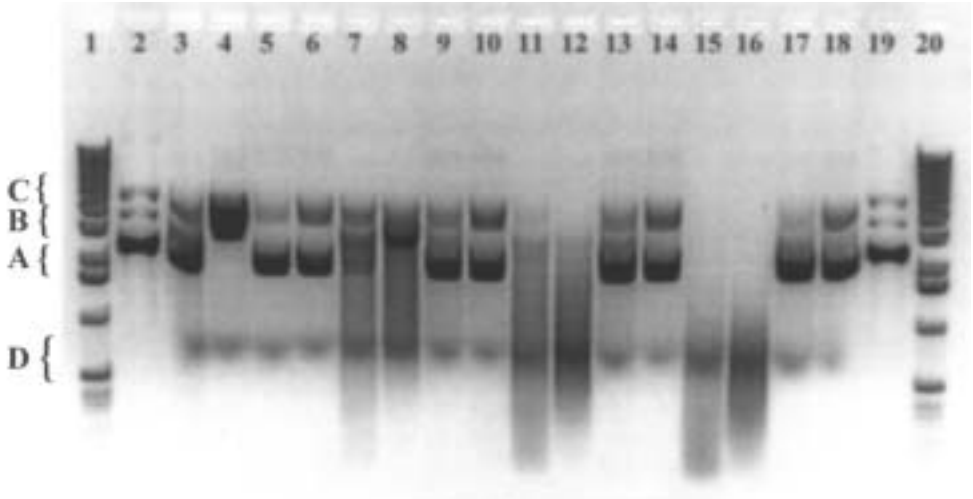

FIG. 3. Effect of GI extracts on lipoplexes and uncomplexed "free" DNA. Lanes 1 and 20, 1 kb standard; lanes 2 and 19, DNA (control); lanes 3–18, free or complexed DNA after incubation with stomach or ileum extracts as described in Table 1. All lipoplex preparations were formed using 1:1 *N*-[2,3-(dioleoyloxy)propyl]-*N,N,N*-trimethylammonium chloride/1,2-dioleoyl-*sn*-3-phosphoethanolamine (DOTAP/DOPE) at a 3:1 cationic lipid/DNA phosphate charge ratio. Forms of DNA: A, supercoiled; B, linear; C, nicked circular; and D, digested.

TABLE 2
Lipoplex Formulations for the Incubation Studies of Figure 4[a]

Lane	Ratio DOTAP/cholate/DOPE	Cholate no.
4	1:2:3	5
5	2:1:3	5
6	0:1:1	5
7	1:2:3	6
8	2:1:3	6
9	0:1:1	6

[a]DOTMA, *N*-[2,3-(dioleyloxy)propyl]-*N,N,N*-trimethylammonium chloride; DOPE, 1,2-dioleoyl-*sn*-3-phosphoethanolamine.

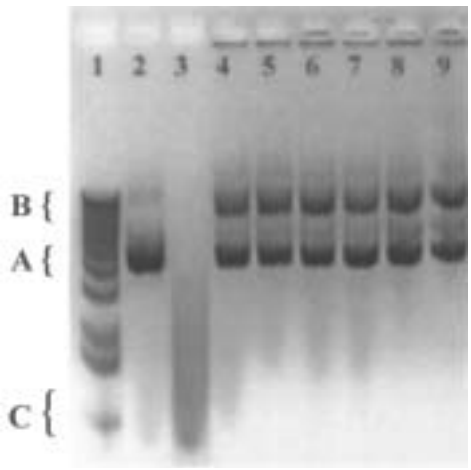

FIG. 4. Effect of ileum extracts on cholate-based lipoplexes. Lane 1, 1 kb standard; lane 2, DNA (control); lane 3, DNA after incubation with the ileum extract; lanes 4–9, lipoplex DNA after incubation with the ileum extract. Lipid/DNA complexes were formed at a 3:1 cationic lipid/DNA phosphate charge ratio using varying combinations of DOTAP, cholate amphiphile, and DOPE (see Table 2). All ileum extract incubations were performed for 30 min at 37°C. Forms of DNA: A, supercoiled; B, linear; C, digested. See Figure 3 for abbreviations.

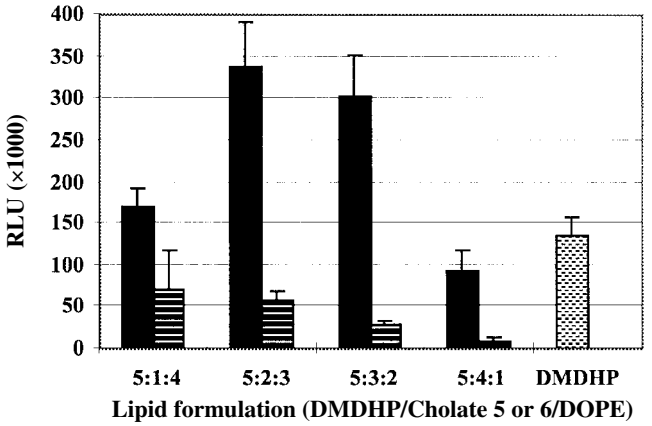

FIG. 5. DNA transfection of NIH 3T3 cells using cholate lipids 5 and 6. Solid bars represent formulations incorporating cholate **5** and dashed bars represent formulations incorporating cholate **6**. *N,N*-bis(2-hydroxyethyl)-*N*-[2,3-(dimyristoyloxy)propyl]-*N*-methylammonium chloride (DMDHP) was formulated as a 1:1 mixture with DOPE. All lipoplex preparations were formulated at a 4:1 molar ratio of DMDHP/DNA phosphate. Results are summarized as the means ($n = 4$) and standard deviation of total luciferase relative light units (RLU) obtained from cells lysed after administration of 1 μg DNA. See Figure 3 for other abbreviation.

mising the transfection activity of the principal transfection agent.

We have disclosed a convenient and readily adaptable synthesis of new C(3)-functionalized cholic acid analogs. Co-formulation of these lipids did not compromise the gastroprotection of DNA imparted by a lipoplex preparation. These modified lipoplexes were also shown to be active in a transfection experiment. The present study demonstrates that cationic lipid-complexation of DNA serves to protect the polynucleotide from GI degradation and represents the first step toward development of orally administered gene medicines.

ACKNOWLEDGMENTS

We are grateful to the Cystic Fibrosis Foundation and Genteric for support of this work. EJN is thankful for a fellowship from Genteric. We thank Kathleen Galligan for DNA preparation and Dr. Stephen Rothman and Dr. Hsein Tseng for helpful discussions.

REFERENCES

1. Pahdha, H.S. and Lemoine, N.R. (1996) Gene Therapy in Gastroenterology, *Gut 38*, 161–165.
2. Caplen, N.J., Alton, E.W., Middleton, P.G., Dorin, J.R., Stevenson, B.J., Gao, X., Durham. S.R., Jeffery, P.K., Hosdson, M.E., and Coutelle, C. (1995) Liposome-Mediated Cftr Gene Transfer to the Nasal Epithelium of Patients with Cystic Fibrosis, *Nature Med. 1*, 39–46.
3. Gill, D.R., Southern, K.W., Moddord, K.A., Sedon, T., Huang, L., Sorgi, F., Thomson, A., MacVinish, L.J., Ratcliff, R., Bilton, D., *et al.* (1997) A Placebo-Controlled Study of Liposome-Mediated Gene Transfer to the Nasal Epithelium of Patients with Cystic Fibrosis, *Gene Therapy 4*, 199–209.
4. MacGregor, R.R., Boyer, J.D., Ugen, K.E., Lacy, K.E., Gluckman, S.J., Bagarazzi, M.L., Chattergoon, M.A., Baine, Y., Higgins, T.J., Ciccarelli, R.B., *et al.* (1998) First Human Trial of a DNA-Based Vaccine for Treatment Of Human Immunodeficiency Virus Type 1 Infection: Safety and Host Response, *J. Infect. Dis. 178*, 92–100.
5. Dunbar, C.E., Cottler-Fox, M., O'Shaughnessy, J.A., Doren, S., Carter, C., Berenson, R., Brown, S., Moen, R.C., Greenblatt, J., and Stewart, F.M. (1995) Retrovirally Marked Cd34-Enriched Peripheral Blood and Bone Marrow Cells Contribute to Long-Term Engraftment After Autologous Transplantation, *Blood 85*, 3048–3057.
6. Schmid, R.M., Weidenbach, H., Draenert, G.F., Lerch, M.M., Liptay, S., Schorr, J., Beckh, K.H., and Adler, G.Z. (1994) Liposome-Mediated Gene Transfer into the Rat Oesophagus, *Gastroenterology 32*, 665–670.
7. During, M.J., Xu, R., Young, D., Kaplitt, M.G., Sherwin, R.S., and Leone, P. (1998) Peroral Gene Therapy of Lactose Intolerance Using an Adeno-Associated Virus Vector, *Nature Med. 4*, 1131–1135.
8. Jones, D.H., Clegg, J.C.S., and Farrar, G.H. (1998) Oral Delivery of Micro-Encapsulated DNA Vaccines, *Dev. Biol. Stand. 92*, 149–155.
9. Roy, K., Mao, H.Q., Huang, S-K., and Leong, K.W. (1999) Oral Gene Delivery with Chitosan—DNA Nanoparticles Generates Immunologic Protection in A Murine Model of Peanut Allergy, *Nature Med. 5*, 387–391.
10. Jain, K.K. (1998) *Textbook of Gene Therapy*, pp. 36–50, Hogrefe & Huber, Seattle.
11. Felgner, P.L., Gadek, T.R., Holm, M., Roman, R., Chan, H.W.,

Wenz, M., Northrop, J.P., Ringold, G.M., and Danielsen, M. (1987) Lipofection: A Highly Efficient, Lipid-Mediated DNA-Transfection Procedure, *Proc. Natl. Acad. Sci. USA 84*, 7413–7417.
12. Miller, A.D. (1998) Cationic Liposomes for Gene Therapy, *Angew. Chem. Int. Ed. 37*, 1768–1785.
13. Hope, M.J., Mui, B., Ansell, S., and Ahkong, Q.F. (1998) Cationic Lipids, Phosphatidylethanolamine and the Intracellular Delivery of Polymeric, Nucleic Acid-Based Drugs, *Molec. Membr. Biol. 15*, 1–14.
14. Felgner, P.L., Barenholz, Y., Behr, J.P., Cheng, S.H., Cullis, P., Huang, L., Jessee, J.A., Seymour, L., Szoka, F.C., Thierry, A.R., *et al.* (1997) Nomenclature for Synthetic Gene Delivery Systems, *Human Gene Ther. 8*, 511–512.
15. Dowling, R.H. (1972) The Enterohepatic Circulation*, Gastroenterology 62*, 122–129.
16. Swaan, P.W., Szoka, F.C., and Øie, S. (1996) Use of the Intestinal and Hepatic Bile Acid Transporters for Drug Delivery, *Adv. Drug Del. Rev. 20*, 59–82.
17. Wess, G., Kramer, W., Schubert, G., Enhsen, A., Baringhaus, K.H., Glombik, H., Muller, S., Bock, K., Kleine, H., John, W., *et al.* (1993) Synthesis of Bile Acid-Drug Conjugates—Potential Drug Shuttles for Liver Specific Targeting, *Tetrahedron Lett. 34*, 819–822.
18. Walker, S., Sofia, M.J., Kakarla, R., Kogan, N.A., Wierichs, L., Longley, C.B., Bruker, K., Axelrod, H.R., Midha, S., Babu, S., and Kahne, D. (1996) Cationic Facial Amphiphiles: A Promising Class of Transfection Agents, *Proc. Natl. Acad. Sci. USA 93*, 1585–1590.
19. Swaan, P.W., Hillgren, K.M., Szoka, F.C., and Øie, S. (1997) Enhanced Transepithelial Transport of Peptides by Conjugation to Cholic Acid Bioconjugate, *Chemistry 8*, 520–525.
20. Leventis, R., and Silvius, J.R. (1990) Interactions of Mammalian Cells with Lipid Dispersions Containing Novel Metabolizable Cationic Amphiphiles, *Biochim. Biophys. Acta 1023*, 124–132.
21. German, M.S., and Wang, J. (1994) The Insulin Gene Contains Multiple Transcriptional Elements That Respond to Glucose, *Mol. Cell Biol. 14*, 4067–4075.
22. Gouin, S. and Zhu, X.X. (1996) Synthesis of 3α- and 3β-Dimers from Selected Bile Acids, *Steroids 61*, 664–669.
23. Wess, G., Kramer, W., Bartmann, W., Enhsen, A., Glombik, H., Mullner, S., Bock, K., Dries, A., Kleine, H., and Schmidt, W. (1992) Modified Bile Acids—Preparation of 7-α,12α-Dihydroxy-3α-cholanic and 7-α,12α-Dihydroxy-3α-(2-hydroxyethoxy)- 5β-cholanic Acid and Their Biological Activity, *Tetrahedron Lett. 33*, 195–198.
24. Bonar-Law, R.P., Davis, A.P., and Sanders, J.K.M. (1990) New Procedures for the Selectively Protected Cholic Acid Derivatives—Regioselective Protection of the 12α-OH Group, and *Tert*-Butyl Esterification of the Carboxy Group, *J. Chem. Soc., Perk. Trans.*, 2245–2250.
25. Gao, X., and Huang, L. (1991) A Novel Cationic Liposome for the Efficient Transfection of Mammalian Cells, *Biochem. Biophys. Res. Commun. 179*, 280–285.
26. Caplen, N.J., Kinrade, E., Sorgi, F., Gao, X., Gruenert, D., Geddes, D., Coutelle, C., Huang, L., Alton, E.W., and Williamson, R. (1995) *In Vitro* Liposome-Mediated DNA Transfection of Epithelial Cell Lines Using the Cationic Liposome DC-Chol/DOPE, *Gene Therapy 9*, 603–613.
27. Goldfine, I.D., German, M.S., Tseng, H.-C., Wang, J., Bolaffi, J.L. Chen, J-W., Olson, D.C. and Rothman, S.S. (1995) The Endocrine Secretion of Human Insulin and Growth Hormone By Exocrine Glands of the Gastrointestinal Tract, *Nature Biotechnol. 15*, 1378–1382.
28. Tokuda, Y., Nakamura, T., Satonaka, K., Maeda, S., Doi, K., Babu, S., and Sugiyama, T. (1990) Fundamental Study on the Mechanism of DNA Degradation in Tissues Fixed in Formaldehyde, *J. Clin. Pathol. 43*, 748–751.
29. Gershon, H., Ghirlando, R., Guttman, S.B., and Minsky, A. (1993) Mode of Formation and Structural Features of DNA–Cationic Liposome Complexes Used for Transfection, *Biochemistry 32*, 7143–751.
30. Leventis, R., and Silvius, J.R. (1990) Interactions of Mammalian Cells with Lipid Dispersions Containing Novel Metabolizable Cationic Amphiphiles, *Biochim. Biophys. Acta 1023*, 124–132.
31. Bennett, M.J., Aberle, A.M., Balasubramaniam, R.P., Malone, J.G., Malone, R.W., and Nantz, M.H. (1997) Cationic Lipid-Mediated Gene Delivery to Murine Lung: Correlation of Lipid Hydration with *in vivo* Transfection Activity, *J. Med. Chem. 40*, 4069–4078.
32. Murphy, J.E., Uno, T., Hamer, J.D., Cohen, F.E., Dwarki, V., and Zuckerman, R.N. (1998) A Combinatorial Approach to the Discovery of Efficient Cationic Peptidoreagents for Gene Delivery, *Proc. Natl. Acad. Sci. USA 95*, 1517–1522.
33. Hendrix, T.R. (1980) in *Medical Physiology* (Mountcastle, V.B., ed.) pp. 1255–1288, C.V. Mosby Co., St. Louis.
34. DMDHP is the cationic lipid component of the commercially available transfection reagent TransFast™ (Promega Corporation, Madison, WI); see also: Nantz, M.H., Bennett, M.J., and Balasubramaniam, R.P. U.S. Patent 5,824,812.

[Received February 1, 2000, and in revised form and accepted May 11, 2000]

Liver and Intestinal Fatty Acid-Binding Protein Expression Increases Phospholipid Content and Alters Phospholipid Fatty Acid Composition in L-Cell Fibroblasts

Eric J. Murphy[a,*], Daniel R. Prows[b], Thomas Stiles[a], and Friedhelm Schroeder[a]

[a]Department of Physiology and Pharmacology, Texas A & M University, TVMC, College Station, Texas 77843-4466, and
[b]Division of Pharmacology and Medicinal Chemistry, University of Cincinnati, College of Pharmacy, Cincinnati, Ohio 45267-0004

ABSTRACT: Although fatty acid-binding proteins (FABP) differentially affect fatty acid uptake, nothing is known regarding their role(s) in determining cellular phospholipid levels and phospholipid fatty acid composition. The effects of liver (L)- and intestinal (I)-FABP expression on these parameters were determined using stably transfected L-cells. Expression of L- and I-FABP increased cellular total phospholipid mass (nmol/mg protein) 1.7- and 1.3-fold relative to controls, respectively. L-FABP expression increased the masses of choline glycerophospholipids (ChoGpl) 1.5-fold, phosphatidylserine (PtdSer) 5.6-fold, ethanolamine glycerophospholipids 1.4-fold, sphingomyelin 1.7-fold, and phosphatidylinositol 2.6-fold. In contrast, I-FABP expression only increased the masses of ChoGpl and PtdSer, 1.2- and 3.1-fold, respectively. Surprisingly, both L- and I-FABP expression increased ethanolamine plasmalogen mass 1.6- and 1.1-fold, respectively, while choline plasmalogen mass was increased 2.3- and 1.7-fold, respectively. The increase in phospholipid levels resulted in dramatic 48 and 33% decreases in the cholesterol-to-phospholipid ratio in L- and I-FABP expressing cells, respectively. L-FABP expression generally increased polyunsaturated fatty acids, primarily by increasing 20:4n-6 and 22:6n-3, while decreasing 18:1n-9 and 16:1n-7. I-FABP expression generally increased only 20:4n-6 proportions. Hence, expression of both I- and L-FABP differentially affected phospholipid mass, class composition, and acyl chain composition. Although both proteins enhanced phospholipid synthesis, the effect of L-FABP was much greater, consistent with previous work suggesting that these two FABP differentially affect lipid metabolism.

Paper no. L8406 in *Lipids 35*, 729–738 (July 2000).

The cytosolic fatty acid-binding protein (FABP) superfamily is comprised of immunologically distinct proteins that share similar structures, overlapping ligand specificity, and considerable sequence homology. Why some tissues and cell types contain multiple FABP is not known. For example, intestinal-FABP (I-FABP), a 15.1 kDa cytosolic protein, is found in the columnar epithelial cells of the small intestine, where it constitutes 2–4% of the total cytosolic protein (1). I-FABP expression also varies depending upon developmental stage, diet, and position of the cells along the longitudinal axis of the intestinal tract (2). Liver-FABP (L-FABP), a 14.2 kDa protein, is also found in intestinal enterocytes, where it accounts for 2% of the total cytosolic protein, as well as in the liver, where it accounts for 3–5% of the total cytosolic protein (2–4). The N-terminus of both proteins is blocked by acetylation consistent with the intracellular localization (5). I- and L-FABP have a similar affinity for fatty acids (3,6,7), although some studies suggest that L-FABP has a greater affinity for polyunsaturated fatty acids (PUFA), such as arachidonic acid, than I-FABP (8). This is consistent with our finding that endogenous L-FABP isolated from rat liver contains a substantial quantity of PUFA (9). Furthermore, I- and L-FABP not only bind fatty acids but also are thought to bind long-chain fatty acyl CoA with a high affinity (10–12). In addition, L-FABP binds a number of lipophilic ligands including prostaglandins (13), hydroperoxy- and hydroxyeicosatetraenoic acids (14), heme (15), and warfarin (16). Although suggestive of function, ligand binding alone has not allowed discrimination of the respective physiological role(s) for the different FABP in altering cellular lipid metabolism.

To better assess the physiological function of these FABP in cells, L-FABP (17,18) and I-FABP (19) were stably expressed in L-cell fibroblasts. In these cells, L-FABP (18,20) but not I-FABP expression (19–21) increased fatty acid uptake, whereas both proteins increased the apparent fatty acid cytoplasmic diffusion coefficient (20). A recent study in murine stem cells suggests that the cellular differentiation state affects I-FABP-induced fatty acid uptake, with I-FABP expression enhancing fatty acid uptake only in undifferentiated cells (22). Furthermore, expression of L-FABP or I-FABP dif-

*To whom correspondence should be addressed at Section on Brain Physiology and Metabolism, National Institute on Aging, Building 10 Room 6C103, Bethesda, MD 20892. E-mail: murphye@mail.nih.gov

Abbreviations: CerPCho, sphingomyelin; ChoGpl, choline glycerophospholipid; ER, endoplasmic reticulum; EtnGpl, ethanolamine glycerophospholipid; FABP, fatty acid binding protein; FAME, fatty acid methyl ester; GLC, gas–liquid chromatography; HPLC, high-performance liquid chromatography; I-FABP, intestinal-FABP; L-FABP, liver-FABP; MUFA, monounsaturated fatty acid; PlsCho, choline plasmalogen; PlsEtn, ethanolamine plasmalogen; PtdEtn, phosphatidylethanolamine; PtdIns, phosphatidylinositol; PtdOH, phosphatidic acid; PtdSer, phosphatidylserine; PUFA, polyunsaturated fatty acid; TLC, thin-layer chromatography.

ferentially affected targeting of exogenous fatty acids for esterification into specific lipid pools (18,19,21). This enhancement of fatty acid targeting is supported by studies showing that both L-FABP (10,23,24) and I-FABP (24) stimulate phosphatidic acid (PtdOH) synthesis *in vitro*, although L-FABP has a more robust effect on synthesis than I-FABP (24). In other studies, expression of adipocyte-FABP in Chinese hamster ovary cells enhanced fatty acid uptake and esterification into cellular lipids 1.5- and 2.0-fold, respectively, compared to nontransfected cells (25). Expression of heart-FABP in a human breast cancer cell line increased fatty acid uptake nearly 1.7-fold compared to control cells but did not increase the targeting of fatty acids to either neutral lipids or phospholipids (26). Thus, studies using transfected cell lines suggest that FABP differentially affect fatty acid uptake, cytoplasmic diffusion, and targeting (18–22).

Despite these findings, whether L-FABP and I-FABP expression differentially affects phospholipid mass, class composition, or phospholipid fatty acid composition is not known. We report that L-FABP, and to a lesser extent I-FABP, expression differentially increased L-cell phospholipid mass, including plasmalogen mass, resulting in a dramatic decrease in the cholesterol-to-phospholipid ratio. Likewise, L-FABP, and to a lesser extent I-FABP, expression altered phospholipid fatty acid composition, suggesting that these proteins not only enhance phospholipid synthesis but also can modulate fatty acyl chain composition.

MATERIALS AND METHODS

Cells. Murine L-cell fibroblasts (L arpt⁻tk⁻) were stably transfected with the cDNA encoding for either I-FABP (19) or L-FABP (17,18). The transfected cells express these proteins at similar levels as determined by quantitative Western blotting (17–19). Control and transfected cells were grown to confluency in Higuchi medium containing 10% fetal bovine serum (Hyclone, Logan, UT) (27).

Lipid extraction. Lipids were extracted from confluent control and transfected cells using *n*-hexane/2-propanol (3:2 vol/vol) (28,29). Before extraction, the cell culture medium was removed and the cells were washed twice with ice-cold phosphate-buffered saline. Following removal of the last wash, the cell plate was floated on liquid N_2 to minimize acylhydrolase activity during cell removal (30). The cell plate was removed from the liquid N_2, 2 mL of 2-propanol was added, and the cells were removed from the plate by scraping. The 2-propanol containing the cells was transferred to a tube containing 6 mL of *n*-hexane. The cell plate was washed with another 2-mL aliquot of 2-propanol, which was transferred to the tube containing the *n*-hexane, resulting in *n*-hexane/2-propanol (3:2 vol/vol).

Cell extracts were centrifuged at 2,500 rpm to pellet the denatured protein and other cellular debris. The lipid-containing organic phase was decanted and stored under a $N_{2(g)}$ atmosphere at –80°C until analysis. These storage conditions limit oxidation of lipids, including PUFA, as demonstrated previously (29,31–33). The residual protein pellet was dried overnight at room temperature.

Phospholipid separation. Before separating the phospholipid classes by high-performance liquid chromatography (HPLC), the sample volume was reduced under a stream of $N_{2(g)}$ and the samples were filtered through a Nylon 66 0.2-μm filter (Ranin, Emeryville, CA). The filtered sample was then dried to completeness and redissolved in a known volume of HPLC-grade *n*-hexane/2-propanol (3:2 vol/vol).

The HPLC system consisted of a Beckman 125 pump module, a Beckman 166 UV/Vis detector (Fullerton, CA), and a column heater (Jones Chromatography, Littleton, CO) containing a Phenomenex Selectosil column (5 μm, 4.6 × 250 mm, Torrance, CA) maintained at 34°C. The eluant absorbance was monitored at 205 nm.

The phospholipids were separated using a binary gradient of (A) *n*-hexane/2-propanol (3:2 vol/vol) and (B) *n*-hexane/2-propanol/water(56.7:37.8:5.5 by vol). Initial solvent conditions were 65% A/35% B with a step gradient to 100% B over 75 min. This method separates all of the major phospholipids including phosphatidylserine (PtdSer) and phosphatidylinositol (PtdIns) (34). The ethanolamine glycerophospholipid (EtnGpl) and choline glycerophospholipid (ChoGpl) fractions were quantitatively divided into two equal parts, one of which was used to quantify phospholipid mass by assaying lipid phosphorus (35). The other half was dried under $N_{2(g)}$ and exposed to HCl vapor for 15 min to cleave the vinyl ether linkage of the plasmalogen subclasses (36). The latter fractions were re-separated by HPLC and the glycerophospholipid and lysophospholipid fractions collected and quantified by assaying for lipid phosphorus (35). All other phospholipid fractions were also quantified by analysis of lipid phosphorus (35).

The neutral lipid fraction from the phospholipid separation was saved and separated using a binary solvent system consisting of *n*-hexane/2-propanol/acetic acid (98.7:1.2:0.1) and *n*-hexane (18,37). The column used was a Selectosil column (5 μm, 4.6 × 250 mm) maintained at 55°C. Data were collected using the Dionex UI-120 (Sunnyvale, CA) analog-to-digital interface. The unesterified cholesterol mass was calculated by converting absorbance at 205 nm from peak area to mass using a standard curve.

Thin-layer chromatography (TLC). Phospholipid fatty acid composition was analyzed in individual phospholipids separated by TLC. Silica gel G plates (Analtech, Newark, DE) were heat-activated at 110°C for 1 h and samples streaked onto the plates. The developing solvent was chloroform/methanol/water (65:25:4 by vol). This solvent system separates the PtdIns from the PtdSer as well as the ChoGpl from the sphingomyelin (CerPCho) (38). Bands were visualized using 1 mM 6-*p*-toluidino-2-naphthalene sulfonic acid dissolved in 50 mM Tris (pH 7.4) (39). Bands corresponding to authentic lipid standards were scraped into screw-top test tubes and subjected to base-catalyzed transesterification.

Transesterification. Methanol was added to the individual phospholipid fractions, which were subjected to base-catalyzed transesterification, converting the phospholipid acyl chains to fatty acid methyl esters (FAME) (40). This method

of transesterification avoids formation of dimethylacetals and oxidative side reactions common with acid-catalyzed methods. FAME were extracted from the methanol by using 2 mL of *n*-hexane, and the *n*-hexane phase containing the FAME was removed. The lower phase was re-extracted two more times with 2-mL aliquots of *n*-hexane, and these washes were combined with the original aliquot.

Gas–liquid chromatography (GLC). FAME were separated by GLC and quantified using flame-ionization detection. Individual fatty acids were identified using FAME standards (Nu-Chek-Prep, Elysian, MN). Relative correction factors for fatty acids were established using standards and based upon a set concentration of 17:0 added prior to analysis. Detector response was linear within the sample concentration range for all of the fatty acids.

The GLC system consisted of a GLC-14A (Shimadzu, Kyoto, Japan) equipped with an SP-2330 capillary column (0.32 mm i.d. × 30 m length, Supelco, Bellefonte, PA). Column temperature was maintained at 185°C, with the injector and detector temperature set at 220°C. The split ratio was 40:1. Peak area data were collected using a Dionex UI-120 analytical-to-digital interface and converted to peak area using Dionex PeakNet software.

Protein assay. Proteins were measured using a modified dye-binding assay (41). The dried protein residue from the extracts was digested overnight in 0.2 M KOH at 65°C. Following digestion, aliquots were used to measure the protein concentration by converting absorbances to concentrations using a bovine serum albumin standard curve.

Statistics. All groups were compared by a one-way analysis of variance and Tukey-Kramer multiple comparisons posttest using Instat II (GraphPad, San Diego, CA). All values are expressed as means ± SD. Statistical significance was defined as $P < 0.05$. The *n* is defined as the number of cultures used to determine each data point.

RESULTS

Total phospholipid mass. The effect of L- and I-FABP expression on total cellular phospholipid mass (nmol/mg protein) was determined in L-cells expressing L-FABP and I-FABP at similar levels. Total phospholipid mass was increased from 266 ± 53 in control cells to 452 ± 26 and 343 ± 23 for L-FABP- and I-FABP-expressing cells, respectively. Values represent means ± SD, $n = 4$. I-FABP expression increased total cellular phospholipid mass 1.3-fold compared to control cells, but this increase was significantly less than the 1.7-fold increase observed with L-FABP expression. Thus, FABP expression differentially affected phospholipid mass in L-cells.

Endoplasmic reticulum (ER)-synthesized individual phospholipid class mass. Changes in total cellular phospholipid mass are not indicative of changes in the mass of individual phospholipid classes. To assess the effects of I- and L-FABP expression on the mass of individual phospholipids formed in the ER, phospholipids were resolved using HPLC and their individual masses calculated. In the I-FABP-expressing cells, the masses of PtdSer and ChoGpl were elevated 3.1- and 1.2-fold, respectively, compared to the control (Table 1). In contrast to I-FABP-expressing cells, L-FABP expression increased the mass of every major phospholipid class relative to control cells, but the magnitudes of these changes were greater than those for I-FABP-expression. In L-FABP-expressing cells, EtnGpl mass was increased 1.4-fold, ChoGpl mass was elevated 1.5-fold compared to control, whereas PtdIns and PtdSer masses were increased 2.6- and 5.6-fold, respectively, compared to the control. Relative to I-FABP-expressing cells, PtdIns and PtdSer masses were increased 3.3- and 1.8-fold in L-FABP-expressing cells, respectively. Lastly, in L-FABP expressing cells, CerPCho mass was increased 1.7- and 1.5-fold relative to control and I-FABP-expressing cells, respectively. Thus, L-FABP expression increased phospholipid mass in L-cells to a much greater extent than I-FABP expression, indicating that these two FABP had differential effects on phospholipid metabolism.

Peroxisomal and ER-synthesized plasmalogen mass. The effects of L- and I-FABP expression on plasmalogen levels were determined. [Plasmalogens are phospholipids containing a vinyl ether linkage in the *sn*-1 position that are synthesized by steps involving both peroxisomes and ER; they have a role in lipid-mediated signal transduction (42–45)]. In I-FABP-expressing cells, ethanolamine plasmalogen (PlsEtn)

TABLE 1
Effect of I- and L-FABP Expression on Phospholipid Mass and Composition in L-cells[a]

	Phospholipid mass (nmol/mg protein)			Phospholipid composition (mol%)		
Phospholipid class	Control	I-FABP	L-FABP	Control	I-FABP	L-FABP
EtnGpl	72.5 ± 8.3	79.5 ± 11.2	101.1 ± 4.7*,**	25.6 ± 1.5	23.2 ± 3.3	22.3 ± 1.0
LysoPtdEtn	5.1 ± 1.9	7.4 ± 1.6	5.3 ± 2.8	1.8 ± 1.6	1.9 ± 0.8	1.5 ± 0.6
PtdIns	10.9 ± 3.3	8.7 ± 4.7	28.6 ± 3.7*,**	3.8 ± 0.9	2.5 ± 1.4	6.3 ± 0.8*,**
PtdSer	4.4 ± 1.3	13.6 ± 4.0*	24.6 ± 3.8*,**	1.6 ± 0.5	3.9 ± 1.1	5.5 ± 0.8*
ChoGpl	153.9 ± 9.4	193.5 ± 7.9*	231.2 ± 14.3*,**	54.5 ± 0.7	56.4 ± 2.3	51.1 ± 3.2*,**
CerPCho	31.0 ± 2.5	35.7 ± 7.9	53.8 ± 8.8*,**	11.1 ± 1.5	10.4 ± 2.2	11.9 ± 1.9
LysoPtdCho	4.6 ± 1.9	5.0 ± 2.9	6.2 ± 1.4	1.6 ± 0.6	1.5 ± 0.9	1.4 ± 0.3

[a]Values are expressed as means ± SD, $n = 4$. A single asterisk (*) indicates significantly different from the control; a double asterisk (**) indicates significantly different from I-FABP-expressing cells, $P < 0.05$. Abbreviations: I-FABP, intestinal fatty acid-binding protein; L-FABP, liver fatty acid-binding protein; EtnGpl, ethanolamine glycerophospholipid; lysoPtdEtn, lysophosphatidylethanolamine; PtdIns, phosphatidylinositol; PtdSer, phosphatidylserine; ChoGpl, choline glycerophospholipid CerPCho, sphingomyelin; lysoPtdCho, lysophosphatidylcholine.

mass was increased 1.1-fold in these cells (Table 2). In contrast, PlsEtn mass was increased in L-FABP-expressing cells 1.6- and 1.4-fold compared to the control and I-FABP-expressing cells, respectively. Similarly, the choline plasmalogen (PlsCho) levels were also differentially affected by I-FABP and L-FABP expression. In I-FABP-expressing cells, the acid-labile ChoGpl, PlsCho, was increased 1.7-fold relative to the control. However, L-FABP expression increased PlsCho mass 2.3- and 1.3-fold compared to the control and I-FABP-expressing cells, respectively. These data also indicate that L-FABP, and to a lesser extent I-FABP, expression increased both the EtnGpl and ChoGpl acid-stable fractions, which contain mainly the diacyl phosphatidyl fraction. Thus, both I- and L-FABP expression increased PlsEtn and PlsCho levels, although only L-FABP expression appeared specifically to affect PlsEtn formation.

Phospholipid class composition. Although both L- and I-FABP expression dramatically increased total phospholipid mass and differentially affected the masses of individual phospholipid classes, these data do not provide information regarding the relative distribution of the individual phospholipids. Therefore, the effect of L- and I-FABP expression on L-cell phospholipid composition was determined from the phospholipid mass data in Table 1. Expression of I-FABP had no effect on the phospholipid percentage composition compared to control cells (Table 1). In contrast, L-FABP expression produced marked changes in phospholipid percentage composition relative to both control and I-FABP-expressing cells (Table 1). PtdSer and PtdIns proportions were increased 3.4- and 1.7-fold, respectively, compared to the control. Both PtdIns and ChoGpl proportions were altered with respect to I-FABP-expressing cells, with the ChoGpl proportion decreased in L-FABP-expressing cells by 10% and the PtdIns increased 2.5-fold. ChoGpl proportions were decreased 6% in L-FABP expressing cells relative to control.

L- and I-FABP expression also differentially affected ChoGpl and EtnGpl subclass composition (Table 2). L-FABP expression increased the proportion of acid-labile EtnGpl, PlsEtn, relative to the acid-stable fraction consisting primarily of phosphatidylethanolamine (PtdEtn) (Table 2). As such, the proportion of the acid-stable fraction was also significantly reduced compared to either control or I-FABP-expressing cells. In contrast, I-FABP and L-FABP expression increased the proportion of acid-labile ChoGpl, PlsCho, compared to the control. Hence, L-FABP expression differentially affected phospholipid composition in L-cells relative to I-FABP and control cells, suggesting a specific increase in PtdSer and PtdIns relative to the other phospholipids.

Free cholesterol to phospholipid ratio. Earlier studies from this laboratory demonstrated a change in the biophysical membrane dynamics in L-FABP-expressing cells (17,20,46), although such data are limited for I-FABP expressing cells (20). Because of the large changes in phospholipid mass in these FABP-expressing cells, the cholesterol-to-phospholipid ratio was determined. Unesterified (free) cholesterol values (nmol/mg protein) were 73 ± 5, 69 ± 11, and 65 ± 6 for control, L-FABP-, and I-FABP-expressing cells, respectively. The cholesterol- to-phospholipid ratio was 0.28 ± 0.02, 0.15 ± 0.02, and 0.19 ± 0.02 for the control, L-FABP-, and I-FABP-expressing cells, respectively. In I-FABP-expressing cells, the cholesterol-to-phospholipid ratio was significantly decreased, 32% compared to the control, whereas in L-FABP-expressing cells this significant reduction was nearly 50%. Furthermore, similar to the effects on phospholipid metabolism, the extent of the decrease in the cholesterol-to-phospholipid ratio was significantly greater in L-FABP-expressing cells than I-FABP-expressing cells. Because there was little change in the free cholesterol levels, the change in the cholesterol-to-phospholipid ratio was primarily the result of increased phospholipid mass. Nonetheless, these results indicate that this ratio, which is a major determinant of membrane structure, was decreased in L- and I-FABP-expressing cells. These results are consistent with previous reports of increased membrane fluidity in L-FABP-expressing cells (17,20,46).

Phospholipid fatty acid composition. In addition to the cholesterol-to-phospholipid ratio and phospholipid composition, the other major determinant of membrane structure is the phospholipid fatty acid composition. The effect of L- and I-FABP expression on the phospholipid fatty acid composition was determined for the EtnGpl, ChoGpl, PtdIns, and PtdSer (Tables 3–6) in L-FABP-expressing, I-FABP-expressing, and control L-cells.

For EtnGpl, expression of either protein increased the mole percentage of 18:0 and 20:3n-6 1.3- and 1.9-fold, respectively, whereas only L-FABP expression increased the mole percentage of 22:6n-3 (Table 3). Because of the limited increase in PUFA, there was no significant change in the PUFA/saturated fatty acid index, and there was a decrease in the unsaturated/saturated fatty acid index in both L- and I-FABP-expressing cells. Hence, the net result of either L- or I-

TABLE 2
Effect of I- and L-FABP Expression on Plasmalogen Composition and Mass in L-Cells[a]

Phospholipid class		Composition of glycerophospholipid class (mol%)			Mass of glycerophospholipid subclass (nmol/mg protein)		
		Control	I-FABP	L-FABP	Control	I-FABP	L-FABP
Etn	acid stable	64.4 ± 0.6	62.7 ± 1.1	59.3 ± 1.8*,**	41.2 ± 0.4	49.9 ± 0.9*	60.0 ± 1.1*,**
	acid labile	35.6 ± 0.6	37.3 ± 1.1	40.7 ± 1.8*,**	22.7 ± 0.4	29.6 ± 0.9*	41.1 ± 1.1*,**
Cho	acid stable	91.3 ± 0.9	88.5 ± 2.1*	87.6 ± 1.6*	135.9 ± 1.6	171.1 ± 3.7*	200.9 ± 5.2*,**
	acid labile	8.6 ± 0.9	11.6 ± 1.9*	12.4 ± 1.6*	13.0 ± 1.6	22.4 ± 3.7*	30.3 ± 5.3*,**

[a]Values are expressed as means ± SD, $n = 4$. A single asterisk (*) indicates significantly different from the control; a double asterisk (**) indicates significantly different from I-FABP-expressing cells, $P < 0.05$. Etn, ethanolamine; Cho, choline; for other abbreviations see Table 1.

TABLE 3
Effect of I- and L-FABP Expression on EtnGpl Fatty Acid Composition

Fatty acid	Control	L-FABP expressors	I-FABP expressors
16:0	5.78 ± 0.55	4.65 ± 0.74	6.51 ± 0.66
16:1	1.58 ± 0.09	0.34 ± 0.12*	0.63 ± 0.43*
18:0	22.25 ± 3.69	28.71 ± 1.02*	28.21 ± 1.93*
18:1n-9	42.25 ± 5.72	37.08 ± 1.23	39.49 ± 1.26
18:2n-6	2.85 ± 0.59	2.90 ± 0.39	3.34 ± 0.38
18:3n-6	0.35 ± 0.19	0.11 ± 0.13	0.30 ± 0.25
18:3n-3	0.39 ± 0.04	0.25 ± 0.11	0.12 ± 0.14
20:0	0.50 ± 0.09	0.67 ± 0.13	0.61 ± 0.28
20:1	3.67 ± 0.72	2.14 ± 0.47*	1.41 ± 0.35*
20:2n-6	0.37 ± 0.06	0.21 ± 0.07	0.19 ± 0.16
20:3n-6	0.80 ± 0.03	1.48 ± 0.13*	1.60 ± 0.18*
20:4n-6	9.12 ± 1.80	11.25 ± 0.51	11.11 ± 1.67
22:3n-3	1.33 ± 1.02	0.45 ± 1.01	BLD
22:4n-6	1.74 ± 0.78	1.90 ± 0.14	1.28 ± 0.31
22:6n-3	4.09 ± 1.80	6.56 ± 0.63*	4.73 ± 0.76
24:0	1.09 ± 0.55	0.29 ± 0.40	BLD
Saturated	29.21 ± 2.26	34.92 ± 0.92*	35.72 ± 2.14*
MUFA	47.50 ± 5.70	39.91 ± 1.61*	41.58 ± 2.02
PUFA	21.56 ± 5.53	25.17 ± 0.99	22.67 ± 1.19
n-6	15.08 ± 2.81	17.91 ± 0.36	17.82 ± 1.74
n-3	6.08 ± 2.25	7.26 ± 0.83	4.85 ± 0.70
MUFA/saturated	1.63 ± 0.31	1.14 ± 0.08*	1.17 ± 0.12*
PUFA/saturated	0.74 ± 0.11	0.72 ± 0.03	0.64 ± 0.06
Unsat/saturated	2.40 ± 0.24	0.87 ± 0.08*	1.80 ± 0.16*
n-3/n-6	0.40 ± 0.14	0.41 ± 0.05	0.28 ± 0.06
PUFA/MUFA	0.45 ± 0.18	0.63 ± 0.05	0.55 ± 0.04

[a]Values are mole percentage and represent means ± standard deviation, $n \geq 3$. A single asterisk (*) indicates significantly different from the control, $P < 0.05$. BLD, below limit of detection, MUFA, monounsaturated fatty acid; PUFA, polyunsaturated fatty acid; for other abbreviations see Table 1.

TABLE 4
Effect of I- and L-FABP Expression on ChoGpl Fatty Acid Composition

Fatty acid	Control	L-FABP expressors	I-FABP expressors
16:0	23.45 ± 1.05	23.36 ± 1.95	23.72 ± 1.28
16:1	6.33 ± 0.29	3.85 ± 0.67*	4.37 ± 0.69*
18:0	15.40 ± 2.21	17.33 ± 0.68	17.62 ± 1.10
18:1n-9	47.41 ± 0.67	44.72 ± 1.24*	44.69 ± 0.60*
18:2n-6	1.85 ± 0.03	2.97 ± 0.13*	2.81 ± 0.22*
18:3n-6	0.25 ± 0.14	0.24 ± 0.12	0.08 ± 0.10
18:3n-3	0.04 ± 0.03	0.09 ± 0.08	BLD
20:0	0.27 ± 0.06	0.34 ± 0.04	0.39 ± 0.10
20:1	1.10 ± 0.22	1.44 ± 0.32	1.48 ± 0.08
20:2n-6	0.12 ± 0.01	0.29 ± 0.03*	0.26 ± 0.07*
20:3n-6	0.35 ± 0.04	0.76 ± 0.05	1.16 ± 0.84
20:4n-6	1.03 ± 0.26	2.52 ± 0.24*,**	1.87 ± 0.40*
22:0	0.19 ± 0.05	0.22 ± 0.03	0.35 ± 0.14
22:3n-3	0.42 ± 0.28	0.15 ± 0.34	BLD
22:4n-6	0.57 ± 0.19	0.32 ± 0.02	0.40 ± 0.29
22:6n-3	0.39 ± 0.24	0.98 ± 0.09*	0.70 ± 0.16
22:5	0.51 ± 0.06	0.26 ± 0.15	BLD
24:1	0.11 ± 0.08	0.03 ± 0.05	BLD
Saturated	39.27 ± 1.22	41.51 ± 1.16*	42.08 ± 0.54*
MUFA	54.96 ± 0.38	50.17 ± 0.67*	50.64 ± 1.21*
PUFA	5.77 ± 0.86	8.32 ± 0.76*	7.28 ± 1.21
n-6	4.71 ± 0.79	7.25 ± 0.63*	6.58 ± 1.08*
n-3	1.06 ± 0.17	1.06 ± 0.17	0.70 ± 0.16
MUFA/saturated	1.40 ± 0.05	1.21 ± 0.05*	1.20 ± 0.04*
PUFA/saturated	0.15 ± 0.02	0.20 ± 0.02*	0.17 ± 0.03
Unsat/saturated	1.55 ± 0.08	1.41 ± 0.07*	1.38 ± 0.03*
n-3/n-6	0.22 ± 0.05	0.15 ± 0.02*	0.11 ± 0.01*
PUFA/MUFA	0.10 ± 0.01	0.17 ± 0.01*	0.14 ± 0.03*

[a]Values are mole percentages and represent means ± standard deviation, $n \geq 3$. A single asterisk (*) indicates significantly different from the control; double asterisk (**) indicates significantly different from I-FABP-expressing cells, $P < 0.05$. For abbreviations see Table 1 and 3.

FABP expression on the EtnGpl fatty acid composition was an increase in saturated fatty acids despite a small, but significant increase in specific PUFA.

Changes observed in ChoGpl were similar to those observed in EtnGpl (Table 4). Of the PUFA, 20:4n-6 and 22:6n-3 mole percentages were increased 2.4- and 2.5-fold in L-FABP- expressing cells, but only the 20:4n-6 mole percentage was elevated in I-FABP-expressing cells. Both proteins significantly elevated the proportion of the n-6 fatty acids relative to the control. Although the percentages of these PUFA were changed in I-FABP-expressing cells, only L-FABP expression significantly elevated PUFA levels and led to an increase in the PUFA/saturated fatty acid index. Because both proteins decreased the mole percentage of 18:1n-9 and 16:1n-7, there was a net decrease in monounsaturated fatty acids (MUFA), resulting in an overall decrease in the unsaturated/saturated fatty acid index. Thus, L- and I-FABP expression altered ChoGpl fatty acid composition, although L-FABP expression appeared to elicit a larger effect.

For PtdSer, expression of either protein had dramatic effects on the fatty acid composition (Table 5). In L-FABP-expressing cells, several PUFA were increased including 2.7-and 1.4-fold increases in 20:3n-6 and 20:4n-6, respectively, relative to the control. These changes, including an increase in 22:6n-3 above the level of detection in L-FABP-expressing cells, resulted in a 2.3-fold increase in PUFA and a 2.4-fold increase in the PUFA/saturated fatty acid index. Even though there is a large decrease in the proportions of 18:1n-9, 16:1n-7, and 18:0 in L-FABP-expressing cells, and to a lesser extent in I-FABP-expressing cells, the 16:0 proportion increased twofold in L-FABP-expressing cells, leaving the overall proportion of saturated fatty acids unchanged in L-FABP-expressing cells relative to control and I-FABP-expressing cells. Thus, in the PtdSer fraction, L-FABP-increased the amount of PUFA, thereby increasing the PUFA/saturated fatty acid index; however, the marked decrease in MUFA left the unsaturated/saturated fatty acid index unchanged. I-FABP expression, on the other hand, had limited effects on PtdSer fatty acid composition, although there was a significant decrease in MUFA/saturated fatty acid index.

L- or I-FABP expression had limited effects on PtdIns fatty acid composition (Table 6). L- and I-FABP expression increased 16:0 proportions nearly 1.8-fold compared to the control. L-FABP-expressing cells had a decreased mole percentage of 18:1n-9; whereas I-FABP-expressing cells had an increase in 18:2n-6 mole percentage. Although the effects by either protein were limited, in both, the overall amount of saturated fatty acids increased, causing a significant decrease in the unsaturated/saturated fatty acid index relative to control.

TABLE 5
Effect of I- and L-FABP Expression on PtdSer Fatty Acid Composition

Fatty acid	Control	L-FABP expressors	I-FABP expressors
16:0	5.02 ± 1.57	10.14 ± 1.07*,**	6.56 ± 0.68
16:1	1.94 ± 0.81	BLD	0.47 ± 0.27*
18:0	50.41 ± 1.86	41.48 ± 2.16*,**	48.27 ± 1.30
18:1n-9	35.97 ± 0.88	27.70 ± 0.54*	30.12 ± 2.30*
18:2n-6	1.93 ± 0.21	3.39 ± 1.30	2.25 ± 0.21
18:3n-6	2.16 ± 0.12	1.27 ± 1.12	0.04 ± 0.10*
20:0	0.50 ± 0.10	1.44 ± 0.23	0.13 ± 0.19
20:1	BLD	1.86 ± 0.33	0.84 ± 0.09
20:2n-6	BLD	1.17 ± 0.30	1.58 ± 1.09
20:3n-6	0.69 ± 0.14	1.90 ± 0.69*,**	0.51 ± 0.24
20:4n-6	1.47 ± 0.51	2.05 ± 0.13**	1.40 ± 0.14**
22:0	BLD	2.69 ± 0.78*	1.75 ± 0.34*
22:1	BLD	0.31 ± 0.30*,**	2.97 ± 0.59*
22:4n-6	BLD	1.38 ± 0.16*,**	BLD
22:6n-3	BLD	3.20 ± 0.30*	3.10 ± 0.49*
Saturated	55.93 ± 0.82	55.75 ± 2.05	58.64 ± 1.61
MUFA	37.71 ± 0.94	29.87 ± 0.26*	32.18 ± 1.99*
PUFA	6.36 ± 0.67	14.38 ± 2.31*,**	9.18 ± 0.86
n-6	6.36 ± 0.67	11.17 ± 2.53*,**	5.94 ± 0.35
n-3	0	3.20 ± 0.30*	3.24 ± 0.56*
MUFA/saturated	0.67 ± 0.02	0.54 ± 0.02*	0.55 ± 0.05*
PUFA/saturated	0.11 ± 0.02	0.26 ± 0.05*,**	0.16 ± 0.01
Unsat/saturated	0.79 ± 0.02	0.80 ± 0.07	0.71 ± 0.05
n-3/n-6	0.00 ± 0.00	0.30 ± 0.10*,**	0.54 ± 0.07*
PUFA/MUFA	0.17 ± 0.02	0.48 ± 0.08*,**	0.29 ± 0.04

[a]Values are mole percentages and represent means ± standard deviation, $n \geq 3$. A single asterisk (*) indicates significantly different from the control; double asterisk (**) indicates significantly different from I-FABP-expressing cells, $P < 0.05$. For abbreviations see Table 1 and 3.

TABLE 6
Effect of I- and L-FABP Expression on PtdIns Fatty Acid Composition

Fatty acid	Control	L-FABP expressors	I-FABP expressors
16:0	4.00 ± 0.69	7.71 ± 1.65*	7.20 ± 0.90*
16:1	0.81 ± 0.52	1.02 ± 0.33	0.67 ± 0.26
18:0	33.94 ± 0.65	34.86 ± 2.20	34.10 ± 1.82
18:1n-9	43.06 ± 4.06	35.28 ± 2.78*	40.93 ± 2.86
18:2n-6	0.92 ± 0.11	1.74 ± 0.50	2.17 ± 0.58*
18:3n-6	0.74 ± 0.68	0.40 ± 0.29	BLD
18:3n-3	0.07 ± 0.09	BLD	BLD
20:0	0.16 ± 0.03	0.48 ± 0.06	0.39 ± 0.10
20:1	1.38 ± 0.28	1.42 ± 0.81	0.96 ± 0.66
20:2n-6	0.37 ± 0.06	0.11 ± 0.21	0.49 ± 0.21
20:3n-6	1.13 ± 0.14	1.77 ± 0.88	1.47 ± 0.10
20:4n-6	9.69 ± 1.17	11.30 ± 1.45	8.22 ± 1.75
22:4n-6	0.69 ± 0.78	0.68 ± 0.65	1.12 ± 0.54
22:6n-3	1.42 ± 0.88	1.84 ± 0.96	1.47 ± 0.22
Saturated	36.78 ± 2.79	43.04 ± 2.17*	41.68 ± 1.11*
MUFA	45.26 ± 4.05	37.90 ± 2.28*	42.56 ± 2.96
PUFA	13.57 ± 1.95	17.84 ± 1.06*	14.95 ± 2.04
n-6	12.12 ± 1.19	16.00 ± 1.83	13.48 ± 2.10
n-3	1.45 ± 0.86	1.84 ± 0.96	1.47 ± 0.22
MUFA/saturated	1.24 ± 0.15	0.88 ± 0.09*	1.02 ± 0.09
PUFA/saturated	0.37 ± 0.05	0.41 ± 0.03	0.36 ± 0.04
Unsat/saturated	1.61 ± 0.12	1.29 ± 0.11*	1.38 ± 0.06*
n-3/n-6	0.12 ± 0.05	0.12 ± 0.07	0.11 ± 0.03
PUFA/MUFA	0.30 ± 0.06	0.47 ± 0.04*	0.36 ± 0.07

[a]Values are mole percentages and represent means ± standard deviation, $n \geq 3$. A single asterisk (*) indicates significantly different from the control; double asterisk (**) indicates significantly different from I-FABP-expressing cells, $P < 0.05$. For abbreviations see Table 1 and 3.

The decrease in the mole percentage of 18:1n-9 in L-FABP-expressing cells resulted in a net decrease in MUFA, leading to a decrease in the MUFA/saturated fatty acid index and an increase in the PUFA/MUFA index, illustrating that even though there were no significant changes in individual PUFA, there was nonetheless a net increase in PUFA.

In summary, both L-FABP and I-FABP expression altered phospholipid acyl chain composition, although L-FABP expression appeared to have a greater effect than I-FABP expression. In general, L-FABP expression increased PUFA, predominantly through a 1.5- to 2.5-fold increase in 22:6n-3 and a 1.4- to 2.4-fold increase in 20:4n-6 proportions relative to the control. MUFA was decreased, resulting in a decrease in the unsaturated/saturated fatty acid index but an increase in the PUFA/saturated fatty acid index. In I-FABP-expressing cells, there was a 6–15% decrease in MUFA along with limited changes in PUFA, resulting in a decrease in the unsaturated/saturated fatty acid index. Hence, L-FABP and I-FABP expression differentially affected L-cell phospholipid fatty acid composition.

DISCUSSION

The physiological role(s) proposed for FABP include fatty acid uptake, intracellular metabolism, cellular growth, and differentiation (2,12). Previously, we showed that I- and L-FABP expression in L-cells differentially affects fatty acid uptake (21) and targets exogenous fatty acids for esterification into distinct lipid pools (18,19,21). However, both I- and L-FABP increase the apparent fatty acid intracellular diffusion coefficient (20), indicating both proteins are involved in intracellular fatty acid trafficking, consistent with results showing that FABP stimulate fatty acid transfer between membranes *in vitro* (47,48). Because both I- and L-FABP differentially stimulate an increase in PtdOH synthesis (24), this suggests that both I- and L-FABP expression in L-cells may affect not only phospholipid mass but also the phospholipid acyl chain composition. To determine if I- and L-FABP expression differentially affects these properties, cells expressing either L-FABP or I-FABP and control cells were grown under the same conditions, and the phospholipid acyl chain composition, phospholipid, and cholesterol mass were analyzed.

Phospholipid levels. Prior studies suggested that L-FABP expression, but not I-FABP expression, increased phospholipid mass in L-cells (18,19). In contrast, we show here that L-FABP, and to a lesser extent I-FABP, expression increased total cellular phospholipid mass compared with the control. These data with transfected cells are supported by results showing that L-FABP had a significantly greater effect on PtdOH biosynthesis *in vitro* than I-FABP (24). When the individual phospholipid classes were separated, the effect of I-FABP was limited to increased ChoGpl and PtdSer mass

(Table 1). On the other hand, L-FABP expression increased the mass of all the major phospholipids between 1.4- and 5.6-fold, depending upon the phospholipid class (Table 1). Previous results suggested only CerPCho, ChoGpl, and EtnGpl mass was increased in L-cells expressing L-FABP (18); however, results presented here clearly indicate a robust effect on both PtdIns and PtdSer mass. Thus, L-FABP markedly increased phospholipid mass of all the phospholipid classes, whereas I-FABP expression had a limited effect on total phospholipid mass; and these changes were limited to two phospholipid classes.

Both I- and L-FABP-expressing cells had altered plasmalogen mass and proportions relative to control cells (Table 2). L-FABP expression significantly increased the mass of PlsCho and PlsEtn to a much greater extent than I-FABP expression. Similarly, both proteins differentially increased the mass of the acid-stable fraction. Thus, by analyzing the ChoGpl and EtnGpl subclasses, it became evident that these proteins elevated both the acid-stable and acid-labile fractions relative to the control, indicating I- and L-FABP facilitated not only plasmalogen biosynthesis but also PtdEtn and PtdCho synthesis. Because plasmalogens have a role in lipid-mediated signal transduction (42–44), FABP may support not only the synthesis of PtdIns but also of other phospholipids involved in cell signaling.

Phospholipid composition. In L-cells, expression of L-FABP but not I-FABP significantly altered the phospholipid percentage composition. In L-FABP-expressing cells, total cellular phospholipid composition was dramatically changed, with proportions (mol%) of both PtdIns and PtdSer increased and ChoGpl proportions decreased (Table 1). These results are consistent with data showing plasma membrane phospholipid composition is altered in L-FABP-expressing L-cells (46). We also report an alteration in the composition of ChoGpl and EtnGpl subclasses (Table 2). In L-FABP-expressing cells, PlsEtn proportions, expressed as mole percentage of EtnGpl, were increased. In contrast, I-FABP expression had no effect on the composition of the EtnGpl subclasses. These results indicate that PlsEtn synthesis was increased at the expense of the predominantly diacyl subclass, PtdEtn. In contrast, both I- and L-FABP expression increased PlsCho proportions, once again with a decrease mainly in the PtdCho subclass. Clearly, there was a profound effect on plasmalogen biosynthesis, with the increase in PlsCho proportions suggesting an increase in the utilization of PlsEtn to form the PlsCho (49,50). This increase in PlsCho proportions is important as PlsCho is the active plasmalogen pool involved in signal transduction (42–44,50,51).

Possible mechanisms for enhanced phospholipid synthesis. Several mechanisms may account for the observed increases in phospholipid levels. The general increase in phospholipid mass in the L-FABP-expressing cells may be the result of elevated PtdOH biosynthesis, since L-FABP stimulates PtdOH synthesis *in vitro* (10,23,24). This appears plausible as PtdOH is the central and key intermediate for the Kennedy pathway (52,53). The reported difference in the magnitude of stimulation by L-FABP and I-FABP *in vitro* (24) may account, in part, for the reduced effect of I-FABP expression on L-cell phospholipid mass. In addition, L-FABP, and not I-FABP, has been reported to be localized in the ER as well as the cytosol (12). It is also quite possible that L-FABP affected other enzymes in the Kennedy pathway, in particular, the portion of the pathway involved in PtdIns and PtdSer biosynthesis. These two phospholipids were selectively elevated, suggesting L-FABP expression enhanced more than just PtdOH synthesis and may have stimulated activity of key enzymes in the Kennedy pathway.

Both I- and L-FABP expression increased plasmalogen mass in L-cells. Plasmalogen synthesis requires both peroxisomal (54,55) and microsomal (56–58) steps. Formation of the 1-*0*-alkyl linkage occurs in the peroxisome (54,55), whereas the desaturation of the 1-*0*-alkyl moiety occurs in the microsome (56–58). Because L-FABP has been detected in the ER but not in peroxisomes (12), FABP expression more likely stimulates the microsomal as compared to peroxisomal pathways. However, because L-FABP increased 22:6n-3 proportions to a greater extent than I-FABP and because 22:6n-3 formation is peroxisome-dependent (59), increased plasmalogen mass may merely be the result of an overall increase in peroxisomal function, stimulated to a greater degree by L-FABP expression than I-FABP expression. This postulated increase in peroxisomal function may be correlated with increased fatty acid uptake in L-FABP-expressing cells and the enhancement of peroxisome proliferator-activated receptor activity by L-FABP (60).

Alternatively, because the final steps for plasmalogen biosynthesis are microsomal (56–58), I- and L-FABP expression may also increase desaturase activity. Such a mechanism is consistent with the known (10,23,24) and proposed effects on Kennedy pathway enzymes. Furthermore, expression of either protein dramatically increased levels of PlsCho, which is made using PlsEtn as the direct precursor (49,50). Regardless of whether I- and L-FABP expression enhanced either the peroxisomal steps or the microsomal steps of plasmalogen synthesis or both, expression of either protein increased plasmalogen levels. This elevation in plasmalogens may be very important as plasmalogens are active components of several cascades involved in lipid-mediated signal transduction (42–44, 50,51,61).

Free cholesterol to phospholipid ratio. We also report a large decrease in the cholesterol to phospholipid ratio. Similar to all of the other effects of I- and L-FABP expression on lipid metabolism, L-FABP decreased the cholesterol-to-phospholipid ratio to a greater extent than I-FABP. The decrease in this ratio is consistent with another study indicating L-FABP expression decreased this ratio (17). Furthermore, the lateral membrane mobility in L-FABP expressing cells is reduced (20), consistent with a decrease in the cholesterol-to-phospholipid ratio. The reduction in this parameter may account for the observed decrease in acyl chain order in these cells (17,46).

Phospholipid acyl chain composition. Lastly, expression of either L- or I-FABP caused significant changes in the phospholipid fatty acid composition (Tables 3–6). In general, the effect of FABP expression on phospholipid fatty acids was a decrease in MUFA and an increase in PUFA. For L-FABP, this included a 1.5- to 2.5-fold increase in 22:6n-3 and a 1.4- to 2.4-fold increase in 20:4n-6 proportions (mol%) relative to control. In contrast, I-FABP expression produced limited increases in 20:4n-6 proportions along with a 6–15% decrease in the MUFA. These changes are consistent with binding affinity data showing a preferential binding of PUFA to L-FABP compared to I-FABP (8). Because I- and L-FABP bind both fatty acids and fatty acyl-CoA with a high affinity, these proteins may facilitate interactions of fatty acids and fatty acyl-CoA with CoA-dependent and CoA-independent acyltransferases (62). Within the cellular milieu, L-FABP may exhibit preferential binding for PUFA over MUFA, similar to that observed *in vitro* (8), accounting for the differential effects on PUFA composition in I- and L-FABP-expressing cells. Taken in context with the increased levels of particular phospholipids involved in lipid-mediated signal transduction, an increase in the amount of 20:4n-6 in the phospholipids would increase the amount of 20:4n-6 potentially liberated during signal transduction. This increase in the potential availability of 20:4n-6 could profoundly affect cellular function.

In summary, both L- and I-FABP expression increased total cellular phospholipids; however, the extent of this increase was significantly different between L- and I-FABP-expressing cells. L- and I-FABP expression also differentially affected individual phospholipid levels and phospholipid composition. We speculate that both L- and I-FABP stimulated an increase in phospholipid biosynthesis *via* the Kennedy pathway by affecting not only PtdOH biosynthesis, but also specific enzymes in the pathway, thereby accounting for the increased PtdSer and PtdIns mass. Furthermore, L- and I-FABP increased plasmalogen mass, perhaps indicating an increase in peroxisomal function or ER function or both, especially in the L-FABP-expressing cells. The increased phospholipid levels, in the absence of elevated cholesterol mass, resulted in a substantial decrease in the cholesterol to phospholipid ratio. Lastly, both proteins altered the phospholipid fatty acid composition by increasing the mole percentage of PUFA at the expense of MUFA. In conclusion, L- and I-FABP expression in L-cells differentially enhanced phospholipid synthesis and altered phospholipid fatty acid composition. These findings extend the previously reported differential effect of L- and I-FABP expression on fatty acid uptake (18–21) and targeting (18,19,21). However, the dramatic effects on phospholipid pools involved in cell signaling as well as an increase in 20:4n-6 proportions suggest that FABP may have an important role in maintaining lipid pools used in lipid-mediated signal transduction. Our results suggest L-FABP has a greater role in this process than I-FABP.

ACKNOWLEDGMENTS

We thank Cindy Murphy for the typed preparation of this manuscript. This work was supported by a U.S. Public Health Service grant from the National Institutes of Health, #DK 41402, to Friedhelm Schroeder.

REFERENCES

1. Glatz, J.F.C., and van der Vusse, G.J. (1990) Cellular Fatty Acid Binding Proteins: Current Concepts and Future Directions, *Mol. Cell Biochem. 98,* 237–251.
2. Veerkamp, J.H., Peeters, R.A., and Maatman, R.G.H.J. (1991) Structural and Functional Features of Different Types of Cytoplasmic Fatty Acid-Binding Proteins, *Biochim. Biophys. Acta 1081,* 1–24.
3. Nemecz, G., Hubbell, T., Jefferson, J.R., Lowe, J.B., and Schroeder, F. (1991) Interaction of Fatty Acids with Recombinant Rat Intestinal and Liver Fatty Acid-Binding Proteins, *Arch. Biochem. Biophys. 286,* 300–309.
4. Börchers, T., and Spener, F. (1994) Fatty Acid Binding Proteins, in *Current Topics in Membranes,* pp. 261–294, Academic Press, Inc., New York.
5. Gordon, J.I., Alpers, D.H., Ockner, R.K., and Strauss, A.W. (1983) The Nucleotide Sequence of Rat Liver Fatty Acid Binding Protein mRNA, *J. Biol. Chem. 258,* 3356–3363.
6. Nemecz, G., Jefferson, J.R., and Schroeder, F. (1991) Polyene Fatty Acid Interactions with Recombinant Intestinal and Liver Fatty Acid-Binding Proteins, *J. Biol. Chem. 266,* 17112–17123.
7. Cistola, D.P., Sacchettini, J.C., Banaszak, L.J., Walsh, M.T., and Gordon, J.I. (1989) Fatty Acid interactions with Rat Intestinal and Liver Fatty Acid-Binding Proteins Expressed in *Escherichia coli:* A Comparative ^{13}C NMR Study, *J. Biol. Chem. 264,* 2700–2710.
8. Richieri, G.V., Ogata, R.T., and Kleinfeld, A.M. (1994) Equilibrium Constants for the Binding of Fatty Acids with Fatty Acid-Binding Proteins from Adipocyte, Intestine, Heart, and Liver Measured with the Fluorescent Probe ADIFAB, *J. Biol. Chem. 269,* 23918–23930.
9. Murphy, E.J., Edmondson, R.D., Russell, D.H., Colles, S., and Schroeder, F. (1999) Isolation and Characterization of Two Distinct Forms of Liver Fatty Acid Binding Protein from the Rat, *Biochim. Biophys. Acta 1436,* 413–425.
10. Hubbell, T., Behnke, W.D., Woodford, J.K., and Schroeder, F. (1994) Recombinant Liver Fatty Acid Binding Protein Interacts with Fatty Acyl-coenzyme A, *Biochemistry 33,* 3327–3335.
11. Frolov, A., and Schroeder, F. (1997) Time-Resolved Fluorescence of Intestinal and Liver Fatty Acid Binding Proteins: Role of Fatty Acyl CoA and Fatty Acid, *Biochemistry 36,* 505–517.
12. McArthur, M.J., Atshaves, B.P., Frolov, A., Foxworth, W.D., Kier, A.B., and Schroeder, F. (1999) Cellular Uptake and Intracellular Trafficking of Long Chain Fatty Acids, *J. Lipid Res. 40,* 1371–1383.
13. Dutta-Roy, A.K., Gopalswamy, N., and Trulzsch, D.V. (1987) Prostaglandin E1 Binds to Z Protein of Rat Liver, *Eur. J. Biochem. 162,* 615–619.
14. Raza, H., Pongubala, J.R., and Sorof, S. (1989) Specific High Affinity Binding of Lipoxygenase Metabolites of Arachidonic Acid by Liver Fatty Acid Binding Protein, *Biochem. Biophys. Res. Commun. 161,* 448–455.
15. Vincent, S.H., and Muller-Eberhard, U. (1985) A Protein of the Z Class of Liver Cytosolic Proteins in the Rat That Preferentially Binds Heme, *J. Biol. Chem. 260,* 14521–14528.
16. Myszka, D.G., and Swenson, R.P. (1991) Identification by Photoaffinity Labeling of Fatty Acid-Binding Protein as a Potential Warfarin Receptor in Rat Liver, *J. Biol. Chem. 266,* 20725–20731.

17. Jefferson, J.R., Powell, D.M., Rymaszewski, Z., Kukowska-Latallo, J., Lowe, J.B., and Schroeder, F. (1990) Altered Membrane Structure in Transfected Mouse L-Cell Fibroblasts Expressing Rat Liver Fatty Acid Binding Protein, *J. Biol. Chem. 265,* 11062–11068.
18. Murphy, E.J., Prows, D.R., Jefferson, J.R., and Schroeder, F. (1996) Liver Fatty Acid Binding Protein Expression in Transfected Fibroblasts Stimulates Fatty Acid Uptake and Metabolism, *Biochim. Biophys. Acta 1301,* 191–196.
19. Prows, D.R., Murphy, E.J., Moncecchi, D., and Schroeder, F. (1996) Intestinal Fatty Acid-Binding Protein Expression Stimulates Fibroblast Fatty Acid Esterification, *Chem. Phys. Lipids 84,* 47–56.
20. Murphy, E.J. (1998) L-FABP and L-FABP Expression Increases NBD-Stearate Uptake and Cytoplasmic Diffusion in L Cells, *Am. J. Physiol. 275,* G244–G249.
21. Prows, D.R., Murphy, E.J., and Schroeder, F. (1995) Intestinal and Liver Fatty Acid Binding Proteins Differentially Affect Fatty Acid Uptake and Esterification in L-cells, *Lipids 30,* 907–910.
22. Atshaves, B.P., Foxworth, W.B., Frolov, A., Roths, J.B., Kier, A.B., Oetama, B.K., Piedrahita, J.A., and Schroeder, F. (1998) Cellular Differentiation and I-FABP Protein Expression Modulate Fatty Acid Uptake and Diffusion, *Am. J. Physiol. 274,* C633-C644.
23. Vancura, A., and Haldar, D. (1992) Regulation of Mitochondrial and Microsomal Phospholipid Synthesis by Liver Fatty Acid-Binding Protein, *J. Biol. Chem. 267,* 14353–14359.
24. Jolly, C.A., Hubbell, T., Behnke, W.D., and Schroeder, F. (1997) Fatty Acid Binding Protein: Stimulation of Microsomal Phosphatidic Acid Formation, *Arch. Biochem. Biophys. 341,* 112–121.
25. Sha, R.S., Kane, C.D., Xu, Z.H., Banaszak, L.J., and Bernlohr, D.A. (1993) Modulation of Ligand-Binding Affinity of the Adipocyte Lipid-Binding Protein by Selective Mutation—Analysis *in vitro* and *in situ*, *J. Biol. Chem. 268,* 7885–7892.
26. Buhlmann, C., Borchers, T., Pollak, M., and Spener, F. (1999) Fatty Acid Metabolism in Human Breast Cancer Cells (MCF7) Transfected with Heart-Type Fatty Acid Binding Protein, *Mol. Cell Biochem. 199,* 41–48.
27. Higuchi, K. (1970) An Improved Chemically Defined Culture Medium for Strain L Mouse Cells Based on Growth Responses to Graded Levels of Nutrients Including Iron and Zinc, *J. Cell Physiol. 75,* 65–72.
28. Hara, A., and Radin, N.S. (1978) Lipid Extraction of Tissues with a Low-Toxicity Solvent, *Anal. Biochem. 90,* 420–426.
29. Murphy, E.J., Rosenberger, T.A., and Horrocks, L.A. (1997) Effects of Maturation on the Phospholipid and Phospholipid Fatty Acid Compositions in Primary Rat Cortical Astrocyte Cell Cultures, *Neurochem. Res. 22,* 1205–1213.
30. Demediuk, P., Anderson, D.K., Horrocks, L.A., and Means, E.D. (1985) Mechanical Damage to Murine Neuronal-Enriched Cultures During Harvesting: Effects on Free Fatty Acids, diglycerides, Na^+,K^+-ATPase, and Lipid Peroxidation, *In Vitro Cell. Develop. Biol. 21,* 569–574.
31. Murphy, E.J., and Horrocks, L.A. (1993) Composition of the Phospholipids and Their Fatty Acids in the ROC-1 Oligodendroglial Cell Line, *Lipids 28,* 67–71.
32. Murphy, E.J., and Horrocks, L.A. (1993) Effects of Differentiation on the Phospholipid and Phospholipid Fatty Acid Compositions of N1E-115 Neuroblastoma Cells, *Biochim. Biophys. Acta 1167,* 131-136.
33. Murphy, E.J., Haun, S.E., Rosenberger, T.A., and Horrocks, L.A. (1995) Altered Lipid Metabolism in the Presence and Absence of Extracellular Ca^{2+} During Combined Oxygen-Glucose Deprivation in Primary Astrocyte Cultures, *J. Neurosci. Res. 42,* 109–116.
34. Dugan, L.L., Demediuk, P., Pendley II, C.E., and Horrocks, L.A. (1986) Separation of Phospholipids by High Pressure Liquid Chromatography: All Major Classes Including Ethanolamine and Choline Plasmalogens, and Most Minor Classes, Including Lysophosphatidylethanolamine, *J. Chromatogr. 378,* 317–327.
35. Rouser, G., Siakotos, A., and Fleischer, S. (1969) Quantitative Analysis of Phospholipids by Thin Layer Chromatography and Phosphorus Analysis of Spots, *Lipids 1,* 85–86.
36. Murphy, E.J., Stephens, R., Jurkowitz-Alexander, M., and Horrocks, L.A. (1993) Acidic Hydrolysis of Plasmalogens Followed by High-Performance Liquid Chromatography, *Lipids 28,* 565–568.
37. Murphy, E.J., Rosenberger, T.A., and Horrocks, L.A. (1996) Separation of Neutral Lipids by High-Performance Liquid Chromatography: Quantification by Ultraviolet, Light Scattering and Fluorescent Detectors, *J. Chromatogr. B 685,* 9–14.
38. Nakagawa, Y., and Waku, K. (1988) Phospholipids, in *Neuromethods 7. Lipids and Related Compounds* (Boulton, A.A., Baker, G.B., and Horrocks, L.A., eds.), pp. 149–178, Humana Press, Clifton.
39. Jones, M., Keenan, R.W., and Horowitz, P. (1982) Use of 6-*p*-Toluidino-2-naphthalenesulfonic Acid to Quantitate Lipids After Thin-Layer Chromatography, *J. Chromatogr. 237,* 522–524.
40. Brockerhoff, H. (1975) Determination of the Positional Distribution of Fatty Acids in Glycerolipids, *Methods Enzymol. 35,* 315–325.
41. Bradford, M. (1976) A Rapid and Sensitive Method for the Quantitation of Microgram Quantities of Protein Utilizing the Principle of Protein-Dye Binding, *Anal. Biochem. 72,* 248–254.
42. Horrocks, L.A., Harder, H.W., Mozzi, R., Goracci, G., Francescangeli, E., Porcellati, S., and Nenci, G.G. (1986) Receptor Mediated Degradation of Choline Plasmalogen and Glycerophospholipid Methylation: A New Hypothesis, in *Enzymes of Lipid Metabolism, Vol. 2* (Freysz, L., Dreyfus, H., Massarelli, R., and Gatt, S., eds.), pp. 707–711, Plenum Press, New York.
43. Horrocks, L.A., Yeo, Y.K., Harder, H.W., Mozzi, R., and Goracci, G. (1986) Choline Plasmalogens, Glycerophospholipid Methylation, and Receptor-Mediated Activation of Adenylate Cyclase, in *Advances in Cyclic Nucleotide Protein Phosphorylation Research, Vol. 20* (Greengard, P., and Robinson, G.A., eds.), pp. 263–292, Raven Press, New York.
44. McHowat, J., and Liu, S. (1997) Interleukin-1β Stimulates Phospholipase A_2 Activity in Adult Rat Ventricular Myocytes, *Am. J. Physiol. 272 (Cell Phys. 41),* C450–C456.
45. McHowat, J., Liu, S., and Creer, M.H. (1998) Selective Hydrolysis of Plasmalogen Phospholipids by Ca^{2+}-Independent PLA_2 in Hypoxic Ventricular Myocytes, *Am. J. Physiol. 274 (Cell Phys. 43),* C1727–C1737.
46. Woodford, J.K., Jefferson, J.R., Wood, W.G., Hubbell, T., and Schroeder, F. (1993) Expression of Liver Fatty Acid Binding Protein Alters Membrane Lipid Composition and Structure in Transfected L-Cell Fibroblasts, *Biochim. Biophys. Acta 1145,* 257–265.
47. Storch, J., and Bass, N.M. (1990) Transfer of Fluorescent Fatty Acids from Liver and Heart Fatty Acid-Binding Proteins to Model Membranes, *J. Biol. Chem. 265,* 7827–7831.
48. Hsu, K.-T. and Storch, J. (1996) Fatty Acid Transfer from Liver and Intestinal Fatty Acid-Binding Proteins to Membranes Occurs by Different Mechanisms, *J. Biol. Chem. 271,* 13317–13323.
49. Paltauf, F. (1994) Review: Ether Lipids in Biomembranes, *Chem. Phys. Lipids 74,* 101–139.
50. Lee, T.-C. (1998) Review: Biosynthesis and Possible Biological Functions of Plasmalogens, *Biochim. Biophys. Acta 1394,* 129–145.
51. Gross, R.W. (1995) Myocardial Phospholipase A_2, *J. Lipid Mediators Cell Signalling 12,* 131–137.

52. Thompson Jr., G.A. (1973) Phospholipid Metabolism in Animal Tissues, in *Form and Function of Phospholipids (B.B.A. Library, Vol. 3)* (Ansell, G.B., Hawthorne, J.N., and Dawson, R.M.C., eds.), 2nd edn., pp. 67–96, Elsevier Scientific Publishing Co., Amsterdam.
53. van den Bosch, H., and Vance, D.E. (1997) Editorial, *Biochim. Biophys. Acta 1348,* 1–2.
54. Hajra, A.K., Burke, C.L., and Jones, C.L. (1979) Subcellular Localization of Acyl Coenzyme A: Dihydroxyacetone Phosphate Acyltransferase in Rat Liver Peroxisomes (microbodies), *J. Biol. Chem. 254,* 10896–10900.
55. Singh, H., Beckman, K., and Poulos, A. (1993) Exclusive Localization in Peroxisomes of Dihydroxyacetone Phosphate Acyltransferase and Alkyl-dihydroxyacetone Phosphate Synthase in Rat Liver, *J. Lipid Res. 34,* 467–477.
56. Hajra, A.K., and Bishop, J.E. (1992) Glycerolipid Biosynthesis in Peroxisomes *via* the Acyl Dihydroxyacetone Phosphate Pathway, *Ann. NY Acad. Sci. 386*, 170–182.
57. van den Bosch, H., Schutgens, R.B.H., Wanders, R.J.A., and Tager, J.M. (1992) Biochemistry of Peroxisomes, *Annu. Rev. Biochem. 61,* 157–197.
58. van den Bosch, H., Schrakamp, G., Hardeman, D., Zomer, A.W.M., Wanders, R.J.A., and Schutgens, R.B.H. (1993) Ether Lipid Synthesis and Its Deficiency in Peroxisomal Disorders, *Biochimie 75,* 183–189.
59. Sprecher, H., Chen, Q., and Yin, F.Q. (1999) Regulation of the Biosynthesis of 22:5n-6 and 22:6n-3: A Complex Intracellular Process, *Lipids 34,* S153–S156.
60. Wolfrum, C., Ellinghaus, P., Fobker, M., Seedorf, U., Assmann, G., Borchers, T., and Spener, F. (1999) Phytanic Acid Is Ligand and Transcriptional Activator of Murine Liver Fatty Acid Binding Protein, *J. Lipid Res. 40,* 708–714.
61. Hirashima, Y., Farooqui, A.A., Mills, J.S., and Horrocks, L.A. (1992) Identification and Purification of Calcium-Independent Phospholipase A_2 from Bovine Brain Cytosol, *J. Neurochem. 59,* 708–714.
62. Yamashita, A., Sugiura, T., and Waku, K. (1997) Acyltransferases and Transacylases Involved in Fatty Acid Remodeling of Phospholipids and Metabolism of Bioactive Lipids in Mammalian Cells, *J. Biochem. 122,* 1–16.

[Received December 1, 1999, and in revised form April 28, 2000; revision accepted May 15, 2000]

Do Glycerolipids Display Lateral Heterogeneity in the Thylakoid Membrane?

Sylvie Duchêne and Paul-André Siegenthaler*

Laboratoire de Physiologie Végétale, Université de Neuchâtel, CH-2007 Neuchâtel, Switzerland

ABSTRACT: The lateral heterogeneity of lipids in the thylakoid membrane has been questioned for over 20 yrs. It is generally believed that glycerolipids are asymmetrically distributed within the plane of the membrane. In the present investigation, we isolated several thylakoid membrane domains by using sonication followed by separation in an aqueous dextran–polyethylene glycol two-phase system. This technique, which avoids detergent treatments, allowed us to obtain stroma and grana lamellae vesicles as well as grana central core and grana margin vesicles from thylakoids. The relative distribution of the four lipid classes, i.e., monogalactosyldiacylglycerol, digalactosyldiacylglycerol, sulfoquinovosyldiacylglycerol, and phosphatidylglycerol, was found to be statistically identical in all four thylakoid fractions and in whole thylakoids. Similarly, the relative amount of fatty acids in each individual lipid and the eight main phosphatidylglycerol molecular species was identical in all thylakoid membrane fractions tested as well as in the intact thylakoid membrane. Based on presently available procedures for obtaining thylakoid subfractions that are unable to discriminate microdomains within the membrane, it is concluded that glycerolipids are evenly distributed within the plane of the thylakoid membrane. These data are discussed in terms of "bulk" and "specific" lipids.

Paper no. L8426 in *Lipids 35,* 739–744 (July 2000).

Glycerolipids are major components of the thylakoid membrane. They consist of four classes: monogalactosyldiacylglycerol (MGDG), digalactosyldiacylglycerol (DGDG), sulfoquinovosyldiacylglycerol (SQDG), and phosphatidylglycerol (PG). These lipids are characteristic of photosynthetic membranes. Galactolipids (MGDG and DGDG) represent about 80 mol% of total lipids and are therefore considered to be the most abundant membrane lipids in the world. In addition, they are characterized by an exceptionally high content of trienoic acids, mainly, α-linolenic acid; additionally, in the so-called 16:3-plants, hexadecatrienoic acid is found in MGDG. SQDG is enriched in palmitic acid (35 mol%), whereas PG contains a unique fatty acid, *trans*-Δ^3-hexadecenoic acid (e.g., 1,2). The fatty acid composition of these glycerolipids is unique and gives rise to a great number of molecular species (3,4). It is surprising that, up to now, none or only a few of these lipid molecular species have been assigned to a specific location in the membrane or to a specific role in the photosynthetic function.

During the past years, several attempts have been made to determine whether, in a manner similar to proteins, acyl lipids are also asymmetrically distributed in the plane of the thylakoid membrane (TM). Among them, the following approaches have been used: (i) mild solvent extraction of freeze-dried membranes (e.g., 5); (ii) fractionation of subchloroplast particles enriched in photosystem I (PSI) or photosystem II (PSII) activities (e.g., 6); (iii) separation of appressed (granal) and nonappressed (stromal) regions of thylakoids (e.g., 7–10); (iv) purification of the membrane protein complexes (e.g., 11–19); (v) detection of glycerolipids by using antibodies directed to individual lipids bound to the surface of the TM, to subchloroplast particles, or to individual proteins (e.g., 20–22, and references therein); (vi) reconstitution of photosynthetic structures and activities with lipids (for a review, see Ref. 23). The general conclusions of these studies are that glycerolipids are asymmetrically distributed within the plane of the TM, although the lateral heterogeneity of thylakoid proteins is much more pronounced than that of lipids (for a review, see Ref. 1).

Several studies argue for this conclusion. For instance, one molecule of MGDG (and possibly one molecule of PG) was found to bind one PSII reaction center complex (18). Furthermore, the fatty acids of these two lipids are much more saturated (50% of the total fatty acids) than those in the bulk lipids of thylakoid and PSII membranes (10% of the total fatty acids). The removal of DGDG from isolated light-harvesting chlorophyll *a/b* protein complex (LHCII) renders the complex unable to form two- or three-dimensional crystals. The ability to crystallize is completely restored by the addition of DGDG at a ratio of about four molecules of DGDG per polypeptide for three-dimensional crystallization, suggesting the existence of several binding sites at the periphery of the trimeric complexes (24). The sulfolipid SQDG was found to be associated with the coupling factor complex (CF_0–CF_1) of spinach (16). This suggests that this acidic glycolipid is

*To whom correspondence should be addressed at Laboratoire de Physiologie Végétale, Université de Neuchâtel, Rue Emile-Argand 13, CH-2007 Neuchâtel, Switzerland. E-mail: Paul-Andre.Siegenthaler@bota.unine.ch

Abbreviations: B3, grana lamellae vesicles; B3-420S, grana central core vesicles (or central core of the appressed region); Chl, chlorophyll; DGDG, digalactosyldiacylglycerol; F695, fluorescence at 695 nm; F740, fluorescence at 740 nm; LHCII, light harvesting chlorophyll *a/b* protein complex; MGDG, monogalactosyldiacylglycerol; PG, phosphatidylglycerol; 420S, grana margin vesicles; SQDG, sulfoquinovosyldiacylglycerol; TM, thylakoid membranes; T3, stroma lamellae vesicles.

firmly bound to the ATP-synthetase complex and may play a special role in the mechanism of energy coupling. Several examples show the involvement of PG molecular species in the maintenance of the structure and function of the TM. In lipid-depleted LHCII, only PG containing 16:1 (3t), but not PG containing 16:0 fatty acids, induced reoligomerization from monomer forms of LHCII (25). In addition, PG is involved in the stacking of thylakoids (23).

Because most of the above methods, especially those for obtaining subchloroplast particles, involved the use of detergents, which are known to partially extract and/or displace lipids (8), in the present investigation we isolated the TM in several domains by using sonication followed by separation in an aqueous dextran–polyethylene glycol two-phase system (26). When comparing the content and the characteristics of lipids in TM, stroma lamellae vesicles (T3) and grana lamellae vesicles (B3), grana central core vesicles (B3-420S) and grana margin vesicles (420S), our results indicate that, considering the domains tested in this investigation, no lateral heterogeneity occurred in the TM.

EXPERIMENTAL PROCEDURES

Preparation of thylakoid vesicles. Spinach plants (*Spinacia oleracea* L.) were grown in a growth chamber at 20°C with a light period of 12 h and incident light intensity of 400 μE/m^2/s. Thylakoids were prepared from leaves according to Andreasson *et al.* (27). After the final centrifugation, the thylakoid preparation was suspended for 45 min in 10 mM sodium phosphate buffer (pH 7.4), 5 mM NaCl, and 100 mM sucrose supplemented with 1 mM $MgCl_2$ to allow a complete stacking of the membranes before fragmentation, then adjusted to 4 mg chlorophyll (Chl)/mL. T3, B3, B3-420S, and 420S were obtained by essentially following the procedure described by Wollenberger *et al.*, (28): (i) thylakoids were mixed with two polymers (5.6 dextran and 5.6% polyethylene glycol), then sonicated on ice (6 × 30 s, with 1-min resting intervals); the mixture was submitted to a series of three partition steps in the same aqueous dextran–polyethylene glycol two-phase system allowing the separation of T3 and B3; (ii) polymers were added to the B3 fraction, and the mixture was sonicated (14 × 30 s, with 1-min resting intervals); then a series of three partition steps in the same aqueous dextran–polyethylene glycol two-phase system allowed the separation of B3-420S and 420S. The four vesicle preparations were diluted 4 to 5 times with the initial suspension medium and centrifuged at 100,000 × *g* for 30 min to remove polymers. The pellets were resuspended in 10 mM sodium phosphate buffer (pH 7.4), 5 mM NaCl, 1 mM $MgCl_2$, and 100 mM sucrose, then adjusted to 1 mg Chl/mL.

Chemical analyses. Total lipids were extracted by adding 4 mL chloroform/methanol (53:37, vol/vol) and 2 mL 0.5 M KCl to the thylakoid suspension (150 μL). This resulted in a two-phase system. The lipids of the lower phase were separated by thin-layer chromatography on silica gel plates (precoated silica gel plates, no. 5626; Merck, Darmstadt, Germany) in two dimensions. Then, MGDG, DGDG, SQDG, and PG were methylated and the resulting fatty acid methyl esters separated and identified by gas–liquid chromatography (29). Molecular species of PG were identified in the TM fraction, T3, and B3-420S by high-performance liquid chromatography following the procedure described by Kito *et al.*, (30), modified by Xu and Siegenthaler, (4). Chl concentration was determined according to Bruinsma (31). The relative content of Chl *a* and *b* was estimated (32).

Photosynthetic activities. Fluorescence emission spectra at 77 K of thylakoid preparations were determined (33).

RESULTS

Characterization of thylakoid domains. Table 1 shows a few biochemical characteristics of the TM and the derived thylakoid domains, i.e., T3, B3, B3-420S, and 420S. When total glycerolipids, i.e., the sum of MGDG, DGDG, SQDG, and PG, were expressed in nmol/mg Chl, μg/mg Chl, or nmol/nmol Chl, the data did not display significant differences between TM and the different fractions. Though there are no statistical values available for expressing the content of total glycerolipids as a function of proteins (nmol/mg protein or μg/mg protein), Table 1 shows that the difference between the values characterizing the TM, grana, and stroma lamellae did not exceed 13.5%. On the basis of the standard deviations calculated for the level of total glycerolipids/Chl, this difference cannot be considered as significant.

As shown by other authors (28), the Chl *a/b* ratio was the highest in stroma lamellae and the lowest in the grana central core. The low-temperature emission of fluorescence at 695 and 740 nm reflects the relative amount of PSII and PSI in the different thylakoid fraction. In Table 1, we see that the thylakoid membrane was slightly enriched in PSII (F_{695}/F_{740} = 1.2, where F_{695} is the fluorescence at 695 nm and F_{740} is the fluorescence at 740 nm). When TM was fractionated in distinct domains, the two photosystems were not distributed uniformly. B3 and B3-420S, which are enriched in PSII, displayed the highest F_{695}/F_{740} ratio values, whereas T3 exhibited a very low value. The 420S had intermediate F_{695}/F_{740} ratio values. Altogether, these results confirmed that the foregoing thylakoid fractions, which originate from different TM domains, are distinct and well-defined, as described in the literature (34).

Composition of lipids, fatty acids, and PG molecular species. The composition in lipid classes (MGDG, DGDG, SQDG, and PG) of four TM domains compared to that of the whole membrane is shown in Table 2. The relative amount of each lipid, expressed as mole percentage, in TM was similar to the values published in the literature (1). The relative distribution of the four lipid classes in T3 and B3, as well as in B3-420S and 420S, was statistically identical. This shows that these domains displayed the same relative lipid distribution as that observed in the whole TM. In a similar fashion, the relative amount of fatty acids in each individual lipid was identical in the four TM domains as well as in the whole TM (Table 3).

TABLE 1
Biochemical Characteristics of Thylakoid Membrane Domains

Membrane characteristic	Thylakoid membrane domain[a]				
	TM	T3	B3	B3-420S	420S
Total glycerolipids					
nmol/mg Chl	1641 ± 162 (n = 7)	1788 ± 272 (n = 10)	1586 ± 40 (n = 4)	1601 ± 151 (n = 11)	1806 ± 116 (n = 4)
μg/mg Chl[b,c]	1319 ± 130	1437 ± 219	1275 ± 32	1287 ± 121	1452 ± 93
nmol/nmol Chl[c,d]	1.48 ± 0.15	1.61 ± 0.24	1.43 ± 0.04	1.45 ± 0.13	1.63 ± 0.10
nmol/mg protein	560	520	590	ND[e]	ND
μg/mg protein	450	420	470	ND	ND
Protein[f]					
μg/mg Chl	2900	3400	2700	ND	ND
Chl *a*/*b* (n = 12)	2.8 ± 0.1	4.0 ± 0.1	2.2 ± 0.1	2.1 ± 0.1	2.6 ± 0.2
F_{695}/F_{740} ratio	1.2 ± 0.2 (n = 12)	0.3 ± 0.1 (n = 12)	3.9 ± 0.3 (n = 7)	4.6 ± 1.5 (n = 10)	2.4 ± 0.9 (n = 4)

[a]TM, thylakoid membranes; T3, stroma lamellae vesicles; B3, grana lamellae vesicles; B3-420S, grana central core vesicles; 420S, grana margin vesicles; F695/F740, ratio of fluorescence at 695 nm compared to fluoresence at 740 nm; Chl, chlorophyll.
[b]Total glycerolipids expressed in μg/mg Chl were calculated by taking into consideration the molecular weight of each lipid class and the relative amount of each lipid class in the thylakoid membrane.
[c]The number of experiments (n) for the calculation of the standard deviation is the same as that indicated in the second line of this table.
[d]Total glycerolipids expressed in nmol/nmol Chl was calculated by taking into consideration the molecular weights of chlorophyll *a* and *b* and the Chl *a*/*b* ratio.
[e]ND, not determined.
[f]Protein content is from Albertsson *et al.* (26).

It is well established that in spinach plants, a chilling-resistant species, thylakoids contain 10 molecular species of PG, three of them, 18:3/16:1(3t), 18:3/16:0 and 16:0/16:1(3t), being prominent (3,4). PG molecular species were determined only in two thylakoid domains, i.e., T3 and B3-420S, because of the lack of material in the other fractions. Concerning the eight main PG molecular species, there were no differences between the two fractions and the TM (Table 4).

DISCUSSION

The four TM domains (T3, B3, B3-420S, and 420S) used in this study were obtained after a series of sonication and repeated partition steps in an aqueous dextran–polyethylene glycol two-phase system. Compared to other techniques using detergents to solubilize the membrane, the two-phase system technique offers real advantages, namely, in avoiding unverifiable displacement and selective extraction of lipids, which generally occurs in the presence of detergents and therefore may generate biased conclusions.

According to the pioneering work of Murphy and Woodrow, (9) and Gounaris *et al.*, (7), who used a similar experimental approach to isolate B3 and T3, TM was found to display considerable lateral heterogeneities in the distribution of all major membrane components, including lipids. On the contrary, the present results show quite clearly that the relative distribution of the four lipid classes (MGDG, DGDG, SQDG, and PG), as well as the relative amount of fatty acids in each individual lipid and the main PG molecular species, was statistically identical in all four thylakoid fractions and in intact thylakoids. This finding is quite important for understanding the molecular organization of lipids in the TM and argues in favor of the existence of two types of lipid molecules, i.e., the bulk lipids and the specific lipid molecules. This hypothesis was first proposed in 1980 (35) and subsequently refined (36,37).

TABLE 2
Composition in Lipid Classes of Four Thylakoid Membrane Domains[a]

Thylakoid fractions	Lipid class[b] (mol%)			
	MGDG	DGDG	SQDG	PG
TM (n = 7)	50 ± 1	28 ± 2	9 ± 1	13 ± 2
T3 (n = 10)	51 ± 1	28 ± 3	9 ± 1	12 ± 2
B3 (n = 4)	47 ± 4	27 ± 2	12 ± 3	14 ± 3
B3-420S (n = 11)	49 ± 6	29 ± 3	10 ± 3	12 ± 2
420S (n = 4)	52 ± 1	28 ± 2	10 ± 2	10 ± 1

[a]MGDG, monogalactosyldiacylglycerol; DGDG, digalactosyldiacylglycerol; SQDG, sulfoquinovosyldiacylglycerol; PG, phosphatidylglycerol; for other abbreviations see Table 1.
[b]The mol% values are calculated from the data shown in Table 1. For each thylakoid fraction, the 100% values corresponded to the sum of the four acyl lipids.

TABLE 3
Fatty Acid Composition of the Four Lipid Classes in Various Thylakoid Membrane Domains

Acyl lipid Thylakoid fraction	Fatty acid[a] (mol%)						
	16:0	16:1(3t)	16:3	18:0	18:1	18:2	18:3
MGDG							
TM (n = 7)	Tr	Tr	17.6 ± 0.6	Tr	Tr	2.3 ± 0.4	80.1 ± 0.9
T3 (n = 10)	Tr	Tr	17.8 ± 0.6	Tr	Tr	2.4 ± 0.5	79.8 ± 0.9
B3 (n = 4)	Tr	Tr	16.7 ± 1.0	Tr	Tr	2.3 ± 0.1	81.0 ± 0.8
B3-420S (n = 11)	Tr	Tr	17.8 ± 0.5	Tr	Tr	2.5 ± 0.5	79.7 ± 1.3
420S (n = 4)	Tr	Tr	17.7 ± 1.4	Tr	Tr	2.9 ± 0.3	79.4 ± 3.8
DGDG							
TM (n = 8)	5.9 ± 0.6	Tr	2.8 ± 0.2	Tr	Tr	2.5 ± 0.3	88.8 ± 1.5
T3 (n = 10)	5.9 ± 0.7	Tr	2.9 ± 0.2	Tr	Tr	2.5 ± 0.4	88.7 ± 1.6
B3 (n = 4)	8.6 ± 3.4	Tr	2.6 ± 0.1	Tr	Tr	2.5 ± 0.3	86.3 ± 2.0
B3-420S (n = 11)	5.5 ± 1.2	Tr	2.8 ± 0.2	Tr	Tr	2.7 ± 0.4	89.0 ± 2.1
420S (n = 4)	5.5 ± 1.6	Tr	2.7 ± 0.1	Tr	Tr	3.0 ± 0.2	88.8 ± 1.9
SQDG							
TM (n = 8)	41.1 ± 1.6	Tr	1.7 ± 0.3	Tr	Tr	9.0 ± 0.8	48.2 ± 1.8
T3 (n = 10)	41.6 ± 0.2	Tr	1.5 ± 0.6	Tr	Tr	9.1 ± 1.0	47.8 ± 1.3
B3 (n = 4)	44.5 ± 1.9	Tr	1.3 ± 0.1	Tr	Tr	7.5 ± 2.0	46.6 ± 3.5
B3-420S (n = 11)	41.9 ± 0.9	Tr	1.6 ± 0.2	Tr	Tr	9.6 ± 1.1	46.9 ± 2.4
420S (n = 4)	41.4 ± 2.9	Tr	1.6 ± 0.3	Tr	Tr	10.5 ± 1.6	46.5 ± 6.6
PG							
TM (n = 8)	16.0 ± 0.5	38.0 ± 1.1	0	Tr	Tr	6.4 ± 0.7	39.6 ± 0.9
T3 (n = 11)	16.1 ± 0.6	37.7 ± 0.9	0	Tr	Tr	7.3 ± 1.0	38.9 ± 1.2
B3 (n = 4)	15.2 ± 2.2	37.4 ± 2.0	0	Tr	Tr	7.0 ± 1.3	40.4 ± 2.2
B3-420S (n = 11)	15.3 ± 0.4	40.0 ± 1.5	0	Tr	Tr	6.6 ± 0.6	38.1 ± 1.3
420S (n = 4)	14.1 ± 2.3	39.1 ± 1.2	0	Tr	Tr	7.1 ± 0.9	39.7 ± 1.3

[a]Tr, traces (less than 1 mol%). Results are expressed in mol% for each lipid class. For TM, 100% values corresponded in nmol/mg Chl to 825 ± 89 for MGDG, 450 ± 57 for DGDG, 140 ± 12 for SQDG, and 214 ± 45 for PG; for T3 fraction, to 924 ± 143, 501 ± 103, 158 ± 20, and 214 ± 43; for B3 fraction, to 745 ± 38, 428 ± 13, 190 ± 20, and 222 ± 64; for B3-420S, to 774 ± 101, 474 ± 77, 163 ± 62, and 190 ± 43; for 420S fraction, to 944 ± 53, 510 ± 47, 181 ± 26, and 171 ± 11. For other abbreviations see Tables 1 and 2.

The bulk lipids predominate in the TM and fill the spaces between the various proteins. They can be considered as having a structural role. For instance, they offer a hydrophobic matrix to the proteins and pigments and, owing to their high degree of unsaturation, confer an appropriate fluidity to the membrane. In addition, MGDG, which is the major lipid in the TM, can form, under certain conditions, nonbilayer configurations and therefore influence the structure and the photosynthetic function of the membrane (38). The analyses of lipids in the different domains of the membrane (Tables 2–4) concern the bulk lipids and reveal that the level of the four lipid classes (MGDG, DGDG, SQDG, and PG), the nature of their acyl chains, and the main molecular species of PG are identical in B3 and T3, as well as in B3-420S and 420S.

By contrast, the specific lipids are by nature less abundant than the bulk lipids, but especially much more saturated than the bulk lipids (15,18,19). These specific lipid molecules can be considered as functional or strategic lipids. They are involved in specific interactions with proteins, resulting in an appropriate maintenance of the conformation and/or orientation of protein molecules in the membrane and high photosynthetic performances. These lipids are encountered in the four lipid classes and display specific functions. For instance, MGDG sustains charge separation (18), DGDG induces three-dimensional crystallization of the LHCII (24), and SQDG is associated with the structure and function of the coupling factor complex (16). In addition, specific molecules of PG have been reported to be involved in oligomerization of LHCII (25), the stacking of thylakoids (23), and the support of the electron flow activity (39,40). The specific lipid molecules are, of course,

TABLE 4
Composition in PG Molecular Species of Four TM Domains[a]

Thylakoid fraction	Molecular species (mol%)							
	18:3/16:1(3t)	18:3/16:0	18:2/16:1(3t)	18:2/16:0	18:1/16:1(3t)	16:0/16:1(3t)	18:1/16:0	16:0/16:0
TM (n = 8)	61.8 ± 4.3	10.6 ± 1.8	5.2 ± 2.7	6.0 ± 1.6	2.8 ± 1.4	9.6 ± 1.1	1.2 ± 0.7	2.8 ± 1.9
T3 (n = 11)	63.2 ± 4.8	11.1 ± 1.3	4.5 ± 1.6	6.0 ± 1.7	2.4 ± 1.1	9.7 ± 2.1	1.6 ± 1.5	1.5 ± 1.4
B3-420S (n = 11)	64.2 ± 4.9	9.7 ± 1.1	5.3 ± 2.1	5.7 ± 1.7	2.8 ± 1.7	9.5 ± 1.3	1.4 ± 0.8	1.4 ± 1.5

[a]The 100% values correspond to 209 ± 35 nmol PG/mg Chl for TM, 208 ± 37 nmol PG/mg Chl for T3, and 185 ± 31 nmol PG/mg Chl for B3-420S; n = number of experiments. The 18:0/16:1(3t) and 18:0/16:0 PG molecular species were found only in trace amounts. For abbreviations see Tables 1 and 2.

concentrated at different locations in the membrane where they are associated with their interacting protein(s). But, owing to their scarcity, they do not change the global composition and the distribution of the four classes of lipids between the membrane domains considered in this study (Tables 1–4).

In conclusion, we propose that the current model of thylakoid membrane lipid composition is one that contains simultaneously bulk and specific lipids. Current experimental evidence (as described in this investigation) indicates that only the latter ones display lateral heterogeneity in the membrane.

ACKNOWLEDGMENTS

This research was supported in part by the Swiss National Science Foundation (grants number 31.336 93.92 and 31.432 97.95). The authors thank very much Per-Åke Albertsson and his collaborators for help and advice in preparing thylakoid vesicles. This work is part of a doctoral program that has been carried out by Sylvie Duchêne in the Laboratoire de Physiologie végétale, Université de Neuchâtel, Switzerland.

REFERENCES

1. Siegenthaler, P.A. (1998) Molecular Organization of Acyl Lipids in Photosynthetic Membranes of Higher Plants, in *Lipids in Photosynthesis: Structure, Function and Genetics* (Siegenthaler, P.A., and Murata, N., eds.), Vol. 6, pp. 119–144, Kluwer Academic Publishers, Dordrecht.
2. Dubacq, J.P., and Trémolières, A. (1983) Occurrence and Function of Phosphatidylglycerol Containing Δ^3-*trans*-Hexadecenoic Acid in Photosynthetic Lamellae, *Physiol. Vég. 21*, 293–312.
3. Nishihara, M., Yokota, K., and Kito, M. (1980) Lipid Molecular Species Composition of Thylakoid Membranes, *Biochim. Biophys. Acta 617,* 12–19.
4. Xu, Y.N., and Siegenthaler, P.-A. (1996) Phosphatidylglycerol Molecular Species of Photosynthetic Membranes Analyzed by High-Performance Liquid Chromatography: Theoretical Considerations, *Lipids 31*, 223–229.
5. Costes, C., Bazier, R., and Lechevallier, D. (1972) Rôle Structural des lipides dans les membranes des chloroplastes de Blé, *Physiol. Vég. 10*, 291–317.
6. Ouijja, A., Farineau, N., Cautrel, C., and Guillot-Salomon, T. (1988) Biochemical Analysis and Photosynthetic Activity of Chloroplasts and Photosystem II Particles from a Barley Mutant Lacking Chlorophyll *b*, *Biochim. Biophys. Acta 932*, 97–106.
7. Gounaris, K., Sundby, C., Andersson, B., and Barber, J. (1983) Lateral Heterogeneity of Polar Lipids in the Thylakoid Membranes of Spinach Chloroplasts, *FEBS Lett. 156*, 170–174.
8. Henry, L.E.A., Mikkelsen, J.D., and Møller, B.L. (1983) Pigment and Acyl Lipid Composition of Photosystem I and II Vesicles and of Photosynthetic Mutants in Barley, *Carlsberg Res. Commun. 48*, 131–148.
9. Murphy, D.J., and Woodrow, I.E. (1983) Lateral Heterogeneity in the Distribution of Thylakoid Membrane Lipid and Protein Components and Its Implications for the Molecular Organization of Photosynthetic Membranes, *Biochim. Biophys. Acta 725*, 104–112.
10. Bednarz, J., Radunz, A., and Schmid, G.H. (1988) Lipid Composition of Photosystem I and II in the Tobacco Mutant *Nicotiana tabacum* NC 95, *Z. Naturforsch. 43c*, 423–430.
11. Heinz, E., and Siefermann-Harms, D. (1981) Are Galactolipids Integral Components of the Chlorophyll–Protein Complexes in Spinach Thylakoids? *FEBS Lett. 124*, 105–111.
12. Trémolières, A., Dubacq, J.P., Ambard-Bretteville, F., and Rémy, R. (1981) Lipid Composition of Chlorophyll–Protein Complexes, *FEBS Lett. 130*, 27–31.
13. Rémy, R., Trémolières, A., Duval, J.C., Ambard-Bretteville, F., and Dubacq, J.P. (1982) Study of the Supramolecular Organisation of Light Harvesting Chlorophyll Protein (LHCP), *FEBS Lett. 137*, 271–275.
14. Doyle, M.F., and Yu, C.A. (1985) Preparation and Reconstitution of a Phospholipid Deficient Cytochrome b_6-f Complex from Spinach Chloroplasts, *Biochem. Biophys. Res. Commun. 131*, 700–706.
15. Gounaris, K., and Barber, J. (1985) Isolation and Characterisation of a Photosystem II Reaction Center Lipoprotein Complex, *FEBS Lett. 188*, 68–72.
16. Pick, U., Gounaris, K., Weiss, M., and Barber, J. (1985) Tightly Bound Sulpholipids in Chloroplast CF_0–CF_1, *Biochim. Biophys. Acta 808*, 415–420.
17. Sigrist, M., Zwillenberg, C., Giroud, C., Eichenberger, W., and Boschetti, A. (1988) Sulfolipid Associated with the Light-Harvesting Complex Associated with Photosystem II Apoproteins of *Chlamydomonas reinhardtii, Plant Sci. 58*, 15–23.
18. Murata, N., Higashi, S.-I., and Fujimura, K. (1990) Glycerolipids in Various Preparations of Photosystem II from Spinach Chloroplasts, *Biochim. Biophys. Acta 1019*, 261–268.
19. Trémolières, A., Dainese, P., and Bassi, R. (1994) Heterogeneous Lipid Distribution Among Chlorophyll-Binding Proteins of Photosystem II in Maize Mesophyll Chloroplasts, *Eur. J. Biochem. 221*, 721–730.
20. Radunz, A. (1981) Application of Antibodies in the Analysis of Structural Configuration of Thylakoid Membranes, *Ber. Dtsch. Bot. Ges. 94*, 477–489.
21. Voss, R., Radunz, A., and Schmid, G.H. (1992) Binding of Lipids onto Polypeptides of the Thylakoid Membrane. I. Galactolipids and Sulpholipid as Prosthetic Groups of Core Peptides of the Photosystem II Complex, *Z. Naturforsch. 47c*, 406–415.
22. Kruse, O., and Schmid, G.H. (1995) The Role of Phosphatidylglycerol as a Functional Effector and Membrane Anchor of the D_1-Core Peptide from Photosystem II Particles of the Cyanobacterium *Oscillatoria chalybea, Z. Naturforsch. 50c*, 380–390.
23. Trémolières, A., and Siegenthaler, P.A. (1998) Reconstitution of Photosynthetic Structures and Activities with Lipids, in *Lipids in Photosynthesis: Structure, Function and Genetics* (Siegenthaler, P.A., and Murata, N., eds.), Vol. 6, pp. 175–189, Kluwer Academic Publishers, Dordrecht.
24. Nussberger, S., Dörr, K., Wang, D.N., and Kühlbrandt, W. (1993) Lipid-Protein Interactions in Crystals of Plant Light-Harvesting Complex, *J. Mol. Biol. 234*, 347–356.
25. Krupa, Z., Williams, J.P., Khan, M.U., and Huner, N.P.A. (1992) The Role of Acyl Lipids in Reconstitution of Lipid-Depleted Light-Harvesting Complex II from Cold-Hardened and Non-hardened Rye, *Plant Physiol. 100*, 931–938.
26. Albertsson, P.A., Andreasson, E., Stefansson, H., and Wollenberger, L. (1994) Fractionation of Thylakoid Membrane, in *Aqueous Two-Phase Systems* (Walter, H., and Johansson, G., eds.) *Methods in Enzymology,* Vol. 228, pp. 469–482, Academic Press, New York.
27. Andreasson, E., Svensson, P., Weibull, C., and Albertsson, P.A. (1988) Separation and Characterization of Stroma and Grana Membranes—Evidence for Heterogeneity in Antenna Size of Both Photosystem I and Photosystem II, *Biochim. Biophys. Acta 936*, 339–350.
28. Wollenberger, L., Stefansson, H., Yu, S.-H., and Albertsson, P.-A. (1994) Isolation and Characterization of Vesicles Originating from the Chloroplast Grana Margins, *Biochim. Biophys. Acta 1184*, 93–102.
29. Xu, Y.N., and Siegenthaler, P.-A. (1997) Low Temperature Treatments Induce an Increase in the Relative Content of Both

Linolenic and Δ^3-*trans*-Hexadecenoic Acids in Thylakoid Membrane Phosphatidylglycerol of Squash Cotyledons, *Plant Cell Physiol. 38*, 611–618.
30. Kito, M., Takamura, H., Narita, H., and Urade, R. (1985) A Sensitive Method for Quantitative Analysis of Phospholipid Molecular Species by High-Performance Liquid Chromatography, *J. Biochem. 98*, 327–331.
31. Bruinsma, J. (1961) A Comment on the Spectrophotometric Determination of Chlorophyll, *Biochim. Biophys. Acta 52*, 576–578.
32. Lichtenthaler, H.K. (1987) Chlorophylls and Carotenoids: Pigments in Photosynthetic Biomembranes, in *Plant Cell Membranes* (Packer, L., and Douce, R., eds.), *Methods in Enzymology,* Vol. 148, pp. 350–382, Academic Press, New York.
33. Siegenthaler, P.A., Sutter, J., and Rawyler, A. (1988) The Transmembrane Distribution of Galactolipids in Spinach Thylakoid Inside-out Vesicles Is Opposite to That Found in Intact Thylakoids, *FEBS Lett. 228*, 94–98.
34. Albertsson, P.A. (1995) The Structure and Function of the Chloroplast Photosynthetic Membrane—A Model for the Domain Organization, *Photosynth. Res. 46*, 141–149.
35. Rawyler, A., and Siegenthaler, P.A. (1980) Role of Lipids in Function of Photosynthetic Membranes Revealed by Treatment with a Lipolytic Acyl Hydrolase, *Eur. J. Biochem. 110*, 179–187.
36. Siegenthaler, P.A., and Rawyler, A. (1986) Acyl Lipids in Thylakoid Membranes: Distribution and Involvement in Photosynthetic Functions, in *Encyclopedia of Plant Physiology* (Staehelin, L.A., and Arntzen, C., eds.), Vol. 19, New Series, pp. 693–705, Springer-Verlag, Berlin.
37. Siegenthaler, P.A., and Trémolières, A. (1998) Role of Acyl Lipids in the Function of Higher Plants' Photosynthetic Membranes, in *Lipids in Photosynthesis: Structure, Function and Genetics* (Siegenthaler, P.A., and Murata, N., eds.), Vol. 6, pp. 145–173, Kluwer Academic Publishers, Dordrecht.
38. Murphy, D.J. (1986) The Molecular Organisation of the Photosynthetic Membranes of Higher Plants, *Biochim. Biophys. Acta 864*, 33–94.
39. Siegenthaler, P.A., Rawyler, A., and Smutny, J. (1989) The Phospholipid Population Which Sustains the Uncoupled Non-Cyclic Electron Flow Activity is Localized in the Inner Monolayer of the Thylakoid Membrane, *Biochim. Biophys. Acta 975*, 104–111.
40. Duchêne, S., Smutny, J., and Siegenthaler, P.A. (2000) The Topology of Phosphatidylglycerol Populations Is Essential for Sustaining Photosynthetic Electron Flow Activities in Thylakoid Membranes, *Biochim. Biophys. Acta 1463*, 115–120.

[Received December 30, 1999, and in final revised form and accepted May 12, 2000]

Dietary n-3 Long-Chain Polyunsaturated Fatty Acid Deprivation, Tissue Lipid Composition, *ex vivo* Prostaglandin Production, and Stress Tolerance in Juvenile Dover Sole (*Solea solea* L.)

J.A. Logue[a], B.R. Howell[b], J.G. Bell[c], and A.R. Cossins[a,*]

[a]School of Biological Sciences, University of Liverpool, Liverpool L69 3BX, [b]CEFAS, Conwy Laboratory, Conwy, North Wales, LL32 8UB, and [c]Institute of Aquaculture, University of Stirling, Stirling FK9 4LA, Scotland, United Kingdom

ABSTRACT: Larval Dover sole fed an *Artemia* diet supplemented with n-3 long-chain (C_{20} + C_{22}) polyunsaturated fatty acids (PUFA) are known to be more resistant to low-temperature injury. Here we explore the relationship between tissue fatty acid composition and tolerance of stressful environmental conditions over the larval and early juvenile periods. *Artemia* nauplii supplemented with n-3 long-chain PUFA-deficient and PUFA-enriched oil emulsions were fed to two groups of larvae. Whole body tissue samples from the resulting PUFA-deficient and -enriched juveniles possessed 12.1 and 21.9% n-3 long-chain PUFA, respectively. These differences were at the expense of C_{18} PUFA, while proportions of saturated fatty acids, monounsaturated fatty acids, and total PUFA were unaffected. Brain and eye tissues from the PUFA-deficient fish contained lower levels of 22:6n-3, known to be important for optimal nervous system function, incorporating instead a range of fatty acids of lower unsaturation. PUFA-deprived juveniles showed substantially greater mortality when exposed to a combination of low temperature and low salinity, as well as to high temperature and to hypoxia. After adaptation to the different diets, both dietary groups were fed a common formulated feed high in n-3 long-chain PUFA. Tissue PUFA in both groups progressively increased to the same high value, with a consequent loss of the differences in cold-susceptibility. These correlated changes support a link between dietary manipulation of n-3 long-chain PUFA and development of a stress-sensitive phenotype. PUFA deprivation had no detectable effect upon static hydrocarbon order of purified brain membranes (as assessed by fluorescence polarization) but was associated with an increase in the whole-body content of prostaglandins. We conclude that susceptibility to environmental stress is responsive to dietary n-3 long-chain PUFA manipulation, possibly due to altered tissue development or the overproduction of eicosanoids.

Paper no. L8404 in *Lipids 35,* 745–755 (July 2000).

*To whom correspondence should be addressed at Integrative Biology Research Division, School of Biological Sciences, Derby Building, University of Liverpool, P.O. Box 147, Liverpool, L69 3BX, United Kingdom.
E-mail: cossins@liverpool.ac.uk

Abbreviations: AA, arachidonic acid (20:4n-6); ANOVA, analysis of variance; DHA, docosahexaenoic acid; DPH, 1,6-diphenyl-1,3,5-hexatriene (22:6n-3); EPA, eicosapentaenoic acid (20:5n-3); GLC, gas–liquid chromatography; ICES, International Council for Exploration of the Seas; MUFA, monounsaturated fatty acids; PC, phosphatidylcholine; PE, phosphatidylethanolamine; PGE, prostaglandin E; PUFA, polyunsaturated fatty acid; SFA, saturated fatty acid; TLC, thin-layer chromatography.

Resistance of fish to biotic and abiotic environmental stress is heavily dependent upon health and physical condition, and circumstances leading to a loss of condition may significantly affect survival. The control of whole organism environmental tolerance has practical significance in aquaculture of marine fish larvae where the emphasis has focused on maximizing larval numbers at the expense of larval condition. Consequently, it is common for artificially reared marine fish to display reduced resistance to environmental stress when compared with wild-caught individuals. It seems clear, for some commercially important species at least, that larval production techniques have not yet been properly optimized, nor have the factors that contribute to reduced larval quality been identified.

There is evidence that whole-animal resistance to thermal stress is linked to the biophysical structure and lipid composition of cellular membranes (1). The primary lesion of thermal damage has been identified as a disruption of the physical structure of cellular membranes. Secondary effects such as loss of barrier properties and subsequent increased permeability may be followed by tertiary effects caused by impairment of important homeostatic processes, notably respiration and neuromuscular coordination, leading ultimately to death (1). The brain is certainly critical in defining thermal limits in adult fish since direct manipulations of brain temperature can ameliorate or enhance the early symptoms of thermal damage without effects on other body functions (2). The principal evidence in support of the lipid theory of acquired thermotolerance comes from the correlated changes in thermotolerance during thermal acclimation of fish with changes in the lipid saturation and biophysical structure ("fluidity") of brain membranes (3,4).

Neuronal tissue is somewhat unusual in that its lipid requirements for successful development, differentiation, and function are quite specific. The cell membranes of these tissues are enriched in n-3 long-chain (C_{20} + C_{22}) polyunsaturated fatty acids (PUFA), particularly docosahexaenoic acid (DHA, 22:6n-3). In fish retina DHA can exceed 50% of the total fatty acids in membrane phospholipids (5). Studies on rats have shown this pool of specific membrane PUFA may be highly conserved during starvation or dietary manipulation (6), but restriction of these lipids during early life stages

may have serious consequences for nervous system development. A good example is the effect of DHA deficiency upon visual performance at low light intensities in juvenile herring (7). Deficiency during development resulted in decreased levels of 22:6n-3 in retinal phospholipid molecular species, which correlated with a reduced feeding ability at low light intensities. This depression in feeding efficiency of the juvenile would have effects upon growth rate and subsequent survival. In humans, functional impairment caused by a dietary insufficiency in early life stages may not be rectified by subsequent sufficiency (8), suggesting some interference with the ontogenetic progression of neuronal cells and tissue into an otherwise functional system.

Dietary lipid deficiency may also have additional adverse effects, including the overproduction of certain PUFA-derived eicosanoids. Eicosanoids are cellular mediators involved in a whole range of transient signaling events and are formed from both n-3 and n-6 long-chain PUFA (9,10). Enhanced levels of the bioactive 2-series eicosanoids (e.g., prostaglandin E_2, PGE_2) derived from arachidonic acid (AA, 20:4n-6) are implicated in a host of pathological conditions, including thrombosis, tumor growth, atherosclerosis, and immune inflammatory disorders (11,12). However, high levels of dietary eicosapentaenoic acid (EPA, 20:5n-3) and DHA are thought to ameliorate these effects by reducing the synthesis of AA-derived eicosanoids (13).

Successful rearing of marine fish larvae requires specific fatty acid supplementation of the diet (14). In contrast to terrestrial food webs, the marine food chain is rich in n-3 long-chain PUFA, particularly 20:5n-3 and 22:6n-3, produced by the basal unicellular phytoplanktonic algae (15). As a result marine fish have no endogenous capacity for essential long-chain PUFA production and are entirely dependent upon dietary provision. Recent work has demonstrated that the survival of juvenile Dover sole, *Solea solea,* to low temperatures (5°C) is improved by supplementation of their *Artemia* diet with n-3 long-chain PUFA-enriched emulsions. Thus, the larval and juvenile diet appears to define the thermotolerance of subsequent stages (16). This offers a very clear-cut model with which to explore the influences of larval nutrition upon environmental stress resistance (i.e., quality) of both larval and subsequent life history stages. We have thus fed larval and juvenile Dover sole *Artemia* diets enriched with high or low n-3 long-chain PUFA contents and assessed their tolerance to high and low lethal temperatures and to hypoxia.

MATERIALS AND METHODS

Larval rearing procedures. All fish-handling and experimental procedures were performed in accordance with and under the control of the Home Office 1986 Animal Procedures Act (U.K.), and reviewed by the Natural Environmental Research Council (U.K.). Sole larvae were hatched from the same batch of naturally spawned eggs from a captive broodstock maintained under the conditions described by Baynes *et al*. (17). The eggs were incubated at 12 ± 1°C. Two to three days after hatching the yolk-sac larvae were transferred to 60-cm diameter mat-black rearing tanks containing 60 L of seawater. Each tank was gently aerated through a single diffuser block and received a continuous supply of fresh seawater. Illumination was provided by fluorescent lights set to follow the ambient photoperiod. Similarly, temperature changes followed approximately the natural cycle and increased from 14 to 18°C during the rearing period.

Following eye pigmentation and opening of the mouth, larvae were fed newly-hatched *Artemia* nauplii for 5 d before the introduction of the variously enriched *Artemia*. Food was added twice daily in sufficient quantity to provide excess at all times. The *Artemia* cysts were hatched at 28°C for 24 h in 80 L cylindroconical tanks. The nauplii were enriched for 24 h in identical tanks stocked with 150 nauplii per mL. The lipid emulsion was added during the morning and evening at a rate of 150 mg emulsion/L/100,000 nauplii. *Artemia* harvested during the morning were stored at 4–5°C until used.

Larval and juvenile feeding regimes. Two 60-L rearing tanks were each stocked with about 3,000 yolk-sac larvae hatched from the same batch of eggs. After an initial 4–5 d period of feeding on newly hatched *Artemia* nauplii of San Francisco origin, larvae were subsequently fed Great Salt Lake *Artemia* which had been previously enriched for 24 h with different lipid emulsions. One diet was supplemented with a lipid emulsion containing high proportions of n-3 long-chain PUFA (high-PUFA) [30/4/C/5 (order code); International Council for Exploration of the Seas (ICES) standard emulsions, Laboratory of Aquaculture and *Artemia* Research Centre, Ghent, Belgium] and the other enriched with a low-PUFA (θ/-/C/3; ICES) emulsion of equal lipid content. Batches of sole were also reared on *Artemia* enriched with the low-PUFA emulsion to which had been added high proportions of EPA (EPA/25/C; ICES). These standard reference emulsions facilitate comparisons in marine aquaculture research, and the quantities used were based upon what is known of the dietary lipid requirements for marine fish.

Fifty-five days after hatching, when approximately 3 cm in length, all fish were transferred to weaning tanks of a similar design and weaned onto a common formulated feed (agglomerated weaning diet, 98042 size 0.8–1.4 mm; SSF, Bergen, Norway) which also contained high proportions of n-3 long-chain PUFA (18).

Stress tests. Juveniles were subjected to short-term stress tests at intervals pre- and postweaning. Each challenge involved abrupt transfer from the rearing tanks to experimental tanks with sea water of (i) low temperature and low salinity (3°C, 10‰), (ii) high temperature (32°C), and (iii) hypoxia (10% oxygen saturation). Tests were carried out using mesh-bottomed trays, divided into compartments (0.6 L), held in the experimental tank. Conditions in each of the tray compartments mirrored those of the whole tank. For each experiment, groups of fish from each dietary treatment were simultaneously transferred to the experimental tanks. At intervals of 2–3 h, groups of 20 fish were successively removed to a recovery tank of ambient temperature and salinity (16–17°C,

30 ± 2‰), where they were allowed to recover for 24 h before survival was assessed. For hypoxia experiments, the oxygen content of the experimental tank was reduced by bubbling with oxygen-free N_2 gas. Fine control of P_{O_2} was achieved with an oxygen meter in the tank and a flow meter on the N_2 gas supply. P_{O_2} was uniform throughout the experimental tank.

Lipid extraction and fatty acid analysis. Fatty acid compositional analysis was performed for lipid emulsions, enriched *Artemia* diets, and whole carcass of the larval and juvenile Dover sole throughout the rearing period. Sole were stunned by a blow to the head and killed by bisection of the spinal cord. Carcasses were chopped, blended, and homogenized in 1–5 mL of water, and total lipid was extracted following the method of Bligh and Dyer (19). Lipids were separated by silica gel thin-layer chromatography (TLC) using a neutral solvent of hexane/diethyl ether/acetic acid (80:20:2, by vol). The polar lipids at the origin (primarily phospholipids) were eluted by washing with 2:1 chloroform/methanol (vol/vol) containing 0.005% butylated hydrooxytoluene, dried under flowing N_2 gas, and methylated by heating at 100°C with 14% boron trifluoride–methanol complex (20). The fatty acid methyl esters were analyzed by gas–liquid chromatography (GLC; 610 Series F.I.D. gas chromatograph; ATI Unicam, Cambridge, United Kingdom) on a free fatty acid phase fused-silica capillary column, 30 m × 0.25 mm (J&W Scientific, PhaseSep, Clwyd, United Kingdom). The methyl esters were identified by comparing peak retention times with those of known standards whose identity had been confirmed by mass spectrometry (courtesy of Dr. D. Tocher, University of Stirling). The fatty acid composition of whole eye and brain phospholipids was also assessed. Phospholipids were separated by two-dimensional TLC (21) using solvent systems of chloroform/methanol/7 M ammonia (103:40:7, by vol) and chloroform/methanol/acetone/acetic acid/water (47:16:63:16:8, by vol) in the first and second directions, respectively. Phospholipids were revealed by spraying with Rhodamine 6G, and phosphatidylcholine (PC) and phosphatidylethanolamine (PE) fractions were collected and processed for GLC analysis.

Assessment of brain membrane order. Whole brain membrane samples were prepared by modification of established procedures (22,23). All procedures were carried out at 0–4°C. Three replicate groups of 20 sole (length 40–50 mm) from each dietary treatment were stunned by a blow to the head and their spinal cords severed. Brains were rapidly removed, placed in 15 mL of ice-cold isolation medium (280 mM sucrose, 2 mM EDTA, 20 mM imidazole, pH 7.4), cut, blended, and homogenized before centrifugation at 1000 × *g* for 10 min. The supernatant was centrifuged at 12,000 × *g* for 30 min, and the upper white portion of the pellet was gently resuspended and homogenized in 15 mL of lysing medium (1 mM EDTA, 10 mM imidazole pH 7.4) before centrifugation at 20,000 × *g* for 30 min. The resulting crude synaptosomal pellet was then resuspended by gentle homogenization in 2.5 mL 10 mM imidazole pH 7.4.

Membrane biophysical order was determined by steady-state fluorescence polarization on a PC1 spectrofluorometer (ISS Inc., Urbana, IL) using anisotropy measurements of the probe 1,6-diphenyl-1,3,5-hexatriene (DPH) (24). A small aliquot of the brain membrane preparation was added to 2.5 mL of 0.1 M potassium phosphate buffer (pH 7.1) in a 10-mm pathlength quartz cuvette to give an optical density of 0.10 at 500 nm. Two microliters of 2 mM DPH dissolved in tetrahydrofuran was added while mixing with a pipette. The probe was left to equilibrate with the membranes for 10 min at room temperature prior to the polarization assays. The temperature of the cuvette block was controlled to ±0.1°C by circulating water from a computer-controlled thermostated bath. Polarization scans were performed from 5 to 40°C at a rate of increase of 1°C/min. The measurement temperature within the cuvette was recorded to ±0.1°C by computer *via* a digital thermistor probe.

Extraction and enzyme immunoassay of prostaglandins. Gill tissue from six fish and whole carcass samples were taken for prostaglandin analysis after the feeding of the different *Artemia* diets. Gill tissue is a major source of prostaglandins, thought here to be involved in cellular osmoregulatory function (13). Samples were weighed and then homogenized in 3 mL Hanks balanced salt solution (without calcium) containing 0.45 mL absolute ethanol and 0.15 mL 2M formic acid. Homogenates were then frozen in liquid nitrogen and stored at −20°C. Eicosanoid extraction and measurement of total PGE content were as given in Bell *et al*. (13). Total PGE was determined using a commercial enzyme immunoassay kit for PGE_2 (SPI-Bio, Massy, France).

Statistical analysis. Fatty acid composition, fish length, and prostaglandin data were analyzed using one-way analysis of variance (ANOVA). For stress test data, the numbers surviving at each time period were modeled as a binomially distributed random variable within a generalized linear model (25) of time and dietary effects. This model was fitted with a probit link with time expressed on a log scale to base 2, with zero time given the value zero on the log scale. Hence:

$$\text{number of survivors at time } t = \text{number of fish} \times \Phi(a + b \log_2 t) \quad [1]$$

where Ø is the normal distribution function and the intercept *a* depends on the dietary treatment. Model terms were tested assuming a chi-square distribution for the decrease in the deviance following the introduction of a model term.

RESULTS

Dietary lipids and effects upon tissue fatty acid composition. Total lipid fatty acid compositions of the low-PUFA and high-PUFA emulsions are shown in Table 1. The high-PUFA emulsion possessed appreciable proportions of EPA and DHA, whereas the low-PUFA emulsion contained no n-3 long-chain PUFA. The effects of these emulsions on *Artemia* lipid composition are shown in Table 2. *Artemia* fed the PUFA-deficient diet contained small proportions of 20:5n-3 but negligible amounts of other long-chain PUFA. In contrast, the n-3 PUFA-enriched *Artemia* contained considerable amounts of

TABLE 1
Total Lipid Fatty Acid Composition of the Low-PUFA and High-PUFA Emulsions Fed to *Artemia*[a]

Fatty acid	Low PUFA	High PUFA
14:0	48.1 (1.3)	12.6 (0.6)
16:0	22.1 (0.0)	12.3 (0.5)
16:1n-7		3.6 (0.1)
18:0	5.9 (0.5)	3.1 (0.5)
18:1n-9	14.7 (1.0)	14.6 (1.8)
18:1n-7		2.4 (0.4)
18:2n-6	8.8 (2.1)	6.6 (1.8)
20:5n-3		10.2 (0.6)
22:1n-11		2.8 (0.7)
22:5n-3		5.2 (0.6)
22:6n-3		24.7 (3.1)
Saturated	24.2 (1.4)	72.0 (1.5)
MUFA	14.7 (1.0)	24.1 (2.2)
PUFA	9.5 (2.4)	47.9 (3.7)
n-3 LC PUFA[b]	—	40.1 (4.1)
n-3/n-6	0.1 (0.0)	6.6 (2.2)

[a]Values are means for three different samples and are given as weight % (±SD) of total composition. Only fatty acids present at >2% are shown.
[b]n-3 long-chain (LC) polyunsaturated fatty acids (PUFA) refers to total n-3 C_{20} + C_{22} PUFA; MUFA, monounsaturated fatty acid.

both 20:5n-3 and 22:6n-3. The elevated proportions of 20:5n-3 and more especially 22:6n-3 in the common formulated diet fed to both treatment groups after weaning are also shown in Table 2.

TABLE 2
Total Lipid Fatty Acid Composition of *Artemia* Diets Enriched by the Lipid Emulsions and Common Formulated Feed Weaning Diet[a]

	Enriched *Artemia* preweaning diets			Common
Fatty acid	Low PUFA	High PUFA	Low + EPA[b]	weaning diet[c]
14:0	7.2 (0.0)	2.0 (0.1)	3.9 (0.4)	6.0 (0.7)
16:0	15.4 (0.1)	13.3 (0.7)	10.5 (0.9)	20.9 (1.6)
16:1n-7	3.9 (0.1)	4.6 (0.3)	3.2 (0.2)	3.7 (0.4)
18:0	6.6 (0.3)	5.7 (0.4)	2.8 (0.6)	2.6 (0.2)
18:1n-9	22.2 (0.2)	22.7 (1.2)	16.3 (0.9)	11.4 (0.8)
18:1n-7	8.5 (0.1)	9.4 (0.5)	4.4 (0.2)	2.6 (0.2)
18:2n-6	7.7 (0.1)	6.8 (0.4)	6.8 (0.4)	11.7 (1.4)
18:3n-3	20.3 (0.1)	20.0 (0.7)	18.3 (0.1)	2.1 (0.0)
18:4n-3	2.3 (0.1)	2.0 (0.4)		
20:1n-9				4.6 (1.2)
20:5n-3	3.8 (0.0)	9.1 (0.4)	31.0 (1.7)	8.1 (0.3)
22:1n-11				6.0 (2.0)
22:6n-3		5.6 (0.1)		16.7 (1.9)
Saturated	29.1 (0.3)	20.9 (1.1)	17.1 (1.9)	29.6 (1.4)
MUFA	34.6 (0.3)	36.7 (1.9)	24.4 (0.9)	28.3 (4.2)
PUFA	36.9 (0.2)	47.8 (1.7)	58.3 (2.7)	42.1 (3.2)
n-3 LC PUFA	6.6 (0.1)	18.9 (0.8)	31.3 (2.0)	26.3 (0.9)
n-3/n-6	2.9 (0.1)	4.5 (0.3)	7.2 (0.5)	2.4 (0.2)

[a]Values are means for three different samples and are given as weight % (±SD) of total composition. Only fatty acids present at >2% are shown.
[b]Low + EPA refers to *Artemia* enriched with the low-PUFA emulsion to which had been added high proportions of eicosapentaenoic acid (EPA, 20:5n-3).
[c]Formulated feed weaning diet was fed to all fish 55 d after hatching. For abbreviations, see Table 1.

Whole carcass phospholipid fatty acid compositions of each treatment group were determined over the full larval stage (days 9–55 after hatching) and up to 70 d after weaning. Dietary lipid composition had a major influence on membrane phospholipid content; during the *Artemia* feeding stage, fish fed the PUFA-enriched diet possessed 21.9% n-3 long-chain PUFA compared to 12.1% for the deficient sole, with correspondingly greater proportions of the C_{18} PUFA 18:2n-6 and 18:3n-3 in the latter (Table 3). By contrast, the proportions of saturated fatty acids (SFA), monounsaturated fatty acids (MUFA), and total PUFA were very similar. Also shown for comparison are data for wild-caught sole of similar size. These fish contained 5% greater proportion of SFA and much smaller proportions of MUFA. Of particular significance is the greater proportion of n-3 long-chain PUFA, even compared to those reared in the laboratory with high-PUFA food; thus 22:6n-3 constituted over 30% of all fatty acids in the wild specimens, compared to only 10% for the PUFA-enriched reared fish. Wild fish also possessed negligible levels of C_{18} PUFA.

Figure 1 shows how the proportions of the different fatty acid classes for whole carcass polar lipids of the sole varied over the full rearing period. All fish were adapted to the same n-3 long-chain PUFA-rich agglomerated diet (Table 2) 55 d after hatching. For reference, metamorphosis occurred approximately 20 d posthatching. There was little difference between the two treatment groups during the entire rearing period, although the low-PUFA group possessed elevated proportions of PUFA and reduced proportions of MUFA during the early postweaning phase.

TABLE 3
Effects of Enriched *Artemia* Diets on Whole Body Polar Lipid Composition of Preweaned Dover Sole[a]

	Dietary groups of lab-reared Dover sole			
Fatty acid	Low PUFA	High PUFA	Low + EPA[b]	Wild sole[c]
14:0	2.1 (0.2)		2.2 (0.2)	
16:0	17.0 (1.1)	17.7 (1.2)	19.0 (0.8)	19.8 (0.5)
16:1	2.6 (0.1)	3.8 (0.9)	2.6 (0.2)	3.8 (0.2)
18:0	9.3 (0.6)	9.5 (0.8)	10.6 (0.9)	13.4 (0.3)
18:1n-9	18.5 (1.2)	17.3 (1.5)	18.4 (1.4)	9.6 (0.4)
18:1n-7	7.8 (0.4)	9.5 (0.9)	8.7 (0.5)	3.3 (0.4)
18:2n-6	10.9 (0.7) ↑	5.4 (0.3)	5.4 (0.2)	
18:3n-3	13.4 (1.7) ↑	8.4 (1.3)	6.4 (1.5)	
20:4n-6	2.6 (0.4)	2.5 (0.3)		2.4 (0.0)
20:5n-3	5.9 (0.8) ↓	8.1 (1.5)	12.0 (2.5)	8.1 (0.6)
22:5n-3	2.2 (0.6) ↓	3.8 (0.5)	5.1 (0.8)	4.0 (0.4)
22:6n-3	3.3 (0.8) ↓	10.0 (1.4)	6.1 (2.1)	30.5 (1.8)
Saturated	28.4 (1.7)	28.7 (2.0)	31.8 (1.4)	34.8 (0.8)
MUFA	29.8 (1.8)	31.6 (1.8)	30.8 (1.9)	17.6 (0.8)
PUFA	41.8 (2.6)	39.7 (3.5)	37.4 (3.0)	47.6 (1.6)
n-3 LC PUFA	12.1 (1.9)	21.9 (2.8)	23.1 (2.9)	42.6 (1.0)
n-3/n-6	1.7 (0.2)	3.4 (0.6)	3.8 (0.4)	9.7 (1.5)

[a]Values are means for three different samples and are given as weight % (±SD) of total composition. Only fatty acids present at >2% are shown.
[b]Low + EPA refers to *Artemia* enriched with the low-PUFA emulsion to which had been added high proportions of EPA. For abbreviations, see Tables 1 and 2.
[c]The composition of wild-caught sole of comparable size is also given.

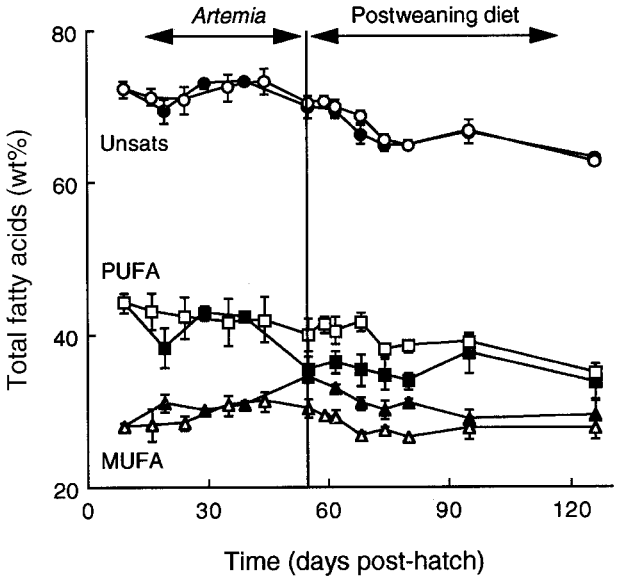

FIG. 1. Proportions of monounsaturated (MUFA; △, ▲), polyunsaturated (PUFA; □, ■), and total unsaturated (unsats) fatty acids (○, ●) in Dover sole whole carcass polar lipids during the *Artemia* and postweaning feeding periods. Fish were fed either low-PUFA (△, □, ○)- or high-PUFA (▲, ■, ●)-enriched *Artemia* diets. Data points represent means from three replicate samples and are given as weight % (±SD) of total fatty acid composition.

Figure 2 shows the proportion of n-3 long-chain PUFA during the rearing period. During the *Artemia* feeding stage, the high-PUFA juveniles possessed high proportions (20–25%) of these fatty acids, whereas the low-PUFA sole contained much lower proportions (11–14%). Upon weaning at day 55, when all fish were fed the same PUFA-rich diet, PUFA levels in the previously deficient sole progressively increased over 30 d, leading to a convergence in the n-3 long-chain PUFA contents.

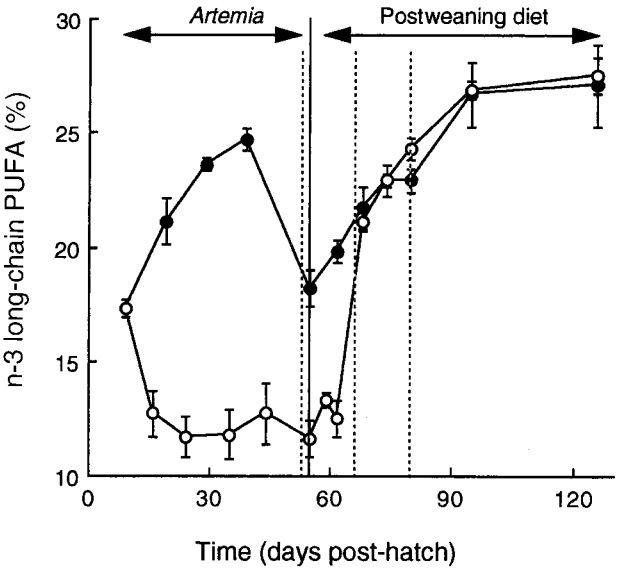

FIG. 2. n-3 Long-chain PUFA content of sole whole carcass polar lipids during the *Artemia* and postweaning feeding periods. Fish were fed either low-PUFA (○)- or high-PUFA (●)-enriched *Artemia* diets. Data points represent means from three replicate samples and are given as weight % (±SD) of total fatty acid composition. Solid line represents transfer from the different *Artemia* diets to the common weaning diet (day 55). Dashed lines indicate time points for the low-temperature and low-salinity stress tests shown in Figure 3. For abbreviation, see Figure 1.

Temperature and hypoxic stress tests. Results for combined low-temperature and low-salinity stress tests, performed at preweaning and 2 and 4 wk postweaning (indicated by vertical dashed lines in Fig. 2), are shown in Figure 3. Statistical analysis of the data (Table 4) showed that before weaning (Fig. 3A), the high-PUFA sole were significantly more resistant than the low-PUFA group. Here, 50% mortality was evident after 4.3 h in the low-PUFA group and 10.6 h in the high-PUFA group. After 2 wk of being fed the same postweaning diet (Fig. 3B), tolerance in the low-PUFA fish increased with a 50% mortality of 7.0 h compared to 9.8 h in the high-PUFA group, yet the difference was still significant (Table 4). However, at 4 wk postweaning (Fig. 3C), there was no significant difference (Table 4) between the two groups, i.e., 50% mortality at ~10.5 h. Thus, the low-PUFA group had increased resistance similar to that of the high-PUFA group. Similarly, results from a hypoxia stress test (Fig. 4) for preweaned sole showed that members of the high-PUFA group were significantly more resistant (Table 5); 50% mortality occurred at 14.1 h compared to 8.9 h in the low-PUFA group. Treatment groups were also tested at high lethal temperature (32°C, results not shown) with identical results, that is, the high-PUFA sole were more tolerant.

EPA supplementation. To ascertain whether other n-3 long-chain PUFA can substitute for 22:6n-3 in promoting stress resistance, batches of sole larvae were fed *Artemia* enriched with the low-PUFA emulsion to which had been added high proportions of EPA. This EPA-enriched diet contained high levels of EPA but no DHA (Table 2). Effects of this diet on Dover sole lipid composition are shown in Table 3 and Figure 5. First, proportions of n-3 long-chain PUFA in the high- and EPA-enriched sole were very similar, 21.9 and 23.1%, respectively (Table 3). Very high proportions of EPA were evident in the EPA-enriched fish (Fig. 5A). Proportions of DHA were low and more comparable to the low-PUFA fish (Fig. 5B). On feeding the DHA-rich postweaning diet, the proportion of EPA fell rapidly to be replaced by DHA.

Stress resistance of the EPA-enriched fish was compared to the zero- and high-PUFA sole for hypoxia (Fig. 4) and combined low temperature and low salinity (Fig. 6). The

TABLE 4
Statistical Analysis of Survival Data for Low-PUFA and High-PUFA Sole Subjected to Low Temperature/Salinity Stress Tests[a]

Stress test period	df	X^2	Probability[b]	Significance
Prewean	1	66.0	<0.001	S
2 wk Postwean	1	11.1	<0.001	S
4 wk Postwean	1	0.7	<0.5	NS

[a]Results shown in Figure 3.
[b]See the Materials and Methods section for details of statistical analysis. S, significant; NS, not significant; for other abbreviation, see Table 1.

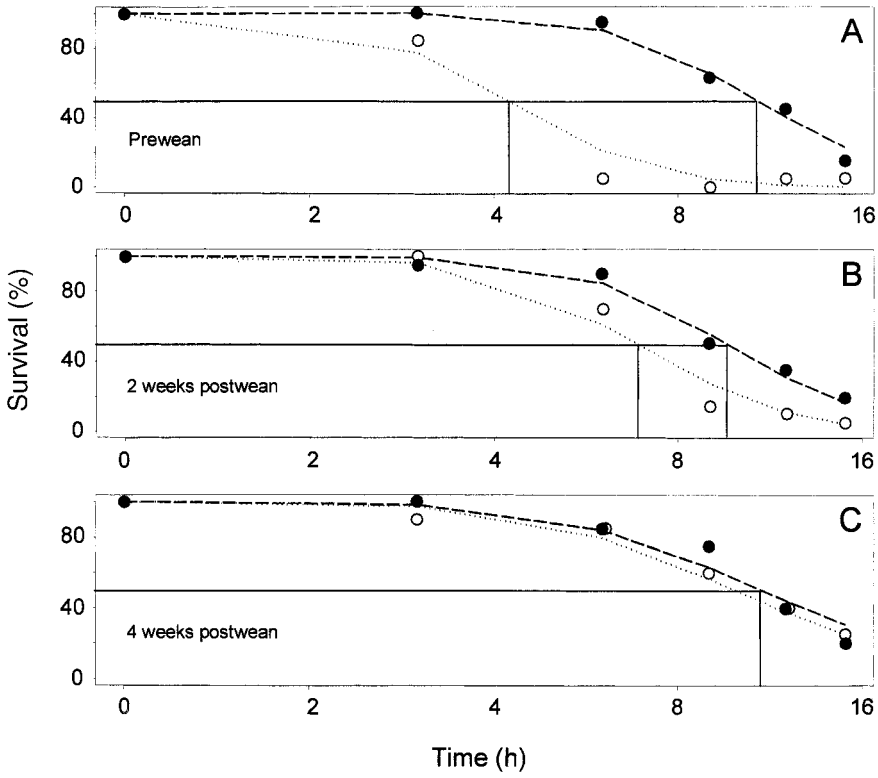

FIG. 3. Effect of dietary treatment on stress tolerance of Dover sole subjected to low temperature and low salinity (3°C, 10‰). Fish were fed either low-PUFA (○)- or high-PUFA (●)-enriched *Artemia* diets. Each data point is for 20 fish. Results are given for experiments performed before weaning (A) and 2 wk (B) and 4 wk (C) postweaning. For abbreviation, see Figure 1.

EPA-enriched fish possessed similar high resistance in each test, similar to that of the high-PUFA sole, indicating that a high dietary EPA content also confers the stress-resistant phenotype. Statistical analysis (Table 5) showed the significant differences between the low-PUFA and both n-3 PUFA-enriched groups accounted for nearly all of the dietary effects, implying no difference between the EPA and high-PUFA treatments.

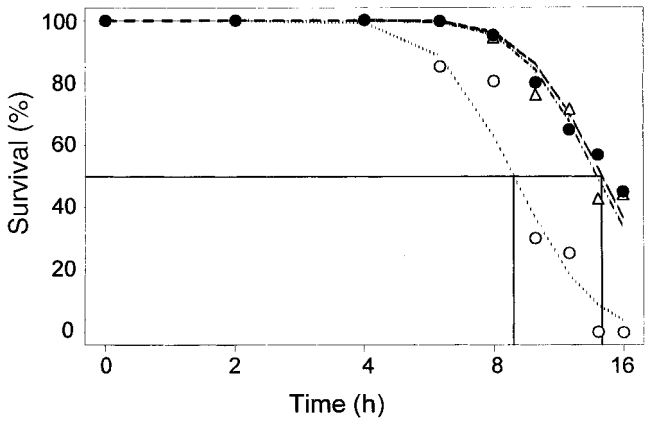

FIG. 4. Effect of dietary treatment on stress tolerance of Dover sole subjected to hypoxia (10% full aeration). Fish were fed either low-PUFA (○), high-PUFA (●), or low-PUFA + eicosapentaenoic acid (EPA; △)-enriched *Artemia* diets. Each data point is for 20 fish. For other abbreviation, see Figure 1.

Brain and eye lipids. The proportions of long-chain PUFA in brain and eye phospholipids from the different dietary groups are shown in Figure 7. The small size of the eye prevented the quantification of retinal fatty acid composition alone, but 70% of total eye phospholipids in marine fish are retinal (7). As with whole carcass composition, dietary restriction of DHA severely reduced its deposition in these tissues. For PE of the eye, 22:6n-3 accounted for 12% of the total fatty acids in the low-PUFA sole (L, Fig. 7A), compared to 35% in the high-PUFA supplemented fish (H). This is compensated for by incorporation of a range of other C_{20} and C_{22}

TABLE 5
Statistical Analysis of Survival Data for Dietary Treated Sole Groups Subjected to Stress Tests[a]

Stress test	Effect	df	X^2	Probability[b]	Significance
Hypoxia[c]	Diet	2	64.1	<0.001	S
	Low vs. EPA/High	1	63.9	<0.001	S
Low temp.	Diet	2	345.8	<0.001	S
Salinity[d]	Low vs. EPA/High	1	313.8	<0.001	S

[a]Data for sole fed low-PUFA, high-PUFA or EPA-enriched *Artemia* diets.
[b]See the Materials and Methods section for details of statistical analysis.
[c]Results shown in Figure 4.
[d]Results shown in Figure 6. For abbreviations, see Tables 1 and 2.

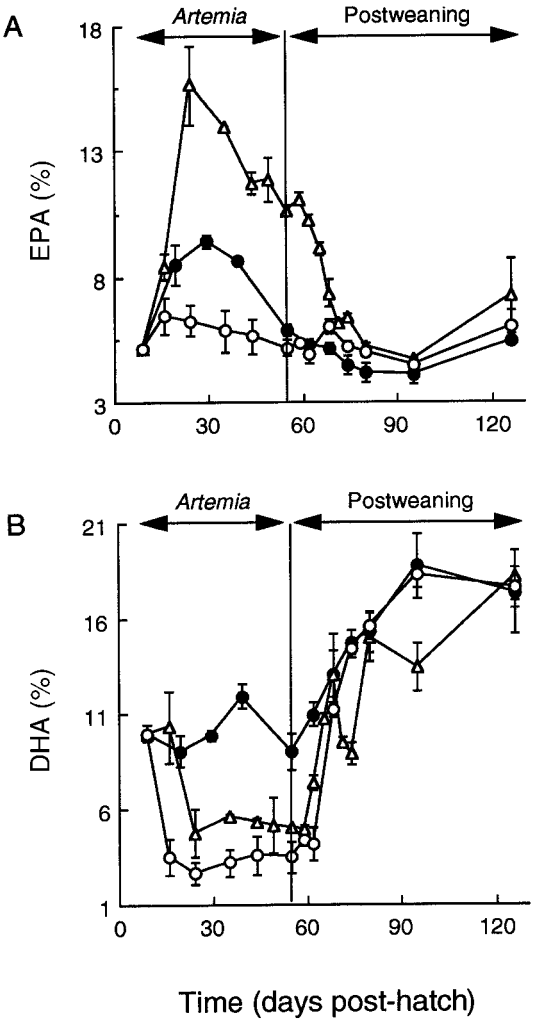

FIG. 5. EPA (A) and DHA (B) content of sole whole carcass polar lipids during the *Artemia* and postweaning feeding periods. Fish were fed either low-PUFA (○), high-PUFA (●), or low-PUFA + EPA (△) enriched *Artemia* diets. Data points represent means from three replicate samples and are given as weight % (±SD) of total fatty acid composition. For abbreviations, see Figures 1 and 4.

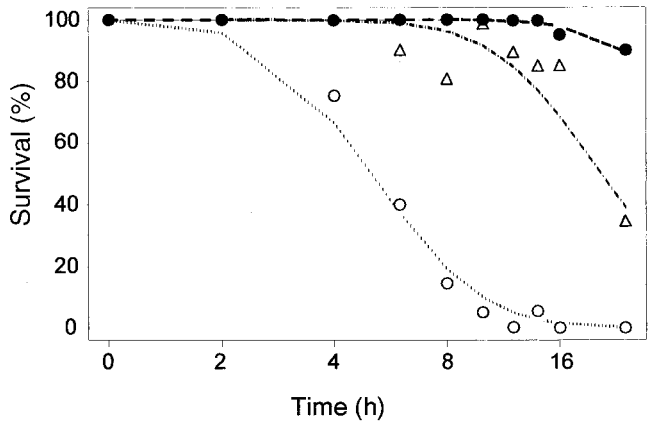

FIG. 6. Effect of dietary treatment on stress tolerance of Dover sole subjected to low temperature and low salinity (3°C, 10‰). Fish were fed either low-PUFA (○), high-PUFA (●), or low-PUFA + EPA (△)-enriched *Artemia* diets. Each data point is for 20 fish. For abbreviations, see Figures 1 and 4.

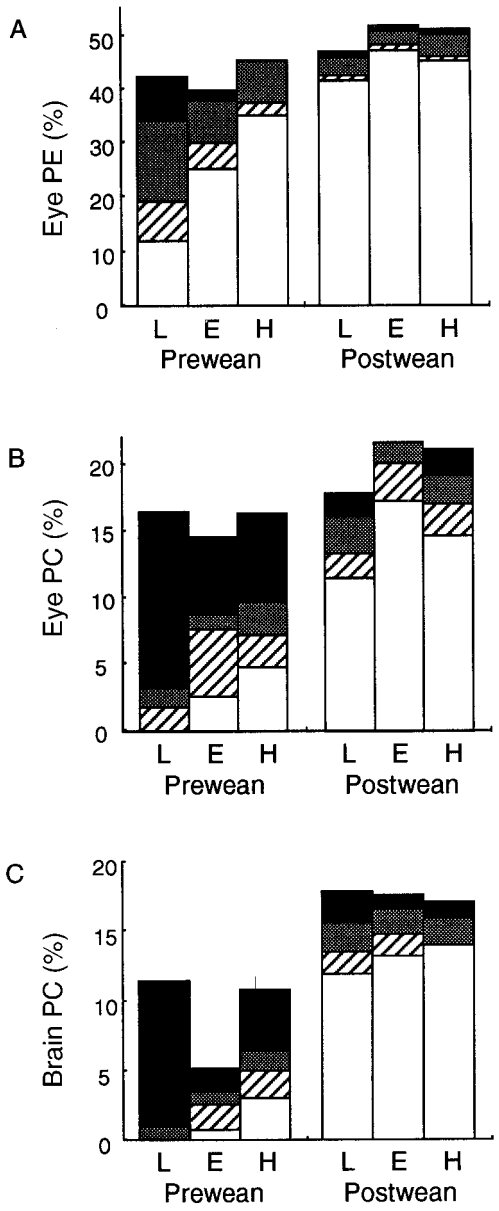

FIG. 7. Effect of dietary treatment on the PUFA content of eye and brain membrane phospholipids in Dover sole. The data show the proportions of 22:6n-3 (open bar), 20:5n-3 (lined bar), other C_{20} + C_{22} PUFA (stippled bar), and C_{18} PUFA (closed bar) within eye phosphatidylethanolamine, PE (A), and eye (B) and brain phosphatidylcholine, PC (C). Compositions are given both preweaning and postweaning for sole fed the low-PUFA (L), low-PUFA + EPA (E), and high-PUFA (H) *Artemia* diets. Values shown are percentages of total fatty acids in the sample, e.g., in 7A, H postwean, 22:6n-3 + 20:5n-3 + other C_{20} + C_{22} PUFA = 50% of total fatty acids. For abbreviations, see Figures 1 and 4.

PUFA, including 20:5n-3 (7.3%), 22:5n-3 (3.5%), 20:4n-6 (5.0%), and 20:3n-6 (5.2%). The low-PUFA fish also possessed elevated proportions of the C_{18} PUFA 18:2n-6 and 18:3n-3. Following weaning, however, levels of 22:6n-3 increased appreciably to over 40% for all groups, with other PUFA being present in only small amounts.

Similarly, 22:6n-3 was completely absent in PC from the eye of the low-PUFA sole (L, Fig. 7B), with 20:5n-3 (1.9%)

and 20:4n-6 (1.4%) being the only long-chain unsaturates present. This was compensated by greatly increased proportions of 18:2n-6 and 18:3n-3. The EPA (E) and high-PUFA (H) sole also contained significant amounts of C_{18} PUFA in PC, presumably as a result of the low levels of $C_{20} + C_{22}$ fatty acids found in these lipids preweaning. Following weaning, proportions of DHA for all treatment groups increased largely at the expense of C_{18} PUFA. The composition for brain membrane phospholipids reflected those of the eye, with similar changes after weaning (Fig. 7C).

Finally, preweaning sole reared on the low-PUFA + EPA (E) diet did not contain particularly enhanced proportions of 20:5n-3 in their neural membranes compared to the other groups (Fig. 7A–C). This may be surprising considering the amount of 20:5n-3 in the diet (Table 2) and that incorporated into whole carcass lipids (Fig. 5A). The low levels of 20:5n-3 indicated this PUFA could not functionally replace 22:6n-3 to any great extent in membranes of the nervous system. Rather, high dietary 20:5n-3 appeared to result in an increase in the proportions of 22:6n-3 in neural tissue membranes, particularly in PE lipids.

Comparison of membrane lipid order. The effects of dietary manipulation of tissue phospholipid composition upon membrane biophysical order, as measured by steady-state fluorescence anisotropy using DPH as probe, are shown in Figure 8. The profiles were approximately linear with no difference between treatments either in the values of anisotropy or the profile over the full range of measurement temperatures.

Gill and whole carcass PG production. The levels of PGE ($PGE_2 + PGE_3$) found in gill tissue homogenates and whole carcass homogenates are given in Table 6. No differences were found for gill tissue, but there was a significant difference in the carcass values, with the PUFA-deficient sole possessing more than double the levels of PGE found in the high-PUFA group. Immunoreactive prostaglandin values were low for the carcass, pg/g as compared to ng/g for the gills, as skeletal muscle is not particularly active in eicosanoid production. However, homogenization of the skin, kidney, brain, heart, and other organs will all yield eicosanoids of different types and ratios.

TABLE 6
Prostaglandin E Content of Gill and Whole Body Samples from Dover Sole Fed Low-PUFA and High-PUFA Enriched *Artemia*[a]

Tissue	Low-PUFA	High-PUFA	Probability[b]
Gill	17.0 (5.5)	22.1 (4.9)	0.301
Whole body	277.3 (50.5)	124.3 (29.7)	0.002

[a]Values given are means for three different gill samples, each comprising gills from six fish, and four different carcass samples, ±SD. Units are ng/g gill and pg/g carcass.
[b]Statistical analysis was performed by one-way analysis of variance. For abbreviation, see Table 1.

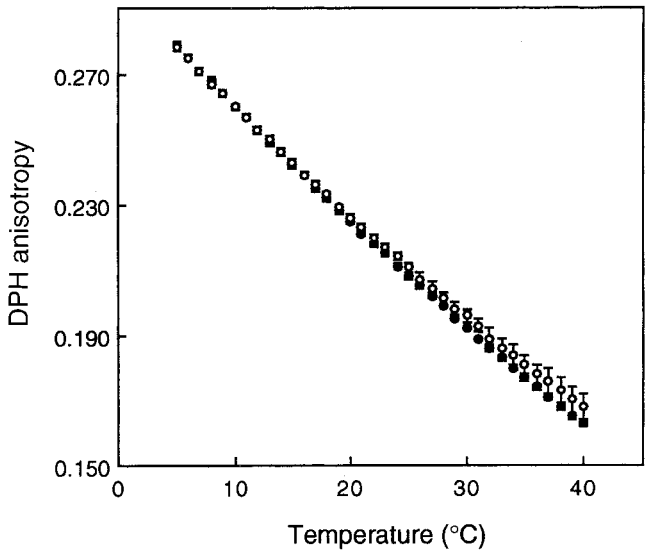

FIG. 8. Effects of dietary treatment upon physical order of brain membrane fractions. Results are shown for the preweaned sole fed the low-PUFA (○) and high-PUFA (●)-enriched *Artemia* diets. Membrane order was determined by steady-state fluorescence anisotropy using the probe 1,6-diphenyl-1,3,5-hexatriene. Data points represent means ± SD from three different membrane preparations. For abbreviation, see Figure 1.

DISCUSSION

Effects of dietary PUFA manipulation upon whole carcass fatty acid composition. The fatty acid composition of membrane phospholipids of Dover sole larvae and juveniles is substantially affected by dietary lipid composition. Larvae fed a diet low in n-3 long-chain PUFA possessed lower proportions of these fatty acids in their tissue phospholipids with correspondingly higher proportions of the C_{18} PUFA, 18:2n-6 and 18:3n-3. However, the overall proportions of SFA, MUFA, and total PUFA were largely unaffected by diet, as shown by other studies (26,27), and were constant throughout the larval and juvenile periods.

Correlating dietary treatment with stress resistance. Larvae and juveniles deprived of dietary n-3 long-chain PUFA in our study possessed reduced tolerance to combined low temperature and low salinity, high temperature, and hypoxia. The sensitivity to stress is general and not specific to cold. Furthermore, as n-3 long-chain PUFA content increased on restoration of these fatty acids in the postweaning diet, so does their capacity to withstand these stresses. Stress resistance is clearly not fixed in the very early stages of life but is subject to change according to the dietary experiences of the fish, the critical feature being the proportion of n-3 long-chain PUFA.

DHA, which is the most abundant long-chain PUFA found in the high-PUFA Dover sole (Table 3), is thought to be crucial in early development of neural tissues. However, dietary provision of 20:5n-3 as the principal n-3 long-chain PUFA confers the stress-resistant phenotype with equal potency to 22:6n-3. Although 20:5n-3 in the EPA-enriched fish is incorporated into whole body tissues in large amounts, there was no evidence of large-scale incorporation into the membranes of the nervous system. Thus, 20:5n-3 does not directly replace 22:6n-3 in these highly polyunsaturated membranes. Instead,

the capacity to synthesize 22:6n-3 from 20:5n-3, albeit limited, appears to be sufficient to bolster levels of 22:6n-3 within neural membrane lipids. Similarly, in the absence of high proportions of 22:6n-3 or 20:5n-3, a range of C_{18} and C_{20} fatty acids of lower unsaturation was incorporated into the neural tissues of the PUFA-deficient sole. However, given their stress susceptibility, it follows that these alternative fatty acids are unable to fulfill the functional role of the absent 22:6n-3. Thus, the stress resistance phenotype appears correlated with high proportions of 22:6n-3 alone in neural tissue, with stress susceptibility associated with low proportions of 22:6n-3, irrespective of other long-chain PUFA that may be present.

Despite the provision of an *Artemia* diet enriched with a PUFA-containing emulsion, the resulting sole juveniles still contained much lower proportions of n-3 long-chain PUFA (21.9%) than wild-caught fish (42.6%). The natural diet of wild sole (20–30 mm), predominantly copepods, is richer in long-chain PUFA, particularly DHA, than artificial feeds (27,28). Although we were unable to test the stress tolerance of wild-caught fish, we predict on the basis of our PUFA deprivation experiments that it would exceed that of reared sole fed the PUFA-enriched *Artemia*. It is therefore likely that commercial rearing diets for marine fish larvae based on enriched *Artemia* nauplii are suboptimal, both in the sense that they fail to achieve sufficiently high levels of PUFA supplementation and that the physiological condition of the resulting larvae is less than maximal.

A neural mechanism underlying long-chain PUFA-induced stress tolerance. It is unlikely that the observed differences in tolerance were due to a deficiency in energy provision as both the low- and high-PUFA emulsions used in this study contained similar lipid contents (29), and growth rates were not significantly different between groups (measurements of weight tested by one way ANOVA, data not shown). It is therefore more likely that the protective effects of dietary long-chain PUFA provision are linked to the specific functions of these molecules within biological systems.

The n-3 long-chain PUFA, particularly 22:6n-3, are found in high proportions in the neural tissue membranes of all vertebrates. This is especially true for marine fish species, where 22:6n-3 can constitute over 60% of total fatty acids in retinal PE lipids (5,30,31). These high levels are thought to be crucial for optimal nervous system function (32), but their exact role within these membranes and the reason for their essentiality are unclear. Such highly unsaturated, bulky components may lend themselves to the regulation of bilayer physical and barrier properties (33–35) while maintaining functionality of these excitable tissues (36,37).

Removal of these fatty acids from the diets of fully formed adults tends to have little effect either on neuronal lipid composition or performance because the nervous system tenaciously conserves its lipid complement (6). However, restriction of essential lipid supply during the early life stages may have much more serious effects. Growth, development, and differentiation of neuronal tissue require the provision of large quantities of essential nutrients, and restriction of supply would directly affect these processes and the functional properties of the resulting nervous system. This principle is clearly demonstrated by the effect of 22:6n-3 deprivation upon the feeding ability of herring juveniles at low light intensities (7). Similarly, aquaculture of marine flatfish larvae is associated with a high incidence of abnormal pigmentation. A proposed cause is an impaired nervous and/or visual system, whereby visual signals in the eye, brain, or other regions of the neural network are processed incorrectly, resulting in a discrepancy between the shade of the fish and that of its environment. This condition can be improved or resolved by increasing dietary 22:6n-3 provision (29,38,39).

Overproduction of eicosanoids. We show here an increase in total PGE (PGE_2 + PGE_3) production in homogenates of PUFA-deprived juvenile sole carcass. PGE_2 are derived from AA and PGE_3 from EPA. Despite the large excess of EPA over AA found in all fish cells, PGE_2 tends to be the predominant PGE homolog produced in fish tissues (9,10,40). Even when fish are fed high-EPA diets, little or no increase in PGE_3 production is observed (40,41). Furthermore, the PGE_2 antibody used for the detection of PGE in this study has a 100% reactivity with PGE_2 but only a 43% cross-reactivity with PGE_3. Thus it is likely that differences in prostaglandin synthetic capacity reported here are due predominantly to elevated PGE_2 in the low-PUFA group. The 2-series PG are the most bioactive eicosanoids, overproduction of which is implicated in many pathophysiological conditions (11).

In addition to acting as a precursor for PGE_3, EPA also competitively inhibits the production of PGE_2 from AA (42). Consequently, the ratio of AA/EPA (20:4n-6/20:5n-3) influences the rate and type of eicosanoids produced in some systems. An imbalance in the proportions of dietary n-3 and n-6 PUFA may possibly offset the balance of their respective eicosanoids, resulting in enhanced PGE_2 production and consequent physiological abnormalities *in vivo*. We show that the ratio of n-3/n-6 fatty acids was indeed significantly different, with values of 1.7 and 3.4 for the low- and high-PUFA sole, respectively. Feeding Atlantic salmon smolts a diet enriched with n-6 fatty acids resulted in a high n-6/n-3 acyl chain ratio in body tissues but a nonsignificant change in A23187-stimulated PGE_2 production *in vitro* (43). Associated with this diet were severe tissue lesions of the heart and increased mortality when animals were subjected to handling and transportation stress (44).

In summary, we have demonstrated that feeding a diet deficient in n-3 long-chain PUFA causes Dover sole larvae to lose resistance to common abiotic stressors such as high temperature, hypoxia, and combined low temperature and low salinity. This deficiency was reversible since adapting to a diet high in n-3 long-chain PUFA increased stress resistance compared to that observed in high-PUFA-fed control fish. These correlated changes support a link between dietary manipulation of n-3 long-chain PUFA and development of a stress-sensitive phenotype. The low levels of neural tissue n-3 PUFA and/or possibly enhanced production of 2-series PG

associated with n-3 long-chain PUFA deprivation are associated with this stress susceptibility during the critical larval and early juvenile periods.

The dietary effects reported here are not limited to artificial feeding conditions imposed during aquaculture but may also occur under natural conditions. Marine phytoplankton is frequently dominated by a limited number of species. Whereas the lipids of dinoflagellates contain high proportions of 22:6n-3, diatoms and green algae contain predominantly C_{16} fatty acids (14). Adequate dietary provision of 22:6n-3 in early larval stages of marine fish therefore depends critically upon the species composition of the algal community at the base of the food web, which can vary both spatially and temporally (28,45). Blooms of 22:6n-3-deficient diatoms during the larval period would result in low levels of these fatty acids within body tissues, leading to a reduced general fitness, increased susceptibility to natural environmental stresses, and consequent increased mortality rate. Thus, dietary input of essential long-chain PUFA may have important consequences for recruitment of juveniles into natural fisheries as well as being vital for the continued success of marine aquaculture.

ACKNOWLEDGMENTS

This work was supported by a grant from the Ministry of Agriculture, Fisheries and Food, United Kingdom. We thank Terry Beard and John Hallam for fish husbandry and Mike Nicholson for advice with statistical analysis.

REFERENCES

1. Cossins, A.R., and Bowler, K. (1987) *The Temperature Biology of Animals,* Chapman & Hall, London.
2. Friedlander, M.J., Kotchabhakdi, N., and Prosser, C.L. (1976) Effects of Cold and Heat on Behaviour and Cerebellar Function in Goldfish, *J. Comp. Physiol. 112,* 19–45.
3. Logue, J.A., Tiku, P., and Cossins, A.R. (1995) Heat Injury and Resistance Adaptation in Fish, *J. Therm. Biol. 20,* 191–197.
4. Logue, J.A., DeVries, A.L., Fodor, E., and Cossins, A.R. (2000) Lipid Compositional Correlates of Temperature-Adaptive Interspecific Differences in Membrane Physical Structure, *J. Exp. Biol. 203,* 2105–2115.
5. Bell, M.V., and Tocher, D.R. (1989) Molecular-Species Composition of the Major Phospholipids in Brain and Retina from Rainbow Trout *(Salmo gairdneri)*—Occurrence of High Levels of Di-(n-3)polyunsaturated Fatty Acid Species, *Biochem. J. 264,* 909–915.
6. Wiegand, R.D., Koutz, C.A., Stinson, A.M., and Anderson, R.E. (1991) Conservation of Docosahexaenoic Acid in Rod Outer Segments of Rat Retina During n-3 and n-6 Fatty Acid Deficiency, *J. Neurochem. 57,* 1690–1699.
7. Bell, M.V., Batty, R.S., Dick, J.R., Fretwell, K., Navarro, J.C., and Sargent, J.R. (1995) Dietary Deficiency of Docosahexaenoic Acid Impairs Vision at Low Light Intensities in Juvenile Herring (*Clupea harengus* L.), *Lipids 30,* 443–449.
8. Crawford, M.A. (1993) The Role of Essential Fatty-Acids in Neural Development—Implications for Perinatal Nutrition, *Am. J. Clin. Nutr. 57,* S703–S710.
9. Bell, J.G., Tocher, D.R., and Sargent, J.R. (1994) Effect of Supplementation with 20:3(n-6), 20:4(n-6) and 20:5(n-3) on the Production of Prostaglandins E and F of the 1-, 2- and 3-Series in Turbot *(Scophthalmus maximus)* Brain Astroglial Cells in Primary Culture, *Biochim. Biophys. Acta 1211,* 335–342.
10. Tocher, D.R., and Sargent, J.R. (1987) The Effects of Calcium Ionophore A23187 on the Metabolism of Arachidonic and Eicosapentaenoic Acids in Neutrophils from a Marine Teleost Fish Rich in (n-3) Polyunsaturated Fatty Acids, *Comp. Biochem. Physiol. 87B,* 733–739.
11. Kinsella, J.E., Lokesh, B., Broughton, S., and Whelan, J. (1990) Dietary Polyunsaturated Fatty Acids and Eicosanoids—Potential Effects on the Modulation of Inflammatory and Immune Cells—An Overview, *Nutrition 6,* 24–44.
12. Lands, W. (1993) Eicosanoids and Health, *Ann. NY Acad. Sci. 676,* 46–59.
13. Bell, J.G., Farndale, B.M., Dick, J.R., and Sargent, J.R. (1996) Modification of Membrane Fatty Acid Composition, Eicosanoid Production, and Phospholipase A Activity in Atlantic Salmon *(Salmo salar)* Gill and Kidney by Dietary Lipid, *Lipids 31,* 1163–1171.
14. Bell, M., and Sargent, J. (1996) Lipid Nutrition and Fish Recruitment, *Mar. Ecol. Prog. Ser. 134,* 315–316.
15. Sargent, J.R., Bell, M.V., Bell, J.G., Henderson, R.J., and Tocher, D.R. (1995) Origins and Functions of n-3 Polyunsaturated Fatty Acids in Marine Organisms, in *Phospholipids: Characterization, Metabolism and Novel Biological Applications* (Ceve, G., and Paltauf, F., eds.) pp. 248–259, AOCS Press, Champaign
16. Howell, B., Beard, T.W., and Hallam, J.D. (1995) The Effect of Diet Quality on the Low-Temperature Tolerance of Juvenile Sole, *Solea solea* (L.), International Council for the Exploration of the Sea, CM 1995/F13.
17. Baynes, S.M., Howell, B.R., and Beard, T.W. (1993) A Review of Egg Production by Captive Sole, *Solea solea* (L.), *Aquacult. Fish Manage. 24,* 171–180.
18. Howell, B.R. (1997) A Re-appraisal of the Potential of the Sole, *Solea solea* (L.), for Commercial Cultivation, *Aquaculture 155,* 355–365.
19. Bligh, E.G., and Dyer, W.J. (1959) A Rapid Method of Total Lipid Extraction and Purification, *Can. J. Biochem. Physiol. 37,* 911–917.
20. Morrison, W.R., and Smith, L.M. (1964) Preparation of Fatty Acid Methyl Esters and Dimethylacetals from Lipids with Boron Fluoride–Methanol, *J. Lipid Res. 5,* 600–608.
21. Lee, J.A., and Cossins, A.R. (1990) Temperature Adaptation of Biological Membranes: Differential Homeoviscous Responses in Brush-Border and Basolateral Membranes of Carp Intestinal Mucosa, *Biochim. Biophys. Acta 1026,* 195–203.
22. Cossins, A.R., and Prosser, C.L. (1982) Variable Homeoviscous Responses of Different Brain Membranes of Thermally Acclimated Goldfish, *Biochim. Biophys. Acta 687,* 303–309.
23. Behan-Martin, M.K., Jones, G.R., Bowler, K., and Cossins, A.R. (1993) A Near-Perfect Temperature Adaptation of Bilayer Order in Vertebrate Brain Membranes, *Biochim. Biophys. Acta 1151,* 216–222.
24. Jones, G.R., and Cossins, A.R. (1990) Physical Methods of Study, in *Liposomes: A Practical Approach* (New, R.R.C., ed.) pp. 183–220, IRL Press, Oxford.
25. McCullagh, P., and Nelder, J.A. (1989) *Generalized Linear Models,* 2nd edn., Chapman and Hall, London.
26. Navarro, J., Batty, R., Bell, M., and Sargent, J. (1993) Effects of Two *Artemia* Diets with Different Contents of Polyunsaturated Fatty Acids on the Lipid Composition of Larvae of Atlantic Herring *(Clupea harengus), J. Fish Biol. 43,* 503–515.
27. Shields, R.J., Bell, J.G., Luizi, F.S., Gara, B., Bromage, N.R., and Sargent, J.R. (1999) Natural Copepods Are Superior to Enriched *Artemia* Nauplii as Feed for Halibut Larvae *(Hippoglossus hippoglossus)* in Terms of Survival, Pigmentation and Retinal Morphology: Relation to Dietary Essential Fatty Acids, *J. Nutr. 129,* 1186–1194.
28. Fraser, A.J., Sargent, J.R., Gamble, J.C., and Seaton, D.D.

(1989) Formation and Transfer of Fatty Acids in an Enclosed Marine Food Chain Comprising Phytoplankton, Zooplankton and Herring (*Clupea harengus* L.) Larvae, *Mar. Chem. 27,* 1–18.
29. Sargent, J., McEvoy, L., Estevez, A., Bell, G., Bell, M., Henderson, J., and Tocher, D. (1999) Lipid Nutrition of Marine Fish During Early Development: Current Status and Future Directions, *Aquaculture 179,* 217–229.
30. Tocher, D.R., and Harvie, D.G. (1988) Fatty Acid Compositions of the Major Phosphoglycerides from Fish Neural Tissues—(n-3) and (n-6) Polyunsaturated Fatty Acids in Rainbow Trout *(Salmo gairdneri)* and Cod *(Gadus morhua)* Brains and Retinas, *Fish Physiol. Biochem. 5,* 229–239.
31. Bell, M.V., and Dick, J.R. (1991) Molecular Species Composition of the Major Diacyl Glycerophospholipids from Muscle, Liver, Retina and Brain of Cod *(Gadus morhua), Lipids 26,* 565–573.
32. Bourre, J.M., Bonneil, M., Clement, M., Dumont, O., Durand, G., Lafont, H., Nalbone, G., and Piciotti, M. (1993) Function of Dietary Polyunsaturated Fatty Acids in the Nervous System, *Prostaglandins Leukotrienes Essent. Fatty Acids 48,* 5–15.
33. Applegate, K.R., and Glomsett, J.A. (1991) Effect of Acyl Chain Unsaturation on the Packing of Model Diacylglycerols in Simulated Monolayers, *J. Lipid Res. 32,* 1645–1655.
34. Rabinovitch, A.L., and Ripatti, P.O. (1991) On the Conformational, Physical Properties and Functions of Polyunsaturated Acyl Chains, *Biochim. Biophys. Acta 1085,* 53–62.
35. Baenziger, J., Jarrell, H., and Smith, I. (1992) Molecular Motions and Dynamics of a Diunsaturated Acyl Chain in a Lipid Bilayer—Implications for the Role of Polyunsaturation in Biological Membranes, *Biochemistry 31,* 3377–3385.
36. Wiedmann, T.S., Pates, R.D., Beach, J.M., Salmon, A., and Brown, M.F. (1988) Lipid Protein Interactions Mediate the Photochemical Function of Rhodopsin, *Biochemistry 27,* 6469–6474.
37. Litman, B., and Mitchell, D. (1996) A Role for Phospholipid Polyunsaturation in Modulating Membrane Protein Function, *Lipids 31,* S193–S197.
38. Reitan, K.I., Rainuzzo, J.R., and Olsen, Y. (1994) Influence of Live Feed on Growth, Survival and Pigmentation of Turbot Larvae, *Aquacult. Int. 2,* 33–48.
39. McEvoy, L., Naess, T., Bell, J., and Lie, O. (1998) Lipid and Fatty Acid Composition of Normal and Malpigmented Atlantic Halibut *(Hippoglossus hippoglossus)* Fed Enriched *Artemia*: A Comparison with Fry Fed Wild Copepods, *Aquaculture 163,* 237–250.
40. Bell, J.G., Tocher, D.R., MacDonald, F.M., and Sargent, J.R. (1995) Diets Rich in Eicosapentaenoic Acid and Gamma-Linolenic Acid Affect Phospholipid Fatty Acid Composition and Production of Prostaglandins E1, E2 and E3 in Turbot *(Scopthalmus maximus),* a Species Deficient in Delta 5-Fatty Acid Desaturase, *Prostaglandins Leukotrienes Essent. Fatty Acids 53,* 279–286.
41. Bell, J.G., Tocher, D.R., Farndale, B.M., Cox, D.I., McKinney, R.W., and Sargent, J.R. (1997) The Effect of Dietary Lipid on Polyunsaturated Fatty Acid Metabolism in Atlantic Salmon *(Salmo salar)* Undergoing Parr-Smolt Transformation, *Lipids 32,* 515–525.
42. Whelan, J. (1996) Antagonistic Effects of Dietary Arachidonic Acid and n-3 Polyunsaturated Fatty Acids, *J. Nutr. 126,* S1086–S1091.
43. Bell, J.G., Dick, J.R., and Sargent, J.R. (1993) Effect of Diets Rich in Linoleic or α-Linolenic Acid on Phospholipid Fatty Acid Composition and Eicosanoid Production in Atlantic Salmon *(Salmo salar), Lipids 28,* 819–826.
44. Bell, J.G., McVicar, A.H., Park, M.T., and Sargent, J.R. (1991) High Dietary Linoleic Acid Affects the Fatty Acid Compositions of Individual Phospholipids from Tissues of Atlantic Salmon *(Salmo salar)*—Association with Stress Susceptibility and Cardiac Lesion, *J. Nutr. 121,* 1163–1172.
45. Kattner, G., Gercken, G., and Eberlein, K. (1983) Development of Lipids During a Spring Plankton Bloom in the Northern North Sea, *Mar. Chem. 14,* 149–162.

[Received November 30, 1999, and in revised form April 19, 2000; revision accepted May 18, 2000]

Long-Term Feeding of Dietary Oils Alters Lipid Metabolism, Lipid Peroxidation, and Antioxidant Enzyme Activities in a Teleost (*Anabas testudineus* Bloch)

Sheelu Varghese and Oommen V. Oommen*

Endocrinology and Biochemistry Division, Department of Zoology, University of Kerala, Kariavattom-695 581, Kerala, India

ABSTRACT: *Anabas testudineus* (climbing perch), average body weight 21 ± 1 g, were maintained in culture tanks and fed a 35% protein feed plus an additional supplementation of three dietary oils (20% each of coconut oil, palm oil, or cod liver oil). Body weight gain was similar among all groups. However, several hepatic lipogenic enzymes such as malic enzyme (ME), NADP-isocitrate dehydrogenase (ICDH), glucose 6-phosphate dehydrogenase (G6PDH), 6-phosphogluconate dehydrogenase (6PGDH) and β-hydroxy-β-methyl glutaryl CoA reductase (HMG CoA reductase) were assayed, and they responded differently. Hepatic ME and G6PDH activities showed a significant decrease in the coconut oil and palm oil groups, but there was no significant change in ICDH activity. The 6PGDH activities were reduced, whereas HMG CoA reductase activity was increased in the palm oil-treated group. Cholesterol synthesis in the liver and muscle increased in the palm oil-treated group, but liver phospholipids did not show any significant change in fish supplemented with oils rich in saturated fatty acids. Triacylglycerol and free fatty acid concentrations were high in the coconut oil- and palm oil-supplemented groups. Lipid peroxidation products such as thiobarbituric acid-reactive substances and conjugated dienes decreased in the same two groups. Antioxidant potential was high in all groups as evidenced by increased activity of superoxide dismutase, glutathione peroxidase, and glutathione content. The results of this study indicate that in fish, dietary lipids depress hepatic lipogenic activity as well as lipid peroxidation products by maintaining high levels of antioxidant enzymes.

Paper no. L8293 in *Lipids 35,* 757–762 (July 2000).

Lipids in fish contain comparatively high levels of polyunsaturated fatty acids (PUFA) of the n-3 series that provide diets of high nutritional value. Lipid metabolism in fish is not simply a matter of availability of dietary fatty acids. Physiological processes such as growth, metabolism, behavior, and even more particularly the structural and functional integrity of the cellular membranes are dependent on these macromolecules (1,2). Experiments with dietary treatments have shown that a strong parallel exists between fatty acids of the diet and the enzymes of intermediary metabolism. Generally, commercial fish diets are rich in fat and low in carbohydrate and protein, and their influences on metabolic pathways have been frequently studied (3,4). However, alteration in body lipid content by dietary manipulation is least understood even though lipids serve as the principal depot of energy reserves for metabolic process (5).

Lipid at a level of 10–20% in fish diet gives an optimal growth rate, but an intraspecific variation exists in the ability of fish to utilize lipid as a source of energy (6). For many fish long-chain n-3 fatty acids must be supplied in the diet. Inclusion of fish oil rich in eicosapentaenoic acid (EPA, 20:5n-3) and docosahexaenoic acid (DHA, 22:6n-3) in fish feed is now common as such oils are usually available. Moreover, fish oil rich in n-3 fatty acids in the diet can produce farmed fish with a greater content of these fatty acids in their lipids. Fish oil often gives better growth rates when compared to other oils in the diet (7). The productivity and cost effectiveness of a commercial culture farm is highly dependent on the availability of a cheaper diet. However, the commonly used ingredients such as fish meal and fish oil are expensive due to the world's limited resources (8).

Coconut oil, which is rich in saturated fatty acids (92%) and also contains 2% PUFA and 6% monounsaturated fatty acids (MUFA), is a main cooking oil in India. Of that 92%, lauric acid (12:0) constitutes 47%, myristic acid (14:0) 18%, and palmitic acid (16:0) 9%. Palm oil, a major edible oil used worldwide, contains 10% PUFA, 40% MUFA, and 50% saturated fatty acids. Among the saturated fatty acids are palmitic acid, 47%; lauric acid, 0.1–0.5%; and myristic acid, 0.09–0.15%. Cod liver oil, which is rich in PUFA of the n-3 series, should have a greater impact on *in vivo* lipid metabolism in farmed fish.

Oxidative metabolism in fish is regulated by diet (9,10) and free radicals are generated as a result of normal metabolism. They are controlled to a great extent by antioxidant enzymes, primarily by a glutathione-dependent system (11). Reports on ectotherms suggest the occurrence of a strong defense mecha-

*To whom correspondence should be addressed.
E-mail: oommen@md2.vsnl.net.in

Abbreviations: 6PGDH, 6 phosphogluconate; ANOVA, analysis of variance; DHA, docosahexaenoic acid; EPA, eicosapentaenoic acid; GPx, glutathione peroxidase; GR, glutathione reductase; G6PDH, glucose-6-phosphate dehydrogenase; HMG CoA reductase, β-hydroxy-β-methyl glutaryl CoA reductase; H/M ratio, ratio between HMG CoA and mevalonate; ICDH, isocitrate dehydrogenase; MUFA, monounsaturated fatty acid; ME, malic enzyme; PUFA, polyunsaturated fatty acid; SOD, superoxide dismutase; TAG, triacylglycerols; TBARS, thiobarbituric acid-reactive substances.

nism against free radical attack (12,13). In this study of the teleost *Anabas testudineus* (climbing perch), our objective is to analyze the role of edible oils rich in either saturated fatty acids or unsaturated fatty acids on lipogenic enzymes, lipid turnover, lipid peroxidation, and antioxidant enzyme activities.

MATERIALS AND METHODS

Fish were collected from fresh water ecosystems. Female *A. testudineus* weighing 21 ± 1 g were selected and kept in large storage tanks, where they were acclimated in constantly flowing water at 25 ± 2°C for a month prior to experimentation. Fish were fed with a 35% protein feed prepared in the laboratory by mixing 57.2% fish meal, 43.5% groundnut oil cake, 6.7% rice bran, 2% tapioca powder, 0.02% vitamin mix, and antioxidant (50 mg α-tocopherol/kg diet); this mixture was ground and reconstituted into pellets (14), and fed once daily *ad libitum*. Prior to experimental feeding, fish were weighed individually and mean values were noted. Acclimated fish were divided into four groups of eight each (n = 8) and kept in aquarium tanks (24″ × 12″ × 12″). The tanks were subjected to the natural photoperiod. Group I fish, fed the standard 35% protein feed, served as control. Groups II, III, and IV fish were fed a pelletized diet prepared in the laboratory by mixing, respectively, 20% (wt/vol) of coconut oil, palm oil, or cod liver oil into the 35% protein feed. Fish feeds were then stored at –20°C to avoid oxidation. The fish were fed once daily *ad libitum* and maintained on the respective diets for a period of 60 d. They were deprived of feed 24 h before sampling. Fish were weighed individually, and mean values were noted to assess the differences in weight gain.

Sampling and fractionation. Fish were killed by severing the spinal column posterior to the brain. The liver, heart, and muscle were removed immediately. Perfused liver was taken for biochemical analysis. The gall bladder was removed carefully from the liver. The liver was perfused *via* the hepatic vein with Hanks balanced salt solution containing 10 mM HEPES and 1 mM EDTA with a 20-gauge needle fitted to a perfusion apparatus to remove blood from the tissue (15). Muscle samples were taken from a similar position above the lateral line and in front of the dorsal fin (nape region). All the samples were stored at –20°C until analyzed.

Biochemical analyses. The activities of major lipogenic enzymes were determined in the liver and heart. The activities of malic enzyme (ME) and isocitrate dehydrogenase (ICDH) were assayed by the method of Ochoa (16,17). Glucose-6-phosphate dehydrogenase (G6PDH) activity was determined by the method of Kornberg and Horecker (18) and 6-phosphogluconate dehydrogenase (6PGDH) activity by the method of Horecker and Smyrniotis (19). β-Hydroxy-β-methyl glutaryl CoA reductase (HMG CoA reductase) was determined by the method of Rao and Ramakrishnan (20) from the ratio between HMG CoA and mevalonate (H/M ratio). Extraction of total lipid from the liver and muscle was performed by the method of Folch *et al.* (21). From these extracts aliquots were used for the quantitative estimation of cholesterol by the method of Abell *et al.* (22); free fatty acids by the method of Falhot *et al.* (23); and triacylglycerols (TAG) and phospholipids by the methods of Weidman and Schonfeld (24).

The rate of lipid peroxidation in the liver was determined by quantitative estimation of thiobarbituric acid-reactive substances (TBARS) and conjugated dienes by the method of John and Steven (25) and hydroperoxides by that of Mair and Hall (26). The changes in the antioxidant defense system were determined by studying superoxide dismutase (SOD) by the method of Kakkar *et al.* (27), glutathione peroxidase (GPx) activity according to Lawrence and Burk (28), glutathione reductase (GR) by the procedure of David and Richard (29), and glutathione content by the method of Patterson and Lazarow (30). Total protein was estimated by the biuret method of Gornall *et al.* (31) with bovine serum albumin as reference standard. Absorbance was determined using an ultraviolet (UV)-visible spectrophotometer (UV-1601; Shimadzu, Kyoto, Japan).

Statistical analysis. An SPSS (Chicago, IL) setup was used for statistical analysis. Significance of difference among groups was determined by one-way analysis of variance (ANOVA) with Duncan's multiple range test at the level of $P < 0.05$ (32). In all of these cases comparison was made between control group and groups fed with different dietary oils.

RESULTS

The average body weight after supplementation of different oils in the diet did not show any significant difference among groups (Table 1). ME, a major lipogenic enzyme involved in fatty acid biosynthesis, decreased in the liver of coconut oil- and palm oil-treated animals. In heart, ME activity was unaffected by dietary manipulation. In liver, ICDH activity was not affected by diet; in heart there was increased activity associated with palm oil and cod liver oil diets but there was no

TABLE 1
Average Body Weight Before and After Supplementation of Different Dietary Oils[a]

	Group I	Group II	Group III	Group IV
Initial body weight (g)	21.21 ± 1.14[a]	21.56 ± 1.21[a]	20.91 ± 0.87[a]	21.01 ± 1.13[a]
Final body weight (g)	32.51 ± 0.35[a]	32.33 ± 0.43[a]	32.43 ± 0.44[a]	32.51 ± 0.92[a]

[a]Results expressed as mean ± SD (n = 8). The significant difference between the groups was analyzed by one-way analysis of variance (ANOVA). Mean values with different superscript roman letters are significantly different ($P < 0.05$) as determined by Duncan's multiple range test. Group I, control; Group II, 20% coconut oil; Group III, 20% palm oil; Group IV, 20% cod liver oil.

TABLE 2
Effect of Different Dietary Oils on Lipogenic Enzymes of *Anabas testudineus* (climbing perch)[a]

Parameters analyzed	Group I	Group II	Group III	Group IV
Malic enzyme (L)	1.37 ± 0.27[a]	0.95 ± 0.13[b]	0.82 ± 0.35[b]	1.43 ± 0.49[a]
Malic enzyme (H)	1.7 ± 0.5[a]	1.89 ± 0.12[a]	2.16 ± 0.6[a]	1.92 ± 0.4[a]
Isocitrate dehydrogenase (L)	3.72 ± 0.8[a]	3.05 ± 0.54[a]	3.52 ± 0.76[a]	3.32 ± 0.4[a]
Isocitrate dehydrogenase (H)	6.0 ± 0.48[a]	6.58 ± 0.4[a,b]	7.61 ± 0.68[c]	6.78 ± 0.64[b]
G6PDH (L)	0.1 ± 0.01[a]	0.09 ± 0.01[b]	0.05 ± 0.009[c]	0.08 ± 0.02[b]
6PGDH (L)	0.12 ± 0.01[a]	0.1 ± 0.01[a,b]	0.08 ± 0.01[c]	0.12 ± 0.02[a]
H/M ratio	5.07 ± 0.33[a]	4.43 ± 0.98[a]	2.19 ± 0.66[b]	4.78 ± 0.36[a]

[a]Results expressed as mean ± SD (n = 8). Values are IU/mg protein except for HMG CoA/mevalonate ratio. For HMG CoA reductase activity high HMG CoA/mevalonate ratio shows low enzyme activity. The significant difference between the groups was analyzed by one-way ANOVA. Mean values of different superscript roman letters significantly different ($P < 0.05$) as determined by Duncan's multiple range test. Group I, control; Group II, 20% coconut oil; Group III, 20% palm oil; Group IV, 20% cod liver oil. L, liver; H, heart; G6PDH, glucose-6-phosphate dehydrogenase; 6PGDH, 6-phosphogluconate; H/M ratio, ratio between HMG CoA (β-hydroxy-β-methyl glutaryl CoA) and mevalonate. For other abbreviation see Table 1.

significant difference in coconut oil-fed fish. G6PDH activity in liver was reduced significantly in all oil-fed groups. In the liver, 6PGDH activity decreased only in the palm oil-treated group. In the palm oil-treated group HMG CoA reductase activity was increased compared to the control group, suggesting an increased cholesterol biosynthesis whereas in all other groups no significant changes were observed (Table 2).

Lipid profile analysis showed that total cholesterol in the liver and muscle increased in the palm oil-treated group, and no alteration was found in the coconut oil- and cod liver oil-treated groups. Phospholipids in the liver were unaffected by consumption of oil rich in saturated fat whereas an increased concentration was found in the cod liver oil-treated group. In muscle, dietary treatment did not cause any alteration in phospholipid concentration. Coconut oil and palm oil feeding increased TAG concentration in the liver whereas cod liver oil supplementation did not cause any change. On the other hand, all treatments with dietary oils increased TAG concentrations in muscle. Free fatty acid concentration in the liver increased in all groups compared to control whereas in muscle, dietary treatment of oils had no significant effect on the free fatty acid content (Table 3).

Lipid peroxidation products such as TBARS and conjugated dienes decreased significantly in liver of the coconut oil- and palm oil-treated animals. Hydroperoxides in the liver showed decreased concentrations only in palm oil-treated group.

The activity of SOD and GPx increased in all oil fed groups. The glutathione content in the liver also showed an increase in all oil-fed groups (Table 4).

DISCUSSION

The growth of fish and food conversion efficiency vary with physiological as well as environmental factors (33). In the present study the groups of fish fed diets supplemented with lipids had similar growth rates as in control fish fed with 35% protein feed. Many different experimental approaches using carbohydrate, protein, or lipid and their effects on PUFA in fish species have been reviewed (1,10,34). However, the action of dietary fat on lipogenic enzymes and on lipid peroxidation in fish is not understood. Supplementation of diet with carbohydrate, protein, or lipid invariably affects the synthesis and degradation of various lipid classes (9,35,36). In this study the major lipogenic enzymes responded differentially to the dietary fat content in various tissues. ME, which is involved in fatty acid biosynthesis in converting malate to pyruvate with subsequent generation of extramitochondrial

TABLE 3
Effect of Different Dietary Oils on Various Lipid Classes of *A. testudineus*[a]

Parameters analyzed	Group I	Group II	Group III	Group IV
Cholesterol (L)	4.75 ± 0.92[a]	4.83 ± 0.93[a]	7.23 ± 0.97[b]	4.2 ± 0.35[a]
Cholesterol (M)	0.73 ± 0.15[a]	0.76 ± 0.09[a]	0.95 ± 0.05[b]	0.76 ± 0.15[a]
Phospholipids (L)	108.84 ± 18.5[a]	121.06 ± 6.9[a]	112.23 ± 2.57[a]	139.19 ± 11.09[b]
Phospholipids (M)	30.07 ± 6.7[a]	30.44 ± 2.62[a]	33.43 ± 1.14[a]	34.44 ± 2.89[a]
Triglycerides (L)	3.1 ± 0.95[a]	4.67 ± 0.57[b]	5.14 ± 0.34[b]	2.93 ± 0.49[a]
Triglycerides (M)	0.21 ± 0.05[a]	0.33 ± 0.05[b]	0.4 ± 0.02[c]	0.33 ± 0.075[b]
Free fatty acids (L)	2.47 ± 0.28[a]	5.37 ± 0.91[b]	3.96 ± 0.61[c]	7.89 ± 1.04[d]
Free fatty acids (M)	0.27 ± 0.05[a]	0.31 ± 0.05[a]	0.29 ± 0.03[a]	0.32 ± 0.04[a]

[a]Results expressed as mean ± SD (n = 8). Values are mg/g tissue for liver and muscle samples. The significant difference between the groups was analyzed by one-way ANOVA. Mean values of different superscript roman letters significantly different ($P < 0.05$) as determined by Duncan's multiple range test. Group I, control; Group II, 20% coconut oil; Group III, 20% palm oil; Group IV, 20% cod liver oil. For abbreviations see Tables 1 and 2.

TABLE 4
Effect of Different Dietary Oils on Lipid Peroxidation and Antioxidant Enzyme Activities in the Liver of *A. testudineus*[a]

Parameters analyzed	Group I	Group II	Group III	Group IV
Malondialdehyde (μM/g tissue)	22.34 ± 3.4[a]	12.38 ± 1.65 b	17.18 ± 4.2 c	22.92 ± 2.88[a]
Hydroperoxides (μM/g tissue)	35.3 ± 0.4[a]	35.1 ± 0.72[a]	33.7 ± 0.73[b]	35.2 ± 1.02[a]
Conjugated dienes (μM/g tissue)	45.5 ± 6.0[a]	31.01 ± 4.8[b]	38.6 ± 8.23[c]	28.5 ± 5.4[b]
Superoxide dismutase (IU/mg protein)	0.42 ± 0.04[a]	1.3 ± 0.26[b]	2.5 ± 0.7[c]	1.9 ± 0.5[d]
Glutathione peroxidase (IU/mg protein)	0.01 ± 0.004[a]	0.26 ± 0.02[b]	0.21 ± 0.02[c]	0.3 ± 0.03[d]
Glutathione reductase (IU/mg protein)	0.02 ± 0.001[a]	0.03 ± 0.001[b]	0.02 ± 0.002[c]	0.04 ± 0.003[d]
Glutathione content (mM/100 g tissue)	33.14 ± 11.8[a]	64.83 ± 6.73[b]	121.40 ± 9.92[c]	94.67 ± 12.27[d]

[a]Results expressed as mean ± SD ($n = 8$). The significant difference between the groups was analyzed by one-way ANOVA. Mean values of different superscript letters are significantly different ($P < 0.05$) as determined by Duncan's multiple range test. Group I, control; Group II, 20% coconut oil; Group III, 20% palm oi; Group IV, 20% cod liver oil. For abbreviations see Tables 1 and 2.

NADPH, was significantly reduced in liver with a diet rich in saturated fat, whereas in heart tissue there was no significant change. It is reported that when more fat is absorbed from the intestine the activities of major lipogenic enzymes are reduced (9). The cytosolic ICDH is suggested as an important source of reducing equivalents for fatty acid biosynthesis. In this experiment liver ICDH activity was unaltered irrespective of the nature of the fat present in the diet. The other two enzymes involved in the oxidative phase of pentose-phosphate pathway, G6PDH and 6PGDH, responded differentially to dietary fat content. The G6PDH activity is an excellent model system to analyze the regulation of intracellular metabolism by dietary fat since it participates in multiple metabolic pathways such as lipogenesis, cellular growth and reductive biosynthesis. It also has a direct influence on detoxification reactions (37). Supplementation with three different oils reduced the activity of this enzyme in the liver. This is in broad agreement with other observations in different fish species, as reviewed by Greene and Selivonchick (1). The 6PGDH activity in the liver was not affected by coconut oil and cod liver oil treatment, but a decreased activity was associated with dietary palm oil. HMG CoA reductase, the rate-limiting enzyme involved in the cholesterol biosynthesis pathway and responsible for the synthesis of isoprenoid precursor mevalonate, was unaltered by coconut oil and cod liver oil treatment. However, in the palm oil-supplemented group hepatic HMG CoA reductase activity increased, indicating increased cholesterol biosynthesis.

In this experiment most of the lipogenic enzymes decreased in the liver when more fat was absorbed. In heart muscle no such correlation could be found in lipogenic enzyme activity. It has been reported that absorbed fat is the most important factor in influencing the activity of lipogenic enzymes. Even though absorption and utilization of fat may vary with species, physiological status, food intake and absorbed fat are generally and negatively correlated with lipogenic enzyme activity (9,33).

In this study, only the livers of the 20% palm oil-treated group had higher cholesterol content compared to other groups. This may be due to increased cholesterol biosynthesis as evident from increased HMG CoA reductase activity.

In *A. testudineus,* supplementation of oil rich in saturated fat does not alter phospholipid concentration in the liver whereas cod liver oil treatment increases the concentration. In muscle, treatment with different dietary oils does not produce any change. The increase in the phospholipid content of the liver of cod liver oil-treated animals may be because of the incorporation of long-chain PUFA into phospholipids. The primary storage molecules in higher bony fish are TAG (36). In our study, the TAG content in the liver was high only in fish fed with a diet high in saturated fat, indicating the probable presence of saturated fat as circulating TAG, whereas in muscle all dietary oil treatments led to an increased TAG concentration.

In the liver, free fatty acids concentration increased in all treated groups. A corresponding increase was not observed in muscle. The increase in free fatty acids in the liver of the group fed 20% cod liver oil may have taken place postmortem, as enzyme activity could be emphasized by additional cellular phospholipids. In the two saturated fat-treated groups, the hydrolysis of stored TAG probably caused an increased concentration of free fatty acids (39).

The overall physiological functions in a cell are dependent on the integrity of membranes. Fluidity of membranes is directly correlated with membrane function and is maintained by the integrity of lipids combined with other macromolecules. Membrane lipids undergo autoxidation, leading to reactive oxygen and nitrogen radicals that affect the structural and functional integrity of plasma membranes. A strong defense mechanism that exists against free radical attack in mammals is SOD, which converts O_2 into H_2O_2 (40). Another vital defense against lipid peroxidation is glutathione-dependent enzymes that can metabolize the H_2O_2 involved in the initiation of lipid peroxidation. A paucity of information is available to elucidate the action of dietary fat on lipid peroxidation and antioxidant enzyme activity in fish. Among the lipid classes, the most susceptible substrates undergoing autoxidation are those rich in PUFA, and there may be greater chances of lipid peroxidation leading to the generation of reactive oxygen species. In the present study, lipid peroxidation products such as TBARS and conjugated dienes decreased significantly when more saturated fat was being absorbed. Meanwhile, in the PUFA-treated group, a high level of TBARS was observed since these fatty acids are the obvious

substrates for lipid peroxidation. However, a possible deleterious effect in cellular function can be ruled out because of the high levels of antioxidant enzymes in all of the experimental animals in this study. In addition, glutathione, a tripeptide and an intracellular reductant involved in the cellular defense system, also increased with increased fat absorption.

In summary, these results suggest that supplemented dietary fat is well utilized and has pronounced influences on the regulation of lipogenic enzymes assayed. The important observation from the present study is that supplemental fat in the diet reduces lipid peroxidation products by maintaining high levels of antioxidant enzymes such as SOD and GPx in *A. testudineus.*

ACKNOWLEDGMENTS

We thank Krishnamoorthy Kalyanaraman, Department of Statistics, for statistical analysis and interpretation of data and Dr. Raj Mohan, Department of Biochemistry, University of Kerala, for the critical reading of the manuscript. This work was supported by a grant to Dr. Oommen V. Oommen from the Department of Science and Technology, Government of India (SP/SO/C11/95).

REFERENCES

1. Greene, D.H.S., and Selivonchick, P.D. (1987) Lipid Metabolism in Fish, *Prog. Lipid Res. 26*, 53–85.
2. Sheridan, M.A., and Kao, H.Y. (1998) Regulation of Metamorphosis-Associated Changes in the Lipid Metabolism of Selected Vertebrates, *Am. Zool. 38*, 350–368.
3. Hilton, J.W., and Atkinson, J.L. (1982) Response of Rainbow Trout (*Salmo gairdneri*) to Increased Levels of Available Carbohydrate in Practical Trout Diets, *Br. J. Nutr. 47,* 597–607.
4. Shimeno, S., Kheyyali, D., and Shikata, T. (1995) Metabolic Response to Dietary Lipid to Protein Ratios in Common Carp, *Fish Sci. 61*, 1995.
5. Sargent, J.R., Bell, J.G., Bell, M.V., Henderson, R.J., and Tocher, D.R. (1993) The Metabolism of Phospholipids and Polyunsaturated Fatty Acids in Fish, in *Coastal and Estuarine Studies* (Lahlou, B., and Vitiello, P., eds.), pp. 103–124, American Geophysical Union, Washington, DC.
6. Cowey, C.B., and Sargent, J.R. (1979) Nutrition, in *Fish Physiology* (Hoar, W.S., Randall, D.J., and Brettl, J.R., eds.), pp. 1–69, Academic Press, London.
7. Bell, G.J., McVicar, A.H., Moira, P.T., and Sargent, J.R. (1991) High Dietary Linoleic Acid Affects the Fatty Acid Compositions of Individual Phospholipids from Tissues of Atlantic Salmon (*Salmo salar*): Association with Stress Susceptibility and Cardiac Lesion, *J. Nutr. 121*, 1163–1172.
8. James, D.G. (1994) Fish as Food: Present Utilisation and Future Prospects, *Omega-3 News 9*, 1–4.
9. Arnesen, P., Krogdahl, A., and Kristiansen, I.O. (1993) Lipogenic Enzyme Activities in Liver of Atlantic Salmon (*Salmo salar* L.), *Comp. Biochem. Physiol. 105B*, 541–546.
10. Christiansen, D.C., and Klungsoyr, L. (1987) Metabolic Utilisation of Nutrients and the Effects of Insulin in Fish, *Comp. Biochem. Physiol. 88B,* 701–711.
11. Otto, D.M.E., and Moon, T.W. (1996) Endogenous Antioxidant Systems of Two Teleost Fish, the Rainbow Trout and the Black Bullhead, and the Effect of Age, *Fish Physiol. Biochem. 15*, 349–358.
12. Han, T.J., and Liston, J. (1989) Lipid Peroxidation Protection Factors in Rainbow Trout (*Salmo gairdnerii*) Muscle Cytosol, *J. Food Sci. 54*, 809–813.
13. Stephan, G., Guillaume, J., and Lamour, F. (1995) Lipid Peroxidation in Turbot (*Scophthalmus maximus*) Tissue: Effect of Dietary Vitamin E and Dietary n-6 or n-3 Polyunsaturated Fatty Acids, *Aquaculture 130*, 251–268.
14. Hardy, R. (1980) Fish Feed Formulation, in *FAO/UNDP Training Course in Fish Feed Technology*, p. 8, Seattle.
15. Tocher, D.R., Bell, G.J., Dick, J.R., and Sargent, J.R. (1997) Fatty Acyl Desaturation in Isolated Hepatocytes from Atlantic Salmon (*Salmo salar*): Stimulation by Dietary Borage Oil Containing γ-Linolenic Acid, *Lipids 32*, 1237–1247.
16. Ochoa, S. (1955) Isocitric Dehydrogenase System (TPN) from Pig Heart, *Methods Enzymol. 1*, 699.
17. Ochoa, S. (1955) "Malic" Enzyme, *Methods Enzymol. 1*, 739.
18. Kornberg, A., and Horecker, B.L. (1967) Glucose-6-phosphate Dehydrogenase, *Methods Enzymol. 1*, 322.
19. Horecker, B.L., and Smyrniotis, P.Z. (1967) 6-Phosphogluconic Dehydrogenase, *Methods Enzymol. 1*, 323.
20. Rao, A.V., and Ramakrishnan, S. (1975) Indirect Assessment of Hydroxymethyl Glutaryl CoA Reductase (NADPH) Activity in Liver Tissue, *Clin. Chem. 21*, 1523.
21. Folch, J., Lee, M., and Sloane-Stanley, G.H. (1957) A Simple Method for the Isolation and Purification of Total Lipids from Animal Tissue, *J. Biol. Chem. 226*, 497–509.
22. Abell, L.L., Levy, B.B., and Kendall, F.E. (1952) A Simplified Method for the Estimation of Total Cholesterol in Serum and Demonstration of Its Specificity, *J. Biol. Chem. 195*, 357.
23. Falholt, K., Lund, B., and Falholt, W. (1973) An Easy Calorimetric Micromethod for Routine Determination of Free Fatty Acids in Plasma, *Clin. Chim. Acta 46*, 105–111.
24. Weidman, S.W, and Schonfeld, G. (1963) Lipids and Lipoprotein, in *Gradwhol's Clinical Laboratory Methods and Diagnosis* (Sonnenwirth, A.C., and Jarett, L., eds.), pp. 284–286, 288–289, The C.V. Mosby Company, St. Louis.
25. John, A.B., and Steven, D.A. (1978) Microsomal Lipid Peroxidation, *Methods Enzymol. 52*, 302–310.
26. Mair, R.D., and Hall, T. (1977) Inorganic Peroxides, *Intersciences 2*, 532–534.
27. Kakkar, P., Das, B., and Viswanathan, P.N. (1984) A Modified Spectrophotometric Assay of Superoxide Dismutase, *Ind. J. Biochem. Biophys. 21*, 130–132.
28. Lawrence, R.A., and Burk, R.E. (1976) Glutathione Peroxidase Activity in Selenium-Deficient Rat Liver, *Biochem. Biophys. Res. Commun. 17*, 952–958.
29. David, M., and Richard, J.S. (1983) Glutathione Reductase, *Methods Enzymol. Anal. 3*, 258–265.
30. Patterson, J.W., and Lazarow, A. (1955) Determination of Glutathione, in *Methods of Biochemical Analysis* (Glick, D., ed.), pp. 259–278, Intersciences, New York.
31. Gornall, A.G., Bardawill, C.J., and David, M.M. (1949) Determination of Serum Protein by Means of Biuret Reaction, *J. Biol. Chem. 177,* 751–766.
32. Duncan, D.B. (1955) Multiple Range and Multiple F Test, *Biometrics 11*, 1–42.
33. Lin, H., Romsos, D.R., Tack, P.I., and Leveille, G.A. (1977) Influence of Dietary Lipid on Lipogenic Enzyme Activities in Coho Salmon *Oncorhynchus kisutch* (Walbaum), *J. Nutr. 107*, 846–854.
34. Henderson, R.J., and Tocher, D.R. (1987) The Lipid Composition and Biochemistry of Fresh Water Fish, *Prog. Lipid Res. 26*, 281–347.
35. Craig, S.R., Neill, W.H., and Gatlin, D.M. (1995) Effects of Dietary Lipids and Environmental Salinity on Growth, Body Composition and Cold Tolerance of Juvenile Red Drum *(Sciaenops ocellatus), Fish Physiol. Biochem. 14,* 49–61.
36. Likimani, T.A., and Wilson, R.P. (1982) Effects of Diet on Lipogenic Enzyme Activities in Channel Catfish Hepatic and Adipose Tissue, *J. Nutr. 112*, 112–117.

37. Horton, A.A., and Fairhurst, S. (1987) Lipid Peroxidation and Mechanism of Toxicity, in *Critical Reviews in Toxicology* (Golnerg, L., ed.), pp. 27–77, CRC Press, Boca Raton.
38. Sheridan, M.A. (1988) Lipid Dynamics in Fish: Aspects of Absorption, Transportation, Deposition and Mobilisation, *Comp. Biochem. Physiol. 90B*, 679–690.
39. Addison, R.F., Ackman, R.G., and Hingley, J. (1969) Free Fatty Acids of Herring Oils: Possible Derivation from Both Phospholipids and Triglycerides in Fresh Herring, *J. Fish. Res. Board Can. 26*, 1577–1583.
40. Fridovich, I. (1997) Superoxide Anion Radical (O_2^-), Superoxide Dismutase, and Related Matters, *J. Biol. Chem. 272*, 18515–18517.

[Received June 28, 1999, and in final revised form June 3, 2000; revision accepted June 7, 2000]

Effect of Low-to-Moderate Amounts of Dietary Fish Oil on Neutrophil Lipid Composition and Function

D.A. Healy[a], F.A. Wallace[b], E.A. Miles[b], P.C. Calder[b], and P. Newsholme[a,*]

[a]Department of Biochemistry, The Conway Institute of Biomolecular and Biomedical Research, University College Dublin, Belfield, Dublin 4, Ireland, and [b]Institute of Human Nutrition, University of Southampton, Southampton SO16 7PX, United Kingdom

ABSTRACT: Although essential to host defense, neutrophils are also involved in numerous inflammatory disorders including rheumatoid arthritis. Dietary supplementation with relatively large amounts of fish oil [containing >2.6 g eicosapentaenoic acid (EPA) plus 1.4 g docosahexaenoic acid (DHA) per day] can attenuate neutrophil functions such as chemotaxis and superoxide radical production. In this study, the effects of more moderate supplementation with fish oil on neutrophil lipid composition and function were investigated. The rationale for using lower supplementary doses of fish oil was to avoid adverse gastrointestinal problems, which have been observed at high supplementary concentrations of fish oil. Healthy male volunteers aged <40 yr were randomly assigned to consume one of six dietary supplements daily for 12 wk ($n = 8$ per treatment group). The dietary supplements included four different concentrations of fish oil (the most concentrated fish oil provided 0.58 g EPA plus 1.67 g DHA per day), linseed oil, and a placebo oil. The percentages of EPA and DHA increased (both $P < 0.05$) in neutrophil phospholipids in a dose-dependent manner after 4 wk of supplementation with the three most concentrated fish oil supplements. No further increases in EPA or DHA levels were observed after 4 wk. The percentage of arachidonic acid in neutrophil phospholipids decreased ($P < 0.05$) after 12 wk supplementation with the linseed oil supplement or the two most concentrated fish oil supplements. There were no significant changes in *N*-formyl-met-leu-phe-induced chemotaxis and superoxide radical production following the dietary supplementations. In conclusion, low-to-moderate amounts of dietary fish oil can be used to manipulate neutrophil fatty acid composition. However, this may not be accompanied by modulation of neutrophil functions such as chemotaxis and superoxide radical production.

Paper no. L8303 in *Lipids 35,* 763–768 (July 2000).

Polymorphonuclear granulocytes (neutrophils) are derived from stem cells and mature in the bone marrow. Upon activation, neutrophil responses include adherence to endothelial cells, migration into inflamed tissue (chemotaxis), and production of superoxide radicals (1–4). Toxic metabolites of superoxide such as hydrogen peroxide (H_2O_2), hypochlorous acid (HOCl), and hydroxyl radicals ($OH^{\bullet}$) play an important role in the ability of neutrophils to kill invading microorganisms. The neutrophil is also capable of releasing the toxic contents of granules, which include elastase, collagenase, myeloperoxidase and lysozyme, upon activation. The combination of superoxide radical metabolites and granule-derived toxins provides a potent defense against invading microorganisms.

Although essential to host defense, neutrophils have been implicated in the pathology of several inflammatory disorders (1,3,5). This appears to be due to the same set of metabolites and toxins which are involved in host defense. Supplementing the diet with fish oil has been shown to attenuate neutrophil functions such as superoxide radical production (6,7) and chemotaxis (8,9). Many authors have reported moderate improvement in several inflammatory disorders including psoriasis (10) and rheumatoid arthritis (11) after dietary supplementation with fish oil and suggest that this might be, in part, due to reduced neutrophil responsiveness. Interest in such effects of fish oil stemmed from the observation that populations that ingest relatively large amounts of oily fish and marine mammals in the diet (e.g., Eskimos) have a lower incidence of inflammatory disorders than populations which consume little or no oily fish (12). The beneficial effect of fish oil on neutrophil function has been attributed to the n-3 polyunsaturated fatty acids (PUFA), eicosapentaenoic acid (EPA; 20:5n-3), and docosahexaenoic acid (DHA; 22:6n-3), which are found in relatively high concentrations in fish oil. Arachidonic acid (ARA; 20:4n-6), a member of the alternative n-6 PUFA family, can be metabolized to a variety of pro-inflammatory mediators, and may itself be a pro-inflammatory second messenger (13). It is believed that EPA competes with ARA for use as substrate in several important pathways, resulting in reduced production of pro-inflammatory products of ARA (14–17). This competitive inhibition by EPA of ARA metabolism is due to the similarity in structure between the molecules, and may explain in part the anti-inflammatory effect of fish oil.

Numerous studies have used large amounts of fish oil (up to 9.4 g EPA plus 5 g DHA per day) to attenuate neutrophil function (6–9,18,19). However, the amounts of fish oil used

*To whom correspondence should be addressed.
E-mail: philip.newsholme@ucd.ie

Abbreviations: ARA, arachidonic acid; DHA, docosahexaenoic acid; DMSO, dimethyl sulfoxide; EPA, eicosapentaenoic acid; fMLP, *N*-formyl-met-leu-phe; HBSS, Hank's balanced salt solution; LA, linoleic acid; LTB_4, leukotriene B_4; PBS, phosphate-buffered saline; PUFA, polyunsaturated fatty acids; SOD, superoxide dismutase.

are not practical or sustainable, and some volunteers experienced gastrointestinal symptoms such as diarrhea and mild steatorrhea (9). It would seem reasonable to assume that such an extreme dietary regime would not achieve widespread acceptance for long-term use. The aim of this study was to determine whether dietary supplementation with lower amounts of fish oil could be used to bring about both structural and functional changes to neutrophils.

MATERIALS AND METHODS

Materials. Diazomethane, Histopaque-1077, cytochrome c, cytochalasin B, catalase, Hank's balanced salt solution (HBSS) with calcium and magnesium, *N*-formyl-met-leu-phe (fMLP), superoxide dismutase, and phosphate-buffered saline (PBS) tablets were all purchased from Sigma Chemical Co. (Poole, Dorset, United Kingdom). All solvents were from Fuher Scientific Ltd. (Loughborough, Leicestershire, United Kingdom). Lysis buffer (autoclaved and filter-sterilized) was prepared by dissolving 37.2 mg EDTA, 8.29 g NH_4Cl, and 1.00 g $KHCO_3$ (all from Sigma) in 1 L of distilled water.

Subjects and study design. Healthy male volunteers, with a mean age of 23.8 ± 0.8 yr (range 18–39), were randomly assigned to receive one of six dietary supplements (n = 8 subjects per group, no difference in mean age between groups). Each volunteer consumed nine capsules of oil (1 capsule = 1 g) daily for 12 wk. The subjects were instructed not to change their diets or lifestyles during the course of the study. None of the volunteers reported any side effects during or after the supplementation period. Fasting blood samples (40 mL) were taken from the volunteers prior to the beginning of supplementation (baseline) and after 4, 8, and 12 wk of supplementation; a final blood sample was taken 8 wk after the end of supplementation.

Compositions of the dietary supplements. The dietary supplements contained the following oil mixtures: (i) Placebo oil: comprised of 80% palm oil and 20% soybean oil [The fatty acid composition of this oil mix mimics closely that of the average United Kingdom diet (20)]; (ii) tuna oil; (iii) a 50:50 mix of tuna oil and placebo oil; (iv) a 25:75 mix of tuna oil and placebo oil; (v) a 12.5:87.5 mix of tuna oil and placebo oil; and (vi) linseed oil. Table 1 shows the fatty acid composition of each of the dietary supplements.

Neutrophil isolation. Whole heparinized blood was carefully layered onto an equal volume of Histopaque-1077 and then centrifuged at 600 × g for 15 min. The plasma and mononuclear cell layers were aspirated off. Contaminating erythrocytes were removed by washing with lysis buffer (prepared as described above) twice (10 min each wash), and the purified neutrophils were then finally washed and resuspended in HBSS containing calcium and magnesium. Neutrophils were counted with a Coulter Counter (Coulter Electronics Ltd., Luton, Bedforshire, United Kingdom) and adjusted to the appropriate concentration.

Superoxide generation. The superoxide dismutase (SOD) inhibitable reduction of cytochrome c was used to measure production of superoxide radicals by neutrophils. Neutrophils (1×10^6) were incubated with cytochalasin B (final concentration 10.4 μM); dissolved in dimethyl sulfoxide (DMSO), catalase (final concentration 35 IU/mL), and cytochrome c (final concentration 1.5 mg/mL) for 5 min at 37°C. The cells were then stimulated with 100 nM fMLP, and the rate of superoxide generation was followed for 10 min by determining the change in absorbance of the reaction mixture at 550 nm using a kinetic microtiter plate reader; initial rates of superoxide production were obtained over the first 3 min only. The final reaction volume was 200 μL. SOD was included in the reaction mix in some determinations (at a concentration of 10 units/mL) to demonstrate that cytochrome c reduction was superoxide-dependent. Neutrophils incubated with HBSS, 35 IU/mL catalase, 10.4 μM cytochalasin B, and 1.5 mg/mL cytochrome c, ONLY, did not produce measurable amounts of superoxide.

Neutrophil chemotaxis. Neutrophil chemotaxis was assayed in a modified Boyden chamber. The wells of the 96-well plate contained a 100-nM solution of fMLP in HBSS.

TABLE 1
Fatty Acid Composition of Dietary Supplements[a]

	Supplement					
Fatty acid	PO	LO	100% TO	50% TO	25% TO	12.5% TO
14:0	2.1 (0.6)	0.4 (0.4)	6.0 (1.0)	4.9 (1.7)	5.1 (1.4)	1.5 (0.8)
16:0	34.9 (1.7)	7.0 (0.3)	22.8 (1.7)	29.6 (2.1)	30.3 (0.4)	33.5 (2.0)
16:1n-7	2.0 (1.0)	0.2 (0.2)	5.3 (2.0)	4.3 (0.5)	3.3 (0.8)	2.6 (0.8)
18:0	3.7 (0.1)	6.5 (2.0)	6.7 (1.7)	5.0 (0.1)	4.5 (0.6)	4.9 (0.6)
18:1n-9	33.8 (2.7)	18.9 (1.4)	15.5 (1.4)	25.2 (4.7)	27.3 (1.8)	32.6 (2.2)
18:2n-6	18.9 (0.5)	16.9 (0.7)	2.4 (0.7)	12.0 (1.5)	14.4 (1.8)	17.4 (0.8)
18:3n-3	1.8 (0.4)	45.9 (1.0)	1.6 (0.1)	2.1 (0.7)	2.3 (0.8)	2.3 (0.4)
20:2n-6		2.0 (1.1)				
20:4n-6		1.7 (0.2)	2.3 (0.4)	2.2 (0.7)		
20:5n-3			6.4 (1.1)	3.3 (0.8)	1.9 (0.6)	0.7 (0.4)
22:5n-3			0.8 (0.4)			
22:6n-3			18.5 (1.9)	8.7 (1.1)	3.7 (0.6)	2.3 (0.4)

[a]Values shown are percentage of fatty acids present and are means of three determinations; values in brackets are SEM. Abbreviations: PO, placebo oil; LO, linseed oil; TO, tuna oil.

Neutrophils (suspended in HBSS at a concentration of 3×10^6 cells per well) were separated from the fMLP by a 5-μm pore filter (purchased from Neuro Probe Inc., Gaithersburg, MD). The chamber was incubated for 1 h at 37°C. Chemotaxis was measured as the number of neutrophils migrating across the filter into the wells containing fMLP. Neutrophils were counted using a Coulter counter. The number of migrated cells in control wells was in the range of 2.8×10^4 to 5.0×10^4 cells per well. Mean values of migrated cells in control wells (i.e., no fMLP) did not change at any time point for any dietary supplement (data not shown).

Neutrophil fatty acid composition. Neutrophil lipids were extracted by addition of 5 vol of a 2:1 chloroform/methanol mixture to the neutrophil suspension (containing 15×10^6 cells per sample) in PBS. The tubes were sealed under nitrogen to prevent lipid oxidation, vortexed vigorously, and then centrifuged at 400 × *g* for 10 min. After collection of the solvent phase, any remaining lipids in the aqueous phase were extracted using 3 vol of pure chloroform. The solvent phases containing lipids were pooled and then washed twice with 0.88% KCl solution in order to remove traces of water. The lipid extract was dried down completely under nitrogen. The lipids were resuspended in 100 μL of methanol, and 1 mL of 0.5 M KOH was added. The lipids were sealed under nitrogen and saponified by incubation at 80–90°C for about 4 h. After this time, the mixture was allowed to cool to room temperature, and 50 μL of 5 M H_2SO_4 was added to bring the mixture to ~pH 7. The fatty acids were then extracted as in the initial lipid extraction phase and finally dissolved in ~10 μL methanol. Fatty acids were methylated by addition of 200 μL of diazomethane in ether. After 20 min, the samples were dried down completely under nitrogen. The fatty acid methyl esters were redissolved in hexane and separated by gas chromatography in a Hewlett-Packard 6890 gas chromatograph (Hewlett-Packard, Avondale, PA) fitted with a 30 m × 0.32 mm BPX70 capillary column, film thickness 0.25 μm. Helium at 2.0 mL/min was used as the carrier gas, and the split/splitless injector was used with a split/splitless ratio of 10:1. Injector and detector temperatures were 170 and 250°C, respectively. The column oven temperature was maintained at 170°C for 12 min after sample injection and was programmed to then increase from 170 to 200°C at 5°C/min before being maintained at 200°C for 15 min. The separation was recorded with HP GC Chem Station software (Hewlett-Packard). Fatty acid methyl esters were identified by comparison with standards run previously.

Statistical analysis. The effect of dietary supplementation was assessed by using analysis of variance and suitable post-hoc tests; a significance level of $P < 0.05$ was used.

RESULTS

Neutrophil fatty acid composition. Significant increases in the proportions of both EPA and DHA were observed after dietary supplementation with the 100, 50, and 25% tuna oils (Fig. 1A,B,C and Fig. 2A,B,C). The content of both n-3

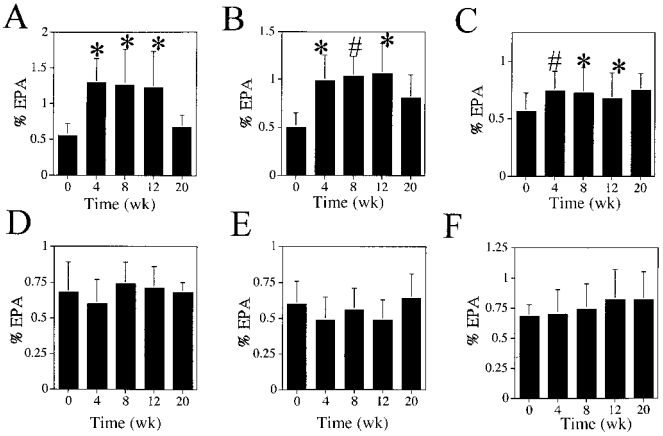

FIG. 1. The effect of 9 g/d of 100% tuna oil (A), 50% tuna oil (B), 25% tuna oil (C), 12.5% tuna oil (D), placebo oil (E), and linseed oil (F) on neutrophil eicosapentaenoic acid (EPA) content. In each case, neutrophil EPA content was determined prior to supplementation (0 wk), during supplementation (at 4, 8, and 12 wk), and after an 8-wk post-supplementation washout period (20 wk). Results are expressed as means percentage EPA found in neutrophil lipids ± SD ($n = 8$). $^*P < 0.05$, $^\#P < 0.01$ vs. value at 0 wk (one-way analysis of variance).

PUFA was maximal after 4 wk of dietary supplementation. The other supplements had no effect on neutrophil EPA or DHA content (Fig. 1D,E,F and Fig. 2D,E,F). There were significant linear correlations ($P < 0.0001$) between the amounts of EPA and DHA provided per day by the dietary supplements and the proportions of EPA and DHA, respectively, in neutrophil lipids (Fig. 3). A significant decrease in neutrophil ARA was observed after supplementation with the 100 and 50% tuna oils and the linseed oil (Fig. 4A,B,F). The decrease occurred after 8 wk supplementation in each case, and was maximal at 12 wk for the linseed oil supplement (Fig.

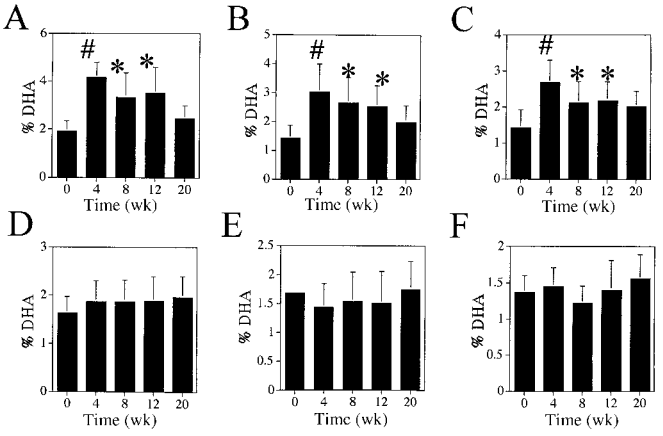

FIG. 2. The effect of 9 g/d of 100% tuna oil (A), 50% tuna oil (B), 25% tuna oil (C), 12.5% tuna oil (D), placebo oil (E), and linseed oil (F) on neutrophil docosahexaenoic acid (DHA) content. In each case, neutrophil DHA content was determined prior to supplementation (0 wk), during supplementation (at 4, 8 and 12 wk), and after an 8-wk post-supplementation washout period (20 wk). Results are expressed as means percentage DHA found in neutrophil lipids ± SD ($n = 8$). $^*P < 0.05$, $^\#P < 0.01$ vs. value at 0 wk (one-way analysis of variance).

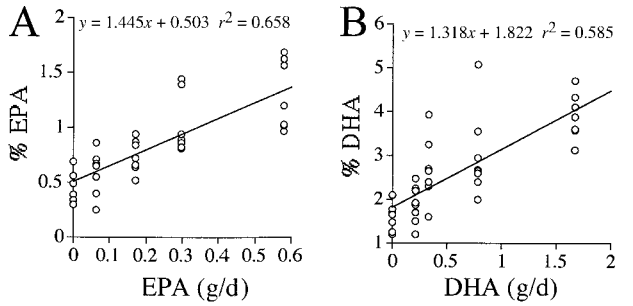

FIG. 3. The effect of EPA and DHA dose on EPA and DHA levels in neutrophil lipids after 4 wk supplementation. The relationship between the daily amounts of EPA and DHA provided by the dietary supplements and the proportions of those fatty acids in neutrophil lipids was determined by calculating Spearman's correlation coefficient (*r*). (A) EPA dose vs. phospholipid EPA; (B) DHA dose vs. phospholipid DHA. See Figures 1 and 2 for abbreviations.

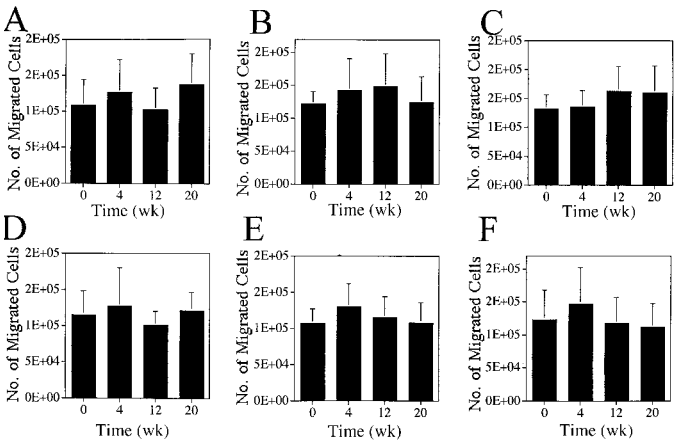

FIG. 5. The effect of 9 g/d of 100% tuna oil (A), 50% tuna oil (B), 25% tuna oil (C), 12.5% tuna oil (D), placebo oil (E), and linseed oil (F) on chemotaxis by neutrophils stimulated with 100 nM *N*-formyl-met-leu-phe (fMLP). Neutrophil chemotaxis was assessed prior to supplementation (0 wk), during supplementation (at 4, 8, and 12 wk), and after an 8-wk postsupplementation washout period (20 wk). Results are expressed as means number of neutrophil migrations occurring per hour ± SD ($n = 8$). Not significant vs. value at 0 wk (one-way analysis of variance).

4A,B,F). The other supplements had no effect on neutrophil ARA content (Fig, 4C,D,E).

Neutrophil superoxide generation and chemotaxis. The dietary supplements did not significantly affect neutrophil chemotaxis or superoxide radical generation (initial rate and total production) (Figs. 5–7).

DISCUSSION

Neutrophil fatty acid composition was found to change in a dose-dependent fashion. The changes observed after tuna oil supplementation in this study are in agreement with the findings of studies where larger amounts of fish oil were used to supplement the diets of healthy volunteers (14,20). For example, provision of 1.4–4.2 g EPA plus 0.9–1.4 g DHA per day resulted in an increase of EPA content in neutrophils from 1.2 ± 0.2 to 3.2 ± 0.7% ($P < 0.05$) after 2 wk and an increase in DHA content from 1.9 ± 0.8 to 2.7 ± 0.8% ($P < 0.05$) after 12 wk (20). In the present study, provision of up to 0.58 g EPA plus 1.7 g DHA per day resulted in an increase in the EPA content of neutrophils from 0.55 ± 0.17 to 1.29 ± 0.34% ($P < 0.05$) and an increase in the DHA content from 1.92 ± 0.41 to 4.16 ± 0.63% ($P < 0.05$) after 4 wk supplementation, and remained so without increasing for the ensuing 8 wk.

The linseed oil supplement was included in the study because it contains a high concentration of α-linolenic acid

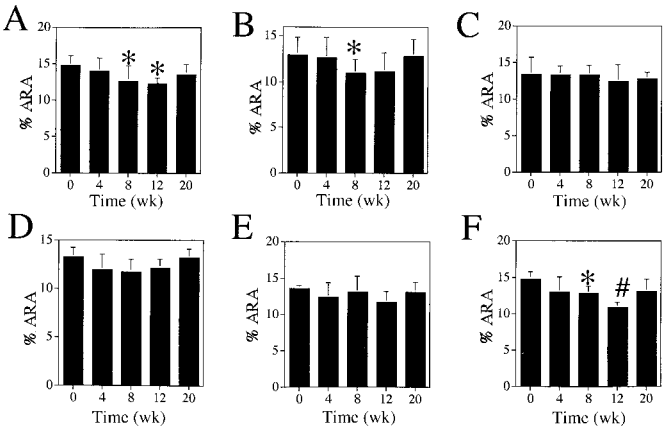

FIG. 4. The effect of 9 g/d of 100% tuna oil (A), 50% tuna oil (B), 25% tuna oil (C), 12.5% tuna oil (D), placebo oil (E), and linseed oil (F) on neutrophil arachidonic acid (ARA) content. Neutrophil ARA content was determined prior to supplementation (0 wk), during supplementation (at 4, 8, and 12 wk), and after an 8-wk postsupplementation washout period (20 wk). Results are expressed as means percentage ARA in neutrophil lipids ± SD ($n = 8$). $^{*}P < 0.05$, $^{\#}P < 0.01$ vs. value at 0 wk (one-way analysis of variance).

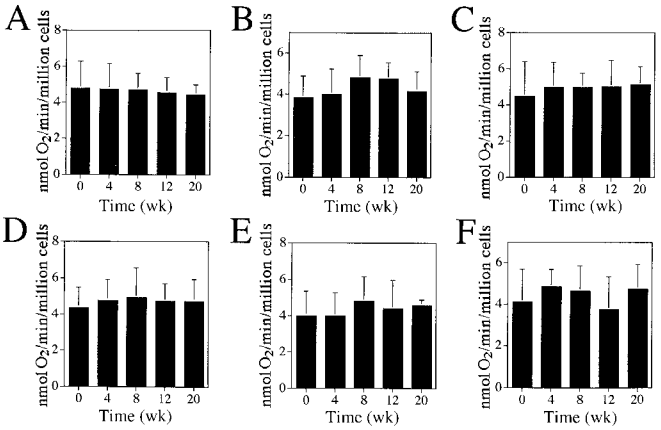

FIG. 6. The effect of 9 g/d of 100% tuna oil (A), 50% tuna oil (B), 25% tuna oil (C), 12.5% tuna oil (D), placebo oil (E), and linseed oil (F) on initial rate of superoxide generation by neutrophils stimulated with 100 nM fMLP. Initial rate of superoxide generation was determined prior to supplementation (0 wk), during supplementation (at 4, 8, and 12 wk) and after an 8-wk postsupplementation washout period (20 wk). Results are expressed as mean nanomoles superoxide produced per minute per million cells ± SD ($n = 8$). Not significant vs. value at 0 wk (one-way analysis of variance). See Figure 5 for abbreviation.

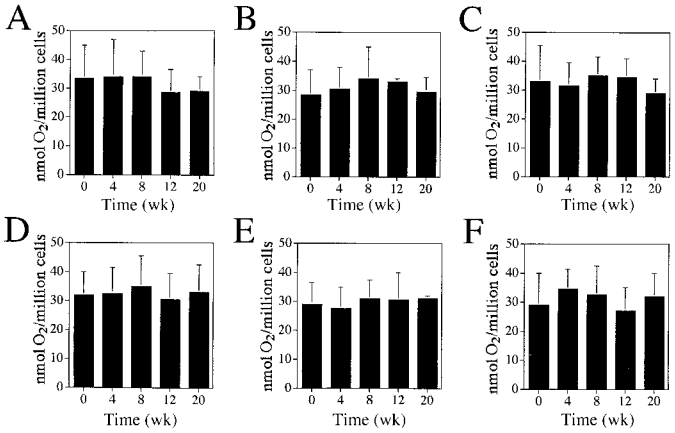

FIG. 7. The effect of 9 g/d of 100% tuna oil (A), 50% tuna oil (B), 25% tuna oil (C), 12.5% tuna oil (D), placebo oil (E), and linseed oil (F) on total superoxide generation by neutrophils stimulated with 100 nM fMLP. Superoxide generation was determined prior to supplementation (0 wk), during supplementation (at 4, 8, and 12 wk), and after an 8-wk postsupplementation washout period (20 wk). Results are expressed as means nmoles superoxide generated per million cells ± SD (n = 8). Not significant vs. value at 0 wk (one-way analysis of variance). See Figure 5 for abbreviation.

(α-LA; 18:3n-3), which is a precursor of both EPA and DHA *in vivo*. It was speculated that supplementation with the linseed oil would lead to increased biosynthesis of EPA and DHA *in vivo*, with a subsequent increased incorporation of EPA and DHA into neutrophil lipids. However, the results showed that provision of up to 4 g extra α-LA per day had no effect on neutrophil lipid EPA or DHA levels. The linseed oil significantly decreased the amount of ARA found in the neutrophil lipids. This may be due to an inhibitory effect of α-LA on ARA biosynthesis from linoleic acid.

Despite the changes in neutrophil composition observed after tuna oil supplementation, there were no concomitant changes in neutrophil superoxide radical formation or chemotaxis following exposure to an inflammatory stimulus (100 nM fMLP). This is in contrast to other studies where amounts of fish oil providing more than 2.6 g EPA plus 1.4 g DHA per day were ingested, resulting in significant changes in neutrophil functions (6,7,9,14,18,19,21,22). High doses of fish oil led to significantly decreased superoxide production in response to phorbol myristic acid (PMA) (6) or opsonized zymosan (7), and also significantly reduced the chemotactic response to stimulants including leukotriene B_4 (LTB_4) (21), autologous serum (18,19), and fMLP (18,19,22). Other neutrophil functions attenuated by fish oil supplementation include LTB_4 production (9,21) and ARA release (21) following stimulation by the calcium ionophore A23187. However, other studies using lower amounts of fish oil have reported no effect of fish oil on neutrophil superoxide production and adhesion following stimulation with fMLP, PMA, or opsonized zymosan (23,24).

Due to limited availability of neutrophils in the present study, only two functional parameters were studied in detail, namely superoxide production and chemotaxis in response to fMLP. It is possible that the level of fish oil supplementation in the present study did alter other parameters of function, but these were not assessed.

The results obtained here suggest that supplementation of the diet with low-to-moderate amounts of fish oil daily may be of little benefit in the treatment of inflammatory disorders. However, several points regarding this assessment need to be addressed. First, during this study the volunteers were instructed to maintain their normal diet and lifestyle. Therefore, the n-6 PUFA intake of the volunteers remained unchanged. It has been speculated that the high n-6 PUFA of the modern Western diet may not be optimal for the expression of the anti-inflammatory effects of the n-3 PUFA (25). Although the n-6/n-3 PUFA ratio of the neutrophils was significantly decreased by the fish oil supplementation, it may still be too high for any anti-inflammatory effect of the fish oil to be evident. Also it has been shown that LA inhibits the incorporation of dietary n-3 PUFA into human (26) and rat (25) immune cell lipids. Therefore, a moderate increase in n-3 PUFA intake combined with a decrease in n-6 PUFA intake may produce significant anti-inflammatory effects. This remains to be investigated. Second, in this study, the effect of low-to-moderate fish oil supplementation on neutrophil responses was examined in young males, whereas older subjects are more vulnerable to inflammatory diseases. The possibility that fish oil may behave differently among individuals of different ages cannot be excluded.

Moderate fish oil supplementation of the diet may have an important role to play in the therapy of inflammatory disorders when used as an adjunct to conventional pharmacological therapy. Several studies have shown drug-sparing effects of fish oil when used in conjunction with drugs in the treatment of rheumatoid arthritis (27,28). Use of multicomponent therapy for inflammatory disorders may be of greater benefit than drug use alone. This is especially important where existing drug-based treatments result in significant toxicity.

ACKNOWLEDGMENTS

This research was supported in part by a grant to PCC from the BBSRC (Grant No. 51/FO5696) and a grant to PN from Enterprise Ireland (SC/1997/249). DAH is supported by funding from Enterprise Ireland and FAW holds a Rank Prize Fund Studentship.

REFERENCES

1. Muid, R.E., Twomey, B.M., and Dale, M.M. (1994) The Neutrophil Leucocyte, *Textbook of Immunopharmacology,* Chapter 3, Blackwell Scientific Publications, Oxford, United Kingdom.
2. Weiss, S.J. (1989) Tissue Destruction by Neutrophils, *New Engl. J. Med. 320,* 365–376.
3. Smith, J.A. (1994) Neutrophils, Host Defense, and Inflammation: A Double-Edged Sword, *J. Leucocyte Biol. 56,* 672–686.
4. Chanock, S.J., El Benna, J., Smith, R.M., and Babior, B.M. (1994) The Respiratory Burst Oxidase, *J. Biol. Chem. 269,* 24519–24522.
5. Babior, B.M. (1978) Oxygen-Dependent Microbial Killing by Phagocytes (Part 1), *New Engl. J. Med. 298,* 659–668.
6. Luostarinen, R., and Saldeen, T. (1996) Dietary Fish Oil Decreases Superoxide Generation by Human Neutrophils: Relation

to Cyclooxygenase Pathway and Lysosomal Enzyme Release, *Prostaglandins Leukotrienes Essent. Fatty Acids 55,* 167–172.
7. Varming, K., Schmidt, E.B., Svaneborg, N., Moller, J.M., Lervang, H.H., Grunnet, N., Jersild, C., and Dyerberg, J. (1995) The Effect of n-3 Fatty Acids on Neutrophil Chemiluminescence, *Scand. J. Clin. Lab. Invest. 55,* 47–52.
8. Sperling, R.I. (1991) Effects of Dietary Fish Oil on Leukocyte Leukotriene and PAF Generation and on Neutrophil Chemotaxis, *World Rev. Nutr. Diet. 66,* 391–400.
9. Sperling, R.I., Benincaso, A.I., Knoell, C.T., Larkin, J.K., Austen, K.F., and Robinson, D.R. (1993) Dietary n-3 Polyunsaturated Fatty Acids Inhibit Phosphoinositide Formation and Chemotaxis in Neutrophils, *J. Clin. Invest. 91,* 651–660.
10. Ziboh, V.A., Cohen, K.A., Ellis, C.N., Miller, C., Hamilton, T.A., Kragballe, K., Hydrick, C.R., and Voorhees, J.J. (1986) Effects of Dietary Supplementation of Fish Oil on Neutrophil and Epidermal Fatty Acids. Modulation of Clinical Course of Psoriatic Subjects, *Arch. Dermatol. 122,* 1277–1282.
11. Kremer, J.M., Lawrence, D.A., Jubiz, W., DiGiacomo, R., Rynes, R., Bartholomew, L.E., and Sherman, M. (1990) Dietary Fish Oil and Olive Oil Supplementation in Patients with Rheumatoid Arthritis: Clinical and Immunologic Effects, *Arthr. Rheum. 33,* 810–820.
12. Schmidt, E.B., and Dyerberg, J. (1989) n-3 Fatty Acids and Leucocytes, *J. Intern. Med. 225,* 151–158 (Suppl. 1).
13. Abramson, S.B., Leszczynska-Piziak, J., and Weissmann, G. (1991) Arachidonic Acid as a Second Messenger: Interactions with a GTP-Binding Protein of Human Neutrophils, *J. Immunol. 147,* 231–236.
14. Chilton, F.H., Patel, M., Fonteh, A.N., Hubbard, W.C., and Triggiani, M. (1993) Dietary n-3 Fatty Acid Effects on Neutrophil Lipid Composition and Mediator Production (influence of duration and dosage), *J. Clin. Invest. 91,* 115–122.
15. Terano, T., Hirai, A., Tamura, Y., Kumagai, A., and Yoshida, S. (1987) Effect of Dietary Supplementation of Highly Purified Eicosapentaenoic Acid and Docosahexaenoic Acid on Arachidonic Acid Metabolism in Leukocytes and Leukocyte Function in Healthy Volunteers, *Adv. Prostaglandin Thromboxane Leukotriene Res. 17,* 880–885.
16. Sipka, S., Dey, I., Buda, C., Csongor, J., Szegedi, G., and Farkas, T. (1989) The Mechanism of Inhibitory Effect of Eicosapentaenoic Acid on Phagocytic Activity and Chemotaxis of Human Neutrophil Granulocytes, *Clin. Immunol. Immunopathol. 52,* 257–270.
17. Kragballe, K., Voorhees, J.J., and Goetzl, E.J. (1987) Inhibition by Leukotriene B_5 of Leukotriene B_4-Induced Activation of Human Keratinocytes and Neutrophils, *J. Invest. Dermatol. 88,* 555–558.
18. Schmidt, E.B., Varming, K., Pedersen, J.O., Lervang, H.H., Grunnet, N., Jersild, C., and Dyerberg, J. (1992) Long-Term Supplementation with n-3 Fatty Acids, II: Effect on Neutrophil and Monocyte Chemotaxis, *Scand. J. Clin. Lab. Invest. 52,* 229–236.
19. Schmidt, E.B., Pederson, J.O., Ekelund, S., Grunnet, N., Jersild, C., and Dyerberg, J. (1989) Cod Liver Oil Inhibits Neutrophil and Monocyte Chemotaxis in Healthy Males, *Atherosclerosis 77,* 53–57.
20. Gibney, M.J., and Hunter, B. (1993) The Effects of Short- and Long-Term Supplementation with Fish Oil on the Incorporation of n-3 Polyunsaturated Fatty Acids into Cells of the Immune System in Healthy Volunteers, *Eur. J. Clin. Nutr. 47,* 255–259.
21. Lee, T.H., Hoover, R.L., Williams, J.D., Sperling, R.I., Ravalese, J., III, Spur, B.W., Robinson, D.R., Corey, E.J., Lewis, R.A., and Austen, K.F. (1985) Effect of Dietary Enrichment with Eicosapentaenoic and Docosahexaenoic Acids on *in vitro* Neutrophil and Monocyte Leukotriene Generation and Neutrophil Function, *New Engl. J. Med. 312,* 1217–1224.
22. Luostarinen, R., Siegbahn, A., and Saldeen, T. (1992) Effect of Dietary Fish Oil Supplemented with Different Doses of Vitamin E on Neutrophil Chemotaxis in Healthy Volunteers, *Nutr. Res. 12,* 1419–1430.
23. Guarini, P., Bellavite, P., Biasi, D., Carletto, A., Galvani, S., Caramaschi, P., Bambara, L.M., and Corrocher, R. (1998) Effects of Dietary Fish Oil and Soy Phosphatidylcholine on Neutrophil Fatty Acid Composition, Superoxide Release, and Adhesion, *Inflammation 22,* 381–391.
24. Schmidt, E.B., Varming, K., Moller, J.M., Bulow Pedersen, I., Madsen, P., and Dyerberg, J. (1996) No Effect of a Very Low Dose of n-3 Fatty Acids on Monocyte Function in Healthy Humans, *Scand. J. Clin. Lab. Invest. 56,* 87–92.
25. James, M.J., and Cleland, L.G. (1997) Dietary n-3 Fatty Acids and Therapy for Rheumatoid Arthritis, *Semin. Arthritis Rheum. 27,* 85–97.
26. Cleland, L.G., James, M.J., Neumann, M.A., D'Angelo, M., and Gibson, R.A. (1992) Linoleate Inhibits EPA Incorporation from Dietary Fish Oil Supplements in Human Subjects, *Am. J. Clin. Nutr. 55,* 395–399.
27. Kjeldsen-Kragh, J., Lund, J.A., Riise, T., Finnanger, B., Haaland, K., Finstad, R., Mikkelsen, K., and Førre, Ø. (1992) Dietary Omega-3 Fatty Acid Supplementation and Naproxen Treatment in Patients with Rheumatoid Arthritis, *J. Rheumatol. 19,* 1531–1536.
28. Kremer, J.M., Lawrence, D.A., Petrillo, G.F., Litts, L.L., Mullaly, P.M., Rynes, R.I., Skocker, R.P., Parhami, N., Greenstein, N.S., Fuchs, B.R., *et al.* (1995) Effects of High-Dose Fish Oil on Rheumatoid Arthritis After Stopping Nonsteroidal Antiinflammatory Drugs, *Arthritis Rheum. 38,* 1107–1114.

[Received July 2, 1999, and in final revised form May 25, 2000; final revision accepted June 7, 2000]

Preferential Loss of Visceral Fat Following Aerobic Exercise, Measured by Magnetic Resonance Imaging

E. Louise Thomas[a,*], Audrey E. Brynes[b], John McCarthy[c], Anthony P. Goldstone[d], Joseph V. Hajnal[a], Nadeem Saeed[a], Gary Frost[b], and Jimmy D. Bell[a]

[a]The Robert Steiner MR Unit, MRC Clinical Sciences Centre, [b]Department of Nutrition and Dietetics and [d]Endocrine Unit, Imperial College School of Medicine, Hammersmith Hospital, and [c]The National Sports Medicine Institute of the United Kingdom, London, England

ABSTRACT: The aim of this study was to use whole-body magnetic resonance imaging (MRI) together with biochemical and anthropometric measurements to study the influence of regular moderate exercise with no dietary intervention on adipose tissue distribution in nonobese healthy women. We found significant decreases in both total (28.86 ± 2.24 vs. 27.00 ± 2.27 liters, $P < 0.05$) and regional fat depots (visceral fat: 1.68 ± 0.21 vs. 1.26 ± 0.18 liters, $P < 0.01$) using whole-body MRI despite no significant change in body weight, body mass index, or the waist-to-hip ratio. Interestingly, no changes in body fat content were found using anthropometry or impedance. There was a significant increase in high density lipoprotein cholesterol (1.58 ± 0.06 vs. 1.66 ± 0.08 mmol/L $P < 0.02$) following exercise although there were no changes in other blood lipids such as triglycerides. In summary, moderate aerobic exercise over a period of 6 mon resulted in a preferential loss in visceral fat in nonobese healthy women, and this may help to explain some of the health benefits associated with regular and moderate physical activity.

Paper no. L8300 in *Lipids 35*, 769–776 (July 2000).

The health benefits of regular exercise are well-established (1,2). However, results regarding the effect of exercise on adipose tissue are conflicting (3,4). Many studies have shown the effect of exercise and diet on the amount and distribution of adipose tissue (3), but the effect of exercise alone on different adipose tissue depots is less well-studied. Furthermore, many studies examining the effects of exercise on body morphology and composition have used overweight or obese subjects, given that they appear to be more likely to benefit from a change in physical activity. Less is known, however, regarding the effect of a moderate amount of aerobic exercise on body fat content in nonobese healthy women.

*To whom correspondence should be addressed at Robert Steiner MRI Unit, Imperial College School of Medicine, Hammersmith Hospital, Du Cane Road, London, W12 OHS, United Kingdom. E-mail: louise.thomas@ic.ac.uk

Abbreviations: BASES, British Association of Sports and Exercise Science; BMI, body mass index; CI, confidence interval; CT, computer-assisted tomography; CV, coefficient of variation; DHEAS, dehydroepiandrosterone sulfate; HDL-C, high density lipoprotein cholesterol; LDL-C, low density lipoprotein cholesterol; MRI, magnetic resonance imaging; NEFA, nonesterified fatty acid; SHBG, sex hormone-binding globulin; VeO_2, ventilatory oxygen equivalent; VO_2 max, maximal rate of oxygen consumption; WHR, waist-to-hip ratio.

A number of techniques have been applied to the study of body fat content following exercise. Underwater weighing and anthropometry are often used, although these indirect techniques can be used to measure total body fat, they cannot be used to assess regional fat depots such as visceral fat (5,6). Computer-assisted tomography (CT) allows the direct measurement of visceral fat, but owing to the radiation dose involved, only single slices tend to be acquired (6). Magnetic resonance imaging (MRI) provides an accurate measure of body fat content as well as a direct measure of visceral fat content. MRI has previously been applied to studies which have shown changes in regional and total body fat in obese women following a combination of energy restriction and exercise (7,8).

In this study we used whole-body MRI together with biochemical and anthropometric measurements to determine the influence of regular moderate exercise with no dietary intervention on adipose tissue distribution in nonobese sedentary healthy women.

SUBJECTS AND METHODS

Written informed consent was obtained from all volunteers. Permission for this study was obtained from the Ethics Committee of the Royal Postgraduate Medical School, Hammersmith Hospital, London (REC. 92/3995).

Thirty women were initially recruited; data from the 17 who completed all parts of the study are presented in this paper. Thirteen women did not complete the study, mainly because they were a young, mobile population, and many of whom moved out of the area and thus were unable to attend the gym used for their exercise to be monitored. Regular attendance at a specific gym was an essential prerequisite for participation in this study.

Seventeen nonobese, premenopausal healthy (previously nonexercising) female volunteers (mean age: 32.6 ± 1.8 yr; range: 25–45 yr) were studied before and after 6 mon of three times per week aerobic exercise. Volunteers were recruited for this study following advertisements placed in local newspapers. All women were interviewed by the senior investigator prior to inclusion in the study. The primary motivation given by the women joining the study was to improve their

fitness. Exclusion criteria included a history of obesity, dieting, or eating disorders, any form of medication including the contraceptive pill, smoking, or a previous history of regular exercise. Each woman served as her own control for the purpose of this study.

Regional and total body fat contents were measured by whole-body MRI. Body fat content was also measured by bioelectric impedance and skinfold anthropometry. Exercise records were regularly obtained from all the volunteers to ensure compliance with the exercise regime. Dietary intake was also measured at the beginning and at the end of the study to ensure that volunteers were not restricting their energy intake.

MRI and analysis. Subjects were imaged lying prone in a Picker 1.0T HPQ system (Marconi Medical Systems, Cleveland, OH) with a rapid T_1 weighted spin-echo sequence (TR 36 ms, TE 14 ms) (9). Subjects were scanned from their fingertips to their toes by acquiring 10-mm thick transverse images with a 30-mm gap between slices in the arms and legs and a 10-mm gap in the torso (10). Images were analyzed using an image segmentation software program that employs a threshold range and a contour-following algorithm with an interactive image-editing facility (11). The total internal fat content of each subject was subdivided into visceral and nonvisceral (i.e., intramuscular, pericardial, and fat from depots other than visceral fat) internal body fat. Visceral fat content was obtained by quantifying fat signals in the slices from the femoral heads to the slice containing the top of the liver or the base of the lungs (T10). Subcutaneous fat in these slices was labeled as abdominal subcutaneous fat. All other internal fat was labeled as nonvisceral internal fat. The coefficient of variation (CV) varies between different depots, but the data analysis method is generally highly reproducible, 3% internal fat, 5% visceral fat, and less than 1% for total, subcutaneous, subcutaneous abdominal, fat and bone marrow fat, respectively.

Exercise testing. All participants were assessed for their physical fitness at the National Sports Medicine Institute of the United Kingdom (Exercise Physiology Laboratory) before starting and at regular intervals throughout the study. Prior to testing, each subject completed a standard health questionnaire (Par-Q) to inform the physiologist of any health details that might influence the test results or her participation (12).

Physiological assessment. Following informed consent, all subjects were assessed for cardiorespiratory fitness at the beginning of the study. The measurements on each visit to the test facility included resting lung function and the maximal rate of oxygen consumption (VO_2 max).

Resting lung function. This was measured using a standard bellows Vitalograph (Vitalograph Ltd., Buckinghampshire, United Kingdom). Standard measures of forced vital capacity and forced expiratory volume in 1 s were made. Established tables of normative values (of age-, height-, and sex-matched individuals) were used for comparison (Vitalograph Ltd.).

VO_2 max. Each subject performed an incremental treadmill walking test at a constant 5 km/h, where the slope was increased by 2.5% every 2 min (Astrand protocol). All subjects were encouraged to continue the test to volitional exhaustion (or their measured peak capacity). Expired air was analyzed continuously for percentages of oxygen and carbon dioxide and minute ventilation (volume of air per minute) to measure oxygen consumption using an on-line metabolic cart [Jaeger Eos Sprint, Erich Jaeger (U.K.) Ltd.]. Subjects rated their perceived exertion using an unmodified Borg Scale in the last 30 s of each treadmill stage (13). The subject's heart rate was monitored continuously throughout the test (by using a Hewlett-Packard 43120A combined three-lead electrocardiogram monitor/defibrillator). The subject's resting (seated) heart rate was recorded before the test and her recovery (seated) heart rate 3 min immediately posttest. British Association of Sport and Exercise Science (BASES) guidelines were followed for all calibration and testing protocols (14). All measurements were carried out by the same accredited (BASES) exercise physiologist (JM). The CV of repeated VO_2 measurement in the laboratory is less than 2% (gas analyzer accuracy level = 0.1%). The CV for VO_2 measurements for any given individual on a day-to-day basis was approximately 3%.

Exercise. (i) Prescription. The results of the baseline cardiorespiratory test were used to ensure all subjects performed the same level of exercise. All participants were requested to perform three exercise sessions per week for a minimum of 30-min duration each time at an intensity corresponding to 60–70% of their individual VO_2max (derived from graphs of their VO_2 max vs. heart rate).

(ii) Progression. Because the individuals included in this study had not previously exercised and may therefore increase their VO_2 max quite quickly, it was necessary to retest everyone at 12 wk to ensure that their personalized "training zone" had not altered owing to improved fitness. All tests were scheduled to coincide with the individual's phase of their menstrual cycle and similar time of day from the baseline assessment. A new heart rate training zone was prescribed for those who had improved their fitness, to maintain the 60–70% of VO_2 max level of work in all their exercise classes for the duration of the study.

Exercise classes. Exercise classes consisted of pre-set aerobic routines including step-classes and aerobic exercise to music. All subjects were educated as to the correct use of heart rate monitors and how to exercise within their training zone. During the exercise period, all subjects were provided with ambulatory heart rate monitors (Polar/Cardiosport, Cardiosport Healthcare Technology Limited, Chichester, United Kingdom) and training diaries. The participants were asked to record their exercising heart rate at 10-min intervals during the organized classes. Each participant achieved and maintained her prescribed heart rate as instructed—maintenance was achieved by individual attenuation of the workload where necessary throughout the class. The attenuation was reinforced by visits from the researchers to the fitness establishment, during laboratory test sessions, and by periodic telephone contact. Activities outside the classes included danc-

ing (classes), swimming, jogging, and cycling for a small minority of participants and occurred mainly with subjects that were away for short periods of time, e.g., holidays. Guidelines were given in written format about forms of exercise and the required intensities.

Dietary analysis. Each volunteer completed a 7-d dietary diary at the beginning and at the end of the 6-mon exercise study, using methodology validated by Bingham *et al.* (15). Subjects were given a standard booklet containing written instruction on prospectively recording their food intake, which was also backed up by verbal advice. Portion sizes were estimated using handy household measures. The diaries were then returned and the volunteers contacted by telephone if clarification of intake was needed. Dietary analysis was carried out using a standard database (Dietplan 5, Forest Field Software, Horsham, West Sussex, United Kingdom) containing all data from current food tables (16).

Indirect calorimetry. Energy expenditure was measured using a Deltatrac II indirect calorimeter (S.W. Vickers Ltd., Kent, United Kingdom). The calorimeter was calibrated using standard gas before every subject, and alcohol burning was performed once a month. Weight was measured to the nearest 0.5 kg (Seka Scales, West Germany) and height to the nearest centimeter using a standometer. Measurements lasted 23 ± 2.3 min (means ± SEM) excluding a 5-min run-in period and were carried out in the morning after a 12-h overnight fast.

Skinfold anthropometry. Anthropometric assessment was obtained on each subject by a single trained observer (AB). Measurements of weight, height, waist and hip circumference, and skinfold thicknesses from the triceps, biceps, subscapular, and suprailiac regions were obtained. Percentage total body fat was calculated for each individual using standard methods (17).

Bioelectric impedance. Body fat content was measured by bioelectrical impedance analysis using the Bodystat 1500 Unit (Bodystat, Isle of Man Ltd., United Kingdom).

Biochemical analysis. Blood was obtained from each volunteer following a 12-h overnight fast. Serum was assayed for total cholesterol and triglycerides (enzymatic method, Technicon Dax system, Bayer Diagnostics, Leverkusen, Germany), high density lipoprotein cholesterol (HDL-C; direct measurement, RIAXT machine; Biostat Diagnostics, Cheshire, United Kingdom), and low density lipoprotein cholesterol (LDL-C) was calculated using the Friedwald formula. Serum was also assayed for insulin by immunoradiometric assay (guinea pig antiinsulin antibody; Scottish Antibody Production Unit, Carluke, Lanarkshire, Scotland). Plasma glucose was measured using an automated glucose analyzer (RA-1000; Technicon Instrument Co. Ltd., Basingstoke, United Kingdom).

Sex hormone-binding globulin (SHBG) was measured using an automated assay employing enzyme tracer and chemiluminescent endpoints [Immulite Diagnostic Products Corporation (DPC), Los Angeles, CA]. Testosterone and dehydroepiandrosterone sulfate (DHEAS) were measured using the St. Thomas's Extraction Assay (Chelsea Kits, London, United Kingdom). Free testosterone index was calculated by dividing testosterone (nmol/L) by SHBG (nmol/L) and multiplying by 100. C-peptide was measured using an enzyme immunometric assay (Immulite, DPC) is presented as the ratio of C-peptide to insulin, which is a good marker of insulin resistance. Cortisol levels were assessed using a TDX FPIA (fluorescence polarization immunoassay) (Abbott, IL). Serum nonesterified fatty acids (NEFA) were measured using a colorimetric assay (Wako, Osaka, Japan). Plasma leptin was measured using a double-antibody radioimmunoassay (Linco Research, St. Charles, MO). CV values for these assays were <10%. Samples were collected and stored till the end of the study, then analyzed in a single batch.

Statistical analysis. All data from the 17 women who completed the study are presented as means ± SEM. Possible differences before and after exercise were tested for using the Student's paired *t*-test. Significance was taken as $P < 0.05$; 95% confidence intervals (CI) are provided in parentheses. Because of the relatively small number of subjects and the possibility of a nonnormal distribution, these data were also analyzed using nonparametric statistics (Wilcoxon Signed Rank Test), with no difference in the results. Pearson product movement correlation coefficients (*r*) were used to assess the relationship between variables.

RESULTS

Results are presented from the 17 women who completed the study. There were no significant differences at baseline between the women who completed the study and those who dropped out (results not shown). The compliance rate of the subjects completing the study over the 6 mon was approximately 93% with occasional holiday and illness periods causing minor disruptions. On average, during a given 7-d period, each subject performed three classes of 40-min duration (heart rate within required training zone—i.e., excluding warm-up and cool-down periods). On a few occasions two subjects performed additional exercise sessions—but when averaged over the 6-mon period, 3 d-per-wk was standard.

Fitness. Following the 6-mon exercise training, there was an improvement in fitness, with significant increases in VO_2 max [36.35 ± 1.87 vs. 40.23 ± 1.33 mL/kg/min, $P < 0.05$ (95% CI −7.00– −0.75)] and maximal ventilation [87.12 ± 3.29 vs. 96.23 ± 4.21 L/min, $P < 0.01$ (95% CI −15.50– −2.73)]. There was also a significant decrease in heart rate recovery [113.8 ± 2.1 vs. 106.8 ± 2.4 beats/min, $P < 0.05$ (95% CI, 0.67–12.03)] (Table 1). There was no significant change in mean VeO_2 (ventilatory oxygen equivalent), which would have been expected to decrease with improving fitness.

Indirect calorimetry. There was no change in resting metabolic rate, measured by indirect calorimetry [1345 ± 56 vs. 1305 ± 78 kcal (95% CI, 162.11–204.37)] or in respiratory quotient [0.85 ± 0.02 vs. 0.84 ± 0.02 (95% CI, −0.04–0.08)] after 6 mon of aerobic exercise.

Dietary intake. No subjects were excluded because of dieting, as there was good agreement between recorded dietary

TABLE 1
Changes in Fitness Post-exercise[a]

	Pre-exercise (n = 17)	Post-exercise (n = 17)	Significance	95% CI
VO_2max (mL/kg/min)	36.35 ± 1.87	40.23 ± 1.33	$P < 0.05$	7.00––0.75
VeO_2	32.06 ± 1.04	30.65 ± 0.96	NS	–1.49–4.31
Maximal ventilation (L/min)	87.12 ± 3.29	96.23 ± 4.21	$P < 0.01$	–15.50––2.73
Heart rate recovery (beats/min)	113.2 ± 2.1	106.8 ± 2.4	$P < 0.05$	0.67–12.03

[a]Results presented as means ± SEM and 95% confidence interval (CI). NS, not significant. VD_2 max, maximal rate of oxygen consumption.

intake and resting metabolic rate (RMR) × 1.5 physical activity ratio (PAR) activity factor ($r = 0.78$, $P < 0.05$). There were no significant changes in daily calorific intake by 7-d food diaries [1920.0 ± 179.62 vs. 1971.0 ± 146.24 kcal/d (95% CI, –264.86–162.86)] following the 6-mon exercise protocol. Furthermore, levels of protein [14.39 ± 0.95 vs. 15.61 ± 1.48% (95% CI, –4.26–1.80)], carbohydrate [49.46 ± 2.36 vs. 51.43 ± 2.18% (95% CI, –7.18–3.23)] and fat [32.20 ± 2.36 vs. 29.47 ± 2.71% (95% CI, –3.98–9.44)] did not change significantly over the 6-mon period. The macronutrient content did not differ from the normal United Kingdom diet.

Body morphology. There was no significant change in body weight following 6 mon of exercise. Furthermore, body composition measurements by impedance and anthropometry did not significantly change following 6 mon of exercise (Table 2). Similarly, there were no significant changes in waist circumference, the waist-to-hip ratio (WHR), or the body mass index (BMI) after exercise.

Significant decreases in both total and some regional fat depots were observed with whole-body MRI (Table 3). There was a 6.4% decrease in the absolute amount of total body fat present [pre: 28.9 ± 2.2 vs. post: 27.0 ± 2.3 liters, $P < 0.05$ (95% CI, 0.49–3.21)]. There were also significant decreases (–4.6 and –16.8%) in the amount of subcutaneous [24.6 ± 1.9 vs. 23.4 ± 1.9 liters, $P < 0.05$ (95% CI, 0.10–2.15)] and internal fat [4.3 ± 0.4 vs. 3.6 ± 0.3 liters, $P < 0.01$ (95% CI, 0.33–1.12)], respectively. The biggest decrease was in the level of visceral fat (Fig. 1), which was reduced by 25% following exercise [1.7 ± 0.2 vs. 1.3 ± 0.2 liters, $P < 0.01$, (95% CI, 0.22–0.64)]. There was also a decrease of 11.5% in the level of non-visceral internal fat [2.6 ± 0.2 vs. 2.3 ± 0.2 liters, $P < 0.05$ (95% CI, 0.04–0.56)]. The change in the level of subcutaneous fat from the abdominal region was not significant [6.1 ± 0.6 vs. 5.7 ± 0.5 liters (95% CI, –0.08–0.90)].

Biochemistry. A significant increase in plasma HDL-C levels [1.58 ± 0.06 vs. 1.66 ± 0.08 mmol/L (60.11 ± 2.59 vs. 62.95 ± 3.12 mg/dL), $P < 0.02$ (95% CI, –0.18– –0.02)] was observed following exercise. However, there were no significant changes in total or LDL-C, plasma triglycerides, plasma glucose, or insulin (Table 4). Furthermore, there were no significant changes in NEFA, cortisol, testosterone (or free testosterone), C-peptide/insulin ratio, DHEAS, or SHBG following exercise (Table 4). There was no significant change in leptin levels following exercise.

Relationship between variables. There was a significant correlation between serum insulin and visceral fat both before ($r = 0.81$, $P < 0.01$) and after ($r = 0.54$, $P < 0.02$) exercise. There was also a significant correlation between abdominal subcutaneous fat and insulin before ($r = 0.71$, $P < 0.01$) but not after exercise. Interestingly, although there was no change in waist circumference with exercise, there was a significant correlation between waist circumference and visceral fat both pre- ($r = 0.78$, $P < 0.01$) and post-exercise ($r = 0.82$, $P < 0.01$). There were no significant correlations between visceral fat and the WHR either before or after exercise. There were no significant correlations between visceral fat and HDL-C, cortisol,

TABLE 2
Changes Post-exercise[a]

	Pre-exercise (n = 17)	Post-exercise (n = 17)	Significance	95% CI
Weight (kg)	68.2 ± 2.5	67.6 ± 2.7	NS	–1.16–1.39
BMI (kg/m^2)	24.5 ± 0.8	24.4 ± 0.8	NS	–0.39–0.52
Waist/hip	0.7 ± 0.01	0.7 ± 0.01	NS	–0.01–0.02
Body fat (%) (anthropometry)	30.3 ± 1.1	29.5 ± 1.2	NS	–1.18–2.19
Body fat (%) (impedance)	28.0 ± 1.5	28.9 ± 1.5	NS	–2.81–1.00
Body fat (%) (MRI[b])	29.9 ± 1.3	28.1 ± 1.4	$P < 0.01$	0.75–3.32

[a]Results presented as means ± SEM and 95% CI. BMI, body mass index. For other abbreviations see Table 1.
[b]Magnetic resonance imaging (MRI). For comparison with the anthropometry and impedance data, it is necessary to convert the absolute fat measurement in liters to a percentage. Therefore, MRI data in liters (Table 3) are converted to percentage body fat using the following equations (11): body fat in kg = [body fat in liters] × 0.9 [1]/% body fat = [(body fat in kg)/(body weight)] × 100 × 0.8 [2]. The factor 0.9 in Equation 1 is the widely accepted value for the density of adipose tissue in kg/L and is required to convert volume of fat in liters to mass of fat in kilograms. In Equation 2, the factor 0.8 accounts for the fat content of adipose tissue and is required to convert from fractional adipose tissue content to percentage fat in the body.

TABLE 3
Body Fat Content by Whole-Body MRI Expressed in Liters[a]

	Pre-exercise (n = 17)	Post-exercise (n = 17)	Mean % change	Significance	95% CI
Total fat	28.9 ± 2.2	27.0 ± 2.3	–6.4	$P < 0.05$	0.49—3.21
Subcut fat	24.6 ± 1.9	23.4 ± 1.9	– 4.6	$P < 0.05$	0.10—2.15
Abdo fat	6.1 ± 0.6	5.7 ± 0.5	–6.7	NS	–0.08—0.90
Internal fat	4.3 ± 0.4	3.6 ± 0.3	–16.8	$P < 0.001$	0.33—1.12
Visceral fat	1.7 ± 0.2	1.3 ± 0.2	–25.0	$P < 0.001$	0.22—0.64
Nonvisceral internal fat	2.6 ± 0.2	2.3 ± 0.2	–11.5	$P < 0.05$	0.04—0.56

[a]Results presented as means ± SEM and 95% CI. Subcut = subcutaneous; abdo = abdominal subcutaneous fat. For other abbreviations see Tables 1 and 2.

C-peptide/insulin, or NEFA before or after exercise. The correlations between visceral fat and DHEAS ($r = -0.41$, $P < 0.05$), and SHBG ($r = 0.72$, $P < 0.01$) and testosterone ($r = -0.46$, $P < 0.05$) were only significant following exercise.

DISCUSSION

In this study we showed that a moderate exercise program (only 3 h a week) had a significant effect on the body fat content of nonobese sedentary healthy women. Furthermore there was a preferential loss of fat from certain fat depots. These changes were observed even though there were no significant changes in body weight, BMI, waist circumference, or WHR.

The changes in body fat content reported in this cohort of subjects were only detected using whole-body MRI, probably because MRI is the only technique that can measure total and regional adipose tissue directly. Anthropometry and impedance only provide an indirect measure of body fat and are therefore unable to detect regional changes. Furthermore, the most significant changes detected in this study were from internal fat depots which overall correspond to <20% of total body fat. Therefore, even a significant decrease in fat from a small depot may be missed in the total body fat measurement.

Numerous studies have examined the effects of exercise on total body fat content. However, there is a paucity of information regarding the impact of exercise on specific body fat depots. This is partly because many research protocols include dietary restriction/modification in addition to the exercise regime. Also the technique(s) used to measure body fat may not allow separation of different body fat compartments. In our study we used a protocol which only included aerobic exercise, with no dietary restriction, with fat depots assessed directly by MRI. The results showed that a preferential loss of visceral fat followed a 6-mon regime of aerobic exercise.

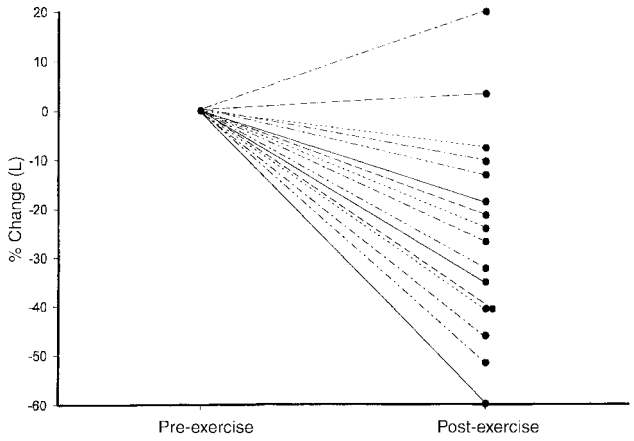

FIG. 1. Percentage change in visceral fat (in liters) for each volunteer following 6 mon aerobic exercise training.

Results from the present study are similar to those reported by Treuth *et al.* (6) with obese volunteers but differ from those of Despres *et al.* (18), who showed preferential loss of subcutaneous abdominal fat without changes in visceral fat following a set exercise regimen. Furthermore, in a separate study Schwartz *et al.* (19) showed exercise led to overall body fat loss, including visceral fat. These apparent differences regarding the effects of exercise on body fat depots may be due to a number of factors, including scanning methodology, exercise regime (aerobic or resistance), and choice of volunteers (lean or obese; pre- or postmenopausal).

To study regional changes in adipose tissue, it is essential to use direct imaging techniques such as CT or MRI. However, it is important that sufficient data be collected from the whole region of interest so that subtle changes are not missed or overinterpreted. A change or lack of change reported using single slice CT or MRI scans from a selected region of the abdomen might not reflect the effect of the intervention on the entire adipose tissue depot. Indeed, it has previously been shown that a single CT scan obtained at the level of the umbilicus contains a substantial amount of retroperitoneal fat, which is less metabolically active than other visceral fat depots (20). It has therefore been suggested that changes occurring in the entire visceral fat depot may be diluted out by the presence of the less-active retroperitoneal fat in the single slice (19). Factors like this can have a profound effect on the final results. Similarly, exercise protocols and choice of volunteers appear to be important and should be taken into account when comparing different published studies. Nevertheless, our results and those from other groups clearly suggest that different body fat depots are affected differently by environmental stresses such as exercise and diet.

The possible underlying mechanism(s) responsible for the

TABLE 4
Biochemical Measurements[a]

	Pre-exercise (n = 17)	Post-exercise (n = 17)	Significance	95% CI
Total cholesterol, mmol/L (mg/dL)	4.37 ± 0.13 (166.25 ± 4.85)	4.37 ± 0.12 (165.93 ± 4.48)	NS	–0.22–0.16
Triglycerides, mmol/L (mg/dL)	0.67 ± 0.05 (25.36 ± 1.84)	0.75 ± 0.04 (28.60 ± 1.42)	NS	–0.20–0.04
HDL cholesterol, mmol/L (mg/dL)	1.58 ± 0.07 (60.11 ± 2.59)	1.66 ± 0.08 (62.95 ± 3.12)	$P < 0.05$	–0.18– –0.02
LDL cholesterol, mmol/L (mg/dL)	2.38 ± 0.13 (94.29 ± 4.38)	2.48 ± 0.11 (90.39 ± 4.82)	NS	–0.16–0.34
HDL/LDL	0.66 ± 0.04	0.74 ± 0.08	NS	–0.24–0.08
Glucose, mmol/L	5.1 ± 0.1	5.1 ± 0.2	NS	–0.25–0.43
Serum insulin, mU/L	15.3 ± 2.6	13.1 ± 1.9	NS	–4.18–0.23
Cortisol, nmol/L	294 ± 28	313 ± 28	NS	–105.04–68.10
Testosterone, nmol/L	1.9 ± 0.1	2.0 ± 0.1	NS	–0.41–0.12
DHEAS, µmol/L	6.3 ± 0.7	7.2 ± 0.9	NS	–2.00–0.19
SHBG, nmol/L	62 ± 6	58 ± 8	NS	–19.84–26.92
C-peptide/insulin	483.1 ± 36.2	493.0 ± 29.9	NS	–557.65– –412.06
Leptin, ng/mL	13.0 ± 2.5	10.6 ± 1.6	NS	–5.84–16.38
NEFA, µmol/L	466.2 ± 60.8	570.7 ± 76.1	NS	–239.22–30.14

[a]Results presented as means ± SEM and 95% CI. Lipid data are expressed in both mmol/L and mg/dL. DHEAS, dehydroepiandrosterone sulfate; SHBG, sex hormone-binding globulin; NEFA, nonesterified fatty acid; HDL, high density lipoprotein; LDL, low density lipoprotein; for other abbreviation see Table 1.

preferential loss of fat from certain fat depots are not fully understood. Fat depots differ metabolically and may be controlled differently by environmental and genetic factors. Indeed, visceral and subcutaneous fats are known to be differentially affected by glucocorticoids, sex hormones, insulin, and adrenergic hormones (21). Changes in a number of these hormones occur with exercise, including cortisol secretion and in the balance of sex hormones (22). However, we found no changes in cortisol or sex hormone levels following exercise in the present study, suggesting the influence of an alternative factor. It is possible that the decrease in fat cell size reported to occur following exercise is greater in visceral fat than subcutaneous fat (23). For example, norepinephrine stimulates lipolysis more actively in visceral fat than in subcutaneous adipose tissue, mainly due to differences in adrenoreceptor levels (24). It has been reported that a preferential mobilization of abdominal subcutaneous fat is related to the initial size of the depot (8,25). Clearly complex interactions between a number of factors result in differential fat metabolism, which requires further investigation.

An interesting finding arising from using whole-body MRI was the fact that there was a significant decrease in nonvisceral internal fat depot (internal fat from regions other than visceral fat) with exercise. A substantial part of this fat depot arises from adipose tissue between muscle fibers (extracellular skeletal muscle fat). These changes may be important, particularly in light of the potential influence of muscle triglycerides on insulin sensitivity (26). The extra-muscular fat depot is perhaps the least well-understood adipose depot in the body, in part because of the difficulty in measuring it accurately. Although the MRI technique used in the present study was not optimized for measuring this depot, we were still able to detect significant changes with exercise, suggesting that MRI techniques may play an important role in the study of this fat depot. Further work is required to determine if extracellular skeletal muscle fat is an independent factor in the modulation of insulin sensitivity.

There was a significant correlation between the level of visceral fat and waist circumference both before and after exercise. This would appear to confirm the suggestion that waist circumference as opposed to WHR is a more suitable surrogate measure of visceral fat (27). However, there was a significant reduction in visceral adipose tissue, there were no significant changes in either waist circumference or abdominal subcutaneous fat following exercise. This would suggest that the relationship between waist circumference and visceral fat content is not straightforward. Indeed in this study we found a stronger correlation between abdominal subcutaneous fat and waist circumference ($r = 0.90$, $P < 0.01$) than for visceral fat and waist circumference ($r = 0.78$, $P < 0.01$). In nonobese women, such as those included in this study, abdominal subcutaneous fat makes up a far greater proportion of the area described by the waist circumference than visceral fat. A significant change in the waist circumference will not likely be seen unless there is a significant reduction in abdominal subcutaneous fat. The findings of this and a previous study highlight the potential problem of using surrogate measures of visceral fat (21).

The significant loss of visceral fat (25%; Table 3) explains some of the positive effects of moderate exercise on health (e.g., the increase in plasma HDL-C levels). The beneficial effects of exercise on plasma lipid levels have been well-documented (28). Trained individuals generally have higher levels of plasma HDL-C and lower levels of triglycerides than control subjects. Furthermore, plasma HDL-C levels increase following exercise over a period of months, a finding we confirmed in the present study. However, there were no changes

in plasma triglycerides. In some ways it is not surprising that there were not more significant changes in the biochemical profile. The volunteers' plasma lipid levels and those of their other metabolites were all within the normal range, so they would not necessarily be expected to change significantly with exercise alone. We found no significant changes in leptin levels before and after exercise. The greatest percentage change in fat was visceral. Previous studies have shown that visceral fat produces considerably less leptin than subcutaneous fat (29).

In summary, in this study we demonstrated that a moderate amount of aerobic exercise, without dietary restriction, produces a significant preferential loss of MRI-measured visceral fat content. In the future, we hope to determine the effects of different types of exercise regimes on different fat depots and their relationship to health benefits.

ACKNOWLEDGMENTS

Financial support from the Medical Research Council and Marconi Medical Systems are gratefully acknowledged. We thank all of the volunteers who took part in this study and The Women's Gym (in particular Myriam Thompson and Thuvia Jones) for their cooperation. We also thank Dr. Basant Puri, Simon Taylor-Robinson, Gabby Jenkinson, and Po-Wah So from the MRI unit for their assistance. Finally we thank Biochemical Endocrinology, Hammersmith Hospital for performing the hormone assays and the Oxford Lipid Metabolism Group, Radcliffe Infirmary, Oxford for performing the NEFA assay. APG is a U.K. Medical Research Council Training Fellow.

REFERENCES

1. Folsom, A.R., Arnett, D.K., Hutchinson, R.G., Liao, F., Clegg, L.X., and Cooper, L.S. (1997) Physical Activity and Incidence of Coronary Heart Disease in Middle-Aged Women and Men, *Med. Sci. Sports Exercise 29*, 901–909.
2. Richter, E.A., Turcotte, L.P., Hespel, P., and Kiens, B. (1992) Metabolic Responses to Exercise, *Diabetes Care 15*, 1767–1774.
3. Miller, W.C., Koceja, D.M., and Hamilton, E.J. (1997) A Meta-Analysis of the Past 25 Years of Weight Loss Research Using Diet, Exercise or Diet Plus Exercise Intervention, *Int. J. Obesity 21*, 941–947.
4. Tremblay, A., Despres, J.P., Leblanc, C., and Bouchard, C. (1984) Sex Dimorphism in Fat Loss in Response to Exercise-Training, *J. Obes. Wt. Reg. 3*, 193–203.
5. Nelson, M.E., Fiatarone, M.A., Layne, J.E., Trice, I., Economos, C.D., Fielding, R.A., Ma, R., Pierson, R.N., and Evans, W.J. (1996) Analysis of Body-Composition Techniques and Models for Detecting Change in Soft Tissue with Strength Training, *Am. J. Clin. Nutr. 63*, 678–686.
6. Treuth, M.S., Hunter, G.R., Kekes-Szabo, T., Weinsier, R.L., Goran, M.I., and Berland, L. (1995) Reduction in Intra-Abdominal Adipose Tissue After Strength Training in Older Women, *J. Appl. Physiol. 78*, 1425–1431.
7. Ross, R., Pedwell, H., and Rissanen, J. (1995) Effects of Energy Restriction and Exercise on Skeletal Muscle and Adipose Tissue in Women as Measured by Magnetic Resonance Imaging, *Am. J. Clin. Nutr. 61*, 1179–1185.
8. Ross, R., and Rissanen, J. (1994) Mobilization of Visceral and Subcutaneous Adipose Tissue in Response to Energy Restriction and Exercise, *Am. J. Clin. Nutr. 60*, 695–703.
9. Barnard, M.L., Schwieso, J.E., Thomas, E.L., Bell, J.D., Saeed, N., Frost, G., Bloom, S.R., and Hajnal, J.V. (1996) Evaluation of Magnetic Resonance Imaging Techniques for Analysis of Body Fat Distribution, *NMR Biomed. 9*, 156–164.
10. Thomas, E.L., Saeed, N., Hajnal, J.V., Brynes, A.E., Goldstone, A.P., Frost, G., and Bell, J.D. (1998) Magnetic Resonance Imaging of Total Body Fat, *J. Appl. Physiol. 85*, 1778–1785.
11. Saeed, N., Barnard, M.L., Hajnal, J.V., Thomas, E.L., Bell, J.D., and Young, I.R. (1996) Automated Fat, Bone Marrow and Bone Segmentation from MR Scans Using Knowledge-Based Image Processing, *Proceedings of the Fourth Annual Meeting of the Society for Magnetic Resonance 1635,* held in New York, published in Berkeley.
12. Shephard, R.J. (1988) PAR-Q: Physical Activity Readiness Questionnaire, *Sports Med. 5*, 185–195.
13. Borg, G. (1970) Perceived Exertion as an Indicator of Somatic Stress, *Scand. J. Rehab. Med. 2*, 92–98.
14. *Physiological Testing Guidelines*, 3rd edn., British Association of Sport and Exercise Sciences, 1997, London.
15. Bingham, S.A., Gill, C., Welch, A., Day, K., Cassidy, A., Khaw, K.T., Sneyd, M.J., Key, T.J.A., Roe, L., and Day, N.E. (1994) Comparison of Dietary Assessment Methods in Nutritional Epidemiology: Weighed Records vs. 24 h Recalls, Food Frequency Questionnaire, and Estimated Records, *Br. J. Nutr. 72*, 619–643.
16. Holland, B., Welch, A.A., Unwin, I.D., Buss, D.H., Paul, A.A., and Southgate, D.A.T. (1991) *McCance and Widdowson's—The Composition of Foods,* 5th rev. and extended edition, RSC and Ministry of Agriculture Fisheries and Food, UK Government, London.
17. Durnin, J.V.G., and Womersley, J. (1974) Body Fat Assessment from Total Body Density and Its Estimate from Skinfold Thicknesses: Measurements on 481 Men and Women Aged from 16 to 72 Years, *Br. J. Nutr. 32*, 77–87.
18. Despres, J.P., Pouliot, M.C., Moorjani, S., Nadeau, A., Tremblay, A., Lupien, P.J., Theriault, G., and Bouchard, C. (1991) Loss of Abdominal Fat and Metabolic Response to Exercise Training in Obese Women, *Am. J. Physiol. 24*, E159–E167.
19. Schwartz, R.S., Cain, K.C., Shuman, W.P., Larson, V., Stratton, J.R., Beard, J.C., Kahn, S.E., Cerqueira, M.D., and Abrass, I.B. (1992) Effect of Intensive Endurance Training on Lipoprotein Profiles in Young and Older Men, *Metabolism 41*, 649–654.
20. Rossner, S., Bo, W.J., Hiltbrandt, E., Hinson, W., Karstaedt, N., Santago, P., Sobol, W.T., and Crouse, J.R. (1990) Adipose Tissue Determinations in Cadavers—A Comparison Between Cross-Sectional Planimetry and Computed Tomography, *Int. J. Obes. 14*, 893–902.
21. Abate, N., and Garg, A. (1995) Heterogeneity in Adipose Tissue Metabolism: Causes, Implications and Management of Regional Adiposity, *Prog. Lipid Res. 34*, 53–70.
22. Kraemer, W.J., Staron, R.S., Hagerman, F.C., Hikida, R.S., Fry, A.C., Gordon, S.E., Nindl, B.C., Gothshalk, L.A., Volek, J.S., Marx, J.O., Newton, R.U., and Hakkinen, K. (1998) The Effects of Short-Term Resistance Training on Endocrine Function in Men and Women, *Eur. J. Appl. Physiol. 78*, 69–76.
23. Tremblay, A., Despres, J.P., and Bouchard, C. (1985) The Effects of Exercise Training on Energy Balance and Adipose Tissue Morphology and Metabolism, *Sports Med. 2*, 223–233.
24. Efendic, S. (1970) Catecholamines and Metabolism of Human Adipose Tissue. 3. Comparison Between the Regulation of Lipolysis in Omental and Subcutaneous Adipose Tissue, *Acta Med. Scand. 187*, 477–483.
25. Martin, M.L., and Jensen, M.D. (1991) Effects of Body Fat Distribution on Regional Lipolysis in Obesity, *J. Clin. Invest. 88*, 609–613.
26. Pan, D.A., Lillioja, S., Kriketos, A.D., Milner, M.R., Baur, L.A.,

Bogardus, C., Jenkins, A.B., and Storlien, L.H. (1997) Skeletal Muscle Triglyceride Levels Are Inversely Related to Insulin Action, *Diabetes 46*, 983–988.
27. Han, T.S., and Lean, M.E.J. (1998) Self-Reported Waist Circumference Compared with the "Waist Watcher" Tape-Measure to Identify Individuals at Increased Health Risk Through Intra-Abdominal Fat Accumulation, *Br. J. Nutr. 80*, 81–88.
28. Durstine, J.L., and Haskell, W.L. (1994) Effects of Exercise Training on Plasma Lipids and Lipoproteins, *Exercise Sport Sci. Rev. 22*, 477–521.
29. Montague, C.T., Prins, J.B., Sanders, L., Digby, J.E., and O'Rahilly, S. (1997) Depot- and Sex-Specific Differences in Human Leptin mRNA Expression: Implications for the Control of Regional Fat Distribution, *Diabetes 46*, 342–347.

[Received July 1, 1999, and in final revised form February 22, 2000; revision accepted May 1, 2000]

Conjugated Linoleic Acid Supplementation in Humans: Effects on Body Composition and Energy Expenditure

Kirsten L. Zambell, Nancy L. Keim*, Marta D. Van Loan, Barbara Gale, Paloma Benito, Darshan S. Kelley, and Gary J. Nelson

U.S. Department of Agriculture/Western Human Nutrition Research Center, University of California, Davis, California 95616

ABSTRACT: Recent animal studies have demonstrated that dietary conjugated linoleic acid (CLA) reduces body fat and that this decrease may be due to a change in energy expenditure. The present study examined the effect of CLA supplementation on body composition and energy expenditure in healthy, adult women. Seventeen women were fed either a CLA capsule (3 g/d) or a sunflower oil placebo for 64 d following a baseline period of 30 d. The subjects were confined to a metabolic suite for the entire 94 d study where diet and activity were controlled and held constant. Change in fat-free mass, fat mass, and percentage body fat were unaffected by CLA supplementation (0.18 ± 0.43 vs. 0.09 ± 0.35 kg; 0.01 ± 0.64 vs. –0.19 ± 0.53 kg; 0.05 ± 0.62 vs. –0.67 ± 0.51%, placebo vs. CLA, respectively). Likewise, body weight was not significantly different in the placebo vs. the CLA group (0.48 ± 0.55 vs. –0.24 ± 0.46 kg change). Energy expenditure (kcal/min), fat oxidation, and respiratory exchange ratio were measured once during the baseline period and during weeks 4 and 8 of the intervention period. At all three times, measurements were taken while resting and walking. CLA had no significant effect on energy expenditure, fat oxidation, or respiratory exchange ratio at rest or during exercise. When dietary intake was controlled, 64 d of CLA supplementation at 3 g/d had no significant effect on body composition or energy expenditure in adult women, which contrasts with previous findings in animals.

Paper no. L8437 in *Lipids 35,* 777–782 (July 2000).

Conjugated linoleic acid (CLA) refers to a group of linoleic acid isomers in which the double bonds are conjugated. The double bonds, each of which may be in the *cis* or *trans* configuration, can be in any position on the carbon chain but are usually in the 9 and 11 or 10 and 12 positions, giving rise to at least eight theoretical isomers in mixed CLA preparations. CLA is found naturally in foods such as grilled ground beef (1) and some dairy products (2). The estimated consumption of CLA by adults in the United States is 1 g/person/d (2).

CLA has been reported to be protective against atherosclerosis in rabbits (3) and to suppress mammary carcinogenesis in rats (4–6) when the animals were fed diets supplemented with CLA. Recently, the addition of CLA to the diet of mice has reportedly caused a decrease in body fat (7–11). Studies with adipocytes exposed to exogenous CLA showed reduced lipoprotein lipase activity, reduced levels of triglyceride and glycerol inside the cells, and increased glycerol levels outside the cells (8,10). These data suggest that CLA may reduce body fat by affecting key enzymes involved in lipid mobilization and storage.

Although CLA caused a decrease in body fat in mice, overall body weight was either unchanged (8,9) or decreased (7,10,11). Supplementation studies in rats showed no effect of CLA on body weight (body fat was not measured) (4–6). The body weight decrease and the reduction in body fat may be countered by an increase in lean body mass and body water (8,9). Changes in body composition could also be due to changes in energy intake and/or expenditure. Energy intake was unaffected (7) or reduced (8,11) in mice on a CLA-supplemented diet. The effects of CLA on energy expenditure have not been fully studied.

Despite the previous results in animal models, the effect of CLA in humans has not been thoroughly studied. In the study reported here, we observed the effects of CLA supplementation (3 g/d/person) on body composition and energy expenditure in healthy women. The dosage of CLA used was threefold higher than the reported daily consumption for American adults (2). This amount is similar to that used in previous animal and human studies, and it is within the reasonable range for a healthy, non-vegan adult.

MATERIALS AND METHODS

Subjects. Seventeen women, 20–41 yr of age, completed the entire 94-d study. Subject selection criteria included being a healthy nonsmoker, premenopausal with normal menstrual cycles, and free of any abnormal physiological conditions or diseases. Prior to being selected for the study, all subjects completed medical and dietary histories, physical examination, urinary test for pregnancy, resting electrocardiogram, and a standard battery of blood tests. Participation was by informed consent. The study protocol was approved by the Human Subject Committees of the U.S. Department of Agriculture and the University of California, Davis.

*To whom correspondence should be addressed at USDA/Western Human Nutrition Research Center, Department of Exercise Science, University of California, Davis, CA 95616. E-mail: nkeim@whnrc.usda.gov

Abbreviations: CLA, conjugated linoleic acid; DXA, dual x-ray absorptiometry; FFM, fat-free mass; RER, respiratory exchange ratio; TOBEC, total body electrical conductivity; VCO_2, carbon dioxide production; VO_2, oxygen consumption.

Subjects lived in the metabolic suite at the Western Human Nutrition Research Center, 24 h/d, 7 d/wk for 94 d of the study. Times for meals and routine daily activities were standardized to keep the activities similar throughout the study. Routine activities included a daily outdoor walk (2 mi/d) and other forms of outdoor exercise.

Experimental design. This randomized, blind, and placebo-controlled study was conducted with two cohorts (9 in the first cohort and 8 in the second) since the metabolic suite could not accommodate 17 subjects at once. The duration of each cohort was 94 d, consisting of a 30-d baseline period followed by a 64-d intervention period during which either CLA or placebo capsules were administered. During the baseline period, all subjects received a daily placebo containing sunflower oil to become accustomed to taking the capsules. On day 31, 10 subjects were randomly assigned to the group receiving supplemental CLA (approximately 1% of calories, ~3 g/d) for the remainder of the study. The seven remaining subjects served as controls and consumed placebo capsules for the entire study.

CLA capsules were obtained from Pharmanutrients, Inc. (Lake Bluff, IL). CLA constituted approximately 65% of the total fatty acids in the capsule with the remainder consisting primarily of oleic acid. Isomer composition of the CLA was determined by gas chromatography and found to be 22.6% *trans*-10,*cis*-12; 23.6% *cis*-11,*trans*-13; 17.6% *cis*-9,*trans*-11; 16.6% *trans*-8,*cis*-10; 7.7% *trans*-9,*trans*-11 and *trans*-10,*trans*-12; 11.9% other isomers. The placebo capsule contained 72.6% linoleic acid with the remainder consisting mainly of palmitic, stearic, and oleic acids and no detectable CLA isomers. The capsules used were identical in appearance and were packaged in the same manner.

Dietary intake. The subject's diets were equivalent to the American Heart Association's Step II Diet containing the reference daily intake for all known nutrients with 30% of calories from fat, 15% from protein and 55% from carbohydrate. The energy intake of each subject was estimated using the Harris-Benedict equation. During the baseline period, the energy intake was adjusted if body weight changed by ±3% over time. The ratio of saturated, monounsaturated, and polyunsaturated fat was 1:1:1 for both placebo and intervention groups with saturated fat, linoleic acid, and other n-6 polyunsaturated fat held constant among the two groups. The cholesterol content of the diets was between 250 and 300 mg/d.

Body weight and composition. Subjects were weighed daily by a member of the nursing staff in the morning, after urinating to empty their bladders and before ingesting breakfast. Subjects wore standard hospital gowns for all weight measurements.

Body composition was determined three times per week by total body electrical conductivity (TOBEC) measured by an HA-2 body composition analyzer (EM-SCAN, Springfield, IL). This method exploits the difference in the electrical conductivity of fat vs. fat-free tissue to estimate fat-free mass (FFM). Body fat mass was determined by subtracting FFM from body weight. This method has been validated in our laboratory and shown to produce values for FFM similar to that estimated by hydrostatic weighing in humans (12) and carcass analysis in pigs (13). All measurements were taken before breakfast.

Body composition was also determined by using dual x-ray absorptiometry (DXA) (DPX, software package 3.63, Lunar Corp., Madison, WI) at three times during the study—baseline and twice during the supplementation period. DXA directly measures fat mass and FFM by passing a small quantity of x-rays through the body. The change in fat mass and FFM was calculated by subtracting the baseline DXA measurement from the final measurement. Owing to the exposure of the subjects to x-rays, DXA could not be used on a more frequent basis throughout the study.

To avoid reporting spurious changes in body weight and composition that may be due to the menstrual cycle, we analyzed body weight and composition data by fitting a regression line to the plot of each variable vs. time for the baseline and intervention periods. The change in body weight or composition was determined by multiplying the slope of the regression line by the number of days in the baseline or intervention period.

Energy expenditure and utilization. Metabolic rate and respiratory exchange ratio (RER) were determined from measurements of oxygen consumption (VO_2) and carbon dioxide production (VCO_2). The gas exchange measurements were made with an automated respiratory gas exchange system (2900; SensorMedics, Anaheim, CA). The system was calibrated with standard gas mixtures and the calibration was verified at intervals throughout the collection periods. Subjects wore inflatable facemasks that were connected to the gas analyzers *via* a tubing assembly. Energy expenditure was calculated from VO_2 and VCO_2 using the equations of Weir (14). A correction factor for urinary nitrogen output was made by estimating a nitrogen excretion rate of 0.01 g/min. This estimate was based on dietary nitrogen intake, fecal nitrogen losses (~1 g/d) and insensible nitrogen losses (~1 g/d). Fat oxidation (g/min) was calculated using the equation of Frayn (15).

Energy expenditure was measured once during the baseline period and twice during the intervention period (weeks 4 and 8). Following an overnight fast, subjects rested quietly in a comfortable chair for 30 min, then respiratory gas exchange was measured for 20 min intervals: first, while resting in a seated position, then, during steady-state walking on a treadmill at 60% VO_2max (at time intervals of 5–25 and 30–50 min).

Statistical methods. Values are reported as means ± SEM. Data represent combined data for all subjects because statistical analysis showed no effect of cohort. To compare subject characteristics among placebo and CLA groups *t*-tests were used. Analysis of variance was used to determine the effect of CLA on changes in body weight and composition. The baseline rate of change was used as a covariate in the model. Analysis of variance was used to determine the effect of CLA, time, and the interaction of CLA and time on energy expenditure parameters. To adjust for differences in body size among

subjects, body FFM was used as a covariate in the analysis. The probability level for significance was set at $P < 0.05$. All statistical analyses were performed using the Statistical Analysis System (SAS Institute Inc., Cary, NC).

RESULTS

Subject characteristics at start of intervention. Physical and metabolic characteristics of the subjects at the end of the baseline period are listed in Table 1. Mean values for age, body weight, height, FFM, percentage body fat, resting metabolic rate, and RER were similar for the groups prior to the CLA supplementation.

Change in body weight and composition. Dietary energy intake was similar during baseline and supplementation periods for both the placebo and CLA groups (Table 2). Daily CLA supplementation did not cause a significant change in body weight after 64 d of intervention compared to the placebo group (Fig. 1; Table 3). In using the TOBEC method, there were no significant differences in body composition among the CLA and placebo groups (Table 3). Likewise, body composition results from the DXA method indicated that CLA had no effect on body fat mass (–0.19 ± 0.67 vs. –0.49 ± 0.44 kg change, placebo vs. CLA) or body FFM (0.17 ± 0.40 vs. 0.07 ± 0.24 kg change, placebo vs. CLA).

Energy expenditure and utilization. The energy expenditure and fat oxidation data were adjusted for differences in FFM by using FFM as a covariate. During the baseline period, energy expenditure (kcal/min) was similar between placebo and CLA groups while resting and exercising (Fig. 2). No significant effects of CLA were observed at 4 or 8 wk of intervention during rest or while walking. An expected increase in energy expenditure was observed with the onset of walking in both placebo and CLA groups at all timepoints.

As with energy expenditure, fat oxidation (g/min) was similar between the placebo and CLA groups at rest and while exercising during the baseline period (Fig. 2). CLA had no significant effect on fat oxidation during resting or walking at 4 or 8 wk of intervention. Because of the increase in energy expenditure associated with walking, fat oxidation was higher while walking as compared to rest at all three timepoints.

In both the CLA and placebo groups, the RER increased with the onset of walking (5–25 min) but gradually dropped as walking progressed (30–50 min; Fig. 3). When an average value for the 20-min rest and 50-min walk periods was calculated, there was no significant effect of CLA on the RER during resting or walking (data not shown).

DISCUSSION

Healthy, adult women, fed a CLA mixture daily for 64 d, showed no significant change in FFM, fat mass, or percentage body fat compared to the placebo group (Table 2). These findings contrast markedly with previously reported human and animal studies in which diets were supplemented with CLA. Medstat Research Ltd. (16) performed the only other known study in which CLA was fed to humans. The Medstat Research study reported a 20% decrease in body fat after 12 wk of CLA supplementation (~1.8 g/d) in free-living, healthy men and women. There are several differences between the present study and the Medstat study that might explain the discrepancy. First, in the present study, body composition was

TABLE 1
Subject Characteristics Prior to CLA Supplementation[a]

Subject	Age (yr)	Weight (kg)	Height (m)	BMI (kg/m^2)	FFM (kg)	Body fat (%)	RMR (kcal/d)	RER (VCO_2/VO_2)
Placebo group								
#33	27	55.3	1.67	19.8	37.7	31.8	1,147.7	0.83
#35	22	63.5	1.65	23.3	42.8	32.6	1,263.7	0.82
#36	26	63.4	1.73	21.2	45.2	28.8	1,391.7	0.84
#37	36	57.6	1.65	21.2	43.0	25.4	1,398.5	0.81
#39	25	63.4	1.78	20.0	49.0	22.8	1,340.0	0.86
#42	29	89.0	1.74	29.4	52.8	40.7	1,370.3	0.89
#45	41	54.7	1.65	20.1	38.1	30.4	903.3	0.89
Mean ± SEM	29.4 ± 2.5	63.8 ± 4.4	1.69 ± 0.02	22.2 ± 1.3	44.1 ± 2.1	30.3 ± 2.2	1,259.3 ± 68.1	0.85 ± 0.01
CLA group								
#29	31	67.5	1.67	24.2	45.0	33.3	1,324.8	0.86
#30	20	64.3	1.67	23.1	45.8	28.9	1,401.2	0.86
#31	24	57.9	1.55	24.1	39.5	31.8	1,218.3	0.88
#32	23	62.3	1.65	22.9	48.2	22.7	1,347.6	0.87
#34	27	61.8	1.59	24.4	39.2	36.4	1,217.4	0.85
#38	28	65.7	1.66	23.8	44.9	31.7	1,340.0	0.86
#40	25	77.7	1.77	24.8	50.0	35.6	1,331.8	0.81
#41	24	55.2	1.65	20.3	39.9	27.7	1,252.4	0.78
#43	29	64.7	1.72	21.9	47.9	25.9	1,537.6	0.84
#47	41	54.1	1.52	23.4	34.6	36.1	1,129.0	0.79
Mean ± SEM	27.2 ± 1.8	63.1 ± 2.1	1.64 ± 0.02	23.2 ± 0.5	43.5 ± 1.6	31.0 ± 1.5	1,310.0 ± 35.9	0.84 ± 0.01

[a]No significant differences were observed between the placebo and CLA groups. BMI, body mass index; FFM, fat-free mass; RMR, resting metabolic rate; RER, respiratory exchange ratio; CLA, conjugated linoleic acid.

TABLE 2
Dietary Energy Intake During Baseline and CLA Supplementation[a]

	Placebo (kcal/d) (n = 7)	CLA (kcal/d) (n = 10)
Baseline	2,070.0 ± 116.8	2,109.4 ± 25.0
Supplementation	2,054.3 ± 108.5	2,109.2 ± 26.6

[a]Baseline refers to the last 2 wk of the baseline period (days 17–30) whereas supplementation refers to the entire supplementation period (days 31–94). There were no statistical differences within or among groups. For abbreviation see Table 1.

TABLE 3
The Effect of CLA Supplementation on Body Weight and Composition[a]

	Placebo (n = 7) (change over 64 d)	CLA (n = 10) (change over 64 d)	P
Weight (kg)	0.48 ± 0.55	–0.24 ± 0.46	0.35
Fat-free mass (kg)	0.18 ± 0.43	0.09 ± 0.35	0.88
Fat mass (kg)	0.01 ± 0.64	–0.19 ± 0.53	0.82
Body fat (%)	0.05 ± 0.62	–0.67 ± 0.51	0.39

[a]Body composition measurements were made using the TOBEC (total body electrical conductivity) method. For abbreviation see Table 1.

measured three times per week throughout the entire study using a whole-body measurement, TOBEC. In the Medstat study, body composition was measured once every 4 wk using infrared technology on the bicep of the better arm. Second, the Medstat study included males and females but did not break down the results by gender so the effect of CLA on body composition in women was not reported. Third, the present study was conducted in a metabolic suite so diet and activity could be controlled and held constant throughout, whereas the Medstat study was a free-living study with no documented evidence of activity or diet intake levels. Fourth, the isomer composition of the CLA supplement in the Medstat study was not reported and may be different from the present study. Therefore, it is difficult to interpret the body composition data from the Medstat study and compare them to the present data.

Previous work with mice (7–11), rats (17), and pigs (18) showed a decrease in body fat with consumption of a CLA mixture. Several studies have also shown an increase in FFM with a supplemental CLA mixture (7–9). All of these studies used weanling or adolescent animals that were still growing and changing in body composition. There are data to suggest that CLA may affect growing animals differently from adults by depressing body fat accumulation *via* a reduction in preadipocyte number when given during periods of growth (19). The subjects in the present study were weight-stable adults with steady body compositions prior to CLA supplementation (Table 1). Unfortunately, there are no studies currently available reporting the effect of dietary CLA on body weight and composition in an adult animal model.

Consumption of a CLA mixture also had no effect on body weight in adult women in the present study (Table 3; Fig. 1). Although the placebo group had a tendency to gain weight while the CLA group lost weight, the changes were very small and within the measurement variability. This finding is consistent with previous human and animal studies in which body weight remained stable, or the increase in body weight was similar between CLA and placebo groups. The Medstat study also showed no significant change in body weight after 12 wk of CLA supplementation in humans (16). In general, a dietary CLA mixture (0.05–1.5%, by weight, for 6–36 wk) had no effect on body weight or feed intake in rats (4,5,20,21)

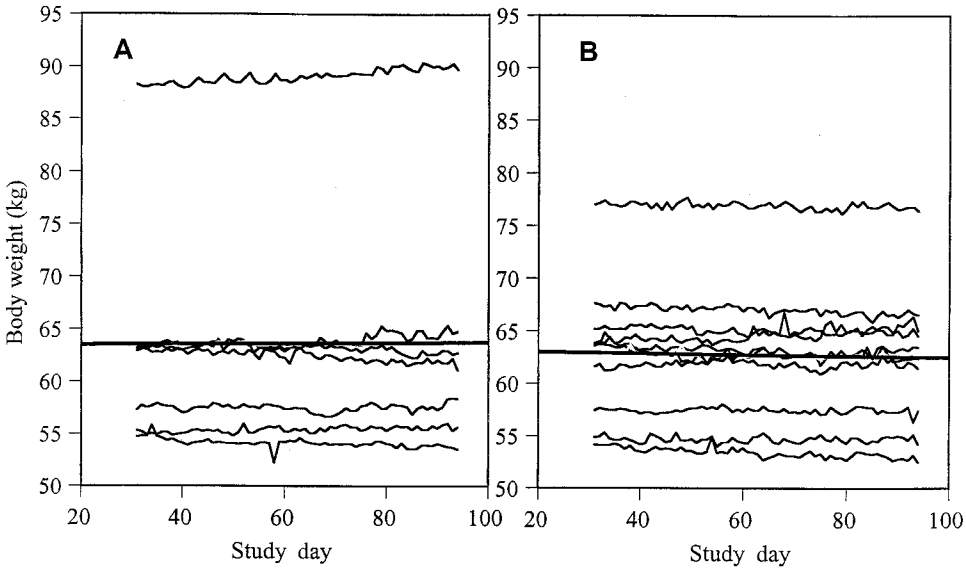

FIG. 1. Daily body weights (kg) during the conjugated linoleic acid (CLA) supplementation period (days 31–94) of the placebo (A; n = 7) and CLA (B; n = 10) groups. The bold line indicates the regression line for the average daily weight in each group.

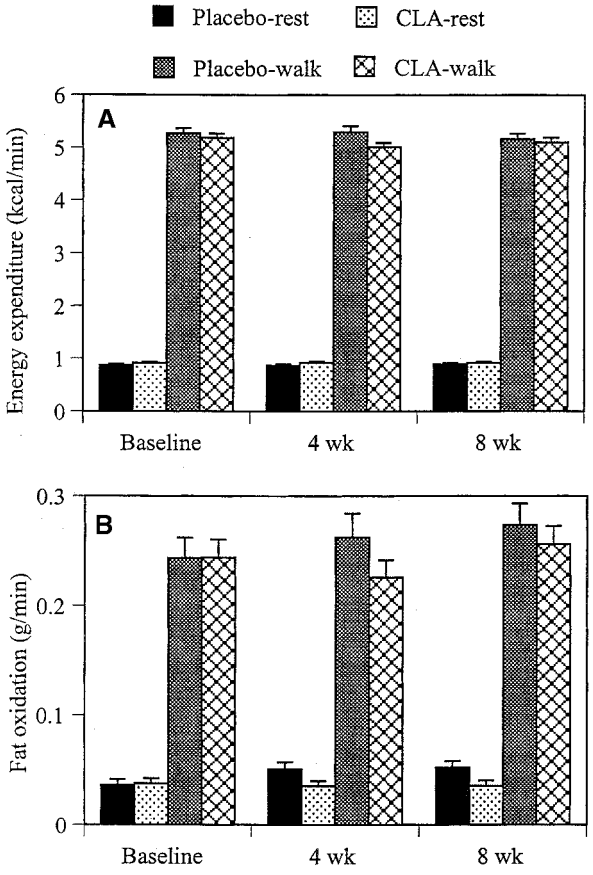

FIG. 2. The effect of CLA on energy expenditure (A) and fat oxidation (B) at baseline, 4 or 8 wk of intervention during resting and walking. Energy expenditure and fat oxidation were adjusted for fat-free mass. The bars represent means ± SEM for all subjects because statistical analysis showed no effect of cohort; $n = 7$ for placebo group, $n = 10$ for CLA group. No significant differences were found when placebo and CLA groups were compared during rest or during exercise. For abbreviation see Figure 1.

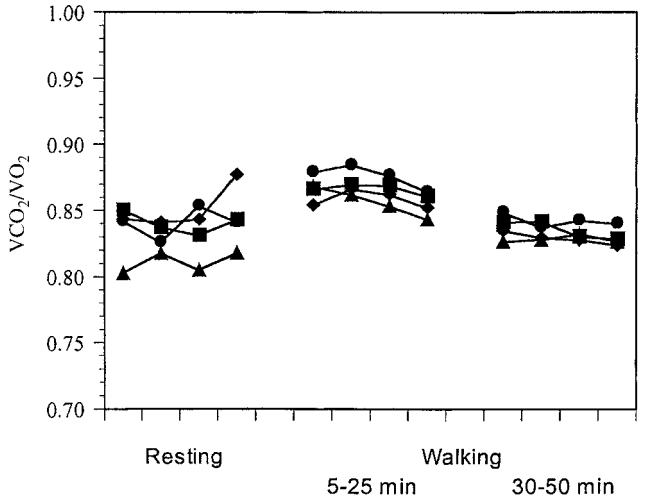

FIG. 3. The effect of CLA on the respiratory exchange ratio at baseline or 8 wk of intervention during resting and walking. Each point represents the average of five 1-min data collections. No significant differences were found when placebo and CLA groups were compared at baseline (● and ■, respectively) or 8 wk (▲ and ◆, respectively) during rest or exercise; $n = 7$ for placebo group and $n = 10$ for CLA group. For abbreviation see Figure 1.

or rabbits (3). Decreases in body weight due to consumption of a CLA mixture (0.25–1.2% for 4–6 wk) have been observed in mice, however, they were associated with a decrease in food intake (9,10). The short duration of the mice studies may have confounded the body weight results since a decrease in food intake has been observed during the first few weeks of CLA supplementation (11). The authors suggested that the addition of CLA may have caused an initial decrease in the palatability of the diet. Overall, the data are consistent with the idea that feeding a mixture of CLA isomers does not significantly affect body weight in humans or rodents when food intake is maintained.

Energy expenditure was unaffected by consumption of a CLA mixture in adult women as well (Fig. 2). A previous animal study suggested that CLA might decrease body fat by increasing overall energy expenditure (11). During the sixth week of CLA supplementation, energy expenditure (kcal/d) was significantly higher in the CLA-fed mice vs. the placebo group. However, the CLA-supplemented mice also exhibited a decrease in feed intake compared to controls. Therefore, it is difficult to determine if the observed changes in body composition were due to the decrease in food intake or the increase in energy expenditure.

There was no effect of consumption of a CLA mixture on fat oxidation during rest or while walking (Fig. 2). The effect of supplemental CLA on fat oxidation has not been measured previously. Based on earlier studies with adipocytes exposed to a CLA mixture, we expected to observe an increase in fat oxidation. Exposure to a mixture of CLA isomers reduces lipoprotein lipase activity and enhances lipolysis, causing a reduction in the intracellular triglyceride and glycerol concentrations (8,9). Muscle carnitine palmitoyltransferase activity was also stimulated in mice fed a CLA mixture (8) suggesting increased fatty acid oxidation in the muscle tissue. Although carnitine palmitoyltransferase activity was increased, fat oxidation was not directly measured. CLA has also been shown to increase hepatic lipid concentrations, suggesting that nonoxidized fatty acids are routed to the liver (22). Thus, CLA may increase triglyceride recycling (triglycerides broken down in the adipose tissue and reformed in the liver) without affecting fatty acid oxidation.

The onset of walking did lead to an increase in fat oxidation vs. the resting state in both the placebo and CLA groups (Fig. 2). This is to be expected since working muscles burn more fatty acids for energy during exercise than at rest. An expected transient increase in the RER with the onset of walking was also observed in both placebo and CLA groups (Fig. 3). Walking at 60% VO_2max increased the energy expenditure of the subjects by about fivefold (Fig. 2). However, the mean RER (over the 50-min walk) was not different from the RER at rest in both treatment groups.

It should be noted that the CLA supplement used in the present experiment was not pure and included a number of isomers along with the presumed biologically active form, *trans*-10,*cis* 12 (9). In the present study, the *trans*-10,*cis*-12 isomer was the most abundant isomer, along with the *cis*-11,*trans*-13 (~23% for each), in the CLA supplement. However, previous studies that observed changes in body composition in mice employed CLA supplements that consisted of 40–45% *trans*-10,*cis*-12 (7,9–11). Although feeding CLA containing 44 or 79% *trans*-10,*cis*-12 to mice resulted in similar reductions in percentage body fat (9), it is possible that 23% of the active isomer may be below the threshold level necessary to elicit body composition changes. Further studies using various levels of the pure isomers would be useful to understand fully the metabolic effect of dietary CLA.

In conclusion, consumption of a CLA mixture at 1% of calories had no significant effect on body composition or energy expenditure in healthy women after 64 d of intervention. These results are in marked contrast to previous animal studies which used adolescent, growing animals for supplementation studies.

ACKNOWLEDGMENTS

We would like to thank Theresa Barbieri for technical support; Carlene Gibbons for study coordination; Illona Ellingwood and nursing staff for weight measurements; Kathy Bourdet for dietary planning; Vicky Jen and dietary staff for meal preparation; and Ginny Gildengorin for statistical consultation.

REFERENCES

1. Ha, Y.L., Grimm, N.K., and Pariza, M.W. (1987) Anticarcinogens from Fried Ground Beef: Heat Altered Derivatives of Linoleic Acid, *Carcinogenesis 8,* 1881–1887.
2. Ha, Y.L., Grimm, N.K., and Pariza, M.W. (1989) Newly Recognized Anticarcinogenic Fatty Acids: Identification and Quantification in Natural and Processed Cheeses, *J. Agric. Food Chem. 37,* 75–81.
3. Lee, K.N., Kritchevsky, D., and Pariza, M.W. (1994) Conjugated Linoleic Acid and Atherosclerosis in Rabbits, *Atherosclerosis 108,* 19–25.
4. Ip, C., Chin, S.F., Scimeca, J.A., and Pariza, M.W. (1991) Mammary Cancer Prevention by Conjugated Dienoic Derivative of Linoleic Acid, *Cancer Res. 51,* 6118–6124.
5. Ip, C., Singh, M., Thompson, H.J., and Scimeca, J.A. (1994) Conjugated Linoleic Acid Suppresses Mammary Carcinogenesis and Proliferative Activity of the Mammary Gland in the Rat, *Cancer Res. 54,* 1212–1215.
6. Ip, C., Briggs, S.P., Haegele, A.D., Thompson, H.J., Storkson, J., and Scimeca, J.A. (1996) The Efficacy of Conjugated Linoleic Acid in Mammary Cancer Prevention Is Independent of the Level or Type of Fat in the Diet, *Carcinogenesis 17,* 1045–1050.
7. DeLany, J.P., Blohm, F., Truett, A.A., Scimeca, J.A., and West, D.B. (1999) Conjugated Linoleic Acid Rapidly Reduces Body Fat Content in Mice Without Affecting Energy Intake, *Am. J. Physiol. 276,* R1172–R1179.
8. Park, Y., Albright, K.J., Liu, W., Storkson, J.M., Cook, M.E., and Pariza, M.W. (1997) Effect of Conjugated Linoleic Acid on Body Composition in Mice, *Lipids 32,* 853–858.
9. Park, Y., Albright, K.J., Storkson, J.M., Liu, W., Cook, M.E., and Pariza, M.W. (1999) Changes in Body Composition in Mice During Feeding and Withdrawal of Conjugated Linoleic Acid, *Lipids 34,* 243–248.
10. Park, Y., Storkson, J.M., Albright, K.J., Liu, W., and Pariza, M.W. (1999) Evidence That the *trans*-10,*cis*-12 Isomer of Conjugated Linoleic Acid Induces Body Composition Changes in Mice, *Lipids 34,* 235–241.
11. West, D.B., DeLany, J.P., Camet, P.M., Blohm, F., Truett, A.A., and Scimeca, J. (1998) Effects of Conjugated Linoleic Acid on Body Fat and Energy Metabolism in the Mouse, *Am. J. Physiol. 275,* R667–R672.
12. Van Loan, M.D., Keim, N.L., and Belko, A.Z. (1990) Body Composition Assessment of a General Population using Total Body Electrical Conductivity (TOBEC), in *Sports, Medicine and Health (*Hermans, G.P.H., ed.), Elsevier Science Publishers B.V., Amsterdam, pp. 665–670.
13. Keim, N.L., Mayclin, P.L., Taylor, S.J., and Brown, D.L. (1988) Total-body Electrical Conductivity Method for Estimating Body Composition: Validation by Direct Carcass Analysis of Pigs, *Am. J. Clin. Nutr. 47,* 180–185.
14. Weir, J.B.deV. (1949) New Methods for Calculating Metabolic Rate with Special Reference to Protein Metabolism, *J. Physiol. 109,* 1–9.
15. Frayn, K.N. (1983) Calculation of Substrate Oxidation Rates *in Vivo* from Gaseous Exchange, *J. Appl. Physiol. 55,* 628–634.
16. Thom, E. (1997) A Pilot Study with the Aim of Studying the Efficacy and Tolerability of Tonalin CLA on the Body Composition in Humans, Medstat Research Ltd., Lillestrøm, Norway.
17. Sisk, M., Azain, M.J., Hausman, D.B., and Jewell, D.E. (1998) Effect of Conjugated Linoleic Acid on Fat Pad Weights and Cellularity in Sprague-Dawley and Zucker Rats, *FASEB J. 12,* A536.
18. Cook, M.E., Jerome, D.L., Crenshaw, T.D., Buege, D.R., Pariza, M.W., Albright, K.J., Schmidt, S.P., Scimeca, J.A., Lofgren, P.A., and Hentges, E.J. (1998) Feeding Conjugated Linoleic Acid Improves Feed Efficiency and Reduces Carcass Fat in Pigs, *FASEB J. 12,* A836.
19. Satory, D.L., and Smith, S.B. (1999) Conjugated Linoleic Acid Inhibits Proliferation but Stimulates Lipid Filling of Murine 3T3-L1 Preadipocytes, *J. Nutr. 129,* 92–97.
20. Moya-Camerena, S.Y., Vanden Heuvel, J.P., and Belury, M.A. (1999) Conjugated Linoleic Acid Activates Peroxisome Proliferator-Acitvated Receptor α and β Subtypes but Does Not Induce Hepatic Peroxisome Proliferation in Sprague-Dawley Rats, *Biochim. Biophys. Acta 1436,* 331–342.
21. Scimeca, J.A. (1998) Toxicological Evaluation of Dietary Conjugated Linoleic Acid in Male Fischer 344 Rats, *Food Chem. Toxicol. 36,* 391–395.
22. Belury, M.A., and Kempa-Staczko, A. (1997) Conjugated Linoleic Acid Modulates Hepatic Lipid Composition in Mice, *Lipids 32,* 199–204.

[Received January 14, 2000, and in revised form May 30, 2000; revision accepted June 7, 2000]

Conjugated Linoleic Acid Supplementation in Humans: Effects on Circulating Leptin Concentrations and Appetite

Edward A. Medina[a], William F. Horn[b], Nancy L. Keim[b], Peter J. Havel[c], Paloma Benito[b], Darshan S. Kelley[b], Gary J. Nelson[b], and Kent L. Erickson[a,*]

[a]Department of Cell Biology and Human Anatomy, School of Medicine, [b]U.S. Department of Agriculture/Western Human Nutrition Research Center, and [c]Department of Nutrition, University of California, Davis, California 95616

ABSTRACT: Conjugated linoleic acid (CLA) has been demonstrated to reduce body fat in animals. However, the mechanism by which this reduction occurs is unknown. Leptin may mediate the effect of CLA to decrease body fat. We assessed the effects of 64 d of CLA supplementation (3 g/d) on circulating leptin, insulin, glucose, and lactate concentrations in healthy women. Appetite was assessed as a physiological correlate of changes in circulating leptin levels. Analysis of plasma leptin concentrations adjusted for adiposity by using fat mass as a covariate showed that CLA supplementation significantly decreased circulating leptin concentrations in the absence of any changes of fat mass. Mean leptin levels decreased over the first 7 wk and then returned to baseline levels over the last 2 wk of the study in the CLA-treated group. Appetite parameters measured at around the time when the greatest decreases in leptin levels were observed showed no significant differences between supplementation and baseline determinations in the CLA-supplemented group or between the CLA and placebo-supplemented groups. There was a nonsignificant trend for mean insulin levels to increase toward the end of the supplementation period in CLA-treated subjects. CLA did not affect plasma glucose and lactate over the treatment period. Thus, 64 d of CLA supplementation in women produced a transient decrease in leptin levels but did not alter appetite. CLA did not affect these parameters in a manner that promoted decreases of adiposity.

Paper no. L8438 in *Lipids 35,* 783–788 (July 2000).

Conjugated linoleic acid (CLA) is the generic name for a group of positional and geometric conjugated dienoic isomers of linoleic acid. CLA has received considerable attention for its anticarcinogenic (1) and antiatherogenic activities (2,3). More recently CLA has been demonstrated to reduce body fat in mice (4–6) and lower glucose and insulin levels in genetically obese Zucker fatty (fa/fa) rats (7). However, CLA has also been shown to increase plasma insulin levels in mice (4). Because CLA supplementation is being considered for the treatment and prevention of obesity and diabetes, it would be useful to determine the effects of CLA on plasma insulin and glucose levels in humans.

The mechanism by which CLA exerts its effects on body composition is unknown. *In vitro* studies suggest that CLA reduces body fat by acting directly on adipocytes to enhance lipolysis and decrease lipoprotein lipase activity (5). However, it is also possible that CLA mediates reductions of body fat through leptin, the *ob* gene product that regulates adiposity through decreases of food intake and increases in metabolic rate (8–11). Leptin has also been shown to directly stimulate lipolysis in adipose tissue explants (12) and cultured adipocytes (13,14). CLA has been shown to decrease food intake and increase metabolic rate to varying degrees in mice (5,6,15). Thus, increases of plasma leptin concentrations could indeed mediate the effect of CLA to reduce body fat.

In this study, we sought to assess the effects of 9 wk of CLA supplementation on circulating leptin levels in healthy women. Because a number of studies indicate that insulin (16) and insulin-mediated glucose metabolism (17) regulate leptin production by adipose tissue as well as changes of circulating leptin concentrations in response to energy intake (18–20) and energy restriction (21,22), plasma insulin and glucose concentrations were measured throughout the study. Appetite was assessed as physiological correlate of changes in leptin production.

MATERIALS AND METHODS

Subjects and study design. Twenty-four women were recruited for this study, and 17 women completed it. Potential subjects completed a medical and physical examination, standard blood test, diet history, assessment of eating behavior to rule out eating disorders, and a urine test for pregnancy. Subjects selected for inclusion were all healthy, nonsmoking women between the ages of 20 and 41 yr of age and with normal menstrual cycles. Subjects lived in the metabolic suite at the Western Human Nutrition Research Center, University of California (Davis, CA) 24 hr/d, 7 d/wk for the entire study, which consisted of a 30-d stabilization period followed by a 64-d intervention period. At the end of the baseline period,

*To whom correspondence should be addressed at the Department of Cell Biology and Human Anatomy, University of California, School of Medicine, One Shields Ave., Davis, CA 95616-8643. E-mail: klerickson@ucdavis.edu

Abbreviations: AUC, area under the curve; BMI, body mass index; CLA, conjugated linoleic acid; PPAR-γ, peroxisome proliferator activated receptor-γ.

10 subjects were randomly assigned to receive a CLA supplement and 7 were assigned to receive a sunflower oil placebo. The subjects and technical/support staff were blinded as to the treatment assignments.

At the beginning of the intervention period, 3 g/d (approximately 1% of daily energy intake) of CLA was given in the form of a treatment capsule from Pharmanutrients, Inc. (Lake Bluff, IL) until the study was completed. Of the fatty acids in the capsules 65% were CLA isomers, and gas chromatography showed that the isomer composition was 22.6% *trans*-10, *cis*-12; 23.6% *cis*-11,*trans*-13; 17.6% *cis*-9,*trans*-11; 16.6% *trans*-8,*cis*-10; 7.7% *trans*-9,*trans*-11 and *trans*-10,*trans*-12; and 11.9% other isomers. Placebo capsules made from sunflower oil contained 72.6% linoleic acid and no detectable CLA; they were taken during the baseline period by all subjects and during the intervention period by the control group. The CLA and placebo capsules were identical in appearance.

Both baseline and intervention diets met the Recommended Daily Allowance for all known nutrients and were matched with respect to energy as a percentage of calories from carbohydrate, protein, and fat (55, 15, and 30%, respectively). The caloric intake of each subject was estimated with the Harris-Benedict equation and intake adjusted during the baseline period to maintain body weight. The diet was provided as a rotating 5-d menu. Four meals were served daily. Meal times were set at 8:30–9:00 A.M. for breakfast, 12:00–12:30 P.M. for lunch, 5:00–5:30 P.M. for dinner, and 7:00–7:30 P.M. for evening snack. Subjects walked 2 mi twice daily; this and other activities were controlled carefully throughout the study. For all subjects, blood was collected between 7:00–8:00 A.M. by antecubital venipuncture after an overnight fast. Weight was assessed daily before breakfast. All subjects gave their informed consent. The study protocol was approved by the Human Subjects Committees of the U.S. Department of Agriculture and the University of California, Davis.

Appetite assessment. Appetite was assessed with the use of visual analog scales. Subjects marked their answers on a line displayed on the screen of a handheld computer (Palm Pilot©). Feelings of hunger, fullness, and prospective consumption (an assessment of the amount of food that could be eaten) were reported hourly from 7:00 A.M. to 10:00 P.M.; the area under the curve (AUC) was then calculated from the responses. Baseline appetite was assessed during the third week of the baseline period, and treatment effects were measured after 6 wk of intervention. Appetite measurements were performed every other day for three replicates. The same menu days of the baseline test were chosen as the measurement days for the treatment period.

Assays. Leptin concentrations in the plasma were determined with radioimmunoassay kits (Linco Research, St. Louis, MO) as previously described (23). For human leptin, the intra- and interassay coefficients were <8%. Plasma insulin concentrations were measured with a specific radioimmunoassay for human insulin (ICN Diagnostic Div., ICN, Costa Mesa, CA) according to the method of Yalow and Berson with minor modifications (24). Plasma glucose and lactate concentrations were measured with a YSI 2300 StatPlus Glucometer (Yellow Springs Instruments, Yellow Springs, OH).

Data analysis. A linear model with time taken as a repeated measure was used to determine the effects of CLA on appetite, plasma leptin, glucose, and lactate levels. The leptin data were also analyzed after adjustment for body fat mass by including body fat mass as a covariate in the model. The fat mass values utilized were obtained as previously described (25). These analyses were performed using the Statistical Analysis System (SAS Institute, Inc., Cary, NC). Owing to the wide variation in fasting insulin levels between subjects, the insulin data were analyzed as the percentage change in insulin from baseline levels for each subject. To determine the effect of CLA on plasma insulin levels, the AUC (trapezium rule) for the percentage change in insulin levels was calculated for each subject, and the mean AUC for the CLA and placebo-supplemented groups were compared by a two sample *t*-test. Data are expressed as the mean ± SEM. The probability level for significance was set at $P < 0.05$, and a Bonferroni adjustment applied to multiple comparisons where appropriate.

RESULTS

Effect of CLA on plasma leptin concentrations. Leptin levels initially decreased and then returned to baseline levels in CLA-treated subjects (Table 1, Fig. 1A). Analysis of plasma leptin concentrations adjusted for adiposity by using fat mass as a covariate showed that CLA supplementation significantly decreased leptin levels ($P = 0.05$). Adiposity-adjusted leptin levels tended to be low at 33 d and were decreased significantly after 49 d in the CLA-supplemented group compared to the placebo-supplemented group and baseline values ($P = 0.02$ and $P = 0.04$, respectively). From the low point at 49 d, leptin concentrations in the CLA-treated group increased until they returned to near-baseline levels by the end of the study. After 57 d of supplementation, mean leptin levels in the CLA-treated group, although lower, were not significantly different from leptin levels in the placebo-treated group or from baseline values ($P = 0.12$ and $P = 0.17$, respectively). Since plasma leptin levels were not assessed between 33 and 49 d, the maximal effect of CLA on plasma leptin levels could have occurred during this time period. Changes of absolute and plasma leptin concentrations normalized as the ratio of leptin to fat mass or percentage fat mass in the CLA-supplemented group (Table 1) were similar to changes of adiposity-adjusted leptin concentrations. For example, mean absolute leptin levels were at their lowest point after 49 d of CLA supplementation. Over the entire supplementation period, CLA tended to decrease absolute and normalized plasma concentrations of leptin ($P = 0.10$). All of the observed changes in leptin concentrations occurred in the absence of detectable changes of fat mass (25) and body mass index (BMI) (Table 1).

Effect of CLA on plasma insulin, glucose, and lactate concentrations. There was a nonsignificant trend for mean plasma insulin levels to increase in CLA-treated subjects

TABLE 1
Mean BMI; Absolute and Normalized Plasma Leptin, Insulin, Glucose, and Lactate Concentrations; and Mean Change During 63 d of Treatment with Placebo or CLA[a]

	Baseline	33-d Treatment	49-d Treatment	57-d Treatment	63-d Treatment
BMI (kg/m^2)					
Placebo	22.2 ± 1.3	22.1 ± 1.2	22.6 ± 1.6	22.1 ± 1.4	22.2 ± 1.4
Δ		−0.05 ± 0.07	0.0 ± 0.1	−0.1 ± 0.2	0.1 ± 0.2
CLA	23.2 ± 0.5	23.3 ± 0.5	23.0 ± 0.5	23.1 ± 0.5	23.1 ± 0.5
Δ		−0.05 ± 0.07	−0.2 ± 0.1	−0.1 ± 0.1	−0.1 ± 0.1
Leptin (ng/mL)					
Placebo	16.7 ± 4.3	15.5 ± 5.0	16.8 ± 5.9	16.2 ± 5.0	15.7 ± 4.6
Δ		−0.2 ± 0.8	1.0 ± 1.6	−0.6 ± 1.6	−1.0 ± 1.8
CLA	16.0 ± 2.5	13.3 ± 2.4	12.9 ± 2.3[a,b]	13.8 ± 2.2	15.1 ± 3.6
Δ	−2.8 ± 0.7	−3.2 ± 0.6	−2.3 ± 1.1	0.3 ± 1.8	
Leptin/fat mass (ng/mL/kg)					
Placebo	0.79 ± 0.12	0.73 ± 0.11	0.76 ± 0.15	0.76 ± 0.09	0.76 ± 0.11
Δ		0.02 ± 0.02	0.05 ± 0.08	−0.03 ± 0.08	−0.03 ± 0.11
CLA	0.83 ± 0.10	0.67 ± 0.07[a]	0.66 ± 0.08[a]	0.68 ± 0.07	0.78 ± 0.15
Δ		−0.16 ± 0.07	−0.17 ± 0.04	−0.14 ± 0.07	0.02 ± 0.08
Leptin/% fat mass (ng/mL)					
Placebo	0.51 ± 0.10	0.51 ± 0.10	0.51 ± 0.13	0.50 ± 0.10	0.50 ± 0.10
Δ		0.03 ± 0.02	0.03 ± 0.05	−0.01 ± 0.05	−0.01 ± 0.07
CLA	0.52 ± 0.07	0.43 ± 0.06	0.41 ± 0.06[b]	0.43 ± 0.05	0.52 ± 0.10
Δ		−0.09 ± 0.04	−0.10 ± 0.03	−0.09 ± 0.04	0.03 ± 0.05
Insulin (pmoles/L)					
Placebo	64.6 ± 13.2	55.6 ± 8.3	71.5 ± 13.2	54.2 ± 9.0	70.1 ± 13.2
Δ		−14.6 ± 6.9	1.4 ± 4.2	−10.4 ± 6.9	5.6 ± 6.3
CLA	54.9 ± 10.4	50.7 ± 5.6	65.3 ± 13.2	60.4 ± 8.3	65.3 ± 6.3
Δ		−3.5 ± 6.3	10.4 ± 6.3	6.3 ± 8.3	10.4 ± 10.4
Glucose (mmoles/L)					
Placebo	4.11 ± 0.17	4.05 ± 0.21	4.25 ± 0.24	3.92 ± 0.29	4.08 ± 0.22
Δ		−0.10 ± 0.17	0.10 ± 0.19	−0.18 ± 0.23	−0.02 ± 0.17
CLA	4.04 ± 0.09	4.04 ± 0.18	4.01 ± 0.16	4.11 ± 0.19	4.1 ± 0.23
Δ		−0.01 ± 0.11	−0.03 ± 0.11	0.07 ± 0.14	0.06 ± 0.18
Lactate (mmoles/L)					
Placebo	2.25 ± 0.29	2.11 ± 0.40	3.06 ± 0.59	2.36 ± 0.17	2.43 ± 0.21
Δ		−0.14 ± 0.46	0.62 ± 0.54	0.11 ± 0.33	0.18 ± 0.22
CLA	2.39 ± 0.34	2.68 ± 0.34	2.89 ± 0.29	2.78 ± 0.39	2.33 ± 0.23
Δ		0.29 ± 0.37	0.49 ± 0.42	0.39 ± 0.62	−0.06 ± 0.48

[a]Mean ± SEM; $n = 7$ for placebo and $n = 10$ for CLA. Treatment change (Δ) values represent mean change from baseline; BMI, body mass index; CLA, conjugated linoleic acid. [a]$P < 0.05$ vs. baseline. [b]$P < 0.05$ vs. placebo.

(Table 1 and Fig. 1B). The mean percentage change in insulin levels from baseline increased over the last 2 wk of the study in the CLA-supplemented group; this change coincided with the increase in leptin from the low point in leptin concentrations at 49 d (Figs. 1A and 1B). The mean AUC for the percentage change in insulin levels from baseline was 1039 ± 708 and −208 ± 895 for the CLA and placebo-supplemented groups, respectively. Although the difference in the mean AUC between the two groups was not significant ($P = 0.17$), it is possible that significance would have been attained with a larger sample size. CLA did not have any effect on plasma glucose ($P = 0.524$) and lactate concentrations ($P = 0.845$) (Table 1).

Effect of CLA on appetite. The AUC ratings during the baseline and supplementation periods for hunger, fullness, and prospective consumption showed that none of the three appetite measures was significantly affected by CLA treatment (Table 2). In addition, an approximately equal number of subjects had increased or decreased hunger, fullness, or prospective consumption in the CLA and placebo-supplemented groups (data not shown).

DISCUSSION

The present study is the first to examine the effects of CLA supplementation on circulating leptin levels in humans. CLA supplementation significantly decreased leptin concentrations without any detectable changes of body fat mass. After 7 wk of treatment, in the CLA-supplemented group, circulating leptin concentrations were at their lowest point. Thereafter, over the last 2 wk of intervention, leptin concentrations rose to pretreatment levels. These data are consistent with a recent study, which showed that plasma leptin concentrations tended to decrease in CLA-treated mice maintained on a high-fat diet (4). In mice fed a diet of 1% CLA by weight, plasma leptin levels were significantly decreased after 6 wk of treatment but did not differ from controls after 8 wk. However, since the 1% CLA diet decreased several different fat depots by greater

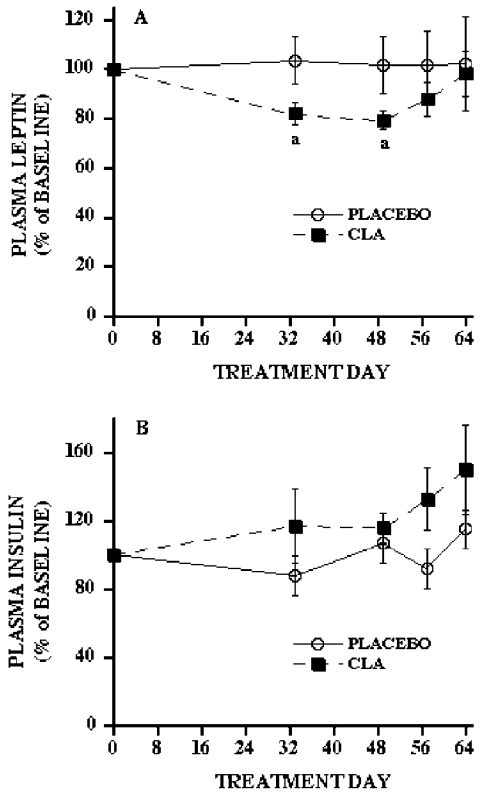

FIG. 1. Percentage change in leptin (A) and insulin (B) concentrations from baseline levels in conjugated linoleic acid (CLA) and placebo-supplemented subjects. Blood samples were collected after an overnight fast at baseline and at days 33, 49, 57, and 63 of intervention. Leptin and insulin concentrations were assessed by radioimmunoassay. Mean ± SEM; $n = 7$ for placebo and $n = 10$ for CLA. $^aP < 0.05$ vs. baseline.

than 50% after 6 wk of treatment, it is possible that the decreased leptin levels resulted from a reduction of body fat in the mice. However, by the end of that study, while overall fat mass decreased nearly 43%, leptin levels no longer differed from control levels. Thus, it is possible, like the present study, that CLA had effects on leptin levels that were independent of changes in fat mass.

To assess whether CLA-mediated changes in leptin levels were related to changes in appetite, self-ratings of hunger, fullness, and prospective consumption were determined. We have previously reported that in energy-restricted human females, subjects with lower leptin concentrations and greater percentage decreases in circulating leptin reported greater feelings of hunger, desire to eat, and prospective consumption than those with higher leptin concentrations and smaller decreases in leptin (26). In the present study, although appetite parameters were measured at around the time when the greatest decreases in leptin levels were observed, there were no significant differences between supplementation and baseline determinations in the CLA-supplemented group or between the CLA and placebo-supplemented groups. It is possible that there were undetected changes in appetite that were related to the decrease in leptin levels; the subjective assessment of appetite may be a gross measure that does not pick

TABLE 2
Mean Ratings of Hunger, Fullness, and Prospective Consumption[a]

	Baseline	After 6 wk of treatment
Hunger (AUC as mm·h)		
Placebo	486 ± 59	467 ± 50
CLA	508 ± 77	518 ± 64
Fullness (AUC as mm·h)		
Placebo	798 ± 75	
CLA	716 ± 56	727 ± 32
Prospective consumption (AUC as mm·h)		
Placebo	514 ± 97	500 ± 72
CLA	531 ± 83	568 ± 61

[a]Summarized mean of area under the curve (AUC) ± SEM for 16 hourly inquiries throughout the day; $n = 7$ for placebo and $n = 10$ for CLA.

up subtle changes in appetite. However, in the present study, in contrast to the previous one, the subjects were on a maintenance rather than an energy-restricted diet. Therefore, the decreases of circulating leptin levels were much more modest (~20%) in the present study than during energy restriction (~50–70%). It is also possible that other physiological changes, in addition to decreases in leptin concentration, are required to mediate changes of appetite. Although changes in leptin levels have been shown to modulate energy expenditure (8–11), it was also not affected in the present study by CLA treatment despite the changes in circulating leptin concentrations (25). Thus, the physiological significance of the changes that were observed in circulating leptin levels are not clear.

Plasma insulin levels tended to increase in CLA-treated subjects over the last 2 wk of the supplementation period. This change coincided with the increase in leptin concentrations from their low point at 49 d. A recent study showed that changes in plasma leptin correlate with changes of fasting plasma insulin independent of changes of BMI or percentage body fat (27). It was also demonstrated that insulin administration, at doses producing increments of insulin within the physiological range, increases circulating leptin concentrations in humans (28, 29). Thus, it is possible that the increase in insulin levels mediated the return of leptin concentrations to baseline levels. A trend for circulating insulin levels to increase with CLA supplementation was recently demonstrated in rodents by DeLany and colleagues (4). They reported that plasma insulin levels of CLA-fed mice tended to increase over the treatment period but did not reach significance until after 8 wk. Similar to the present study, this change in insulin levels occurred about 1 wk following the greatest difference in leptin levels between CLA-treated and control mice, and it also coincided with the increase in leptin to control levels. Thus, for both studies, it is possible that increases in insulin levels influenced circulating leptin concentrations.

The increase in insulin levels may have been part of a homeostatic response to counter the effect of CLA to decrease leptin. There are other possible explanations for the transient effect of CLA on circulating leptin concentrations. Initially, as suggested by a recent *in vitro* study (7), CLA could have acted as a ligand that activated peroxisome proliferator-acti-

vated receptor-γ (PPAR-γ). In turn, activation of PPAR-γ has been demonstrated to decrease leptin gene expression in rodents (30) and an adipocyte cell line (31). An event that could have occurred later during the intervention is demonstrated by a study in which rats fed a 1% CLA diet incorporated the *cis*-9,*trans*-11-isomer into membrane phospholipids of mammary epithelial cells (1). The investigators suggested that the incorporation of CLA into phospholipids could have various effects on signal transducing pathways. It is conceivable that altered signaling affected leptin production as CLA incorporation into adipocyte membranes increased.

In summary, 64 d of CLA supplementation in women produced a transient decrease in leptin levels but did not alter appetite or energy expenditure. These results are counter to what would be expected if CLA were able to reduce body fat in humans as it does in animals.

ACKNOWLEDGMENTS

We thank Kimber Stanhope, Peter Taylor and Wing Tung Chau for technical assistance, John Beckmeyer for computer programming assistance, nursing staff and clinical chemistry support staff for assistance with blood drawing and processing, Ginny Gildengorin and Bruce Mackey for statistical consultation. This work was supported by the United States Department of Agriculture, NIH grants DK 50129, DK 35747, the Juvenile Diabetes Association, the American Diabetes Association, and the California Breast Cancer Research Program of the University of California, 1RB-0404. E.A.M. was supported by a Medical Scholars Award from the American Diabetes Association and NIH grant DK09950-01.

REFERENCES

1. Ip, C., Scimeca, J.A., and Thompson, H.J. (1994) Conjugated Linoleic Acid. A Powerful Anticarcinogen from Animal Fat Sources, *Cancer 74*, 1050–1054.
2. Lee, K.N., Kritchevsky, D., and Pariza, M.W. (1994) Conjugated Linoleic Acid and Atherosclerosis in Rabbits, *Atherosclerosis 108*, 19–25.
3. Nicolosi, R.J., Rogers, E.J., Kritchevsky, D., Scimeca, J.A., and Huth, P.J. (1997) Dietary Conjugated Linoleic Acid Reduces Plasma Lipoproteins and Early Aortic Atherosclerosis in Hypercholesterolemic Hamsters, *Artery 22*, 266–277.
4. DeLany, J.P., Blohm, F., Truett, A.A., Scimeca, J.A., and West, D.B. (1999) Conjugated Linoleic Acid Rapidly Reduces Body Fat Content in Mice Without Affecting Energy Intake, *Am. J. Physiol. 276*, R1172–R1179.
5. Park, Y., Albright, K.J., Liu, W., Storkson, J.M., Cook, M.E., and Pariza, M.W. (1997) Effect of Conjugated Linoleic Acid on Body Composition in Mice, *Lipids 32*, 853–858.
6. West, D.B., DeLany, J.P., Camet, P.M., Blohm, F., Truett, A.A., and Scimeca, J. (1998) Effects of Conjugated Linoleic Acid on Body Fat and Energy Metabolism in the Mouse, *Am. J. Physiol. 275*, R667–R672.
7. Houseknecht, K.L., Vanden Heuvel, J.P., Moya-Camarena, S.Y., Portocarrero, C.P., Peck, L.W., Nickel, K.P., and Belury, M.A. (1998) Dietary Conjugated Linoleic Acid Normalizes Impaired Glucose Tolerance in the Zucker Diabetic Fatty *fa/fa* Rat, *Biochem. Biophys. Res. Commun. 244*, 678–682.
8. Woods, S.C., Seeley, R.J., Porte, D., Jr., and Schwartz, M.W. (1998) Signals That Regulate Food Intake and Energy Homeostasis, *Science 280*, 1378–1383.
9. Chen, G., Koyama, K., Yuan, X., Lee, Y., Zhou, Y.T., O'Doherty, R., Newgard, C.B., and Unger, R.H. (1996) Disappearance of Body Fat in Normal Rats Induced by Adenovirus-Mediated Leptin Gene Therapy, *Proc. Natl. Acad. Sci. USA 93*, 14795–14799.
10. Pelleymounter, M.A., Cullen, M.J., Baker, M.B., Hecht, R., Winters, D., Boone, T., and Collins, F. (1995) Effects of the Obese Gene Product on Body Weight Regulation in ob/ob Mice, *Science 269*, 540–543.
11. Halaas, J.L., Gajiwala, K.S., Maffei, M., Cohen, S.L., Chait, B.T., Rabinowitz, D., Lallone, R.L., Burley, S.K., and Friedman, J.M. (1995) Weight-Reducing Effects of the Plasma Protein Encoded by the Obese Gene, *Science 269*, 543–546.
12. Siegrist-Kaiser, C.A., Pauli, V., Juge-Aubry, C.E., Boss, O., Pernin, A., Chin, W.W., Cusin, I., Rohner-Jeanrenaud, F., Burger, A.G., Zapf, J., and Meier, C.A. (1997) Direct Effects of Leptin on Brown and White Adipose Tissue, *J. Clin. Invest. 100*, 2858–2864.
13. Wang, M.Y., Lee, Y., and Unger, R.H. (1999) Novel Form of Lipolysis Induced by Leptin, *J. Biol. Chem. 274*, 17541–17544.
14. Fruhbeck, G., Aguado, M., and Martinez, J.A. (1997) *In Vitro* Lipolytic Effect of Leptin on Mouse Adipocytes: Evidence for a Possible Autocrine/Paracrine Role of Leptin, *Biochem. Biophys. Res. Commun. 240*, 590–594.
15. Park, Y., Albright, K.J., Storkson, J.M., Liu, W., Cook, M.E., and Pariza, M.W. (1999) Changes in Body Composition in Mice During Feeding and Withdrawal of Conjugated Linoleic Acid, *Lipids 34*, 243–248.
16. Saad, M.F., Khan, A., Sharma, A., Michael, R., Riad-Gabriel, M.G., Boyadjian, R., Jinagouda, S.D., Steil, G.M., and Kamdar, V. (1998) Physiological Insulinemia Acutely Modulates Plasma Leptin, *Diabetes 47*, 544–549.
17. Mueller, W.M., Gregoire, F.M., Stanhope, K.L., Mobbs, C.V., Mizuno, T.M., Warden, C.H., Stern, J.S., and Havel, P.J. (1998) Evidence That Glucose Metabolism Regulates Leptin Secretion from Cultured Rat Adipocytes, *Endocrinology 139*, 551–558.
18. Schoeller, D.A., Cella, L.K., Sinha, M.K., and Caro, J.F. (1997) Entrainment of the Diurnal Rhythm of Plasma Leptin to Meal Timing, *J. Clin. Invest. 100*, 1882–1887.
19. Havel, P.J., Townsend, R., Chaump, L., and Teff, K. (1999) High-Fat Meals Reduce 24-h Circulating Leptin Concentrations in Women, *Diabetes 48*, 334–341.
20. Havel, P.J. (1999) Mechanisms Regulating Leptin Production: Implications for Control of Energy Balance [Editorial; comment], *Am. J. Clin. Nutr. 70*, 305–306.
21. Dubuc, G.R., Phinney, S.D., Stern, J.S., and Havel, P.J. (1998) Changes of Serum Leptin and Endocrine and Metabolic Parameters After 7 Days of Energy Restriction in Men and Women, *Metabolism 47*, 429–434.
22. Boden, G., Chen, X., Mozzoli, M., and Ryan, I. (1996) Effect of Fasting on Serum Leptin in Normal Human Subjects, *J. Clin. Endocrinol. Metab. 81*, 3419–3423.
23. Landt, M., Gingerich, R.L., Havel, P.J., Mueller, W.M., Schoner, B., Hale, J.E., and Heiman, M.L. (1998) Radioimmunoassay of Rat Leptin: Sexual Dimorphism Reversed from Humans, *Clin. Chem. 44*, 565–570.
24. Yalow, R.S., and Berson, S.A. (1960) Immunoassay of Endogenous Plasma Insulin in Man, *J. Clin. Invest. 39*, 1157–1175.
25. Zambell, K.L., Keim, N.L., Van Loan, M.D., Gale, B., Benito, P., Kelley, D.S., and Nelson, G.J. (2000) Conjugated Linoleic Acid Supplementation in Humans: Effects on Body Composition and Energy Expenditure, *Lipids 35*, 777–782.
26. Keim, N.L., Stern, J.S., and Havel, P.J. (1998) Relation Between Circulating Leptin Concentrations and Appetite During a Prolonged, Moderate Energy Deficit in Women, *Am. J. Clin. Nutr. 68*, 794–801.
27. Havel, P.J., Kasim-Karakas, S., Mueller, W., Johnson, P.R.,

Gingerich, R.L., and Stern, J.S. (1996) Relationship of Plasma Leptin to Plasma Insulin and Adiposity in Normal Weight and Overweight Women: Effects of Dietary Fat Content and Sustained Weight Loss, *J. Clin. Endocrinol. Metab. 81*, 4406–4413.
28. Saladin, R., De Vos, P., Guerre-Millo, M., Leturque, A., Girard, J., Staels, B., and Auwerx, J. (1995) Transient Increase in Obese Gene Expression After Food Intake or Insulin Administration, *Nature 377*, 527–529.
29. Cusin, I., Sainsbury, A., Doyle, P., Rohner-Jeanrenaud, F., and Jeanrenaud, B. (1995) The Ob Gene and Insulin. A Relationship Leading to Clues to the Understanding of Obesity, *Diabetes 44*, 1467–1470.
30. Zhang, B., Graziano, M.P., Doebber, T.W., Leibowitz, M.D., White-Carrington, S., Szalkowski, D.M., Hey, P.J., Wu, M., Cullinan, C.A., Bailey, P., *et al.* (1996) Down-Regulation of the Expression of the Obese Gene by an Antidiabetic Thiazolidinedione in Zucker Diabetic Fatty Rats and *db/db* Mice, *J. Biol. Chem. 271*, 9455–9459.
31. Kallen, C.B., and Lazar, M.A. (1996) Antidiabetic Thiazolidinediones Inhibit Leptin (ob) Gene Expression in 3T3-L1 Adipocytes, *Proc. Natl. Acad. Sci. USA 93*, 5793–5796.

[Received January 14, 2000, and in revised form May 30, 2000; revision accepted June 7, 2000]

Determination of the Conjugated Linoleic Acid-Containing Triacylglycerols in New Zealand Bovine Milk Fat

Nicholas P. Robinson* and Alastair K.H. MacGibbon

New Zealand Dairy Research Institute, Palmerston North, New Zealand

ABSTRACT: Reversed-phase high-performance liquid chromatography (HPLC) with ultraviolet (UV) detection at 233 nm was used to separate, quantify, and identify the triacylglycerols (TAG) of milk fat that contain conjugated linoleic acid (CLA). The absorbance at 233 nm was substantially due to CLA-TAG (chromatography of some representative TAG devoid of CLA, such as tripalmitin and triolein, showed poor responses at 233 nm, 1/800th that of CLA-TAG). A CLA molar extinction coefficient at 233 nm of 23,360 L mol^{-1} cm^{-1} and an HPLC UV response factor were obtained from a commercially available *cis*-9,*trans*-11-CLA standard. This molar extinction coefficient was only 86% of reported literature values. Summation of all chromatographic peaks absorbing at 233 nm using the corrected response factor gave good agreement with independent determinations of total CLA by gas chromatography and UV spectrophotometry. This agreement allowed quantification of individual CLA-TAG peaks in the HPLC separation of a typical New Zealand bovine milk fat. Three CLA-containing TAG, CLA-dipalmitin, CLA-oleoyl-palmitin and CLA-diolein, were prepared by interesterification of tripalmitin with the respective fatty acid methyl esters and used to assign individual peaks in the reversed-phase chromatography of total milk fat, of which CLA-oleoyl-palmitin was coincident with the largest UV peak. Band fractions from argentation thin-layer chromatography of total milk fat were similarly employed to identify five predominant CLA-TAG groups in total milk fat: CLA-disaturates, CLA-oleoyl-saturates, CLA-vaccenyl-saturates, CLA-vaccenyl-olein, and CLA-diolein.

Paper no. L8386 in *Lipids 35*, 789–796 (July 2000).

Ruminant fats are the most important natural source of conjugated linoleic acid (CLA). The high natural levels in ruminant depot fat originate partly from bacteria in the rumen (1), of which *Butyrivibrio fibrisolvens* is the most widely known. In milk fat, the level is further enhanced by the activity of 9-desaturase on *trans*-11-vaccenic acid (2), and humans apparently have a similar facility. CLA isomeric mixtures, synthesized by alkaline isomerization of linoleic acid, have been of recent import owing to their broad physiological impact in animal models: the evidence indicates protective effects against mammary cancer (3,4) and atherosclerosis (5), and a role in depot fat reduction while increasing lean body mass (6). These are the reasons for the intense interest in the distribution, synthesis, and concentration of CLA.

A knowledge of the triacylglycerols (TAG) containing CLA within milk fat is important in terms of both the mechanism of TAG synthesis and TAG digestibility. Milk fat is a complex natural substance. It contains TAG made from over 400 detectable fatty acids (7,8), of which CLA constitutes only about 1% by mass (8). To elucidate this complex array of TAG, there have been many detailed separations, often involving gas chromatography (GC) or reversed-phase (RP) high-performance liquid chromatography (HPLC) (10–13). An RP-HPLC separation of typical New Zealand milk fat has been reported previously by this group (14); when detected by evaporative light scattering, milk fat separated into 61 peaks, based on total acyl chain length (Carbon Number), number of double bonds, and, surprisingly, double bond configuration (*cis*- or *trans*-). A key finding (14) was the accuracy with which differences in HPLC retention time could be used to identify molecular groups. As most of the major TAG were discernible within a given Partition Number, and samples of separate molecular groups were available from argentation thin-layer chromatography (Ag-TLC), there was a sound basis on which to assign whole sets of chemically related TAG.

If TAG detection is on the basis of mass only (such as flame ionization or evaporative light scattering), it is unlikely to give any specific indication of the TAG that contain CLA—the concentrations are either too low or the peaks are likely to be overwhelmed by other, more dominant TAG with the same retention time. However, CLA has a particular advantage—conjugated dienoic fatty acids are highly absorptive of ultraviolet (UV) light around 233 nm (15–20), whereas the other fatty acids of milk fat have generally low absorptivities at this wavelength (21,22). Methods are already available in which this property of conjugated dienoic acids is exploited (21–24), and some of these have provided valuable information about the positional and geometric isomers of transmethylated CLA in a range of biological samples. However, little work has been conducted on intact CLA-TAG, and no study has to our

*To whom correspondence should be addressed at New Zealand Dairy Research Institute, Private Bag 11-029, Palmerston North, New Zealand.
E-mail: nick.robinson@nzdri.org.nz

Abbreviations: Ag-TLC, argentation thin-layer chromatography; CLA, conjugated linoleic acid; ELSD, evaporative light-scattering detector/detection; FAME, fatty acid methyl ester; GC, gas chromatography; HPLC, high-performance liquid chromatography; L, linoleic acid; O, oleic acid; P, palmitic acid; RP, reversed-phase; S, stearic acid; SPE, solid phase extraction; TAG, triacylglycerol; TBME, *tert*-butyl methyl ether; UV, ultraviolet; V, vaccenic acid.

knowledge described the CLA-TAG of bovine milk fat.

At the CLA absorbance maximum of 233 nm (15,16), an opportunity was foreseen to specifically detect CLA-TAG in milk fat, without the complication of the many other TAG. In addition, we hypothesized that UV detection, with its proven linear dynamic range, would provide absolute concentrations of individual TAG containing CLA.

The aims of this study therefore were fourfold: to obtain a practical HPLC separation and detection of CLA-TAG in total milk fat using UV detection; to determine if all or most of the absorbance at 233 nm was due to CLA-TAG; to obtain accurate quantitative information from HPLC about the level of some specific CLA-TAG in milk fat; and to use HPLC and Ag-TLC to assign identities to those TAG containing CLA. We report here an existing reversed-phase HPLC method for which we have added UV detection at 233 nm to monitor the elution of CLA-containing TAG. As a precursor to quantification of individual HPLC peaks, the level of total CLA observed by HPLC was confirmed by static UV-visible spectrophotometry and fatty acid methyl ester–GC (FAME–GC). Finally, an HPLC analysis of bands from Ag-TLC of total milk fat is described, providing a means to identify the components of many of the peaks arising from detection at 233 nm.

EXPERIMENTAL PROCEDURES

Reagents and samples. All solvents (BDH, Poole, United Kingdom) were of HPLC grade and were used as received. Helium and nitrogen (Oxygen Free grade) gas were supplied by BOC Gases (Palmerston North, New Zealand). Tripalmitin (99% grade), 1,2-dipalmitin (racemic, 99%), and 2-linoleoyl-1,3-dipalmitin (PLP, 99% grade) were obtained from Sigma-Aldrich Pty. Limited (Castle Hill, Australia). Triolein (99%+) and methyl linoleate were obtained from Nu-Chek-Prep (Elysian, MN). CLA was available in various grades of isomeric purity: an isomeric mixture of *cis,trans-/trans,cis*-9,11- and *cis,trans-/trans,cis*-10,12-isomers was obtained from Sigma-Aldrich Pty. Limited; a 75–78% *cis*-9,*trans*-11 and a 97% *cis*-9,*trans*-11 grade were obtained from Matreya Inc. (Pleasant Gap, PA). Diazomethane was used to methylate both the Sigma-Aldrich CLA for interesterification and the Matreya CLA for absorbance measurements, by an established procedure (25). Oxalyl chloride was supplied by BDH. The TAG standard, 2-elaidoyl-1,3-distearin, was synthesized, and the ratio of stearic to elaidic acid confirmed by FAME analysis. Milk fat samples were obtained from the New Zealand Dairy Research Institute, Palmerston North, or were typical commercial samples.

Ag-TLC. Ag-TLC experiments were performed according to a previously reported procedure (26). TAG samples were typically 10 mg in size. Some modification to the published method was made for isolation of the TAG: silica from a recovered band was washed with *tert*-butylmethyl ether (TBME)/hexane (1:1, 2 × 2 mL), and the sample solution was put through a solid phase extraction (SPE) cartridge (SI type, BondElut, Varian, Harbor City, CA), before evaporating to dryness.

UV/visible absorbance measurements. UV/visible absorbance measurements were carried out on a Jasco V-560 Spectrophotometer, calibrated with the internal calibration function. Spectrometer settings were all controlled by the computer software. Absorbance measurements, performed in isooctane solution (1 cm quartz cell) were obtained from the mean of three individual readings. Molar extinction coefficients were calculated (27) from a plot of absorbance vs. concentration (for CLA, at four concentrations that ranged from 0.003 to 0.043 g/L), by multiplying the slope of the resulting plot by the molecular weight of CLA. Total CLA determination at 233 nm was performed according to the AOCS Official Method (23), also using the Jasco V-560 Spectrophotometer. β-Carotene absorbance measurements were performed on a 50 μg/L solution in isooctane.

CLA-TAG preparation. The basis of the following interesterification procedure was described by Marangoni and Rousseau (28). The procedure involves heating a TAG in the presence of a FAME and sodium metal, and the net effect is substitution of one or more of the TAG fatty acids by the methyl-esterified fatty acid. The reaction is not regioselective, and is sensitive to both water and the proportions of reagents, but it has the advantage of simplicity, cheap reagents, and minimal workup. Thus, a three-necked round bottom 250 mL flask, flushed with N_2 gas, was charged with isooctane (15 mL) and tripalmitin (0.483 g, 0.60 mmol). Dissolution of tripalmitin was incomplete at ambient temperature. Methyl conjugated linoleate (Sigma-Aldrich; mixture of *cis*- and *trans*-9,11- and 10,12-, 0.326 g, 1.11 mmol) was added by Pasteur pipette. Sodium metal (0.009 g, 0.39 mmol), prewashed with hexane, was added to the three-necked flask. The mixture was heated to gentle reflux and maintained there for 30 min, during which time it turned from colorless to yellow/gold. The boiling point of isooctane, 98–99°C at ambient pressure, assisted the progress of the reaction. Sodium is molten at this temperature and readily provided fresh metal surfaces to catalyze the reaction. The reaction mixture was allowed to cool. While taking care to leave the sodium metal in the reactor flask, the mixture was poured into a separatory funnel containing aqueous ammonium chloride (saturated solution, 50 mL). TBME (50 mL) was used to rinse the reactor flask, and the rinses were added to the separatory funnel. The organic layer was washed with aqueous sodium bicarbonate (1% solution, 50 mL) and saturated sodium chloride solution (50 mL), dried (solid sodium sulfate, anhydrous), and filtered. Solvent removal under reduced pressure gave a pale yellow oil (0.776 g). TLC indicated the presence of FAME, TAG, free fatty acids, and diacylglycerols. A TAG fraction was obtained by SPE, using aminopropyl cartridges to remove free fatty acids, and SI (silica) cartridges to remove FAME and diacylglycerols. Tripalmitin and the mono-CLA, di-CLA, and tri-CLA TAG were separated by Ag-TLC, using chloroform/toluene (1:1) as eluant (26). FAME analysis of the band at R_f 0.44 confirmed the presence of a group of mono-CLA-dipalmitic TAG (all regioisomers assumed), whereas

the di-CLA-monopalmitic TAG were identified in the band at R_f 0.22. Tripalmitin was detected at R_f 0.66. A mixture of regioisomeric TAG containing linoleic acid was also prepared by the same method. The synthesis of 3-CLA-1,2-dipalmitin was achieved by reacting CLA (Matreya, 75-78% 9*Z*,11*E* isomer; 92+% 9,11 isomers, 0.348g, 1.24 mmol) with oxalyl chloride (120 μL, 1.37 mmol) in dry dichloromethane to generate the acyl chloride of CLA. The solvent was removed under reduced pressure, and to the flask containing CLA acyl chloride were added pyridine (1 mL, 12.36 mmol), dichloromethane (5 mL) and 1,2-dipalmitin (0.700 g, 1.23 mmol). The P-P-CLA product was isolated by the same extraction procedure described above for interesterification. Silica column chromatography (25 g silica), using 5% step changes in eluant from 0–15% TBME in hexane, gave two fractions (combined mass 0.238 g) that contained P-P-CLA. The first of these fractions was adjudged purer than the second by silica TLC, and was thus used for RP-HPLC, where it gave a single peak that agreed well with the mono-CLA-dipalmitin obtained from interesterification. Further purification of the first silica column fraction by Ag-TLC gave a white solid residue that, after FAME-GC analysis, gave a molar ratio of two P groups to one CLA. FAME-GC also confirmed that neither set of preparative conditions, acyl chloride synthesis or interesterification, had altered the original ratios of 9,11-CLA or 10,12-CLA isomers.

GC. FAME were obtained by transmethylation of TAG samples, according to the procedure of MacGibbon (29). Separation of FAME and CLA isomers was carried out on a Shimadzu GC 17A (Shimadzu Corporation, Kyoto, Japan) equipped with a flame-ionization detector, operated at 250°C, with hydrogen supplied at 50 mL/min, and air at 500 mL/min. Hydrogen was used as carrier gas at a flow rate of 1.2 mL/min. The capillary column was a BPX70, 50 m × 0.22 mm i.d., film thickness 0.25 μm (SGE Incorporated, Austin, TX). The column was operated at 50°C for 1.5 min, then the temperature was increased at 3°C/min until the final temperature of 220°C was reached, where it was held for a further 10 min. Routinely, 0.2 μL of each sample solution was injected, constituting approximately 0.5 μg FAME. Response factors were calculated relative to P, using values from Ackman and Sipos (30) and Bannon *et al.* (31).

HPLC. RP-HPLC was performed on an LC Module 1 Plus (Waters Associates, Milford, MA), following a previously described method (14), with the addition of in-line detection at 233 nm. HPLC sample solutions were prepared by dissolving an aliquot (50 mg) of the melted fat sample in 1,2-dichloroethane/acetonitrile (2:1, 10 mL, final fat concentration 5 mg/mL). Filtration through a polytetrafluoroethylene syringe filter into an autosampler vial (1 mL size) gave a clear, pale yellow solution. The injection volume for a total milk fat sample was 20 μL (total fat injected 100 μg). Larger injections of total milk fat, of the order of 300 μg (as described in Fig. 1), can also be used and provide improved ratios of UV signal to noise, but we note that sample solutions more concentrated than 5 mg/mL require the addition of neat 1,2-dichloroethane to dissolve all TAG. When total milk fat TAG (12.8 mg) were separated by Ag-TLC, band extracts were reconstituted in 1,2-dichloroethane (0.2 mL), and the injection volume was 20 μL. The chromatography column was a Waters Nova-

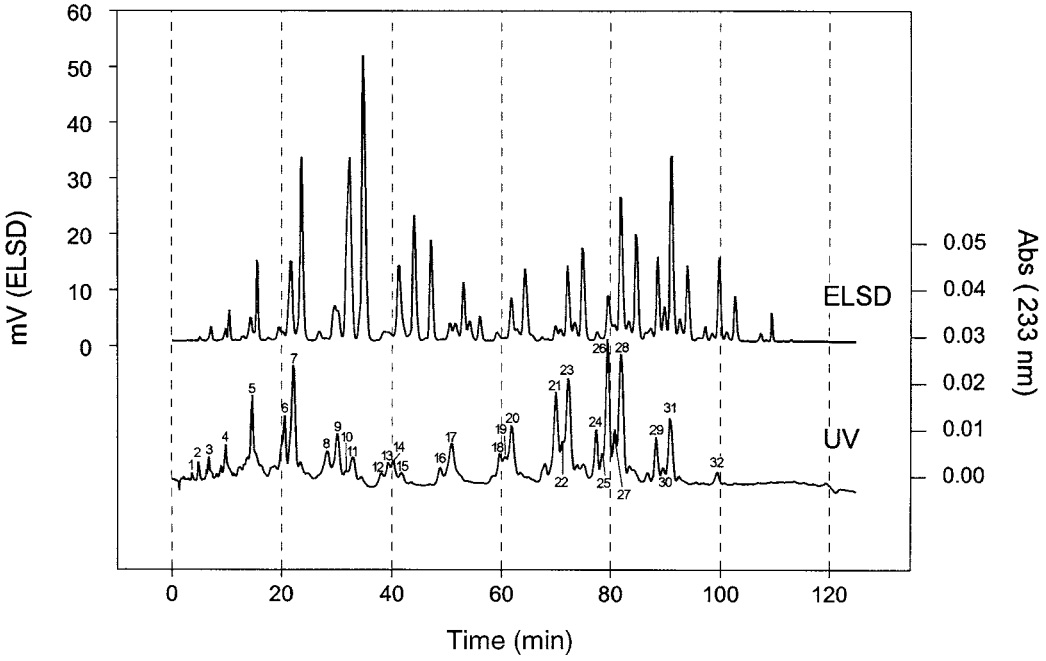

FIG. 1. High-performance liquid chromatography (HPLC) separation of total milk fat (317 μg injection) on a Waters Nova-Pak™ C18 reversed-phase column, 4 μm, 3.9 × 150 mm, with evaporative light-scattering detection (ELSD) and ultraviolet (UV) 233 nm detection. Peak numbers used in the UV trace pertain to those in Table 1.

Pak™ C18 (4 μm, 3.9 × 150 mm), with a pre-column module containing inserts of the same bonded phase. The column temperature was maintained at 20°C by water circulated from a bath to a column jacket. TAG were serially detected by UV at 233 nm (Waters 486 detector) and ELSD (Alltech 500; Alltech Associates Inc., Deerfield, IL). The time difference between UV and ELSD was of the order of 5 s. Nitrogen gas was supplied to the ELSD at a pressure of 80 psi, and the nitrogen flow at the nebulizer was maintained at 2.00 standard liters per minute, generating a nebulizer gas pressure of 32 psi. The solvent pressure at the nebulizer was typically less than 10 psi, and the ELSD drift tube temperature was set at 70°C. Peak data, collected at a sampling rate of 2 points/s, were acquired through a BUS/LACE interface and analyzed using Millennium^{32}™ software (Waters Associates, Milford, MA). The mobile phase gradient program was as previously described (14). During each cycle of the pump gradient program, the baseline absorbance at 233 nm increased with increasing dichloromethane content, generating a significant slope in the baseline. To remove this slope, a blank sample was injected and the blank data were subtracted from the sample data.

RESULTS AND DISCUSSION

A single injection of total milk fat TAG (317 μg), with serial detection at 233 nm and by ELSD, is shown in Figure 1. Three important features were evident from the overlaid traces: first, there was a wide variety of UV-absorbing species; second, the most dominant peaks by mass (ELSD) did not necessarily have any UV absorbance (for example, the biggest peak in the ELSD trace, at a retention time of 35 min, corresponds to only a small UV peak); and third, many of the clusters of UV peaks were very similar in shape and spacing to those of the ELSD data. The data indicated that the TAG detected by UV and ELSD had been separated in similar ways, and that if most of the UV absorbance was due to CLA, then it was widely distributed among the TAG of milk fat. It was suspected that both were true, but proof of the specificity of the 233 nm absorbance for CLA, and of whether the summed UV peaks accounted for all the CLA, was required before any individual peaks could be quantified.

Total CLA quantification. There were two aspects to the determination. The question of whether TAG without CLA accounted for any significant absorbance of a peak was addressed by HPLC analysis of some common TAG, representative of those found in milk fat, with detection at 233 nm. The resulting absorbances were small compared to CLA-TAG. Tripalmitin, triolein, 2-elaidoyl-1,3-distearin, and 2-linoleoyl-1,3-dipalmitin gave UV peak responses that were 1/500 that of the "standard" CLA-P-P/P-CLA-P (synthesized with CLA from Sigma-Aldrich) prepared by interesterification, although a purer CLA standard later showed that this factor should be closer to 1/800. 2-Linoleoyl-1,3-dipalmitin, with methylene-interrupted double bonds, gave a response that was only 20% higher than tripalmitin. In a similar observation, Brown and Snyder (24) reported that trilinolein does not absorb appreciably at 233 nm, and that its extinction coefficient is similar to that of tristearin. In a report by Angers *et al.* (32), total milk fat TAG were detected by UV at 220 nm; at this wavelength the TAG containing CLA may have represented the predominant signals, but the authors did not indicate that. Repeating the HPLC procedure of Angers *et al.* in our own laboratory gave a trace that was dominated by the same signals as had occurred at 233 nm.

To further indicate the low absorbance of non-CLA-TAG, and to estimate their combined absorbance in a total milk fat sample, a hydrogenated milk fat sample was analyzed by HPLC. Of 24 peaks detected by ELSD, only the two largest (identified as P-S-S/S-P-S and S-S-S) were detected at 233 nm, and their combined UV area was only 2% of the summed UV area commonly observed for total milk fat. It was therefore provisionally concluded that the total absorbance of peaks detected at 233 nm was greater than 95% CLA-TAG.

A second consideration was whether the HPLC peaks observed at 233 nm accounted for all the CLA-TAG. For quantification of individual peaks at 233 nm to be meaningful and accurate, the summed UV absorbance from a sample trace had to agree with independent measures of total CLA. This would address the possibility of some underlying baseline absorbance (due to CLA-TAG) being missed by integration and therefore not included in the quantification. Injections of 1,2-dichloroethane solvent blanks indicated no UV-absorbing signals after a breakthrough peak at 1.4 min. A set of 12 fat samples of known CLA content were independently analyzed by FAME-GC and the AOCS spectrophotometric method (23) and compared with the results from HPLC peak summation. To allow valid comparison, the HPLC UV detector response at 233 nm was determined using a CLA standard of stated purity, 97% 9*Z*,11*E* (Matreya), although methylation of the standard was required for chromatography. The molar extinction coefficient of this CLA free fatty acid standard as received was 24,400 L mol^{-1}cm^{-1} in isooctane, 10% lower than two previous reports of 26,600 L mol^{-1}cm^{-1} in carbon disulfide solution (15) and 27,000 L mol^{-1}cm^{-1} in isooctane solution (16), although in each report the methyl ester of CLA was described. For other commercial CLA samples ε_{233} was significantly lower; for the Nu-Chek-Prep methyl conjugated linoleate, ε_{233} was 15,300 L mol^{-1}cm^{-1}; for the Matreya 75–78% 9*Z*,11*E* CLA (free fatty acid), ε_{233} was 22,100 L mol^{-1}cm^{-1}. After methylation, we observed a slightly lower molar extinction coefficient of 23,360 L mol^{-1}cm^{-1}, and an HPLC UV peak area of 1.23×10^6 mAbs × s (units of peak area) per nanomole methyl-CLA. If the literature values are taken as more accurate, this HPLC peak response should be corrected to 1.42×10^6 mAbs × s per nanomole methyl-CLA.

On comparison with FAME-GC and AOCS measurements, the corrected UV detector response (1.42×10^6 mAbs × s per nanomole CLA, multiplied by the mass of CLA methyl ester to provide a mass percentage of CLA in the sample) gave better agreement. The correlation of each independent method with these samples is shown in Figure 2. The

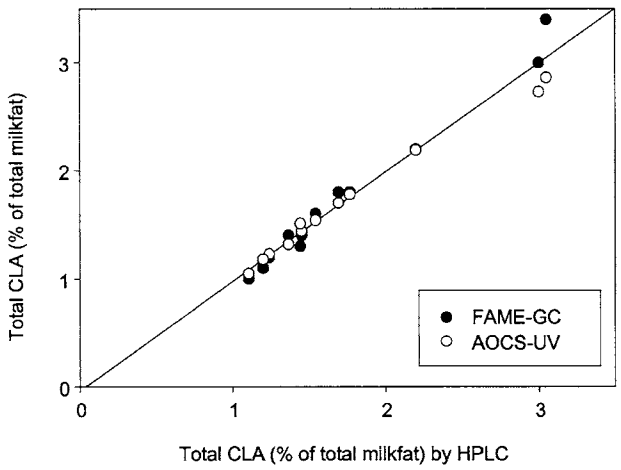

FIG. 2. Total conjugated linoleic acid (CLA) (% of total milk fat fatty acids) determined by HPLC, fatty acid methyl ester-gas chromatography (FAME-GC) and American Oil Chemists' Society (AOCS)-UV (23) methods. Total CLA by HPLC is calculated from a corrected response factor using the literature value for ε_{233} of 27,060 L $mol^{-1}cm^{-1}$. For abbreviations see Fig. 1.

AOCS method is potentially susceptible to absorbance from other non-CLA compounds, such as carotenoids, in milk fat. UV measurements of β-carotene solutions at 233 nm, at concentrations typically found in milk fat (approximately 10 mg/kg), indicated that β-carotene accounted for less than 1% of the total absorbance of a typical milk fat sample by the AOCS method. Literature reports indicated ε_{233} for β-carotene of 13,400 (33), similar in magnitude to ε_{233} for CLA, but the low concentrations of β-carotene in milk fat (1/1000th that of CLA) accounted for its small contribution to total absorbance.

The good agreement of summed UV 233 nm absorbance with total CLA and the finding of minimal interference from non-CLA-TAG at 233 nm provided some confidence for the quantification of individual CLA-TAG peaks in a typical commercial milk fat sample (described below and in Table 1). For comparison, FAME-GC data of the same milk fat sample are described in Table 2.

Peak identification. If the TAG of total milk fat were made up of randomly distributed fatty acids, CLA at the level of 1% would produce only minute quantities of di-CLA and tri-CLA TAG due to statistical probability. The positional selectivities of fatty acids in milk fat, such as short chains preferentially at the *sn*-3 position, further limit multiple esterification by a single fatty acid. These two premises simplified the framework for identification of CLA-TAG, for which it was assumed that practically all CLA-TAG were singly esterified with CLA. Thus, for the three groups of CLA-TAG reference compounds prepared by chemical synthetic means, we focused primarily on the mono-CLA compounds. The first of these "standards," mono-CLA-dipalmitin, was prepared by the two independent routes of interesterification of tripalmitin with the methyl ester of CLA followed by Ag-TLC separation, and reaction of the acyl chloride of CLA with 1,2-dipalmitin. An Ag-TLC plate depicting the TAG generated from the latter experiment is shown in Figure 3. HPLC analysis of the mono-CLA-dipalmitin from each experiment consistently gave a single peak that was in agreement with peak 28 in Figure 1.

TABLE 1
Conjugated Linoleic Acid Triacylglycerols (CLA-TAG) in Total Milk Fat

Peak number	Mass% of sample[a]	Identity	Typical ret. time (min)
1	Trace[b]	CLA, 6:0, 4:0[c]	3.7
2	Trace	CLA, 8:0, 4:0	4.9
3	0.02	CLA, 10:0, 4:0	6.8
4	0.03	CLA, 12:0, 4:0	9.8
5	0.09	CLA, 14:0, 4:0	14.7
6	0.08	CLA, 18:1[d], 4:0	20.6
7	0.19	CLA, 16:0, 4:0	22.2
8	0.07	CLA, 18:1, 6:0	28.4
9	0.09	CLA, 12:0, 10:0	30.2
10	0.02	CLA, 14:0, 8:0	31.7
11	0.05	CLA, 16:0, 6:0	33.0
12	0.03	CLA, 18:1, 8:0	38.1
13	0.05	CLA, 12:0, 12:0; CLA, 14:0, 10:0	39.4
14	0.05	CLA, 16:0, 8:0	40.3
15	0.03	CLA, 18:0, 6:0	41.8
16	0.04	CLA, 18:1, 10:0	48.8
17	0.12	CLA, 14:0, 12:0; CLA, 16:0, 10:0	50.9
18	0.06	CLA, 18:1, 12:0	59.7
19	0.05[e]	CLA, 18:1*t*, 12:0	60.7
20	0.15	CLA, 14:0, 14:0; CLA, 16:0, 12:0	61.9
21	0.22	CLA, 18:1, 14:0	70.0
22	0.06[e]	CLA, 18:1*t*, 14:0	71.3
23	0.26	CLA, 16:0, 14:0; CLA, 18:0, 12:0	72.4
24	0.11	CLA, 18:1, 18:1	77.4
25	0.04[e]	CLA, 18:1*t*, 18:1	78.5
26	0.28	CLA, 18:1, 16:0	79.5
27	0.09[e]	CLA, 18:1*t*, 16:0	80.8
28	0.30	CLA, 16:0, 16:0; CLA, 18:0, 14:0	82.0
29	0.08	CLA, 18:1, 18:0	88.4
30	0.03[e]	CLA, 18:1*t*, 18:0	89.6
31	0.15	CLA, 16:0, 18:0	90.9
32	0.03	CLA, 18:0, 18:0	99.4

[a]Calculated from 100 × (observed area/1.42×10^6) × (molecular weight of the CLA-TAG)/(total injection mass in ng).
[b]Indicates 0.01% or less.
[c]Fatty acid composition: no specific regioisomers are implied by the nomenclature, although it is well known that the short-chains 4:0 and 6:0 are almost exclusively at *sn*-position 3.
[d]18:1 is *cis*-9 oleic acid; vaccenic acid is indicated as 18:1*t*.
[e]An impure CLA-TAG peak. The concentration of the CLA-TAG listed is therefore overestimated when measured from a trace of the total milk fat. Argentation thin-layer chromatography indicated that there are unidentified CLA-TAG with coincident retention times underlying the CLA-TAG described.

A second interesterification, from which 10 TAG products (excluding regioisomers) were possible, was carried out by reacting tripalmitin with methyl conjugated linoleate and methyl oleate. The reaction produced detectable amounts of three CLA-TAG: CLA-P-P, CLA-P-O, and CLA-O-O (and their respective regioisomers). These were separated by Ag-TLC into three bands. Small amounts of P-CLA-CLA, O-CLA-CLA, and CLA-CLA-CLA and their respective regioisomers were also produced.

FAME analysis of the Ag-TLC bands confirmed the identities of bands at R_f = 0.02 as CLA-O-O and R_f = 0.14 as

TABLE 2
Fatty Acids of the Total Milk Fat Shown in Figure 1

Fatty acid	Mass% of sample[a]	Fatty acid	Mass% of sample[a]
4:0	3.7	16:0	28.9
6:0	2.3	16:1	1.8
8:0	1.3	17:0	0.7
10:0	2.9	17:1	0.4
10:1	0.3	18:0	11.5
12:0	3.3	18:1	21.2
14:0	11.2	18:2	1.4
14:1	0.9	18:2 conj.[b]	1.2
15:0	1.3	18:3	0.8

[a]Measured as fatty acid methyl esters by gas chromatography (for conditions see Experimental Procedures section), but reported as fatty acid weight percentage of total fatty acids. The values do not add to 100%. Minor fatty acids—predominantly branched chains, saturated, and unsaturated isomers—have been omitted.
[b]Conjugated linoleic acid.

CLA-P-O. CLA-O-O coincided with the peak numbered 24 in Figure 1, and CLA-P-O coincided with peak 26. This "standard mixture" was also a useful indicator of the R_f values of these TAG in the Ag-TLC separation of total milk fat described below.

To enable a more comprehensive assignment of CLA-TAG, nine bands from Ag-TLC of total milk fat (depicted in Fig. 3) were recovered for analysis by RP-HPLC. Analysis of Ag-TLC band 6, equivalent at R_f 0.48 to the CLA-P-P standard, provided a strong indication that a series of mono-CLA-disaturated TAG had been isolated (Fig. 4), as the dominant peak was in good agreement with CLA-P-P, and the periodic spacing of other peaks was in agreement with that previously observed for two carbon spacings of other TAG in milk fat

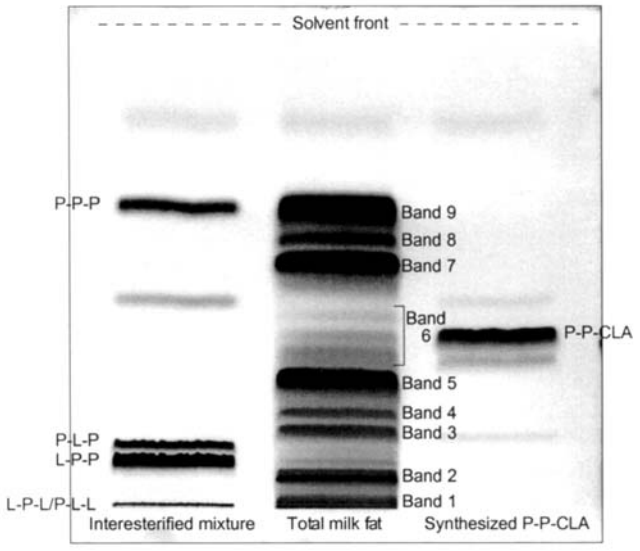

FIG. 3. Argentation thin-layer chromatography (Ag-TLC) plate of a L-P-P/P-L-P regioisomeric mixture obtained by interesterification (left lane), total milk fat triacylclycerols (TAG) (middle lane), and CLA-P-P obtained from the reaction of 1,2-dipalmitin with CLA (right lane) P, palmitic acid; L, linoleic acid; for other abbreviation see Figure 2.

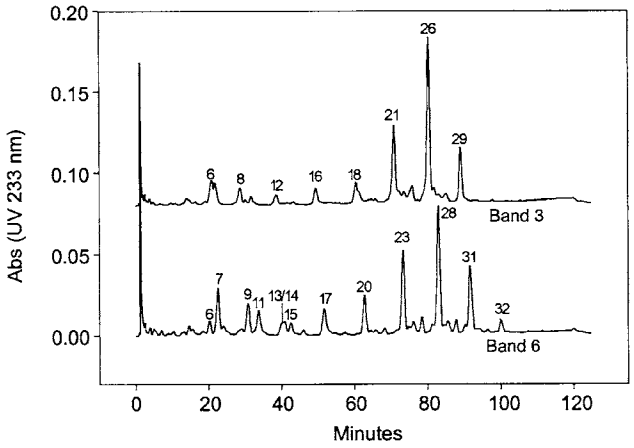

FIG. 4. Reversed-phase HPLC separation, with UV 233 nm detection, of the two major CLA-TAG groups in total milk fat, obtained from Ag-TLC of total milk fat. TAG of Band 6 are of the type mono-CLA-disaturate, and in Band 3 are of the type mono-CLA-oleoyl-saturate. Peak numbers correspond to those in Figure 1 and Table 1. For abbreviations see Figures 1–3.

(14). Complete recovery of all regioisomers of mono-CLA-disaturated TAG from band 6 was ensured by using the mono-CLA-dipalmitin regioisomeric mixture to indicate the R_f of these CLA-TAG on the plate. No UV absorbances were observed in Ag-TLC bands 7, 8, and 9.

The other major series of CLA-TAG occurred at R_f 0.09, between bands 2 and 3, which we propose was the series CLA-oleoyl-saturates (Fig. 4), and at R_f 0.02, band 1, which we propose was CLA-O-O. Some small UV peaks were observed in bands 2 and 5 that suggest the presence of CLA-V-O and CLA-V-saturate TAG respectively (where V = vaccenic acid), but these were not independently confirmed with proven CLA-TAG compounds. The chain-length-based separation of all TAG under Ag-TLC conditions, as described previously (26), was noted here also for CLA-TAG: mono-CLA-disaturated TAG, for example, were spread over a wide area of the plate from R_f 0.27 to R_f 0.48 and the HPLC results indicated that this separation pertained to fatty acid length. The observed R_f of mono-CLA-disaturated TAG, approximately midway between *cis*-monoenoic TAG (band 5) and *trans*-monoenoic TAG (band 7) was in accord with reported behavior of methyl esters of *cis*-monoenoic, *trans*-monoenoic, and conjugated *cis, trans*-dienoic fatty acids, in similar eluant mixtures (34).

Although di-CLA-monopalmitin was isolated by Ag-TLC after the interesterification of tripalmitin with methyl conjugated linoleate, and its elution during RP-HPLC noted at a retention time of 70 min, no HPLC signals detected by UV 233 nm pertaining to di-CLA-monosaturate TAG were observed in the corresponding bands from Ag-TLC of total milk fat.

In RP-HPLC the regioisomeric mixture of CLA-P-P/P-CLA-P was coincident with a commercial standard P-L-P, indicating that under RP conditions, conjugated double bonds behaved very similarly to methylene-interrupted double bonds, and that, as previously reported (14), regioisomeric

TAG were not resolved by this RP-HPLC method. This was confirmed after co-injection of a regioisomeric mixture of L-P-P and P-L-P. The regioisomeric mixture was obtained from interesterification and Ag-TLC, and the identities of bands at R_f = 0.13, 0.10, and 0.00 (Fig. 3, far-left lane) were established by FAME-GC, which indicated ratios of P/L = 2:1, 2:1, and 1:2, respectively. The observations were also confirmed by co-injection of a mixture of L-P-P and CLA-P-P, which gave only one signal by ELSD.

In summary, the absorbance of UV-detected peaks at 233 nm was shown to be substantially due to CLA-TAG. Two independent methods of total CLA quantification were employed to obtain good agreement with total CLA determination by HPLC, and this was a necessary step for quantification of particular CLA-TAG separated by HPLC. The highest-purity CLA standard available is adequate for determining an HPLC UV peak response at 233 nm, although we recommend that the CLA molar extinction coefficient at 233 nm be verified and a correction be made, if needed, before using it as the sole basis for quantification.

The range of TAG in total milk fat containing CLA was found to be wide. Although the broad groups of CLA-TAG isolated from Ag-TLC were less numerous than the other TAG, this is mostly by virtue of one fatty acid being fixed. Indeed, within each Ag-TLC band, the CLA-TAG displayed a similarly wide variety of total carbon chain lengths as the regular TAG. By using proposed identities deduced from the commercial standards, synthesized standards, and Ag-TLC bands, a summary of CLA-TAG in the major peaks of a UV trace is given in Table 1, along with an estimated concentration in a typical New Zealand bovine milk fat. The most prominent CLA-TAG were of the type mono-CLA-disaturated and CLA-oleoyl-saturated, as might be predicted from the known dominant concentrations of saturated and oleic fatty acids in milk fat.

These conclusions indicate a challenging task for those wishing to concentrate CLA in milk fat, without either first hydrolyzing it from the glycerol backbone or substantially boosting the natural level.

ACKNOWLEDGMENTS

This work was supported by research grants from the Public Good Science Fund (contract no. DRI801) and the New Zealand Dairy Board (project A1022-2). The authors also acknowledge Bertram Fong for FAME-GC analyses, Daina Grant and Dr. Justin Bendall for technical assistance, Sarah Kappely for assistance with graphical material, and Dr. Mike Boland for reviewing the manuscript.

REFERENCES

1. Harfoot, C.G., and Hazlewood, G.P. (1997) Lipid Metabolism in the Rumen, in *The Rumen Microbial Ecosystem* (Hobson P.N., and Stewart C.S., eds.), pp. 383–426, Blackie Academic and Professional Press, London.
2. Salminen, I., Mutanen, M., Jauhiainen, M., and Aro A. (1998) Dietary *trans*-Fatty Acids Increase Conjugated Linoleic Acid Levels in Human Serum, *J. Nutr. Biochem. 9*, 93–98.
3. Ip, C., Chin, S.F., Scimeca, J.A., and Pariza, M.W. (1991) Mammary Cancer Prevention by Conjugated Dienoic Derivative of Linoleic Acid, *Cancer Res. 51*, 6118–6124.
4. Ip, C., Singh, M., Thompson, H.J., and Pariza, M.W. (1994) Conjugated Linoleic Acid Suppresses Mammary Carcinogenesis and Proliferative Activity of the Mammary Gland in the Rat, *Cancer Res. 54*, 1212–1215.
5. Lee, K.N., Kritchevsky, D., and Pariza, M.W. (1994) Conjugated Linoleic Acid and Atherosclerosis in Rabbits, *Atherosclerosis 108*, 19–25.
6. Pariza, M.W., Park, Y., Cook, M., Albright, K., and Liu, W. (1996) Conjugated Linoleic Acid (CLA) Reduces Body Fat, *FASEB J. 10*, A560.
7. Jensen, R.G., Ferris, A.M., and Lammi-Keefe, C.J. (1991) The Composition of Milkfat, *J. Dairy Sci. 74*, 3228–3243.
8. Creamer, L.K., and MacGibbon, A.K.H. (1996) Some Recent Advances in the Basic Chemistry of Milk Proteins and Lipids, *Int. Dairy J. 6*, 539–568.
9. Fraga, M.J., Fontecha, J., Lozada, L., and Juárez M. (1998) Silver Ion Adsorption Thin Layer Chromatography and Capillary Gas Chromatography in the Study of the Composition of Milk Fat Triglycerides, *J. Agric. Food Chem. 46*, 1836–1843.
10. Laakso, P. (1996) Analysis of Triacylglycerols—Approaching the Molecular Composition of Natural Mixtures, *Food Rev. Int. 12*, 199–250.
11. Spanos, G.A., Schwartz, S.J., van Breemen, R.B., and Huang, C.-H. (1995) High-Performance Liquid Chromatography with Light-Scattering Detection and Desorption Chemical-Ionization Tandem Mass Spectrometry of Milk Fat Triacylglycerols, *Lipids 30*, 85–90.
12. Gresti, J., Bugaut, M., Maniongui, C., and Bezard, J. (1993) Composition of Molecular Species of Triacylglycerols in Bovine Milk Fat, *J. Dairy Sci. 76*, 1850–1869.
13. Ruiz-Sala, P., Hierro, M.T.G., Martinez-Castro, I., and Santa-Maria, G. (1996) Triglyceride Composition of Ewe, Cow and Goat Milk, *J. Am. Oil Chem. Soc. 73*, 283–293.
14. Robinson, N.P., and MacGibbon, A.K.H. (1998) The Composition of New Zealand Milk Fat Triacylglycerols by Reversed-Phase High-Performance Liquid Chromatography, *J. Am. Oil Chem. Soc. 75*, 993–999.
15. Chipault, J.R., and Hawkins, J.M. (1959) The Determination of Conjugated *cis-trans* and *trans-trans* Methyl Octadecadienoates by Infrared Spectroscopy, *J. Am. Oil Chem. Soc. 36*, 535–539.
16. Scholfield, C.R. (1973) Infrared Absorption of Methyl *cis*-9, *trans*-11-, and *trans*-10,*cis*-12-Octadecadienoates, *J. Am. Oil Chem. Soc. 51*, 33–34.
17. Emken, E.A., Scholfield, C.R., Davison, V.L., and Frankel, E.N. (1967) Separation of Conjugated Methyl Octadecadienoate and Trienoate Geometric Isomers by Silver-Resin Column and Preparative Gas–Liquid Chromatography, *J. Am. Oil Chem. Soc. 44*, 373–375.
18. Tolberg, W.E., and Wheeler, D.H. (1958) *Cis,trans*-Isomerization of Conjugated Linoleates by Iodine and Light, *J. Am. Oil Chem. Soc. 35*, 385–388.
19. Scholfield, C.R. (1972) Hydrogenation of *cis*-9,*cis*-12-, *cis*-9,*trans*-12- and *trans*-9,*trans*-12-Octadecadienoates, *J. Am. Oil Chem. Soc. 49*, 583–585.
20. Body, D.R., and Shorland, F.B. (1965) The Geometric Isomers of Conjugated Octadecadienoates from Dehydrated Methyl Ricinoleate, *J. Am. Oil Chem. Soc. 42*, 5–8.
21. Sehat, N., Yurawecz, M.P., Roach, J.A.G., Mossoba, M.M., Kramer, J.K.G., and Ku, Y. (1998) Silver-Ion High-Performance Liquid Chromatographic Separation and Identification of Conjugated Linoleic Acid Isomers, *Lipids 33*, 217–221.
22. Sehat, N., Kramer, J.K.G., Mossoba, M.M., Yurawecz, M.P., Roach, J.A.G., Eulitz, K., Morehouse, K.M., and Ku, Y. (1998) Identification of Conjugated Linoleic Acid Isomers in Cheese

by Gas Chromatography, Silver-Ion High-Performance Liquid Chromatography and Mass Spectral Reconstructed Ion Profiles. Comparison of Chromatographic Elution Sequences, *Lipids 33*, 963–971.
23. AOCS (1989) *Official Methods and Recommended Practices of the American Oil Chemists' Society*, 4th edn. (Firestone, D., ed.), American Oil Chemists' Society Press, Champaign, Official Method Ti 1a-64.
24. Brown, H.G., and Snyder, H.E. (1982) Conjugated Dienes of Crude Soy Oil: Detection by UV Spectrophotometry and Separation by HPLC, *J. Am. Oil Chem. Soc. 59*, 280–283.
25. Vogel, A.I. (1959) *Textbook of Practical Organic Chemistry Including Qualitative Organic Analysis*, 3rd edn., pp. 969–971, Longmans, New York.
26. Robinson, N.P., and MacGibbon, A.K.H. (1998) Separation of Milk Fat Triacylglycerols by Argentation Thin-Layer Chromatography, *J. Am. Oil Chem. Soc. 75*, 783–788.
27. Skoog, D.A., and Leary, J.J. (1992) *Principles of Instrumental Analysis*, 4th edn., p. 124, Saunders College Publishing, Fort Worth.
28. Marangoni, A.G., and Rousseau, D. (1995) Engineering Triacylglycerols: The Role of Interesterification, *Trends Food Sci. Technol. 6*, 329–335.
29. MacGibbon, A.K.H. (1988) Modified Method of Fat Extraction for Solid Fat Content Determination, *NZ J. Dairy Sci. Technol. 23*, 399–403.
30. Ackman, R.G., and Sipos, J.C. (1964) Application of Specific Response Factors in the Gas Chromatographic Analysis of Methyl Esters of Fatty Acids with Flame Ionization Detectors, *J. Am. Oil Chem. Soc. 41*, 377–378.
31. Bannon, C.D., Craske, J.D., and Hilliker, A.E. (1986) Analysis of Fatty Acid Methyl Esters with High Accuracy and Reliability. V. Validation of Theoretical Relative Response Factors of Unsaturated Esters in the Flame Ionization Detector, *J. Am. Oil Chem. Soc. 63*, 105–110.
32. Angers, P., Tousignant, É., Boudreau, A., and Arul, J. (1998) Regiospecific Analysis of Fractions of Bovine Milk Fat Triacylglycerols with the Same Partition Number, *Lipids 33*, 1195–1201.
33. Schwerter, U., and Isler, O. (1967) Vitamins Acid Carotene, in *The Vitamins* (Sebrell, W.H., and Harris, R.S., eds.), Vol. 1, 2nd edn., p. 73, Academic Press, New York.
34. Parodi, P.W. (1977) Conjugated Octadecadienoic Acids in Milk Fat, *J. Dairy Sci. 60*, 1550–1553.

[Received November 12, 1999, and in final revised form June 5,

2000; revision accepted June 7, 2000]

Gas Chromatography—High Resolution Selected-Ion Mass Spectrometric Identification of Trace 21:0 and 20:2 Fatty Acids Eluting with Conjugated Linoleic Acid Isomers

John A.G. Roach[a,*], Martin P. Yurawecz[a], John K.G. Kramer[b], Magdi M. Mossoba[a], Klaus Eulitz[a], and Yuoh Ku[a]

[a]U.S. Food and Drug Administration, Washington, DC 20204, and [b]Southern Crop Protection, Food Research Center, Agriculture and Agri-Food Canada, Guelph, Ontario, Canada N1G 5C9

ABSTRACT: High-resolution selected-ion recording (SIR) of the exact molecular ion mass was used to confirm unambiguously the presence of conjugated linoleic acid (CLA) derivatives in biological matrices and standard mixtures and to differentiate non-CLA derivatives from CLA derivatives in the CLA region of the gas chromatogram. The success of this method was based on the selectivity of the SIR technique and its sensitivity, which was comparable to that of flame-ionization detection. A minor fatty acid methyl ester (FAME) was identified as methyl heneicosanoate (21:0), and six isomers of 20:2 FAME were found to elute in the CLA region. Isomerization of a standard CLA mixture resulted in a non-CLA flame-ionization response eluting in the CLA region of the gas chromatogram. It is therefore recommended that the identification of minor CLA isomers in natural products or biological matrices should include their direct confirmation by mass spectrometry

Paper no. L8385 in *Lipids 35*, 797–802 (July 2000).

Analysis of fatty acid methyl esters (FAME) by gas chromatography (GC) using long capillary columns and a flame-ionization detector (FID) has become the generally accepted method for the determination of the fatty acid composition of natural products and standard compounds (1). Identification of the FAME peaks often is performed solely by comparison of the retention times with those of known standards. However, independent direct confirmation of identity by alternative techniques is essential to establish definitive assignments, particularly of minor or co-eluting FAME peaks. Comparable sensitivity to GC–FID is generally a problem with alternative detectors, such as ultraviolet (UV) (1) or infrared (2,3). Although an electron impact mass spectrometry (EIMS) detector has adequate sensitivity, unsaturated FAME provide similar EI mass spectra that are of little use in distinguishing between isomers because the double bonds tend to migrate along the carbon chain under EI conditions (4). On the other hand, high-resolution selected-ion recording (SIR) mass spectrometry (MS) can provide unambiguous molecular weight confirmation for targeted analytes by GC–EIMS as demonstrated for drug residue analysis (5).

The direct GC–EIMS SIR confirmation of identity of unspecified minor conjugated linoleic acid (CLA) isomers in natural products is simple and unambiguous. In contrast, two recent reports on CLA isomers in cheese lipids included CLA-methyl ester (CLA-ME) GC peaks that were only tentatively assigned (6,7). Silver-ion high-performance liquid chromatography (HPLC) with UV detection at 234 nm was shown to be effective in separating and identifying individual CLA isomers (8–10), but this technique could not identify interfering FAME that do not absorb at 234 nm but that are found in the CLA region of the gas chromatogram. Furthermore, it is difficult to compare all the peaks observed in the CLA isomers in the GC–EIMS and Ag^+–HPLC chromatograms. A detailed positional analysis of the double bonds of fatty acids must be subsequently performed using one of several fatty acid derivatives other than FAME, such as dimethyloxazoline (DMOX) derivatives; see reviews (11–14).

In the present study high-resolution MS with the SIR technique is presented as a rapid and sensitive technique to confirm directly the presence of minor CLA-ME isomers in natural products and to distinguish them from interfering fatty acids or unknowns in the CLA region of the gas chromatogram without additional sample treatment.

MATERIALS AND METHODS

The ME of heneicosanoic acid (21:0), 99% purity, was purchased from Sigma (St. Louis, MO). A mixture of CLA as

*To whom correspondence should be addressed at U.S. Food and Drug Administration, 200 C St. SW, Washington, DC 20204.
E-mail: JRoach@CFSAN.FDA.GOV

Abbreviations: CLA, conjugated linoleic acid; DMOX, dimethyloxazoline; EIMS, electron impact mass spectrometry; FAME, fatty acid methyl esters; FID, flame-ionization detector; GC, gas chromatography; HPLC, high-performance liquid chromatography; ME, methyl ester; MS, mass spectrometry, SIR, selected-ion recording; UV, ultraviolet.

ME, 99% purity, was obtained from Nu-Chek-Prep, Inc. (Elysian, MN). A 10% solution of trimethylsilyldizomethane in hexane was obtained from TCI America (Portland, OR). Cheeses were purchased locally. All solvents were distilled-in-glass quality.

Extraction of lipids and preparation of fatty acid derivatives. Cheese was extracted with diethyl ether/petroleum ether (1:1) after homogenization with ethyl alcohol in the presence of potassium oxalate as described previously (6). Total cheese lipids were methylated using anhydrous $NaOCH_3$/methanol (6,15). DMOX derivatives were prepared as described (6).

GC–FID. The gas chromatograph (model 5890 Series II; Hewlett-Packard, Palo Alto, CA) was equipped with an FID, a fused-silica capillary column (100 m × 0.25 mm i.d. × 0.2 m film CP-Sil 88; Chrompack, Inc., Raritan, NJ), hydrogen as carrier gas at a head pressure of 26 psi, a split vent flow of 20 mL/min, and a septum purge of 2.4 mL/min. All injections were under data system control with an auto-injector and a glass split injector insert packed with silanized glass wool. The injection port temperature was 250°C. The oven temperature program was: 75°C for 2 min after injection, 5°C/min to 180°C, held at 180°C for 33 min, then 4°C/min to 225°C, and held at 225°C for 43.8 min.

GC–EIMS. Low- and high-resolution mass spectra were recorded with a double-focusing magnetic sector instrument (Autospec Q; Micromass, Wythenshawe, United Kingdom). The gas chromatograph (Hewlett-Packard 5890 Series II) used hydrogen carrier gas at 26 psi and a 100-m CP-Sil 88 fused-silica capillary column. Split vent flow was 100 mL/min, and septum purge flow was 3.0 mL/min. Injections were manual, split or splitless into a double-gooseneck glass injector insert at an injection port temperature of 220°C. The oven temperature program was: 75°C for 2 min after injection, 5°C/min to 170°C, held at 170°C for 40 min, 5°C/min to 220°C, and held at 220°C for 20 min. Transfer line temperature was 220°C, and the ion source temperature was 250°C. Filament trap current was 400 μA at 70 eV.

RESULTS AND DISCUSSION

In a recent study of CLA isomers in cheese (6), a partial FID profile was reported of the CLA-ME region from total cheese FAME using a 100-m polar fused-silica capillary column. The identity of the most intense of the minor ME peaks was not confirmed and was tentatively labeled 11*t*,13*c*-18:2? (6). The correct identity is reported next.

SIR of the molecular ions of CLA and of related FAME at a resolution of 10,000 provided accurate retention times of the CLA-ME isomers, with enhanced analyte sensitivity and selectivity (5). The SIR molecular ion profile of CLA-ME at *m/z* 294.2559 recorded for the same total cheese FAME is shown in Figure 1B. The CLA components of a commercial CLA-ME standard (Nu-Chek-Prep) are shown for comparison in Figure 1C. Most importantly, this comparison established the relative retention times of the four major positional *cis/trans*- and the previously identified *cis,cis*- and *trans,trans*- CLA-ME isomers (16).

A careful reexamination of the major non-CLA-ME peak (labeled A*) in the FID chromatogram of cheese FAME (Fig. 1A) revealed a spectrum with a weak molecular ion at *m/z* 340 and fragmentation consistent with methyl heneicosanoate (21:0) (Fig. 2A). The identity of this FAME (A*) in cheese lipids was subsequently confirmed as 21:0 by comparison of its retention time and mass spectrum (Fig. 2B) with that of a standard 21:0 ME analyzed under identical conditions.

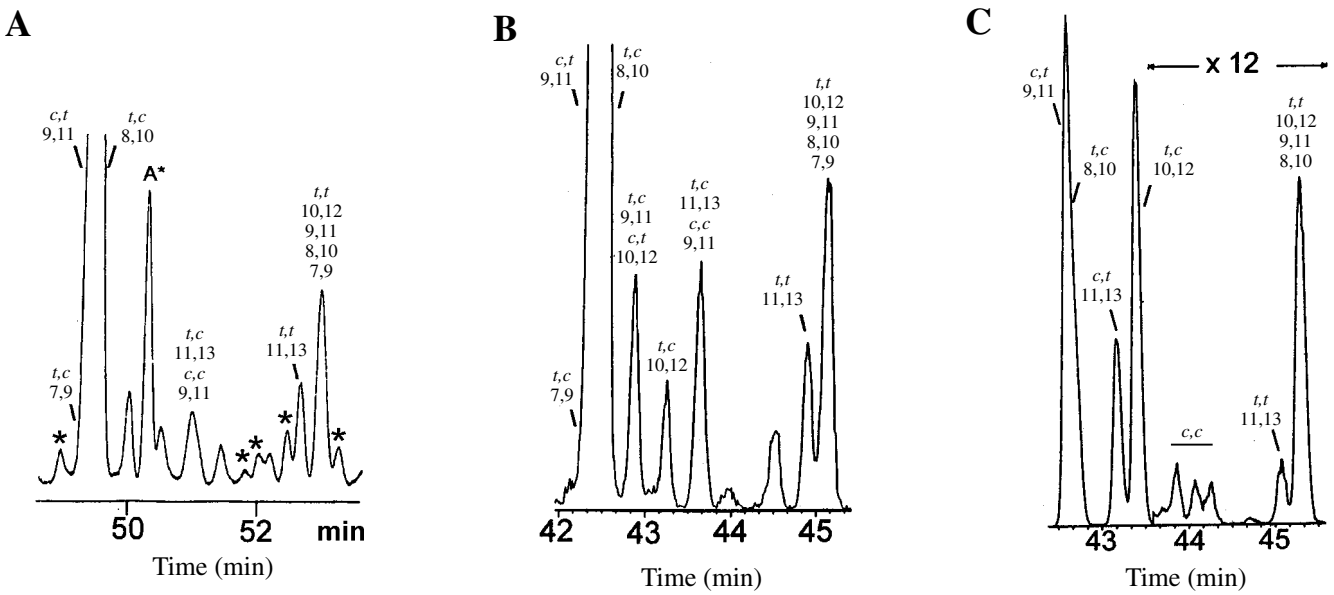

FIG. 1. Comparison of (A) a partial gas chromatography–flame-ionized detector (GC–FID) chromatogram of total cheese fatty acid methyl esters (FAME) with (B) the same conjugated linoleic acid-methyl ester (CLA-ME) region obtained by high-resolution selected-ion recording (SIR) at *m/z* 294.2559 for total cheese FAME and (C) a standard CLA-ME mixture obtained from Nu-Chek-Prep Inc. (Elysian, MN). Peaks not found in the SIR chromatogram of cheese FAME (B) are not isomers of CLA and are indicated by an asterisk (*) in Figure 1A. The most intense FID peak not found in the SIR data is indicated by A* in Figure 1A. The peaks adjacent to peak A* in Figure 1A are labeled in Figure 1B.

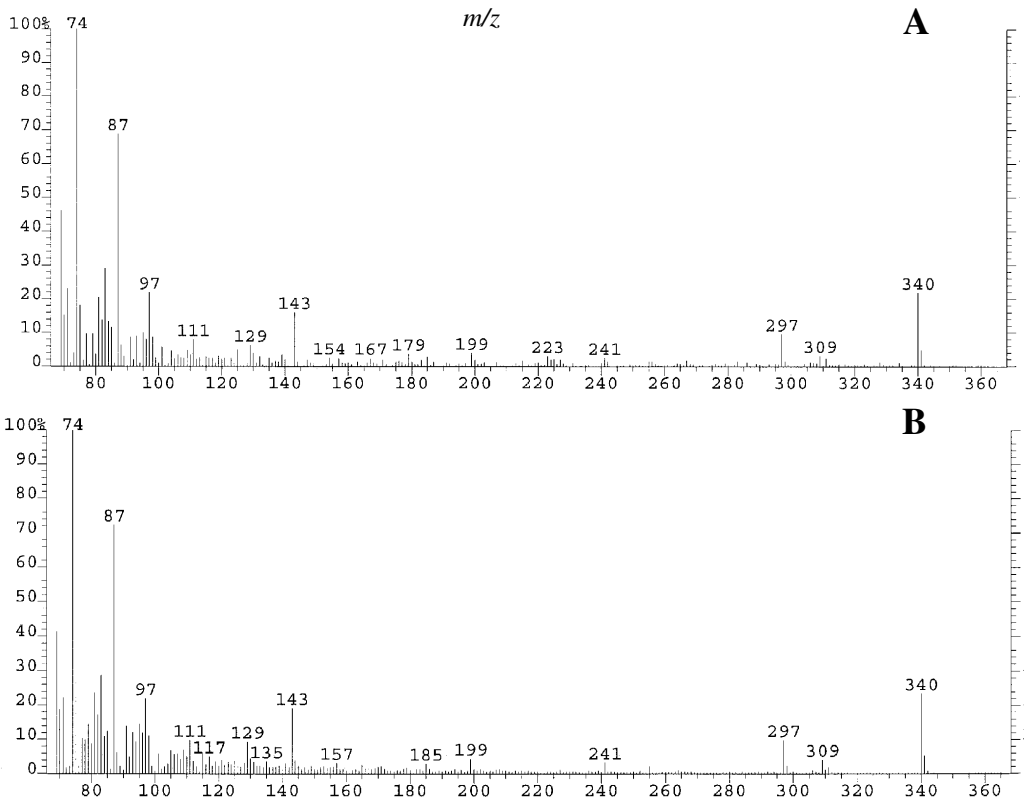

FIG. 2. Low-resolution GC–mass spectrum of (A) the peak labeled A* in Figure 1A, and (B) methyl heneicosanoate (21:0) standard recorded under identical GC–electron impact mass spectrometry conditions. For abbreviation see Figure 1.

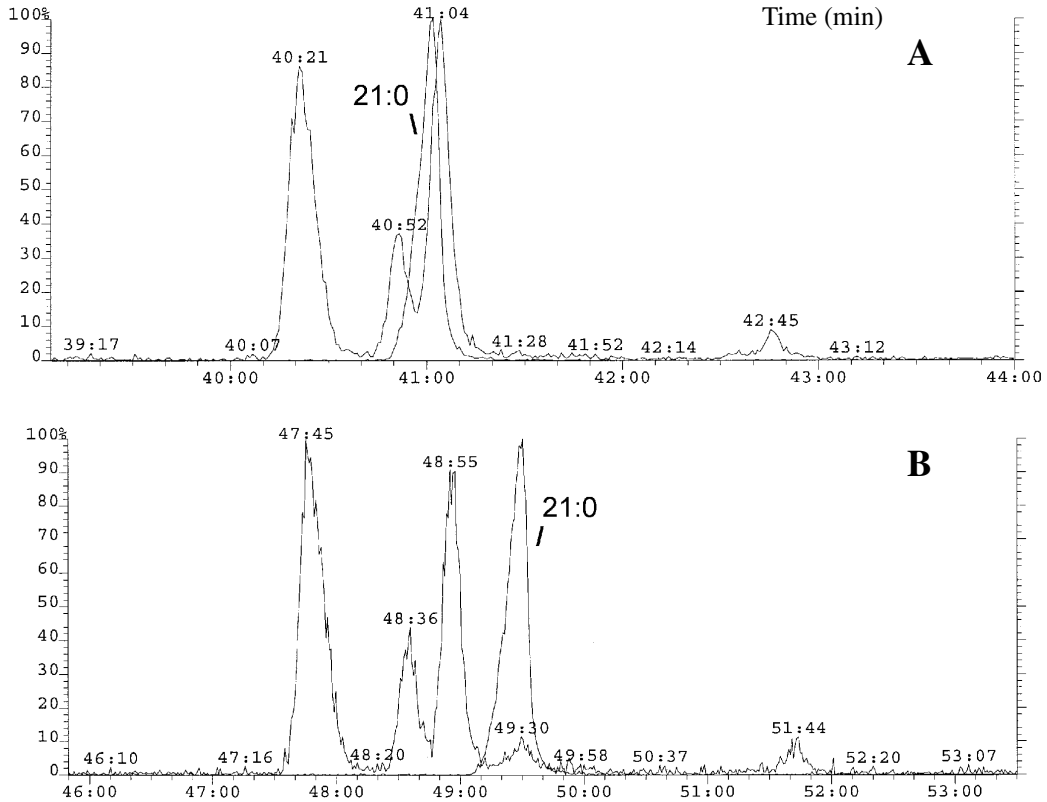

FIG. 3. Low-resolution reconstructed ion profiles of the molecular ions of a mixture of the methyl esters of the commercial CLA mixture (*m/z* 294) and 21:0 (*m/z* 340). The gas chromatograph was operated at 180°C (A) and 170°C (B). For abbreviation see Figure 1.

The

21:0 FAME was previously reported (16) as co-eluting with 8*cis*,10*cis*-18:2 in the gas chromatogram of sphingomyelins isolated from heart and liver lipids of pigs fed CLA. The assignment was made based on comparing the retention time of this GC peak with that of a known standard of 21:0, analyzed under identical GC conditions. However, no attempt was made to confirm its identity by MS in that study (16).

At first it appeared as though we were dealing with two different FAME in the sphingomyelin fractions and in cheese lipids, since a similar 100-m SP-Sil 88 column was used, but the relative retention times were different. We failed to appreciate the effect of differences in temperature programming on the relative retention times of different FAME. Figure 3 shows the differences in the relative retention times obtained between 21:0 and the standard CLA-ME mixture when co-injected and analyzed at 180 (Fig. 3A) and 170°C (Fig. 3B). Ion profiles for the respective molecular ions of methyl CLA, *m/z* 294, and 21:0, *m/z* 340, were extracted from low-resolution GC–EIMS full-scan data to prepare Figure 3. At 180°C, 21:0 eluted between 11*cis*,13*trans*-18:2 and 10*trans*,12*cis*-18:2 (Fig. 3A) as observed in the total cheese FAME (6), whereas at 170°C, 21:0 co-eluted with the *cis,cis* CLA isomers as reported in the analysis of the sphingomyelins (16).

High-resolution multiple ion screening for the molecular ions of other FAME that may possibly elute in the CLA retention time window detected signals only for the *m/z* 322.2872 ion, suggesting the presence of several 20:2 isomers in the CLA region (Fig. 4). These signals were two orders of magnitude less than the combined signal recorded for the 9*cis*,11*trans* and 8*trans*,10*cis* CLA-ME isomers in cheese. Screenings for the molecular ions of 18:1, 18:3, 18:4, 19:1, 19:2, 19:3, 20:0, 20:1, and 20:3 within the CLA-ME window were negative. The major 20:2 FAME in cheese was 11*cis*,14*cis*-20:2, which eluted after the CLA region (Fig. 4B). Although the apparent 20:2 FAME signals were significantly smaller than the signals for the principal isomers of CLA in cheese, they did have the potential to interfere with the determination of the minor isomers of CLA either as FAME or DMOX derivatives. No structural identification of the much weaker 20:2 isomers as DMOX derivatives was attempted. A prior separation of the 18:2 and 20:2 would be required, because of interference and low concentrations of the minor 18:2 and 20:2 isomers.

The SIR technique proved invaluable in unambiguously establishing the identity of CLA-DMOX derivatives in the GC–FID chromatogram and in revealing the presence of interferences in the GC–FID data. Careful adjustment of the column temperature resulted in a good agreement of the rela-

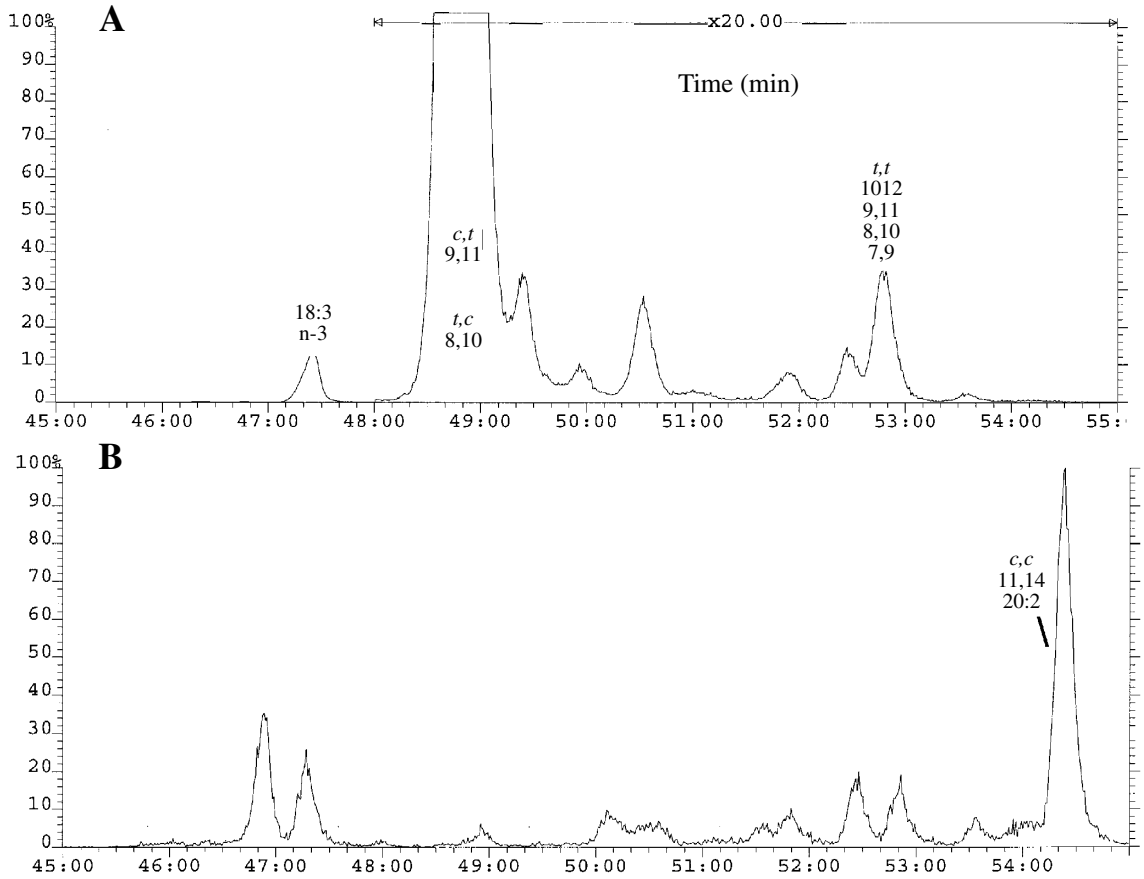

FIG. 4. High-resolution selected ion profiles of *m/z* 294.2559 (A) and *m/z* 322.2872 (B) recorded for total cheese FAME. The signals recorded for *m/z* 322 are on the order of 1% of the 294 signal recorded for the principal CLA peak and represent the co-elution of the 9*cis*,11*trans*- and

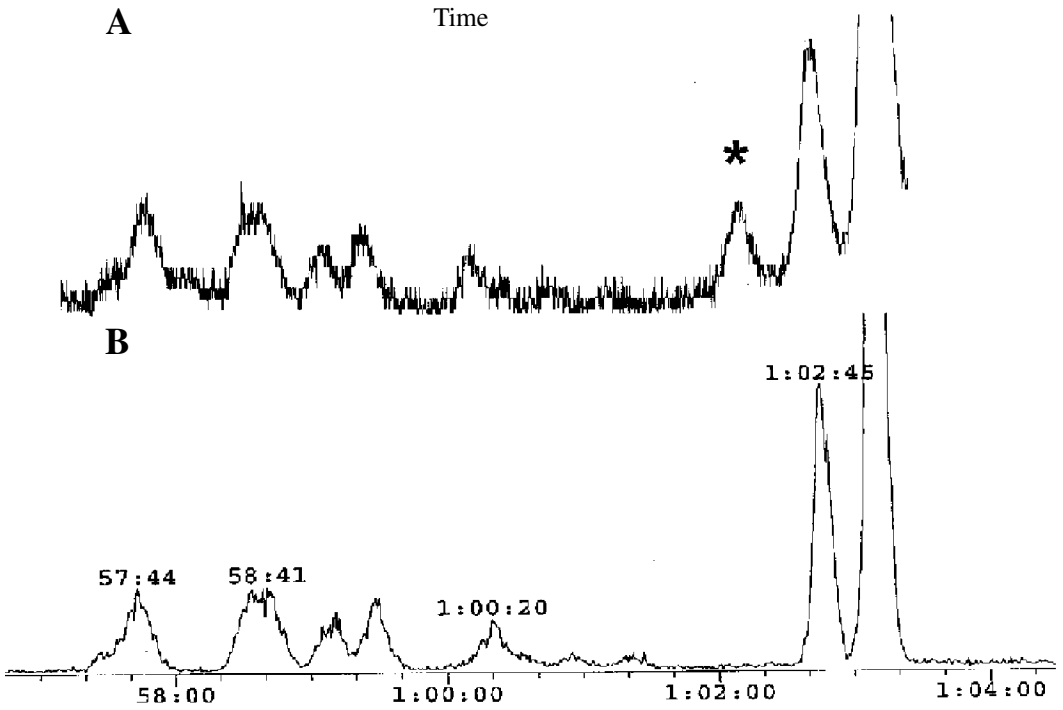

FIG. 5. (A) A partial GC–FID chromatogram of the dimethyloxazoline (DMOX) derivatives of an isomerized CLA mixture prepared as described previously (9), and (B) a high-resolution SIR chromatogram for the same isomerized CLA mixture at *m/z* 333.3032, the molecular ion for CLA-DMOX. The same test portion was injected at the same concentration under closely matched GC conditions. The peak labeled with an asterisk (*) in the FID (A) trace was not a CLA-DMOX. See Figure 1 for other abbreviations.

tive retention time data recorded by GC–FID and GC–EIMS for an isomerized standard CLA mixture described previously (9) (Fig. 5). The data shown in Figure 5A represent the GC–FID analysis of DMOX derivatives from the isomerized CLA mixture (9), whereas high-resolution SIR mass spectral data at *m/z* 333.3032 (molecular ion for 18:2 DMOX derivative) are shown in Figure 5B. The relative retention times of the different CLA-DMOX derivatives in the GC–FID and GC–EIMS chromatograms were in good agreement, except for an extraneous unknown FID peak, labeled by an asterisk (*) in Figure 5A, which is clearly absent in Figure 5B, and hence is not a DMOX derivative of CLA.

The results of this study clearly demonstrate the importance of routinely checking GC–FID data of FAME for correct molecular weight assignments by monitoring their molecular ions in the SIR mode. In the analysis of total cheese FAME, a minor peak in the CLA region of the GC–FID chromatogram was confirmed as 21:0 FAME. In addition, a presumed CLA–DMOX derivative in the FID analysis of an isomerized CLA mixture was likewise determined by SIR to be an extraneous FID response. It is highly recommended that future analyses of the minor CLA isomers from natural products of biological matrices include a demonstration of unequivocal identification of the CLA isomers by using high-resolution SIR MS.

REFERENCES

1. Christie, W.W., *Gas Chromatography and Lipids: A Practical Guide* (1989), Oily Press, Ayr, Scotland.
2. White, R. (1990) Chromatography/Fourier Transform Infrared Spectroscopy and Its Applications, in *Practical Spectroscopy, Series 10*, Marcel Dekker Inc., New York.
3. Reedy, G.T., and Mossoba, M.M. (1998) FTIR and Hyphenated IR Techniques for the Analysis of Foods, in *Spectral Methods in Food Analysis* (Mossoba, M.M., ed.), pp. 325–396, Marcel Dekker Inc., New York.
4. Bieman, K. (1962) *Mass Spectrometry Organic Chemical Applications*, pp. 83–84, McGraw-Hill, New York.
5. Sphon, J.A. (1978) Use of Mass Spectrometry for Confirmation of Animal Drug Residues, *J. Assoc. Off. Anal. Chem. 61*, 1247–1252.
6. Sehat, N., Kramer, J.K.G., Mossoba, M.M., Yurawecz, M.P., Roach, J.A.G., Eulitz, K., Morehouse, K.M., and Ku, Y. (1998) Identification of Conjugated Linoleic Acid Isomers in Cheese by Gas Chromatography, Silver-Ion High-Performance Liquid Chromatography and Mass Spectral Reconstructed Ion Profiles. Comparison of Chromatographic Elution Sequences, *Lipids 33*, 963–971.
7. Lavillonnière, F., Martin, J.C., Bougnoux, P., and Sébédio, J.-L. (1998) Analysis of Conjugated Linoleic Acid Isomers and Content in French Cheeses, *J. Am. Oil Chem. Soc. 75*, 343–352.
8. Sehat, N., Yurawecz, M.P., Roach, J.A.G., Mossoba, M.M., Kramer, J.K.G., and Ku, Y. (1998) Silver-Ion High-Performance Liquid Chromatographic Separation and Identification of Conjugated Linoleic Acid Isomers, *Lipids 33*, 217–221.
9. Eulitz, K., Yurawecz, M.P., Sehat, N., Fritsche, J., Roach, J.A.G., Mossoba, M.M., Kramer, J.K.G., Adlof, R.O., and Ku, Y. (1999) Preparation, Separation, and Confirmation of the Eight Geometrical *cis/trans* Conjugated Linoleic Acid Isomers 8,1.0- Through 11,13-18:2, *Lipids 34*, 873–877.
10. Kramer, J.K.G., Sehat, N., Fritsche, J., Mossoba, M.M., Eulitz, K., Yurawecz, M.P., and Ku, Y. (1999) Separation of Conjugated Fatty Acid Isomers, in *Advances in Conjugated Linoleic Acid Research* (Yurawecz, M.P., Mossoba, M.M., Kramer,

J.K.G., Pariza, M.W., and Nelson, G.J., eds.), Vol. 1, pp. 83–109, AOCS Press, Champaign.
11. Spitzer, V. (1997) Structure Analysis of Fatty Acids by Gas Chromatography–Low Resolution Electron Impact Mass Spectrometry of Their 4,4-Dimethyloxazoline Derivatives—A Review, *Prog. Lipid Res. 35*, 387–408.
12. Christie, W.W. (1998) Gas Chromatography–Mass Spectrometry Methods for Structural Analysis of Fatty Acids, *Lipids 33*, 343–353.
13. Roach, J.A.G., Yurawecz, M.P., Mossoba, M.M., and Eulitz, K. (1999) Gas Chromatography–Mass Spectrometry of Lipids, in *Spectral Properties of Lipids* (Hamilton, R.J., and Cast, J., eds.), pp. 191–234, Sheffield Academic Press, Sheffield, England.
14. Roach, J.A.G. (1999) Identification of CLA Isomers in Food and Biological Extracts by Mass Spectrometry, in *Advances in Conjugated Linoleic Acid Research* (Yurawecz, M.P., Mossoba, M.M., Kramer, J.K.G., Pariza, M.W., and Nelson, G.J., eds.), Vol. 1, pp. 126–140, AOCS Press, Champaign.
15. Kramer, J.K.G., Fellner, V., Dugan, M.E.R., Sauer, F.D., Mossoba, M.M., and Yurawecz, M.P. (1997) Evaluating Acid and Base Catalysts in the Methylation of Milk and Rumen Fatty Acids with Special Emphasis on Conjugated Dienes and Total *trans* Fatty Acids, *Lipids 32*, 1219–1228.
16. Kramer, J.K.G., Sehat, N., Dugan, M.E.R., Mossoba, M.M., Yurawecz, M.P., Roach, J.A.G., Eulitz, K., Aalhus, J.L., Schaefer, A.L., and Ku, Y. (1998) Distributions of Conjugated Linoleic Acid (CLA) Isomers in Tissue Lipid Classes of Pigs Fed a Commercial CLA Mixture Determined by Gas Chromatography and Silver-Ion High-Performance Liquid Chromatography, *Lipids 33*, 549–558.

[Received November 9, 1999, and in revised form February 21, 2000; revision accepted March 6, 2000]

COMMUNICATION

A Comparison of Lycopene and Astaxanthin Absorption from Corn Oil and Olive Oil Emulsions

Richard M. Clark*, Lili Yao, Li She, and Harold C. Furr

Department of Nutritional Sciences, U-17, University of Connecticut, Storrs, Connecticut 06269-4017

ABSTRACT: The effect of different oils on the absorption of carotenoids was investigated in mesenteric lymph duct cannulated rats. Sixteen treatment emulsions containing increasing concentrations of either lycopene (LYC) or astaxanthin (AST) (5, 10, 15, 20 μmol/L) were prepared with olive oil or corn oil and continuously infused into the duodenum of the rat. Absorption of carotenoids into the mesenteric lymph duct was determined. Absorption of LYC and AST from both oils increased with the amount infused into the duodenum. The average recovery of AST in the lymph from the olive oil emulsion was 20% but was decreased to 13% from emulsions containing corn oil. Lycopene was not as well absorbed as AST. The average recovery of LYC was 6% from olive oil emulsions but only 2.5% when infused with corn oil. The LYC used in this study was isolated from tomato paste and was primarily in the all-*trans* form. We did not observe any significant isomerization of all-*trans* LYC to 9-*cis* LYC during absorption. We conclude that the type of oil with which a carotenoid is consumed can influence its absorption.

Paper no. L8416 in *Lipids 35*, 803–806 (July 2000).

Compared to other dietary lipids, carotenoids are not well absorbed, and factors influencing carotenoid absorption are poorly understood (see recent reviews 1–4). Because carotenoids are lipid soluble, the amount and type of lipid with which they are consumed may influence their absorption. Several studies have shown that concurrent consumption of dietary lipid significantly increases carotenoid absorption (5–8). Although the presence of dietary lipid appears to be a key factor in carotenoid absorption, information on the effect of different types of lipid on absorption of carotenoids is relatively sparse.

Hollander and Ruble (9) measured the disappearance of β-carotene from micellar perfusates in rat intestinal loops. The disappearance rate from perfusates containing polyunsaturated fatty acids (PUFA) (linoleic acid and linolenic acid) was lower than when oleic acid was added to the perfusate (9). In assuming that disappearance rates are an index of absorption, these results suggest that the unsaturated fatty acid composition of a diet can influence carotenoid absorption. The purpose of this study was to further investigate the influence of dietary lipid on carotenoid absorption by comparing the absorption of lycopene (LYC) and astaxanthin (AST) from a polyunsaturated triacylglycerol emulsion containing corn oil to their absorption from a monounsaturated triacylglycerol emulsion made with olive oil.

*To whom correspondence should be addressed.
E-mail: RCLARK@CANR.CAG.UCONN.EDU

Abbreviations: AST, astaxanthin; CRBP, cellular retinol-binding protein type II; HPLC, high-pressure liquid chromatography; LYC, lycopene; PUFA,

MATERIALS AND METHODS

Animals and surgical procedure. Male Holtzman albino rats obtained from Harlan Sprague Dawley (Indianapolis, IN) and weighing 300–350 g at the time of surgery were used. A feeding tube was placed into the duodenum and the major mesenteric lymph duct was cannulated. Surgery and animal care were conducted as previously described (10) and were approved by The University of Connecticut Institutional Animal Care and Use Committee.

Following surgery, the animals were placed in a warm, dark environment and allowed to recover for about 36 h. During recovery animals had access to water and received intraduodenally a glucose/electrolyte solution (Pedialyte; Ross Laboratories, Columbus, OH) at 2.0 mL/h. After recovery, treatment emulsions were infused into the duodenum for 12 h at a rate of 2.0 mL/h . The lymph was collected during the final 6 h of infusion for analysis. Lymph was stored at −70°C until analyzed.

Preparation of carotenoid stock solutions. Stock solutions of the two carotenoids were prepared and used within 48 h. Lycopene was purified from tomato paste on a 5% water-weakened alumina column eluted with hexane/ethyl acetate (95:5 vol/vol). Solvent was removed under reduced pressure and a stock solution of LYC prepared in dichloromethane. Astaxanthin was a gift from Dr. Harry Frank (University of Connecticut, Storrs, CT). A stock solution of AST also was prepared with dichloromethane. The concentration of carotenoid in each stock solution was determined by absorption spectroscopy. Astaxanthin concentration was estimated at 466 nm ($E^{1\%}_{1\ cm}$ = 2135) and LYC concentration was estimated at 472 nm ($E^{1\%}_{1\ cm}$ = 3450) (11).

Treatment emulsions. The basic treatment emulsion consisted of a buffer solution (115 mmol/L NaCl, 5.0 mmol/L KCl, 6.8 mmol/L Na_2HPO_4, and 16.5 mmol/L NaH_2PO_4), 10 mmol/L sodium taurocholate (Sigma Chemical, St. Louis, MO) and 3.0% (wt/vol) olive oil or tocopherol-stripped corn oil (ICN, Costa Mesa, CA) with different concentrations of AST or LYC.

Treatment emulsions were prepared by placing olive oil or corn oil in a round-bottomed flask and adding an appropriate amount of carotenoid stock solution to the oil. The carotenoid, either AST or LYC, and oil were mixed, and the solvent was removed with a stream of nitrogen. Sodium taurocholate and buffer were added to the lipid/carotenoid mixture. The contents of the flask then were emulsified using a probe sonicator producing approximately 40 watts output for 15 s, repeated four or five times until no lipid droplets were observed. An aliquot of the emulsion was extracted three times with hexane and the final concentration of carotenoid in the emulsion determined by high-pressure liquid chromatography (HPLC) as described below for lymph analysis.

Carotenoid analysis of lymph. Lymph samples were thawed to room temperature and an aliquot taken for analysis. To extract the carotenoids, dichloromethane/methanol (2:1, vol/vol) containing an internal standard, ethyl-β-apo-8′-carotenoate (Fluka, Ronkonkoma, NY), and lymph were placed in a separatory funnel at a solvent to lymph ratio of 9:1 (vol/vol) and stored in the dark at 4°C for 4–6 h. The bottom phase was removed and saved. Methanol at 1.5 times and dichloromethane at six times the original volume were added to the upper phase. The separatory funnel was again stored for several hours in the dark at 4°C. After phase separation the bottom phase was removed and combined with the original bottom phase. Preliminary studies showed that further extraction of the upper phase with a salt solution and solvents, as called for in the original extraction method of Folch *et al.* (12), did not improve the recovery of carotenoids from lymph.

Samples were prepared for injection into the HPLC by removing the solvent from the lipid extract under reduced pressure and redissolving the residue in dichloroethane/2-propanol (1:1 vol/vol). Carotenoids then were separated by HPLC using a Waters C18 Resolve column (15 cm × 3.9 mm; Millipore, Milford MA.) with an Upchurch C18 guard column (Upchurch Scientific, Oak Harbor, WA). An isocratic mobile phase consisting of acetonitrile/dichloromethane/methanol/*n*-butanol/ammonium acetate (90:15:10:0.1:0.1, by vol) was used for analysis of LYC and an isocratic mobile phase of methanol/water (98:2, vol/vol) was used for AST analysis. The carotenoids and ethyl-β-8′-carotenate were identified and quantified at a wavelength of 450 nm.

Fatty acid analysis of treatment emulsions and lymph. A 200-μL aliquot of treatment emulsion or lymph was used for fatty acid analysis. Fatty acids in the aliquot were prepared for analysis by direct transmethylation in methanol/hexane (4:1, vol/vol) in the presence of acetyl chloride (13). The fatty acid methyl esters were separated by gas–liquid chromatography on a Supelcowax 10 fused-silica capillary column (30 m, 0.53 mm i.d.: Supelco, Bellefonte, PA), and identification of individual fatty acids was based on comparison of retention times with known standards.

Statistical arrangement of treatments. This study was a completely randomized design with treatments in a $2 \times 2 \times 4$ factorial arrangement. The 16 treatment emulsions contained either olive oil or corn oil with one of four different concentrations of LYC or AST (5, 10, 15, 20 μmol/L). There were three rats per treatment. Data were analyzed as a three-way analysis of variance using the General Linear Model procedure in SAS (14).

RESULTS AND DISCUSSION

The carotenoids used in this study were chosen because they have very different physical properties. Astaxanthin, a 3,3′ dihydroxy-4,4′-diketo derivative of β-carotene, was selected because it is a polar xanthophyll. Astaxanthin is a major carotenoid in marine animals with strong quenching activity against singlet oxygen and is an active scavenger of reactive oxygen species (15). Although AST is important in aquaculture, very little is known about its absorption by mammals. Mice fed a diet containing AST have significant levels of AST in the plasma which suggests that AST is readily absorbed (16). The second carotenoid used in this study was LYC, a nonpolar open-chained isomer of β-carotene associated with numerous health benefits such as prevention of cardiovascular disease and cancers of the prostate or gastrointestinal tract (17).

The fatty acid composition of a representative test emulsion containing each of the oils and the lymph collected from the rats intraduodenally infused with each of these emulsions is shown in Table 1. The fatty acids in the lymph reflect the fatty acids of the treatment emulsions. However, the lymph contained a greater proportion of palmitic acid and arachidonic

TABLE 1
Fatty Acids of Test Emulsions and Lymph Collected from Rats Infused with the Emulsions[a]

	Treatment emulsions		Mesenteric lymph	
Fatty acid	Olive oil	Corn oil	Olive oil	Corn oil
16:0	12.0	11.2	17.4	22.6
16:1n-7	0.8	0.2	1.3	1.5
18:0	3.8	2.2	4.2	7.8
18:1n-9	65.3	26.3	55.9	19.6
18:2n-6	14.5	58.2	15.5	40.5
18:3n-3	0.8	0.9	0.5	1.3
20:4n-6	—	—	3.3	5.1

[a]Values are weight percentage (wt%) distributions of fatty acid methyl esters.

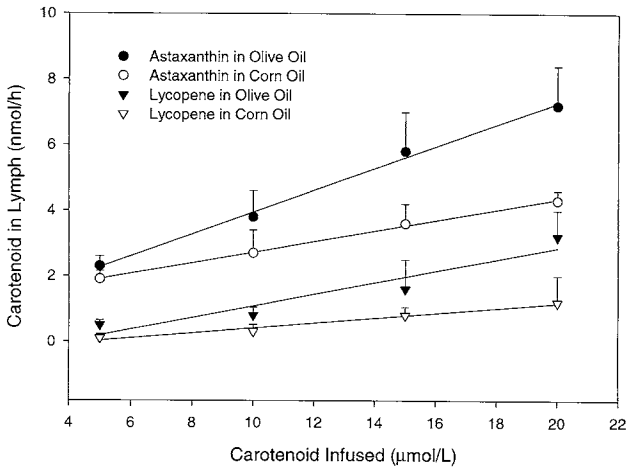

FIG. 1. Relationship between concentration of carotenoid continuously infused into the duodenum at the rate of 2.0 mL/h and concentration of carotenoid recovered per hour in the mesenteric lymph. The lymph samples were collected from 6 to 12 h after the initiation of infusion. These samples represent absorption under steady-state conditions. Each point is the mean ± SD from three individual rats. For both carotenoids, there was a significant ($P < 0.05$) linear relationship between the amount of carotenoid infused and the amount absorbed.

acid than the original emulsions. The additional fatty acids in the lymph may have originated from endogenous sources such as biliary phospholipids, or cells sloughed from the intestine. The major differences in the fatty acid composition of both the emulsions and lymph were the much greater amount of linoleic acid associated with the corn oil treatment and the greater amount of oleic acid associated with the olive oil treatment.

The results of the study are shown in Figure 1. There was a significant ($P < 0.05$) linear relationship between the amount of carotenoid infused into the duodenum and the amount recovered in the lymph. AST was more efficiently absorbed than LYC, and both carotenoids were significantly ($P < 0.05$) better absorbed from olive oil than from corn oil emulsions.

The calculated efficiencies of absorption are presented in Table 2. To calculate absorption efficiencies, conditions of steady-state absorption were assumed. Absorption efficiency was defined as the amount of carotenoid recovered in the lymph per hour divided by the amount infused into the duodenum per hour. In an earlier study with lymph duct cannulated rats, we observed that carotenoids reached a plateau or steady-state transport into the lymph by 6 h of continuous infusion of the carotenoid emulsions (18). Based on the results of this earlier study, lymph samples in the current study were collected from 6 to 12 h after the initiation of intraduodenal infusions and therefore represent steady-state absorption.

The efficiency of AST absorption from olive oil averaged 20% with individual samples having a range of 14 to 28%. In a similar study with rats the xanthophyll canthaxanthin was absorbed from olive oil emulsions with approximately the same efficiency as AST in this study (18). The efficiency of AST absorption from emulsions with corn oil was less than with olive oil and averaged only 13% with a range of values from individual samples of 9 to 25%.

LYC was not as well absorbed as AST. The absorption of LYC from olive oil emulsions averaged only 6% with a range of 3 to 11%. Absorption of LYC was further reduced to 2.5% with a range of 0.7 to 6.5% when infused with corn oil.

The less efficient absorption of AST and LYC from corn oil in the current study is consistent with the earlier observation that PUFA reduced the rate of disappearance of β-carotene from perfused rat intestinal loops. In the earlier study β-carotene disappearance was decreased by 15% from a linoleic acid or linolenic acid micellar perfusate when compared to oleic acid micellar perfusate (9). The mechanism for decreased carotenoid absorption when dispersed in PUFA is unknown.

There are several potential intraluminal and intracellular events where dietary oils could influence carotenoid absorption. Oils high in PUFA might promote carotenoid oxidation in the intestinal chyme resulting in less carotenoid available for absorption. Another explanation may be that the transfer of carotenoid from lipid emulsions containing large amounts of PUFA to mixed bile salt micelles is reduced. Incorporation into bile salt micelles appears to be a required step for carotenoid absorption (19). After carotenoids are transferred to mixed bile salt micelles, it has been suggested that micelles containing PUFA are larger in size than micelles containing saturated fatty acid and that the larger micelles diffuse more slowly through the unstirred water layer adjacent to the enterocyte, thereby decreasing the rate of carotenoid absorption (9). Another possibility is the two oils contain different amounts of stanols and phytosterols, which are known to interfere with the absorption of carotenoids (20).

Once carotenoids are absorbed into the enterocyte, intracellular processing of the carotenoid may be altered. Recently, β-carotene 15,15′-dioxygenase activity and cellular

TABLE 2
Recovery of Carotenoids in the Lymph[a]

	Amount of carotenoid intraduodenally infused							
	10 nmol/h		20 nmol/h		30 nmol/h		40 nmol/h	
Treatment	Amount	Percent	Amount	Percent	Amount	Percent	Amount	Percent
Astaxanthin (olive oil)	2.3 ± 0.3	23	3.8 ± 0.8	19	5.8 ± 1.2	19	7.2 ± 1.2	18
Astaxanthin (corn oil)	1.7 ± 0.2	17	2.7 ± 0.7	14	3.6 ± 0.6	12	4.3 ± 0.3	11
Lycopene (olive oil)	0.5 ± 0.2	5	0.8 ± 0.2	4	1.7 ± 0.9	6	3.2 ± 0.2	8
Lycopene (corn oil)	0.2 ± 0.1	2	0.3 ± 0.2	2	0.8 ± 0.3	3	1.2 ± 0.8	3

retinol-binding protein type II (CRBP II) level were observed to increase in response to dietary unsaturated triacylglycerol in the rat intestine (21). Altered dioxygenase activity and level of CRBP II would influence absorption of carotenoids that are cleaved to vitamin A. There may be other events influenced by dietary lipid that affect carotenoid uptake and transport through the enterocyte.

Finally, it should be noted that we did not observe isomerization of LYC during absorption by the rat. Significant amounts of *cis* LYC are present in human plasma even when dietary LYC is mostly in the all-*trans* form (17). The source of the *cis* isomers is unknown. Isomerization of all-*trans* β-carotene to the 9-*cis* form during absorption has been suggested (22) and might also explain the presence of *cis* LYC in human plasma. The HPLC chromatogram of the treatment emulsions showed that LYC was primarily in the all-*trans* form, and the chromatograms from the lymph were essentially identical. Because the HPLC method used in this study would not fully resolve geometric isomers of LYC, we are cautious in providing precise values for *cis* isomers of LYC. However, we estimate the *cis* isomers of LYC to be less than 10% of the total LYC in emulsions or lymph.

In conclusion, AST and LYC were absorbed in a dose-dependent manner with the xanthophyll (AST) more efficiently absorbed than the nonpolar hydrocarbon carotenoid (LYC). To our knowledge this is the first report that has directly measured absorption of AST by mammals. Both carotenoids were less efficiently absorbed from corn oil than from olive oil suggesting that the type of lipid with which a carotenoid is absorbed will influence its absorption. Additional research is needed to identify the mechanism responsible for the decreased absorption with corn oil.

ACKNOWLEDGMENTS

The authors wish to thank Gregory Richards for his technical assistance and Dr. Harry Frank, Department of Chemistry, University of Connecticut, for the gift of astaxanthin. Supported in part by Federal Funds available through provisions of the Hatch Act and U.S. Department of Agriculture Competitive Grant 92-37200-7703. This work constitutes Scientific Contribution No.1926 of the Storrs Agricultural Experiment Station, The University of Connecticut, Storrs, CT.

REFERENCES

1. Furr, H.C., and Clark, R.M. (1997) Intestinal Absorption and Tissue Distribution of Carotenoids, *J. Nutr. Biochem. 8*, 364–377.
2. Parker, R.S. (1996) Absorption, Metabolism, and Transport of Carotenoids, *FASEB J. 10*, 542–551.
3. Erdman, J.W., Jr., Bierer, T.L., and Gugger, E.T. (1993) Absorption and Transport of Carotenoids, *Ann. NY Acad. Sci. 691*,76–85.
4. Olson, J.A. (1994) Absorption, Transport, and Metabolism of Carotenoids in Humans, *Pure Appl. Chem. 66*, 1011–1016.
5. Dimitrov, N.V., Meyer, C., Ullrey, D.E., Chenoweth, W., Michelakis, A., Malone, W., Boone, C., and Fink, G. (1988) Bioavailability of β-Carotene in Humans, *Am. J. Clin. Nutr. 48*, 298–304.
6. Roels, O.A., Trout, M., and Dujacquier, R. (1958) Carotenoid Balances on Boys in Ruanda Where Vitamin A Deficiency Is Prevalent, *J. Nutr. 65*, 115–127.
7. Prince, M.R., and Frisoli, J.K. (1993) Beta-Carotene Accumulation in Serum and Skin, *Am. J. Clin. Nutr. 57*, 175–181.
8. Shiau, A., Mobarhan, S., Stacewicz-Sapuntzakis, M., Benya, R., Liao, Y., Ford, C., Bowen, P., Friedman, H., and Frommel, T.O. (1994) Assessment of the Intestinal Retention of Beta-Carotene in Humans, *J. Am. Coll. Nutr. 13*, 369–375
9. Hollander, D., and Ruble, P.E., Jr. (1978) Beta-Carotene Absorption: Bile, Fatty Acid, pH, and Flow Rate Effects on Transport, *Am. J. Physiol. 235*:E686–E691.
10. Hageman, S.H., She, L., Furr, H.C., and Clark, R.M. (1999) Excess Vitamin E Decreases Canthaxanthin Absorption in the Rat, *Lipids 34*, 627–631.
11. Furr, H.C., Barua, A.B. and Olson, J.A. (1992) Retinoids and Carotenoids, in *Modern Chromatographic Analysis of Vitamins* (Nelis, H.J., Lambert, W.E., and De Leenheer, A.P., eds.), pp. 1–71, Marcel Dekker, New York.
12. Folch, J., Lees, M., and Sloane-Stanley, G.H. (1957) A Simple Method for the Isolation and Purification of Total Lipids from Animal Tissues, *J. Biol. Chem. 226*, 497–509.
13. Lepage, G., and Roy, C. (1986) Direct Transesterification of All Classes of Lipids in a One-Step Reaction, *J. Lipid Res. 27*, 114–120.
14. SAS Institute Inc. (1993) *SAS User's Guide: Statistics*, SAS Institute, Cary.
15. Wataru, M. (1991) Biological Functions and Activities of Animal Carotenoids, *Pure Appl. Chem. 63*, 141–146.
16. Chew, B.P., Park, J.S., Wong, M.W., and Wong, T.S. (1999) A Comparison of the Anticancer Activities of Dietary Beta-Carotene, Canthaxanthin and Astaxanthin in Mice *in vivo, Anticancer Res. 19*, 1849–1853.
17. Clinton, S.K. (1998) Lycopene: Chemistry, Biology, and Implications for Human Health and Disease, *Nutr. Rev. 56*, 35–51.
18. Clark, R.M., Yao, L., She, L., and Furr, H.C. (1998) A Comparison of Lycopene and Canthaxanthin Absorption: Using the Rat to Study the Absorption of Non-Provitamin A Carotenoids, *Lipids 33*, 159–163.
19. El-Gorab, M., Underwood, B.A., and Loerch, J.D. (1975) The Roles of Bile Salts in the Uptake of Beta-Carotene and Retinol by Rat Everted Gut Sacs, *Biochim. Biophys. Acta 401*, 265–277.
20. Nguyen, T. (1999) The Cholesterol-Lowering Action of Plant Stanol Esters, *J. Nutr. 129*, 2109–2112.
21. During, A., Nagao, A., and Terao, J. (1998) β-Carotene 15,15′ Dioxygenase Activity and Cellular Retinol-Binding Protein Type II Level Are Enhanced by Dietary Unsaturated Triacylglycerols in Rat Intestines, *J. Nutr. 128*, 1614–1619.
22. Tamia, H., Morinobu, T., Murata, T., Manago, M., and Mino, M. (1995) 9-*cis* β-Carotene in Human Plasma and Blood Cells After Ingestion of β-Carotene, *Lipids 30*, 493–498.

[Received December 13, 1999, and in revised form June 5, 2000; revision accepted June 7, 2000]

ARTICLE

Follow-Up of the Δ4 to Δ16 *trans*-18:1 Isomer Profile and Content in French Processed Foods Containing Partially Hydrogenated Vegetable Oils During the Period 1995–1999. Analytical and Nutritional Implications

Robert L. Wolff[a,*], Nicole A. Combe[b], Frédéric Destaillats[a], Carole Boué[a,b], Dietz Precht[c], Joachim Molkentin[c], and Bernard Entressangles[a]

[a]ISTAB and [b]ITERG, Talence, France, and [c]Bundesanstalt für Milchforschung, Kiel, Germany

ABSTRACT: A survey of the total content of *trans*-18:1 acids and their detailed profile in French food lipids was conducted in 1995–1996, and 1999. For this purpose, 37 food items were chosen from their label indicating the presence of partially hydrogenated vegetable oils (PHVO) in their ingredients. The content as well as the detailed profile of these isomers was established by a combination of argentation thin-layer chromatography and gas–liquid chromatography (GLC) on long polar capillary columns. With regard to the mean *trans*-18:1 acid contents of extracted PHVO, a significant decrease was observed between the two periods, i.e., from 26.9 to 11.8% of total fatty acids. However, only minor differences were noted in the mean relative distribution profiles of individual *trans*-18:1 isomers with ethylenic bonds between positions Δ4 and Δ16 for the two periods. The predominant isomer was Δ9-18:1 (elaidic) acid, in the wide range 15.2–46.1% (mean, 27.9 ± 7.2%) of total *trans*-18:1 acids, with the Δ10 isomer ranked second, with a mean of 21.3% (range, 11.6 to 27.4%). The content of the unresolved Δ6 to Δ8 isomer group was higher than the Δ11 isomer (vaccenic acid), representing on average 17.5 and 13.3%, respectively. Other isomers Δ4, Δ5, Δ12, Δ13/Δ14, Δ15, and Δ16, were less than 10% each: 1.0, 1.6, 7.4, 7.1, 1.8, and 1.0%, respectively. However, considering individual food items, it was noted that none of the extracted PHVO were identical to one another, indicating a considerable diversity of such fats available to the food industry. A comparison of data for French foods with similar data recently established for Germany indicates that no gross differences occur in PHVO used by food industries in both countries. Estimates for the absolute mean consumption of individual isomers from ruminant fats and PHVO are made for the French population and compared to similarly reconstructed hypothetical profiles for Germany and North America. Differences occur in the total intake of *trans*-18:1 acids, but most important, in individual *trans*-18:1 isomer intake, with a particular increase of the Δ6–Δ8 to Δ10 isomers with increasing consumption of PHVO. It is inferred from the present and earlier data that direct GLC of fatty acids is a faulty procedure that results (i) in variable underestimates of total *trans*-18:1 acids, (ii) in a loss of information as regards the assessment of individual isomeric *trans*-18:1 acids, and (iii) in the impossibility of comparing data obtained from human tissues if the relative contribution of dietary PHVO and ruminant fats is not known.

Paper no. L8460 in *Lipids 35,* 815–825 (August 2000).

The industrial use of partially hydrogenated vegetable oils (PHVO) in food processing has been and is still a matter of debate among nutritionists (1–5), owing to the presence in more or less high amounts of unsaturated fatty acids with ethylenic bonds in the *trans* configuration. The conversion of *cis* ethylenic bonds to *trans* and positional isomers by catalytic hydrogenation is aimed at producing fats with superior physical properties and stability toward autoxidation (6). The *trans*-18:1 isomers are by far the major constituents of the so-called *trans* fatty acids that in fact embrace mono-, di-, and triunsaturated fatty acids with one *trans* double bond or more, at variable positions along the hydrocarbon chain, each with a particular metabolic fate (7,8). Regarding the *trans*-18:1 isomers, their presence in PHVO would not be particularly extraordinary, because "natural" foods derived from ruminant milk and meat, and these natural foods themselves, contain exactly the same individual *trans*-18:1 isomers, yet in different proportions, as PHVO (9). From time immemorial, humans have consumed such isomers, not to mention the widespread *trans*-3 16:1 isomer, a major constituent of the *sn*-2 position of chloroplastic diacylglycerophosphorylglycerol (10), and consequently present in all green vegetables, and also in ruminant milk fats (Destaillats, F., Wolff, R.L., Precht, D., and Molkentin, J., unpublished data).

Following the conclusions of some epidemiological and nutritional studies published in the early 1990s, manufacturers in many countries, e.g., France, Germany, Austria, Denmark, and Canada, have been producing margarines with lower contents of *trans* isomers (11–15). Except for the cheapest margarines we could find in France in 1999, imported from the Netherlands, some of which contained partially hydrogenated fish oils (not analyzed here), all popular French margarine brands exhibited no or rather low contents

*To whom correspondence should be addressed at ISTAB, Université Bordeaux 1, Ave. des Facultés, 33405 Talence Cedex, France.
E-mail: r.wolff@istab.u-bordeaux.fr

Abbreviations: Ag-TLC, argentation thin-layer chromatography; FAME, fatty acid methyl ester; GLC, gas–liquid chromatography; PHVO, partially hydrogenated vegetable oils.

of *trans*-18:1 acids. This is probably because fully hydrogenated oils and/or tropical fats instead of PHVO are used in their manufacture (some are still labeled as containing hydrogenated vegetable oils). However, it was not known whether "hidden fats" (those used in food processing) had followed this trend, and the present study was aimed at determining the level as well as the detailed profile of individual *trans*-18:1 isomers in French processed foods labeled as containing PHVO. Recently, Ratnayake *et al*. (15) estimated that the major contribution to the *trans* fatty acid intake by Canadians was from hidden fats, not from margarines.

The analytical methods used here involve a combination of argentation thin-layer chromatography (Ag-TLC) and gas–liquid chromatography (GLC) on 100-m polar capillary columns operated under optimal temperature and carrier gas pressure conditions. This procedure, though time-consuming, allows resolution of practically all major individual *trans*-18:1 isomers with no interferences with any other overlapping fatty acids, as well as accurate quantitation. This contrasts with so-called "optimized" methods based on single GLC runs (16,17) that lead to elution of *trans*-18:1 isomers under an asymmetrical and uneven peak, more or less well separated from oleic acid, and that obviously do not allow any accurate insight into the distribution profile of individual isomers.

Although the analysis of 21 French food items purchased locally in supermarkets in 1999, and of 16 items purchased earlier (1995–1996), showed that the mean contents of *trans*-18:1 isomers in food lipids for the two periods were somewhat different, their mean relative profiles were rather similar, differing in detail only. This allows establishment of a mean profile for these PHVO and comparison with corresponding data for German margarines and shortenings. To our knowledge, no similar studies have been published on PHVO used as ingredients in food processing. Thus, data presented here appear of general use to accurately estimate the consumption of individual *trans*-18:1 isomers in European countries where food consumption or disappearance data are known.

EXPERIMENTAL PROCEDURES

Samples. Twenty-one food items with labels indicating the presence of PHVO were purchased locally in supermarkets near Bordeaux (France) in May 1999. They included, among others, 11 different dehydrated soups. Another set of 16 foods, also labeled as containing PHVO, was purchased earlier in the same region during 1995 and 1996.

Fat extraction. For dehydrated soups and other food items containing less than 10% water, a representative sample of foods, or the whole item, was homogenized with a household electric grinder. Forty grams of the resulting powder or homogenate was extracted for 4 h in an all-glass Soxhlet extractor using *ca*. 200 mL of petroleum ether (b.p. 40–60°C). For foods with a higher water content, a smaller portion of the homogenates (*ca*. 10 g) was extracted according to Folch *et al.* (18), with methanol being added first and the sample dispersed with a 20 M Ultraturrax homogenizer (Janke & Kunkel GmbH & Co. KG, Staufen, Germany) before adding chloroform and performing a second homogenization with the Ultraturrax. After removal of the solvent in a rotary evaporator at 45°C, fats were transferred with a small volume of hexane into 5-mL vials and stored at 4°C until use.

Fatty acid methyl esters (FAME) preparation. FAME were prepared by vigorously shaking for 1 min a mixture of 5 mL hexane containing approximately 500 mg of fat and 300 µL of a 0.5 N sodium methoxide solution with further incubation at 50°C for 10 min and frequent shaking. After completion of the reaction, 1 mL of a 5% (wt/vol) aqueous solution of NaCl was added, and the upper layer was withdrawn and stored in stoppered glass tubes at 4°C until use. Completeness of the reaction was regularly checked for each category of foods by TLC using hexane/diethyl ether (90:10, vol/vol) as the solvent.

Fractionation of FAME by Ag-TLC. FAME were fractionated according to the number and geometry of double bonds by TLC on silica-gel plates impregnated with $AgNO_3$. The plates were prepared by immersion in a 5% solution of $AgNO_3$ in acetonitrile as described by Wolff (19). The developing solvent was the mixture hexane/diethyl ether (90:10, vol/vol). At the end of the chromatographic runs, the plates were briefly air-dried, sprayed with a solution of 2′,7′-dichlorofluorescein, and viewed under ultraviolet light (234 nm). Generally, the *trans*-band was quite well separated from the *cis*-band, and no cross-contaminations occurred. The bands corresponding to the saturated and *trans*-monoenoic acids were scraped off into aluminum foil, and the gel from the two bands was transferred into the same test tube. To the gel were added successively 1.5 mL of methanol, 2 mL of hexane, and 1.5 mL of a 5% (wt/vol) aqueous solution of NaCI (19). Thorough mixing followed each addition. After standing for *ca*. 1 min, the hexane phase was withdrawn almost quantitatively and concentrated under a light stream of N_2. The residue was dissolved in a small volume of hexane for further GLC analysis. Palmitic and stearic acids, determined by total fatty acid analysis before performing Ag-TLC fractionation, were used as internal standards to calculate the content of *trans*-18:1 isomers (19).

Analysis of FAME by GLC. Analyses of total *trans*-18:1 acids by GLC were performed with a CP 9003 chromatograph (Chrompack, Middelburg, The Netherlands) equipped with a flame-ionization detector and a split injector that were maintained at 250°C. A 50 m × 0.25 mm i.d. CP-Sil 88 fused-silica capillary column (stationary phase: 100% cyanopropyl polysiloxane, 0.20 µm film thickness; Chrompack) was used and operated isothermally at 190˚C. Helium was the carrier gas with an inlet pressure of 100 kPa (split ratio, 1:50). The chromatograph was coupled with an SP 4290 integrator equipped with the memory module (Spectra Physics, San Jose, CA).

Analysis of individual *trans*-18:1 isomer fractions isolated by Ag-TLC was performed by using a gas chromatograph CP 9000 (Chrompack) with a split injector, a flame-ionization detector, and a fused-silica capillary column (100 m × 0.25 mm) coated with 0.20 µm CP-Sil 88 (Chrompack) under the following conditions: H_2 as the carrier gas; injector temperature

255°C; and detector temperature 280°C. Monoenoic TLC fractions were analyzed isothermally at 172°C with a column head pressure of 160 kPa (split ratio 1:50).

Identification of individual isomeric *trans* octadecenoates was achieved by comparison of retention times with FAME standards of the 18:1 isomers Δ6, Δ7, Δ9, Δ11, Δ12, Δ13, and Δ15 (Sigma, St. Louis, MO). *Trans*-18:1 acids isolated from butterfat were used as a secondary standard (20). Integration and quantitation were accomplished with an HP 3365 II ChemStation system (Hewlett-Packard, Palo Alto, CA). Calibration of GLC data included the conversion from FAME to free fatty acids. Thus, results expressing absolute concentrations are given as g/100 g of total fatty acids.

RESULTS AND DISCUSSION

Individual trans-*18:1 acids in PHVO prepared from French foods*. In the past, the only means to analyze individual *trans*-18:1 isomers in complex FAME mixtures (e.g., prepared from ruminant fats or PHVO) was to isolate these components, often by a combination of argentation chromatography and preparative GLC, and to submit them to an oxidative cleavage (21). The resulting fragments were further analyzed by GLC, allowing quantitation of individual isomers. A drawback of this procedure was that the shortest volatile fragments were prone to losses, and correction factors had to be applied to compensate for the unequal response of the flame-ionization detector *vis à vis* methylene and carboxylic groups. However, until recently, this analytical procedure was frequently applied to PHVO from several countries to gain insight into the *trans*- as well as the *cis*-18:1 isomer distributions (22–30).

Yet, very early after the advent of capillary columns, encouraging results (31) had demonstrated the potentiality of this material in the resolution of individual 18:1 isomers. Chromatograms published as early as 1966 (31) were of better quality than many chromatograms published nowadays. However, the use of long capillary columns (100 m) operated at rather low temperatures became a routine procedure only after 1995 (20,32,33). Despite the remarkable improvement that was achieved with this procedure, the isolation of the *trans*-monoenoic acid fraction by argentation chromatography (most often, Ag-TLC) is still a prerequisite, for many *trans*-18:1 isomers overlap *cis*-18:1 isomers (34,35). Without this fractionation, inaccurate data (always underestimates) are obtained (35), particularly when 50-m instead of 100-m columns are used, or when these columns are operated at too high a temperature. Unfortunately, there are no unique factors to correct published data obtained in such a way, as the correction factor varies with the *trans*-18:1 isomer profile in the range 1.2–1.8, depending on the fat analyzed (e.g., PHVO vs. ruminant fats) (35).

In the present study, FAME prepared from all food samples were processed through the Ag-TLC/GLC procedure to establish their *trans*-18:1 acid content and profile. Data for food items analyzed in 1995 and 1996 are given in Table 1, and those for foods analyzed in 1999 in Tables 2 and 3. From our experience with foods analyzed during the first period, we knew that the profiles of *trans*-18:1 acids were highly

TABLE 1
***Trans*-18:1 Isomeric Acid Content and Profile in Some Food Items Labeled as Containing Partially Hydrogenated Vegetable Oils Commercialized in France in 1995–1996**

Sample	Total content[a]	Isomeric distribution[b]							
		Δ6–Δ8	Δ9	Δ10	Δ11	Δ12	Δ13/14	Δ15	Δ16
Cake	23.0	20.5	24.3	21.9	14.0	8.1	8.4	1.6	1.2
Cake	13.0	21.1	22.8	21.7	13.9	8.2	9.2	1.8	1.4
Cake	18.8	21.5	25.1	20.3	14.1	8.6	7.7	1.5	1.2
Cereals	36.6	20.7	29.0	22.5	14.3	7.4	5.2	0.5	0.3
Roasted bread	21.2	17.7	33.1	24.0	13.9	6.3	4.2	0.5	0.4
Brioche	34.8	17.7	32.5	22.2	14.1	7.5	5.3	0.5	0.2
Crackers	15.2	20.3	20.9	18.6	15.1	9.5	12.5	1.7	1.4
Cornflour	52.1	18.5	26.8	20.6	14.8	8.5	8.1	1.5	1.2
Puff pastry	61.0	17.5	23.0	23.0	14.7	9.5	9.8	1.5	1.0
Toasted bread	20.8	17.2	25.8	25.0	16.9	8.2	7.0	ND[c]	ND
Bread	15.6	21.7	30.3	26.6	12.6	5.2	3.6	ND	ND
Cereals	21.2	24.0	28.8	24.4	12.3	6.3	4.2	ND	ND
Cake	13.9	16.7	25.5	23.2	14.3	9.2	8.7	1.4	1.0
Brioche	24.5	20.5	35.8	20.5	11.9	6.4	4.1	0.4	0.4
Cookies	23.0	25.8	38.9	24.1	8.0	2.3	0.9	ND	ND
Rolled cake	35.9	19.7	25.6	23.4	14.3	8.0	7.2	1.2	0.6
Mean	26.9	20.1	28.0	22.6	13.7	7.5	6.6	0.9	0.6
S.D.	13.4	2.4	5.0	2.0	1.9	1.8	2.9	0.7	0.5
Minimum	13.0	16.7	20.9	18.6	8.0	2.3	0.9	ND	ND
Maximum	61.0	25.8	38.9	26.6	16.9	9.5	12.5	1.8	1.4

[a]Weight percentage relative to total fatty acids.
[b]Weight percentage of individual isomers or group of isomers relative to total *trans*-18:1 acids. The Δ4 and Δ5 isomers were not recorded.
[c]ND, not detected.

TABLE 2
***Trans*-18:1 Isomeric Acid Content and Profile in Some Food Items Labeled as Containing Partially Hydrogenated Vegetable Oils Commercialized in France in 1999**

Sample	Total content[a]	Isomeric distribution[b]									
		Δ4	Δ5	Δ6–Δ8	Δ9	Δ10	Δ11	Δ12	Δ13/14	Δ15	Δ16
Melba toast	16.5	0.7	1.6	15.4	40.6	17.6	9.5	4.5	8.8	0.9	0.5
Sandwich	3.7	3.4	10.9	38.5	21.3	11.6	0.4	6.4	4.9	1.5	1.2
Muesli	2.0	0.9	1.1	21.4	32.4	21.2	10.3	5.9	5.0	0.8	1.1
Crackers	0.1	3.5	4.5	8.6	21.4	17.6	8.8	7.7	22.0	2.9	3.2
Crackers	2.2	0.8	0.6	9.2	23.0	22.2	18.0	9.2	11.6	3.1	2.3
Crackers	17.4	0.5	0.6	14.7	25.8	23.8	16.7	8.6	6.8	1.6	1.1
Crackers	15.8	0.4	0.5	9.5	15.2	27.4	25.0	11.5	8.8	1.0	0.9
Pizza paste	16.6	0.1	0.3	13.6	46.1	21.0	10.8	4.9	2.6	0.4	0.2
Cake	12.6	0.5	1.0	11.7	18.7	21.6	18.5	11.7	12.4	2.1	1.7
Cake	22.4	0.2	0.9	15.8	18.4	21.7	18.9	11.5	10.1	1.5	1.1
Mean	10.9	1.1	2.2	15.8	26.3	20.6	13.7	8.2	9.3	1.6	1.3
S.D.	8.1	1.3	3.3	8.8	10.2	4.2	7.0	2.8	5.3	0.9	0.9
Minimum	0.1	0.1	0.3	8.6	15.2	11.6	0.4	4.5	2.6	0.4	0.2
Maximum	22.4	3.5	10.9	38.5	46.6	27.4	25.0	11.7	22.0	3.1	3.2

[a]Weight percentage relative to total fatty acids.
[b]Weight percentage of individual isomers or group of isomers relative to total *trans*-18:1 acids.

variable. To understand whether there was a relationship between the nature of the foods and the PHVO used to manufacture them, we analyzed eleven samples of dehydrated soups in 1999, where PHVO have no obvious roles in the structure of the food, except that they are solid at ambient temperature and resistant to oxidation. Not one of the extracted fats was identical to another one (Table 3). Evidently, the extracted fats may not be exactly representative of the added PHVO, as some ingredients also naturally contain some fat. If this fat is derived from beef or mutton, or from milk, then a small part of the *trans*-18:1 isomers may come from these food constituents.

For the two periods considered, the mean *trans*-18:1 isomer contents are 26.9 (range, 13.0–61.0%) and 11.9% (range, 0.1–27.0%), respectively, of total fatty acids (Tables 1–3). This difference does not strongly indicate that hydrogenation habits have changed in the meantime. The categories of foods analyzed at the two periods were somewhat different, and for a given category, the brands differed too. However, PHVO with very high *trans*-18:1 acid levels (>30%) seem to have disappeared in 1999. Regarding the profile of these isomers, in 1999 as well as in 1995–1996, foods with identical *trans*-18:1 isomers are exceptional, which means either that food processors had and still have access to a very wide range of

TABLE 3
***Trans*-18:1 Isomeric Acid Content and Profile in Some Dehydrated Soups Labeled as Containing Partially Hydrogenated Vegetable Oils Commercialized in France in 1999**

Sample[a]	Total content[b]	Isomeric distribution[c]									
		Δ4	Δ5	Δ6–Δ8	Δ9	Δ10	Δ11	Δ12	Δ13/14	Δ15	Δ16
DS01	20.6	0.4	0.6	18.5	31.1	22.7	13.4	6.8	5.3	0.8	0.4
DS04	5.9	0.6	0.3	12.8	45.5	21.7	10.8	4.7	2.5	0.7	0.4
DS06	10.0	0.9	1.2	16.0	27.2	21.3	14.7	7.4	8.2	1.8	1.3
DS07	27.0	0.5	1.1	17.3	20.9	20.7	14.6	10.4	10.9	2.3	1.3
DS08	10.8	0.5	0.8	14.9	31.5	21.3	15.3	7.0	6.6	1.2	0.9
DS09	6.6	0.6	0.6	16.8	28.0	17.1	8.2	4.4	3.3	18.6	2.6
DS10	4.3	2.1	1.6	18.9	30.1	20.5	10.9	6.1	5.2	3.1	1.6
DS12	12.8	0.2	0.4	16.6	33.5	23.9	12.6	7.2	4.9	0.6	0.3
DS13	9.1	1.2	1.7	13.7	36.8	20.7	12.2	5.9	5.1	1.6	1.2
DS14	24.8	0.4	0.9	18.0	21.7	20.5	14.7	10.2	10.8	1.8	1.1
DS15	8.0	2.4	2.5	12.5	29.0	19.7	15.2	6.2	5.5	4.6	2.5
Mean	12.7	0.9	1.1	16.0	30.5	20.9	13.0	6.9	6.2	3.4	1.2
S.D.	7.8	0.7	0.7	2.2	6.8	1.7	2.3	1.9	2.7	5.2	0.8
Minimum	4.3	0.2	0.4	12.5	30.9	17.1	8.2	4.7	2.5	0.6	0.3
Maximum	27.0	2.1	2.5	18.9	45.5	23.9	15.3	10.4	10.9	18.6	2.6

[a]Twenty-two dehydrated soups (DS) were analyzed for their *trans*-18:1 acid content, and half of them were chosen at random and analyzed for their *trans*-18:1 isomeric acid profiles.
[b]Weight percentage relative to total fatty acids.
[c]Weight percentage of individual isomers or group of isomers relative to total *trans*-18:1 acids.

TABLE 4
Comparison of the Relative Distribution Profile of Isomeric *trans*-18:1 Acids in Partially Hydrogenated Vegetable Oils Prepared from French Foods During Two Periods with Corresponding Data for German Margarines and Related Products

	France														Germany									
	1999 survey						1995–1996 survey				Both periods				1994–1996 survey[a]									
	Dehydrated soups (n = 11)			Other food items (n = 10)			All food items[b] (n = 16)				All food items (n = 37)				Conventional margarines (n =46)			Shortenings and cooking fats (n = 16)			Dietary and reformulated fats (n = 31)			
Isomer	Mean	SD	Min	Max	Mean	SD	Min	Max	Mean	SD	Min	Max	Mean	SD	Min	Max	Mean	SD	Min	Max	Mean	SD	Min	Max
Δ4	0.9	0.7	0.2	2.1	1.1	1.3	0.1	3.5	ND[c]	ND	ND	ND	1.0	1.0	0.1	3.5	0.3	0.3	0.0	1.6	0.5	0.6	0.0	2.6	2.4	2.2	0.0	8.0
Δ5	1.1	0.7	0.4	2.5	2.2	3.3	0.3	10.9	ND	ND	ND	ND	1.6	2.3	0.3	10.9	0.7	0.2	0.3	1.3	0.8	0.5	0.3	2.4	2.4	1.9	0.0	7.7
Δ6–Δ8	16.0	2.2	12.5	18.9	15.8	8.8	8.6	38.5	19.5	2.4	16.2	25.0	17.5	5.2	8.6	38.5	18.5	3.6	9.4	24.1	14.6	3.3	5.1	18.9	14.3	4.9	4.1	28.2
Δ9	30.5	6.8	30.9	45.5	26.3	10.2	15.2	46.1	27.2	4.9	20.2	37.7	27.9	7.2	15.2	46.1	23.7	5.1	9.1	34.2	25.5	6.0	15.3	39.8	21.9	5.2	9.0	31.2
Δ10	20.9	1.7	17.1	23.9	20.6	4.2	11.6	27.4	22.0	1.9	18.1	25.8	21.3	2.7	11.6	27.4	20.7	3.1	8.7	26.1	20.2	2.2	15.7	24.2	21.2	4.3	11.0	30.8
Δ11	13.0	2.3	8.2	15.3	13.7	7.0	0.4	25.0	13.3	1.9	7.8	16.4	13.3	3.9	0.4	25.0	13.4	3.2	6.1	21.1	14.7	4.3	7.6	25.4	14.8	5.0	7.5	29.7
Δ12	6.9	1.9	4.7	10.4	8.2	2.6	4.5	11.7	7.2	1.8	2.2	9.2	7.4	2.1	2.2	11.7	10.9	3.5	5.1	18.8	11.4	3.4	2.8	15.8	10.0	4.5	3.0	21.5
Δ13/14	6.2	2.7	2.5	10.9	9.3	5.1	2.6	22.0	6.4	2.8	0.9	12.1	7.1	3.8	0.9	22.0	9.4	4.7	3.4	32.5	9.6	3.4	3.7	16.1	9.5	5.5	3.0	27.6
Δ15	3.4	5.2	0.6	18.6	1.6	0.9	0.4	3.1	0.9	0.7	ND	1.7	1.8	3.0	ND	18.6	1.5	0.7	0.5	5.2	1.6	0.7	0.0	2.5	1.5	1.1	0.0	4.4
Δ16	1.2	0.8	0.3	2.6	1.3	0.9	0.2	3.2	0.6	0.5	ND	1.4	1.0	0.8	ND	3.2	1.1	1.1	0.3	7.8	1.0	0.4	0.0	1.7	2.0	2.5	0.0	12.2

[a]Data from Ref. 38.
[b]Data normalized at 97.0% to compensate for the absence of quantitation of the Δ4 and Δ5 isomers at that period.
[c]Not determined.

such fats or that blending is a current practice. Also, this means that analysis of only a few food items in dietary survey studies is unlikely to be representative of a "mean PHVO." Sampling of foods thus must be wide enough to take into account the great variability of the *trans*-18:1 isomer profile in PHVO.

Comparison with German PHVO. In the present study, we observed that the mean relative profile established for dehydrated soups was nearly identical to that established for other food items in 1999 (Fig. 1 and Table 4). Moreover, combining results for dehydrated soups and other food items for the period 1999 gives a mean profile that only differs in details from that established for foods analyzed in 1995–1996 (Fig. 2). Averaging all *trans*-18:1 isomers profiles (n = 37) leads to a mean profile thought to accurately represent a "mean PHVO" present in foods consumed by French people. This profile is compared in Table 4 and Figure 3 to the mean profiles established for margarines on the one hand, and shortenings and frying fats on the other hand, commercialized in Germany (36–38). Differences are visible, e.g., between margarines and foods, which may be attributed to different hydrogenated oils being used in each category. The influence of the source of oil on the pattern of *trans*-18:1 isomers, which also depends on the conditions of processing, is well known. Also, it may be reasonably hypothesized that hidden PHVO in foods may be derived from cheaper raw materials than in margarines (e.g., rapeseed oil vs. sunflower oil).

When all French and German samples are considered, it appears on average that the Δ9 isomer (elaidic acid) is the predominant isomer in all categories of foods and that it may vary in the approximate range 9–46% (Table 4), averaging 22–30%. The Δ10 isomer is ranked second, at *ca.* 21% (range, 8.7–30.8%). In contrast to elaidic acid, and with few exceptions only, the proportion of the latter isomer is remarkably constant from one category of food to another. The unresolved Δ6 to Δ8 group represents *ca.* 16%, which is higher than the content of vaccenic acid that accounts for approximately 14%. Considering the Δ6 to Δ8 group, it is likely that the Δ8 is the predominant isomer (22–30). All other isomers are less than 10%, and appear rather variable quantitatively. Special attention, however, should be paid to the late-eluting Δ12, Δ13 + Δ14, Δ15, and Δ16 isomers. These isomers have often been neglected, although from Ag-TLC they are accessible without difficulties on 50-m capillary columns operated at moderately high temperatures, that is, allowing reasonable times of analysis. Finally, the minor Δ4 and Δ5 isomers, which are the earliest-eluting components of the *trans*-18:1 fractions, are not always easily quantitated (e.g., not reported for French foods analyzed in 1995–1996), as they may not be taken into account by integrators when the quantity of *trans*-18:1 FAME injected is not appropriate for their detection. This also holds for the Δ15 and Δ16 isomers.

In Figure 4, the relative *trans*-18:1 isomer profile of PHVO as established in the present study for French foods is compared with that of ruminat fats. For the latter profile, data from Wolff (19,39), Bayard and Wolff (40), and Wolff *et al*.

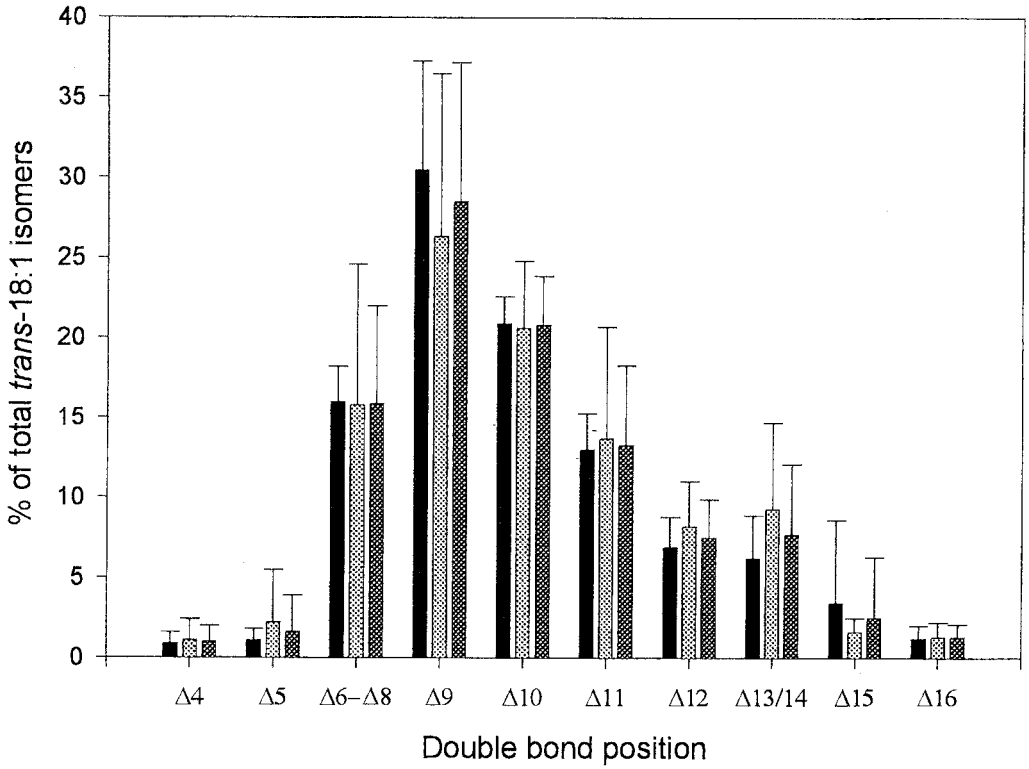

FIG. 1. Relative isomeric distribution (mean ± SD) of individual *trans*-18:1 isomers prepared from partially hydrogenated vegetable oils extracted from foods purchased in France in 1999. Black bars, dehydrated soups (n = 11); light grey bars, other food items (n = 10); dark grey bars, all samples (n = 21).

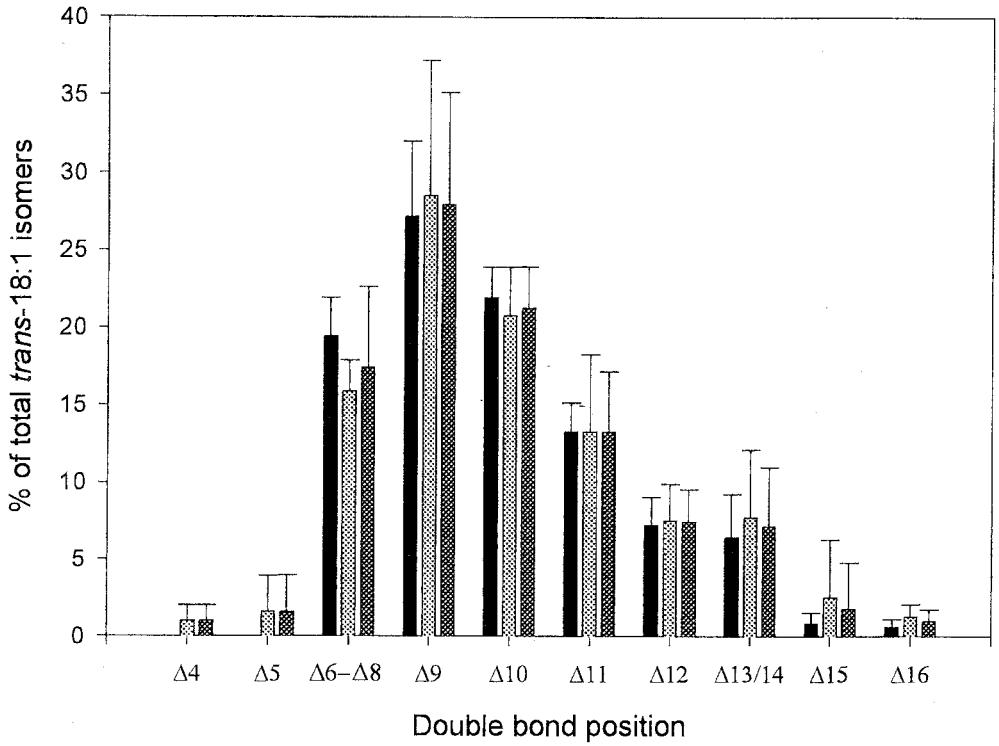

FIG. 2. Comparison of the relative isomeric distribution (mean ± SD) of individual *trans*-18:1 isomers prepared from partially hydrogenated vegetable oils extracted from foods purchased in France in 1995–1996 (black bars, n = 16) and in 1999 (light grey bars, n = 21); all samples for both periods (dark grey bars, n = 37).

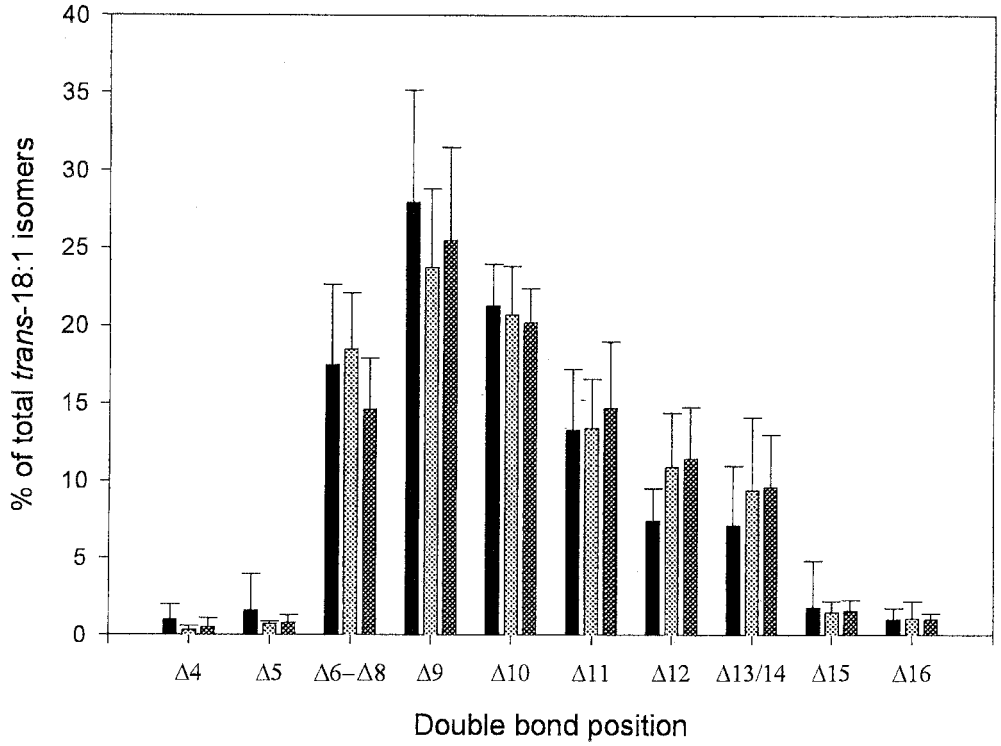

FIG. 3. Comparison of the relative isomeric distribution (mean ± SD) of individual *trans*-18:1 isomers prepared from partially hydrogenated vegetable oils extracted from foods purchased in France (black bars, $n = 37$) with corresponding data for German margarines (light grey bars, $n = 46$) and shortenings and cooking fats (dark grey bars, $n = 16$) purchased in 1994.

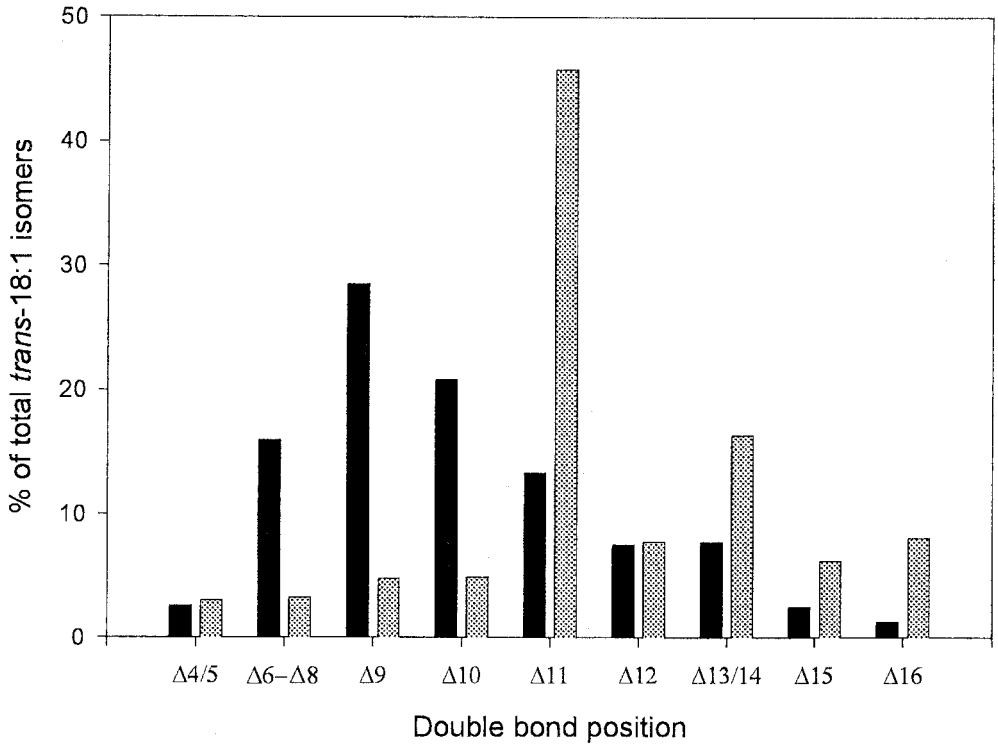

FIG. 4. Relative isomeric distribution of individual *trans*-18:1 isomers prepared from partially hydrogenated vegetable oils extracted from foods purchased in France (black bars, $n = 37$) and from ruminant fats (grey bars, essentially calculated from data in Refs. 39–41; see text, however).

(41) for France were used, with additional new data for individual isomers of French ruminant fats not available previously (Precht, D., Molkentin, J., Destaillats, F., and Wolff, R.L., unpublished data). In fact, totaling *trans*-18:1 isomers from all ruminant fats (taking into account their respective share in the French diet) leads to a profile almost undistinguishable from that of French or German bovine milk fat alone (results not shown; see Refs. 9 and 42, however). The differences between PHVO and ruminant fats are obvious, with a shift of the bulk of *trans*-18:1 acids toward low Δ positions of the ethylenic bond in PHVO as compared to ruminant fats. More than two-thirds of total *trans*-18:1 isomers have their ethylenic bond between the Δ4 and Δ10 positions in PHVO, whereas the great majority (>65%) of *trans*-18:1 isomers have their ethylenic bond at position Δ11 and farther in ruminant fats.

Nutritional and analytical implications. The dissimilarity in the distribution of *trans*-18:1 isomers from the two dietary sources becomes even more apparent when the absolute profile of the daily intake of *trans*-18:1 isomers is constructed (Fig. 5). The French profile is based on a mean daily intake of 1.5 g of *trans*-18:1 acids from ruminant fats (39), and 1 g from PHVO (43). Vaccenic acid represents approximately one-third (800 mg) of the total, originating mostly from ruminant fats. The contribution of PHVO to the intake of vaccenic acid is small and is far below that attributable solely to seasonal variations of the quantity of vaccenic acid in bovine milk fat. Depending on the feed, 100 g of milk fatty acids contains from *ca.* 1 (barn feeding) to almost 3 g (pasture feeding) of vaccenic acid (44). A similar influence of diet also affects the Δ12 to Δ16 isomers. On the other hand, the amounts of Δ6 to Δ10 isomers vary little with the feed of the cattle, and the contribution of PHVO to the intake of these isomers is crucial.

The model shown in Figure 5 can be extended to other countries. For Germany, where an estimated mean intake of 3.0 g/person/d appears reasonable (45), half of which coming from ruminant fats and the other half from PHVO, the diagram shown in the center of Figure 5 is obtained. The increase of the Δ6 to Δ10 part becomes more conspicuous, with little effect on the Δ11 to Δ16 part, even if the difference in *trans*-18:1 acid intake between German and French people is 0.5 g/person/d.

Extrapolation of our data to North America (Canada and the United States) is also interesting. *Trans*-fatty acid consumption by Canadian and U.S. people has been reviewed several times (46–49), and considerable discrepancies between estimates were noted. These show in particular the weakness of food frequency questionnaires to assess the *trans*-fatty acid consumption, resulting in *ca.* two to three times less than assessments based on disappearance and consumption data, or estimates based on the *trans*-18:1 acid content in human milk obtained by Ag-TLC coupled with GLC or related procedures (reviewed in Ref. 50). As a matter of comparison with France and Germany, we have chosen a value of 7.0 g/person/d, which should be realistic, of which

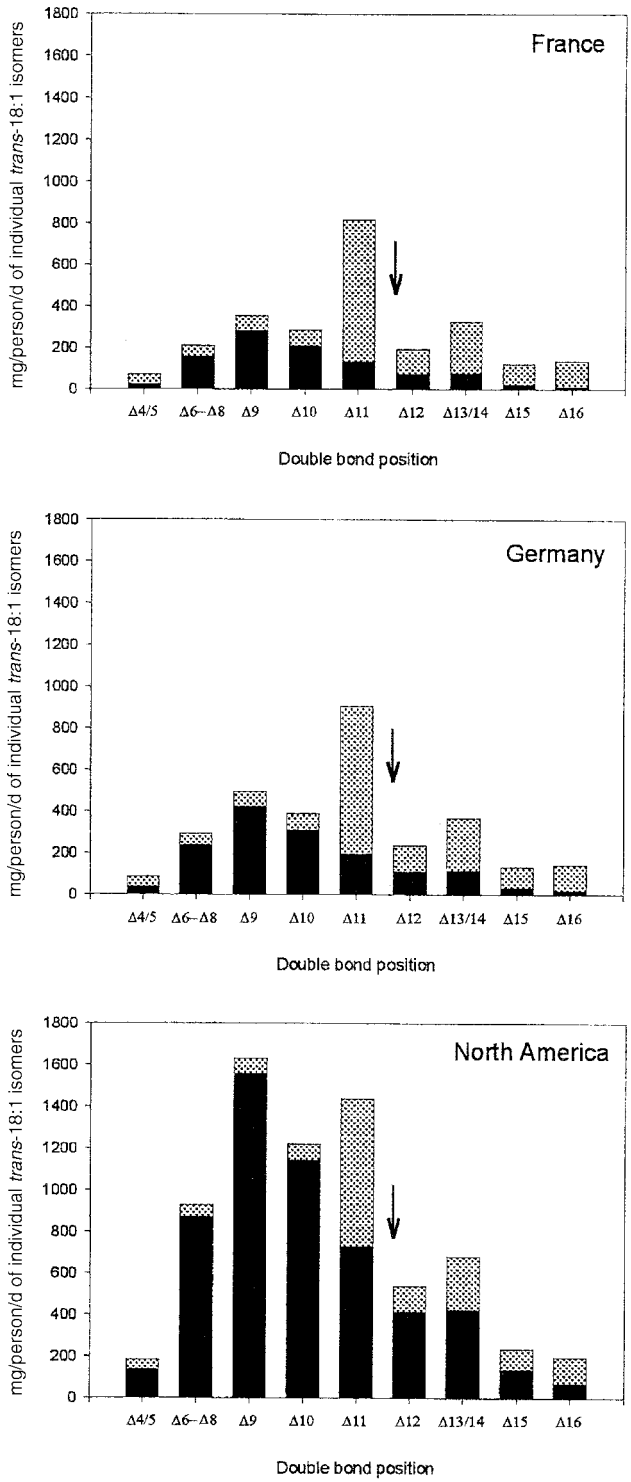

FIG. 5. Estimated absolute per capita daily intake of individual *trans*-18:1 acids in France (top), Germany (center), and North America (bottom). Black bars: contribution by partially hydrogenated vegetable oils; grey bars, contribution by ruminant fats. The arrows show the limit between visible (left side) and masked (right side) isomers that occurs during direct gas–liquid chromatography on 50-m columns.

1.5 g (approximately 20% of the total) would come from ruminant fats. These values allow construction of the diagram on the bottom of Figure 5. The preponderance of elaidic acid

among other *trans*-18:1 acids becomes obvious, and this contrasts with data for France or Germany (top and central diagrams in Fig. 5). There is a difference not only in the total intake of *trans*-18:1 isomers but also in the distribution of individual isomers. The latter diagram compares well with those published by Emken (51) for the United States, and by Ratnayake (28) for Canada. However, it is likely that in these two countries, the raw materials that are hydrogenated may not be the same as in European countries (e.g., soybean in the United States, canola in Canada). Thus, small differences between our predictive diagram and the true distribution in North American diets should probably occur.

We repeatedly pointed out (3,34,35,45,48) the faulty use of direct GLC to assess the *trans*-18:1 acid content in foods or biological samples. The diagrams in Figure 5 once again examplify how direct GLC leads to unavoidable underestimates, and hence, to erroneous data. On 50-m columns systematically, or on 100-m columns operated at too high a temperature, isomers with a Δ12 ethylenic bond (or at best, the Δ13 plus Δ14 critical pair) and all other isomers with ethylenic bonds still further along the chain elute under oleic and *cis*-vaccenic acids and even after them. Isomers lost in this way are those to the right of the arrows in Figure 5. These isomers are not taken into account because only the Δ6 to Δ11 (or Δ12, at least in part) are more or less well separated from oleic acid and integrated. The proportion of these isomers relative to total *trans*-18:1 acids varies with the proportions of PHVO and ruminant fats in the sample to be analyzed, with underestimates in the range 8–67% (35,36). Clearly, direct GLC determinations of *trans*-18:1 isomeric acids only allow gross estimates that are of little use, unreliable, and inaccurate.

An example will help to illustrate why case-control studies for ischemic heart diseases based on direct GLC are unable to lead to reliable conclusions. Let us imagine two groups, one consuming mostly ruminant fats with little PHVO (group A), and the other one, principally PHVO with little ruminant fats (group B). Admittedly, no differences are found in the content of *trans*-18:1 isomers determined by direct GLC in their adipose tissue, say 2.0% of total fatty acids in both groups. The conclusion, based on a wealth of statistical treatments, will lead to an absence of relationships between diets and effects. In fact, the true proportion of *trans*-18:1 isomers in group A would be 2.0 × 1.5 = 3.0%, whereas in group B, the corresponding value would be 2.0 × 1.3 = 2.6%, with 1.5 and 1.3 being the mean correction factors for consideration of the masked *trans*-18:1 isomers (35). Possibly, the difference would then be significant. Conversely, two different percentages of *trans*-18:1 isomers in the adipose tissue of group A (1.8%) and group B (2.1%), here too established by direct GLC and considered statistically different, may be identical: group A, 1.8 × 1.5 = 2.7%, and group B, 2.1 × 1.3 = 2.7%. This clearly demonstrates that an accurate knowledge of all individual *trans*-18:1 isomers is imperative before drawing any conclusions as to their effects in case-control studies based on data obtained by direct GLC. Because this has never been done, the problem of the potential harmfulness or harmlessness of these isomers must be considered unresolved and remains a fully open question.

Retrospectively, considering conclusions based on "mixed-up *trans*-fatty acids" determined in such a way, one should rather critically look at the methodology before accepting the findings. Moreover, it possibly is not the quantity of *trans*-18:1 isomers that should be questioned, but their intimate profile, only accessible by Ag-TLC/GLC with specifically optimized GLC operating conditions. Surprisingly, with rare exceptions employing the Ag-TLC/GLC procedure (52), in practically none of the case-control studies published so far was a chromatogram given showing the resolution of *trans*-18:1 isomers, and eventually other *trans*-fatty acids. Consequently, suspicion should be cast on their conclusions.

ACKNOWLEDGMENTS

The authors thank Mrs. Birte Fischer, Mrs. Bärbel Krumbeck, Mrs. Laurence Fonseca, and Mrs. Pascale Nonatel for their contribution to the analytical work. Frédéric Destaillats was funded by an ADERA grant and the Bundesanstalt für Milchforschung.

REFERENCES

1. Report of the Expert Panel on *trans* Fatty Acids and Coronary Heart Disease (1995) *Trans* Fatty Acids and Coronary Heart Disease Risk, *Am. J. Clin. Nutr. 62*, 655S–708S.
2. *Trans* Fatty Acids, *The Report of the British Nutrition Foundation Task Force*, British Nutrition Foundation, London, 1995.
3. Precht, D., and Molkentin, J. (1995) *Trans* Fatty Acids: Implications for Health, Analytical Methods, Incidence in Edible Fats and Intake, *Nahrung 39*, 343–374.
4. Stender, S., Dyerberg, J., Hølmer, G., Ovesen, L., and Sandström, B. (1995) The Influence of *trans* Fatty Acids on Health: A Report from the Danish Nutrition Council, *Clin. Sci. 88*, 375–392.
5. Aro, A. (1998) Epidemiological Studies of *trans* Fatty Acids and Coronary Heart Disease, in Trans *Fatty Acids in Human Nutrition* (Sébédio, J.-L., and Christie, W.W., eds.), pp. 235–260, Oily Press, Dundee.
6. Ackman, R.G., and Mag, T.K. (1998) *Trans* Fatty Acids and the Potential for Less in Technical Products, in Trans *Fatty Acids in Human Nutrition* (Sébédio, J.-L., and Christie, W.W., eds.), pp. 35–58, Oily Press, Dundee.
7. Hølmer, G. (1998) Biochemistry of *trans*-Monoenoic Acids, in Trans *Fatty Acids in Human Nutrition* (Sébédio, J.-L., and Christie, W.W., eds.), pp. 163–189, Oily Press, Dundee.
8. Sébédio, J.-L., and Chardigny, J.M. (1998) Biochemistry of *trans* Polyunsaturated Acids, in Trans *Fatty Acids in Human Nutrition* (Sébédio, J.-L., and Christie, W.W., eds.), pp. 191–215, Oily Press, Dundee.
9. Wolff, R.L., Precht, D., and Molkentin, J. (1998) Occurrence and Distribution Profile of *trans*-18:1 Acids in Edible Fats of Natural Origin, in Trans *Fatty Acids in Human Nutrition* (Sébédio, J.-L., and Christie, W.W., eds.), pp. 1–33, Oily Press, Dundee.
10. Ohnishi, M., and Thompson, G.A., Jr. (1991) Biosynthesis of the Unique *trans* Δ^3-Hexadecenoic Acid Component of Chloroplast Phosphatidylglycerol: Evidence Concerning Its Site and Mechanism of Formation, *Arch. Biochem. Biophys. 288*, 591–599.
11. Bayard, C.C., and Wolff, R.L. (1995) *Trans*-18:1 Acids in French Tub Margarines and Shortenings: Recent Trends, *J. Am. Oil Chem. Soc. 72*, 1485–1489.

12. Fritsche, J., and Steinhart, H. (1997) *Trans* Fatty Acid Content in German Margarines, *Fett/Lipid 6*, 214–217.
13. Henninger, M., and Ulberth, F. (1996) *Trans* Fatty Acids in Margarines and Shortenings Marketed in Austria, *Z. Lebensm.-Unters.-Forsch. 203*, 210–215.
14. Ovesen, L., Leth, T., and Hansen, K. (1996) Fatty Acid Composition of Danish Margarines and Shortenings, with Special Emphasis on *trans* Fatty Acids, *Lipids 31*, 971–975.
15. Ratnayake, W.M.N., Pelletier, G., Hollywood, R., Bacler, S., and Leyte, D. (1998) *Trans* Fatty Acids in Canadian Margarines: Recent Trends, *J. Am. Oil Chem. Soc. 75*, 1587–1594.
16. Duchateau, G.S.M.J.E., van Oosten, H.J., and Vasconcellos, M.A. (1996) Analysis of *cis*- and *trans*-Fatty Acid Isomers in Hydrogenated and Refined Vegetable Oils by Capillary Gas–Liquid Chromatography, *J. Am. Oil Chem. Soc. 73*, 275–282.
17. Bysted, A., Cold, S., and Hølmer, G. (1999) An Optimized Method for the Fatty Acid Analysis, Including Quantification of *trans* Fatty Acids, in Human Adipose Tissue by Gas–Liquid Chromatography, *Scand. J. Clin. Lab. Invest. 59*, 205–214.
18. Folch, J., Lees, M., and Sloane-Stanley, G.M. (1957) A Simple Method for the Isolation of Total Lipids from Animal Tissues, *J. Biol. Chem. 226*, 497–509.
19. Wolff, R.L. (1994) Contribution of *trans*-18:1 Acids from Ruminant Fats to European Diets, *J. Am. Oil Chem. Soc. 71*, 277–283.
20. Wolff, R.L., and Bayard, C.C. (1995) Improvement in the Resolution of Individual *trans*-18:1 Isomers by Capillary Gas–Liquid Chromatography: Use of a 100-m CP-Sil 88 Column, *J. Am. Oil Chem. Soc. 72*, 1197–1201.
21. Scholfield, C.R. (1979) Analysis and Physical Properties of Isomeric Fatty Acids, in *Geometrical and Positional Fatty Acid Isomers* (Emken, E.A., and Dutton, H.J., eds.), pp. 17–52, American Oil Chemists' Society, Champaign.
22. Dutton, H.J. (1979) Hydrogenation of Fats and Its Significance, in *Geometrical and Positional Fatty Acid Isomers* (Emken, E.A., and Dutton, H.J., eds.), pp. 1–16, American Oil Chemists' Society, Champaign.
23. Carpenter, D.L., and Slover, H.T. (1973) Lipid Composition of Selected Margarines, *J. Am. Oil Chem. Soc. 50*, 372–376.
24. Parodi, P.W. (1976) Composition and Structure of Some Consumer-Available Edible Fats, *J. Am. Oil Chem. Soc. 53*, 372–376.
25. Ohlrogge, J.B., Emken, E.A., and Gulley, R.M. (1981) Human Tissue Lipids: Occurrence of Fatty Acid Isomers from Dietary Hydrogenated Oils, *J. Lipid Res. 22*, 955–960.
26. Marchand, C.M. (1982) Positional Isomers of *trans*-Octadecenoic Acids in Margarines, *Can. Inst. Food Sci. Technol. J. 15*, 196–199.
27. Smallbone, B.W., and Sahasrabudhe, M.R. (1985) Positional Isomers of *cis*- and *trans*-Octadecenoic Acids in Hydrogenated Vegetable Oils, *Can. Inst. Food Sci. Technol. J. 18*, 174–177.
28. Chen, Z.Y., Ratnayake, W.M.N., Fortier, L., and Cunnane, S.C. (1995) Similar Distribution of *trans* Fatty Acid Isomers in Partially Hydrogenated Vegetable Oils and Adipose Tissue of Canadians, *Can. J. Physiol. Pharmacol. 73*, 718–723.
29. Chen, Z.Y., Pelletier, G., Hollywood, R., and Ratnatake, W.M.N. (1995) *Trans* Fatty Acid Isomers in Canadian Human Milk, *Lipids 30*, 15–21.
30. Ratnayake, W.M.N., and Chen, Z.-Y. (1996) *Trans*, n-3, and n-6 Fatty Acids in Canadian Human Milk, *Lipids 31 (Suppl.)*, 279–282.
31. Kuemmel, D.F., and Chapman, D.R. (1966) Analysis of Methyl Octadecenoate and Octadecadienoate Isomers by Combined Liquid–Solid and Capillary Gas–Liquid Chromatography, *Anal. Chem. 38*, 1611–1614.
32. Molkentin, J., and Precht, D. (1995) Optimized Analysis of *trans*-Octadecenoic Acids in Edible Fats, *Chromatographia 41*, 267–272.
33. Wolff, R.L., and Precht, D. (1998) Comments on the Resolution of Individual *trans*-18:1 Isomers by Gas–Liquid Chromatography, *J. Am. Oil Chem. Soc. 75*, 421–422.
34. Wolff, R.L. (1998) Simple Methods for the Identification and Quantification by GLC of Most Individual *trans*-18:1 Isomers Present in Foods and Human Tissues, *Lipid Technol. 11*, 16–18.
35. Wolff, R.L., Combe, N.A., Precht, D., Molkentin, J., and Ratnayake, W.M.N. (1998) Accurate Determination of *trans*-18:1 Isomers by Capillary Gas–Liquid Chromatography on Cyanoalkyl Polysiloxane Stationary Phases, *Oléagineux, Corps Gras, Lipides 5*, 295–299.
36. Precht, D., and Molkentin, J. (1997) Vergleich der Fettsäuren und der Isomerenverteilung der *trans*-C18:1-Fettsäuren von Milchfett, Margarine, Back-, Brat- und Diätfetten, *Kiel. Milchwirtsch. Forschungber. 49*, 17–34.
37. Molkentin, J., and Precht, D. (1995) Determination of *trans*-Octadecenoic Acids in German Margarines, Shortenings, Cooking and Dietary Fats by Ag-TLC/GC, *Z. Ernährungswiss. 34*, 314–317.
38. Molkentin, J., and Precht, D. (1996) Isomeric Distribution and Rapid Determination of *trans*-Octadecenoic Acids in German Brands of Partially Hydrogenated Edible Fats, *Nahrung 40*, 297–304.
39. Wolff, R.L. (1995) Content and Distribution of *trans*-18:1 Acids in Ruminant Milk and Meat Fats. Their Importance in European Diets and Their Effect on Human Milk, *J. Am. Oil Chem. Soc. 72*, 259–272.
40. Bayard, C.C., and Wolff, R.L. (1996) Analysis of the *trans*-18:1 Isomer Content and Profile in Edible Refined Beef Tallow, *J. Am. Oil Chem. Soc. 73*, 531–533.
41. Wolff, R.L., Bayard, C.C., and Fabien, R.J. (1995) Evaluation of Sequential Methods for the Determination of Butterfat Fatty Acid Composition with Emphasis on *trans*-18:1 Acids. Application to the Study of Seasonal Variations in French Butters, *J. Am. Oil Chem. Soc. 72*, 1471–1483.
42. Precht, D., and Molkentin, J. (1996) Rapid Analysis of the Isomers of *trans*-Octadecenoic Acid in Milk Fat, *Int. J. Dairy Sci. 6*, 781–809.
43. Boué, C., Combe, N., Billeaud, C., Mignerot, C., Entressangles, B., Théry, G., Geoffrion, H., Brun, J.L., Dallay, D., and Leng, J.J. (2000) *Trans* Fatty Acids in Adipose Tissue of French Women in Relation to Their Dietary Sources, *Lipids 35*, 561–566 (2000).
44. Precht, D., and Molkentin, J. (1997) Effect of Feeding on *trans* Positional Isomers of Octadecenoic Acid in Milk Fats, *Milchwissenschaft 52*, 564–568.
45. Precht, D., and Molkentin, J. (1999) C18:1, C18:2 and C18:3 *trans* and *cis* Fatty Acid Isomers Including Conjugated *cis* Δ9, *trans* Δ11 Linoleic Acid (CLA) as Well as Total Fat Composition of German Human Milk Lipids, *Nahrung 43*, 233–244.
46. Enig, M.G., Atal, S., Keeney, M., and Sampugna, J. (1990) Isomeric *trans* Fatty Acids in the U.S. Diet, *J. Am. Coll. Nutr. 9*, 471–486.
47. Hunter, J.E., and Applewhite, T.H. (1991) Reassessment of *trans* Fatty Acid Availability in the US Diet, *Am. J. Clin. Nutr. 54*, 363–369.
48. Craig-Schmidt, M.C. (1998) Worldwide Consumption of *Trans*-Fatty Acids, in Trans *Fatty Acids in Human Nutrition* (Sébédio, J.-L., and Christie, W.W., eds.), pp. 59–113, Oily Press, Dundee.
49. Allison, D.B., Egan, K., Barraj, L.M., Caughman, C., Infante, M., and Heimbach, J.T. (1999) Estimated Intakes of *trans* Fatty and Other Fatty Acids in the US Population, *J. Am. Diet. Assoc. 99*, 166–174.
50. Wolff, R.L., Precht, D., and Molkentin, J. (1998) *Trans*-18:1 Acid Content and Profile in Human Milk Lipids. Critical Survey

of Data in Connection with Analytical Methods, *J. Am. Oil Chem. Soc. 75*, 661–671.
51. Emken, E.A. (1981) Metabolic Aspects of Positional Monounsaturated Fatty Acids Isomers, *J. Am. Oil Chem. Soc. 58*, 278–283.
52. Seppänen-Laakso, T., Laakso, I., Backlund, P., Vanhanen, H., and Viikari, J. (1996) Elaidic and *trans*-Vaccenic [*sic*] Acids in Plasma Phospholipids as Indicators of Dietary Intake of 18:1 *trans*-Fatty Acids, *J. Chromatogr. B. 687*, 371–378.

[Received February 8, 2000, and in revised form June 5, 2000; revision accepted June 22, 2000]

Smoking Influences the Association Between Apolipoprotein E and Lipids: The National Heart, Lung, and Blood Institute Family Heart Study

Luc Djoussé[a,*], Richard H. Myers[a], Hilary Coon[b], Donna K. Arnett[c], Michael A. Province[d], and R. Curtis Ellison[a]

[a]Section of Preventive Medicine & Epidemiology, Evans Department of Medicine, Boston University School of Medicine, Boston, Massachusetts, [b]Department of Psychiatry, University of Utah, Salt Lake City, Utah, [c]Division of Epidemiology, University of Minnesota, Minneapolis, Minnesota, and [d]Division of Biostatistics, Washington University, St. Louis, Missouri

ABSTRACT: Apolipoprotein E allele 4 (apo ε_4) and smoking each have been associated with an unfavorable lipid profile. We used data collected on 1,472 subjects in the National Heart, Lung, and Blood Institute Family Heart Study to assess whether smoking interacts with apo ε_4 to influence the levels of plasma lipids. We dichotomized smoking and apo ε_4 and used analysis of covariance to estimate the means of lipids. Smokers had lower body mass index, were younger, and consumed less fruits and vegetables. Among individuals without apo ε_4, comparing nonsmokers with smokers, mean low density lipoprotein cholesterol (LDL) was 129.3 and 134.4 mg/dL, respectively, for women and 126.1 and 127.6 mg/dL, respectively, for men. Among subjects with an apo ε_4 allele, corresponding means were 132.0, and 152.9 mg/dL, respectively, for women and 131.3 and 137.3 mg/dL, respectively, for men (P for interaction <0.001 for women and 0.11 for men). A similar interaction was observed for total cholesterol among women ($P = 0.02$). This study shows a statistically significant effect modification of the relation of apo ε_4 to LDL and total cholesterol by smoking among women. Smoking may enhance genetic susceptibility to an unfavorable lipid profile among subjects with apo ε_4.

Paper no. L8482 in *Lipids 35*, 827–831 (August 2000).

Elevated low density lipoprotein cholesterol (LDL) and triglycerides and low levels of high density lipoprotein cholesterol (HDL) are established risk factors for coronary heart disease (CHD) (1–6). Plasma levels of LDL, HDL, and triglycerides are influenced by both genetic and environmental factors. Genetic polymorphism of apolipoprotein (apo) E, a protein found in very low density lipoprotein and HDL, is common. The major isoforms E2, E3, and E4 are coded by the alleles ε_2, ε_3, and ε_4, respectively. Apo ε_4 has been associated with increased risk of CHD (7–8), raised LDL (9–12) and triglycerides (11), and lower HDL (11). Contrary to apo ε_4, which is a nonmodifiable risk factor for cardiovascular disease, cigarette smoking is a modifiable risk factor which can be targeted for preventive interventions. Smoking is also associated with increased LDL (13–19) and triglycerides (20), and with decreased HDL (19). The effects of smoking on LDL may be mediated through decreased activity of lipoprotein lipase (21). In this study, we have used data collected in the National Heart, Lung, and Blood Institute (NHLBI) Family Heart Study to evaluate whether smoking and apo ε_4 interact to influence the levels of LDL, HDL, and triglycerides among women and men.

MATERIALS AND METHODS

Study population. The NHLBI Family Heart Study is a multicenter, population-based study designed to identify and evaluate genetic and nongenetic determinants of CHD, preclinical atherosclerosis, and cardiovascular risk factors. A detailed description of the methods and design has been reported (22). Subjects in this study are members of families from previously established population-based cohort studies: the Framingham Heart Study in Framingham, Massachusetts; the Atherosclerosis Risk in Communities (ARIC) cohorts in North Carolina and Minnesota; and the Utah Health Family Tree Study in Salt Lake City, Utah. In 1993–1995, groups of individuals participating in each of the four studies were selected at random and invited to furnish an updated family health history that contained information on their parents, children, and siblings. Of 4,679 individuals contacted, responses were obtained from 3,150 (67%); their other family members were then contacted, and self-reported health data were obtained from 22,908 other family members (86% of those contacted). Of the families furnishing data, 588 were chosen at random and 657 were chosen because of higher than expected CHD rates among family members. All members of these families were invited to come to one of the four study clinics for clinical evaluation. The evaluation included a detailed medical and lifestyle history, obtained through interview. All interviewers were trained centrally and required periodic certification; standardization of interviews was facilitated by periodic review of taped interviews, and by frequent circulation of the distributions of responses obtained by different interviewers and different centers, with prompt corrective actions taken when nonstandardized interviewing

*To whom correspondence should be addressed at Boston University School of Medicine, Room B-612, 715 Albany St., Boston MA 02118.
E-mail: ldjousse@bu.edu

Abbreviations: Apo ε_4, apolipoprotein E allele ε_4; ARIC, Atherosclerosis Risk in Communities; BMI, body mass index; CHD, coronary heart disease; HDL, high density lipoprotein cholesterol; LDL, low density lipoprotein cholesterol; Ln: natural logarithm; NHLBI, National Heart, Lung, and Blood Institute; PCR, polymerase chain reaction.

techniques were detected. The study protocol was reviewed and approved by the Institutional Review Boards of each of the participating institutions.

Blood collection and assays. All participants were asked to fast for 12 h before their arrival at the study center. Evacuated tubes without additives were used to collect samples for lipids; blood samples were then spun at 3,000 × *g* for 10 min at 4°C. Sera were stored at −70°C until shipment to a central laboratory at the Fairview-University Medical Center in Minneapolis, Minnesota, for processing. LDL was estimated using the method of Friedewald *et al.* (23) except for subjects with triglycerides above 400 mg/dL, whose LDL was measured by ultracentrifugation. Total cholesterol and triglycerides concentrations were measured by a Roche COBAS FARA high-speed centrifugal analyzer (Roche Diagnostic Systems, Montclair, NJ). HDL cholesterol was measured after precipitation of the other lipoprotein fractions by dextran sulfate (24).

Apo E genotyping was performed using polymerase chain reaction (PCR) to amplify a 267 base-pairs fragment from exon 4 of the apo E gene (25). The PCR product was digested with the HhaI restriction endonuclease (an isoschizomer of CfoI), which resulted in a specific banding pattern for the three isoforms of the apo E protein when they were separated by polyacrylamide gel electrophoresis and then silver-stained. Information on cigarette smoking was obtained by the question "Do you now smoke cigarettes?" Classification of smoking was based on the dichotomous answer to this question.

Other variables. Anthropometric data were collected with subjects wearing scrub suits. A balance scale was used to measure body weight, and height was measured using a wall-mounted vertical ruler. Information on alcohol intake (drinks per week) and physical activity (minutes per day of leisure activity) was obtained by interview. Calorie intake and fruit and vegetable consumption (servings per week) were assessed using a food frequency questionnaire (26,27) administered by a trained interviewer. The proportion of calories from fat was calculated by dividing the number of calories from total fat by total calories. Estrogen use by women was obtained by interview and by review of all medications being taken (brought to the clinic).

Statistical analysis. Apo E phenotype was determined among 1,744 subjects. Of these, 272 were excluded because of (i) $\varepsilon_2/\varepsilon_4$ genotype (41 subjects), (ii) current treatment for hyperlipidemia (41 subjects), or (iii) missing covariates (190 subjects). Because women have higher HDL levels and estrogen use is an important predictor of both LDL and HDL, we performed gender-specific analyses. Current cigarette smoking and apo ε_4 were dichotomized, and the following categories were generated: (i) absence of apo ε_4 and no smoking, (ii) absence of apo ε_4 and smoking, (iii) presence of apo ε_4 and no smoking, and (iv) presence of apo ε_4 and smoking. We used analysis of covariance to estimate the means of lipid values according to the above categories. Adjustment was made for age, age^2, calories from total fat, fruit and vegetable intake, body mass index (BMI), all on continuous scale, and estrogen use for women. For HDL cholesterol, further adjustment was made for alcohol intake and physical activity. Additional analyses using 5-yr age categories and quintiles of BMI and calories from fat yielded similar results. Because the distributions of triglycerides were markedly skewed, we used natural logarithmic-transformed values for the analyses. A product term (smoking × apo ε_4) was used in the multivariate model to assess the interaction. To assess the influence of menopause, we conducted additional analyses among women stratified by menopausal status. We used a bootstrap technique (300 replications) to adjust the variance for familial correlation. All analyses were performed using SAS (28).

RESULTS

Of the 1,472 subjects included in the analysis, 783 were women and 689 were men. The age range was 25 to 93 years for women [mean (SD): 56.4 (11.0) yr] and 25 to 91 years for men [mean (SD): 56.2 (11.1) yr]. The prevalence of current smoking was 13.7% for women and 14.4% for men. The frequency distributions of apolipoprotein $\varepsilon_2/\varepsilon_2$, $\varepsilon_2/\varepsilon_3$, $\varepsilon_3/\varepsilon_4$, $\varepsilon_4/\varepsilon_4$, and $\varepsilon_3/\varepsilon_3$ were 0.5, 11.1, 26.2, 2.9, and 59.3%, respectively. Table 1 presents gender-specific characteristics of the study population by apo ε_4 and smoking status. Among women without apo ε_4, smokers had lower BMI ($P = 0.08$), were younger ($P = 0.01$), had higher calories from fat ($P = 0.007$), and consumed fewer fruits and vegetables ($P = 0.08$). Among females with apo ε_4, smoking was associated with younger age ($P = 0.08$), lower BMI ($P = 0.03$), and lower consumption of fruits and vegetables ($P = 0.001$). [Female smokers were less likely to use estrogen compared with nonsmokers, but these results were not statistically significant ($P = 0.41$ for women without apo ε_4 and $P = 0.25$ for women with apo ε_4), Table 1.] For males, smoking was associated with younger age irrespective of apo ε_4 status ($P = 0.05$) and was related to lower BMI ($P = 0.01$), greater calories from fat ($P = 0.001$), and lower consumption of fruits and vegetables ($P = 0.003$) among subjects without apo ε_4.

Table 2 presents adjusted means of lipids according to the combination of apo ε_4 and smoking status. Compared with subjects who lacked apo ε_4 and who were not current smokers, current smoking and the presence of apo ε_4 were individually associated with a slight increase of LDL (4 and 2%, respectively, for women; 1 and 4%, respectively, for men), whereas the presence of both apo ε_4 and current smoking was associated with much larger increases of LDL (18 and 9% for women and men, respectively; P for interaction < 0.001 for women and 0.11 for men). The joint presence of smoking and apo ε_4 was associated with 7% increases of total cholesterol in both women and men (P for interaction = 0.02 for women and 0.14 for men). Among women, compared with the category of nonsmoking and absence of ε_4, smoking alone and apo ε_4 alone were associated with a 6 and 13% decrease in HDL, respectively, whereas the joint presence of smoking and apo ε_4 was associated with a 17% decrease in HDL. Corresponding values for men were 7, 6, and 11% decrease of HDL with smoking alone, apo ε_4 alone, and joint presence of smoking and apo ε_4, respectively (P for interaction = 0.99 for women and 0.22 for men). For the ratio of total cholesterol to HDL, the highest values were among women and

TABLE 1
Baseline Characteristics of 1,472 Participants of the NHLBI Family Heart Study (1994–1996) According to the Presence of Apolipoprotein ε_4 and Smoking Status

Apolipoprotein ε_4[a]	—	—	+	+
Cigarette smoking	—	+	—	+
Women	(n = 479)	(n = 79)	(n = 197)	(n = 28)
Age (yr)	57.5 ± 10.8[b]	54.0 ± 11.9[b]	55.0 ± 10.9	51.2 ± 11.2
Body mass index (kg/m^2)	28.8 ± 6.7	27.4 ± 5.8	28.6 ± 6.5[b]	25.9 ± 5.2[b]
Fruit and vegetable intake (servings/week)	16.0 ± 9.2	12.8 ± 8.7	15.3 ± 7.8[b]	9.8 ± 6.6[b]
Calories from fat (%)	29.7± 6.9[b]	32.0 ± 7.6[b]	29.3 ± 7.5	31.2 ± 7.3
Estrogen usage	31.1	26.6	32.0	21.4
Postmenopausal status (%)	77	71	64	68
Men	(n = 417)	(n = 70)	(n = 173)	(n = 29)
Age (Y)	57.3 ± 11.0[b]	53.1 ± 11.4[b]	55.4 ± 10.9[b]	49.8 ± 9.0[b]
Body mass index (kg/m^2)	28.4 ± 4.4[b]	27.0 ± 4.8[b]	28.7 ± 4.5	27.8 ± 4.2
Fruit and vegetable intake (servings/week)	13.5 ± 8.2[b]	10.4 ± 6.7[b]	13.1 ± 7.7	13.0 ± 13.0
Calories from fat (%)	30.7 ± 7.7[b]	33.9 ± 7.4[b]	32.7 ± 7.9	32.0 ± 6.4

[a]+ and — indicate presence and absence, respectively, of the corresponding variable; apolipoprotein ε_4 is considered present if at least one allele of ε_4 is present. NHLBI, National Heart, Lung, and Blood Institute.
[b]$P < 0.05$ comparing smokers with nonsmokers within category of apolipoprotein ε_4.

men who had apo ε_4 and smoked. There were no major changes of mean triglycerides according to smoking and apo ε_4 in either gender (Table 2). Additional analysis restricted to postmenopausal women revealed a stronger interaction between smoking and apo ε_4 for LDL and total cholesterol (Table 3).

DISCUSSION

Studies have reported a positive association between apolipoprotein ε_4 and plasma LDL and triglycerides (9–12). In addition, smoking has been shown to be associated with an increase in plasma LDL and triglycerides, and a decrease in HDL (13–20,29,30). Physiologic mechanisms by which different isoforms of apo E influence plasma cholesterol have been described: triglyceride-rich particles containing apo ε_4 are removed faster by the liver; the faster clearance of apo ε_4-rich particles results in downregulation of LDL receptors and subsequent increased level of plasma cholesterol (31). On the other hand, inconsistent findings have been reported on the mechanisms by which smoking may influence LDL cholesterol. Some authors have suggested that the effect of smoking on LDL is mediated through a reduction of lipoprotein lipase (21,32), whereas others have reported no difference in lipoprotein lipase activity between smokers and nonsmokers (33,34). Plasma lipases are important regulators of plasma lipoprotein composition. Lipoprotein lipase is a catalyst for triglyceride-rich lipoprotein hydrolysis and enables blood clearance of triglycerides. Hepatic lipase has been shown to be activated

TABLE 2
Multivariate Adjusted Means (SE) of Lipids According to Smoking Habit and Presence of Apolipoprotein ε_4 (at least one ε_4 allele) Among 1,472 Participants of the NHLBI Family Heart Study (1994–1996)[a]

Apolipoprotein ε_4[b]		—	—	+	+	P for
Cigarette smoking		—	+	—	+	interaction[c]
	n for women	479	79	197	28	
	n for men	417	70	173	29	
Low density cholesterol (mg/dL)	Women	129.3 (1.6)	134.4 (4.0)	132.0 (2.5)	152.9 (6.8)	0.00002
	Men	126.1 (1.7)	127.6 (4.2)	131.3 (2.6)	137.3 (6.4)	0.11
Total cholesterol (mg/dL)	Women	217.6 (1.9)	223.9 (4.6)	218.9 (2.9)	232.7 (7.8)	0.02
	Men	200.8 (1.8)	199.8 (4.5)	207.9 (2.8)	212.3 (6.9)	0.14
High density cholesterol (mg/dL)	Women	56.7 (0.6)	53.5 (1.0)	49.6 (1.6)	47.3 (2.7)	0.99
	Men	42.5 (0.5)	39.5 (0.8)	40.0 (1.2)	37.9 (1.9)	0.22
Total cholesterol to high density cholesterol ratio	Women	4.1 (0.1)	4.8 (0.1)	4.4 (0.1)	5.1 (0.2)	0.48
	Men	5.0 (0.1)	5.3 (0.2)	5.5 (0.1)	5.9 (0.3)	0.73
Ln [triglycerides] (mg/dL)[d]	Women	4.92 (0.02)	5.08 (0.06)	4.96 (0.04)	4.97 (0.10)	0.16
	Men	4.93 (0.03)	4.92 (0.07)	5.08 (0.04)	5.01 (0.10)	0.32

[a]Adjustment for age, age^2, calories from fat (%), fruit and vegetable consumption, body mass index, and estrogen for women; alcohol intake and physical activity were added in the model for high density lipoprotein cholesterol. For abbreviation see Table 1.
[b]+ and — indicate presence and absence, respectively, of the corresponding variable.
[c]Interaction between smoking and apolipoprotein ε_4.
[d]Natural logarithmic-transformed.

TABLE 3
Multivariate Adjusted Means (SE) of Lipids According to Smoking Habit and Presence of Apolipoprotein ε_4 (at least one ε_4 allele) Among 570 Postmenopausal Women in the NHLBI Family Heart Study (1994–1996)[a]

Apolipoprotein ε_4[b]		—	—	+	+	*P* for
Cigarette smoking		—	+	—	+	interaction[c]
	n	368	56	127	19	
Low density cholesterol (mg/dL)		132.6 (1.9)	132.7 (4.9)	135.0 (3.3)	160.2 (8.5)	0.00000
Total cholesterol (mg/dL)		224.5 (2.2)	223.6 (5.7)	226.6 (3.8)	241.9 (9.8)	0.0005
High density cholesterol (mg/dL)		59.3 (0.8)	52.6 (2.1)	54.3 (1.4)	49.7 (3.6)	0.59
Total cholesterol to high density cholesterol ratio		4.1 (0.1)	4.6 (0.2)	4.5 (0.1)	5.1 (0.3)	0.28
Ln [triglycerides] (mg/dL)[d]		4.9 (0.03)	5.1 (0.06)	5.1 (0.04)	5.1 (0.11)	0.25

[a]Adjustment for age, age^2, calories from fat (%), fruit and vegetable consumption, body mass index, and estrogen for women; alcohol intake and physical activity were added in the model for high density lipoprotein cholesterol. Numbers of premenopausal women were inadequate for separate analyses.
[b]+ and — indicate presence and absence, respectively, of the corresponding variable.
[c]Interaction between smoking and apolipoprotein ε_4.
[d]Natural logarithmic-transformed. For abbreviation see Table 1.

among smokers (33). This enzyme plays a role in converting very low density lipoprotein to LDL (35). An experimental study has shown that blood exposure to smoking leads to inhibition of lecithin:cholesterol acyl transferase (36). In addition, nicotine exerts hyperlipidemic effects by increasing the synthesis of triglyceride-rich lipoproteins (18).

In the present study, we demonstrated that cigarette smoking significantly modified the relation of apo ε_4 to LDL and total cholesterol among women. Although not statistically significant, the trend was suggestive of greater risk of higher LDL and total cholesterol among male smokers with apo ε_4. We are not aware of any previous study that assessed whether smoking interacts with apo ε_4 to influence plasma LDL, HDL, and triglycerides. Our results are consistent with previous reports indicating that both smoking and apo ε_4 are associated with increased LDL and total cholesterol (9–12,29,30).

In this study, subjects with apo ε_4 and current smoking status were on average younger than subjects in the other three groups. One possible explanation is that subjects with the apo ε_4 isoform who smoked may have died at a younger age from cardiovascular diseases than subjects without apo ε_4. If this hypothesis were true, our measure of effect would have been underestimated. The findings observed among women are not likely to be explained by estrogen use; the fact that women were not aware of their apolipoprotein genotype precludes differential estrogen use among women with ε_4 allele. The lack of statistically significant difference in the frequency distribution of estrogen use across smoking-ε_4 cross-classification in our data supports this hypothesis. Our results are unlikely to be influenced by recall bias, as subjects in this study were not aware of their apo E phenotype and thus were unlikely to show differential reporting of smoking habits. Furthermore, the use of standardized questionnaires and trained interviewers may have further minimized any information bias, which might have threatened the validity of this study.

In conclusion, this study shows that smoking modifies the relation of apo ε_4 to LDL among women; among men, there is a trend toward a similar relation. Subjects with apo ε_4 who smoke are at greater risk of CHD, elevated LDL, triglycerides, and lower HDL. Smoking cessation measures should be directed toward any smoker but should be enhanced among those with apo ε_4.

ACKNOWLEDGMENTS

Support was partially provided by the National Heart, Lung, and Blood Institute cooperative agreement grants U01 HL56563, U01 HL56564, U01 HL56565, U01 HL56566, U01 HL56567, U01 HL56568, U01 HL56569. This paper is presented on behalf of the investigators of the NHLBI Family Heart Study. Participating institutions and principal staff of the study are as follows: Forsyth County/University of North Carolina/Wake Forest University: Gerardo Heiss, Stephen Rich, Greg Evans; James Pankow; H.A. Tyroler, Jeannette T. Bensen, Catherine Paton, Delilah Posey, and Amy Haire; University of Minnesota Field Center: Donna K. Arnett, Aaron R. Folsom, Larry Atwood, James Peacock, and Greg Feitl; Boston University/Framingham Field Center: R. Curtis Ellison, Richard H. Myers, Yuqing Zhang, Andrew G. Bostom, Luc Djoussé, Jemma B. Wilk, and Greta Lee Splansky; University of Utah Field Center: Steven C. Hunt, Roger R. Williams (deceased), Paul N. Hopkins, Hilary Coon, and Jan Skuppin; Coordinating Center, Washington University, St. Louis: Michael A. Province, D.C. Rao, Ingrid B. Borecki, Yuling Hong, Mary Feitosa, Jeanne Cashman, and Avril Adelman; Central Biochemistry Laboratory, University of Minnesota: John H. Eckfeldt, Catherine Leiendecker-Foster, Michael Y. Tsai, and Greg Rynders; Central Molecular Laboratory, University of Utah: Mark F. Leppert, Jean-Marc Lalouel, Tena Varvil, Lisa Baird; National Heart, Lung, & Blood Institute—Project Office: Phyliss Sholinsky, Millicent Higgins (retired), Jacob Keller (retired), Sarah Knox, and Lorraine Silsbee.

REFERENCES

1. Laakso, M. (1996) Lipids and Lipoproteins as Risk Factors for Coronary Heart Disease in Non-Insulin-Dependent Diabetes Mellitus, *Ann. Med. 28*, 341–345.
2. Allen, J.K., Young, D.R., Blumenthal, R.S., Moy, T.F., Yanek, L.R., Wilder, L., Becker, L.C., and Becker, D.M. (1996) Prevalence of Hypercholesterolemia Among Siblings of Persons with Premature Coronary Heart Disease. Application of the Second Adult Treatment Panel Guidelines, *Arch. Int. Med. 156*, 1654–1660.
3. Schaefer, E.J., Lichtenstein, A.H., Lamon-Fava, S., McNamara, J.R., and Ordovas, J.M. (1995) Lipoproteins, Nutrition, Aging, and Atherosclerosis, *Am. J. Clin. Nutr. 61*, 726S–740S.
4. Poulter, N.R. (1990) Major Risk Factors for Coronary Heart Dis-

ease in Hypertension: Implications for Management. *J. Hum. Hypertens. 4, Suppl. 3*:3–6.
5. Manninen, V., Elo, M.O., Frick, M.H., Haapa. K., Heinonen, O.P., Heinsalmi, P., Helo, P., Huttunen, J.K., Kaitaniemi, P., and Koskinen, P. (1988) Lipid Alterations and Decline in the Incidence of Coronary Heart Disease in the Helsinki Heart Study, *JAMA 260*, 641–651.
6. Castelli, W.P. (1996) Lipids, Risk Factors and Ischaemic Heart Disease, *Atherosclerosis 124*, S1–S9.
7. Wilson, P.W., Schaefer, E.J., Larson, M.G., and Ordovas, J.M. (1996) Apolipoprotein E Alleles and Risk of Coronary Disease. A Meta-analysis, *Arterioscler. Thromb. Vasc. Biol. 16*, 1250–1255.
8. Tiret, L., de Knijff, P., Menzel, H.J., Ehnholm, C., Nicaud, V., and Havekes, L.M. (1994) ApoE Polymorphism and Predisposition to Coronary Heart Disease in Youths of Different European Populations. The EARS Study. European Atherosclerosis Research Study, *Arterioscler. Thromb. 14*, 1617–1624.
9. Gomez-Coronado, D., Alvarez, J.J., Entrala, A., Olmos, J.M., Herrera, E., and Lasuncion, M.A. (1999) Apolipoprotein E Polymorphism in Men and Women from Spanish Population: Allele Frequencies and Influence on Plasma Lipids and Apolipoproteins, *Atherosclerosis 147*, 167–176.
10. Boer, J.M., Ehnholm, C., Menzel, H.J., Havekes, L.M., Rosseneu, M., O'Reilly, D.S., and Tiret, L. (1997) Interactions Between Lifestyle-Related Factors and the ApoE Polymorphism on Plasma Lipids and Apolipoproteins. The EARS Study. European Atherosclerosis Research Study, *Arterioscler. Thromb. Vasc. Biol. 17*, 1675–1681.
11. Kataoka, S., Robbins, D.C., Cowan, L.D., Go, O., Yeh, J.L., Devereux, R.B., Fabsitz, R.R., Lee, E.T., Welty, T.K., Thomas, K., and Howard, B.V. (1996) Apolipoprotein E Polymorphism in American Indians and Its Relation to Plasma Lipoproteins and Diabetes: The Strong Heart Study, *Arterioscler. Thromb. Vasc. Biol. 16*, 918–925.
12. Murakami, K., Shimizu, M., Yamada, N., Ishibashi, S., Shimano, H., Yazaki, Y., and Akanuma, Y. (1993) Apolipoprotein E Polymorphism Is Associated with Plasma Cholesterol Response in a 7-Day Hospitalization Study for Metabolic and Dietary Control in NIDDM, *Diabetes Care 16*, 564–569.
13. Muscat, J.E., Harris, R.E., Haley, N.J., and Wynder, E.L. (1991) Cigarette Smoking and Plasma Cholesterol, *Am. Heart. J. 121*, 141–147.
14. Lee, K.S., Park, C.Y., Meng, K.H., Bush, A., Lee, S.H., Lee, W.C., Koo, J.W., and Chung, C.K. (1998) The Association of Cigarette Smoking and Alcohol Consumption with Other Cardiovascular Risk Factors in Men from Seoul, Korea, *Ann. Epidemiol. 8*, 31–38.
15. Butowski, P., and Winder, A. (1998) The Early Cardiovascular Toll of Cigarette Smoking in Dyslipidemic Patients in the United Kingdom, *Eur. J. Med. Res. 3,* 189–193.
16. Namekata, T., Moore, D.E., Suzuki, K., Mori, M., Knopp, R.H., Marcovina, S.M., Perrin, E.B., Hughes, D.A., Hatano, S., and Hayashi, C. (1997) Biological and Lifestyle Factors, and Lipid and Lipoprotein Levels Among Japanese Americans in Seattle and Japanese Men in Japan, *Int. J. Epidemiol. 26*, 1203–1213.
17. Vincelj, J., Sucic, M., Bergovec, M., Sokol, I., Mirat, J., Romic, Z., Lajtman, Z., Bergman-Markovic, B., and Bozikov, V. (1997) Serum Total, LDL, HDL Cholesterol and Triglycerides Related to Age, Gender and Cigarette Smoking in Patients with First Acute Myocardial Infarction, *Coll. Antropol. 21*, 517–524.
18. Ashakumary, L., and Vijayammal, P.L. (1997) Effect of Nicotine on Lipoprotein Metabolism in Rats, *Lipids 32*, 311–315.
19. Whitehead, T.P., Robinson, D., and Allaway, S.L. (1996) The Effects of Cigarette Smoking and Alcohol Consumption on Blood Lipids: A Dose-Related Study on Men, *Ann. Clin. Biochem. 33*, 99–106.
20. Craig, W.Y., Palomaki, G.E., and Haddow, J.E. (1989) Cigarette Smoking and Serum Lipid and Lipoprotein Concentrations: An Analysis of Published Data, *Br. Med. J. 298*, 784–788.
21. Freeman, D.J., Caslake, M.J., Griffin, B.A., Hinnie, J., Tan, C.E., Watson, T.D., Packard, C.J., and Shepherd, J. (1998) The Effect of Smoking on Post-Heparin Lipoprotein and Hepatic Lipase, Cholesteryl Ester Transfer Protein and Lecithin:Cholesterol Acyl Transferase Activities in Human Plasma, *Eur. J. Clin. Invest. 28*, 584–591.
22. Higgins, M., Province, M., Heiss, G., Eckfeldt, J., Ellison, R.C., Folsom, A.R., Rao, D.C., Sprafka, J.M., and Williams, R. (1996) NHLBI Family Heart Study: Objectives and Design, *Am. J. Epidemiol. 143*, 1219–1228.
23. Friedewald, W.T., Levy, R.I., and Fredrickson, D.S. (1972) Estimation of the Concentration of Low-Density Lipoprotein Cholesterol in Plasma, Without Use of the Preparative Ultracentrifuge, *Clin. Chem. 18*, 499–502.
24. Warnick, G.R., Benderson, J., and Albers, J.J. (1982) Dextran Sulfate-Mg^{2+} Precipitation Procedure for Quantitation of High-Density-Lipoprotein Cholesterol, *Clin. Chem. 28*, 1379–1388.
25. Reymer, P.W., Groenemeyer, B.E., van de Burg, R., and Kastelein, J.J. (1995) Apolipoprotein E Genotyping on Agarose Gels, *Clin. Chem. 41*, 1046–1047.
26. Willett, W.C., Sampson, L., Stampfer, M.J., Rosner, B., Bain, C., Witschi, J., Hennekens, C.H., and Speizer, F.E. (1985) Reproducibility and Validity of a Semiquantitative Food Frequency Questionnaire, *Am. J. Epidemiol. 122*, 51–65.
27. Rimm, E.B., Giovannucci, E.L., Stampfer, M.J., Colditz, G.A., Litin, L.B., and Willett, W.C. (1992) Reproducibility and Validity of an Expanded Self-Administered Semiquantitative Food Frequency Questionnaire Among Male Health Professionals, *Am. J. Epidemiol. 135*, 1114–1126.
28. *SAS/STAT User's Guide* (1989), version 6, 4th edn., Vol. 2, pp. 1071–1126, SAS Institute, Cary, NC.
29. Freeman, D.J., and Packard, C.J. (1995) Smoking and Plasma Lipoprotein Metabolism, *Clin. Sci. 89*, 333–342.
30. Brischetto, C.S., Connor, W.E., Connor, S.L., and Matarazzo, J.D. (1983) Plasma Lipid and Lipoprotein Profiles of Cigarette Smokers from Randomly Selected Families: Enhancement of Hyperlipidemia and Depression of High-Density Lipoprotein, *Am. J. Cardiol. 52*, 675–680.
31. Tikannen, M.J., Huttunen, J.K., Ehnholm, C., and Pietinen, P. (1990) Apolipoprotein E4 Homozygosity Predisposes to Serum Cholesterol Elevation During High Fat Diet, *Arteriosclerosis 10*, 285–288.
32. Freeman, D.J., Griffin, B.A., Murray, E., Lindsay, G.M., Gaffney, D., Packard, C.J., and Shepherd, J. (1993) Smoking and Plasma Lipoproteins in Man: Effects on Low Density Lipoprotein Cholesterol Levels and High Density Lipoprotein Subfraction Distribution, *Eur. J. Clin. Invest. 23*, 630–640.
33. Moriguchi, E.H., Fusegawa, Y., Tamachi, H., and Goto, H. (1991) Effects of Smoking on HDL Subfractions in Myocardial Infarction Patients: Effects on Lecithin-Cholesterol Acyl Transferase and Hepatic Lipase, *Clin. Chim. Acta. 195*, 139–143.
34. Eliasson, B., Mero, N., Taskinen, M.R., and Smith, U. (1997) The Insulin Resistance Syndrome and Postprandial Lipid Intolerance in Smokers, *Atherosclerosis 129*, 79–88.
35. Packard, C.J., and Shepherd, J. (1993) Lipoprotein Metabolism in Lipase Deficient States: Studies in Primary and Secondary Hyperlipidemia, *Biochem. Soc. Trans. 21*, 503–506.
36. McCall, M.R., van den Berg, J.J., Kuypers, F.A., Tribble, D.L., Krauss, R.M., Knoff, L.J., and Forte, T.M. (1994) Modification of LCAT Activity and HDL Structure. New Links Between Cigarette Smoke and Coronary Heart Disease Risk, *Arterioscler. Thromb. 14*, 248–253.

[Received March 8, 2000, and in revised form June 5, 2000; revision accepted June 12, 2000]

Variability of the Intestinal Uptake of Lipids Is Genetically Determined in Mice

M. Keelan[a], D.Y. Hui[b], G. Wild[c], M.T. Clandinin[a], and A.B.R. Thomson[a]

[a]Nutrition and Metabolism Research Group, Department of Medicine, Division of Gastroenterology, University of Alberta, Edmonton, Alberta, T6G 2C2 Canada, [b]Department of Pathology and Laboratory Medicine, University of Cincinnati College of Medicine, Cincinnati, Ohio 45267, and [c]Department of Medicine, Division of Gastroenterology, McGill University Health Centre, Montréal, Québec, H3G 1A4 Canada

ABSTRACT: The response of the plasma cholesterol concentration to changes in dietary lipids varies widely in humans and animals. There are variations in the *in vivo* absorption of cholesterol between different strains of mice. This study was undertaken in three strains of inbred mice to test the hypotheses that: (i) there are strain differences in the *in vitro* uptake of fatty acids and cholesterol and (ii) the adaptability of the intestine to respond to variations in dietary lipids is genetically determined. An *in vitro* intestinal ring technique was used to assess the uptake of medium- and long-chain fatty acids and cholesterol into jejunum and ileum of adult DBA/2, C57BL6, and C57L/J mice. The jejunal uptake of cholesterol was similar in C57L/J, DBA/2, or C57BL6 fed *ad libitum* a low-fat (5.7% fat, no cholesterol) chow diet. This is in contrast to a previous demonstration that *in vivo* cholesterol absorption was lower in C57L/J than in the other murine strains. The jejunal uptake of several long-chain fatty acids was greater in DBA/2 fed for 4 wk the high-fat (15.8% fat and 1.25% cholesterol) as compared with the low-fat diet. Furthermore, on the high-fat diet, the uptake of many long-chain fatty acids was higher in DBA/2 than in C57BL6 or C57L/J. The differences in cholesterol and fatty acid uptake were not explained by variations in food uptake, body weight gain, or the weight of the intestine. In summary: (i) there are strain differences in the *in vitro* intestinal uptake of fatty acids but not of cholesterol; (ii) a high-fat diet enhances the uptake of long-chain fatty acids in only one of the three strains examined in this study; and (iii) the pattern of strain- and diet-associated alterations in the *in vivo* absorption of cholesterol differs from the pattern of changes observed *in vitro*. We speculate that genetic differences in cholesterol and fatty acid uptake are explained by variations in the expression of protein-mediated components of lipid uptake.

Paper no. L8234 in *Lipids 35*, 833–837 (August 2000)

The response of the plasma cholesterol concentration to changes in dietary lipids varies widely in humans and in animals (1–8). Alterations in the efficiency of cholesterol absorption can account for differences in serum cholesterol concentrations between hypo- and hyper-responding rabbits after feeding a cholesterol-rich diet (9). Using human intestinal biopsy samples, Safonova and co-workers (10) demonstrated that cholesterol uptake is clustered into low, medium, and high rates. The suggestion that cholesterol absorption might be regulated by specific gene(s) was strengthened by the recent study by Carter and co-workers using inbred strains of mice (11). They showed that cholesterol absorption measured with an *in vivo* fecal recovery technique varied between mouse strains under low dietary fat conditions. Furthermore, there were different changes between strains in cholesterol absorption observed in response to feeding a high-fat/cholesterol diet.

This study was undertaken to determine (i) if the initial uptake step in cholesterol absorption varied between three inbred mouse strains and in response to a high-fat diet and (ii) if the variability in cholesterol uptake also included the uptake of fatty acids. The results support the hypothesis that the specific gene(s) controlling cholesterol uptake are different from those which influence the uptake of long-chain fatty acids and that the adaptation of lipid uptake in response to alterations in dietary fats is also regulated by genetic factors. Furthermore, the reported genetically influenced differences in the *in vivo* absorption of cholesterol cannot be explained by variations in the uptake step demonstrated *in vitro*.

METHODS

Animals and diets. The C57BL6 and DBA/2 mice were purchased from Harlan Bioproducts (Indianapolis, IN), and C57L/J mice were obtained from The Jackson Laboratories (Bar Harbor, ME). Male chimeric mice derived from cholesterol esterase gene-targeted embryonic stem cells, with a 129/SvEv genetic background, were mated with female Black Swiss mice (12). Heterozygotes from different parents were mated with female Black Swiss mice. Black Swiss and 129/SvEv mice were obtained from Taconic Farms (Germantown, NY). Animals with the normal cholesterol esterase genotype were selected for the current study. The mice were housed in a temperature- and humidity-controlled room with a 12-h light/dark cycle for at least 7 d before experiments. Female mice between the ages of 10 and 12 wk were used for all ex-

*To whom correspondence should be addressed at Department of Gastroenterology, University of Alberta, 519 Robert Newton Research Building, Edmonton, Alberta T6G 2C2, Canada. E-mail: alan.thomson@ualberta.ca

Abbreviations: BBM, brush border membrane; FAT, fatty acid transporter; UWL, unstirred water layer.

periments. The mice were fed either the basal nonpurified low-fat chow diet (Teklad LM485; Madison, WI) containing 5.7% fat and no cholesterol or a high-fat/high-cholesterol nonpurified diet (Purina Mouse Chow 5015 supplemented with 7.5% cocoa butter and 1.25% cholesterol to yield final concentrations of 15.8% fat and 1.25% cholesterol). Mice were fed *ad libitum* the high-fat/high-cholesterol diet for at least 4 wk, and up until the morning that the transport studies were performed. All experimental protocols described in the text were reviewed and approved by the Institutional Animal Care and Use Committee of the University of Cincinnati and the Health Sciences Animal Welfare Committee of the University of Alberta, in compliance with Guide for Care and Use of Laboratory Animals and the Canadian Committee on Animal Care, respectively.

Probe and marker compounds. [^{3}H]-inulin was used as a nonabsorbable marker to correct for the adherent mucosal fluid volume. The [^{14}C]-labeled probes included lauric acid (12:0), palmitic acid (16:0), stearic acid (18:0), oleic acid (18:1), linoleic acid (18:2n-6), linolenic acid (18:3n-3), and cholesterol. D- and L-glucose uptake was assessed as a control for the anticipated changes in lipid uptake. Unlabeled and [^{14}C]-labeled probes were supplied by Sigma Co. (St. Louis, MO) and New England Nuclear (Boston, MA), respectively. Probes were shown by the manufacturer to be more than 99% pure by high-performance liquid chromatography.

Tissue preparation and determination of uptake rates. The *in vitro* uptake into everted intestinal rings was examined in mouse jejunum and ileum. Animals were weighed at the time of sacrifice. Animals were anesthetized by the intraperitoneal injection of Euthanyl® (pentobarbital, 35 mg/kg body weight; MTC Pharmaceuticals, Mississauga, Ontario, Canada). A midline incision was made into the peritoneal cavity. The ligament of Treitz, which marks the proximal end of the jejunum, was clamped and cut. The small intestine was pulled out until it reached the ileocecal junction, which marks the distal end of the ileum. The whole length of small intestine was removed rapidly. In these studies, the jejunum was represented by the proximal third and the ileum by the distal third of the removed intestine; the middle third of the intestine was discarded.

The intestine was everted and cut into small rings of approximately 3 mm each, which were immersed immediately in pre-incubation beakers containing oxygenated Krebs-bicarbonate buffer (pH 7.2) at 37°C (13). The rings were allowed to equilibrate for approximately 5 min prior to commencement of the uptake studies. Nutrient uptake was initiated by the timed transfer of everted tissue rings into a shaking water bath (37°C) containing 5-mL plastic vials with oxygenated Krebs buffer plus [^{3}H]-inulin and one of the following [^{14}C]-labeled substrates: 0.1 mM fatty acids (12:0, 16:0, 18:0, 18:1, 18:2, 18:3), 0.05 mM cholesterol. The long-chain fatty acids and cholesterol were solubilized in 20 mM taurocholic acid. The uptake of glucose was also assessed to establish whether strain differences in lipid uptake also influenced the active carrier-mediated uptake of a water-soluble nutrient: the concentrations of D-glucose were 4, 8, 16, 32, and 64 mM, and L-glucose 16 mM. After incubation for 5 min, the uptake of nutrient was terminated by pouring the vial contents onto filters on an Amicon vacuum filtration manifold (Millipore Canada Ltd., Nepean, Ontario, Canada) maintained under suction, followed by washing the jejunal or ileal rings with ice-cold saline. The tissue was dried overnight at 55°C to a constant weight. The dry weight of tissues was determined, and the tissues were saponified with 0.75 N NaOH. Scintillation fluid was added, and radioactivity was determined by means of an external standardization technique to correct for variable quenching of the two isotopes.

Expression of the results. The rates of uptake were expressed as nanomoles of substrate taken up per milligram dry weight of tissue per minute (nmol·mg tissue^{-1}·min^{-1}). The values obtained from the dietary groups are reported as the means ± SEM for results obtained from five to six animals in each group.

Glucose uptake kinetics were determined by fitting the observed data points to the Michaelis-Menten equation and by nonlinear regression analysis using the Sigma Plot (Jandel Scientific, San Rafael, CA) program for best fit curves. As variance increased with the size of the y-axis variable (rate of uptake of glucose), data points were weighted in proportion to the reciprocal of the within-concentration estimates of variance (14).

Analysis of variance was used to test for a difference between the five dietary groups. Individual differences were determined using a Student Neuman-Keuls multiple range test. A value of $P < 0.05$ was accepted as statistically significant.

RESULTS

There were no differences between the three strains of mice in the rates of jejunal or ileal uptake of cholesterol when the animals were fed either chow or the high-fat diet (Table 1). When fed chow, the jejunal uptake of 12:0 was highest and 18:3 was lowest in the C57L/J mice as compared with the other animals, whereas the ileal uptake of 18:0 was highest. When the animals were fed the high-fat diet, the jejunal uptake of 16:0, 18:2, and 18:3 was highest in DBA/2, and the ileal uptakes of 16:0 and 18:1 were also highest in this strain. In C57L/J fed chow or the high-fat diet, the jejunal uptake of 12:0 was greater than in DBA/2 or C57BL6.

The chow and high-fat/cholesterol diets were not isocaloric, but the animals were fed *ad libitum* and there were no differences in food intake (Table 2). The rate of body weight gain was lower in C57L/J fed either chow or the high-fat diet, as compared with DBA/2 or C57BL6. The variations in fatty acid uptake were not due to any differences in the animals' food intake, the weight of the intestine, or the weight of the mucosa (Table 2).

A curvilinear relationship was noted between glucose concentration and uptake (data not shown). In the jejunum the rate of uptake of L-glucose was unchanged by diet or by the strain of mouse. In the ileum, uptake of L-glucose was lower in C57L/J mice fed the basal diet. When the high-fat diet was fed, the uptake of L-glucose was higher in C57L/J than in the other two strains. After correcting for the minor differences in passive uptake, there were no differences in the maximal transport rate (V_{max}) or the apparent Michaelis affinity constant (K_m) for jejunal or ileal glucose uptake between DBA/2, C57BL6, or C57L/J (Table 3).

TABLE 1
Effect of Dietary Lipids on the *in vitro* Uptake of Lipids in Different Strains of Mice[a]

	Chow diet			High-fat/cholesterol diet		
Lipid	DBA/2[b]	C57BL6[b]	C57L/J[c]	DBA/2	C57BL6	C57L/J
Jejunum						
Fatty acids						
12:0	11.1 ± 2.1	16.1 ± 1.0[a]	18.3 ± 1.2[a]	11.3 ± 1.5	13.8 ± 1.1	17.5 ± 2.2[a]
16:0	2.3 ± 0.4	2.5 ± 0.3	2.0 ± 0.3	4.1 ± 0.6[a]	2.3 ± 0.3[a]	2.8 ± 0.4[a]
18:0	2.0 ± 0.4	1.9 ± 0.3	1.6 ± 0.2	2.7 ± 0.3	2.1 ± 0.2	2.2 ± 0.5
18:1	2.2 ± 0.4	2.0 ± 0.4	2.3 ± 0.2	3.2 ± 0.4	2.1 ± 0.2	2.3 ± 0.4
18:2	1.7 ± 0.4	2.0 ± 0.3	1.5 ± 0.2	3.4 ± 0.5[c]	1.8 ± 0.3[a]	1.2 ± 0.3[a]
18:3	2.0 ± 0.2	1.7 ± 0.2	1.0 ± 0.2[a,b]	3.2 ± 0.5[c]	1.8 ± 0.3[a]	2.0 ± 0.5[a]
Cholesterol	0.6 ± 0.2	0.4 ± 0.1	0.7 ± 0.2	0.8 ± 0.4	0.7 ± 0.4	0.5 ± 0.1
Ileum						
Fatty acids						
12:0	17.2 ± 2.9	13.0 ± 1.9	9.1 ± 1.5	21.8 ± 2.8	12.8 ± 1.3[a]	15.8 ± 1.9
16:0	1.8 ± 0.6	1.7 ± 0.3	1.2 ± 0.3	3.8 ± 0.8[c]	0.9 ± 0.2[a]	1.8 ± 0.5[a]
18:0	1.1 ± 0.2	1.7 ± 0.2	2.4 ± 0.5[a]	2.2 ± 0.4	1.4 ± 0.4	1.6 ± 0.3
18:1	1.5 ± 0.6	0.9 ± 0.1	2.1 ± 0.6	3.0 ± 0.6	1.2 ± 0.3[a]	1.6 ± 0.3[a]
18:2	1.0 ± 0.2	0.8 ± 0.2	1.5 ± 0.5	2.3 ± 0.8	0.9 ± 0.5	1.6 ± 0.4
18:3	1.2 ± 0.2	1.6 ± 0.2	1.4 ± 0.5	2.9 ± 0.6	2.7 ± 0.8	1.6 ± 0.3
Cholesterol	0.8 ± 0.4	0.4 ± 0.1	0.3 ± 0.2	0.6 ± 0.3	0.6 ± 0.1	0.2 ± 0.1

[a]Means ± SEM, nmol·100 mg^{-1}·min^{-1}·0.1 mM^{-1}. [a]$P < 0.05$, vs. DBA/2. [b]$P < 0.05$, vs. C57BL6. [c]$P < 0.05$, high-cholesterol diet vs. standard chow diet.
[b]Harlan Bioproducts (Indianapolis, IN).
[c]The Jackson Laboratories (Bar Harbor, ME).

TABLE 2
Effect of Dietary Lipids on Animal Characteristics[a]

	Chow diet			High-fat/cholesterol diet		
	DBA/2	C57BL6	C57L/J	DBA/2	C57BL6	C57L/J
Food intake (g/mouse/d)	3.5 ± 0.2	5.4 ± 1.3	3.5 ± 0.6	2.5 ± 0.5	7.4 ± 1.2	2.9 ± 0.5
Body weight gain (g/mouse/d)	0.39 ± 0.10	0.22 ± 0.04	0.00 ± 0.02[a,b]	0.24 ± 0.09	0.34 ± 0.07	0.07 ± 0.04[b]
Jejunum						
Mucosa (mg/cm)	2.5 ± 0.5	4.1 ± 1.1	4.4 ± 0.5	4.6 ± 0.9	3.5 ± 0.6	4.1 ± 0.7
Remainder of intestine (mg/cm)	3.3 ± 0.3	2.4 ± 0.2	4.5 ± 0.6	4.2 ± 0.9	2.9 ± 0.3	3.2 ± 0.4
Ileum						
Mucosa (mg/cm)	1.7 ± 0.4	2.4 ± 0.4	1.7 ± 0.3	3.0 ± 0.6	2.8 ± 0.6	2.7 ± 0.5
Remainder of intestine (mg/cm)	1.9 ± 0.3	3.5 ± 0.8	1.7 ± 0.3	1.8 ± 0.2	2.5 ± 0.6	2.0 ± 0.2

[a]Significance: [a]$P < 0.05$, vs. DBA/2. [b]$P < 0.05$, vs. C57BL6. See Table 1 for company sources.

TABLE 3
Effect of Dietary Lipids on *in vitro* Uptake of Glucose in Different Strains of Mice[a]

	Standard chow diet			High-cholesterol diet		
	DBA/2	C57BL6	C57L/J	DBA/2	C57BL6	C57L/J
Jejunum						
V_{max}	441 ± 143	653 ± 136	1121 ± 357	685 ± 119	652 ± 214	815 ± 107
K_m	11.9 ± 4.2	7.9 ± 3.7	12.2 ± 3.2	3.3 ± 1.2	10.6 ± 3.0	7.9 ± 2.7
Ileum						
V_{max}	450 ± 119	851 ± 194	559 ± 198	777 ± 210	445 ± 129	232 ± 70
K_m	8.0 ± 0.6	4.9 ± 2.8	9.0 ± 3.0	8.6 ± 2.5	7.8 ± 5.6	4.0 ± 0.6

[a]V_{max}, maximal transport rate (nmol·mg $tissue^{-1}$·min^{-1}); K_m, apparent Michaelis constant (mM). These values are not statistically different from each other ($P > 0.05$) and represent the means ± SEM of estimates calculated from individual animals. See Table 1 for company sources.

DISCUSSION

The topic of the intestinal absorption of lipids has been reviewed (15,16). Once cholesterol or long-chain fatty acids have been solubilized in bile salt micelles in the intestinal lumen, they diffuse across the intestinal unstirred water layer (UWL). The lipids then partition from the micelle, either directly into the lipophilic enterocyte brush border membrane (BBM) or into an aqueous phase, and then diffuse across the BBM. There also may be a carrier-mediated component to the uptake of fatty acids and cholesterol (7,8,10,17–20).

There was no difference in the initial step of cholesterol uptake observed between the three murine strains (Table 1). The greater *in vitro* uptake of 12:0 into the jejunum of C57L/J fed chow or the high-fat diet suggests but does not prove that the UWL resistance is lower in these animals than in the DBA/2 or C57BL6 mice (21). The measurement of the uptake of fatty acid 12:0 is not the ideal measure of UWL resistance, and the value of the diffusion coefficient for cholesterol under these conditions is unknown. Thus, the BBM permeability of cholesterol in C57L/J is either similar to or higher than in the two other strains of mice. This is in contrast to the lower *in vivo* absorption of cholesterol in the C57L/J mice when fed either the low-fat chow or the high-fat diet (11). Thus, the strain differences in the intestinal absorption of cholesterol observed *in vivo* (11) cannot be explained simply on the basis of variations in the uptake step when studied *in vitro.* Although these strain differences in the *in vivo* as compared with *in vitro* absorption of cholesterol may result from the presence of bile, an intact blood circulation, diet, or desquamated cells, the possibility exists that there may be genetic variations related to the process of digestion of the luminal lipids prior to absorption by the enterocytes, intracellular metabolism, or transport out of the enterocyte.

Genetic differences in the lipid uptake of long-chain fatty acids have not been reported. In this study the mice fed chow did not display major differences in jejunal or ileal uptake of long-chain fatty acids, but, when fed the high-fat diet, the uptake of most fatty acids was greater in DBA/2 than in C57BL6 or C57L/J mice (Table 1). DBA/2 mice also had a greater uptake of lipids when fed the high- as compared with the low-fat diet. This suggests that uptake of long-chain fatty acids is also genetically influenced and that the pattern is different from changes observed in the *in vivo* absorption of cholesterol (11). Of note, the uptake of only some fatty acids was affected by strain differences. This argues for the change in the uptake process not being the result of a general alteration in the lipophilic properties of the BBM, which would have been expected to have altered the uptake of all lipids. Instead, the finding of the change in the uptake of only some fatty acids argues in favor of there being BBM or cytosolic proteins mediating the uptake of only some lipids, or having a greater affinity for the transport of some lipids. Furthermore, the variability in lipid uptake between the three strains when fed chow was different when they were fed the high-fat diet. This suggests that there may be involvement of a protein-mediated component in lipid absorption, as has been proposed by others (7,19,21–23).

Feeding a sunflower oil-enriched diet upregulated fatty acid transporter (FAT) mRNA 2.6-fold over feeding a medium-chain triglyceride-enriched diet (21). The increases in linoleic acid and linolenic acid uptake in DBA/2 mice after fat and cholesterol feeding reported in the present study may be associated with the upregulation of FAT. The binding of several long-chain fatty acids (stearic acid, oleic acid, arachidonic acid) to FAT was not significantly different from each other (22), but studies were not done on linoleic acid, linolenic acid, docosahexaenoic acid, or short-chain fatty acids. Furthermore, the differences in lipid uptake between strains fed the low-fat vs. the high-fat diet raise the possibility that there may be several genes modifying cholesterol and long-chain fatty acid uptake.

The uptake of glucose is mediated by a sodium-dependent transporter in the BBM, SGLT1 (24). The activity of SGLT1 may be influenced by the lipophilic properties of the BBM (25). For this reason, we speculated that if the strain-associated alterations in cholesterol and long-chain fatty acid absorption were on the basis of changes in the lipophilic properties of the BBM, then glucose uptake also might have been influenced. However, there was no effect of strain differences on the values of the V_{max} or K_m for glucose uptake (Table 3). Therefore, this also suggests that the mechanism(s) responsible for the strain-associated change in the uptake of cholesterol and long-chain fatty acids is not a process caused by generalized alterations in the lipophilic properties of the BBM.

The lower rate of body weight gain in C57L/J as compared with DBA/2 or C57BL6 fed either chow or the high-fat diet occurred despite similar amounts of food being ingested (Table 2).The lower rate of uptake of some long-chain fatty acids in C57L/J fed the high-fat diet may have contributed in part to their lower body weight gain as compared with DBA/2, in which fatty acid uptake and weight gain were both higher. However, this would not explain the greater weight gain in C57BL6 than C57L/J, since there were similar rates of fatty acid uptake (Table 1). Presumably, the lower rate of weight gain in C57L/J was due to lower total lipid absorption, and not just to lower rates of lipid uptake. This speculation of the difference between murine strains and the *in vitro* fatty acid uptake vs. *in vivo* absorption is supported by the variations between the *in vivo* absorption and the *in vitro* uptake of cholesterol, in which absorption was lowest in C57L/J (11) but *in vitro* uptake was similar in the three strains (Table 1).

In this study we did not determine which protein-mediated component might be responsible for the strain-associated variations in fatty acid uptake observed when the mice were fed the low- or the high-fat diets. The failure of some strains to modify their lipid uptake when switched from a high- to a low-fat diet leads us to speculate that dietary lipid modification is likely to be a successful therapeutic strategy to modify the exogenous contribution of lipids to hyperlipidemia only in those strains which are genetically capable of modifying

their lipid absorption in response to dietary lipid changes. We speculate that these genetically determined differences in cholesterol and fatty acid uptake and absorption also may exist in humans and may be responsible for known variations in cholesterol absorption between individuals (i.e., hypo- and hyper-responsiveness), as well as their variable responses to a high-cholesterol/lipid diet (1–6,9,10,18). If a marker could be discovered in humans for high rates of lipid uptake and absorption, this would potentially lead the way to screening young persons before the development of hyperlipidemia. Such a marker also would be useful to determine which persons with hyperlipidemia would be most likely to respond to dietary treatment with a low-fat/cholesterol diet. Finally, finding the gene products responsible for the variations in cholesterol and fatty acid uptake and absorption would open the way to the development of targeted therapeutic agents which could reduce the absorption of lipids for the treatment of hyperlipidemia or obesity.

ACKNOWLEDGMENTS

The authors wish to express their appreciation to Cindy Anaka and Rachel Jacobs for word-processing skills and to Scott Lindeman for technical assistance. This work was supported in part by grants from the Medical Research Council (Canada), the Dairy Bureau (Canada), and the Crohn's and Colitis Foundation of Canada, and the National Institutes of Health Grant # DK40917 and # DK46405. Dr. G. Wild is a senior research scholar of Les Fonds de la Recherche en Sante du Quebec.

REFERENCES

1. Aubert, R., Perdereau, D., Roubiscoul, M., Herzog, J., and Lemonnier, D. (1988) Genetic Variations in Serum Lipid Levels of Inbred Mice and Response to Hypercholesterolemic Diet, *Lipids 23*, 48–54.
2. Bhattacharyya, A.K., Baker, H.N., Eggen, D.A., Malcolm, G.T., Roheim, P.S., and Strong, J.P. (1989) Effect of Cholesterol Feeding on Lipolytic Activities in High- and Low-Responding Rhesus Monkeys, *Arteriosclerosis 9*, 380–389.
3. Bhattacharyya, A.K., and Eggen, D.A. (1988) Studies on the Mechanisms of High Intestinal Absorption of Cholesterol and Campesterol in High-Responding Rhesus Monkeys, *Atherosclerosis 72*, 109–114.
4. Kirk, E.A., Moe, G.L., Caldwell, M.T., Lernmark, J.A., Wilson, D.L., and LeBoeuf, R.C. (1995) Hyper- and Hypo-Responsiveness to Dietary Fat and Cholesterol Among Inbred Mice: Searching for Level and Variability Genes, *J. Lipid Res. 36*, 1522–1532.
5. McNamura, D.J., Kolb, R., Parker, T.S., Batwin, H., Simon, P., Brown, C.D., and Ahrens, E.H. (1987) Heterogeneity of Cholesterol Responsiveness in Man, *J. Clin. Invest. 79*, 1729–1739.
6. Mahley, R.W., Weisgraber, K.H., and Innerarity, T.L. (1974) Canine Lipoproteins and Atherosclerosis II. Characterization of the Plasma Lipoproteins Associated with Atherogenic and Nonatherogenic Hyperlipidemia, *Circ. Res. 35*, 722–733.
7. Thurnhofer, H.J., Schnabel, J., Betz, M., Lipka, G., Pidgeon, C., and Hauser, H. (1991) Cholesterol-Transfer Protein Located in the Intestinal Brush-Border Membrane. Partial Purification and Characterization, *Biochim. Biophys. Acta 1064*, 275–286.
8. Lipka, G., Schulthess, G., Thurnhofer, H., Wacker, H., Wehrli, E., Zeman, K., Weber, F.E., and Hauser, H. (1995) Characterization of Lipid Exchange Proteins Isolated from Small Intestinal Brush Border Membrane, *J. Biol. Chem. 270*, 5917–5925.
9. Overturf, M.L., Smith, S.A., and Gotto, A.M. (1990) Dietary Cholesterol Absorption and Sterol and Bile Acid Excretion in Hypercholesterolemia-Resistant White Rabbits, *J. Lipid Res. 31*, 2019–2027.
10. Safonova, I.G., Sviridov, D.D., Roytman, A., Rytikov, F.M., Dolgov, V.V., Nano, J.L., Rampal, P., and Repin, V.S. (1993) Cholesterol Uptake in the Human Intestine, *Biochim. Biophys. Acta 1166*, 313–316.
11. Carter, C.P., Howles, P.N., and Hui, D.Y. (1997) Genetic Variation in Cholesterol Absorption Efficiency Among Inbred Strains of Mice, *J. Nutr. 127*, 1344–1348.
12. Howles, P.N., Carter, C.P., and Hui, D.Y. (1996) Dietary Free and Esterified Cholesterol Absorption in Cholesterol Esterase (bile salt-stimulated lipase) Gene-Targeted Mice, *J. Biol. Chem. 271*, 7196–7202.
13. Perin, N., Keelan, M., Clandinin, M.T., and Thomson, A.B.R. (1997) Ontogeny of Intestinal Absorption Adaptation in Rats in Response to Isocaloric Changes in Dietary Lipids, *Am. J. Physiol. 273*, G713–G720.
14. Fingerote, R.J., Doring, K.A., and Thomson, A.B.R. (1994) Gradient for Glucose and Linoleic Acid Uptake Along the Crypt-Villus Axis of Rabbit Jejunal Brush Border Membrane Vesicles, *Lipids 29*, 117–127.
15. Tso, P. (1994) Intestinal Lipid Absorption, in *Physiology of the Gastrointestinal Tract*, pp. 1867–1907, Raven Press, New York.
16. Thomson, A.B.R., Schoeller, C., Keelan, M., Smith, L., and Clandinin, M.T. (1993) Lipid Absorption: Passing Through the Unstirred Layers, Brush Border Membrane and Beyond, *Can. J. Physiol. Pharm. 71*, 531–555.
17. Schroeder, F., Jefferson, J.R., Powell, D., Incerpi, S., Woodford, J.K., Colles, S.M., Myers-Payne, S., Emge, T., Hebbell, T., and Moncecchi, D. (1993) Expression of Rat L-FABP in Mouse Fibroblasts: Role in Fat Absorption, *Mol. Cell. Biochem. 123*, 73–83.
18. Paigen, B. (1995) Genetics of Responsiveness to High-Fat and High-Cholesterol Diets in the Mouse, *Am. J. Clin. Nutr. 62*, 458S–462S.
19. Schoeller, C., Keelan, M., Mulvey, G., Stremmel, W., and Thomson, A.B.R. (1995) Oleic Acid Uptake into Rat and Rabbit Jejunal Brush Border Membrane, *Biochim. Biophys. Acta 1236*, 51–64.
20. Stremmel, W. (1988) Uptake of Fatty Acids by Jejunal Mucosal Cells Is Mediated by a Fatty Acid-Binding Membrane Protein, *J. Clin. Invest. 82*, 2001–2010.
21. Poirier, H., Degrace, P., Niot, I., Bernard, A., and Besnard, P. (1996) Localization and Regulation of the Putative Membrane Fatty-Acid Transporter (FAT) in the Small Intestine. Comparison with Fatty Acid-Binding Proteins (FABP), *Eur. J. Biochem. 238*, 368–373.
22. Baille, A.G.S., Coburn, C.T., and Abumrad, N.A. (1996) Reversible Binding of Long-Chain Fatty Acids to Purified FAT, the Adipose CD36 Homolog, *J. Membr. Biol. 153*, 75–81.
23. Ibrahimi, A., Sfeir, Z., Magharaie, H., Amri, E., Grimaldi, P., and Abumrad, N.A. (1996) Expression of the CD36 Homolog (FAT) in Fibroblast Cells: Effect on Fatty Acid Transport, *Proc. Natl. Acad. Sci. USA 93*, 2646–2651.
24. Hediger, M.A., and Rhoads, D.B. (1994) Molecular Physiology of Sodium-Glucose Cotransporters, *Physiol. Rev. 74*, 993–1026.
25. Meddings, J.B., and Theisen, S. (1989) Development of Rat Jejunum: Lipid Permeability, Physical Properties, and Chemical Composition, *Am. J. Physiol. 256*, G931–G940.

[Received April 12, 1999, and in final revised form January 21, 2000; revision accepted January 28, 2000]

Electrospray Ionization Mass Spectrometric Analyses of Changes in Tissue Phospholipid Molecular Species During the Evolution of Hyperlipidemia and Hyperglycemia in Zucker Diabetic Fatty Rats

Fong-Fu Hsu, Alan Bohrer, Mary Wohltmann, Sasanka Ramanadham, Zhongmin Ma, Kevin Yarasheski, and John Turk*

Medicine Department Mass Spectrometry Facility, Division of Diabetes, Endocrinology, and Metabolism, Washington University School of Medicine, St. Louis, MO 63110

ABSTRACT: The Zucker diabetic fatty (ZDF) rat is a genetic model of type II diabetes mellitus in which males homozygous for nonfunctional leptin receptors (fa/fa) develop obesity, hyperlipidemia, and hyperglycemia, but rats homozygous for normal receptors (+/+) remain lean and normoglycemic. Insulin resistance develops in young fa/fa rats and is followed by evolution of an insulin secretory defect that triggers hyperglycemia. Because insulin secretion and insulin sensitivity are affected by membrane phospholipid fatty acid composition, we have determined whether metabolic abnormalities in fa/fa rats are associated with changes in tissue phospholipids. Electrospray ionization mass spectrometric analyses of glycerophosphocholine (GPC) and glycerophosphoethanolamine (GPE) molecular species from tissues of prediabetic (6 wk of age) and overtly diabetic (12 wk) fa/fa rats and from +/+ rats of the same ages indicate that arachidonate-containing species from heart, aorta, and liver of prediabetic fa/fa rats made a smaller contribution to GPC total ion current than was the case for +/+ rats. There was a correspondingly larger contribution from species with *sn*-2 oleate or linoleate substituents in fa/fa heart and aorta. The relative contributions of arachidonate-containing GPC species increased in these tissues as fa/fa rats aged and were equal to or greater than those for +/+ rats by 12 wk. For heart and aorta, relative contributions from GPE species with *sn*-2 arachidonate or docosahexaenoate substituents to the total ion current increased and those from species with *sn*-2 oleate or linoleate substituents fell as fa/fa rats aged, but these tissue lipid profiles changed little with age in +/+ rats. GPC and GPE profiles for brain, kidney, sciatic nerve, and red blood cells were similar among fa/fa and +/+ rats at 6 and 12 wk of age, and pancreatic islets from fa/fa and +/+ rats exhibited similar GPC and GPE profiles at 12 wk of age. Under-representation of arachidonate-containing GPC and GPE species in some fa/fa rat tissues at 6 wk could contribute to insulin resistance, but depletion of islet arachidonate-containing GPC and GPE species is unlikely to explain the evolution of the insulin secretory defect that is well-developed by 12 wk of age.

Paper no. L8469 in *Lipids 35*, 839–854 (August 2000).

*To whom correspondence should be addressed at Box 8127, Washington University School of Medicine, 660 S. Euclid Ave., St. Louis, MO 63110. E-mail: jturk@imgate.wustl.edu

Abbreviations: CAD, collisionally activated dissociation; ESI, electrospray ionization; GPC, glycerophosphocholine; GPE, glycerophosphoethanolamine; HPLC, high-performance liquid chromatography; IDDM, insulin-dependent diabetes mellitus; NIDDM, non-insulin-dependent diabetes mellitus; NP, normal phase; MS, mass spectrometry; PBS, phosphate-buffered saline; ZDF, Zucker diabetic fatty.

The Zucker diabetic fatty (ZDF) rat (1–22) is a genetic model of non-insulin-dependent diabetes mellitus (NIDDM), in which metabolic abnormalities arise from a mutation in the intracellular domain of the receptor for leptin (6,7), an adipocyte hormone that signals fat store content (23,24). Males homozygous for this mutation (fa/fa) become obese and diabetic, but males of the same genetic background with wild-type receptors (+/+) remain lean and normoglycemic. As in human NIDDM (25,26), insulin resistance develops in fa/fa rats, but normoglycemia is initially maintained by compensatory insulin hypersecretion (2–5,11). Progressive elevations in blood free fatty acid and triglyceride concentrations begin at 7–8 wk in male fa/fa rats, and, at 9–10 wk, an insulin secretory defect develops that triggers hyperglycemia (3,11).

Insulin secretory defects in fa/fa rats include increased basal secretion, blunted responses to glucose, abnormalities in secretory pulsations, and defective modulation of secretion by fatty acids (2–5,8). There is also a loss of β-cell mass *via* apoptosis as fa/fa rats age (15,18,19). Abnormal accumulation of lipids in fa/fa rat islets is implicated in these abnormalities. Modest accumulation of triglycerides in islets of young fa/fa rats contributes to insulin hypersecretion, and marked islet triglyceride accumulation as the rats age impairs secretion and increases β-cell sensitivity to injurious stimuli (3,5,8,9,11–14,16–20). Accumulation of the sphingolipid ceramide in islets of older fa/fa rats contributes to β-cell apoptosis (18,19).

Accumulation of complex lipids in fa/fa rat islets is driven by hyperlipidemia and increased expression of lipid biosynthetic enzymes, including glycerol-3-phosphate acyltransferase (9,17), which catalyzes an early step in *de novo* synthesis of triglycerides and other glycerolipids (27). ZDF fa/fa rat islets overexpress serine palmitoyltransferase (18,19), which catalyzes

the first step in *de novo* synthesis of ceramide. Islet glycerophospholipid composition may affect secretion (28–31), but these molecules have not been extensively studied in ZDF rats. Normal rat and human β-cells are enriched in arachidonate-containing glycerophosphocholine (GPC) and glycerophosphoethanolamine (GPE) species (32–34). Such molecules may serve as substrates for phospholipases in β-cell signaling (35–38), in which arachidonate hydrolysis from phospholipids may amplify secretagogue-induced rises in cytosolic [Ca^{2+}] and insulin release (39–43).

Arachidonate-containing phospholipids also may play structural roles in β-cells. The β-cell secretory granule and plasma membranes are enriched in GPE species with a *sn*-1 vinyl ether linkage and esterified arachidonate in the *sn*-2 position (34). Such polyunsaturated plasmenylethanolamines facilitate fusion of membrane bilayers (44,45) and of β-cell secretory granule and plasma membranes (34,46). Interference with biosynthesis of arachidonate-containing plasmenylethanolamines can induce apoptosis (47), and conditions that induce loss of arachidonate from islet GPE lipids (48) induce β-cell apoptosis (49). A decline in arachidonate-containing phospholipids might thus impair β-cell secretion or survival.

Insulinoma cells undergo loss of arachidonate-containing phospholipid species when cultured in arachidonate-poor medium, and this is associated with reduced insulin secretion (50,51). These effects are partially reversed by culture with arachidonic acid (51). This raises the possibility that islet β-cells might be affected by blood lipid content. The hyperlipidemia that develops in fa/fa rats might cause replacement of arachidonate in β-cell phospholipids with more saturated substituents, and this could impair β-cell survival or secretion. The phospholipid composition of tissues subject to diabetic complications might be similarly affected. A decline in tissue phospholipid arachidonate content occurs in a rat model of insulin-dependent diabetes mellitus (IDDM) induced by streptozotocin (52).

We have used electrospray ionization mass spectrometry (ESI/MS), a powerful tool for determining phospholipid structures (34,53–55), to examine GPC and GPE lipid species in tissues from prediabetic and diabetic ZDF fa/fa rats and from age-matched, nondiabetic +/+ rats.

EXPERIMENTAL PROCEDURES

Materials. Phospholipid standards were obtained from Avanti (Birmingham, AL); organic solvents from Burdick and Jackson (Muskegee, MI); LiOH and buffer salts from Sigma (St. Louis, MO); high-performance liquid chromatography (HPLC) columns from Alltech (Deerfield, IL); and collagenase from Boehringer Mannheim (Indianapolis, IN).

Experimental animals. Animal studies were approved by the Washington University Animal Studies committee and conformed to accepted standards. ZDF fa/fa and +/+ rats were obtained from Genetic Models (Indianapolis, IN). Rats were fed Purina Formulab 5008 high-fat chow *ad libitum*, which contains 23% crude protein, 6.5% crude fat, 4% crude fiber, 8% ash, and 2.5% added minerals. ZDF fa/fa rats consume about 15–30 g daily and +/+ rats about 12–15 g daily. The diet lipid composition is 280 ppm cholesterol, 1.37% linoleic acid, 0.09% linolenic acid, 0.01% arachidonic acid, 0.29% n-3 fatty acids, 2.51% saturated fatty acids, and 2.32% monounsaturated fatty acids.

Plasma measurements. Blood was collected at 9:00–10:00 A.M. by vascular puncture with a syringe containing 50 μL of 15% Na_2EDTA. Plasma and red blood cells were separated by centrifugation. Plasma glucose was measured by the glucose oxidase method, and plasma triacylglycerol was measured with a Sigma kit (GPO-Trinder procedure no. 337), as described (3).

Collection and processing of pancreatic islets and other tissues. Rats were anesthetized with intraperitoneal sodium pentobarbital and islets isolated after pancreatic excision, collagenase digestion, and centrifugation through a discontinuous Ficoll gradient (32–34,56). Islet phospholipids were extracted by the method of Bligh and Dyer (57). Heart, brain, liver, kidney, and sciatic nerve were excised and placed on ice in conical polypropylene tubes containing phosphate-buffered saline (PBS) without added Ca^{2+} or Mg^{2+}. Tissues were rinsed twice (ice-cold PBS), transferred to silanized glass beakers, and minced. Minced tissues were transferred to conical polypropylene tubes and rinsed (five times, ice-cold PBS) to remove blood. Minced tissues were drained, blotted, weighed, and transferred to conical glass tubes containing chloroform/methanol (1:1, vol/vol), homogenized, vortex-mixed, and incubated on ice (2 h) before completing lipid extraction by adding PBS (0.375 vol/vol) of chloroform/methanol (1:1), centrifugation (900 × *g*, 5 min) to separate phases, and collection of the chloroform-rich, lipid-containing lower phase.

Normal-phase HPLC isolation of GPE and GPC lipids from phospholipid extracts. GPE and GPC lipids were isolated from extracts by normal-phase HPLC (32–34) on a silicic acid HPLC column (LiChrospher Si-100, 10 μm particle size, 250 × 4.6 mm; Alltech) in a solvent system consisting of a gradient between solvent mixtures A and B, the compositions of which were hexane/isopropanol/water (100:100:3, by vol) and (100:100:7, by vol), respectively. Initial solvent composition (100% A/0% B) was maintained for 6 min (flow 2 mL/min) and followed by a linear gradient over 24 min to the final composition (50% A/50% B) to isolate GPE (8 min retention time) and GPC (55 min retention time).

Determination of acid-lability of phospholipids. Acid-lability was determined (32–34,58) after dividing samples into two aliquots and concentrating to dryness. One was treated with acid (1 N HCl in methanol/chloroform, 1:1, vol/vol, 1 mL, 45 min, room temperature) and the other sham-treated (chloroform/methanol, 1:1, vol/vol, 1 mL). Samples were neutralized (1 M Na_2CO_3, 0.5 mL), extracted (chloroform, 1 mL), concentrated, reconstituted (methanol/chloroform, 1:9, vol/vol, 0.1 mL), and analyzed by ESI/MS. Acid-stable diacyl- and alkylacyl-lipids appear in acid- and sham-treated sample spectra, but acid-labile plasmalogens do not appear in acid-treated sample spectra.

MS. ESI/MS was performed on a Finnigan (San Jose, CA) TSQ-7000 triple stage quadrupole mass spectrometer with

ESI source controlled by Finnigan ICIS software. Phospholipids were dissolved (1–5 pmol/μL) in methanol/chloroform (9:1, vol/vol) containing LiOH (2–5 pmol/μL). GPC lipids were analyzed in positive- and GPE lipids in negative-ion mode (34,55). Samples were infused (1 μL/min) into the ESI source with a Harvard syringe pump. Electrospray needle and skimmer were operated at ground potential. To acquire positive or negative ions, respectively, electrospray chamber and the glass capillary entrance were operated at positive or negative potentials; positive or negative potentials were applied to the glass capillary exit; and positive or negative potentials were placed on the tube lens. The heated capillary temperature was 250°C. For collisionally activated dissociation (CAD), precursor ions were selected in the first quadrupole and accelerated (32–36 eV) into a collision chamber containing argon (2.2–2.5 mtorr). Product ions were analyzed by *m/z* value in the final quadrupole. Spectra were acquired with a signal-averaging protocol in profile mode (one scan/3 s).

Statistical analyses. Student's *t*-test was used to compare two groups, and multiple groups were compared by one-way analysis of variance with *post-hoc* Newman-Keul's analyses.

RESULTS

Age-related changes in blood glucose and triglyceride concentrations in ZDF rats. Lean ZDF rats homozygous for functional leptin receptors (+/+) maintained normal blood glucose (Fig. 1A) and triacylglycerol (Fig. 1B) concentrations at 6 and 12 wk of age. In contrast, obese ZDF rats homozygous for nonfunctional leptin receptors (fa/fa) exhibited significant increases in both blood glucose and triacylglycerol concentrations between 6 and 12 wk, and the 12-wk rats were hyperglycemic and hypertriglyceridemic (Fig. 1), as reported by others (3,11). We determined whether age-related changes in blood lipid concentrations were associated with changes in tissue phospholipid species by ESI/MS analyses of GPC and GPE lipids.

GPC lipids from ZDF rat heart. Figure 2 illustrates ESI/MS spectra of Li^+ adducts of GPC lipids from hearts of +/+ rats at 6 (Fig. 2A) and 12 wk (Fig. 2C) of age and from fa/fa rats of the same ages (Fig. 2B and D). CAD and tandem MS (Fig. 3) were used to identify GPC species in these mixtures. In tandem spectra of Li^+ adducts of GPC lipids, the headgroup is identified by ions reflecting loss of phosphocholine with Li (loss of 189) or with H (loss of 183^+) (55), and ions reflecting these losses are present in each spectrum in Figure 3. Identities of fatty acid substituents are reflected by ions, reflecting loss of trimethylamine plus either the *sn*-1 or *sn*-2 substituent as a free fatty acid. The relative abundance of the former ion exceeds that of the latter (55).

In GPC ESI/MS spectra for extracts from hearts of +/+ rats and from 12-wk fa/fa rats, the most abundant $[M + Li]^+$ ion oc-

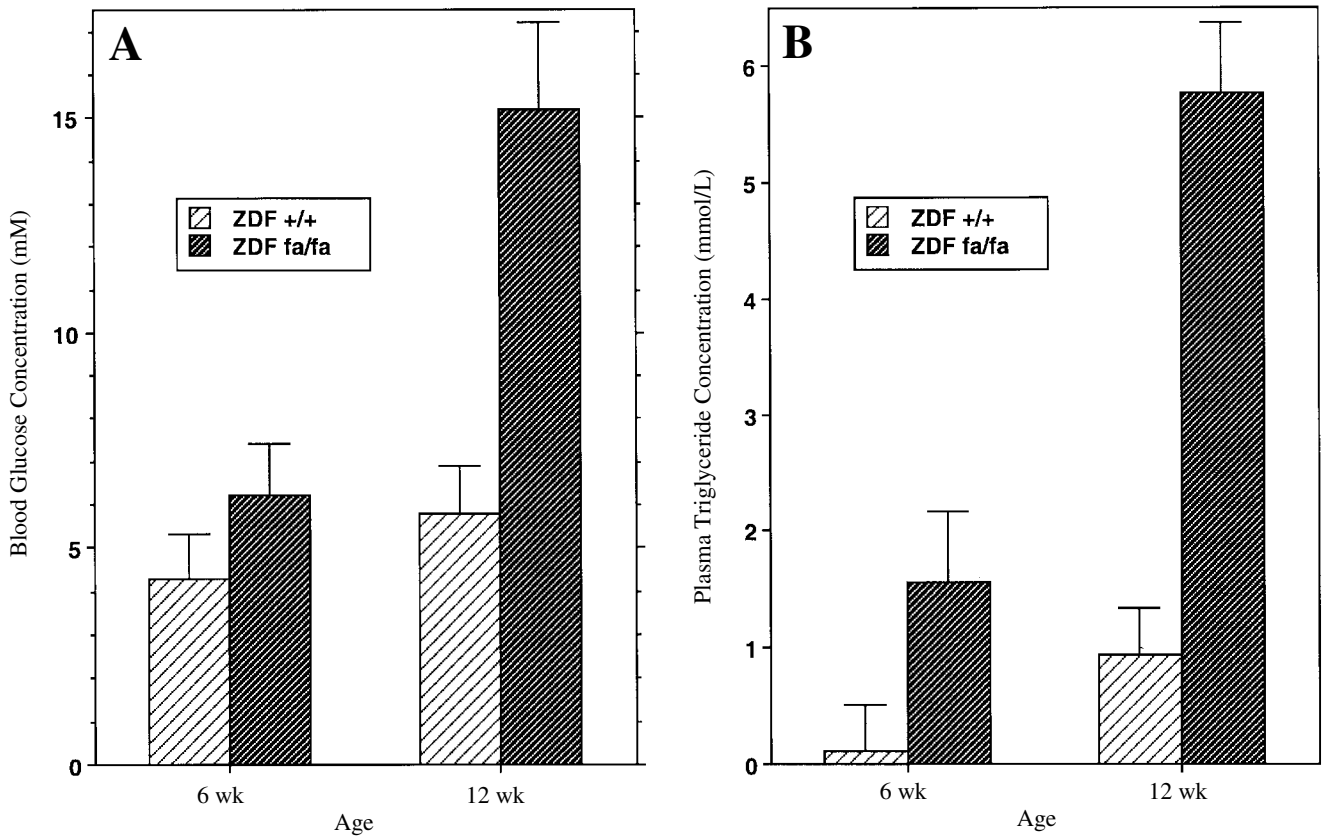

FIG. 1. Blood glucose and triglyceride concentrations in Zucker diabetic fatty (ZDF) rats of various ages. Blood glucose (A) or triglyceride (B) concentrations were determined in ZDF +/+ (light bars) or ZDF fa/fa (dark bars) rats at 6 (left set of bars in each panel) or 12 (right set of bars in each panel) wk of age. Means values ± SEM are displayed ($n = 6$).

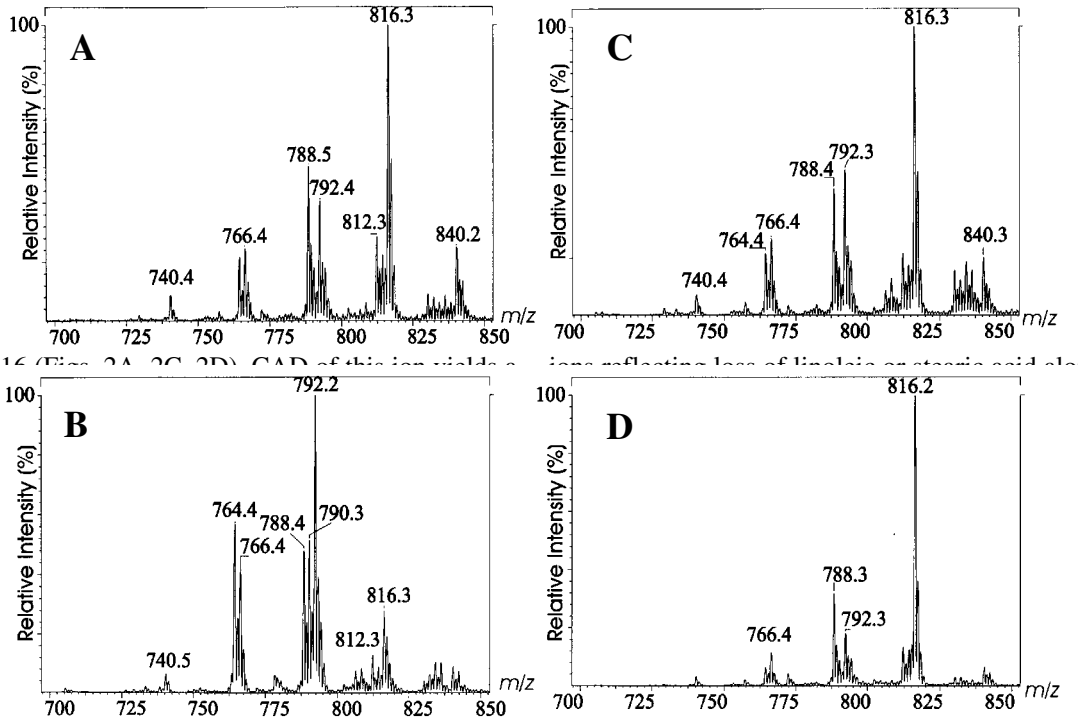

FIG. 2. Electrospray ionization (ESI) positive-ion mass spectrometric (MS) analysis of Li^+ adducts of glycerophosphocholine (GPC) lipids from hearts of ZDF rats. Phospholipids extracted from hearts of 6-wk-old (A and B) or 12-wk-old (C and D) ZDF +/+ (A and C) or ZDF fa/fa (panels B and D) rats were analyzed by normal-phase high-performance liquid chromatography (NP-HPLC) to isolate GPC lipids, which were then analyzed by ESI/MS as Li^+

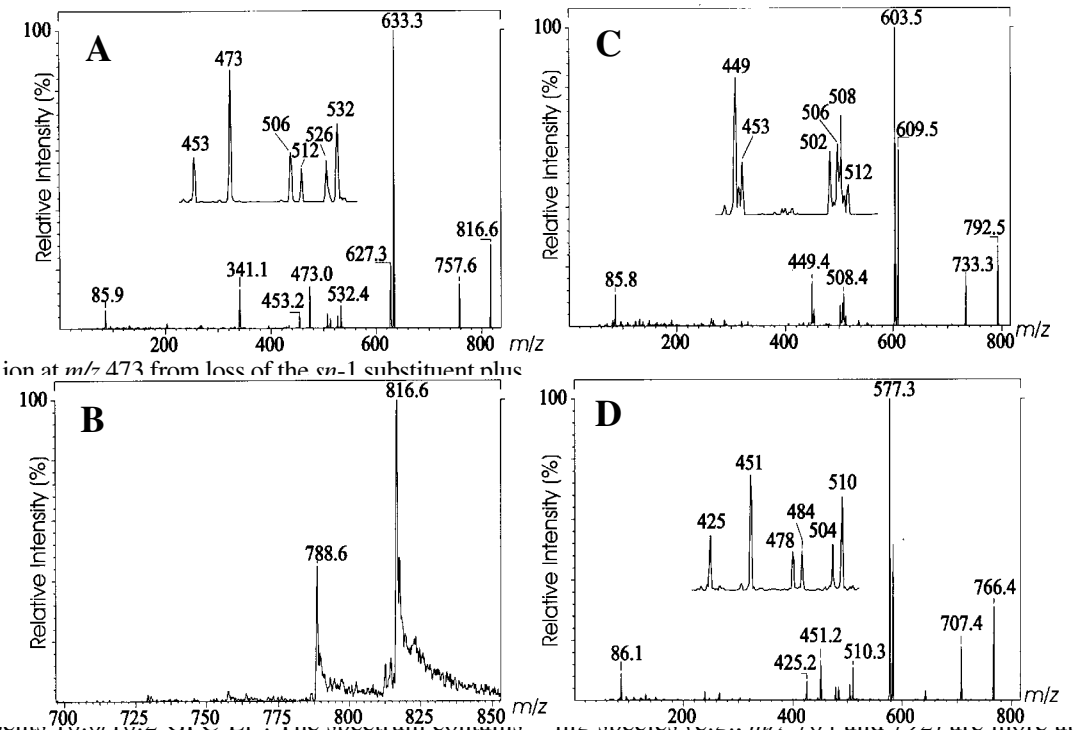

FIG. 3. Tandem mass spectra obtained from collisionally activated dissociation (CAD) of $[M + Li]^+$ ions of GPC lipids from hearts of ZDF rats. ESI/MS was performed as in Figure 2, and $[M + Li]^+$ ions at *m/z* 816 (A: 18:0/20:4-GPC), 792 (C: 18:0/18:2-GPC), or 766 (D: 16:0/18:1-GPC) were isolated in the first quadrupole and subjected to CAD. Product ions were then analyzed in the final quadrupole. B: (20:4) represents a tandem MS scanning experiment performed with the GPC-Li^+ mixture from hearts of 12-wk ZDF fa/fa rats in which parent ions were identified that yielded a product ion at *m/z* 473 upon CAD. See Figures 1 and 2 for other abbreviations.

those representing arachidonate-containing species (e.g., *m/z* 816) less abundant than for the 12-wk rats. The relative abundances of ions reflecting both oleate- (e.g., *m/z* 766) and linoleate-containing (e.g., *m/z* 764 and 792) species are lower in heart GPC mixtures from 12-wk fa/fa rats than in mixtures from +/+ rats, and the relative contribution of arachidonate-containing species to the GPC $[M + Li]^+$ ion current is correspondingly higher in 12-wk fa/fa rats.

GPE lipids from ZDF rat heart. Figure 4 illustrates ESI/MS analyses of $[M - H]^-$ ions of GPE lipids from hearts of +/+ rats at 6 (Fig. 4A) and 12 wk (Fig. 4C) of age and from fa/fa rats of the same ages (Fig. 4D). Ions representing plasmenylethanolamine species are designated with asterisks in Figure 4, based on acid-lability studies (32–34). Plasmalogens are acid-labile, and ions representing them are not observed upon ESI/MS analyses of acid-treated samples. Diacyl-GPE species are acid-stable. CAD and tandem MS (Fig. 5) were used to identify GPE species in the mixtures illustrated in Figure 4.

In GPE ESI/MS spectra for heart extracts from +/+ and 12-wk fa/fa rats, the most abundant $[M - H]^-$ ion occurs at *m/z* 790, and the species represented by this ion is acid-stable, indicating that it is not a plasmalogen. The tandem spectrum of this ion (Fig. 5A) contains ions at *m/z* 140 and 196, representing a dehydration product of the GPE moiety and phosphoethanolamine anion (34,54,58), respectively, and these ions identify the headgroup. The spectrum also contains stearate (*m/z* 283) and docosahexaenoate (*m/z* 327) anions and an ion (*m/z* 480) reflecting loss of docosahexaenoate as a ketene, thus identifying the parent as 18:0/22:6-GPE.

In GPE ESI/MS spectra for heart extracts from 6-wk fa/fa rats, the most abundant $[M - H]^-$ ion occurs at *m/z* 766, and the species represented by this ion is acid-stable, indicating that it is not a plasmalogen. The tandem spectrum of this ion (Fig. 5B) contains arachidonate (*m/z* 303) and stearate (*m/z* 283) anions and ions reflecting loss of arachidonate as a ketene (*m/z* 480) or as a free fatty acid (*m/z* 462). These features identify the parent as 18:0/20:4-GPE.

An $[M - H]^-$ ion at *m/z* 722 is observed in ESI/MS spectra of GPE mixtures from hearts of all four groups of animals (Fig. 4), and an $[M - H]^-$ ion at *m/z* 742 is prominent in the mixture from 6-wk fa/fa rats (Fig. 4B). The latter represents an acid-stable and the former an acid-labile species. CAD of the $[M - H]^-$ ion at *m/z* 742 yields a tandem spectrum (Fig. 5C) that identifies the parent as 18:0/18:2-GPE. The spectrum contains linoleate (*m/z* 279) and stearate (*m/z* 283) anions and ions reflecting loss of linoleate as a ketene (*m/z* 480) or as a free fatty acid (*m/z* 462).

TABLE 1
Glycerophosphocholine (GPC) Lipid Species Identified in ZDF Rat Heart by Positive Ion ESI/MS[a]

	ZDF rat heart GPC lipid species ($[M + Li]^+$)				Relative abundance in percentage			
m/z	Combined chain length	*sn*-1 linkage	Double bonds	Major species	6-wk +/+	12-wk +/+	6-wk fa/fa	12-wk fa/fa
738	32	a	1	16:0a/16:1	0.0 ± 0.0	0.0 ± 0.0	7.2 ± 3.1	0.0 ± 0.0
740	32	a	0	16:0a/16:0	13.6 ± 5.4	7.1 ± 3.1	22.3 ± 8.1	4.1 ± 1.0
764	34	a	2	16:0a/18:2	39.4 ± 9.6	26.2 ± 0.6	51.6 ± 9.7	8.2 ± 2.1
766	34	a	1	16:0a/18:1	45.3 ± 9.2	26.7 ± 0.4	74.2 ± 9.9	11.6 ± 0.7
780	36	e	1	18:0e/18:1	4.0 ± 2.0	0.0 ± 0.0	8.2 ± 4.1	0.0 ± 0.0
788	36	a	4	16:0a/20:4	54.2 ± 1.4	42.3 ± 0.4	26.6 ± 9.2	32.7 ± 1.6
790	36	a	3	18:1a/18:2	25.1 ± 1.8	15.6 ± 1.3	26.7 ± 9.8	9.2 ± 1.3
792	36	a	2	18:0a/18:2	66.5 ± 9.4	58.8 ± 7.4	89.5 ± 10.5	19.2 ± 1.1
794	36	a	1	18:0a/18:1	26.3 ± 5.2	20.4 ± 1.8	46.2 ± 9.1	7.4 ± 1.3
806	38	e	2	18:0e/20:2	1.6 ± 0.4	4.1 ± 2.0	20.2 ± 6.1	0.0 ± 0.0
812	38	a	6	16:0a/22:6	23.3 ± 3.1	21.2 ± 1.1	6.3 ± 3.1	17.2 ± 3.1
814	38	a	5	18:1a/20:4	19.3 ± 3.2	17.1 ± 1.0	3.1 ± 1.4	11.3 ± 2.4
816	38	a	4	18:0a/20:4	100 ± 0.0	100 ± 0.0	14.6 ± 7.4	100 ± 0.0
840	40	a	6	18:0a/22:6	24.5 ± 0.6	19.6 ± 0.4	08.6 ± 0.4	12.1 ± 3.2
Percentage of ion current represented by species with *sn*-2:								
				18:1	17.1 ± 4.5	12.9 ± 1.3	30.5 ± 6.2**	7.8 ± 0.5
				18:2	29.6 ± 3.5	28.9 ± 3.9	40.0 ± 6.1*	12.1 ± 3.9**
				20:4	39.2 ± 6.1	43.9 ± 1.9	10.5 ± 4.6**	61.9 ± 2.2*
				22:6	10.7 ± 3.1	11.2 ± 1.1	3.5 ± 1.1*	12.6 ± 3.3

[a]Zucker diabetic fatty (ZDF) rat heart lipid extracts were analyzed by normal-phase high-performance liquid chromatography (NP-HPLC) to isolate GPC lipids, which were analyzed by electrospray ionization/mass spectrometry (ESI/MS) as Li^+ adducts as in Figure 2. Relative abundances of $[M + Li]^+$ ions at tabulated *m/z* values were determined from total positive ion current profiles of 32 spectra from eight animals and are expressed as means values (±SEM). $[M + Li]^+$ ions were subjected to collisionally activated dissociations (CAD) and tandem MS to identify molecular species. The combined chain length and number of double bonds in fatty side chains are tabulated, as are chain length and double-bond number for each substituent of the major species at each *m/z* value. At some *m/z* values, more than one isomer was observed. The designation "e" denotes an *sn*-1 alkyl ether linkage and "a" an *sn*-1 acyl linkage. For each condition, contributions of species containing an *sn*-2 oleate (18:1), linoleate (18:2), arachidonate (20:4), or docosahexaenoate (22:6) fatty acid residue to the total tabulated ion current are indicated. For 18:1-containing species, only the value for 6-wk fa/fa rats differed significantly from the other three groups. For 18:2- and for 20:4-containing species, the values for 6-wk fa/fa rats differed significantly from those for the other three groups, and this was also true for the value for the 12-wk fa/fa rats. For 22:6-containing species, the value for the 6-wk fa/fa animals differed significantly from those for the other three groups. For the fa/fa rats, values denoted with an asterisk (*) differed from those of the +/+ rats with a *P* value of less than 0.05, and values denoted with a double asterisk (**) differed from those of the +/+ rats with a *P* value of less than 0.01.

CAD of the $[M - H]^-$ ion at *m/z* 722 yields a tandem spectrum (Fig. 5D) that, in conjunction with acid-lability studies, identifies the parent as 16:0p/20:4-GPE, where "p" denotes an *sn*-1 plasmenyl linkage. This spectrum contains arachidonate anion (*m/z* 303), an ion (*m/z* 259) reflecting loss of CO_2 from arachidonate anion, and ions reflecting loss of arachidonate as a ketene (*m/z* 435) or as a free fatty acid (*m/z* 418). Tandem spectra of other $[M - H]^-$ ions in the heart GPE mixtures illustrated in Figure 4 identified the components summarized in Table 2.

Figure 4 and Table 2 indicate that relative abundances of major GPE $[M - H]^-$ ions are similar in +/+ rat heart lipid extracts at 6 and 12 wk. In contrast, heart GPE $[M - H]^-$ profiles change with age in fa/fa rats. For 6-wk fa/fa rats, ions representing linoleate-containing species (e.g., *m/z* 714 and 742) are more abundant and those representing docosahexaenoate-containing species (e.g., *m/z* 790) less abundant than for 12-wk rats. As for GPC, there is thus a shift of heart GPE with age toward species with longer, more unsaturated substituents in fa/fa but not in +/+ rats.

GPC and GPE lipids from ZDF rat aorta and liver. ESI/MS analyses of GPC and GPE species from +/+ rat aorta exhibited little change with age (not shown). Age-related changes in distribution of both GPC and GPE species were observed in fa/fa rats (Fig. 6, Table 3). For GPC, the relative contribution of arachidonate-containing species (e.g., *m/z* 816) to total $[M + Li]^+$ ion current increased and that of species containing monounsaturated *sn*-2 substituents (e.g., *m/z* 738) declined with age in fa/fa rat aorta mixtures (Figs. 6A, 6B, and upper substituents (e.g., *m/z* 738 and 766) to $[M + Li]^+$ ion current decreased, and the contribution of arachidonate-containing species increased with age (Figs. 7A, 7B, upper part of Table 4). Age-related changes in distribution of GPE species were not observed in fa/fa rat liver, and GPE $[M - H]^-$ profiles were similar at 6 and 12 wk (Figs. 7C, 7D, lower part of Table 4).

GPC and GPE lipids from ZDF rat pancreatic islets, red blood cells, kidney, sciatic nerve, and brain. ESI/MS profiles of GPC $[M + Li]^+$ and GPE $[M - H]^-$ ions did not change appreciably with age in pancreatic islets isolated from +/+ rats, and, at 12 wk, islets from fa/fa rats exhibited profiles of GPC and GPE ions similar to those for +/+ islets (Fig. 8, Table 5). In red blood cells, kidney, sciatic nerve, and brain there was also little change with age in GPC or GPE lipid profiles and little difference between +/+ and fa/fa rats (not shown).

DISCUSSION

GPC and GPE lipid profiles in cardiovascular tissues of male fa/fa rats change as the rats age from 6 to 12 wk, a period during which hyperlipidemia and hyperglycemia develop. Cardiovascular GPC and GPE lipid profiles are relatively constant with age in +/+ rats. In GPC mixtures from heart and aorta of 6-wk fa/fa rats, arachidonate-containing species contribute a smaller fraction of $[M + Li]^+$ total ESI/MS ion current than is the case for 6-wk +/+ rats. Oleate- and linoleate-containing species contribute a correspondingly larger fraction of GPC $[M + Li]^+$ ion current for heart and aorta for 6-wk

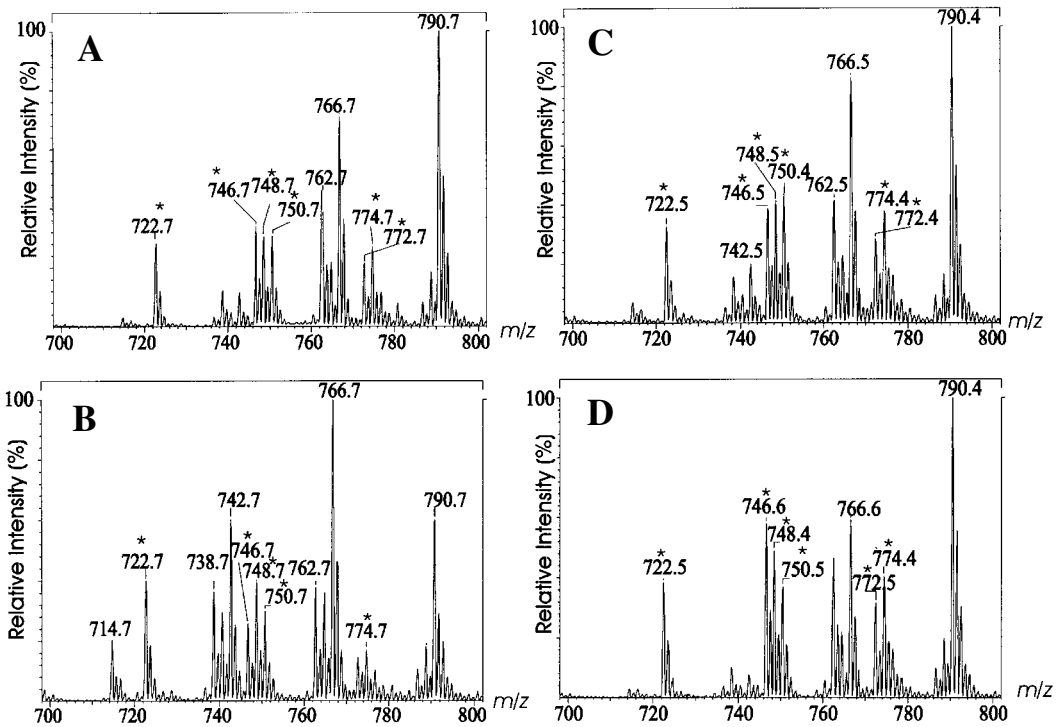

FIG. 4. ESI negative-ion MS analyses of GPE lipids from hearts of ZDF rats. Phospholipids extracted from hearts of 6-wk-old (A and B) or 12-wk-old (C and D) ZDF +/+ (A and C) or ZDF fa/fa (B and D) rats were analyzed by NP-HPLC to isolate GPE lipids, which were then analyzed by ESI/MS as $[M - H]^-$ ions. Peaks designated with asterisks were not observed when the GPE mixture was treated with acid before ESI/MS analysis. See Figures 1 and 2 for other abbreviations.

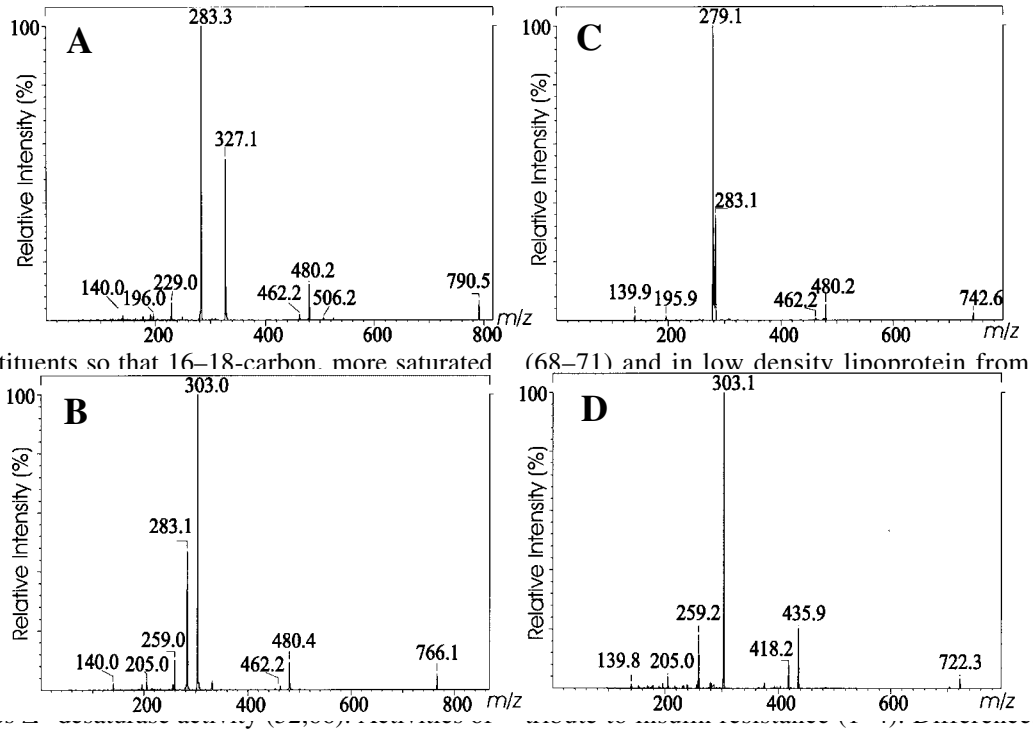

GPE *sn*-2 substituents so that 16–18-carbon, more saturated (68–71) and in low density lipoprotein from NIDDM and

FIG. 5. Tandem spectra obtained from CAD of $[M - H]^-$ ions of GPE lipids from hearts of ZDF rats. ESI/MS was performed as in Figure 4, and $[M - H]^-$ ions at *m/z* 790 (A: 18:0/22:6-GPE), 766 (B: 18:0/20:4-GPE), 742 (C: 18:0/18:2-GPE), or 722 (D: 16:0p/20:4-GPE) were isolated in the first quadrupole and subjected to CAD. Product ions were then analyzed in the final quadrupole. See Figures 1–3 for abreviations.

Δ^9- and Δ^6-desaturases are also reduced in experimental diabetes, and insulin corrects these defects (66). In streptozotocin-diabetes, the arachidonate content of heart GPC declines progressively (63), while in ZDF fa/fa rat hearts, the relative abundance of arachidonate-containing GPC species is diminished only at 6 wk. By 12 wk, the contribution of arachidonate-containing species to GPC $[M + Li]^+$ ion current for ZDF fa/fa rats rises to values equal to or exceeding those for +/+ rats.

Differences between the diabetic state induced by β-cell toxins and that in ZDF fa/fa rats include the fact that toxins induce IDDM from insulin deficiency. ZDF fa/fa rats develop NIDDM characterized by insulin resistance, hyperinsulinemia, and hyperlipidemia. ZDF fa/fa rats also lack functional leptin receptors, which influence lipogenic enzyme expression (3,9,12–14,16,17–20). In ZDF fa/fa rats, hepatic Δ^6- and Δ^5-desaturase activities rise between 6 and 12 wk, and hepatic Δ^5-desaturase capacity doubles, achieving levels exceeding those of lean littermates (67). While the arachidonate content of liver microsomal lipids for ZDF fa/fa rats is lower than that for lean littermates at 6 wk, it rises to levels exceeding that of lean littermates by 12 wk (67). These changes are similar in character to those in contribution of arachidonate-containing GPC species to $[M + Li]^+$ ion current that we observe in fa/fa rat heart, aorta, and liver.

In contrast to the reduced tissue phospholipid arachidonate content in rodent IDDM (52,59–64), increased arachidonate is observed in platelet phospholipids in human NIDDM GPE lipid profiles between ZDF fa/fa and +/+ rats are not observed in all tissues, and heterogeneity in fatty acid compositional abnormalities occurs in other diabetes models. Brain (63) and kidney (59) phospholipids do not undergo fatty acid compositional changes in rodent IDDM, but such changes do occur in heart (63) and aorta (62). We observe no differences in GPC or GPE profiles in pancreatic islets from 12-wk ZDF fa/fa rats compared to those from +/+ rats, suggesting that depletion of arachidonate-containing GPE and GPC species in islet cell membranes is not likely to explain the fa/fa rat insulin secretory defect.

ACKNOWLEDGMENTS

This work was supported by grants from the U.S. Public Health Service (R37-DK34388, P41-RR00954, P60-DK20579, PO1-HL57278, and P30-K56341), the American Diabetes Association, and the Juvenile Diabetes Foundation (No. 996003). We are grateful to Denise Kampwerth for excellent secretarial assistance.

REFERENCES

1. Peterson, R.G., Shaw, W.N., Neal, M., Little, L.A., and Eichberg, J. (1990) Zucker Diabetic Fatty Fat as a Model for Non-insulin-dependent Diabetes Mellitus, *ILAR News 32,* 16–19.
2. Sturis, J., Pugh, W.L., Tang, J., Ostrega, D.M., Polonsky, J.S., and Polonsky, K.S. (1994) Alterations in Pulsatile Insulin Secretion in the Zucker Diabetic Fatty Rat, *Am. J. Physiol. 267,* E250–E259.
3. Lee, Y., Hirose, H., Ohneda, M., Johnson, J.H., McGarry, J.D., and Unger, R.H. (1994) Beta-Cell Lipotoxicity in the Pathogene-

TABLE 2
Glycerophosphoethanolamine (GPE) Lipid Species Identified in ZDF Rat Heart by Negative ion ESI/MS[a]

	ZDF rat heart GPE lipid species ([M – H]⁻)				Relative abundance in percentage			
m/z	Combined chain length	*sn*-1 linkage	Double bonds	Major species	6-wk +/+	12-wk +/+	6-wk fa/fa	12-wk fa/fa
700	34	p	1	16:0p/18:1	0.0 ± 0.0	0.0 ± 0.0	0.0 ± 0.0	0.0 ± 0.0
714	34	a	2	16:0a/18:2	6.1 ± 2.0	6.5 ± 0.5	22.0 ± 0.6	1.5 ± 0.7
716	34	a	1	16:0a/18:1	1.5 ± 0.4	2.2 ± 0.6	5.6 ± 2.4	1.4 ± 0.6
722	36	p	4	16:0p/20:4	26.0 ± 4.1	30.7 ± 1.4	30.5 ± 4.1	37.6 ± 1.7
726	36	p	2	18:1p/18:1	0. ± 0.0	1.5 ± 0.5	0.0 ± 0.0	1.0 ± 0.5
728	36	p	1	18:0p/18:1	0.0 ± 0.0	0.0 ± 0.0	0.0 ± 0.0	0.0 ± 0.0
738	36	a	4	16:0a/20:4	17.5 ± 1.8	16.0 ± 0.3	35.1 ± 3.1	9.2 ± 1.3
740	36	a	3	18:1a/18:2	7.5 ± 0.5	10.5 ± 1.6	35.0 ± 1.1	2.5 ± 0.5
742	36	a	2	18:0a/18:2	19.3 ± 5.2	23.4 ± 1.4	68.2 ± 8.0	8.4 ± 1.1
744	36	a	1	18:0a/18:1	0.0 ± 0.0	2.5 ± 0.6	0.0 ± 0.4	1.5 ± 0.6
746	38	p	6	16:0p/22:6	27.1 ± 6.1	33.2 ± 5.3	19.3 ± 6.4	53.2 ± 3.1
748	38	p	5	18:1p/20:4	27.3 ± 3.2	38.5 ± 2.4	28.1 ± 7.4	46.3 ± 1.4
750	38	p	4	18:0p/20:4	26.5 ± 4.3	41.0 ± 1.3	22.6 ± 5.6	34.5 ± 1.5
762	38	a	6	16:0a/22:6	44.4 ± 2.4	40.5 ± 0.5	31.2 ± 6.5	47.6 ± 0.5
764	38	a	5	18:1a/20:4	23.0 ± 2.0	24.6 ± 1.4	33.4 ± 2.7	20.5 ± 0.6
766	38	a	4	18:0a/20:4	87.0 ± 13.0	89.6 ± 6.4	100 ± 0.0	57.4 ± 1.6
772	40	p	7	18:1p/22:6	18.5 ± 4.6	22.6 ± 6.4	12.6 ± 4.4	29.3 ± 1.4
774	40	p	6	18:0p/22:6	23.5 ± 7.6	31.4 ± 7.1	15.5 ± 3.5	36.6 ± 4.4
790	40	a	6	18:0a/22:6	96.0 ± 4.0	100 ± 0.0	50.0 ± 6.9	100 ± 0.0
Percentage of ion current represented by species with *sn*-2:								
				18:1	0.3 ± 0.1	1.3 ± 0.6	0.9 ± 0.3	0.6 ± 0.2
				18:2	6.9 ± 2.5	6.9 ± 0.9	24.7 ± 4.9	2.5 ± 0.8
				20:4	46.0 ± 3.1	46.2 ± 1.9	47.0 ± 3.1	42.1 ± 1.1
				22:6	46.5 ± 3.9	44.3 ± 2.1	25.3 ± 2.9	54.7 ± 1.9

[a]ZDF rat heart extracts were analyzed by NP-HPLC to isolate GPE lipids, which were analyzed as [M – H]⁻ ions by ESI/MS as in Figure 4. Relative abundances of [M – H]⁻ ions were determined from total negative ion current profiles of 32 spectra from eight animals and are expressed as mean values ± SEM. [M – H]⁻ ions were subjected to CAD and tandem MS to identify molecular species. The combined chain length and number of double bonds in fatty side chains are tabulated, as are chain length and double-bond number for each substituent of the major species at each *m/z* value. At some *m/z* values, more than one isomer was observed. The designation "p" denotes an *sn*-1 vinyl ether (plasmalogen) linkage. All other GPE lipid species had two acyl substituents. For each condition, contributions of species containing an *sn*-2 oleate (18:1), linoleate (18:2), arachidonate (20:4), or docosahexaenoate (22:6) fatty acid residue to the total tabulated ion current are indicated. For 18:1- and for 20:4-containing species, there were no significant differences among the four groups. For 18:2- and for 22:6-containing species, the values for 6-wk fa/fa rats differed significantly from those for the other three groups. See Table 1 for abbreviations.

sis of Non-insulin-Dependent Diabetes Mellitus of Obese Rats. Impairment in Adipocyte-beta-cell Relationships, *Proc. Natl. Acad. Sci. USA 91,* 10878–10882.
4. Tokuyama, T., Sturis, J., DePaoli, A.M., Takeda, J., Stoffel, M., Tang, J., Sun, X., Polonsky, K., and Bell, G.I. (1995) Evolution of β-Cell Dysfunction in the Male Zucker Diabetic Fatty Rat, *Diabetes 44,* 1447–1457.
5. Milburn, J.L., Hirose, H., Lee, Y.H., Nagasawa, Y., Oguwa, A., Ohneda, M., BeltrandelRiio, H., Newgard, C.B., Johnson, J.H., and Unger, R.H. (1995) Pancreatic Beta Cells in Obesity. Evidence for Induction of Functional Morphololgic and Metabolic Abnormalities by Increased Long-Chain Fatty Acids, *J. Biol. Chem. 270,* 1295–1299.
6. Phillips, M.S., Liu, Q., Hammond, H.A., Dugan, V., Hey, P.J., Caskey, C.T., and Hess, J.F. (1996) Leptin Receptor Missense Mutation in the Fatty Zucker Rat, *Nature Gen. 13,* 18–19.
7. Iida, M., Murakami, T., Ishida, K., Mizuno, Z., Kuwajima, M., and Shima, K. (1996) Substitution at Codon 269 (glutamine to proline) of the Leptin Receptor cDNA Is the Only Mutation Found in the Zucker Fatty (fa/fa) Rat, *Biochem. Biophys. Res. Commun 224,* 567–604.
8. Hirose, H., Lee, Y.H., Inman, L.R., Nagasawa, Y., Johnson, J.H., and Unger, R.H. (1996) Defective Fatty Acid-Mediated Beta-Cell Compensation in Zucker Diabetic Fatty Rats. Pathogenic Implications for Obesity-Dependent Diabetes, *J. Biol. Chem. 271,* 5633–5637.
9. Lee, Y., Hirose, H., Zhou, Y.-T., Esser, V., McGarry, J.D., and Unger, R.H. (1997) Increased Lipogenic Capacity of the Islets of Obese Rats. A Role in the Pathogenesis of NIDDM, *Diabetes 46,* 408–413.
10. Cockburn, B.N., Ostrega, D.M., Sturis, J., Kubstrap, C., Polonsky, K.S., and Bell, G.I. (1997) Changes in Pancreatic Islet Glucokinase and Hexokinase Activities with Increasing Age, Obesity, and the Onset of Diabetes, *Diabetes 46,* 1434–1439.
11. Shimabukuro, M., Ohneda, M., Lee, Y., and Unger, R. (1997) Role of Nitric Oxide in Obesity-Induced Beta-Cell Disease, *J. Clin. Invest. 100,* 290–295.
12. Shimabukuro, M., Koyama, K., Lee, Y., and Unger, R.H. (1997) Leptin or Troglitazone-Induced Lipopenia Protects Islets from Interleukin 1β Cytotoxicity, *J. Clin. Invest. 100,* 1750–1754.
13. Shimabukuro, M., Koyama, K., Chen, G., Wang, M.-Y., Trieu, F., Lee, Y., Newgard, C.B., and Unger, R.H. (1997) Direct Antidiabetic Effect of Leptin Through Triglyceride Depletion of Tissues, *Proc. Natl. Acad. Sci. USA 94,* 4637–4641.
14. Zhou, Y.-T., Shimabukuro, M., Koyama, K., Lee, Y., Wang, M.-Y., Trieu, F., Newgard, C.B., and Unger, R.H. (1997) Induction by Leptin of Uncoupling Protein-2 and Enzymes of Fatty Acid Oxidation, *Proc. Natl. Acad. Sci. USA 94,* 6386–6390.
15. Pick, A., Clark, J., Kubstrup, C., Levisetti, M., Pugh, W., Bonner-Weir, S., and Polonsky, K. (1998) Role of Apoptosis in Failure of Beta-Cell Mass Compensation for Insulin Resistance and Beta-Cell Defects in the Male Zucker Diabetic Fatty Rat, *Diabetes 47,*

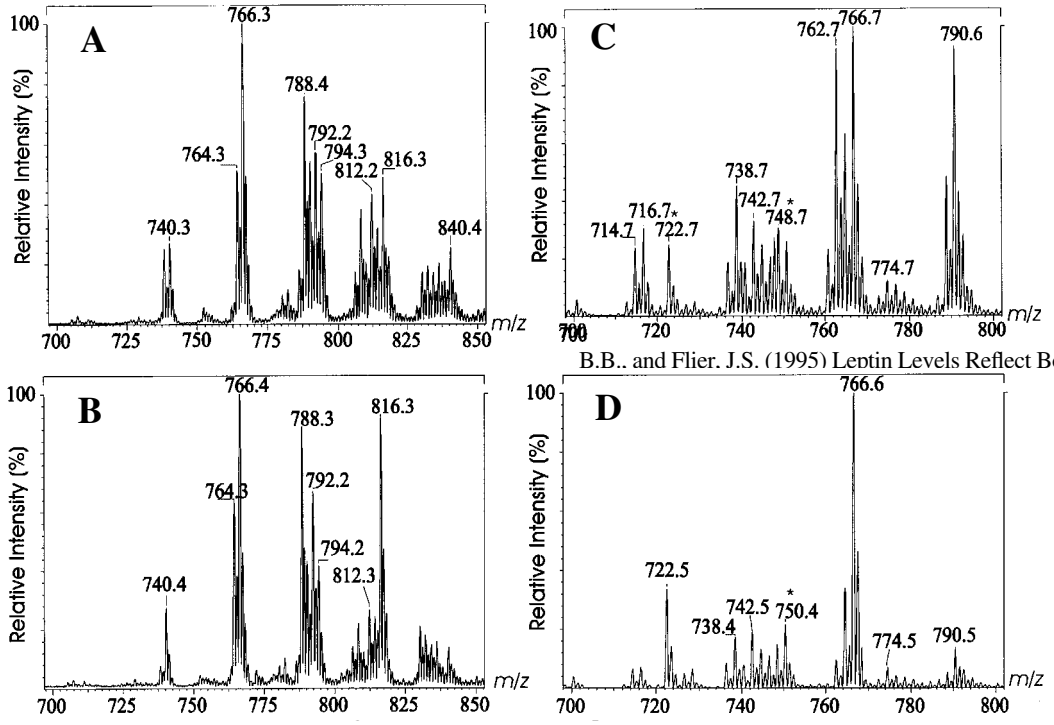

FIG. 6. ESI/MS analyses of $[M + Li]^+$ ions of GPC lipids and of $[M - H]^-$ ions of GPE lipids from aorta of ZDF fa/fa rats. Phospholipid extracts from aortae of 6-wk-old [A (rat aorta: GPC-Li^+) and C (rat aorta: GPE $[M - H]^-$) or 12-wk-old [B (rat aorta: GPC-Li^+) and D (rat aorta: GPE $[M - H]^-$)] ZDF fa/fa rats were analyzed by NP-HPLC to isolate GPC (A and B) or GPE (C and D) lipids, which were then analyzed as $[M + Li]^+$ or $[M- H]^-$ ions, respectively. See Figures 1 and 2 for abbreviations.

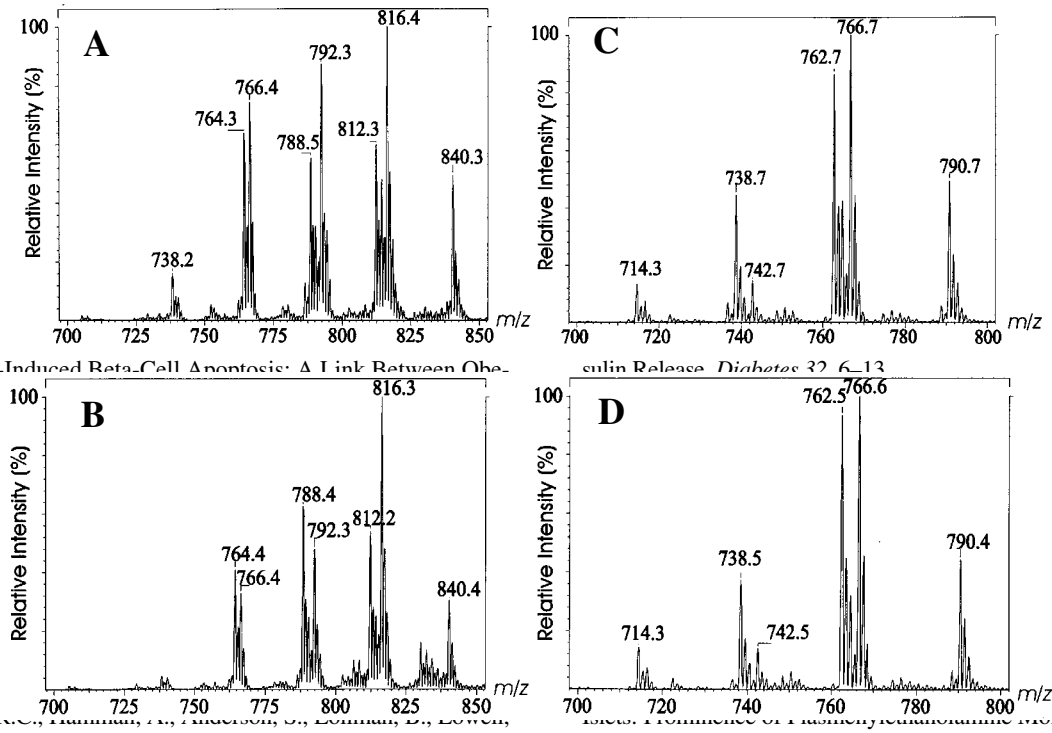

FIG. 7. ESI/MS analyses of $[M + Li]^+$ ions of GPC lipids and of $[M - H]^-$ ions of GPE lipids from liver of ZDF fa/fa rats. Phospholipid extracts from livers of 6-wk-old (A and C) or 12-wk-old (B and D) ZDF fa/fa rats were analyzed by NP-HPLC to isolate GPC (A and B) or GPE (C and D) lipids, which were then analyzed as $[M + Li]^+$ or $[M - H]^-$ ions, respectively.

358–364. B.B., and Flier, J.S. (1995) Leptin Levels Reflect Body Lipid Con-

Fatty Acid-Induced Beta-Cell Apoptosis: A Link Between Obe- sulin Release, *Diabetes* 32, 6–13

29. Frederich, R.C., Hamann, A., Anderson, S., Löllmann, B., Lowell, Islets: Prominence of Plasmenylethanolamine Molecular Species,

TABLE 3
GPC and GPE Lipid Species Identified in ZDF fa/fa Rat Aorta by ESI/MS[a]

	ZDF rat aorta GPC lipid species ($[M + Li]^+$)				Relative abundance in percentage	
m/z	Combined chain length	*sn*-1 linkage	Double bonds	Major species	6-wk fa/fa	12-wk fa/fa
738	32	a	1	16:0a/16:1	27.5 ± 2.5	7.5 ± 0.5
740	32	a	0	16:0a/16:0	29.6 ± 2.4	29.6 ± 2.4
764	34	a	2	16:0a/18:2	29.4 ± 9.6	69.2 ± 4.6
766	34	a	1	16:0a/18:1	100 ± 0.0	95.0 ± 5.0
780	36	e	1	18:0e/18:1	14.3 ± 4.0	9.1 ± 1.8
788	36	a	4	16:0a/20:4	53.1 ± 9.8	83.3 ± 2.9
790	36	a	3	18:1a/18:2	27.7 ± 9.4	43.8 ± 1.4
792	36	a	2	18:0a/18:2	32.3 ± 9.2	70.4 ± 3.8
794	36	a	1	18:0a/18:1	42.6 ± 9.4	41.1 ± 1.0
806	38	e	2	18:0e/20:2	8.3 ± 3.4	7.2 ± 3.1
812	38	a	6	16:0a/22:6	20.3 ± 6.1	20.2 ± 1.9
814	38	a	5	18:1a/20:4	12.1 ± 4.2	20.1 ± 2.0
816	38	a	4	18:0a/20:4	23.5 ± 8.0	96.0 ± 4.0
840	40	a	6	18:0a/22:6	12.5 ± 4.6	13.6 ± 0.4
Percentage of ion current represented by species with *sn*-2:						
				18:1	43.1 ± 6.5	23.9 ± 1.1
				18:2	16.0 ± 3.5	30.2 ± 1.9
				20:4	19.2 ± 6.1	32.9 ± 1.2
				22:6	5.7 ± 3.1	5.5 ± 1.1

	ZDF rat aorta GPE lipid species ($[M - H]^-$)				Relative abundance in percentage	
m/z	Combined chain length	*sn*-1 linkage	Double bonds	Major species	6-wk fa/fa	12-wk fa/fa
700	34	p	1	16:0p/18:1	5.1 ± 1.9	1.5 ± 0.5
714	34	a	2	16:0a/18:2	39.3 ± 4.1	7.1 ± 0.9
716	34	a	1	16:0a/18:1	46.4 ± 8.4	7.2 ± 0.6
722	36	p	4	16:0p/20:4	19.4 ± 4.1	32.6 ± 1.9
726	36	p	2	18:1p/18:1	3.2 ± 1.4	2.0 ± 0.8
728	36	p	1	18:0p/18:1	4.1 ± 1.6	3.0 ± 1.4
738	36	a	4	16:0a/20:4	54.5 ± 2.1	17.5 ± 0.6
740	36	a	3	18:1a/18:2	26.4 ± 1.5	8.3 ± 0.6
742	36	a	2	18:0a/18:2	43.3 ± 5.9	20.4 ± 1.4
744	36	a	1	18:0a/18:1	34.0 ± 5.1	14.6 ± 1.6
746	38	p	6	16:0p/22:6	11.6 ± 4.1	5.2 ± 2.3
748	38	p	5	18:1p/20:4	17.3 ± 5.2	14.4 ± 0.4
750	38	p	4	18:0p/20:4	17.7 ± 4.3	20.5 ± 0.5
762	38	a	6	16:0a/22:6	79.2 ± 6.4	7.5 ± 1.5
764	38	a	5	18:1a/20:4	61.1 ± 1.2	33.6 ± 1.4
766	38	a	4	18:0a/20:4	100 ± 0.0	100 ± 0.0
772	40	p	7	18:1p/22:6	7.0 ± 2.6	1.6 ± 1.1
774	40	p	6	18:0p/22:6	10.2 ± 4.6	3.4 ± 1.4
790	40	a	6	18:0a/22:6	71.5 ± 9.5	12.0 ± 2.0
Percentage of ion current represented by species with *sn*-2:						
				18:1	13.3 ± 2.1	8.0 ± 0.4
				18:2	17.5 ± 3.5	12.1 ± 0.9
				20:4	41.3 ± 1.1	70.3 ± 2.9
				22:6	27.2 ± 4.9	9.1 ± 3.6

[a]ZDF fa/fa rat aorta lipid extracts were analyzed by NP-HPLC to isolate GPC and GPE lipids, which were analyzed by positive-ion ESI/MS as Li^+ adducts and by negative-ion ESI/MS as $[M - H]^-$ ions, respectively. Relative abundances of $[M + Li]^+$ or $[M - H]^-$ ions at tabulated *m/z* values were determined from total-ion current profiles of 32 spectra from eight animals and are expressed as means values ± SEM. $[M + Li]^+$ or $[M - H]^-$ ions were subjected to CAD and tandem MS to identify molecular species, which are designated in Tables 1 and 2. For each condition, contributions of species containing an *sn*-2 oleate (18:1), linoleate (18:2), arachidonate (20:4), or docosahexaenoate (22:6) fatty acid residue to the total tabulated ion current are indicated. For GPC lipids, the values for 6- and 12-wk rats differed significantly for 18:1-, 18:2-, and 20:4-containing species but not for 22:6-containing species. For GPE lipids, the values for 6- and 12-wk rats differed significantly for 20:4- and 22:6-containing species but not for 18:1- or 18:2-containing species. See Tables 1 and 2 for abbreviations.

TABLE 4
GPC and GPE Lipid Species Identified in ZDF fa/fa Rat Liver by ESI/MS[a]

	ZDF rat liver GPC lipid species ($[M + Li]^+$)				Relative abundance in percentage	
m/z	Combined chain length	*sn*-1 linkage	Double bonds	Major species	6-wk fa/fa	12-wk fa/fa
738	32	a	1	16:0a/16:1	20.0 ± 1.9	5.0 ± 1.5
740	32	a	0	16:0a/16:0	11.6 ± 3.4	3.1 ± 0.4
764	34	a	2	16:0a/18:2	39.4 ± 9.6	56.2 ± 8.6
766	34	a	1	16:0a/18:1	88.5 ± 11.5	40.4 ± 5.0
780	36	e	1	18:0e/18:1	17.3 ± 6.0	1.5 ± 0.6
788	36	a	4	16:0a/20:4	28.4 ± 7.8	69.3 ± 5.9
790	36	a	3	18:1a/18:2	15.7 ± 6.4	30.8 ± 4.4
792	36	a	2	18:0a/18:2	54.3 ± 9.2	61.4 ± 8.8
794	36	a	1	18:0a/18:1	33.6 ± 1.4	14.1 ± 1.9
806	38	e	2	18:0e/20:2	0.0 ± 0.0	4.5 ± 2.1
812	38	a	6	16:0a/22:6	30.3 ± 8.1	49.2 ± 4.9
814	38	a	5	18:1a/20:4	24.1 ± 6.2	28.1 ± 2.0
816	38	a	4	18:0a/20:4	50.2 ± 24.3	100 ± 0.0
840	40	a	6	18:0a/22:6	28.1 ± 9.6	30.6 ± 1.4
Percentage of ion current represented by species with *sn*-2:						
				16:0 or 16:1 or 18:1	37.8 ± 2.5	13.1 ± 0.4
				18:2	24.4 ± 4.4	29.9 ± 4.5
				20:4	22.8 ± 2.1	40.0 ± 1.9
				22:6	12.9 ± 2.1	16.1 ± 2.5

	ZDF rat liver GPE lipid species ($[M - H]^-$)				Relative abundance in percentage	
m/z	Combined chain length	*sn*-1 linkage	Double bonds	Major species	6-wk fa/fa	12-wk fa/fa
714	34	a	2	16:0a/18:2	18.3 ± 0.6	18.1 ± 2.9
716	34	a	1	16:0a/18:1	12.4 ± 1.6	3.5 ± 1.6
722	36	p	4	16:0p/20:4	0.0 ± 0.0	1.6 ± 0.8
738	36	a	4	16:0a/20:4	47.5 ± 3.1	39.0 ± 2.6
740	36	a	3	18:1a/18:2	3.4 ± 1.5	9.3 ± 0.6
742	36	a	2	18:0a/18:2	18.3 ± 0.5	16.4 ± 1.9
750	38	p	4	18:0p/20:4	3.7 ± 1.3	3.1 ± 1.3
762	38	a	6	16:0a/22:6	81.2 ± 7.4	76.5 ± 9.5
764	38	a	5	18:1a/20:4	44.1 ± 3.2	31.6 ± 1.4
766	38	a	4	18:0a/20:4	100 ± 0.0	100 ± 0.0
774	40	p	6	18:0p/22:6	0.0 ± 0.0	1.5 ± 0.4
790	40	a	6	18:0a/22:6	45.5 ± 3.5	40.0 ± 5.0
Percentage of ion current represented by species with *sn*-2:						
				18:1	3.4 ± 0.5	1. ± 0.5
				18:2	10.9 ± 1.1	12.9 ± 2.9
				20:4	51.9 ± 1.2	51.7 ± 2.9
				22:6	33.8 ± 1.6	34.4 ± 4.6

[a]ZDF fa/fa rat liver lipid extracts were analyzed and the results tabulated as in Table 3. For each condition, contributions of GPC lipid species containing an *sn*-2 saturated or mononusaturated species (16:0, 16:1, or 18:1) or containing *sn*-2 linoleate (18:2), arachidonate (20:4), or docosahexaenoate (22:6) fatty acid residue to the total tabulated ion current are indicated. The values for 6- and 12-wk rats differed significantly for GPC species containing an *sn*-2 saturated or monounsaturated substituent and for species containing *sn*-2 arachidonate but not for species containing *sn*-2 linoleate or docosahexaenoate. For each condition, contributions of GPE lipid species containing an *sn*-2 oleate (18:1), linoleate (18:2), arachidonate (20:4), or docosahexaenoate (22:6) fatty acid residue to the total tabulated ion current are indicated. Values for 6- and 12-wk rats did not differ significantly for GPE species containing any of these substituents. See Tables 1 and 2 for abbreviations.

TABLE 5
GPC and GPE Lipid Species Identified in ZDF Rat Pancreatic Islets by ESI/MS[a]

ZDF rat islet GPC lipid species ([M + Li]$^+$)					Relative abundance in percentage	
m/z	Combined chain length	*sn*-1 linkage	Double bonds	Major species	12-wk +/+	12-wk fa/fa
738	32	a	1	16:0a/16:1	6.5 ± 0.5	6.5 ± 2.5
740	32	a	0	16:0a/16:0	24.0 ± 5.4	17.6 ± 4.4
764	34	a	2	16:0a/18:2	63.4 ± 9.6	79.2 ± 9.6
766	34	a	1	16:0a/18:1	87.5 ± 9.0	67.0 ± 4.0
780	36	e	1	18:0e/18:1	4.3 ± 2.0	2.1 ± 1.0
788	36	a	4	16:0a/20:4	83.5 ± 6.8	81.5 ± 1.5
790	36	a	3	18:1a/18:2	43.7 ± 5.4	47.6 ± 6.4
792	36	a	2	18:0a/18:2	69.3 ± 6.2	68.4 ± 4.8
794	36	a	1	18:0a/18:1	39.1 ± 1.4	23.1 ± 0.7
806	38	e	2	18:0e/20:2	7.3 ± 3.4	4.5 ± 2.1
812	38	a	6	16:0a/22:6	12.3 ± 0.4	20.2 ± 1.9
814	38	a	5	18:1a/20:4	24.1 ± 1.2	30.1 ± 9.0
816	38	a	4	18:0a/20:4	97.0 ± 3.0	86.0 ± 9.0
840	40	a	6	18:0a/22:6	14.5 ± 3.6	19.6 ± 6.4
Percentage of ion current represented by species with *sn*-2:						
				18:1	22.7 ± 4.9	17.1 ± 2.9
				18:2	30.3 ± 3.1	35.0 ± 3.9
				20:4	35.8 ± 2.1	34.6 ± 3.2
				22:6	4.7 ± 1.1	8.7 ± 4.1

ZDF rat islet GPE lipid species ([M – H]$^-$)					Relative abundance in percentage	
m/z	Combined chain length	*sn*-1 linkage	Double bonds	Major species	12-wk +/+	12-wk fa/fa
700	34	p	1	16:0p/18:1	13.5 ± 5.9	9.5 ± 3.5
714	34	a	2	16:0a/18:2	8.3 ± 3.1	9.1 ± 3.9
716	34	a	1	16:0a/18:1	9.4 ± 4.4	11.2 ± 3.6
722	36	p	4	16:0p/20:4	25.4 ± 6.1	24.6 ± 3.9
726	36	p	2	18:1p/18:1	20.2 ± 6.4	8.5 ± 3.8
728	36	p	1	18:0p/18:1	22.1 ± 4.6	15.0 ± 5.4
738	36	a	4	16:0a/20:4	17.5 ± 2.1	21.5 ± 2.6
740	36	a	3	18:1a/18:2	10.4 ± 2.5	10.3 ± 3.6
742	36	a	2	18:0a/18:2	30.3 ± 5.9	25.4 ± 1.4
744	36	a	1	18:0a/18:1	20.5 ± 3.1	16.6 ± 3.6
746	38	p	6	16:0p/22:6	8.6 ± 3.1	11.2 ± 3.3
748	38	p	5	18:1p/20:4	24.3 ± 5.2	29.4 ± 5.4
750	38	p	4	18:0p/20:4	56.7 ± 9.3	53.5 ± 6.5
762	38	a	6	16:0a/22:6	11.2 ± 3.4	17.5 ± 3.5
764	38	a	5	18:1a/20:4	27.1 ± 3.2	29.6 ± 4.4
766	38	a	4	18:0a/20:4	100 ± 0.0	100 ± 0.0
772	40	p	7	18:1p/22:6	7.0 ± 2.6	10.6 ± 3.1
774	40	p	6	18:0p/22:6	17.2 ± 4.6	15.4 ± 4.4
790	40	a	6	18:0a/22:6	25.5 ± 2.5	29.0 ± 4.0
Percentage of ion current represented by species with *sn*-2:						
				18:1	11.7 ± 4.1	8.5 ± 3.4
				18:2	15.1 ± 1.5	11.9 ± 3.9
				20:4	56.8 ± 4.4	60.5 ± 6.9
				22:6	14.9 ± 1.9	17.5 ± 4.6

[a]ZDF rat pancreatic islets lipid extracts were analyzed and the results tabulated as in Table 3. No significant differences between the +/+ and fa/fa rats were observed. See Tables 1 and 2 for abbreviations.

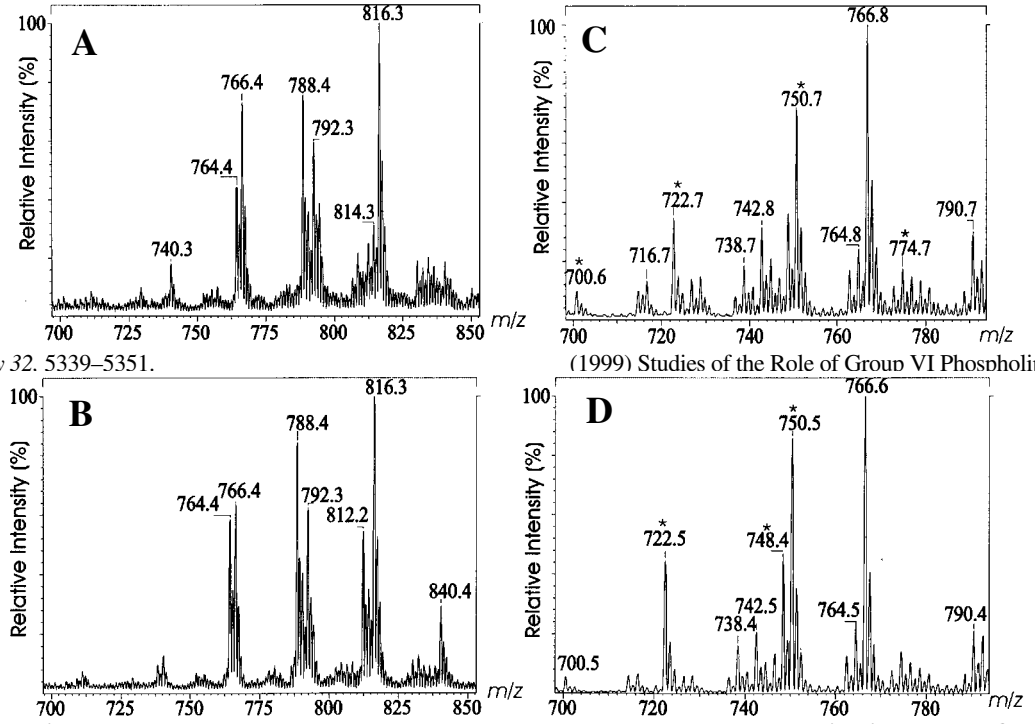

FIG. 8. ESI/MS analyses of $[M + Li]^+$ ions of GPC lipids and of $[M - H]^-$ ions of GPE lipids from pancreatic islets ZDF rats. Phospholipid extracts from isolated pancreatic islets from 12-wk-old ZDF +/+ (A and B) or ZDF fa/fa (C and D) rats were analyzed by NP-HPLC to isolate GPC (panels A and B) or GPE (C and D) lipids, which were then analyzed as $[M + Li]^+$ or $[M - H]^-$ ions, respectively. See Figues 1 and 2 for abbreviations.

1565–1573.

36. Jolly, Y.C., Major, C., and Wolf, B.A. (1993) Transient Activation of Calcium-Dependent Phospholipase A_2 by Insulin Secretagogues in Isolated Pancreatic Islets, *Biochemistry 32,* 337–346.
37. Konrad, R.J., Major, C.D., and Wolf, B.A. (1994) Diacylglycerol Hydrolysis to Arachidonic Acid Is Necessary for Insulin Secretion from Isolated Pancreatic Islets. Sequential Actions of Diacylglycerol and Monoacylglycerol Lipases, *Biochemistry 33,* 13284–13294.
38. Metz, S.A., Draznin, B., Sussman, K.E., and Leitner, J.W. (1987) Unmasking of Arachidonate Induced Insulin Release by Removal of Extracellular Calcium. Arachidonic Acid Mobilizes Cellular Calcium in Islets of Langerhans, *Biochem. Biophys. Res. Commun. 142,* 251–258.
39. Wolf, B., Turk, J., Sherman, W., and McDaniel, M. (1986) Intracellular Ca^{2+} Mobilization by Arachidonic Acid. Comparison with Myo-inositol 1,4,5-Triphosphate in Isolated Pancreatic Islets, *J. Biol. Chem. 261,* 3501–3510.
40. Wolf, B.A., Pasquale, S.M., and Turk, J. (1991) Free Fatty Acid Accumulation in Secretagogue Stimulated Pancreatic Islets and Effects of Arachidonate on Depolarization-Induced Insulin Secretion, *Biochemistry 30,* 6372–6379.
41. Ramanadham, S., Gross, R.W., and Turk, J. (1992) Arachidonic Acid Induces an Increase in Cytosolic Calcium Concentration in Single Pancreatic Islet Beta Cells, *Biochem. Biophys. Res. Commun. 184,* 647–653.
42. Ramanadham, S., Gross, R.W., Han, X., and Turk, J. (1993) Inhibition of Arachidonate Release by Secretagogue-Stimulated Pancreatic Islets Suppresses Both Insulin Secretion and the Rise in Beta-Cell Cytosolic Calcium Concentration, *Biochemistry 32,* 337–346.
43. Ramanadham, S., Hsu, F.-F., Bohrer, A., Ma, Z., and Turk, J. (1999) Studies of the Role of Group VI Phospholipase A_2 (iPLA$_2$) in Pancreatic Islet Phospholipid Metabolism, *Biochemistry 32,* 5339–5351.
44. Ramanadham, S., Hsu, F.-F., Zhang, S., Jin, C., Bohrer, A., Song, Y., Ma, Z., Bao, S., Gross, R.W., and Turk, J. (2000) Characterization and Role of Calcium-Independent Phospholipase A_2 in Normal Pancreatic Islets, Pancreatic Beta-Cells and Transplantable Beta-Cell Tumors, *J. Lipid Res. 41,* 415–434.
45. Ramanadham, S., Ma, Z., Bohrer, A., Zhang, S., Gross, R.W., and Turk, J. (1998) Calcium-Independent Phospholipase A_2 in Human Pancreatic Islets and Carcinoma Cells. Lipid Substrates and Immunological Identification of Immunoreactive Enzyme Vidual Isoforms, *Biochemistry 34,* 12193–12203.
46. Han, X., Ramanadham, S., Turk, J., and Gross, R.W. (1998) Reconstitution of Membrane Fusion Between Pancreatic Islet Secretory Granules and Plasma Membranes. Catalysis by a Protein Constituent Recognized by a Monoclonal Antibody Directed Against Glyceraldehyde-3-phosphate Dehydrogenase, *Biochim. Biophys. Acta 1414,* 95–107.
47. Surette, M.E., Winkler, J.D., Fonteh, A.N., and Chilton, F.H. (1996) Relationship Between Arachidonate-Phospholipid Remodeling and Apoptosis, *Biochemistry 35,* 9187–9196.
48. Nowatzke, W., Ramanadham, S., Hsu, F.-F., Ma, Z., Bohrer, A., and Turk., J. (1998) Mass Spectrometric Evidence That Agents Which Cause Loss of Ca^{2+} from Intracellular Compartments Induce Hydrolysis of Arachidonic Acid from Pancreatic Islet Membrane Phospholipids by a Mechanism That Does Not Require a Rise in Cytosolic Ca^{2+} Concentration, *Endocrinology 139,* 4073–4085.
49. Zhou, Y., Teng, D., Drayluk, F., Ostrega, D., Roe, M.W., Philipson, L., and Polonsky, K.S. (1998) Apoptosis in Insulin-Secreting Cells. Evidence for the Role of Intracellular Ca^{2+} Stores and Arachidonic Acid Metabolism, *J. Clin. Invest. 101,* 1623–1632.
50. Ramanadham, S., Wolf, M., Li, B., Bohrer, A., and Turk, J. (1997) Glucose-Responsivity and Expression of an ATP-Stimulatable, Ca^{2+}-Independent Phospholipase A_2 Enzyme in Clonal Insulinoma Cell Lines, *Biochim. Biophys. Acta 1344,* 153–164.
51. Ramanadham, S., Hsu, F.-F., Zhang, S., Bohrer, A., Ma, Z., and Turk, J. (2000) Electrospray Ionization Mass Spectrometric Analysis of INS-1 Insulinoma Cell Phospholipids. Comparison to Pancreatic Islets and Effects of Fatty Acid Supplementation on Phospholipid Composition and Insulin Secretion, *Biochim. Biophys. Acta 1484,* 251–256.
52. Holman, R.T., Johnson, S.B., Gerrard, J.M., Mauer, S.M., Kupcho-Snadber, S., and Brown, D.M. (1983) Arachidonic Acid Defi-

ciency in Streptozotocin Induced Diabetes, *Proc. Natl. Acad. Sci. USA 80,* 2375–2379.
53. Han, X., and Gross, R.W. (1994) Electrospray Ionization Mass Spectrometric Analysis of Human Erythrocyte Membrane Phospholipids, *Proc. Natl. Acad. Sci. USA 91,* 10635–10639.
54. Han, X., and Gross, R.W. (1995) Structural Determination of Picomole Amounts of Phospholipids *via* Electrospray Ionization Tandem Mass Spectrometry, *J. Am. Soc. Mass Spectrom. 6,* 1202–1210.
55. Hsu, F.-F., Bohrer, A., and Turk, J. (1998) Formation of Lithiated Adducts of Glycerophosphocholine Lipids Facilitates Their Identification by Electrospray Ionization Tandem Mass Spectrometry, *J. Am. Soc. Mass Spectrom. 9,* 516–526.
56. McDaniel, M.L., Colca, J.R., Kotagal, N., and Lacy, P.E. (1983) A Subcellular Fractionation Approach for Studying Insulin Release Mechanisms and Calcium Metabolism in Islets of Langerhans, *Methods Enzymol. 98,* 182–200.
57. Bligh, E.G., and Dyer, W.J. (1959) A Rapid Method of Total Lipid Extraction and Purification, *Can. J. Biochem. Physiol. 37,* 911–917.
58. Murphy, R.C., and Harrison, K.A. (1994) Fast Atom Bombardment Mass Spectrometry of Phospholipids, *Mass Spectrom. Rev. 13,* 57–76.
59. Huang, Y.S., Horrobin, D.F., Manaku, M.S., Mitchell, J., and Ryan, M.A. (1984) Tissue Phospholipid Fatty Acid Composition in the Diabetic Rat, *Lipids 19,* 367–370.
60. Gudbjarnason, S., El-Hage, A.N., Whitehurst, V.E., Simental, F., and Balzas, T. (1987) Reduced Arachidonic Acid Levels in Major Phospholipids of Heart Muscle in the Diabetic Rat, *J. Mol. Cell. Cardiol. 19,* 1141–1146.
61. Takahashi, R., Morse, N., and Horrobin, D.F. (1988) Plasma, Platelet, and Aorta Fatty Acids Composition in Response to Dietary n-6 and n-3 Fats Supplementation in a Rat Model of Non-Insulin Dependent Diabetes, *J. Nutr. Sci. Vitaminol. 34,* 413–421.
62. Dang, A.Q., Faas, F.H., Lee, J.A., and Carter, W.J. (1988) Altered Fatty Acid Composition in the Plasma, Platelets, and Aorta of the Streptozotocin Induced Diabetic Rat, *Metabolism 37,* 1065–1072.
63. Hu, Q., Ishii, E., and Nakagawa, Y. (1994) Differential Changes in Relative Levels of Arachidonic Acid in Major Phospholipids from Rat Tissues During Progression of Diabetes, *J. Biochem. 115,* 405–408.
64. Kuwahara, Y., Yanagishita, T., Konno, N., and Katagiri, T. (1997) Changes in Microsomal Membrane Phospholipids and Fatty Acids and in Activities of Membrane-Bound Enzyme in Diabetic Rat Heart, *Basic Res. Cardiol. 92,* 214–222.
65. Sprecher, H., Lutria, D.L., Mohammed, B.S., and Baykousheva, S.P. (1995) Reevaluation of the Pathways for the Biosynthesis of Polyunsaturated Fatty Acids, *J. Lipid Res. 36,* 2471–2477.
66. Poisson, J.-P.G., and Cunnane, S.C. (1991) Long Chain Fatty Acid Metabolism in Fasting and Diabetes. Relation Between Altered Desaturase Activity and Fatty Acid Composition, *J. Nutr. Biochem. 2,* 60–70.
67. Blond, J.-P., Henchiri, C., and Bezard, J. (1989) Delta-6 and Delta-5 Desaturase Activities in Liver from Obese Zucker Rats at Different Ages, *Lipids 24,* 389–395.
68. Kalofoutis, A., and Lekakis, J. (1981) Changes in Platelet Phospholipids in Diabetes Mellitus, *Diabetologia 21,* 540–543.
69. Morita, I., Takahashi, R., Ito, H., Orimo, H., and Murota, S. (1983) Increased Arachidonic Acid Content in Platelet Phospholipids from Diabetic Patients, *Prostaglandins Leukotrienes Med. 11,* 33–41.
70. Takahashi, R., Morita, I., Saito, Y., Ito, H., and Murota, S. (1984) Increased Arachidonic Acid Incorporation into Platelet Phospholipids in Type 2 (non-insulin-dependent) Diabetes, *Diabetologia 26,* 134–137.
71. Prisco, D., Rogasi, P.G., Paniccia, R. Abbate, R., Gensini, G.F., Pinto, S., Vanni, D., and Neri Serneri, G.G. (1989) Altered Membrane Fatty Acid Composition and Increased Thromboxane A_2 Generation in Platelets from Patients with Diabetes Mellitus, *Prostaglandins Leukotrienes Essent. Fatty Acids 35,* 15–23.
72. Rabini, R.A., Fumelli, P., Galassi, R., Dousset, N., Taus, M., Ferretti, G., Mazzanti, L., Curatola, G., Solera, M.L., and Valdiguie, P. (1994) Increased Susceptibility to Lipid Oxidation of Low-Density Lipoproteins and Erythrocyte Membranes from Diabetic Patients, *Metabolism 43,* 1470–1474.
73. Wijendran, V., Bendel, R.B., Couch, S.C., Philipson, E.H., Thomsen, K., Zhang, X., and Lammi-Keefe, C.J. (1999) Maternal Plasma Phospholipid Polyunsaturated Fatty Acids in Pregnancy With and Without Gestational Diabetes Mellitus. Relations with Maternal Factors, *Am. J. Clin. Nutr. 70,* 53–61.
74. Field, C.J., Ryan, E.A., Thomson, A.B.R., and Clandinin, M.T. (1988) Dietary Fat and the Diabetic State Alter Insulin Binding and the Fatty Acyl Composition of the Adipocyte Plasma Membrane, *Biochem. J. 253,* 417–424.
75. Field, C.J., Ryan, E.A., Thomson, A.B.R., and Clandinin, M.T. (1990) Diet Fat Composition Alters Membrane Phospholipid Composition, Insulin Binding, and Glucose Metabolism in Adipocytes from Control and Diabetic Animals, *J. Biol. Chem. 265,* 11143–11150.
76. Borkman, M., Storlien, L.H., Pan, D.A., Jenkins, A.B., Chisholm, D.J., and Campbell, L.V. (1993) The Relation Between Insulin Sensitivity and the Fatty Acid Composition of Skeletal Muscle Phospholipids, *N. Engl. J. Med. 328,* 238–244.
77. Pan, D.A., Lillioja, S., Milner, M.R., Kriketos, A.D., Baur, L.A., Bogaardus, C., and Storlien, L.H. (1995) Skeletal Muscle Membrane Lipid Composition Is Related to Adiposity and Insulin Action, *J. Clin. Invest. 96,* 2802–2808.

[Received February 18, 2000, and in final revised form May 9, 2000; revision accepted June 7, 2000]

Response of Urinary Lipophilic Aldehydes and Related Carbonyl Compounds to Factors That Stimulate Lipid Peroxidation *in vivo*

A. Saari Csallany*, Song-Suk Kim, and Daniel D. Gallaher

Department of Food Science and Nutrition, University of Minnesota, St. Paul, Minnesota 55108

ABSTRACT: Peroxidation of lipids results in the formation of a number of aldehydic and other carbonyl-containing secondary degradation products. The effect of peroxidative stimuli mediated by vitamin E deficiency, a diet high in polyunsaturated fatty acids (containing cod liver oil), and carbon tetrachloride administration on urinary excretion of a number of lipophilic aldehydes and related carbonyl compounds was examined in rats. These secondary lipid peroxidation products were measured as 2,4-dinitrophenylhydrazine derivatives. All three treatments increased urinary excretion of secondary lipid peroxidation products, although the pattern of excretion of these products varied somewhat among the treatments. Significant increases were found in butanal, hexanal, octanal, butan-2-one, pentan-2-one, hex-2-enal, hepta-2,4-dienal, 4-hydroxyhex-2-enal, 4-hydroxyoct-2-enal, 4-hydroxynon-2-enal, and a number of unidentified carbonyl compounds. These results suggest that urinary excretion of these lipophilic secondary lipid peroxidation products is a useful and noninvasive marker of whole-body lipid peroxidation.

Paper no. L8350 in *Lipids 35*, 855–862 (August 2000).

All organisms have evolved antioxidant defense systems to tolerate mild oxidative stress, which can result from either depletion of antioxidants or from excess production of free radicals and reactive oxygen species such as superoxide, singlet oxygen, hydrogen peroxide, and hydroxy free radicals. However, severe oxidative stress can produce cell damage and tissue injury by reaction of free radicals and active oxygen species with essential cell constituents (1,2). It is well-known that frequent cellular targets of free radicals are membrane lipids, resulting in lipid peroxidation. This potentially deleterious reaction can be controlled in part by antioxidants that scavenge free radicals. Among the antioxidant defense systems, vitamin E (*RRR*-α-tocopherol) is the most effective endogenous lipid-soluble antioxidant for protecting cell membranes from peroxidative damage (3,4). The antioxidant activity of this vitamin is related to its scavenging action of peroxyl radicals by hydrogen donation. A number of *in vivo* and *in vitro* studies have shown that vitamin E deficiency results in lipid peroxidation and the formation of fatty acid peroxides and a number of secondary aldehydic degradation products (5–8).

It is also well-known that the n-3 and n-6 polyunsaturated fatty acids (PUFA) containing lipids are highly oxidizable. Furthermore, increasing the content of these fatty acids in tissues and cells by dietary manipulation can readily modify the extent of cellular oxidative damage, thereby increasing the amount of endogenous peroxidation of lipids (9,10). Dietary lipids have been shown to induce extensive modification in the fatty acid composition of cell membranes and various cellular functions (11,12). Recently diets rich in fish oils which contain n-3 PUFA (20:5, eicosapentaenoic acid and 22:6, docosahexaenoic acid) were recommended for the treatment and prevention of atherosclerosis and heart disease (13,14). However, increasing incorporation of n-3 PUFA into membrane fatty acids potentiates the susceptibility of cellular membranes to lipid peroxidation (15–17). Besides vitamin E deficiency and high-PUFA diets, certain chemical agents such as the hepatotoxic carbon tetrachloride (CCl_4) are known to induce lipid peroxidation *in vivo* (18).

The decomposition of lipid hydroperoxides in biological systems leads to formation of a variety of saturated and unsaturated aldehydes and other carbonyl compounds (19,20). The main mechanism for their formation is the so-called beta-cleavage reaction of lipid alkoxyl radicals (21). Evidence indicates that certain of these aldehydes, including malondialdehyde (MDA), hydroxyaldehydes, and other short-chain carbonyl compounds, contribute to peroxidative cell damage by inhibiting DNA, RNA, and protein synthesis, inhibiting respiration and depleting glutathione, among other effects (22). These aldehydes are sufficiently long-lived to damage target molecules distant from the site of their formation (23,24) and are capable of impairing protein function, inhibiting protein synthesis, causing cell lysis and affecting cellular reproductive integrity (25–27).

*To whom correspondence should be addressed at Department of Food Science and Nutrition, 1334 Eckles Ave., St. Paul, MN 55108.
E-mail: ascsalla@tc.umn.edu

Abbreviations: CCl_4, carbon tetrachloride; CH_2Cl_2, dichloromethane; CLO, cod liver oil; CO, corn oil; DNPH, 2,4-dinitrophenylhydrazine; –E, vitamin E deficiency; HE, high vitamin E; HHE, 4-hydroxyhex-2-enal; HNE, hydroxynon-2-enal; HOE, 4-hydroxyoct-2-enal; HPLC, high-performance liquid chromatography; MDA, malondialdehyde; NE, normal vitamin E; NONPOL, nonpolar carbonyl compounds; POL, polar carbonyl compounds; PUFA, polyunsaturated fatty acids; TLC, thin-layer chromatography.

Previous experiments in this laboratory showed the existence of a number of lipophilic aldehydes and related carbonyl compounds in normal rat and human urine. These included butanal; butan-2-one; pentan-2-one; hex-2-enal; hexanal; hepta-2,4-dienal; hept-2-enal; octanal; non-2-enal; deca-2,4-dienal; 4-hydroxyhex-2-enal; and 4-hydroxynon-2-enal (28). In the present experiment, the effect of lipid peroxidative stress in the form of vitamin E deficiency, a high-PUFA diet, and CCl_4 administration on the urinary excretion of lipophilic aldehydes and related carbonyl compounds was determined in rats.

MATERIALS AND METHODS

Chemicals and supplies. 2,4-dinitrophenylhydrazine (DNPH), hexanal, and sodium tungstate were obtained from Sigma Chemical Company (St. Louis, MO); pentan-2-one (97%), hept-2-enal (97%), hepta-2,4-dienal (90%), decanal, and deca-2,4-dienal from Aldrich Chemical Co. (Milwaukee, WI); hydrochloric acid, high-performance liquid chromatography (HPLC)-grade acetone, methanol, dichloromethane, hexane, and water from EM Science (Gibbstown, NJ); sulfuric acid from Mallinckrodt Inc. (Paris, KY); and alkaline picrate reagent from Sigma Diagnostics (St. Louis, MO). DNPH derivatives of butanal, butanone, hexanal, octanal, non-2-enal, 4-hydroxyhex-2-enal, and 4-hydroxynon-2-enal were a gift from Dr. Esterbauer, University of Graz (Graz, Austria). Pentan-2-one, hept-2-enal, hepta-2,4-dienal, and deca-2,4-dienal DNPH derivatives were synthesized from pure standards and purified by repeated recrysta1ization from methanol (29). Silica gel thin layer chromatographic (TLC) plates (Silica gel 60, aluminum-backed 20 cm × 20 cm, 0.2 mm thickness) were purchased from Alltech Associates Inc. (Deerfield, IL). Amicon cell equipped with a YCO5 Diaflo Ultrafilter was obtained from Amicon Corp. (Beverly, MA).

Diet ingredients. Anhydrous d(+)-dextrose, vitamin-free casein, vacuum-distilled corn oil, and cod liver oil were obtained from United States Biochemical Corp. (Cleveland, OH). Salt mixture 4179, vitamin E free vitamin mixture (vitamin A acetate, 500,000 I.U./g, 1.80; vitamin D_2 calciferol, 850,000 I.U./g, 0.125; inositol, 5.0; choline chloride, 75.0; menadione, 2.250; biotin, 0.020; *p*-aminobenzoic acid, 5.0; ascorbic acid, 45.0; niacin, 4.250; riboflavin, 1.0; pyridoxine hydrochloride, 1.0; thiamin hydrochloride, 1.0; calcium pantothenate, 3.0; folic acid, 0.090; vitamin B_{12}, 0.00135; dextrose, 855.46365), and *RRR*-α-tocopheryl acetate were purchased from ICN Biochemicals Inc. (Aurora, OH).

Animals. Four groups of eight or nine Sprague-Dawley female weanling rats were fed one of the following diets: a diet containing 8% vacuum-distilled corn oil as the fat source that was adequate in all respects except for vitamin E (–E group) (30); the same diet supplemented with a normal amount of vitamin E (30 mg/kg *RRR*-α-tocopheryl acetate) (NE group); the diet supplemented with 300 mg/kg *RRR*-α-tocopheryl acetate (HE group); a diet containing 5% corn oil, 3% cod liver oil, and 30 mg/kg *RRR*-α-tocopheryl acetate (CLO group). After 19 wk, six rats from the NE and HE groups received 100 μL CCl_4/100 g body weight by gavage.

Urine collection. At the end of the experiment, the animals were individually held in stainless steel metabolic cages and fasted for 48 h with access to water *ad libitum.* Urine samples were collected during the second 24 h of fasting and stored at –70°C.

Instrumentation. The HPLC system consisted of an Altex Model 11OA solvent metering pump, an Altex Model 1lOA sample injector (Beckman Instruments, Berkeley, CA), a Spectra-Physics Model SPS4OO UV/VIS detector, and a Spectra-Physics Model SP4100 computing integrator (Spectra-Physics, Arlington, IL). The HPLC separations were performed on an Ultrasphere ODS C_{18} reverse-phase column (25 cm × 4.6 mm i.d., 5 μm particle size) (Altex) with a 2 cm × 2 mm i.d. guard column (Chrom Tech, Apple Valley, MN). Samples were filtered through a 0.2-μm polyvinylidene difluoride filter (Chrom Tech) prior to injection. A Spectronic 20 spectrophotometer (Bausch & Lomb, Rochester, NY) was used for urinary creatinine assay.

Measurement of urinary lipophilic aldehydes and carbonyl compounds. Urine analysis was carried out as previously described by Kim *et al.* (31). Briefly, the method includes ultrafiltration of urine to remove compounds with molecular masses larger than 500 dalton using Amicon cells, synthesis of 2,4-dinitrophenylhydrazone (DNP-hydrazone) derivatives of urinary aldehydes and carbonyl compounds, extraction of the DNPH-hydrazones with dichloromethane (CH_2Cl_2) and preliminary separation of nonpolar compounds (NONPOL) and polar carbonyl compounds (POL) on silica gel TLC plates developed with CH_2Cl_2. Separation and quantitation of the hydrazones were achieved by HPLC on a reverse-phase C_{18} column in two different solvent systems. NONPOL were eluted using methanol/water (75:25, vol/vol) and POL using methanol/water (50:50, vol/vol). Identification of DNPH hydrazones was accomplished by cochromatography with pure standards in three different solvent systems (31). The limit of detection was 1 ng.

Measurement of urinary creatinine. Creatinine concentration was determined in duplicate samples by the method of Sonnenwirth and Jarett (32).

Statistical analysis. Data were presented as means ± SEM. Significant differences between means were determined using analysis of variance coupled with Student-Newman-Keuls method. Student's *t*-test and paired *t*-tests were used to compare the values for other groups. A P-value <0.05 was considered significant for all analysis.

RESULTS AND DISCUSSION

Effect of dietary vitamin E. Typical HPLC chromatograms for NONPOL and POL excreted by vitamin E-deficient rats are shown in Figures 1 and 2, respectively. Fourteen NONPOL were separated by HPLC, and nine were identified: butanal, butan-2-one, pentan-2-one, hex-2-enal, hexanal, hepta-2,4-dienal, hept-2-enal, octanal, and oct-2-enal. There were five unidentified compounds. Thirteen POL were detected and

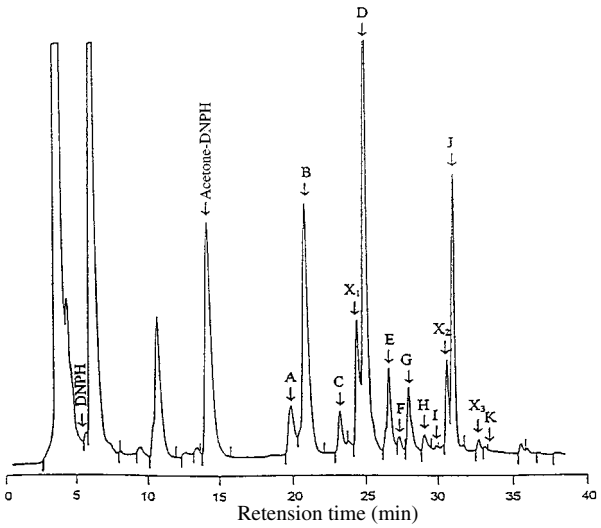

FIG. 1. High performance liquid chromatography (HPLC) separation of 2,4-dinitrophenylhydrazine (DNPH) derivatives of urinary lipophilic nonpolar aldehydes and related carbonyl compounds from a vitamin E-deficient (–E) rat. A, butanal; B, butan-2-one; D, pentan-2-one; F, hex-2-enal; G, hexanal; H, hepta-2,4-dienal; I, hept-2-enal; K, octanal; X_3, oct-2-enal; C, E, J, X_1, X_2, unidentified. Separation conditions: Ultrasphere ODS column (4.6 mm × 25 cm, 5 μm), isocratic elution with methanol/water (75:25, vol/vol) for 10 mm, followed by a linear gradient from methanol/water (75:25, vol/vol) to methanol for 30 min, flow rate; 0.8 mL/min, detector wave length; 378 nm, injected volume, l00 μL.

two were identified: 4-hydroxyhex-2-enal (HHE) and 4-hydroxyoct-2-enal (HOE). 4-Hydroxynon-2-enal (HNE) was detected and identified only in animals treated with CCl_4. Figs. 3 and 4 show differences in the urinary excretion of

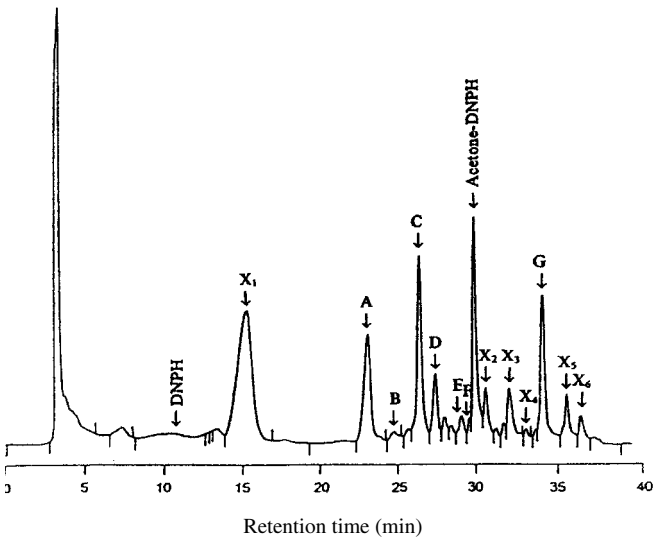

FIG. 2. HPLC separation of DNPH derivatives of urinary lipophilic polar aldehydes and related carbonyl compounds from a –E rat. E, 4-hydroxyhex-2-enal; X_4, 4-hydroxyoct-2-enal; A, B, C, D, F, G, X_1, X_2, X_3, X_5, and X_6, unidentified. Separation conditions: Ultrasphere ODS column (4.6 mm × 25 cm, 5 μm), isocratic elution with methanol/water (50:50, vol/vol) for 10 mm, followed by a linear gradient from methanol/water (50:50, vol/vol) to methanol for 30 min, flow rate; 1.0 mL/min, detector wave length; 378 nm, injected volume; l00 μL. See Figure 1 for abbreviations.

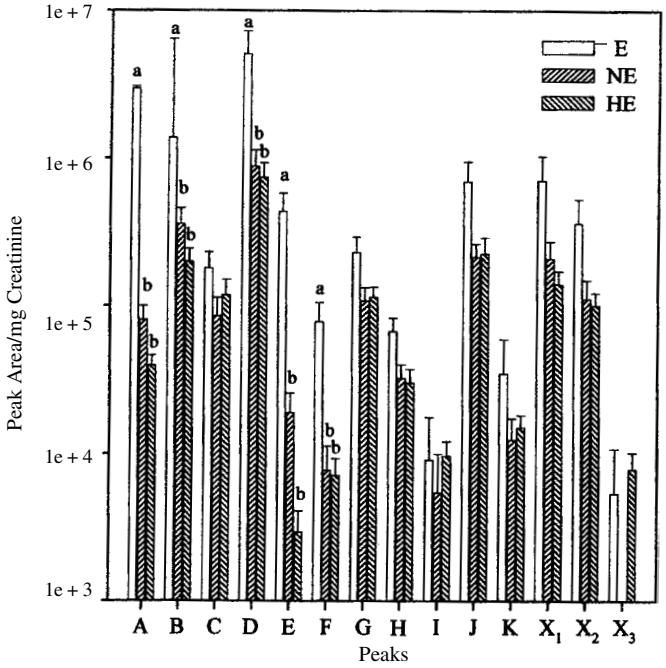

FIG. 3. Comparison of the DNPH derivatives of urinary nonpolar aldehydes and related carbonyl compounds from rats –E, normal vitamin E (NE), and high vitamin E (HE) diets. A, butanal; B, butane-2-one; D, pentane-2-one; F, hex-2-enal; G, hexanal; H, hepta-2,4-dienal; I, hept-2-enal; K, octanal; X_3, oct-2-enal; C, E, J, X_1, X_2, unidentified. Values represent means ± SEM of six to nine animals per dietary group and are expressed on a logarithmic scale. Different letters denote significant differences between groups by Student-Newman Keuls method ($P < 0.05$). See Figure 1 for abbreviations.

NONPOL and POL on the –E, NE, and HE diets. There was a general tendency for the excretion of NONPOL to be greater on the –E diet compared to the NE and HE diets; these differences were statistically significant for butanal, butan-2-one, pentan-2-one, hex-2-enal, and unidentified compound E (Fig. 3). There were no significant differences in excretion between the rats fed the NE and HE diets for any compound. The effect of vitamin E status on the excretion of POL is shown in Figure 4. All 14 POL showed increased concentrations in the urine due to vitamin E deficiency compared to animals given the NE and HE diets; however, significant increases were found only for HOE and unidentified compounds A, C, D, and X_2. Variations in urinary NONPOL and POL concentrations were much greater between individual animals in vitamin E deficiency than in animals fed the NE and HE diets. High variability in urinary excretion of lipid peroxidation products in vitamin E deficiency was found previously (33). This may be due to variations in depletion rate among individual animals (34). Urinary excretion of the sum of NONPOL and POL was significantly greater ($P < 0.05$) in the –E group than in the NE and HE groups (Tables 1 and 2).

Others have found increases in certain lipophilic aldehydes as a result of dietary lack of vitamin E. Yosino *et al.* (35) found hexanal and HNE in the plasma and liver of vitamin E-deficient rats. Elevated levels of HNE were found in the retina in vitamin E-deficient rats and dogs (8). *In vitro* oxidation of

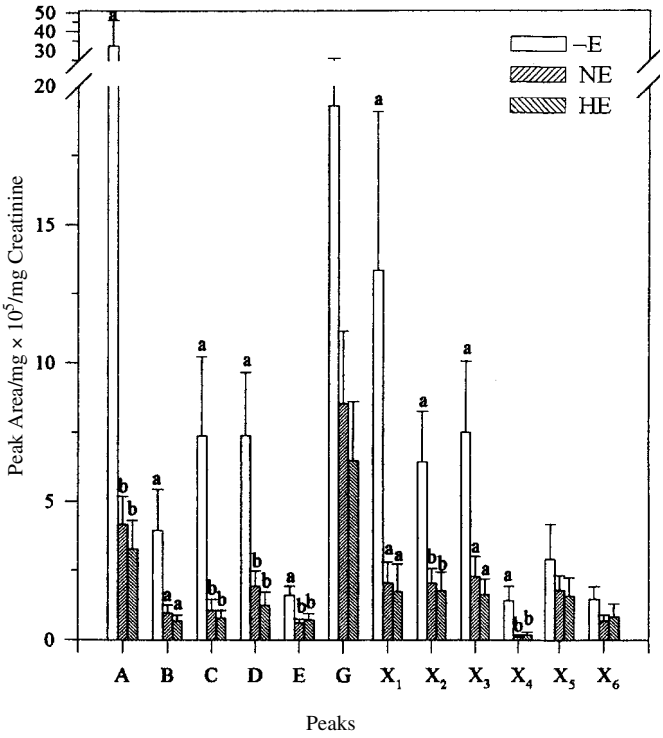

FIG. 4. Comparison of the DNPH derivatives of urinary polar aldehydes and related carbonyl compounds from rats fed –E, NE, and HE diets. E, 4-hydroxyhex-2-enal; X_4, 4-hydroxyoct-2-enal; A, B, C, D, G, X_1, X_2, X_3, X_5 and X_6, unidentified. Values represent means ± SEM of 6–9 animals per dietary group. Different letters denote significant differences between groups by Student-Newman Keul's method ($P < 0.05$).

vitamin E-depleted human low density lipoproteins yielded butanal, propanal, hexanal, 2,4-heptadienal, HHE, HNE, and HOE (36). In the present experiment, the increased oxidative stress caused by vitamin E deficiency resulted in increases in the urine in many of the same lipophilic secondary oxidation products. This demonstrates that oxidation products formed by *in vitro* lipoprotein oxidation are also formed *in vivo* under oxidizing conditions.

A quantitative estimation of urinary excretion of the NONPOL and POL compounds from animals fed NE, –E, and HE diets are shown in Tables 1 and 2. There was approximately twice the concentration of POL as NONPOL compounds. The compounds excreted in greatest amounts in the –E fed animals were the POL compounds A, C, D, G, X_1, X_2, and X_3 and the NONPOL compounds A (butanal), D (pentan-2-one), B (butan-2-one), E, J, and X_1. Although no HNE was detected in these animals, it was found in animals administered CCL_4 (see below).

Effect of dietary PUFA. Excretion of NONPOL and POL for CO- and CLO-fed rats is illustrated in Figures 5 and 6, respectively. All 13 NONPOL except butan-2-one (B) and all 10 POL except the two unidentified compounds B and X_1 were in greater concentration in the urine of the high n-3 CLO animals compared to the CO group. The increases in NONPOL were significant for hexanal (G), hepta-2, 4-dienal (H), oct-2-enal (X_3), and three unidentified compounds C, E, and

TABLE 1
Quantitative Estimate of Nonpolar Lipophilic Urinary Excretion Products (ng/mg creatinine) from Rats Fed a Control (NE), Vitamin E-Deficient (–E), High Vitamin E (HE), High-PUFA (CLO) Diets, or Treated with Carbon Tetrachloride (CCl_4)

Nonpolar compounds[a]	NE	–E	HE	CLO	CCL_4
A (butanal)	10.3	37.8*[b]	5.1	14.0	11.8
B (butan-2-one)	46.0	175.9*	25.5	38.7	44.3
C	12.1	25.6	16.9	33.8*	69.1**
D (pentan-2-one)	134.7	774.2*	113.1	175.8	134.9
E	3.1	72.4*	0.5	10.7*	14.4
F (hex-2-enal)	1.4	14.1*	1.3	3.2	28.6*
G (hexanal)	19.7	41.7	20.8	52.7*	85.4*
H (hept-2,4-dienal)	6.3	13.1	5.9	16.8	23.5*
I (hept-2-enal)	1.0	1.7	1.8	2.6	2.8
J	44.9	145.7	47.4	65.7	106.4*
K (octanal)	2.8	7.9	3.4	5.1	2.0
X_1	47.3	159.3	31.8	60.1	38.2
X_2	25.3	82.3	22.8	95.1**	47.8
X_3 (oct-2-enal)	0.2	1.1	1.6	0.7*	5.4
Total	355.1	1,552.8*	279.9	575.0	614.6

[a]Compounds were separated and identified by high-performance liquid chromatography (HPLC). Quantitation was based on 1 ng hexanal = peak area of 2000 and assumed a similar molar extinction coefficient for all compounds (Ref. 56). Molecular weights for unknown compounds were estimated based on extrapolation from molecular weights of adjacent known compounds.
[b]Significantly different from the control group; *$P < 0.05$, **$P < 0.01$. PUFA, polyunsaturated fatty acids; CLO, cod liver oil.

TABLE 2
Quantitative Estimate of Polar Lipophilic Urinary Excretion Products (ng/mg Creatinine) from Rats Fed a NE, –E, HE, High-PUFA (CLO) Diets or Treated with CCl_4

Nonpolar compounds[a]	NE	–E	HE	CLO	CCL_4
A	104.7	821.3*[b]	82.4	123.3	178.4
B	24.3	98.7	17.2	23.8	39.5
C	26.8	185.1*	20.0	61.1	80.3*
D	48.7	185.9*	31.2	50.5	128.0
E (HHE)	12.5	32.5*	14.6	50.3*	206.9*
G	215.1	485.5	163.3	474.0*	698.7*
H (HNE)	n.d.	n.d.	n.d.	n.d.	47.9*
X_1	52.0	335.8	44.0	28.6	86.8
X_2	51.4	161.8*	44.6	123.4	142.7*
X_3	57.7	189.0	41.3	105.7	210.1*
X_4 (HOE)	3.1	35.0*	4.5	31.3*	43.5*
X_5	45.2	73.1	40.0	93.5	165.9*
X_6	17.1	36.8	20.6	48.7*	216.7
Total	658.6	2,640.5*	523.7	1,214.2	2,245.4*

[a]Compounds were separated and identified by HPLC. Quantitation was based on 1 ng hexanal = peak area of 2000 and assumed a similar molar extinction coefficient for all compounds (Ref. 57). Molecular weights for unknown compounds were estimated based on extrapolation from molecular weights of adjacent known compounds. Abbreviations: n.d., not detected.
[b]Significantly different from the control group; *$P < 0.05$. HHE, 4-hydroxyhex-2-enal; HNE, hydroxynon-2-enal; HOE, 4-hydroxyoct-2-enal. See Table 1 for other abbreviations.

X_2. The significant increase of hepta-2, 4-dienal (H) reflects the decomposition of n-3 fatty acids. Among POL compounds, HHE (E), HOE (X_4), and two unidentified compounds G and X_6 were significantly increased compared to the control. Although total urinary NONPOL and POL were

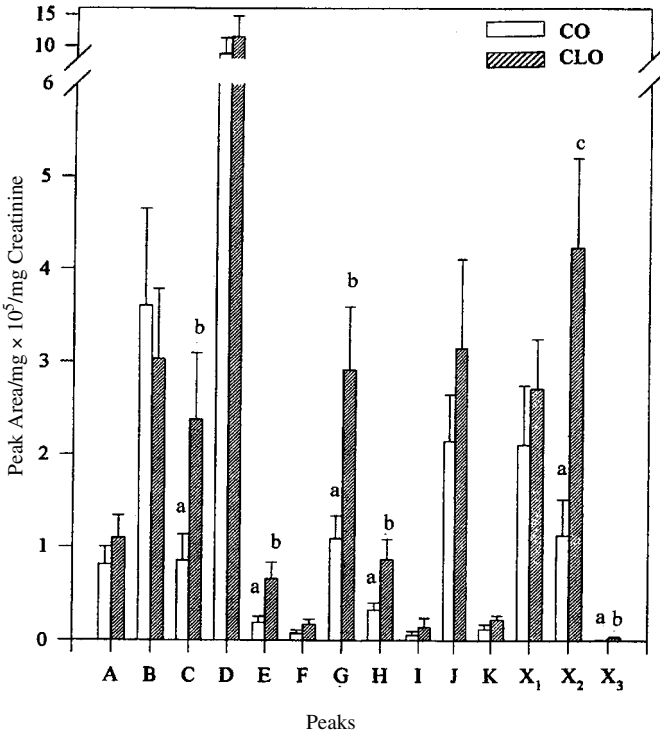

FIG. 5. Comparison of the DNPH derivatives of urinary nonpolar aldehydes and related carbonyl compounds from rats fed either a normal diet containing 8% corn oil (CO) or a polyunsaturated fatty acids (PUFA) diet containing 3% cod liver oil (CLO) and 5% CO. A, butanal; B, butan-2-one; D, pentan-2-one; F, hex-2-enal; G, hexanal; H, hepta-2,4-dienal; I, hept-2-enal; K, octanal, X_3, oct-2-enal; C, E, J, X_1, X_2, unidentified. Values represent means ± SEM of nine and six animals in CO and CLO groups, respectively. Statistical significant difference is determined by Student's *t*-test; a vs. b, $P < 0.05$ and a vs. c, $P < 0.01$. See Figure 1 for abbreviations.

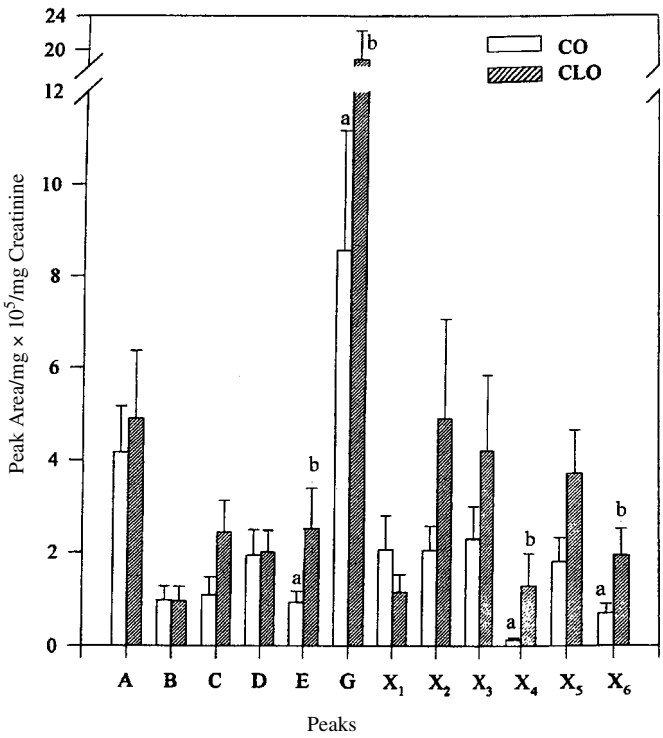

FIG. 6. Comparison of the DNPH derivatives of urinary polar aldehydes and related carbonyl compounds from rats fed either a normal diet containing 8% CO or a PUFA diet containing 3% CLO and 5% CO. E, 4-hydroxyhex-2-enal; X4, 4-hydroxyoct-2-enal; A, B, C, D, G, X_1, X_2, X_3, X_5, and X_6, unidentified. Values represent means ± SEM of nine and six animals in CO and CLO groups, respectively. Statistical significance of difference is determined by Student's *t*-test; a vs. b, $P < 0.05$. See Figures 1 and 5 for abbreviations.

increased in the CLO-fed rats compared to the CO control (NE) group, due to high variability within groups, these differences did not achieve statistical significance (Tables 1 and 2).

It is well-established that feeding diets containing cod liver oil or other fish oils increases incorporation of n-3 PUFA into plasma lipids and cell membranes (37–39). Studies *in vivo* and *in vitro* (40–42) demonstrated that cellular membranes and tissues containing relatively high amounts of n-3 PUFA-containing phospholipids become more vulnerable to peroxidative damage. Saito and Nakatsugawa (43) found that lipid peroxides increased in rat liver microsomal fatty acids after consumption of a fish oil diet. In addition, incorporation of n-3 PUFA into the lipids of cultured cells enhanced the cellular susceptibility to oxidants, especially H_2O_2 (44,45). Recent studies also showed that a fish oil-enriched diet induced vitamin E deficiency in animals and increased lipid peroxides in human plasma (46,47). Thus, the greater excretion of urinary lipophilic aldehydes and carbonyl compounds in rats fed cod liver oil diet found here is consistent with these observations by other investigators.

Effect of CCl_4 administration. CCl_4 administration induces liver damage due to peroxidation of hepatic lipids by CCl_3• and CCl_3O_2•, free radical metabolites of CCl_4 (48). DNPH-reactive carbonyl compounds have been detected in membrane phospholipids of hepatic endoplasmic reticulum in CCl_4-treated rats (49), and increased concentrations of HNE have been demonstrated in liver homogenates from CCl_4-treated mice and in liver microsomes peroxidized with CCl_4 (50). Further, numerous secondary lipid peroxidative products, including HHE, alkanals, alkenals, and ketones, were found both *in vivo* and *in vitro* in studies using mice liver extracts, isolated rat hepatocytes, or rat liver microsomes (51,52). CCl_4 administration in the present study yielded generally greater urinary excretion of lipophilic aldehydes and carbonyl compounds (Figs. 7 and 8), consistent with an enhanced lipid peroxidation *in vivo*. Following CCl_4 intubation, 11 of the 14 NONPOL and all 13 POL had a tendency to be in greater concentration in the urine. Hex-2-enal (F), hexanal (G), hepta-2,4-dienal (H), and unidentified compounds C and J were significantly greater in NONPOL and HHE (E), HNE (H), HOE (X_4), and unidentified compounds C, G, X_2, X_3, and X_5 were significantly greater in POL compared to controls (Figs. 7 and 8). Total urinary excretion of NONPOL and POL was increased in animals treated with CCl_4; however, due to high variability within groups, only the urinary excretion of POL was statistically different from the control (NE) group (Ta-

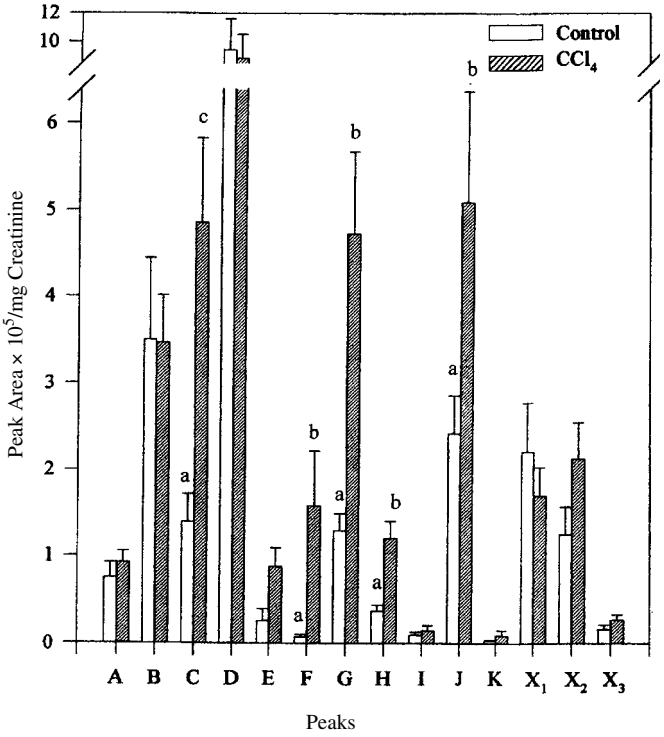

FIG. 7. Comparison of the DNPH derivatives of urinary nonpolar aldehydes and related carbonyl compounds from rats fed a normal control diet and the control diet group treated with carbon tetrachloride (CCl_4). A, butanal; B, butan-2-one; D, pentan-2-one; F, hex-2-enal; G, hexanal; H, hepta-2,4-dienal; I, hept-2-enal; K, octanal; X_3, oct-2-enal; C, E, J, X_1, X_2, unidentified. Values represent means ± SEM of 10 animals per group. Statistical significance of difference is determined by paired *t*-test; a vs. b, $P < 0.05$ and a vs. c, $P < 0.01$. See Figure 1 for abbreviations.

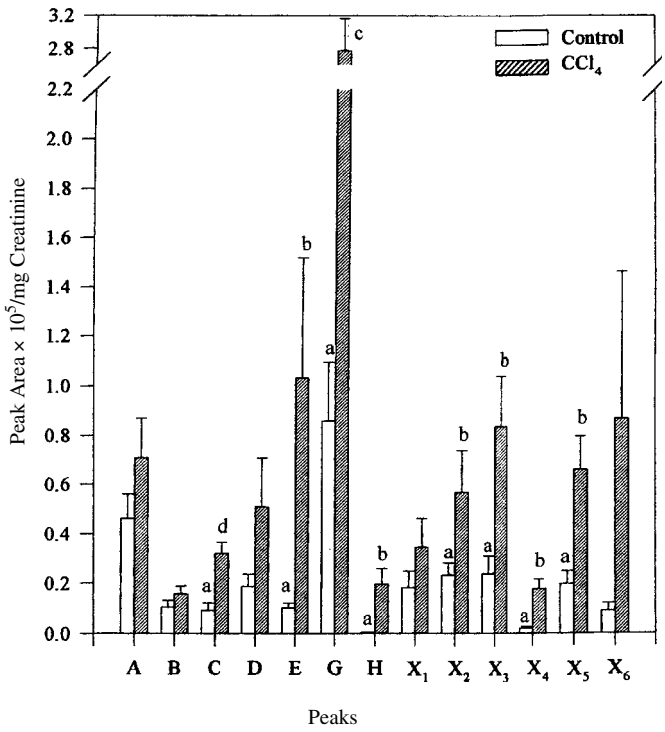

FIG. 8. Comparison of the DNPH derivatives of urinary polar aldehydes and related carbonyl compounds from rats fed a normal control diet and the control diet group treated with CCl_4. E, 4-hydroxyhex-2-enal; H, 4-hydroxynon-2-enal; X4, 4-hydroxyoct-2-enal; A, B, C, D, G, X_1, X_2, X_3, X_5, and X_6, unidentified. Values represent means ± SEM of 10 animals per group. Statistical significance of difference is determined by paired *t*-test; a vs. b, $P < 0.05$; a vs. c, $P < 0.01$; and a vs. d, $P < 0.001$. See Figures 1 and 7 for abbreviations.

bles 1 and 2). These results are consistent with those of Dhanakoti and Draper (53), who found increased urinary MDA excretion due to CCl_4 administration. The increased concentrations of some urinary lipophilic aldehydes and carbonyl compounds in CCl_4-intoxicated rats in this study indicate that these secondary lipid peroxidative products enter the bloodstream and ultimately are excreted into the urine.

The major forms of urinary HHE and HNE are as mercapturic acid conjugates (54,55), which are not detected using the present method. Thus, it appears that the peroxidizing action of CCl_4 increases production of HHE, HNE, and possibly HOE *in vivo* to levels that exceed the ability to form mercapturic acid conjugates. The result is excretion of these compounds in the urine in a form that is detectable by the present method (e.g., free form or as amino acid conjugates). Consequently, the total quantity of HHE and HNE excreted in the urine must exceed that which was measured here, perhaps substantially.

A collation of the results of the pro-oxidant effects of vitamin E deficiency, high dietary PUFA, and CCl_4 administration on the excretion of the urinary lipophilic nonpolar and polar aldehydes and related carbonyl compounds is presented in Tables 1 and 2. For each treatment, there was a greater excretion of urinary total POL than total NONPOL. The profile of excretion differed somewhat among the treatments. Overall, –E led to the greatest urinary excretion of both NONPOL and POL. However, with the exception of butan-2-one, excretion of every compound was increased in at least two of three of the treatments. The excretion of the vast majority of the compounds was increased in all three treatments. Thus, in each case, these secondary *in vivo* peroxidation products clearly accumulated in tissues and were excreted to some extent in the urine.

In summary, peroxidative stimuli mediated by vitamin E deficiency, high PUFA, and CCl_4 administration in rats induced lipid peroxidation *in vivo* and resulted in increased urinary excretion of a number of lipophilic aldehydes and related carbonyl compounds. These secondary lipid peroxidation products were measured as 2,4-dinitrophenylhydrazine derivatives by HPLC. Measurement of the urinary excretion of these compounds would appear to be a useful and noninvasive index of lipid peroxidation *in vivo*.

ACKNOWLEDGMENTS

Published as paper No. 22,609 of the contribution series of the Minnesota Agricultural Experiment Station on research conducted under Project No. 18-085 supported by Hatch funds, and by the U.S. Agency for International Development, Contract no. 608-0160.

REFERENCES

1. De Groot, H. (1994) Reactive Oxygen Species in Tissue Injury, *Hepatogastroenterol 41,* 328–332.
2. Halliwell, B. (1994) Free Radicals and Antioxidants: A Personal View, *Nutr. Rev. 52,* 253–265.
3. Packer, L. (1991) Protective Role of Vitamin E in Biological Systems, *Am. J. Clin. Nutr. 53 (Suppl. 4),* 1050S–1055S.
4. Burton, G.W. (1994) Vitamin E: Molecular and Biological Function, *Proc. Nutr. Soc. 53,* 251–262.
5. Maellaro, E., Casini, A.F., Bello, B.D., and Comporti, M. (1990) Lipid Peroxidation and Antioxidant Systems in the Liver Injury Produced by Glutathione-Depleted Agents, *Biochem. Pharmacol. 39,* 1513–1521.
6. Niki, E., Yamamoto, Y., Komuro, E., and Sato, K. (1991) Membrane Damage Due to Lipid Oxidation, *Am. J. Clin. Nutr. 53,* 201S–205S.
7. Blanchflower, W.J., Walsh, D.M., Kennedy, S., and Kennedy, D.G. (1993) A Thermospray Mass Spectrometric Assay for Fe-Induced 4-Hydroxynonenal in Tissues, *Lipids 28,* 261–264.
8. Dratz, E.A., Garnsworth, C.F., Loew, E.C., Stephens, R.J., Thomas, D.W., and Van Kuijk, F.J.G.M. (1989) Products of *in vivo* Peroxidation Are Present in Tissues of Vitamin E-Deficient Rats and Dogs, *Ann. N.Y. Acad. Sci. 570,* 46–60.
9. Cosgrove, J.P., Church, D.F., and Pryor, W.A. (1987) The Kinetics of the Autoxidation of Polyunsaturated Fatty Acids, *Lipids 22,* 299–304.
10. Wills, E.D. (1985) The Role of Dietary Components in Oxidative Stress in Tissues, in *Oxidative Stress* (Sies, H., ed.) pp. 197–216, Academic Press, London.
11. Spector, A.A., and Yorek, M.A. (1985) Membrane Lipid Composition and Cellular Function, *J. Lipid Res. 26,* 1015–1035.
12. Hart, C.M., Tolson, J.K., and Block, E.R. (1991) Supplemental Fatty Acids Alter Lipid Peroxidation and Oxidant Injury in Endothelial Cells, *Am. J. Physiol. 260,* L481–L488.
13. Smith, D.L., Willis, A.L., Nguyen, N., Conner, D., Zahedi, S., and Fulks, J. (1989) Eskimo Plasma Constituents, Dihomo-γ-linolenic Acid, Eicosapentaenoic Acid, and Docosahexaenoic Acid Inhibit the Release of Atherogenic Mitogens, *Lipids 24,* 70–75.
14. Zöllner, N., and Tatò, F. (1992) Fatty Acid Composition of the Diet: Impact on Serum Lipids and Atherosclerosis, *Clin. Invest. 70,* 968–1009.
15. Hu, M.L., Frankel, E.N., Leibovitz, B.E., and Tappel, A.L. (1989) Effect of Dietary Lipids and Vitamin E on *in vitro* Lipid Peroxidation in Rat Liver and Kidney Homogenates, *J. Nutr. 119,* 1574–1582.
16. Kaasgaard, S.G., Homer, G., Hoy, C.E., Behrens, W.A., and Beare-Rogers, J. L. (1992) Effects of Dietary Linseed Oil and Marine Oil on Lipid Peroxidation in Monkey Liver *in vivo* and *in vitro, Lipids 27,* 740–745.
17. Lamers, J.M., Hartog, J.M., Guarnieri, C., Vaona, I., Verdouw, P.D., and Koster, J.F. (1988) Lipid Peroxidation in Normotic and Ischaemic-Reperfused Heart of Fish Oil and Lard Fat Fed Pigs, *J. Mol. Cell Cardiol. 20,* 605–615.
18. Connor, H.D., Thurman, R.G., Galizi, M.D., and Mason, R.P. (1986) The Formation of a Novel Free Radical Metabolite from CCl_4 in the Perfused Rat Liver and *in vivo, J. Biol. Chem. 261,* 4542–4548.
19. Schauenstein, E. (1967) Autoxidation of Polyunsaturated Esters in Water: Chemical Structure And Biological Activity of the Products, *J. Lipid Res. 8,* 417–428.
20. Benedetti, A., Comporti, M., and Esterbauer, H. (1980) Identification of 4-Hydroxynonenal As a Cytotoxic Product Originating from the Peroxidation of Liver Microsomal Lipids, *Biochim. Biophys. Acta 620,* 281–96.
21. Esterbauer, H., Zollner, H., and Schaur, R.J. (1990) Aldehydes Formed by Lipid Peroxidation: Mechanisms of Formation, Occurrence, and Determination, in *Membrane Lipid Peroxidation* (Vigo-Pelfrey, C., ed.) pp. 240–268, CRC Press, Boca Raton.
22. Esterbauer, H., Schaur, R.J., and Zollner, H. (1991) Chemistry and Biochemistry of 4-Hydroxynonenal, Malonaldehyde, and Related Aldehydes, *Free Rad. Biol. Med. 11,* 81–128.
23. Comporti, M. (1989) Three Models of Free Radical-Induced Cell Injury, *Chem.-Biol. Interact. 72,* 1–56.
24. Eckl, P.M., Ortner, A., and Esterbauer, H. (1993) Genotoxic Properties of 4-Hydroxyalkenals and Analogous Aldehydes, *Mutat. Res. 290,* 183–192.
25. Witz, G. (1989) Biological Interactions of α,β-Unsaturated Aldehydes, *Free Rad. Biol. Med. 7,* 333–349.
26. Kanazawa, K., and Ashida, H. (1991) Target Enzymes on Hepatic Dysfunction Caused by Dietary Products of Lipid Peroxidation, *Arch. Biochem. Biophys. 288,* 71–78.
27. Comporti, M. (1993) Lipid Peroxidation: Biopathological Significance, *Molec. Aspects Med. 14,* 199–207.
28. Kim, S.-S., Gallaher, D.D., and Csallany, A.S. (1999) Lipophilic Aldehydes and Related Carbonyl Compounds in Rat and Human Urine, *Lipids 34,* 489–496.
29. Cheronis, N.D., and Entrikin, I.B. (1961) Derivatives of Aldehydes, in *Semimicro Qualitative Organic Analysis,* pp. 388–401, Interscience, Ltd., London.
30. Lee, H.-S., Shoeman, D.W., and Csallany, A.S. (1992) Urinary Response to *in vivo* Lipid Peroxidation Induced by Vitamin E Deficiency, *Lipids 27,* 124–128.
31. Kim, S.-S., Gallaher, D.D., and Csallany, A.S. (1999) Lipophilic Aldehydes and Related Carbonyl Compounds in Rat and Human Urine, *Lipids 34,* 489–496.
32. Sonnenwirth, A.C., and Jarett, L. (1980) *Gradwhohl's Clinical Laboratory Methods and Diagnosis,* Vol. 1, pp. 507–509, St. Louis.
33. Lee, H.-S., Shoeman, D.W., and Csallany, A.S. (1992) Urinary Response to *in vivo* Lipid Peroxidation Induced by Vitamin E Deficiency, *Lipids 27,* 124–128.
34. Packer, L., and Landvik, S. (1989) Vitamin E: Introduction to Biochemistry and Health Benefits, *Ann. N.Y Acad. Sci. 570,* 1–6.
35. Yoshino, K., Sano, M.. Fujita, M., and Tomita. I. (1990) Studies on the Formation of Aliphatic Aldehydes in the Plasma and Liver of Vitamin E-Deficient Rats, *Chem. Pharm. Bull. 38,* 2212–2215.
36. Esterbauer, H., Gunther, J., Quehenberger, O., and Koller, E. (1987) Autoxidation of Human Low Density Lipoprotein: Loss of Polyunsaturated Fatty Acids and Vitamin E and Generation of Aldehydes, *J. Lipid Res. 28,* 495–509.
37. Snijders, C.P., Schouten, J.A., De Jong, A.P., and Van Der Veen, E.A. (1984) Effect of Dietary Cod-Liver Oil on the Lipid Composition of Human Erythrocyte Membranes, *Scand. J. Clin. Lab, Invest. 44,* 39–46.
38. Javouhey, A., Rocquelin, G., Rochette, L., and Juaneda, P. (1990) Comparative Effects of Equivalent Intakes of 18:3 (n-3) and of Marine (n-3) Fatty Acids on Rat Cardiac Phospholipid Contents and Fatty Acid Compositions, *Nutr. Res. (N.Y.) 10,* 291–301.
39. Rao, C.V., Zang, E., and Reddy, B.S. (1993) Effect of High Fat Corn Oil, Olive Oil, and Fish Oil on Phospholipid Fatty Acid Composition in Male F344 Rats, *Lipids 28,* 441–447.
40. Van Den Boom, M.A.P., Wassink, M.G., Roelofsen, B., De Fouw, N.J., and Op Den Kamp, J.A.F. (1996) The Influence of a Fish Oil-Enriched Diet on the Phospholipid Fatty Acid Turnover in the Rabbit Red Cell Membrane *in vivo, Lipids 31,* 285–293.
41. Burns, A., Lin, Y., Gibson, R., and Jamieson, D. (1991) The Effect of a Fish Oil-Enriched Diet on Oxygen Toxicity and Lipid Peroxidation in Mice, *Biochem. Pharmacol. 42,* 1353–1360.

42. Van Den Berg, J.J.M., De Fouw, N.J., Kuypers, F.A., Roelofsen, B., Houtsmuller, U.M.T., and Op Den Kamp, J.A.F. (1991) Increased n-3 Polyunsaturated Fatty Acid Content of Red Blood Cells from Fish Oil-Fed Rabbits Increases *in vitro* Lipid Peroxidation, But Decreases Hemolysis, *Free Radical Biol. Med. 11,* 393–399.
43. Saito, M., and Nakatsugawa, K. (1994) Increased Susceptibility of Liver to Lipid Peroxidation After Ingestion of a High Fish Oil Diet, *Internat. J. Vit. Nutr. Res. 64,* 144–151.
44. Spitz, D.R., Kinter, M.T., Kehrer, J.P., and Roberts, R.J. (1992) The Effect of Monosaturated and Polyunsaturated Fatty Acids on Oxygen Toxicity in Cultured Cells, *Pediatr. Res. 32,* 366–372.
45. Hart, C.M., Tolson, J.K., and Block, E.R. (1991) Supplemental Fatty Acids Alter Lipid Peroxidation and Oxidant Injury in Endothelial Cells, *Am. J. Physiol. 260,* L481–L488.
46. Javouhey-Donzel, A., Guenot, L., Maupoil, V., Rochette, L., and Rocquelin, G. (1993) α-Linolenic Acid and Marine n-3 Fatty Acids, *Lipids 28,* 651–655.
47. Nair, P.P., Judd, J.T., Berlin, E., Taylor, P.R., Shami, S., Sainz, E., and Bhagavan, H.N. (1993) Dietary Fish Oil-Induced Changes in the Distribution of α-Tocopherol, Retinol, and β-Carotene in Plasma, Red Blood Cells, and Platelets: Modulation by Vitamin E, *Am. J. Clin. Nutr. 58,* 98–102.
48. Cheeseman, K.H., Albano, E.F., Tomasi, A., and Slater, T.F. (1985) Biochemical Studies on the Metabolic Activtion of Halogenated Alkanes, *Environ. Health Perspect. 64,* 85–101.
49. Benedetti, A., Fulceri, R., Ferrali, M., Ciccoli, L., Esterbauer, H., and Comporti, M. (1982) Detection of Carbonyl Function in Phospholipids of Liver Microsomes in CCl_4- and $BrCCl_3$-Poisoned Rats, *Biochim. Biophys. Acta 712,* 628–638.
50. Goldring, C., Casini, A.F., Maellaro, E., Bello, B.D., and Comporti, M. (1993) Determination of 4-Hydroxynonenal by High-Performance Liquid Chromatography with Electrochemical Detection, *Lipids 28,* 141–145.
51. Poli, G., Cheeseman, K.H., Biasi, F., Chiarpotto, E., Dianzani, M.U., Esterbauer, H., and Slater, T.F. (1989) Promethazine Inhibits the Formation of Aldehydic Products of Lipid Peroxidation But Not Covalent Binding Resulting from the Exposure of Rat Liver Fractions to CCl_4, *Biochem. J. 264,* 527–532.
52. Poli, G., Dianzani, M.U., Cheeseman, K.H., Slater, T.F., Lang, J., and Esterbauer, H. (1985) Separation and Characterization of the Aldehydic Products of Lipid Peroxidation Stimulated by Carbon Tetrachloride or ADP-Iron in Isolated Rat Hepatocytes and Rat Liver Microsomal Suspensions, *Biochem. J. 227,* 629–638.
53. Dhanakoti, S.N., and Draper, H.H. (1987) Response of Urinary Malonaldehyde to Factors That Stimulate Lipid Peroxidation *in vivo, Lipids 22,* 643–646.
54. Alary, J., Bravais, F., Cravedi, J.P., Debrauwer, L., Rao, D., and Bones, G. (1995) Mercapturic Acid Conjugates as Urinary End Metabolites of the Lipid Peroxidation Product 4-Hydroxy-2-nonenal in the Rat, *Chem. Res. Toxicol. 8,* 34–39.
55. Winter, C.K., Segall, H.J., and Jones, A.D. (1987) Distribution of *trans*-4-hydroxy-2-hexenal and Tandem Mass Spectrometric Detection of Its Urinary Mercapturic Acid in the Rat, *Drug Metab. Dispos. 15,* 608–612.
56. Esterbauer, H., and Zollner, H. (1989) Methods for Determination of Aldehydic Lipid Peroxidation Products, *Free Rad. Biol. Med. 7,* 197–203.
57. Esterbauer, H., and Zollner, H. (1989) Methods for Determination of Aldehydic Lipid Peroxidation Products, *Free Rad. Biol. Med. 7,* 197–203.

[Received August 26, 1999, and in final revised form and accepted June 5, 2000]

n-3 Fatty Acid Deficiency Decreases Phosphatidylserine Accumulation Selectively in Neuronal Tissues

Jillonne Hamilton, Rebecca Greiner, Norman Salem Jr., and Hee-Yong Kim*

Section of Mass Spectrometry, Laboratory of Membrane Biochemistry and Biophysics, National Institute on Alcohol Abuse and Alcoholism, National Institutes of Health, Rockville, Maryland 20852

ABSTRACT: We have previously shown that the docosahexaenoate (22:6n-3) status in membrane phospholipids influences the biosynthesis and accumulation of phosphatidylserine (PS) in brain microsomes and C6 glioma cells. In the present study, we investigated whether the observed effect of membrane docosahexaenoic acid status on PS accumulation is universal or occurs specifically in neuronal tissues. We observed that rat brain cortex, brain mitochondria, and olfactory bulb, where 22:6n-3 is highly concentrated, contain significantly higher levels of PS in comparison to liver and adrenal, where 22:6n-3 is a rather minor component. Phospholipid molecular species analysis revealed that in brain cortex, mitochondria, and olfactory bulb 18:0,22:6n-3 was the most abundant species representing 45–65% of total PS. In nonneuronal tissues such as liver and adrenal, 18:0,20:4n-6 was the major PS species. Dietary depletion of n-3 fatty acids during prenatal and postnatal developmental periods decreased the brain 22:6n-3 content by more than 80%, with a concomitant increase in 22:5n-6 in all tissues. Under these conditions, an approximately 30–35% reduction in total PS in rat brain cortex, brain mitochondria, and olfactory bulb was observed, while PS levels in liver and adrenal were unchanged. The observed reduction of PS content in neuronal membranes appears to be due to a dramatic reduction of 18:0,22:6n-3-PS without complete replacement by 18:0,22:5n-6-PS. These results establish that variations in membrane 22:6n-3 fatty acid composition have a profound influence on PS accumulation in neuronal tissues where 22:6n-3 is abundant. These data have implications in neuronal signaling events where PS is believed to play an important role.

Paper no. L8490 in *Lipids 35,* 863–869 (August 2000).

Docosahexaenoic acid (22:6n-3) is the major polyunsaturated fatty acid in neuronal membranes (1,2). This lipid profile appears to be rigorously maintained, and increasing evidence suggests that maintenance of high levels of 22:6n-3 is necessary for optimal neural development and function (3–5). Phosphatidylserine (PS), the major anionic phospholipid class in biomembranes, is particularly enriched with this fatty acid (1,2). PS is synthesized from pre-existing molecules of phosphatidylcholine (PC) or phosphatidylethanolamine (PE) *via* base-exchange of L-serine with either choline or ethanolamine (6–8). The reaction, which is catalyzed by base-exchange enzymes, is energy independent and stimulated by Ca^{2+}. In mammalian cells, at least two distinct enzymes located in the endoplasmic reticulum or mitochondria-associated membrane are responsible, phosphatidylserine synthase I (PSS I) and phosphatidylserine synthase II (PSS II) (9,10). PPS I utilizes primarily PC as the substrate for the base-exchange reaction, while PSS II utilizes only PE as the substrate (11). Once formed, PS can be exported into the mitochondria and become decarboxylated to PE by phosphatidylserine decarboxylase, which is found in the inner mitochondria membrane (12).

The importance of PS revolves around its functions in cellular events, such as translocation of protein kinases to the plasma membrane and apoptosis. For example, it is known that PS interacts selectively with the cystine-rich amino-terminal end of Raf-1 kinase (13,14) and facilitates translocation of Raf-1 to the plasma membrane. Translocation of Raf-1 to the plasma membrane is one of the first steps necessary to transduce growth factor signaling (15). PS also participates in the translocation of protein kinase C to the membrane for activation (16). Apoptosis, or programmed cell death, is a physiological phenomenon that occurs extensively in the developing central nervous system, but can also occur in many pathological conditions (17). During apoptosis, PS, which is normally found in the inner leaflet of the plasma membrane, appears in the outer leaflet (18). The outer leaflet PS may serve as a signal for noninflammatory engulfment of apoptotic cells (19). PS is also important in protein-lipid interactions, an example being the recently reported human serum deprivation response gene, that encodes for a specific PS-binding protein (20). In addition to the role of PS in cellular signaling events, it may also be useful in treating neurological disorders such as Alzheimer's disease (21) and amnesia (22). Thus, dietary signals, which can regulate the level of membrane PS, may also serve to regulate these PS functions.

We have previously reported that depletion of 22:6n-3 fatty acid leads to a decrease in PS biosynthesis and a reduc-

*To whom correspondance should be addressed at Section of Mass Spectrometry, LMBB, NIAAA, NIH, 12420 Parklawn Drive, Rm. 158, Rockville, MD 20852. E-mail: hykim@nih.gov

Abbreviations: 20:4n-6, arachidonic acid; 22:6n-3, docosahexaenoic acid; 22:5n-6, docosapentaenoic acid; 22:4n-6, docosatetraenoic acid; 18:3n-3, α-linolenic acid; ESI/MS, electrospray ionization/mass spectrometry; GC, gas chromatography; HPLC/MS, high-performance liquid chromatography/mass spectrometry; PC, phosphatidylcholine; PE, phosphatidylethanolamine; PS, phosphatidylserine; PSS, phosphatidylserine synthase.

tion of PS in brain microsomes (23). Furthermore, we have reported that enrichment of membrane phospholipids with 22:6n-3 significantly promotes incorporation of this fatty acid into PS and the synthesis of PS by serine base exchange, leading to increased PS levels (24). Others have shown that intraamniotic injection of ethyl-docosahexaenoate increases brain 22:6n-3 as well as PS content in rats (25). In this study, we determine whether modulation of PS accumulation, due to the 22:6n-3 status, is a general phenomenon or occurs specifically in tissues where 22:6n-3 concentration is particularly high. Phospholipid composition of various rat tissues and organelles including brain cortex, olfactory bulb, adrenal gland, liver, and brain mitochondrial fractions in both n-3-adequate and n-3-deficient rats were examined using electrospray high-performance liquid chromatography/mass spectrometry (HPLC/MS). The data establish that PS levels are considerably higher in neuronal tissues in comparison to non-neuronal tissues and that n-3-deficiency results in a dramatic reduction of PS only in neuronal cells.

MATERIALS AND METHODS

Materials. Deuterium-labeled or nonlabeled phospholipid standards and brain PS were purchased from or custom-synthesized by Avanti Polar Lipids (Alabaster, AL). All solvents were HPLC grade, and purchased from EM Scientific (Gibbstown, NJ), or Burdick & Jackson (Muskegon, MI). BF_3/methanol was obtained from Alltech (Deerfield, IL). Fiske and Subbarow reagent was purchased from Sigma (St. Louis, MO). Deuterated phospholipid standards used for quantitation were calibrated by phosphorus assay (26) and gas chromatography (GC) analysis.

Animals and tissue preparation. Procedures for the rearing of animals were previously described in detail (27). Briefly, 21-d-old Long-Evans rats (Charles River, Portage, MI) were randomized into two groups and began consuming one of two experimental diets. The two experimental diets were designed to contain only one primary fatty acid variable, α-linolenic acid (18:3n-3). Safflower oil contributed adequate and identical amounts of linoleic acid (18:2n-6) to both diets. A small amount of flaxseed oil was added to provide α-linolenate in the n-3-adequate diet. Thus, 18:3n-3 was 3.1% of total fatty acids in the n-3-adequate diet and 0.04% in the n-3-deficient diet. The male offspring of these rats, denoted as the F2 generation, were weaned to the diet of the dam and maintained on these diets throughout the study. At 8 wk of age, F2 generation rats consuming the n-3-deficient diet had an 82% decrease in 22:6n-3 compared to rats consuming the n-3-adequate diet. All animal procedures were approved by the National Institute on Alcohol Abuse and Alcoholism (LMBB OC09).

The brain mitochondrial fractions were prepared according to Cotman (28), with slight modifications. Homogenates of rat brain were prepared in a solution of 0.32 M sucrose with 10 mM tris HCl and 1 mM EDTA (pH 7.3) and centrifuged at 1,000 × *g* for 5 min to remove nuclei and unbroken cells. The resulting supernatant was transferred and centrifuged at 11,000 × *g* for 20 min to provide a supernatant and a pellet. The pellet was suspended in 30 mL of 0.32 M sucrose, and centrifuged at 11,000 × *g* for 20 min. To isolate the mitochondrial fraction, the resulting pellet was suspended in a 12% Ficoll solution, a 7.5% Ficoll solution was placed on top of the 12% layer, and 0.32 M sucrose buffer was placed on top of the 7.5% layer and centrifuged at 100,000 × *g* for 60 min. The mitochondrial fraction precipitated at the bottom and was collected, washed with phosphate-buffered saline, and stored at −70°C until further use. A protein assay was performed using the bicinchoninic acid reagent (29), and lipids were extracted according to the method of Bligh and Dyer (30). For phospholipid molecular species analysis, internal standards, d_{35}-18:0,20:4-PC and PE, and d_{35}-18:0,22:6-PS, were added prior to lipid extraction. Similarly, tissue samples of brain cortex, liver, adrenal gland, and olfactory bulb were homogenized and aliquots were removed for protein assay (29) and lipid extraction (30).

Fatty acid analysis. Lipids were extracted in the presence of tricosanoic acid (23:0) as the internal standard, and fatty acids were determined by GC analysis after transmethylation as previously described (31). The content of each individual fatty acid was expressed as a weight percentage of total fatty acids. Fatty acids were identified by the retention times of known fatty acid standards, and the content of each individual fatty acid was expressed as a weight perentage of total fatty acids.

PS molecular species analysis by HPLC/MS. Phospholipid molecular species were separated and determined using reversed-phase HPLC/electrospray ionization-mass spectrometry (ESI-MS) with a C18 column (150 × 20 mm, 5 µm; Phenomenex, Torrance, CA) as described previously (32). Separation was accomplished using a mobile phase containing water; 0.5% ammonium hydroxide in methanol; and hexane, changing from 12:88:0 to 0:88:12 in 17 min after holding the initial composition for 3 min at a flow rate of 0.4 mL/min (33). A Hewlett Packard HPLC-MS Series 1100 MSD instrument (Palo Alto, CA) was employed to detect the separated phospholipid molecular species. For electrospray ionization, the drying gas temperature was 350°C while the drying gas flow rate and nebulizing gas pressure were 13 L/min and 32 psi, respectively. The capillary voltage was set at 4000 V, and the exit voltage was set at 200 V. Quantification was based on the area ratio calculated against the internal standard of the same phospholipid class. Identification of molecular species was based on the mono- and diglyceride ion peaks as described previously (32). Quantification was based on the area ratio calculated against the internal standard of the same phospholipid class using diglyceride ions.

The HPLC-ESI/MS method employed for phospholipid molecular species analysis was validated by phosphorus assay with 16:0,18:1-PS and a commercial preparation of brain PS (Avanti Polar Lipids). The amounts of 16:0,18:1-PS in aliquots of a standard stock solution were determined by phosphorus assay (26) performed in triplicate. Separately, the

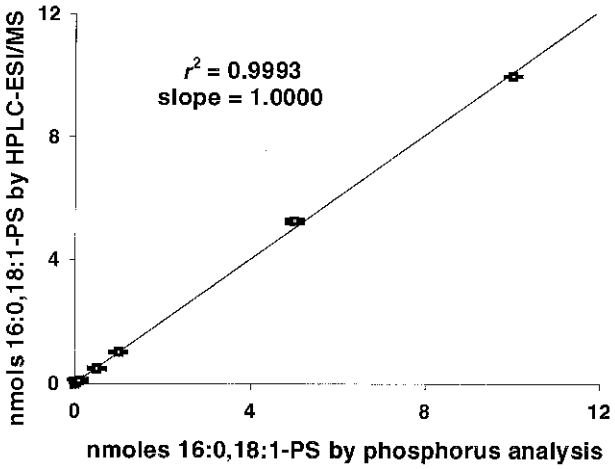

FIG. 1. Correlation between 16:0,18:1-PS content determined by phospholipid molecular species method using d_{35}-18:0,22:6-PS as an internal standard and by phosphorus analysis. Representative data from two experiments are shown. PS, phosphatidylserine.

16:0,18:1-PS amount was determined by phospholipid molecular species analysis using HPLC-ESI/MS after addition of d_{35}-18:0,22:6-PS as an internal standard. The results obtained by these two independent methods were in good agreement in the 50–10,000 pmol range (Fig. 1). To validate the HPLC-ESI/MS method for analysis of phospholipid mixtures, aliquots of a commercial brain PS mixture were analyzed by GC, HPLC-ESI/MS, and phosphorus assay. Total PS contents determined by HPLC-ESI/MS and phosphorus assay were comparable, as shown in Table 1. When fatty acid contents obtained by GC analysis were converted to mol% and compared with species data, consistent results were obtained (Table 1), indicating that the HPLC-ESI/MS method can be generally applied to the analysis of PS molecular species in biological mixtures.

Phospholipid class separation followed by phosphorus assay. Phospholipid classes were separated employing normal-phase chromatography with a silica column (100 × 2 mm i.d., 3 μm; Thompson, Springfield, VA). Separation was accomplished using a mobile phase containing isopropyl alcohol, water, and hexane, changing from 54.4:3.7:41.9 to 51.6:8.6:39.8, respectively, in 14 min after holding the initial composition for 8 min at a flow rate of 0.5 mL/min (34). Fractions were collected from the olfactory bulb and subjected to phosphorus analysis (26).

Statistical analysis. Statistical differences between n-3-adequate and n-3-deficient animals were assessed by the Student's *t*-test.

RESULTS

Effect of n-3 deficiency on the total lipid composition. As expected, fatty acid analysis indicated that in neuronal tissues of n-3-adequate animals, 22:6n-3 levels were high. Brain cortex, brain mitochondria, and the olfactory bulb contained ap-

TABLE 1
Molecular Species and Fatty Acid Content of Standard Bovine Brain Phosphatidylserine

HPLC-ESI/MS analysis		Fatty acyl contents evaluated by GC and HPLC-ESI/MS		
PS	nmol ± SD	FA	GC (mol%)[b]	LC/MS (mol%)[c]
16:0,18:1n-9	0.14 ± 0.03	16:0	1.62 ± 0.09	1.94 ± 0.04
16:0,22:2n-6	0.53 ± 0.04	18:0	42.54 ± 0.31	38.60 ± 0.48
16:0,22:6n-3	0.19 ± 0.01	18:1n-9	33.32 ± 0.13	34.29 ± 0.59
18:0,18:1n-9	7.91 ± 0.45	20:1n-9	2.50 ± 0.08	2.73 ± 0.12
18:0,20:1n-9	0.60 ± 0.06	20:3n-6	0.47 ± 0.01	0.59 ± 0.14
18:0,20:3n-6	0.28 ± 0.06	20:4n-6	2.04 ± 0.10	2.68 ± 0.22
18:0,20:4n-6	1.14 ± 0.33	22:2n-6	0.90 ± 0.04	1.18 ± 0.04
18:0,22:4n-6	0.99 ± 0.17	22:4n-6	3.68 ± 0.06	3.86 ± 0.35
18:0,22:5n-6	1.55 ± 0.17	22:5n-6	2.99 ± 0.03	3.38 ± 0.28
18:0,22:6n-3	4.00 ± 0.35	22:6n-3	9.46 ± 0.18	9.81 ± 0.25
18:0,24:4n-6	0.30 ± 0.04	24:4n-6[d]	0.58 ± 0.07	0.65 ± 0.05
18:1,18:1n-9	2.79 ± 0.12			
18:1,20:1n-9	0.65 ± 0.06			
18:1,20:4n-6	0.18 ± 0.01			
18:1,22:4n-6	0.70 ± 0.15			
18:1,22:6n-3	0.23 ± 0.05			
22:6,22:6n-3	0.03 ± 0.01			
Total PS by HPLC-ESI/MS	22.22 ± 0.24			
Total PS by phosphorus assay	24.30 ± 3.33[a]			

[a]Data expressed as nmol phosphorus ± SD.
[b]mol% ± SD determined by GC.
[c]mol% ± SD calculated from HPLC-ESI/MS data.
[d]Identified by relative retention behavior under an isothermal condition. Abbreviations: HPLC-ESI/MS, high-performance liquid chromatography-electroscopy ionization/mass spectrometry; GC, gas chromatography; PS, phosphatidylserine; FA, fatty acid.

TABLE 2
Fatty Acid Distribution of Selected Fatty Acids from Olfactory Bulb, Brain Cortex, Brain Mitochondria, Adrenal Gland, and Liver from n-3-Adequate and n-3-Deficient Rats[a]

	Olfactory bulb		Brain cortex		Brain mitochondria		Adrenal		Liver	
FA	Adequate	Deficient	Adequate	Deficient	Adequate	Deficient	Adequate	Deficient	Adequate	Deficient
16:0	24.9 ± 2.7	25.8 ± 3.1	20.6 ± 0.9	20.3 ± 0.8	20.1 ± 0.2	19.7 ± 1.1	21.3 ± 3.0	21.4 ± 2.4	22.7 ± 1.34	23.0 ± 0.9
18:0	20.1 ± 1.8	18.4 ± 2.1	21.7 ± 0.3	21.6 ± 0.4	22.9 ± 0.3	24.2 ± 3.3	15.1 ± 3.3	14.4 ± 2.2	17.4 ± 1.1	18.4 ± 1.3
18:1n-9	16.3 ± 1.1	16.8 ± 0.6	16.6 ± 0.8	15.4 ± 0.3	14.0 ± 0.4	12.9 ± 1.3	18.2 ± 2.8	17.7 ± 3.0	12.1 ± 1.5	10.8 ± 1.9
20:4n-6	9.6 ± 0.7	9.1 ± 1.0	10.7 ± 0.4	11.4 ± 0.3[b]	12.7 ± 0.6	13.6 ± 0.9	15.0 ± 4.0	14.8 ± 2.7	16.9 ± 1.0	18.6 ± 1.7
22:4n-6	2.6 ± 0.4	2.9 ± 0.6	3.0 ± 0.1	3.9 ± 0.2[c]	2.7 ± 0.0	3.5 ± 0.3	4.9 ± 0.8	6.5 ± 1.7[c]	0.3 ± 0.0	0.6 ± 0.1[c]
22:5n-3	0.14 ± 0.0	ND	0.1 ± 0.0	ND	0.1 ± 0.0	ND	0.6 ± 0.1	0.1 ± 0.0	0.5 ± 0.1	ND
22:5n-6	1.9 ± 0.2	13.0 ± 0.8[c]	0.6 ± 0.1	12.6 ± 0.3[c]	0.9 ± 0.0	13.1 ± 1.3[c]	1.7 ± 0.2	3.3 ± 0.3	0.5 ± 0.1	5.8 ± 0.8[c]
22:6n-3	15.7 ± 1.8	2.2 ± 0.1[c]	15.3 ± 0.6	2.5 ± 0.1[c]	16.8 ± 0.2	2.2 ± 0.1[c]	1.3 ± 0.3	0.3 ± 0.2[b]	7.1 ± 0.7	0.5 ± 0.0[c]

[a]Data are expressed as percentage of total fatty acid ± SD from six different animals.
[b]Significantly different from n-3-adequate rats at $P < 0.01$.
[c]Significantly different from n-3-adequate rats at $P < 0.001$. ND, not detected.

proximately twice as much 22:6n-3 as liver and 12 times more than the adrenal gland (Table 2). The most abundant polyunsaturated fatty acid in liver and adrenal gland was arachidonic acid (20:4n-6), and the adrenal also contained a significant amount of docosatetraenoic acid (22:4n-6). An n-3 fatty acid deficiency resulted in a dramatic reduction in 22:6n-3 for all tissues with concomitant increases in docosapentaenoic acid (22:5n-6) (Table 2). The decrease in 22:6n-3, in all tissues except adrenal, was mostly compensated for by increases in 22:5n-6. In the case of the adrenal, total 22:5n-6 content of deficient rats exceeded the 22:6n-3 content of n-3-adequate rats. In brain cortex, 20:4n-6 was significantly higher in the n-3-deficient animals. For adrenal, liver, and brain mitochondria, 22:4n-6 was also increased with n-3 fatty acid deficiency. Total phospholipid content, as determined by phosphorus assay, was not significantly changed by n-3-deficiency in any of the tissues examined (Table 3). The phospholipid to protein ratio was highest in brain cortex, followed by brain mitochondria and olfactory bulb, and lowest in adrenal and liver (Table 3).

Effect of n-3 deficiency on the phospholipid molecular species profile. Molecular species analysis of PS indicated that neuronal tissues contain significantly higher levels of PS in comparison to nonneuronal cells (Table 4). In the n-3-adequate animals, brain cortex, brain mitochondria, and olfactory bulb contained approximately 24, 12, and 9 times more PS than adrenal gland or liver, respectively, when the data were expressed as nmol/mg protein (Table 4). In terms of molecular species, 18:0,22:6n-3-PS was the most abundant, constituting 45–65% of total PS in neuronal tissues. In adrenal and liver, however, 18:0,20:4n-6-PS was the most abundant species, making up approximately half of total PS (Table 4).

The effect of n-3 deficiency on total PS content expressed as an absolute value normalized to protein content is shown in Table 4 and Figure 2A. The PS content was greatest in brain cortex (129 ± 5.4 nmol/mg protein) followed by brain mitochondria and olfactory (72.2 ± 3.5 and 49.2 ± 2.5 nmol/mg protein) (Fig. 2A). Adrenal and liver PS amounts were 5.4 ± 0.3 and 5.5 ± 0.2 nmol/mg protein, respectively. Dietary depletion of n-3 fatty acids resulted in an approximately 30% reduction in total PS for neuronal tissues, but did not alter PS levels in adrenal or liver (Fig. 2A). Due to the low phospholipid/protein ratio in the olfactory bulb, the percentage of PS normalized to total phosphorus was higher than that of cortex or mitochondria (Table 3 and Fig. 2B). However, the decrease of PS was consistently observed in neuronal tissues of n-3-deficient animals. The largest decrease in PS (38%) occurred in brain cortex; the proportion of PS (expressed as % of total phospholipid) in brain cortex for control rats was 12.3 ± 0.4%, which is similar to a previously reported value of 10.2 ± 0.1% (35), and was reduced to 7.6 ± 0.4% in the n-3 deficient rats. In the olfactory bulb, PS was reduced from 16.8 ± 0.3 to 11.7 ± 0.3%, while in brain mitochondria, PS was reduced from 8.3 ± 0.4 to 6.5 ± 0.7%. The percentages of PS in adrenal and liver of n-3-adequate animals were 2.4 ± 0.1 and 3.0 ± 0.1%, respectively, which are similar to previously reported values (35,36). Unlike the neuronal tissues, there was no significant decrease in the PS percentage for the adrenal gland or liver.

In neuronal tissues, but not adrenal and liver, di-polyunsaturated species of PS were detected (Table 4). The brain cortex, brain mitochondria, and olfactory bulb of n-3-adequate animals contained 22:6,22:6n-3 and 22:4,22:6n-3-PS, and/or 22:5,22:5-PS species (Table 4). Also present in the brain cortex of n-3-adequate animals was 22:5,22:6-PS (Table 4). While significantly less, 22:4,22:6n-3 and/or 22:5,22:5-PS was present in n-3-deficient animals in all neu-

TABLE 3
Total Phosphorus Content of Olfactory Bulb, Brain Cortex, Brain Mitochondria, Adrenal Gland, and Liver from n-3-Adequate and n-3-Deficient Rats[a]

	Adequate	Deficient
Olfactory bulb	286 ± 34	267 ± 21
Brain cortex	1,039 ± 27	1,142 ± 180
Brain mitochondria	865 ± 190	786 ± 152
Adrenal	221 ± 14	232 ± 33
Liver	180 ± 27	174 ± 7.0

[a]Data are expressed as nmole phosphorus/mg protein ± SD from three different animals.

TABLE 4
Phosphatidylserine Molecular Species of Olfactory Bulb, Brain Cortex, Brain Mitochondria, Adrenal Gland, and Liver from n-3-Adequate and n-3-Deficient Rats

	Olfactory bulb		Brain cortex		Brain mitochondria		Adrenal		Liver	
PS	Adequate	Deficient	Adequate	Deficient	Adequate	Deficient	Adequate	Deficient	Adequate	Deficient
16:0,18:1n-9	1.1 ± 0.1[a]	0.8 ± 0.0	1.5 ± 0.3	1.5 ± 0.2	0.8 ± 0.0	0.6 ± 0.0	ND	ND	ND	ND
16:0,20:4n-6	0.4 ± 0.0	0.3 ± 0.0	0.6 ± 0.0	0.3 ± 0.0	0.4 ± 0.0	0.1 ± 0.0[d]	0.4 ± 0.01	0.5 ± 0.1	0.8 ± 0.1	0.4 ± 0.0[d]
16:0,22:4n-6	ND[b]	ND	ND	ND	ND	ND	ND	ND	ND	0.9 ± 0.1[d]
16:0,22:5[e]	1.4 ± 0.2	5.0 ± 0.3[d]	ND	1.6 ± 0.2[d]	ND	0.7 ± 0.1[c]	ND	ND	ND	ND
16:0,22:6n-3	8.1 ± 1.3	1.0 ± 0.2[d]	3.3 ± 0.4	0.2 ± 0.0[d]	1.3 ± 0.2	0.2 ± 0.1[c]	ND	ND	ND	ND
18:0,18:1n-9	6.4 ± 2.1	4.3 ± 0.3	13.3 ± 1.0	9.6 ± 0.7	5.0 ± 0.7	3.6 ± 0.8	0.3 ± 0.0	0.4 ± 0.0[c]	0.1 ± 0.0	0.2 ± 0.0[d]
18:0,20:4n-6	3.0 ± 0.7	3.3 ± 0.4	12.0 ± 0.6	8.1 ± 0.7[c]	3.0 ± 0.2	3.4 ± 0.5	3.2 ± 0.2	3.2 ± 0.1	2.9 ± 0.2	3.1 ± 0.1
18:0,22:4n-6	ND	ND	4.2 ± 0.5	4.8 ± 0.6	5.7 ± 0.2	4.3 ± 1.0	0.4 ± 0.0	0.3 ± 0.0	ND	0.1 ± 0.0[c]
18:0,22:5[e]	1.4 ± 0.5	8.6 ± 0.4[d]	6.8 ± 0.6	33.4 ± 1.5[d]	ND	25.0 ± 3.4[d]	ND	ND	ND	0.7 ± 0.1[d]
18:0,22:6n-3	23.1 ± 2.4	6.0 ± 0.9[d]	66.0 ± 4.1	14.9 ± 2.0[d]	46.0 ± 2.4	8.0 ± 0.7d	0.1 ± 0.0	ND[d]	1.6 ± 0.1	0.2 ± 0.0[d]
18:1,18:1n-9	1.2 ± 0.3	1.3 ± 0.3	2.2 ± 0.2	2.5 ± 0.3	1.8 ± 0.2	1.9 ± 0.4	0.4 ± 0.0	0.5 ± 0.0	ND	ND
18:1,20:4n-6	ND	ND	3.0 ± 0.5	2.0 ± 0.2	0.7 ± 0.2	0.5 ± 0.1	0.6 ± 0.1	ND[c]	ND	ND
18:1,22:5[e]	ND	1.2 ± 0.3[d]	ND	3.3 ± 0.3[c]	ND	0.2 ± 0.0[c]	ND	ND	ND	ND
18:1,22:6n-3	1.4 ± 0.4	ND[d]	6.0 ± 0.5	1.2 ± 0.6[d]	1.6 ± 0.1	0.1 ± 0.0[d]	ND	ND	ND	ND
22:6,22:4n-6	1.2 ± 0.2	0.3 ± 0.1[c]	7.4 ± 0.3	1.9 ± 0.2[d]	1.5 ± 0.3	0.6 ± 0.1[c]	ND	ND	ND	ND
and/or										
22:5,22:5[e]										
22:6,22:5[e]	ND	0.4 ± 0.1[d]	0.3 ± 0.0	0.9 ± 0.1[d]	ND	0.2 ± 0.0[d]	ND	ND	ND	ND
22:6,22:6n-3	0.5 ± 0.1	ND[c]	2.4 ± 0.2	0.04 ± 0.0[d]	0.7 ± 0.1	ND[c]	ND	ND	ND	ND
Total PS	49.2 ± 2.5	32.6 ± 1.0[d]	129.0 ± 5.4	86.3 ± 4.7[d]	72.2 ± 3.5	51.1 ± 5.8[c]	5.4 ± 0.3	4.9 ± 0.2	5.5 ± 0.2	5.5 ± 0.1

[a]Data are expressed as nmol/mg protein ± SD from six different animals.
[b]ND, not detected.
[c]Significantly different from n-3-adequate rats at $P < 0.01$.
[d]Significantly different from n-3-adequate rats at $P < 0.001$. See Table 1 for abbreviation.
[e]The current HPLC-ESI/MS technique could not distinguish PS species containing 22:5n-6 from those with 22:5n-3.

ronal tissues, and di-22:6n-3 was detected only in brain cortex. In all neuronal tissues from n-3-deficient animals, the 22:5,22:6-PS species increased slightly but significantly, presumably due to the increased content of 22:5n-6 by dietary manipulation. The current HPLC-ESI/MS technique could not distinguish PS species containing 22:5n-6 from those with 22:5n-3.

DISCUSSION

The molecular species composition of membrane phospholipids is a determinant of the biochemical and biophysical properties of cell membranes with consequences for the function and activity of membrane-bound proteins (37,38). Dietary α-linolenate deficiency has been shown to induce dramatic modifications in membrane lipid composition, mainly by decreasing 22:6n-3 and increasing 22:5n-6 (1,2,39,40). This leads to a number of functional changes such as alterations in enzymatic activities (41,42), suboptimal retinal and brain development (4,43–45), and poorer performance in learning-related tasks (27,46). Low levels of 22:6n-3 have also been correlated with peroxisomal disorders associated with severe and progressive neurological deterioration (47).

The present study demonstrates that dietary n-3 fatty acids positively modulate PS accumulation in neuronal tissues. Previous work with rats fed a balanced or an n-3 polyunsaturated fatty acid-deficient diet showed that PS accumulation eventually decreases (–22%) at 24 mon in the hippocampus of rats fed the deficient diet (48). Also, intraamniotic injection with ethyl esters of 22:6n-3 has been shown to increase the PS content in rat pup brains (25). In a study of herring raised on either a 22:6n-3 supplemented diet (4.3%) or one lacking in 22:6n-3, it was found that total PS decreased in the retina of fish fed the 22:6n-3 deficient diet; the loss of 22:6n-3 was most pronounced in di-22:6n-3 species (49). Furthermore, the phospholipid composition of cerebral cortex in "sudden infant death syndrome" infants fed breast milk contained 39% more PS in comparison to formula-fed infants (50). The ranges of 18:3n-3 and 22:6n-3 in breast milk were 0.5–1.2 and 0.1–0.5%, respectively, whereas the formula contained 0.4% of 18:3n-3 and no 22:6n-3 (50). These reports and our earlier studies (23,24) corroborate with the present finding that 22:6n-3 is a potent modulator of neuronal PS accumulation.

Our current data show that the 18:0,22:6-PS molecular species contributes most to PS accumulation as well as to the reduction of PS in neuronal tissues, suggesting that the biosynthesis of PS may have a substrate specificity for 18:0,22:6 containing PC and/or PE. Alternatively, PS degradation pathways, such as PS decarboxylation, may favor other PS molecular species in comparison to 18:0,22:6-PS. In addition, acylation and/or reacylation reactions may also be in-

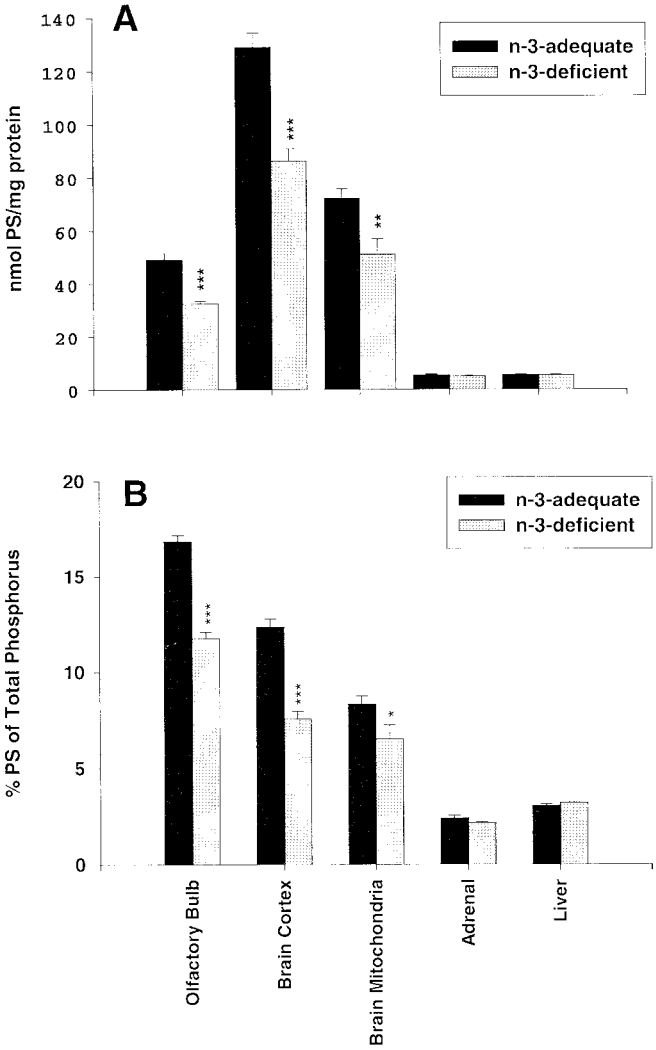

FIG. 2. (A) Absolute levels of PS in olfactory bulb, brain cortex, brain mitochondria, adrenal gland, and liver from n-3-adequate and n-3-deficient rats determined by high-pressure liquid chromatography-electrospray ionization-mass spectrometry phospholipid molecular species analysis and expressed as nmol/mg protein. Representative data from three experiments are shown. (B) Percentage PS normalized to total phosphorus content in olfactory bulb, brain cortex, brain mitochondria, adrenal and liver from n-3-adequate and n-3-deficient rats. $***P < 0.001$, $**P < 0.01$, $*P < 0.05$. Data shown represent the results from two experiments. See Figure 1 for other abbreviations.

volved in enrichment of 22:6n-3 in PS. Under n-3 fatty acid deficiency, the activity of these enzymes may be altered so that 18:0,22:6n-3-PS as well as total PS decrease. Further studies will be necessary to address these issues.

The present study establishes that membrane levels of 22:6n-3 affect PS accumulation selectively in cells where levels of 22:6n-3 are abundant. When 22:6n-3 levels are reduced in these cell membranes, either through prolonged dietary depletion (23) or ethanol treatment (24), PS accumulation decreases. This phenomenon occurs specifically in neuronal cells suggesting that n-3-deficiency may have a profound effect on PS-related signaling events in the nervous system.

ACKNOWLEDGMENTS

The assistance in tissue preparation by Karl Kevala and phospholipid quantitation by SonMi Lee are greatly appreciated.

REFERENCES

1. Salem Jr., N. (1989) New Protective Roles for Selected Nutrients, in *Omega-3 Fatty Acids: Molecular and Biochemical Aspects* (Spiller, G., and Scala, J., eds.), pp. 109–228, Alan R. Liss, New York.
2. Salem Jr., N., Kim, H.K., and Yergey, J.A. (1986) Docosahexaenoic Acid: Membrane Function and Metabolism, in *Health Effect of Polyunsaturated Fatty Acids in Seafoods* (Simopoulos, A.P., and Kifer, R.R., eds.), pp. 263–317, Academic Press, New York.
3. Carlson, S.E. (2000) Behavioral Methods Used in the Study of Long-Chain Polyunsaturated Fatty Acids Nutrition in Primate Infants, *Am. J. Clin. Nutr. 71*, 268S–274S.
4. Uauy, R., Birch, E., Birch, D., and Peirano, P. (1992) Visual and Brain Function Measurements in Studies of n-3 Fatty Acid Requirements of Infants, *J. Pediatr. 120*, S168–S180.
5. Hamosh, M., and Salem Jr., N. (1998) Long-Chain Polyunsaturated Fatty Acids, *Biol. Neonate 74*, 106–120.
6. Hubscher, G., Dils, R.R., and Pover, W.F.R. (1959) Studies on the Biosynthesis of Phosphatidylserine, *Biochim. Biophys. Acta 36*, 518–528.
7. Dils, R.R., and Hubscher, G. (1959) Metabolism of Phospholipids III. The Effect of Calcium Ions on the Incorporation of Labeled Choline into Rat-Liver Microsomes, *Biochim. Biophys. Acta 46,* 503–513.
8. Borkenhagen, J.D., Kennedy, E.P., and Fielding, L. (1961) Enzymatic Formation and Decarboxylation of Phosphatidylserine, *J. Biol. Chem. 236*, PC28–PC29.
9. Dennis, E.A., and Kennedy, E.P. (1972) Intracellular Sites of Lipid Synthesis and the Biogenesis of Mitochondria, *J. Lipid Res. 13*, 263–267.
10. Vance, J.E. (1990) Phospholipid Synthesis in a Membrane Fraction Associated with Mitochondria, *J. Biol. Chem. 265*, 7248–7256.
11. Kuge, O., and Nishijima, M. (1997) Phosphatidylserine Synthase I and II of Mammalian Cells, *Biochim. Biophys. Acta 1348*, 151–156.
12. Shiao, Y.-J., Lupo, G., and Vance, J.E. (1995) Evidence That Phosphatidylserine Is Imported into Mitochondria *via* a Mitochondria-Associated Membrane and That the Majority of Mitochondrial Phosphatidylethanolamine Is Derived from Decarboxylation of Phosphatidylserine *J. Biol. Chem. 270*, 11190–11198.
13. Ghosh, S., Xie, W.Q., Quest, A.F.G., Mabrouk, G.M., Strum, J.C., and Bell, R.M. (1994) The Cysteine-Rich Region of Raf-1 Kinase Contains Zinc, Translocates to Liposomes, and Is Adjacent to a Segment That Binds GTP-Ras, *J. Biol. Chem. 269*, 10000–10007.
14. Ghosh, S., Strum, J.C., Sciorra, V.A. Daniel, L., and Bell, R.M. (1996) Raf-1 Kinase Possesses Distinct Binding Domains for Phosphatidylserine and Phosphatidic Acid, *J. Biol. Chem. 271*, 8472–8480.
15. Yuryev, A., and Wennogle, L.P. (1998) The RAF Family: An Expanding Network of Post-Translational Controls and Protein-Protein Interactions, *Cell Res. 2*, 81–98.
16. Mosior, M., and Newton, A.C. (1998) Mechanism of the Apparent Cooperativity in the Interaction of Protein Kinase C with Phosphatidylserine, *Biochem. J. 37*, 17271–17279.
17. Valente, M., and Calabrese, F. (1999) Liver and Apoptosis, *Ital. J. Gastroenterol Hepatol. 1*, 73–77.
18. Martin, S.J., Reutelingsperger, C.P.M., McGahon, A.J., van

Schie, R.C.C.A., La Face, D.M., and Green, D.R. (1995) Early Distribution of Plasma Membrane Phosphatidylserine Is a General Feature of Apoptosis Regardless of the Initiating Stimulus: Inhibition by Overexpression of Bcl-2 and Abl, *J. Exp. Med. 182*, 1545–1556.
19. Fadok, V.A., Voelker, D.R., Campbell, P.A., Cohen, J.J., Bratton, D.L., and Henson, P.M. (1992) Exposure of PS on the Surface of Apoptotic Lymphocytes Triggers Specific Recognition and Removal by Macrophages, *J. Immunol. 148*, 2207–2216.
20. Gustincich, S., Vatt, P., Goruppi, S., Wolf, M., Saccone, S., Della Valle, G., Baggiolini, M., and Schneider, C. (1999) The Human Serum Deprivation Response Gene (SDPR) Maps to 2q32-q33 and Codes for a Phosphatidylserine-Binding Protein, *Genomics 57,* 120–129.
21. Crook, T., Petrie, W., Wells, C., and Massari, D.C. (1992) Effects of Phosphatidylserine in Alzheimer's Disease, *Psychopharm. Bull. 28*, 81–66.
22. Claro, F.T., Silva, R.H., and Frussa-Filho, R. (1999) Bovine Brain Phosphatidylserine Attenuates Scopolamine-Induced Amnesia, *Physiol. Behav. 67*, 551–554.
23. Garcia, M.C., Ward, G., Ma, Y.C., Salem Jr., N., and Kim, H.Y. (1998) Effect of Docosahexaenoic Acid on the Synthesis of Phosphatidylserine in Rat Brain Microsomes and C6 Glioma Cells, *J. Neurochem. 70*, 24–30.
24. Kim, H.Y., and Hamilton, J. (2000) Accumulation of Docosahexaenoic Acid in Phosphatidylserine Is Selectively Inhibited by Chronic Ethanol Exposure in C-6 Glioma Cells, *Lipids 35*, 187–195.
25. Green, P., and Yavin, E. (1995) Modulation of Fetal Rat Brain and Liver Phospholipid Content by Intraamniotic Ethyl Docosahexaenoate Administration, *J. Neurochem. 65*, 2555–2560.
26. Bartlett, G. (1959) Phosphorus Assay in Column Chromatography, *J. Biol. Chem. 234*, 466–468.
27. Greiner, R.S., Moriguchi, T., Hutton, A., Slotnick, B.M., and Salem Jr., N. (1999) Rats with Low Levels of Brain Docosahexaenoic Acid Show Impaired Performance in Olfactory-Based and Spatial Learning Tasks, *Lipids 34 Suppl*., S239–S243.
28. Cotman, C.W. (1974) Isolation of Synaptosomal and Synaptic Plasma Membrane Fractions, in *Methods of Enzymology* (Fleischer, S., and Packer, L., eds.), Vol. 31, pp. 445–452, Academic Press, New York.
29. Smith, P.K., Krohn, R.I., Hermanson, G.T., Mallia, A.K., Gartner, F.H., Provenzano, M.D., Fujimoto, E.K., Goeke, N.M., Olson, B.J., and Klenk, D.C. (1985) Measurement of Protein Using Bicinchoninic Acid, *Anal. Biochem. 150*, 76–85.
30. Bligh, E.G., and Dyer, W.J. (1959) A Rapid Method of Total Lipid Extraction and Purification, *Can. J. Biochem. Physiol. 37*, 911–917.
31. Morrison, W.R., and Smith, L.M. (1961) Preparation of Fatty Acid Methyl Esters and Dimethylacetals from Lipids with Boron Fluoride-Methanol, *J. Lipid Res. 35*, 600–608.
32. Kim, H.Y., Wang, T.C., and Ma, Y.C. (1994) Liquid Chromatography/Mass Spectrometry of Phospholipids Using Electrospray Ionization, *Anal. Chem. 15*, 3977–3982.
33. Ma, Y.C., and Kim, H.Y. (1995) Development of the On-Line High-Performance Liquid Chromatography/Thermospray Mass Spectrometry Method for the Analysis of Phospholipid Molecular Species in Rat Brain, *Anal. Biochem. 226*, 293–301.
34. Tarachi, T.F., Ellingson, J.S., Wu, A., Zimmerman, R., and Rubin, E. (1986) Phosphatidylinositol from Ethanol-Fed Rats Confers Membrane Tolerance to Ethanol, *Proc. Natl. Acad. Sci. USA 83*, 9398–9402.
35. Diagne, A., Fauvel, J., Record, M., Chap, H., and Dousie-Blazy, L. (1984) Studies on Ether Phospholipids II Comparative Composition of Various Tissues from Human, Rat and Guinea Pig, *Biochim. Biophy. Acta 793*, 221–231.
36. Igarashi, Y., and Kimura, T. (1984) Adrenocorticotropic Hormone-Mediated Changes in Rat Adrenal Mitochondrial Phospholipids, *J. Biol. Chem. 259*, 10745–10753.
37. Holub, B.J., and Kuksis, A. (1978) Metabolism of Molecular Species of Diacylglycerolphospholipids, *Adv. Lipid Res. 16*, 1–125.
38. Lynch, D.V., and Thompson, G.A. (1984) Retailored Lipid Molecular Species: A Tactical Mechanism for Modulating Membrane Properties, *Trans. Biochem. Sci. 9*, 442–445.
39. Foot, M., Cruz, T.F., and Clandinin, M.T. (1982) Influence of Dietary Fat on the Lipid Composition of Rat Brain Synaptosomal and Microsomal Membranes, *Biochem. J. 208*, 631–640.
40. Bourre, J.M., Pascal, D., Durand, G., Masson, M., Dumont, O., and Piciotti, M. (1984) Alterations in the Fatty Acid Composition of Rat Brain Cells (neurons, astrocytes and oligodendrocytes) and of Subcellular Fractions (myelin and synaptosomes) Induced by a Diet Devoid of n-3 Fatty Acids, *J. Neurochem. 43*, 342–348.
41. Hargreaves, K.M., and Clandinin, M.T. (1987) Phosphatidylethanolamine Methyltransferase: Evidence for Influence of Diet on Selectivity of Substrate for Methylation in Rat Brain Synaptic Membranes, *Biochim. Biophys. Acta 918*, 97–105.
42. Bourre, J.M., Francois, M., Youyou, A., Dumont, O., Piciotti, M., Pascal, G., and Durand, G. (1989) The Effects of Dietary Alpha-Linolenic Acid on the Composition of Nerve Membranes, Enzymatic Activity, Amplitude of Eletrophysiologic Parameters, Resistance to Poisons and Performance of Learning Tasks in Rats, *J. Nutr. 119*, 1880–1892.
43. Neuringer, M., Anderson, G.J., and Connor, W.E. (1988) The Essentiality of n-3 Fatty Acids for the Development and Function of Retina and Brain, *Annu. Rev. Nutr. 8*, 517–541.
44. Neuringer, M., Reisbick, S., and Janowsky, J. (1994) The Role of n-3 Fatty Acids in Visual and Cognitive Development: Current Evidence and Methods of Assessment, *J. Pediatr. 125*, S39–S47.
45. Birch, E., Birch, D., Hoffman, D., Hale, L., Everest, M., and Uauy, R. (1993) Breast-Feeding and Optimal Visual Development, *J. Pediatr. Ophthalmol Strabismus 30*, 33–38.
46. Yoshida, S., Yasuda, A., Kawazato, H., Sakai, K., Shimada, T., Takeshita, M., Yuasa, S., Kobayashi, T., Watanabe, S., and Okuyama, H. (1997) Synaptic Vesicle Ultrastructual Changes in the Rat Hippocampus Induced by a Combination of Alpha-Linolenate Deficiency and a Learning Task, *J. Neurochem. 3*, 1261–1268.
47. Martinez, M. (1992) Abnormal Profiles of Polyunsaturated Fatty Acids in the Brain, Liver, Kidney and Retina of Patients with Peroxisomal Disorders, *Brain Res. 583,* 171–182.
48. Delion, S., Chalon, S., Guilloteau, D., Lejeune, B., Besnard, J.-C., and Durand, G. (1997) Age-Related Changes in Phospholipid Fatty Acid Composition and Monoaminergic Neurotransmission in the Hippocampus of Rats Fed a Balanced or a n-3 Polyunsaturated Fatty Acid Deficient-Diet, *J. Lipid Res. 38*, 680–688.
49. Bell, M.V., Batty, R.S., Dick, J.R., Fretwell, K., Navarro, J.C., and Sargent, J.R. (1995) Dietary Deficiency of Docosahexaenoic Acid Impairs Vision at Low Light Intensities in Juvenile Herring (*Clupea harengus* L.), *Lipids 30*, 443–449.
50. Farquharson, J., Jamieson, E.C., Abbasi, K.A., Patrick, W.J.A., Logan, R.W., and Cockburn, F. (1995) Effect of Diet on the Fatty Acid Composition of the Major Phospholipids of Infant Cerebral Cortex, *Arch. Dis. Child 72*, 198–203.

[Received March 17, 2000; and in revised form and accepted July 13, 2000]

The Questionable Role of a Microsomal Δ8 Acyl-CoA-Dependent Desaturase in the Biosynthesis of Polyunsaturated Fatty Acids

Qi Chen, Feng Qin Yin, and Howard Sprecher*

Department of Molecular and Cellular Biochemistry, The Ohio State University, Columbus, Ohio 43210, USA

ABSTRACT: Several experimental approaches were used to determine whether rat liver and testes express an acyl-CoA-dependent Δ8 desaturase. When [1-^{14}C]5,11,14-eicosatrienoic acid was injected *via* the tail vein, or directly into testes, it was incorporated into liver and testes phospholipids, but it was not metabolized to other labeled fatty acids. When [1-^{14}C]11,14-eicosadienoic acid was injected, *via* the tail vein or directly into testes, or incubated with microsomes from both tissues, it was only metabolized to 5,11,14-eicosatrienoic acid. When ethyl 5,5,11,11,14,14-d$_6$-5,11,14-eicosatrienoate was fed to rats maintained on a diet devoid of fat, it primarily replaced esterified 5,8,11-eicosatrienoic acid, but not arachidonic acid. No labeled linoleate or arachidonate were detected. Dietary ethyl linoleate and ethyl 19,19,20,20-d$_4$-1,2-^{13}C-11,14-eicosadienoate were about equally effective as precursors of esterified arachidonate. The doubly labeled 11,14-eicosadienoate was metabolized primarily by conversion to 17,17,18,18-d$_4$-9,12-ocatdecadienoic acid, followed by its conversion to yield esterified arachidonate, with a mass four units greater than endogenous arachidonate. In addition, the doubly labeled substrate gave rise to a small amount of arachidonate, six mass units greater than endogenous arachidonate. No evidence was obtained, with the radiolabeled substrates, for the presence of a Δ8 desaturase. However, the presence of an ion, six mass units greater than endogenous arachidonate when doubly labeled 11,14-eicosadienoate was fed, suggests that a small amount of the substrate may have been metabolized by the sequential use of Δ8 and Δ5 desaturases.

Paper no. L8471 in *Lipids 35*, 871–879 (August 2000).

It is generally accepted that 18:3n-3 and 18:2n-6 are metabolized, respectively, to 20:5n-3 and 20:4n-6 *via* pathways requiring the sequential use of position-specific Δ6 and Δ5 desaturases. Klenk and Mohrhauer (1) and Stoffel and his colleague (2,3) presented evidence that the following twenty carbon acids could also be synthesized *via* a pathway requiring a Δ8 desaturase 9,12,15-18:3→11,14,17-20:3→8,11,14,17-20:4→5,8,11,14,17-20:5 and 9,12-18:2→11,14-20:2→8,11,14-20:3→5,8,11,14-20:4. We subsequently reported that, in liver, these pathways were not operative since 11,14-20:2; 11,14,17-20:3; and several other polyunsaturated fatty acids, with their first double bond at position 11, were only desaturated at position 5 (4,5). Subsequent studies supported the concept that a variety of tissues and cells lack a Δ8 desaturase. When [1-^{14}C]18:2n-6 (6) was injected into rat brains, it was metabolized to radioactive 20:4n-6, but small amounts of labeled 20:2n-6 were detected. When [1-^{14}C]20:2n-6 was injected, only trace amounts of labeled 20:4n-6 were detected with 5,11,14-20:3 being the major metabolite. When [3-^{14}C]11,14,17-20:3 was injected into rat brains, a complex labeling pattern was obtained since retroconversion yielded labeled 18:3n-3, which was metabolized to longer chain n-3 fatty acids *via* the pathway independent of a Δ8 desaturase (7). In addition, the substrate was desaturated to 5,11,14,17-20:4. The authors of these two studies (6,7) concluded that a Δ8 desaturase is not used to synthesize n-6 and n-3 fatty acids. When [1-^{14}C]18:3n-3 was incubated with HTC cells (8) and hepatoma cells (9), it was converted to 20:5n-3 and chain elongated to 11,14,17-20:3, which was desaturated to 5,11,14,17-20:4. All of the labeled acids could be synthesized *via* the pathway that did not require a Δ8 desaturase. Maeda *et al.* (10) compared the pathways for the biosynthesis of polyunsaturated fatty acids in a number of cell lines. Again, no evidence was found for a Δ8 desaturase, but both 5,11,14-20:3 and 5,11,14,17-20:4 were detected. Naval *et al.* (11) reported that K562 cells had negligible Δ6 activity. These cells metabolized 18:2n-6 and 18:3n-3, respectively, to 5,11,14-20:3 and 5,11,14,17-20:4, which in turn were chain elongated. If cells lack a Δ6 desaturase the synthesis of labeled 20:4n-6 and 20:5 n-3 requires a Δ8 desaturase. These two 20-carbon acids were not detected.

Although the preponderance of studies present no conclusive evidence for a Δ8 desaturase, several other studies do not support this conclusion. Most notably, studies in Coniglio's laboratory (12,13) have shown that rat and human testes convert small amounts of 11,14-20:2 to 20:4n-6, although the major product is desaturation of the substrate to 5,11,14-20:3. When microsomes from a number of cancer cells were incubated with [1-^{14}C]11,14-20:2, small amounts of a radioactive metabolite were produced having a retention time identical to methyl arachidonate. The 20:3 that was produced had a retention time identical to methyl 5,11,14-20:3, but its structure was not established by degradative techniques (14). More re-

*To whom correspondence should be addressed at Department of Molecular and Cellular Biochemistry, The Ohio State University, 337 Hamilton Hall, 1645 Neil Avenue, Columbus, Ohio 43210. E-mail: sprecher.1@osu.edu

Abbreviations: GC–MS, gas chromatography–mass spectrometry; HPLC, high-performance liquid chromatography; NADPH, reduced nicotinamide adenine dinucleotide phosphate.

cently, Cook *et al.* (15) and Schenck *et al.* (16) reported that when a number of deuterium-labeled acids were incubated with C16 glial cells, or fed to mice, the labeling patterns were consistent with the presence of a Δ8 desaturase.

When 5,11,14-20:3 is produced, conflicting reports exist as to whether it is (17), or is not (18) desaturated to 20:4n-6. In the study reported here, several experimental approaches were used to determine whether liver and testes express a Δ8 desaturase and the metabolic fate of 5,11,14-20:3.

MATERIALS AND METHODS

Materials. Ethyl linoleate and ethyl 11,14-eicosadienoate were obtained from Nu-Chek Prep (Elysian, MN). Both 4,7,10-nonadecatrien-1-ol and 5,11,14-eicosatriynoic acid were synthesized as previously described (19). The 4,7,10-nonadecatrien-1-ol and 10,13-nonadecadien-1-ol, made by 1-carbon chain elongation of linoleic acid, were used as the starting materials to make [1-^{14}C]-labeled 5,11,14-20:3 and 11,14-20:2 (20). Reduction of 5,11,14-eicosatriynoic acid with deuterium, using Lindlars catalyst in ethyl acetate, in the presence of quinoline, gave 5,5,11,11,14,14-d_6-5,11,14-20:3. The chemical purity of the ethyl ester, when analyzed on a 30 m × 0.25 mm i.d. DB-223 capillary column at 185°C (J & W Scientific, Folsum, CA) was 88.4%. The ethyl ester, without further purification, was used for the feeding studies. An aliquot was purified by argentation thin-layer chromatography. Following saponification, the acid was derivatized by reacting it with equal volumes of acetonitrile and *N*-methyl-*N*-(*t*-butyldimethylsilyl)trifluoracetamide at 70°C for 1 h (21). Gas chromatography–mass spectrometry (GC–MS) was carried out with a Hewlett Packard 5890 gas chromatograph, containing a 30 m × 0.25 mm i.d. HP-5 MS column and a 5972 mass selective detector (Avondale, PA). The isotopic purity, as calculated by integration of appropriate M-57 ions, was 78.6% d_6, 19.1% d_5, and 2.5% d_4. The starting material to synthesize 17,17,18,18-d_4-octadecadiynoic acid, which was reduced with Lindlars catalyst was 4,4,5,5-d_4-1-pentanol, prepared as previously described (21). The acid was then converted to 19,19,20,20-d_4-1,2-^{13}C-11,14-20:2 using a sequence of reactions previously described (20). The Na^{13}CN was obtained from Cambridge Isotopes, Andover, MA. The doubly-labeled acid had a chemical purity of 96.8% and the isotopic purity was 94.6% for the M+6 isotopomer, 3.9% for the M+5 isotopomer, and 1.0% for the M+4 isotopomer.

Injection studies. Sodium salts of labeled fatty acids (55 Ci/mol) were dissolved in a 1% solution of bovine serum albumin in isotonic saline. Male weanling rats, maintained on a fat-free diet (Dyets, Bethlehem, PA) for three months, were anesthetized with diethyl ether, and 40 μCi of each fatty acid, in 500 μL, was injected into the tail vein. Each testes was injected with 2 μCi of labeled acid in a volume of 20 μL. After 6 h, the rats were sacrificed and testes and liver lipids were extracted (22). Neutral lipids were separated from phospholipids by the sequential elution of columns packed with Unisil (Clarkson Chemical Co., Williamsport, PA), $CHCl_3$, and MeOH. Phospholipids were transesterified by reaction with 5% anhydrous HCl in MeOH for 1 h at 80°C. Methyl esters were isolated and separated by high-performance liquid chromatography (HPLC) using a 25 cm × 4.6 mm Zorbax ODS column. The column was eluted with acetonitrile/water (85:15, vol/vol) at a flow rate of 1 mL/min. The effluent was mixed with ScintiVerse LC (Fisher, Cincinnati, OH) at 3 mL/min, and radioactivity was measured with a Beckman 171 radioisotope detector (Fullerton, CA). Methyl esters were identified by comparing their retention times with purchased standards (Nu-Chek Prep.) or with compounds made by total synthesis.

Microsomal Incubations. Liver and testes were homogenized in 10 mM KH_2PO_4-0.25 M sucrose buffer, pH 7.4 at 4°C. Microsomes, prepared by differential centrifugation (23), were suspended in the homogenization buffer at 25 mg/mL of protein using the BCA protein kit (Pierce Chemical, Rockford, IL) with bovine serum albumin as a standard. Incubations were carried out with 5 mg of protein in a total volume of 1 mL in 1.5 × 12.5 cm culture tubes at 37°C in a metabolic shaker. Incubations to measure desaturase activity contained 100 mM potassium phosphate buffer (pH 7.4), 10 mM ATP, 2 mM NADH, 0.4 mM CoASH, 10 mM $MgCl_2$ and 100 μM [1-^{14}C]9,12-18:2 with a specific activity of 5 μCi/μmol. Fatty acids were bound to bovine serum albumin at a molar ratio of fatty acid/albumin of 2:1 assuming a molecular weight of 68,000 for albumin. When combined desaturation-chain elongation reactions were assayed, the incubations also contained 2 mM NADPH and 0.4 mM malonyl-CoA. All co-factors were obtained from Sigma (St. Louis, MO). Reactions were terminated by the addition of 0.25 mL of 4 N NaOH and 2.5 mL of MeOH. After 1 h at 37°C, 0.25 mL of 6 N HCl and 5 mL of $CHCl_3$ were added. The tubes were centrifuged, and the solvent from the bottom layer was removed under a stream of N_2. The lipids were transesterified and the methyl esters were analyzed by HPLC as described above.

Feeding studies and fatty acid analysis. Rats, maintained on the fat-free diet for three months, were fed 70 mg/day of one of the three ethyl esters for a period of 14 days, i.e., ethyl linoleate, ethyl 5,5,11,11,14,14-d_6-11,14-20:2, or ethyl 19,19,20,20-d_4-1,2-^{13}C-11,14-20:2. Because of a limited supply of the later compound, rats were fed 70 mg of ethyl 11,14-20:2 on days 3, 7, and 10. After the 14-d feeding period, the rats were sacrificed, the lipids were extracted, and neutral lipids were separated from phospholipids by column chromatography. Phospholipids were separated by thin-layer chromatography using Whatman LK6 plates (Fisher, Cincinnati, OH), which were developed with $CHCl_3$/MeOH/40% methylamine (60:20:5,vol/vol/vol) (24). Phospholipids were detected by spraying the plates with 0.2% (wt/vol) 2′,7′-dichlorofluorescein in ethanol and identified by using phospholipid standards purchased from Avanti (Alabaster, AL). The individual phospholipids were recovered by transferring the silica gel to screw cap tubes, followed by extraction with $CHCl_3$/MeOH/H_2O (5:5:1,vol/vol/vol). The 10 mL of extract,

obtained from two extractions, was washed by addition of 4.5 mL of $CHCl_3$ and 2 mL of H_2O. The tubes were centrifuged, the solvent from the bottom layer was removed under N_2, and the lipids were transesterified. Methyl esters were separated using a Varian 3600 gas chromatograph containing a 30 m × 0.25 mm i.d. DB-223 capillary column. Injections were made in the split mode at 185°C. After 10 min, the oven was programmed to 215°C at 3°C/min to 215°C, where it was maintained until the methyl ester of 22:6n-3 had eluted. For GC–MS, the lipids were saponified, and fatty acids were derivatized by reacting them with equal volumes of acetonitrile and *N*-methyl-*N*-(*t*-butyldimethylsilyl)trifluoracetamide. The isotopic composition was determined by monitoring appropriate M-57 ions.

RESULTS

When [1-^{14}C]-labeled 8,11,14-20:3; 5,11,14-20:3; and 11,14-20:2 were injected *via* the tail vein in duplicate experiments, between 13–15% of the injected radioactivity was recovered in total liver lipids. When the two 20-carbon trienoic acids were injected into testes, between 23–26% of the injected radioactivity was recovered in the total lipid extracts. An average of 54% of the injected radioactivity was recovered in the lipid extracts from testes after injection of [1-^{14}C]11,14-20:2. With all three substrates, and with both tissues, between 76–96% of the radioactivity was phospholipid associated.

When the methyl esters, derived from phospholipids of rats injected with [1-^{14}C]5,11,14-20:3, were separated by HPLC, no radioactive metabolites were produced by either liver (Fig. 1A) or testes (Fig. 1C). Conversely, both liver (Fig. 1B) and testes (Fig. 1D) metabolized [1-^{14}C]8,11,14-20:3 to 5,8,11,14-20:4. Both liver (Fig. 2A) and testes (Fig. 2D) metabolized [1-^{14}C]11,14-20:2 into a single metabolite. Panels B and C of Figure 2 show the HPLC radiochromatograms when [1-^{14}C]-labeled 8,11,14-20:3 and 5,11,14-20:3 were added, respectively, to the phospholipid derived methyl esters from liver. Labeled 8,11,14-20:3 eluted immediately before the metabolite (Fig. 2B), while exogenous [1-^{14}C]5,11,14-20:3 co-eluted with the metabolite (Fig. 2C). Identical results, as shown in panels E and F of Figure 2, were obtained with testes. These results show that in liver and testes 11,14-20:2 is only desaturated to yield 5,11,14-20:3.

When liver microsomes (Fig. 3A) and testes microsomes (Fig. 3D) were incubated with [1-^{14}C]11,14-20:2, a single radioactive metabolite was produced. Again, by adding radioactive [1-^{14}C]-labeled 5,11,14-20:3 and 8,11,14-20:3, it was shown that the metabolite generated by liver microsomes co-eluted with 5,11,14-20:3 (Fig. 3B) and not with 8,11,14-20:3 (Fig. 3C). Using an identical protocol, it was shown that the metabolite generated by testes microsomes co-eluted with 5,11,14-20:3 (Fig. 3E) and not 8,11,14-20:3 (Fig. 3F). The results show that liver and testes microsomes desaturate 11,14-20:2 only to 5,11,14-20:3.

Additional studies with microsomes were carried out to determine whether 5,11,14-20:3 could be produced *via* a reaction sequence starting from linoleate. As shown in Figure 4A, when [1-^{14}C]9,12-18:2 was incubated with microsomes, it was desaturated to 6,9,12-18:3 with loss of enzyme activity after about 10 min. When malonyl-CoA and reduced nicotinamide adenine dinucleotide phosphate (NADPH) were included in the incubation, only small amounts of 6,9,12-18:3 accumulated (Fig. 4A), but the substrate was also chain elongated to 11,14-20:2. By using the internal standard protocol described above, it was shown that the 20:3 was only 8,11,14-20:3. The results suggest, but do not prove, that arachidonate was only synthesized *via* the pathway requiring the sequential use of Δ6 and Δ5 desaturases. When 11,14-20:2 was incubated with microsomes, it was desaturated to 5,11,14-20:3. However, when 11,14-20:2 was produced by chain elongation of 9,12-18:2, no 5,11,14-20:3 was detected. Possibly, when 8,11,14-20:3 is produced, it is a much better substrate for desaturation at position 5 than is 11,14-20:2.

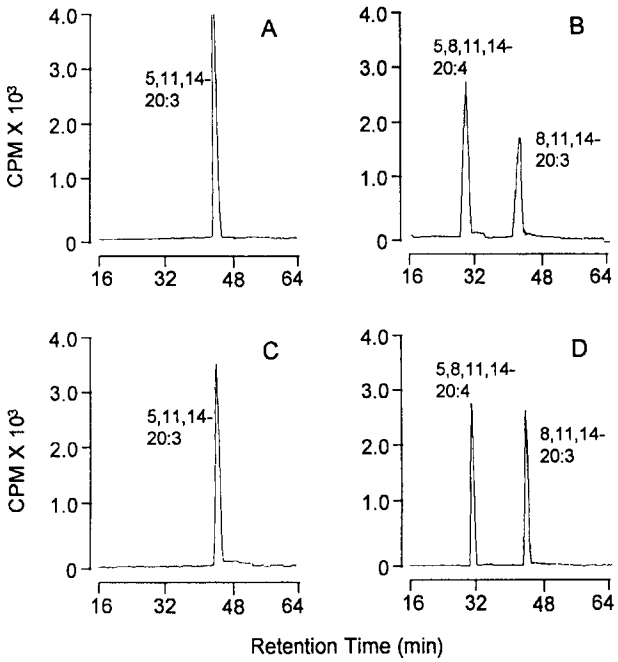

FIG. 1. High-performance liquid chromatography (HPLC) radiochromatograms of the methyl esters derived from liver phospholipids after the tail vein injections of (A) [1-^{14}C]5,11,14-20:3 and (B) [1-^{14}C]8,11,14-20:3. The bottom panels show the corresponding results from testes phospholipids obtained after the intratesticular injections, respectively, of (C) [1-^{14}C]5,11,14-20:3 and (D) [1^{14}C]8,11,14-20:3.

The data with radioactively labeled substrates presents no conclusive evidence for a Δ8 desaturase. To further define how 11,14-20:2 and 5,11,14-20:3 are metabolized, they were fed to rats. The results in Table 1 compare the fatty acid composition of liver phospholipids of rats maintained on the fat-free diet versus when they were fed one of the three experimental acids. Rats maintained on the fat-free diet had the expected high level of 20:3n-9. Two methyl esters eluted between 20:3n-9 and 20:4n-6. By using synthetic standards, it was found that 20:3n-7, a possible palmitoleate metabolite,

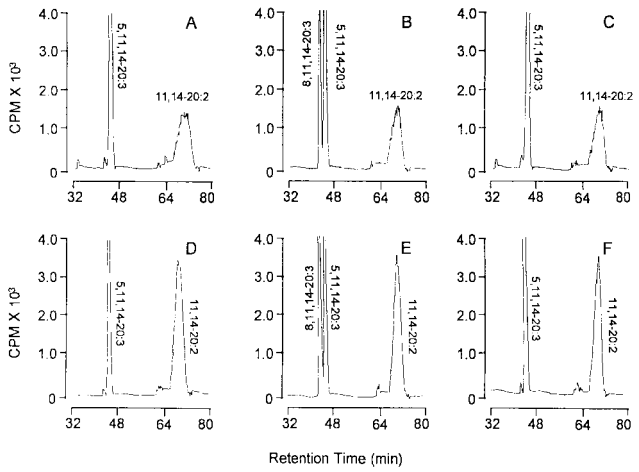

FIG. 2. HPLC radiochromatograms of the methyl esters derived from liver phospholipids after the injection of (A) [1-^{14}C]11,14-20:2 and when (B) [1-^{14}C]8,11,14-20:3 and (C) [1-^{14}C]5,11,14-20:3 were added as external standards. The bottom panels show the corresponding results of testes phospholipids after injection of (D) [1-^{14}C]11,14-20:2 and when (E) [1-^{14}C]8,11,14-20:3 and (F) [1-^{14}C]5,11,14-20:3 were added as external standards. See Figure 1 for abbreviation.

and 5,11,14-20:3 co-eluted. In a similar way, 20:3n-6 and 20:4n-7 co-eluted. These compounds, when detected, are labeled in Table 1 as possible mixtures. When 18:2n-6 was fed, the level of esterified 20:3n-9 decreased with an increase in the 20:4n-6 content.

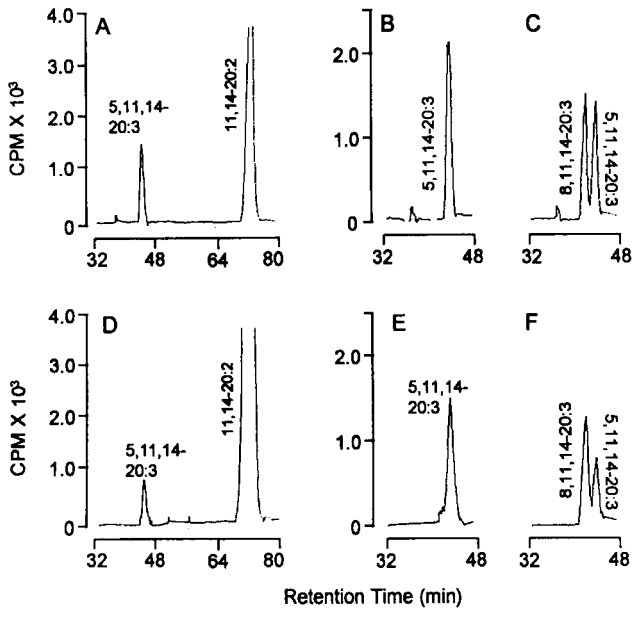

FIG. 3. HPLC radiochromatograms showing the metabolism of (A) [1-^{14}C]11,14-20:2 by liver microsomes as well as when [1-^{14}C]5,11,14-20:3 and (C) [1-^{14}C]8,11,14-20:3 were added as external standards. The bottom panels show, respectively, the metabolism of (D) [1-^{14}C]11,14-20:2 by testes microsomes as well as when exogenous (E) [1-^{14}C]5,11,14-20:3 and (F) [1-^{14}C]8,11,14-20:3 were added. See Figure 1 for abbreviation.

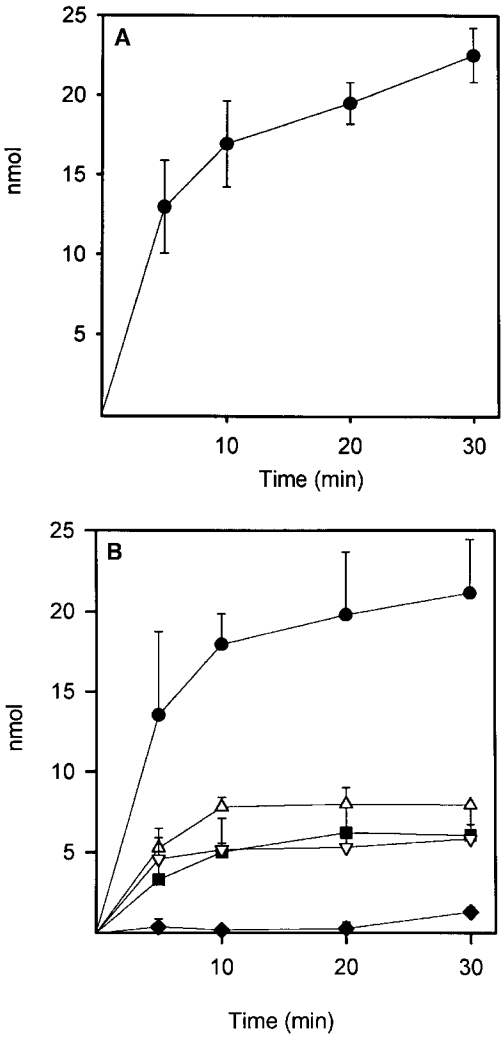

FIG. 4. (A) The metabolism of [1-^{14}C]9,12-18:2 when liver microsomes were incubated without malonyl-CoA and reduced nicotinamide adenine dinucleotide phosphate (NADPH). (B) The time-dependent metabolism of [1-^{14}C]9,12-18:2 when malonyl-CoA and NADPH were included; (●), total nmols of products; (△), 11,14-20:2; (■), 5,8,11,14-20:4; (▽), 8,11,14-20:3; and (◆), 6,9,12-18:3.

When 5,5,11,11,14,14-d$_6$-5,11,14-20:3 was fed, there was a marked decrease in the level of esterified 20:3n-9, but the level of 20:4n-6 was similar to that of the animals fed the fat-free diet. The metabolite labeled as a possible mixture of 20:3n-7:5,11,14-20:3 was isolated by HPLC and shown by GC–MS to be only the dietary acid. When 18:2n-6 and 20:4 n-6 were isolated by HPLC and analyzed by GC–MS, only the unlabeled isotopomers were detected. These *in vivo* studies agree with the radioactive data showing that, although 5,11,14-20:3 is readily incorporated into phospholipids, it is not metabolized to either 18:2n-6 or 20:4n-6. The primary role of 5,11,14-20:3 is to replace esterified 20:3n-9, but not 20:4n-6.

Small amounts of dietary 19,19,20,20-d$_4$-1,2-^{13}C-11,14-20:2 were incorporated into phospholipids, as defined both

TABLE 1
The Fatty Acid Composition (wt %) of Rat Liver Phospholipids[a]

	Dietary fatty acid			
Fatty acid	Fat-free controls	18:2n-6	5,11,14-20:3[b]	11,14 20:2[c]
16:0	16.5 ± 0.7	18.0 ± 1.3	17.4 ± 0.8	18.3 ± 0.7
16:1n-7	5.6 ± 0.4	5.2 ± 1.0	4.0 ± 0.3	4.6 ± 0.1
18:0	17.0 ± 3.5	19.6 ± 1.5	18.1 ± 1.5	18.7 ± 1.2
18:1n-9	11.3 ± 1.7	8.4 ± 0.6	8.7 ± 0.9	7.8 ± 1.0
18:1n-7	7.2 ± 1.3	7.3 ± 0.2	7.6 ± 0.9	6.6 ± 0.7
18:2n-6	2.7 ± 0.1	5.6 ± 0.5	1.2 ± 0.1	3.3 ± 0.9
20:3n-9	12.1 ± 0.4	6.3 ± 0.5	4.8 ± 0.4	5.6 ± 1.0
20:2n-6	—	—	—	4.1 ± 0.5
20:3n-7:5,11,14-20:3	1.3 ± 0.1	1.0 ± 0.1	16.6 ± 0.6	3.5 ± 0.5
20:3n-6:20:4n-7	2.3 ± 0.3	2.5 ± 0.2	0.7 ± 0.3	1.3 ± 0.2
20:4n-6	8.9 ± 1.6	17.0 ± 0.6	10.4 ± 0.8	16.2 ± 1.2
22:5n-6	2.0 ± 0.3	3.0 ± 0.5	2.0 ± 0.4	3.4 ± 0.1
22:6n-3	2.6 ± 0.4	2.2 ± 0.1	2.4 ± 0.1	3.0 ± 0.1
20:3n-9/20:4n-6 ratio	1.4	0.4	0.5	0.3

[a]All results are averages ± the SEM from three animals.
[b]5,5,11,11,14,14-d_6-5,11,14-20:3.
[c]19,19,20,20-d4 -1,2-^{13}C-11,14-20:2.

by gas chromatography (Table 1) and isolation of this compound by HPLC and analysis by GC–MS. The levels of esterified arachidonate were similar to those when linoleate was fed. There are two possible pathways for the synthesis of 20:4n-6 from the dietary acid. First, partial β-oxidation of the substrate results in the loss of the two carbons labeled with C-13, giving rise to 17,17,18,18-d_4-9,12-18:2, which upon conversion to arachidonate, yields an isotopomer four mass units greater than unlabeled 20:4n-6. Second, sequential desaturation of the substrate, at positions 8 and 5, yields an isotopomer six mass units greater than endogenous 20:4n-6. When 18:2n-6 was isolated and analyzed by GC–MS, 76 ± 1% was unlabeled while 24.2 ± 2% contained four deuterium atoms (averages ± SEM of three rats), showing that the dietary acid was partially β-oxidized. The results in Figure 5 show select ion chromatograms of compounds formed by loss of 57 mass units from isotopomers of 20:4n-6. The top trace, at *m/z* = 361, corresponds to the loss of 57 mass units from unlabeled 20:4n-6. The second ion chromatogram at *m/z* = 362 is the M+1 isotopomer of unlabeled 20:4n-6. The third ion chromatogram at *m/z* = 365 is the ion expected for 20:4n-6 labeled with four deuterium and shows that the 17,17,18,18-d_4-9,12-18:2, formed by partial β-oxidation of the dietary acid, is converted to 20:4n-6. The ion trace at *m/z* = 366 is the M+1 isotopomer of 20:4n-6 labeled with four deuterium atoms. The ion chromatogram at *m/z* = 367, corresponds to the M+2 isotopomer of 20:4n-6 labeled with four deuterium atoms. An ion of this composition would also be produced if the substrate was directly converted to arachidonate, giving rise to an isotopomer six mass units greater than unlabeled 20:4n-6. The bottom ion chromatogram at *m/z* = 368 corresponds to the M+1 isotopomer which would be produced from arachidonate six mass units greater than unlabeled

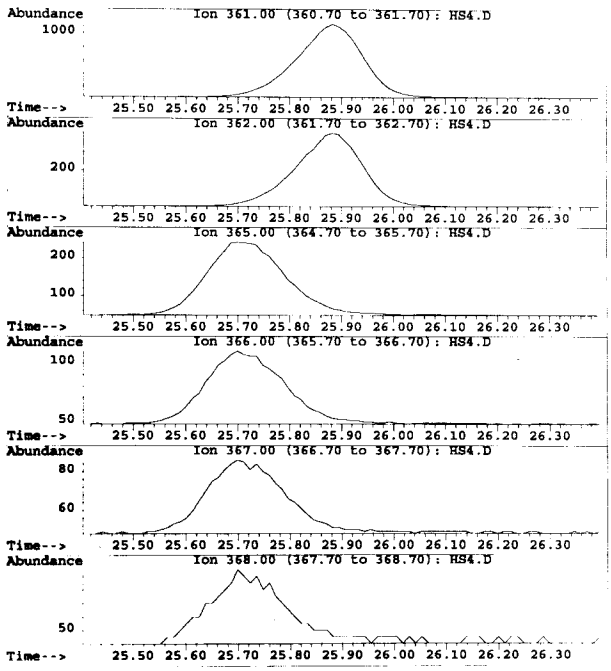

FIG. 5. Ion chromatograms obtained by loss of 57 mass units from arachidonic acid isotopomers when 19,19,20,20-1,2-^{13}C-11,14-20:2 was fed to rats. Ion traces from top to bottom are respectively; *m/z* = 361, endogenous 20:4n-6; *m/z* = 362, the M+1 isotopomer of endogenous arachidonate; *m/z* = 365, the M+4 isotopomer formed by metabolism of the substrate to d_4 linoleate and its conversion to arachidonate; *m/z* = 366 the M+1 isotopomer of d_4-labeled arachidonate; *m/z* = 367, an ion of this composition corresponds to the M+2 isotopomer from d_4-labeled arachidonic acid but it also would be the ion expected by conversion of the substrate directly to arachidonic acid; *m/z* = 368, the M+2 isotopomer expected from arachidonic acid six mass units greater than endogenous arachidonic acid.

TABLE 2
The Amounts (wt%) of 20:3n-9, 20:4n-6, and 5,11,14-20:3 in Individual Liver Phosphoglycerides[a]

	Dietary fatty acid			
Fatty acid	Fat-free controls	18:2n-6	11,14-20:2[a]	5,11,14-20:3[b]
Choline phosphoglycerides				
20:3n-9	11.8 ± 0.2	5.8 ± 0.8	5.2 ± 1.0	3.7 ± 0.4
20:4n-6	5.6 ± 0.8	12.4 ± 1.0	13.1 ± 2.5	7.4 ± 0.5
5,11,14-20:3	—	—	—	18.2 ± 2.3
20:3n-9/20:4n-6 ratio	2.1	0.5	0.5	0.4
Σ20:3n-9 + 20:4n-6	17.4	18.2	18.3	11.1
Ethanolamine phosphoglycerides				
20:3n-9	9.5 ± 0.9	3.6 ± 0.1	3.1 ± 0.7	3.4 ± 0.3
20:4n-6	20.3 ± 1.4	28.4 ± 0.5	26.5 ± 0.3	17.3 ± 1.0
5,11,14-20:3	—	—	—	14.5 ± 1.2
20:3n-9/20:4n-6 ratio	0.5	0.1	0.2	0.1
Σ20:3n-9 + 20:4n-6	29.8	32.0	29.6	20.7
Serine phosphoglycerides				
20:3n-9	6.7 ± 0.7	2.4 ± 0.1	2.3 ± 0.5	2.0 ± 0.1
20:4n-6	17.3 ± 2.3	21.0 ± 1.5	21.1 ± 0.5	10.4 ± 0.1
5,11,14-20:3	—	—	—	16.2 ± 1.4
20:3n-9/20:4n-6 ratio	0.4	0.1	0.2	0.1
Σ20:3n-9 + 20:4n-6	24.0	23.4	23.4	12.4
Inositol phosphoglycerides				
20:3n-9	29.1 ± 0.6	17.8 ± 1.1	17.1 ± 2.3	16.3 ± 0.3
20:4n-6	8.6 ± 1.0	18.0 ± 1.1	19.7 ± 3.3	12.3 ± 0.3
5,11,14-20:3	—	—	—	10.0 ± 1.0
20:3n-9/20:4n-6 ratio	3.3	1.0	0.9	1.3
Σ20:3n-9 + 20:4n-6	37.7	35.8	36.8	28.6

[a]All results are averages ± the SEM from three animals.
[b]19,19,20,20,-d_4-1,2-^{13}C-11,14-20:2
[c]5,5,11,11,14,14-d_6-5,11,14-20:3.

20:4n-6. An ion of this composition would be expected if the substrate was sequentially desaturated at positions 8 and 5. The presence of the ion at *m/z* = 368, coupled with the observation that the ion at *m/z* = 367 was too intense for the M+2 isotopomer derived from d_4-20:4n-6, suggests that small amounts of 11,14-20:2 were metabolized directly to 20:4n-6. By correcting for isotopomer composition of the *m/z* = 367 ion, it was calculated that the isotopic composition of 20:4n-6 was d_0, 81.3 ± 2.7%; d_4 , 17.0 ± 2.4%; and d_6, 1.6 ± 0.3% (averages ± the SEM from three animals). These stable isotope studies suggest that a small amount of the substrate is metabolized to 20:4n-6 *via* a pathway not requiring its partial degradation 9,12-18:2.

The results in Table 2 compare the levels of 20:3n-9, 20:4n-6, and 5,11,14-20:3 in individual phospholipids versus those in total phospholipids (Table 1). There are four points to be made as it relates to this compositional data. First, in the fat-free controls, the 20:3n-9/20:4n-6 ratio differs among the four individual phospholipids. These ratios in the choline-, ethanolamine-, serine-, and inositol-containing phospholipids were, respectively, 2.1, 0.5, 0.4, and 3.3. Second, as expected, when linoleate was added to the diet there was an increase in the amount of 20:4n-6 esterified in all phospholipids, which was accompanied by a reduced level of 20:3n-9. The rank order of the 20:3n-9/20:4n-6 ratio remained the same as was found in the animals raised on the fat-free diet. Third, when 19,19,20,20-d_4-1,2-^{13}C-11,14-20:2 was added to the diet, the amount of 20:4n-6 esterified in individual phospholipids was approximately the same as when linoleate was fed. Based on the isotopic data obtained with the total phospholipids (Fig. 4), the majority of 20:4n-6 was formed by partial β-oxidation of the substrate to 19,19,20,20-d_4-18:2 n-6 followed by its metabolism to 20:4n-6. The 20:3n-9/20:4n-6 ratio in individual phospholipids was approximately the same when linoleate or labeled 20:2n-6 were fed. Indeed, as shown in Table 2, the summed amounts of 20:3n-9 plus 20:4n-6, in individual phospholipids, were approximately the same in animals raised on the fat-free diet vs. when 18:2n-6 or 20:2n-6 were fed. Finally, when 5,5,11,11,14,14-d_6-5,11,14-20:3 was fed, it was incorporated, in rather large amounts, into all four phospholipids. The primary metabolic fate of 5,11,14-20:3 was to replace esterified 20:3n-9 rather than arachidonate. As shown in Table 2, the level of esterified 20:4n-6 in the choline- and ethanolamine-containing phospholipids was about the same in the fat-free controls as when 5,11,14-20:3 was fed. Interestingly, when 5,11,14-20:3 was fed, there was a 40% decrease in the amount of 20:4n-6 esterified in the serine-containing phospholipids, which was accompanied by a 43% increase in the amount of 20:4n-6 esterified in the inositol-containing phospholipids. Since the injection experiments with [1-^{14}C]5,11,14-20:3 showed that it was not metabolized to 20:4n-6 the compositional data suggests that

there was some movement of 20:4n-6 among the phospholipids during the 14 d feeding period.

DISCUSSION

Over the years, several types of studies have contributed to the concept that position-specific desaturases are expressed. These include competitive substrate studies using microsomes (25), and feeding studies (26) using a variety of unsaturated fatty acids. Several types of cells were able to desaturate fatty acids at position 5, but not at position 6 (10,27). However, it was not until molecular techniques evolved that definitive proof was obtained to prove the presence of position specific Δ6 and Δ5 desaturases. Several groups of investigators have cloned and expressed Δ6 desaturases from animals (28–30). The gene product desaturated both linoleate and linolenate (28,29), but not 8,11,14-20:3 (29). Two groups of investigators (31,32) isolated a gene from *Caenorhabditis elegans,* and when it was expressed in yeast, it was shown that the gene product did not desaturate fatty acids at position 6, but it desaturated 8,11,14-20:3 as well as 11,14-20:2 and 11,14,17-20:3 at position 5 (32).

In the study reported here, we confirm the findings of Schlenk *et al*. (18), that 5,11,14-20:3 is not desaturated to 20:4n-6 in either liver or testes. We also confirmed our previous findings that [1-^{14}C]11,14-20:2 is only desaturated in liver to 5,11,14-20:3 (4,5). Our *in vivo* data with testes, as well as with microsomes, also show that the substrate is only desaturated at position 5. Thus, it seems likely, based on the work of Watts and Browse (32), that a single protein in rats desaturates both 8,11,14-20:3 and 11,14-20:2 at position 5.

Our findings with testes, however, are not in agreement with those reported by Albert and Coniglio (12) for rat testes or by Albert *et al.* (13) for human testes as to whether a Δ8 desaturase is expressed in rats. The reason for these discrepancies is not known. Our studies with rat testes differed only slightly from those used by Albert and Coniglio (12). They used rats maintained on a chow diet while our studies were carried out on rats raised on a diet devoid of fat. We selected the later dietary condition since it is well known that in these animals, there is considerable synthesis and esterification of 20:4n-6.

If a Δ8 desaturase is expressed, it is a matter of conjecture when it is used to make polyunsaturated fatty acids. The most conclusive evidence for the presence of this activity is observed when acids, with their first double bond at position 11, are used as substrates (12,13,15,16). In the study reported here, the labeling pattern of 20:4n-6, when 19,19,20,20-d_4-1,2-^{13}C-11,14-20:2 was fed, is consistent with the direct conversion of small amounts of the substrate directly to 20:4n-6. The rationale for using the doubly labeled substrate was that after one cycle of β-oxidation it would yield 17,17,18,18-d_4-9,12-18:2, which upon metabolism to 20:4n-6 would yield the M+4 isotopomer of 20:4n-6. This was the major pathway by which the substrate was metabolized. The possibility exists that when acetate, labeled with C-13 was produced, it was reutilized. If this labeled acetate was used to chain elongate 17,17,18,18-d_4-6,9,12-18:3 when it was produced from 17,17,18,18-d_4-9,12-18:2, a M+6 isotopomer of 20:4n-6 could be produced by the pathway independent of a Δ8 desaturase. Although we cannot rule out this possibility, it seems highly unlikely since M+2 isotopomers of other fatty acids were not detected.

It is very difficult to design experiments to conclusively demonstrate that a Δ8 desaturase is, or is not, used when the initial substrate is either linoleate or linolenate. When linoleate is used as a substrate, both 6,9,12-18:3 and 8,11,14-20:3 are obligatory intermediates in the synthesis of arachidonate, *via* the pathway that is independent of a Δ8 desaturase. When the Δ8 desaturase is required, 11,14-20:2 and 8,11,14-20:3 are obligatory intermediates. None of these intermediates accumulate in large amounts in tissue lipids. When [3-^{14}C]-labeled 11,14-20:2, 11,14,17-20:3, or stable isotopes of these two acids are used as substrates, their primary metabolic fate is one cycle of β-oxidation to yield linoleate and linolenate, which may then be metabolized *via* the Δ8 desaturase independent pathway (4,5,7,15,16). If 11,14-20:2 is synthesized *in vivo,* under normal physiological conditions, what is its metabolic fate, i.e., desaturation at position 8, or partial β-oxidation to yield linoleate? Interestingly, when Bridges and Coniglio (33) studied the metabolism of [1-^{14}C]9,12-18:2 to longer chain n-6 polyunsaturated fatty acids in testes, no labeled 11,14-20:2 was detected. Their studies (12), like ours, present no evidence for the presence of a hepatic Δ8 desaturase. Then, is there any condition when it might be advantageous for cells to express a Δ8 desaturase? If cells were devoid of Δ6 desaturase activity, the expression of a Δ8 desaturase would provide an optional way to synthesize 20:4n-6 and 20:5n-3. Naval *et al.* (11) reported that K562 leukemic cells lack a Δ6 desaturase, but they metabolized linoleate to 5,11,14-20:3 and linolenate to 5,11,14,17-20:4, a finding which would not be expected if the cells express a Δ8 desaturase. Recently, Wallis and Browse (34) reported the isolation of a Δ8 desaturase from *Euglena gracilis* with a high degree of homology with Δ6 and Δ5 desaturases isolated from *Caenhorabditis elegans*. A conclusive answer as to whether mammals do or do not express a Δ8 desaturase may well require the molecular techniques, which have just recently been used as they relate to defining the number and specificities of other acyl-CoA-dependent desaturases.

In these studies, the addition of linoleate to the diet resulted as expected, in a decrease in the level of esterified 20:3n-9 accompanied by an increased level of esterified 20:4n-6 in all phospholipids. Both the synthesis of 20:4n-6 from 18:2n-6, as well as its use as a substrate for phospholipid biosynthesis, are processes localized primarily in the endoplasmic reticulum (35,36). Although the 20:3n-9/20:4n-6 ratio varied among phospholipids, the addition of labeled 11,14-20:2 to the diet resulted in an increase in the level of esterified 20:4n-6 in all phospholipids, similar to what was observed when linoleate was fed. The primary pathway of 11,14-20:2 metabolism was partial β-oxidation to yield

linoleate. Based on studies with 22- and 24-carbon n-3 and n-6 polyunsaturated fatty acid, the degradation of 11,14-20:2 to linoleate takes place in peroxisomes (37,38). Since the levels of esterified 20:4n-6 were similar when 18:2n-6 and 11,14-20:2 were fed, the findings imply that when 18:2n-6 is produced from 11,14-20:2 in peroxisomes, it preferentially moves to the endoplasmic reticulum for use in fatty acid and phospholipid biosynthesis, rather than continued peroxisomal degradation.

Interestingly 5,11,14-20:3 was metabolized quite differently than was 11,14-20:2. The structures of 5,8,11-20:3; 5,8,11,14-20:4; and 5,11,14-20:3 are similar. The sole anabolic fate of dietary 5,11,14-20:3, when fed to animals raised on a fat-free diet, was direct esterification and in this regard it replaced 5,8,11-20:3 and not arachidonate. Labeled linoleate or arachidonate were not produced from the 5,5,11,11,14,14-d_6-5,11,14-20:3. Two pathways exist in both peroxisomes and mitochondria for degrading fatty acids with their first double bond at position 5 (39). With 5,11,14-20:3 as substrate, the pathway using only the enzymes of saturated fatty acid degradation, yields 3,9,12-18:3 after one cycle of degradation. The pathway using $\Delta^{3,5}$-$\Delta^{2,4}$-dienoyl-CoA isomerase and NADPH-dependent 2,4-dienoyl-CoA isomerase would convert 5,11,14-20:3 to 9,12-18:2 after one cycle of β-oxidation. Both of these enzymes have been purified from peroxisomes (40,41). Failure to detect labeled 18:2n-6 or 20:4n-6 suggests that the pathway using these two enzymes was of marginal significance. Conflicting reports exist in the literature as to the relative roles of these two pathways in the mitochondrial degradation of fatty acids with their first double bond at position 5 (42,43). Our results may be explained in two possible ways. First, if 5,11,14-20:3 is primarily degraded by mitochondria, *via* either pathway, it would probably be completely degraded without the accumulation of intermediates (39). Alternatively, if peroxisomes are the primary intracellular site for degradation, most likely the first cycle of β-oxidation used only the enzymes of saturated fatty acid degradation so that labeled 18:2n-6 was not produced.

ACKNOWLEDGMENTS

This study was supported by HIH Grant DK48744 and a Grant from Wyeth Nutritionals International, Philadelphia, PA.

REFERENCES

1. Klenk, E., and Mohrhauer, H. (1960) Untersuchungen über den Stoffwechsel der Polyenfettsäuren bei der Ratte, *Hoppe-Seyler's Z. Physiol. Chem. 320*, 218–232.
2. Stoffel, W. (1963) Der Stoffwechsel der Ungesättigten Fettsauren, I Zur Biosynthese Hochungesättigter Fettsäuren, *Hoppe-Seyler's Z. Physiol. Chem. 333*, 71–88.
3. Stoffel, W., and Ach, K.-L. (1964) Der Stoffwechsel der Ungesättigten Fettsäuren, II Eigenschaften des Kettenverlängernden Enzyms Zur Frage der Biohydrogenierung der Ungesättigten Fettsauren, *Hoppe-Seyler's Z. Physiol. Chem. 337*, 123–132.
4. Ullman, D., and Sprecher, H. (1971) An *In Vitro* and *In Vivo* Study of the Conversion of Eicosa-11,14-dienoic Acid to Eicosa-5,11,14-trienoic Acid and the Conversion of Eicosa-11-enoic Acid to Eicosa-5,11-dienoic Acid, *Biochim. Biophys. Acta 248*, 186–197.
5. Sprecher, H., and Lee, C.-J. (1975) The Absence of an 8-Desaturase in Rat Liver: A Reevaluation of Optional Pathways for the Metabolism of Linoleic and Linolenic Acids, *Biochim. Biophys, Acta 388*, 113–125.
6. Dhopeshwarkar, G.A., and Subramanian, C. (1976) Intracranial Conversion of Linoleic Acid to Arachidonic Acid: Evidence for Lack of Δ^8 Desaturase in the Brain, *J. Neurochem. 26*, 1175–1179.
7. Dhopeshwarkar, G.A., and Subramanian, C. (1976) Biosynthesis of Polyunsaturated Fatty Acids in the Developing Brain II. Metabolic Transformations of Intracranially Administered [3-^{14}C]Eicosatrienoic Acid, Evidence for Lack of Δ^8 Desaturase, *Lipids 11*, 689–692.
8. Alaniz, M.J.T. de, Gómez Dumm, I.N.T. de, and Brenner, R.R. (1976) The Action of Insulin and Bibutyryl Cyclic AMP on the Biosynthesis of Polyunsaturated Acids of the α-Linolenic Acid Family in HTC Cells, *Mol. Cell Biochem. 12*, 3–8.
9. Alaniz, M.J.T. de, and Brenner, R.R. (1976) Effect of Different Carbon Sources on the Biosynthesis of Polyunsaturated Fatty Acids of the α-Linolenic Acid Family in Culture of Minimal Deviation Hepatoma 7288 Cells, *Mol. Cell Biochem. 12*, 81–87.
10. Maeda, M., Doi, O., and Akamatsu, Y. (1978) Metabolic Conversions of Polyunsaturated Fatty Acids in Mammalian Cells, *Biochim. Biophys. Acta 530*, 153–164.
11. Naval, J., Martínez-Lorenzo, M.J., Marzo, I., Desportes, P., and Piñeiro, A. (1993) Alternative Route for the Biosynthesis of Polyunsaturated Fatty Acids in K562 Cells, *Biochem. J. 281*, 841–845.
12. Albert, D.H., and Coniglio, J.G. (1977) Metabolism of Eicosa-11,14-dienoic Acid in Rat Testes Evidence for Δ^8-Desaturase Activity, *Biochim. Biophys. Acta 489*, 390–396.
13. Albert, D.H., Rhamy, R.K., and Coniglio, J.G. (1979) Desaturation of Eicosa-11,14-dienoic Acid in Human Testes, *Lipids 14*, 498–500.
14. Nagazawa, I., and Mead J.F. (1976) *In Vitro* Activity of the Fatty Acyl Desaturases of Human Cancerous and Noncancerous Tissues, *Lipids 11*, 79–82.
15. Cook, H.W., Byers, D.M., Palmer, F.B.St.C., Spence, M.W., Rakoff, H., Duval, S.M., and Emken, E.A. (1992) Alternate Pathways in the Desaturation and Chain Elongation of Linolenic Acid, 18:3 (n-3), in Cultured Glioma Cells, *J. Lipid Res. 32*, 1265–1273.
16. Schenck, P.A., Rakoff, H., and Emken E.A. (1996) Δ^8 Desaturation *in vivo* of Deuterated Eicosatrienoic Acid by Mouse Liver, *Lipids 31*, 593–600.
17. Takagi, T. (1965) The Dehydrogenation of All-*cis*-5,11,14-Eicosatrienoic Acid to Arachidonic Acid, *Bull. Chem. Soc. Jpn. 38*, 2055–2057.
18. Schlenk, H., Sand, D.M., and Gellerman, J.L. (1970) Nonconversion of 5,11,14-Eicosatrienoic Acid into Arachidonic Acid by Rats, *Lipids 5*, 575–577.
19. Evans, R.W., and Sprecher, H. (1985) Total Synthesis and Spectral Characterization of 5,8,14-Icosatrienoic Acid and 5,11,14-Icosatrienoic Acid, *Chem. Phys. Lipids 38*, 327–342.
20. Sprecher, H., and Sankarappa, S. (1982) Synthesis of Radiolabeled Fatty Acids, *Methods Enzymol. 86*, 357–366.
21. Luthria, D.L., and Sprecher, H. (1993) Synthesis of Ethyl Arachidonate-19,19,20,20-d_4 and Ethyl Dihomo-γ-linolenate-19,19,20,20,-d_4, *Lipids 28*, 853–856.
22. Folch, J., Lees, M., and Sloane Stanley, G.H. (1957) A Simple Method for the Isolation and Purification of Total Lipids from Animal Tissue, *J. Biol. Chem. 226*, 497–509.
23. Bernert, J.T., and Sprecher, H. (1975) Studies to Determine the Role Rates of Chain Elongation and Desaturation Play in Regu-

lating the Unsaturated Fatty Acid Composition of Rat Liver Phospholipids, *Biochim. Biophys. Acta 398*, 354–363.
24. Hadjiagapiou, C., and Spector A.A. (1987) Docosahexaenoic Acid Metabolism and Effect on Prostacyclin Production in Endothelial Cells, *Arch. Biochem. Biophys. 253*, 1–12.
25. Brenner, R.R., and Peluffo, R.O. (1966) Effect of Saturated and Unsaturated Fatty Acids on the Desaturation *In Vitro* of Palmitic, Stearic, Oleic, Linoleic and Linolenic Acids, *J. Biol. Chem. 241*, 5213–5219.
26. Holman, R.T. (1986) Nutritional and Biochemical Evidences of Acyl Interaction with Respect to Essential Fatty Acids, *Prog. Lipid. Res. 25*, 29–39.
27. Dunbar, L.M., and Bailey, J.M. (1975) Enzyme Deletions and Essential Fatty Acid Metabolism in Cultured Cells, *J. Biol. Chem. 250*, 1152–1153.
28. Cho, H.P., Nakamura, M.T., and Clarke, S.D. (1999) Cloning, Expression, and Nutritional Regulation of the Mammalian Δ-6 Desaturase, *J. Biol. Chem. 274*, 471–477.
29. Aki, T., Shimada, Y., Inagaki, K., Higashimoto, H., Kawamoto, S., Shigeta, S., and Suzuki, O. (1999) Molecular Cloning and Functional Characterization of Rat Delta-6 Fatty Acid Desaturase, *FEBS Lett. 255*, 575–579.
30. Napier, J.A., Hey, S.J., Lacey, D.J., and Shewry, P.R. (1998) Identification of a *Caerorhabditis elegans* Δ^6-Fatty-acid-desaturase by Heterologous Expression in *Saccharomyces cerevisiae*, *Biochem. J. 330*, 611–614.
31. Michaelson, L.V., Napier, J.A., Lewis, M., Griffiths, G., Lazarus, C.M., and Stobart, A.K. (1998) Functional Identification of a Fatty Acid Delta 5 Desaturase Gene from *Caerorhabditis elegans*, *FEBS Lett. 439*, 215–218.
32. Watts, J.L., and Browse, J. (1999) Isolation and Characterization of a Δ^5-Fatty Acid Desaturase from *Caerorhabditis elegans, Arch. Biochem. Biophys. 362*, 175–182.
33. Bridges, R.B., and Coniglio, J.G. (1970) The Metabolism of Linoleic and Arachidonic Acids in Rat Testes, *Lipids 5*, 628–635.
34. Wallis, J.G., and Browse, J. (1999) The Δ^8-Desaturase of *Euglena gracilis*: An Alternate Pathway for Synthesis of 20-Carbon Polyunsaturated Fatty Acids, *Arch. Biochem. Biophys. 365*, 307–316.
35. Lands, W.E.M., Inoue, M., Sugiura, Y., and Okuyama, H. (1982) Selective Incorporation of Polyunsaturated Fatty Acids into Phosphatidylcholine by Rat Liver Microsomes, *J. Biol. Chem. 257*, 14968–14972.
36. Dircks, L., and Sul, H.S. (1999) Acyltransferases of *de novo* Glycerophospholipid Biosynthesis, *Prog. Lipid Res. 38*, 461–479.
37. Christensen, E., Woldseth, B., Hagve, T.-A., Poll-The, B.T., Wanders, R.J.A., Sprecher, H., Stokke, O., and Christopherson, B.O. (1993) Peroxisomal β-Oxidation of Polyunsaturated Fatty Acids in Human Fibroblasts. The Polyunsaturated and the Saturated Long Chain Fatty Acids are Retroconverted by the Same Acyl-CoA Oxidase, *Scand. J. Clin. Lab. Invest. 536 (Suppl. 215),* 61–74.
38. Moore, S.A., Hurt, E., Yoder, E., Sprecher, H., and Spector, A.A. (1995) Docosahexaenoic Acid Synthesis in Human Skin Fibroblasts Involves Peroxisomal Retroconversion of Tetracosahexaenoic Acid, *J. Lipid. Res. 36*, 2433–2443.
39. Kunau, W.-H., Dommes, V., and Schulz, H. (1995) Beta-Oxidation of Fatty Acids in Mitochondria, Peroxisomes and Bacteria: a Century of Continued Progress, *Prog. Lipid Res. 34*, 267–342.
40. He, X.-Y., Shourky, K., Chu, C., Yang, J., Sprecher, H., and Schulz, H. (1995) Peroxisomes Contain $\Delta^{3,5}$-$\Delta^{2,4}$-dienoyl-CoA Isomerase and Thus Possess All Enzymes Required for the β-Oxidation of Unsaturated Fatty Acids by a Novel Reductase-Dependent Pathway, *Biochem. Biophys. Res. Commun. 2215*, 15–21.
41. Geisbrecht, B.V., Liang, X., Morrell, J.C., Schulz, H., and Gould, S.J. (1999) The Mouse Gene PDCR Encodes a Peroxisomal Delta (2), Delta (4)-dienoyl-CoA Reductase, *J. Biol. Chem. 274*, 25814–25820.
42. Tserng, K.-Y., Jin, S.-J., and Chen, L.-S. (1996) Reduction Pathway of *cis*-5 Unsaturated Fatty Acids in Intact Rat-liver and Rat-heart Mitochondria: Assessment with Stable-Isotope-Labelled Substrates, *Biochem. J. 313*, 581–588.
43. Shoukry, K., and Schulz, H. (1998) Significance of the Reductase-Dependent Pathway for the Beta-Oxidation of Unsaturated Fatty Acids with Odd-Numbered Double Bonds. Mitochondrial Metabolism of 2-*trans*-5-*cis*-Octadienoyl-CoA, *J. Biol. Chem. 273*, 6892–6899.

[Received February 22, 2000; accepted June 20, 2000]

Triacylglycerols of the Red Microalga *Porphyridium cruentum* Can Contribute to the Biosynthesis of Eukaryotic Galactolipids

Inna Khozin-Goldberg[a], Hu Zheng Yu[a], Daniel Adlerstein[a,b], Shoshana Didi-Cohen[a], Yair M Heimer[a], and Zvi Cohen[a,*]

[a]Microalgal Biotechnology Laboratory, The Albert Katz Department of Dryland Biotechnologies, Jacob Blaustein Institute for Desert Research, Sde-Boker Campus 84990, Israel, and [b]The Department of Chemistry, Ben-Gurion University of the Negev, Beer-Sheva, Israel

ABSTRACT: A mutant of the red microalga *Porphyridium cruentum* was selected on the basis of impaired growth at suboptimal temperatures (15 vs. 25°C). Fatty acid and lipid analyses revealed diminished proportions of eicosapentaenoic acid (from 41 to 30%) and of the eukaryotic molecular species (from 38 to 28% of monogalactosyldiacylglycerol (MGDG) and elevated proportion (10 vs. 2%) of triacylglycerols (TAG) in the mutant, as compared with the wild type. Pulse labeling of the wild type cells with radioactive fatty acid precursors indicated an initial incorporation of the fatty acids into phosphatidylcholine (PC) and TAG. Following the pulse, the label of PC and TAG decreased with time (from 25 to 5% of the total dpm in TAG) while that of chloroplastic polar lipids, mainly MGDG, continued to increase. In the mutant, however, the labeling of TAG after the pulse was higher (30% of the total dpm) than that of the wild type and decreased only slightly to 20%. This may indicate that in *P. cruentum*, TAG can contribute to the biosynthesis of eukaryotic species of MGDG.

Paper no. L8444 in *Lipids 35*, 881–889 (August 2000).

The complex biosynthetic pathways leading to the formation of the polyunsaturated fatty acid (PUFA) 18:3n-3 in higher plants' leaf lipids were reviewed by Browse and Somerville (1). The model consists of a prokaryotic pathway and a eukaryotic pathway. In the former, the fatty acids, which are synthesized *de novo* in plastids, are used as building blocks for the production of chloroplastic lipids. These lipids are characterized by the presence of a C_{16} acyl group at the *sn*-2 position of the glycerol moiety of the lipid. In the eukaryotic pathway, acyl, groups, which are synthesized *de novo* in the chloroplast, are exported from the chloroplast to the cytoplasm and incorporated into phospholipids. After desaturation, most of the diacylglycerol (DAG) moieties of the phospholipids are transported back into the chloroplast to be galactosylated and further desaturated (1). These galactolipids typically contain a C_{18} acyl group at their *sn*-2 position. DAG can also be acylated in the cytoplasm at their *sn*-3 position by a diacylglycerolacyltransferase (DAGAT) to produce (TAG). It is generally accepted that this reaction is not reversible and that TAG are end products that do not participate in any known pathway of fatty acid or lipid metabolism (1).

Although PUFA of leaf lipids and many algae contain 16 or 18 carbon atoms, some algae are unique in producing PUFA with longer carbon chains, such as 20:4n-6 [arachidonic acid (AA)], 20:5n-3 [eicosapentaenoic acid, (EPA)], and 22:6n-3 [docosahexaenoic acid, (DHA)]. The biosynthetic pathways leading to the production of 18:3n-3 in algae are believed to be similar to those suggested for higher plants (2). However, the biosynthesis of C_{20} and C_{22} PUFA from C_{18} fatty acids in algae is still rather obscure (3,4). Following our study of EPA biosynthesis in *Porphyridium cruentum* (5), one of its promising sources (5,6), we recently proposed (7,8) several possible pathways leading to the biosynthesis of EPA in *P. cruentum*. In the major, n-6 pathway (Scheme 1), 18:2-bound phosphatidylcholine (PC) is converted to 20:4n-6-PC by a sequence of reactions that includes a Δ6 desaturation, an elongation step, and a Δ5 desaturation. In the minor n-3 pathway (not shown), first 18:2-PC is apparently desaturated to 18:3n-3-PC, which is further converted to 20:5n-3-PC, presumably by the same enzymes involved in the n-6 pathway. The products of both pathways are exported, as their DAG constituents, to the chloroplast to be galactosylated into the respective monogalactosyldiacylglycerol (MGDG) molecular species. Apparently, 20:4n-6 is also imported from an extrachloroplastic lipid and inserted into the *sn*-1 position to form 20:4/16:0 MGDG, which is structurally analogous to prokaryotic species of higher plants' galactolipids. The source of 20:4 for prokaryotic lipids and its mode of transfer from the cyto-

*To whom correspondence should be addressed at Microalgal Biotechnology Lab., The Albert Katz Department of Dryland Biotechnologies, Jacob Blaustein Institute for Desert Research, Sde-Boker Campus 84990, Israel. E-mail: cohen@bgumail.bgu.ac.il

Abbreviations: AA, arachidonic acid; C_n fatty acid, fatty acid with *n* carbon atoms; DAG, diacylglycerol; DAGAT, diacylglycerol acyltransferase; DGDG, digalactosyldiacylglycerol; EPA, eicosapentaenoic acid (20:5n-3); MGDG, monogalactosyldiacylglycerol; PC, phosphatidylcholine; PUFA, polyunsaturated fatty acid; TAG, triacylglycerol; WT, wild type; X:Y, a fatty acyl group containing X carbon atoms and Y double bonds (*cis*). Pairs of numbers representing the fatty acids, when separated by a slash, designate the components in the *sn*-1 and *sn*-2 positions, respectively, of the molecular species.

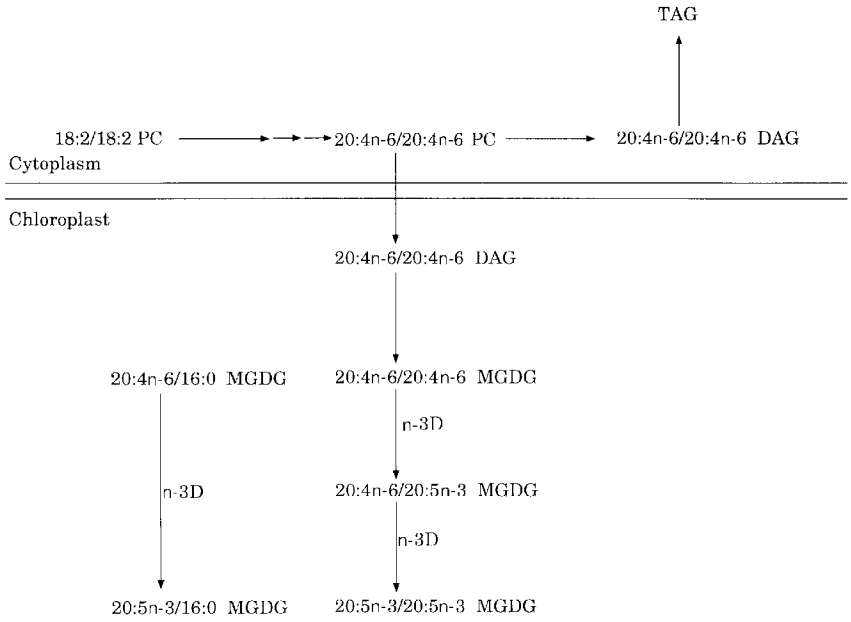

SCHEME 1

plasm to the chloroplast still are not clear. The 20:4n-6 in both eukaryotic and prokaryotic molecular species of MGDG can be further desaturated to EPA by a chloroplastic n-3 desaturase (8).

Elucidation of the biosynthesis of PUFA in higher plants was made possible by the use of mutants of *Arabidopsis thaliana,* deficient in various steps of the biosynthesis (1). Similar mutants could be very valuable tools in the elucidation of biosynthetic pathways of long-chain PUFA in algae. Indeed, using a mutant deficient in EPA production, Schneider *et al.* (9) pointed to the existence of an extrachloroplastic Δ17 desaturase in *Nannochloropsis*. Wada *et al.* (10) showed that PUFA are necessary for growth and tolerance to photoinhibition in cyanobacteria at low temperatures. Based on the assumption that in *P. cruentum* EPA fulfills a role similar to that of 18:3n-3 in cyanobacteria and *Arabidopsis* (11), we employed the strategy utilized by Wada and Murata (12) to select for chill-sensitive mutants of *P. cruentum.* We anticipated that some mutants deficient in EPA biosynthesis could be found. Indeed, we describe here the successful selection of an EPA-deficient mutant of *P. cruentum* that is sensitive to low temperature and provides some biochemical characterization. Based on the data we have obtained, we suggest that TAG participate in the eukaryotic pathway of EPA biosynthesis in *P. cruentum*. Furthermore, HZ3 is the first described mutant of a higher or lower plant, that appears to be deficient in the ability to utilize TAG for lipid biosynthesis.

MATERIALS AND METHODS

Organism and Culture Conditions. Porphyridium cruentum strain 1380.1d was obtained from the Göttingen Algal Culture Collection (Göttingen, Germany) and was grown on Jones' medium (13) as previously described (11) in Erlenmeyer flasks under an air/CO_2 (99:1) atmosphere at 25°C, unless otherwise stated. The flasks were placed in an incubator shaker and illuminated from above at a light intensity of 115 μmol quanta m^{-2} s^{-1}. Cultures were grown exponentially (with proper dilution) for at least 4 d prior to the onset of the experiment.

Selection of mutants. Cultures of *P. cruentum* in the logarithmic phase of growth ($1.4 \cdot 10^7$ cells mL^{-1}) were treated with 1-methyl-3-nitro-1-nitroso guanidine at a final concentration of 25 μg mL^{-1}) for 30 min. This concentration of the mutagen caused less than 5% survival. The surviving cells were plated on solid medium at a density that resulted in about 200 colonies per 90 × 15 mm plate. Then they were incubated at 25°C for 15 d. The surviving colonies were then plated onto two plates using toothpicks and incubated at 25 and 15°C, respectively. Colonies that failed to show appreciable growth at 15°C as compared to wild type (WT) cells were scored and inoculated into a small volume of liquid medium in test tubes and incubated at 25°C. When the cultures of the putative chill-sensitive lines reached comparable density, as judged by observation, the low-temperature screening was repeated by streaking equal volumes of the scored cultures on sectors of two plates side by side with aliquots of WT cultures treated similarly. One of the plates was incubated at 25°C and the other at 15°C. Cell lines that were inhibited at 15°C as compared to the WT were scored again and the screening was repeated once more.

Pulse label experiments. Ammonium salts of (1-^{14}C)AA (5 μCi, specific activity 58 mCi/mmol) (Amersham, Little Chalfont, United Kingdom), (1-^{14}C)linoleic acid (25 μCi, specific activity 53 mCi/mmol), and (1-^{14}C) α-linolenic acid (25 μCi, specific activity 53 mCi/mmol) (NEN Research

Products, Mississauga, Ontario, Canada) were used in this work. Cultures were pulse-labeled for 30 min, centrifuged, washed twice with label-free medium, resuspended in one-half of the original volume, and cultivated as previously described (11). Aliquots were taken at various times after the end of the pulse. Experiments were repeated three times. The data in the figures depict the average of duplicate analyses in a representative experiment.

Nitrogen starvation. Cultures were resuspended in nitrate-free medium for 3 d. Ferric ammonium citrate was substituted with ferric citrate. After 2 d of nitrogen starvation, the cultures were labeled for 24 h with 5 μCi [1-^{14}C]AA and resuspended in label-free control medium. Labeling of lipids and their fatty acids was determined at various times.

Lipid extraction and analysis. Lipids were extracted using the procedure of Bligh and Dyer (14). Fatty acid methyl esters of total and individual lipids were obtained by transmethylation with 2% sulfuric acid in methanol. Fatty acid methyl esters were separated by reversed-phase high-performance liquid chromatography (HPLC) on an RP-18, 5 μm (250 mm, Lichrospher 100; Merck, Darmstadt, Germany) column using a solvent system of methanol/acetonitrile/water, 76:12:12 (by vol), detected at 205 nm, and identified using authentic standards. Radioactivity of individual peaks was determined by a Flo-One\Beta series A-100 detector (Radiomatic Instruments and Chemical Co., Inc., Tampa, FL). Distribution of radioactivity among individual lipids was assessed by thin-layer chromatography (TLC) on 10 × 10 cm plates (Silica Gel 60, 0.25 mm thickness, Macherey-Nagel, Duren, Germany). Two-dimensional separations of polar lipids were carried out using a solvent system of chloroform/methanol/water, 65:25:4 (by vol) for the first direction and chloroform/methanol/1-ethylpropylamine/concentrated ammonia, 65:35:0.5:5 (by vol) for the second direction. To estimate distribution of label in neutral lipids, aliquots of total lipid extracts were separated by TLC using a solvent system of petroleum ether/diethyl ether/acetic acid, 80:20:1 (by vol). Lipids were visualized by brief exposure to I_2 vapors. Radioactivity was detected by autoradiography with x-ray films (X-OMAT AR; Kodak, Rochester, NY) exposed to the TLC plates for 17 h. Lipid spots were scraped directly into scintillation vials containing 1 mL of methanol, a scintillation cocktail was added, and radioactivity was measured in a liquid scintillation counter (Rackbeta LKB, model 1217; Wallac Oy, Turku, Finland). MGDG and digalactosyldiacylglycerol (DGDG) extracted from the silica gel plates were separated to the constituent molecular species by reverse-phase HPLC (column as mentioned above) with a solvent mixture of methanol/water, 95:5 (vol/vol) (15) on a Waters (Millipore, Milford, MA) chromatograph, equipped with ultraviolet and radioactivity detectors.

RESULTS

Selection of mutants and growth characteristics. By comparing the growth of putative mutants of *P. cruentum* on agar plates at 15 and 25°C to that of the WT, we were able to select a series of mutants defective in growth at low temperatures. We chose the HZ3 mutant for further studies. The growth characteristics of the mutant and the WT at two temperatures are summarized in Figure 1. The growth of the mutant line at 15°C and at the optimal growth temperature of 25°C was severely inhibited. At 30°C however, inhibition of the mutant line could be observed only when cultures of low density biomass were compared, whereas at higher density, mutant cultures attained a final cell concentration similar to that of the WT cultures (data not shown).

Lipid and fatty acid composition. The proportion of TAG in the HZ3 mutant increased from 2 (in the WT) to 10% (of total fatty acids) with MGDG decreasing from 37 to 32% (Table 1). The proportion of EPA decreased from 41% (of total fatty acids) in the WT to 30% in the mutant, while the proportions of 16:0, 18:2, 18:3n-6 and 20:4n-6 increased (Table 1). The most affected lipids in the mutant were TAG, where the proportion of EPA decreased from 17 to 5%, and MGDG, with a decrease from 63 to 47%. In *P. cruentum*, the molecular species of DGDG and sulfoquinousyl diacylglycerol (SQDG) are almost entirely of prokaryotic structure, i.e., they contain C_{20} (or C_{18}) and C_{16} fatty acids in the *sn*-1 and *sn*-2 positions, respectively, while those of MGDG are partly eukaryotic and contain C_{20} fatty acids in both positions. Since MGDG was predominantly affected by the mutation, we suspected that only the synthesis of eukaryotic species was impaired. Therefore, separated MGDG and DGDG into their constituent molecular species. Indeed, the proportion of the major eukaryotic molecular species of MGDG, 20:5/20:5, decreased while that of the prokaryotic species 18:2/16:0, 20:4/16:0, and 20:5/16:0 increased (Table 2). The composition of DGDG, however, was not significantly changed. We have interpreted this as an indication that the mutation affected the eukaryotic pathway.

Incorporation of exogenously supplied radiolabeled fatty acids. Using exogenously supplied radiolabeled fatty acids, we

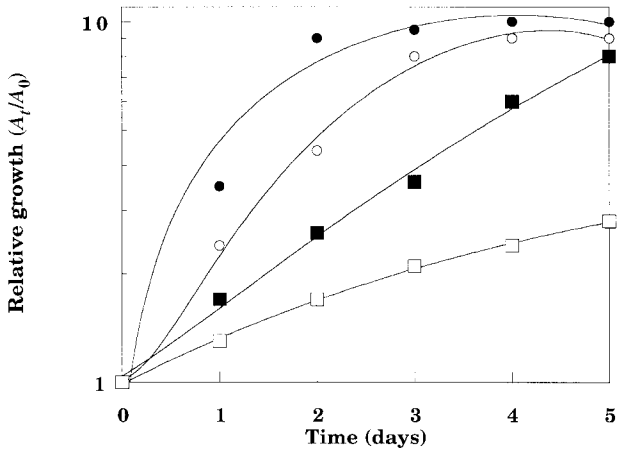

FIG. 1. Growth (expressed as chlorophyll concentration relative to day 0) of wild type (filled symbols) and HZ3 mutant (open symbols) of *Porphyridium cruentum* cultivated at 25 (circles) and 15°C (squares) and at a light intensity of 100 μmol quanta m^{-2} sec^{-1}.

TABLE 1
Lipid and Fatty Acid Composition of Wild Type and HZ3 Mutant of *P. cruentum* at 25°C[a]

			Fatty acid composition (% of fatty acids)									
Strain	Lipid	% of total lipids	16:0	16:1[b]	18:0	18:1 n-9	18:2 n-6	18:3 n-6	20:2 n-6	20:3 n-6	20:4 n-6	20:5 n-3
WT	Biomass	100	25.9	7.6	0.3	0.3	4.9	0.8	0.3	0.5	17.9	41.3
HZ3		100	30.4	7.7	0.4	0.4	7.5	1.2	0.3	0.7	22.3	30.3
WT	MGDG	37	26.2	0.8	0.3	0.3	4.1	0.1	—	0.1	5.5	62.6
HZ3		32	32.0	2.2	0.5	1.0	9.3	0.2	—	0.3	7.2	47.0
WT	DGDG	22	45.9	—	0.5	0.5	5.2	0.1	—	0.1	2.1	45.3
HZ3		22	50.1	0.3	0.5	0.5	4.1	0.1	—	0.1	2.9	41.2
WT	SQDG	13	49.8	0.7	1.3	0.9	1.5	—	2.0	0.2	4.4	37.1
HZ3		14	53.5	0.2	1.3	0.9	2.0	—	2.2	0.3	3.7	32.5
WT	PC	9	26.9	0.6	0.8	1.0	3.6	3.1	0.1	1.7	56.6	4.6
HZ3		7	18.5	0.9	0.9	0.8	2.0	3.0	0.1	1.9	67.7	3.7
WT	PE	2	35.0	2.3	4.4	2.8	3.4	3.4	—	0.2	33.7	13.4
HZ3		4	45.6	0.4	1.5	0.8	1.2	5.6	—	1.2	33.5	8.9
WT	PG	9	23.5	40.3	0.6	0.5	0.7	—	—	—	2.5	35.0
HZ3		6	25.4	49.9	0.9	0.3	1.0	0.1	0	0	6.2	30.0
WT	PI	2	54.0	1.7	1.3	1.5	29.6	1.2	0	0.5	5.8	3.2
HZ3		2	53.4	0.9	2.8	1.6	24.6	1.8	0	0.8	12.5	1.1
WT	PA	5	15.5	1.5	3.0	1.7	2.9	2.2	0	1.4	63.4	7.4
HZ3		3	16.6	0.8	1.5	1.0	2.1	2.8	—	1.5	68.2	3.9
WT	TAG	2	21.2	1.6	2.0	1.1	20.9	1.7	—	0.7	32.7	17.4
HZ3		10	24.6	1.7	1.2	1.4	24.6	2.2	—	1.4	37.9	4.8

[a]The data shown represent mean values with a range of less than 5% for major peaks (over 10% of fatty acids) and 15% for minor peaks, of three independent samples, each analyzed in duplicate.
[b]Sum of two isomers. In PG 16:1Δ3*t* constituted 36.5 and 35.5% of fatty acids in WT and HZ3, respectively. Abbreviations: WT, wild type; MGDG, monogalactosyldiacylglycerol; DGDG, dialactosyldiacylglycerol; SQDG, sulfoquinovosyldiacylglycerol; PC, phosphatidylcholine; PE, phosphatidylethanolamine; PG, phosphatidylglycerol; PI, phosphatidylinositol; PA, phosphatidic acid; TAG, triacylglycerol.

recently showed (8) that 18:2 is converted to EPA through a major n-6 and a minor n-3 (not shown) pathway in *P. cruentum* (Scheme 1). Thus, to obtain more insight into the biosynthesis of EPA in the mutant, WT and mutant cells were pulse-labeled with [^{14}C]18:2n-6 or [^{14}C]20:4n-6 and the redistribution of label in the lipids and fatty acids was followed.

Incorporation of [1-^{14}C]linoleic acid. Immediately after the pulse of [^{14}C]18:2, most of the label in both the WT and the HZ3 mutant was in PC and TAG (Fig. 2A,B). Total counts did not change significantly in both cases. In the WT, the label in the lipids decreased with time in favor of chloroplastic lipids (Fig. 2C,D). While the label of PC in the mutant decreased in time in a similar pattern to that of the WT, the extent of label in TAG was relatively stable and decreased much more slowly over a period of 22 h (Fig. 2). In TAG of the WT, most of the radioactivity coming from 18:2 disappeared after 22 h, whereas in the mutant, the decrease was much milder (Fig. 3). Radiolabeled 20:4n-6, which appeared after 4 h, accumulated faster in the mutant than in the WT. In MGDG of the mutant, 18:2 was more highly labeled, whereas 20:4 and 20:5 were less than in the WT (Fig. 4).

In comparison to the WT the molecular species analysis of MGDG of the mutant revealed a delay in the accumulation of radioactivity and eventually a decrease in all eukaryotic species, (Fig. 5). The proportion of the labeled prokaryotic species 20:4n-6/16:0 and 20:5n-3/16:0 was similar to that of the WT while that of 18:2/16:0 increased.

We also labeled the WT and the mutant with [1-^{14}C]18:3n-3. The label pattern was rather similar to that obtained following the incorporation of radioactive 18:2 (data not shown).

Incorporation of [1-^{14}C]arachidonic acid (AA). At the end of the pulse, PC of the WT was the most highly labeled lipid,

TABLE 2
Molecular Species Composition of Galactolipids of Wild Type and HZ3 Mutant of *P. cruentum*[a]

		Molecular species composition (% of total)					
Culture	Lipid	20:5/20:5	20:4/20:5	20:4/20:4	20:5/16:0	20:4/16:0	18:2/16:0
WT	MGDG	37.7	2.5	tr	55.5	0.8	3.5
HZ3	MGDG	22.6	2.2	tr	55.9	2.8	16.5
WT	DGDG	tr	—	—	94.2	0.7	5.1
HZ3	DGDG	tr	—	—	94.6	1.6	3.8

[a]Galactolipids were isolated by 2D thin-layer chromatography. Molecular species of galactolipids were separated by reversed phase high-performance liquid chromatography as detailed in the Materials and Methods section and are arranged in the order of their elution. The data shown represent mean values with a range of less than 10% for major peaks of three independent samples. See Table 1 for abbreviations.

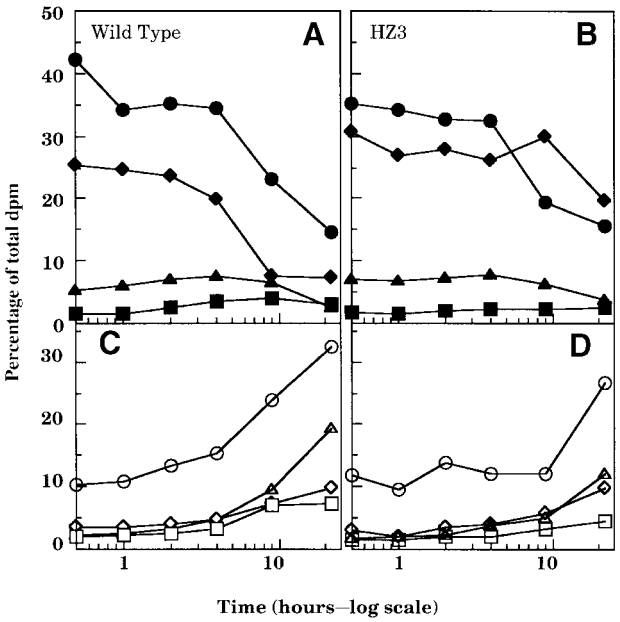

FIG. 2. Redistribution of radioactivity in lipids of wild type and HZ3 mutant of *P. cruentum* after labeling with 25 μCi of [1-^{14}C]linoleic acid. Lipids were separated by two-dimensional thin-layer chromatography, ●, phosphatidylcholine (PC); ◆, triacylglycerol (TAG); ■, phosphatidylethanolamine (PE); ▲, phosphatidylinositol (PI); ○, monogalactosyldiacylglycerol (MGDG); △, digalactosyldiacylglycerol (DGDG); ◇, sulfoquinovosyldiacylglycerol (SQDG); □, phosphatidylglycerol (PG).

accounting for 76% of total radioactivity, while TAG constituted only 9% (Fig. 7). Gradually, the label in these lipids decreased to 15 and 1%, respectively. In the mutant, the label of PC was slightly less at the end of the pulse, but much higher after 22 h (22 vs. 15%). The label of mutant TAG was higher than that of the WT throughout the time course and showed very little decrease. Chloroplastic lipids of the mutant were more highly labeled in the first 2 h, in comparison to the WT, but less labeled after 22 h. In the mutant, the fatty acid composition of total lipids and MGDG showed a decrease in the conversion of 20:4n-6 to 20:5 (data not shown).

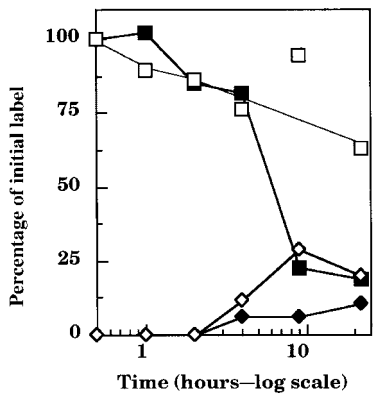

FIG. 3. Redistribution of radioactivity in fatty acids of TAG of wild type (filled symbols) and HZ3 mutant (open symbols) after labeling with [1-^{14}C]linoleic acid. Data presented as percentage of initial label. Fatty acids were determined by radio-high-performance liquid chromatography, ■, 18:2; ◆, 20:4n-6. For abbreviation see Figure 2.

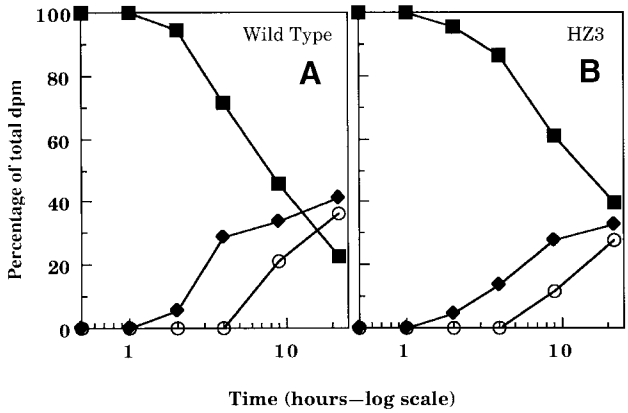

FIG. 4. Redistribution of radioactivity in fatty acids of MGDG of wild type and mutant after labeling with [1-^{14}C]linoleic acid. ■, 18:2; ◆, 20:4n-6, ○, 20:5n-3. For abbreviation, see Figure 2.

Recovery from nitrogen starvation. Under nitrogen starvation, cells of *P. cruentum* accumulate TAG (16). Thus, to evaluate the extent of the involvement of TAG in the biosynthesis of eukaryotic MGDG, we studied growth resumption following recovery from nitrogen starvation. When nitrogen is replenished, growth is resumed and chloroplastic lipids, especially eukaryotic MGDG, are actively produced (16,17). AA was used for labeling since it is one of the major fatty acids of TAG, especially under nitrogen starvation. Furthermore, the acyl moieties exported from the cytoplasm are predominantly C_{20} fatty acids, AA and EPA. We resuspended cultures of WT and HZ3 *P. cruentum* in nitrogen-free medium and kept them in this medium for 3 d. Two d after the medium change, the cultures were labeled with [1-^{14}C]AA for 24 h, as

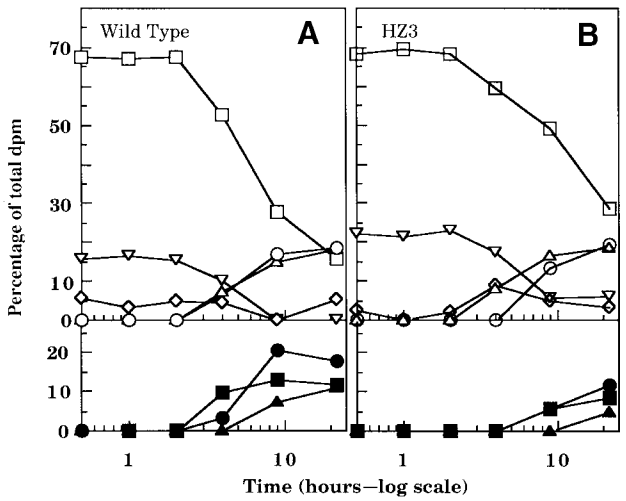

FIG. 5. Redistribution of radioactivity in molecular species of MGDG of wild type and HZ3 mutant after labeling with [1-^{14}C]linoleic acid. □, 18:2/16:0; ○, 20:4/16:0; ▽, 20:4/18:2; △, 20:5/16:0; ◇, 20:5/18:2; ■, 20:4/20:4; ●, 20:4/20:5; ▲, 20:5/20:5. See Figure 2 for abbreviation.

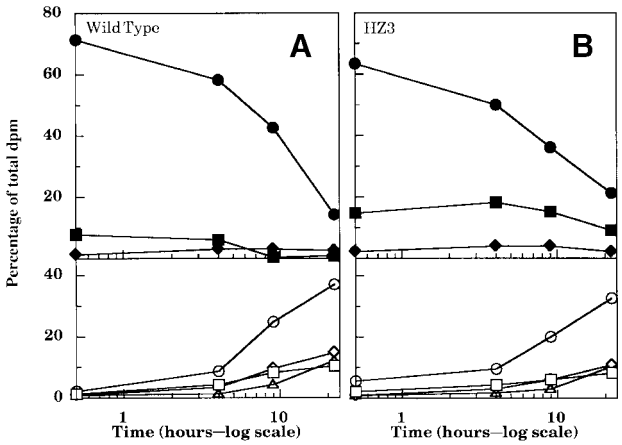

FIG. 6. Redistribution of radioactivity in lipids of wild type and HZ3 mutant *P. cruentum* after labeling with 10 μCi [1-^{14}C]20:4n-6. ●, PC; ◆, TAG; ■, PE; ○, MGDG; △, DGDG; ◇, SQDG; □, PG. See Figure 2 for abbreviations.

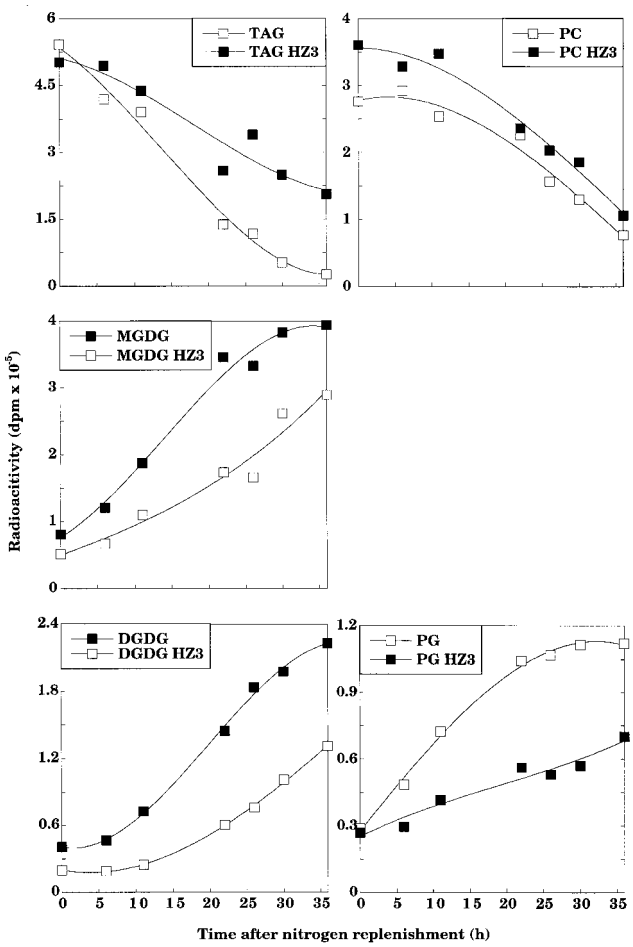

FIG. 7. Transfer of radioactivity from cytoplasmic (TAG and PC) to chloroplastic (MGDG, DGDG, and PG) lipids in wild type and HZ3 mutant *P. cruentum* following recovery from nitrogen starvation and labeling with 5 μCi [1-^{14}C]20:4n-6. See Figure 2 for abbreviations.

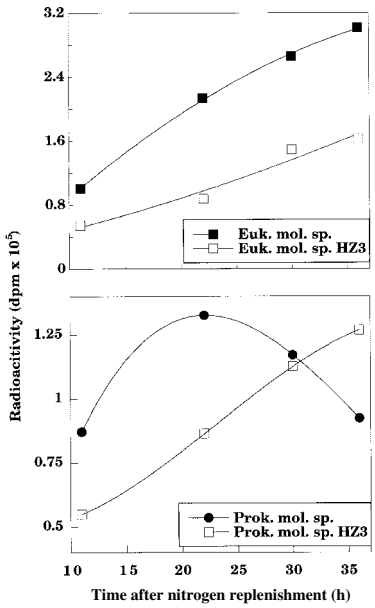

FIG. 8. Increase in label of prokaryotic (prok.) and eukaryotic (euk.) molecular species (mol. sp.) of MGDG in wild type and HZ3 mutant *P. cruentum* following recovery from nitrogen starvation and labeling with 5 μCi [1-^{14}C]20:4n-6. See Figure 2 for abbreviation.

preliminary studies have shown that after that period, TAG were already maximally labeled. Following the pulse, there were no significant differences between the level of radioactivity incorporated into the WT and the mutant, or in the distribution of the label between cytoplasmic and chloroplastic lipids (Figs. 7,8). However, with time, the label in the cytoplasmic lipids of the WT declined faster than that of the mutant, while that of the chloroplastic lipids increased to a greater extent in the WT compared to the mutant. After 36 h, WT cytoplasmic lipids retained only 15% of total counts in comparison to 40% in the mutant (data not shown). While PC of both cultures lost about 70% of their label, WT TAG lost 95% of its original label in comparison to only 59% in the mutant (Fig. 7). Molecular species analysis of MGDG showed that, whereas the prokaryotic species (20:4n-6/16:0 and 20:5n-3/16:0) were similarly labeled throughout the time course, there were large differences in the labeling of the eukaryotic species. Labeling of all the eukaryotic species (20:4n-6/20:4n-6, 20:4n-6/20:5n-3, 20:5n-3/18:2, and mostly 20:5n-3/20:5n-3) of the mutant was about half of the WT (Fig. 8).

DISCUSSION

C_{18} PUFA contribute to chill tolerance in higher plants (18) and cyanobacteria (19). In *P. cruentum*, the proportion of the main PUFA, EPA, increases in MGDG, its major depot, from 10% at 30°C to 51% at 20°C (17). This is reflected in an enhancement in the proportion of the ultimate eukaryotic molecular species, 20:5/20:5, from 6 to 40%. Furthermore, we have shown that the proportion of EPA at each temperature is

correlated with growth rate (11). We have thus hypothesized that the comparison of the growth rates at optimal and low temperatures would be a tool for the isolation of mutants of *P. cruentum* deficient in EPA content. Indeed, we were able to select such mutants. One of these mutants, HZ3, displayed the most severe growth impairment at reduced temperatures (Fig. 1) and was selected for further studies. The lipid and fatty acid analysis of the HZ3 mutant indicated a reduced level of eukaryotic molecular species of MGDG, which could be the consequence of a deficiency in the eukaryotic pathway. The reduced growth rate at 15°C (Fig. 1) of the HZ3 mutant and the low level of EPA, suggest that this fatty acid may have a role in the growth of microalgae at lower temperatures. However, further studies are required in order to exclude the possibility that the inhibition of growth and the impairment of lipid metabolism are not the result of a pleiotropic effect of a single mutation or the result of two or more independent mutations.

The labeling experiments with each of the different radioactive fatty acids revealed that mutant TAG accumulated a higher percentage of the initial label and were severely limited in turning over the label in comparison to the WT. One may argue that the higher TAG content of the HZ3 mutant represents a larger pool size, which is responsible for the delay in the turnover of the label. However, some decrease would have been expected in the first h after the pulse, but there was no decrease whatsoever in the label of mutant TAG for the first 10 h (Figs. 2,6). Under nitrogen starvation, the TAG content was similar in the WT and the mutant, and yet the same differences were observed (Fig. 7). That the disappearance of label from PC in the mutant was similar to that of the WT indicates that any contribution of DAG moieties of PC to the eukaryotic pathway is not impaired. We interpret our *in vivo* radiolabeling studies as showing that, in addition to PC, there is a notable contribution of TAG to the synthesis of chloroplastic lipids of *P. cruentum*. Possibly, the mutant is deficient in its ability to mobilize DAG (or acyl) moieties from TAG for the production of eukaryotic molecular species of MGDG. In oilseeds, which accumulate PUFA, TAG share a common DAG pool with phospholipids, primarily with PC. The conversion of DAG to TAG in oil-accumulating tissues is generally considered to be unidirectional (1) and TAGs are regarded metabolically as end-products that are used only as an energy store. However, Garces *et al.* (20) showed that when the growth temperature of developing sunflower seeds is reduced, the oleate acyl groups of TAG are superseded by linoleates. Recently, Stobart *et al.* (21) obtained evidence that supports a transacylation mechanism that can account for the TAG turnover in microsomal membranes of developing safflower seeds.

Nevertheless, we cannot exclude the possibility that the genetic lesion occurred in a different site that is responsible for the production of a component requiring high levels of eukaryotic MGDG. In the mutant, lower levels of this component would require lower levels of eukaryotic MGDG, resulting in a down regulation of the contribution of TAG to the production of these molecular species.

Under nitrogen starvation, much of the acyl flux of *P. cruentum* is diverted from the production of chloroplastic lipids, predominantly eukaryotic MGDG, to the accumulation of TAG (16). Replenishing the nitrogen to the algal cells results in a quick return to exponential growth. This, in turn, requires the synthesis of new chloroplastic membranes. The massive transfer of label from TAG to eukaryotic MGDG supports our hypothesis that C_{20} PUFA deposited in TAG of *P. cruentum* can be utilized as a reservoir for the swift production of eukaryotic MGDG when necessary.

Algal TAG are generally characterized by saturated and monounsaturated fatty acids, thought to serve as storage material (22). These characteristics seem to be common to most algal species studied for their potential to produce C_{20} PUFA. The TAG of the eustigmatophyte *Nannochloropsis*, an EPA producer, contains mainly 14:0, 16:0, and 16:1 (23). Similar findings were reported for other EPA-producing algae such as *Monodus subterraneus* (24) and *Phaeodactylum tricornutum* (25). Likewise, the TAGs of the DHA-rich cryptomonad *Chroomonas salina* (26) are almost entirely made of C_{18} fatty acids. However, certain algae are able to produce TAG rich in EPA and AA, e.g., *Ectocarpus fasciculatus* (27), *Pavlova lutheri* (28), *Nitzschia frigida,* and *Melosira antartica* (29). A high content of AA in TAG appears to be a feature of many, if not all, rhodophytes. Thus, the proportion of AA in TAG was reported to be 36% in *Chondrus crispus*, 49% in *Polysiphonia lanosa* (30), 40 to 64% in various *Gracilaria* sp. (31), and 33% in *P. cruentum* (as well as 17% EPA) (11). The ability of *P. cruentum* to utilize its TAG may explain the unique fatty acid composition of these lipids. However, it remains to be seen whether other microalgae having PUFA-rich TAG are able to utilize their TAG for similar purposes.

At present, we have no data to support any hypothesis concerning the mechanism by which the reutilization of TAG may take place. Nonetheless, several possibilities can be considered: i) a transacylation of monoacylglycerol by TAG to produce two molecules of DAG (21); (ii) a lipase activity that hydrolyzes TAG to DAG; and (iii) a DAGAT activity that is also capable of operating in the reverse direction. However, in the case of the latter, one would have expected a lower than normal level of TAG since this enzyme is likely to affect the incorporation of label into TAG, not just its turnover.

In higher plants, especially in *Arabidopsis*, mutants deficient in the production of either the prokaryotic or the eukaryotic molecular species of chloroplastic lipids demonstrated normal behavior at normal or low temperatures. Furthermore, it was shown that these mutants were able to ameliorate the damage to their membranes by adjusting the fatty acid flux leading to the prokaryotic and the eukaryotic pathways (32). In higher plants, the ultimate prokaryotic molecular species of MGDG, 18:3/16:3, differs from the eukaryotic species, 18:3/18:3, by only two carbon atoms. We speculate that for this reason, prokaryotic and eukaryotic molecular species of MGDG of higher plants are, to a certain extent, interchangeable. In *P. cruentum,* however, the eukaryotic molecular species, 20:5/20:5, contain four more carbon atoms and five more double bonds than the prokaryotic species, 20:5/16:0.

P. cruentum is found mainly in shallow marshes where temperature fluctuations are rapid and more pronounced than in deeper water bodies. The increase in the proportion of EPA in MGDG at low temperatures, and especially in that of the eukaryotic component of MGDG, 20:5/20:5, could possibly be attributed to the organism's attempt to cope with the stress inflicted by sudden drops in temperature. However, the *de novo* synthesis of EPA is apparently not fast enough to accommodate the increased demand for EPA. When *P. cruentum* was labeled with radioactive acetate, labeled EPA appeared only after 10 h (data not shown, see also Fig. 4). We hypothesize that TAG can be utilized as a buffering system for 20:4- and 20:5-containing DAG, which can be mobilized relatively rapidly for the production of eukaryotic molecular species of the major chloroplastic lipid MGDG. The role of these PUFA is not just maintenance of membrane fluidity. In various algae, enhanced n-3 desaturation was shown to be correlated with the activity of photosystem I (33). This hypothesis is supported by the work of Wanner and Kost (34) who found that rapid formation of cellular membranes from lipid bodies of different intracellular localization (cytoplasmic oil bodies and chloroplastic plastoglobules) has been observed during regeneration of starved cells of *P. cruentum*.

ACKNOWLEDGMENTS

This research was supported in part by the Israeli ministry of art and sciences. I.K-G. was supported in part by a fellowship from the Israeli ministry of absorption. Contribution No. 128 from the Laboratory for Microalgal Biotechnology, Jacob Blaustein Institute for Desert Research.

REFERENCES

1. Browse, J., and Somerville, C.R. (1991) Glycerolipid Synthesis: Biochemistry and Regulation, *Annu. Rev. Plant Mol. Biol. 42*, 467–506.
2 Norman, H.A., Smith, L.A., Lynch, D.V., and Thompson, G.A. (1985) Effects of Low-Temperature Stress on the Metabolism of Phosphatidylglycerol Molecular Species in *Dunaliella salina*, *Arch. Biochem. Biophys. 24*, 157–167.
3. Arao, T., Sakaki, T., and Yamada, M. (1994) Biosynthesis of Polyunsaturated Lipids in the Diatom, *Phaeodactylum tricornutum*, *Phytochemistry 36*, 629–635.
4 Arao, T., and Yamada, M. (1994) Biosynthesis of Polyunsaturated Fatty Acids in the Marine Diatom, *Phaeodactylum tricornutum*, *Phytochemistry 35*, 1177–1181.
5. Cohen, Z., Norman, H.A., and Heimer, Y.M. (1995) Microalgae as a Source of Omega-3 Fatty Acids, in Plants in Human Nutrition, *World Review of Nutrition and Dietetics* (Simopoulos A.P., ed.) Vol. 77, pp. 1–31, Karger, Basel.
6. Simopoulos, A.P. (1991) ω-3 Fatty Acids in Health and Disease and in Growth and Development, *Am. J. Clin. Nutr. 54*, 438–463.
7. Shiran, D., Khozin, I., Heimer, Y.M., and Cohen, Z. (1996) Elucidation of the Biosynthesis of EPA in *Porphyridium cruentum*. I: The Use of Externally Supplied Fatty Acids, *Lipids 31*, 1277–1282.
8. Khozin, I., Adlerstein, D., Bigogno, C., Heimer, Y.M., and Cohen, Z. (1997) Elucidation of the Biosynthesis of EPA in the Microalga *Porphyridium cruentum* II: Radiolabeling Studies, *Plant Physiol. 114*, 223–230.
9. Schneider, J.C., Livne, A., Sukenik, A., and Roessler, P.G. (1995) A Mutant of *Nannochloropsis* Deficient in Eicosapentaenoic Acid Production, *Phytochemistry 40*, 807–814.
10. Wada, H., Gombos, Z., Sakamoto, T., and Murata, N. (1992) Genetic Manipulation of the Extent of Desaturation of Fatty Acids in Membrane Lipids in the Cyanobacterium *Synechocystis* PCC6803, *Plant Cell Physiol. 33*, 535–540.
11. Cohen, Z., Vonshak, A., and Richmond, A. (1988) Effect of Environmental Conditions of Fatty Acid Composition of the Red Alga *Porphyridium cruentum*: Correlation to Growth Rate, *J. Phycol. 24*, 328–332.
12. Wada, H., and Murata, N. (1989) *Synechocystis* PCC 6803 Mutants Defective in Desaturation of Fatty Acids, *Plant Cell Physiol. 30*, 971–978.
13. Jones, R.E., Speer, L., and Kury, W. (1983) Studies on the Growth of the Red Alga *Porphyridium cruentum*, *Physiol. Plant. 16*, 636–643.
14. Bligh, E.G., and Dyer, W.J. (1959) A Rapid Method for Total Lipid Extraction and Purification, *Can. J. Biochem. 37*, 911–917.
15. Lynch, D.V., Gundersen, R.E., and Thompson, G.A. (1983) Separation of Galactolipid Molecular Species by High Performance Liquid Chromatography, *Plant Physiol. 72*, 903–905.
16. Cohen, Z. (1990) The Production Potential of Eicosapentaenoic Acid and Arachidonic Acid of the Red Alga *Porphyridium cruentum*, *J. Am. Oil Chem. Soc. 67*, 916–920.
17. Adlerstein, D., Khozin, I., Bigogno, C., and Cohen, Z. (1997) The Effect of Growth Temperature and Culture Density on the Molecular Species Composition of the Galactolipids in the Red Microalga *Porphyridium cruentum* (Rhodophyta), *J. Phycol. 33*, 975–979.
18. Miquel, M., James, D., Dooner, J., and Browse, J. (1993) *Arabidopsis* Requires Polyunsaturated Lipids for Low-temperature Survival, *Proc. Natl. Acad. Sci. U.S.A. 90*, 6208–6212.
19. Wada, H., Gombos, Z., and Murata, N. (1990) Enhancement of Chilling Tolerance of a Cyanobacterium by Genetic Manipulation of Fatty Acid Desaturation, *Nature 347*, 200–203.
20. Garces, R., Sarmiento, C., and Mancha, M. (1994) Oleate from Triacylglycerols Is Desaturated in Cold-induced Developing Sunflower (*Helianthus annuus* L.) Seeds, *Planta 193*, 473–477.
21. Stobart, K., Mancha, M., Lenman, M., Dahlqvist, A., and Stymne, S. (1997) Triacylglycerols are Synthesized and Utilized by Transacylation Reactions in Microsomal Preparations of Developing Safflower (*Carthamus tinctorius* L.) Seeds, *Planta 203*, 58–66.
22. Henderson, R.J., Hodgson, P., and Harwood, J.L. (1990) Differential Effects of the Substituted Pyridazinone Herbicide Sandoz 9785 on Lipid Composition and Biosynthesis in Photosynthetic and Non-photosynthetic Marine Microalgae. II. Fatty Acid Composition, *J. Exp. Bot. 41*, 729–736.
23. Sukenik, A., and Carmeli, Y. (1990) Lipid Synthesis and Fatty Acid Composition in *Nannochloropsis* sp. (Eustimatophyceae) Grown in a Light-Dark Cycle, *J. Phyc. 26*, 464–469.
24. Cohen, Z. (1994) Production Potential of Eicosapentaenoic Acid by *Monodus subterraneus*, *J. Am. Oil Chem. Soc. 71*, 941–945.
25. Yongmanitchai, W., and Ward, O.P. (1991) Growth of and Omega-3 Fatty Acid Production by *Phaeodactylum tricornutum* Under Different Culture Conditions, *Appl. Environ. Microbiol. 57*, 419–425.
26. Henderson, R.J., and McKinley, E.E. (1992) Radiolabeling Studies of Lipids in the Marine Cryptomonad *Chroomonas salina* in Relation to the Fatty Acid Desaturation, *Plant Cell Physiol. 33*, 395–406.
27. Makewicz, A., Gribi, C., and Eichenberger, W. (1997) Lipids of *Ectocarpus fasciculatus* (Phaeophyceae). Incorporation of [1-^{14}C]Oleate and the Role of TAG and MGDG in Lipid Metabolism, *Plant Cell Physiol. 38*, 952–60.

28. Eichenberger, W., and Gribi, C. (1997) Lipids of *Pavlova lutheri*: Cellular Site and Metabolic Role of DGCC, *Phytochemistry 45*, 1561–1567.
29. Falk-Peterson, S., Sargent, J.R., Hegseth, E.N., Hop, H., and Oklodkov, Y.B. (1998) Lipid and Fatty Acid Composition in Ice Algae and Phytoplankton from the Marginal Ice Zone in the Barents Sea, *Polar Biology 20*, 41–47.
30. Pettitt, T.R., Jones, A.L., and Harwood, J.L. (1989) Lipids of the Marine Red Algae, *Chondrus crispus* and *Polysiphonia lanosa*, *Phytochemistry 28*, 2053–2058.
31. Araki, S., Sakurai, T., Oohusa, T., Kayama, M., and Nizsizawa, K. (1990) Content of Arachidonic and Eicosapentaenoic Acids in Polar Lipid from *Gracilaria* (Gracilariales, Rhodophyta), *Hydrobiologia 204/205*, 513–519.
32. Browse, J., and Somerville, C.R. (1994) Glycerolipids, in *Arabidopsis* (Meyerowitz, E.M., and Sormerville, C.R., eds.) pp. 881–912, Cold Spring Harbor Laboratory Press, Plainview.
33. Klyachko-Gurvich, G., Tsoglin, L.N., Doucha, J., Kopetskii, J., Shebalina, B.I., and Semenenko, V.E. (1999) Desaturation of Fatty Acids as an Adaptive Response to Shifts in Light Intensity, *Physiol. Plant. 107*, 240–249.
34. Wanner, G., and Kost, H.P. (1984) "Membrane Storage" of the Red Alga *Porphyridium cruentum* During Nitrate and Sulfate Starvation, *Z. Pflanzenphysiol. 113*, 251–262.

[Received January 18, 2000, and in revised form May 30, 2000; revision accepted June 15, 2000]

Intravenously Injected [1-^{14}C]Arachidonic Acid Targets Phospholipids, and [1-^{14}C]Palmitic Acid Targets Neutral Lipids in Hearts of Awake Rats

Eric J. Murphy[1],*, Thad A. Rosenberger, Casey B. Patrick, and Stanley I. Rapoport

Section on Brain Physiology and Metabolism, National Institute on Aging, National Institutes of Health, Bethesda, Maryland 20892-1582

ABSTRACT: The differential uptake and targeting of intravenously infused [1-^{14}C]palmitic ([1-^{14}C]16:0) and [1-^{14}C]arachidonic ([1-^{14}C]20:4n-6) acids into heart lipid pools were determined in awake adult male rats. The fatty acid tracers were infused (170 μCi/kg) through the femoral vein at a constant rate of 0.4 mL/min over 5 min. At 10 min postinfusion, the rats were killed using pentobarbital. The hearts were rapidly removed, washed free of exogenous blood, and frozen in dry ice. Arterial blood was withdrawn over the course of the experiment to determine plasma radiotracer levels. Lipids were extracted from heart tissue using a two-phase system, and total radioactivity was measured in the nonvolatile aqueous and organic fractions. Both fatty acid tracers had similar plasma curves, but were differentially distributed into heart lipid compartments. The extent of [1-^{14}C]20:4n-6 esterification into heart phospholipids, primarily choline glycerophospholipids, was elevated 3.5-fold compared to [1-^{14}C]16:0. The unilateral incorporation coefficient, *k**, which represents tissue radioactivity divided by the integrated plasma radioactivity for heart phospholipid, was sevenfold greater for [1-^{14}C]20:4n-6 than for [1-^{14}C]16:0. In contrast, [1-^{14}C]16:0 was esterified mainly into heart neutral lipids, primarily triacylglycerols (TG), and was also found in the nonvolatile aqueous compartment. Thus, in rat heart, [1-^{14}C]20:4n-6 was primarily targeted for esterification into phospholipids, while [1-^{14}C]16:0 was targeted for esterification into TG or metabolized into nonvolatile aqueous components.

Paper no. L8403 in *Lipids 35,* 891–898 (August 2000).

While it is well-established that phospholipid breakdown is accelerated during myocardial ischemia (1–3), until recently the roles of phospholipids and their constitutive fatty acids in lipid-mediated signal transduction and membrane turnover in the heart were poorly understood. A number of signal transduction mechanisms in the heart function through a phospholipase A_2-mediated release of arachidonic acid (20:4n-6). In rat ventricular myocytes, interleukin-1β (IL-1β) activates the plasmalogen selective phospholipase A_2 through a receptor-linked mechanism, resulting in increased 20:4n-6 levels (4). Tumor necrosis factor-α also increases phospholipase A_2 activity in rat ventricular myocytes, although the phospholipase A_2 which is activated is apparently different from that activated by IL-1β (5). Angiotensin II stimulates the release of both 20:4n-6 and inositol phosphates through activation of multiple receptor subtypes involving increased phospholipase A_2 and phospholipase C activity (6). The β_2-adrenergic receptor stimulation leads to 20:4n-6 release through activation of a cytosolic phospholipase A_2 (7). Furthermore, the heart has an active phosphoinositide pathway that responds to α-1-adrenergic and muscarinic receptor stimulation (8,9). This pathway is partially regulated by lysophosphatidylcholine levels, with its activity decreasing with increasing levels (10). This suggests that, lysophosphatidylcholine produced by phospholipase A_2-mediated hydrolysis of choline glycerophospholipids (ChoGpl) regulates another lipid-mediated signal transduction system in the heart. Despite the role of 20:4n-6 in heart lipid-mediated signal transduction, the uptake and targeting of this fatty acid in the heart are controversial.

The mammalian heart uses palmitic acid (16:0) as a primary source of metabolic energy *via* β-oxidation (11), but the heart also takes up polyunsaturated fatty acids such as 20:4n-6 (12). The uptake rate and ultimate deposition of fatty acids depend, in part, upon chain length (11). Palmitic acid, a saturated fatty acid, is targeted for esterification into triacylglycerol (TG) pools and used to meet energy demands (11, 13). Oleic acid, a monounsaturated fatty acid, is also taken up by heart and is targeted for esterification into TG (14). Uptake and targeting of these fatty acids toward β-oxidation are decreased with high glucose levels (15). However, when glucose levels are in the physiologic range, saturated and monounsaturated fatty acids are esterified into TG and used almost exclusively for β-oxidation (13–15).

In contrast, the ultimate fate of 20:4n-6 in heart is unclear. A number of studies in isolated hearts or isolated myocytes

[1]National Research Council Senior Fellow.

*To whom correspondence should be addressed at Section on Brain Physiology and Metabolism, National Institute on Aging, National Institutes of Health, Building 10, Room 6C103, Bethesda, MD 20892.
E-mail: murphye@mail.nih.gov

Abbreviations: CE, cholesteryl esters; CerPCho, sphingomyelin; ChoGpl, choline glycerophospholipids; DG, diacylglycerols; EtnGpl, ethanolamine glycerophospholipids; FFA, free fatty acids; IL-1β, interleukin-1β; *k**, unilateral incorporation coefficient; PET, positron emission tomography; PlsCho, choline; PlsEtn, ethanolamine plasmalogen; PtdIns, phosphatidylinositol; PtdOH, phosphatidic acid; PtdSer, phosphatidylserine; TG, triacylglycerols; TLC, thin-layer chromatography.

suggest that esterification of 20:4n-6 into lipid pools is concentration-dependent (12,16). For instance, in a perfused isolated heart model, when the concentration of 20:4n-6 in the perfusate is high, it is preferentially esterified into myocyte TG (12,16), while when the concentration is low, it is preferentially esterified into phospholipids (12). Regardless, very little 20:4n-6 is used for β-oxidation, thereby conserving this fatty acid for other uses (12). This conservation is consistent with the utilization of 20:4n-6 in lipid-mediated signal transduction. Other studies in myocytes have shown that 20:4n-6 and other polyunsaturated fatty acids are esterified into the TG pool much more than into phospholipid pools (17). Under these experimental conditions, the heart did not elongate or desaturate the fatty acids, suggesting that it lacks the high levels of enzymic activity for these functions (17). Results also indicate that 20:4n-6 found in heart is not formed from linoleic acid but rather arises from direct uptake from the circulation (17). Thus, the targeting of 20:4n-6 in heart remains unclear. These conflicting results suggest that 20:4n-6 uptake and targeting need to be reexamined in the heart.

Others have used perfused heart models or isolated myocytes to study 20:4n-6 uptake and targeting, but these models may not represent the situation found *in vivo*. Therefore, we examined 20:4n-6 uptake and targeting, as compared to 16:0, by intravenously infusing awake adult male rats with either [1-^{14}C]20:4n-6 or [1-^{14}C]16:0 and quantifying the uptake and deposition of each tracer into different heart lipid pools. By using high specific activity tracers, unlabeled plasma fatty acid levels were unaltered (18). We found that [1-^{14}C]20:4n-6 was largely esterified into rat heart phospholipids, whereas [1-^{14}C]16:0 was preferentially esterified into heart TG and found in the nonvolatile aqueous fraction representing by-products of β-oxidation.

MATERIALS AND METHODS

Animals. Male Sprague-Dawley rats (200 g) were obtained from Charles River Laboratories (Wilmington, DE) and maintained *ad libitum* on standard laboratory rat chow and water prior to surgery. This study was conducted in accordance with the National Institutes of Health Guidelines for the Care and Use of Laboratory Animals (NIH publication 80-23), under a protocol approved by the National Institute of Child Health and Development's Institutional Animal Care and Use Committee.

Animal surgery. Unfasted rats were anesthetized with respired halothane (1–3%), and their femoral artery and vein were catherized with polyethylene tubing (PE-50). Following catheter insertion, the wound was closed using standard surgical staples and the area anesthetized with xylocaine (1%). The rats were wrapped in plaster body casts, taped to wooden blocks, and maintained postoperatively in a quiet temperature-controlled environment that kept body temperature at 37°C for 3 h prior to infusion. Seven out of eight rats survived (88%) the surgical procedure.

Awake rats were infused with 170 μCi/kg of either [1-^{14}C]20:4n-6 or [1-^{14}C]16:0 into the femoral vein over 5 min, using a constant rate infusion pump (Harvard Apparatus Co., South Natick, MA). Throughout the experimental period, arterial blood samples (200 μL) were taken to determine plasma radioactivity. Fifteen minutes from the start of infusion, the rats were killed using sodium pentobarbital (100 mg/kg, i.v.). The hearts were rapidly removed, bisected, and residual blood was removed by rinsing with ice-cold 0.9% KCl. After blotting, the hearts were frozen in dry ice.

Preparation of radiotracer. Radiotracers (Moravek Biochemical, Brea, CA) were prepared by taking an aliquot of either tracer in ethanol and evaporating the ethanol under a constant stream of N_2 at 50°C. Radiotracer purity was assessed by thin-layer chromatography (TLC) and found to be >97% pure for each tracer. The fatty acid tracers were individually solubilized in 5 mM HEPES (pH 7.4) buffer containing fatty acid free-bovine serum albumin (50 mg/mL; Sigma Chemical Co., St. Louis, MO). Solubilization was facilitated by sonication in a bath sonicator for 10 min. Radioactivity was determined using liquid scintillation counting and adjusted to 100 μCi/mL. The appropriate amount of radiotracer was prepared for each animal to administer 170 μCi/kg (18).

Plasma extraction. Arterial blood samples, taken at predetermined time points during the infusion period, were stored on ice for up to 10 min before separating the plasma by centrifugation using a Beckman microfuge (Fullerton, CA). Plasma lipids were extracted by transferring a 100-μL aliquot of plasma into a tube containing 3 mL of chloroform/methanol (2:1, vol/vol), then vortexing. The addition of 0.63 mL of 0.9% KCl to these tubes resulted in two phases, which were thoroughly mixed and allowed to separate overnight in a −20°C freezer. The upper phase was removed and the lipid-containing lower phase was rinsed with 0.63 mL of theoretical upper phase to remove any water-soluble contaminants (19). Phase separation was facilitated by centrifugation at 1500 rpm and 0°C in a refrigerated Sorvall RT 6000 B centrifuge (DuPont Instruments, Wilmington, DE). The upper phase was discarded, the lower phase was dried, and its radioactivity quantified using a Packard 2200 CA Tricarb liquid scintillation counter (Packard Instruments, Downers Grove, IL).

Heart extraction. Frozen heart tissue was weighed, minced, and extracted in a Tenbroeck tissue homogenizer using a two-phase system (19). Briefly, the tissue mass (g) was multiplied by a correction factor of 1.28 to convert it to an equivalent value expressed in mL (20). This value represented 1 vol. The minced tissue was placed in the homogenizer and 17 vol of chloroform/methanol (2:1, vol/vol) added. Tissue was homogenized to a fine particulate-like powder. The solvent was removed and the homogenizer rinsed with 2 vol of chloroform/methanol (2:1, vol/vol). The rinse was added to the original sample, and 4 vol of 0.9% KCl solution added to this combined lipid extract. After vigorous mixing, phase separation was facilitated by centrifugation as described above. The upper phase and proteinaceous interface were removed and saved in a 20-mL glass scintillation vial. The lower organic phase was washed twice with 2 mL of theoretical upper phase, with phase separation facilitated by cen-

trifugation between washes. The washes were removed and combined with the previously removed upper phase. The washed lower phase was dried under a stream of nitrogen and the lipids redissolved in 1 mL of *n*-hexane/2-propanol (3:2, vol/vol) containing 5.5% H_2O.

Aqueous fraction. The aqueous fraction was processed for liquid scintillation counting by first being dried at 80°C for 18 h to remove $^{14}CO_2$. The dried material was then solubilized in 2 mL of Soluable (Packard Instruments) in tightly capped scintillation vials heated at 80°C for 2 h. Radioactivity was determined after addition of 10 mL of Ready-Solv (Beckman Instruments) using a Packard 2200 CA Tricarb liquid scintillation counter.

TLC. Phospholipids and neutral lipids were separated by TLC. For each separation, 100 µL of sample was spotted onto a TLC plate. Phospholipids were separated on heat-activated Whatman silica gel-60 plates (20 × 20 cm, 250 µm) developed in chloroform/methanol/acetic acid/water (60:30:3:1, by vol). This solvent system resolves cardiolipin, phosphatidic acid (PtdOH), and ethanolamine glycerophospholipids (EtnGpl) but not phosphatidylinositol (PtdIns) and phosphatidylserine (PtdSer). Neutral lipids were separated using heat-activated silica G plates (Analtech, Newark, DE) developed in petroleum ether/diethyl ether/acetic acid (70:30:1.3, by vol) (21). This solvent system resolves cholesteryl esters (CE) and TG. Lipid fractions were determined using authentic standards (Doosan-Serday, Englewood Cliffs, NJ, and Nu-Chek-Prep, Elysian, MN).

Bands corresponding to PtdOH, EtnGpl, combined PtdIns/PtdSer, ChoGpl, and sphingomyelin (CerPCho) were scraped into 20-mL liquid scintillation vials, and 0.5 mL H_2O was added followed by 10 mL of Beckman Ready-Solv. After mixing, the samples were quantified by liquid scintillation counting at least 1 h after the addition of the Ready-Solv. Bands corresponding to TG, CE, diacylglycerol (DG), and free fatty acids (FFA) also were scraped into 20-mL scintillation vials and counted as described above.

Plasmalogens. Fatty acid esterification into choline and ethanolamine plasmalogen was also determined. ChoGpl and EtnGpl were separated by TLC, the phospholipids removed by scraping, and the phospholipids extracted from the silica using *n*-hexane/2-propanol (3:2, vol/vol) containing 5.5% H_2O. The extraction was 97–98% efficient based on the recovery of radioactivity. The ChoGpl and EtnGpl fractions were dried under a stream of nitrogen and exposed to HCl vapor for 15 min to hydrolyze the vinyl ether linkage (22). The samples were redissolved in solvent, and the acid-labile and -stable fractions were separated by high-performance liquid chromatography (22) and collected in 20-mL scintillation vials. The solvent was evaporated and the radioactivity determined as described above.

Unilateral incorporation coefficient of labeled fatty acid. Integrated areas for the plasma radioactivity curves were determined using the trapezoidal method (Sigma Plot; Jandel Scientific, San Rafael, CA). Total radioactivity for each individual heart fraction was normalized to the wet weight (g ww) and divided by the integrated area of plasma radioactivity. This calculation essentially normalizes the tissue radioactivity to the exposure of plasma tracer. The resulting coefficient is called the unilateral incorporation coefficient or k^*, with values expressed as s^{-1} (23). Hence, the k^* represents the radioactivity of each fraction normalized to the amount of presented radioactivity in the plasma. The following equation was used to calculate the k^*:

$$k^* = c^*_{\text{tissue}} \Big/ \int_0^T c^*_{\text{plasma}}\, dt \qquad [1]$$

where k^* = incorporation coefficient of tracer into a heart compartment, c^*_{tissue} = tracer radioactivity in the heart compartment, c^*_{plasma} = tracer radioactivity in the plasma, and T = time of tissue sampling.

Statistical analysis. Statistical analysis was done using a two-tailed Student's *t*-test or one-way analysis of variance coupled with Tukey-Kramer multiple comparisons test when appropriate. Statistical significance was defined at $P < 0.05$. For the [^{14}C]20:4n-6 group, $n = 4$, and for the [^{14}C]16:0 group, $n = 3$. Data are given as means ± standard deviation.

RESULTS

Plasma curves. Infusion of [1-^{14}C]20:4n-6 or [1-^{14}C]16:0 for 5 min produced a rapid increase in total organic plasma radioactivity, followed by a decline in radioactivity which was indistinguishable between the two tracers (Fig. 1). Tracer plasma half-lives were 81 ± 1 and 79 ± 1 s for [1-^{14}C]20:4n-6 and [1-^{14}C]16:0, respectively. The average areas under the curve were also equivalent, 1061 ± 223 and 1184 ± 59 nCi × mL plasma^{-1} × min^{-1} for [1-^{14}C]20:4n-6 and [1-^{14}C]16:0, respectively. The bulk of this radioactivity (>95%) was found in the plasma FFA fraction, with only minor amounts found esterified to plasma lipids (data not shown).

[1-^{14}C]16:0 and [1-^{14}C]20:4n-6 radioactivity. Total radioactivity of [1-^{14}C]20:4n-6 and [1-^{14}C]16:0 in heart tissue, 15 min after infusion began, was determined by measuring the radioactivity in the combined organic and dried aqueous phases (Table 1). Total radioactivity for [1-^{14}C]20:4n-6 was twofold greater than for [1-^{14}C]16:0. In the lipid-containing organic fraction, [1-^{14}C]20:4n-6 radioactivity was threefold higher relative to [1-^{14}C]16:0. There was no significant difference between radioactivities in the dried aqueous phase.

TABLE 1
Incorporated [1-^{14}C]16:0 and [1-^{14}C]20:4n-6 into Rat Heart[a]

	Radioactivity (µCi/g ww)		
	Total	Aqueous (nonvolatile)	Organic
[^{14}C]16:0 ($n = 3$)	0.34 ± 0.11	0.14 ± 0.06	0.20 ± 0.13
[^{14}C]20:4n-6 ($n = 4$)	0.68 ± 0.18*	0.06 ± 0.02	0.61 ± 0.19*

[a]Values represent means ± SD. *Statistical significance, $P < 0.05$, using a two-tailed Student's *t*-test. Abbreviation: ww, wet weight.

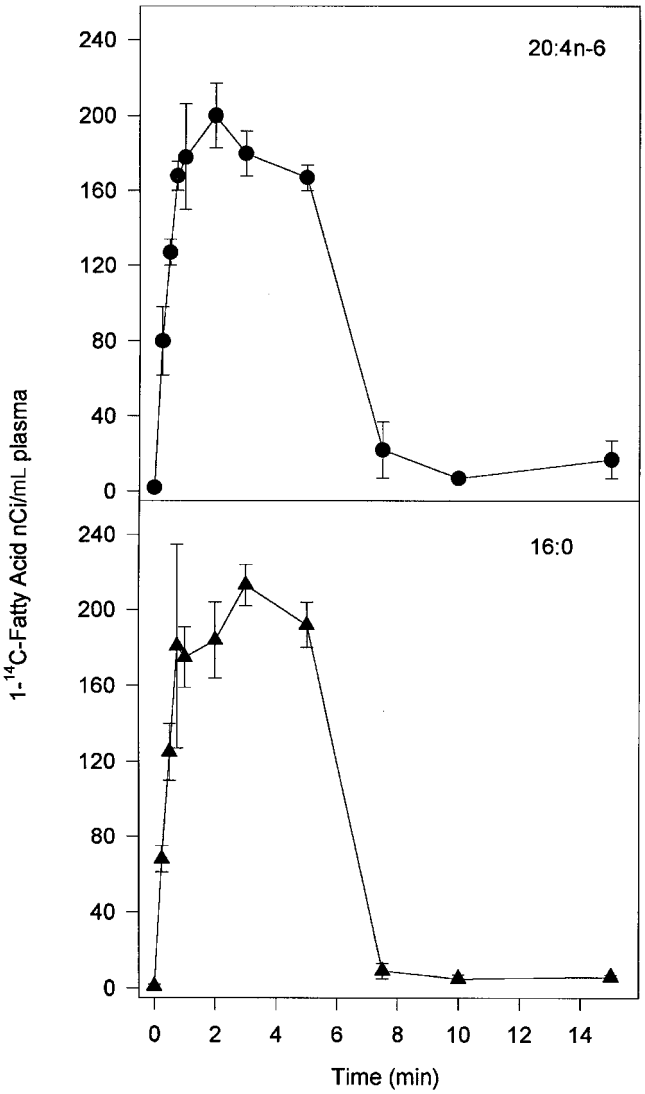

FIG. 1. Plasma curves for [1-^{14}C]20:4n-6 and [1-^{14}C]16:0. Values are expressed as nCi/mL plasma and represent means ± SD, $n = 3$.

Thus, [1-^{14}C]20:4n-6 was found primarily in the organic fraction, where 91% of the total tissue radioactivity was found. For [1-^{14}C]16:0, 60% of the total tissue radioactivity was found in the organic fraction. Furthermore, calculating the percentage extraction of each radiotracer by the heart from the total amount infused, the percentage oxidation was 0.37 ± 0.11 and 0.16 ± 0.06% ($P = 0.0292$) for 20:4n-6 and 16:0, respectively.

k*. The differences between [1-^{14}C]20:4n-6 and [1-^{14}C]-16:0 levels in heart may have arisen from preferential fatty acid extraction from plasma. To assess this possibility, radioactivity in different heart compartments was normalized to net exposure to plasma tracer, by calculating the unilateral incorporation coefficient for each tracer, *k** (Eq. 1). The *k** was calculated for total heart (combined organic and nonvolatile aqueous fractions), the lipid-containing organic fraction, and for the nonvolatile aqueous compartments (Table 2). The organic fraction was then fractionated into phospholipid, esterified neutral lipid, and FFA fractions, and *k** were calculated for these pools (Table 2). In the total heart, *k** was 2.2-fold greater for [1-^{14}C]20:4n-6 than for [1-^{14}C]16:0. There was no significant difference between the tracers in *k** in the aqueous compartment. For the organic fraction, *k** was 3.3-fold greater for [1-^{14}C]20:4n-6 than for [1-^{14}C]16:0. When the organic fraction was divided into its phospholipid and esterified neutral lipid compartments, differences were very apparent (Table 2). In the phospholipid fraction, *k** was 7.5-fold greater for [1-^{14}C]20:4n-6 than for [1-^{14}C]16:0. In the FFA compartment, *k** was over fivefold greater for [1-^{14}C]20:4n-6 than for [1-^{14}C]16:0. It was difficult to ascertain whether this increase in free [1-^{14}C]20:4n-6 represented fatty acid available for esterification or fatty acid that had been released by phospholipase A_2 during heart removal. There was no significant difference between the *k** for each tracer for the neutral lipid fraction. In any case, [1-^{14}C]20:4n-6 was more rapidly incorporated into the heart organic fraction than was [1-^{14}C]16:0, and this disparity was largely accounted for by a 7.5-fold greater *k** into heart phospholipids.

Incorporation coefficients were then calculated for different lipid classes (Table 3). In the phospholipids, *k** was larger for [1-^{14}C]20:4n-6 than for [1-^{14}C]16:0 in all fractions except PtdOH. Most notable was a 12.3-fold greater *k** for incorporation into the ChoGpl. Similar in magnitude was the ninefold greater *k** for [1-^{14}C]20:4n-6 relative to [1-^{14}C]16:0 in the combined PtdIns/PtdSer fraction. In esterified neutral lipids, the only difference was in the DG fraction, where *k** for [1-^{14}C]20:4n-6 was fivefold greater than that for [1-^{14}C]16:0. The values of *k** for the individual lipid classes confirm that [1-^{14}C]20:4n-6 was incorporated selectively into the phospholipid classes and that there was no difference between *k** for [1-^{14}C]20:4n-6 and [1-^{14}C]16:0 into neutral lipid fractions except for the DG fraction.

Distribution of [1-^{14}C]16:0 and [1-^{14}C]20:4n-6. The percentage distribution of radioactive fatty acids that were esterified into the neutral and phospholipid fractions was calculated by dividing an individual *k** by total *k** (Table 2). A significantly greater percentage of [1-^{14}C]20:4n-6 was esterified into the total phospholipid fraction compared to [1-^{14}C]16:0. In contrast, the percentage of [1-^{14}C]16:0 esterified into neutral lipids was threefold greater than that for [1-^{14}C]20:4n-6, despite a similar incorporation coefficient (Table 2). A greater percentage of [1-^{14}C]20:4n-6 was found as unesterified or free fatty acid compared to [1-^{14}C]16:0. These results confirm the selective targeting of [1-^{14}C]20:4n-6 for esterification into phospholipids, while [1-^{14}C]16:0 was targeted for esterification into neutral lipids.

To better understand these differences, the phospholipid and neutral lipid fractions were further separated into individual classes, and the percentage distribution of individual values of *k** relative to total *k** was determined (Table 3). For the neutral lipids, [1-^{14}C]16:0 was found primarily in TG. The percentage of [1-^{14}C]16:0 in the TG was increased 7.2-fold greater than for [1-^{14}C]20:4n-6. Distribution of radioactivity into CE was not significantly different between the radiola-

TABLE 2
Unilateral Incorporation Coefficient, *k, and Distribution of Total Radioactivity for Fractions from Rat Heart[a]**

	$k^* \times 10^{-3}$		Total k^* (%)	
	[^{14}C]16:0	[^{14}C]20:4n-6	[^{14}C]16:0	[^{14}C]20:4n-6
Fractions[b]				
Total	4.91 ± 1.78	10.68 ± 1.77*		
Organic	2.91 ± 2.02	9.59 ± 1.78*	56.0 ± 21.1	89.8 ± 6.7*
Aqueous	2.03 ± 0.82	1.09 ± 0.71	44.0 ± 21.1	10.2 ± 6.7*
Organic fraction[c]				
Phospholipid	0.87 ± 0.46	6.51 ± 0.91*	17.6 ± 5.0	61.4 ± 5.8*
Neutral lipid	1.67 ± 1.45	0.87 ± 0.17	31.0 ± 16.2	8.1 ± 0.7*
Free fatty acid	0.36 ± 0.13	1.89 ± 0.51*	7.5 ± 2.1	17.5 ± 3.4*

[a]Incorporation coefficients are expressed as s^{-1} and represent means ± SD. Percentage of total k^* was calculated by dividing individual k^* for each fraction by the total k^* and represents means ± SD. *Statistical significance, $P < 0.05$, using a two-tailed Student's *t*-test.
[b]Values under this heading represent distribution of radioactivity in all of the fractions.
[c]Values under this heading represent the major fraction found in the organic fraction under the heading "Fractions."

beled fatty acids, although there was a 2.5-fold increase in the percentage of [1-^{14}C]20:4n-6 in the DG fraction compared to [1-^{14}C]16:0. Whether this DG fraction represents an anabolic or catabolic intermediate is not clear.

Because [1-^{14}C]20:4n-6 was found mainly in phospholipids (Table 3), the distribution of radioactive fatty acids into individual phospholipid classes was evaluated. In the ChoGpl, the percentage of [1-^{14}C]20:4n-6 was 5.7-fold greater than for [1-^{14}C]16:0. Similarly, in the combined PtdIns/PtdSer fraction, [1-^{14}C]20:4n-6 percentages were increased 4.3-fold over the percentage of [1-^{14}C]16:0 in the same fraction. The smallest difference was seen in the CerPCho fraction, while the EtnGpl fractions were not different between groups. Thus, [1-^{14}C]20:4n-6 was preferentially targeted for esterification into phospholipids and found primarily in the ChoGpl fraction.

The vast proportion of heart arachidonic acid is found in choline and ethanolamine plasmalogens (24,25). To determine if [1-^{14}C]20:4n-6 and [1-^{14}C]16:0 were also targeted to the plasmalogens, the distributions of [1-^{14}C]20:4n-6 and of [1-^{14}C]16:0 in choline (PlsCho) and ethanolamine plasmalogens (PlsEtn) were measured. Only a small proportion of either fatty acid tracer was found in plasmalogen subclasses. For PlsEtn, 1.6 ± 0.1% and 1.9 ± 0.7% of total heart radioactivity was found in this subclass for [1-^{14}C]20:4n-6 and [1-^{14}C]16:0, respectively. In the PlsCho subclass, 2.4 ± 0.6 and 2.2 ± 1.7% of the total radioactivity were present for the [1-^{14}C]20:4n-6 and [1-^{14}C]-16:0 infused rats, respectively. These results indicate that within the 15-min time frame of this study, there was limited pulse labeling of plasmalogens by either fatty acid tracer.

TABLE 3
Unilateral Incorporation Coefficients, *k, and Distribution of Radioactivity for Individual Lipid Classes[a]**

	$k^* \times 10^{-3}$		Total k^* (%)	
	[^{14}C]16:0	[^{14}C]20:4n-6	[^{14}C]16:0	[^{14}C]20:4n-6
Phospholipids				
EtnGpl	0.32 ± 0.16	0.74 ± 0.19*	6.5 ± 1.9	6.9 ± 0.8
ChoGpl	0.41 ± 0.19	5.04 ± 0.70*	8.4 ± 2.4	47.6 ± 5.1*
PtdIns/PtdSer	0.06 ± 0.04	0.54 ± 0.09*	1.2 ± 0.3	5.1 ± 0.8*
PtdOH	0.04 ± 0.02	0.05 ± 0.03	0.5 ± 0.3	0.5 ± 0.3
CerPCho	0.03 ± 0.01	0.13 ± 0.03*	0.5 ± 0.1	1.3 ± 0.3*
Neutral lipids				
TG	1.52 ± 1.33	0.42 ± 0.10	28.0 ± 14.9	3.9 ± 0.3*
DG	0.08 ± 0.04	0.40 ± 0.09*	1.6 ± 0.6	3.8 ± 0.5*
CE	0.08 ± 0.08	0.04 ± 0.03	1.5 ± 1.1	0.4 ± 0.2

[a]Incorporation coefficients are expressed as s^{-1} and represent means ± SD. Percentage of total k^* was determined by dividing individual compartment k^* by the total k^* and represents means ± SD. *Statistical significance, $P < 0.05$, using a two-tailed Student's *t*-test. Abbreviations: EtnGpl, ethanolamine glycerophospholipids; ChoGpl, choline glycerophospholipids; PtdIns, phosphatidylinositol; PtdSer, phosphatidylserine; PtdOH, phosphatidic acid; CerPCho, sphingomyelin; TG, triacylglycerols; DG, diacylglycerols; CE, cholesteryl esters.

DISCUSSION

Because of the increasing recognition of the importance of phospholipids and their fatty acids in heart function and structure (4,5,8,10, 26,27), we quantified incorporation coefficients and targeting of [1-^{14}C]20:4n-6 and [1-^{14}C]16:0 in heart, using intravenous infusion of tracer in awake adult male rats. Previously, this method was used to quantify fatty acid incorporation and turnover rates for various fatty acids in the brains of awake adult rats (28,29). Because the quantity of radiotracer injected does not alter the plasma concentration of the infused fatty acid, this model avoids artifacts that may result from elevating plasma fatty acid levels above normal physiological levels (18,23,29). This avoids possible problems related to the observed concentration dependence for 20:4n-6 targeting in isolated hearts and myocytes (12,16,17).

In heart, saturated and monounsaturated fatty acids are utilized as the primary energy source, consistent with the fact that the heart has a tremendous capacity for fatty acid uptake and esterification (11,15). Palmitic acid is targeted for esterification into TG pools (12,13,16) or is used for β-oxidation directly (16). Oleic acid is also targeted to neutral lipids; nearly 80% of the oleic acid is localized in TG in both isolated perfused hearts and isolated myocytes (14). Our results confirm that 16:0 is preferentially esterified into the neutral lipid compartment, with the neutral lipids accounting for over 30% of the total radioactivity and into the nonvolatile aqueous pool accounting for 44% of the total radioactivity (Table 2). However, in contrast to other reports, we found nearly 18% of total [1-^{14}C]16:0 esterified into the heart phospholipid pools (Table 2). This value is similar to that reported in isolated myocytes, where 18% of the fatty acid is found in myocyte phospholipids, although this distribution in myocytes was not calculated from total radioactivity; thus the contribution of the aqueous radioactivity to the total radioactivity was not included (12). In isolated working rat heart, 9.5% of 16:0 in the lipid fraction is esterified into heart phospholipids (16). This value is not very different from ours, considering the difference in models. Thus, although [1-^{14}C]16:0 was esterified into heart phospholipids in awake rats, it was primarily targeted to the neutral lipid fraction where it was esterified into TG, or it was metabolized to products found in the nonvolatile aqueous phase.

In various isolated heart models and myocyte preparations, 20:4n-6 uptake and targeting appear to be linked to fatty acid availability (12,16,17). In isolated working rat heart, nearly all 20:4n-6 taken up from the perfusate (20:4n-6 concentration 1.2 mM) enters TG, with only 14% going into phospholipids (16). However, the 20:4n-6 concentration used in this study (16) is supraphysiologic, as the free 20:4n-6 concentration in rats *in vivo* is on the order of 16 μM (30). Consistent with these observations, much lower concentrations of 20:4n-6 (0.02–0.4 μM) are targeted almost exclusively in isolated rat myocytes to TG (82.3%), whereas only 12.3% is esterified into phospholipids (17). However, in isolated adult rat myocytes, 39% of the labeled 20:4n-6 in the lipid fraction is found in phospholipids when the medium 20:4n-6 concentration is 20 μM, but at a medium concentration of 5 nM; over 71% of the labeled 20:4n-6 is esterified into phospholipids (12). Clearly, targeting of 20:4n-6 is concentration-dependent in these models, suggesting a need to reevaluate 20:4n-6 uptake and targeting in an intact awake animal using physiologically relevant concentrations of each fatty acid.

In contrast to published results, we report that [1-^{14}C]-20:4n-6 was targeted selectively into heart phospholipids (60% of total radioactivity) in awake adult male rats (Table 2) and found primarily in ChoGpl (Table 3). Only 9% of the total radiotracer in heart at 15 min was found in the nonvolatile aqueous phase, compared with nearly 41% for [1-^{14}C]16:0. This suggests that [1-^{14}C]20:4n-6 was minimally metabolized to water-soluble nonvolatile compounds and was conserved relative to [1-^{14}C]16:0. Using the same fatty acid model, nearly 40% of the [1-^{14}C]16:0 found in the brain following infusion had been metabolized to slowly-disappearing nonvolatile aqueous phase compounds, mainly glutamate and aspartate (31). In rats infused with [20-^{18}F]20:4n-6 at radiotracer levels, 72.9% of the labeled 20:4n-6 in heart was found in the organic fraction and the majority of that radioactivity in the phospholipid fraction (32). In isolated heart models or myocytes, 20:4n-6 also appears to be conserved (12) and minimally metabolized by β-oxidation (12,17). Our data support these results. We also found that [1-^{14}C]20:4n-6 had a greater incorporation coefficient and was taken up to a greater extent by the heart than [1-^{14}C]16:0 (Tables 1 and 2), although our calculations did not take into account the complete conversion of 16:0 to CO_2. The published values for plasma fatty acid concentrations are 16.1 ± 0.9 and 161.3 ± 7.0 nmol × mL^{-1} for 20:4n-6 and 16:0, respectively (30), a 10-fold difference in the cold fatty acid concentrations. Using the unilateral incorporation coefficient determined in this study (Table 2), the incorporation of cold 20:4n-6 and 16:0 was 0.152 ± 0.002 and 0.758 ± 0.011 nmol × mL^{-1} × s^{-1} ($P <$ 0.0001), respectively. This is only a fivefold difference in uptake despite a 10-fold difference in availability, suggesting that there are selective processes for the uptake of 20:4n-6 from the plasma. These results indicate that in awake rats, relatively more cold 20:4n-6 appeared to have been extracted by the heart from the plasma than cold 16:0 and that this extracted 20:4n-6 was mainly esterified into phospholipids, despite a 10-fold greater availability of cold 16:0 in the plasma (30).

One mechanism that may explain the differential targeting of [1-^{14}C]20:4n-6 and [1-^{14}C]16:0 in heart could be the different affinities of CoA-dependent and -independent acyltransferase and transacylases for these two fatty acids (33). In rabbit heart, a cytosolic CoA-dependent acyltransferase exists which selectivity acylates 20:4n-6 onto ChoGpl (34). This might explain our observation that [^{14}C]20:4n-6 was preferentially esterified into ChoGpl (Table 3). Furthermore, this enzyme is highly selective for 20:4n-6 and is not found in the liver, suggesting it is localized solely in heart (34). In contrast, the CoA-independent acyltransferase does not exhibit

any substrate selectivity (34), suggesting that our observed differences in fatty acid targeting were accounted for by a heart-specific, 20:4n-6 selective, cytosolic CoA-dependent acyltransferase, which targets fatty acids primarily into ChoGpl.

The importance of the ethanolamine and choline plasmalogen subclasses in lipid-mediated signal transduction has become more apparent in heart since the isolation and characterization of a plasmalogen-selective phospholipase A_2 from heart (35–37). Further, because the plasmalogen subclass comprises a large proportion of ChoGpl and EtnGpl in mammalian heart (24,25,38,39) and because the *sn*-2 position contains a large proportion of heart 20:4n-6, we determined [1-^{14}C]20:4n-6 distribution into the PlsCho and PlsEtn. In awake rats, very little (<3%) [1-^{14}C]20:4n-6 was esterified into the PlsCho or PlsEtn. A plausible explanation for these results is that ether lipid biosynthesis *de novo* proceeds at a rate in heart that is much slower than the experimental time frame used. Indeed, heart plasmalogen biosynthesis *de novo* occurs on the order of hours, with no newly formed plasmalogen evident until up to 3 h after infusion of [1-^{3}H]-hexadecanol (40). This certainly may account for the minimal amount of [1-^{14}C]20:4n-6 found in the plasmalogens if the majority of the 20:4n-6 is esterified into plasmalogens during the synthetic process as opposed to esterification into lysoplasmenylcholine or to a direct transfer by a transacylase (33).

Lastly, because of the preferential targeting of [1-^{14}C]-20:4n-6 to phospholipid pools and the lack of appreciable alternative metabolism *via* other pathways, [^{11}C]20:4n-6 infusion coupled with positron emission tomography (PET) could be used to clinically study dynamic phospholipid turnover in heart. Past human heart studies using [^{11}C]palmitate with PET scanning have focused on the β-oxidation aspect of myocardial fatty acid metabolism (41,42); however, our findings suggest that these studies could be extended to examine lipid-mediated signal transduction in diseased human heart using [^{11}C]20:4n-6.

In summary, upon entering the heart, [1-^{14}C]20:4n-6 was predominantly esterified into ChoGpl, while [1-^{14}C]16:0 was targeted for esterification into TG or found in the nonvolatile aqueous fraction. The k^* for phospholipids was sevenfold greater for [1-^{14}C]20:4n-6 compared to [1-^{14}C]16:0, while there was no difference in values of k^* for esterified neutral lipids. Thus, in the awake adult rat, where the normal plasma fatty acid levels were maintained, there was a differential targeting of [1-^{14}C]20:4n-6 and [1-^{14}C]16:0 into distinct heart lipid pools. This suggests that fatty acid targeting in heart is based upon function. Further, this differential targeting suggests that 20:4n-6 and 16:0 have substantially different roles in heart metabolism and function.

ACKNOWLEDGMENTS

We thank Cindy Murphy for the typed preparation of this manuscript. This work was supported in part by a senior fellowship awarded by the National Research Council to EJM.

REFERENCES

1. Gunn, M.D., Sen, A., Chang, A., Willerson, J.T., Buja, L.M., and Chien, K.R. (1985) Mechanisms of Accumulation of Arachidonic Acid in Cultured Myocardial Cells During ATP Depletion, *Am. J. Physiol. 249*, H1188–H1194.
2. Freyss-Beguin, M., Millanvoye-Van Brussel, E., and Duval, D. (1989) Effect of Oxygen Deprivation on Metabolism of Arachidonic Acid by Cultures of Rat Heart Cells, *Am. J. Physiol. 257 (Heart Circ. 26)*, H444–H451.
3. Miyazaki, Y., Gross, R.W., Sobel, B.E., and Saffitz, J.E. (1990) Selective Turnover of Sarcolemmal Phospholipids with Lethal Cardiac Myocyte Injury, *Am. J. Physiol. 259 (Cell Physiol. 28)*, C325–C331.
4. McHowat, J., and Liu, S. (1997) Interleukin-1β Stimulates Phospholipase A_2 Activity in Adult Rat Ventricular Myocytes, *Am. J. Physiol. 272 (Cell Phys. 41)*, C450–C456.
5. Liu, S.J., and McHowat, J. (1998) Stimulation of Different Phospholipase A_2 Isoforms by TNF-α and IL-1β in Adult Rat Ventricular Myocytes, *Am. J. Physiol. 275 (Heart Circ. 44)*, H1462–H1472.
6. Lokuta, A.J., Cooper, C., Gaa, S.T., Wang, H.E., and Rogers, T.B. (1994) Angiotensin II Stimulates the Release of Phospholipid-Derived Second Messengers Through Multiple Receptor Subtypes in Heart Cells, *J. Biol. Chem. 269*, 4832–4838.
7. Pavoine, C., Magne, S., Sauvadet, A., and Pecker, F. (1999) Evidence for a β2-Adrenergic/Arachidonic Acid Pathway in Ventricular Cardiomyocytes. Regulation by the β1-Adrenergic/cAMP Pathway, *J. Biol. Chem. 274*, 628–637.
8. Meij, J.T.A., and Lamers, J.M.J. (1989) Alpha-1-adrenergic Stimulation of Phosphoinositide Breakdown in Cultured Neonatal Rat Ventricular Myocytes, *Mol. Cell Biochem. 88*, 73–75.
9. de Chaffoy de Courcelles, D. (1989) Is There Evidence of a Role of the Phosphoinositol-Cycle in the Myocardium? *Mol. Cell Biochem. 88*, 65–72.
10. Liu, S.-Y., Yu, C.-H., Hays, J.-A., Panagia, V., and Dhalla, N.S. (1997) Modification of Heart Sarcolemmal Phosphoinositide Pathway by Lysophosphatidylcholine, *Biochim. Biophys. Acta 1349*, 264–274.
11. DeGrella, R.F., and Light, R.J. (1980) Uptake and Metabolism of Fatty Acids by Dispersed Adult Rat Heart Myocytes. I. Kinetics of Homologous Fatty Acids, *J. Biol. Chem. 255*, 9731–9738.
12. Hohl, C.M., and Rosen, P. (1987) The Role of Arachidonic Acid in Rat Heart Cell Metabolism, *Biochim. Biophys. Acta 921*, 356–363.
13. Klein, M.S., Goldstein, R.A., Welch, M.J., and Sobel, B.E. (1979) External Assessment of Myocardial Metabolism with [^{11}C]Palmitate in Rabbit Hearts, *Am. J. Physiol. 237*, H51–H57.
14. Tamboli, A., O'Looney, P., Vander Maten, M., and Vahouny, G.V. (1983) Comparative Metabolism of Free and Esterified Fatty Acids by the Perfused Rat Heart and Rat Cardiac Myocytes, *Biochim. Biophys. Acta 750*, 404–410.
15. DeGrella, R.F., and Light, R.J. (1980) Uptake and Metabolism of Fatty Acids by Dispersed Adult Rat Heart Myocytes. II. Inhibition of Albumin and Fatty Acid Homologues, and the Effect of Temperature and Metabolic Reagents, *J. Biol. Chem. 255*, 9739–9745.
16. Saddik, M., and Lopaschku, G.D. (1991) The Fate of Arachidonic Acid and Linoleic Acid in Isolated Working Rat Hearts Containing Normal or Elevated Levels of Coenzyme A, *Biochim. Biophys. Acta 1086*, 217–224.
17. Hagve, T.-A., and Sprecher, H. (1989) Metabolism of Long-Chain Polyunsaturated Fatty Acids in Isolated Cardiac Myocytes, *Biochim. Biophys. Acta 1001*, 338–344.
18. Freed, L.M., Wakabayashi, S., Bell, J.M., and Rapoport, S.I. (1994) Effect of Inhibition of β-Oxidation on Incorporation of

[U-^{14}C]Palmitate and [1-^{14}C]Arachidonate into Brain Lipids, *Brain Res. 645*, 41–48.
19. Folch, J., Lees, M., and Sloane-Stanley, G.H. (1957) A Simple Method for the Isolation and Purification of Total Lipids from Animal Tissues, *J. Biol. Chem. 226*, 497–509.
20. Radin, N.S. (1988) Lipid Extraction, in *Neuromethods 7 Lipids and Related Compounds* (Boulton, A.A., Baker, G.B., and Horrocks, L.A., eds.) pp. 1–62, Humana Press, Clifton, NJ.
21. Marcheselli, V.L., Scott, B.L., Reddy, T.S., and Bazan, N.G. (1988) Quantitative Analysis of Acyl Group Composition of Brain Phospholipids, Neutral Lipids, and Free Fatty Acids, in *Neuromethods 7 Lipids and Related Compounds* (Boulton, A.A., Baker, G.B., and Horrocks, L.A., eds.) pp. 83–110, Humana Press, Clifton, NJ.
22. Murphy, E.J., Stephens, R., Jurkowitz-Alexander, M., and Horrocks, L.A. (1993) Acidic Hydrolysis of Plasmalogens Followed by High-Performance Liquid Chromatography, *Lipids 28*, 565–568.
23. Kimes, A.S., Sweeney, D., London, E.D., and Rapoport, S.I. (1983) Palmitate Incorporation into Different Brain Regions in the Awake Rat, *Brain Res. 274*, 291–301.
24. Gross, R.W. (1984) High Plasmalogen and Arachidonic Acid Content of Canine Myocardial Sarcolemma: A Fast Atom Bombardment Mass Spectroscopic and Gas Chromatography–Mass Spectroscopic Characterization, *Biochemistry 23*, 158–165.
25. Gross, R.W. (1985) Identification of Plasmalogen as the Major Phospholipid Constituent of Cardiac Sarcoplasmic Reticulum, *Biochemistry 24*, 1662–1668.
26. Kang, J.X., Xiao, Y.-F., and Leaf, A. (1995) Free, Long-Chain, Polyunsaturated Fatty Acids Reduce Membrane Electrical Excitability in Neonatal Rat Cardiac Myocytes, *Proc. Natl. Acad. Sci. USA 92*, 3997–4001.
27. Honore, E., Barhanin, J., Attali, B., Lesage, F., and Lazdunski, M. (1994) External Blockade of the Major Cardiac Delayed-Rectifier K^+ Channel (Kv1.5) by Polyunsaturated Fatty Acids, *Proc. Natl. Acad. Sci. USA 91*, 1937–1944.
28. Rapoport, S.I., Purdon, D., Shetty, H.U., Grange, E., Smith, Q., Jones, C., and Chang, M.C.J. (1997) *In Vivo* Imaging of Fatty Acid Incorporation into Brain to Examine Signal Transduction and Neuroplasticity Involving Phospholipids, *Ann. NY Acad. Sci. 620*, 56–74.
29. Robinson, P.J., Noronha, J., DeGeorge, J.J., Freed, L.M., Nariai, T., and Rapoport, S.I. (1992) A Quantitative Method for Measuring Regional *in vivo* Fatty Acid Incorporation into and Turnover Within Brain Phospholipids: Review and Critical Analysis, *Brain Res. Rev. 17*, 187–214.
30. Chang, M.C.J., Bell, J.M., Purdon, A.D., Chikhale, E.G., and Grange, E. (1999) Dynamics of Docosahexaenoic Acid Metabolism in the Central Nervous System: Lack of Effect of Chronic Lithium Treatment, *Neurochem. Res. 24*, 399–406.
31. Gnaedinger, J.M., Miller, J.C., Latker, C.H., and Rapoport, S.I. (1988) Cerebral Metabolism of Plasma [^{14}C]Palmitate in Awake Adult Rat: Subcellular Localization, *Neurochem. Res. 13*, 21–29.
32. Nagatsugi, F., Hokazono, J., Sasaki, S., and Maeda, M. (1996) 20-[^{18}F]Fluoroarachidonic Acid: Tissue Biodistribution and Incorporation into Phospholipids, *Biol. Pharm. Bull. 19*, 1316–1321.
33. Yamashita, A., Sugiura, T., and Waku, K. (1997) Acyltransferases and Transacylases Involved in Fatty Acid Remodeling of Phospholipids and Metabolism of Bioactive Lipids in Mammalian Cells, *J. Biochem. 122*, 1–16.
34. Needleman, P., Wyche, A., Sprecher, H., Elliott, W.J., and Evers, A. (1985) A Unique Cardiac Cytosolic Acyltransferase with Preferential Selectivity for Fatty Acids That Form Cyclooxygenase/Lipooxygenase Metabolites and Reverse Essential Fatty Acid Deficiency, *Biochim. Biophys. Acta 836*, 267–273.
35. Hazen, S.L., Stuppy, R.J., and Gross, R.W. (1990) Purification and Characterization of Canine Myocardial Cytosolic Phospholipase A_2. A Calcium-Independent Phospholipase with Absolute *sn*-2 Regiospecificity for Diradyl Glycerophospholipids, *J. Biol. Chem. 265*, 10622–10630.
36. Hazen, S.L., and Gross, R.W. (1991) ATP-Dependent Regulation of Rabbit Myocardial Cytosolic Calcium-Independent Phospholipase A_2, *J. Biol. Chem. 266*, 14526–14534.
37. Hazen, S.L., and Gross, R.W. (1993) The Specific Association of a Phosphofructokinase Isoform with Myocardial Calcium-Independent Phospholiase A_2. Implications for the Coordinated Regulation of Phospholipolysis and Glycolysis, *J. Biol. Chem. 268*, 9892–9900.
38. Das, D.K., Maulik, N., and Jones, R.M. (1994) Gas Chromatography–Mass Spectroscopic Detection of Plasmalogen Phospholipids in Mammalian Heart, in *Lipid Chromatographic Analysis* (Shibamoto, T., ed.) pp. 317–345, Marcel Dekker, Inc., New York.
39. Scherrer, L.A., and Gross, R.W. (1989) Subcellular Distribution, Molecular Dynamics and Catabolism of Plasmalogens in Myocardium, *Mol. Cell Biochem. 88*, 97–105.
40. Ford, D.A., and Gross, R.W. (1994) The Discordant Rates of *sn*-1 Aliphatic Chain and Polar Head Group Incorporation into Plasmalogen Molecular Species Demonstrate the Fundamental Importance of Polar Head Remodeling in Plasmalogen Metabolism in Rabbit Myocardium, *Biochemistry 33*, 1216–1222.
41. Geltman, E.M. (1994) Assessment of Myocardial Fatty Acid Metabolism with 1-^{11}C-Palmitate, *J. Nucl. Cardiol. 1*, S15–S22.
42. Lerch, R.A., Ambos, H.D., Bergmann, S.R., Welch, M.J., Ter-Pogossian, M.M., and Sobel, B.E. (1981) Localization of Viable, Ischemic Myocardium by Positron-Emission Tomography with ^{11}C-Palmitate, *Circulation 64*, 689–699.

[Received November 30, 1999, and in final revised form May 4, 2000; revision accepted June 22, 2000]

Conjugated Linoleic Acid Suppresses Triglyceride Accumulation and Induces Apoptosis in 3T3-L1 Preadipocytes

M. Evans[a], C. Geigerman[a], J. Cook[a], L. Curtis[b], B. Kuebler[b], and M. McIntosh[a,*]

[a]Department of Nutrition and Foodservice Systems, University of North Carolina-Greensboro, Greensboro, North Carolina 27402 and [b]Department of Biology, High Point University, High Point, North Carolina

ABSTRACT: Four sets of experiments were conducted to examine the influence of conjugated linoleic acid (CLA) isomers during proliferation and differentiation of cultures of 3T3-L1 preadipocytes using physiological culturing conditions. Cultures treated with either albumin [bovine serum albumin (BSA) vehicle] or linoleic acid (LA) served as controls. For the proliferation study (Expt.1), cells were cultured in media containing a crude mixture of CLA isomers or pure LA at 0, 10, 50, or 200 μM for 4 d. Preadipocyte proliferation (cell number, ^{3}H-thymidine incorporation into DNA) decreased as the level of CLA increased in the cultures. In contrast, LA had no impact on DNA synthesis. In Experiment 2a, postconfluent cultures were grown in media containing a crude mixture of CLA isomers or LA at 0, 10, 50, or 200 μM for the next 6 d. Postconfluent cultures supplemented with 50–200 μM CLA had less triglyceride (TG) and were smaller in size than cultures supplemented with similar amounts of LA. In Experiment 2b, postconfluent cultures supplemented with 200 μM of a crude mixture of CLA isomers or LA were harvested on days 1, 3, 6, or 9. Differences in TG content of cultures supplemented with 200 μM CLA compared to control and LA-supplemented cultures became apparent after 3 d of culture. Experiments 3a and 3b examined whether the fatty acid vehicle (BSA vs. ethanol) or the vitamin E status (±0.2 mM α-tocopherol) of the cultures altered CLA's impact on preadipocyte TG content. In Experiment 3a, ethanol-treated cultures had more TG than non-ethanol-treated cultures regardless of the fatty acid treatment. In Experiment 3b, cultures treated with 100 μM of either a crude mixture of CLA or the *trans*-10, *cis*-12 CLA isomer without supplemental vitamin E for 6 d had less TG than CLA-treated cultures containing vitamin E. In Experiment 4, postconfluent cultures were grown in media containing 100 μM LA or either a crude mixture of CLA isomers or the *trans*-10,*cis*-12 CLA isomer for 24–96 h to assess CLA's influence on the cell cycle and indices of apoptosis. Cultures treated with 100 μM CLA for 24–96 h had more apoptotic cells than BSA- or LA-treated cultures. Furthermore, cultures treated for 48 h with CLA had fewer cells in the S-phase than control cultures. The effects of the *trans*-10,*cis*-12 CLA isomer were more pronounced than those of the crude mixture of CLA isomers. These data suggest that CLA may exert its antiobesity effects by inhibiting proliferation, attenuating TG content, and/or inducing apoptosis in (pre)adipocytes.

Paper no. L8418 in *Lipids 35,* 899–910 (August 2000).

Conjugated linoleic acid (CLA) consists of a group of positional and geometric fatty acid isomers that are derived from linoleic acid (LA) (18:2n-6). CLA occurs naturally in ruminant meats, pasteurized cheeses, and dairy products and therefore is a dietary constituent of many Americans. However, health organizations continue to recommend we limit our intake of these animal products. Thus, as we decrease our consumption of animal fats, CLA consumption also decreases. Ironically, consumption of a crude mixture of CLA isomers by rodents has been shown to have a variety of health benefits, including anticarcinogenic (1), antiatherogenic (2,3), antidiabetic (4), and antiobesity actions (4–9). As an antiobesity agent, mice and pigs fed low levels of CLA (<1.5%, w/w) had less body fat and more lean body mass than controls (5–8,10–12). Furthermore, Park *et al*. (6) demonstrated that mature 3T3-L1 adipocytes treated with 20–200 μM CLA for 2 d had less triglyceride (TG) content and lipoprotein lipase (LPL) activity compared to control cultures. Moreover, Park *et al.* (7) recently found that the *trans*-10,*cis*-12 isomer of CLA is the bioactive isomer responsible for reducing adipocyte LPL activity and TG content. In contrast, Satory and Smith (13) showed that post-confluent cultures of differentiating 3T3-L1 preadipocytes treated with a crude mixture of CLA treatment had greater rates of lipogenesis [↑ lipogenesis; effective concentration that reduces activity by 50% (EC_{50}) ~ 18 μM] and more TG than nontreated cultures. However, CLA attenuated proliferation of preconfluent preadipocytes at concentrations as low as 1.7 μM. In contrast, Brodie *et al*. (14) demonstrated that 25–100 μM CLA inhibited both proliferation and differentiation (↓ glycerol-3-phosphate dehydrogenase activity; EC_{50} ~ 35 μM) of cultures of 3T3-L1 preadipocytes. Nevertheless, the culturing conditions used in these last two studies raise questions about the physiological relevance and interpretations of these data.

*To whom correspondence should be addressed at Department of Nutrition and Foodservice Systems, University of North Carolina at Greensboro, P.O. Box 26170, Greensboro, NC 27402-6170. E-mail: mkmcinto@uncg.edu

Abbreviations: AA, arachidonic acid; ANOVA, analysis of variance; BCA, bicinchoninic acid; BCS, bovine calf serum; BSA, bovine serum albumin; CLA, conjugated linoleic acid; DAG, diacylglycerol; DMEM, Dulbecco's modified Eagle's medium; DMSO, dimethyl sulfoxide; EC_{50}, effective concentration that reduces activity by 50%; FBS, fetal bovine serum; HBSS, Hank's balanced salt solution; HMDS, hexamethyldisilazane; LA, linoleic acid; LDH, lactate dehydrogenase; LPL, lipoprotein lipase; PBS, phosphate-buffered saline; PI, propidium iodide; PPAR-γ2, peroxisome proliferating activated receptor-γ2; SEM, scanning electron microscopy; TG, triglyceride.

These data suggest that the antiobesity actions of a crude mixture of CLA isomers may be due to the direct influence of CLA on preadipocyte growth and differentiation. However, the results of these preadipocyte studies are conflicting and may be due to differences in experimental conditions. Moreover, the physiological relevance of the studies by Satory and Smith (13) and Brodie *et al.* (14) are not clear since they used ethanol or dimethyl sulfoxide (DMSO) as the delivery vehicle for the fatty acids, whereas, *in vivo,* free fatty acids are transported by albumin. Furthermore, these authors did not include antioxidants in the media to prevent fatty acid peroxidation. Therefore, we investigated the influence of CLA on the growth and differentiation of cultures of 3T3-L1 preadipocytes using a physiological delivery method, e.g., using albumin as the fatty acid vehicle and supplementing the cultures with 0.2 mM α-tocopherol to protect CLA from peroxidation. Cultures treated with LA served as fatty acid controls to determine if CLA's effects are unique to its geometric structure or a generic effect of unsaturated fatty acids.

EXPERIMENTAL PROCEDURES

Cell model. Pre- (Expt. 1) and postconfluent (Expts. 2–4) monolayers of 3T3-L1 preadipocytes were used as the cellular model for these studies (see Fig. 1 for details). The 3T3-L1 preadipocytes are a nontransformed cell line, which is a continuous substrain of Swiss albino 3T3 murine cells developed through clonal expansion (15). These cells can be converted from a preadipose to adipose-like phenotype when appropriately stimulated. Furthermore, transplantation studies with this cell line demonstrate normal development of fat cells at the site of implantation. Lastly, these cells are capable of differentiating in culture in response to agents that induce adipose tissue differentiation *in vivo*.

Experimental designs and culture conditions (Fig. 1). As outlined in Figure 1, Experiment 1 was designed to examine the influence of continual supplementation of preconfluent, proliferating cultures with various doses of a crude mixture of CLA isomers and pure LA during the first 4 d of the preadipocyte proliferation program. The objective of Experiment 2a was to investigate the impact of continual supplementation of postconfluent, differentiating cultures with various doses of a crude mixture of CLA isomers and pure LA during the first 6 d of preadipocyte differentiation into mature adipocytes. The purpose of Experiment 2b was to assess the time course of supplementation with 200 μM of a crude mixture of CLA isomers and pure LA over the entire differentiation program (days 1–9). The objectives of Experiment 3 were to determine if the vehicle [bovine secum albumin (BSA) vs. ethanol] and the vitamin E status (±0.2 mM α-tocopherol) of the cultures influenced CLA's effects on adipogenesis based on conflicting data from several recent reports (13,14). Experiment 4 examined potential mechanisms by which a crude mixture of CLA or the *trans*-10, *cis*-12 CLA isomer may attenuate preadipocyte differentiation, including cell cycle arrest and apoptosis using flow cytometry and nuclear staining techniques.

CLA or LA was complexed to 7.5% fatty acid-free BSA (w/w; 4:1 molar ratio of fatty acid/BSA) and added to the cultures on day −6 to preconfluent, proliferating cultures and day 1 to postconfluent, differentiating cultures (Fig. 1) based on protocol used in Dr. Steven Clarke's lab (University of Texas, Austin, TX: personal communication). The mixture of crude isomers of CLA (major isomers includes 41% *cis*- or *trans*- 9, 11 isomers; 44% *trans*-10,*cis*-12 isomers; and 10% *cis*-10, *cis*-12 isomers according to the manufacturers), and the pure LA were obtained from Nu-Chek-Prep (Elysian, MN). The *trans*-10,*cis*-12 CLA isomer (98+% pure according to the manufacturers) was obtained from Matreya, Inc. (Pleasant Gap, PA). Since we did not analyze CLA and LA for their purity, we realize that other isomers could be present in each fatty acid. All treatments contain 0.2 mM α-tocopherol (Sigma Chemical

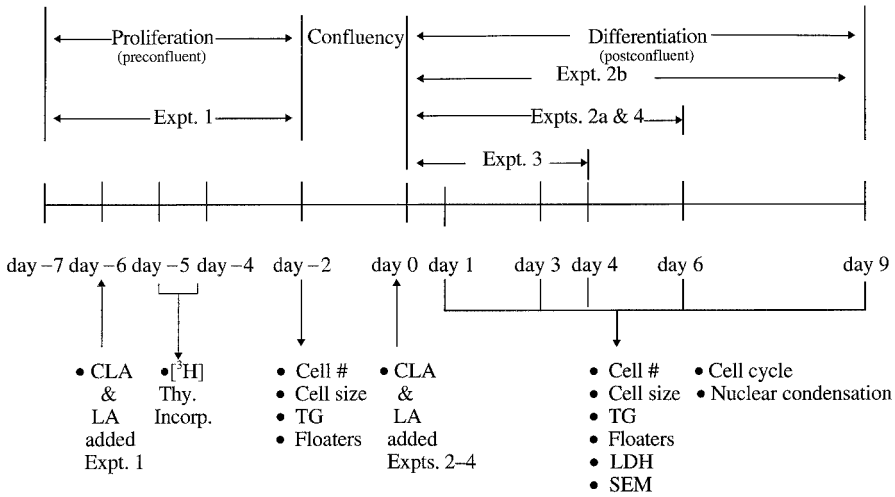

FIG. 1. Design of experiments. Abbreviations: CLA, conjugated linoleic acid; LA, linoleic acid; [^{3}H]-thy incorp, [^{3}H]-thymidine incorporation; TG, triglyceride; LDH, lactate dehydrogenase; floaters, nonadherent cells floating in media; SEM, scanning electron microscopy; Expt., experiment.

Co., St. Louis, MO) to prevent lipid peroxidation unless otherwise indicated (e.g., Expt. 3) based on protocol used in Dr. Steven Clarke's lab (personal communication). Media were changed at 2-d intervals and fresh fatty acids added to each medium change until the day of harvest. Each treatment combination per experiment was conducted in triplicate and repeated at least once (e.g., $n = 6$) unless otherwise indicated.

Cells were seeded at a density of $3.3 \times 10^3/cm^2$ in 12-well plates and cultured in Dulbecco's modified Eagle's medium (DMEM), 10% bovine calf serum (BCS), 0.2 mM α-tocopherol (only Expt. 1), and antibiotics until confluent. Two days postconfluence, the cells were stimulated to differentiate with DMEM containing 10% fetal bovine serum (FBS) (charcoal-stripped to remove endogenous fatty acids), 10 µg/mL insulin, 0.5 mM isobutylmethylxanthine, 0.1 µM dexamethasone, 0.2 mM α-tocopherol (except Expt. 3), and 1% antibiotics. On day 3 of differentiation, the above media were replaced with DMEM, 10% stripped FBS, 2.5 µg/mL insulin, 0.2 mM α-tocopherol, and 1% antibiotics. From day 5 onward, media containing DMEM, 10% stripped FBS, 0.2 mM α-tocopherol, and 1% antibiotics were used.

For DNA staining and cell cycle analysis, cells were seeded at 3.3×10^3 cells per cm^2 in six-well culture plates and grown to confluence. Forty-eight hours after reaching confluence, cultures were treated with differentiation media containing 100 µM of each fatty acid. Cells were harvested and/or stained at 24-, 48-, 72-, and 96-h intervals for DNA cell cycle analysis and Hoechst staining.

[^{3}H]-thymidine incorporation (Expt. 1). The 3T3-L1 preadipocytes were plated in 200 µL of proliferation media (DMEM, 10% BCS, 10 mM HEPES, and antibiotics) at a density of $3.3 \times 10^3/cm^2$ in 96-well plates (1.1×10^3 cells/well). Twenty-four hours later, the media were removed and proliferation media containing either 0, 10, 50, or 200 µM of a crude mixture of CLA isomers or pure LA were added to the cultures. When the control cultures had reached approximately 30% confluence (~56 h after seeding), 0.5 µCi of [^{3}H]-thymidine (methyl[^{3}H]-thymidine; specific activity 248 GBq/mmol; NEN, Boston, MA) was added to each well. After ~18 h of incubation, the cultures were frozen at −70°C for 1 h and then thawed at room temperature to promote cell lysis. The DNA from each well was then transferred to filters by a cell harvesting system (Flow Laboratories-Skatron A/S, Lier, Norway), placed in scintillation vials containing 3 mL scintillation fluid, and counted on a Beckman LS 6000 Coulter Counter (Beckman Instruments, Palo Alto, CA).

Cell number and size (Expts. 1–4). Adherent and floating cells were counted and sized using a Coulter Multisizer IIE (Coulter Corp., Miami, FL). Spent media containing floating cells were removed at each media change and on the day of harvest and centrifuged at 500 × *g*. The supernatant was removed and saved for lactate dehydrogenase (LDH) analysis in Experiment 2a. The remaining cell pellet was resuspended in phosphate-buffered saline (PBS) and the number of cells counted. Viability of floating cells was assessed by trypan blue exclusion using a hemacytometer. Adherent cells were harvested in a cell counting solution (25 mM glucose, 0.154 M NaCL, 0.01 M NaH_2PO_4 [monobasic], 5 mM EDTA, 2% albumin, pH 7.4) and counted and sized on the Coulter Multisizer.

TG content (Expts. 2 and 3). TG content was measured using a commercially available colorimetric kit (Sigma #339-10; Sigma Chemical Co.) and modified for cell culture as previously described (16). This procedure employs enzymatic hydrolysis of glycerol and fatty acids. The glycerol is then measured by enzyme coupled reduction of a dye that absorbs light at 500 nm and can be quantified spectrophotometrically.

Protein content (Expts. 1 and 2). Protein was measured using the bicinchoninic acid (BCA) assay (Pierce, Rockford, IL). This assay measures the reduction of Cu^{2+} to Cu^+ by protein in an alkaline medium, thereby forming a tetradentate-Cu^+ complex. The Cu^+ ions then chelate with two molecules of BCA which absorbs light at 562 nm and can be quantified spectrophotometrically.

LDH activity (Expt. 2). The presence of LDH in the spent media relative to its activity in adherent cells has been used as an index of cell necrosis and a late indicator of apoptotic cell death (17). However, it does not distinguish between the two processes involved in cell death. Spent media removed from cell monolayers at the time of each medium replenishment and the day of cell harvest were frozen at −20°C. Adherent cells were rinsed twice with Hank's balanced salt solution (HBSS), scraped into 0.5 mL ice-cold sucrose buffer (29 mM sucrose, 73 µM TRIS, 24 µM EDTA, 0.02% β-mercaptoethanol), and stored at −70°C. The resulting extract was sonicated with two 5-s bursts and centrifuged for 30 min at 1600 × *g* at 4°C and the supernatant assayed for LDH activity. LDH activity in cell extracts and spent media was determined spectrophotometrically at 25°C by measuring the oxidation of NADH at 340 nm in the presence of pyruvate (18). Data are presented as the cumulative LDH activity after 6 d of treatment with CLA, LA, or albumin (controls) per mg protein (1 mU/mg protein = nmol of NADH oxidized per min per mg protein).

Scanning electron microscopy (SEM) (Expt. 2). 3T3-L1 monolayers were grown and treated until day 6 of differentiation on inserts (Falcon) that fit into individual wells where the media and solutions for processing were applied. Cells on inserts were fixed with 2% glutaraldehyde in 0.1 M cacodylate in 0.1 M sucrose buffer for 1 h. Cells were rinsed with cacodylate-sucrose buffer prior to postfixation for 1 h in 1% osmium tetroxide. Cells were then rinsed with 0.1 M piperazine-*N*-*N*′-bis[2-ethane sulfonic acid] buffer and refrigerated until being processed for SEM. The inserts with attached cells were processed for SEM by chemically drying with hexamethyldisilazane (HMDS). They were dehydrated in a series of ethanol dilutions (70, 85, 95, and 100%) for 5 min each. Next, they were placed in HMDS and dried overnight under vacuum. After drying, the insert membranes with attached cells were placed on aluminum stubs and coated with gold in a SPI Module' Sputter coater. Samples were examined with a JSM-35CF scanning electron microscope. Images at 480× and 2000× magnification were recorded on Type 52 Polaroid film.

Propidium iodide (PI) staining (Expt. 4). Cultured cells were trypsinized at harvest and rinsed once in a washing solution containing Dulbecco's Ca^{2+}, Mg^{2+} free PBS (Sigma) and 1% FCS. The cell pellet was then fixed with 70% ice-cold absolute ethanol. Samples were stored at −20°C until all harvests were collected, then removed from storage, pelleted, and washed once with washing solution. Pellets were resuspended and stained for 30 min at room temperature with PI (Sigma) (50 µg/mL), RNase (Sigma; 0.2 µg/mL), and immediately analyzed by flow cytometry on a FACSCalibur flow cytometer (Becton Dickinson Immunocytometry Systems, San Jose, CA).

DNA cell cycle analysis (Expt. 4). Samples from adherent cultures were analyzed on a FACSCalibur flow cytometer equipped with a 15 mW air-cooled 488 nm argon-ion laser. PI fluorescence was collected using linear amplification, FL2 area (A) and width (W) to permit doublet discrimination. A minimum of 10,000 events was collected for each DNA histogram with a low flow rate (112 µL/min) for optimal peak resolution. Doublet contamination was minimal; therefore analysis was done on all histogram events without gating. A noise threshold of about 20% of the G_1 peak fluorescence intensity was established to reduce nonspecific signal. Measurements were made with CellQuest (BDIS) and ModFit LT Software (Verify Software House, Topsham, ME).

Hoechst staining (Expt. 4). All staining was performed in the cell culture dish and all fluid changes were performed gently in order to prevent loss of loosely attached cells. Media were removed, and the monolayer was fixed with Baker's formalin (37% formaldehyde, 10% $CaCl_2$) at 4°C for 5 min. Cells were rinsed with HBSS, stained with Hoechst 33258 (Sigma; 8 µg/mL in HBSS) for 10 min, and rinsed again with buffer. Cells were then treated with one drop of 50% glycerol and coverslipped.

Fluorescence microscopy and photography of nuclear condensation (Expt. 4). A preliminary study was conducted using the 24-h serum starvation technique described by Magun *et al.* (19) to induce nuclear condensation in cultures of differentiating 3T3-L1 preadipocytes. Three different researchers that were blinded to the treatments examined the cultures. In our preliminary study, cultures supplemented with either 0, 1, 5, or 10% FBS for the first 24 h of the differentiation program had 52.0, 36.1, 7.2, and 1.2% of their cells demonstrating chromatin condensation, respectively. An Olympus IX70 microscope (Olympus, Melville, NY) equipped with an inverted reflected light fluorescence observation attachment was used to view and photodocument nuclear condensation. Cell monolayers were subjected to ultraviolet excitation and observed with a 20× objective. A cooled CCD camera (Spot; Diagnostic Instruments Inc., Sterling Heights, MI) integrated with the microscope was used to capture digitized cell images. All image acquisitions were controlled by Adobe Photoshop 5.0 software (Adobe Systems, Inc., San Jose, CA) and printed on color paper for subsequent quantification of cell number and nuclear condensation.

Statistical analyses. Data were analyzed by the Least Squares ANOVA General Linear Models Procedures (PROC GLM) of SAS (SAS Institute, Cary, NC). For Experiments 1–3, a two-way analysis of variance (ANOVA) was conducted and their interactions (fatty acid × dose in Expts. 1 and 2; fatty acid × vehicle in Expt. 3a; fatty acid × vitamin E status in Expt. 3b) were compared for significance at the $P < 0.05$ level. For Experiment 4, a three-way ANOVA was conducted, and the fatty acid by dose interactions within each treatment period (e.g., 24, 48, 72, and 96 h) were compared for significance at the $P < 0.05$ level. The means ± SE of the treatment interactions and their statistical differences are presented in the figures and Table 1. (Means not sharing common letters are significantly different.)

TABLE 1
Effect of Treating Cultures of Differentiating 3T3-L1 Preadipocytes for 24, 48, 72, or 96 h with 100 µM LA, a Crude Mixture of Mixed CLA, or the 10,12 Isomer of CLA (10,12-CLA) on the Percentage of Cells in the G_1, S, and G_2M Phases of the Cell Cycle[a]

		Length of treatment (h)			
Phase	Treatment	24	48	72	96
G_1	BSA	56.2 ± 2.3 b	70.5 ± 0.7 a	81.9 ± 0.9 b	83.5 ± 0.4 c
	LA	54.6 ± 2.0 a,b	71.0 ± 0.6 a	81.4 ± 1.1 b	84.6 ± 0.6 c
	Mixed CLA	54.0 ± 2.2 a,b	71.9 ± 0.5 a,b	80.6 ± 0.4 b	80.1 ± 0.7 b
	10,12-CLA	52.8 ± 1.6 a	73.0 ± 0.4 b	78.6 ± 0.5 a	77.2 ± 1.8 a
S	BSA	18.5 ± 0.7 a	13.9 ± 1.0 b	5.6 ± 1.6 a	3.3 ± 0.2 a
	LA	18.8 ± 1.2 a	13.3 ± 1.0 b	5.8 ± 1.2 a	2.7 ± 0.4 a
	Mixed CLA	18.6 ± 0.3 a	11.4 ± 1.0 a	6.5 ± 0.8 a	6.8 ± 0.4 b
	10,12-CLA	20.1 ± 1.0 a	10.5 ± 0.8 a	6.1 ± 0.9 a	9.2 ± 1.1 c
G_2M	BSA	25.3 ± 2.9 a	15.6 ± 0.4 a	12.5 ± 0.7 a	13.2 ± 0.2 a
	LA	26.5 ± 2.0 a	15.7 ± 0.4 a	12.7 ± 0.5 a	12.7 ± 0.2 a
	Mixed CLA	27.3 ± 2.4 a	16.7 ± 0.8 a	13.0 ± 0.8 a	13.0 ± 0.3 a
	10,12-CLA	27.1 ± 2.2 a	16.4 ± 0.9 a	15.3 ± 0.4 b	13.6 ± 0.7 a

[a]Cultures were treated continuously and harvested after 24, 48, 72, or 96 h of treatment. Means (±SEM; $n = 6$) not sharing a common letter are significantly different ($P < 0.05$). BSA, bovine serum albumin; LA, linoleic acid; CLA, conjugated linoleic acid.

RESULTS

Experiment 1: Proliferation (days –6 to –2); dose response (Figs. 2 and 3). (i) Cell number and size. Proliferating cultures supplemented with 10 and 50 μM of a crude mixture of CLA isomers and pure LA had fewer cells than control cultures (Fig. 2). At the 200 μM level, cultures supplemented with CLA had fewer cells than those supplemented with LA. Neither cell size nor the number of floating cells in spent media (viable and dead cells) was influenced by either fatty acid (data not shown).

(ii) *DNA synthesis.* [^{3}H]thymidine incorporation into DNA decreased as the level of a crude mixture of CLA isomers in proliferating cultures increased (Fig. 3). In contrast, cultures treated with LA had similar amounts of [^{3}H]thymidine incorporation.

Experiment 2a: Differentiation (days 1–6); dose response (Figs. 4–8). (i) TG content. The TG content/10^6 cells of differentiating cultures of 3T3-L1 preadipocytes increased as the level of LA increased in the cultures (Fig. 4). In contrast, the TG content of CLA-treated cultures was similar to the BSA controls. Cultures treated with 50 and 200 μM of a crude mixture of CLA isomers had less TG than 50 and 200 μM LA-treated cultures.

(ii) *Cell size.* Adipocyte size decreased as the level of a crude mixture of CLA isomers in differentiating cultures increased (Fig. 5). In contrast, adipocyte size was not affected by LA treatment.

(iii) *Cell viability.* Cultures supplemented with 50–200 μM of a crude mixture of CLA isomers had slightly more floating cells than control and LA-supplemented cultures (Fig. 6). Furthermore, LDH activity in the spent media of CLA-treated cultures was greater than control and LA-treated cultures. This effect of CLA was most pronounced at the 200 μM level (Fig. 7).

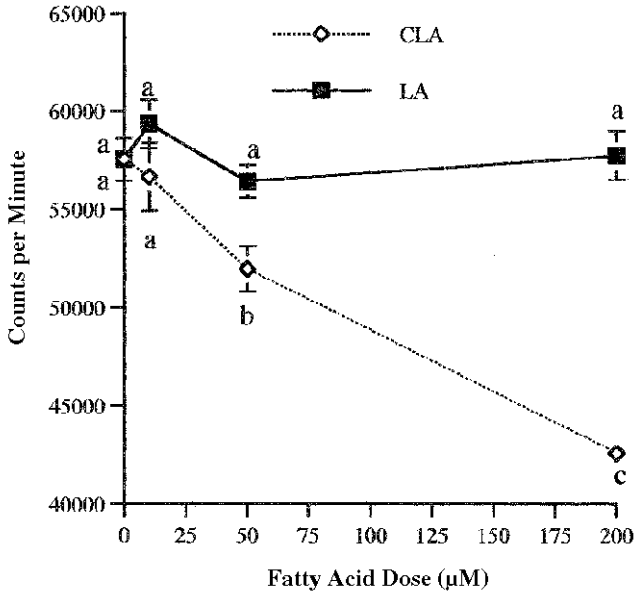

FIG. 3. The influence of a crude mixture of CLA isomers and LA on [^{3}H]-thymidine incorporation into DNA in cultures of proliferating 3T3-L1 preadipocytes. Cultures were treated with 0–200 μM CLA or LA continuously and harvested after 4 d of treatment. Means (±SEM; n = 6) not sharing a common letter are significantly different ($P < 0.05$). See Figure 1 for abbreviations.

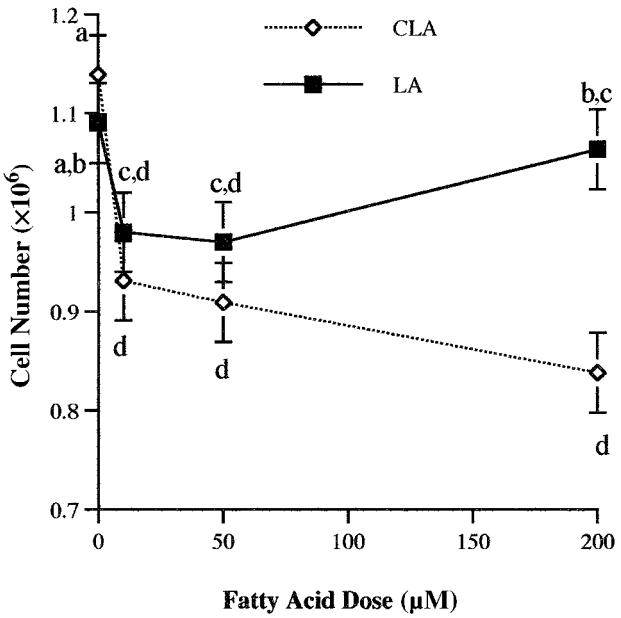

FIG. 2. The influence of a crude mixture of CLA isomers and LA on the number of cells in cultures of proliferating 3T3-L1 preadipocytes. Cultures were treated with 0–200 μM CLA or LA continuously and harvested after 4 d of treatment. Means (±SEM; n = 10–12/treatment) not sharing a common letter are significantly different ($P < 0.05$). See Figure 1 for abbreviations.

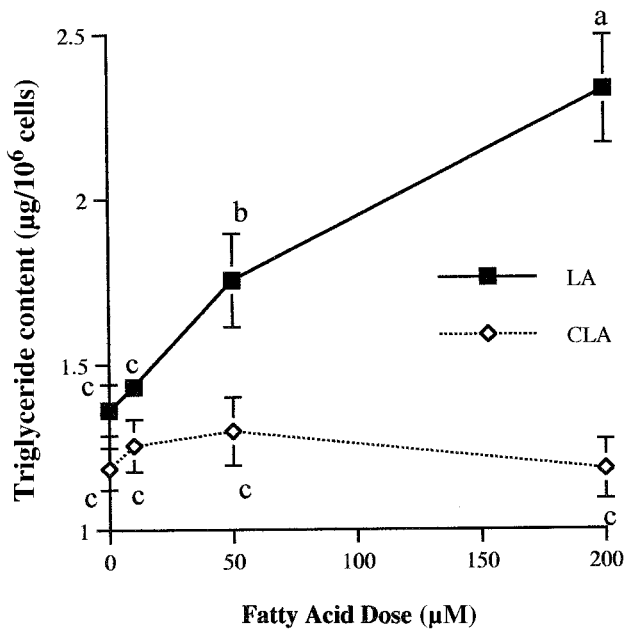

FIG. 4. The effect of increasing doses of a crude mixture of CLA isomers or LA on TG content on day 6 of postconfluent cultures of differentiating 3T3-L1 preadipocytes. Cultures were treated with 0–200 μM CLA or LA continuously and harvested after 6 d of treatment. Means (±SEM; n = 6) not sharing a common letter are significantly different ($P < 0.05$). See Figure 1 for abbreviations.

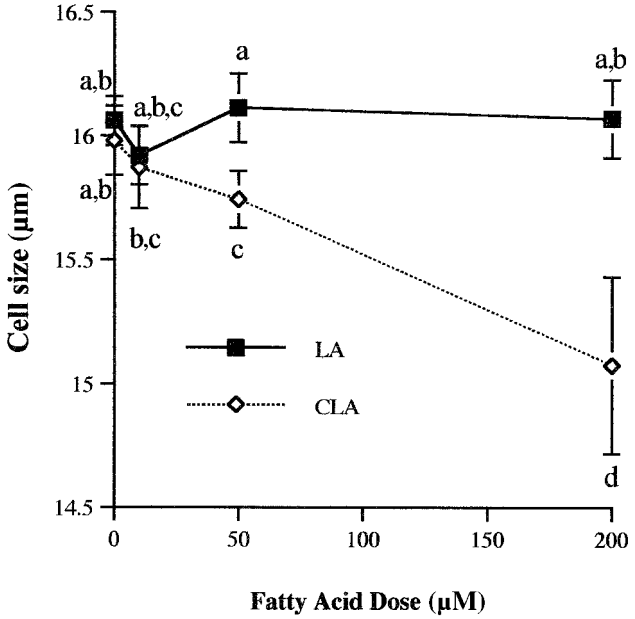

FIG. 5. The effect of increasing doses of a crude mixture of CLA isomers or LA on mean cell size on day 6 of postconfluent cultures of differentiating 3T3-L1 preadipocytes. Cultures were treated with 0–200 μM CLA or LA continuously and harvested after 6 d of treatment. Means (±SEM; $n = 6$) not sharing a common letter are significantly different ($P < 0.05$). See Figure 1 for abbreviations.

(iv) SEM micrographs (480×). SEM of the cultures revealed normal cell morphology for the control cultures (Fig. 8; 0 μM LA and CLA). Cells were fibroblastic in shape with numerous microvilli and sharp-pointed lamellipodia. At 50 μM LA, some cells still retained a flattened fibroblastic appearance. However, number and length of microvilli per cell appeared decreased. Also, the number of rounded-up cells had increased remarkably, indicative of mitosis or lipid accumulation. At 50 μM of a crude mixture of CLA isomers, there were still some flattened cells, but there were large numbers of small, rounded cells that appeared lumpy in appearance. Microvilli were also decreased. At 200 μM LA, cells retained some of the fibroblastic characteristics and some cells still had microvilli. The number of rounded-up cells increased in cultures supplemented with 200 μM LA. Several large, round, and smooth vesicles can be seen. We speculate that these are lysed lipid droplets that remained after washing and prior to cell fixation. At 200 μM CLA, no cells with typical characteristics were seen. Large numbers of cells were found that appeared to be blebbing, a characteristic of apoptotic cells. Images photographed at 2000× (data not shown) confirmed this membrane blebbing that appeared in cultures treated with both 50 and 200 μM CLA. As was observed in the 200 μM LA cultures, a number of small, round, and smooth vesicles presumed to be lysed lipid droplets can be seen in the 200 μM CLA cultures.

Experiment 2b: Differentiation (days 1–9); time course. Differences in TG and protein contents of cultures supplemented with 200 μM of a crude mixture of CLA isomers compared to control and LA-supplemented cultures became appar-

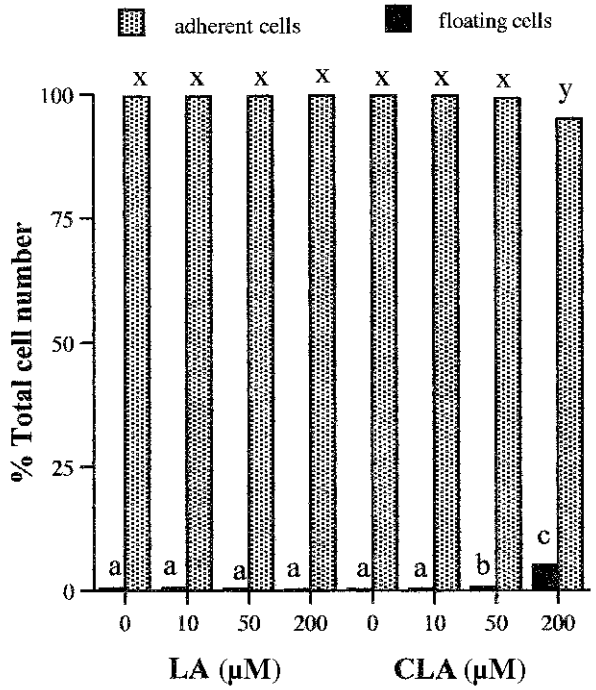

FIG. 6. The effect of increasing doses of a crude mixture of CLA isomers or LA on the number of floaters vs. adherent cells on day 6 of postconfluent cultures of differentiating 3T3-L1 preadipocytes. Cultures were treated with 0–200 μM CLA or LA continuously and harvested after 6 d of treatment. Means (±SEM; $n = 6$) not sharing a common letter are significantly different ($P < 0.05$). See Figure 1 for abbreviations.

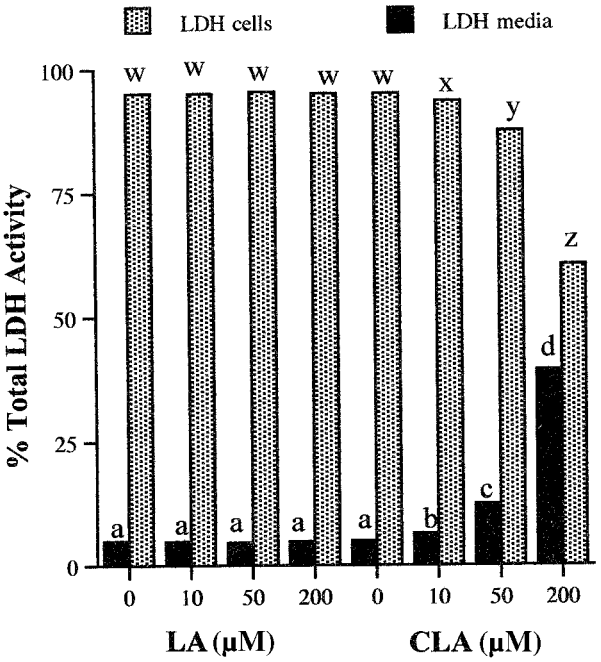

FIG. 7. The effect of increasing doses of a crude mixture of CLA isomers or LA on lactate dehydrogenase (LDH) activity in the media and in the adherent cells on day 6 of postconfluent cultures of differentiating 3T3-L1 preadipocytes. Cultures were treated with 0–200 μM CLA or LA continuously and harvested after 6 d of treatment. Media were collected at each medium change and LDH activity determined so that the cumulative LDH activity during the entire 6 d could be determined. Means (±SEM; $n = 6$) not sharing a common letter are significantly different ($P < 0.05$). See Figure 1 for other abbreviations.

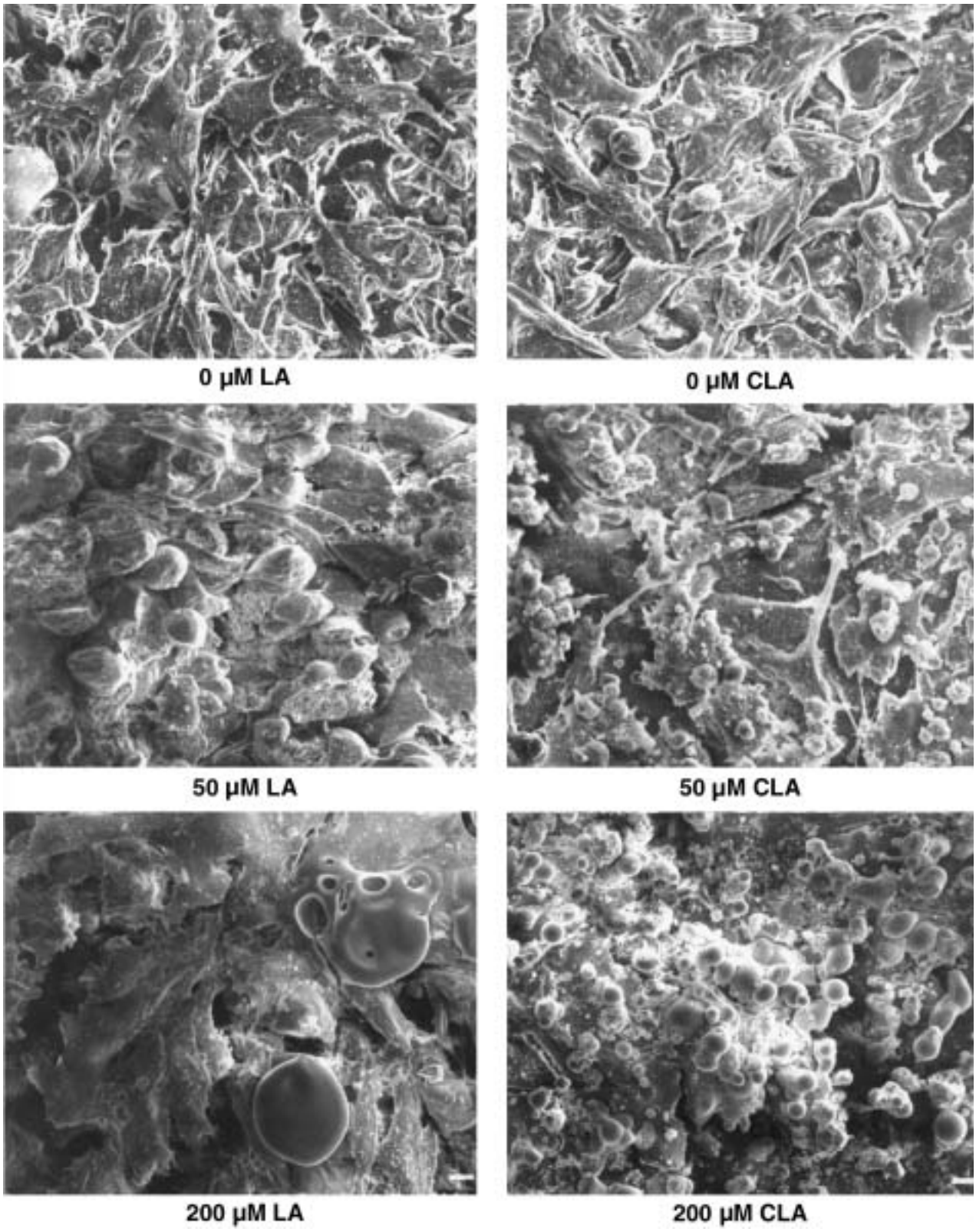

FIG. 8. Scanning electron micrographs of postconfluent cultures of differentiating 3T3-L1 preadipocytes treated with either a crude mixture of CLA isomers or LA for 6 d. Cultures were treated with 0–200 μM CLA or LA continuously and harvested on day 6. Magnification (480×) is the same in all photographs. Representative samples that were taken from at least two different cultures in each treatment group were similar in appearance. See Figure 1 for abbreviations.

ent after 3 d of culture (data not shown). For example, cultures supplemented with either 200 μM of a crude mixture of CLA isomers or pure LA had 0.6 ± 0.03 and 1.0 ± 0.05 μg TG/10^6 cells, respectively, after 3 d of treatment. By day 9, CLA-supplemented cultures had 36 and 32% less TG and protein content, respectively, than the LA-supplemented cultures.

Experiment 3a: Differentiation (days 1–6); ethanol vs. BSA as vehicle (Fig. 9). Cultures in which ethanol was used as the vehicle to deliver the fatty acids had more TG than treatment-matched cultures in which BSA was used as the vehicle (Fig. 9). No treatment by vehicle interactions was observed.

Experiment 3b: Differentiation (days 1–6); ± vitamin E supplementation (Fig. 10). Fatty acid-treated cultures supplemented with 0.2 mM α-tocopherol had more TG than non-supplemented cultures (Fig. 10). This was particularly evident for cultures treated with the crude mixture of CLA isomers. Within vitamin E treatments, cultures treated with the *trans*-10,*cis*-12 isomer of CLA had the lowest amount of TG/10^6 cells compared to the other cultures.

Experiment 4: Differentiation (days 1–4); nuclear condensation (Fig. 11) and cell cycle analyses (Fig. 12, Table 1). (i) Indices of apoptosis. The percentage of adherent cells exhibiting nuclear condensation was higher in the CLA-treated cultures for all treatment periods compared to the control and LA-treated cultures. This apoptotic effect of CLA was clearly evident after only 24 h of treatment (Fig. 11). The *trans*-10, *cis*-12 isomer of CLA was more effective than a crude mixture of CLA isomers in inducing nuclear condensation after 72 and 96 h of treatment. The percentage of adherent cells in

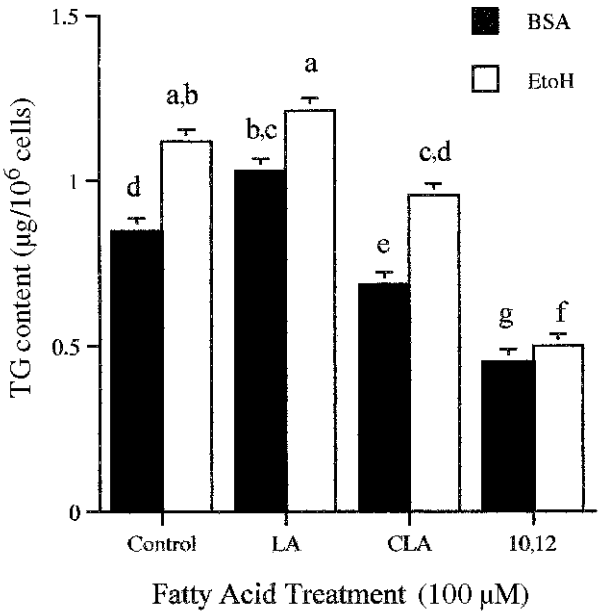

FIG. 9. The effect of using either bovine serum albumin (BSA) or ethanol (EtoH) to deliver either 100 μM of LA, a crude mixture of CLA isomers, or the *trans*-10, *cis*-12 isomer of CLA (10,12-CLA) on TG content on day 6 of postconfluent cultures of differentiating 3T3-L1 preadipocytes. Cultures were treated continuously and harvested after 6 d of treatment. Means (±SEM; $n = 6$) not sharing a common letter are significantly different ($P < 0.05$). See Figure 1 for other abbreviations.

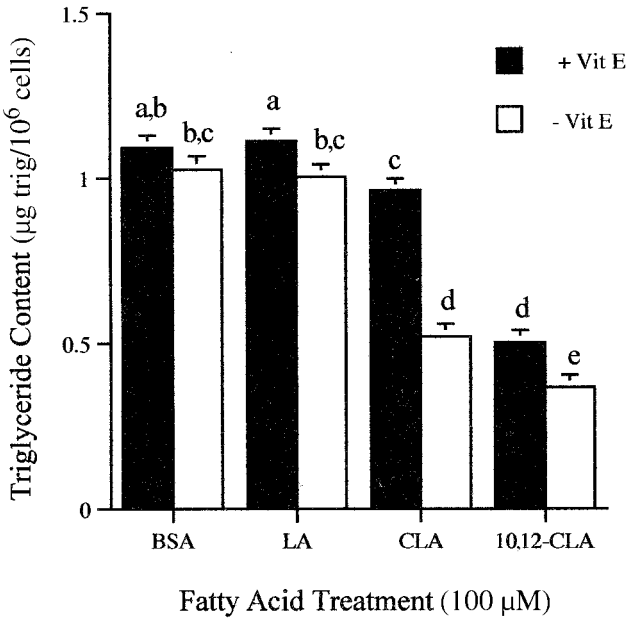

FIG. 10. The effect of 0.2 mM vitamin E (vit E) supplementation on cultures treated with either 100 μM of LA, a crude mixture of CLA isomers, or the *trans*-10, *cis*-12 isomer of CLA (10,12-CLA) on TG content on day 6 of postconfluent cultures of differentiating 3T3-L1 preadipocytes. Cultures were treated continuously and harvested after 6 d of treatment. Means (±SEM; $n = 6$) not sharing a common letter are significantly different ($P < 0.05$). See Figure 1 for abbreviations.

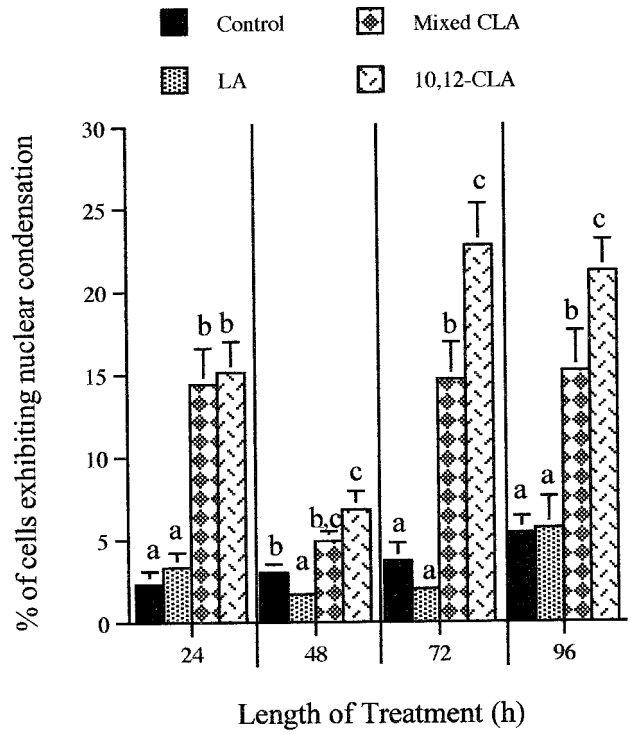

FIG. 11. The effect of treating cultures for either 24, 48, 72, or 96 h with either 100 μM of LA, a crude mixture of mixed-CLA isomers, or the *trans*-10,*cis*-12 isomer of CLA (10,12-CLA) on the percentage of cells exhibiting nuclear condensation (i.e., apoptotic) in postconfluent cultures of differentiating 3T3-L1 preadipocytes. Cultures were treated continuously and harvested after 24, 48, 72, or 96 h of treatment. Means (±SEM; $n = 6$) not sharing a common letter are significantly different ($P < 0.05$). See Figure 1 for abbreviations.

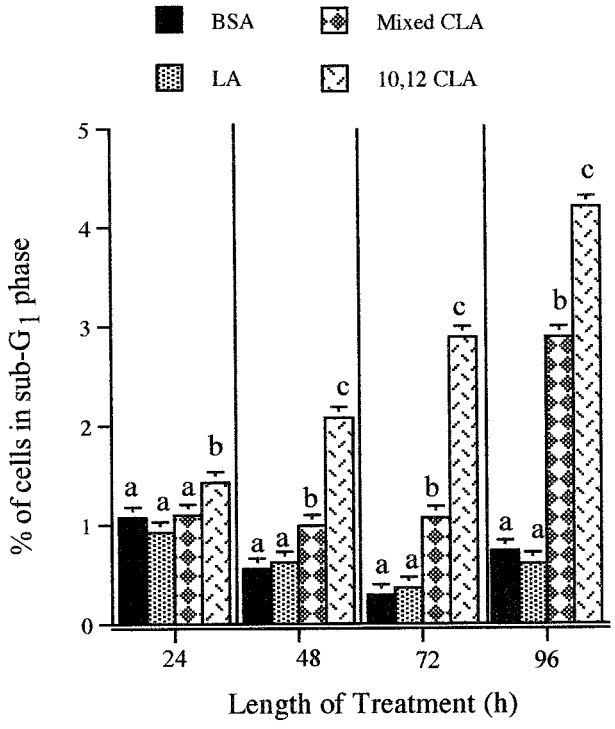

FIG. 12. The effect of treating cultures for either 24, 48, 72, or 96 h with either 100 μM of LA, a crude mixture of mixed-CLA isomers, or the *trans*-10,*cis*-12 isomer of CLA (10,12-CLA) on the percentage of cells in the sub-G1 phase of the cell cycle (i.e., apoptotic) in postconfluent cultures of differentiating 3T3-L1 preadipocytes. Cultures were treated continuously and harvested after 24, 48, 72, or 96 h of treatment. Means (±SEM; $n = 6$) not sharing a common letter are significantly different ($P < 0.05$). See Figure 1 and 9 for abbreviations.

the sub-G_1 phase of the cell cycle, another measurement of apoptosis, was higher in the CLA-treated cultures for all treatment periods compared to the control and LA-treated cultures (Fig. 12). As with the nuclear condensation data, the *trans*-10,*cis*-12 isomer of CLA was more effective than the crude mixture of CLA isomers in increasing the percentage of cells in the sub-G_1 phase.

(ii) Cell cycle analyses. Data on the influence of BSA, LA, a crude mixture of CLA isomers, and the *trans*-10,*cis*-12 isomer of CLA on the G_1, S, and G_2M phase of the cell cycle are presented in Table 1. With the exception of the 48-h treatment period, cultures treated with the *trans*-10,*cis*-12 isomer of CLA had fewer cells in the G_1 phase of the cell cycle than the BSA or control cultures. Cultures treated with CLA for 48 h had fewer cells in the S phase than BSA or control cultures. In contrast, cultures treated with CLA for 96 h had more cells in the S phase than BSA or control cultures. Cultures treated for 72 h with *trans*-10,*cis*-12 CLA had more cells in the G_2M phase of the cell cycle than the other treatments.

DISCUSSION

The present study provides direct evidence that CLA attenuates preadipocyte proliferation and TG content in monolayer cultures of 3T3-L1 (pre)adipocytes. Moreover, these data demonstrate that the *trans*-10,*cis*-12 isomer is a major antiadipogenic isomer of CLA. To our knowledge, this is also the first time that the *trans*-10,*cis*-12 isomer of CLA has been shown to cause apoptosis, assessed by nuclear condensation and cells in the sub-G_1 peak of the cell cycle, in postconfluent cultures of 3T3-L1 preadipocytes. These data provide further support for the concept that the antiobesity effects of a crude mixture of CLA isomers observed in mice (5–8,10) and pigs (11,12) may indeed be due to the direct actions of the *trans*-10,*cis*-12 isomer of CLA on adipose tissue mass and cellularity. The crude mixture of CLA isomers used in this study contained 41% 9–11 (an unknown mixture of *cis-trans* and *trans-cis*) isomers, 44% *trans*-10,*cis*-12 isomers, and 10% *cis*-10,*cis*-12 isomers according to the analyses by the supplier, Nu-Chek-Prep. Therefore, in Experiments 1 and 2, it was not clear which of the isomers reduced preadipocyte growth and TG content compared to LA. Furthermore, other isomers of CLA may have also been present in these CLA preparations, since we did not confirm the fatty acid isomer profiles ourselves. However, when comparing the effects of the crude mixture of CLA isomers to that of the *trans*-10,*cis*-12 CLA isomer on TG content in Experiment 3 (Figs. 9 and 10), the *trans*-10,*cis*-12 CLA isomer was 36–50% more potent than the crude mixture of CLA isomers within respective treatments. This reduced potency of the crude mixture of CLA isomers corresponds to its lower content of the *trans*-10,*cis*-12 isomer (e.g., 44%). Furthermore, the *trans*-10,*cis*-12 isomer of CLA was generally more potent than the crude mixture of CLA isomers in inducing nuclear condensation (e.g., ~7 vs. 35% in Fig. 11) and the percentage of cells in the sub-G1 phase of the cell cycle (e.g., ~27 vs. 64% in Fig. 12). In support of our findings, a recent study by Park *et al.* (7) demonstrated that the *trans*-10,*cis*-12 isomer of CLA is the antiadipogenic isomer in mature 3T3-L1 adipocytes. They found that the *trans*-10,*cis*-12 isomer decreased LPL activity and increased lipolysis to a greater extent than the crude mixture of CLA isomers from Nu-Chek-Prep. In contrast, the *cis*-9,*trans*-11 isomer of CLA, which has anticarcinogenic actions (20), had no influence on mature adipocytes. In further support of these data, we have preliminary data demonstrating that the *cis*-9,*trans*-11 isomer of CLA actually increases TG content of differentiating cultures of 3T3-L1 (pre)adipocytes. When taken together, these data suggest that the *trans*-10,*cis*-12, not the *cis*-9,*trans*-11, isomer of CLA may attenuate adipocyte cellularity and mass by reducing preadipocyte differentiation, inducing apoptosis, and promoting adipocyte delipidiation.

These data also demonstrated that CLA supplementation attenuates the growth (e.g., decreased cell number and ^3H-thymidine incorporation into DNA) of preconfluent cultures of 3T3-L1 preadipocytes using a physiological method to deliver fatty acids (i.e., complexed to albumin) to monolayer cultures of preadipocytes. The inhibitory effect of a crude mixture of CLA isomers on preadipocyte growth during the proliferation program is in agreement with Brodie *et al.* (14)

and Satory and Smith (13), who used either DMSO or ethanol to deliver CLA to the cultures. However, they reported that LA also reduced preadipocyte proliferation, whereas we found no effect of LA on thymidine incorporation and only a small effect of LA on cell number. These differences in the effects of CLA on proliferation may be due to the organic solvent used to deliver fatty acids to cell cultures vs. using a more physiological carrier such as albumin. This difference in vehicles employed to deliver fatty acids may also explain why these researchers found that CLA and LA suppressed proliferation at much lower concentrations (i.e., 1.7 μM) than we did (i.e., 10–50 μM). Alternatively, the inclusion of vitamin E in our study may have reduced the peroxidation of LA and CLA in the cultures. Peroxidized lipids can undoubtedly influence cell growth. For this reason, many researchers using unsaturated fatty acids in cell culture supplement the media with an antioxidant such as α-tocopherol. In support of this concept, data in Figure 10 demonstrated that LA- and CLA-treated cultures without additional vitamin E during differentiation have significantly less TG/10^6 cells compared to vitamin E-supplemented cultures.

These CLA-mediated changes in preadipocyte TG content were accompanied by a dose-dependent increase in indices of growth arrest (e.g., decreased protein content and cell numbers) and cell death (e.g., floating cells and LDH activity in the media, morphological changes indicative of membrane blebbing, nuclear condensation, cells in the sub-G_1 peak of the cell cycle). It is unclear whether these effects of CLA are due to a direct influence on regulators of growth and/or differentiation or perhaps more general cytotoxic or apoptotic effects. Unfortunately, the LDH assay does not discriminate between apoptosis and cytotoxicity (17). However, it is possible that CLA treatment increases apoptosis or cell detachment, thereby increasing the number of floating cells or cell bodies that release their LDH into the media before, during, or after cell harvest.

Several studies with normal mammary cells (21) and transformed cells, including MFC-7 human breast cancer cell lines (22), indicate that CLA may inhibit growth by inducing cell cycle arrest (1). These data suggest that CLA may inhibit preadipocyte proliferation and/or differentiation by a similar mechanism. In agreement with this concept, we found cell number and DNA synthesis were lower in cultures treated with a crude mixture of CLA isomers compared to cultures treated with LA. Furthermore, differentiating cultures treated for 48 h with CLA had fewer cells in the S-phase of the cell cycle. However, cultures treated for 96 h actually had a greater percentage of cells in the S-phase than control cultures. Therefore, CLA appears to have its greatest impact on cell growth during the proliferative program and the clonal expansion phase of 3T3-L1 adipogenesis.

Alternatively, CLA could be influencing cell growth by inducing programmed cell death or apoptosis. Since post-confluent 3T3-L1 preadipocytes undergo several rounds of replication during the first 48 h of the differentiation program, induction of apoptosis may be a potential mechanism by which CLA attenuates adipogenesis. This hypothesized antiadipogenic mechanism of CLA could result in smaller and/or fewer adipocytes containing less lipid. The three indicators of apoptosis used in this study that suggest CLA induces apoptosis were: (i) nuclear condensation; (ii) cells in the sub-G_1 peak of the cell cycle; and (iii) floating cells and LDH activity in the media. Morphological changes observed using SEM were characteristic of membrane blebbing in cultures treated with CLA, also supporting an apoptotic mechanism of action of CLA. In support of this concept, Ip *et al*. (21) found that CLA, not LA, inhibited the growth of normal mammary epithelial cells by inducing apoptosis. Surprisingly, we found that a crude mixture of CLA isomers has no influence on the cell cycle nor the number of floating cells in the media of cultures of preconfluent, proliferating 3T3-L1 preadipocytes (data not shown). Therefore, CLA's apoptotic effects seem to be most pronounced in postconfluent, differentiating cultures of preadipocytes. Interestingly, we have preliminary data demonstrating that the *cis*-9,*trans*-11 isomer of CLA does not influence these indices of cell growth. This observation provides further support for the concept that the antiadipogenic effects of CLA are mediated by the *trans*-10,*cis*-12 isomer of CLA.

CLA also could be impacting cell growth and/or differentiation by altering cellular membrane phospholipid composition and phospholipid metabolism to intracellular signals. Indeed, feeding diets rich in CLA to cattle (23) or humans (9) alters the lipid content and the fatty acid composition of their milk. CLA is incorporated into mouse forestomach (24) and rat mammary (25) tumor phospholipids and neutral lipids. Furthermore, supplementing preadipocyte cultures with CLA influences the types and amounts of cellular fatty acids (13). For example, the percentage of arachidonic acid (AA), a precursor to prostaglandins that stimulate lipogenesis [e.g., prostaglandin I_2 is a ligand for peroxisome proliferating activated receptor-γ2 (PPAR-γ2)], was reduced by >50% in CLA-treated cultures of 3T3-L1 preadipocytes (13). Moreover, incorporation of fatty acids into phospholipid membranes is known to alter the activities of enzymes involved in signal transduction processes (26). Therefore, CLA could be displacing certain fatty acids associated with membrane phospholipids such as AA, thereby decreasing intracellular signals such as diacylglycerol (DAG), inositol triphosphate, and AA. These phospholipid-derived signals are know to influence numerous signaling cascades that alter cellular metabolism including intracellular calcium, protein kinase activity, and PPAR-γ2. Interestingly, Brodie *et al*. (14) found that CLA-treated cultures had lower levels of mRNA expression of PPAR-γ2 and fatty acid binding protein. Alternatively, CLA-derived phospholipids may generate CLA-specific eicosanoids that suppress adipogenesis and/or induce apoptosis.

Finally, CLA could be attenuating TG content by causing lipid peroxidation. This theory is based on our finding that supplementation of CLA-containing cultures with 0.2 mM α-tocopherol significantly reduced CLA's attenuation of TG content in postconfluent cultures. In support of this theory,

O'Shea *et al*. (27) demonstrated that treatment of cultures of human MCF-7 and SW480 cancer cells with a crude mixture of CLA isomers increases lipid peroxidation (thiobarbitiuric acid-reactive substance) and induced the activities of several antioxidant enzymes. Schonberg and Krokan (28) also found that treatment of cultures of lung adenocarcinoma and gliablastoma cells with up to 40 μM of mixed CLA isomers significantly increased lipid peroxidation. The formation of peroxides was abolished by the addition of 30 μM α-tocopherol to the media. However, cell growth was not completely restored by α-tocopherol, suggesting that lipid peroxidation was only partially responsible for CLA's suppression of cell growth. In contrast, several studies have found no effect of CLA on lipid peroxidation *in vivo* (25) or *in vitro* (29). Furthermore, both the *cis*-9,*trans*-11 and the *trans*-10,*cis*-12 isomers were found to be resistant to peroxidation catalyzed by hydoperoxide (30). Alternatively, it is conceivable that the *trans*-10,*cis*-12 isomer of CLA simply has a decreased capacity for esterification into TG.

In conclusion, these data demonstrate that CLA attenuates 3T3-L1 preadipocyte proliferation and TG content compared to LA-treated cultures. Potential mechanisms responsible for CLA's antiadipogenic actions to be examined in future studies include: (i) induction of apoptosis; (ii) alterations in phospholipid signals that impact cell growth and differentiation; (iii) influence on lipid peroxidation; and (iv) impaired esterification of the *trans*-10,*cis*-12 isomer of CLA.

REFERENCES

1. Belury, M. (1995) Conjugated Dienoic Linoleate: A Polyunsaturated Fatty Acid with Unique Chemoprotective Properties, *Nutr. Rev. 53,* 83–89.
2. Lee, K., Kritchevsky, D., and Pariza, M. (1994) Conjugated Linoleic Acid and Atherosclerosis in Rabbits, *Atherosclerosis 108,* 19–25.
3. Nicolosi, R., Rogers, E., Kritchevsky, D., Scimeca, J., and Huth, P. (1997) Dietary Conjugated Linoleic Acid Reduces Plasma Lipoproteins and Early Aortic Atherosclerosis in Hypercholesterolemic Hamsters, *Artery 22,* 266–277.
4. Houseknecht, K., Heuvel, J., Moya-Camarena, S., Portocarrero, C., Peck, L., Nickel, K., and Belury, M. (1998) Dietary Conjugated Linoleic Acid Normalizes Impaired Glucose Tolerance in Zucker Diabetic Fatty fa/fa Rat, *Biochem. Biophys. Res. Commun. 244,* 678–682.
5. West, D., Delany, J., Camet, P., Blohm, F., Truett, A., and Scimeca, J. (1998) Effects of Conjugated Linoleic Acid on Body Fat and Energy Metabolism in the Mouse, *Am. J. Physiol. 275,* R667–R672.
6. Park, Y., Albright, K., Liu, W., Storkson, J., Cook, M., and Pariza, M. (1997) Effect of Conjugated Linoleic Acid on Body Composition in Mice, *Lipids 32,* 853–858.
7. Park, Y., Storkson, J., Albright, K., Liu, W., and Pariza, M. (1999) Evidence that *trans*-10, *cis*-12 Isomer of Conjugated Linoleic Acid Induces Body Composition Changes in Mice, *Lipids 34,* 235–241.
8. Park, Y., Albright, K., Storkson, J., Liu, W., Cook, M., and Pariza, M. (1999) Changes in Body Composition in Mice During Feeding and Withdrawal of Conjugated Linoleic Acid, *Lipids 33,* 243–248.
9. Park, Y., McGuire, M., Behr, R., McGuire, M., Evans, M., and Schultz, T. (1999) High-Fat Dairy Product Consumption Increases Δ-9*c*,11*t*-18:2 (rumenic acid) and Total Lipid Concentration of Human Milk, *Lipids 34,* 543–549.
10. DeLany, J., Blohm, F., Truett, A., Scimeca, J., and West, D. (1999) Conjugated Linoleic Acid Rapidly Reduces Body Fat Content in Mice Without Affecting Energy Intake, *Am. J. Physiol. 276,* R1172–R1179.
11. Cook, M., Jerome, D., Crenshaw, T., Buege, P., Pariza, M., Albright, K., Schmidt, S., Scimeca, J., Lotgren, P., and Hentges, E. (1999) Feeding Conjugated Linoleic Acid Improves Feed Efficiency and Reduces Carcass Fat in Pigs, 27th Steenbock Symposium, *Adipocyte Biology and Hormone Signaling Symposium,* June 7–9, p. 67.
12. Ostrowska, E., Muralitharan, M., Cross, R., Bauman, D., and Dunshea, F. (1999) Dietary Conjugated Linoleic Acids Increase Lean Tissue and Decrease Fat Deposition in Growing Pigs, *J. Nutr. 129,* 2037–2042.
13. Satory, D., and Smith, S. (1999) Conjugated Linoleic Acid Inhibits Proliferation but Stimulates Lipid Filling of Murine 3T3-L1 Preadipocytes, *J. Nutr. 129,* 92–97.
14. Brodie, A., Manning, V., Ferguson, K., Jewell, D., and Hu, C.Y. (1999) Conjugated Linoleic Acid Inhibits Differentiation of Pre- and Post-Confluent 3T3-L1 Preadipocytes but Inhibits Cell Proliferation Only in Pre-confluent Cells, *J. Nutr. 129,* 602–606.
15. MacDougald, O., and Lane, D. (1995) Transcriptional Regulation of Gene Expression During Adipocyte Differentiation, *Annu. Rev. Biochem. 64,* 345–373.
16. McIntosh, M., Lea-Currie, R., Geigerman, C., and Pasevouros, L. (1999) Dehydroepiandrosterone Alters the Growth of Stromal-Vascular Cells from Human Adipose Tissue, *Int. J. Obesity 23,* 595–602.
17. Loo, D., and Rillema, J. (1998) Measurement of Cell Death, in *Methods in Cell Biology.* Vol. 57, pp. 251–263, Academic Press, New York.
18. Glascott, P., Gilfor, E., and Farber, J. (1992) Effects of Vitamin E on the Killing of Cultured Hepatocyte by *tert*-Butyl Hydroperoxide, *Mol. Pharmacol. 41,* 1055–1102.
19. Magun, R., Boone, D., Tsang, B., and Sorisky, A. (1998) The Effect of Adipocyte Differentiation on the Capacity of 3T3-L1 Cells to Undergo Apoptosis in Response to Growth Factor Deprivation, *Int. J. Obes. 22,* 567–571.
20. Ip, C., Banni, S., Angioni, E., Carta, G., McGinley, J., Thompson, H., Barbano, D., and Bauman, D. (1999). Conjugated Linoleic Acid-Enriched Butter Fat Alters Mammary Gland Morphogenesis and Reduces Cancer Risk in Rats, *J. Nutr. 129,* 2135–2142.
21. Ip, M., Masso-Welch, P., Shoemaker, S., Shea-Eaton, W, and Ip, C. (1999). Conjugated Linoleic Acid Inhibits Proliferation and Induces Apoptosis of Normal Rat Mammary Epithelial Cells in Primary Culture, *Exp. Cell Res. 250,* 22–34.
22. Shultz, T., Chew, B., and Seaman, W. (1992) Differential Stimulatory and Inhibitory Responses of Human MCF-7 Breast Cancer Cells to Linoleic Acid and Conjugated Linoleic Acid in Culture, *Anticancer Res. 12,* 2143–2146.
23. Chouinard, P., Corneau, L., Bardano, D., Metzeger, L., and Bauman, D. (1999) Conjugated Linoleic Acids Alter Milk Fatty Acid Composition and Inhibit Milk Fat Secretion in Dairy Cows, J. *Nutr. 129,* 1579–1584.
24. Ha, Y., Storkson, J., and Pariza, M. (1990) Inhibition of Benzopyrene-Induced Mouse Forestomach Neoplasia by Conjugated Dienoic Derivative of Linoleic Acid, *Cancer Res. 50,* 1097–1101.
25. Ip, C., Chin, S., Scimeca, J. and Pariza, M. (1991) Mammary Cancer Prevention by Conjugated Dienoic Derivative of Linoleic Acid, *Cancer Res. 51,* 6118–6124.
26. Graber. R., Sumida, C., and Nunez, J. (1994) Fatty Acids and Cell Signal Transduction, *J. Lipid Mediators Cell Signalling 9,* 91–116.

27. O'Shea, M., Stanton, C., and Devery, R. (1999) Antioxidant Enzyme Defense Responses of Human MCF-7 and SW480 Cancer Cells to Conjugated Linoleic Acid, *Anticancer Res. 19,* 1953–1960.
28. Schonberg, S., and Krokan, H. (1995) The Inhibitory Effect of Conjugated Dienoic Derivatives (CLA) of Linoleic Acid on the Growth of Human Tumor Cell Lines Is in Part Due to Increased Lipid Peroxidation, *Anticancer Res. 15,* 1241–1246.
29. Cunningham, D., Harrison, L., and Schultz, T. (1997) Proliferative Responses of Normal Human Mammary and MCF-7 Breast Cancer Cells to Linoleic Acid, Conjugated Linoleic Acid and Eicosanoid Synthesis Inhibitors in Culture, *Anticancer Res. 17,* 197–204.
30. Bielski, B., Arudi, R., and Sutherland, M. (1983) A Study of the Reactivity of H_2O_2 with Unsaturated Fatty Acids, *J. Biol. Chem. 258,* 4759–4761.

[Received December 13, 1999, and in final revised form June 12, 2000; revision accepted June 20, 2000]

Incorporation and Metabolism of *Trans* 20:5 in Endothelial Cells. Effect on Prostacyclin Synthesis

C. Loï[a], J.M. Chardigny[a,*], C. Cordelet[a], L. Leclere[a], M. Genty[a], C. Ginies[b], J.P. Noël[c], and J.L. Sébédio[a]

INRA, [a]Unité de Nutrition Lipidique and [b]Laboratoire de Recherche sur les Arômes, 21034 Dijon, France, and [c]CEA-Saclay, Service des Molécules Marquées, 91191 Gifsur Yvette, France

ABSTRACT: To study the ability of long-chain *trans* fatty acids (FA) to be incorporated and metabolized into endothelial cells, bovine aortic endothelial cells were incubated with medium enriched eicosapentaenoic acid (EPA) bound to albumin (M2) or one of its geometrical isomers: 20:5 5*c*,8*c*,11*t*,14*c*,17*c* (M3), 20:5 5*c*,8*c*,11*c*,14*c*,17*t* (M4), or 20:5 5*c*,8*c*,11*t*,14*c*,17*t* (M5). After 48 h of incubation, supernatant and cells were harvested and their lipids were analyzed, including prostacyclin synthesis. EPA and 22:5n-3 of endothelial cells incubated with M2 were, respectively, three and two times higher than in control cells (incubated in M1, without any fatty acid added), whereas 22:6n-3 increased only in the supernatant, suggesting its release after biosynthesis. However, 18:2n-6 and 22:4n-6 decreased (about 30%). *Trans* 20:5 isomers represented 4.7, 3.9, and 5.2% of total phospholipid FA in endothelial cells incubated with M3, M4, and M5, respectively. They were elongated into *trans* 22:5 and *trans* 24:5, as revealed by gas chromatography–mass spectrometry and gas chromatography–Fourier transform infrared analysis. In cells incubated with M2, M3, M4, and M5, prostacyclin synthesis was inhibited by 49.0, 62.5, 60.5, and 72.0%, respectively. This effect may be due to less available arachidonic acid in the cells and to a competition between EPA isomers and AA at the level of cyclooxygenase pathway, as it was demonstrated that 20:5 Δ17*t* was metabolized by this enzyme.

Paper no. L8457 in *Lipids 35*, 911–918 (August 2000).

Trans isomers of n-3 polyunsaturated fatty acids (FA) are formed during heat treatment of vegetable oils including deodorization or deep-frying treatments (1–3). Geometrical isomers of linolenic acid are present in human food such as dietary oils, low-calorie spreads (4–6) or infant formulas (7–9). As a consequence, the major geometrical isomers of 18:3n-3, i.e., the 18:3 9*c*,12*c*,15*t* (18:3 Δ15*t*) and the 18:3 9*t*,12*c*,15*c* were found in several human tissues such as serum (10), milk (11), plasma, and platelets (12). Furthermore, *trans* 18:3 can be desaturated and elongated into *trans* 20:5 (13,14). Indeed, 20:5 5*c*,8*c*,11*c*,14*c*,17*t* (20:5 Δ17*t*) formed from the 18:3 Δ15*t,* was found in human platelets (12,15), plasma (12), and umbilical vein endothelial cells (Loï, C., and Chardigny, J.M., unpublished data).

In rat platelets, this *trans* 20:5 seems to be recognized as arachidonic acid (AA), its structural analog (16). Since endothelial cells play a crucial role by maintaining hemostasis (AA) (17) and protecting against thrombogenesis, we wondered (i) whether, in these cells, 20:5 Δ17*t* is recognized as AA, the major precursor of eicosanoid synthesis and (ii) whether 20:5 Δ17*t* has the same effects as its *cis* homolog, eicosapentaenoic acid (EPA).

Several studies reported that the incorporation of EPA into endothelial cell lipids leads to its conversion into 22:5n-3 (18–20) and induces (i) an increase in nitric oxide (NO) production and intracellular free calcium concentration (21), (ii) an increase of the release of endothelium-derived relaxing factors (22), and (iii) a decrease in AA content and in synthesis of eicosanoids such as prostacyclin (PGI_2) (18,23–25) or prostaglandin (PG) E_2 (26). Kanayasu *et al.* (27) also demonstrated that EPA may act as an endogenous inhibitor of angiogenesis under various pathological conditions. Thus, incorporation of EPA in endothelial cell lipids has been extensively studied, but no data are available so far on the incorporation of geometrical isomers of EPA, i.e., 20:5 5*c*,8*c*,11*t*,14*c*,17*c* (20:5 Δ11*t*), 20:5 5*c*,8*c*,11*t*,14*c*,17*t* (20:5 Δ11*t*,17*t*), and 20:5 Δ17*t*.

Thus, the aims of this study were (i) to explore the ability of *trans* 20:5 to be incorporated and metabolized by bovine aortic endothelial cells (BAEC), (ii) to evaluate if the position or the number of the *trans* double bonds influences the metabolic effects of these *trans* FA, (iii) to assess if the incorporation of these *trans* FA influences PGI_2 synthesis, and (iv) to compare the metabolism of 20:5 Δ17*t* with that of AA, its structural analog.

MATERIAL AND METHOD

EPA and AA were purchased from Sigma (L'Isle d'Abeau, France). The 20:5 Δ11*t*, the 20:5 Δ17*t*, and the 20:5 Δ11*t*,17*t*

*To whom correspondence should be addressed at INRA, Unité de Nutrition Lipidique, 17, rue Sully, BP 86510, 21065 Dijon Cedex, France.
E-mail: chardign@dijon.inra.fr

Abbreviations: AA, arachidonic acid; BAEC, bovine aortic endothelial cells; DHA, docosahexaenoic acid; DMOX, dimethyloxazoline derivative; DPA, docosapentaenoic acid; EPA, eicosapentaenoic acid; FA, fatty acids; FCS, fetal calf serum; FTIR, Fourier transform infrared; GC, gas chromatography; HPLC, high-performance liquid chromatography; NO, nitric oxide; PG, prostaglandin; PGI, prostacyclin; RV, retention volume; SFA, saturated fatty acid; 18:3 Δ15*t*, 18:3 9*c*,12*c*,15*t*; 20:5 Δ11*t*, 20:5 5*c*,8*c*,11*t*,14*c*,17*c*; 20:5 Δ17*t*, 20:5 5*c*,8*c*,11*c*,14*c*,17*t*; 20:5 Δ11*t*,17*t*, 20:5 5*c*,8*c*,11*t*,14*c*,17*t*.

were synthesized as methyl esters (28,29) and saponified (30) prior to being bound to a delipidated human serum albumin (Sigma).

[1-^{14}C]-Radiolabeled AA (specific activity 2.04 GBq/mmol) was purchased from NEN, Life Sciences (Les Ulis, France). [18-^{14}C]-Radiolabeled 20:5 Δ17*t* (specific activity 1.96 GBq/mmol) and [18-^{14}C]-radiolabeled EPA (specific activity 1.96 GBq/mmol) were obtained by total synthesis (31). These three FA were diluted with their respective unlabeled homologs to obtain specific activities required for our experiments.

Endothelial cell growing factor and trypsin were purchased from Sigma and Biochrom KG (Berlin, Germany), respectively. Medium M199, antibiotics, and fetal calf serum (FCS) were supplied by Polylabo (Strasbourg, France). The collagenase was obtained from Boehringer (Grenoble, France).

Cell cultures. Endothelial cells were isolated from bovine aortae (obtained from freshly slaughtered animals) by scraping the luminal surface with a razor blade, and were then dispersed by treatment with collagenase (0.02% in phosphate-buffered saline containing 0.011 M of glucose) for 15 min at 37°C, under gentle shaking. The cells were sedimented (200 × *g* for 5 min), plated in complete Medium 199 [with Earle's salt, 30 μM/mL of endothelial cell growing factor, 20% heat-inactivated FCS, penicillin (100 U/mL), and streptomycin (100 μg/mL)] on 25-cm^2 tissue culture dishes (Falcon, Primaria). They were incubated at 37°C under an atmosphere containing 5% CO_2 and 95% air. Subcultures were performed with trypsin and by scraping the dishes with a plastic spatula. As for primary cultures, cells were sedimented and plated in complete Medium 199 on 25-cm^2 dishes. The cells were identified as endothelial cells by morphology and by immunofluorescent staining for von Willebrand factor. They were used at confluence in the second passage.

Preparation of media enriched with different FA. Tenfold-concentrated FA solutions, as compared to the final FA concentration, were prepared by incubating delipidated bovine serum albumin with EPA (M2), 20:5 Δ11*t* (M3), 20:5 Δ17*t* (M4), 20:5 Δ11*t*,17*t* (M5), [1-^{14}C]AA (0.74 GBq/mmol, M6), [18-^{14}C]EPA (0.74 GBq/mmol, M7), [18-^{14}C]20:5 Δ17*t* (0.74 GBq/mmol, M8), and without any fatty acid (= control = M1) for 5 h at 37°C under N_2 and gently shaking. The final FA/albumin ratio was 2:1. Then, the solutions were diluted with Medium 199, 20% FCS; filtered; and added to the cells at confluence. Incubations were carried out for 48 h.

Lipid analysis. At the end of the incubation period, lipids of cell supernatant from pools of two dishes were extracted according to the method of Folch *et al.* (32). The free FA were separated from the other lipid classes by thin-layer chromatography, transmethylated (33), and analyzed by gas chromatography (GC) (BPX70, 50 × 0.33 i.d., film thickness 0.25 μm, SGE, Melbourne, Australia) using a Hewlet-Packard 5890 series II gas chromatograph (Avondale, PA), fitted with a splitless injector and a flame-ionization detector. Both were maintained at 250°C. The oven temperature was programmed from 60 to 185°C (20°C/min) for 35 min and then from 185 to 220°C (20°C/min).

Cells (pools from two dishes) were rinsed with phosphate-buffered saline solution and scraped off into methanol. Lipids were extracted according to Folch *et al.* (32). Phospholipids of half the samples were separated from neutral lipids by the method of Kaluzny *et al*. (34), and their FA were transmethylated (33) and analyzed by GC. The remaining methyl esters of these phospholipid FA were separated by high-performance liquid chromatography (HPLC) (column: Nucleosil C18, 5 μM, 250 × 4.6, mobile phase: acetonitrile at 1 mL/min) in order to obtain the 20:5 + 22:6 fraction [F1, retention volume (RV) of 6 mL], the 20:4 + 22:5 fraction (F2, RV of 7.2 mL), and the 22:4 + 24:5 fraction (F3, RV of 8.7 mL). F2 and F3 were then divided into two samples. One was analyzed by GC (HP5890 gas chromatograph, BPX70, 30 m × 0.25 mm i.d., film thickness 0.25 μm; SGE) coupled with Fourier-transform infrared (FTIR) spectrometry (FTS 60A; Biorad, Cambridge, MA) and fitted with a splitless injector maintained at 250°C. The oven temperature was programmed from 60 to 200°C (20°C/min). The second samples of F2 and F3 were reacted to form dimethyloxazoline derivatives (DMOX) (35). Briefly, the fractions were evaporated to dryness under nitrogen. Next, 100 μL of 2-amino-2 methyl-1-propanol was added before heating at 170°C for 8 h. DMOX derivatives were extracted twice using dichloromethane. After washing by distilled water, DMOX derivatives were injected onto an HP5 wall-coated capillary column (30 m × 0.25 mm i.d., film thickness 0.25 μm) interfaced with a MSD5970 quadrupole mass spectrometer (Hewlett-Packard). The oven temperature was programmed from 50 to 240°C at a rate of 20°C/min. The mass spectrometer was operated in electron impact mode at an ionization energy of 70 eV.

Phospholipids of the remaining half of the samples were separated from neutral lipids, the different phospholipid classes were separated by HPLC (column: Lichrosorb Si60, 5 μm, 250 mm × 4 mm) (36), and their FA were transmethylated and analyzed by GC as described above.

Prostaglandin synthesis analysis. Cells incubated for 48 h with M1, M2, M3, M4, and M5 were stimulated for 15 min at 37°C with [1-^{14}C]AA (20 μM, 0.55 GBq/mmol) to assess if incorporation of geometrical isomers of EPA has an influence on PGI synthesis from exogenous AA. Cells and supernatant were harvested. Radiolabeled AA metabolites were extracted using octadecyl-silica minicolumns (Amprep; Amersham, Courtaboeuf, France) (37) and analyzed with a reversed-phase-HPLC technique (38,39), slightly modified in our laboratory. Separation of PG from the other eicosanoids and unmetabolized AA was performed on a Nucleosil-C18 (5 μm, 4.6 × 250 mm) column (Interchim, France). Solvent A was acetonitrile and solvent B was water acidified to pH 3 with acetic acid. PG were eluted isocratically at a flow rate of 1 mL/min over 40 min with 31% solvent A/69% solvent B. Following elution of the PG, the concentration of acetonitrile was increased to 100% over 45 min and then maintained at 100% for 10 min. The column effluent was collected in 1-mL fractions and radioactivity determined by liquid scintillation spectrometry. Unlabeled 6-keto ($PGF_{1\alpha}$), (PGD_2), and AA were used as standards to identify the chromatogram peaks. They

were detected using an ultraviolet detector (Varian 9050, Palo Alto, CA). Absorbance was monitored at 207 nm for the first 50 min and then at 220 nm.

*[18-^{14}C]20:5 Δ17*t *metabolism.* BAEC at confluence (second generation) were stimulated for 15 min at 37°C with [18-^{14}C]20:5 Δ17*t* (20 μM, 0.55 GBq/mmol) to assess if these cells are able to metabolize this *trans* isomer of EPA in PG. Eicosanoid extraction and analysis were performed as described above.

Cyclooxygenase inhibition. BAEC at confluence (second generation) were incubated for 5 min at 37°C with indomethacin [5 μM diluted in ethanol (0.5% of total medium volume)], a specific inhibitor of the cyclooxygenase (40). Then they were incubated with [18-^{14}C]20:5 Δ17*t* (20 μM, 0.55 GBq/mmol) for 15 min at 37°C to assess PG synthesis. Analyses were performed as described above.

Statistical analysis. The results were analyzed using the NCSS package (Kaysville, UT). An analysis of variance with a Newman-Keuls test at one-factor term was performed to compare the different groups. Results are expressed as mean ± standard deviation.

RESULTS

FA profile of BAEC phospholipids. As shown in Table 1 and Figure 1, BAEC incorporated the different 20:5 fatty acids added in the culture medium. Unknown compounds named Y1 and W1 (M3), Y and W (M4), and Y2 and W2 (M5) were detected. Mass spectra of the DMOX derivatives of these molecules revealed that they are 22:5n-3 (Y, Y1, Y2, Fig. 2A) and 24:5 isomers (W, W1, W2, Fig. 2B), as it is shown in Figure 3B with the IR spectrum of Y revealing the presence of a *trans* double bond.

FA incorporation in the different phospholipid classes was also assessed, and there was no difference between 20:5 Δ17*t*, EPA, and AA incorporation into phosphatidylethanolamine and phosphatidylcholine.

Composition of cell supernatant free FA. Table 2 shows that the FA added to the initial medium and their 22:5 metabolites were found in all cell supernatants. Only the 24:5 isomer produced from the 20:5 Δ17*t* was detected.

There was an increase in AA ($P < 0.001$), 22:4n-6, and sum of n-6 FA ($P < 0.01$) in M2 and M4 media. Docosahexaenoic acid (DHA) content was increased in M2, M4, and M5 media compared to the control (M1).

PGI_2 synthesis. Figure 4 shows that incorporation of EPA, 20:5 Δ11*t*, 20:5 Δ17*t,* and 20:5 Δ11*t*,17*t* in BAEC inhibited PGI_2 synthesis from exogenous AA by 49.0, 62.5, 60.5, and 71.9%, respectively. The effect of the di-*trans* isomer was more potent than that of the other FA. The effects of the different mono-*trans* isomers were similar.

*20:5 Δ17*t *metabolism.* Figures 5B and C present chromatograms of the 20:5 Δ17*t* metabolites from BAEC stimulated with [18-^{14}C]20:5 Δ17*t* (20 μM, 0.55 GBq/mmol) in the presence (C) or absence (B) of indomethacin (5 μM).

BAEC were able to metabolize 20:5 Δ17*t* into compounds where synthesis was inhibited by indomethacin. Furthermore, the Δ17 *trans* isomer of EPA was metabolized into nonpolar

TABLE 1
Phospholipid Fatty Acid Composition (wt% of total phospholipid fatty acids, means ± SEM of 12 determinations) in BAEC Incubated with Medium M199 (M1) Enriched With Different Fatty Acids: EPA (M2), 20:5 Δ11*t* (M3), 20:5 Δ17*t* (M4), or 20:5 Δ11*t*,17*t* (M5)[a]

	M1	M2	M3	M4	M5
Saturated	44.11 ± 3.52[a]	42.04 ± 3.15[a]	41.15 ± 2.43[a]	42.63 ± 3.48[a]	43.57 ± 3.66[a]
MUFA	22.95 ± 2.90[a]	21.58 ± 1.57[a]	21.38 ± 1.11[a]	21.37 ± 2.51[a]	20.01 ± 1.70[a]
18:2n-6	2.59 ± 0.43[a]	1.74 ± 0.16[b]	2.07 ± 0.26[c]	1.78 ± 0.30[b]	1.94 ± 0.26[b,c]
20:4n-6	8.04 ± 1.73[a]	6.35 ± 0.79[b]	8.76 ± 0.79[a]	7.26 ± 0.97[b]	7.99 ± 0.89[b]
22:4n-6	0.66 ± 0.16[a]	0.69 ± 0.10[a]	0.73 ± 0.11[a]	0.86 ± 0.12[b]	0.89 ± 0.10[b]
Sum n-6	13.78 ± 1.75[a]	10.74 ± 1.24[b]	14.33 ± 0.81[a]	12.44 ± 1.35[a,b]	13.35 ± 1.21[a,b]
EPA	2.21 ± 0.36[a]	6.80 ± 0.72[b]	1.69 ± 0.26[c]	1.11 ± 0.19[d]	1.26 ± 0.23[c,d]
22:5n-3	4.57 ± 0.75[a]	9.05 ± 1.46[b]	4.83 ± 0.73[a]	4.28 ± 0.91[a]	4.78 ± 0.76[a]
Δ11*t*	0.00[a]	0.00[a]	4.70 ± 0.42[b]	0.00[a]	0.00[a]
Y1	0.00[a]	0.00[a]	0.56 ± 0.15[b]	0.00[a]	0.00[a]
W1	0.00[a]	0.00[a]	0.08 ± 0.01[b]	0.00[a]	0.00[a]
Δ17*t*	0.00[a]	0.00[a]	0.00[a]	3.94 ± 0.76[b]	0.00[a]
Y	0.00[a]	0.00[a]	0.00[a]	3.94 ± 0.96[b]	0.00[a]
W	0.00[a]	0.00[a]	0.00[a]	0.34 ± 0.08[b]	0.00[a]
Δ11*t*,17*t*	0.00[a]	0.00[a]	0.00[a]	0.00[a]	5.20 ± 0.47[b]
Y2	0.00[a]	0.00[a]	0.00[a]	0.00[a]	1.04 ± 0.16[b]
W2	0.00[a]	0.00[a]	0.00[a]	0.00[a]	0.08 ± 0.01[b]
22:6n-3	3.94 ± 0.57[a]	2.75 ± 0.47[b]	4.20 ± 0.41[a]	3.32 ± 0.60[c]	3.88 ± 0.36[a]
24:5	0.11 ± 0.12[a]	0.40 ± 0.27[b]	0.23 ± 0.03[a]	0.18 ± 0.04[a]	0.19 ± 0.02[a]
Sum n-3[b]	10.87 ± 1.55[a]	18.79 ± 2.44[b]	16.24 ± 1.09[b]	16.72 ± 2.94[b]	16.30 ± 1.19[b]

[a]Values in rows having different roman superscript letters are significantly different ($P < 0.01$). EPA, eicosapentaenoic acid; SEM, standard error of the mean; MUFA, monounsaturated fatty acid; BAEC, bovine aortic endothelial cells; 20:5 Δ11*t*, 20:5 5*c*,8*c*,11*t*,14*c*,17*c*; 20:5 Δ17*t*, 20:5 5*c*,8*c*,11*c*,14*c*,17*t*; 20:5 Δ11*t*,17*t*, 20:5 5*c*,8*c*,11*t*,14*c*,17*t*.

[b]Including *cis* and *trans* isomers.

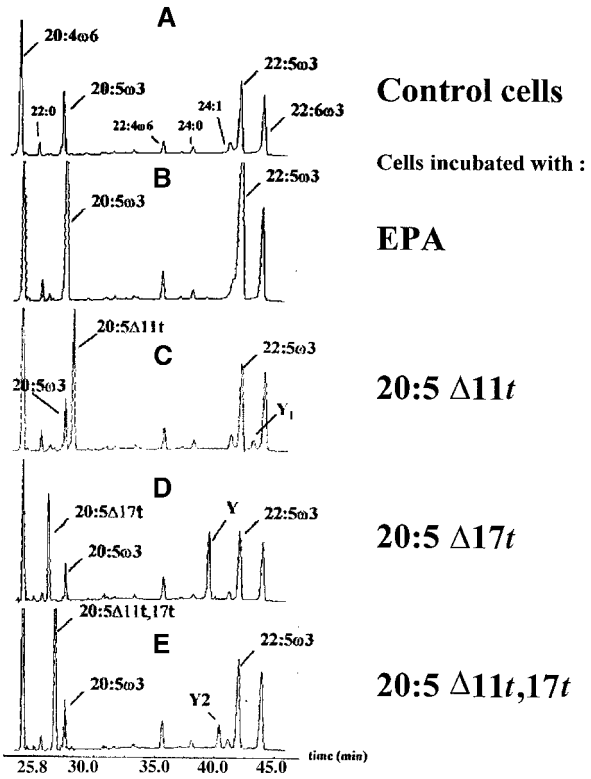

FIG. 1. Incorporation of *trans* 20:5 in bovine aortic endothelial cell phospholipids and elongation in *trans* 22:5. Part of gas–liquid chromatograms of phospholipid fatty acid methyl esters of cells incubated for 48 h with 12.5 μM of bovine delipidated albumin and 25 μM of eicosapentaenoic acid (B), 20:5 Δ11*t* (20:5 5*c*,8*c*,11*t*,14*c*,17*c*) (C), 20:5 Δ17*t* (20:5 5*c*,8*c*,11*c*,14*c*,17*t*) (D), 20:5 Δ11*t*,17*t* (20:5 5*c*,8*c*,11*t*,14*c*, 17*t*) (E), or only albumin (control, A).

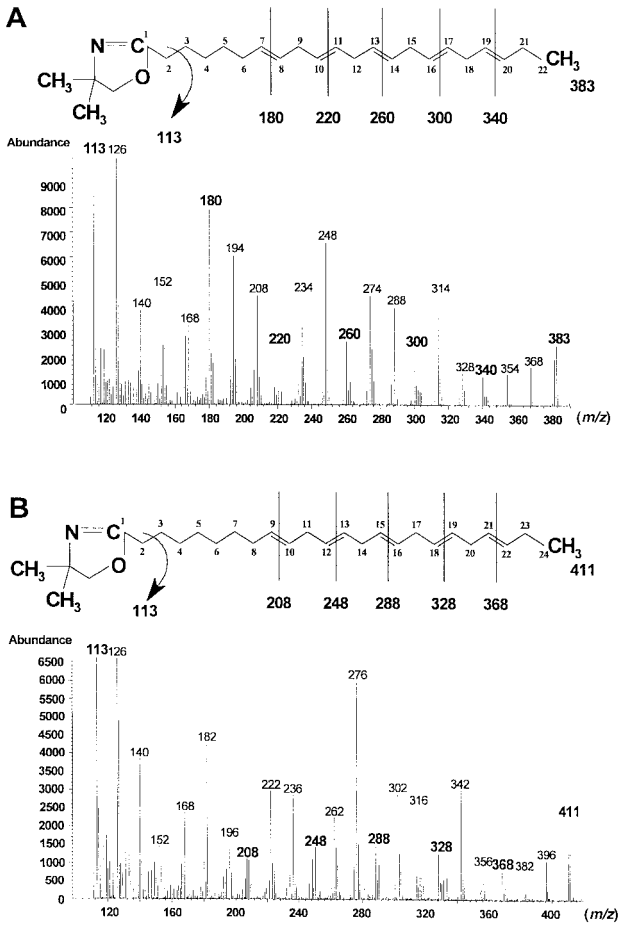

FIG. 2. Mass spectra of dimethyloxazoline derivatives of Y (22:5 7*c*,10*c*,13*c*,16*c*,19*c*) (A) and W (24:5 9*c*,12*c*,15*c*,18*c*,21*t*) (B). Mass spectra of Y1 and Y2 (22:5 7*c*,10*c*,13*t*,16*c*,19*c* and 22:5 7*c*,10*c*,13*t*,16*c*,19*t*, respectively) are identical to that of Y, those of W1 and W2 (24:5 9*c*,12*c*,15*t*,18*c*,21*c* and 24:5 9*c*,12*c*,15*t*,18*c*,21*t*, respectively) are similar to that of W.

metabolites, as illustrated by several peaks with a retention volume of 50 to 75 mL.

DISCUSSION

Effect of 20:5 incorporation on n-3 FA metabolism. As already shown with EPA (20–22), BAEC are able to incorporate *trans* 20:5 FA (Fig. 1). This incorporation induced a decrease in EPA content in cell phospholipids. Furthermore, BAEC were able to elongate these *trans* isomers of EPA into *trans* 22:5 (Table 1, Figs. 2A, 3A) named, Y_1 (from 20:5 Δ11*t*), Y (from 20:5 Δ17*t*) and Y_2 (from 20:5 Δ11*t*,17*t*) and into *trans* 24:5 (Figs. 2B, 3B). Y has already been detected in tissues of rats fed a diet enriched with heated oil (13,41), but it has never been identified. However, it has been suspected to be a FA that is intermediate between the 20:5 Δ17*t* and the 22:6 4*c*,7*c*,10*c*,13*c*,16*c*,19*t* in the desaturation and elongation cascade. On the other hand, the *trans* 24:5 are not desaturated into 24:6, and it seems that there is no retroconversion into *trans* 22:6 as it is not detected in the cell phospholipids or in cell supernatant. An elongation in such long-chain FA has already been demonstrated in human umbilical vein endothelial cells for the n-6 family of FA (42).

When analyzed on a BPX70 capillary column, the geometrical isomers of 22:5 (Fig. 1) and 24:5 (data not shown) are eluted in the same order as those of 20:5. This particularity has already been observed by Piconneaux (43). Results of GC analyses of radiolabeled (data not shown) or unlabeled FA of endothelial cell phospholipids, in GC–mass spectrometry and GC-FTIR plus the fact that BAEC were incubated with only one *trans* FA at a time, allow us to say that Y is the 22:5 7*c*,10*c*,13*c*,16*c*,19*t*; W is the 24:5 9*c*,12*c*,15*c*,18*c*,21*t*, Y1 is the 22:5 7*c*,10*c*,13*t*,16*c*,19*c*; W1 is the 24:5 9*c*,12*c*,15*t*,18*c*,21*c*; Y2 is the 22:5 7*c*,10*c*,13*t*,16*c*,19*t*; and W2 is the 24:5 9*c*,12*c*,15*t*,18*c*,21*t*.

In phospholipids from BAEC incubated with EPA, we observed a decrease of the content of DHA; therefore, we expected an increase of this metabolite, as it is a desaturation and elongation product of EPA, which was present in large quantities. In fact, most of the synthesized DHA should be released in the medium as its content was increased in the supernatant of the cells. These results are in agreement with those of Achard *et al.* (44).

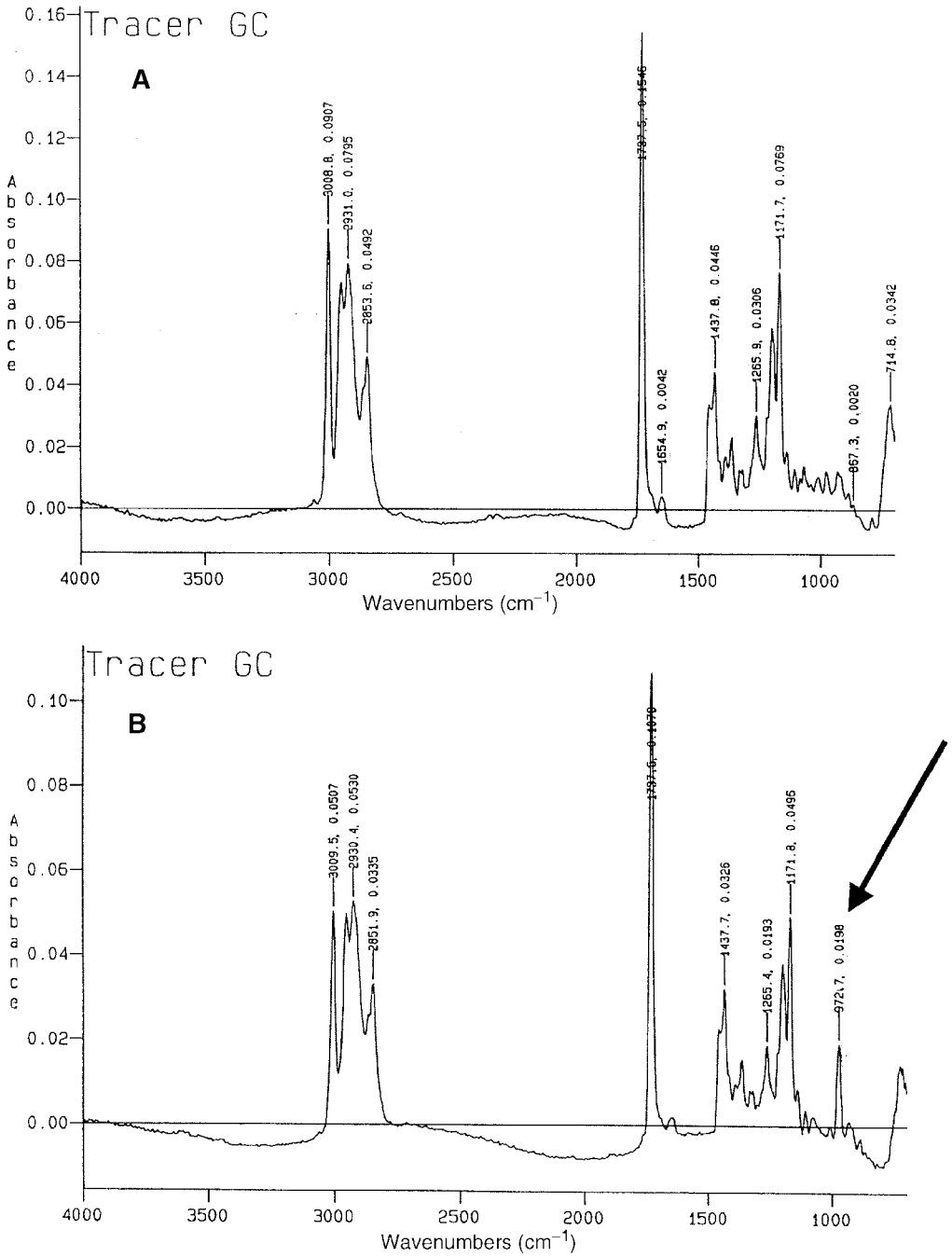

FIG. 3. Gas–liquid chromatography–Fourier transform infrared spectra of dimethyloxazoline derivatives of 22:5n-3 (A) and Y (B). (A) reveals the presence of a highly desaturated fatty acid (3008.8 cm^{-1} for δ = CH). (B) shows a highly desaturated fatty acid (3009.5 cm^{-1} for δ = CH) with a *trans* ethylenic bond (972.7 cm^{-1} for δ = CH).

Similarly, cells incubated with 20:5 Δ17*t* showed a decrease in their DHA content and an increase of DHA in their supernatant. This is one of the similarities found between the cells incubated with a medium enriched with EPA and those with 20:5 Δ17*t*. Another difference is that the 20:5 Δ17*t* was as much converted into Y as was EPA into 22:5n-3. Hence, it would be of interest to compare the effects of cells enriched with EPA on platelet regulation to cells enriched with 20:5 Δ17*t*.

Effect of 20:5 incorporation on n-6 FA metabolism. Influence on PGI_2 synthesis. The 20:5 incorporation induced a decrease in 18:2n-6 content in cell phospholipids. Its content in supernatants was unchanged. Furthermore, AA was also decreased in phospholipids of cells incubated with EPA, 20:5 Δ17*t,* and 20:5 Δ11*t*,17*t*. Such a decrease was already reported with EPA (18,24–26,45,46). This may be due to a competition between 20:5 and 20:4 for incorporation in phospholipids.

TABLE 2
Percentage (means ± SEM of three determinations) of Free Fatty Acids (wt% of total fatty acids) in the Super-natant of the Incubated BAEC[a]

	M1	M2	M3	M4	M5
Saturated	47.25 ± 3.58[a]	32.09 ± 1.82[b]	38.50 ± 1.66[b]	34.83 ± 1.11[b]	49.95 ± 2.90[a]
MUFA	22.4 ± 3.22[a,b]	24.95 ± 0.3[b,c]	28.21 ± 0.67[c]	27.17 ± 0.85[b,c]	19.63 ± 0.43[a]
18:2	2.46 ± 0.36	2.3 ± 0.1	2.35 ± 0.12	2.34 ± 0.1	2.44 ± 0.09
20:4n-6	0.95 ± 0.42[a]	3.18 ± 0.36[b]	1.39 ± 0.07[a]	3.23 ± 0.25[b]	1.65 ± 0.03[a]
22:4n-6	0.18 ± 0.18	0.35 ± 0.01	0.25 ± 0.04	0.42 ± 0.06	0.19 ± 0.07
Sum n-6	5.68 ± 1.05[a]	8.08 ± 0.63[b]	5.92 ± 0.31[a]	7.76 ± 0.52[b]	4.86 ± 0.22[a]
EPA	0.24 ± 0.13[a]	15.49 ± 1.99[b]	0.34 ± 0.1[a]	0.48 ± 0.06[a]	0.43 ± 0.05[a]
22:5 Δ11*t*	0 ± 0[a]	0 ± 0[a]	10.41 ± 2.72[b]	0 ± 0[a]	0 ± 0[a]
20:5 Δ17*t*	0 ± 0[a]	0 ± 0[a]	0 ± 0[a]	7.44 ± 0.74[b]	0 ± 0[a]
20:5 Δ11*t*,17*t*	0 ± 0[a]	0 ± 0[a]	0 ± 0[a]	0 ± 0[a]	13.12 ± 1.97[a]
22:5n-3	0.36 ± 0.16[a]	2.85 ± 0.38[b]	0.48 ± 0.09[a]	1.15 ± 0.14[a]	0.76 ± 0.27[a]
Y1	0 ± 0[a]	0 ± 0[a]	0.11 ± 0.03[b]	0 ± 0[a]	0 ± 0[a]
Y	0 ± 0[a]	0 ± 0[a]	0 ± 0[a]	1.56 ± 0.31[b]	0 ± 0[a]
Y2	0 ± 0[a]	0 ± 0[a]	0 ± 0[a]	0 ± 0[a]	0.78 ± 0.20[a]
22:6n-3	0.31 ± 0.32[a]	2.24 ± 0.2[b]	0.98 ± 0.18[a,c]	1.76 ± 0.24[b,c]	1.75 ± 0.46[b,c]
24:5n-3	0.18 ± 0.18	0.22 ± 0.06	0.11 ± 0.03	0.12 ± 0.03	0.14 ± 0.03
W	0 ± 0[a]	0 ± 0[a]	0 ± 0[a]	0.23 ± 0.03[b]	0 ± 0[a]
Sum n-3[b]	2.86 ± 0.41[a]	21.26 ± 2.55[b]	13.03 ± 3.16[b]	13.21 ± 1.51[b]	17.51 ± 2.91[b]

[a]Values in rows having different roman superscript letters are significantly different ($P < 0.01$). See Table 1 for abbreviations.
[b]Including *cis* and *trans* isomers.

Consequently, free AA may be released from the cells, and this explains the increase of its content in the supernatant of cells incubated with the 20:5. On the other hand, in phospholipids from cells which have incorporated 20:5 with a *trans* double bond at the Δ17 position, the elongation of AA into 22:4 was greater than for the other cell phospholipids. These changes in n-6 FA content in cell phospholipids correspond to a lesser availability of AA to be metabolized into PGI_2. Consequently, 20:5 incorporation could influence endothelial cell function.

These observations could partially explain the inhibitory effect of EPA and *trans* 20:5 incorporation in cells on PGI_2 synthesis, as exogenous AA enters in competition, at the level of the cyclooxygenase metabolism, with the other FA released from membrane phospholipids. However, it is of interest to know if 22:5 isomers or 20:5 FA are responsible for this inhibition. Indeed, Bénistant *et al.* (47) observed that inhibition of PGI_2 synthesis in endothelial cells treated with docosapentaenoic acid (DPA) might depend on EPA formed by retroconversion of DPA.

Metabolism of 20:5 Δ17t. Figure 5 shows that endothelial cells were able to metabolize 20:5 Δ17*t* into two unknown compounds with RV close to those of 6-keto $PGF_{1\alpha}$ and PGD_2. Using indomethacin as a specific inhibitor of the cyclooxygenase showed that these compounds were produced by this enzymatic pathway. Consequently, these metabolites may be *trans* isomers of Δ17-6-keto-$PGF_{1\alpha}$ (stable metabolite of PGI_2) and PGD_2, but only determination of their chemical structure would confirm this hypothesis. As it was already demonstrated in platelets (16), it seems that 20:5 Δ17*t* is recognized as AA, its structural analog, by the cyclooxygenase. A competition at the level of this enzyme could also explain the inhibitory effect of its incorporation on PGI_2 synthesis.

In contrast, the Δ17 *trans* isomer of EPA was more metabolized in nonpolar compounds than AA. Their RV were similar to those of hydroxyacids. It would be of interest to incubate endothelial cells with nordihydroguaiaretic acid and/or baicalein prior to stimulating them with 20:5 Δ17*t* in order to assess if these compounds are synthesized by 5-, 12- or 15-lipoxygenase.

In conclusion, the present study shows that *trans* 20:5 can be incorporated in endothelial cells and elongated into *trans* 22:5 and *trans* 24:5. The 20:5 Δ17*t*, which is the major 20:5 isomer found in human tissues, was as much converted in Y and W as was EPA into 22:5n-3 and 24:5. The differences observed between the *trans* 20:5 groups show that there is an in-

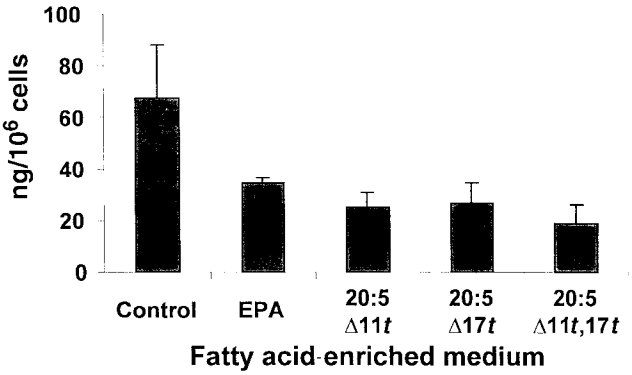

FIG. 4. Prostacyclin (PGI_2) synthesis inhibition in cells incubated for 48 h with medium enriched with different *trans* 20:5 (25 μM) or not (control). Cells were stimulated for 15 min at 37°C with radiolabeled arachidonic acid. PGI_2 was quantified by reversed phase-high-performance liquid chromatography (RP-HPLC) as described in the Material and Methods section.

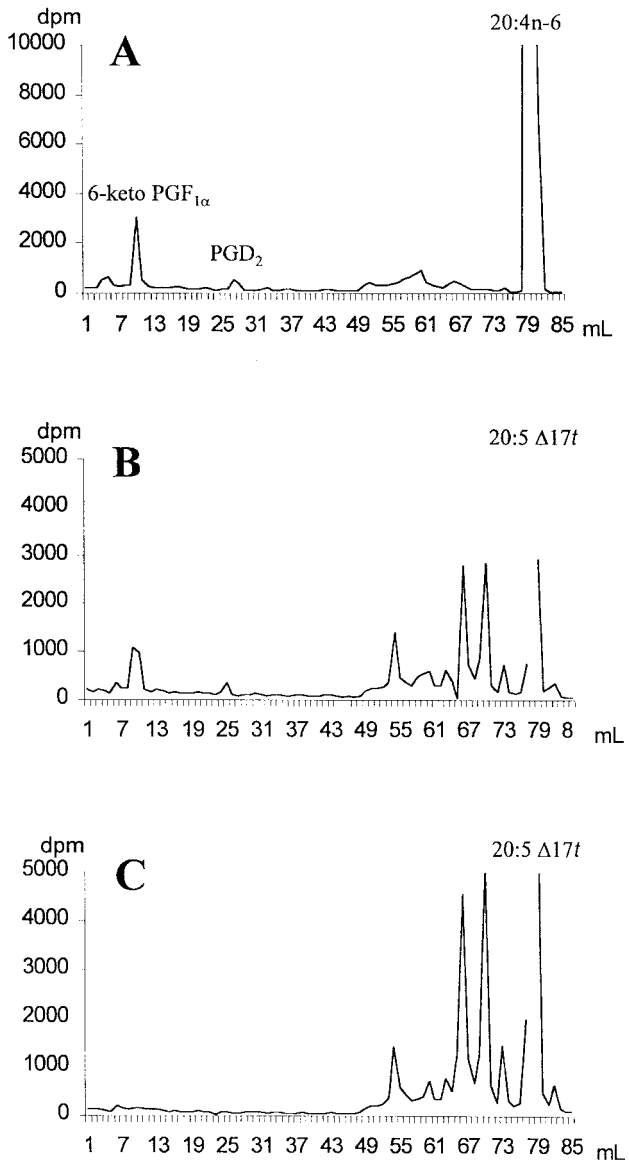

FIG. 5. HPLC profile of radio-labeled eicosanoids resolved using RP-HPLC. Cells were incubated for 15 minutes at 37°C with (A) [1-^{14}C]arachidonic acid (20 μM, 0.55 GBq/mmol) and (B) [18-^{14}C]20:5 Δ17*t* (20 μM, 0.55 GBq/mmol). (C) Cells were incubated for 5 min at 37°C with 5 μM of indomethacin prior to being stimulated for 15 min with [18-^{14}C]-20:5 Δ17*t* (20 μM, 0.55 GBq/mmol). See Figures 1 and 4 for other abbreviations.

fluence of the position of the *trans* double bond on the metabolism of these *trans* FA. An inhibitory effect on PGI_2 synthesis due to the 20:5 FA incorporation can be explained by (i) a decrease in 18:2n-6 and 20:4n-6 (except with M3) and an increase in 22:4n-6 (M4 and M5), which leads to less available AA for the cyclooxygenase pathway and (ii) the fact that the 20:5 Δ17*t* (and possibly the other *trans* 20:5) competes with the 20:4n-6 at the level of the cyclooxygenase step. Further studies are required to assess if there is a competitive inhibition between these two FA, to identify whether 20:5 Δ11*t* and 20:5 Δ11*t*17*t* are metabolized by the same enzymes, to determine the chemical structures of these metabolites, and to understand the mechanism of action of these *trans* 20:5.

ACKNOWLEDGMENTS

The authors gratefully acknowledge the region of Burgundy and Lesieur Alimentaire for their financial support. C. Loï was funded by a fellowship from INRA and the region of Burgundy, France.

REFERENCES

1. Ackman, R.G., and Hooper, S.N. (1974) Linolenic Acid Artifacts from Deodorization of Oils, *J. Am. Oil Chem. Soc. 51*, 42–49.
2. Sébédio, J.L., Grandgirard, A., and Prevost, J. (1988) Linoleic Acid Isomers in Heat Treated Sunflower Oils, *J. Am. Oil Chem. Soc. 65*, 362–366.
3. Grandgirard, A., Sébédio, J.L., and Fleury, J. (1984) Geometrical Isomerization of Linolenic Acid During Heat Treatment of Vegetable Oils, *J. Am. Oil Chem. Soc. 61*, 1563–1568.
4. Sébédio, J.L., Grandgirard, A., Septier, C., and Prevost, J. (1987) État d'Altération de Quelques Huiles de Friture Prélevées en Restauration, *Rev. Fr. Corps Gras 1*, 15–18.
5. Wolff, R.L., and Sébédio, J.L. (1991) Geometrical Isomers of Linolenic Acid in Low-Calorie Spreads Marketed in France, *J. Am. Oil Chem. Soc. 68*, 719–725.
6. Chardigny, J.M., Sébédio, J.L., and Berdeaux, O. (1996) *Trans* Polyunsaturated Fatty Acids: Occurrence and Nutritional Implications, *Adv. Applied Lipid Res. 2*, 1–33.
7. O'Keefe, S.F., Willey, V., and Gaskins, S. (1994) Geometrical Isomers of Essential Fatty Acids in Liquid Infant Formulas, *Food Res. Int. 27*, 7–13.
8. Chardigny, J.M., Wolff, R.L., Mager, E., Bayard, C.C., Sébédio, J.L., Martine, L., and Ratnayake, W.M.N. (1996) Fatty Acid Composition of French Infant Formulas with Emphasis on the Content and Detailed Profile of *Trans* Fatty Acids, *J. Am. Oil Chem. Soc. 73*, 1595–1601.
9. Ratnayake, W.M.N., Chardigny, J.M., Wolff, R.L., Bayard, C. C., Sébédio, J. L., and Martine, L. (1997) Essential Fatty Acids and Their *Trans* Geometrical Isomers in Powdered and Liquid Infant Formulas Sold in Canada, *J. Pediatr. Gastroenterol. Nutr. 25*, 400–407.
10. Wolff, R.L. (1995) Recent Applications of Capillary Gas–Liquid Chromatography to Some Difficult Separations of Positional or Geometrical Isomers of Unsaturated Fatty Acids, in *New Trends in Lipid and Lipoprotein Analysis* (Sébédio, J.-L., and Perkins, E.G., eds.) pp. 147–180, AOCS Press, Champaign.
11. Chardigny, J.M., Wolff, R.L., Mager, E., Sébédio, J.L., Martine, L., and Juaneda, P. (1995) *Trans* Mono- and Polyunsaturated Fatty Acids in Human Milk, *Eur. J. Clin. Nutr. 49*, 523–531.
12. Sébédio, J.L., Mensink, R.P., Chardigny, J.M., Beaufrère, B., Vermunt, S., Armstrong, R.A., Christie, W.W., Niemelä, J., Hénon, G., and Riemersma, R.A. (1999) Nutritional and Health Impact of *Trans*-Polyunsaturated Fatty Acids in European Populations, the *TRANS*LinE Study. Design, Method, Baseline Characteristics and Adherence to Dietary Interventions, *Eur. J. Clin. Nutr. 53*, 1–10.
13. Grandgirard, A., Piconneaux, A., Sébédio, J.L., O'Keefe, S.F., Semon, E., and Le Quéré, J.L. (1989) Occurrence of Geometrical Isomers of Eicosapentaenoic and Docosahexaenoic Acids in Liver Lipids of Rats Fed Heated Linseed Oil, *Lipids 24*, 799–804.
14. Chardigny, J.M., Sébédio, J.L., Grandgirard, A., Martine, L., Berdeaux, O., and Vatèle, J. M. (1996) Identification of Novel *Trans* Isomers of 20:5n-3 in Liver Lipids of Rats Fed Heated Oil, *Lipids 31*, 165–168.

15. Chardigny, J.M., Sébédio, J.L., Juaneda, P., Vatèle, J.M., and Grandgirard, A. (1993) Occurrence of n-3 *Trans* Polyunsaturated Fatty Acids in Human Platelets, *Nutr. Res. 13*, 1105-1111.
16. Loï, C., Chardigny, J.M., Berdeaux, O., Vatèle, J.M., Poullain, D., Noël, J.P., and Sébédio, J.L. (1998) Effects of Three *Trans* Isomers of Eicosapentaenoic Acid on Rat Platelet Aggregation and Arachidonic Acid Metabolism, *Thromb. Haemostasis. 80*, 656–661.
17. De Angelis, E., Moss, S.H., and Pouton, C.W. (1996) Endothelial Cell Biology and Culture Methods for Drug Transport Studies, *Adv. Drug Delivery Rev. 18*, 193–218.
18. Spector, A., Kaduce, T.L., Figard, P.H., Norton, K.C., Hoak, J.C., and Czervionke, R.L. (1983) Eicosapentaenoic Acid and Prostacyclin Production by Cultured Human Endothelial Cell, *J. Lipid Res. 24*, 1595–1604.
19. Garcia, M.C., Sprecher, H., and Rosenthal, M.D. (1990) Chain Elongation of Polyunsaturated Fatty Acids by Vascular Endothelial Cells: Studies with Arachidonate Analogues, *Lipids 25*, 211–215.
20. Rosenthal, M.D., Garcia, M.C., Jones, M.R., and Sprecher, H. (1991) Retroconversion and Δ^4 Desaturation of Docosatetraenoate [22:4(n-6)] and Docosapentaenoate [22:5(n-3)] by Human Cells in Culture, *Biochim. Biophys. Acta 1083*, 29–36.
21. Okuda, Y., Kawashima, K., Sawada, T., Tsurumaru, K., Asano, M., Suzuki, S., Soma, M., Nakajima, T., and Yamashita, K. (1997) Eicosapentaenoic Acid Enhances Nitric Oxide Production by Cultured Human Endothelial Cells, *Biochem. Biophys. Res. Commun. 232*, 487–491.
22. Shimokawa, H., and Vanhoutte, P.M. (1989) Dietary ω3 Fatty Acids and Endothelium-Dependent Relaxation in Porcine Coronary Artery, *Am. J. Physiol. 256*, H968–H973.
23. Hornstra, G., Christ-Hazelhof, E., Haddeman, E., Ten Hoor, F., and Nugteren, D.H. (1981) Fish Oil Feeding Lowers Thromboxane and Prostacyclin Production by Rat Platelets and Aorta and Does Not Result in the Formation of Prostaglandin I_3, *Prostaglandins 21*, 727–738.
24. Morita, I., Saito, Y., Chang, W.C., and Murota, S. (1983) Effects of Purified Eicosapentaenoic Acid on Arachidonic Acid Metabolism in Cultured Murine Aortic Smooth Muscle Cells, Vessel Walls and Platelets, *Lipids 18*, 42–49.
25. Hadjiagapiou, C., Kaduce, T.L., and Spector, A. (1986) Eicosapentaenoic Acid Utilization by Bovine Aortic Endothelial Cells: Effects on Prostacyclin Production, *Biochim. Biophys. Acta 875*, 369–381.
26. Raederstorff, D., and Maser, U. (1992) Influence of an Increased Intake of Linoleic Acid on the Incorporation of Dietary (n-3) Fatty Acids in Phopholipids and on Prostanoid Synthesis in Rat Tissues, *Biochim. Biophys. Acta 1165*, 194–200.
27. Kanayasu, T., Morita, I., Nakao-Hayashi, J., Asuwa, N., Fujisawa, C., Ishii, T., Ito, H., and Murota, S. (1991) Eicosapentaenoic Acid Inhibits Tube Formation of Vascular Endothelial Cells *in Vitro*, *Lipids 26*, 271–276.
28. Vatèle, J.M., Dong Doan, H., Chardigny, J.M., and Sébédio, J.L. (1994) *Trans* Polyunsaturated Fatty Acids. Part 1—Synthesis of Methyl (5*Z*,8*Z*,11*Z*,14*Z*,17*E*)-Eicosapentaenoate and Methyl (4*Z*,7*Z*,10*Z*,13*Z*,16*Z*,19*E*)-Docosahexaenoate, *Chem. Phys. Lipids 74*, 185–193.
29. Vatèle, J.M., Dong Doan, H., Fenet, B., Chardigny, J.M., and Sébédio, J.L. (1995) Synthesis of Methyl (5*Z*,8*Z*,11*E*,14*Z*,17*Z*)- and (5*Z*,8*Z*,11*E*,14*Z*,17*E*)-Eicosapentaenoate (EPA Δ11*t* and EPA Δ11*t*,17*t*), *Chem. Phys. Lipids 78*, 65–70.
30. Lamothe, F., Peyronel, D., Sergent, M., Iatrides, M.C., Artaud, J., and Phan-Tan-Luu, R. (1988) Saponification of Oils Rich in Polyunsaturated Fatty Acids: Optimization of Conditions by Response Surface Methodology, *J. Am. Oil Chem. Soc. 65*, 652–658.
31. Eynard, T., Poullain, D., Vatèle, J.M., Noël, J.P., Chardigny, J.M., and Sébédio, J.L. (1998) Synthesis of Methyl (5*Z*,8*Z*,11*Z*,14*Z*,17*Z*)- and (5*Z*,8*Z*,11*Z*,14*Z*,17*E*)-[18-^{14}C]Eicosapentaenoate, *J. Labelled Comp. Radiopharm. 41*, 411–421.
32. Folch, J., Lees, M., and Sloane Stanley, G.H. (1957) A Simple Method for the Isolation and Purification of Total Lipids from Animal Tissues, *J. Biol. Chem. 226*, 497–509.
33. Morrison, W.R., and Smith, L.M. (1964) Preparation of Fatty Acid Methyl Esters and Dimethylacetals from Lipids with Boron Fluoride–Methanol, *J. Lipid Res. 5*, 600–608.
34. Kaluzny, M.A., Duncan, L.A., Merritt, M.V., and Epps, D.E. (1985) Rapid Separation of Lipid Classes in High Yield and Purity Using Bonded Phase Columns, *J. Lipid Res. 26*, 135–140.
35. Dobson, G., and Christie, W.W. (1996) Structural Analysis of Fatty Acids by Mass Spectrometry of Picolinyl Esters and Dimethyloxazoline Derivatives, *Trends Anal. Chem. 15*, 130–137.
36. Juanéda, P., Rocquelin, G., and Astorg, P.O. (1990) Separation and Quantification of Heart and Liver Phospholipid Classes by High-Performance Liquid Chromatography Using a New Light-Scattering Detector, *Lipids 25*, 756–759.
37. Powell, W.S. (1980) Rapid Extraction of Oxygenated Metabolites of Arachidonic Acid from Biological Samples Using Octadecylsilyl Silica, *Prostaglandins 20*, 947–957.
38. Wohlfeil, E.R., and Campbell, W.B. (1997) 25-Hydroxycholesterol Enhances Eicosanoid Production in Cultured Bovine Coronary Artery Endothelial Cells by Increasing Prostaglandin G/H Synthase-2, *Biochim. Biophys. Acta 1345*, 109–120.
39. Alhenc-Gelas, F., Tsai, S.J., Callahan, K.S., Campbell, W.B., and Johnson, A. (1982) Stimulation of Prostaglandin Formation by Vasoactive Mediators in Cultured Human Endothelial Cells, *Prostaglandins 24*, 723–742.
40. Salari, H., Braquet, P., and Borgeat, P. (1984) Comparative Effects of Indomethacin, Acetylenic Acids, 15-HETE, Nordihydroguaiaretic Acid and BW755C on the Metabolism of Arachidonic Acid in Human Leukocytes and Platelets, *Prostaglandins Leukotrienes Med. 13*, 53–60.
41. Grandgirard, A., Piconneaux, A., Sebedio, J.L., and Julliard, F. (1998) *Trans* Isomers of Long-Chain n-3 Polyunsaturated Fatty Acids in Tissue Lipid Classes of Rats Fed with Heated Linseed Oil, *Reprod. Nutr. Dev. 38*, 17–29.
42. Rosenthal, M.D., and Hill, J.R. (1984) Human Vascular Endothelial Cells Synthesize and Release 24- and 26-Carbon Polyunsaturated Fatty Acids, *Biochim. Biophys. Acta 795*, 171–178.
43. Piconneaux, A. (1987) Etude de la Désaturation et de l'Elongation *in Vivo* d'Isomères Géométriques de l'Acide Linolénique, Ph.D. Thesis, University of Burgundy.
44. Achard, F., Benistant, C., and Lagarde, M. (1995) Interconversions and Distinct Metabolic Fate of Eicosapentaenoic, Docosapentaenoic and Docosahexaenoic Acids in Bovine Aortic Endothelial Cells, *Biochim. Biophys. Acta 1255*, 260–266.
45. Takayama, H., Gimbrone, M.A., and Schafer, A. (1987) Preferential Incorporation of Eicosanoid Precursor Fatty Acids into Human Umbilical Vein Endothelial Cell Phospholipids, *Biochim. Biophys. Acta 922*, 314–322.
46. Achard, F., Gilbert, M., Benistant, C., Benslama, S., Dewitt, D.L., Smith, W.L., and Lagarde, M. (1997) Eicosapentaenoic and Docosahexaenoic Acids Reduce PGH Synthase 1 Expression in Bovine Aortic Endothelial Cells, *Biochem. Biophys. Res. Commun. 241*, 513–518.
47. Bénistant, C., Achard, F., Ben Slama, S., and Lagarde, M. (1996) Docosapentaenoic Acid (22:5n-3): Metabolism and Effect on Prostacyclin Production in Endothelial Cells, *Prostaglandins Leukotrienes Essent. Fatty Acids 55*, 287–292.

[Received February 1, 2000, and in revised form May 26, 2000; revision accepted June 28, 2000]

Kinetic Properties of *Penicillium cyclopium* Lipases Studied with Vinyl Esters

Henri Chahinian[a], Lylia Nini[a], Elisabeth Boitard[b], Jean-Paul Dubès[b], Louis Sarda[c,*], and Louis-Claude Comeau[a]

[a]Laboratoire de Chimie Biologique Appliquée, Faculté des Sciences et Techniques, St-Jérôme, 13397 Marseille Cedex 20, France, [b]Université de Provençe, CTM-CNRS (UPR 7461) Faculté St-Charles, 13331 Marseille Cedex 3, France, and [c]Laboratoire de Biochimie, Faculté St-Charles, Université de Provence, 13331 Marseille Cedex 3, France

ABSTRACT: *Penicillium cyclopium* produces two lipases with different substrate specificities. Lipase I is predominantly active on triacylglycerols whereas lipase II hydrolyzes mono- and diacylglycerols but not triacylglycerols. In this study, we compared the kinetic properties of *P. cyclopium* lipases and human pancreatic lipase, a classical triacylglycerol lipase, by using vinyl esters as substrates. Results indicate that *P. cyclopium* lipases I and II and human pancreatic lipase hydrolyze solutions of vinyl propionate or vinyl butyrate at high relative rates compared with emulsions of the same esters, although, in all cases, maximal activity is reached in the presence of emulsified particles, at substrate concentrations above the solubility limit. It appears that partially water-soluble short-chain vinyl esters are suitable substrates for comparing the activity of lipolytic enzymes of different origin and specificity toward esters in solution and in emulsion.

Paper no. L8467 in *Lipids 35,* 919–925 (August 2000).

Penicillium cyclopium produces two extracellular lipases that have been isolated and characterized at the molecular and biochemical levels (1–4). Lipase I is produced mainly in stationary culture. It hydrolyzes short-, medium-, and long-chain triacylglycerols and has low activity on mono- and diacylglycerols. Its N-terminal amino acid sequence is similar to that of lipases of *P. expansum* (5) and *P. solitum* (6). Lipase II is predominantly produced in shaken culture (7). It hydrolyzes mono- and diacylglycerols but has almost no activity toward triacylglycerols. It is a glycosylated enzyme of the same size and substrate specificity as the partial acylglycerol lipase from *P. camembertii*. The N-terminal sequences of *P. cyclopium* lipase II and *P. camembertii* lipase are similar and differ from that of *P. cyclopium* lipase I (8). Because of their difference in substrate specificity, the kinetic properties of lipases I and II from *P. cyclopium* cannot be directly compared using the same acylglycerol substrate.

As shown earlier by Brockerhoff (9,10), vinyl esters, which contain a highly electrophilic alcohol moiety, are good substrates of porcine pancreatic triacylglycerol lipase. Recently, Yamaguchi and Mase (11) used vinyl laurate to measure the activity of *P. camembertii* lipase. Vinyl esters also have been widely used in recent studies of lipase-catalyzed transfer reactions (12–14). Unlike tributyrin and dioctanoin, which are used to specifically determine the activity of *P. cyclopium* lipases I and II, short-chain vinyl esters like vinyl propionate and vinyl butyrate are partially soluble in water and therefore can be used to study the interfacial activity of lipases by measuring the rates of enzymatic hydrolysis of the ester substrate in solution and in emulsion. In this communication, we report the results of comparative kinetic studies of *P. cyclopium* and human pancreatic lipases carried out with vinyl esters.

EXPERIMENTAL PROCEDURES

Solubility of vinyl esters. The solubilities of vinyl propionate and vinyl butyrate in aqueous solution were estimated by the turbidimetric method. Increasing amounts of vinyl propionate (0–600 μL) or vinyl butyrate (0–400 μL) were added to 30 mL of 2.5 mM Tris-HCl buffer (pH 7.0) in the absence or presence of 100 mM NaCl. (NaCl is generally added at the concentration of 100 or 150 mM to aqueous suspensions of tributyrin or tripropionin routinely used to assay triacylglycerol activity.) The vinyl ester was dispersed by mechanical stirring for 2 min under the same conditions as used in the potentiometric assay of lipase activity with the pH-stat (see below). The optically clear solution or turbid emulsion of vinyl ester was transferred into a 3-mL spectrophotometer cell (Uvicord II), and absorbance was read at 600 nm (Fig. 1). The absorbance increased as soon as insoluble particles were formed in oversaturated solutions of ester. The concentrations of saturated solutions of vinyl propionate and vinyl butyrate are 86 mM (8.6 g L^{-1}) and 22 mM (2.5 g L^{-1}), respectively. These concentrations correspond to the addition of 280 μL and 85 μL of ester, respectively, into 30 mL of Tris buffer used in the potentiometric assay. The solubility limits of the vinyl esters are the same in the absence and presence of 100 mM NaCl. The solubility limit of vinyl laurate, determined by the same method, is as low as 0.25 mM ($6 \cdot 10^{-2}$ g L^{-1}), which corresponds to the addition of 2 μL of ester into 30 mL

*To whom correspondence should be addressed at Laboratoire de Biochimie, Case Postale 65, Faculté des Sciences St-Charles, Université de Provençe, 3 Place Victor Hugo, 13331 Marseille Cedex 3, France.

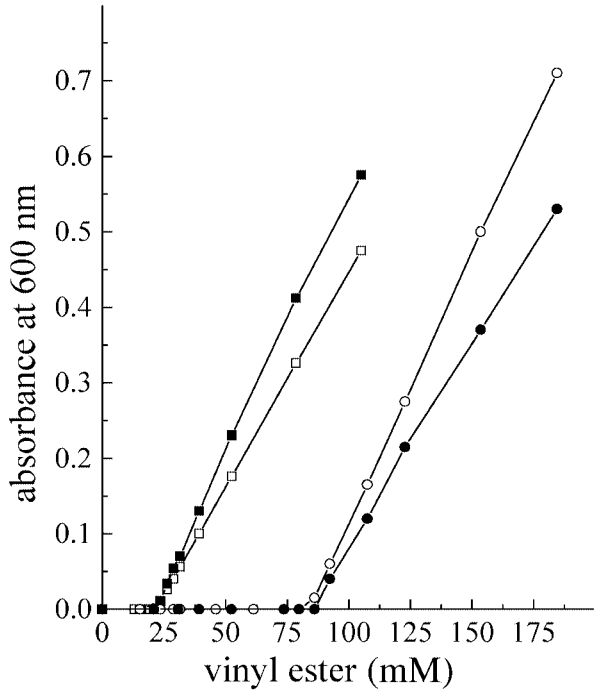

FIG. 1. Determination of the solubility limits of vinyl propionate and vinyl butyrate by the turbidimetric method. Vinyl propionate (○,●) and vinyl butyrate (□,■) were dispersed by mechanical stirring for 2 min at 25°C in 2.5 mM Tris-HCl buffer (pH 7.0) in the absence (○,□) and presence (●,■) of 100 mM NaCl. The absorbance of solutions and emulsions of the vinyl esters was read at 600 nm.

of Tris buffer. Finally, the solubility limit of tripropionin is 10 mM (2.4 g L^{-1} or 70 μL in 30 mL of Tris buffer) in the absence and presence of NaCl.

Enzymatic hydrolysis of vinyl esters. Hydrolysis of vinyl propionate and vinyl butyrate by *P. cyclopium* lipases and human pancreatic lipase was followed potentiometrically at 25°C for 5 min with a pH-stat (TTT 80 Radiometer, Copenhagen, Denmark). Released acid was titrated at pH 7.0 with 0.02 M NaOH. Kinetic studies were performed with increasing amounts of ester ranging from 0 to 500 μL (0–153 mM) of vinyl propionate and from 0 to 300 μL (0–78 mM) of vinyl butyrate in 30 ml of Tris buffer, pH 7.0, in the absence and presence of 100 mM NaCl. The concentration of the vinyl ester in the lipase assay system was expressed as millimoles per liter at concentrations below and above the solubility limit. Enzymatic hydrolysis of vinyl laurate or tripropionin was measured under the same conditions as above with amounts of ester ranging from 0 to 300 μL (0–37.5 mM) and from 0 to 180 μL (0–25 mM), respectively, in 30 mL of 2.5 mM Tris buffer, pH 7.0, in the presence of 100 mM NaCl. Correction was made for partial dissociation of lauric acid at pH 7.0, assuming an apparent pK_a of 7.4. Lipolytic activity on olive oil emulsified with gum arabic was assayed as described previously (7). In all cases, enzyme activity was expressed as lipase units. One unit corresponds to the release of one microequivalent of acid per minute. The amount of enzyme used to determine lipolytic activity potentiometrically was equivalent to 10 lipase units measured at a substrate concentration ensuring maximum enzyme activity (V_{max}). All assays were performed in duplicate with less than 5% deviation. Experiments were performed to check that *P. cyclopium* and human pancreatic lipases are resistant to acetaldehyde, the unavoidable by-product released in lipolysis reactions with vinyl esters. The rates of lipase-catalyzed hydrolysis of vinyl propionate was measured as described above, in the absence and presence of 100 mM NaCl, with an amount of acetaldehyde ranging from 0.5 to 30 mM added to the assay system prior to enzyme. Experiments were performed with saturated ester solutions and with emulsions at ester concentrations ensuring maximal lipolytic activity. In all cases, activity was not affected by acetaldehyde.

Enzymes. Penicillium cyclopium lipases I and II were prepared at the laboratory as reported previously (4,7). The specific activities of lipases I and II, measured at pH 7.0 and 25°C on emulsified tributyrin and dioctanoin, were 8,000 and 1,100 units mg^{-1}, respectively. Human pancreatic lipase, with a specific activity of 6,500 units mg^{-1} measured on emulsified tributyrin at pH 7.0 and 25°C, and human pancreatic colipase were gifts from Dr. F. Carrière (Marseille, France). Protein was estimated with the colorimetric method of Lowry *et al.* using bovine serum albumin as standard protein (15).

Chemicals. Vinyl propionate, vinyl butyrate, vinyl laurate, tripropionin, tributyrin, and acetaldehyde were from Sigma-Aldrich-Fluka (St-Quentin-Fallavier, France). Dioctanoin was prepared at the laboratory by chromatographic separation of a partial enzymatic hydrolysate of trioctanoin, as described previously (7). Olive oil was from local origin.

RESULTS AND DISCUSSION

Hydrolysis of vinyl laurate by P. cyclopium *lipases and human pancreatic lipase.* The emulsion of vinyl laurate was prepared in 30 mL of 2.5 mM Tris-HCl buffer pH 7.0 containing 100 mM NaCl with amounts of ester ranging from 0 to 300 μL (0–37.5 mM), and the rates of hydrolysis by lipases I and II were measured at pH 7.0 with the pH-stat. The specific activities of *P. cyclopium* lipases I and II were 2,100 and 3,200 units mg^{-1}, respectively. The specific activity of human pancreatic lipase, measured at pH 8.0, was 450 units mg^{-1} (Table 1). In all cases, half-maximal activity was obtained in the presence of 30 μL of vinyl laurate in the reaction system, which corresponds to 3.75 mM.

Hydrolysis of vinyl propionate by P. cyclopium *lipases.* The effect of increasing concentration of vinyl propionate on enzyme activity is presented in Figure 2. It can be observed from the curves of Figures 2A and 2B that the activity of lipases I and II is maximum (V_{max}) at substrate concentrations above the solubility limit, both in the absence and presence of 100 mM NaCl. The specific activities of lipases I and II are 950 and 1,250 units mg^{-1}, respectively (Table 1). The relative rates of hydrolysis of a saturated solution of vinyl propionate by lipases I and II amount to 0.45 V_{max} and 0.30 V_{max}, respectively, in the absence of NaCl, and to 0.90 V_{max} and 0.85 V_{max},

TABLE 1
Specific Activity of *Penicillium cyclopium* Lipases I and II and Human Pancreatic Lipase[a]

	P. cyclopium lipase I	*P. cyclopium* lipase II	Human pancreatic lipase
Vinyl propionate	950	1,200	960
Vinyl butyrate	3,000	2,000	750
Vinyl laurate	2,100	3,200	450
Tripropionin	1,250	0	4,000
Tributyrin	8,000	0	9,500
Trioctanoin	4,200	50	6,500
Olive oil	3,700	0	4,000
Dioctanoin	500	1,100	ND

[a]Activity is determined at 25°C against emulsions of vinyl propionate, vinyl butyrate, vinyl laurate, tripropionin, tributyrin, trioctanoin, olive oil, and dioctanoin at the optimal ester concentration and is expressed as lipase units. Specific activity is expressed as unit per mg of protein. Activities of *P. cyclopium* lipases I and II were measured at pH 7.0 and those of human pancreatic lipase at pH 8.0. ND, not determined.

respectively, in the presence of NaCl. Finally, from the curves of Figures 2A and B one sees that activity increases steadily with substrate concentration and that no abrupt increase occurs at at the point of saturation of the aqueous phase (86 mM). It appears that in this substrate system *P.cyclopium* lipases do not display interfacial activation.

Hydrolysis of vinyl butyrate by P. cyclopium *lipases.* The effect of increasing concentration of vinyl butyrate on the rate of hydrolysis of vinyl butyrate by *P. cyclopium* lipases I and II is shown in Figure 3. As previously found with vinyl propionate, the two lipases display maximal activity (V_{max}) on emulsified ester. The specific activities of the two lipases are 3,000 and 2,100 units mg^{-1}, respectively, both in the absence and presence of 100 mM NaCl. Lipases I and II are active on solutions of vinyl butyrate in the presence of sodium chloride. Activities against a saturated solution of vinyl butyrate amount to 0.90 V_{max} and 0.35 V_{max}, respectively. Surprisingly, lipase I hydrolyzes solutions of vinyl butyrate in the absence of sodium chloride whereas, under the same conditions, lipase II is almost inactive on the vinyl ester. The minimum concentration of sodium chloride allowing maximal activity on soluble vinyl butyrate is around 10 mM (data not shown).

Hydrolysis of vinyl propionate and vinyl butyrate by human pancreatic lipase. Kinetic studies were performed with human pancreatic lipase under the same conditions as above except that colipase was systematically added to the reaction system in 5 M excess to lipase. Results are shown in Figure 4. The specific activities of human pancreatic lipase calculated from the maximal activity (V_{max}), measured against emulsified vinyl propionate and vinyl butyrate, are 960 and 750 units mg^{-1}, respectively (Table 1). Human pancreatic lipase hydrolyzes solutions of vinyl propionate (Fig. 4A) and vinyl butyrate (Fig. 4B) in the presence of NaCl but at a lower relative rate than *P. cyclopium* lipases. The relative rates of hydrolysis of saturated solutions of vinyl propionate and vinyl butyrate amount to 0.60 V_{max} and 0.30 V_{max}, respectively. NaCl has little effect on the rate of hydrolysis of the solutions of the vinyl esters. As found with *P. cyclopium*

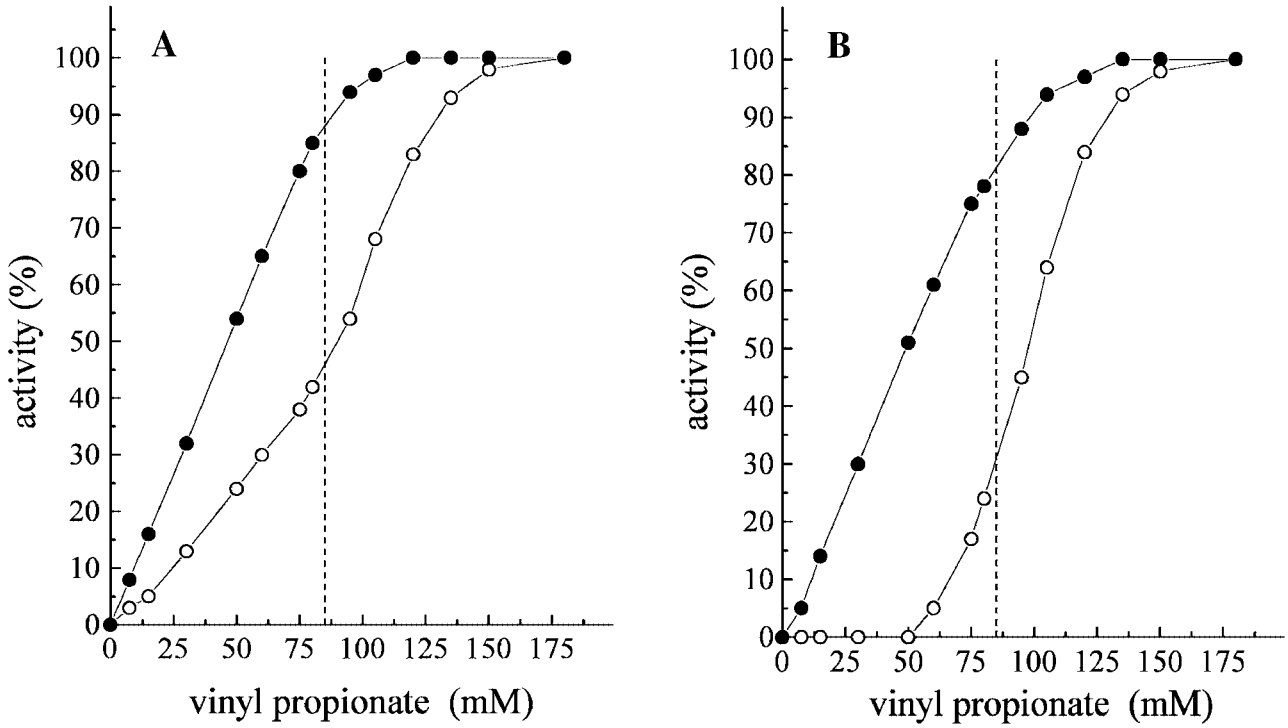

FIG. 2. Effect of substrate concentration on the rate of hydrolysis of vinyl propionate by *Penicillium cyclopium* lipase I (A) and II (B). Activity is expressed as percentage of maximal activity (V_{max}) measured at optimal ester concentration. The dotted line indicates the solubility of vinyl propionate (86 mM). Activity was determined at pH 7.0 and 25°C in 2.5 mM Tris-HCl buffer in the absence (○) and presence (●) of 100 mM NaCl.

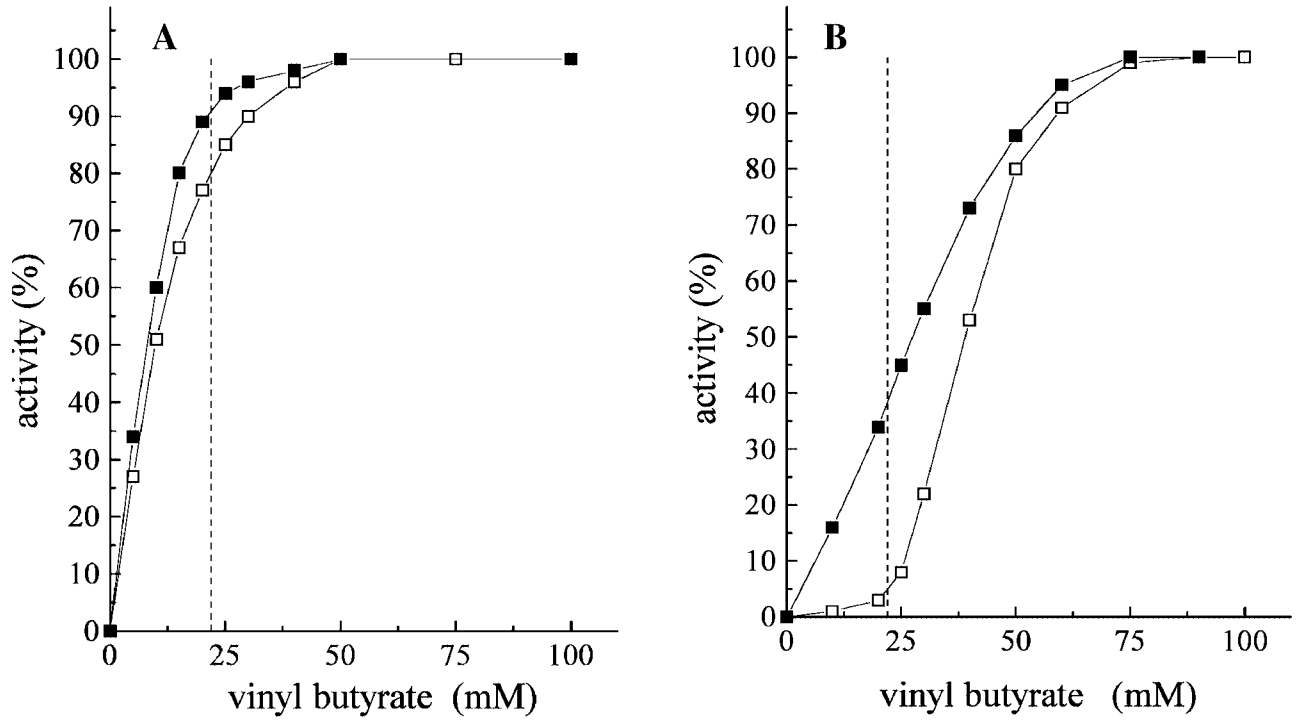

FIG. 3. Effect of substrate concentration on the rate of hydrolysis of vinyl butyrate by *Penicillium cyclopium* lipase I (A) and II (B). Assays were performed as described in Figure 2. The solubility of vinyl butyrate is indicated by the dotted line. Experiment performed in absence (□) and presence (■) of 100 mM NaCl.

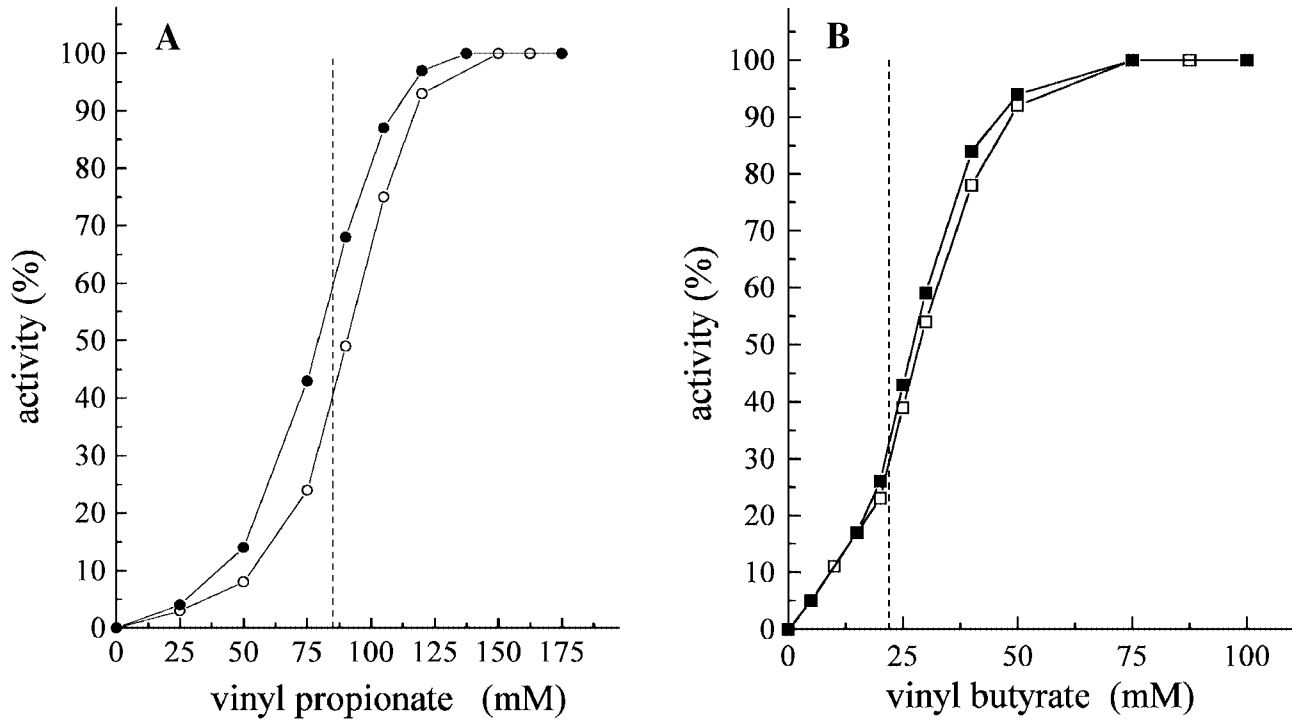

FIG. 4. Effect of substrate concentration on the rate of hydrolysis of (A) vinyl propionate and (B) vinyl butyrate by human pancreatic lipase. Assays were performed as described in Figure 2 except that enzymatic hydrolysis was measured at pH 8.0. Symbols are the same as in Figure 1, and dotted lines are as in Figures 2 and 3.

lipases I and II, the activity of pancreatic lipase increases with substrate concentration irrespective of the physical state of the vinyl ester, and in this assay system, the pancreatic lipase does not display interfacial activation.

Hydrolysis of tripropionin by P. cyclopium *lipase I and by human pancreatic lipase.* Results of comparative kinetic studies of the hydrolysis of tripropionin by triacylglycerol lipases from *P. cyclopium* (lipase I) and from human pancreas are shown in Figure 5. Curves of Figure 5A confirm the well-documented capacity of classical pancreatic triacylglycerol lipases from higher mammals to hydrolyze tripropionin in solution in the presence of NaCl (13,14). The relative rate of hydrolysis of a solution of tripropionin at saturating concentration is around 0.70 V_{max} compared with the maximal activity against an emulsion of the triacylglycerol (specific activity: 4,000 units mg^{-1}). In the absence of sodium chloride, the shape of the curve is unchanged although the curve is shifted toward higher concentrations of substrate. The same observations can be made from the curves representing the effect of substrate concentration on the rate of hydrolysis of tripropionin by *P. cyclopium* lipase I (Fig. 5B). The specific activity of lipase I calculated from the activity measured on emulsified tripropionin is 1,200 units mg^{-1} (Table 1).

It can be concluded from the results presented above that the triacylglycerol lipases from *P. cyclopium* (lipase I) and from human pancreas and the partial acylglycerol lipase from *P. cyclopium* (lipase II) hydrolyze short- and long-chain vinyl esters at high relative rates compared with their respective specific substrates (Table 1). Therefore, vinyl esters are suitable for comparing the hydrolytic activity of lipases of various origins and specificities. All lipases studied here display maximal activity against emulsions of vinyl esters. However, they hydrolyze solutions of slightly water-soluble short-chain vinyl esters, namely, vinyl propionate and vinyl butyrate, at variable relative rates compared with emulsions. Addition of NaCl to the reaction system enhances enzyme enzymatic lipolysis although it does not affect the solubility limit of the esters (Fig. 1).

The patterns of substrate concentration dependency of the rates of hydrolysis (*V/S* curves) of vinyl propionate, vinyl butyrate or tripropionin by *P. cyclopium* lipases or human pancreatic lipase (Figs. 2–5) do not show an abrupt increase in activity at the point of saturation of the solution, which corresponds to the transition from soluble to emulsified substrate. The lipases do not show the classical phenomenon of interfacial activation under the conditions used for assaying activity. In the kinetic studies reported in Figures 2–5, the *V/S* curves deviate from the shape of a rectangular hyperbola derived from the classical Michaelis-Menten model. For example, Figures 6A and B show double reciprocal plots (V^{-1}/S^{-1}) of the *V/S* curves shown in Figures 3A and 4A which are representative of the hydrolysis of vinyl butyrate by *P. cyclopium* lipase I and of vinyl propionate by human pancreatic lipase, respectively. It can be seen that the V^{-1}/S^{-1} curves are composed of two straight lines intersecting at the substrate concentration corresponding to the solubility limit of the substrate. Taken together, these observations are reminiscent of the results of studies of lipase-catalyzed hydrolysis of solu-

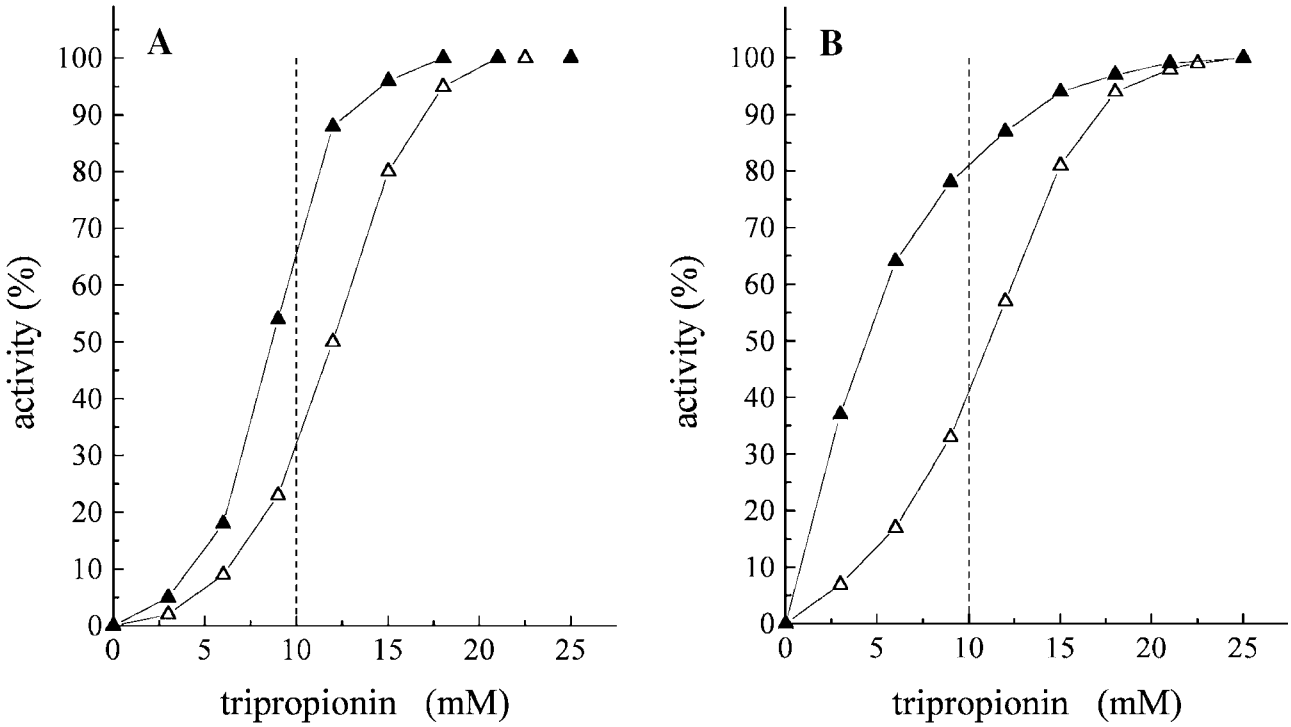

FIG. 5. Effect of substrate concentration on the rate of hydrolysis of tripropionin by (A) human pancreatic lipase and (B) *Penicillium cyclopium* lipase I. Assays were performed at 25°C and pH 7.0 (lipase I) or pH 8.0 (pancreatic lipase) in 2.5 mM Tris-HCl buffer in the absence (△) and presence (▲) of 100 mM NaCl. The solubility of tripropionin is indicated by the dotted line.

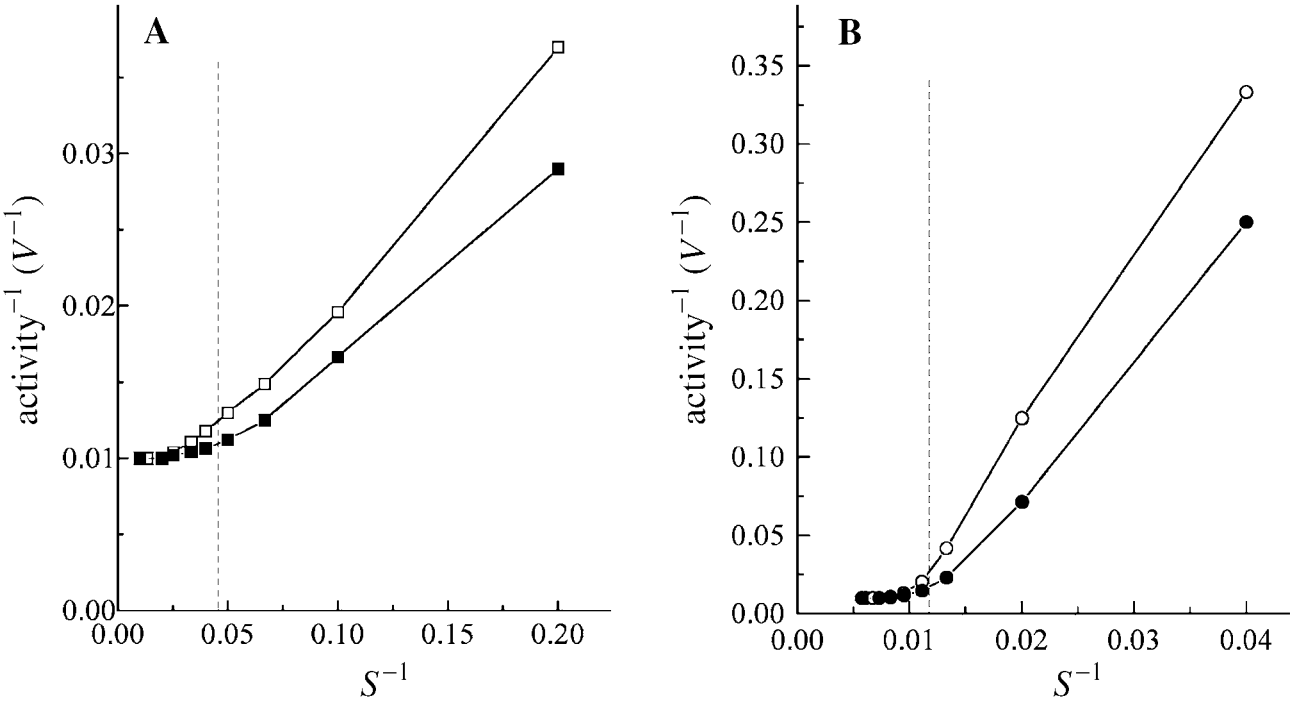

FIG. 6. Double reciprocal plots (V^{-1}/S^{-1}) for the hydrolysis of solution and emulsion (A) of vinyl butyrate by *Penicillium cyclopium* lipase I and (B) of vinyl propionate by human pancreatic lipase. Experimental data are taken from Figures 3A and 4A, respectively. Substrate concentration and relative activity are expressed as in Figures 2–5. Symbols are the same as in Figure 1.

tions of tributyrin or *p*-nitrophenyl butyrate. As reported recently, guinea pig pancreatic lipase, a type 2 pancreatic-related protein active on both triacylglycerols and phospholipids, shows high relative activity on solutions of tributyrin in the presence of NaCl and is not interfacially activated (18). Kinetic studies of *Candida antarctica* lipase B with solutions and emulsions of *p*-nitrophenyl butyrate have shown that the enzyme does not display interfacial activation, whereas lipase from *Thermomyces* (*Humicola*) *lanuginosa* shows unambiguous interfacial activation in the same assay system. The very low solubilities of tributyrin (0.4 mM) and *p*-nitrophenyl butyrate (1 mM) make it difficult to know whether the substrate molecules dispersed in the aqueous phase are in the monomeric or/and aggregated form; this information is needed to interpret the mode of action of the enzymes on soluble esters. It can be hypothesized that the irregularities of the *V/S* curves observed in the kinetic studies of lipase-catalyzed hydrolysis of solutions and emulsions of short-chain vinyl esters might reflect changes of the affinity constants and kinetic parameters due to phase transitions from monomers to micelles in optically clear solutions and from micelles to particles at ester concentrations beyond the solubility limit. The solubility limits of vinyl propionate (86 mM) and vinyl butyrate (22 mM), which are high compared with those of tributyrin and *p*-nitrophenyl butyrate, should allow further experimental determination of the physical state of the ester molecules in solution and provide valuable information on lipase-substrate interaction in view to interpret the lipase-catalyzed hydrolysis of soluble esters.

ACKNOWLEDGMENTS

The authors thank Dr. Frédéric Carrière (CNRS, Marseille, France) and Dr. Akio Sugihara (Municipal Technical Research Institute, Osaka, Japan) for their valuable contributions and Professor David Attwood (Department of Pharmacy, The University of Manchester, United Kingdom) and Professor Henri Tachoire (Department of Physical Chemistry, University of Marseille, France) for helpful discussions during the preparation of the manuscript. Financial support from the European Community is acknowledged.

REFERENCES

1. Iwai, M., Okumura, S., and Tsujisaka, Y. (1975) The Comparison of the Properties of Two Lipases from *Penicillium cyclopium* Westring, *Agr. Biol. Chem. 39*, 1063–1070.
2. Okumura, S., Iwai, M., and Tsujisaka, Y. (1980) Purification and Properties of Partial Glyceride Hydrolase of *Penicillium cyclopium* M1, *J. Biochem. 87*, 205–211.
3. Isobe, K., Akiba, T., and Yamaguchi, S. (1988) Crystallization and Characterization of Lipase from *Penicillium cyclopium, Agr. Biol. Chem. 52*, 41–47.
4. Ibrik, A., Chahinian, H., Rugani, N., Sarda, L., and Comeau, L.C. (1998) Biochemical and Structural Characterization of Triacylglycerol Lipase from *Penicillium cyclopium*, *Lipids 33*, 377–384.
5. Stocklein, W., Sztajer, H., Menge, U., and Schmid, R.D. (1993) Purification and Properties of a Lipase from *Penicillium expansum*, *Biochim. Biophys. Acta 1168*, 181–189.
6. Gulomova, K., Ziomek, E., Schrag, J.D., Davranov, K., and Cygler, M. (1996) Purification and Characterization of a *Penicillium* sp. Lipase Which Discriminates Against Diglycerides, *Lipids 31,* 379–384.
7. Chahinian, H., Vanot, G., Ibrik, A., Rugani, N., Sarda, L., and Comeau, L.C. (2000) Production of Extracellular Lipases by

Penicillium cyclopium Purification and Characterization of a Partial Acylglycerol Lipase, *Biosci. Biotechnol. Biochem. 64,* 215–222.
8. Isobe, K., and Nokihara, K., (1993) Primary Structure Determination of Mono- and Diacylglycerol Lipase from *Penicillium camembertii*, *FEBS Lett. 320*, 101–106.
9. Brockerhoff, H. (1968) Substrate Specificity of Pancreatic Lipase, *Biochim. Biophys. Acta 159*, 296–303.
10. Brockerhoff, H. (1970) Substrate Specificity of Pancreatic Lipase. Influence of the Structure of Fatty Acids on the Reactivity of Esters, *Biochim. Biophys. Acta 212,* 92–101.
11. Yamaguchi, S., and Mase, T. (1991) Purification and Characterization of Mono- and Diacylglycerol Lipase Isolated from *Penicillium camembertii* U-150, *Appl. Microbiol. Biotechnol. 34*, 720–725.
12. Kaga, H., Siegmund, B., Neufellner, E., Faber, K., and Paltauf, F. (1994) Stabilization of *Candida* Lipase Against Acetaldehyde by Adsorption on Celite, *Biotechnol. Lett. 8*, 369–374.
13. Weber, H.K., Stecher, H., and Faber, K. (1995) Sensitivity of Microbial Lipases to Acetaldehyde Formed by Acyl-Transfer Reactions from Vinyl Esters, *Biotechnol. Lett. 17*, 803–806.
14. Kita, Y., Takebe, Y., Murata, K., Naka, T., and Akai, S. (1996) Vinyl Acetate as a Novel Highly Reactive and Reliable Acyl Donor for Enzymatic Resolution of Alcohols, *Tetrahedron Lett. 37*, 1369–1372.
15. Lowry, O.H., Rosebrough, N.J., Farr, A.L., and Randall, R.J. (1951) Protein Measurement with the Folin-Phenol Reagent, *J. Biol. Chem. 193*, 265–275.
16. Entressangles, B., and Desnuelle, P. (1970) Action of Pancreatic Lipase on Aggregated Glyceride Molecules in an Isotropic System, *Biochim. Biophys. Acta 159*, 285–295.
17. Verger, R. (1997) Interfacial Activation of Lipases: Facts and Artifacts, *TIBTECH. 15*, 32–38.
18. Hjorth, A., Carrière, F., Cudrey, C., Wöldike, H., Boel, E., Lawson, D.M., Ferrato, F., Cambillau, C., Dodson, G.G., Thim, L., and Verger, R. (1993) A Structural Domain (the lid) Found in Pancreatic Lipase Is Absent in the Guinea Pig (Phospho)lipase, *Biochemistry 32*, 4702–4707.
19. Martinelle, M., Holmquist, M., and Hult, K. (1995) On the Interfacial Activation of *Candida antarctica* Lipase A and B as Compared with *Humicola lanuginosa* Lipase, *Biochim. Biophys. Acta 1258*, 272–276.

[Received February 14, 2000, and in revised form May 30, 2000; revision accepted June 23, 2000]

COMMUNICATION

Fetal Erythrocyte Phospholipid Polyunsaturated Fatty Acids Are Altered in Pregnancy Complicated with Gestational Diabetes Mellitus

Vasuki Wijendran[a], Robert B. Bendel[b], Sarah C. Couch[a], Elliot H. Philipson[c], Sunita Cheruku[a], and Carol J. Lammi-Keefe[a,*]

Departments of [a]Nutritional Sciences and [b]Animal Sciences, University of Connecticut, Storrs, Connecticut 06269, and [c]Department of Obstetrics and Gynecology, Hartford Hospital, Hartford, Connecticut, 06102

ABSTRACT: Insulin resistance and altered maternal metabolism in gestational diabetes mellitus (GDM) may impair fetal arachidonic acid (AA) and docosahexaenoic acid (DHA) status. The objectives were to test the hypothesis that fetal polyunsaturated fatty acids would be altered with GDM and identify factors related to fetal phospholipid (PL) AA and DHA. Maternal and cord vein erythrocyte PL fatty acids were determined in GDM (n = 13) and healthy pregnant women (controls, n = 12). Cord vein erythrocyte PL AA and DHA concentrations were significantly lower in GDM vs. controls. Maternal blood hemoglobin A_1C was inversely correlated to fetal erythrocyte PL DHA and AA in controls and GDM (n = 25). Pregravid body mass index was negatively associated with fetal PL DHA. The data support the hypothesis that there is impairment in fetal accretion of DHA and AA in GDM.

Paper no. L8366 in *Lipids 35,* 927–931 (August 2000).

Arachidonic acid (20:4n-6, AA) and docosahexaenoic acid (22:6n-3, DHA) play important roles in fetal growth and development (1,2). The ability of the fetus and neonate to synthesize long-chain polyunsaturated fatty acids (LC-PUFA) from precursor essential fatty acids (EFA) is relatively low (3,4). Thus, placental transfer of maternal AA and DHA is likely the major source for fetal accretion of these LC-PUFA *in utero* (4,5). Therefore, alterations in maternal polyunsaturated fatty acid (PUFA) metabolism and placental transfer during gestation would significantly impact fetal accretion of these essential PUFA.

EFA metabolism is altered in pathologies characterized by insulin resistance, such as insulin-dependent diabetes mellitus (6) and obesity (7). Further, impairment in placental transfer of AA *in vitro* in perfused placentas of women with insulin-dependent diabetes mellitus has been reported (8). Gestational diabetes mellitus (GDM) is a pathological condition in which glucose intolerance is recognized for the first time during pregnancy (9). Insulin resistance and alterations in maternal metabolism during the third trimester in pregnancy complicated with GDM (10,11) may alter placental transfer and fetal LC-PUFA accretion. To our knowledge, fetal PUFA status in pregnancy complicated with diet-treated GDM has not been studied. Therefore, the current study was undertaken with the following objectives: (i) to test the hypothesis that fetal phospholipid (PL) PUFA will be altered in pregnancy complicated with GDM and (ii) to determine maternal factors associated with fetal PL AA and DHA.

METHODS

Subjects and study design. Thirteen women diagnosed with GDM and 12 healthy pregnant women (controls) participated in this study. Criteria for subject recruitment and diagnosis of GDM have been previously reported (12,13). Women with GDM in this study were treated with diet which consisted of individualized diet plans following the recommendations for normal pregnancy (14).

Maternal erythrocyte PL fatty acids, fasting plasma insulin concentration, and blood hemoglobin A_1C (HbA_1C) were determined at term in women with GDM and controls. Cord vein erythrocyte PL fatty acids were determined at delivery in all subjects.

Data collection. Fasting maternal blood samples were collected at 36–39 wk gestation. Maternal blood (~10 mL) was sampled from the antecubital vein and collected in EDTA-containing tubes. Cord vein blood samples were collected into heparinized syringes using a double-clamp procedure. Maternal and cord vein erythrocytes were separated from plasma by centrifugation (1500 × g at 4°C for 10 min), portioned, and immediately stored at –80°C until analysis.

*To whom correspondence should be addressed at Department of Nutritional Sciences, U-17, University of Connecticut, Storrs, CT 06269-4017.
E-mail: clammi@canr.uconn.edu.

Abbreviations: AA, arachidonic acid; ANOVA, analysis of variance; BMI, body mass index; DHA, docosahexaenoic acid; EFA, essential fatty acid; GDM, gestational diabetes mellitus; HbA_1C, hemoglobin A_1C; LA, linoleic acid; LC-PUFA, long-chain polyunsaturated fatty acid; LNA, linolenic acid; PL, phospholipid; P/S, polyunsaturated to saturated fatty acid ratio; PUFA, polyunsaturated fatty acid; SFA, saturated fatty acid.

Maternal dietary PUFA intake during the third trimester was assessed using three 24-h recalls and analyzed using the University of Minnesota Nutrition Data System (NDS 2.91; Minneapolis, MN).

Sample analysis. Erythrocyte lipid was extracted by the Dodge and Phillips method (15). Methodologies for the separation of lipid classes, preparation of fatty acid methyl esters, and identification and quantification of individual fatty acids were previously published (12).

Statistical analysis. All statistical analyses were performed using the Statistical Analysis System software (16). The normal distribution assumption was checked for all the variables. Variables which were not normally distributed were log-transformed. One-way analysis of variance (ANOVA) was used to determine differences between the group means for the maternal descriptive data, age, parity, pregravid body mass index (BMI), length of gestation, fasting plasma insulin concentration (μU/mL), HbA_1C, neonatal data, and maternal dietary PUFA intake. Group differences in cord vein erythrocyte PL fatty acids were assessed using one-way ANOVA and analysis of covariance with maternal blood HbA_1C as the covariate. Paired *t*-tests were performed to compare cord vein with maternal vein PL linoleic acid (LA), linolenic acid (LNA), AA, and DHA (wt%). Pearson correlation and linear regression analyses were performed to study the associations of maternal plasma PL PUFA, HbA_1C, insulin concentration, pregravid body mass index (BMI), parity, and length of gestation to cord vein erythrocyte AA and DHA.

RESULTS

Maternal and neonatal characteristics of the study population are shown in Table 1. Women with GDM gained less weight during gestation compared with controls. GDM women had higher fasting plasma insulin concentration and blood HbA_1C than the controls at 36–39 wk gestation. Neonatal birth weight, birth length, ratio of birth weight to birth length, and head circumference adjusted for length of gestation and sex of the infant did not differ between the two groups.

Maternal mean estimated dietary intake of PUFA during the third trimester is shown in Table 2. Macronutrient and individual fatty acid intake of the controls and GDM have been reported (12). Women with GDM had significantly higher dietary intake of AA, eicosapentaenoic acid (20:5n-3, EPA), and DHA compared with controls.

Maternal and cord vein erythrocyte fatty acids are presented in Table 3. Cord vein erythrocyte PL (wt% and μg/mL) n-6 and n-3 LC-PUFA were different for GDM vs. controls. AA and DHA (wt% and μg/mL) were lower (by approximately 28%, $P = 0.02$ and 37%, $P = 0.005$ in wt%, respectively) in the cord vein erythrocyte of women with GDM than the controls. Further, cord vein erythrocyte PL (wt% and μg/mL), ∑n-6 PUFA, ∑n-3 PUFA, and DHA sufficiency index (ratio of 22:6n-3 to 22:5n-6 wt%) were lower in women with GDM compared with controls. In contrast, saturated fatty acids (SFA), 16:0, 18:0, and ∑SFA (wt%) were higher by approximately 12% ($P = 0.05$), 33% ($P = 0.02$), and 21%

TABLE 1
Maternal and Neonatal Characteristics of the Study Population[a]

	Control ($n = 12$)	GDM ($n = 13$)
Age (yr)	30.25 ± 1.43	32.70 ± 1.28
Race[b]		
Black	1	2
Hispanic	1	2
White	10	9
Parity[b]		
0	6	7
1	2	4
2	3	1
3	1	1
Length of gestation (wk)	40.30 ± 0.32	39.53 ± 0.31
Pregravid BMI (kg/m^2)	23.97 ± 1.28	24.85 ± 1.23
Weight gain (kg)	18.01 ± 1.73[a]	12.89 ± 1.55[b]
Insulin[c] (μU/mL)	10.07 ± 2.42[a]	14.26 ± 1.98[b]
HbA_1C[d] (%)	4.86 ± 0.16[a]	5.19 ± 0.14[b]
Neonatal birth weight (g)	3359.66 ± 98.11	3611.83 ± 101.66
Neonatal birth length (cm)	51.80 ± 0.66	52.32 ± 0.68
Neonatal birth weight (g)/ birth length (cm) ratio	64.85 ± 1.66	69.02 ± 1.72
Neonatal head circumference (cm)	33.98 ± 0.53	34.49 ± 0.50

[a]Least square mean ± SEM
[b]Subject distribution.
[c]Fasting plasma insulin concentration at term (36–39 wk gestation).
[d]Glycosylated blood hemoglobin at term (36–39 wk gestation). Different superscript roman letters indicate significant differences between groups, $P \leq 0.05$. GDM, gestational diabetes mellitus; BMI, body mass index; HbA_1C, hemoglobin A_1C.

TABLE 2
Mean Maternal Estimated Dietary Fatty Acid Intake During the Third Trimester[a]

Nutrient	Controls (n = 12)	GDM (n = 13)
18:2n-6 (g/d)	11.0 ± 1.3	10.5 ± 1.2
20:4n-6 (mg/d)	95.4 ± 16.4[a]	139.7 ± 14.7[b]
18:3n-3 (g/d)	1.1 ± 0.1	1.1 ± 0.1
20:5n-3 (mg/d)	20.5 ± 11.6[a]	51.0 ± 10.4[b]
22:6n-3 (mg/d)	37.9 ± 35.5[a]	86.0 ± 31.7[b]
EFA[b] (% energy)	5.6 ± 0.7	6.2 ± 0.6
PUFA[c] (% energy)	5.7 ± 0.7	6.4 ± 0.7
P/S[d]	0.5 ± 0.1	0.5 ± 0.1

[a]Least square mean ± SEM.
[b]EFA, total essential fatty acids (∑18:2n-6,18:3n-3).
[c]PUFA, total polyunsaturated fatty acids (∑n-6, n-3 fatty acids).
[d]P/S, ratio of polyunsaturated to saturated fatty acids. Different superscript roman letters indicate significant differences between groups $P \leq 0.05$. See Table 1 for other abbreviation.

(P = 0.02), respectively, in cord vein erythrocyte in GDM subjects relative to controls. Cord vein erythrocyte PL P/S (polyunsaturated to saturated fatty acid wt%) ratio was lower in women with GDM than controls.

Cord vein erythrocyte PL (wt%) LA and LNA were significantly lower compared with maternal PL LA and LNA, respectively, in controls and GDM (Table 3). On the other hand, their long-chain derivatives, AA and DHA (wt%) were higher in the cord vein erythrocyte PL than the maternal vein PL AA and DHA (wt%), respectively, in controls. In contrast, in women with GDM, PL DHA (wt%) was significantly lower in cord vein erythrocyte PL than the maternal PL DHA. A similar trend was observed in the fetal–maternal difference for erythrocyte PL AA (wt%) in women with GDM.

Maternal plasma PL AA (wt%) was positively associated with fetal erythrocyte PL AA wt% (r = 0.83, P = 0.003, n = 12) in controls. Similarly, maternal plasma PL DHA (wt%) showed significant positive correlation with fetal erythrocyte PL DHA wt% (r = 0.62, P = 0.04, n = 12) in controls. In contrast, in GDM women there was a trend for a negative association between maternal plasma PL DHA and fetal erythrocyte PL DHA wt% (r = –0.54, P = 0.08, n = 13). There was no correlation between maternal plasma and fetal erythrocyte PL AA wt% in women with GDM (r = –0.10, P = 0.77, n = 13).

Maternal glucose control, measured by blood HbA_1C at 36–39 wk gestation, showed a significant negative association with fetal erythrocyte PL DHA and AA wt% (r = –0.53, P = 0.02, and r = –0.51 and P = 0.03, respectively) in controls and GDM combined (n = 25). Additionally, maternal pregravid BMI (kg/m^2) was inversely related to fetal erythrocyte PL DHA wt% (r = –0.45, P = 0.05, n = 25).

DISCUSSION

The current study demonstrates decreased DHA and AA (wt% and μg/mL) in cord vein erythrocyte PL in GDM treated with diet compared with controls. The decrease in the LC-PUFA in fetal erythrocyte PL was accompanied by higher proportions of SFA in women with GDM. Fetal erythrocytes play a key role in the provision of maternal LC-PUFA, particularly DHA and n-3 LC-PUFA, to the fetus (17). Placental transfer of maternal LC-PUFA to the fetus may occur *via* exchange with fetal erythrocyte membranes and preferential enrichment of erythrocyte membrane PL with DHA and AA (17). Given the potential significance of this transport mechanism, lower DHA and AA in the cord vein erythrocyte PL provide evidence for impaired fetal accretion of these LC-PUFA in pregnancy complicated with GDM.

In controls, enrichment of AA and DHA in fetal erythrocyte PL relative to maternal PL AA and DHA (wt%), respectively, is consistent with the findings of previous studies (18,19). However, in women with GDM, lower fetal PL DHA compared with maternal PL DHA (wt%) and a lack of fetal–maternal difference for PL AA (wt%) suggest that placental transfer of maternal LC-PUFA during the third trimester may have been altered in GDM. Further, higher maternal dietary intake of DHA and AA and elevated maternal PL DHA in GDM women compared with controls, coupled with lack of correlation between maternal and fetal PL DHA and AA in GDM, support the above hypothesis.

In women with GDM, fetal erythrocyte total fatty acid concentration in PL was lower compared with controls (189.2 ± 28.5 vs. 251.3 ± 30.4 μg/mL, respectively), whereas maternal PL total fatty acids were elevated (573.7 ± 85.8 vs. 460.4 ± 103.2, respectively). Decrease in the absolute concentrations of PL per unit cholesterol in cord erythrocytes membranes and/or impairment in the assimilation of fatty acids into cord erythrocyte membrane PL in GDM subjects due to altered erythrocyte membrane function may underlie these changes. Whether these changes in fatty acid concentrations of cord erythrocyte membranes lead to alterations in oxygen-carrying capacity of fetal erythrocytes and other erythrocyte membrane-related functions in GDM needs to be investigated.

Maternal glycemic control in the third trimester and pregravid BMI were associated with fetal erythrocyte PL DHA in this study population. GDM subjects treated with diet in the present study had blood HbA_1C values within the accepted clinical range of 4–6% (9), indicating that glucose control was not severely compromised. However, maternal blood HbA_1C was significantly elevated in GDM women compared with controls, suggesting moderate impairment of glucose control in GDM. Further, there was little overlap for individual HbA_1C values between GDM and control subjects. These findings point to altered blood glucose control in women with GDM relative to controls as an important maternal factor associated with the lower fetal LC-PUFA status in GDM. Additionally, the present study suggests that pregravid obesity may be an independent maternal factor associated with impaired *in utero* DHA accretion in the fetus. This finding warrants further investigation.

In summary, fetal cord vein erythrocyte PL (wt% and μg/mL) AA, DHA, ∑n-6, and ∑n-3 PUFA were lower in women with diet-treated GDM than the controls. Maternal blood HbA_1C and pregravid BMI were inversely related to

TABLE 3
Maternal and Fetal Erythrocyte PL Fatty Acids in Controls (n = 12) and Women with GDM (n = 13)[a]

Fatty acids	Group	Wt%		Conc. (μg/mL)	
		Maternal erythrocyte	Cord vein erythrocyte	Maternal erythrocyte	Cord vein erythrocyte
SFA					
16:0	C	24.71 ± 0.69	25.82 ± 1.89^{a}	112.93 ± 27.80	66.06 ± 7.28
	GDM	24.62 ± 0.58	29.41 ± 1.68^{b}	143.68 ± 23.13	50.06 ± 6.46
18:0	C	12.52 ± 0.41	14.63 ± 2.11^{a}	58.14 ± 11.88	37.11 ± 4.94
	GDM	12.08 ± 0.34	21.93 ± 1.87^{b}	69.20 ± 9.88	34.96 ± 4.38
Total SFA	C	37.81 ± 0.79	41.09 ± 3.45^{a}	173.64 ± 40.29	104.71 ± 12.01
	GDM	37.27 ± 0.66	52.29 ± 3.06^{b}	216.33 ± 33.52	86.67 ± 10.65
MUFA					
16:1	C	0.94 ± 0.09	1.14 ± 0.17	4.17 ± 0.95	2.69 ± 0.27
	GDM	0.77 ± 0.07	1.11 ± 0.15	4.54 ± 0.79	2.32 ± 0.24
18:1	C	17.11 ± 0.40	12.92 ± 0.95	78.73 ± 17.57	33.12 ± 4.26
	GDM	16.96 ± 0.33	10.43 ± 0.84	95.00 ± 14.62	22.82 ± 3.77
Total MUFA	C	18.46 ± 0.43	14.33 ± 1.08	84.80 ± 18.77	33.46 ± 4.36
	GDM	18.14 ± 0.36	11.77 ± 0.95	104.55 ± 15.62	25.71 ± 3.86
PUFA n-6					
18:2	C	11.43 ± 0.55^{A}	3.70 ± 0.24^{B}	53.02 ± 11.44	9.48 ± 1.20^{a}
	GDM	10.77 ± 0.46^{A}	3.17 ± 0.22^{B}	61.36 ± 9.52	6.61 ± 1.06^{b}
20:2	C	0.47 ± 0.02	0.28 ± 0.01^{a}	2.16 ± 0.38	0.74 ± 0.08^{a}
	GDM	0.43 ± 0.02	0.24 ± 0.01^{b}	2.41 ± 0.32	0.54 ± 0.08^{b}
20:3	C	2.03 ±0.09	2.94 ± 0.28	9.41 ± 2.08	7.66 ± 1.09
	GDM	1.90 ± 0.08	2.45 ± 0.25	10.86 ± 1.73	5.43 ± 0.97
20:4	C	14.78 ± 0.49^{A}	19.81 ± 1.60^{a,B}	68.70 ± 14.35	50.45 ± 6.32^{a}
	GDM	15.23 ± 0.41	14.35 ± 1.50^{b}	86.59 ± 11.94	32.67 ± 5.60^{b}
22:4	C	5.78 ± 0.28	6.58 ± 0.52^{a}	27.42 ± 4.91	16.99 ± 2.01^{a}
	GDM	5.61 ± 0.22	4.39 ± 0.48^{b}	31.44 ± 3.85	10.55 ± 1.84^{b}
22:5	C	2.66 ± 0.24	4.48 ± 1.31	11.83 ± 4.09	10.75 ± 3.15
	GDM	3.11 ± 0.20	7.50 ± 1.16	18.45 ± 3.41	12.41 ± 2.79
Total n-6	C	36.52 ± 0.73	37.81 ± 2.31^{a}	169. 49 ± 36.11	96.08 ± 11.59^{a}
	GDM	37.05 ± 0.61	31.73 ± 2.05^{b}	211.11 ± 30.05	67.35 ± 10.28^{b}
PUFA n-3					
18:3	C	0.20 ± 0.01^{a}	Trace	0.93 ± 0.18	Trace
	GDM	0.16 ± 0.01^{b}	Trace	0.89 ± 0.15	Trace
20:5	C	0.27 ± 0.03	0.15 ± 0.04	1.28 ± 0.38	0.37 ± 0.06
	GDM	0.26 ± 0.03	0.13 ± 0.04	1.48 ± 0.31	0.26 ± 0.07
22:5	C	2.14 ± 0.14	0.69 ± 0.06	9.87 ± 2.13	1.80 ± 0.22
	GDM	2.04 ± 0.11	0.60 ± 0.06	11.54 ± 1.78	1.41 ± 0.24
22:6	C	4.38 ± 0.31^{a,A}	5.70 ± 0.50^{a,B}	20.38 ± 5.52	14.82 ± 1.86^{a}
	GDM	4.88 ± 0.26^{b,A}	3.60 ± 0.44^{b,B}	27.83 ± 4.60	8.38 ± 1.65^{b}
Total n-3	C	6.99 ± 0.40	6.57 ± 0.58^{a}	32.45 ± 8.11	17.09 ± 2.13^{a}
	GDM	7.33 ± 0.33	4.08 ± 0.52^{b}	41.73 ± 6.75	9.49 ± 1.89^{b}
Total PUFA	C	43.51 ± 0.99	44.38 ± 2.77a	201.94 ± 44.10	113.16 ± 13.55^{a}
	GDM	44.39 ± 0.82	35.81 ± 2.46^{b}	252.84 ± 36.69	76.83 ± 12.01^{b}
P/S	C	1.16 ± 0.05	1.09 ± 0.09^{a}		
	GDM	1.20 ± 0.04	0.79 ± 0.08^{b}		
DHASI	C	1.80 ± 0.18	1.42 ± 0.19^{a}		
	GDM	1.63 ± 0.15	0.81 ± 0.17^{b}		

[a]Least square means ± SEM. Different superscript lowercase roman letters indicate significant differences between groups, $P \leq 0.05$; different superscript capital roman letters indicate significant differences between maternal and core vein PL fatty acids (wt%), $P \leq 0.05$. Abbreviations: SFA, saturated fatty acids; total SFA, sum of 12:0, 14:0, 16:0, 18:0, 20:0, and 22:0; MUFA, monounsaturated fatty acids; total MUFA, sum of 16:1, 18:1, and 20:1; total n-6 PUFA, sum of 18:2, 18:3, 20:2, 20:3, 20:4, 22:4, and 22:5n-6; total n-3 PUFA, sum of 18:3, 20:5, 22:5, and 22:6n-3; total PUFA, sum of n-6 plus n-3 PUFA; DHASI, docosahexaenoic acid sufficiency index (22:6n-3/22:5n-6); PL, phospholipid; GDM, gestational diabetes mellitus; C, control. See Tables 1 and 2 for other abbreviations.

fetal erythrocyte PL DHA (wt%). Further studies are needed to understand the mechanisms underlying the alterations in fetal LC-PUFA metabolism in GDM and obesity and their long-term implications for the offspring of mothers with GDM.

ACKNOWLEDGMENTS

The authors wish to thank Patricia O'Connell and Brunnella Ibarralo from the Diabetes Lifecare Center at Hartford Hospital for their help with patient recruitment, and the staff at the Department of Obstetrics and Gynecology at Hartford Hospital for their help with car-

rying out the research protocol. We are grateful to the subjects who participated in this study. Supported in part by Hartford Hospital, Hartford, CT, the Kraft/General Foods Predoctoral Fellowship Program, contract 93-37200-8876 from the U.S. Department of Agriculture Research Service, and the University of Connecticut Research Foundation.

REFERENCES

1. Crawford, M.A., Doyle, W., Drury, P., Lennon, A., Costeloe, K., and Leighfield, M. (1989) n-6 and n-3 Fatty Acids During Early Human Development, *J. Intern. Med. 225* (suppl.), 159–169.
2. Neuringer, M., Anderson, G.J., and Connor, W.E. (1988) The Essentiality of n-3 Fatty Acids for the Development and Function of the Retina and Brain, *Annu. Rev. Nutr. 8,* 517–541.
3. Salem, N., Wegher, B., Mena, P., and Uauy, R. (1996) Arachidonic and Docosahexaenoic Acids Are Biosynthesized from Their 18-Carbon Precursors in Human Infants, *Proc. Natl. Acad. Sci. USA 93,* 49–54.
4. Feldman, M., Vanaerde, J.E., and Clandinin, M.T. (1992) Lipid Accretion in the Fetus and Newborn, in *Fetal and Neonatal Physiology* (Polin, A., ed.) pp. 299–314, W.B. Saunders Co., Philadelphia.
5. Haggarty, P., Ashton, J., Joynson, M., Abramovich, D.R., and Page, K. (1999) Effect of Maternal Polyunsaturated Fatty Acid Concentration on Transport by the Human Placenta, *Biol. Neonate. 75,* 350–359.
6. Holman, R.T., Johnson, S.B., Gerrard, J.M., Mauer, S.M., Kupcho-Sandberg, S., and Brown, D.M. (1983) Arachidonic Acid Deficiency in Streptozotocin-Induced Diabetes, *Proc. Natl. Acad. Sci. USA 80,* 2375–2379.
7. Phinney, S.D., Davis, P.G., Johnson, S.B., and Holman R.T. (1991) Obesity and Weight Loss Alter Polyunsaturated Lipids in Humans, *Am. J. Clin. Nutr. 53,* 831–838.
8. Kuhn, D.C., Crawford, M.A., Stuart, M.J., Botti, J.J., and Demers, L.M. (1990) Alterations in Transfer of Arachidonic Acid in Placentas of Diabetic Pregnancies, *Diabetes 39,* 914–918.
9. National Diabetes Data Group (1977) Classification and Diagnosis of Diabetes Mellitus and Other Categories of Glucose Intolerance, *Diabetes 28,* 1039–1057.
10. Kautzky-Willer, A., Prager, R., Waldhausl, W., Pacini, G., Thomaseth, K., Wagner, O.F., Ulm, M., Streli, C., and Ludvik, B. (1997) Pronounced Insulin Resistance and Inadequate Beta-Cell Secretion Characterize Lean Gestational Diabetes During and After Pregnancy, *Diabetes Care 20,* 1717–1723.
11. Knopp, R.H., Montes, A., Childs, M., Li, J.R., and Mabuchi, H. (1981) Metabolic Adjustments in Normal and Diabetic Pregnancy, *Clin. Obstet. Gynecol. 24,* 21–49.
12. Wijendran, V., Bendel, R.B., Couch, S.C., Philipson, E.H., Thomsen, K., Zhang, X., and Lammi-Keefe, C.J. (1999) Maternal Plasma Phospholipid Polyunsaturated Fatty Acids in Pregnancy With and Without Gestational Diabetes Mellitus: Relations with Maternal Factors, *Am. J. Clin. Nutr. 70,* 53–61.
13. O'Sullivan, J.B., and Mahan, C.M. (1967) Criteria for the Oral Glucose Tolerance Test in Pregnancy, *Diabetes 13,* 278–285.
14. American Diabetes Association (1986) Nutrient Recommendations and Principles for Individuals with Diabetes Mellitus, *Diabetes Care 10,* 121–132.
15. Dodge, J., and Phillips, G. (1967) Composition of Phospholipids and of Phospholipid Fatty Acids and Aldehydes in Human Red Cells, *J. Lipid. Res. 8,* 667–675.
16. SAS Institute, Inc. (1986) *SAS User's Guide: Statistics,* SAS Institute, Inc., Cary, NC.
17. Ruyle, M., Connor, W.E., Anderson, G.J., and Lowensohn, R.I. (1990) Placental Transfer of Essential Fatty Acids in Humans: Venous-Arterial Difference for Docosahexaenoic Acid in Fetal Umbilical Erythrocytes, *Proc. Natl. Acad. Sci. USA 87,* 7902–7906.
18. Crawford, M.A. (1977) Fetal Accumulation of Long-Chain Polyunsaturated Fatty Acids, in *Function and Biosynthesis of Lipids* (Bazan, N.G., Brenner, R.R., and Giusto, N.M. eds.), pp. 135–143, Plenum Press, New York.
19. Friedman, Z., Danon, A., and Lamberth, E.L. (1978) Cord Blood Fatty Acid Composition in Infants and Their Mothers During the Third Trimester, *J. Paediatr. 92,* 461–466.

[Received October 6, 1999, and in final revised form June 15, 2000; revision accepted June 22, 2000]

REVIEW

Current Methods for the Identification and Quantitation of Ceramides: An Overview

Aida E. Cremesti* and Anthony S. Fischl[1]

The University of Rhode Island, Department of Food Science and Nutrition, West Kingston, Rhode Island 02892

ABSTRACT: Ceramides are key compounds in the metabolism of sphingolipids and are emerging as important second messengers for various cellular processes including cell cycle arrest, differentiation, senescence, apoptosis, and others. Because of their important biological functions, exact analysis of their molecular species and concentrations is crucial for elucidating their function and metabolism. Toward this goal, several methods have been developed for the identification and quantitation of cellular ceramide levels. Methods have been developed utilizing thin-layer or high-performance liquid chromatography. Mass spectrometry also has become increasingly utilized. The *Escherichia coli* diacylglycerol kinase assay is one of the most frequently used techniques for ceramide quantitation. This review presents a current summary of methods used for the identification and quantitation of ceramides.

Paper no. L8419 in *Lipids 35*, 937–945 (September 2000).

The major role of phospholipids and sphingolipids was previously thought to be structural, whereby they establish a barrier for cell permeability and form a matrix for the association of membrane proteins (1,2). With the discovery that sphingosine acts as a potent inhibitor of protein kinase C (3), sphingolipids were thrust into a central role in signal transduction and cell regulation. Various experimental approaches have suggested that ceramide is a key signaling molecule generated in response to a variety of stresses that mediate growth arrest, differentiation, senescence, apoptosis, or an immune response (4–10). Recently, ceramides and sphingoid bases (SB) have been shown to be involved in the stress response of the yeast *Saccharomyces cerevisiae* to heat shock (11–13). Sphingolipids are involved in various aspects of the stress responses and metabolism in yeast (reviewed in Ref. 10). Ceramide has been proposed to be the intracellular mediator of some agents like γ-interferon, dexamethasone, tumor necrosis factor-α (TNF-α), interleukin-1β, and vitamin D_3 (6,7). These agents induce the hydrolysis of plasma membrane sphingomyelin (SM) by a sphingomyelinase, followed by the downstream activation of several cellular targets that mediate the cellular actions of ceramides.

Lipid-dependent cell signaling represents a rapidly expanding field. The growing interest in this field and its significance makes an accurate and quantitative determination of intracellular second messengers both necessary and desirable. It is difficult to isolate free ceramide quantitatively and in completely pure form since its content in biological materials is quite low, being less than 1% of the total extractable lipids (14). However, because ceramides are key compounds in the metabolism of sphingolipids and are thought to be important second messengers, exact analysis of their molecular species and concentrations would seem to be crucial for elucidating their function and metabolism. Toward this goal, several methods have been developed for the identification and quantitation of cellular ceramide levels utilizing a wide variety of analytical and enzymological techniques. And although every method has its advantages and inherent weaknesses, recent reports have raised serious questions about the validity of some of the most frequently used methods for ceramide quantitation (15–17). The following review presents a summary of the various methods and techniques used for the identification and quantification of ceramides in different types of tissues and cells.

The use of chromatography for ceramide quantitation. Structurally, ceramide consists of a long-chain amino alcohol, referred to as SB or long-chain base (LCB), covalently linked *via* an amide linkage to a fatty acyl chain (Fig. 1). The SB and fatty acid could vary in length, degree of unsaturation or hydroxylation, giving rise to a very complex and diverse group of molecules, the ceramides. These lipid molecules have proven to be very difficult to study due to their apolar nature, enormous diversity, and relatively low levels in biological samples.

The lack of a chromophore in the ceramide molecule makes it impossible to identify these molecules using ultraviolet (UV) detection. Various methods have been developed based on the derivatization of ceramides with fluorescent or

*To whom correspondence should be addressed at Memorial Sloan-Kettering Cancer Center, Box 254, 430 East 67th St., New York, NY 10021. E-mail: cremesta@mskcc.org

[1]Current address: Lilly Research Laboratories, Eli Lilly and Company, Indianapolis, IN.

Abbreviations: DAG, diacylglycerol; DHS, dihydrosphingosine; ELSD, evaporative light-scattering detector; ESI, electrospray ionization; GC, gas chromatography; HFA, hydroxy fatty acid; HPLC, high-performance liquid chromatography; LCB, long-chain base; MS, mass spectrometry; MS/MS, tandem MS; NHFA, nonhydroxy fatty acid; NP-HPLC, normal-phase HPLC; RP, reversed-phase; SB, sphingoid bases; SM, sphingomyelin; SPT, serine palmitoyl transferase; TLC, thin-layer chromatography; TNF, tumor necrosis factor; UV, ultraviolet.

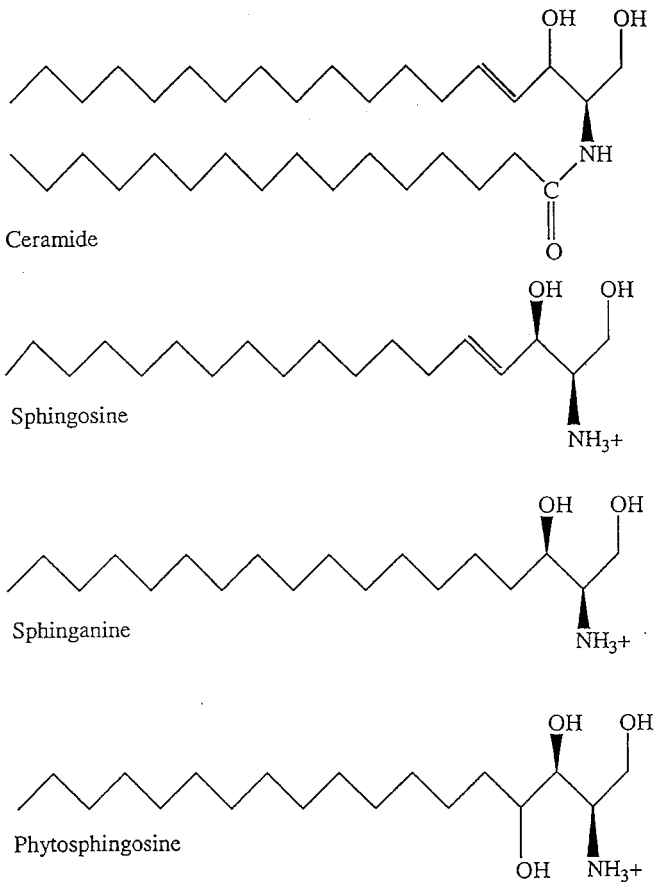

FIG. 1. Chemical structure of ceramide and sphingoid bases.

UV-absorbing compounds and the subsequent identification and quantitation of the derivatized ceramides. The use of high-performance liquid chromatography (HPLC) has been reported for the quantitation of ceramides; however, the full potential of this analytical tool for the separation and quantitation of ceramides has yet to be achieved. HPLC has been used owing to its rapidity, reproducibility, and sensitivity in addition to the high degree of resolution attained with the use of the proper stationary and mobile phases.

Iwamori *et al.* (14) were the first to develop a method for the derivatization of ceramides with benzoyl chloride or benzoyl anhydride, leading to the production of *N*-acyl derivatives which absorb UV light strongly in the 230–280 nm range, depending on the type of ceramide. Benzoylation was achieved by incubation with benzoyl chloride or benzoyl anhydride and pyridine for 3 h at 70°C. For ceramides containing nonhydroxy fatty acids (NHFA), benzoyl anhydride was preferred because the *N*-acyl benzoyl derivatives of ceramides overlapped with methyl benzoate, a by-product of the reaction with benzoyl chloride, on thin-layer chromatography (TLC) and HPLC. For hydroxy fatty acid (HFA)-containing ceramides, treatment with benzoyl chloride was necessary to achieve perbenzoylation, and prolonged reaction times of 4 h were necessary because the 2-hydroxy group of the fatty acid moiety would interfere in the formation of the *N,N*-acyl benzoyl derivative due to steric hindrance (14). Ceramides were separated by normal-phase (NP) HPLC with a silica gel column using hexane/ethyl acetate (94:6, vol/vol) or 0.05% methanol in pentane as mobile phase. Authors reported a recovery of 85–90% for various ceramides, and the response was linear within the 10–100 nanomole range (14). This method allowed for the quantitative determination of ceramide levels in various samples (14,18). Recently, a modified version of this method was used for quantifying ceramide levels in the yeast *S. cerevisiae* using hexane/dioxane (93:7, vol/vol) as mobile phase and a Lichrosorb silica column (Micro Pak, Varian Associates, Palo Alto, CA) as stationary phase (19). However, despite its good quantitative results, this procedure is cumbersome and time-consuming. The reaction is very sensitive to water, and even traces have to be removed to achieve complete benzoylation. The chemicals involved, benzoyl chloride and pyridine, have to be prepared fresh each time and stored and handled anhydrously. These chemicals are extremely toxic, and benzoyl chloride is carcinogenic. Also, radioactive ceramide has to be prepared and used as an internal standard in order to determine the recovery and percentage of benzoylation for quantitation purposes. For derivatization to be of optimal use, the reaction should yield only one derivative per analyte, and the derivative should be resistant to hydrolysis, solvolysis, and thermal decomposition (20). A major disadvantage of most derivatization procedures is the low stability of the derivatized products, which demands that samples not be stored for prolonged times and analysis be done shortly after derivatization (18).

The use of fluorescent tags to label and quantify ceramides has been reported as well. Previati *et al.* (21) developed a method for determining ceramide levels after coupling of the free oxydril group of ceramide to the carboxylic group of the fluorescent label 6-methoxy-α-methyl-2-naphthalene acetic acid. The reaction was achieved after prolonged incubation at –20°C under anhydrous conditions. The authors reported an 80% yield after 3 h of incubation. Separation of ceramides was achieved by using an Econosphere CN column (Phase Sep, a subsidiary of Waters, Inc., Milford, MA) as stationary phase with a gradient of isopropanol in hexane as mobile phase. Linearity was reported in the 5–100 ng range with fluorescent detection and 50–5000 ng with UV absorbance (21). However, inhibition of the reaction could arise from the oxydril group of phospholipids, which necessitates some extra purification steps before the initiation of the reaction to remove interfering lipids and optimize the reaction conditions (21). In addition, radioactive internal standards should be used in order to determine the percentage conversion and recovery of the reaction. Yano *et al.* (22) developed a method for the quantitative analysis of molecular species of ceramide and dihydroceramide by reversed-phase (RP) chromatography. Various *N*-acyl- chain-containing ceramides were synthesized as standards and derivatized with anthroyl-cyanide, a fluorescent reagent. The derivatization process was conducted in the presence of acetonitrile/dichloromethane containing quinuclidine at 4°C overnight. Anthroyl derivatives

of ceramide and dihydroceramide were analyzed with HPLC using a Lichrosorb PR-18 column with a fluorescence detector. Isocratic mode of elution was used with acetonitrile/methanol/ethyl acetate (12:1:7, by vol) as mobile phase and a flow rate of 1.2 mL/min. Successful separation of 17 different species of ceramide and dihydroceramide was achieved in a 40-min run. Species were separated according to fatty acid chain length and SB backbone, whereby retention times increased with increasing number of carbon atoms in the fatty acid chain. The linear range for quantification was reported to be from 1 to 18 picomoles of ceramide. This method could be useful for elucidating the functions of particular subspecies of ceramide since it can effectively separate them. However, long incubation times for successful derivatization pose a drawback. Santana *et al.* (23,24) used a modification of the method developed by Merrill *et al.* (25) for determining sphingosine levels and used it for the quantification of ceramide. The procedure is based on the fact that ceramide can be deacylated to generate free sphingosine, which in turn can be derivatized with *O*-phthaldehyde reagent to form a fluorescent compound. Lipids were separated on a Nova pack C-18 RP-HPLC column (Waters, Inc.) run isocratically with methanol/5 mM potassium phosphate (90:10, vol/vol) at 0.6 mL/min. A fluorescence detector at 340 nm excitation and 455 nm emission wavelength was used to identify ceramides.

The full potential of the resolving power of HPLC in the separation and analysis of simple and complex lipid classes from tissues was not achieved until the introduction of the evaporative light-scattering detector (ELSD), which is a mass detector. The use of ELSD for ceramide detection and quantitation could offer a unique approach which would enable direct analysis without any prior derivatizations (26). There are many advantages to the use of ELSD for the analysis of lipid classes. This type of detector is ideal for the analysis of solutes which do not have a UV chromophore, where the chromophore has a low extinction coefficient, or where the mobile phase contains a chromophore (27). The ELSD is designed to separate nonvolatile solute particles from a volatile eluant. By using this detector, the solvent emerging from the HPLC column is evaporated in a stream of nitrogen gas; the solute does not evaporate and passes in the form of minute droplets through a light beam which is reflected and refracted. The amount of scattered light is measured and bears a relationship to the mass of the sample (26). Quantitation with ELSD can be achieved since the response is a function of mass. However, the relationship is generally not linear (27). The use of this detector has greatly simplified the separation of lipid classes. This type of detector has been used with a ternary gradient pump system to separate all simple and complex lipids from tissues in a single chromatographic run (28). For this, ELSD has become the method used most often in the detection of lipids by HPLC. Several methods based on ELSD have been reported for the identification and quantitation of ceramides. Gildenast and Lasch (29) have used ELSD for the detection of ceramides from stratum corneum lipid extracts. They developed a NP-HPLC method using Lichrospher silica as stationary phase and ethanol/hexane (1:19, vol/vol) as mobile phase. Samples were concentrated with the use of a semipreparative HPLC column in order to make the ceramides detectable from those extracts (Fig. 2). This method was sensitive enough to separate ceramide type III, containing NHFA, from ceramide type IV, containing HFA, which is more polar. Wells *et al.* (13) developed a NP-HPLC method with ELSD using

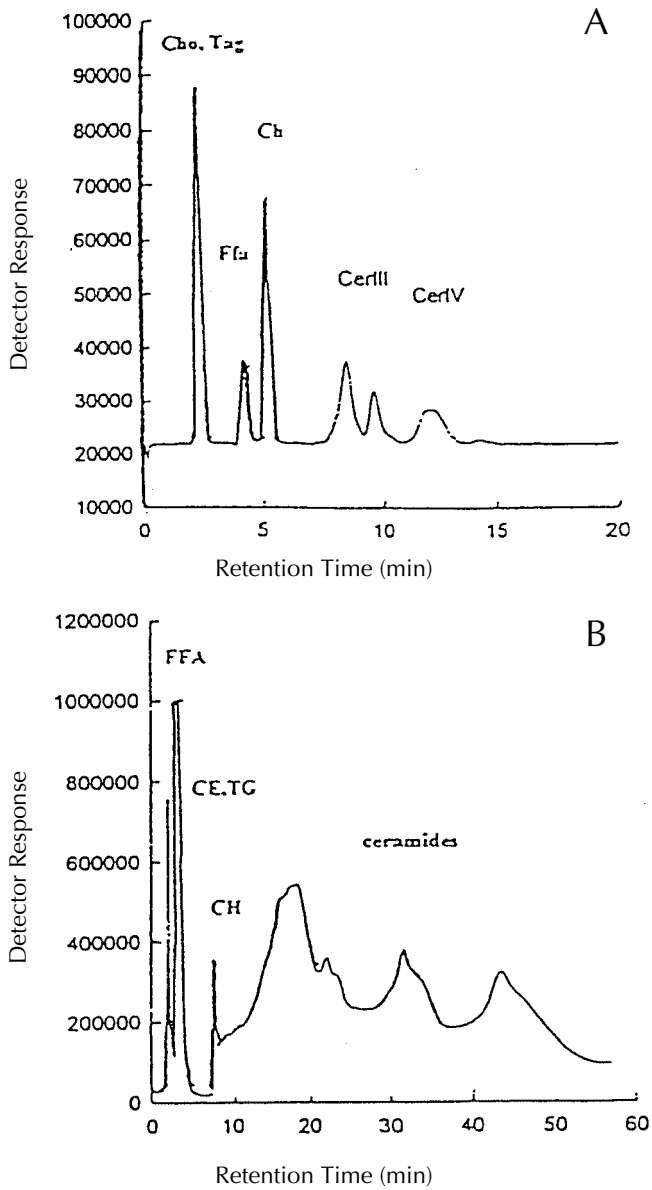

Lichrosorb silica gel column as the stationary phase and a gra-

FIG. 2. Separation and identification of ceramides with evaporative light-scattering detection (ELSD) from stratum corneum lipid extracts by Gildenast and Lasch (29). (A) Analytical high-performance liquid chromatography (HPLC) run of reference lipids using a mobile phase of hexane/ethanol 19:1. (B) Semipreparative HPLC run of enriched ceramide fraction. Mobile phase: hexane/ethanol 29:1. Abbreviations in A: Ffa: free fatty acid; Cho: cholesterol oleate; Tag: triacylglycerols (triolein); Ch: cholesterol; CerIII: ceramide type III (nonhydroxy fatty acid-containing); CerIV: ceramide type IV (fatty acid-containing). Abbreviations in B: FFA: free fatty acids; CE: cholesteryl ester; CH: cholesterol (free sterol); TG: triacylglycerol. Reprinted from *Biochim. Biophys. Acta, 1346,* Gildenast, T., and Lasch, J., Isolation of Ceramide from Human Stratum Corneum Lipid Extract, pp. 69–74, (1997), with permission from Elsevier Science.

dient mobile phase consisting of various proportions of methanol in chloroform. This method is fast, does not require any preliminary purifications, and can be used to identify and quantitate ceramides in crude lipid extracts, provided the appropriate authentic standards are used. McNabb *et al.* (30) were the first to develop an NP-HPLC method to separate ceramides and SB simultaneously using an ELSD detector. Methods for the quantitation of SB have been mainly limited to derivatization techniques (25). Van Veldhoven *et al.* (31) also developed an enzymatic assay to quantitate sphingosine after converting it to ceramide by acylation and using the *E. coli* diacylglycerol (DAG) kinase assay. McNabb *et al.* (30) achieved separation of ceramides from SB in yeast lipid extracts on both silica gel and diol bonded phase columns with an isocratic flow of chloro-

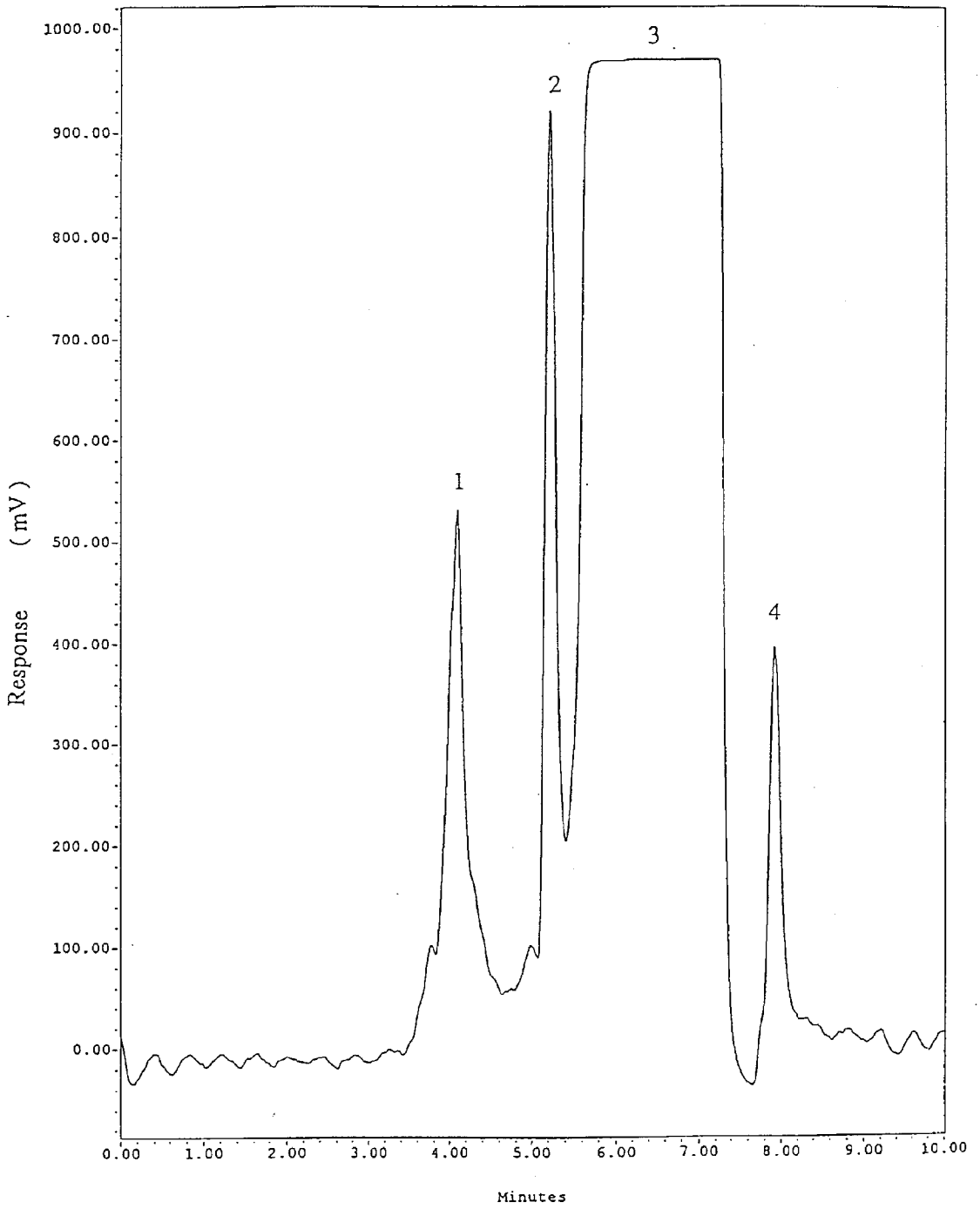

FIG. 3. Chromatograms of lipid extracts from yeast obtained by McNabb *et al.* (27). Lipids were separated on a silica gel column and a mobile phase of chloroform/ethanol/triethylamine/formic acid and detected using an ELSD detector. Peaks: 1, hydroxy fatty acid ceramide; 2, C-2 ceramide; 3, sphingolipid; 4, phytosphingosine. Peaks were identified by comparison of retention times to those of pure authentic standards. See Figure 2 for other abbreviations.

form/ethanol/triethylamine/formic acid (90:10:1:1, by vol) at a flow rate of 0.5 mL/min. Figure 3 shows a chromatogram of a typical complex yeast lipid extract obtained by McNabb *et al.* (30). The method was capable of separating ceramides containing HFA and NHFA and ceramides with fatty acids of varying chain lengths (30). The authors reported sensitivity in the nanomole to picomole range. This is the first method developed capable of separating several subspecies of ceramides and SB in a single run.

A major disadvantage for the quantification of lipids by ELSD is the lack of a simple rectilinear relationship between sample size and the response (28). The nature of the lipid sample and the mobile phase also will exert an effect. However, if calibration is performed with the appropriate standards, high precision and accuracy can be achieved (28). HPLC-based methods offer sensitivity, excellent resolution, reproducibility, and short analysis times. Resolution could be improved by the use of smaller-sized particles for the stationary phase and various modifiers for the mobile phase. Also, sensitive methods could be developed that would allow the separation of various subspecies of ceramides, varying in fatty acid chain length, or the nature, degree of unsaturation or degree of hydroxylation of the SB. RP-HPLC could be particularly useful for the separation of various types of LCB (25).

Much more common in the literature are methods for the separation and isolation of ceramides based on TLC techniques (32–36). Lipid extracts are usually subject to mild alkaline hydrolysis followed by TLC separation on silica gel plates with different proportions of chloroform/methanol/acetic acid. Identification of ceramides is usually done by staining with copper sulfate in orthophosphoric acid or 8-anilino-1-naphthalene sulfonic acid and quantitation is done by densitometry (34). Frequently, various radioactive precursors have been used for labeling cells and following their incorporation into radioactive ceramide (37–41). Motta *et al.* (34) optimized a method based on TLC separation of lipid extracts derived from human stratum corneum cells, followed by scanning densitometry for the identification and quantitation of various types of ceramides using TLC silica gel plates and chloroform/methanol/glacial acetic acid (190:9:1, by vol) as mobile phase (34). This method was sensitive enough to separate ceramides into five different fractions based on the presence or absence of hydroxyl groups in the fatty acid or long-chain base moieties. However, separation of the ceramide species could not be achieved by a single TLC run and required separation of the ceramide fraction first, concentration, and a second TLC run (34). Although this method is sensitive and quantitative significant problems are associated with it. Preparative TLC is sensitive to sample overload and is time-consuming and cumbersome. Also, the capacity of high-performance TLC is too low to separate substantial amounts of ceramides, a drawback for the use of this method for preparative operations. In this respect, HPLC is more efficient and provides a higher recovery.

Radiolabeling of sphingolipid metabolites by various radioactive precursors and subsequent extraction and separation by TLC has been widely used for ceramide identification and quantitation (19,37–40,42). However, care should be taken with the choice of radioactive precursor. The use of tritiated [^{3}H]palmitate would introduce a heavy bias toward the palmitate-containing sphingolipids. Also, radioactive palmitate might be metabolized through other pathways, such as β-oxidation, leading to the production of radioactive by-products, especially with the use of [^{14}C]palmitate. [^{3}H]dihydrosphingosine (DHS) has been shown to be taken up readily into the cells and utilized to make all known classes of complex sphingolipids (37). Uptake of [^{3}H]DHS is greatly enhanced by using detergents and by blocking the synthesis of endogenous DHS with inhibitors of serine palmitoyl transferase (SPT), the first enzyme in the *de novo* biosynthesis of sphingolipids. Labeling with [^{3}H]serine has also been used for separation of ceramides (23,24,42) since it is used by SPT for the synthesis of long-chain SB. Usually, growing cells are incubated with the radioactive precursor for varying lengths of time after which lipids are extracted and isolated on TLC plates. Quantitation is done by scanning the amount of radioactivity with phosphor imagers or incubation of the plates with X-ray film, identifying the spots, scraping them, and estimating the amount of radioactivity by liquid scintillation counting. Santana *et al.* (23,24) used this technique to quantitate ceramides and SM in HL-60 cells after labeling cells with [^{3}H]serine for 24–48 h, followed by alkaline hydrolysis to remove phosphatidylserine that might interfere with separation on TLC. These techniques allow for the identification of ceramides but are not an accurate depiction of the actual amount of ceramide present in the cells. Since not all the radioactive precursor is taken up into the cells and since the synthesis of nonradioactive endogenous precursors cannot be stopped, it becomes impossible to determine the exact amount of ceramide produced by the cells. These methods are more applicable to pulse-chase type of experiments, in studies on the relative amounts of ceramide produced in cells grown under different conditions, or in monitoring the transport and metabolism of lipids (42), rather than determining the exact amount of ceramides formed by the cell *per se*. Thus, even though ceramide labeling with tritiated precursors has been widely used, it does not provide real mass data, and care should be taken with the choice of radioactive precursor. If the precursor chosen is a fatty acid, it will co-extract with the labeling products and the separation of sphingolipids from glycerolipids cannot be achieved in a single TLC run, thus requiring either a glycerolipid hydrolysis step to remove the radioactive fatty acid in the aqueous phase, or several TLC steps to achieve the separation. Also, these studies often require very large amounts of starting material, extensive chromatographic separations, prolonged incubation times, and have very low yields of radiolabeled products, in addition to the low sensitivity and detection limits characteristic of TLC.

The use of mass spectrometry (MS) for ceramide quantification. MS is a powerful tool for determining the levels of endogenous physiologically active compounds because of its high level of sensitivity and selectivity. MS identifies a mole-

cule on the basis of its mass to charge ratio (*m/z*). Electrospray ionization MS (ESI/MS) and tandem MS (ESI–MS/MS collision-induced decomposition) have been successfully used for several years mainly for the analysis of proteins and peptides (17) and have more recently been extended to the analysis of other molecular species, such as carbohydrates and glycolipids (43,44). Rubino *et al.* (45) used fast atom bombardment, precursor and fragment ion analysis MS to characterize the fatty acid and LCB composition of a complex mixture of ceramides obtained from beef brain lipid extracts. Precursor ion analysis allowed recognition of ceramides with 14 different fatty acid chains. Kerwin *et al.* (44) have used positive and negative ion electrospray MS and MS/MS (tandem MS) to identify glycerophospholipid and ceramide headgroups and their alkyl, alkenyl, and acyl constituents. In ESI, molecules are injected onto the electrospray interface as dilute solutions to obtain positive ions. These ions are usually formed by protonation of covalent analytes or by dissociation of ionic compounds. Gu *et al.* (46) developed a method for the separation and quantification of ceramides based on ESI–MS/MS technique where collision-induced decomposition of ceramides produced ions of different spectra that were identified and compared to those of standards (46). The authors reported sufficient resolution and sensitivity with this technique to allow the detection of subpicomolar amounts from samples (15,46), requiring minimal amounts of starting biological material. This method is rapid and sensitive enough to determine the relative amounts of sphingosine and sphinganine subspecies of ceramide using C-2 ceramide as an internal standard. Authors separated and identified several species of ceramide differing in fatty acid chain length and degree of unsaturation of the SB backbone. However, this technique was used for determining ceramide levels in cells only after the crude lipid extracts were subject to silica gel chromatography to remove polar lipids that would interfere with the ESI–MS analysis and suppress the signal (15,46). Care should be taken in preparing the samples because overdilution of cellular lipids would result in a high degree of variation in the detected signal intensities. This necessitated that fractions be concentrated on silica gel columns, separated, and redissolved in the right amount of solvent before subjecting to ESI–MS (46). Watts *et al.* (15) used this method to determine ceramide levels in cells following the activation of the Fas receptor, and in cells following treatment with TNF (17), and were able to quantitate ceramides from as little as 2.5 $\times 10^7$ cells. Mano *et al.* (47) developed a liquid chromatography-ionspray tandem MS (LC/MS/MS) technique for ceramide quantification. Separation of lipid classes, which preceded MS/MS, was done on a C-18 silica gel RP column using HPLC with a gradient mobile phase of ammonium formate/methanol/tetrahydrofuran (47) (Fig. 4). However; the presence of a stream splitter was necessary before the ionspray interface because the sensitivity of ionspray MS is greatly reduced with high solute concentrations (47). This method allowed for the quantification of ceramides over a range of 0.1–100 ng/10^4 cells. Couch *et al.* (48) have even utilized an atmospheric pressure chemical ionization MS method for determining ceramide

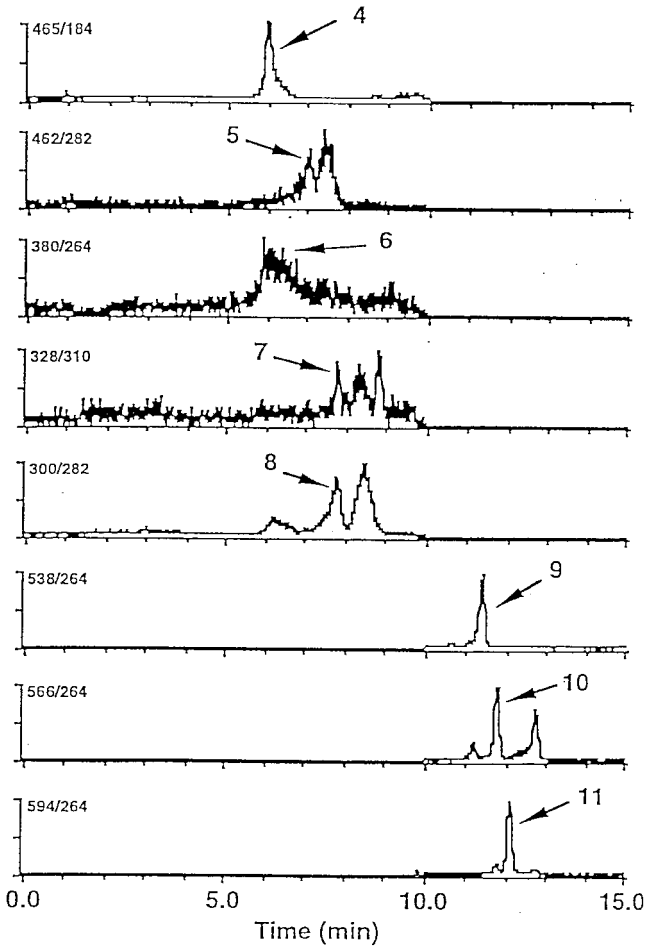

FIG. 4. Typical chromatograms of endogenous sphingolipid metabolites in HL-60 cells obtained by Mano *et al.* (47) using liquid chromatography–ion spray tandem mass spectrometry (MS/MS). Separation of lipid classes which preceded MS/MS was done on a C-18 silica gel reversed-phase column with a gradient mobile phase of formate/ methanol/tetrahydrofuran. (4) Sphingosyl phosphoryl choline; (5) psychosine; (6) sphingosine-1-phosphate; (7) dimethylsphingosine; (8) sphingosine; (9) C-16 ceramide; (10) C-18 ceramide; (11) C-20 ceramide. Numbers on the upper left indicate the *m/z* of precursor ion (first number) and product ion (second number). Figure reprinted by permission of Academic Press, Orlando, FL, from Mano, M., Oda, Y., Yamada, K., Asakawa, N., and Katayana, K. (1997) Simultaneous Quantitative Determination Method for Sphingolipid Metabolites by LC/Electrospray Ionization Tandem Mass Spectrometry, *Anal. Biochem. 244*, 291–300.

levels following RP-HPLC which gave significant structural information and differentiated ceramides on the basis of their fatty acid constituents (48). Kuksis *et al.* (43) developed an HPLC assay using chloride attachment negative chemical ionization MS for detection of glyceryl esters and ceramides in plasma samples. Carboxyl or hydroxyl groups of lipids were derivatized by trimethyl or *tert*-butyl dimethyl chlorosilane, after phospholipase C treatment of plasma. The lipids were separated on a RP column with 20–90% propionitrile in acetonitrile containing 1% dichloromethane. However, the mass spectra yielded only a single peak for ceramide, and the results were not quantitative in nature for ceramide. The au-

thors reported an overestimation of the more saturated short-chain ceramide and an underestimation of the long-chain ceramides (43).

Gaudin *et al.* (49) developed a method for the separation and structural identification of ceramides. The authors achieved separation of ceramides using nonaqueous RP chromatography on a Kromasil C18 column (Eka Nobel, Bohus, Sweden) with 5 μm particle size and a gradient mobile phase of 100% methanol to methanol/0.2% acetone and a flow rate of 0.4 mL/min. Furthermore, they used a gas chromatography (GC)/MS approach to confirm the structures deduced from their HPLC analysis. GC/MS analysis was done after cleavage of ceramides by acidic methanolysis and conversion of the products to volatile trimethylsilyl derivatives. Methanolysis was necessary to convert the fatty acid moiety in ceramide to fatty acid methyl esters and release the LCB (48). For the GC, a gradient of acetonitrile/tetrahydrofuran (95:5, vol/vol) to acetonitrile/tetrahydrofuran/ propanol (63:35:5, by vol) in 30 min was used having triethylamine and formic acid as modifiers. The method was capable of identifying three types of fatty acids: saturated, unsaturated, and hydroxy-saturated fatty acids. They were also capable of analyzing three types of LCB: sphingosine, dihydrosphingosine, and phytosphingosine (49). Gaudin *et al.* (49) used this technique to confirm and identify the composition and structures of commercially available ceramides and SB, but did not apply this technique to the analysis of ceramides in biological samples. Karlsson *et al.* (50) used atmospheric pressure chemical ionization MS with NP-chromatography to separate and identify species of SM. Their method was capable of determining SM molecular masses as well as their LCB and fatty acid (saturated and unsaturated) compositions.

MS is a very powerful analytical tool and provides important structural information. This would be essential in determining the particular molecular species of ceramides that are involved in cellular responses since evidence has shown that not all isomers of ceramides are biologically active (6). However, MS is generally nonquantitative in nature unless appropriate internal standards are utilized. Watts *et al.* (16) have discussed some of the shortcomings of MS analysis of lipids. They pointed out that the mass obtained for a molecule should not serve as the sole basis for its identification and that fragmentation analysis is needed when complex lipid mixtures from biological extracts are analyzed (16). Also, MS involves the use of very expensive equipment and requires the knowledge and expertise of skilled analysts to use and interpret results which have limited its use in many applications in sphingolipid research, even though it has become increasingly utilized.

The use of biochemical assays for ceramide quantification. One of the most frequently used assays for ceramide quantification is the *E. coli* DAG assay (4,11,41,51). This enzyme was first identified, partially purified and characterized by Schneider and Kennedy in 1970 (52), who were also the first to show that *E. coli* DAG kinase effectively utilized ceramides as well as DAG as substrate. Later, this enzyme was overexpressed in a plasmid-bearing *E. coli* strain which accounted for 10–15% of membrane proteins and subsequently used as a source of the enzyme for the quantification of DAG by converting it to [^{32}P]phosphatidic acid in the presence of [γ-^{32}P]ATP (53,54). It was observed that the enzyme was also capable of converting ceramide to [^{32}P]ceramide-phosphate (52–54) as well, and the assay was subsequently used for the quantification of ceramides after correction for conversion and recovery. DAG kinase catalyzes the transfer of the γ-phosphate group of ATP to the free 3′ hydroxyl group of diglyceride and the 1′ hydroxyl group of ceramide and requires the presence of a fatty acid linked through an acyl bond to an amino group. Lipids from tissue samples are usually extracted using the Bligh and Dyer (55) or Folch *et al.* (56) procedure, dried, and incubated with DAG kinase and [γ-^{32}P] ATP in the presence of the detergent β-octylglucoside in a mixed micelle assay (4,11,51). Products are reextracted, spotted on silica gel TLC plates, and developed with chloroform/methanol/acetic acid (65:15:5, by vol) and then subjected to autoradiography or phosphor imaging and quantified (4,11,31,53,54). Although this assay has been widely used, several drawbacks exist and could affect the enzymatic conversion and lower the reliability of the procedure (15,16,57). The enzyme source, either a crude membrane fraction (54,57) or a chromatographically purified enzyme (54,57) available commercially (4,11,51), could contain contaminating lipases that would contribute to increased background by carrying undesirable substrates into the product (21). Perry and Hannun (57) have emphasized the importance of the enzyme source in the validity of the assay. They argue that a lyophilized preparation of the enzyme available commercially can be activated by a ganglioside, leading to incorrect determination of ceramide levels. They also recommend the use of C6–C12 ceramide as an internal standard in order to determine percentage conversion for quantitative purposes. The use of C2 ceramide is not recommended since it is a poor substrate for the DAG kinase (57). Also, the source of [γ-^{32}P] ATP should be highly pure, since impurities in the ATP preparation could inhibit the enzyme (54), so this reagent must be prepared and monitored with care. Accurate determination of the specific activity of ATP is also crucial since this radionucleotide has a very short half-life, and samples should be prepared and used while fresh where the [γ-^{32}P] ATP has a very high specific activity. Another disadvantage of this assay is the use of the very high energy radionucleotide which mandates certain precautions. The assay becomes very cumbersome if a phosphor imager is not available because the radioactive spots have to be scraped and subjected to scintillation counting. Van Veldhoven *et al.* (58) evaluated the phosphorylation of ceramides by the *E. coli* DAG kinase enzyme in an octylglucoside/phosphatidylglycerol mixed micelle assay. They reported that ceramides containing NFH were phosphorylated quantitatively over a broad range from 25 to 2,000 picomoles, whereas the conversion of HFA ceramide was not quantitative.

Perry and Hannun (57) have elaborated on the kinetics of the enzyme, pointing out that proper use of the assay necessi-

tates the use of excess enzyme in order to avoid Michaelis-Menten kinetics and achieve a complete and quantitative conversion of the ceramide to ceramide-1-phosphate. Under Michaelis-Menten conditions, the enzyme becomes limiting and hence subject to factors that affect the velocity of the reaction and the affinity of the enzyme and alter its activity (57). Although this technique has been very widely used for ceramide quantification, recent reports have raised serious questions about the validity of this approach (15,16). Watts *et al.* (15) have used this assay in conjunction with an MS approach to determine ceramide levels in cells following the activation of the Fas receptor which has been associated with elevation in ceramide levels and apoptosis (6). The authors reported elevated ceramide levels when using the DAG kinase assay but could not detect elevations with MS. They concluded that increases in ceramide levels observed were due to fluctuations in DAG kinase activity rather than changes in the endogenous ceramide levels *per se*. Others have attributed these conflicting results to the use of a commercially available lyophilized preparation of the enzyme which appears to be activated by certain lipids (57).

Although discrepancies in the reported results using the DAG kinase assay in various cell systems exist, this method cannot be completely dismissed but should be used with caution. The need for new, reliable, and accurate methods for identification and quantitation of ceramides becomes evident in light of the increasing body of literature attributing important biological roles to ceramides. The choice of method for ceramide quantitation would depend on the purpose of the study, as well as the availability of resources and skilled personnel.

ACKNOWLEDGMENTS

This work was supported by grant GM 49214 from the National Institutes of Health. We thank Thomas McNabb for his comments on this manuscript.

REFERENCES

1. Carman, G.M., and Henry, S.A. (1989) Phospholipid Biosynthesis in Yeast, *Annu. Rev. Biochem. 58*, 635–669.
2. Carman, G.M., and Zeimetz, G.M. (1996) Regulation of Phospholipid Biosynthesis in the Yeast *Saccharomyces cerevisiae*, *J. Cell Biochem. 272*, 13293–13296.
3. Hannun, Y., Loomis, C.R., Merrill, A.H., and Bell, R.M. (1986) Sphingosine Inhibition of PKC Activity and of Phorbol Dibutyrate Binding *in vitro* and Human Platelets, *J. Biol. Chem. 262*, 12604–12609.
4. Gamard, C.J., Dbaibo, G.S., Liu, B., Obeid, L., and Hannun, Y. (1997) Selective Involvement of Ceramide in Cytokine-Induced Apoptosis, *J. Biol. Chem. 272*, 16474–16481.
5. Okazaki, T., Kondo, T., Kitano, T., and Tashima, M. (1998) Diversity and Complexity of Ceramide Signaling in Apoptosis, *Cell Signal. 10*, 685–692.
6. Hannun, Y.A. (1996) Function of Ceramide in Coordinating Cellular Responses to Stress, *Science 272*, 1855–1858.
7. Obeid, L.M., and Hannun, Y.A. (1995) Ceramide: A Stress Signal and Mediator of Growth Suppression and Apoptosis, *J. Cell Biochem. 58,* 191–198.
8. Fishbein, J.D., Dobrowsky, R.T., Bielawska, A., Garrett, S., and Hannun, Y.A. (1993) Ceramide-Mediated Growth Inhibition and CAPP Are Conserved in *Saccharomyces cerevisiae*, *J. Biol. Chem. 268*, 9255–9261.
9. Venable, M.E., Lee, Y.L., Smith, M.J., Bielawska, A., and Obeid, L.M. (1995) Role of Ceramide in Cellular Senescence, *J. Biol. Chem. 67*, 27–38.
10. Dickson, R. (1998) Sphingolipid Functions in *Saccharomyces cerevisiae*: Comparison to Mammals, *Annu. Rev. Biochem. 67*, 27–48.
11. Jenkins, G.M., Richards, A., Wahl, T., Mao, C., Obeid, L., and Hannun, Y. (1997) Involvement of Yeast Sphingolipids in the Heat Stress Response of *Saccharomyces cerevisiae, J. Biol. Chem. 272*, 32566–32572.
12. Dickson, R.C., Nagiec, E.T., Skypek, M., Tillman, P., Wells, G.B., and Lester, R.L. (1997) Sphingolipids Are Potential Heat Stress Signals in *Saccharomyces cerevisiae*, *J. Biol. Chem. 272,* 30196–30200.
13. Wells, G., Dickson, R., and Lester, R. (1998) Heat-Induced Elevation of Ceramides in *Saccharomyces cerevisiae via de novo* Synthesis*, J. Biol. Chem. 273*, 7235–7243.
14. Iwamori, M., Costello, C., and Moser, H. (1979) Analysis and Quantitation of Free Ceramide-Containing Nonhydroxy and 2-Hydroxy Fatty Acids and Phytosphingosine, *J. Lipid Res. 20,* 86–96.
15. Watts, J.D., Gu, M., Polverino, A., Patterson, S., and Aebersold, R. (1997) On the Complexities of Ceramide Changes in Cells Undergoing Apoptosis: Lack of Evidence for a Second Messenger Function in Apoptosis Induction, Cell Death and Differentiation, *Proc. Natl . Acad. Sci. USA 94*, 7292–7296.
16. Watts, J.D., Aebersold, R., Polverino, A.J., Patterson, S.D., and Gu, M. (1999) Ceramide Second Messengers and Ceramide Assays, *TIBS 24*, 228.
17. Watts, J.D., Gu, M., Patterson, S.D., Aebersold, R., and Polverino, A.J. (1999) On the Complexities of Ceramide Changes in Cells Undergoing Apoptosis: Lack of Evidence for a Second Messenger Function in Apoptotic Induction, *Cell Death Differen. 6*, 105–114.
18. Sugita, M., Iwamori, M., Evans, J., McCluer, R.H., Dulaney, J.T., and Moser, H. (1974) HPLC of Ceramides: Application to Analysis in Human Tissues and Demonstration of Ceramide Excess in Farber's Disease, *J. Lipid Res. 15*, 223–226.
19. Nagiec, M., Nagiec, E., Baltisberger, J., Wells, G., Lester, R., and Dickson, R. (1997) Sphingolipid Synthesis as a Target of Antifungal Drugs, *J. Biol. Chem. 272*, 9809–9817.
20. Weston, A.R., and Brown, P.R. (1997) *HPLC and CE Principles and Practice*, pp. 28–42, Academic Press, San Diego.
21. Previati, M., Bertolaso, L., Tramain, M., Bertagnolo, V., and Capitani, S. (1996) Low Nanogram Range Quantification of Diglycerides and Ceramide by HPLC, *Anal. Biochem. 233*, 108–114.
22. Yano, M., Kishida, E., Muneyuki, Y., and Masuzawa, Y. (1998) Quantitative Analysis of Ceramide Molecular Species by High-Performance Liquid Chromatography, *J. Lipid Res. 39*, 2091–2097.
23. Santana, P., Fanjul, L.F., and Galaretta, C.M.R. (1998) *Methods in Molecular Biology: Phospholipid Signaling Protocols*, Vol. 105, pp. 217–221, Humana Press Inc., Totowa, NJ.
24. Santana, P., Galaretta, C.M.R., and Fanjul, L.F. (1998) *Methods in Molecular Biology: Phospholipid Signaling Protocols*, Vol. 105, pp. 223–231, edited by Ian M. Bird, Humana Press Inc., Totowa, NJ.
25. Merrill, A.H., Jr., Wang, E., Mullins, R.E., Jamison, W.C., Nimkar, S., and Liotta, D.C. (1988) Quantitation of Free Sphingosine in Liver by High-Performance Liquid Chromatography, *Anal. Biochem. 171*, 373–381.
26. Christie, W. (1985) Rapid Separation and Quantification of Lipid Classes by HPLC and Mass (light-scattering) Detection,

J. Lipid Res. 26, 507–512.
27. McNabb, T.J., Cremesti, A.E., Brown, P.R., and Fischl, A.S. (1999) High-Performance Liquid Chromatography/Evaporative Light-Scattering Detector Techniques for Neutral, Polar, and Acidic Lipid Classes: A Review of Methods and Detector Models, *Sem. Food Anal. 4*, 53–70.
28. Christie, W., and Urvine, R.A. (1995) Separation of Lipid Classes from Plant Tissues by HPLC on Chemically Bonded Stationary Phases, *J. High Resolut. Chromatogr. 18*, 97–100.
29. Gildenast, T., and Lasch, J. (1997) Isolation of Ceramide from Human Stratum Corneum Lipid Extract, *Biochim. Biophys. Acta 1346*, 69–74.
30. McNabb, T., Cremesti, A., Brown, P., and Fischl, A. (1999) The Separation and Direct Detection of Ceramides and Sphingoid Bases by Normal-Phase High-Performance Liquid Chromatography and Evaporative Light Scattering Detection, *Anal. Biochem. 276*, 242–250.
31. Van Veldhoven, P.D., Bishop, R.W., and Bell, R.M. (1989) Enzymatic Quantification of Sphingosine in the Picomole Range in Cultured Cells, *Anal. Biochem. 183*, 177–189.
32. Bose, R., Chen, P., Loconti, A., Grullich, C., Abrams, J., and Kolesnick, R. (1998) Ceramide Generation by the Reaper Protein Is Not Blocked by the Caspase Inhibitor p35, *J. Biol. Chem. 273*, 28852–28859.
33. Robson, K.J., Stewart, M.E., Michelson, S., Lazao, N.D., and Downing, D.T. (1994) 6-Hydroxy-4-sphingenine in Human Epidermal Ceramides, *J. Lipid Res. 35*, 2060–2068.
34. Motta, S., Monti, M., Sesana, S., Caputo, R., Carelli, S., and Ghidoni, R. (1993) Ceramide Composition of the Psoriatic Scale, *Biochim. Biophys. Acta 1182*, 147–151.
35. Haak, D., Gable, K., Beeler, T., and Dunn, T. (1997) Hydroxylation of *Saccharomyces cerevisiae* Ceramide Requires sur2p and scs7p, *J. Biol. Chem. 272*, 29704–29710.
36. Selvam, R., and Radin, N.S. (1981) Quantitation of Lipids by Charring on Thin-Layer Plates and Scintillation Quenching: Application to Ceramide Determination, *Anal. Biochem. 112*, 338–345.
37. Reggiori, F., Canivence-Gansel, E., and Conzelmann, A. (1997) Lipid Remodeling Leads to the Introduction and Exchange of Defined Ceramides on GPI Proteins in the ER and Golgi of *Saccharomyces cerevisiae*, *EMBO J. 16*, 3506–3518.
38. Sipos, G., Reggiori, F., Vionnet, C., and Conzelmann, A. (1997) Alternative Lipid Remodeling Pathways for Glycophosphatidylinositol Membrane Anchors in *Saccharomyces cerevisiae*, *EMBO J. 16*, 3494–3505.
39. Mandala, S., Thornton, R., Rosenbach, M., Milligan, J., Calvo, M., Bull, H.B., and Kurtz, M.B. (1997) Khafrefungin, a Novel Inhibitor of Sphingolipid Synthesis, *J. Biol. Chem. 272*, 32709–32714.
40. Tepper, A.D., DeCock, J.G., Vreiss, E., Borst, J., and Blitterswijk, W. (1997) CD95, Fas Induced Ceramide Formation Proceeds with Slow Kinetics and Is Not Blocked by Caspase-3/cp32 Inhibition, *J. Biol. Chem. 272*, 24308–24312.
41. Gomez-Munoz, A., Waggoner, D., O'Brien, L., and Brindley, D.N. (1995) Interaction of Ceramides, Sphingosine and Sphingosine 1-Phosphate in Regulating DNA Synthesis and PLD Activation, *J. Biol. Chem. 272*, 26318–26325.
42. Mandala, S., Thornton, R., Tu, Z., Kurtz, M., Nickels, J., Broach, J., Menzeleev, R., and Spiegel, S. (1997) Sphingoid Base 1-Phosphate Phosphatase: A Key Regulator of Sphingolipid Metabolism and Stress Response, *Proc. Natl. Acad. Sci. USA 95*, 150–155.
43. Kuksis, A., Marai, L., and Myher, J.J. (1991) Plasma Lipid Profiling by Liquid Chromatography with Chloride-Attachment Mass Spectrometry, *Lipids 26*, 240–245.
44. Kerwin, J.L., Tuininga, A.A., and Ericsson, L.H. (1994) Identification of Molecular Species of Glycerophospholipids and Sphingomyelin Using Electrospray Mass Spectrometry, *J. Lipid Res. 35*, 1102–1114.
45. Rubino, F.M., Zecca, L., and Sonnino, S. (1994) Characterization of a Complex Mixture of Ceramides by Fast Atom Bombardment and Precursor and Fragment Analysis Tandem Mass Spectrometry, *Biol. Mass Spectrom. 23*, 82–90.
46. Gu, M., Kerwin, J., Watts, J.D., and Aebersold, R. (1997) Ceramide Profiling of Complex Lipid Mixtures by Electrospray Ionization Mass Spectrometry, *Anal. Biochem. 244*, 347–356.
47. Mano, M., Oda, Y., Yamada, K., Asakawa, N., and Katayana, K. (1997) Simultaneous Quantitative Determination Method for Sphingolipid Metabolites by LC/Electrospray Ionization Tandem Mass Spectrometry, *Anal. Biochem. 244*, 291–300.
48. Couch, L.H., Churchwell, M.I., Doerge, D.R., Tolleson, W.H., and Howard, P.C. (1997) Identification of Ceramides in Human Cells Using LC with Determination by APCI, *Rapid Commun. Mass Spectrom. 11*, 504–512.
49. Gaudin, K., Chaminade, P., Baillet, A., Ferrier, D., Bleton, J., Gousaud, S., and Tchapla, A. (1999) Contribution to Liquid Chromatographic Analysis of Cutaneous Ceramides, *J. Liq. Chromatogr. Rel. Technol. 22*, 379–400.
50. Karlsson, A., Michelsen, P., and Goran, O. (1998) Molecular Species of Sphingomyelin: Determination by High-Performance Liquid Chromatography/Mass Spectrometry with Electrospray and High-Performance Liquid Chromatography/Tandem Mass Spectrometry with Atmospheric Pressure Chemical Ionization, *J. Mass Spectrom. 33*, 1192–1198.
51. Wu, W., McDonough, V.M., Nickels, J.T., Ko, J., Fischl, A.S., Vales, T.R., Merrill, A.H., Jr., and Carman, G.M. (1995) Regulation of Lipid Biosynthesis in *Saccharomyces cerevisiae* by Fumonisin B1, *J. Biol. Chem. 270*, 13171–13178.
52. Schneider, G., and Kennedy, E.P. (1970) Partial Purification and Properties of Diglyceride Kinase from *E. coli*, *Biochim. Biophys. Acta 441*, 201–212.
53. Preiss, J., Loomis, C.R., Bishop, R.W., Stein, R., Niedel, J.E., and Bell, R. (1986) Quantitative Measurement of *sn*-1,2 DAG in Platelets, Hepatocytes, and Normal ras and sis-Transformed Normal Rat Kidney Cells, *J. Biol. Chem. 261*, 8597–8600.
54. Preiss, J.E., Loomis, C.R., Bell, R.M., and Niedel, J. (1987) Quantitative Measurement of *sn*-1,2 Diacylglycerols, *Methods Enzymol. 141*, 295–301.
55. Bligh, E.G., and Dyer, W.J. (1959) A Rapid Method of Total Lipid Extraction and Purification, *Can. J. Biochem. Physiol. 37*, 911–917.
56. Folch, J., Lees, M., and Sloane-Stanley, G.H. (1957) A Simple Method for the Isolation and Purification of Total Lipid from Animal Tissues, *J. Biol. Chem. 226*, 497–509.
57. Perry, D.K., and Hannun, Y.A. (1999) The Use of Diglyceride Kinase for Quantifying Ceramide, *TIBS 24*, 226–227.
58. Van Veldhoven, P., Bishop, R.W., Yurivich, D.A., and Bell, R.M. (1995) Ceramide Quantitation: Evaluation of a Mixed Micellar Assay Using *E. coli* Diacylglycerol Kinase, *Biochem. Mol. Biol. Int. 36*, 21–30.

[Received December 13, 1999, and in final revised form May 12, 2000; revision accepted June 13, 2000]

Autoxidation of Methyl Linoleate: Identification of the Bis-allylic 11-Hydroperoxide

Alan R. Brash*

Department of Pharmacology, Vanderbilt University, Nashville, Tennessee 37232

ABSTRACT: Based on the understanding of lipid peroxidation as a free radical chain reaction, over 50 yr ago the three primary products of linoleic acid autoxidation were predicted to be the 9-, 11-, and 13-hydroperoxides. The 9- and 13-hydroperoxides were found at the time, but formation of 11-hydroperoxylinoleate or any other bis-allylic fatty acid hydroperoxide has not been reported heretofore as a product of lipid peroxidation reactions. In vitamin E-controlled autoxidation of methyl linoleate, the 11-hydroperoxy derivative was identified as the next most prominent primary peroxidation product after the 9- and 13-hydroperoxides. It was present in approximately 5–10% of the abundance of the 9- or 13-hydroperoxide. The structures of 11-hydroperoxylinoleate and its 11-hydroxy derivative were established by high-pressure liquid chromatography, ultraviolet spectroscopy, gas chromatography–mass spectroscopy, and ^{1}H nuclear magnetic resonance spectroscopy. The 11-hydroperoxide was not detectable in the absence of α-tocopherol, indicating that efficient trapping of the 11-peroxyl radical as the hydroperoxide is critical to permitting its accumulation.

Paper no. L8520 in *Lipids 35,* 947–952 (September 2000).

Following development of the concepts of lipid peroxidation as a free radical chain reaction in the 1940s (reviewed in Ref. 1), attempts were made to characterize the nature of the primary peroxidation products of the prototypical polyunsaturated lipid, linoleic acid. It follows from an understanding of tautomerism of the initial free radical that three positions are available for reaction with molecular oxygen, namely, C9, C11, and C13 (Scheme 1).

In studying the products from linoleic acid, Bergstrom and colleagues found the expected 9- and 13-hydroperoxides, whereas the 11-hydroperoxide was not detected (2,3). It was uncertain at the time whether the 11-hydroperoxide was formed in very low yield and/or was highly unstable and thus could not be isolated. In further studies over the years, the allylic nonconjugated 8- and 14-hydroperoxylinoleates were isolated as autoxidation products (4), but detection of the 11-hydroperoxide remained elusive (e.g., Refs. 4–6). The present report describes conditions for the isolation of the bis-allylic hydroperoxide from autoxidation of methyl linoleate.

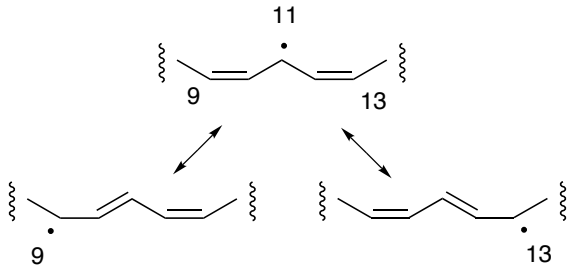

SCHEME 1

EXPERIMENTAL PROCEDURES

Materials. Methyl linoleate was purchased from Nu-Chek-Prep Inc. (Elysian, MN). Autoxidation products with conjugated diene chromophores were quantified by ultraviolet (UV) spectroscopy (ε = 23,000 M^{-1} cm^{-1} at 235 nm). Vitamin E (α-tocopherol; Sigma Chemical Co., St. Louis, MO) was quantified by using a value of $E_{1\%}$ = 76 at 292 nm in ethanol, (i.e., 100 μg/mL gives an absorbance of 0.76 at 292 nm).

Autoxidation conditions. Reactions were run essentially as described by Peers and Coxon (7) using mixtures of methyl linoleate and 5% by weight of α-tocopherol. The mixture (0.25–0.6 g) was taken to dryness in a 1-L flask, flushed with oxygen, and kept for several days in an oven at 35–37°C. The sample was flushed again with oxygen, usually every day. After 3 d, the sample was examined daily by UV spectroscopy: the whole sample was dissolved in 10 mL dichloromethane, and the UV spectrum of a 5-μL aliquot was recorded in 2 mL of methanol using a Beckman DU-7 (Fullerton, CA) scanning spectrophotometer. Reaction was continued as a dry film under oxygen until ≈20% conversion to conjugated diene was evident from UV spectroscopy. After several days, the distinct 292 nm absorbance of α-tocopherol became less evident and the sample was replenished with an additional 5% α-tocopherol by weight.

High-pressure liquid chromatography (HPLC) analyses. Autoxidized methyl linoleate was analyzed by straight-phase (SP)-HPLC using a Beckman 5 μm silica column and a sol-

*Address correspondence at Department of Pharmacology, Vanderbilt University, 23rd Ave at Pierce, Nashville, TN 37232-6602.
E-mail: alan.brash@mcmail.vanderbilt.edu

Abbreviations: GC–MS, gas chromatography–mass spectrometry; HETE, hydroxyeicosatetraenoic acid; NMR, nuclear magnetic resonance; RP-HPLC, reversed-phase high-pressure liquid chromatography; SP-HPLC, straight-phase HPLC; TMS, trimethylsilyl; UV, ultraviolet.

vent of hexane/isopropanol 100:1 or 100:0.5 (vol/vol). For analytical work, the products were monitored by on-line detection using a Hewlett-Packard 1040A diode array UV detector (Palo Alto, CA). For collection of products, samples of up to 4 mg total of hydroperoxide products (and including in the sample larger amounts of unchanged methyl linoleate) were injected on an Alltech (Deerfield, IL) 10 µm semipreparative silica column (25 × 1 cm) eluted with hexane/isopropanol (100:0.5, vol/vol) at a flow rate of 5 mL/min. For collection of products, the column effluent was monitored using a Spectrophysics (San Jose, CA) variable wavelength UV detector set at 210 nm. Reversed-phase (RP)-HPLC analysis and purification of 0.5-mg aliquots of the novel product were carried out using a Beckman Ultrasphere 5 µ ODS column (25 × 0.46 cm) with an Upchurch guard column and a solvent system of methanol/water, 85:15 (vol/vol). Final purification by SP-HPLC was carried out on aliquots of up to 0.5 mg per injection using the Beckman analytical silica column and the hexane/isopropanol 100:1 (vol/vol) solvent.

Derivatization. Hydrogenation of 5–10 µg of hydroxy fatty acid methyl ester was carried out by bubbling hydrogen through a suspension of platinum oxide (*ca.* 1 mg) in 100 µL ethanol for 2 min followed by addition of water and extraction with ethyl acetate. Trimethylsilyl (TMS) ether derivatives were prepared by treatment with bis(trimethylsilyl)trifluoracetamide (10 µL) and pyridine (5 µL) for 15 min at room temperature. Subsequently, the reagents were evaporated under a stream of nitrogen and the samples dissolved in hexane for gas chromatography–mass spectrometry (GC–MS) analysis.

GC–MS. Mass spectra were recorded in the electron impact mode using a Hewlett-Packard HP5980 engine mass spectrometer operated at 70 eV and coupled to a Hewlett-Packard 5890 gas chromatograph equipped with an SPB-1 fused-silica capillary column of 5 or 15 m × 0.25 mm inner diameter. Samples were injected on column at an oven temperature of 150°C, and after 1 min the temperature was programmed to 300°C at 10 or 20°C/min.

Nuclear magnetic resonance (NMR) analyses. Spectra were recorded in deuterated benzene using a Bruker 400 MHz instrument (Billerica, MA). Chemical shifts are reported in relation to tetramethylsilane (δ 0.0).

RESULTS

Isolation of a novel product. SP-HPLC analysis of vitamin E-controlled autoxidation reactions of methyl linoleate showed the formation of 13- and 9-hydroperoxy products and one distinct minor product that chromatographed between the two main peaks (Fig. 1). In contrast to the major 13- and 9-hydroperoxides, the minor product did not contain a conjugated diene chromophore and was detectable only at lower wavelengths in the UV. The unreduced product was collected from injections of the autoxidation mixture on a semipreparative SP-HPLC column. Following reduction of the hydroperoxides, the retention times of all the products on SP-HPLC increased, and the minor product shifted its chromatographic mobility and now eluted with the 9-hydroxylinoleate (Fig. 2A), or, on a silica column from a different manufacturer (Alltech), as a peak in the tail of the 9-hydroxylinoleate (not shown).

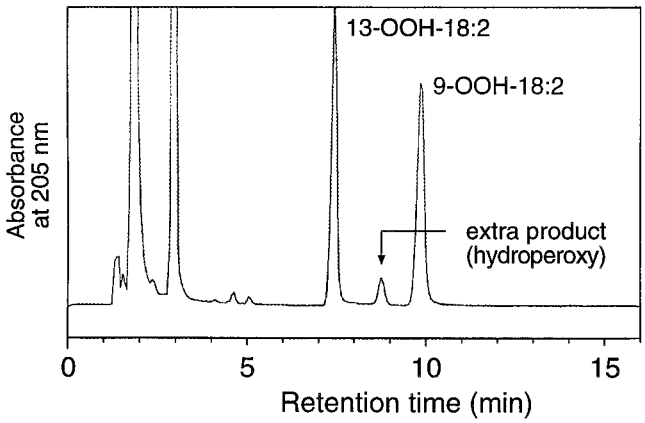

FIG. 1. Straight-phase high-pressure liquid chromatographic (SP-HPLC) analysis of autoxidized methyl linoleate. Vitamin E-controlled autoxidation of methyl linoleate was analyzed on an Alltech (Deerfield, IL) silica column (25 × 0.46 cm) using a solvent of hexane/isopropanol (100:0.5, vol/vol) eluted at 2 mL/min with ultraviolet detection at 205 nm. The large peak near the solvent front is methyl linoleate and the second large peak at 3 min is α-tocopherol. The novel product is marked as "extra product, (hydroperoxy)."

On the RP-HPLC system used for further purification (Fig. 2B), the novel product (as the hydroperoxide or the hydroxy derivative) eluted at ≈10 mL, substantially earlier than the combined peak of 9- and 13-hydro(per)oxides (retention volume ≈13 mL), allowing complete removal of these contaminants from the semipreparative SP-HPLC. The hydroperoxy and hydroxy derivatives of the new product were not resolved from each other on RP-HPLC; they formed shoulders of the same chromatographic peak. Prior to GC–MS and NMR analyses, the new product was finally re-purified as the hydroperoxide or hydroxy derivative by SP-HPLC. It was recovered in a yield of approximately 5–10% relative to one of two main products, or up to a 5% yield of the combined products. About 0.5–0.75 mg of 11-hydroperoxide was recovered pure from autoxidations that gave 7.5 mg each of purified 9- and 13-hydroperoxides.

Spectral analyses. When analyzed as the methyl ester TMS ether of the triphenylphosphine-reduced (hydroxy) derivative, the novel product had a similar mass spectrum to 9- and 13-hydroxylinoleates. The most prominent ions were present at *m/z* 382 (M^+, 35% relative abundance), *m/z* 311 ($M - C_5H_{11}$, 48%), *m/z* 225 (C9–C18, base peak), and *m/z* 130 (55% relative abundance). The differences from the spectra of the 9- and 13-hydroxylinoleates were in ion abundances, making it difficult to distinguish the different compounds with the double bonds still present. The position of the hydroxyl group in the new product was established unambiguously from the mass spectrum of the methyl ester TMS ether derivative of the hydrogenated product (Fig. 3). The

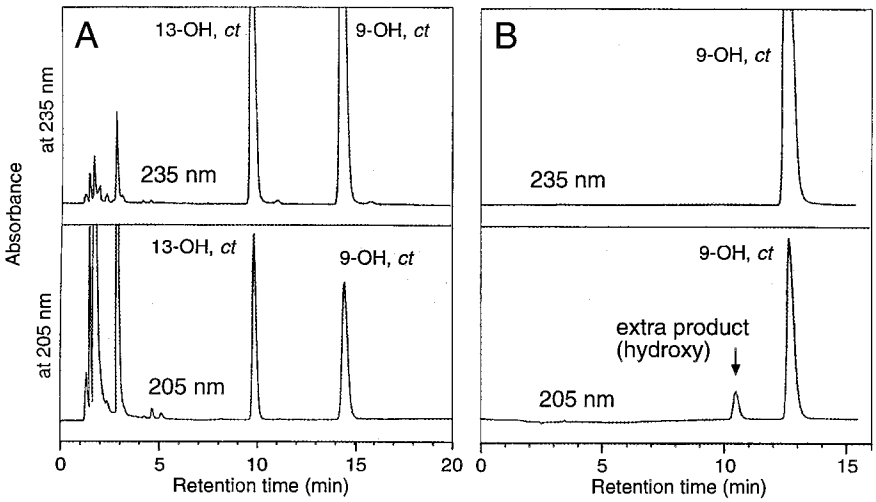

FIG. 2. SP-HPLC and reversed-phase (RP)-HPLC analyses of hydroxylinoleate methyl esters. (A) Following reduction with triphenylphosphine to the corresponding hydroxy products, the sample shown in Figure 1 was analyzed by SP-HPLC using the identical chromatographic conditions. The absorbance scales at 205 and 235 nm are set at identical values [0.35 absorbance units (AU) full scale]. (B) The peak of 9-hydroxylinoleate methyl ester collected from SP-HPLC was chromatographed on RP-HPLC using a Beckman 5 μm ODS Ultrasphere column (25 × 0.46 cm; Fullerton, CA) and a solvent of methanol/water (85:15, vol/vol) with a flow rate of 1 mL/min. The absorbance scales at 205 and 235 nm are set at identical values (0.5 AU full scale). For abbreviation see Figure 1.

base peak was recorded at *m/z* 73. The two most prominent ions above *m/z* 100 were the two α-cleavage ions at *m/z* 287 and 201 (26 and 62% relative abundance, respectively). This establishes the position of the hydroxyl group at C-11. Other structurally significant ions were recorded at *m/z* 371 (M – 15, <0.5% relative abundance), *m/z* 355 (M – 31, <0.5%), and *m/z* 339 (M – 47, 1%). Additional prominent ions above *m/z* 100 were *m/z* 258 [M – 128, 7%, an ion that

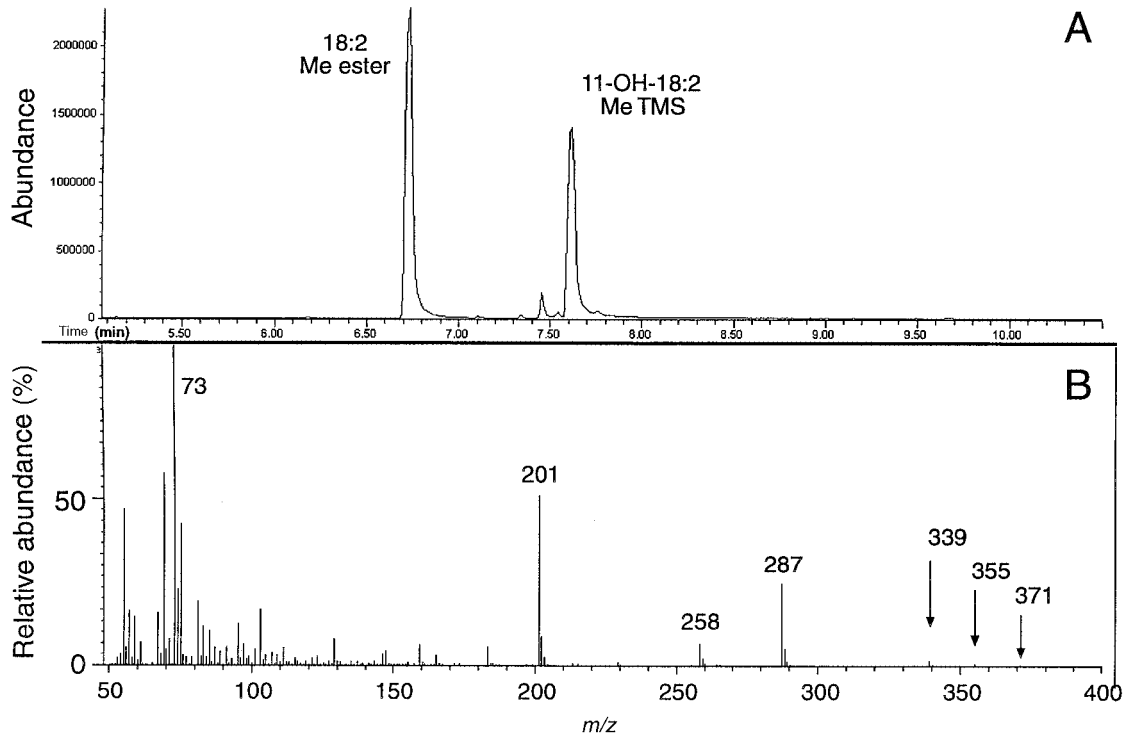

FIG. 3. Gas chromatography–mass spectrometry analysis of hydrogenated 11-hydroxylinoleate, methyl ester trimethylsilyl (TMS) ether derivative. Panel A shows the total ion chromatogram. The largest peak is methyl stearate (18:2 Me ester) formed by loss of the C-11 hydroxyl during hydrogenation. (B) The mass spectrum of the methyl ester TMS ether derivative of 11-hydroxy-stearate (11-OH-18:2 MeTMS) is shown.

had the same chromatographic profile as the major diagnostic ions in the GC peak; it may represent migration of the TMS group to the ester carbonyl followed by cleavage at C-10/C-11 and elimination of the fragment OHC–$(CH_2)_6$–CH_3], *m/z* 183 (6%), *m/z* 159 (7%), *m/z* 129 (8%), and *m/z* 103 (16%).

The ^{1}H NMR spectra of the 11-hydroperoxide and the 11-hydroxylinoleate are in accord with the spectral characteristics reported for the bis-allylic arachidonate products, 13-hydroxyeicosatetraenoic acid (13-HETE) (8) and 10-HETE (9). Most notably, the geminal hydro(pero)xy proton at C-11 has a chemical shift unusually far downfield and it appears among the olefinic protons (Fig. 4). In the hydroxy derivative (Fig. 4B), H11 occurs at 5.37 ppm as a double triplet. The triplet is accounted for by the equivalent coupling to H10 and H12 (J = 8.5 Hz), while a 3.5 Hz coupling that splits the triplet occurs between the geminal H11 proton and the proton on the hydroxyl group itself; the latter is a doublet (J = 3.5 Hz) at 1.00 ppm. The C-11 geminal proton reverted to a simple triplet upon exchange of the hydroxyl proton with D_2O, with concomitant elimination of the hydroxyl signal at 1.00 ppm. In the hydroperoxide, H11 appears as a clean triplet at 5.75 ppm (Fig. 4A) accounted for by the equal couplings to H10 and H12. An additional 3.5 Hz coupling can occur through the oxygen atom in the hydroxy derivative, but no significant long-range coupling is possible through both oxygens of the hydroperoxide.

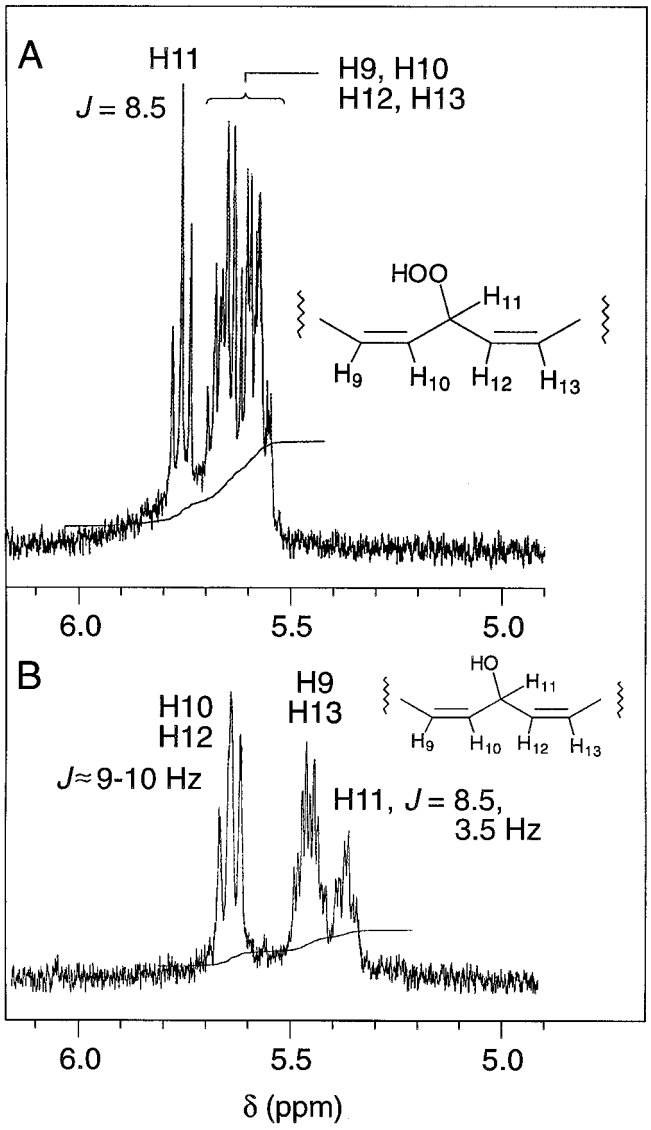

FIG. 4. Olefinic and H11 protons in the ^{1}H nuclear magnetic resonance spectra (400 MHz) of 11-hydroperoxy- and 11-hydroxylinoleate methyl esters in d_6-benzene. The two panels show the signals from H9, H10, H11, H12, and H13 of (A) 11-hydroperoxylinoleate, and (B) 11-hydroxylinoleate.

The spectrum of 11-hydroxylinoleate has the four olefinic protons resolved into two pairs, permitting assessment of the double-bond configurations. As the signals from H10 and H12 at 5.65 ppm are superimposed, the olefinic region centered on C11 must be symmetrical. The slightly broad triplet of H10/H12 (almost a doublet of doublets) is caused by the partially superimposed couplings of 8.5 Hz to the geminal proton H11 ($J_{10,11} = J_{11,12}$) and the ≈10 Hz coupling across the double bonds ($J_{9,10} = J_{12,13}$). The latter defines the two double bonds as *cis*.

^{1}H NMR (400 MHz, in deuterated benzene, using 7.24 ppm for the residual protons in the solvent) gave for 11-hydroperoxylinoleate methyl ester (ppm): δ 0.95 (*t*, 3 protons, H18), 1.2–1.5 (*m*, 14 protons, H4, H5, H6, H7, H15, H16, H17), 1.65 (*p*, 2 protons, H3), 2.2 (*m*, 6 protons, H2, H8, H14), 3.45 (*s*, 3 protons, C$\underline{H}_3$O), 5.55–5.7 (*m*, 4 protons, H9, H10, H12, H13), 5.75 (*t*, 1 proton, H11, $J_{9,10} = J_{11,12}$ = 8.5 Hz), 7.55 (*s*, 1 proton, –OO$\underline{H}$). For 11-hydroxylinoleate methyl ester (ppm): δ 0.95 (*t*, 3 protons, H18), 1.0 (*d*, 1 proton, <1 in area, –OH, $J_{11,-OH}$ = 3.5 Hz), 1.2–1.4 (*m*, 14 protons, H4, H5, H6, H7, H15, H16, H17), 1.6 (*p*, 2 protons, H3), 2.2 (*m*, 6 protons, H2, H8, H14), 3.45 (*s*, 3 protons, C$\underline{H}_3$O), 5.37 (*dt*, 1 proton, H11, $J_{10,11} = J_{11,12}$ = 8.5 Hz, $J_{11,-OH}$ = 3.5 Hz), 5.45 (*m*, 2 protons, H9, H13), 5.65 (*t/dd*, 2 protons, H10, H12, J ≈ 8.5–10 Hz).

The 11-hydroperoxy and 11-hydroxy products do not contain a conjugate diene chromophore yet their UV spectra can be distinguished from the spectrum of linoleate and from each other (Fig. 5). A similar extension to the end absorbance of the nonconjugated chromophore was reported for bis-allylic 7-, 10-, and 13-HETE (10).

Autoxidation in the absence of vitamin E. In autoxidation of a dry film of methyl linoleate in the absence of α-tocopherol (analyzed after ≈15% conversion to conjugated diene), the SP-HPLC profile showed prominent peaks for the 9- and 13-hydroperoxides with both *cis-trans* and *trans-trans* conjugated dienes (Fig. 6). The 11-hydroperoxide was not visible, even though, based on retention time, it should have appeared as a peak in the tail of the 13-hydroperoxy-9-*trans*,11-*trans*-linoleate. When the peak and tail of the *trans-trans* 13-hydroperoxide were collected from SP-HPLC and examined on RP-HPLC at 205 and 235 nm, there was no trace of a product with the chromatographic and spectral characteristics of 11-hydroperoxylinoleate methyl ester.

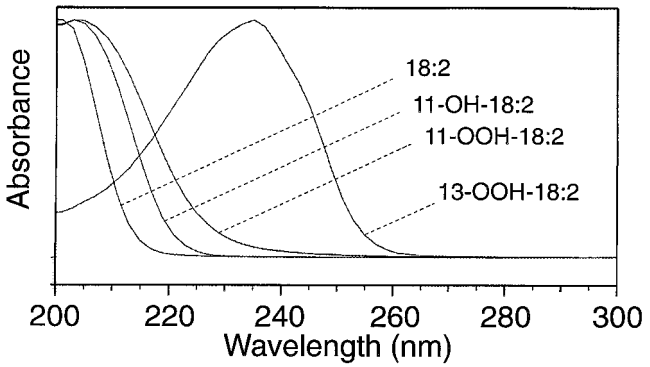

FIG. 5. Ultraviolet spectra of methyl linoleate and its 11-hydroperoxy and 11-hydroxy derivatives. Spectra were recorded using a Hewlett-Packard 1040A diode array detector (Palo Alto, CA) during an RP-HPLC run in methanol/water (85:15 vol/vol) solvent (or 100% methanol for methyl linoleate, 18:2). To avoid saturation of the signal at the low wavelengths, the maximal absorbance at 205 nm was kept below 0.5 AU; spectra at the apex and on the upslope of chromatographic peaks were indistinguishable, confirming that there was no significant saturation of the signal in these spectra. The spectrum of 13-hydroperoxylinoleate is included for comparison. The spectra are normalized to λ_{max} and do not convey relative molar extinction values. Previous studies suggest that at 205 nm the bis-allylic products and the nonconjugated fatty acid derivatives have similar molar absorptions (Ref. 10), estimated here as around 10,000 for the linoleic acid derivatives. For abbreviations see Figure 2.

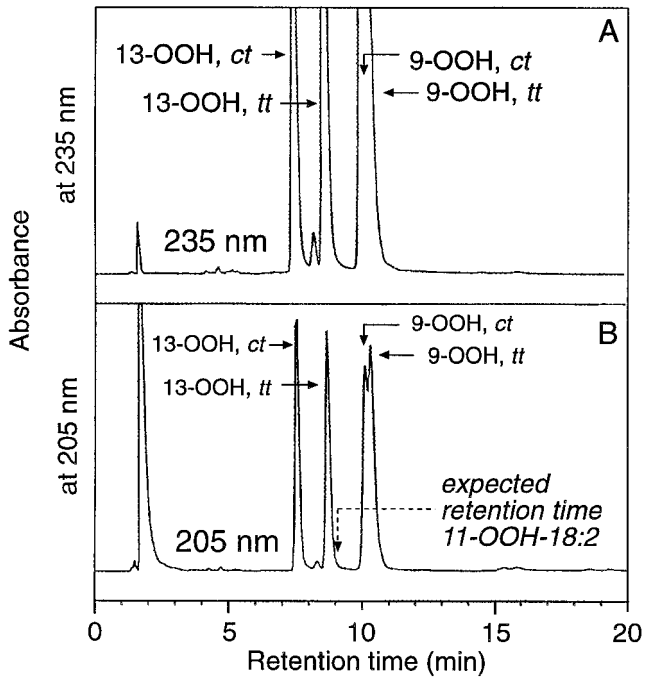

FIG. 6. SP-HPLC analysis of methyl linoleate autoxidized in the absence of vitamin E. Chromatographic conditions were identical to those given in the legend of Figure 1. The absorbance scales at 205 and 235 nm are set at identical values (0.35 AU full scale). See Figures 1 and 2 for abbreviations.

DISCUSSION

The presence of α-tocopherol in the autoxidation of methyl linoleate allowed detection of a previously unrecognized primary product of lipid peroxidation, the bis-allylic 11-hydroperoxide. Efficient trapping of peroxyl radicals by α-tocopherol and other hydrogen atom donors is known to suppress the isomerization of the *cis-trans* conjugated 9- and 13-hydroperoxyl radicals and thus reduce the formation of *trans-trans* isomers and other secondary products (cf. Figs. 1 and 6) (7,11). This activity also appears to be the basis of the trapping and preservation of the bis-allylic product. The critical competition is at the peroxyl radical stage. The relatively unstable bis-allylic peroxyl radical is formed as originally predicted (1,2,12). If vitamin E is present, the peroxyl radical is trapped; the bis-allylic hydroperoxide product is stable under the conditions of its formation, and it does not convert to the 9- and 13-hydroperoxides. If vitamin E is not present, the 11-peroxyl radical fragments and re-adds molecular oxygen to give the thermodynamically more stable conjugated diene peroxyls, which then go on to the 9- and 13-hydroperoxide products.

In the course of relatively recent experiments on the oxygenation of polyunsaturated fatty acids, bis-allylic hydroxy or hydroperoxy products have been found as enzymatic products. The first report was of the occurrence of the 13-hydroxyeicosapentaenoic acid in the marine red algae *Lithothamnion corallioides* and *L. calcareum* (8). As a product of linoleic acid metabolism in *L. corallioides* (13), 11*R*-hydroxylinoleate was subsequently found. Later in the 1990s, bis-allylic product(s) were detected as hydroxy derivatives in cytochrome P450 reactions (10,14,15) and in the myoglobin-catalyzed monooxygenation of linoleic acid (16), and as hydroperoxide products of the manganese-containing lipoxygenase of the fungus *Gäumannomyces graminis* (17) and of the 8*R*-lipoxygenase domain of the peroxidase-lipoxygenase fusion protein from the coral *Plexaura homomalla* (18).

The bis-allylic 11-hydroperoxylinoleate derivative is fairly stable to chromatographic and other analytical manipulations, provided the sample is not subjected to low pH (10,14). For methyl esters, as in the present study, there is no need to acidify during chromatography or HPLC. For long-chain free fatty acids the pK_a values are approximately pH 7–8 for the parent fatty acids (19,20) and probably in the region of pH 6–7 for the monohydro(pero)xy products, so it is not necessary to acidify to pH 3–4 to achieve an efficient extraction. The long-term stability of these products is similar to other fatty acid hydroperoxides. A sample of oxidized linoleate methyl ester kept in the −20°C freezer for 4 yr (in ethanol in the presence of α-tocopherol from the original autoxidation) contained a similar proportion of the 11-hydroperoxide as freshly autoxidized methyl linoleate.

Under the appropriate conditions, formation and accumulation of bis-allylic products can be expected for other polyunsaturated lipids. As evidence of this, several years ago we detected the 10,15-dihydro(pero)xyeicosatrienaoate among the primary oxygenation products in the vitamin E-controlled autoxidation of 15-hydroxyeicosa-8,11,13-trienoate methyl ester (Brash, A.R., and Boeglin, W.E., unpub-

lished observations). At the time there was some doubt as to the origin of this bis-allylic hydroperoxy derivative, but it is now evident that its formation as a primary oxygenation product is no longer in question.

ACKNOWLEDGMENTS

I thank Dr. Ned Porter for discussions on bis-allylic oxygenation, Dr. Thomas M. Harris for comments on the NMR spectra, Sam Saleh for acquiring the spectra, Betty Fox for help with the mass spectrometry, and the reviewers for helpful comments. This work was supported by NIH grant GM-53638.

REFERENCES

1. Uri, N. (1961) Physico-chemical Aspects of Autoxidation, in *Autoxidation and Antioxidants* (Lundberg, W.O., ed.), Vol. I, pp. 55–106, John Wiley, Interscience, New York.
2. Bergström, S. (1945) Autoxidation of Linoleic Acid, *Nature 156,* 717–718.
3. Bergström, S., Blomstrand, R., and Laurell, S. (1950) On the Autoxidation of Linoleic Acid in Aqueous Colloidal Solution, *Acta Chem. Scand. 4,* 245–250.
4. Haslbeck, F., Grosch, W., and Firl, J. (1983) Formation of Hydroperoxides with Unconjugated Diene Systems During Autoxidation and Enzymic Oxygenation of Linoleic Acid, *Biochim. Biophys. Acta 750,* 185–193.
5. Chan, H.W.-S., and Levett, G. (1976) Autoxidation of Methyl Linoleate. Separation and Analysis of Isomeric Mixtures of Methyl Linoleate Hydroperoxides and Methyl Hydroxylinoleates, *Lipids 12,* 99–104.
6. Roberts, D.H. (1982) I. Vinyl Cyclopropyl Bromides as Precursors to Fatty Acid Hydroperoxides. II. Minor Oxidation Products of Methyl Linoleate, Ph.D. Thesis in Chemistry, Duke University, Durham.
7. Peers, K.F., and Coxon, D.T. (1983) Controlled Synthesis of Monohydroperoxides by α-Tocopherol Inhibited Autoxidation of Polyunsaturated Lipids, *Chem. Phys. Lipids 32,* 49–56.
8. Guerriero, A., D'Ambrosio, M., and Pietra, F. (1990) Novel Hydroxyicosatetraenoic and Hydroxyicosapentaenoic Acids and a 13-Oxo Analog. Isolation from a Mixture of the Calcareous Red Algae *Lithothamnion corallioides* and *Lithothamnion calcareum* of Brittany Waters, *Helv. Chim. Acta 73,* 2183–2189.
9. Yeola, S.N., Saleh, S.A., Brash, A.R., Prakash, C., Taber, D.F., and Blair, I.A. (1996) Synthesis of 10(*S*)-Hydroxyeicosatetraenoic Acid: a Novel Cytochrome P-450 Metabolite of Arachidonic Acid, *J. Org. Chem. 61,* 838–841.
10. Brash, A.R., Boeglin, W.E., Capdevila, J.H., Suresh, Y., and Blair, I.A. (1995) 7-HETE, 10-HETE, and 13-HETE Are Major Products of NADPH-Dependent Metabolism of Arachidonic Acid in Rat Liver Microsomes. Analysis of Their Stereochemistry and the Stereochemistry of Their Acid-Catalyzed Rearrangement, *Arch. Biochem. Biophys. 321,* 485–492.
11. Porter, N.A., Weber, B.A., Weenen, H., and Khan, J.A. (1980) Autoxidation of Polyunsaturated Lipids. Factors Controlling the Stereochemistry of Product Hydroperoxides, *J. Am. Chem. Soc. 102,* 5597–5601.
12. Khan, N.A., Lundberg, W.O., and Khan, J.A. (1954) Displacement Analysis of Lipids. IX. Products of the Oxidation of Methyl Linoleate, *J. Am. Chem. Soc. 76*, 1179–1784.
13. Hamberg, M., Gerwick, W.H., and Åsen, P.A. (1992) Linoleic Acid Metabolism in the Red Alga *Lithothamnion corallioides*: Biosynthesis of 11(*R*)-Hydroxy-9(*Z*),12(*Z*)-octadecadienoic Acid, *Lipids 27,* 487–493.
14. Oliw, E.H., Brodowsky, D., Hörnsten, L., and Hamberg, M. (1993) Bis-allylic Hydroxylation of Polyunsaturated Fatty Acids by Hepatic Monooxygenases and Its Relation to the Enzymatic and Nonenzymatic Formation of Conjugated Hydroxy Fatty Acids, *Arch. Biochem. Biophys. 300,* 434–439.
15. Oliw, E.H. (1993) Bis-allylic Hydroxylation of Linoleic Acid and Arachidonic Acid by Human Hepatic Monooxygenases, *Biochim. Biophys. Acta 1166,* 258–263.
16. Hamberg, M. (1997) Myoglobin-Catalyzed Bis-allylic Hydroxylation and Epoxidation of Linoleic Acid, *Arch. Biochem. Biophys. 344,* 194–199.
17. Hamberg, M., Su, C., and Oliw, E. (1998) Manganese Lipoxygenase. Discovery of a Bis-allylic Hydroperoxide as Product and Intermediate in a Lipoxygenase Reaction, *J. Biol. Chem. 273,* 13080–13088.
18. Boutaud, O., and Brash, A.R. (1999) Purification and Catalytic Activities of the Two Domains of the Allene Oxide Synthase-Lipoxygenase Fusion Protein of the Coral *Plexaura homomalla*, *J. Biol. Chem. 274,* 33764–33770.
19. Bild, G.S., Ramadoss, C.S., and Axelrod, B. (1977) Effect of Solvent Polarity on the Activity of Soybean Lipoxygenase Isozymes, *Lipids 12,* 732–735.
20. Glickman, M.H., and Klinman, J.P. (1996) Lipoxygenase Reaction Mechanism: Demonstration That Hydrogen Abstraction from Substrate Precedes Dioxygen Binding During Catalytic Turnover, *Biochemistry 35,* 12882–12892.

[Received May 1, 2000, and in revised form August 7, 2000; revision accepted August 8, 2000]

Synthesis of 9,12-Dioxo-10(*Z*)-dodecenoic Acid, a New Fatty Acid Metabolite Derived from 9-Hydroperoxy-10,12-octadecadienoic Acid in Lentil Seed (*Lens culinaris* Medik.)

Bernd A.W. Gallasch and Gerhard Spiteller*

Organische Chemie I, Universität Bayreuth, 95440 Bayreuth, Germany

ABSTRACT: The previously unknown linoleic acid peroxidation product 9,12-dioxo-10(*Z*)-decenoic acid (***Z*5**) was detected in lentil seed flour (*Lens culinaris* Medik.) by electron impact mass spectrometry (EI-MS) after derivatization with pentafluorobenzyl-hydroxylamine-hydrochloride, methylation of acidic groups with diazomethane, and protection of hydroxylic groups with *N*-methyl-*N*-trimethylsilyl-trifluoroacetamide. The structure of the natural product was confirmed by synthesis of ***Z*5**, 9,12-dioxo-10(*E*)-decenoic acid, and derivatives. EI-MS, nuclear magnetic resonance and gas chromatographic data of these compounds and synthetic intermediates are discussed.

Paper no. L8479 in *Lipids 35*, 953–960 (September 2000).

Lipid peroxidation processes induced by lipoxygenase (LOX; EC 1.13.11.12) are reported to occur in plant systems; they were observed for instance in germinating cereals, in wheat flour suspensions (1–3), and in legumes (4). Linoleic acid is transformed by LOX to 9-hydroperoxy-10,12-octadecadienoic acid (9-HPODE) or 13-hydroperoxy-9,11-octadecadienoic acid (13-HPODE) depending on LOX type and conditions. Further oxidation and decay of HPODE generate aldehydes, e.g., 4-hydroxynonenal (4-HNE), 9-oxononanoic acid, and 2,4-decadienal, along with other products (5,6). Some of these compounds show biological activity (7–9). An excellent method for trapping aldehydic products is the reaction with pentafluorobenzylhydroxylaminehydrochloride (PFBHA·HCl) added to reaction or extraction mixtures (10,11). The pentafluorobenzyloximes are generated under very mild conditions [3 h at room temperature (RT)]. Their electron impact (EI) mass spectra often show a characteristic fragmentation pattern (12).

*To whom correspondence should be addressed at Organische Chemie I, Universitätsstrasse 30, 95440 Bayreuth, Germany.
E-mail: gerhard.spiteller@uni-bayreuth.de

Abbreviations: CC, column chromatography; DMO, dimethyldioxirane; DMS, dimethylsulfide; EI-MS, electron impact mass spectrometry; GC–EI-MS, gas chromatography–electron impact mass spectrometry; HNE, 4-hydroxynonenal; HPODE, hydroperoxyoctadecadienoic acid; LOX, lipoxygenase; MCPBA, metachloroperbenzoic acid; MSTFA, *N*-methyl-*N*-trimethylsilyl trifluoroacetamide; NMR nuclear magnetic resonance; PCC, pyridinium chlorochromate; PFBHA·HCl, pentafluorobenzyloxime hydrochloride; PFBO, pentafluorobenzyloxime; RI, retention index; RT, room temperature; TEG, triethyleneglycol; TLC, thin-layer chromatography; TPP, tetraphenylporphine; UV, ultraviolet; XOD, xanthine oxidase.

Hamberg and Gotthammar (13) found that among other reactions 9-HPODE suffered transformation to 12,13-epoxy-9-hydroxy-10-octadecenoic acid, which was degraded by hydrolysis to 9,12,13-trihydroxy-10-octadecenoic acid (14). This compound was cleaved oxidatively to 9-hydroxy-12-oxo-10-dodecenoic acid (**4**) by reaction with $NaIO_4$ (15) or $Pb(OAc)_4$ (16). Recently, Gardner (17) and Noordermeer *et al.* (18) identified **4** to be an enzymic product after incubation experiments of 13*S*-HPODE with LOX-1 protein preperations from soybean and alfalfa. Loidl-Stahlhofen *et al.* (19) and Mlakar and Spiteller (20) detected **4** in traces after autoxidation of linoleic acid in the form of its 12-*O*-2,3,4,5,6-pentafluorobenzyloximino-9-trimethylsilyloxy-10(*E*)-dodecenoic acid methyl ester derivative ($M^{+\cdot}$ = 509). In this paper we describe the structure of the new metabolite 9,12-dioxo-10(*Z*)-decenoic acid and its *E* isomer.

EXPERIMENTAL PROCEDURES

Materials. If not otherwise marked, all reagents were purchased from Aldrich, Fluka, or Sigma (Deisenhofen, Germany). All solvents, except MeOH, were freshly distilled and dried with Alox B and $LiAlH_4$, if required. Dry MeOH was prepared by continuous distillation over Mg. *N*-Methyl-*N*-trimethylsilyl-trifluoroacetamide (MSTFA) was obtained from Machery-Nagel (Düren, Germany). An etheral solution of diazomethane was freshly prepared. A solution of 2,2-dimethyldioxirane in acetone was prepared according to Adam *et al.* (21). Photolysis was carried out with a 500 W Hg-lamp from LOT-Oriel (Darmstadt, Germany).

Chromatographic and instrumental methods. Gas chromatography (GC) was performed with a United Technologies Packard Model 438 gas chromatograph equipped with a methyl silicone capillary column DB-5 (30 m × 0.32 mm, film thickness 0.1 μm) from J&W Scientific (Mainz-Kastel, Germany), column head pressure 60 kPa. Hydrogen was used as carrier gas. Linear retention indices (RI) were calculated (22). GC–electron impact mass spectrometry (EI-MS) was carried out with a Finnigan MAT 95 mass spectrometer (Bremen, Germany) connected to a Hewlett-Packard 5890 series II gas chromatograph equipped with a methyl silicone capillary column DB-5ms (30 m × 0.32 mm, film thickness 0.32 μm) from

J&W Scientific. The nuclear magnetic resonance (NMR) spectra were acquired on an AM 300 Bruker NMR instrument (Rheinstetten, Germany) at 300 MHz for ^{1}H and 75 MHz for ^{13}C NMR, under standard conditions.

Indices of derivatives. Derivatization of the functional groups is indicated by addition of Latin letters to the compound number with respect to derivatization type. The first letter indicates derivatization of the acidic group at C-1 (**a**, methoxy; **a′**, ethoxy; **c**, trimethylsilyloxy). The second letter indicates derivatization of the functional group at the last carbon atom (**b**, pentafluorobenzyloximino, **c**, either MSTFA addition product to an aldehyde or trimethylsilyloxy product of a hydroxy function). The third letter indicates derivatization of the hydroxyl or oxo group in the chain (**b**, pentafluorobenzyloximino; **c**, trimethylsilyloxy).

Incubation experiments with lentil seed flour and structure elucidation by GC–MS. Freshly milled lentil seed flour (10 g) was stirred with 55.8 mg linoleic acid as substrate in 200 mL 0.067 M phosphorus buffer at pH 5.6 for 1 h at room temperature (RT). Twenty-five mL CH_2Cl_2, 50 mL MeOH, and 100 mg PFBHA·HCl were added to 20-mL aliquots to prepare a homogenous solution (23) and to transform carbonyl groups to their pentafluorobenzyloximes. After 3 h of incubation time and centrifugation the supernatant was separated. Two layers were obtained by addition of 25 mL H_2O and 25 mL CH_2Cl_2 to the supernatant. The solvent was removed from the organic layer *in vacuo*. The residue was subjected to saponification by treatment with 10 mL sodium methylate (1 M in MeOH) followed by neutralization with methanolic HCl (2 N in MeOH). After washing and removal of the solvent, acidic groups were protected by reaction with an etheral diazomethane solution, then hydroxy groups were trimethylsilylated with MSTFA (30 μL, 1 h, RT). The obtained samples were ready for GC and GC–EI-MS without removal of excess reagent.

Synthesis of the known starting compounds 12-hydroxy-10-dodecenoic acid or its methyl ester (**2** or **2a**) was carried out by formylation of undecenoic acid or its methyl ester (**1** or **1a**) according to Metzger and Biermann (24).

*Synthesis of 9,10-epoxy-12-hydroxydodecanoic acid (**3**).* Seven grams of 4-chloroperbenzoic acid [containing 70% metachloroperbenzoic acid (MCPBA), 20% water, and 10% metachlorobenzoic acid] was dissolved in 100 mL CH_2Cl_2 to separate the 4-chloroperbenzoic acid from water. After removing the solvent of the organic layer *in vacuo,* the residue was redissolved in 70 mL dry CH_2Cl_2. Fifty mL of the dried solution (Na_2SO_4) corresponding to 4 g (26 mmol) 4-chloroperbenzoic acid were added dropwise to 4.48 g (20.9 mmol) **2** in 50 mL dry CH_2Cl_2 at 0°C and stirred for 2 h at RT. A column head was prepared by addition of 25 g silica 60 (40–63 μm) and removal of the solvent. Fast column chromatography (CC) was carried out on 400 g silica 60 (40–63 μm) with 2.5 L cyclohexane/ethylacetate (1:2, vol/vol) resulting in 4.09 g (17.8 mmol) **3** (yield = 85%, by GC). After preparative thin-layer chromatography (TLC) of 400 mg of the epoxides on silica 60 with cyclohexane/ethylacetate (2:1 vol/vol) 200 mg (0.9 mmol) ***Z*3** (R_f = 0.39) and 50 mg (0.2 mmol) ***E*3** (R_f = 0.55) were obtained, corresponding to the *E*/*Z*-ratio of the primary product. ^{1}H NMR 300 MHz ($CDCl_3$) δ ppm ***Z*3**: 3.77 (2H, *dt, J* = 6.6*,* 1.4 Hz*,* on C12), 2.85 (1H, *m*, on C-10), 2.78 (1H, *td, J* = 5.5, 2.4 Hz, on C-9, *cis*), 2.33 (2H, *t, J* = 6.4 Hz), 1.95, 1.68 (2H, *m*, on C-11), 1.62 (2H, *m*, on C-8), 1.51 (2H, *m*, on C-7), 1.41 (2H, *m*, on C-3), 1.25–1.35 (6H, on C-4, C-5, C-6); ^{13}C NMR (75 MHz, $CDCl_3$) δ ppm ***Z*3**: 178.7 (C-1), 60.1 (C-12), 58.3 (C-9), 56.9 (C-10), 34.1 (C-11), 33.8 (C-2), 31.8 (C-8), 29.0, 28.8, C-4, C-5, C-6, 25.8 (C-7), 24.5 (C-3).

*Synthesis of methyl 9,10-epoxy-12-hydroxydodecanoate (**3a**).* Thirty-five mL (2.8 mmol) 2,2-dimethyldioxirane (DMO) in acetone (0.07 M) was added to 500 mg (2.2 mmol) **2a** and stirred at 0°C for 1 h. The solvent was removed *in vacuo* at RT. The residue (**3a**) was used without further purification (yield> 95% by GC). ^{1}H NMR 500 MHz ($CDCl_3$) δ ppm **3a**: 3.72 (2H, *brd*, on C-12), 3.61 (3H, *brt*, –O–CH_3), 2.80 (1H, *brdt*, on C-10), 2.72 (1H, *brdt*, on C-9), 2.24 (2H, *brt*, on C-2), 1.89, 1.65 (2H, *m*, on C-11), 1.56 (2H, *m*, on C-8), 1.47 (2H, *brt*, on C-7), 1.37 (2H, *brt*, on C-3), 1.22–1.35 (6H, *brt*, on C-4, C-5, C-6); ^{13}C NMR (125 MHz, $CDCl_3$) δ ppm **3a**: 59.8 (C-12), 58.2 (C-9), 56.8 (C10), 51.4 (–O–CH_3), 34.2 (C-11), 33.9 (C-2), 31.8 (C-8), 29.0, 28,8 C-4, C-5, C-6, 25.8 (C-7), 24.7 (C-3), C-1 not determined; retention index (RI) **3ac** (DB-5) = 2020. EI–MS data are given in Table 1.

*Synthesis of methyl 9-hydroxy-12-oxo-10(*E*)-dodecenoate (**E*4a*) and methyl 9,12-dioxo-10(*E*)-dodecenoate (**E*5a*).* Eighty mg (0.33 mmol) **3a** were added dropwise to 194 mg (0.9 mmol) pyridinium chlorochromate (PCC) dissolved in 5 mL dry CH_2Cl_2 and stirred for 1 h at RT. After addition of 30 mL dry Et_2O and 16 h stirring at RT, the black gum was extracted with dry ether. After derivatization of hydroxyl groups with MSTFA, the ratio of the main products ***E*4a**/***E*5a** was deduced by GC integrals to be ~ 1:1. Yield after preparative TLC on SiO_2 plates from Fluka with cyclohexane/ethylacetate (3:1, vol/vol) was 17 mg (0.07 mmol, yield = 21%) of ***E*4a** and 12 mg (0.05 mmol, yield = 15%) of ***E*5a**. ^{1}H NMR 300 MHz ($CDCl_3$) δ ppm ***E*4a**: 9.55 (1 H, *d, J = 7.85* Hz), 6.80 (1H, *dd, J = 15.87, 4.66* Hz, on C-10), 6.30 (1H, *dd, J* = 15.87, 7.85 Hz, on C-11), 4.40 (1H, *brtdd*, on C-9), 3.63 (3H, *s*, –O–CH_3), 2.28 (2H, *brt*, on C-2), 1.5–1.8 (8H, *m*, C-3, C-4, C-5, C-6); ^{13}C NMR 75 MHz ($CDCl_3$) δ ppm ***E*4a**: 193.5 (C-12), 170.6 (C-1), 158.9 (C-10), 130.6 (C-11), 71.0 (C-9), 53.4 (–O–CH_3), 36.4 (C-8), 34.0 (C-2), 29.0, 28.9 C-4, C-5, C-6, 25.0 (C-7), 24.7 (C-3); RI ***E*4abc** (DB-5) = 2521, 2561; EI-MS data are given in Table 1. EI-MS data of **4ac** were in agreement with those published by Gardner (17).

^{1}H NMR 300 MHz ($CDCl_3$) δ ppm ***E*5a**: 9.80 (1H, *d, J* = 6.98 Hz, on C12), 6.85 (1H, *d, J = 16.25* Hz, on C10), 6.55 (1H, *dd, J* = 16.26, 6.82 Hz, on C-11), 3.62 (3H, *s*, –O–CH_3), 2.67 (2H, *brt, J* = 7.29 Hz, on C-2), 1.5–1.7 (8H, *m*, on C-3, C-4, C-5, C-6); ^{13}C NMR 75 MHz ($CDCl_3$) δ ppm ***E*5a**: 193.5 (C-12), 144.8 (C-10), 137.3 (C-11), 51.4 (–O–CH_3), 41.1 (C-8), 33.9 (C-2), 28.9, 28.8 C-4, C-5, C-6, 24.7 (C-3), 23.5 (C-7); C-1 and C-9 not determined; RI ***E*5abc** (DB-5) = 2706; EI–MS data shown in Table 1.

*Synthesis of 9,12-dioxo-10(Z)-dodecenoic acid (**Z5**).* Four mg tetraphenylporphine (TPP) was added to 30 mg (0.14 mmol) 8-[2-furyl]-octadecanoic acid **(7)** in 20 mL CH_2Cl_2 at −78°C. The reaction mixture was photolyzed for 4 h under a mild stream of oxygen. Photolysis was terminated by addition of 100 μL dimethylsulfide (DMS) at −78°C for 10 min. Complete conversion of **7** to ***Z5*** was proven by ^1H and ^{13}C NMR after removal of the excess DMS *in vacuo* and redissolving the residue in $CDCl_3$.

^1H NMR 300 MHz ($CDCl_3$) δ ppm ***Z5***: 10.18 (1H, *d, J* = 7.13 Hz, on C-12), 6.90 (1H, *d, J* = 11.82 Hz, on C-10), 6.14 (1H, *dd*, on C-11), 2.59 (2H, *t, J* = 7.26 Hz, on C-2), 2.29 (2H, *brdt, J* = 7.40, 2.20 Hz, on C-8), 1.2–1.7 (8H, *m*); ^{13}C NMR 75 MHz ($CDCl_3$) ppm ***Z5***: 200.7 (C-9), 192.6 (C-12), 178.5 (C-1), 140.2 (C-10), 137.8 (C-11), 40.3 (C-8), 33.9 (C-2), 28.9, 28.7 C-4, C-5, C-6, 24.5 (C-3), 23.4 (C-7); RI ***Z5*abc** (DB-5) = 2664, 2679; to obtain pentafluorobenzyloxime derivatives an aliquot of the crude extract was treated with 0.1 M solution of PFBHA·HCl in MeOH/H_2O (1:1, vol/vol) for 3 h at RT. Monooximes (R_f = 0.48) and dioximes (R_f = 0.65) of **5** were separated by preparative TLC on SiO_2-TLC plates from Fluka with cyclohexane/ethylacetate (3:1, vol/vol). EI-MS data of derivatives are given in Table 1.

*Synthesis of ethyl 8-[2-furyl]-8-oxo-octanoate (**9a′**).* Thionyl chloride (0.3 mL) was added to a solution of 170 mg (0.84 mmol) monoethyl suberate from Lancaster (Eastgate, England) in 10 mL CH_2Cl_2 under N_2 at RT. Excess of $SOCl_2$ was removed in a mild stream of dry N_2. The resulting monoethyl suberate monochloride was used without further purification. Sixty-three mL dry furan (0.84 mmol), (0.84 mmol), was added to a suspension of 670 mg (0.14 mol) $AlCl_3$ and 212 mg (0.84 mmol) monoethyl suberate monochloride in 10 mL CH_2Cl_2 under dry N_2 and stirred overnight. The reaction mixture was poured onto 20 g ice. $Al(OH)_3$ was redissolved by addition of concentrated HCl. After distribution between H_2O and CH_2Cl_2 (2 × 20 mL), the CH_2Cl_2 solution was dried (Na_2SO_4) and CH_2Cl_2 removed *in vacuo*. IR spectrum **9a′**: 3017 cm^{-1} (aromatic C–H), 2937 cm^{-1} (aliphatic C–H), 1733 cm^{-1} (ester C=O), 1677 cm^{-1} (carbonyl C=O), and 1569 cm^{-1} (aromatic C=C vibrations). The product was used for Wolff-Kishner reduction without further purification (yield 90%, by GC). RI **9a′** (DB-5) = 1920; EI-MS data are given in Table 1.

Synthesis of 8-[2-furyl]-octanoic acid (**7**). Three hundred mg (76 mmol) **9a′**, 100 μL $N_2H_4 \cdot H_2O$ (85 %) from Merck (Hohenbrunn, Germany), 170 mg powdered KOH ,and 10 mL triethylene glycol (TEG) were boiled at 180°C for 2 h. After cooling to RT, 20 mL H_2O was added. The solution was acidified with HCl and distributed between H_2O and CH_2Cl_2 (2 × 20 mL). The washed CH_2Cl_2 solution was dried over Na_2SO_4. CH_2Cl_2 was evaporated *in vacuo*. After preparative TLC, 96 mg (0.58 mmol) 8-[2-furyl]-octanoic acid was obtained (yield = 69%). IR spectrum **7**: broad band at 2800 to 3500 cm^{-1} (acidic O–H), and bands at 2935 cm^{-1} (aliphatic C–H), 1704 cm^{-1} (broad, carbonyl C=O), 1490 and 1560 cm^{-1} (aromatic C=C vibrations). ^1H NMR 300 MHz ($CDCl_3$) δ ppm **7**: 7.28 (1H, *d, J* = Hz, on C-12), 6.26 (1H, *dd, J* = Hz, on C-11), 5.98 (1 H, *dd*, *J* = Hz, on C-10), 2.63 (2H, *brt, J* = Hz, on C-8), 2.36 (2H, *brt, J* = Hz, on C-2) 1.66 (4H, *brt*, on C-3, C-7), 1.35 (6H, *m*, on C-4, C-5, C-6); ^{13}C NMR 75 MHz ($CDCl_3$) δ ppm **7a**: 180.6 (C-1), 156.3 (C-9), 150.6 (C-12), 109.9 (C-11),

TABLE 1
RI values and EI-MS Data of Derivatized Compounds [DB-5, from 80 (3 min isothermal) to 280°C, 15 min isothermal, 60 kPa column head pressure]

Compound[a]	RI (DB-5)	M	*m/z* (relative intensity %)
3ac	2020	316	301 (M – 15, 1), 285 (3), 271 (7), 239 (6), 159 (15), 131 (49), 103 (75), 73 (59), 75 (100)
3cc	2100	374	359 ($M^{+\cdot}$ – 15, 1), 343 (1), 329 (8), 147 (11), 131 (25), 129 (18), 117 (9), 103 (41), 75 (61), 73 (100)
4abc	2521, 2561	509	509 ($M^{+\cdot}$, 2), 494 (5), 478 (5), 352 (74), 328 (29), 312 (41), 181 (44), 73 (100)
4acc	2317, 2321	513	513 ($M^{+\cdot}$,1), 498 (1), 482 (1), 423 (2), 416 (2), 386 (11), 356 (100), 254 (5), 228 (5), 184 (5), 147 (5), 134 (5), 119 (5), 110 (3), 73 (58)
***E*5a**	1963, 2061	240	240 ($M^{+\cdot}$,1), 223 (1), 211 (11), 209 (10), 208 (7), 158 (18), 115 (41), 87 (100), 84 (17), 83 (20), 81 (24), 74 (47), 59 (29), 55 (72)
***E*5ab**	2621	435	435 ($M^{+\cdot}$,1), 404 (4), 306 (1), 293 (11), 278 (8), 181 (100)
***Z*5abb**	3005, 3010	630	630 ($M^{+\cdot}$,1), 599 (3), 449 (8), 433 (21), 418 (3), 401 (23), 181 (100)
***E*5abb**	3080, 3085	630	630 ($M^{+\cdot}$,1), 599 (2), 488 (3), 449 (1), 433 (13), 418 (6), 406 (1), 181 (100)
***Z*5abc**	2664, 2679	507	507 ($M^{+\cdot}$, 4), 492 (2), 476 (4), 378 (16), 364 (35), 310 (100), 181 (68), 73 (86)
***E*5abc**	2706	507	identical to ***Z*5abc**
7a	1619	224	224 ($M^{+\cdot}$, 31), 206 (2), 193 (17), 181 (3), 137 (11), 123 (28), 95 (98), 87 (10), 82 (43), 81 (100), 74 (11), 73 (37), 59 (30)
9a′	1920	252	252 ($M^{+\cdot}$, 1), 230 (2), 165 (6), 148 (11), 123 (11), 110 (100), 95 (67)

[a]Derivatization of the functional groups is indicated by addition of Latin letters to the compound number in respect of derivatization type. The first letter indicates derivatization of the acidic group at C-1 (**a**, methoxy; **a′**, ethoxy; **c**, trimethylsilyloxy). The second letter indicates derivatization of the functional group at the last carbon atom (**b**, pentafluorbenzyloximino; **c**, MSTFA adduct to aldehyde group or trimethylsilyloxy). The third letter indicates derivatization of the hydroxyl or oxo group in the chain (**b**, pentafluorbenzyloximino; **c**, trimethylsilyloxy). Compound structures are illustrated in Schemes 2 and 3. DB-5 column from J&W Scientific (Maiz-Kastel, Germany). Abbreviations: EI-MS, electron impact-mass spectrometry; MSTFA, *N*-methyl-*N*-trimethylsilyl-trifluoroacetamide; RI, retention index.

104.5 (C-10), 34.0 (C-2), 28.8, 27.9, 27.8 C-4, C-5, C-6, C-7, C-8, 24.5 (C-3); RI **7a** (DB-5) = 1619; EI-MS data are given in Table 1.

Mass spectra of derivatives. In order to identify free fatty acids as well as methyl esters derived by saponification, different derivatives of the natural and synthetic products [**4** and 9,12-dioxo-10-dodecenoic acid (**5**)] were prepared by reaction with PFBHA·HCl, MSTFA, and diazomethane according to literature data.

RESULTS AND DISCUSSION

In an investigation of lipid peroxidation in lentil seed flour (*Lens culinaris* Medik.), we trapped aldehydes by addition of PFBHA·HCl). Samples were withdrawn from the extract at 10-min intervals and investigated by GC. We detected, in the C_{24} to C_{28} RI region of gas chromatograms, with increasing incubation time, increasing amounts of four peaks representing pentafluorobenzyloximes (PFBO) (25). The reconstituted ion current of a GC run is reproduced in Figure 1.

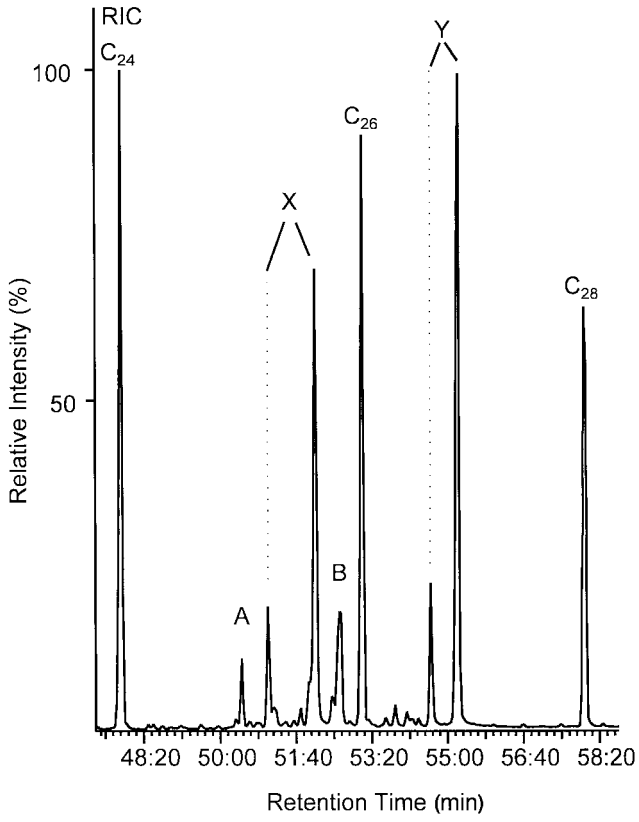

FIG. 1. Reconstituted ion current of the C_{24} to C_{28} region after extraction of lipids and derivatization with pentafluorobenzyloxime hydrochloride, saponification with 1 M NaDMe, and trimethylsilylation with *N*-methyl-*N*-trimethylsilyl trifluoroacetamide (C_{24}, C_{26}, C_{28} = linear hydrocarbons; A = di-(2-ethylhexyl)phthalate (solvent impurity); B = methyl 9,12,13-tris-(trimethylsilyloxy)-10-octadecenoate; X = methyl 12-*O*-2,3,4,5,6-pentafluorobenzyloximino-9-trimethylsilyloxy-10(*E*)-dodecenoate (***E*4abc**); Y = methyl 12-*O*-2,3,4,5,6-pentafluorobenzyloximino-9-trimethylsilyloxy-8,10(*Z*)-dodecadienoate (***Z*5abc**).

The peaks marked X were identified to correspond to *anti*- and *syn*-oxime derivatives of 9-hydroxy-12-oxo-10-dodecenoic acid according to their mass spectra (Fig. 2) and RI values (19). Both peaks marked Y showed nearly identical mass spectra (Fig. 3) and resembled those of X. The main difference in mass spectra of compounds X and Y is a shift of the molecular ions (509 to 507 *m/z*) and the fragment ions of 312 to 310 *m/z*. The presence of a pentafluorobenzyloxime in Y was confirmed by peaks at M – 181 (*m/z* 326) and M – 197 (*m/z* 310) as well as a peak at *m/z* 181, corresponding to the pentyfluorobenzyl ion itself.

The generation of the ion m/z 364 (Fig. 3) is explained by loss of a $–(CH_2)_6–COOCH_3$ side chain forming a 1,3-disubstituted pyridinium ion (Scheme 1), that of *m/z* 378 by benzylic cleavage. Presence of a trimethylsilyloxy group was recognized by the intense peaks at mass 73 and 75. Thus, it was assumed that compound Y might be a further oxidation product of 9-hydroxy-12-oxo-10-dodecenoic acid, obtained by transformation of the hydroxy group into an oxo function, which might have suffered enolization by reaction with MSTFA. Therefore, the original structure of compound Y (Fig. 3) **5** was tentatively deduced to be 9,12-dioxo-10-dodecenoic acid with unknown configuration of the double bond.

To prove the deduced structure of compound Y, **5** had to be synthesized. Since generation of **5** was visualized to be an oxidation product of **4**, synthesis of **5** was envisaged by oxidation from **4**, which is distinguished from 4-HNE only by exchange of the C_5H_{11} residue by $(CH_2)_6–COOH$. Thus, we followed, for synthesis of ***E*4** the route to 4-HNE published by Gardner *et al.* (26), except we started with 10-undecenoic acid **1** as precursor. In a second modification, we used PCC as an oxidant instead of periodine in order to carry out the reaction in nonaquous medium. We reacted **1** with formaldehyde to generate a mixture of *cis/trans* 12-hydroxy-9-dodecenoic acid **2** (24) (Scheme 2). This acid was transformed with DMO (21) or 4-chloroperbenzoic acid to **3**. Compound **3** was then oxidized to ***E*4** and 9,12-dioxo-10(*E*)-dodecenoic acid (***E*5**). Complete oxidation of **3** or ***E*4** to ***E*5** with PCC failed since most of ***E*4** was cyclized to **6** in the acidic medium, which spontaneously eliminated water to **7**, proven by ^{1}H NMR spectroscopy. When ***E*4** was dissolved in unstabilized $CDCl_3$ due to the presence of traces of HCl it was converted within a few hours to **7** as deduced by NMR measurements (data not shown).

Synthesis of ***Z*5** was achieved *via* the furan derivative **7**, which was synthesized by acylation of furan, followed by Wolff-Kishner reduction (Scheme 3). Compound **7** was subjected to a photolytic oxidation in analogy to a reaction described by Wasserman and Lipshitz (27) and Saito *et al.* (28) to the endoperoxide **8**, which suffered cleavage to *cis* 9,12-dioxo-10-dodecenoic acid ***Z*5** by treatment with DMS at –70°C. The latter isomerizes to its *trans* isomer by treatment with ultraviolet (UV)-light at RT. Reaction of **8** with DMS at RT generates the *trans* isomer directly.

The configuration of double bonds at C-10/C-11 was determined in the synthetic samples by NMR. Since the syn-

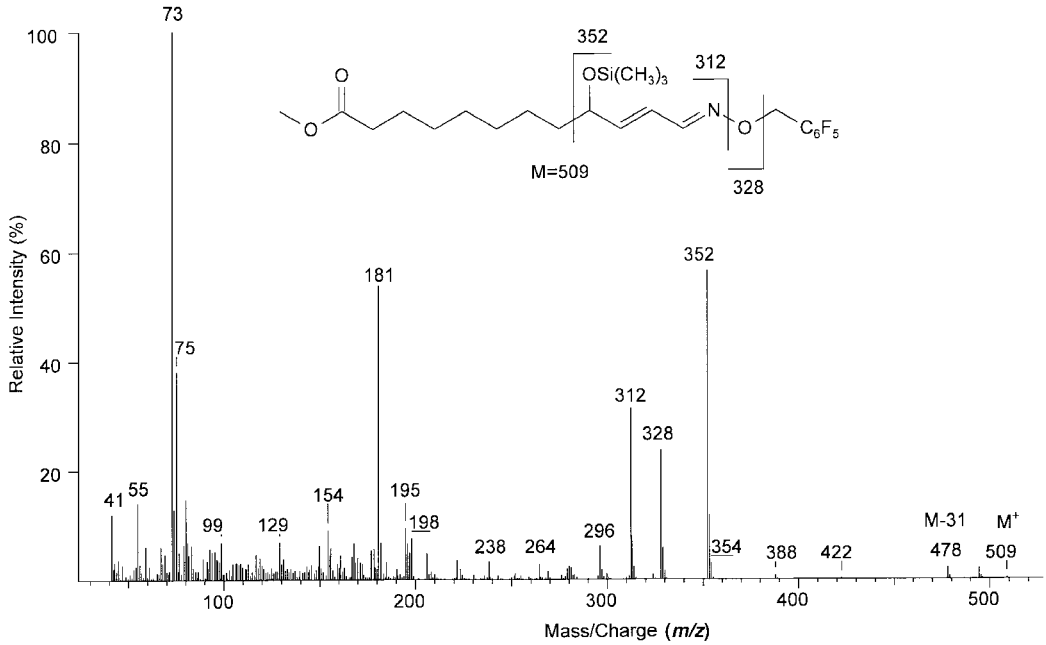

FIG. 2. Mass spectrum of (***E*4abc**). For abbreviation see Figure 1.

thetic isomers of ***E*5** and ***Z*5** show different RI values, it was possible to identify the natural isomers. The large RI difference observed for the two isomers of **4abc** and **5abc**, respectively, was found to be caused by the *E/Z* isomers of the C=N bond of the oximes (*syn/anti* isomers) and not by C=C isomerism. Compound **4** occurs in lentil seed flour incubations only in the form of its *E*-isomer, whereas **5** is generated only in the *Z*-isomeric form. This was unambigiously proven by synthesis and purification of three authentic *E* and *Z* aldehydes ***E*4**, ***E*5** and ***Z*5** and their derivatives.

Compound **5** is an oxidation product of compound **4**. **4** is the counterpart of 4-HNE [exchange of C_5H_{11} with $(CH_2)_6$-COOH]; 4-HNE was detected in enzyme suspensions of soybean (17) and alfalfa (18). Its genesis was derived from 9-HPODE (29–32). Following the deductions in these papers, the precursor of **4** is visualized to be 13-HPODE.

Compound ***E4*** is stable at room temperature, in solid form or in solutions, in the absence of protic reagents. In contrast, we have not been able to isolate ***Z4*** since it spontaneously cyclized to **7** during PCC oxidation. The oxidation of **7** to com-

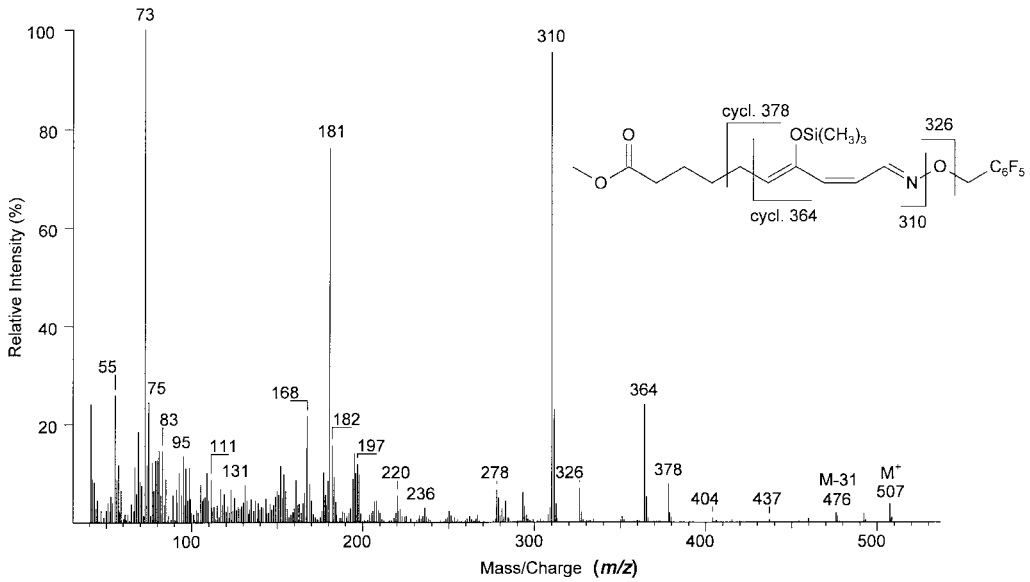

FIG. 3. Mass spectrum of (***Z*5abc**). For abbreviation see Figure 1.

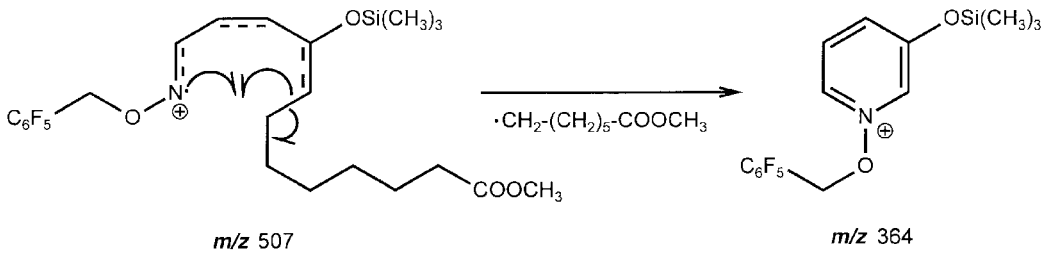

SCHEME 1

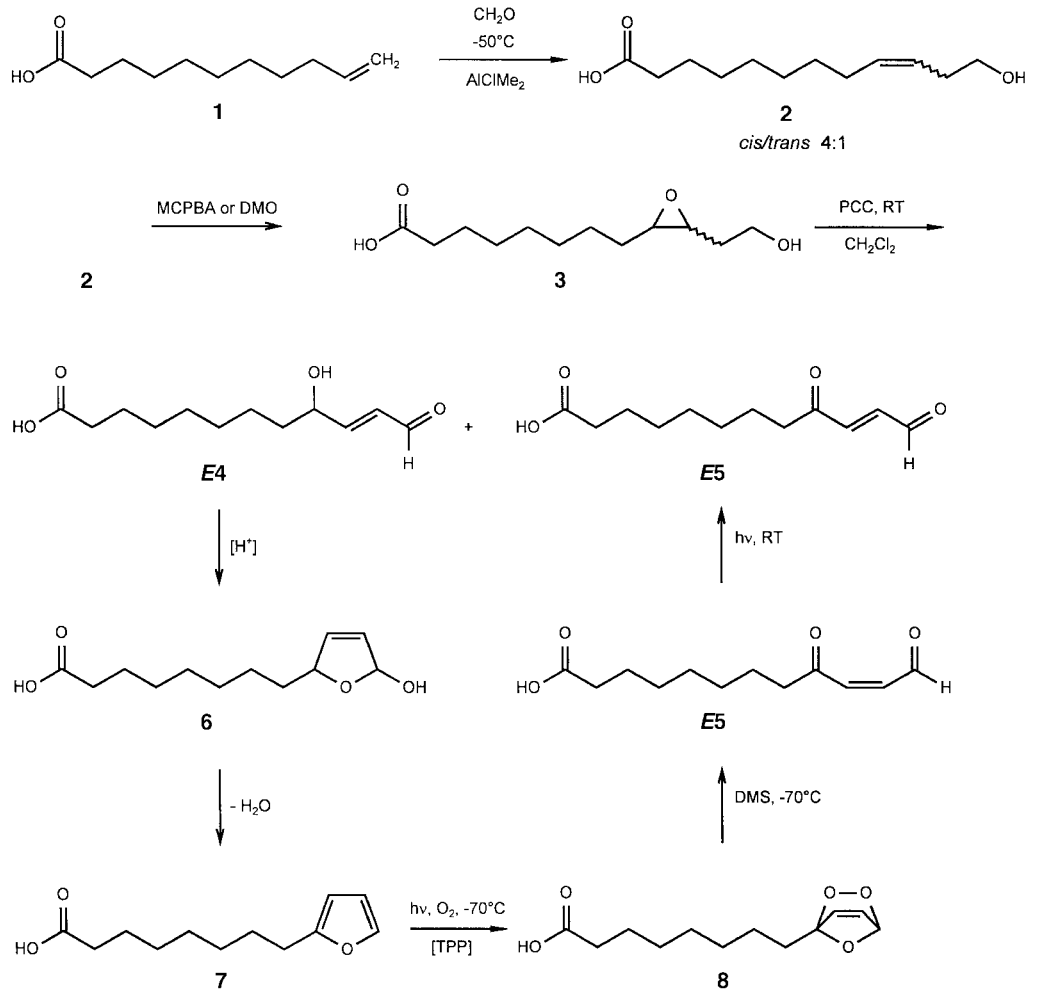

SCHEME 2

pound ***Z*5** (Scheme 2) by oxygen with UV-light in presence of a suitable sensitizer at –70°C resembles the opening of a furan ring by xanthine oxidase (XOD; EC 1.1.3.22) described by Kellog and Fridovich (33). The described synthesis of ***Z*5** mimics this pathway (Scheme 4). Therefore, it might be possible that **5** is generated in a similar way in lentils by XOD activity.

Treatment of **5** with diazomethane [even for only 10 s (34) and by cooling], still does not produce characterized side products if the aldehyde group is not protected. However, methylation of the free acid with diazomethane was achieved without side reactions after derivatization of the aldehyde group with PFBHA·HCl.

Yamaguchi *et al.* (35) described that **4** inhibits phospholipase A. Compound **5** is very sensitive to nucleophilic or electrophilic attack. Owing to the accumulation of functional

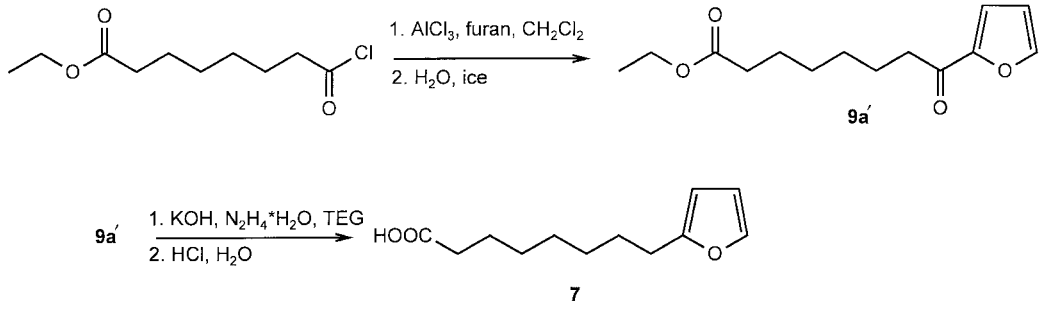

SCHEME 3

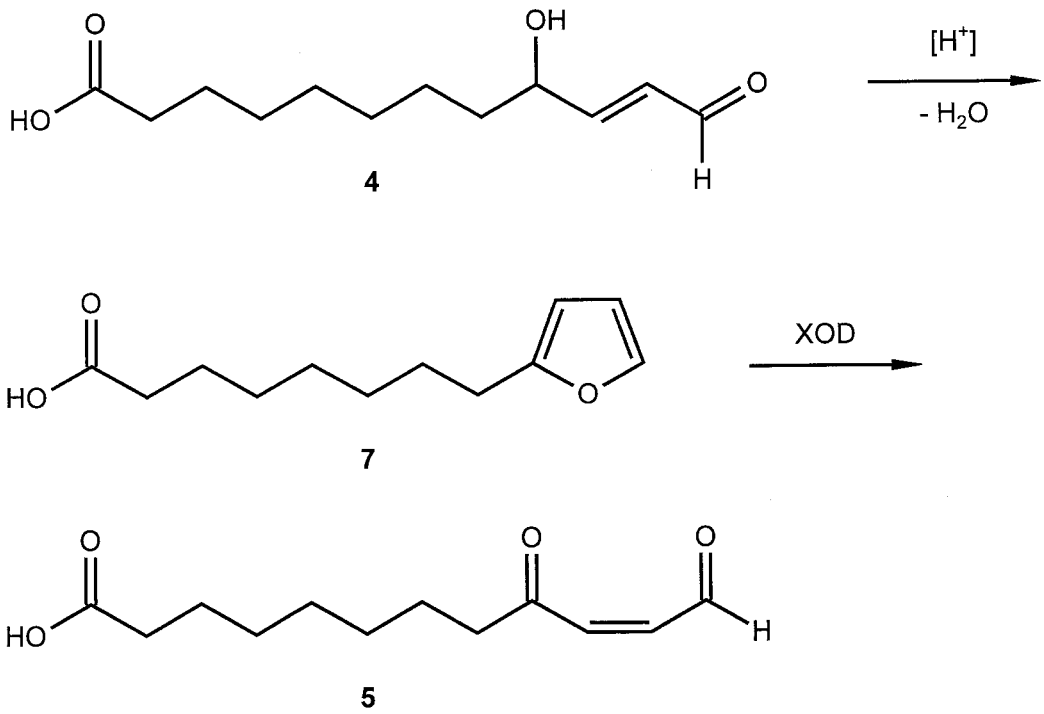

SCHEME 4

groups, this compound might show activity in biological material. The synthesis of **5** reported in this paper offers the possibility to elucidate its physiological effects in plant chemistry.

ACKNOWLEDGMENTS

We are obliged to Werner Kern for preparation of solvents and diazomethane, Markus Seitz for experimental assistance, Dr. Joseph Reiner and Marco Burkhard for NMR spectra, and Michael Glaeßner for MS spectra. We thank Deutsche Forschungsgemeinschaft, Fonds der chemischen Industrie and Fischer Stiftung for financial support.

REFERENCES

1. Graveland, A. (1970) Enzymic Oxidations of Linoleic Acid and Glycerol-1-monolinoleate in Doughs and Flour–Water Suspensions, *J. Am. Oil Chem. Soc. 47*, 352–361.
2. Graveland, A. (1973) Analysis of Lipoxygenase Nonvolatile Reaction Products of Linoleic Acid in Aqueous Cereal Suspensions by Urea Extraction and Gas Chromatography, *Lipids 8,* 599–606.
3. Graveland, A. (1973) Enzymic Oxidation of Linoleic Acid in Aqueous Wheat Flour Suspensions, *Lipids 8*, 606–611.
4. Chang, P.R.Q., and McCurdy, A.R. (1985) Lipoxygenase Activity in Fourteen Legumes, *Can. Inst. Food Sci. Technol. J. 18*, 144–160.
5. Crombie, L., Morgan, D.O., and Smith, E.H. (1991) An Isotopic Study (^1H and ^{18}O) of the Enzymic Conversion of Linoleic Acid into Colneleic Acid with Carbon Chain Fracture: The Origin of Shorter Chain Aldehydes, *J. Chem. Soc. Perkin Trans. 1*, 567–575.
6. Wendel, T., and Jüttner, F. (1996) Lipoxygenase-Mediated Formation of Hydrocarbons and Unsaturated Aldehydes in Fresh Water Diatoms, *Phytochemistry 41*, 1445–1449.
7. Miralto, A., Barone, G., Romano, G., Poulet, S.A., Ianora, A., Russo, G.L., Buttino, I., Mazzarella, G., Laabir, M., *et al.* (1999)

The Insidious Effect of Diatoms on Copepod Reproduction, *Nature 402*, 173–176.
8. Esterbauer, H., Ertl, A., and Scholz, N. (1976) The Reaction of Cysteine with α,β-Unsaturated Aldehydes, *Tetrahedron 32*, 285–289.
9. Esterbauer, H., Schaur, R.J., and Zollner, H. (1991) Chemistry and Biochemistry of 4-Hydroxynonenal, Malondialdehyde and Related Aldehydes, *Free Radical Biol. Med. 11*, 81–128.
10. van Kujik, F.J.G.M., Thomas, D.W., Stephens, R.J., and Dratz E.A. (1986) Occurrence of 4-Hydroxyalkenals in Rat Tissues Determined as Pentafluorobenzyl Oxime Derivatives by Gas Chromatography–Mass Spectrometry, *Biochem. Biophys. Res. Commun. 39*, 144–149.
11. Hoffmann, G.F., and Sweetman, L. (1991), *O*-(2,3,4,5,6-Pentafluorobenzyl)oxime-trimethylsilyl Ester Derivatives for Sensitive Identification and Quantitation of Aldehydes, Ketones and Oxoacids in Biological Fluids, *Clin. Chim. Acta 199*, 237–242.
12. Spiteller, G., Kern, W., and Spiteller, P. (1999) Investigation of Aldehydic Lipid Peroxidation Products by Gas Chromatography–Mass Spectrometry, *J. Chromatogr. A 843*, 29–98.
13. Hamberg, M., and Gotthammar, B. (1973) A New Reaction of Unsaturated Fatty Acid Hydroperoxides: Formation of 11-Hydroxy-12,13-epoxy-9-octadecenoic Acid from 13-Hydroperoxy-9,11-octadecenoic Acid, *Lipids 8*, 737–744.
14. Hamberg, M., and Hamberg, G. (1996) Peroxygenase-Catalyzed Fatty Acid Epoxidation in Cereal Seeds. Sequential Oxidation of Linoleic Acid into 9(*S*),12(*S*),12(*S*)-Trihydroxy-10(*E*)-octadecenoic Acid, *Plant Physiol. 110*, 807–815.
15. Cardellina, J.H., II, and Moore, R.E. (1980) Malyngic Acid, a New Fatty Acid from *Lyngbya majuscula, Tetrahedron 36*, 993–996.
16. Grechkin, A.N., Kuramshin, R.A., Latypov, S.K., Savonova, Y.Y., Gafarova, T.E., and Ilyasov, A.V. (1991) Hydroperoxides of α-Ketols. Novel Products of the Plant Lipoxygenase Pathway, *Eur. J. Biochem. 199*, 451–457.
17. Gardner, H.W. (1998) 9-Hydroxy-traumatin, a New Metabolite of the Lipoxygenase Pathway, *Lipids 33*, 745–749.
18. Noordermeer, M.A., Veldink, G.A., and Vliegenthart, J.F.G (1999) Alfalfa Contains Substantial 9-Hydroperoxide Lyase Activity and a 3-*Z*:2*E*-enal Isomerase, *FEBS Lett. 443*, 201–204.
19. Loidl-Stahlhofen, A., Hannemann, K., and Spiteller, G. (1994) Generation of α-Hydroxyaldehydic Compounds in the Course of Lipid Peroxidation, *Biochim. Biophys Acta 1213*, 140–148.
20. Mlakar, A., and Spiteller, G. (1994) Reinvestigation of Lipid Peroxidation of Linoleic Acid, *Biochim. Biophys Acta 1214*, 209–220.
21. Adam, W., Bialas, J., and Hadjiarapoglou, L. (1991) A Convenient Preparation of Acetone Solutions of Dimethyldioxirane, *Chem. Ber. 124*, 2377.
22. van den Dool, H., and Kratz, P.D. (1963) A Generalization of the Retention Index System Including Linear Temperature Programmed Gas–Liquid Partition Chromatography, *J. Chrom. atogr. 11*, 463–471.
23. Bligh, E.G., and Dyer, W.J. (1956), A Rapid Method of Total Lipid Extraction and Purification, *Can. J. Biochem. Physiol. 37*, 911–917.
24. Metzger, J.O., and Biermann, U. (1992) Alkylaluminum Chloride Catalyzed Ene Reactions of Formaldehyde with Unsaturated Carboxylic Acids, Esters and Alcohols, *Synthesis*, 463–465.
25. Gallasch, B.A.W. (1998) Untersuchungen pflanzlicher Fettsäureoxidationsprodukte mittels GC/FID/MSD-Kopplung, Ph.D. Thesis, Universität Bayreuth, Bayreuth, pp. 36–40.
26. Gardner, H.W., Bartelt, R.J., and Weisleder, D. (1992) A Facile Synthesis of 4-Hydroxy-2(*E*)-nonenal, *Lipids 27*, 686–689.
27. Wasserman, H.H., and Lipshitz, B.H. (1979) Reactions of Singlet Oxygen with Heterocyclic Systems, in *Singlet Oxygen* (Wasserman, H.H., and Murray, R.W., eds.), Organic Chemistry–A Series of Monographs, Vol. 40, pp. 429–509, Academic Press, New York.
28. Saito, I., Kuo, Y.H., and Matsuura, T. (1986) Photoinduced Reactions. 168. Photooxygenation of Furans in the Presence of Trimethylsilyl Cyanide. Oxidative Cyanation of Furans, *Tetrahedron Lett. 27*, 2757–2760.
29. Gardner, H.W., Weisleder, D., and Plattner, R.D. (1991) Hydroperoxide Lyase and Other Hydroperoxide-metabolizing Activity in Tissues of Soybean, *Glycine max., Plant Physiol. 97*, 1059–1072.
30. Gardner, H.W., and Hamberg, M. (1993) Oxygenation of (3*Z*)-Nonenal to (2*E*)-4-Hydroxy-2-nonenal in the Broad Bean (*Vicia faba* L.), *J. Biol. Chem. 268*, 6971–6977.
31. Takamura, H., and Gardner, H.W. (1996) Oxygenation of (3*Z*)-Alkenal to (2*E*)-4-Hydroxy-2-alkenal in Soybean Seed (*Glycine max* L.), *Biochim. Biophys. Acta 1303*, 83–91.
32. Gardner, H.W., and Grove, M.J. (1998) Soybean Lipoxygenase-1 Oxidizes 3*Z*-Nonenal. A Route to 4*S*-Hydroperoxy-2*E*-Nonenal and Related Products, *Plant Physiol. 116*, 1359–1366.
33. Kellog, E.W., III, and Fridovich, I. (1975) Superoxide, Hydrogen Peroxyde, and Singlet Oxygen in Lipid Peroxidation by a Xanthine Oxidase System, *J. Biol. Chem. 250*, 8812–8817.
34. Hamberg, M., and Fahlstadius, P. (1989) Allene Oxidase Cyclase: A New Enzyme in Plant Lipid Metabolism, *Arch. Biochem. Biophys 276*, 518–526.
35. Yamaguchi, K., Nakamura, T., and Toyomizu, M. (1981) Inhibition of Phospholipase A by Oxidized Lipid, *Kyushu Daigaku Nogakubu Gakugei Zasshi 35*, 71–80.

[Received March 3, 2000, and in revised form July 19, 2000; revision accepted July 28, 2000]

Formation of 8-Oxo-2′-deoxyguanosine in the DNA of Human Diploid Fibroblasts by Treatment with Linoleic Acid Hydroperoxide and Ferric Ion

Takao Kaneko* and Shoichi Tahara

Tokyo Metropolitan Institute of Gerontology, Itabashi-ku, Tokyo 173-0015, Japan

ABSTRACT: Lipid peroxides are suggested to be related to the occurrence of a variety of diseases including cancer and atherosclerosis. We examined whether lipid peroxides cause oxidative damage to DNA in intact cells. Linoleic acid hydroperoxide (LOOH) and ferric chloride were used at concentrations at which separate treatment had no effect on the formation of 8-oxo-2′-deoxyguanosine (8-oxodG) in DNA or the survival rate of cultured human diploid fibroblasts, TIG-7. The amount of 8-oxodG in the cellular DNA increased significantly when TIG-7 cells were treated concurrently with LOOH and ferric chloride. In a LOOH concentration-dependent manner 8-oxodG was formed. However, no significant induction of the activities of superoxide dismutases, catalase, or glutathione peroxidase was observed under these conditions. The formation of 8-oxodG by lipid hydroperoxides seems to be due to the generation of reactive species other than superoxide radicals and hydrogen peroxide. These results indicate that some species formed during the reaction of lipid hydroperoxides with ferric ion can cause oxidative damage to DNA.

Paper no. L8491 in *Lipids 35,* 961–965 (September 2000).

Amounts of dietary lipids have been suggested to be related to mortality in the case of cancers of some organs, such as breast, colon, kidney, and pancreas (1,2); and lipid peroxides, oxidative products formed when lipids are subjected to oxidative stress, are often considered as a cause of these cancers. Furthermore, lipid peroxides have also been suggested to play roles in atherosclerosis and aging (3). Unsaturated fatty acids are readily oxidized to form their hydroperoxides by both atmospheric oxygen and singlet oxygen. Lipid peroxidation also takes place *in vivo* through the controlled oxidation of unsaturated lipids catalyzed by lipoxygenases. It is known that DNA is damaged during lipid peroxidation (4). Damage to DNA is strongly suggested to be involved in the etiology of a variety of diseases such as cancer and aging because it induces mutagenesis of DNA if it is not repaired. Unsaturated fatty acid hydroperoxides have been reported to cause the cleavage of DNA strands (5) and the formation of fluorescent products in the presence of metal ions (6). Further, it has been reported that autoxidation mixtures of unsaturated fatty acids cause oxidative damage to calf thymus DNA in homogeneous solutions to form 8-oxo-2′-deoxyguanosine (8-oxodG) (7,8). 8-OxodG is a major product of oxidative damage to DNA bases and is thought to be a typical marker of oxidative damage in organisms. The attack of hydroxyl radicals on the C-8 position of the guanine base forms 8-oxodG, which has also been found in DNA after the *in vivo* reaction of DNA with mutagens or carcinogens such as nitrosoamines (9). Thus, DNA damage, such as the formation of 8-oxodG or strand breaks, induced by lipid peroxides appears to be involved in mutagenesis and carcinogenesis. However, lipid peroxides should be present in cellular membranes, since lipid peroxides are lipophilic except for small molecular weight aliphatic aldehydes. It is unclear whether compounds produced during lipid peroxidation actually influence nuclear and/or mitochondrial DNA in cells. To clarify this point, we studied the effect of polyunsaturated fatty acid hydroperoxide, a primary product of lipid peroxidation, on the formation of 8-oxodG in the DNA of cultured human diploid fibroblasts, TIG-7.

MATERIALS AND METHODS

Materials. Nuclease P1 and alkaline phosphatase from *Escherichia coli* were purchased from Sigma Chemical Co. (St. Louis, MO). Ribonucleases T1 and A were obtained from Boehringer Mannheim (Indianapolis, IN) and proteinase K was from E. Merck (Darmstadt, Germany). Wako Pure Chemicals Industries (Osaka, Japan) provided 8-oxodG and polyethylene glycol (PEG; molecular weight: 7,300–9,000) was from Nacalai Tesque Inc. (Kyoto, Japan). Eagle's minimum essential medium (MEM) was purchased from Nissui Pharmaceutical Co. (Tokyo, Japan), and fetal bovine serum (FBS) was from Moregate (Melbourne, Australia). Linoleic acid hydroperoxide (LOOH) was prepared by oxidation of linoleic acid with soybean lipoxygenase-1, and 13-(*S*)-hydroperoxy-9*Z*,11*E*-octadecadienic acid, a main isomer, was purified by

*To whom correspondence should be addressed at Tokyo Metropolitan Institute of Gerontology, 35-2 Sakaecho, Itabashiku, Tokyo 173-0015, Japan. E-mail: kaneko@center.tmig.or.jp

Abbreviations: dG, 2′-deoxyguanosine; ECD, electrochemical detection; FBS, fetal bovine serum; GPx, glutathione peroxidase; HPLC, high-performance liquid chromatography; 8-oxodG, 8-oxo-2′-deoxyguanosine; LOOH, linoleic acid hydroperoxide; MEM, minimum essential medium; PEG, polyethylene glycol; SDS, sodium dodecyl sulfate; SOD, superoxide dismutase; UV, ultraviolet.

high-performance liquid chromatography (HPLC) before use (10). All other chemicals were of analytical grade and used without further purification. The water used in this study was treated with Chelex 100 to remove trace amounts of transient metal ions such as iron ion.

Cell culture. Human embryonic fibroblasts TIG-7 (11), established in the Tokyo Metropolitan Institute of Gerontology, were grown at 37°C in Eagle's MEM supplemented with 10% FBS in 10 cm plastic dishes under a humidified atmosphere of 5% CO_2 and 95% air. Cells at confluency were incubated in Earle solution, pH 7.2, containing LOOH (10–50 μM) solubilized in ethanol and/or 10 μM ferric chloride ($FeCl_3$) at 37°C for 3 h. The final ethanol concentration was less than 0.1% and had no effect on cells. Earle solution is a buffered solution whose only organic compound is glucose. The influence of components such as FBS in the growth medium is expected to be excluded in the system using Earle solution.

Isolation of DNA from TIG-7 cells. DNA was isolated by the sodium iodide and polyethylene glycol method. In brief, cells (*ca*. 5×10^6) incubated in Earle solution containing LOOH and/or $FeCl_3$ were harvested by trypsinization followed by centrifugation at 1,000 rpm for 5 min. Cell pellets were washed twice with phosphate-buffered saline (pH 7.2), resuspended in 50 μL of an aqueous solution of proteinase K (25 mg/mL) and 300 μL of 1% sodium dodecyl sulfate (SDS)/1 mM EDTA (pH 8.0), and incubated at 37°C for 1 h under an argon atmosphere. The resulting solution was mixed with 300 μL of 7 M NaI and 600 μL of isopropyl alcohol and kept at –20°C for 10 min. The mixture was then centrifuged at 14,000 rpm for 20 min. The pelleted DNA was rinsed twice with 70% ethanol and dissolved in 200 μL of 0.01 × SSC (saline-sodium citrate) buffer. Ribonucleases T1 (40 units) and A (80 μg) were added to the crude DNA solution, and the mixture was incubated at 37°C for 1 h under an argon atmosphere. Following incubation, 300 μL of chloroform/isoamyl alcohol (25:1, vol/vol) was added and mixed, and the mixture was centrifuged at 14,000 rpm for 10 min. The aqueous phase was transferred to another tube and mixed with 200 μL of 13% PEG solution containing 1.6 M NaCl, and the mixture was left overnight at 4°C. The mixture was then centrifuged at 14,000 for 20 min, and the DNA was rinsed twice with 70% ethanol and dissolved in 30–50 μL of water treated with Chelex 100. The concentration and purity of the DNA were determined by ultraviolet (UV) absorption as described previously (12).

Hydrolysis of DNA and quantitation of 8-oxodG. DNA, isolated as described above, was hydrolyzed to prepare nucleosides. Acetate buffer (pH 4.8, 20 mM, 25 μL) containing 25 μg DNA and 2 μg of nuclease P1 was incubated at 37°C for 30 min under an argon atmosphere. Then, 3 μL of 1 M Tris-HCl (pH 7.4) and 0.3 units of alkaline phosphatase were added and the mixture was incubated at 37°C for 20 min under an argon atmosphere. The mixture was filtered through an Ultrafree-MC filter (Millipore Co., Bedford, MA) and the filtrate was applied to HPLC equipped with a Symmetry C18 column (particle size, 3.5 μm; 4.6 × 75 mm; Waters Co., Milford, MA). The mobile phase was 12.5 mM citrate buffer (pH 5.1) containing 6% methanol, and the flow rate was 0.8 mL/min. 8-OxodG was detected by electrochemical detection (ECD; ESA Coulochem II 5200; Bedford, MA) using an analytical cell model 5011 (Detector I, 150 mV; Detector II, 350 mV). Oxidative damage to DNA is expressed as the molar ratio of 8-oxodG to 10^5 deoxyguanosine (dG). The amount of dG was calculated from the absorption at 260 nm in the same sample as measured with a UV detector.

Biochemical analysis. Superoxide dismutase (SOD) activity was assayed by the method of Oyanagi (13), catalase activity by the method of Aebi (14), and glutathione peroxidase (GPx) activity by the method of Flohé and Günzler (15). Protein content was measured by the method of Bradford (16).

Statistical analysis. Data are expressed as means ± SD. Scheffe *F*-test was used for the statistical analysis of the data. Differences were considered significant when the probability (*P*) values were less than 0.05.

RESULTS

Damage to TIG-7 cells by LOOH and ferric ion. The survival rate of TIG-7 cells incubated in Earle solution was not affected up to 4 h (survival rate: 99.9 ± 1.9%). Although the survival rates did not change when TIG-7 cells were incubated in Earle solution containing 50 μM LOOH for 3 h, treatment with 100 μM LOOH reduced the survival rate (Table 1). On the other hand, treatment with $FeCl_3$, even at 100 μM, had no effect on the cell survival rate. The rate was decreased by concurrent treatment with LOOH and $FeCl_3$ as shown in Table 1. The 8-oxodG content (0.342 ± 0.066 8-oxodG/10^5 dG) in cellular DNA was slightly increased by incubation with 50 μM LOOH, but the change was not significant (Table 2). On the other hand, incubation of the cells with 25 μM $FeCl_3$ produced a slight increase in 8-oxodG content in cellular DNA (0.386 ± 0.128 8-oxodG/10^5 dG). As shown in Figure 1, concurrent treatment with 10 μM LOOH and 10 μM ferric ion produced a significant elevation in the 8-oxodG content in the DNA of TIG-7 cells (0.587 ± 0.105 8-oxodG/10^5 dG). The content of 8-oxodG in the DNA of TIG-7 cells treated with 10 μM ferric ion and 50 μM LOOH rose further (0.764 ± 0.258 8-oxodG/10^5 dG). If ferric ions

TABLE 1
Effect of Incubation with LOOH and Ferric Ion on the Survival of TIG-7 Cells[a]

Concentration (μM)	Survival (%)		
	LOOH	$FeCl_3$	LOOH/$FeCl_3$
0	100.0 ± 6.7	100.0 ± 3.0	100.0 ± 5.4
10	101.2 ± 7.6	100.7 ± 10.2	102.5 ± 13.3
25	100.1 ± 4.8	102.8 ± 15.1	96.8 ± 12.7
50	94.7 ± 16.9	99.7 ± 3.9	88.5 ± 5.9
100	63.3 ± 11.0*	94.4 ± 16.5	37.9 ± 9.4*

[a]Cells were incubated in Earle solution containing different concentrations of linoleic acid hydroperoxide (LOOH) and/or $FeCl_3$ at 37°C for 3 h. Results show the means ± SD of four separate experiments performed in duplicate. *Significantly different from the control (0 μM) value at $P < 0.01$.

TABLE 2
Increase in 8-OxodG in the DNA of TIG-7 Cells Treated with LOOH or Ferric Ion[a]

Concentration (μM)	8-OxodG/10^5 dG	
	LOOH	$FeCl_3$
0	0.317 ± 0.062	0.317 ± 0.062
10	0.316 ± 0.039	0.335 ± 0.035
25	0.307 ± 0.054	0.386 ± 0.128
50	0.342 ± 0.066	0.560 ± 0.185*

[a]Cells were incubated in Earle solution containing different concentrations of LOOH or $FeCl_3$ at 37°C for 3 h. The content of 8-oxo-2′-deoxyguanosine (8-oxodG) in the DNA was measured by a high-performance liquid chromatography–electrochemical detection system as described in the Materials and Methods section. Results show the means ± SD of four separate experiments performed in duplicate. *Significantly different from the control (0 μM) value at $P < 0.01$. See Table 1 for other abbreviation.

adhere to the surface of cellular membranes or pass through cellular membranes into the cytosol, they may catalyze the oxidation of DNA during the isolation of DNA from cells. To check this possibility, $FeCl_3$ was added to cell suspensions in an aqueous solution of proteinase K and SDS/EDTA, and then the DNA was isolated. However, the addition of $FeCl_3$ did not change the amount of 8-oxodG in the isolated DNA (0.314 ± 0.104 8-oxodG/10^5 dG).

Effect of LOOH and ferric ion on antioxidant enzyme activity in TIG-7 cells. To clarify whether reactive oxygen species are primarily involved in the formation of 8-oxodG in DNA of cells treated with LOOH and ferric ion, the induction of antioxidant enzyme activities was examined. All the enzyme activities measured showed a tendency to increase with concurrent treatment with LOOH and ferric ion, but the increases were not significant as shown in Table 3.

DISCUSSION

Artificial oxidation is always a serious problem during the isolation of oxidized products of biological molecules such as DNA, lipids, and proteins. In particular, the guanine bases in DNA are easily oxidized during the isolation of DNA from animal tissues or cultured cells and during the hydrolysis of DNA to produce nucleosides or bases (17–22). Phenol and atmospheric oxygen are proposed to be responsible for the formation of 8-oxodG during these procedures (23). In this study, incubation with enzymes during the isolation and hydrolysis of DNA was performed under an argon atmosphere. Furthermore, sodium iodide and isopropyl alcohol were used instead of phenol, sodium chloride, and ethanol for the extraction of crude DNA from samples treated with proteinase K and SDS. The water used in these experiments was treated with Chelex 100 resin to remove trace amounts of iron ions.

Chemical agents that enhance free radical reactions in membranes may accelerate oxidative damage not only to lipids but also to DNA. That is, some products formed during

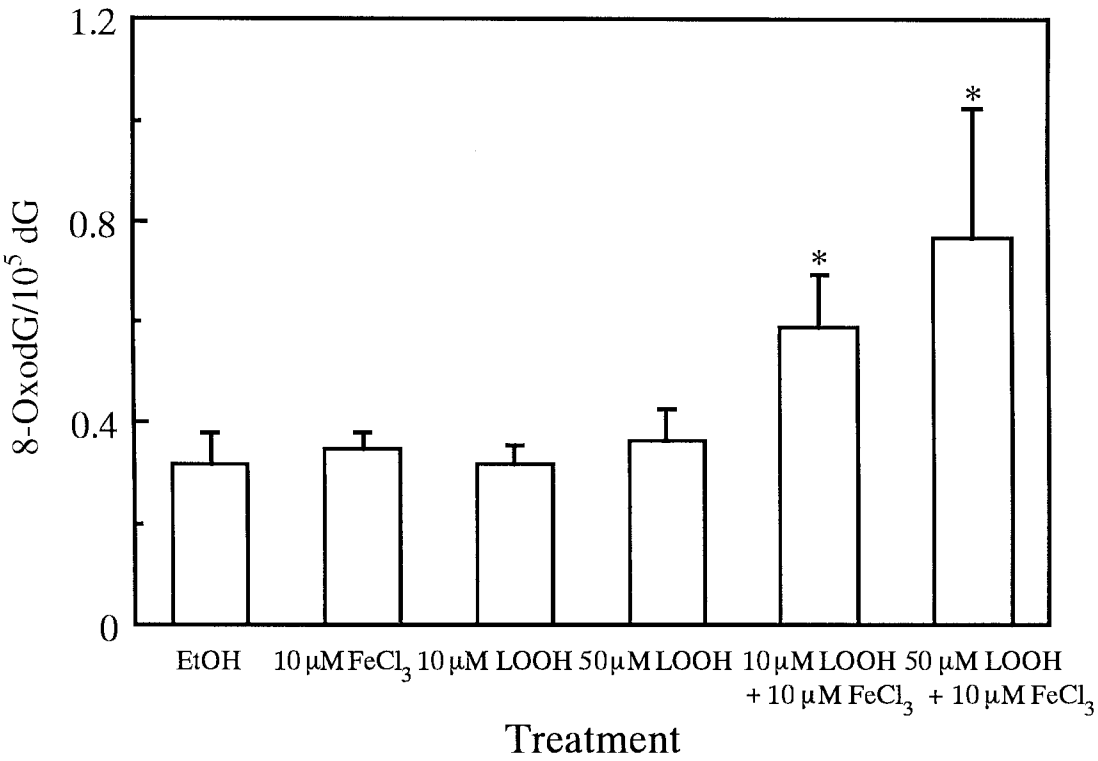

FIG. 1. Formation of 8-oxo-2′-deoxyguanosine (8-oxodG) in the DNA of cultured human diploid fibroblasts TIG-7 by treatment with linoleic acid hyproperoxide (LOOH) and/or ferric ion. Cells were incubated in Earle solution containing 10 μM $FeCl_3$ and/or 10 μM or 50 μM LOOH at 37°C for 3 h. Results represent the means ± SD of four experiments performed in duplicate. *Significantly different from the control value obtained by separate treatment with LOOH or $FeCl_3$ at $P < 0.01$.

TABLE 3
Effect of Treatment with LOOH and $FeCl_3$ on the Activities of SOD, Catalase, and GPx in TIG-7 Cells[a]

	Enzyme activity (U/mg protein)				
Treatment	Total SOD	Mn SOD	CuZn SOD	Catalase	GPx
Control	166.8 ± 44.1	122.9 ± 25.6	44.0 ± 22.0	2.157 ± 0.461	0.038 ± 0.008
$FeCl_3$	170.9 ± 12.7	119.3 ± 13.0	51.6 ± 15.5	2.125 ± 0.776	0.040 ± 0.003
LOOH	162.3 ± 31.2	121.6 ± 15.6	45.7 ± 17.7	2.176 ± 0.952	0.041 ± 0.013
$FeCl_3$/LOOH	195.1 ± 72.8	137.1 ± 59.5	58.0 ± 16.5	2.476 ± 0.904	0.044 ± 0.008

[a]Cells were incubated in Earle solution containing 50 μM LOOH and 10 μM $FeCl_3$ at 37°C for 3 h. Values represent the means ± SD of four experiments. SOD, superoxide dismutase; GPx, glutathione peroxidase. See Table 1 for other abbreviation.

lipid peroxidation may cause oxidative stress to DNA, because lipid peroxides have been found to cause DNA damage such as strand breaks (24). Furthermore, it has been reported that calf thymus DNA exposed to autoxidized methyl linolenate in solution or in liposomes forms 8-oxodG (8). In this study, we found that unsaturated fatty acid hydroperoxides such as LOOH, primary products of lipid peroxidation, caused oxidative damage to cellular DNA in the presence of ferric ion. As shown in Figure 1, concurrent treatment of TIG-7 cells with LOOH (10 or 50 μM) and $FeCl_3$ (10 μM) induced 8-oxodG formation in a LOOH dose-dependent manner. Ferric ion was essential to the formation of 8-oxodG in the DNA of TIG-7 cells treated with LOOH because treatment with LOOH alone produced little change in the amount of 8-oxodG in the cellular DNA. If ferric ions are attached to the surface of cellular membranes, or if they pass through the cellular membrane into the cytosol, the DNA molecules may encounter ferric ions when the cells are homogenized and this may accelerate the formation of 8-oxodG. To examine this effect of ferric ions, we added $FeCl_3$ (final concentration: 10 μM) to cell suspensions containing proteinase K, SDS, and extracted cellular DNA. The amounts of 8-oxodG were not elevated by the addition of ferric ions. Furthermore, the possibility that the DNA in dead cells might be oxidized by ferric ions to produce 8-oxodG was excluded by the finding that the 8-oxodG contents in cellular DNA, treated concurrently with 10 μm LOOH and 10 μm $FeCl_3$, were elevated without a decrease in the cell survival rate. These results indicate that the concurrent existence of LOOH and ferric ion enhances the formation of 8-oxodG in cellular DNA. Lipid hydroperoxides have been reported to induce DNA strand breaks in cultured human lung fibroblasts (25) and human lymphocytes (26). From this study, it was found that lipid hydroperoxides not only cause DNA strand breaks but also the oxidation of DNA bases.

Lipid hydroperoxides are effectively reduced by GPx or glutathione S-transferase in cells to the corresponding alcohols (27). However, if these antioxidant enzyme activities are lowered or hydroperoxide contents overcome the defense ability, hydroperoxides will exert their harmful effects upon biological systems. Lipid hydroperoxides are readily decomposed in the presence of transient metal ions to form alkyl peroxyl radicals, alkoxyl radicals, and hydroxyl radicals. Since lipids are present in membranes in biological systems, endogenous lipid hydroperoxides should be located mostly within membranes. Lipid hydroperoxides added to the medium are thought to be present in membranes if they are incorporated into cells. Thus, species formed by the decomposition of lipid hydroperoxides must shift to the cytosol to cause damage to DNA. The fact that 8-oxodG was formed in cellular DNA in the concurrent presence of LOOH and ferric ion indicates that hydroxyl radicals are finally formed in this system. If superoxide radical and/or hydrogen peroxide is the primary product formed in this system, then the induction of antioxidant enzyme activities, such as SOD, catalase and GPx, might be observed. However, the activities of these enzymes are only slightly increased by concurrent treatment with LOOH and ferric ion, and these changes are not significant. Thus, superoxide or hydrogen peroxide may not be present as the primary cause of DNA oxidation.

The mechanism of oxidative DNA damage in cellular systems by unsaturated fatty acid hydroperoxides and ferric ion is unclear at present. However, the formation of 8-oxodG indicates the involvement of hydroxyl radicals in this system. The production of hydroxyl radicals is well known in the reaction of various hydroperoxides with transition metal ions (28). However, it is hardly considered that hydroxyl radicals have a direct influence on DNA in nuclei or mitochondria even if they are formed from the decomposition of LOOH. On the other hand, alkyl peroxyl radicals have been reported to be generated from the reaction of organic hydroperoxide and heme iron, to be a major cytotoxic species against gram-positive bacteria, and to be stably generated at steady concentrations for 30 min or longer (29). Furthermore, it has also been shown that the alkyl peroxyl radicals generated by the reaction of alkyl hydroperoxide with hemoglobin cause single-strand breaks (30). Alkyl peroxyl radicals may be generated in our reaction system. Further research is needed to clarify more precisely the reactive species in this reaction.

REFERENCES

1. Carroll, K.K. (1998) Obesity as a Risk Factor for Certain Types of Cancer, *Lipids 33,* 1055–1059.
2. Carroll, K.K. (1991) Dietary Fats and Cancer, *Am. J. Clin. Nutr. 53,* 10645–10675.
3. Ames, B.N. (1983) Dietary Carcinogens and Anticarcinogens. Oxygen Radicals and Degenerative Diseases, *Science 221,* 1256–1264.

4. Fraga, C.G., and Tappel, A.L. (1988) Damage to DNA Concurrent with Lipid Peroxidation in Rat Liver Slices, *Biochem. J. 252,* 893–896.
5. Inouye, S. (1984) Site-specific Cleavage of Double-strand DNA by Hydroperoxide of Linoleic Acid, *FEBS Lett. 172,* 231–234.
6. Fujimoto, K., Neff, W.E., and Frankel, E.N. (1984) The Reaction of DNA with Lipid Oxidation Products, Metals and Reducing Agent, *Biochim. Biophys. Acta 795,* 100–107.
7. Kasai, H., and Nishimura, S. (1988) Formation of 8-Hydroxydeoxyguanosine in DNA by Auto-oxidized Unsaturated Fatty Acids, in *Medical, Biochemical and Chemical Aspects of Free Radicals* (Hayaishi, O., Niki, E., Kondo, M., and Yoshikawa, T., eds.) pp. 1021–1023, Elsevier, Amsterdam.
8. Park, J.-W., and Floyd, R.A. (1992) Lipid Peroxidation Products Mediate the Formation of 8-Hydroxydeoxyguanosine in DNA, *Free Radical Biol. Med. 12,* 245–250.
9. Kasai, H. (1997) Analysis of a Form of Oxidative DNA Damage, 8-Hydroxy-2′-deoxyguanosine, as a Marker of Cellular Oxidative Stress During Carcinogenesis, *Mutat. Res. 387,* 147–163.
10. Kaneko, T., and Matsuo, M. (1984) Isomerization of Linoleic Acid Hydroperoxides Under Argon and Under Degassed Conditions, *Chem. Bull. Pharm. (Tokyo) 32,* 332–335.
11. Yamamoto, K., Kaji, K., Kondo, H., Matsuo, M., Shibata, Y., Tasaki, Y., Utakoji, T., and Ooka, H. (1991) A New Human Male Diploid Cell Strain, TIG-7: Its Age-Related Changes and Comparison with a Matched Female TIG-1 Cell Strain, *Exp. Gerontol. 26,* 525–540.
12. Kaneko, T., Tahara, S., and Matsuo, M. (1996) Non-linear Accumulation of 8-Hydroxy-2′-deoxyguanosine, a Marker of Oxidized DNA Damage, During Aging, *Mutat. Res. 316,* 277–285.
13. Oyanagi, Y. (1984) Reevaluation of Assay Methods and Establishment of Kit for Superoxide Dismutase Activity, *Anal. Biochem. 142,* 290–296.
14. Aebi, H. (1984) Catalase *in Vitro*, *Methods Enzymol. 105,* 121–126.
15. Flohé, L., and Günzler, W.A. (1984) Assays of Glutathione Peroxidase, *Methods Enzymol. 105,* 114–120.
16. Bradford, M.M. (1976) A Rapid and Sensitive Method for the Quantitation of Microgram Quantities of Protein Utilizing the Principle of Protein–Dye Binding, *Anal. Biochem. 72,* 248–254.
17. Floyd, R.A., West, M.S., Eneff, K.L., Schneider, J.E., Wong, P.K., Tingey, D.T., and Hogsett, W.E. (1990) Conditions Influencing Yield and Analysis of 8-Hydroxy-2′-deoxyguanosine in Oxidative Damaged DNA, *Anal. Biochem. 188,* 155–158.
18. Claycamp, H.G. (1992) Phenol Sensitization of DNA to Subsequent Oxidative Damage in 8-Hydroxyguanine Assays, *Carcinogenesis 13,* 1289–1292
19. Adachi, S., Zeisig, M., and Möller, L. (1995) Improvements in the Analytical Method for 8-Hydroxydeoxyguanosine in Nuclear DNA, *Carcinogenesis 16,* 253–258.
20. Herbert, K.E., Evans, M.D., Finnegan, M.T., Farooq, S., Mistry, N., Podmore, I.D., Farmer, P., and Lunec, J. (1996) A Novel HPLC Procedure for the Analysis of 8-Oxoguanine in DNA, *Free Radical Biol. Med. 20,* 467–473.
21. Helbock, H.J., Beckman, K.B., Shigenaga, M.K., Walter, P.B., Woodall, A.A., Yeo, H.C., and Ames, B.N. (1998) DNA Oxidation Matters: The HPLC–Electrochemical Detection Assay of 8-Oxo-deoxyguanosine and 8-Oxo-guanine, *Proc. Natl. Acad. Sci. USA 95,* 288–293.
22. Cadet, J., D'Ham, C., Douki, T., Pouget, J.P., Ravanat, J.L., and Sauvaigo, S. (1998) Facts and Artifacts in the Measurement of Oxidative Base Damage to DNA, *Free Radical Res. Commun. 29,* 541–550.
23. Kasai, H., Crain, P.F., Kuchino, Y., Nishimura, S., Ootsuyama, A., and Tanooka, H. (1986) Formation of 8-Hydroxyguanine Moiety in Cellular DNA by Agents Producing Oxygen Radicals and Evidence for Its Repair, *Carcinogenesis 7,* 1849–1851.
24. Yang, M.-H., and Schaich, K.M. (1996) Factors Affecting DNA Damage Caused by Lipid Hydroperoxide and Aldehydes, *Free Radical Biol. Med. 20,* 225–236.
25. Kozumbo, W.J., Hanley N.M., Agarwal, S., Thomas, M.J., and Madden, M.C. (1996) Products of Ozonized Arachidonic Acid Potentiate the Formation of DNA Single Strand Breaks in Cultured Human Lung Cells, *Environ. Mol. Mutagen. 27,* 185–195.
26. Weitberg, A.B., and Corvese, D. (1989) Hydroxy- and Hydroperoxy-6,8,11,14-Eicosatetraenoic Acids Induce DNA Strand Breaks in Human Lymphocytes, *Carcinogenesis 10,* 1029–1031.
27. Flohé, L. (1982) Glutathione Peroxidase Brought into Focus, in *Free Radicals in Biology V* (Pryor, W.A., ed.) pp. 223–254, Academic Press, New York.
28. Minotti, G., and Aust, S.D. (1987) The Requirement for Iron (III) in the Initiation of Lipid Peroxidation by Iron (II) and Hydrogen Peroxide, *J. Biol. Chem. 262,* 1098–1104.
29. Akaike, T., Sato, K., Ijiri, S., Miyamoto, Y., Kohno, M., Ando, M., and Maeda, H. (1992) Bactericidal Activity of Alkyl Peroxyl Radicals Generated by Heme-Iron-Catalyzed Decomposition of Organic Peroxides, *Arch. Biochem. Biophys. 294,* 55–63.
30. Sawa, T., Akaike, T., Kida, K., Fukushima, Y., Takagi, K., and Maeda, H. (1998) Lipid Peroxyl Radicals from Oxidized Oils and Heme-Iron: Implication of a High-Fat Diet in Colon Carcinogenesis, *Cancer Epidemiol. Biomarkers Prevention 7,* 1007–1012.

[Received March 3, 2000; and in revised form and accepted July 6, 2000]

Lipid Peroxidation as Determined by Plasma Isoprostanes Is Related to Disease Severity in Mild Asthma

Lisa G. Wood[a], Dominic A. Fitzgerald[b,1], Peter G. Gibson[c], David M. Cooper[b], and Manohar L. Garg[a,*]

[a]Discipline of Nutrition and Dietetics, Faculty of Medicine and Health Sciences, University of Newcastle, Newcastle, New South Wales, 2308, Australia, [b]Department of Paediatrics, John Hunter Children's Hospital, Rankin Park, New South Wales, 2305, Australia, and [c]Airway Research Centre, Department of Respiratory Medicine, John Hunter Hospital, Rankin Park, New South Wales, 2305, Australia

ABSTRACT: Oxidative stress is believed to play an important role in the pathophysiology of asthma. Recently discovered F2-isoprostanes, of which 8-iso-$PGF_{2\alpha}$ is the most well-known isomer, have emerged as the most reliable marker of *in vivo* oxidative stress. The aim of this study was to examine 8-iso-$PGF_{2\alpha}$ as a biomarker of oxidative stress in mild asthma in relation to endogenous and dietary antioxidant protection. Total (free and esterified) plasma 8-iso-$PGF_{2\alpha}$, plasma dietary antioxidants (vitamins E and C, β-carotene, Zn, and Se), and erythrocyte antioxidant enzyme activities (glutathione peroxidase and superoxide dismutase) were measured in 15 mild asthmatics and 15 age- and sex-matched controls. Total plasma 8-iso-$PGF_{2\alpha}$ levels [median (quartile 1 – quartile 3)] were significantly increased in the asthmatics [213 pg/mL (122–455) vs. 139 pg/mL (109–174), P = 0.042]. The 8-iso-$PGF_{2\alpha}$ levels were found to be associated with clinical asthma severity (P = 0.044) and inhaled corticosteroid use (P = 0.027) in asthmatics. No differences were observed in the plasma dietary antioxidant vitamins. The asthmatics had significantly lower plasma levels of Zn (P = 0.027) and Se (P = 0.006). Plasma Se correlated negatively with 8-iso-$PGF_{2\alpha}$ (r = –0.725, P = 0.002). No differences between the groups were observed for glutathione peroxidase or superoxide dismutase, however, superoxide dismutase activity was negatively associated with asthma severity (P = 0.042). In conclusion, oxidative stress is increased in mild asthmatics, as reflected by increased plasma levels of 8-iso-$PGF_{2\alpha}$ and a deficiency in plasma Zn and Se. The isoprostane 8-iso-$PGF_{2\alpha}$ may provide a useful tool in intervention studies aimed at improving clinical status in asthma.

Paper no. L8398 in *Lipids 35,* 967–974 (September 2000).

Oxidative stress is believed to play an important role in the pathophysiology of asthma (1,2), which is characterized by many factors such as bronchial hyperresponsiveness, increased vascular permeability with edema of airway walls, mucus hypersecretion with small airway plugging, and infiltration by inflammatory cells (1). Inflammatory cells that are sequested and activated in asthmatic airways include mast cells, macrophages, eosinophils, neutrophils, lymphocytes, and platelets (1). These cells release a variety of mediators that are involved in the inflammatory response, including a range of toxic reactive oxygen species (ROS), such as the superoxide, hydrogen peroxide, and hydroxyl radicals (1,2). These ROS can have many detrimental effects on airway function such as peroxidation of membrane lipids, leading to epithelial cell disruption and/or death; DNA damage; alteration in important biomolecules such as surface receptor proteins and enzymes; enhanced release of arachidonic acid from membranes causing smooth muscle contraction; impaired β-adrenergic responsiveness; increased airway reactivity and secretions; and increased vascular permeability (1). Many of these effects will contribute to the variable and reversible airway narrowing that is characteristic of asthma, suggesting that ROS may contribute to the pathophysiology of the disease by several different mechanisms.

Evidence for the occurrence of oxidative stress in asthma includes: increased exhaled hydrogen peroxide and nitric oxide (3,4), increased thiobarbituric acid-reactive substances (TBARS) (2), decreased Trolox equivalent antioxidant capacity (TEAC) (2), altered status of antioxidant enzymes [glutathione peroxidase (GSHPx), superoxide dismutase (SOD), and catalase] (4–8) and their cofactors (Se and Zn) (5,6,9), decreased vitamin E (4,10), decreased vitamin C (10), increased generation of ROS from inflammatory cells *in vitro* (11), and decreased levels of lipoperoxidation substrates (12). Although measurements such as the *in vitro* TBARS test, breath alkane levels, hydroperoxides, conjugated dienes, and others are satisfactory in many circumstances, they have met criticism by a number of investigators, particularly when examining oxidative stress *in vivo* (13,14). These tests have limited specificity and/or sensitivity for oxidative stress or

[1]Present address: Department of Respiratory Medicine, New Children's Hospital, Parramatta, New South Wales, 2124, Australia.

*To whom correspondance should be addressed at Discipline of Nutrition and Dietetics, Faculty of Medicine & Health Sciences, University of Newcastle, Callaghan, NSW, 2308, Australia.
E-mail: ndmg@medicine.newcastle.edu.au

Abbreviations: BHT, butylated hydroxytoluene; EIA, enzyme immunoassay; FEV1, forced expiratory volume in one second; FVC, forced vital capacity; GC–MS, gas chromatography–mass spectrometry; GSHPx, glutathione peroxidase; Hb, hemoglobin; HPLC, high-performance liquid chromatography; ICP–MS, inductively coupled plasma–mass spectrometry; 8-iso-$PGF_{2\alpha}$, isomer of F2-isoprostane; MDA, malondialdehyde; ROS, reactive oxygen species; SEM, standard error of the mean; SOD, superoxide dismutase; TBARS, thiobarbituric acid-reactive substance; TEAC, Trolox equivalent antioxidant capacity; TxB_2, tritium-labeled thromboxane.

may be unreliable when applying the techniques to human subjects (14).

Isoprostanes, a recently discovered marker of oxidative stress, can be measured in plasma, urine, or other biological fluids (15–18), and overcome many of the methodological problems surrounding other markers. They are prostaglandin-like compounds produced *in vivo via* the cyclooxygenase-independent free radical-catalyzed oxidation of arachidonic acid (16). The most well-known isomer is 8-iso-$PGF_{2\alpha}$. Isoprostanes are now accepted to be the most accurate and reliable marker of oxidative stress, because they are structurally stable, are produced *in vivo*, and are present in relatively high concentrations (16). Indeed, as a marker of oxidative stress, the 8-iso-$PGF_{2\alpha}$ determination of carbon tetrachloride-induced lipid peroxidation is believed to be 20 times more sensitive than measurement of TBARS (17). Furthermore, isoprostane levels have been shown to increase in experimental models of injury, and can be suppressed using antioxidants (16).

The aim of this study was to examine oxidative stress in mild asthma using plasma 8-iso-$PGF_{2\alpha}$ as a biomarker and to examine antioxidant defenses in asthmatics, by studying both endogenous (erythrocyte GSHPx and SOD) and dietary (plasma vitamins E and C, β-carotene, Zn, and Se) antioxidant protection.

MATERIALS AND METHODS

Subject recruitment. Fifteen asthmatic subjects and 15 age- and gender-matched healthy controls were recruited for the study. All asthmatics studied had attended asthma clinics at the John Hunter Hospital and undergone pulmonary function testing in our laboratory. The diagnosis of asthma was made by a respiratory physician based upon a history of episodic respiratory symptoms, a doctor's prior diagnosis of asthma, the use of inhaled asthma therapy (β_2 agonists, corticosteroids, cromolyn, long-acting β_2 agonists), and all patients demonstrated a >12% improvement in their forced expiratory volume in 1 s (FEV1) in response to bronchodilator in our pulmonary function laboratory (19,20). All patients were clinically stable from an asthma viewpoint. Specifically, none had required oral corticosteroids for 3 mon prior to participation in this study. None had altered their preventive medications in the 4 wk prior to enrollment. The exclusion criteria were (i) age less than 5 yr (unable to perform reproducible spirometry), (ii) vitamin supplements taken in the last 4 wk, (iii) presence of other diseases known to be associated with elevated oxidative stress (cancer, diabetes, arthritis, or cystic fibrosis). Informed written consent was obtained from the subjects and/or their guardians. Ethics approval was obtained from the Hunter Area Health Service and the University of Newcastle Human Research Ethics Committees.

Subject characteristics. Each subject was assessed by a respiratory physician, who administered a questionnaire to assess current symptoms and treatment, past severity, and prior hospitalization. Subsequently, each subject's asthma severity was classfied as infrequent episodic, frequent episodic, or persistent, using standard criteria (19) (Table 1). All subjects were clinically stable when assessed. Routine pulmonary function tests were performed in all subjects using a spirometer (Medgraphics 1085D Breeze™ cardiorespiratory diagnostic software 1991, St. Paul, MN) with established normal values (21). FEV1 and forced vital capacity (FVC) were recorded and compared to predicted values. Height was measured with a Holtain, Crymych, Dyfed stadiometer. Weight was recorded using GEC/Avery digital scales (model number 824/890). Blood was collected in EDTA-coated tubes for full blood counts, performed using a Coulter Gen-S analyzer.

Vitamins and minerals. Blood samples were collected in EDTA-coated tubes and then centrifuged at 3,000 rpm at 4°C for 10 min. Plasma was collected and frozen at –70°C within half an hour of blood collection. Plasma levels of vitamins A and E and β-carotene were separated on a reversed-phase high-performance liquid chromatography (HPLC) column and measured using a variable wavelength ultraviolet (UV)-visible detector. Samples were thawed, mixed with ethanol to precipitate proteins, and vortexed; then hexane was added. After vortexing again, samples were centrifuged and the hexane phase removed and injected into an HPLC column [lab-packed Whatman ODS 3 (5 µm) 300 × 3.5 mm i.d.], with a flow rate of 1 mL/min, run time of 20 min, at ambient temperature. At 0.01 min, vitamin A was measured at 310 nm; at 5.5 min, vitamin E was measured at 280 nm; and at 9.0 min, β-carotene was measured at 450 nm. Plasma vitamin C was separated on a reversed-phase HPLC column and measured using an electrochemical detector. Samples were mixed with trichloracetic acid to precipitate proteins, vortexed, and centrifuged; and the supernatant was injected into an HPLC column [lab-packed Whatman ODS 3 (5 µm) 150 × 3.5 mm i.d.], with a flow rate of 1 mL/min, run time of 15 min, at ambient temperature. Measurements were made with an amperometric electrochemical detector with potential +0.6 V vs. Ag/AgCl reference electrode. Plasma levels of zinc, selenium, and copper were analyzed by inductively coupled plasma–mass spectrometry (ICP–MS). Samples were diluted in an ammonium EDTA-based diluent in a quantitative appli-

TABLE 1
Classification of Asthma

	Infrequent episodic	Frequent episodic	Persistent
Frequency of asthma exacerbation	< Every 6 wk	At least every 4–6 wk	Symptoms on most days
Use of bronchodilators	Not needed between exacerbations	< 3 Times weekly	Most days
Interval preventative therapy	Not required	May be required	Always required

cation. Platinum and rhodium were used as internal standards in the diluent. Calibration was by additions calibration in a pooled plasma base.

Total (free and esterified) 8-iso-$PGF_{2\alpha}$ assays. Blood samples were collected in EDTA-coated tubes, containing reduced glutathione (Sigma Chemical Company, St. Louis, MO) as an antioxidant. The samples were centrifuged at 3,000 rpm at 4°C for 10 min. The plasma fraction was removed and stored at −70°C in tubes precoated with butylated hydroxytoluene (BHT) (Sigma) for 8-iso-$PGF_{2\alpha}$ analysis. To an aliquot of plasma, a known amount of tritium-labeled thromboxane B_2 (TxB_2) (Amersham, Arlington Heights, IL) was added, to allow determination of recovery rate after purification procedure. Ethanol was added, the sample was chilled at 4°C, then centrifuged at 1,500 × *g* for 10 min to remove the precipitated proteins. The supernatant was decanted, an equal volume of 15% KOH was added and the resultant solution incubated at 40°C for 1 h, to cleave any esterified isoprostane. The sample was diluted with H_2O, then the pH was lowered with HCl to below 4.0. The sample was passed through a Sep-Pak C-18 reversed-phase cartridge (Waters, Milford, MA) which had been activated by rinsing with methanol, then H_2O. After passing the sample through, the cartridge was rinsed again with H_2O, then hexane. Finally, the 8-iso-$PGF_{2\alpha}$ was eluted with ethyl acetate containing 1% methanol. This solvent was evaporated using N_2, and the sample reconstituted with assay buffer. Purified sample was added to aqueous biodegradable counting scintillant (Amersham), and counted using a liquid scintillation counter, to determine recovery rates. A quantity of the remaining portion was analyzed with an 8-isoprostane enzyme immunoassay kit (Cayman Chemical, Ann Arbor, MI). Absorbance values were measured by using a plate reader and a wavelength of 405 nm, and the raw data were corrected for recovery. The assay was validated by adding a series of known amounts of pure 8-iso-$PGF_{2\alpha}$ standard to equal volumes of purified plasma. The concentration of total 8-iso-$PGF_{2\alpha}$ in these samples was determined by using enzyme immunoassay (EIA). A high correlation (0.99) was obtained between the known amounts of pure 8-iso-$PGF_{2\alpha}$ added and the concentration determined by EIA. The antiserum used in this assay has a 100% cross-reactivity with 8-iso-$PGF_{2\alpha}$; 0.2% each with $PGF_{2\alpha}$, $PGF_{3\alpha}$, PGE_1, and PGE_2; and 0.1% with 6-keto-$PGF_{1\alpha}$. The detection limit of the assay is 4 pg/mL. This kit has been used to measure 8-iso-$PGF_{2\alpha}$ concentration in human plasma, bronchoalveolar lavage, and other fluids (15,18,22).

GSHPx enzyme assay. Whole blood was collected into EDTA-coated tubes and centrifuged at 8,500 × *g* at 4°C for 10 min. Plasma was discarded, and cells were washed with 10 vol of ice-cold buffer (50 mM Tris-HCl, pH 7.5, containing 5 mM EDTA and 1 mM dithiothreitol). Samples were centrifuged again at 8,500 × *g* at 4°C for 10 min, and supernatant was discarded. Cells were then lysed by adding exactly 4 vol of ice-cold deionized water. After centrifuging again at 8,500 × *g* at 4°C for 10 min, supernatant was collected and stored at −70°C for analysis. Erythrocyte GSHPx activities were measured using a GPx-340 spectrophotometric assay kit (Bioxytech; OXIS International, Portland, OR), to obtain values in units per mL. The hemoglobin (Hb) concentration of the samples was also measured using Sigma Kit No. 525 for Total Hemoglobin, to allow erythrocyte GSHPx activity to be expressed as units per g of Hb.

SOD enzyme assay. Whole blood was collected into EDTA-coated tubes, and centrifuged at 3,000 rpm at 4°C for 10 min. The erythrocyte pellet was separated and stored at −70°C before analysis. The erythrocyte pellet was thawed and resuspended in 4 vol of ice-cold water and vortexed thoroughly. Ice-cold extraction reagent (ethanol/chloroform, 62.5:37.5 vol/vol) was added to the erythrocyte suspension and vortexed for 30 s. Samples were centrifuged at 3,000 × *g* at 4°C for 10 min. The upper phase was collected and stored at −70°C for analysis. Erythrocyte Zn/Cu-SOD activities were measured using SOD-525 spectrophotometric assay kit (Bioxytech; OXIS International), to obtain values in units per mL. The Hb concentration of the samples was also measured using Sigma Kit No. 525 for Total Hemoglobin, to allow erythrocyte Zn/Cu-SOD activity to be expressed as units per mg of Hb.

Dietary intake. Dietary intake was assessed using the 24-h recall method (23). Analysis of food records was conducted using the Diet/1 Nutrient Calculation Software, which is based on the 1992 Australian food tables and the composition of Australian manufactured foods (24). The mean intakes of energy, protein, fat, carbohydrates, fiber, retinol, β-carotene, vitamin A equivalents, vitamin C, iron, and zinc for each subject group were determined from these.

Statistical analysis. Results were analyzed using a standard computer statistical package (Minitab Inc. Version 12 for Windows 1997, State College, PA). Data were tested for normality using the Anderson-Darling test. Statistical comparisons were performed using the paired Student *t*-test for normally distributed data and the Wilcoxon paired test for nonparametric data. Correlations between variables were studied by linear regression, with calculation of Pearson's correlation coefficient for normal data, and Spearman's rank correlation coefficient for nonparametric data. Subgroup analysis was done using the Kruskal-Wallis test for nonparametric variables and the analysis of variance test for normal variables (25). The mean ± standard error is reported for normal data; for nonparametric data the median (quartile 1 – quartile 3) is reported. Differences were considered significant when $P < 0.05$.

RESULTS

Demographic data are reported for 15 asthmatic subjects (median age 14.0 yr) and 15 age- and sex-matched healthy controls (median age 14.0 yr) (Table 2). There were no significant differences between the mean height or weight of the two groups. Pulmonary function testing revealed no difference in lung function between the groups as indicated by the percentage predicted FEV1, percentage predicted FVC, and

TABLE 2
Characteristics of Healthy Controls and Asthmatics

Variable	Controls (n = 15)	Asthmatics (n = 15)	P value
Sex (M/F)	8/7	8/7	
Age (yr)[a]	14.0 (11.0–29.0)	14.0 (11.0–29.0)	1.000
<18 yr	9	9	
≥ 18 yr	6	6	
Smoking status (Y/N)	0/15	0/15	
Height (cm)[b]	164.0 ± 3.8	165.7 ± 4.7	0.576
Weight (kg)[b]	60.8 ± 4.6	62.1 ± 6.4	0.754
%FEV1[b]	102.7 ± 2.7	99.5 ± 4.3	0.533
%FVC[b]	102.5 ± 3.0	103.6 ± 4.4	0.836
FEV1/FVC (%)[b]	86.1 ± 1.8	82.7 ± 1.8	0.164
White cell count (10^9/L)[a]	5.8 (5.6–6.3)	6.9 (5.0–8.4)	0.167
Neutrophil count (10^9/L)[b]	2.91 ± 0.23	3.21 ± 0.30	0.260
Eosinophil count (10^9/L)[a]	0.20 (0.10–0.23)	0.30 (0.20–0.40)	0.014

[a]Non-parametric data analyzed by using Wilcoxon paired test. Values reported are median (quartile 1 – quartile 3).
[b]Normal data analyzed using Student's paired *t*-test. Values reported are mean ± SEM.

FEV1/FVC (Table 2). Subjects were classified as infrequent episodic, frequent episodic, and persistent asthmatics (Table 3) (19).

As expected, the peripheral blood eosinophil count was significantly higher in the asthmatic group (P = 0.014) than in the controls, indicative of the disease often being atopic in nature (Table 2). Eosinophil count was associated with clinical asthma severity (P = 0.032) and inhaled corticosteroid use (P = 0.003).

Total (free and esterified) plasma 8-iso-$PGF_{2\alpha}$ levels were found to be elevated in the asthmatics compared to the controls (P = 0.042) (Fig. 1). The 8-iso-$PGF_{2\alpha}$ levels were associated with clinical asthma severity (P = 0.044) and inhaled corticosteroid use (P = 0.027) in asthmatics (Figs. 2A and 2B). All subjects had normal lung function (Table 2), and no correlation was observed between total 8-iso-$PGF_{2\alpha}$ levels and lung function. There was no relationship between lung function and disease severity.

Plasma levels of Zn and Se were both significantly lower in the asthmatics (P = 0.027 and 0.006, respectively) (Table 4), with Se levels correlating negatively with total plasma 8-iso-$PGF_{2\alpha}$ levels (r = –0.725, P = 0.002). Erythrocyte SOD activity was lower in the asthmatics, with this difference approaching significance (P = 0.076). SOD activity was negatively associated with clinical severity of asthma (P = 0.042), with the more severely asthmatic subjects having reduced SOD activity. There was, however, no significant difference in the erythrocyte activity levels of GSHPx and no association between GSHPx activity and clinical severity.

Plasma levels of the dietary antioxidants β-carotene and vitamins E and C were similar in the two groups. There was no correlation between total plasma 8-iso-$PGF_{2\alpha}$ and plasma dietary antioxidants. Dietary analysis indicates that there was no significant difference in the nutrient intake of the groups (Table 5).

DISCUSSION

This study demonstrated reduced levels of plasma Zn and Se, increased total plasma 8-iso-$PGF_{2\alpha}$ levels, and a negative cor-

TABLE 3
Clinical Characteristics of Asthmatics

Clinical severity, *n* (%)	Infrequent episodic	7 (47)
	Frequent episodic	4 (27)
	Persistent	4 (27)
Current medications, *n* (%)	Short-acting β_2-agonist	12 (80)
	Long-acting β_2-agonist	1 (7)
	Cromoglycate	2 (13)
	Ipratropium	1 (7)
	Inhaled corticosteroid	5 (33)
	Fluticasone propionate, 125 µg	3 (20)
	Budesidonide, 200–600 µg	2 (13)
Oral corticosteroid use for asthma in past 2 yr, *n* (%)		5 (33)
Duration of asthma, yr[a]		10.0 (8.0–16.0)

[a]Values reported are median (quartile 1 – quartile 3).

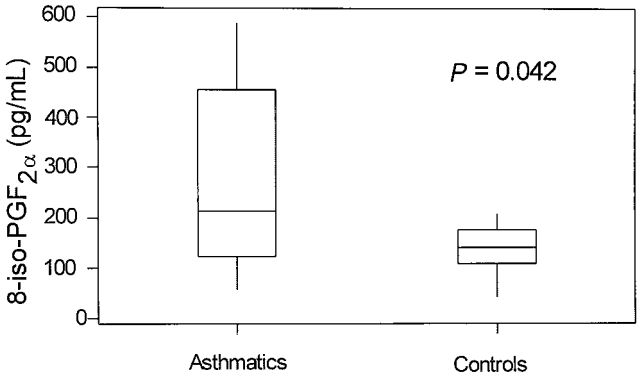

FIG. 1. Total plasma 8-iso-$PGF_{2\alpha}$ levels in 15 asthmatics vs. 15 age- and gender-matched controls. Plot shows medians and interquartile ranges (quartile 1 – quartile 3).

relation between plasma 8-iso-$PGF_{2\alpha}$ and Se levels in mild asthmatics, providing further evidence that oxidative stress is elevated in asthma. Moreover, this study showed a positive association between asthma severity and the level of total plasma 8-iso-$PGF_{2\alpha}$ and a negative association between asthma severity and erythrocyte SOD enzyme activity. By implication, simple dietary antioxidant supplementation may provide adjunctive therapy for asthmatics, especially those more severely affected.

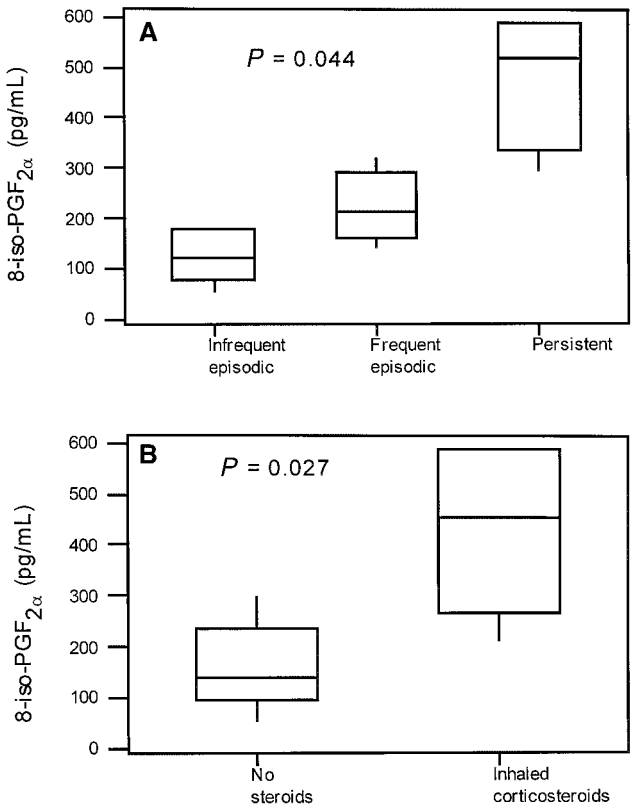

FIG. 2. (A) Total plasma 8-iso-$PGF_{2\alpha}$ levels in asthmatics with infrequent episodic (n = 7), frequent episodic (n = 4), and persistent (n = 4) asthma. An association between 8-iso-$PGF_{2\alpha}$ and asthma severity is observed (P = 0.044). (B) Total plasma 8-iso-$PGF_{2\alpha}$ levels in steroid-naïve asthmatics (n = 10) vs. asthmatics using inhaled corticosteroids (n = 5). An association between 8-iso-$PGF_{2\alpha}$ and steroid use is observed (P = 0.027). Plots show medians and interquartile ranges (quartile 1 – quartile 3).

Inflammation of the airways is believed to be a main contributor to oxidative stress in asthma (1). Inflammatory cells that may release ROS into asthmatic airways include mast cells, macrophages, neutrophils lymphocytes, platelets, and, in particular, eosinophils (1). In our study, the higher eosinophil count in the asthmatics and the association between eosinophil count and asthma severity demonstrate that severity of asthma is related to the degree of inflammation. Furthermore, the positive association demonstrated between eosinophil count and inhaled corticosteroid use indicates that inflammation persists despite steroid use in these patients.

As inflammation is persistent and increases with disease severity in the asthmatics, it is not surprising that we observed an elevation in oxidative stress, as measured by plasma 8-iso-$PGF_{2\alpha}$ levels, and a positive association between 8-iso-$PGF_{2\alpha}$ levels and asthma severity. A similar trend was recently reported by Montuschi *et al.* (18), who reported elevated 8-iso-$PGF_{2\alpha}$ levels in breath condensate of asthmatics, with 8-iso-$PGF_{2\alpha}$ levels increasing as asthma severity increased. The positive association we observed between 8-iso-$PGF_{2\alpha}$ levels and inhaled corticosteroid use also agrees with the work of Montuschi *et al.* (18), who reported higher 8-iso-$PGF_{2\alpha}$ in breath condensate of severe asthmatics using oral steroids, compared to mild asthmatics who were steroid-naive. In contrast, studies using other indices of oxidative stress have reported inhibition of oxidation in response to steroid use (3,26). In our study, it is likely that 8-iso-$PGF_{2\alpha}$ concentrations remained elevated in patients using inhaled corticosteroids because the treatment had not effectively controlled their asthma, resulting in residual inflammation and oxidative stress. Studies examining the relationship between steroid use, residual inflammation, and oxidative stress are warranted.

As isoprostanes have also been observed to be potent vasoconstrictory agents in rat lungs (27), one can speculate about their contribution to the airway narrowing that is characteristic of asthma. Although the situation in humans *in vivo* may be different, the full impact of elevated isoprostane levels on pulmonary function remains to be established, and isoprostanes may prove to have an important biological role as well as being an important *in vivo* marker of oxidative stress.

While there is evidence suggesting 8-iso-$PGF_{2\alpha}$ may also be produced enzymatically by cyclooxygenase activity in some cells and tissues (28), this does not appear to occur in humans *in vivo* (29). Thus, this marker is still believed to be an accurate indicator of oxidative stress (30). The EIA methodology used in this study to measure 8-iso-$PGF_{2\alpha}$ provides an inexpensive, accessible alternative to analysis by gas chromatography–mass spectrometry (GC–MS). The values of total 8-iso-$PGF_{2\alpha}$ we observed in normal plasma using the EIA method are similar to those obtained by Morrow *et al.* using GC–MS (31). As discussed by Morrow and Roberts (16), GC–MS assay is expensive and labor-intensive and uses technology that is not widely available. Thus, the use of spe-

TABLE 4
Biochemical Markers—Plasma Levels of 8-iso-$PGF_{2\alpha}$, Vitamin E, Vitamin C, β-Carotene, Vitamin A, Zn, Se, Cu, and Erythrocyte Levels of GSHPx and SOD Activity

Biochemical marker	Controls	Asthmatics	*P* value
8-Iso-$PGF_{2\alpha}$ (pg/mL)[a]	139 (109 – 174)	213 (122 – 455)	0.042
Vitamin E (μmol/L)[a]	17 (14 – 21)	17 (15 – 20)	0.900
Vitamin C (μmol/L)[b]	57.2 ± 7.4	54.2 ± 7.1	0.562
β-Carotene (μmol/L)[a]	0.4 (0.2 – 0.6)	0.3 (0.2 – 0.6)	0.701
Vitamin A (μmol/L)[a]	1.6 (1.4 – 1.9)	1.6 (1.3 – 1.9)	0.286
Zn (μmol/L)[b]	12.8 ± 0.4	11.5 ± 0.4	0.027
Se (μmol/L)[b]	1.35 ± 0.06	1.16 ± 0.08	0.006
Cu (μmol/L)[a]	14.5 (13.0 – 16.2)	14.1 (12.3 – 17.9)	0.932
GSHPx (U/g Hb)[b]	18.2 ± 1.3	19.8 ± 1.1	0.361
SOD (U/mg Hb)[b]	2.03 ± 0.07	1.85 ± 0.06	0.076

[a]Non-parametric data analyzed by using Wilcoxon paired test. Values reported are median (quartile 1 – quartile 3).
[b]Normal data analyzed using Student's paired *t*-test. Values reported are mean ± SEM. GSHPx, glutathione peroxidase; SOD, superoxide dismutase; Hb, hemoglobin.

cific immunoassays has expanded research in this area, with several studies using the EIA methodology recently being reported (15,18,22).

Our data showed a significant deficiency in plasma Zn levels in asthmatics, supporting results from other researchers (32). Zn plays an important role as an antioxidant, with the probable mechanisms being stabilization of sulfhydryl groups to prevent intramolecular disulfide formation, displacement of bound Cu and Fe to prevent electron transfer, and reduction of free radical production in neutrophils (33). Thus, the consequence of Zn deficiency in the asthmatics is reduced antioxidant protection.

Zn is also a cofactor for the antioxidant enzyme, Cu,Zn-SOD. Located primarily in the cytosol and mitochondria of cells, SOD catalyzes the dismutation of the superoxide anion into oxygen and hydroperoxide, which is then acted upon by GSHPx to form water. The activity and synthesis of this enzyme, however, are not decreased by dietary Zn deficiency (34), as Zn can be replaced at the structural site by other metals. Previous studies of SOD activity in asthmatics are inconsistent, with both decreased activity (7,26) and increased activity (8) being reported. These data are difficult to compare owing to variations in disease severity and differences in the cell types and blood components being measured. In our study, erythrocyte SOD activity was not significantly reduced in the asthmatics. There was, however, a negative association between SOD activity and asthma severity. This suggests that SOD levels are only diminished in the case of severe oxidative stress, when the oxidant burden exceeds the host's ability to upregulate antioxidant enzyme protection.

The asthmatic subjects in our study also had low plasma Se levels, supporting results of other researchers, who have reported decreased levels of Se in whole blood (5,9), plasma/serum (6,9), and erythrocytes (6). Se is an essential component of the GSHPx enzyme, necessary for both its synthesis and activity. Thus, many reports have linked Se deficiency to a decrease in GSHPx activity (5,6). Our data, however, which are also supported by other researchers (9,26), showed no deficiency in erythrocyte GSHPx activity despite low plasma Se levels. This suggests that Se has another func-

TABLE 5
Nutrient Intake of Healthy Controls and Asthmatics

Nutrient/kg body weight	Controls	Asthmatics	*P* value
Energy (kJ)[a]	171.3 ± 12.4	158.6 ± 10.7	0.360
Protein (g)[a]	1.7 ± 0.2	1.3 ± 0.1	0.116
%Protein[a]	16.9 ± 1.0	14.7 ± 0.9	0.119
Fat (g)[a]	1.5 ± 0.2	1.3 ± 0.2	0.415
%Fat[b]	32 (30 – 36)	31 (21 – 41)	0.496
Carbohydrate (g)[a]	5.1 ± 0.4	5.1 ± 0.3	0.948
%Carbohydrate[a]	49.7 ± 2.4	53.9 ± 3.1	0.269
Fiber (g)[a]	0.35 ± 0.03	0.34 ± 0.01	0.981
Vitamin A (μg)[a]	6.8 ± 1.1	7.0 ± 1.1	0.926
β-Carotene (μg)[b]	42.6 (18.1 – 90.6)	16.7 (11.0 – 36.1)	0.164
Vitamin C (mg)[b]	1.7 (1.1 – 3.4)	2.0 (1.3 – 3.3)	0.932
Iron (mg)[a]	0.22 ± 0.02	0.20 ± 0.02	0.442
Zinc (mg)[b]	0.20 (0.10 – 0.28)	0.11 (0.09 – 0.18)	0.201

[a]Normal data analyzed using Student's paired *t*-test. Values reported are mean ± SEM.
[b]Non-parametric data analyzed using Wilcoxon paired test. Values reported are median (quartile 1 – quartile 3).

tion, independent of its association with GSHPx. The negative correlation observed between Se and total plasma 8-iso-$PGF_{2\alpha}$ levels suggests that Se has a role as an antioxidant. In humans, only about 10% of total erythrocyte Se is bound to GSHPx (35). Much of the remaining Se is incorporated into several different selenoproteins, most of which have redox functions, suggesting that an antioxidant role is likely. Selenoprotein P is one such protein, which has been identified as having a protective effect against oxidation (36). In the case of Se deficiency, as observed in our asthmatics, it is possible that while the available Se is used to maintain GSHPx activity, the production and activity of other selenoproteins such as Selenoprotein P have been reduced, thereby reducing overall antioxidant protection. In future studies, measurement of these selenoproteins will be important if the role of Se in asthma is to be better understood.

Plasma concentrations of vitamins C and E and β-carotene in the asthmatics showed no deficiencies compared to the controls. Although some have found similar results (37), others have shown a decrease in plasma levels of vitamin C (38) and erythrocyte vitamin E (4). This inconsistency may be due to differences in the dietary intake and/or asthma severity of the subjects in each study. In our study, patients had relatively mild disease (no subjects required oral steroids). Also, the dietary analysis indicates that the nutrient intake of the asthmatics in our study was similar to the control group. Thus, while the presence of ROS was apparently elevated in the asthmatics, the utilization of these antioxidant vitamins was not increased. This suggests that the mechanisms described above, involving the minerals Se and Zn, may be the first line of antioxidant defense in asthma. Alternatively, another recent report (10) suggested that peripheral blood markers may be less sensitive than direct lung measurements. Thus, plasma antioxidant levels may be a poor reflection of local antioxidant defenses in the lung and while plasma antioxidant vitamin levels are normal, deficiencies may be occurring in the lung lining fluid. This highlights the importance of directly measuring the antioxidant defenses in the lung in future studies.

In conclusion, this study indicates that oxidative stress is elevated and contributes to the clinical severity of asthma, with a deficiency in plasma Se and Zn being usual. As these minerals have been shown to play an important role in antioxidant defense, it would be sensible to supplement asthmatic patients with these nutrients, in order to minimize the effects of oxidant stress. A previous report of Se supplementation improving antioxidant defenses and clinical symptoms in asthmatics (39) is encouraging and suggests that further investigation of oxidative stress during Se and Zn supplementation is warranted. The discovery of 8-iso-$PGF_{2\alpha}$ as the best indicator of oxidative stress *in vivo* allows examination of the effects of future antioxidant interventions in asthmatics.

ACKNOWLEDGMENTS

Supported by a National Health and Medical Research Council Biomedical Postgraduate Research Scholarship. Assistance with sample collection received from Dr. Jodi Hilton, Dr. Larry Roddick, Majella Maher, and Robyn Hankin, John Hunter Children's Hospital. Assistance with sample processing received from Brett Griffin, University of Newcastle.

REFERENCES

1. Barnes, P.J. (1990) Reactive Oxygen Species and Airway Inflammation, *Free Radical Biol. Med. 9*, 235–243.
2. Rahman, I., Morrison, D., Donaldson, K., and MacNee, W. (1996) Systemic Oxidative Stress in Asthma, COPD and Smokers, *Am. J. Respir. Crit. Care Med. 154,* 1055–1060.
3. Horvarth, I., Donnelly, L.E., Kiss, A., Kharitonov, S.A., Lim, S., Chung, K.F., and Barnes, P.J. (1998) Combined Use of Exhaled Hydrogen Peroxide and Nitric Oxide in Monitoring Asthma, *Am. J. Respir. Crit. Care Med. 158*, 1042–1046.
4. Mohan, I.K., and Das, U.N. (1997) Oxidant Stress, Antioxidants, Nitric Oxide and Essential Fatty Acids in Bronchial Asthma, *Med. Sci. Res. 25*, 307–309.
5. Flatt, A., Pearce, N., Thomson, C.D., Sears, M., Robinson, M.F., and Beasley, R. (1990) Reduced Selenium in Asthmatic Subjects in New Zealand, *Thorax 45*, 95–99.
6. Kadrabova, J., Madaric, A., Kovakicova, Z., Podivinsky, F., Ginter, E., and Gazdik, F. (1996) Selenium Status Is Decreased in Patients with Intrinsic Asthma, *Biol. Trace Elem. Res. 52*, 241–248.
7. Smith, L.J., Shamsuddin, M., Sporn, P.H.S., Denenberg, M., and Anderson, J. (1997) Reduced Superoxide Dismutase in Lung Cells of Patients with Asthma, *Free Radical Biol. Med. 22*, 1301–1307.
8. Kurosawa, M., Kobayashi, H., and Nakano, M. (1993) Cu-Zn Superoxide Dismutase Activities in Platelets from Stable Bronchial Asthmatic Patients, *Int. Arch. Allergy Immunol. 101*, 61–65.
9. Stone, J., Hinks, L.J., Beasley, R., Holgate, S.T., and Clayton, B.A. (1989) Reduced Selenium Status of Patients with Asthma, *Clin. Sci. 77*, 495–500.
10. Kelly, F.J., Mudway, I., Blomberg, A., Frew, A., and Sandstrom, T. (1999) Altered Lung Antioxidant Status in Patients with Mild Asthma, *Lancet 354*, 482–483.
11. Cluzel, M., Damon, M., Chanez, P., Bousquet, J., Crastes de Paulet, A., Michel, F.B., and Bodard, P. (1987) Enhanced Alveolar Cell Luminol-dependent Chemiluminescence in Asthma, *J. Allergy Clin. Immunol. 80*, 195–201.
12. Chilvers, E.R., Garratt, H., Whyte, M.K.B., Fink, R., and Ind, P.W. (1989) Absence of Circulating Products of Oxygen-Derived Free Radicals in Acute Severe Asthma, *Eur. Respir. J. 2*, 950–954.
13. Pincemail, J., Defraigne, J.O., and Limet, R. (1996) Oxidative Stress in Clinical Situations—Fact or Fiction? *Eur. J. Anaesthesiol. 13*, 219–234.
14. Halliwell, B., and Grootveld, M. (1987) The Measurement of Free Radical Reactions in Humans, *FEBS Lett. 213*, 9–14.
15. Montuschi, P., Ciabattoni, G., Paredi, P., Pantelidis, P., du Bois, R.M., Kharitonov, S.A., and Barnes, P.J. (1998) 8-Isoprostane as a Biomarker of Oxidative Stress in Interstitial Lung Diseases, *Am. J. Respir. Crit. Care Med. 158*, 1524–1527.
16. Morrow, J.D., and Roberts, L.J. (1997) The Isoprostanes—Unique Bioactive Products of Lipid Peroxidation, *Prog. Lipid Res. 36*, 1–21.
17. Awad, J.A., Roberts, L.J., Burk, R.F., and Morrow, J.D. (1996) Isoprostanes—Prostaglandin-like Compounds Formed *in vivo* Independently of Cyclooxygenase, *Gastroenterol. Clin. North America 25*, 409–427.
18. Montuschi, P., Corradi, M., Ciabattoni, G., Nightingale, J., Kharitonov, S.A., and Barnes, P.J. (1999) Increased 8-Isoprostane, a Marker of Oxidative Stress, in Exhaled Condensa-

tion in Asthma Patients, *Am. J. Respir. Crit. Care Med. 160*, 216–220.
19. Anonymous (1998) *Asthma Management Handbook,* 4th edn., National Asthma Campaign, Melbourne, Australia.
20. Norzila, M.Z., Fakes, K., Henry, R.L., Simpson, J., and Gibson, P.G. (2000) Interleukin 8 Secretion and Neutrophil Recruitment Accompanies Induced Sputum Eosinophil Activation in Children with Acute Asthma*, Am. J. Respir. Crit. Care Med. 161*, 769–774.
21. Knudson, R.J., Slatin, R.C., Lebowitz, M.D., and Burrows, B. (1976) The Maximal Expiratory Flow-Volume Curve: Normal Standards, Variability and Effects of Age*, Am. Rev. Respir. Dis. 113*, 587–600.
22. Collins, C.E., Quaggiotto, P., Wood, L., O'Loughlin, E.V., Henry, R.L., and Garg, M.L. (1999) Elevated Plasma Levels of F2α Isoprostane in Cystic Fibrosis, *Lipids. 34*, 551–556.
23. Block, G. (1982) A Review of Validations of Dietary Assessment Methods, *A. J. Epidemiol. 115*, 492–505.
24. Goodhill, C., Diet/1 Nurient Calculation Software, 20 Westborne St., Highgate Hill, Brisbane, Queensland, Australia, 4101.:(c) Xyris Software, 1992.
25. Bland, M. (1987) *An Introduction to Medical Statistics*, 1st edn., pp. 216–240, Oxford University Press, Oxford.
26. DeRaeve, H.R., Thunnissen, F.B.M.J., Kaneko, F.T., Guo, F.H., Lewis, M., Kavuru, M.S., Secic, M., Thomassen, M.J., and Erzurum, S.C. (1997) Decreased Cu,Zn-SOD Activity in Asthmatic Airway Epithelium: Correction by Inhaled Corticosteroid *in vivo, Am. J. Physiol. 272 (Lung Cell. Mol. Physiol. 16),* L148–L154.
27. Kang, H.K., Morrow, J.D., Roberts, L.J., Newman, J.H., and Banerjee, M. (1993) Airway and Vascular Effects of 8-Epi-prostaglandin F2α in Isolated Perfused Rat Lung*, J. Appl. Physiol. 74*, 460–465.
28. Klein, T., Reutter, F., Schweer, H., and Nusing, R.M. (1997) Generation of the Isoprostane 8-Epi-prostaglandin F_2 alpha *in vitro* and *in vivo via* the Cyclooxygenases*, J. Pharmacol. Exp. Ther. 282*, 1658–1665.
29. Pratico, D., Basili, S., Vieri, M., Cordova, C., Violi, F., and Fitzgerald, G.A. (1998) Chronic Obstructive Pulmonary Disease Is Associated with an Increase in Urinary Levels of Isoprostane F2α III, an Index of Oxidant Stress*, Am. J. Respira. Crit. Care Med. 158*, 1709–1714.
30. Delanty, N., Reilly, M., Pratico, D., Fitzgerald, D.J., Lawson, J.A., and Fitzgerald, G.A. (1996) 8-Epi-PGF2α Specific Analysis of an Isoeicosanoid as an Index of Oxidant Stress *in vivo, Br. J. Clin. Pharmacol. 42*, 15–19.
31. Morrow, J.D., Frei, B., Longmire, A.W., Gaziano, J.M., Lynch, S.M., Shyr, Y., Strauss, W.E., Oates, J.A., and Roberts, L.J. (1995) Increase in Circulating Products of Lipid Peroxidation (F2-isoprostanes) in Smokers, *N. Engl. J. Med. 332*, 198–203.
32. Malvy, J.M.D., Lebranchu, Y., Richard, M.J., Arnaud, J., and Favier, A. (1993) Oxidative Metabolism and Severe Asthma in Children, *Clin. Chem. Acta 218*, 117–120.
33. Bray, T.M., and Bettger, W.J. (1990) The Physiological Role of Zinc as an Antioxidant, *Free Radical Biol. Med. 8*, 281–291.
34. Taylor, C.G., Bettger, W.J., and Bray, T.M. (1988) The Effect of Dietary Zinc or Copper Deficiency on the Primary Free Radical Defense System in Rats, *J. Nutr. 118*, 613–621.
35. Behne, D., and Wolters, W. (1979) Selenium Content and Glutathione Peroxidase Activity in the Plasma and Erythrocytes of Non-pregnant and Pregnant Women, *J. Clin. Chem. Clin. Biochem. 17*, 133–135.
36. Burk, R.F., Hill, K.E., Awad, J.A., Morrow, J.D., and Lyons, P.R. (1995) Liver and Kidney Necrosis in Selenium-Deficient Rats Depleted of Glutathione, *Lab. Invest. 72*, 723–730.
37. Powell, C.V.E., Nash, A.A., Powers, H.J., and Primhak, R.A. (1994) Antioxidant Status in Asthma, *Pediatr. Pulmonol. 18,* 34–38.
38. Aderele, W.I., Ette, S.I., Oduwole, O., and Ikpeme, S.J. (1985) Plasma Vitamin C (ascorbic acid) Levels in Asthmatic Children, *Afr. J. Med. Sci. 14*, 115–120.
39. Hasselmark, L., Malmgren, R., Zetterstrom, O., and Unge, G. (1993) Selenium Supplementation in Intrinsic Asthma, *Allergy 48,* 30–36.

[Received November 29, 1999, and in revised form June 2, 2000; revision accepted July, 2000]

Comparison of Growth and Fatty Acid Metabolism in Rats Fed Diets Containing Equal Levels of γ-Linolenic Acid from High γ-Linolenic Acid Canola Oil or Borage Oil

John D. Palombo,[a,*] Stephen J. DeMichele[b], Jim-Wen Liu[b], Bruce R. Bistrian[a], and Yung-Sheng Huang[b]

[a]Departments of Surgery and Medicine, Beth Israel Deaconess Medical Center and Harvard Medical School, Boston, Massachuetts 02215, and [b]Strategic Discovery R&D, Ross Products Division, Abbott Laboratories, Columbus, Ohio 43219

ABSTRACT: We have utilized transgenic technology to develop a new source of γ-linolenic acid (GLA) using the canola plant as a host. The aim of the present study was to compare the growth and fatty acid metabolism in rats fed equal amounts of GLA obtained from the transgenic canola plant relative to GLA from the borage plant. Young male Sprague-Dawley rats (n = 10/group) were randomized and fed a purified AIN93G diet (10% lipid by weight) containing either a mixture of high GLA canola oil (HGCO) and corn oil or a control diet containing borage oil (BO) for 6 wk. GLA accounted for 23% of the triglyceride fatty acids in both diets. Growth and diet consumption were monitored every 2–3 d throughout the study. At study termination, the fatty acid composition of the liver and plasma phospholipids was analyzed by gas chromatography. The growth and diet consumption of the HGCO group were similar to the BO group. There were no adverse effects of either diet on the general health or appearance of the rats, or on the morphology of the major organs. There was no significant difference between the diet groups for total percentage of n-6 polyunsaturated fatty acids present in either the total or individual phospholipid fractions of liver or plasma. The relative percentage of GLA and its main metabolite, arachidonic acid, in each phospholipid fraction of liver or plasma were also similar between groups. The percentage of 18:2n-6 in liver phosphatidylethanolamine and phosphatidylinositol/serine was higher ($P < 0.05$) and 22:5n-6 was lower in the HGCO group than the BO group. This finding could be attributed to the higher 18:3n-3 content in the HGCO diet than the BO diet. Results from this long-term feeding study of rats show for the first time that a diet containing transgenically modified canola oil was well-tolerated, and had similar biological effects, i.e., growth characteristics and hepatic metabolism of n-6 fatty acids, as a diet containing borage oil.

Paper no. L8525 in *Lipids 35*, 975–981 (September 2000).

Conversion of the essential fatty acid, linoleic acid (18:2n-6), to γ-linolenic acid (GLA, 18:3n-6) and dihomo-γ-linolenic acid (DHGLA, 20:3n-6) is rate-limited by Δ6 desaturase activity. GLA may become essential under certain pathological conditions that depress Δ6 desaturase activity and reduce production of DHGLA and its anti-inflammatory metabolites, prostaglandin E_1 (PGE_1) and 15-hydroxy-eicosatrienoic acid (15-HETrE) (1–3). A chronic imbalance between the fatty acids DHGLA and arachidonic acid and their respective derivatives (PGE_1 and 15-HETrE, vs. the 2-series of prostaglandins) has been proposed to be one contributing factor in the etiology of some inflammatory and cardiovascular disorders (4). In this regard, dietary studies have shown that provision of GLA to bypass Δ6 desaturase alleviated pathologic conditions associated with low levels of PGE_1 and 15-HETrE (5,6). More recently, experimental (7,8) and clinical studies (9) have revealed that supplementation of nutritional formulas with a combination of eicosapentaenoic (20:5n-3) and GLA can favorably reduce an inflammatory response while promoting vasodilation and oxygen delivery following acute lung injury.

These beneficial effects have increased the demand for GLA-enriched oils. At the present time, the predominant sources of GLA are oils from plants such as borage, evening primrose, and black currant. Since all GLA-containing oils on the market are relatively expensive due to large fluctuations in availability, and production and purification costs, there is a need for more economical sources of GLA. For this purpose, we have utilized transgenic technology to develop a new source of GLA using the canola plant as a host. The production of GLA in the canola plant starts with oleic acid (18:1n-9) and requires two desaturation steps at the Δ12 and Δ6 positions. Recently, cDNA clones encoding Δ12 and Δ6 desaturases from *Mortierella alpina* have been identified (10). By recombinant expression of both desaturases, the yield of GLA from the modified canola plant can range from 22 to 45% of the total fatty acids.

The aim of the present study was to compare, for the first time, the growth and fatty acid metabolism in rats fed diets containing equal levels of GLA from high GLA canola oil (HGCO) or borage oil (BO) for 6 wk. We also determined the fatty acid composition of the principal phospholipid fractions

*To whom correspondence should be addressed at Department of Surgery, Beth Israel Deaconess Medical Center, 21-27 Burlington Avenue, 503C, Boston, MA 02215.
E-mail: jpalombo@caregroup.harvard.edu

Abbreviations: ANOVA, analysis of variance; BO, borage oil; DHGLA, dihomo-γ-linolenic acid; GLA, γ-linolenic acid; GLC, gas–liquid chromatography; 15-HETrE, 15-hydroxy-eicosatrienoic acid; HGCO, high GLA canola oil; PC, phosphatidylcholine; PE, phosphatidylethanolamine; PGE_1, prostaglandin E_1; PI/PS, phosphatidylinositol/serine; PUFA, polyunsaturated fatty acids; TLC, thin-layer chromatography.

of liver and plasma and triglycerides in epididymal adipose at study termination to compare the dietary effects on the metabolism of the principal n-6 fatty acids in these tissues.

MATERIALS AND METHODS

The study design was approved by the Institute Animal Care and Use Committee. The care of the animals was in accordance with the guidelines set forth by the National Institute of Health's, *Guide for the Care and Use of Laboratory Animals*. Pathogen-free male (78–100 g) Sprague Dawley rats (Taconic Farms, Germantown, NY) were housed in plastic cages (two rats per cage) and maintained on a 12-h light-dark cycle in a temperature- and humidity-controlled room.

After a 2-d acclimatization period, the rats were weighed and randomly assigned to receive a semisynthetic diet supplemented with 10% by weight of HGCO or BO (n = 10/group). Each diet was prepared at Ross Products Division (Columbus, OH) using a fat-free purified powder diet (AIN93G; Harlan Teklad, Madison, WI) fortified with vitamins and minerals according to recently established guidelines (11). The fatty acid compositions of the original HGCO oil and the two diets (HGCO and BO) are presented in Table 1. The HGCO was blended with corn oil (54:46, w/w) to approximate the relative percentages of GLA (23%) and LA (36%) in the BO. The percentage of α-linolenic acid (18:3n-3) was 1.1 and 0.3% in the HGCO and BO diets, respectively. Both HGCO and BO were extracted and processed in similar methods by the same processor (POS Pilot Plant Corp., Saskatoon, Canada). The mean total nonsaponifiable fractions in HGCO and BO were 1.7 and 1.6 g/100 g oil, respectively, while the mean total tocopherols were 922 and 763 mg/kg oil, respectively.

Gas chromatographic analysis of diet samples taken before and after the 6-wk feeding period indicated that no significant changes in the relative percentages of the fatty acids had occurred during the study period. Aliquots of each diet were stored under N_2 in sealed, plastic bags at –20°C. Every second or third day fresh aliquots of diet were weighed into clean, stainless steel feeders that hung vertically within the cages. Using this system, diet spillage within the cage was minimal. The rats were allowed free access to the diets and water during the study. Body weights and diet consumption were measured every 2–3 d throughout the study period. The rats' appearance and behavior were observed daily for signs of diet intolerance or toxicity.

TABLE 1
Principal Triglyceride Fatty Acids of Original HGCO and Study Diets[a]

Fatty acid	HGCO	HGCO diet	BO diet
16:0	4.2	8.3	10.8
18:0	3.7	2.8	4
18:1n-9	21.6	20.4	15.5
18:1n-7	3.4	2.1	0.7
18:2n-6	26.0	38.7	36.4
18:3n-6	37.0	23.3	22.6
18:3n-3	1.3	1.1	0.3
22:1n-9		0.4	2.9

[a]Expressed as the mole percentage of total fatty acids identified. HGCO, high γ-linolenic acid-canola oil; BO, borage oil.

After 6 wk of feeding, food was withheld from the animals overnight prior to study termination. Under pentobarbital anesthesia (50 mg/kg intraperitoneally), the abdomen was opened and blood drawn from the vena cava into heparinized syringes. The whole blood was centrifuged at 2500 × g at 4°C for 10 min to isolate the plasma. All rats were subjected to gross necropsy. The liver, kidneys, spleen, heart, and epididymal fat were excised, examined and weighed. Samples of plasma, liver, and epididymal fat were stored under N_2 at –20°C for compositional analysis of phospholipid or triglyceride fatty acids.

Fatty acid analysis of triglyceride and individual phospholipid fractions (10). Total tissue lipids were extracted immediately after samples had been thawed. Liver, epididymal tissue, plasma, and diet powder were extracted with chloroform/methanol, 2:1 (vol/vol). The extraction solvent mixture of each sample was allowed to stand in the refrigerator overnight. Saline was added to separate the chloroform and aqueous phase. Samples were centrifuged and the chloroform layer was transferred into Teflon-lined screw cap tubes. The chloroform was then evaporated at 40°C under N_2 and the lipid residues were redissolved in chloroform. The total lipid extracts were separated by thin-layer chromatography (TLC) into their neutral and phospholipid classes using LHPK Silica Gel on 10 × 20 cm plates with a thickness of 200 μm (Whatman, Fairfield, NJ). Neutral lipids were developed for 12 min with hexane/ethyl ether/glacial acetic acid, 70:30:1 (by vol). The solvent system for the phospholipids was chloroform/ethanol/de-ionized water/triethylamine, 4:5:1:5 (by vol). After visualization by spraying with 2,7-dichlorofluorescin in 2% ethanol, the areas corresponding to triglycerides and total phospholipids were scraped off the neutral TLC plate, and phosphatidylethanolamine (PE), phosphatidylinositol/serine (PI/PS), and phosphatidylcholine (PC) were obtained from the phospholipid plate. All lipid fractions were derivatized by methylation with 12% boron trifluoride in methanol. For fatty acid quantitation, a known amount of triheptadecanoin (17:0) was added as the internal standard to each lipid fraction. The fatty acid methyl esters obtained from each lipid fraction were extracted in hexane and analyzed by gas–liquid chromatography (GLC).

A Hewlett-Packard 6890 series GLC (Palo Alto, CA) was set up with the following conditions: Omegawax 320™ capillary column (Supelco, Bellefonte, PA), 30 m × 0.32 mm i.d., 0.25 μm film; helium carrier gas; flame-ionization detector; pulsed splitless injection mode; injector 205°C; detector 235°C; column 120°C for 1 min, then raised 4°C/min to 205°C and held for 25 min. A sample volume of 2 μL was injected and analyzed with Hewlett-Packard ChemStation software version G2070AA. Peaks were identified based upon the relative responses of an external standard of pure fatty acid methyl esters.

Statistics. Descriptive and inferential statistics were computed on all continuous data for each parameter. The sample size was based primarily on the historical adequacy in similar studies using this model (12,13). Group differences were determined by *t* test and repeated measures of analysis of variance (ANOVA) across time points. Tukey's test was used for *post hoc* comparison of means of significant ANOVA. Estimates and 95% confidence intervals for group differences at each time point were also computed. Statistical significance was set at a P value less than 0.05.

RESULTS

The control (BO) and experimental (HGCO) diets were well tolerated throughout the study. There was no evidence of adverse effects of the diets with regard to the general appearance or behavior of the animals based on daily observations. The growth of the rats from each treatment group was similar. Initial and final body weights, mean body weight trends, and mean cumulative weight gain (288 vs. 286 g per rat for HGCO vs. BO groups, respectively) for each group were similar (Fig. 1). Diet consumption (Fig. 2) was also similar between treatment groups throughout the 6 wk study. The mean total consumption (±SD) of the HGCO and BO diets per two rats per cage over 6 wk was 2.13 (± 0.23) and 2.20 kg (± 0.14), respectively. Results from an earlier pilot study of Sprague-Dawley rats fed either the HGCO and BO diet for 3 wk revealed that the mean (±SD) outputs of fecal fat over three separate 48 h collections were similar for each diet group (0.07 ± 0.01 g/d for each group) (Palombo, J., unpublished observation).

Gross postmortem examination of the major organs did not reveal any adverse treatment effects. The mean liver weight (±SD) was not significantly different between diet groups (11.1 ± 1.1 vs. 11.5 ± 0.9 g for the HGCO and BO groups, respectively). In addition, mean weights (g) of heart (1.5 vs. 1.5), kidneys (2.7 vs. 2.7) or spleen (1.2 vs. 1.1) were similar for the HGCO vs. BO group, respectively.

Principal fatty acids in liver phospholipids. The effects of feeding either the HGCO or BO diets on the composition of n-6 fatty acids in the total and individual liver phospholipids are shown in Tables 2–5. There was no difference between diets for the total percentage of n-6 polyunsaturated fatty acids (PUFA) present in either the total (Table 2) or individual (Tables 3–5) phospholipid fractions. The relative percentages of 18:2n-6 and 18:3n-6 in the liver total phospholipids (Table 2) and PC fraction (Table 3) were also similar for both diets. The percentage of 18:2n-6 in liver PE (Table 4) and PI/PS (Table 5) was significantly higher ($P < 0.05$) in the HGCO diet group as compared with the BO group. The percentage of 20:3n-6 in the total phospholipids was slightly lower in the HGCO group than the BO group (Table 2); however, the percentages of 20:3n-6 in the individual phospholipid fractions (Tables 3–5) were similar between diets. There were no diet-induced differences in the percentages of 20:4n-6 and 22:4n-6 present in the total or individual phospholipids. The percentage of 22:5n-6, the end-product of the n-6 series of PUFA, in the HGCO group was significantly lower ($P < 0.05$) in the total phospholipids and each phospholipid fraction (Tables 2–5) in comparison with the BO group.

The percentage of total n-3 PUFA in each phospholipid fraction of liver was similar across the two diets. However, we observed small differences between the two diets for percentages of 22:5n-3 and 22:6n-3 within the phospholipid frac-

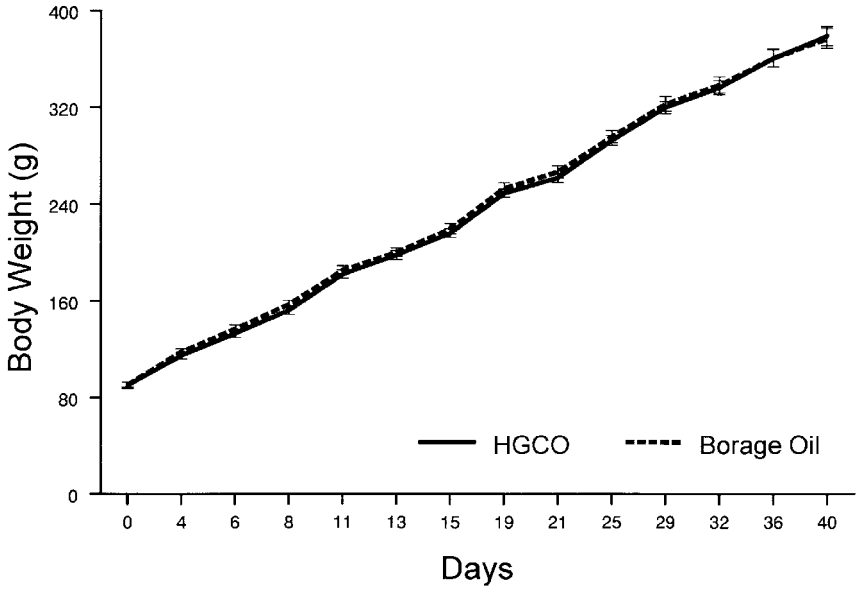

FIG. 1. Cumulative body weight gain (g) over 6 wk. Data points represent the mean ± SD for 10 male Sprague-Dawley rats fed an AIN93G diet containing 10% by weight high γ-linolenic acid (GLA) canola oil (HGCO) or borage oil for 6 wk.

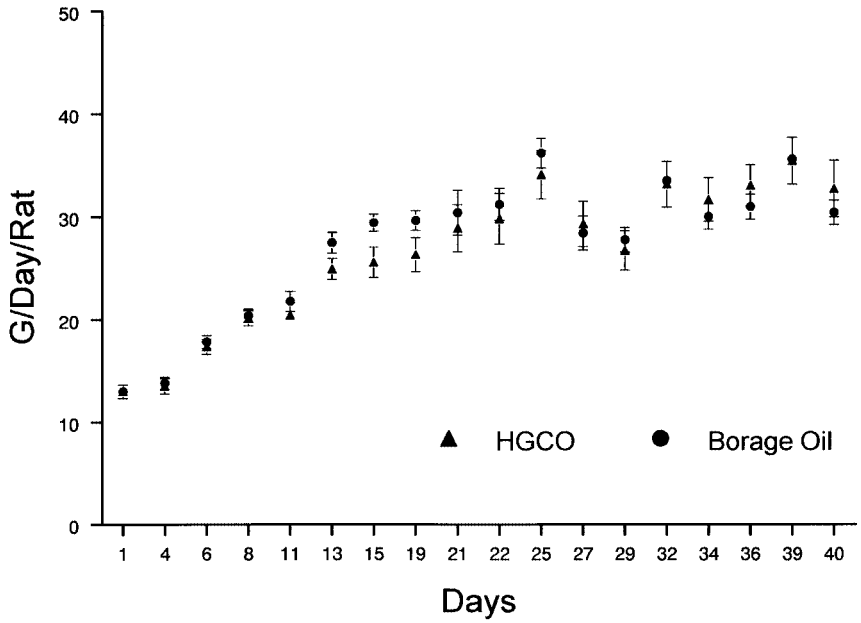

FIG. 2. Mean ± SD food consumption (g) per rat over 6 wk. Data points represent the calculated intake per rat of AIN93G diet containing 10% by weight HGCO or borage oil over a 2–3 d period (n = 10/group). See Figure 1 for abbreviations.

tions. Specifically, the relative percentage of 22:5n-3 was significantly higher, while the concurrent percentage of 22:6n-3 was lower in the total phospholipids (Table 2), and the PC (Table 3) and PE (Table 4) fractions from the HGCO group compared with the BO group. The mean percentage of 22:6n-3 in the PI/PS fraction of livers from the HGCO group was also lower as compared with the BO diet group (Table 5). Total monounsaturates (i.e., primarily the sum of 18:1n-9 and 18:1n-7) in the PC and PE fractions were higher in livers from rats fed the HGCO diet as compared with those from the BO diet group. The percentage of total saturates in each phospholipid fraction was similar between the treatment groups.

Principal fatty acids in plasma phospholipids. The effects of feeding either the HGCO or BO diets on the composition of n-6 fatty acids in the total and individual plasma phospholipids are shown in Tables 6–9. The total n-6 PUFA, n-3 PUFA, monounsaturates, and saturates in the total (Table 6) and individual (Tables 7–9) fractions of phospholipids were similar between diet groups. The relative percentages of individual n-6 PUFA, i.e., 18:2n-6, 18:3n-6, 20:3n-6, 20:4n-6,

TABLE 2
Fatty Acid Composition of Liver Total Phospholipids After 6 wk

Fatty acid	HGCO diet[a]	BO diet
16:0	24.5 ± 1.0	24.0 ± 1.1
18:0	24.7 ± 1.7	26.4 ± 2.4
18:1n-9	3.4 ± 0.3	3.0 ± 0.2*
18:1n-7	4.1 ± 0.5	2.9 ± 0.2*
18:2n-6	11.3 ± 0.9	10.3 ± 1.4
18:3n-6	0.6 ± 0.1	0.6 ± 0.1
20:2n-6	0.6 ± 0.2	0.4 ± 0.1*
20:3n-6	1.0 ± 0.1	1.4 ± 0.4*
20:4n-6	23.5 ± 1.7	23.4 ± 1.6
22:4n-6	1.3 ± 0.1	1.4 ± 0.3
22:5n-6	0.4 ± 0.2	1.4 ± 0.6*
22:5n-3	0.7 ± 0.1	0.4 ± 0.1*
22:6n-3	0.9 ± 0.2	1.2 ± 0.2*
Total saturates	50.5 ± 1.9	51.4 ± 2.6
Total monounsaturates	9.1 ± 0.8	8.1 ± 0.5
Total n-6 polyunsaturates	38.7 ± 2.0	38.9 ± 2.3
Total n-3 polyunsaturates	1.6 ± 0.3	1.6 ± 0.3

[a]Mean relative mole percentage ± SD, n = 10/group. *$P < 0.05$ by t test vs. HGCO group. See Table 1 for abbreviations.

TABLE 3
Fatty Acid Composition of Liver Phosphatidylcholine After 6 wk

Fatty acid	HGCO diet[a]	BO diet
16:0	27.7 ± 1.4	27.1 ± 2.0
18:0	17.2 ± 1.8	17.5 ± 4.4
18:1n-9	3.1 ± 0.4	2.7 ± 0.3*
18:1n-7	3.1 ± 0.5	2.0 ± 0.2*
18:2n-6	7.8 ± 0.8	7.7 ± 1.4
18:3n-6	0.7 ± 0.1	0.8 ± 0.2
20:3n-6	0.8 ± 0.1	0.9 ± 0.3
20:4n-6	34.0 ± 1.6	34.2 ± 3.9
22:4n-6	1.2 ± 0.1	1.1 ± 0.3
22:5n-6	0.5 ± 0.1	1.8 ± 0.9*
22:5n-3	0.8 ± 0.1	0.4 ± 0.1*
22:6n-3	1.2 ± 0.3	1.6 ± 0.3*
Total saturates	45.5 ± 1.9	45.2 ± 5.0
Total monounsaturates	7.2 ± 0.9	5.9 ± 0.5*
Total n-6 polyunsaturates	45.2 ± 1.7	46.8 ± 4.9
Total n-3 polyunsaturates	2.1 ± 0.4	2.1 ± 0.3

[a]Mean relative mole percentage ± SD, n = 10/group. *$P < 0.05$ by t test vs. HGCO group. See Table 1 for abbreviations.

TABLE 4
Fatty Acid Composition of Liver Phosphatidylethanolamine After 6 wk

Fatty acid	HGCO diet[a]	BO diet
16:0	19.9 ± 1.1	20.0 ± 1.6
18:0	26.2 ± 6.1	29.8 ± 6.9
18:1n-9	3.0 ± 0.4	2.5 ± 0.4*
18:1n-7	3.3 ± 0.6	1.9 ± 0.3*
18:2n-6	6.2 ± 1.1	4.6 ± 1.1*
18:3n-6	0.6 ± 0.1	0.6 ± 0.1
20:3n-6	0.9 ± 0.1	1.0 ± 0.4
20:4n-6	29.5 ± 4.4	26.8 ± 4.5
22:4n-6	2.5 ± 0.3	2.8 ± 0.6
22:5n-6	1.0 ± 0.2	3.4 ± 1.4*
22:5n-3	1.8 ± 0.3	1.1 ± 0.3*
22:6n-3	2.6 ± 0.6	3.2 ± 0.3*
Total saturates	46.8 ± 6.1	50.3 ± 5.9
Total monounsaturates	7.5 ± 0.9	5.7 ± 0.8*
Total n-6 polyunsaturates	41.2 ± 5.4	39.6 ± 5.5
Total n-3 polyunsaturates	4.4 ± 0.8	4.4 ± 0.5

[a]Mean relative mole percentage ± SD, $n = 10$/group. *$P < 0.05$ by t test vs. HGCO group. See Table 1 for abbreviations.

TABLE 6
Fatty Acid Composition of Plasma Total Phospholipids After 6 wk

Fatty acid	HGCO diet[a]	BO diet
16:0	27.9 ± 1.2	27.1 ± 1.5
18:0	19.8 ± 1.2	21.5 ± 1.1
18:1n-9	2.8 ± 0.2	2.7 ± 0.2
18:1n-7	2.6 ± 0.4	1.8 ± 0.2*
18:2n-6	7.6 ± 0.6	7.6 ± 0.9
18:3n-6	0.6 ± 0.4	0.9 ± 0.8
20:3n-6	0.8 ± 0.1	1.0 ± 0.3
20:4n-6	29.1 ± 2.8	28.4 ± 1.6
22:4n-6	1.0 ± 0.2	1.2 ± 0.3
22:5n-6	0.1 ± 0.1	0.8 ± 0.8
22:5n-3	0.6 ± 0.2	0.3 ± 0.0*
22:6n-3	0.7 ± 0.2	0.9 ± 0.3
Total saturates	49.4 ± 2.0	50.0 ± 1.6
Total monounsaturates	9.6 ± 1.0	8.5 ± 0.9
Total n-6 polyunsaturates	40.1 ± 2.6	40.4 ± 2.1
Total n-3 polyunsaturates	0.9 ± 0.2	1.0 ± 0.3

[a]Mean relative mole percentage ± SD, $n = 10$/group. *$P < 0.05$ by t test vs. HGCO group. See Table 1 for abbreviations.

22:4n-6, and 22:5n-6, in the total phospholipids were similar between the HGCO and BO diet groups (Table 6). The percentage of 18:2n-6 in the PI/PS fraction of plasma was slightly higher for the HGCO group than the BO group (3.4 vs. 2.5%, respectively).

As observed in the liver, the percentages of 22:5n-3 in the total phospholipids (Table 6) and PC fraction (Table 7) of the plasma from the HGCO group were slightly higher ($P < 0.05$) than the corresponding levels of 22:5n-3 from the BO group. Unlike the liver, there was no significant difference in the relative percentage of 22:6n-3 in any phospholipid fraction between the groups.

Epididymal triglyceride fatty acids. The percentages of 18:2n-6, 20:3n-6, 20:4n-6, and 22:4n-6 in the epididymal triglycerides of the HGCO group were similar to the corresponding levels in the BO group (Table 10). The mean percentage of triglyceride 18:3n-6 was slightly higher (11.9 vs. 10.1%, $P < 0.05$) in the BO group than the HGCO group.

DISCUSSION

These data represent the first dietary studies undertaken to evaluate the biological effects of transgenic HGCO in mammals. The results revealed that, when feeding equal amounts of GLA from either HGCO or BO, no significant differences were observed in growth characteristics and diet consumption by the rats over 6 wk. In addition, there was no evidence of any adverse effect of feeding a diet containing HGCO on the rats' appearance, behavior, or organ morphology.

In both plasma and liver total phospholipids, we observed no significant changes in the levels of 18:3n-6, 20:4n-6, or 22:4n-6 in rats fed the HGCO diet as compared to those fed

TABLE 5
Fatty Acid Composition of Liver Phosphatidylinositol/Serine After 6 wk

Fatty acid	HGCO diet[a]	BO diet
16:0	8.7 ± 1.0	7.0 ± 0.9*
18:0	47.9 ± 7.6	53.4 ± 5.6
18:1n-9	1.7 ± 0.3	1.7 ± 0.2
18:1n-7	0.9 ± 0.2	0.7 ± 0.2
18:2n-6	2.5 ± 0.4	1.6 ± 0.3*
20:3n-6	1.3 ± 0.3	1.6 ± 0.7
20:4n-6	31.1 ± 6.2	27.1 ± 4.6
22:4n-6	1.3 ± 0.4	1.4 ± 0.3
22:5n-6	0.4 ± 0.2	1.1 ± 0.3*
22:5n-3	0.7 ± 0.2	0.6 ± 0.2
22:6n-3	0.7 ± 0.2	1.1 ± 0.4*
Total saturates	57.5 ± 7.0	61.3 ± 5.1
Total monounsaturates	4.0 ± 0.5	3.9 ± 0.4
Total n-6 polyunsaturates	37.1 ± 6.7	33.1 ± 5.3
Total n-3 polyunsaturates	1.4 ± 0.3	1.7 ± 0.5

[a]Mean relative mole percentage ± SD, $n = 10$/group. *$P < 0.05$ by t test vs. HGCO group. See Table 1 for abbreviations.

TABLE 7
Fatty Acid Composition of Plasma Phosphatidylcholine After 6 wk

Fatty acid	HGCO diet[a]	BO diet
16:0	29.0 ± 1.3	28.1 ± 1.5
18:0	18.2 ± 1.0	19.9 ± 1.0*
18:1n-9	2.9 ± 0.3	2.7 ± 0.2
18:1n-7	2.9 ± 0.4	2.0 ± 0.2*
18:2n-6	8.6 ± 0.9	8.5 ± 1.0
20:1n-9	0.5 ± 0.1	0.7 ± 0.1*
20:3n-6	0.9 ± 0.1	1.1 ± 0.3*
20:4n-6	32.5 ± 1.9	31.3 ± 1.4
22:4n-6	1.2 ± 0.1	1.3 ± 0.3
22:5n-6	0.3 ± 0.1	1.5 ± 0.9
22:5n-3	0.6 ± 0.1	0.3 ± 0.0*
22:6n-3	0.9 ± 0.2	1.3 ± 0.2
Total saturates	47.7 ± 1.5	48.7 ± 1.5
Total monounsaturates	6.8 ± 0.7	6.0 ± 0.5
Total n-6 polyunsaturates	43.9 ± 1.6	43.8 ± 1.5
Total n-3 polyunsaturates	1.6 ± 0.3	1.5 ± 0.3

[a]Mean relative mole percentage ± SD, $n = 10$/group. *$P < 0.05$ by t test vs. HGCO group. See Table 1 for abbreviations.

TABLE 8
Fatty Acid Composition of Plasma Phosphatidylethanolamine After 6 wk[a]

Fatty acid	HGCO diet[a]	BO diet
14:0	2.5 ± 0.7	2.2 ± 0.9
16:0	21.1 ± 4.0	20.4 ± 2.9
18:0	29.5 ± 4.4	30.9 ± 1.7
18:1n-9	5.3 ± 1.4	4.9 ± 0.6
18:1n-7	2.1 ± 0.9	1.8 ± 0.4
18:2n-6	6.5 ± 1.6	5.8 ± 0.6
18:3n-6	2.3 ± 1.3	2.0 ± 0.5
18:3n-3	1.1 ± 0.3	1.0 ± 0.3
20:1n-9	2.7 ± 1.6	2.2 ± 0.5
20:3n-6	0.7 ± 0.4	0.8 ± 0.3
20:4n-6	18.3 ± 6.5	22.7 ± 3.0
22:4n-6	4.3 ± 1.6	4.6 ± 1.9
Total saturates	55.1 ± 4.8	54.2 ± 4.2
Total monounsaturates	10.2 ± 1.4	8.9 ± 1.0
Total n-6 polyunsaturates	32.9 ± 9.3	36.6 ± 4.8
Total n-3 polyunsaturates	1.1 ± 0.3	1.0 ± 0.3

[a]Mean relative mole percentage ± SD, n = 10/group. See Table 1 for abbreviations.

TABLE 10
Fatty Acid Composition of Epididymal Triglycerides After 6 wk

Fatty acid	HGCO diet[a]	BO diet
16:0	19.9 ± 2.2	19.9 ± 1.2
18:0	2.1 ± 0.2	2.3 ± 0.3
18:1n-9	20.7 ± 1.6	19.3 ± 1.5
18:1n-7	2.4 ± 0.3	1.5 ± 0.1*
18:2n-6	29.2 ± 2.7	29.0 ± 1.7
18:3n-6	10.1 ± 1.4	11.9 ± 1.4*
18:3n-3	1.0 ± 0.2	0.5 ± 0.1*
20:3n-6	1.5 ± 0.2	1.7 ± 0.2
20:4n-6	2.7 ± 0.5	3.1 ± 0.5
22:4n-6	0.4 ± 0.1	0.5 ± 0.1
Total saturates	23.8 ± 2.2	24.7 ± 0.8
Total monounsaturates	29.9 ± 2.2	28.9 ± 1.5
Total n-6 polyunsaturates	45.0 ± 4.0	45.7 ± 2.1
Total n-3 polyunsaturates	1.3 ± 0.2	0.7 ± 0.1

[a]Mean relative mole percentage ± SD, n = 10/group. *$P < 0.05$ by t test vs. HGCO group. See Table 1 for abbreviations.

the BO diet. Similar findings were reported by Raederstorff and Moser in a GLA feeding study comparing BO with primrose oil (14). They found no changes in liver GLA and DHGLA levels within groups given equal amounts of dietary GLA from either oil source, indicating that the relative percentages of GLA and DHGLA in tissue phospholipids are dependent upon the GLA content in the diet, but not on the oil source of GLA. The only exception in the present study was that we found that the percentage of 20:3n-6 in liver total phospholipids from the rats given the BO diet was slightly higher than that in rats fed the HGCO diet (1.4 vs 1.0, $P < 0.05$) (Table 2). However, there were no dietary differences in the relative percentage of 20:3n-6 present in the liver PC, PE, or PI/PS fractions (Tables 3–5), suggesting that this may have been a statistical anomaly.

When fatty acid profiles within individual liver phospholipids were examined more closely, we observed minor changes in the relative percentage of several fatty acids in rats fed diets containing HGCO as compared to BO. For example, the levels of 18:2n-6 in PE (Table 4) and PI/PS (Table 5) were increased in the HGCO group. The elevation of 18:2n-6 may indicate a decrease in the hepatic Δ6 desaturation of 18:2n-6 in rats fed the HGCO diet. This could be due to competition for binding of Δ6 desaturase by 18:3n-3, which was present in higher amounts in the HGCO diet as compared with the BO diet (1.1 vs. 0.3, Table 1). A greater ratio of n-3/n-6 is known to suppress the metabolism of n-6 fatty acids given that n-3 PUFA are the preferred substrates for the Δ6-desaturase binding (15,16) and acyltransferase (17). The above finding was not unexpected as our main objective was to maintain the ratio of comparable levels of n-6 PUFA (18:2n-6 and 18:3n-6) in both diets. As a consequence the n-3/n-6 fatty acids were not balanced. In addition to an increase in 18:2n-6, we have also observed a decrease in the levels of 22:5n-6 in rats fed the HGCO diet as compared with rats fed the BO diet (Tables 2–5). This finding, in the absence of differences in levels of 18:3n-6, 20:3n-6, 20:4n-6, and 22:4n-6, suggests that any inhibition on desaturation of 18:2n-6 after feeding the HGCO diet may exclusively affect the levels of its end metabolite, 22:5n-6. In this regard, Sprecher *et al.* (18) have proposed a revised pathway for the biosynthesis of 22:5n-6, which requires elongation of 22:4n-6 to 24:4n-6 followed by Δ6 desaturation to 24:5n-6, which in turn undergoes partial β-oxidation to 22:5n-6. Thus, preferential binding of n-3 vs. n-6 fatty acids at this later Δ6 desaturation step would result in decreased production of 22:5n-6 as observed in the liver phospholipids for the HGCO group. Similar changes in 22:5n-6 have been reported by others who also fed diets with equal amounts of GLA, but unbalanced n-3/n-6 fatty acids (14). It should be noted, however, that the level of 22:5n-6 represents only a minor fraction of the overall PUFA content in liver lipids.

TABLE 9
Fatty Acid Composition of Plasma Phosphatidylinositol/Serine After 6 wk

Fatty acid	HGCO diet[a]	BO diet
16:0	11.7 ± 1.6	10.1 ± 1.6*
18:0	40.4 ± 3.4	41.2 ± 5.2
18:1n-9	2.0 ± 0.3	1.8 ± 0.4
18:1n-7	1.1 ± 0.2	0.8 ± 0.2*
18:2n-6	3.4 ± 0.8	2.5 ± 0.4*
18:3n-6	0.6 ± 0.2	0.6 ± 0.1
20:1n-9	0.7 ± 0.2	0.7 ± 0.1
20:3n-6	1.0 ± 0.2	1.3 ± 0.5
20:4n-6	34.6 ± 2.8	34.4 ± 3.2
22:4n-6	0.8 ± 0.2	0.8 ± 0.4
Total saturates	53.0 ± 3.6	52.3 ± 5.2
Total monounsaturates	4.4 ± 1.8	3.4 ± 0.6
Total n-6 polyunsaturates	42.4 ± 3.4	43.8 ± 4.6
Total n-3 polyunsaturates	0.4 ± 0.8	0.7 ± 1.0

[a]Mean relative mole percentage ± SD, n = 10/group. *$P < 0.05$ by t test vs. HGCO group. See Table 1 for abbreviations.

In summary, the growth and hepatic metabolism of the principal n-6 fatty acids was similar between rats fed diets containing the same amounts of fat (10%, by weight) and GLA (23% of total fats) whether the source of GLA was HGCO or BO. Additional bioequivalency studies are now warranted to determine the effects of long-term feeding (i.e., >12 wk) of diets containing HGCO on clinically relevant biochemical and hematologic parameters.

ACKNOWLEDGMENTS

The authors gratefully acknowledge the technical assistance of Emil Bobik, Lu-Te Chuang, Kathy Dailey, and Christine Hastilow for this study.

REFERENCES

1. Brenner, R.R. (1981) Nutritional and Hormonal Factors Influencing Desaturation of Essential Fatty Acids, *Prog. Lipid Res. 20*:41–48.
2. Das, U.N., Horrobin, D.F., Begin, M.E., Huang, Y-S., Cunnane, S.C., Manku, M.S., and Nassar, B.A. (1988) Clinical Significance of Essential Fatty Acids, *Nutrition 4*, 337–341.
3. Ziboh, V.A., and Fletcher, M.P. (1992) Dose-Response Effects of Dietary γ-Linolenic Acid-Enriched Oils on Human Polymorphonuclear-Neutrophil Biosynthesis of Leukotriene B_4, *Am. J. Clin. Nutr. 55*, 39–45.
4. Wu, D., and Meydani, S.N. (1996) γ-Linolenic Acid and Immune Function, in *γ-Linolenic Acid: Metabolism and Its Roles in Nutrition and Medicine* (Huang, Y.-S., and Mills, D.E., eds.) pp. 106–117, AOCS Press, Champaign.
5. Horrobin, D.F. (1992) Gamma-Linolenic Acid: An Intermediate in Essential Fatty Acid Metabolism with Potential as an Ethical Pharmaceutical and as a Food, *Rev. Contemp. Pharmacother. 1*, 1–45.
6. Leventhal, L.J., Boyce, E.G., and Zurier, R.B. (1993) Treatment of Rheumatoid Arthritis with γ-Linolenic Acid, *Ann. Intern. Med. 119*, 867–873.
7. Palombo, J.D., DeMichele, S.J., Boyce, P.J., Lydon, E.E., Liu, J.-W., Huang, Y.-S., Forse, R.A., Mizgerd, J.P., and Bistrian, B.R. (1999) Effect of Short-Term Enteral Feeding with Eicosapentaenoic and γ-Linolenic Acids on Alveolar Macrophage Eicosanoid Synthesis and Bactericidal Function in Rats, *Crit. Care Med. 27*, 1908–1915.
8. Mancuso, P., Whelan, J., DeMichele, S.J., Snider, C.C., Guszcza, J.A., Claycombe, K.J., Smith, G.T., Gregory, T.J., and Karlstad, M.D. (1997) Effects of Eicosapentaenoic and γ-Linolenic Acid on Lung Permeability and Alveolar Macrophage Eicosanoid Synthesis in Endotoxic Rats, *Crit. Care Med. 25*, 523–532.
9. Gadek, J.E., DeMichele, S.J., Karlstad, M.D., Pacht, E.R., Donahoe, M., Albertson, T.E., Van Hoozen, C., Wennberg, A.K., Nelson, J.L., and Noursalehi, M. (1999) Effect of Enteral Feeding with Eicosapentaenoic Acid, γ-Linolenic Acid, and Antioxidants in Patients with Acute Respiratory Distress Syndrome, *Crit. Care Med. 27*, 1409–1420.
10. Huang, Y.S., Chaudhary, S., Thurmond, J.M., Bobik, E.G., Jr., Yuan, L., Chan, G.M., Kirchner, S.J., Mukerji, P., and Knutzon, D.S. (1999) Cloning of Delta 12- and Delta 6-Desaturases from *Mortierella alpina* and Recombinant Production of Gamma-Linolenic Acid in *Saccharomyces cerevisiae*, *Lipids 34*, 649–659.
11. Reeves, P.G., Nielsen, F.H., and Fahey, G.C., Jr. (1993) AIN-93 Purified Diets for Laboratory Rodents: Final Report of the American Institute of Nutrition ad hoc Writing Committee on the Reformulation of the AIN76A Rodent Diet, *J. Nutr. 123*, 1939–1951.
12. Palombo, J.D., DeMichele, S.J., Boyce, P.J., Noursalehi, M., Forse, R.A., and Bistrian, B.R. (1998) Metabolism of Dietary α-Linolenic Acid vs. Eicosapentaenoic Acid in Rat Immune Cell Phospholipids During Endotoxemia, *Lipids 33*, 1099–1105.
13. Palombo, J.D., DeMichele, S.J., Lydon, E.E., Gregory, T.J., Banks, P.L.C., Forse, R.A., and Bistrian, B.R. (1996) Rapid Modulation of Lung and Liver Macrophage Phospholipid Fatty Acids in Endotoxemic Rats by Continuous Enteral Feeding with n-3 and γ-Linolenic Acids, *Am. J. Clin. Nutr. 63*, 208–219.
14. Raederstorff, D., and Moser, U. (1992) Borage and Primrose Oil Added to Standardized Diets Are Equivalent Sources for γ-Linolenic Acid in Rats, *Lipids 27*, 1018–23.
15. Holman, R.T. (1964) Nutritional and Metabolic Interrelationships Between Fatty Acids, *Fed. Proc. 23*, 1062–67.
16. Stubbs, C.D., and Smith, A.D. (1984) The Modification of Mammalian Membrane Polyunsaturated Fatty Acid Composition in Relation to Membrane Fluidity and Function, *Biochim. Biophys. Acta 779*, 89–137.
17. Lands, W.E.M., Morris, A., and Libelt, B. (1990) Quantitative Effects of Dietary Polyunsaturated Fats on the Composition of Fatty Acids in Rat Tissues, *Lipids 25*, 505–516.
18. Sprecher, H., Luthria, D., Baykousheva, S.P., and Mohammed, B.S. (1996) Pathways for the Biosynthesis of Polyunsaturated Fatty Acids, in *γ-Linolenic Acid*: *Metabolism and Its Roles in Nutrition and Medicine*, AOCS Press, Champaign, pp. 14–21.

[Received May 4, 2000, and in revised form July 21, 2000; revision accepted July 27, 2000]

Calcium Deficiency Modifies Polyunsaturated Fatty Acid Metabolism in Growing Rats

Carlos A. Marra* and María J.T. de Alaniz

INIBIOLP (Instituto de Investigaciones Bioquímicas de La Plata), CONICET-UNLP, Facultad de Ciencias Médicas, Universidad Nacional de La Plata, La Plata, Argentina

ABSTRACT: Fatty acid desaturase activities were determined in liver microsomes from calcium-deficient rats and compared to calcium-sufficient ones. The calcium-deprived diet (0.5 g/kg) administered for 60 d caused a 30% inhibition in the Δ5 desaturase activity and a 45–55% decrease in Δ6 and Δ9, respectively, facts that cannot be attributed to a reduction in food intake. *In vitro* addition of calcium, ethyleneglycol-bis(β-aminoethyl ether)*N,N*-tetraacetic acid, and/or cytosol fractions from control or calcium-deficient rats to microsomes from both groups of animals indicates that the reduced desaturase capacities would be the consequence of an indirect effect of calcium deprivation. The present work shows that the reduced unsaturated fatty acid biosynthesis might be the result of modifications in the physicochemical properties of microsomal membranes. Such changes could also be derived from the inhibition of phospholipase A_2 activity induced by calcium deficiency.

Paper no. L8344 in *Lipids 35,* 983–990 (September 2000).

A series of experimental reports carried out either in animals (1–3) or in human populations (4–9) shows a clear correlation between serum concentrations of metal cations and cardiovascular diseases. The effect of dietary manipulations of mineral components on the development of atherosclerosis and related diseases suggests that the nonsaturated fatty acid metabolism is clearly influenced by its metabolic actions. Previous works have documented that metal cations play an important role in polyunsaturated fatty acid biosynthesis and degradation. The availability of zinc is essential for linoleic acid metabolism, probably at both desaturation and elongation steps (10–14). These early findings were then corroborated by other authors (15–17). Similarly, the effect of magnesium as an essential cofactor in the fatty acid oxidative desaturation reactions was previously reported (1,18). The Δ5 and Δ9 desaturation steps are also particularly influenced by the level of copper, which has an opposite effect to that of zinc (19–26). It was also demonstrated that sodium loading increases arachidonic acid metabolism by means of prostaglandins from series two. At the same time, a hypernatriuretic diet modifies arachidonic acid content in liver lipids through the increment in the Δ5 and Δ6 liver microsomal desaturase activities (27,28). Recently, a peroxidiferric intermediate was found to be required for the Δ9 desaturation reaction (29). The crucial role of iron in the desaturation process is now well-established (24–26,30). Selenium and cadmium are also involved in fatty acid desaturation in mammals (31–33).

Regarding the effect of calcium, Huang *et al.* (1) reported that the levels of 18:3n-6 fatty acid in calcium-deficient rats are elevated, whereas those of 20:4n-6 are diminished. These results were interpreted as an indication of a reduced elongation capacity. On the other hand, we demonstrated a close correlation between calcium levels and fatty acyl composition of lipids from hepatoma culture cells (34) or rat liver microsomes (35), suggesting that the desaturase activities would be under a calcium-dependent regulatory effect. Taking into account that there are previous studies dealing with the involvement of various metal ions in polyunsaturated fatty acid transformation, and considering the potential regulatory action of calcium in the metabolism of the nonsaturated fatty acids, it is surprising that the possible effect of calcium deficiency on fatty acid desaturase reactions still remains unexplored. For this reason, it was our aim to investigate the fatty acid desaturase capacity in liver microsomes from calcium-deficient (CD) rats compared to the calcium-sufficient (S) ones.

MATERIALS AND METHODS

Fatty acids and other chemicals. Unlabeled fatty acids were obtained from Nu-Chek-Prep, Inc. (Elysian, MN). ATP (disodium salt), NADH, *N*-acetylcysteine, CoA (lithium salt), snake venom (*Crotalus atrox*, western diamondback rattlesnake), and sodium deoxycholate (grade II) were purchased from Sigma Chemical Co. (St. Louis, MO). Phospholipids were obtained from Serdary Research Laboratories (London, Ontario, Canada). The following radioactive fatty acids were supplied by Amersham International (Buckinghamshire, United Kingdom) (specific activity as mCi/mmol and percent degree of radiochemical purity are, respectively, indicated in parentheses): [1-^{14}C]palmitic (58.0, 99), [1-^{14}C]stearic (56.5, 98), [1-^{14}C]linoleic (55.5, 99), [1-^{14}C]α-

*To whom correspondence should be addressed at Facultad de Medicina, Universidad Nacional de La Plata, 60 y 120 (1900) La Plata, Argentina. E-mail: camarra@atlas.med.unlp.edu.ar

Abbreviations: CD, calcium-deficient; GLC, gas–liquid chromatography; EGTA, ethyleneglycol-bis(β-aminoethyl ether)-*N,N*-tetraacetic acid; PC, phosphatidylcholine; S, sufficient (control); SEM, standard error of the mean; RP-HPLC, reversed-phase high-performance liquid chromatography; TLC, thin-layer chromatography.

linolenic (57.0, 99), and [1-^{14}C]eicosa-8,11,14-trienoic (58.5, 99). [1-^{14}C]Palmitoyl-CoA (57.0, 99) and [1-^{14}C]eicosa-8,11,14-trienoyl-CoA (52.2, 98) were purchased from New England Nuclear Research Products (Boston, MA). The concentration and degrees of purity of the fatty acids were routinely checked by liquid scintillation counting and gas–liquid chromatography (GLC) of their fatty acid methyl esters prepared in the presence of internal standard (eicosa-11-monoenoic acid). Fatty acids were appropriately diluted in absolute ethanol (Riedel-de Haen, Seelze, Germany) and stored in the dark at –20°C under an atmosphere of N_2 until used. Solvents for high-performance liquid chromatography (HPLC) were provided by Carlo Erba (Milano, Italy). Other chemicals used were supplied by commercial sources.

Animal treatment. Female Wistar rats from Comisión Nacional de Energía Atómica (Buenos Aires, Argentina) weighing 170 ± 10 g were bred and maintained on a control diet (Cargill type "C," Rosario, Argentina) throughout gestation and lactation. The dams were housed in plastic cages (one animal per cage) in a vivarium kept at 22 ± 1°C with a 12-h light/dark cycle and a relative humidity of 60 ± 10%. After weaning, 24 female pups (weighing 47 ± 4 g/animal) were randomly divided into two groups of 12 animals each, and fed *ad-libitum* either on a CD diet (group CD) or on a balanced diet (group S). The composition of the CD diet, prepared in our laboratory, was reported in detail in a previous paper (35). The Ca^{2+} content (0.5 g/kg), was determined by a Shimadzu Atomic Absorption Spectrophotometer AA-630-12 (Shimadzu Corp., Kyoto, Japan) following the mineralization procedure described elsewhere (36). Control animals were fed a standard balanced diet supplemented with 5.0 g/kg calcium in order to supply the mineral at a level equivalent to that recommended by the American Institute of Nutrition for the Formulation of the AIN-93 Purified Diets for Laboratory Rodents (37). The content of Ca^{++} in drinking water (given *ad-libitum*) was determined either by atomic absorption or by calcium-selective electrode Orion model 93-20 (Orion Research Inc., Cambridge, MA), and it was generally below 15 ppm. During the feeding period, body weight, water consumption, and food intake were determined every day. Samples of blood were collected in order to determine plasma calcium levels. Food intake and water consumption, relative to body weight, were not significantly different between the groups of animals at the time the rats were killed (after the 60-d feeding period). CD animals grew at a similar rate for the initial 20 d of feeding, then they grew at a reduced rate until day 59 when differences between groups became significant. In order to avoid individual differences among animals, as might result from an *ad-libitum* feeding, on day 59 all rats were fasted for 24 h, re-fed with the corresponding diet for 2 h, and then killed by decapitation without prior anesthesia 12 h after the refeeding period.

All diet components used were purchased from Carlo Erba or Mallinckrodt Chem. Works (NY). The casein was depleted of calcium by ethyleneglycol-bis(β-aminoethyl ether)*N*,*N*-tetraacetic acid (EGTA) treatment and then defatted with boiling acetone. The calcium content in the extracted casein was negligible. Animal maintenance and handling were in accordance with the National Institute for Health's Guide for the Care and Use of Laboratory Animals (38).

Microsomal suspensions. Livers from S and CD rats were rapidly excised and immediately placed in an ice-cold homogenizing medium (39). The homogenates were processed individually at 1°C, and the microsomal fractions were separated by differential centrifugation at 110,000 × *g* as previously described (39). Microsomal pellets were resuspended in a cold homogenizing solution to a final protein concentration of 30–40 mg/mL. Cytosol samples (110,000 × *g* supernatant fractions) from S and CD rats were also collected and stored at –80°C under N_2 atmosphere until further use.

Preparation of labeled phosphatidylcholine ([^{14}C]PC). The procedure to obtain labeled PC was developed in our laboratory after assaying different experimental conditions. Briefly, a suspension of liver microsomes from a female Wistar rat (150 ± 20 g body weight), obtained as described above, was incubated at 30°C in a metabolic shaker in the proportion of 5 mg microsomal protein/mL of incubation medium, which consisted of 0.1 M potassium phosphate buffer (pH: 7.40), 0.1 M $MgCl_2$, 10 mM Na_2ATP, 1 mM CoA (lithium salt), 5 mM *N*-acetylcysteine, 0.5 mM lysophosphatidylcholine, and 0.5 mM [1-^{14}C]eicosa-8,11,14-trienoic acid. The lysophospholipid was previously scattered, under carefully controlled temperature, in cold potassium buffer plus 0.1 mM sodium deoxycholate (grade II) by means of three 20-s sonication periods with a Heat System-Ultrasonic Sonicator model W-220F (Plainview, NY) equipped with a 1/8-inch diameter microtip at 50% output. The labeled fatty acid was prepared as follows: an aliquot of the acid was evaporated to dryness under N_2, neutralized with ammonium hydroxide, and diluted in pure propylenglycol. After vigorous vortexing at 30°C for 3 min, an aliquot from this preparation was directly transferred to the incubation medium. An hour later, under continuous agitation, the biosynthesis was stopped by the addition of 5 mL chloroform/methanol (2:1, vol/vol) according to Folch *et al.* (40). The total lipid extract was concentrated under vacuum at low temperature, and further fractionated by preparative HPLC according to the method of Patton *et al.* (41) with minor modifications. [^{14}C]PC was separated on a 150 × 4.0 mm Bio-Sil ODS 5S column (Bio-Rad, Richmond, CA) and eluted with 50 mM choline chloride in methanol/water/acetonitrile (90:5:5.8, by vol) at a flow rate of 1.5 mL/min, using a Merck-Hitachi L-6200 Intelligent Delivery System (Darmstadt, Germany). Detection was performed by absorption at 205 nm using an L-4200 Ultraviolet-Visible Detector (Merck-Hitachi). The PC fraction was identified on the basis of its retention time relative to authentic standards. Di-20:1n-9-PC was used for quantification. Once the phospholipid was identified, the corresponding eluate was carefully collected and concentrated under vacuum at low temperature. Samples were taken for phosphorus measurements (42) and liquid scintillation counting in a Wallac Rackbeta Liquid Scintillation Counter (Turku, Finland) with 92% efficiency for ^{14}C. The specific activity, ranging from 21 to 27

mCi/mmol, was routinely obtained by this procedure. Similar results were obtained by purification of the PC fraction in preparative thin-layer chromatography (TLC) on Silicagel G-60 plates (Riedel-de Haen) following the method described elsewhere (43,44).

Phospholipase A_2 activity assay. Phospholipase A_2 activity was determined with [^{14}C]PC (24.0 mCi/mmol, 99% pure) as substrate according to the method of Hirata *et al.* (45) with the modifications described as follows. The phospholipid was dispersed in the incubation medium by three 20-s sonication periods (small probe, 50% maximum intensity). The reaction mixture contained (0.5 mL total volume) 1.5 mM radioactive substrate, 50 mM Tris/glycylglycine buffer at pH 8.0, and 0.1 mM sodium deoxycholate (grade II). After preincubation at 37°C for 1 min, the assay was started by the addition of 20–40 μg of protein. Under these conditions, the reaction was completely linear up to 30 min. It was stopped after 10 min incubation by the addition of 3 mL isopropyl alcohol/heptane/1 N H_2SO_4 (40:10:1, by vol) followed by 2 mL distilled water, plus 2 mL of petroleum ether containing 5 μg/tube unlabeled eicosatrienoic acid, thorough mixing and incubation for 10 min at room temperature. Unlabeled eicosatrienoic acid was added to facilitate the extraction of [1-^{14}C]20:3n-6. Labeled fatty acids, released by the action of phospholipase, were recovered from the upper phase (at least 95% yield) and counted by liquid scintillation. Blanks consisting of boiled samples (10 min at 100°C) were routinely run in all incubations. Formation of unlabeled lysophosphatidylcholine was routinely checked by recovering the phospholipids from the aqueous phase and identifying of the lipid components by TLC as described previously (43,44).

Assay for in vitro *fatty acid desaturation.* Each fatty acid (16:0, 18:0, 18:2n-6, 18:3n-3, or 20:3n-3) was diluted to a specific activity of 0.20–0.25 μCi/mol with the respective pure unlabeled fatty acid. The assay procedure was as follows: 1.25 mg of microsomal protein was incubated in an open test tube with 100 nmol of diluted labeled substrate in a Dubnoff shaker at 37°C for 10 min. The total volume of the incubation medium was 0.8 mL; it consisted of 0.04 M potassium phosphate buffer (pH: 7.40), 0.15 M KCl, 0.25 M sucrose, 0.04 M NaF, 1.3 mM ATP, 0.06 mM CoA, 0.7 mM *N*-acetylcysteine, 0.87 mM NADH, and 5 mM $MgCl_2$. In some cases free fatty acids were replaced by the corresponding acyl-CoA esters (CoA was omitted in these incubations). The reaction was stopped with 1.0 mL of 10% potassium hydroxide in ethanol and the mixture was saponified at 80°C for 45 min under N_2 atmosphere. The unsaponifiable lipids were extracted twice with 2 mL hexane and discarded. The remaining lipids were acidified with 0.3 mL of concentrate HCl and extracted three times with 2 mL hexane. The organic solvent of each sample was pooled and evaporated to dryness at low temperature under vacuum. The fatty acids were then dissolved in the chromatographic mobile phase (methanol/water/acetic acid; 85:15:0.2, by vol), and separated by reversed-phase (RP)-HPLC in an apparatus equipped with a L-6200 Solvent Delivery System and a L-4200 UV/VIS Detector set at 205 nm from Merck-Hitachi as previously described (46). A 250 × 4.6 mm Econosil C-18 column (Alltech Associates, Deerfield, IL), coupled to a 10 × 4 mm guard column (packed similarly) was used at a flow rate of 0.9 mL/min. The peaks were identified on the basis of their retention times relative to appropriate fatty acid standards. Radioactivity was continuously detected by a Radiomatic Model Flo-One/Beta Radioactivity Flow Detector from Packard Instruments (Downers Grove, IL) using Ultima Flo-M liquid scintillation cocktail (Packard Instruments).

Other analytical determinations and statistical treatment of the data. Calcium content in liver microsomal suspensions was determined after mineralization (36) by atomic absorption as described above. The protein content was determined by the micromethod of Lowry *et al.* (47) with crystalline serum albumin as standard. All values represent the mean of three to six individual determinations (assayed in duplicate or triplicate) ± SEM. In order to test the statistical significance of numerical differences in results, data were analyzed by either the Student's *t*-test or by analysis of variance, with the aid of the GB-STAT Professional Statistics Program (version 4.0) from Dynamic Microsystems Inc. (Silver Springs, FL).

RESULTS

In previous papers we demonstrated that the CD diet here employed evokes a significant decrease in the calcium content of various rat tissues and subcellular fractions including microsomes (35,48). Table 1 shows that in these kinds of calcium-depleted microsomes, the fatty acid desaturase activities are strongly depressed compared to the ones found in microsomes from sufficient rats. The *in vitro* biosynthesis of arachidonic acid from labeled eicosa-8,11,14-trienoate was reduced 30%, whereas the Δ6 desaturation of both linoleic and α-linolenic acids was diminished 40 and 45%, respectively. The formation of monoenoates from either palmitic or stearic acids was significantly reduced (45–55%), indicating that Δ9 desaturation capacity was also decreased in CD microsomes.

In order to investigate the possible direct effect of calcium deficiency on the fatty acid desaturase system, an experiment was designed in which free calcium ions were added to CD microsomes in excess amount with respect to the content of the cation determined in the control microsomal suspensions. Atomic absorption measurements performed on S and CD microsomes demonstrated that the CD diet evoked a decrease in the total calcium content from 0.026 ± 0.001 μmol Ca/mg protein in control animals up to 0.015 ± 0.01 μmol in sufficient ones. Cytosolic fractions from CD rats were also significantly affected, showing a 40% decrease with respect to the values determined in S rats (0.008 μmol Ca/mg protein). Taking into account that the effect of calcium deprivation could be reverted by the cation itself or by the presence of another unknown soluble-factor (calcium-dependent), supernatants from 110,000 × *g* centrifuged liver homogenates were also added. EGTA addition was performed to investigate if the in-

TABLE 1
Fatty Acid Desaturase Activities in Liver Microsomes from S or CD Rats

Desaturase enzymes	Substrate/product	Liver microsomes S	Liver microsomes CD	$P <$
Δ 5	20:3n-6/20:4n-6	0.88 ± 0.03[a]	0.61 ± 0.02*	0.01
Δ 6	18:2n-6/18:3n-6	0.56 ± 0.03	0.34 ± 0.01*	0.001
Δ 6	18:3n-3/18:4n-3	0.26 ± 0.02	0.14 ± 0.01*	0.001
Δ 9	16:0/16:1	0.24 ± 0.03	0.11 ± 0.01*	0.001
Δ 9	18:0/18:1	0.29 ± 0.02	0.15 ± 0.01*	0.001

[a]Results are expressed as nmol of substrate transformed/min·mg of microsomal protein, and they correspond to the mean ± 1 SEM of six independent determinations. Enzyme activities were determined as described in the Materials and Methods section. *Significantly different with respect to the corresponding control value. S, control; CD, calcium-deficient.

TABLE 2
Effect of the Incubation Medium Supplementation on the Fatty Acid Desaturase Activities of Liver Microsomes from S or CD Rats

Microsomes	Additions	Desaturase activities[a] (nmol product/min·mg microsomal protein) Δ 9	Δ 6	Δ 5
S	None	0.30 ± 0.05[b]	0.61 ± 0.04	0.73 ± 0.09
S	Cytosol S[c]	0.29 ± 0.07	0.57 ± 0.08	0.69 ± 0.10
S	Cytosol CD[c]	0.32 ± 0.05	0.53 ± 0.13	0.80 ± 0.08
S	EGTA[d]	0.28 ± 0.04	0.60 ± 0.05	0.77 ± 0.06
S	$CaCl_2$[e]	0.34 ± 0.08	0.64 ± 0.07	0.75 ± 0.11
CD	None	0.16 ± 0.03*	0.38 ± 0.07*	0.48 ± 0.10*
CD	Cytosol S[c]	0.14 ± 0.02*	0.31 ± 0.05*	0.51 ± 0.12*
CD	Cytosol CD[c]	0.13 ± 0.01*	0.35 ± 0.03*	0.45 ± 0.05*
CD	EGTA[d]	0.17 ± 0.03*	0.32 ± 0.07*	0.48 ± 0.04*
CD	$CaCl_2$[e]	0.15 ± 0.03*	0.34 ± 0.04*	0.50 ± 0.06*

[a]The substrates used to determine the enzyme activities were [1-^{14}C]palmitic, [1-^{14}C]linoleic, and [1-^{14}C]eicosa-8,11,14-trienoic acids for Δ9, Δ6 and Δ5 desaturases, respectively.
[b]Results are expressed as mean ± SEM of four independent determinations.
[c]0.5 mg of liver microsomal protein/tube.
[d]0.5 μM final concentration.
[e]1 μM final concentration.
*Significantly different ($P < 0.01$) respect to the corresponding control assay. Incubation details were described in Materials and Methods section. EGTA, ethyleneglycol-bis(β-aminoethylether)*N,N*-tetraacetic acid. See Table 1 for other abbreviations.

hibitory effect observed on the desaturase system could be augmented by *in vitro* sequestering of the total free calcium present in the microsomal suspension. As shown in Table 2, *in vitro* calcium restitution—in excess amount with respect to control levels—was unable to restore the diminished desaturase capacity in any of the cases. No significant changes were observed due to the addition of cytosolic fractions or to an excess of EGTA.

In our laboratory, it was demonstrated that the acyl-S-CoA synthetase activity was significantly increased in CD rats (35,48). It is also well known that the formation of acyl-S-CoA esters is an obligatory step in the desaturation process (49,50). In spite of the fact that the supply of activated substrates was guaranteed in CD animals, the possibility that a defined calcium level would be necessary in a step subsequent to the activation process should not be discarded. For that reason, an experiment designed to highlight this question was performed. Results shown in Table 3 indicate that the fatty acid desaturase activities in microsomal suspensions from CD rats remain significantly depressed even after replacing free fatty acids by their corresponding acyl-S-CoA esters with or without the addition of calcium ions.

Table 4 shows the results obtained of phospholipase A_2 activities in different fractions from livers of S or CD rats. In homogenates and microsomes, the calcium deprivation caused a significant loss of activity (~80%) in both fractions. In contrast, the activity of cytosol was not significantly modified. Calcium addition partially restored the phospholipase A_2 activity in homogenate from CD rats, whereas in microsomes the addition of calcium not only restored the enzyme activity but also produced a significant increment (25%) with respect to the basal level. Although the amount of EGTA added was enough to bind the free calcium present in the fractions studied completely, none of them showed a significant decrease in their phospholipase A_2 activity under this treatment. Moreover, the addition of an EGTA excess to the cytosol from both S or CD rats—prior to the enzyme assay—led to a slight increase in the phospholipase activity.

Table 3
Desaturase Activities in Fatty Acyl-CoA Esters of Microsomal Suspensions from S or CD Rats.

	Desaturase activities (nmol product/min·mg microsomal protein)			
	Δ 9		Δ 5	
Substrates	S	CD	S	CD
16:0	0.25 ± 0.03[a]	0.13 ± 0.02*	—	—
16:0-S-CoA	0.22 ± 0.04	0.12 ± 0.03*	—	—
16:0-S-CoA + $CaCl_2$[b]	0.21 ± 0.05	0.10 ± 0.02*	—	—
20:3n-6	—	—	0.66 ± 0.04	0.47 ± 0.02*
20:3n-6-S-CoA	—	—	0.65 ± 0.06	0.42 ± 0.04*
20:3n-6-S-CoA + $CaCl_2$[b]	—	—	0.70 ± 0.04	0.44 ± 0.05*

[a]Results are expressed as the mean ± SEM of six independent determinations. Enzyme activities were determined as described in the Materials and Methods section. [b]1 μM final concentration. *Significantly different ($P < 0.01$) with respect to the corresponding control assay. See Table 1 for abbreviation.

TABLE 4
Phospholipase A_2 Activity in Liver Fractions from S or CD Rats

		Enzyme activity (dpm 10^3/mg protein)	
Fractions	Additions	S	CD
Cytosol	None	193.4 ± 6[a]	182.0 ± 14
	$CaCl_2$[b]	175.1 ± 9	149.9 ± 17
	EGTA[c]	220.6 ± 11	211.2 ± 9
Homogenate	None	3,002.2 ± 182	545.8 ± 80*
	CaCl2[b]	2,971.4 ± 76	1,195.3 ± 44*
	EGTA[c]	766.9 ± 106	635.0 ± 81
Microsomes	None	2,245.3 ± 51	461.7 ± 39*
	$CaCl_2$[b]	2,439.8 ± 60	3,033.5 ± 67*
	EGTA[c]	371.4 ± 39	311.2 ± 101

[a]Results are expressed as the mean ± SEM of six independent determinations. Incubation conditions were described in the Materials and Methods section.
[b]Calcium was added at a final concentration of 0.50 μM for cytosolic fraction, 3 mM for homogenates, and 1 μM for microsomes.
[c]EGTA was added at 3 mM final concentration in all assays. * Significantly different ($P < 0.001$) with respect to the corresponding control assay. See Tables 1 and 2 for abbreviations.

DISCUSSION

It is evident that calcium deprivation leads to a general inhibition of the fatty acid desaturase activities in rat liver microsomes (Table 1). Previous studies from our laboratory have extensively shown the effect of several hormones and nutritional conditions on polyunsaturated fatty acid metabolism in rats (49,51). Fasting and energy restriction profoundly modify desaturase activities and, as reported previously, the gain in body weight is directly involved in this regulatory effect (49,51–53). Taking into account these considerations, a decreased desaturase activity for CD rats compared with the S rats (paired-fed controls) can therefore be ascribed to calcium deprivation and not to a decreased food intake. This finding is consistent with Ca involvement in the liver microsomal desaturase reactions. However, results from Table 2 led us to discard, rather confidently, the direct effect of this cation on the desaturase enzyme itself or on other components involved in the transport of electrons to the terminal component. Currently, no experimental evidence has been presented related to the possible role of Ca as a desaturase cofactor and/or any other role of this cation as an essential part in the catalytic process. Results in this paper showed that *in vitro* addition of an excess of calcium to the microsomal suspension was unable to restore the inhibition evoked by CD diet. Moreover, no effect was observed even in the presence of cytosolic proteins; and no additional inhibitory effect was found after complexing the available calcium with excess EGTA. Previous experiments from our laboratory demonstrated that glucocorticoids can induce a soluble second messenger recovered as a low molecular weight peptide in the 110,000 × *g* supernatant fraction from liver cell homogenates. The addition of this factor modulates desaturase activities in *in vitro* enzyme assays (39,54,55). It was our aim to investigate if calcium deprivation could modify desaturase activity through a similar mechanism of action. Several investigations have described the dramatic influence exerted by Ca level modification on the calmodulin-mediated events, and it is well-known that a depletion of only 5–10% of the total cytosolic calcium is sufficient to substantially modify several cellular processes (56,57). The results presented here (Table 2) discard this mechanism of action since the addition of cytosol S to CD microsomes was un-

able to restore Δ9, Δ5, or Δ6 desaturase activities. On the other hand, calcium deficiency would not modify straightforwardly the desaturase activities through the inhibition of the coupled electron transport chain since the electron flux, produced from the NADH to the desaturase, is not a limiting factor for the reaction. It was demonstrated that the lowest step is located at the desaturase itself (58,59), where a variety of stimuli exert their regulatory effects.

The fact that the effect of calcium deprivation on the desaturase activity was also observed using acyl-S-CoA as substrate (Table 3) clearly demonstrates that acylation was not the rate-limiting reaction for this regulatory phenomenon, though considering that acyl CoA synthetase activity significantly increases under calcium deficiency (35).

It seems therefore that the effect of calcium deficiency on the desaturase activity may be produced by an indirect modification, which would involve another metabolic event. We also hypothesized that the inhibition of phospholipase A_2 would be able to diminish the substrate supply for desaturation in CD rats. However, if this consideration were valid in the whole animal, it would not be the same for *in vitro* determinations in which free fatty acids are used as substrates. Results in Table 4 led us to recognize that the alterations found in phospholipase A_2 activity under a CD diet modify the acylation/deacylation cycles, altering the physicochemical properties of the microsomal membranes. Experimental evidence would confirm this hypothesis. Storch and Schachter (60) demonstrated that calcium ions decrease the lipid fluidity of isolated rat hepatocyte plasma membranes by altering the hydrophobic interior of the bilayer. These authors also suggested that the change in the fluorescent anisotropy results from the activation of the Ca-dependent phospholipase A_2, located in the hepatocyte plasma membrane. The increase in this enzyme activity may result in the cleavage and loss of polyunsaturated fatty acids (mainly arachidonate) from membrane phospholipids and the subsequent reduction of the fluidity (60). On the other hand, we demonstrated in a recent study that calcium-deficiency evoked a significant increment in the fluidity of rat liver microsomal membrane as determined by the rotational mobility of the probe diphenylhexatriene (35). We also proved that the CD diet produced an important increase in saturated fatty acids (palmitic and stearic) in both neutral and polar lipid fractions of liver microsomes (35). An important increment of linoleic acid in both lipid fractions with a concomitant decrease in the polyunsaturated fatty acids of the n-3 and n-6 families also led to a significant decrease in the double-bond unsaturation index, suggesting a loss of the desaturation capacity in the liver microsomes from CD rats (35). Several interlipid and lipid/protein relationships were also affected by deprivation of this cation, including those parameters closely associated to the physical state of the membrane. In CD rats, the proportion of cholesterol, usually associated with a decreased membrane fluidity, was significantly reduced compared to S rats (35). This experimental evidence, together with the results shown in Table 4, supports the direct involvement of the altered calcium-dependent phospholipase A_2 in those changes observed on the physicochemical properties of microsomal membranes. So far, it is well known (49,51,58,61–63) that there exists a clear dependence between desaturase activities and membrane fluidity. Such dependence may result, as suggested by Brenner *et al.* (64), in a self-regulatory process by which an increased fluidity leads to a depletion in the nonsaturated fatty acid biosynthesis and *vice versa*.

These findings are supported by a recent report by Kan *et al.* (65) and Xing and Insel (66), who stated that calcium increase in cytosol gives rise to the release of arachidonic acid into the nucleus by means of phospholipase A_2 translocation to the nuclear envelope. Arachidonic acid increment would evoke the subsequent increase in prostacyclin synthesis (65,66). This fact may be related to the stimulated transcription of desaturase genes described by Landschulz *et al.* (67). Then, the decrease in calcium availability would imply a reduced transcription rate of fatty acid desaturase genes. Currently, we are working to gain insight into this mechanism.

In summary, we found that calcium deprivation in rats brings about a thorough alteration in the quality and/or quantity of the fatty acids acylated to neutral and polar lipid fractions from liver microsomal membranes. At least part of these modifications can be attributed to the inhibition of the calcium-dependent phospholipase A_2. The general inhibition observed in the desaturase activities would be the consequence of an adaptable phenomenon to the increased membrane fluidity, evoked by the calcium deficiency.

Literature dealing with the relationship between calcium deprivation and fatty acid metabolism in humans has been recently reviewed (68). Calcium loss in bones of elderly people is closely related to membrane transport alterations and several changes in lipid composition (69). Recently, mortality studies have demonstrated that these kinds of alterations may be far more dangerous than the calcium loss itself, since in women with osteoporosis most deaths are due to either vascular diseases or non-related bone abnormalities (68). We think that the interaction between fatty acid metabolism and calcium levels deserves more investigation since it offers novel approaches for the understanding of human illnesses, which in fact, involve both fields of study.

ACKNOWLEDGMENTS

The authors are grateful to Norma Cristalli for her excellent technical assistance and to Norma Tedesco for language revision. This study was supported in part by grants from CONICET, ANPCyT, and CIC, Argentina.

REFERENCES

1. Huang, Y.S., McAdoo, K.R., Mitchell, J., and Horrobin, D.F. (1983) Effects of Calcium Deprivation on n-6 Fatty Acid Metabolism in Growing Rats, *Biochem. Med. Metab. Biol. 40*, 61–67.
2. Ouchi, Y., Tabata, R.E., Stergiopoulos, K., Sato, F., Hattori, A., and Orino, H. (1990) Effect of Dietary Magnesium on Develop-

ment of Atherosclerosis in Cholesterol-Fed Rabbits, *Atherosclerosis 10*, 732–737.
3. Chetty, K.N., Walker, J., Brown, K., and Ivie, G.W. (1993) The Effects of Dietary Calcium and Chlordecone on Cholinesterase, Triglycerides, Low Density Lipoproteins, and Cholesterol in Serum of Rat, *Arch. Environ. Contam. Toxicol. 24*, 365–367.
4. Margetts, B.M. (1986) Recent Developments in the Etiology and Treatment of Hypertension: Dietary Calcium, Fat and Magnesium, *Am. J. Clin. Nutr. 44*, 704–705.
5. Van Beresteyn, E.C., Schaafsma, G., and De Waard, H (1986) Oral Calcium and Blood Pressure: A Controlled Intervention Trial, *Am. J. Clin. Nutr. 44*, 883–888.
6. Oster, O., and Prellwitz, W. (1990) Selenium and Cardiovascular Disease, *Biol. Trace Elem. Res. 24*, 91–103.
7. Bazarre, T.L., Scarpino, A., Sigmon, R., Marguart, L.F., Wu, S.M., and Izurieta, M. (1993) Vitamin-Mineral Supplement Use and Nutritional Status of Athletes, *J. Am. Coll. Nutr. 12*, 162–169.
8. Hermann, J., Arquitt, A., and Hanson, C. (1993) Relationship Between Dietary Minerals, Plasma Lipids and Glucose Among Older Adults, *J. Nutr. Elder. 12*, 1–14.
9. Ripa, S., and Ripa, R. (1994) Zinc and Atherosclerosis, *Minerva Med. 85*, 647–654.
10. Cunnane, S.C., Huang, Y.S., Horrobin, D.F., and Davignon, J. (1981) Role of Zinc in Linoleic Acid Desaturation and Prostaglandin Synthesis, *Prog. Lipid Res. 20*, 157–160.
11. Cunnane, S.C., and Horrobin, D.F. (1981) Probable Role of Zinc in the Mobilization of Dihomo-γ-linolenic Acid and in the Desaturation of Linoleic Acid, *Prog. Lipid Res. 20*, 835–837.
12. Huang, Y.S., Cunnane, S.C., Horrobin, D.F., and Davignon, J. (1982) Most Biological Effects of Zinc Deficiency Corrected by Gamma-Linolenic Acid (18:3 omega 6) but Not by Linoleic Acid (18:2 omega 6), *Atherosclerosis 41*, 193–207.
13. Cunnane, S.C., and Horrobin, D.F. (1985) Zinc Deficiency, Reduced Food Intake and Essential Fatty Acids, *J. Nutr. 115*, 500–503.
14. Ayala, S., and Brenner, R.R. (1983) Essential Fatty Acid Status in Zinc Deficiency: Effect on Lipid and Fatty Acid Composition, Desaturation Activity and Structure of Microsomal Membranes of Rat Liver and Testes, *Acta Physiol. Latinoam. 33*, 193–204.
15. Dib, A., and Carreau, J.P. (1986) Effects of Gamma-Linolenic Acid Supplementation on Lipogenesis Regulation in Pregnant Zinc-Deficient Rat and Fetus, *Int. J. Biochem. 18*, 1053–1056.
16. Ayala, S., and Brenner, R.R. (1987) Effect of Zinc Deficiency on the *in vivo* Biosynthesis of Fatty Acids of the Linoleic Series in the Rat, *Acta Physiol. Pharmacol. Latinoam. 37*, 321–330.
17. Kudo, N., Nakagawa, Y., and Waku, K. (1990) Effects of Zinc Deficiency on the Fatty Acid Composition and Metabolism in Rats Fed Fat-Free Diet, *Biol. Trace Elem. Res. 24*, 49–60.
18. Mahfouz, M.M., and Kumerow, F.A. (1989) Effect of Magnesium Deficiency on Δ6 Desaturase Activity and Fatty Acid Composition of Rat Liver Microsomes, *Lipids 24*, 727–732.
19. Wahle, K.W.J., and Davies, N.T. (1975) Effect of Dietary Copper Deficiency in the Rat on Fatty Acid Composition of Adipose Tissue and Desaturase Activity of Liver Microsomes, *Br. J. Nutr. 34*, 105–112.
20. Cunnane, S.C., Horrobin, D.F., Manku, M.S., and Oka, M. (1981) Interactions of Zinc with Prostaglandins E_1 and E_2 in Vascular Smooth Muscle, *Prog. Lipid Res. 20*, 261–264.
21. Cunnane, S.C. (1981) Zinc and Copper Interact Antagonistically in the Regulation of Linoleic Acid Metabolism, *Prog. Lipid Res. 20*, 601–603.
22. Cunnane, S.C., McAdoo, K.R., and Prohaska, J.R. (1986) Lipid and Fatty Acid Composition of Organs from Copper-Deficient Mice, *J. Nutr. 116*, 1248–1256.
23. Cunnane, S.C. (1989) Modulation of Long Chain Fatty Acid Unsaturation by Dietary Copper, *Adv. Exp. Med. Biol. 258*, 183–195.
24. Cunnane, S.C. (1991) Are Copper and Iron Required for Δ9 Desaturation of Fatty Acids? *Nutr. Rev. 49*, 225–226.
25. Johnson, S.B., Kramer, T.R., Briske-Anderson, M., and Holman, R.T. (1989) Fatty Acid Pattern of Tissue Phospholipids in Copper and Iron Deficiencies, *Lipids 24*, 141–145.
26. Cunnane, S.C. (1991) Possible Requirement for Iron and Copper in Δ9 Desaturation of Long-chain Fatty Acids, *Nutr. Rev. 49*, 387–389.
27. Narce, M., Minouni, V., and Poisson, J.P. (1992) Effect of Sodium Loading (3% NaCl) on Arachidonic Acid Biosynthesis in Rat Liver Microsomes, *Prostaglandins Leukotrienes Essent. Fatty Acids 47*, 193–197.
28. Narce, M., and Poisson, J.P. (1985) *In vitro* Study of Delta-6 and Delta-5-Desaturation of Linoleic and Dihomo-Gamma-Linolenic Acids in WKY Rats on a High-Sodium Diet, *C.R. Seances Soc. Biol. Fil. 179*, 732–740.
29. Broadwater, J.A., Ali, J., Loehr, T.M., Sanders-Loehr, J., and Fox, B.G. (1998) Peroxidiferric Intermediate of Stearoyl-Acyl Carrier Protein Delta 9 Desaturase: Oxidase Reactivity During Single Turnover and Implications for the Mechanism of Desaturation, *Biochemistry 37*, 14664–14671.
30. Rao, G.A., Crane, R.T., and Larkin, E.C. (1983) Reduction of Hepatic Stearoyl-CoA Desaturase Activity in Rats Fed Iron-Deficient Diets, *Lipids 18*, 573–575.
31. Infante, J.P. (1986) Vitamin E and Selenium Participation in Fatty Acid Desaturation. A Proposal for an Enzymatic Function of These Nutrients, *Mol. Cell. Biochem. 69*, 93–108.
32. Kudo, N., Nakagawa, Y., and Waku, K. (1990) The Effect of Cadmium on the Composition and Metabolism of Hepatic Fatty Acids in Zinc-Adequate and Zinc-Deficient Rats, *Toxicol. Lett. 50*, 203–212.
33. Kudo, N., and Waku, K. (1996) Cadmiun Supresses Delta 9 Desaturase Activity in Rat Hepatocytes, *Toxicology 114*, 101–111.
34. Marra, C.A., and Alaniz, M.J.T. de (1997) Role of Calcium Ionophore and Phospholipase A_2-Inhibitors on the Fatty Acid Composition of Hepatoma Tissue Culture Cells and Lipid Secretion, *Med. Sci. Res. 25*, 59–62.
35. Marra, C.A., and Alaniz, M.J.T. de (1999) Acyl-CoA Synthetase Activity in Liver Microsomes from Calcium-Deficient Rats, *Lipids 34*, 343–354.
36. Alto, L., and Dhalla, N.S. (1979) Myocardial Cation Contents During Induction of Calcium Paradox, *Am. J. Physiol. 237*, H713–H719.
37. Reeves, P.G., Nielsen, F.H., and Fahey, G.C., Jr. (1993) AIN-93 Purified Diets for Laboratory Rodents: Final Report of the American Institute of Nutrition *ad hoc* Writing Committee on the Reformulation of the AIN-76A Rodent Diet, *J. Nutr. 123*, 1939–1951.
38. National Research Council (1985) *Guide for the Care and Use of Laboratory Animals*, Publication No. 85-23 (rev.), National Institute of Health, Bethesda, MD.
39. Marra, C.A., Alaniz, M.J.T. de, and Brenner, R.R. (1986) Modulation of Δ6 and Δ5 rat Liver Microsomal Desaturase Activities by Dexamethasone-Induced Factor, *Biochim. Biophys. Acta 879*, 388–393.
40. Folch, J., Lees, M., and Stanley, G.A.S. (1957) A Simple Method for the Isolation and Purification of Total Lipids from Animal Tissues, *J. Biol. Chem. 226*, 497–509.
41. Patton, G.M., Fasulo, J.M., and Robins, S.J. (1982) Separation of Phospholipids and Individual Molecular Species of Phospholipids by High-Performance Liquid Chromatography, *J. Lipid Res. 23*, 190–196.
42. Chen, P.S., Toribara, T.Y., and Warner, H. (1956) Microdetermination of Phosphorus, *Anal. Chem. 33*, 1405–1406.
43. Neskovic, N.M., and Kostic, D.M. (1968) Quantitative Analysis

of Rat Liver Phospholipids by a Two-Step Thin-Layer Chromatography Procedure, *J. Chromatogr. 35*, 297–300.
44. Marra, C.A., and Alaniz, M.J.T. de (1992) Incorporation and Metabolic Conversion of Saturated and Unsaturated Fatty Acids in SK-Hep$_1$ Hepatoma Cells in Culture, *Mol. Cell. Biochem. 117*, 107–118.
45. Hirata, F., Schiffmann, E., Venkatasubramanian, K., Salomon, D., and Exelrod, J. (1980) A Phospholipase A_2 Inhibitory Protein in Rabbit Neutrophile Induced by Glucocorticoids, *Proc. Natl. Acad. Sci. USA 77*, 2533–2536.
46. Garda, H.A., Leikin, A.I., and Brenner, R.R. (1992) Determination of Fatty Acid Desaturase Activities by RP-HPLC, *An. Asoc. Quim. Argent. 80*, 365–371.
47. Lowry, O.H., Rosebrough, M.J., Farr, A.J., and Randall, R.J. (1951) Protein Measurement with the Folin Phenol Reagent, *J. Biol. Chem. 193*, 275–295.
48. Marra, C.A., and Alaniz, M.J.T. de, Effect of Calcium Deficiency on Acyl-CoA Synthetase Activity in Microsomes from Various Rat Tissue, *Acta Physiol. Pharmacol. Latinoam.*, in press.
49. Brenner, R.R. (1981) Nutritional and Hormonal Factors Influencing Desaturation of Essential Fatty Acids, *Prog. Lipid Res. 20*, 41–48.
50. Sprecher, H. (1983) The Mechanism of Fatty Acid Chain Elongation and Desaturation in Animals, in *High and Low Erucic Acid Rapeseed Oil* (Kramer, J.D.G., Souer, F.D., and Pigden, W.J., eds.) pp. 385–411, Academic Press, New York.
51. Brenner, R.R. (1987) Polyunsaturated Fatty Acid Metabolism and Its Regulation, in *Recent Advances in Essential Fatty Acid Research* (Das, V.N., ed.) Vol. I, pp. 5–18, Academic Publication, India.
52. Marín, M.C., De Tomás, M.E., Serres, C., and Mercuri, O. (1995) Protein-Energy Malnutrition During Gestation and Lactation in Rats Affects Growth Rate, Brain Development, and Essential Fatty Acid Metabolism, *J. Nutr. 125*, 1017–1024.
53. Marín, M.C., and Alaniz, M.J.T. de (1998) Relationship Between Dietary Oil During Gestation and Lactation and Biosynthesis of Polyunsaturated Fatty Acids in Control and in Malnourished Dam and Pup Rats, *J. Nutr. Biochem. 9*, 388–395.
54. Marra, C.A., Alaniz, M.J.T. de, and Brenner, R.R. (1988) A Dexamethasone-Induced Protein Stimulates Δ9 Desaturase Activity in Rat Liver Microsomes, *Biochim. Biophys. Acta 958*, 93–98.
55. Alaniz, M.J.T. de, and Marra, C.A. (1992) Glucocorticoid and Mineralocorticoid Hormones Depress Liver Δ5 Desaturase Activity Through Different Mechanism, *Lipids 27*, 599–604.
56. Reinhart, P.H., Taylor, W.M., and Bygrave, F.L. (1984) The Role of Calcium Ions in the Mechanism of Action of α-Adrenergic Agonists in Rat Liver, *Biochem. J. 223*, 1–13.
57. Salesse, R., and Garnier, J. (1984) Adenylate Cyclase and Membrane Fluidity. The Repressor Hypothesis, *Mol. Cell. Biochem. 60*, 17–31.
58. Brenner, R.R., Garda, H., Leikin, A.I., and Pezzano, H. (1980) Effect of Temperature on the Structure of Rat Liver Microsomes Studied by Electron Spin Resonance, Fluorescence and Activity of Enzymes Involved in Fatty Acid Biosynthesis, *Acta Physiol. Latinoam. 30*, 225–238.
59. Garda, H., and Brenner, R.R. (1982) Effect of Induced Phase Transitions on the Glucose-6-phosphate Activity and Electron Transport of Rat Liver Microsomes, *Acta Physiol Latinoam. 32*, 31–52.
60. Storch, J., and Schachter, D. (1985) Calcium Alters the Acyl Chain Composition and Lipid Fluidity of Rat Hepatocyte Plasma Membrane *in vitro, Biochim. Biophys. Acta 812*, 473–484.
61. Garda, H.A., and Brenner, R.R. (1984) Short-Chain Aliphatic Alcohols Increase Rat-Liver Microsomal Membrane Fluidity and Affect the Activities of Some Microsomal Membrane-Bound Enzymes, *Biochim. Biophys. Acta 769*, 160–170.
62. Garda, H.A., and Brenner, R.R. (1985) *In vitro* Modification of Cholesterol Content of Rat Liver Microsomal. Effects upon Membrane Fluidity and Activities of Glucose-6-phosphatase and Fatty Acid Desaturation Systems, *Biochim. Biophys. Acta 819*, 45–54.
63. Leikin, A.I., and Brenner, R.R. (1987) Cholesterol-Induced Microsomal Changes Modulate Desaturase Activities, *Biochim. Biophys. Acta 922*, 294–303.
64. Brenner, R.R. (1984) Effect of Unsaturated Acids on Membrane Structure and Enzyme Kinetics, *Prog. Lipid Res. 23*, 69–96.
65. Kan, H., Ruan, Y., and Malik, K.U. (1996) Involvement of Mitogen-Activated Protein Kinase and Translocation of Cytosolic Phospholipase A_2 to the Nuclear Envelope in Acetylcholine-Induced Prostacyclin Synthesis in Rabbit Coronary Endothelial Cells, *Mol. Pharmacol 50*, 1139–1147.
66. Xing, M., and Insel, P.A. (1996) Protein Kinase C-Dependent Activation of Cytosolic Phospholipase A_2 and Mitogen-Activated Protein Kinase by Alpha 1-Adrenergic Receptors in Maderi-Darbey Canine Kidney Cells, *J. Clin. Invest. 97*, 1302–1310.
67. Landschulz, K.T., Jump, D.B., Mac Dougald, O.A., and Lane, M.D. (1994) Transcriptional Control of the Stearoyl-CoA Desaturase-1 Gene by Polyunsaturated Fatty Acids, *Biochem. Biophys. Res. Commun. 200*, 763–768.
68. Kruger, M.C., and Horrobin, D.F. (1997) Calcium Metabolism, Osteoporosis, and Essential Fatty Acids: A Review, *Prog. Lipid Res. 36*, 131–151.
69. Alisio, A., Canas, F., De Bronia, D.H., Pereira, R., and Tolosa de Talamoni, N. (1997) Effect of Vitamin D Deficiency on Lipid Composition and Calcium Transport in Basolateral Membrane Vesicles from Chick Intestine, *Biochem Mol. Biol. Int. 42*, 339–347.

[Received August 30, 1999, and in revised form May 19, 2000; accepted July 20, 2000]

Response of Plasma Lipids to Dietary Cholesterol and Wine Polyphenols in Rats Fed Polyunsaturated Fat Diets

Lucie Frémont*, Marie T. Gozzelino, and Alain Linard

Laboratoire de Nutrition et Sécurité Alimentaire, INRA-CRJ, 78352 Jouy-en-Josas Cedex, France

ABSTRACT: This experiment was designed to evaluate the effects of dietary red wine phenolic compounds (WP) and cholesterol on lipid oxidation and transport in rats. For 5 wk, weanling rats were fed polyunsaturated fat diets (n-6/n-3 = 6.4) supplemented or not supplemented with either 3 g/kg diet of cholesterol, 5 g/kg diet of WP, or both. The concentrations of triacylglycerols (TAG, $P < 0.01$) and cholesterol ($P < 0.0002$) were reduced in fasting plasma of rats fed cholesterol despite the cholesterol enrichment of very low density lipoprotein + low density lipoprotein (VLDL + LDL). The response was due to the much lower plasma concentration of high density lipoprotein (HDL) (–35%, $P < 0.0001$). In contrast, TAG and cholesteryl ester (CE) accumulated in liver (+120 and +450%, respectively, $P < 0.0001$). However, the cholesterol content of liver microsomes was not affected. Dietary cholesterol altered the distribution of fatty acids mainly by reducing the ratio of arachidonic acid to linoleic acid ($P < 0.0001$) in plasma VLDL + LDL (–35%) and HDL (– 42%) and in liver TAG (–42%), CE (–78%), and phospholipids (–28%). Dietary WP had little or no effect on these variables. On the other hand, dietary cholesterol lowered the α-tocopherol concentration in VLDL + LDL (–40%, $P < 0.003$) and in microsomes (–60%, $P < 0.0001$). In contrast, dietary WP increased the concentration in microsomes (+21%, $P < 0.0001$), but had no effect on the concentration in VLDL + LDL. Cholesterol feeding decreased ($P < 0.006$) whereas WP feeding increased ($P < 0.0001$) the resistance of VLDL + LDL to copper-induced oxidation. The production of conjugated dienes after 25 h of oxidation ranged between 650 (WP without cholesterol) and 2,560 (cholesterol without WP) μmol/g VLDL + LDL protein. These findings show that dietary WP were absorbed at sufficient levels to contribute to the protection of polyunsaturated fatty acids in plasma and membranes. They could also reduce the consumption of α-tocopherol and endogenous antioxidants. The responses suggest that, in humans, these substances may be beneficial by reducing the deleterious effects of a dietary overload of cholesterol.

Paper no. L8353 in *Lipids 35*, 991–999 (September 2000).

*To whom correspondence should be addressed at LNSA, INRA-CRJ, 78352 Jouy-en-Josas Cedex, France. E-mail: Myriam.Defrance@jouy.inra.fr

Abbreviations: ANOVA, analysis of variance; apo, apolipoprotein; CE, cholesteryl ester; CVD, cardiovascular diseases; HDL, high density lipoprotein; HDL-C, HDL cholesterol; LCAT, lecithin:cholesterol acyltransferase; LDL, low density lipoprotein; PL, phospholipid; PUFA, polyunsaturated fatty acids; TAG, triacylglycerol; VLDL, very low density lipoprotein; WP, wine phenolic compounds.

Moderate consumption of red wine is considered to decrease morbidity and mortality due to cardiovascular diseases (CVD) (reviewed in Ref. 1). The protection seems partly due to ethanol (reviewed in Ref. 2) through a hemostatic mechanism and an increase in plasma levels of high density lipoprotein (HDL) (3–5), but there is some evidence that the nonalcoholic fraction of wine plays an important role in cardioprotection (6). This fraction contains large amounts of phenolic compounds, mainly flavonoids, which favorably influence several biological mechanisms such as oxidation of polyunsaturated fatty acids (PUFA) and platelet aggregation involved in the development of CVD. These substances mainly act by scavenging free radicals and chelating metal ions (7,8). The beneficial effect of flavonoids on human health is supported by epidemiological studies showing an inverse relationship between dietary intake and coronary heart disease (9–11).

In 1993, Frankel *et al.* (12) showed that phenolic substances in Californian red wine protected human low density lipoprotein (LDL) from copper-catalyzed oxidation. The authors showed that the effect was due not only to flavonoids but also to resveratrol (3,4′,5-trihydroxystilbene) present at low amounts in some red wines (13). The biological properties of this compound were confirmed in further studies (14,15). By using total or alcohol-free red wine, *ex-vivo* experiments demonstrated the favorable effects of moderate consumption (16–22).

It may be advantageous to increase the dietary intake of PUFA since they are believed to reduce risk factors associated with CVD such as thrombosis and hyperlipemia (23). However, it should be taken into consideration that the enrichment of body fluids and membranes in highly oxidizable PUFA may increase the consumption of endogenous antioxidants. We recently found that the resistance of very low density lipoprotein (VLDL) + LDL to lipid peroxidation was much lower in rats fed PUFA than in rats fed monounsaturated fatty acids. The consumption of diets supplemented with two defined flavonoids, quercetin and catechin, which are found in red wine, protected PUFA and increased the α-tocopherol content of liver microsomes in rats fed PUFA (24).

The resistance of LDL to lipid peroxidation may also be linked to cholesterol status since this compound is involved

in the etiology of CVD. The intake of high amounts of dietary cholesterol may induce changes in concentrations and composition of plasma and liver lipids, which modify the properties of lipoproteins such as resistance to lipid peroxidation. In humans, plasma lipoproteins derived from hypercholesterolemic patients are more susceptible to lipid peroxidation than those from normal subjects (25). Hence, supplementation of diet with antioxidant compounds such as polyphenols is potentially beneficial. Moreover, these substances may lower the cholesterol content of plasma. Such an effect was found in rats fed tea catechins and their gallate esters, which inhibit intestinal absorption by reducing solubility in mixed micelles (26).

This study was undertaken to determine whether responses to dietary wine phenolic compounds (WP) were influenced by the presence of cholesterol in high-PUFA diets. For this purpose, we compared diet-induced changes in plasma and liver lipids in weanling rats. In particular, we investigated the effects of dietary supplementation on the susceptibility of VLDL + LDL to lipid peroxidation and on the concentration of α-tocopherol in plasma and liver.

MATERIALS AND METHODS

All the chemicals used were of analytical reagent grade and were purchased from Sigma-Aldrich (Saint Quentin Fallavier, France).

Animals and diets. Male Wistar rats (IFFA Credo, L'Arbresle, France) bred in our laboratory were maintained at 22 ± 1°C with a 12 h light/dark cycle, with free access to water and food. The nutrient composition of experimental diets has been previously reported (27). The fat source (100 g/kg diet) was a mixture of oils rich in PUFA (75% sunflower oil, 25% sardine oil). This mixture provided 52% n-6 PUFA including 51.9% linoleic acid (18:2n-6), and 0.1% arachidonic acid (20:4n-6). They also provided 8.1% n-3 PUFA including 3% eicosapentaenoic acid (20:5n-3) and 3.2% docosahexaenoic acid (22:6n-3). Rats were randomly distributed into four groups of 18 animals each, just after weaning (21 d old) in a 2 × 2 factorial design. Two groups of rats were fed the diets without cholesterol whereas the other two received the same diets containing 3 g/kg diet cholesterol (previously dissolved in the oil mixture). One diet with cholesterol and one diet without cholesterol were supplemented with 5 g/kg diet of a dry powder of red wine (Cabernet Sauvignon grape variety) from the Institut National de la Recherche Agronomique (Montpellier, France). One liter of red wine produced 2 g of dry powder (WP) containing 0.98 g/g of total polyphenols. The main components (per g of WP) were monomeric flavonols (catechin + epicatechin) 8.6 mg; free anthocyanins (including 52% malvidin-3 glucoside), 52.4 mg; phenolic acids (including 19.5% caftaric acid), 8.7 mg; and proanthocyanidols expressed as catechin, 480 mg. One gram of WP contained 235 mg *trans*-resveratrol (M_r = 228) as analyzed according to Jeandet *et al.* (28).

The French instructions 88-123 concerning ordinance 87-848 about animal experimentation rules were followed.

After 5 wk of dietary treatment, rats were food-deprived for a night before weighing and killing by decapitation between 0800 and 0900. Blood was collected on heparin sodium salt (100 mg/L), and a mixture of 2 mmol/L benzamidin and 200 mmol/L gentamycin was added as preservative. Plasma samples from each group, obtained after low-speed centrifugation, were randomly pooled three by three into six subgroups. After adding 2 g/L Chelex-100 (Biorad, Ivry sur Seine, France) to remove traces of contaminating transition metals and aprotinin (100 kallikrein inhibitory units/L), plasma samples were stored at –80°C until analysis. Liver was rapidly removed, rinsed with ice-cold 150 mmol/L NaCl, blotted and weighed. Individual aliquots were freeze-clamped and stored at –80°C.

Lipoprotein isolation. Lipoprotein classes were isolated by sequential ultracentrifugation at 145,000 × *g* according to Havel *et al.* (29) using saline solutions stored on Chelex-100 (3 g/L) to remove traces of contaminating transition metals. As both VLDL (precursor of LDL) and LDL undergo lipid peroxidation and as rats have relatively small amounts of LDL (30), the following two fractions were isolated: VLDL + LDL, d < 1.050 kg/L and HDL, d = 1.050–1.21 kg/L, after a 20- and a 36-h centrifugation, respectively.

Preparation of liver membranes. All operations were performed at 4°C. Liver tissue was rinsed with ice-cold EDTA/NaCl 6 mmol/L: 150 mmol/L), minced with scissors, and homogenized in 2 mL/g of buffer (10 mmol/L Tris-HCl, 250 mmol/L sucrose, and 1 mmol/L EDTA, pH 7.4) using a Polytron homogenizer (PT 1200 Kinematica, Bioblock, Strasbourg, France). An aliquot was filtered through a nylon gauze and centrifuged at 500 × *g* for 5 min. The supernatant was centrifuged at 15,000 × *g* for 15 min followed by centrifugation of the supernatant at 105,000 × *g* for 60 min. The pellet termed "microsomes" was suspended in the same buffer at a protein concentration of 2 g/L and stored at –80°C.

Chemical analysis. Liver lipids were extracted from homogenate according to Folch *et al.* (31) using 6 mL of chloroform/methanol (2:1, vol/vol) for 1.5 mL homogenate. After washing twice, the lower chloroform phase was dried under nitrogen and resolubilized in 0.25 mL of 2-propanol. Liver triacylglycerol (TAG) and cholesterol (total and free) were quantified by enzymatic colorimetric tests (240052 and 1442341 Boehringer Mannheim, Meylan, France). The phospholipid (PL) content was estimated from the phosphorus content (P × 25) determined by the method of Bartlett (32). Plasma and lipoprotein TAG and cholesterol concentrations were directly measured using the same tests. HDL cholesterol (HDL-C) was determined in the fraction (d 1.050–1.21 kg/L) isolated from a defined volume of plasma. VLDL + LDL cholesterol was estimated as the difference between total cholesterol and HDL-C. The protein concentration of liver, lipoproteins, and plasma samples was determined by the method of Bradford (33) using the Biorad Protein assay (Biorad, Richmond, CA) with bovine serum albumin (fraction V) as standard. The HDL composition was determined by measuring amounts of components: free cholesterol, cholesteryl esters (CE), TAG, PL, and protein in

isolated HDL. Amounts of CE were calculated as the difference between total HDL-C and HDL free cholesterol multiplied by 1.7. The plasma HDL concentration (g/L) was calculated by adding weights of components.

Fatty acid composition. Methyl esters were prepared and analyzed by gas–liquid chromatography using a bonded fused-silica capillary column (Carbowax 20M, 50 m × 0.3 mm i.d.) and a flame-ionization detector as previously described (27).

Tocopherol analysis. Lipids were extracted from total plasma and HDL according to Burton *et al.* (34) by mixing the sample (0.5 mL), water (0.5 mL), and absolute ethanol (1 mL) in a glass tube. After adding *n*-hexane (1 mL), the mixture was stirred using a vortex for 50 s, and the organic phase was separated by centrifugation. The aqueous phase was re-extracted, and the hexane extract was dried under N_2 and resolubilized in a defined volume of hexane. The sample was analyzed by high-performance liquid chromatography using a Microporasil column (300 × 3.9 mm, 10 μm i.d.) supplied by Waters (Milford, MA). The mobile phase was *n*-hexane/ethyl acetate (100:7.5, vol/vol) at a flow rate of 1 mL/min. Detection was performed with a Hitachi spectrofluorimeter (model F-2000; Tokyo, Japan) with excitation at 290 nm and fluorescence emission at 330 nm. Quantification was performed with external standards of dl-α-tocopherol. The VLDL + LDL α-tocopherol concentration was calculated as the difference between total plasma and HDL concentration. The same procedure was used for analysis in liver fractions, but 1 mL of sodium dodecylsulfate aqueous solution (100 mmol/L) was added to 0.5 mL of either homogenate (100 mg fresh tissue) or microsomes (1 mg protein). Then, ethanol (2 mL) and *n*-hexane (2 mL) were added to extract α-tocopherol.

Oxidation of lipoproteins. The kinetics of conjugated diene formation in the VLDL + LDL fraction were followed by continuous monitoring of the 234-nm absorption according to Esterbauer *et al.* (35). Just before use, the lipoprotein was filtered through a 0.2-mm Millipore filter (Saint-Quentin en Yvelines, France) to remove Chelex, and lipoprotein aliquots (25 mg protein/L) in oxygenated phosphate-buffered saline (10 mmol/L, pH 7.4) were incubated at 37°C with 5 μmol/L $CuSO_4$. The increase of absorbance was recorded every 15 min for 24 h in a Uvikon 930 spectrophotometer (Kontron, Montigny le Bretonneux, France). The maximum diene concentration was determined from the difference between the absorbance at the maximum slope of the absorbance curve and the absorbance at time zero using the extinction coefficient for conjugated dienes at 234 nm [ε = 29,500 L/(mol · cm)].

Statistical analysis. Values are presented as means and SEM with significance set at $P < 0.05$. One-way analysis of variance (ANOVA) was used to compare the four group means. Two-way ANOVA was used to test effects of supplementation with cholesterol and WP and their interaction on variables. The differences between means were tested using least significant differences when the *F*-value was significant. The statistical computer program was Super ANOVA (Abacus Concepts, Berkeley, CA).

RESULTS

There were no significant differences among dietary groups for final body weight (no supplementation, control group, 353.7 ± 8.7 g; group fed cholesterol, 346.7 ± 7.5 g; group fed WP, 346.1 ± 9.6 g; group fed cholesterol + WP, 351.8 ± 10.3 g). As shown in Table 1, the dietary intake of cholesterol significantly lowered plasma levels of TAG ($P < 0.01$), total cholesterol ($P < 0.0002$), and HDL-C ($P < 0.0001$) and HDL-C to total cholesterol ratios ($P < 0.0001$). However, it increased the cholesterol to protein ratio in the VLDL + LDL fraction (+60%, $P < 0.005$).

The dietary-induced changes in HDL were assessed by quantifying the components of the fraction isolated by centrifugation (Table 2). Dietary cholesterol, but not WP, significantly reduced the plasma HDL concentration from 235–258 mg/L to 160 mg/L ($P < 0.0001$). Hence, the amounts of cholesterol carried by plasma HDL were 40–55% lower than in rats fed diets without cholesterol. The distribution of fatty acids in HDL was influenced by dietary cholesterol (and WP for 20:4n-6). The decreasing effect of dietary cholesterol on the proportion of arachidonic acid (20:4n-6) was compensated by opposite changes in the proportion of the precursor. As a result, the ratios of 20:4n-6 to 18:2n-6, unaffected by dietary WP, were lowest in rats fed cholesterol (1.05 vs. 1.75, $P < 0.0001$).

The lipid content of liver (Table 1) was affected by dietary cholesterol, but not by WP. The response, as opposed to that of plasma, was reflected by the 20% higher liver weight in rats fed cholesterol (10.2 ± 0.20 vs. 8.6 ± 0.14 g; $P < 0.0001$). This was mainly due to the accumulation of TAG (+120%, $P < 0.0001$) and cholesterol (+450%, $P < 0.0001$). In contrast, the PL content of liver was slightly lower (–10%, $P < 0.0002$).

Cholesterol feeding lowered the α-tocopherol concentration of plasma by about 40% ($P < 0.0001$) whereas it did not influence that of total liver. Relative to protein, the cholesterol content of microsomes was unaffected by either dietary supplementation, but the α-tocopherol content was lower in rats fed cholesterol (–60%) and higher in rats fed WP (+21%), $P < 0.0001$ for both compared to unsupplemented counterparts.

The kinetics of conjugated diene formation during copper-catalyzed oxidation of VLDL + LDL showed striking differences among groups for resistance to lipid peroxidation (Fig. 1). The amounts produced at 25 h oxidation were highest in rats fed cholesterol without WP (2560 μmol/g VLDL + LDL protein) whereas they were 75% lower in rats fed WP without cholesterol (cholesterol effect, $P < 0.006$; WP effect, $P < 0.0001$) (Table 1). The distribution of fatty acids in VLDL + LDL was influenced by dietary cholesterol but not by WP (Table 3). The highest response to cholesterol concerned 20:4n-6, which was reduced by almost 30% ($P < 0.0001$). This was compensated by higher proportions of 18:1n-9 and 18:2n-6.

WP supplementation had little or no effect on the distribution of fatty acids in liver esterified lipids (Table 4). In contrast, the response to cholesterol supplementation was significant ($P < 0.0001$ for almost all fatty acids). TAG incorporated less saturated fatty acids (–23%) and 20:4n-6 (–40%), but

TABLE 1
Effects of Cholesterol and Wine Polyphenols (WP) Supplementation on Lipids and a-Tocopherol in Plasma and Liver of Rats Fed Diets Rich in Polyunsaturated Fatty Acids[a,b]

	– Cholesterol		+ Cholesterol		Pooled	*P* values[c]	
	– WP	+ WP	– WP	+ WP	SEM	Chol	WP
Plasma			(mmol/L)				
Triacylglycerol	1.11[a]	0.98[a,b]	0.91[b]	0.88[b]	0.06	0.01	NS
Total cholesterol	1.47[a]	1.36[a]	1.07[b]	1.05[b]	0.08	0.0002	NS
HDL-C	1.16[a]	1.11[a]	0.59[b]	0.65	0.05	0.0001	NS
HDL-C/total C	0.81[a]	0.81[a]	0.55[b]	0.62[b]	0.03	0.0001	NS
			(μmol/L)				
Total α-tocopherol	13.06[a]	13.68[a]	8.04[b]	7.60[b]	0.40	0.0001	NS
HDL α-tocopherol	8.15[a]	8.48[a]	4.09[b]	4.56[b]	0.31	0.0001	0.01
			μmol/mg (VLDL + LDL) protein				
Cholesterol	6.05[b]	5.20[c]	9.84[a]	8.17[a,c]	1.07	0.005	NS
			μmol/mg (VLDL + LDL) protein				
Dienes (25 h)	1902[a]	650[c]	2560[a]	1419[b]	204.6	0.006	0.0001
α-tocopherol	92.4[a]	87.6[a,b]	76.5[b]	75.7[b]	4.16	0.003	NS
Total liver			(μmol/g)				
Triacylglycerols	12.56[b]	13.74[b]	28.62[a]	27.91[a]	0.74	0.0001	NS
Total cholesterol	6.25[b]	6.54[b]	33.96[a]	35.21[a]	1.35	0.0001	NS
Free cholesterol	4.22[b]	4.55[b]	5.12[a]	5.16[a]	0.14	0.0001	NS
Phospholipids	39.26[a]	37.88[a]	35.49[b]	34.80[b]	0.80	0.0002	NS
			(nmol/g)				
α-Tocopherol	67.47	74.88	66.96	68.14	3.09		
Liver microsomes			(μmol/g protein)				
Cholesterol	205.40	214.4	212.3	222.0	5.62		
α-Tocopherol	1.30[b]	1.64[a]	0.76[d]	0.99[c]	0.05	0.0001	0.0001

[a]Diets were supplemented (+) or not supplemented (–) with 0.3% cholesterol, 0.5% WP, or both.
[b]Values are means; $n = 6$ (pooled samples with three rats per pool) for plasma; $n = 18$ (individual samples) for liver (total and microsomes). Within a row, values with no common roman superscript differ at $P < 0.05$.
[c]Two-way analysis of variance: Chol, significant influence of cholesterol supplementation; WP, significant influence of WP supplementation; there was no significant Chol × WP interaction for any dietary group. NS, not significant ($P < 0.05$); HDL-C, high density lipoprotein cholesterol.

TABLE 2
Effects of Cholesterol and WP Supplementation on Plasma HDL Concentration and Composition in Rats Fed Diets Rich in Polyunsaturated Fatty Acids[a,b]

	– Cholesterol		+ Cholesterol		Pooled	*P* values[c]		
	– WP	+ WP	– WP	+ WP	SEM	Chol	WP	Chol × WP
mg/dL plasma								
Triacylglycerol	3.90[a]	2.58[b]	2.69[b]	2.62[b]	0.17	0.002	0.0004	0.001
Free cholesterol	8.34[a]	7.01[a]	3.51[b]	3.65[b]	3.22	0.0001	NS	0.04
Cholesteryl ester	62.35[a]	60.92[a]	32.69[b]	36.47[b]	2.95	0.0001	NS	NS
Phospholipid	67.83[a]	56.41[b]	32.20[b]	34.84[c]	8.73	0.0001	NS	NS
Protein	115.87[a]	108.02[a]	86.90[b]	86.34[b]	2.76	0.0001	NS	NS
Total HDL	258.3[a]	234.9[a]	158.0[b]	163.9[b]	8.73	0.0001	NS	NS
mol/100 mol fatty acids								
16:0 + 18:0	25.67[b,c]	26.21[a,c]	28.93[a]	25.83[c]	1.00	NS	NS	NS
Monounsaturated[d]	7.43[b,c]	7.04[c]	8.88[a]	7.68[a,c]	0.47	0.04	NS	NS
18:2n-6	22.28[a]	20.93[a]	28.10[b]	28.04[b]	1.12	0.0001	NS	NS
20:4n-6	36.91[a]	38.48[a]	27.85[c]	30.83[b]	0.68	0.0001	0.003	NS
Total n-3[e]	6.95[a]	6.63[a,c]	5.66[b]	6.53[b,c]	0.19	0.002	NS	0.006
20:4/18:2	1.66[a]	1.84[a]	0.99[b]	1.10[b]	0.09	0.0001	NS	NS

[a]Diets were supplemented (+) or not supplemented (–) with 0.3% cholesterol, 0.5% WP, or both.
[b]Values are means; $n = 6$ (pooled samples with three rats per pool). Within a row, values with no common roman superscript differ at $P < 0.05$.
[c]Two-way analysis of variance. Chol × WP, interaction. See Table 1 for other abbreviations.
[d]Consist of 16:1n-9/n-7, 18:1n-9/n-7.
[e]Consist of 20:5, 22:5, 22:6.

TABLE 3
Effects of Cholesterol and WP Supplementation on the Fatty Acid Composition of Plasma (VLDL + LDL) in Rats Fed Diets Rich in Polyunsaturated Fatty Acids[a,b]

	– Cholesterol		+ Cholesterol		Pooled	*P* value[c]
	– WP	+ WP	– WP	+ WP	SEM	Chol
	mol/100 mol					
16:0 + 18:0	26.75[a]	27.03[a]	24.00[b]	24.25[a]	0.29	0.0001
18:1n-9	13.28[b]	13.35[b]	17.08[a]	17.06[a]	0.30	0.0001
18:2n-6	37.82[b]	37.72[b]	39.84[a]	39.62[a]	0.39	0.0001
20:4n-6	7.22[a]	7.39[a]	5.21[b]	5.24[b]	0.02	0.0001
Total n-3[d]	11.05[a]	10.60[a]	8.97[b]	9.30[b]	0.27	0.0001
Others[e]	3.88[a]	3.90[a]	4.88[b]	5.53[b]	0.13	0.0001
20:4/18:2	1.19[a]	0.20[a]	0.13[b]	0.13[b]	0.01	0.0001

[a]Diets were supplemented (+) or not supplemented (–) with 0.3% cholesterol, 0.5% WP, or both.
[b]Values are means; $n = 6$ (pooled samples with 3 rats per pool). Within a row, values with no common roman superscripts are significantly different at $P < 0.05$.
[c]Two-way analysis of variance. There was no significant influence of dietary WP for any dietary groups. VLDL, very low density lipoprotein; LDL, low density lipoprotein; for other abbreviations see Table 1.
[d]Consist of 18:3, 20:5, 22:5, 22:6.
[e]Consist of 16:1n-9/n-7, 18:1n-7, 18:3n-6, 20:3n-6, 22:4n-6.

more n-3 PUFA (+29%). In CE, the 62% lower proportion of saturated fatty acids and 20:4n-6 was compensated by the higher proportion of 18:1n-9, 18:2n-6, and n-3 PUFA. The fatty acid composition of PL was moderately affected by dietary treatments. However, the proportion of 20:4n-6 was 20% lower in cholesterol-fed rats. In the three lipid classes, the response was reflected by the lower 20:4n-6 to 18:2n-6 ratio. Figure 2 represents the liver content of major fatty acyl chains incorporated in esterified lipids (as calculated from Tables 1 and 4). Supplementation with cholesterol dramatically enhanced the amounts of acyl chains present in CE (from 2 to 25 μmol/g liver, $P < 0.0001$) and in TAG (from 38 to 81 μmol/g liver, $P < 0.0001$). In contrast, WP supplementation did not alter these variables. PL amounts were not or were only slightly influenced by dietary treatments and the response contrasted with that of other esters (from 74 to 67 μmol/g liver, $P < 0.001$). This was mainly due to the decreasing effect of dietary cholesterol ($P < 0.0001$) on 20:4n-6 (–26%) and n-3 PUFA (–17%) and of dietary wine on 18:2n-6 (–12%).

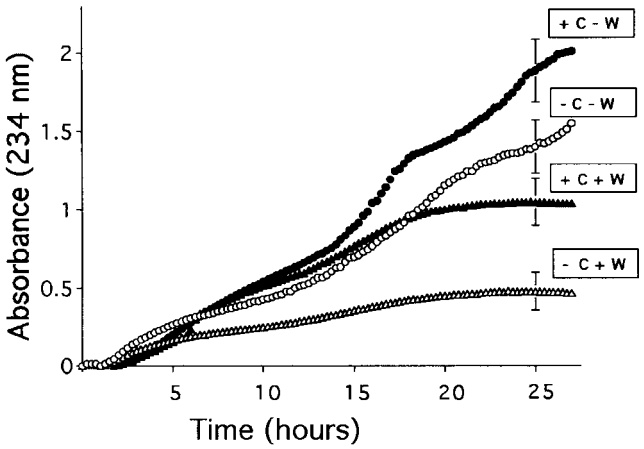

FIG. 1. Kinetics of copper-catalyzed oxidation of very low density lipoprotein + low density lipoprotein in rats fed diets not supplemented or supplemented with cholesterol (C) and red wine polyphenols (W). The changes in absorbance at 234 nm were continuously monitored and recorded every 15 min. The initial absorbance was subtracted from all data. Each value of each curve represents the mean of six pooled samples (3 rats per pool). With the exception of that at 25 h, the bars showing SEM have been omitted for clarity. At 25 h, there was a significant difference among groups for the effect of dietary C ($P < 0.006$) and W ($P < 0.0001$) without interaction. Amounts of dienes are given in Table 1.

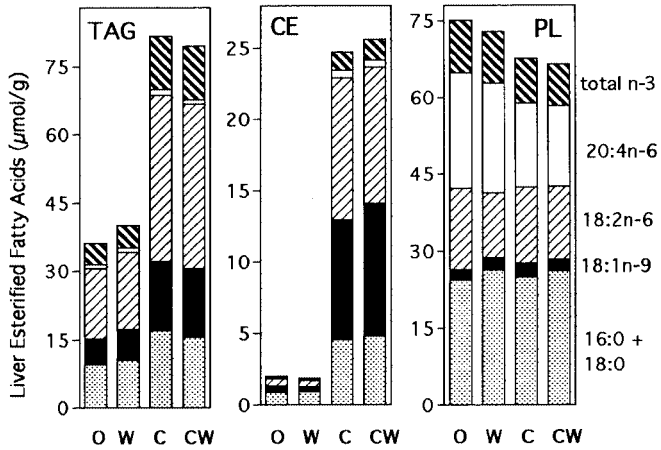

FIG. 2. Amounts of major fatty acids in liver-esterified lipids (μmol/g fresh tissue). Values were calculated using data from Tables 1 and 3 considering that triacylglycerol (TAG), cholesteryl ester (CE), and phospholipid (PL) contain 3, 1, and 2 mol fatty acid/mol ester, respectively. Esterified cholesterol is total cholesterol minus free cholesterol. Letters in abcissa represent dietary groups: not supplemented (O) or supplemented with wine polyphenols (W), cholesterol (C), cholesterol and wine polyphenols (CW). Values are mean ($n = 18$). Bars showing SEM have been omitted for clarity. There was a significant difference among groups for 1) the effect of dietary C on the acyl chain content of TAG and CE ($P < 0.0001$ except 20:4n-6 in TAG, $P < 0.0002$) and of PL ($P < 0.0001$ for 20:4n-6 and total n-3, $P < 0.03$ for 18:1n-9; 2) for the effect of dietary W on the 18:2n-6 content of PL ($P < 0.0003$).

TABLE 4
Effects of Cholesterol and WP Supplementation on the Fatty Acid Composition of Hepatic Esterified Lipids in Rats Fed Diets Rich in Polyunsaturated Fatty Acids[a,b]

	Triacylglycerol							
	– Cholesterol		+ Cholesterol		Pooled	*P* value[c]		
Fatty acid	– WP	+ WP	– WP	+ WP	SEM	Chol	WP	Chol × WP
	mol/100 mol							
16:0 + 18:0	25.29[a]	25.72[a]	19.86[b]	18.88[b]	0.50	0.0001	NS	NS
18:1n-9	15.01[c]	16.42[b]	17.59[a]	17.99[a]	0.35	0.0001	NS	NS
18:2n-6	40.82[b]	40.68[b]	42.69[a]	43.08[a]	0.31	0.0001	NS	NS
20:4n-6	2.16[b]	2.41[b]	1.42[c]	1.28[c]	0.08	0.0001	NS	NS
Total n-3[d]	8.81[b]	8.58[b]	12.52[a]	12.84[a]	0.50	0.0001	NS	NS
Others[e]	7.90[a]	6.20[b,c]	5.92[c]	5.93[c]	0.29	0.0003	0.005	0.005
20:4/18:2	0.05[a]	0.06[a]	0.03[b]	0.03[b]	0.01	0.0001	NS	0.03
	Phospholipid							
	– Cholesterol		+ Cholesterol		Pooled	*P* value[c]		
Fatty acid	– WP	+ WP	– WP	+ WP	SEM	Chol	WP	Chol × WP
	mol/100 mol							
16:0 + 18:0	30.95[c]	34.51[b]	35.06[a,b]	37.67[a]	0.93	0.0002	0.001	NS
18:1n-9	2.77[c]	3.17[b]	3.81[a]	3.17[b]	0.09	0.0001	NS	0.0001
18:2n-6	20.07[a]	16.78[b]	20.91[a]	20.31[a]	0.55	0.0002	0.0008	0.02
20:4n-6	28.77[a]	28.44[a]	23.12[b]	22.78[b]	0.56	0.0001	NS	NS
Total n-3[d]	13.12[a]	13.14[a]	12.17[b]	11.72[b]	0.27	0.0001	NS	NS
Others[e]	4.32[b]	3.95[c]	4.92[a]	4.34[b]	0.13	0.003	0.005	NS
20:4/18:2	1.43[b]	1.69[a]	1.11[c]	1.12[c]	0.05	0.0001	0.006	0.02
	Cholesteryl ester							
	– Cholesterol		+ Cholesterol		Pooled	*P* value[c]		
Fatty acid	– WP	+ WP	– WP	+ WP	SEM	Chol	WP	Chol × WP
	mol/100 mol							
16:0 + 18:0	41.82[b]	46.31[a]	16.25[c]	16.33[c]	1.13	0.0001	0.04	NS
18:1n-9	20.09[c]	18.42[c]	29.34[b]	32.36[a]	0.63	0.0001	NS	0.0004
18:2n-6	23.26[b]	20.60[c]	35.08[a]	33.22[a]	0.75	0.0001	0.003	NS
20:4n-6	4.41[b]	4.95[a]	1.90[c]	1.78[c]	0.18	0.0001	NS	NS
Total n-3[d]	3.47[c]	3.17[c]	4.46[b]	5.01[a]	0.14	0.0001	NS	0.004
Otherse	6.95[c]	6.55[c]	12.98[a]	11.29[b]	0.40	0.0001	0.01	NS
20:4/18:2	0.19[b]	0.24[a]	0.05[c]	0.05[c]	0.01	0.0001	0.03	0.03

[a]Diets were supplemented (+) or not supplemented (–) with 0.3% cholesterol, 0.5% WP, or both.
[b]Values are means expressed as mol per 100 mol of total fatty acids; $n = 18$. Within a row, values with no common roman superscripts differ at $P < 0.05$.
[c]Two-way analysis of variance. For abbreviations see Tables 1 and 2.
[d]Consist of 18:3, 20:5, 22:5, 22:6.
[e]Consist of 16:1n-9/n-7, 18:1n-7, 18:3n-6, 20:3n-6, 22:4n-6.

DISCUSSION

The major findings of this study are the opposing responses of plasma and liver lipids to dietary cholesterol. Paradoxically, cholesterol feeding induced a reduction of total plasma cholesterol levels despite the cholesterol enrichment of the VLDL + LDL fraction. The overall hypocholesterolemic effect was due to the reduction of HDL which, in rats, are the main vehicles of plasma CE. They are mainly synthesized in plasma through the action of lecithin:cholesterol acyltransferase (LCAT) with large differences between species for the substrate specificity. Thus in rat, the LCAT reaction produces predominantly 20:4n-6 CE (36,37). The accumulation of CE in plasma HDL is believed to result from the deficiency of a lipid transfer protein that, in humans, transfers HDL CE to lipoproteins of lower density (38). Moreover, the plasma LDL levels are low because rats have an efficient mechanism for hepatic clearance of chylomicrons and VLDL remnants from the circulation (30).

The level and type of dietary fats largely influence the lipid content of plasma. In rats, dietary long-chain n-3 PUFA reduce both TAG and cholesterol plasma concentrations (39,40). Such effects were observed in rats fed 10% safflower oil diets (rich in 18:2n-6) when 50% of the lipid source was

replaced by fish oil. The addition of 1% cholesterol to diets did not impair the response to long-chain n-3 PUFA but increased the plasma cholesterol content and the liver weight (41). Our data are consistant with that obtained by Lu and Wu (42) in rats fed diets resembling that of this study (10% fat with 42% PUFA and a n-6 to n-3 ratio of about 5). The addition of 1% cholesterol to diets induced a reduction of plasma TAG, cholesterol, and HDL levels and an increase of liver TAG and CE levels. The authors suggested that most of the cholesterol transported into the blood stream from the gut was immediately removed from the circulation by the liver. Indeed, the activity of the hepatic acyl-CoA:cholesterol acyltransferase, which catalyzes the formation of cholesteryl esters, is high in rats fed fish oils (43), and cholesterol feeding increases the activity (44). This lead to an hepatic overload of CE. The hepatic accumulation of TAG reported in rats fed diets rich in n-6 PUFA without fish oil supplemented with cholesterol was ascribed to the reduction of fatty acid oxidation and to the stimulation of TAG synthesis (45). In this study, the intake of dietary fish oils, which reduce the hepatic synthesis of TAG (46), did not impair the hepatic accumulation. The concentration of fish oils in diet could be insufficient to neutralize the response to dietary cholesterol.

The present findings suggest that the lowering effect of dietary cholesterol on the HDL content of plasma was linked to the availability of 20:4n-6. Indeed, dietary cholesterol alters the metabolism of hepatic fatty acids by inhibiting the conversion of 18:2n-6 to 20:4n-6 (47). Moreover, dietary cholesterol accentuates the inhibitory effects of long-chain n-3 PUFA on the desaturation of 18:2n-6 (41). In this study, this was reflected by the lower 20:4n-6 to 18:2n-6 ratio in either class of liver lipids as well as in plasma lipids. The reduction of the hepatic pool of 20:4n-6 could be partly responsible for the lower PL content of liver. Despite a greater liver weight, the amounts of 20:4n-6 in the whole tissue were slighty lower than in unsupplemented counterparts (167 μmol vs. 192 μmol).

In plasma, the reduction of 20:4n-6 likely affected the PL class thereby decreasing the production of HDL CE through the LCAT reaction. In total HDL, the amounts of 20:4n-6 reached about 27 μmol/100 dL plasma with cholesterol-free diets whereas they were lowered to 10 μmol/100 dL plasma with cholesterol-supplemented diets. The reduction in the synthesis of HDL could also be due to dysfunctions in the liver metabolism in response to lipid accumulation. This could impair the synthesis of apolipoproteins (apo) and their association with lipid fractions.

The proportion of 18:2n-6, which is considered as the primary predictor of oxidative susceptibility of LDL (48), was only 5% higher in VLDL + LDL from rats fed cholesterol as compared to unsupplemented counterparts. Accordingly, the increasing effect of dietary cholesterol on the production of dienes could be linked in a minor way, to the 18:2n-6 content of particles. The cholesterol enrichment of particles likely enhanced their susceptibility to oxidation. Such an effect was reported in the case of rabbits fed diets containing 2% cholesterol (49). On the other hand, the oxidizability of lipoproteins is partly dependent on the concentration of substances having antioxidant properties. Quantitatively, the main lipophilic antioxidant associated with particles is α-tocopherol. Hence, the reducing effect of dietary cholesterol on the α-tocopherol content of VLDL + LDL could also contribute to the production of higher amounts of dienes.

Feeding WP resulted in a lower oxidizability of VLDL + LDL fatty acids. The highly significant response suggests that the assay mixture contained wine antioxidants. They could be either bound to particles or solubilized in their aqueous environment. As was the case previously (14), the VLDL + LDL fraction was not dialyzed after isolation so as to prevent the loss of soluble antioxidants. Actually, with diets similar to that of this study, we observed that the intake of dietary quercetin and catechin inhibited the formation of conjugated dienes in VLDL + LDL. In other studies, epicatechin administered orally to Wistar rats was found to decrease the oxidizability of plasma. The compound exhibited antioxidative activity even after intestinal absorption and metabolic conversion (50).

The intestine can also absorb the phenolic substances of red wine. In humans consuming red wine, Furhman *et al.* (17) found that LDL were enriched in phenolic compounds whereas their capacity to undergo peroxidation induced by copper ions was reduced. Further studies showed that the response was not due to alcohol intake. Thus, a significant increase in plasma antioxidant potential and polyphenol concentration was found in humans consuming alcohol-free red wine (21). The protective effects of WP against atherosclerosis were demonstrated in apo E-deficient mice in which LDL are highly susceptible to oxidation and aggregation. Indeed, dietary supplementation with red wine or its polyphenolic compounds, quercetin and catechin, lowered the susceptibility of their LDL to oxidation and inhibited the development of aortic lesions (51).

The wine powder used in this study contained anthocyanins. These flavonoid pigments, which are strong antioxidants (52), are partially absorbed (53). The major fraction of wine polyphenols consists of proanthocyanidols which are oligomers and polymers of flavonols. In wine, a fraction is present as condensed tannins containing three to five subunits, which are potent metal chelators (1). Moreover, they may reduce the intestinal absorption of cholesterol (54).

It is not known whether the oxidizability of VLDL + LDL is linked to the plasma HDL content. However, it should be taken into consideration that not only *in vitro* (55) but also *in vivo*, HDL have been found to protect LDL. The effect might be related to that of HDL-associated antioxidants such as α-tocopherol and paraoxonase, which can destroy oxidized lipids (56). Moreover, HDL are potent scavengers of free radicals (57). In rabbits, cholesterol-feeding reduced the plasma HDL concentration, suggesting that this effect could contribute to the formation of atherosclerotic lesions (49).

In liver microsomes, there were no major differences between groups for the cholesterol content and for the distribution of fatty acids (assuming that liver PL are representative

of membrane PL). The α-tocopherol enrichment of microsomes in rats supplemented with WP is consistent with previous findings using diets enriched with defined flavonoids (14). This suggests that the cholesterol-induced reduction of α-tocopherol in membranes could be partially prevented by dietary WP.

Even if the present findings cannot be extrapolated to the human situation, they provide useful informations about responses to the intake of dietary wine polyphenols. They prove that these compounds, which are potent antioxidants, are absorbed at sufficient levels to contribute to the protection of PUFA in plasma and membranes, thereby sparing α-tocopherol and endogenous antioxidants. In particular, they suggest that the intake of dietary wine polyphenols is beneficial more especially when feeding high cholesterol diets.

ACKNOWLEDGMENTS

The authors thank Dr. Michel Bourzeix and Dr. Véronique Cheynier (INRA, Montpellier) for the gift of wine powder and Dr. Philippe Jeandet (Laboratoire d'Oenologie, Reims) for measuring the resveratrol content.

REFERENCES

1. Soleas, G.J., Diamandis, E.P., and Goldberg D.M. (1997) Wine as a Biological Fluid : History, Production and Role in Disease Prevention, *J. Clin. Lab. Anal. 11*, 287–313.
2. Rimm, E.B., Klatsky, A., Grabble, D., and Stampfer, M.J. (1996) Review of Moderate Alcohol Consumption and Reduced Risk of Coronary Heart Disease: Is the Effect due to Beer, Wine, or Spirits? *Br. Med. J. 312*, 731–736.
3. Renaud, S., and De Lorgeril, M. (1992) Wine, Alcohol, Platelets, and the French Paradox for Coronary Heart Disease, *Lancet 339*, 1523–1526.
4. Gaziano, J.M., Buring, J.E., Breslow, J.L., Goldhaber, S.Z., Rosner, B., Van Denburgh, M., Willet, W., and Hennekens, C.H. (1993) Moderate Alcohol Intake, Increased Levels of High-Density Lipoprotein and Its Subfractions, and Decreased Risk of Myocardial Infarction, *N. Engl. J. Med. 329*, 1829–1834.
5. Lavy, A., Fuhrman, B., Markel, A., Dankner, G., Ben-Amotz, A., Presser, D., and Aviram, M. (1994) Effect of Dietary Supplementation of Red and White Wine on Human Blood Chemistry Hematology and Coagulation: Favorable Effect of Red Wine on Plasma High-Density Lipoprotein, *Ann. Nutr. Metab. 38*, 287–294.
6. St. Leger, A.S., Cochrane, A.L., and Moore, F. (1979) Factors Associated with Cardiac Mortality in Developed Countries with Particular Reference to the Consumption of Wine, *Lancet 1*, 1017–1020.
7. Cook, N.C., and Samman, S. (1996) Flavonoids–Chemistry, Metabolism, Cardioprotective Effects, and Dietary Sources, *J. Nutr. Biochem. 7*, 66–76.
8. Rice-Evans, C.A., Miller, N.J., and Paganga, G. (1997) Antioxidant Properties of Phenolic Compounds, *Trends Plant Sci. 2*, 152–159.
9. Hertog, M.G.L., Feskens, E.J.M., Hollman, P.C.H., Katan, M.B., and Kromhout, D. (1993) Dietary Antioxidant Flavonoids and Risk of Coronary Heart Disease: The Zutphen Elderly Study, *Lancet 342*, 1007–1011.
10. Keli, S.O., Hertog, M.G.L., Feskens, E.J.M., and Kromhout, D. (1996) Dietary Flavonoids, Antioxidant Vitamins, and Incidence of Stroke: The Zutphen Study, *Arch. Intern. Med. 156*, 637–642.
11. Knekt, P., Järvinen, R., Reunanen, A., and Maatela, J. (1996) Flavonoid Intake and Coronary Mortality in Finland: a Cohort Study, *Br. Med. J. 312*, 478–481.
12. Frankel, E.N., Kanner, J., German, B.J., Parks, E., and Kinsella, J.E. (1993) Inhibition of Oxidation of Human Low-Density Lipoprotein by Phenolic Substances in Red Wine, *Lancet 34*, 454–457.
13. Frankel, E.N., Waterhouse, A.L., and Kinsella, J.E. (1993) Inhibition of Human LDL Oxidation by Resveratrol, *Lancet 341*, 1103–1104.
14. Belguendouz, L., Frémont, L., and Linard, A. (1997) Resveratrol Inhibits Metal Ion-Dependent and Independent Peroxidation of Porcine Low-Density Lipoproteins, *Biochem. Pharmacol. 53*, 1347–1355.
15. Soleas, G.J., Diamandis, E.P., and Goldberg, D.M. (1997) Resveratrol: A Molecule Whose Time Has Come? and Gone? *Clin. Biochem. 30*, 91–113.
16. Abu-Amsha, R., Croft, K.D., Puddey, I.B., Proudfoot, J.M., and Beilin, L.J. (1996) Phenolic Content of Various Beverages Determines the Extent of Inhibition of Human Serum and Low-Density Lipoprotein Oxidation *in vitro*: Identification and Mechanism of Action of Some Cinnamic Acid Derivatives from Red-Wine, *Clin. Sci. 91*, 449–458.
17. Fuhrman, B., Lavy, A., and Aviram, M. (1995) Consumption of Red Wine with Meals Reduces the Susceptibility of Human Plasma and Low-Density Lipoprotein to Lipid Peroxidation, *Am. J. Clin. Nutr. 61*, 549–554.
18. Kondo, K., Matsumoto, A., Kurata, H., Tanahashi, H., Koda, H., Amachi, T., and Itakura, H. (1994) Inhibition of Oxidation of Low-Density Lipoprotein with Red Wine, *Lancet 344*, 1152.
19. Miyagi, Y., Miwa, K., and Inoue, H. (1997) Inhibition of Human Low-Density Lipoprotein Oxidation by Flavonoids in Red-Wine and Grape Juice, *Am. J. Cardiol. 80*, 1627–1631.
20. Nigdikar, S.V., Williams, N.R., Griffin, B.A., and Howard, A.N. (1998) Consumption of Red Wine Polyphenols Reduces the Susceptibility of Low-Density Lipoproteins to Oxidation *in vivo*, *Am. J. Clin. Nutr. 68*, 258–265.
21. Serafini, M., Maiani, G., and Ferro-Luzzi, A. (1998) Alcohol-Free Red Wine Enhances Plasma Antioxidant Capacity in Humans, *J. Nutr. 128*, 1003–1007.
22. Whitehead, T.P., Robinson, D., Allaway, S., Syms, J., and Hale, A. (1995) Effect of Red Wine Ingestion on the Antioxidant Capacity of Serum, *Clin. Chem. 41*, 32–35.
23. Goodnight, S.H., Harris, W.S., Connor, W.E., and Illingworth, D.R. (1982) Polyunsaturated Fatty Acids, Hyperlipidemia, and Thrombosis, *Arteriosclerosis 2*, 87–113.
24. Frémont, L., Gozzelino, M.T., Franchi, M.P., and Linard, A. (1998) Dietary Flavonoids Reduce Lipid Peroxidation in Rats Fed Polyunsaturated or Monounsaturated Fat Diets, *J. Nutr. 128*, 1495–1502.
25. Lavy, A., Brook, G.J., Dankner, G., Amotz, A.B., and Aviram, M. (1991) Enhanced *in vitro* Oxidation of Plasma Lipoproteins Derived from Hypercholesterolemic Patients, *Metabolism 40*, 794–799.
26. Ikeda, I., Imasato, Y., Sasaki, E., Nakayama, M., Nagao, H., Takeo, T., Yayabe, F., and Sugano, M. (1992) Tea Catechins Decrease Micellar Solubility and Intestinal Absorption of Cholesterol in Rats, *Biochim. Biophys. Acta 1127*, 141–146.
27. Frémont, L., and Gozzelino, M.T. (1996) Dietary Sunflower Oil Reduces Plasma and Liver Triacylglycerols in Fasting Rats and Is Associated with Decreased Liver Microsomal Phosphatidate Phosphohydrolase Activity, *Lipids 31*, 871–878.
28. Jeandet, P., Breuil, A.C., Adrian, M., Weston, L.A., Debord, S., Meunier, P., Maume, G., and Bessis, R. (1997) HPLC Analysis of Grapevine Phytoalexins Coupling Photodiode Array Detec-

tion and Fluorometry, *Anal. Chem. 69*, 5172–5177.
29. Havel, R.J., Eder, H.A., and Bragdon, J.H. (1955) The Distribution and Chemical Composition of Ultracentrifugally Separated Lipoproteins in Human Serum, *J. Clin. Invest. 34*, 1345–1353.
30. Oschry, Y., and Eisenberg, S. (1982) Rat Plasma Lipoproteins: Reevaluation of a Lipoprotein System in an Animal Devoid of Cholesteryl Ester Transfer Activity, *J. Lipid Res. 23*, 1099–1106.
31. Folch, J., Lees, M., and Sloane Stanley, G.H. (1957) A Simple Method for the Isolation and Purification of Total Lipides from Animal Tissues, *J. Biol. Chem. 226*, 497–509.
32. Bartlett, G.R. (1959) Phosphorus Assay in Column Chromatography, *J. Biol. Chem. 234*, 466–468.
33. Bradford, M.M. (1976) A Rapid and Sensitive Method for the Quantitation of Microgram Quantities of Protein Utilizing the Principle of Protein-Dye Binding, *Anal. Biochem. 72*, 248–254.
34. Burton, G.W., Webb, A., and Ingold, K.U. (1985) A Mild, Rapid, and Efficient Method of Lipid Extraction for Use in Determining Vitamin E/Lipid Ratios, *Lipids 20*, 29–39.
35. Esterbauer, H., Striegl, G., Puhl, H., and Rotheneder, M. (1989) Continuous Monitoring of *in vitro* Oxidation of Human Low Density Lipoprotein, *Free Rad. Res. Comms 6*, 67–75.
36. Grove, D., and Pownall, H.J. (1991) Comparative Specifity of Plasma Lecithin:Cholesterol Acyltransferase from Ten Animal Species, *Lipids 26*, 416–420.
37. Liu, M., and Bagdade, J.D. (1995) Specificity of Lecithin:Cholesterol Acyltransferase and Atherogenic Risk: Comparative Studies on the Plasma Composition and *in vitro* Synthesis of Cholesteryl Esters in 14 Vertebrate Species, *J. Lipid Research 36*, 1813–1824.
38. Ha, Y.C., and Barter, P.J. (1982) Differences in Plasma Cholesteryl Ester Transfer Activity in Sixteen Vertebrate Species, *Comp. Biochem. Physiol. 71B*, 265–269.
39. Wong, S., Reardon, M.F., and Nestel, P.J. (1985) Reduced Triglycerides Formation from Long-Chain Polyenoic Fatty Acids in Rat Hepatocytes, *Metabolism 34*, 900–905.
40. Balasubramaniam, S., Simons, L.A., Chang, S., and Hickie, J. B. (1985) Reduction in Plasma Cholesterol and Increase in Biliary Cholesterol by a Diet Rich in n-3 Fatty Acids in the Rat, *J. Lipid Res. 26*, 684–689.
41. Huang, Y.S., Nassar, B.A., and Horrobin, D.F. (1986) Changes of Plasma Lipids and Long-Chain n-3 and n-6 Fatty Acids in Plasma, Liver, Heart and Kidney Phospholipids of Rats Fed Variable Levels of Fish Oil with or Without Cholesterol Supplementation, *Biochim. Biophys. Acta 879*, 22–27.
42. Lu, Y.F., and Wu, H.L. (1994) Effect of Monounsaturated Fatty Acids Under Fixed P/S and n-6/n-3 Ratios on Lipid Metabolism, *J. Nutr. Sci. Vitaminol. 40*, 189–200.
43. Chautan, M., Chanussot, F., Portugal, H., Pauli, A.M., and Lafont, H. (1990) Effects of Salmon Oil and Corn Oil on Plasma Lipid Level and Hepato-Biliary Cholesterol Metabolism in Rats, *Biochim. Biophys. Acta 879*, 22–27.
44. Mitropoulos, K.A., Venkatessen, S., and Balasubramaniam, S. (1980) On the Mechanism of Regulation of Hepatic Hydroxy-3-methyl Glutaryl Coenzyme A Reductase and of Acyl Coenzyme A: Cholesterol Acyltransferase by Dietary Fat, *Biochim. Biophys. Acta, 619*, 247–257.
45. Fungwe, T.V., Cagen, L.M., Cook, G.A., Wilcox, H.G., and Heimberg, M. (1993) Dietary Cholesterol Stimulates Hepatic Biosynthesis of Triglyceride and Reduces Oxidation of Fatty Acids in the Rat, *J. Lipid Res. 34*, 933–941.
46. Al-Shurbaji, A., Larsson-Backström, C., Berkglund, L., Eggertsen, G., and Björkhem, I. (1991) Effect of n-3 Fatty Acids on the Key Enzymes Involved in Cholesterol and Triglyceride Turnover in Rat Liver, *Lipids 26*, 385–389.
47. Garg, M. L., Snoswell, A.M., and Sabine, J.R. (1985) Effect of Dietary Cholesterol on Cholesterol Content and Fatty Acid Profiles of Rat Liver and Plasma, *Nutr. Rep. Int. 32*, 117–127.
48. Wander, R.C., Du, S.H., and Thomas, D.R. (1998) Influence of Long-Chain Polyunsaturated Fatty Acids on Oxidation of Low Density Lipoprotein, *Prostaglandins, Leukotriences Essent. Fatty Acids 59*, 143–151.
49. Nenseter, M.S., Gudmundsen, O., Malterud, K.E., Berg, T., and Drevon C.A. (1994) Effect of Cholesterol Feeding on the Susceptibility of Lipoproteins to Oxidative Modification, *Biochim. Biophys. Acta. 1213*, 207–214.
50. Da Silva, E.L., Piskula, M., and Terao, J. (1998) Enhancement of Antioxidative Ability of Rat Plasma by Oral Administration of (–)-Epicatechin, *Free Radical Biol. Med. 24*, 1209–1216.
51. Hayek, T., Fuhrman, B., Vaya, J., Rosenblat, M., Belinky, P., Coleman, R., Elis, A., and Aviram, M. (1997) Reduced Progression of Atherosclerosis in Apolipoprotein E-Deficient Mice Following Consumption of Red Wine, or its Polyphenols Quercetin or Catechin, Is Associated with Reduced Susceptibility of LDL to Oxidation and Aggregation, *Arterioscler. Thromb. Vasc. Biol. 17*, 2744–2752.
52. Tsuda, T., Shiga, K., Ohshima, K., Kawakishi, S., and Osawa, T. (1996) Inhibition of Lipid Peroxidation and the Active Oxygen Radical Scavenging Affect of Anthocyanin Pigments Isolated from Phaseolus vulgaris, *L. Biochem. Pharmacol. 52*, 1033–1039.
53. Lapidot, T., Harel, S., Granit, R., and Kanner, J. (1998) Bioavailability of Red Wine Anthocyanins as Detected in Human Urine, *J. Agric. Food Chem. 46*, 4297–4302.
54. Tebib, K., Besançon, P., and Rouanet, J.M. (1994) Dietary Grape Seed Tannins Affect Lipoproteins, Lipoprotein Lipases and Tissue Lipids in Rats Fed Hypercholesterolemic Diets, *J. Nutr. 124*, 2451– 2457.
55. Parthasarathy, S., Barnett, J., and Fong, L.G. (1990) High-Density Lipoprotein Inhibits the Oxidative Modification of Low-Density Lipoprotein, *Biochim. Biophys. Acta 1044*, 275–283.
56. Watson, A.D., Berliner, J.A., Hama, S.Y., La Du, B.N., Faull, K.F., Fogelman, A.M., and Navab, M. (1995) Protective Effect of High Density Lipoprotein Associated Paraoxonase—Inhibition of the Biological Activity of Minimally Oxidized Low Density Lipoprotein, *J. Clin. Invest. 96*, 2882–2891.
57. Singh, K., Chander, R., and Kapoor, N.K. (1997) High Density Lipoprotein Subclasses Inhibit Low Density Lipoprotein Oxidation, *Indian J. Biochem. Biophys. 34*, 313–318.

[Received September 15, 1999, and in final revised form July 6, 2000; revision accepted August 7, 2000]

The Effect of Low α-Linolenic Acid Diet on Glycerophospholipid Molecular Species in Guinea Pig Brain

J.-P. Kurvinen[a,b], A. Kuksis[a], A.J. Sinclair[c,*], L. Abedin[c], and H. Kallio[b]

[a]Banting and Best Department of Medical Research, University of Toronto, Toronto, Ontario M5G 1L6, Canada, [b]Department of Biochemistry and Food Chemistry, University of Turku, FIN-20014 Turku, Finland, and [c]The Royal Melbourne Institute of Technology University, Melbourne Victoria 3001, Australia

ABSTRACT: The changes in guinea pig brain (cerebrum) glycerophospholipid molecular species resulting from a low α-linolenic acid (ALA) diet are described. Two groups of six guinea pigs were raised from birth to 16 wk of age on either an n-3 deficient diet containing 0.01 g ALA/100 g diet or n-3 sufficient diet containing 0.71 g ALA/100 g diet. Molecular species of diradyl glycerophosphoethanolamine (GroPEtn), glycerophosphocholine, glycerophosphoserine, and glycerophosphoinositol were analyzed by high-performance liquid chromatography with on-line electrospray ionization mass spectrometry (HPLC/ESI/MS). Alkenylacyl GroPEtn species were determined by comparing spectra before and after mild acid treatment while diacyl- and alkylacyl species were distinguished by HPLC/ESI/MS. The proportions of phospholipid classes and of the diradyl GroPEtn subclasses were not altered by diet changes. The main polyunsaturated molecular species of diradyl GroPEtn subclasses and of phosphatidylcholine and phosphatidylserine (PtdSer) contained 16:0, 18:0, or 18:1 in combination with docosahexaenoic acid (DHA, 22:6n-3), docosapentaenoic (DPA, 22:5n-6), or arachidonic acid (ARA, 20:4n-6). A significant proportion of DPA containing species were present in both diet groups, but in n-3 fatty acid deficiency, the proportion of DPA increased and DHA was primarily replaced by DPA. The combined value of main DHA and DPA containing species in the n-3 deficient group ranged from 91–111% when compared with the n-3 sufficient group, indicating a nearly quantitative replacement. The n-3 fatty acid deficiency did not lower the content of ARA containing molecular species of PtdSer of the guinea pig brain as reported previously for the rat brain. The molecular species of phosphatidylinositol were not altered by n-3 fatty acid deficiency. The present data show that the main consequence of a low ALA diet is the preferential replacement of DHA-containing molecular species by DPA-containing molecular species in alkenylacyl- and diacyl GroPEtn and PtdSer of guinea pig brain.

Paper no. L8448 in Lipids 35, 1001–1009 (September 2000).

Previous studies have shown (1–4) that a low n-3 polyunsaturated fatty acid (PUFA) content in an infant diet may lead to disorders in visual and cognitive development, but the biochemical basis for this observation has remained obscure. Decreasing α-linolenic acid (ALA) content in formula led to a reduced proportion of docosahexaenoic acid (DHA) in phospholipids, while the level of docosapentaenoic acid (DPA) was increased (5). These changes in infant brain or other tissues are not easily investigated. However, there are some post mortem studies that show a reduced DHA level in the brain of formula fed infants when compared with breast-fed infants (6–8). In animal studies (9,10), n-3 fatty acid deficiency strongly reduces the proportion of DHA and increases that of DPA in the nervous system. In the rat, n-3 deficiency has been reported (11) to reduce the total PUFA content of brain phosphatidylserine (PtdSer), and DHA has been suggested to be a modulator of brain PtdSer biosynthesis. A basic strategy for investigating the role of brain DHA in neurological functions has been to manipulate tissue levels of DHA and evaluate appropriate functional endpoints (12–14). It has been shown that an artificial rearing method with a low n-3 fat diet can produce rats with brain DHA reduced by 50% in the first generation and more than 90% in the second generation (15). Reductions of even more than this were achieved in three generations of guinea pigs reared normally (16). Most previous studies have been based on analyses of the total fatty acid content of different phospholipid classes, which may conceal specific effects upon individual molecular species that may be important in overall membrane function. Therefore, the present study describes the changes in glycerophospholipid molecular species of guinea pig brain (cerebrum) caused by low dietary ALA content.

MATERIALS AND METHODS

Materials. All solvents were high-peformance liquid chromatography (HPLC) or reagent grade and were purchased from

*To whom correspondence should be addressed at The Royal Melbourne Institute of Technology University, GPO Box 2476V, Melbourne Victoria 3001, Australia. E-mail: andrew.sinclair@rmit.edu.au

Abbreviations: a, alkylacyl; ACN, acyl carbon number; ALA, α-linolenic acid (18:3n-3); ARA, arachidonic acid (20:4n-6); CL, cardiolipin; DB, double bond; DHA, docosahexaenoic acid (22:6n-3); DPA, docosapentaenoic acid (22:5n-6); GroPCho, glycerophosphocholine; GroPEtn, glycerophosphoethanolamine; GroPIns, glycerophosphoinositol; GroPSer, glycerophosphoserine; HPLC, high-performance liquid chromatography; HPLC/ESI/MS, high-performance liquid chromatography/electrospray ionization/mass spectrometry; p, alkenylacyl; PtdCho, phosphatidylcholine; PtdEtn, phosphatidylethanolamine; PtdIns, phosphatidylinositol; PtdSer, phosphatidylserine; PUFA, polyunsaturated fatty acid; TLC, thin-layer chromatography.

Caledon Chemicals (Toronto, Canada). All reagents used were of reagent grade or better quality. Sep-Pak®-silica cartridges were purchased from Waters Corporation (Milford, MA). Lipid standards: bovine brain galactocerebrosides (type I and type II), bovine brain galactocerebroside sulfate, bovine heart cardiolipin, 1,2-dimyristoyl-*sn*-glycero-3-phosphocholine, 1,2-dimyristoyl-*sn*-glycero-3-phosphoethanolamine, 1,2-palmitoyl-*sn*-glycero-3-phosphocholine, 1,2-dipalmitoyl-*sn*-glycero-3-phosphoethanolamine, 1,2-dipalmitoyl-*sn*-glycero-3-phosphoserine, bovine brain sphingomyelin, and bovine liver phosphatidyl inositol were purchased from Sigma Chemical Co. (St. Louis, MO).

Animals and diets. Two groups of six pigmented female guinea pigs (English short hair), raised from mothers maintained on two different diets for the last one-third of pregnancy, were fed from birth to 16 wk of age. The diets, fed to guinea pigs *ad libitum,* differed in fatty acid composition, providing an n-3 fatty acid sufficient diet group and n-3 deficient diet group (Table 1). The lipid content of both diets was 10% (w/w) and the triacylglycerols in the diets contained n-6 fatty acids and n-3 fatty acids, entirely in the form of linoleic acid (18:2n-6) and ALA (18:3n-3), respectively. The proportion of linoleic acid in both diets was 16% of the total fatty acids, while that of ALA was 7.1% in the sufficient diet and 0.1% in the deficient diet. DHA or arachidonic acid (ARA) were not present in either of the diets.

Sample preparation. At the end of the feeding period, animals were sacrificed using CO_2 asphyxiation. The brain was removed, washed in saline and the cerebrum was divided into halves along the midline. Lipids from one half of the homogenized cerebrum were extracted overnight in chloroform/methanol (2:1, vol/vol) containing 10 mg/mL butylated hydroxytoluene as an antioxidant using 50 mL of solvent per gram of brain. The extraction mixture was filtered and filtrate washed with saline (20% of filtrate volume). After phase separation, the organic phase was evaporated under vacuum. Oil residue was redissolved in chloroform and evaporation was repeated to remove any remaining water. The final residue was stored in chloroform solution.

TABLE 1
Fatty Acid Composition of n-3 Fatty Acid Sufficient Diet and n-3 Fatty Acid Deficient Diet Fed to Two Groups of Six Guinea Pigs[a]

Fatty acid	n-3 Sufficient diet	n-3 Deficient diet
8:0	1.9	6.1
10:0	1.6	5.0
12:0	11.5	36.4
14:0	4.6	14.0
16:0	6.1	8.9
16:1	0.2	0.1
18:0	4.6	8.9
18:1	42.7	3.1
18:2n-6	16.1	16.2
18:3n-3	7.1	0.1
18:2/18:3	2.3/1	161/1

[a]Results expressed as % of total fatty acids.

Separation of phospholipid classes. To avoid coelution of glycolipids with phospholipids, brain total lipid extracts were fractionated into neutral lipids, glycolipids, and phospholipids by normal phase silica gel column chromatography prior to phospholipid class separation by thin-layer chromatography (TLC). Approximately 15 mg of brain total lipid extract was loaded into a commercial Sep-Pak® cartridge and lipid classes were separated by step-wise elution. Neutral lipids were eluted with 10 mL $CHCl_3$ containing 1% acetic acid to facilitate the elution of free fatty acids. Glycolipids were then eluted by 20 mL acetone/methanol (14:1, vol/vol), followed by elution of phospholipids by 10 mL methanol. The elution system was developed by testing with lipid standards and the purity of brain lipid fractions obtained was checked by HPLC/electrospray ionization/mass spectrometry (HPLC/ESI/MS) method. Phospholipid classes were separated by TLC using boric acid impregnated silica gel G plates prepared in the laboratory. A slurry of silica gel (0.5 g/mL) was prepared in 2.4% (wt/vol) boric acid solution and a layer of 250 µm spread on 20 × 20 cm glass plates. Before use, the plates were air dried and activated at 120°C for 1 h. Plates were developed in a solvent system consisting of chloroform/ethanol/water/triethylamine (30:35:6:35, by vol) (17). Lipid bands were visualized by spraying with 0.1% 2′7′-dichlorofluorescein in ethanol and phospholipids were extracted with chloroform/methanol (2:1, vol/vol) followed by removal of staining reagent by 2% $KHCO_3$ (wt/vol).

Fatty acid analysis. Phospholipid fractions, obtained by TLC separation, were transmethylated using 6% sulfuric acid in methanol for 2 h at 80°C. Fatty acid methyl esters of each phospholipid class were analyzed by a HP 5880 (Hewlett-Packard, Palo Alto, CA) gas–liquid chromatograph equipped with SP-2380 column (15 m × 0.25 mm i.d., 0.20 µm film thickness) and a flame-ionization detector. Column oven temperature was set to rise after 0.5 min from 100 to 130°C (20°C/min) and from 130 to 240°C (5°C/min). Transmethylated fatty acids were identified by comparing retention times with known fatty acid methyl esters used as external standards.

HPLC/ESI/MS apparatus. The HPLC/ESI/MS system consisted of a Hewlett-Packard 1090 liquid chromatograph connected to a Hewlett-Packard 5989A quadrupole mass spectrometer equipped with a nebulizer-assisted electrospray interface. Samples were introduced into the HPLC system by autoinjector and components were separated on a silica column (Supelcosil LC-Si, 5 µm, 250 mm × 4.6 mm i.d.; Supelco Inc., Bellefonte, PA). The solvent system consisted of solvent mixtures A (chloroform/methanol/30% ammonium hydroxide, 80:19.5:0.5, by vol) and B (chloroform/methanol/water/30% ammonium hydroxide, 60:34:5.5:0.5, by vol) (18). The column was eluted at 1 mL/min with a linear gradient starting with 100% solvent A and changing to 100% solvent B in 14 min after holding the starting composition for 3 min. The final composition was held for 10 min. HPLC effluent was split 1:50 using a commercial splitter (LC Packings) to deliver suitable flow to the electrospray interface. Full scan mass

spectra ranging from *m/z* 400–1300 were collected in negative and positive ionization mode.

Analysis of phospholipid molecular species. Molecular species of diradyl glycerophosphoethanolamine (GroPEtn), glycerophosphocholine (GroPCho), glycerophosphoserine (GroPSer), and glycerophosphoinositol (GroPIns) were analyzed by injecting approximately 8–10 μg of brain total lipid extract directly into the HPLC/ESI/MS system. GroPCho species were analyzed in positive ionization mode while other species were analyzed in negative ion mode. Phosphatidylcholine (PtdCho), phosphatidylserine (PtdSer), and phosphatidylinositol (PtdIns) were distinguished directly by HPLC/ESI/MS according to chromatographic retention times of phospholipid classes and molecular weights of individual molecular species. Alkenylacyl, diacyl, and alkylacyl subclasses of GroPEtn were determined by analyzing samples before and after mild acid treatment performed to hydrolyze the vinyl ether bond of alkenylacyl species. Alkenylacyl species could then be calculated by subtracting spectra derived from the samples after acid treatment from spectra obtained before acid treatment. Diacyl and alkylacyl species of GroPEtn were distinguished using spectra derived from the acid treated sample. To hydrolyze alkenylacyl GroPEtn species, an aliquot of total lipid extract was dried down and treated with 200 μL of 2 M methanolic HCl for 30 min at room temperature (19,20). After the acid treatment, the sample was dried down and reconstituted in HPLC solvent A for analysis. 1,2-dimyristoyl-*sn*-glycero-3-phosphoethanolamine (25 μg/mL) and 1,2-dimyristoyl-*sn*-glycero-3-phosphocholine (25 μg/mL), which were not present in brain lipid extracts, were added to samples as internal standards prior to analysis. An average of three analyses of each sample was used to calculate the results. The relative responses for analyzed phospholipid classes in negative ionization mode were determined by co-injecting known concentrations of phospholipid standards into HPLC/ESI/MS system, and response factors were calculated relative to GroPEtn.

Statistical analyses. Significant differences in fatty acid composition and phospholipid molecular species composition between dietary groups were tested using a one-way analysis of variance with a significance level of 0.05 (*P*-values).

RESULTS

Fatty acid composition. The PUFA composition of different phospholipid classes of guinea pig brain (cerebrum) is presented in Table 2. The proportion of PUFA varied from 7.8 to 39.3% as a percentage of total fatty acids in phospholipids depending on phospholipid class, with the most polyunsaturated classes being diradyl GroPEtn and PtdIns. The proportion remained constant regardless of diet in all brain phospholipid classes ($P > 0.05$). There were clearly significant differences between diet groups in proportions of DHA and DPA in all phospholipid classes. The minor differences in some other PUFA also existed with significance level of 0.05 as indicated in Table 2. In all cases, the percentage of DPA in the n-3 fatty acid deficient group equaled approximately the corresponding percentage of DHA in the n-3 fatty acid sufficient group, indicating a nearly quantitative replacement of DHA by DPA. Conversely, the proportion of DHA in the n-3 fatty acid deficient group was lower than that of DPA in the n-3 sufficient group. In phosphatidylethanolamine (PtdEtn), PtdCho, PtdSer, and PtdIns the combined values of percentages of DHA and DPA in the n-3 fatty acid sufficient group were 13.8, 1.9, 14.2, and 1.6% (percentage of total fatty acids), respectively. The corresponding values in the n-3 fatty acid deficient group were 11.0, 1.5, 12.0, and 1.1%, respectively, indicating that the combined value of these fatty acids remained nearly constant regardless of the n-3 fatty acid deficiency.

Analysis of phospholipid molecular species. Phospholipid classes were clearly resolved by the HPLC system used. Neutral lipids eluted at the beginning of the run and gave a very weak response in negative ionization mode. In the negative ion mode, glycolipids followed by cardiolipin, were seen to elute between 5 and 10 min, after which the acidic phospholipids were eluted in the order of PtdEtn, PtdIns, and PtdSer (Fig. 1A). In the positive ionization mode, PtdCho was seen to elute in 15–17 min, clearly resolved from sphingomyelin eluting in 18.5–19.5 min and lysoPtdCho in 23–25 min. PtdEtn gave a weak response in positive ionization mode, but was well separated from PtdCho in retention time. PtdCho and sphingomyelin were not detected in negative ionization mode even as the chloride adducts $[M + 35]^-$. In negative ionization mode, the response factors for PtdSer and PtdIns relative to PtdEtn were determined by co-injecting known concentrations of each phospholipid class standard compounds. PtdSer and PtdIns were detected with higher sensitivity than PtdEtn and the correction factors were 0.35 and 0.42 relative to PtdEtn, respectively. By using internal standards in positive and negative ionization mode and correction factors in negative ionization mode, the relative proportions of phospholipid classes in brain lipid extracts were calculated. The distribution of phospholipids between different phospholipid classes was not affected by diet changes as indicated in Table 3. The relative proportions of diradyl GroPEtn subclasses were also unaffected by diet changes (Table 3). An example of mass spectra averaged over diradyl GroPEtn peak in total lipid extract and in acid hydrolyzed total lipid extract is given in Figure 2. These spectra demonstrate the hydrolysis of the vinyl ether bond of alkenylacyl GroPEtn in acid treatment. The peak at *m/z* 774 in Figure 2A represents alkenylacyl GroPEtn 40:6p [acyl carbon number (ACN):double bond (DB)]. In spectrum derived from the acid treated sample (Fig. 2B), there is no peak at a corresponding *m/z* value indicating the total hydrolysis of the vinyl ether bond. The highest intensity peak at *m/z* 750 in Figure 2A represents 38:4 alkenylacyl GroPEtn (38:4p) and 38:5 alkylacyl GroPEtn (38:5a) in total lipid extract. After acid hydrolysis, the low intensity peak at *m/z* 750 represents alkylacyl GroPEtn (38:5a), which remains intact during acid treatment. The main diacyl GroPEtn species 40:6, 38:4, 40:5, and 40:4 at *m/z* values 790, 766, 792, and 794, respectively, are also

TABLE 2
Polyunsaturated Fatty Acid Composition of Cerebrum Glycerophospholipid Classes from Guinea Pigs Fed Either with n-3 Fatty Acid Sufficient Diet or with n-3 Fatty Acid Deficient Diet[a]

	PtdEtn		PtdCho	
Fatty acid	n-3 Sufficient diet	n-3 Deficient diet	n-3 Sufficient diet	n-3 Deficient diet
n-6 PUFA				
18:2n-6	0.7 ± 0.05	1.3 ± 0.1	1.2 ± 0.08[a]	3.1 ± 0.1[b]
20:2n-6	0.3 ± 0.03	0.5 ± 0.07	0.2 ± 0.02	0.5 ± 0.07
20:3n-6	1.2 ± 0.03	1.0 ± 0.09	0.3 ± 0.01[a]	0.5 ± 0.08[b]
20:4n-6	16.0 ± 0.7	14.8 ± 0.4	3.4 ± 0.2	3.1 ± 0.5
22:4n-6	6.0 ± 0.6	5.5 ± 0.9	0.8 ± 0.03	0.8 ± 0.03
22:5n-6	4.7 ± 1.1[a]	9.5 ± 2.4[b]	0.6 ± 0.06[a]	1.3 ± 0.03[b]
n-3 PUFA				
22:5n-3	0.5 ± 0.05	ND	ND	ND
22:6n-3	9.1 ± 0.5[a]	1.5 ± 0.5[b]	1.3 ± 0.2[a]	0.2 ± 0.06[b]
Total	38.5 ± 3.1	34.1 ± 4.6	7.8 ± 0.6	9.5 ± 0.9

	PtdSer		PtdIns	
Fatty acid	n-3 Sufficient diet	n-3 Deficient diet	n-3 Sufficient diet	n-3 Deficient diet
n-6 PUFA				
18:2n-6	0.3 ± 0.2	0.8 ± 0.3	0.4 ± 0.3[a]	1.3 ± 0.2[b]
20:2n-6	ND	ND	ND	ND
20:3n-6	1.2 ± 0.1[a]	1.7 ± 0.1[b]	0.6 ± 0.06	0.7 ± 0.01
20:4n-6	4.3 ± 0.8	6.2 ± 1.6	35.0 ± 4.3	29.7 ± 2.7
22:4n-6	3.0 ± 0.8[a]	5.1 ± 1.0[b]	1.7 ± 0.7	1.0 ± 0.2
22:5n-6	4.7 ± 1.6[a]	10.3 ± 0.3[b]	0.5 ± 0.1[a]	1.0 ± 0.08[b]
n-3 PUFA				
22:5n-3	0.2 ± 0.2	0.3 ± 0.1	ND	ND
22:6n-3	9.5 ± 2.0[a]	1.7 ± 0.3[b]	1.1 ± 0.1[a]	0.1 ± 0.05[b]
Total	23.2 ± 5.7	26.1 ± 3.7	39.3 ± 5.6	33.8 ± 3.2

[a]Results expressed as mol% of total fatty acids in each phospholipid class, mean ± SD ($n = 6$). Different superscript roman letters indicate significant differences between diet groups ($P < 0.05$). PtdCho, phosphatidylcholine; PtdEtn, phosphatidylethanolamine; PtdIns, phosphatidylinositol; PtdSer, phosphatidylserine; PUFA, polyunsaturated fatty acid.

unaffected by acid hydrolysis as shown in Figure 2. In total lipid extract, alkylacyl and alkenylacyl species of GroPEtn with different degrees of unsaturation exist at the same *m/z* value. The alkylacyl and diacyl GroPEtn remaining after acid hydrolysis can be distinguished by differences in the *m/z* values. The acid hydrolysis together with use of internal standard, thus, enables the complete separation of diradyl GroPEtn species with minimal sample preparation. 1-lyso-*sn*-GroPEtn species formed during acid hydrolysis partly coeluted with PtdSer (Fig. 1B), but were easily distinguished according to molecular weight. Figure 1C shows the spectrum averaged over the lysoGroPEtn peak in Figure 1B, showing the lysoGroPEtn species containing PUFA in the *sn*-2 position. In the spectrum, ARA is the most abundant PUFA in the *sn*-2 position of alkenylacyl GroPEtn molecular species, which is in accordance with ARA being the most abundant PUFA in the diradyl GroPEtn molecular species (Table 2).

Phospholipid molecular species in brain. A low ALA diet affected mainly the polyunsaturated GroPEtn and GroPSer molecular species. Although GroPCho was an abundant phospholipid class (Table 3), it was not affected as strongly as GroPEtn and GroPSer since it had a smaller proportion of polyunsaturated molecular species (Tables 4 and 5). GroPIns molecular species were not affected by n-3 fatty acid deficiency (Table 5).

Table 4 lists the polyunsaturated molecular species of diradyl GroPEtn containing at least four DB in the n-3 fatty acid

TABLE 3
Composition of Cerebrum Phospholipids from Guinea Pigs Fed Either with n-3 Fatty Acid Sufficient Diet or with n-3 Fatty Acid Deficient Diet[a]

Phospholipid class	n-3 Sufficient diet	n-3 Deficient diet
PtdCho	36.2 ± 3.2	38.8 ± 6.4
PtdSer	8.5 ± 0.5	8.1 ± 1.2
PtdIns	6.6 ± 0.8	6.4 ± 0.7
Diradyl GroPEtn total	48.6 ± 2.5	46.8 ± 4.6
Alkenylacyl GroPEtn	31.8 ± 7.0	29.3 ± 7.9
Diacyl GroPEtn	15.6 ± 6.7	16.3 ± 7.5
Alkylacyl GroPEtn	1.2 ± 0.5	1.1 ± 0.6

[a]Results expressed as weight % of total phospholipid, mean of ± SD ($n = 6$). GroPEtn, glycerophosphoethanolamine. For other abbreviations see Table 2.

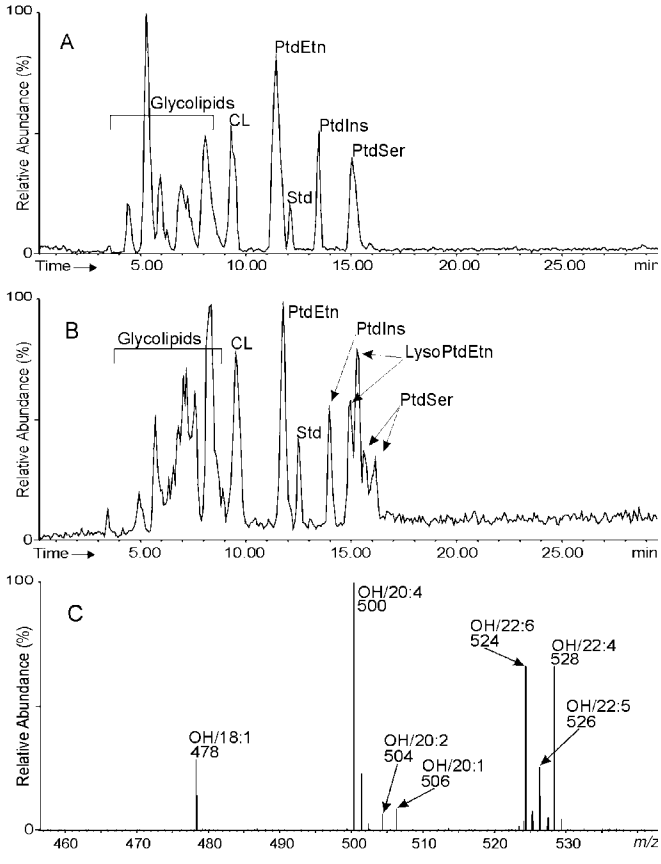

FIG. 1. High-performance liquid chromatography/electrospray ionization/mass spectrometry (HPLC/ESI/MS) analysis of guinea pig brain phospholipids. (A) Total negative ion chromatogram of brain total lipid extract showing the separation of glycolipids and cardiolipin from phospholipids and elution order of separated glycerophospholipid classes. (B) Total negative ion chromatogram of acid hydrolyzed brain total lipid extract demonstrating the appearance of *sn*-1-lysoPtdEtn species after HCl-hydrolysis of alkenylacyl GroPEtn species. (C) Mass spectrum averaged over lysoPtdEtn peak in Figure 1B showing lysoPtdEtn species containing unsaturated fatty acids in *sn*-2 position. The major species are: OH/18:1, OH/20:4, OH/20:2, OH/20:1, OH/22:6, OH/22:5, and OH/22:4, respectively. See the Materials and Methods section for chromatographic conditions. Abbreviations: CL, cardiolipin; PtdEtn, phosphatidylethanolamine; PtdIns, phosphatidylinositol; PtdSer, phosphatidylserine; Std, internal standard.

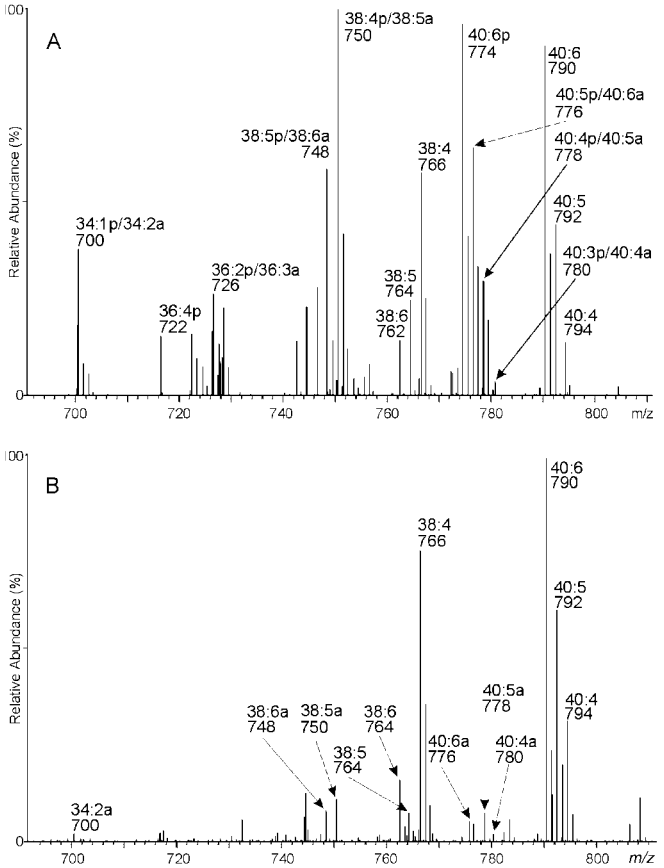

FIG. 2. Mass spectra of molecular species of diradyl GroPEtn in guinea pig brain extract as obtained by HPLC/ESI/MS analysis. (A) Mass spectrum of total diradyl GroPEtn species in the total lipid extract. (B) Mass spectrum of diradyl GroPEtn species in brain lipid extract after acid destruction of alkenylacyl GroPEtn species. The major species are: 34:2a, 16:0′-18:2; 34:1p/34:2a, 16:0″-18:1/16:0′-18:2; 36:4p, 16:0″-20:4; 36:2p/36:3a, 18:0″-18:2/18:1′-18:2; 38:5p/38:6a, 16:0″-22:5/16:0′-22:6; 38:4p/38:5a, 18:0″-20:4/16:0′-22:5; 38:6, 16:0-22:6; 38:5, 16:0-22:5; 38:4, 18:0-20:4; 40:6p, 18:0″-22:6; 40:5p/40:6a, 18:0″-22:5/18:0′-22:6; 40:4p/40:5a, 18:0″-22:4/18:0′-22:5; 40:3p/40:4a, 18:0″-22:3/18:0′-22:4; 40:6, 18:0-22:6; 40:5, 18:0-22:5; 40:4, 18:0-22:4. GroPEtn, glycerophosphoethanolamine. See Figure 1 for other abbreviations.

sufficient and n-3 deficient diet groups. The fatty acid combinations for each ACN:DB class are listed in the decreasing order of probability on the basis of fatty acid composition of phospholipid classes (Table 2). The total proportion of these polyunsaturated molecular species varied from 67.3 to 84.8% (mol% of total molecular species) in diradyl GroPEtn species and remained constant regardless of diet differences. Table 5 shows the corresponding species of diacyl GroPCho, GroPSer, and GroPIns. The combined proportion of polyunsaturated species was also unaffected by diet treatment in these phospholipid classes. The PtdCho contained less polyunsaturated molecular species than other phospholipid classes, while PtdIns consisted almost entirely of molecular species with four or more DB in esterified fatty acid chains (Table 5). The effect of n-3 fatty acid deficiency on molecular species of GroPIns was not detected, although a significant difference in proportions of DHA and DPA fatty acids between diet groups was observed (Table 2). In the alkylacyl GroPEtn subclass, the only significant differences observed were the decreases in 38:6 and 40:6 (ACN:DB) and increases in 40:4 species by n-3 fatty acid deficiency (Table 4). Despite relatively high deviation, it may be concluded that, unlike in other diradyl GroPEtn subclasses, DHA containing species are mainly replaced by 22:4n-6 containing species in alkylacyl-GroPEtn. In all other phospholipid classes, the proportion of DHA containing species was always decreased on the n-3 fatty acid deficient diet, while the proportion of DPA containing species was increased (Tables 4 and 5). A significant proportion of DPA containing molecular species was also present in brains of n-3 sufficient diet group animals, but the

TABLE 4
Polyunsaturated Molecular Species of Cerebrum Diacyl, Alkenylacyl, and Alkylacyl GroPEtn from Guinea Pigs Fed with n-3 Fatty Acid Sufficient Diet or with n-3 Fatty Acid Deficient Diet[a]

		Phospholipid class					
		Diacyl GroPEtn		Alkenylacyl GroPEtn		Alkylacyl GroPEtn	
ACN/DB	Molecular species[b]	n-3 Sufficient diet	n-3 Deficient diet	n-3 Sufficient diet	n-3 Deficient diet	n-3 Sufficient diet	n-3 Deficient diet
36:4	16:0/20:4n-6 18:2/18:2 16:1/20:3n-6	1.7 ± 0.9	2.7 ± 0.6	4.4 ± 1.0	5.2 ± 1.4	ND	ND
38:7	16:1/22:6n-3	ND	ND	1.4 ± 1.4	0.3 ± 0.4	ND	ND
38:6	16:0/22:6n-3 18:2/20:4n-6 16:1/22:5n-6	5.3 ± 0.4[a]	1.2 ± 0.4[b]	5.1 ± 1.4[a]	0.6 ± 0.5[b]	10.4 ± 6.0[a]	2.2 ± 1.9[b]
38:5	16:0/22:5n-6 18:1/20:4n-6 18:2/20:3n-6	5.3 ± 2.7[a]	10.4 ± 0.7[b]	10.1 ± 1.1[a]	14.7 ± 1.2[b]	16.3 ± 6.8	15.4 ± 6.7
38:4	18:0/20:4n-6 16:0/22:4n-6 18:1/20:3n-6 18:2/20:2n-6	21.5 ± 2.8	24.6 ± 3.3	16.9 ± 2.2	19.1 ± 1.5	12.6 ± 8.4	16.8 ± 5.6
40:7	18:1/22:6n-3 18:2/22:5n-6	2.0 ± 1.0[a]	0.6 ± 0.4[b]	2.0 ± 0.9[a]	0.2 ± 0.2[b]	ND	ND
40:6	18:0/22:6n-3 18:1/22:5n-6 18:2/22:4n-6	26.4 ± 5.0[a]	7.1 ± 0.9[b]	14.8 ± 1.0[a]	5.3 ± 1.8[b]	15.1 ± 5.8[a]	6.6 ± 2.8[b]
40:5	18:0/22:5n-6 18:1/22:4n-6	13.7 ± 2.5[a]	32.0 ± 1.9[b]	9.2 ± 1.1[a]	19.0 ± 1.1[b]	13.8 ± 4.8	17.8 ± 4.3
40:4	18:0/22:4n-6	6.8 ± 1.9	6.2 ± 3.5	6.2 ± 2.0[a]	8.9 ± 1.5[b]	1.8 ± 3.4[a]	8.5 ± 4.9[b]
	Total	82.7 ± 17.2	84.8 ± 11.7	70.1 ± 12.1	73.3 ± 9.6	70.0 ± 35.2	67.3 ± 26.2

[a]Results expressed as mol% of total molecular species in each phospholipid class, mean ± SD (n = 6). Different superscript roman letters indicate significant differences between diet groups ($P < 0.05$).
[b]Fatty acid combinations listed in the order of decreasing probability according to fatty acid composition of phospholipid classes. ACN, acyl carbon number; DB, double bond. See Table 3 for other abbreivation.

level was further increased by a factor of approximately two in n-3 deficiency (Tables 4 and 5). In addition to alkylacyl GroPEtn, an increase in 18:0/22:4n-6 species was also observed in alkenylacyl GroPEtn and in PtdCho and PtdSer. In all cases there were more DPA containing species in the n-3 fatty acid deficient diet group than corresponding DHA containing species in the n-3 sufficient group. Conversely, the proportion of DPA containing molecular species in the n-3 sufficient group always exceeded the corresponding proportion of DHA containing species in the n-3 fatty acid deficient diet group. The combined proportion of molecular species containing DHA or DPA, calculated separately for 38 and 40 acyl carbons, containing species in the n-3 fatty acid sufficient group ranged from 91 to 111% when compared with the corresponding value in the n-3 deficient group (Tables 4 and 5). The result indicates a nearly quantitative replacement of DHA containing species by DPA species. There were no significant differences in proportions of main ARA containing species between diet groups in any phospholipid classes. These data suggest the main consequence of n-3 fatty acid deficiency to be the replacement of DHA fatty acid containing phospholipid molecular species by DPA containing species in guinea pig cerebrum.

DISCUSSION

Deficiency of n-3 fatty acids in infant nutrition has been shown to affect neurobehavioral development and visual acuity (2–4). However, studying the changes of lipid composition in the human nervous system is restricted to post mortem studies (6–8). Therefore, studying these changes is most easily conducted using animal models. Rhesus monkeys, deprived of 18:3n-3 during development, have lower than normal neural accumulation of DHA (21,22). If fed 18:2n-6,

TABLE 5
Polyunsaturated Molecular Species of PtdCho, PtdSer, and PtdIns from the Cerebrum of Guinea Pigs Fed With n-3 Fatty Acid Sufficient or n-3 Fatty Acid Deficient Diet[a]

		Phospholipid class					
		PtdCho		PtdSer		PtdIns	
ACN/DB	Molecular species[b]	n-3 Sufficient diet	n-3 Deficient diet	n-3 Sufficient diet	n-3 Deficient diet	n-3 Sufficient diet	n-3 Deficient diet
36:4	16:0/20:4n-6 18:2/18:2 16:1/20:3n-6	6.7 ± 0.4	7.6 ± 0.6	ND	ND	9.5 ± 1.7	11.7 ± 2.2
38:6	16:0/22:6n-3 18:2/20:4n-6 16:1/22:5n-6	3.9 ± 0.5[a]	0.9 ± 0.3[b]	0.3 ± 0.3	ND	0.2 ± 0.4	0.4 ± 0.4
38:5	16:0/22:5n-6 18:1/20:4n-6 18:2/20:3n-6	4.2 ± 0.5[a]	6.4 ± 0.2[b]	1.7 ± 1.6	2.0 ± 2.1	9.8 ± 1.5	10.2 ± 3.3
38:4	18:0/20:4n-6 16:0/22:4n-6 18:1/20:3n-6 18:2/20:2n-6	7.8 ± 0.9	7.2 ± 0.5	4.2 ± 1.4	5.3 ± 1.0	76.7 ± 2.4	76.6 ± 3.9
40:7	18:1/22:6n-3 18:2/22:5n-6	2.0 ± 0.4[a]	0.6 ± 0.1[b]	ND	ND	ND	ND
40:6	18:0/22:6n-3 18:1/22:5n-6 18:2/22:4n-6	5.7 ± 0.6[a]	2.6 ± 0.6[b]	36.9 ± 6.4[a]	8.8 ± 1.6[b]	ND	ND
40:5	18:0/22:5n-6 18:1/22:4n-6	3.3 ± 0.6[a]	5.2 ± 0.3[b]	20.8 ± 5.1[a]	46.1 ± 6.8[b]	ND	ND
40:4	18:0/22:4n-6	1.6 ± 0.3[a]	2.5 ± 0.5[b]	7.9 ± 0.7[a]	12.4 ± 2.5[b]	ND	ND
	Total	35.2 ± 4.2	33.0 ± 3.1	71.8 ± 15.5	74.6 ± 14.0	96.2 ± 4.3	98.9 ± 7.6

[a]Results expressed as mol% of total molecular species in each phospholipid class, mean ± SD (n = 6). Different superscript roman letters indicate significant differences between diet groups ($P < 0.05$).
[b]Fatty acid combinations listed in the order of decreasing probability according to fatty acid composition of phospholipid classes. ACN, acyl carbon number; DB, double bond. For other abbreviations see Table 2.

neural DHA is replaced by DPA (21,22). The n-3 deficient animals are physically healthy and grow normally in contrast to n-6 deficient animals, but they have lower visual development, higher reactivity, and longer look duration compared with monkeys fed n-3 fatty acids (21,22). Attempts to deplete mammals, such as rats and monkeys, of retinal n-3 fatty acids by dietary manipulation (chow-feeding), however, have led to limited success (23,24). Since the guinea pig is the only mammal studied that can be almost completely depleted of retinal DHA by dietary manipulation, it has been suggested (16) that it metabolizes n-3 fatty acids differently from rats and monkeys. Thus, optimal retinal function was achieved in the guinea pig where the retinal DHA level was even lower than that of rats and monkeys raised on n-3 deficient diets. In the present study, therefore, we analyzed molecular species of the glycerophospholipids of brains (cerebrum) of guinea pigs maintained either on an n-3 fatty acid sufficient or an n-3 deficient diet. The complete analysis of molecular species of all glycerophospholipid classes and diradyl GroPEtn subclasses and to fatty acid analyses were performed to monitor the changes in proportions of phospholipid classes and molecular species.

The molecular species composition of the phospholipids of a developing guinea pig brain has been reported by Burdge and Postle (25). Only the choline and ethanolamine glycerophospholipids were examined. The results obtained in the later gestational stages (40 and 68 d) for the molecular species of these phospholipids were not unlike those just described for the mature guinea pig brain on the n-3 sufficient diet. The present study confirms our previous finding (26,27) that in n-3 deficiency, 22:6n-3 is primarily replaced by 22:5n-6. The replacement of DHA containing phospholipid molecular species took place similarly in the diradyl GroPEtn and in PtdCho and PtdSer. In contrast, the ARA rich PtdIns and ARA containing molecular species of other glycerophospholipids were not affected. The present data obtained for the

phospholipid molecular species of whole brain (cerebellum) of guinea pig differ from the data obtained for rat brain microsomes (11). This does not necessarily imply that rat brain responds to n-3 fatty acid deficiency differently than guinea pig brain, as it is well established that fatty acid composition of various subcellular lipid fractions within the same species may differ. Garcia *et al*. (11) studied rat brain microsomes, where the major arachidonoyl species (18:0/20:4n-6 GroPSer) decreased while the minor arachidonoyl species (16:0/20:4n-6 GroPSer) remained unaffected. In the diacyl GroPEtn, the major arachidonic acid-containing species (16:0/20:4n-6 and 18:0/20:4n-6) remained unchanged, while the minor species (18:1/20:4n-6 GroPEtn) was increased fourfold. The various diradyl GroPEtn subclassses responded to the n-3 deficiency in a similar manner as also noted by Zhang *et al*. (28), who examined the pineal phospholipids of the rat brain. The ARA-containing PtdCho species remained unaffected by n-3 deficiency in our studies or in the studies reported by Garcia *et al.* (11), who did not examine the molecular species of the PtdIns of rat brain microsomes.

It has been concluded that the distribution of PtdEtn and PtdCho species between the monolayers of single lamellar vesicles is modulated by acyl chain composition as well as packing requirements of polar head groups of mixed phospholipids (29). The cooperativity of the phase transition of GroPCho bilayer decreased as unsaturation increased from 16:0/18:1 to 16:0/20:4 or to 16:0/22:6 GroPCho (30). The effect of acyl chain packing in the PtdCho bilayer on the equilibrium concentration of metarhodopsin II in a reconstituted system consisting of different diacyl GroPCho bilayers has also been studied (31). The results indicated that an increasing degree of unsaturation in the *sn*-2 position of PtdCho leads to a more permissive bilayer with better capability to accommodate expanded protein in the metarhodopsin II state (31). In a similar study, a difference between 16:0/22:6 and 16:0/20:4 GroPCho vesicles was observed in respect of metarhodopsin II formation (32). In the present study, the DHA in the *sn*-2 position of phospholipid molecular species in guinea pig brain was mainly replaced by DPA as an aftermath of the n-3 fatty acid deficient diet. Based on the above discussion, it may be postulated that changes in phospholipid molecular species caused by n-3 fatty acid deficiency may have an effect on those reactions in the brain that are dependent on interaction between cell membrane and integral membrane proteins.

The biosynthesis of PtdSer in mammalian cells takes place primarily through the serine base exchange reaction (33). The serine exchange enzyme catalyzes the calcium-dependent, energy-independent incorporation of L-serine in exchange for a choline or ethanolamine headgroup. The serine base exchange enzyme is located in the endoplasmic reticulum, mainly from where the freshly synthesized PtdSer is transferred to mitochondria where it can be decarboxylated to PtdEtn (34). PtdEtn may be further converted to PtdCho by stepwise methylation (35,36). The serine base exchange enzyme of rat brain has been isolated and characterized (37) and several factors have been reported to regulate the synthesis of PtdSer in brain (38,39). Although we did not specifically investigate the effect of DHA on the synthesis of PtdSer in guinea pig cerebrum, we can nevertheless comment upon the potential conversion of PtdSer into PtdEtn. A comparison of the major molecular species of the PtdCho or PtdEtn with PtdSer would appear to exclude a direct precursor-product relationship, although a limited base exchange cannot be excluded. The high level of the 1-stearoyl-2-docosahexaenoyl (18:0/22:6n-3 GroPSer) molecular species in the brain may reflect preference for serine exchange enzyme for 22:6n-3 containing phospholipids. Any more significant base exchange would have to be accompanied or followed by a remodeling of the molecular species by acyl exchange.

In this study, the effect of a low ALA diet on glycerophospholipid molecular species in guinea pig brain was investigated. In conclusion, the study shows that a low ALA diet led to an extensive replacement of the DHA containing glycerophospholipid species by DPA containing molecular species in the guinea pig brain. Specifically, dietary deficiency of n-3 fatty acids mainly affected the molecular species of alkenylacyl and diacyl GroPEtn and PtdSer, while PtdCho was affected less and PtdIns remained unchanged. The proportions of the phospholipid classes and the subclasses of the ethanolamine containing phospholipids also remained unchanged. The selective replacement of DHA by DPA is unprecedented and requires further study.

ACKNOWLEDGMENTS

This research was supported by funds from The Academy of Finland, Helsinki, Finland; Jenny and Antti Wihuri Foundation, Helsinki, Finland; The Ontario Heart Foundation, Toronto, Ontario; The Medical Research Council of Canada, Ottawa, Ontario; The Grains Research and Development Corporation, Australia; and Meadow Lea Foods Ltd, Australia. Dr. Amir Ravandi and Dr. Jyrki Ågren are thanked for kind guidance and assistance in mass spectrometric and gas chromatographic analyses.

REFERENCES

1. Weisinger, H.S., Vingrys, A.J., Bui, B.V., and Sinclair, A.J. (1999) Effects of Dietary n-3 Fatty Acid Deficiency and Repletion in the Guinea Pig Retina, *Invest. Opthalmol. Vis. Sci. 40*, 327–338.
2. Carlson, S.E., and Neuringer, M. (1999) Polyunsaturated Fatty Acid Status and Neurodevelopment: A Summary and Critical Analysis of the Literature, *Lipids 34*, 171–178.
3. Jacobson, S.W. (1999) Assessment of Long-Chain Polyunsaturated Fatty Acid Nutritional Supplementation on Infant Neurobehavioral Development and Visual Acuity, *Lipids 34*, 151–160.
4. Willatts, P., Forsyth, J.S., Di Modugno, M.K., Varma, S., and Colvin, M. (1998) Effect of Long-Chain Polyunsaturated Fatty Acids in Infant Formula on Problem Solving at 10 Months of Age, *Lancet 352*, 688–691.
5. Jensen, C.L., Chen, H., Fraley, J.K., Anderson, R.E., and Heird, W.C. (1996) Biochemical Effects of Dietary Linoleic/α-Linolenic Acid Ratio in Term Infants, *Lipids 31,* 107–113.
6. Makrides, M., Neumann, M.A., Byard, R.W., Simmer, K., and Gibson, R.A. (1994) Fatty Acid Composition of Brain, Retina,

and Erythrocytes in Breast- and Formula-Fed Infant, *Am. J. Clin. Nutr. 60,*189–194.
7. Martinez, M. (1992) Tissue Levels of Polyunsaturated Fatty Acids During Early Human Development, *J. Pediatr. 120,* S129–S138.
8. Farquaharson, J., Jamieson, E.C., Abbasi, K.A., Patrick, W.J., Logan, R.W., and Cockburn, F. (1995) Effect of Diet on the Fatty Acid Composition of the Major Phospholipids of Infant Cerebral Cortex, *Arch. Dis. Child. 72,* 198–203.
9. Clandinin, M.T. (1999) Brain Development and Assessing the Supply of Polyunsaturated Fatty Acid, *Lipids 34*, 131–137.
10. Fernstrom, J.D. (1999) Effects of Dietary Polyunsaturated Fatty Acids on Neuronal Function, *Lipids 34*, 161–169.
11. Garcia, M.C., Ward, G., Ma, Y.-C., Salem, N., Jr., and Kim, H.-Y. (1998) Effect of Docosahexaenoic Acid on the Synthesis of Phosphatidyl Serine in Rat Brain Microsomes and C6 Glioma Cells, *J. Neurochem. 70*, 24–30.
12. Crawford, M.A., Doyle, W., Leaf, A., Leighfield, M., Ghebremeskel, K., and Phylactos, A. (1993) Nutrition and Neurodevelopmental Disorders, *Nutr. Health 9*, 81–97.
13. Salem, N., Jr., and Ward, G.R. (1993) Are Omega 3 Fatty Acids Essential Nutrients for Mammals?, *World Rev. Nutr. Diet 72*, 128–147.
14. Martinez, M. (1995) Polyunsaturated Fatty Acids in the Developing Human Brain, Erythrocytes and Plasma in Peroxisomal Disease: Therapeutic Implications*, J. Inherit. Metab. Dis. 18* (Suppl. 1), 61–75.
15. Ward, G., Woods, J., Reyzer, M., and Salem, N. Jr. (1996) Artificial Rearing of Infant Rats on Milk Formula Deficient in n-3 Essential Fatty Acids: A Rapid Method for the Production of Experimental n-3 Deficiency, *Lipids 31*, 71–77.
16. Weisinger, H.S., Vingrys, A.J., and Sinclair, A.J. (1996) The Effect of Docosahexaenoic Acid on the Electroretinogram of the Guinea Pig, *Lipids 31*, 65–70.
17. Leray, C., and Pelletier, X. (1987) Thin-Layer Chromatography of Human Platelet Phospholipids with Fatty Acid Analysis, *J. Chromatogr. 420*, 411–416.
18. Ravandi, A., Kuksis, A., Myher, J.J., and Marai, L. (1995) Determination of Lipid Ester Ozonides and Core Aldehydes by High-Performance Liquid Chromatography with On-Line Mass Spectrometry, *J. Biochem. Biophys. Methods 30*, 271– 285.
19. Pugh, E.L., Kates, M., and Hanahan, D.J. (1977) Characterization of the Alkyl Ether Species of Phosphatidylcholine in Bovine Heart, *J. Lipid Res. 18*, 710–715.
20. Khaselev, N., and Murphy, R.C. (1999) Susceptibility of Plasmenyl Glycerophosphoethanolamine Lipids Containing Arachidonate to Oxidative Degradation, *Free Radical Biol. Med. 26*, 275–284.
21. Lin, D.S., Connor, W.E., Anderson, G.J., and Neuringer, M. (1990) Effects of Dietary n-3 Fatty Acids on the Phospholipid Molecular Species of Monkey Brain, *J. Neurochem. 55*, 1200–1207.
22. Carlson, S.E. (1999) *Abstracts of the 23rd World Congress and Exhibition of the International Society for Fat Research,* Brighton, England, October 3–7, pp. 53–54.
23. Connor, W.E., Neuringer, M., and Reisbick, S. (1992) Essential Fatty Acids: The Importance of n-3 Fatty Acids in the Retina and Brain, *Nutr. Rev. 50*, 21–29.
24. Bazan, N.G., Rodriguez de Turco, E.B., and Gordon, W.C. (1993) Pathways for the Uptake and Conservation of Docosahexaenoic Acid in Photoreceptors and Synapses: Biochemical and Autoradiographic Studies, *Can. J. Physiol. Pharmacol. 71*, 690–698.
25. Burdge, G.C., and Postle, A.D. (1995) Phospholipid Molecular Species Composition of Developing Fetal Guinea Pig Brain, *Lipids 30*, 719–724.
26. Weisinger, H.S., Vingrys, A.J., and Sinclair, A.J. (1995) Dietary Manipulation of Long-Chain Polyunsaturated Fatty Acids in the Retina and Brain of Guinea Pigs, *Lipids 30*, 471–473.
27. Abedin, L., Lien, E.L., Vingrys, A.J., and Sinclair, A.J. (1999) The Effects of Dietary α-Linolenic Acid Compared with Docosahexaenoic Acid on Brain, Retina, Liver, and Heart in the Guinea Pig, *Lipids 34*, 475–482.
28. Zhang, H., Hamilton, J.H., Salem, N., Jr., and Kim, H.Y. (1998) n-3 Fatty Acid Deficiency in the Rat Pineal Gland: Effects on Phospholipid Molecular Species Composition and Endogenous Levels of Melatonin and Lipoxygenase Products, *J. Lipid Res. 39*, 1397–1403.
29. Lentz, B.R., and Litman, B.J. (1978) Effect of Head Group on Phospholipid Mixing in Small, Unilamellar Vesicles: Mixtures of Dimyristoylphosphatidylcholine and Dimyristoylphosphatidylethanolamine, *Biochemistry 17*, 5537–5543.
30. Litman, B.J., Lewis, E.N., and Levin, I.W. (1991) Packing Characteristics of Highly Unsaturated Bilayer Lipids: Raman Spectroscopic Studies of Multilamellar Phosphatidylcholine Dispersions, *Biochemistry 30*, 319–324.
31. Mitchell, D.C., Straume, M., and Litman, B.J. (1992) Role of *sn*-1-Saturated, *sn*-2-Polyunsaturated Phospholipids in Control of Membrane Receptor Conformational Equilibrium: Effects of Cholesterol and Acyl Chain Unsaturation on the Metarhodopsin I ↔ Metarhodopsin II Equilibrium, *Biochemistry 31*, 662–670.
32. Litman, B.J., and Mitchell, D.C. (1996) A Role for Phospholipid Polyunsaturation in Modulating Membrane Protein Function, *Lipids 31*, S193–S197.
33. Kanfer, J.N., and McCartney, D. (1991) Sphingosine and Unsaturated Fatty Acids Modulate the Base Exchange Enzyme Activities of Rat Brain Membranes, *FEBS Lett. 291*, 63–66.
34. Corazzi, L., Pistolesi, R., Carlini, E., and Arienti, G. (1993) Transport of Phosphatidylserine from Microsomes to the Inner Mitochondrial Membrane in Brain Tissue, *J. Neurochem. 60*, 50–56.
35. Blusztajn, J.K., Zeisel, S.H., and Wurtman, R.J. (1979) Synthesis of Lecithin (Phosphatidylcholine) from Phosphatidylethanolamine in Bovine Brain, *Brain Res. 179*, 319–327.
36. Crews, F.T., Hirata, F., and Axelrod, J. (1980) Identification and Properties of Methyltransferases That Synthesize Phosphatidylcholine, *J. Neurochem. 34*, 1491–1498.
37. Suzuki, T.T., and Kanfer, J.N. (1985) Purification and Properties of an Ethanolamine-Serine Base Exchange Enzyme of Rat Brain Microsomes, *J. Biol. Chem. 260*, 1394–1399.
38. Corazzi, L., Pistolesi, R., and Arienti, G. (1991) The Fusion of Liposomes to Rat Brain Microsomal Membranes Regulates Phosphatidylserine Synthesis, *J. Neurochem. 56*, 207–212.
39. Kanfer, J.N., and McCartney, D. (1993) Modulation of the Serine Base Exchange Enzyme Activity of Rat Brain Membranes by Amphiphilic Cations and Amphiphilic Anions, *J. Neurochem. 60*, 1228–1235.

[Received January 20, 2000, and in revised form on July 10, 2000; revision accepted July 21, 2000]

Dietary Docosahexaenoic Acid Affects Stearic Acid Desaturation in Spontaneously Hypertensive Rats

Marguerite M. Engler[a,]*, Sandrine H. Bellenger-Germain[b], Mary B. Engler[a], Michel M. Narce[b], and Jean-Pierre G. Poisson[b]

[a]Laboratory of Cardiovascular Physiology, Department of Physiological Nursing, University of California, San Francisco, California 94143-0610, and [b]UPRES Lipides et Nutrition, Université de Bourgogne, Faculté des Sciences Mirande, BP 47870, 21078 Dijon Cedex, France

ABSTRACT: Docosahexaenoic acid (DHA, 22:6n-3) is an n-3 polyunsaturated fatty acid which attenuates the development of hypertension in spontaneously hypertensive rats (SHR). The effects of DHA on delta-9-desaturase activity in hepatic microsomes and fatty acid composition were examined in young SHR. Two groups of SHR were fed either a DHA-enriched diet or a control diet for 6 wk. Desaturase activity and fatty acid composition were determined in hepatic microsomes following the dietary treatments. Delta-9-desaturase activity was decreased by 53% in DHA-fed SHR and was accompanied by an increase in 16:0 and a reduction in 16:1n-7 content in hepatic microsomes. The DHA diet also increased the levels of eicosapentaenoic acid (20:5n-3) and DHA. The n-6 fatty acid content was also affected in DHA-fed SHR as reflected by a decrease in gamma-linolenic acid (18:3n-6), arachidonic acid (20:4n-6), adrenic acid (22:4n-6), and docosapentaenoic acid (22:5n-6). A higher proportion of dihomo-gamma-linolenic acid (20:3n-6) and a lower proportion of 20:4n-6 is indicative of impaired delta-5-desaturase activity. The alterations in fatty acid composition and metabolism may contribute to the antihypertensive effect of DHA previously reported.

Paper no. L8459 in *Lipids 35,* 1011–1015 (September 2000).

Alterations in fatty acid biosynthesis and metabolism may contribute to the pathogenesis of hypertension (1–4). Fatty acids are incorporated into tissues and organs and influence cell membrane properties important to physiological functions such as blood pressure regulation. Fatty acid composition can affect membrane fluidity, intracellular signaling, and the activity of membrane-bound receptors and enzymes (5–7).

Fatty acid composition is dependent on hepatic metabolism through a sequence of desaturation and elongation steps. One major pathway of tissue fatty acid biosynthesis begins with desaturation of palmitic acid (16:0) and stearic acid (18:0) (8). Delta-9-desaturase is the key enzyme necessary for the conversion of palmitic to palmitoleic acid (16:1n-7) and stearic to oleic acid (18:1n-9). Delta-6 and delta-5 desaturase enzymes are required for the metabolism of essential fatty acids, linoleic (18:2n-6) and alpha-linolenic (18:3n-3), to long-chain polyunsaturated fatty acids. Hormonal and dietary factors can affect the activity of delta-9-, delta-6-, and delta-5-desaturases, which alters monounsaturated and polyunsaturated fatty acid composition (9,10).

Risk factors linked to coronary heart disease including hypertension, diabetes, and aging have also been associated with impaired delta-6 and delta-5 desaturase activities (4,8,11–14). Fish oil rich in long-chain n-3 fatty acids, eicosapentaenoic (EPA, 20:5n-3) and docosahexaenoic (DHA, 22:6n-3) acids, reportedly offers a protective effect against coronary artery disease by lowering blood pressure, modulating inflammatory and thrombotic responses, and reducing plasma lipid levels (15–20). We have recently shown that DHA alone has a blood pressure-lowering effect in spontaneously hypertensive rats (SHR), which is associated with an increase in n-3 fatty acids in plasma, tissues, and organs (21,22). Previous studies have demonstrated a reduction in hepatic delta-6- and delta-5-desaturase activities in SHR (1,2). Moreover, supplementation with EPA and DHA also decreased delta-6- and delta-5-desaturase activities in SHR hepatocytes and affected n-6 polyunsaturated fatty acid composition (23,24). Increased levels of 18:1n-9 in total liver lipids have been evidenced in SHR compared to Wistar Kyoto (WKY) rats (4). It is not known whether dietary DHA influences delta-9-desaturase activity in SHR.

The purpose of this study was to determine the effects of dietary DHA on hepatic microsomal delta-9 desaturation of stearic acid in hypertension. To investigate whether the metabolism of fatty acids is altered by dietary DHA, hepatic microsomal fatty acid composition was also determined in SHR.

MATERIALS AND METHODS

Animals and diets. Male SHR aged 7 wk, obtained from Harlan (Indianapolis, IN) were randomized into two groups and housed in cages at constant temperature (26°C) and lighting (12 h light/12 h dark cycle). Diets and water were provided

*To whom correspondence should be addressed at University of California, San Francisco, Laboratory of Cardiovascular Physiology, Department of Physiological Nursing, 2 Kirkham St., Room N631, Box 0610, San Francisco, CA 94143-0610. E-mail: marguerite.engler@nursing.ucsf.edu

Abbreviations: CO, control diet; DHA, docosahexaenoic acid; EPA, eicosapentaenoic acid; SHR, spontaneously hypertensive rats; WKY, Wistar Kyoto.

ad libitum. The rats were fed one of two diets for 6 wk. The purified fat-free basal mix diets contained a combination of corn and soybean oils (Research Diets Inc., New Brunswick, NJ) as the fat component; however, the experimental diet also consisted of a DHA-enriched oil (DHASCO®; Martek Biosciences Corp., Columbia, MD). The dietary constituents included (g/kg): corn starch, 423; sucrose, 231; casein, 150; cellulose, 50; fat, 50 (control diet, corn oil/soybean oil: 25:25; experimental diet, corn oil/soybean oil/DHASCO: 15:15:20); maltodextrin 10, 40; mineral mix, 23; calcium phosphate, 13; vitamin mix, 10; calcium carbonate, 5.5; and DL-methionine, 2.3. The fatty acid composition of the control and experimental diets is shown in Table 1. The diets were stored at 0°C and provided fresh daily. At the end of the dietary treatments, SHR were anesthetized with halothane (5%) in a mixture of oxygen and nitrous oxide. Liver tissue was excised quickly and rinsed in cold saline. The samples were placed immediately in dry ice and then stored at −70°C until analysis. All experimental procedures were reviewed and conducted according to the guidelines of the Committee on Animal Research at the University of California, San Francisco.

Desaturation assays. Liver tissue (3 g) was washed in ice-cold 0.15 mol/L NaCl, cut into thin slices, homogenized at 4°C in a Potter-Elvejhem homogenizer with 6 vol of 0.05 mol/L phosphate buffer (pH 7.4) and 0.25 mol/L sucrose solution. All subsequent operations were performed at the same temperature. The crude homogenate was centrifuged at 13,000 × *g* for 30 min in a Beckman model J-21B centrifuge, JA 20 rotor (Beckman Instruments, Palo Alto, CA); the pellet was then discarded and the supernatant was centrifuged again at 105,000 × *g* for 60 min in a Beckman model L8-55 ultracentrifuge, Ti 60 rotor, to obtain the microsomal pellet. The microsomal fraction was resuspended in 0.4 mL supernatant and 0.8 mL of 0.05 mol/L phosphate buffer (pH 7.4) and 0.25 mol/L sucrose solution. All subsequent enzymatic assays (delta-9-desaturase activity) and composition analysis used these microsomal membrane fractions. Microsomal protein concentrations were estimated by the method of Layne (25) with fatty acid-free crystalline bovine serum albumin as a standard. The delta-9 desaturation by liver microsomes was measured by estimation of the percentage of conversion of ^{14}C stearic acid to its corresponding product, ^{14}C oleic acid. Before enzyme activity measurement, [1-^{14}C]stearic acid (1-^{14}C 18:0; 50 mCi/mmol, 98% pure; NEN Life Products-France SA, Le Blanc Mesnil, France) was diluted in ethanol (Prolabo, Paris, France) to a specific activity of 5 mCi/mmol with the corresponding unlabeled fatty acid (Sigma Chemical Co, St. Louis, MO). Under such conditions the reaction was linear, proportional to the time of incubation and protein concentration (26). Before the incubation, the microsomes were preincubated at 37°C for 3 min. The incubations were then performed in duplicate (with good reproducibility in terms of results) in open shaking flasks, at 37°C for 15 min, with 5 mg microsomal protein in a total volume of 2.1 mL in each flask containing 150 µmol/L phosphate buffer (pH 7.4), 7.4 µmol ATP (pH 7.4), 1 µmol CoA, 2.5 µmol NADPH, 10 µmol $MgCl_2$, and 0.05 µmol (1-^{14}C 18:0). The coenzymes and other reagents were pure products from Sigma or Merck (Darmstadt, Germany). The desaturation reaction was terminated by addition of 15 mL $CHCl_3$/MeOH (1:1, vol/vol). Then, the incubation mixtures were saponified for 20 min at 80°C. The transesterification was performed by addition of 2 mL 14% boron trifluoride (Sigma Chemical Co.) in methanol and incubated at 80°C for 20 min, according to Slover and Lanza (27). After addition of 2 mL 35% sodium chloride, the fatty acid methyl esters were extracted two times with 1 mL isooctane (Carlo Erba, Milan, Italy). The samples were kept in 2 mL at −20°C under nitrogen. The distribution of radioactivity between substrates and products was determined by the reverse-phase high-performance liquid chromatography technique described by Narce *et al.* (28) using a Waters Set (510 HPLC pump and 410 differential refractometer; Millipore, Molsheim, Germany) equipped with a Merck Lichrocart column (Superspher RP 18, 250 × 4 mm i.d.; Merck). Analyses were carried out isocratically using acetonitrile/water (95:5, vol/vol) as the mobile phase at a flow rate of 1.0 mL/min. The fatty acid methyl ester mixtures were dissolved in pure acetone before injection. To collect the ^{14}C radioactive methyl ester fractions, the solvent obtained from the detector was recovered and the radioactivity was directly measured in the solvent by liquid scintillation counting twice for 5 min (Ultimagold; Packard Instrument, Rungis, France) in 20 mL Zinsser polyethylene vials (Frankfurt, Germany) with a Packard Tri-Carb Model 1900 TR liquid scintillation analyzer. Counting efficiencies were estimated by external standardization. The fatty acid methyl esters were identified according to their retention times by comparison with "cold" reference standards (Nu-Chek-Prep, Elysian, MN). The specific activity, expressed as pmol converted per min per mg microsomal protein, was calculated from the conversion percentage determined from the radioactivity distribution percentage of total fatty acids. A control assay with addition of microsomes, but also 15 mL $CHCl_3$/MeOH (1:1, vol/vol),

TABLE 1
Fatty Acid Composition of Control (CO) and Experimental (DHA) Diets[a]

Fatty acid	CO	DHA
10:0	2.5	0.2
12:0	22.3	21.6
14:0	0.6	3.3
16:0	7.7	7.5
16:1n-7	—	0.5
18:0	1.9	1.6
18:1n-9	13.5	14.7
18:1n-7	0.6	0.5
18:2n-6	33.1	21.4
18:3n-3	2.8	1.8
20:4n-6	—	—
20:5n-3	—	—
22:6n-3	—	8.8

[a]Values represent % of total fatty acids. —, fatty acid not detected, 15–18% could not be identified; CO, control diet; DHA, docosahexaenoic acid.

was done at time 0 of the reaction and no desaturation was observed.

Lipid analysis. Fatty acid composition of total liver lipids in microsomes was determined by gas–liquid chromatography of methyl esters. Briefly, total lipids were extracted by the method of Folch *et al*. (29), saponified, and methylated by the method of Slover and Lanza (27) at 80°C for 20 min. Fatty acid methyl esters were then extracted with 2 mL isooctane, separated by gas–liquid chromatography in a Packard, Model 417 gas–liquid chromatograph equipped with a flame-ionization detector and a 30-m capillary glass column coated with Carbowax 20M. Conditions were as follows: oven, 194°C; and injector and ionization detector, 240°C. Helium was used as the carrier gas, with a flow rate of 0.4 mL/min. Quantitative analysis was achieved with reference to the internal standards (Nu-Chek-Prep) by means of a DELSI ENICA 31 (Delsi Nermag Instruments, Rungis, France). The percentage of total fatty acid was given by weight for the fatty acids of main interest.

Statistical analysis. Results are shown as mean ± SEM for control and DHA groups. Statistical significance of differences between means was assessed using the Student's *t*-test. Values were considered significant when P was less than 0.05.

RESULTS

Hepatic desaturase activity. The effect of dietary DHA on delta-9-desaturase activity in hepatic microsomes when stearic acid (18:0) was used as a substrate is shown in Table 2. In SHR fed the DHA diet, the activity of 18:1n-9 delta-9-desaturation was significantly decreased, approximately 53%, compared to activity in control SHR.

Hepatic microsomal fatty acid composition. The fatty acid composition of hepatic microsomal total lipids is presented in Table 3. DHA-fed SHR had a higher percentage of 16:0 compared to control SHR. Interestingly, no significant difference in microsomal 18:0 and 18:1(n-9 + n-7) levels was found between groups. A marked reduction in n-6 fatty acids 18:3n-6, 20:4n-6, 22:4n-6, and 22:5n-6 was observed in hepatic microsomes in DHA-fed SHR. This was accompanied with a significant increase in 20:3n-6, which is consistent with impaired delta-5-desaturase activity. The DHA diet also increased levels of n-3 fatty acids, 20:5n-3 (EPA) and 22:6n-3 (DHA) by 8.5- and 3.3-fold, respectively. A reduction in 18:3n-3 and 22:5n-3 levels was found in DHA-fed SHR compared to control SHR.

TABLE 2
Delta-9-desaturase (D9D) Activity for 18:0 to 18:1n-9 in Hepatic Microsomes of SHR Fed the CO or DHA Diets[a]

Enzyme	CO	DHA
D9D activity (pmol/min/mg protein)	82.0 ± 6.0	38.3 ± 3.3*
Conversion percentage	12.3 ± 0.9	5.7 ± 0.5*

[a]SHR, spontaneously hypertensive rats. See Table 1 for other abbreviations. *$P < 0.01$.

TABLE 3
Total Fatty Acid Composition of Liver Microsomes from SHR Fed the CO or DHA Diets[a]

Fatty acid	CO	DHA
14:0	0.47 ± 0.09	0.29 ± 0.02
16:0	19.30 ± 0.47	21.25 ± 0.19*
16:1n-7	1.79 ± 0.58	1.28 ± 0.01
18:0	13.70 ± 1.05	13.91 ± 0.18
18:1(n-7 + n-9)	10.51 ± 0.82	9.51 ± 0.37
18:2n-6	15.89 ± 0.90	16.12 ± 0.36
18:3n-6	0.27 ± 0.04	0.11 ± 0.01**
18:3n-3	0.28 ± 0.03	0.16 ± 0.01**
20:2n-6	0.29 ± 0.04	0.23 ± 0.01
20:3n-6	0.63 ± 0.09	1.84 ± 1.00**
20:4n-6	28.04 ± 0.80	13.10 ± 0.49**
20:5n-3	0.19 ± 0.03	1.62 ± 0.06**
22:4n-6	0.65 ± 0.07	0**
22:5n-6	0.58 ± 0.10	0.25 ± 0.06*
22:5n-3	1.42 ± 0.13	0.52 ± 0.03**
22:6n-3	5.94 ± 0.54	19.78 ± 0.56**

[a]Results are shown as mean of 4 rats ± SEM for control and DHA groups. *$P < 0.05$ and **$P < 0.01$: DHA group as compared with control group. See Tables 1 and 2 for abbreviations.

DISCUSSION

Several experimental studies have demonstrated that alterations in tissue fatty acid metabolism are associated with hypertension (1–4). Increasing evidence suggests that dietary fish oils, EPA and DHA, have an antihypertensive effect (15–17). Our recent investigation shows that the attenuation of high blood pressure in DHA-fed SHR (13 wk old) is associated with profound changes in the fatty acid composition of the vasculature, liver, and organs involved in blood pressure regulation (22). We observed an increase in hepatic levels of 18:0 and a decrease in 18:1n-9 indicative of inhibition of delta-9-desaturase activity. This result is attributed to dietary DHA since a previous investigation found decreased levels of 18:0 and increased levels of 18:1n-9 in total liver lipids of 13-wk-old SHR compared to WKY rats fed standard chow (4).

In the present study, the direct effects of dietary DHA on delta-9-desaturase activity and fatty acid composition was investigated in hepatic microsomes of SHR. This is the first study known to examine the influence of dietary DHA on delta-9-desaturase in SHR. A recent investigation reported that DHA administered by gastric intubation for 10 d in normotensive rats decreased delta-9-desaturase mRNA by 70% (30). Our results demonstrate that delta-9-desaturase activity is reduced by 53% in microsomes of DHA-fed SHR. This finding is supported by the fatty acid compositional changes of 16:0 and 16:1n-7 in hepatic microsomes of DHA-fed SHR even though 16:1n-7 levels are not statistically significant. There is, however, a 30% reduction in the ratio of 16:1n-7/16:0 in the DHA fed SHR compared to control SHR, which is a better reflection of the depressed delta-9-desaturase activity. The rise in 16:0 is significant, especially since this fatty acid is a major constituent in hepatic microsomes as well as total liver lipids (22). Saturated fatty acids have several functions in cell physiology including production and storage

of energy, lipid transport, synthesis of membrane lipids, and modification of membrane proteins (6). In a previous study, we have shown that total liver lipids were increased in SHR fed a standard diet, with a concomitant increase of 18:1n-9 (4). The decreased delta-9-desaturation, due to dietary DHA evidenced in the present work indicates that, in fact, such a diet tends to modify the altered delta-9-desaturation to the level observed in nonhypertensive rats. Such a result is of interest, related to the hypotensive effect of DHA. However, the limited delta-9-desaturase activity was not consistent with changes in 18:0 and 18:1n-9 in hepatic microsomes in contrast to our previous results in total liver lipids (22). This apparent discrepancy could be related to the compositional difference of microsomes and total lipids. Total liver lipids also contain storage lipids, which may modify their composition in response to dietary changes. Consequently, the more stable membrane structural lipids in microsomes are less affected. Other enzyme systems involved in lipid metabolism such as acyltransferase or fatty acid synthetase may maintain 18:0 and 18:1n-9 levels at the microsomal level, despite impairment of delta-9-desaturase activity. This could also reflect strong membrane stability of saturated and monounsaturated fatty acids.

The supplementation of DHA in the diet increased the proportion of DHA by 3.3-fold in hepatic microsomes. This finding is comparable to our previous results in total liver lipids of SHR fed a DHA-enriched diet (22). In the present study, a marked increase was also observed in the level of EPA in DHA-fed SHR. Since EPA is not preformed or available in the diet, the data suggests that DHA is retroconverted to EPA in hepatic microsomes. This has been demonstrated in a previous study in isolated rat hepatocytes (31). The elevation in EPA content in SHR may be of significance since EPA is a precursor for vasoactive eicosanoids.

Dietary DHA affected the composition of long-chain n-6 polyunsaturated fatty acids 18:3n-6, 20:4n-6, 22:4n-6, and 22:5n-6 in SHR. Other investigators have shown that dietary fish oil rich in both EPA and DHA increases the profile of serum and hepatic microsomal n-3 fatty acids in Sprague-Dawley rats at the expense of n-6 polyunsaturated fatty acids (32). The present study shows that DHA alone has an influence on the fatty acid composition of hepatic microsomes in favor of n-3 fatty acids in SHR. Our findings of increased levels of 20:3n-6 and decreased content of 20:4n-6 are indicative of impaired delta-5-desaturase activity induced by dietary DHA. A previous investigation demonstrated that hepatic delta-5-desaturase activity is depressed in SHR aged 13 wk fed an EPA- and DHA-enriched diet for 9 wk (24). We also reported a concomitant increase in 20:3n-6 and a reduction in 20:4n-6 in hepatocyte total lipids.

Alterations in the fatty acid composition of hepatic microsomes of DHA-fed SHR may influence the supply of long-chain unsaturated fatty acids to other tissues such as the kidney, which is involved in the pathogenesis of hypertension. Numerous epidemiological and experimental studies have suggested that dietary n-3 fatty acids have a beneficial effect on the development of kidney diseases (33,34). By giving a supplement of purified EPA, DHA, or corn oil, we have demonstrated that increasing levels of n-3 fatty acids in membranes affects the uptake and intracellular metabolism of fatty acids as well as membrane fluidity in the kidney (35). We have also shown that dietary DHA increases n-3 fatty acids and reduces the levels of n-6 fatty acids in the vasculature and organs of SHR (22). The resulting physiochemical changes in membrane structure may modify cellular responses important to blood pressure regulation. The n-3 fatty acids reportedly modulate intracellular calcium concentrations in vascular smooth muscle in SHR (36–38). This may explain why DHA elicits a vasorelaxant response in SHR aorta (39). A similar effect in systemic arteries would decrease vascular resistance and lower blood pressure. Another recent study demonstrated that dietary DHA affects the renin-angiotensin-aldosterone system in SHR by reducing adrenal synthesis of aldosterone (21). The results from these studies may be related to the effects of dietary DHA on desaturation and unsaturated fatty acid composition in SHR.

In conclusion, dietary DHA decreases delta-9-desaturase activity in hepatic microsomes in SHR and tends to modify it to the level observed in nonhypertensive rats. The DHA diet also produced increased proportions of n-3 fatty acids in hepatic microsomes at the expense of long-chain n-6 fatty acids in SHR. It is possible that dietary DHA influences cellular membrane properties and function as a result of the fatty acid compositional changes. These effects may be important to blood pressure regulation in SHR.

ACKNOWLEDGMENTS

This work was supported in part by the National Institutes of Health grant #HL 55038. We thank Diane Heininger (San Francisco) for preparation of this manuscript and Joseph Gresti (Dijon) for helpful suggestions in performing chromatography analysis.

REFERENCES

1. Narce, M., and Poisson, J.-P. (1984) *In Vitro* Study of Delta-6 and Delta-5 Desaturation of Linoleic and Dihomogammalinolenic Acids During Development of Hypertension and in Relation to Age in Spontaneously Hypertensive and Normotensive Rats, *C.R. Soc. Biol. 178,* 458–466.
2. Singer, P., Wirth, M., Gerike, U., Godicke, W., and Moritz, V. (1984) Age Dependent Alterations of Linoleic, Arachidonic and Eicosapentaenoic Acids in Renal and Medulla of Spontaneously Hypertensive Rats, *Prostaglandins 27,* 375–390.
3. Watanabe, Y., Huang, Y.-S., Simmons, V.A., and Horrobin, D.F. (1989) The Effect of Dietary n-6 and n-3 Polyunsaturated Fatty Acids on Blood Pressure and Tissue Fatty Acid Composition in Spontaneously Hypertensive Rats, *Lipids 24,* 638–644.
4. Narce, M., and Poisson, J.-P. (1995) Age-Related Depletion of Linoleic Acid Desaturation in Liver Microsomes from Young Spontaneously Hypertensive Rats, *Prostaglandins Leukotrienes Essent. Fatty Acids 52,* 59–63.
5. Spector, A.A., and Yorek, M.A. (1985) Membrane Lipid Composition and Cellular Function, *J. Lipid Res. 26,* 1015–1035.
6. Spector, A.A. (1999) Essentiality of Fatty Acids, *Lipids 34 (Supplement),* S1–S3.
7. Foucher, C., Narce, M., Nasr, L., Delachambre, M.-C., and Pois-

son, J.-P. (1997) Liver Microsomal Membrane Fluidity and Microsomal Desaturase Activities in Adult Spontaneously Hypertensive Rats, *J. Hypertens. 15,* 863–869.
8. Poisson, J.-P., and Cunnane, S.C. (1991) Long-Chain Fatty Acid Metabolism in Fasting and Diabetes: Relation Between Altered Desaturase Activity and Fatty Acid Composition, *J. Nutr. Biochem. 2,* 60–70.
9. Brenner, R.R. (1989) Factors Influencing Fatty Acid Chain Elongation and Desaturation, in *The Role of Fats in Human Nutrition* (Vergroesen, A.J., and Crawford, M., eds.) pp. 45–79, Academic Press, New York.
10. Poisson, J.-P. (1989) Essential Fatty Acid Metabolism in Diabetes, *Nutrition 5,* 263–266.
11. Mimouni, V., and Poisson, J.-P. (1990) Spontaneous Diabetes in BB Rats: Evidence for Insulin Dependent Liver Microsomal Delta-6 and Delta-5 Desaturase Activities, *Horm. Metab. Res. 22,* 405–407.
12. Hrelia, S., Bordoni, A., Celadon, M., Turchetto, E., Biagi, P.L., and Rossi, C.A. (1989) Age Related Changes in Linoleate and α-Linolenate Desaturation by Rat Liver Microsome, *Biochem. Biophys. Res. Commun. 163,* 348–355.
13. Biagi, P.L., Bordoni, A., Hrelia, S., Celadon, M., and Horrobin, D.F. (1991) Gamma-Linolenic Acid Dietary Supplementation Can Reverse the Aging Influence on Rat Liver Microsome Delta-6-desaturase Activity, *Biochim. Biophys. Acta 1083,* 187–192.
14. Ulmann, L., Blond, J.P., Maniongui, C., Poisson, J.-P., Durand, G., Bezard, J., and Pascal, G. (1991) Effects of Age and Dietary Essential Fatty Acids on Desaturase Activities and on Fatty Acid Composition of Liver Microsomal Phospholipids of Adult Rats, *Lipids* 26, 127–133.
15. Knapp, H.R., and Fitzgerald, G.A. (1989) The Antihypertensive Effects of Fish Oil: A Controlled Study of Polyunsaturated Fatty Acid Supplements in Essential Hypertension, *New Engl. J. Med. 320,* 1037–1043.
16. Bonaa, K.H., Bjerve, K.S., Straume, B., Gram, I.T., and Thelle, D. (1990) Effect of Eicosapentaenoic and Docosahexaenoic Acids on Blood Pressure in Hypertension, *New Engl. J. Med. 322,* 795–801.
17. Morris, M.C., Sacks, F., and Rosner, B. (1993) Does Fish Oil Lower Blood Pressure? A Meta-Analysis of Controlled Trials, *Circulation 88,* 523–533.
18. Nordoy, A. (1999) Dietary Fatty Acids and Coronary Heart Disease, *Lipids 34 (Supplement),* S19–S22.
19. Calder, P.C. (1999) Dietary Fatty Acids and the Immune System, *Lipids 34 (Supplement),* S137–S140.
20. Sellmayer, A., Hrboticky, N., and Weber, P.C. (1999) Lipids and Vascular Function, *Lipids 34 (Supplement),* S13–S18.
21. Engler, M.M., Engler, M.B., Goodfriend, T.L., Ball, D.L., Yu, Z., Su, P., and Kroetz, D.L. (1999) Docosahexaenoic Acid Is an Antihypertensive Nutrient That Affects Aldosterone Production in SHR, *Proc. Soc. Exp. Biol. Med. 221,* 32–38.
22. Engler, M.M., Engler, M.B., Kroetz, D.L., Boswell, K.D.B., Neeley, E., and Krassner, S.M. (1999) The Effects of a Diet Rich in Docosahexaenoic Acid on Organ and Vascular Fatty Acid Composition in Spontaneously Hypertensive Rats, *Prostaglandins Leukotrienes Essent. Fatty Acids 61,* 289–296.
23. Narce, M., Asdrubal, P., Delachambre, M.-C., Gresti, J., and Poisson, J.-P. (1995) Influence of Spontaneous Hypertension on n-3 Delta-6-desaturase Activity and Fatty Acid Composition of Rat Hepatocytes, *Mol. Cell. Biochem. 152,* 7–12.
24. Narce, M., Frenoux, J.M., Dardel, V., Foucher, C., Germain, S., Delachambre, M.-C., and Poisson, J.-P. (1997). Fatty Acid Metabolism, Pharmacological Nutrients and Hypertension, *Biochimie 79,* 135–138.
25. Layne, E. (1957) Spectrophotometric and Turbidimetric Methods for Measuring Proteins, in *Methods in Enzymology* (Colowick, S.P., and Kaplan, N.O., eds.) pp. 447–454, Academic Press, New York.
26. Narce, M., Poisson, J.-P., Belleville, J., and Chanussot, B. (1992). Depletion of Delta-9 Desaturase (EC-1.14.99.5) Enzyme Activity in Growing Rat During Dietary Protein Restriction, *Br. J. Nutr. 68,* 627–637.
27. Slover, H.T., and Lanza, E. (1979) Quantitative Analysis of Food Fatty Acids by Capillary Gas Chromatography, *J. Am. Oil Chem. Soc. 56,* 933–943.
28. Narce, M., Gresti, J., and Bezard, J. (1988) Methods for Evaluating the Bioconversion of Radioactive Polyunsaturated Fatty Acids by Use of Reverse-Phase Liquid Chromatography, *J. Chromatogr. 448,* 249–264.
29. Folch, J., Lees, M. and Sloane-Stanley, G.H. (1957) A Simple Method for Isolation and Purification of Total Lipids from Animal Tissues, *J. Biol. Chem. 226,* 497–509.
30. Lochsen, T., Ormstad, H., Braud, H., Brodal, B., Christiansen, E.N., and Osmundsen, H. (1999) Effects of Fish Oil and n-3 Fatty Acids on the Regulation of Delta-9-Fatty Acid Desaturase mRNA and -Activity in Rat Liver, *Lipids 34 (Supplement),* S221–S222.
31. Gronn, M., Christensen, E., Hagve, T.A., and Christophersen, B.O. (1992). Effects of Dietary Purified Eicosapentaenoic Acid (20:5 (n-3)) and Docosahexaenoic Acid (22:6 (n-3)) on Fatty Acid Desaturation and Oxidation in Isolated Rat Liver Cells, *Biochim. Biophys. Acta 1125,* 35–43.
32. Garg, M.L., Thomson, A.B., and Clandinin, M.T. (1990) Interactions of Saturated, n-6 and n-3 Polyunsaturated Fatty Acids to Modulate Arachidonic Acid Metabolism, *J. Lipid Res. 31,* 271–277.
33. De Caterina, R., Endres, S., Kristensen, S.D., and Schmidt, E.B. (1994) n-3 Fatty Acids and Renal Diseases, *Am. J. Kidney Dis. 24,* 397–415.
34. Plotnick, A.N. (1996) The Role of Omega-3 Fatty Acids in Renal Disorders, *J. Am. Vet. Med. Assoc. 209,* 906–910.
35. Hagve, T.-A., Woldseth, B., Brox, J., Narce, M., and Poisson, J.-P. (1998) Membrane Fluidity and Fatty Acid Metabolism in Kidney Cells from Rats Fed Purified Eicosapentaenoic Acid or Purified Docosahexaenoic Acid, *Scand. J. Clin. Lab. Invest. 58,* 187–194.
36. Engler, M.B., Ma, Y.-L., and Engler, M.M. (1999) Calcium-Mediated Mechanisms of Eicosapentaenoic Acid-Induced Relaxation in Hypertensive Rat Aorta, *Am. J. Hypertens. 12,* 1225–1235.
37. Smith, J.M., Paulson, D.J., and Labak, S. (1992). Effects of Dietary Fish Oil on Rb^+ Efflux from Aorta of Stroke Prone Spontaneously Hypertensive Rats, *J. Hypertens. 8,* 369–375.
38. Chin, J.P., and Dart, A.M. (1995) How Do Fish Oils Affect Vascular Function? *Clin. Exp. Pharmacol. Physiol. 22,* 71–81.
39. Engler, M.B., Engler, M.M., and Ursell, P.C. (1994) Vasorelaxant Properties of n-3 Polyunsaturated Fatty Acids in Aortas from Spontaneously Hypertensive and Normotensive Rats, *J. Cardiovasc. Risk 1,* 75–80.

[Received February 4, 2000, and in revised form June 12, 2000; revision accepted July 27, 2000]

Secretion of Hepatic Lipase by Perfused Liver and Isolated Hepatocytes

Xavier Galan, Monique Q. Robert, Miquel Llobera, and Ignasi Ramírez*

Departament de Bioquímica i Biologia Molecular, Facultat de Biologia, Universitat de Barcelona, Barcelona, E-08071 Spain

ABSTRACT: Hepatic lipase is found in liver and in adrenal glands and ovaries. Because in adult rats, neither adrenals nor ovaries synthesize this enzyme, it is assumed that the liver is the origin of their hepatic lipase. Our aim was to study the secretion of hepatic lipase by the liver. We observed that plasma of both fed and fasted rats contained hepatic lipase activity. This activity was significantly correlated with that in the liver. Isolated livers, perfused with heparin-free medium, secreted fully active hepatic lipase to the perfusate. The addition of heparin resulted in a rapid and larger release of hepatic lipase to the perfusate. In isolated hepatocytes, heparin did not affect the secretion of hepatic lipase mass, although it increased the stability of the enzyme activity. To study the degradation of hepatic lipase by hepatocytes, protein synthesis was blocked with cycloheximide, and both secreted and intracellular hepatic lipases were analyzed by Western blotting. We observed that the amount of hepatic lipase secreted equaled the decrease of intracellular mass. The total mass of the enzyme (inside and outside the cells) remained constant, at least for 90 min. In the next experiment, 0.7 nM ^{125}I-hepatic lipase was added to hepatocyte suspensions, and the appearance of trichloracetic acid-soluble products was analyzed. Only 12% of the radioactivity added was associated with the cells after 90 min of incubation, and less than 2% of the hepatic lipase added was degraded. Although the association was decreased in the presence of heparin, the amount of ^{125}I-hepatic lipase degraded was not affected. Taking all these results into account, we propose a model for the continuous secretion of hepatic lipase by the liver.

Paper no. L8382 in *Lipids 35,* 1017–1026 (September 2000).

Rat hepatic lipase is a 476-amino acid glycoprotein with two potential sites for *N*-glycosylation (1). This enzyme belongs to a lipase gene family that includes lipoprotein lipase and pancreatic lipase (1,2). The first studies on the function of hepatic lipase, performed in whole animals treated with specific antibodies, revealed that the enzyme was involved in the metabolism of remnant lipoproteins (3) and of triglyceride-rich high density lipoproteins-2 (HDL_2) (4). As a result of the hydrolysis of both triglycerides and phospholipids, hepatic lipase promotes the uptake of HDL cholesterol by the liver (5) and generates pre-β_1 HDL (6). These particles appear to be the first acceptor of cellular cholesterol (see Ref. 7 for review). The relevance of hepatic lipase in lipoprotein metabolism was emphasized by the observation that total plasma cholesterol level was decreased in transgenic rabbits over-expressing human hepatic lipase compared to nontransgenic littermates (8). However, in mice strains with targeted inactivation of the hepatic lipase gene, only a mild dyslipemia was reported (9). Similarly, only a moderate hyperlipemia appeared in humans with identified hepatic lipase deficiency (10). Recent kinetic studies made in hepatic lipase-deficient mice provide *in vivo* evidence of the significant role of hepatic lipase in the selective delivery of HDL-cholesteryl esters to the liver (11).

By using immunocytochemistry, most hepatic lipase molecules were seen in the Space of Disse of the hepatic sinusoid (12–14). These enzyme molecules are synthesized and secreted by hepatocytes (15). The secretion of hepatic lipase was initially studied in isolated rat liver parenchymal cells (16), and in primary cultures of rat hepatocytes (17). Three conclusions arose from these early studies: (i) continuous secretion required protein synthesis, (ii) heparin induced a two- to fourfold increase in the secretion of hepatic lipase activity, and (iii) secretion required glycosylation. Later studies attempted to characterize the intracellular processing of the enzyme (15,18), the role of heparin (19,20), and the relevance of glycosylation for the activation/secretion process (21,22).

Adrenal glands and ovaries also contain hepatic lipase (23). In the former, it was immunolocalized in capillaries of the zona fasciculata (24), and in the latter it was seen in thin-walled blood vessels of theca interna of the follicles, corpora lutea, and interstitial cells (25). Since neither adrenal glands (26) nor ovaries (27) in the adult rat synthesize hepatic lipase, it is assumed that the enzyme is produced in the liver. Here we report direct evidence of the constitutive secretion of hepatic lipase by the liver.

EXPERIMENTAL PROCEDURES

Experiments in whole animals. Wistar rats were obtained from our own colony. At the age of 60 d, animals (either fed of fasted for 24 h) were killed by decapitation. The blood was

*To whom correspondence should be addressed at Departament de Bioquímica i Biologia Molecular, Facultat de Biologia, Universitat de Barcelona, Diagonal 645, 08071-Barcelona, Spain.
E-mail: sunyer@porthos.bio.ub.es

Abbreviations: BSA, bovine serum albumin; HDL_2, high density lipoproteins-2; K_D, dissociation constant; LRP, receptor-related protein; PAGE, polyacrylamide gel electrophoresis; PBS, phosphate-buffered saline; SDS, sodium dodecyl sulfate; TCA, trichloracetic acid.

collected in heparinized vials and plasma was obtained by centrifugation (30 min at 10,000 × *g* at 4°C). The liver was immediately frozen in liquid N_2. Liver homogenates were made with 10 mM Hepes pH 7.5 containing 1 mM EDTA and 1 mM dithiothreitol in a Polytron homogenizer (Kinematica GmbH, Luzern, Switzerland). Homogenates were clarified by centrifugation (10 min at 10,000 × *g* at 4°C). Clarified supernatants and blood plasma were kept at –40°C and used to determine hepatic lipase activity.

Experiments in perfused livers. Rats were anesthetized with sodium pentobarbital 60 mg/kg (i.p.). The portal vein was cannulated, and the liver was perfused for 10 min with washing solution [bicarbonate-containing isotonic buffer supplemented with 5.5 mM glucose and 1% albumin (28), maintained at 37°C] at a flow rate of 40 mL/min. During this time, the liver was carefully isolated and placed in a perfusion chamber as described (29). The perfusion was then made to recirculate with 50 mL of fresh buffer with or without heparin (5 units/mL). At selected times, a sample of the perfusate (0.4 mL) was obtained and kept at –40°C and used for further assays. At the end of the perfusion, the liver was homogenized as indicated above. Clear supernatants were kept at –40°C. Lactate dehydrogenase activity was determined as described by Vassault (30).

Hepatocyte isolation and incubation. Hepatocytes were isolated according to the methods of Peinado-Onsurbe *et al.* (28). Before incubation, cells were rinsed twice with an amino acid- and vitamin-containing buffer (buffer D in Ref. 31), and finally suspended at a density of 2.5×10^6 cells/mL in the same buffer supplemented with heparin (5 units/mL) when indicated. After isolation, cells were immediately used for incubations, which were carried out in a rotatory water bath at 37°C under O_2/CO_2 (19:1) atmosphere. At indicated times, a sample was taken and the cells were precipitated by centrifugation at 12,000 × *g* for 10 s. The medium was immediately frozen and stored at –40°C for no more than 1 mon. The cells were disrupted by sonication in lysis buffer (1 mM EDTA, 1 mM dithiothreitol, 10 mM Hepes pH 7.5 containing 10 milliunits/mL aprotinin, 25 mM benzamidine, 1 μM leupeptin, 1 μM pepstatin, 0.2 mM phenylmethyl sulfonyl fluoride, 5 units/mL heparin, and 1.5 % Triton X-100). After centrifugation (10 min, 1,000 × *g* at 4°C), the supernatant was stored at –40°C for further analysis, always for less than 1 mon. The storage conditions affected neither hepatic lipase activity nor the relative amount of hepatic lipase, as determined by Western blot. Viability of the cells was routinely determined by the Trypan blue exclusion test, and sometimes by lactate dehydrogenase release (30). Preparations with initial cell viability lower than 90% were discarded.

Hepatic lipase activity was determined by the method of Ehnholm *et al.* (32) as previously described (29). One unit of enzyme activity was defined as the amount of enzyme that released 1 μmol of oleate per min at 25°C.

Thermal stability of hepatic lipase. To quantify the effect of heparin on the thermal stability of hepatic lipase activity in solution, we first obtained the enzyme from perfused rat livers. Isolated livers were perfused, in recirculation conditions, for 30 min at 37°C with 50 mL of buffer D. Heparin was not included during perfusion to avoid any residual amount of heparin in control conditions. The perfusate containing hepatic lipase activity (5.9 mU/mL) was divided in two halves. One was adjusted to a final heparin concentration of 5 U/mL; the other did not receive heparin. Both were then placed into a water bath at 37°C and at selected times a sample was taken and kept in ice-cold water until the incubation was terminated. Then, the remaining hepatic lipase activity was determined. We had previously observed that hepatic lipase activity was stable at 4°C. In some experiments the perfusate was diluted with conditioned medium (in which hepatocytes had been incubated for 3 h at 37°C) with or without heparin, with similar results. The inactivation constants were estimated by adjusting the decay curves to a negative exponential ($a_t = a_0\, e^{-kt}$), where a_t is the activity remaining at time t, a_0 is the activity at time zero, and k is the inactivation constant. The inactivation constants were used to correct enzyme activity in medium for inactivation as described by Peinado-Onsurbe *et al.* (33).

Hepatic lipase purification and antibodies. Hepatic lipase was purified from heparin perfusates from rat livers by a combination of heparin-Sepharose and diethylaminoethyl-Sepharose chromatography according to Waite *et al.* (34). The hepatic lipase appeared homogeneous in 10%-polyacrylamide gels upon silver staining (not shown). Rabbit anti-rat hepatic lipase antiserum was obtained as previously described (35).

Western blot analysis. Incubation medium (6.25 μL diluted 1:4 in sampling buffer), cell lysates (25 μL diluted 1:2 in sampling buffer), or liver perfusates (4.17 μL diluted 1:4 in sampling buffer) were run in 10%-polyacrylamide gels in denaturing and reducing conditions (36). The separate proteins were then transferred to Immobilon-P membranes (Millipore, Milford, MA) by electroblotting. After transfer, the membranes were soaked in blocking solution [2% bovine serum albumin (BSA) in phosphate-buffered saline (PBS)] for 90 min at 37°C, rinsed [5 × 5 min in 100 mL of rinsing solution: 1% sodium dodecyl sulfate (SDS), 1% Triton X-100, and 0.5% defatted powdered-milk in PBS] and incubated overnight at 4°C with the primary antibody [rabbit anti-rat hepatic lipase serum diluted 1:1000 in buffer A (0.1% SDS, 0.1% Triton X-100, and 0.5% defatted powdered-milk in PBS) supplemented with 5% BSA and 0.5% gelatin]. The membranes were rinsed as indicated above and incubated for 30 min at room temperature with the secondary antibody [biotin-labeled goat anti-rabbit IgG (Vector, Burlingame, CA) diluted 1:5000 in buffer A]. After rinsing as above, the membranes were incubated with the ABC-complex [VECTASTAIN (ABC-kit); Vector] and developed with the ECL-system (Amersham, Arlington Heights, IL). Films were analyzed with Phoretix 1D Gel Analysis software (Newcastle upon Tyne, United Kingdom) after scanning in an Epson GT-8500 (Epson Iberica, Barcelona, Spain). In each gel, a lane was loaded with a constant amount of hepatic lipase to correct for differences in the results. In experiments with isolated cells, the final densitometric quantifications were referred to 10^6 cells to make the results comparable.

Analysis of ^{125}I-hepatic lipase and ^{125} I-lipoprotein lipase degradation. Purified rat hepatic lipase was labeled as described for lipoprotein lipase by Wallinder *et al.* (37); ^{125}I-labeled bovine milk lipoprotein lipase was obtained from Dr. T. Olivecrona (University of Umeå, Sweden). Hepatocytes (2.5×10^6 cells/mL, 2 mL final volume) were incubated in the presence of 70 ng of ^{125}I-labeled hepatic lipase (891 cpm/ng), or 10 ng of ^{125}I-labeled lipoprotein lipase (12,689 cpm/ng), in an incubation medium with or without heparin (5 U/mL). The concentration of labeled hepatic lipase was 0.7 nM and that of labeled lipoprotein lipase was 0.1 nM. At indicated times 0.2-mL samples were taken and the medium was immediately separated from the cells by centrifugation (1 min, 13,000 × *g* at 4°C). The cells were rinsed twice in ice-cold fresh buffer. The amount of 10% trichloracetic acid (TCA)-soluble and 10% TCA-precipitable radioactivity was measured in both medium and cells.

Animal care. All experimental procedures were approved by The Committee on Animal Care of the University of Barcelona.

RESULTS

Several reports indicate that hepatic lipase is present not only in liver, adrenal glands, and ovaries but also in plasma (38). We showed that the activity in plasma is affected by fasting, as is the activity in liver (39). To study the relationship between hepatic lipase activity in liver and plasma we determined these activities in animals either fed or fasted for 24 h. Figure 1 shows the individual values obtained in this study. There was a significant ($P < 0.001$) linear relationship between both parameters. In overnight-fasted humans, significant correlation between pre- and post-heparin (which may reflect liver activity) hepatic lipase activities was also reported (40).

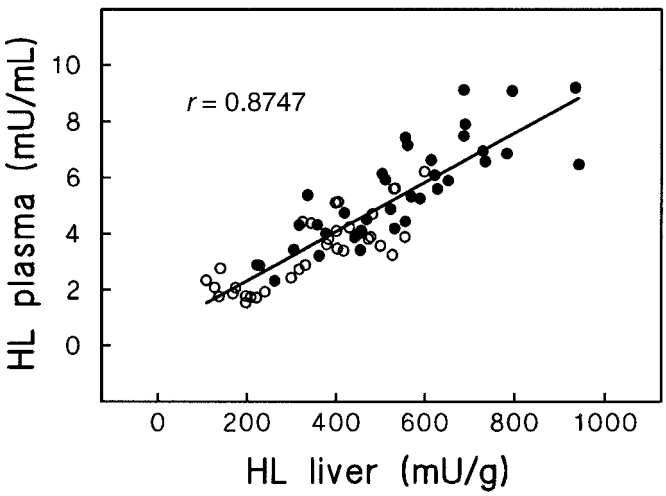

FIG. 1. Relationship between hepatic lipase activity in liver and plasma. Hepatic lipase (HL) activity was measured in the liver and plasma of rats either fed (●) or fasted for 24 h (○) before sacrifice. The mean ± SE for the hepatic lipase in the liver of fed and fasted rats was 548 ± 30 and 346 ± 24 mUnits/g, respectively ($P < 0.001$). In plasma the activity was 5.58 ± 0.30 and 3.40 ± 0.22 mUnits/mL for fed and fasted animals, respectively ($P < 0.001$).

In the next experiment, we analysed the secretion of hepatic lipase by isolated livers perfused with a recirculated medium. Figure 2 shows that the liver continuously released hepatic lipase to the perfusion medium. After 30 min of perfusion, we recovered 295 mUnits of hepatic lipase in the perfusate. This accounted for nearly 10% of the whole system hepatic lipase activity (released + residual). There was also release of lactate dehydrogenase, but the activity recovered in the perfusate at the end of the experiment accounted for only 0.02% of the whole system activity. The addition of heparin resulted in a rapid release of hepatic lipase to the perfusate, which accounted for 70% of the whole system activity after 30 min of perfusion. The release of lactate dehydrogenase was not affected by heparin (the symbols corresponding to these results cannot be observed in the figure because they overlap with those corresponding to nonheparin-perfused liver).

Released hepatic lipase appeared in SDS–polyacrylamide gel electrophoresis (PAGE) gels as a single band with an apparent M_r of 55,000 (Fig. 2). At zero time there was no detectable hepatic lipase in the perfusate, but 5 min afterward a tiny band was observed, the intensity of which increased as the perfusion continued. In the presence of heparin, a large amount of hepatic lipase was observed in the perfusate in the first sample obtained. When the activity (μUnits loaded to the gels) to mass (densitometric arbitrary units) ratio was calculated, we found no differences between heparin-free and heparin-containing perfusates. At 30 min of perfusion this ratio was 0.024 ± 0.002 and 0.022 ± 0.001, respectively. Identical values were obtained at every time studied (data not shown).

Next, we studied the secretion of hepatic lipase by isolated hepatocytes. Secreted hepatic lipase appeared in SDS–PAGE gels as a single band with an apparent M_r of 55,000 (Fig. 3), which is similar to the values reported by others in several cell systems (15,18). We identified two forms of hepatic lipase inside the cells with apparent M_r 52,000 and 55,000 (Fig. 3). By immunoprecipitating ^{35}S-labeled hepatic lipase, Laposata *et al.* (15) and Cisar and Bensadoun (18) also identified two intracellular forms of hepatic lipase, corresponding to the fully and partially glycosylated forms of the enzyme. The bands of higher M_r observed in cell lysates were biotin-containing proteins since these bands were also observed when the membranes were incubated without the specific primary antibody, but with the biotin-detecting ABC-reagent.

Since the early studies of Schoonderwoerd *et al.* (41), it has been known that heparin increases by nearly twofold the amount of hepatic lipase activity secreted from isolated hepatocytes. We found that the amount of hepatic lipase secreted after 3 h of incubation was not affected by heparin (Fig. 3). The scanning of the gels indicated that differences were nonsignificant (67 ± 9 and 72 ± 5 densitometric units in the medium of cells incubated without and with heparin, respectively). Heparin did not affect the amount of either intracellular forms (33 ± 2 and 22 ± 3 densitometric units for the 55,000 and 52,000 forms of hepatic lipase in cells incubated without heparin; 31 ± 1 and 19 ± 1 densitometric units for each form

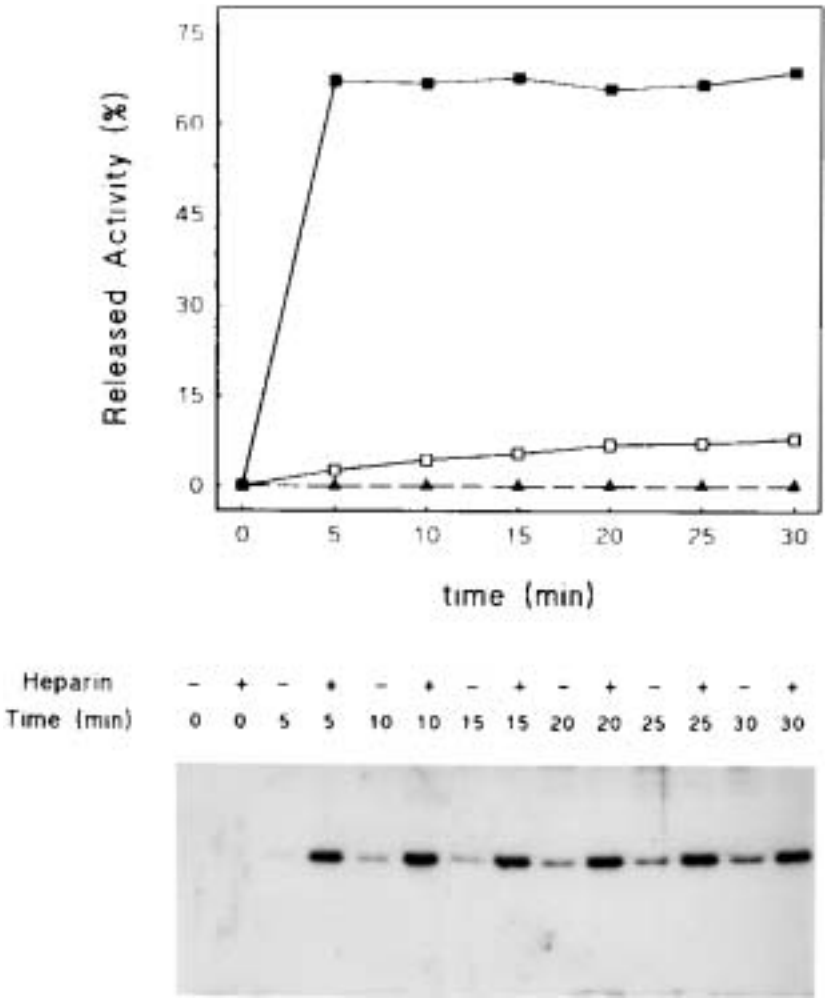

FIG. 2. The secretion of hepatic lipase in perfused livers is increased by heparin. Upper panel: isolated livers were perfused at 37°C with 50 mL of medium containing (■,▲) or not containing (□,△) 5 Units heparin/mL in a recirculatory system. Hepatic lipase (■,□) and lactate dehydrogenase (▲,△) released to the perfusate were determined at the indicated times. (△ cannot be observed because they overlap with ▲.) At the end of the perfusion the liver was homogenized to determine the residual activity. Results are the mean of two livers perfused in each condition and are expressed as percentage of released activity compared to the total (released after 30 min + residual) activity to make the results of hepatic lipase and lactate dehydrogenase comparable. Lower panel: hepatic lipase mass in perfusate obtained at the indicated times from livers perfused with or without heparin was analyzed by Western blot. The result shown corresponds to one of the livers perfused in each condition. The second liver was also analyzed with identical results, but these are not shown in this figure.

of hepatic lipase in cells incubated with heparin). However, when activity was measured, we observed that heparin had increased the hepatic lipase activity secreted to the incubation medium 4.3-fold (Fig. 4A). Since the active conformation of hepatic lipase is rather unstable in solution (32,41), we studied whether thermal inactivation could explain the differences between the mass and the activity detected in the medium. First, we determined the inactivation constants of soluble hepatic lipase (obtained from isolated livers perfused without heparin to avoid any exposure of the enzyme to this molecule) in the presence or the absence of heparin. As shown in Figure 4B, heparin decreased the inactivation rate constant. When these inactivation constants were used to correct the measured activity in medium, no significant differences were found in the corrected activity secreted by cells incubated with or without heparin (Fig. 4C).

The time course of hepatic lipase secretion, when protein synthesis was either allowed or blocked by the addition of 20 μM cycloheximide, is shown in Figure 5. Cycloheximide addition resulted in a progressive decline in the rate of hepatic lipase secretion. This is in accordance with previous results (16; and many others thereafter). The effect became significant after 45 min of incubation. At 90 min, the activity/mass ratio in the medium was 0.024 and 0.025 for control and cy-

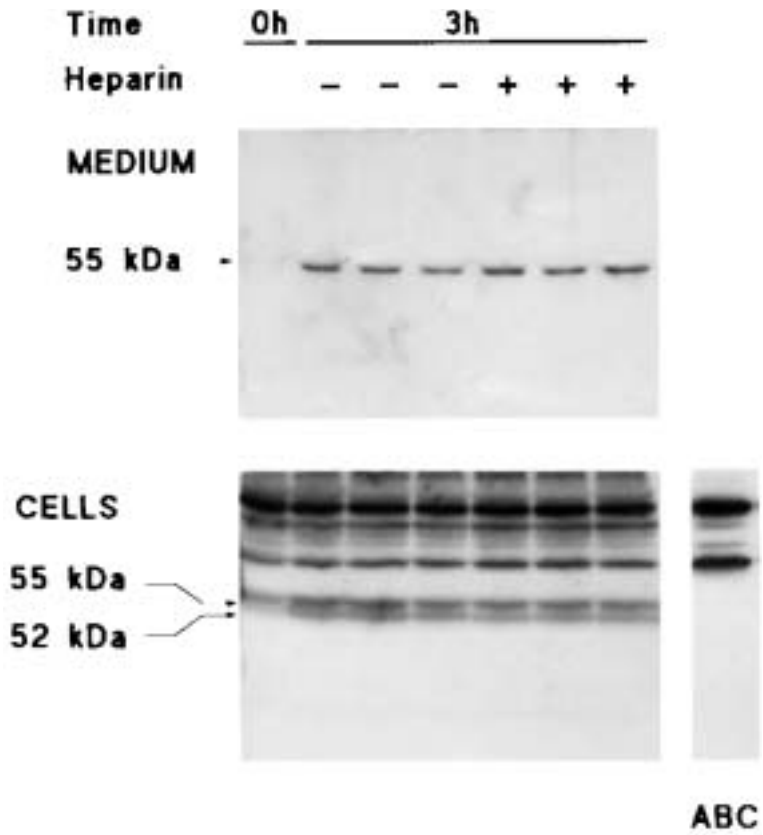

FIG. 3. Heparin does not increase the amount of hepatic lipase secreted by rat hepatocytes. Hepatocytes were incubated in the absence or in the presence of 5 Units heparin/mL. At zero time and after 3 h of incubation, samples were obtained. The cells were separated from the medium by centrifugation, and the amount of hepatic lipase was determined by Western blot analysis. Incubation medium (6.25 µL) or cell lysate (25 µL) was loaded in each lane (upper and lower panels, respectively). ABC lane corresponds to a membrane containing the transferred proteins from zero-time cells, incubated without the primary antibody but with the secondary antibody and the ABC-reagent (Vector, Burlingame, CA).

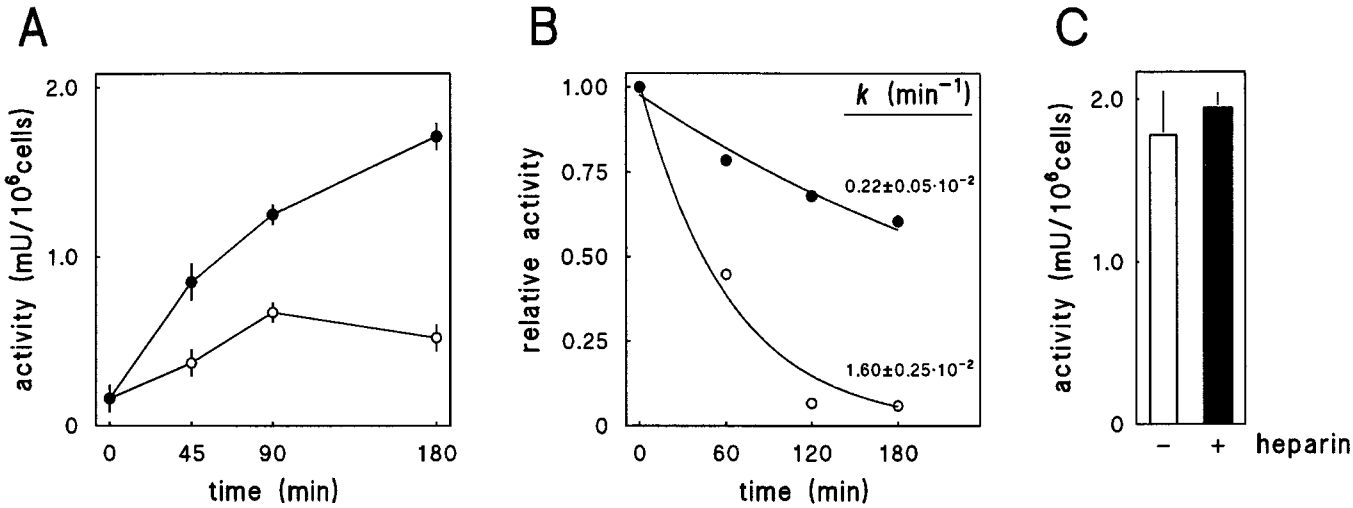

FIG. 4. The apparent effect of heparin on the secretion of hepatic lipase is a consequence of stabilization of enzyme activity. (A) The amount of hepatic lipase activity secreted by hepatocytes incubated at 37°C in the absence (○) or in the presence of 5 Units heparin/mL (●) was determined at the indicated incubation times. The results are the mean ± SE of triplicate values. (B) The thermal stability of the activity of hepatic lipase released from nonheparin-perfused livers was determined at 37°C either in the absence (○) or in the presence (●) of added heparin (5 Units/mL). The inactivation constants (k) were obtained by fitting the decay curves to a negative exponential (rel act = e^{-kt}). (C) The inactivation constant values were used to correct the apparently secreted activity (panel A) by inactivation (see the Experimental Procedures section). This panel shows the corrected activity accumulated in the medium after 3 h of incubation in the absence or in the presence of heparin.

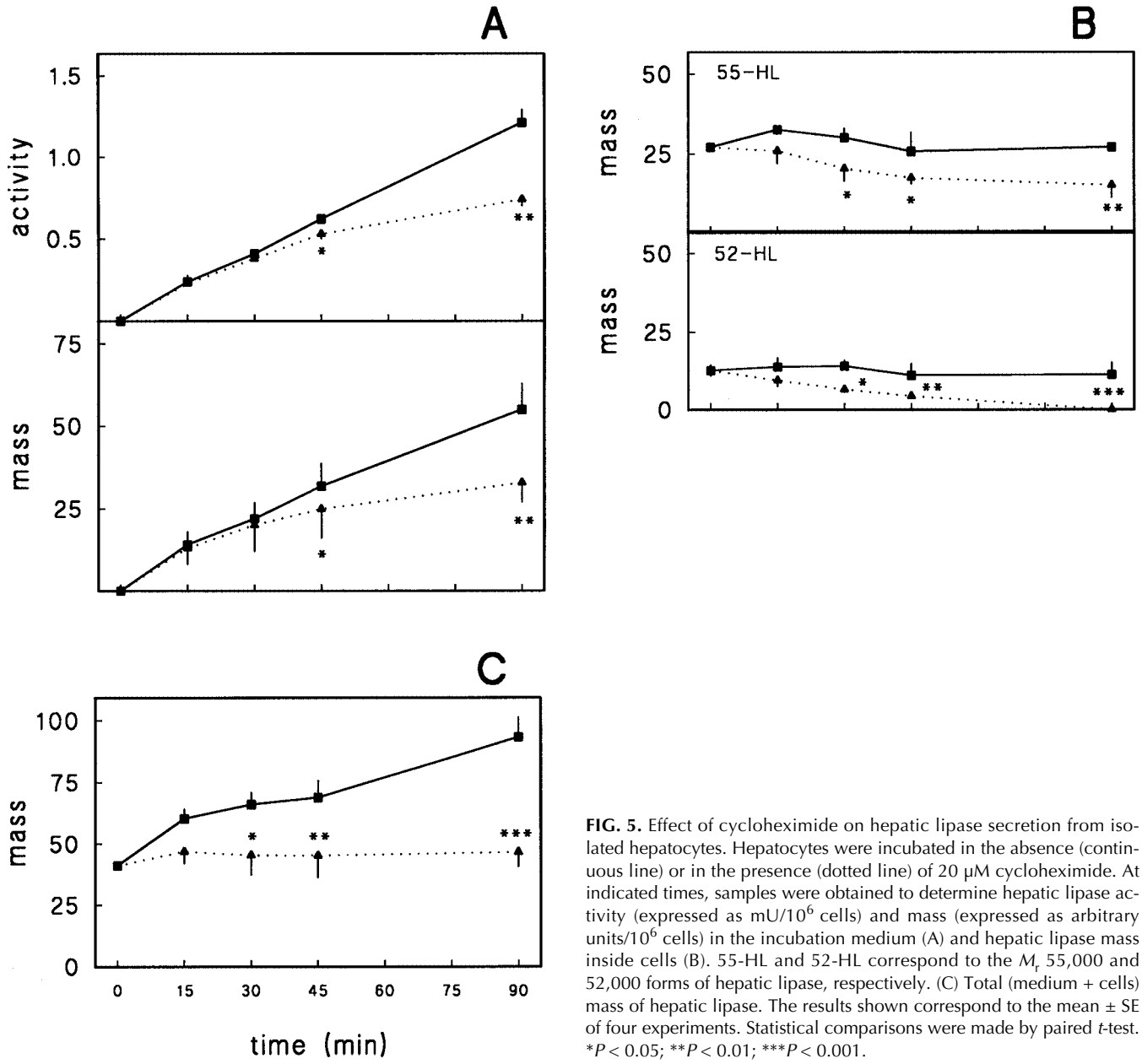

FIG. 5. Effect of cycloheximide on hepatic lipase secretion from isolated hepatocytes. Hepatocytes were incubated in the absence (continuous line) or in the presence (dotted line) of 20 μM cycloheximide. At indicated times, samples were obtained to determine hepatic lipase activity (expressed as mU/10^6 cells) and mass (expressed as arbitrary units/10^6 cells) in the incubation medium (A) and hepatic lipase mass inside cells (B). 55-HL and 52-HL correspond to the M_r 55,000 and 52,000 forms of hepatic lipase, respectively. (C) Total (medium + cells) mass of hepatic lipase. The results shown correspond to the mean ± SE of four experiments. Statistical comparisons were made by paired *t*-test. $^*P < 0.05$; $^{**}P < 0.01$; $^{***}P < 0.001$.

cloheximide-incubated cells, respectively. This indicates that cycloheximide did not affect the catalytic properties of the secreted enzyme molecules. Regarding intracellular hepatic lipase, in cells incubated without cycloheximide, the amount of each of the intracellular forms remained constant throughout the incubation period. However, in cells exposed to cycloheximide, the M_r 52,000 form was almost completely absent at 90 min, whereas the amount of the M_r 55,000 form was 50% decreased. Total hepatic lipase mass (the sum of that in medium and both intracellular forms) increased linearly in control cells throughout the incubation time. Indeed, the total amount of hepatic lipase did not increase in the cells exposed to cycloheximide, but it did not decrease either.

We also studied the effect of heparin on the degradation of ^{125}I-labeled hepatic lipase, exogenously added to isolated hepatocytes. To minimize interferences due to release of endogenous unlabeled hepatic lipase, we estimated first, from results shown in Figures 4 and 5, the amount of enzyme that was spontaneously released to the incubation medium. Jansen and Bensadoun (42) reported a specific activity for the purified enzyme of 45 mmol/h/mg protein. If we assume that this also corresponds to the specific activity of the enzyme released from hepatocytes, we can calculate that after 3 h incubation the amount of hepatic lipase released may reach nearly 0.07 nM [this calculation assumes that the amount of corrected activity secreted after 3 h is 2 mU/10^6 cells, a cell density of 2.5×10^6 cells/mL, and a M_r of the protein moiety of the enzyme of 53,222 (1)]. Therefore, we added 0.7 nM ^{125}I-hepatic lipase in these experiments. For comparison, the degradation of 0.1 nM ^{125}I-labeled lipoprotein lipase was

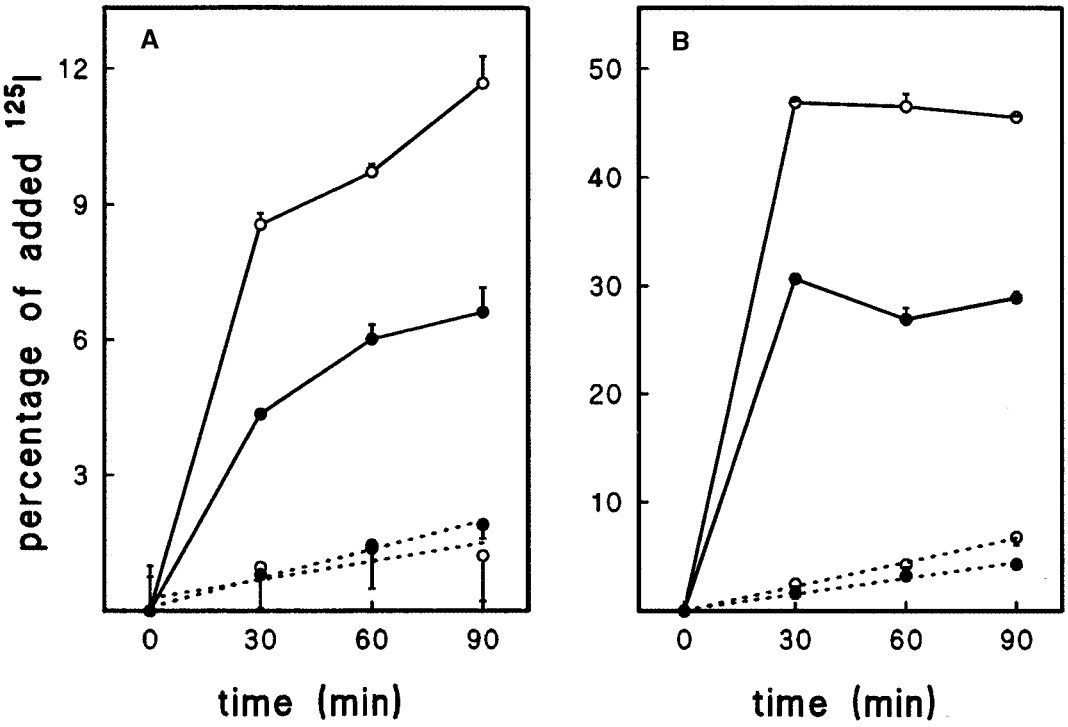

FIG. 6. Heparin does not affect degradation of added ^{125}I-labeled hepatic lipase. (A) Hepatocytes were incubated with 0.7 nM of ^{125}I-labeled hepatic lipase and either in the absence (○) or in the presence of 5 units-heparin/mL (●). At the indicated times, a sample was obtained to determine the amount of cell-associated (continuous lines) and the degraded (dotted lines) ^{125}I- labeled hepatic lipase. The results are the mean SE of triplicate values. (B) For comparison, another set of cells were incubated with 0.1 nM ^{125}I-labeled lipoprotein lipase instead of ^{125}I-labeled hepatic lipase.

studied. The results are shown in Figure 6. After 90 min of incubation, hepatocytes had taken up nearly 12% of the ^{125}I-hepatic lipase. Heparin decreased the uptake to about 6%. Only a very minor proportion of the radioactivity appeared as TCA-soluble (degraded) end products (less than 2%). Heparin did not affect this proportion. The estimated rate constants of ^{125}I-labeled hepatic lipase degradation were 0.014 ± 0.006 and 0.021 ± 0.002%/min in cells incubated in the absence and in the presence of heparin, respectively (nonsignificant differences). Isolated hepatocytes also took up ^{125}I-lipoprotein lipase and heparin decreased this uptake. The estimated rate constant of ^{125}I-labeled lipoprotein lipase degradation was decreased by heparin (0.074 ± 0.004 and 0.048 ± 0.003%/min in cells incubated in the absence and in the presence of heparin, respectively, $P < 0.01$). Heparin-sensitive pathways for uptake and degradation of active lipoprotein lipase in perfused livers have already been described (43).

DISCUSSION

Although hepatic lipase is synthesized in parenchymal liver cells (15,18), most of the enzyme molecules are found in the extracellular space (24). Schoonderwoerd *et al.* (44) found that heparin-sensitive sites accounted for most of the extracellular hepatic lipase binding sites. In agreement with these results, we observed that the perfusion of isolated livers with heparin released about 70% of the whole liver activity. Similar results were previously obtained in several laboratories (28,44).

Two different lines of evidence indicate that the liver continuously releases hepatic lipase to the circulation. The first is indirect: there was a highly significant correlation between hepatic lipase activity in liver and plasma. The second is more direct: isolated livers secreted hepatic lipase to the perfusate when they were perfused in the absence of heparin. This cannot be attributed to leakage of intracellular enzyme due to tissue damage because lactate dehydrogenase release was almost negligible. Furthermore, since the activity to mass ratio was similar in nonheparin and in heparin perfusates, we conclude that the spontaneously secreted enzyme was fully active.

From data in Figure 2 we calculated a secretion rate of 10 mUnits/min/liver. In heparin perfusates we recovered 2,065 mUnits (mean of two experiments). Since it is conceivable that the spontaneously secreted enzyme comes from that bound to some extracellular site [and among these sites, heparin-sensitive ones are the majority (44)], we may calculate a fractional turnover rate of 4.8×10^{-3} min^{-1}. This value predicts a half-residence time of about 150 min for the enzyme in the extracellular space. Cisar and Bensadoun (18) studied the intracellular processing of hepatic lipase in FU5AH rat hepatoma cells. They obtained a half-residence time of hepatic lipase inside the cells of nearly 60 min, which is in keeping with the results reported by Laposata *et al.* (15) concerning the process-

ing of this enzyme in nontransformed rat hepatocytes. The comparison of our predicted half-residence time in the extracellular space with that described for the processing of the enzyme inside hepatocytes explains why most of the enzyme molecules are found in the extracellular space.

In order to maintain a steady-state number of enzyme molecules in the extracellular space, the amount of hepatic lipase released to the perfusate (or to the blood stream in the whole animal) has to be replaced by new enzyme molecules synthesized in hepatocytes. Our results indicate that freshly isolated rat hepatocytes, incubated in amino acid- and vitamin-containing medium, maintain steady-state amounts of hepatic lipase inside the cells for several hours and that these cells continuously, and linearly, secrete active hepatic lipase at a rate of 10–12 μU/min × 10^6 cells (obtained from data in Fig. 4). It is known that adult rat liver contains about 10^9 hepatocytes (45). Thus, we may estimate a secretion rate of 10–12 mU/min × (whole liver), which is similar to the rate of hepatic lipase secretion obtained in perfusion experiments (see above).

Although heparin was reported to increase the amount of hepatic lipase secreted from hepatocytes (17), we observed that the apparent effect on secreted activity was actually the result of stabilization of the active conformation. Neither when the amount of secreted hepatic lipase mass was determined nor when the secreted activity was corrected by inactivation did heparin produce a significant effect.

Cisar *et al.* (20) studied the short-term effect of heparin on hepatic lipase secretion in a hepatoma cell line. They found that heparin increased the secretion of hepatic lipase mass because it decreased the degradation of both newly synthesized hepatic lipase and ^{125}I-labeled hepatic lipase added to the culture medium. They also reported the presence of a class of high-affinity binding sites on the cell surface [dissociation constant (K_D) 10^{-7} M]. A similar dissociation constant for the binding of hepatic lipase to purified low density lipoprotein receptor-related protein (LRP) was described more recently (46). These authors concluded that LRP mediates internalization and degradation of ^{125}I-labeled hepatic lipase by cultured cells, and that surface proteoglycans are also required. In all these cultured cell systems, heparin might prevent degradation by displacing hepatic lipase from its binding sites, which suggests that, as proposed for the lipoprotein lipase processing in avian adipocytes (47), degradation requires the passage of the enzyme by the cell surface.

In contrast to these results, we observed that a very minor proportion of added ^{125}I-labeled hepatic lipase was degraded in our cell system. In these experiments we added 0.7 nM ^{125}I-hepatic lipase, a concentration much lower than that used by Cisar *et al.* (20). In these conditions, given the K_D value for the association to LRP, one may expect a low binding of the enzyme to the cells, as we observed. Although heparin displaced some of the cell-associated enzyme, it did not affect the amount of enzyme degraded. We estimated that hepatic lipase produced endogenously reached an even lower concentration in the medium. Therefore, most of the enzyme that reached the cell surface might dissociate from binding sites and remain free in solution. This explains why there was no effect of heparin on the amount of enzyme released to the medium. If retention of hepatic lipase at the cell surface is required for degradation, we would expect to find no degradation of endogenous hepatic lipase in our cell system. In fact, we did not observe any decrease in the total amount of hepatic lipase in cells exposed to cycloheximide (Fig. 5), which indicates that there was no degradation of endogenous hepatic lipase.

It can be argued that, provided we used the cells immediately after isolation, the isolation procedure could have destroyed proteoglycans of the cell surface. However, we observed that these cells bound and degraded ^{125}I-lipoprotein lipase and that heparin decreased both binding and degradation of ^{125}I-lipoprotein lipase. Furthermore, the amount of ^{125}I-lipoprotein lipase bound to the cells that was displaced by heparin corresponded to that predicted by the K_D and association rate constant for the interaction of purified lipoprotein lipase with heparan sulfate (48). In addition, kinetics of binding and degradation of ^{125}I-lipoprotein lipase obtained in our experiments agree with those obtained in perfused livers (43).

Other arguments could explain the discrepancy concerning degradation of endogenous hepatic lipase. One is that the rate of hepatic lipase production may be much higher in hepatoma cells than in hepatocytes. Another is the fact that cultured cells produce a matrix around them, which is missing in freshly isolated cells. Although it was reported (13,49) that, in intact liver, most of extracellular hepatic lipase localizes at the Space of Disse associated apparently to the hepatocyte microvilli, the fixation techniques used in those reports did not allow for a precise identification of the structures at which the immunogold particles are bound, when samples are observed at 15,000× magnification. In fact, Vilaró (50), at a much higher magnification (75,000–127,000×), observed that most of the gold particles are actually associated with collagen-like fibers of the extracellular matrix. Binding of hepatic lipase to secreted fibers may contribute to explain why degradation of hepatic lipase was observed in cell culture (20,46), but not in freshly isolated cell suspensions.

Based on the results presented here, together with those reported in the literature and discussed above, we propose a model for the processing of hepatic lipase in the whole liver. Hepatocytes continuously secrete active hepatic lipase to the Space of Disse, where enzyme molecules are retained by extracellular matrix proteins. Some of the enzyme molecules in this extracellular compartment may eventually bind to LRP and return to hepatocytes, where they can be degraded (Scheme 1, where UG = unglycosylated; HL = hepatic lipase; and 52 and 55 refer, respectively, to molecular sizes of 52,000 and 55,000). Most of the secreted molecules will be released to the blood stream. Released enzyme molecules are then available to adrenal glands and ovaries, where they may contribute to the uptake of HDL-cholesterol.

This model predicts that the size of the extracellular pool of hepatic lipase is controlled primarily by the rate of secretion from hepatocytes. Literature shows some examples of this relationship. Both the amount of heparin-releasable hepatic li-

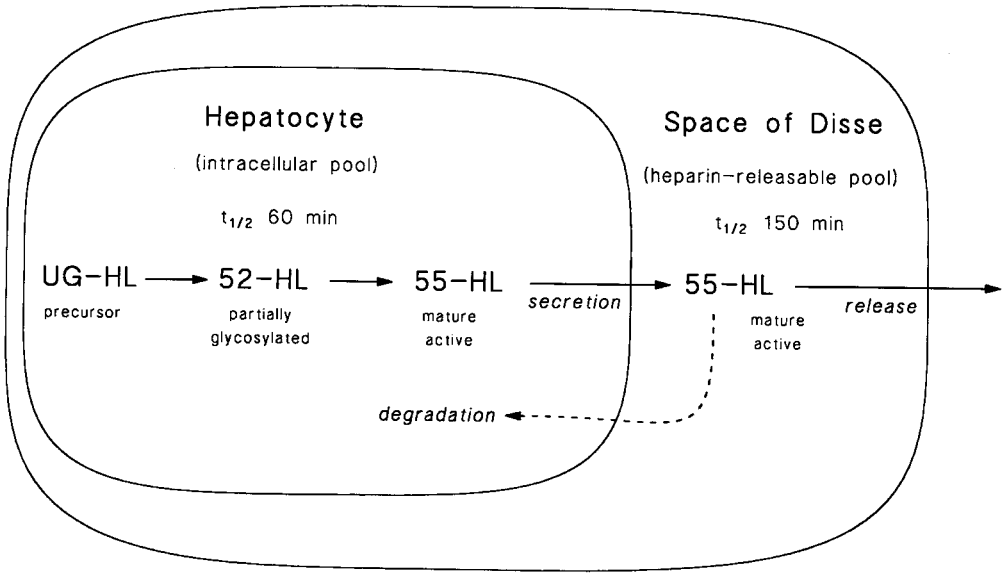

SCHEME 1

pase (51) and the secretion rate from isolated hepatocytes (52) are lower in corticosteroid-treated than in control rats. Short-term fasting (24 h) reduces both the amount of heparin-releasable activity in perfused livers and the secretion rate from isolated hepatocytes (28). This model does not exclude that other factors also contribute to control the amount of extracellular hepatic lipase, as it was previously proposed (52).

ACKNOWLEDGMENTS

We express our gratitude to Dr. Thomas Olivecrona (University of Umeå, Sweden) for the ^{125}I-labeled lipoprotein lipase and to Robin Rycroft for the editorial help. This work was supported by grants (PB91-0803 and PB92-0548) from D.G.I.C.Y.T. (Ministerio de Educación y Ciencia, Spain).

REFERENCES

1. Komaromy, M.C., and Schotz, M.C. (1987) Cloning of Rat Hepatic Lipase cDNA: Evidence for a Lipase Gene Family, *Proc. Natl. Acad. Sci. USA 84*, 1526–1530.
2. Kirchgessner, T.G., Chaut, J.C., Heinzmann, C., Etienne, J., Guilhot, S., Svenson, K., Ameis, D., Pilon, C., D'Auriol, L., Andalibi, A., *et al*. (1989) Organization of the Human Lipoprotein Lipase Gene and Evolution of the Lipase Gene Family, *Proc. Natl. Acad. Sci. USA 86*, 9647–9651.
3. Landin, B., Nilsson, A., Twu, J.S., and Schotz, M.C. (1984) A Role for Hepatic Lipase in Chylomicron and High Density Lipoprotein Phospholipid Metabolism, *J. Lipid Res. 25*, 559–563.
4. Jansen, H., van Tol, A., and Hülsmann, W.C. (1980) On the Metabolic Function of Heparin-Releasable Liver Lipase, *Biochem. Biophys. Res. Commun. 92*, 53–59.
5. Marques-Vidal, P., Azéma, C., Collet, X., Vieu, C., Chap, H., and Perret, B. (1994) Hepatic Lipase Promotes the Uptake of HDL Esterified Cholesterol by the Perfused Rat Liver: A Study Using Reconstituted HDL Particles of Defined Phospholipid Composition, *J. Lipid Res. 35*, 373–384.
6. Barrans, A., Collet, X., Barbaras, R., Jaspard, B., Manent, J., Vieu, C., Chap, H., and Perret, B. (1994) Hepatic Lipase Induces the Formation of Pre-β_1 High Density Lipoprotein (HDL) from Triacylglycerol-rich HDL_2. A Study Comparing Liver Perfusion to *in vitro* Incubation with Lipases, *J. Biol. Chem. 269*, 11572–11577.
7. Fielding, C.J., and Fielding, P.E. (1995) Molecular Physiology of Reverse Cholesterol Transport, *J. Lipid Res. 36*, 211–228.
8. Fan, J., Wang, J., Bensadoun, A., Lauer, S.J., Dang, Q., Mahley, R.W., and Taylor, J.M. (1994) Overexpression of Hepatic Lipase in Transgenic Rabbits Leads to a Marked Reduction of Plasma High Density Lipoproteins and Intermediate Density Lipoproteins, *Proc. Natl. Acad. Sci. USA 91*, 8724– 8728.
9. Homanics, G.E., De Silva, H.V., Osada, J., Zhang, S.H., Wong, H., Borensztajn, J., and Maeda, N. (1995) Mild Dyslipidemia in Mice Following Targeted Inactivation of the Hepatic Lipase Gene, *J. Biol. Chem. 270*, 2974–2980.
10. Breckenridge, W.C., Little, J.A., Alaupovic, P., Wang, C.S., Kuksis, A., Kakis, G., Lindgren, F., and Gardiner, G. (1982) Lipoprotein Abnormalities Associated with a Familial Deficiency of Hepatic Lipase, *Atherosclerosis 45*, 161–179.
11. Lambert, G., Amar, M.J.A., Martin, P., Fruchart-Najib, J., Föger, B., Shamburek, R.D., Brewer, H.B., Jr., and Santamarina-Fojo, S. (2000) Hepatic Lipase Deficiency Decreases the Selective Uptake of HDL-Cholesteryl Esters *in vivo, J. Lipid Res. 41*, 667–672.
12. Kuusi, T., Nikkilä, E.A., Virtanen, I., and Kinnunen, P.K.J. (1979) Localization of the Heparin-Releasable Lipase *in situ* in the Rat Liver, *Biochem. J. 181*, 245–246.
13. Breedveld, B., Schoonderwoerd, K., Verhoeven, A.J.M., Willemsen, R., and Jansen, H. (1997) Hepatic Lipase Is Localized at the Parenchymal Cell Microvilli in Rat Liver, *Biochem. J. 321*, 425–430.
14. Sanan, D.A., Fan, J., Bensadoun, A., and Taylor, J.M. (1997) Hepatic Lipase Is Abundant on Both Hepatocyte and Endothelial Cell Surfaces in the Liver, *J. Lipid Res. 38*, 1002–1013.
15. Laposata, E.A., Laboda, H.M., and Strauss, J.F., III (1987) Hepatic Lipase. Synthesis, Processing, and Secretion by Isolated Rat Hepatocytes, *J. Biol. Chem. 262*, 5333–5338.
16. Jansen, H., Kalman, C., Zonneveld, A.J., and Hülsmann, W.C. (1979) Secretion of Triacylglycerol Hydrolase Activity by Isolated Parenchymal Rat Liver Cells, *FEBS Lett. 98*, 299–302.
17. Leitersdorf, E., Stein, O., and Stein, Y. (1984) Synthesis and Secretion of Triacylglycerol Lipase by Cultured Rat Hepatocytes, *Biochim. Biophys. Acta 794*, 261–268.

18. Cisar, L.A., and Bensadoun, A. (1987) Characterization of the Intracellular Processing and Secretion of Hepatic Lipase in FU5AH Rat Hepatoma Cells, *Biochim. Biophys. Acta 927*, 305–314.
19. Busch, S.J., Martin, G.A., Barnhart, R.L., and Jackson, R.L. (1989) Heparin Induces the Expression of Hepatic Triglyceride Lipase in a Human Hepatoma (HepG2) Cell Line, *J. Biol. Chem. 264*, 9527–9532.
20. Cisar, L.A., Melford, K.H., Sensel, M., and Bensadoun, A. (1989) Heparin Decreases the Degradation Rate of Hepatic Lipase in Fu5AH Rat Hepatoma Cells. A Model for Hepatic Lipase Efflux from Hepatocytes, *Biochim. Biophys. Acta 1004*, 196–204.
21. Verhoeven, A.J.M., and Jansen, H. (1990) Secretion of Rat Hepatic Lipase Is Blocked by Inhibition of Oligosaccharide Processing at the Stage of Glucosidase I, *J. Lipid Res. 31*, 1883–1893.
22. Stahnke, G., Davis, R.C., Doolittle, M.H., Wong, H., Schotz, M.C., and Will, H. (1991) Effect of N-Linked Glycosylation on Hepatic Lipase Activity, *J. Lipid Res. 32*, 477–484.
23. Jansen, H., and De Greef, W.J. (1981) Heparin-Releasable Lipase Activity of Rat Adrenals, Ovaries and Testes, *Biochem. J. 196*, 739–745.
24. Persoon, N.L.M., Hülsmann, W.C., and Jansen, H. (1986) Localization of the Salt-Resistant Heparin-Releasable Lipase in the Rat Liver, Adrenal and Ovary, *Eur. J. Cell Biol. 41*, 134–137.
25. Hixenbaugh, E.A., and Paavola, L.G. (1991) Heterogeneity Among Ovarian Blood Vessels—Endogenous Hepatic Lipase Is Concentrated in Blood Vessels of Rat Corpora Lutea, *Anat. Rec. 230*, 291–306.
26. Doolittle, M.H., Wong, H., Davis, R.C., and Schotz, M.C. (1987) Synthesis of Hepatic Lipase in Liver and Extrahepatic Tissues, *J. Lipid Res. 28*, 1326–1334.
27. Hixenbaugh, E.A., Sullivan, T.R., Jr., Straus, J.F., III, Laposata, E.A., Komaromy, M., and Paavola, L.G. (1989) Hepatic Lipase in Rat Ovary. Ovaries Cannot Synthesize Hepatic Lipase But Accumulate It from the Circulation, *J. Biol. Chem. 264*, 4222–4230.
28. Peinado-Onsurbe, J., Soler, C., Galan, X., Poveda, B., Soley, M., Llobera, M., and Ramírez, I. (1991) Involvement of Catecholamines in the Effect of Fasting on Hepatic Endothelial Lipase Activity in the Rat, *Endocrinology 129*, 2599–2606.
29. Burgaya, F., Peinado, J., Llobera, M., and Ramírez, I. (1989) Hepatic Endothelial Lipase Activity in Neonatal Rat Liver, *Biosci. Rep. 9*, 559–564.
30. Vassault, A. (1983) Lactate Dehydrogenase: UV-Method with Pyruvate and NADH, in *Enzymes 1: Oxidoreductases, Transferases* (Bergmeyer, J., and Grassl, M., eds.) Vol. III, pp. 118–126, VCH Verlagsgessellschaft, Weinheim.
31. Burgaya, F., Peinado, J., Vilaró, S., Llobera, M., and Ramírez, I. (1989) Lipoprotein Lipase Activity in Neonatal-Rat Liver Cell Types, *Biochem. J. 259*, 159–166.
32. Ehnholm, C., Shaw, W., Greten, H., and Brown, W.V. (1975) Purification from Human Plasma of a Heparin-Released Lipase with Activity Against Triglycerides and Phospholipids, *J. Biol. Chem. 250*, 6756–6764.
33. Peinado-Onsurbe, J., Soler, C., Soley, M., Llobera, M., and Ramírez, I. (1992) Lipoprotein Lipase and Hepatic Lipase Activities Are Differentially Regulated in Isolated Hepatocytes from Neonatal Rats, *Biochim. Biophys. Acta 1125*, 82–89.
34. Waite, M., Thuren, T.Y., Wilcox, R.W., Sisson, P., and Kucera, G.L. (1991) Purification and Substrate Specificity of Rat Hepatic Lipase, in *Methods in Enzymology* (Denis, E.A., ed.), Vol. 197, pp. 331–339, Academic Press, New York.
35. Julve, J., Robert, M.Q., Llobera, M., and Peinado-Onsurbe, J. (1996) Hormonal Regulation of Lipoprotein Lipase Activity from 5-day-old Rat Hepatocytes, *Mol. Cell. Endocrinol. 116*, 97–104.
36. Laemmli, U.K. (1970) Cleavage of Structural Proteins During the Assembly of the Head of Bacteriophage T4, *Nature 227*, 680–685.
37. Wallinder, L., Peterson, J., Olivecrona, T., and Bengtsson-Olivecrona, G. (1984) Hepatic and Extrahepatic Uptake of Intravenously Injected Lipoprotein Lipase, *Biochim. Biophys. Acta 795*, 513–524.
38. Peterson, J., Olivecrona, T., and Bengtsson-Olivecrona, G. (1985) Distribtion of Lipoprotein Lipase Between Plasma and Tissues: Effect of Hypertriglyceridemia, *Biochim. Biophys. Acta 837*, 262–270.
39. Galan, X., Llobera, M., and Ramírez, I. (1994) Lipoprotein Lipase and Hepatic Lipase in Wistar and Sprague-Dawley Rat Tissues. Differences in the Effects of Gender and Fasting, *Lipids 29*, 333–336.
40. Glaser, D.S., Yost, T.J., and Eckel, R.H. (1992) Preheparin Lipoprotein Lipolytic Activities—Relationship to Plasma Lipoproteins and Postheparin Lipolytic Activities, *J. Lipid Res. 33*, 209–214.
41. Schoonderwoerd, K., Hülsmann, W.C., and Jansen, H. (1981) Stabilization of Liver Lipase *in vitro* by Heparin or by Binding to Non-parenchymal Liver Cells, *Biochim. Biophys. Acta 665*, 317–321.
42. Jansen, G.L., and Bensadoun, A. (1981) Purification, Stabilization, and Characterization of Rat Hepatic Lipase, *Anal. Biochem. 113*, 246–252.
43. Vilaró, S., Llobera, M., Bengtsson-Olivecrona, G., and Olivecrona, T. (1988) Lipoprotein Lipase Uptake by the Liver: Localization, Turnover, and Metabolic Role, *Am. J. Physiol. 254*, G711–G722.
44. Schoonderwoerd, K., Verhoeven, A.J.M., and Jansen, H. (1994) Rat Liver Contains a Limited Number of Binding Sites for Hepatic Lipase, *Biochem. J. 302*, 717–722.
45. Berry, M.N., Edwards, A.M., and Barritt, G.J. (1991) *Isolated Hepatocytes Preparation, Properties and Applications*, pp. 52–53, Elsevier, Amsterdam.
46. Kounnas, M.Z., Chappell, D.A., Wong, H., Argraves, W.S., and Strickland, D.K. (1995) The Cellular Internalization and Degradation of Hepatic Lipase Is Mediated by Low Density Lipoprotein Receptor-Related Protein and Requires Cell Surface Proteoglycans, *J. Biol. Chem. 270*, 9307–9312.
47. Cisar, L., Hoogewerf, A.J., Cupp, M., Rapport, C.A., and Bensadoun, A. (1989) Secretion and Degradation of Lipoprotein Lipase in Cultured Adipocytes. Binding of Lipoprotein Lipase to Membrane Heparan Sulfate Proteoglycans Is Necessary for Degradation, *J. Biol. Chem. 264*, 1767–1774.
48. Lookene, A., Chevreuil, O., Ostergaard, P., and Olivecrona, G. (1996) Interaction of Lipoprotein Lipase with Heparin Fragments and with Heparan Sulfate: Stoichiometry, Stabilization, and Kinetics, *Biochemistry 35*, 12155–12163.
49. Vilaró, S., Ramírez, I., Bengtsson-Olivecrona, G., Olivecrona, T., and Llobera, M. (1988) Lipoprotein Lipase in Liver. Release by Heparin and Immunocytochemical Localization, *Biochim. Biophys. Acta 959*, 106–117.
50. Vilaró, S. (1986) Lipoprotrein Lipase in Liver. Induction, Characterization, and Localization., Ph.D. Thesis, University of Barcelona, Barcelona.
51. Jansen, H., and Hülsmann, W.C. (1975) On Hepatic and Extrahepatic Postheparin Serum Lipase Activities and the Influence of Experimental Hypercortisolism and Diabetes on These Activities, *Biochim. Biophys. Acta 398*, 337–346.
52. Schoonderwoerd, K., Hülsmann, W.C., and Jansen, H. (1983) Regulation of Liver Lipase. I. Evidence for Several Regulatory Sites, Studied in Corticotrophin-treated Rats, *Biochim. Biophys. Acta 754*, 279–283.

[Received November 1, 1999, and in revised form May 30, 2000; revision accepted July 20, 2000]

Study of Individual *trans*- and *cis*-16:1 Isomers in Cow, Goat, and Ewe Cheese Fats by Gas–Liquid Chromatography with Emphasis on the *trans*-Δ3 Isomer

Frédéric Destaillats[a], Robert L. Wolff[a,*], Dietz Precht[b], and Joachim Molkentin[b]

[a]Institut des Sciences et Techniques des Aliments de Bordeaux, Talence, France, and [b]Bundesanstalt für Milchforschung, Kiel, Germany

ABSTRACT: Low-temperature gas–liquid chromatography (GLC) was applied to study the distribution profiles of isomeric *trans*- and *cis*-hexadecenoic acids in ruminant (cow, goat, and ewe) milk fat after their fractionation by argentation thin-layer chromatography (Ag-TLC). The fat was extracted from cheeses (12 samples of each species), the most common foods made with goat and ewe milks. The predominant *trans*-16:1 isomer is palmitelaidic acid (the Δ9 isomer), but it does not exceed one-third of the total group, which itself represents 0.17% (cow), 0.16% (goat), and 0.26% (ewe) of the total fatty acids. The *trans*-Δ3 16:1 isomer, which is reported for the first time in ruminant lipids and which likely comes from the animals' feed, is present at a level of *ca.* 10% of the *trans*-16:1 acid group. Otherwise, all isomers with their ethylenic bond between positions Δ4 and Δ14 are observed in the three species studied, roughly showing the same relative distribution pattern. Quantitatively, the *trans*-16:1 isomers only represent *ca.* 5% of the sum of the *trans*-16:1 plus *trans*-18:1 isomers, and they appear of little importance in comparison. It is inferred from this and recent studies that some previously reported data that were established for consumption assessments dealt in fact mainly with iso-17:0 acid, which was confused with (and added to) *trans*-Δ9 (palmitelaidic) acid; consequently, these results were large overestimates. Regarding the *cis*-16:1 acids, the Δ9 isomer is the prominent constituent as expected, but the second-most important isomer is the Δ13 isomer. It does not appear that *trans*-16:1 isomers are from ruminant milk fats of great nutritional importance as compared with *trans*-18:1 isomeric acids. As for *trans*-18:1 isomers, the combination Ag-TLC/GLC is a necessary procedure to quantitate *trans*-16:1 acids accurately and reliably. Ag-TLC allows removal of interfering branched 17:0 acids and *cis*-16:1 acids, and low-temperature GLC permits an accurate measurement of all individual isomers most of which with baseline resolution.

Paper L8463 in *Lipids 35,* 1027–1032 (September 2000).

In some earlier reports on the possible health effects of *trans* fatty acid consumption, dietary *trans*-16:1 isomers were alleged to be a potential cause in the etiology of ischemic heart diseases (1,2). Such isomers may indeed be present in the human diet; the main sources would be partially hydrogenated fish oils (3) and ruminant fats (4–10), but partially hydrogenated vegetable oils would be negligible (3,10) because native vegetable oils contain only very small amounts of unsaturated C_{16} acids.

However, the overlap of *trans*-16:1 isomers and branched 17:0 acids [mainly iso and anteiso forms, and also other methyl-hexadecanoic acids (3,6–10)] during gas–liquid chromatography (GLC) on highly polar columns (generally used in the study of *trans* fatty acids) is a pitfall that is well known to gas chromatographers (3,6–10) and that precludes any reliable conclusions based on single chromatographic runs of fatty acids containing both *trans*-16:1 isomers and branched 17:0 acids, as well as *cis*-16:1 isomers. Moreover, little is known about the nature (position of the ethylenic bonds) and the distribution of individual *trans*-16:1 isomers in ruminant fats. These fats (particularly cow milk fat) are important dietary sources of *trans* fatty acids in many European countries (9,11,12). The little information that has appeared about isomeric distribution of *trans*-16:1 isomers in bovine milk fats was published 30 yr ago by Hay and Morrison (4), who used a combination of argentation thin-layer chromatography (Ag-TLC), preparative GLC, oxidative cleavage, and further GLC of the resulting fragments, and more recently by Precht and Molkentin (10), who used Ag-TLC and low-temperature GLC on 100-m capillary columns. Other *trans*-16:1 acid profiles have been reported for steer perinephric fat (5), for margarines, cooking fats, and shortenings containing partially hydrogenated fish oil (3), and for human milk (10).

Another common error made by nutritionists is to consider *trans*-16:1 isomers as being limited to a single component, palmitelaidic (*trans*-9 16:1) acid, probably because this is the only *trans*-hexadecenoate isomer commercially available as a standard. On 50-m columns coated with 100% cyanopropylpolysiloxane stationary phases as well as also on 100-m columns not operated under optimized conditions, palmitelaidic acid exactly coincides with the branched iso-17:0 (methyl-15-hexadecanoic) acid (3,9,10). In ruminant fats, in particular, the latter acid accounts for 0.3 to 0.5% of total fatty acids, depending on the cattle feed (13). The confusion between these two acids may explain why high levels of *trans*-

*To whom correspondence should be addressed at ISTAB, Université Bordeaux 1, Avenue des Facultés, 33405 Talence Cedex, France.
E-mail: r.wolff@istab.u-bordeaux.fr

Abbreviations: Ag-TLC, argentation thin-layer chromatography; FAME, fatty acid methyl ester; FFA, free fatty acid; GLC, gas–liquid chromatography; TMSH, trimethyl sulfonium hydroxide.

16:1 acids are reported in some nutritional or food survey studies (14). In fact, as already demonstrated 30 yr ago (4), as well as in recent studies (3,10), the *trans*-16:1 acid group encompasses several isomers, the major one being indeed palmitelaidic acid. Further, the other *trans*-16:1 isomers partly overlap with anteiso-17:0 and 17:0 acids, even on a 100-m column operated at low oven temperatures of 120 to 125°C (3,10).

The purpose of the present study was to quantitate each individual *trans*-16:1 isomer in ruminant milk fats. We chose cheeses as starting material, with the assumption that their fatty acid compositions are representative of the corresponding milks, i.e., from cow, goat, and ewe. The cheeses, which were purchased in May–June, are supposed to be representative mostly of spring milks in the case of cow milk. Data for *trans*-16:1 isomers were already partially available for cow milk fat [$n = 27$ (3) and $n = 3$ (10)]. In particular, the whole group of *trans*-16:1 isomers represents between 0.05 and 0.25% of the total fatty acids, averaging *ca*. 0.13% (3). We report here on the detailed *trans*- as well as *cis*-16:1 isomeric acid profiles of fat from French cheeses manufactured with cow, goat, and ewe milk. The analytical method used for this purpose involves a combination of Ag-TLC and GLC on 100% cyanopropyl-polysiloxane-coated 100-m capillary columns operated under optimal temperature and carrier gas pressure. Also evidence is given for the first time on *trans*-Δ3 16:1 acid occurring in ruminant milk fats, likely originating from the animals' feed (green parts of plants). It is common knowledge that the *trans*-Δ3 16:1 acid is a major constituent of chloroplast diacylglycerylphosphorylglycerol (15).

EXPERIMENTAL PROCEDURES

Samples. Three lots each of 12 different cheeses made with cow, goat, and ewe milks (produced in France) were purchased locally in supermarkets near Bordeaux (France) in May–June 1999. Frozen spinach leaves were bought in a supermarket in Kiel (Germany). Genuineness of the cheese samples was ascertained by establishing the 12:0/10:0 acid ratios (11).

Fat extraction. Cheese fat was extracted according to Wolff *et al*. (16) using isopropanol and hexane. Representative portions of the cheeses (*ca*. 40 g) were homogenized in a mortar with a pestle, and 5 g of the homogenate was dispersed in 10 mL of isopropanol in a Teflon-coated beaker with an Ultraturrax T25 (Janke & Kunkel GmbH & Co. KG, Staufen, Germany). A sufficient amount of anhydrous Na_2SO_4 and 15 mL of hexane were then added, and a second dispersion was carried out with the Ultraturrax. The suspension was then filtered on a glass column containing a lower layer of anhydrous Na_2SO_4 and an upper layer of Celite 545 (*ca*. 2 cm height each). The lipid solution was eluted three times successively with 25-mL portions of hexane/isopropanol (3:2, vol/vol) and collected in a 250-mL flask. After the solvents were removed in a rotary evaporator at 45°C, the fat was weighed and then transferred into 5-mL vials and stored at 4°C until use.

Fatty acid methyl ester (FAME) preparation. As cheese fats may contain a higher amount of free fatty acids (FFA), the fat acidity of all 36 samples was determined according to International Dairy Federation standard 6B (17). In contrast to methylation with trimethyl sulfonium hydroxide (TMSH), sodium methoxide does not transform FFA into FAME. To choose a suitable transesterification method, we prepared FAME from cheese fat samples having a particularly high FFA content by using both methods. However, the results showed that the fatty acid composition was not significantly influenced by FFA contents. Compared to the TMSH method, the sodium methoxide procedure as used with our samples was more precise. The following procedure was thus chosen. FAME were prepared by vigorously shaking for 3 min a mixture of 1.2 mL *n*-heptane, 0.3 mL of a 10% fat solution in *n*-heptane, and 30 µL of a 2 N sodium methoxide solution in methanol. After centrifugation, the supernatant was directly used for GLC analysis. For Ag-TLC, a 20% fat solution was used. The fat solutions used for FAME preparation were obtained by blending equal amounts of fats from each of the 12 cheeses from a given species. Data reported here are thus for composite samples.

Fractionation of FAME by Ag-TLC. FAME were fractionated according to the number and geometry of double bonds by TLC on silica-gel plates prepared by immersion in a 20% aqueous solution of $AgNO_3$ as described by Precht and Molkentin (18). The developing solvent was the mixture *n*-heptane/diethyl ether (90:10, vol/vol). At the end of the chromatographic runs, the plates were briefly air-dried, lightly sprayed with a solution of 2′,7′-dichlorofluorescein, and viewed under ultraviolet light (234 nm). The *trans*- and *cis*-monoenoic acid bands were scraped off separately and eluted several times with diethyl ether. Complete evaporation of the combined eluates of each fraction was achieved with a light stream of N_2. The residues were dissolved in an appropriate volume of *n*-heptane for further GLC analysis.

Analysis of FAME by GLC. The total fatty acid composition covering *ca*. 70 fatty acids in the carbon chain length range of 4:0 to 24:0 was determined by GLC analysis of the methyl esters on a CP 9001 chromatograph (Chrompack, Middelburg, The Netherlands) equipped with a split injector (split ratio, 1:50) and a flame-ionization detector, using a 25-m capillary CP-Wax 58 CB column (0.25 mm i.d., 0.20 µm film depth; Chrompack). The operating conditions were: H_2 as the carrier gas at an inlet pressure of 40 kPa; injector and detector temperature, 265°C; oven program: 50°C, 1 min, then 5°C/min to 225°C, 15 min isothermal, and finally 5°C/min to 260°C. Calibration of the individual fatty acids was achieved using the reference material CRM 164 obtained from the Community Bureau of Relevence, Commission of the European Communities (Brussels, Belgium).

Analyses of the *cis* and *trans* isomers in total FAME as well as of individual *cis*- and *trans*-16:1 isomer fractions isolated by Ag-TLC were performed using a gas chromatograph CP 9000 (Chrompack) with a split injector, a flame-ionization detector, and a fused-silica capillary column (100 m × 0.25 mm i.d.) coated with 0.20 µm CP-Sil 88 (Chrompack)

under the following conditions: H_2 as the carrier gas; injector temperature 255°C; detector temperature 280°C. The unfractionated FAME were analyzed isothermally at 172°C with a column head pressure of 160 kPa (split ratio, 1:50). Monoenoic TLC fractions were analyzed isothermally at a lower temperature, 120°C, with a column head pressure of 220 kPa (split ratio, 1:25), as described earlier (3,10). Under these conditions, elution of *cis*- as well as *trans*-16:1 isomers took approximately 100 min.

The calibration of positional isomers of the *trans*-16:1 and *trans*-18:1 acids present in the *trans*-monoenoate fraction was achieved with the isomer *trans*-Δ11 18:1, which had been quantitated by stearic acid in the isothermal chromatography of the unfractionated FAME on the CP-Sil 88 column. Stearic acid was determined beforehand by total FAME analysis on the CP-Wax 58 CB column. Further, the *cis*-16:1 and -17:1 isomers found in the *cis*-monoenoate fraction were calibrated by *cis* 9-17:1 acid, which could be determined in the isothermal chromatogram of unfractionated FAME (10). Calibration of GLC data included the conversion from methyl esters to FFA. Thus, results expressing absolute concentrations are given as g/100 g or mg/100 g of total fatty acids.

Identification of individual isomeric *trans*- and *cis*-hexadecenoic acids was achieved according to Precht and Molkentin (3,9,10), except for the *trans*-Δ3 16:1 acid (see below). Integration and quantitation were accomplished with a HP 3365 II ChemStation system (Hewlett-Packard, Palo Alto, CA).

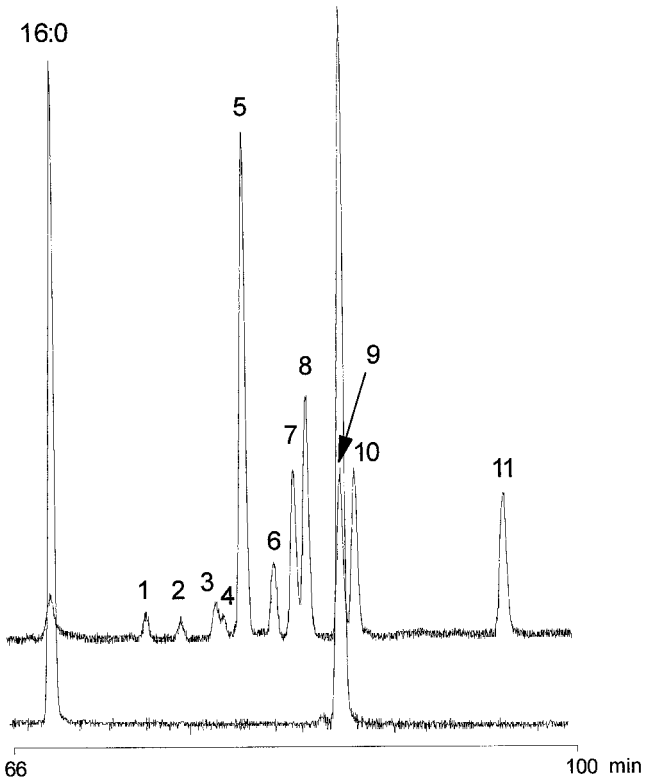

FIG. 1. Representative chromatogram of *trans*-isomeric hexadecenoic acid methyl esters prepared from ewe cheese fat (upper chromatogram) and spinach leaf lipid extract (lower chromatogram, spiked with methyl palmitate for time calibration) and fractionated by argentation thin-layer chromatography prior to analysis by low-temperature gas–liquid chromatography on a 100-m CP-Sil 88 capillary column (Chrompack, Middelburg, The Netherlands) operated 120°C, with H_2 as the carrier gas at an inlet pressure of 220 kPa. Peak numbering as in Table 1.

RESULTS AND DISCUSSION

Figure 1 shows a typical gas chromatogram of *trans*-16:1 isomers prepared from ewe milk fat after Ag-TLC fractionation followed by low-temperature GLC. Baseline resolution of most peaks could only be achieved by reducing the temperature to 120°C, resulting in 100-min analysis times. *Trans*-16:1 fractions from the three species studied here were qualitatively similar. Identifications were made according to Precht and Molkentin (3,10), using in particular a corresponding fraction isolated from hydrogenated fish oil as a secondary standard. In addition to peaks identified in this way (Δ4 to Δ14), a supplementary peak was observed that preceded the Δ13 isomer (arrow in Fig. 1). A possibility for the structure of this peak was *trans*-Δ3 16:1, as we knew that a *trans*-Δ3 18:1 standard elutes just before the Δ15 18:1 *trans* isomer (10,19; Wolff, R.L., and Destaillats, F., unpublished data). This also seemed logical, as the *trans*-3 16:1 isomer is a normal constituent of plant lipids, being more specifically esterified to the *sn*-2 position of diacylglycerophosphorylglycerol in chloroplasts (13), and hence present in the cattle feed. Also, Ackman and Macpherson (6) suspected its presence in butterfat.

To test this hypothesis, we isolated *trans*-Δ3 16:1 acid from lipids extracted by the method of Folch *et al.* (20) from frozen spinach leaves by Ag-TLC of the FAME. Although we saw no band between the saturated and *cis*-monoenoic acid fractions, where *trans*-3 16:1 acid was expected to migrate (21), we scraped off the gel between these two fractions and eluted its content. This intermediate fraction contained a single peak, *trans*-Δ3 16:1 acid, which coeluted with the unknown component in the *trans*-monoenoic acid fraction isolated from ruminant milk fat (Fig. 1). The experiment was repeated with *trans*-Δ3 16:1 acid isolated from fresh leaves of *Araucaria araucana* (monkey puzzle tree), *Pinus pinaster* (maritime pine), and *Aster tongolensis*, the latter plant being known for its particularly high level of *trans*-Δ3 16:1 acid. The unknown peak is thus the *trans*-Δ3 16:1 isomer. This peculiar isomer does not seem to have been reported previously in ruminant fats, or more generally, in herbivore fats, although the hypothesis of its presence in the latter source was put forth as early as 1964 (22). Because *A. tongolensis* also contains a *trans*-Δ3 18:1 acid (Aitzetmüller, K., personal communication), we looked for its presence among ruminant *trans*-18:1 isomers, but we could not detect it. A dietary origin of *trans*-Δ3 16:1 acid, rather than a β-oxidation of the Δ5 *trans*-18:1 acid (a very minor isomer in milk fats), is the most probable explanation for the presence of that isomer. Interestingly, human milk lipids are devoid of the *trans*-Δ3 isomer, although all other *trans*-16:1 isomers are present in that source (10).

Table 1 displays the relative proportions of individual

TABLE 1
Relative Distribution of *trans*-Positional Isomers of Hexadecenoic Acid in Cow, Goat, and Ewe Cheese Fat

Peak number[a]	Double bond position[b]	Weight % of total[c]		
		Cow	Goat	Ewe
1	Δ4	1.8	2.7	1.5
2	Δ5	1.6	1.8	1.8
3	Δ6/Δ7	4.1	5.2	3.6
4	Δ8	2.5	3.7	2.6
5	Δ9	31.7	26.6	31.1
6	Δ10	4.6	6.6	5.5
7	Δ11	7.3	9.6	9.0
8	Δ12	11.0	14.6	13.3
9	Δ3	14.7	8.6	12.6
10	Δ13	10.0	9.5	9.9
11	Δ14	10.8	11.1	9.0

[a]Peak numbers refer to Figure 1.
[b]The position of the double bond is counted from the carboxylic end.
[c]Values established with composite samples (see Experimental Procedures section).

trans-16:1 isomers established in cow, goat, and ewe milk fats. The first remark concerns the level of palmitelaidic acid, which represents only one-fourth to one-third of total *trans*-16:1 isomers. This observation supports older estimates established by oxidative cleavage of monoenoic fatty acids, which indicate similar or slightly higher values, 33 and 46% for two samples of cow milk fat (4). This observation also agrees with recent results for German bovine milk fat (10). In taking into account the range indicated above, this acid represents on average 0.04% of total fatty acids. A second point is that the content of the Δ3 isomer is not negligible, as it is ranked second to fourth, depending on the species, with values in the range 8.6–14.7% of the *trans*-16:1 fraction. Other isomers with contents in the same approximate range are the Δ12, Δ13, and Δ14 isomers. Isomers with their ethylenic bond between the carboxylic group and the Δ9-position (Δ4 to Δ8) are practically all less than 5%, with the Δ10 isomer showing a somewhat intermediate range (*ca.* 5–7%).

The *cis*-16:1 isomer group is much simpler than the corresponding *trans* fraction with only six visible peaks instead of 11 (Fig. 2). As expected, palmitoleic (*cis*-9 16:1) acid is by far the major isomer (two-thirds and more) (Table 2). However, in contrast to what occurs in most plants and animals, as well as in human milk fat (10), the second major isomer is not the Δ7 isomer, but the Δ13 isomer. As regards the *cis*-18:1 isomers, it is known that the Δ15 isomer is derived from α-linolenic (9,12,15-18:3) acid by biohydrogenation (23). However, in ruminant milk fats, this isomer is present at levels not exceeding 1% of total *cis*-18:1 acids (Precht, D., Molkentin, J., Destaillats, F., and Wolff, R.L., unpublished data). A possibility is that the *cis*-Δ13 16:1 isomer derives from the *cis*-Δ15 18:1 isomer by β-oxidation, but another possibility would be the biohydrogenation of 16:3n-3 (7,10,13-16:3) acid, also a common constituent of plant lipids. This possibility could also hold for the *trans*-16:1 isomers. It should be noted that the *cis*-Δ7, -Δ9, and -Δ13 16:1 isomers give three peaks that are quite well separated on 50-m CP-Sil 88 columns after Ag-TLC fractionation (see, e.g., Ref. 11, where the Δ13 isomer was tentatively and erroneously assigned the structure Δ11).

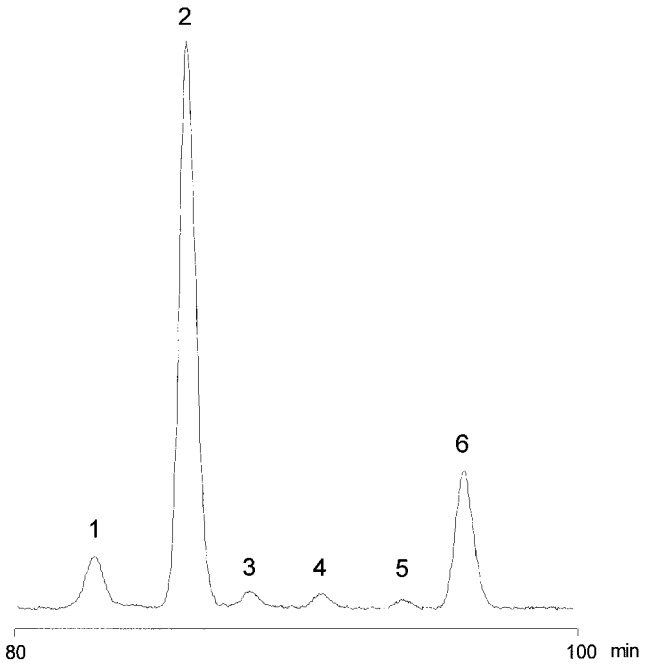

FIG. 2. Representative chromatogram of *cis*-isomeric hexadecenoic acid methyl esters prepared from ewe cheese fat and fractionated by argentation thin-layer chromatography prior to analysis by low-temperature gas–liquid chromatography on a 100-m CP-Sil 88 capillary column (commercial source and operating conditions as in Fig. 1). Peak numbering as in Table 2.

A comparison of the different *trans*- and *cis*-16:1 acid relative distributions immediately shows a profound similarity between the three species analyzed here (Tables 1 and 2). As expected, with the exception of the exogenous *trans*-Δ3 isomer, the bulk of *trans*-16:1 isomeric acids has its double bonds between positions Δ9 and Δ14, in the same way that *trans*-18:1 acids have their ethylenic bonds mostly between positions Δ11 and Δ16. The similarity between the three profiles (Table 1) suggests that the same biosynthetic pathways operate in the formation of the *trans*-16:1 acids, although it is

TABLE 2
Relative Distribution of *cis*-Positional Isomers of Hexadecenoic Acid in Cow, Goat, and Ewe Cheese Fat

Peak number[a]	Double bond position[b]	Weight % of total[c]		
		Cow	Goat	Ewe
1	Δ7	3.3	7.8	5.9
2	Δ9	82.0	66.0	74.6
3	Δ10	0.9	3.6	2.5
4	Δ11	3.4	3.1	2.8
5	Δ12	1.4	2.1	2.4
6	Δ13	9.0	17.3	11.8

[a]Peak numbers refer to Figure 2.
[b]The position of the double bond is counted from the carboxylic end.
[c]Values established with composite samples (see Experimental Procedures section).

not possible to decide whether they originate from *trans*-18:1 isomers by β-oxidation, or by biohydrogenation of 16:3n-3 acid from the feed. Both mechanisms might operate as well.

Regarding the absolute concentrations of *trans*-16:1 acids in French cheese fat samples, the following amounts could be established: cow, 0.17; goat, 0.16; and ewe, 0.26 g/100 g (results not shown). These values are in the range determined by Precht and Molkentin (3) for German cow milk fat under various feeding conditions. For the major isomer, palmitelaidic acid, we found 54, 41, and 80 mg/100 g of total fatty acids for cow, goat, and ewe, respectively. However, it should be stressed that *trans*-16:1 isomers only represent from 4.2 (cow milk) to 5.6% (goat milk) of the sum *trans*-16:1 plus *trans*-18:1 acids (practically all *trans*-monoenoic acids; results not shown). Thus they are very minor isomers in ruminant milk fats. As for the *trans*- and *cis*-18:1 isomers, accurate and reliable determinations of *trans*- and *cis*-16:1 isomers can only be obtained by using the Ag-TLC/GLC combination. Direct GLC cannot distinguish between all components, as many peak overlaps between the *cis*- and *trans*-16:1 acids occur, in addition to those with branched-17:0 acids. Clearly, data obtained by direct GLC are inaccurate and unreliable, owing in particular to a confusion between *trans*-Δ9 16:1 and iso-17:0 acids. Determination of the *trans*-16:1 as well as the *trans*-18:1 isomers by single GLC runs without Ag-TLC prefractionation is thus a faulty procedure (24). However, in the former case, large overestimates are obtained, whereas in the latter case, underestimates of variable amplitude are made (25). This can be examplified by data reported in the industry-sponsored TRANSFAIR study (14). In that study, the so-called *trans*-Δ9 16:1 acid reached almost 0.8% of total fatty acids in some instances. In comparison with our data, this represents overestimates by as much as 2,000%. This undoubtedly is due to the fact that iso-17:0 acid (major) and *trans*-Δ9 16:1 acid (minor) were both reported as *trans*-16:1 isomers. Regarding the *trans*-18:1 isomers, we reported elsewhere (25) that data from the same study were underestimates by *ca.* 35%. In both cases, assessments resemble more haphazard assessments than accurate measurements. The same would hold for data relating to beef fat (14,26).

Regarding the consumption of *trans*-16:1 acids by the French population, for whom an intake of 1.5 g/p/d of *trans*-18:1 acids from ruminant fats is admitted (7,11), our results would imply that the consumption of total *trans*-16:1 isomers (5% of total *trans*-monoenoic acids) would not exceed 0.08 g/p/d. Of these, at most *ca*. 0.03 g/p/d (one-third) should correspond to the sole *trans*-9 16:1 isomer. In the TRANSFAIR study (27), the estimate for this isomer was 0.36 g/p/d, that is, 12 times more than our own determination based on the Ag-TLC/GLC procedure. Interestingly, our consumption estimate is supported by studies from Combe *et al*. (28,29) who employed the Ag-TLC/GLC procedure and found 0.08% of total *trans*-16:1 acids in the milk of lactating French women, and 0.06% in the adipose tissue of nonparturient women (0.10% in parturient women and in men).

Finally, it should be emphasized that the use of low-temperature conditions in operating the 100-m column (i.e., 120°C), which are not commonly employed, is a simple alternative to the formerly used oxidative cleavage of 16:1 isomers isolated by Ag-TLC and preparative GLC, and further analysis of the resulting fragments by GLC (4,5). The 18:1 isomeric acids isolated along with the 16:1 acids can be analyzed during the same GLC run but with long retention times of *ca*. 3.5 h (Precht, D., Molkentin, J., Destaillats, F., and Wolff, R.L., unpublished data).

ACKNOWLEDGMENTS

The authors thank Birte Fischer and Bärbel Krumbeck for their contribution to the analytical work. Elodie Pasquier contributed to the preparation of the *trans*-3 16:1 acid fraction from *Araucaria araucana* and *Pinus pinaster* leaves. Professor Kurt Aitzetmüller kindly donated a sample of plant oil from *Aster tongolensis*. F. Destaillats was funded by an ADERA (Association pour le Développement de l'Enseignement et des Recherches auprès des Universirés, des Centres de Recherche, et des Entreprises d'Aquitaine) grant and Bundesanstalt für Milchforschung, Kiel.

REFERENCES

1. Thomas, L.H., and Winter, J.A. (1987) Ischaemic Heart Disease and Consumption of Hydrogenated Marine Oils, *Hum. Nutr.: Food Sci. Nutr. 41F*, 153–165.
2. Thomas, L.H., Olpin, S.O., Scott, R.G., and Wilkins, M.P. (1987) Coronary Heart Disease and the Composition of Adipose Tissue Taken at Biopsy, *Hum. Nutr.: Food Sci. Nutr. 41F*, 167–172.
3. Molkentin, J., and Precht, D. (1997) Occurrence of *trans*-C16:1 Acids in Bovine Milkfats and Partially Hydrogenated Edible Fats, *Milchwissenschaft 52*, 380–385.
4. Hay, J.D., and Morrison, W.R. (1970) Isomeric Monoenoic Fatty Acids in Bovine Milk Fat, *Biochim. Biophys. Acta 202*, 237–243.
5. Hay, J.D., and Morrison, W.R. (1973) Positional Isomers of *cis* and *trans* Monoenoic Fatty Acids from Ox (steer) Perinephric Fat, *Lipids 8*, 94–95.
6. Ackman, R.G., and Macpherson, E.J. (1994) Coincidence of *cis*- and *trans*-Monoethylenic Fatty Acids Simplifies the Open-Tubular Gas–Liquid Chromatography of Butyl Esters of Butter Fatty Acids, *Food Chem. 50*, 45–52.
7. Wolff, R.L. (1994) Contribution of *trans*-18:1 Acids from Ruminant Fats to European Diets, *J. Am. Oil Chem. Soc. 71*, 277–283.
8. Alonso, L., Fontecha, J., Lozada, L., Fraga, M.J., and Juarez, M. (1999) Fatty Acid Composition of Caprine Milk: Major, Branched-Chain, and *trans* Fatty Acids, *J. Dairy Sci. 82*, 878–884.
9. Precht, D., and Molkentin, J. (1999) C18:1, C18:2 and C18:3 *trans* and *cis* Fatty Acid Isomers Including Conjugated *cis* Δ9, *trans* Δ11 Linoleic Acid (CLA) as Well as Total Fat Composition of German Human Milk Lipids, *Nahrung 43*, 233–244.
10. Precht, D., and Molkentin, J. (2000) Identification and Quantitation of *cis*/*trans*-16:1 and -17:1 Fatty Acid Positional Isomers in German Human Milk Lipids by TLC–Gas Chromatography–Mass Spectrometry, *Eur. J. Lipid Sci. Technol. 102*, 102–113.
11. Wolff, R.L. (1995) Content and Distribution of *trans*-18:1 Acids in Ruminant Milk and Meat Fats. Their Importance in European Diets and Their Effect on Human Milk, *J. Am. Oil Chem. Soc. 72*, 259–272.
12. Wolff, R.L., Precht, D., and Molkentin, J. (1998) *Trans*-18:1 Acid Content and Profile in Human Milk Lipids. Critical Survey

of Data in Connection with Analytical Methods, *J. Am. Oil Chem. Soc. 75*, 661–671.
13. Precht, D. (1990) Quantitativer Nachweis von Milchfett in Schokolademischungen I: Bestimmung von Milchfettanteilen in Kakaobutter, *Fat Sci. Technol. 92*, 153–161.
14. Aro, A., Antoine, J.M., Pizzoferrato, L., Reykdal, O., and van Poppel, G. (1998) *Trans* Fatty Acids in Dairy and Meat Products from 14 European Countries: The TRANSFAIR Study, *J. Food Comp. Anal. 11*, 150–160.
15. Ohnishi, M., and Thompson, G.A., Jr. (1991) Biosynthesis of the Unique *trans* Δ^3-Hexadecenoic Acid Component of Chloroplast Phosphatidylglycerol: Evidence Concerning Its Site and Mechanism of Formation, *Arch. Biochem. Biophys. 288*, 591–599.
16. Wolff, R.L., Bayard, C.C., and Fabien, R.J. (1995) Evaluation of Sequential Methods for the Determination of Butterfat Fatty Acid Composition with Emphasis on *trans*-18:1 Acids. Application to the Study of Seasonal Variations in French Butters, *J. Am. Oil Chem. Soc. 72*, 1471–1483.
17. International Dairy Federation (1989) IDF Standard 6B: Determination of Fatty Acid, IDF, Brussels, Belgium.
18. Molkentin, J., and Precht, D. (1996) Isomeric Distribution and Rapid Determination of *trans*-Octadecenoic Acids in German Brands of Partially Hydrogenated Edible Fats*, Nahrung 40*, 297–304.
19. Gunstone, F.D., Ismail, I.A., and Lie Ken Jie, M.S.F. (1967) Thin-Layer and Gas–Liquid Chromatographic Properties of the *cis* and *trans* Methyl Octadecenoates and of Some Acetylenic Esters, *Lipids 1*, 376–385.
20. Folch, J., Lees, M., and Sloane-Stanley, G.M. (1957) A Simple Method for the Isolation and Purification of Total Lipids from Animal Tissues, *J. Biol. Chem. 226*, 497–509.
21. Lamberto, M., and Ackman, R.G. (1994) Confirmation by Gas Chromatography/Mass Spectrometry of Two Unusual *trans*-3-Monoethylenic Fatty Acids from the Nova Scotian Seaweed *Palmaria palmata* and *Chondrus crispus*, *Lipids 29*, 441–444.
22. Weenink, R.O., and Shorland, F.B. (1964) The Isolation of *trans*-3-Hexadecenoic Acid from the Lipids of Red-Clover (*Trifolium pratense*) Leaves, *Biochim. Biophys. Acta 84*, 613–614.
23. Kemp, P., White, R.W., and Lander, D.J. (1975) The Hydrogenation of Unsaturated Fatty Acids by Five Bacterial Isolates from the Sheep Rumen, Including a New Species, *J. Gen. Microbiol. 90*, 100–114.
24. Leth, T., Ovesen, L., and Hansen, K. (1998) Fatty Acid Composition of Meat from Ruminants, with Special Emphasis on *trans* Fatty Acids, *J. Am. Oil Chem. Soc. 75*, 1001–1005.
25. Wolff, R.L., Combe, N.A., Destaillats, F., Boué, C., Precht, D., Molkentin, J., and Entressangles, B. (2000) Follow-Up of the Δ4 to Δ16 *trans*-18:1 Isomer Profile and Content in French Processed Foods Containing Partially Hydrogenated Vegetable Oils During the Period 1995–1999. Analytical and Nutritional Implications, *Lipids 35*, in press.
26. Wolff, R.L., Combe, N.A., Precht, D., Molkentin, J., and Ratnayake, W.M.N. (1998) Accurate Determination of *trans*-18:1 Isomers by Capillary Gas–Liquid Chromatography on Cyanoalkyl Polysiloxane Stationary Phases, *Oléagineux, Corps Gras, Lipides 5*, 295–299.
27. Hulshof, K.F., van Erp-Baart, M.A., Anttolainen, M., Becker, W., Church, S.M., Couet, C., Hermann-Kunz, E., Kesteloot, H., Leth, T., Martins, I., *et al.* (1999) Intake of Fatty Acids in Western Europe with Emphasis on *trans* Fatty Acids: The TRANSFAIR Study, *Eur. J. Clin. Nutr. 53*, 143–157.
28. Combe, N.A., Billeaud, C., Mazette, S., Entressangles, B., and Sandler, B. (1995) *Trans* Fatty Acids (TFA) in Human Milk Reflect Animal or Vegetable TFA Consumption in France, *Pediatric Res. 37*, 304 A (abstract).
29. Combe, N., Judde, A., Boué, C., Billeaud, C., Entressangles, B., Dallay, D., Leng, J.J., and Baste, J.C. (1998) Composition en Acides Gras *trans* du Tissu Adipeux d'une Population Française et Origines Alimentaires de ces Acides Gras *trans*, *Oléagineux, Corps Gras, Lipides 5*, 142–148.

[Received February 10, 2000, and in revised form July 10, 2000; revision accepted July 14, 2000]

Determination of the Phospholipid/Lipophilic Compounds Ratio in Liposomes by Thin-Layer Chromatography Scanning Densitometry

S. Rodríguez, M.V. Cesio, H. Heinzen*, and P. Moyna

Cátedra de Farmacognosia y Productos Naturales, Facultad de Química, Universidad de la República, Montevideo, Uruguay

ABSTRACT: The determination of the ratio of phospholipid/lipophilic compounds in liposomes was achieved after thin-layer chromatography (TLC) by measuring the spot intensities of dipalmitoyl phosphatidylcholine and the lipophilic compound. The liposome components under study were separated on one TLC plate, developed in two steps, and detected after charring the plate with specific visualization reagents. The method shows good reproducibility and provides a simple way to quantify the level of lipophilic compound incorporated in the liposome bilayer.

Paper no. L8324 in *Lipids 35*, 1033–1036 (September 2000)

Liposomes have been used as model systems for studying the interaction of the phospholipid-bilayer with individual components of the cell membrane such as proteins or other lipids. The simplicity of the system provides a suitable model for the study of such interactions within the cellular membrane framework, since the effects due to other membrane components are avoided (1). They have also been used to study the interaction of lipids exogenous to the cell membrane with the bilayer, for example, the potential biological activity of compounds such as triterpenes (2,3). The inclusion of sterols and other lipophilic molecules in the bilayers introduces concentration-dependent changes in properties such as phase transition, permeability, and fluidity, which could relate to their biological activity (1–7).

During our study on the influence of wax triterpenes on the phase transition of dipalmitoyl phosphatidylcholine (DPPC) liposomes (2), we faced the problem of quantifying the amount of compound included in the liposome bilayer. The point, which has received only scant attention (8), is not trivial. Erroneous evaluation of this parameter could lead to misinterpretation of the observed effects. In spite of this, the great majority of scientific communications assume that the lipophilic compound under study is completely included in the bilayer (3,4,9,10). The results obtained during our studies indicate that this is not always the case (2).

To address this issue, we developed a thin-layer chromatography (TLC)-scanning based method. TLC-scanning is particularly suitable for the quantification of lipophilic substances such as triterpenoids, sterols, and lecithins within mixtures. Such a method only requires a TLC separation of the components, avoiding most of the possible interferences while having very high sensitivity. We have previously applied direct TLC-densitometric quantification to a number of natural products, e.g., cuticular waxes (11), carbohydrates (12), steroidal alkaloids (13), and terpenes in essential oils (14). The measured refraction values are linearly dependant on the applied concentration, and the unknown concentration can be calculated from the standard curves. In all the cases, the results presented high accuracy and reproducibility.

MATERIALS AND METHODS

Materials and apparatus. Aluminum or plastic-supported silica gel G TLC plates were obtained from Macherey Nagel (Düren, Germany) or Merck (Darmstadt, Germany). Solvents were all analytical grade and redistilled in glass prior to use. DPPC was purchased from Aldrich Chemical Co. (Milwaukee, WI). Cholesterol was obtained by recrystallization from ethanol of a commercial sample. Lupeol and taraxerol were isolated from the cuticular wax of *Colletia paradoxa* Spr. (15,16), ursolic acid was isolated from apple (*Malus domestica* fruit) cuticular wax (17), and uvaol was obtained by reduction of ursolic acid (15). Betulin was purchased from Sigma Chemical Co. (St. Louis, MO). The densitometer was a Flying Spot Shimadzu TLC Scanner 9000 (Kyoto, Japan) operating in the visible range ($\lambda = 560$ nm), in the zig-zag and refraction mode. The gas chromatograph was a Shimadzu GC-6AM, using a SE-52 fused-silica column (0.25 mm thickness, 25 m) with N_2 as the carrier gas. The temperature program was 120°C for 4 min; 10°C/min to 280°C; 50 min at 280°C.

Treatment of liposomes. Liposomes were prepared according to Bangham (18). Fifteen micromoles of DPPC, along with the desired amount of the compound under study, were dissolved in 10 mL of chloroform and rotary-evaporated to

*To whom correspondence should be addressed at Cátedra de Farmacognosia y Productos Naturales, Facultad de Química, Universidad de la República, Avda. General Flores 2124 CC 1157, Montevideo, Uruguay.
E-mail: heinzen@bilbo.edu.uy

Abbreviations: DPPC, dipalmitoyl phosphatidylcholine; FAME, fatty acid methyl ester; GC, gas chromatography; TLC, thin-layer chromatography; TMSi, trimethylsilyl.

obtain a thin film on the bottom of a 25-mL round-bottomed flask. After breaking vacuum under nitrogen, 1.00 mL of water at 50°C and a 2-mm round glass bead were added. The suspension was vortexed for 1 min and sonicated for 5 min. The sample was checked with an optical microscope for the presence of nonincorporated crystals. The suspension of liposomes was first filtered through cotton to remove crystals and nonliposomal particles. The filter was then washed with distilled water (3 × 5 mL), and the combined washes were pooled together with the filtrate. Finally, the sample was freeze-dried, and the residue was dissolved in 1 mL of dichloromethane.

Quantification. In a typical experiment, 1, 2, 4, 6, and 8 μL of a DPPC solution (1 mg/mL) were spotted with a micropipette on a 20 × 20 cm TLC plate, together with 1, 2, 4, 6, and 8 μL of a solution containing 1 mg/mL of the triterpene or steroid under study. Triplicates of 2 μL of the liposome problem solution were spotted in between both calibration curves. The plate was then developed twice, first using $CHCl_3/CH_3OH/NH_4OH$ 2% (70:30:5) for an 8-cm run followed by $CHCl_3$ (for cholesterol and monotriterpenols) or $CHCl_3/(CH_3)_2CO$ (95:5) (for triterpene diols and acids) in the same direction for the full plate (18 cm).

The plate was cut at the first solvent front. The lower 10 cm was sprayed with ammonium molybdate/perchloric acid reagent (19) and heated for 10 min at 110°C to detect and quantify the phospholipids with the densitometer at λ = 560 nm. The area values were recorded. The top part of the plate was sprayed with $CuSO_4/H_3PO_4$ reagent and heated for 5 min at 110°C for cholesterol and taraxerol, 6 min at 110°C for ursolic acid, and 10 min at 110°C for uvaol. The spot intensities were measured and recorded as reported (11,12,14).

Gas chromatography (GC) analysis. Five milligrams of the liposome problem solution was heated for 5 min at 60°C with 1 mL of methanol/BF_3 reagent (Aldrich). The solvent was evaporated and the residue trimethylsilylated using 0.5 mL of trimethylsilyl (TMSi) imidazole/pyridine (1:2) at 60°C for 1 h. The resulting solution was injected into the gas chromatograph operating under the described conditions.

Data treatment. The values for each class of compound were graphed by means of a linear correlation (11–14). The concentrations in the problems were calculated, averaged, and expressed as the molar ratio of (lipophilic compound)/(DPPC + lipophilic compound).

RESULTS

The different polarities of phospholipids and sterol-like molecules established the need for a two-solvent system. With this procedure, lecithins were easily separated from nonpolar lipids by TLC with very good resolution ($R_{f\text{ of DPPC}} = 0.25$; $R_{f\text{ of cholesterol}} = 0.75$; $R_{f\text{ of ursolic acid}} = 0.60$).

The ammonium molybdate/perchloric acid reagent provided the best results for the visualization of phospholipids. Draggendorf reagent was also assessed for the quantification of these compounds, but it was half as sensitive. Care must be taken when using the ammonium molybdate/perchloric acid reagent since it decomposes very easily. It must be prepared 24 h prior to use, and it is usable for 3 wk when kept in the refrigerator, under nitrogen, and in dark bottles. For the quantification of steroids and triterpenoids, the detection agent of choice was $CuSO_4/H_3PO_4$, as previously reported (12).

Exact amounts of the tested compounds were spotted on a TLC plate along with three samples of the liposome solution. Both groups of components were measured with the TLC scanner. The plates were read transversely so all the spots were read at the same time ± 2 min, avoiding differential charring of the compounds. The observed areas and the concentration of compounds spotted were graphed by means of linear correlation.

The coefficients of variation were calculated employing only curves with $r > 0.992$ for the DPPC and $r > 0.999$ for the triterpenoid (or steroid). The data obtained for each of the values were averaged. The values corresponded to a coefficient of variation ≤3% for the phospholipid, and ≤1% for the triterpenoid (or sterols). The reproducibility of the measurements on the same DPPC spot was assayed by measuring the same spot 30 times. The values were then averaged and the coefficient of variation was <3%. The reproducibility of the measured data was assessed by performing the analysis of DPPC/cholesterol, 12% liposomes in three different plates. The resulting values showed a coefficient of variation of 4%. The incorporation levels in DPPC liposomes of the different tested compounds (Scheme 1) are summarized in Table 1.

GC provides an alternative to the present methodology; however, direct determination of the compounds is not possible and derivatization is necessary. Phospholipids were quantitatively converted to the corresponding fatty acid methyl esters (FAME) by BF_3-catalyzed methanolysis of the mixture. Cholesterol can be determined without derivatization or as TMSi derivative. Triterpenols were also analyzed as TMSi derivatives. In the case of polyfunctional triterpenes, it is advisable to prepare their TMSi derivatives overnight, since

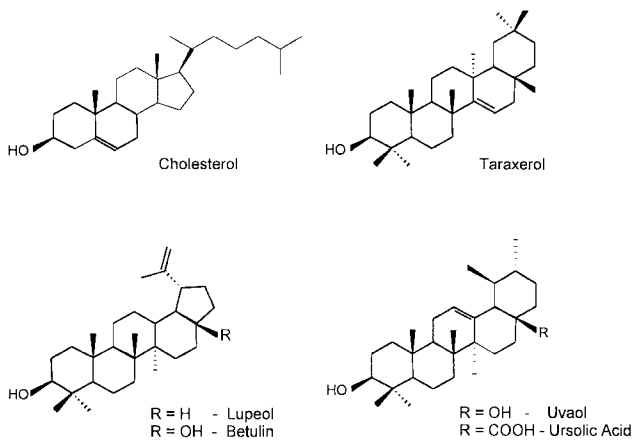

SCHEME 1

TABLE 1
Quantitation of Liposome Components by Thin-Layer Chromatography[a]

Entry	Compound	Incorporation level	
		Theoretical[b]	Experimental[c]
1	Cholesterol	0.12	0.12
2	Taraxerol	0.12	0.05
3	Lupeol	0.25	0.12
4	Ursolic acid	0.10	0.05
5	Uvaol	0.25	0.09
6	Betulin	0.25	0.10
7	Cholesterol + betulin	0.30 + 0.30	0.30 + 0.12

[a]The numbers are given as the molar ratios of the incorporated molecule to the total components (dipalmitoyl phosphatidylcholine and incorporated molecule).
[b]Expected amount of triterpene (or sterol) included in the liposomes.
[c]TLC measured ratio of compounds included in liposomes.

some compounds (betulin) can decompose when heated in the normal derivatization protocol (15). For hydroxyacids, the procedure was similar. The acid function was methylated during the transesterification step, and the TMSi derivative was prepared in a second reaction.

In a single GC run, the phospholipid fatty acids (as FAME) were separated from sterol and triterpene TMSi derivatives. The different retention times of the compounds under study were as follows: (i) myristic acid, 15 min; palmitic acid, 17 min; linoleic acid, 18 min; oleic acid, 18.5 min; stearic acid, 19 min; (ii) cholesterol, 35 min; taraxerol, 38 min; uvaol, 52 min; betulin, 54 min; and ursolic acid compounds listed under (i) were analyzed as the methyl ester derivatives, (ii) as TMSi derivatives, and (iii) as TMSi methyl ester derivatives. Tetracosane was employed as an internal standard, and a correction factor was applied due to the differential responses of the flame-ionization detector (FID) to each lipophilic compound depending on their oxidation degree and structure (20). A GC run was completed in 70 min, and calculations were simple since the phospholipid, DPPC, had only one fatty acid component. If more complex lipids are used, calculations must be adjusted.

DISCUSSION

The accurate measurement of the precise amounts of lipophilic compound incorporated into membranes is crucial for the rigorous understanding of the resulting changes in the physicochemical properties of liposomes. It has been assumed that the total amount of a compound blended with the phospholipid is completely included within the bilayer, but this is not always the case. Although cholesterol achieves complete incorporation in the bilayer (Table 1, entry 1) (2), triterpenes such as ursolic acid or uvaol only attain low incorporation levels (Table 1, entries 4 and 5). Recent studies on the dynamic properties of DPPC and ursolic acid 1:0.3 liposomes have been reported (3); however, our results show that the highest attained incorporation of ursolic acid in the liposome bilayer (Table 1, entry 4) was close to 5% molar ratio.

The TLC method achieves an accurate determination of the concentration of sterols and steroid-like molecules within phospholipid bilayers in a single analysis, without prior derivatization. The method can be applied to liposomes formed by complex phospholipids or containing more than one lipophilic compound. The study of the changes of DPPC-cholesterol liposomes that include another lipophilic compound can provide interesting information, and might be nearer the biological membrane model. Table 1, entry 7 shows the case of a simultaneous triple determination. In addition, the method is not limited to steroid-like molecules and can be applied to any lipophilic compound as long as its concentration can be determined by TLC. As an example, the incorporation levels of β-diketones and resorcinols in liposomes was also determined in our laboratory (21).

GC provides an alternative method for the simultaneous quantification of lipophilic compounds and phospholipids present in bilayers; however, it presents some major drawbacks. Analysis of each sample requires two derivatization steps that make the process more tedious and time consuming. In addition, it requires the use of correction factors for the FID response, which have to be experimentally established. A major advantage of TLC scanning is that the compound under study is the one used as the internal standard, a situation that is not possible with GC. Furthermore, while the determination of a complex phospholipid by TLC implies determining only one compound, with the GC methodology, the concentration of all fatty acid components should be established.

In summary, the TLC-scanning method reported herein provides a fast, convenient, and accurate way of determining the incorporation of lipophilic compounds in the bilayer. Furthermore, the method is not limited to the case of DPPC-triterpene liposomes, and more complex systems can be analyzed. This technique allows determining the actual incorporation level of a lipophilic compound in the bilayer, and consequently it permits a more rigorous understanding of the observed associated effects.

REFERENCES

1. Eibl, H. (1984) Phopholipids as Functional Constituents of Biomembranes, *Angew. Chem. Int. Ed. Engl. 23*, 257–271.
2. Rodríguez, S., Garda, H.A., Heinzen, H., and Moyna, P. (1997) Effect of Plant Monofunctional Pentacyclic Triterpenes on the Dynamic and Structural Properties of Dipalmitoylphosphatidylcholine Bilayers, *Chem. Phys. Lipids 89*, 119–130.
3. Han, S.K., Ko, Y.I., Park, S.J., Jin, I.J., and Kim,Y.M. (1997) Oleanolic Acid and Ursolic Acid Stabilize Liposomal Membranes, *Lipids 32*, 769–773.
4. Nes, W.D., and Heftmann, E. (1981) A Comparison of Triterpenes and Sterols as Membrane Constituents, *J. Nat. Prod. 44*, 377–400.
5. Nagumo, A., Sato, I., and Suzuki, Y. (1991) Electron Spin Resonance Studies of Phosphatidylcholine Interacted with Cholesterol and with a Hopanoid in Liposomal Membrane, *Chem. Pharm. Bull. 39*, 3071–3074.
6. Cavagnetto, F., Relini, A., Mirghani, Z., Gliozza, A., Bertoia, D., and Gambacorta, A. (1992) Molecular Packing Parameters of Bipolar Lipids, *Biochim. Biophys. Acta 1107*, 273–281.
7. Stillwell, W., Brengle, B., Blecher, D., and Wassall, S.R. (1987)

Comparison of the Effects of ABA and IAA on Phospholipid Bilayers, *Phytochemistry 26*, 3145–3150.
8. Piretti, M.V., Pagliuca, G., and Vasina, M. (1987) Proposal of an Analytical Method for the Study of the Oxidation Products of Membrane Lipids, *Anal. Biochem. 167*, 358–361.
9. Coster, H.G.L., and Laver, D.R. (1986) The Effect of Benzyl Alcohol and Cholesterol on the Acyl Chain Order and Alkane Solubility of Bimolecular Phosphatidylcholine Membranes, *Biochim. Biophys. Acta 861*, 406–412.
10. Cabral, D.J., Small, D.M., Lilly, H.S., and Hamilton, J.A. (1987) Transbilayer Movement of Bile Acids in Model Membranes, *Biochemistry 26*, 1801–1804.
11. Cesio, V., Heinzen, H., Servetto, C., Torres, M., and Moyna, P. (1996) Rapid Determination of Lactose Intolerance, *Quím. Anal. 15*, 140–143.
12. Davyt, D., Pandolfi, E., Heinzen, H., Troche, L., and Moyna, P. (1995) TLC Scanning of Wheat Seed Waxes, *An. Asoc. Quím. Argentina 83*, 1–4.
13. Ferreira, F., Moyna, P., Soule, S., and Vázquez, A. (1993) Rapid Determination of *Solanum* Alkaloids by TLC-Scanning, *J. Chromatogr. A 653*, 380–384.
14. Rossini, C., Pandolfi, E., Dellacassa, E., and Moyna, P. (1995) Determination of 1,8-Cineole in *Eucalyptus* Oil by TLC and Densitometry, *J. Assoc. Off. Anal. Chem. (int.) 78*, 115–117.
15. Heinzen, H. (1993) Chemische Transformationen und Ökologie Triterpenoider Waschen, Dr. rer.nat Thesis, Cuiviller Verlag, Gottingen, Germany.
16. Moyna, P., Heinzen, H., Laborde, E., and Ramos, G. (1983) Epicuticular Wax of *Colletia paradoxa* (Spreng), *Phytochemistry 22*, 1283–1285
17. Buckingham, J. (ed.) (1994) *Dictionary of Natural Products,* Vol. 1, A–C, Chapman & Hall, New York.
18. Bangham, A.D., Hill, M.W., and Miller, N.G.A. (1974) Preparation and Use of Liposomes as Models of Biological Membranes, in *Methods in Membrane Biology* (Korn, E.D., ed.) Plenum Press, New York, pp. 1–68.
19. Stahl, E. (1966) *Thin Layer Chromatography*, 2nd edn., Springer Verlag, New York, p. 886.
20. Moyna, P., and García, M. (1983) Chemical Composition of Oat Seed Epicuticular Wax, *J. Sci. Food Agric. 34*, 209–211.
21. Rodríguez, S. (1995) Estudio de la Variación de las Propiedades de Bicapas Lipídicas en Presencia de Isósteros del Colesterol, M.S. Thesis, Universidad de la República, Montevideo, Uruguay.

[Received July 30, 1999; and in revised form June 20, 2000; revision accepted June 27, 2000]

Deuterium Uptake and Plasma Cholesterol Precursor Levels Correspond as Methods for Measurement of Endogenous Cholesterol Synthesis in Hypercholesterolemic Women

Nirupa R. Matthan[a], Mahmoud Raeini-Sarjaz[a], Alice H. Lichtenstein[b], Lynne M. Ausman[b], and Peter J.H. Jones[a,*]

[a]School of Dietetics and Human Nutrition, McGill University, Macdonald Campus, Ste-Anne-de-Bellevue, Québec, Canada H9X 3V9, and [b]Jean Mayer USDA Human Nutrition Center on Aging at Tufts University, Boston, Massachusetts 02111

ABSTRACT: To assess the validity of two techniques used to measure human cholesterol synthesis, the rate of uptake of deuterium (D) into plasma free cholesterol (FC), and plasma cholesterol precursor (squalene, lanosterol, desmosterol and lathosterol) levels were compared in 14 women [65–71 yr with low density lipoprotein-cholesterol (LDL-C) ≥ 3.36 mmol·L^{-1}]. Subjects consumed each of six diets for 5-wk periods according to a randomized crossover design. The experimental diets included a baseline diet (39% energy as fat, 164 mg chol·4.2 MJ^{-1}) and five reduced-fat diets (30% of energy as fat), where two-thirds of the fat was either soybean oil; squeeze, tub or stick margarines; or butter. Fractional and absolute synthesis rates (FSR and ASR) of FC were determined using the deuterium incorporation (DI) method, while cholesterol precursor levels were measured using gas–liquid chromatography. Data were pooled across diets for each variable and correlation coefficients were calculated to determine if associations were present. There was good agreement among levels of the various cholesterol precursors. In addition, FSR in pools/d (p·d^{-1}) and ASR in grams/d (g·d^{-1}) were strongly associated with lathosterol (r = 0.72 and 0.71, P = 0.0001), desmosterol (r = 0.75 and 0.75, P = 0.0001), lanosterol (r = 0.67 and 0.67), and squalene (r = 0.69 and 0.68) when levels of the precursors were expressed as μmol·$mmol^{-1}$ C. Significant but lower correlations were observed between the D uptake and plasma cholesterol precursor levels when the latter were expressed in absolute amounts (μmol·L^{-1}). The wide range of fatty acid profiles of the experimental diets did not influence the degree of association between methods. In conclusion, the DI method and levels of some cholesterol precursors correspond as methods for short-term measurement of cholesterol synthesis.

Paper no. L8503 in *Lipids 35,* 1037–1044 (September 2000).

Cholesterol homeostasis is maintained by regulatory mechanisms that balance input and output so as to prevent net accumulation of cholesterol (1). Alterations in homeostasis, resulting in elevated circulating cholesterol concentrations, are associated with undesirable plasma lipid responses that increase the risk of developing cardiovascular disease (CVD) (2,3). A factor known to influence *de novo* cholesterogenesis is dietary fat modification (4–6). Several techniques have been used to measure cholesterol synthesis in humans, including sterol balance (7–11), kinetic approaches (12,13), activity of the enzyme 3-hydroxyl-3-methylglutaryl coenzyme A (HMG-CoA) reductase (14,15), and cholesterol precursor levels (14,16–22). More recent approaches include the mass isotopomer distribution analysis (MIDA) (23–25) and deuterium incorporation (DI) methodology (26–31).

The sterol balance method provides an accurate value for biosynthesis once internal sterol pools have equilibrated, but has the disadvantage of being laborious, requiring complete stool collections and accuracy in recording food intake (32). Kinetic studies with [^{13}C]cholesterol provide detailed information about pool sizes, distribution, and formation rates of cholesterol, but require prolonged measurement intervals consistent with metabolic steady state (6). Determination of the activity of HMG-CoA reductase, the rate-limiting enzyme in the synthetic pathway of cholesterol, provides an index of cholesterol synthesis over the short term, but is restricted by the need for a liver biopsy (15). Sterol precursor levels in plasma, including mevalonic acid (16,17), squalene (14,18), lanosterol (14,19), desmosterol (14,20) and lathosterol (14,21,22), are alternate indicators of synthesis; however, the sensitivity of these techniques is still under investigation. The MIDA technique, despite its advantages, is invasive, requiring indwelling catheters for delivery of isotope label, serial blood sampling, and lengthy data analysis with elaborate mathematical processing (6).

Alternatively, the deuterium (D) uptake method, capable of directly measuring the rate of incorporation of D from body water into newly formed cholesterol (26–31), offers a safe, noninvasive alternative for detecting changes in cholesterol synthesis rates over short periods of time. This method

*To whom correspondence should be addressed at School of Dietetics and Human Nutrition, Faculty of Agricultural and Environmental Sciences, McGill University, Macdonald Campus, 21,111 Lakeshore Road, Ste-Anne-de-Bellevue, Québec, Canada H9X 3V9.
E-mail: jonesp@macdonald.mcgill.ca

Abbreviations: ASR, absolute synthesis rate; C, cholesterol; CVD, cardiovascular disease; D, deuterium; DI, deuterium incorporation; D_{max}, maximum number of deuterium molecules; FC, free cholesterol; FSR, fractional synthesis rate; HMG-CoA, 3-hydroxyl-3-methylglutaryl coenzyme A; MIDA, mass isotopomer distribution analyses; TC, total cholesterol.

has been validated against levels of plasma mevalonic acid (33), sterol balance (32), and MIDA (34) techniques; however, a direct comparison between DI and the commonly used cholesterol precursor level assessment method has not been performed. Thus, the objective of the present investigation was to determine whether levels of some cholesterol precursors (squalene, lanosterol, desmosterol, and lathosterol) correlate with the D uptake method for measurement of endogenous cholesterogenesis. The study was originally designed to assess the effect of different *trans* and fatty acid profiles on cholesterol synthesis. The specific effects induced by the diet change are reported elsewhere. Here, the focus of attention will be to determine whether an association exists between the two methods.

MATERIALS AND METHODS

Subjects. Fourteen postmenopausal, middle-aged to elderly, moderately hypercholesterolemic (low density lipoprotein-cholesterol ≥ 3.36 mmol·L^{-1}) women (65–71 yr) were recruited as previously described (35). Subjects had no family history of premature CVD, nor showed any signs of hepatic, renal, thyroid, or intestinal disease. None of the subjects was taking any medication known to alter lipid metabolism such as lipid-lowering drugs, β-blockers, diuretics, or hormones. The protocol was reviewed and approved by the Human-Investigation Review Committee of New England Medical Center and Tufts University. All potential subjects were given a verbal and written description of the study prior to obtaining written consent.

Study design and diets. Subjects were given, in a double-blind fashion, each of six diets for 5-wk periods, separated by washout periods ranging from 2 to 4 wk. The experimental diets included a baseline diet designed to approximate that currently consumed in the United States (39% energy as fat, 164 mg cholesterol·4.2 MJ^{-1}), and five reduced fat diets (30% of energy) where two-thirds of the total fat was provided by either soybean oil or soybean oil-based margarines in the squeeze, tub, or stick forms, as well as butter. All food and drink were provided by the Metabolic Research Unit of the Jean Mayer U.S. Department of Agriculture Human Nutrition Research Center on Aging at Tufts University (Boston, MA) to be consumed on-site or packaged for take-out. Energy intakes of the subjects were tailored to individual requirements, as verified by the ability to maintain stable body weight. Analysis of the macronutrient, fatty acid, and cholesterol content of the diets was carried out by Covance Laboratories (Madison, WI) and Best Foods Research and Engineering Center (Union, NJ). These compositions are given in Table 1. Levels of the cholesterol precursors proposed to be measured in plasma were not detected in the different diets.

Protocol and analyses. During the final week of each dietary phase, fasting blood samples were collected in tubes containing EDTA (0.15%). This was immediately followed by administration of an oral dose of D_2O (1.2 g per kg total body water). Twenty-four hours postdose, another fasting blood sample was collected. Plasma was separated, aliquoted, and frozen at −80°C until further analysis.

Cholesterol precursor analyses. Plasma total cholesterol (TC) concentrations were analyzed using enzymatic procedures (36,37). The precursor sterols were quantified using gas–liquid chromatography (GLC). An internal standard containing 150 μL of 5α-cholestane was added to 1 mL of plasma. The sample, in duplicate, was then saponified for 1 h at 100°C, with 0.5 M methanolic potassium hydroxide in 15-mL Teflon-capped glass tubes. After saponification, samples were allowed to cool to room temperature, followed by the addition of 2.5 mL of distilled water and 3 mL petroleum ether to each tube. The tubes were vortexed, centrifuged at 1500 × *g* for 15 min, and the upper layers containing the non-saponifiable materials were transferred into clean glass tubes. The extraction procedure was repeated twice. Combined extracts were then dried down under nitrogen and resuspended in 1 mL of chloroform. A sample volume of 2 μL was injected into a gas–liquid chromatograph equipped with a flame-ionization detector (HP 5890, Series II; Hewlett Packard, Palo Alto, CA) using a 30-m capillary column (SAC-5; Supelco, Bellefonte, PA). Injector and detector temperatures were 300 and 310°C, respectively. A multiramp oven temperature program was used. The initial temperature, 80°C, was held for 1 min and then increased to 120°C at a rate of 20°/min. After

TABLE 1
Composition of Experimental Diets as Determined by Chemical Analysis[a]

Constituent	Soybean oil	Squeeze margarine	Tub margarine	Stick margarine	Butter	Baseline
	Total daily energy intake (%)					
Protein	15.7	17.1	16.3	16.7	16.9	16.8
Carbohydrate	55.8	51.7	52.9	53.5	53.9	44.6
Fat	28.5	31.2	30.8	29.7	29.1	38.6
Saturated fatty acids	7.3	8.6	8.4	8.5	16.7	15.5
Monounsaturated fatty acids[b]	8.1	8.1	8.0	8.5	8.1	15.1
Polyunsaturated fatty acids[b]	12.5	13.5	11.1	6.3	2.4	6.9
Trans fatty acids	0.6	0.9	3.3	6.7	1.3	1.7
Cholesterol (mg·4.2 MJ^{-1})	65.9	68.0	70.3	66.5	121.0	163.8

[a]Because of rounding, percentages may not total 100%.
[b]Only *cis* isomers are included.

15 min, the temperature was further increased to 269°C at a rate of 20°/min and held for 25 min. The final temperature of 320°C was reached using a rate of 20°/min and held for 5 min. Peaks of interest were identified by comparison with authentic standards (Supelco).

Deuterium uptake analyses. Additional plasma aliquots were used to determine D enrichment in body water and free cholesterol (FC) as previously described (26–31). Briefly, lipids were extracted (38) and FC was separated by thin-layer chromatography using petroleum ether/ethyl ether/acetic acid (135:15:1.5, by vol). FC was eluted with hexane/chloroform/ethyl ether (5:2:1, by vol) and dried under a stream of nitrogen. The purified cholesterol was converted into water and carbon dioxide by combustion over cupric oxide and silver wire at 520°C for 2 h. In addition, pre- and post-D_2O samples diluted twofold and tenfold, respectively, to produce D enrichments within detectable ranges on the mass spectrometer, were distilled into zinc-containing tubes. This enabled measurement of D enrichment of plasma water. The combustion water from FC and plasma was then vacuum-distilled into Pyrex™ tubes containing zinc reagent and reduced to hydrogen D gas by heating at 520°C for 30 min. D enrichment of the gas was analyzed by isotope ratio mass spectrometry (VG isomass 903 D; Cheshire, England). The instrument was calibrated daily using water standards of known isotopic composition. Values were expressed relative to the enrichment of standard mean ocean water in parts per mil (‰). The per mil designation was used because of the relatively small enrichments encountered. Duplicate samples for each subject were analyzed concurrently against a single set of standards. Maximum acceptable precision for D was 5‰ at enrichments over 500‰, and 2‰ at enrichments below 200‰.

Fractional synthesis rate (FSR) of FC, defined as the proportion of the central or M_1 pool replaced daily by newly synthesized cholesterol, was calculated as the change in product enrichment over time divided by the maximum possible enrichment, based on a linear rate of uptake of label into cholesterol over time (27,29). The equation used was:

$$\text{FSR–FC } \left(\text{p}\cdot\text{d}^{-1}\right) = \frac{\delta \text{ cholesterol (\%)}}{\delta \text{ plasma water (\%)} \times 0.478} \qquad [1]$$

where δ is the difference in D enrichment over 24 h. Model parameters and assumptions underlying the use of D_2O as a tracer for FSR measurements have been described previously (27,29). Absolute synthesis rate (ASR) of FC, which is an approximation of the daily production of newly synthesized cholesterol expressed in grams/day ($g\cdot d^{-1}$), was derived by multiplying the FSR–FC by M_1 pool size and a factor of 0.33. The M_1 pool size was calculated using Goodman's equation (39), which takes into account subjects' body weights, plasma TC and triglyceride concentrations. The factor of 0.33 was included to account for the proportion of FC in the overall plasma TC pool.

Statistical analysis. Prior to analyses, the distribution of each outcome variable was checked for normality (Proc Univariate, SAS version 6.12; SAS Institute Inc., Cary, NC) and, if necessary, the appropriate transformations were performed. Data were pooled across diets for each variable and Pearson's correlation coefficients were determined to test for associations between variables, with significance set at $P < 0.05$ (Proc Corr, SAS version 6.12; SAS Institute Inc.). Untransformed data are presented in text and tables as means ± SD.

RESULTS

This study was originally designed to determine the effect of changes in dietary fatty acid composition on endogenous cholesterol synthesis. However, it is the purpose of the present study to focus on the association between plasma levels of cholesterol precursors and D uptake as indicators of cholesterol synthesis. The results of the diet-induced changes in cholesterol synthesis have been reported elsewhere (40). Nevertheless, it was deemed appropriate to provide these values in summary form to be read only as background information. Table 2 lists the pooled mean (±SD) plasma concentrations of total cholesterol, its precursors, as well as FSR and ASR of free cholesterol. The range of values for each variable is in good agreement with those previously reported for humans (14,20,22,41,42).

Table 3 summarizes the correlations between the various cholesterol precursors when expressed as $\mu mol\cdot L^{-1}$ or $\mu mol\cdot mmol^{-1}$ of cholesterol (C). In general, good agreement was observed between concentrations of all four precursors (range from $r = 0.88$ to 0.95). Figure 1 depicts the relation between FSR ($p\cdot d^{-1}$) obtained using the DI method and plasma concentrations of squalene, lanosterol, desmosterol, and lathosterol (expressed as either $\mu mol\cdot L^{-1}$ or $\mu mol.mmol^{-1}$ C). Higher correlations ($P = 0.0001$) were obtained between FSR

TABLE 2
Pooled Mean Values for Total Cholesterol, Its Precursors, FSR, and ASR[a]

Variable	Concentration range	Mean ± SD
Total cholesterol		
$mmol\cdot L^{-1}$	4.32–8.25	6.28 ± 0.84
Squalene		
$mmol\cdot L^{-1}$	0.01–2.77	0.74 ± 0.58
$\mu mol\cdot mmol^{-1}$ [b]	0.13–45.37	12.11 ± 10.05
Lanosterol		
$\mu mol\cdot L^{-1}$	0.39–5.36	1.78 ± 1.08
$\mu mol\cdot mmol^{-1}$ [b]	5.98 –103.13	28.78 ± 19.36
Desmosterol		
$\mu\mu mol\cdot L^{-1}$	0.41–6.09	2.47 ± 1.45
$\mu mol\cdot mmol^{-1}$ [b]	7.18–110.74	40.08 ± 24.62
Lathosterol		
$\mu mol\cdot L^{-1}$	6.12–32.53	13.63 ± 4.47
$\mu mol\cdot mmol^{-1}$ [b]	81.52–625.93	220.82 ± 84.37
FSR		
$p\cdot d^{-1}$	0.01–0.22	0.07 ± 0.03
ASR		
$g\cdot d^{-1}$	0.06–1.71	0.61 ± 0.28

[a]Data were pooled across diets for all subjects ($n = 14$).
[b]Relative to concentration of total cholesterol. FSR, fractional synthesis rate; ASR, absolute synthesis rate.

TABLE 3
Correlation Among Various Cholesterol Precursors Expressed as Absolute (μmol·L^{-1}) or Relative (μmol·mmol^{-1} C) Concentrations

Cholesterol precursor[a]	Correlation coefficient (r^b)	
	μmol·L^{-1}	μmol·mmol^{-1} [c]
Squalene vs. lanosterol	0.92	0.93
Squalene vs. desmosterol	0.94	0.95
Squalene vs. lathosterol	0.90	0.90
Lanosterol vs. desmosterol	0.88	0.89
Lanosterol vs. lathosterol	0.91	0.93
Desmosterol vs. lathosterol	0.89	0.90

[a]Data were pooled across diets for all subjects (n = 14).
[b]$P < 0.0001$.
[c]Relative to concentration of total cholesterol. C, cholesterol.

and plasma concentrations of desmosterol (r = 0.71 and 0.75) and lathosterol (r = 0.68 and 0.72). Significant (P = 0.0001), but lower associations were observed between FSR and squalene (r = 0.67 and 0.69), and FSR and lanosterol (r = 0.65 and 0.67). The total amount of cholesterol synthesized per day (ASR) was also computed and correlated with absolute (μmol·L^{-1}) or relative (mol·mmol^{-1} C) concentrations of the cholesterol precursors (Fig. 2). Similar to the FSR data, we found that desmosterol (r = 0.75 and 0.75) and lathosterol (r = 0.71 and 0.76) were better correlated with ASR than were squalene (r = 0.68 and r = 0.69) and lanosterol (r = 0.67 and 0.69). Overall, concentrations of the precursors were found to correlate better with FSR and ASR, when expressed relative to cholesterol (μmol·mmol^{-1} C) than when expressed in absolute amounts (μmol·L^{-1} of plasma).

DISCUSSION

A variety of methods exists for measuring human cholesterol biosynthesis. These methods vary in the duration needed to attain equilibrium, and thus represent either a short-term or longer-term picture into *de novo* cholesterogenesis (6). Among the short-term approaches, both the D uptake and cholesterol precursor assessment methods offer potential advantages over other indices of cholesterol formation rates. However, a direct cross-comparison of these techniques has not been carried out. We present new evidence that the D uptake method corresponds well with levels of the cholesterol precursors—lathosterol, desmosterol, lanosterol, and squalene. In addition, the degree of association was not influenced by the differing fatty acid composition of the experimental diets.

The rationale for using plasma levels of cholesterol precursors as indicators of cholesterol synthesis stems from the assumption that these compounds leak into plasma lipoproteins at rates proportional to their formation in the cholesterol synthetic pathway (14). On the other hand, the DI method is based on the incorporation of deuterated water tracer into *de novo* cholesterol from a precursor pool of body water, which is in equilibrium with NADPH (27). Labeled water equilibrates quickly between the intracellular site of cholesterogenesis and extracellular body fluid. Thus, newly synthesized cholesterol is derived from a pool of known enrichment that can be determined by measuring either urine, saliva or plasma. Despite the different assumptions of each method, both are considered valid tools to assess changes in endogenous cholesterogenesis under various physiological and pathological conditions (20,22,29,30,41).

Comparatively, plasma cholesterol precursor concentrations and the D uptake method each offer advantages and disadvantages. The former method is rapid and easy, but values obtained are relative indicators of synthetic rates. In contrast, results obtained by the D uptake method yield a direct measure of net synthesis. However, this method has its drawbacks, both procedural and theoretical. Technically, the DI method is labor intensive, requiring lengthy multistage sample preparation. Theoretically, the major concern is establishing the maximum number of D molecules (D_{max}) incorporated per molecule of newly synthesized cholesterol. Over the long term, D_{max} has been shown to increase, as the acetyl-CoA pool begins to incorporate D. However, over the short term it has been established that D_{max} fluctuates between the narrow range of 20 and 22 (n = 7 hydrogen from water and 14 from NADPH). Thus, the D uptake method is considered a valid and reliable indicator of endogenous cholesterol synthesis when measurements are made around 24 h.

Similarly, the cholesterol precursor assessment method has been criticized because differences in plasma levels of the precursors could be a mere consequence of varying number of lipoprotein acceptor particles in the plasma compartment (18). It has been suggested that expressing plasma levels of precursors relative to the levels of free or total cholesterol would be a more valid index of cholesterol synthesis, as it would account for these differences in number of lipoprotein acceptor particles (18). Indeed, we found stronger correlations between levels of cholesterol precursors and the D uptake method when precursor levels were calculated relative to plasma cholesterol concentrations. In addition, our results indicate that desmosterol and lathosterol were more closely associated with FSR and ASR, while squalene and lanosterol showed significant but smaller associations. Since a certain degree of accumulation of precursors must occur inside the cells before there is a significant leakage into circulation, and given that there is a high capacity to convert squalene and lanosterol into other cholesterol intermediates, it seems reasonable that these early intermediates in the cholesterol synthetic pathway would be associated to a lesser degree than intermediates formed at later stages of the pathway.

Our results demonstrate that the D uptake method correlates well with some plasma cholesterol precursor levels. While this association demonstrates the strength of the relation between the two methods, it does not indicate the agreement between them. The Bland and Altman (43) technique is considered an accurate statistical method for assessing agreement between two methods as it plots the difference among the methods against their mean. Unfortunately, this type of analysis could not be performed in the present study given the

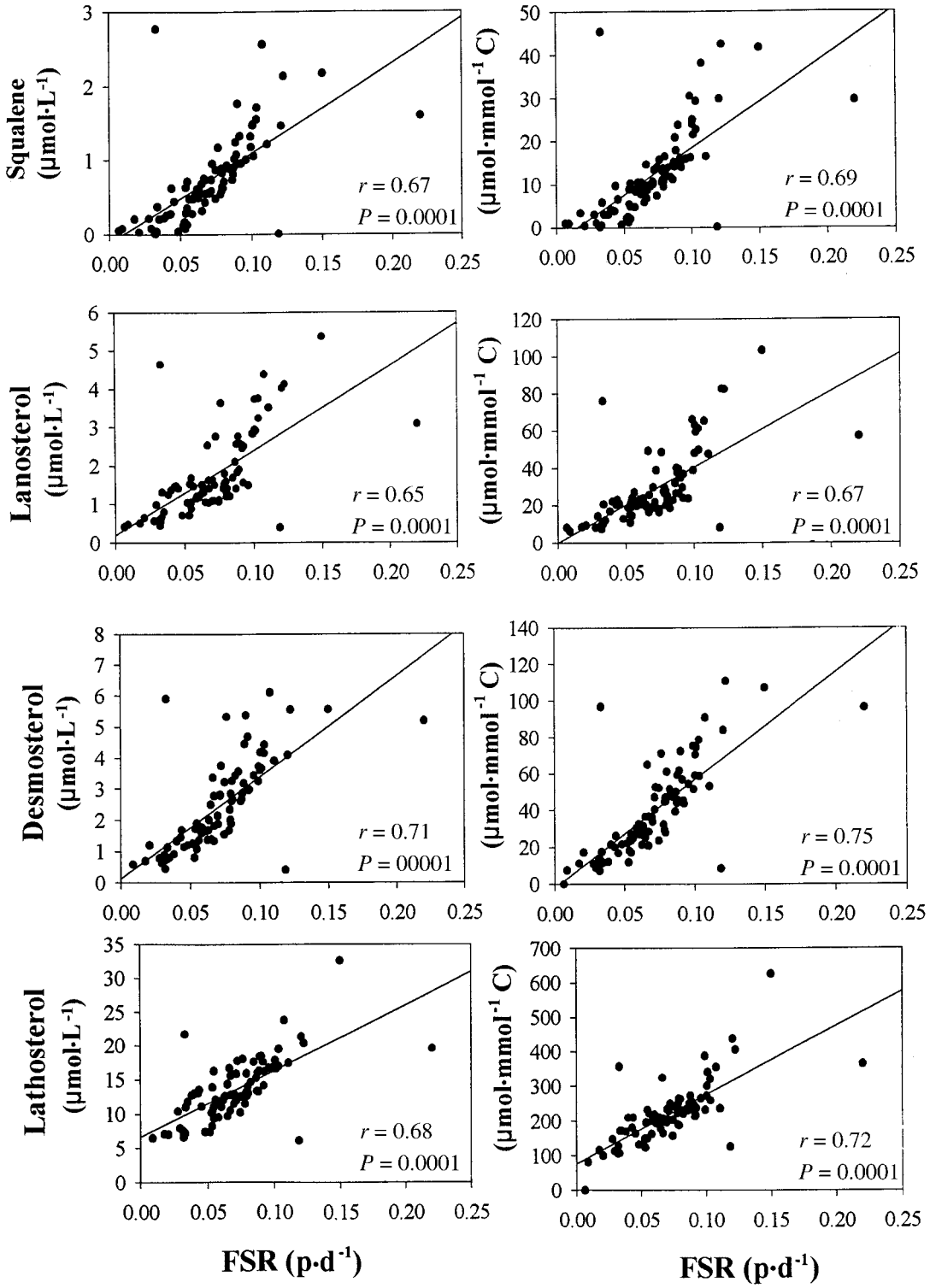

FIG. 1. Correlation between fractional synthesis rate (FSR) ($p \cdot d^{-1}$) and concentrations of different precursors to cholesterol expressed as $\mu mol \cdot L^{-1}$ and $\mu mol \cdot mmol^{-1}$ of cholesterol (C). Data were obtained from 14 subjects and pooled across the six diets for each variable.

different units of measurements for each method. However, using the above technique, good agreement has been demonstrated between the DI method and sterol balance (33) and MIDA (34) techniques. In addition, plasma levels of some of the precursors have also been validated against HMG-CoA reductase (14) and sterol balance (21). Thus in their own right, the accuracy of the D uptake and plasma cholesterol precursor levels has been established. Consequently, it is felt

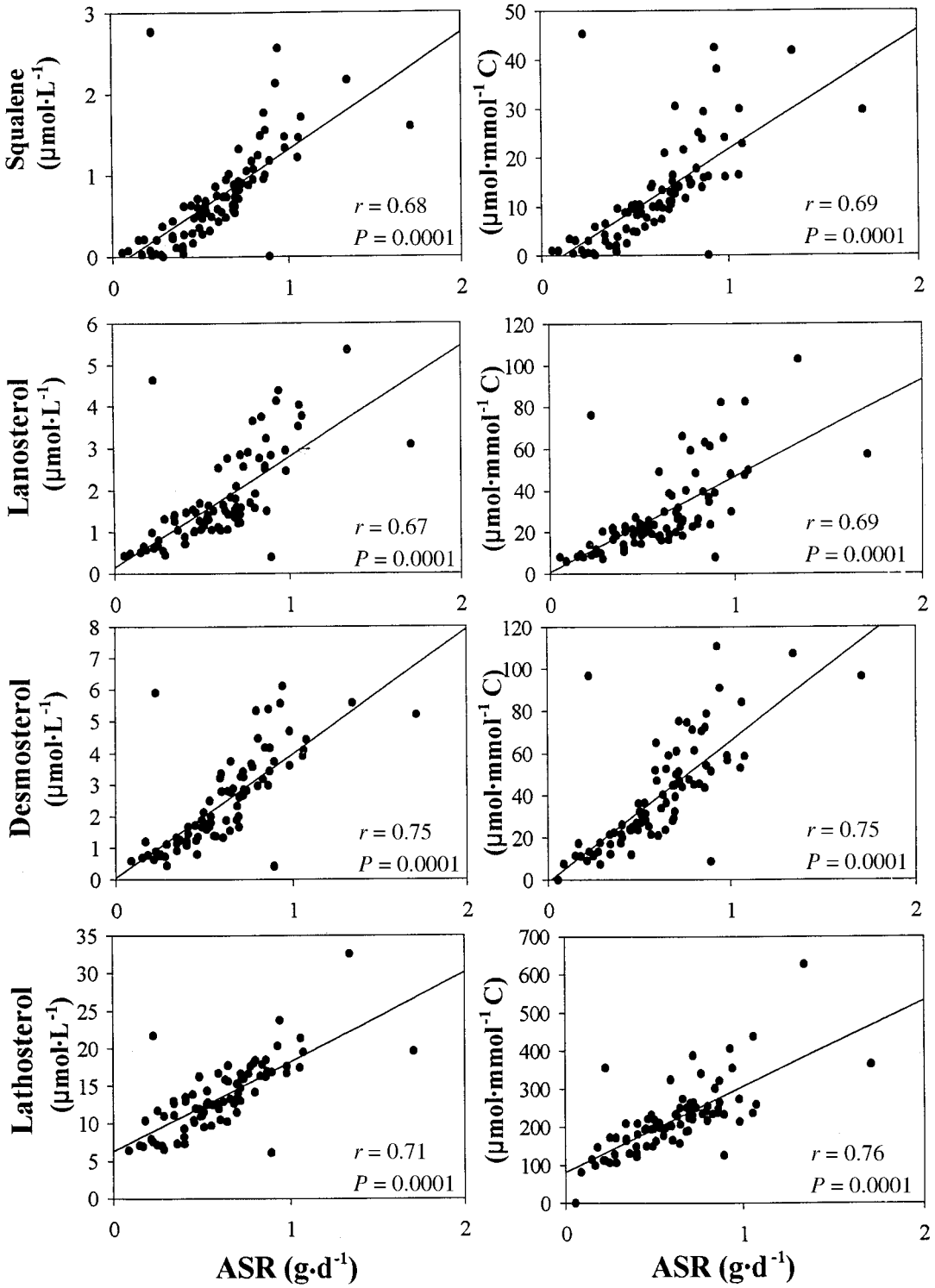

FIG. 2. Correlation between absolute synthesis rate (ASR) ($g \cdot d^{-1}$) and concentrations of different precursors to cholesterol expressed as $\mu mol \cdot L^{-1}$ and $\mu mol \cdot mmol^{-1}$ of C. Data was obtained from 14 subjects and pooled across the six diets for each variable. See Figure 1 for other abbreviation.

that the association observed in this study provides evidence that both methods are reliable and suitable for relatively uninvasive, short-term detection of cholesterol synthesis. Furthermore, these methodologies can be used to study factors known to influence human cholesterol metabolism and consequently the risk of developing CVD.

ACKNOWLEDGMENTS

This work was supported by grants from the National Institute of Health (Grant number: HL-54727) and Medical Research Council of Canada. We are indebted to the staff of the Metabolic Research Unit for the expert care provided to the study subjects. We would also like to acknowledge the cooperation of the study subjects, without whom this investigation would not be possible.

REFERENCES

1. Pfohl, M., Naoumova, R.P., Kim, K.D., and Thompson, G.R. (1998) Use of Cholesterol Precursors to Assess Changes in Cholesterol Synthesis Under Non-Steady-State Conditions, *Eur. J. Clin. Invest. 28,* 491–496.
2. LaRosa, J.C., Hunninghake, D., Bush, D., Criqui, M.H., Getz, G.S., Gotto, A.M., Jr., Grundy, S.M., Rakita, L., Robertson, R.M., and Weisfeldt, M.L. (1990) The Cholesterol Facts. A Summary of the Evidence Relating Dietary Fats, Serum Cholesterol, and Coronary Heart Disease. A Joint Statement by the American Heart Association and the National Heart, Lung, and Blood Institute. The Task Force on Cholesterol Issues, American Heart Association, *Circulation 81,* 1721–1733.
3. Ulbricht, T.L.V., and Southgate, D.A.T. (1991) Coronary Heart Disease: Seven Dietary Factors, *Lancet 338,* 985–992.
4. Rudney, H., and Sexton, R.C. (1986) Regulation of Cholesterol Biosynthesis, *Annu. Rev. Nutr. 6,* 245–272.
5. Mazier, P.M.J., and Jones, P.J.H. (1991) Dietary Fat Quality and Circulating Cholesterol Levels in Humans: A Review of Actions and Mechanisms, *Prog. Food Nutr. Sci. 15,* 21–41.
6. Jones, P.J.H. (1997) Regulation of Cholesterol Biosynthesis by Diet in Humans*, Am. J. Clin. Nutr. 66,* 438–446.
7. Avigan, J., and Steinberg, D. (1965) Sterol and Bile Acid Excretion in Man and the Effect of Dietary Fat, *J. Clin. Invest. 44,* 1845–1856.
8. Connor, W.E., Witiak, D.T., Stone, D.H., and Armstrong, M. L. (1969) Cholesterol Balance and Fecal Neutral Steroid and Bile Acid Excretion in Normal Men Fed Dietary Fats of Different Fatty Acid Composition*, J. Clin. Invest. 48,* 1363–1375.
9. Nestel, P.J., Havenstein, N., Whyte, H.M., Scott, T.J., and Cook, L.J. (1973) Lowering of Plasma Cholesterol and Enhanced Sterol Excretion with the Consumption of Polyunsaturated Ruminant Fats, *N. Engl. J. Med. 288,* 379–382.
10. Grundy, S.M., and Ahrens, E.H. Jr. (1970) The Effects of Unsaturated Dietary Fats on Absorption, Excretion, Synthesis, and Distribution of Cholesterol in Man, *J. Clin. Invest. 49,* 1135–1152.
11. Glatz, J.F., and Katan, M.B. (1993) Dietary Saturated Fatty Acids Increase Cholesterol Synthesis and Fecal Steroid Excretion in Healthy Men and Women*, J. Clin. Invest. 23,* 648–655.
12. Ferezou, J., Rautureau, J., Coste, T., Gouffier, E., and Chevallier, F. (1982) Cholesterol Turnover in Human Cholesterol Lipoproteins: Studies with Stable and Radioactive Isotopes, *Am. J. Clin. Nutr. 36,* 235–244.
13. Schwartz, C.C., Zech, L.A., VandenBroek, J.M., and Cooper, P.S. (1993) Cholesterol Kinetics in Subjects with Bile Fistula. Positive Relationship Between Size of the Bile Acid Precursor Pool and Bile Acid Synthetic Rate, *J. Clin. Invest. 91,* 923–938.
14. Bjorkhem, I., Miettinen, T., Reihner, E., Ewerth, S., Angelin, B., and Einarsson, K. (1987) Correlation Between Serum Levels of Some Cholesterol Precursors and Activity of HMG-CoA Reductase in Human Liver, *J. Lipid Res. 28,* 1137–1143.
15. Carulli, N., Tripodi, A., and Carubbi, F. (1989) Assay of HMG-CoA Reductase Activity in the Evaluation of Cholesterol Synthesis in Man, *Clin. Chim. Acta 183,* 77–81.
16. Parker, T.S., McNamara, D.J., Brown, C., Kolb, R., Ahrens, E.H., Jr., Alberts, A.W., Tobert, J., Chen, J., and De Schepper, P.J. (1984) Plasma Mevalonate as a Measure of Cholesterol Synthesis in Man, *J. Clin. Invest. 74,* 795–804.
17. Parker, T.S., McNamara, D.J., Brown, C., Garrigan, O., Kolb, R., Batwin, H., and Ahrens, E.H., Jr. (1982) Mevalonic Acid in Human Plasma: Relationship of Concentration and Circadian Rhythm to Cholesterol Synthesis Rates in Man, *Proc. Natl. Acad. Sci. USA 79,* 3037–3041.
18. Miettinen, T.A. (1982) Diurnal Variation of Cholesterol Precursors Squalene and Methyl Sterols in Human Plasma Lipoproteins, *J. Lipid Res. 23,* 466–473.
19. Miettinen, T.A. (1985) Precursor Sterols Related to Cholesterol Synthesis, in *Proceedings of the NATO Meeting, Coordinate Regulation of Cholesterol Metabolism, Santa Fe, NM,* (Sanghvi, A., ed.), pp. 87–106, University of Pittsburgh School of Medicine, Pittsburgh.
20. Uusitupa, M.I.J., Miettinen, T.A., Happonen, P., Ebeling, T., Turtola, H., Voutilainen, E., and Pyorala, K. (1992) Lathosterol and Other Noncholesterol Sterols During Treatment of Hypercholesterolemia with Lovastatin Alone and with Cholestyramine or Guar Gum*, Arterioscler. Thromb. 12,* 807–813.
21. Kempen, H.J.M., Glatz, J.F.C., Gevers Leuven, J.A., van der Voort, H.A., and Katan, M.B. (1988) Serum Lathosterol Concentration Is an Indicator of Whole-Body Cholesterol Synthesis in Humans, *J. Lipid Res. 29,* 1149–1155.
22. Duane, W.C. (1995) Serum Lathosterol Levels in Human Subjects Reflect Changes in Whole Body Cholesterol Synthesis Induced by Lovastatin but Not Dietary Cholesterol, *J. Lipid Res. 36,* 343–348.
23. Hellerstein, M.K. (1985) Methods for Measurement of Fatty Acid and Cholesterol Metabolism, *Curr. Opin. Lipidol. 6,* 172–181.
24. Lee, W.N., Bassilian, S., Guo, Z., Schoeller, D., Edmond, J., Bergner, E.A., and Byerley, L.O. (1994) Measurement of Fractional Lipid Synthesis Using Deuterated Water (^2H_2O) and Mass Isotopomer Analysis, *Am. J. Physiol. 266,* E372–E383.
25. Neese, R.A., Faix, D., Kletke, C., Wu, K., Wang, A.C., Shackleton, C.H., and Hellerstein, M.K. (1993) Measurements of Endogenous Synthesis of Plasma Cholesterol in Rats and Humans Using MIDA, *Am. J. Physiol. 264,* E136–E147.
26. Taylor, C.B., Mikkelson, B., Anderson, J.A., Forman, D.T., Asdel, A.K., and Ho, K.J. (1966) Human Serum Cholesterol Synthesis Measured Using the Deuterium Label, *Arch. Pathol. 81,* 213–231.
27. Jones, P.J.H., Leitch, C.A., Li, Z.C., and Connor, W.E. (1993) Human Cholesterol Synthesis Measurement Using Deuterated Water: Theoretical and Procedural Considerations, *Arterioscler. Thromb. 13,* 247–253.
28. Deske, D.J., and Dietschy, J.M. (1980) Regulation of Rates of Cholesterol Synthesis *in Vivo* in the Liver and Carcass of the Rat Measured Using [^{3}H] Water*, J. Lipid Res. 21,* 364–376.
29. Jones, P.J.H., Scanu, A.M., and Schoeller, D.A. (1988) Plasma Cholesterol Synthesis Using Deuterated Water in Humans: Effects of Short Term Food Restriction, *J. Lab. Clin. Med. 111,* 627–633.
30. Jones, P.J.H., Lichtenstein, A.H., and Schaefer, E.J. (1994) Interaction of Dietary Fat Type and Cholesterol Level on Cholesterol Synthesis Measured Using Deuterium Incorporation*, J. Lipid Res. 35,* 1093–1101.
31. Jones, P.J.H., Pappu, A.S., Hatcher, L., Li, Z.C., Illingworth, D.R., and Connor, W.E. (1996) Dietary Cholesterol Feeding Suppresses Human Cholesterol Synthesis Measured by Deuterium Incorporation and Urinary Mevalonic Acid Levels, *Atheroscler. Thromb. 16,* 1222–1228.
32. Jones, P.J.H., Ausman, L.M., Croll, D.H., Feng, J.Y., Schaefer, E.A., and Lichtenstein, A.H. (1998) Validation of Deuterium In-

corporation Against Sterol Balance for Measurement of Human Cholesterol Biosynthesis, *J. Lipid Res. 39,* 1111–1117.
33. Jones, P.J.H., Pappu, A.S., Illingworth, D.R., and Leitch, C.A. (1992) Correspondence Between Plasma Mevalonic Acid Levels and Deuterium Uptake in Measuring Human Cholesterol Synthesis, *Eur. J. Clin. Invest. 22,* 609–613.
34. Di Buono, M., Jones, P.J.H., Beaumier, L., and Wykes, L. (1999) Deuterium Incorporation (DI) and Mass Isotopomer Distribution Analysis (MIDA) Give Similar Estimates of Cholesterol Biosynthesis over 24 Hours, *FASEB J. 13,* 444.11 (abs.).
35. Lichtenstein, A.H., Ausman, L.M., Jalbert, S.M., and Schaefer, E.J. (1999) Effects of Different Forms of Dietary Hydrogenated Fats on Serum Lipoprotein Cholesterol Levels, *New Engl. J. Med. 340,* 1933–1940.
36. Havel, R.J., Eder, H.A., and Bragdon, J.H. (1955) Distribution and Chemical Composition of Ultracentrifugally Separated Lipoproteins in Human Serum, *J. Clin. Invest. 34,* 1345–1353.
37. McNamara, J.R., and Schaefer, E.J. (1987) Automated Enzymatic Standardized Lipid Analyses for Plasma and Lipoprotein Fractions, *Clin. Chim. Acta 166,* 1–8.
38. Folch, J., Lees, M., and Sloane Stanley, G.H. (1957) A Simple Method for the Isolation and Purification of Total Lipids from Animal Tissues, *J. Biol. Chem. 226,* 497–509.
39. Goodman, D.S., Noble, R.P., and Dell, R.B. (1973) Three-Pool Model of the Long-Term Turnover of Plasma Cholesterol in Man, *J. Lipid Res. 14,* 178–188.
40. Matthan, N.R., Ausman, L.M., Lichtenstein, A.H., and Jones, P.J.H. (2000) Hydrogenated Fat Consumption Affects Cholesterol Synthesis Rates in Moderately Hypercholesterolemic Women, *J. Lipid Res. 41,* 834–839.
41. Jones, P.J.H., Lichtenstein, A.H., Schaefer, E.J., and Namchuk, G.L. (1994) Effect of Dietary Fat Selection on Plasma Cholesterol Synthesis in Older, Moderately Hypercholesterolemic Humans, *Arterioscler. Thromb. 14,* 542–548.
42. Cuchel, M., Schwab, U.S., Jones, P.J.H., Vogel, S., Lammi-Keefe, C., Li, Z., Ordovas, J., McNamara, J.R., Schaefer, E.J., and Lichtenstein, A.H. (1996) Impact of Hydrogenated Fat Consumption on Endogenous Cholesterol Synthesis and Susceptibility of Low-Density Lipoprotein Cholesterol to Oxidation in Moderately Hypercholesterolemic Individuals, *Metabolism 45,* 241–247.
43. Bland, J.M., and Altman, D.G. (1986) Statistical Methods for Assessing Agreement Between Two Measures of Clinical Measurement, *Lancet 1,* 307–310.

[Received April 4, 2000, and in revised form August 1, 2000; revision accepted August 10, 2000]

COMMUNICATION

Antioxidant Reactions of α-Tocopherolhydroquinone

Daniel C. Liebler* and Jeanne A. Burr

Department of Pharmacology and Toxicology and Southwest Environmental Health Sciences Center, College of Pharmacy, The University of Arizona, Tucson, Arizona 85721-0207

ABSTRACT: α-Tocopherolhydroquinone (TQH_2) is a product of α-tocopherol oxidation/reduction that exerts antioxidant effects in biological systems. TQH_2 inhibited autoxidation of methyl linoleate initiated by peroxyl radicals derived from thermolysis of 2,2′-azobis(2,4-dimethylvaleronitrile) in acetonitrile. TQH_2 oxidation yielded α-tocopherolquinone (TQ) as a major product and 2,3-epoxy-α-tocopherolquinone and 5,6-epoxy-α-tocopherolquinone as minor products. Each TQH_2 consumed approximately two peroxyl radicals in the course of the oxidation. The data suggest that TQH_2 scavenges peroxyl radicals primarily by electron transfer to form TQ and secondarily by addition-elimination to form the epoxyquinones.

Paper no. L8493 in *Lipids 35*, 1045–1047 (September 2000).

Antioxidant reactions of α-tocopherol (vitamin E: TH) with peroxyl radicals generate 8a-substituted tocopherones and epoxytocopherones as initial products. The former hydrolyze to α-tocopherolquinone (TQ), which also is a product of TH oxidation by several other types of oxidants. Several reports indicate that TQ is present in tissues, although the reported levels vary (1–9). Previous work in our laboratory suggested that much of the TQ formed in tissues is present as the two-electron reduction product α-tocopherolhydroquinone (TQH_2) (10). Although TQH_2 is at the same oxidation state as TH, it is a hydroquinone rather than a chroman-6-ol. Nevertheless, TQH_2 would be expected to display antioxidant properties similar to TH and structurally analogous ubiquinols.

An interesting recent finding is that TQ undergoes reduction by NAD(P)H:quinone oxidoreductase (DT-diaphorase) to yield TQH_2 (11). Cells expressing the enzyme and supplemented with TQ displayed increased resistance to oxidant challenges, and this protection paralleled the reduction of TQ to TQH_2. Thus, TQH_2 may contribute to biological antioxidant protection by exerting direct antioxidant effects in cells. To further explore the potential role of TQH_2 as a cellular antioxidant, we have studied the antioxidant reactions of TQH_2 in chemically defined solution systems. Here we report that TQH_2 reacts with peroxyl radicals to generate TQ as the principal reaction product. Identification of epoxyquinone reaction products indicates that competing reactions also occur.

EXPERIMENTAL PROCEDURES

Reagents. TQH_2 was synthesized by $NaBH_4$ reduction of TQ as described previously (12). TQH_2 was prepared fresh immediately prior to each experiment. Preparation of TQ, 5,6-epoxy-α-tocopherolquinone (TQE_1), and 2,3-epoxy-α-tocopherolquinone (TQE_2) was done as described previously (10). The compound 2,2′-azobis(2,4-dimethylvaleronitrile) (AMVN) was obtained from Polysciences, Inc. (Warrington, PA). Methyl linoleate was from Nu-Chek-Prep, Inc. (Elysian, MN).

Kinetics of TQH_2 and methyl linoleate oxidation. Reactions contained 200 μmol methyl linoleate, 0.4 μmol TQH_2, and 20 μmol AMVN in 3 mL acetonitrile at 50°C. Aliquots (10 μL) were taken at 2-min intervals, diluted with 1 mL acetonitrile, and analyzed by ultraviolet (UV)-visible spectroscopy. Methyl linoleate oxidation was monitored by the appearance of conjugated dienes at 235 nm. TQH_2 and TQ were monitored by absorbances at 292 and 268 nm, respectively. The stoichiometry of AMVN-initiated TQH_2 oxidation by peroxyl radicals in acetonitrile was measured by the inhibited autoxidation method of Boozer *et al.* (13), as modified in our laboratory (14). Butylated hydroxytoluene (4-methyl-2,6-di-*tert*-butylphenol) was used as an antioxidant standard with an assigned stoichiometry value *n* of 2.0.

Analysis of TQH_2 oxidation products. Products of TQH_2 oxidation were analyzed by gas chromatography–mass spectrometry (GC–MS) as trimethylsilyl ethers following extraction and derivatization as previously described (10).

RESULTS AND DISCUSSION

Peroxyl radical-dependent oxidation of TQH_2 in homogeneous acetonitrile solution at 50°C was initiated with the azo initiator AMVN, which produces peroxyl radicals by thermolysis and oxygen addition . Oxidation of TQH_2 by AMVN-derived peroxyl radicals resulted in near-quantitative conversion of TQH_2 to TQ, as assessed by UV spectroscopic analysis of the reaction mixtures. TQ displays distinctive doublet absorbance maxima at 262 and 268 nm, whereas TQH_2 dis-

*To whom correspondence should be addressed at Department of Pharmacology and Toxicology, College of Pharmacy, The University of Arizona, P.O. Box 210207, Tucson, AZ 85721-0207.
E-mail: liebler@pharmacy.arizona.edu

Abbreviations: AMVN, 2,2′-azobis(2,4-dimethyvaleronitrile); GC–MS, gas chromatography–mass spectrometry; TH, α-tocopherol; TQ, α-tocopherolquinone; TQE_1, 5,6-epoxy-α-tocopherol-quinone; TQE_2, 2,3-epoxy-α-tocopherolquinone; TQH_2, α-tocopherolhydroquinone; UV, ultraviolet.

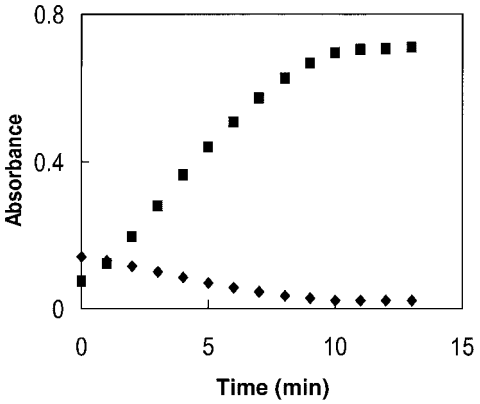

FIG. 1. Time course of 2,2′-azobis(2,4-dimethylvaleronitrile) (AMVN)-initiated α-tocopherolhydroquinone (TQH_2) disappearance (292 nm, ◆) and α-tocopherolquinone (TQ) appearance (268 nm, ■) in acetonitrile at 50°C.

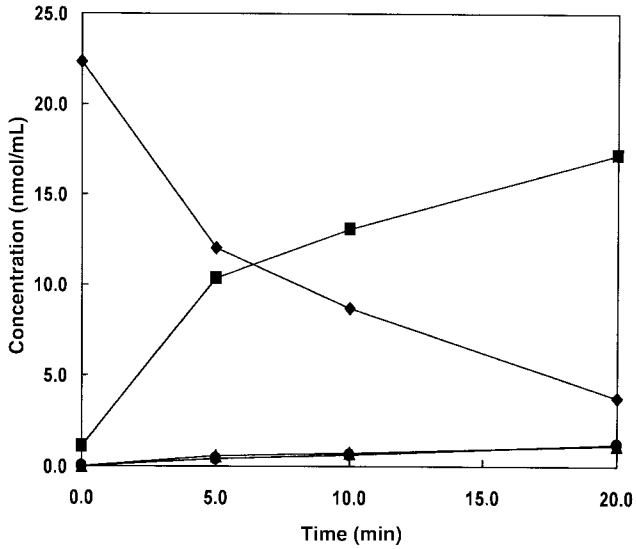

FIG. 2. Time course of TQH_2 (◆), TQ (■), 5,6-epoxy-α-tocopherolquinone (●), and 2,3-epoxy-α-tocopherolquinone (▲) in AMVN-initiated oxidation containing methyl linoleate (67 mM) and TQH_2 (0.13 mM). Products were analyzed by gas chromatography–mass spectrometry with selected ion monitoring. See Figure 1 for abbreviation.

plays a less intense absorbance maximum at 292 nm. Upon AMVN-initiated oxidation, absorbance for TQH_2 at 292 nm rapidly declined and absorbance of TQ at 268 nm concomitantly increased (Fig. 1).

TQH_2 inhibited AMVN-initiated methyl linoleate oxidation in acetonitrile at 50°C. By using the inhibited autoxidation method, a rate of chain initiation R_i of 0.0082 ± 0.0001 mM min^{-1} was measured and a stoichiometric factor n of 1.933 ± 0.223 ($n = 4$) was calculated for TQH_2, indicating that two peroxyl radicals are scavenged for each molecule of TQH_2 oxidized. GC–MS analysis of the reaction mixture indicated that TQ and TQH_2 were the principal species present throughout the reaction and that TQ was converted almost entirely to TQH_2 (Fig. 2). In GC–MS analyses, formation of small amounts of the epoxyquinones TQE_1 and TQE_2 were detected (Fig. 2). Quantitation of $TQE_{1/2}$ formation based on selected ion monitoring with stable isotope-labeled internal standards indicated that at 20 min of oxidation, TQ, TQE_1, and TQE_2 accounted for 87, 6, and 6%, respectively, of the TQH_2 oxidized.

Our data indicate that TQH_2 acts as a chain-breaking antioxidant with efficiency similar to that of TH, when measured by antioxidant stoichiometry. This result is consistent with previous reports that TQH_2 acts as an antioxidant in liposomes and submitochondrial particles (12), in low density lipoprotein (16), and in intact cells (11). The antioxidant stoichiometry for radical scavenging measured in our studies is approximately 10-fold above that measured by Shi *et al.* (17). The difference in the measured values evidently was attributable to the different conditions under which the measurements were made. Shi *et al.* employed a lower concentration of the AMVN initiator and conducted the reaction at a lower temperature. Both differences are expected to reduce the rate of generation of peroxyl radicals from AMVN and to reduce the efficiency of the reaction of the semiquinone intermediate $TQH^{\cdot}$ with peroxyl radicals. As demonstrated previously (16,17), oxidation of this semiquinone by oxygen to produce TQ and superoxide appears to be a facile reaction. Another possible reaction in this system is the dismutation of two $TQH^{\cdot}$ semiquinone radicals to TQ and TQH_2. This would appear not to be a significant reaction in our experiments, as it would have reduced the measured antioxidant stoichiometry to values below two. However, as with redox cycling of the semiquinone, dismutation would be disfavored under conditions where rapid generation of AMVN-derived peroxyl radicals efficiently trapped the semiquinone. These considerations underscore the importance of competing autoxidation and radical-trapping reactions to the antioxidant action of TQH_2.

Our data indicate that the principal reaction of TQH_2 with peroxyl radicals probably proceeds either by electron transfer/deprotonation or by hydrogen abstraction to form TQ (Scheme 1). (For clarity, only the mechanism of formation TQE_2 is depicted in detail. The formation of TQE_1 would proceed by an analogous mechanism.) However, the formation of $TQE_{1/2}$ suggests that a radical addition/elimination reaction also occurs. In this mechanism, a peroxyl radical adds to the hydroquinone and the unstable peroxide adduct rearranges to the epoxyquinone with concomitant elimination of an alcohol (Scheme 1). This addition/elimination mechanism also has been invoked to explain the formation of β-carotene epoxides in peroxyl radical oxidations (18). The addition/elimination mechanism results in the same net consumption of radicals as the TQ-forming pathway (i.e., two peroxyl radicals trapped for each epoxyquinone formed from TQH_2) and thus is also consistent with the measured antioxidant stoichiometry of TQH_2. One interesting aspect of epoxyquinone formation is that TQE_1 and TQE_2 are formed in equal amounts by TQH_2 oxidation, in contrast to the yields of these epoxides in TH oxidations, where TQE_2 usually is formed in a twofold excess over TQE_1 (14,19–21). This probably reflects the relative ease of attack of peroxyl radicals at either C-2 or C-6 of the TQH_2 ring, in contrast to the apparent preference for attack at C-5 over C-7 in

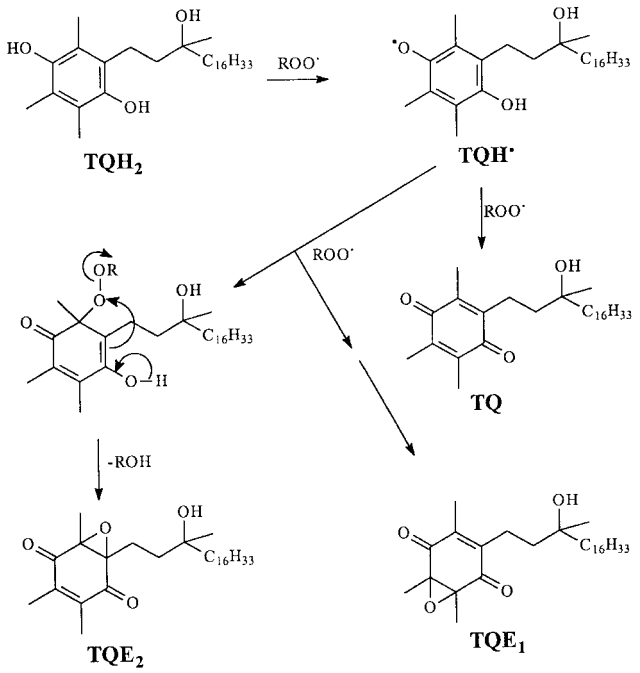

SCHEME 1

TH (C-5 and C-7 in TH are equivalent to C-2 and C-6, respectively, in TQH_2) (22).

In summary, our data indicate that TQH_2 scavenges peroxyl radicals primarily by an electron transfer mechanism that yields TQ as the major product. TQH_2 thus could contribute to antioxidant protection in biological membranes and lipoproteins. Interestingly, Neuzil *et al.* (16) demonstrated that TQH_2 contributed to antioxidant protection of low density lipoprotein by reducing tocopheroxyl radicals formed by oxidation of TH. This suggests that TQH_2 may contribute to antioxidant protection both by directly scavenging peroxyl radicals and by driving redox cycles of TH. Further work to explore these relationships is ongoing in our laboratory.

ACKNOWLEDGEMENT

This work was supported in part by U.S. National Institutes of Health grants CA84452 and ES06694.

REFERENCES

1. Bieri, J.G., and Tolliver, T.J. (1981) On the Occurrence of α-Tocopherolquinone in Rat Tissue, *Lipids 16*, 777–778.
2. Csallany, A.S., Draper, H.H., and Shah, S.N. (1962) Conversion of *d*-α-Tocopherol-^{14}C to Tocopheryl-*p*-quinone *in vivo*, *Arch. Biochem. Biophys. 98*, 142–145.
3. Ham, A.J.L., and Liebler, D.C. (1995) Vitamin E Oxidation in Rat Liver Mitochondria, *Biochemistry 34*, 5754–5761.
4. Hayashi, T., Kanetoshi, A., Nakamura, M., Tamura, M., and Shirahama, H. (1992) Reduction of α-Tocopherolquinone to α-Tocopherolhydroquinone in Rat Hepatocytes, *Biochem. Pharmacol. 44*, 489–493.
5. Howell, S.K., and Wang, Y.M. (1982) Quantitation of Physiological α-Tocopherol, Metabolites, and Related Compounds by Reversed-Phase High-Performance Liquid Chromatography, *J. Chromatogr. 227*, 174–180.
6. Kohar, I., Baca, M., Suarna, C., Stocker, R., and Southwell-Keely, P.T. (1995) Is α-Tocopherol a Reservoir for α-Tocopherolhydroquinone? *Free Radical Biol. Med. 19*, 197–207.
7. Murphy, M.E., and Kehrer, J.P. (1987) Simultaneous Measurement of Tocopherols and Tocopheryl Quinones in Tissue Fractions Using High-Performance Liquid Chromatography with Redox Cycling Electrochemical Detection, *J. Chromatogr. 421*, 71–82.
8. Pascoe, G.A., Duda, C.T., and Reed, D.J. (1987) Determination of α-Tocopherol and α-Tocopherolquinone in Small Biological Samples by High-Performance Liquid Chromatography with Electrochemical Detection, *J. Chromatogr. 414*, 440–448.
9. Vatassery, G.T., and Smith, W.E. (1987) Determination of α-Tocopherolquinone (vitamin E quinone) in Human Serum, Platelets, and Red Cell Membrane Samples, *Anal. Biochem. 167*, 411–417.
10. Liebler, D.C., Burr, J.A., Philips, L., and Ham, A.J.L. (1996) Gas Chromatography–Mass Spectrometry Analysis of Vitamin E and Its Oxidation Products, *Anal. Biochem. 236*, 27–34.
11. Siegel, D., Bolton, E.M., Burr, J.A., Liebler, D.C., and Ross, D. (1997) The Reduction of α-Tocopherolquinone by Human NAD(P)H:Quinone Oxidoreductase: The Role of α-Tocopherol Hydroquinone as a Cellular Antioxidant, *Mol. Pharmacol. 52*, 300–305.
12. Bindoli, A., Valente, M., and Cavallini, L. (1985) Inhibition of Lipid Peroxidation by α-Tocopherolquinone and α-Tocopherolhydroquinone, *Biochem. Int. 10*, 753–761.
13. Boozer, C.E., Hammond, G.S., Hamilton, C.S., and Sen, J.N. (1955) Air Oxidation of Hydrocarbons. II. The Stoichiometry and Fate of Inhibitors in Benzene and Chlorobenzene, *J. Am. Chem. Soc. 77*, 3233–3237.
14. Liebler, D.C., and Burr, J.A. (1995) Antioxidant Stoichiometry and the Oxidative Fate of Vitamin E in Peroxyl Radical Scavenging Reactions, *Lipids 30*, 789–793.
15. Niki, E. (1990) Free Radical Initiators as Source of Water- or Lipid-Soluble Peroxyl Radicals, *Methods Enzymol. 186*, 100–108.
16. Neuzil, J., Witting, P.K., and Stocker, R. (1997) α-Tocopheryl Hydroquinone Is an Efficient Multifunctional Inhibitor of Radical-Initiated Oxidation of Low Density Lipoprotein Lipids, *Proc. Natl. Acad. Sci. USA 94*, 7885–7890.
17. Shi, H., Noguchi, N., and Niki, E. (1999) Comparative Study on Dynamics of Antioxidative Action of α-Tocopheryl Hydroquinone, Ubiquinol, and α-Tocopherol Against Lipid Peroxidation, *Free Radical Biol. Med. 27*, 334–346.
18. Kennedy, T.A., and Liebler, D.C. (1991) Peroxyl Radical Oxidation of β-Carotene: Formation of β-Carotene Epoxides, *Chem. Res. Toxicol. 4*, 290–295.
19. Liebler, D.C., Baker, P.F., and Kaysen, K.L. (1990) Oxidation of Vitamin E: Evidence for Competing Autoxidation and Peroxyl Radical Trapping Reactions of the Tocopheroxyl Radical, *J. Am. Chem. Soc. 112*, 6995–7000.
20. Liebler, D.C., and Burr, J.A. (1992) Oxidation of Vitamin E During Iron-Catalyzed Lipid Peroxidation: Evidence for Electron-Transfer Reactions of the Tocopheroxyl Radical, *Biochemistry 31*, 8278–8284.
21. Ham, A.J.L., and Liebler, D.C. (1997) Antioxidant Reactions of Vitamin E in the Perfused Rat Liver: Product Distribution and Effect of Dietary Vitamin E Supplementation, *Arch. Biochem. Biophys. 339*, 157–164.
22. Liebler, D.C. (1993) The Role of Metabolism in the Antioxidant Function of Vitamin E, *Crit. Rev. Toxicol. 23*, 147–169.

[Received March 21, 2000, and in revised form July 6, 2000; revision accepted July 20, 2000]

Biotransformation of Linoleic Acid by *Clavibacter* sp. ALA2: Heterocyclic and Heterobicyclic Fatty Acids

Harold W. Gardner[a], Ching T. Hou[b,*], David Weisleder[c], and Wanda Brown[b]

[a]Bioactive Agents Research, [b]Oil Chemical Research, and [c]Analytical Chemical Services, National Center for Agricultural Utilization Research, ARS, USDA, Peoria, Illinois 61604

ABSTRACT: *Clavibacter* sp. ALA2 transformed linoleic acid into a variety of oxylipins. In previous work, three novel fatty acids were identified, (9*Z*)-12,13,17-trihydroxy-9-octadecenoic acid and two tetrahydrofuran-(di)hydroxy fatty acids. In this report, we confirm the structures of the tetrahydrofuran-(di)hydroxy fatty acids by nuclear magnetic resonance as (9*Z*)-12-hydroxy-13,16-epoxy-9-octadecenoic acid and (9*Z*)-7,12-dihydroxy-13,16-epoxy-9-octadecenoic acid. Three other products of the biotransformation were identified as novel heterobicyclic fatty acids, (9*Z*)-12,17;13,17-diepoxy-9-octadecenoic acid, (9*Z*)-7-hydroxy-12,17;13,17-diepoxy-9-octadecenoic acid, and (9*Z*)-12,17;13,17-diepoxy-16-hydroxy-9-octadecenoic acid. Thus, *Clavibacter* ALA2 effectively oxidized linoleic acid at C-7, -12, -13, -16, and/or -17.

Paper no. L8514 in *Lipids 35*, 1055–1060 (October 2000).

In previous work (1) biotransformation of linoleic acid by *Clavibacter* sp. ALA2 produced a number of products, among which (9*Z*)-12,13,17-trihydroxy-9-octadecenoic acid (**7**) was the predominant metabolite. Among the other metabolites, two tetrahydrofuran fatty acids were identified by gas chromatography–mass spectrometry (GC–MS), microchemical techniques, and preliminary nuclear magnetic resonance (NMR) data (2). In this report, these latter tetrahydrofuran fatty acids are fully confirmed by complete ^{1}H NMR and ^{13}C NMR analyses. In addition, two other unknowns, "unknown 3" and "unknown 5" (2), were isolated and identified as heterobicyclic fatty acids, (9*Z*)-12,17;13,17-diepoxy-9-octadecenoic acid (**1**) and (9*Z*)-12,17;13,17-diepoxy-7-hydroxy-9-octadecenoic acid (**4**), respectively. In addition, a positional isomer of **4** was identified, (9*Z*)-12,17;13,17-diepoxy-16-hydroxy-9-octadecenoic acid (**6**).

*To whom correspondence should be addressed at National Center for Agricultural Utilization Research, ARS, USDA, 1815 N. University Street, Peoria, IL 61604. E-mail: houct@mail.ncaur.usda.gov

Abbreviations: ANS, Na 8-anilino-1-napthalenesulfonate; CS, chemical shift; EI–MS, electron impact–mass spectrum; GC, gas chromatography; GC–MS, gas chromatography–mass spectrometry; HPLC, high-performance liquid chromatography; NMR, nuclear magnetic resonance; OTMSi, trimethylsilyloxy ether; RT, retention time; TLC, thin-layer chromatography; UV, ultraviolet.

MATERIALS AND METHODS

Production and purification of products. The bioconversion of linoleic acid by *Clavibacter* sp. ALA2, separation of the products fatty acids into fractions by high-performance liquid chromatography (HPLC), and preparation of chemical derivatives were described previously (2). Incubation of 0.22 g linoleic acid/50 mL for 4–5 d afforded about a 60% yield of products. Thin-layer chromatography (TLC) of HPLC-fractionated products as their methyl ester derivatives was completed with Silica Gel 60 F_{254} plates (20 × 20 × 250 μm, Merck, Darmstadt, Germany), and detection of compounds was done with a nondestructive spray reagent, 0.1% aqueous 8-anilino-1-naphthalenesulfonic acid (ANS) (Eastman Kodak, Rochester, NY) as sodium salt, followed by viewing under long-wave ultraviolet (UV). TLC developing solvents were: solvent A, hexane/diethyl ether (1:1, vol/vol); solvent B, hexane/ethyl acetate (6:4, vol/vol); solvent C, hexane/diethyl ether (9:1, vol/vol); and solvent D, ethyl acetate/hexane (6:4, vol/vol). TLC bands were scraped with a razor blade and recovered by ethyl acetate elution.

Spectral and microchemical methods. GC–MS of methyl esters or methyl esters/trimethylsilyloxy ethers (OTMSi) was completed as described previously (3). Fatty esters oxidatively cleaved by $KMnO_4$/acetic acid were separated by the same GC–MS system described (3), except the temperature programming was modified to 65°C to 260°C at 10°C/min in order to accommodate the short-chain esters . Less than obvious mass spectral fragment ions were analyzed by Xcalibur HighChem Mass Frontier Software from Finnigan Corporation (San Jose, CA). NMR spectra were obtained with a Bruker model ARX-400 spectrometer (Billerica, MA) equipped with a 5 mm $^{13}C/^{1}H$ dual probe (^{1}H NMR, 400 MHz; ^{13}C NMR, 100 MHz). NMR spectra were recorded with $CDCl_3$ as internal standard and solvent. Chemical shifts of the carbons were determined by heteronuclear multiple quantum correlation spectroscopy.

Fatty acids were methyl esterified for 30 s with diazomethane in diethyl ether/methanol (9:1, vol/vol). Hydroxyls were converted into OTMSi derivatives for 30 min with trimethylchlorosilane (Applied Sciences, State College, PA)/hexamethyldisilazane (Sigma, St Louis, MO)/anhydrous pyridine (3:2:2, vol/vol/vol), followed by evaporation of the

reagent with a stream of nitrogen and solvation in hexane. Methyl esterified samples were hydrogenated by stirring in 2 mL methanol under a hydrogen atmosphere with 20 mg 5% palladium on calcium carbonate catalyst (Aldrich, Milwaukee, WI). Double bonds were oxidatively cleaved with 12 mg $KMnO_4$ in 0.3 mL acetic acid at 37°C for 1 h (4).

RESULTS AND DISCUSSION

Biotransformation products of linoleic acid. Fatty acid products were separated by HPLC as described previously (2). The HPLC fractions were methyl esterified with diazomethane, and the unknown fractions previously separated by HPLC (2) were further purified and identified in this communication. A representative total product mixture analyzed by GC–MS is shown in Figure 1. Relative amounts of products varied somewhat depending on culture conditions. For structures of *Clavibacter* sp. ALA2 oxylipins derived from linoleic acid see Scheme 1.

*(9Z)-12,17;13,17-Diepoxy-9-octadecenoic acid (**1**).* The fatty acid methyl ester previously referred to as "unknown 3" [see Fig. 1 in Hou *et al.* (2)] was analyzed by GC–MS showing that it was largely one component, but included four minor impurities ranging in amounts of 1–4%, compared to the main component. Methyl esterified HPLC fraction isolated as described previously (2) containing **1** (16 mg) was purified by TLC developing with solvent A. From the main band, detected by ANS spray (R_f = 0.72), 5.4 mg was recovered. GC–MS showed that this component was one peak [15.1 min retention time (RT)] (**1**, methyl ester). This methyl ester afforded the following electron impact-mass spectrum (EI-MS) *m/z* (relative intensity): 324 $[M]^+$ (0.1), 293 $[M - CH_3O]^+$ (0.8), 282 $[M - CH_2CO]^+$ (1), 165 (0.8), 150 (1), 127 [ether bicyclic ring, $M - CH_2CH{=}CH(CH_2)_7COOCH_3]^+$ (100), 99 (8), 85 (6), 81 (13), 67 (9), 55 (10). Treatment of **1** (methyl ester) with either 15 mg of $NaBH_4$/0.5 mL methanol or OTMSi reagent resulted in no change in the GC–MS profile; therefore, this fatty acid possessed neither aldehyde, ketone, nor hydroxyl moiety.

Fatty acid (methyl ester) **1** was hydrogenated, and this product had a slightly longer retention time by gas chromatography (GC) and a mass spectrum with more intense fragment ions, also showing a gain in the molecular ion of two hydrogens (EI–MS) *m/z* (relative intensity): 326 $[M]^+$ (0.3), 308 $[M - H_2O]^+$ (0.7), 295 $[M - CH_3O]^+$ (9), 284 $[M - CH_2CO]^+$ (34), 283 $[M - CH_3CO]^+$ (21), 277 $[M - CH_3O - H_2O]^+$ (5), 266 (4), 255 (16), 242 (34), 227 (13), 223 (20), 195 (18), 185 (11), 184 (12), 152 (26), 127 [ether bicyclic ring, $M - CH_2CH{=}CH(CH_2)_7COOCH_3]^+$ (20), 112 (32), 98 (93), 81 (56), 74 (31), 69 (42), 67 (50), 55 (100). This confirmed the presence of one double bond.

A portion of **1** (methyl ester, 0.1 mg) was oxidatively

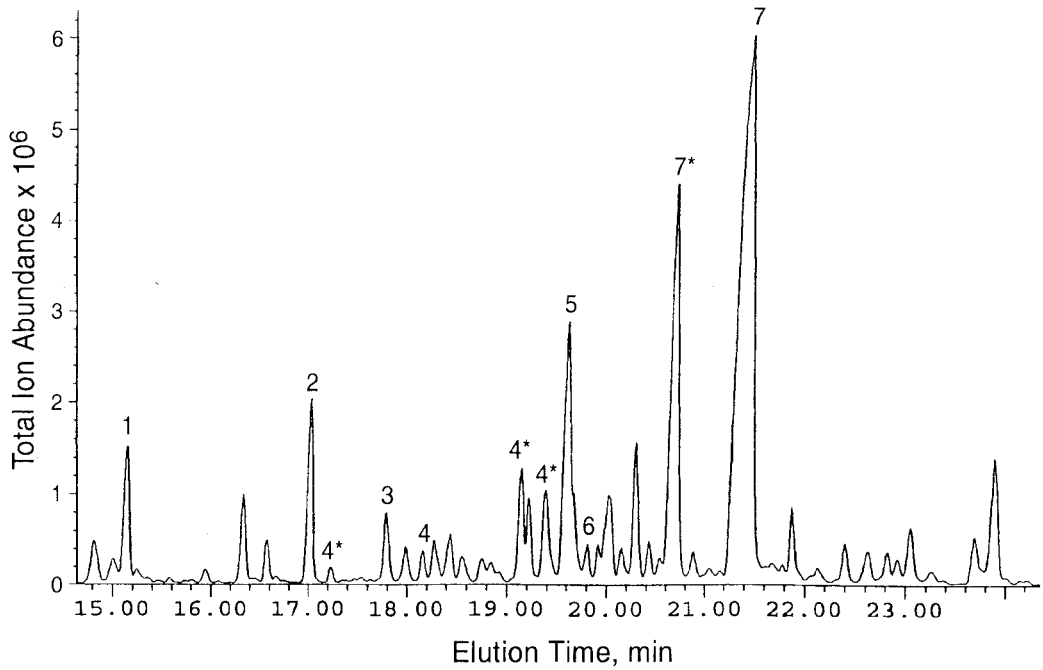

FIG. 1. GC–MS of a total mixture of products [as methyl esters/trimethylsilyloxy (OTMSi) ethers] from bioconversion of linoleic acid by *Clavibacter* ALA2. Peak numbering corresponds to the numbered identity of the isolated fatty acids (see Scheme 1). Numbers with asterisks identify possible isomers that possessed mass spectra very similar to the isomer identified in this study (plain number). Not shown is unconverted linoleic acid (methyl ester) eluting at a retention time of 12.3 min amounting to 26% (total ionization) of all peaks analyzed. Culture conditions were as described previously (2), except for some modifications to the culture medium. Culture medium (per L): dextrose, 5 g; K_2HPO_4, 5 g; yeast extract, 5 g; soybean flour, 5 g; $MgSO_4{\cdot}7H_2O$, 0.5 g; $FeSO_4{\cdot}7H_2O$, 0.5 g; $ZnSO_4$, 0.014 g; $MnSO_4{\cdot}H_2O$, 0.008 g; and nicotinic acid, 0.01 g. The medium was adjusted to pH 6.8 with dilute phosphoric acid. Linoleic acid (0.22 g) was incubated with 50 mL culture medium.

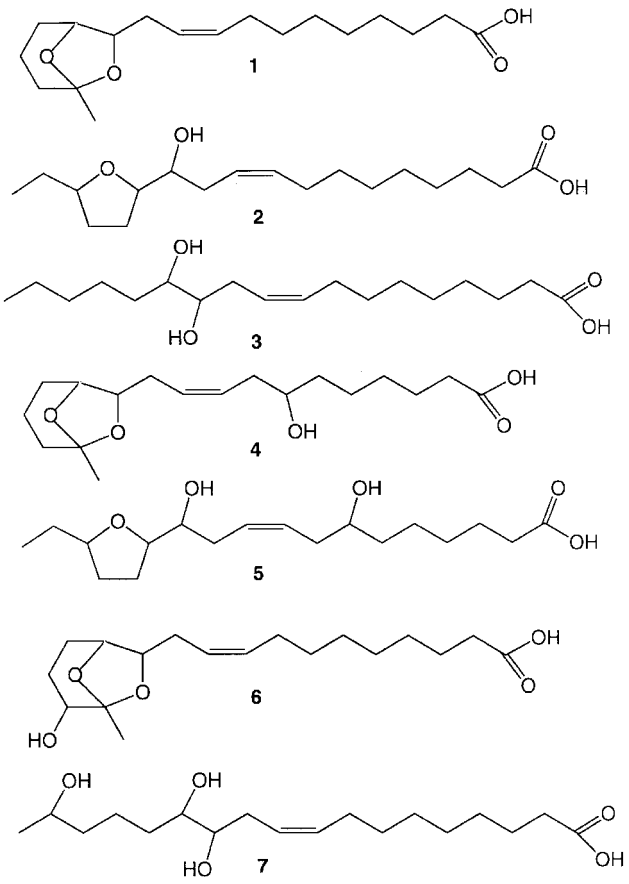

SCHEME 1

cleaved with $KMnO_4$/acetic acid, and reesterified with diazomethane. GC–MS of the oxidation mixture afforded two major peaks. The first at 9.2 min RT gave a mass spectrum that was consistent with methyl 3,8;4,8-diepoxy-nonanoate (EI–MS) *m/z* (relative intensity): 200 $[M]^+$ (0.7), 169 $[M - OCH_3]^+$ (11), 158 $[M - CH_2CO]^+$ (65), 157 $[M - CH_3CO]^+$ (27), 141 $[M - COOCH_3]^+$ (15), 130 (20), 129 (100), 127 [ether bicylic ring, $M - CH_2COOCH_3]^+$ (11), 116 (13), 98 (56), 81 (14), 74 (8), 71 (10), 70 (11), 59 (11), 55 (18), 43 $[CH_3CO]^+$ (93). The second GC peak at 11.9 min was identical to standard dimethyl nonanedioate. Therefore, a double bond is located at C-9,10.

^1H and ^{13}C NMR of **1** suggested that the compound was a heterobicyclic fatty acid (Tables 1 and 2). The singlet multiplicity of the terminal methyl showed that there was no coupling with C-17, and the chemical shift of C-17 by ^{13}C NMR was consistent with its diether functionality. The ^{13}C resonance assignment for the C-15 methylene of **1** at the unusual chemical shift of δ17.1 is consistent with a heterobicyclic structure based on the predicted chemical shift of δ16.0 assigned to C-15 in the ^{13}C NMR shift prediction module of ChemIntosh (Bio-Rad, Richmond, CA). The introduction of a hydroxyl group at C-16 in (9*Z*)-12,17;13,17-diepoxy-16-hydroxy-9-octadecenoic acid (see below) causes a downfield shift of the C-15 methylene to δ25.5, verifying the initial assignment. The H-12 resonance is a triplet because of coupling to the freely rotating H-11 protons. Coupling between H-12 and H-13 is not observed, indicating that the configuration of the ethers between C-12 and -13 was *threo*. The *threo* configuration causes the dihedral angle of the protons to be 90 degrees with the preferred chair-form of the six-membered ring giving the lack of coupling. The *threo* configuration was consistent with that found for the dihydroxyls at C-12 and -13 for a product discussed later, 12,13-dihydroxy-9-octadecenoic acid. The H-13 resonance appears as a broad singlet. The dihedral angle for H-13 and either of the H-14 protons is about 60 degrees, resulting in small unresolved splittings of the H-13 signal. The coupling constant for C-9,10 of 10.9 Hz was consistent with (*Z*)-double bond geometry.

*(9Z)-13,16-Epoxy-12-hydroxy-9-octadecenoic acid (**2**).* Fatty acid **2**, previously identified as "unknown 4" [see Fig. 1 in Hou *et al.* (2)], was structurally characterized by GC–MS and microchemical methods, including preliminary ^1H NMR data indicating a terminal ethyl group (2).

Further work with this fraction by GC–MS of its OTMSi derivative showed that it was a mixture containing about 50% of the compound previously identified as "unknown 4." This fraction (as methyl ester) was further purified by TLC using development by solvent A, affording 5.0 mg of **2** (R_f = 0.50). GC–MS indicated that the recovered material was a single component [see Hou *et al.* (2) for additional structural proof of **2**, including mass spectral data of **2** and its derivatives]. Isolate **2** was analyzed by NMR. The structure of **2** (methyl ester) was confirmed by complete ^1H and ^{13}C NMR data (Tables 1 and 2). The double bond at C-9 was determined to be (9*Z*) because of the ^{13}C NMR chemical shift at C-8 of 27.3 δ (5).

*12,13-Dihydroxy-9-octadecenoic acid (**3**).* The methyl ester OTMSi derivative of **3** was tentatively identified by an excellent comparison of its mass spectrum and GC RT (17.82 min) with the identical compound obtained by soybean epoxide hydrolase action on vernolic acid [(12*S*,13*R*,9*Z*)-12,13-epoxy-9-octadecenoic acid from Sigma, St Louis, MO]. It is known that *cis*-epoxides are hydrolyzed by epoxide hydrolase into *threo*-dihydroxyls (6). On the other hand, $NaBH_4$ reduction of the α-ketol obtained from allene oxide synthase action on the 13-hydroperoxide of linoleic acid gave two separable isomers of (9*Z*)-12,13-dihydroxy-9-octadecenoic acid (as methyl ester/OTMSi derivative) composed of *erythro* and *threo* diols at retention times of 17.82 and 18.05 min (7). Therefore, the isomer detected in the *Clavibacter* product was the *threo*-12,13-dihydroxy; that is, either (12*R*,13*R*) or (12*S*,13*S*).

*(9Z)-12,17;13,17-Diepoxy-7-hydroxy-9-octadecenoic acid (**4**), and (9Z)-12,17;13,17-diepoxy-16-hydroxy-9-octadecenoic acid (**6**).* The fatty acid methyl ester referred to as "unknown 5" [see Fig. 1 in Hou *et al.* (2)] was analyzed by GC–MS as its methyl ester or methyl ester/OTMSi ether showing that it was a mixture. Analysis of the mass spectra indicated that most of the GC peaks were isomers of two principal compounds; a number of other minor compounds were found with unrelated mass spectra. A portion of this HPLC

TABLE 1
^{1}H NMR Spectral Data[a] for Fatty Acid Products (as Methyl Esters)[b]

	1			2			4			5			6		
Carbon no.	δ	mult.	Hz	δ	mult.	Hz	δ	mult.	Hz	δ	mult.	Hz	δ	mult.	Hz
2	2.28	*t*		2.28	*t*		2.29	*t*		2.30	*t*		2.29	*t*	
3	1.59	*m*		1.60	*m*		1.61	*m*		1.61	*m*		1.60	*m*	
4	1.28	*m*		1.28	*m*		1.28	*m*		1.33	*m*		1.29	*m*	
5	1.28	*m*		1.28	*m*		1.28	*m*		1.33	*m*		1.29	*m*	
6	1.28	*m*		1.28	*m*		1.40	*m*		1.33	*m*		1.29	*m*	
7	1.28	*m*		1.28	*m*		3.62	*m*		3.54	*m*		1.29	*m*	
8	2.01	*dt*		2.01	*m*		2.19	*m*		2.13	*m*		2.02	*m*	
9	5.48	*dt*	10.9	5.46	*m*		5.50	*m*	10.9	5.60	*m*		5.49	*dt*	10.9
10	5.33	*dt*	10.9	5.46	*m*		5.45	*m*	10.9	5.60	*m*		5.33	*dt*	10.9
11	a2.19	*m*		2.19	*m*		a2.19	*m*		2.28	*m*		a2.22	*m*	
	b2.29	*m*					b2.29	*m*					b2.29	*obs*	
12	3.99	*t*	6.8	3.42	*m*		4.00	*t*	6.8	3.44	*m*		3.90	*t*	6.8
13	4.12	*brs*		3.82	*ddd*		4.12	*brs*		3.83	*m*		4.12	*brs*	
14	1.79	*m*		a1.47	*m*		1.80	*m*		a1.47	*m*		2.02	*m*	
				b1.94	*m*					b1.98	*m*				
15	a1.42	*m*		1.60	*m*		a1.45	*obs*		1.55	*m*		a1.50	*m*	
	b1.59	*obs*					b1.57	*obs*					b1.60	*obs*	
16	1.59	*m*		3.82	*ddd*		1.61	*m*		3.83	*m*		3.45	*app,s*	
17	—			a1.45	*m*		—			a1.48	*m*		—		
				b1.60	*m*					b1.65	*m*				
18	1.41	*s*		0.89	*t*		1.42	*s*		0.90	*t*		1.39	*s*	
OCH_3	3.64	*s*		3.64	*s*		3.65	*s*		3.65	*s*		3.65	*s*	
OTMSi	—			—			0.09	*s*		—			0.11	*s*	

[a]Chemical shift (ppm), δ; multiplicity (br, broad; d, doublet; m, multiplet; obs, obscured; s, singlet; t, triplet); coupling constant, Hz.
[b]Fatty esters 4 and 6 were analyzed as their trimethylsilyloxyethers (OTMSi). NMR, nuclear magnetic resonance.

fraction, as methyl esters, was purified by TLC using solvent B. The main band at $R_f = 0.37$ (15 mg) was found by GC–MS to be a mixture of two different fatty acids, which subsequently were identified as **4** (methyl ester) and the other as the methyl ester of **6**. A second band at $R_f = 0.47$ (7.5 mg) was shown by GC–MS to be one major and three minor peaks having mass spectra consistent with **4** (methyl ester/OTMSi ether). As shown in Figure 1, there are a number of peaks identified as **4*** that gave mass spectra similar to **4** (methyl ester/OTMSi ether). The third band at $R_f = 0.53$ (1.7 mg) was unrelated material that comprised two main peaks and a few minor ones as assessed by GC–MS.

The main TLC band described above ($R_f = 0.37$), comprising two main components, was selected for further separation, but it was determined that the two could not be separated by conventional TLC. However, it was found that the two compounds could be readily separated by "chemical chromatography" (3). A portion of this TLC fraction (4.5 mg) was silylated and the OTMSi derivative was separated by TLC using three-fold development with solvent C. Two main bands at $R_f = 0.20$ and 0.26 were isolated. As assessed by GC–MS, the band at $R_f = 0.20$ (1.7 mg) was the OTMSi ether/methyl ester of **4** with a very minor satellite peak indicative of conversion of a OTMSi group into hydroxyl. The ^{1}H NMR data are listed in Table 1; interpretation of the data for H-12, H-13 is the same as described for fatty ester **1**; that is, a *threo* configuration of the ethers at C-12 and -13. The mass spectrum of **4** (methyl ester/OTMSi ether) was indicative of its structure (EI–MS) *m/z* (relative intensity): 397 [M – CH_3]$^+$ (0.1), 381 [M – CH_3O]$^+$ (0.9), 283 [M – $(CH_2)_5COOCH_3$]$^+$ (1), 231 [CHOTMSi$(CH_2)_5COOCH_3$]$^+$

TABLE 2
^{13}C NMR Chemical Shifts (ppm), δ[a], for Fatty Acid Products (as Methyl Esters)

Carbon	Fatty ester				
no.	**1**	**2**	**4**[c]	**5**	**6**
1	172.2	174.3	174.2	174.3	174.3
2	34.0	34.0	34.0	34.0	34.1
3	24.9	24.9	24.9	24.9	24.9
4	29.0*	29.1*	29.3	29.2	29.1*
5	29.0*	29.1*	25.3*	25.4	29.1*
6	29.1*	29.1*	37.2**	37.2	29.1*
7	29.5*	29.5*	72.4	70.9	29.5*
8	27.4**	27.3	37.3**	35.4	27.4
9	132.6	132.5	25.7*	128.5*	132.8
10	124.6	125.1	25.6*	128.6*	124.4
11	33.7***	31.5**	34.8	31.3**	33.4
12	79.5****	73.9	79.7***	73.8	78.3**
13	78.2****	80.7***	78.6***	80.7***	77.8**
14	27.8**	28.5****	27.8	28.5****	23.9
15	17.1	28.4****	17.1	28.4****	25.5
16	34.8***	81.2***	35.8	81.5***	69.4
17	107.9	31.9**	107.7	31.9**	108.1
18	25.0	10.3	25.1	10.3	21.8
OCH_3	51.4	51.4	51.4	51.4	51.4
OTMSi[b]	—	—	0.43	—	0.11

[a]Chemical shifts marked by *, **, *** or **** are interchangeable.
[b]Fatty esters **4** and **6** were analyzed as their OTMSi ethers.
[c]Hydrogenated sample. See Table 1 for abbreviations.

(100), 199 (11), 171 (11), 155 (6), 133 (8), 127 [ether bicyclic ring, M – $CH_2CH{=}CHCH_2CHOTMSi(CH_2)_5COOCH_3]^+$ (89), 113 (11), 99 (11), 81 (57), 73 $[TMSi]^+$ (81), 55 (16).

As described above, the band obtained by "chemical chromatography" at R_f = 0.26 (0.5 mg) was found by GC–MS to be one component identified as **6** (methyl ester/OTMSi ether, see NMR data, Tables 1 and 2). Interpretation of the H-12 and H-13 resonance indicates a *threo* configuration as described for **1** and **4** (methyl ester). The mass spectrum of **6** (methyl ester/OTMSi ether) gave useful marker ions for determining molecular weight, but many of the fragment ions were difficult to interpret. Thus, Xcalibur software from Finnigan was used to interpret some of the ions affording diagnostic fragments, some of which located the hydroxyl at C-16. The data is given as follows (EI–MS) *m/z* (relative intensity): 412 $[M]^+$ (0.1), 381 $[M - CH_3O]^+$ (0.3), 379 $[M - H_2O - CH_3]^+$ (0.4), 352 $[TMSiOCH{\cdot}(CH_2)_2CH^+CH{=}CHCH{=}CH(CH_2)_7\text{-}COOCH_3]$ (8), 309 (2), 291 (2), 262 (4), 236 $[{\cdot}CH_2CH^+CH{=}CHCH{=}CH(CH_2)_7COOCH_3]$ (41), 215 [ether bicyclic ring containing one OTMSi group, M – $CH_2CH{=}CH(CH_2)_7\text{-}COOCH_3]^+$ (14), 195 (8), 181 (16), 168 (11), 155 (44), 143 (33), 116 $[{\cdot}CH_2CH{=}O^+TMSi]$ (100), 101 $[CH_2{=}CHO^+{=}Si(CH_3)_2]$ (76), 73 $[TMSi]^+$ (86), 55 (26). A mass spectrum of **6** (methyl ester) afforded some diagnostic ions as follows (numerous ions of lower *m/z* are not listed) (EI-MS) *m/z* (relative intensity): 309 $[M - CH_3O]^+$ (3), 291 $[M - CH_3O - H_2O]^+$ (3), 280 $[O{=}CH(CH_2)_2CH{\cdot}CH^+CH_2CH{=}\ CH(CH_2)_7\text{-}COOCH_3]$ (3), 262 (12), 248 (14), 236 $[{\cdot}CH_2\text{-}CH^+CH{=}\ CHCH{=}CH(CH_2)_7\ COOCH_3]$ (43), 143 [hydroxylated ether bicyclic ring, M – $CH_2CH{=}CH(CH_2)_7COOCH_3]^+$ (62). A third minor TLC band at R_f = 0.32 (0.2 mg) was isomeric **6** (methyl ester/OTMSi ether) with a slightly smaller retention time compared to the former; this fraction was not characterized further.

Another portion (9.2 mg) of the main band (R_f = 0.37 containing mixed methyl esters of **4** and **6**) was hydrogenated, and the same "chemical chromatography" procedure described in the preceding paragraphs was completed. TLC of the methyl ester/OTMSi ether using twofold development with solvent C afforded 5.6 mg hydrogenated **4** (methyl ester/OTMSi ether; R_f = 0.22), 1.8 mg hydrogenated **6** (methyl ester/OTMSi ether; R_f = 0.30), and 0.5 mg of another isomer of hydrogenated **6** (methyl ester/OTMSi ether; R_f = 0.35) with a slightly smaller GC RT. The mass spectrum of hydrogenated **4** (methyl ester/OTMSi ether) showed there was a gain of two hydrogens (i.e., one double bond) as follows (EI–MS) *m/z* (relative intensity): 399 $[M - CH_3]^+$ (0.1), 383 $[M - CH_3O]^+$ (1), 324 $[M - TMSiOH]^+$ (0.6), 285 $[M - (CH_2)_5COOCH_3]^+$ (3), 282 (11), 264 (7), 253 (4), 231 $[CHOTMSi(CH_2)_5COOCH_3]^+$ (67), 195 $[285 - TMSiOH]^+$ (45), 171 (9), 159 (12), 149 (34), 127 (25), 98 (32), 81 (54), 73 $[TMSi]^+$ (100), 67 (25), 55 (33). The ^{13}C NMR data for hydrogenated **4** (methyl ester) is shown in Table 2. As described for **1**, the chemical shift of C-17 at δ107.7 in **4** was indicative of diether carbon. The unusual methylene chemical shift of C-15 at δ17.1 is consistent with the heterobicyclic structure as explained previously for **1**.

The mass spectrum of the principal isomer of hydrogenated **6** (methyl ester/OTMSi ether) gave useful ions suggesting its molecular weight (an increase of two indicating one double bond) and the position of the 16-hydroxyl as follows (EI-MS) *m/z* (relative intensity): 414 $[M]^+$ (0.3), 381 $[M - CH_3 - H_2O]^+$ (0.4), 354 $[TMSiOCH{\cdot}(CH_2)_2CH^+CH{=}CH(CH_2)_9COOCH_3]$ (11), 311 (5), 293 (3), 264 (3), 250 (2), 207 (2), 169 (6), 155 (33), 143 (29), 133 (28), 116 $[{\cdot}CH_2CH{=}O^+TMSi]$ (100), 101 $[CH_2{=}CHO^+{=}Si(CH_3)_2]$ (70), 73 $[TMSi]^+$ (59), 55 (23). Both ^1H NMR and ^{13}C NMR of hydrogenated **4** and **6** (methyl ester/OTMSi ether) decisively showed that one double bond in each compound was saturated.

In the data given above it can be seen that **4** and **6** both have at least one hydroxyl group from the observation that both compounds were derivatized as OTMSi ethers. The unsilylated compounds both had an apparent molecular weight of 340 from observation of *m/z* 309 $[M - CH_3O]^+$, which is the theoretical *m/z* 72 less than that of corresponding ions of the mono-silylated derivatives. A coupling constant of 10.9 Hz (Table 1) showed that the double bond was (*Z*) for both **4** and **6**.

To demonstrate the position of the double bond, the methyl ester/OTMSi of **4** was oxidatively cleaved with $KMnO_4$ and then derivatized with diazomethane and silylating reagent. Five cleavage products were found for **4**. The earliest eluting peak was identical to the $KMnO_4$ oxidation fragment obtained from **1**; that is, a spectrum suggesting methyl 3,8;4,8-diepoxy-nonanoate. The second and third peaks were relatively small; the former gave a mass spectrum consistent with dimethyl heptanedioate and the third was unknown. The mass spectrum of the fourth peak was consistent with dimethyl nonenedioate, possibly from hydroxyl elimination, and the fifth peak was very indicative of dimethyl 3-OTMSi-nonanedioate as follows (EI–MS) *m/z* (relative intensity): 289 $[M - CH_3]^+$ (22), 273 $[M - CH_3O]^+$ (1), 257 $[M - CH_3O - CH_3]^+$ (12), 231 $[M - CH_2COOCH_3]^+$ (12), 225 (10), 215 (16), 202 (9), 183 (45), 175 $[CHOTMSiCH_2COOCH_3]^+$ (62), 159 (38), 155 (34), 151 (49), 133 (46), 123 (19), 105 (17), 89 (84), 73 (100), 59 (32), 55 (23). Together these data were very suggestive of a 9,10-double bond.

$KMnO_4$ oxidation of **6** (methyl ester/OTMSi ether) afforded two main cleavage products after treating with diazomethane and silylating reagent. The first GC–MS peak was identical to standard dimethyl nonanedioate and the second peak was consistent with methyl 3,8;4,8-diepoxy-nonanoate additionally possessing one OTMSi group as follows (EI–MS) *m/z* (relative intensity): 273 $[M - CH_3]^+$ (12), 257 $[M - CH_3O]^+$ (2), 245 (4), 228 (14), 185 (10), 169 (8), 155 (34), 143 (32), 116 (82), 101 (100), 87 (10), 74 (18), 73 $[TMSi]^+$ (56), 59 (17), 55 (13). Therefore, these data indicate a 9,10-double bond.

*(9Z)-13,16-Epoxy-7,12-dihydroxy-9-octadecenoic acid (**5**).* Fatty acid **5** was previously identified as "unknown 6" [see Fig. 1 in Hou *et al.* (2)]. In the previous work, the structure was determined by GC–MS and microchemical methods. The terminal ethyl group was indicated by preliminary ^1H

NMR data; that is, triplet multiplicity of the C-18 methyl group (2).

From the HPLC fraction (2) **5** was isolated by TLC developing with solvent D (R_f = 0.32). GC–MS of its OTMSi derivative indicated that the recovered methyl ester (14 mg) was one component [see Hou *et al.* (2) for additional structural proof of **5**, including mass spectral data of **5** and its derivatives]. The structure of **5** (methyl ester) was confirmed by complete ^{1}H and ^{13}C NMR data (Tables 1 and 2). The ^{1}H NMR resonance pattern for the C-9 and -10 protons was very similar to that of **2**, so it was surmised that this olefin was also (9*Z*).

The fatty acids identified in this study and previous work (1,2) showed that *Clavibacter* ALA2 is especially efficient at oxidizing C-12, -13 and -17 with hydroxyl groups. To a lesser extent hydroxyls also occurred at C-7 and -16. It seems probable that these oxidations are catalyzed by cytochromes P450. Since fatty acid **3** was exclusively the *threo* isomer some stereospecificity of the oxidations at C-12 and -13 was indicated; however, we did not complete studies on absolute stereoconfiguration. Since all the fatty acids reported in this study have either an ether or hydroxyl functionality at C-12 and -13, it is a reasonable assumption that these products may also possess the *threo* configuration at these carbons. Although not proved, it would appear that conversion into heterocyclic and heterobicyclic fatty acids occurs as a subsequent step from precursor hydroxyl fatty acids, such as **7**. In regard to the heterobicyclic fatty acids, it would appear that oxidation of the 17-hydroxyl to a 17-ketone may precede cyclization. Incubation of **7** with *Clavibacter* ALA2 should resolve this question.

ACKNOWLEDGMENT

We thank Dr. Mark Berhow at the National Center for Agricultural Utilization Research for assistance with Xcalibur mass spectral software.

REFERENCES

1. Hou, C.T. (1996) A Novel Compound, 12,13,17-Trihydroxy-9(*Z*)-octadecenoic Acid, from Linoleic Acid by a New Microbial Isolate *Clavibacter* sp. ALA2, *J. Am. Oil Chem. Soc. 73*:1359–1362.
2. Hou, C.T., Gardner, H., and Brown, W. (1998) Production of Polyhydroxy Fatty Acids from Linoleic Acid by *Clavibacter* sp. ALA2, *J. Am. Oil Chem. Soc. 75*:1483–1487.
3. Gardner, H.W. (1998) 9-Hydroxy-traumatin, a New Metabolite of the Lipoxygenase Pathway, *Lipids 33*:745–749.
4. Hamberg, M., Herman, R.P., and Jacobsson, U. (1986) Stereochemistry of Two Epoxy Alcohols from *Saprolegnia parasitica, Biochim. Biophys. Acta 879*:410–418.
5. Lie Ken Jie, M.S.F., and Cheng, A.K.L. (1993) Confirmation of the Carbon Chemical Shifts of Ethylenic Carbon Atoms in Methyl Ricinoleate and Methyl Ricinelaidate, *Nat. Prod. Lett. 3*:65–69.
6. Blée, E., and Schuber, F. (1992) Regio- and Enantioselectivity of Soybean Fatty Acid Epoxide Hydrolase, *J. Biol. Chem. 267*:11881–11887.
7. Pan, Z., Durst, F., Werck-Reichhart, D., Gardner, H.W., Camara, B., Cornish, K., and Backhaus, R.A. (1995) The Major Protein of Guayule Rubber Particles Is a Cytochrome P450. Characterization Based on cDNA Cloning and Spectroscopic Analysis of the Solubilized Enzyme and Its Reaction Products, *J. Biol. Chem. 270*:8487–8494.

[Received April 19, 2000, and in revised form and accepted September 4, 2000]

Production of Eicosapentaenoic Acid by a Recombinant Marine Cyanobacterium, *Synechococcus* sp.

Reiko Yu[a,*], Akiko Yamada[a], Kazuo Watanabe[a], Kazunaga Yazawa[a], Haruko Takeyama[b], Tadashi Matsunaga[b], and Ryuichiro Kurane[c]

[a]Sagami Chemical Research Center, Sagamihara, Kanagawa 229-0012, Japan, [b]Tokyo University of Agriculture and Technology, Department of Biotechnology, Koganei, Tokyo 184-8588, Japan, and [c]National Institute of Bioscience and Human Technology, Agency of Industrial Science and Technology, Japan

ABSTRACT: The eicosapentaenoic acid (EPA) synthesis gene cluster from an EPA-producing bacterium, *Shewanella* sp. SCRC-2738, was cloned into a broad-host range vector, pJRD215, and then introduced into a marine cyanobacterium, *Synechococcus* sp. NKBG15041c, by conjugation. The transconjugant cyanobacteria produced 3.7 ± 0.2% (2.24 ± 0.13 mg/L) EPA (n-3) and 2.5 ± 0.2% (1.49 ± 0.06 mg/L) eicosatetraenoic acid (n-3) of the total fatty acids when the cells were cultured at 23°C at a light intensity of 1,000–1,500 Lux. The EPA and eico-satetraenoic acid contents of the cells were increased to 4.6 ± 0.6% (3.86 ± 1.11 mg/L) and 4.7 ± 0.3% (3.86 ± 0.82 mg/L), and 7.5 ± 0.3% (1.76 ± 0.10 mg/L) and 5.1 ± 0.2% (1.19 ± 0.06 mg/L) when they were cultured at low temperature (18°C) and at lower light intensity (40 Lux), respectively.

Paper no. L8450 in *Lipids 35*, 1061–1064 (October 2000).

The n-3 group of polyunsaturated fatty acids (PUFA), in particular eicosapentaenoic acid (20:5n-3, EPA) and docosahexaenoic acid (22:6n-3) have received much attention for their importance in keeping the human circulation and nervous systems in a healthy condition (1,2). Moreover, these compounds are also essential nutrients to larval marine fish (3). At present, the main sources of dietary EPA are marine fish and algae such as *Porphyridium* and *Nannochloropsis* (4,5). Marine cyanobacteria like *Synechococcus* are widely distributed in the sea and have important roles as primary producers in the marine food chain. Utilization of these cyanobacteria for purposes of fish culture is convenient, because they are bioavailable as whole cells without any extraction. However, marine cyanobacteria do not produce EPA. Therefore, by introducing an EPA synthesis gene cluster to marine cyanobacteria, it is expected that they might be a valuable source of n-3 fatty acids for fish culture.

The EPA synthesis gene cluster [approximately 38 kb, composed of nine open reading frames (ORF) (Yamada, A., Yu, R., Watanabe, K., Yazawa, K., and Konda, K., unpublished data)] was isolated from a marine bacterium, *Shewanella* sp. SCRC-2738 (6,7). In previous work, we confirmed that a marine cyanobacterium, *Synechococcus* sp. NKBG042902, produced EPA after the introduction of an EPA synthesis gene cluster (8). However, plasmid pJRDEPA, including all nine ORF of this gene cluster, was unstable in the cells, and the total amount of EPA produced was low. In this paper, we demonstrate EPA production by a transgenic marine cyanobacterium, *Synechococcus* sp. NKBG15041c (9), carrying a plasmid containing the essential ORF for EPA synthesis and its enhancement under different growth conditions.

EXPERIMENTAL PROCEDURES

Strains and plasmids. A marine cyanobacterium, *Synechococcus* sp. NKBG15041c, isolated from a Japanese coastal area, was used as a host strain. It was cultured in BG11 medium (American Type Culture Collection catalog, medium no. 617) supplemented with 3% (wt/vol) NaCl (BG11-M) under aerobic conditions with continuous light at 23°C unless otherwise stated. *Escherichia coli* JM109 and S17-1 (10) were cultured under aerobic conditions in LB medium [10 g/L Bacto-tryptone 5 g/L Bacto-yeast extract, both from Difco (Detroit, MI) and 10 g/L NaCl] at 37 or 25°C. Cloning vector pBSIIKS(+) (Stratagene, La Jolla, CA) and broad-host range vector pJRD215 (10.2 kb, containing Km^r and Sm^r genes; 11) were used in this work. As the source of the EPA synthesis gene cluster, pEPA (46.6 kb; 7,8) was used. pEPA is a plasmid that is carrying an EPA synthesis gene cluster (GenBank accession number, U73935) isolated from *Shewanella* sp. SCRC-2738.

Construction of pJRDEPA-S. DNA constructs were produced using standard methods. Restriction enzymes were purchased from New England Biolabs (Beverly, MA) and Takara Shuzo (Kyoto, Japan). At first, the subcloning of essential ORF (2,5,6,7, and 8) for EPA production from pEPA was carried out. A 8,398 bp *Xba*I-*Spe*I fragment (23,045–31,443 bp, containing the 3′ end of ORF6, ORF7, and the 5′ end of ORF8), a 10,731 bp *Xba*I-*Xba*I fragment (12,314–23,045 bp, containing the 3′ end of ORF3, ORF4, 5 and the 5′ of ORF6), and a 1,071 bp *Spe*I-*Nhe*I fragment (31,443– 32,514 bp, containing the 3′ end

*To whom correspondence should be addressed at Sagami Chemical Research Center, 4-4-1, Nishi-Ohnuma, Sagamihara, Kanagawa 229-0012, Japan. E-mail: ryuscrc@ce.mbn.or.jp

Abbreviations: EPA, eicosapentaenoic acid; GLC, gas–liquid chromatography; GC–MS, gas chromatography–mass spectrometry; ORF, open reading frame; PUFA, polyunsaturated fatty acid; TLC, thin-layer chromatography.

of ORF8) of the EPA synthesis gene cluster were cloned in order into the *Xba*I-*Spe*I, *Xba*I site, and *Spe*I sites of pBSIIKS(+), respectively. The resultant plasmid was named ΔX4XbNh/pBS. After digestion with *Not*I, ΔX4XbNh/pBS was treated with T4 DNA polymerase (Takara Shuzo) to make blunt ends, and then cut with *Xho*I to obtain fragment A. For ORF2, a fragment cut out from R/pSTV28 [a plasmid containing ORF2, 7,951–9,129 bp, in pSTV28 (Takara Shuzo, Kyoto, Japan)] with *Eco*RI and *Pst*I, was cloned into the *Eco*RI-*Pst*I site of pBSIIKS(+) to obtain R/pBS. After treatment with *Pst*I and T4 DNA polymerase, a *Xho*I linker was inserted into R/pBS. Then, fragment B was obtained from R/pBS by XhoI digestion. Fragments A and B were cloned into the *Xho*I-*Stu*I and *Xho*I sites of pJRD215 by *in vitro* packaging (PackageneR Lambda DNA Packaging System; Promega, Madison, WI) and by using a DNA ligation kit (Takara Shuzo), respectively. The final plasmid constructed was designated as pJRDEPA-S (Scheme 1).

Conjugal gene transfer to the cyanobacterium. Conjugal gene transfer to the cyanobacterium was carried out as previously reported (8) with some modifications. Cyanobacterial cells at the mid-growth phase were centrifuged, washed with BG11-M medium, and then resuspended in fresh medium. Freshly transformed *E. coli* S17-1 cells harboring pJRDEPA-S were collected from Luria broth plates containing 50 μg kanamycin/mL and 50 μg streptomycin/mL, and then suspended in BG11-M medium. Suspensions of cyanobacterial cells and *E. coli* cells were mixed in the cell number ratio of 1:10 (cyanobacterium/*E. coli*) and then spotted onto dried BG11 plates supplemented with 15 mM NaCl. After 48 h of incubation under light, the cells were collected from the plates with BG11-M medium, and then streaked on BG11-M plates containing 75 μg kanamycin/ mL to select cyanobacterial transconjugants.

Gas–liquid chromatography (GLC). Fatty acid methyl esters were prepared from the lyophilized cyanobacterial cells or *E. coli* cells by treatment with 5% methanolic hydrochloric acid (12). The fatty acid methyl esters, which were purified by using thin-layer chromatography (TLC), were analyzed by GLC. The analytical conditions were as previously reported (8), with minor modifications.

Fatty acid methyl esters prepared from *Shewanella* sp. SCRC-2738 that had been confirmed to contain EPA and 20:4n-3 (12) and EPA methyl ester (Sigma Chemical Co., St.Louis, MO) were used as standard samples. Heneicosanoic acid (21:0) was also used as an internal standard.

GC–mass spectrometry (GC–MS). PUFA methyl ester fractions were prepared from the fatty acid methyl esters by $AgNO_3$-TLC (12), and then subjected to GC–MS. The analytical conditions were previously reported (8) with minor modifications.

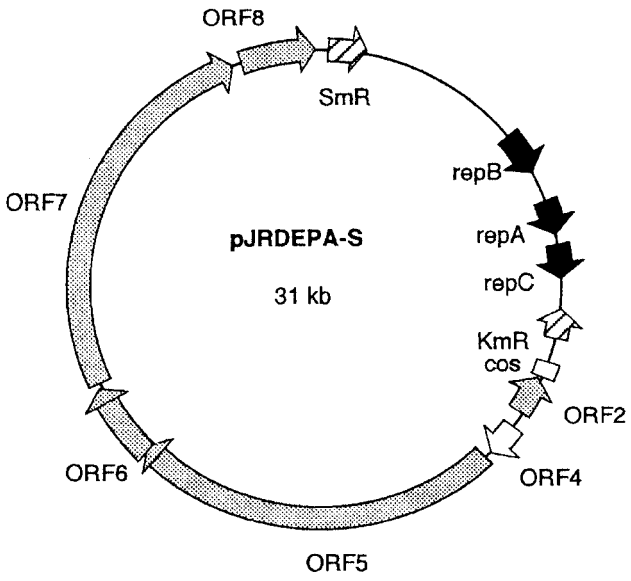

SCHEME 1

RESULTS AND DISCUSSION

Construction of a plasmid containing an EPA synthesis gene cluster and EPA production in E. coli. Functional analysis of each ORF in the EPA synthesis gene cluster isolated from SCRC-2738 indicated that five (ORF2, 5, 6, 7, and 8) of the nine ORF were required for EPA synthesis in *E. coli* (Yamada, A., Yu, R., Watanabe, K., Yazawa, K., and Kondo, K., unpublished data). In this experiment, after excluding noncoding regions present both upstream and downstream of the ORF, five essential ORF and one nonessential ORF (ORF4) for EPA synthesis were ligated into pJRD215. With this procedure, plasmid pJRDEPA-S (Scheme 1) is approximately 17 kb shorter than pJRDEPA. To determine the EPA productivity of pJRDEPA-S, it was transferred into *E. coli* JM109. The fatty acid methyl esters of the JM109 were analyzed with GLC and GC–MS. The EPA content in the total fatty acids reached 5.7%, i.e., more than that of pEPA (less than 4.5%; 7), although the copy number was lower in *E. coli* cells (data not shown). This suggested reduction in the size of the EPA synthesis gene cluster enhanced the EPA productivity.

EPA production by cyanobacterial cells. Fatty acid methyl esters prepared from the total wild type cyanobacterial cells and transconjugant cells harboring pJRDEPA-S were analyzed by GLC (Table 1). For the transconjugant, there were two novel peaks that were never detected in wild-type, corresponding to authentic 20:4n-3 and EPA (20:5n-3), respectively. The methyl esters of total fatty acids and PUFA were analyzed by GC–MS (Table 1). For the two GLC peaks mentioned above, ion peaks were detected at *m/z* 318 and 316, consistent with the molecular weights of 20:4 and 20:5, respectively, and an ion peak at *m/z* 79, typical of polyunsaturated fatty acids was also seen (data not shown). Therefore, it was confirmed that the transgenic cyanobacterium was able to produce EPA and 20:4n-3 on the introduction of pJRDEPA-S.

In comparing with the wild-type cyanobacteria, percentages of 18:1n-9 and 18:2n-6 to total fatty acids were lower in the transconjugant (Table 1). The decrease might be correlated to production of EPA and 20:4n-3.

EPA production in cyanobacterial cells under different culture conditions. The cyanobacterial transconjugant harboring

TABLE 1
Fatty Acid Composition (% of total fatty acid) of Wild-Type *Synechococcus* sp. NKBG15041c and a Transconjugant Harboring pJRDEPA-S Under Different Growth Conditions[a]

	Transconjugant (pJRDEPA-S)			Wild-type
Fatty acid	Condition A	Condition B	Condition C	Condition A
Shorter than 16:0	1.8 ± 0.8	3.5 ± 1.0	10.3 ± 0.2	7.4 ± 0.1
16:0	37.2 ± 0.8	38.3 ± 0.7	38.7 ± 1.4	37.6 ± 1.6
16:1n-7	12.0 ± 0.5	10.2 ± 0.3	12.2 ± 0.4	13.4 ± 1.0
18:0	1.0 ± 0.1	0.9 ± 0.1	0.7 ± 0.1	1.0 ± 0.2
18:1n-9	13.4 ± 0.2	9.4 ± 1.6	9.9 ± 0.4	19.5 ± 1.2
18:2n-6	13.4 ± 0.5	8.6 ± 0.8	7.6 ± 0.1	15.5 ± 0.7
18:3n-3	7.0 ± 0.0	2.7 ± 0.1	6.7 ± 0.7	6.4 ± 0.5
20:4n-3	2.5 ± 0.2	5.1 ± 0.2	4.7 ± 0.3	ND
20:5n-3, EPA	3.7 ± 0.2	7.5 ± 0.3	4.6 ± 0.6	ND
Others	8.6 ± 0.9	15.0 ± 1.4	9.3 ± 2.4	3.1 ± 0.6

[a]Condition A: 23°C, 1,000–1,500 Lux, 14 d; Condition B: 23°C, *ca.* 40 Lux, 48 d; Condition C: 18°C, 800–1,000 Lux, 22 d (with shaking at 100 rpm). For conditions A–C $n = 3$. Abbreviation, ND, not detected.

pJRDEPA-S was cultured at different growth temperatures and light intensities. Table 1 shows the major fatty acid compositions of the transconjugant and wild type grown at 18 and 23°C, and at high and low light intensities. In the case of culture at 18°C, flasks were shaken at 100 rpm to compensate for biased illumination. The transconjugant grown at 18°C exhibited higher EPA content and higher absolute yield (4.6 ± 0.6%; 3.86 ± 1.11 mg/L) than when grown at 23°C (3.7 ± 0.2%; 2.24 ± 0.13 mg/L). The increase of EPA content associated with a decrease of culture temperature was also observed in the experiments using *E. coli* JM109 carrying pEPA at 20 and 25°C (7). It seems that these tendencies might be related to chilling tolerance by accumulation of PUFA into cell membranes (13,14). For the transconjugant grown at 18°C, the increase of EPA productivity might also be affected by aeration. In a marine cyanobacterium, *Synechococcus* sp. NKBG042902, harboring pJRDEPA, the EPA content in the total fatty acids was 0.7 ± 0.2% at 17°C (8). With a different cyanobacterial host and a shortened plasmid, the EPA content increased to eightfold more than in the previous work.

When the light intensity was lowered to 40 Lux, the transconjugant exhibited the highest content of EPA (7.5 ± 0.3%). Its absolute yield, however, was lower than that of the transconjugant cultured at 23°C (1.76 ± 0.10 mg/L), even though given a longer culture period (Table 1). The cause of this phenomenon is not clear. The cells might find a more suitable condition to synthesize EPA under weak light intensity because the light-induction of photosynthetic systems does not fully function (15,16).

In SCRC-2738 or *E. coli* with the EPA synthesis gene cluster introduced, as high content of 20:4n-3 as that of the cells in this study was not observed (12; Yamada, A., Yu, R., Watanabe, K., Yazawa, K., and Kondo, K., unpublished data). This tendency may depend on the fatty acid composition intrinsic to the particular organisms. According to the hypothetical pathway for the EPA synthesis in SCRC-2738 (17), 18:3n-3, which is present in considerable amounts in cyanobacteria (Table 1; 18), is a likely precursor of 20:4n-3 or EPA.

In the previous work, pJRDEPA was shown to be unstable in *Synechococcus* sp. NKBG042902 (8). In contrast, pJRDEPA-S was maintained well in NKBG15041c. This stability may be attributed to the size of plasmid and host characteristics of NKBG15041c, carrying no native plasmids to compete against introduced plasmids (19).

In this paper, we demonstrated that a transgenic marine cyanobacteria produced EPA and 20:4n-3, and the productivity was changed related to culture conditions. We need more precise optimization of culture condition to make them useful on a large scale. These transgenic cyanobacteria may also be useful in elucidating the synthetic pathway of EPA in bacteria, because they make precursors to EPA such as 20:4n-3 (17), and undergo regulation by factors such as temperature, osmotic pressure and light intensity (13,14,16).

ACKNOWLEDGMENTS

This work was performed as a part of The Industrial Science and Technology Project, Technology Development of Biological Resources in Bioconsorcia supported by the New Energy and Industrial Technology Development Organization (NEDO). The authors wish to thank Shizuo Mohara for the GC–MS analysis.

REFERENCES

1. Abbey, M., Clifton, P., Kestin, M., Belling, B., and Nestel, P. (1990) Effects of Fish Oil on Lipoproteins, Lecithin:Cholesterol Acyltransferase, and Lipid Transfer Protein Activity in Humans, *Atherosclerosis 10,* 85–94.
2. Simpoulos, A.P. (1999) Essential Fatty Acids in Health and Chronic Disease, *Am. J. Nutr. 70,* 560S–569S.
3. Watanabe, K., Sezaki, K., Yazawa, K., and Hino, A. (1992) Nutritive Fortification of the Rotifer *Brachionus plicatilis* with Eicosapentaenoic Acid-Producing Bacteria, *Nippon Suisan Gakkaishi 58,* 271–276.
4. Cohen, Z., Norman, H.A., and Heimer, Y.M. (1995) Microalgae as a Source of ω3 Fatty Acids, in *Plants in Human Nutrition* (Simopoulos, A.P., ed.) pp. 1–31, Karger, Basel.
5. Cohen, Z. (1990) The Production Potential of Eicosapentaenoic Acid and Arachidonic Acids by the Red Alga *Porphyridium cruentum, J. Am. Oil Chem. Soc. 67,* 916–920.

6. Yazawa, K., Araki, K., Watanabe, K., Ishikawa, C., Inoue, A., Kondo, K., Watabe, S., and Hashimoto, K. (1988) Eicosapentaenoic Acid Productivity of the Bacteria Isolated from Fish Intestine, *Nippon Suisan Gakkaishi 54,* 1835–1838.
7. Yazawa, K. (1996) Production of Eicosapentaenoic Acid from Marine Bacteria, *Lipids 31,* S297–S300.
8. Takeyama, H., Takeda, D., Yazawa, K., Yamada, A., and Matsunaga, T. (1997) Expression of the Eicosapentanoic Acid Synthesis Gene Cluster from *Shewanella* sp. in a Transgenic Marine Cyanobacterium, *Synechococcus* sp., *Microbiology 143*, 2725–2731.
9. Sode, K., Tatara, M., Burgess, J., and Matsunaga, T. (1992) Conjugative Gene Transfer in Marine Cyanobacteria: *Synechococcus* sp. and *Pseudoanabaena* sp., *Appl. Microbiol. Biotechnol. 37,* 369–373.
10. Simon, R., Priefer, U., and Puhler, A. (1983) A Broad Host Range Mobilization System for *in vivo* Genetic Engineering: Transposon Mutagenesis in Gram Negative Bacteria, *Bio/Technology 118,* 640–659.
11. Davison, J., Heusterspreute, M., Chevalier, N., Ha-Thi, V., and Brunel, F. (1987) Vectors with Restriction Site Banks. V. pJRD215, a Wide-Host-Range Cosmid Vector with Multiple Cloning Sites, *Gene 51,* 275–280.
12. Watanabe, K., Ishikawa, C., Yazawa, K., Kondo, K., and Kawaguchi, A. (1996) Fatty Acid and Lipid Composition of an Eicosapentaenoic Acid-Producing Marine Bacterium, *J. Mar. Biotechnol. 4,* 104–112.
13. Wada, H., Gombos, Z., and Murata, N. (1990) Enhancement of Chilling Tolerance of a Cyanobacterium by Genetic Manipulation of Fatty Acid Desaturation, *Nature 347,* 200–203.
14. Murata, N., and Wada, H. (1995) Acyl-Lipid Desaturases and Their Importance in the Tolerance and Acclimation to Cold of Cyanobacteria, *Biochem. J. 308,* 1–8.
15. Golden, S.S. (1994) Light-Responsive Gene Expression and the Biochemistry of the Photosystem II Reaction Center, in *Advances in Photosynthesis: The Molecular Biology of Cyanobacteria* (Bryant, D.A., ed.) pp. 693–714, Kluwer Academic Publishers, Dordrecht.
16. Cohen, Z., Vonshak, A., and Richmond, A. (1988) Effect of Enviromental Conditions on Fatty Acid Composition of the Red Alga *Porphyridium cruentum*: Correlation to Growth Rate, *J. Phycol. 24,* 328–332.
17. Watanabe, K., Yazawa, K., Kondo, K., and Kawaguchi, A. (1997) Fatty Acid Synthesis of an Eicosapentaenoic Acid-Producing Bacterium: *De novo* Synthesis, Chain Elongation, and Desaturation Systems, *J. Biochem. 122,* 467–473.
18. Murata, N., and Nishida, I. (1987) Lipids of Blue-Green Algae (cyanobacteria), in *The Biochemistry of Plants* (Stumpf, P.K., ed.) Vol. 9, pp. 315–347, Academic Press, New York.
19. Takeyama, H., Burgess, J.G., Sudo, H., Sode, K., and Matsunaga, T. (1991) Salinity-Dependent Copy Number Increase of a Marine Cyanobacterial Endogenous Plasmid, *FEMS Microbiol. Lett. 90,* 95–98.

[Received January 24, 2000, and in revised form August 21, 2000; revision accepted August 28, 2000]

Dietary Conjugated Linoleic Acid Did Not Alter Immune Status in Young Healthy Women[1]

D.S. Kelley[a,*], P.C. Taylor[a], I.L. Rudolph[a], P. Benito[a], G.J. Nelson[a], B.E. Mackey[b], and K.L. Erickson[c]

[a]U.S. Department of Agriculture, Agricultural Research Service, Western Human Nutrition Research Center, University of California, Department of Nutrition, Davis, California, [b]Western Regional Research Center, Albany, California, and [c]University of California, Department of Cell Biology and Human Anatomy, School of Medicine, Davis, California

ABSTRACT: The purpose of this study was to examine whether conjugated linoleic acid (CLA) supplementation in human diets would enhance indices of immune status as reported by others for animal models. Seventeen women, 20–41 yr, participated in a 93-d study conducted in two cohorts of 9 and 8 women at the Metabolic Research Unit of Western Human Nutrition Research Center. Seven subjects were fed the basal diet (19, 30, and 51% energy from protein, fat, and carbohydrate, respectively) throughout the study. The remaining 10 subjects were fed the basal diet for the first 30 d, followed by 3.9 g CLA (Tonalin)/d for the next 63 d. CLA made up 65% of the fatty acids in the Tonalin capsules, with the following isomeric composition: *t*10,*c*12, 22.6%; *c*11,*t*13, 23.6%; *c*9,*t*11, 17.6%; *t*8,*c*10, 16.6%; and other isomers 19.6%. Most indices of immune response were tested at weekly intervals, three times at the end of each period (stabilization/intervention); delayed-type hypersensitivity (DTH) to a panel of six recall antigens was tested on study day 30 and 90; all subjects were immunized on study day 65 with an influenza vaccine, and antibody titers were examined in the sera collected on day 65 and 92. None of the indices of immune status tested (number of circulating white blood cells, granulocytes, monocytes, lymphocytes, and their subsets, lymphocytes proliferation in response to phytohemagglutinin, and influenza vaccine, serum influenza antibody titers, and DTH response) were altered during the study in either dietary group. Thus, in contrast to the reports with animal models, CLA feeding to young healthy women did not alter any of the indices of immune status tested. These data suggest that short-term CLA supplementation in healthy volunteers is safe, but it does not have any added benefit to their immune status.

Paper no. L8543 in *Lipids 35*, 1065–1071 (October 2000).

Conjugated linoleic acid (CLA) is a mixture of the isomers of the 18:2 fatty acids that have conjugated double bonds. One of the prominent isoforms of CLA is the 9-*cis* and 11-*trans* (9*c*,11*t*-18:2) isomer. This isomer, rumenic acid, is found naturally in beef and dairy products. Several other isomers of CLA are produced industrially during the processing of vegetable oils. The most abundant among these isomers include the 8*t*,10*c*-18:2, 10*t*,12*c*-18:2, and11*c*,13*t*-18:2. In addition, there are several other minor isomers.

Feeding a mixture of the CLA isomers was found to provide several health benefits in animal models, including anticancer (1–8), antiatherogenic (9,10), and antidiabetogenic actions (11). It has also been reported to decrease body fat while increasing muscle (12,13) and bone mass (14). Additionally, it has been reported to block the endotoxin-induced suppression of growth (15,16) and to alter several indices of immune status (17–19). For example, feeding diets containing CLA to experimental animals enhanced *ex vivo* splenocyte proliferation, IL-2 production, delayed-type hypersensitivity (DTH) response, and macrophage phagocytosis (16–18). In contrast, other investigators found no effect of CLA feeding on lymphocyte proliferation (17), DTH (18), and tumor necrosis factor α (TNF α) production (19). Others report a decrease in the production of IL-2, IL-6, and TNF α, and the macrophage phagocytic activity by the feeding of diets containing CLA (7,19). Overall, the observed effects of dietary CLA on immune functions in animal models have been variable.

Despite the variability in data from animals and the lack of data from humans, there are healthy people who are eager to supplement their diets with CLA. We do not know if supplementation of human diets with CLA has any beneficial health effects, or even if it is safe. Therefore, the purpose of this study was to determine whether it is safe to supplement human diets with CLA, and if it will enhance human immune status. We conducted this study with healthy adults rather than with a group having compromised immune status, because we wanted to know if there are any added benefits from CLA supplementation. We examined the effect of feeding a mixture of CLA isomers on a number of indices of immune status, such as lymphocyte subsets and proliferation, DTH, and influenza antibody titers in young healthy women.

[1]Parts of data included here were published as an abstract for the Experimental Biology 2000, meeting.

*To whom correspondence should be addressed at USDA/ARS/WHNRC, Department of Nutrition, University of California Davis, One Shields Ave., Davis, CA 95616. E-mail: dkelley@whnrc.usda.gov

Abbreviations: BMI, body mass index; CD, cluster differentiation; CLA, conjugated linoleic acid; CI, 95% confidence intervals; CT, cytotoxic T lymphocytes; DTH, delayed-type hypersensitivity; GM, geometric mean; IL, interleukin; LPS, lipopolysaccharide; MRU, metabolic research unit; NK, natural killer; PBMNC, peripheral blood mononuclear cells; PHA, phytohemagglutinin; PPAR, peroxisomal proliferation activation receptor; RDA, recommended dietary allowance; TNF α, tumor necrosis factor α; USDA, U.S. Department of Agriculture; WBC, white blood cells.

MATERIALS AND METHODS

Subjects and study design. Seventeen healthy women were selected to participate in two cohorts of a 93-d metabolic research unit study after a physical and clinical evaluation by a physician. Nine women (5 CLA group and 4 control group) participated in the first cohort (January 25 to April 28, 1998), and eight women (5 CLA group and 3 control group) participated in the second cohort (September 8 to December 10, 1998). Subjects were randomly assigned to the two groups, but to increase the power in the CLA group, we purposely assigned more subjects to the CLA group. They were all nonsmokers and non–drug-users and had body weights within 110–120% of ideal body weight (1983 Metropolitan Life Insurance Co.). Mean body weights, age, and body mass index for the study subjects are given in Table 1.

The study protocol was approved by the human use committees of the University of California, Davis, and the U.S. Department of Agriculture (USDA), Houston, TX. The study lasted for 93 d, although because of other scheduled procedures, no immunological tests were conducted after study day 92. All subjects were immunized on day 65 with a trivalent 1997–1998 influenza vaccine (Connaught Laboratories Inc., Swiftwater, PA). All subjects remained on the premises of the metabolic suite of the Western Human Nutrition Research Center for the duration of the study, except when going for daily walks (2 mi, twice daily) or other scheduled outings. Subjects were under supervision when going out of the metabolic unit. They consumed only those foods prepared by the staff of the unit. As shown in Figure 1, all study participants were fed a basal diet supplemented with a placebo (sunflower oil 3.9 g/d) for the first 30 d, after which they were divided into two groups; 7 subjects consumed the basal diet for the entire period of the study (control group), while for the remaining 10 subjects, a mixture of CLA isomers (3.9 g/d) replaced the placebo supplement from study days 31 to 93 (CLA group). We used a mixture of CLA isomers because that is what has been used in animal studies, and because purified isomers of CLA for human feeding trials were not available at the time the study was conducted. The body weights of the subjects were maintained within 2% of their initial body weights throughout the study by adjusting their caloric intake if necessary.

The nutrient content of the diets was calculated using USDA Handbook 8 (20); all known nutrients were at or above the recommended dietary allowance (RDA) level, and were not different between the two diets. Diets contained 1 × RDA of vitamin E from natural foods. An additional 100-mg capsule of α-tocopherol (Bronson Pharmaceutical, St. Louis, MO) was supplemented every 5 d to reduce the increased oxidative stress from CLA supplementation. The proportion of energy from protein, fat, and carbohydrate in both diets was 19, 30, and 51%, respectively. Diets were organized according to a 5-d rotating menu, comprised of 3 meals and a postdinner snack. Specific menus were designed so that the fat would consist of saturated, monounsaturated, and polyunsaturated types providing 10% energy for both the control and intervention groups. Tonalin (gift from Pharmanutrient, Inc., Lake Bluff, IL) was the source of CLA. It was served as capsules by replacing an equivalent amount of the placebo oil. Both Tonalin and placebo oil capsules were administered to the subjects before each meal (breakfast, lunch, and dinner) under the supervision of the kitchen staff. As shown in Table 2, CLA isomers made up 65 wt% of the total fatty acids present in Tonalin, while other fatty acids made up the remaining 35%. The fatty acid composition of Tonalin and the placebo oil (sunflower) is given in Table 2. The major isomers of CLA present in Tonalin, expressed as a percentage of total CLA were: *t*10,*c*12, 22.6%; *c*11,*t*13, 23.6%; *c*9,*t*11, 17.6%; *t*8,*c*10, 16.6%; and other isomers 19.6%. Placebo capsules were made from sunflower oil containing 72.6% linoleic acid and no detectable CLA.

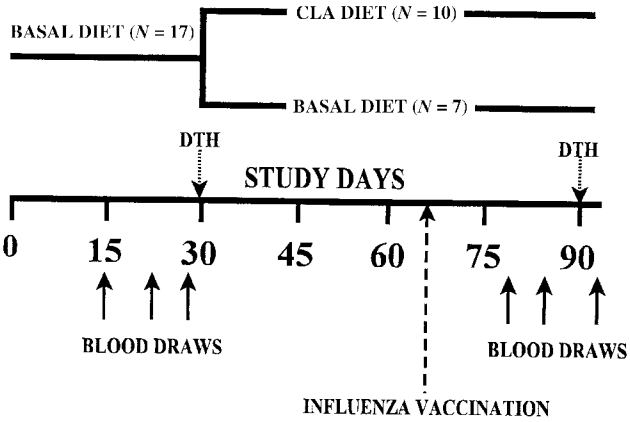

FIG. 1. Study design. Blood samples drawn on study day 15, 22, 29 (stablization period), and 78, 85, 92 (intervention period) were used to determine immune cell numbers and functions. DTH, delayed-type hypersensitivity response; CLA, conjugated linoleic acid.

Laboratory procedures. Blood samples were collected between 0700 and 0800 after an overnight fast on study days 15, 22, 29, 78, 85, and 92 by antecubital venipuncture into evacuated tubes containing heparin for cell culture experiments, EDTA for blood cell count and phenotypic analysis, and no anticoagulant for preparation of sera.

Blood cell count and lymphocyte phenotypic analysis. For each blood draw, a complete and differential cell count was performed using a Serono Baker Automated System (Model 9000 diff; Allentown, PA). Phenotypic analysis for B [cluster differentiation (CD) 19+ or CD19+], T (CD3+), helper (CD3+, CD4+), suppressor (CD3+,CD8+), natural killer (NK) (CD3–, CD16+,56+), and cytotoxic T (CT)(CD3+,CD16+, 56+) lym-

TABLE 1
Characteristics of Subjects[a]

	CLA group (n = 10)	Control group (n = 7)
Age (yr)	27.0 ± 1.8	29.3 ± 2.6
Weight (kg)	63.1 ± 2.1	63.2 ± 4.3
Body mass index (kg/m^2)	23.6 ± 0.5	21.9 ± 1.2

[a]Data shown are mean ± SEM. None of the characteristics were different between the two groups. CLA, conjugated linoleic acid.

TABLE 2
Fatty Acid Composition of Tonalin® CLA and Placebo (sunflower oil) Capsules

Fatty acid	Tonalin CLA[a]	Placebo[a]
14:0	0.25 ± 0.01	
16:0	4.71 ± 0.03	6.23 ± 0.10
16:1n-9	0.12 ± 0.01	
18:0	1.95 ± 0.02	4.09 ± 0.02
18:1n-9	24.70 ± 0.20	16.39 ± 0.02
19:0	0.20 ± 0.01	
18:2n-6	2.29 ± 0.03	72.57 ± 0.03
20:1n-9	0.24 ± 0.08	
9*c*,11*t*-18:2	11.43 ± 0.07	
8*t*,10*c*-18:2	10.79 ± 0.12	
11*c*,13*t*-18:2	15.29 ± 0.31	
10*t*,12*c*-18:2	14.69 ± 0.09	
8*c*,10*c*-18:2	1.38 ± 0.05	
9*c*,11*c*-18:2	1.59 ± 0.05	
10*c*,12*c*-18:2	2.45 ± 0.05	
11*c*,13*c*-18:2	1.32 ± 0.10	
11*t*,13*t* and 8*t*,10*t*-18:2	0.97 ± 0.04	
9*t*,11*t* and 10*t*,12*t*-18:2	5.02 ± 0.04	
20:2n-6	0.11 ± 0.03	
20:3n-6		0.29 ± 0.02
22:0		0.71 ± 0.06
Total	99.92 ± 0.08	100.00 ± 0.00
Unidentified	0.08 ± 0.08	

[a]Values given as means ± SD (n = 5). See Table 1 for abbreviation. Tonalin was a gift from Pharmanutrient, Inc. (Lake Bluff, IL).

phocytes was done with a Becton-Dickinson FACStar flow cytometer (San Jose, CA) as previously reported (21). Briefly, whole blood collected in EDTA-containing vacutainer tubes was transferred into tubes containing fluorochrome-labeled monoclonal antibodies against specific CD antigens. After incubation for 30 min, the red cells were lysed with formaldehyde and removed by washing the leukocytes twice with Dulbecco's phosphate-buffered saline (PBS) without calcium and magnesium. The stained cells were fixed in 1% paraformaldehyde prior to analysis with the flow cytometer. A total of 10,000 lymphocytes were counted to determine their percentage distribution as lymphocyte subsets.

Isolation and culture of peripheral blood mononuclear cells (PBMNC). The PBMNC were isolated using Histopaque-1077 as previously reported (22). The culture medium used was RPMI-1640 (Gibco, Grand Island, NY) containing 10% autologous serum and L-glutamine (2 mmol/L), penicillin (100 KU/L), streptomycin (100 mg/L), and gentamicin (20 mg/L). One hundred microliters of the culture medium containing 1×10^5 PBMNC was added to each well of a 96-well flat-bottom culture plate, followed by an additional 100 μL of the culture medium with or without phytohemagglutinin (PHA; Sigma Chemical Co., St. Louis, MO), or influenza vaccine (Connaught Laboratories Inc.). Cells treated with PHA (0, 1.25, 2.5, 5.0, 10.0, and 20.0 mg/L) were cultured for 72 h, and those treated with influenza vaccine (0, 1/250, 1/500, 1/1000, 1/2000, and 1/4000) were cultured for 120 h. [^{3}H]Thymidine, 37 K Bq, in 50 μL, was added to each well during the last 24 h of cell culture. Cells were collected on filter strips, and the radioactivity was determined using a Packard β-gas counter (Hewlett-Packard Co., Palo Alto, CA). [^{3}H]thymidine incorporation into cellular DNA (Bq/1000 cell) was used as the index of PBMNC proliferation.

DTH skin testing. DTH was tested by intradermally injecting a battery of six recall antigens (tuberculin, mumps, tetanus, candida, streptokinase, and trichophyton) as previously described (22), and the induration diameters in mm were determined 48 h after the application of the antigens. An induration of 4 mm or more was considered positive. The total induration was determined by adding all the positive responses. The antigen score indicates the number of positive responses to the test antigens.

Serum antibody titers. The antibody titers were determined by using the hemagglutination inhibition assay (23) and the viral strains AH1N1, AH3N2, and B/Habrin (strains included in the vaccine). Results for antibody titers are expressed as the geometric mean of the antibody titers, with 95% confidence intervals.

Data analysis. The data from the two cohorts were combined for a repeated measures ANOVA using the SAS PROC MIXED procedure (24). Day, diet, and the interaction between them were considered the fixed effects, while cohort, diet × cohort, subjects within diet × cohort, and diet × cohort × day were the random effects. The period 1 (stabilization) vs. period 2 (intervention) × diet contrast was partitioned out of the day × diet effect. Pooled means ± SEM for the three measurements made at the ends of stabilization (day 15, 22, and 29) and intervention (day 78, 85, and 92) periods are shown in the Results section. Changes in the parameters examined are considered significant for $P < 0.05$ unless stated otherwise.

RESULTS

Both diets provided 19, 30, and 51% energy from protein, fat, and carbohydrates, respectively. The average daily caloric intake was approximately 2100 Kcal (2117 ± 191, mean ± SD) and was not significantly different between the two groups. Fatty acid composition of the diets is shown in Table 3. Fatty acids other than CLA and linoleic acid were not significantly different between the two diets. The control diet contained a nondetectable amount of CLA, while in the CLA diet, CLA isomers were 5.28% of the total fatty acids. The linoleic acid content of the control diet was about 5% higher than that in the CLA diet. This was because the placebo supplement contained sunflower oil, which contained 73 wt% linoleic acid.

Effect of CLA on circulating white blood cells (WBC). The number of total circulating WBC and their specific subgroups, at the ends of periods 1 (stabilization) and 2 (intervention), are shown in Table 4. This table shows that the number of total WBC, granulocytes, monocytes, and lymphocytes in both groups remained unchanged throughout the study. Also unchanged were the numbers of circulating B, NK, total T, helper, suppressor, and CT lymphocytes in both groups.

Effect of CLA on PBMNC proliferation. The influence of dietary CLA on the proliferation of lymphocytes cultured

TABLE 3
Fatty Acid Composition (wt%) of Experimental Diets

Fatty acid	Diet w/o suppl.[a]	Diet + placebo[a]	Diet + CLA[a]
11:00	0.38 ± 0.15	0.39 ± 0.18	0.40 ± 0.23
12:0	0.67 ± 0.40	0.70 ± 0.45	0.70 ± 0.43
14:0	3.29 ± 1.12	3.14 ± 1.25	3.11 ± 1.19
14:1n-7	0.18 ± 0.04	0.19 ± 0.03	0.18 ± 0.04
14:1n-5	0.32 ± 0.04	0.32 ± 0.05	0.30 ± 0.06
15:0	0.34 ± 0.13	0.33 ± 0.13	0.32 ± 0.13
16:0	19.04 ± 1.00	18.19 ± 1.23	17.99 ± 1.30
16:1*t*	0.13 ± 0.01		
16:1n-9	1.14 ± 0.25	1.07 ± 0.22	1.06 ± 0.23
17:0	0.38 ± 0.09	0.35 ± 0.08	0.35 ± 0.08
18:1n-7 DMA	0.28 ± 0.00	0.26 ± 0.00	0.26 ± 0.00
18:0	8.24 ± 0.99	7.91 ± 0.94	7.77 ± 0.93
18:1*t*, all isomers	5.23 ± 2.28	4.96 ± 2.24	4.58 ± 1.86
18:1n-9	25.13 ± 2.35	24.34 ± 2.40	25.23 ± 2.27
18:1n-7	1.24 ± 0.21	1.19 ± 0.20	1.21 ± 0.20
18:1n-5	0.98 ± 0.52	1.08 ± 0.35	1.06 ± 0.34
19:0			0.11 ± 0.00
18:2*tt*			0.25 ± 0.01
18:2n-6	29.85 ± 2.85	32.97 ± 2.31	27.56 ± 2.30
20:0	0.14 ± 0.02	0.15 ± 0.03	0.14 ± 0.02
18:3n-3	1.83 ± 0.31	1.74 ± 0.27	1.71 ± 0.28
20:1n-9	0.26 ± 0.00	0.26 ± 0.00	0.26 ± 0.00
9*c*,11*t* and 8*t*,10*c*-18:2	0.23 ± 0.00		2.22 ± 0.62
11*c*,13*t*-18:2			1.34 ± 0.42
10*t*,12*c*-18:2			1.30 ± 0.40
9*t*,11*t* and 10*t*,12*t*-18:2			0.44 ± 0.13
20:3n-6	0.25 ± 0.13	0.28 ± 0.15	0.30 ± 0.13
20:4n-6	0.19 ± 0.04	0.20 ± 0.00	0.20 ± 0.04
24:0	0.24 ± 0.00	0.25 ± 0.00	0.24 ± 0.00
Total	98.69 ± 0.52	98.71 ± 0.58	98.86 ± 0.39
Unidentified	1.31 ± 0.52	1.29 ± 0.59	1.14 ± 0.39

[a]Values given as means ± SD (n = 5). DMA, dimethylacetate; see Table 1 for other abbreviation.

with different concentrations of a T cell mitogen, PHA, and a B cell antigen, influenza vaccine are shown in Tables 5 and 6, respectively. Increasing the concentration of PHA increased lymphocyte proliferation, with the maximum attained at a PHA concentration of 10 mg/L. At all PHA concentrations, the proliferation of lymphocytes was not different between periods one and two in both dietary groups. B lymphocyte proliferation in response to the influenza vaccine increased with the increasing concentration of the vaccine, the maximum being attained at a dilution of 1/1000 in both groups (Table 6). B cell proliferation in response to influenza vaccine in period two was significantly higher ($P < 0.05$) than that in period one in both groups. This increase in proliferation was caused by the immunization with the same vaccine on day 65. Thus, CLA feeding did not alter proliferation of either T or B lymphocytes.

Effect of CLA on DTH skin response. The induration responses were examined 48 h after the intradermal injection of six recall antigens on study days 28 and 90. All 17 subjects responded to mumps, tetanus, and candida antigens. The data from the other three antigens (trichophyton, streptokinase, and tuberculin purified derivative) were pooled, because fewer than 25% of the subjects responded to each of these antigens (data not shown). The induration score (sum of induration) and the antigen score (number of antigens testing positive) did not differ from study days 30 to 92 in either group (Table 7). The induration in response to individual antigens also did not change during the course of the study.

CLA feeding and serum influenza antibody titers. The pre- (day 65) and postimmunization (day 92) serum antibody titers against the three strains (AH1N1, AH3N2, B/Habrin) of influenza virus for both groups of subjects are shown in Table 8. For all three viral strains, the pre-immunization antibody titers were not different between the two groups. Immunization caused approximately 2-, 4-, and 10-fold increases in the concentration of circulating antibodies against AH3N2, B/Habrin, and AH1N1, respectively, in both groups. The increases in the antibody titers between the CLA and control group also were not different. The results shown regarding antibody titers in Table 8 were obtained with the hemagglutination inhibition assay; however, the results from enzyme-linked immunosorbent assay also lead to the same conclusion (data not shown).

DISCUSSION

The purpose of this study was to examine whether CLA supplementation of human diets would stimulate indices of human immunity as previously reported for animals (16–19).

TABLE 4
Effects of CLA Feeding on Circulating WBC[a]

	CLA group (n = 10)		Control group (n = 7)	
Cell type	Period 1	Period 2	Period 1	Period 2
WBC[1]	6.91 ± 0.68	6.51 ± 0.50	5.94 ± 0.37	5.50 ± 0.45
PMN[1]	4.08 ± 0.58	3.66 ± 0.38	3.28 ± 0.24	2.86 ± 0.32
% of WBC	57.57 ± 1.91	55.38 ± 2.02	55.21 ± 1.66	51.69 ± 3.12
Monocytes[1]	0.42 ± 0.04	0.44 ± 0.05	0.40 ± 0.04	0.38 ± 0.04
% of WBC	6.22 ± 0.43	6.45 ± 0.69	6.81 ± 0.73	7.03 ± 0.80
Lymphocytes[1]	2.42 ± 0.13	2.45 ± 0.16	2.25 ± 0.15	2.23 ± 0.21
% of WBC	36.21 ± 1.73	38.06 ± 2.00	37.98 ± 1.81	41.08 ± 2.88
B (CD19+)[1]	0.29 ± 0.04	0.30 ± 0.04	0.24 ± 0.03	0.27 ± 0.03
NK (CD3–, 16+,56+)[1]	0.25 ± 0.05	0.19 ± 0.03	0.26 ± 0.06	0.23 ± 0.05
T (CD3+)[1]	1.87 ± 0.10	1.98 ± 0.13	1.74 ± 0.13	1.76 ± 0.15
Helper (CD3+, 4+)[1]	1.21 ± 0.09	1.30 ± 0.12	1.08 ± 0.09	1.13 ± 0.10
Suppressor (CD3+,8+)[1]	0.59 ± 0.04	0.61 ± 0.06	0.60 ± 0.06	0.58 ± 0.06
CT (CD3+, 16+, 56+)[1]	0.07 ± 0.01	0.06 ± 0.01	0.09 ± 0.01	0.08 ± 0.01

[a]Abbreviations: WBC, white blood cells; PMN, polymorphonuclear leukocytes; CD, cluster designation; NK, natural killer; CT, cytotoxic T lymphocytes: for other abbreviations see Table 1. Superscript 1 indicates cell number x 10^{-9}/L. Data shown for period 1 are the pooled mean and SEM for study days 15, 22, and 29, and for period 2 are the pooled mean and SEM for study days 78, 85, and 92. None of these variables were different between the two groups, nor were they altered by CLA supplementation.

TABLE 5
Effects of CLA Feeding on Proliferation (Bq/1000 cells) of PBMNC Cultured with PHA[a]

	CLA group (n = 10)		Control group (n = 7)	
PHA (mg/L)	Period 1	Period 2	Period 1	Period 2
0.00	0.04 ± 0.01	0.04 ± 0.01	0.05 ± 0.01	0.05 ± 0.01
1.25	2.39 ± 0.97	2.32 ± 0.80	3.35 ± 1.26	3.08 ± 0.94
2.50	14.38 ± 2.50	15.53 ± 1.93	12.21 ± 2.13	13.85 ± 2.20
5.00	21.55 ± 2.39	22.92 ± 2.16	18.47 ± 1.74	19.32 ± 2.59
10.00	24.31 ± 2.57	27.07 ± 2.67	21.49 ± 1.93	23.03 ± 2.62
20.00	24.06 ± 2.41	26.21 ± 2.48	21.51 ± 1.41	21.86 ± 1.81

[a]Abbreviations: PBMNC, peripheral blood mononuclear cells; Bq, Becquerel; PHA, phytohemagglutinin. See Table 1 for other abbrevation. Data for periods one and two represent the same study days as in Table 4. At all PHA concentrations, PBMNC proliferation in both groups did not change during the study.

The concentration of CLA in the basal diet used in our study was nondetectable, while in the CLA-supplemented diet, it was 5.3 wt% of the total fatty acids (providing approximately 1.5% of daily energy intake). Thus, the CLA concentration used in our study was comparable to that used in many of the animal studies. However, the isomeric composition of the CLA used in our study was different from that reported for the animal studies. Most of the animal studies report that *c*9,*t*11-18:2, and *t*10,*c*12-18:2 made up about 80% of all the CLA isomers (3,8). In our study, these two isomers were only about 40% of all isomers. The CLA used in our study was prepared by refluxing a natural oil (safflower oil), while a mixture of the synthetic isomers of CLA was used in many of the animal studies. At the time we conducted this study, synthetic isomers of CLA for human consumption were not available. The difference in isomeric composition may also be due to inaccurate identification of CLA isomers in some of the other studies. The acid-catalyzed methylation causes isomerization of CLA isomers (25,26). In our study, we used sodium-methoxide for fatty acid methylation, thus avoiding this problem (25,26).

None of the indices of immunity tested (number of circulating

TABLE 6
CLA Feeding Does Not Alter the Proliferation (Bq/10^6 cells) of PBMNC Cultured with Influenza Vaccine[a]

	CLA group (n = 10)		Control group (n = 7)	
Vaccine concentration	Period 1	Period 2	Period 1	Period 2
0.00	54 ± 15	52 ± 15	62 ± 16	53 ± 10
1/250	563 ± 163	1183 ± 225	527 ± 252	1110 ± 324
1/500	1226 ± 290	2297 ± 439	1439 ± 408	2499 ± 615
1/1000	1519 ± 345	2255 ± 477	1897 ± 502	2544 ± 554
1/2000	1307 ± 314	1866 ± 432	1610 ± 488	2070 ± 507
1/4000	812 ± 230	1382 ± 345	1134 ± 390	1584 ± 522

[a]See Tables 1 and 5 for abbreviations and data presentations. *In vivo* immunization with the vaccine on day 65 caused a significant ($P < 0.05$) increase in the proliferation of PBMNC cultured with all concentrations of the same vaccine *in vitro* during period two; however, there was no effect of CLA on this response.

TABLE 7
Effect of CLA Feeding on Delayed-Type Hypersensitivity Response (DTH)[a]

	CLA group (n = 10)		Control group (n = 7)	
	Study day 30	Study day 90	Study day 30	Study day 90
Mumps (mm)	16.8 ± 3.4	22.3 ± 3.1	17.1 ± 2.5	15.6 ± 2.5
Tetanus (mm)	10.4 ± 3.1	12.1 ± 1.3	10.4 ± 2.6	13.4 ± 2.4
Candida (mm)	18.5 ± 1.4	18.5 ± 2.6	16.3 ± 3.8	17.9 ± 4.4
Other antigens (mm)	3.2 ± 0.7	6.2 ± 1.3	6.4 ± 1.2	16.5 ± 3.0
Sum induration (mm)	48.9 ± 5.4	59.1 ± 6.1	50.2 ± 6.2	63.4 ± 11.4
Antigen score	2.8 ± 0.3	3.6 ± 0.3	3.4 ± 0.2	3.9 ± 0.3

[a]DTH response to six recall antigens (mumps, tetanus, candida, trichophyton, streptokinase, and PPD) was determined 48 h after their intradermal injections. Data shown are mean ± SEM. CLA feeding did not alter the DTH response. See Table 1 for abbreviation.

TABLE 8
Effect of CLA Feeding on Serum Influenza Antibody Titers[a]

		CLA group (n = 10)		Control group (n = 7)	
Viral strain	Study day	GM	CI	GM	CI
AH1N1	65	53	30–92	47	25–90
	92	520	297–911	510	268–971
AH3N2	65	70	24–202	37	13–110
	92	149	51–433	144	49–425
B/Habrin	65	46	29–74	72	41–127
	92	160	100–257	290	165–510

[a]GM, geometric mean; CI, 95% confidence intervals. See Table 1 for other abbreviation. All subjects were immunized with influenza vaccine on day 65. Immunization significantly ($P < 0.05$) increased the antibody titers for all three viral strains in both groups. However, the increase in antibody titers was not significantly different between the two groups.

WBC, lymphocytes within different subsets, T and B lymphocyte proliferation, DTH, and serum antibody titers) were stimulated by CLA supplementation of the diets. Our results, showing no change in human lymphocyte proliferation with CLA supplementation are at variance with those of others who found increases in this response in mice, rats, and chickens (7,16,18). However, our results are in agreement with those of other investigators (17) who failed to detect an increase in splenocyte proliferation in mice fed CLA-containing diets for 6 wk. Similarly, our results regarding antibody production, DTH, and lymphocyte phenotypic analysis are consistent with the results from animal studies (16,18,27). While CLA supplementation did not improve any of the indices of immune status tested, it did not have any adverse effects either.

The discrepancy between our results and those obtained from animal models may simply be due to species' differences. Perhaps humans do not respond to CLA the same way rats, mice, and chickens do. One of the perceived mechanisms by which CLA exerts its health effects in animal models is through the induction of peroxisomal proliferation activation receptor (PPAR)-responsive genes in the liver (28). Humans appear to be resistant to peroxisome proliferation, and the promotor region of the human acetyl-CoA oxidase is resistant to transcriptional regulation by PPAR (29). Thus, inadequacy of the PPAR and their response elements may be why CLA failed to stimulate immune response in our human study. Even in the animal models, the effects of CLA on immune response have been only modest and have ranged from inhibition to stimulation. Based on these results, CLA does not seem to be a strong modulator of the immune response. Most of the animal experiments with CLA have involved growing animals, and in one study, the effects of CLA were less pronounced in the older mice than in the younger mice (18). It is possible that CLA did not stimulate indices of immune status in our study subjects because they were healthy adults, but it may stimulate them in growing human subjects, or in those with a compromised immune status. Another explanation may be that different isomers of CLA have opposing effects, and they may neutralize the effects of each other. Studies with purified isomers of CLA are needed to address this issue.

Other results from this study demonstrated that CLA supplementation did not affect body weight, fat-free mass, fat mass, percent body fat, or energy expenditure (30). Nor did it alter appetite, or the serum concentrations of insulin, glucose and lactic acid (31). There was a transient decrease in the concentration of serum leptin; however, it was not maintained until the end of the study (31). Taken together, the results from our study suggest that short-term supplementation of the diets of healthy adult humans with a mixture of CLA isomers is safe; however, there is no added benefit to the immune status and body composition. It is possible that CLA isomers have some health benefits to humans with a compromised immune status, or that one or more of the purified isomers may be beneficial to healthy adults. Until such information is obtained, CLA supplementation to improve human immune status or body composition should not be recommended.

ACKNOWLEDGMENTS

The authors are appreciative of the support provided by the dietary and nursing staff of the MRU in conducting this study. We thank the volunteers who participated in the study, the Bioanalytical Laboratory for sample processing, Health Services Department of California in Berkeley for determining influenza antibody titers, and Pharmanutrient, Inc. for donating the Tonalin oil.

REFERENCES

1. Ha, Y.L., Storkson, J., and Pariza, M.W. (1987) Inhibition of Benz-(a) pyrene-Induced Mouse Forestomach Neoplasia by Conjugated Linoleic Acid, *Cancer Res. 50*, 1097–1101.
2. Ip, C., Singh, M., Thompson, H.J., and Scimeca, J.A. (1994) Conjugated Linoleic Acid Suppresses Mammary Carcinogenesis and Proliferative Activity of the Mammary Gland in the Rat, *Cancer Res. 54*, 1212–1215.
3. Ip, C., Chin, S.F., Scimeca, J.A., and Pariza, M.W. (1991) Mammary Cancer Prevention by Conjugated Dienoic Derivative of Linoleic Acid, *Cancer Res. 51*, 6118–6124.
4. Ip, C., Jiang, C., Thompson, H.J., and Scimeca, J.A (1997) Retention of Conjugated Linoleic Acid in Mammary Gland Is Associated with Tumor Inhibition During the Post-Initiation Phase of Carcinogenesis, *Carcinogenesis 18*, 755–759.
5. Visonneau, S., Cesano, A., Tepper, S.A., Scimeca, J.A., Santoli, D., and Kritchevsky, D. (1997) Conjugated Linoleic Acid Suppresses the Growth of Human Breast Adenocarcinoma Cells in SCID Mice, *Anticancer Res. 17*, 969–974.
6. Liew, C., Schut, H.A.J., Chin, S.F., Pariza, M.W., and Dashwood, R.H. (1995) Protection of Conjugated Linoleic Acids Against 2-Amino, 3-Methylimidazo[4,5-f] Quinoline Induced Colon Carcinogenesis in F-344 Rat: A Study of Inhibitory Mechanisms, *Carcinogenesis 16*, 3037–3043.
7. Chew, B.P., Wong, T.S., Schultz, T.D., and Magnuson, N.S. (1997) Effects of Conjugated Dienoic Derivatives of Linoleic Acid and β-Carotene in Modulating Lymphocyte and Macrophage Function, *Anticancer Res. 17*, 1099–1106.
8. Schultz, T.D., Chew, B.P., Seaman, W.R., and Leudecke, L.O. (1992) Inhibitory Effects of Conjugated Dienoic Acid and Derivatives of Linoleic Acid and β-Carotene on the *in vitro* Growth of Human Cancer Cells, *Cancer Lett. 63*, 125–133.
9. Lee, K.N., Kritchevsky, D., and Pariza, M.W. (1994) Conjugated Linoleic Acid and Atherosclerosis in Rabbits, *Atherosclerosis 108*, 19–25.
10. Nicolosi, R.J., Rogers, E.J., Kritchevsky, D., Scimeca, J.A., and Hut, P.J. (1997) Dietary Conjugated Linoleic Acid Reduces Plasma Lipoproteins and Early Aortic Atherosclerosis in Hypercholesterolemic Hamsters, *Artery 22*, 266–277.
11. Houseknecht, K.L., Vanden, H.J.P., Moya-Camarena, S.Y., Porpocarrero, C.P., Beck, L.W., Nickel, K.P., and Belury, M.A. (1998) Dietary Conjugated Linoleic Acid Normalizes Impaired Glucose Tolerance in the Zucker Diabetic Fatty fa/fa Rat, *Biochem. Biophys. Res. Commun. 244*, 678–682.
12. Park, Y., Albright, K.J., Liu, W., Storkson, J.M., Cool, M.E., and Pariza, M.W. (1997) Effect of Conjugated Linoleic Acid on Body Composition in Mice, *Lipids 32*, 853–858.
13. Dugan, M.E.R., Aalus, J.L., Schaefer, A.L., and Kramer, J.K.G. (1997) The Effects of Conjugated Linoleic Acid on Fat and Lean Repartitioning and Feed Conversion in Pigs, *Can. J. Anim. Sci. 77*, 723–725.
14. Li, Y., and Watkins, B.A. (1998) Conjugated Linoleic Acids Alter Bone Fatty Acid Composition and Reduce ex vivo Bone Prostaglandin E_2 Biosynthesis in Rats Fed n-6 and n-3 Fatty Acids, *Lipids 33*, 417–425.
15. Miller, C.C., Park, Y., Pariza, M., and Cook, M.E. (1994) Feeding Conjugated Linoleic Acid to Animals Partially Overcomes the Catabolic Responses Due to Endotoxin Injection, *Biochem. Biophys. Res. Commun. 198*, 1107–1112.
16. Cook, M.E., Miller, C.C., Park, Y., and Pariza, M. (1993) Immune Modulation by Altered Nutrient Metabolism, Nutritional Control of Immune-Induced Growth Depression, *Poult. Sci. 72*, 1301–1305.
17. Wong, M.W., Chew, B.P., Wong, T.S., Hosick, H.L., Boylston, T.D., and Schultz, T.D. (1997) Effects of Dietary Conjugated Linoleic Acid on Lymphocyte Function and Growth of Mammary Tumors in Mice, *Anticancer Res. 17*, 987–994.
18. Hayek, M.J., Han, S.N., Wu, D., Watkins, B.A., Meydani, M., Dorsey, J.L., Smith, D.E., and Meydani, S.K. (1999) Dietary Conjugated Linoleic Acid Influences the Immune Response of Young and Old C57BL/6NCrIBR Mice, *J. Nutr. 129*, 32–38.
19. Turek, J.J., Li, Y., Schoenlein, I.A., Allen, K.G.D., and Watkins, B.A. (1998) Modulation of Macrophage Cytokine Production by Conjugated Linoleic Acid Is Influenced by the Dietary n-6:n-3 Fatty Acid Ratio, *J. Nutr. Biochem. 9*, 258–266.
20. U.S. Department of Agriculture (1987) *Composition of Foods*, U.S. Government Printing Office, Washington, DC, [Revised Agriculture Handbook no. 8.1–8.14.]
21. Kelley, D.S., Taylor, P.C., Nelson, G.J., Schmidt, P.C., Mackey, B.E., and Kyle, D. (1997) Effects of Dietary Arachidonic Acid on Human Immune Response, *Lipids 32*, 449–456.
22. Kelley, D.S., Taylor, P.C., Nelson, G.J., and Mackey, B.E. (1998) Dietary Docosahexaenoic Acid and Immunocompetence in Young Healthy Men, *Lipids 33*, 559–566.
23. Hierholzer, J.C., Suggs, M.T., and Hall, E.C. (1969) Standardized Viral Hemagglutination and Hemagglutination Tests. II. Description and Statistical Evaluation, *Appl. Microbiol. 18*, 824–833.
24. Littell, R.C., Milliken, G.A., Stroup, W.W., and Wolfinger, R.D. (1996) *SAS^{TM} System for Mixed Models*, SAS Institute Inc., Cary, NC, p. 633.
25. Kramer, J.K.G., Fellner, V., Dugan, M.E.R, Sauer, F.D., Mossoba, M.M., and Yurawecz, M.P. (1997) Evaluating Acid and Base Catalysis in the Methylation of Milk and Rumen Fatty Acids with Special Emphasis on Conjugated Dienes and Total *trans* Fatty Acids, *Lipids 32*, 1219–1228.
26. Kramer, J.K.G., Sehat, N., Dugan, M.E.R., Mossoba, M.M., Yurawecz, M.P., Roach, J.A.G., Eulitz, K., Aalhus, J.L., Schaefer, A.L., and Ku, Y. (1998) Distribution of Conjugated Linoleic Acid (CLA) Isomers in Tissue Lipid Classes of Pigs Fed a Commercial CLA Mixture Determined by Gas Chromatography and Silver Ion High-Performance Liquid Chromatography, *Lipids 33*, 549–558.
27. Sugano, M., Tsujita, A., Yamasaki, M., Noguchi, M., and Yamada, K. (1998) Conjugated Linoleic Acid Modulates Tissue Levels of Chemical Mediators and Immunoglobulins, *Lipids 33*, 521–527.
28. Moya-Camarena, S.Y., and Belury, M.A (1999) Species Differences in the Metabolism and Regulation of Gene Expression by Conjugated Linoleic Acid, *Nutr. Rev. 57*, 336–340.
29. Woodyatt, N.J., Lambe, K.J., Myers, K.A., Dougwood, J.D., and Roverts, R.A. (1999) The Peroxisome Proliferator (PP) Response Element Upstream the Human Acyl CoA Oxidase Gene Is Inactive Among a Sample Human Population: Significance of Species Differences in Response to PPs, *Carcinogenesis 20*, 369–372.
30. Zambell, K.L., Keim, N.L., van Loan, M., Gale, B., Benito, P., Kelley, D.S., and Nelson, G.J. (2000) Conjugated Linoleic Acid Supplementation in Humans: Effect on Body Composition and Energy Expenditure, *Lipids 35*, 777–782.
31. Medina, E.A., Horm, W.F., Keim, N.L., Havel, P.J., Benito, P., Kelley, D.S., Nelson, G.J., and Erickson, K.L. (2000) Conjugated Linoleic Acid Supplementation in Humans: Effect on Circulating Leptin Concentrations and Appetite, *Lipids 35*, 783–788.

[Received May 31, 2000, and in revised form August 11, 2000; accepted August 18, 2000]

Absorption by Rats of Tocopherols Present in Edible Vegetable Oils

Trine Porsgaard* and Carl-Erik Høy

Department of Biochemistry and Nutrition and Center for Food Research, Technical University of Denmark, 2800 Lyngby, Denmark

ABSTRACT: The absorption of tocopherols (α, γ, and δ) and fatty acids from rapeseed (RO), soybean (SOO), and sunflower (SUO) oil, both from the natural oils and from the oils following moderate heating (180°C for 15 min), was measured in lymph-cannulated rats. Oils were administered as emulsions through a gastrostomy tube, and lymph samples were collected for 24 h. The composition of tocopherols in oils and lymph fractions was measured by high-performance liquid chromatography, and fatty acids were measured by gas–liquid chromatography. The highest accumulated transport of α-tocopherol was observed after SUO administration, the lowest after SOO, with RO in between, corresponding to their relative contents (41.6 ± 8.8, 32.7 ± 5.0, and 24.9 ± 4.3 μg at 24 h after administration of SUO, RO, and SOO, respectively). The calculated recoveries (in %) 24 h after oil administration were 21.4 ± 4.5, 45.7 ± 7.0, and 78.8 ± 13.5 for SUO, RO, and SOO, respectively, suggesting that the absorption efficiency decreased when the α-tocopherol concentration increased. The recovery of α-tocopherol was higher than the recoveries of γ- and δ-tocopherol, indicating that the different tocopherols were not absorbed to the same extent or with similar rates. No differences between unheated and heated oils were observed in the absorption of tocopherols, whereas heating led to lower absorption of fatty acids, thus showing no direct association between absorption of tocopherols and fatty acids.

Paper no. L8425 in *Lipids 35,* 1073–1078 (October 2000).

Vitamin E is the major lipid-soluble antioxidant present in membranes and is important for the protection of polyunsaturated fatty acids against peroxidative damage, and thereby also for the normal function of membranes (1–3). Vitamin E is the term used for eight naturally occurring molecules, four tocopherols and four tocotrienols (named α, β, γ, and δ), all exhibiting vitamin E activity. The biological activities of the tocopherols differ, with α-tocopherol being the most active (4,5).

Tocopherols are absorbed together with other lipid-soluble components in the intestine. The presence of bile salts for micelle formation is important for the absorption (6,7). Disease states with impaired bile salt and pancreatic enzyme secretion lead to malabsorption of dietary fat and also of the lipid-soluble vitamins (8,9). Data based on mechanistic studies with everted intestinal sacs indicate that absorption into the enterocytes takes place by a passive diffusion process at the highest rate in the medial portion of the small intestine (10). On the other hand, studies by Kelleher *et al*. (11) and Brink *et al.* (12) using fecal excretion as a measure of unabsorbed tocopherol amounts showed decreased absorption at high dose levels compared to lower dose levels. The absorbed tocopherols are secreted into the lymphatics associated with chylomicrons (13,14), although small amounts can be transported from the intestine *via* the portal vein, but this is only a minor pathway under normal circumstances (15). From the lymphatics chylomicrons enter the circulation where they are catabolized. Lipoprotein lipase in the endothelial lining transfers fatty acids from chylomicrons to the tissues along with a minor part of the tocopherols (16), while the major part is absorbed together with chylomicron remnants into the liver and secreted in very low density lipoprotein (17,18).

Generally, tocopherol absorption is measured in two ways, either by measuring the unabsorbed part remaining in the intestine and feces or by estimating the level of absorbed tocopherol in the body. Infusion of radiolabeled tocopherols or large amounts of unlabeled standards followed by estimation of the amount transported in lymph is widely used to measure absorbed amounts (13,15,19,20). Vegetable oils are among the richest sources of vitamin E in the diet (21,22). In the present study, we investigated the absorption measured as lymphatic transport in rats of tocopherols as well as of fatty acids from three vegetable oils: rapeseed (RO), soybean (SOO), and sunflower (SUO). This study focuses on the absorption efficiencies of tocopherols in naturally occurring concentrations in edible oils. Furthermore, the effect of moderate heating, simulating household heating with fresh oils, on tocopherol absorption was examined since heating is known to reduce the tocopherol content (23). To our knowledge no groups have compared the absorption of tocopherols present in natural amounts in vegetable oils and related the effects of heating to absorption.

EXPERIMENTAL PROCEDURES

Animals. The following experiment was approved by the Danish Committee for Animal Experiment. Male Wistar rats

*To whom correspondence should be addressed at Department of Biochemistry and Nutrition, The Technical University of Denmark, Building 224, DK-2800 Lyngby, Denmark. E-mail: trine@mimer.be.dtu.dk

Abbreviations: HPLC, high-performance liquid chromatography; RO, rapeseed oil; SOO, soybean oil; SUO, sunflower oil.

were fed a standard nonpurified diet (Altromin No. 1324, Chr. Petersen A/S, Ringsted, Denmark) containing 4% fat and 75 mcg Vitamin E per g diet before the experiment. They were subjected to surgery as described previously (24) and fasted until the following day. Five (SOO, SUO, heated RO, and heated SOO) or six (RO, heated SUO) rats were used in each group.

Administration of oil and collection of lymph. On the postoperative day, the experiment was started by collection of a baseline fraction of lymph from –1 to 0 h. At time zero, a sonicated emulsion of 0.3 mL (corresponding to 270 mg) oil and 0.3 mL of a solution containing 20 mM taurocholate (Sigma Chemical Company, St. Louis, MO) and 10 mg/mL choline (Sigma Chemical Company) in distilled water was injected through the feeding tube followed by 0.6 mL saline, and the infusion of saline was continued at 2 mL/h. Lymph was collected in tubes in 1-h fractions for the following 8 h and a combined fraction was obtained from 8 to 23 h followed by a 1-h fraction from 23 to 24 h after administration of fat. The tubes contained 100 μL of a 10% (wt/vol) Na_2-EDTA-solution (E. Merck, Darmstadt, Germany) and they were frozen immediately after collection and kept at –20°C until analysis.

Analysis of tocopherol contents in oil and lymph. The following oils were used for the experiment: a low α-linolenic rapeseed oil (seed selected by DLF-Trifolium, St. Heddinge, Denmark; oil refined at the Department of Biotechnology, DTU, Lyngby), and a soybean and a sunflower oil (Aarhus Olie A/S, Aarhus, Denmark). The oils were heated in a stainless steel pan at 180°C in a 5-mm layer for 15 min. The unheated oils and corresponding heated oils were administered to rats as described above. Tocopherols (α, γ, and δ) in oils were determined by high-performance liquid chromatography (HPLC) as described in Porsgaard *et al.* (24).

Tocopherols (α, γ, and δ) in lymph samples were determined by the method of Kaplan *et al.* (25) after the following sample preparation performed in the dark. The values were not corrected for the baseline lymph tocopherol values. All solvents used were of HPLC-grade. Lymph (200 μL) together with 200 μL α-tocopherol acetate (133.7 μg/mL ethanol) as internal standard was extracted twice with 3 mL hexane alternating with centrifugation (5 min, 4000 rpm, room temperature, Heraeus Megafuge 1.0). The supernatants were combined and evaporated under vacuum for 40 min at 25°C in a Christ Alpha RVC vacuum-centrifuge. The residue was reconstituted in 150 μL acetonitrile/chloroform (80:40, vol/vol), filtered, and transferred to colored vials before injection of 80 μL into the HPLC. The HPLC system consisted of the following equipment purchased from Waters Corporation (Milford, MA): a programmable 490 ultraviolet detector measuring at 292 nm, an automated 717 sample injector, and a model 510 pump with a Supelcosil LC-18 column (25 cm × 4.6 mm, 5 μm, Supelco, Bellefonte, PA). The mobile phase consisted of acetonitrile/chloroform/2-propanol/water (78:16:3.5:2.5, by vol) at a flow rate of 2 mL/min. The concentrations of individual tocopherols were determined from standard curves using the internal standard.

Fatty acids in oils and lymph. The fatty acid composition of triacylglycerols in oils and lymph was determined as described in Porsgaard *et al.* (24). The fatty acid composition of the oils before as well as following heating is presented in Table 1.

Statistics. The results were presented as means ± SEM. Absorbed amounts of tocopherols in lymph after administration of different oils as well as the fractional absorption of different tocopherols were compared with one-way analysis of variance using the Jandel SigmaStat statistical package (Jan-

TABLE 1
Fatty Acid Composition (mol%) of Oils[a]

Fatty acid	Rapeseed	Heated rapeseed	Soybean	Heated soybean	Sunflower	Heated sunflower
16:0	4.7	4.8	12.3	12.9	7.7	7.7
16:1	0.3	0.2	ND[b]	ND	ND	0.1
18:0	1.7	1.8	4.2	4.4	4.2	4.1
18:1n-9	58.4	57.4	21.9	21.8	23.8	25.1
18:1n-7	3.0	3.0	1.5	1.5	0.8	0.8
18:2n-6	22.7	22.9	50.6	49.7	60.6	59.5
18:3n-3	6.2	6.5	7.8	7.9	1.3	1.1
20:0	0.6	0.6	0.5	0.5	0.4	0.3
20:1n-9	1.3	1.2	0.2	0.2	ND	0.2
22:0	0.3	0.2	0.3	0.3	0.5	0.5
22:1n-9	0.3	0.4	ND	ND	ND	ND
24:0	0.8	0.9	0.8	1.0	0.8	0.5
∑SAFA[c]	8.1	8.3	18.1	19.1	13.6	13.1
∑MUFA[d]	63.3	62.2	23.6	23.5	24.6	26.2
∑PUFA[e]	28.9	29.4	58.4	57.6	61.9	60.6

[a]The values represent the mean of three determinations.
[b]ND, not detected.
[c]∑SAFA = ∑saturated fatty acids.
[d]∑MUFA = ∑monounsaturated fatty acids.
[e]∑PUFA = ∑polyunsaturated fatty acids.

del Corporation, Erkrath, Germany). The correlation between tocopherol concentrations in oils and absorbed amounts was tested by Pearson correlation analysis. Differences were considered significant if the P value was <0.05.

RESULTS

Tocopherol content of oils. The content of total and individual tocopherols varied between RO, SOO, and SUO (Table 2). SUO contained the highest amount of α-tocopherol followed by RO and SOO. SOO had the highest content of γ- and δ-tocopherol. Heating of oils had only a minor effect on the tocopherol content.

Lymphatic transport of tocopherols. A significant positive correlation between the amounts of α-tocopherol transported in lymph and the content in the oils was observed ($P = 0.003$, $r = 0.95$) with the highest transport observed after SUO, the lowest after SOO, and with RO in between (Fig. 1). The accumulated amounts of individual tocopherols transported at 8 and 24 h after oil administration are shown in Table 3. The amount of α-tocopherol transported 8 h after administration of SUO was higher than the amount transported after SOO, heated SOO, and heated RO. In contrast to the differences observed at 8 h, the values for accumulated transport of α-tocopherol at 24 h did not show any significant differences, suggesting that differences in the content between the oils were counterbalanced by differences in absorbed amounts. This was further elucidated in the calculated recoveries of administered tocopherols at 8 and 24 h (Table 4). Eight hours after administration of SUO and heated SUO, the α-tocopherol recovery was significantly lower compared to the recovery after administration of the other four oils. Furthermore, the recovery of α-tocopherol after SOO was higher than the recovery after RO and heated RO. These differences were also observed 24 h after administration.

No differences were observed in the absorption of γ-tocopherol between RO and SOO when calculated in actual amounts (Table 3), even though the amount in SOO was almost twice as high as in RO.

When the absorption of individual tocopherols was compared, differences were observed suggesting that α-, γ-, and δ-tocopherol were not absorbed to the same extent or with similar rates. Eight hours after administration, a significantly higher recovery of administered amounts was observed for α-tocopherol compared to γ- and δ-tocopherol after SOO administration. This was also seen at 24 h together with similar differences after heated SOO administration. Differences in the absorption of α- and γ-tocopherol were observed 24 h after administration of RO and heated RO.

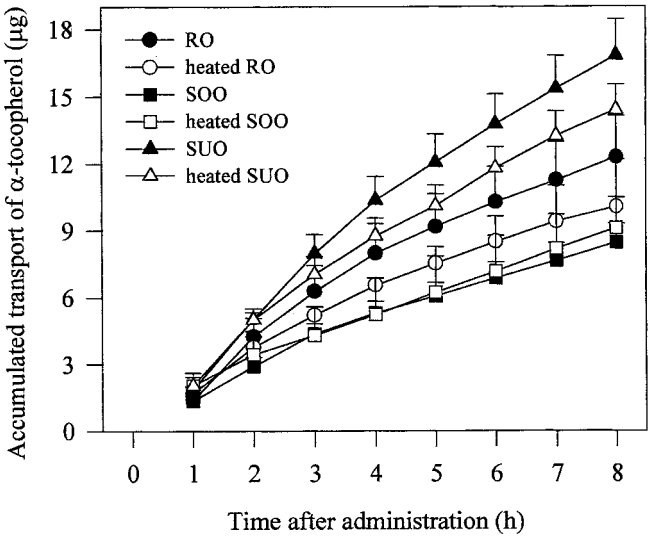

FIG. 1. Accumulated lymphatic transport (μg) of α-tocopherol in rats after administration of oils that had or had not been heated. Values represent means ± SEM (n = 5 or 6). RO, rapeseed oil; SOO, soybean oil; SUO, sunflower oil.

The absorption of tocopherols from heated and unheated oils showed no differences for any of the oils, suggesting that heating did not affect the absorption of tocopherols.

Absorption of fatty acids. The dominant fatty acid in SUO and SOO was linoleic acid, representing 61 and 51% of total fatty acids, respectively, while lower in RO (23%). On the other hand, RO contained 58% oleic acid (Table 1). The absorption of total fatty acids at 24 h after administration of unheated oils amounted to more than 100% (Table 4), indicating that the rats were able to digest and absorb these oils and thereby also were assumed to be able to absorb tocopherols. The absorption of total fatty acids from heated oils was lower than from unheated oils, but this did apparently not affect the absorption of tocopherols as no differences were observed between unheated and heated oils. The observed differences in absorption of fatty acids from unheated and heated oils were commented upon in Porsgaard *et al.* (24).

TABLE 2
Content of Tocopherols (T) in Each Dosage of Oil (μg T/0.3 mL)[a]

	Rapeseed	Heated rapeseed	Soybean	Heated soybean	Sunflower	Heated sunflower
α-T	72	68	32	37	194	177
γ-T	92	78	171	163	ND	ND
δ-T	26	23	96	94	20	22
Total T	190	169	299	294	214	199

[a]The values represent the mean of two determinations. For abbreviation see Table 1.

DISCUSSION

Absorption of vitamin E has received great attention because of the essentiality of this vitamin in the protection of polyunsaturated fatty acids against peroxidation. In this study we investigated the absorption in rats of individual tocopherols (α, γ, and δ) occurring at their natural levels in three different vegetable oils by following the lymphatic transport for 24 h after oil administration. The highest accumulated amount of α-tocopherol transported in lymph at 8 and 24 h was observed after administration of SUO and the lowest after SOO, corre-

TABLE 3
Accumulated Lymphatic Amounts (μg) of α-, γ-, and δ-Tocopherols at 8 and 24 h After Administration of Fat[a]

	Rapeseed		Heated rapeseed		Soybean		Heated soybean		Sunflower		Heated sunflower	
	Mean	SEM	Mean	SEM	Mean	SEM	Mean	SEM	Mean	SEM	Mean	SEM
α-T												
8 h	12.3	1.8	10.1[b]	0.4	8.5[b]	0.9	9.1[b]	3.1	16.8	1.6	14.4	1.1
24 h	32.7	5.0	26.4	2.2	24.9	4.3	27.5	6.0	41.6	8.8	38.2	4.0
γ-T												
8 h	10.3	2.3	8.5	0.6	12.9	2.5	12.5	5.4	ND		ND	
24 h	15.8	4.1	12.7	0.6	16.5	2.9	16.6	5.9	ND		ND	
δ-T												
8 h	ND		ND		9.2	1.9	8.4	3.3	ND		ND	
24 h	ND		ND		9.8	1.4	9.6	3.9	ND		ND	

[a]The values represent the means ± SEM of five or six rats. The doses administered are given in Table 2.
[b]Mean values were significantly lower than those for sunflower oil, $P < 0.05$. For abbreviations See Tables 1 and 2.

sponding to the relative amounts in the oils. On the other hand, when recoveries of administered amounts of α-tocopherol were compared, SUO showed the lowest recovery indicating that the absorption efficiency decreased with high contents of tocopherol in the oil. This resulted in recoveries of administered α-tocopherol amounts of 21.4 ± 4.5, 45.7 ± 7.0, and 78.8 ± 13.5% at 24 h after SUO, RO, and SOO administration, respectively. The content of γ-tocopherol in SOO was nearly twice the amount in RO, but no statistically significant differences in recoveries were observed (9.7 ± 1.7% at 24 h after SOO administration compared to 17.1 ± 4.4% after RO).

Gallo-Torres *et al.* (26) proposed that the nature of the accompanying fat might influence the lymphatic absorption of tocopherols. Increased levels of linoleic acid depressed the lymphatic absorption in rats of vitamin E, suggesting that polyunsaturated fatty acids have a negative influence on the absorption of vitamin E. In our study, we compared the absorption of three oils normally applied in household frying, and all three oils were rich in unsaturated fatty acids. The highest content of linoleic acid was in SUO, but it cannot alone account for the observed differences in recoveries between oils because SOO also contained high amounts of this fatty acid.

Tocopherol absorption has been examined in many studies. It was suggested that tocopherols were absorbed into the enterocytes through a passive diffusion process (10). Kelleher *et al.* (11) showed that the absorption of radioactive α-tocopherol in rats was decreased when the dose was increased and suggested that some kind of saturable process existed limiting the absorption at high dose levels. This was also observed by Brink *et al.* (12), who compared the absorption measured from fecal excretion of tocopheryl acetate added in three different concentrations. Bjørneboe *et al.* (13) measured a lymphatic recovery of 15 ± 9% after intraduodenal feeding

TABLE 4
Amount of α-, γ-, and δ-Tocopherols and Total Fatty Acids in Lymph Compared to the Infused Amount (% recovery) at 8 and 24 h After Administration of Fat[a]

	Rapeseed		Heated rapeseed		Soybean		Heated soybean		Sunflower		Heated sunflower	
	Mean	SEM	Mean	SEM	Mean	SEM	Mean	SEM	Mean	SEM	Mean	SEM
α-T												
8 h	17.2[b]	2.6	14.8[b]	0.6	26.8	2.7	24.8	8.5	7.2[c]	1.6	8.2[c]	1.6
24 h	45.7[b]	7.0	38.8[b]	3.2	78.8	13.5	82.0	18.9	21.4[c]	4.5	21.5[c]	2.3
γ-T												
8 h	11.2	2.5	9.0	2.1	7.6[d]	1.5	7.7	3.3	ND		ND	
24 h	17.1[e]	4.4	1.62[e]	0.7	9.7[d]	1.7	11.2[d]	4.5	ND		ND	
δ-T												
8 h	ND		ND		9.5[d]	1.9	9.0	3.6	ND		ND	
24 h	ND		ND		10.2[d]	1.4	11.7[d]	5.1	ND		ND	
FA												
24 h	116.9	6.6	78.5[f]	7.4	103.4	4.6	96.6	9.0	103.0	5.2	74.0[f]	7.5

[a]The values represent the means ± SEM of five or six rats.
[b]Mean values were significantly lower than those for soybean oil in the same row, $P < 0.05$.
[c]Mean values were significantly lower than those for the other oils in the same row, $P < 0.05$.
[d]Mean values were significantly lower than those for α-tocopherol in the same oil, $P < 0.001$.
[e]Mean values were significantly lower than those for α-tocopherol in the same oil, $P < 0.05$.
[f]Mean values were significantly lower than those for the corresponding unheated oil, $P < 0.01$. FA, fatty acids; for other abbreviations see Tables 1 and 2.

of 10 mg α-tocopherol in soybean oil to rats compared with a recovery of 22 ± 8% after 1 mg α-tocopherol showing slightly higher recovery after the low dose, but the difference was not statistically significant. Traber *et al.* (14) found that the efficiency of α-tocopherol absorption was decreased when the amount given to rats was increased. The results from these studies and those obtained in the present study suggest that the absorption efficiency decreases when the tocopherol concentration increases, but further studies are needed to clarify the underlying mechanisms.

The observed tocopherol recoveries in rats vary widely between different studies. When administered as ^{3}H-α-tocopherol in micellar solution a mesenteric lymphatic recovery of 42% was observed after 24 h (15), while Traber *et al.* (14) found 65% of the administered α-tocopherol in thoracic duct lymph. The 24-h thoracic duct lymph recovery of α-tocopherol measured by Ikeda *et al.* (20) was 25%. In intestinal loops an α-tocopherol absorption of 32% over 6 h was measured (27). Brink *et al.* (12) measured absorption efficiencies between 73 and 90% by feces collection. These large differences in recoveries may be the result of different ways of administering the tocopherols as well as different ways of measuring the absorption. Often, very high doses of vitamin E are administered and, as discussed above, this could affect the relative absorption.

Interest has concentrated on α-tocopherol because of its high biological activity, but γ-tocopherol is also important because it constitutes a considerable amount of the daily intake. When present in different amounts during infusion, almost similar lymphatic recoveries were found in rats for α- and γ-tocopherol, indicating that the absorption of these two tocopherols was independent of each other (14). In another study, Traber *et al.* (28) found that in humans α- and γ-tocopherol were absorbed and secreted in chylomicrons with equal efficiencies. Pearson and Barnes (27) observed similar absorption of α- and γ-tocopherol from intestinal loops in rats, while the absorption of δ-tocopherol was more than 15 times lower. In mesenteric lymph γ-tocopherol was found to be absorbed to an extent 15% lower than that of α-tocopherol (19). We found a significantly lower absorption of γ-tocopherol compared to α-tocopherol after RO administration and lower absorption of γ- and δ-tocopherol after SOO administration, suggesting that in our model there was discrimination between different tocopherols during the absorption.

The moderate heating procedure applied in our experiment had limited effect on tocopherol contents in the oils (Table 2). Previously, it was shown that heating decreased the tocopherol content in rapeseed oil (23), but this oil was exposed to a more severe heating procedure, including stirring and heating for 4 h. The absorption of fatty acids from unheated oils was higher than 100% (Table 4), indicating lymphatic transport of endogenous fatty acids in addition to the exogenous administered fatty acids (29). Heating of oils decreased the absorption of total fatty acids (the decrease was significant after administration of RO and SOO, $P < 0.01$), caused among other things by the formation of polymers during heating. In contrast to this, the absorption of tocopherols was unaffected by heating, indicating that there was no direct association between the absorption of fatty acids and tocopherols.

This study has shown that within the range of concentrations in vegetable oils, there is an increase in efficiency of tocopherol absorption at low dietary levels, although there is still a positive correlation between the amounts of tocopherols absorbed in lymph and the concentrations in the oils. The results emphasize the importance of investigating the absorption of tocopherols from natural sources. Moderate heating of RO, SOO, and SUO has no effect on tocopherol absorption, while fatty acid absorption is reduced following heating of SUO and RO.

ACKNOWLEDGMENTS

The authors wish to thank Kirsten Nielsen and Bente Pedersen for technical assistance, Steen Balchen, Department of Biotechnology, DTU, for refining the low α-linolenic rapeseed oil, and Robert G. Nielsen, Biotechnological Institute, Kolding, for heating oils. Financial support was given from the Danish Programme for Advanced Food Technology (FØTEK 2) and from The Danish Research Councils.

REFERENCES

1. Burton, G.W., Joyce, A., and Ingold, K.U. (1983) Is Vitamin E the Only Lipid-Soluble, Chain-Breaking Antioxidant in Human Blood Plasma and Erythrocyte Membranes? *Arch. Biochem. Biophys. 221*, 281–290.
2. Chow, C.K. (1985) Vitamin E and Blood, *World Rev. Nutr. Diet. 45*, 133–166.
3. Ingold, K.U., Webb, A.C., Witter, D., Burton, G.W., Metcalfe, T.A., and Muller, D.P.R. (1987) Vitamin E Remains the Major Lipid-Soluble, Chain-Breaking Antioxidant in Human Plasma Even in Individuals Suffering Severe Vitamin E Deficiency, *Arch. Biochem. Biophys. 259*, 224–225.
4. Burton, G.W., and Ingold, K.U. (1986) Vitamin E: Application of the Principles of Physical Organic Chemistry to the Exploration of Its Structure and Function, *Acc. Chem. Res. 19*, 194–201.
5. Sheppard, A.J., Pennington, J.A.T., and Weihrauch, J.L. (1992) Analysis and Distribution of Vitamin E in Vegetable Oils and Foods, in *Vitamin E in Health and Disease* (Packer, L., and Fuchs, J., eds.) pp. 9–31, Marcel Dekker, Inc., New York.
6. Gallo-Torres, H.E. (1970) Obligatory Role of Bile for the Intestinal Absorption of Vitamin E, *Lipids 5*, 379–384.
7. MacMahon, M.T., and Thompson, G.R. (1970) Comparison of the Absorption of a Polar Lipid, Oleic Acid, and a Non-Polar Lipid, α-Tocopherol from Mixed Micellar Solutions and Emulsions, *Eur. J. Clin. Invest. 1*, 161–166.
8. MacMahon, M.T., and Neale, G. (1970) The Absorption of α-Tocopherol in Control Subjects and in Patients with Intestinal Malabsorption, *Clin. Sci. 38*, 197–210.
9. Sokol, R.J., Reardon, M.C., Accurso, F.J., Stall, C., Narkewicz, M., Abman, S.H., and Hammond, K.B. (1989) Fat-Soluble-Vitamin Status During the First Year of Life in Infants with Cystic Fibrosis Identified by Screening of Newborns, *Am. J. Clin. Nutr. 50*, 1064–1071.
10. Hollander, D., Rim, E., and Muralidhara, K.S. (1975) Mechanism and Site of Small Intestinal Absorption of α-Tocopherol in the Rat, *Gastroenterology 68*, 1492–1499.
11. Kelleher, J., Davies, T., Smith, C.L., Walker, B.E., and Losowsky, M.S. (1972) The Absorption of α-Tocopherol in the

Rat. I. The Effect of Different Carriers and Different Dose Levels, *Internat. J. Vit. Nutr. Res. 42*, 394–402.
12. Brink, E.J., Haddeman, E., and Tijburg, L.B. (1996) Vitamin E Incorporated into a Very-Low-Fat Meal Is Absorbed from the Intestine of Young Rats, *Br. J. Nutr. 75*, 939–948.
13. Bjørneboe, A., Bjørneboe, G.-E.A., Bodd, E., Hagen, B.F., Kveseth, N., and Drevon, C.A. (1986) Transport and Distribution of α-Tocopherol in Lymph, Serum and Liver Cells in Rats, *Biochim. Biophys. Acta 889*, 310–315.
14. Traber, M.G., Kayden, H.J., Green, J.B., and Green, M.H. (1986) Absorption of Water-Miscible Forms of Vitamin E in a Patient with Cholestasis and in Thoracic Duct-Cannulated Rats, *Am. J. Clin. Nutr. 44*, 914–923.
15. MacMahon, M.T., Neale, G., and Thompson, G.R. (1971) Lymphatic and Portal Venous Transport of α-Tocopherol and Cholesterol, *Eur. J. Clin. Invest. 1*, 288–294.
16. Traber, M.G., Olivecrona, T., and Kayden, H.J. (1985) Bovine Milk Lipoprotein Lipase Transfers Tocopherol to Human Fibroblasts During Triglyceride Hydrolysis *in Vitro, J. Clin. Invest. 75*, 1729–1734.
17. Bjørneboe, A., Bjørneboe, G.-E.A., and Drevon, C.A. (1987) Serum Half-Life, Distribution, Hepatic Uptake and Biliary Excretion of α-Tocopherol in Rats, *Biochim. Biophys. Acta 921*, 175–181.
18. Traber, M.G., Ingold, K.U., Burton, G.W., and Kayden, H.J. (1988) Absorption and Transport of Deuterium-Substituted 2*R*,4′*R*,8′*R*-α-Tocopherol in Human Lipoproteins, *Lipids 23*, 791–797.
19. Peake, I.R., Windmueller, H.G., and Bieri, J.G. (1972) A Comparison of the Intestinal Absorption, Lymph and Plasma Transport, and Tissue Uptake of α- and γ-Tocopherols in the Rat, *Biochim. Biophys. Acta 260*, 679–688.
20. Ikeda, I., Imasato, Y., Sasaki, E., and Sugano, M. (1996) Lymphatic Transport of α-, γ- and δ-Tocotrienols and α-Tocopherol in Rats, *Internat. J. Vit. Nutr. Res. 66*, 217–221.
21. Bieri, J.G. (1984) Sources and Consumption of Antioxidants in the Diet, *J. Am. Oil Chem. Soc. 61*, 1917–1918.
22. Syväoja, E.-L., Piironen, V., Varo, P., Koivistoinen, P., and Salminen, K. (1986) Tocopherols and Tocotrienols in Finnish Foods: Oils and Fats, *J. Am. Oil Chem. Soc. 63*, 328–329.
23. Kishida, E., Oribe, M., and Kojo, S. (1990) Relationship Among Malondialdehyde, TBA-Reactive Substances, and Tocopherols in the Oxidation of Rapeseed Oil, *J. Nutr. Sci. Vitaminol. 36*, 619–623.
24. Porsgaard, T., Zhang, H., Nielsen, R.G., and Høy, C.-E. (1999) Absorption in Rats of Rapeseed, Soybean, and Sunflower Oils Before and Following Moderate Heating, *Lipids 34*, 727–732.
25. Kaplan, L.A., Miller, J.A., Stein, E.A., and Stampfer, M.J. (1990) Simultaneous, High-Performance Liquid Chromatographic Analysis of Retinol, Tocopherols, Lycopene, and α- and β-Carotene in Serum and Plasma, *Methods Enzymol. 189*, 155–167.
26. Gallo-Torres, H.E., Weber, F., and Wiss, O. (1971) The Effect of Different Dietary Lipids on the Lymphatic Appearance of Vitamin E, *Internat. J. Vit. Nutr. Res. 41*, 504–515.
27. Pearson, C.K., and Barnes, M.M. (1970) Absorption of Tocopherols by Small Intestinal Loops of the Rat *in Vivo, Internat. J. Vit. Res. 40*, 19–22.
28. Traber, M.G., Burton, G.W., Hughes, L., Ingold, K.U., Hidaka, H., Malloy, M., Kane, J., Hyams, J., and Kayden, H.J. (1992) Discrimination Between Forms of Vitamin E by Humans With and Without Genetic Abnormalities of Lipoprotein Metabolism, *J. Lipid Res. 33*, 1171–1182.
29. Porsgaard, T., Straarup, E.M., and Høy, C.-E. (1999) Lymphatic Fatty Acid Absorption Profile During 24 Hours After Administration of Triglycerides to Rats, *Lipids 34*, 103–107.

[Received December 23, 1999, and in revised form July 6, 2000; revision accepted August 18, 2000]

Escherichia coli Sepsis Increases Hepatic Apolipoprotein B Secretion by Inhibiting Degradation

Hope W. Phetteplace[a], Natalia Sedkova[a], Ken-Ichi Hirano[b], Nicholas O. Davidson[b], and Susan P. Lanza-Jacoby[a,*]

[a]Department of Surgery, Jefferson Medical College, Philadelphia, Pennsylvania 19107, and [b]Department of Medicine, University of Chicago, Chicago, Illinois 60637

ABSTRACT: Sepsis leads to hypertriglyceridemia in both humans and animals. Previously, we reported that plasma very low density lipoprotein apolipoprotein (apo) B and hepatic production of apoB increased during *Escherichia coli* sepsis. The present experiments were undertaken to determine whether the altered hepatic secretion of apoB was associated with an increase in synthesis or a decrease in degradation rate. Sepsis was induced in male, Lewis rats (225–275 g) by intravenous injection of 3.8×10^8 live *E. coli* colonies/100 g body. Twenty-four hours later rats were sacrificed, and primary hepatocytes were prepared and incubated overnight with ^{35}S-methionine. Hepatocytes from *E. coli*-treated rats secreted twice as much apoB-48 and total apoB than the hepatocytes from control rats. *Escherichia coli* sepsis increased cellular triglyceride mass by 86%, which was due to a stimulation in triglyceride synthesis from newly synthesized fatty acids, measured by ^3H_2O incorporation into triglycerides. The apoB synthesis rate, apoB mRNA levels, and apoB mRNA editing were not altered during *E. coli* sepsis. The pulse-chase experiments showed that the rate of apoB degradation decreased in *E. coli*-treated rats. These findings demonstrate that the secretion of apoB is regulated posttranslationally during *E. coli* sepsis by decreasing the degradation of newly synthesized apoB, which contributes to the development of hypertriglyceridemia.

Paper no. L8372 in *Lipids 35*, 1079–1085 (October 2000).

Gram-negative sepsis continues to be a serious complication in hospitalized patients with major trauma injuries or surgery (1,2). Normal metabolic processes, including lipid and lipoprotein metabolism, are altered (3,4). A prominent feature of the disordered lipid metabolism is an early rise in plasma triglycerides (TG) accompanied by an increase in hepatic production of lipids (5,6).

Hypertriglyceridemia may result from (i) decreased clearance of TG lipoproteins, (ii) increased synthesis of hepatic TG, (iii) increased synthesis and secretion of apolipoprotein (apoB)-containing lipoprotein particles, (iv) decreased hepatic uptake of lipoprotein remnant particles, and/or (v) decreased activities of low density lipoprotein (LDL) receptor. Previously we showed that increased production of very low density lipoprotein (VLDL)-TG and reduced clearance contributed to the development of hypertriglyceridemia of gram-negative sepsis (5–7). The defect in TG clearance during *E. coli* sepsis is attributable in part to reduced activities of lipoprotein lipase (LPL) in skeletal muscles, heart, and adipose tissues (5). The hypertriglyceridemia is characterized by an increased number of VLDL particles (8) with a normal composition of TG. The higher concentration of circulating VLDL in the *E. coli*-treated rats was associated with increased hepatic production of total apoB relative to the control rats (9).

The purpose of this study was to investigate the regulatory mechanisms by which *E. coli* sepsis increased hepatic production of apoB. In rats the liver is capable of synthesizing both forms of apoB; apoB-48 is formed by RNA editing of apoB-100 RNA. We used freshly isolated hepatocytes in suspension or in primary culture from *E. coli*-treated rats to measure the rate of secretion and synthesis of apoB-48 and apoB-100 and the synthesis of TG and total cholesterol. The molecular regulation of apoB was evaluated by measuring mRNA levels and RNA editing. Because degradation can also modify secretion of apo, we measured the recovery of newly synthesized apoB using pulse-chase studies.

MATERIALS AND METHODS

Male, Lewis inbred rats (225–275 g) were used in all experiments. They were maintained in the animal facility under standard conditions (12 h light/12 h dark cycle) and allowed free access to a standard rat chow (Purina 5001, Ralston-Purina, St. Louis, MO) for at least 1 wk prior to the beginning of each study. All experiments were performed in accordance with the guidelines of the National Institute of Health and with a proto-

*To whom correspondence should be addressed at Department of Surgery, Jefferson Medical College, Room 603 College Bldg., 1025 Walnut St., Philadelphia, PA 19107. E-mail: Susan.Lanza-Jacoby@mail.tju.edu

Abbreviations: apo, apolipoprotein; BSA, bovine serum albumin; ELISA, enzyme-linked immunosorbent assay; LDL, low density lipoprotein; LPL lipoprotein lipase; RT-PCR, reverse transcription-polymerase chain reaction; TG, triglyceride; TNF, tumor necrosis factor; TNF-α, tumor necrosis factor alpha; VLDL, very low density lipoprotein.

col approved by the Thomas Jefferson University Animal Care and Use Committee.

Escherichia coli Type 25922 (American Type Tissue Culture Collection, Rockville, MD) was used to induce sepsis. Rats in the *E. coli*-treated group received intravenously (i.v.) 3.8×10^8 colonies/100 g body weight. Control rats received i.v. sterile 0.9% NaCl. Food was removed from both groups after inducing sepsis, and hepatocytes were isolated 24 h later.

The hepatocytes were isolated following the procedure of Seglen (10) and were suspended in Waymouth's medium containing 0.2% bovine serum albumin (BSA) and 0.1 nM insulin, pH 7.4, gentamycin and streptomycin/penicillin (basal medium). Hepatocyte yield was approximately 1.5 to 2.0×10^8 cells/liver. Damaged cells were removed by centrifugation through Percoll and then washed twice with basal medium (11). More than 85% of the cells isolated excluded trypan blue. The hepatocytes were then counted and incubated in 125-mL polypropylene Erlenmeyer flasks at approximately 3×10^6 cells/mL.

Measurement of secreted apoB. Primary hepatocyte cultures were prepared for secretion studies. Approximately 1.75 to 2×10^6 cells were plated on 60 × 15 mm culture dishes and allowed to adhere for 2–4 h. Adherent cells were washed with basal medium and reincubated with the RPMI-1640 medium containing 0.38 mM leucine, 1.3 mM lysine, 2.4 mM glutamine, 1.8 mM choline chloride, 50 μM methionine; 28 mM glucose, 0.2% BSA, 0.1 nM insulin, 50 μg/mL gentamicin, and 100 μg/mL streptomycin plus 40 μCi of ^{35}S-methionine for 14 h at 37°C in 95% O_2/5% CO_2. After incubation, medium was collected for measurement of apoB secretion. Cells were washed twice with phosphate-buffered saline (PBS), then 0.3 mL of solubilization buffer [0.01 M sodium phosphate buffer (pH 7.4), 0.125 M sodium chloride, 0.5% Triton X-100, 0.5% sodium deoxycholate, 0.5% lithium dodecyl sulfate, 0.5% BSA (fatty acid-free) plus protease inhibitors (1 mM phenyl methyl sulfonyl fluoride, 1 mM EDTA, 1 mM benzamidine, 10 μg/mL leupeptin, 1 μM Aprotinin)] was added to the cells and they were transferred to a microcentrifuge tube.

The solubilized cells were sonicated and apoB was immunoprecipitated and separated by gel electrophoresis as described by Tripp *et al.* (9).

Measurement of mRNA and mRNA editing. Total RNA from hepatocytes was extracted using the method of Chomczynski and Sacchi (12). RNA was separated by 1% agarose-formaldehyde gel, stained with ethidium bromide to verify equal loading of RNA, and transferred to nylon membranes for Northern analysis.

ApoB cDNA was isolated, purified, and radiolabeled with ^{32}P-dCTP using a random priming kit (RPN1601Z, Amersham; Arlington Heights, IL). The blot was hybridized with the radiolabeled cDNA overnight at 42°C. After hybridization the membrane was washed several times with SSC (0.15 M NaCl/0.15 M Na citrate, pH 7.4)/SDS solutions at 55°C and the membranes were exposed to XAR-5 film at –70°C. After exposing the film, the membrane was stripped and re-hybridized with S-14 as a control probe. The intensity of the bands on the film for apoB and S-14 was quantified by scanning densitometry.

The editing of apoB was determined as previously described (13). Briefly, 2 to 10 μg of total RNA was treated with DNase as described by Giannoni *et al.* (14), and approximately 100 ng was used for reverse transcription-polymerase chain reaction (RT-PCR). Each sample was checked for DNA contamination by running a negative control with rTth. To exclude PCR product contamination, each reaction had an additional tube with all of the above buffers and enzymes, but without RNA. An aliquot of the PCR products was analyzed on a 2% agarose gel to confirm the expected 275 base pair apoB amplification product. RT-PCR products were purified by spin kit columns (Quigen, Studio City, CA), and apoB editing was assayed by primer extension. The extension products were resolved on an 8% denaturing polyacrylamide gel, dried, and exposed at –80°C with enhancing screens. The autoradiographs were scanned by laser densitometry.

ApoB synthesis and degradation. Freshly isolated hepatocytes were used in these studies to determine differences in basal apoB synthesis between *E. coli*-treated and control rats. To measure the synthesis of apoB, the freshly isolated hepatocytes were preincubated in RPMI-1640 medium without methionine and then pulsed with 50 μCi/mL ^{35}S-methionine for 15 min. Aliquots (1 mL) of the cells plus medium were taken for immunoprecipitation, and 750 μL of solubilization buffer was added. The immunoprecipitation procedure was the same as listed for the secretion experiments, except that 600–800 μL of the sonicated homogenate were analyzed.

Degradation of apoB was measured by pulsing freshly isolated hepatocytes as described above. Then the cells were washed three times with RPMI-1640 and incubated in RPMI-1640 plus 10 mM L-methionine for the times indicated in Table 1. ApoB from cells plus medium were identified by immunoprecipitation as described previously (9).

De novo *triglyceride and total cholesterol synthesis.* Freshly isolated hepatocytes (2.5×10^6 cells/mL) were incubated with ^3H_2O (0.5 mCi/mL) for 60 min at 37°C in 95% O_2/5% CO_2. Incorporation of ^3H_2O into TG and total cholesterol was measured

TABLE 1
Effect of *Escherichia coli* Bacteremia on the Recovery[a] of Labeled Total apoB from Cell and Medium After 45- to 180-min Chase Periods[b]

	Chase times (min)		
Group	45	90	180
Control	89 ± 5	70 ± 4	39 ± 3
E. coli-treated	96 ± 6	89 ± 5*	75 ± 4*

[a]Freshly isolated hepatocytes were pulsed with ^{35}S-methionine (50 μCi/mL) for 15 min. After pulse the cells were washed with fresh medium and chased with unlabeled methionine for selected time periods. Labeled apolipoprotein (apo) B was determined in cells plus medium by immunoprecipation and sodium dodecyl sulfate polyacrylamide gel electrophoresis. Bands from gels corresponding to apoB were quantitated by scintillation counting.

[b]The data presented are expressed as a mean percentage ± SEM of the ^{35}S-methionine incorporated into cellular total apoB at the end of the 15-min pulse for three independent experiments performed in triplicate. Asterisk (*): differs significantly ($P \leq 0.05$) from control.

in the cells plus medium by extracting total lipids and separating the lipid classes by thin-layer chromatography as described previously (5). After the 60-min incubation, lipids were extracted from the cell pellet and were used for mass determination of TG and total cholesterol (5).

Enzyme-linked immunosorbent assay (ELISA) and protein determination. A competitive ELISA using a goat anti-rat apoB antibody was performed according to the procedure developed by Wong and Pino (15,16).

Total protein of the radiolabeled cellular homogenates from secretion and synthesis experiments was determined using the method of Lowry *et al.* (17).

Statistics. Each sample was analyzed in triplicate. Results are expressed as average of averages ± standard error of the mean (SEM). All data were statistically analyzed by unpaired *t*-test.

RESULTS

ApoB secretion. Steady-state secretion of apoB from primary hepatocyte from control and *E. coli*-treated rats was determined by incubation overnight in RPMI-1640 plus ^{35}S-methionine. Cellular protein was not significantly different due to sepsis (control = 2.26 ± 0.34 and *E. coli*-treated = 2.03 ± 0.37 mg/mL). The secretion of apoB, as measured by immunoprecipitation and separation by gel electrophoresis, indicated that the *E. coli*-treated rats secreted more than twice as much apoB-48 ($P < 0.05$) as the hepatocytes from the control rats, which led to a twofold increase in total apoB secreted into the medium (Fig. 1A). There were no significant differences in cellular ^{35}S-labeled apoB (Fig. 1B).

ApoB synthesis, apoB mRNA, apoB editing. To determine whether the increased secretion of apoB was related to increased synthesis, freshly isolated hepatocytes were pulsed for 15 min with ^{35}S-methionine, and the incorporation of radiolabel into cells plus medium was measured by immunoprecipitation and gel electrophoresis. In our previous studies with *E. coli* bacteremia we found that freshly isolated hepatocytes in suspension cultures maintained the disturbances in lipid metabolism that were observed *in vivo* (5,6,18). Moreover, our findings demonstrated that the *E. coli*-induced increase in apoB secretion observed in perfused livers was also present when primary hepatocytes were cultured overnight (9). Approximately 40 min is required for newly synthesized apoB to be secreted in measurable amounts in the medium (19). Thus, the amount of ^{35}S-labeled apoB represents initial cellular synthesis. As shown in Figure 2, there were no significant differences in the incorporation of ^{35}S-methionine into apoB-48 or apoB-100 in hepatocytes from control and *E. coli*-treated rats. Total apoB concentrations, as measured by ELISA in cells plus medium (control = 1.40 ± 0.6 μg/mL; *E. coli*-treated = 1.25 ± 0.5 μg/mL), were similar, indicating that the pool size of these apo was not altered during sepsis.

We next evaluated apoB mRNA and apoB editing since the increase in apoB secretion may be due to changes in mRNA levels or the proportion of apoB mRNA that encoded for apoB-48 and apoB-100. As indicated in Figure 3, *E. coli* bacteremia did not alter apoB mRNA levels, as measured by Northern analyses on hepatocyte total RNA. ApoB editing, as expressed as % TAA, did not differ between the two groups (control = 50 ± 1, *E. coli*-treated = 52 ± 1) (Fig. 4).

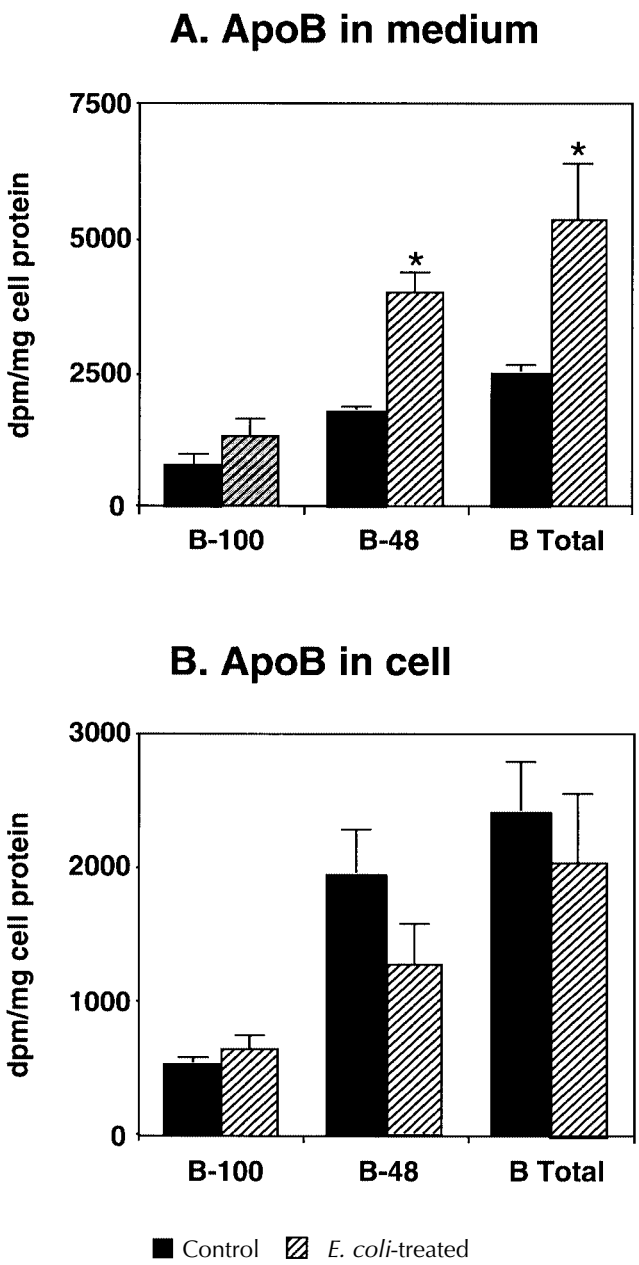

FIG. 1. Secretion of apolipoprotein (apo) B-48, apoB-100, and total apoB from primary hepatocytes from control and *Escherichia coli*-bacteremic rats. Primary cultured hepatocytes from control and *E. coli*-treated rats were prepared as described in the Materials and Methods section and cultured with RPMI medium containing 0.2% bovine serum albumin plus 40 μCi of ^{35}S-methionine for 14 h. After incubation, media and cells were prepared for immunoprecipitation and labeled apoB-48 and apoB-100 were separated by sodium dodecyl sulfate/polyacrylamide gel electrophoresis. Data were calculated as the average radioactivity of six experiments in which apoB was assayed in triplicate; bars represent the average of averages ± SEM. Asterisk (*) differs significantly ($P \leq 0.05$) from control.

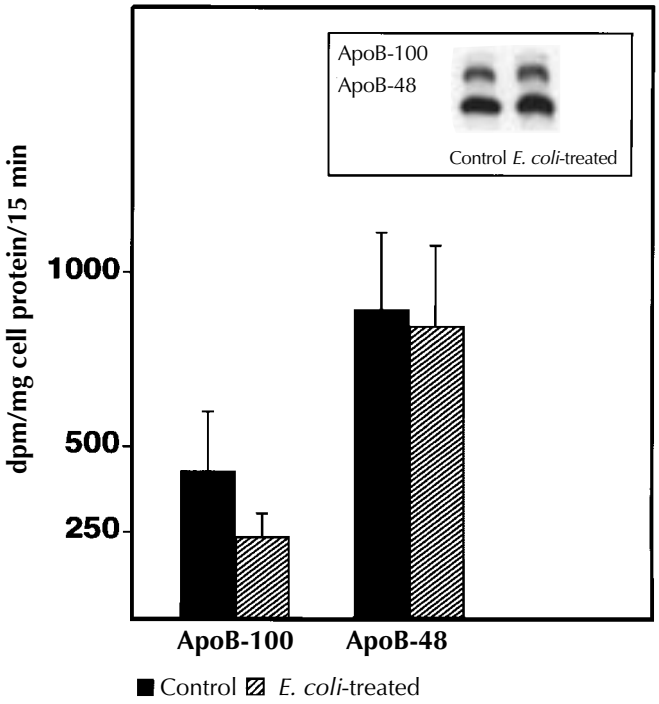

FIG. 2. Initial synthesis of apoB-48 and apoB-100 in freshly isolated hepatocytes from control and *E. coli*-bacteremic rats. Freshly isolated hepatocytes were pulse-labeled for 15 min by adding 50 μCi/mL of ^{35}S-methionine. The insert shows a representative autoradiograph of apoB-100 and apoB-48. Data were calculated as the average radioactivity of 6 experiments in which apoB was assayed in triplicate; bars represent the average of averages ± SEM. Asterisk (*) differs significantly ($P \leq 0.05$) from control. For abbreviations see Figure 1.

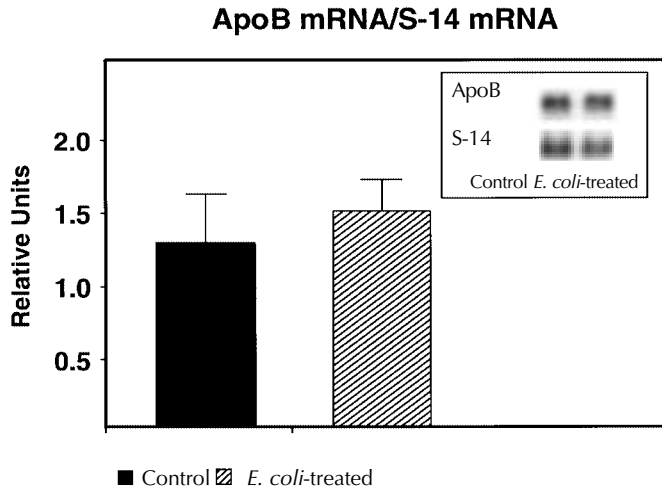

FIG. 3. Northern analysis of apoB mRNA and S-14 nRNA from freshly isolated hepatocytes from control and *E. coli*-bacteremic rats. RNA was separated on 1% agarose-formaldehyde gel, transferred to nylon membranes, hybridized to ^{32}P-labeled cDNA, and exposed to film. ApoB mRNA signal was quantified by densitometric analysis and normalized to S-14 signal. The insert shows a representive autoradiograph of apoB mRNA. Data were calculated as the average radioactivity of six experiments in which apoB was assayed in triplicate; bars represent the average of averages ± SEM. For abbreviations see Figure 1.

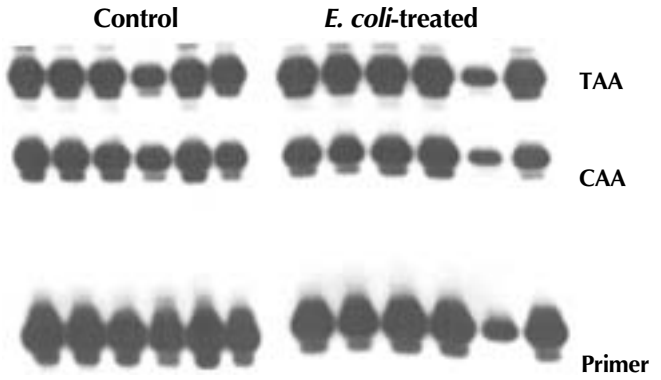

FIG. 4. ApoB mRNA editing in freshly isolated hepatocytes from control and *E. coli*-bacteremic rats. RNA was treated with DNase and used for reverse transcription-polymerase chain reaction (PCR). Purified PCR products were subject to primer extension analysis to demonstrate the proportion of edited (TAA) vs. unedited (CAA) apoB cDNA. For abbreviations see Figure 1.

Since apoB synthesis or changes in apoB mRNA were not altered in freshly isolated hepatocytes, we investigated whether a decrease in the rate of degradation could account for the increase in secretion rate. Pulse-chase studies were conducted to measure the degradation of the newly synthesized apoB. The recovery of labeled apoB in hepatocytes plus media was measured over time. After 180 min more labeled apoB remained in the hepatocytes plus their media from the *E. coli*-treated rats than the hepatocytes from the control rats (Table 1).

De novo *synthesis of TG and total cholesterol.* The availability of lipids is thought to have a role in regulating apoB degradation and secretion. We determined TG and total cholesterol synthesis from newly synthesized fatty acids and the content of TG and total cholesterol in hepatocytes. Syntheses of TG and total cholesterol were three- and sixfold higher, respectively, in hepatocytes from *E. coli*-treated rats than control rats (Fig. 5). These increases in synthesis were accompanied by similar increases in the content of hepatocyte TG and total cholesterol (Fig. 6).

DISCUSSION

One of the first metabolic responses to sepsis is the elevation in plasma TG. Plasma TG and apoB levels are elevated over twofold (5,8). The initial rise in TG results from an increase in hepatic production of VLDL-TG. The increase in the number of VLDL particles in the plasma is due to an increase in hepatic production of apoB and a decrease in the clearance of VLDL remnants (6–9). The present experiment explores the mechanisms for the altered apoB production during *E. coli* sepsis using an isolated hepatocyte system.

We have found that primary cultured hepatocytes from *E. coli*-treated rats secreted over twofold more apoB, which is consistent with previous findings in our laboratory using i*n vivo* and *in situ* liver perfusion systems (9). Cytokines such as tumor necrosis factor α(TNF-α) may mediate the hyper-

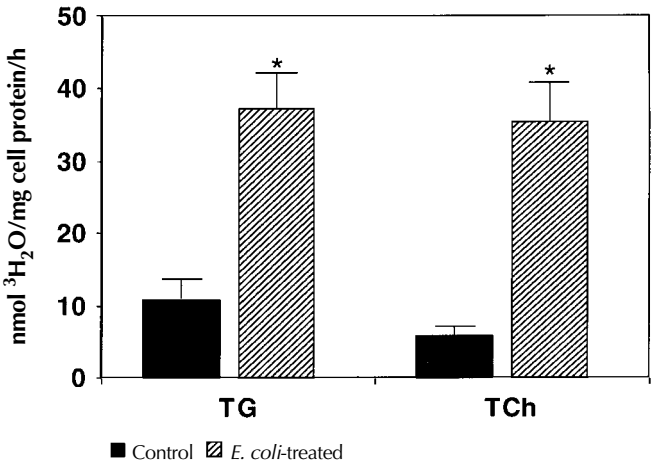

FIG. 5. *De novo* triglyceride (TG) and total cholesterol (TCh) synthesis in freshly isolated hepatocytes from control and *E. coli*-bacteremic rats. Hepatocytes were incubated with ^3H_2O (0.5 mCi/mL) for 60 min at 37°C in 95% O_2/5% CO_2. Total lipids were extracted in cell plus medium. Incorporated of ^3H_2O into TG and TCh was measured after separation by thin-layer chromatography as described in the Materials and Methods section. Bars are means ± SEM from four separate experiments which were conducted in triplicate. Asterisk (*) differs significantly ($P \leq 0.05$) from control. For abbreviations see Figure 1.

lipidemia of infection and sepsis (20). *Escherichia coli* bacteremia (6) and endotoxemia (18) produced an elevation in serum TNF-α within 60 to 90 min after administration. TNF also led to a rapid rise in serum VLDL within 45–90 min that was due to an initial increase in hepatic secretion of VLDL (20). Yet, treatment of *E. coli*-bacteremic rats with anti-TNF antibody did not prevent the rise in VLDL-TG (6).

The altered secretion of apoB in primary hepatocytes from *E. coli*-treated rats was not associated with changes in the synthesis rate or mRNA levels in the freshly isolated cells.

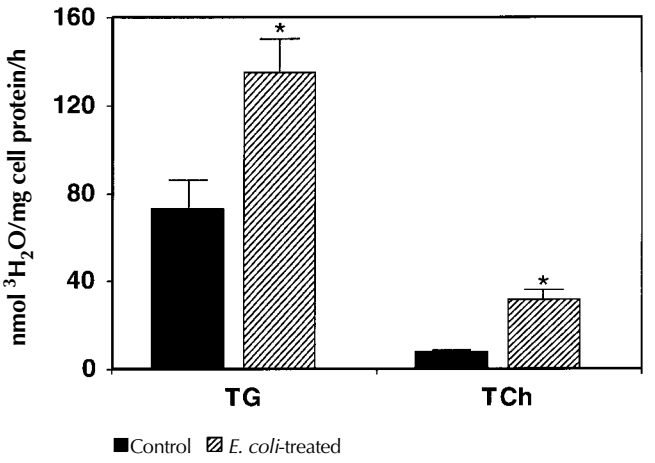

FIG. 6. TG and TCh mass in freshly isolated hepatocytes from control and *E. coli*-bacteremic rats. Hepatocytes were incubated for 60 min at 37°C in 95% O_2/5% CO_2; total lipids were extracted in cell plus medium for mass determination of TG and TCh. Bars are means ± SEM from four separate experiments which were conducted in triplicate. Asterisk (*) differs significantly ($P \leq 0.05$) from control. For abbreviations see Figures 1 and 5.

These findings agree with those of Delers *et al.* (21) who found that rats injected with mouse recombinant TNF had no change in the levels of apoB mRNA in the liver. Other investigators have shown in rat primary cultured hepatocytes and Hep G2 cells that the apoB message is relatively stable during changing metabolic situations in which apoB secretion is altered (22,23).

Posttranscriptional editing of apoB-100 mRNA in the livers of rodents produces apoB-48, so that both B-100 and B-48 are secreted (24–26). The increased secretion of apoB-48 from the primary cultured hepatocytes from the *E. coli*-treated rats could not be attributed to changes in apoB editing. Fasting has been shown to affect apoB editing (27). In this study we observed that fasting reduced apoB mRNA editing in both control and *E. coli*-treated rats compared with fed rats even though the total amount of apoB mRNA did not change (Lanza-Jacoby, S., unpublished observation). Hepatocytes used in the present study were from fasted rats and were considered to remain in a fasted state relative to mRNA concentration and apoB synthesis. Davis *et al.* (28) found that synthesis in cultured hepatocytes obtained from rats fasted for 3 d was not changed by addition of glucose to the medium.

Since apoB mRNA, synthesis, and editing did not account for the increased secretion of apoB, we investigated whether posttranslational mechanisms were involved. Studies from rat hepatocytes and HepG2 cells have indicated that intracellular degradation regulates the secretion of apoB (28,29). Degradation was evaluated in freshly isolated hepatocytes, which may lead to higher degradation rates than primary hepatocytes. However, the relative differences in degradation rates between control and *E. coli*-treated rats are evident in the freshly isolated hepatocytes. Our results indicate that degradation of apoB in the hepatocyte from the *E. coli*-treated rats was less than half the value of control rats, which would account for the increased secretion of apoB. Hormones such as insulin and glucocorticoids alter apoB secretion in primary cultured hepatocytes by regulating apoB degradation (23,29). Plasma concentration of insulin, glucagon, and glucocorticoids are elevated in this *E. coli* septic model (5,6), which may account, in part, for the increased secretion of apoB. Insulin decreased apoB secretion in cultured rat hepatocytes by reducing synthesis and degradation (19). In contrast, dexamethasone increased apoB secretion in rat cultured hepatocytes by increasing synthesis of apoB-48 and apoB-100 and decreasing intracellular degradation of newly synthesized apoB (22).

Degradation of apoB may be modified by altering TG synthesis and availability (30,31). Several studies in rabbit hepatocytes and HepG2 cells have demonstrated that the availability of TG protected apoB from degradation and thus increased apoB secretion (32–34). During sepsis the amount of *de novo* synthesized fatty acids incorporated into TG and total cholesterol is increased leading to an accumulation of these lipids in cells, which could facilitate lipoprotein assembly and secretion. Previously we also demonstrated that the activities of glycerol-3-phosphate acyltransferase and phosphatidate phos-

phohydrolase, key rate-limiting enzymes in TG synthesis, are elevated in hepatocytes from *E. coli*-treated rats (18).

Recently, the LDL receptor was shown to have a role in posttranslational regulation of apoB (35). ApoB secretion was increased in primary hepatocytes in the absence of the LDL receptor because degradation of apoB-100 and apoB-48 were reduced (35). We observed that the LDL receptor protein is downregulated in hepatocytes from *E. coli*-treated rats (Lanza-Jacoby, S., Phetteplace, H., and Sedkova, A., unpublished observations), which may also account for the decrease in apoB degradation.

Posttranslational changes in apoB metabolism increased secretion and contributed to the hypertriglyceridemia of sepsis. The twofold increase in apoB secretion correlated with a twofold rise in plasma apoB concentration. The physiological function of the hyperlipoproteinemia is not well understood. Recent reports have suggested that the rise in plasma lipoproteins may have a protective role by modifying the bioavailability and clearance of bacteria (36). Several mechanisms are involved in maintaining the elevation in plasma lipoproteins during sepsis (5–9). The onset of bacteremia leads to increased production of VLDL-TG arising from increased synthesis of lipids (5,6,8). During the course of the septic episode the clearance of TG decreases due to altered transcriptional regulation of LPL (5,37). The present studies explain how *E. coli* sepsis increases the plasma concentration of VLDL particles by decreasing the degradation of apoB, thus stimulating hepatic production of apoB-containing lipoproteins.

ACKNOWLEDGMENTS

The authors wish to thank Dr. Edward A. Fisher of Mount Sinai School of Medicine, New York, NY, for the gift of the apoB cDNA and Dr. Laurence Wong, Louisiana State University Medical Center for the goat anti-rat apoB antibody. We also thank Dr. Wong for his advice concerning the apoB ELISA. This study was supported by Grant No. GM31828 to S.L.J. from the National Institutes of General Medical Sciences and grants DK 56260 and HL 38180 to N.O.D.

REFERENCES

1. Bone, R.C. (1994) Sepsis and Its Complications: The Clinical Problem, *Crit. Care Med. 22,* S8–S11.
2. Natanson, C., Hoffman, W.D., Suffredini, A.F., Eichacker, P.Q., and Danner, R.L. (1994) Selected Treatment Strategies for Septic Shock Based on Proposed Mechanisms of Pathogenesis, *Ann. Inter. Med. 120,* 771–783.
3. Kispert, P., and Caldwell, M.D. (1989) Metabolic Changes in Sepsis and Multiple Organ Failure, in Dietch, E.A. (ed.) *Multiple Organ Failure: Pathophysiology and Basic Concepts of Therapy*, pp. 104–125, Thieme Medical Public, New York.
4. Gallin, J.I., Kay, D., and O'Leary W.M. (1969) Serum Lipids in Infection, *N. Engl. J. Med. 281*, 1081–1086.
5. Lanza-Jacoby, S., and Tabares, A. (1990) Triglyceride Kinetics, Tissue Lipoprotein Lipase, and Liver Lipogenesis in Septic Rats, *Am. J. Physiol. 258*, E678–E685.
6. Lanza-Jacoby, S., Phetteplace, H., Sedkova, N., and Knee, G. (1998) Sequential Alterations in Tissue Lipoprotein Lipase, Triglyceride Secretion Rates, and Serum Tumor Necrosis Alpha During *E. coli* Bacteremic Sepsis in Relation to the Development of Hypertriglyceridemia, *Shock 9*, 46–51.
7. Phetteplace, H., Maniscalco M., and Lanza-Jacoby, S. (1994) The Catabolism of Apolipoprotein B from Very Low Density Lipoprotein and Triglyceride-Rich Lipoprotein Remnants in Fasted Septic Rats, *Shock 1*, 227–220.
8. Lanza-Jacoby, S., Wong, S.H., Tabares, A., Baer, D., and Schneider, T. (1992) Disturbances in the Composition of Plasma Lipoproteins During Gram-Negative Sepsis in the Rat, *Biochim. Biophys. Acta 1124*, 233–240.
9. Tripp, R.T., Tabares, A., Wang, H., and Lanza-Jacoby, S. (1993) Altered Hepatic Production of Apolipoproteins B and E in the Fasted Septic Rat: Factors in the Development of Hypertriglyceridmia, *J. Surg. Res. 55*, 465–472.
10. Seglen, P.O. (1976) Preparation of Isolated Rat Liver Cells, in *Methods in Cell Biology*, (Prescott, D.M, ed.), Vol. 13, pp. 29–83, Academic, San Diego.
11. Berry, M.N., Edwards, A.M., Barritt, G.J., Grivell, M.B., Halls, H.J., Gannon, B.J., and Friend, D.S. (1991) High-yield Preparation of Isolated Hepatocytes from Rat Liver, in *Isolated Hepatocytes: Preparation, Properties and Applications, Laboratory Techniques in Biochemistry and Molecular Biology*, (Burdon R.H., and van Knippenberg, P.H. eds.), Vol. 21, pp. 15–58, Elsevier, New York.
12. Chomczynski, P., and Sacchi, N. (1987) Single-Step Method of RNA Isolation by Guanidinium Thiocyanate-Phenol-Chloroform Extraction, *Anal. Biochem. 162*, 156–159.
13. Teng, B., Verp, M., Salmon, J., and Davidson, N.O. (1990) Apolipoprotein B Messenger RNA Editing Is Developmentally Regulated and Widely Expressed in Human Tissues, *J. Biol. Chem. 265*, 20616–20620.
14. Giannoni, F., Field, F.J., and Davidson, N.O. (1994) An Improved Reverse Transcription-Polymerase Chain Reaction Method to Study Apolipoprotein Gene Expression in Caco-2 cells, *J. Lipid Res. 35*, 340–350.
15. Wong, L., and Pino, R.M. (1987) Biogenesis of Very-Low-Density Lipoproteins in Rat Liver, *Eur. J. Biochem. 164*, 357–367.
16. Wong, L. (1989) Contribution of Endosomes to Intrahepatic Distribution of Apolipoprotein B and Apolipoprotein E, *Eur. J. Cell. Physiol. 141*, 441–452.
17. Lowry, O.H., Rosebrough, N.J., Farr, A.L., and Randall, R.J. (1951) Protein Measurements with Folin-Phenol Reagent, *J. Biol. Chem. 193*, 256–275.
18. Lanza-Jacoby, S., and Rosato, E.L. (1994) Regulatory Factors in the Development of Fatty Infiltration of the Liver During Gram-Negative Sepsis, *Metabolism 43*, 691–696.
19. Sparks, J.D., and Sparks C.E. (1990) Insulin Modulation of Hepatic Synthesis and Secretion of Apolipoprotein B by Rat Hepatocytes, *J. Biol. Chem. 265*, 8854–8862.
20. Krauss, R.M., Grunfeld, C., Doerrler, W.T., and Feingold, K.R. (1990) Tumor Necrosis Factor Acutely Increases Plasma Levels of Very Low Density Lipoproteins of Normal Size and Composition, *Endocrinology 127*, 1016–1021.
21. Delers, F., Mangeney, M., Raffa, D., Vallet-Colom, I., Daveau, M., Tran-Quang, N., Davrinches, C., and Chambaz, J. (1989) Changes in Rat Liver mRNA for Alpha-1-Acid-Glycoprotein, Apolipoprotein E, Apolipoprotein B and Beta-Actin After Mouse Recombinant Tumor Necrosis Factor Injection, *Biochem. Biophys. Res. Comm. 161*, 81–88.
22. Wang, C.N., McLeod, R.S., Yao, Z., and Brindley, D.N. (1995) Effects of Dexamethasone on the Synthesis, Degradation, and Secretion of Apolipoprotein B in Cultured Rat Hepatocytes, *Arterioscler. Thromb. Vasc. Biol. 15*, 1481–1491.
23. Pullinger, C.E., North, J.D., Teng, B-B., Rifici, V.A., Ronchild de Brito, A.E., and Scott, J. (1989) The Apoprotein B Gene Is

Constitutively Expressed in Hep G2 Cells: Regulation of Secretion by Oleic Acid, Albumin, and Insulin, and Measurement of Half-life, *J. Lipid Res. 30*, 1065–1076.
24. Elovson, J., Huang, Y.O., Baker, N., and Kannan, R. (1981) Apolipoprotein B Is Structurally and Metabolically Heterogeneous in the Rat, *Proc. Natl. Acad. Sci. USA 78*, 157–161.
25. Davidson, N.O., Powell, L.M., Wallis, S.C., and Scott, J. (1988) Thyroid Hormone Modulates the Introduction of a Stop Codon in Rat Liver Apolipoprotein B Messenger RNA, *J. Biol. Chem. 263*, 13482–13485.
26. Chen, S.-H., Habib, G., Yang, C.-Y., Gu, Z.-W., Lee, B.R., Weng, S.-A., Silberman, S.R., Cai, S.-J., Deslypere, J.P., Rosseneu, M., *et al*. (1987) Apolipoprotein B-48 Is the Product of a Messenger RNA with an Organ-Specific In-frame Stop Codon, *Science 238*, 363–366.
27. Leighton J.K., Joyner, J., Zamarripa, J., Deines, M., and Davis, R.A. (1990) Fasting Decreases Apolipoprotein B mRNA Editing and the Secretion of Small Molecular Weight ApoB by Rat Hepatocytes: Evidence That the Total Amount of Apo B Secreted Is Regulated Post-Transcriptionally, *J. Lipid Res. 31*, 1663–1668.
28. Davis, R.A., Boogaerts, J.R., Borchardt, R.A., Malone-McNeal, M., and Archambault-Schexnayder, J. (1985) Intrahepatic Assembly of Very Low Density Lipoproteins: Varied Synthetic Response of Individual Apolipoproteins to Fasting, *J. Biol. Chem. 260*, 14137–14144.
29. Borchardt, R.A., and Davis, R.A. (1987) Intrahepatic Assembly of Very Low Density Lipoproteins. Rate of Transport Out of the Endoplasmic Reticulum Determines Rate of Secretion, *J. Biol. Chem. 262*, 16394–16402.
30. Davis, R.A., and Boogaerts, J.R. (1982) Intrahepatic Assemby of Very Low Density Lipoproteins: Effect of Fatty Acids on Triacylglycerol and Apolipoprotein Synthesis, *J. Biol. Chem. 257*, 10908–10913.
31. Boogaerts, J.R., Malone-McNeal, M., Archambault-Schexnayder, J., and Davis, R.A. (1984) Dietary Carbohydrate Induces Lipogenesis and Very Low-Density Lipoprotein Synthesis, *Am. J. Physiol. 246 (Endocrinol. Metab. 9)*, E77–E83.
32. Kosykh, V.A., Novikov, I.N., Trakht, N., Podrez, E.A., Victorov, A.V., Repin, V.S., and Smirov, V.N. (1991) Effect of Chylomicron Remnants on Cholesterol Metabolism in Cultured Rabbit Hepatocytes: Very Low Density Lipoprotein and Bile Acid Production, *Lipids 26*, 799–805.
33. Wu, X., Sakata, N., Dixon, J., and Ginsberg, H.N. (1994) Exogenous VLDL Stimulates Apolipoprotein B Secretion from HepG2 Cells by Both Pre- and Post-translational Mechanisms, *J. Lipid Res. 35*, 1200–1210.
34. Ooyen, C., Zecca, A., Zanelli, T., and Catapano, A.L. (1997) Decreased Intracellular Degradation and Increased Secretion of apo B-100 in Hep G2 Cells After Inhibition of Cholesteryl Ester Synthesis, *Atherosclerosis 130*, 143–152.
35. Twisk. J., Gillian-Daniel, D.L., Tebon, A., Wang, L., Barrett, P.H.R., and Attie, A.D. (2000) The Role of the LDL Receptor in Apolipoprotein B Secretion, *J. Clin. Invest. 105*, 521–532.
36. Read, T.E., Harris, H.W., Grunfeld, C., Feingold, K.R., Kane, J.P. and Rapp, J.H. (1993) The Protective Effect of Serum Lipoproteins Against Bacterial Lipopolysaccharide, *Eur. Heart J. 14(Suppl.)*, 125–129.
37. Lanza-Jacoby, S., Sedkova, N., Phetteplace, H., and Perrotti, D. (1997) Sepsis-Induced Regulation of Lipoprotein Lipase Expression in Rat Adipose Tissue and Soleus Muscle, *J. Lipid Res. 38*, 69–78.

[Received October 18, 1999, and in revised form May 9, 2000; revision accepted July 7, 2000]

Table 2. Apo B and apo E mass of cell plus media as measured by ELISA

	μg/mg protein	
.	Control	Septic
Apo B	1.40±0.6	1.25±0.5
Apo E	0.81±0.25	0.93±0.16

.Values are mean±S.D. n=9 for apo B and n=4 for apo E.

PLEASE NOTE:

The above table was:
a) not called out in text
b) there was no hard-copy run out

PLEASE ADVISE: Robbie/TS

Cu^{2+}-Induced Low Density Lipoprotein Peroxidation Is Dependent on the Initial O_2 Concentration: An O_2 Consumption Study

John K. Lodge[a,*], Maret G. Traber[b], and Peter J. Sadler[a,1]

[a]Department of Chemistry, Birkbeck College, University of London, Gordon House and Christopher Ingold Laboratories, London WC1H OPP, United Kingdom, and [b]Linus Pauling Institute, Oregon State University, Corvallis, Oregon 97331-6512

ABSTRACT: Atherosclerotic plaques form in the arterial intima, where low density lipoprotein (LDL) is thought to be oxidatively modified at sites which may contain catalytic amounts of copper in the presence of low O_2 tension. We have investigated O_2 consumption during LDL peroxidation induced by Cu^{2+} ions *in vitro* and found two phases: a lag phase followed by a phase of rapid O_2 consumption. The length of the lag phase was dependent on Cu^{2+} and on initial O_2 concentrations; increasing either decreased the lag time; however, LDL concentration had no effect. LDL-induced Cu^{2+} reduction, however, was not affected by low initial O_2 concentrations, suggesting that O_2 is not required for LDL-mediated reduction of Cu^{2+}. Following the lag phase, O_2 consumption was dependent upon LDL or initial O_2 concentrations; Cu^{2+} concentrations had little effect, suggesting that the propagation phase is more dependent on the presence of LDL lipids and O_2 as substrates for the reaction. In summary, LDL peroxidation takes place in the presence of Cu^{2+} at low O_2 tension; however, the reaction is dependent upon initial O_2 concentrations; increases shorten the lag phase and accelerate O_2 consumption.

Paper no. L8251 in *Lipids 35*, 1087–1092 (October 2000).

Oxidation of polyunsaturated fatty acids (peroxidation) is a complex chain reaction, and can be initiated by either free radicals or lipoxygenase enzymes (1). Peroxidation involves a rearrangement of double bonds forming conjugated diene systems and the uptake of O_2, leading to the production of various isomeric hydroperoxides. The reaction is sustained, in the presence of O_2, by the abstraction of hydrogens from nearby lipids. Consequently, a single initiating event can lead to the formation of many hydroperoxide molecules. A commonly cited hypothesis for the pathogenesis of atherosclerosis involves formation of oxidatively modified low density lipoproteins (LDL) in the artery wall as a result of lipid peroxidation (2,3).

The precise initiating event in LDL peroxidation *in vivo* remains unclear; however, the addition of Cu^{2+} ions is a commonly used technique to induce these reactions *in vitro*. Indeed, Cu^{2+}-modified LDL shares properties with LDL oxidized by cells, a process that is also believed to involve transition metal ions (4,5). Significant amounts of copper have been detected in atherosclerotic plaques (6–8), and catalytic amounts of copper and iron are released from the intima after mechanical disruption (9), highlighting a possible role for transition metal-induced lipid peroxidation in the pathogenesis of atherosclerosis. However, markers of copper-induced LDL oxidation in atherosclerotic plaques have suggested that copper has a role only at an advanced stage (10).

In vivo LDL is thought to be peroxidized only when trapped within the arterial wall (2). The microenvironment of the arterial intima is such that O_2 saturation (11) and pH are low. Oxygen saturation may be lower here than surrounding tissues as a result of increased O_2 consumption by the growing atheroma (2,11), or by the altered permeability of the artery wall, caused by endothelial damage.

Although O_2 is fundamental to lipid peroxidation, few studies investigating O_2 uptake during LDL oxidation *in vitro* have been carried out. Oxygen consumption during LDL peroxidation has been measured (12–14); however, variations in response to O_2 saturation were not evaluated. In this study we have investigated the role of O_2 in Cu^{2+}-induced LDL peroxidation, and in particular, the role of the initial O_2 concentration in determining lag time and propagation rates.

MATERIALS AND METHODS

LDL isolation. LDL was isolated from heparinized blood of nonfasted, healthy, normolipidemic volunteers by fast protein liquid chromatography (FPLC) as described previously (15), using a modification of published methods (16,17). Occasionally, LDL was concentrated from plasma by precipitation with phosphotungstate and magnesium, as previously described (15,18), then purified by FPLC. The protein content of the pooled LDL fractions was determined by a variation of the Lowry method (Total protein–micro, Sigma diagnostics). The LDL solution was converted to molarity using an apoprotein

*To whom correspondence should be addressed at School of Biological Sciences, University of Surrey, Guildford, Surrey GU2 7XH, UK.
E-mail: j.lodge@surrey.ac.uk

[1]Present address: Department of Chemistry, University of Edinburgh, West Mains Road, Edinburgh EH9 3JJ, UK.

Abbreviations: apoB, apoprotein B; FPLC, fast protein liquid chromatography; LDL, low density lipoprotein; PBS, phosphate-buffered saline; UV, ultraviolet.

B (apoB) molecular size of 500,000. LDL was stored in sealed vials at 4°C and used within 2 d of isolation.

O_2 uptake. Oxygen uptake was followed using a Clarke-type O_2 electrode (Rank Brothers, Cambridge, England). The platinum electrode was polished, and the semipermeable membrane changed every other day prior to use. The electrode was calibrated to a chart-recorder using air-saturated phosphate-buffered saline (PBS) pH 7.4 as the 100% O_2 mark; the 0% O_2 mark was achieved by addition of sodium dithionate crystals to the PBS. The final volume of the reaction cell was 3600 μL. The percentage O_2 was converted to molarity, taking air-saturated buffer to contain 240 μM O_2 according to published approximate values (19,20).

LDL peroxidation. At the start of the experiment, after setup of the electrode, PBS (0.1 M phosphate, 0.15 M NaCl, pH 7.4) was added to the chamber and allowed to air-equilibrate for 10 min. LDL, at the requisite concentration, was then added, and the top placed on the chamber. The recorder was set at the 100% O_2 mark. After a baseline was recorded, Cu^{2+} was added *via* injection through the plug, and the O_2 consumption was followed. For various experiments, either the LDL concentration was varied (0.01–0.106 μM) keeping the Cu^{2+} concentration constant (2.77 μM), or the Cu^{2+} concentration was varied (0.27–5.53 μM), while the LDL concentration was kept constant (0.052 μM). In other experiments the initial O_2 concentration was varied (480-43 μM) *via* degassing with helium or bubbling with pure O_2, while the LDL and Cu^{2+} concentrations were kept constant (0.054 and 2 μM, respectively), and the temperature sustained at 24°C.

Cu^+ formation. LDL-mediated Cu^{2+} reduction was measured photometrically using the specific Cu^+ probe bathocuprione. The bathocuprione:Cu^+ complex exhibits a maximum at 480 nm (ε = 9047 M^{-1} cm^{-1}) (21). Bathocuprione (300 μM) was incubated with LDL (100 μg/mL ~0.2 μM) in PBS at pH 7.4. The reaction was followed after addition of Cu^{2+} (15 μM). Experiments were performed with air-saturated PBS, or that which was degassed with helium to ~20% of the original O_2 concentration as measured with the O_2 electrode. The ultraviolet (UV) cuvette was sealed and the cap coated with petroleum jelly (Vaseline) to prevent O_2 exchange.

UV spectroscopy. Electronic absorption spectroscopy was carried out on a PerkinElmer Lambda 16 spectrometer using 0.5 mL of solution in 1-cm pathlength cells. Parallel conjugated diene assays were undertaken *via* measurement of absorbance at 234 nm. Similar concentrations of LDL and Cu^{2+} were used as described in the above sections.

Kinetics. Kinetic analyses of O_2 consumption data were carried out during the propagation phase. Rates were determined from the gradient of the line from $\ln(a - x)$ vs. t, where $(a - x)$ is the O_2 concentration at time t, minus the initial O_2 concentration.

RESULTS

Oxygen uptake during Cu^{2+}-induced LDL peroxidation typically shows a lag phase of slow consumption followed by an increased O_2 consumption phase, then a second phase of slow consumption. These phases are comparable to the characterized lag, propagation, and termination phases identified with a conjugated diene assay (22) under similar conditions used in this study.

Varying LDL concentration. To estimate the effect of LDL concentration on O_2 uptake, the final LDL concentration in the reaction chamber was varied from 0.01 to 0.106 μM, while the Cu^{2+} concentration was kept constant at 2.77 μM (Fig. 1). Lag times were unaffected by LDL concentrations and were all approximately 50 min. However, each curve plateaued at a different point, dependent upon the initial LDL concentration such that the final O_2 concentration decreased with increasing LDL concentration. A conjugated diene assay from similar experiments (data not shown) also revealed that lag time was unchanged, but that the maximal absorbance at 234 nm increased with increasing LDL concentrations.

Varying Cu^{2+} concentration. To evaluate the effect of copper on O_2 consumption, the LDL concentration was kept constant (0.053 μM), and the Cu^{2+} concentration was varied from 0.27 to 5.53 μM (Fig. 2). Oxygen consumption curves were parallel for each Cu^{2+} concentration, and after 250 min all curves were at a similar level.

Varying the initial O_2 concentration. To evaluate the rates of O_2 consumption when O_2 is limiting or in excess, the LDL and Cu^{2+} concentrations were kept constant (0.053 and 2.77 μM, respectively), and the initial O_2 concentration was varied from 43 to 480 μM (18–200% of control) (Fig. 3). When the initial O_2 concentration was 240 μM (100%, air-saturated solution) or higher, O_2 consumption plateaued at 100 min,

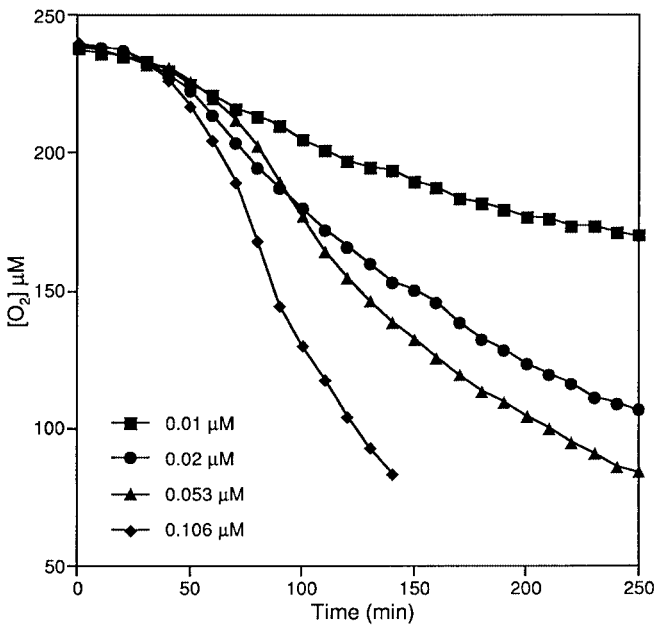

FIG. 1. Varying the low density lipoprotein (LDL) concentration affects O_2 consumption during Cu^{2+}-catalyzed peroxidation of LDL. The LDL concentration was varied as shown with a fixed Cu^{2+} concentration of 2.77 μM and an initial O_2 concentration of 240 μM at 24°C. Shown are representative traces of at least duplicate independent experiments.

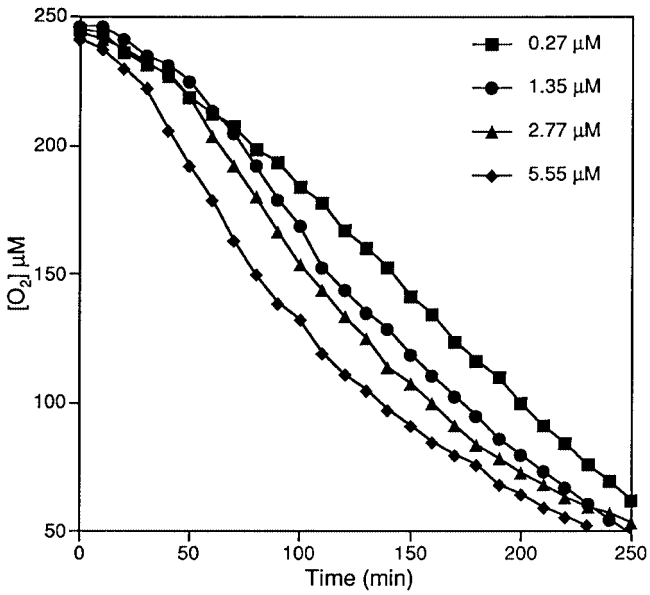

FIG. 2. Varying the Cu^{2+} concentration affects O_2 consumption during Cu^{2+}-catalyzed peroxidation of LDL. The Cu^{2+} concentration is varied as shown with a fixed LDL concentration of 0.053 μM and an initial O_2 concentration of 240 μM at 24°C. Shown are representative traces of at least duplicate independent experiments. See Figure 1 for abbreviation.

and the reaction did not result in complete O_2 depletion. This was not the case when the initial O_2 concentration was lower. Here the O_2 consumption following the lag phase was slow and came to an abrupt halt because the O_2 had been depleted

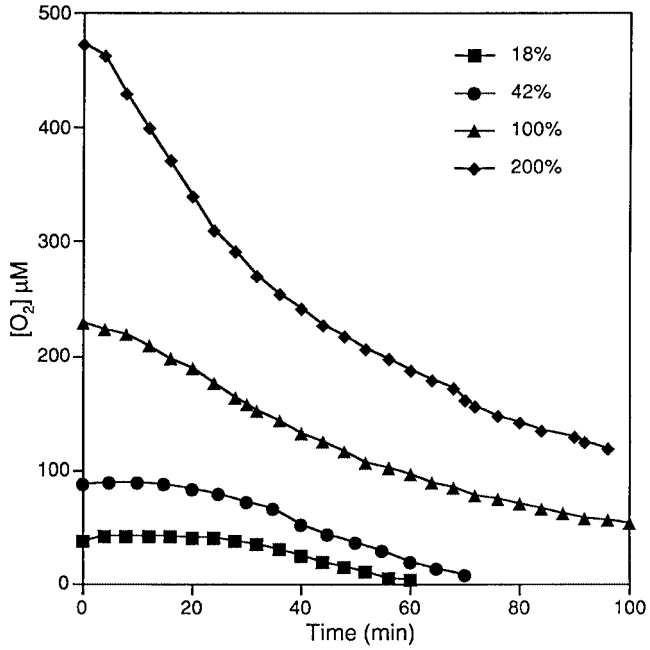

FIG. 3. Varying the initial O_2 concentration affects O_2 consumption during Cu^{2+}-catalyzed peroxidation of LDL. The initial O_2 concentration was varied as shown. Cu^{2+} and LDL concentrations are 2.77 and 0.053 μM, respectively, at 24°C. Representative traces of at least duplicate independent experiments are shown. See Figure 1 for abbreviation.

in the chamber. Addition of O_2 at this stage resulted in immediate O_2 uptake, at a similar rate to that observed prior to O_2 depletion (data not shown).

O_2 consumption lag times. Figure 4 shows graphically the effect of the above variables on the lag time of Cu^{2+}-mediated LDL peroxidation measured by O_2 consumption. While increasing the LDL concentration (Fig. 4A) had no effect on lag time, increasing Cu^{2+} concentration (Fig. 4B), or initial O_2 concentration (Fig. 4C) decreased the lag time. Indeed, there was a linear correlation between lag-time and Cu^{2+} concentration over the range studied ($r^2 = 0.973$), while increasing the initial O_2 concentration caused an exponential decrease in the lag time ($r^2 = 0.95$).

O_2 consumption rates. In order to obtain O_2 consumption rates, the O_2 uptake over a given period during the propagation phase was calculated as $d[O_2]/dt$. Oxygen uptake increased linearly with increasing LDL ($r^2 = 0.968$) (Fig. 5A) or exponentially with increasing initial O_2 concentration ($r^2 = 0.98$) (Fig. 5C). Increasing the Cu^{2+} concentration also linearly increased oxygen uptake ($r^2 = 0.982$) but not markedly (Fig. 5B); a fivefold increase in Cu^{2+} concentration did not even double the rate of O_2 consumption. Also the intercept of this graph (Fig. 5B) did not go through zero indicating that in the absence of Cu^{2+}, O_2 is consumed. In a control experiment with no added Cu^{2+}, O_2 was consumed at a steady rate, but only after a long lag time. The rate of this consumption is shown on the graph as the zero Cu^{2+} point.

Cu^+ formation. Since LDL is known to reduce Cu^{2+} and this may be an important step in the initiation process, LDL-mediated Cu^{2+} reduction was investigated at low initial concentrations of O_2. Figure 6 shows a typical experiment, comparing Cu^+ formation in control (air-saturated) and at low initial O_2 concentrations. No differences between the two treatments are seen, suggesting that LDL reduces Cu^{2+} equally well at normal and low O_2 concentrations. These data indicate that O_2 is not required for LDL-mediated reduction of Cu^{2+} to Cu^+.

DISCUSSION

In this study we investigated various parameters which could modulate the time course of Cu^{2+}-mediated LDL peroxidation by monitoring O_2 consumption. We demonstrate here that varying the Cu^{2+} concentration and the initial O_2 concentration, but not the LDL concentration, will affect peroxidation lag times. During the propagation phase, O_2 consumption rates are dependent upon LDL concentration and initial O_2 concentration, but do not vary much with Cu^{2+} concentration.

Although the importance of O_2 concentrations in peroxidation reactions is unquestionable, there have been very few reports in which the uptake of O_2 during LDL peroxidation was measured, and even fewer which have studied this reaction under various levels of O_2 saturation. This is surprising, given that the arterial intima, the probable site of LDL oxidative modification, is a site of low O_2 saturation (11,23). Since it is likely that LDL *in vivo* is peroxidized under conditions of low O_2 saturation, it is important to investigate how the initial O_2 concentration modulates LDL peroxidation.

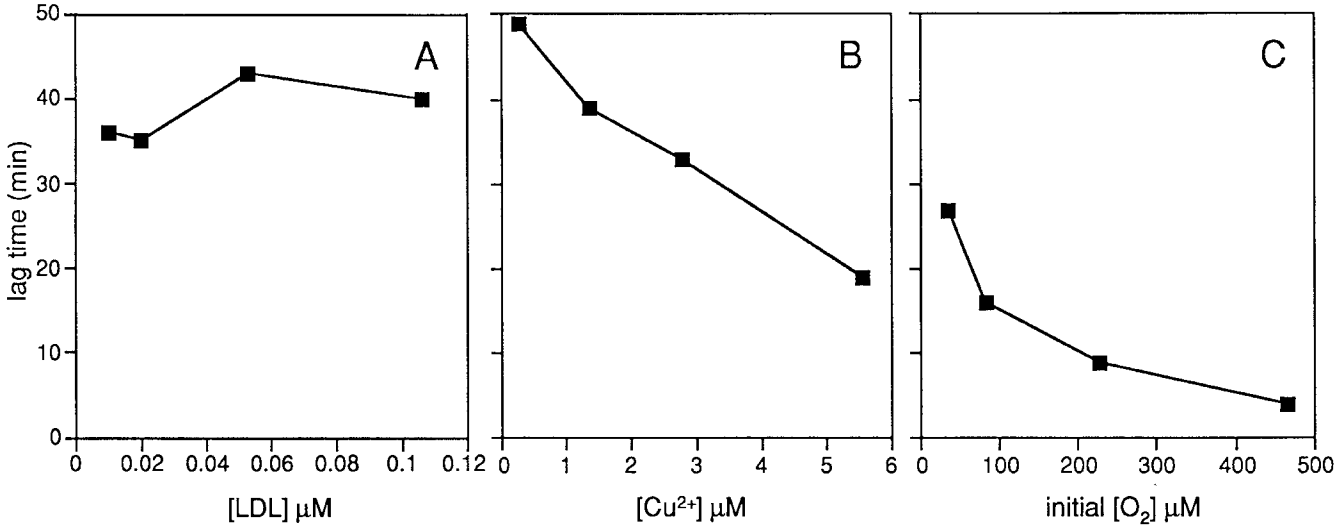

FIG. 4. Graphs showing the relationship between the reaction parameters and the lag-times of O_2 consumption during Cu^{2+}-catalyzed LDL peroxidation. Conditions are for Figures 1–3. Average values are shown from at least duplicate measurements. (A) Varying LDL concentration; (B) varying Cu^{2+} concentration; (C) varying initial O_2 concentration. Significance values for linear or exponential fits are given in the text. See Figure 1 for abbreviation.

A major observation in this study is that the lag times and O_2 consumption rates were both dependent upon the initial O_2 concentrations. At low initial O_2 concentrations the lag-phases were extended and the subsequent peroxidation rates were low (Figs. 3 and 4C). As initial O_2 concentrations increased, lag times shortened and peroxidation rates increased. Since Cu^{2+} and LDL concentrations also affected these variables, certain assumptions can be drawn regarding each phase in LDL peroxidation and are discussed in the following sections.

The lag phase. The lag times were dependent upon both initial O_2 concentrations and copper concentrations; low concentrations of either prolonged the lag times. Interestingly, lag times were not dependent upon LDL concentrations over the ranges studied (Figs. 1 and 4A); LDL concentrations were varied over 10-fold while the lag times remained relatively constant between 35 and 40 min. Since the initiation event in Cu^{2+}-induced LDL oxidation is thought to involve Cu^{2+} reduction, it is likely then that the lowest LDL concentration used was sufficient to reduce all the Cu^{2+} to Cu^{+}. Lynch and Frei (21) showed that at a constant Cu^{2+} concentration, increasing the LDL concentration beyond a certain limit resulted in no further Cu^{2+} reduction; 0.025 μM LDL (~10 μg/mL) was sufficient to reduce 10 μM Cu^{2+}. Thus, in their experiments a 400-fold excess of Cu^{2+} was reduced by

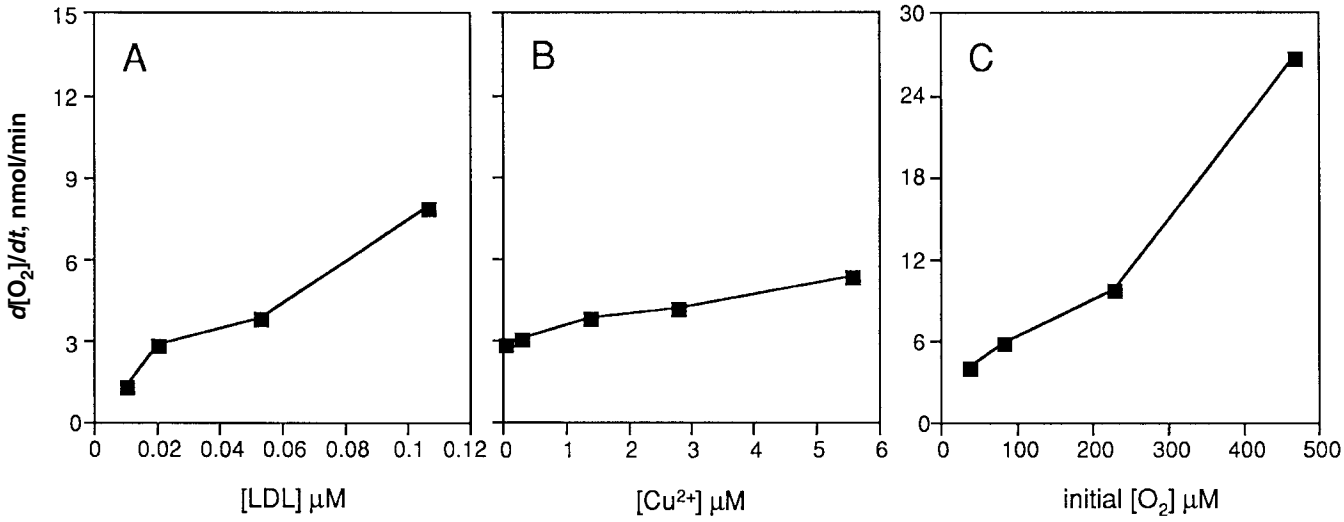

FIG. 5. Graphs showing the relationship between the reaction parameters and the rates of O_2 consumption during Cu^{2+}-catalyzed LDL peroxidation. Conditions are for Figures 1–3. Rates are taken as $d[O_2]/dt$ (nmol O_2 consumed/min) for a given period during the propagation phase. Average values are shown from at least duplicate measurements. (A) Varying LDL concentration; (B) varying Cu^{2+} concentration; (C) varying initial O_2 concentration. Significance values for linear or exponential fits are given in the text. See Figure 1 for abbreviation.

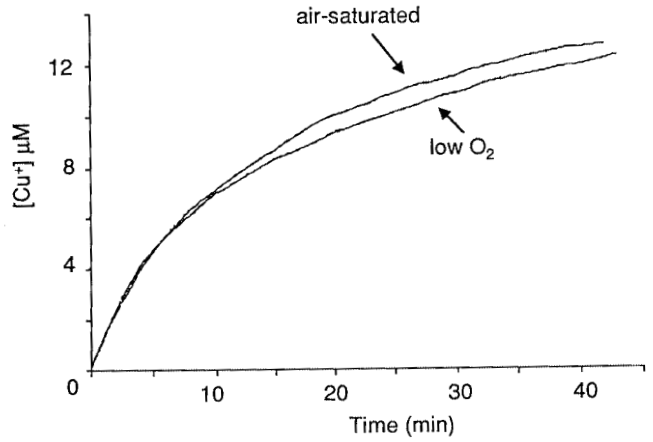

FIG. 6. Low initial O_2 concentration does not affect LDL-mediated Cu^{2+} reduction. Cu^+ formation was measured using the specific probe bathocuprione (300 μM) with LDL (100 μg/mL) and Cu^{2+} (15 μM) in either air-saturated (100% or 240 μM) or O_2 depleted (18% or 43 μM) buffer. See Figure 1 for abbreviation.

LDL, in our experiments the maximal excess of Cu^{2+} was only 280-fold.

The mechanism for Cu^{2+}-induced LDL oxidation is unknown. Reduction of Cu^{2+} may be important, and the reductant for Cu^{2+} in LDL has been proposed to be α-tocopherol (24,25), although lipid hydroperoxides may play a role (27,28). LDL also binds copper , and a number of these binding sites are believed to be reactive (29). It has been shown that peroxidation of LDL lipids only proceeds with normal kinetics when Cu^{2+} binds preferentially to sites on apoB that contain histidine residues, and that these sites are not involved in Cu^{2+} reduction (29). LDL-mediated Cu^{2+} reduction was unaffected by a low initial O_2 concentration (Fig. 6); however, the lag times were dependent on initial O_2 concentrations (Figs. 3, 4C). Thus, O_2 must be involved in the initiating event, but not with Cu^{2+} reduction. One potential explanation is the formation of a reactive intermediate species between copper and O_2; however, no direct evidence is presented here. One would expect that if the initiating species were derived from a reaction between Cu^+ and O_2, then adding Cu^+ directly would be highly prooxidant. Studies have shown this not to be the case. Cu^+ does not oxidize LDL efficiently, and antagonizes α-tocopherol depletion and lipid peroxidation under certain conditions (30).

Therefore, it is likely that a radical chain event involving O_2 occurs upon Cu^{2+} reduction, the number of reactive species formed being proportional to the O_2 and Cu^{2+} concentrations, hence a requirement for LDL-induced Cu^{2+} reduction.

The propagation phase. The propagation phase immediately follows the lag phase, and it is characterized by a rapid increase in hydroperoxide formation and, as shown in these experiments, O_2 consumption. All variables tested appeared to affect the rate of O_2 uptake during this phase; however, varying Cu^{2+} concentration had the smallest effect (Fig. 2). Increasing the copper concentration has been shown previously to increase the rate of peroxidation (28), however, in those systems O_2 was not limiting. Presumably, because Cu^{2+} was in excess over the LDL concentration, further increases in Cu^{2+} had little effect as excess radicals had been generated. Indeed the rate of hydroperoxide formation has been shown to depend on the ratio of bound Cu^{2+} to LDL (31).

It is interesting that increasing the LDL concentration increased the rate of peroxidation (Figs. 1, 5A). In this respect LDL is behaving as a prooxidant species, although it has been shown that LDL particles do not rapidly exchange radicals (32). It appears that LDL concentrations (or to be more specific, LDL polyunsaturated fatty acids) are rate-limiting for peroxidation. This is not surprising since LDL is the substrate. Indeed, total O_2 consumption was proportional to the LDL concentration (Fig. 1). Interestingly though, Noguchi *et al.* (14) proposed from their studies that a proportion of oxygen uptake by oxidizing LDL could not be accounted for by conjugated diene or total peroxides. Similarly, O_2 concentration is a dependent factor and is also a substrate. Oxygen is required both for the initial reactive species and for the formation of hydroperoxides.

Similar findings were reported by Hatta and Frei (33) and Reaven *et al.* (34) who both found decreased rates of LDL oxidation at lower O_2 concentrations, indicating that O_2 concentration is a rate-limiting factor for LDL peroxidation.

The termination phase. The rate of O_2 consumption only slows during the termination phase, suggesting that hydroperoxide formation is still occurring, but the extent of hydroperoxide breakdown must exceed formation. This termination phase is dependent upon the LDL concentration. This is not surprising since LDL is the substrate for the reaction, hence when the substrate reaches low concentrations then the rate of reaction must slow. In following this rationale it would be expected that as the O_2 concentration falls (as it is being consumed in the reaction vessel) the rate of O_2 uptake and hence peroxidation would also fall. This was clearly not the case (Fig. 3). When the initial O_2 concentration was low, O_2 uptake came to an abrupt stop when the O_2 concentration in the reaction vessel fell below a critical level (1.5%). The rate of O_2 consumption only decreases when the LDL polyunsaturated fatty acid concentration is low, that is, when the termination phase begins.

These findings possibly have *in vivo* implications since atherosclerotic lesions are known to be ischemic, engorged with LDL lipids, and contain redox active transition metals. In such circumstances peroxidation could readily occur, and will not be limited by low O_2 concentrations.

ACKNOWLEDGMENT

This work was supported by the British Heart Foundation.

REFERENCES

1. Halliwell, B., and Gutteridge, J.M.C. (1998) *Free Radicals in Biology and Medicine,* Clarendon Press, Oxford, pp. 289–296.
2. Steinberg, D., Parthasarathy, S., Carew, T.E., Khoo, J.C., and Witztum, J.L. (1989) Beyond Cholesterol. Modifications of

Low-Density Lipoprotein That Increase Its Atherogenicity, *New Engl. J. Med. 320,* 915–924.
3. Esterbauer, H., Gebicki, J., Puhl, H., and Jurgens, G. (1992) The Role of Lipid Peroxidation and Antioxidants in Oxidative Modification of LDL, *Free Radical Biol. Med. 13,* 341–390.
4. Sparrow, C.P., and Olszewski, J. (1993) Cellular Oxidation of Low Density Lipoprotein Is Caused by Thiol Production in Media Containing Transition Metal Ions, *J. Lipid Res. 34,* 1219–1228.
5. Heinecke, J.W., Kawamura, M., Suzuki, L., and Chait, A. (1993) Oxidation of Low Density Lipoprotein by Thiols: Superoxide-Dependent and -Independent Mechanisms, *J. Lipid Res. 34,* 2051–2061.
6. Smith, C., Mitchinson, M.J., Aruoma, O.I., and Halliwell, B. (1992) Stimulation of Lipid Peroxidation and Hydroxyl-Radical Generation by the Contents of Human Atherosclerotic Lesions, *Biochem. J. 286,* 901–905.
7. Swain, J., and Gutteridge, J.M.C. (1995) Prooxidant Iron and Copper, with Ferroxidase and Xanthine Oxidase Activities in Human Atherosclerotic Material, *FEBS Lett. 368,* 513–515.
8. Lamb, D.J., Mitchinson, M.J., and Leake, D.S. (1995) Transition Metal Ions Within Human Atherosclerotic Lesions Can Catalyse the Oxidation of Low Density Lipoprotein by Macrophages, *FEBS Lett. 374,* 12–16.
9. Evans, P.J., Smith, C., Mitchinson, M.J., and Halliwell, B. (1995) Metal Ion Release from Mechanically Disrupted Human Arterial Wall. Implications for the Development of Atherosclerosis, *Free Radical Res. 23,* 465–469.
10. Leuwenburgh, C., Rasmussen, J.E., Hsu, F.F., Mueller, D.M., Penathur, S., and Heinecke, J.W. (1997) Mass Spectrometric Quantification of Markers for Protein Oxidation by Tyrosyl Radical, Copper, and Hydroxyl Radical in Low Density Lipoprotein Isolated from Human Atherosclerotic Plaques, *J. Biol. Chem. 272,* 3530–3535.
11. Hajjar, D.P., Faber, I.C., and Smith, S.C. (1988) Oxygen Tension Within the Arterial Wall: Relationship to Altered Bioenergetic Metabolism and Lipid Accumulation, *Arch. Biochem. Biophys. 262,* 375–380.
12. Laranjinha, J.A.N., Almedia, L.M., and Madeira, V.M.C. (1994) Reactivity of Dietary Phenolic Acids With Peroxyl Radicals: Antioxidant Activity Upon Low Density Lipoprotein Peroxidation, *Biochem. Pharmacol. 48,* 487–494.
13. Noguchi, N., Gotoh, N., and Niki, E. (1993) Dynamics of the Oxidation of Low Density Lipoprotein Induced by Free Radicals, *Biochim. Biophys. Acta 1168,* 348–357.
14. Noguchi, N., Numano, R., Kaneda, H., and Niki, E. (1998) Oxidation of Lipids in Low Density Lipoprotein Particles, *Free Radical Res. Comm. 29,* 43–52.
15. Lodge, J.K. (1993) NMR Investigations of Lipoprotein Modifications, Ph.D. Thesis, University of London, London, pp. 29–74.
16. Ha, Y.C., and Barter, P.J. (1985) Rapid Separation of Plasma Lipoproteins by Gel Permeation Chromatography on Agarose Gel Superose 6B, *J. Chromatogr. Biomed. Appl. 341,* 154–159.
17. Cole, T., Kitchens, R., Daugherty, A., and Schonfeld, G. (1988) *FPLC Biocomm. 4,* 4–6.
18. Burstein, M., and Scholnick, H.R. (1973) Lipoprotein-Polyanion-Metal Interactions, *Adv. Lipid Res. 11,* 67–108.
19. Vanderkooi, J.M., Maniara, G., Green, T.J., and Wilson, D.F. (1987) An Optical Method for Measurement of Dioxygen Concentration Based Upon Quenching of Phosphorescence, *J. Biol. Chem. 262,* 5476–5482.
20. Yomo, T., Urabe, I., and Okado, H. (1989) Enzymatic Method for Measuring the Absolute Value of Oxygen Concentration, *Anal. Biochem. 179,* 124–126.
21. Lynch, S.M., and Frei, B. (1995) Reduction of Copper, but Not Iron, by Human Low Density Lipoprotein (LDL). Implications for Metal Ion-Dependent Oxidative Modification of LDL, *J. Biol. Chem. 270,* 5158–5163.
22. Esterbauer, H., Dieber-Rotheneder, M., Waeg, G., Striegl, G., and Jurgens, G. (1990) Biochemical, Structural and Functional Properties of Oxidized Low-Density Lipoprotein, *Chem. Res. Toxicol. 3,* 77–92.
23. Crawford, D.W., and Blankenhorn, D.H. (1991) Arterial Wall Oxygenation, Oxyradicals, and Atherosclerosis, *Atherosclerosis 89,* 97–108.
24. Kontush, A., Meyer, S., Finckh, B., Kohlschutter, A., and Beisiegel, U. (1996) α-Tocopherol as a Reductant for Cu(II) in Human Lipoproteins, *J. Biol. Chem. 271,* 11106–11112.
25. Perugini, C., Seccia, M., Bagnati, M., Cau, C., Albano, E., and Bellomo, G. (1998) Different Mechanisms are Progressively Recruited to Promote Cu(II) Reduction by Isolated Human Low-Density Lipoprotein Undergoing Oxidation, *Free Radical Biol. Med. 25,* 519–528.
26. Patel, R., Svistunenko, D., Wilson, M.T., and Darley-Usmar, V. (1997) Reduction of Cu(II) by Lipid Hydroperoxides: Implications for the Copper-Dependent Oxidation of Low-Density Lipoprotein, *Biochem. J. 322,* 85–92.
27. Kuzuya, M., Yamada, K., Hayashi, T., Funaki, C., Naito, M., Asai, K., and Kuzuya, F. (1992) Role of Lipoprotein–Copper Complex in Copper-Catalyzed Peroxidation of Low-Density Lipoprotein, *Biochim. Biophys. Acta 1123,* 334–341.
28. Gieseg, S.P., and Esterbauer, H. (1994) Low Density Lipoprotein Is Saturable by Pro-Oxidant Copper, *FEBS Lett. 343,* 188–194.
29. Wagner, P., and Heinecke, J.W. (1997) Copper Ions Promote Peroxidation of Low Density Lipoprotein Lipid by Binding to Histidine Residues of Apolipoprotein B100, but They Are Reduced at Other Sites on LDL, *Arterioscler. Thromb. Vasc. Biol. 17,* 3338–3346.
30. Bagnati, M., Bordone, R., Perugini, C., Cau, C., Albano, E., and Bellomo, G. (1998) Cu(I) Availability Paradoxically Antagonizes Antioxidant Consumption and Lipid Peroxidation During the Initiation of Copper-Induced LDL Oxidation, *Biochem. Biophys. Res. Comm. 253,* 235–241.
31. Pinchuk, I., Schnitzer, E., and Lichtenberg, D. (1998) Kinetic Analysis of Copper-Induced Peroxidation of LDL, *Biochim. Biophys. Acta 1389,* 155–172.
32. Thomas, M.J., Chen, Q., Franklin, C., and Rudel, L.L. (1997) A Comparison of the Kinetics of Low-Density Lipoprotein Oxidation Initiated by Copper or by Azobis (2-amidinopropane), *Free Radical Biol. Med. 23,* 927–935.
33. Hatta, A., and Frei, B. (1995) Oxidative Modification and Antioxidant Protection of Human Low Density Lipoprotein at High and Low Oxygen Partial Pressures, *J. Lipid Res. 36,* 2383–2393.
34. Reaven, P.D., Ferguson, E., Navab, M., and Powell, F.L. (1994) Susceptibility of Human LDL to Oxidative Modification. Effects of Variations in β-Carotene Concentration and Oxygen Tension, *Arterioscler. Thromb. 14,* 1162–1169.

[Received May 3, 1999, and in revised form May 3, 2000; revision accepted August 12, 2000]

Adaptation of Composition and Biophysical Properties of Phospholipids to Temperature by the Crustacean, *Gammarus* spp.

Eila Lahdes[a], Gabor Balogh[b], Elfrieda Fodor[b], and Tibor Farkas[b,*]

[a]Finnish Institute of Marine Research, FIN-00930 Helsinki, Finland, and [b]Institute of Biochemistry, Biological Research Center, Hungarian Academy of Sciences, H-6701 Szeged, Hungary

ABSTRACT: The compositions of lipid classes as well as the molecular species composition of subclasses (diacyl, alkylacyl, and alkenylacyl forms) of choline and ethanolamine phosphoglycerides in marine amphipod crustaceans, *Gammarus* spp., collected in the Baltic Sea at 8 and 15°C, were studied in relation to environmental temperature. The structural order of phospholipid multibilayers was also determined. Environmental temperature had little effect on fatty acid composition. The level of some polyunsaturated fatty acids, such as 20:4, even increased in choline and ethanolamine phosphoglycerides at 15°C. Ethanolamine phosphoglycerides were rich in alkenylacyl forms, especially in crustaceans collected at 15°C. The accumulation of *sn*-1 monoenic, *sn*-2 polyenic diacyl, alkyl, and alkenylacyl phosphatidylethanolamines and diacyl phosphatidylcholines was observed at 8°C. The phospholipid vesicles of crustaceans collected at 8°C were more disordered than expected compared to those obtained from animals collected at 15°C. It was concluded that, in addition to variations in the levels of *sn*-1 monoenic and *sn*-2 polyenic phospholipid molecular species with temperature, ethanolamine plasmalogens may play a role in controlling membrane biophysical properties in marine amphipod crustaceans.

Paper no. L8470 in *Lipids 35*, 1093–1098 (October 2000).

An inherent property of cells in poikilothermic animals is their capacity to adjust the physicochemical characteristics of their membranes to prevailing temperatures. The so-called homeoviscous adaptation of membrane fluidity was first described by Sinensky in *Escherichia coli* (1), and this observation was extended to numerous invertebrate (2–4) and poikilothermic vertebrate species, from fish to birds (5,6). In fish, during adaptation to reduced temperatures, unsaturation of the constituent fatty acids increases (7–9), with the polar head group as well as the molecular species composition of membrane phospholipids being reorganized. Hazel *et al.* (10) demonstrated that exposure to cold results in an increase of a wedge-shaped phospholipid, phosphatidylethanolamine (PE), in the membranes of the gills of rainbow trout. This response was shown to occur with freshwater planktonic crustaceans (11), but not with marine calanoid copepods collected around Norway and India (2). One of the most spectacular changes taking place with phosphatidylcholines (PC) and PE during the adaptation of fish to reduced temperature is the accumulation of monoenoic fatty acid in the *sn*-1 position of the molecule combined with a polyunsaturated fatty acid in position *sn*-2 (6,12). A monounsaturated fatty acid in position *sn*-1 increases the surface area which the molecule occupies in a monolayer by about 25–30% relative to its saturated homolog (13), which renders these structures ideal for controlling membrane order during thermal adaptation. Indeed, model experiments have proved that this type of phospholipids increases membrane fluidity at reduced temperatures in fish phospholipids and membranes (6).

Whereas all of these data were obtained for fish, little information is available to show whether the same response to temperature occurs in invertebrates. The nematode *Caenorhabditis elegans* also accumulates monoenoic fatty acid in position *sn*-1 of its phospholipids when grown at reduced temperatures (14). We showed earlier that the PE of the cold-adapted marine shrimps from Norway were richer in 18:1/22:6 than those collected in the southern Mediterranean Sea (15). In the present paper, the fatty acid composition of phospholipids, the molecular species composition of the two major phospholipids, PC and PE, as well as the fluidity of phospholipid vesicles obtained from a Baltic Sea amphipod crustacean, *Gammarus* spp. collected from different thermal environments, are compared. It is hoped that studying the molecular composition of membrane phospholipids in invertebrates that are evolutionally or seasonally adapted to extreme temperatures will shed some light on the strategies followed by the vertebrates and invertebrates in order to preserve the structural and functional integrity of their membranes under various thermal conditions.

MATERIAL AND METHODS

Animals. *Gammarus* spp. were collected near the Archipelago Research Institute in the Archipelago Sea (the Baltic Sea) (60°15.25′ N, 21°57.30′ E) in spring (May) and summer

*To whom correspondence should be addressed.
E-mail: epa@nucleus.szbk.u-szeged.hu

Abbreviations: DPH, 1,6-diphenyl 1,3,5-hexatriene; HPLC, high-performance liquid chromatography; PC, phosphatidylcholine; PE, phosphatidylethanolamine; TLC, thin-layer chromatography.

(August) at temperatures of 8 and 15°C, respectively. The salinity remained at the constant level of 6 ppt except in early spring after the melting of the ice, when it was *ca.* 0.5 ppt lower. Animals were sampled from a belt of *Fucus vesiculosus,* which grew freely on the sandy bottom. The depth to the bottom was 1.5–2 m. The animals were kept in aerated, filtered (using Whatman GF/C glass fiber filter) sea water at the *in situ* temperature for 24 h in order to empty their guts before quick-freezing in liquid nitrogen in a small volume of filtered sea water. Sea water was used after the observation that samples were better preserved in liquid. The storage temperature of the samples was –80°C. The populations consisted of *G. oceanicus*, *G. locusta*, and *G. zaddachi*. Because we wanted to see the variation in membrane characteristics in an existing *Gammarus* community between seasons rather than between individuals, species and sexes were not separated. *Gammarus* spp. have a wide geographical distribution in the littoral zones from the Arctic region in the north to the east coast of North America in the west. In general, they tolerate well the changes in salinity and temperature, as one would expect considering their wide geographical distribution (16).

Analytical techniques. Lipids were extracted using chloroform/methanol (2:1, vol/vol) according to Folch *et al.* (17). Silicic acid column chromatography was used to separate neutral and polar lipids. Chloroform eluted the neutral and methanol the polar lipids. The lipids were stored in benzene containing 0.01% butylated hydroxytoluene at –70°C until processing. Fatty acid methyl esters were separated on a FFAP column (0.25 mm i.d. capillary column of 30 m length from Supelco, Bellefonte, PA) in a Hewlett-Packard Model 6890 gas chromatograph, after transesterification in absolute methanol containing 5% HCl at 80°C. Peaks were identified with the aid of authentic standards such as those marketed by Sigma (St. Louis, MO).

Phospholipids were segregated according to polar head groups by thin-layer chromatography (TLC) following the method of Fine and Sprecher (18). PC and PE, after visualization with 5-amino 8-naphthalene sulfonic acid in methanol under ultraviolet light, were eluted with chloroform/methanol/H_2O (50:50:1, by vol). The purified phospholipids were then digested with phospholipase C (Sigma) and the obtained diradylglycerols were converted to fluorescent anthroyl derivatives as described by Takamura and Kito (19). Diacyl, alkylacyl, and alkenylacyl subclasses were separated on TLC and further segregated into molecular species on a Supelcosil LC-18 column (1 mm i.d. and 30 cm in length, Supelco) as well as on a C-8 column (1 mm i.d., 30 cm in length, Supelco) using a Hitachi Merck high-performance liquid chromatograph (HPLC) equipped with a fluorescent detector and acetonitrile/isopropanol (80:20, vol/vol) and methanol/water/acetonitrile (93:5:2, by vol) as solvent. Peaks were identified using authentic standards and also on an HPLC–mass spectrometer (Shimadzu SCL-10Avp connected to a Shimadzu LCMS-QP8000 mass spectrometer) using the same columns and solvents. A known amount of derivatized 12:0/12:0 was added to the spots on the TLC plate to quantify the phospholipid subclasses. The 12:0/12:0 was selected as internal standard because it did not overlap with any molecular species in the sample.

The fluidity of phospholipid vesicles was determined using 1,6-diphenyl 1,3,5-hexatriene (DPH) (Molecular Probes, Eugene, OR) in tetrahydrofuran in a molecular ratio of 1:1000 (lipid/fluorescent probe). Approximately 250 mg of phospholipids was evaporated under high vacuum onto the wall of a test tube, and the film was rehydrated in 3 mL of 20 mM Tris-HCl (pH 7.4) buffer under vigorous vortexing. The steady-state fluorescence anisotropy parameter was measured on a T-format fluorescence spectrometer (Quanta Master QM-1; Photon Technology International, Princeton, NJ) as $R_{ss} = [(R_V/R_H) - 1]/[(R_V/R_H) + 2]$, where R_V and R_H are the ratios of the intensities detected in the two emission channels with the excitation polarizer in the vertical and horizontal position, respectively. The excitation and emission wavelengths were 360 and 430 nm. The temperature of the sample was controlled by a circulating water bath and measured directly in the cuvettes with a platinum electrode. Measurements were made between 5 and 40°C using a heating rate of 0.4°C/min.

RESULTS

Table 1 shows the fatty acid composition of the neutral and polar lipids (phospholipids) of *Gammarus* spp. acclimatized to two extreme temperatures, 8 and 15°C, respectively. In general, the distribution of the fatty acids in lipids is similar to that found within gammarides such as *G. duebeni* (20,21), i.e., the level of 22:6 is lower than that of 20:5. Except for palmitoleic acid, the environmental temperature had little effect on the fatty acid composition of the separated lipid classes. Palmitoleic acid was more abundant in the triglycerides of crustaceans collected at 8°C than in those collected at 15°C. Since the fatty acid composition of the food triglycerides represents more or less the fatty acid composition of neutral lipids, it is possible that the animals at 8°C consumed food more rich in this acid. It is interesting, however, that it did not accumulate in polar lipids. Higher levels of 20:5 and 22:6 in neutral lipids at 8°C might also indicate increased uptake of these fatty acids. The linoleic (18:2), arachidonic (20:4), and eicosapentaenoic acids (20:5) in polar lipids responded to environmental temperature in the opposite sense than expected: their level was higher at 15°C than at 8°C. In contrast, the level of docosahexaenoic acid (22:6) remained unchanged. Owing to this and to the high content of 18:0 in cold-acclimatized animals (13.7 vs. 4.3%), the ratio of saturated to unsaturated fatty acids was considerably higher in phospholipids at 8°C. Both PC and PE showed little response to temperature, except 16:0 in PC at 15°C (25 vs. 20%). The presence of dimethylacetals in PE indicates the presence of ether lipids (Table 1).

Table 2 shows the subgroup composition of the major phospholipids, PC and PE. The PC fraction consisted of only diacyl forms, but in the PE fraction the ether lipids dominated. The level of ethanolamine plasmalogens was higher in animals collected from warmer environments (52.2 vs.

TABLE 1
Fatty Acid (FA) Composition (%) of Major Lipid Classes[a] in *Gammarus* spp.

		8°C				15°C			
	FA	NL	PL	PC	PE	NL	PL	PC	PE
	14:0	2.6	2.9	2.1	1.6	3.2	2.5	3.2	2.6
	14:1	0.4	ND	0.7	0.4	1.8	3.4	ND	0.7
DMA	16:0	ND	4.1	0.6	3.5	1.8	3.7	1.7	3.2
	16:0	18.3	18.6	20.1	17.4	20.1	16.4	24.6	13.1
	16:1n-7	21.3	4.7	4.1	1.9	5.3	1.5	4.7	3.5
	16:2	1.0	2.6	2.5	1.5	2.5	3.3	ND	1.4
DMA	18:0	ND	2.5	0.3	4.6	ND	2.1	ND	6.1
DMA	18:1	ND	3.0	0.4	3.3	ND	ND	ND	2.2
	18:0	5.6	13.7	25.0	15.3	14.3	4.3	23.5	15.5
	18:1n-9	10.6	9.1	13.5	8.4	10.9	7.8	11.7	7.4
	18:1n-7	5.7	0.5	3.0	1.8	3.3	1.2	ND	1.5
	18:2n1-6	2.2	3.5	3.0	5.5	6.4	4.8	5.2	4.4
	18:3n-3	1.3	2.0	0.9	1.1	3.7	1.8	1.3	1.2
	20:1n-9	2.2	3.6	0.9	ND	4.9	2.3	1.5	0.9
	20:4n-6	1.8	3.6	1.7	3.5	3.7	9.3	4.1	6.9
	20:3n-3	0.3	1.2	1.3	1.9	0.9	1.1	ND	2.4
	20:4n-3	0.4	0.4	2.3	0.7	0.5	0.6	3.3	1.7
	20:5n-3	16.2	12.6	6.5	10.0	12.6	18.0	6.6	10.6
	22:5n-6	0.7	1.4	1.5	1.8	ND	2.0	ND	1.9
	22:5n-3	ND	ND	1.4	2.0	ND	ND	ND	ND
	22:6n-3	9.5	10.2	4.4	11.6	2.7	11.7	4.6	10.0

[a]NL, neutral lipids; PL, phospholipids; PC, choline phosphoglycerides; PE, ethanolamine phosphoglycerides; DMA, dimethylacetal; ND, not detected.

68.2%). Chapelle and Benson (22) also reported high levels of ethanolamine plasmalogens in the gills of some marine decapods.

Eighteen to 20 different molecular species were separated from both phospholipids, but only the most characteristic ones are listed in Table 3. In diacyl PC the fraction 16:0/18:1 was the major component followed by 16:0/16:0. There was a seasonal variation in the levels of these species: at 8°C the levels of 16:0/18:1 and 16:0/16:0 were roughly half of those found at 15°C. The sum of the disaturated species (16:0/16:0 + 18:0/18:0) was 21 vs. 13.9% in the warm- and cold-adapted states, respectively. In diacyl PE the fraction 16:0/18:1 was also the dominant species, and its level also varied slightly with the environmental temperature: it rose from 17.7% in cold-adapted specimens to 22.1% in warm-adapted ones. In contrast to diacyl PC, 16:0/16:0 did not vary with temperature in diacyl PE. The ratios 18:1/20:5, 18:1/22:6, and 18:1/20:4 also varied with temperature in such a way that they were represented by higher values at the lower environmental temperature. It is important to note that the sum of *sn*-1 monoenic, *sn*-2 polyenic species in both PC and PE was roughly three to four times higher in the cold-adapted state than the warm-adapted state.

Twenty to 25 different molecular species were also detected in the alkylacyl and alkenylacyl forms of PE, some of them in amounts less than 0.1%; they are therefore not listed in Table 4. In the alkenylacyl form almost all the molecular

TABLE 2
Subgroup Composition of Choline and Ethanolamine Phosphoglycerides in *Gammarus* spp. Acclimatized to 8 or 15°C (as %)

	Phosphatidylcholine		Phosphatidylethanolamine	
	15°C	8°C	15°C	8°C
Diacyl	100	100	8.3	19.5
Alkylacyl	ND[a]	ND	23.5	28.3
Alkenylacyl	ND	ND	68.2	52.2

[a]ND, not detected.

TABLE 3
The Major Molecular Species in Diacylphosphatidylcholines and Diacylphosphatidylethanolamines of *Gammarus* spp. Acclimatized to 15 and 8°C (as %)

	Phosphatidylcholine		Phosphatidylethanolamine	
	15°C	8°C	15°C	8°C
18:1/20:5[a]	1.3	7.4	6.5	12.8
16:0/20:5	1.4	3.8	3.6	3.4
18:1/22:6[a]	0.8	2.6	1.4	4.8
16:0/22:6	1.9	2.0	9.4	8.2
18:1/20:4[a]	1.5	2.9	2.4	5.8
16:0/20:4	1.9	1.8	6.4	3.5
18:0/20:5	0.7	1.6	4.0	5.1
18:0/22:6	1.5	7.9	4.2	6.9
16:0/18:2	9.0	13.5	7.8	8.1
18:0/20:4	1.9	0.4	4.3	2.4
18:1/18:1	0.8	3.6	8.1	7.7
16:0/18:1	48.0	29.3	22.1	17.7
16:0/16:0	19.1	11.5	4.2	3.9
18:1/18:0	3.0	1.1	3.8	2.1
16:0/18:0	1.9	2.4	0.1	1.1
REST	7.9	12.7	6.5	—
ΣMONO/POLY[b]	3.6	12.8	10.3	29.4

[a]The presence of the reverse isomers cannot be excluded.
[b]ΣMONO/POLY represents the sum of the molecular species containing monounsaturated fatty acid in the *sn*-1 position and polyunsaturated fatty acid in the *sn*-2 position.

TABLE 4
Major Molecular Species in Ether Forms of Phosphatidylethanolamine from *Gammarus* spp. Acclimatized to 15 or 8°C (as %)

	Alkylacyl		Alkenylacyl	
	15°C	8°C	15°C	8°C
18:1a/20:5	7.2	4.5	6.0	17.5
16:0a/20:5	24.9	5.4	5.1	10.0
18:1a/22:6	ND	12.0	8.3	13.3
16:0a/22:6	ND	28.5	8.3	5.8
18:1a/22:5	ND	0.2	0.5	3.0
18:1a/20:4	5.8	1.1	4.9	2.4
16:0a/20:4	4.9	3.8	5.8	3.7
18:0a/20:5	8.0	1.5	9.6	5.7
18:0a/22:6	26.9	20.6	16.4	16.9
18:0a/20:4	2.4	1.4	5.0	4.6
16:0a/18:1	ND	ND	9.9	ND
16:0a/16:0	ND	ND	2.7	ND
REST	19.4	21.0	17.5	17.6
ΣMONO/POLY	7.2	16.7	14.8	36.6

[a]Abbreviations: a, alcohol; ND, not detected.
[b]ΣMONO/POLY represents the sum of the molecular species containing monounsaturated fatty alcohol in the *sn*-1 position and polyunsaturated fatty acid in the *sn*-2 position.

species and their sum (36.6%) containing monoenic fatty alcohol in position *sn*-1 and polyenic fatty acid in position *sn*-2 were more abundant in cold-adapted animals (except 18:1a/20:4, where "a" represents alcohol) than in warm-adapted ones, and their sum was even higher than in the diacyl forms (36.6 vs. 29.4%). Alkylacyl PE from animals collected at 8°C were also rich in these species. Molecular species containing a saturated fatty alcohol in position *sn*-1 and a polyenic fatty acid in position *sn*-2 varied inconsistently with temperature, levels of some of them being higher, i.e., 16:0a/22:6 in alkylacyl PE (0.0 vs. 28.5%), or 16:0a/20:5 in alkenylacyl PE (5.1 vs. 10.0%), whereas the levels of alkylacyl 16:0a/20:5 and 16:0a/20:4 PE were lower at 8°C. Neither alkylacyl nor alkenylacyl 18:0a/20:4 showed any response to environmental temperature.

Measurement of the structural order of phospholipid vesicles revealed less ordered, more fluid structures in the case of the cold-adapted specimens (Fig. 1), indicating that *Gammarus* is capable of regulating membrane fluidity according to the environmental temperature. In fact there is an "overfluidization" of phospholipid structures in the cold: equal R_{SS} values were measured at 20°C in cold-adapted specimens instead of 15°C.

DISCUSSION

The experimental animals were collected directly from natural surroundings. Accordingly, in evaluating the results, the temperature history of the animals should be considered. In spring the water temperature increased over a short period from a value of almost zero to the temperature existing at the sampling time. It is possible that the spring animals were still adapted to a somewhat lower temperature than that of the sampling temperature. In summer a more stable temperature had prevailed for a longer period.

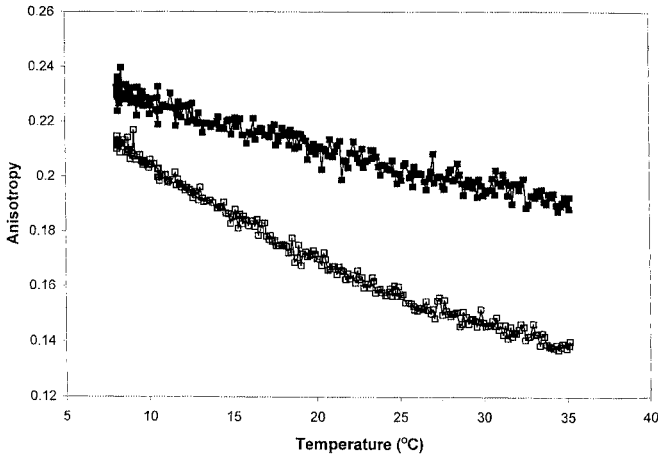

FIG. 1. Temperature dependency of the fluorescence anisotropy, R_{SS}, of 1,6-diphenyl 1,3,5-hexatriene embedded in phospholipid vesicles obtained from *Gammarus* spp. acclimatized to spring (8°C) and summer (15°C) temperatures. Filled squares: phospholipids from 15°C; open squares: phospholipids from 8°C.

Despite only a small variation in the fatty acid composition of phospholipids, the present result shows a drastic difference in the fluidity of phospholipid vesicles obtained from spring and summer *Gammarus*. In earlier studies it was proven that differences in dietary lipids have only a minor effect on the fluidity of fish membranes (15,23). On the basis of these observations we conclude that temperature has a major impact on the physicochemical characteristics of *Gammarus* spp. also. Lipids taken up with food might have been similar in both 8- and 15°C-adapted specimens as judged from similarities in the fatty acid composition of neutral lipids (Table 1). It is interesting that palmitoleic acid, abundant in triglycerides, did not appear in polar lipids. The presence of palmitoleic and eicosapentaenoic acids might indicate the presence of diatoms in the diets of these crustaceans.

Based on observations made of the membranes of vertebrates having different body temperatures (5) it was expected that the R_{SS} values of phospholipid vesicles would also be similar at the respective body temperatures in *Gammarus* spp. Figure 1 shows, however, that an overfluidization takes place at the level of isolated phospholipids. Similar overfluidization was observed in the branchial microsomal membranes, but not in the neural membranes, of the antarctic amphipod *Orchomene plebs* adapted to –1.2°C and Baltic Sea isopod, *Saduria entomon*, adapted to +4°C (3). On the other hand, only a partial compensation was observed in the plasma membranes of leg muscles from a cold stenothermic crustacean, *Cancer pagurus*, and with the same membranes of a less cold stenothermic crustacean, *Carcinus maenas* (4). A possible explanation for the observation presented in Figure 1 is that we used total phospholipids, a mixture of phospholipids from different membranes, devoid of other membrane components such as proteins and sterols which might have rendered these structures more rigid. A study in progress shows that the cholesterol content of the mitochondrial membranes of the winter-active *Gammarus* spp. was 5.2 and 6.2% of the total lipids

in spring and summer animals, respectively. In general, cholesterol has a stabilizing effect on the membranes, but its role in membrane fluidity is a matter of controversy (24).

The increased fluidity of *Gammarus* at 8°C cannot be explained on the basis of the fatty acid composition of total phospholipids. The level of polyunsaturated fatty acids was almost identical at both temperatures. The ratio of saturated/unsaturated fatty acid, which is often regarded as an index of membrane fluidity, was higher in cold due to the high level of 18:0 (0.54 vs. 0.36). The striking difference between the molecular species compositions is that levels of 16:0/16:0 PC as well as of 1-monoenic, 2-polyenic species of PC and PE (Tables 3 and 4), first of all 18:1/20:5, are higher in specimens collected at 8°C (Table 3). The kink at the ninth carbon atom of 18:1 combined with the extended configuration of 22:5 and 22:6 (25) in PE with a reduced level of 16:0/16:0 in PC in cold-adapted ones might be at least partly sufficient to increase membrane disorder and to compensate for the effect of reduced temperature on chain ordering. It thus appears that *Gammarus* follows the same strategy to control membrane fluidity in the cold as do the fish species investigated so far (6,12), namely *Gammarus* also accumulates *sn*-1 monoenic and *sn*-2-polyenic phospholipid molecular species at reduced temperatures. The accumulation of these species cannot be traced back to differences in food ingested at the two temperatures because the fatty acid composition of triglycerides, which is supposed to represent the fatty acid composition of food, is also similar, except for the higher level of palmitoleic acid in the cold (Table 1). It must be mentioned that these crustaceans are active also at 8°C. It has been shown earlier that winter-active crustacean species have a better ability to adjust their membrane composition to prevailing conditions (11,26).

We believe that the increase in the levels of 1-monoenic, 2-polyenic molecular species cannot fully explain the differences in the fluidities of *Gammarus* living at 8 and 15°C. Model experiments using a mixture of synthetic 16:0/22:6 PC and synthetic 18:1/22:6 PE, and using 2-, 12-anthroyloxy stearic acid, and 16-anthroyloxy palmitic acid showed that 18:1/22:6 PE exerted the greatest disordering effect at the level above the twelfth carbon atom in the bilayer and almost no effect was seen in the hydrophobic core with 16-anthroyloxy palmitic acid (6). Considering that DPH distributes evenly in the bilayer and that the difference in the levels of total 1-monoenic, 2-polyenic molecular species is only 14%, the involvement of some other membrane component must be considered.

A determination of subclass composition of PE showed a 20% decrease in the level of alkenylacyl species at 8°C (Table 2). Ethanolamine plasmalogens have been shown to reduce the ordering of bilayers in other systems (27). From these observations the conclusion may be tentatively drawn that, besides the above-mentioned phospholipid molecular species, *Gammarus* utilizes ethanolamine plasmalogens, for this purpose so far undescribed elements, to adjust membrane fluidity to the prevailing temperature.

However, the question arises as to how these crustaceans maintain the bilayer structure of their membranes with such high contents of ether lipids. These lipids are prone to form so-called non-bilayer structures. The highest level of ethanolamine plasmalogens was demonstrated from the brain, where they amount to 40–60% of the ethanolamine phosphoglycerides (28) in contrast to 68% in the ethanolamine phosphoglycerides of *Gammarus* spp. (Table 2). A possible explanation could be that these crustaceans utilize some proteins capable of arranging phospholipids, otherwise only forming non-bilayer phases, into a bilayer phase arrangement. The existence of such proteins has already been described in other systems (29–31).

ACKNOWLEDGMENTS

The authors wish to thank Carita Sunell for her field work, and Erika Zukic, Judith Baunoch, and Tuovi Vartio for their excellent work in the laboratory. This research was funded by the Finnish Academy of Sciences and the Hungarian Academy of Sciences as a bilateral exchange grant to Eila Lahdes.

REFERENCES

1. Sinensky, M. (1974) Homeoviscous Adaptation—A Homeostatic Process That Regulates the Viscosity of Membrane Lipids in *Escherichia coli, Proc. Natl. Acad. Sci. USA 71*, 522–525.
2. Farkas, T., Storebakken, T., and Bhosle, N.B. (1989) Composition and Physical State of Phospholipids in Calanoid Copepods from India and Norway, *Lipids 24*, 619–622.
3. Lahdes, E.O., Kivivuori, L.A., and Lehti-Koivunen, S.M. (1993) Thermal Tolerance and Fluidity of Neuronal and Branchial Membranes of an Antarctic Amphipod (*Orchomene plebs*): A Comparison with a Baltic Isopod (*Saduria entomon*), *Comp. Biochem. Physiol. 105A*, 463–470.
4. Cuculescu, M., Hyde, D., and Bowler, K. (1995) Temperature Acclimation of Marine Crabs: Changes in Plasma Membrane Fluidity and Lipid Composition, *J. Therm. Biol. 20*, 207–222.
5. Behan-Martin, M.K., Jones, G.R., Bowler, K., and Cossins, A.R. (1993) A Near Perfect Temperature Adaptation of Bilayer Order in Vertebrate Brain Membranes, *Biochim. Biophys. Acta 1151*, 216–222.
6. Fodor, E., Jones, R.H., Buda, C., Kitajka, K., Dey, I., and Farkas, T. (1995) Molecular Architecture and Biophysical Properties of Phospholipids During Thermal Adaptation in Fish: An Experimental and Model Study, *Lipids 30*, 1119–1126.
7. Cossins, A.R. (1977) Adaptation of Biological Membranes to Temperature. The Effect of Temperature Acclimation of Goldfish upon Viscosity of Synaptosomal Membranes, *Biochim. Biophys. Acta 470*, 395–471.
8. Farkas, T., Csengeri, I., Majoros, F., and Oláh, J. (1980) Metabolism of Fatty Acids in Fish. III. Combined Effect of Environmental Temperature and Diet on Formation and Deposition of Fatty Acids in the Carp, *Cyprinus carpio* Linneatus, *Aquaculture 20*, 29–40.
9. Sellner, P.A., and Hazel, J.R. (1982) Time Course of Changes in Fatty Acid Composition of Gills of Rainbow Trout (*Salmo gairdneri*) During Thermal Acclimation, *J. Exp. Zool. 221*, 159–168.
10. Hazel, J.R., and Carpenter, R. (1985) Rapid Changes in the Phospholipid Composition of Gill Membranes During Thermal Acclimation of the Rainbow Trout, *Salmo gairdneri, J. Comp. Physiol. B 155*, 597–602.
11. Farkas, T., Nemecz, G., and Csengeri, I. (1984) Differential Response of Lipid Metabolism and Membrane Physical State by

an Actively and Passively Overwintering Planktonic Crustacean, *Lipids 19*, 436–442.
12. Dey, I., Buda, C., Wiik, T., Halver, J.E., and Farkas, T. (1993) Molecular Structure and Structural Composition of Phospholipid Membranes in Livers of Marine and Freshwater Fish in Relation to Temperature, *Proc. Natl. Acad. Sci. USA 90*, 7498–7502.
13. Zabelinskii, S.A., Brovtsyna, N.B., Cheboterova, M.A., Gorbunova, O.B., and Krivchenko, A.I. (1995) Comparative Investigation of Lipid and Fatty Acid Composition of Fish Gills and Mammalian Lungs. A Model of the Membrane Lipid Component Areas, *Comp. Biochem. Physiol. 111B*, 127–140.
14. Tanaka, T., Ikita, K., Ashida, T., Motoyama, Y., Yamaguchi, Y., and Satouchi, K. (1996) Effects of Growth Temperature on the Fatty Acid Composition of the Free-Living Nematode *Caenorhabditis elegans, Lipids 31*, 1173–1178.
15. Farkas, T., Dey, I., Buda, C., and Halver, J.E. (1994) Role of Phospholipid Molecular Species in Maintaining Lipid Membrane Structure in Response to Temperature, *Biophys. Chem. 50*, 147–155.
16. Segerstråle, S.G. (1959) Synopsis of Data on the Crustaceans *Gammarus locusta*, *Gammarus oceanicus, Pontoporeia affinis* and *Corophium volutator* (Amphipoda Gammarides), *Soc. Sci. Fenn. Commentat. Biol. 20*, 1–23.
17. Folch, J., Lees, M., and Sloane-Stanley, G.H. (1957) A Simple Method for the Isolation and Purification of Total Lipids from Animal Tissue, *J. Biol. Chem. 226*, 497–509.
18. Fine, J.B., and Sprecher, H. (1982) Unidimensional Thin-Layer Chromatography of Phospholipids on Boric Acid Impregnated Plates, *J. Lipid Res. 13*, 660–663.
19. Takamura, H., and Kito, M. (1991) A Highly Sensitive Method for Quantitative Analysis of Phospholipid Molecular Species by High Performance Liquid Chromatography, *J. Biochem. 109*, 436–439.
20. Dawson, M.E., Morris, R.J., and Lockwood, A.P.M. (1984) Some Combined Effect of Temperature and Salinity on Water Permeability and Gill Lipid Composition in the Amphipod *Gammarus duobeni, Comp. Biochem. Physiol. 78A*, 729–735.
21. Clarke, A., Skadsheim, A., and Holmes, L.J. (1985) Lipid Biochemistry and Reproductive Biology in Two Species of Gammaridae (Crustacea: Amphipoda), *Marine Biol. 88*, 247–263.
22. Chapelle, S., and Benson, A.A. (1986) Studies on the Plasmalogens of Crustacean Gills, *Comp. Biochem. Physiol. 85B*, 507– 510.
23. Roy, R., Fodor, E., Kitajka, K., and Farkas, T. (1999) Fatty Acid Composition of the Ingested Food Only Slightly Affects Physicochemical Properties of Liver Total Phospholipids and Plasma Membranes in Cold-Adapted Freshwater Fish, *Fish Physiol. Biochem. 20*, 1–11.
24. Pruitt, N.L. (1990) Adaptations to Temperature in the Cellular Membranes of Crustaceans. Membrane Structure and Metabolism, *J. Therm. Biol. 15*, 1–8.
25. Applegate, K.R., and Glomset, G. (1991) Effect of Acyl-Chain Unsaturation on the Conformation of Model Diacylglycerols: A Computer Modeling Study, *J. Lipid Res. 31*, 1665–1668.
26. Pruitt, N.L. (1988) Membrane Lipid Composition and Overwintering Strategy in Thermally Acclimated Crayfish, *Am. J. Physiol. 254*, R870–R876.
27. Demediuk, P., Cowan, D.L., Moscatelli, E.A. (1983) Effects of Plasmenylethanolamine on the Dynamic Properties of the Hydrocarbon Region of Mixed Phosphatidylcholine-Phosphatidylethanolamine Aqueous Dispersions. A Spin Label Study, *Biochim. Biophys. Acta 730*, 263–270.
28. Sastry, P.S. (1985) Lipids of Nervous Tissue: Composition and Metabolism, *Progr. Lipid Res. 24*, 69–176.
29. Taraschi, T.F., Kruijff, B., De Verkleij, A., and van Echteld, C.J.A. (1982) Effect of Glycophorin on Lipid Polymorphism. A ^{31}P-NMR Study, *Biochim. Biophys. Acta 685*, 153–161.
30. Williams, W.P. (1998) The Physical Properties of Thylakoid Membrane Lipids and Their Relation to Photosynthesis, in *Lipids in Photosynthesis: Structure, Function and Genetics* (Siegenthaler, P.A., and Murata, N., eds.) pp. 103–118, Kluwer Academic Publishers, Amsterdam.
31. Simidjief, L., Stoylova, S., Amenitsch, H., Javorfi, T., Mustardy, L., Laggner, P., Holzenburg, A., and Garab, G. (2000) Self-Assembly of Large, Ordered Lamellae from Non-bilayer and Integral Membrane Proteins *in vitro, Proc. Natl. Acad. Sci. USA*, in press.

[Received February 22, 2000, and in revised form June 20, 2000; revision accepted July 5, 2000]

Cold Acclimation or Grapeseed Oil Feeding Affects Phospholipid Composition and Mitochondrial Function in Duckling Skeletal Muscle

François Chaînier, Damien Roussel, Bruno Georges, Roger Meister*, Jean-Louis Rouanet, Claude Duchamp, and Hervé Barré

Laboratoire de Physiologie des Régulations Energétiques, Cellulaires et Moléculaires (Unité Mixte de Recherches 5578 Centre National de la Recherche Scientifique - Université Lyon 1), F-69622 Villeurbanne Cedex, France

ABSTRACT: The phospholipid fatty acid (FA) composition and functional properties of skeletal muscle and liver mitochondria were examined in cold-acclimated (CA, 4°C) ducklings. Phospholipid FA of isolated muscle mitochondria from CA birds were longer and more unsaturated than those from thermoneutral (TN, 25°C) reared ducklings. The rise in long-chain and polyunsaturated FA (PUFA, mainly 20:4n-6) was associated with a higher State 4 respiration rate and a lower respiratory control ratio (RCR). Hepatic mitochondria, by contrast, were much less affected by cold acclimation. The cold-induced changes in phospholipid FA profile and functional properties of muscle mitochondria were reproduced by giving TN ducklings a diet enriched in grapeseed oil (GO, rich in n-6 FA), suggesting a causal relationship between the membrane structure and mitochondrial functional parameters. However, hepatic mitochondria from ducklings fed the GO diet also showed an enrichment in long-chain PUFA but opposite changes in their biochemical characteristics (lower State 4, higher RCR). It is suggested that the differential modulation of mitochondrial functional properties by membrane lipid composition between skeletal muscle and liver may depend on muscle-specific factors possibly interacting with long-chain PUFA and affecting the proton leakiness of mitochondrial membranes.

Paper no. L8546 in *Lipids 35,* 1099–1106 (October 2000).

When chronically exposed to cold, most endotherms are able to enhance their metabolic capacity to generate heat to compensate for the rise in heat loss and maintain homeothermy. Small rodents are thus well known to develop nonshivering thermogenic (NST) capacity in the cold (1). Some species of birds, including chickens, ducks, and penguins, can also develop NST in response to cold acclimation or acclimatization (2–5). This remarkable adaptation to cold exposure differs from the situation in mammals, as birds lack the specialized thermogenic brown adipose tissue (BAT) of newborn mammals, hibernators, and small rodents (6–8). In the absence of BAT, skeletal muscle appears as the main site of cold-induced NST (9).

Muscle NST may be based on a loose-coupling of mitochondrial oxidative phosphorylation controlled by fatty acids (FA) on the basis of results obtained with isolated mitochondria in cold-acclimated (CA) ducklings (3,10,11). These studies have contributed to clarify the earlier observation of loose-coupled mitochondria and possible involvement of FA in CA birds (12,13). The molecular mechanisms of such loose-coupling are still unclear, but involve an increase (+40%) in the mitochondrial membrane conductance to protons in CA ducklings (11). No uncoupling protein with protonophoric properties similar to those expressed in mammalian tissues has yet been described in CA birds (7,8). Nevertheless, because phospholipid membranes are inherently leaky to protons (14,15) and the degree of proton leak correlates with the composition in unsaturated FA (16,17), a change in the phospholipid composition of mitochondrial membrane may contribute to the increased leakiness of mitochondrial membranes in CA ducklings. Differences in nonphosphorylating respiratory rates of isolated mitochondria from various species have already been related to mitochondrial phospholipid composition (18). Consistent with this idea is the observation that in CA rats, the membranes of BAT mitochondria contain more polyunsaturated FA (PUFA), possibly contributing to the thermogenic activation of BAT mitochondria (19). Furthermore, an enrichment of membranes with PUFA obtained through changes in the lipid composition of the diet was associated with an increased skeletal muscle oxygen consumption (20).

The aim of this study was therefore to assess whether the development of skeletal muscle NST in CA ducklings was accompanied by changes in the FA composition of tissue membranes. In a first experiment with whole tissues, we found that there was an enrichment in PUFA in skeletal muscle phospholipids of CA ducklings. In a second experiment, we examined whether the cold-induced changes in phospholipid composi-

*To whom correspondence should be addressed at Laboratoire de Physiologie des Régulations Energétiques, Cellulaires et Moléculaires, (UMR 5578 CNRS-Université Lyon 1), Faculté des Sciences, 43 bld. du 11 Novembre 1918, bât 404, F-69622 Villeurbanne Cedex, France.
E-mail: meister@physio.univ-lyon1.fr

Abbreviations: ANOVA, analysis of variance; BAT, brown adipose tissue; CA, cold acclimated; FA, fatty acid; FOG, fast-oxidative glycolytic; GO, grapeseed oil; MUFA, monounsaturated fatty acid; NST, nonshivering thermogenesis; PUFA, polyunsaturated fatty acid; RCR, respiratory control ratio; SFA, saturated fatty acid; TN, thermoneutral control ducklings; U.A.R., Usine d'Alimentation Rationnelle.

tion were causally related to the functional characteristics of isolated mitochondria. To this purpose, mitochondrial membrane FA composition was altered at thermoneutrality by changing the lipid composition of the diet (21). The consequences of a diet supplemented with grapeseed oil rich in n-6 FA on the phospholipid composition and functional properties of hepatic and muscle mitochondria were thus examined in ducklings kept at thermoneutrality and compared to those observed after cold acclimation.

MATERIALS AND METHODS

Animals. Animals were cared for under the French Code of Practice for the Care and Use of Animals for Scientific Purposes, and the experimental protocols were approved by the French Ministry of Agriculture Ethics Committee (section animals). Male Muscovy ducklings (*Cairina moschata* L., pedigree R51, Institut National de la Recherche Agronomique, France) were obtained from a commercial stockbreeder (Ets Grimaud, France). They were fed *ad libitum* with a commercial mash (Genthon 5A; Genthon, Cheyssieu, France, see Table 1) and had free access to water. From 1 wk of age, ducklings were assigned to experimental groups.

A first batch of ducklings was divided into two groups; one was kept at 25°C and constituted the thermoneutral (TN) control group, while the other one was reared in the cold (4°C) and constituted the CA group. These birds were kept on the Genthon 5A commercial mash. This cold-acclimation schedule was shown to stimulate the development of skeletal muscle NST by 5 wk of age (6,9). Ducklings were killed by decapitation and tissues (gastrocnemius muscle and liver) were sampled and frozen in liquid nitrogen and kept at −70°C until FA analysis of total tissue phospholipids.

Following the results of the first experiment, a second batch of ducklings was divided into three experimental groups. Two groups of TN or CA ducklings were fed *ad libitum* with a commercial mash [UAR 115; Usine d'Alimentation Rationnelle (U.A.R.), Villemoisson, France]. A third group of ducklings kept at thermoneutrality was fed with the UAR 115 mash supplemented with 6.5% (w/w) grapeseed oil (GO; U.A.R.). Composition and energy content of diets are presented in Table 1. By 5 wk of age, ducklings were killed by decapitation. As the CA group grew a little bit more slowly (Fig. 1), they were killed a few days later at the same body weight as the TN and GO groups. Red internal gastrocnemius, rich in slow-oxidative and fast-oxidative glycolytic (FOG) fibers, white external gastrocnemius, rich in fast glycolytic and FOG fibers (22), and liver samples were taken and used for the analysis of mitochondrial function and FA composition of mitochondrial phospholipids. Photoperiod was 8 h/16 h (light/dark). Food consumption and body weight of ducklings were measured daily.

Isolation of skeletal muscle mitochondria. Internal and external gastrocnemius muscle and liver samples were rapidly taken out, freed of fat and connective tissues, and mixed in a cold isolation medium with a Teflon glass homogenizer. Mus-

TABLE 1
Fatty Acid Composition (in %) of Diets

	Genthon 5A	UAR 115	GO diet
14:0	3.49	0.31	0.15
14:1n-7	0.24	0.06	0.03
16:0	15.68	11.39	8.46
16:1n-9	0.26	0.07	0.04
16:1n-7	1.13	1.00	0.42
18:0	5.76	2.78	3.37
18:1n-9	27.98	22.02	20.28
18:1n-7	1.30	1.41	1.00
18:2n-6	37.98	49.61	60.52
20:0	0.41	0.41	0.30
20:1n-9	2.28	5.10	2.21
20:2n-6	0.15	0.19	0.12
20:3n-6	0.19	0.05	0.07
22:0	—	0.04	0.05
20:4n-6	0.05	0.17	0.07
20:5n-3	—	0.67	0.26
24:0	0.10	0.28	0.17
24:1n-9	—	0.20	0.06
22:5n-3	—	0.12	—
22:6n-3	0.20	1.38	0.54
Total SFA	25.24	15.21	12.50
Total MUFA	33.78	29.86	24.04
Total PUFA	39.25	52.19	61.58
Total n-6	38.64	50.02	60.78
Total n-3	0.92	2.17	0.80
n-3/n-6	0.02	0.04	0.01
Unsaturation index[a]	1.14	1.42	1.50
Mean chain length[b]	17.08	17.47	17.57
Lipid content (%)	4.5	3.5	9.5
Energetic value[c] (kcal/g)	4.20	3.38	3.74

[a]Unsaturation index = $(\sum m_i \cdot n_i)/100$, where m_i is the mole percentage and n_i is the number of C–C double bonds of the fatty acid *i*.
[b]Mean chain length index = $(\sum m_i \cdot n_i)/100$, where m_i is the mole percentage and n_i is the number of C of the fatty acid *i*.
[c]Energetic value has been calculated according to 4 kcal/g for digestible proteins and carbohydrates and 9 kcal/g for digestible lipids. GO, grapeseed oil; SFA, saturated fatty acid; MUFA, monounsaturated fatty acid; PUFA, polyunsaturated fatty acid.

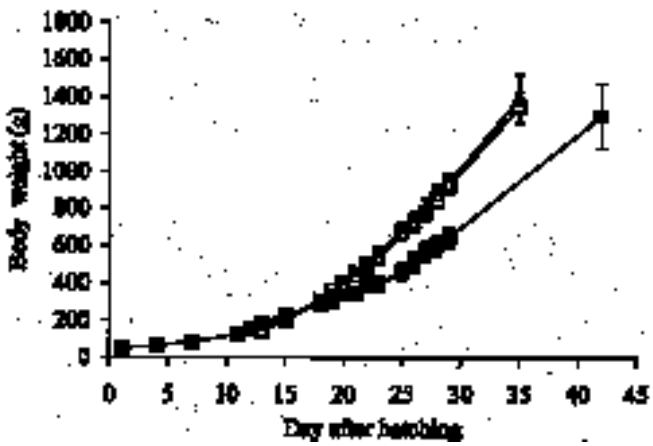

FIG. 1. Effects of grapeseed oil (GO) feeding or cold acclimation on growth rate. GO ducklings reared at thermoneutrality (△) and CA ducklings (■) are compared with thermoneutral controls (□). Values are means ± SE (n = 7).

cle intermyofibrillar mitochondria and liver mitochondria were isolated as described previously (10,11).

Lipid analysis. Tissue and mitochondrial total lipids were extracted according to Folch *et al*. (23). Residual water of the extracts was removed by oil-vacuum. The lipid extracts were weighed, diluted in chloroform, and stored at –20°C until use.

Phospholipids and triglycerides from tissue extracts were separated by thin-layer chromatography on silica gel (G60 plates) using diisopropyl ether as migration solvent. Phospholipids were recovered by scratching the gel and then methylating according to Slover and Lanza (24) before FA analysis.

The FA analysis of phospholipids from mitochondrial extracts was performed with total lipids because the presence of tri- and diglycerides was found negligible, and only traces of cholesterol were detected. The FA of total lipids were therefore assumed to be those of phospholipids. Methylation was performed according to Lepage and Roy (25) using acetylchloride.

FA methyl esters were stored in hexane (high-performance liquid chromatography grade). Gas–liquid chromatography of FA methyl esters was performed using a Chrompack CP9001 chromatograph (Chrompack, Middelburg, The Netherlands) equipped with a 50-m capillary column (CP-Sil 88, 0.25 mm internal diameter) and Chrompack Maestro2 integrator software. The split injector was at 270°C and the flame-ionization detector at 260°C. Temperature program was 150°C for 8 min, rising to 185°C by 10°C/min, 185°C for 10 min, rising to 200°C by 10°C/min, and then 200°C for 20 min. Nitrogen was used as carrier gas (100 kPa). FA were identified by comparison with commercially available standards (Supelco, Bellefonte, PA).

Mitochondrial respiration and enzymatic activities. The respiration of isolated mitochondria (0.5 mg mitochondrial protein/mL) was determined polarographically with a Clark oxygen electrode (oxygraph Gilson 5/6 H), in a glass cell of 1.5 mL volume, thermostated at 25°C as described previously (10,11). The ATP synthesis of mitochondria was determined by the bioluminescence procedure of Wibom *et al*. (26) at 25°C with some modifications as described previously (11). The cytochrome oxidase activity of isolated mitochondria was determined polarographically as described elsewhere (10). As the protein/lipid ratio remained unchanged in all the experiments (data not shown), the specific activity of the enzymes was expressed per mg of protein.

Statistics and chemicals. Data are presented as means ± SE. One-way or two-way analysis of variance (ANOVA) and post-ANOVA Fisher PLSD tests and Student's *t* tests were used to determine significant differences between groups. Statistical difference was accepted at $P < 0.05$.

Solvent of analytical grade for lipids extraction and analysis was from SDS (Peypin, France); the other chemicals were purchased from Sigma.

RESULTS

Experiment 1: Effect of cold acclimation on the FA composition of tissue phospholipids. At the time of killing, TN ducklings were slightly heavier than CA birds (1.43 ± 0.03 vs. 1.20

TABLE 2
Fatty Acid Composition (in %) of Total Phospholipids from Gastrocnemius Muscle and Liver in Thermoneutral (TN) or Cold-Acclimated (CA) Ducklings[a]

	Gastrocnemius muscle		Liver	
	TN	CA	TN	CA
16:0	12.6 ± 0.3	11.9 ± 0.2*	23.6 ± 0.4	21.2 ± 1.3*
16:1n-7	—	—	0.4 ± 0.1	0.7 ± 0.1*
18:0	17.5 ± 0.4	19.3 ± 0.1*	18.4 ± 0.3	19.3 ± 0.4
18:1n-9	19.8 ± 0.7	16.6 ± 0.4*	11.3 ± 0.4	13.6 ± 1.0*
18:1n-7	0.7 ± 0.1	0.5 ± 0.1	1.0 ± 0.1	1.2 ± 0.1
18:2n-6	16.0 ± 0.4	15.5 ± 0.3	8.4 ± 0.6	9.1 ± 1.2
20:3n-6	1.5 ± 0.1	1.1 ± 0.1*	2.4 ± 0.2	2.7 ± 0.5
20:4n-6	11.2 ± 0.4	14.2 ± 0.3*	21.1 ± 0.6	19.3 ± 2.9
22:4n-6	3.9 ± 0.2	4.1 ± 0.1	1.8 ± 0.1	1.3 ± 0.1*
22:5n-6	2.9 ± 0.1	3.1 ± 0.1	3.6 ± 0.2	2.7 ± 0.2*
22:5n-3	1.4 ± 0.1	1.5 ± 0.2	0.5 ± 0.1	0.8 ± 0.1*
22:6n-3	1.5 ± 0.1	2.4 ± 0.2*	1.9 ± 0.1	1.9 ± 0.3
Total SFA	31.9 ± 0.6	33.2 ± 0.2*	42.4 ± 0.3	40.9 ± 0.9
Total MUFA	20.7 ± 0.7	17.3 ± 0.4*	13.9 ± 0.5	16.7 ± 0.9*
Total PUFA	39.4 ± 0.9	43.0 ± 0.3*	42.2 ± 0.4	41.0 ± 1.7
Total n-6	36.0 ± 0.7	38.7 ± 0.2*	37.3 ± 0.6	35.5 ± 1.4
Total n-3	3.3 ± 0.2	4.4 ± 0.1*	3.1 ± 0.3	3.5 ± 0.3
n-3/n-6	0.092 ± 0.004	0.113 ± 0.004*	0.082 ± 0.006	0.097 ± 0.007
Unsaturation index	1.51 ± 0.04	1.66 ± 0.01*	1.70 ± 0.02	1.65 ± 0.09

[a]Values are mean ± SE from six (gastrocnemius) or five (liver) animals kept on the Genthon 5A diet. *$P < 0.05$ vs. TN. Fatty acids representing a small proportion of the total are not shown but values are included when possible in the totals presented. See Table 1 for abbreviations.

± 0.03 kg, $P < 0.05$) despite a lower food intake by 5 wk of age (106 ± 3 vs. 139 ± 4 kcal·kg$^{-0.75}$·d^{-1}). The FA profile of tissue phospholipids (Table 2) differed between the two tissues, the gastrocnemius muscle being poorer in saturated fatty acids (SFA) but richer in monounsaturated fatty acids (MUFA) than the liver. In the gastrocnemius muscle, cold acclimation led to a marked increase in the proportion of total PUFA and to a lesser extent of SFA at the expense of total MUFA. The cold-induced rise in total PUFA was mainly accounted for by 20:4n-6, and to a lesser extent by 22:4n-6 and 22:6n-3. The unsaturation index of total phospholipids was thus higher in skeletal muscle from CA than from TN ducklings. In liver, by contrast, the cold-induced rise in long-chain PUFA was not observed, and there was only a slight increase in the proportion of total MUFA mainly accounted for by 18:1n-9 FA in CA ducklings. The unsaturation index of liver phospholipids was similar between TN and CA ducklings.

Experiment 2: Effect of GO diet or cold on food intake and growth rate. Despite differences in the energy content of the diet, TN and GO ducklings had a similar energy intake by 5 wk of age (441 ± 3 and 439 ± 12 kcal·kg$^{-0.75}$·d^{-1}, respectively) and grew at similar rates (Fig. 1). Again, the energy intake of CA ducklings was higher (496 ± 5 kcal·kg$^{-0.75}$·d^{-1}) and their growth rate lower than those of the ducklings kept at thermoneutrality.

Experiment 2: Effect of GO diet or cold on the FA profile of mitochondrial phospholipids. Whatever the diet or cold-acclimation status, the FA composition of mitochondrial phospholipids differed between tissues (Table 3). As seen in the composition of tissue phospholipids, there were more SFA and less PUFA in the phospholipids of mitochondria isolated from liver than from gastrocnemius muscles. Mitochondrial phospholipids from the red internal part of the gastrocnemius muscle were richer in PUFA than those from the white part. Despite these differences, the unsaturation indexes were similar in the three tissues studied, mainly because of the differences in the pattern of n-6 FA. The content in 20:4n-6 was higher in hepatic than in muscle mitochondria, while the 18:2n-6 was the most abundant FA in muscle mitochondria. The n-3/n-6 ratio was similar in the three tissues.

The mitochondrial FA profile was differentially affected by cold acclimation in liver and skeletal muscles. In both parts of the gastrocnemius muscle, a higher unsaturation index and a longer mean chain length were observed in CA ducklings. These parameters reflected the increased proportion of PUFA (especially 20:4n-6, and to a lesser extent

TABLE 3
Fatty Acid Composition (in %) of Total Phospholipids from Mitochondria of Internal, External Gastrocnemius Muscle, and Liver in TN, CA, and GO-Supplemented Ducklings[a]

	Internal gastrocnemius			External gastrocnemius			Liver		
	TN	CA	GO	TN	CA	GO	TN	CA	GO
14:1n-7	1.2 ± 0.1	1.5 ± 0.3	1.1 ± 0.2	2.6 ± 0.4	2.5 ± 0.4	2.0 ± 0.3	0.1 ± 0.0	0.1 ± 0.0	0.1 ± 0.0
16:0	10.5 ± 0.3^{a}	8.2 ± 0.2^{b}	8.8 ± 0.2^{b}	12.2 ± 0.4^{a}	9.5 ± 0.3^{b}	10.9 ± 0.4^{c}	19.0 ± 0.8	19.3 ± 0.6	17.9 ± 0.5
16:1n-9	0.2 ± 0.0	0.1 ± 0.0	0.2 ± 0.0	0.3 ± 0.1	0.2 ± 0.0	0.3 ± 0.0	0.4 ± 0.0	0.3 ± 0.0	0.3 ± 0.03
16:1n-7	0.4 ± 0.0^{a}	0.3 ± 0.0^{b}	0.2 ± 0.0^{c}	0.6 ± 0.1^{a}	0.4 ± 0.0^{b}	0.2 ± 0.0^{c}	0.9 ± 0.1^{a}	0.9 ± 0.1^{a}	0.3 ± 0.0^{b}
18:0	19.1 ± 0.4^{a}	21.7 ± 0.2^{b}	21.5 ± 0.3^{b}	15.1 ± 0.3^{a}	18.4 ± 0.2^{b}	17.2 ± 0.3^{c}	16.2 ± 0.3^{a}	17.0 ± 0.2^{a}	18.9 ± 0.3^{b}
18:1n-9	13.1 ± 0.5^{a}	10.8 ± 0.3^{b}	8.2 ± 0.3^{c}	16.5 ± 0.6^{a}	13.8 ± 0.4^{b}	10.7 ± 0.3^{c}	15.2 ± 0.4^{a}	16.9 ± 0.6^{b}	8.7 ± 0.5^{c}
18:1n-7	3.5 ± 0.1^{a}	3.7 ± 0.1^{a}	2.6 ± 0.1^{b}	3.7 ± 0.1^{a}	4.2 ± 0.1^{b}	2.6 ± 0.1^{c}	1.8 ± 0.1^{a}	1.6 ± 0.1^{a}	1.1 ± 0.1^{b}
18:2n-6	20.2 ± 0.2^{a}	19.4 ± 0.7^{a}	23.9 ± 0.8^{b}	20.7 ± 0.3^{a}	20.1 ± 0.9^{a}	25.7 ± 1.0^{b}	10.1 ± 0.3^{a}	9.0 ± 0.3^{b}	15.2 ± 0.4^{c}
20:0	0.3 ± 0.0^{a}	0.2 ± 0.0^{b}	0.3 ± 0.0^{c}	0.2 ± 0.0^{a,b}	0.2 ± 0.0^{a}	0.3 ± 0.0^{b}	0.1 ± 0.0	0.1 ± 0.0	0.1 ± 0.0
20:1 + 18:3n-3	0.6 ± 0.0^{a}	0.6 ± 0.0^{a}	0.4 ± 0.0^{b}	0.6 ± 0.0^{a}	0.6 ± 0.0^{a}	0.4 ± 0.0^{b}	0.4 ± 0.0^{a}	0.4 ± 0.0^{a}	0.3 ± 0.0^{b}
20:2n-6	0.5 ± 0.0^{a}	0.4 ± 0.0^{b}	1.0 ± 0.0^{c}	0.5 ± 0.0^{a}	0.4 ± 0.0^{a}	1.1 ± 0.1^{b}	0.4 ± 0.0^{a}	0.3 ± 0.0^{a}	1.0 ± 0.1^{b}
22:0	0.8 ± 0.0^{a}	0.6 ± 0.1^{b}	0.5 ± 0.0^{b}	0.9 ± 0.1^{a}	0.7 ± 0.1^{b}	0.6 ± 0.1^{b}	2.1 ± 0.2	1.8 ± 0.2	1.4 ± 0.3
20:4n-6	12.4 ± 0.5^{a}	16.3 ± 0.7^{b}	15.7 ± 0.6^{b}	9.4 ± 0.4^{a}	12.2 ± 0.4^{b}	12.1 ± 0.6^{b}	18.1 ± 0.4^{a}	17.9 ± 0.7^{a}	20.8 ± 0.6^{b}
20:5n-3	1.0 ± 0.1^{a}	0.6 ± 0.0^{b}	0.3 ± 0.0^{c}	1.0 ± 0.0^{a}	0.7 ± 0.0^{b}	0.4 ± 0.0^{c}	0.7 ± 0.1^{a}	0.6 ± 0.1^{a}	0.2 ± 0.0^{b}
22:4n-6	1.9 ± 0.1^{a}	2.5 ± 0.1^{b}	2.8 ± 0.1^{c}	1.8 ± 0.1^{a}	2.5 ± 0.1^{b}	2.9 ± 0.2^{b}	1.4 ± 0.1^{a}	1.5 ± 0.1^{a}	2.2 ± 0.1^{b}
22:5n-6	1.2 ± 0.1^{a}	1.2 ± 0.1^{a}	2.1 ± 0.1^{b}	1.2 ± 0.1^{a}	1.3 ± 0.1^{a}	2.3 ± 0.2^{b}	1.6 ± 0.1^{a}	1.3 ± 0.2^{a}	3.0 ± 0.1^{b}
22:5n-3	1.3 ± 0.1^{a}	1.2 ± 0.1^{a}	1.0 ± 0.1^{b}	1.4 ± 0.1	1.4 ± 0.1	1.2 ± 0.1	0.6 ± 0.0	0.5 ± 0.0	0.5 ± 0.0
22:6n-3	6.0 ± 0.3^{a}	6.5 ± 0.2^{a}	4.7 ± 0.3^{b}	6.3 ± 0.4^{a}	7.0 ± 0.3^{a}	4.9 ± 0.4^{b}	6.4 ± 0.4	6.4 ± 0.4	5.6 ± 0.4
Total SFA	31.0 ± 0.4	31.0 ± 0.2	31.4 ± 0.3	28.6 ± 0.3	29.0 ± 0.2	29.2 ± 0.2	37.8 ± 0.5	38.5 ± 0.4	38.5 ± 0.4
Total MUFA	18.6 ± 0.7^{a}	16.6 ± 0.4^{b}	12.4 ± 0.3^{c}	23.9 ± 0.9^{a}	21.3 ± 0.4^{b}	15.8 ± 0.3^{c}	18.6 ± 0.6^{a}	20.0 ± 0.6^{a}	10.5 ± 0.6^{b}
Total PUFA	44.7 ± 0.6^{a}	48.2 ± 0.5^{b}	51.7 ± 0.3^{c}	42.4 ± 0.8^{a}	45.9 ± 0.4^{b}	50.8 ± 0.8^{c}	39.3 ± 0.7^{a}	37.8 ± 0.9^{a}	48.6 ± 0.8^{b}
Total n-6	34.4 ± 0.5^{a}	37.5 ± 0.5^{b}	42.9 ± 0.3^{c}	31.9 ± 0.4^{a}	34.3 ± 0.5^{b}	41.4 ± 0.5^{c}	30.3 ± 0.4^{a}	28.8 ± 0.6^{a}	40.1 ± 0.6^{b}
Total n-3	8.3 ± 0.4^{a}	8.3 ± 0.2^{a}	6.0 ± 0.3^{b}	8.7 ± 0.5^{a}	9.1 ± 0.4^{a}	6.5 ± 0.5^{b}	7.7 ± 0.4^{a}	7.5 ± 0.3^{a}	6.3 ± 0.4^{b}
n-3/n-6	0.24 ± 0.01^{a}	0.22 ± 0.01^{a}	0.14± 0.01^{b}	0.27 ± 0.02^{a}	0.27 ± 0.01^{a}	0.16 ± 0.01^{b}	0.25 ± 0.0^{a}	0.26 ± 0.01^{a}	0.16 ± 0.01^{b}
Unsaturation index	1.71 ± 0.03^{a}	1.86 ± 0.02^{b}	1.82 ± 0.03^{b}	1.67 ± 0.04^{a}	1.81 ± 0.02^{b}	1.79 ± 0.05^{b}	1.70 ± 0.03^{a}	1.67 ± 0.04^{a}	1.87 ± 0.03^{b}
Mean chain length	18.4 ± 0.0^{a}	18.5 ± 0.0^{b}	18.5 ± 0.0^{b}	18.2 ± 0.1^{a}	18.4 ± 0.0^{b}	18.4 ± 0.1^{b}	18.4 ± 0.0^{a}	18.4 ± 0.0^{a}	18.5 ± 0.1^{b}

[a]Values are means ± SE ($n = 7$). FA representing less than 0.4% are not shown, but are taken into account for the calculation of the totals. Each tissue value with a different roman superscript is significantly different ($P < 0.05$), two-way analysis of variance (ANOVA) and Fisher post-ANOVA test. See Tables 1 and 2 for abbreviations.

22:4n-6). The proportion of 22:6n-3 was not significantly increased in mitochondrial phospholipids. The rise in long-chain PUFA was somehow compensated for by a decrease in the proportion of MUFA (especially 18:1n-9) and an increase in the mean chain length of SFA (rise in 18:0 and drop in 16:0). In liver, by contrast, the rise in long-chain PUFA was not observed, and cold acclimation induced only minor changes in mitochondrial FA profile, i.e., a slight increase in 18:1, compensated for by a decrease in 18:2n-6. The n-3/n-6 ratio was not affected by cold acclimation in the three tissues.

Contrary to cold acclimation, the GO diet at thermoneutrality affected the three tissues studied similarly and induced a nonspecific increase in the proportion of all n-6 phospholipid FA. In muscle mitochondria, these increases were at least up to the levels observed in CA ducklings. Consequently, in muscle mitochondria of GO ducklings, the mean chain length and the unsaturation index reached the values observed in CA ducklings, while in hepatic mitochondria, these parameters were higher than in both TN and CA ducklings. In the three tissues of GO ducklings, the increased proportion of n-6 FA was compensated for by a decreased proportion of MUFA and the n-3/n-6 ratio was markedly decreased.

Experiment 2: Effect of cold acclimation or GO diet on the biochemical characteristics of isolated mitochondria. Cold acclimation affected the functional characteristics of skeletal muscle mitochondria (Table 4), especially in the red part of gastrocnemius, but not those of liver mitochondria (Table 5). In both parts of the gastrocnemius muscle, there was a higher State 4 respiratory rate, and consequently a lower respiratory control ratio (RCR) in CA than in TN ducklings. The ADP/O ratio was, however, not affected by cold acclimation. The specific (per mg mitochondrial protein) ATP synthesis was higher in muscle mitochondria from CA ducklings, but the specific cytochrome oxidase activity was unaffected. Because of a higher amount of mitochondrial proteins in skeletal muscles of CA ducklings, the total oxidative capacity and ATP production capacity per organ were increased by cold acclimation in both skeletal muscles.

The GO diet affected the functional characteristics of hepatic and skeletal muscle mitochondria differently. In liver, the GO diet led to a higher ADP/O ratio and a higher RCR due to a lower respiratory State 4 as compared with ducklings fed the standard diet. The other parameters remained unchanged. In both parts of the gastrocnemius muscle, the GO diet induced a lower RCR due to a higher respiratory State 4 than in control TN ducklings. The specific ATP synthesis activity was intermediate between that of TN and CA ducklings, but because of the increased mitochondrial amount, the total ATP production per gram of muscle reached the level observed after cold acclimation. Taken together, present results

TABLE 4
Respiratory and Functional Parameters of Mitochondria from Internal and External Gastrocnemius Muscle in TN, CA, and GO-Supplemented Ducklings[a]

	Internal gastrocnemius[b]			External gastrocnemius[b]			P^c		
	TN	CA	GO	TN	CA	GO	Effect of treatment	Effect of muscle type	Interaction treatment × muscle type
State 4	23.0 ± 1.8	26.8 ± 1.0	26.7 ± 1.9	21.8 ± 1.0	26.4 ± 1.6	25.0 ± 1.0	<0.05$^{\$,£}$	NS	NS
State 3	116.5 ± 10.0	116.9 ± 3.1	122.3 ± 4.9	121.8 ± 6.2	133.6 ± 6.2	128.1 ± 5.2	ns	NS	NS
RCR	5.05 ± 0.14	4.38 ± 0.15	4.63 ± 0.17	5.62 ± 0.31	5.12 ± 0.27	5.14 ± 0.17	<0.05$^{\$,£}$	<0.01	NS
ADP/O	1.19 ± 0.04	1.15 ± 0.04	1.26 ± 0.02	1.24 ± 0.03	1.30 ± 0.05	1.31 ± 0.02	NS	<0.01	NS
Cytochrome-oxidase specific activity	0.88 ± 0.02	0.88 ± 0.03	0.85 ± 0.02	0.80 ± 0.03	0.80 ± 0.03	0.81 ± 0.03	NS	<0.05	NS
Total cytochrome oxidase activity	53.2 ± 2.5	64.8 ± 6.6	63.9 ± 4.3	34.5 ± 2.5	42.5 ± 3.2	38.3 ± 2.6	<0.05$^{\$,£}$	<0.0001	NS
Mitochondrial proteins	60.8 ± 2.9	74.06 ± 7.1	75.5 ± 4.5	43.2 ± 3.1	53.1 ± 3.4	48.0 ± 4.4	<0.05$^{\$,£}$	<0.0001	NS
Specific ATP-synthesis	66.7 ± 6.5	85.2 ± 2.4	78.9 ± 5.6	84.1 ± 7.5	100.9 ± 8.6	92.2 ± 4.5	<0.05$^{\$}$	<0.01	NS
Total ATP production	4.16 ± 0.56	6.58 ± 0.86	6.00 ± 0.60	3.57 ± 0.34	5.42 ± 0.50	4.47 ± 0.51	<0.01$^{\$,£}$	<0.05	NS

[a]The respiratory reaction medium contained 200 mM sucrose, 5 mM KH_2PO_4, and 20 mM Tris-HCl, pH 7.4 with a final fatty-acid-free bovine serum albumin concentration of 2 mg/mL (0.2% wt/vol). The controlled state of respiration (State 4) was initiated by the addition of 5 mM succinate (sodium salt) in the presence of rotenone (5 μM) and the active state of respiration (state 3) was initiated by the addition of 100 μM ADP. The method of Estabrook (44) was used for the calculation of State 4 and state 3 respiration and the respiratory control ratio (RCR). The latter respiratory parameter is a measure of the degree of control imposed on oxidation by phosphorylation. ADP/O ratio was calculated by using the total oxygen consumed during phosphorylation of a pulse of ADP added to initiate state 3 respiration.

[b]Values are means ± SE. State 4 and State 3 in nmol O/min/mg protein, ADP/O in nmol ADP/nmol O, cytochrome-oxidase specific activity in μmol O/min/mg protein, total cytochrome-oxidase activity in μmol O/min/g muscle, mitochondrial proteins in mg protein/g muscle, specific ATP-synthesis in pmol ATP/min/μg protein, and total ATP production in μmol ATP/min/g muscle.

[c]Values of two-way ANOVA. [$]Significant difference between CA and TN; [£]significant difference between GO and TN; NS, nonsignificant ($P > 0.05$). See Tables 1, 2, and 3 for other abbreviations.

TABLE 5
Respiratory and Functional Parameters of Mitochondria Liver in TN, CA, and GO-Supplemented Ducklings[a]

	Liver		
	TN	CA	GO
State 4	11.4 ± 1.0[a,b]	12.3 ± 0.7[a]	9.0 ± 0.9[b]
State 3	51.3 ± 4.9	53.5 ± 2.5	48.4 ± 3.4
RCR	4.49 ± 0.28[a]	4.37 ± 0.09[a]	5.47 ± 0.33[b]
ADP/O	1.39 ± 0.02[a]	1.44 ± 0.02[a]	1.52 ± 0.02[b]
Cytochrome-oxidase specific activity	0.42 ± 0.04	0.39 ± 0.02	0.31 ± 0.04
Total cytochrome-oxidase activity	81.1 ± 8.3	85.5 ± 4.9	66.9 ± 5.3
Mitochondrial proteins	195.2 ± 19.2	217.4 ± 6.4	222.3 ± 14.3
Specific ATP-synthesis	29.4 ± 3.0	31.6 ± 4.0	27.5 ± 3.0
Total ATP production	5.67 ± 0.69	6.84 ± 0.82	5.31 ± 0.61

[a]Values are means ± SE (n = 7). State 4 and State 3 in nmol O/min/mg protein, ADP/O in nmol ADP/nmol O, cytochrome-oxidase specific activity in µmol O/min/mg protein, total cytochrome-oxidase activity in µmol O/min/g muscle, mitochondrial proteins in mg protein/g muscle, specific ATP-synthesis in pmol ATP/min/µg protein and total ATP production in µmol ATP/min/g muscle. Each tissue means with a different roman superscript is significantly different ($P < 0.05$), one-way ANOVA and Fisher post-ANOVA test. See Tables 1, 2, and 3 for abbreviations.

showed that in skeletal muscles, but not in liver, the GO diet at thermoneutrality globally mimicked the changes in the mitochondrial lipid composition and biochemical parameters induced by cold acclimation.

DISCUSSION

Two main results emerged from the present study. First, CA ducklings showed alterations in the lipid composition of skeletal muscle membranes leading to an increased proportion of long-chain PUFA. Second, the enrichment of mitochondrial phospholipids with n-6 PUFA, created by giving ducklings kept at thermoneutrality a diet rich in GO, partly reproduced the alterations in the functional properties of skeletal muscle mitochondria observed in CA ducklings.

Present results clearly show that cold acclimation altered the FA composition of tissue and mitochondrial phospholipids in the gastrocnemius muscle. Indeed, there was a higher proportion of the longer and more unsaturated FA (mainly 20:4n-6) in tissue and mitochondrial phospholipids from gastrocnemius muscle of CA than in those of TN ducklings resulting in increased (+10%) unsaturation index and mean chain length of membrane FA. By contrast, these changes in FA profile were not observed in liver mitochondria. We do not favor the possibility that the difference between liver and skeletal muscle is related to the fact that these tissues experience different temperatures during cold acclimation. Although living at low temperature indeed results in increased unsaturation in ectotherms (see Ref. 27 for a recent review), the difference between liver and skeletal muscle temperature is likely to be small in endothermic ducklings and would not exceed a few degrees. This is far less than the thermal challenge used to induce phospholipid changes in ectotherms. A similar enrichment in PUFA resulting in an increase in the total FA unsaturation index of mitochondrial phospholipids has been described in the thermogenic BAT of rodents (19). By contrast, there was a decrease in the proportion of total unsaturated FA in heart mitochondria from CA rats (28), mainly resulting from a rise in the proportion of 18:0 and a decrease in that of 18:1. No marked changes in the unsaturation index of phospholipid FA have been reported in hepatic mitochondria of CA rodents (29). These results therefore indicate a tissue-specific modulation of the FA composition of membrane phospholipids toward an enrichment in long-chain PUFA in the thermogenic organs (BAT or skeletal muscles) of endotherms. Such enrichment in long-chain PUFA in mitochondrial membranes of CA ducklings suggests specific roles of these FA in the biophysical properties of these membranes. It is indeed generally accepted that changes in FA profile of biological membranes alter the fluidity, leakiness to protons, and may contribute to the modulation of the activity of membrane-bound enzymes (30–33).

The FA composition of mitochondrial phospholipids could be altered by giving ducklings kept at thermoneutrality a diet rich in GO, providing more n-6 PUFA. This diet composition, rich in 18:2n-6, was chosen in order to provide ducklings with the FA that were the most affected by cold acclimation as shown in the first experiment with total tissue phospholipids (Table 2). Results of experiment 2 indicate that in birds, as in mammals (21), the mitochondrial membrane FA composition can be manipulated by the FA composition of the diet. However, the enrichment in membrane PUFA is lower than what could be expected from the diet composition, indicating some homeostatic control of the membrane lipid composition already noted by others (34). Because the diet similarly affected the FA profile of mitochondrial phospholipids of the three tissues investigated, it follows that the tissue-specific changes observed after cold acclimation are precisely regulated and, for instance, are not dependent on the higher food intake or alterations in the supply of blood lipids (35). These changes may therefore reflect active processes controlling the incorporation of specific long-chain highly unsaturated FA into

membranes for particular metabolic and thermogenic purposes. Thyroid hormones are good candidates for the modulation of phospholipid composition in CA ducklings. Indeed, they are known to increase 20:4n-6 and decrease 18:2n-6 (36,37) and concomitantly increase the unsaturation index (38). Furthermore, they are suspected to play a role in the development of NST in birds (4,5).

Cold acclimation as well as GO feeding, both leading to an enrichment of mitochondrial phospholipids in n-6 FA, similarly altered the functional properties of isolated skeletal muscle mitochondria. In both cases, there was an increase in State 4 respiration rates and a decrease in respiratory control, indicating a lower degree of control imposed on oxidation by the phosphorylation. Similar loose-coupling of muscle mitochondria in CA ducklings has already been reported (11,22) and has been related to an increase in mitochondrial membrane conductance to protons (11). The present results support the hypothesis that the FA composition of ducklings' mitochondrial membranes may contribute, at least in part, to an increased proton leak across mitochondrial inner membrane. In mammals as well, the degree of proton leak is correlated with the composition in unsaturated FA (16,17) and differences in nonphosphorylating respiratory rates of isolated mitochondria from various species are related to mitochondrial phospholipid composition (18). However, the PUFA composition of mitochondrial membranes may not be the only factor responsible for the altered coupling of muscle mitochondria as similar changes in FA composition induced by the GO diet were observed in liver mitochondria, while there were opposite changes in mitochondrial characteristics (decreased State 4, increased RCR). This difference is difficult to interpret, but may possibly be related to the muscle-specific expression of mitochondrial membrane proteins interacting with membrane phospholipids and modulating membrane proton leakiness. This hypothesis is based on the recent description of an uncoupling protein 3 expressed at high levels in mammalian skeletal muscles and BAT, but not in hepatocytes (39,40) although the presence of a similar protein in duckling muscle is still not demonstrated. It is also based on the observation that reconstituted liposomes of differing fatty acid composition do not exhibit differences in proton leak (41), while in intact mitochondria, differences in FA composition affect membrane proton leakiness (17). It is therefore tentatively postulated that a muscle-specific avian uncoupling protein, the protonophoric activity of which may be potentiated by the FA composition of the mitochondrial membrane, contributes to the functional properties of muscle mitochondria induced by either cold acclimation or the GO diet. More studies are required to confirm the existence and clarify the regulatory activity of such protein.

On an other hand, the lipid composition of mitochondrial membranes may be important in modulating the activity of membrane-bound enzymes, and the enrichment in PUFA induced by cold acclimation was indeed related to an increase of the ATP synthesis in skeletal muscles. The ATPase complex activity was already shown to be regulated by the chain length and the degree of unsaturation of membrane FA (42). The GO diet had less clear-cut effects on the ATP synthesis, despite marked changes in membrane PUFA, possibly because the proportion of the 18:2n-6 was also markedly increased. In rats, the ATP-synthase activity was indeed shown to be inversely related to the content in 18:2n-6 (43). A specific role of the 20:4n-6 or longer n-6 FA in modulating these activities remains to be clarified.

In conclusion, this study showed that in CA young birds, there is a muscle-specific enrichment of mitochondrial phospholipids in long and unsaturated FA. Similar changes do not occur in liver mitochondria. Feeding a GO diet rich in n-6 PUFA induced similar changes in lipid composition and mitochondrial functional activity in skeletal muscles as did cold acclimation. It is suggested that the FA composition of mitochondrial membranes may contribute to the increased proton leakiness of muscle mitochondria observed in CA ducklings, but that muscle-specific factors control this effect.

ACKNOWLEDGMENTS

This work was supported by a grant from the Université Claude Bernard, and the Centre National de la Recherche Scientifique (CNRS). François Chaînier was in receipt of a Ministère de l'Education National, de l'Enseignement Supérieur et de la Recherche fellowship.

REFERENCES

1. Jansky, L. (1971) Participation of Body Organs During Nonshivering Heat Production, *Biol. Rev. 48*, 85–132.
2. El Halawani, M.E., Wilson, W.D., and Burger, R.E. (1971) Cold Acclimation and the Role of Catecholamines in Body Temperature Regulation in Male Leghorns, *Poult. Sci. 49*, 621–632.
3. Barré, H., Nedergaard, J., and Cannon, B. (1986) Increased Respiration in Skeletal Muscle Mitochondria from Cold-Acclimated Ducklings: Uncoupling Effects of Free Fatty Acids, *Comp. Biochem. Physiol., B 85*, 343–348.
4. Duchamp, C., Barré, H., Delage, D., Rouanet, J.L., Cohen-Adad, F., and Minaire, Y. (1989) Nonshivering Thermogenesis and Adaptation to Fasting in King Penguin Chicks, *Am. J. Physiol. 257*, R744–R751.
5. Duchamp, C., Marmonier, F., Denjean, F., Lachuer, J., Eldershaw, T.P., Rouanet, J.L., Morales, A., Meister, R., Benistant, C., Roussel, D., and Barré, H. (1999) Regulatory, Cellular and Molecular Aspects of Avian Muscle Nonshivering Thermogenesis, *Ornis Fennica 76*, 151–165.
6. Barré, H., Cohen-Adad, F., Duchamp, C., and Rouanet, J.L. (1986) Multilocular Adipocytes from Muscovy Ducklings Differentiated in Response to Cold Acclimation, *J. Physiol. (Lond.) 375*, 27–38.
7. Saarela, S., Hissa, R., Pyörnilä, A., Harjula, R., Ojanen, M., and Orell, M. (1989) Do Birds Possess Brown Adipose Tissues? *Comp. Biochem. Physiol., A 92A*, 219–228.
8. Denjean, F., Lachuer, J., Cohen-Adad, F., Barré, H., and Duchamp, C. (1999) Are the Mammalian-Like Uncoupling Proteins 1 and 2 Expressed in Cold-Acclimated Muscovy Ducklings? *Ornis Fennica 76*, 167–175.
9. Duchamp, C., and Barré, H. (1993) Skeletal Muscle as the Major Site of Nonshivering Thermogenesis in Cold-Acclimated Ducklings, *Am. J. Physiol. 265*, R1076–R1083.
10. Barré, H., Berne, G., Brebion, P., Cohen-Adad, F., and Rouanet, J.L. (1989) Loose-Coupled Mitochondria in Chronic Glu-

cagon-Treated Hyperthermic Ducklings, *Am. J. Physiol. 256*, R1192–R1199.
11. Roussel, D., Rouanet, J.L., Duchamp, C., and Barré, H. (1998) Effects of Cold Acclimation and Palmitate on Energy Coupling in Duckling Skeletal Muscle Mitochondria, *FEBS Lett. 439*, 258–262.
12. Skulachev, V.P., and Maslov, S.P. (1960) The Role of Nonphosphorylating Oxidation in Temperature Regulation, *Biochemistry (Moscow) 25*, 1058–1064.
13. Levachev, M.M., Mishukova, E.A., Sivkova, V.G., and Skulachev, V.P. (1965) Energy Metabolism in the Pigeon During Self-Warming After Hypothermia, *Biokhimiia 30*, 864–874.
14. Garlid, K.D., Beavis, A.D., and Ratkje, S.K. (1989) On the Nature of Ion Leaks in Energy-Transducing Membranes, *Biochim. Biophys. Acta 976*, 109–120.
15. Brown, G.C., and Brand, M.D. (1991) On the Nature of the Mitochondrial Proton Leak, *Biochim. Biophys. Acta 1059*, 55–62.
16. Porter, R.K., Hulbert, A.J., and Brand, M.D. (1996) Allometry of Mitochondrial Proton Leak: Influence of Membrane Surface Area and Fatty Acid Composition, *Am. J. Physiol. 271*, R1550–R1560.
17. Brookes, P.S., Buckingham, J.A., Tenreiro, A.M., Hulbert, A.J., and Brand, M.D. (1998) The Proton Permeability of the Inner Membrane of Liver Mitochondria from Ectothermic and Endothermic Vertebrates and from Obese Rats: Correlations with Standard Metabolic Rate and Phospholipid Fatty Acid Composition, *Comp. Biochem. Physiol. 119B*, 325–334.
18. Brand, M.D., Couture, P., Else, P.L., Withers, K.W., and Hulbert, A.J. (1991) Evolution of Energy Metabolism. Proton Permeability of the Inner Membrane of Liver Mitochondria Is Greater in a Mammal Than in a Reptile, *Biochem. J. 275*, 81–86.
19. Senault, C., Yazbeck, J., Goubern, M., Portet, R., Vincent, M., and Gallay, J. (1990) Relation Between Membrane Phospholipid Composition, Fluidity and Function in Mitochondria of Rat Brown Adipose Tissue. Effect of Thermal Adaptation and Essential Fatty Acid Deficiency, *Biochim. Biophys. Acta 1023*, 283–289.
20. Early, R.J., and Spielman, S.P. (1995) Muscle Respiration in Rats Is Influenced by the Type and Level of Dietary Fat, *J. Nutr. 125*, 1546–1553.
21. Ayre, K.J., and Hulbert, A.J. (1996) Dietary Fatty Acid Profile Influences the Composition of Skeletal Muscle Phospholipids in Rats, *J. Nutr. 126*, 653–662.
22. Duchamp, C., Cohen-Adad, F., Rouanet, J.L., and Barré, H. (1992) Histochemical Arguments for Muscular Nonshivering Thermogenesis in Muscovy Ducklings, *J. Physiol. (Lond.) 457*, 27–45.
23. Folch, J., Lees, M., and Sloane Stanley, G.H. (1957) A Simple Method for the Isolation and Purification of Total Lipides from Animal Tissues, *J. Biol. Chem. 226*, 497–509.
24. Slover, H.J., and Lanza, E. (1979) Quantitative Analysis of Food Fatty Acids by Capillary Gas Chromatography, *J. Am. Oil Chem. Soc. 56*, 953–962.
25. Lepage, G., and Roy, C.C. (1986) Direct Transesterification of All Classes of Lipids in a One-Step Reaction, *J. Lipid Res. 27*, 114–120.
26. Wibom, R., Lundin, A., and Hultman, E. (1990) A Sensitive Method for Measuring ATP-Formation in Rat Muscle Mitochondria, *Scand. J. Clin. Lab. Invest. 50*, 143–152.
27. Hulbert, A.J., and Else, P.L. (1999) Membranes as Possible Pacemakers of Metabolism, *J. Theor. Biol. 199*, 257–274.
28. Steffen, D.G., and Platner, W.S. (1976) Subcellular Membrane Fatty Acids of Rat Heart After Cold Acclimation or Thyroxine, *Am. J. Physiol. 231*, 650–654.
29. Mak, I.T., Shrago, E., and Elson, C.E. (1983) Modification of Liver Mitochondrial Lipids and of Adenine Nucleotide Translocase and Oxidative Phosphorylation by Cold Adaptation, *Biochim. Biophys. Acta 722*, 302–309.
30. Field, C.J., and Clandinin, M.T. (1984) Modulation of Adipose Tissue Fat Composition by Diet: A Review, *Nutr. Res. 4*, 743–755.
31. Daum, G. (1985) Lipids of Mitochondria, *Biochim. Biophys. Acta 822*, 1–42.
32. Yeagle, P.L. (1989) Lipid Regulation of Cell Membrane Structure and Function, *FASEB J. 3*, 1833–1842.
33. Merrill, A.H., Jr., and Schroeder, J.J. (1993) Lipid Modulation of Cell Function, *Annu. Rev. Nutr. 13*, 539–559.
34. Gibson, R.A., McMurchie, E.J., Charnock, J.S., and Kneebone, G.M. (1984) Homeostatic Control of Membrane Fatty Acid Composition in the Rat After Dietary Lipid Treatment, *Lipids 19*, 942–951.
35. Benistant, C., Duchamp, C., Cohen-Adad, F., Rouanet, J.L., and Barré, H. (1998) Increased *in vitro* Fatty Acid Supply and Cellular Transport Capacities in Cold-Acclimated Ducklings *(Cairina moschata), Am. J. Physiol. 275*, R683–R690.
36. Gompertz, D., and Greenbaum, A.L. (1966) The Effects of Thyroxine on the Pattern of Fatty Acid Synthesis in Rat Liver, *Biochim. Biophys. Acta 116*, 441–459.
37. Faas, F.H., Carter, W.J., and Wynn, J. (1972) Effect of Thyroxine on Fatty Acid Synthesis *in vitro, Endocrinology 91*, 1481–1492.
38. Clejan, S., Collipp, P.J., and Maddaiah, V.T. (1980) Hormones and Liver Mitochondria: Influence of Growth Hormone, Thyroxine, Testosterone, and Insulin on Thermotropic Effects of Respiration and Fatty Acid Composition of Membranes, *Arch. Biochem. Biophys. 203*, 744–752.
39. Vidal-Puig, A., Solanes, G., Grujic, D., Flier, J.S., and Lowell, B.B. (1997) UCP3: An Uncoupling Protein Homologue Expressed Preferentially and Abundantly in Skeletal Muscle and Brown Adipose Tissue, *Biochem. Biophys. Res. Commun. 235*, 79–82.
40. Boss, O., Samec, S., Paoloni-Giacobino, A., Rossier, C., Dulloo, A., Seydoux, J., Muzzin, P., and Giacobino, J.P. (1997) Uncoupling Protein-3: a New Member of the Mitochondrial Carrier Family with Tissue-Specific Expression, *FEBS Lett. 408*, 39–42.
41. Brookes, P.S., Hulbert, A.J., and Brand, M.D. (1997) The Proton Permeability of Liposomes Made from Mitochondrial Inner Membrane Phospholipids: No Effect of Fatty Acid Composition, *Biochim. Biophys. Acta 1330*, 157–164.
42. Bruni, A., van Dijck, P.W., and de Gier, J. (1975) The Role of Phospholipid Acyl Chains in the Activation of Mitochondrial ATPase Complex, *Biochim. Biophys. Acta 406*, 315–328.
43. Jumelle-Laclau, M., Rigoulet, M., Averet, N., Leverve, X., Dubourg, L., Carbonneau, A., Clerc, M., and Guerin, B. (1993) Relationships Between Age-Dependent Changes in the Effect of Almitrine on H(+)-ATPase/ATPsynthase and the Pattern of Membrane Fatty Acid Composition, *Biochim. Biophys. Acta 1141*, 90–94.
44. Estabrook, R.W. (1967) Mitochondrial Respiratory Control and the Polarographic Measurement of ADP:O Ratios, *Methods Enzymol. 10*, 41–47.

[Received June 2, 2000, and in revised form and accepted September 8, 2000]

Effect of n-3 Fatty Acid Deficiency on Fatty Acid Composition and Metabolism of Aminophospholipids in Rat Brain Synaptosomes

Atsushi Ikemoto[a,*], Masayo Ohishi[a], Noriaki Hata[b], Yoshihisa Misawa[b], Yoichi Fujii[a], and Harumi Okuyama[a]

[a]Department of Biological Chemistry, Faculty of Pharmaceutical Sciences, Nagoya City University, Nagoya 467-8603, Japan, and [b]Applied Research Department, Harima Chemicals, Inc., Tsukuba 300-26, Japan

ABSTRACT: Docosahexaenoic acid (DHA, 22:6n-3) is one of the major polyunsaturated fatty acids esterified predominantly in aminophospholipids such as ethanolamine glycerophospholipid (EtnGpl) and serine glycerophospholipid (SerGpl) in the brain. Synaptosomes prepared from rats fed an n-3 fatty acid-deficient safflower oil (Saf) diet had significantly decreased 22:6n-3 content with a compensatory increased 22:5n-6 content when compared with rats fed an n-3 fatty acid-sufficient perilla oil (Per) diet. When the Saf group was shifted to a diet supplemented with safflower oil plus 22:6n-3 (Saf + DHA) after weaning, 22:6n-3 content was found to be restored to the level of the Per group. The uptake of [^{3}H]ethanolamine and its conversion to [^{3}H]EtnGpl did not differ significantly among the three dietary groups, whereas the formation of [^{3}H]lysoEtnGpl from [^{3}H]ethanolamine was significantly lower in the Saf group than in the other groups. The uptake of [^{3}H]serine, its incorporation into [^{3}H]SerGpl, and the conversion into [^{3}H]EtnGpl by decarboxylation of [^{3}H]SerGpl did not differ among the three dietary groups. The observed decrease in lysoEtnGpl formation associated with a reduction of 22:6n-3 content in rat brain synaptosomes by n-3 fatty acid deprivation may provide a clue to reveal biochemical bases for the dietary fatty acids–behavior link.

Paper no. L8384 in *Lipids 35*, 1107–1115 (October 2000).

Polyunsaturated fatty acids (PUFA) derived from n-6 or n-3 fatty acids are fundamental components of structural membrane lipids in the central nervous system. These PUFA, mainly arachidonic acid (20:4n-6) and docosahexaenoic acid (DHA, 22:6n-3), can be derived from essential fatty acid precursors, linoleic (18:2n-6) and α-linolenic acids (18:3n-3), which must be supplied from dietary sources in mammals (1–3). A reduction in 22:6n-3 content and a small but significant increase in 20:4n-6 content caused by dietary deprivation of n-3 fatty acids for long periods (e.g., through two generations) were shown to cause impaired retinal function and learning ability as well as altered behavior and drug sensitivity in rodents (4–9). These results suggest that 22:6n-3 plays an important role in the maintenance of normal neural functions, for which n-6 PUFA cannot compensate. However, the extent of dietary modification of fatty acid composition and its effect on phospholipid metabolism have not been well defined.

In the brain, 22:6n-3 is particularly enriched in aminophospholipids such as ethanolamine glycerophospholipid (EtnGpl) and serine glycerophospholipid (SerGpl). Recently, it was suggested that bioactive metabolites of 22:6n-3 are not responsible for its functions in the brain but that 22:6n-3-containing aminophospholipids are critical for optimal neural function and structure (10). We have reported that dietary n-3 fatty acid deficiency and a learning task synergistically induce ultrastructural changes in synapse in the hippocampus (11) and some functional changes in the brain microsomal membrane surfaces (12). EtnGpl has been described to be associated with a specific protein in phospholipid bilayer. For example, EtnGpl is preferentially located in the extracellular leaflet in acetylcholine receptor-rich membranes (13). SerGpl in membranes is known to be an essential cofactor for the activation of protein kinase C (14). Several lines of evidence have shown that SerGpl regulates the activity of various enzymes such as diacylglycerol kinase (15), Na^+, K^+-ATPase (16), and nitric oxide synthase (17), and acts as a ligand in recognition of apoptotic cells (18).

In previous studies we demonstrated that in rat pheochromocytoma PC12 cells, nerve growth factor (NGF)-induced neurite outgrowth was enhanced by 22:6n-3 but suppressed by 20:4n-6 (19). The 20:4n-6 also reduced incorporation of [^{3}H]ethanolamine into EtnGpl *via* suppression of [^{3}H]ethanolamine uptake into the cells whereas 22:6n-3 had no effect (19,20). On the other hand, 22:6n-3, but not 20:4n-6, increased SerGpl and EtnGpl synthesis from [^{3}H]serine in PC12 cells irrespective of NGF-induced differentiation (20). En-

*To whom correspondence should be addressed at Department of Biological Chemistry, Faculty of Pharmaceutical Sciences, Nagoya City University, 3-1 Tanabedori, Mizuhoku, Nagoya 467-8603, Japan.
E-mail: aikemoto@phar.nagoya-cu.ac.jp

Abbreviations: ANOVA, analysis of variance; BSS, balanced salt solution; ChoGpl, choline glycerophospholipid; DHA, docosahexaenoic acid (22:6n-3); EtnGpl, ethanolamine glycerophospholipid; NGF, nerve growth factor; PBS, phosphate-buffered saline; Per, perilla oil; PLA, phospholipase A; PtdIns, phosphatidylinositol; PUFA, polyunsaturated fatty acid; Saf, safflower oil; SerGpl, serine glycerophospholipid; TLC, thin-layer chromatography.

hancement by 22:6n-3 of SerGpl synthesis from [^{3}H]serine has been observed in C6 glioma cells (21). These results from *in vitro* cultured cells suggest that 22:6n-3 enhances but 20:4n-6 suppresses both aminophospholipid synthesis and neurite elongation.

In vivo studies using autoradiographic methods led to apparently inconsistent conclusions; brain phospholipid synthesis was lowered, but protein synthesis was enhanced by n-3 fatty acid deficiency (22,23). However, a methodological problem was pointed out about specific radioactivity of the direct precursor pool of phospholipid synthesis (24), and we observed no significant changes in protein synthesis in the rat brain under n-3 fatty acid deficiency (25).

In this study we investigated the effect of reduction of 22:6n-3 content on aminophospholipid metabolism using synaptosomes prepared from rats under n-3 fatty acid deficiency. The data presented here demonstrate that, unlike in cultured cells and *in vivo* autoradiographic results, dietary n-3 fatty acid deficiency does not affect aminophospholipid synthesis evaluated using [^{3}H]ethanolamine and [^{3}H]serine as precursors, but suggest that turnover of EtnGpl to lysoEtnGpl is lowered.

EXPERIMENTAL PROCEDURES

Materials. The ethyl ester of 22:6n-3 (>95% pure) was produced by Harima Chemicals, Inc. (Tsukuba, Japan). Percoll was purchased from Pharmacia Biotech (Uppsala, Sweden). [1-^{3}H]Ethanolamine hydrochloride (28 Ci/mmol) and [^{3}H(G)] L-serine (27.5 Ci/mmol) were purchased from Amersham (Buckingham, United Kingdom) and Moravek Biochemicals Inc. (Brea, CA), respectively. Silica Gel 60G thin-layer chromatography (TLC) plates were purchased from Merck (Darmstadt, Germany).

Animals and diets. All procedures for animal use were approved by the Center for Laboratory Animals, Faculty of Pharmaceutical Sciences, Nagoya City University. The semipurified diet (Clea Japan Inc., Tokyo, Japan) contained, by weight, 47% corn starch, 24.6% milk casein, 2% α-starch, 8% cellulose powder, 5% sucrose, 2% vitamin mixture, 6% mineral mixture, 0.4% DL-methionine, 0.6% choline chloride, and 5% of the indicated oil. The fatty acid compositions of diets supplemented with the oils are shown in Table 1. Female Wistar rats (F_0) (SLC Co., Shizuoka, Japan) at 4 wk of age were fed a safflower oil (Saf) or perilla oil (Per) diet for 2 mon. The rats (F_0) were mated at 11 wk of age and the litters (F_1) were weaned at 3 wk. The male pups (F_1) fed the Saf diet were divided randomly into two groups. One group was fed the same Saf diet and the other group was fed a diet supplemented with 4.5% Saf plus 0.5% 22:6n-3 (Saf + DHA). The male pups (F_1) from the Per diet group were fed the same Per diet. The male rats (F_1) at 19 wk of age were used for the experiments.

Preparation of rat brain synaptosomes. The 19-wk-old rats (F_1) were decapitated, and the brains were isolated rapidly. The synaptosomes were prepared by a Percoll gradient procedure (26) as follows. The brains were homogenized in 10 vol of buffer composed of 0.32 M sucrose, 5 mM Hepes pH 7.4, and 0.1 mM EGTA. The homogenate was centrifuged at 1,100 × *g* for 5 min, and the supernatant was layered on a discontinuous two-step Percoll density gradient composed of equal volumes of 10 and 23% (w/w) Percoll. The density gradient separations were performed by centrifugation at 15,000 × *g* for 30 min. The synaptosomes were banded at the interfacial fractions found between 10 and 23% Percoll. The synaptosomal fractions were isolated and centrifuged at 15,000 × *g* for 10 min. The pellets obtained were suspended in balanced salt solution (BSS; 128 mM NaCl, 2.4 mM KCl, 1.2 mM $MgSO_4$, 1.2 mM KH_2PO_4, 10 mM Hepes pH 7.4, 10 mM D-glucose) and centrifuged at 15,000 × *g* for 10 min to remove the remaining Percoll. The pellets obtained were suspended in BSS and used immediately for the experiments. The purity of synaptosomes was checked by marker enzymes as described previously (27). Protein concentration was determined using a bicinchoninic acid reagent (28).

TABLE 1
Fatty Acid Composition of Diets[a]

Fatty acid	Safflower oil diet	Safflower oil + DHA diet	Perilla oil diet
16:0	6.6	5.9	6.8
18:0	2.4	2.2	2.3
18:1	13.5	12.1	21.9
18:2n-6[b]	76.8	69.1	13.2
18:3n-3	0.2	0.2	54.7
20:5n-3	ND	0.5	ND
22:6n-3	ND	9.5	ND
n-6/n-3[c]	>300	6.79	0.24

[a]The fatty acid composition of the diets (% of total fatty acids, w/w) was analyzed by gas–liquid chromatography. ND, not detected (below 0.05% of the total); DHA, docosahexaenoic acid.
[b]The position of the double bond numbered from the methyl terminus is designated as n-6 or n-3.
[c]n-6/n-3 indicates the ratio of the total n-6 fatty acids/total n-3 fatty acids.

Analysis of fatty acid composition. Synaptosomal lipids were extracted three times with chloroform/methanol according to the method of Bligh and Dyer (29). The lipid classes were separated by silica gel TLC with chloroform/methanol/acetic acid/formic acid/water (70:30:12:4:2, by vol) as the developing solvent. The regions corresponding to individual phospholipids were scraped off, and phospholipids were extracted from the silica gel twice with chloroform/methanol/3% NH_4OH (6:5:1, by vol) and then once with chloroform/methanol (2:1, by vol). Fatty acids were converted to their methyl esters by treatment with 5% HCl in methanol and were quantified by capillary column gas–liquid chromatography using heptadecanoic acid as an internal standard as described previously (4).

Ethanolamine and serine uptake by synaptosomes. Synaptosomes containing 200 μg of protein were preincubated at 37°C for 5 min in BSS. The uptake assay was started by adding 0.25–1.0 μM [^{3}H]ethanolamine (2 Ci/nmol) or [^{3}H]serine (2 Ci/nmol) at a final volume of 0.5 mL. After incubation at 37°C for 5 min, the suspension was centrifuged at 15,000 × *g* at 2°C for 10 min. The pellet was washed three times with ice-cold BSS and the synaptosome-associated radioactivity was measured.

Incorporation of [^{3}H]ethanolamine and [^{3}H]serine into aminophospholipids. Synaptosomes containing 200 μg of protein were preincubated at 37°C for 5 min in BSS. After the addition of 2 μCi/mL [^{3}H]ethanolamine or 3 μCi/mL [^{3}H]serine in a final volume of 0.5 mL, the mixture was incubated at 37°C for 0.5 to 4.0 h. The reactions were stopped by addition of 2 vol of methanol, and the synaptosomal lipids were extracted three times with chloroform/methanol according to the method of Bligh and Dyer (29). The lipids were separated by TLC with chloroform/methanol/acetic acid/water (25:15:4:2, by vol) as the developing solvent. The regions corresponding to individual phospholipids were scraped into scintillation vials, the contents of silica gel were adjusted to the same amounts, and the radioactivities were measured using a liquid-scintillation counter (LSC-5100; Aloka, Tokyo, Japan) by using the optimized scintillation cocktail (30). For the pulse-chase experiments, synaptosomes were incubated for 1 h with 2 μCi/mL [^{3}H]ethanolamine. After the pulse-labeling, the BSS was removed and the synaptosomes were washed three times. Then the buffer was replaced with BSS containing 1 mM unlabeled ethanolamine, and the synaptosomes were incubated for 0.5 to 4.0 h.

Statistics. Results were compared by one-way analysis of variance followed by a Bonferroni multiple comparison test. A difference was considered significant at $P < 0.05$.

RESULTS

Fatty acid composition of synaptosomal phospholipids. Among the three dietary groups, weight gain, litter size, brain weight, and synaptosomal protein were not significantly different (data not shown). Table 2 shows the fatty acid composition of choline glycerophospholipid (ChoGpl) in rat brain synaptosomes. Total fatty acid contents of ChoGpl (μg/mg protein) were not significantly different among the three groups. The major fatty acids in ChoGpl were saturated and monounsaturated fatty acids (>85%), which did not differ among the three groups. The contents of PUFA in ChoGpl were relatively small, but in the Saf group, 22:6n-3 was lower and 20:4n-6, 22:4n-6, and 22:5n-6 were significantly higher compared with the Per and the Saf + DHA groups.

Fatty acid compositions of EtnGpl and SerGpl are presented in Tables 3 and 4, respectively. Total fatty acid contents per protein in EtnGpl and SerGpl were not significantly different among the three dietary groups. The aminophospholipids contained relatively higher amounts of PUFA. In the Saf group, n-3 fatty acid deficiency led to marked decreases of 22:6n-3 in both EtnGpl and SerGpl as compared with the Per and the Saf + DHA groups. The total PUFA contents were similar; in the Saf group the marked decrease in 22:6n-3 was compensated for by increases in 22:4n-6 and 22:5n-6 in both aminophospholipids. In the Saf + DHA group, the level of 22:5n-6 was similar to that in the Per group in both EtnGpl and SerGpl, while the level of 22:4n-6 was intermediate between those of the Saf and the Per groups. EtnGpl contained relatively higher amounts of 20:4n-6 than SerGpl. In both

TABLE 2
Fatty Acid Composition of Choline Glycerophospholipid in Brain Synaptosomes[a]

Fatty acid	Saf	Saf + DHA	Per
	(% of total fatty acids)		
16:0 DMA	0.25 ± 0.14	0.18 ± 0.03	0.22 ± 0.06
16:0	38.35 ± 1.52	39.95 ± 2.51	39.56 ± 1.20
18:0 DMA	0.21 ± 0.11	0.18 ± 0.04	0.18 ± 0.03
18:1 DMA	0.38 ± 0.39	0.22 ± 0.08	0.22 ± 0.14
18:0	15.13 ± 0.27	14.70 ± 0.83	14.89 ± 0.51
18:1	31.26 ± 1.12	32.61 ± 1.81	33.20 ± 1.75
18:2n-6	0.89 ± 0.10^b	1.30 ± 0.13^a	0.88 ± 0.06^b
20:0	0.25 ± 0.02	0.25 ± 0.05	0.23 ± 0.02
20:1	1.37 ± 0.08	1.37 ± 0.23	1.27 ± 0.12
20:3n-6	0.18 ± 0.07	0.24 ± 0.00	0.32 ± 0.03
20:4n-6	6.01 ± 0.47^a	4.28 ± 0.51^b	3.71 ± 0.55^b
22:0	0.17 ± 0.12	0.27 ± 0.06	0.21 ± 0.06
22:1	0.10 ± 0.07	0.15 ± 0.02	0.13 ± 0.03
22:4n-6	0.94 ± 0.09^a	0.49 ± 0.07^b	0.30 ± 0.07^c
22:5n-6	1.91 ± 0.37^a	0.17 ± 0.03^b	0.05 ± 0.07^b
22:5n-3	ND^b	ND^b	0.19 ± 0.04^a
22:6n-3	1.83 ± 0.24^b	2.98 ± 0.54^a	3.66 ± 0.76^a
24:0	0.32 ± 0.04	0.34 ± 0.05	0.30 ± 0.06
Total fatty acids (μg/mg of protein)	124 ± 21	119 ± 15	125 ± 21

[a]Synaptosomes were prepared from rats fed semipurified diets supplemented with safflower oil (Saf), safflower oil plus DHA (Saf + DHA), or perilla oil (Per). Values represent means ± SD for four rats. DMA, dimethylacetal; for other abbreviations see Table 1. Values of the same fatty acid with different roman superscripts are significantly different ($P < 0.05$) in one-way analysis of variance (ANOVA) using Bonferroni's test.

TABLE 3
Fatty Acid Composition of Ethanolamine Glycerophospholipid in Brain Synaptosomes[a]

Fatty acid	Saf	Saf + DHA	Per
	(% of total fatty acids)		
16:0 DMA	4.41 ± 0.18	4.46 ± 0.73	4.76 ± 0.65
16:0	5.30 ± 0.64	4.86 ± 0.69	5.16 ± 0.38
18:0 DMA	8.28 ± 0.67	8.77 ± 0.33	8.35 ± 0.80
18:1 DMA	3.72 ± 0.24	4.66 ± 0.66	3.89 ± 0.64
18:0	21.24 ± 0.46^a	19.89 ± 0.75^b	20.25 ± 0.36^a
18:1	14.96 ± 2.46	17.87 ± 2.83	18.90 ± 1.14
18:2n-6	0.35 ± 0.10	0.44 ± 0.05	0.21 ± 0.18
20:0	0.39 ± 0.05^a	0.39 ± 0.06^a	0.27 ± 0.01^b
20:1	2.53 ± 0.39^b	3.11 ± 0.37^a	2.87 ± 0.28^a
20:3n-6	0.40 ± 0.03^b	0.58 ± 0.08^a	0.54 ± 0.03^a
20:4n-6	12.93 ± 0.26^a	10.08 ± 0.81^b	8.65 ± 0.73^c
22:0	0.20 ± 0.14	0.20 ± 0.18	0.29 ± 0.01
22:1	0.07 ± 0.06	0.12 ± 0.10	0.13 ± 0.02
22:4n-6	6.77 ± 0.73^a	4.88 ± 1.12^{a,b}	2.01 ± 1.76^b
22:5n-6	7.40 ± 0.92^a	0.12 ± 0.14^b	0.34 ± 0.60^b
22:5n-3	0.13 ± 0.09	ND	0.71 ± 0.62
22:6n-3	8.76 ± 1.31^b	17.19 ± 4.43^a	20.00 ± 1.33^a
24:0	1.28 ± 0.11	1.26 ± 0.10	1.13 ± 0.11
Total fatty acids (μg/mg of protein)	110 ± 21	105 ± 14	108 ± 16

[a]Synaptosomes were prepared from rats fed semipurified diets supplemented with Saf, Saf + DHA, or Per. Values represent means ± SD for four rats. Values of the same fatty acid with different roman superscripts are significantly different ($P < 0.05$) in one-way ANOVA using Bonferroni's test. For abbreviations see Tables 1 and 2.

TABLE 4
Fatty Acid Composition of Serine Glycerophospholipid in Brain Synaptosomes[a]

Fatty acid	Saf	Saf + DHA	Per
	(% of total fatty acids)		
16:0 DMA	0.04 ± 0.09	0.12 ± 0.25	0.06 ± 0.07
16:0	1.32 ± 0.18	1.30 ± 0.30	1.31 ± 0.25
18:0 DMA	0.08 ± 0.16	0.20 ± 0.30	0.12 ± 0.15
18:1 DMA	0.07 ± 0.14	0.19 ± 0.22	0.03 ± 0.06
18:0	43.69 ± 0.72	41.83 ± 1.11	42.52 ± 1.15
18:1	20.14 ± 2.42[b]	22.04 ± 2.15[b]	27.71 ± 0.64[a]
18:2n-6	0.07 ± 0.08	0.12 ± 0.14	0.12 ± 0.08
20:0	0.60 ± 0.06	0.67 ± 0.15	0.45 ± 0.30
20:1	2.13 ± 0.09	2.11 ± 0.32	1.54 ± 1.05
20:3n-6	0.38 ± 0.27	0.48 ± 0.32	0.67 ± 0.16
20:4n-6	4.07 ± 0.24[a]	3.63 ± 0.22[b]	2.70 ± 0.23[c]
22:0	0.74 ± 0.51	1.20 ± 0.33	0.78 ± 0.53
22:1	0.41 ± 0.28	0.71 ± 0.13	0.46 ± 0.31
22:4n-6	4.53 ± 0.61[a]	2.36 ± 1.60[b]	1.32 ± 0.59[b]
22:5n-6	11.74 ± 1.48[a]	0.91 ± 0.67[b]	0.42 ± 0.17[b]
22:5n-3	ND[b]	ND[b]	0.42 ± 0.28[a]
22:6n-3	8.76 ± 0.82[c]	20.59 ± 0.21[a]	18.29 ± 1.25[b]
24:0	0.91 ± 0.22	1.16 ± 0.36	0.81 ± 0.08
Total fatty acids (μg/mg of protein)	41.2 ± 5.1	43.5 ± 3.8	42.8 ± 4.6

[a]Synaptosomes were prepared from rats fed semipurified diets supplemented with Saf, Saf + DHA, or Per. Values represent means ± SD for four rats. Values of the same fatty acid with different roman superscripts are significantly different ($P < 0.05$) in one-way ANOVA using Bonferroni's test. For abbreviations see Tables 1 and 2.

aminophospholipids, the 20:4n-6 level in the Saf group was 1.5-fold higher than the Per group, whereas its level in the Saf + DHA group was intermediate between the Saf and the Per groups.

Phosphatidylinositol (PtdIns) had the highest content of 20:4n-6 among the major phospholipid classes (Table 5); the 20:4n-6 content in the Saf group was 13% higher than in the Per group. However, C_{22} PUFA content was relatively low and was affected relatively little by the dietary n-3 fatty acid deficiency, although a significantly lower 22:6n-3 content and concomitantly higher 22:4n-6 and 22:5n-6 contents were observed in the Saf group as compared with the other phospholipids.

TABLE 5
Fatty Acid Composition of Phosphatidylinositol in Brain Synaptosomes[a]

Fatty acid	Saf	Saf + DHA	Per
	(% of total fatty acids)		
16:0	8.47 ± 1.58	8.92 ± 1.49	10.29 ± 0.72
18:0	42.78 ± 1.49	41.37 ± 0.60	42.71 ± 2.39
18:1	9.50 ± 1.33	10.69 ± 1.99	10.39 ± 1.40
20:4n-6	34.19 ± 1.48[a]	32.59 ± 1.19[b]	30.21 ± 1.68[c]
22:4n-6	0.62 ± 0.11[a]	ND[b]	ND[b]
22:5n-6	1.98 ± 0.22[a]	ND[b]	ND[b]
22:6n-3	2.45 ± 0.08[b]	6.43 ± 0.76[a]	6.40 ± 0.90[a]
Total fatty acids (μg/mg of protein)	9.98 ± 1.62	9.45 ± 1.31	0.43 ± 1.06

[a]Synaptosomes were prepared from rats fed semipurified diets supplemented with Saf, Saf + DHA, or Per. Values represent means ± SD for four rats. Values of the same fatty acid with different superscripts are significantly different ($P < 0.05$) in one-way ANOVA using Bonferroni's test. For abbreviations see Tables 1 and 2.

Ethanolamine and serine uptake by synaptosomes. The uptake of ethanolamine and serine by synaptosomes increased linearly for up to 10 min at concentrations of 0.25 to 1.0 μM (data not shown). Therefore, we compared the uptake of ethanolamine and serine among the three dietary groups after 5 min of incubation (Fig. 1). The uptake of ethanolamine at 0.25 to 1.0 μM did not differ among the three dietary groups (Fig. 1A). Similarly, serine uptake was not different among the three

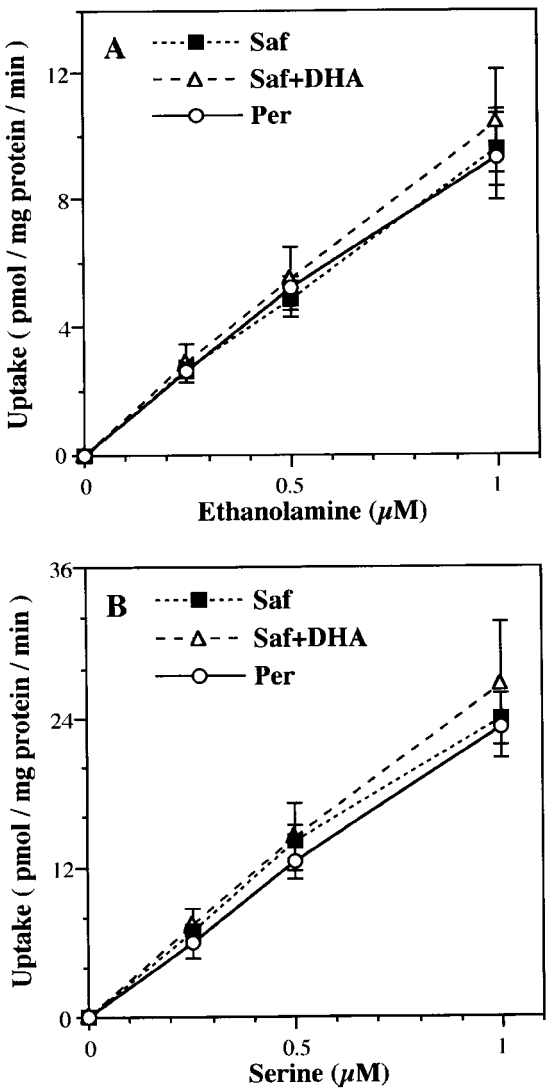

FIG. 1. Ethanolamine and serine uptake by brain synaptosomes. Synaptosomes prepared from rats fed semipurified diets supplemented with safflower oil (Saf), safflower oil plus DHA (Saf + DHA) or perilla oil (Per) were incubated with [^{3}H]ethanolamine (A) or [^{3}H]serine (B) at the indicated concentration for 5 min. The radioactivities associated with the synaptosomes were measured as described in the text. Values represent means ± SD for six rats.

dietary groups (Fig. 1B). Thus, n-3 fatty acid deficiency did not affect ethanolamine and serine uptake by synaptosomes.

Incorporation of [^{3}H]ethanolamine into aminophospholipids. The incorporation of [^{3}H]ethanolamine into [^{3}H]EtnGpl and its conversion to [^{3}H]lysoEtnGpl increased linearly for up to 2 and 4 h, respectively (Fig. 2). Incorporation of [^{3}H]ethanolamine into [^{3}H]EtnGpl after 1 h incubation was not significantly different among the three dietary groups (Fig. 3A). However, the formation of [^{3}H]lysoEtnGpl was significantly lower by about 20% in the Saf group than in the Per and Saf + DHA groups (Fig. 3B). Synaptosomes were first pulse-labeled for 1 h with [^{3}H]ethanolamine, then incubated for an additional 4 h in the presence of 1 mM unlabeled ethanolamine (Fig. 4). The lysoEtnGpl/EtnGpl ratio decreased with time, which is a type of label kinetics indicating an EtnGpl–lysoEtnGpl precursor–product relationship, i.e., a simultaneous decline of [^{3}H]EtnGpl and an increase of [^{3}H]lysoEtnGpl.

Incorporation of [^{3}H]serine into aminophospholipids. The incorporation of [^{3}H]serine into [^{3}H]SerGpl and its conversion to [^{3}H]EtnGpl by decarboxylation increased linearly for up to 2 and 4 h, respectively (Fig. 5). The formation of [^{3}H]lysoEtnGpl from [^{3}H]serine-derived [^{3}H]EtnGpl was essentially negligible (lower than 100 dpm per 200 μg of protein) during 4 h incubation (data not shown). The incorporation of [^{3}H]serine into [^{3}H]SerGpl for 1 h incubation did not differ among the three dietary groups (Fig. 6A). Similarly, the conversion of [^{3}H]SerGpl to [^{3}H]EtnGpl by decarboxylation was not significantly different among the three dietary groups (Fig. 6B). Thus, n-3 fatty acid deficiency did not affect [^{3}H]SerGpl synthesis from [^{3}H]serine and its conversion to [^{3}H]EtnGpl in synaptosomes.

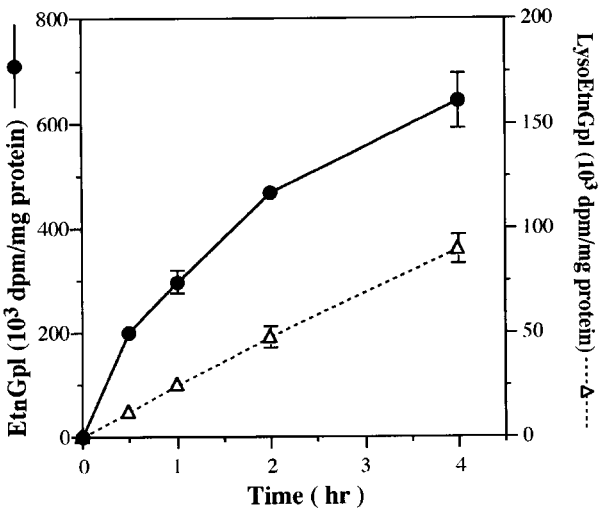

FIG. 2. Time course of incorporation of [^{3}H]ethanolamine into aminophospholipids in brain synaptosomes. Synaptosomes prepared from rats fed a conventional chow were incubated with 2 μCi/mL [^{3}H]ethanolamine for 0.5 to 4.0 h. The radioactivities incorporated into ethanolamine glycerophospholipid (EtnGpl) and lysoEtnGpl were measured as described in the text. Values represent means ± SD for four rats. In some cases error bars are included within the symbols.

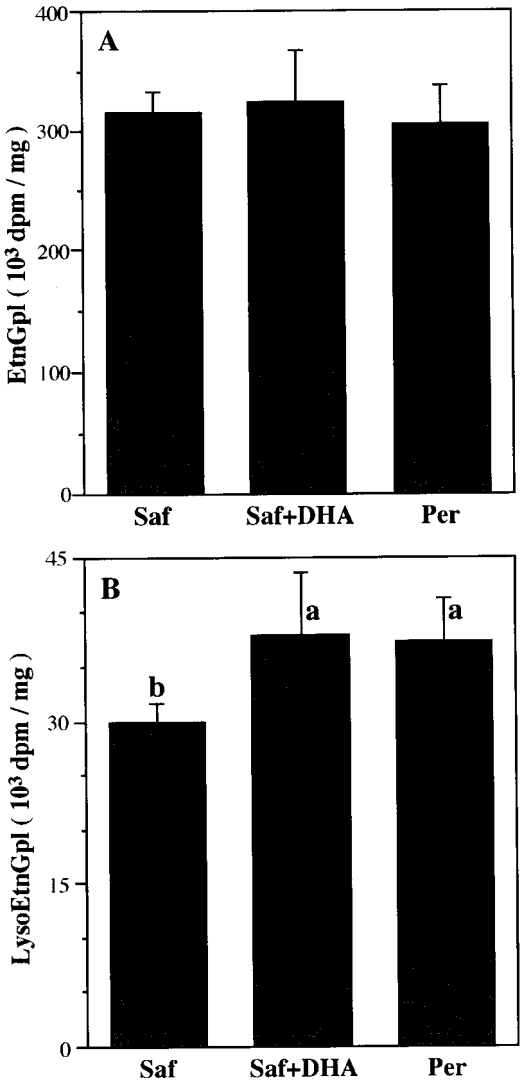

FIG. 3. Effect of dietary fatty acid status on incorporation of [^{3}H]-ethanolamine into aminophospholipids in brain synaptosomes. Synaptosomes prepared from rats fed semipurified diets supplemented with Saf, Saf + DHA, or Per were incubated with 2 μCi/mL [^{3}H]ethanolamine for 1 h. The radioactivities incorporated into EtnGpl (A) and lysoEtnGpl (B) were measured as described in the text. Values represent means ± SD for six rats. Values with different superscripts are significantly different ($P < 0.05$) in one-way analysis of variance using Bonferroni's test. For abbreviations see Figures 1 and 2.

DISCUSSION

In the previous study using cultured PC12 cells, 20:4n-6 added to the medium decreased ethanolamine uptake in a dose-dependent manner (20). The 20:4n-6 treatment resulted in a three- to fivefold increase in 20:4n-6 content (17–20% of total fatty acids vs. 5.8–6.6% in the control) with a concomitant decrease in 18:1 content (about 60% decrease compared with the control) in membrane phospholipids (19). In brain synaptosomes prepared from rats fed one of the three diets, the n-3 fatty acid-deficient (Saf), n-3 fatty acid-replenished (Saf + DHA), or n-3 fatty acid-sufficient (Per) diet, the up-

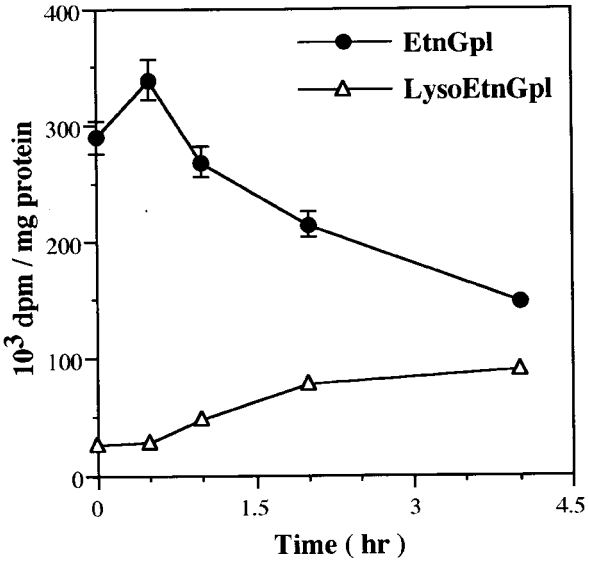

FIG. 4. Effect of exogenous unlabeled ethanolamine on [^{3}H]EtnGpl and [^{3}H]lysoEtnGpl in synaptosomes prelabeled with [^{3}H]ethanolamine. Synaptosomes prepared from rats fed a conventional chow were incubated with 2 μCi/mL [^{3}H]ethanolamine for 1 h. The pulse medium was removed and the synaptosomes were incubated in chase medium with 1 mM unlabeled ethanolamine, for 0.5–4.0 h. At the time intervals indicated, lipids were extracted and the level of [^{3}H]EtnGpl and [^{3}H]lysoEtnGpl were determined as described in the text. Each point represents the mean ± SD of four rats. In some cases error bars are included within the symbols.

take of aminophospholipid precursors such as ethanolamine and serine was not affected by altered n-6 and n-3 PUFA profiles in membrane phospholipids. The 20:4n-6 contents in the Saf group were 1.62-, 1.49-, and 1.51-fold greater in ChoGpl,

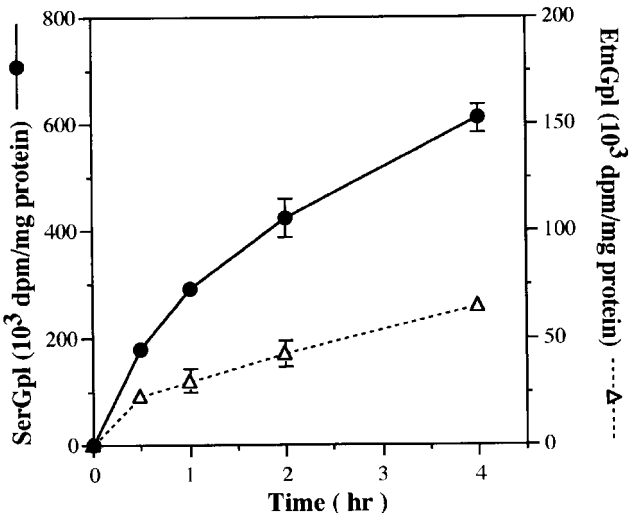

FIG. 5. Time course of incorporation of [^{3}H]serine into aminophospholipids in brain synaptosomes. Synaptosomes prepared from rats fed a conventional chow were incubated with 2 μCi/mL [^{3}H]serine for 0.5 to 4.0 h. The radioactivities incorporated into serine glycerophospolipid (SerGpl) and EtnGpl were measured as described in the text. Values represent means ± SD for four rats. In some cases error bars are included within the symbols. For other abbreviations see Figures 1 and 2.

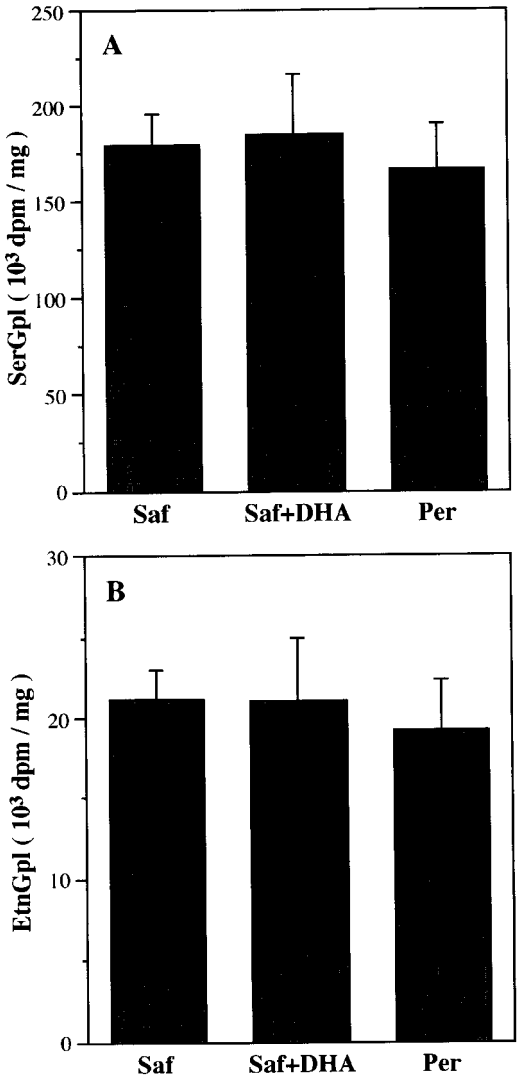

FIG. 6. Effect of dietary fatty acid status on incorporation of [^{3}H]serine into aminophospholipids in brain synaptosomes. Synaptosomes prepared from rats fed semipurified diets supplemented with Saf, Saf + DHA, or Per were incubated with 2 μCi/mL [^{3}H]serine for 1 h. The radioactivities incorporated into SerGpl (A) and EtnGpl (B) were measured as described in the text. Radioactivity in lysoEtnGpl was negligible (< 100 dpm/200 μg protein). Values represent means ± SD for six rats. For abbreviations see Figures 1, 2, and 5.

EtnGpl, and SerGpl, respectively, compared with the Per group. These changes were relatively smaller than those with PC12 cells cultured in the presence of 20:4n-6. The total PUFA contents in synaptosomes did not differ among the three dietary groups, whereas significant increases in PUFA contents and concomitant decreases in 18:1 contents were detected in PC12 cells treated with 20:4n-6 (about 60% low compared with the control). Differential extents of fatty acid modification and difference in cell types may account for the observed difference in aminophospholipid metabolism between PC12 cells and synaptosomes. Moreover, the differential effects may arise from the different method of fatty

acid modification between the *in vivo* and the *in vitro* experiments.

Although the [^{3}H]ethanolamine uptake and incorporation into EtnGpl in synaptosomes were not affected by n-3 fatty acid deficiency, the formation of [^{3}H]lysoEtnGpl, a probable deacylation product of [^{3}H]EtnGpl, was 20% less in the Saf group compared with the Per group. Moreover, the lower [^{3}H]lysoEtnGpl formation was restored by supplementing the Saf group with 22:6n-3 after weaning. This is the first demonstration of altered phospholipid metabolism observed in synaptosomes from rats nutritionally manipulated with respect to n-6 and n-3 fatty acid status.

At least four enzymatic pathways could be involved in the altered [^{3}H]lysoEtnGpl contents: (i) degradation by phospholipase A_1 (PLA_1), (ii) degradation by phospholipase A_2 (PLA_2), (iii) transfer of the acyl-moiety of EtnGpl to other phospholipids by transacylase, and (iv) lysophospholipase. PLA_1 preferentially hydrolyzing EtnGpl in the presence of Mg^{2+} has been observed in the soluble fraction of bovine brain (31), but this enzyme preferentially hydrolyzes phosphatidic acid in the absence of Mg^{2+} (32).

Several different PLA_2 enzymes exist in the mammalian brain (33,34). They are classified into two subtypes, Ca^{2+}-dependent and Ca^{2+}-independent, based on their catalytic dependence on Ca^{2+}. In Ca^{2+}-dependent subtypes, cytosolic PLA_2 preferentially hydrolyzes arachidonate-containing molecular species (34). Type II secretory PLA_2, another Ca^{2+}-dependent subtype found in rat brain, has no specificity for the acyl-chain of phospholipids *in vitro* but can hydrolyze arachidonate from membrane phospholipids by physiological stimuli in intact cells (35). Group IV Ca^{2+}-independent PLA_2 is considered to function in membrane phospholipid remodeling such as 20:4n-6 incorporation and redistribution (36). Plasmalogen-selective and Ca^{2+}-independent PLA_2 has been observed in bovine brain cytosol (37), but its specificity for acyl chains remains to be clarified. In this study, [^{3}H]lysoEtnGpl formation was correlated with 22:6n-3 levels but not 20:4n-6 levels in aminophospholipids of the three dietary groups (Table 3 and Fig. 3B). Therefore, the substrate specificity of PLA reported previously could not account for the difference in [^{3}H]lysoEtnGpl formation. Moreover, n-3 deficiency does not affect brain contents and composition of phospholipid or plasmalogen content (4,8), therefore phospholipid and plasmalogen content could not account for our results.

Transacylase activity using diacylphospholipids as acyl donors for the transacylation of lysophospholipids has been observed in human brain homogenate (38). This enzyme transfers radiolabeled acyl chains from the *sn*-2 position of EtnGpl to lysoChoGpl. Lysophospholipase (38) may also affect lysoEtnGpl formation in brain synaptosomes. In the hamster heart, newly imported ethanolamine is preferentially utilized for EtnGpl biosynthesis (39) and newly synthesized EtnGpl may be remodeled by deacylation–reacylation. Although SerGpl-derived EtnGpl is preferentially deacylated and reacylated in cultured rat hepatocytes (40), the formation of EtnGpl by SerGpl decarboxylation in rat brain synaptosomes is relatively low compared with that in hepatocytes (40) and PC12 cells (20). It is suggested that CDP-ethanolamine:diacylglycerol ethanolaminephosphotransferase shows selectivity for 22:6n-3-containing species (41), and that 22:6n-3-containing EtnGpl is mainly synthesized *de novo* (41), whereas 20:4n-6 is introduced into phospholipids mainly through the remodeling pathway (42). The physiological roles of deacylation of newly synthesized EtnGpl in fatty acid remodeling are not yet clear.

Treatment of PC12 cells with 60 μM 22:6n-3 led to a fivefold increase in 22:6n-3 levels and a concomitant decrease in 18:1 (about 60% decrease compared with control) in membrane phospholipids (19). As a result, 22:6n-3 treatment increased C_{22} PUFA content (fivefold) and incorporation of [^{3}H]serine into SerGpl in PC12 cells (20). Phospholipids containing C_{22} PUFA are selectively used for the synthesis of SerGpl by a base exchange reaction (43,44). This step may contribute to the 22:6n-3 level which was significantly higher in the Saf + DHA group relative to the Per group in SerGpl but not EtnGpl. Garcia *et al.* reported that n-3 fatty acid deficiency led to a decrease in both C_{22} PUFA-containing SerGpl and a decrease in incorporation of [^{3}H]serine into SerGpl in rat brain microsomes (21). However, the incorporation of [^{3}H]serine into SerGpl in synaptosomes was not affected by n-3 fatty acid deficiency in this study (Fig. 6). In the Saf group, the markedly lower 22:6n-3 content was compensated for by higher n-6 C_{22} PUFA contents in phospholipids. As a result, total PUFA contents in individual phospholipids in synaptosomes were not different among the three dietary groups. The observed differences may be attributable to the differences between types of fractions, synaptosomes vs. microsomes.

In summary, n-3 fatty acid deficiency in synaptosomes induced by a Saf diet does not affect the uptake of aminophospholipid precursors such as ethanolamine and serine by synaptosomes and their incorporation into aminophospholipids such as EtnGpl and SerGpl. However, n-3 fatty acid deficiency leads to significantly lower formation of [^{3}H]lysoEtnGpl through [^{3}H]EtnGpl newly synthesized from [^{3}H]ethanolamine in synaptosomes. Detailed analysis of molecular species of [^{3}H]lysoEtnGpl and determination of these enzymes are necessary to correlate the observed changes in lysoEtnGpl formation with many types of enzymes involved in EtnGpl metabolism.

ACKNOWLEDGMENTS

This work was supported in part by Special Coordination Funds for Promoting Science and Technology from the Science and Technology Agency of Japan and by a Scientific Research Grant from the Ministry of Education, Science, Sports and Culture of Japan.

REFERENCES

1. Bazan, N.G. (1990) Supply of n-3 Polyunsaturated Fatty Acids and Their Significance in the Central Nervous System, in *Nutri-*

tion and the Brain (Wurtman, R.J., and Wurtman, J.J., eds.) Vol. 8, pp. 1–24, Raven Press, New York.
2. Pawlosky, R.J, Ward, G., and Salem, N., Jr. (1996) Essential Fatty Acid Uptake and Metabolism in the Developing Rodent Brain, *Lipids 31,* S103–S107.
3. Green, P., and Yavin, E. (1993) Elongation, Desaturation, and Esterification of Essential Fatty Acids by Fetal Rat Brain *in vivo, J. Lipid Res. 34,* 2099–2107.
4. Yamamoto, N., Saito, M., Moriuchi, A., Nomura, M., and Okuyama, H. (1987) Effect of the Dietary α-Linolenate/Linoleate Balance on Lipid Compositions and Learning Ability of Rats, *J. Lipid Res. 28,* 144–151.
5. Yamamoto, N., Hashimoto, A., Moriuchi, A., Takemoto, Y., Okuyama, H., Nomura, M., Kitajima, R., Togasi, T., and Tamai, Y. (1988) Effect of the Dietary α-Linolenate/Linoleate Balance on Lipid Compositions and Learning Ability of Rats. II. Discrimination Process, Extinction Process, and Glycolipid Compositions, *J. Lipid Res. 29,* 1013–1021.
6. Yamamoto, N., Okaniwa, Y., Mori, S., Nomura, M., and Okuyama, H. (1991) Effect of the High α-Linolenate Diet on the Learning Ability of Aged Rats, *J. Gerontol. 46,* B17–B22.
7. Watanabe, I., Kato, M., Aonuma, H., Hashimoto, A., Naito, Y., Moriuchi, A., and Okuyama, H. (1987) Effect of Dietary α-Linolenate/Linoleate Balance on the Lipid Composition and Electroretinographic Responses in Rats, *Adv. Biosci. 62,* 563–570.
8. Bourre, J.M., Francois, M., Youyou, A., Dumont, O., Piciotti, M., Pascal, G., and Durand, G. (1989) The Effects of Dietary α-Linolenic Acid on the Composition of Nerve Membranes, Enzymatic Activity, Amplitude of Electrophysiological Parameters, Resistance to Poisons and Performance of Learning Tasks in Rats, *J. Nutr. 119,* 1880–1892.
9. Nakashima, Y., Yuasa, S., Hukamizu, Y., Okuyama, H., Ohhara, T., Kameyama, T., and Nabeshima, T. (1993) Effect of a High Linoleate and a High α-Linolenate Diet on General Behavior and Drug Sensitivity in Mice, *J. Lipid. Res. 34,* 239–247.
10. Salem, N., Jr., and Niebylski, C.D. (1995) The Nervous System Has Absolute Molecular Species Requirement for Proper Function, *Mol. Membr. Biol. 12,* 131–134.
11. Yoshida, S., Yasuda, A., Kawazato, H., Sasaki, K., Shimada, T., Takeshita, M., Yuasa, S., Kobayashi, T., Watanabe, S., and Okuyama, H. (1997) Synaptic Vesicle Ultrastructural Changes in the Rat Hippocampus Induced by a Combination of α-Linolenate Deficiency and a Learning Task, *J. Neurochem. 68,* 1261–1268.
12. Yoshida, S., Miyazaki, M., Takeshita, M., Yuasa, S., Kobayashi, T., Watanabe, S., and Okuyama, H. (1997) Functional Changes of Rat Brain Microsomal Membrane Surface After Learning Task Depending on Dietary Fatty Acids, *J. Neurochem. 68,* 1269–1277.
13. Barrantes, F.J. (1993) Structural-Functional Correlates of the Nicotinic Acetylcholine Receptor and Its Lipid Microenvironment, *FASEB J. 7,* 1460–1467.
14. Newton, A.C., and Keranen, L.M. (1994) Phosphatidyl-L-serine Is Necessary for Protein Kinase C's High-Affinity Interaction with Diacylglycerol-Containing Membranes, *Biochemistry 33,* 6651–6658.
15. Sakane, F., Yamada, K., Imai, S., and Kanoh, H. (1991) Porcine 80-kDa Diacylglycerol Kinase Is a Calcium-Binding and Calcium/Phospholipid-Dependent Enzyme and Undergoes Calcium-Dependent Translocation, *J. Biol. Chem. 266,* 7096–7100.
16. Stekhoven, F.M., Tijmes, J., Umeda, M., Inoue, K., and De Pont, J.J. (1994) Monoclonal Antibody to Phosphatidylserine Inhibits Na^+/K^+-ATPase Activity, *Biochim. Biophys. Acta 1194,* 155–165.
17. Calderon, C., Huang, Z.H., Gage, D.A., Sotomayor, E.M., and Lopez, D.M. (1994) Isolation of a Nitric Oxide Inhibitor from Mammary Tumor Cells and Its Characterization as Phosphatidylserine, *J. Exp. Med. 180,* 945–958.
18. Fadok, V.A., Voelker, D.R., Campbell, P.A., Cohen, J.J., Bratton, D.L., and Henson, P.M. (1992) Exposure of Phosphatidylserine on the Surface of Apoptotic Lymphocytes Triggers Specific Recognition and Removal by Macrophages, *J. Immunol. 148,* 2207–2216.
19. Ikemoto, A., Kobayashi, T., Watanabe, S., and Okuyama, H. (1997) Membrane Fatty Acid Modifications of PC12 Cells by Arachidonate or Docosahexaenoate Affect Neurite Outgrowth but Not Norepinephrine Release, *Neurochem. Res. 22,* 671–678.
20. Ikemoto, A., Kobayashi, T., Emoto, K., Umeda, M., Watanabe, S., and Okuyama, H. (1999) Effect of Docosahexaenoic and Arachidonic Acids on the Synthesis and Distribution of Aminophospholipids During Neuronal Differentiation of PC12 Cells, *Arch. Biochem. Biophys. 364,* 67–74.
21. Garcia, M.C., Ward, G., Ma, Y.-C., Salem, N., Jr., and Kim, H.-Y. (1998) Effect of Docosahexaenoic Acid on the Synthesis of Phosphatidylserine in Rat Brain Microsomes and C6 Glioma Cells, *J. Neurochem. 70,* 24–30.
22. Gazzah, N., Gharib, A., Croset, M., Bobillier, P., Lagarde, M., and Sarda, N. (1995) Decrease of Brain Phospholipid Synthesis in Free-Moving n-3 Fatty Acid Deficient Rats, *J. Neurochem. 64,* 908–991.
23. Giaume, M., Gay, N., Baubet, V., Gharid, A., Durand, G., Bobillier, P., and Sarda, N. (1994) n-3 Fatty Acid Deficiency Increases Brain Protein Synthesis in the Free-Moving Adult Rat, *J. Neurochem. 63,* 1995–1998.
24. Rapoport, S.I. (1995) Docosahexaenoate Turnover in Brain Phospholipids, *J. Neurochem. 65,* 1903–1905.
25. Sato, A., Osakabe, T., Ikemoto, A., Watanabe, S., Kobayashi, T., and Okuyama, H. (1999) Long-term n-3 Fatty Acid Deficiency Induces No Substantial Change in the Rate of Protein Synthesis in Rat Brain and Liver, *Biol. Pharm. Bull. 22,* 775–779.
26. Dunkley, P.R., Heath, J.W., Harrison, S.M., Jarvie, P.E., Glenfield, P.J., and Rostas, A.P. (1988) A Rapid Percoll Gradient Procedure for Isolation of Synaptosomes Directly from an S1 Fraction: Homogeneity and Morphology of Subcellular Fractions, *Brain Res. 441,* 59–71.
27. Tsutsumi, T., Yamauchi, E., Suzuki, E., Watanabe, S., Kobayashi, T., and Okuyama, H. (1995) Effect of a High α-Linolenate and High Linoleate Diet on Membrane-Associated Enzyme Activities in Rat Brain—Modulation of Na^+, K^+-ATPase Activity at Suboptimal Concentrations of ATP, *Biol. Pharm. Bull. 18,* 664–670.
28. Smith, P.K., Krohn, R.I., Hermanson, G.T., Mallia, A.K., Gartner, F.H., Provenzano, M.D., Fujimoto, E.K., Goeke, N.M., Olson, B.J., and Blenk, D.C. (1985) Measurement of Protein Using Bicinchoninic Acid, *Anal. Biochem. 150,* 76–85.
29. Bligh, E.G., and Dyer, W.J. (1959) A Rapid Method of Total Lipid Extraction and Purification, *Can. J. Biochem. Physiol. 37,* 911–917.
30. Okuyama, H., and Wakil, S.J. (1973) Positional Specificities of Acyl Coenzyme A: Glycerophosphate and Acyl Coenzyme A: Monoacylglycerophosphate Acyltransferases in *Escherichia coli, J. Biol. Chem. 248,* 5197–5205.
31. Pete, M.J., Ross, A.H., and Exton, J.H. (1995) Purification and Properties of Phospholipase A_1 from Bovine Brain, *J. Biol. Chem. 269,* 19494–19500.
32. Higgs, H.N., and Glomset, J.A. (1996) Purification and Properties of a Phosphatidic Acid-Preferring Phospholipase A_1 from Bovine Testis, *J. Biol. Chem. 271,* 10874–10883.
33. Farooqui, A.A., Yang, H.-C., Rosenberger, T.A., and Horrocks, L.A. (1997) Phospholipase A_2 and Its Role in Brain Tissue, *J. Neurochem. 69,* 889–901.

34. Dennis, E.A. (1997) The Growing Phospholipase A_2 Superfamily of Signal Transduction Enzymes, *Trends Biochem. Sci. 22,* 1–2.
35. Matsuzawa, A., Murakami, M., Atsumi, G., Imai, K., Prados, P., Inoue, K., and Kudo, I. (1996) Release of Secretory Phospholipase A_2 from Rat Neuronal Cells and Its Possible Function in the Regulation of Catecholamine Secretion, *Biochem. J. 318,* 701–709.
36. Dennis, E.A. (1997) Function and Inhibition of Intracellular Calcium-Independent Phospholipase A_2, *J. Biol. Chem. 272,* 16069–16072.
37. Farooqui, A.A., Yang, H.-C., and Horrocks, L.A. (1995) Plasmalogens, Phospholipases A_2 and Signal Transduction, *Brain Res. Rev. 21,* 152–161.
38. Ross, B.M., and Kish, S.J. (1994) Characterization of Lysophospholipid Metabolizing Enzymes in Human Brain, *J. Neurochem. 63,* 1839–1848.
39. McMaster, C.R., and Choy, P.C. (1992) Newly Imported Ethanolamine is Preferentially Utilized for Phosphatidylethanolamine Biosynthesis in the Hamster Heart, *Biochim. Biophys. Acta 1124,* 13–16.
40. Samborski, R.W., and Vance, D.E. (1993) Phosphatidylethanolamine Derived from Phosphatidylserine Is Deacylated and Reacylated in Rat Hepatocytes, *Biochim. Biophys. Acta 1167,* 15–21.
41. Onuma, Y., Masuzawa, Y., Ishima, Y., and Waku, K. (1984) Selective Incorporation of Docosahexaenoic Acid in Rat Brain, *Biochim. Biophys. Acta 793,* 80–85.
42. Yamashita, A., Sugiura, T., and Waku, K. (1997) Acyltransferases and Transacylases Involved in Fatty Acid Remodeling of Phospholipids and Metabolism of Bioactive Lipids in Mammalian Cells, *J. Biochem. 122,* 1–16.
43. Holbrook, P.G., and Wurtman, R.J. (1990) Calcium-Dependent Incorporation of Choline into Phosphatidylcholine (PC) by Base-Exchange in Rat Brain Membranes Occurs Preferentially with Phospholipid Substrates Containing Docosahexaenoic Acids [22:6(n-3)], *Biochim. Biophys. Acta 1046,* 185–188.
44. Ellingson, J.S., and Seenaish, B. (1994) The Selective Use of Stearoyl-Polyunsaturated Molecular Species of Phosphatidylcholine and Phosphatidylethanolamine for the Synthesis of Phosphatidylserine, *Biochim. Biophys. Acta 1213,* 113–117.

[Received November 8, 1999, and in revised form July 27, 2000; revision accepted August 18, 2000]

Further Characterization of Rat Dihydroceramide Desaturase: Tissue Distribution, Subcellular Localization, and Substrate Specificity[1]

Catherine Causeret[2], Luc Geeraert[2,3], Gerd Van der Hoeven, Guy P. Mannaerts, and Paul P. Van Veldhoven*

Katholieke Universiteit Leuven, Faculteit Geneeskunde, Departement Moleculaire Celbiologie, Afdeling Farmakologie, B-3000 Leuven, Belgium

ABSTRACT: The introduction of the double bond in the sphingoid backbone of sphingolipids occurs at the level of dihydroceramide *via* an NADPH-dependent desaturase, as discovered in permeabilized rat hepatocytes. In the rat, the enzyme activity, which has now been further characterized, appeared to be mostly enriched in liver and Harderian gland. By means of subcellular fractionation of rat liver homogenates and density gradient separation of microsomal fractions, the desaturase was localized to the endoplasmic reticulum. Various detergents were inhibitory to the enzyme, and maximal activities were obtained in the presence of NADPH and when the substrate was complexed to albumin. In the presence of albumin, the chain length of the fatty acid of the truncated dihydroceramides hardly affected the activity. Finally, in view of a likely evolutionary relationship between desaturases and hydroxylases, the formation of hydroxylated intermediates was analyzed. No evidence for their presence was found under our assay conditions.

Paper no. L8364 in *Lipids 35*, 1117–1125 (October 2000).

Although the major portion of sphingoid bases found in sphingolipids contains a 4-*trans* double bond in mammals, for some time it was neither clear whether this double bond is added at the level of sphinganine (D-*erythro*-2-amino-1,3-octadecanediol) or of dihydroceramide (*N*-acyl-sphinganine), nor known where in the cell and by which mechanism this reaction takes place. Based on incorporation studies with labeled sphinganine, dihydroceramide, or serine (1–3) and on the cellular effects of fumonisin B1 (4,5), a toxin produced by *Fusarium moniliforme* that blocks the acylation of sphingoid bases (4,6), it was established that dihydroceramide is an intermediate in the *de novo* synthesis of sphingolipids. Dihydroceramide, generated by acylation of sphinganine, is subsequently converted into ceramide. Until recently, the nature of the enzyme responsible for the introduction of the double bond was obscure.

By comparing the release of labeled water from the truncated dihydroceramide analog, *N*-hexanoyl-[4,5-^{3}H]sphinganine, in intact and permeabilized rat hepatocytes, we could evaluate the importance of NADPH in the formation of ceramide, a cofactor pointing to a role for a desaturase (7,8). This idea was further sustained by the effect of specific inhibitors and electron-donors/acceptors (8), indicating that the dihydroceramide desaturase (DHCD) complex consists of a flavin-containing cytochrome (cyt) b_5 reductase, a heme-containing cyt b_5, and a nonheme-containing desaturase (see Fig. 1 for an overview of the biosynthesis of ceramide). Independently, Michel *et al*. (9), who investigated the influence of NADH on the metabolism of *N*-[1-^{14}C]octanoyl-sphinganine in rat liver microsomes, reached similar conclusions. In their hands, however, NADH and NADPH worked equally well (9), whereas in permeabilized rat hepatocytes, NADH was effective only in the presence of ATP (8).

Upon liver fractionation, the desaturase activity was recovered mainly in the microsomal fraction (8). This would be consistent with an association with endoplasmic reticulum (ER) vesicles, also the subcellular site of sphinganine-*N*-acyltransferase (10,11), the enzyme generating the substrate for the desaturase reaction. Desaturation rates of *N*-C_6-[4,5-^{3}H]sphinganine (where C_6 = hexanoyl) in rat liver homogenates under optimized conditions reached only 30% of those observed in intact hepatocytes (8). Contributing factors were postulated to be an exchange reaction that occurs in intact cells (8,12), whereby the short chain of the truncated substrate is replaced by a more physiological long-chain fatty acid, and nonoptimal delivery of the substrate, complexed to albumin, to the enzyme in broken systems. In the present report, the tissue distribution of DHCD in the rat and the subcellular localization of the activity in rat liver were investigated. To further optimize the assay, the use of substrate/de-

[1]In part presented at the Conférence Jacques Monod "Cell lipids: Topology, transport and signalling functions," Aussois, May 1997 (France); Van Veldhoven, P.P. "Ceramide biosynthesis: Characterisation of the conversion of dihydroceramide to ceramide."

[2]Contributed equally to this study.

[3]Present address: Janssen Research Foundation, Beerse, Belgium.

*To whom correspondence should be addressed at Katholieke Universiteit Leuven, Campus Gasthuisberg, Afd. Farmakologie, Herestraat, B-3000 Leuven, Belgium. E-mail: paul.vanveldhoven@med.kuleuven.ac.be

Abbreviations: BSA, bovine serum albumin; C_6, hexanoyl; C_x, acyl chain containing *x* carbon atoms; CHAPS, 3-[(3-cholamidopropyl)dimethylammonio]-1-propanesulfonate; CMC, critical micellar concentration; Cyt, cytochrome; DHCD, dihydroceramide desaturase; ER, endoplasmic reticulum; Mops, morpholino propane sulfonic acid; sphinganine, D-*erythro*-2-amino-1,3-octadecanediol; sphingenine: D-*erythro*-2-amino-1,3-4*E*-octadecenediol; TLC, thin-layer chromatography.

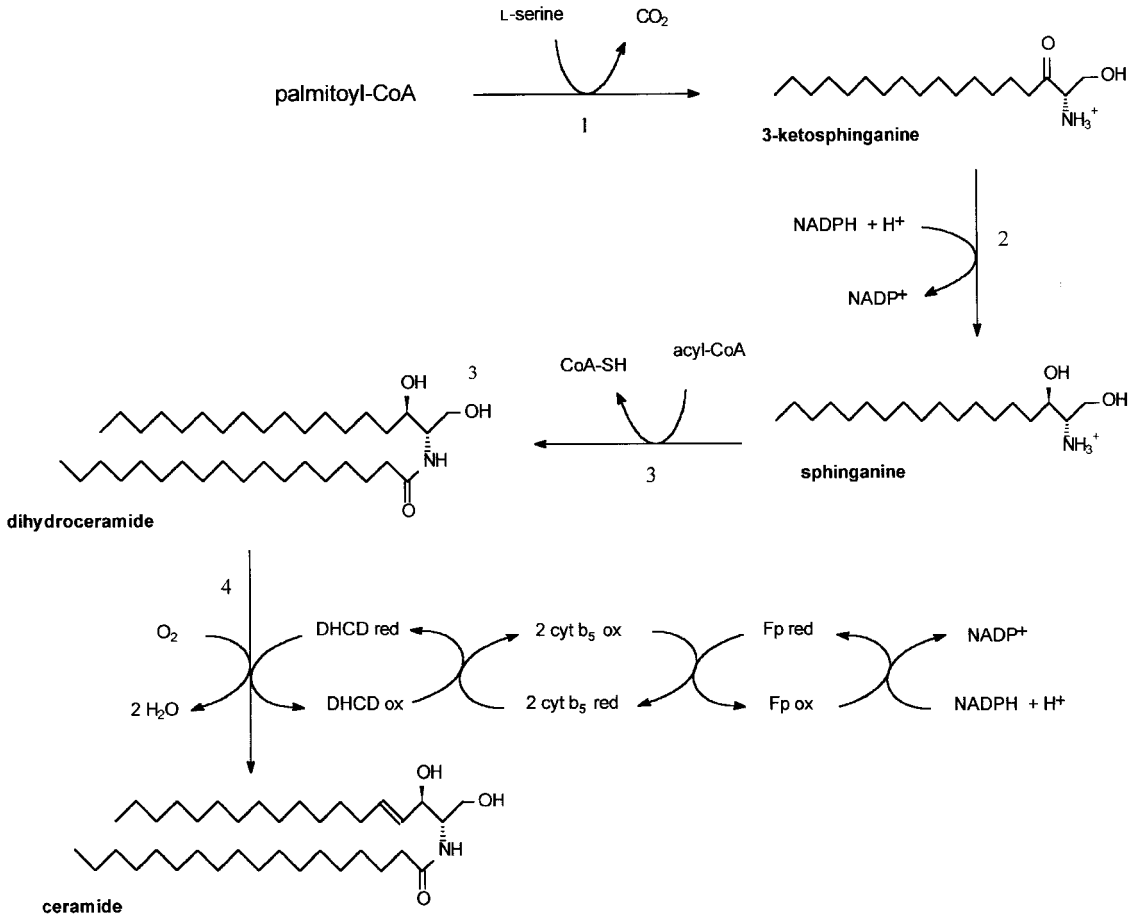

FIG. 1. Biosynthesis of ceramide. The pathway depicted shows the current view of ceramide biosynthesis whereby the following enzymes are involved: (1) serine palmitoyl-CoA transferase; (2) 3-ketosphinganine reductase; (3) sphinganine-*N*-acyltransferase; (4) dihydroceramide desaturase (DHCD). The desaturation of dihydroceramide is catalyzed by an enzyme complex consisting of a flavoprotein (Fp), a cytochrome (cyt) b_5, and a desaturase, and is driven by NADPH.

tergent micelles and the specifity toward the *N*-acyl chain length of the dihydroceramide substrate were evaluated. Finally, the role of NADPH vs. NADH as cofactor was studied whereby the formation of possibly hydroxylated intermediates was analyzed.

MATERIALS AND METHODS

Materials. Analytical-grade solvents and biochemicals were purchased from commercial suppliers. Anhydrous solvents were obtained from Fluka (Buchs, Switzerland). Sphingolipids, *N*-dodecyl sarcosine (Sarkosyl), *N*-dodecyl- and *N*-tetradecyl-*N*,*N*-dimethyl-3-ammonio-1-propane sulfonate were from Sigma; 3-[(3-cholamidopropyl)dimethylammonio]-1-propanesulfonate (CHAPS), cyclodextrins, dodecylmaltoside, octanoyl-*N*-methylglucamide (MEGA-8), octylglucoside, sucrose monolaurate, Thesit [dodecylpoly(ethyleneglycolether)$_n$; where $n \approx 9$], Triton X-100, and protease inhibitors were from Boehringer (Mannheim, Germany); lauryl-*N*,*N*-dimethylamine *N*-oxide (*N*,*N*-dimethyl-*N*-dodecylamine oxide) was from Serva (Heidelberg, Germany); and *N*-octanoyl-β-D-glucosamine, *N*-octyl *N*,*N*-dimethyl-3-ammonio-1-propane sulfonate, and decylmaltoside were from Calbiochem (LaJolla, CA).

Preparation of substrates. [4,5-^{3}H]Sphinganine, obtained as a side product of the acidic hydrolysis of tritiated dihydrosphingomyelin (13), was purified by silica gel chromatography and mixed with unlabeled sphinganine, prepared by hydrogenation of sphingenine (D-erythro-2-amino-1,3-4*E*-octadecenediol; Ref. 14), and purified in the same way as the labeled compound, to obtain a specific activity of 86.7 μCi/μmol. Radiochemical purity was more than 95% as determined by thin-layer chromatography (TLC: silica G60 Alugram plates; Machery-Nagel, Düren, Germany) using chloroform/methanol/2 M NH_4OH (60:30:5, by vol; solvent A) and chloroform/methanol/water (60:35:8, by vol; solvent B). Concentrations of sphinganine solutions were determined by means of derivatization with trinitrobenzenesulfonic acid (15). *N*-[1-^{14}C]C_6-sphinganine, *N*-C_6-sphinganine, *N*-C_6-sphingenine, and *N*-C_6-4*D*-hydroxysphinganine were synthesized as described before (8). Truncated tritiated dihydroceramides were obtained by acylation of [4,5-^{3}H]sphinganine using either the appropriate anhydrides (for *N*-

C_2- and *N*-C_6-sphinganine) as described (8,15,16) or acyl chlorides (for *N*-C_4 and *N*-C_8-sphinganine) as adapted from Reference 17. The other dihydroceramide analogs (*N*-C_{10}-, *N*-C_{12}-, *N*-C_{14}-, and *N*-C_{16}-sphinganine) were generated by means of diethyl phosphorocyanidate (18) as condensing reagents. Briefly, fatty acids were dissolved in anhydrous dimethylformamide/dichloromethane (2:1, vol/ vol), to 20 mM, followed by addition of a fivefold molar excess (over fatty acids) of triethylamine and of an equimolar amount of diethyl phosphorocyanidate. After incubation for 5 min, an aliquot of this mixture was mixed with 1 vol of 10 mM [4,5-^{3}H]sphinganine [in dimethylformamide/dichloromethane (2:1, vol/vol)], and allowed to react for 2 h at room temperature. Acylation of sphinganine appeared to be almost complete as revealed by TLC analysis [solvent C: chloroform/methanol/acetic acid (90:10:1, by vol)]. All acylated products were subjected to an alkaline hydrolysis (15) to remove any formed *O*-acylester, extracted into chloroform and, if necessary, purified by preparative TLC in solvent C. Yields ranged between 90 and 95% when using diethyl phosphorocyanidate. The radiochemical purity of the different dihydroceramides was more than 97% as determined by TLC (solvents C and A). Lipids were transiently visualized by iodine vapor followed by specific spraying (ninhydrin-cupric nitrate, molybdenum blue reagent) and/or charring (19). Labeled lipids were scraped into 0.5 mL of 1% (wt/vol) sodium dodecyl sulfate, and radioactivity was measured in a liquid scintillation counter after adding 4 mL of Optifluor and corrected for background radioactivity.

Subcellular fractionation and marker enzyme analysis. Maintenance and treatment of male Wistar rats were approved by the local Institutional Ethics Committee. Animals (body weight approximately 200 g) were fasted overnight and killed by decapitation. The tissues were removed and homogenized in 0.25 M sucrose/5 mM morpholino propane sulfonic acid (Mops) pH 7.2/0.1% (vol/vol) ethanol. Liver homogenates were fractionated as described before (13). The microsomal fraction was further separated by means of sucrose density gradient centrifugation. Optimal resolution was obtained by layering an aliquot (2.5 mL) of a microsomal fraction derived from 2.5 g of rat liver on top of a 25–75% (wt/vol) linear sucrose gradient (18 mL), containing 5 mM Mops pH 7.2/0.1% (vol/vol) ethanol, and supported by a cushion of 75% (wt/vol) sucrose (2.5 mL). The gradient was spun at 4°C in a Beckman 55.2 Ti fixed-angle rotor for 2 h at 100,000 × *g* (slow acceleration mode). After centrifugation, gradient fractions were collected starting from the bottom by means of a needle connected to a peristaltic pump. Measurements of protein and most marker enzymes were done according to the modifications described previously: protein (20), glutamate dehydrogenase (20), acid phosphatase (20), glucose-6-phosphatase (20), 5′-nucleotidase (21), galactosyltransferase (13), and urate oxidase (22). Catalase was assayed as in Reference 23, but the final assay volume was reduced to 2.6 mL. Alkaline phosphatase activities were followed kinetically at 400 nm (ε = 18,300 $cm^{-1} \cdot M^{-1}$) after a 5-min preincubation of the samples at pH 10.5 with Mg and Zn ions. Final assay concentrations were 50 mM glycine-NaOH pH 10.5/2 mM $MgCl_2$/20 μM Zn acetate/0.1% (wt/vol) Triton X-100/2 mM *p*-nitrophenyl-phosphate (final volume of 0.5 mL). For a comprehensive review on tissue fractionation and the use of marker enzymes, see Reference 24.

DHCD. Desaturase activity measurements were based on the formation of tritiated water using *N*-C_6-[4,5-^{3}H]sphinganine as substrate. Assays on tissue homogenates and subcellular fractions were done exactly as described before (8). Briefly, 200 μL of sample, appropriately diluted in homogenization medium, was mixed with 800 μL of reaction mixture (final concentrations: 40 μM *N*-C_6-[4,5-^{3}H]-sphinganine [1:1 molar complex with bovine serum albumin (BSA)], 20 mM Bicine pH 8.5, 50 mM NaCl, 2 mM NADPH), and the mixture was incubated for 20 minutes at 37°C. After adding 100 μL of 8% (wt/vol) BSA, the mixture was acidified with 100 μL of 72% (wt/vol) trichloroacetic acid. Denatured proteins were removed by centrifugation; and a 0.8-mL aliquot of the supernatant, adjusted to pH 5.5 with 1 M Na_2HPO_4, was applied to a C_{18} solid-phase extraction column (500 mg Bond Elut; Varian). The amount of label not retained, corrected for the presence of non-volatile tritium (8), was taken as a measure for the desaturation reaction. For the analysis of N-acyl chain length specificity and the influence of detergents in microsomal fractions, volumes of the assay and stop solutions were reduced twofold.

In some experiments, the C_{18}-Bond Elut columns were further washed with methanol to elute bound lipids. The methanol fractions were dried and separated on silica G60 glass plates (solvent A). The following R_f values were found: *N*-C_6-sphinganine 0.90; *N*-C_6-sphingenine 0.86; *N*-C_6-4*D*-hydroxysphinganine 0.81; sphinganine 0.46; sphingenine 0.54; 4*D*-hydroxysphinganine 0.30–0.34.

In some experiments, *N*-[1-^{14}C]C_6-sphinganine alone or mixed with *N*-C_6-[4,5-^{3}H]sphinganine was used as substrate. In addition to the above described analysis, the protein/lipid precipitate after acidification was subjected to chloroform/methanol extraction, followed by phase separation. The organic phase was analyzed by TLC using borate-impregnated silica G60 Alugram plates (8) which were developed twice (solvent D; chloroform/methanol 9:1, vol/vol) in order to separate *N*-C_6-sphinganine (R_f 0.62) from *N*-C_6-sphingenine (R_f 0.44) and *N*-C_6-4*D*-hydroxysphinganine (R_f 0.04).

RESULTS AND DISCUSSION

To find a suitable tissue to study the subcellular localization of the desaturase and to use as starting material for the isolation of the desaturase complex, the tissue distribution of DHCD was analyzed in the rat. As shown in Table 1, a rather unusual picture emerged: liver and Harderian gland contained the highest activities. The role of the desaturase in the eye gland is not clear. This sebaceous gland is known to be very lipid-rich and particularly active in ether lipid synthesis (25). Since the formation of vinylether lipids is also dependent on the action of a desaturase complex, called Δ1-alkyl desaturase (26), one could argue that this desaturase contributes to the

TABLE 1
Tissue Distribution of Dihydroceramide Desaturase (DHCD) in Rat[a]

Tissue	Activity	
	pmol/min·g	pmol/min·mg protein
Liver	548	2.30
Harderian gland	382	3.09
Kidney	101	0.55
Lung	58	0.37
Intestinal mucosa	42	0.49
Spleen	29	0.19
Testis	27	0.33
Cerebrum	26	0.44
Cerebellum	25	0.27
Muscle	13	0.11
Pancreas	9	0.05
Heart	6	0.03
Thymus	6	0.05

[a]Rat tissues were homogenized in 0.25 M sucrose/5 mM morpholino propane sulfonic acid pH 7.2/0.1 % (vol/vol) ethanol in the presence of a cocktail of protease inhibitors from Boehringer (Mannheim, Germany) (0.2 mM EDTA, 0.1 mM Pefabloc, 4 μM bestatin, 2 μM E-64, 1 μM pepstatin A, and 1 mM benzamidine) and assayed for desaturase activity by using *N*-hexanoyl-[4,5-^{3}H]sphinganine as substrate as described in the Materials and Methods section. Results are averages of values obtained in two separate experiments. Control experiments in which the protease inhibitors were not or were separately added to the medium to prepare the homogenates did not reveal significant differences in rat liver (data not shown).

dihydroceramide desaturation. However, both complexes differ with regard to stereochemistry and cofactor requirement, Δ1-alkyl desaturase introducing *cis*-bonds and being NADH dependent (see also Ref. 8).

Based on the tissue distribution data, liver was chosen to study the subcellular site of dihydroceramide desaturation. Upon cell fractionation by differential centrifugation, the majority of the activity was recovered in the microsomal fraction, and the distribution profile resembled that of the ER-markers, glucose-6-phosphatase and esterase (Fig. 2). Further separation of the vesicles present in the microsomal fraction by means of sucrose density gradient centrifugation followed by DHCD and marker enzyme measurements revealed that the desaturase is associated with ER-vesicles enriched in glucose-6-phosphatase activity (designated as class c vesicles) (27) (Fig. 3). Vesicles derived from the plasma membrane or the Golgi apparatus appeared to contain (virtually) no desaturase activity. These data are in agreement with the findings of Michel and van Echten-Deckert (28) who reported an enrichment of the (NADH-dependent) DHCD in purified ER-vesicles, but not in purified Golgi fractions of rat liver. Proteolysis experiments have indicated that the catalytic site(s) of the complex face the cytosol (28).

Hence, the enzymes catalyzing the first four steps in the synthesis of ceramide—serine-palmitoyl-CoA transferase (11), 3-ketosphinganine reductase (11), sphinganine *N*-acyltransferase (11,29), and DHCD–all co-localize to the ER and their active sites face the cytosol (11,28,29). How the substrate is presented to the desaturase remains unknown, however. One might envision that dihydroceramide, formed by the N-acyltransferase, becomes inserted in the outer leaflet of the lipid bilayer and reaches the desaturase by lateral diffusion. As a consequence, the use of a substrate, complexed to albumin, may not be physiologically meaningful. This argument was also used to explain the lower desaturation rates in broken systems (8). Therefore, in an attempt to further optimize the assay, various detergents were screened for their ability to support the desaturation reaction in rat liver microsomal fractions. Most detergents, tested in the assay at a concentration equaling their critical micellar concentration (CMC), resulted in very poor activities, except for some nonionic compounds such as octylglucoside, decyl- or dodecylmaltoside, and sucrose monolaurate (Table 2; Fig. 4). However, rates obtained in the presence of these detergents were still substantially lower than those obtained with the albumin-complexed substrate. The zwitterionic detergent CHAPS, employed by Michel *et al.* (9), displayed a sharp optimum well below its CMC value. When present at concentrations above their CMC value, nonionic detergents were even more inhibitory (Fig. 4). When added to assay mixtures containing albumin-bound substrate, all detergents tested also lowered the activity, even at concentrations equaling their CMC values (data not shown).

Despite this thorough screening of detergents, none resulted in higher activities than those measured in the presence of albumin. Also the use of dihydroceramide/cyclodextrin complexes was not succesful (Table 2). Therefore, the influence of the N-acyl chain length was analyzed in the hope to find a better substrate. As shown in Figure 5, the activities obtained with the different truncated dihydroceramides did not dramatically differ, but tended to decrease with longer chain lengths. The N-butyryl derivative was the best substrate. A much more drastic influence of the N-acyl chain length was reported by Michel *et al.* (9), who showed that the (NADH-dependent) activity with *N*-C_8-sphinganine is approximately 10-fold higher than that with *N*-C_{12}- or *N*-C_{16}-sphinganine. This difference might be related to the way these substrates were delivered: ethanol/dodecane solubilization followed by dilution in aqueous medium and sonication (9) vs. albumin in our experiments. Presumably the length of the N-acyl chain will not markedly modulate the binding of truncated dihydroceramides to albumin. Although addition of [4,5-^{3}H]sphinganine to rat hepatocytes resulted in the production of labeled water (8), sphinganine was not desaturated by rat liver microsomal fractions under our assay condition (data not shown). This finding is in agreement with earlier data (5) and shows that the desaturase recognizes the presence of the amide bond. At the primary hydroxyl group of the substrate, some substitutions are allowed since truncated dihydrosphingomyelin can be desaturated (9); truncated dihydroceramide-1-phosphate, however, did not appear to be a substrate (data not shown).

Because Michel *et al.* (9) reported that NADH and NADPH could support the desaturation of dihydroceramide equally well, the requirement for NADPH vs. NADH was reinvestigated in the presence of albumin and some detergents. NADH was effective, but in all conditions tested, NADPH resulted in higher activities (Table 2), confirming our initial observations (8). Furthermore, the NADPH-dependent

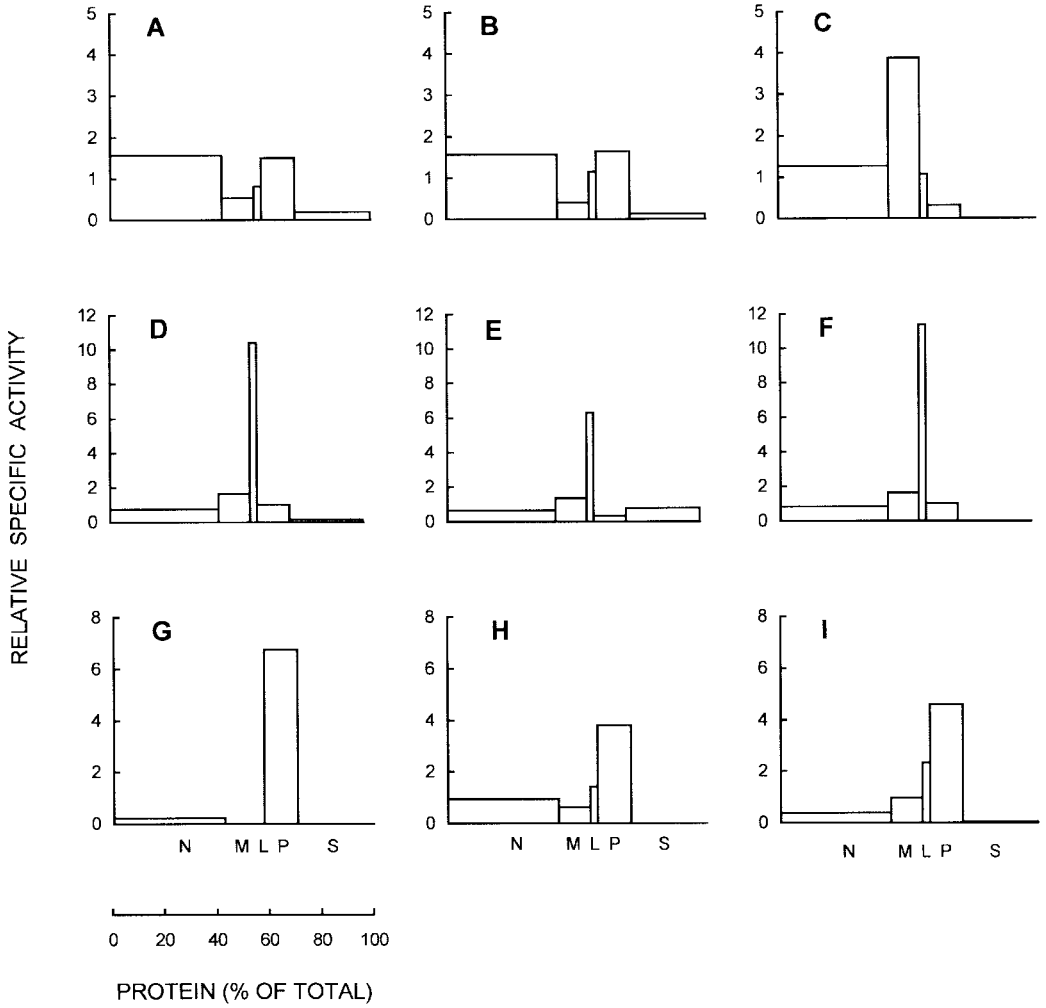

FIG. 2. Subcellular distribution of DHCD in rat liver. A rat liver homogenate was fractionated into a nuclear (N), a heavy mitochondrial (M), a light mitochondrial (L), a microsomal (P), and a cytosolic (S) fraction. In each fraction marker enzymes, DHCD, and protein were measured. Results are expressed as relative specific activities (RSA) vs. the cumulative percentage of protein. To calculate the percent activity of a marker in a particular fraction compared to the total homogenate, one has to multiply the RSA value with the percent protein present in that fraction (for N, M, L, P, and S, the percent proteins were 42.8, 12.3, 2.7, 12.9, and 29.3). The following markers were measured (in parentheses are indicated: recovery; activity, expressed in U per g of liver whereby a unit is defined as μmol substrate used per min; subcellular site): (A) 5′-nucleotidase (100%; 13.1 U/g; plasma membrane); (B) alkaline phosphatase (99.7%; 614 mU/g; plasma membrane); (C) glutamate dehydrogenase (109%; 327 U/g; mitochondria); (D) acid phosphatase (97.8%; 10.7 U/g; lysosomes); (E) catalase (89.9%; 79.0 U/g; peroxisomal matrix); (F) urate oxidase (98.9%; 3.17 U/g; peroxisomal core); (G) galactosyl transferase (96.9%; 3.41 mU/g; *trans*-Golgi apparatus); (H) glucose-6-phosphatase (101%; 28.4 U/g; endoplasmic reticulum); (I) DHCD (94.9%; 0.58 mU/g); not shown, lactate dehydrogenase (100%; 307 U/g; cytosol); and protein (95.1%; 235 mg/g). A similar histogram for DHCD was obtained in another fractionation experiment in which fewer marker enzymes were analyzed. For abbreviation see Figure 1.

activity was not further increased by addition of NADH (data not shown). Also when *N*-[1-^{14}C]C_6-sphinganine was used as substrate, followed by separation of substrate and the produced *N*-[1-^{14}C]C_6-sphingenine on borate-impregnated plates, as done by Michel *et al.* (9), NADPH appeared to be a better cofactor (data not shown).

Most likely, the NADPH-dependent desaturase, as reported in this paper and before (8), and the NADH-dependent desaturase described by others (9,28), reflect the activity of the same complex. Nevertheless, some discrepancies exist that are not readily explainable. In addition to the above-mentioned difference with respect to NADPH and NADH, reported K_m values differ substantially, being 6.1 μM for *N*-C_6-sphinganine (8) vs. 340 μM for *N*-C_8-sphinganine (9). It is unlikely that this difference is due only to the slight difference in N-acyl chain length. On the other hand, it cannot be excluded that substrate delivery is a critical factor as already mentioned above. Also the NADH-dependent reaction rates,

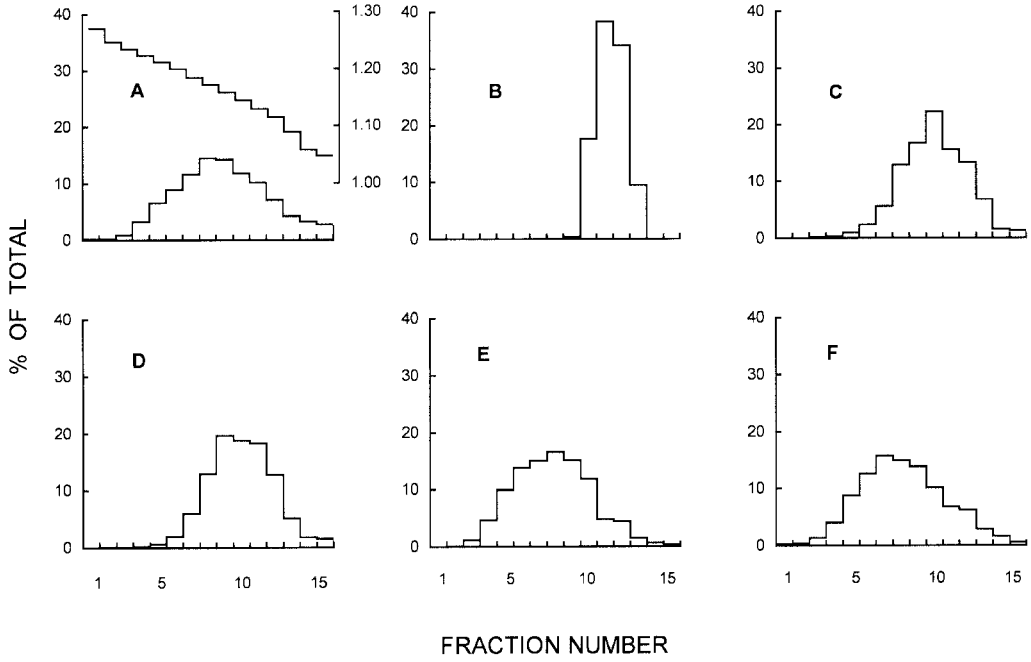

FIG. 3. Subfractionation of a microsomal fraction by sucrose density gradient centrifugation. A microsomal fraction, prepared from rat liver by differential centrifugation, was subfractionated on a sucrose density gradient as described in the Materials and Methods section. The gradient fractions were analyzed for refraction, marker enzymes, DHCD, and protein. Results of a representative experiment are shown and expressed as percentages of total recovered gradient activity or content present in each fraction. Panels represent the following marker (recoveries indicated in parentheses): (A) protein (95.5%); (B) galactosyl transferase (71.0%); (C) alkaline phosphatase (91.8%); (D) 5′-nucleotidase (110%); (E) glucose-6-phosphatase (98.0%); (F) DHCD (102%). Density of the fractions is shown in the insert of panel A. For abbreviation see Figure 1.

as calculated from the data reported by Michel *et al*. (9), appear to be approximately 30-fold higher than the NADPH-dependent rates obtained under our conditions, raising some concern about the validity of the different assays. In our assay the release of water from carbons 4 and 5 from the sphinganine backbone is followed. The other assay relies on a difference in the mobility of truncated ^{14}C-labeled ceramide and dihydroceramide upon chromatography on borate-impregnated plates. However, metabolic alterations other than 4,5-desaturation of dihydroceramide, such as a 8,9-desaturation that was recently discovered in plants (30), will result in similar mobility changes. In mammals, only a small portion of the sphingolipids contains a 4D-hydroxysphinganine backbone, but the introduction of this 4-hydroxy group, if occurring at the level of dihydroceramide and if happening in mammals, will alter the mobility of and can also cause the release of tritium from *N*-C_6-[4,5-^{3}H]sphinganine. Likewise, hydroxylation of (dihydro)ceramide in the fatty acid moiety cannot be excluded, the more since lauramide diethanolamine (*N*-dodecanoyl-diethanolamine), a compound used in cosmetics and showing some resemblance to ceramide, is hydroxylated at position 11 or 12 of the fatty acid by rat liver microsomes (31). Other (theoretical) metabolic conversions of the truncated dihydroceramide, like desaturation of the fatty acid chain, a hydroxylation at the ω-end of the sphinganine moiety or at the α-carbon of the fatty acid, would also result in mobility changes. To reveal whether dihydroceramide can undergo such conversions, microsomal fractions were incubated with *N*-C_6-[4,5-^{3}H]sphinganine and/or *N*-[1-^{14}C]C_6-sphinganine in the presence of NADH or NADPH, followed by analysis of the water-soluble and water-insoluble reaction products. In our hands, due to tailing of the (labeled) substrate during separations on borate-impregnated plates, it was difficult to obtain accurate values for the desaturation product which migrates somewhat slower than the substrate. Despite this problem, the reaction rates based on the release of tritiated water or the formation of ^{14}C-labeled *N*-C_6-sphingenine did not differ by more than 40% (data not shown). The different TLC analyses performed showed some hydrolysis of the substrate and product to sphinganine and sphingenine, respectively, but did not reveal the occurrence of hydroxylated intermediates, either at the sphinganine or (dihydro)ceramide level. These findings by no means exclude hydroxylation of sphingolipids in mammalian systems since these reactions might be dependent on other assay conditions, substrates, or enzyme sources. In yeast, the enzyme responsible for the 4-hydroxylation of sphingolipids has recently been characterized (Sur2p), but it is not clear yet at which level, sphinganine or dihydroceramide, the 4-hydroxy group is introduced (32). Since Sur2p appears to be a member of the hydroxy-

TABLE 2
Effect of Detergents on Dihydroceramide Desaturase[a]

Solubilizing agent[b]	Reported CMC		Activity (% of control)	
	mM	% (wt/vol)	1 × CMC	5 × CMC
Triton X-100	0.25	0.016	13	11
Thesit	0.1	0.006	23	10
Brij-35	0.1	0.012	13	9.3
Octylglucoside	25	0.73	8.5	ND
Decylmaltoside	1.6	0.008	27	8.0
Dodecylmaltoside	0.15	0.008	24	6.1
Sucrose monolaurate	0.2	0.01	27	21
LDAO	2.1	0.05	28	8.2
CHAPS	6.5	0.40	3.0	0
N-Octyl-DMAPS	330	9.24	18	5.6
N-Dodecyl-DMAPS	3	0.10	10	2.4
Sodium dodecylsulfate	8.1	0.24	0.3	ND
N-Dodecyl sarcosine	14.6	0.43	0[c]	ND
α-Cyclodextrin			18[d]	
β-Cyclodextrin			20[d]	

[a]Microsomal fractions were prepared from rat liver homogenates and assayed for DHCD using *N*-hexanoyl-[4,5-^{3}H]sphinganine as substrate (0.5 mL final assay volume). The substrate (20 nmol), dissolved in 2.5 μL of ethanol, was added either to an albumin solution (final concentration 40 μM) or to a detergent solution (final concentrations equaling one or five times the reported critical micelle concentration (CMC) of the detergents (34), unless otherwise indicated). After adjusting the volumes, the reaction mixture containing NADPH or NADH was added and reactions were started by adding the microsomal fraction. Activities are expressed as percentage of the control activity determined in the presence of NADPH and substrate bound to an equimolar concentration of albumin. Most values are averages of two determinations, done with different batches of microsomal fractions. The control activity was 282 ± 16 pmol/min·microsomal fraction derived from 1 g of liver [mean ± SEM (n = 6)]. With NADH, activities were on the average 1.7-fold lower in albumin-containing reaction mixtures [161 ± 30; mean ± SEM (n = 3)]. In the presence of detergents, NADH resulted likewise in lower activities (data not shown). Appropriate controls indicated that the lower activities in the presence of detergents or cyclodextrins were not due to inadequate substrate solubilization. For other abbreviation see Table 1.
[b]DMAPS, *N*,*N*-dimethyl-3-ammonio-1-propane sulfonate; ND, not determined; LDAO, lauryl-*N*,*N*-dimethylamine *N*-oxide; CHAPS, 3-[(3-cholamidopropyl)dimethylammonio]-1-propanesulfonate.
[c]When measured at *N*-dodecyl sarcosine/substrate molar ratios varying between 1 and 6, activities reached 55% of the control value.
[d]Activities obtained at a substrate/cyclodextrin molar ratio of 0.5.

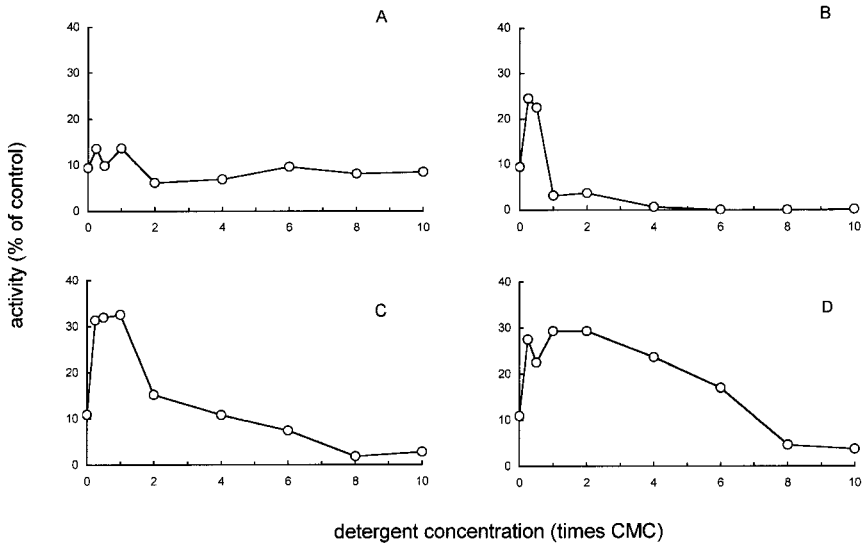

FIG. 4. Influence of detergents on DHCD activity. DHCD activities were measured in microsomal fractions using *N*-hexanoyl-[4,5-^{3}H]sphinganine as substrate and NADPH as cofactor in a final volume of 0.5 mL in the presence of different detergents, Triton X-100 (A), 3-[(3-cholamidopropyl)dimethylammonio]-1-propanesulfonate (B), decylmaltoside (C), sucrose monolaurate (D), and dodecylmaltoside (not shown; similar curve as in C). Concentrations of the detergents are expressed as times their reported critical micelle concentration (CMC) values (see Table 2). Data are expressed as percentage of the activities obtained with substrate in the presence of an equimolar concentration of albumin (288 ± 47 pmol/min·microsomal fraction derived from 1 g of liver; mean ± SEM; n = 3). Dissolution of the substrates was checked by removing and counting a 5-μL aliquot of the reaction mixtures just before adding the microsomal fraction. For the detergents shown, substrate solubilization became complete between 0.5 and 1 times the CMC values. For abbreviation, see Figure 1.

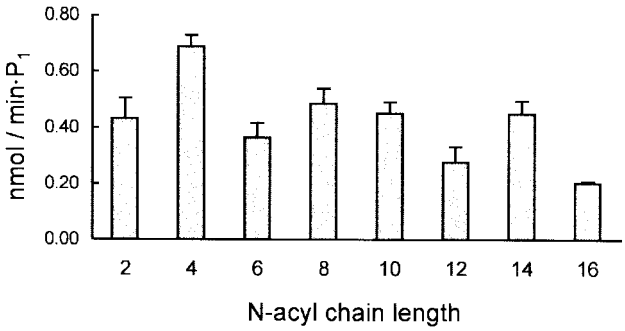

FIG. 5. Influence of *N*-acyl chain length of dihydroceramide analogs on DHCD activity. DHCD activities were measured in microsomal fractions using 40 μM of truncated dihydroceramides differing in their N-acyl chain length (number of carbon atoms indicated in the abscissa), bound to an equimolar concentration of albumin. NADPH was used as cofactor and final assay volumes were 0.5 mL. Data are means ± SEM of values obtained with three different microsomal fractions. P_1: microsomal fraction derived from 1 g of liver. For abbreviation see Figure 1.

lase/desaturase family (33), this raises the interesting possibility that the introductions of the 4-*trans* double bond (major pathway in mammals) and of the 4-hydroxy group (major pathway in yeast) in sphingoid bases are evolution-related processes.

ACKNOWLEDGMENTS

Research was supported by grants from the "Fonds voor Wetenschappelijk Onderzoek—Vlaanderen G.0240.98" and from the "InterUniversitaire AttractiePolen P4/23". Catherine Causet was supported by fellowships from the "Institut Français pour la Nutrition–IFN" and the "Fondation Singer Polignac".

REFERENCES

1. Ong, D.E., and Brady, R.N. (1973) *In vivo* Studies on the Introduction of the 4-*t*-Double Bond of the Sphingenine Moiety of Rat Brain Ceramides, *J. Biol. Chem. 248*, 3884–3888.
2. Merrill, A.H., Jr., and Wang, E. (1986) Biosynthesis of Long-Chain (sphingoid) Bases from Serine by LM Cells. Evidence for Introduction of the 4-*trans*-Double Bond After *de novo* Biosynthesis of *N*-Acylsphinganine(s), *J. Biol. Chem. 261*, 3764–3769.
3. Stoffel, W., and Bister, K. (1974) Studies on the Desaturation of Sphinganine. Ceramide and Sphingomyelin Metabolism in the Rat and in BHK 21 Cells in Tissue Culture, *Hoppe-Seyler's Z. Physiol. Chem. 355*, 911–923.
4. Rother, J., van Echten, G., Schwarzmann, G., and Sandhoff, K. (1992) Biosynthesis of Sphingolipids: Dihydroceramide and Not Sphinganine Is Desaturated by Cultured Cells, *Biochem. Biophys. Res. Commun. 189*, 14–20.
5. Merrill, A.H., Jr., van Echten, G., Wang, E., and Sandhoff, K. (1993) Fumonisin B1 Inhibits Sphingosine (sphinganine) *N*-Acyltransferase and *de novo* Sphingolipid Biosynthesis in Cultured Neurons *in situ*, *J. Biol. Chem. 268*, 27299–27306.
6. Wang, E., Norred, W.P., Bacon, C.W., Riley, R.T., and Merrill, A.H., Jr. (1991) Inhibition of Sphingolipid Biosynthesis by Fumonisins. Implications for Diseases Associated with *Fusarium moniliforme*, *J. Biol. Chem. 266*, 14486–14490.
7. Geeraert, L., Mannaerts, G.P., and Van Veldhoven, P.P. (1995) Conversion of Dihydroceramide to Ceramide: Involvement of a Desaturase, *Arch. Intern. Physiol. Biochim. 103*, B69.
8. Geeraert, L., Mannaerts, G.P., and Van Veldhoven, P.P. (1997) Conversion of Dihydroceramide to Ceramide: Involvement of a Desaturase, *Biochem. J. 327*, 125–132.
9. Michel, C., van Echten-Deckert, G., Rother, J., Sandhoff, K., Wang, E., and Merrill, A.H., Jr. (1997) Characterization of Ceramide Synthesis. A Dihydroceramide Desaturase Introduces the 4,5-*trans*-Double Bond of Sphingosine at the Level of Dihydroceramide, *J. Biol. Chem. 272*, 22432–22437.
10. Walter, V.P., Sweeney, K., and Morre, D.J. (1983) Neutral Lipid Precursors for Gangliosides Are Not Formed by Rat Liver Homogenates or by Purified Cell Fractions, *Biochim. Biophys. Acta 750*, 346–352.
11. Mandon, E.C., Ehses, I., Rother, J., van Echten, G., and Sandhoff, K. (1992) Subcellular Localization and Membrane Topology of Serine Palmitoyltransferase, 3-Dehydrosphinganine Reductase, and Sphinganine *N*-Acyltransferase in Mouse Liver, *J. Biol. Chem. 267*, 11144–11148.
12. Ridgway, N.D., and Merriam, D.L. (1995) Metabolism of Short-Chain Ceramide and Dihydroceramide Analogues in Chinese Hamster Ovary (CHO) Cells, *Biochim. Biophys. Acta 1256*, 57–70.
13. Van Veldhoven, P.P., and Mannaerts, G.P. (1991) Subcellular Localization and Membrane Topology of Sphingosine-Phosphate Lyase in Rat Liver, *J. Biol. Chem. 266*, 12502–12507.
14. Schwarzmann, G. (1978) A Simple and Novel Method for Tritium Labeling of Gangliosides and Other Sphingolipids, *Biochim. Biophys. Acta 529*, 106–114.
15. Van Veldhoven, P.P., Bishop, W.R., and Bell, R.M. (1989) Enzymatic Quantification of Sphingosine in the Pmole Range in Cultured Cells, *Anal. Biochem. 183*, 177–189.
16. De Ceuster, P., Mannaerts, G.P., and Van Veldhoven, P.P. (1995) Identification and Subcellular Localization of Sphinganine-Phosphatases in Rat Liver, *Biochem. J. 311*, 139–146.
17. Weiss, B., and Raizman, P. (1958) Synthesis of Long Chain Fatty Acid Amides of Sphingosine and Dihydrosphingosine, *J. Am. Chem. Soc. 80*, 4657–4658.
18. Shioiri, T., Yokoyama, Y., Kasai, Y., and Yamada, S. (1976) Reaction of Diethyl Phosphorocyanidate (DEPC) with Carboxylic Acids. A New Synthesis of Carboxylic Esters and Amides, *Tetrahedron 32*, 2211–2217.
19. Sherma, J. (1972) Detection Reagents for Paper and/or Thin-layer Chromatography, in *Handbook of Chromatography, Volume II* (Zweig, G., and Sherma, J., eds.), pp. 105–173, CRC Press, Cleveland.
20. Van Veldhoven, P.P., Baumgart, E., and Mannaerts, G.P. (1996) Iodixanol (Optiprep™), an Improved Density Gradient Medium for the Iso-osmotic Isolation of Rat Liver Peroxisomes, *Anal. Biochem. 237*, 17–23.
21. Van Veldhoven, P.P., Brees, C., and Mannaerts, G.P. (1991) D-Aspartate Oxidase, a Peroxisomal Enzyme in Liver of Rat and Man, *Biochim Biophys. Acta 1073*, 203–208.
22. Van Veldhoven, P.P., Just, W.W., and Mannaerts, G.P. (1987) Permeability of the Peroxisomal Membrane to Cofactors of β-Oxidation: Evidence for the Presence of a Pore-forming Protein, *J. Biol. Chem. 262*, 4310–4318.
23. Baudhuin, P., Beaufay, H., Rahman-Li, Y., Sellinger, O.Z., Wattiaux, R., Jacques, P., and de Duve, C. (1964) Tissue Fractionation Studies. 17. Intracellular Distribution of Monoamine Oxidase, Aspartate Aminotransferase, Alanine Aminotransferase, D-Amino Acid Oxidase and Catalase in Rat-Liver Tissue, *Biochem. J. 92*, 179–184.
24. de Duve, C., and Beaufay, H. (1981) A Short History of Tissue Fractionation, *J. Cell Biol. 91*, 293–299.
25. Rock, C.O. (1977) Harderian Gland, in *Lipid Metabolism in Mammals,* (Snyder, F., ed.), Vol. 2, pp. 311–321, Plenum Press, New York.

26. Paltauf, F. (1983) Biosynthesis of 1-*O*-(1′-alkenyl)Glycerolipids (plasmalogens), in *Ether Lipids*: *Biochemical and Biomedical Aspects* (Mangold, H.K., and Paltauf, F., eds.), pp. 107–128, Academic Press, New York.
27. Beaufay, H., Amar-Costesec, A., Thinès-Sempoux, D., Wibo, M., Robbi, M., and Berthet, J. (1974) Analytical Study of Microsomes and Isolated Subcellular Membranes from Rat Liver. 3. Subfractionation of the Microsomal Fraction by Isopycnic and Differential Centrifugation in Density Gradients, *J. Cell Biol. 61*, 213–231.
28. Michel, C., and van Echten-Deckert, G. (1997) Conversion of Dihydroceramide to Ceramide Occurs at the Cytosolic Face of the Endoplasmic Reticulum, *FEBS Lett. 416*, 153–155.
29. Hirschberg, K., Rodger, J., and Futerman, A.H. (1993) The Long-Chain Sphingoid Base of Sphingolipids Is Acylated at the Cytosolic Surface of the Endoplasmic Reticulum in Rat Liver, *Biochem. J. 290*, 751–757.
30. Sperling, P., Zähringer, U., and Heinz, E. (1998) A Sphingolipid Desaturase from Higher Plants. Identification of a New Cytochrome b5 Fusion Protein, *J. Biol. Chem. 273*, 28590–28596.
31. Merdink, J., Decosta, K., Mathews, J.M., Jones, C.B., Okita Rice, J., and Okita, R.T. (1996) Hydroxylation of Lauramide Diethanolamine by Liver Microsomes, *Drug Metab. Disp. 24*, 180–186.
32. Haak, D., Gable, K., Beeler, T., and Dunn, T. (1997) Hydroxylation of *Saccharomyces cerevisiae* Ceramides Requires Sur2p and Scs7p, *J. Biol. Chem. 272*, 29704–29710.
33. Van De Loo, F.J., Broun, P., Turner, S., and Somerville, C. (1995) An Oleate 12-Hydroxylase from *Ricinus communis* L. Is a Fatty Acyl Desaturase Homolog, *Proc. Natl. Acad. Sci. USA 92*, 6743–6747.
34. Neugebauer, J.M. (1990) Detergents: An Overview, *Methods Enzymol. 182*, 239–253.

[Received October 1, 1999, and in revised form May 19, 2000; revision accepted August 1, 2000]

Identification of the Pathway of α-Oxidation of Cerebronic Acid in Peroxisomes

Rajat Sandhir, Mushfiquddin Khan, and Inderjit Singh*

Department of Pediatrics, Medical University of South Carolina, Charleston , South Carolina 29425

ABSTRACT: Cerebronic acid (2-hydroxytetracosanoic acid), an α-hydroxy very long-chain fatty acid (VLCFA) and a component of cerebrosides and sulfatides, is unique to nervous tissues. Studies were carried out to identify the pathway and the subcellular site involved in the oxidation of cerebronic acid. The results from these studies revealed that cerebronic acid was catabolized by α-oxidation to CO_2 and tricosanoic acid (23:0). Studies with subcellular fractions indicated that cerebronic acid was α-oxidized in fractions having particulate bound catalase and enzyme systems for the β-oxidation of VLCFA (e.g., lignoceric acid), suggesting peroxisomes as the subcellular organelle responsible for α-oxidation of cerebronic acid. Etomoxir, an inhibitor of mitochondrial fatty acid oxidation, had no effect on cerebronic acid α-oxidation. Further, cerebronic acid oxidation was found to be dependent on the presence of NAD^+ but not FAD, NADPH, ATP, Mg^{2+}, or CoASH. Intraorganellar localization studies indicated that the enzyme system for the α-oxidation of cerebronic acid was associated with the peroxisomal limiting membranes. Studies on cultured fibroblasts from normal subjects and patients with peroxisomal disorders indicated an impairment of α-oxidation of cerebronic acid in cell lines that lack peroxisomes [e.g., Zellweger syndrome (ZS)]. On the other hand, α-oxidation of cerebronic acid was found to be normal in cell lines from X-linked adrenoleukodystrophy, adult Refsum disease, and rhizomelic chondrodysplasia punctata. Our results clearly demonstrate that α-oxidation of α-hydroxy VLCFA (cerebronic acid) is a peroxisomal function and that this oxidation is impaired in ZS. Furthermore, this α-oxidation enzyme system is distinct from the one for the α-oxidation of β-carbon branched-chain fatty acids (e.g., phytanic acid).

Paper no. L8363 in *Lipids 35,* 1127–1133 (October 2000).

α-Hydroxy long-chain and α-hydroxy very long-chain fatty acids (VLCFA) are characteristically abundant in brain and other nervous tissue as components of cerebrosides and sulfatides, most of which are found in myelin (1). These constitute α-hydroxy derivatives of C_{18} to C_{26} straight carbon-chain saturated and/or monounsaturated fatty acids (2). The α-hydroxy fatty acids are derived from corresponding nonhydroxy fatty acids by an enzyme system (fatty acid α-hydroxylase) present in brain microsomes. However, Kishimoto *et al.* (2) were not able to detect free cerebronic acid or cerebronoyl-CoA, an intermediate in the synthesis of α-hydroxy fatty acid containing ceramides and cerebrosides. This indicates that cerebronic acid, synthesized by fatty acid α-hydroxylase from lignoceric acid, is directly transferred to sphingosine for the synthesis of ceramide. This in turn is converted to cerebrosides and sulfatides by enzymes present in the endoplasmic reticulum-Golgi (3). Cerebronic acid is released from cerebronic acid-containing lipids by enzymes present in lysosomes. Sulfatides are degraded to cerebrosides by sulfatidase, followed by the conversion of cerebrosides to ceramides by cerebrosidase. Ceramides, in turn, are degraded to sphingosine and fatty acids by ceramidase. Although the detailed steps in the degradation of straight-chain and branched-chain fatty acids have been elucidated (4–6), the mechanism and subcellular site of oxidation of 2-hydroxy fatty acids remains uncertain. α-Hydroxy fatty acids probably cannot undergo β-oxidation because of the presence of a hydroxyl group at their α-carbon. The degradation of α-hydroxy fatty acids, derived from corresponding nonhydroxy fatty acids, to odd-numbered fatty acids with one less carbon atom was previously shown in a series of *in vivo* experiments (7,8). Using rat brain preparations, Levis and Mead (9) subsequently showed *in vitro* conversion of α-hydroxy fatty acids to fatty acids one carbon shorter, by rat brain microsomal preparations *via* oxidative decarboxylation. Interestingly, they also observed that the liver microsomes were not active toward α-oxidation of α-hydroxy fatty acids**.** Understanding the pathway and subcellular site for oxidation of cerebronic acid, 2-hydroxy VLCFA, is important as they are the major components of myelin lipids. Furthermore, VLCFA and branched-chain fatty acids are known to accumulate in excessive amounts in peroxisomal disorders in various tissues because of a deficiency in their catabolic activities in peroxisomes (5,6,10–12).

Therefore, the purpose of the present studies was to elucidate the pathway and subcellular organelle responsible for the oxidation of cerebronic acid and its metabolism in peroxisomal disorders. These studies report that cerebronic acid was

*To whom correspondence should be addressed at Medical University of South Carolina, Department of Pediatrics, 171 Ashley Ave., Charleston, SC 29425. E-mail: singhi@musc.edu

Abbreviations: DMEM, Dulbecco's modified Eagle's minimum essential medium; BCS, bovine calf serum; MOPS, 3-(*N*-morpholino)propanesulfonic acid; PBr_3, phosphorus tribromide;PMSF, phenylmethylsulfonyl fluoride; RCDP, rhizomelic chondrodysplasia punctata; RD, Refsum disease; VLCFA, very long-chain fatty acid; X-ALD, X-linked adrenoleukodystrophy; ZS, Zellweger syndrome.

α-oxidized to CO_2 and a fatty acid with one carbon atom short in peroxisomes. This activity is present in the limiting membrane of peroxisomes and was deficient in cells from Zellweger syndrome (ZS) and peroxisome-deficient cells, but not in cells from patients with other peroxisomal disorders, e.g., X-linked adrenoleukodystrophy (X-ALD), Refsum disease (RD), and rhizomelic chondrodysplasia punctata (RCDP). The normal activity of cerebronic acid α-oxidation in cell lines from RD patients, having a defect in phytanic acid oxidation, a requirement of NAD^+ only as compared to other cofactor requirements for phytanic acid oxidation, and a localization of oxidation activity in the peroxisomal-limiting membranes as compared to the matrix localization of phytananoyl-CoA hydroxylase (12), clearly indicates that the enzyme system for α-oxidation of cerebronic acid is different from the one responsible for the α-oxidation of phytanic acid to pristanic acid.

MATERIALS AND METHODS

Cell lines. ZS (GM 00228), X-ALD (04934), RD (03896), and RCDP (11347) skin fibroblast cell lines were obtained from the NIGMS Human Genetic Mutant Cell Repository (Camden, NJ). Other cell lines from patients with peroxisomal disorders (ZS, X-ALD, and RCDP) and from control healthy subjects were established in this laboratory.

Materials. Nycodenz was obtained from Accurate Chemical and Scientific Corp. (Westbury, NY). Cytochrome c, α-cyclodextrin, FAD, NAD, desulfo-CoA, ATP, L-carnitine, L-malate, imidazole, sucrose, antipain, leupeptin, pepstatin, phenylmethylsulfonyl fluoride (PMSF), dithiothreitol, and coenzyme A were purchased from Sigma Chemical Co. (St. Louis, MO). Bromine and phosphorus tribromide (PBr_3) were obtained from Aldrich Chemical Co. (Milwaukee, WI). Etomoxir was obtained from Research Biochemicals, Inc. (Natick, MA). [1-^{14}C]Palmitic acid (50 mCi/mmol) and K^{14}CN (55 mCi/mmol) were purchased from American Radiolabeled Chemicals, Inc. (St. Louis, MO). 2-Hydroxytetracosanoic (cerebronic) acid and tetracosanoic (lignoceric) acid were obtained from Matreya Inc. (Pleasant Gap, PA). Dulbecco's modified Eagle's minimum essential medium (DMEM), trypsin-EDTA, and Hank's balanced salt solution were obtained from GIBCO BRL (Grand Island, NY). Bovine calf serum (BCS) was from Hyclone (Logan, UT).

Methods. (i) Synthesis of [1-^{14}C]cerebronic acid from [1-^{14}C]lignoceric acid. [1-^{14}C]Lignoceric acid with a specific activity of 54.5 mCi/mmol was synthesized and characterized as described in our earlier publication (13). [1-^{14}C]Lignoceric acid (1 mCi) was allowed to melt in a screw-capped (16 × 100 mm) glass tube equipped with a stirring bar at 80°C. PBr_3 (5 μL) was slowly added, in the bottom of this tube. Bromine (8 μL) was added dropwise in the bottom of the tube with stirring, and the tube was closed immediately after addition of the final drop of bromine. The tube was then left at room temperature for 20 h, after which water (1 mL) was added to the reaction mixture and tube was left open in a well-ventilated fume hood at room temperature overnight. The product was extracted three times with 3-mL portions of ether. The combined ether extracts were washed with water and then evaporated to dryness. The radioactive product, α-bromolignoceric acid, was obtained in quantitative yield as examined by thin-layer chromatography (TLC)-radioscanning. α-Bromolignoceric acid was converted to the corresponding α-hydroxy acid as described earlier (14) with some modifications on a micro scale. The crude product was treated with 1.2 mL 95% ethanol, having 2 mg KOH/mL, and refluxed for 24 h. Alcohol was removed under nitrogen, 2 mL water was added, and the content was acidified with 2 N HCl. The product was extracted five times with 5-mL portions of ethers. The combined pool of ether was washed once with water, and solvent was removed. The labeled compounds were identified by TLC and co-TLC [K6 silica gel 60 plates; solvent system, hexane/ether/acetic acid 50:50:1 (by vol)] with nonradioactive standards (obtained either commercially or prepared in our laboratory). The desired compound, 2-hydroxylignoceric acid, was purified by TLC as described above and the yield was 20%. A fraction of the radiolabeled product was converted to the methyl ester by treatment with 1.5% (vol/vol) H_2SO_4 in anhydrous methanol at 80°C for 2 h. The product was compared by TLC and was found to be identical to the corresponding authentic nonradioactive methyl cerebronate.

(ii) Fibroblast cell culture. Cell lines were grown in DMEM supplemented with 15% BCS in a 5% CO_2 air atmosphere at 37°C (15). Cells were harvested by trypsinization 3–4 d after they reached confluence and were washed with Hank's balanced salt solution. The cells were then suspended in DMEM supplemented with 15% BCS and incubated for 1 h at 37°C, following which they were centrifuged, washed, and suspended in Hank's balanced salt solution prior to use.

(iii) Glial cell culture. Mixed glial cell cultures were established from 1- to 2-d-old rat pups as previously described (16). Cells were maintained in DMEM containing 5% glucose, 10% BCS, and antibiotic/antimycotic mixture. After 10 d of culture, microglia were removed by shaking for 2 h in an orbital shaker at 200 rpm. The medium was changed and the flask was again shaken for 24 h at 240 rpm. The detached cells, predominantly oligodendrocytes, were further purified from microglia by seeding on petri dishes for 30–60 min. The nonattached cells (oligodendrocytes) were further cultured on poly-L-lysine-coated plates. The flasks containing the remaining cells, astrocytes, were trypsinized (0.1% trypsin in 10 mM Tris-EDTA saline, pH 7.4) and seeded for studies.

(iv) Isolation of peroxisomes from rat liver. Liver peroxisomes were prepared from Sprague-Dawley rats (200–250 g) by the procedure described previously (17). Briefly, livers were homomogenized in a buffer (0.25 M sucrose, 1 mM EDTA, 0.5 μg leupeptin, 0.5 μg antipain, 0.7 μg pepstatin/mL, 0.2 mM PMSF, and 0.1% ethanol in 3 mM imidazole, pH 7.4) and fractionated by differential centrifugation to prepare the light mitochondrial fraction (the "lambda" fraction). Peroxisomes from the lambda fraction were prepared by isopycnic equilibrium centrifugation on a continuous gradient of

0–50% (wt/vol) Nycodenz with 55% Nycodenz as cushion. The gradient fractions were collected from the bottom of the tubes, and subcellular fractions were analyzed by their respective marker enzymes: catalase for peroxisomes (18), cytochrome c oxidase for mitochondria (19), and NADPH cytochrome c reductase for microsomes (20).

(v) Preparation of peroxisomal matrix and membranes. Isolated peroxisomes were sedimented by centrifugation to remove Nycodenz, and the peroxisomal pellet was washed with a homogenization buffer. Peroxisomes were lysed by incubating with digitonin (0.2 mg/mL) for 1 h at 4°C and then centrifuged at 50,000 rpm for 1 h in a Beckman 70 Ti rotor. Separation of membrane and matrix was confirmed by measuring catalase activity. Catalase activity was mainly present in the peroxisomal matrix fraction.

(vi) Assay for activation and oxidation of [1-^{14}C] fatty acids. Activation of fatty acids by ligase to fatty acyl CoA was measured as described previously (21). The reaction mixture (0.25 mL) contained 4.96 μM [1-^{14}C] fatty acid (150,000 dpm), 10 mM ATP, 80 μM CoASH, 30 mM KCl, 5 mM $MgCl_2$, and 0.05 mM dithiothreitol in 30 mM 3-(*N*-morpholino)propanesulfonic acid (MOPS)-HCl, pH 7.8. The reaction was terminated by addition of Dole's reagent (isopropyl alcohol/heptane/1 N H_2SO_4, 40:10:1 by vol). Denatured protein was removed by centrifugation, followed by addition of 0.45 mL water and 0.8 mL heptane. The aqueous layer was washed three times with heptane and radioactivity in the aqueous layer was counted.

α-Oxidation of cerebronic acid to $C_{23:0}$ fatty acid was measured as $^{14}CO_2$, released from [1-^{14}C]cerebronic acid according to methods described previously for α-oxidation of phytanic acid (22). Briefly, 0.25 mL of the reaction mixture contained 4.96 μM [1-^{14}C] fatty acid (150,000 dpm), 30 mM KCl, 5 mM $MgCl_2$, 8.5 mM ATP, 0.25 mM NAD^+, 0.08 mM CoASH, and 1 mg of α-cyclodextrin in 20 mM MOPS-HCl buffer, pH 7.8. The reaction was started by addition of the peroxisomal fraction and was incubated at 37°C and stopped with 50 μL of 5 N H_2SO_4 after 1 h. $^{14}CO_2$ was collected in KOH-wetted cotton by shaking overnight, and radioactivity was measured. β-Oxidation of [1-^{14}C] labeled fatty acids to acetate was measured as previously described (10). The reaction mixture contained 4.96 μM [1-^{14}C] fatty acid (150,000 dpm), 30 mM KCl, 5 mM $MgCl_2$, 8.5 mM ATP, 0.25 mM NAD^+, 0.17 mM FAD, 2.5 mM L-carnitine, 0.08 mM CoASH, and 1 mg of α-cyclodextrin in 20 mM MOPS-HCl buffer, pH 7.8. The oxidation was stopped by addition of 0.625 mL 1 M KOH in methanol, and the denatured protein was removed by centrifugation. The supernatant was incubated at 60°C for 1 h, neutralized with 0.125 mL of 6 N HCl, and partitioned with chloroform and methanol. The amount of radioactivity in the aqueous phase was taken as an index of [1-^{14}C] fatty acid oxidized to acetate. Fatty acid substrates used for activation and oxidation were solubilized with α-cyclodextrin (23). Fatty acids were first dried under nitrogen and then suspended in homogenization buffer containing α-cyclodextrin (20 mg/mL) and sonicated for 30 min.

RESULTS AND DISCUSSION

The oxidation of cerebronic acid was studied in subcellular organelles purified by differential and isopycnic gradient techniques (17) from rat liver. Figure 1 shows that peroxisomes, mitochondria, and microsomes were resolved from each other in the Nycodenz gradient as judged by the distribution of the marker enzymes: catalase for peroxisomes, cytochrome c oxidase for mitochondria, and NADPH cytochrome c reductase for microsomes. Cerebronic acid α-oxidation activity was essentially observed to be localized in fractions that paralleled the distribution of catalase, a well-established peroxisomal marker**.** The peroxisomes prepared by the method described here were approximately 97% pure with minor contamination of mitochondria (0.5%) and microsomes (2.83%) as described by Fujiki *et al.* (24). The specific activities for oxidation of cerebronic acid and other fatty acids are presented in Table 1. Specific activities for α-oxidation of cerebronic acid were 16 and 17 times higher in the peroxisomal fraction compared to the mitochondrial and microsomal fractions, respectively. Lignoceric acid β-oxidation, a peroxisomal function (5), was observed to be localized mainly in peroxisomes. Consistent with previous reports, palmitic acid was oxidized both in peroxisomes and mitochondria (10,15). These results indicated that the site for α-oxidation of cerebronic acid was peroxisomes.

To further establish the subcellular site for α-oxidation of cerebronic acid, we examined the effect of Etomoxir, an inhibitor of mitochondrial fatty acid oxidation, on the oxidation of cerebronic, lignoceric, and palmitic acids in human cultured skin fibroblasts (Table 2). As expected, the β-oxidation of palmitic acid was inhibited by Etomoxir in fibroblasts. On the other hand, Etomoxir had no effect on the oxidation of cerebronic and lignoceric acids, further confirming the observation that cerebronic acid is α-oxidized in an organelle other than mitochondria. The observed higher specific activity of α-oxidation of cerebronic acid in purified peroxisomes and the lack of effect of Etomoxir on the oxidation of cerebronic acid suggest that the catabolism of cerebronic acid is a peroxisomal function.

Activation of fatty acid to its CoA-ester is an obligatory step for oxidation. However, we failed to detect any acyl-CoA synthetase activity for cerebronic acid in subcellular fractions

TABLE 1
α- and β-Oxidation of Fatty Acids in Subcellular Fractions from Rat Liver[a]

	Cerebronic acid	Lignoceric acid	Palmitic acid
	(nmol/h/mg protein)		
Homogenates	0.259 ± 0.02	0.35 ± 0.06	3.28 ± 0.99
Microsomes	0.142 ± 0.01	0.01 ± 0.01	0.14 ± 0.05
Mitochondria	0.152 ± 0.05	0.18 ± 0.09	11.66 ± 2.62
Peroxisomes	2.422 ± 0.25	1.49 ± 0.32	3.52 ± 0.75

[a]Subcellular fractions were prepared from rat liver, and the α- and β-oxidation of fatty acids was measured as described in the Materials and Methods section. Values are mean ± SD for four separate experiments. Protocol for studies with animals were approved by the Institutional Review Board and conform to accepted standards.

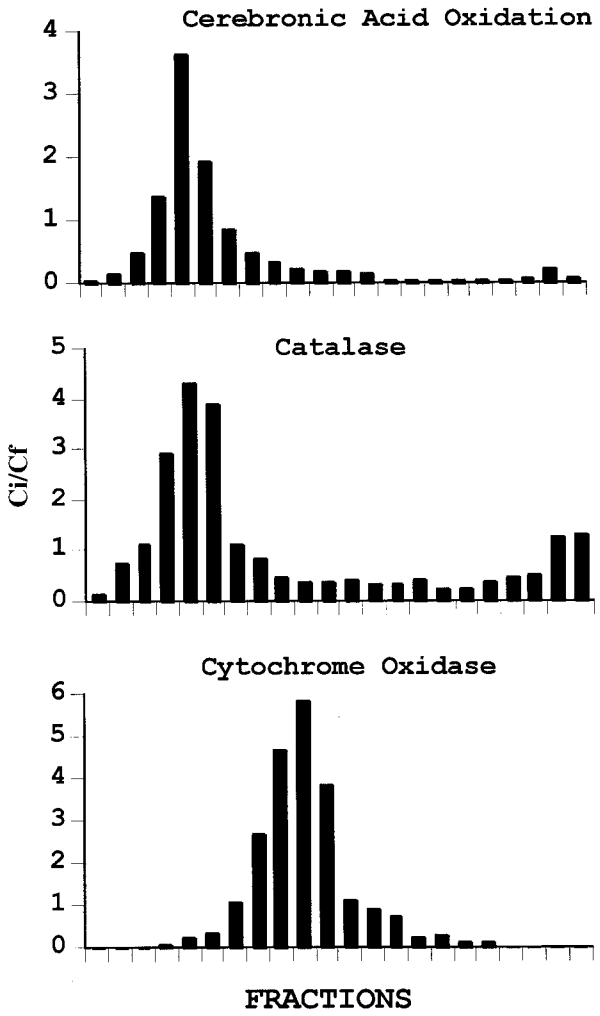

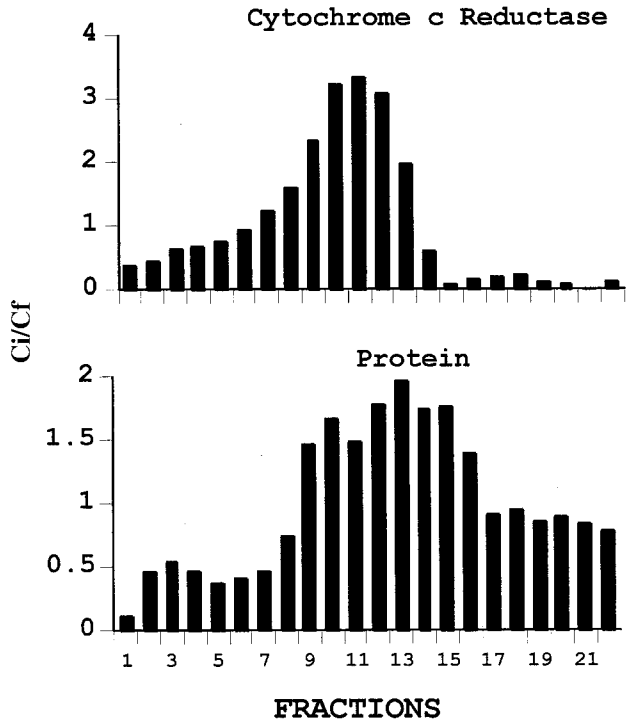

FIG. 1. Subcellular localization of cerebronic acid oxidation in rat liver. Rat liver was fractionated by differential and density gradient centrifugation as described in the Materials and Methods section. The distribution of subcellular organelles in the gradient was analyzed by their marker enzymes, catalase for peroxisomes, cytochrome c oxidase for mitochondria, and NADPH cytochrome c reductase for microsomes. The relative concentration is derived by dividing the actual concentration of the enzyme in a particular fraction by the concentration of the enzyme that would be observed if the enzyme were homogeneously distributed throughout the gradient. These results are averages of three gradients. Cerebronic acid oxidation was carried out as described in the Materials and Methods section.

from rat liver (data not shown). In order to confirm the observation that conversion of cerebronic acid to its CoA derivative was not prerequisite for its α-oxidation, we studied the effect of desulfo-CoA (a nonfunctional CoA analog that cannot form a thioester bond with fatty acid) on cerebronic acid oxidation. Consistent with the requirement for activation to acyl-CoA derivative for β-oxidation, the desulfo-CoA inhibited the oxidation of lignoceric and palmitic acids (Fig. 2),

TABLE 2
Effect of Etomoxir on the Oxidation of Fatty Acids in Human Skin Fibroblasts[a]

	Fatty acid oxidation (pmol/h/mg protein)	
	Etomoxir (–)	Etomoxir (+)
Cerebronic acid	333.35 ± 37.21	313.46 ± 46.45
Lignoceric acid	353.26 ± 29.43	309.57 ± 38.04
Phytanic acid	118.96 ± 23.27	120.21 ± 20.39
Palmitic acid	1142.94 ± 55.26	80.28 ± 19.20

[a]Fatty acid oxidation was studied in human cultured skin fibroblasts. The cells suspended in Hank's balanced salt solution were incubated in the presence of 10 μM Etomoxir for 30 min and the oxidation of labeled fatty acids was measured as described in the Materials and Methods section. Values are mean ± SD for three separate experiments.

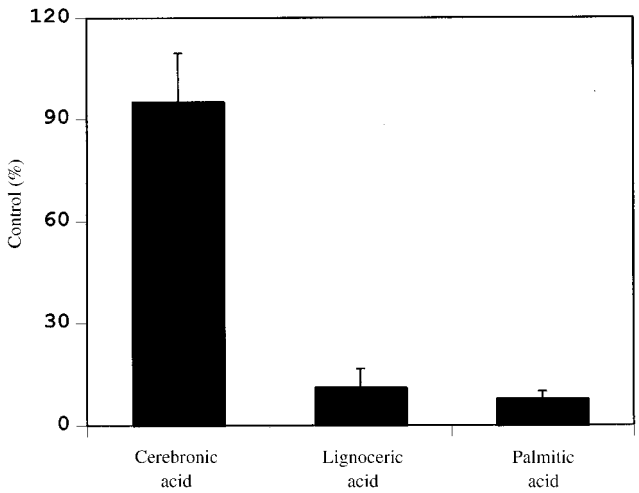

FIG. 2. Effect of desulfo-CoA on the oxidation of fatty acids in purified peroxisomes. Rat liver peroxisomes were prepared, and the rate of oxidation of fatty acids was studied in the presence of 50 μM desulfo-CoA as described in the Materials and Methods section. Data are presented as mean ± SD for three separate experiments.

whereas, it had no effect on the α-oxidation of cerebronic acid (Fig. 2). Furthermore, we investigated the cofactor requirements for the enzyme system for α-oxidation of cerebronic acid (Fig. 3). The α-oxidation of cerebronic acid was observed to be dependent on the presence of NAD whereas ATP, Mg^{2+}, CoASH, FAD, and NADPH did not support the α-oxidation of cerebronic acid. Based on these results, it appears that cerebronic acid oxidation is NAD-dependent for its oxidative decarboxylation to CO_2 and C_{n-1} fatty acid and that cerebronic acid did not need to be activated to its CoA-ester. An earlier study by Akanuma and Kishimoto (25) was also unable to detect cerebronyl-CoA while studying the mechanism of hydroxylation of VLCFA. These observations indicate that α-oxidation of cerebronic acid does not require its activation to CoA derivative. It may be possible that for decarboxylation, free cerebronic acid rather than its CoA derivative is the substrate. Formation of the odd carbon-chain fatty acid as an intermediate in degradation of 2-hydroxy fatty acids has already been established (26,27). Moreover, it is well documented that peroxisomes have a distinct matrix and limiting membrane (5). Enzyme systems for activation of straight-chain fatty acids (e.g., palmitic acid and lignoceric acid) and branched-chain fatty acids (e.g., phytanic acid and pristanic acid) are localized in the peroxisomal-limiting membrane, and enzyme systems for β-oxidation of straight-chain fatty acids and α-oxidation of branched-chain fatty acids are localized in the peroxisomal matrix (5). It was found that the enzyme systems involved in the oxidation of cerebronic acid were associated with the peroxisomal-limiting membrane and not with the matrix (Fig. 4). This supports the observation that the enzymes involved in the α-oxidation of cerebronic acid are different from those of phytanic acid (12). The α-oxidation of phytanic acid involves at least two steps: α-hydroxylation and α-decarboxylation. Furthermore, contrary to cerebronic acid oxidation, which required NAD, the oxidation of phytanic acid and 2-hydroxyphytanic acid does not need NAD. Phytanic acid (3,7,11,15-tetramethylhexadecanoic acid) is a branched-chain fatty acid that undergoes α-oxidation yielding pristanic acid (2,6,10,14-tetramethylpentadecanoic acid) with 2-hydroxyphytanoyl-CoA as an intermediate (12,28,29). We have previously demonstrated that the subcellular localization of phytanic acid α-oxidation systems is in the peroxisomes (30). We and others have also reported that phytanic acid oxidation activity is deficient in cells from patients with RD, due to mutation in phytanoyl-CoA α-hydroxylase gene (31–33); RCDP, due to abnormality in the PEX 7 gene product, a protein required for targeting phytanic acid oxidase to peroxisomes (34); and in ZS cells due to lack of peroxisomes (5). Moreover, the activity of 2-hydroxyphytanic acid oxidation was also deficient in cells from ZS patients and the levels of 2-hydroxyphytanic acid were higher in plasma of these patients (35). The different substrate specificity (free fatty acid vs. acyl-CoA), cofactor requirement (NAD vs. 2-ketoglutarate-dependent dioxygenase cofactors), intraperoxisomal localization (membrane vs. matrix), and observed differential α-oxidation (normal vs. deficient in RD and RCDP human skin fibroblasts cell lines) indicate that the enzymes responsible for α-oxidation of phytanic acid and cerebronic acid have different properties. Furthermore, the oxidation of 2-hydroxyphytanic acid involves an oxidase that requires oxygen and produces H_2O_2 (36). In the present study, we failed to detect any H_2O_2 production during cerebronic acid α-oxidation (data not shown).

In order to understand the metabolism of 2-hydroxy VLCFA in peroxisomal disorders, oxidation of cerebronic acid along with lignoceric acid and phytanic acid was studied in human cultured skin fibroblasts from patients with peroxisomal disorders. Consistent with previous observations, the α-oxidation of phytanic acid was deficient in cell lines from ZS, RD, and RCDP patients. Cerebronic acid oxidation in X-ALD, RD, and RCDP was normal (Table 3). However, ZS

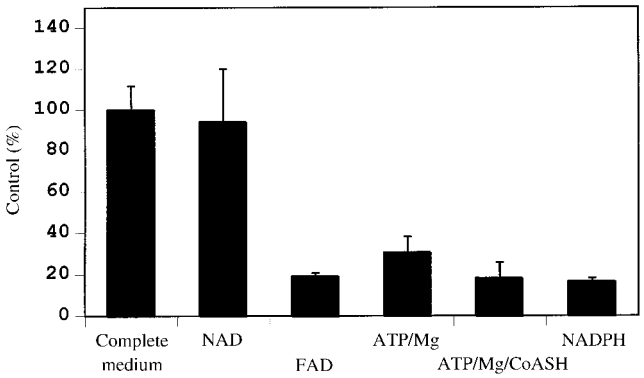

FIG. 3. Cofactor requirements for cerebronic acid oxidation by rat peroxisomes. Oxidation of cerebronic acid was studied in the presence of complete medium containing ATP, CoASH, $MgCl_2$, NAD, FAD, and L-carnitine and then in the presence of individual cofactors as shown on the X-axis and described in the Materials and Methods section. Values are mean ± SD for three separate experiments.

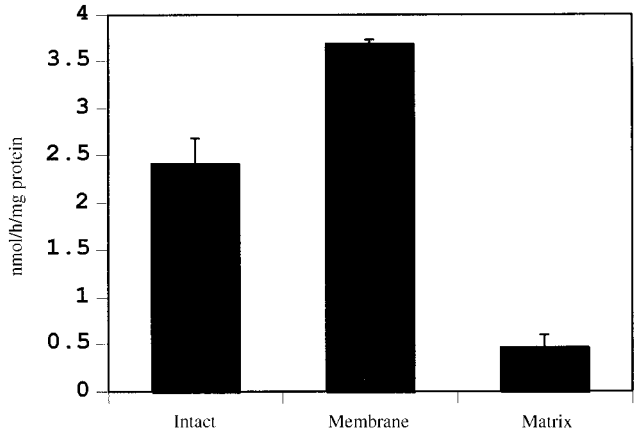

FIG. 4. Intraorganellar localization of cerebronic acid oxidation. Peroxisomal membrane and matrix fractions were prepared from rat liver peroxisomes, and cerebronic acid oxidation activity was studied as described in the Materials and Methods section. Catalase activity was assayed in membrane and matrix to monitor the percent lysis. Catalase activity was found mainly in the matrix. Values are mean ± SD for three separate experiments.

TABLE 3
Fatty Acid Oxidation Ratios in Fibroblasts from Control Subjects and Patients with Peroxisomal Disorders[a]

	Fatty acid oxidation		
	Cerebronic/palmitic	Lignoceric/palmitic	Phytanic/palmitic
Control	0.363 ± 0.050	0.36 ± 0.05	0.036 ± 0.005
ZS	0.184 ± 0.021	0.03 ± 0.02	0.002 ± 0.002
X-ALD	0.321 ± 0.035	0.09 ± 0.03	0.036 ± 0.006
RD	0.296 ± 0.030	0.30 ± 0.04	0.007 ± 0.003
RCDP	0.334 ± 0.017	0.30 ± 0.01	0.008 ± 0.002

[a]Fatty acid oxidation was studied in cultured human skin fibroblasts suspended in Hank's balanced salt solution as described in the Materials and Methods section. Values are mean ± SD for four separate experiments and are expressed as ratio of cerebronic acid or lignoceric acid or phytanic acid to palmitic acid oxidation. ZS, Zellweger syndrome; X-ALD, X-linked adrenoleukodystrophy; RD, Refsum disease; RCDP, rhizomelic chondrodysplasia punctata.

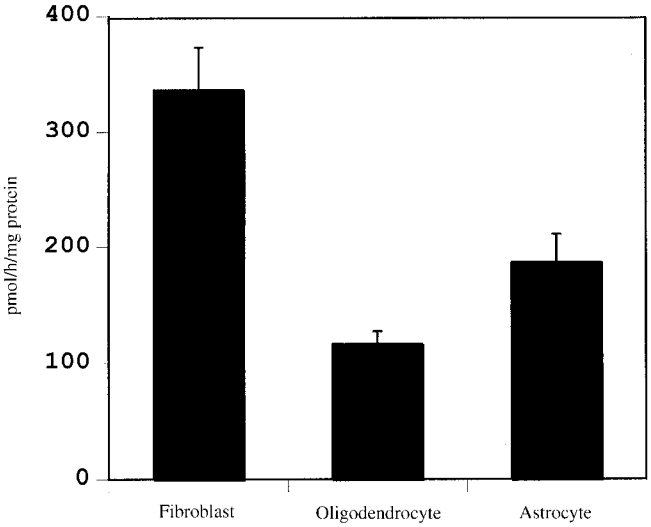

FIG. 5. Oxidation of cerebronic acid in glial cells. Oligodendrocytes and astrocytes were isolated from rat brain and cerebronic acid oxidation was studied as described in the Materials and Methods section. Values are mean ± SD for three separate experiments.

cells from human skin fibroblasts had a significant level of cerebronic acid α-oxidation activity (approximately 50% of the normal control). As expected, lignoceric acid oxidation activity was normal in RD and RCDP, but deficient in ZS by approximately 92%. At present, we do not fully understand the basis of such a high residual activity of cerebronic acid oxidation in cell lines that lack peroxisomes. It may be possible that cerebronic acid decarboxylase is relatively stable as compared to other peroxisomal proteins in cell lines that lack peroxisomes. The partial loss of activity for α-oxidation of cerebronic acid in ZS indicates that some level of cerebronic acid may accumulate in ZS tissue/patients; however, no report is yet available on the accumulation of 2-hydroxy VLCFA in peroxisomal disorders. It may be of interest to monitor levels of 2-hydroxy VLCFA in the brain of ZS patients. The pathological significance of impaired oxidation of cerebronic acid is not clear, as no report is available regarding the toxic effects of α-hydroxy fatty acids. Recently, 2-hydroxy long-chain fatty acids have been demonstrated to have antiviral activity (37). Cerebronic acid oxidation was also studied in the primary glial cells (oligodendrocytes and astrocytes) since cerebronic acid is a major fatty acid of cerebroside and sulfatide in the nervous system (Fig. 5). It was observed that both oligodendrocytes and astrocytes oxidize cerebronic acid and that the specific activity was higher in astrocytes as compared to oligodendrocytes. Consistent with our previous observations for β-oxidation of nervonic acid (13), the cerebronic acid α-oxidation activity in human skin fibroblasts was also higher than in oligodendrocytes and astrocytes (Fig. 5).

In summary, the studies reported here clearly demonstrate that 2-hydroxy VLCFA (cerebronic acid) are catabolized by α-oxidation in peroxisomes and that this enzyme system seems to be different from that which α-oxidizes phytanic acid.

ACKNOWLEDGMENTS

We would like to thank Dr. Avtar Kaur Singh for reviewing the manuscript and Lucinda Burridge for typing the manuscript. The study is supported by grants from the National Institutes of Health (NS-22576, NS-34741 and NS-37766).

REFERENCES

1. Kishimoto, Y., and Radin, N.S. (1963) Occurrence of 2-Hydroxy Fatty Acids in Animal Tissues, *J. Lipid Res. 4*, 139–143.
2. Kishimoto, Y., Akanuma, H., and Singh, I. (1979) Fatty Acid α-Hydroxylation and Its Relation to Myelination, *Mol. Cell. Biochem. 28*, 93–105.
3. Singh, I., and Kishimoto, Y. (1982) Brain-specific Ceramide Synthesis Activity: Change During Brain Maturation and in Jimpy Mouse Brain, *Brain Res. 232*, 500–505.
4. Kunau, W.H., Dommes, V., and Schulz, H. (1995) β-Oxidations of Fatty Acids in Mitochondria, Peroxisomes, and Bacteria: A Century of Continued Progress, *Prog. Lipid Res. 34*, 267–342.
5. Singh, I. (1997) Biochemistry of Peroxisomes, *Mol. Cell. Biochem. 167,* 1–29.
6. Singh, I., Pahan, K., Dhaunsi, G.S., Lazo, O., and Ozand, P. (1993) Phytanic Acid α-Oxidation, *J. Biol. Chem. 268*, 9972–9979.
7. Fulco, A.J., and Mead, J.F. (1961) The Biosynthesis of Lignoceric, Cerebronic and Nervonic Acids, *J. Biol. Chem. 236*, 2416–2420.
8. Hajra, A.K., and Radin, N.S. (1963) Biosynthesis of Odd- and Even-numbered Cerebroside Fatty Acids: Evidence for Two Routes, *Biochim. Biophys. Acta 70*, 97–99.
9. Levis, G.M., and Mead, J.F. (1964) An α-Hydroxy Acid Decarboxylase in Brain Microsomes, *J. Biol. Chem. 239*, 77–80.
10. Singh, I., Moser, A.N., Goldfischer, S., and Moser, H.W. (1984) Lignoceric Acid Is Oxidized in the Peroxisomes: Implications for the Zellweger Cerebro-hepato-renal Syndrome and Adrenoleukodystrophy, *Proc. Natl. Acad. Sci. USA 81*, 4203–4207.
11. Wanders, R.J., van Roermund, C.W.T., van Wijland, M.J.A., Schutgens, R.B.H., Heikoops, J., van den Bosch, H., Schram, A.W., and Tager, J.M. (1987) Peroxisomal Fatty Acid β-Oxidation in Relation to the Accumulation of Very Long Chain Fatty Acids in Cultured Skin Fibroblasts with Zellweger Syndrome and Other Peroxisomal Disorders, *J. Clin. Invest. 80*, 1778–1783.

12. Mihalik, S.J., Rainville, A.M., and Watkins, P.A. (1995) Phytanic Acid α-Oxidation in Rat Liver Peroxisomes: Production of α-Hydroxyphytanoyl-CoA and Formate Is Enhanced by Dioxygenase Cofactors, *Eur. J. Biochem. 232*, 545–551.
13. Sandhir, R., Khan, M., Chahal, A., and Singh, I. (1998) Localization of Nervonic Acid β-Oxidation in Human and Rodent Peroxisomes: Impaired Oxidation in Zellweger Syndrome and X-Linked Adrenoleukodystrophy, *J. Lipid Res. 39*, 2161–2171.
14. Sweet, R.S., and Estes, F.L. (1956) 2-Hexadecenoic Acid and Related Compounds, *J. Org. Chem. 21*, 1426–1429.
15. Lazo, O., Contreras, M., Hashmi, M., Stanley, W., Irazu, C., and Singh, I. (1988) Peroxisomal Lignoceroyl-CoA Ligase Deficiency in Childhood Adrenoleukodystrophy and Adrenomyeloneuropathy, *Proc. Natl. Acad. Sci. USA 85,* 7647–7651.
16. McCarthy, K., and DeVellis, J. (1980) Preparation of Separate Astroglial and Oligodendroglial Cell Cultures from Rat Cerebral Tissue, *J. Cell. Biol. 85,* 890–902.
17. Lazo, O., Contreras, M., and Singh, I. (1991) Effect of Ciprofibrate on the Activation and Oxidation of Very Long Chain Fatty Acids, *Mol. Cell. Biochem. 100*, 159–167.
18. Baudhuin, P., Beaufy, Y., Rahman Li, O., Sellinger, Z., Wattiaux, R., Jacques, P., and de Duve, C. (1964) Tissue Fractionation Studies: Intracellular Distribution of Monoamine Oxidase, Aspartate Aminotransferase, Alanine Aminotransferase, D-Amino Acid Oxidase and Catalase in Rat Liver Tissue, *Biochem. J. 92,* 179–184.
19. Coopertein, S.J., and Lazarow, A. (1951) A Microspectrophotometric Method for the Determination of Cytochrome Oxidase, *J. Biol. Chem. 189*, 665–670.
20. Beaufay, H., Amar-Cotesec, A., Feytmans, E., Thines-Sempoux, D., Wibo, M., Robbi, M., and Berthet, J. (1974) Analytical Study of Microsomes and Isolated Subcellular Membranes from Rat Liver, *J. Cell Biol. 61*, 188–200.
21. Singh, I., Singh, R., Bhushan, A., and Singh, A.K. (1985) Lignoceroyl-CoA Ligase Activity in Rat Brain Microsomal Fraction: Topographical Localization and Effect of Detergents and α-Cyclodextrin, *Arch. Biochem. Biophys. 236*, 418–426.
22. Singh, I., Lazo, O., Kalipada, P., and Singh, A.K. (1992) Phytanic Acid α-Oxidation in Human Skin Fibroblasts, *Biochim. Biophys. Acta 1180*, 221–224.
23. Singh, I., and Kishimoto, Y. (1983) Effect of Cyclodextrin and the Solubilization of Lignoceric Acid, Ceramide, and Cerebroside, and on the Enzymatic Reactions Involving These Compounds, *J. Lipid Res. 24*, 662–665.
24. Fujiki, Y., Fowler, S., Shio, H., Hubbard, A.L., and Lazarow, P.B. (1982) Polypeptide and Phospholipid Composition of the Membrane of Rat Liver Peroxisomes: Comparison with Endoplasmic Reticulum and Mitochondrial Membranes, *J. Cell Biol. 93*, 103–110.
25. Akanuma, H., and Kishimoto, Y. (1979) Synthesis of Ceramides and Cerebrosides Containing Both α-Hydroxy and Nonhydroxy Fatty Acids from Lignoceroyl-CoA by Rat Brain Microsomes, *J. Biol. Chem. 254*, 1050–1056.
26. Mead, J.F., and Levis, G.M. (1963) A 1 Carbon Degradation of the Long Chain Fatty Acids of Brain Sphingolipids, *J. Biol. Chem. 238*, 1634–1636.
27. Lippel, K., and Mead, J.F. (1968) Alpha-oxidation of 2-Hydroxystearic Acid *in vitro, Biochim. Biophys. Acta 152*, 669–680.
28. Verhoeven, N.M, Wanders, R.J.A., Poll-The, B.T., Saudubray, J.-M., and Jakobs, C. (1998) The Metabolism of Phytanic Acid and Pristanic Acid in Man: A Review, *J. Inher. Metab. Dis. 21*, 697–728.
29. Wanders, R.J.A., van Grunsven, E.G., and Jansen, G.A. (2000) Lipid Metabolism in Peroxisomes: Enzymology, Functions and Dysfunctions of the Fatty Acid α- and β-Oxidation Systems in Humans, *Biochem. Soc. Trans. 28 (part 2),* 141–149.
30. Pahan, K., Khan, M., and Singh, I. (1996) Phytanic Acid Oxidation: Normal Activation and Transport Yet Defective α-Hydroxylation of Phytanic Acid in Peroxisomes from Refsum Disease and Rhizomelic Chondrodysplasia Punctata, *J. Lipid Res. 37*, 1137–1143.
31. Mihalik, S.J., Morrell, J.C., Kim, D., Sacksteder, K.A., and Watkins, P.A. (1997) Identification of PAHX, a Refsum Disease Gene, *Nature Genet. 17*, 185–189.
32. Jansen, G.A., Ofman, R., Ferdinandusse, S., Ijlst, L., Muijsers, A.O., Skjeldal, O.H., Stokke, O., Jakobs, C., Besley, G.T.N., Wraith, J.E., *et al*. (1997) Refsum Disease is Caused by Mutations in the Phytanoyl-CoA Hydroxylase Gene, *Nature Genet. 17*, 190–193.
33. Chahal, A., Khan, M., Pai, S.G., Barbosa, E., and Singh, I. (1998) Restoration of Phytanic Acid Oxidation in Refsum Disease Fibroblasts from Patients with Mutations in the Phytanoyl-CoA Hydroxylase Gene, *FEBS Lett. 429*, 119–122.
34. Braverman, N., Steel, G., Obie, C., Moser, A., Moser, H., Gould, S.J., and Valle, D. (1997) Human *PEX7* Encodes the Peroxisomal PTS2 Receptor and is Responsible for Rhizomelic Chondrodysplasia Punctata, *Nature Genet. 15*, 369–375.
35. Ten Brink, H.J., Schor, D.S.M., Kok, R.M., Poll-The, B.T., Wanders, R.J.A., and Jacobs, C. (1992) Phytanic Acid Alpha-oxidation: Accumulation of 2-Hydroxyphytanic Acid and Absence of 2-Oxophytanic Acid in Plasma from Patients with Peroxisomal Disorders, *J. Lipid Res. 33*, 1449–1457.
36. Wanders, R.J., van Roermund, C.W., Schor, D.S., ten Brink, H.J., and Jakobs, C. (1994) 2-Hydroxyphytanic Acid Oxidase Activity in Rat and Human Liver and Its Deficiency in the Zellweger Syndrome, *Biochim. Biophys. Acta 1227*, 177–182.
37. Harper, D.R., Gilbert, R.L., Oconnor, T.J., Kinchington, D., Mahmood, N., Mcilhinney, R.A.J., and Jeffries, D.J. (1996) Antiviral Activity of 2-Hydroxy Fatty Acids, *Antiviral Chem. Chemother. 7*, 138–141.

[Received September 26, 1999, and in revised form July 5, 2000; revision accepted August 18, 2000]

Novel Lipidic Enaminones from a C_{18} Keto-allenic Ester

Marcel S.F. Lie Ken Jie* and Maureen M.L. Lau

Department of Chemistry, The University of Hong Kong, Hong Kong, China

ABSTRACT: Primary amines (ammonia, methyl, propyl, octyl, octadecyl, phenyl, benzyl, phenethyl) including methyl esters of amino acids (glycine, DL-alanine, L-valine, L-leucine, L-tyrosine, and L-methionine), and secondary amines (dimethyl, diethyl, dipropyl, diisopropyl, dioctyl, and diphenyl) attack regiospecifically the central carbon atom of the allene system of methyl 12-keto-9,10-octadecadienoate (**1**) to give the corresponding lipidic enaminone derivatives (**2–21**) with an average yield of 77%. The E- and Z-configuration of the enaminone system of these novel lipid derivatives was confirmed by infrared and nuclear magnetic resonance spectroscopic techniques. Primary amines furnished Z-enaminones, while secondary amines gave E-enaminones.

Paper no. L8498 in *Lipids 35*, 1135–1145 (October 2000)

We have recently reported the synthesis of pyrazole fatty esters from a C_{18} keto-allenic ester, methyl 12-oxo-9,10-octadecadienoate (Scheme 1). The latter compound was obtained by the isomerization of methyl 12-oxo-9-octadecynoate (1). The allenic

$$CH_3(CH_2)_5\text{-}CO\text{-}CH{=}C{=}CH\text{-}(CH_2)_7COOCH_3$$

SCHEME 1

system adjacent to the keto function in this compound makes this substrate a very reactive functional group for nucleophilic addition reactions. During such nucleophilic addition reactions, the attack is specific at the central carbon atom of the allene system (i.e., the C-10 of the alkyl chain of the fatty ester). Regiospecific addition products can therefore be obtained. When the nucleophile is an (alkyl or aryl) amine, the resulting product is an enaminone.

Enaminones are important synthetic intermediates and are particularly useful in heterocyclic chemistry (2). The addition reactions of cyclic enaminones with Grignard reagents have been recently reported (3). Many organic compounds containing the enaminone system have been shown to possess potent biological activities. For example, methyl 4-[(*p*-chlorophenyl) amino]-6-methyl-2-oxo-3-cyclohexen-1-oate exhibits anticonvulsant activities with a remarkable lack of neurotoxicity (4). Pyrrolidino-, isoquinolino-, and indolo-enaminones have been shown to inhibit cyclooxygenase and 5-lipoxygenase as determined in bovine thrombocytes and polymorphonuclear leukocytes, respectively (5).

Of interest is the reduction of an enaminone to give a diamino alcohol, which is a key intermediate in the large-scale synthesis of Ritonavir (a human immunodeficiency virus protease inhibitor) (6).

The chemistry of enaminones has been extensively described (7,8). Despite the importance of this organic functional group, no lipid molecule containing an enaminone system has been reported in the chemical literature. This paper presents the first synthesis of a number of C_{18} enaminone fatty ester derivatives. To reflect the high reactivity of the α-keto-allene system toward amines, reactions with amino acids are also included in this study. The configuration of the double bond of the enaminone system is determined by a combination of spectroscopic techniques.

MATERIALS AND METHODS

Column chromatographic separation was performed on neutral aluminum oxide (Merck, Art. 1077, 70–230 mesh ASTM) as the adsorbent using gradient elution with mixtures of *n*-hexane/diethyl ether in various proportions as the mobile phase. The column run was monitored by thin-layer chromatography (TLC) analysis of the eluent. Infrared (IR) spectra were recorded on a Bio-Rad FTS-165 Fourier-transform IR spectrometer. Samples were run as neat films on NaCl plates. Nuclear magnetic resonance (NMR) spectra were recorded on a Bruker Avance DPX_{300} (300 MHz) or Avance DRX (500 MHz) Fourier-transform NMR spectrometer (Bruker, Fallanden, Switzerland) from solutions in deuteriochloroform ($CDC1_3$) (0.2–0.3 mM) with tetramethylsilane (TMS) as the internal reference standard. Chemical shifts are given in δ-values in ppm downfield from TMS ($\delta_{TMS} = 0$ ppm). Mass spectral analyses were carried out on a Finnigan MAT-95 (Finnigan Corp., San Jose, CA). Methyl 12-oxo-9,10-octadecadienoate (**1**) was obtained by $NaHCO_3$ isomerization of methyl 12-hydroxy-9-octadecynoate. The latter compound was pre-

*To whom correspondence should be addressed at Department of Chemistry, The University of Hong Kong, Pokfulam Road, Hong Kong.
E-mail: hrsclkj@hkucc.hku.hk

Abbreviations: HRMS, high-resolution mass spectral analysis; IR, infrared; NMR, nuclear magnetic resonance; 2D-NOESY, two-dimensional nuclear Overhauser enhancement spectroscopy; TLC, thin-layer chromatography; TMS, tetramethylsilane.

pared by bromination/dehydrobromination of ricinoleic acid, which was obtained from castor oil. The procedures for the synthesis of compound **1** are described elsewhere (1).

General procedure for the synthesis of C_{18} enaminone derivatives as exemplified by the reaction of methyl 12-oxo-9,10-octadecadienoate with ammonia. A mixture of methyl 12-oxo-9,10-octadecadienoate (**1**, 0.5 g, 1.6 mmol), ethanol (95%, 30 mL), and ammonium hydroxide (35% w/w of ammonia in water, 0.3 mL, 19.5 mmol) was stirred at room temperature for 3 h. Water (30 mL) was added, and the reaction mixture was extracted with diethyl ether (3 × 30 mL). The ethereal extract was washed with brine (20 mL) and dried over anhydrous Na_2SO_4. The filtrate was evaporated to give pure methyl 10-amino-12-oxo-10*Z*-octadecenoate (**2**, 0.43 g, 86%) as a viscous liquid. TLC on silica: R_f = 0.4 (*n*-hexane/diethyl ether, 1:1 vol/vol, as developer); IR (NaCl, neat): 3413 (*m*, N-H), 3184 (*m*, N-H), 2930, 2857, 1741, 1615, 1529, 1462, 1436, 1361, 1245, 1198, 1172, 1100, 1025, 882, and 725 cm^{-1}; ^1H NMR ($CDCl_3$, δ_H) 0.88 (*t*, *J* = 6.7 Hz, 3H, C*H*$_3$), 1.2–1.7 (*m*, 20H, C*H*$_2$), 2.11 (*t*, *J* = 7.7 Hz, 2H, 9-*H*), 2.26 (*t*, *J* = 7.7 Hz, 2H, 13-*H*), 2.30 (*t*, *J* = 7.5 Hz, 2H, 2-*H*), 3.67 (*s*, 3H, COOC*H*$_3$), 5.03 (*s*, 1H, 11-*H*), and 9.79 (*br. s*, 2H, N-*H*); ^{13}C NMR ($CDCl_3$, δ_C) 14.10 (C-18), 22.58 (C-17), 24.88 (C-3), 25.96 (C-14), 27.94 (C-8), 29.04, 29.11, 29.26 (C-15), 31.77 (C-16), 34.05 (C-2), 36.44 (C-9), 42.57 (C-13), 51.47 (COO*C*H$_3$), 94.57 (C-11), 165.00 (C-10), 174.28 (*C*OOCH$_3$), and 200.15 (C-12); high-resolution mass spectral analysis (HRMS), found: M^+, 325.2620, $C_{19}H_{35}NO_3$ requires 325.2617.

This reaction procedure (performed in ethanol at room temperature) was suitable for the following nucleophiles: methylamine, propylamine, dimethylamine, diethylamine, dipropylamine, diisopropylamine, phenylamine, benzylamine, and phenethylamine. In the case where the nucleophile was either octylamine, octadecylamine, dioctylamine, or diphenylamine, the reaction was performed in chloroform instead of ethanol under reflux. And for the reactions involving the HCl salts of the methyl esters of amino acids (glycine, DL-alanine, L-valine, L-leucine, L-tyrosine, and L-methionine), the reactions were performed in methanol under reflux in the presence of triethylamine. An excess amount of amine (about fivefold molar equivalent) to compound **1** was used in each case. After isolation of the reaction products, the unreacted amine was removed either by reduced pressure distillation or by washing the isolated product mixtures with dilute HCl. The final purification of the enaminone derivatives was carried out by alumina column chromatography (gradient elution using a mixture of *n*-hexane and diethyl ether). The results of the spectroscopic and spectrometric analyses of the various derivatives (**3–21**) are listed below.

Methyl 10-methylamino-12-oxo-10Z-octadecenoate (**3**, 84% yield). TLC on silica: R_f = 0.4 (*n*-hexane/diethyl ether, 1:1 vol/vol, as developer); IR (NaCl, neat): 3455 (*w*, N-H), 2929, 2856, 1739, 1610, 1580, 1520, 1436, 1358, 1249, 1171, 727 cm^{-1}; ^1H NMR ($CDCl_3$, δ_H) 0.87 (*t*, *J* = 6.7 Hz, 3H, C*H*$_3$), 1.2–1.7 (*m*, 20H, CH$_2$), 2.15–2.25 (*m*, 4H, 9-*H* and 13-*H*), 2.31 (*t*, *J* = 7.5 Hz, 2H, 2-*H*), 2.93 (*d*, *J* = 5.3 Hz, 3H, N-C*H*$_3$), 3.67 (*s*, 3H, COOC*H*$_3$), 4.96 (*s*, 1H, 11-*H*), 10.86 (*br. s*, 1H, N-*H*); ^{13}C NMR ($CDCl_3$, δ_C) 14.19 (C-18), 22.67 (C-17), 24.97 (C-3), 26.51 (C-14), 27.69 (C-8), 29.14, 29.19, 29.21 (N-*C*H$_3$), 29.37, 29.46, 31.81 (C-16), 31.87 (C-9), 34.12 (C-2), 42.23 (C-13), 51.53 (COO*C*H$_3$), 93.76 (C-11), 168.05 (C-10), 174.32 (*C*OOCH$_3$), and 198.26 (C-12); HRMS, found: M^+, 339.2774, $C_{20}H_{37}NO_3$ requires 339.2773.

Methyl 12-oxo-10-propylamino-10Z-octadecenoate (**4**, 80% yield). TLC on silica: R_f = 0.7 (*n*-hexane/diethyl ether, 1:1 vol/vol, as developer); IR (NaCl neat): 3455 (*w*, N-H), 2930, 2857, 1741, 1608, 1580, 1514, 1463, 1436, 1359, 1238, 1170, 1094, 1023, 727 cm^{-1}; ^1H NMR ($CDCl_3$, δ_H) 0.88 (*t*, *J* = 6.7 Hz, 3H, C*H*$_3$), 0.99 (*t*, *J* = 7.4 Hz, 3H, N-CH$_2$CH$_2$C*H*$_3$), 1.2–1.7 (*m*, 22H, C*H*$_2$), 2.15–2.25 (*m*, 4H, 9-*H* and 13-*H*), 2.31 (*t*, *J* = 7.5 Hz, 2H, 2-*H*), 3.1–3.2 (*m*, 2H, N-C*H*$_2$), 3.67 (*s*, 3H, COOC*H*$_3$), 4.93 (*s*, 1H, 11-*H*), 10.98 (*br. s*, 1H, N-*H*); ^{13}C NMR ($CDCl_3$, δ_C) 11.49 (N-CH$_2$CH$_2$*C*H$_3$), 14.12 (C-18), 22.60 (C-17), 23.47 (N-CH$_2$*C*H$_2$), 24.91 (C-3), 26.31 (C-14), 28.02, 29.08, 29.13, 29.19, 29.32, 29.42, 31.80 (C-16), 32.02 (C-9), 34.05 (C-2), 42.16 (C-13), 44.43 (N-*C*H$_2$), 51.44 (COO*C*H$_3$), 93.51 (C-11), 167.14 (C-10), 174.22 (*C*OOCH$_3$), and 197.99 (C-12); HRMS, found: M^+, 367.3086, $C_{22}H_{41}NO_3$ requires 367.3086.

Methyl 10-octylamino-12-oxo-10Z-octadecenoate (**5**, 35% yield). TLC on silica: R_f = 0.3 (*n*-hexane/diethyl ether, 4:1 vol/vol, as developer); IR (NaCl neat): 3462 (*w*, N-H), 2928, 2856, 1741, 1608, 1580, 1513, 1465, 1436, 1359, 1282, 1259, 1169, 1091, 1024, 803, 725 cm^{-1}; ^1H NMR ($CDCl_3$, δ_H) 0.88 (*t*, merged, 3H, C*H*$_3$), 0.89 (*t*, merged, 3H, C*H*$_3$), 1.2–1.7 (*m*, 32H, C*H*$_2$), 2.13–2.25 (*m*, 4H, 9-*H* and 13-*H*), 2.31 (*t*, *J* = 7.5 Hz, 2H, 2-*H*), 3.1–3.2 (*m*, 2H, N-C*H*$_2$), 3.67 (*s*, 3H, COOC*H*$_3$), 4.93 (*s*, 1H, 11-*H*), 10.98 (*br. s*, 1H, N-*H*); ^{13}C NMR ($CDCl_3$, δ_C) 14.09 (C-18 and N-[CH$_2$]$_7$*C*H$_3$), 22.59, 22.65, 24.89 (C-3), 26.31 (C-14), 28.01, 29.08, 29.14, 29.30, 29.41, 30.21, 31.80, 31.82, 32.01 (C-9), 34.03 (C-2), 42.14 (C-13), 42.73 (N-*C*H$_2$), 51.40 (COO*C*H$_3$), 93.46 (C-11), 167.05 (C-10), 174.17 (*C*OOCH$_3$), and 197.92 (C-12); HRMS found: M^+, 437.3865, $C_{27}H_{51}NO_3$ requires 437.3869.

Methyl 10-octadecylamino-12-oxo-10Z-octadecenoate (**6**, 20% yield). TLC on silica: R_f = 0.7 (*n*-hexane/diethyl ether, 1:1 vol/vol, as developer); IR (NaCl neat) 3463 (*w*, N-H), 2926, 2854, 1742, 1608, 1581, 1513, 1466, 1436, 1367, 1282, 1241, 1197, 1170, 1091, 1026, 802, 724 cm^{-1}; ^1H NMR ($CDCl_3$, δ_H) 0.8–0.95 (*m*, 6H, 18-*H* and N-[CH$_2$]$_{17}$C*H*$_3$), 1.2–1.6 (*m*, 52H, C*H*$_2$), 2.13–2.25 (*m*, 4H, 9-*H* and 13-*H*), 2.31 (*t*, *J* = 7.5 Hz, 2H, 2-*H*), 3.2–3.25 (*m*, 2H, N-C*H*$_2$), 3.67 (*s*, 3H, COOC*H*$_3$), 4.92 (*s*, 1H, 11-*H*), 10.95 (*br. t*, 1H, N-*H*); ^{13}C NMR ($CDCl_3$, δ_C) 14.26 (C-18 and N-[CH$_2$]$_{17}$*C*H$_3$), 22.72 (C-17), 22.84 (C-17′, *N*-octadecyl), 25.03 (C-3), 26.45 (C-14), 27.06, 28.14, 29.22, 29.26, 29.45, 29.51, 29.56, 29.62, 29.75, 29.81, 29.85, 30.35, 31.92, 32.07, 32.16 (C-9), 34.18 (C-2), 42.30 (C-13), 42.88 (N-*C*H$_2$), 51.58 (COO*C*H$_3$), 93.57 (C-11), 167.19 (C-10), 174.36 (COOCH$_3$), and 198.11 (C-12); HRMS, found: M^+, 577.5432, $C_{37}H_{71}NO_3$ requires 577.5434.

Methyl 12-oxo-10-phenylamino-10Z-octadecenoate (**7**,

80% yield). TLC on silica: R_f = 0.7 (*n*-hexane/diethyl ether, 1:1 vol/vol, as developer); IR (neat) 3461 (*w*, N-H), 3064 (arom. C-H), 3031 (arom. C-H), 2929, 2856, 1740, 1612, 1596, 1573, 1506, 1362, 1254, 1096, 1027, 752, 698 cm^{-1}; ^1H NMR ($CDCl_3$, δ_H) 0.89 (*t, J* = 6.7 Hz, 3H, CH_3), 1.2–1.7 (*m*, 20H, CH_2), 2.25–2.35 (*m*, 6H, 2-*H*, 9-*H* and 13-*H*), 3.66 (*s*, 3H, $COOCH_3$), 5.19 (*s*, 1H, 11-*H*), 7.05–7.40 (*m*, 5H, Ph-*H*), 12.54 (*s*, 1H, N-*H*); ^{13}C NMR ($CDCl_3$, δ_C) 14.12 (C-18), 22.59 (C-17), 24.87 (C-3), 26.09 (C-14), 28.06, 28.91, 28.97, 29.02, 29.10, 29.28, 31.78 (C-16), 31.86 (C-9), 34.04 (C-2), 42.49 (C-13), 51.44 ($COOCH_3$), 95.90 (C-11), 125.20 (C-2′ and C-6′ arom.), 125.67 (C-4′ arom.), 129.09 (C-3′ and C-5′ arom.), 138.75 (C-1′ arom.), 164.73 (C-10), 174.23 ($COOCH_3$), and 199.55 (C-12); HRMS, found: M^+, 401.2933, $C_{25}H_{39}NO_3$ requires 401.2930.

Methyl 10-benzylamino-12-oxo-10Z-octadecenoate (**8**, 84% yield). TLC on silica: R_f = 0.3 (*n*-hexane/diethyl ether, 7:3 vol/vol, as developer); IR (neat) 3455 (*v w*, N-H), 3064 (arom. C-H), 3029 (arom. C-H), 2929, 2856, 1739, 1607, 1577, 1512, 1454, 1365, 1323, 1283, 1234, 1170, 1090, 1029, 751, 732, 697, 665 cm^{-1}; ^1H NMR ($CDCl_3$, δ_H) 0.88 (*t, J* = 6.7 Hz, 3H, 18-*H*), 1.2–1.75 (*m*, 20H, CH_2), 2.17–2.29 (*m*, 4H, 9-*H* and 13-*H*), 2.30 (*t, J* = 7.5 Hz, 2H, 2-*H*), 3.66 (*s*, 3H, $COOCH_3$), 4.45 (*d, J* = 6.3 Hz, 2H, N-CH_2), 5.03 (*s*, 1H, 11-*H*), 7.2–7.35 (*m*, 5H, Ph-*H*), 11.27 (*br. t*, 1H, N-*H*); ^{13}C NMR ($CDCl_3$, δ_C) 14.10 (C-18), 22.58 (C-17), 24.87 (C-3), 26.17 (C-14), 28.04, 29.06, 29.28, 29.35, 31.77 (C-16), 31.94 (C-9), 34.04 (C-2), 42.27 (C-13), 46.47 (N-CH_2), 51.44 ($COOCH_3$), 94.32 (C-11), 126.82 (C-2′ and C-6′ arom.), 127.40 (C-4′ arom.), 128.77 (C-3′ and C-5′ arom.), 139.19 (C-1′ arom.), 166.89 (C-10), 174.23 ($COOCH_3$), and 198.72 (C-12); HRMS, found: M^+, 415.3088, $C_{26}H_{41}NO_3$ requires 415.3086.

Methyl 12-oxo-10-phenethylamino-10Z-octadecenoate (**9**, 85% yield). TLC on silica: R_f = 0.4 (*n*-hexane/diethyl ether, 1:1 vol/vol, as developer); IR (neat) 3315 (*w*, N-H), 3064 (arom. C-H), 3028 (arom. C-H), 2929, 2856, 1739, 1605, 1575, 1511, 1455, 1087, 1030, 749, 700 cm^{-1}; ^1H NMR ($CDCl_3$, δ_H) 0.88 (*t, J* = 6.6 Hz, 3H, 18-*H*), 1.2–1.7 (*m*, 20H, CH_2), 2.07 (*t, J* = 7.8 Hz, 2H, 9-*H*), 2.23 (*t, J* = 6.6 Hz, 2H, 13-*H*), 2.30 (*t, J* = 7.5 Hz, 2H, 2-*H*), 2.88 (*t, J* = 7.5 Hz, 2H, N-CH_2CH_2), 3.4–3.5 (*m*, 2H, N-CH_2) 3.66 (*s*, 3H, $COOCH_3$), 4.92 (*s*, 1H, 11-*H*), 7.17–7.3 (*m*, 5H, Ph-*H*), 11.04 (*br. t*, 1H, N-*H*); ^{13}C NMR ($CDCl_3$, δ_C) 14.11 (C-18), 22.59 (C-17), 24.88 (C-3), 26.37 (C-14), 27.92, 29.06, 29.10, 29.28, 29.37, 31.78 (C-16), 31.90 (C-9), 34.05 (C-2), 37.05 (N-CH_2CH_2), 42.23 (C-13), 44.57 (N-CH_2), 51.46 ($COOCH_3$), 93.77 (C-11),126.65 (C-4′ arom.), 128.63 (C-2′ and C-6′ arom.), 128.77 (C-3′ and C-5′ arom.), 138.49 (C-1′ arom.), 166.86 (C-10), 174.26 ($COOCH_3$), and 198.35 (C-12); HRMS, found: M^+, 429.3245, $C_{26}H_{43}NO_3$ requires 429.3243.

Methyl 10-(methoxycarbonylmethyl-amino)-12-oxo-10Z-octadecenoate (**10**, 90% yield). TLC on silica: R_f = 0.4 (*n*-hexane/diethyl ether, 1:1 vol/vol, as developer); IR (neat) 3480 (*w*, N-H), 2930, 2856, 1741, 1613, 1575, 1512, 1436, 1209 cm^{-1}; ^1H NMR ($CDCl_3$, δ_H) 0.88 (*t, J* = 6.7 Hz, 3H, 18-*H*), 1.20–1.70 (*m*, 20H, CH_2), 2.13 (*t, J* = 7.8 Hz, 2H, 9-*H*), 2.26 (*t, J* = 7.6 Hz, 2H, 13-*H*), 2.31 (*t, J* = 7.5 Hz, 2H, 2-*H*), 3.67 (*s*, 3H, $COOCH_3$), 3.77 (*s*, 3H, amino ester $COOCH_3$), 4.03 (*d, J* = 6.2 Hz, 2H, N-CH_2), 5.06 (*s*, 1H, 11-*H*), 11.04 (*t, J* = 5.7 Hz, 1H, N-*H*); ^{13}C NMR ($CDCl_3$, δ_C) 14.10 (C-18), 22.58 (C-17), 24.88 (C-3), 26.06 (C-14), 27.78, 29.06, 29.09, 29.12, 29.26, 29.31, 31.77 (C-16), 31.88 (C-9), 34.03 (C-2), 42.39 (C-13), 44.34 (N-*C*H), 51.45 ($COOCH_3$), 52.49 (amino ester $COOCH_3$), 95.12 (C-11), 165.60 (C-10), 169.74 (amino ester $COOCH_3$), 174.22 ($COOCH_3$), and 199.41 (C-12); HRMS, found: M^+, 397.2829, $C_{22}H_{39}NO_5$ requires 397.2828.

Methyl 10-(1-methoxycarbonyl-ethylamino)-12-oxo-10Z-octadecenoate (**11**, 87% yield). TLC on silica: R_f = 0.4 (*n*-hexane/ diethyl ether, 1:1 vol/vol, as developer); IR (neat) 3480 (*w*, N-H), 2930, 2857, 1741, 1611, 1582, 1458, 1436, 1205, 1170, 1147 cm^{-1}; ^1H NMR ($CDCl_3$, δ_H) 0.88 (*t, J* = 6.7 Hz, 3H, 18-*H*), 1.25–1.70 (*m*, 20H, CH_2), 1.5 (*d, J* = 7 Hz, 3H, amino ester CH_3), 2.10–2.20 (*m*, 2H, 9-*H*), 2.27 (*t, J* = 7.6 Hz, 2H, 13-*H*), 2.31 (*t, J* = 7.5 Hz, 2H, 2-*H*), 3.67 (*s*, 3H, $COOCH_3$), 3.75 (*s*, 3H, amino ester $COOCH_3$), 4.20–4.30 (*m*, 2H, N-C*H*), 5.02 (*s*, 1H, 11-*H*), 11.02 (*d, J* = 8.5 Hz, 1H, N-*H*); ^{13}C NMR ($CDCl_3$, δ_C) 14.21 (C-18), 19.56 (N-CH-*C*H_3), 22.68 (C-17), 24.99 (C-3), 26.00 (C-14), 28.25, 29.17, 29.20, 29.36, 29.46, 31.87 (C-16), 32.04 (C-9), 34.15 (C-2), 42.43 (C-13), 51.29 (N-*C*H), 51.57 ($COOCH_3$), 52.66 (amino ester $COOCH_3$), 95.01 (C-11), 165.30 (C-10), 172.93 (amino ester $COOCH_3$), 174.36 ($COOCH_3$), and 199.38 (C-12); HRMS, found: M^+, 411.2984, $C_{23}H_{42}NO_5$ requires 411.2985.

Methyl 10-(1-methoxycarbonyl-2-methyl-propylamino)-12-oxo-10Z-octadecenoate (**12**, 77% yield). TLC on silica: R_f = 0.5 (*n*-hexane/diethyl ether, 1:1 vol/vol, as developer); IR (neat) 3465 (*w*, N-H), 2930, 2856, 1741, 1610, 1583, 1508, 1437, 1264, 1199, 1145 cm^{-1}; ^1H NMR ($CDCl_3$, δ_H) 0.88 (*t, J* = 6.7 Hz, 3H, 18-*H*), 1.00 and 1.02 (*d, J* = 6.9 and 7.0 Hz, 3H each, amino ester CH_3), 1.20–1.70 (*m*, 20H, CH_2), 2.07-2.14 (*m*, 2H, 9-*H*), 2.17–2.27 (*m*, 1H, amino ester N-CH-C*H*), 2.27 (*t, J* = 7.7 Hz, 2H, 13-*H*), 2.31 (*t, J* = 7.5 Hz, 2H, 2-*H*), 3.67 (*s*, 3H, $COOCH_3$), 3.73 (*s*, 3H, amino acid $COOCH_3$), 3.94 (*dd, J* = 9.8 and 5.8 Hz, 1H, N-C*H*), 5.02 (*s*, 1H, 11-*H*), 11.16 (*d, J* = 9.7 Hz, 1H, N-*H*); ^{13}C NMR ($CDCl_3$, δ_C) 14.17 (C-18), 18.11 and 19.29 (amino ester CH_3), 22.65 (C-17), 24.97 (C-3), 26.02 (C-14), 28.18 (C-8), 29.14, 29.17, 29.35, 29.40, 31.82 (C-16), 31.87 (N-CH-*C*H), 32.10 (C-9), 34.12 (C-2), 42.47 (C-13), 51.54 ($COOCH_3$), 52.32 (amino ester $COOCH_3$), 61.65 (N-*C*H), 95.05 (C-11), 165.83 (C-10), 172.07 (amino ester $COOCH_3$), 174.33 ($COOCH_3$), and 199.22 (C-12); HRMS, found: M^+, 439.3293, $C_{25}H_{45}NO_5$ requires 439.3298.

Methyl 10-(1-methoxycarbonyl-3-methyl-butylamino)-12-oxo-10Z-octadecenoate (**13**, 90% yield). TLC on silica: R_f = 0.5 (*n*-hexane/diethyl ether, 1:1 vol/vol, as developer); IR (neat) 3459 (*w*, N-H), 2930, 2857, 1741, 1611, 1583, 1507, 1437, 1368, 1247, 1198, 1149, 1089 cm^{-1}; ^1H NMR ($CDCl_3$, δ_H) 0.88 (*t, J* = 6.8 Hz, 3H, 18-*H*), 0.92 and 0.97 (*d, J* = 6.1 Hz, 3H each, amino ester CH_3), 1.25–1.80 (*m*, 23H, CH_2), 2.06–2.14 (*m*, 2H, 9-*H*), 2.27 (*t, J* = 7.7 Hz, 2H, 13-*H*), 2.31

(*t, J* = 7.5 Hz, 2H, 2-*H*), 3.67 (*s*, 3H, COOCH_3), 3.77 (*s*, 3H, amino ester COOCH_3), 4.10–4.20 (*m*, 1H, N-C*H*), 5.01 (*s*, 1H, 11-*H*), 10.97 (*d, J* = 8.9 Hz, 1H, N-*H*); ^{13}C NMR ($CDCl_3$, δ_C) 14.21 (C-18), 22.02 and 22.86 (amino ester *C*H_3), 22.68 (C-17), 24.78 (C-3), 25.00 (N-CH-CH_2-*C*H), 25.98 (C-14), 28.19, 29.18, 29.20, 29.36, 29.46, 31.86 (C-16), 32.12 (C-9), 34.16 (C-2), 42.29 (N-CH-*C*H_2), 42.45 (C-13), 51.59 (COO*C*H_3), 52.33 (amino ester COO*C*H_3), 54.44 (N-*C*H), 95.06 (C-11), 165.69 (C-10), 172.99 (amino ester *C*OOCH_3), 174.36 (*C*OOCH_3), and 199.33 (C-12); HRMS, found: M^+, 453.3452, $C_{26}H_{47}NO_5$ requires 453.3454.

Methyl 10-[2-(4-hydroxy-phenyl)-1-methoxycarbonyl-ethyl-amino]-12-oxo-10Z-octadecenoate (**14**, 89% yield). TLC on silica: R_f = 0.7 (*n*-hexane/diethyl ether, 1:5 vol/vol, as developer); IR (neat) 3453 (*w*, N-H), 3212 (*v. br.*, O-H), 3023 (arom. C-H), 2929, 2855, 1746, 1592, 1511, 1435, 1362, 1275, 1167, 824 cm^{-1}; ^{1}H NMR ($CDCl_3$, δ_H) 0.88 (*t, J* = 6.7 Hz, 3H, 18-*H*), 1.10–1.60 (*m*, 20H, CH_2), 1.96 (*t, J* = 7.3 Hz, 2H, 9-*H*), 2.26 (*t, J* = 7.6 Hz, 2H, 13-*H*), 2.32 (*t, J* = 7.4 Hz, 2H, 2-*H*), 2.95 (*dd, J* = 8.4 and 13.8 Hz, 1H, N-CH-CH_2), 3.08 (*dd, J* = 4.3 and 13.9 Hz, 1H, N-CH-CH_2), 3.68 (*s*, 3H, COOCH_3), 3.70 (*s*, 3H, amino acid COOCH_3), 4.31 (*ddd, J* = 4.5, 8.9, and 8.9 Hz, 1H, N-C*H*), 4.97 (*s*, 1H, 11-*H*), 6.76 (*d, J* = 8.3 Hz, 2H, 3′-*H* and 5′-*H* arom.), 7.00 (*d, J* = 8.3 Hz, 2H, 2′-*H* and 6′-*H* arom.), 11.14 (*d, J* = 9.5 Hz, 1H, N-*H*); ^{13}C NMR ($CDCl_3$, δ_C) 14.21 (C-18), 22.67 (C-17), 24.91 (C-3), 26.50 (C-14), 27.97, 29.11, 29.30, 29.35, 31.77 (C-16), 32.08 (C-9), 34.16 (C-2), 39.22 (N-CH-*C*H_2), 42.33 (C-13), 51.73 (COO*C*H_3), 52.68 (amino ester COO*C*H_3), 58.06 (N-*C*H), 95.14 (C-11), 115.80 (C-3′ and C-5′ arom.), 126.64 (C-1′ arom.), 130.51 (C-2′ and C-6′ arom.), 156.38 (C-4′ arom.), 166.50 (C-10), 171.69 (amino ester *C*OOCH_3), 174.84 (*C*OOCH_3), and 199.59 (C-12); HRMS, found: M^+, 503.3249, $C_{29}H_{45}NO_6$ requires 503.3247.

Methyl 10-(1-methoxycarbonyl-3-methylsulfanyl-propyl-amino)-12-oxo-10Z-octadecenoate (**15**, 87% yield). TLC on silica: R_f = 0.4 (*n*-hexane/diethyl ether, 1:1 vol/vol, as developer); IR (neat) 3469 (*w*, N-H), 2929, 2856, 1741, 1610, 1583, 1508, 1437, 1269, 1197, 1171 cm^{-1}; ^{1}H NMR ($CDCl_3$, δ_H) 0.88 (*t, J* = 6.6 Hz, 3H, 18-*H*), 1.25–1.70 (*m*, 20H, CH_2), 2.09 (*s*, 3H, S-CH_3), 2.12–2.20 (*m*, 4H, S-CH_2CH_2 and 9-H), 2.27 (*t, J* = 7.7 Hz, 2H, 13-*H*), 2.31 (*t, J* = 7.5 Hz, 2H, 2-*H*), 2.55–2.64 (*m*, 2H, S-CH_2), 3.67 (*s*, 3H, COOCH_3), 3.75 (*s*, 3H, amino ester COOCH_3), 4.40 (*m*, 1H, N-C*H*), 5.04 (*s*, 1H, 11-*H*), 11.01 (*d, J* = 9.5 Hz, 1H, N-*H*); ^{13}C NMR ($CDCl_3$, δ_C) 14.10 (C-18), 15.22 (S-*C*H_3), 22.57 (C-17), 24.90 (C-3), 25.88 (C-14), 28.08, 29.07, 29.09, 29.23, 29.34, 30.07 (S-*C*H_2), 31.74 (C-16), 32.08 and 32.20 (C-9/S-CH_2-*C*H_2), 34.05 (C-2), 42.31 (C-13), 51.46 (COO*C*H_3), 52.60 (amino ester COO*C*H_3), 53.96 (N-*C*H), 95.31 (C-11), 165.97 (C-10), 172.18 (amino ester *C*OOCH_3), 174.26 (*C*OOCH_3), and 199.47 (C-12); HRMS, found: M^+, 471.3019, $C_{25}H_{45}NSO_5$ requires 471.3018.

*Methyl 10-dimethylamino-12-oxo-10*E*-octadecenoate* (**16**, 82% yield). TLC on silica: R_f = 0.3 (*n*-hexane/diethyl ether, 1:1 vol/vol, as developer); IR (NaCl neat) 2929, 2856, 1739, 1635, 1543, 1438, 1417, 1402, 1377, 1366, 1238, 1198, 1171, 1141, 1089, 1012, 973, 881, 845, 780, 725, 667 cm^{-1}; ^{1}H NMR ($CDCl_3$, δ_H) 0.87 (*t, J* = 6.7 Hz, 3H, 18-*H*), 1.2–1.7 (*m*, 20H, CH_2), 2.25–2.35 (*m*, 6H, 2-*H*, 9-*H* and 13-*H*), 2.96 (*s*, 6*H*, N-CH_3), 3.66 (*s*, 3H, COOCH_3), 4.96 (*s*, 1H, 11-*H*); ^{13}C NMR ($CDCl_3$, δ_C) 14.22 (C-18), 22.71 (C-17), 25.08 (C-3), 26.26 (C-14), 28.33, 28.83, 29.23, 29.37, 29.42, 30.01 (C-9), 31.95 (C-16), 34.23 (C-2), 39.71 (N-*C*H_3), 44.86 (C-13), 51.55 (COO*C*H_3), 94.37 (C-11), 166.04 (C-10), 174.48 (*C*OOCH_3), and 197.11 (C-12); HRMS found: M^+, 353.2959, $C_{21}H_{39}NO_3$ requires 353.2930.

*Methyl 10-diethylamino-12-oxo-10*E*-octadecenoate* (**17**, 82% yield). TLC on silica: R_f = 0.5 (*n*-hexane/diethyl ether, 1:1 vol/vol, as developer); IR (NaCl neat) 2928, 2855, 1740, 1634, 1537, 1460, 1379, 1358, 1198, 1171, 1140, 1090, 1076 cm^{-1}; ^{1}H NMR ($CDCl_3$, δ_H) 0.87 (*t, J* = 6.6 Hz, 3H, 18-*H*), 1.18 (*t, J* = 7.0 Hz, 6H, N-CH_2CH_3), 1.2–1.7 (*m*, 20H, CH_2), 2.2–2.35 (*m*, 4H, 2-*H* and 13-*H*), 2.93 (*br. s*, 2H, 9-*H*), 3.28 (*t, J* = 7 Hz, 4H, N-CH_2), 3.65 (*s*, 3H, COOCH_3), 5.01 (*s*, 1H, 11-*H*); ^{13}C NMR ($CDCl_3$, δ_C) 13.08 (N-CH_2CH_3), 14.12 (C-18), 22.64 (C-17), 24.98 (C-3), 26.26 (C-14), 28.58 (C-9), 29.11, 29.13, 29.29, 29.33, 31.89 (C-16), 34.05 (C-2), 43.70 (N-*C*H_2), 44.80 (C-13), 51.30 (COO*C*H_3), 93.14 (C-11), 164.34 (C-10), 174.11 (*C*OOCH_3), and 196.30 (C-12); HRMS found: M^+, 381.3241, $C_{23}H_{43}NO_3$ requires 381.3243.

*Methyl 12-oxo-10-dipropylamino-10*E*-octadecenoate* (**18**, 81% yield). TLC on silica: R_f = 0.5 (*n*-hexane/diethyl ether, 1:1 vol/vol, as developer); IR (NaCl neat) 2957, 2930, 2873, 2856, 1741, 1635, 1535, 1463, 1367, 1297, 1247, 1197, 1172, 1140, 1090, 1041, 984, 892, 782, 753, 726, 663 cm^{-1}; ^{1}H NMR ($CDCl_3$, δ_H) 0.82–0.96 (*m*, 9H, 18-*H* and N-$CH_2CH_2CH_3$), 1.24–1.68 (*m*, 24H, CH_2), 2.23–2.33 (*m*, 4H, 2-*H* and 13-*H*), 2.93 (*br. s*, 2H, 9-*H*), 3.5 (*t, J* = 7.8 Hz, 4H, N-CH_2), 3.66 (*s*, 3H, COOCH_3), 4.97 (*s*, 1H, 11-*H*); ^{13}C NMR ($CDCl_3$, δ_C) 11.36 (N-CH_2CH_2CH_3), 14.16 (C-18), 22.65 (C-17), 25.01 (C-3), 26.25 (C-14), 28.61 (C-9), 29.09, 29.17, 29.28, 29.33, 30.02, 31.88 (C-16), 34.15 (C-2), 44.87 (C-13), 51.45 (COO*C*H_3), 51.74 (N-*C*H_2), 93.53 (C-11), 164.85 (C-10), 174.38 (*C*OOCH_3), and 196.53 (C-12); HRMS found: M^+, 409.3537, $C_{25}H_{47}NO_3$ requires 409.3556.

*Methyl 10-diisopropylamino-12-oxo-10*E*-octadecenoate* (**19**, 82% yield). TLC on silica: R_f = 0.5 (*n*-hexane/diethyl ether, 1:1 vol/vol, as developer); IR (neat) 2930, 2856, 1741, 1635, 1531, 1457, 1371, 1242, 1131, 1085, 804 cm^{-1}; ^{1}H NMR ($CDCl_3$, δ_H) 0.87 (*t, J* = 6.7 Hz, 3H, 18-*H*), 1.25–1.7 (*m*, 32H, CH_2 and N-CH-CH_3), 2.25–2.35 (*m*, 4H, 2-*H* and 13-*H*), 2.99 (*br. s*, 2H, 9-*H*), 3.66 (*s*, 3H, COOCH_3), 3.8–3.95 (*m*, 2H, N-C*H*), 5.18 (*s*, 1H, 11-*H*); ^{13}C NMR ($CDCl_3$, δ_C) 14.11 (C-18), 20.79 (N-CH-*C*H_3), 22.61 (C-17), 24.97 (C-3), 26.29 (C-14), 29.12, 29.28, 29.29, 29.74, 29.94, 31.83 (C-16), 34.11 (C-2), 45.23 (C-13), 47.49 (N-*C*H), 51.41 (COO*C*H_3), 96.67 (C-11), 163.90 (C-10), 174.33 (*C*OOCH_3), and 195.95 (C-12); HRMS, found: M^+, 409.3541, $C_{25}H_{47}NO_3$ requires 409.3556.

*Methyl 10-dioctylamino-12-oxo-10*E*-octadecenoate* (**20**, 95% yield). TLC on silica: R_f = 0.7 (*n*-hexane/diethyl ether,

1:1 vol/vol, as developer); IR (neat) 2954, 2927, 2855, 1742, 1638, 1536, 1467, 1371, 1246, 1198, 1169, 1139, 1091, 946, 754, 723 cm^{-1}; ^1H NMR ($CDCl_3$, δ_H) 0.8–0.9 (*m*, 9H, 18-*H* and N-$[CH_2]_7CH_3$), 1.2–1.7 (*m*, 44H, CH_2), 2.2–2.3 (*m*, 4H, 2-*H* and 13-*H*), 2.91 (*br. s*, 2H, 9-*H*), 3.15 (*t, J* = 7.7 Hz, 4H, N-CH_2) 3.66 (*s*, 3H, $COOCH_3$), 4.96 (*s*, 1H, 11-*H*); ^{13}C NMR ($CDCl_3$, δ_C) 14.25 (C-18), 22.76, 22.79 (C-17), 22.82, 25.13 (C-3), 26.41 (C-14), 27.12 (C-9), 28.06, 28.91, 28.97, 29.02, 29.10, 29.28, 31.93 (C-16), 34.26 (C-2), 45.02 (C-13), 51.56 ($COOCH_3$), 93.52 (C-11), 164.84 (C-10), 174.48 ($COOCH_3$), and 196.58 (C-12); HRMS, found: M^+, 549.5116, $C_{35}H_{67}NO_3$ requires 549.5121.

*Methyl 10-diphenylamino-12-oxo-10*E*-octadecenoate* (**21**, 40% yield). TLC on silica: R_f = 0.3 (*n*-hexane/diethyl ether, 4:1 vol/vol, as developer); IR (neat) 3069 (arom. C-H), 3035 (arom. C-H), 2928, 2855, 1739, 1658, 1585, 1547, 1490, 1451, 1435, 1268, 1199, 1171, 1132, 1076, 1027, 757, 697 cm^{-1}; ^1H NMR ($CDCl_3$, δ_H) 0.86 (*t, J* = 6.8 Hz, 3H, 18-*H*), 1.1–1.7 (*m*, 20H, CH_2), 2.19 (*t, J* = 7.5 Hz, 2H, 13-*H*), 2.27 (*t, J* = 7.6 Hz, 2H, 2-*H*), 2.8–2.9 (*m*, 2H, 9-*H*), 3.66 (*s*, 3H, $COOCH_3$), 5.41 (*s*, 1H, 11-*H*), 7.13–7.45 (*m*, 10H, Ph-*H*); ^{13}C NMR ($CDCl_3$, δ_C) 14.08 (C-18), 22.54 (C-17), 24.92 (C-3), 25.12 (C-14), 28.83, 28.93, 29.04, 29.07, 29.47, 29.77 (C-9), 31.71 (C-16), 34.11 (C-2), 44.65 (C-13), 46.47 (N-CH_2), 51.42 ($COOCH_3$), 94.32 (C-11),125.87 (C-4′ arom.), 127.64 (C-2′ and C-6′ arom.), 129.36 (C-3′ and C-5′ arom.), 145.51 (C-1′ arom.), 165.05 (C-10), 174.23 ($COOCH_3$), and 198.82 (C-12); HRMS, found: M^+, 477.3240, $C_{31}H_{43}NO_3$ requires 477.3243.

RESULTS AND DISCUSSION

The nucleophiles used in the reactions with the keto-allene ester, methyl 12-oxo-9,10-octadecadienoate (**1**), were either primary alkyl and aryl amines including methyl esters of amino acids or secondary alkyl and aryl amines (Scheme 2). The reactions of compound **1** with the short-chain primary alkylamines (ammonia, methylamine, and propylamine) and aryl amines (phenylamine, benzylamine, and phenethylamine) were achieved at room temperature in ethanol in high yield. However, owing to the poor solubility of octylamine and octadecylamine in ethanol, the reactions involving these reactants were conducted in chloroform under reflux with the keto-allene substrate (**1**) to give the corresponding enaminones **5** and **6** in 35 and 20% yield, respectively. The reactions with HCl salts of the methyl esters of amino acids (glycine, DL-alanine, L-valine, L-leucine, L-tyrosine, L-methionine) were performed in methanol (reflux for 3 h) with an average yield of 87%.

The reactions of most of the secondary alkyl (dimethyl, diethyl, dipropyl, and diisopropyl) amines with compound **1** were also readily achieved in ethanol at room temperature (average 83%), except those involving dioctyl and diphenyl amine. Again owing to the poor solubility of the last two reactants, these reactions were carried out in chloroform (under reflux for 3 h) where dioctylamine gave a 95% and diphenylamine furnished a 40% yield of the corresponding enaminones. The overall average yield of the enaminone derivatives (**2–21**) obtained from these reactions was 82%.

A weak N-H stretching vibration of enaminones derived from primary amines (compounds **2–15**) appeared at about 3460 cm^{-1} in the IR spectra. The stretching vibration of the keto carbonyl group in the enaminone derivatives containing an N-H bond (**2–15**) was found to be 20–30 cm^{-1} lower in wavenumbers than enaminones (**16–21**) derived from secondary amines. This observation indicates that enaminone derivatives (**2–15**) formed from primary amines with the C_{18} keto allene have the N-H group hydrogen-bonded to the oxygen atom of the keto group at C-12 to give a Z-configuration to the double bond (9). Enaminones derived (**16–21**) from secondary amines have the E-configuration with the nitrogen and its attached groups placed in a less sterically hindered position of the molecule. The general structures of these E- and Z-derivatives are shown in Scheme 2.

The enaminone system was confirmed by proton and carbon NMR spectroscopic analyses. In the ^1H NMR spectral analysis the proton at the C-11 olefinic carbon atom appeared as a singlet at about δ_H 5.0, whereas the protons of the methylene group adjacent to the keto function (13-*H*) gave a characteristic triplet at δ_H 2.1–2.2, which merged with the signal of the 2-*H* protons. The carbon NMR spectral analysis showed the effect of the nitrogen atom on the shifts of the olefinic carbon (C-10), which appeared much more downfield (δ_C 164–168) than the other olefinic carbon atom (C-11, at δ_C 93–95) adjacent to the keto group. The carbon shift of the keto carbonyl appeared at about δ_C 197–200. All these shifts were in close agreement with data reported in the literature for various enaminones (10–15). The *N*-alkyl, *N*-aryl groups and the various amino acid residues incorporated in the enaminone system of compounds **2–21** were readily identified by proton and carbon NMR spectral analyses. The ^{13}C-^1H homonuclear correlation spectroscopy and heteronuclear multiple bond correlation spectroscopy spectra of compound **2** are shown in Figures 1 and 2, respectively.

Of significance was the carbon shift of C-9, i.e., the methylene group attached to the double bond of the enaminone system, of compounds **2–15**. The carbon shift of this methylene group appeared at about δ_C 32. Such downfield shift position for a methylene group adjacent to a double bond is normally observed for olefins with a *trans* double bond. The result therefore showed that the C-9 methylene group was in the *anti* position relative to the keto function of the enaminone. As a result, this would signify a Z-configuration for the double bond of the enaminone system, and thus support the proposal that the incoming nucleophile occupied the same side as that of the keto group. This arrangement would therefore allow the hydrogen of the N-H to be hydrogen-bonded to the keto group. In the ^{13}C NMR spectra of compounds **16–21**, no additional signal was found in the region of δ_C 32, except those for C-2 (δ_C 34) and C-16 (δ_C 31.8). The shift of the C-9 carbon atom of compounds **16–21** appeared to fall within the "methylene envelope" region of δ_C 27–30. From this differ-

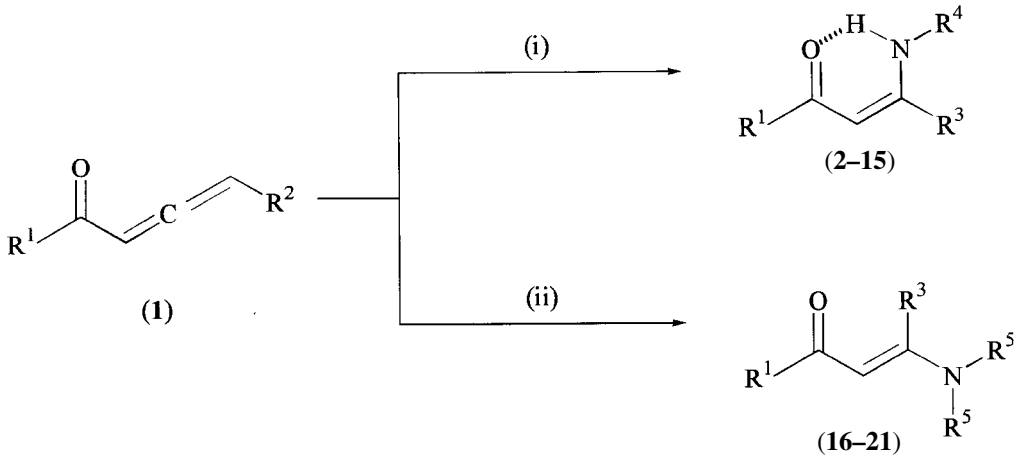

$R^1 = CH_3(CH_2)_5$; $R^2 = (CH_2)_7COOCH_3$; $R^3 = (CH_2)_8COOCH_3$

Reagents and conditions: (i) R^4NH_2, EtOH, room temperature (RT) [or $CHCl_3$, reflux (for octylamine and octadecylamine); or Et_3N, CH_3OH, reflux (for HCl salts of methyl esters of amino acids)]; (ii) $(R^5)_2NH$, EtOH, RT [or $CHCl_3$, reflux (for dioctylamine and diphenylamine)].

Compound	R^4	Compound	R^4	Compound	R^5
2	H				
3	CH_3	**10**	CH_2COOCH_3	**16**	CH_3
4	$(CH_2)_2CH_3$				
5	$(CH_2)_7CH_3$	**11**	$-CH(CH_3)COOCH_3$	**17**	CH_2CH_3
6	$(CH_2)_{17}CH_3$	**12**	$-CH(CH(CH_3)_2)COOCH_3$	**18**	$(CH_2)_2CH_3$
7	C_6H_5	**13**	$-CH(CH_2CH(CH_3)_2)COOCH_3$	**19**	$CH(CH_3)_2$
8	$CH_2C_6H_5$	**14**	$-CH(CH_2\text{-}p\text{-}C_6H_4OH)COOCH_3$	**20**	$(CH_2)_7CH_3$
9	$(CH_2)_2C_6H_5$	**15**	$-CH((CH_2)_2SCH_3)COOCH_3$	**21**	C_6H_5

SCHEME 2

ence in spectral detail, it could be implied that the alkanoate chain was attached to the double bond of the enaminone system in a *cis* manner. This would therefore place the alkanoate chain on the same side of the keto group. The nitrogen and its attached groups would therefore be found *anti* to the keto group. A number of reports have studied the various tautomeric forms of enaminones (2,11,14), but no relevant information from such studies could be extracted to assist in the confirmation of the enaminones (**2–21**) under study. It was therefore decided to conduct further NMR experiments on these derivatives.

To confirm the stereochemistry of the E- and Z-enaminone system, two-dimensional nuclear Overhauser enhancement spectroscopy (2D-NOESY) experiments were conducted on these derivatives. Compounds **16–21** showed a distinct interaction between the 11-*H* and the protons of the groups attached to the nitrogen atom. This result confirmed that the nitrogen and its attached groups were on the same side as that

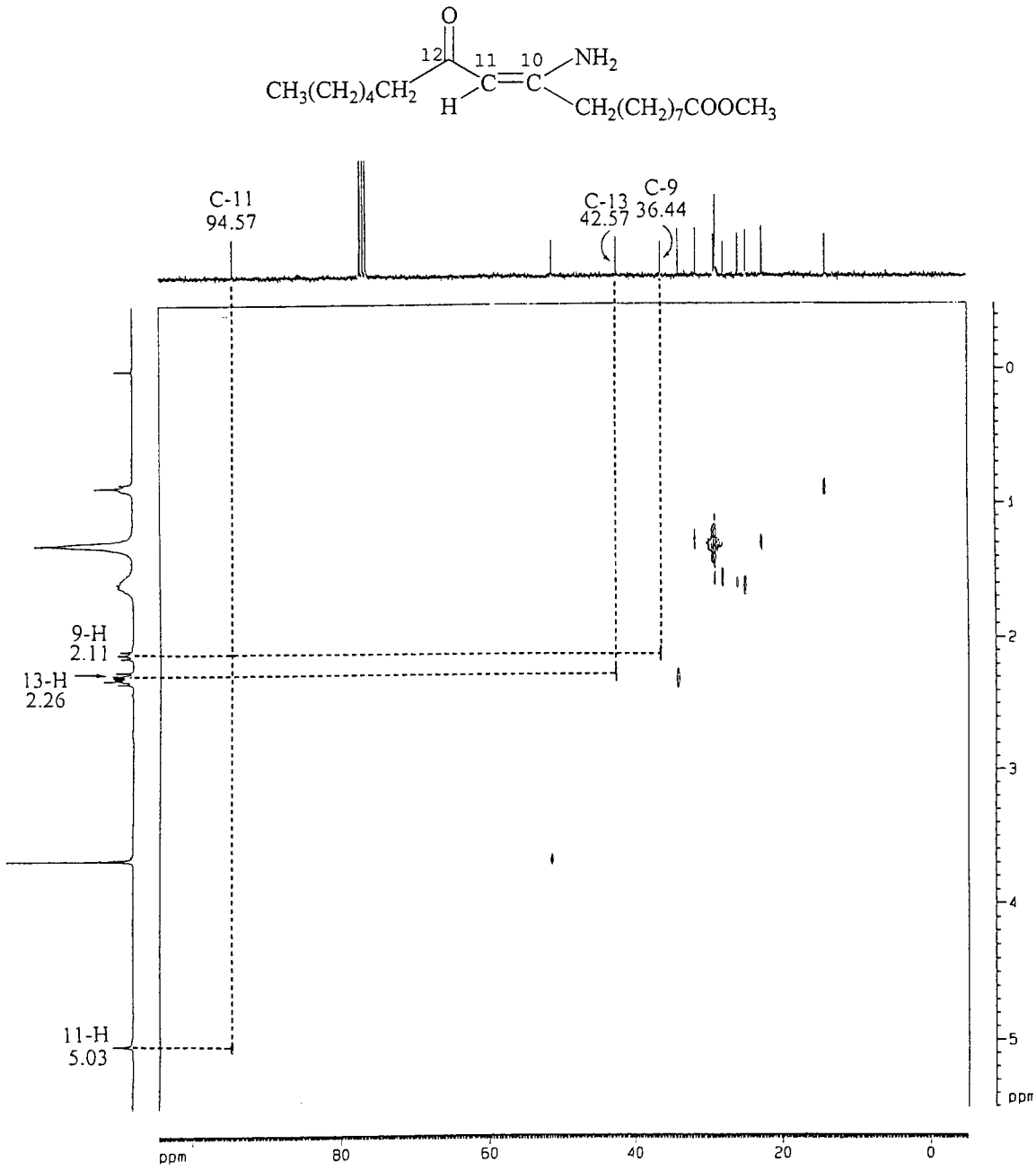

FIG. 1. ^{13}C-^{1}H homonuclear correlation spectroscopy spectrum of methyl 10-amino-12-oxo-10*Z*-octadecenoate (**2**).

of the 11-*H* of the double bond, thus placing the nitrogen atom on the *anti* position relative to the keto group (hence, an E-configuration). When the 2D-NOESY experiments were carried out on compounds **2–15**, no such interactions between the 11-*H* proton were found with protons from groups attached to the nitrogen. This observation showed that the nitrogen and its attached group were too far apart from the 11-*H* to interact. The situation would be so when the nitrogen atom was placed *anti* to the 11-*H* proton and on the same side as the keto group. From these NOESY experiments, it can therefore be concluded that the enaminones derived from primary amines (compounds **2–15**) have a Z-configuration, and enaminones derived from secondary amines (compounds **16–21**) have an E-configuration at the double bond.

The results of the high resolution mass spectral analyses of compounds **2–21** confirmed the molecular weight (formula) of each derivative. The results of the electron impact (EI) mass spectral analyses of compounds **2–21** are presented in Table 1. One significant peak (M – 85), resulting from the cleavage of the C-12/C-13 (adjacent to the keto group), was characteristic in almost every spectrum (ion fragment *a*). This result indicated the position of the keto group at the C-12 position. This fact was further confirmed

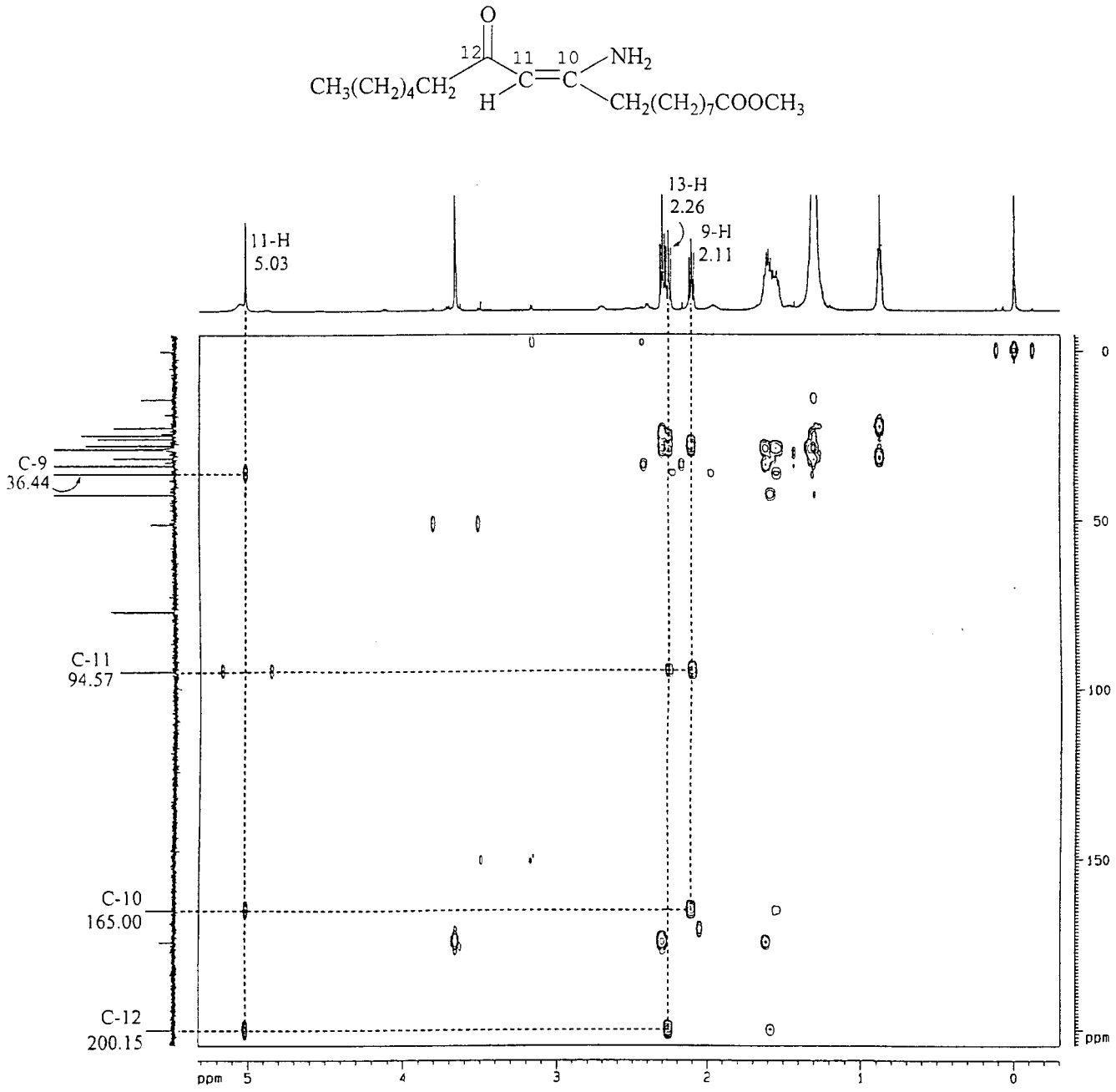

FIG. 2. Heteronuclear multiple bond correlation spectroscopy spectrum of methyl 10-amino-12-oxo-10*Z*-octadecenoate (**2**).

by the peak at $m/z = 113$ (ion fragment *c*) and from ion fragment *b* in most cases. Ion fragment *d*, which resulted from the cleavage of the allylic C-C bond (C-9/C-10), was also a significant peak in most spectra. However, in the case of compounds **12–21** (which contain either a phenyl or an amino ester group near the enaminone system), the mass spectra of these derivatives gave some very intense peaks due to the loss of the phenyl group or part of the ester group. No definite cleavage pattern could be recognized, which would allow the structure of these molecules to be further confirmed.

This work shows that the central atom of a conjugated keto-allene system in compound **1** was very reactive to nucleophilic attack by primary and secondary alkyl and aryl amines (including amino acid esters) to give the corresponding lipidic enaminones.

ACKNOWLEDGMENTS

This work was supported by the Lipid Research Fund, the Research Grants Committee of the University of Hong Kong, and the Research Grant Council of Hong Kong.

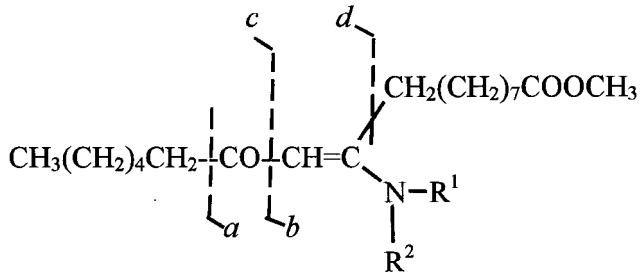

TABLE 1
Mass Spectral Results of C_{18} Enaminones (ion fragments *m/z* and relative abundance in parentheses)

Compound	R^1	R^2	M^+	M – 31	*a*	*b*	*c*	*d*	Others
2	H	H	325 (28)	294 (9)	240 (100)	212 (5)	113 (10)	154 (5)	268 (15), 255 (22), 182 (61), 169 (10), 112 (28), 99 (55)
3	H	CH_3	339 (27)	308 (16)	254 (100)	226 (3)	113 (69)	168 (5)	282 (9), 212 (11), 196 (50), 183 (24), 149 (11), 126 (16)
4	H	$(CH_2)_2CH_3$	367 (43)	336 (25)	282 (100)	254 (23)	113 (6)	196 (9)	310 (20), 224 (59), 21 1(33), 154 (28), 141 (81), 126 (22), 99 (35)
5	H	$(CH_2)_7CH_3$	437 (39)	406 (22)	352 (100)	324 (39)	113 (8)	266 (34)	380 (21), 353 (21) ,310 (19) ,294 (57), 281 (26), 224 (42), 211 (25), 196 (20), 168 (51), 154 (50)
6	H	$(CH_2)_{17}CH_3$	577 (69)	546 (26)	492 (100)	464 (59)	113 (9)	406 (57)	520 (26), 450 (37), 434 (62), 421 (67), 364 (23), 351 (32), 336 (30), 308 (68), 294 (55), 224 (25)
7	CH_3	CH_3	353 (12)	322 (14)	268 (100)	240 (9)	113 (3)	182 (7)	296 (5), 226 (10), 210 (33), 197 (18), 127 (32), 112 (19), 85 (42)
8	CH_2CH_3	CH_2CH_3	381 (20)	350 (16)	296 (100)	268 (85)	113 (61)	210 (7)	364 (21), 324 (4), 238 (30), 199 (23), 183 (26), 155 (44), 150 (49), 140 (27), 100 (28)
9	$(CH_2)_2CH_3$	$(CH_2)_2CH_3$	409 (29)	378 (22)	324 (97)	296 (100)	113 (4)	238 (8)	392 (21), 380 (21), 352 (5), 266 (20), 253 (19), 168 (13), 141 (29), 126 (9), 99(11)
10	$CH(CH_3)_2$	$CH(CH_3)_2$	409 (11)	378 (9)	324 (12)	296 (100)	113 (2)	238 (0)	366 (80), 352 (0), 266 (0), 254 (25), 166 (4),140 (6)
11	$(CH_2)_7CH_3$	$(CH_2)_7CH_3$	549 (17)	518 (12)	464 (83)	436 (100)	113 (3)	378 (37)	533 (15), 492 (4), 465 (27), 450 (23), 422 (1), 406 (12), 294 (12), 280 (23), 266 (59), 168 (13), 154(8)
12	H	C_6H_5	401 (76)	370 (14)	316 (71)	288 (0)	113 (0)	230 (4)	344 (4), 284 (36), 274 (38), 258 (69), 245 (75), 175 (100), 160 (34), 133 (63), 93 (49), 77 (47)

Continued

TABLE 1
(Continued)

Compound	R^1	R^2	M^+	M – 31	*a*	*b*	*c*	*d*	Others
13	H	$CH_2C_6H_5$	415 (42)	384 (10)	330 (72)	302 (29)	113 (0)	244 (5)	358 (11), 272 (31), 259 (37), 202 (15), 189 (44), 174 (16), 160 (14), 147 (37), 146 (22), 91 (100)
14	H	$(CH_2)_2C_6H_5$	429 (12)	398 (12)	344 (38)	316 (8)	113 (4)	258 (3)	372 (7), 338 (100), 286 (16), 273 (24), 226 (9), 203 (18), 182 (23), 161 (8), 105 (40), 91 (7)
15	C_6H_5	C_6H_5	477 (76)	446 (24)	392 (69)	364 (88)	113 (9)	306 (17)	420 (4), 360 (20), 334 (50), 321 (52), 274 (100), 230 (27), 208 (31), 169 (19), 118 (10)
16	H	CH_2COOCH_3	397 (14)	366 (11)	312 (35)	284 (0)	113 (16)	226 (43)	340 (12), 254 (33), 199 (14), 184 (27), 171 (100), 156 (23), 142 (22), 129 (57)
17	H	$CHCOOCH_3$ | CH_3	411 (45)	380 (27)	326 (99)	298 (17)	113 (5)	240 (25)	354 (21), 324 (22), 268 (58), 255 (39), 198 (28), 196 (20), 185 (100), 170 (29), 156 (20), 143 (50), 84 (15)
18	H	$CHCOOCH_3$ | $CH(CH_3)_2$	439 (39)	408 (25)	354 (68)	326 (9)	113 (10)	268 (18)	396 (21), 382 (18), 380 (97), 310 (13), 296 (43), 283 (35), 224 (100), 213 (44), 198 (13), 184 (11), 171 (21), 154 (12) 115 (40), 99 (20)
19	H	$CHCOOCH_3$ | $CH_2CH(CH_3)_2$	453 (23)	422 (19)	368 (45)	340 (13)	113 (4)	282 (17)	410 (18), 396 (18), 394 (61), 324(16), 310 (25), 254 (10), 241 (100), 198 (8), 171 (32), 129 (27)
20	H	$CHCOOCH_3$ | $CH_2C_6H_4OH$	503 (2)	472 (6)	418 (8)	390 (0)	113 (4)	332 (3)	446 (0), 397 (26), 396 (100), 364 (7), 360 (4), 326 (26), 309 (10), 284 (6), 240 (7), 170 (24), 107 (6)
21	H	$CHCOOCH_3$ | $CH_2CH_2SCH_3$	471 (28)	440 (20)	386 (44)	358 (0)	113 (7)	300 (18)	424 (27), 414 (12), 410 (41), 397 (17), 340 (14), 328 (27), 268 (14), 254 (24), 241 (100), 184 (7), 171 (52), 156 (14), 147 (14), 129 (37), 61 (23)

REFERENCES

1. Lie Ken Jie, M.S.F., and Lau, M.M.L. (1999) Ultrasound Assisted Synthesis of Pyrazole Fatty Ester Derivatives from a Key C_{18} Keto-allenic Ester, *Chem. Phys. Lipids 101*, 237–242.
2. Greenhill, J.V. (1977) Enaminones, *Chem. Soc. Rev. 6*, 277–294.
3. Shawe, T.T., Hansen, D.B., Peet, K.A., Prokopowicz, A.S., Robinson, P.M., Cannon, A., Dougherty, K.E., Ross, A.A., and Landino, L.M. (1997) Addition Reactions of Cyclic *s-trans*-Enaminones with Grignard Reagents, *Tetrahedron 53*, 1547–1556.
4. Edafiogho, I.O., Hinko, C.N., Chang, H., Moore, J.A., Mulzac, D., Nicholson, J.M., and Scott, K.R. (1992) Synthesis and Anticonvulsant Activity of Enaminones, *J. Med. Chem. 35*, 2798–2805.
5. Dannhardt, G., Bauer, A., and Nowe, U. (1998) Synthesis and Pharmacological Activity of Enaminones Which Inhibit Both Bovine Cyclooxygenase and 5-Lipoxygenase, *J. Prakt. Chem./Chem.-Ztg. 340*, 256–263.
6. Haight, A.R., Stuk, T.L., Allen, M.S., Bhagavatula, L., Fitzgerald, M., Hannick, S.M., Kerdesky, F.A.J., Menzia, J.A., Parekh, S.I., Robbins, T.A., *et al.* (1999) Reduction of an Enaminone: Synthesis of the Diamino Alcohol Core of Ritonavir, *Org. Process Res. Develop. 3*, 94–100.
7. Lue, P., and Greenhill, J.V. (1996) Enaminones in Heterocyclic Synthesis, *Adv. Heterocyclic Chem. 67*, 207–343.
8. Bol'shedvorskaya, R.L., Pavlova, G.A., Gavrilov, L.D., Alekseeva, N.V., and Vereshchagin, L.I. (1972) Nucleophilic Addition of Amines to α-Allenic and β-Acetylenic Ketones, *J. Org. Chem. USSR 8*, 1927–1930.
9. Vdovenko, S.I., Gerus, I.I., and Gorbunova, G. (1993) α, β-Unsaturated Enamino-ketones with Trifluoromethyl Groups. Infrared Spectra and Structure, *J. Chem. Soc. Perkin Trans. 2*, 559–562.
10. de la Cal, T., Cristobal, B.I., Cuadrado, P., Gonzalez, A., and Pulido, F.J. (1989) Addition of Organocuprates to Ketoketenimines. Synthesis of β-Enaminoketones, *Synth. Commun. 19*, 1039–1045.
11. Kashima, C., Aoyama, H., Yamamoto, Y., Nishio, T., and Yamada, K. (1975) Nuclear Magnetic Resonance Spectral Study of β-Aminoenones, *J. Chem. Soc. Perkin Trans. 2*, 665–670.
12. Kozerski, L., and Dabrowski, J. (1972) ASIS and Protonation Studies of the Rotational Isomerism of Enamino Aldehydes and Ketones, *Org. Mag. Reson. 4*, 253–258.
13. Azzaro, M., Geribaldi, S., Videau, B., and Chastrette, M. (1984) Principal Component Analysis of the ^{13}C NMR Spectra of Enamino Ketones, *Org. Mag. Reson. 22*, 11–15.
14. Zhuo, J.C. (1996) ^{17}O NMR Spectroscopic Study of Tertiary Enaminones, *Mag. Reson. Chem. 34*, 595–602.
15. Zhuo, J.C., (1997) ^{1}H, ^{13}C and ^{17}O NMR Spectroscopic Studies of Acyclic and Cyclic *N*-Aryl Enaminones: Substituent Effects and Intramolecular Hydrogen Bonding, *Mag. Reson. Chem. 35*, 311–322.

[Received March, 27, 2000, and in revised form and accepted August 29, 2000]

Comparison of Silver-Ion High-Performance Liquid Chromatographic Quantification of Free and Methylated Conjugated Linoleic Acids

Ewa Ostrowska[a,b], Frank R. Dunshea[b], Morley Muralitharan[c], and Reginald F. Cross[a,*]

[a]School of Engineering and Science, Swinburne University of Technology, Hawthorn, Victoria 3122, Australia, [b]Agriculture Victoria, Victorian Institute of Animal Science, Werribee, Victoria 3030, Australia, and [c]Charles Sturt University, Wagga Wagga, NSW 2650, Australia

ABSTRACT: Silver-ion high-performance liquid chromatography was used to fractionate a mixture of conjugated linoleic acid (CLA) isomers (as the free fatty acids, CLAFFA) in commercial CLA mixtures and biological samples. Due to the unchanged retention mechanism, it was assumed that the elution order of the isomers remained the same as that of methyl esters separated on the same column. The most abundant isomers, *cis/trans* 10,12-18:2 and *cis/trans* 9,11-18:2, were separated better as free acids on a single column than in the methyl ester form. Quantification of the CLA standard was used as the reference profile to evaluate different methylation methods commonly used to prepare CLA methyl esters for quantitation. Acid- and base-catalyzed derivatization methods resulted in CLA intraisomerization and losses in total conjugated dienes content. Acid (HCl and BF_3) methylations significantly elevated the level of *trans,trans* isomers and significantly reduced the *cis/trans* isomers. Base methylation, tetramethylguanidine/methanol, resulted in loss of *trans,trans* isomers, and a substantial loss of total underivatized conjugated dienes. Other catalysts such as the trimethylsilyldiazomethane produced additional peaks of unidentified artifacts. The analysis of CLAFFA appears to provide more accurate quantification of CLA isomers in commercial and biological samples.

Paper no. L8452 in *Lipids 35,* 1147–1153 (October 2000).

Conjugated linoleic acid (CLA) comprises a mixture of positional and geometric isomers of linoleic acid (*cis,cis*-9,12-octadecadienoic acid) with conjugated double bonds (1). These conjugated dienes were found to be responsible for many biological properties that relate to health. One of the most important is the anticarcinogenic activity in both the *in vivo* and *in vitro* models that is often attributed to the *cis,trans* 9,11 isomer of CLA, abundant in products of ruminant origin (2–5). CLA was demonstrated to possess antiatherogenic properties in hamsters (6) and antidiabetic properties in the Zucker diabetic fatty acid *fa/fa* rats (7). It was also found to reduce the catabolic effects of immune stimulation in mice, rats, and chickens (8,9). Another biological effect of CLA relates to fat accreation and nutrient partitioning. CLA significantly reduces body fat and increases lean body mass in rats and mice (10–12) and in farm animals such as pigs (13). The fat metabolism and body composition are thought to be influenced by the *trans,cis* 10,12 isomer (2,14,15).

Although the effects of CLA have been investigated for a number of years, its mechanism of action is poorly understood. This can be largely attributed to the methods used in the past to analyze these acids. The most common means of analysis, gas chromatography (GC), produced overlapping peaks of major isomers of CLA, the *cis/trans*-9,11 and *cis/trans*-8,10 and their geometric isomers (*cis,cis* and *trans,trans*). For optimal quantification, long columns are required and these are associated with prolonged retention times. Furthermore, GC separation requires fatty acids to be in a methyl ester form, which is less polar and more volatile in comparison to the parent form. Some derivatization methods can be time consuming and can also result in small losses of unconverted acids (16). Derivatization of acids in biological samples raises the possibility of interisomerization (conversion between unconjugated linoleic acid and CLA due to shifts in double bonds), resulting in inaccurate CLA isomer data (17). Additionally, biological samples may contain allylic hydroxy oleate (AHO), which is a secondary oxidation product of oleic acid. AHO undergoes reactions during exposure to strong acids such as HCl and BF_3 resulting in artifacts and increased levels of CLA (18). Recently, it was reported that 20:2 conjugated fatty acid isomers synthesized by alkali isomerization eluted in the region of the silver-ion high-performance liquid chromatography (Ag^+-HPLC) chromatogram close to the geometric CLA isomers (19). Therefore, the selection of methylation method is crucial to successfully quantifing acids such as CLA.

In recent years, a method has been developed which involves the use of Ag^+-HPLC (19–21). In commercial mix-

*To whom correspondence should be addressed at the School of Engineering and Science, Swinburne University of Technology, P.O. Box 218, Hawthorn, Victoria 3122, Australia. E-mail: rcross@swin.edu.au

Abbreviations: ACN, acetonitrile; Ag^+-HPLC, silver-ion high-performance liquid chromatography; AHO, allylic hydroxy oleate; CLA, conjugated linoleic acid; *cis/trans*, all the CLA isomers having a *cis,trans* or *trans,cis* configuration; CLAFFA, conjugated linoleic acid as the free fatty acids; FAME, fatty acid methyl esters; FFA, free fatty acid; GC, gas chromatography; TAG, triacylglycerol; TMG, tetramethylguanidine; TMS, trimethylsilyldiazomethane.

tures, it allows for well-resolved separation of three groups of geometric isomers of CLA (*trans,trans*, *cis/trans,* and *cis,cis*) under isocratic conditions. Within each group, there is further separation into positional isomers 13,15-18:2; 12,14-18:2; 11,13-18:2; 10,12-18:2; 9,11-18:2; 8,10-18:2; and 7,9-18:2. The separation of the positional isomers improves by connecting silver columns in series (19,22).

Most recently, we have demonstrated that the same Ag^+-HPLC may be adapted to analyze CLA as the free fatty acids (CLAFFA), thus eliminating the need to methylate prior to assay (23). In addition to the potential waste of time and resources in the event of a separate methylation process, there are also questions about loss and modification of the isomer distribution that occur during methylation that have been frequently discussed in the literature. Thus, in this present study, single-column Ag^+-HPLC was used to evaluate the effect of derivatization methods on CLA distribution and the extent of intraisomerization (conversion of one isomer of CLA to another). The results have been compared to the distribution of CLA in the standard mixture that was separated using the same column, but different mobile phase compositions. The effect of different methylation procedures on interisomerization of CLA and other fatty acids present in biological samples was not investigated in the current study. The identity of isomers found in biological samples was also not investigated.

MATERIALS AND METHODS

Materials and reagents. A mixture of CLA isomers in free acid form and CLA methyl esters (FAME) were obtained from Sigma (St. Louis, MO). The commercial mixture of CLA (55%) and a mixture of *trans,cis* 10,12 (45%) and *cis,trans* 9,11 (43%) isomers were obtained from Natural Lipids Ltd. (Hovdebygda, Norway). All solvents and chemicals were reagent grade.

Animals and diets. Ethics approval for this investigation was given by the Animal Experimentation Ethics Committee of the Victorian Institute of Animal Science in July 1997, permit number 1755. Samples of adipose tissue and longissimus muscle were obtained from pigs (Large White gilts × Landrace) fed *ad libitum* for 8 wk with diets containing 5.5 g of CLA per kg diet (13).

Lipid extraction, saponification, and preparation of fatty acid esters. Total lipids were extracted with chloroform/methanol (2:1, vol/vol) as described previously by Folch *et al.* (24). A mild saponification method was employed for fats extracted from adipose and muscle tissues of pigs (25). In that paper it was demonstrated that the use of strong acids and bases and elevated temperatures can lead to altered isomer distributions. However, mild conditions of saponification (low temperatures and minimal base concentrations) are possibly the least likely to alter the CLA distribution.

FAME were prepared by methylating in 15-mL tubes with Teflon-lined screw caps under N_2. HCl/methanol (26) was heated for 1 h at 80°C or at room temperature for 30 min. Tetramethylguanidine (TMG)/methanol (27) and BF_3 (28) were heated for 2 min at 100°C. Trimethylsilyldiazomethane (TMS) catalyzed transesterification (29) was carried out at room temperature for 30 min. Solvents were removed by stream of nitrogen and the acids were dissolved in 1 mL of hexane.

Ag^+-HPLC conditions. A ChromSpher 5 Lipids analytical silver-impregnated column (4.6 × 250 mm i.d. stainless steel; 5 µm particle size; Chrompack, Bridgewater, NJ) was used. The column was protected by a 3.0 × 10 mm i.d. guard column containing the same stationary phase. HPLC analyses were performed with a Varian (Walnut Creek, CA) isocratic solvent delivery system equipped with a 9012 pump, a Polychrom 9065 diode array detector (recently replaced by a Prostar 330 photodiode array detector), and a Star Workstation (recently upgraded to version 5.3 Star software). All measurements were taken at 234 nm. Samples were introduced *via* a Rheodyne (Cotati, CA) 8125 injector fitted with a 5-µL injection loop. A Timberline column heater maintained the temperature at 30°C for all runs. Minimum tubing diameters and distances were used between the injector and detector.

Integration and quantitation. Self-consistent integration procedures were adopted for all quantitation. Hence, notwithstanding a far smaller degree of resolution than is always desirable for quantitation, the integration procedures utilized and thus the results of this study are highly relevant to all who use Ag^+-HPLC for CLA quantitation, whether as CLAFFA or CLA FAME. It is indeed particularly useful for the quantitation to have been done under the same conditions of resolution as used by others.

Fractionation of CLA FAME by Ag^+-HPLC. Separation of total CLA methyl esters was performed according to Sehat *et al.* (21) protocol. Mobile phase consisted of 0.1% vol/vol acetonitrile (ACN) in hexane and the solvent flow was set to 1.0 mL/min. CLA content in the sample size ranged from 5 to 10 µg. Four analyses from one of the methylation methods and two analyses of underivatized CLA were performed on each day. The experiment was carried out over 6 d, 1 d for each of six methylation methods.

Fractionation of CLAFFA by Ag^+-HPLC. The standard CLA mixture of FFA was separated using a mobile phase consisting of hexane, ACN, and glacial acetic acid. The investigated concentrations of those cosolvents varied from 0–5% vol/vol for ACN and 0–5% vol/vol for acetic acid. The reproducibility of the separation was very sensitive to small changes in concentration of acetic acid and more so to the concentration of ACN, possibly due to its low solubility in hexane. Therefore, the ACN/acetic acid/hexane mix was stirred thoroughly before use. The column was equilibrated with the new solvent mix for at least 30 min before sample injection, and every run was repeated four times or until reproducible retention times were obtained.

Statistical analyses. Different methylation methods were compared by an analysis of variance using Genstat (30) adjusted for the blocking factor of the day of assay. Thus, error variation was commonly estimated using between-assay variability from every day. One assay method (CLA methyl esters purchased from Sigma) was unreported, but was included

TABLE 1
Comparison of the Effect of Different Methylation Procedures on Three Geometric Groups of CLA (% area)[a]

Geometric groups	Average area (%)[b] Free acids	BF_3	TMS[f]	HCl (80°C)	HCl[d]	TMG[f]	SED
tt	0.86	1.05**	1.06**	3.21**	1.49**	0.56**	0.026
ct	23.9	23.6**	23.7**	20.8**	23.0**	23.7**	0.048
cc	0.29	0.32^{NS}	0.30^{NS}	0.98**	0.55**	1.58**	0.017
ct/tt[c]	27.7	23.5**	22.2**	15.4**	6.50**	41.0**	0.012[e]
ct/cc[c]	82.6	73.7^{+}	78.4^{NS}	21.4**	40.7**	14.5**	0.019[e]
tt/cc[c]	2.98	3.28^{NS}	3.53**	3.27^{NS}	2.65^{NS}	0.35**	0.019[e]

[a]Significance for comparison of methylation method to free acid analysis using the many-one *t* statistics technique (31). $^{NS}P > 0.10$; $^{+}P < 0.10$; $^{*}P < 0.05$; $^{**}P < 0.01$.
[b]The area of each peak was divided by the sum of all the peaks except for the artifacts to calculate percentages. The average percentage was calculated for each geometric group.
[c]The ratios of the geometric groups are presented as geometric means.
[d]Methylated at room temperature for 30 min.
[e]After log transformation. SED, standard errors of differences.
[f]TMS, trimethylsilyldiazomethane; TMG, tetramethylguanidine.

in the analysis to increase the residue degrees of freedom from 20 to 24. The isomers' distribution in the CLA mixture was treated as the control and compared to the treatment mean of CLA distribution resulting from each methylation method. For this type of analyses, the many-one *t* statistics technique was appropriate (31), as it takes into account that five methods are being compared to the control. The ratios of the positional groups presented in Table 1 were analyzed as log values for more heterogeneous distribution of residuals and presented in the form of geometric means.

RESULTS AND DISCUSSION

Fractionation of CLAFFA. Recently, we reported successful separation of the FFA on a commercially available silver-impregnated column (23). In that study, we attempted first to separate the FFA using the method of Sehat *et al.* (21). However, the CLA isomers were not eluted in 2 h. High concentrations of the strong solvent (ACN) removed the CLA from the stationary phase, but even moderate ACN concentrations destroyed the separation. On the other hand, the addition of a competing acid (acetic acid) reduced the run times as desired, but did not interfere with the separation. Hence, it was clear that the acetic acid was an excellent mobile phase additive for the removal of the carboxylic acid end of the CLA from the abundant surface silanols on the stationary phase, but a very poor strong solvent for the removal of the CLA double bonds from the Ag^+ ions in the stationary phase. ACN was the opposite of this. Thus, it is clear that the retention mechanism in the separation of FFA and separation of methyl esters of CLA was in both cases due to interactions of double bonds with Ag^+ ions. The additional interactions of the free acid group with the excess silanols on the stationary phase of the column were canceled out with the addition of the competing acid (glacial acetic acid) (23). Furthermore, from Figures 1A and 1B, notwithstanding the statistically significant differences between them, the gross distribution of species in the two chromatograms can be seen to be qualitatively indistinguishable. Without the detailed analysis to follow, it would not be possible to differentiate between the distributions. The amounts of the major isomers are so different from each other that any change in order of elution is improbable in the extreme. These chromatograms (Figs. 1A and 1B) were run on the Sigma standard mix of FFA and our esters (methylated by the BF_3 method). Chromatograms on the Sigma standard mixes of FFA and methyl esters were related in exactly the same way. Hence, the order of elution of the isomers of CLA must be assumed to be the same for the CLA and the methyl esters. Mobile phase conditions chosen in this study consisted of 2.5% vol/vol acetic acid and 0.025% vol/vol ACN, although the conditions may need to be optimized for individual columns since there appears to be batch-to-batch variations in the stationary phases supplied. Under the chosen conditions, the separation was equivalent to the separation of CLA methyl esters described by Sehat *et al.* (21), but the most abundant and the isomers thought to be biologically active, *cis/trans* 10,12 and *cis/trans* 9,11, were almost baseline-resolved (see Fig. 1A vs. 1B).

Intraisomerization of CLA due to methylation procedures. To study the extent of CLA intraisomerization, an assumption was made that the free acids analyzed using Ag^+-HPLC represented a true distribution of CLA content and resulted in 100% recovery of conjugated dienes. The results presented in Table 2 show the difference in the composition of all the positional and geometric isomers of CLA present in the commercial mixture resulting from commonly used methylation methods. Statistical analysis showed that there was a highly significant difference among all methylation methods tested ($P < 0.001$). All catalysts contributed to changes to the isomer distribution and the overall loss of total CLA. In terms of the recovery of total CLA, the boron trifluoride method was the most suitable method with 1.6% ($P < 0.10$) loss of conjugated dienes. TMS- and HCl-catalyzed reactions (reaction carried out at ambient temperature) produced the second-smallest losses of total CLA with 8% ($P < 0.05$) and 8.9% ($P < 0.05$), respectively. The remaining HCl (at 80°C) and TMG resulted in a highly significant loss of total CLA (20 and 29%, respectively).

All acid catalysts were associated with significantly increased levels of *trans,trans* isomers of CLA and significantly lower levels of *cis/trans* isomers (Table 2). For example, HCl methylation at 80°C resulted in approximately 70% ($P < 0.01$) recovery of both the *cis/trans* 8,10-18:2 and 9,11-18:2 isomers (Table 1). Three- and fivefold increases in *trans,trans* 8,10-18:2 and 9,11-18:2 were obtained, respectively. The method was also associated with the formation of artifacts (Fig. 1C). Sehat *et al.* (21) identified the additional peaks formed during HCl methylation as positional allylic methoxy derivatives formed due to acid and heat treatment.

Several investigators detected changes in the CLA isomer distribution pattern due to the combination of acid and heat, but limited data were presented to confirm the extent of intraisomerization of CLA due to lack of chromatographic resolution (18). It was claimed that the isomerization of the conju-

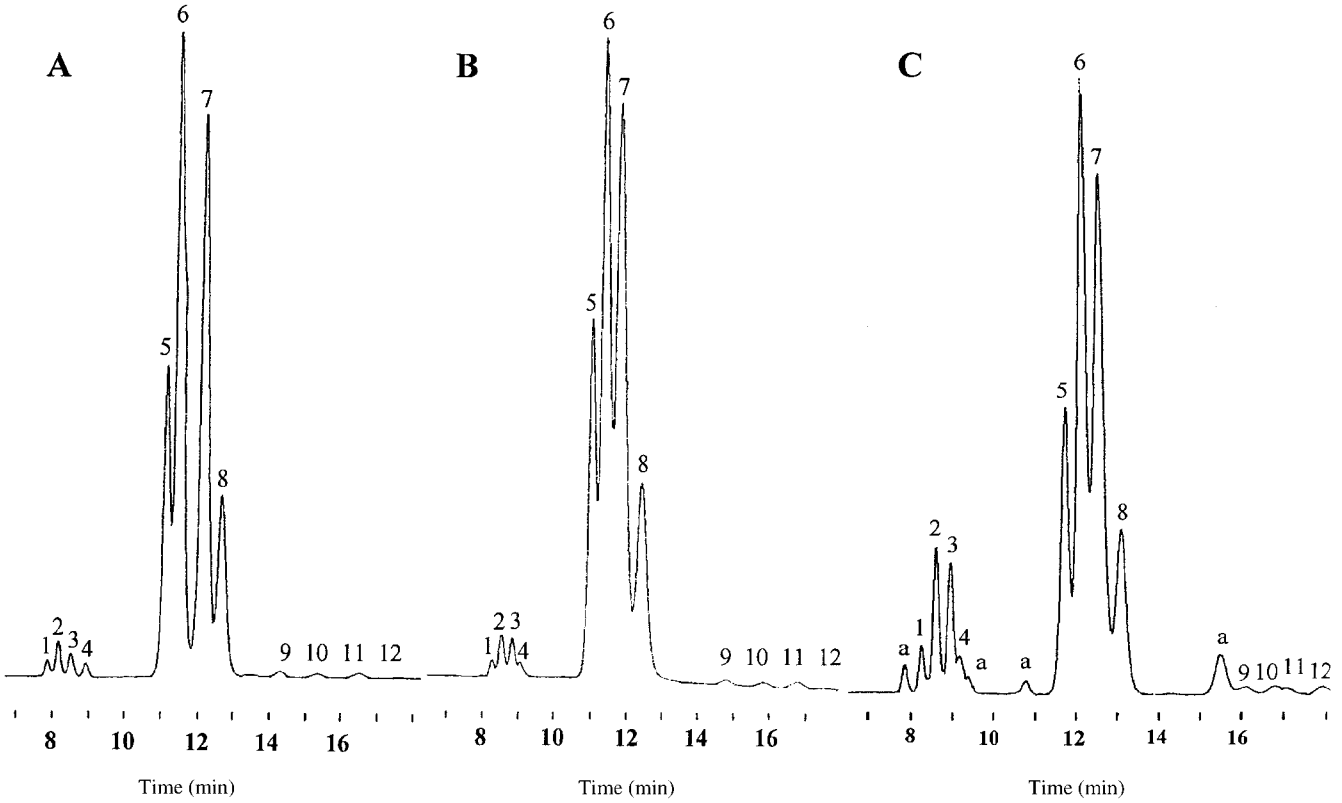

FIG. 1. (A) Ag^+ ion chromatogram of the Sigma standard conjugated linoleic acid (CLA) mixture using 2.5% vol/vol acetic acid and 0.025% vol/vol acetonitrile at 1mL/min flow. (B) CLA standard mixture derivatized with BF_3, 0.1% vol/vol acetonitrile at 1 mL/min. (C) CLA standard mixture derivatized with HCl at 80°C for 1 h, 0.1% vol/vol acetonitrile at 1mL/min. The individual isomers are: 1, *t,t*-11,13; 2, *t,t*-10,12; 3, *t,t*-9,11; 4, *t,t*-8,10; 5, *c/t*-11,13; 6, *c/t*-10,12; 7, *c/t*-9,11; 8, *c/t*-8,10; 9, *c,c*-11,13; 10, *c,c*-10,12; 11, *c,c*-9,11; and 12, *c,c*-8,10. Peaks labeled "a" correspond to unidentified artifacts not present in reference standards.

TABLE 2
Comparison of the Effect of Different Methylation Procedures on CLA Composition (% area)[a]

	Isomer (%)[b]						
Isomer	Free acids	BF_3	TMS	HCl (80°C)	HCl[d]	TMG	SED
t,t-11,13	0.60	0.70*	0.68**	1.50**	1.32**	0.51*	0.030
t,t-10,12	1.30	1.61**	1.60**	4.93**	2.50**	0.74**	0.043
t,t-9,11	0.96	1.21**	1.21**	4.75**	1.40**	0.54**	0.042
t,t-8,10	0.57	0.70^{+}	0.72**	1.58**	0.79**	0.46*	0.038
c/t-11,13	15.2	14.6^{NS}	14.5^{NS}	12.5**	12.9**	12.8**	0.314
c/t-10,12	34.7	33.3**	34.0^{NS}	29.7**	35.1^{NS}	31.6**	0.314
c/t-9,11	33.8	35.3*	34.3^{NS}	30.6**	32.3*	33.9^{NS}	0.460
c/t-8,10	11.7	11.4^{NS}	$12.^{NS}$	10.4*	11.5^{NS}	13.2**	0.366
c,c-11,13	0.37	0.45^{NS}	0.39^{NS}	2.79**	0.81**	2.79**	0.037
c,c-10,12	0.29	0.31^{NS}	0.29^{NS}	0.34**	0.60**	2.06 *	0.032
c,c-9,11	0.40	0.49*	0.44^{NS}	0.62**	0.62**	1.17**	0.034
c,c-8,10	0.09	0.03**	0.07^{NS}	0.24**	0.23**	0.27**	0.017
c/t-10,12/*c/t*-9,11	1.03	0.94**	0.99^{NS}	0.97*	1.09*	0.93**	0.020
Artifacts[c]	0.00	0.00^{NS}	3.53**	3.35**	1.27**	0.00^{NS}	0.083
Recovery (%)	100	98.4^{NS}	92.0*	79.5**	91.1*	70.9**	2.854

[a]Significance for comparison of methylation method to free acid analysis using the many-one *t* statistics technique (31). $^{NS}P > 0.10$; $^{+}P < 0.10$; $^{*}P < 0.05$; $^{**}P < 0.01$.
[b]The area of each peak was divided by the sum of all the peaks except for the artifacts to calculate percentages.
[c]Sum of all artifacts divided by the sum of all the peaks.
[d]Methylated at room temperature for 30 min. See Table 1 for abbreviations.

gated dienes during acid-catalyzed methanolysis can be minimized by carrying out reactions at room temperature (17,32, 33). HCl in methanol at room temperature yielded a significantly higher level of total *trans,trans* fatty acids (+73%, $P < 0.01$) than in any other method and the control, but was reduced approximately twofold compared to the same reaction carried out at a higher temperature (Table 2). Consequently, the level of *cis/trans* isomers was higher than in the high-temperature HCl methylating procedure, although still significantly reduced when compared to the true distribution (−4%, $P < 0.01$).

Werner *et al.* (17) investigated the effect of temperature on CLA isomer composition in the methanolic boron trifluoride methylating procedure. The effects on both the intraisomerization of CLA and interisomerization of linoleic acid and CLA were negligible. In the present study, a significant increase in the average content of *trans,trans* isomers (+22%, $P < 0.01$) was observed at a short incubation time of 2 min at a high temperature (100°C) and the *cis/trans* was significantly reduced by 1% ($P < 0.01$) whereas *cis,cis* isomers were not affected. The ratio of the *cis/trans* 9,11 and *cis/trans* 10,12 (Table 1) was significantly different from the controls (0.94 vs. 1.03, respectively), but this could be attributed to poorly resolved peaks compared with the baseline-resolved underivatized sample.

Base catalysis by TMG results did not yield artifacts, but significant changes in CLA composition were recorded. The levels of *trans,trans* and *cis/trans* isomers were significantly reduced (−35%, $P < 0.01$ and −1%, $P < 0.01$, respectively), whereas the levels of *cis,cis* isomers were increased fourfold ($P < 0.01$). Consequently, the ratios of *trans,trans* and *cis/trans* to the *cis,cis* groups were much lower (Table 2). Therefore, this method is unsuitable for the analysis of CLA.

The extent of intraisomerization was minimized with TMS methanolysis, although the level of all *trans,trans* isomers was significantly higher (+20%, $P < 0.01$) than the levels recorded for the underivatized reference mixture of CLA. The changes in the *cis/trans* and *cis,cis* isomer composition were minimal, but not significantly different from the underivatized sample. However, the method produced several additional peaks. The identity and the origin of these artifacts were not investigated.

Eulitz and co-workers (34) reported intraisomerization of CLA methyl esters as a result of reaction with *p*-toluenesulfinic acid and I_2. The reaction resulted in migration of the double bonds and formation of eight geometric isomers of the 11,13-, 10,12-, 9,11-, and 8,10-octadecadienoic acid methyl esters, which were partially separated using three columns connected in series. The geometric isomers of the 10,12-isomer were not resolved and the *trans,cis* 9,11 coeluted with the *cis,trans* 8,10 isomer. The coelution of the *cis,trans* 8,10 methyl ester with the *trans,cis* 9,11 methyl ester has not been reported previously, possibly due to the absence of the *trans,cis* 9,11 isomer in commercial mixtures of CLA.

Separation of CLA from biological samples in the FFA form. Commercial sources of CLA occur in a FFA form. The biologically occuring CLA are, however, present in triacylglycerols (TAG) (35). The fatty acids present as TAG need to be freed from the molecules of glycerol by the process of saponification prior to methylation and analysis. The process of saponification may also involve the use of heat in the presence of strong bases and strong acids and may contribute to the isomerization of CLA. The effect can be minimized by adopting milder conditions (25) but, as it was shown in this study, even the reactions carried out at room temperature and using weaker acid can result in modification of the isomer distribution. However, eliminating the methylation (if it were to be carried out as a second, separate reaction from the saponification), would certainly enable us to establish a less erroneous distribution of CLA in biological samples. Where saponification and methylation are achieved in one step (16), it is possible that errors are incurred similar to those in the separate methylation under comparable conditions. However, this needs to be determined experimentally.

Figure 2 shows an example of a single column Ag^+-HPLC separation of CLA derived from pig tissue and in the free acid form. The identities of the labeled CLA isomers in Figures 2A and 2B were assigned on the basis of coincidence of retention with the known isomers in the standard Sigma mix. It should be noted that retention times and resolution of the CLA mixtures were found to be subject to sample size, as has been reported in other studies. Furthermore, loss of retention over time as the columns aged necessitated frequent checking of the standards. The identities of the *cis/trans* 10,12 and *cis/trans* 9,11 major isomers were confirmed by spiking the sample with the reference mixture of those two isomers (Fig. 2C). The identities of the remaining isomers were based on the relative elution order. The CLA isomer distribution of the commercial sample shown in Figure 2A (CLA 55% wt/vol; Natural Lipid Ltd.) was as follows: 0.17% *trans,trans*-12,14; 0.42% *trans,trans*-11,13; 1.96% *trans,trans*-10,12; 2.07% *trans,trans*-9,11; 0.43% *trans,trans*-8,10; 0.30% *trans,trans*-7,9; 0.37% *cis/trans*-12,14; 17.94% *cis/trans*-11,13; 30.49% *cis/trans*-10,12; 24.65% *cis/trans*-9,11; 14.52% *cis/trans*-8,10; 0.88% *cis,cis*-11,13; 2.71% *cis,cis*-10,12; 2.21% *cis,cis*-9,11; and 0.74% *cis,cis*-8,10. The commercial mixture of CLA was supplemented in pigs' diets at concentrations of 0–5.5 mg/kg of diet. The effect of CLA supplementation on CLA isomer distribution in pig tissue will be discussed elsewhere. Peaks 8, 9, 10, and 11 in Figure 2B corresponded to the isomers found in the standards (Fig. 2C); however, the presence of additional peaks could suggest the separation of the *trans,cis* and *cis,trans* isomers. Therefore, the conjugated double-bond geometry and position as well as the purity of these isomers in biological samples need to be confirmed by GC-direct deposition-Fourier transform infrared and GC-electron impact–mass spectrometry.

The resolution of the peaks, especially of the most abundant isomers in the *cis/trans* group, appears to be dependent on its concentration in the sample (22). With lower levels of *trans,cis*-10,12 compared to the *cis,trans*-9,11 found in intramuscular fat of pigs (Fig. 2B), the separation is more difficult due to the great differences in the relative amounts. We found that the resolution between the overlapping peaks can be fur-

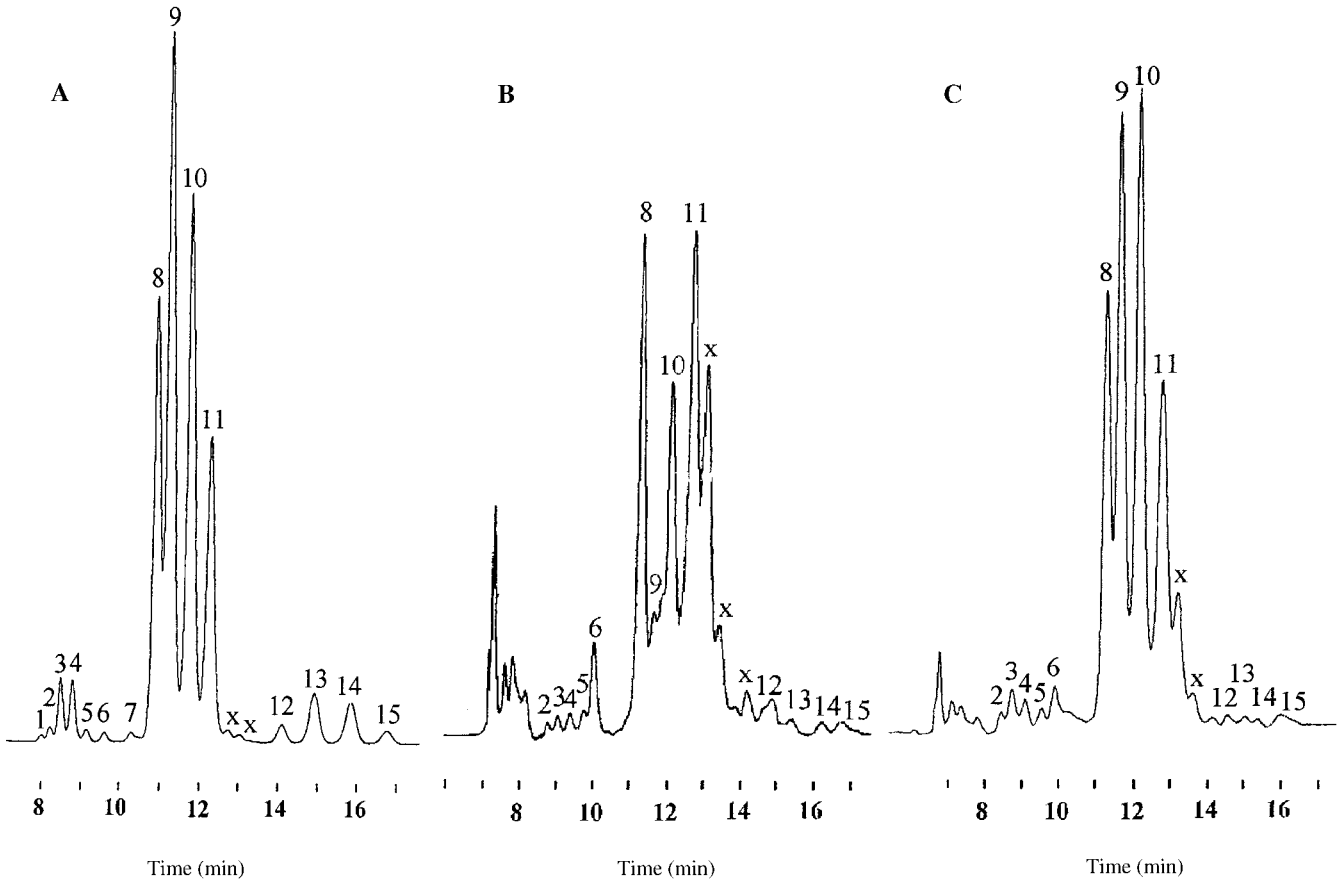

FIG. 2. (A) Ag^+ ion chromatogram of a commercial CLA solution that was added to pigs' diets (55% wt/vol; National Lipid Ltd., Hovdebygda, Norway). (B) A typical chromatogram of the pig muscle sample. (C) Muscle sample spiked with CLA isomer reference. Samples were separated using 2.5% vol/vol acetic acid and 0.025% vol/vol acetonitrile at 1 mL/min flow. The individual isomers are thought to be: 1, *t,t*-12,14; 2, *t,t*-11,13; 3, *t,t*-10,12; 4, *t,t*-9,11; 5, *t,t*-8,10; 6, *t,t*-7,9; 7, *c/t*-12,14; 8, *c/t*-11,13; 9, *c/t*-10,12; 10, *c/t*-9,11; 11, *c/t*-8,10; and possibly *t,c*-9,11; 12, *c,c*-11,13; 13, *c,c*-10,12; 14, *c,c*-9,11; and 15, *c,c*-8,10. Peaks labeled "x" correspond to isomers not present in the standards. See Figure 1 for abbreviation.

ther improved by adjusting the mobile phase conditions, e.g., removing the ACN from the mobile phase and lowering the concentration of acetic acid to 1.5% vol/vol (data not shown). Another way is to increase the number of columns used. Recently, Sehat *et al*. (19) reported the use of up to six columns connected in series in order to improve separation of CLA isomers present in beef tissue. Since addition of competing acid to the mobile phase improves the separation of CLA in the free acid form, similar separation resulting from tandem-column chromatography could be achieved with a smaller number of columns.

CONCLUSION

The present study shows that the composition of CLA was significantly affected by the catalyst used in the methylation procedure. Furthermore, CLA methylation appears to be sensitive to temperature changes that can result in the formation of artifacts. Boron trifluoride and TMS were the most appropriate methylation procedures, boron trifluoride achieving the best recovery and TMS the most accurate distribution. However, both methods were associated with significantly increased levels of *trans,trans* isomers and in the case of TMS, formation of unidentified artifacts. Therefore, direct injection of the mildly saponified lipids to the FFA is likely to be the most accurate method of quantifying CLA isomers. This should, in turn, aid in understanding the mechanisms responsible for the diverse biological functions reported for CLA, due to more confident measurements of CLA isomer distributions.

ACKNOWLEDGMENTS

Ewa Ostrowska gratefully acknowledges a Swinburne University Postgraduate Research Award and the support of the Pig Research and Development Corporation. The authors also wish to thank Kym Butler for his advice and assistance with the statistical analysis.

REFERENCES

1. Morrison, R.T., and Boyd, R.N. (1959) *Organic Chemistry*, p. 49, Allyn and Bacon, Boston.
2. Belury, M.A. (1995) Conjugated Dienoic Linoleate: A Polyunsaturated Fatty Acid with Unique Chemoprotective Properties, *Nutr. Rev. 53*, 83–89.
3. Ha, Y.L., Grimm, N.K., and Pariza, M.W. (1987) Anticarcinogens from Fried Ground Beef: Heat-Altered Derivatives of Linoleic Acid, *Carcinogenesis 8*, 1881–1887.

4. Ip, C., Singh, M., Thompson, H.J., and Scimeca, J.A. (1994) Conjugated Linoleic Acid Suppresses Mammary Carcinogenesis and Proliferative Activity of the Mammary Gland in the Rat, *Cancer Res. 54*, 1212–1215.
5. Ip, C., Chin, S.F., Scimeca, J.A., and Pariza, M.W. (1991) Mammary Cancer Prevention by Conjugated Dienoic Derivative of Linoleic Acid, *Cancer Res. 51*, 6118–6124.
6. Nicolosi, R.J., Rogers, E.J., Knichevski, D., Scimeca, J.A., and Huth, P.J. (1997) Dietary Conjugated Linoleic Acid Reduces Plasma Lipoproteins and Early Aortic Artherogenesis in Hypercholesterolemic Hamsters, *Artery 22*, 266–277.
7. Houseknecht, K.L., Vanden Heuvel, J.P., Moya-Camarena, S.Y., Portocarrero, C.P., Peck, L.W., Nickel, K.P., and Belury, M.A. (1998) Dietary Conjugated Linoleic Acid Normalizes Impaired Glucose Tolerance in the Zucker Diabetic Fatty *fa/fa* rat [published erratum appears in *Biochem. Biophys. Res. Commun*. 1998 June 29; *247(3)*:911], *Biochem. Biophys. Res. Commun. 244*, 678–682.
8. Cook, M.E., Miller, C.C., Park, Y., and Pariza, M. (1993) Immune Modulation by Altered Nutrient Metabolism: Nutritional Control of Immune-Induced Growth Depression, *Poult. Sci. 72*, 1301–1305.
9. Miller, C.C., Park, Y., Pariza, M.W., and Cook, M.E. (1994) Feeding Conjugated Linoleic Acid to Animals Partially Overcomes Catabolic Responses Due to Endotoxin Injection, *Biochem. Biophys. Res. Commun. 198*, 1107–1112.
10. Albright, K., Liu, K.L., Storkson, J.M., Hentges, E., Lofgren, P., Simeca, J., Cook, M.E., and Pariza, M. (1996) Body Composition Repartitioning Following the Removal of Dietary Conjugated Linoleic Acid, *J. Anim. Sci. 74*, 152.
11. Chin, S.F., Storkson, J.M., Albright, K.J., Cook, M.E., and Pariza, M.W. (1994) Conjugated Linoleic Acid Is a Growth Factor for Rats as Shown by Enhanced Weight Gain and Improved Feed Efficiency, *J. Nutr. 124*, 2344–2349.
12. Park, Y., Albright, K.J., Liu, W., Storkson, J.M., Cook, M.E., and Pariza, M.W. (1997) Effect of Conjugated Linoleic Acid on Body Composition in Mice, *Lipids 32,* 853–858.
13. Ostrowska, E., Muralitharan, M., Cross, R.F., Bauman, D.E., and Dunshea, F.R. (1999) Dietary Conjugated Linoleic Acids Increase Lean Tissue and Decrease Fat Deposition in Growing Pigs, *J. Nutr. 129*, 2037–2042.
14. Bretillon, L., Chardigny, J.M., Gregoire, S., Berdeaux, O., and Sebedio, J.L. (1999) Effects of Conjugated Linoleic Acid Isomers on the Hepatic Microsomal Desaturation Activities *in vitro, Lipids 34*, 965–969.
15. Park, Y., Storkson, J.M., Albright, K.J., Liu, W., and Pariza, M.W. (1999) Evidence That the *trans*-10,*cis*-12 Isomer of Conjugated Linoleic Acid Induces Body Composition Changes in Mice, *Lipids 34*, 235–241.
16. Kramer, J.K., Gellner, V., Dugan, M.E., Sauer, F.D., Mossoba, M.M., and Yurawecz, M.P. (1997) Evaluating Acid and Base Catalysts in the Methylation of Milk and Rumen Fatty Acids with Special Emphasis on Conjugated Dienes and Total *trans* Fatty Acids, *Lipids 32*, 1219–1228.
17. Werner, S.A., Luedecke, L.O., and Shultz, T.D. (1992) Determination of Conjugated Linoleic Acid and Isomer Distribution in Three Cheddar-type Cheeses: Effect of Cheese Cultures, *J. Agric. Food Chem. 40*, 1817–1821.
18. Yurawecz, M.P., Hood, J.K., Roach, J.A., Mossoba, M.M., Daniels, D.H., Ku, Y., Pariza, M.W., and Chin, S.F. (1994) Conversion of Allylic Hydroxy Oleate to Conjugated Linoleic Acid and Methoxy Oleate by Acid-catalyzed Methylation Procedures, *J. Am. Oil Chem. Soc. 71*, 1149–1155.
19. Sehat, N., Rickert, R., Mossoba, M.M., Kramer, J.K., Yurawecz, M.P., Roach, J.A., Adlof, R.O., Morehouse, K.M., Fritsche, J., Eulitz, K.D., *et al*. (1999) Improved Separation of Conjugated Fatty Acid Methyl Esters by Silver Ion–High-Performance Liquid Chromatography, *Lipids 34*, 407–413.
20. Adlof, R., and Lamm, T. (1998) Fractionation of *cis*- and *trans*-Oleic, Linoleic, and Conjugated Linoleic Fatty Acid Methyl Esters by Silver Ion High-Performance Liquid Chromatography, *J. Chromatogr. A 799*, 329–332.
21. Sehat, N., Yurawecz, M.P., Roach, J.A., Mossoba, M.M., Kramer, J.K.G., and Ku, Y. (1998) Silver-Ion High-Performance Liquid Chromatographic Separation and Identification of Conjugated Linoleic Acid Isomers, *Lipids 33*, 217–221.
22. Rickert, R., Steinhart, H., Fritsche, J., Sehat, N., Yurawecz, M.P., Mossoba, M.M., Roach, J.A., Eulitz, K., Ku, Y., and Kramer, J.K. (1999) Enhanced Resolution of Conjugated Linoleic Acid Isomers by Tandem-Column Silver-Ion High-Performance Liquid Chromatography, *J. High Resolut. Chromatogr. 22*, 144–148.
23. Cross, R.F., Ostrowska, E., Muralitharan, M., and Dunshea, F.R. (2000) Mixed Mode Retention and the Use of Competing Acid for the Ag-HPLC Analysis of Underivatized Conjugated Linoleic Acids, *J. High Resolut. Chromatogr. 23*, 317–323.
24. Folch, J., Lees, M., and Sloane Stanley, G.H. (1957) A Simple Method for the Isolation and Purification of Total Lipids from Animal Tissues, *J. Biol. Chem. 226*, 497–509.
25. Banni, S., Day, B.W., Evans, R.W., Coprongiu, F.P., and Lombardi, B. (1994) Liquid Chromatographic-Mass Spectrometric Analysis of Conjugated Diene Fatty Acids in a Partially Hydrogenated Fat, *J. Am. Oil Chem. Soc. 71*, 1321–1325.
26. Stoffel, W., Chu, F., and Ahrens, E.H. (1959) Analysis of Long-Chain Acid by Gas–Liquid Chromatography, *Anal. Chem. 31*, 307–308.
27. Schuchardt, U., and Lopes, O.C. (1988) Tetramethylguanidine Catalyzed Transesterification of Fats and Oils: A New Method for Rapid Determination of Their Composition, *J. Am. Oil Chem. Soc. 65*, 1940–1941.
28. *Official Methods of Analysis of AOAC International*, 16th edn., 1995, Method 969.33, Association of Official Analytical Chemists, Arlington.
29. Hashimoto, N., Aoyama, T., and Shioiri, T. (1981) A Simple Efficient Preparation of Methyl Esters with Trimethylsilyldiazomethane (TMSCHN2) and Its Application to Gas Chromatographic Analysis of Fatty Acids, *Chem. Pharm. Bull. 29*, 1475–1478.
30. Payne, R.W., Lane, P.W., and Genstat 5 Committee (1993) *Genstat 5 Reference Manual*, pp. 76–80, Oxford Science Publications, Oxford.
31. Miller, R.G. (1981) *Simultaneous Statistical Inference*, pp. 76–80, Springer-Verlag, New York.
32. Jiang, J., Bjorck, L., Fonden, R., and Emanuelson, M. (1996) Occurrence of Conjugated *cis*-9, *trans*-11-Octadecadienoic Acid in Bovine Milk: Effects of Feed and Dietary Regimen, *J. Dairy Sci. 79*, 438–445.
33. van den Berg, J.J., Cook, N.E., and Tribble, D.L. (1995) Reinvestigation of the Antioxidant Properties of Conjugated Linoleic Acid, *Lipids 30*, 599–605.
34. Eulitz, K., Yurawecz, M.P., Sehat, N., Fritsche, J., Roach, J.A., Mossoba, M.M., Kramer, J.K.G., Adlof, R.O., and Ku, Y. (1999) Preparation, Separation, and Confirmation of the Eight Geometrical *cis/trans* Conjugated Linoleic Acid Isomers 8,10- Through 11,13-18:2, *Lipids 34*, 873–877.
35. Ip, C., Banni, S., Angioni, E., Carta, G., McGinley, J., Thompson, H.J., Barbano, D., and Bauman, D. (1999) Conjugated Linoleic Acid-Enriched Butter Fat Alters Mammary Gland Morphogenesis and Reduces Cancer Risk in Rats, *J. Nutr. 129*, 2135–2142.

[Received January 24, 2000, and in revised form June 22, 2000; accepted August 22, 2000]

Characterization of Caldarchaetidylglycerol Analogs, Dialkyl-type and Trialkyl-type, from *Thermoplasma acidophilum*

Ikuko Uda[a,*], Akihiko Sugai[a], Yuko H. Itoh[b], and Toshihiro Itoh[a]

[a]Division of Chemistry, Center for Natural Science, Kitasato University, Kanagawa 228-8555, Japan, and
[b]Department of Bioengineering, Faculty of Engineering, Soka University, Tokyo 192-8577, Japan

ABSTRACT: The structures of three kinds of phospholipids (PL-X, PL-Y, and PL-T) isolated from *Thermoplasma acidophilum* have been characterized. The core lipid of PL-Y was caldarchaeol, and that of PL-X was archaeol. The composition of the hydrocarbon chains of the PL-T core lipid was C_{20} phytane and C_{40} isoprenoid in a molar ratio of 2 to 1. The major molecular species of the C_{40} isoprenoid was acyclic without the cyclopentane ring. These three kinds of intact phospholipids commonly had glycerophosphate residues as polar head groups. The structure of PL-T was characterized as trialkyl-type caldarchaetidylglycerol, PL-Y as caldarchaetidylglycerol, and PL-X as archaetidylglycerol.

Paper no. L8569 in *Lipids 35*, 1155–1157 (October 2000).

The membrane lipid structures of Archaea are basically ether-type, such as derivatives of archaeol, 2,3-di-*O*-phytanyl-*sn*-glycerol, and caldarchaeol, tetra-*O*-di(biphytanyl)diglycerol (1–3). The core lipids of thermoacidophilic Archaea, such as *Sulfolobus* or *Thermoplasma*, are mainly caldarchaeol and their derivatives, and about 10% archaeol (4). As the minor isoprenoid ether core lipid, 3-*O*-phytanyl-*sn*-glycerol and glycerol-trialkyl-glycerol tetraether are also detected in *S. solfataricus* (5). The constituents of the C_{40}-hydrocarbon chains in these caldarchaeols have a wide range of variety, which depends on the number of cyclopentane rings. These hydrocarbon chains contain from a minimum of zero to a maximum of four cyclopentane rings (6,7).

Recently, we have reported the structures of neutral glycolipids of *T. acidophilum*, and all of their core lipids were caldarchaeol (8). The existence of diether-type polar lipids and also the phosphatidyl diether lipid was suggested by two groups (9, 10).

In this paper, we clarified the structures of three intact lipids having glycerophosphate groups attached to caldarchaeol, archaeol, or glycerol-trialkyl-glycerol tetraether (trialkyl-type-caldarchaeol) as core lipids. The last one is a novel phospholipid from *T. acidophilum*.

*To whom correspondence should be addressed at Division of Chemistry, Center for Natural Science, Kitasato University, 1-15-1 Kitasato, Sagamihara, Kanagawa 228-8555 Japan.
E-mail: uda@clas.kitasato-u.ac.jp

Abbreviations: DEA, diethanolamine; EI, electron ionization; FAB-MS, fast atom bombardment-mass spectrometry; GC–MS, gas chromatography–mass spectrometry; GLC, gas–liquid chromatography; GPL-A, gulosyl-caldarchaetidyl-glycerol; HPTLC, high-performance thin-layer chromatography; TLC, thin-layer chromatography.

EXPERIMENTAL PROCEDURES

Organisms and preparation of lipids. Thermoplasma acidophilum (ATCC 27658) was grown aerobically at 59°C in a medium containing inorganic salts, 0.1% yeast extract, and 1% glucose described previously (8,11). The preparation and separation procedures of neutral and acidic lipids were described previously by Uda *et al.* (8). The acidic lipids [1 g in 1.5 mL chloroform/methanol (9:1, vol/vol)] were further fractionated by silicic acid column (36 × 1 cm) chromatography, eluted with a linear gradient of chloroform/methanol from 9:1 (vol/vol) to 1:4 (vol/vol) in a total vol of 600 mL. Five-milliliter fractions were collected. Further purification of acidic lipids [pooled fractions 27–37 in chloroform/methanol/water (1:6:1, by vol)] was performed using reversed-phase column (5 × 1 cm) chromatography eluted with solvent mixture of chloroform/methanol/water. After PL-X was eluted with the solvent of 2:6:1 (by vol), PL-T and PL-Y were eluted together with 3:6:1 (by vol).

Analytical procedures. Analytical procedure of core lipids and hydrocarbon chains were described previously (12,13).

Thin-layer chromatography (TLC) of acidic lipids was performed using boric acid-impregnated high-performance TLC (HPTLC) plates of silica gel (8). Four kinds of solvent systems were used for this study, A: chloroform/methanol/0.2% $CaCl_2$ (55:45:7, by vol), B: chloroform/methanol/1 M NH_4OH (65:35:5, by vol), C: chloroform/methanol (4:1, vol/vol), and D: hexane/diethyl ether/acetic acid (60:40:2, by vol). The TLC of core lipids was performed using an HPTLC plate of silica gel and a double development system, with the first development one-third high with solvent C, and the second development up to the top of the plate with solvent D. Caldarchaeol and archaeol, prepared from *S. solfataricus,* were used as standard substances (14). Lipids were detected by spraying with 18 M H_2SO_4 followed by heating at 150°C. The contents of each lipid in the total cellular lipids were estimated using a Dual-Wavelength Chromato Scanner (CS-930; Shimadzu, Kyoto, Japan).

Fast atom bombardment-mass spectrometry (FAB-MS) was carried out in a positive or negative mode with a matrix

[*m*-nitrobenzylalcohol and diethanolamine (DEA)] using a mass spectrometer (model JMS-AX505H; JEOL, Tokyo, Japan).

Preparation and analytical procedures of glycerophosphate were described previously (15).

Periodate oxidation of lipids was performed using sodium periodate. The resulting products were reduced with sodium borohydride. The resulting periodate oxidation products of acidic lipids were analyzed by FAB-MS.

RESULTS AND DISCUSSION

The acidic lipids were gradually eluted in due order from nonpolar lipids to polar lipids by silicic acid column chromatography. The main phosphoglycolipid, gulosyl-caldarchaetidylglycerol (GPL-A) (10), which occupies 46% of the total lipids, eluted around fraction 40, and its R_f value using solvent A was 0.73. PL-X (R_f = 0.81) and PL-Y (R_f = 0.84) were eluted before GPL-A. Purified PL-X was obtained by reversed-phase column chromatography, and a PL-T and PL-Y mixture was separated further with preparative TLC developed with solvent system B. The R_f values of the lipids by solvent B were as follows: PL-T, 0.56; PL-Y, 0.50; and PL-X, 0.46. The PL-X content in the total cellular lipids, based on the calculation of TLC scanning, was about 5%, and PL-Y was less than 1%. Further, the PL-T content was less than one-tenth of the PL-Y content.

Core lipids obtained from PL-X and PL-Y co-chromatographed on the TLC with archaeol (R_f = 0.80) and caldarchaeol (R_f = 0.55), respectively. An unknown core lipid (R_f = 0.73) was detected in PL-T. The gas chromatogram of the hydrocarbon chain from PL-X showed only one peak. Its gas chromatography–mass spectrometry (GC–MS) (electron ionization, EI) spectrum showed a peak for $[M]^+$ at *m/z* 282, which was identified as $C_{20}H_{42}$ phytane. The hydrocarbon chain from PL-Y showed four peaks in the gas chromatogram corresponding to the same C_{40} hydrocarbon chains detected in *S. solfataricus* (7). The peaks for $[M]^+$, obtained from the GC–MS (EI) spectra, at *m/z* 562, 560, 558, and 556 were identified as $C_{40}H_{82}$ (acyclic), $C_{40}H_{80}$ (monocyclic), $C_{40}H_{78}$ (bicyclic), and $C_{40}H_{76}$ (tricyclic), respectively. The average cyclization percentages of each hydrocarbon chain in caldarchaeol, calculated from the peak area of the gas chromatograms, are shown in Table 1. The gas chromatogram, of the hydrocarbon chain from PL-T showed the peaks of both C_{20} and C_{40} hydrocarbons, and their molar ratio was 2 to 1. Distribution of the cyclopentane rings in the PL-T core lipid is shown in Table 1. The main molecular species of the C_{40} hydrocarbon chain of the PL-T core lipid did not contain a cyclopentane ring (C_{40} acyclic). One mole of the core lipid of PL-T was constructed with two moles of glycerol, two moles of C_{20} phytane, and one mole of C_{40} hydrocarbon. These results were according to the data for glycerol-trialkyl-glycerol tetraether (trialkyl-type caldarchaeol) from *S. solfataricus* (5).

PL-X, PL-Y, and PL-T were positive for Dittmer reagent. The molar ratios of phosphorus content vs. the core lipid for each lipid were all 1:1 by phosphorus measurement assay (16). The polar head groups of PL-X, PL-Y, and PL-T were identified as glycerol-3-phosphate by comparison with the result of GPL-A, according to TLC, gas–liquid chromatography (GLC) analysis, and enzymatic assay.

The negative FAB-MS spectrum of PL-X showed a molecular ion peak at 805.6 as *m/z* $[M - H]^-$ corresponding to the structure of archaetidylglycerol. The proposed structure of PL-X was consistent with the phosphoryl-diether lipid structure previously suggested (10). The positive FAB-MS spectrum of PL-Y showed molecular ion peaks at *m/z* 1456, 1478, and 1561, corresponding to $[M + H]^+$, $[M + Na]^+$, and $[M + DEA + H]^+$, respectively. In the case of using DEA as a matrix, a characteristic ion peak *m/z* $[M + DEA + H]^+$ (M + 106) was observed, and the molecular weight [M] of PL-Y was estimated to be 1455. A negative FAB-MS spectrum of PL-Y showed a molecular ion peak at 1454 as *m/z* $[M - H]^-$, corresponding to the structure of caldarchaetidylglycerol with a core lipid composed of C_{40} acyclic, as the major molecular species. The molecular ion $[M - H]^-$ at *m/z* 1454 was according to the values calculated from the proposed structure of PL-Y. The negative FAB-MS spectrum of PL-T always showed a molecular ion at 1456, which was two mass units larger than that of PL-Y at any experimental conditions. These results strongly supported the proposed structure of PL-T, which was caldarchaetidylglycerol (trialkyl-type) composed of one mole of a C_{40} acyclic-hydrocarbon chain and two moles of C_{20} phytane.

The FAB-MS of periodate oxidation products of these phospholipids showed that the molecular ion of the degradation products was 30 ($-CH_2O$) mass units less than that of intact PL-X, PL-Y, and PL-T. These values completely overlapped the theoretically calculated values.

The core lipids of PL-X and PL-Y were identified as archaeol and caldarchaeol, respectively, and that of PL-T was trialkyl-type caldarchaeol, by comparison of the R_f values on TLC, the GLC patterns, and the GC-MS spectra with the stan-

TABLE 1
Distribution of Cyclopentane Rings in Core Lipids from *Thermoplasma acidophilum*

	C_{40} (%)					Average cyclization[a]
	Acyclic	Monocyclic	Bicyclic	Tricyclic	Tetracyclic	
PL-Y	70.8	13.3	13.2	2.6	ND[b]	0.48
PL-T	70.0	16.5	13.5	<0.1	ND	0.44

[a]Average cyclization: (% monocyclic + 2 × % bicyclic + 3 × % tricyclic + 4 × % tetracyclic) × 10^{-2}.
[b]ND: not detected.

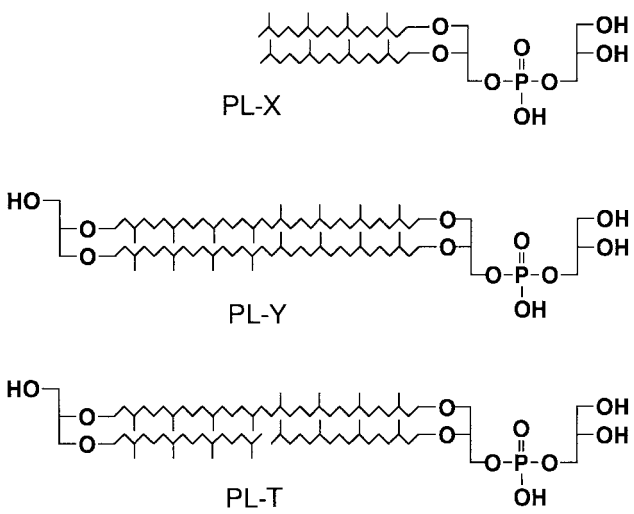

FIG. 1. Proposed structures of PL-X, PL-Y, and PL-T. The core lipid of PL-T is composed of two moles of C_{20} phytane and one mole of acyclic C_{40} hydrocarbon chains. Which hydrocarbon chain binds with the *sn*-2 or *sn*-3 hydroxy group of glycerol is not clear.

dard substances. The phosphate-base constituting these lipids was *sn*-glycerol-3-phosphate in each case. Consequently, it became clear that the PL-X of the *T. acidophilum* is archaetidylglycerol, PL-Y is caldarchaetidylglycerol, and PL-T is caldarchaetidylglycerol (trialkyl-type). The proposed structures of PL-X, PL-Y, and PL-T are shown in Figure 1.

Two types of intact lipid constituents of trialkyl-type caldarchaeol core lipid were also reported in *S. acidocaldarius*, which have inositolphosphates as their polar head groups, bonded to one or both sides of the core lipid (17). In *T. acidophilum*, the trialkyl-type caldarchaeol core lipid was detected not only in PL-T but also in fraction 60, obtained by silicic acid column chromatography. It is assumed to be a lipid having glycerophosphates bonded to both sides of the core lipid. Those lipids might exist in membrane lipids of *T. acidophilum*, which is important to consider concerning their metabolism, and PL-T might be an intermediate in the biosynthesis process from PL-X to PL-Y.

ACKNOWLEDGMENT

The authors greatly appreciate Naoya Tsutsumi for his technical assistance.

REFERENCES

1. Gambacorta, A., Gliozzi, A., and De Rosa, M. (1995) Archaeal Lipids and Their Biotechnological Applications, *World J. Microbiol. Biotechnol. 11*, 115–131.
2. Nishihara, M., Morii, H., and Koga, Y. (1987) Structure Determination of a Quartet of Novel Tetraether Lipids from *Methanobacterium thermoautotrophicum*, *J. Biochem. 101*, 1007–1015.
3. De Rosa, M., and Gambacorta, A. (1988) The Lipids of Archaebacteria, *Prog. Lipid Res. 27*, 153–175.
4. Langworthy, T.A. (1982) Lipids of Bacteria Living in Extreme Environments, in *Current Topics in Membranes and Transport*, Vol. 17, pp. 45–77, Academic Press, New York.
5. De Rosa, M., Gambacorta, A., Nicolaus, B., Chappe, B., and Albrecht, P. (1983) Isoprenoid Ethers; Backbone of Complex Lipids of the Archaebacterium *Sulfolobus solfataricus, Biochim. Biophys. Acta 753*, 249–256.
6. De Rosa, M., De Rosa, S., and Gambacorta, A. (1977) ^{13}C-NMR Assignments and Biosynthetic Data for the Ether Lipids of *Caldariella, Phytochemistry 16*, 1909–1912.
7. De Rosa, M., Gambacorta, A., Nicolaus, B., Sodano, S., and Bu'Lock, J.D. (1980) Structural Regularities in Tetraether Lipids of *Caldariella* and Their Biosynthetic and Phyletic Implications, *Phytochemistry 19*, 833–836.
8. Uda, I., Sugai, A., Kon, K., Ando, S., Itoh, Y.H., and Itoh, T. (1999) Isolation and Characterization of Novel Neutral Glycolipids from *Thermoplasma acidophilum, Biochim. Biophys. Acta 1439*, 363–370.
9. Langworthy, T.A., Smith P.F., and Mayberry, W.R. (1972) Lipids of *Thermoplasma acidophilum*, *J. Bacteriol. 112*, 1193–1200.
10. Swain, M., Brisson, J.-R., Sprott, G.D., Cooper, F.P., and Patel, G.B. (1997) Identification of β-L-Gulose as the Sugar Moiety of the Main Polar Lipid *Thermoplasma acidophilum*, *Biochim. Biophys. Acta 1345*, 56–64.
11. Darland, G., Brock, T.D., Samsonoff W., and Conti, S.F. (1970) A Thermophilic, Acidophilic Mycoplasma Isolated from a Coal Refuse Pile, *Science 170*, 1416–1418.
12. Furuya, T., Nagumo, T., Itoh T., and Kaneko, H. (1980) A Thermophilic Acidophilic Bacterium from Hot Spring, *Agric. Biol. Chem. 44*, 517–521.
13. Sugai, A., Uda, I., Kurosawa, N., Shimizu, A., Ikeguchi, M., Itoh, Y.H., and Itoh, T. (1995) The Structure of the Core Polyol of the Ether Lipid from *Sulfolobus acidocaldarius*, *Lipids 30*, 339–344.
14. De Rosa, M., Esposito, E., Gambacorta, A., Nicolaus, B., and Bu'Lock, J.D. (1980) Effects of Temperature on Their Lipid Composition of *Caldariella acidophila*, *Phytochemistry 19*, 827–831.
15. Uda, I., Sugai, A., Shimizu, A., Itoh, Y.H., and Itoh, T. (2000) Glucosylcaldarchaetidylglycerol, a Minor Phosphoglycolipid from *Thermoplasma acidophilum, Biochim. Biophys. Acta 1484*, 83–86.
16. Sugai, A., Sakuma, R., Fukuda, I., Itoh, Y.H., and Itoh, T. (1992) Improved Method for Determining Soybean Phospholipid Composition by Two-dimensional TLC-phosphorus Assay, *J. Jpn. Oil Chem. Soc. 41*, 1029–1034.
17. Sugai, A., Uda, I., Kon, K., Ando, S., Itoh, Y.H., and Itoh, T. (1996) Structural Identification of Minor Phosphoinositol Lipids in *Sulfolobus acidocaldarius N-8*, *J. Jpn. Oil Chem. Soc. 45*, 327–333.

[Received June 23, 2000, and in revised form and accepted August 7, 2000]

The Effect of Maternal Diets on the Mean Melting Points of Human Milk Fatty Acids

Sir:

Triacylglycerols (TAG) are synthesized in the rough endoplasmic reticulum of the secreting cells of the mammary gland. The TAG must be liquid at body temperature for formation of microdroplets in the cell, for fusion of these into droplets, and for secretion of the droplets as globules (1). The core of the globule is TAG, and most of these must be liquid. The liquidity of TAG is related to their structure and to the melting points (MP) of the fatty acids (FA). For example: the MP of 16:0 is 63°C; 18:1*t*, 44°C; and 18:1*c*, 16°C. The MP of 16:0–16:0–16:0 is 66°C, 16:0–16:0–18:1, 37°C, and 16:0–18:1–18:1, 24°C (2).

The diets of lactating women contain wide-ranging amounts of the major FA: 10:0, 12:0, 14:0, 16:0, 18:0, 18:1*t*, 18:1*c*, 18:2, and 18:3. Changes in diets alter the kinds and amounts of the FA, and as a result, the TAG in milk (3). It would appear that ingestion of large quantities of FA with MP above 38°C, which includes all of those listed above except 10:0, 18:1*c*, 18:2, and 18:3, would raise the MP of milk TAG. In addition, the production of 10:0–14:0, which are synthesized in the mammary gland, is stimulated by maternal diets high in carbohydrate, and this should increase the MP of milk TAG. However, the influence of changes in the maternal diet on the liquidity or MP of milk fat has not been reported. In this paper we provide the mean melting points (MMP) of the FA in milks from women who consumed a variety of diets.

Holman *et al.* (4) developed a measure of liquidity or fluidity of membranes. They calculated the MMP of FA in plasma phospholipids. They found, for example, that the MMP was 14.8°C for normal American omnivores and 21.3°C for patients with multiple sclerosis. The authors briefly described their method for calculating MMP. The contribution of the molar fraction of the MP of each FA was determined. All increments were summed and the MMP calculated. One of us (RGJ) was told (Holman, R.T., personal communication) to add 100 to each FA-MP so as to avoid negative numbers. Dr. Frank D. Gunstone (personal communication) evaluated our method for calculating MMP and simplified the procedure. A description of the procedure follows: (i) Determine the mol% of each FA. We used only the major milk FA listed above. Inclusion of all FA had little effect. (ii) Multiply each mol% by the (MP + 100) of each FA to obtain MP fractions. See Reference 2 for MP. (iii) Sum the MP fractions and subtract 100 to obtain the MMP of the FA mixture.

The contents of the major FA in milks from women on different diets and the MMP of their FA are shown in Table 1. The diets in the paper by Insull *et al.* (5) were given sequentially to a patient, and their effects on the FA profiles of her milk samples determined. The ingestion of 228 g of corn oil/d increased the 18:2 + 18:3 of her milk from 9.0 to 42.0%, while the MMP dropped markedly. Milks from the Nigerian (6,7), Tanganyikan (8), and Bedouin women (8) contained FA with MMP close to body temperature. Lauric (12:0) and 14:0 contents were high in these milks because their synthesis in the mammary gland is increased by the consumption of large quantities of dietary carbohydrates. The fat contents and volumes of milk were not reported so we do not know if those high MMP affected the secretion of milk fat. The MMP of the milks from mothers who ate diets high in 18:1*t* (9) were lower than those who did not. This may be caused by their lower contents of 14:0. The fat contents of the milks were; high, 18:1*t*, 4.51; and low, 4.14%. The low MMP in milks from the mothers on vegetarian diets (10) were caused by the relatively large amount of 18:2, 28.8%, therein. The milk fat contents were; vegetarian, 3.1 and omnivorian, 4.2%. These were not significantly different when tested by the Wilcoxon rank sum method. However, this large difference may be biologically important. These results illustrate the value of determining and reporting the fat contents of the milks when FA are analyzed. The milks from all mothers, including those on unusual diets, had MMP at or below body temperature, thus all the milk fats should be liquid.

The maintenance of milk TAG liquidity regardless of the ingestion of large quantities of FA with high MP indicates the ability of the mammary gland to synthesize TAG with the required MP and to incorporate them into milk fat globules. Human milk TAG are unique in that about 70% of the 16:0 are esterified to the *sn*-2 position (3,11–13). Based on their study, Winter *et al.* (11) stated that the amounts of 16:0 and 18:0 in TAG of human milk fat appear to be modulated by nonrandom distributions of 18:1*c* and 18:2 or 8:0–12:0, so that the fat is liquid at body temperatures. The small quantities of trisaturated TAG in human milk (11) will be dissolved in the liquid TAG. The acyltransferase systems in the gland are able to combine the FA into TAG that will be liquid at

Paper no. L8526 in *Lipids 35*, 1159–1161 (October 2000).

Abbreviations: FA, fatty acids; MP, melting point; MMP, mean melting point; TAG, triacylglycerol.

TABLE 1
The Composition (wt%) and Mean Melting Points (MMP °C) of the Fatty Acids (FA) in Milk Triacylglycerols from Lactating Women on Various Diets

	U.S. (Ref. 5)[a]		Nigeria (Refs. 6,7)[b]		Indigenous (Ref. 8)[c]				U.S. (Ref. 9)[d] *trans* 18:1		U.S. (Ref. 10)[e]	
Fatty acid	*Ad lib.*	Corn oil	Fulani	Yoruba	Tanganyikan	Jordan	Bedouin	Lebanese	Low	High	Vegetarian	Non-Vegetarian
10:0	1.0	1.0	3.9	2.1	—	—	—	—	—	—	1.6	1.6
12:0	6.0	3.0	18.4	31.4	11.5	7.2	5.0	5.8	3.5	2.7	7.1	5.5
14:0	9.0	2.0	13.9	9.0	12.7	9.7	8.5	7.0	6.6	4.2	8.2	6.5
16:0	25.0	14.0	21.5	20.1	17.5	22.2	26.7	24.0	27.9	23.9	15.3	20.5
16:1	2.0	1.0	2.0	3.1	1.4	3.0	4.5	2.0	2.9	2.5	1.7	3.4
18:0	8.0	3.0	3.8	3.4	6.0	4.3	7.9	7.1	7.1	7.3	4.5	8.1
18:1*t*	—	—	—	—	—	—	—	—	1.8	6.5	—	—
18:1*c*	34.0	31.0	21.5	20.8	39.6	33.5	35.4	39.6	31.6	33.4	26.9	34.7
18:2	9.0	45.0	10.0	8.2	1.0	15.2	6.3	11.3	14.4	13.0	28.8	14.5
18:3	—	—	0.5	—	—	—	—	—	—	—	2.8	1.9
MMP °C FA	37.3	17.2	38.9	39.2	38.7	32.9	37.1	34.3	35.4	34.0	25.6	31.5

[a]Hospital patient received 228 g corn oil/d during Dietary Period VI. 18:3 included in 18:2.
[b]Nigerian donors. Diets high in carbohydrates, low in fat and protein.
[c]Tanganyikan: 75% of calories from carbohydrates, dietary fat mainly vegetables. Jordan: Fat mainly vegetable with variable amounts of soybean oils. Bedouin: Fat mainly from animals. Lebanese: Fat about 75% vegetable, mostly olive oil.
[d]Controlled feeding trial.
[e]Samples from recognized groups. Milks from both groups contained 0.2% 8:0.

body temperature. This occurs even though changes in the maternal diet alter the amounts of FA in the TAG (3). Preferential retention of polyunsaturated FA was observed in the milk lipids containing higher levels of 10.0–14:0 [Refs. 7 and 8 in Table 1 (14)]. A reasonable explanation is that these are needed to maintain fat liquidity.

A desaturase that converts 18:0 to 18:1 has been found in the mammary gland of dairy cattle (1) but not in the human gland. We made a thorough search and found no evidence that the desaturase exists in the gland. In humans, most of the desaturation occurs in the liver (15). The conjugated linoleic acid 9*c*,11*t*-18:2 was found in human serum when vaccenic (11*t*-18:1) acid was fed (16). However, this desaturation probably occurred in the liver. The conversion of 11*t*-18:1 to 9*c*,11*t*-18:2 in humans was recently confirmed using deuterated FA (17). This desaturation appears to be a major pathway, but it is not available in the human mammary gland.

Thus, it is evident the secreting cell tends to incorporate patterns of FA into TAG that will produce lipid droplets, and ultimately fat globules, that are liquid at body temperature. How might this selection mechanism work? A clue may be provided by bovine milk fat, which contains about 5% of a high-melting (55°C) TAG fraction containing about 75% 16:0 and 18:0 (18). These data make it quite unlikely that the discrimination depends on the melting property of each TAG molecule, but more plausibly on the capacity of an accumulating liquid TAG droplet to dissolve newly synthesized molecules of TAG. In this manner, a certain small proportion of high-melting molecules would be expected to dissolve in the growing liquid droplet. Beyond that amount, additional high-melting molecules apparently are rejected and may undergo FA exchange to make them extractable or acceptable as to the melting point. We conceive of the rough endoplasmic reticulum membrane system as the most likely site for this MP discrimination process (19). It is well established that the endoplasmic reticulum is the site of TAG synthesis in the lactating cell (1,20), and a mechanism for accumulation of TAG within the bilayer of the endoplasmic reticulum membrane has been postulated (see Fig. 4 in Ref. 21). Maintaining liquidity in the hydrophobic region of this membrane appears essential to gathering of TAG into droplets. These considerations lead to the prediction that the yield of milk fat is dependent on melting properties of the FA available for TAG synthesis. We did not have information about the fat contents of most of the milks in Table 1.

To summarize, the MMP of milk FA from women who consumed a variety of test and indigenous diets were lower than or near body temperature. The MMP of milk FA from women who consumed high-carbohydrate diets were near 37.5°C. Liquidity of the FA was maintained. The results indicate the ability of the mammary gland to synthesize TAG that will be liquid at body temperature. Our results are probably applicable to other particles that transport TAG, such as chylomicrons.

ACKNOWLEDGMENTS

We thank the Mead Johnson Nutritional Group, Ross Products Division, Abbott Laboratories, and Wyeth-Ayerst International, who provided the funds for the preparation of this paper and the purchase of reprints.

REFERENCES

1. Timmen, H., and Patton, S. (1988) Milk Fat Globules: Fatty Acid Composition, Size and *in vivo* Regulation of Fatty Liquidity, *Lipids 23*, 685–689.

2. Gunstone, F.D., Harwood, J.L., and Padley, F.B. (1994) Dictionary Section, in *The Lipid Handbook*, 2nd ed., Chapman and Hall, New York.
3. Jensen, R.G. (1996) The Lipids in Human Milk, *Prog. Lipid Res 35*, 53–92.
4. Holman, R.T., Johnson, S.B., and Kokmen, E. (1989) Deficiencies of Polyunsaturated Fatty Acids and Replacement by Nonessential Fatty Acids in Multiple Sclerosis, *Proc. Natl. Acad. Sci. USA 86*, 4720–4724.
5. Insull, W., Jr., Hirsch, J., James, T., and Ahrens, E.H., Jr. (1959) The Fatty Acids of Human Milk. II. Alterations Produced by Manipulation of Caloric Balance and Exchange of Dietary Fats, *J. Clin. Invest. 38*, 443–450.
6. Schmeits, B.L., Okolo, S.N., VanderJagt, D.J., Huang, Y.-S., Chuang, L.-T., Mata, J.R., Tsin, A.T.C., and Glew, R.H. (1999) Content of Lipid Nutrients in the Milk of Fulani Women, *J. Hum. Lact. 15*, 113–120.
7. Glew, R.H., Omone, J., Vignetti, S., D'Amico, M., and Evans, R.W. (1995) Fatty Acid Composition of Breast Milk Lipids of Nigerian Women, *Nutr. Res.15*, 477–489.
8. Read, W.W.C., Lutz, P.G., and Tashjian, A. (1965) Human Milk Lipids II. The Influence of Dietary Carbohydrates and Fat on the Fatty Acids of Mature Milk. A Study in Four Ethnic Groups, *Am. J. Clin. Nutr. 17*, 180–183.
9. Craig-Schmidt, M.C., Weete, J.D., Faircloth, S.A., Wickwire, M.A., and Livant, E.J. (1984) The Effect of Hydrogenated Fat in the Diet of Nursing Mothers on Lipid Composition and Prostaglandin Content of Human Milk, *Am. J. Clin. Nutr. 39*, 778–786.
10. Specker, B.L., Wey, H.E., and Miller, D. (1987) Differences in Fatty Acid Composition of Human Milk in Vegetarian and Nonvegetarian Women: Long-Term Effect of Diet, *J. Pediatr. Gastroenterol. Nutr. 6*, 764–768.
11. Winter, C.H., Hoving, E.B., and Muskiet, F.A.J. (1993) Fatty Acid Composition of Human Milk Triglyceride Species. Possible Consequences for Optimal Structures of Infant Formula Triglycerides, *J. Chromatogr. 616*, 9–24.
12. Martin, J.-C., Bougnoux, P., Antoine, J.-M., and Lanson, M. (1993) Triacylglycerol Structure of Human Colostrum and Mature Milk, *Lipids 28*, 637–643.
13. Kallio, H., and Rua, P. (1994) Distribution of the Major Fatty Acids of Human Milk Between *sn*-2 and *sn*-1,3 Positions of Triacylglycerols, *J. Am. Oil. Chem. Soc. 71*, 985–992.
14. Schmeits, B.L., VanderJagt, D.J., Okolo, S.N., Huang, Y.S., and Glew, R.H. (1999) Selective Retention of n-3 and n-6 Fatty Acids in Human Milk Lipids the Face of Increasing Proportions of Medium-Chain Length (C10–C14) Fatty Acids, *Prostaglandins Leukotrienes Essent. Fatty Acids 61*, 219–224.
15. Barber, M.C., Clegg, R.A., Travers, M.T., and Vernon, R.G. (1997) Lipid Metabolism in the Lactating Mammary Gland, *Biochim. Biophys. Acta 1347*, 101–126.
16. Salminen, I., Mutanen, M., Jauhiainen, M., and Aro, A. (1998) Dietary *trans* Fatty Acids Increase Conjugated Linoleic Acid Levels in Human Serum, *J. Nutr. Biochem. 9*, 93–98.
17. Adlof, R.S., Duval, S., and Emken, E.A. (2000) Biosynthesis of Conjugated Linoleic Acid in Humans, *Lipids 35*, 131–135.
18. Patton, S., and Keeney, P.G. (1958) The High-Melting Triglyceride Fraction from Milk Fat, *J. Dairy Sci. 41*, 1288–1289.
19. Mather, I.H., and Keenan, T.W. (1998) Origin and Secretion of Milk Lipids, *J. Mam. Gland Biol. Neoplasia 3*, 259–273.
20. Keon, B.H., Ankrapp, D.P., and Keenan, T.W. (1994) Cytosolic Lipoprotein Particles from Milk Secreting Cells Contain Fatty Acid Synthase and Interact with Endoplasmic Reticulum, *Biochim. Biophys. Acta 1215*, 327–336.
21. Long, C.A., and Patton, S. (1978) Formation of Intracellular Fat Droplets: Interrelation of Newly Synthesized Phosphatidylcholine and Triglyceride in Milk, *J. Dairy Sci. 61*, 1392–1399.

Robert G. Jensen*
Department of Nutritional Sciences
University of Connecticut
186 Chaffeeville Rd.
Storrs, Connecticut 06268-2637

Stuart Patton
Center for Molecular Genetics
University of California, San Diego
La Jolla, California 92093

[Received May 5, 2000, and in revised form August 24, 2000; revision accepted September 1, 2000]

*To whom correspondence should be addressed.
E-mail: rjensen@uconnvm.uconn.edu

Development in Lipid Analysis: Some New Extraction Techniques and *in situ* Transesterification

Ana I. Carrapiso* and Carmen García

Laboratory of Food Technology, Extremadura University, 10071 Cáceres, Spain

ABSTRACT: The development of methods for analyzing fatty acids that provide rapid and reliable results is currently in great demand. Recently, different lipid extraction procedures such as microwave or supercritical fluid extraction have been researched. Both procedures avoid the use of large volumes of solvents and provide rapid lipid isolations. Only a few papers have reported work on microwave extraction, but many studies about supercritical fluid extraction have been carried out and have been gaining acceptance within the scientific community. Avoiding the lipid isolation step, by synthesizing fatty acid esters by simultaneous lipid extraction and derivatization through *in situ* reactions, has also been proposed. The saving of time and reagents is significant. Owing to the differences among the procedures, some knowledge of their characteristics is essential in order to improve methods and achieve reliable and accurate results. Clearly, results depend on factors such as the type of catalysis selected, the use of nonpolar solvents, heating applied during the synthesis, and the degree of suitability of the procedure chosen for the particular features of each sample.

Paper no. L8465 in *Lipids 35,* 1167–1177 (November 2000).

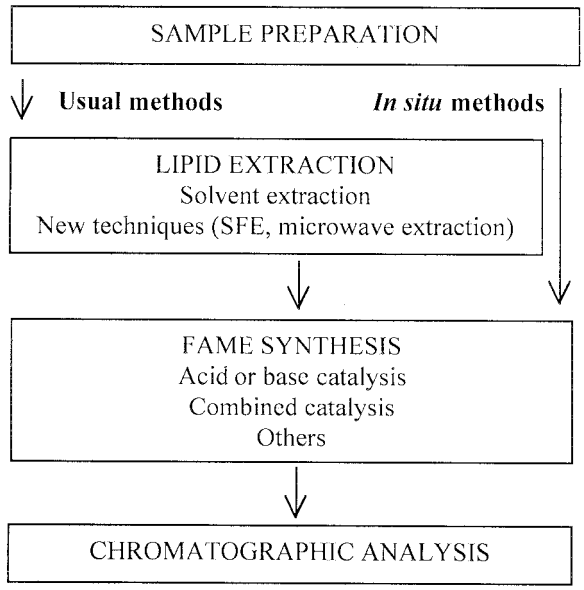

SCHEME 1

In recent years, the analysis of fatty acids has gained in importance because of their nutritional and health implications. The beneficial relation between n-3 fatty acids and chronic diseases such as atherosclerosis (1) or rheumatoid arthritis (2) has been known for a number of years. In addition, the accuracy and the usefulness of fatty acid analysis to determine fat content have been the focus of recent works (3,4) and have brought about the new fat definition of the Nutrition and Labeling Education Act (NLEA) (5).

Fatty acids are determined mainly by gas–liquid chromatography and flame-ionization detectors (FID). In accordance with fatty acid characteristics, chromatographic analysis is applied to fatty acid esters such as methyl (6,7), isopropyl (8) or butyl esters (9) instead of fatty acids since the analysis is more accurate and selective. Fatty acid methyl esters (FAME) are prepared more often than others in biological tissues and foods because of the lower temperatures required to change their volatility, thus improving peak shape and resolution for the more common fatty acids (14:0–22:0). To avoid interference in the FAME synthesis, lipids are usually extracted from samples with organic solvents. The whole procedure is time-consuming and expensive, and therefore several options have been attempted to make it easier. Some knowledge of these methods and their performance in lipid extraction and FAME synthesis is required before one can decide which method to use.

In line with these facts, the present work reviews (i) advances in isolating lipids (focusing on microwave and supercritical fluid extractions) and in synthesizing FAME (focused on *in situ* synthesis) (Scheme 1) with respect to their feasibility to obtain accurate and reliable results and (ii) critical conditions and limitations of their application. Since most attention is paid to *in situ* transesterification methods, this review will be restricted to research related to total fatty acid composition. The reader will need to consult alternative procedures if separation and characterization of individual lipid classes is desired.

EXTRACTION METHODS: NEW TECHNIQUES

Currently, a large number of methods are available for extracting lipids from biological materials. Most of them use or-

*To whom correspondence should be addressed at Tecnología de los Alimentos, Facultad de Veterinaria, Universidad de Extremadura, Avda. de la Universidad s/n, 10071 Cáceres, Spain. E-mail: acarrapi@unex.es

Abbreviations: AOAC, Association of Official Analytical Chemists; FAME, fatty acid methyl ester; NLEA, Nutrition and Labeling Education Act; S-CO_2, supercritical CO_2; SFE, supercritical fluid extraction; TLC, thin-layer chromatography; TMG, tetramethylguanidine.

ganic solvents, usually in mixtures such as chloroform and methanol, as in the Bligh and Dyer (10) and Folch *et al.* (11) procedures. These methods often produce large amounts of hazardous solvent wastes and are generally cumbersome. Automated extraction equipment such as the Soxhlet or Goldfisch apparatus has been successfully described (12,13), but they require long extraction times. The interest in lipid extraction and the lack of efficiency found in some cases have led to continual research on this topic (13,14). Furthermore, the need for easier and quicker analyses has prompted the development of new techniques. Among them, the more outstanding have been in the use of microwaves and supercritical fluids as well as fatty acid extraction combined with ester synthesis in a single step.

The use of microwaves. The use of microwaves for isolating lipids has recently been reported. To date, their application has been limited and focused only on the digestion of samples for measuring trace metals (15–17), and on the extraction of organic contaminants (18–22). However, microwave technology has allowed the development of rapid, safe, and cheap methods for extracting lipids and does not require samples devoid of water (23).

The feasibility of microwave irradiation for extracting lipid was first reported in the mid-1980s. Ganzler *et al.* (24) developed a microwave extraction method that proved to be more effective than the conventional procedure in isolating lipids and pesticides from seeds, foods, feeds, and soil. This improvement was obtained by irradiating the mixture of a sample and an appropriate solvent several times for 30 s each. Recently, extraction equipment that combines microwave energy with small volumes of solvents has appeared, resulting in the procedure known as microwave-assisted extraction. Results from various types of biological samples obtained by this method were qualitatively and quantitatively compared to the Folch *et al.* method (11) in feeds and powdered rat for all classes of lipids (25), and these were also similar to a solvent extraction method with a previous hydrolysis in milk and egg powders and meat samples (23). Partial extraction without solvents has also been useful in studying qualitatively fatty acids from adipose tissue (26), although this method has a limited application: it is appropriate only for samples with a high lipid content, and a validation must be performed because fatty acid profiles can vary according to the extraction method and its efficiency (27).

Although treatments with microwave energy can result in lipid oxidations and in quantitative modifications in the fatty acid composition (28), these changes seem to be imperceptible in the usual conditions (26,29,30). In fact, the irradiation provides selective heating of the sample–solvent mixture, and hence lipids may undergo conditions even less adverse than in some solvent extraction procedures which include heating.

Furthermore, microwave technology can be used for performing chemical reactions, such as hydrolysis (31,32), FAME synthesis (33) and *in situ* derivatizations (extraction and simultaneous reaction) such as ethylations (34).

Up to now, only a few studies about microwave lipid extraction have been reported. However, in view of its growing use for isolating organic compounds and its significant advantages, the future introduction and dissemination of microwave equipment seem to be assured for lipid extraction.

The use of supercritical fluids. Supercritical fluid extraction (SFE) has received increasing attention as an alternative to conventional extraction methods (35). Not only is there a significant reduction in the use of organic solvents but concern about waste is also avoided. Although the time reduction is not so great as in some microwave procedures, SFE has gained much more widespread acceptance. It potentially causes fewer adverse conditions to the fatty acids owing to the low temperature of the extractant fluid, usually supercritical carbon dioxide (S-CO_2).

Several conditions must be improved to achieve suitable and reliable results (36). Optimal temperature and pressure are critical because they affect the extraction yield (37–39) and the extract composition (39,40). Extractions that use only S-CO_2 usually yield good recoveries of nonpolar lipids (41). However, polar lipids may remain unextracted because of their lower solubility in S-CO_2, and therefore samples containing a certain quantity of these types of lipids (e.g., milk) may present extraction difficulties. To improve the extraction of nonpolar lipids, the polarity of S-CO_2 can be varied by using solvents such as methanol, ethanol, or even water. Several researchers have reported that lipid solubility in S-CO_2 is greatly increased by adding ethanol, and some phospholipids are extracted at levels directly proportional to the added ethanol (42,43). The presence of water dissolved in the supercritical fluid also increases the solubility of polar compounds, and it has been used successfully to analyze several dairy products (44). Sample preparation must be considered as well. Particle size affects lipid recovery since it influences the surface area of sample exposed to S-CO_2 (36). The moisture content of samples also affects the extraction efficiency by conditioning their surface structure (45). High moisture content reduces S-CO_2-sample contact owing to the pasty consistency of samples, and moisture acts as a barrier to the diffusion of S-CO_2 in the sample as well as the diffusion of lipids outside the sample (46). In this way, an increase in lipid recovery with decreased moisture content has been demonstrated in wet samples such as meat (47) and fish (48), although moisture does not affect extractability at a low content (48–51). Therefore, samples with high moisture content are usually freeze-dried before the S-CO_2 extraction to improve efficiency (38,47,48,51,52).

Several researchers have compared SFE with conventional extraction methods. Ikushima *et al*. (51) reported yields similar to those from a hot hexane extraction. An S-CO_2 method obtained recoveries of 97–100% when compared to a Soxhlet extraction in potato chips and puff-dried products (53), seeds and seed meals (54), and several other food products (55). King *et al*. (56) concluded that there were no significant differences between fatty acids extracted with an SFE method and with the solvent extraction step of the NLEA procedure in beef samples. Berg *et al*. (57) showed that results for total fat

and several lipid classes in meat coincided with those from the Bligh and Dyer procedure (10), and yields reported by Maness *et al*. (58) and Melinz *et al*. (59) seem to be similar to those obtained with conventional methods. Likewise, fatty acid contents determined by an SFE method and by an acid hydrolysis solvent extraction procedure were comparable in beef and bakery samples (60). Cheung *et al*. (39) showed significantly higher recoveries of lipid and fatty acid contents with SFE than with a chloroform and methanol Soxhlet extraction in seaweeds. Dionisi *et al*. (44) reported satisfactory results for fat content and fatty acid profiles in several dairy products, although for other samples the recovery was only between 83.1 and 96.4%. Similarly, Zou *et al*. (61) showed that SFE and conventional extraction (acid hydrolysis and diethyl ether extraction) were statistically equivalent for some bakery products, whereas for others (cereal matrices subjected to baking or toasting) the treatment by acid hydrolysis released some bound fat not otherwise available for extraction.

Results mentioned above show that SFE could replace solvent extraction methods in a large variety of samples. In fact, SFE has recently been included in the recommended methods from the Association of Official Analytical Chemists (AOAC) to extract fat from oilseed (62). However, for materials with strong interactions between lipids and matrix, methods involving alkaline or acid pretreatment could be required. Furthermore, the simultaneous extraction and FAME synthesis have been reported (63–65), and the feasibility of combining lipases with S-CO_2 to synthesize esters *in situ* has been demonstrated (66,67). At the moment the main shortcomings are the cost of supercritical extraction equipment, the extraction of nonfat material such as water (46,49,68,69), and incomplete lipid extractions under some conditions. Consequently, further development is needed since each biological system is unique. Conditions must be investigated and improved in order to optimize yields for each sample type.

The in situ *synthesis of FAME. In situ* ester synthesis has also been a focus of attention. Although it was proposed as early as 1963 (70), most procedures have been performed for only a few years. The separate lipid extraction step is avoided, and fatty acids are simultaneously extracted and transesterified, allowing for a significant reduction in the length of the total procedure, for a saving of time and work, and for the use of minimal sample amounts. The use of reagents and solvents is reduced, the analysis is less expensive and easier, and the concern about waste disposal is avoided. Moreover, the temperature and reaction time required for the synthesis do not seem to be increased after elimination of the separate lipid extraction step. Therefore, lipids experience fewer adverse conditions than in conventional procedures that include the lipid extraction step and subsequent derivatization. Many studies demonstrate that *in situ* procedures often bear comparison with conventional methods, and fat can be estimated using an internal standard. In spite of important limitations such as the restriction to analyzing only total fatty acids from samples, these procedures offer the chance to derivatize fatty acids from the separate lipid classes scraped from thin-layer chromatography (TLC) plates.

FAME SYNTHESIS AND *IN SITU* PROCEDURES

General considerations. Before performing the FAME synthesis, a certain knowledge about reaction principles is required so that accurate and reliable results will be obtained by using brief procedures for each sample type. Derivative reactions are usually catalyzed by acidic or basic media (Table 1), but they can also occur in the presence of diazomethane or other catalysts. The reactions usually occur with the following: (i) free fatty acids in media with acid pH (Eq. 1) or with diazomethane (Eq. 2). The reaction is called esterification or methylation.

$$R'-CO-CH + CH_3-OH \overset{H^+}{\rightleftharpoons} R'-CO-OCH_3 + HOH \quad [1]$$

$$R'-CO-OH + CH_2N_2 \longrightarrow R'-CO-OCH_3 + N_2 \quad [2]$$

(ii) fatty acids included in complex lipids by *O*-acyl bonds (ester) (e.g., triacylglycerols, phospholipids) in acid or basic media. The reaction is called transesterification or transmethylation (also known as alcoholysis or methanolysis) (Eq. 3).

$$R'-CO-OR'' + CH_3-OH \overset{H^+ \text{ or } OCH_3^-}{\rightleftharpoons} R'-CO-OCH_3 + R''-OH \quad [3]$$

(iii) fatty acids from N-acyl complex lipids (amine) in acid medium (Eq. 4), although special considerations have to be taken into account.

$$R'-CO-NHR'' + CH_3-OH \overset{H^+}{\rightleftharpoons} R'-CO-OCH_3 + R''-NH_2 \quad [4]$$

Given that most fatty acids in biological samples are included in triacylglycerols and phospholipids, the derivatization of fatty acids from samples is mainly a transesterification. Hence transesterification often refers to FAME synthesis from fatty acid mixtures. The term *in situ* is used when the derivatization occurs without a previous extraction step to isolate lipids, not only from tissue matrixes, but also from other matrixes such as adsorbents from TLC.

The two main concerns in performing *in situ* reactions are lipid solubilization (advisable to achieve fast and complete reactions) and prevention of the interference of water or other

TABLE 1
Characteristic of Catalytic Medium in Esterification/Transesterification Reactions

	Acidic	Basic
Temperature	High	Ambient
Time	Minutes–hours	Seconds–minutes
Esterifying power	Medium–high	No
Transesterifying power	Low	High
Risk of saponification	Low	High
Water interference	Low	High

compounds. Therefore, sample features must be considered to decide which is the best solvent, whether a previous step is required to achieve samples devoid of water, and what type of catalyst can be applied.

The effectiveness of the solvent depends on its ability to solubilize lipids (and specifically nonpolar lipids due to their limited solubility in the methanolic medium used for the synthesis) and to create a one-phase system with lipids, methanol, and other reagents. If water is present, it must also be integrated into the system. When a derivatization method is performed with isolated lipids, problems usually do not appear because water is absent, but in using *in situ* procedures water is not always excluded. Above specific water levels, triacylglycerols, particularly those with long-chain saturated fatty acids, tend to precipitate and react much more slowly (71) in media that include most frequently used solvents, although this drawback has not been reported with dioxane (71, 72). In this way, 10% water in an alkaline methanolic medium with hexane is enough to interfere noticeably with the reaction (73). In acidic methanolic media with toluene, FAME recovery remains unaffected in the presence of 5 (74) or 20% water (75), although 40 μL (larger than the sample weight) (76) and 100 mg (about 20–100% of the sample weight) (77) cause a drastic interference.

The concern for water content depends not only on the catalyst and the moisture content of the sample but also on its lipid content, which determines the sample amount required and thus the amount of water introduced. Moreover, water may interfere with the reactions since it is a stronger electron donor than methanol. Hence *in situ* synthesis must be carried out in samples with low moisture contents, or after removing water to below critical limits. This pretreatment adds the advantage of facilitating the penetration of solvents and is often used prior to the lipid extraction (7), although in some samples the extraction yield may be reduced as a consequence of the alteration of the physical structure of the matrix (78). In performing *in situ* FAME synthesis, different procedures have been used to remove water. 2,2′-Dimethoxypropane, a reagent which has been used as methylating reagent (79), was successfully utilized as a water scavenger, but spurious peaks on the chromatograms were ascribed to the unreacted reagent (76,80). These peaks can be avoided by removing both the acetone produced in the reaction and the unreacted 2,2′-dimethoxypropane before adding the catalyst, so that the mixture with the catalyst is prevented and the artifacts are absent (81,82). Oven-drying procedures can bring about alterations in unsaturated fatty acids (75,78), so when pretreatment is necessary, freezing-drying the samples is mainly chosen for removing water.

In choosing the catalytic reagent, some sample characteristics must be considered, such as the occurrence of free fatty acids and the type of bond of the fatty acids linked, the feasibility of using strong heating conditions, and the accuracy required. Most *in situ* derivatization procedures are similar to those applied to lipid extracts (Table 2).

Catalysis with diazomethane. This reagent provides fast esterifying reactions, but it shows no ability to catalyze transesterifying reactions in the usual conditions. Its use has been limited owing to its short shelf life and the great care required in handling it. Its feasibility through *in situ* methods for quantifying plasma free fatty acids more quickly (about 15 min) than conventional methods (extraction, fractionation, and esterification steps) has been reported (83), although the bibliographic values shown as comparison were larger than those obtained by using this procedure.

Basic catalysis. Derivatizations performed in the presence of basic catalysts have advantages such as their speed (84–86) and the mild heating conditions needed, which can be as low as room temperature (71,72,87). For these reasons, this type of catalysis is recommended in samples with short-chain fatty acids, such as milk fats or coconut oil, given that these fatty acids are highly volatile and conventional methods fail in quantifying them (88). It is also a useful alternative to acid-catalyzed reactions when samples contain acid-labile fatty acids, e.g., those with cyclopropene rings, epoxyl groups, or some conjugated unsaturations, present in some vegetable tissues (6).

However, alkali-based transesterification has two main shortcomings. First, free fatty acids (71,89,90) and sphingolipids (91) remain unreacted. Second, esters undergo saponification reactions. In the presence of methoxide, water yields free hydroxide ions (Eq. 5).

$$CH_3O^- + H_2O \rightleftharpoons CH_3OH + OH^- \quad [5]$$

In the presence of these ions, the hydrolysis of sample esters

TABLE 2
Characteristics of the Main Catalysts Used in *in situ* Esterification/Transesterification

	Acid in methanol			Alkali in methanol	
Reagents	HCl	H_2SO_4	BF_3	$NaOCH_3$	TMG
Concentration	5%	1–2%	6–14%	0′2–2 N	1:4 (vol/vol)
Temperature	60°C–refluxing			Ambient–refluxing	
Time of reaction	30 min–2 h		2–60 min	s–1 h	s–5 min
Form of starting material	Gas/liquid	Liquid	Gas	Metal	Liquid
Ease of preparation	No	Yes	No	No	Yes
Introduction of water	No	Yes	No	No	Yes
Danger of preparation	Yes	No	Yes	Yes	No

and the newly generated FAME occurs (Eq. 6). It is irreversible because the carboxylate ion is not subjected to nucleophilic attack by the alcohol as a consequence of its negative charge (6). Furthermore, Na^+ or K^+ ions join with it to form soap, which can promote emulsifications and delays in the FAME extraction (92).

$$R'-CO-OR'' + OH^- \longrightarrow R'-CO-O^- + H-OR'' \quad [6]$$

According to Suter *et al*. (71), 6% water in samples is stoichiometrically enough to cause a complete saponification, and so these methods are usually influenced by the belief that the complete absence of water is a prerequisite. However, more than 80 yr ago Reid, Anderson, and Pardee proved that base-catalyzed transesterification is about 1,500 times faster than saponification (71). This fact was later confirmed by Glass (89), and this enables suitable FAME recoveries even in the presence of water, provided that the reaction has been stopped before significant saponification has taken place (71,92), usually by adding HCl to neutralize the pH of the medium.

Nonpolar solvents used in *in situ* alkali-based transesterification have been hexane (73), petroleum benzine (87), and dioxane (71,72), although others can be applied. Despite the fact that dioxane integrates water better in the reaction medium, it has a flaw: in using polar columns, it can be confused or overlapped with methyl butyrate (71). Chloroform should be excluded because in the presence of methoxide it presumably produces dichlorocarbene, which can react with the double bonds of unsaturated fatty acids (6).

Solubilization and the subsequent reaction of lipids are usually performed without problems. However, when fatty acids remain partially unsolubilized and unreacted, an increase in the temperature or in the time of reaction is not advised owing to the occurrence of saponification and degradation in unsaturated fatty acids. As a feasible option in samples with enclosed lipids, such as meat and dry meat, solubilization can be achieved by first refluxing samples in dimethylformamide (71,72).

Among the reagents used for *in situ* base-catalyzed reactions, sodium methoxide has been the most widely used. It is prepared by adding sodium metal in dry methanol (Eq. 7), and it can be stored for some months.

$$2CH_3OH + 2Na \longrightarrow 2Na^+OCH_3^- + H_2 \quad [7]$$

Initially, sodium methoxide was applied *in situ* to rapeseeds with satisfactory results (93). Long *et al*. (73) used sodium methoxide and hexane in dry grain and dairy products at 80°C for 10 min, and found that the results were reproducible and quantitatively comparable to those from the AOAC method (ether extraction before FAME synthesis with KOH and methanolic BF_3) (94) for all the determinations, both as individual and as total FAME. Later, Cantellops *et al*. (95) performed a similar method in infant formula powder, with results comparable to those from the AOAC method (96) (also ether extraction, KOH, and methanolic BF_3), although some differences in the contents of some groups of fatty acids were reported. Suter *et al*. (71,72) applied sodium methoxide to a wide variety of foods at room temperature for 60–90 s with dioxane as the nonpolar solvent; the work focused on the fat content determination (by conversion of FAME content to triacylglycerols), and *in situ* values were almost comparable to those from official methods.

A special type of alkaline catalyst is the organic base reagent. Not only are these reagents strong bases used as catalysts for transesterification reactions, but they also react with free fatty acids, being easily pyrolyzed in the injection port of the gas chromatograph to yield methyl esters (6,97). In this way, tetramethylguanidine (TMG) seems to be suitable for performing *in situ* derivatizations. Schuchardt and Lopes (85) used it in refined and in degummed fats and oils. Heating for 2 min at 100°C was enough to obtain more than 99% FAME yield (determined by ^1H nuclear magnetic resonance spectroscopy) even in the presence of 6.7% free fatty acids, and therefore the authors suggest that guanidinium carboxylate (formed by the joining of free fatty acids and the guanidinium ion) can be attacked by methanol before the injection. The procedure did not induce *trans*-isomerization in unsaturated fatty acids, according to the infrared spectra, and fatty acid profiles were comparable to those obtained using methanolic BF_3. Marx and Stender (87) also applied *in situ* TMG and petroleum benzine (nonpolar solvent) to oilseeds, and in most cases results for the fatty acid contents were similar to those obtained using a conventional method.

Acid catalysis. The ability to catalyze derivatization from all the fatty acids (free or linked) has led to a widespread use of acid catalysis. However, heating is required and the reaction time needed is longer than in basic catalysis. In samples containing sugar, a chromatographic peak eluted just after lauric (12:0) acid methyl ester. This peak corresponds with methyl levulinate, which appears when this type of sample is subjected to heating in an acid medium and later esterified (Eq. 8) (98). In any case, these reactions involve mainly a gravimetric hazard in lipid extraction procedures with previous acid hydrolysis (99), given that in chromatographic analysis the methyl levulinate peak can be identified.

Different solvents have been used in performing *in situ* acid-based methods: hexane (100–102), tetrahydrofuran (79), benzene (74,75,79,103,104), toluene (75,77,79,105), and chloroform (75). Pentane, hexane, or isooctane were not beneficial when used to replace benzene (74), and benzene and toluene extracted FAME better than chloroform (75). Owing to the toxicity of benzene, several researchers have preferred toluene. Although the peak for toluene can overlap the peaks for short-chain FAME, no problems were reported in analyzing milk fat (75), although quantitative results were not suitable.

In samples with enclosed lipids and therefore slow FAME synthesis, the reaction time may be increased because no saponification appears. Harsh conditions (high temperatures, heating for long time) can cause degradation in fatty acids,

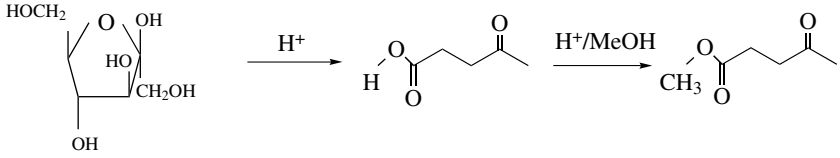

Fructose (levulose) Levulinic acid Methyl levulinate [8]

but mild conditions yield low FAME recoveries. Hence, heating must be tailored to the minimal requirement, which varies as a result of the procedure applied (e.g., catalyst, nonpolar solvent, reagent ratio) and is also a consequence of the type of samples (106). The main concern is water interference, as mentioned above, although the derivatization is affected to a lesser extent than in basic catalysis. Hydrogen chloride, sulfuric acid, and boron trifluoride in methanol are the reagents used most frequently for *in situ* reactions.

Methanolic hydrogen chloride (HCl) is, according to some authors, the best general purpose esterifying agent. It is the most widely mentioned one being used in *in situ* procedures, probably because it is affected less by small amounts of water. With regard to its drawbacks, its unstability in storage, its inconvenient preparation, and the production of artifacts under certain conditions (101,107) must be mentioned. Methanolic HCl is usually prepared by bubbling dry gaseous hydrogen chloride into methanol, but adding acetyl chloride to anhydrous methanol has been preferred for performing *in situ* procedures. The methyl acetate which is generated does not interfere with FAME synthesis at this concentration, but the reagent is useful only for a week (6).

The *in situ* acid-based procedures are quite varied, both in the heating and in the use of nonpolar solvents, and therefore the accuracy of the results has been different. After heating with benzene for 2 h at 70°C, Outen *et al*. (103) quantified fatty acids with an accuracy similar to that of a conventional method (hexane extraction after basic hydrolysis and reaction with methanolic HCl) in feeds, digesta, and feces from sheep. Suitable results in mammalian tissues were also obtained by Shimasaki *et al*. (82) using a similar method. Lepage and Roy (104) successfully applied methanolic HCl and benzene at 100°C for 60 min to fatty acid standards and triacylglycerols in mammalian tissues. The same procedure was later used in all classes of lipids, obtaining FAME yields higher than in the transesterification of lipid extracts (74), and in plasma fatty acids (108). After heating at 80°C for an hour, Browse *et al*. (76) reported low recoveries (15–20% lower than the conventional method) in fresh leaf tissues, probably owing to the absence of a nonpolar solvent during the reaction and the incomplete FAME extraction before adding the internal standard. Sukhija and Palmquist (75) improved the method of Outen *et al*. (103) and achieved results which were quantitatively comparable to those of the conventional method in feedstuffs and feces, although only the fatty acid profile was similar in milk fat. Ulberth and Henninger (77) replaced benzene with toluene in analyzing in fats, oils, and processed foods, obtaining fatty acid contents higher than these in the conventional method with acid hydrolysis and ether extraction but lower than others with chloroform and methanol extraction. Comparable results were obtained with the same procedure in fish oil capsules and fish fillets (105). Bohnert *et al*. (102) applied methanolic HCl and hexane at 100°C for an hour to infant formulae, producing results statistically comparable to those obtained by chloroform and methanol extraction and methanolic HCl catalysis. Sönnichsen and Müller (109) reported a low recovery (70–83%) by using two internal standards in fungal mycelia after heating at 100°C for an hour with hexane, although no comparison to an established method was included. In any case, these authors propose a correction factor to quantify the total fatty acid content.

Methanolic HCl has also been used *in situ* in methods employing milder heating conditions to selectively methylate plasma free fatty acids, this adaptation was made because they are esterified much faster than other lipids being transesterified. After heating at 25°C for 45 min, Lepage and Roy (110) reported results similar to those obtained with the conventional method, and no significant hydrolysis of standards of triacylgylcerols, cholesterol esters, and phospholipids was found. Welz *et al*. (101) (who also heated samples at 25°C for 45 min) confirmed the feasibility of a similar method in human plasma, rat liver microsomes, and encapsulated fish oil; and they found that trioleate, cholesterol esters, and lecithin were converted into FAME to a neglectible extent (less than 3%). In any case, the low margin of error allowed in these methods is an important shortcoming.

Catalysis with methanolic sulfuric acid is similar to that one previously described. This reagent has been widely used because of its long shelf life and easy and safe preparation, and some researchers consider it to be the most useful. Decomposition of polyunsaturated fatty acids may occur if the reagent is used carelessly or under certain conditions (6), as with acidic reagents (111).

Methanolic sulfuric acid was applied *in situ* by Dugan *et al*. (112) in biological materials with diethyl ether at a low temperature. The method was also successfully used in seed crops and flour (113), and 98% recovery was obtained in tripalmitin after heating for a rather long time (3 h at 95°C) (114). Harrington and D'Arcy-Evans (115) performed an *in situ* method to synthetize large amounts of FAME from sunflower seeds, resulting in a yield larger than that from a conventional method (hexane extraction). However, the length of time for both procedures was long (above 4 h at 100°C for the catalysis). Dahmer *et al.* (100) used a short reaction time (20 min at 90°C) and hexane as the nonpolar solvent, and obtained only 70% recovery from soybean seeds, probably owing to insufficient heating. Garcés and Mancha (80) also carried out a method with methanolic sulfuric acid

and several solvents in fresh plant tissues with different water and lipid contents, reporting results comparable to those obtained by using the Hara and Radin procedure (116).

Methanolic boron trifluoride (BF_3) is one of the most commonly used catalysts for FAME preparation because of its high esterifying power, although this does not necessarily mean that this reagent is the best (7). In fact, methanolic BF_3 is toxic, expensive, and relatively unstable in storage. It is prone to the formation of artifacts (117), and the use of old or too highly concentrated solutions may result in the loss of large amounts of polyunsaturated fatty acids (6). Furthermore, this reagent is quickly destroyed in the presence of water, and therefore must be applied to water-free samples (118). In fact, most *in situ* procedures involving BF_3 have been performed in samples devoid of large amounts of water, such as lipids from TLC plates or freeze-dried samples.

Initially, *in situ* derivatization by using methanolic BF_3 was reported successfully on microorganisms (70). Later, Ohta *et al*. (119) treated plasma lipids contained in silica gel scraped from TLC plates at 100°C for 30 min, reporting results that were quantitatively similar to those from a conventional method. Sattler *et al*. (118) demonstrated that their method (110°C for 90 min) provided recoveries higher than the conventional procedure [lipid extraction with Folch *et al.* (11) method and also methanolic BF_3] in the main lipoprotein classes. Later, Sattler *et al*. (120) successfully applied the method to lipoprotein and macrophage lipid subclasses scraped from TLC plates. House *et al*. (121) reported a high FAME yield in soy oil after heating it with benzene at 100°C for 45 min, but recoveries in foodstuffs were unsatisfactory owing to inconsistent results and distorted fatty acid profiles, probably due to the presence of water in the samples. Rule (106) showed, by heating at 80°C for 2 h without a nonpolar solvent, a similar effectiveness to that of a conventional method [extraction by Bligh and Dyer method (10) and FAME synthesis with BF_3] in adipose tissue and muscle, and a higher recovery in liver from lambs.

Methanolic aluminum chloride can be considered as an atypical acid catalyst: it provides pH values below 1, but shows no ability to derivatizate free fatty acids. Segura (122) investigated its *in situ* application (at 100°C for 60 min) in milk, several vegetable oils, and in the presence of silica gel. Although fatty acid values seem to be suitable, aluminum chloride has no advantage over the much faster basic catalysts.

Acid catalysis after alkali-catalyzed reaction. As was mentioned above, acid catalysis has significant advantages over basic catalysis. To overcome the large reaction time needed, the consecutive use of basic and acid reagents was proposed. Fatty acids from triacylglycerols are saponified or transesterified by fast reactions in basic media, and free fatty acids are later esterified in an acid medium, making use of its esterifying power, which is higher than transesterifying. The first process may consist of a hydrolysis (e.g., KOH in ethanol), but more often it is a transesterification (e.g., methanolic KOH, NaOH, or sodium methoxide). In the subsequent acid catalysis, sulfuric acid may be used, but BF_3 is usually preferred because of its higher esterifying power. The reduction of time in the combined procedure quickly gave these methods popularity. Moreover, they are especially useful for analyzing *N*-acyl lipids. Basic catalysis is unsuitable for it, and the rigorous conditions required for the FAME synthesis in acid medium led to the formation of artifacts from the long-chain bases. Therefore, when both the fatty acid and base components have to be analyzed, an aqueous alkaline hydrolysis before acid catalysis is preferred (6).

In situ procedures with methanolic BF_3 after an alkali-based catalysis have been reported by several researchers. Lambert and Moss (123) found that fatty acid from bacterial suspensions could be determinated by *in situ* derivatization. Divakaran and Ostrowski (124) applied methanolic sodium hydroxide to fish eggs for 10 min of refluxing prior to the methanolic BF_3 catalysis for 2–3 min, and no significant differences were reported for most individual fatty acid contents with respect to a conventional method [solvent extraction method (94) and the same catalysis]. Guillou *et al*. (125) applied the same method to brook charr tissues. Results in liver and skin were similar to those obtained with the AOAC (126) method, and in flesh samples the *in situ* procedure showed significantly higher fatty acid contents. Park and Goins (90) used a similar method (heating for 10 min at 90°C during the two steps) in several foodstuffs and obtained fatty acid profiles similar to those obtained by using a conventional procedure (no quantification was included).

Final considerations. In spite of the general assumption that lipid extraction is required to obtain usable results, numerous studies about *in situ* FAME preparation seem to contradict this. Owing to the great advantages of saving the extraction step prior to the FAME synthesis, *in situ* procedures mean a significant advance to the widespread application of fatty acid analysis. However, some considerations must be taken into account.

When the type of catalysis chosen is appropriate and conditions are favorable (water content suitable; the heating and the amount of sample and reagents adapted; the use of nonpolar solvents), no obstacle appears in theory to obtaining results which are qualitatively and quantitatively comparable to those from conventional methods. In fact, lipids do not undergo any further adverse conditions, and the lipid extraction can be even more exhaustive since samples are subjected to acid or basic treatments and extraction with mixtures of polar (methanol) and nonpolar solvents while heating is applied. Therefore, digestion, extraction, and derivatization are all included in one step; thus, the experimental error is potentially less. Nevertheless, in real conditions samples often include some amount of water or lipids that remain unreacted (e.g., owing to strong bonds with the matrix), and in some cases the pretreatment required to obtain reliable and accurate values can lead to awkward procedures. In any case, *in situ* methods seem to be a feasible and useful option in most samples, and advantages are especially significant for samples that are prone to forming emulsions during lipid extraction (the saving of time is significant) or for analyzing fatty acids when

only small sample sizes are available (e.g., lipids from plasma or from TLC). However, prior to their application, some knowledge of their shortcomings and how to avoid them is advisable. Research about the selected method and each type of sample may be conducted for the kind of reaction to be adapted. In addition, although *in situ* synthesis is usually carried out in the presence of an acidic reagent, the use of basic catalysis, which provides much faster reactions, should be attempted. Hence a good knowledge about sample characteristics and the shortcomings of each type of catalysis seems to be essential in order to achieve accurate and reliable results using brief analytical procedures.

ACKNOWLEDGMENTS

We thank to the Junta de Extremadura (Consejería de Educación y Juventud) and the Fondo Social Europeo for their support.

REFERENCES

1. Kinsella, J.E., Shimp, J.L., Mai, J., and Weihrauch, J. (1977) Fatty Acid Content and Composition of Freshwater Finfish, *J. Am. Oil Chem. Soc. 54*, 424–429.
2. Soberman, R. (1990) The Effects of Fish Oil on Connective Tissue Metabolism and Connective Tissue Disease, in *Omega-3 Fatty Acids in Health and Disease* (Lees, R.S., and Karel, M., eds.), pp. 87, Marcel Dekker, New York.
3. Schul, D., Tallmadge, D., Burress, D., Ewald, D., Berger, B., and Henry, D. (1998) Determination of Fat in Olestra-Containing Savory Snack Products by Capillary Gas Chromatography, *J. AOAC Int. 81*, 848–868.
4. Pendl, R., Bauer, M., Caviezel, R., and Schulthess, P. (1998) Determination of Total Fat in Foods and Feeds by the Caviezel Method, Based on a Gas Chromatographic Technique, *J. AOAC Int. 81*, 907–917.
5. *Federal Register 58,* 631–2964 (1993).
6. Christie, W.W. (1993) Preparation of Ester Derivatives of Fatty Acids for Chromatographic Analysis, in *Advances in Lipid Methodology–Two* (Christie, W.W., ed.), pp. 69–112, The Oily Press, Dundee.
7. Liu, K.-S. (1994) Preparation of Fatty Acid Methyl Esters for Gas Chromatographic Analysis of Lipids in Biological Materials, *J. Am. Oil Chem. Soc. 71*, 1179–1187.
8. Peuchant, E., Wolff, R., Salles, C., and Jensen, R. (1989) One-Step Extraction of Human Erythrocyte Lipids Allowing Rapid Determination of Fatty Acid Composition, *Anal. Biochem. 181*, 341–344.
9. Iverson, J.L., and Sheppard, A.J. (1977) Butyl Ester Preparation for Gas–Liquid Chromatographic Determination of Fatty Acids in Butter, *J. AOAC Int. 60*, 284–288.
10. Bligh, E.G., and Dyer, W.J. (1959) A Rapid Method of Total Lipid Extraction and Purification, *Can. J. Biochem. Physiol. 37*, 911–917.
11. Folch, J., Lees, M., and Sloane-Stanley, G.H. (1957) A Simple Method for the Isolation and Purification of Total Lipids from Animal Tissues, *J. Biol. Chem. 226*, 497–509.
12. Dobush, G.R., Ankney, D., and Krementz, D.G. (1985) The Effect of Apparatus, Extraction Time, and Solvent Type on Lipid Extractions of Snow Geese, *Can. J. Zool. 63*, 1917–1920.
13. Brooks, S.P.J., Ratnayake, W.M.N., Lampi, B.J., and Hollywood, R. (1998) Measuring Total Lipid Content in Rat Carcasses: A Comparison of Commonly Employed Extraction Methods, *J. Agr. Food Chem. 46*, 4214–4217.
14. Erickson, M.C. (1993) Lipid Extraction from Channel Catfish Muscle: Comparison of Solvent Systems, *J. Food Sci. 58*, 84–89.
15. Buldini, P.L., Cavalli, S., and Trifiro, A. (1997) State-of-the-Art Ion Chromatographic Determination of Inorganic Ions in Food, *J. Chromatogr. 789*, 529–548.
16. Huffer, J.W., Westcott, J.E., Miller, L.V., and Krebs, N.F. (1998) Microwave Method for Preparing Erythrocytes for Measurement of Zinc Concentration and Zinc Stable Isotope Enrichment, *Anal. Chem. 70*, 2218–2220.
17. Radlinger, G., and Heumann, K.G. (1998) Iodine Determination in Food Samples Using Inductively Coupled Plasma Isotope Dilution Mass Spectrometry, *Anal. Chem. 70*, 2221–2224.
18. Marcato, B., and Vianello, M. (2000) Microwave-Assisted Extraction by Fast Sample Preparation for the Systematic Analysis of Additives in Polyolefins by High-Performance Liquid Chromatography, *J. Chromatogr. 869*, 285–300.
19. Molins, C., Hogendoorn, E.A., Dijkman, E., Heusinkveld, H.A., and Baumann, R.A. (2000) Determination of Linuron and Related Compounds in Soil by Microwave-Assisted Solvent Extraction and Reversed-Phase Liquid Chromatography with UV Detection, *J. Chromatogr. 869*, 487–496.
20. Pedersen, S.N., and Lindholst, C. (1999) Quantification of the Xenoestrogens 4-*tert*-Octylphenol and Bisphenol A in Water and in Fish Tissue Based on Microwave Assisted Extraction, Solid-Phase Extraction and Liquid Chromatography–Mass Spectrometry, *J. Chromatogr. 864*, 17–24.
21. Pensado, L., Casais, C., Mejuto, C., and Cela, R. (2000) Optimization of the Extraction of Polycyclic Aromatic Hydrocarbons from Wood Samples by the Use of Microwave Energy, *J. Chromatogr. 869*, 505–513.
22. Pino, V., Ayala, J.H., Afonso, A.M., and Gonzalez, V. (2000) Determination of Polycyclic Aromatic Hydrocarbons in Marine Sediments by High-Performance Liquid Chromatography After Microwave-Assisted Extraction with Micellar Media, *J. Chromatogr. 869*, 515–522.
23. Paré, J.R.J., Matni, G., Bélanger, J.M.R., Li, K., Rule, C., and Thibert, B. (1997) Use of the Microwave-Assisted Process in Extraction of Fat from Meat, Dairy, and Egg Products Under Atmospheric Pressure Conditions, *J. AOAC Int. 80*, 928–933.
24. Ganzler, K., Salgo, A., and Valko, K. (1986) Microwave Extraction. A Novel Sample Preparation Method for Chromatography, *J. Chromatogr. 371*, 299–306.
25. Leray, C., Gric, T., Gutbier, G., and Bnouham, M. (1995) Microwave Oven Extraction Procedure for Lipid Analysis in Biological Samples, *Analusis 23*, 65–67.
26. De Pedro, E., Casillas, M., and Miranda, C.M. (1997) Microwave Oven Application in the Extraction of Fat from the Subcutaneous Tissue of Iberian Pig Ham, *Meat Sci. 45*, 45–51.
27. Carpenter, D.E., Ngeh-Ngwainbi, J., and Lee, S. (1993) Lipid Analysis, in *Methods for Analysis for Nutrition Labeling* (Sullivan, D.M., and Carpenter, D.E., eds.), pp. 85–104, AOAC International, Arlington.
28. Yoshida, H., Hiroka, N., and Kajimoto, G. (1990) Microwave Energy Effects on Quality of Some Seed Oils, *J. Food Sci. 55*, 1412–1416.
29. Hearn, T.L., Sgoutas, S.A., Sgoutas, D.S., and Hear, J.A. (1987) Stability of Polyunsaturated Fatty Acids After Microwave Cooking of Fish, *J. Food Sci. 52*, 1430–1431.
30. Yoshida, H., and Kajimoto, G. (1989) Effects of Microwave Energy on the Tocopherols of Soybean Seeds, *J. Food Sci. 54*, 1596–1600.
31. Taketomi, T., Hara, A., Uemura, K., Kurahashi, H., and Sugiyama, E. (1996) A Microwave-Mediated Saponification of Galactosylceramide and Galactosylceramide I3-Sulfate and Identification of Their Lyso-Compounds by Delayed Extrac-

tion Matrix-Assisted Laser Desorption Ionization Time-of-Flight Mass Spectrometry, *Biochem. Biophys. Res. Commun. 224*, 462–467.
32. Dayal, B., and Ertel, N.H. (1998) Rapid Hydrolysis of Bile Acid Conjugates Using Microwaves: Retention of Absolute Stereochemistry in the Hydrolysis of (25R) 3α,7α,12α-Trihydroxy-5β-cholestan-26-oyltaurine, *Lipids 33*, 333–338.
33. Banerjee, P., Dawson, G., and Dasgupta, A. (1992) Enrichment of Saturated Fatty Acid Containing Phospholipids in Sheep Brain Serotonin Receptor Preparations: Use of Microwave Irradiation for Rapid Transesterification of Phospholipids, *Biochim. Biophys. Acta 1110*, 65–74.
34. Rodriguez, I., Santamarina, M., Bollain, M.H., Mejuto, M.C., and Cela, R. (1997) Speciation of Organotin Compounds in Marine Biomaterials After Basic Leaching in a NonFocused Microwave Extractor Equipped with Pressurized Vessels, *J. Chromatogr. 774*, 379–387.
35. Randolph, T.W. (1990) Supercritical Fluid Extractions in Biotechnology, *Trends Biotechnol. 8*, 78–82.
36. Eller, F.J., and King, J.W. (1996) Determination of Fat Content in Foods by Analytical SFE, *Sem. Food Anal. 1*, 145–162.
37. De Filippi, R. (1982) Carbon Dioxide as a Solvent: Application to Fats, Oils and Other Materials, *Chem. Ind. 19*, 390–394.
38. Yamaguchi, K., Murakami, M., Nakano, H., Konosu, S., Kokura, T., Yamamoto, H., Kosaka, M., and Hata, K. (1986) Supercritical Carbon Dioxide Extraction of Oils from Antarctic Krill, *J. Agr. Food Chem. 34*, 904–907.
39. Cheung, P.C.K., Leung, A.Y.H., and Ang, P.O. (1998) Comparison of Supercritical Carbon Dioxide and Soxhlet Extraction of Lipids from a Brown Seaweed, *Sargassum hemiphyllum* (Turn.) C. Ag., *J. Agr. Food Chem. 46*, 4228–4232.
40. Merkle, J.A., and Larick, D.K. (1995) Fatty Acid Content of Supercritical Carbon Dioxide Extracted Fractions of Beef Fat, *J. Food Sci. 60*, 959–962.
41. List, G.R., Friedrich, J.P., and King, J.W. (1989) Supercritical CO_2 Extraction and Processing of Oilseeds, *Oil Mill Gaz. 95*, 28–34.
42. Cocero, M.J., and Calvo, L. (1996) Supercritical Fluid Extraction of Sunflower Seed Oil with CO_2–Ethanol mixtures, *J. Am. Oil Chem. Soc. 73*, 1573–1578.
43. Montarini, L., King, J.W., List, G.R., and Rennick, K.A. (1996) Selective Extraction of Phospholipid Mixtures by Supercritical Carbon Dioxide and Cosolvents, *J. Food Sci. 61*, 1230–1233.
44. Dionisi, F., Hug, B., Aeschlimann, J.M., and Houllemar, A. (1999) Supercritical CO_2 Extraction for Total Fat Analysis of Food Products, *J. Food Sci. 64*, 612–615.
45. Stahl, E., Quirin, K.W., and Gerard, D. (1988) *Dense Gases for Extraction and Refining*, Springer-Verlag, Berlin.
46. Dunford, N.T., and Temelli, F. (1997) Extraction Conditions and Moisture Content of Canola Flakes as Related to Lipid Composition of Supercritical CO_2 Extracts, *J. Food Sci. 62*, 155–159.
47. King, J.W., Johnson, H.J., and Friedrich, J.P. (1989) Extraction of Fat Tissue from Meat Products with Supercritical Carbon Dioxide, *J. Agr. Food Chem. 37*, 951–954.
48. Dunford, N.T., Temelli, F., and Leblanc, E. (1997) Supercritical CO_2 Extraction of Oil and Residual Proteins from Atlantic Mackerel (*Scomber scombrus*) as Affected by Moisture Content, *J. Food Sci. 62*, 289–294.
49. Snyder, M., Friedrich, J.P., and Christianson, D.D. (1984) Effect of Moisture and Particle Size on the Extractability of Oils from Seeds with Supercritical CO_2, *J. Am. Oil Chem. Soc. 61*, 1851–1856.
50. Christianson, D.D., Friedrich, J.P., List, G.R., Warner, K., Bagley, E.B., Stringfellow, A.C., and Inglett, G.E. (1984) Supercritical Fluid Extraction of Dry-Milled Corn Germ with Carbon Dioxide, *J. Food Sci. 49*, 229–232, 272.
51. Ikushima, Y., Saito, N., Hatakeda, K., Ito, S., Asano, T., and Goto, T. (1986) A Supercritical Carbon Dioxide Extraction from Mackarel (*Scomber japonicus*) Powder: Experiment and Modelling, *Bull. Chem. Soc. Jpn. 59*, 3709–3713.
52. Temelli, F., LeBlanc, E., and Fu, L. (1995) Supercritical CO_2 Extraction of Oil from Atlantic Mackerel (*Scomber scombrus*) and Evaluation of Protein Functionality, *J. Food Sci. 60*, 703–706.
53. Myer, L., Damian, J., Liescheski, P., and Tehrani, J. (1992) Étude Comparative d'Extractions par un Fluide à Phase Supercritique et par la Méthode de Soxhlet, *Spectra 2000 165*, 57–63.
54. Taylor, S.L., King, J.W., and List, G.R. (1993) Determination of Oil Content in Oilseeds by Analytical Supercritical Fluid Extraction, *J. Am. Oil Chem. Soc. 70*, 437–439.
55. Hopper, M.L., King, J.W., Johnson, J.H., Serino, A.A., and Butler, R.J. (1995) Multivessel Supercritical Fluid Extraction of Food Items in Total Diet Study, *J. AOAC Int. 78*, 1072–1079.
56. King, J.W., Eller, F.J., Snyder, J.M., Johnson, J.H., McKeith, F.K., and Stites, C.R. (1996) Extraction of Fat from Ground Beef for Nutrient Analysis Using Analytical Supercritical Fluid Extraction, *J. Agr. Food Chem. 44*, 2700–2704.
57. Berg, H., Magard, M., Johansson, G., and Mathiasson, L. (1997) Development of a Supercritical Fluid Extraction Method for Determination of Lipid Classes and Total Fat in Meats and Its Comparison with Conventional Methods, *J. Chromatogr. 785*, 345–352.
58. Maness, N.O., Chrz, D., Pierce, T., and Brusewitz, G.H. (1995) Quantitative Extraction of Pecan Oil from Small Samples with Supercritical Carbon Dioxide, *J. Am. Oil Chem. Soc. 72*, 665–669.
59. Melinz, R., Fister, S., and Pfannhauser, W. (1997) Determination of Fat Content in Food by Extraction with Supercritical Carbon Dioxide, *Ernaehrung 21*, 557–561.
60. Eller, F.J., and King, J.W. (1998) Supercritical CO_2 Extraction of Fat: Comparison of Gravimetric and GC-FAME Methods, *J. Agr. Food Chem. 46*, 3657–3661.
61. Zou, W., Lusk, C., Messer, D., and Lane, R. (1999) Fat Contents of Cereal Foods: Comparison of Classical with Recently Developed Extraction Techniques, *J. AOAC Int. 82*, 141–150.
62. AOAC (1997) *Official Methods and Recommended Practices,* 1996–1997 edn., Am 3-96, Association of Official Analytical Chemists, Arlington.
63. Gharaibeh, A.A., and Voorhees, K.J. (1996) Characterization of Lipid Fatty Acids in Whole-Cell Microorganisms Using *in situ* Supercritical Fluid Derivatization/Extraction and Gas chromatography/Mass Spectrometry, *Anal. Chem. 68*, 2805–2810.
64. Cummins, M.T., and Wells, R.J. (1997) *In Situ* Derivatisation and Extraction of Volatile Fatty Acids Entrapped on Anion-Exchange Resin from Aqueous Solutions and Urine as a Test Matrix Using Pentafluorobenzyl Bromide in Supercritical Carbon Dioxide, *J. Chromatogr. Biomed. Sci. Appl. 694*, 11–19.
65. McDaniel, L.H., and Taylor, L.T. (1999) Esterification of Decanoic Acid During Supercritical Fluid Extraction Employing Either Methanol-Modified Carbon Dioxide or a Methanol Trap, *J. Chromatogr. 858*, 201–207.
66, Snyder, J.M., King, J.W., and Jackson, M.A. (1997) Analytical Supercritical Fluid Extraction with Lipase Catalysis: Conversion of Different Lipids to Methyl Esters and Effect of Moisture, *J. Am. Oil Chem. Soc. 74*, 585–588.
67. Taylor, S.L., Eller, F.J., and King, J.W. (1997) A Comparison of Oil and Fat Content in Oilseeds and Ground Beef Using Su-

percritical Fluid Extraction and Related Analytical Techniques, *Food Res. Int. 30*, 365–370.
68. Hardardottir, I., and Kinsella, J.E. (1988) Extraction of Lipid and Cholesterol from Fish Muscle with Supercritical Fluids, *J. Food Sci. 53*, 1656–1658.
69. Chao, R.R., Mulvaney, S.J., Bailey, M.E., and Fernando, L.N. (1991) Supercritical CO_2 Conditions Affecting Extraction of Lipid and Cholesterol from Ground Beef, *J. Food Sci. 56*, 183–187.
70. Abel, K., de Schmertzing, H., and Peterson, J.I. (1963) Classification of Microorganisms by Analysis of Chemical Composition. Feasibility of Utilizing Gas Chromatography, *J. Bacteriol. 85*, 1039–1044.
71. Suter, B., Grob, K., and Pacciarelli, B. (1997) Determination of Fat Content and Fatty Acid Composition Though 1-min Transesterification in the Food Sample: Principles, *Z. Lebensm. Unters. Forsch. A 204*, 252–258.
72. Suter, B., Grob, K., Pacciarelli, B., and Novosalac, A. (1997) Determination of Fat Content and Fatty Acid Composition Through 1-min Transesterification in the Food Sample. II. Solubilization of the Fat, Results, *Mitt. Geb. Lebensmittelunters. Hyg. 88*, 259–276.
73. Long, A.R., Massie, S.J., and Tyznik, W.J. (1988) Rapid Direct Extraction Derivatization Method for the Determination of Acylglycerol Lipids in Selected Samples Matrices, *J. Food Sci. 53*, 940–942, 959.
74. Lepage, G., and Roy, C.C. (1986) Direct Transesterification of All Classes of Lipids in a One-Step Reaction, *J. Lipid Res. 27*, 114–120.
75. Sukhija, P.S., and Palmquist, D.L. (1988) Rapid Method for Determination of Total Fatty Acid Content and Composition of Feedstuffs and Feces, *J. Agr. Food Chem. 36*, 1202–1206.
76. Browse, J., McCourt, P.J., and Somerville, C.R. (1986) Fatty Acid Composition of Leaf Lipids Determined After Combined Digestion and Fatty Acid Methyl Ester Formation from Fresh Tissue, *Anal. Biochem. 152*, 141–145.
77. Ulberth, F., and Henninger, M. (1992) One-Step Extraction/Methylation Method for Determining the Fatty Acid Composition of Processed Foods, *J. Am. Oil Chem. Soc. 69*, 174–177.
78. Williams, K.C., Barlow, C.G., Brock, I., and Rodgers, L.J. (1995) Use of Autoclaving in the Preparation of Homogenates for Determining the Proximate Chemical and Fatty Acid Composition of Fish, *J. Sci. Food Agr. 69*, 451–456.
79. Tserng, K.Y., Kliegman, R.M., Miettinen, E.L., and Kalhan, S.C. (1981) A Rapid, Simple, and Sensitive Procedure for the Determination of Free Fatty Acids in Plasma Using Glass Capillary Column Gas–Liquid Chromatography, *J. Lipid Res. 22*, 852–858.
80. Garcés, R., and Mancha, M. (1993) One-Step Lipid Extraction and Fatty Acid Methyl Esters Preparation from Fresh Plant Tissues, *Anal. Biochem. 211*, 139–143.
81. Kramer, J.K.G., and Hulan, H.W. (1976) Artifacts Produced During Acid-Catalyzed Methanolysis of Esterol Esters, *J. Lipid Res. 17*, 674–676.
82. Shimasaki, H., Phillips, F.C., and Privett, O.S. (1977) Direct Transesterification of Lipids in Mammalian Tissue for Fatty Acid Analysis *Via* Dehydratation with 2,2′-Dimethoxypropane, *J. Lipid Res. 18*, 540–543.
83. Pace-Asciak, C.R. (1989) One-Step Rapid Extractive Methylation of Plasma Nonesterified Fatty Acids for Gas Chromatographic Analysis, *J. Lipid Res. 30*, 451–454.
84. Ayorinde, F.O., Clifton, J., Jr., Afolabi, O.A., and Sheppard, R.L. (1988) Rapid Transesterification and Mass Spectrometric Approach to Seed Oil Analysis, *J. Am. Oil Chem. Soc. 65*, 942–948.
85. Schuchardt, U., and Lopes, O.C. (1988) Tetramethylguanidine Catalyzed Transesterification of Fats and Oils: A New Method for Rapid Determination of Their Composition, *J. Am. Oil Chem. Soc. 65*, 1940–1941.
86. Ichihara, K., Shibahara, A., Yamamoto, K., and Nakayama, T. (1996) An Improved Method for Rapid Analysis of the Fatty Acids of Glycerolipids, *Lipids 31*, 535–539.
87. Marx, F., and Stender, A. (1997) Rapid Micro Methods for the GLC Determination of Fat Content and Fatty Acid Composition in Seeds Rich in Lipids, *Fett / Lipid 99*, 25–28.
88. Christopherson, S.W., and Glass, R.L. (1969) Preparation of Milk Fat Methyl Esters by Alcoholysis in an Essentially Non Alcoholic Solution, *J. Dairy Sci. 52*, 1289–1293.
89. Glass, R.G. (1971) Alcoholysis, Saponification and the Separation of Fatty Acids Methyl Esters, *Lipids 6*, 919–922.
90. Park, P.W., and Goins, R.E. (1994) *In Situ* Preparation of Fatty Acid Methyl Esters for Analysis of Fatty Acid Composition in Foods, *J. Food Sci. 59*, 1262–1266.
91. MacGee, J., and Williams, M.G. (1981) Preparation of Sphingolipid Fatty Acid Methyl Esters for Determination by Gas–Liquid Chromatography, *J. Chromatogr. 205*, 281–288.
92. Bannon, C.D., Brenn, G.J., Craske, J.D., Hai, N.T., Harper, N.L., and O'Rouke, K.L. (1982) Analysis of Fatty Acid Methyl Esters with High Accuracy and Reliability. III. Literature Review of and Investigations into the Development of Rapid Procedures for the Methoxide-Catalysed Methanolysis of Fats and Oils, *J. Chromatogr. 247*, 71–89.
93. Hougen, F.W., and Bodo, V. (1973) Extraction and Methanolysis of Oil from Whole or Crushed Rapeseed for Fatty Acid Analysis, *J. Am. Oil Chem. Soc. 50*, 230–234.
94. AOAC (1984) *Official Methods of Analysis,* 17th edn. (Williams, S., ed.), Association of Official Analytical Chemists, Washington, DC.
95. Cantellops, D., Reid, A.P., Eitenmiller, R.R., and Long, A.R. (1999) Determination of Lipids in Infant Formula Powder by Direct Extraction Methylation of Lipids and Fatty Acid Methyl Esters (FAME) Analysis by Gas Chromatography, *J. AOAC Int. 82*, 1128–1139.
96. Association of Official Analytical Chemists (1995) *Official Methods of Analysis,* 16th edn., Method 996.01, AOAC International, Gaitherburg, MD.
97. Fourie, P.C., and Basson, D.S. (1990) Application of a Rapid Transesterification Method for Identification of Individual Fatty Acids by Gas Chromatography on Three Different Nut Oils, *J. Am. Oil Chem. Soc. 67*, 18–20.
98. Eller, F.J. (1999) Interference by Methyl Levulinate in Determination of Total Fat in Low-Fat, High-Sugar Products by Gas Chromatographic Fatty Acid Methyl Ester (GC-FAME) Analysis, *J. AOAC Int. 82*, 766–769.
99. Conway, E.S., and Adams, M. (1975) Fats and Oils. Determination of Fat in Body Tissues and in Food Mixtures, *J. AOAC Int. 58*, 23–27.
100. Dahmer, M.L., Fleming, P.D., Collins, G.B., and Hildebrand, D.F. (1989) A Rapid Screening Technique for Determining the Lipid Composition of Soybean Seeds, *J. Am. Oil Chem. Soc. 66*, 543–547.
101. Welz, W., Sattler, W., Leis, H., and Malle, E. (1990) Rapid Analysis of Non-Esterified Fatty Acids as Methyl Esters from Different Biological Specimens by Gas Chromatography After One-Step Esterification, *J. Chromatogr. 526*, 319–329.
102. Bohnert, B., Braun, M., Winter, H., and Flück, B. (1997) Direct Esterification Method for Analysis of Long-Chain Polyunsaturated Fatty Acids (LC-PUFAs) in Infant Formulae, *Z. Lebensm. Unters Forsch. A 204*, 27–31.
103. Outen, G.E., Beever, D.E., and Fenlon, J.S. (1976) Direct Methylation of Long-Chain Fatty Acids in Feeds, Digesta and Feces Without Prior Extraction, *J. Sci. Food Agr. 27*, 419–425.
104. Lepage, G., and Roy, C.C. (1984) Improved Recovery of Fatty

Acid Through Direct Transesterification Without Prior Extraction or Purification, *J. Lipid Res. 25*, 1391–1396.
105. Ulberth, F., and Henninger, M. (1995) Determination of the Fatty Acid Profile of Fish by a One-Step Extraction/Methylation Method, *Fat Sci. Technol. 97*, 77–80.
106. Rule, D.C. (1997) Direct Transesterification of Total Fatty Acids of Adipose Tissue, and of Freeze-dried Muscle and Liver with Boron-trifluoride in Methanol, *Meat Sci. 46*, 23–32.
107. Patton, J.S. (1981) Gastrointestinal Lipid Digestion, in *Physiology of the Gastrointestinal Tract (*Johnson, L.R., ed.), pp. 1123–1146, Raven Press, New York.
108. Lepage, G., Levy, E., Ronco, N., Smith, L., Galeano, N., and Roy, C.C. (1989) Direct Transesterification of Plasma Fatty Acids for the Diagnosis of Essential Fatty Acid Deficiency in Cystic Fibrosis, *J. Lipid Res. 30*, 1483–1490.
109. Sönnichsen, M., and Müller, B.W. (1999) A Rapid and Quantitative Method for Total Fatty Acid Analysis of Fungi and Other Biological Samples, *Lipids 34*, 1347–1349.
110. Lepage, G., and Roy, C.C. (1988) Specific Methylation of Plasma Nonesterified Fatty Acids in a One-Step Reaction, *J. Lipid Res. 29*, 227–230.
111. Morrison, W.R., and Smith, L.M. (1964) Preparation of Fatty Acid Methyl Esters and Dimethylacetals from Lipids with Boron Fluoride-Methanol, *J. Lipid Res. 5*, 600–608.
112. Dugan, L.R., McGinnins, G.W., and Vahedra, D.V. (1966) Low Temperature Direct Methylation of Lipids in Biological Materials, *Lipids 1*, 305–311.
113. Welch, R.W. (1975) A Micro-Method for the Estimation of Oil Content and Composition in Seed Crops, *J. Sci. Food Agr. 28*, 635–639.
114. Welsh, R.W. (1975) Fatty Acids Composition of Grain from Winter and Spring Sown Oats, Barley and Wheat, *J. Sci. Food Agr. 26*, 429–432.
115. Harrington, K.J., and D'Arcy-Evans, C. (1985) A Comparison of Conventional and *in Situ* Methods of Transesterification of Seed Oil from a Series of Sunflower Cultivars, *J. Am. Oil Chem. Soc. 62*, 1009–1013.
116. Hara, A., and Radin, N.S. (1978) Lipid Extraction of Tissues with a Low-Toxicity Solvent, *Anal. Biochem. 90*, 420–426.
117. Dawidowicz, E.A., and Thompson, T.E. (1971) Artifacts Produced by Boron Trifluoride Methanolysis of a Synthetic Lecithin Containing Cyclopropane Fatty Acids (1-2-dihydrosterculoyl-3-*sn*-phosphatidylcholine), *J. Lipid Res. 12*, 636–637.
118. Sattler, W., Puhl, H., Hayn, M., Kostner, G., and Esterbauer, H. (1991) Determination of Fatty Acids in the Main Lipoprotein Classes by Capillary Gas Chromatography: BF_3/Methanol Transesterification of Lyophilized Samples Instead of Folch Extraction Gives Higher Yields, *Anal. Biochem. 198*, 184–190.
119. Ohta, A., Mayo, M.C., Kramer, N., and Lands, W.E.M. (1990) Rapid Analysis of Fatty Acids in Plasma Lipids, *Lipids 25*, 742–747.
120. Sattler, W., Reicher, H., Ramos, P., Panzenboeck, U., Hayn, M., Esterbauer, H., Malle, E., and Kostner, G.M. (1996) Preparation of Fatty Acid Methyl Esters from Lipoprotein and Macrophage Lipid Subclasses on Thin-Layer Plates, *Lipids 31*, 1302–1310.
121. House, S.D., Larson, P.A., Johnson, R.R., De Vries, J.W., and Martin, D.L. (1994) Gas Chromatographic Determination of Total Fat Extracted from Food Samples Using Hydrolysis in the Presence of Antioxidant, *J. AOAC Int. 77*, 960–965.
122. Segura, R. (1988) Preparation of Fatty Acid Methyl Esters by Direct Transesterification of Lipids with Aluminium Chloride–Methanol, *J. Chromatogr. 441*, 99–113.
123. Lambert, M.A., and Moss, C.W. (1983) Comparison of the Effects of Acid and Base Hydrolysis on Hydroxyl and Cyclopropane Fatty Acids in Bacteria, *J. Clin. Microbiol. 18*, 1370–1377.
124. Divakaran, S., and Ostrowski, A.C. (1989) Fatty Acid Analysis of Fish Eggs Without Solvent Extraction, *Aquaculture 80*, 371–375.
125. Guillou, A., Sourcy, P., and Khalil, M. (1996) Preparation of Fatty Acid Methyl Esters from Brook Charr Tissues: Comparison of a Classical and Direct Method, *Fett/Lipid 98*, 18–21.
126. AOAC (1990) *Official Methods of Analysis of the Association of Official Analytical Chemists,* 15th edn. (Helrich, K., ed.), Method 969.33, Association of Official Analytical Chemists, Arlington.

[Received February 17, 2000, and in final revised form June 30, 2000; revision accepted October 10, 2000]

Polyunsaturated Fatty Acids in Plasma Lipids of Obese Children With and Without Metabolic Cardiovascular Syndrome

Tamás Decsi*, Györgyi Csábi, Katalin Török, Éva Erhardt, Hajnalka Minda, István Burus, Szilárd Molnár, and Dénes Molnár

Department of Paediatrics, University of Pécs, Pécs, H-7623 Hungary

ABSTRACT: Previously we reported significantly higher values of γ-linolenic acid (GLA, 18:3n-6), dihomo-γ-linolenic acid (DHGLA, 20:3n-6), and arachidonic acid (20:4n-6) in plasma lipid classes in obese children than in nonobese controls. In the present study, fatty acid composition of plasma phospholipids (PL) and sterol esters (STE) was determined by high-resolution capillary gas–liquid chromatography in obese children with and without metabolic cardiovascular syndrome [MCS: defined as simultaneous presence of (i) dyslipidemia, (ii) hyperinsulinemia, (iii) hypertension, and (iv) impaired glucose tolerance] and in nonobese controls. Fatty acid composition of PL and STE lipids did not differ between obese children without MCS and controls. Obese children with MCS exhibited significantly lower linoleic acid (LA, 18:2n-6) values in PL (17.43 [2.36], % wt/wt, median [range from the first to the third quartile]) than obese children without MCS (19.14 [3.49]) and controls (20.28 [3.80]). In contrast, PL GLA values were significantly higher in obese children with (0.13 [0.08]) than in those without MCS (0.08 [0.04]), whereas STE GLA values were higher in obese children with MCS (1.04 [0.72]) than in controls (0.62 [0.48]). DHGLA values in PL were significantly higher in obese children with MCS (4.06 [0.74]) than in controls (2.69 [1.60]). The GLA/LA ratio was significantly higher, whereas the AA/DHGLA ratio was significantly lower in obese children with MCS than in obese children without MCS and in controls. In this study, LA metabolism was affected only in obese children with but not in those without MCS. In obese children with MCS, Δ6-desaturase activity appeared to be stimulated, whereas Δ5-desaturase activity appeared to be inhibited. Disturbances in LA metabolism may represent an additional health hazard within the multifaceted clinical picture of MCS.

Paper no. L8486 in *Lipids 35,* 1179–1184 (November 2000).

Prevalence of childhood obesity is high and still increasing in many affluent countries. In children and adolescents investigated from 1988 to 1991 in the United States, the prevalence of overweight based on body mass index was 11% according to the 95th and 22% according to the 85th percentile cutoff points (1). In Hungary, the prevalence of childhood obesity defined as body mass index exceeding the 90th percentile is around 13% (2). The long-term morbidity and mortality associated with childhood obesity are closely connected to the cardiovascular and metabolic status detectable in the pediatric age group (3). Therefore, identification of cardiovascular risk factors in obese children is of practical importance.

Previously we found significantly higher percentage contributions of the n-6 long-chain polyunsaturated fatty acids (LCPUFA), γ-linolenic acid (GLA, 18:3n-6), dihomo-γ-linolenic acid (DHGLA, 20:3n-6), and arachidonic acid (AA, 20:4n-6) to the fatty acid composition of plasma lipid classes in obese children than in nonobese controls (4). Since LCPUFA are prone to lipid peroxidation, their enhanced availability in circulating lipids may represent a further risk factor of atherogenesis in obese children. Moreover, nonphysiological LCPUFA content of membrane lipids may also influence receptor functions and signal transduction.

However, data on LCPUFA status in obese subjects are controversial. A significantly lower percentage contribution of AA to plasma phospholipids (PL) was reported in obese than in nonobese adults in one study (5), whereas in another study significantly higher AA values in plasma sterol esters (STE) were found in obese adults than in controls (6). The clear controversy between data obtained in apparently similar studies comparing fatty acids in obese vs. nonobese subjects might be explained by interindividual differences in LCPUFA status in obesity.

Accumulating evidence suggests that a clustering of risk factors such as abdominal adiposity, hyperinsulinemia, impaired glucose tolerance, dyslipidemia and high blood pressure is characteristic of a group of obese individuals who have an especially high risk for cardiovascular morbidity (for recent reviews see Refs. 7,8). The clustering of risk factors is already detectable in the pediatric age group (9,10). In a recent epidemiological survey, we found 9% prevalence of the metabolic cardiovascular syndrome (MCS)—defined as simultaneous presence of (i) dyslipidemia, (ii) hyperinsulinemia, (iii) hypertension, and (iv) impaired glucose tolerance—in obese children referred to medical attention (11). Here we report fatty acid composition of plasma PL and STE lipids in obese children with and without MCS and in nonobese controls.

*To whom correspondence should be addressed at Department of Paediatrics, University of Pécs, József A. u. 7., H-7623 Pécs, Hungary.
E-mail: decsi@apacs.pote.hu

Abbreviations: AA, arachidonic acid; DHGLA, dihomo-γ-linolenic acid; EFA, essential fatty acid; GLA, γ-linolenic acid; LA, linoleic acid; LCPUFA, long-chain polyunsaturated fatty acid; MCS, metabolic cardiovascular syndrome; PL, phospholipid; PUFA, polyunsaturated fatty acid; STE, sterol ester.

SUBJECTS AND METHODS

The investigations were carried out with obese children referred to the Outpatient Clinic for Obesity of the Department of Paediatrics, University of Pécs (Pécs, Hungary), because of their overweight. The children were free of other known illnesses, were not dieting, and were not participating in physical training programs. The cohort of control children was recruited from children referred to the general outpatient clinic of our department for routine investigations. The study was carried out in accordance with the Declaration of Helsinki II and with approval of the ethics committee of the University of Pécs. Informed parental consent was obtained for each child before enrollment in the study.

Anthropometric measurements were carried out by the same investigator. Body weight was determined to the nearest 0.5 kg with the child dressed only in underwear and wearing no shoes. Height was measured to the nearest 0.1 cm by a Holtain stadiometer (Holtain Limited, Crymich, Dyfed, Britain). The waist and hip circumferences were measured with the subject in the supine position. Body fat was estimated according to Parizková and Roth (12) from five skinfold thicknesses measured on the left side of the body three consecutive times with the help of a Holtain caliper. Lean body mass was calculated by subtracting body fat from actual body weight. Relative body weight was calculated as the ratio between actual body weight and the ideal body weight for age, gender, and height (13). The pubertal stage of the children was determined according to Tanner (14).

Blood pressure was measured according to published recommendations (15) at least five times in each subject on five separate days by the same observer, using a mercury-gravity manometer with proper cuff size in standard conditions. If the average of the five blood pressure values was above the 95th percentile for age and sex, 24-h ambulatory blood pressure monitoring was carried out. Those children whose mean arterial blood pressure values exceeded the 95th percentile value for height and sex (16) were considered to be hypertensive.

Blood samples were taken from the antecubital vein in the fasting state early in the morning. Blood was collected into tubes containing 2 mg/mL EDTA for triglyceride, cholesterol, high-density lipoprotein cholesterol, plasma glucose, and insulin determinations, and into another tube for fatty acid analysis. The samples were centrifuged immediately at 4°C and plasma was stored at –20°C until analysis. Plasma samples were thawed only once.

Plasma glucose concentrations were determined by the glucose oxidase method (17). Plasma insulin concentrations were measured with commercially available radioimmunoassay kits (Isotope Institute of the Hungarian Academy of Sciences, Budapest, Hungary). With this method, the cutoff value for insulin was 18.7 μU/mL (95th percentile value of 100 healthy children). The oral glucose tolerance test consisted of oral administration of glucose (1.75 g/kg body weight, maximum 75 g) followed by plasma glucose and insulin determinations at 30, 60, 90, 120, and 180 min. The test results were evaluated according to published criteria (18,19). Ethical considerations did not allow us to carry out oral glucose tolerance tests in the control subjects.

Triglyceride and cholesterol were determined with an enzymatic kit (Boehringer Mannheim, Mannheim, Germany). High-density lipoprotein cholesterol was measured by the precipitation method of Steele *et al.* (20). Plasma cholesterol, high-density lipoprotein cholesterol, and triglyceride were considered high or low when they fell above or below the recommended value of the Hungarian Lipid Consensus Conference (21): cholesterol 5.2 mmol/L, high-density lipoprotein cholesterol 0.9 mmol/L, and triglyceride 1.5 mmol/L.

Altogether, 180 obese and 239 nonobese children participated in the epidemiological survey investigating the prevalence of MCS (11). We considered children as obese if their body weights exceeded the normal weight for height by more than 20%, and if body fat content was higher than 25% in males and 30% in females. Finally, MCS was diagnosed in 16 of the obese and none of the nonobese children. To the 16 obese children with MCS, 16 obese children who fulfilled none or only one of the four aforementioned criteria of MCS and 16 nonobese control children were assigned by computer-generated simple randomization. This sample size allowed the detection of differences of one standard deviation with an 80% chance at a 5% significance level. Owing to technical reasons, a plasma sample for fatty acid analysis was not available for one obese child with MCS; therefore, one further obese child without MCS was entered into the study.

For fatty acid analysis, plasma lipids were extracted from 0.25 mL plasma with chloroform/methanol (22) after addition of internal standards (phosphatidyl- and cholesteryl pentadecanoic acid, 15:0). Lipid classes were separated on silica gel plates (Nr. 5721; E. Merck, Darmstadt, Germany) with one 18-cm run of hexane/diethlyether/chloroform/acetic acid (105:30:15:15, by vol). Fatty acids in plasma PL and STE were transesterified with methanol and hydrochloric acid (23). Fatty acid methyl esters were determined by high-resolution capillary gas–liquid chromatography using a Finnigan 9001 chromatograph (Finnigan/Tremetrics Inc., Austin, TX) with split injection (ratio: 1 to 15) and a flame-ionization detector. A cyanopropyl column of 40 m length (DB-23, J&W Scientific, Folsom, CA) was used. The temperature program was the following: initial temperature 100°C for 0.1 min, temperature increase by 40°C min^{-1} up to 180°C, 1-min isotherm period, temperature increase by 2°C min^{-1} up to 200°C, 1-min isotherm period, temperature increase by 10°C min^{-1} up to 240°C, 9.9-min isotherm period. The constant linear velocity was 0.3 m s^{-1} (referred to 100°C). Identification of fatty acids was secured by comparison with authentic standards (Nu-Chek-Prep, Elysian, MN).

Results were evaluated with SPSS for Windows, Release 7.5 (SPSS Inc., Chicago, IL). All data except fatty acids have been presented as mean ± SD and were evaluated by analysis of variance followed by the least significant difference comparison test to compare mean values of subgroups. The fatty acid data are presented as median and range from the first to

the third quartile values, because skewed distributions were found especially in fatty acids present at lower concentrations. Fatty acids were analyzed by the Kruskal-Wallis nonparametric analysis of variance followed by Mann-Whitney's two-sided rank test to compare median values of subgroups. Differences were regarded as statistically significant at $P < 0.05$.

RESULTS

Neither obese children without MCS nor controls were absolutely free from cardiovascular risk factors: dyslipidemia, hyperinsulinemia, and impaired glucose tolerance were seen in one, one, and two obese children without MCS, respectively, whereas one control child exhibited dyslipidemia. The subjects' characteristics are shown in Table 1. Sex did not differ among the three groups. The children investigated were in puberty, median Tanner stages for pubic hair/genitalia development were between 3 and 5 in the six subgroups formed on the basis of gender and study stratification. Age did not differ between obese children with and without MCS, whereas control subjects were significantly older than obese children. Body weight, body mass index, and waist/hip ratio were significantly higher in both groups of obese children than in controls, and they were significantly higher in obese children with than in those without MCS. Relative body weight and body fat were significantly higher in both groups of obese children than in controls. Lean body mass was significantly higher in obese children with MCS than in obese children without MCS and in controls. Height was significantly lower in obese children without MCS than in controls. Both systolic and diastolic blood pressures were significantly higher in obese children with MCS than in obese children without MCS and in controls. Plasma triglyceride, cholesterol, and insulin concentrations were significantly higher in obese children with MCS than in obese children without MCS and in controls. Plasma high-density lipoprotein cholesterol and glucose concentrations did not differ among the three groups.

TABLE 1
Characteristics of the Subjects[a]

	Obese, MCS (n = 15)	Obese, no MCS (n = 17)	Control (n = 16)
Sex (male:female)	11:4	11:6	10:6
Age (yr)	13.4 ± 2.1[f]	14.4 ± 2.4[b]	16.2 ± 1.0[b,f]
Weight (kg)	95.5 ± 15.2[d,f]	78.3 ± 17.4[d,e]	60.6 ± 9.2[e,f]
RBW (%)	177 ± 23[f]	163 ± 42[g]	103 ± 10[f,g]
BMI (kg/m^2)	34.2 ± 3.1[b,f]	30.4 ± 6.2[b,g]	20.7 ± 1.9[f,g]
BF (%)	37.8 ± 2.2[f]	36.3 ± 5.9[g]	25.6 ± 5.7[f,g]
LBM (kg)	58.9 ±11.0[b,d]	49.5 ± 9.9[b]	45.8 ± 8.4[d]
Waist/hip ratio	0.88 ± 0.07[b,f]	0.84 ± 0.05[b,d]	0.77 ± 0.06[d,f]
Height (cm)	167 ± 12	161 ± 12[b]	171 ± 9[b]
Systolic BP (mm Hg)	135 ± 6[f,g]	116 ± 9[f]	115 ± 7[g]
Diastolic BP (mm Hg)	83 ± 5[f,g]	69 ± 8[f]	69 ± 8[g]
Triglyceride[b] (mmol/L)	1.67 ± 0.54[d,f]	1.03 ± 0.29[f]	1.06 ± 0.40[d]
Cholesterol[b] (mmol/L)	4.71 ± 0.97[b,c]	4.09 ± 0.65[b]	3.77 ± 0.94[c]
HDL-cholesterol[b] (mmol/L)	1.39 ± 0.19	1.32 ± 0.24	1.33 ± 0.26
Glucose (mmol/L)	4.81 ± 0.64	4.51 ± 0.87	4.49 ± 0.75
IRI (μU/mL)	30.5 ± 14.4[f,g]	10.6 ± 4.3[f]	8.9 ± 4.5[g]

[a]Values are mean ± SD. Means in a row sharing a common roman superscript (b–g) are significantly different ([b,c]$P < 0.05$, [d,e]$P < 0.01$, [f,g]$P < 0.001$) using analysis of variance followed by Student's unpaired t test; MCS, metabolic cardiovascular syndrome; RBW, relative body weight; BMI, body mass index; BF, body fat content; LBM, lean body mass; BP, blood pressure; HDL-cholesterol, high-density lipoprotein cholesterol; IRI, fasting immunoreactive insulin.
[b]Cutoff points of cholesterol, HDL-cholesterol, and triglyceride in children were set by the Hungarian Lipid Consensus Conference (21) as 5.2, 0.9, and 1.5 mmol/L, respectively.

The fatty acid composition of plasma PL and STE lipids is shown in Table 2. Values of total saturated fatty acids in PL were significantly higher in obese children with MCS than in obese children without MCS and in controls. Percentage contributions of palmitoleic acid (16:1n-7) to both PL and STE lipids were significantly higher in obese children with MCS than in obese children without MCS and in controls. In contrast, values of vaccenic acid (18:1n-7) in the PL fraction were significantly lower in obese children with MCS than in obese children without MCS and in controls. Total monounsaturated fatty acid values did not differ among the three groups.

Percentage contribution of linoleic acid (LA, 18:2n-6) to PL was significantly lower in obese children with MCS than in obese children without MCS and in controls. In contrast, PL GLA values were significantly higher in obese children with than in those without MCS, and STE GLA values were significantly higher in obese children with MCS than in controls. Contribution of DHGLA to PL was significantly higher in obese children with MCS than in controls. Neither AA nor α-linolenic acid (18:3n-3) and docosahexaenoic acid (22:6n-3) values differed among the three groups. There were no differences in the values of the intermediary metabolites [eicosatrienoic acid (20:3n-3), eicosapentaenoic acid (20:5n-3), docosapentaenoic acid (22:5n-3)] of docosahexaenoic acid synthesis (data not shown).

Product/substrate ratios for n-6 LCPUFA biosynthesis are compared among the three groups in Table 3. The ratios of GLA to LA as well as the ratio of GLA plus DHGLA to LA were higher in PL in obese children with than in those without MCS, and were higher in STE in obese children with MCS than in obese children without MCS and in controls. In contrast, the ratio of AA to DHGLA was significantly lower in both PL and STE in obese children with MCS than in obese children without MCS and in controls. The ratio of AA to LA, i.e., the ratio reflecting the activity of the whole pathway of AA synthesis, did not differ among the three groups.

DISCUSSION

In the present study, fatty acid composition of plasma PL and STE lipids was investigated in obese children with and without MCS and in nonobese controls. We defined MCS as simultaneous presence of four well-established cardiovascular risk factors (dyslipidemia, hyperinsulinemia, impaired glucose tolerance, and hypertension). The clustering of these risk factors is strongly related to morbidity and mortality (7,8), and obese children with MCS represent about 1% of the

TABLE 2
Major Fatty Acids of Plasma Phospholipids and Sterol Esters in Obese Children With and Without MCS and in Controls[a]

	Phospholipids			Sterol esters		
Fatty acid	Obese, MCS	Obese, no MCS	Control	Obese, MCS	Obese, no MCS	Control
Saturated fatty acids						
16:0	27.64 (3.08)	26.31 (2.05)	27.34 (1.58)	12.95 (2.73)	11.26 (2.11)	11.37 (1.57)
18:0	16.15 (2.28)	14.88 (1.62)	15.26 (3.10)	1.61 (1.94)	1.61 (0.19)	1.47 (0.85)
Total	47.24 (5.91)[b,d]	45.69 (3.11)[b]	44.35 (3.03)[d]	16.26 (5.82)	14.20 (3.47)	14.22 (2.44)
Monounsaturated fatty acids						
16:1n-7	0.63 (0.36)[d,e]	0.44 (0.15)[d]	0.37 (0.13)[e]	3.77 (1.33)[d,f]	2.15 (0.73)[d]	1.69 (0.66)[f]
18:1n-9	9.35 (2.91)	7.53 (1.36)	8.27 (1.45)	17.47 (5.92)	15.59 (5.40)	15.63 (3.62)
18:1n-7	1.13 (0.23)[b,d]	1.26 (0.35)[b]	1.45 (0.26)[d]	1.06 (0.21)	1.22 (0.30)	1.18 (0.36)
Total	13.91 (3.59)	12.48 (2.44)	12.71 (1.73)	23.45 (5.48)	19.67 (6.37)	19.64 (4.58)
n-6 Polyunsaturated fatty acids						
18:2n-6	17.43 (2.36)[b,c]	19.14 (3.49)[b]	20.28 (3.80)[c]	48.81 (1.14)	52.55 (7.71)	52.79 (7.58)
18:3n-6	0.13 (0.08)[d]	0.08 (0.04)[d]	0.09 (0.10)	1.04 (0.72)[b]	0.79 (0.29)	0.62 (0.48)[b]
20:2n-6	0.55 (0.08)	0.57 (0.12)	0.53 (0.08)	0.18 (0.08)	0.17 (0.05)	0.13 (0.10)
20:3n-6	4.06 (1.74)[b]	3.40 (1.00)	2.69 (1.60)[b]	0.99 (0.46)	0.90 (0.12)	0.78 (0.33)
20:4n-6	11.30 (6.69)	13.26 (5.46)	12.86 (3.37)	6.50 (5.36)	9.23 (4.42)	8.62 (3.14)
22:4n-6	0.51 (0.26)	0.57 (0.20)	0.50 (0.19)	0.10 (0.17)	0.05 (0.20)	0.11 (0.12)
22:5n-6	0.40 (0.25)	0.48 (0.21)	0.39 (0.25)	0.08 (0.05)	0.06 (0.03)	0.07 (0.03)
∑ n-6 LCPUFA[b]	16.57 (8.76)	18.52 (6.34)	17.13 (3.55)	8.25 (5.70)	10.54 (4.43)	9.50 (3.04)
n-3 Polyunsaturated fatty acids						
18:3n-3	0.08 (0.05)	0.09 (0.04)	0.08 (0.04)	0.22 (0.04)	0.24 (0.10)	0.25 (0.12)
22:6n-3	2.02 (1.95)	2.74 (1.33)	2.60 (1.40)	0.34 (0.33)	0.46 (0.23)	0.51 (0.22)
∑ n-3 LCPUFA[c]	3.21 (2.59)	3.42 (1.91)	3.38 (1.51)	0.56 (0.60)	0.58 (0.20)	0.69 (0.25)

[a] Values are % wt/wt [median (range from the first to the third quartile)]. Obese, MCS: $n = 15$, obese, no MCS: $n = 17$, control: $n = 16$, MCS denotes metabolic cardiovascular syndrome. Medians in a row sharing a common roman superscript (b,c,d,e,f) are significantly different ([b,c]$P < 0.05$, [d,e]$P < 0.01$, [f]$P < 0.001$) using the Kruskal-Wallis analysis of variance followed by Mann-Whitney's two-sided rank test.
[b]Total n-6 long-chain polyunsaturated fatty acids (LCPUFA) denotes (20:2n-6 + 20:3n-6 + 20:4n-6 + 22:4n-6 + 22:5n-6).
[c]Total n-3 LCPUFA denotes (20:5n-3 + 22:5n-3 + 22:6n-3). For abbreviations see Table 1.

teenager population, at least in our country (2,11). Therefore, further delineation of the metabolic status of obese children with MCS is of practical importance.

The major finding of the present study is the significant difference observed in n-6 polyunsaturated fatty acid (PUFA) values between obese children with MCS, on the one hand, and obese children without MCS and controls, on the other hand. In spite of significantly lower values of the precursor fatty acid, LA, values of GLA and DHGLA were significantly higher in obese children with MCS than in obese children without MCS or in controls. This fatty acid pattern is consistent with—but does not prove—an enhanced conversion of LA to its longer-chain metabolites in obese children with MCS. However, values of the principal n-6 LCPUFA, AA, did not differ among the three groups.

The interpretation of the data obtained in this study is complicated by the fact that the control subjects proved to be significantly older than the obese children investigated. For three major reasons, however, we do not think that this unintentional selection bias could have influenced the results obtained to any significant extent. First, pubertal status did not differ among the groups, and it is puberty which might be linked to most of the age-related issues in teenagers. Second, we did not find any significant difference in the fatty acid composition of plasma PL and STE lipids between children aged 10 to <15 yr and >15 yr in a previous study carried out in a sizable cohort of healthy children (24). Third, age did not differ between obese children with and without MCS, and it is difficult to assume such age-related influences that would, in parallel, (i) mask differences between obese children with-

TABLE 3
Product/Substrate Ratios of n-6 LCPUFA Biosynthesis in Plasma Phospholipids and Sterol Esters of Obese Children With and Without MCS and in Controls[a]

	Phospholipids			Sterol esters		
Ratio	Obese, MCS	Obese, no MCS	Control	Obese, MCS	Obese, no MCS	Control
18:3n-6/18:2n-6	0.007 (0.005)[d]	0.004 (0.002)[d]	0.004 (0.005)	0.021 (0.011)[b,c]	0.016 (0.007)[b]	0.012 (0.011)[c]
(18:3n-6 + 20:3n-6)/18:2n-6	0.25 (0.13)[b]	0.19 (0.05)[b]	0.16 (0.08)	0.04 (0.02)[b,c]	0.04 (0.001)[b]	0.03 (0.02)[c]
20:4n-6/20:3n-6	2.79 (0.86)[d,e]	3.73 (1.58)[d]	4.32 (1.65)[e]	6.49 (2.91)[d,e]	9.73 (4.24)[d]	11.21 (3.30)[e]
20:4n-6/18:2n-6	0.62 (0.45)	0.66 (0.34)	0.58 (0.22)	0.14 (0.08)	0.16 (0.08)	0.16 (0.06)

[a]Values are % wt/wt [median (range from the first to the third quartile)]. Obese, MCS: $n = 15$; obese, no MCS: $n = 17$; control: $n = 16$. Medians in a row sharing a common superscript (b,c,d,e) are significantly different ([b,c]$P < 0.05$, [d]$P < 0.01$, [e]$P < 0.001$) using the Kruskal-Wallis analysis of variance followed by Mann-Whitney's two-sided rank test. For abbreviations see Tables 1 and 2.

out MCS and controls, and (ii) cause differences between obese children with MCS and controls. It is also to be noted that not only body fat contents but also lean body masses were significantly higher in obese children than in the controls in the present study. Higher accumulation rate of lean tissues usually accompanies enhanced deposition of fat in obese children, and it remains to be clarified whether expansion of lean tissues contributes, in part, to the metabolic complications of obesity.

Metabolism of n-6 PUFA has been investigated in various experimental models of obesity (25–29). In the Zucker rat model of monogenic obesity, significantly reduced LA, significantly enhanced DHGLA, and significantly reduced AA values were found in total liver lipids, liver PL, and total microsomal liver lipids in the genetically obese (fa/fa) as compared to the genetically lean (Fa/–) animals investigated at the ages of 6, 9, and 12 wk (26). The AA/DHGLA ratios were consistently lower in the obese than in the lean animals, whereas the AA/LA ratios showed inconsistent results depending on the lipid class and age investigated. Another extensive study comparing phospholipid fatty acid composition of nine different tissues demonstrated higher DHGLA/LA and lower AA/DHGLA ratios in genetically obese as compared to lean Zucker rats (27). In a mouse model of multigenic obesity, reduced LA, enhanced DHGLA but similar AA values were found in the obese as compared to the lean animals (28).

In the ob/ob mouse model of obesity, significantly reduced LA but significantly enhanced DHGLA and AA values were reported (25). In another study in ob/ob mice, significant enhancement of the Δ6-desaturase index (DHGLA/LA) and significant reduction of the Δ5-desaturase index (AA/DHGLA) were reported (29). These latter findings are in close agreement with the product/substrate ratios found in obese children with MCS in the present study. The multifaceted results seen in animal experiments as well as in human studies *(vide infra)* inspired the concept of AA maldistribution, i.e., a shift of AA from PL to STE lipids in obesity (30). In the present study, however, AA values showed similar patterns among the three groups both in PL and STE lipids.

Several nutritional and hormonal factors play a role in the regulation of EFA desaturation (31,32). On the one hand, insulin has been reported to be a potent activator of the Δ6-desaturase enzyme (33–36), and the obese children with MCS in this study were, by definition, hyperinsulinemic. On the other hand, hypertriglyceridemia was associated with diminished AA values in various animal tissues investigated (37), and many obese children with MCS in this study had elevated plasma triglyceride values.

It is tempting to speculate that the net effect of various hormonal and metabolic factors influencing Δ6- and Δ5-desaturase enzyme activities may differ among obese individuals with different degrees of the metabolic complications accompanying obesity. The data obtained in the present study indicate that the presence or absence of hyperinsulinemia and dyslipidemia (among other possible factors) in a group of obese subjects is associated with significant differences in plasma essential fatty acids (EFA) and PUFA values. When we recently reviewed human data on the effect of overnutrition on EFA metabolism (38), we found striking controversies between apparently similar studies. For instance, significantly lower AA values in plasma PL were found in obese than in nonobese adults in one study (5), whereas significantly higher AA values in plasma STE were reported for obese than for nonobese adults in another study (6). Moreover, significantly lower erythrocyte membrane phosphatidylethanolamine AA values were found in obese French children than in nonobese controls (39), whereas previously we reported significantly higher plasma PL and STE AA values in obese Hungarian children than in nonobese controls (4). These apparently contradictory results may well be explained by differences in the metabolic status of the obese subjects studied.

The data obtained in the present study allow two practical conclusions to be drawn. First, the significantly higher contribution of saturated fatty acids to plasma PL in obese children with MCS than in obese children without MCS and in controls provides further link between high saturated fatty acid intake and cardiovascular morbidity in obesity. Second, alterations of PUFA metabolism appear to be characteristic of certain subsets of the obese population but not necessarily to obesity itself. The pathophysiological consequences of the alterations observed in n-6 PUFA metabolism in obese children with MCS are unclear; however, nonphysiological availability of n-6 LCPUFA (e.g., that of DHGLA for eicosanoid synthesis) may represent an additional health hazard within the multifaceted clinical picture of MCS.

Children with MCS represent a well-defined and relatively sizable cohort of the obese population. Further investigations on fatty acid status in this subgroup of obese individuals may yield valuable data for better understanding of the alterations of fatty acid metabolism in obesity. It is to be emphasized, however, that fatty acid composition of plasma lipid classes as well as product/substrate ratios calculated on this basis represent only an indirect indicator of EFA metabolism. Today both sophisticated stable isotope techniques (40) and cloning of the Δ6-desaturase enzyme (41) provide novel research tools for further studies on EFA and PUFA metabolism in obesity.

ACKNOWLEDGMENTS

The project was supported by the Hungarian National Research Fund (OTKA T 031948 for T.D., and T 026663 and T 033066 for D.M.) and by the Hungarian Ministry of Welfare (T-02377/2000 for T.D. and T-07 100/99 for É.E.).

REFERENCES

1. Troiano, R.P., Flegal, K.M., Kuczmarski, R.J., Campbell, S.M., and Johnson, C.L. (1995) Overweight Prevalence and Trend for Children and Adolescents. The National Health and Nutrition Examination Surveys, 1963 to 1991, *Arch. Pediatr. Adolesc. Med. 149,* 1085–1091.
2. Dóber, I. (1996) The Prevalence of Obesity and Super Obesity Among School Children of Pécs in the 1990s, *Anthrop. Közl. 38,* 149–155.

3. Must, A., Jacques, P.F., Dallal, G.E., Bajema, C.J., and Dietz, W.H. (1992) Long-term Morbidity and Mortality of Overweight Adolescents, *N. Engl. J. Med. 327,* 1350–1355.
4. Decsi, T., Molnár, D., and Koletzko, B. (1996) Long-chain Polyunsaturated Fatty Acids in Plasma Lipids of Obese Children, *Lipids 31,* 305–311.
5. Phinney, S.D., Davis, P.G., Johnson, S.B., and Holman, R.T. (1991) Obesity and Weight Loss Alter Serum Polyunsaturated Lipids in Humans, *Am. J. Clin. Nutr. 53*, 831–838.
6. Rössner, S., Walldius, G., and Björvell, H. (1989) Fatty Acid Composition in Serum Lipids and Adipose Tissue in Severe Obesity Before and After Six Weeks of Weight Loss, *Int. J. Obes. 13*, 603–612.
7. Baillie, G.M., Sherer, J.T., and Weart, C.W. (1998) Insulin and Coronary Artery Disease: Is Syndrome X the Unifying Hypothesis? *Ann. Pharmacother. 32,* 233–247.
8. Liese, A.D., Mayer-Davies, E.J., and Haffner, S.M. (1998) Development of the Multiple Metabolic Syndrome: An Epidemiological Perspective, *Epidemiol. Rev. 20,* 157–172.
9. Arslanian, S., and Suprasongsin, C. (1996) Insulin Sensitivity, Lipids and Body Composition in Childhood: Is Syndrome X Present? *J. Clin. Endocrinol. Metab. 81,* 1058–1062.
10. Chen, W., Srinivasan, S.R., Elkasabany, A., and Berenson, G.S. (1999) Cardiovascular Risk Factors Clustering Features of Insulin Resistance Syndrome (Syndrome X) in a Biracial (Black-White) Population of Children, Adolescents, and Young Adults: The Bogalusa Heart Study, *Am. J. Epidemiol. 150,* 667–674.
11. Csábi, G., Török, K., Jeges, S., and Molnár, D. (2000) Presence of Metabolic Cardiovascular Syndrome in Obese Children, *Eur. J. Pediatr. 159,* 91–94.
12. Parizková, J., and Roth, Z. (1972) Assessment of Depot Fat in Children from Skinfold Measurements by Holtain Caliper, *Hum. Biol. 44*, 613–616.
13. Moore, D.J., Durie, P.R., Forstner, G.G., and Pencharz, P.B. (1985) The Assessment of Nutritional Status in Children, *Nutr. Res. 5*, 797–799.
14. Tanner, J.M. (1962) *Growth at Adolescence*, 2nd edn., Blackwell Scientific Publications, Oxford, p. 325.
15. Task Force on Blood Pressure Control in Children, National Heart, Lung, and Blood Institute, Bethesda, Maryland (1987) Report of the Second Task Force on Blood Pressure Control in Children—1987, *Pediatrics 79,* 1–25.
16. Soergel, M., Kirschstein, M., and Busch, C. (1997) Oscillometric Twenty-four-hour Ambulatory Blood Pressure Values in Healthy Children and Adolescents: A Multicenter Trial Including 1141 Subjects, *J. Pediatr. 130,* 178–184.
17. Braham, D., and Tinder, P. (1972) An Improved Reagent for the Determination of Blood Glucose by the Oxidase System, *Analyst 97*, 142–146.
18. Guthrie, R.A., Guthrie, D.W., and Murthy, D.Y.N. (1973) Standardization of Oral Glucose Tolerance Test and Criteria for the Diagnosis of Chemical Diabetes in Children, *Metabolism 22,* 275–282.
19. Alberti, K.G.M.M. (1995) Impaired Glucose Tolerance—Fact or Fiction, *Diab. Med. 13,* S6–S8.
20. Steele, B.W., Rochler, D.F., Azar, N.M., Blaszkowszki, T.B., Ruba, K., and Dempsey, M.E. (1976) Enzymatic Determination of Cholesterol in High Density Lipoprotein Fractions Prepared by a Precipitation Technique, *Clin. Chem. 22,* 98–102.
21. Romics, L., Szollár, L., and Zajkás, G. (1993) Management of Arteriosclerosis-related Lipid Metabolism Disorders. Recommendations of the Hungarian Lipid Consensus Conference [in Hungarian with English summary], *Orv. Hetil. 134,* 227–238.
22. Folch, J., Lees, M., and Sloane Stanley, G.H. (1957) A Simple Method for the Isolation and Purification of Total Lipids from Animal Tissues, *J. Biol. Chem. 226*, 497–509.
23. Stoffel, W., Chu, F., and Ahrens, E.H. (1959) Analysis of Long-Chain Fatty Acids by Gas–Liquid Chromatography, *Anal. Chem. 31*, 307–308.
24. Decsi, T., and Koletzko, B. (1994) Fatty Acid Composition of Plasma Lipid Classes in Healthy Subjects from Birth to Young Adulthood, *Eur. J. Pediatr. 153*, 520–525.
25. Cunnane, S.C., Manku, M.S., and Horrobin, D.F. (1985) Essential Fatty Acids in the Liver and Adipose Tissue of Genetically Obese Mice: Effect of Supplemental Linoleic and Gamma-linolenic Acids, *Br. J. Nutr. 53*, 441–448.
26. Blond, J.-P., Henchiri, C., and Bézard, J. (1989) Δ6 and Δ5 Desaturase Activities in Liver from Obese Zucker Rats at Different Ages, *Lipids 24,* 389–395.
27. Guesnet, P., Bourre, J.-M., Guerre-Millo, M., Pascal, G., and Durand, G. (1990) Tissue Phospholipid Fatty Acid Composition in Genetically Lean (Fa/–) or Obese (fa/fa) Zucker Female Rats on the Same Diets, *Lipids 25*, 517–522.
28. Phinney, S.D., Fisler, J.S., Tang, A.B., and Warden, C.H. (1994) Liver Fatty Acid Composition Correlates with Body Fat and Sex in a Multigenic Mouse Model of Obesity, *Am. J. Clin. Nutr. 60,* 61–67.
29. Clandinin, M.T., Cheema, S., Pehowich, D., and Field, C.J. (1996) Effect of Polyunsaturated Fatty Acids in Obese Mice, *Lipids 31,* S13–S22.
30. Phinney, S.D. (1996) Arachidonic Acid Maldistribution in Obesity, *Lipids 31,* S271–S274.
31. Brenner, R.R. (1981) Nutritional and Hormonal Factors Influencing Desaturation of Essential Fatty Acids, *Progr. Lipid Res. 20*, 41–47.
32. Brenner, R.R. (1991) Endocrine Control of Fatty Acid Desaturation, *Biochem. Soc. Trans. 18*, 773–775.
33. Brenner, R.R. (1977) Regulatory Function of Delta-6-desaturase—Key Enzyme of Polyunsaturated Fatty Acids Synthesis, *Adv. Exp. Med. Biol. 83*, 85–101.
34. Holman, R.T., Johnson, S.B., Gerrard, J.M., Mauer, S.M., Kupcho-Sandberg, S., and Brown, D.M. (1983) Arachidonic Acid Deficiency in Streptozocin-Induced Diabetes, *Proc. Natl. Acad. Sci. USA 80*, 2375–2379.
35. Huang, Y.S., Horrobin, D.F., Manku, M.S., Mitchell, J., and Ryan, M.A. (1984) Tissue Phospholipid Fatty Acid Composition in the Diabetic Rat, *Lipids 19*, 367–370.
36. Borkman, M., Storlien, L.H., Pan, D.A., Jenkins, A.B., Chisholm, D.J., and Campbell, L.V. (1993) The Relation Between Insulin Sensitivity and the Fatty Acid Composition of Skeletal-Muscle Phospholipids, *N. Engl. J. Med. 328,* 238–244.
37. Cunnane, S.C., Huang, Y.-S., and Manku, M.S. (1985) Triacylglycerol Content of Arachidonic Acid Varies Inversely with Total Triacylglycerol in Liver and Plasma, *Biochim. Biophys. Acta 876*, 183–186.
38. Decsi, T., Molnár, D., and Koletzko, B. (1998) The Effect of Under- and Overnutrition on Essential Fatty Acid Metabolism in Childhood, *Eur. J. Clin. Nutr. 52,* 541–548.
39. Frelut, M.L., Therond, P., Camuso, M.C., Benali, K., Cathelineau, L., and Navarro, J. (1994) Inhibited Plasma Delta 6 Desaturase Activity and Abnormal Membrane Essential Fatty Acid Pattern in Obese Children. Impact of Weight Loss (abstract), *Acta Paediatr. Hung. 34,* 219.
40. Demmelmair, H., Sauerwald, T., Koletzko, B., and Richter, T. (1997) New Insights into Lipid and Fatty Acid Metabolism *via* Stable Isotopes, *Eur. J. Pediatr. 156 Suppl. 1,* S70–S74.
41. Cho, H.P., Nakamura, M.T., and Clarke, S.D. (1999) Cloning, Expression, and Nutritional Regulation of the Mammalian Delta-6 Desaturase, *J. Biol. Chem. 274,* 471–477.

[Received March 14, 2000, and in revised form September 5, 2000; revision accepted September 27, 2000]

Fatty Acid Chain Length and Degree of Unsaturation Are Inversely Associated with Serum Triglycerides

Sameline Grimsgaard[a,*], Kaare H. Bønaa[a], and Kristian S. Bjerve[b]

[a]Institute of Community Medicine, University of Tromsø, N-9037 Tromsø, Norway, and [b]Department of Clinical Chemistry, Regional Hospital, University of Trondheim, N-7006 Trondheim, Norway

ABSTRACT: Little is known about the association between dietary fatty acids and serum triglyceride concentrations. Plasma fatty acids may reflect dietary intake and can be used to study the relationship between concentrations of individual fatty acids and serum lipids. We examined the cross-sectional relationship of plasma fatty acids with serum nonfasting triglyceride and total cholesterol concentrations. Relative concentrations of individual plasma phospholipid fatty acids were determined by gas–liquid chromatography among 4,158 men aged 40–42 yr, who participated in a population study. The pattern of associations between individual fatty acids and cholesterol was different from that between individual fatty acids and triglyceride concentrations. All fatty acids displayed positive associations with total cholesterol concentration except linoleic acid, which was inversely related to cholesterol. In contrast, associations between individual fatty acids and triglyceride concentrations differed in strength and direction depending on both carbon chain length and the degree of unsaturation. Concentrations of very long chain (20 carbon atoms or more) saturated, monounsaturated, and n-3 polyunsaturated fatty acids showed significant inverse associations with triglycerides, whereas shorter fatty acids within these classes were positively associated with triglyceride concentrations. The present data suggest that the associations between concentrations of serum triglycerides and plasma phospholipid fatty acids depend on both fatty acid chain length and the degree of unsaturation.

Paper no. L8466 in *Lipids 35,* 1185–1193 (November 2000).

Serum triglyceride concentration is probably an independent risk factor for coronary heart disease (1), and the increased risk seems to start at relatively low concentrations of triglycerides (2). Dietary supplementation with n-3 polyunsaturated fatty acids decreases serum triglyceride concentrations (3). Little is known about the effects of other dietary fats (4), although a meta-analysis indicated that dietary polyunsaturated fat lowered triglycerides compared with monounsaturated fat (5).

There is an increasing awareness that individual fatty acids within the saturated, monounsaturated, and n-6 and n-3 polyunsaturated fatty acid classes may have different effects on serum lipid and lipoprotein concentrations (6). Dietary fat intake is difficult to measure, and blood concentrations of fatty acids may be used to examine the relationship between individual fatty acids and serum lipids. Plasma concentrations of essential n-6 and n-3 polyunsaturated fatty acids are highly correlated with dietary intake (7–9). Concentrations of nonessential fatty acids are less reliable indicators of diet because they reflect dietary consumption as well as fatty acid synthesis and metabolism. Nevertheless, plasma concentrations of palmitic, stearic, and monounsaturated fatty acids correlated with intake of saturated fat in individuals consuming a Western diet (7,8), probably because of their common sources in milk products and animal fat (10). In addition, high concentrations of eicosatrienoic (20:3n-9) and dihomo-γ-linolenic (20:3n-6) acids may reflect a diet relatively rich in saturated fatty acids (11,12).

Studies examining the relationship of blood concentrations of individual fatty acids with serum triglycerides and total cholesterol are not consistent (13–18). Most studies included few subjects (13–15), or measured a limited number of fatty acids (13,15,17,18).

We analyzed the association of individual plasma phospholipid fatty acids with serum concentrations of total cholesterol and triglycerides among 4,158 men aged 40–42 yr. This large data set allowed a detailed investigation of the relationship between plasma fatty acids and serum triglycerides and total cholesterol in a population consuming a Western diet.

METHODS

Subjects. In 1988–1989, all men and women aged 40–42 yr living in Nordland county, Norway, were invited to a health screening organized by the National Health Screening Service, the University of Tromsø, and the local health authorities (19). Plasma phospholipid fatty acids were quantitated in men, of whom 5,492 were invited and 4,302 participated (78%). Measurements of plasma phospholipid fatty acids were missing in 144 men, leaving 4,158 for the analysis. A second questionnaire was completed by 3,590 men; thus the analysis on certain variables is restricted. The Norwegian Data Inspectorate considered legal and ethical issues and approved the study. The subjects gave informed consent.

*To whom correspondence should be addressed at Department of Pharmacoepidemiology and Pharmacy Practice, University of Tromsø, N-9037 Tromsø, Norway. E-mail: sameline@farmasi.uit.no

Abbreviations: BMI, body mass index; LDL, low density lipoprotein; VLDL, very low density lipoprotein.

Questionnaires. The letter of invitation gave information about the survey and included a questionnaire about previous cardiovascular disease and smoking habits (yes/no). Leisure time physical activity was graded from I to IV according to which of the following categories would best describe the participant's usual level of physical activity. I: reading or watching television or other sedentary activity; II: walking, cycling or other forms of exercise at least 4 h/wk; III: participation in recreational sports, heavy gardening etc. for at least 4 h/wk; IV: participation in hard training or sports competitions regularly several times a week. Categories III and IV were merged in our analysis. A nurse checked the questionnaire for logical inconsistencies and incomplete items at the examination and obtained information about time since last meal. A second questionnaire, covering alcohol consumption and dietary habits, was handed out at the screening site and returned by mail. Alcohol consumption was categorized from I to VI. I: teetotaler; consumption of alcohol equivalent to 5 units of alcohol (1 unit equals 9 g of alcohol) II: no times last year; III: a few times last year; IV: 1 or 2 times per month; V: 1 or 2 times per week; and VI: 3 times per week or more. We merged categories V and VI in the analysis. Two questions about habitual consumption of lean and fat fish for dinner meals were categorized from I to V. I: less than once weekly; II: once weekly; III: twice weekly; IV: three times weekly; V: four times weekly or more. We merged the two questions into four categories covering total weekly consumption of lean and fat fish for dinner. The questionnaire also assessed present use of fish oil supplements (yes/no).

Measurements. Body weight was measured on an electronic scale with subjects wearing light inner clothing and no shoes, and height was measured to the nearest centimeter. Body mass index (BMI) was calculated as the body weight in kilograms divided by the square of the height in meters (kg/m^2). Systolic and diastolic blood pressure were measured by an automatic device (Dinamap, Critikon, Tampa) (19). A nonfasting blood sample was collected and analyzed in fresh serum for total cholesterol and triglycerides at the Central Laboratory, Ullevål Hospital, Oslo. The analyses were performed by an enzymatic colorimetric method (20,21), on a Hitachi 737 Automatic Analyzer (Boehringer Mannheim, Mannheim, Germany) with reagents from the manufacturer. Measurement precision, expressed as the coefficient of variation, was 3% for both serum total cholesterol and triglycerides.

EDTA plasma was stored at –80°C for a maximum of 2 yr before phospholipid fatty acids (14:0, 16:0, 18:0, 20:0, 22:0, 24:0, 16:1, 18:1, 20:1, 22:1, 24:1, 20:3n-9, 18:2n-6, 20:2n-6, 20:3n-6, 20:4n-6, 22:4n-6, 22:5n-6, 18:3n-3, 20:5n-3, 22:5n-3 and 22:6n-3) were quantitated by gas–liquid chromatography as described previously (22). The coefficients of variation for individual fatty acids estimated from replicate analyses (n = 55) of a serum sample ranged from 3.3 to 6.6%. Fatty acids were measured as relative concentrations (mol%). *Trans*-fatty acids were not measured.

Statistical analysis. All variables were normally distributed except serum triglycerides and plasma 20:5n-3, which were right-skewed. Log transformation had minor impact on the results, and we therefore used untransformed data in the analysis. Pearson correlation coefficients were computed to evaluate the relationships between concentrations of individual plasma phospholipid fatty acids. We used simple linear regression analysis to predict change and 95% confidence interval in serum triglyceride and total cholesterol concentrations by 1 standard deviation increase in fatty acid concentration. Next, we developed multiple linear regression models to examine independent associations between individual fatty acids and serum lipids. Fatty acids significantly associated with serum triglycerides and total cholesterol in univariate analysis were considered for inclusion in the regression models. We included up to two fatty acids from each fatty acid class. Within each fatty acid class we chose the fatty acid which had the strongest positive and inverse relationship with triglycerides (18:0, 22:0, 16:1, 24:1, 20:3n-6, 22:6n-3) and total cholesterol (22:0, 22:1, 20:3n-9, 18:2n-6, 22:4n-6), and where intercorrelations between fatty acids were less than r = 0.60. Fatty acids significantly associated with triglycerides and total cholesterol, respectively, were retained in the models. Finally, we adjusted for BMI and evaluated the effects of potential confounding variables, such as physical activity, alcohol consumption, daily smoking, and time since last meal. Residual analyses confirmed the model assumptions (23). Differences between means were tested by two sample t-tests. Two-sided P-values < 0.05 were considered statistically significant. The SAS software package was used (24).

RESULTS

Characteristics of study participants are shown in Table 1. Among the 4,158 men, 34% had serum total cholesterol concentrations ≥6.50 mmol/L, and 24% had nonfasting triglycerides >2.50 mmol/L. A history of myocardial infarction, angina pectoris, stroke, diabetes mellitus, or use of antihypertensive drugs was reported by 176 men. Fish consumption was relatively high, and 26% were present users of fish oil supplements. Nonfasting serum triglyceride level decreased with time since last meal (Table 2). Plasma phospholipid palmitic (16:0), palmitoleic (16:1), 20:3n-9, 20:3n-6, eicosapentaenoic (20:5n-3), and docosahexaenoic (22:6n-3) acids increased, whereas linoleic (18:2n-6) acid concentrations decreased slightly when time since last meal increased (data not shown).

Interrelationships between concentrations of plasma phospholipid fatty acids. Concentrations of very long chain (20–24 carbon atoms) fatty acids within the saturated and n-3 polyunsaturated fatty acid classes were highly intercorrelated (Table 3). Very long chain polyunsaturated fatty acids of the n-3 class were positively correlated with very long chain monounsaturated fatty acids and inversely correlated with fatty acids of the n-6 class.

Univariate relationship of plasma phospholipid fatty acids with serum nonfasting triglycerides and total cholesterol. Concentrations of stearic (18:0) acid, 16:1, and 20:3n-6

TABLE 1
Characteristics of Study Participants: 4,158 Men 40–42 yr Old

Characteristic	Mean ± SD or %
Serum total cholesterol (mmol/L)	6.12 ± 1.16
Serum nonfasting triglycerides (mmol/L)	1.98 ± 1.22
Systolic blood pressure (mm Hg)	133 ± 14
Diastolic blood pressure (mm Hg)	81 ± 10
Body mass index (kg/m^2)	25.3 ± 3.2
Daily smoking	46
Leisure time physical activity	
Sedentary	23
Moderate	52
Regular/hard training	25
Alcohol consumption[a]	
Teetotaler	4
≥5 units of alcohol	
< Once yearly	20
A few times yearly	45
1 or 2 times monthly	24
1 or 2 times weekly or more	7
Lean or fat fish for dinner[b]	
< Twice weekly	34
Twice weekly	30
Three times weekly	22
Four times weekly or more	14

[a] n = 3,501.
[b] n = 3,530.

showed strong positive associations with triglyceride concentrations (Table 4 and Figs. 1,2). Very long chain saturated, monounsaturated, and n-3 polyunsaturated fatty acids, particularly lignoceric (24:0) acid, nervonic (24:1) acid, and 22:6n-3, were inversely associated with triglycerides. Both fatty acid chain length and the degree of unsaturation were related to triglyceride concentrations (Table 5). The association between triglycerides and chain length appeared to be stronger than the association between triglycerides and degree of unsaturation. Very long chain saturated and monounsaturated fatty acids were positively associated with total cholesterol and inversely associated with triglyceride concentrations (Table 4 and Fig. 1). The associations of saturated and monounsaturated fatty acids with triglycerides differed depending on carbon chain length, whereas all saturated and monounsaturated fatty acids were positively associated with total cholesterol. The associations of fatty acids with triglyceride concentrations were generally stronger than the associations with total cholesterol. The compound 18:2n-6 was the only fatty acid showing a significant inverse association with cholesterol concentrations.

TABLE 2
Nonfasting Serum Triglycerides According to Time Since Last Meal in 4,158 Men

Time since last meal (h)	n	Serum triglycerides (mmol/L), mean ± SD
0	850	2.11 ± 1.23
1	1204	2.08 ± 1.20
2	792	2.04 ± 1.30
3	509	1.88 ± 1.18
4	375	1.75 ± 1.16
5	178	1.60 ± 0.87
6	75	1.40 ± 0.98
7	22	1.26 ± 0.74
8	11	1.82 ± 1.02
9	128	1.66 ± 1.28
Missing	14	2.30 ± 2.10

Multivariate relationship of plasma phospholipid fatty acids with serum nonfasting triglycerides and total cholesterol. Fatty acids explained 19% of the variance in triglyceride concentration (Table 6, model I). Concentrations of 18:0, 16:1, 24:1, and 20:3n-6 were independently associated with triglycerides. The associations remained significant when controlling for BMI, physical activity, and alcohol consumption (Table 6, model II). The n-3 fatty acids were not significantly associated with triglycerides when 24:1 was included in the multiple regression model. There was interaction between alcohol consumption and 16:1 in prediction of triglycerides. Concentrations of 16:1 increased significantly when alcohol consumption increased (P = 0.0001, data not shown). The association between 16:1 and triglyceride concentrations weakened with increasing alcohol consumption, and 16:1 was not significantly associated with triglycerides among men in the highest category of alcohol consumption. The strongest association between concentrations of 16:1 and triglycerides was observed among nondrinkers (data not shown).

Fatty acids explained 7% of the variance in total cholesterol concentration (Table 6, model I). Concentration of 18:2n-6 was not significantly associated with cholesterol after adjustment for BMI (Table 6, model II). Adjustment for daily smoking did not affect the results of the multiple regression analyses. Both stratified and adjusted analyses showed that time since last meal did not influence the relationship of plasma phospholipid fatty acids with serum triglycerides and total cholesterol.

Consumption of fish products, plasma phospholipid fatty acids, and serum triglycerides. Use of fish oil supplements and the level of habitual fish consumption were positively associated with concentrations of gondoic (20:1) acid, erucic (22:1) acid, 24:1, and n-3 fatty acids (all $P < 0.001$) (data not shown). Present users of fish oil had 10% lower mean triglyceride concentration compared with nonusers (P = 0.0001). In multiple regression analysis, fish consumption was inversely associated with serum triglyceride concentrations after adjustment for BMI (P = 0.047). Fish consumption was not significantly associated with serum triglyceride concentrations when 24:1 or 22:6n-3 was added to the regression model.

DISCUSSION

This study shows that fatty acid chain length, as well as the degree of unsaturation, is associated with serum nonfasting triglyceride concentrations. Very long chain fatty acids of the saturated, monounsaturated, and n-3 classes were inversely associated with triglycerides, and the associations increased

TABLE 3
Correlations Between Levels of Plasma Phospholipid Fatty Acids (mol%) in 4,158 Men[a]

	Fatty acid																					
Fatty acid	16:0	18:0	20:0	22:0	24:0	16:1	18:1	20:1	22:1	24:1	20:3n-9	18:2n-6	20:2n-6	20:3n-6	20:4n-6	22:4n-6	22:5n-6	18:3n-3	20:5n-3	22:5n-3	22:6n-3
14:0	0.11	−0.04	0.01	0.08	−0.03	0.20	0.14	0.06	0.07	−0.03	0.14	−0.13	0.09	0.14	−0.11	0.08	0.07	0.07	0.03	0.03	−0.05
16:0		−0.60	−0.14	−0.14	−0.05	0.46	0.23	−0.19	−0.20	0.06	0.19	−0.35	−0.04	0.09	0.05	−0.07	−0.01	−0.12	−0.01	−0.02	−0.02
18:0			−0.07	−0.12	−0.14	−0.32	−0.16	0.00	−0.06	−0.18	−0.10	0.14	−0.01	0.12	−0.03	−0.21	−0.03	0.03	−0.02	0.02	0.01
20:0				0.80	0.65	−0.16	−0.29	−0.21	0.25	0.56	−0.16	−0.05	0.19	−0.11	−0.04	0.37	−0.12	0.09	−0.07	−0.07	−0.03
22:0					0.62	−0.27	−0.31	−0.22	0.31	0.41	−0.17	0.04	0.15	−0.15	−0.04	0.53	−0.13	−0.12	−0.13	−0.18	−0.12
24:0						−0.23	−0.27	−0.36	−0.01	0.71	−0.15	−0.09	0.21	0.00	0.05	0.24	−0.07	−0.13	−0.07	−0.05	−0.08
16:1							0.60	0.06	−0.08	−0.17	0.53	−0.35	0.21	0.32	0.05	0.08	0.29	0.30	−0.02	0.08	−0.08
18:1								−0.01	−0.22	−0.30	0.59	−0.09	0.20	0.24	−0.03	−0.02	0.27	0.18	−0.26	−0.04	−0.32
20:1									0.52	−0.04	−0.02	−0.29	−0.13	−0.26	−0.19	−0.08	−0.01	0.08	0.65	0.27	0.41
22:1										0.25	−0.07	−0.23	−0.07	−0.32	−0.21	0.34	0.02	−0.06	0.46	0.16	0.32
24:1											−0.20	−0.46	0.08	−0.24	−0.05	0.16	−0.18	−0.19	0.37	0.25	0.36
20:3n-9												−0.26	0.23	0.45	0.31	0.21	0.51	0.06	−0.18	0.00	−0.26
18:2n-6													0.02	−0.08	−0.26	−0.07	−0.11	0.17	−0.64	−0.53	−0.62
20:2n-6														0.37	−0.07	0.26	0.21	0.14	−0.27	−0.04	−0.21
20:3n-6															0.37	0.07	0.47	0.00	−0.40	−0.13	−0.34
20:4n-6																0.15	0.39	−0.20	−0.19	−0.09	−0.18
22:4n-6																	0.31	−0.05	−0.14	−0.12	−0.17
22:5n-6																		−0.01	−0.23	−0.02	−0.22
18:3n-3																			−0.08	−0.01	−0.14
20:5n-3																				0.47	0.72
22:5n-3																					0.65

[a]Pearson correlation coefficients between relative concentrations (mol%) of fatty acids. Values > |0.03|, |0.04| and |0.05| are significant at $P < 0.05$, $P < 0.01$, and $P < 0.001$, respectively.

in magnitude with increasing fatty acid chain length. Interestingly, individual very long chain saturated and monounsaturated fatty acids were positively associated with total cholesterol and inversely associated with triglyceride concentrations. This observation has to our knowledge not been reported previously.

Associations of fatty acids with nonfasting triglycerides were not influenced by time since last meal. The analysis can reflect that plasma phospholipid fatty acids explain a component of the interindividual variability in serum triglyceride levels, which is not determined by time since last meal.

Dietary supplementation with very long chain n-3 fatty acids decreases liver very low density lipoprotein (VLDL) synthesis (25) and serum triglyceride concentrations (3). Studies in rats showed that 20:5n-3 increased mitochondrial β-oxidation and reduced fatty acid substrate for VLDL synthesis (26). Mitochondria, the major sites for fatty acid oxidation, are poor oxidizers of very long chain fatty acids (27), but proliferated during dietary supplementation with very long chain n-3 fatty acids (28). Based on these observations we speculate that very long chain saturated and monounsaturated fatty acids stimulate mitochondrial proliferation, whereby fatty acid oxidation increases and VLDL triglycerides decrease. Contrasting fatty acids of the saturated, monounsaturated and n-3 classes, n-6 fatty acids displayed no distinct pattern of association with triglycerides.

We found that concentrations of very long chain monounsaturated and n-3 fatty acids were positively associated with habitual fish consumption and inversely associated with serum triglycerides. Others have reported that the level of fish consumption and triglyceride concentrations were inversely related (14,29). In previous cross-sectional studies however, concentrations of 20:5n-3 were both positively (13), and inversely (14) associated with serum triglycerides.

Cross-sectional studies indicate that plasma phospholipid levels of essential polyunsaturated fatty acids reflect dietary intake (7–9). Dietary supplementation studies confirm that plasma phospholipid concentrations of 18:2n-6, 18:1, 20:5n-3, and 22:6n-3 are sensitive to changes in dietary intake of these fatty acids (30,31). The origins of very long chain saturated and monounsaturated fatty acids are less clear. They may be metabolic products of shorter fatty acids. Fish and fish oils contain 20:1 and 22:1 as well as n-3 fatty acids (10), and one cross-sectional study showed that plasma phospholipid concentrations of 24:1, 20:5n-3, and 22:6n-3 were positively associated with fish consumption (14). It is possible that concentrations of very long chain monounsaturated fatty acids reflect dietary fish and fish oil intake.

In the present study, the inverse associations of 22:1 and 24:1 with triglycerides were stronger than the association of 22:6n-3 with triglyceride concentrations. When 22:1 or 24:1 was added to a regression model including only 22:6n-3, the explained variability in triglycerides increased significantly. This indicates that very long chain monounsaturated fatty acids are independently associated with triglyceride concentrations and are not merely indicators of dietary n-3 fatty acids.

TABLE 4
Concentrations of Plasma Phospholipid Fatty Acids, and Change in Serum Nonfasting Triglycerides and Total Cholesterol by One Standard Deviation (SD) Increase in Fatty Acid Concentration in 4,158 Men

Fatty acid	Mean ± SD (mol%)	Predicted mean change (95% CI) Triglycerides (mmol/L)	Total cholesterol (mmol/L)
Saturated fatty acids[a]	44.10 ± 1.34	0.02 (–0.02, 0.06)	0.16 (0.13, 0.19)
Myristic, 14:0	0.36 ± 0.13	0.10 (0.07, 0.14)	0.08 (0.05, 0.11)
Palmitic, 16:0	26.64 ± 1.54	0.00 (–0.03, 0.04)	0.01 (–0.03, 0.04)
Stearic, 18:0	13.89 ± 0.94	0.27 (0.24, 0.31)	0.07 (0.04, 0.11)
Arachidic, 20:0	0.50 ± 0.13	–0.26 (–0.29, –0.22)	0.10 (0.06, 0.13)
Behenic, 22:0	1.87 ± 0.58	–0.23 (–0.27, –0.19)	0.17 (0.14, 0.21)
Lignoceric, 24:0	0.85 ± 0.28	–0.28 (–0.32, –0.24)	0.05 (0.01, 0.08)
Monounsaturated fatty acids[b]	10.71 ± 1.32	0.06 (0.03, 0.10)	0.06 (0.02, 0.09)
Palmitoleic, 16:1	0.37 ± 0.19	0.25 (0.22, 0.29)	0.11 (0.08, 0.15)
Oleic, 18:1	8.52 ± 1.25	0.19 (0.15, 0.22)	0.00 (–0.03, 0.04)
Gondoic, 20:1	0.27 ± 0.13	–0.06 (–0.10, –0.02)	0.10 (0.06, 0.13)
Erucic, 22:1	0.15 ± 0.13	–0.13 (–0.17, –0.09)	0.19 (0.15, 0.22)
Nervonic, 24:1	1.39 ± 0.54	–0.33 (–0.36, –0.29)	0.03 (–0.01, 0.06)
Eicosatrienoic acid, 20:3n-9	0.11 ± 0.07	0.20 (0.16, 0.24)	0.18 (0.15, 0.22)
n-6 fatty acids[c]	34.74 ± 3.67	0.12 (0.08, 0.15)	–0.12 (–0.15, –0.09)
Linoleic, 18:2n-6	23.44 ± 3.65	0.05 (0.02, 0.09)	–0.15 (–0.18, –0.11)
Eicosadienoic, 20:2n-6	0.38 ± 0.07	0.13 (0.09, 0.17)	0.15 (0.12, 0.18)
Dihomo-γ-linolenic, 20:3n-6	2.46 ± 0.67	0.39 (0.35, 0.43)	0.10 (0.06, 0.14)
Arachidonic, 20:4n-6	7.87 ± 1.39	–0.03 (–0.07, 0.01)	–0.03 (–0.07, 0.00)
Adrenic, 22:4n-6	0.50 ± 0.27	–0.03 (–0.07, 0.01)	0.20 (0.17, 0.24)
Docosapentaenoic, 22:5n-6	0.09 ± 0.05	0.20 (0.17, 0.24)	0.11 (0.07, 0.15)
n-3 fatty acids[d]	10.34 ± 3.31	–0.17 (–0.20, –0.13)	0.04 (0.01, 0.08)
α-Linolenic, 18:3n-3	0.18 ± 0.09	0.10 (0.06, 0.13)	0.01 (–0.03, 0.04)
Eicosapentaenoic, 20:5n-3	2.39 ± 1.75	–0.14 (–0.18, –0.10)	0.05 (0.01, 0.08)
Docosapentaenoic, 22:5n-3	1.22 ± 0.24	–0.15 (–0.18, –0.11)	0.00 (–0.03, 0.04)
Docosahexaenoic, 22:6n-3	6.54 ± 1.67	–0.17 (–0.20, –0.13)	0.04 (0.00, 0.07)

[a]Saturated fatty acids include 14:0, 16:0, 18:0, 20:0, 22:0, 24:0.
[b]Monounsaturated fatty acids include 16:1, 18:1, 20:1, 22:1, 24:1.
[c]n-6 fatty acids include 18:2n-6, 20:2n-6, 20:3n-6, 20:4n-6, 22:4n-6, 22:5n-6.
[d]n-3 fatty acids include 18:3n-3, 20:5n-3, 22:5n-3, 22:6n-3. Abbreviation: CI, confidence interval.

Plasma phospholipid concentrations of 18:0, 16:1, and 20:3n-6 displayed independent positive associations with triglyceride concentrations. The observation finds support in the Paris Prospective Study, where plasma concentrations of 16:1 and 20:3n-6 were positively associated with triglycerides (16). A dietary intervention trial showed that serum triglyceride concentration increased significantly on an 18:0-enriched diet, compared with a diet rich in 18:2n-6 (32). Plasma concentrations of 18:0 and 16:1 were positively associated with dietary saturated fat in cross-sectional studies (7,8), and 20:3n-6 increased on a saturated fat diet (11). Thus, plasma concentrations of 18:0, 16:1, and 20:3n-6 appear to reflect dietary saturated fat to some extent.

Alcohol consumption may be a potential confounder in the relationship between 16:1 and triglycerides, since alcohol intake is associated with high levels of 16:1 (16,33,34) and serum triglycerides (35). In the present study the association between 16:1 and triglycerides remained significant when controlling for alcohol intake, but residual confounding may remain since we used a rather crude estimate of alcohol intake. However, stratified analyses showed that the association between 16:1 and triglycerides was particularly strong among teetotalers and those who consumed alcohol less than yearly or a few times yearly. It appears that the association between 16:1 and triglycerides does not depend on alcohol intake.

Serum nonfasting triglycerides are subject to larger intraindividual variation than are total cholesterol concentrations (36), and this will tend to dilute any association between triglycerides and concentrations of fatty acids. We found that fatty acids explained 19% of the variability in triglyceride, and 7% of the variability in total cholesterol concentrations. Therefore, the biological association of plasma phospholipid fatty acids with serum triglycerides appears to be stronger than the association with total cholesterol.

In the present study, plasma phospholipid concentrations of 22:0, 22:1, and 20:3n-9 were independently and positively associated with serum total cholesterol concentrations. It is not clear which factors determine plasma concentrations of 22:0, 22:1, and 20:3n-9. They may be metabolic products of shorter saturated fatty acids. Fish products can be a source of 22:1, as noted above. When dietary intake of polyunsaturated fat is low, the metabolic conversion of 18:1 to 20:3n-9 increases (12). High levels of plasma 20:3n-9 may thus reflect a diet relatively rich in saturated fat.

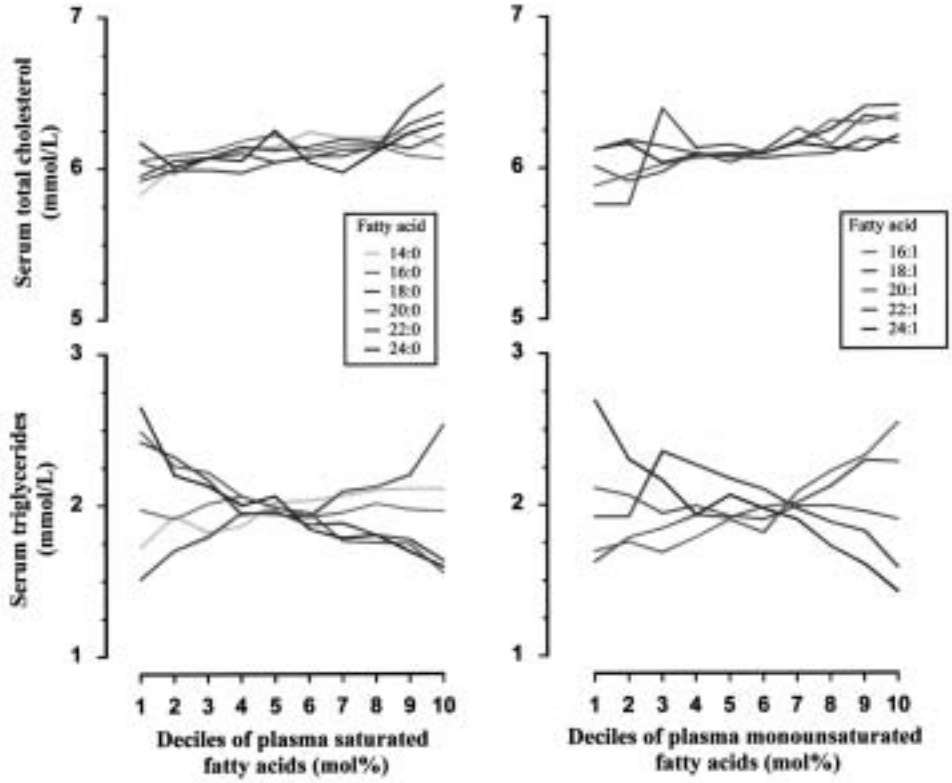

FIG. 1. Mean serum total cholesterol (upper panels) and triglyceride (lower panels) concentrations by deciles of plasma phospholipid saturated (left panels) and monounsaturated (right panels) fatty acids.

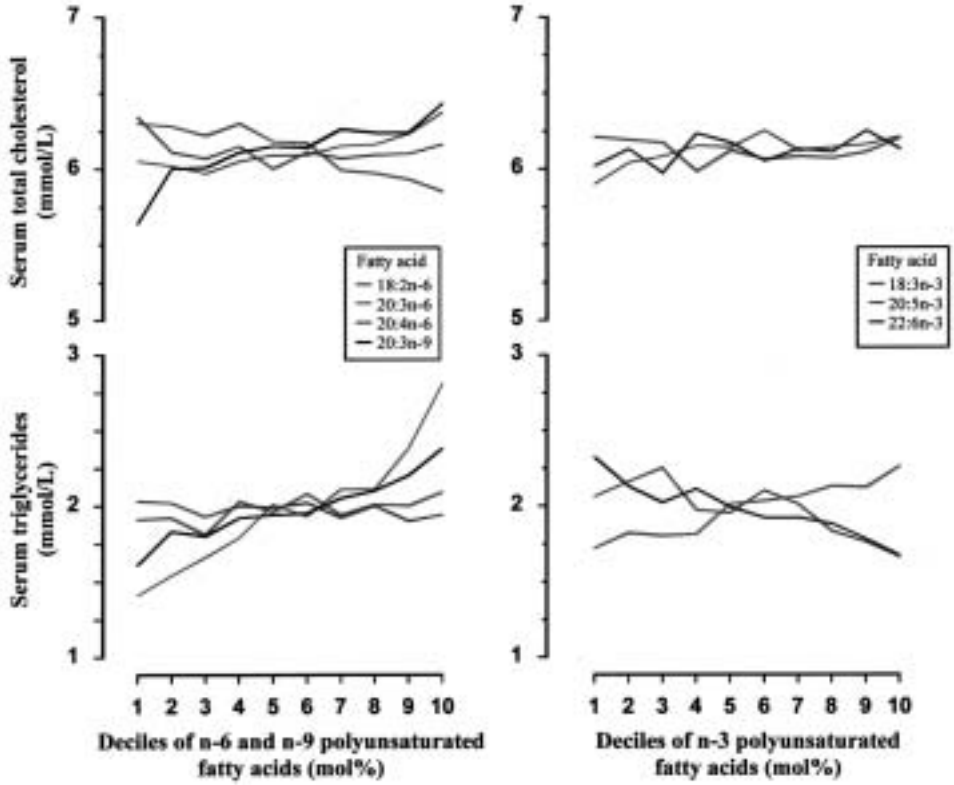

FIG. 2. Mean serum total cholesterol (upper panels) and triglyceride (lower panels) concentrations by deciles of plasma phospholipid n-6 and n-9 polyunsaturated (left panels) and n-3 polyunsaturated (right panels) fatty acids.

TABLE 5
Concentrations of Plasma Phospholipid Fatty Acids and Change in Serum Nonfasting Triglyceride Concentrations According to Fatty Acid Chain Length and Number of Double Bonds in 4,158 Men

Fatty acid group	Mean ± SD (mol%)	Change in triglycerides[a] (mmol/L)
Carbon chain length[b]		
C_{20}	13.99 ± 2.11	–0.02 (–0.06, 0.02)
C_{22}	10.37 ± 1.93	–0.24 (–0.28, –0.20)
C_{24}	2.24 ± 0.76	–0.33 (–0.37, –0.30)
Number of double bonds[c]		
4	8.37 ± 1.46	–0.03 (–0.07, 0.01)
5	3.70 ± 1.87	–0.15 (–0.18, –0.11)
6	6.54 ± 1.67	–0.17 (–0.20, –0.13)

[a]Values are predicted mean change (95% CI) by one SD increase in fatty acid concentration.
[b]C_{20} = 20:0 + 20:1 + 20:3n-9 + 20:2n-6 + 20:3n-6 + 20:4n-6 + 20:5n-3. C_{22} = 22:0 + 22:1 + 22:4n-6 + 22:5n-6 + 22:5n-3 + 22:6n-3. C_{24} = 24:0 + 24:1.
[c]4 = 20:4n-6 + 22:4n-6. 5 = 22:5n-6 + 20:5n-3 + 22:5n-3. 6 = 22:6n-3. For abbreviations see Table 4.

Plasma concentrations of 18:2n-6 are correlated with dietary intake (7,8). We found that 18:2n-6 concentrations were inversely associated with total cholesterol. Small observational studies failed to detect any association between 18:2n-6 and total cholesterol (13,15). Larger studies however, found that plasma (16,18) and adipose tissue (37,38) concentrations of 18:2n-6 were inversely associated with total cholesterol. These data are supported by feeding experiments showing that dietary 18:2n-6 decrease total and low density lipoprotein (LDL) cholesterol concentrations (6), supposedly by increasing liver LDL receptor activity (39).

Our findings are strengthened by the population-based study design, the relatively high participation rate, and large sample size. The study was conducted among men in a narrow age range consuming a Western diet, and the results need confirmation among women and other age groups. We did not measure *trans*-fatty acids, and it is not known how they may influence the results. Relative concentrations (proportions) of fatty acids were used in the analysis. The use of proportions is problematic since an increase in one proportion is associated with a decrease in some other proportion(s). However, as seen in Table 2, most correlations between fatty acids in-

TABLE 6
Multiple Linear Regression Analysis of Serum Nonfasting Triglycerides and Total Cholesterol in 4,158 Men[a]

Predictor variable	Model I	Model II
	Triglycerides (mmol/L)	
Fatty acid (mol%)		
18:0	0.29 (0.25, 0.33)	0.25 (0.21, 0.29)
16:1	0.24 (0.20, 0.28)	0.18 (0.14, 0.23)
24:1	–0.18 (–0.22, –0.14)	–0.22 (–0.26, –0.19)
20:3n-6	0.24 (0.20, 0.28)	0.15 (0.11, 0.19)
Body mass index (kg/m^2)		0.28 (0.24, 0.31)
Physical activity (1–3)[b]		–0.16 (–0.21, –0.11)
Alcohol consumption (0–4)[b]		0.05 (0.01, 0.09)
Adjusted R^2 (%)	19	25[c]
	Total cholesterol (mmol/L)	
Fatty acid (mol%)		
22:0	0.17 (0.13, 0.21)	0.17 (0.13, 0.20)
22:1	0.13 (0.09, 0.17)	0.15 (0.11, 0.19)
20:3n-9	0.20 (0.17, 0.24)	0.19 (0.16, 0.23)
18:2n-6	–0.07 (–0.11, –0.04)	–0.02 (–0.05. 0.02)
Body mass index (kg/m^2)		0.20 (0.17, 0.23)
Physical activity (1–3)[b]		–0.10 (–0.14, –0.05)
Adjusted R^2 (%)	7	11[d]

[a]Values are predicted mean change (95% CI) by one SD increase in predictor variable and by one category increase in physical activity and alcohol consumption. See Table 4 for abbreviations.
[b]See Table 1 for categories of physical activity and alcohol consumption.
[c]n = 3499.
[d]n = 4,155.

cluded in the present analyses were not particularly strong. We therefore believe the findings reflect biologic differences between individual fatty acids and not simply the interrelationship between proportions of fatty acids. Many associations of individual fatty acids with serum triglyceride and total cholesterol concentrations weakened after adjustment for BMI. It is, however, questionable whether adjustment for BMI is appropriate, since plasma phospholipid fatty acids and BMI may be intermediate variables in the relationship of dietary fat with serum cholesterol and triglycerides.

In summary, the present data show that there are major differences with regard to both the strength and the direction of the association between serum triglyceride concentrations and individual fatty acids within the same fatty acid class. These results suggest that the association between triglycerides and fatty acid depends on both fatty acid chain length and degree of unsaturation.

ACKNOWLEDGMENTS

This work was financially supported by the Norwegian Research Council and the University of Tromsø, Norway. The study was conducted in collaboration with the National Health Screening Service, Oslo, Norway.

REFERENCES

1. Hokanson, J.E., and Austin, M.A. (1996) Plasma Triglyceride Level Is a Risk Factor for Cardiovascular Disease Independent of High-Density Lipoprotein Cholesterol Level: A Meta-analysis of Population-based Prospective Studies, *J. Cardiovasc. Risk. 3*, 213–219.
2. Jeppesen, J., Hein, H.O., Suadicani, P., and Gyntelberg, F. (1998) Triglyceride Concentration and Ischemic Heart Disease: An Eight-year Follow-up in the Copenhagen Male Study, *Circulation 97*, 1029–1036.
3. Harris, W.S. (1997) n-3 Fatty Acids and Serum Lipoproteins: Human Studies, *Am. J. Clin. Nutr. 65*, 1645S–1654S.
4. Mensink, R.P., and Katan, M.B. (1992) Effect of Dietary Fatty Acids on Serum Lipids and Lipoproteins. A Meta-analysis of 27 Trials, *Arterioscler. Thromb. 12*, 911–919.
5. Gardner, C.D., and Kraemer, H.C. (1995) Monounsaturated Versus Polyunsaturated Dietary Fat and Serum Lipids. A Meta-analysis, *Arterioscler. Thromb. Vasc. Biol. 15*, 1917–1927.
6. Kris Etherton, P.M., and Yu, S. (1997) Individual Fatty Acid Effects on Plasma Lipids and Lipoproteins: Human Studies, *Am. J. Clin. Nutr. 65*, 1628S–1644S.
7. Nikkari, T., Luukkainen, P., Pietinen, P., and Puska, P. (1995) Fatty Acid Composition of Serum Lipid Fractions in Relation to Gender and Quality of Dietary Fat, *Ann. Med. 27*, 491–498.
8. Ma, J., Folsom, A.R., Shahar, E., and Eckfeldt, J.H. (1995) Plasma Fatty Acid Composition as an Indicator of Habitual Dietary Fat Intake in Middle-aged Adults. The Atherosclerosis Risk in Communities (ARIC) Study Investigators, *Am. J. Clin. Nutr. 62* , 564–571.
9. Andersen, L.F., Solvoll, K., and Drevon, C.A. (1996) Very-long-chain n-3 Fatty Acids as Biomarkers for Intake of Fish and n-3 Fatty Acid Concentrates, *Am. J. Clin. Nutr. 64*, 305–311.
10. Padley, F.B., Gunstone, F.D., and Harwood, J.L. (1994) Occurrence and Characteristics of Oils and Fats, in *The Lipid Handbook* (Gunstone, F.D., Harwood, J.L., and Padley, F.B., eds.) pp. 47–223, Chapman & Hall, London.
11. Lasserre, M., Mendy, F., Spielmann, D., and Jacotot, B. (1985) Effects of Different Dietary Intake of Essential Fatty Acids on C20:3ω6 and C20:4ω6 Serum Levels in Human Adults, *Lipids 20*, 227–233.
12. Siguel, E.N., and Maclure, M. (1987) Relative Activity of Unsaturated Fatty Acid Metabolic Pathways in Humans, *Metabolism 36*, 664–669.
13. Miettinen, T.A., Naukkarinen, V., Huttunen, J.K., Mattila, S., and Kumlin, T. (1982) Fatty-Acid Composition of Serum Lipids Predicts Myocardial Infarction, *Br. Med. J. Clin. Res. Ed. 285*, 993–996.
14. Bønaa, K.H., Bjerve, K.S., and Nordøy, A. (1992) Habitual Fish Consumption, Plasma Phospholipid Fatty Acids, and Serum Lipids: The Tromsø Study, *Am. J. Clin. Nutr. 55*, 1126–1134.
15. De Backer, G., De Craene, I., Rosseneu, M., Vercaemst, R., and Kornitzer, M. (1989) Relationship Between Serum Cholesteryl Ester Composition, Dietary Habits and Coronary Risk Factors in Middle-aged Men, *Atherosclerosis 78*, 237–243.
16. Cambien, F., Warnet, J.M., Vernier, V., Ducimetiere, P., Jacqueson, A., Flament, C., Orssaud, G., Richard, J.L., and Claude, J.R. (1988) An Epidemiologic Appraisal of the Associations Between the Fatty Acids Esterifying Serum Cholesterol and Some Cardiovascular Risk Factors in Middle-aged Men, *Am. J. Epidemiol. 127*, 75–86.
17. Sandker, G.W., Kromhout, D., Aravanis, C., Bloemberg, B.P., Mensink, R.P., Karalias, N., and Katan, M.B. (1993) Serum Cholesteryl Ester Fatty Acids and Their Relation with Serum Lipids in Elderly Men in Crete and The Netherlands, *Eur. J. Clin. Nutr. 47*, 201–208.
18. Rosseneu, M., Cambien, F., Vinaimont, N., Nicaud, V., and De Backer, G. (1994) Biomarkers of Dietary Fat Composition in Young Adults with a Parental History of Premature Coronary Heart Disease Compared with Controls. The EARS Study, *Atherosclerosis 108*, 127–136.
19. Jacobsen, B.K., Stensvold, I., Fylkesnes, K., Kristiansen, I.S., and Thelle, D.S. (1992) The Nordland Health Study. Design of the Study, Description of the Population, Attendance and Questionnaire Response, *Scand. J. Soc. Med. 20*, 184–187.
20. Roschlau, P., Bernt, E., and Gruber, W. (1974) [Enzymatic Determination of Total Cholesterol in Serum (author's transl.)] Enzymatische Bestimmung des Gesamt-Cholesterins im Serum, *Z. Klin. Chem. Klin. Biochem. 12*, 403–407.
21. Eggstein, M., and Kreutz, F.H. (1966) Eine neue Bestimmung der Neutralfette im Blutserum und Gewebe. I. Prinzip, Durchfuhrung und Besprechung der Methode, *Klin. Wochenschr. 44*, 262–267.
22. Bjerve, K.S., Fischer, S., and Alme, K. (1987) Alpha-linolenic Acid Deficiency in Man: Effect of Ethyl Linolenate on Plasma and Erythrocyte Fatty Acid Composition and Biosynthesis of Prostanoids, *Am. J. Clin. Nutr. 46*, 570–576.
23. Kleinbaum, D.G., Kupper, L.L., and Muller, K.E. (1988) *Applied Regression Analyis and Other Multivariate Methods*, 2nd edn., PWS-KENT, Belmont, CA.
24. SAS Institute Inc. (1990) *SAS/STAT User's Guide*, 4th edn., SAS Institute Inc, Cary, NC.
25. Harris, W.S. (1989) Fish Oils and Plasma Lipid and Lipoprotein Metabolism in Humans: A Critical Review, *J. Lipid Res. 30*, 785–807.
26. Willumsen, N., Skorve, J., Hexeberg, S., Rustan, A.C., and Berge, R.K. (1993) The Hypotriglyceridemic Effect of Eicosapentaenoic Acid in Rats Is Reflected in Increased Mitochondrial Fatty Acid Oxidation Followed by Diminished Lipogenesis, *Lipids 28*, 683–690.
27. Mannaerts, G.P., and Van Veldhoven, P.P. (1993) Metabolic Role of Mammalian Peroxisomes, in *Peroxisomes: Biology and Importance in Toxicology and Medicine* (Gibson, G. and Lake, B., eds.) pp. 19–62, Taylor and Francis, London.
28. Frøyland, L., Madsen, L., Vaagenes, H., Totland, G.K., Auwerx,

J., Kryvi, H., Staels, B., and Berge, R.K. (1997) Mitochondrion Is the Principal Target for Nutritional and Pharmacological Control of Triglyceride Metabolism, *J. Lipid Res. 38*, 1851–1858.
29. Jacobsen, B.K., and Thelle, D.S. (1987) The Tromsø Heart Study: Food Habits, Serum Total Cholesterol, HDL Cholesterol, and Triglycerides, *Am. J. Epidemiol. 125*, 622–630.
30. Sacks, F.M., Stampfer, M.J., Munoz, A., McManus, K., Canessa, M., and Kass, E.H. (1987) Effect of Linoleic and Oleic Acids on Blood Pressure, Blood Viscosity, and Erythrocyte Cation Transport, *J. Am. Coll. Nutr. 6*, 179–185.
31. Grimsgaard, S., Bønaa, K.H., Hansen, J.B., and Nordøy, A. (1997) Highly Purified Eicosapentaenoic Acid and Docosahexaenoic Acid in Humans Have Similar Triacylglycerol Lowering Effects, But Divergent Effects on Serum Fatty Acids, *Am. J. Clin. Nutr. 66*, 649–659.
32. Zock, P.L., and Katan, M.B. (1992) Hydrogenation Alternatives: Effects of *trans* Fatty Acids and Stearic Acid Versus Linoleic Acid on Serum Lipids and Lipoproteins in Humans, *J. Lipid Res. 33*, 399–410.
33. Lopes, S.M., Trimbo, S.L., Mascioli, E.A., and Blackburn, G.L. (1991) Human Plasma Fatty Acid Variations and How They Are Related to Dietary Intake, *Am. J. Clin. Nutr. 53*, 628–637.
34. Simon, J.A., Fong, J., Bernert, J.T., Jr., and Browner, W.S. (1996) Relation of Smoking and Alcohol Consumption to Serum Fatty Acids, *Am. J. Epidemiol. 144*, 325–334.
35. Feinman, L., and Lieber, C.S. (1998) Nutrition and Diet in Alcoholism, in *Modern Nutrition in Health and Disease* (Shils, M.E., Olson, J.A., and Shike, M., eds.) Vol. 2, pp. 1081–1101, Lea and Febiger, Philadelphia.
36. Jacobs, D.R., Jr., and Barrett Connor, E. (1982) Retest Reliability of Plasma Cholesterol and Triglyceride. The Lipid Research Clinics Prevalence Study, *Am. J. Epidemiol. 116*, 878–885.
37. Riemersma, R.A., Wood, D.A., Butler, S., Elton, R.A., Oliver, M., Salo, M., Nikkari, T., Vartiainen, E., Puska, P., Gey, F., *et al.* (1986) Linoleic Acid Content in Adipose Tissue and Coronary Heart Disease, *Br. Med. J. Clin. Res. Ed. 292*, 1423–1427.
38. Seidell, J.C., Cigolini, M., Deslypere, J.P., Charzewska, J., and Ellsinger, B.M. (1991) Polyunsaturated Fatty Acids in Adipose Tissue in European Men Aged 38 Years in Relation to Serum Lipids, Smoking Habits, and Fat Distribution, *Am. J. Epidemiol. 134*, 583–589.
39. Dietschy, J.M. (1997) Theoretical Considerations of What Regulates Low-Density-Lipoprotein and High-Density-Lipoprotein Cholesterol, *Am. J. Clin. Nutr. 65*, 1581S–1589S.

[Received February 14, 2000, and in revised form July 19, 2000; revision accepted August 17, 2000]

Discovery of an 11(*R*)- and 12(*S*)-Lipoxygenase Activity in Ovaries of the Mussel *Mytilus edulis*

Gianguido Coffa and Elizabeth M. Hill*

School of Chemistry, Physics and Environmental Science, University of Sussex Falmer, Brighton BN1 9QJ, United Kingdom

ABSTRACT: Eicosanoid biosynthesis was investigated in mussel gonads by incubation of tissue homogenates with radiolabeled arachidonic acid and analysis of the products by radio-high-performance liquid chromatography. No radiolabeled metabolites were formed in homogenates of testes, but two major metabolites were synthesized by ovarian preparations. The radiolabeled metabolites were analyzed by mass spectrometry and chiral chromatography and identified as 11(*R*)-hydroxy-5,8,12,14-eicosatetraenoic acid and 12(*S*)-hydroxy-5,8,10,14-eicosatetraenoic acid. In addition, four other nonlabeled metabolites, formed from endogenous substrates, were detected in ovarian extracts. Their structures, determined by mass spectrometric analysis, were the corresponding 11- and 12-hydroxy analogs formed from eicosapentaenoic acid (11-HEPE and 12-HEPE) and 9-hydroxy-6,10,12,15-octadecatetraenoic acid (9-HOTE) and 13-hydroxy-6,9,11,15-octadecatetraenoic acid formed from stearidonic acid. The biosynthesis of the 11- and 12-hydroxy products was calcium dependent, localized to the 100,000 × *g* supernatant cell fraction, and was inhibited by nordihydroguaiaretic acid, but not inhibited by the prostaglandin synthase inhibitors aspirin and indomethacin, or the monoxygenase inhibitor proadifen. Together these data suggested that both the 11(*R*)- and 12(*S*)-hydroxy products were formed from lipoxygenase-type enzymes. Incubation of homogenates of immature ovaries with eicosapentaenoic acid revealed the major product to be 12-HEPE, whereas in mature ovaries mainly 11-HEPE was formed. Extraction of spawned eggs with methanol revealed that predominantly 11-HEPE and 9-HOTE were formed from endogenous substrates. This study shows that female gonads of the mussel express an 11(*R*)- and 12(*S*)-lipoxygenase activity whose expression is dependent on differentiation of the ovary.

Paper no. L8597 in *Lipids 35,* 1195–1204 (November 2000).

Eicosanoids are biologically active lipid metabolites that are formed from the action of either lipoxygenase, prostaglandin synthase, or cytochrome P450 enzymes on polyunsaturated fatty acids (PUFA) such as arachidonic acid (AA). The biosynthesis and physiological role of eicosanoids have been widely studied in mammals whereas there is less information on the identity and activity of these lipid mediators in lower organisms. A number of studies have reported the biosynthesis and/or activity of eicosanoids in a variety of reproductive processes in aquatic invertebrates (1). Many of these compounds have been identified as hydroperoxyeicosatetraenoic acids (HPETE), or their reduction products hydroxyeicosatetraenoic acids (HETE), which are thought to be stereospecific products of lipoxygenase (LO)-mediated metabolism. Unlike mammalian LO, which tend to form products with the *S* stereochemistry, many invertebrate LO biosynthesize eicosanoids with the *R* configuration. For instance, starfish oocytes have been reported to synthesize 8(*R*)-HETE, which triggers oocyte maturation (meiosis reinitiation) prior to spawning (2). Eggs of the surf clam (*Spisula solidissima*) biosynthesized high levels of 5(*R*)-HETE and 8(*R*)-HETE, although these metabolites did not stimulate oocyte maturation in this species and their physiological role in the surf clam is currently unknown (3). However 5-HETE (chirality not given) was reported to stimulate oocyte maturation in the clam *S. sachalinensis* (4). The LO products 11(*R*)- and 12(*R*)-HETE have been identified in eggs of the sea urchin *Strongylocentrotus purpuratus* although their biological activity was not determined (5). It has been reported that *Hydra magnipapillata* synthesized 11(*R*)-HETE, which inhibited head formation, and 12(*S*)-HETE, which enhanced bud formation in this species (6). 11(*R*)-HETE was also formed in *H. vulgaris* and was shown to promote tentacle regeneration in this hydroid (7). During metamorphosis, larvae of the marine hydroid, *Hydractinia echinata,* synthesize 8(*R*)-HETE, however the biological role of this metabolite has yet to be defined (8). A number of 8-hydroxylated eicosanoid metabolites, including 8(*R*)-HEPE, have been reported to stimulate hatching of barnacle (*Semibalanus balanoides*) embryos (9,10). LO products have been implicated in sperm activation of the polychaete *Arenicola marina* (11). Together, these studies suggest that LO metabolites may play an important role in the reproductive physiology of a number of aquatic invertebrates.

In our laboratory, initial investigations of eicosanoid biosynthesis in different tissues of the mussel, *Mytilus edulis,* identified the gonads as a potent source of hydroxy fatty

*To whom correspondence should be addressed.
E-mail: e.m.hill@sussex.ac.uk

Abbreviations: AA, arachidonic acid; BSTFA, bis(trimethylsilyl)trifluoroacetamide; EPA, eicosapentaenoic acid; GS–MS, gas chromatography–mass spectrometry; 11-HEPE, 11-hydroxy-5,8,12,14,17-EPA; 12-HEPE, 12-hydroxy-5,8,10,14,17-EPA; HETE, hydroxyeicosatetraenoic acid; 9-HOTE, 9-hydroxy-6,10,12,15-octadecatetraenoic acid; 13-HOTE, 13-hydroxy-6,9,11,15-octadecatetraenoic acid; HPETE, hydroperoxyeicosatetraenoic acid; HPLC, high-performance liquid chromatography; IMC, indomethacin; LO, lipoxygenase; NDGA, nordihydroguaiaretic acid; PGB_2, prostaglandin B_2; PUFA, polyunsaturated fatty acid; RP-HPLC, reversed-phase HPLC; SA, stearidonic acid; SP-HPLC, straight-phase HPLC; UV, ultraviolet.

acids. In this study we report on the identity and properties of LO enzymes in the ovaries of *M. edulis.*

MATERIALS AND METHODS

Materials. 5,8,11,14-Eicosatetraenoic acid (AA), 5,11,14,17-eicosapentaenoic acid (EPA), 6,9,12,15-octadecatetraenoic acid (stearidonic acid, SA), indomethacin (IMC), nordihydroguaiaretic acid (NDGA), aspirin, proadifen, baicalein, bis(trimethylsilyl)trifluoroacetamide (BSTFA), 1-methyl-3-nitro-1-nitrosoguanidine, and (–)-menthyl chloroformate were purchased from Sigma Chemical Company (Poole, Dorset, United Kingdom). 1-[^{14}C]-AA (specific activity 2220 Mbq/mmol, radioactive purity >90%) was obtained from Amersham Life Science (Little Chalfont, Buckinghamshire, United Kingdom). (±)11-HETE, (±)12-HETE, and 11(*R*)-HETE were purchased from Cayman Chemical Co. (Ann Arbor, MI), and 12(*S*)-HETE was purchased from Biomol (Plymouth Meeting, PA). Rhodium (5% on alumina) was obtained from Lancaster Synthesis Ltd. (Morecombe, Lancashire, United Kingdom). All solvents used were of high-performance liquid chromatography (HPLC) grade, purchased from Rathburn Chemicals, Ltd. (Walkerburn, United Kingdom).

Animals and preparation of gonads. Mussels (*M. edulis),* length 5–8 cm, were collected between January 1998 and April 1999 from Brighton, East Sussex, United Kingdom, and transported to the laboratory where the gonads were immediately removed and placed on ice. Sex was determined by microscopic examination and gonads were classified as either immature (no gametes visible), partly mature (gonad contains developing gametes), or mature (gonad distended with ripe gametes). For each experiment, gonads were used at identical reproductive stages.

Preparation of gonad homogenates. Gonads (typically 1 gonad/2 mL) were homogenized (30 s, 6000 rpm, Potter-Elvehjem homogenizer; Wheaton Science Products, Millville, NJ) in an ice-cold solution of Tris buffer (50 mM), containing EDTA (5 mM), pepstatin A (0.6 μg/mL), aprotinin (3 μg/mL), and leupeptin (0.6 μg/mL). The tissue preparations were centrifuged at 3,000 × *g* for 5 min, and the supernatants were removed for studies on eicosanoid biosynthesis in crude homogenates.

In some experiments microsomal and cytosolic fractions were prepared as follows. The tissue homogenate was centrifuged at 10,000 × *g* (5°C) for 15 min and the resulting supernatant centrifuged at 100,000 × *g* (5°C) for 1 h. The supernatant (cytosolic extract) was removed and the microsomal pellet washed with Tris buffer (2 × 0.5 mL) and resuspended in Tris buffer at 100 μL/gonad.

Incubation with substrate. Gonad homogenates (1 mL) were incubated with 20 μM (1 μL of 20 mM ethanolic stock) of either AA or EPA followed by 10 mM calcium chloride (10 μL of 1 M aqueous stock). The samples were incubated in a water bath for 30 min at 18–19°C. The reaction was stopped by adding ice-cold methanol (0.3 mL) and the solutions stored at –20°C before eicosanoid extraction. Incubations with boiled homogenates (100°C, 5 min) were used to monitor for nonenzymatic oxidation of substrate. In some experiments radiolabeled [1-^{14}C]AA was used as substrate at a final concentration of 20 μM and 3.7 kBq/mL. In other experiments, homogenates were pre-incubated at 16°C for 15 min with several inhibitors prior to the addition of substrate and calcium. The inhibitors, baicalein (5–30 μM final concentration), NDGA (10–30 μM final concentration), proadifen (30 μM final concentration), aspirin (30 μM final concentration), and IMC (10–25 μM), were added in 1 μL/mL of ethanol carrier.

Collection of eggs. To investigate eicosanoid synthesis in released eggs, mussels were kept in small aquaria with fresh seawater and the spawning was induced by injection of 2.5 mL of KCl (0.5 M) into the mantle cavity. The released eggs of each mussel were then washed and suspended in fresh seawater (2 mL) and divided in two portions, one of which was incubated for 30 min with 20 μM EPA (2 μL of 10 mM ethanolic stock) prior to the addition of methanol (0.3 mL) and the other was incubated with vehicle (2 μL ethanol) prior to the addition of methanol (0.3 mL). The samples where then quickly frozen at –20°C before extraction.

Solid phase extraction of eicosanoids. Prior to extraction, prostaglandin B_2 (PGB_2, 0.4 μg in 40 μL ethanol) was added to each sample as an internal standard. The methanolic samples were centrifuged (3,000 × *g*, 5 min), the supernatants decanted, and the pellets extracted with 0.5 mL methanol. The supernatants were combined and diluted with 16 mL of 17.5 mM ammonium acetate buffer (pH 4). One hundred milligram C_{18} solid phase extraction columns (Waters Corp., Milford, MA) were conditioned with 10 mL of methanol, followed by 10 mL of ammonium acetate buffer. After loading of the sample, the columns were washed with 5 mL of buffer (pH 4) and eicosanoids eluted with 4 mL of methanol. The solvent was removed under vacuum and the residue redissolved in 300 μL of methanol and 300 μL of water pH 5.7 (0.1% acetic acid, pH adjusted with ammonium hydroxide, NH_4OH) for reversed-phase (RP)-HPLC analysis.

RP-HPLC analysis. Samples were analyzed by RP-HPLC using a C_{18} column (5 μM, 4.6 × 150 mm, Nova-Pak; Waters Corp.). Metabolites were detected using a photodiode array detector (996; Waters) followed in series by an on-line radioactivity monitor model (LB 506 C-1; Berthold, Wildbad, Germany). RP-HPLC mobile phase was a mixture of 20% methanol (solvent B) and 80% buffer (0.1% glacial acetic acid buffered to pH 5.7 with NH_4OH) (solvent A) changing to 70% solvent B in 20 min, and increasing to 100% B from 40 to 50 min. Recoveries were monitored by measurement of PGB_2 peak height at 280 nm.

In order to collect samples for further analyses, some incubations were combined prior to HPLC analysis. Where it was necessary to separate and collect closely eluting compounds, the following modified program was used: 40% methanol, 10% acetonitrile, for 20 min, increasing as a step to 50% methanol at 30 min and to 60% at 58 min, with a gradient to 100% from 60 to 70 min. Metabolites were collected from the ultraviolet (UV) detector, the HPLC eluent removed under

vacuum, and the sample redissolved in methanol and stored under oxygen-free nitrogen at –20°C for further analysis.

Gas chromatography–mass spectrometry (GC–MS). Samples, in 10 µL of methanol, were methylated by reaction with an excess of ethereal diazomethane at room temperature for 15 min. The solvent was evaporated and the residues were derivatized to their silyl ethers by addition of 20 µL of BSTFA and 20 µL of pyridine for 15 min at 60°C. The BSTFA was removed under nitrogen and the derivatives redissolved in hexane prior to injection in GC–MS. In addition, an aliquot of some samples was hydrogenated as follows: samples were dissolved in 0.5 mL methanol with 2–5 mg of rhodium (5% on alumina) catalyst. Hydrogen was bubbled through the solution for 15 min (room temperature). Rhodium was removed by centrifugation, the methanol removed under vacuum, and the samples silylated as described above prior to analysis by GC–MS.

Electron ionization mass spectrometry was performed on a Kratos MS890 instrument (Ramsey, NJ) coupled to a Carlo Erba MFC 500 gas chromatograph (Milano, Italy). Samples were injected in splitless mode onto a capillary column (10 m BPX5; SGE Ltd., Milton Keynes, United Kingdom). The injector and source temperatures were 280°C, and the column temperature was increased from 100 to 280°C at a rate of 10°C/min. The accelerating potential was 4 kV, electron energy 70 eV, and the magnetic sector cycled from 600 to 50 amu during 0.8 s.

Steric analysis of 11- and 12-HETE by HPLC. 11- and 12-HETE, obtained from mussel extracts, were purified by RP-HPLC, and methylated as described above. To determine the chiralty of 11-HETE, the methyl ester was converted to the (–)-menthoxycarbonyl derivative by addition of 100 µL of dry toluene, 10 µL of dry pyridine and 5 µL of menthylchloroformate. After 30 min of reaction at room temperature, the solvents were evaporated to dryness under nitrogen and the menthoxycarbonyl derivatives extracted from the solid residue with hexane. The hexane was removed, the sample redissolved in methanol and purified by RP-HPLC (5 µm, 4.6 × 150 mm Waters Nova-Pak C_{18}; solvent methanol/water, 97:3, flow 1 mL/min). The menthoxycarbonyl derivative eluted after ≅8 min. The diastereoisomer was resolved by straight-phase (SP)-HPLC using an Alltech 5-µm silica column (4.6 × 250 mm) and eluting with a mixture *n*-hexane/isopropanol 100:0.1 vol/vol at 1 mL/min. The retention time of 11-HETE from mussel was compared with a racemic mixture of 11-HETE and with 11(*R*)-HETE.

For the chiral analysis of 12-HETE, the methyl ester was resolved by chiral HPLC using a Diacel Chiralcel OD (4.6 × 250 mm) chiral column eluting with a mixture *n*-hexane/isopropanol 99:1 at 1 mL/min. The retention time of 12-HETE from mussel was compared with the racemic mixture and with 12(*S*)-HETE.

RESULTS

Eicosanoid production in male and female gonads. Incubation of [^{14}C]-AA with crude homogenates of partly mature male gonads did not result in the production of any metabolites (Figs. 1A and B). In addition, no radiolabeled or UV-absorbing metabolites were detected when homogenates of either immature or mature male gonads were incubated with radiolabeled substrate (data not shown). However, incubation of crude homogenates of partly mature female gonads of *M. edulis* with [^{14}C]AA resulted in the complete incorporation of radioactive substrate into two major metabolites, designated **I** and **II** (Figs. 1C and 1D). These metabolites were also detected by UV absorption and photodiode array analysis showed that they both contained a chromophore typical of a conjugated diene structure, with a λ_{max} of 235 nm for both metabolites (data not shown). In addition, UV detection showed the presence of three other metabolites that were not radiolabeled (metabolites **III, IV,** and **V**), suggesting they were formed from endogenous substrate. Photodiode array analysis of these metabolites revealed a similar UV spectrum to that of metabolites **I** and **II**. No peaks were formed after incubation of substrate with boiled homogenates suggesting that these five metabolites were not formed from nonenzymatic oxidation (data not shown).

GC–MS analysis of metabolites. The five metabolites produced by homogenates of female gonads were purified by RP-HPLC and analyzed by GC–MS after derivatization to the methyl esters and silyl ethers.

*Metabolite **I**.* GC–MS analysis of **I** [GC retention time (rt) 18.2 min] gave major ions at *m/z* 406 (M^+), *m/z* 391 (M – CH_3), *m/z* 375 (M – OCH_3), and *m/z* 295 (base ion, cleavage between C-12 and C-13) (data not shown). Analysis of the hydrogenated sample (GC rt, 18.6 min) revealed ions at: *m/z* 399 (M – CH_3), *m/z* 383 (M – OCH_3), *m/z* 215 base ion, cleavage at C-12 and loss of $(CH_2)_{10}COOCH_3$, *m/z* 301 cleavage between C-12 and C-13 and loss of $(CH_2)_7CH_3$, and *m/z* 272 cleavage at C-12 and rearrangement of $Si(CH_3)_3$ to the carboxyl group (data not shown). These results are consistent with the structure of 12-hydroxy-5,8,10,14-eicosatetraenoic acid (12-HETE).

*Metabolite **II**.* The mass spectrum of **II** (GC rt, 18.2 min) revealed ions at *m/z* 406 (M^+), *m/z* 391 (M – CH_3), *m/z* 375 (M – OCH_3), and *m/z* 225 (base ion, cleavage between C-10 and C-11). GC–MS analysis of the reduced compound (GC rt, 18.5 min) gave ions at *m/z* 399 (M – CH_3), *m/z* 383 (M – OCH_3), *m/z* 287, cleavage at C-11 and loss of $CH_3(CH_2)_8$, *m/z* 229 base ion, cleavage at C-11 and loss of $(CH_2)_9COOCH_3$, and *m/z* 258 cleavage at C-11 and rearrangement of $Si(CH_3)_3$ to the carboxyl group (data not shown). These results are consistent with the structure of 11-hydroxy-5,8,12,14-eicosatetraenoic acid (11-HETE).

*Metabolite **III**.* GC–MS analysis of metabolite **III** (GC rt, 18.4 min) revealed ions at *m/z* 404 (M^+), *m/z* 389 (M – CH_3), *m/z* 373 (M – OCH_3), and *m/z* 295 (base ion, cleavage between C-12 and C-13). The following ions were observed when the reduced sample was analyzed (GC rt, 18.6 min): *m/z* 399 (M – CH_3), *m/z* 383 (M – OCH_3), *m/z* 215 base ion, cleavage at C-12 and loss of $(CH_2)_{10}COOCH_3$, *m/z* 301 cleavage at C-12 and loss of $(CH_2)_7CH_3$, and *m/z* 272 cleavage at

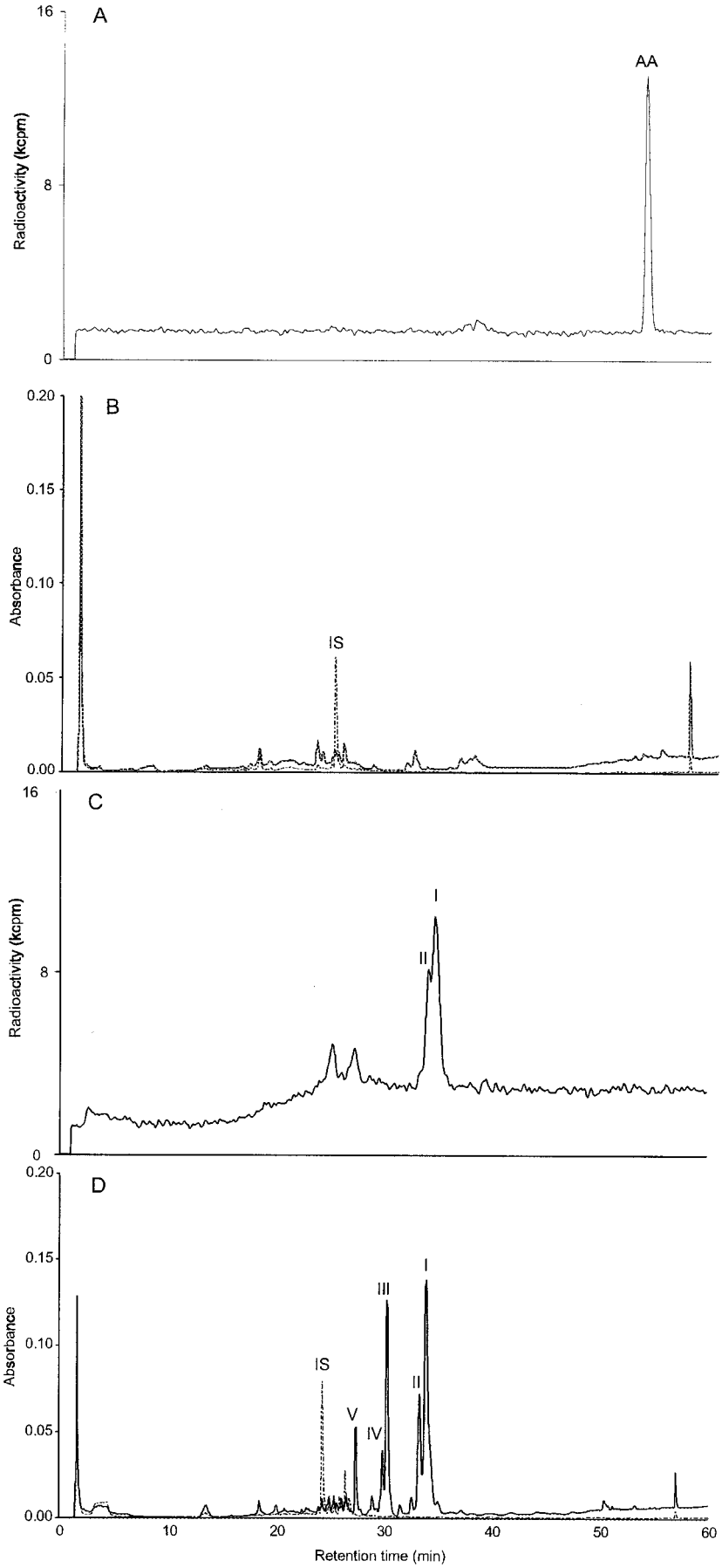

FIG. 1. Reversed-phase high-performance liquid chromatography (RP-HPLC) chromatogram obtained after incubation of mussel gonad tissue preparations with [^{14}C]arachidonic acid. (A) [^{14}C] Radiochromatogram of testis extract; (B) ultraviolet (UV) chromatogram of testis extract (— 235 nm, --- 280 nm); (C) [^{14}C] radiochromatogram of ovary extract; (D) UV chromatogram of ovary extract (— 235 nm, ---280 nm). IS = prostaglandin B_2 (PGB_2) internal standard. Retention time of 11-HETE standard 32.7 min, 12-HETE standard 33.5 min. HETE, hydroxyeicosatetraenoic acid.

C-12 and rearrangement of $Si(CH_3)_3$ to the carboxyl group (data not shown). These results are consistent with the structure of 12-hydroxy-5,8,10,14,17-EPA (12-HEPE).

*Metabolite **IV***. Metabolite **IV** (GC rt, 18.3 min) revealed ions at *m/z* 404 (M^+), *m/z* 389 (M – CH_3), *m/z* 373 (M – OCH_3), and *m/z* 223 (base ion, cleavage between C-10 and C-11). The reduced compound (GC rt, 18.5 min) revealed ions at *m/z* 399 (M – CH_3), *m/z* 383 (M – OCH_3), *m/z* 287 cleavage at C-11 and loss of $CH_3(CH_2)_8$, *m/z* 229 base ion, cleavage at C-11 and loss of $(CH_2)_9COOCH_3$, and *m/z* 258 cleavage at C-11 and rearrangement of $Si(CH_3)_3$ to the carboxyl group (data not shown). These results are consistent with the structure of 11-hydroxy-5,8,12,14,17-EPA (11-HEPE).

*Metabolite **V***. Analysis of this fraction revealed two peaks on GC–MS. Analysis of the major compound (GC rt, 16.6 min) revealed ions at *m/z* 378 (M^+), *m/z* 363 (M – CH_3), *m/z* 347 (M – OCH_3) and *m/z* 223 base ion, cleavage between C-8 and C-9 and loss of $CH_2(CH)_2(CH_2)_4COOCH_3$ (Fig. 2A). The reduced compound (GC rt, 17.1 min) revealed ions at *m/z* 371 (M – CH_3), *m/z* 355 (M – OCH_3), *m/z* 259 base ion, cleavage at C-9 and loss of $CH_3(CH_2)_8$, and *m/z* 229 cleavage at C-9 and loss of $(CH_2)_7COOCH_3$ (Fig. 2B). Assuming the formation of this product from endogenous SA, these results are consistent with the structure of this metabolite as 9-hydroxy-6,10,12,15-octadecatetraenoic acid (9-HOTE).

Analysis of the minor compound (GC rt, 16.6 min) revealed ions at *m/z* 378 (M^+), *m/z* 363 (M – CH_3), *m/z* 347 (M – OCH_3), *m/z* 309 cleavage at C-13 and loss of $CH_3CH_2(CH)_2CH_2$, and *m/z* 223 cleavage at C-8 and loss of $CH_2(CH)_2(CH_2)_4COOCH_3$ (Fig. 3A). After reduction, GC–MS analysis (rt 17.2, min) revealed ions at *m/z* 371 (M – CH_3), *m/z* 355 (M – OCH_3), *m/z* 315 cleavage at C-13 and loss of $CH_3(CH_2)_4$, and *m/z* 173 cleavage at C-13 and loss of $(CH_2)_{11}COOCH_3$ (Fig. 3B). If the precursor substrate was SA, these results are consistent with the structure of this metabolite as 13-hydroxy-6,9,11,15-octadecatetraenoic acid, 13-HOTE.

Steric analyses of 11- and 12-HETE. The chirality of 11-HETE was determined by SP-HPLC analysis of the methyl ester (–)-menthoxycarbonyl derivatives. The racemic standard eluted as two peaks at 11.5 and 12.1 min with the *R* form eluting before the *S* enantiomer (Fig. 4A) similar to a previous report (5). Co-injection of the natural mussel product with the racemic standard resulted in an increase of the *R* enantiomer (Fig. 4B). Analysis of the natural product alone revealed that it predominantly consisted of the *R* enantiomer with less than 1% m/m of the *S* form (Fig. 4C).

The chirality of the 12-HETE metabolite was determined by separation of the methyl ester derivatives on a Chiracel OD column. The racemic mixture of 12-HETE eluted as two peaks at 13.0 and 16.0 min with the *R* enantiomer eluting before the *S* form (Fig. 5A). Co-injection of the mussel natural product resulted in an increase of the *S* form (Fig. 5B). Analysis of the natural product alone revealed that 12-HETE consisted solely of the *S* enantiomer (Fig. 5C).

Eicosanoid production during ovarian development. Initial results with incubation of crude homogenates of ripe ovaries with different PUFA substrates showed that HETE metabolites were only formed from the addition of exogenous substrate (AA) whereas HEPE metabolites were formed even without addition of substrate as well as from addition of exogenous EPA. This suggested the possibility that EPA may be the natural endogenous substrate for biosynthesis of these monohydroxy fatty acids. To investigate changes in the profile of the 11- and 12-hydroxy fatty acids produced during ovarian development, crude homogenates of immature or ripe gonads were incubated with EPA and the resulting eicosanoid profiles analyzed by RP-HPLC. In order to confirm the structures of closely eluting metabolites, RP-HPLC peaks were collected and structures confirmed after GC–MS analysis of the silylated derivatives. In immature female gonads, the major metabolite was 12-HEPE with lesser amounts of 11-HEPE (Fig. 6A). In mature ovaries, the major metabolite produced was 11-HEPE with only low amounts of 12-HEPE present (Fig. 6B).

In order to determine whether these eicosanoids were produced in spawned eggs, mussels were induced to spawn by injection with KCl and spawned eggs were collected, immediately extracted with methanol, and subjected to RP-HPLC analysis. The eicosanoid profile showed high levels of 11-HEPE and HOTE (predominantly the 9-isomer), but low levels of 12-HEPE or HETE (Fig. 6C). There was no increase in the biosynthesis of 11-HEPE when eggs were preincubated with substrate (20 μM EPA, 30 min) prior to extraction (data not shown).

Calcium dependence of the reaction. To determine whether the enzymes involved in the biosynthesis of 11- and 12-HEPE were calcium dependent, crude homogenates of partly mature ovaries (in Tris buffer containing 5 mM EDTA) were incubated with EPA in the presence of different concentrations of calcium. When no calcium was added, only trace amounts of 11- or 12-HEPE were formed. Addition of 10 mM Ca^{2+} or more (final concentration) resulted in maximal response of both enzyme activities (Table 1). These results suggest that the formation of both 11- and 12-HEPE is calcium dependent.

Effects of inhibitors on eicosanoid biosynthesis. The effects of NDGA, baicalein, proadifen, aspirin, and IMC on biosynthesis of 11- and 12-HEPE were investigated. Crude homogenates of partially mature ovaries were preincubated with inhibitors prior to addition of EPA (20 μM) and calcium. Neither aspirin (at 30 μM, an inhibitor of the prostaglandin synthase I isoform) nor IMC (30 μM, a nonselective inhibitor of the prostaglandin synthase pathway) reduced biosynthesis of either eicosanoid. An inhibitor of the cytochrome P450 pathway, proadifen (30 μM), did not inhibit the biosynthesis of either 11- or 12-HEPE. Baicalein is a selective inhibitor of mammalian (platelet) 12(*S*)-LO with an ID_{50} of 0.12 μM (12). In our study, preincubation with 5 μM baicalein did not reduce eicosanoid synthesis but at 20 μM, baicalein inhibited the biosynthesis of 11-HEPE by 54% and only inhibited 12-HEPE biosynthesis by 11% (data not shown). NDGA (10 μM) was the most effective inhibitor and inhibited the biosynthesis of 11-HEPE by 91% and 12-HEPE by 86%.

Cellular localization of the lipoxygenase activity. In order to determine the localization of enzyme activity, 100,000 × *g*

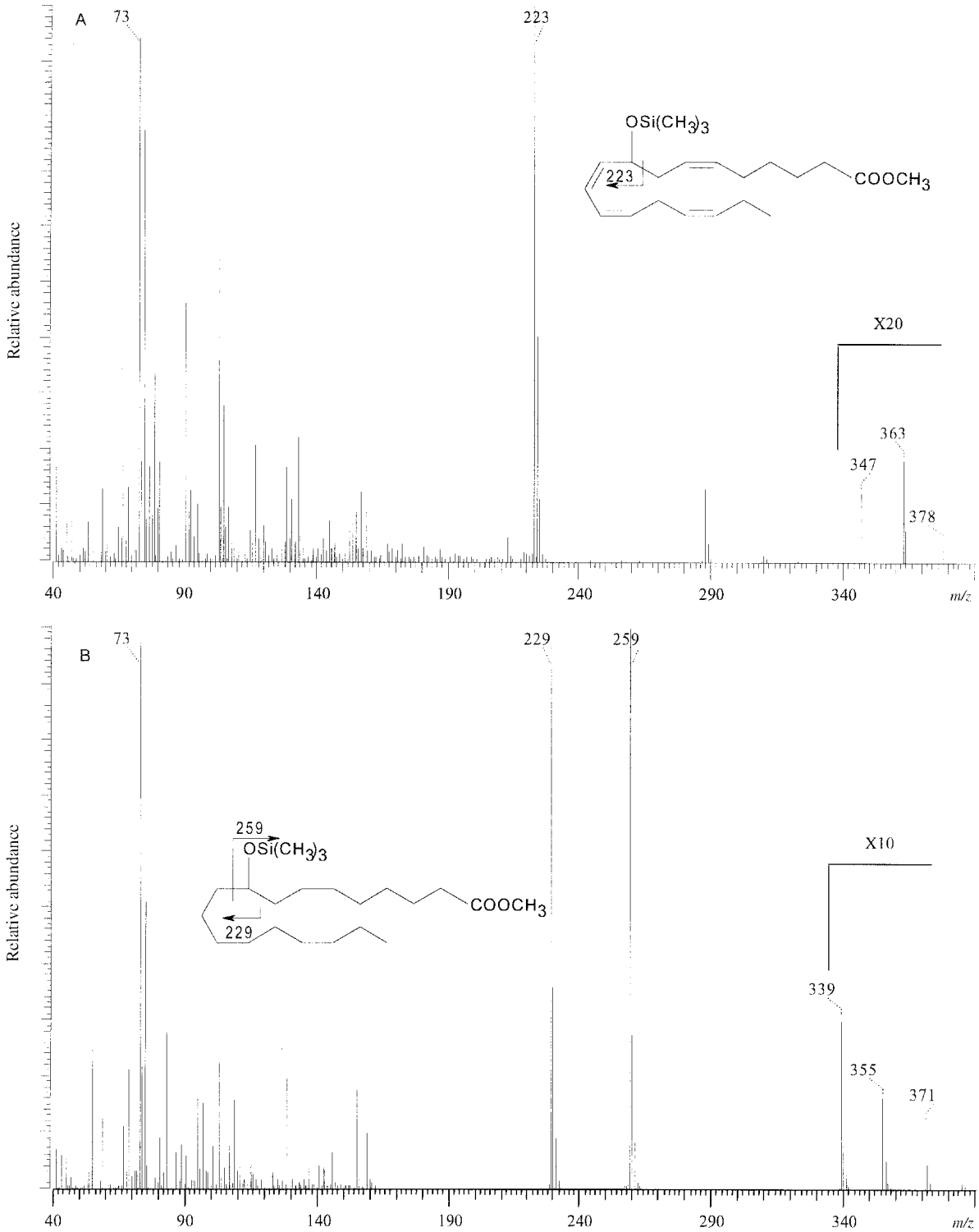

FIG. 2. Gas chromatography–mass spectrometry (GC–MS) analysis of the methyl ester, trimethylsilyl ether of the major compound in the RP-HPLC fraction of metabolite **V**. (A) Native structure; (B) after hydrogenation. See Figure 1 for other abbreviation.

supernatant and pellet preparations were made with partially ripe ovarian tissue. The preparations were incubated with EPA and calcium and the products analyzed by RP-HPLC. Over 96% of both the 11- and 12-LO activity was associated with the 100,000 × *g* supernatant suggesting that both these enzymes were localized in the cell cytosol.

DISCUSSION

This study shows that the synthesis of eicosanoids in the mussel gonad is sex dependent. No eicosanoids were detected in immature or ripe testes, but a number of hydroxy fatty acids were synthesized in mussel ovaries from both endogenously

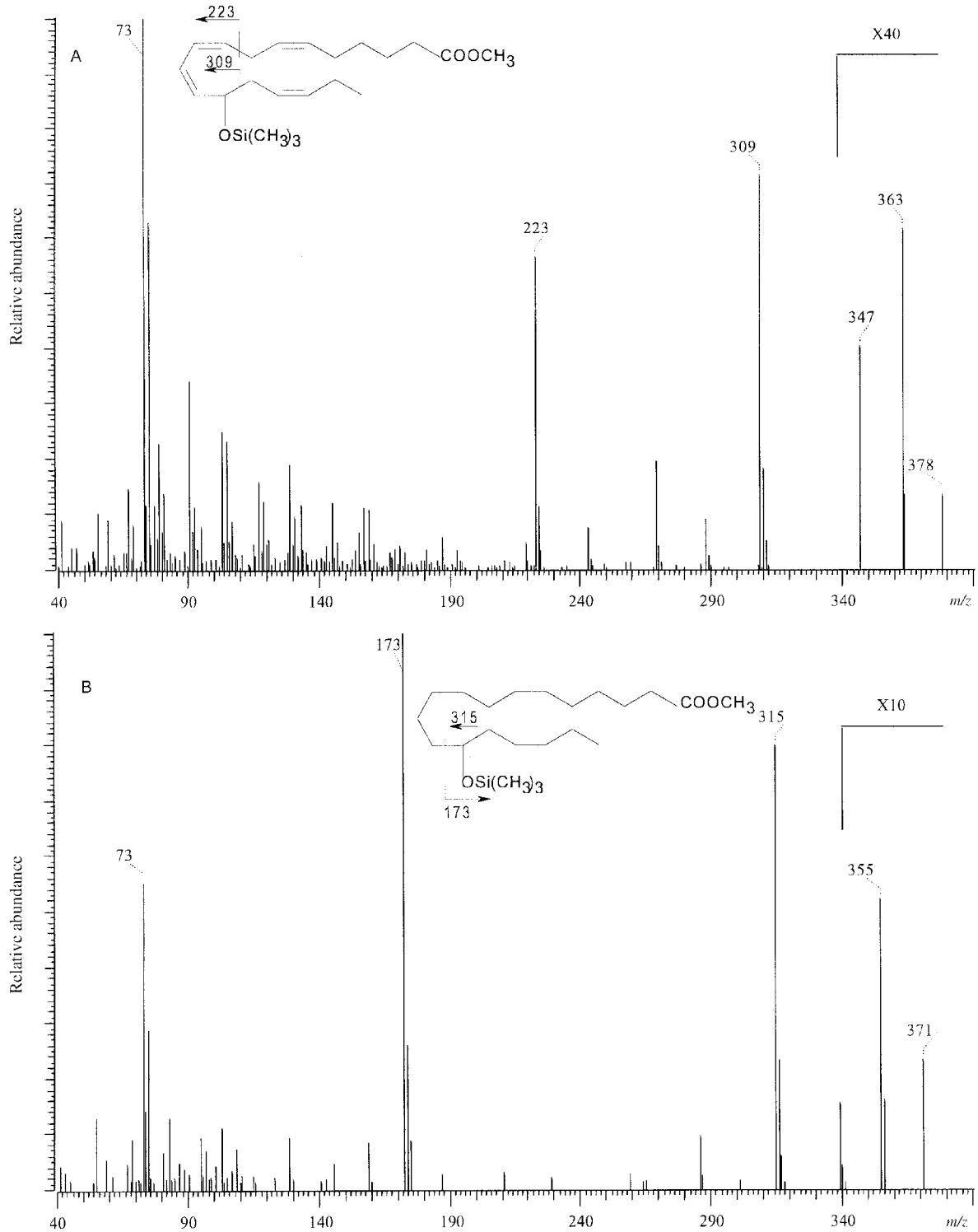

FIG. 3. GC–MS analysis of the methyl ester, trimethylsilyl ether of the minor compound in the RP-HPLC fraction of metabolite **V**. (A) Native structure; (B) after hydrogenation. See Figures 1 and 2 for abbreviations.

and exogenously added substrates. The major metabolites formed from the addition of AA were identified by GC–MS and chiral analyses as 11(*R*)-HETE and 12(*S*)-HETE. The biosynthesis of these metabolites was not inhibited by the prostaglandin synthase inhibitors aspirin and IMC, nor by proadifen, an inhibitor of the cytochrome P450 pathway. Their formation was inhibited by NDGA (10 μM) at a concentration which inhibits mammalian LO enzymes. In addition, unlike the cytochrome P450 and prostaglandin synthase enzymes, the enzymes involved in the biosynthesis of these HETE were localized in the cytosol and not the microsomal fraction, and product formation was calcium dependent. Fur-

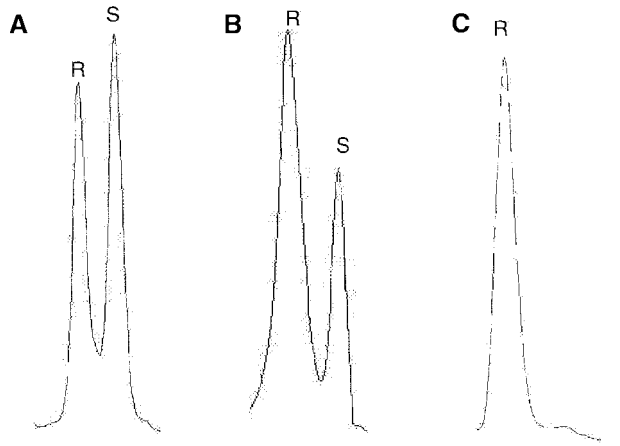

FIG. 4. Chiral analysis of mussel-derived 11-HETE. The methyl ester (–)-menthoxycarbonyl derivatives of standards and samples were analyzed by straight-phase HPLC. (A) Standard racemic 11-HETE; (B) co-injection of mussel-derived 11-HETE with the racemic standard; (C) analysis of mussel 11-HETE alone. See Figure 1 for abbreviations.

thermore, in contrast to many cytochrome P450 metabolites (13), the HETE formed in this study were highly enantiospecific being either all *R* (11-HETE) or all *S* (12-HETE). Together these data suggest that these metabolites are formed from the action of LO enzymes.

The HETE products of LO action in many aquatic invertebrates tend to be of the *R* enantiomer in contrast to most of the HETE products formed by many mammalian tissues. Therefore, the presence of a 12(*S*)-LO is unusual in aquatic invertebrates although a 12(*S*)-LO activity has been reported in *H. magnipapillata* and *Aplysia californica* (6,14). Mammalian platelet 12(*S*)-LO is inhibited by submicromolar concentrations of baicalein (12) but in our study 200-fold higher concentrations of baicalein only resulted in a slight reduction in 12(*S*)-LO activity. Furthermore, the activity of mussel-derived 12(*S*)-LO was calcium dependent unlike that of platelet

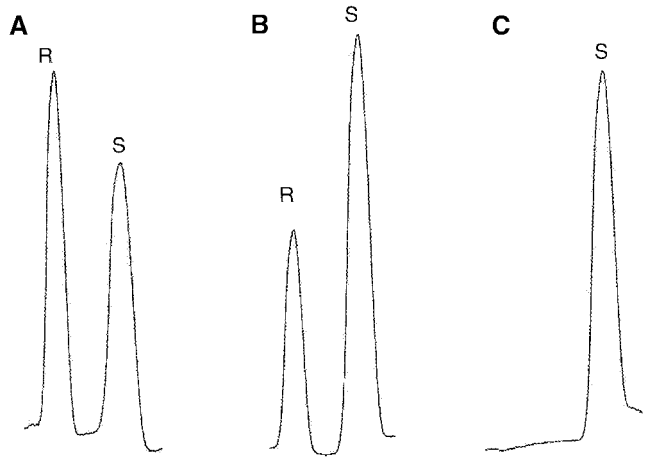

FIG. 5. Chiral analysis of mussel-derived 12-HETE. Methyl ester derivatives of 12-HETE standards and mussel samples were separated on a Chiracel OD column. (A) Standard racemic 12-HETE; (B) co-injection of mussel-derived 12-HETE with the racemic standard; (C) analysis of mussel 12-HETE alone. See Figure 1 for abbreviation.

TABLE 1
The Effect of Calcium Concentration on Lipoxygenase Product Formation[a]

Calcium concentration (mM)	11-HEPE (nmol/30 min)	12-HEPE (nmol/30 min)
0	0.1	0.1
10	2.2	2.2
13	2.1	2.1
15	2.1	2.1

[a]10,000 × *g* homogenates of mussel ovaries (in Tris buffer containing 5 mM EDTA) were incubated with eicosapentaenoic acid (EPA) in the presence of different concentrations of calcium chloride. HEPE products were extracted and quantified by reversed-phase high-performance liquid chromatography. Data are means of two replicate assays. 11-HEPE, 11-hydroxy-5,8,12,14,17-EPA; 12-HEPE, 12-hydroxy-5,8,10,14,17-EPA.

or porcine leukocyte 12(*S*)-LO, which suggested that the mussel enzyme was not the same form as the mammalian 12(*S*)-LO enzymes (15,16). 11(*R*)-LO activity has been reported in two species of *Hydra*, however, unlike mussel 11(*R*)-LO, this activity in *Hydra* was not inhibited by NDGA, which suggests that there are different forms of 11(*R*)-LO enzymes in these two invertebrates (6,7).

There is the possibility that 11(*R*)-HETE and 12(*S*)-HETE could be formed from the same enzyme by abstraction of a co-planar pro-*S* hydrogen atom at either the C-13 or C-10 positions of AA, respectively. However, in our study high concentrations of baicalein inhibited the synthesis of 11(*R*)-HETE much more than 12(*S*)-HETE and, in addition, 12-LO activity predominated in immature ovaries whereas 11-LO was the major activity in ripe ovaries. Together these data suggested that two independent LO enzymes are present in mussel ovaries and that their relative activity is dependent on gonad differentiation.

During incubation of ovary tissue preparations with either exogenous AA or EPA, HOTE metabolites were detected, which could have been formed from endogenous SA. GC–MS analysis of these metabolites showed that they were a mixture of 9- and 13-HOTE. These could be products of an 11-LO activity or, alternatively, 13-HOTE could also be formed by a 12-LO, analogous to the activity of porcine 12(*S*)-LO, which forms alcohols at both the n-9 and n-6 positions of AA and linoleic acid (17).

When spawned eggs were extracted with methanol, both 11-HEPE and HOTE (predominantly 9-HOTE) were formed from endogenous substrate. Incubation of eggs with EPA substrate prior to eicosanoid extraction did not increase biosynthesis of 11-HEPE, which suggested that either the oocyte 11-LO is product-inactivated similar to many other lipoxygenases (18) or that 11-HEPE was formed in surrounding ovarian tissue and diffused into the oocytes prior to spawning. The biosynthesis of eicosanoids from endogenous SA has not been reported before in animal tissues although 13-HOTE has been detected in female gametophytes of the marine alga *Laminaria saccharina* (19). Marine organisms contain high levels of n-3 PUFA and EPA, and to a lesser extent SA, linolenic acid (18:3n-3) as well as AA, are predominant

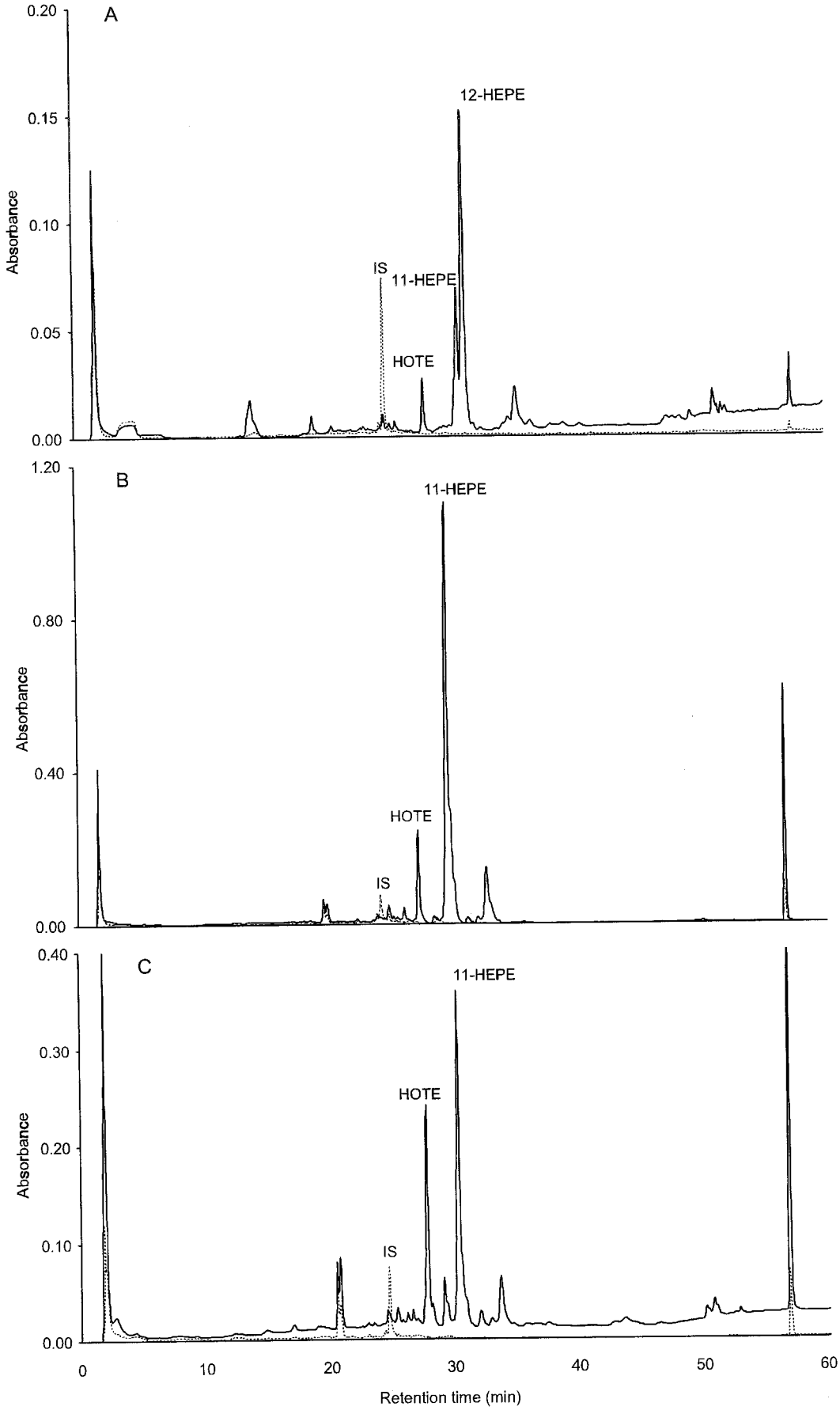

FIG. 6. Eicosanoid biosynthesis during ovarian development. Crude homogenates (10,000 × *g* supernatant) of (A) immature and (B) ripe ovaries were incubated with eicosapentaenoic acid (EPA) (20 μM) and the resulting eicosanoid profile was analyzed by RP-HPLC UV detection. (C) Spawned eggs from one mussel were extracted with methanol and the eicosanoids analyzed by RP-HPLC UV. (— 235 nm, --- 280 nm). IS = PGB_2 internal standard. HOTE, 9- and 13-hydroxyoctadecatetraenoic acids; 11-HEPE, 11-hydoxy-5,8,12,14,17-EPA; 12-HEPE, 12-hydroxy-5,8,1,14,17-EPA. See Figure 1 for other abbreviations.

PUFA in *M. edulis* (20). The detection of only EPA- and SA-, but not AA-derived metabolites suggests either that high levels of EPA and SA substrates are released from oocyte membranes during cell activation and/or that EPA and SA are preferred substrates for mussel LO. The major LO products generated by ionophore activation of sea squirt (*Ciona intestinalis*) tissues were metabolites of EPA rather than AA, suggesting that EPA could be the endogenous substrate for eicosanoid synthesis in some marine organisms (21).

The physiological role of these 11(*R*)-LO and 12(*S*)-LO enzymes in *Mytilus* is unknown at present; however, the isolation of these metabolites in the ovaries and not in the testes suggests a connection with the female reproductive cycle. These results are in contrast to that reported for some other marine invertebrates where LO activity in the testes of the surf clam and the starfish is similar to the activity in the ovaries (3). Our studies, conducted in different periods of the year, have shown that the production of eicosanoids is seasonal; in particular, metabolites of 12(*S*)-LO are the major products in spent and immature ovaries whereas 11(*R*)-LO activity appears to predominate in mature ovaries. 12(*S*)-HETE has been shown to be an important second messenger in a variety of vertebrate and invertebrate cells (6,22,23) and it is possible that metabolites of 12(*S*)-LO may act as second messengers in mussel cells and regulate cell differentiation and gametogenesis in the female gonad. The role of the 11(*R*)-HEPE and/or the HOTE metabolites detected in spawned *Mytilus* oocytes is unclear but the detection of 11(*R*)-LO activity in spawned eggs of the sea urchin suggests this enzyme may also be involved in oocyte function in other species (5).

ACKNOWLEDGMENTS

We thank Professor Alan R. Brash, Vanderbilt University, for advice on the chiral analysis of eicosanoids.

REFERENCES

1. De Petrocellis, L., and Di Marzo, V. (1994) Aquatic Invertebrates Open Up New Perspectives in Eicosanoid Research: Biosynthesis and Bioactivity, *Prostaglandins Leukotrienes Essent. Fatty Acids 51,* 215–229.
2. Meijer, L., Brash, A.R., Bryant, R.W., Ng, K., Maclouf, J., and Sprecher, H. (1986) Stereospecific Induction of Starfish Oocyte Maturation by (8*R*)-Hydroxyeicosatetraenoic Acid, *J. Biol. Chem. 261*, 17040–17047.
3. Hada, T., Swift, L.L., and Brash, A.R. (1997) Discovery of 5*R*-Lipoxygenase Activity in Oocytes of the Surf Clam, *Spisula solidissima*, *Biochim. Biophys. Acta 1346,* 109–119.
4. Varaksin, A.A., Varaksina, G.S., Reunova, O.V., and Latyshev, N.A. (1992) Effect of Serotonin, Some Fatty Acids and Their Metabolites on Reinitiation of Meiotic Maturation in Oocytes of Bivalve *Spisula sachalinensis* (Schrenk), *Comp. Biochem. Physiol. 101C,* 627–630.
5. Hawkins, D.J., and Brash, A.R. (1987) Eggs of the Sea Urchin, *Strongylocentrotus purpuratus*, Contain a Prominent (11*R*) and (12*R*) Lipoxygenase Activity, *J. Biol. Chem. 262,* 7629–7634.
6. Leitz, T., Muller, W., De Petrocellis, L., and Di Marzo, V., (1994) Enantiospecific Synthesis of Bioactive Hydroxyeicosatetraenoic Acids (HETEs) in *Hydra magnipapillata*, *Biochim. Biophys. Acta 1213,* 215–223.
7. Di Marzo, V., De Petrocellis, L., Gianfrani, C., and Cimino, G. (1993) Biosynthesis, Structure and Biological Activity of Hydroxyeicosatetraenoic Acids in *Hydra vulgaris*, *Biochem. J. 295,* 23–29.
8. Leitz, T., Beck, H., Stephan, M., Lehmann, W.D., De Petrocellis, L., and Di Marzo, V. (1994) Possible Involvement of Arachidonic Acid and Eicosanoids in Metamorphic Events in *Hydractinia echinata* (Coelenterata; Hydrozoa), *J. Exp. Zool. 269,* 422–431.
9. Hill, E.M., and Holland, D.L. (1992) Identification and Egg Hatching Activity of Monohydroxy Fatty Acid Eicosanoids in the Barnacle *Balanus balanoides*, *Proc. R. Soc. London B 247,* 41–46.
10. Hill, E.M., Holland, D.L., and East, J. (1993) Egg Hatching Activity of Trihydroxylated Eicosanoids in the Barnacle *Balanus balanoides*, *Biochim. Biophys. Acta 1157,* 297–303
11. Bentley, M.G., and Hardege, J.D. (1996) The Role of a Fatty Acid Hormone in the Reproduction of the Polychaete *Arenicola marina* (L.), *Invertebr. Reprod. Dev. 30,* 159–165.
12. Sekiya, K., and Okuda, H. (1982) Selective Inhibition of Platelet Lipoxygenase by Baicalein, *Biochem. Biophys. Res. Commun. 105,* 1090–1095.
13. Fitzpatrick, F.A., and Murphy, R.C. (1988) Cytochrome P450 Metabolism of Arachidonic Acid. Formation and Biological Actions of Epoxygenases-derived Eicosanoids, *Pharmacol. Rev. 40,* 229–241.
14. Feinmark, S.J., Steel, D.J., Thekkuveetil, A., Abe, M., Li, X.D., and Schwartz, J.H. (1992) *Aplysia californica* Contains a Novel 12-Lipoxygenase Which Generates Biologically Active Products from Arachidonic Acid, *Adv. Exper. Med. Biol. 318,* 159–169.
15. Baba, A., Sakuma, S., Okamoto, H., Inoue, T., and Iwata, H. (1989) Calcium Induces Membrane Translocation of 12-Lipoxygenase in Rat Platelets, *J. Biol. Chem. 264,* 15790–15795.
16. Yoshimoto, T., Miyamoto, Y., Ochi, K., and Yamamoto, S. (1982) Arachidonate 12-Lipoxygenase of Porcine Leukocyte with Activity for 5-Hydroxyeicosatetraenoic Acid, *Biochim. Biophys. Acta 713,* 638–646.
17. Yokoyama, C., Shinjo, F., Yoshimoto, T., Yamamoto, S., Oates, J.A., and Brash, A.R. (1986) Arachidonate 12-Lipoxygenase Purified from Porcine Leukocytes by Immunoaffinity Chromatography and Its Reactivity with Hydroperoxyeicosatetraenoic Acids, *J. Biol. Chem. 261,* 16714–16721.
18. Brash, A.R. (1999) Lipoxygenases: Occurrence, Functions, Catalysis and Acquisition of Substrate, *J. Biol. Chem. 274,* 23679–23682.
19. Rorrer, G.L., Yoo, H.D., Huang, Y.M., Hayden, C., and Gerwick, W.H. (1997) Production of Hydroxy Fatty Acids by Cell Suspension Cultures of the Marine Brown Alga *Laminaria saccharina*, *Phytochemistry 46,* 871–877.
20. Kluytmans, J.H., Boot, J.H., Oudejans, R.C.H.M., and Zandee, D.I. (1985) Fatty Acid Synthesis in Relation to Gametogenesis in the Mussel *Mytilus edulis*, *Comp. Biochem. Physiol. 81B,* 959–963.
21. Knight, J., Taylor, G.W., Wright, P., Clare, A.S., and Rowley, A.F. (1999) Eicosanoid Biosynthesis in an Advanced Deuterostomate Invertebrate, the Sea Squirt (*Ciona intestinalis*), *Biochim. Biophys. Acta 1436,* 467–478.
22. Tang, D.G., Chen, Y.Q., and Honn, K.V. (1996) Arachidonate Lipoxygenases as Essential Regulators of Cell Survival and Apoptosis, *Proc. Natl. Acad. Sci. USA 93,* 5241–5246.
23. Piomelli, D. (1991) Metabolism of Arachidonic Acid in Nervous System of the Marine Mollusk *Aplysia californica*, *Am. J. Physiol. 260,* R844–R848.

[Received July 31, 2000, and in revised form October 3, 2000; revision accepted October 4, 2000]

Evidence for the Mitochondrial Biosynthesis of 3*R*-Hydroxy-5*Z*,8*Z*,11*Z*,14*Z*-eicosatetraenoic Acid in the Yeast *Dipodascopsis uninucleata*

Simon R. Fox[a,*], Mats Hamberg[b], John Friend[a], and Colin Ratledge[a]

[a]University of Hull, Department of Biological Sciences, Hull HU6 7RX, United Kingdom, and [b]Department of Medical Biochemistry and Biophysics, Karolinska Institutet, Stockholm, S-171 77, Sweden

ABSTRACT: The biosynthesis of 3*R*-hydroxy-5*Z*,8*Z*,11*Z*,14*Z*-eicosatetraenoic acid (3*R*-HETE) from arachidonic acid (20:4n-6) by the hyphal-forming yeast, *Dipodascopsis uninucleata,* in cell-free enzyme extracts required CoASH, ATP, NAD^+ and Mg^{2+}; 3*R*-HETE was present as the CoA derivative in enzyme extracts and its biosynthesis was associated with mitochondria. Its synthesis was high from arachidonoyl-CoA (15% conversion of the substrate; 22 nmol mg protein^{-1}·h), but significantly higher from *trans*-2-arachidonoyl-CoA (53 nmol mg protein^{-1}·min). Aspirin, an inhibitor of prostaglandin endoperoxide synthase synthase (cyclooxygenase), did not significantly inhibit 3*R*-HETE biosynthesis in enzyme extracts, as opposed to antimycin A (46% inhibition). The chirality of 3-HETE was 95% *R* and 5% *S*. 3*R*-HETE has the same chirality as the products of peroxisomal enoyl-CoA hydratases of *Neurospora crassa* and *Saccharomyces cerevisiae*; the difference appears to be that in *D. uninucleata* the *R*-enantiomers are synthesized in mitochondria. Exogenously supplied eicosapentaenoic acid was converted to 3-hydroxy 5*Z*,11*Z*,14*Z*,17*Z*-eicosapentaenoic acid by cell-free enzyme extracts though there was no requirement for a 5*Z*,8*Z*-diene structure for the biosynthesis of 3-hydroxylated fatty acids as 3-hydroxy-8*Z*,11*Z*,14*Z,* and 3-hydroxy-11*Z*,14*Z*,17*Z*-eicosatrienoic acids were synthesized from the corresponding fatty acids. We found no evidence for the synthesis of the prostaglandins $F_{2\alpha}$ and E_2.

Paper no. L8523 in *Lipids 35,* 1205–1214 (November 2000).

Currently there is considerable interest in harvesting microorganisms to synthesize valuable secondary products, which may find potential in the pharmaceutical industries. For example, the hyphal-forming yeast *Dipodascopsis uninucleata* was discovered to synthesize the novel fatty acid derivative 3-hydroxy-5*Z*,8*Z*,11*Z*,14*Z*-eicosatetraenoic acid (3-HETE) when incubated with exogenously supplied arachidonic acid (1). Because the synthesis of 3-HETE was inhibited by the inclusion of 1 mM aspirin (*O*-acetylsalicylic acid) in the incubation medium, it seemed possible that one of the enzymes involved in the synthesis of 3-HETE was prostaglandin endoperoxide synthase (PGH synthase), an enzyme well known to be inhibited by such concentrations of aspirin (1). The involvement of PGH synthase or a similar type of enzyme was further supported by the identification of two isomers of the prostaglandin metabolite α-pentanor $PGF_{2\alpha}$-γ-lactone, a breakdown product of prostacyclin (2,3). Evidence was presented suggesting the existence of two further prostaglandins, $PGF_{2\alpha}$ and PGE_2, in the closely related yeast *Dipodascopsis töthii* (4).

Both Kock *et al*. (5,6) and we (7–9) have proposed that the conversion of 20:4n-6 to 3-HETE by *D. uninucleata* involves a modification of the fatty acid β-oxidation cycle. In addition, both we (7,8) and Venter *et al*. (10) have found that the major product (approximately 95%) is the *R*-enantiomer of 3-HETE (7–10). Consequently, a separate hydroxylase for the direct formation of 3*R*-hydroxy-5*Z*,8*Z*,11*Z*,14*Z*-eicosatetraenoic acid (3*R*-HETE) was postulated (10). Interestingly the β-oxidation pathway in fungi is not analogous to that found in mammals and plants. Indeed Kunau *et al*. (11), in a review of β-oxidation, including their own research on this topic, have reported that the 3-hydroxyacyl-CoA intermediates in the fungal β-oxidation pathway have the D-configuration (corresponding to *R*-enantiomers) unlike the mammalian and plant pathways where the intermediates are in the L-configuration (*S*-enantiomers). This then re-opens the possibility that 3*R*-HETE is being formed by β-oxidation in this yeast.

Here we present results from experiments with cell-free enzyme extracts and isolated organelles that indicate that 3*R*-HETE biosynthesis in *D. uninucleata* involves an incomplete β-oxidation process with the intermediates having the same chirality as are found in other fungi. Moreover, this β-oxidation activity in *D. uninucleata* is constitutive and appears to be located in mitochondria, unlike the inducible β-

*To whom correspondence should be addressed at Department of Brassica and Oilseeds Research, John Innes Centre, Norwich Research Park, Norwich, NR4 7UH, United Kingdom. E-mail: Simon.Fox@bbsrc.ac.uk

Abbreviations: 20:3n-6, 8*Z*,11*Z*,14*Z*-eicosatrienoic acid; 20:3n-3, 11*Z*,14*Z*,-17*Z*-eicosatrienoic acid; 20:4n-6, 5*Z*,8*Z*,11*Z*,14*Z*-eicosatetraenoic acid; 20:5n-3, 5*Z*,8*Z*,11*Z*,14*Z*,17*Z*-eicosapentaenoic acid; 20:4n-6-CoA, 5*Z*,8*Z*,-11*Z*,14*Z*-eicosatetraenoyl-CoA; BSA, bovine serum albumin; EI, electron impact; EM, electron microscopy; GC, gas chromatography; 3*R*-HETE, 3*R*-hydroxy-5*Z*,8*Z*,11*Z*,14*Z*-eicosatetraenoic acid; 3*R*-HETE-CoA, 3*R*-hydroxy-5*Z*,8*Z*,11*Z*,14*Z*-eicosatetraenoyl-CoA; HPLC, high-pressure liquid chromatography; int. diam., internal diameter; MS, mass spectrometry; NDGA, nordihydroguaiaretic acid; NS-398, *N*-(2cyclohexyloxy-4-nitrophenyl)-methane sulfonamide; $PGF_{2\alpha}$, prostaglandin $F_{2\alpha}$; PGE_2, prostaglandin E_2; PGH synthase, prostaglandin endoperoxide synthase; RCR, respiratory control ratio; RP, reversed-phase; sp. act., specific activity; TLC, thin-layer chromatography; Tris/HCl, Tris (hydroxymethyl) methylamine hydrochloride; YNB, yeast nitrogen base.

oxidation system, which is located in peroxisomes and specialized microbodies (11). The term "peroxisomes" is used here to refer to organelles containing acyl-CoA oxidase (11).

We reported earlier (7,8) that whole cells of *D. uninucleata* converted both 8*Z*,11*Z*,14*Z*- and 11*Z*,14*Z*,17*Z*-eicosatrienoic acids to their corresponding 3-hydroxy derivatives. We now show that similar reactions are catalyzed by cell-free enzyme extracts. Finally, because of the findings of earlier work with this yeast (1–4), we tried to address the question of whether *D. uninucleata* can be used to synthesize prostaglandins from 20:4n-6.

MATERIALS AND METHODS

Yeast growth. Conical flasks (1 L) containing 400 mL yeast nitrogen base (YNB) medium (7 g YNB, 10 g glucose, and 5 g peptone/L) were inoculated with *Dipodascopsis uninucleata* (UOFS Y128) previously grown on YNB agar plates. After growing at 30°C for 4 d and shaking at 140 rev/min, cultures were filtered through glass wool and the filtrates centrifuged at 10,000 × *g* for 10 min to pellet ascospores. The ascospores were inoculated to give a final concentration of 1.5×10^5 per mL (12) in 400 mL of medium comprising (g/L) glucose, 40 (referred to as 4% glucose medium); YNB (without amino acids), 6.7; peptone, 5; malt extract, 2.4; pH 6. The cultures were maintained at 25°C and 140 rev/min for 48 h. In other experiments, the ascospores were inoculated to the same concentration into an identical medium (400 mL), but one which contained 1% glucose, with YNB (6.7 g/L) without peptone or malt extract (referred to as 1% glucose medium). Likewise, ascospores were also inoculated into a medium (400 mL) containing 1% ethanol as the sole carbon source with YNB (6.7 g/L), but without peptone and malt extract.

Chiral analysis. 3-HETE was isolated from 48-h grown cultures of *D. uninucleata* grown as previously detailed (13). 3-HETE was methylated with diazomethane and catalytically hydrogenated to produce methyl 3-hydroxyeicosanoic acid. This compound was treated with *S*-phenylpropionyl chloride to form the *S*-phenylpropionate ester. The final analysis was carried out by gas chromatography–mass spectrometry (GC–MS) using the *S*-phenylpropionate ester of 3-(*R*,*S*)-hydroxyeicosanoic acid as the reference compound. The reference compound was prepared by anodic coupling of methyl 3(*R,S*)-acetoxy-4-carboxybutanoate (5 mmol; 14) and heptadecanoic acid (15 mmol) in methanol (20 mL) containing sodium methoxide (0.5 mmol). Purification of the saponified and methyl-esterified product by open column silicic acid chromatography afforded methyl 3(*R,S*)-hydroxyeicosanoate as a white solid (0.4 g; 23% yield). The mass spectrum of the Me_3Si derivative showed prominent ions at *m/z* 399 (100%; $M^+ - 15$; loss of $\cdot CH_3$), 341 (6; $M^+ - 73$; loss of $\cdot CH_2–COOCH_3$), 175 (25; $Me_3SiO^+=CH–CH_2–COOCH_3$), 159 (7; $Me_2Si=O^+–CH=CH–COOCH_3$), 89 (14; Me_3SiO^+), and 73 (14; Me_3Si^+). The two enantiomers of methyl 3-acetoxy-4-carboxybutanoate can be easily obtained by resolution of the racemic half ester (14), thus permitting synthesis of the optically active forms of 3-hydroxyeicosanoate.

Preparation of cell-free enzyme extracts. Cells, 5 g wet wt, were harvested by filtration after 24 or 48 h growth. They were washed thoroughly with distilled water before being resuspended in 25 mL 1 mM mercaptoethanol, 5 mM EGTA, 5% (vol/vol) glycerol, and 500 mM Tris (hydroxymethyl) methylamine hydrochloride (Tris/HCl), pH 7.6. The mixture was passed twice through a hydraulic press (Bundenberg, Manchester, United Kingdom) at a pressure of 5.1×10^3 kPa. The homogenate was clarified by centrifugation at 30,000 × *g* for 15 min and the supernatant used as the cell-free enzyme extract (referred to as enzyme extracts; note, these extracts did not contain intact mitochondria). Subsequent incubations were of 1 mL and were maintained at 25°C for 30 min. For experiments with fatty acids the final concentrations were 20:4n-6 (sodium salt), 0.5 mM; 20:4n-6-CoA (Sigma Chemical Co., Poole, United Kingdom), 0.1 mM; CoASH, 0.5 mM; ATP, 5 mM; NAD^+, 0.2 mM; and Mg^{2+}, 1 mM. For analysis of the [^{14}C]acyl-CoA fraction, 18.5 kBq [1-^{14}C]20:4n-6 was included (sp. act. 2,035 MBq/mmol) in an otherwise identical incubation medium (1 mL). For experiments with potential inhibitors of 3-HETE biosynthesis, the final concentration was 1 mM, unless otherwise stated.

Isolation of mitochondria. Cells (10–20 g wet wt) grown on the 4% glucose medium were harvested after 48 h and transferred to extraction buffer (5 mL buffer/1 g wet wt) comprising 0.6 M sucrose, 1 mM EGTA, 0.4% (wt/vol) bovine serum albumin (BSA) (fraction V, essentially fatty acid free; Sigma), 300 mM Tris/HCl, pH 7.4. The mixture was stored on ice for 30 min. Cells were disrupted with a Bead Beater (bead mesh <106 µm; Biospec Products, Bartlesville, OK) during which the apparatus was chilled with dry ice. The homogenate was passed through one layer of muslin, removing most of the beads. Decanting the solution into centrifuge tubes (50 mL) removed the remaining beads. The homogenate was centrifuged at 1,085 × *g* and the supernatant collected and centrifuged at 27,000 × *g* for 10 min. The pellet was resuspended in resuspension medium (50 mL) comprising 0.4 M sucrose, 1 mM EGTA, 0.1% (wt/vol) BSA, 50 mM Tris/HCl, pH 7.4 and centrifuged at 1,085 × *g* for 5 min. The supernatant was recentrifuged at 27,000 × *g* and the pellet resuspended in resuspension medium (1 mL). This was layered onto a discontinuous sucrose gradient comprising 60% (3 mL), 52% (4 mL), 45% (4.5 mL), 41% (4.5 mL), and 30% (3 mL) (vol/vol) sucrose in 10 mM *N*-[2-hydroxyethyl]piperazine-*N*′-[2-ethanesulfonic acid] buffer, pH 7.4. The gradients were centrifuged at 42,000 × *g* for 80 min in a swing-out rotor (3 × 25 mL) at 2°C. Fractions (1 mL) were collected from the bottom of the gradients and used for enzyme assays. In a separate series of experiments, to measure 3-HETE biosynthesis, the organelle bands were removed with a Pasteur pipette from the interfaces between the different sucrose concentrations (*ca*. 2 mL fractions) and diluted to 20–30 mL with resuspension medium. They were pelleted at 27,000 × *g* for 10 min at 2°C. The pellets were resuspended in 4–5 mL

resuspension medium (i.e., containing sucrose as osmoticum). For incubations with fatty acids and cofactors, to measure 3-HETE synthesis, concentrations were as listed for those with enzyme extracts (i.e., incubations of 1 mL). In order to burst mitochondria, they were incubated in resuspension medium but without the sucrose. The respiratory control ratio (RCR) was measured as detailed by Rickwood *et al*. (15) and protein determined using a protein assay kit (Sigma).

Preparation of enoyl-CoA thioesters. *Trans*-2-enoyl derivatives of acyl-CoA thioesters were prepared by incubation of 1.125 U acyl-CoA oxidase (Boehringer Mannheim Ltd., Lewes, United Kingdom) per micromole acyl-CoA in 25 mM potassium phosphate, pH 7.5 at 25°C (Dr. S. Eaton, Institute of Child Health, London, United Kingdom, personal communication). The enoyl-CoA derivatives of acyl-CoA elute immediately before their straight-chain derivatives (16). The reaction, which went to completion after 30 min, was quenched with 100 µL formic acid. The *trans*-2-enoyl-CoA thioesters were purified by high-pressure liquid chromatography (HPLC) on a Lichrosorb 7 RP18 10 × 0.3 cm column (Chrompack International, Middelburg, The Netherlands). HPLC conditions comprised an isocratic gradient of 50 mM KH_2PO_4 (pH 5.6)/acetonitrile (1:1, vol/vol) with a flow rate of 0.5 mL min^{-1} and ultraviolet detection at 260 nm. The fraction containing enoyl-CoA thioesters was stored at –80°C.

Enzyme assays. Spectrophotometric assays were performed at 25°C on a double-beam spectrophotometer. Activities of long-chain acyl-CoA dehydrogenase (17; assayed using arachidonoyl-CoA), acyl-CoA oxidase (18; assayed using arachidonoyl-CoA), long-chain enoyl-CoA hydratase (19; assayed with synthesized *trans*-2-enoyl-CoA thioesters of different chain length and saturation), D-3-hydroxyacyl-CoA dehydrogenase (20; assayed with 3*R*-HETE), 3-ketoacyl-CoA thiolase (21; assayed with a racemic mixture of acetoacetyl-CoA in the reverse direction), fumarase (22), catalase (23), isocitrate lyase (24), malate synthase (25), and $NADP^+$-dependent cytochrome *c* oxidoreductase (26) were determined by established procedures though some of the substrates were altered (as listed).

PGH synthase was assayed in enzyme extracts and microsomal pellets. Microsomes were sedimented at 100,000 × *g* for 90 min from the enzyme extract, giving a brown translucent pellet, and resuspended in resuspension medium. The enzyme PGH synthase was assayed from enzyme extracts as this is the first enzyme in the synthesis of prostaglandins from 20:4n-6 [*viz.* breadown products of prostaglandins had previously been detected in this yeast (3,4)]. The procedure used a polarographic O_2 electrode to measure the decrease in O_2 concentrations upon addition of 20:4n-6 (27). PGH synthase was also assayed by analysis of the products of 20:4n-6 metabolism as detailed by Yamamoto (28) (0.1 mg 20:4n-6, containing 18.5 kBq [1-^{14}C]20:4n-6, sp. act. 2,035 MBq/mmol per mL enzyme extract or microsome preparation). After incubation of extracts (final vol 2 mL) at 25°C for 30 min, the products of [1-^{14}C]20:4n-6 metabolism were extracted (×3) with an equal volume of chloroform and acidified with 50 µL glacial acetic acid. Samples were concentrated to a small volume under N_2 gas prior to separation of polar fatty acids by thin-layer chromatography (TLC) using silica gel G plates (Kieselgel, Anachem, United Kingdom). After application of the samples, the plates were developed at 4°C with the organic phase of the following solvents: ethyl acetate/2,2,4-trimethylpentane/acetic acid/water (110:50:20:100, by vol). ^{14}C was detected by scintillation counting (Bioscan Autochanger 4000, Bioscan Inc., Washington, DC).

Acyl-CoA analysis. The following method is based on that of Watmough *et al*. (16). Enzyme extracts, after incubation with 20:4n-6 and cofactors (final vol 1 mL), were acidified with glacial acetic acid (50 µL) and extracted (×3) with an equal volume of diethyl ether. The organic phases were discarded. Chloroform/methanol (1:2, vol/vol, 9 mL) was added to the aqueous phase and after 40 min protein was precipitated at 40,000 × *g*. The pellet was re-extracted with 1 mL chloroform/methanol. The combined organic phases were concentrated to a small volume and taken up in 1 mL KH_2PO_4 (50 mM, pH 5.6). The sample was injected (200 µL) onto a Lichrosorb 7 RP18 10 × 0.3 cm column. A gradient was run comprising initially 95% KH_2PO_4 (50 mM, pH 5.6), 5% acetonitrile, and a flow rate of 0.5 mL min^{-1}. This was altered to 40% KH_2PO_4 (50 mM, pH 5.6) after 30 min and 60% acetonitrile and maintained for another 20 min. Absorbance of acyl-CoA thioesters was measured at 260 nm.

Fatty acid analysis. For GC with flame-ionization detection, or for GC–MS, samples were subjected to alkaline hydrolysis and extracted (29) before being derivatized by methylation and silylation (30). GC analysis was carried out using a 30 m HP-1 capillary column (Hewlett-Packard, Palo Alto, CA; cross-linked methyl siloxane), internal diameter (int. diam.) 0.25 mm. GC parameters comprised an initial temperature of 200°C with a ramp rate of 2°C min^{-1} to 270°C and with a helium flow rate of 18.7 kPa. 3-HETE was prepared from whole cells of *D. uninucleata* (13) for use as a standard. 3-HETE was identified by the retention time of the compound, 15.00–15.05 min, by GC as described. This method was subsequently used to quantify the compound from incubations with enzyme extracts.

GC–MS was carried out using a Finnigan series 1020 automated GC–mass spectrometer operating in the electron impact mode. GC parameters were: BP-5 25 m fused-silica capillary column (SGE Ltd., Milton Keynes, United Kingdom); helium carrier gas at 13.8 kPa head pressure; 10:1 split; injector temperature, 220°C; initial temperature, 200°C; ramp rate, 2°C min^{-1}; final temperature, 280°C; final time, 10 min; injection volume, 1 µL. MS parameters were: source temperature, 240°C; manifold temperature, 100°C; ionization current, 0.30 A; scan range, 70 amu (arbitary mass units) to 600 amu in 1 s.

RESULTS

Chirality of 3-HETE. 3-HETE was found to be 95% *R* and 5% *S* (Fig. 1). This was in agreement with Venter *et al*. (10) and showed that, as in *Neurospora crassa* and *Saccharomyces cere-*

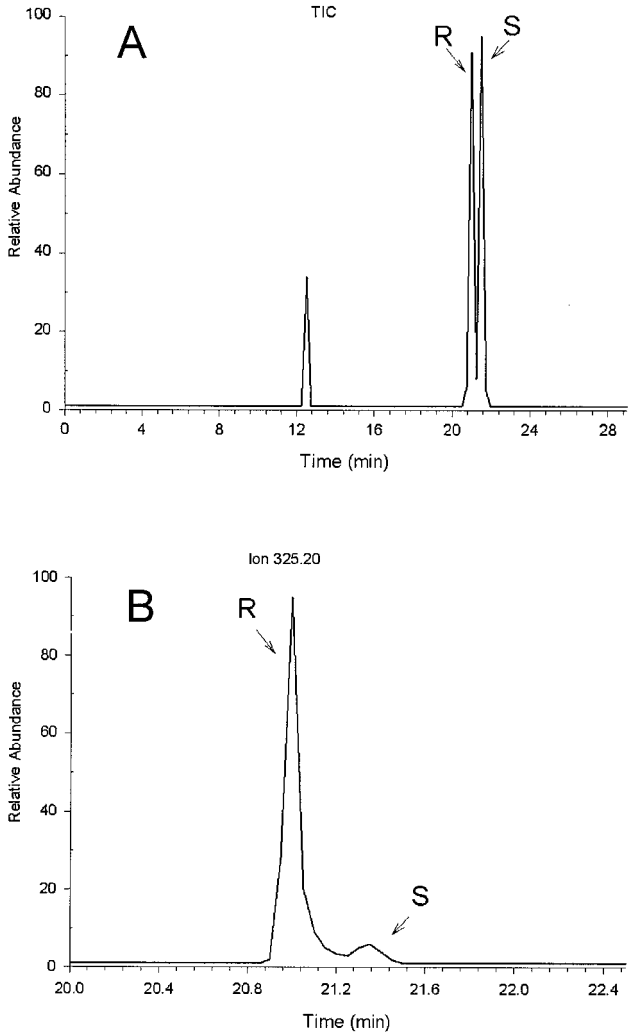

FIG. 1. (A) Total ion chromatogram (TIC) of the separation of the phenylpropionate ester of 3(*R,S*)-hydroxyeicosanoic acid standard by gas chromatography–mass spectrometry (GC–MS). (B) Partial selective ion chromatogram (M^+ = 325) of the GC–MS separation of 3(*R*)-hydroxyeicosanoic acid derived from 3-hydroxy-5*Z*,8*Z*,11*Z*,14*Z*-eicosatetraenoic acid and isolated from the yeast *Dipodascopsis uninucleata* supplied exogenous 20:4n-6 (see Ref. 13). The compound co-chromatographed with the 3(*R*)-hydroxyeicosanoic acid standard. Integration of the peaks from several runs gave an enantiomeric composition of 95% *R* and 5% *S*.

TABLE 1
The Effect of Cofactors of the β-Oxidation System on the Biosynthesis of 3*R*-HETE by Enzyme Extracts of *Dipodascopsis uninucleata* Grown on 4% (wt/vol) Glucose Medium

20:4n-6 added	3*R*-HETE biosynthesis (nmol mg protein^{-1}·h)	Conversion of 20:4n-6 to 3*R*-HETE (%)
None	ND[a]	0
CoASH	0.5[b]	0.1
CoASH, ATP	3.0	0.5
CoASH, ATP, NAD^+	6.4	1.1
CoASH, ATP, NAD^+, Mg^{2+}	15.7	2.6
20:4n-6-CoA added	**3*R*-HETE biosynthesis (nmol mg protein^{-1}·h)**	**Conversion of 20:4n-6-CoA to 3*R*-HETE (%)**
None	22.0	15.0
CoASH, ATP, NAD^+, Mg^{2+}	24.5	19.1

[a]ND, not detected; 3*R*-HETE, 3*R*-hydroxy-5*Z*,8*Z*,11*Z*,14*Z*-eicosatetraenoic acid.
[b]Standard deviations over three experiments were 10–15% of the mean.

visiae, long-chain enoyl-CoA hydratase from *D. uninucleata* generated *R*-3-hydroxy-acyl-CoA thioesters (11). This is unlike the equivalent enzymes of mammalian origin and may explain the potent pharmacological activity of 3*R*-HETE derived from *D. uninucleata* against human neutrophils (31). This is because the *R* chirality of certain monohydroxylated eicosanoids in mammalian cells, e.g., 12*R*-HETE, has been reported to enhance the chemotactic and chemokinetic properties of such molecules (32).

*Biosynthesis of 3*R*-HETE*. Enzyme extracts from cells cultivated on 4% glucose for 48 h did not convert 20:4n-6 to *3R*-HETE unless CoASH was added (Table 1). The subsequent addition of the known cofactors of mitochondrial β-oxidation, namely, ATP, NAD^+, and Mg^{2+}, each led to an increase in the percentage conversion of 20:4n-6 to *3R*-HETE. The increases in *3R*-HETE synthesis after the addition of these cofactors, were statistically significant to $P = 0.02$ (Student's *t*-test). The maximal percentage conversion of 20:4n-6 to *3R*-HETE was 2.6%.

When 20:4n-6-CoA, rather than the free acid, was added to the enzyme extracts there was a statistically significant increase in the rate of conversion to *3R*-HETE ($P = 0.02$, Table 1) compared to 20:4n-6 with CoASH, ATP, NAD^+, and Mg^{2+}. Without additional cofactors, the percentage conversion of 20:4n-6-CoA was 15% (corresponding to a rate of 22 nmol mg protein^{-1}·h) as opposed to 2.6% for 20:4n-6 and all cofactors. Addition of ATP, NAD^+, and Mg^{2+} did not result in a statistically significant increase in the percentage conversion of the substrate 20:4n-6-CoA (19%, $P = 0.1$). Thus it seemed that 20:4n-6 was being activated to its CoA thioester by long-chain acyl-CoA synthetase, an enzyme requiring ATP and Mg^{2+} as cofactors. The increase in *3R*-HETE biosynthesis with NAD^+ suggested that long-chain acyl-CoA dehydrogenase and not acyl-CoA oxidase (no NAD^+ requirement, it uses FAD^+) was responsible for the biosynthesis of the *trans*-2-enoyl-CoA thioester of 20:4n-6-CoA.

Further evidence for the biosynthesis of *3R*-HETE-CoA was obtained by analysis of the acyl-CoA fraction by HPLC (Fig. 2). These fractions, from incubations of enzyme extracts with 20:4n-6 and CoASH, ATP, NAD^+, and Mg^+, yielded a number of peaks. Peak 2 was collected, subjected to alkaline hydrolysis and converted to its methyl silyl derivative. It produced a peak by GC–MS that possessed a mass spectrum identical to that described by Van Dyk *et al.* for *3R*-HETE (1). Therefore, peak 2, which was not observed in the absence of CoASH, was assigned as *3R*-HETE-CoA. Peak 3 was identified as arachidonoyl-CoA by co-elution with the authentic

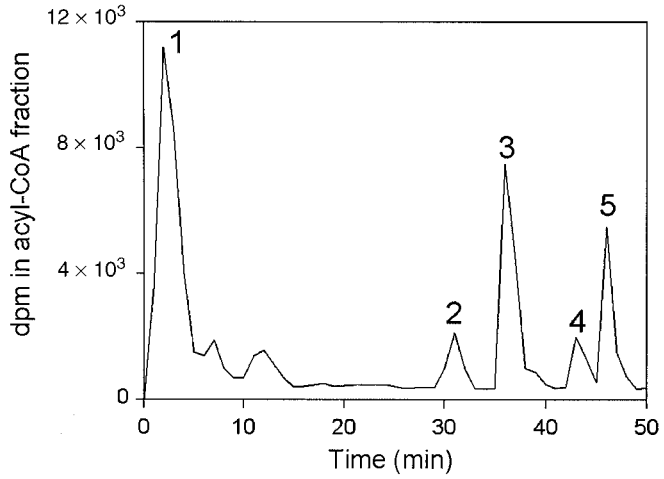

FIG. 2. Radio high-pressure liquid chromatogram of the separation of the [^{14}C] acyl-CoA fraction from enzyme extracts of *D. uninucleata* grown on 4% glucose medium and incubated with [1-^{14}C]20:4n-6, CoASH, ATP, NAD^+, and Mg^{2+}. The identity of the numbered peaks was investigated by GC–MS. For abbreviation see Figure 1.

standard. We were unable to identify the other peaks: we suspect that they included the 3-keto derivative of 20:4n-6-CoA, which would arise from 3*R*-HETE by action of the 3-hydroxyacyl-CoA dehydrogenase as the next enzyme of the β-oxidation cycle.

*Inhibition of 3*R*-HETE biosynthesis.* The conversion of both 20:4n-6 and 20:4n-6-CoA in enzyme extracts to 3*R*-HETE in comparison to controls, where no inhibitors were added, and with all cofactors listed in Table 1 was not significantly inhibited by a range of concentrations of aspirin from 0.1–1 mM (5 and 6%, respectively; experimental error ±10%; fresh solutions of the drug were used due to the instability of aspirin in water) or by 1 mM *N*-(2-cyclohexyloxy-4-nitrophenyl)-methane sulfonamide (NS-398; 4 and 3%, respectively). Both of these compounds are known inhibitors of PGH synthase; evidently, as Van Dyk *et al*. first discovered, aspirin only has inhibitory effects on 3*R*-HETE biosynthesis from added 20:4n-6 in whole cells of *D. uninucleata* (e.g., Ref. 1) rather than enzyme extracts, as in the current work.

The inhibition of 3*R*-HETE biosynthesis from 20:4n-6 and from 20:4n-6-CoA was not significant with aesculetin (1 mM; 11 and 6%, respectively), but was with nordihydroguaiaretic acid (NDGA) (1 mM; 60 and 90%, respectively); both are well-known as lipoxygenase inhibitors. However, we believe that the inhibition recorded with NDGA probably reflected its antioxidative properties, which the compound is known to possess (33).

The inhibition of 3*R*-HETE biosynthesis from 20:4n-6 and 20:4n-6-CoA by antimycin A (0.1 mM) was the second-highest recorded (46 and 64%, respectively). This inhibition suggests some coupled enzyme reactions associated with β-oxidation were still occurring in the cell-free extracts even though such extracts would not contain intact mitochondria. Antimycin A was presumably inhibiting the re-oxidation of NADH by long-chain acyl-CoA dehydrogenase.

Enzyme activities in cells grown in different media. Long-chain acyl-CoA dehydrogenase activity, assayed using arachidonoyl-CoA, was the lowest of the β-oxidation enzymes and was lowest in ethanol-grown cells (Table 2). This may explain the significantly lower rate of synthesis of 3*R*-HETE from 20:4n-6-CoA (22 nmol mg protein^{-1}·h) as opposed to the *trans*-2 derivative of 20:4n-6-CoA. Long-chain enoyl-CoA hydratase, assayed using *trans*-2-arachidonoyl-CoA (*trans*-2-5*Z*,8*Z*,11*Z*,14*Z*-eicosapentaenoyl-CoA), was the most active of these enzymes; the highest rate we recorded was from cells grown on 4% glucose medium of 53 nmol mg protein^{-1}·min. The enzyme was also assayed with other long-chain *trans*-2-acyl-CoA derivatives but there was no significant variation in activity, except with *trans*-2-lignoceroyl-CoA ($C_{24:0}$), 11 nmol mg protein^{-1}.min. Acyl-CoA oxidase activity was absent in extracts from all media. There was no increase in 3*R*-HETE synthesis with enzyme extracts from ethanol-grown cells; this suggested that 3*R*-HETE was not synthesized in

TABLE 2
Enzyme Activity in Cell-Free Enzyme Extracts of *D. uninucleata* After Growth on Different Media[a]

		Growth medium and enzyme activity (nmol·min mg protein^{-1})		
Enzyme*	Time of culture (h)	1% Glucose	4% Glucose	Ethanol
Long-chain acyl-CoA dehydrogenase[b]	24	3	2	<1
	48	3	2	<1
Long-chain enoyl-CoA hydratase[c]	24	40	16	44
	48	32	53	49
D-3-Hydroxy-acyl-CoA dehydrogenase[d]	24	3	8	2
	48	2	3	3
3-Ketoacyl-CoA thiolase[e]	24	3	5	4
	48	4	7	4
Fumarase	24	259	104	113
	48	142	207	117
Catalase	24	<1	<1	<1
	48	<1	<1	<1
Malate synthase	24	29	5	43
	48	8	9	54
Isocitrate lyase	24	7	2	152
	48	3	4	189

[a]Figures represent the average of three experiments. *Also assayed fatty acyl-CoA oxidase but no activity found in any cell-free extract. Standard deviations were ±10–15% of the mean.
[b]Assayed with arachidonoyl-CoA.
[c]Assayed with *trans*-2-arachidonoyl-CoA.
[d]Assayed with 3*R*-HETE.
[e]Assayed with acetoacetyl-CoA. For abbreviation see Table 1.

glyoxysomes or peroxisomes as such growth conditions lead to induction of peroxisome formation.

The activity of D-3-hydroxyacyl-CoA dehydrogenase, assayed using 3*R*-HETE, was the second-lowest of the β-oxidation enzymes, and this activity decreased significantly from 24 to 48 h in cells grown on 4% glucose medium. This may be the factor that leads to accumulation of *3R*-HETE as the rate of formation of 3*R*-HETE has to exceed the rate of its oxidation in order for it to accumulate. 3-Ketoacyl-CoA thiolase activity was likewise low. Ideally this enzyme should have been measured using the 3-keto derivative of arachidonoyl-CoA. The results overall show that glucose did not completely repress β-oxidation activity in *D. uninucleata*, when fatty acid synthesis was occurring; other evidence from electron microscopy (results not shown) revealed an abundance of oil bodies, as well as mitochondria in the 48-h grown cells.

Catalase activity from enzyme extracts of *D. uninucleata* cells grown on either 4% or 1% glucose medium was barely detectable, <1 nmol mg protein^{-1}·min, suggesting peroxisomes had not developed. Malate synthase and isocitrate lyase, glyoxysomal marker enzymes, were present at low activity in glucose-grown cells, but their activity was induced by growth on ethanol, *ca.* 7 and 40–50-fold increased activity, respectively; again there was no inducement of catalase. The glyoxysomal pathway is essential for the synthesis of sugars from C_2 carbon skeletons and glyoxysomes were observed under electron microscopy (EM) (results not shown) from cells grown on ethanol, but not in cells grown on either 4% or 1% glucose medium. We were unable to grow *D. uninucleata* on oils, fatty acids, or methyl esters of fatty acids.

*Location of 3*R*-HETE biosynthesis*. Organelle bands (all from cells grown on 4% glucose medium) occurred at the interfaces between the different sucrose concentrations, as reported in reference 15. These organelle bands are referred to here as bands 1–4, i.e., band 1, 30–41% sucrose interface; band 2, 41–45% interface; band 3, 45–52% interface, and band 4, 52–60% interface. The sucrose gradients appeared to contain two mitochondrial bands (bands 2 and 3). Both were reddish-brown in appearance, presumably due to cytochrome content and identifiable from the peaks of activity for fumarase and NADP$^+$-dependent cytochrome *c* oxidoreductase (Fig. 3). Band 2 had an RCR (the state III to state IV rates of oxygen consumption, a common criterion used to judge the quality of a mitochondrial preparation) of 2.5–3.1, slightly lower than like-extracted mitochondria from *S. cerevisiae* whose mitochondria have an RCR value of *ca.* 4.5 (15). The RCR of band 3 was 1.5–2.5; bands 1 and 4 did not exhibit a positive RCR. Bands 2 and 3 did not contain measurable activities for isocitrate lyase. Bands 2 and 3, viewed under EM by negative-staining (results not shown), contained spherical bodies similar in appearance to the mitochondria described by Mergner *et al.* (34). Low activities of β-oxidation enzymes, apart from long-chain enoyl-CoA hydratase, were associated with bands 2 and 3. Acyl-CoA oxidase activity was absent from the gradients.

As glucose-grown cells do not contain peroxisomes (or glyoxysomes), whose presence in yeasts is induced by growing cells on ethanol, acetate, and fatty acids, we conclude that the mitochondria of these cells were located primarily in bands 2 and 3 after separation by sucrose density gradient centrifugation. No other organelles or subcellular components could be detected in these bands by EM. Thus, the presence of large portions of the endoplasmic reticulum (microsomal fraction) and/or Golgi apparatus in these bands could be ruled out and, from their respiration control ratios, we concluded that the mitochondria in bands 2 and 3 were reasonably pure and free of major amounts of other cellular material.

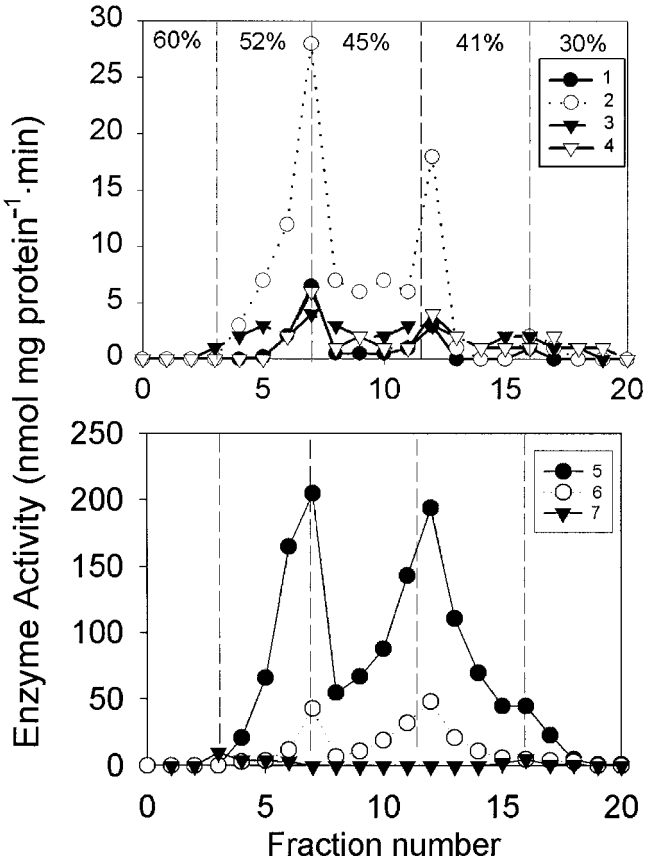

FIG. 3. Distribution of enzymes from *D. uninucleata* cells grown on 4% glucose and fractionated on sucrose gradients to separate cellular organelles. Key: 1, long-chain acyl-CoA dehydrogenase; 2, long-chain enoyl-CoA hydratase; 3, *D*-3-hydroxyacyl-CoA dehydrogenase; 4, ketoacyl-thiolase; 5, fumarase; 6, NADP$^+$-dependent cytochrome *c* oxidoreductase; 7, isocitrate lyase.

When bands 1–4 were each incubated with 20:4n-6, as detailed in the Materials and Methods section, and with addition of all the cofactors listed in Table 1, 3*R*-HETE synthesis was 0.9, 5.2, 7.9, and 0.6 nmol mg protein^{-1}·h in bands 1–4, respectively. The 10-fold higher rate of 3*R*-HETE synthesis in bands 2 and 3 again suggested that it occurred in the mitochondrial reaction. Its biosynthesis was slightly higher when mitochondria were subsequently burst in hypotonic medium (6.2 and 9.5 nmol mg protein^{-1}·h in bands 2 and 3, respectively), which could reflect the impermeability of 20:4n-6-CoA to the membrane and that the acylcarnitine is synthe-

sized *in vivo*. In yeast and animals, carnitine acyltransferases are important regulatory proteins responsible for transporting acyl groups across membranes. The greater increase in 3*R*-HETE biosynthesis in band 3 upon incubation in hypotonic medium may indicate that the latter contained more intact mitochondria than band 2 (it is common to witness both intact and broken organelles in separations of this kind).

Biosynthesis of 3-hydroxyeicosenoic acids by enzyme extracts. The products of 20:3n-6, 20:3n-3, and 20:5n-3 metabolism from enzyme extracts (not containing intact mitochondria) were analyzed as methyl ester silyl ethers by GC and compared with that for the metabolism of 20:4n-6. In each case, upon inclusion of all cofactors listed in Table 1, a peak was detected with a similar retention time to 3*R*-HETE (Fig. 4). These extracts, then analyzed by GC–MS, gave the following mass spectrum results; major ions are reported with our interpretation of structures. In all cases the base ion was *m/z* 73 (silyl group).

(*i*) *20:3n-6. 3-hydroxy-8Z,11Z,14Z-eicosatrienoic acid, (Fig. 5). m/z* 408 [M^+], 393 [$M^+ - 15$], 318 [$M^+ - 90$] and 175 [$(CH_3)_3SiO^+$=CH–CH_2–COO–CH_3]. *m/z* 207, 159 and 105 were not identified.

(*ii*) *20:3n-3. 3-hydroxy-11Z,14Z,17Z-eicosatrienoic acid. m/z* 408 [M^+], 393 [$M^+ - 15$], 318 [$M^+ - 90$] and 175 [$(CH_3)_3SiO^+$=CH–CH_2–COO–CH_3]. Unknown ions included *m/z* 207 and 159.

(*iii*) *20:5n-3. 3-hydroxy-5Z,8Z,11Z,14Z,17Z-eicosapentaenoic acid. m/z* 404 [M^+], 389 [$M^+ - 15$], 314 [$M^+ - 90$] and 175 [$(CH_3)_3SiO^+$=CH–CH_2–COO–CH_3].

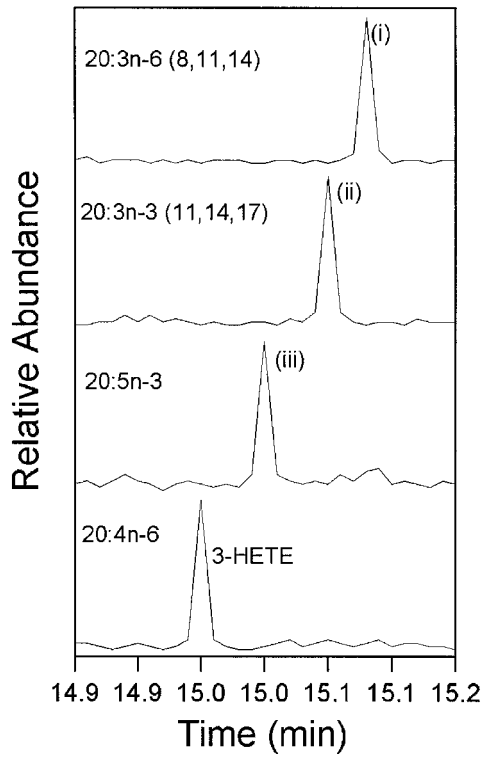

FIG. 4. Comparison of four partial GC chromatograms illustrating the separation of the oxygenated products of four different eicosanoids (as listed) by enzyme extracts of *D. uninucleata* grown on 4% glucose medium. The retention times of the three unknown peaks (i–iii) are shown in relation to one of the products of 20:4n-6 metabolism, 3*R*-hydroxy-5*Z*, 8*Z*,11*Z*,14*Z*-eicosatetraenoic acid. The identities of peaks (i–iii) were analyzed by GC–MS. 3-HETE, 3-hydroxyeicosatetraenoic acid. See Figure 1 for abbreviations.

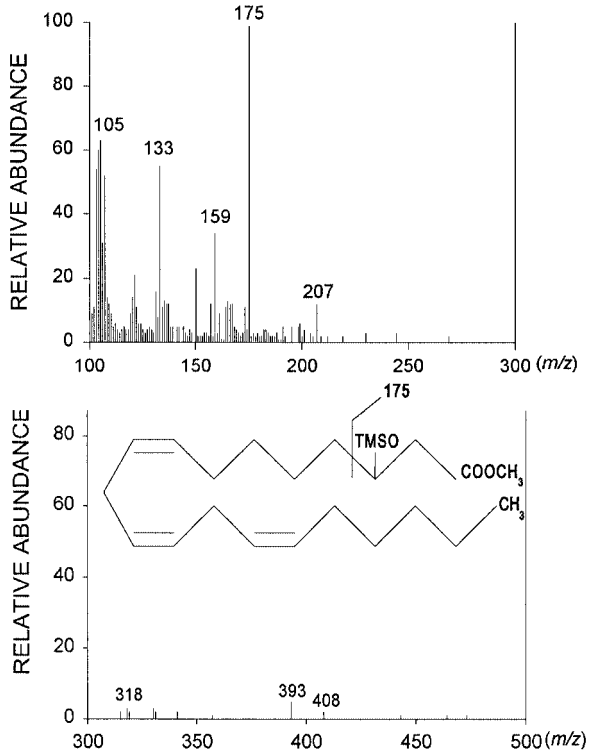

FIG. 5. Electron impact (EI) mass spectrum of the methyl ester silyl ether of 3-hydroxy-8*Z*,11*Z*,14*Z*-eicosatrienoic acid. The compound was isolated from enzyme extracts of *D. uninucleata* incubated with 20:3n-6 and all cofactors listed in Table 1. TMSO, trimethyl silyl ether; for other abbreviation see Figure 1.

In mammalian cells, the degradation of fatty acids with double bonds extending from odd-numbered carbons, such as 20:4n-6, requires additional reactions which result in the saturation of the *cis*-5 double bond and the synthesis of *trans*-2-*cis*-8*Z*,11*Z*,14*Z*-eicosatetraenoic acid (29). However, it now appears that the presence of a 5*Z*,8*Z* diene structure is not required for the synthesis of 3-hydroxyl derivatives of eicosanoids by enzyme extracts of *D. uninucleata*.

Assay of PGH synthase. As previous suggestions (1–4) had been made that the yeast under current study was able to synthesize prostaglandins and that 3*R*-HETE could be an intermediate in this process (1,2), we examined this possibility hoping to corroborate these claims. Prostaglandins are valuable products and their synthesis in microorganisms could be of interest to the pharmaceutical industry. If prostaglandin biosynthesis could be confirmed, then, by extension of the above studies we should be able to elucidate the pathway in greater detail. The first enzyme of prostaglandin biosynthesis is PGH synthase, which introduces dioxygen (O_2) into 20:4n-6 to produce a hydroperoxide at C_{11}. Hence, PGH synthase is often measured using a polarographic O_2 electrode

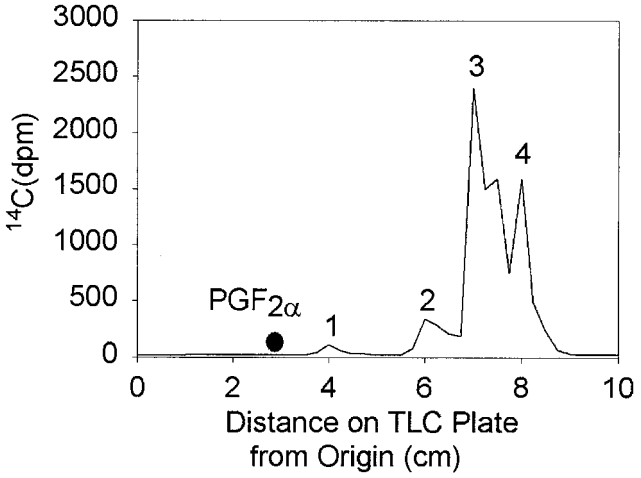

FIG. 6. Separation by thin-layer chromatography (TLC) of the radiochemical products of [1-^{14}C]20:4n-6 metabolism produced by enzyme extracts of *D. uninucleata*. A comparison (●) is given with the R_f of the prostaglandin $PGF_{2\alpha}$. The identities of peaks 1, 2, 3, and 4 were further analyzed by GC–MS. See Figure 1 for other abbreviation.

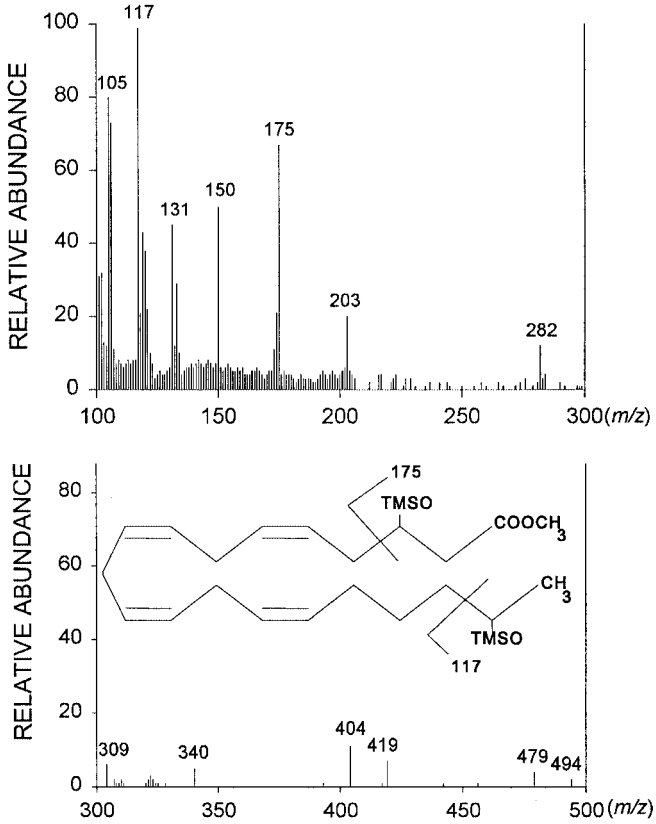

FIG. 7. EI mass spectrum of peak 2 (see Fig. 6) from the TLC separation of the products of [1-^{14}C]20:4n-6 metabolism from enzyme extracts of *D. uninucleata* grown for 48 h on the 4% glucose medium. The compound was assigned as 3,19-di-hydroxy-5*Z*,8*Z*,11*Z*,14*Z*-eicosatetraenoic acid. See Figures 5 and 6 for abbreviations.

(27). We used this method but, upon addition of 20:4n-6 there was no decrease in O_2 concentration in comparison to the control experiment in which no fatty acid was added. This applied to enzyme extracts and microsomal fractions.

A second method to assay PGH synthase, which follows the metabolism of [1-^{14}C]20:4n-6 (Fig. 6), revealed that with enzyme extracts a small peak of radioactivity occurred (peak 1) in a region close to the R_f of the prostaglandin $PGF_{2\alpha}$. Microsomal extracts, the usual location of the enzyme (27,28), did not metabolize 20:4n-6. The [^{14}C]compound(s) of peak 1 were analyzed as methyl silyl derivatives by GC–MS. A peak was detected (Fig. 7) which produced ions at *m/z* 494 [M^+], 479 [$M^+ - 15$], 404 [$M^+ - 90$], 175 [$(CH_3)_3SiO^+$=CH–CH_2–COO–CH_3], 150 [possibly 175 – 15], 117 [$(CH_3)_3SiO^+$=CH–CH_3], and a base ion of 73 [silyl group]. Prominent ions were also detected at *m/z* 340, 282, 203, and 105. The compound was assigned as 3,19-di-hydroxy-5*Z*,8*Z*,11*Z*,14*Z*-eicosatetraenoic acid.

Selective ion searches were made from GC–MS data of methylated and silylated samples from enzyme extracts and microsomal preparations incubated with 20:4n-6, as described in the Materials and Methods section. We also frequently carried out experiments in which 20:4n-6 was added to whole cells of *D. uninucleata*, as described in reference 1, from which we analyzed the oxylipins (results not shown). We were unable to identify the breakdown products of prostacyclin (3), isomers of α-pentanor $PGF_{2\alpha}$-γ-lactone, or any other prostaglandin from any of these samples.

DISCUSSION

Dipodascopsis uninucleata accumulates 3*R*-HETE and other 3-hydroxy fatty acids from exogenously supplied 20:4n-6 and other polyunsaturated fatty acids. These hydroxy-lipins are then considered to play key roles in the growth cycle of the yeast (35,36) and may even involve their conversion to prostaglandins (1–6), which would function as physiologically important molecules as they do in higher animals. The mechanism of 3*R*-HETE formation has remained unclear; the principal routes could be *via* a specific hydroxylase system, perhaps being cytochrome *P*450-dependent, or *via* the β-oxidation cycle which is responsible for fatty acid oxidation in all cell systems. The research group of Kock *et al*. have favored the former explanation (6,10), principally because the chirality of 3-HETE was the *R*-isomer, which was thought to be the opposite of the *S*-isomer that is produced by β-oxidation. However the *S*-enantiomer is only so produced by the fatty acid β-oxidation cycle of plants and animals; in fungi, which include yeasts, it is the *R*-isomer that is found (11). Thus this favors the second option, formation by a β-oxidation system. The results presented here would strongly support this mechanism.

Normally, β-oxidation of fatty acids is considered to occur in specific organelles, i.e., peroxisomes, sometimes known as glyoxysomes. However, such organelles are inducible entities requiring cells to be grown on ethanol, acetic acid, or fatty acids (37). In the absence of peroxisomes, as in cells grown on glucose, cells must carry out vestigial β-oxidation in the mitochondrion as has been shown by Dommes *et al*. (37) for *Candida tropicalis*. Without such a system, cells could not

use exogenous fatty acids, and would not be able to make the transition from growth on glucose to growth on fatty acids. A mitochondrial β-oxidation system is therefore essential and moreover has to be a constituitive cellular activity if cells must oxidize fatty acids *ab initio* prior to, or without, the induction of peroxisome formation.

Such a mitochondrial β-oxidation system has been shown here to occur in *D. uninucleata* and is able to account for the oxidation of a wide range of fatty acids. However, in this particular yeast, the enzymes of the β-oxidation cycle appear not to be closely integrated in their activity and, indeed, in mitochondria in general all such enzymes appear to be separable monofunctional proteins (11,38). It is therefore this imbalance in activities (Table 2) that leads to a faster rate of formation of 3*R*-HETE than its oxidation. Hence 3*R*-HETE accumulates in the mitochondrion. Presumably it must then be translocated from this organelle, probably *via* a carnitine acyltransferase system (38), so that it can exert a physiological role within the cell to control some key aspects of development.

This imbalance in enzyme activities in the β-oxidation cycle of the mitochondrion appears to be greater in older (48 h) cells where our results, with the inhibition of β-oxidation by antimycin A, indicate a possible limitation in the supply of NAD^+ thereby affecting the activity of the long-chain acyl-CoA dehydrogenase. This is the initial enzyme activity of the β-oxidation cycle following activation of 20:4n-6 to its CoA ester by long-chain acyl-CoA synthetase. A similar situation had been observed with mitochondrial extracts from pea cotyledons (Fox, S.R., unpublished work): peas do not synthesize 20:4n-6 or other fatty acids with a Δ^5 *cis* double bond and yet are able to form 3*R*-HETE from 20:4n-6. Thus the partial oxidation of polyunsaturated fatty acids including both representatives of the n-6 and n-3 series may occur in a number of mitochondrial systems all having an imbalance in the sequence of β-oxidation cycle enzymes.

Suggestions that 3*R*-HETE may be a precursor of prostaglandins in this yeast (1,3,4), however, could not be substantiated by this work, although we were able to detect synthesis of 3,19-dihydroxy-5*Z*,8*Z*,11*Z*,14*Z*-eicosatetraenoic acid in cell-free extracts of this yeast incubated with 20:4n-6. This, we presume, will have arisen from 3*R*-HETE as an intermediate possibly *via* an n-1 terminal oxidase system, but this remains speculative. Chromatographically, this metabolite behaved very much like prostaglandin $PGF_{2\alpha}$, which might then account for the earlier suggestions of prostaglandin formation in this yeast (1–6). However, no prostaglandins have been detected in our detailed examination of this yeast, but it is not impossible that some related compounds such as α-pentanor $PGF_{2\alpha}$-γ-lactone may have arisen as minor artifacts (e.g., Ref. 39) from some of the unstable hydroxylipins that this yeast undoubtably can synthesize. Although absence of prostaglandins does not mean they are not occasionally synthesized, the absences of key enzyme activities associated with prostaglandin formation, such as PGH synthase, even after detailed examination suggest that these materials are not produced in this yeast. We therefore conclude, somewhat reluctantly because of the clear interest that would arise from substantiation of the prior claims for the occurrence of prostaglandins in yeasts, that it is unlikely that such entities are being synthesized. Undoubtably though hydroxyeicosanoids are produced and these compounds will almost certainly exert profound effects on yeast cell physiology.

ACKNOWLEDGMENTS

S.R.F. was funded by a grant from The Biotechnology and Biological Sciences Research Council, United Kingdom, awarded to C.R. and J.F. The authors extend their gratitude to Prof. Santosh Nigam for the NS-398, Alan Roberts for help with the GC–MS, and Kath Bulmer, Janice Halder, and Janet Stephenson.

REFERENCES

1. Van Dyk, M.S., Kock, J.L.F., Coetzee, D.J., Augustyn, O.P.H., and Nigam, S. (1991) Isolation of a Novel Arachidonic Acid Metabolite 3-Hydroxy-5,8,11,14-eicosatetraenoic Acid (3-HETE) from the Yeast *Dipodascopsis uninucleata* UOFS-Y128, *FEBS Lett. 283*, 195–198.
2. Van Dyk, M.S., Kock, J.L.F., and Botha, A. (1994) Hydroxy Long-Chain Fatty Acids in Fungi, *World J. Microbiol. Biotech. 10*, 495–504.
3. Kock, J.L.F., Coetzee, D.J., Van Dyk, M.S., Truscott, M., Cloete, F.C., Van Wyk, V., and Augustyn, O.P.H. (1991) Evidence for Pharmacologically Active Prostaglandins in Yeasts, *South Afr. J. Sci. 87*, 73–76.
4. Botha, A., Kock, J.L.F., Van Dyk, M.S., Coetzee, D.J., Augustyn, O.P.H., and Botes, P.J. (1993) Yeast Eicosanoids IV. Evidence for Prostaglandin Production During Ascosporogenesis by *Dipodascopsis töthii*, *System. Appl. Microbiol. 16*, 159–163.
5. Kock, J.L.F., Venter, P., Botha, A., Coetzee, D.J., Botes, P.J., and Nigam, S. (1996) The Production of Biologically Active Eicosanoids by Yeasts, *Prostaglandins Leukotrienes Essent. Fatty Acids 55 (Supplement 1),* 39.
6. Kock, J.L.F., Venter, P., Botha, A., Coetzee, D.J., Botes, P.J., and Nigam, S. (1996) The Production of Biologically Active Eicosanoids by Yeasts, *Prostaglandins Leukotrienes Essent. Fatty Acids 433*, 217–219.
7. Akpinar, A., Fox, S.R., Ratledge, C., and Friend, J. (1996) Biotransformation of Arachidonic Acid and Other Eicosanoids by the Yeast *Dipodascopsis uninucleata*, the Oomycete Fungi *Saprolegnia diclina* and *Leptomitus lacteus* and the Zygomycete Fungus *Mortierella isabellina*, *Prostaglandins Leukotrienes Essent. Fatty Acids 55 (Supplement 1),* 39–42.
8. Akpinar, A., Fox, S.R., Ratledge, C., and Friend, J. (1998) Biotransformation of Arachidonic Acid and Other Eicosanoids by the Yeast *Dipodascopsis uninucleata*, the Oomycete Fungi *Saprolegnia diclina* and *Leptomitus lacteus* and the Zygomycete Fungus *Mortierella isabellina*, *Adv. Exp. Med. Biol. 433*, 231–234.
9. Fox, S.R., Ratledge, C., and Friend, J. (1997) β-Oxidation Forms 3-Hydroxyeicosanoids in the Yeast *Dipodascopsis uninucleata, Prostaglandins Leukotrienes Essent. Fatty Acids 57*, 251.
10. Venter, P., Kock, J.L.F., Kumar, G.S., Botha, A., Coetzee, D.J., Botes, P.J., Bhatt, R.K., Falck, J.R., Schewe, T., and Nigam, S. (1997) Production of 3*R*-Hydroxy-polyenoic Fatty Acids by the Yeast *Dipodascopsis uninucleata*, *Lipids 32*, 1277–1283.
11. Kunau, W.H., Dommes, V., and Schulz, H. (1995) β-Oxidation of Fatty Acids in Mitochondria, Peroxisomes and Bacteria: A Century of Continued Progress, *Prog. Lipid Res. 34*, 267–342.

12. Kock, J.L.F., and Ratledge, C. (1992) Changes in Lipid Composition and Arachidonic Acid Turnover During the Life Cycle of the Yeast *Dipodascopsis uninucleata*, *J. Gen. Microbiol. 139*, 459–464.
13. Fox, S.R., Ratledge, C., and Friend, J. (1997) Optimisation of 3-Hydroxyeicosanoid Biosynthesis by the Yeast *Dipodascopsis uninucleata*, *Biotechnol. Lett. 19*, 155–158.
14. Serck-Hanssen, K. (1956) Optically Active Higher Aliphatic Hydroxy-Compounds, Part III, *Ark. Kemi 10*, 135–149.
15. Rickwood, D., Wilson, M.T., and Darley-Usmar, V.M. (1987) Isolation and Characterization of Intact Mitochondria, in *Mitochondria: A Practical Approach (*Darley-Usmar, V.M., Rickwood, D., and Wilson, M., eds.), pp. 1–16, IRL Press, Oxford.
16. Watmough, N.J., Turnbull, D.M., Sherratt, S.A., and Bartlett, K. (1989) Measurement of the Acyl-CoA Intermediates of β-Oxidation by HPLC with On-Line Radiochemical and Photodiode-Array Detection, *Biochem. J. 262*, 261–269.
17. Dommes, V., and Kunau, W.-H. (1976) A Convenient Assay for Acyl-CoA Dehydrogenases, *Anal. Biochem. 71*, 571–578.
18. Werner, W., Rey, H.G., and Wielinger, H. (1970) Über die Eigenschaften eines Neuen Chromogens für die Blutz United Kingdomerbestimmung nach der GOD/POD-Methode, *Z. Anal. Chem. 252*, 224–228.
19. Binstock, J.F., and Schulz, H. (1981) Fatty Acid Oxidation Complex from *Escherichia coli, Methods Enzymol. 71,* 403–411.
20. Fong, J.C., and Schulz, H. (1977) Purification and Properties of Acyl-Coenzyme A Dehydrogenases from Bovine Liver. Formation of 2-*trans*,4-*cis*-Decadienoyl Coenzyme A, *J. Biol. Chem. 259*, 1789–1797.
21. Middleton, B. (1973) The Oxoacyl Coenzyme A Thiolases of Animal Tissues, *Biochem. J. 132*, 717–730.
22. Hill, R.L., and Bradshaw, R.A. (1969) Fumarase, *Methods Enzymol. 13*, 91–99.
23. Aebi, H. (1974) Katalase, in *Methods of Enzymatic Analysis* (Bergmeyer, H.E., ed.), Vol. 2, pp. 673–684, Verlag Chemie, Weinheim.
24. Armitt, S., McCullough, W., and Roberts, C.F. (1976) Analysis of Acetate Non-Utilizing (acu) Mutants in *Aspergillus nidulans*, *J. Gen. Microbiol. 92*, 263–282.
25. Hock, B., and Beevers, H. (1966) Development and Decline of Glyoxylate-Cycle Enzymes in Watermelon Seedlings (*Citrullus vulgaris* Schrad), *Z. Pflanzenphysiol. 55*, 405–414.
26. Douce, R., Christensen, E.L., and Bonner, W.D., Jr. (1972) Preparation of Intact Plant Mitochondria, *Biochim. Biophys. Acta 275,* 148–160.
27. Van der Ouderaa, F.J.G., and Buytenhek, M. (1982) Purification of PGH Synthase from Sheep Vesicular Glands, *Methods Enzymol. 86*, 60–68.
28. Yamamoto, S. (1982) Purification and Assay of PGH Synthase from Bovine Seminal Vesicles, *Methods Enzymol. 86*, 55–60.
29. Luthria, D.L., Baykousheva, S.P., and Sprecher, H. (1995) Double Bond Removal from Odd Numbered Carbons During Peroxisomal α-Oxidation of Arachidonic Acid Requires Both 2,4-Dienoyl-CoA Reductase and $\Delta^{3,5}$, $\Delta^{2,4}$-Dienoyl-CoA Isomerase, *J. Biol. Chem. 270*, 13771–13776.
30. MacLouf, J., and Rigaud, M. (1982) Open Tubular Glass Capillary Gas Chromatography for Separating Eicosanoids, *Methods Enzymol. 86*, 612–631.
31. Nigam, S., and Kock, J.L.F. (1994) Abstract. 1st International Symposium on Eicosanoids and Their Precursors in Fungi, University of the Orange Free State, Bloemfontein, p. 13.
32. Woollard, P.M., Cunningham, F.M., Murphy, G.M., Camp, R.D.R., Derm, F.F., and Greaves, M.W. (1989) A Comparison of the Proinflammatory Effects of 12 (*R*) and 12 (*S*) Hydroxy-5,8,10,14-eicosatetraenoic Acid in Human Skin, *Prostaglandins 38*, 465–471.
33. Agarwal, R., Wang, Z.Y., and Mukhtar, H. (1991) Nordihydroguaiaretic Acid, an Inhibitor of Lipoxygenase, Also Inhibits Cytochrome-P_{450}-Mediated Monooxygenase Activity in Rat Epidermal and Hepatic Microsomes, *Drug Metab. Dispos. 19,* 620–624.
34. Mergner, W.J., Smith, M.A., and Trump, B.F. (1972) Structural and Functional Effects of the Negative Stains Silicotungstic Acid, Phosphotungstic Acid, and Ammonium Molybdate on Rat Kidney Mitochondria, *Lab. Invest. 27*, 372–383.
35. Kock, J.L.F., Venter, P., Linke, D., Schewe, T., and Nigam, S. (1998) Biological Dynamics and Distribution of 3-Hydroxy Fatty Acids in the Yeast *Dipodascopsis uninucleata* as Investigated by Immunofluorescence Microscopy. Evidence of a Putative Regulatory Role in the Sexual Reproductive Cycle, *FEBS Lett. 427*, 345–348.
36. Kock, J.L.F., Van Wyk, P.W.J., Venter, P., Coetzee, D.J., Smith, D.P., Viljoen, B.C., and Nigam, S. (1999) An Acetylsalicylic Acid-Sensitive Aggregation Phenomenon in *Dipodascopsis uninucleata*, *Antonie van Leeuwenhoek 75*, 261–266.
37. Dommes, P., Dommes, V., and Kunau, W.-H. (1983) α-Oxidation in *Candida tropicalis*. Partial Purification and Biological Function in an Inducible 2,4, Dienoyl-Coenzyme A Reductase, *J. Biol. Chem. 258*, 10846–10852.
38. Ratledge, C. (1994) Biodegradation of Oils, Fats and Fatty Acids, in *Biochemistry of Microbial Degradation (*Ratledge, C., ed.), pp. 89–141, Kluwer Academic Publishers, Dordrecht.
39. Morrow, J.D., and Roberts, L.J. (1994) Mass-Spectrometry of Prostanoids: F_2-Isoprostanes Produced by Non-Cyclooxygenase Free Radical-Catalysed Mechanism, *Methods Enzymol. 233*, 163–174.

[Received May 3, 2000, and in final revised form and accepted September 22, 2000]

Effects of α-Tocopherol and Ascorbyl Palmitate on the Isomerization and Decomposition of Methyl Linoleate Hydroperoxides

E. Marjukka Mäkinen* and Anu I. Hopia

Department of Applied Chemistry and Microbiology, Food Chemistry Division, 00014 University of Helsinki, Finland

ABSTRACT: In order to study antioxidant action on lipid hydroperoxide decomposition, the effects of α-tocopherol (TOH) and ascorbyl palmitate on the decomposition rate and reaction sequences of 9- and 13-*cis,trans* methyl linoleate hydroperoxide (*cis,trans* ML-OOH) decomposition in hexadecane were studied at 40°C. Decomposition of *cis,trans* ML-OOH as well as the formation and isomeric configuration of methyl linoleate hydroxy and ketodiene compounds were followed by high-performance liquid chromatographic analysis. TOH effectively inhibited the decomposition of ML-OOH. The decomposition rate was two times slower at 0.2 mM and more than 10 times slower at 2 and 20 mM of TOH. Ascorbyl palmitate (0.2, 2, and 20 mM) slightly accelerated the decomposition of ML-OOH. Both compounds had an effect on the reaction sequences of ML-OOH decomposition. At high levels TOH inhibited the isomerization of *cis,trans* ML-OOH to *trans,trans* ML-OOH through peroxyl radicals and increased the formation of hydroxy compounds. Further, the majority of the hydroxy and ketodiene compounds formed had a *cis,trans* configuration, indicating that *cis,trans* ML-OOH decomposed through alkoxyl radicals without isomerization. These results suggest that when inhibiting the decomposition of hydroperoxides, TOH can act as a hydrogen atom donor to both peroxyl and alkoxyl radicals. In the presence of ascorbyl palmitate, *cis,trans* ML-OOH decomposed rapidly but without isomerization. In contrast to TOH, the majority of hydroxy compounds were *cis,trans,* but the ketodiene compounds were *trans,trans* isomers. This indicates that ascorbyl palmitate reduced *cis,trans* ML-OOH to the corresponding hydroxy compounds. However, the simultaneous formation of *trans,trans* ketodiene compounds suggests that ML-OOH decomposition, similar to the control sample, also occurred in these samples. Thus, under these experimental conditions, the reduction of ML-OOH to more stable hydroxy compounds did not occur to an extent significant enough to inhibit the radical chain reactions of ML-OOH decomposition.

Paper no. L8515 in *Lipids 35*, 1215–1223 (November 2000).

Lipid hydroperoxides are the primary products of lipid oxidation. They decompose further to a complex mixture of decomposition products (1,2). The damaging effect of lipid oxidation on biological materials as well as the flavor deterioration of foods is, to a significant extent, caused by these decomposition products (3,4). Thus, when studying the effects of lipid oxidation on biological systems, not only the formation of lipid hydroperoxides but also their decomposition rate and reactions need to be clarified. Moreover, in antioxidant research it is important to distinguish between their effects on the formation and decomposition of lipid hydroperoxides. The effect of antioxidants on the stability and decomposition reactions of lipid hydroperoxides in foods, membranes, and other biological systems is still largely unknown.

Previous results of the effects of the α-tocopherol (TOH) and ascorbyl palmitate on the stability of lipid hydroperoxides are controversial. Further, their mechanism of action during hydroperoxide decomposition is not fully understood. Hopia *et al.* (5) showed that TOH inhibits the decomposition of methyl linoleate hydroperoxides (ML-OOH) and suggested that the mechanism may involve the conversion of ML-OOH into more stable hydroxy compounds. Huang *et al.* (6) used hexanal as an indicator of hydroperoxide decomposition in bulk corn oil stripped of natural tocopherols and showed that TOH has a stabilizing effect on lipid hydroperoxides during thermal decomposition at 60°C. Also, Lampi *et al.* (7) showed that TOH reduces the amount of volatile decomposition products of hydroperoxides during the autoxidation of rapeseed oil triacylglycerols. However, this stabilizing effect is highly system dependent as TOH accelerates the decomposition of 13-ML-OOH at 100°C (8).

The reported effects of ascorbyl palmitate on the stability of lipid hydroperoxides are also controversial and depend strongly on the experimental conditions. Schieberle and Grosch (9) showed that ascorbyl palmitate inhibits the breakdown of 13-*cis,trans* ML-OOH in the presence of copper(II) ions by reducing hydroperoxides into their corresponding hydroxy compounds. A stabilizing effect was also found by Von Uhl and Eichner (10) who suggested that ascorbyl palmitate reduces hydroperoxides into more stable hydroxy compounds, which do not continue the radical-intermediated decomposition reactions. On the other hand, O'Brien (11) showed that the decomposition of linoleic acid hydroperoxides in the presence of metal ions is catalyzed by ascorbates.

*To whom correspondence should be addressed at Department of Applied Chemistry and Microbiology, Food Chemistry Division, P.O. Box 27, 00014 University of Helsinki, Finland. E-mail: Marjukka.Makinen@Helsinki.fi

Abbreviations: HPLC, high-performance liquid chromatography; ML-OOH, methyl linoleate hydroperoxides, TOH, α-tocopherol.

The homolytic decomposition of lipid hydroperoxides proceed either through peroxyl or alkoxyl radicals. Due to the high bond dissociation energy of the ROO-H and RO-OH bonds, they are relatively difficult to generate from the preformed hydroperoxides. However, the presence of catalytic quantities of transition metal ions (Eqs. 1 and 2) or other catalyst enhances the formation of these radicals (1).

$$ROOH + M^{n+1} \rightarrow ROO^{\bullet} + H^{+} + M^{n} \quad [1]$$

$$ROOH + M^{n} \rightarrow RO^{\bullet} + OH^{-} + M^{n+1} \quad [2]$$

Antioxidants can retard the radical-mediated decomposition of hydroperoxides by scavenging intermediate radicals, by chelating metal ions, or by reducing hydroperoxides to more stable hydroxy compounds (12). Analysis of selected decomposition products provides specific information about the mechanism of antioxidant action in various sequences of lipid hydroperoxide decomposition.

In this study we compared the effects of two lipid-soluble antioxidants, TOH and ascorbyl palmitate, on the decomposition rate of of 9- and 13-*cis,trans* ML-OOH. To get further information about the effects of these antioxidants on the intermediate radicals and the reaction sequences of ML-OOH decomposition, the isomeric configuration of ML-OOH and the formation and isomeric configuration of selected decomposition products were followed. The effects of antioxidants were studied in purified 9- and 13-*cis,trans* ML-OOH to avoid the consumption of antioxidants in the reactions involving unoxidized material.

MATERIALS AND METHODS

Materials. Methyl linoleate was purchased from Nu-Chek Prep Inc. (Elysian, MN) and TOH from Merck (Darmstadt, Germany). Ascorbyl palmitate and hexadecane were purchased from Sigma Chemicals Co. (St. Louis, MO). Heptane and diethyl ether were from Rathburn (Walkerburn, Scotland) and sodium borohydride from BDH (Poole, United Kingdom).

Preparation of cis,trans *ML-OOH*. Methyl linoleate was oxidized at 40°C in the dark until the oxidation level reached 10–15%. The oxidation was done with 5% TOH to produce only *cis,trans* ML-OOH (13). *Cis,trans* ML-OOH were separated from nonoxidized methyl linoleate and TOH by solid-phase extraction (5). The nonpolar methyl linoleate was first eluted with heptane/diethyl ether (95:5, vol/vol) and then the *cis,trans* ML-OOH fraction was collected with heptane/diethyl ether (85:15, vol/vol). The purity of the *cis,trans* ML-OOH fraction was checked by thin-layer chromatography, and the concentration of *cis,trans* ML-OOH was measured spectrophotometrically at 234 nm (5). As measured by high-performance liquid chromatography (HPLC), a small amount of *cis,trans* hydroxy compounds (0.4–2.5% of total ML-OOH) and *cis,trans* ketodienes (0.8–2.1% of total ML-OOH) was present after solid-phase extraction. The TOH content was less than 0.01 mM as measured by HPLC.

HPLC analysis. Four isomers of ML-OOH, hydroxy, and ketodiene compounds were separated by HPLC. The instrumentation included a model 501 pump equipped with a model 700 autosampler (Waters, Milford, MA). The column was a silica column (25 cm × 2.1 mm, 5 μm; Supelco, Bellefonte, PA) and the elution solvent heptane/diethyl ether (82:18, vol/vol) with a flow rate of 0.4 mL/min. ML-OOH and hydroxy compounds were monitored at 234 nm and ketodienes at 268 nm using a diode array detector (model 996; Waters). The relative standard deviation of six injections was 0.6%.

Identification of the ML-OOH isomers was based on their ultraviolet spectra (14). The retention times of the hydroxy compounds were confirmed by reducing the ML-OOH isomers to their corresponding hydroxy isomers with sodium borohydride (15). Tentative identification of ketodiene geometrical isomers was based on the transition of their maxima in the ultraviolet spectra (14) and on the elution order previously reported by Schieberle *et al.* (16). In the chromatogram (Fig. 1), peaks 1–4 were identified as 13-*cis,trans* ML-OOH, 13-*trans,trans* ML-OOH, 9-*cis,trans* ML-OOH, 9-*trans,trans* ML-OOH and peaks 5–8 as 13-*cis,trans* hydroxy compound, 13-*trans,trans* hydroxy compound, 9-*cis,trans* hydroxy compound and 9-*trans,trans* hydroxy compound. Peaks 9 and 10 were *cis,trans* ketodienes and peaks 11 and 12 were *trans,trans* ketodienes. The amounts of ML-OOH, hydroxy, and ketodiene

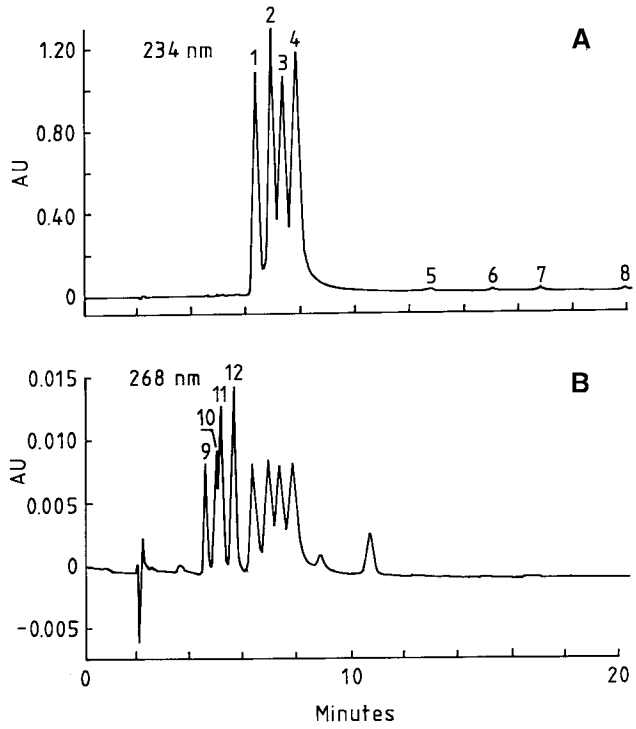

FIG. 1. High-performance liquid chromatograms of methyl linoleate hydroperoxides (ML-OOH) and its decomposition products monitored at 234 nm (A), and 268 nm (B). Peaks 1–4: 13-*cis,trans* ML-OOH, 13-*trans,trans* ML-OOH, 9-*cis,trans* ML-OOH, and 9-*trans,trans* ML-OOH; peaks 5–8: 13-*cis,trans* hydroxy, 13-*trans,trans* hydroxy, 9-*cis,trans* hydroxy, and 9-*trans,trans* hydroxy compounds; peaks 9 and 10: *cis,trans* ketodiene compounds; and peaks 11 and 12: *trans,trans* ketodiene compounds.

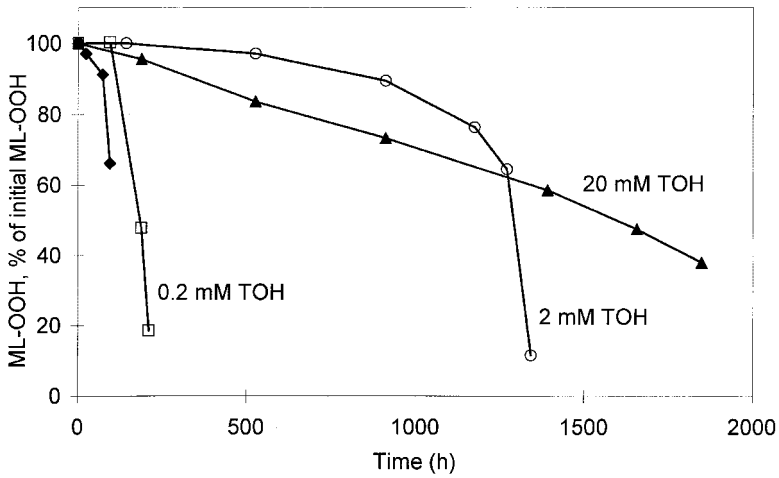

FIG. 2. Effect of α-tocopherol (TOH) on the decomposition of ML-OOH at 40°C. Control (-◆), 0.2 mM TOH (-□-), 2 mM TOH (-○-), and 20 mM TOH (-▲-). For other abbreviation see Figure 1.

compounds were monitored as total areas of four isomer peaks in the chromatograms and then converted to a percentage of the initial content of ML-OOH by using the molar extinction coefficients of 28,600 for ML-OOH (14), 27,200 for hydroxy compounds (14), and 28,000 for ketodienes (17).

Decomposition of cis,trans *ML-OOH.* A solution of *cis,trans* ML-OOH (40 mM) in hexadecane was incubated at 40°C in the dark in screw-capped glass vials (12 mL) with magnetic stirring with or without added antioxidants. The concentrations of TOH and ascorbyl palmitate were 0.2, 2, and 20 mM. Duplicate sample aliquots were taken periodically for HPLC analysis, and each experiment was done in duplicate.

RESULTS

TOH efficiently inhibited the decomposition of ML-OOH (Fig. 2). The inhibition was strongest at 2 mM of TOH. At the higher level of TOH (20 mM), the initial decomposition rate of ML-OOH was higher when compared to 2 mM TOH. In contrast to TOH, ascorbyl palmitate at 2 and 20 mM slightly accelerated the decomposition of ML-OOH (Fig. 3).

Without antioxidants the majority of *cis,trans* ML-OOH isomerized to *trans,trans* ML-OOH prior to decomposition (Fig. 4A). The amount of total ML-OOH started to decrease after a 67-h incubation when only 27% of the total ML-OOH still had the *cis,trans* configuration. Also the majority of hydroxy and ketodiene compounds formed had the *trans,trans* configuration (Figs. 4B and 4C). The level of decomposition products having the *cis,trans* configuration remained at their initial level whereas the level of *trans,trans* decomposition products increased during the decomposition. No differences were seen in the proportions of 9- and 13-isomers of ML-OOH during the decomposition.

At a 2-mM level TOH partly inhibited the isomerization of *cis,trans* ML-OOH to *trans,trans* ML-OOH (Fig. 5A). The

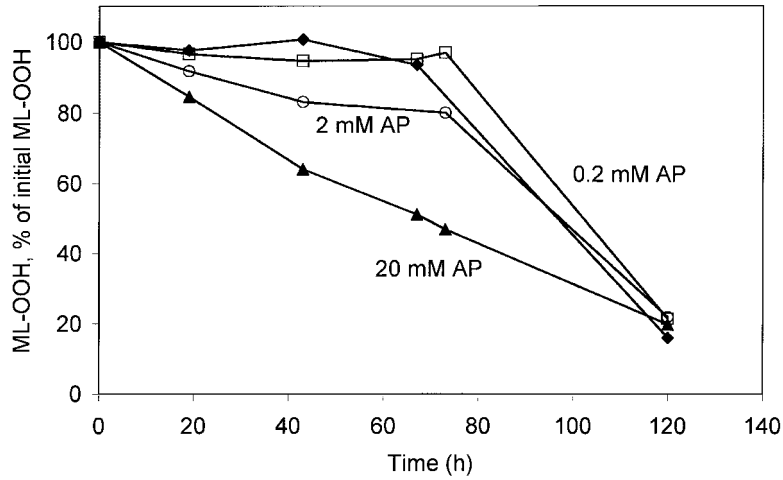

FIG. 3. Effect of ascorbyl palmitate (AP) on the decomposition of ML-OOH at 40°C. Control (-◆-), 0.2 mM AP (-□-), 2 mM AP (-O-), and 20 mM AP (-▲-). For other abbreviation see Table 1.

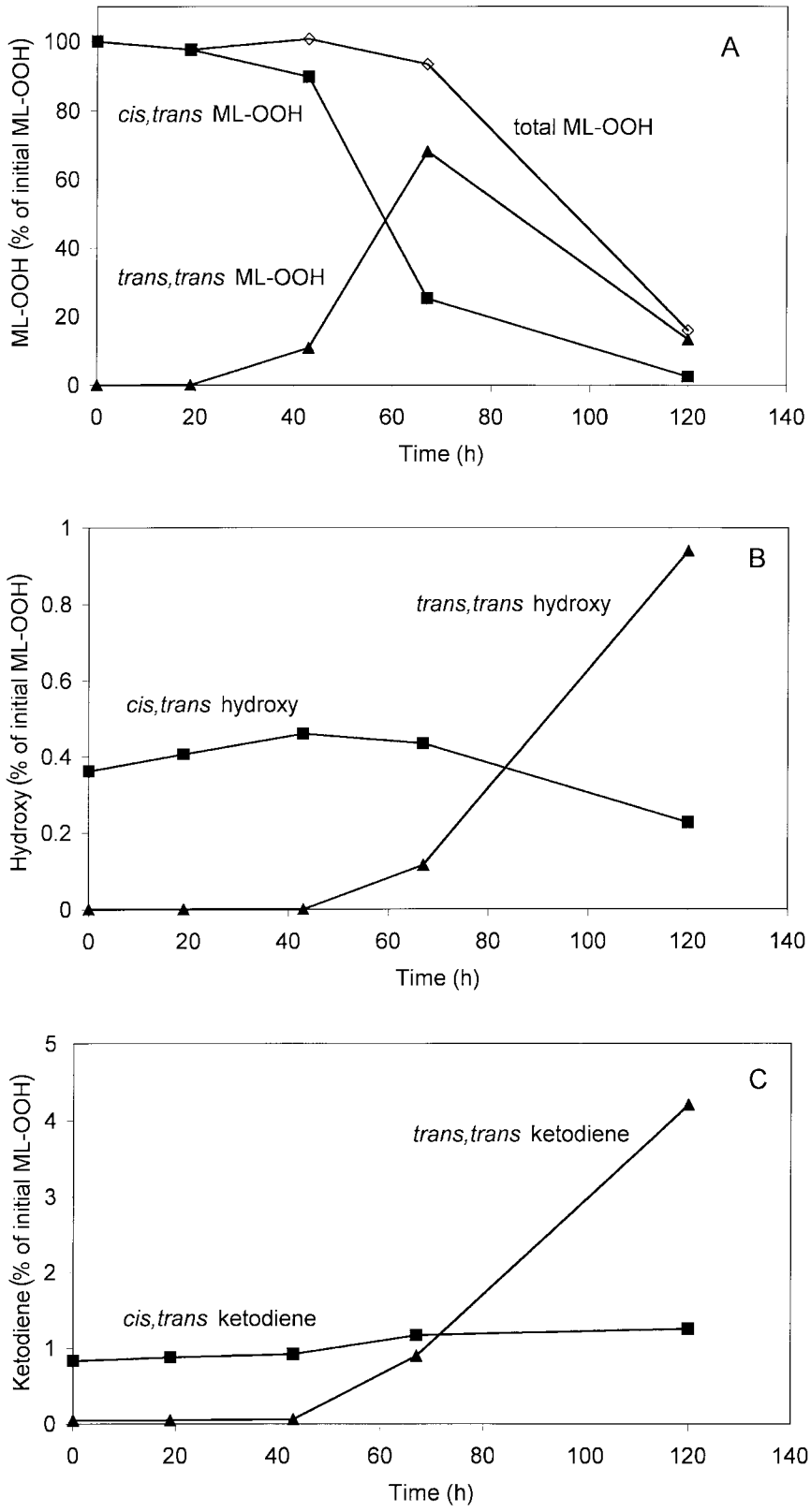

FIG. 4. Decomposition of ML-OOH at 40°C without added antioxidants. (A) ML-OOH, (B) hydroxy compounds, and (C) ketodiene compounds. Total ML-OOH (-◇-), *cis,trans* isomers (-■-), and *trans,trans* isomers (-▲-). For abbreviation see Figure 1.

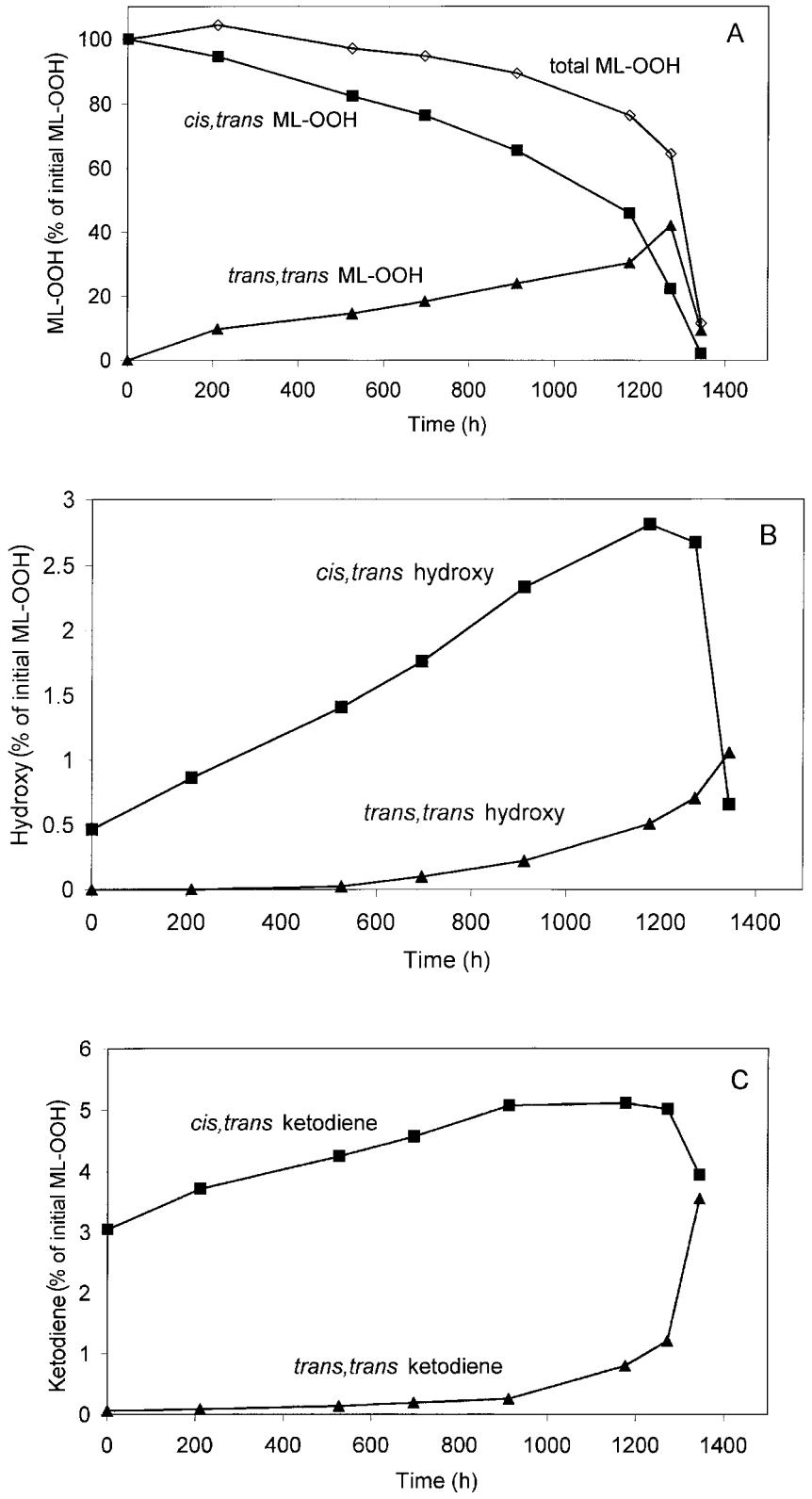

FIG. 5. Decomposition of ML-OOH at 40°C in the presence of 2 mM of α-tocopherol. (A) ML-OOH, (B) hydroxy compounds and (C) ketodiene compounds. Total ML-OOH (-◇-), *cis,trans* isomers (-■-), and *trans,trans* isomers (-▲-). For abbreviation see Figure 1.

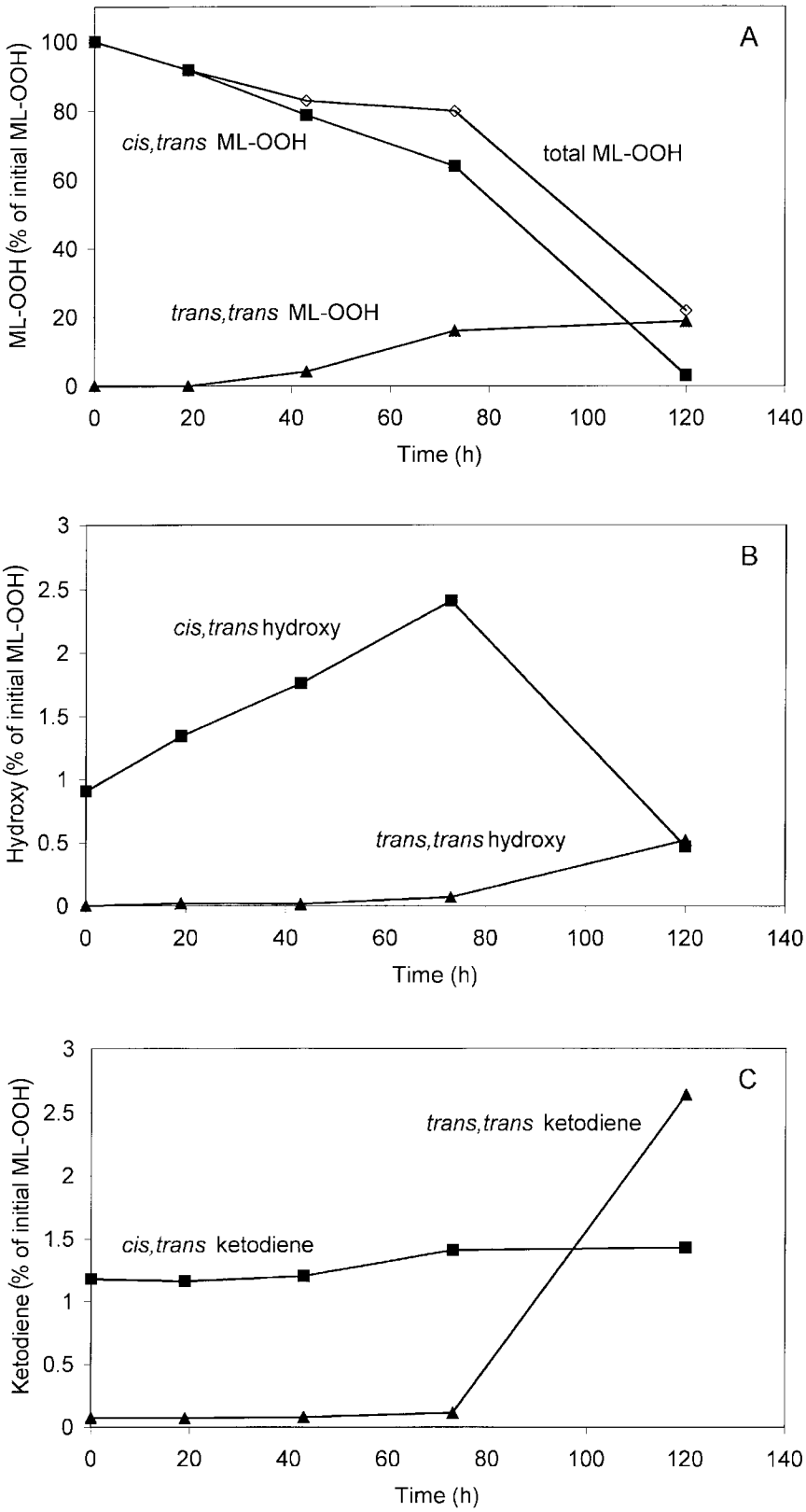

FIG. 6. Decomposition of ML-OOH at 40°C in the presence of 2 mM of ascorbyl palmitate. (A) ML-OOH, (B) hydroxy compounds, and (C) ketodiene compounds. Total ML-OOH (-◇-), *cis,trans* isomers (-■-), and *trans,trans* isomers (-▲-). For abbreviation see Figure 1.

fast decomposition of ML-OOH started after a 1176-h incubation when 61% of the total ML-OOH still had the *cis,trans* configuration. A tenfold increase in TOH (20 mM) completely inhibited the isomerization, and ML-OOH decomposed as *cis,trans* isomers without prior isomerization to *trans,trans* isomers (data not shown). TOH also had a marked effect on the isomeric configuration of decomposition products as the majority of hydroxy and ketodiene compounds had c*is,trans* configuration. Figures 5B and 5C show the isomeric distribution of hydroxy and ketodiene compounds formed in the presence of 2 mM TOH. With 20 mM TOH, more than 90% of the total hydroxy and ketodiene compounds were *cis,trans* isomers during the decomposition of ML-OOH.

In a 2-mM concentration of ascorbyl palmitate *cis,trans* ML-OOH decomposed mainly as *cis,trans* isomers without any change in isomeric configuration (Fig. 6A). Also, most of the hydroxy compounds were *cis,trans* isomers (Fig. 6B). However, the majority of ketodiene compounds were *trans,trans* isomers (Fig. 6C). A tenfold increase in ascorbyl palmitate (20 mM) had similar effects on the isomeric distribution of ML-OOH and its decomposition products (data not shown).

The amount of hydroxy compounds formed during the decomposition of ML-OOH is shown in Table 1 after a fixed time of incubation (67 h) and at a certain level of ML-OOH decomposition (30%). Both TOH and ascorbyl palmitate increased the formation of hydroxy compounds during incubation in a concentration-dependent way. In the presence of ascorbyl palmitate, the amount of hydroxy compounds was already increased at the beginning of the incubation.

DISCUSSION

The effect of antioxidants and pro-oxidants on hydroperoxide decomposition is of great importance in biological systems. This study shows that different antioxidants each have a characteristic effect on further radical chain reactions of hydroperoxides and on the formation of secondary oxidation products.

Both TOH and ascorbyl palmitate had an effect on the decomposition rate of ML-OOH. Under these experimental conditions TOH efficiently inhibited and ascorbyl palmitate slightly accelerated the decomposition of hydroperoxides. The result of TOH is in agreement with the previous result of Hopia *et al.* (5) showing that TOH inhibits the decomposition of a mixture of four ML-OOH isomers at 60°C. However, contradictory results for ascorbyl palmitate's ability to inhibit the decomposition of hydroperoxides have been reported (9,10,18). Clearly the experimental conditions used have a more profound effect on its activity.

TABLE 1
Effects of α-Tocopherol and Ascorbyl Palmitate on the Formation of Hydroxy Compounds During the Decomposition of ML-OOH

Antioxidant concentration	Hydroxy compounds (% of initial ML-OOH)	
	After 67-h incubation	At 30% decomposition level of ML-OOH
α-Tocopherol		
Control	0.4	0.5
0.2 mM	0.6	0.9
2 mM	0.6	3.3
20 mM	0.7	3.5
Ascorbyl palmitate		
Control	0.5	0.7
0.2 mM	0.8	0.8
2 mM	2.2	2.1
20 mM	4.5	3.9

The decomposition of hydroperoxides can proceed either through peroxyl or alkoxyl radicals. If the intermediate radicals are *cis,trans* peroxyl radicals, they have time to rearrange into the thermodynamically more favorable *trans,trans* configurations (19,20,21). As described in Scheme 1, *cis,trans* peroxyl radicals (**2**) are formed from *cis,trans* ML-OOH (**1**). Peroxyl radicals isomerize to *trans,trans* configuration (**4**) through pentadienyl radicals (**3**) and then abstract hydrogen atoms to form *trans,trans* ML-OOH (**5**). *Trans,trans* ML-OOH decompose further into a variety of *trans,trans* decomposition products, such as hydroxy and ketodiene compounds, either through peroxyl or alkoxyl radicals. Thus, if peroxyl radicals are intermediates in the decomposition of *cis,trans* hydroperoxides, the majority of decomposition products have a *trans,trans* configuration in their conjugated diene structure. This was previously shown by Schieberle and Grosch (9) who reported that during the decomposition of 13-*cis,trans* ML-OOH through peroxyl radicals in the presence of copper(II) ions, the majority of ketodiene compounds and some of the hydroxy compounds were *trans,trans* isomers. However, if the decomposition products are formed through more reactive alkoxyl radicals, the original *cis,trans* configuration of hydroperoxide remains in the decomposition product. This was demonstrated earlier by Gardner and Kleiman (22) who showed that the *cis,trans* configuration retained in the decomposition products in cysteine-$FeCl_3$ catalyzed decomposition of *cis,trans* hydroperoxides of linoleic acid. Thus, if the decomposition products of *cis,trans* hydroperoxides still have the *cis,trans* configuration, it indicates that the intermediate radicals of decomposition are alkoxyl radicals.

In this study, the isomerization of *cis,trans* ML-OOH to *trans,trans* ML-OOH was clearly seen in the control sample since the amount of *trans,trans* ML-OOH increased during the incubation. As described above, this isomerization was due to the formation and isomerization of peroxyl radicals. Thus, the importance of peroxyl radicals as intermediates during the decomposition of ML-OOH was demonstrated. TOH at higher levels inhibited this isomerization as no increase in the amount of *trans,trans* ML-OOH was seen. This result indicates that TOH acted as a hydrogen atom donor to *cis,trans* peroxyl radicals before they isomerized to *trans,trans* peroxyl radicals (Scheme 1). Previously Peers *et al.* (13) and Porter (20) showed that TOH acted as a hydrogen atom donor during the autoxidation of methyl linoleate since it increased the *cis,trans* to *trans,trans* ratio of hydroperoxides. TOH may also scavenge other radicals capable of initiating the isomerization and decomposition reac-

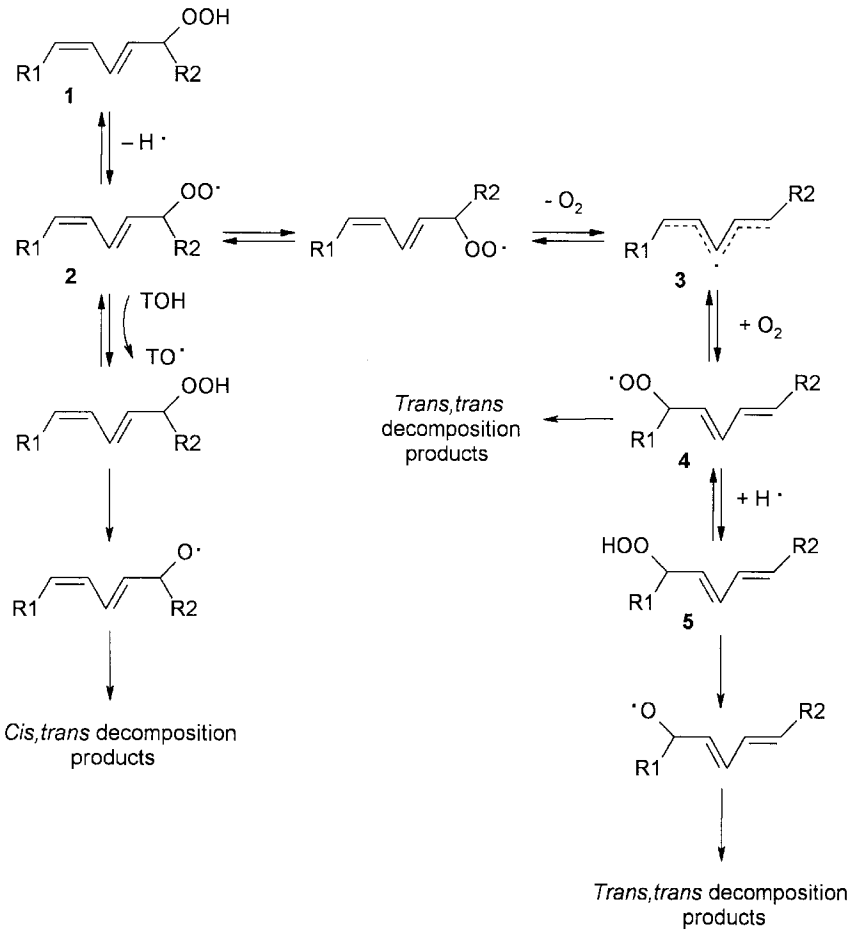

SCHEME 1

tions. However, the scavenging of peroxyl radicals is considered to be the main reaction.

In addition to the isomeric distribution of ML-OOH, TOH had an effect on the isomeric configuration of decomposition products. The majority of hydroxy and ketodiene compounds formed with high levels of TOH had a *cis,trans* configuration, whereas in the control sample most of decomposition products had a *trans,trans* configuration. The high levels of *cis,trans* decomposition products in the presence of TOH indicate that they were formed from *cis,trans* ML-OOH through alkoxyl radicals (Scheme 1), as no isomerization which would occur through peroxyl radicals was seen. Thus, alkoxyl radicals are intermediates during ML-OOH decomposition in the presence of hydrogen donating antioxidants, which can scavenge the peroxyl radicals formed during the decomposition. TOH increased the formation of hydroxy compounds in a concentration dependent way. The mechanism suggested for hydroxy compound formation involves the abstraction of hydrogen atoms by alkoxyl radicals. This reaction pathway may be favored in the presence of strong hydrogen donors such as TOH (Eq. 3) (5):

$$RO^{\bullet} + TOH \rightarrow ROH + TO^{\bullet} \quad [3]$$

Thus the increase in hydroxy formation gives further evidence of the presence of alkoxyl radicals during the decomposition of ML-OOH and of the ability of TOH to donate hydrogen atoms also to these radicals.

The effect of ascorbyl palmitate on ML-OOH decomposition differed markedly from TOH. Ascorbyl palmitate was not capable of inhibiting the decomposition of ML-OOH and at higher levels it even acted as a hydroperoxide decomposer. The analysis of ML-OOH and its decomposition products indicates that the mechanism of action of ascorbyl palmitate is more complex when compared to TOH. As with TOH, most of the of *cis,trans* ML-OOH decomposed without isomerization, but the isomeric configuration of decomposition products was characteristic for ascorbyl palmitate. The majority of hydroxy compounds in the presence of ascorbyl palmitate had a *cis,trans* configuration whereas ketodiene compounds had a *trans,trans* configuration. The increase in the formation of *cis,trans* hydroxy compounds with higher levels of ascorbyl palmitate is obviously due to the direct reduction of *cis,trans* ML-OOH to *cis,trans* hydroxy compounds without radical-intermediated isomerization. The amount of hydroxy compounds was already higher at the early stage of decomposition, which supports this hypothesis. It is interesting to

notice that in contrast to some previous studies (9,10), the reduction of ML-OOH to hydroxy compounds did not have a stabilizing effect on ML-OOH. Thus, under these experimental conditions, the reduction of hydroperoxides to more stable hydroxy compounds did not occur to an extent significant enough to inhibit the radical chain reactions of ML-OOH decomposition. The simultaneous formation of *trans,trans* ketodiene compounds indicates that ML-OOH decomposition similar to control sample occurred in these samples. However, the exact mechanism for ketodiene compound formation is not known at present time. In the literature, both mechanisms through peroxyl and alkoxyl radicals have been suggested (1).

The results of this study show that the stabilizing effect of TOH is partly due to its ability to act as a hydrogen atom donor to both peroxyl and alkoxyl radicals that are formed during the decomposition of hydroperoxides. Under these experimental conditions, ascorbyl palmitate has no stabilizing effect on ML-OOH since the reduction of hydroperoxide to a more stable hydroxy compound does not occur to an extent which inhibits the radical chain reactions of ML-OOH decomposition.

ACKNOWLEDGMENT

This work was financially supported by the Academy of Finland.

REFERENCES

1. Gardner, H.W. (1989) Oxygen Radical Chemistry of Polyunsaturated Fatty Acids, *Free Radical Biol. Med. 7*, 65–86.
2. Frankel, E.N. (1980) Lipid Oxidation, *Prog. Lipid Res. 19*, 1–22.
3. Kubow, S. (1990) Toxicity of Dietary Lipid Peroxidation Products, *Trends Food Sci. Technol. 9*, 67–71.
4. Eriksson, C.E. (1987) Oxidation of Lipids in Food Systems, in *Autoxidation of Unsaturated Lipids* (Chan, H.W.-S., ed.) pp. 207–232, Academic Press Inc., London.
5. Hopia, A., Huang, S.-W., and Frankel, E.N. (1996) Effect of α-Tocopherol and Trolox on the Decomposition of Methyl Linoleate Hydroperoxides, *Lipids 31*, 357–365.
6. Huang, S.-W., Frankel, E.N., and German, J.B. (1994) Antioxidant Activity of α- and γ-Tocopherols in Bulk Oils and in Oil-in-Water Emulsions, *J. Agric. Food Chem. 42*, 2108–2114.
7. Lampi, A.-M., Kataja, L., Kamal-Eldin, A., and Piironen, V. (1999) Antioxidant Activities of α- and γ-Tocopherols in the Oxidation of Rapeseed Oil Triacylglycerols, *J. Am. Oil Chem. Soc. 76*, 749–755.
8. Yamauchi, R., Goto, K., and Kato, K. (1998) Reaction of α-Tocopherol in Heated Bulk Phase in the Presence of Methyl Linoleate (13*S*)-Hydroperoxide or Methyl Linoleate, *Lipids 33*, 77–85.
9. Schieberle, P., and Grosch, W. (1981) Decomposition of Linoleic Acid Hydroperoxides. II. Breakdown of Methyl 13-Hydroperoxy-*cis*-9-*trans*-11-Octadecadienoate by Radicals or Copper II Ions, *Z. Lebensm. Unters. Forsch. 173*, 192–198.
10. Von Uhl, J.C., and Eichner, K. (1990) The Effect of Natural Antioxidants on the Stability of Methyl Linoleate in Model System (in German, abstract in English), *Fat Sci. Technol. 9*, 355–361.
11. O'Brien, P.J. (1969) Intracellular Mechanisms for the Decomposition of a Lipid Peroxide. I. Decomposition of a Lipid Peroxide by Metal Ions, Heme Compounds, and Nucleophiles, *Can. J. Biochem. 47*, 485–492.
12. Frankel, E.N. (1998) *Lipid Oxidation*, pp. 129–160, The Oily Press, Dundee.
13. Peers, K.E., Coxon, D.T., and Chan, H.W-S. (1981) Autoxidation of Methyl Linolenate and Methyl Linoleate: The Effect of α-Tocopherol, *J. Sci. Food Agric. 32*, 898–904.
14. Chan, H.W.-S., and Levett, G. (1977) Autoxidation of Methyl Linoleate. Separation and Analysis of Isomeric Mixtures of Methyl Linoleate Hydroperoxides and Methyl Hydroxylinoleates, *Lipids 12*, 99–104.
15. Hamberg, M., and Samuelsson, B. (1967) On the Specificity of the Oxygenation of Unsaturated Fatty Acids Catalyzed by Soybean Lipoxidase, *J. Biol. Chem. 242*, 5329–5335.
16. Schieberle, P., Tsoukalas, B., and Grosch, W. (1979) Decomposition of Linoleic Acid Hydroperoxides by Radicals. I. Structures of Products of Methyl 13-Hydroperoxy-*cis*,*trans*-9,11-Octadecadienoate, *Z. Lebensm. Unters. Forsch. 168*, 448–456.
17. Fishwick, M.J., and Swoboda, P.A.T. (1977) Measurement of Oxidation of Polyunsaturated Fatty Acids by Spectrophotometric Assay of Conjugated Derivatives, *J. Sci. Food Agric. 28*, 387–393.
18. Alam, M.K., Nakajima, S., and Baba, N. (1996) The Effect of Antioxidants on the Decomposition of Methyl 13-Hydroperoxyoctadecadienoate, *Z. Naturforsch. 51C*, 753–756.
19. Chan, H.W-S., Levett, G., and Matthew, J.A. (1979) The Mechanism of the Rearrangement of Linoleate Hydroperoxides, *Chem. Phys. Lipids 24*, 245–256.
20. Porter, N.A. (1986) Mechanisms for the Autoxidation of Polyunsaturated Lipids, *Acc. Chem. Res. 19*, 262–268.
21. Porter, N.A., Caldwell, S.E., and Mills, K.A. (1995) Mechanism of Free Radical Oxidation of Unsaturated Lipids, *Lipids 30*, 277–290.
22. Gardner, H.W., and Kleiman, R. (1979) Lack of Regioselectivity in Formation of Oxohydroxyoctadecenoic Acids from the 9- or 13-Hydroperoxide of Linoleic Acid, *Lipids 14*, 848–851.

[Received April 26, 2000, and in revised form September 12, 2000; revision accepted September 12, 2000]

Vitamin E and Probucol Reduce Urinary Lipophilic Aldehydes and Renal Enlargement in Streptozotocin-Induced Diabetic Rats

Song-Suk Kim, D.D. Gallaher, and A. Saari Csallany*

Department of Food Science and Nutrition, University of Minnesota, St. Paul, Minnesota 55108

ABSTRACT: Diabetes mellitus is characterized by complications affecting several organs, including the kidney. Lipid peroxidation increases in diabetes and has been implicated in the pathogenesis of diabetic complications. In this study, we examined the ability of two antioxidants, vitamin E and probucol, to reduce lipid peroxidation *in vivo* and renal hypertrophy, an early stage of diabetic nephropathy, in rats. Animals were divided into four groups: non-diabetic, diabetic, diabetic treated with vitamin E, and diabetic treated with probucol. Animals were given antioxidants by intraperitoneal injection after induction of diabetes by streptozotocin injection. After 7 wk, lipid peroxidation *in vivo* was measured by analyzing urinary excretion of lipophilic aldehydes and related carbonyl compounds (LACC) as 2,4-dinitrophenylhydrazones by high-performance liquid chromatography. A number of urinary lipophilic nonpolar and polar aldehydes and related carbonyl compounds were identified, almost all of which increased in diabetes. Antioxidant treatment resulted in significantly decreased excretion of urinary LACC excretion. Antioxidant treatment of diabetic rats reduced renal hypertrophy. There was a high correlation between kidney weight and urinary LACC. Since LACC are accepted markers of lipid peroxidation, these results indicate that antioxidants can reduce the elevated lipid peroxidation of diabetes and may slow the onset of diabetic nephropathy.

Paper no. L7851 in *Lipids 35*, 1225–1237 (November 2000).

Lipid peroxidation has been implicated in a number of pathological conditions that are related to cellular damage induced by the oxidative alteration of polyunsaturated fatty acids (PUFA) (1). Diabetes is one such condition. Elevated lipid peroxidation *in vivo,* as measured by increased malondialdehyde and lipid hydroperoxides, has been observed in plasma (2–4), erythrocytes (5), and retina (6) of diabetic human subjects and rats. Diabetics, over time, often develop complications such as nephropathy, retinopathy, neurological problems, and atherosclerosis. Development of these complications has been proposed to be related to increased reactive oxygen species and to enhanced lipid peroxidation in cellular membranes (7,8). Free radicals, such as superoxide and hydroxyl radicals, may play important roles in the oxidative modification of lipid molecules during diabetes (9,10). Mechanisms that contribute to the peroxidative damage to membrane lipids in diabetes may include not only increased reactive oxygen species but also decreased efficiency of antioxidant defense systems. Diminished serum and erythrocyte antioxidant status has been detected in diabetic rats and human subjects (11–13).

Recently in this laboratory, significant increases of thiobarbituric acid-reactive substances were found in the urine of streptozotocin (STZ)-induced diabetic rats (14). This indicates enhanced lipid peroxidation *in vivo* and the oxidative modification of cellular lipid molecules. Based on this finding, it was speculated that certain secondary lipid peroxidation products, such as lipophilic aldehydes and related carbonyl compounds (LACC), might be excreted in the urine of STZ-induced diabetic rats. The first objective of the present experiment was to examine this hypothesis. The second objective was to evaluate the protective effects after the onset of diabetes of two antioxidants, vitamin E (*RRR*-α-tocopherol) and probucol, on renal hypertrophy, an early stage of diabetic nephropathy.

MATERIALS AND METHODS

Chemicals. 2,4-Dinitrophenylhydrazine (DNPH) and hexanal were obtained from Sigma Chemical Company (St. Louis, MO), pentan-2-one, hept-2-enal, hepta-2,4-dienal, decanal, and deca-2,4-dienal from Aldrich Chemical Co. (Milwaukee, WI), hydrochloric acid and high-performance liquid chromatography (HPLC)-grade acetone, methanol, dichloromethane, hexane, and water from EM Science (Gibbstown, NJ). DNPH derivatives of butanal, butanone, hexanal, octanal, non-2-enal, 4-hydroxyhex-2-enal (HHE), and 4-hydroxynon-2-enal (HNE) were a gift from Dr. Esterbauer, University of Graz

*To whom correspondence should be addressed at Department of Food Science and Nutrition, University of Minnesota, 1334 Eckles Avenue, St. Paul, MN 55108. E-mail: ascsalla@unm.edu

Abbreviations: D, STZ-induced diabetic; DNPH, 2,4-dinitrophenylhydrazine; DNP-hydrazone, 2,4-dinitrophenylhydrazone; HHE, 4-hydroxyhex-2-enal; HNE, 4-hydroxynon-2-enal; HPLC, high-performance liquid chromatography; LACC, lipophilic aldehydes and carbonyl compounds; N, nondiabetic control; NONPOL, nonpolar carbonyl compounds; PKC, protein kinase C; POL, polar carbonyl compounds; PUFA, polyunsaturated fatty acids; STZ, streptozotocin; D+E, vitamin E-treated diabetic; D+P, probucol-treated diabetic; TGF-β, transforming growth factor-β; TLC, thin-layer chromatography.

(Graz, Austria). Pentan-2-one, hept-2-enal, hepta-2,4-dienal, and deca-2,4-dienal DNPH derivatives were synthesized from pure standards and purified by repeated recrystallization from methanol. Silica gel thin-layer chromatographic (TLC) plates (Silica Gel 60, aluminum-backed 20 × 20 cm, 0.2 mm thickness) were purchased from Alltech Associates, Inc. (Deerfield, IL).

Instrumentation. The HPLC system consisted of an Altex Model 110A solvent metering pump, an Altex Model 110A sample injector (Beckman Instruments, Berkeley, CA), a Spectra-Physics Model SP8400 uv/vis detector and a Spectra-Physics Model SP4100 computing integrator (Spectra-Physics, Arlington, IL). The HPLC separations were performed on an Ultrasphere ODS C_{18} reverse phased-column (25 cm × 4.6 mm i.d., 5 μm particle size; Altex, Berkeley, CA) with a 2 cm × 2 mm i.d. guard column (Chrom Tech, Apple Valley, MN). Samples were filtered through 0.2 μm polyvinylidene difluoride membranes (Chrom Tech).

Animal treatment and urine collection. All experimental procedures were conducted in compliance with the University of Minnesota's policy on animal care and use. Four groups of male Wistar rats (Harlan, Indianapolis, IN) weighing 165–190 g (seven animals/group) were used: nondiabetic control (N), STZ-induced diabetic (D), and vitamin E-treated (D+E), or probucol-treated (D+P) diabetic animals. The diet for the N, D, D+E, and D+P groups was the standard AIN-76 diet (15), which provides 50 IU/kg vitamin E as DL-α-tocopheryl acetate. After adaptation to the diet for 4 d, animals in the D, D+E, and D+P groups were injected intraperitoneally with STZ (40 mg/kg body weight in 0.1 M citrate buffer, pH 5.5) (Sigma Chemical Co.). The animals in the N group were given sham injections of citrate buffer only. After confirmation of diabetes by testing for glucose in the urine using glucose oxidase-impregnated strips (Diastix; Miles Inc., Elkhart, IN), the D+E and D+P groups were injected with *RRR*-α-tocopherol (Sigma Chemical Co.) or probucol (Sigma Chemical Co.) intraperitoneally for three consecutive days, respectively. A fourth injection was given 2 wk later. Each injection of α-tocopherol provided approximately 70 times the daily intake. High levels of antioxidants were injected to quickly achieve saturation of blood and tissues with the antioxidant. Animals in the D+E and D+P groups received 79 mg (89 IU) *RRR*-α-tocopherol and 91 mg probucol, respectively, dissolved in 0.5 mL of vacuum-distilled corn oil (Eastman Kodak Co., Rochester, NY). Body weights were determined at the beginning of the experiment, at wk 2, and weekly thereafter. Twenty-four hour food intake was determined once a week at wk 2 and weekly thereafter. At the end of the 7-wk experimental period, urine was collected for 24 h from each animal and stored at −70°C until analysis. Animals were fasted overnight, then anesthetized and blood collected by cardiac puncture. An aliquot of whole blood was taken for determination of glycated hemoglobin and the remainder was centrifuged and the collected plasma was used for glucose and ascorbate analyses. The liver and both kidneys were removed and weighed. Glycated hemoglobin was determined in whole blood by affinity chromatography using a commercial kit (GlycAffin; Isolabs, Akron, OH). Plasma glucose concentration was measured by the hexokinase method (kit #115-A; Sigma Chemical Co.). An aliquot of plasma was diluted 1:4 with 5% meta-phosphoric acid immediately after collection for preservation of ascorbic acid content. Total ascorbate (ascorbate + dehydroascorbate) was subsequently analyzed fluorometrically by the method of Omaye *et al.* (16).

Measurement of urinary LACC. Urine analysis for LACC was carried out by the method of Kim, Gallaher, and Csallany (17,18). Briefly, urine was ultrafiltered to remove compounds with molecular masses larger than 500 daltons using Amicon cells, followed by synthesis of 2,4-dinitrophenylhydrazone (DNP-hydrazone) derivatives of urinary aldehydes and carbonyl compounds, extraction of the DNPH-hydrazones with dichloromethane (CH_2Cl_2) and preliminary separation of nonpolar compounds (NONPOL) and polar carbonyl compounds (POL) by TLC on silica gel plates developed with CH_2Cl_2. Separation and quantitation of the hydrazones was achieved by HPLC on a reversed-phase C_{18} column in two different solvent systems. NONPOL were eluted using methanol/water (75:25, vol/vol) and POL using methanol/water (50:50, vol/vol). Identification of DNP-hydrazones was accomplished by cochromatography with pure standards in three different solvent systems. Urinary excretion of the individual DNPH derivatives of lipophilic nonpolar and polar aldehydes and carbonyl compounds is expressed as the area detected by HPLC per day per 100 g body weight.

Statistical analysis. As the variances among groups were unequal, comparison of the N, D, D+E, and D+P groups was performed by a Kruskal-Wallis analysis of variance on ranks (SigmaStat 1.0; Jandel Scientific, San Rafael, CA). Specific group differences were determined by Student-Newman-Keuls' method or Dunn's method. Pearson correlation coefficients were calculated using group means, although we recognize that this is a nonideal means of correlating log-normalized and nonnormally distributed data. A P-value < 0.05 was considered significant for all analyses.

RESULTS AND DISCUSSION

Growth, food intake, glucose control, ascorbate levels, and organ weights. Diabetic animals had a greater food intake, but lower final body weight than normal animals (Table 1); differences were unaffected by antioxidant treatment. Fasting plasma glucose concentration was greatly elevated in diabetes, confirming the diabetic state. Both antioxidants produced slight but statistically significant reductions in plasma glucose. A reduction in fasting plasma glucose concentration has been found in humans consuming high doses of vitamin E for 3 mon (19), but not in rats fed high doses of either vitamin E or probucol for 6 wk (20). Glycated hemoglobin, an indicator of long-term blood glucose control (21), was elevated to approximately the same degree in all diabetic animals. Ceriello *et al.* (22) reported that vitamin E reduced stable HbA_1 (the major fraction of glycated hemoglobin) after 2

TABLE 1
Changes in Body Weight, Food Intake, Plasma Glucose and Ascorbate, Glycated Hemoglobin, and Organ Weights in Diabetic Rats Treated with Antioxidants for 7 wk[a]

	Normal	Diabetic	Diabetic + vitamin E	Diabetic + probucol
Final body wt (g)	381 ± 23[a]	215 ± 9[b]	229 ± 13[b]	252 ± 20[b]
Food intake (g/d)	24.1 ± 1.0[a]	34.7 ± 1.2[b]	35.8 ± 0.8[b]	34.3 ± 1.5[b]
Plasma glucose (mmol/L)	2.10 ± 0.43[c]	7.64 ± 0.50[a]	5.57 ± 0.67[b]	4.55 ± 0.93[b]
Glycated hemoglobin (%)	6.3 ± 1.0[b]	16.0 ± 0.4[a]	17.4 ± 0.7[a]	16.8 ± 0.4[a]
Plasma ascorbate (mmol/L)	6.39 ± 0.42[a]	1.99 ± 0.36[c]	2.25 ± 0.40[bc]	3.57 ± 0.73[b]
Kidney wt (g/100 g b.w.)	0.75 ± 0.07[c]	1.43 ± 0.02[a]	1.33 ± 0.04[ab]	1.22 ± 0.04[b]
Liver wt (g/100 g b.w.)	3.16 ± 0.20[b]	4.38 ± 0.13[a]	4.31 ± 0.08[a]	4.31 ± 0.15[a]

[a]Values are means ± SEM, $n = 6$ or 7. Within a row, values not sharing a common letter are significantly different ($P < 0.05$).

mon in diabetic subjects, but not after 1 mon; however, they found no effect of vitamin E on fasting plasma glucose concentrations. Paolisso *et al.* (19) found that vitamin E supplementation of type II diabetics for 3 mon reduced both fasting blood glucose concentrations and HbA_1 levels. In our study, a reduction in glycated hemoglobin might have been found with a longer trial period. However, it is possible that antioxidants may reduce fasting glucose levels, but that overall blood glucose control remains unchanged. Thus, the effect of antioxidant treatment during diabetes on glucose control remains uncertain.

Diabetic rats had greatly reduced concentrations of plasma ascorbate compared to normal animals, in agreement with the results of others (24). Treatment of diabetic rats with probucol and, to a lesser extent, vitamin E increased plasma ascorbate, suggesting that treatment of diabetic rats with antioxidants spares ascorbate.

Diabetic rats had heavier kidneys and livers, when expressed per 100 g body weight, than normal animals. In diabetic rats treated with probucol, however, kidneys showed less enlargement than in untreated diabetic rats, and there was a trend toward less renal enlargement in vitamin E-treated diabetic rats. The effect of antioxidants on organ weight was specific to the kidney, as there was no liver weight reduction due to antioxidants. Renal enlargement is one of the first consequences of diabetes and is the earliest event in the development of diabetic nephropathy (24). This growth is characterized in both humans (25) and rats with STZ-induced diabetes (26) by glomerular hypertrophy and basement membrane thickening. The pathological changes of diabetic renal disease are always preceded by this hypertrophy (27). The degree of enlargement strongly correlates with fasting plasma glucose concentrations (28) and with glycated hemoglobin levels (29). In diabetic dogs, improved glycemic control has prevented or regressed renal enlargement. These animals also showed an improved renal morphology compared to animals maintained on poor glycemic control (30). The reduction in renal enlargement by antioxidant treatment in the present study strongly suggests that antioxidants may slow the development of diabetic kidney disease.

Excretion of urinary LACC in diabetes. Typical HPLC separations of 2,4-DNPH derivatives of urinary lipophilic NONPOL and POL aldehydes and carbonyl compounds from STZ-induced diabetic rats are presented in Figures 1 and 2, respectively. Similar HPLC separations were also achieved in the urine of the normal, D+E, and D+P groups. Ten out of 13 NONPOL were identified by using cochromatography in three different solvent systems. These were butanal, butan-2-one, pentan-2-one, hex-2-enal, hexanal, hepta-2,4-dienal, hept-2-enal, octanal, non-2-enal, and deca-2,4-dienal. Two lipophilic polar aldehydes out of eight POL were also identified. These were HHE and HNE.

Comparison of the urinary excretion of lipophilic NONPOL and POL from normal and diabetic rats is presented in Figures 3–10. The results in the figures are presented as box plots because the data were not normally distributed. Eleven compounds, butanal, butan-2-one, pentan-2-one, hexanal, hept-2-enal, octanal, non-2-enal, deca-2,4-dienal, and unidentified compounds C, E, and J, out of 13 total NONPOL detected, were significantly increased in the diabetic group not given antioxidants, compared to excretion of these compounds in the N group (Figs. 3–6). Hex-2-enal (Fig. 5) and hept-2,4-dienal (Fig. 3) tended to be greater in the diabetic group compared to the N group, although these differences did not achieve statistical significance. Elevated levels of urinary lipophilic POL were also observed in the diabetic group compared to the N group, as shown in Figures 7 and 8. Seven of eight lipophilic POL, including the cytotoxic HHE and HNE, were significantly increased in the diabetic group compared to the N group. Unidentified compound G (Fig. 7) showed a trend toward an increase in the diabetic group compared to the N group. The sum of individual NONPOL and POL was significantly increased in the diabetic group compared to the N group, as indicated in Figure 10.

The significant increases in a number of lipophilic NONPOL and POL aldehydes and related carbonyl compounds in the urine of STZ-induced diabetic rats confirm lipid peroxidation *in vivo* and the consequent generation of certain secondary peroxidation products in the diabetic state. Mukherjee *et al.* (31) recently documented elevated lipid peroxidation not only in the pancreas but also in the liver, kidney, and brain tissues of STZ-induced diabetic rats, as measured by increases in thiobarbituric acid-reactive substances. Moreover, significant elevations of saturated aldehydes (hexanal, heptanal, octanal, and decanal) and unsaturated aldehydes (2-butenal, 2,4-pentadienal, 2-octenal, and 2-nonenal) have been

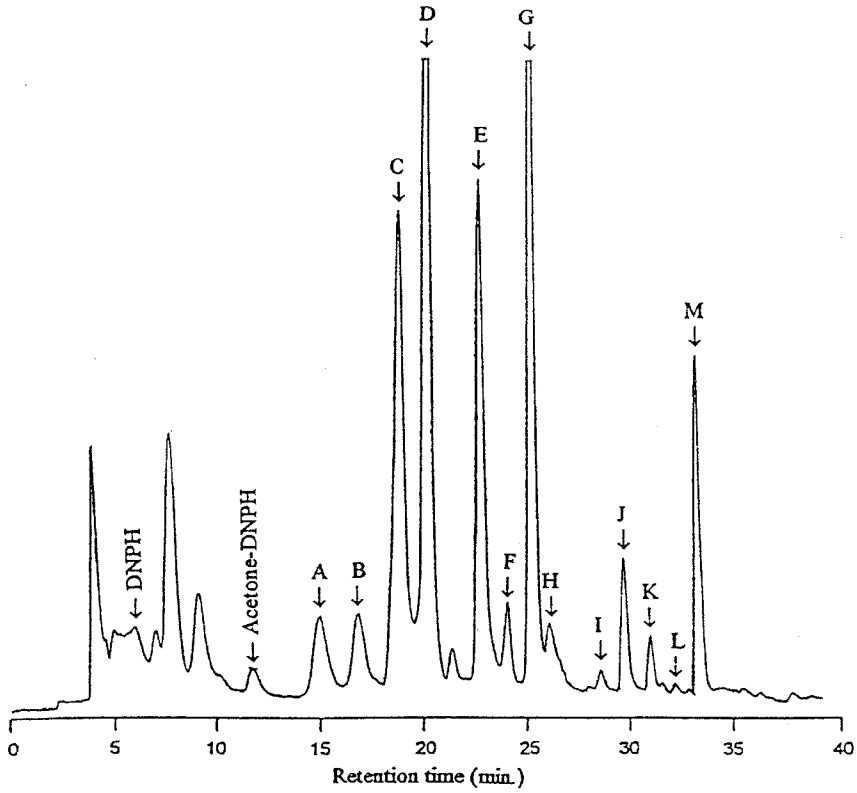

FIG. 1. High-performance liquid chromatography (HPLC) separation of 2,4-dinitrophenyl hydrazine (DNPH) derivatives of urinary nonpolar lipophilic aldehydes and related carbonyl compounds from streptozotocin (STZ)-treated diabetic rats. A, butanal; B, butan-2-one; D, pentan-2-one; F, hex-2-enal; G, hexanal; H, hepta-2,4-dienal; I, hept-2-enal; K, octanal; L, non-2-enal; M, deca-2,4-dienal; C, E, and J, unidentified. Separation conditions: Ultrasphere ODS column (4.6 mm × 25 cm, 5 μm), isocratic elution with 75% methanol in water for 10 min, followed by a linear gradient from 75% methanol in water to 100% methanol for 30 min; flow rate, 0.8 mL/min; detector wavelength, 378 nm; injected volume, 100 μL.

detected in the serum of diabetic human subjects and rats (32). It is established that these lipophilic aldehydes and related secondary peroxidation products can accumulate in cellular membranes and may interact with important biomolecules (33). In particular, HNE is capable of damaging functional proteins, inhibiting enzyme activities, and causing cell lysis in various tissues, at sites beyond where it is produced (34,35). This raises the possibility that the characteristic damage to eyes, kidneys, and arteries seen in diabetes (36,37) may be related to secondary lipid peroxidation products such as lipophilic aldehydes (20).

Effect of antioxidants on urinary excretion of LACC. Treatment of diabetic rats with vitamin E (D+E group) or probucol (D+P group) after the onset of diabetes decreased the urinary excretion of lipophilic NONPOL and POL to varying degrees, as shown in Figures 3 through 9. The unidentified compound E (Fig. 5) and hexanal (Fig. 6) were significantly decreased in the D+E group relative to those in the D group. Excretion of all NONPOL, except butanal, decreased in the D+E group compared to the D group. Six of eight POL exhibited moderate decreases in the D+E group (Figs. 7 and 9). Of particular interest is the significant decrease in HNE excretion observed in the D+E group compared to the D group (Fig. 7).

Excretion of butanal (Fig. 3), pentan-2-one (Fig. 6), hex-2-enal and unidentified compound E (Fig. 5) were significantly decreased in the D+P group compared to those in the D group, and all other lipophilic NONPOL aldehydes and carbonyl compounds tended to decrease. Similar decreases in urinary lipophilic POL were also detected in the D+P group. However, in contrast to vitamin E treatment, probucol treatment had no effect on the excretion of HNE (Fig. 7). Neither antioxidant had an effect on compounds G and F. These results are summarized in Tables 2 and 3.

Both vitamin E and probucol treatment of diabetic rats greatly reduced excretion of the sum of individual NONPOL, as indicated in Figure 10. The D+P group excreted lesser amounts of total NONPOL compared to the D+E group. Probucol treatment also reduced excretion of total POL and there was a tendency toward a reduced excretion with vitamin E treatment. Thus, overall, both antioxidants appeared to

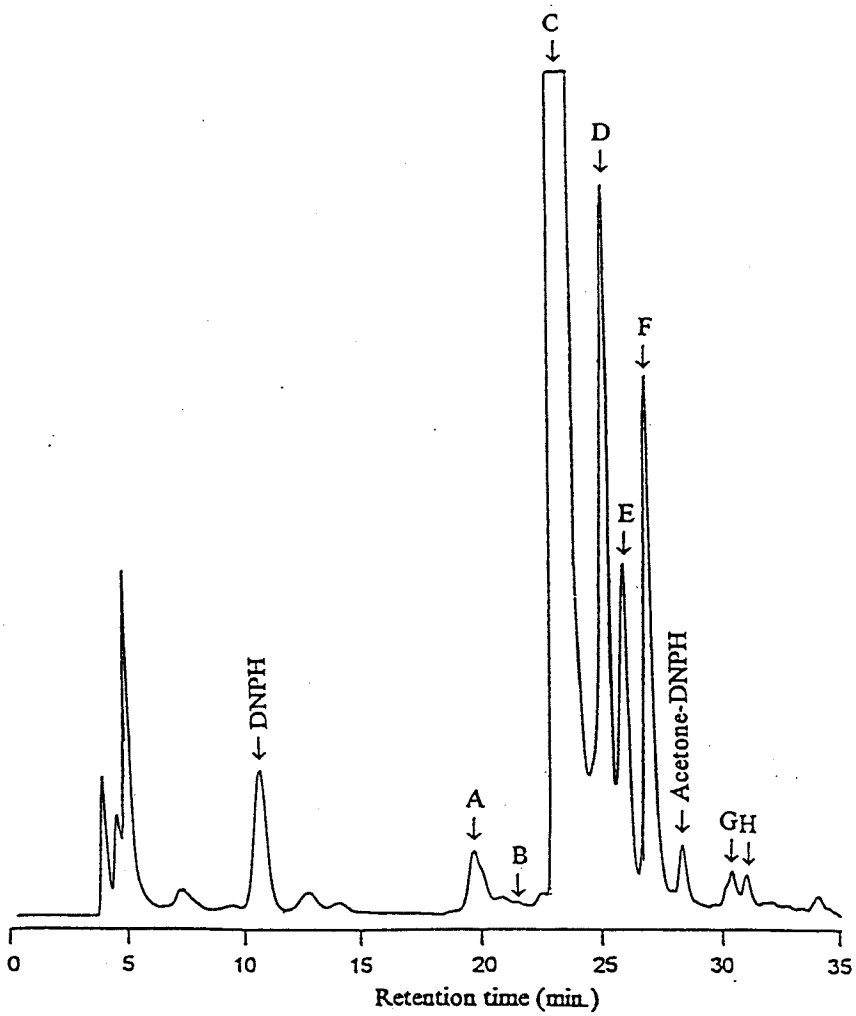

FIG. 2. HPLC separation of DNPH derivatives of urinary lipophilic polar aldehydes and related carbonyl compounds from STZ-treated diabetic rats. E, 4-hydroxyhex-2-enal; H, 4-hydroxynon-2-enal; and A, B, C, D, F, and G, unidentified. Separation conditions: Ultrasphere ODS column (4.6 mm × 25 cm, 5 μm), isocratic elution with 50% methanol in water for 10 min, followed by a linear gradient from 50% methanol in water to 100% methanol for 30 min; flow rate, 1.0 mL/min; detector wavelength, 378 nm; injected volume, 100 μL. See Figure 1 for abbreviations.

be effective at reducing urinary excretion of LACC. However, at the doses used, probucol appeared to be somewhat more effective.

Relationship between urinary LACC and renal enlargement. The relationship between urinary excretion of NONPOL and POL and renal enlargement is shown in Figure 11. There were high correlations between the group means for NONPOL excretion and kidney weight ($r^2 = 0.996$) and POL excretion and kidney weight ($r^2 = 0.990$) when plotted as an exponential curve. Similarly, the correlation, as an exponential curve, between the means of fasting plasma glucose and kidney weight ($r^2 = 0.995$, $P = 0.15$) was high. The correlation between glycated hemoglobin and kidney weight as an exponential was somewhat lower and not statistically significant ($r^2 = 0.88$, $P > 0.05$). The high correlations between the NONPOL and POL and kidney weight would suggest a causal relationship between the level of secondary lipid peroxidation products and renal enlargement.

Kidney failure in diabetes is ultimately caused by glomerulosclerosis as a result of chronic overproduction of mesangial matrix components by glomerular mesangial cells (38). It is now established that increased mesangial expression of the cytokine transforming growth factor-β (TGF-β) is intimately involved in the process of renal hypertrophy and accumulation of mesangial matrix components in diabetes (39). Bioactivation of TGF-β is caused, in part, by activation of protein kinase C (PKC), due to increased synthesis of the PKC activator diacylglycerol (40). An increase in the NADH/NAD^+ ratio appears to be responsible for the increase in diacylglycerol. Potentially, the increase in diacylglycerol

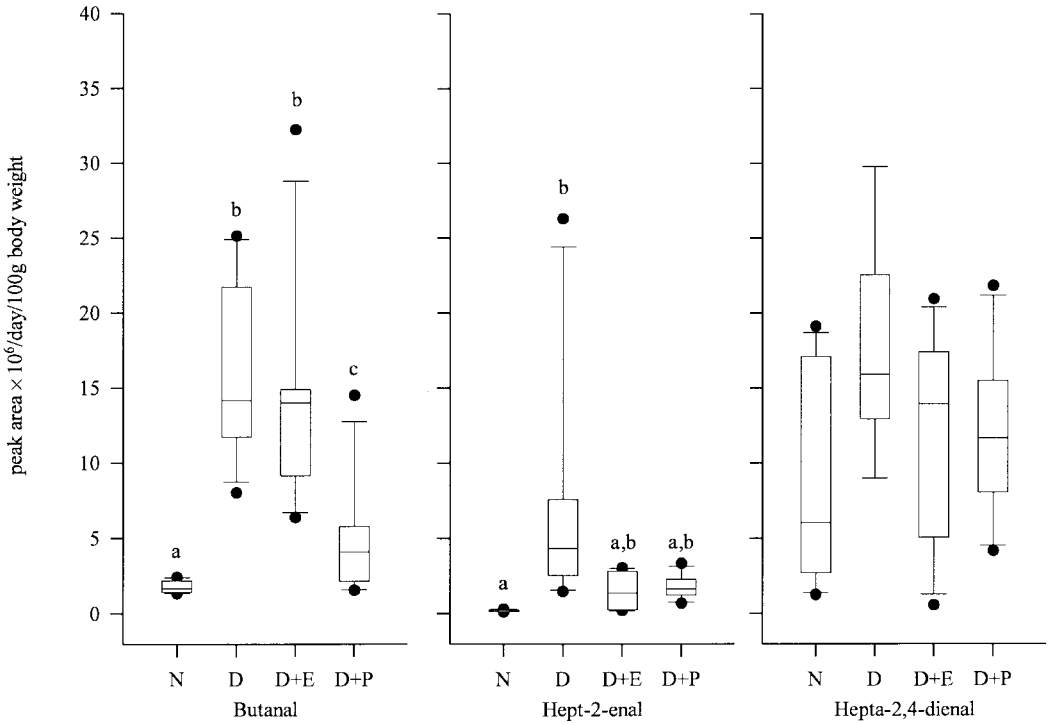

FIG. 3. Comparison of the urinary excretion of butanal, hept-2-enal, and hepta-2,4-dienal DNPH derivatives measured by HPLC from rats in nondiabetic control (N), STZ-treated diabetic (D), vitamin E-treated (D+E), and probucol-treated (D+P) diabetic animals. Values represent seven animals per group. The solid line within each boxplot represents the median. The top and bottom of the box are the 25 and 75% intervals of the data, the top and bottom of the error bars indicates the 5 and 95% interval of the data. Circles above or below the error bars represent data points that exceed the 5 and 95% interval of the data. Different letters denote significant differences ($P < 0.05$) among group medians by the Student-Newman-Keuls' test. See Figure 1 for other abbreviations.

TABLE 2
Effects of Vitamin E and Probucol on the Urinary Excretion of Lipophilic Nonpolar Aldehydes and Related Carbonyl Compounds in Rats

	STZ/nondiabetic[a]	STZ/STZ + E[b]	STZ/STZ + P[c]
A (butanal)	++	–	++
B (butan-2-one)	++	+	+
C (NI)	++	+	+
D (pentan-2-one)	++	+	++
E (NI)	++	++	++
F (hex-2-enal)	+	+	++
G (hexanal)	++	++	+
H (hepta-2,4-dienal)	+	+	+
I (hept-2-enal)	++	+	+
J (NI)	++	+	+
K (octanal)	++	+	+
L (non-2-enal)	++	+	+
M (deca-2,4-dienal)	++	+	+

[a]STZ-treated diabetic vs. nondiabetic control.
[b]STZ-treated diabetic vs. vitamin E-treated diabetic.
[c]STZ-treated diabetic vs. probucol-treated diabetic.
[d]Compounds A through M were separated and identified by high-performance liquid chromatography. Abbreviations: STZ, streptozotocin; E, vitamin E; P, probucol; NI, not identified; ++, significantly increased ($P < 0.05$); +, tendency to be increased, but nonsignificant; –, no significant differences between compared groups.

could be due to increased flux through the polyol pathway, which converts glucose into fructose by way of the intermediate sorbitol *via* an NAD^+-dependent reaction. Under normoglycemic conditions, little glucose is metabolized *via* this pathway. However, during the hyperglycemia that characterizes poorly controlled diabetes, glucose flux through the

TABLE 3
Effects of Vitamin E and Probucol on the Urinary Excretion of Lipophilic Polar Aldehydes and Related Carbonyl Compounds in Rats

	STZ/nondiabetic	STZ/STZ + E	STZ/STZ + P
A (NI)[a]	++	+	+
B (NI)	++	+	+
C (NI)	++	+	+
D (NI)	++	+	+
E (HHE)	++	+	+
F (NI)	++	–	–
G (NI)	+	+	–
H (HNE)	++	++	–

[a]Compounds A through H were separated and identified by HPLC. Abbreviations: HHE, 4-hydroxyhex-2-enal; HNE, 4-hydroxynon-2-enal. See Table 2 for other abbreviations.

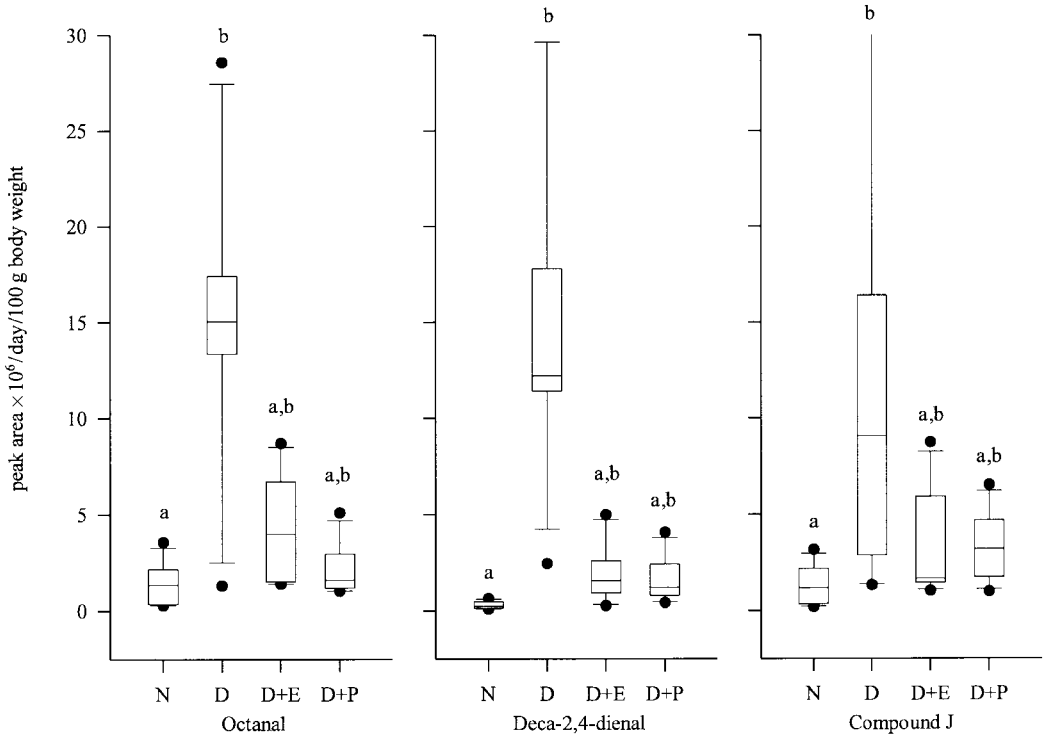

FIG. 4. Comparison of the urinary excretion of octanal, deca-2,4-dienal, and compound J DNPH derivatives measured by HPLC from rats in N, D, D+E, and D+P. Values represent seven animals per group. See Figure 3 for description of boxplot symbols. Different letters denote significant differences ($P < 0.05$) among group medians by Dunn's test. See Figures 1 and 3 for abbreviations.

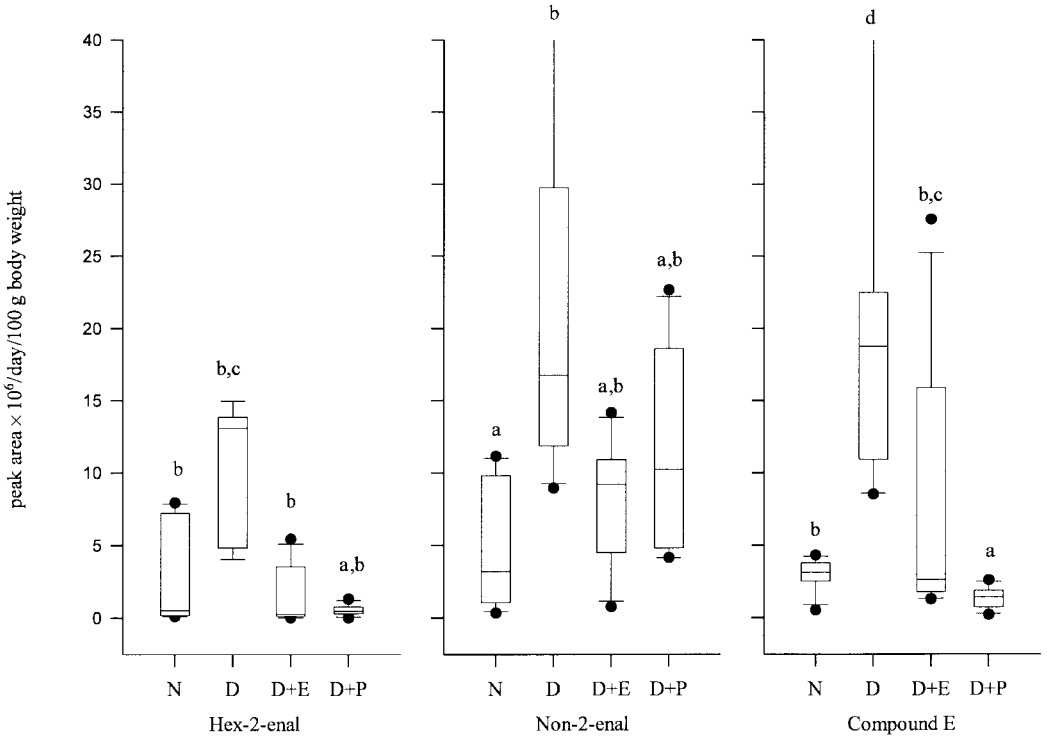

FIG. 5. Comparison of the urinary excretion of hex-2-enal, non-2-enal, and compound E DNPH derivatives measured by HPLC from rats in N, D, D+E, and D+P. Values represent 5–7 animals per group. See Figure 3 for description of boxplot symbols. Different letters denote significant differences ($P < 0.05$) among group medians by Dunn's test. See Figures 1 and 3 for abbreviations.

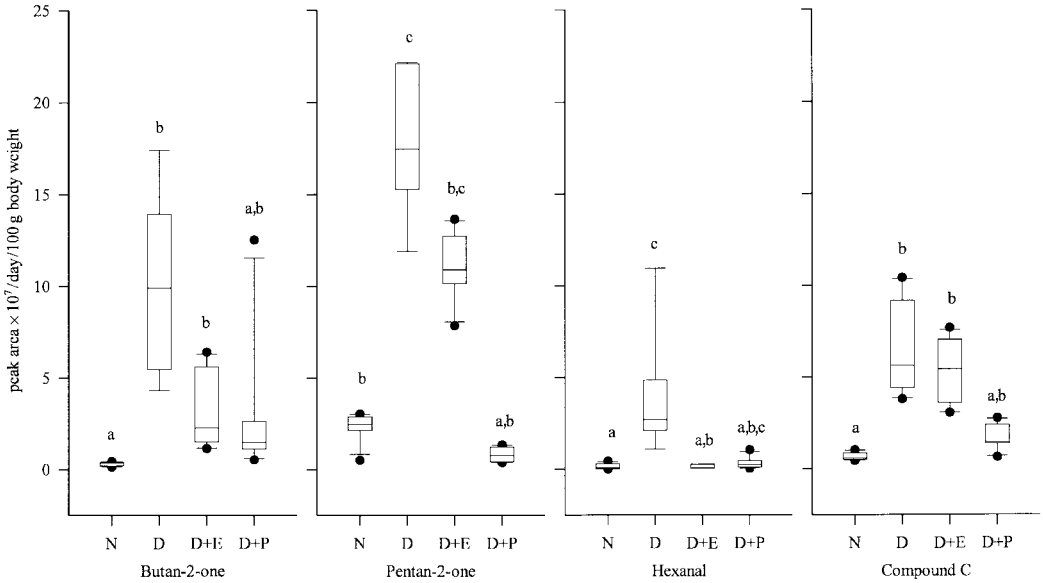

FIG. 6. Comparison of the urinary excretion of butan-2-one, pentan-2-one, hexanal, and compound C DNPH derivatives measured by HPLC from rats in groups N, D, D+E, and D+P. Values represent 5–7 animals per group. See Figure 3 for description of boxplot symbols. Different letters denote significant differences ($P < 0.05$) among group medians by Dunn's test. See Figures 1 and 3 for abbreviations.

polyol pathway may account for as much as one-third of total glucose turnover (41). This can increase the NADH/NAD^+ ratio in tissues that undergo insulin-independent uptake of glucose, such as the kidney. It has recently been demonstrated that numerous other aldehydes, in particular HNE, are excellent substrates for aldose reductase, the first and rate-limiting enzyme in the polyol pathway (42). Indeed, HNE has a K_m for aldose reductase over 1,000-fold lower than that of glucose (43). Thus, in diabetic rats, the increase in HNE, and perhaps of other aldehydic compounds, would contribute to the flux through the polyol pathway. Whether the reduction in these aldehydes by antioxidant treatment is responsible for the at-

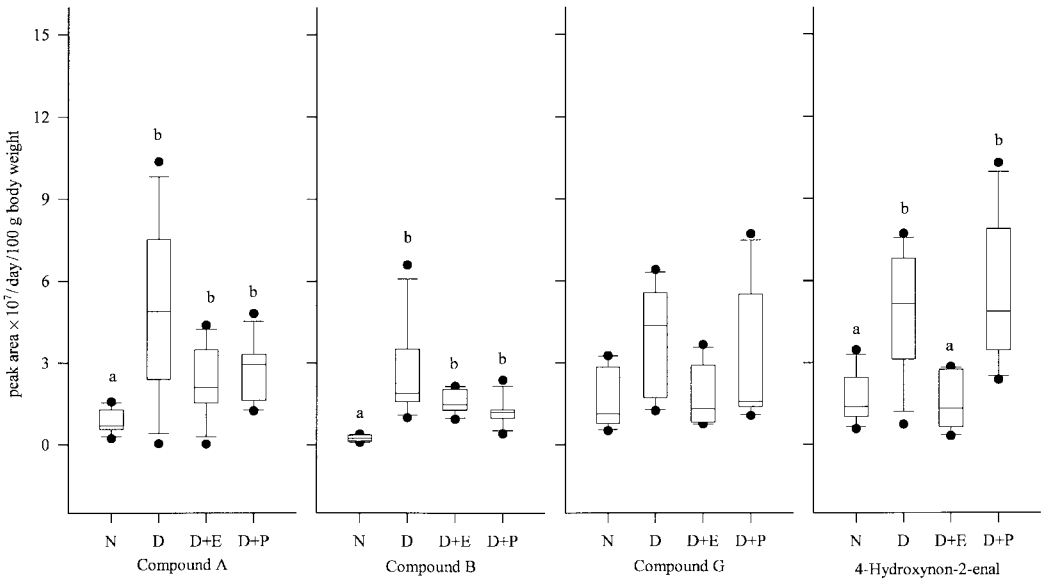

FIG. 7. Comparison of the urinary excretion of 4-hydroxynon-2-enal and the unidentified polar carbonyl compounds A, B, and G DNPH derivatives measured by HPLC from rats in N, D, D+E, and D+P. Values represent seven animals per group. See Figure 3 for description of boxplot symbols. Different letters denote significant differences ($P < 0.05$) among group medians by the Student-Newman-Keuls' test. See Figures 1 and 3 for abbreviations.

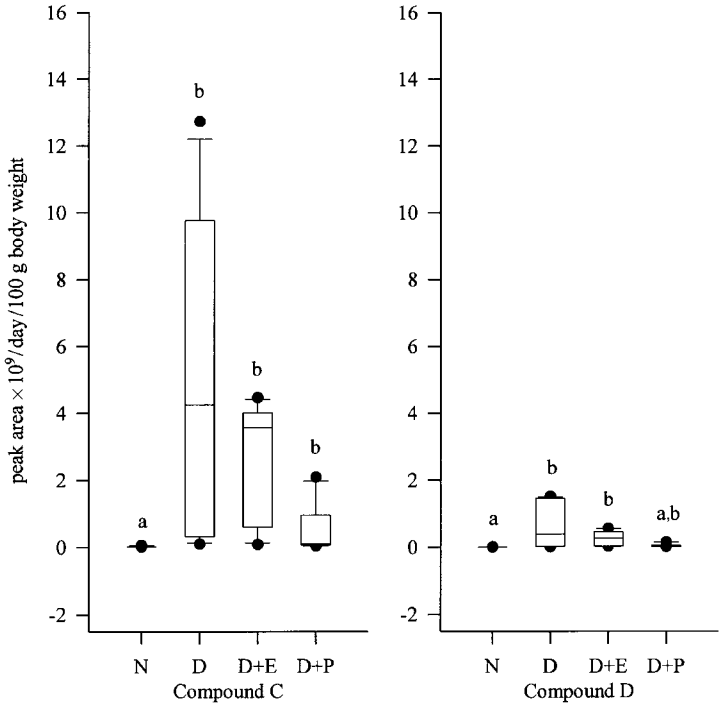

FIG. 8. Comparison of the urinary excretion of the unidentified polar carbonyl compounds C and D DNPH derivatives measured by HPLC from rats in N, D, D+E, and D+P. Values represent 6–7 animals per group. See Figure 4 for description of boxplot symbols. Different letters denote significant differences ($P < 0.05$) among group medians by Dunn's method. See Figures 1 and 4 for abbreviations.

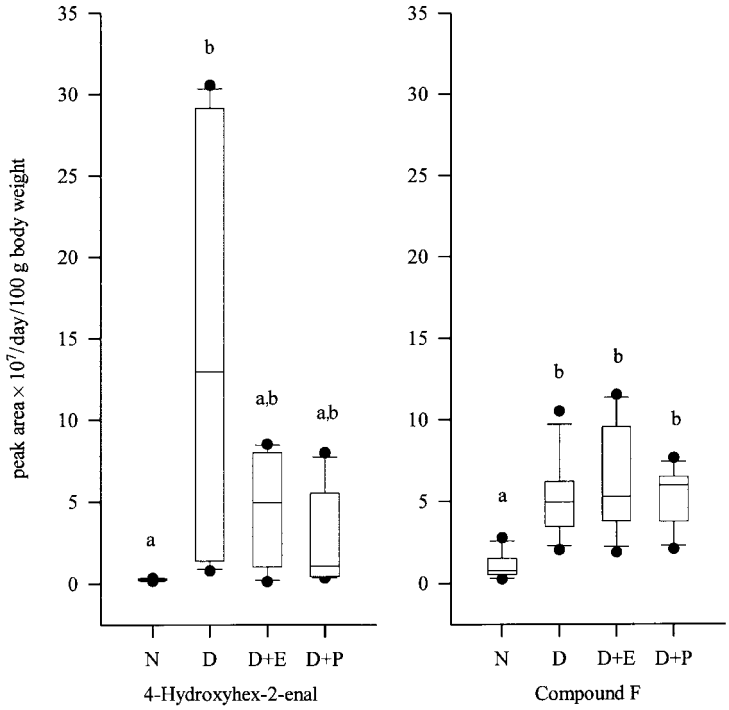

FIG. 9. Comparison of the urinary excretion of the polar carbonyl compounds 4-hydroxyhex-2-enal and the unidentified compound F DNPH derivatives measured by HPLC from rats in N, D, D+E and D+P. Values represent 6–7 animals per group. See Figure 3 for description of boxplot symbols. Different letters denote significant differences ($P < 0.05$) among group medians by Dunn's method. See Figures 1 and 3 for abbreviations.

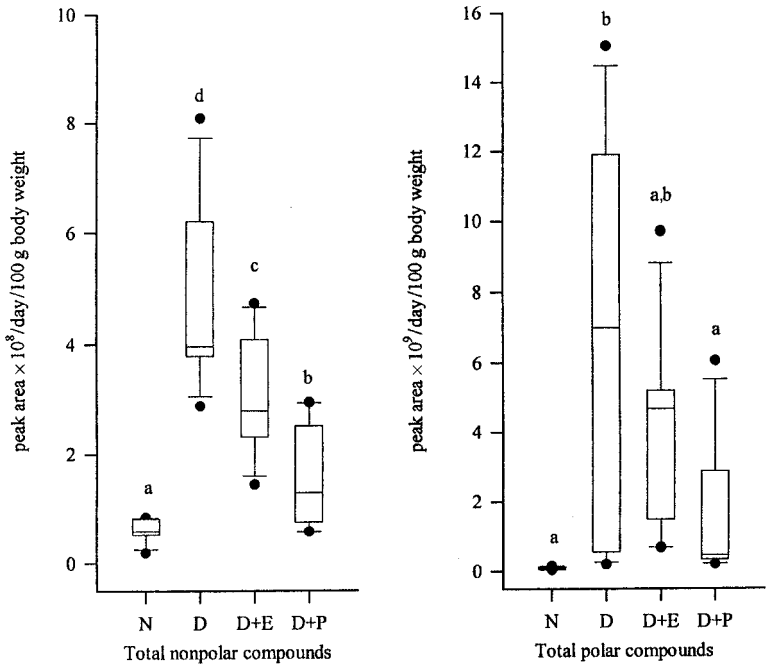

FIG. 10. Comparison of the urinary excretion of total nonpolar and total polar carbonyl compounds-DNPH derivatives measured by HPLC from rats in N, D, D+E, and D+P. Values represent seven animals per group. See Figure 3 for description of boxplot symbols. Different letters denote significant differences ($P < 0.05$) among group medians by the Student-Newman-Keuls' test. See Figures 1 and 4 for abbreviations.

tenuation of renal enlargement by reducing the flux through this pathway is uncertain because of contradictory reports regarding the role of the polyol pathway in renal enlargement. Osterby and Gunderson (44) found that STZ diabetic rats treated with an aldose reductase inhibitor for 6 mon showed less renal enlargement than untreated diabetic rats, whereas Korner *et al.* (45) reported that aldose reductase inhibitor treatment of STZ diabetic rats had no effect on renal enlargement.

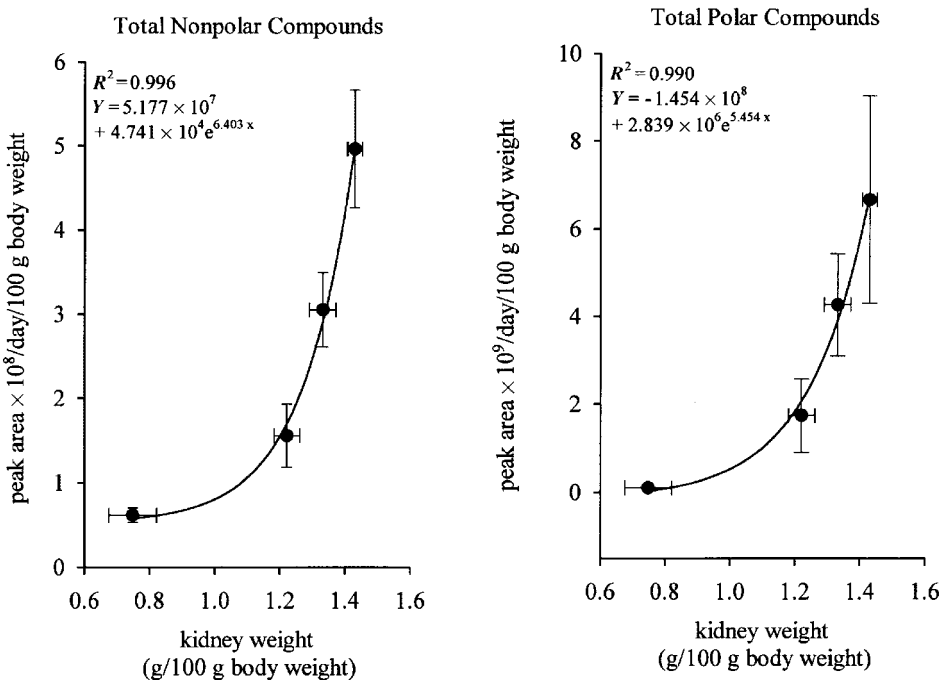

FIG. 11. Correlation between group means of urinary excretion of total nonpolar and total polar carbonyl compounds-DNPH derivatives and kidney weight. Values represent seven animals per group. See Figure 1 for abbreviation.

Recent studies suggest an alternative mechanism by which lipid-soluble antioxidants may inhibit renal enlargement. Kunisaki *et al.* (46) reported that intraperitoneal injections of vitamin E to STZ-induced diabetic rats decreased the membranous (i.e., active form) PKC specific activity and diacylglycerol content in aorta compared to untreated animals. Tran *et al.* (47) found that in cultured endothelial cells vitamin E increased the activity of diacylglycerol kinase, thus increasing conversion of diacylglycerol to phosphatidic acid. These studies raise the possibility that vitamin E, and possibly other lipophilic antioxidants, will lessen renal enlargement by direct activation of diacylglycerol kinase in mesangial cells, which would subsequently reduce diacylglycerol concentrations, leading to a decrease in PKC activity and TGF-β bioactivity. Thus, the mechanism by which antioxidant treatment of diabetic rats lessens renal enlargement is uncertain. Regardless of the mechanism, the results of the present study strongly suggest that antioxidants may be a useful adjunctive therapy for prevention of diabetic renal complications.

Our study confirms that diabetes increases LACC production (the secondary products of peroxidation), and therefore lipid peroxidation *in vivo*. Treatment with antioxidants such as *RRR*-α-tocopherol or probucol provides some protection against this peroxidation, as shown by the reduced urinary excretion of lipophilic aldehydes and related carbonyl compounds. Why diabetes increases lipid peroxidation is, however, uncertain. Based on *in vitro* studies, Wolff *et al.* (48) originally proposed that transition-metal-catalyzed oxidation of glucose was an important source of the oxidative stress of diabetes. More recently, Hunt *et al.* (49) indicated that the oxidation of glucose-protein adducts is the more likely source of oxidants. This is consistent with the results of Al-Abed *et al.* (50), who found that, *in vitro*, formation of advanced glycosylation end products in low density lipoproteins generates 4-hydroxynonenal and 4-hydroxyhexenal, indicating that the "late" products (carbonyl compounds) of the Maillard reaction result in lipid oxidation. These studies implicate high concentrations of glucose in the production of lipid peroxidation products. However, high glucose concentrations may also impair the antioxidant defense system. An *in vitro* study by Kunisaki *et al.* (51) demonstrated that high glucose concentrations reduced the specific binding affinity of *RRR*-α-tocopherol to aortic endothelial cells, potentially resulting in an intracellular vitamin E deficiency and increased levels of hydroperoxides. Further, Jain and Levine (52) reported increased levels of *RRR*-α-tocopheryl quinone, the primary oxidation product of *RRR*-α-tocopherol, in heart ventricles of diabetic rats, indicating an accelerated loss of *RRR*-α-tocopherol for scavenging oxygen radicals. Interestingly, increased vitamin E levels were reported in the liver of STZ-induced diabetic rats (53). This is likely due to the mobilization of *RRR*-α-tocopherol from the adipose tissue to the liver as a result of the high rate of lipolysis associated with the diabetic state (54).

The cholesterol-lowering drug probucol has been suggested to have antioxidant activity based on its chemical structure, in which two butylated hydroxytoluene moieties possess hydrophobic antioxidant activities (55). Fukuda *et al.* (56) suggested that the protective effect of probucol in diabetes may be mediated by its inhibition of oxygen radical generation and therefore reducing lipid peroxidation. It is likely that pre- or posttreatment with probucol could partially inhibit the lipid peroxidation process by its antioxidant action in diabetic conditions.

In the present experiment it was found that after the onset of diabetes, the ability of vitamin E and probucol to prevent formation and urinary excretion of LACC varied. In the urine of rats of the D+E group, significant decreases of hexanal and HNE, the decomposition products of n-6 PUFA, were found. This result may indicate that after the onset of diabetes the antioxidant effect of vitamin E is more effective in reducing the levels of lipid hydroperoxides and peroxy radicals produced from n-6 PUFA in comparison to probucol. Hydroxyaldehydes such as HNE and HHE are believed to cause extensive tissue injury due to their high reactivity with biomolecules (30,57). The action of vitamin E in lowering HNE in diabetic conditions could play an important role in reducing tissue damage related to diabetic complications. Overall, however, vitamin E and probucol were similarly effective in reducing the elevation in urinary excretion of secondary lipophilic products of lipid peroxidation due to diabetes.

ACKNOWLEDGMENTS

Paper no. 98-1-18-0002 of the scientific series of the Minnesota Agricultural Experiment Station on research conducted under the Minnesota Experiment Station project nos. MIN-18-085 and MIN-18-060.

REFERENCES

1. Dargel, R. (1992) Lipid Peroxidation—A Common Pathogenetic Mechanism? *Exp. Toxic. Pathol. 44*, 169–181.
2. Noberasco, G., Odetti, P., Boeri, D., Maiello, M., and Adezati, L. (1991) Malondialdehyde (MDA) Level in Diabetic Subjects. Relationship with Blood Glucose and Glycosylated Hemoglobin, *Biomed. Pharmacother. 45*, 193–196.
3. Griesmacher, A., Kindhauser, M., Andert, S.E., Schreiner, W., Toma, C., Knoebl, P., Pietschmann, P., Prager, R., Schnack, C., Schernthaner, G., and Mueller, M.M. (1995) Enhanced Serum Levels of Thiobarbituric-Acid-Reactive Substances in Diabetes Mellitus, *Am. J. Med. 98*, 469–475.
4. Gallou, G., Ruelland, A., Legras, B., Maugendre, D., Allannic, H., and Cloarec, L. (1993) Plasma Malondialdehyde in Type 1 and Type 2 Diabetic Patients, *Clin. Chim. Acta 241*, 227–234.
5. Jain, S.K., Mcvie, R., Duett, J., and Herbst, J.J. (1989) Erythrocyte Membrane Lipid Peroxidation and Glycosylated Hemoglobin in Diabetes, *Diabetes 38*, 1539–1543.
6. Armstrong, D., and Al-Awadi, F. (1991) Lipid Peroxidation and Retinopathy in Streptozotocin-Induced Diabetes, *Free Radical Biol. Med. 11*, 433–436.
7. Baynes, J.W. (1991) Role of Oxidative Stress in Development of Complications in Diabetes, *Diabetes 40*, 405–412.
8. Gillery, P., Monboisse, J.C., Maquart, F.X., and Borel, J.P. (1989) Does Oxygen Free Radical Increased Formation Explain Long Term Complications of Diabetes Mellitus? *Med. Hypothesis 29*, 47–50.

9. Mullarkey, C.J., Edelstein, D., and Brownlee, M. (1990) Free Radical Generation by Early Glycation Products: A Mechanism for Accelerated Atherogenesis in Diabetes, *Biochem. Biophys. Res. Comm. 173*, 932–939.
10. Hunt, J.V., Smith, C.C.T., and Wolff, S.P. (1990) Autoxidative Glycosylation and Possible Involvement of Peroxides and Free Radicals in LDL Modification by Glucose, *Diabetes 39*, 1420–1424.
11. Asayama, K., Nakane, T., Uchida, N., Hayashibe, H., Dobashi, K., and Nakazawa, S. (1994) Serum Antioxidant Status in Streptozotocin-Induced Diabetic Rat, *Horm. Metab. Res. 26*, 313–315.
12. Asayama, K., Uchida, N., Nakane, T., Hayashibe, H., Dobashi, K., Amemiya, S., Kato, K., and Nakazawa, S. (1993) Antioxidants in the Serum of Children with Insulin-Dependent Diabetes Mellitus, *Free Radical Biol. Med. 15*, 597–602.
13. Jain, S.K., Levine, S.N., Duett, J., and Hollier, B. (1991) Reduced Vitamin E and Increased Lipofuscin Products in Erythrocytes of Diabetic Rats, *Diabetes 40*, 1241–1244.
14. Gallaher, D.D., Csallany, A.S., Shoeman, D.W., and Olson, J.M. (1993) Diabetes Increases Excretion of Urinary MDA Conjugates in Rats, *Lipids 28*, 663–666.
15. American Institute of Nutrition (1980) Second Report of the *Ad Hoc* Committee on Standards for Nutritional Studies, *J. Nutr. 110*, 1726.
16. Omaye, S.T., Turnbull, J.D., and Sauberlich, H.E. (1979) Selected Method for the Determination of Ascorbic Acid in Animal Cells, Tissues, and Fluids, *Methods Enzymol. 62*, 8–9.
17. Csallany, A.S., Kim, S.-S., and Gallaher, D.D. (1996) Lipid Peroxidation *in vivo* Measured by Urinary Excretion of Aldehydes and Hydroxy Aldehydes, in *Proceedings of the 21st World Congress of the International Society for Fat Research*, Vol. 2, pp. 299–301, PJ Barnes & Associates, High Wycombe.
18. Kim, S.-S., Gallaher, D.D., and Csallany, A.S. (1999) Lipophilic Aldehydes and Related Carbonyl Compounds in Rat and Human Urine, *Lipids 34*, 489–496.
19. Paolisso, G., D'Amore, A., Galzerano, D., Balbi, V., Giugliano, D., Varricchio, M., and D'Onofrio, F. (1993) Daily Vitamin E Supplements Improve Metabolic Control but Not Insulin Secretion in Elderly Type II Diabetic Patients, *Diabetes Care 16*, 1433–1437.
20. Morel, D.W., and Chisolm, G.M. (1989) Antioxidant Treatment of Diabetic Rats Inhibits Lipoprotein Oxidation and Cytotoxicity, *J. Lipid Res. 30*, 1827–1834.
21. Bunn, H.F., Gabbay, K.H., and Gallop, P.M. (1978) The Glycosylation of Hemoglobin: Relevance to Diabetes Mellitus, *Science 200*, 21–27.
22. Ceriello, A., Giugliano, D., Quatrano, A., Donzella, C., Dipalo, G., and Lefebvre, P.J. (1991) Vitamin E Reduction of Protein Glycosylation in Diabetes. New Prospect for Prevention of Diabetic Complications? *Diabetes Care 14*, 68–72.
23. Young, I.S., Torney, J.J., and Trimble, E.R. (1992) The Effect of Ascorbate Supplementation on Oxidative Stress in the Streptozotocin Diabetic Rat, *Free Radical Biol. Med. 13*, 41–46.
24. Selby, J.V., FitzSimmons, S., Newman, J.M., Katz, P.P., Sepe S., and Showstack, J. (1990) The Natural History and Epidemiology of Diabetic Nephropathy, *JAMA 263*, 1954–1960.
25. Mogensen, C.E., and Andersen, M.J. (1973) Increased Kidney Size and Glomerular Filtration Rate in Early Juvenile Diabetes, *Diabetes 22*, 706–712.
26. Seyer-Hansen, K. (1976) Renal Hypertrophy in Streptozotocin-Diabetic Rats, *Clin. Sci. Mol. Med. 51*, 551–555.
27. Ziyadeh, F.N. (1993) The Extracellular Matrix in Diabetic Nephropathy, *Am. J. Kidney Dis. 22*, 736–744.
28. Seyer-Hansen, K. (1977) Renal Hypertrophy in Experimental Diabetes: Relation to Severity of Diabetes, *Diabetologia 13*, 141–143.
29. Gallaher, D.D., and Schaubert, D. (1990) The Effect of Dietary Fiber Type on Glycated Hemoglobin and Renal Hypertrophy in the Diabetic Rat, *Nutr. Res. 10*, 1311–1323.
30. Kern, T.S., and Engerman, R.L. (1990) Arrest of Glomerulopathy in Diabetic Dogs by Improved Glycaemic Control, *Diabetologia 33*, 522–525.
31. Mukherjee, B., Mukherjee, J.R., and Chatterjee, M. (1994) Lipid Peroxidation, Glutathione Levels and Changes in Glutathione-Related Enzymes Activities in Streptozotocin-Induced Diabetic Rats, *Immunol. Cell Biol. 72*, 109–114.
32. Novotny, M.V., Yancey, M.F., Stuart, R., Wiesler, D., and Peterson, R.G. (1994) Inhibition of Glycolytic Enzymes by Endogenous Aldehydes: A Possible Relation to Diabetic Neuropathies, *Biochim. Biophys. Acta 1226*, 145–150.
33. Esterbauer, H., Schaur, R.J., and Zollner, H. (1991) Chemistry and Biochemistry of 4-Hydroxynonenal, Malonaldehyde and Related Aldehydes, *Free Radical Biol. Med. 11*, 81–128.
34. Comporti, M. (1993) Lipid Peroxidation. Biopathological Significance, *Molec. Aspec. Med. 14*, 199–207.
35. Witz, G. (1989) Biological Interactions of α,β-Unsaturated Aldehydes, *Free Radical Biol. Med. 7*, 333–349.
36. Ruderman, N.B., and Haudenschild, C. (1984) Diabetes as an Atherogenic Factor, *Prog. Cardiovasc. Dis. 26*, 373–412.
37. Bell, R.H., and Hye, R.J. (1983) Animal Models of Diabetes Mellitus: Physiology and Pathology, *J. Surg. Res. 35*, 433–460.
38. Steffes, M.W., Østerby, R., Chavers, B., and Mauer, S.M. (1989) Mesangial Expansion as a Central Mechanism for Loss of Kidney Function in Diabetic Patients, *Diabetes 38*, 1077–1081.
39. Sharma, K., and Ziyadeh, F.N. (1995) Hyperglycemia and Diabetic Kidney Disease: The Case for Transforming Growth Factor-β as a Key Mediator, *Diabetes 44*, 1139–1146.
40. DeRubertis, F.R., and Craven, P.A. (1994) Activation of Protein Kinase C in Glomerular Cells in Diabetes: Mechanisms and Potential Links to the Pathogenesis of Diabetic Glomerulopathy, *Diabetes 43*, 1–8.
41. Gonzalez, R.G., Barnett, P., Aguayo, J., Cheng, H.M., and Chylack, L.T.J. (1984) Direct Measurement of Polyol Pathway Activity in the Ocular Lens, *Diabetes 33*, 196–199.
42. Vander Jagt, D.L., Kolb, N.S., Vander Jagt, T.J., Chino, J., Martinez, F.J., Hunsaker, L.A., and Royer, R.E. (1995) Substrate Specificity of Human Aldose Reductase: Identification of 4-Hydroxynonenal as an Endogenous Substrate, *Biochim. Biophys. Acta 1249*, 117–126.
43. Vander Jagt, D.L., Torres, J.E., Hunsaker, L.A., Deck, L.M., and Royer, R.E. (1996) Physiological Substrates of Human Aldose and Aldehyde Reductases, in *Enzymology and Molecular Biology of Carbonyl Metabolism 6,* (Weiner, H., Lindahl, R., Crabb, D.W., and Flynn, T.G., eds.) pp. 491–497, Plenum Press, New York.
44. Osterby, R., and Gundersen, H.J. (1989) Glomerular Basement Membrane Thickening in Streptozotocin Diabetic Rats Despite Treatment with an Aldose Reductase Inhibitor, *J. Diabetic Complicat. 3*, 149–153.
45. Korner, A., Celsi, G., Eklof, A.C., Linne, T., Persson, B., and Aperia, A. (1992) Sorbinil Does Not Prevent Hyperfiltration, Elevated Ultrafiltration Pressure and Albuminuria in Streptozotocin-Diabetic Rats, *Diabetologia 35*, 414–418.
46. Kuniski, M., Fumio, U., Nawata, H., and King, G.L. (1996) Vitamin E Normalizes Diacylglycerol-Protein Kinase C Activation Induced by Hyperglycemia in Rat Vascular Tissues, *Diabetes 45 Suppl. 3*, S117–S119.
47. Tran, K., Proulx, P.R., and Chan, A.C. (1994) Vitamin E Suppresses Diacylglycerol (DAG) Level in Thrombin-Stimulated Endothelial Cells Through an Increase of DAG Kinase Activity, *Biochim. Biophys. Acta 1212*, 193–202.
48. Wolff, S.P., Jiang, Z.Y., and Hunt, J.V. (1991) Protein Glyca-

tion and Oxidative Stress in Diabetes Mellitus and Ageing, *Free Radical Biol. Med. 10*, 339–352.
49. Hunt, J.V., Bottoms, M.A., and Mitchinson, M.J. (1993) Oxidative Alterations in the Experimental Glycation Model of Diabetes Mellitus Are Due to Protein–Glucose Adduct Oxidation, *Biochem. J. 291*, 529–535.
50. Al-Abed, Y., Liebich, H., Voelter, W., and Bucala, R. (1996) Hydroxyalkenal Formation Induced by Advanced Glycosylation of Low Density Lipoprotein, *J. Biol Chem. 271*, 2892–2896.
51. Kunisaki, M., Umeda, F., Yamauchi, T., Masakado, M., and Newt, H. (1993) High Glucose Reduces Specific Binding for D-α-Tocopherol in Cultured Aortic Endothelial Cells, *Diabetes 42*, 1138–1146.
52. Jain, S.K., and Levine, S.N. (1995) Elevated Lipid Peroxidation and Vitamin E-Quinone Levels in Heart Ventricles of Streptozotocin-Treated Diabetic Rats, *Free Radical Biol. Med. 18*, 337–341.
53. Sukalski, K.A., Pinto, K.A., and Berntson, J.L. (1993) Decreased Susceptibility of Liver Mitochondria from Diabetic Rats to Oxidative Damage and Associated Increase in α-Tocopherol, *Free Radical Biol. Med. 14*, 57–65.
54. Coppack, S.W., Jensen, M.D., and Miles, J.M. (1994) *In vivo* Regulation of Lipolysis in Humans, *J. Lipid Res. 35*, 177–193.
55. Kuzuya, M., and Kuzuya, F. (1993) Probucol as an Antioxidant and Antiatherogenic Drug, *Free Radical Biol. Med. 14*, 67–77.
56. Fukuda, M., Ikegami, H., Kawaguchi, Y., Sano, T., and Ogihara, T. (1995) Antioxidant, Probucol, Can Inhibit the Generation of Hydrogen Peroxide in Islet Cells Induced by Macrophages and Prevent Islet Cell Destruction in NOD Mice, *Biochem. Biophys. Res. Commun. 209*, 953–958.
57. Esterbauer, H., Zollner, H., and Schaur, R.J. (1988) Hydroxyalkenals: Cytotoxic Products of Lipid Peroxidation, *Atlas Sci. Biochem. 1*, 311–317.

[Received January 15, 1998, and in revised form February 21, 2000; revision accepted September 20, 2000]

The Effect of γ-Interferon to Inhibit Macrophage-High Density Lipoprotein Interactions Is Reversed by 15-Deoxy-$\Delta^{12,14}$-prostaglandin J_2

Steven H. Zuckerman*, Constantinos Panousis, Jacques Mizrahi, and Glenn Evans

Division of Cardiovascular Research, Lilly Research Labs, Indianapolis, Indiana 46285

ABSTRACT: Macrophage activation has been recognized as playing a central role in chronic inflammatory diseases in general and, more specifically, in the vascular wall during the progression of atherosclerotic lesions. Macrophage-activating factors present within the atherosclerotic lesion include the colony-stimulating factors and gamma interferon (IFNγ). In the present study, the effects of IFNγ on macrophage binding and uptake of fluorochrome-labeled high density lipoprotein (HDL) were investigated by flow cytometry and by measuring the amount of the type B scavenger receptors CD36 and scavenger receptor type B (SR-BI) by Northern blot analysis. IFNγ-, but not granulocyte macrophage colony-stimulating factor (GM-CSF)-treated murine peritoneal macrophages displayed a two- to threefold decrease in DiI-labeled HDL uptake. This effect was observed in the absence of a comparable decrease in SR-BI message and protein or CD36 message. This decrease in both HDL binding and uptake was reversed by the peroxisome proliferator-activated receptor gamma (PPARγ) agonist, 15-deoxy-$\Delta^{12,14}$-prostaglandin J_2 (15d-PGJ_2), which also inhibited the IFNγ induction of the β2 integrin CD11a. Furthermore, 15d-PGJ_2 increased the expression of SR-BI and CD36 message and SR-BI protein which was reflected in an increase in HDL binding and uptake. These results suggest a role for PPARγ agonists in modulating the IFNγ-mediated macrophage effector functions relevant to atherosclerotic disease progression.

Paper no. L8497 in *Lipids 35,* 1239–1247 (November 2000).

The macrophage plays a central role in the pathology associated with atherosclerotic lesion development and progression (1–5). The biologic responses mediated by the macrophage are influenced by cytokines, resulting in both autocrine and paracrine regulatory circuits. Gamma interferon (IFNγ) represents one such macrophage-activating factor elaborated by activated Th1-type T cells within the atheroma that could modulate lesion progression (6–8). To this extent, the well-documented effects of IFNγ on macrophage effector functions including induction of inducible nitric oxide synthetase (iNOS), cytokine and protease secretion, increases in class I and II antigen expression, as well as other membrane markers represent effector functions that could impact on lesion development (9,10). More specifically, IFNγ has been demonstrated to downregulate macrophage apolipoprotein (apo) E secretion and lipoprotein receptors, including type I scavenger receptor SR-A, CD36, low density lipoprotein (LDL) receptor-related protein, as well as lipoprotein lipase secretion and cholesterol efflux (11–17). These effects would suggest a contributory role for IFNγ in the progression of atherosclerotic plaque. Consistent with these observations is the report that apo E knockout (KO) mice crossed with IFNγ receptor KO mice resulted in the double homozygote KO having *ca.* 60% reduction in lesion size, lipid accumulation, and cellularity (16). Similar results were observed with CSF-1-deficient mice (18).

One such mechanism for inhibiting IFNγ-mediated macrophage activation involves peroxisome proliferator-activating receptor gamma (PPARγ)/retinoid X receptor, heterodimer nuclear receptors. PPARγ agonists were reported to inhibit IFNγ-iNOS activity, gelatinase, and scavenger receptor A promoter activity by mouse peritoneal macrophages and macrophage cell lines (19,20), as well as phorbol myristate acetate induction of tumor necrosis factor secretion (21), and matrix metalloprotease-9 activity (22) in monocyte-derived macrophages. The demonstration that oxidized LDL upregulate PPARγ expression and that increased PPARγ is observed within atherosclerotic lesions (22–25) clearly suggests the potential for a negative feedback loop for modulating IFNγ-driven processes within the atherosclerotic lesion.

To this extent, the current studies focused on the impact of the PPARγ agonist, 15-deoxy-$\Delta^{12,14}$-prostaglandin J_2 (15d-PGJ_2) (26,27) on IFNγ-regulated processes which could play a role in modulating atherosclerotic lesion progression. As high density lipoprotein (HDL)-cellular interactions can promote cholesterol efflux, the present study was designed to evaluate the effect of IFNγ and PPARγ agonists on this specific interaction. These studies demonstrate that IFNγ decreased both the binding and uptake of fluorochrome-labeled HDL by mouse peritoneal macrophages and that PPARγ agonists blocked these inhibitory effects as well as the IFNγ induction of the β2 integrin CD11a.

*To whom correspondence should be addressed.
E-mail: Zuckerman_Steven@lilly.com

Abbreviations: apo, apolipoprotein; GM-CSF, granulocyte macrophage colony-stimulating factor; HDL, high density lipoprotein; IFNγ, gamma interferon; iNOS, inducible nitric oxide synthetase; KO, knockout; LDL, low density lipoprotein; 15d-PGJ_2, 15-deoxy-^{12,14}-prostaglandin J_2; PPARγ, peroxisome proliferator-activated receptor gamma; RXR, a member of the retinoid nuclear receptor family; SR-BI, scavenger receptor type B.

MATERIALS AND METHODS

Macrophage cultures and flow cytometry assays. Elicited macrophages were obtained 3–4 d following thioglycolate priming of Balb/C mice and were maintained in culture in RPMI 1640 medium supplemented with 2% fetal calf sera (HyClone Laboratories, Logan, UT). Macrophages were stimulated with varying concentrations of recombinant murine IFNγ (BioSource Intl., Camarillo, CA) or recombinant murine granulocyte macrophage colony-stimulating factor (GM-CSF; R&D Systems, Minneapolis, MN) in the presence or absence of 15-d-PGJ_2 (Biomol, Plymouth Meeting, PA). In additional experiments, the effects of other PPARγ agonists on HDL binding including ciglitazone and 12d-PGJ_2 (Biomol) (26,27) were also evaluated. After 48 h culture with the indicated treatments, macrophages were evaluated for changes in DiI (1,1′-dioctadecyl-3,3,3′,3′-tetramethylindocarbocyanine perchlorate), DiI-labeled HDL uptake, Alexa 488-labeled HDL binding, CD11a expression, and phagocytosis. CD11a expression was measured using phycoerythrin-labeled monoclonal antibody (Pharmingen, San Diego, CA). Cells were first washed three times in flow buffer and then were incubated in the same buffer with the antibody at 4 μg/mL on ice for 1 h. Following staining and subsequent washes, cells were detached by a rubber policeman and evaluated by flow cytometry. Parallel cultures were incubated with 50 μg/mL of commercially available human DiI-labeled HDL (for 2–4 h in the existing media) (Intracel Corp., Rockville, MD) or opsonized tetramethylrhodamine-conjugated *Escherichia coli* (Molecular Probes, Eugene, OR). Incubations were performed at 37°C for the indicated period as previously described (28). Human HDL binding to macrophage monolayers was performed at 4°C, using 20–25 μg/mL Alexa 488-labeled HDL prepared following the supplier's recommended protocol (Molecular Probes Alexa 488 protein labeling kit). This binding of Alexa-labeled HDL to macrophages was competed with a 50:1 excess of unlabeled HDL (Intracel Corp.), LDL, acetylated LDL, and fucoidan (data not shown). Following all fluorometric procedures, cells were washed, detached, and evaluated by flow cytometry. All flow cytometry experiments were evaluated on 10,000 individual cells gated for macrophages, based on their forward and side light-scatter profiles. The mean fluorescence intensity was measured using a Becton Dickinson FacSort with Cellquest software (Becton Dickinson, San Jose, CA).

Northern and Western blot analysis. Macrophage cultures with the indicated treatments were lysed at 48 h and processed for RNA and membrane protein. Total RNA and subsequently poly A^+ RNA were isolated using RNA isolation kits (Qiagen, Santa Clarita, CA). Poly A-enriched RNA, 0.5 μg per lane, was separated by 0.7% formaldehyde agarose gels and transferred to Nytran nylon membrane overnight using the turboblotter system (Schliecher and Schuell Inc., Keene, NH). Membranes were prehybridized in hybridization buffer and hybridized with [α-^{32}P]dCTP DNA probes labeled by random primers (Gibco, Grand Island, NY) in fresh hybridization buffer. Scavenger receptor type B (SR-BI), CD36, and CaB45 probes were polymerase chain reaction-amplified using 5′TCCTGAGCCCCGAGAGCCCCTTCCGC, 3′CTGGCTGCGCAGTTGGCAGATGATGGC; 5′CAGCCCAATGGAGCCATC, 3′CAGCGTAGATAGACCTGC; and 5′ AGCTGCTCATGGCCTCTGGTTCTT, 3′ GGTCTCTGAGGTTCCCAAGGACTT primer sets, respectively. Membranes were washed in 2× SSC (saline-sodium citrate buffer) 1% sodium dodecyl sulfate and exposed either to Kodak Biomax-MS film or to phosphoscreen. Quantitation was performed using a phosphoimager (Molecular Dynamics).

Macrophage membrane preparations were obtained following resuspension of detached cells in hypotonic lysis buffer (10 mM Tris pH 7.4, 1 mM EDTA, 5% protease inhibitor cocktail; Sigma Chemical Co., St. Louis, MO) and incubation on ice for 15–30 min. The suspension was then homogenized with a Virtis homogenizer, and the nuclei were removed by centrifugation at 800 × *g* for 10 min. Membranes were then pelleted from the supernatant by ultracentrifugation at 100,000 × *g* for 1 h and resuspended in 40 mM octyl glucoside by stirring on ice for 2–3 h. Solubilized proteins were separated on 8% polyacrylamide Tris-glycine gels (Novex, San Diego, CA), with comparable amounts of protein loaded and were transferred onto nitrocellulose using a semi-dry blotting system. Primary, affinity-purified rabbit anti-human SR-BI antibody (provided by Dr. Sue Acton, Millennium Pharmaceuticals Inc., Cambridge, MA) was incubated at 4°C overnight, and antibody detection was by peroxidase conjugated anti-rabbit IgG followed by enhanced chemiluminescence using Pierce Supersignal Ultra as substrate (Pierce Chemical, Rockford, IL). Preliminary experiments with this antibody demonstrated its cross-reactivity with murine SR-BI.

Nitric oxide measurements. Supernatants from macrophage cultures after 48 h co-culture with IFNγ and varying concentrations of 15d-PGJ_2 were measured for NO levels using the Griess reaction as previously described (29). Briefly, 100-μL aliquots of supernatants were mixed with 100 μL of Griess reagent containing 1% sulfanilamide, 0.1% naphthylethylene diamine dihydrochloride, and 2% phosphoric acid. The optic density change at 10 min was measured at 550 nm and converted to μM concentrations of nitrite based on a sodium nitrite standard curve.

Statistics. Statistical analysis was performed by unpaired (two-tail) *t*-test. Values are reported as means ± SD. The 95% confidence limit was taken as significant ($P < 0.05$).

RESULTS

Elicited murine peritoneal macrophages that had been activated with 1,000 units/mL of IFNγ demonstrated a significant reduction in the uptake of DiI-labeled HDL as evaluated by flow cytometry (Fig. 1A). Whereas untreated control macrophages had a mean fluorescence intensity of 285 fluorescence units, IFNγ resulted in a two- to fourfold decrease in DiI-

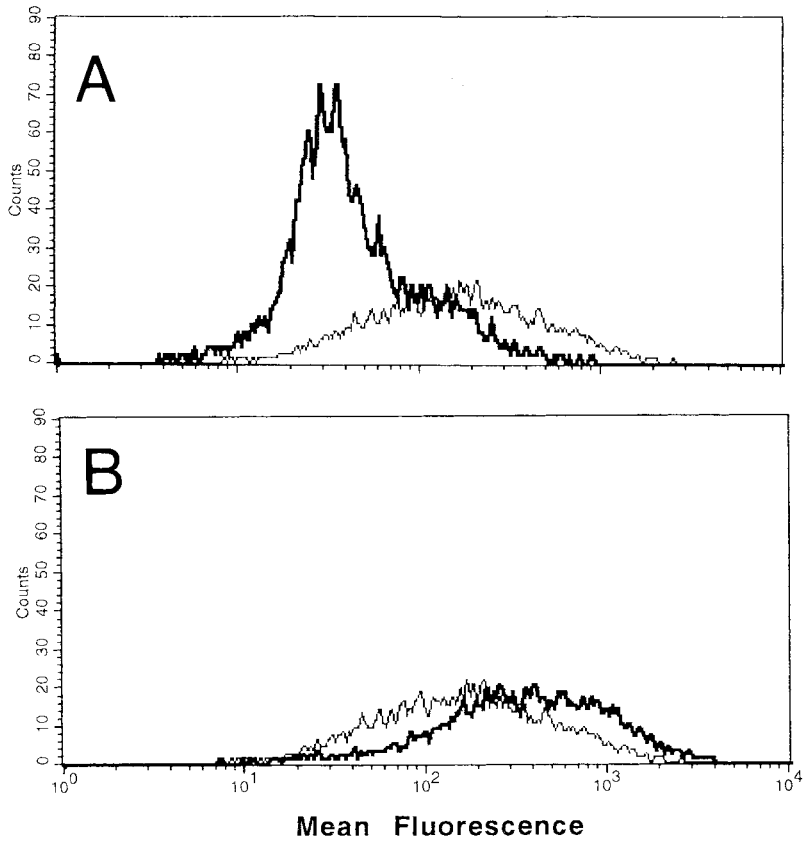

FIG. 1. Effect of macrophage activation on uptake of DiI-labeled high density lipoprotein (HDL). Macrophages were incubated with 1,000 units/mL of gamma interferon (IFNγ) (A) or 10 ng/mL of granulocyte macrophage colony-stimulating factor (GM-CSF) (B) for 48 h prior to challenge with 30 μg/mL of DiI-labeled HDL for 3 h at 37°C. Representative histograms, the mean fluorescence intensity in the control untreated macrophages (thin line) was 283 while IFNγ reduced the mean fluorescence to 72 and GM-CSF (bold lines) increased it to 505.

labeled HDL uptake. This decrease in the uptake of the DiI-labeled HDL was not a general property of activated macrophages as parallel GM-CSF-treated macrophages exhibited an increase in mean fluorescence intensity (Fig. 1B). Therefore, downregulation of DiI-labeled HDL uptake mediated by IFNγ was not a general event associated with macrophage activation.

The signaling pathway and the involvement of PPARγ heterodimer nuclear receptors in the regulation of specific macrophage effector functions modulated by IFNγ such as iNOS induction (19,20) raised the possibility that the IFNγ-mediated effects on HDL interactions could also be modulated through the PPAR pathway. Accordingly, the ability to reverse the IFNγ-mediated decrease in DiI-labeled HDL uptake was investigated using 15d-PGJ_2, a PPARγ agonist. A relevant concentration of 15d-PGJ_2 for the HDL studies was based on the dose response for this compound to inhibit NO accumulation in IFNγ-stimulated macrophage culture supernatants. As evident (Fig. 2) and consistent with previous reports (19,20), 15d-PGJ_2 inhibited in a dose-dependent manner the increase in nitrite detected in culture supernatants by the Griess reagent. Accordingly, a 15d-PGJ_2 concentration of 1.5 μM was chosen for all subsequent experiments. At this concentration, there was no apparent effect of the prostaglandin analog on cellular morphology or viability (data not shown).

The effect of the PPARγ agonist 15d-PGJ_2 on reversing the inhibition of DiI-labeled HDL uptake by IFNγ-activated macrophages was then evaluated at varying concentrations of IFNγ (Fig. 3A). As evident, IFNγ reduced in a dose-dependent manner the uptake of DiI-labeled HDL, and this effect was effectively reversed at all IFNγ concentrations by 15d-PGJ_2. Furthermore, 15d-PGJ_2 by itself resulted in an increase in DiI-labeled HDL uptake. The reduction in DiI-labeled HDL uptake by IFNγ did not reflect a nonspecific effect on all macrophage endocytic or phagocytic processes as uptake of opsonized *E. coli* was not reduced in parallel cultures of activated macrophages, nor was there any apparent nonspecific increase in phagocytosis mediated by 15d-PGJ_2 (Fig. 3B). These results would thus suggest that IFNγ was able to reduce HDL uptake in a dose-dependent manner and that this effect was inhibited by co-culture with the PPARγ agonist 15d-PGJ_2.

In an attempt to directly correlate the changes in DiI-la-

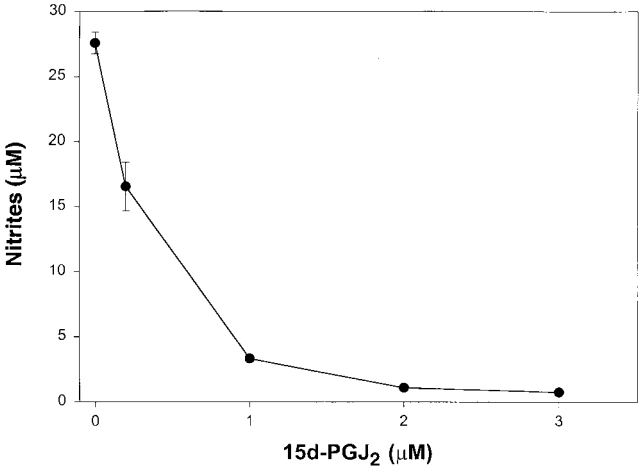

FIG. 2. Effect of the peroxisome proliferator-activated receptor gamma (PPARγ) agonist 15-deoxy-$\Delta^{12,14}$-prostaglandin J_2 (15d-PGJ_2) on inducible nitric oxide synthase (iNOS) activity. Macrophages were incubated with 1,000 units/mL of IFNγ for 48 h in the presence or absence of the indicated concentrations of 15d-PGJ_2. Supernatants were assayed for iNOS activity by measuring nitrite accumulation through the Griess reaction. In the absence of IFNγ, 15d-PGJ_2 treatment did not result in any increase in the basal levels of nitrites detected, which were already below detectable levels. Representative experiment of 3. Brackets indicate standard deviation of the mean based on triplicate cultures. See Figure 1 for other abbreviations.

beled HDL uptake with the expression of HDL receptors, macrophage lysates were evaluated for both CD36 and SR-BI mRNA levels by Northern blot analysis. Macrophage cultures incubated with IFNγ did exhibit a reduction in mRNA levels for both CD36 (Figs. 4A and 4C) and SR-BI (Figs. 5A and 5B). In contrast, parallel cultures incubated with 15d-PGJ_2 alone resulted in an increase in SR-BI and a more significant increase in CD36 message while the combination of IFNγ and 15d-PGJ_2 resulted in type B scavenger receptor message levels similar to the control values. The increases observed in SR-BI and CD36 messages were not related to poly A-enriched RNA loading as there were no differences observed in quantitation of an irrelevant message coding for the Golgi-associated soluble calcium-binding protein, CaB45 (30) (Figs. 4B and 4D). The modest increase observed in the IFNγ-treated cells was also observed with other housekeeping genes including G3PDH (data not shown). Quantitation of the Northern blots by phosphoimager suggested that there was *ca.* tenfold more message for CD36 (Fig. 4C) than SR-BI (Fig. 5B). This quantitative difference between the two type B scavenger receptors was apparent using PCR probes labeled to a comparable specific activity and adding an equal amount of labeled probe into the two hybridizations, suggesting that CD36 is the more abundantly expressed type B scavenger receptor in murine peritoneal macrophages.

Macrophages stimulated with 15d-PGJ_2 also demonstrated changes in SR-BI protein content as evaluated by Western blot analysis (Fig. 5C). While there was no effect observed on SR-BI by IFNγ, 15d-PGJ_2 did result in a twofold increase in SR-BI, and this was also apparent in macrophages cocultured with IFNγ + 15d-PGJ_2. Accordingly, the effects of 15d-PGJ_2 on SR-BI were more apparent at the protein rather than the message levels. While it was not possible to evaluate changes in CD36 protein, due to the absence of an available antibody against murine CD36, HDL binding was evaluated at 4°C using Alexa 488-labeled HDL to distinguish between binding and uptake. Consistent with the increases in SR-BI and CD36 message, 15d-PGJ_2 increased the amount of HDL bound to the macrophage cultures with an apparent threefold increase in the mean fluorescence intensity (Fig. 4E), a magnitude similar to that observed for the increase in CD36 message (Fig. 4C). IFNγ-treated cells did demonstrate a reduction in HDL binding, and this effect was reversed in the presence of 15d-PGJ_2. Therefore, the reductions in SR-BI and CD36 message were consistent with the decrease in Alexa HDL binding while the increases in CD36 and SR-BI message and SR-BI protein by 15d-PGJ_2 were also reflected in an increase in the binding of Alexa-labeled HDL. Furthermore, the effects of 15d-PGJ_2 on increasing HDL binding were also apparent although more modest with two additional PPARγ agonists (Table 1), suggesting that the effects of PPARγ agonists on increasing macrophage binding of HDL are likely to reflect a pharmacologic class effect rather than being unique to a specific agonist structure.

In addition to the IFNγ effects on HDL-macrophage interactions and iNOS induction, other macrophage effector functions relevant to atherosclerotic lesion progression include increases in β2 integrin surface antigen expression. Therefore, the effects of the PPARγ heterodimer pathway on the β2 integrin CD11a were evaluated by flow cytometry. IFNγ, as expected, increased CD11a surface expression in a dose-dependent manner and, as with HDL uptake, these effects were inhibited by 15d-PGJ_2 (Fig. 6). These results clearly demonstrate that PPARγ agonists are capable of modulating both IFNγ-stimulating (CD11a and iNOS activity) and IFNγ-inhibiting (HDL binding and uptake) processes, occurring at

TABLE 1
Effect of PPARγ Agonists on HDL Binding by Murine Peritoneal Macrophages[a]

Treatment	– IFNγ	+ IFNγ
Control	214 (3)	146 (2)
Ciglitazone	288 (7.5)[b]	184 (7.4)[b]
12d-PGJ_2	266 (28)[c]	219 (2)[b]

[a]Ciglitazone and 12 deoxy-$\Delta^{12,14}$-prostaglandin J_2 (12d-PGJ_2) were evaluated at their optimal doses of 3 and 1 μM, respectively. Macrophages were cultured in the presence or absence of 300 units/mL of gamma interferon (IFNγ) with the indicated concentrations of peroxisome proliferator-activated receptor gamma (PPARγ) agonists. Following 48-h incubation, monolayers were washed and incubated for 3 h at 4°C with 25 μg/mL Alexa-labeled high density lipoprotein (HDL). Monolayers were again washed after the binding period, detached, and mean fluorescence intensities (MFI) in triplicate cultures were determined by flow cytometry. In a parallel study, 15d-PGJ_2 increased HDL binding from a control of 204 MFI to 371, and in IFNγ-treated cells from 136 to 289. Parentheses represent the standard deviation of the mean from triplicate cultures.
[b]Differences between the experimental group, and the relative control was significant by a Student's unpaired two-tailed *t*-test ($P < 0.01$).
[c]Or ($P < 0.1$).

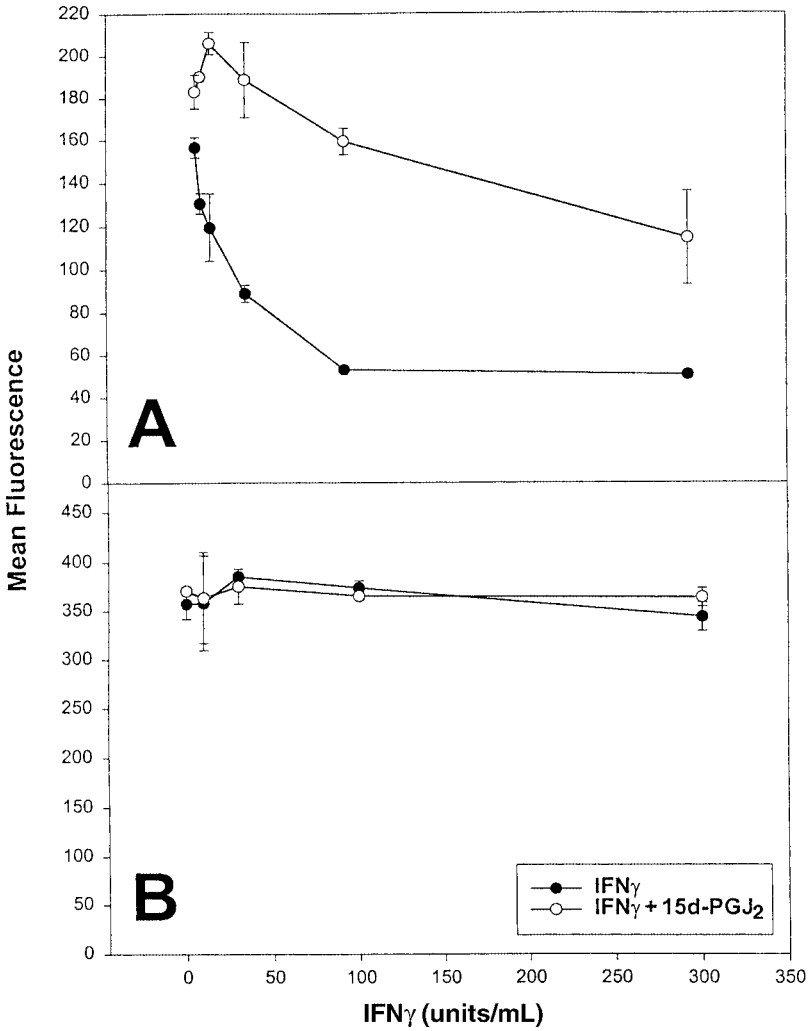

FIG. 3. Reversal of IFNγ-mediated downregulation of DiI-labeled HDL uptake by 15d-PGJ_2. Macrophages in triplicate cultures were incubated with the designated concentrations of IFNγ for 48 h in the presence (○) or absence (●) of 1.5 μM 15d-PGJ_2. Following incubation, macrophage cultures were challenged with DiI-labeled HDL (A) or fluorochrome-labeled opsonized *Escherichia coli* (B) for 3 h or 30 min, respectively, at 37°C. Monolayers were then washed, detached, and evaluated by flow cytometry. Brackets indicate standard deviation of the mean. See Figures 1 and 2 for abbreviations.

the plasma membrane level. In additional experiments, it was apparent that these IFNγ-mediated changes occurred with similar kinetics (Fig. 7). The IFNγ effects on CD11a expression and HDL uptake were apparent by 15 h with further increases (CD11a) or decreases (DiI-HDL) observed at 24 h. Maximal effects for both the reduction in HDL uptake and the increase in CD11a expression were observed by 48 h. With further IFNγ incubation for 72 h, CD11a expression appears to be reduced relative to the 48-h time point while HDL uptake remains inhibited to a comparable degree. These results could suggest that IFNγ within the micro-environment of an atherosclerotic lesion would contribute to plaque progression by increasing β_2 integrin expression and reducing macrophage–HDL interaction, a process likely to be important in reverse cholesterol transport.

DISCUSSION

The demonstration of Th1-type T cells within atherosclerotic lesions suggests a mechanism for the *in situ* activation of both macrophages and macrophage-derived foam cells by exposure to macrophage-activating factors within the microenvironment of the developing atheroma (6–8). In the present study, IFNγ-stimulated murine peritoneal macrophages displayed a reduced uptake of DiI-labeled HDL particles which is maximal by 48 h. This observation is consistent with a previous study, in which IFNγ resulted in a reduction in cholesterol efflux (17). These changes in lipid binding, which are functions attributed to SR-BI (31–33), occurred with only modest changes in SR-BI mRNA and no change in membrane protein. In the previous study from this laboratory, IFNγ had no effect on

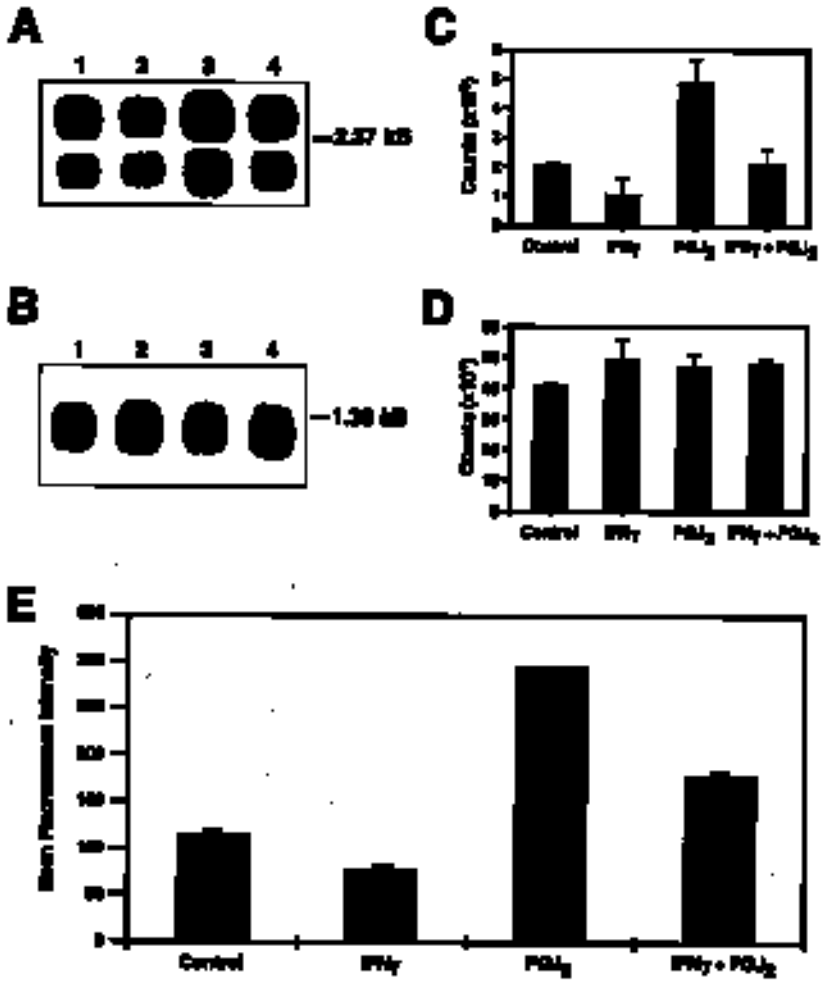

FIG. 4. Effect of IFNγ and 15d-PGJ_2 on CD36 mRNA levels and HDL binding. Macrophage cultures were untreated (lane 1) or incubated for 48 h in the presence of 300 units/mL of IFNγ (lane 2), 1.5 μM 15d-PGJ_2 (lane 3), or 15d-PGJ_2 + IFNγ (lane 4) and lysed for Northern blot analysis based on poly A-enriched mRNA. Nitrocellulose filters were probed with polymerase chain reaction (PCR)-labeled probes specific for CD36 (A), and the Golgi-associated calcium-binding protein Cab45 (B). Quantitation of the hybridized signals for each blot was by phosphoimager analysis (C,D). Band intensities for CD36 were normalized to the band intensity of Cab45 to control for any differences in poly A-enriched mRNA loading. Brackets represent the standard deviation of the mean (n = 3). Parallel cultures were incubated at 4°C with 25 μg/mL Alexa-labeled HDL for 3 h, washed, detached, and evaluated by flow cytometry (E). Brackets indicate the standard deviation of the mean fluorescence intensity in replica cultures. See Figures 1 and 2 for other abbreviations.

SR-BI message levels in macrophage-derived foam cells, whereas in the present study on macrophages that were not lipid-loaded, a modest reduction was observed. Therefore, whether the changes in HDL interactions which occur with IFNγ-activated macrophages reflect changes in functional SR-BI or CD36 which are not apparent when evaluating total protein or message remains to be determined. The more significant effects on DiI-labeled HDL uptake relative to the binding of Alexa labeled HDL would suggest additional effects of IFNγ beyond modulation of type B scavenger receptor levels.

The results of this study demonstrate that the pathway by which IFNγ downregulates HDL uptake is modulated by the PPARγ agonist 15d-PGJ_2, suggesting a role for PPARγ heterodimer nuclear receptors. Involvement of this pathway was supported by the observation that coincubation of macrophages with 1.5 μM 15d-PGJ_2, 12d-PGJ_2, or the unrelated PPARγ agonist ciglitazone resulted in an inhibition of the IFNγ effects on HDL binding. In addition, the present study has also demonstrated that the PPARγ agonist 15d-PGJ_2 was also able to reduce the IFNγ-mediated increases in CD11a expression and iNOS activity. The effect of 15d-PGJ_2 on inhibiting IFNγ-induced CD11a suggests additional IFNγ-regulated pathways modulated through PPARγ agonists. As these activities including iNOS induction are associated with macrophage activation, the ability to specifically inhibit these processes with PPARγ agonists offers therapeutic possibili-

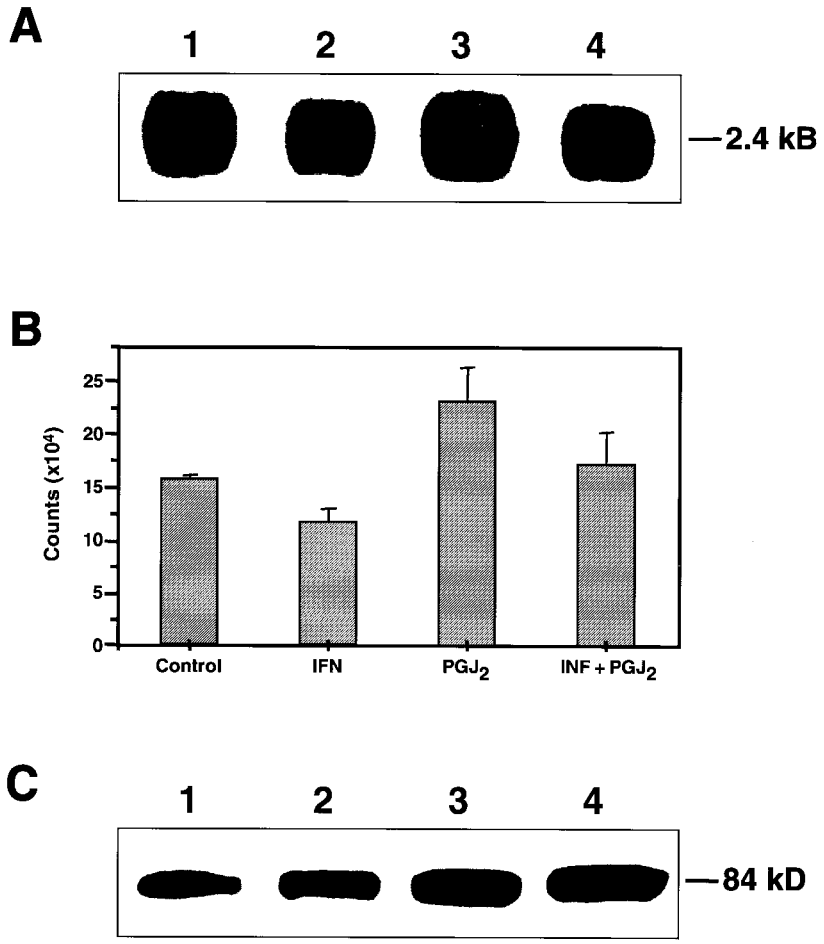

FIG. 5. Effects of IFNγ and 15d-PGJ_2 on SR-BI message and protein. Macrophages were incubated for 48 h in the absence (lane 1) or presence of 300 units/mL of IFNγ (lane 2), 1.5 μM 15d-PGJ_2 (lane 3), or 15d-PGJ_2 + IFNγ (lane 4) and lysed for Northern blot analysis. Poly A-enriched mRNA filters were hybridized with PCR-labeled probes specific for SR-BI (A). Quantitation of the radiolabeled bands was by phosphoimager (B). Band intensities for SR-BI were normalized to the band intensity of Cab45 to control for any differences in poly A-enriched mRNA loading. Brackets indicate standard deviations of the mean, $n = 3$. Parallel cultures were evaluated for SR-BI membrane protein in a membrane fraction following hypotonic lysis. SR-BI was detected by antibody staining using enhanced chemiluminescence (C). For abbreviations see Figures 1, 2, and 4.

ties for impacting the inflammatory aspects of activated macrophage effector functions without compromising functions such as phagocytosis of opsonized microorganisms.

These studies support a role for PPARγ/RXR heterodimers (where RXR is a member of the retinoid nuclear receptor family) in the modulation of macrophage effector functions within the atherosclerotic lesion. Furthermore, the demonstration that PPARγ transcription is increased by oxidized LDL or lipid components (23–25) and also by cytokines including macrophage CSF and GM-CSF (23) suggests an autocrine loop which would ensure maximal expression of PPARγ within an atherosclerotic lesion. Whether the observed increase in DiI-labeled HDL uptake in GM-CSF-treated macrophages in the present study is due to an increase in PPARγ expression remains to be determined.

The additional observations that agonists for this heteronuclear receptor pathway can promote macrophage differentiation as evidenced by increased expression of CD14, CDllb, and CD18 in HL60 cells and CD14 in human monocytes (25) suggest that their role in modulating macrophage effector functions is complex and likely to be dependent upon the state of macrophage activation and differentiation as well as on the relative amounts of other stimuli present within the microenvironment. For example, PPARγ agonists have been reported to decrease SR-A promoter activity in U937 transfectants (19) and the presence of oxidized LDL plus the RXR ligand LG268 increased SR-A message in THP-1 cells (24). These studies as well as the present observations that 15d-PGJ_2 inhibits the IFNγ-mediated decreases in macrophage-HDL interaction and also the induction of CD11a suggest that PPARγ agonists may have a profound effect on the expression of macrophage surface antigens and receptors relevant to the atherosclerotic process.

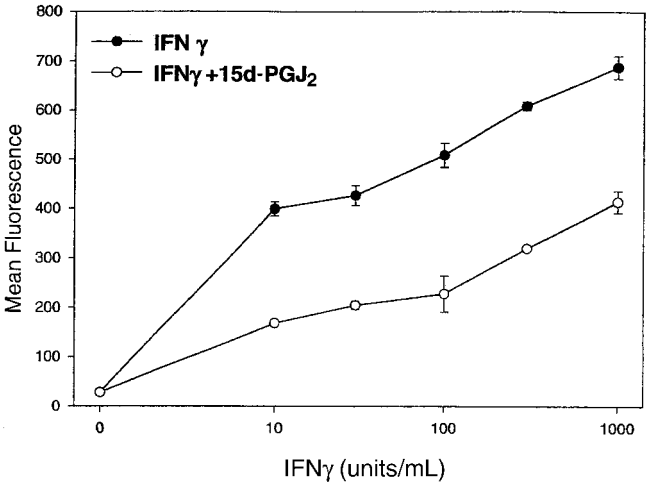

FIG. 6. Inhibition of IFNγ induction of CD11a expression by 15d-PGJ_2. Macrophages were cultured in the absence (●) or presence of 1.5 μM 15d-PGJ_2 (○) at the indicated concentrations of IFNγ. Following 48 h incubation, cultures were stained for CD11a surface expression, and the mean fluoresence intensity was quantitated by flow cytometry. Note inhibition of CD11a expression at all concentrations of IFNγ by the PPARγ agonist. Brackets indicate standard deviation of the mean from triplicate cultures. Representative experiment of 3. See Figures 1 and 2 for abbreviations.

IFNγ by inhibiting apo E secretion (11–13), reducing scavenger receptor activity and cholesterol efflux (14,15,17), promoting macrophage activation (9,10), and as demonstrated in the present study inhibiting macrophage HDL binding would suggest a negative role for this cytokine on the process of reverse cholesterol transport (34–37). Clearly, the reduction in atherosclerotic lesions in the apo E KO mouse when crossed with the IFNγ receptor KO (16) is consistent with its negative role in reverse cholesterol transport. Macrophage-HDL interactions are likely to involve both SR-BI and CD36 (38,39). That IFNγ reduced HDL uptake with only a modest change in SR-BI message and no effect on protein would suggest either an impact on membrane trafficking or function of this receptor through a post-translational modification or, alternatively, downregulation of an HDL receptor distinct from SR-BI. While CD36 would represent a logical candidate, here too, there was only a modest effect on message levels. In distinction, the increase in both the binding of Alexa-labeled HDL and the uptake of DiI-labeled HDL by 15d-PGJ_2 as well as the associated increase in SR-BI protein would suggest that this PPARγ agonist can enhance reverse cholesterol transport by increasing SR-BI and CD36 expression and antagonizing other inflammatory aspects of IFNγ-mediated macrophage activation. The recent demonstration (40) that a CD36 KO mouse had an increase in serum cholesterol primarily within the HDL fraction provides further evidence for the role of this receptor in HDL clearance. Whether PPARγ agonists will modulate HDL binding by macrophages in mice expressing this null mutation remains to be determined. Finally, the global anti-inflammatory effects of PPARγ agonists on macrophages raise the question as to whether more potent agonists of this pathway will promote lesion regression without a negative impact on macrophage effector functions associated with host defense.

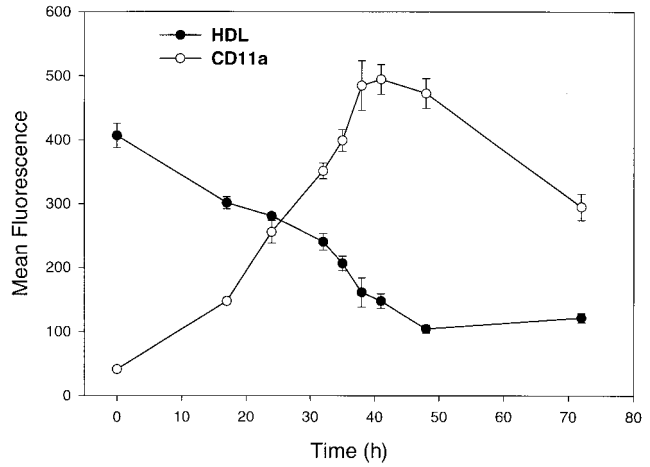

FIG. 7. Kinetics of IFNγ-mediated changes in HDL uptake and CD11a expression. Macrophage cultures in triplicate were incubated with 300 units/mL of IFNγ and at designated intervals were stained for CD11a expression (○) at 4°C or in parallel wells evaluated for the uptake of DiI-labeled HDL at 37°C (●). Parentheses indicate the standard deviation of the mean. See Figure 1 for abbreviations.

ACKNOWLEDGMENTS

The authors wish to thank Dr. Ray Kauffman for his review of our manuscript and Dr. Sue Acton (Millennium Pharmaceuticals Inc.) for providing the antibody against SR-BI.

REFERENCES

1. Ross, R. (1993) The Pathogenesis of Atherosclerosis: A Perspective for the 1990s, *Nature 362,* 801–809.
2. Berliner, J.Z., Navab, M., Fogelman, A.M., Frank, J.S., Demer, L.L., Edwards, P.A., Watson, A.D., and Lusis, A.J. (1995) Atherosclerosis: Basic Mechanisms, Oxidation, Inflammation, and Genetics, *Circulation 91,* 2488–2496.
3. Brown, M.S., and Goldstein, J.L. (1983) Lipoprotein Metabolism in the Macrophage: Implications for Cholesterol Deposition in Atherosclerosis, *Annu. Rev. Biochem. 52,* 223–261.
4. Libby, P., Geng, Y., Aikawa, M., Schoenbeck, U., Mach, F., Clinton, S., Sukhova, G., and Lee, R. (1996) Macrophages and Atherosclerotic Plaque Stability, *Curr. Opin. Lipidol 7,* 330–335.
5. Davies, M., Richardson, P., Woolf, N., Katz, D., and Mann, J. (1993) Risk of Thrombosis in Human Atherosclerotic Plaques: Role of Extracellular Lipid, Macrophage, and Smooth Muscle Cells Content, *Br. Heart J. 69,* 377–381.
6. Hansson, G.K., Holm, J., and Jonasson, L. (1989) Detection of Activated T Lymphocytes in the Human Atherosclerotic Plaque, *Am. J. Pathol. 135,* 169–175.
7. Geng, Y.-J., Holm, J., Nygren, S., Bruzelius, M., Stemme, S., and Hansson, G.K. (1995) Expression of the Macrophage Scavenger Receptor in Atheroma. Relationship to Immune Activation and the T-Cell Cytokine Interferon-γ, *Arterioscler. Thromb. Vasc. Biol. 15,* 1995–2002.
8. Zhou, X., Stemme, S., and Hansson, G.K. (1996) Evidence for a Local Immune Response in Atherosclerosis, *Am. J. Pathol. 149,* 359–366.

9. Nathan, C.F., Murray, H.W., Wiebe, M.E., and Rubin, B.Y. (1983) Identification of Interferon-γ as the Lymphokine That Activates Human Macrophage Oxidative Metabolism and Antimicrobial Activity, *J. Exp. Med. 158,* 670–689.
10. Boehm, U., Klamp, T., Groot, M., and Howard, J.C. (1997) Cellular Responses to Interferon-γ, *Annu. Rev. Immunol. 15,* 749–795.
11. Zuckerman, S.H., Evans, G.F., and O'Neal, L. (1992) Cytokine Regulation of Macrophage Apo E Secretion: Opposing Effects of GM-CSF and TGF-β, *Atherosclerosis 96,* 203–214.
12. Oropeza, R.L., Schreiber, R., and Werb, Z. (1985) Regulation of Apolipoprotein E Expression in Macrophages by γ-Interferon, in *Cellular and Molecular Biology of Lymphokines* (Sorg, C., and Schimpl, S., eds.) pp. 303–307, Academic Press, New York.
13. Garner, B., Baoutina, A., Dean, R.T., and Jessup, W. (1997) Regulation of Serum-Induced Lipid Accumulation in Human Monocyte-Derived Macrophages by Interferon-γ. Correlations with Apolipoprotein E Production, Lipoprotein Lipase Activity, and LDL Receptor-Related Protein Expression, *Atherosclerosis 128,* 47–58.
14. de Villiers, W.J.S., Fraser, I.P., and Gordon, S. (1994) Cytokine and Growth Factor Regulation of Macrophage Scavenger Receptor Expression and Function, *Immunol. Lett. 43,* 73–79.
15. Geng, Y.-J., and Hansson, G.K. (1992) Interferon-γ Inhibits Scavenger Receptor Expression and Foam Cell Formation in Human Monocyte-Derived Macrophages, *J. Clin. Invest. 89,* 1322–1330.
16. Gupta, S., Pablo, A.M., Jiang, X.-C., Wang, N., Tall, A.R., and Schindler, C. (1997) IFN-γ Potentiates Atherosclerosis in Apo E Knock-Out Mice, *J. Clin. Invest. 99,* 2752–2761.
17. Smith, J.D., Trogan, E., Ginsberg, M., Grigaux, C., Tian, J., and Miyata, M. (1995) Decreased Atherosclerosis in Mice Deficient in Both Macrophage Colony-Stimulating Factor (op) and Apolipoprotein E, *Proc. Natl. Acad. Sci. USA 92,* 8264–8268.
18. Rajavashisth, T., Qiao, J.-H., Tripathi, S., Tripathi, J., Mishra, N., Hua, M., Wang, X.-P., Loussararian, A., Clinton, S., Libby, P., and Lusis, A. (1998) Heterozygous Osteopetrotic (op) Mutation Reduces Atherosclerosis in LDL Receptor-Deficient Mice, *J. Clin. Invest. 101,* 2702–2710.
19. Ricote, M., Li, A.C., Willson, T.M., Kelly, C.J., and Glass, C.K. (1998) The Peroxisome Proliferator-Activated Receptor-γ Is a Negative Regulator of Macrophage Activation, *Nature 391,* 79–82.
20. Colville-Nash, P.R., Qureshi, S.S., Willis, D., and Willoughby, D.A. (1998) Inhibition of Inducible Nitric Oxide Synthase by Peroxisome Proliferator-Activated Receptor Agonists: Correlation with Induction of Heme Oxygenase 1, *J. Immunol. 161,* 978–984.
21. Jiang, C., Ting, A.T., and Seed, B. (1998) PPAR-γ Agonists Inhibit Production of Monocyte Inflammatory Cytokines, *Nature 391,* 82–86.
22. Marx, N., Sukhova, G., Murphy, C., Libby, P., and Plutzky, J. (1998) Macrophages in Human Atheroma Contain PPARγ. Differentiation-Dependent Peroxisomal Proliferator-Activated Receptor γ (PPARγ) Expression and Reduction of MMP-9 Activity Through PPARγ Activation in Mononuclear Phagocyes *in vitro, Am. J. Pathol. 153,* 17–23.
23. Ricote, M., Huang, J., Fajas, L., Li, A., Welch, J., Najib, J., Witzum, J.L., Auwerx, J., Palinski, W., and Glass, C.K. (1998) Expression of the Peroxisome Proliferator-Activated Receptor γ (PPARγ) in Human Atherosclerosis and Regulation in Macrophages by Colony-Stimulating Factors and Oxidized Low Density Lipoprotein, *Proc. Natl. Acad. Sci. USA 95,* 7614–7619.
24. Nagy, L., Tontonoz, P., Alvarez, J.G.A., Chen, H., and Evans, R.M. (1998) Oxidized LDL Regulates Macrophage Gene Expression Through Ligand Activation of PPARγ, *Cell 93,* 229–240.
25. Tontonoz, P., Nagy, L., Alvarez, J.G.A., Thomazy, V.A., and Evans, R.M. (1998) PPARγ Promotes Monocyte/Macrophage Differentiation and Uptake of Oxidized LDL, *Cell 93,* 241–252.
26. Kliewer, S.A., Lenhard, J.M., Willison, T.M., Patel, I., Morris, D.C., and Lehmann, J.M. (1995) A Prostaglandin J_2 Metabolite Binds Peroxisome Proliferator-Activated Receptor γ and Promotes Adipocyte Differentiation, *Cell 83,* 813–819.
27. Forman, B.M., Tontonoz, P., Chen, J., Brun, R.P., Spiegelman, B.M., and Evans, R.M. (1985) 15-Deoxy-^{12,14} Prostaglandin J_2 Is a Ligand for the Adipocyte Determination Factor PPARγ, *Cell 83,* 803–812.
28. O'Leary, E.C., Evans, G.F., and Zuckerman, S.H. (1997) *In Vivo* Dexamethasone Effects on Neutrophil Effector Functions in a Rat Model of Acute Lung Injury, *Inflammation 21,* 597–608.
29. Zuckerman, S.H., Ahmari, S.E., Bryan-Poole, N., Evans, G.F., Short, L., and Glasebrook, A.L. (1996) Estriol: A Potent Regulator of TNF and IL-6 Expression in a Murine Model of Endotoxemia, *Inflammation 20,* 581–597.
30. Scherer, P.E., Lederkremer, G.Z., Williams, S., Fogliano, M., Baldini, G., and Lodish, H.F. (1996) Cab45, A Novel (Ca^{2+})-Binding Protein Localized to the Golgi Lumen, *J. Cell Biol. 133,* 257–268.
31. Acton, S., Rigotti, A., Landschulz, K.T., Xu, S., Hobbs, H.H., and Krieger, M. (1996) Identification of Scavenger Receptor SR-BI as a High Density Lipoprotein Receptor, *Science 271,* 518–520.
32. Ji, Y., Jian, B., Wang, N., Sun, Y., de la Llera-Moya, M., Phillips, M.C., Rothblat, G.H., Swaney, J.B., and Tall, A.R. (1997) Scavenger Receptor BI Promotes High Density Lipoprotein-Mediated Cellular Cholesterol Efflux, *J. Biol. Chem 272,* 20982–20985.
33. Jian, B., de la Llera-Moya, M., Ji, Y., Wang, N., Phillips, M.C., Swaney, J.B., Tall, A.R., and Rothblat, G.H. (1998) Scavenger Receptor Class B Type I as a Mediator of Cellular Cholesterol Efflux to Lipoproteins and Phospholipid Acceptors, *J. Biol. Chem. 273,* 5599–5606.
34. Nakagawa, T., Nozaki, S., Nishida, M., Yakub, J.M., Tomiyama, Y., Nakata, A., Matsumoto, K., Funahashi, T., Kameda-Takemura, K., Kurata, Y., Yamashita, S., and Matsuzawa, Y. (1998) Oxidized LDL Increases and Interferon-γ Decreases Expression of CD36 in Human Monocyte-Derived Macrophages, *Arterioscler. Thromb. Vasc. Biol. 18,* 1350–1357.
35. Barter, P.J., and Rye, K.-A. (1996) Molecular Mechanisms of Reverse Cholesterol Transport, *Curr. Opinion Lipidol. 7,* 82–87.
36. Phillips, M.C., Gillotte, K.L., Haynes, M.P., Johnson, W.J., Lund-Katz, S., and Rothblat, G.H. (1998) Mechanism of High Density Lipoprotein-Mediated Efflux of Cholesterol from Cell Plasma Membranes, *Atherosclerosis 137,* S13–S17.
37. Tall, A.R. (1998) An Overview of Reverse Cholesterol Transport, *Eur. Heart J. 19,* A31–A35.
38. Gu, X., Trigatti, B., Xu, S., Acton, S., Babitt, J., and Krieger, M. (1998) The Efficient Cellular Uptake of High Density Lipoprotein Lipids *via* Scavenger Receptor Class B Type I Requires Not Only Receptor-Mediated Surface Binding But Also Receptor Specific Lipid Transfer Mediated by Its Extracellular Domain, *J. Biol. Chem. 273,* 26338–26348.
39. Calvo, D., Gomez-Coronado, D., Suarez, Y., Lasuncion, M.A., and Vega, M.A. (1998) Human CD36 Is a High-Affinity Receptor for the Native Lipoproteins HDL, LDL, and VLDL, *J. Lipid Res. 39,* 777–788.
40. Febbraio, M., Abumrad, N.A., Hajjar, D.P., Sharma, K., Cheng, W., Pearce, S.F.A., and Silverstein, R.L. (1999) A Null Mutation in Murine CD36 Reveals an Important Role in Fatty Acid and Lipoprotein Metabolism, *J. Biol. Chem. 274,* 19055–19062.

[Received March 24, 2000, and in revised form August 21, 2000; revision accepted September 18, 2000]

Human, but Not Bovine, Oxidized Cerebral Spinal Fluid Lipoproteins Disrupt Neuronal Microtubules

M.D. Neely*, L.L. Swift, and T.J. Montine

Department of Pathology, Vanderbilt University, Nashville, Tennessee 37232

ABSTRACT: Cerebral spinal fluid (CSF) lipoproteins have become a focus of research since the observation that inheritance of particular alleles of the apolipoprotein E gene affects the risk of Alzheimer's disease (AD). There is evidence of increased lipid peroxidation in CSF lipoproteins from patients with AD, but the biological significance of this observation is not known. A characteristic of the AD brain is a disturbance of the neuronal microtubule organization. We have shown previously that 4-hydroxy-2(*E*)-nonenal, a major product of lipid peroxidation, causes disruption of neuronal microtubules and therefore tested whether oxidized CSF lipoproteins had the same effect. We exposed Neuro 2A cells to human CSF lipoproteins and analyzed the microtubule organization by immunofluorescence. *In vitro* oxidized human CSF lipoproteins caused disruption of the microtubule network, while their native (nonoxidized) counterparts did not. Microtubule disruption was observed after short exposures (1 h) and lipoprotein concentrations were present in CSF (20 μg/mL), conditions that did not result in loss of cell viability. Importantly, adult bovine CSF lipoproteins, oxidized under identical conditions, had no effect on the microtubule organization of Neuro 2A cells. Comparison of human and bovine CSF lipoproteins revealed similar oxidation-induced modifications of apolipoproteins E and A-I as analyzed by sodium dodecyl sulfate-polyacrylamide gel electrophoresis and Western blotting. Fatty acid analysis revealed substantially lower amounts of unsaturated fatty acids in bovine CSF lipoproteins, when compared to their human counterparts. Our data therefore indicate that oxidized human CSF lipoproteins are detrimental to neuronal microtubules. This effect is species-specific, since equally oxidized bovine CSF lipoproteins left the neuronal microtubule organization unchanged.

Paper no. L8492 in *Lipids 35,* 1249–1257 (November 2000).

Cerebral spinal fluid (CSF) lipoproteins have received increased attention since the discovery that the inheritance of the ε4 allele of the apolipoprotein E (apoE) gene increases the risk of late-onset familial and sporadic Alzheimer's disease (AD) (1). Human CSF lipoproteins consist of a subpopulation of particles, which differ in their physical characteristics as well as protein and lipid composition (2–8). Two types of high density lipoprotein (HDL)-like spherical particles, one enriched in one of the major CSF apolipoproteins, apoE, the other enriched in the second major CSF apolipoprotein, apoA-I, constitute the majority of the CSF lipoproteins (2,3). In addition, other less abundant classes of larger lipoprotein particles have been identified (3–6). Although no genotype-specific differences in the overall protein and lipid composition of CSF lipoproteins ($d < 1.21$ g/mL) were observed (7), the apoE genotype does seem to affect the distribution profile of apoE-containing lipoproteins (5).

There is increasing evidence that oxidative stress and lipid peroxidation in particular play important roles in the pathogenesis of AD (9–19). Lipid peroxidation also has been implicated in another age-related disease, atherosclerosis, where oxidized plasma lipoproteins are thought to contribute to disease progression (for review see Ref. 20). We have observed evidence of increased lipid peroxidation in CSF lipoproteins from AD patients when compared to CSF lipoproteins from non-demented individuals (21). In addition, others have demonstrated increased concentration of the lipid peroxidation product 4-hydroxy-2(*E*)-nonenal (HNE) in CSF of AD patients compared to controls (22). These findings are consistent with the hypothesis that CSF lipoproteins in AD patients are present in an environment favorable for lipid peroxidation or are derived from tissue experiencing lipid peroxidation. In either case, oxidized CSF lipoproteins may act as vehicles to deliver lipid peroxidation products to neurons. Oxidized plasma lipoproteins have been shown to be toxic to a variety of cultured cells, including neurons (23–27). To our knowledge, only one study has examined the potential neurotoxicity of oxidized human CSF lipoproteins (28). The authors observed significant loss of cell viability after 24 h exposures of Neuro 2A cells to *in vitro* oxidized human CSF lipoproteins; however, the mechanism(s) by which the oxidized CSF lipoproteins cause cell death is not known (28).

A hallmark of the AD brain is the change in biochemical and structural features of neuronal microtubules. Abnormal organization and general deficiency of microtubules have been observed in dendrites of neurons in the frontal cortex of AD patients (29–32). Furthermore, in the AD brain, tau, a mi-

*To whom correspondence should be addressed at Vanderbilt University, Department of Pathology, Medical Center North, 1161 21st Street South, Nashville, TN 37232-2561. E-mail: diana.neely@mcmail.vanderbilt.edu

Abbreviations: AAPH, 2,2′-azo-bis-(2-aminopropane) hydrochloride; AD, Alzheimer's disease; apo, apolipoprotein; blotto, 4% dry milk in Tris-buffered saline with 0.05% Tween 20; CNS, central nervous system; CSF, cerebral spinal fluid; DMEM/F12, Dulbecco's Modified Eagle Medium/Nutrient Mixture F-12; HDL, high density lipoproteins; HNE, 4-hydroxy-2(*E*)-nonenal; LDL, low density lipoproteins; PBS, phosphate-buffered saline; PUFA, polyunsaturated fatty acid; SDS-PAGE, sodium dodecyl sulfate-polyacrylamide gel electrophoresis.

crotubule-associated protein, is localized to neuronal somatodendritic region, whereas in the normal brain it is found exclusively in axons (33). Abnormally phosphorylated tau is the major protein component of neurofibrillary tangles (34,35). We have shown previously that some HNE-protein adducts co-localize with neurofibrillary tangles in the AD brain (11,12) and that the lipid peroxidation product HNE causes disruption of the neuronal microtubule network (36). Here, we show that *in vitro* oxidized human CSF lipoproteins cause rapid (within 1 h) disruption of the microtubule organization in Neuro 2A cells. Strikingly, lipoproteins isolated from bovine CSF and oxidized in the same manner did not affect neuronal microtubules.

MATERIAL AND METHODS

Materials. Materials used for cell culture were from Life Technologies (Grand Island, NY). Reagents for sodium dodecyl sulfate-polyacrylamide gel electrophoresis (SDS-PAGE) and Western blotting were obtained from Bio-Rad (Hercules, CA). All other chemicals were from Sigma (St. Louis, MO) unless otherwise indicated.

Case selection and preparation of CSF lipoproteins. Following informed consent, CSF was removed, post mortem, from the lateral ventricles. All autopsies were performed at Vanderbilt University Medical Center within 5 h of death. All individuals had histopathologically confirmed AD (3 patients) or, in controls, age-related changes only (3 subjects). Ventricular fluid (≥8.5 mL), visually free of contamination by blood, was collected. In our extensive experience with human CSF, we have never detected apoB in CSF that was visually free of blood (21,37). After collection, the CSF was immediately sedimented at 1,000 × *g* for 10 min and frozen at −80°C. Ventricular fluid density was raised to $d = 1.210$ g/mL by addition of KBr before centrifugation at 4°C in a Beckman (Fullerton, CA) L8-55 ultracentrifuge using either a 40 rotor at 95,581 × *g* (38,000 rpm) for 42 h or a 50.3 Ti rotor at 165,667 × *g* (48,000 rpm) for 24 h. Floating lipoproteins were recovered by tube slicing and washed once under identical conditions used for initial isolation. The lipoproteins were then dialyzed into phosphate-buffered saline (PBS) and the protein concentration determined by the bicinchoninic acid assay according to the manufacturer's protocol (Pierce, Rockford, IL) except that 0.1% SDS was included in each sample. Frozen adult bovine CSF (guaranteed blood free) was purchased from Pel-Freez (Rogers, AR) and stored at −80°C until use. Isolation and oxidation of bovine CSF lipoproteins were performed exactly as for the human lipoproteins.

Oxidation and analysis of CSF lipoproteins. Lipoproteins were isolated from human and adult bovine CSF, and samples were adjusted to a protein concentration of 40 μg/mL and oxidized with increasing concentrations of 2,2′-azo-bis-(2-aminopropane) hydrochloride (AAPH) (Wako Chemicals, Richmond, VA). AAPH, a water-soluble azo compound that thermally decomposes to produce a constant radical flux, has been used extensively in studies of plasma lipoproteins (38). In order not to lose any metabolites resulting from oxidation, the lipoproteins were not dialyzed after their incubation with AAPH. This was possible because a control solution of 10 mM AAPH (the highest concentration used in our experiments) that had been incubated under identical conditions had no effect on the microtubule organization of Neuro 2A cells. After oxidation, the lipoprotein samples were stored in working aliquots of 50–100 μL at −80°C until use. The effect of lipoprotein oxidation on apoE and apoA-I was analyzed by SDS-PAGE and Western blot analysis. The proteins were separated by electrophoresis in a 12% polyacrylamide gel (39) and stained using the silver nitrate method or transferred to a membrane (#162-0170; Bio-Rad) for Western blot analysis. Nonspecific binding sites on the membrane were blocked with "blotto" (4% dry milk in Tris-buffered saline with 0.05% Tween 20) for at least 3 h at room temperature. The proteins were immunoreacted, first with either a polyclonal anti-human apoE antibody (#A0077; DAKO, Carpinteria, CA) or a polyclonal anti-human apoA-I antibody (#178422; Calbiochem, San Diego, CA), each diluted 500-fold into blotto, and then with an horseradish peroxidase-conjugated anti-rabbit IgG (#A0545; Sigma, St. Louis, MO) diluted 1:4000 into blotto. The signal was visualized with chemiluminescence reagent (#NEL100; New England Nuclear, Boston, MA).

For fatty acid analysis, bovine CSF lipoproteins were isolated from two different 50-mL bovine CSF samples on two different occasions as described above. In one of our analyses, the lipoprotein fraction was divided into two equal samples for analysis, and in the second analysis, the lipoprotein fraction in its totality was lyophilized and delipidated using ethanol/ether. Phospholipids, triglycerides, and cholesteryl esters of the whole samples were separated by thin-layer chromatography (40) and quantified by gas chromatography after fatty acid transmethylation with BF_3/methanol (21,41). Fatty acids were identified by comparison of their retention times with those of known standards, and the lipid mass was determined by comparison with an internal standard (dipentadecanoylphosphatidylcholine, trieicosenoin, or cholesteryl eicosenoate) that was added at the time of delipidation. Approximately 10% of the total isolated lipid fractions was used for each gas chromatographic analysis. In every analysis, the total mass of fatty acid esters exceeded 5 μg, which is the minimum mass we routinely require to ensure accuracy of the analysis (21). Levels of unesterified cholesterol were below detection using a colorimetric method following elution from silica gel (42).

Cell culture and immunocytochemistry. Neuro 2A neuroblastoma cells were purchased from American Type Culture Collection (Rockville, MD). Neuro 2A cells are particularly well suited for cytoskeletal analysis because of their spread morphology and high content of microtubules (36,43). Cells were grown in growth medium [Dulbecco's Modified Eagle Medium/Nutrient Mixture F-12 (DMEM/F12) (1:1) with 10% fetal bovine serum and penicillin-streptomycin at 100 units/mL and 100 μg/mL, respectively]. The day before the experiment, the cells were subcultured and 150 μL of a cell

suspension containing 5×10^4 cells/mL were placed into the wells of 35-mm glass bottom micro well dishes (MatTek Corp., Ashland, MA) and left to adhere for 24 h. The growth medium was then removed and the cells incubated in N2-medium (DMEM/F12 medium containing penicillin-streptomycin and N-2 supplement) overnight, before a 60 min exposure to native (nonoxidized) or oxidized CSF lipoproteins (fraction $d < 1.210$ g/mL) diluted with Earle's balanced salt solution to a final concentration of 20 μg/mL. CSF lipoproteins were used within 4 wk after their isolation and oxidation. Only samples that had never been thawed after the oxidation were used for these experiments. After treatment, the cells were washed and immediately fixed in 4% paraformaldehyde in PBS for 30 min at room temperature. To visualize the microtubules, the cells were permeabilized with 1% Triton X-100 in PBS containing 2% fetal bovine serum for 20 min at room temperature, then incubated with anti-β-tubulin at 0.25 μg/mL (#1111876; Boehringer Mannheim, Indianapolis, IN) in PBS containing 2% fetal bovine serum overnight at 4°C. The secondary antibody (a fluorescein isothiocyanatel-coupled anti-mouse IgG; #55514; Cappel, Durham, NC) was applied at 3 μg/mL in PBS with 2% fetal bovine serum for 2 h at room temperature. The glass slides with the cells were carefully removed from the 35-mm dishes with a razor blade and mounted in ProLong mounting medium (#P-7481; Molecular Probes, Eugene, OR). The microtubules were visualized with a Zeiss Axiovert 135 microscope (Carl Zeiss, Inc., Thornwood, NY) using Plan-Apochromat 63×/1.4 or 100×/1.4 objectives. For semi-quantitative analysis of the microtubule organization, microscope slides were scanned along a fixed y-coordinate using an electronically controlled microscope stage, and the microtubule organization in at least 200 cells per slide was categorized as either normal, mildly disrupted, or severely disrupted. The analysis was done blinded to exposure conditions. Analysis of variance, followed by repeated *t*-tests with Bonferroni correction for multiple comparisons, was used to compare the effects of the different lipoprotein samples.

Cytotoxicity. Cell viability was assessed using a Live/Dead kit containing two different dyes (Molecular Probes) following the manufacturer's protocol. One of these dyes, the cell permeant calcein AM, is cleaved in live cells by intracellular esterases to the fluorescent calcein, thus labeling live cells green. The other dye, ethidium homodimer, enters cells with damaged plasma membranes where it undergoes a 40-fold enhancement of fluorescence upon binding to nucleic acids labeling dead cells red. Neuro 2A cells were incubated with native CSF lipoproteins or lipoproteins that had been oxidized with 0.5, 1, 5, or 10 mM AAPH for 18 h at 37°C. After 40 min, the dyes were added and the cells were incubated for another 20 min, resulting in a total exposure to lipoproteins of 60 min. The cultures were then observed by phase microscopy to find areas of appropriate cell densities. Six such areas per dish were imaged using both fluorescein isothiocyanate and tetramethylrhodamine-5(and-6-) isothiocyanate fluorescence microscopy, and green and red cells were counted manually on the recorded images. Between 1,000 and 2,500 cells were counted per dish. Four experiments with human CSF lipoproteins isolated from two individuals and three experiments with lipoproteins isolated from two different bovine CSF were performed. Viability ≥94% was observed in all cultures analyzed.

RESULTS

Human oxidized CSF lipoproteins disrupt the neuronal microtubule network. Neuro 2A cells were incubated with native (nonoxidized) and *in vitro* oxidized human CSF lipoproteins for 1 h, and their microtubule organization was analyzed by immunocytochemistry. For semiquantitative analysis, the microtubule organization in at least 200 cells per slide was categorized as either normal (Fig. 1A), mildly disrupted (Fig. 1C), or severely disrupted (Fig. 1D). We analyzed the effects of CSF lipoproteins from six different subjects. In all six cases, incubation with native CSF lipoprotein samples left the microtubule organization of Neuro 2A cells unchanged (Fig. 1A; Fig. 2A). In four cases (three control and one AD, all patients had apo E3/E3 genotype) microtubules were only disrupted by the most heavily oxidized lipoproteins (10 mM AAPH). In one case (AD, apo E3/E4 genotype), none of the lipoprotein samples caused significant disruption of the microtubules. In another case (AD, apo E3/E4 genotype) all the oxidized samples, including a lipoprotein sample incubated with 0.1 mM AAPH, but not the native lipoproteins, caused loss of the microtubules.

There was no statistically significant difference in the degree of microtubule disruption caused by oxidized CSF lipoproteins from control and AD patients. Only the most heavily oxidized lipoproteins caused a significant change in the microtubule organization, increasing the number of cells with severely disrupted microtubules from ≤1% in Neuro 2A cultures incubated with native lipoproteins to 39 ± 9.4% ($P < 0.001$) (Fig. 2A). Although our observations suggest a larger variability of the effect on the microtubules by oxidized lipoproteins from patients with AD than from control individuals, the relatively small number of lipoprotein preparations limits our conclusions.

Phase contrast microscopy revealed minor morphological changes in occasional Neuro 2A cells only in cultures exposed to the most heavily oxidized CSF lipoproteins. They manifested themselves as beading, loss of neurites, and rounding of cell bodies. Neuro 2A cell viability was assayed after a 1-h exposure to CSF lipoproteins. We performed seven separate experiments (four with human CSF lipoproteins isolated from two different patients and three with bovine CSF lipoproteins isolated from two different bovine CSF). In all experiments and under all conditions, including native or oxidized lipoproteins, cell viability was ≥94% (data not shown). Therefore, the disruption of the microtubule network by oxidized human CSF lipoproteins was not a consequence of cell death.

Bovine oxidized CSF lipoproteins do not disrupt the neuronal microtubule network. Next, we isolated and oxidized bovine CSF lipoproteins under exactly the same conditions

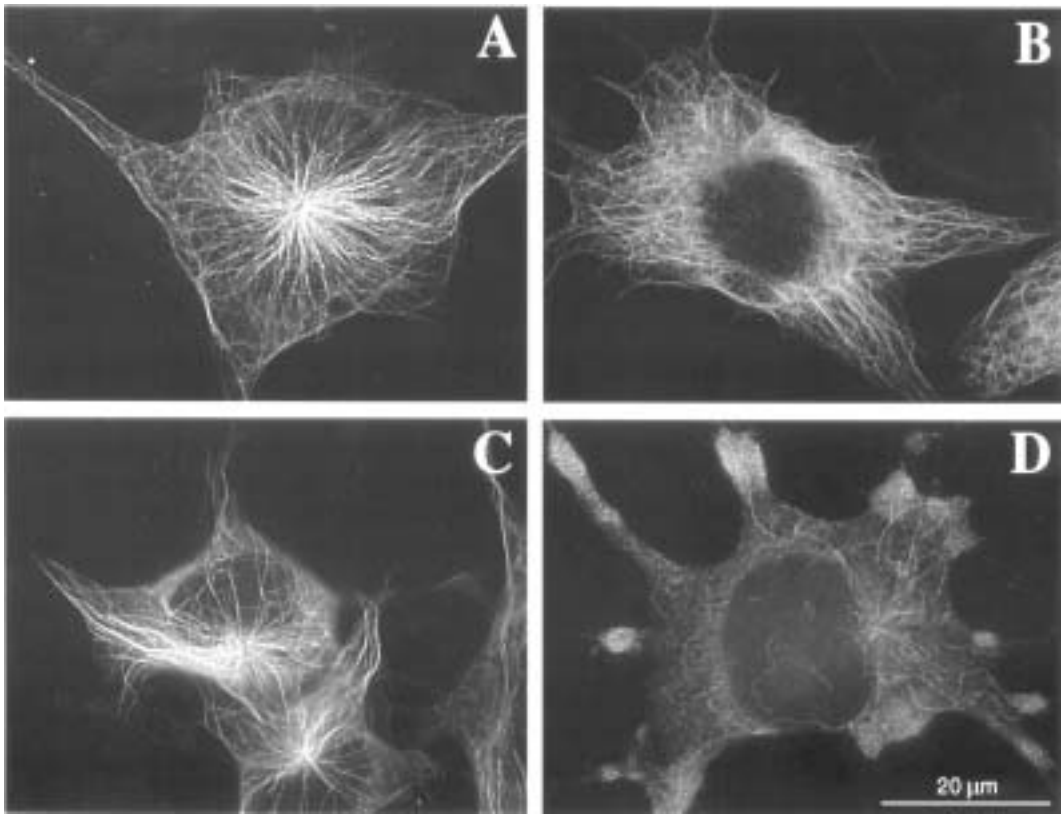

FIG. 1. Oxidized human cerebral spinal fluid (CSF) lipoproteins disrupt neuronal microtubules. Neuro 2A cells were exposed to native and oxidized CSF lipoproteins ($d < 1.21$ g/mL) for 1 h and microtubule organization was analyzed by immunofluorescence using an antibody against β-tubulin. In cells exposed to native human CSF lipoproteins a dense microtubule network radiating from the center to the periphery of the cells can be seen (A). Human CSF lipoproteins that had been oxidized with 10 mM 2,2′-azo-bis-(2-aminopropane) hydrochloride (AAPH) caused microtubule disruption to a varying degree. Neuro 2A cells with mild and severe disruption of the microtubule network are shown in C and D, respectively. Bovine CSF lipoproteins oxidized with 10 mM AAPH had no effect on the microtubule organization in Neuro 2A cells (B). Scale bar = 20 μm.

used for human CSF lipoproteins and analyzed their effect on the microtubules in Neuro 2A cells. In all cases neither native nor any of the oxidized bovine CSF lipoproteins showed a significant effect on the microtubule distribution in Neuro 2A cells (Figs. 1B and 2B). This stands in sharp contrast to the effect of human CSF lipoproteins which, when oxidized with 10 mM AAPH, cause a significant reduction in cells with normal microtubule organization and a significant increase in the number of cells with severely disrupted microtubules (Fig. 2A). This striking difference in the microtubule-disrupting effect of human and bovine oxidized CSF lipoproteins led us to examine the protein and lipid composition of bovine CSF lipoproteins.

Analysis of bovine CSF lipoproteins. Bovine CSF lipoproteins ($d < 1.210$ g/mL) were isolated and analyzed as previously described for human CSF lipoproteins (21). Both total protein and lipid concentrations were lower in bovine than human CSF lipoproteins ($d < 1.210$ g/mL) (protein and lipid concentrations were 21.2 ± 3.3 and 9.4 ± 2.3 for human and 9.1 ± 0.9 and 2.4 ± 0.4 μg/mL for bovine CSF lipoproteins, respectively) (Table 1) (21). The protein to lipid ratio was 3.8 in bovine and 2.3 in human CSF lipoproteins (Table 1) (21). The lipids of the bovine CSF lipoproteins were fractionated by thin-layer chromatography. Similar to human CSF lipoproteins (21), phospholipids constituted the main lipid component (66%) in bovine CSF lipoprotein (Table 1). Phospholipid and cholesteryl ester concentrations were lower in the bovine samples compared to human CSF lipoproteins; triglyceride levels were comparable in the CSF lipoproteins from the two species (Table 1) (21). Unesterified cholesterol levels were below detection in bovine CSF lipoproteins.

The main fatty acids in the phospholipids of bovine CSF lipoproteins were 16:0 (66.5%) and 18:0 (20.8%). The low amount of 18:1 in bovine CSF lipoproteins (0.1%) stands in sharp contrast to its levels (20.9%) in human CSF lipoproteins (21). Linoleate (18:2) is barely detectable (0.1%) and 22:6 is undetectable in the phospholipid fraction of bovine CSF lipoproteins, whereas these two polyunsaturated fatty acids (PUFA) are present in human CSF lipoprotein phospholipid (0.7 and 5.5%, respectively). Arachidonate (20:4) is also present at lower levels in bovine (4.3%) than in human CSF lipoproteins (13.3%), while 18:3 were more prevalent in

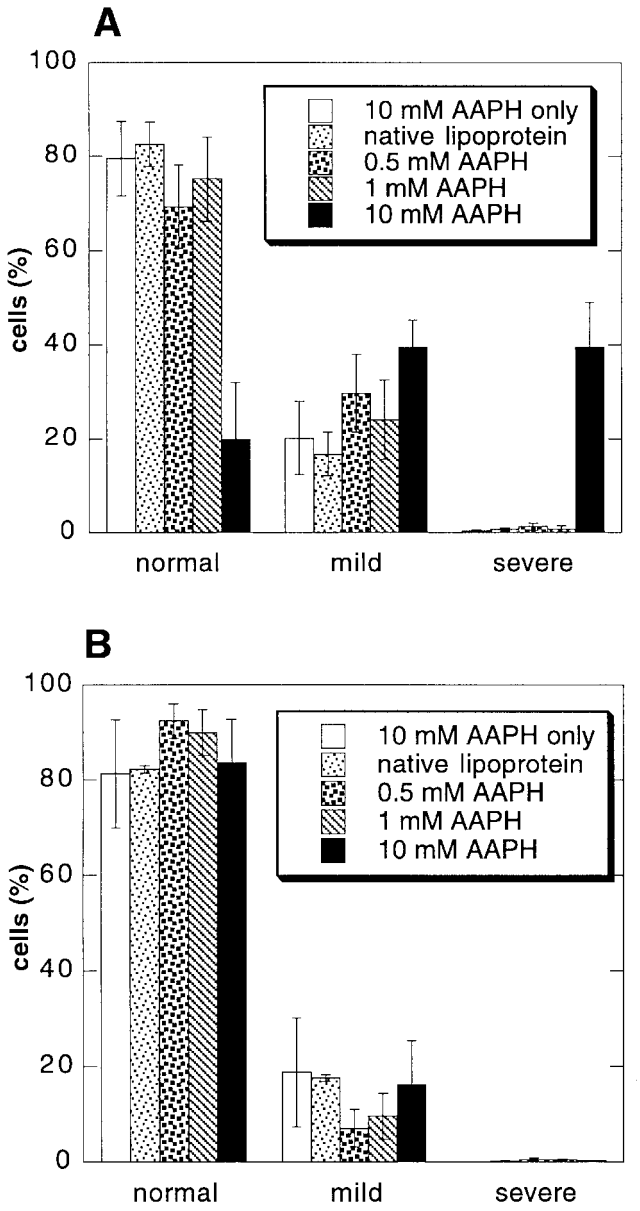

FIG. 2. Comparison of microtubule disruption caused by oxidized human and bovine CSF lipoproteins. The effect of human (A) and bovine (B) CSF lipoproteins ($d < 1.21$ g/mL) on microtubules was compared. In order not to lose any metabolites resulting from oxidation, the lipoproteins were not dialyzed after their incubation with AAPH. This was possible, because a control solution of 10 mM AAPH (without lipoproteins) that had been incubated under identical conditions had no effect on the microtubule organization of Neuro 2A cells (10 mM AAPH only). Neuro 2A cells were incubated with native or oxidized (0.5, 1, and 10 mM AAPH) CSF lipoproteins and microtubule organization was assessed as described in the Materials and Methods section. The majority of the cells incubated with native human or bovine CSF lipoproteins displayed normal microtubule organization characterized by a dense network of microtubules extending to the cell periphery (82.6 ± 4.7% and 85.1 ± 2.9% for human and bovine, respectively). Exposure to the most extensively oxidized human CSF lipoproteins significantly increased the percentage of cells with severely disrupted microtubule networks from ≤1% in cells exposed to native lipoproteins to 39.6 ± 9.4% ($P < 0.001$) (A). Bovine CSF lipoproteins oxidized with 10 mM AAPH, however, did not cause severe microtubule disruption (B). Values are the mean and SEM ($n_{human} = 6$; $n_{bovine} = 3$). See Figure 1 for abbreviations.

bovine (2.2%), than in human (0.2%) CSF lipoprotein phospholipids (21). Overall, the relative levels of monounsaturated fatty acids (0.1%) and PUFA (7.4%) in the phospholipids of bovine CSF lipoproteins were substantially lower than in the human lipoproteins, where the monounsaturated fatty acids and PUFA constitute 20.9 and 19.9%, respectively (Table 1) (21). The relative abundance of the major fatty acids in bovine CSF lipoprotein cholesteryl esters was 16:0 > 14:0 > 18:0. The relative amounts of monounsaturated fatty acids and PUFA again were much smaller (0.1 and 3.5%, respectively) than in the human counterparts, where they make up 34.9 and 29.0% of the total fatty acids, respectively (Table 1) (21). In bovine CSF lipoprotein triglycerides the prevalence of the major fatty acids was 16:0 > 18:0 > 14:0. As in the other two lipid fractions, the unsaturated fatty acids made up a small fraction (3.2%) of the total fatty acids (Table 1). Bovine CSF lipoproteins therefore contain substantially less unsaturated fatty acids than their human counterparts.

Effect of CSF lipoprotein oxidation on apoA-I and apoE. As previously observed, the two main proteins in human and bovine native CSF lipoproteins are apoA-I and apoE (2,44,45) (Fig. 3). The effect of oxidation on human and bovine CSF apolipoproteins was analyzed by SDS-PAGE followed by silver staining (Fig. 3A) and Western blotting (Figs. 3B and C). Oxidation with AAPH concentrations of ≤0.5 mM caused a slight reduction in the electrophoretic mobility of both apoE and apoA-I and the appearance of higher molecular weight protein species (Figs. 3A, B, and C). Oxidation with AAPH concentrations ≥5 mM led to a complete loss of apoE and apoA-I monomer and the appearance of abnormal higher molecular weight protein species that were immunoreactive with antibodies against apoE and apoA-I (Figs. 3A, B, and C). This analysis shows that AAPH induced protein changes were comparable for human and bovine CSF apolipoproteins.

DISCUSSION

To our knowledge, this is the first study to investigate the possible mechanism by which oxidized human CSF lipoproteins cause neurotoxicity. Since one of the pathological hallmarks in AD is a change in neuronal microtubules (29–35) and since we have shown previously that HNE, a major product of lipid peroxidation, causes microtubule disruption, we tested the hypothesis that oxidized CNS lipoproteins disrupt neuronal microtubules. We found that the most heavily oxidized human CSF lipoproteins cause significant disruption of the microtubule network, whereas native and less extensively oxidized lipoproteins had no effect. Microtubule disruption was observed after short exposures (1 h) and at lipoprotein concentrations present in CSF (20 μg/mL) (21). *In vitro* oxidized human CSF lipoproteins have been shown to be toxic to Neuro 2A cells after 24 h exposures (28), but the loss of microtubule organization described here was observed in the absence of cytotoxicity. Therefore, CSF lipoprotein-induced microtubule disruption precedes cell death, but may play a

TABLE 1
Composition of Bovine Cerebral Spinal Fluid (CSF) Lipoproteins[a]

Bovine CSF (d < 1.210 g/mL)	Concentration (μg/mL CSF)	Saturated FA (%)	Monounsaturated FA (%)	Polyunsaturated FA (%)
Protein	9.1 ± 0.9	—	—	—
Phospholipid	1.6 ± 0.3	92.1 ± 0.9	0.1 ± 0.1	7.4 ± 1.5
Triglyceride	0.30 ± 0.06	95.9 ± 4.1	3.2 ± 1.5	0.0
Cholesteryl esters	0.25 ± 0.03	97.0 ± 3.0	0.1 ± 0.1	3.5 ± 2.7
Unesterified Cholesterol	Not detectable	—	—	—
Free fatty acids	0.26 ± 0.02	100 ± 0.0	0.0 ± 0.0	0.0 ± 0.0

[a]Protein and lipids were quantified from three bovine CSF lipoproteins samples (d < 1.210 g/mL). Values are means ± SEM. FA, fatty acid.

mechanistic role in the eventual loss of cell viability. Importantly, while the effect of oxidized human CSF lipoproteins on the neuronal microtubules was dramatic, bovine CSF lipoproteins oxidized under identical conditions left the microtubule organization unchanged.

CSF lipoproteins isolated from AD patients show signs of increased lipid peroxidation when compared with controls (21). However, we did not see microtubule disruption after exposure of Neuro 2A cells to native CSF lipoproteins isolated from AD patients. In addition, the degree of lipoprotein oxidation, as estimated by apolipoprotein modification (this study) or the extent of PUFA consumption (28) necessary to induce disruption of the microtubules, exceeds that observed in CSF lipoproteins isolated from AD patients (21). A similar discrepancy is observed in atherosclerosis. Although many experiments involving *in vitro* oxidized low density lipoprotein (LDL) suggest that oxidation of these lipoproteins plays a role in atherogenesis, the presence of similarly modified LDL has been difficult to demonstrate in plasma (38). The oxidation of LDL is believed to occur locally in the arterial wall; therefore, the oxidized LDL particles may not reach concentrations in the general circulation necessary for detection (20,46). A similar situation may exist in the central nervous system (CNS), where locally induced oxidative changes in CNS lipoproteins do not manifest themselves in CSF.

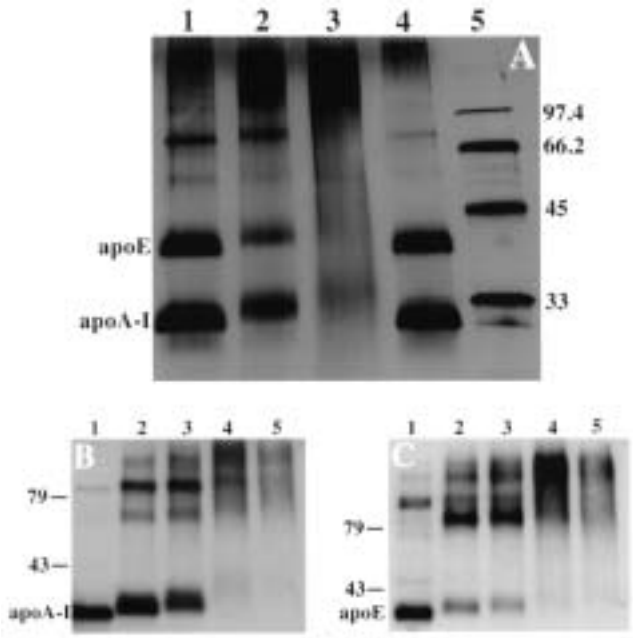

FIG. 3. Analysis of apolipoproteins (apo) in native and oxidized CSF lipoproteins. (A) Bovine CSF lipoproteins (d < 1.21 g/mL) were oxidized with 0.1 (lane 1), 1 (lane 2), and 10 mM AAPH (lane 3) or incubated without AAPH (lane 4) for 18 h at 37°C and the proteins separated by electrophoresis on a 12% sodium dodecyl sulfate-polyacrylamide gel and stained using the silver nitrate method. The protein bands corresponding to native apoE and apoA-I are marked and the molecular weight markers are shown in lane 5. Comparable protein patterns were observed for human CSF lipoproteins (not shown). (B,C) Native (lane 1) or oxidized human CSF lipoproteins (d < 1.21 g/mL) (lanes 2, 3, 4, 5 correspond to 0.5, 1, 5, and 10 mM AAPH, respectively) were separated by electrophoresis on a 12% sodium dodecyl sulfate-polyacrylamide gel and immunoblotted with anti-human apoA-I (B) and anti-human apoE (C) antibodies. The protein bands corresponding to native apoA-I and apoE are indicated and molecular weight markers are shown on the left. Comparable immunoreactivities were observed for bovine CSF lipoproteins (not shown). See Figure 1 for other abbreviations.

CSF lipoproteins have been described as "HDL-like" (2–4). However, differences between plasma HDL particles and CSF lipoproteins exist. The two major apolipoproteins in HDL are apoA-I and apoA-II (47), while in human and bovine CSF lipoproteins (d < 1.21 g/mL) the two main apolipoproteins are apoA-I and apoE (2,44,45). While apoA-I is synthesized in the periphery and presumably transported into the CNS (48), CNS apoE is made and secreted by astrocytes (49). The major fraction of CNS apoE is di-, tri-, or higher sialylated, a posttranslational modification not present in the major portion of human plasma apoE (2,5,7,49,50). In addition to these differences in apolipoproteins, the lipid composition of human CSF lipoproteins shows a greater similarity with brain lipids than with plasma lipoproteins (2,51). These observations underline the importance of the source (CSF vs. plasma) of the lipoproteins when examining their effects on neurons.

Effects of oxidized plasma lipoproteins on neurons have generally been observed after exposures lasting several hours to several days. Necrosis and apoptosis was observed in primary neurons and neuroblastoma cells after 24-h exposures to oxidized LDL at 10 to 100 μg/mL. Neurotoxicity could be inhibited by antioxidants in some cases suggesting that cell damage was mediated through oxidative stress initiated by

oxidized LDL (23–26). These findings demonstrate that *in vitro* neurons can be sensitive to oxidized plasma lipoproteins; however, *in vivo* neurons are unlikely to be exposed to oxidized LDL in the absence of severe disruption of the blood brain barrier (2,3,21,44). Oxidized plasma HDL particles from chicken have been shown to cause neuronal degeneration, disruption of microtubules and hyperphosphorylation of tau (27). These effects were dependent on the aggregation of HDL particles as a result of oxidation (27). We have never observed such aggregates in any of our native or oxidized CSF lipoprotein samples inspected by electron microscopy (not shown). In addition, as discussed above, CSF lipoproteins differ in their protein and lipid composition from plasma HDL. Also, in birds there is no evidence of apoE synthesis (52,53), the apolipoprotein central to the connection between CSF lipoproteins and AD (48,54).

The importance of species differences with respect to the effect of lipoproteins on cellular targets is demonstrated by our observation that human, but not bovine, oxidized CSF lipoproteins caused the disruption of neuronal microtubules. At this point, the reason(s) for the different effect of human and bovine oxidized CSF lipoproteins on microtubules is not clear. It is possible that species differences in apolipoproteins underlie different efficiencies in endocytosis of CSF lipoproteins. Oxidation of human and bovine CSF lipoproteins with AAPH resulted in covalent modifications of apoE and apoA-I and the appearance of higher molecular weight protein species. There was no obvious difference in the degree of these oxidation-induced protein modifications between human and bovine apolipoproteins, suggesting that the human and bovine apolipoproteins are equally susceptible to oxidation. Disruption of microtubules was observed only after incubation with the most heavily oxidized human CSF lipoproteins, which contained little if any native monomeric apolipoproteins. This raises the possibility that oxidized CSF lipoproteins are internalized into neurons by a different mechanism from native CSF lipoproteins. Studies analyzing plasma LDL suggest that oxidized lipoproteins are internalized by endocytotic pathways different from their native counterparts (55). However, the damaging effects of oxidized LDL observed in endothelial cells and erythrocytes are independent of receptor binding and endocytotic uptake of the oxidized LDL (56). In addition, the toxic effects of oxidized LDL on fibroblasts have been observed to lie within the lipid-extractable fraction, again suggesting that receptor-mediated endocytosis may not be required for the cytotoxicity induced by oxidized LDL (57). Similar experiments will have to be performed with the oxidized CSF lipoproteins to analyze the mechanism by which oxidized CSF lipoproteins exert their deleterious effects on neuronal microtubules.

Analysis of bovine CSF lipoproteins revealed substantial differences when compared to their human counterparts. The amount of protein in bovine CSF lipoprotein (9.1 μg/mL CSF) was approximately 50% of that measured in human CSF lipoproteins (21.2 μg/mL CSF; Ref. 21). The mass of lipids associated with CSF lipoproteins was also substantially less in bovine (2.4 μg/mL CSF) than that measured in human CSF (9.4 μg/mL CSF) using exactly the same method (21). To our knowledge this is the first detailed analysis of isolated bovine CSF lipoproteins. One other study quantified some of the lipid components in bovine CSF and reported undetectable triacylglycerol levels and higher cholesterol levels (45). Although the reasons for these differences are not clear, they at least partially might result from differences in biological material used and methods applied. These authors analyzed lipids in whole bovine CSF, while we determined lipid composition of isolated CSF lipoproteins. We used gas chromatography to quantify lipids, while Puppione *et al.* (45) analyzed the lipids using the less sensitive enzymatic kits. This might explain why they were unable to detect triglycerides, while we were able to detect low amounts of these lipids by gas chromatography. We assayed cholesterol levels with two different methods and were unable to detect cholesterol using an enzymatic kit and detected only low levels of cholesterol esters by gas chromatography. The cholesteryl ester levels we measured in bovine CSF lipoproteins (0.25 μg/mL CSF) are comparable to the ones we measured for human CSF lipoproteins (1.2 mg/mL CSF) using the same method when we take into consideration that the total lipid mass is fourfold lower in bovine than in human CSF (21). The higher cholesterol levels reported by Puppione *et al.* (45) might be due to the fact that they used bovine CSF from cows at parturition and postpartum, physiological conditions that the authors show have substantial effects on CSF cholesterol levels.

Another striking difference between human and bovine CSF lipoproteins was the difference in the amount of unsaturated fatty acids. Phospholipids are the main lipid component in human (69%) and bovine (67%) CSF lipoproteins. However, the levels of monounsaturated fatty acids (0.1%) as well as PUFA (7.4%) were much lower in bovine CSF lipoprotein phospholipids than in their human counterparts (20.9% monounsaturated and 19.9% polyunsaturated) (21). The same trend was observed for the triglycerides and cholesteryl esters. The reason for these low levels of unsaturated fatty acids in bovine CSF is difficult to explain given the present lack of knowledge of CSF lipoprotein metabolism. Bovines are ruminants, and PUFA undergo extensive biohydrogenation in the rumen (58); however, in humans the lipid composition of CSF lipoproteins has been shown to be different from plasma lipoproteins (2,51). An explanation for this observation likely has to await further progress in our understanding of brain lipid physiology.

It has been suggested that HNE is one of the molecules responsible for the toxic effects of oxidized LDL, since HNE-modified LDL or HNE by itself could mimic the effects of oxidized LDL (59,60). We have previously shown that HNE causes disruption of neuronal microtubules with a time course and pattern comparable to what we observed after incubation with oxidized human CSF lipoproteins (36). HNE is a product of the peroxidation of the n-6 PUFA 18:2 and 20:4 (61). It is therefore interesting that bovine CSF lipoproteins, which did not disrupt microtubules when oxidized, contained barely de-

tectable levels of 18:2 and very low levels of 20:4, whereas human CSF lipoproteins contain substantial amounts of these two PUFA (21). However, HNE is only one of many products formed during lipoprotein oxidation, and other products of lipoprotein oxidation may mediate the microtubule disruption caused by oxidized human CSF lipoproteins. We did not dialyze the CSF lipoproteins after oxidation in order to retain all oxidation products in our samples. To identify the molecules responsible for certain biological effects caused by oxidized lipoproteins and to analyze their mechanism of action remain a challenge for research in the fields of atherosclerosis and AD.

ACKNOWLEDGMENTS

This work was supported by NIH grants to Dr. Thomas J. Montine (AG00774 and AG16835) and to Dr. D.G. Graham (ES02611), by grants from the Alzheimer's Disease and Related Disorders Association and the American Foundation for Aging Research to Dr. Thomas J. Montine, and by NIH DK26657 (L.L.S.).

REFERENCES

1. Strittmatter, W.J., and Roses, A.D. (1995) Apolipoprotein E and Alzheimer Disease, *Proc. Natl. Acad. Sci. USA 92*, 4725–4727.
2. Pitas, R.E., Boyles, J.K., Lee, S.H., Hui, D., and Weisgraber, K.H. (1987) Lipoproteins and Their Receptors in the Central Nervous System. Characterization of the Lipoproteins in Cerebrospinal Fluid and Identification of Apolipoprotein B,E(LDL) Receptors in the Brain, *J. Biol. Chem. 262*, 14352–14360.
3. Borghini, I., Barja, F., Pometta, D., and James, R.W. (1995) Characterization of Subpopulations of Lipoprotein Particles Isolated from Human Cerebrospinal Fluid, *Biochim. Biophys. Acta 1255*, 192–200.
4. Guyton, J.R., Miller, S.E., Martin, M.E., Khan, W.A., Roses, A.D., and Strittmatter, W.J. (1998) Novel Large Apolipoprotein E-Containing Lipoproteins of Density 1.006–1.060 g/mL in Human Cerebrospinal Fluid, *J. Neurochem. 70*, 1235–1240.
5. Yamauchi, K., Tozuka, M., Hidaka, H., Hidaka, E., Kondo, Y., and Katsuyama, T. (1999) Characterization of Apolipoprotein E-Containing Lipoproteins in Cerebrospinal Fluid: Effect of Phenotype on the Distribution of Apolipoprotein E, *Clin. Chem. 45*, 1431–1438.
6. Ladu, M.J., Gilligan, S.M., Lukens, J.R., Cabana, V.G., Reardon, C.A., Van Eldik, L.J., and Holtzman, D.M. (1998) Nascent Astrocyte Particles Differ from Lipoproteins in CSF, *J. Neurochem. 70*, 2070–2081.
7. Rebeck, G.W., Alonzo, N.C., Berezovska, O., Harr, S.D., Knowles, R.B., Growdon, J.H., Hyman, B.T., and Mendez, A.J. (1998) Structure and Functions of Human Cerebrospinal Fluid Lipoproteins from Individuals of Different APOE Genotypes, *Exp. Neurol. 149*, 175–182.
8. Demeester, N., Castro, G., Desrumaux, C., De Geitere, C., Fruchart, J.C., Santens, P., Mulleners, E., Engelborghs, S., De Deyn, P.P., Vandekerckhove, J., *et al.* (2000) Characterization and Functional Studies of Lipoproteins, Lipid Transfer Proteins, and Lecithin:Cholesterol Acyltransferase in CSF of Normal Individuals and Patients with Alzheimer's Disease, *J. Lipid Res. 41*, 963–974.
9. Markesbery, W.R., and Carney, J.M. (1999) Oxidative Alterations in Alzheimer's Disease, *Brain Pathol. 9*, 133–146.
10. Lovell, M.A., Ehmann, W.D., Butler, S.M., and Markesbery, W.R. (1995) Elevated Thiobarbituric Acid-Reactive Substances and Antioxidant Enzyme Activity in the Brain in Alzheimer's Disease, *Neurology 45*, 1594–1601.
11. Montine, K.S., Kim, P.J., Olson, S.J., Markesbery, W.R., and Montine, T.J. (1997) 4-Hydroxy-2-nonenal Pyrrole Adducts in Human Neurodegenerative Disease, *J. Neuropathol. Exp. Neurol. 56*, 866–871.
12. Montine, K.S., Olson, S.J., Amarnath, V., Whetsell, W.O., Jr., Graham, D.G., and Montine, T.J. (1997) Immunohistochemical Detection of 4-Hydroxy-2-nonenal Adducts in Alzheimer's Disease Is Associated with Inheritance of APOE4, *Am. J. Pathol. 150*, 437–443.
13. Sayre, L.M., Zelasko, D.A., Harris, P.L., Perry, G., Salomon, R.G., and Smith, M.A. (1997) 4-Hydroxynonenal-Derived Advanced Lipid Peroxidation End Products Are Increased in Alzheimer's Disease, *J. Neurochem. 68*, 2092–2097.
14. Montine, K.S., Reich, E., Neely, M.D., Sidell, K.R., Olson, S.J., Markesbery, W.R., and Montine, T.J. (1998) Distribution of Reducible 4-Hydroxynonenal Adduct Immunoreactivity in Alzheimer Disease Is Associated with APOE Genotype, *J. Neuropathol. Exp. Neurol. 57*, 415–425.
15. Montine, T.J., Beal, M.F., Cudkowicz, M.E., O'Donnell, H., Margolin, R.A., Mcfarland, L., Bachrach, A.F., Zackert, W.E., Roberts, L.J., and Morrow, J.D. (1999) Increased CSF F2-Isoprostane Concentration in Probable AD, *Neurology 52*, 562–565.
16. Montine, T.J., Markesbery, W.R., Morrow, J.D., and Roberts, L.J.N. (1998) Cerebrospinal Fluid F_2-Isoprostane Levels Are Increased in Alzheimer's Disease, *Ann. Neurol. 44,* 410–413.
17. Mattson, M.P. (1998) Modification of Ion Homeostasis by Lipid Peroxidation: Roles in Neuronal Degeneration and Adaptive Plasticity, *Trends Neurosci. 21*, 53–57.
18. Kruman, I., Bruce-Keller, A.J., Bredesen, D., Waeg, G., and Mattson, M.P. (1997) Evidence That 4-Hydroxynonenal Mediates Oxidative Stress Induced Neuronal Apoptosis, *J. Neurosci. 17*, 5089–5100.
19. Mark, R.J., Lovell, M.A., Markesbery, W.R., Uchida, K., and Mattson, M.P. (1997) A Role for 4-Hydroxynonenal, an Aldehydic Product of Lipid Peroxidation, in Disruption of Ion Homeostasis and Neuronal Death Induced by Amyloid Beta-Peptide, *J. Neurochem. 68*, 255–264.
20. Esterbauer, H., Schmidt, R., and Hayn, M. (1997) Relationships Among Oxidation of Low-Density Lipoprotein, Antioxidant Protection, and Atherosclerosis, *Adv. Pharmacol. 38*, 425–456.
21. Montine, T.J., Montine, K.S., and Swift, L.L. (1997) Central Nervous System Lipoproteins in Alzheimer's Disease, *Am. J. Pathol. 151*, 1571–1575.
22. Lovell, M.A., Ehmann, W.D., Mattson, M.P., and Markesbery, W.R. (1997) Elevated 4-Hydroxynonenal in Ventricular Fluid in Alzheimer's Disease, *Neurobiol. Aging. 18*, 457–461.
23. Keller, J.N., Hanni, K.B., and Markesbery, W.R. (1999) Oxidized Low Density Lipoprotein Induces Neuronal Death: Implications for Calcium, Reactive Oxygen Species, and Caspases, *J. Neurochem. 72*, 2601–2609.
24. Keller, J.N., Hanni, K.B., Pedersen, W.A., Cashman, N.R., Mattson, M.P., Gabbita, S.P., Friebe, V., and Markesbery, W.R. (1999) Opposing Actions of Native and Oxidized Lipoprotein on Motor Neuron-Like Cells, *Exp. Neurol. 157*, 202–210.
25. Papassotiropoulos, A., Ludwig, M., Naib-Majani, W., and Rao, G.S. (1996) Induction of Apoptosis and Secondary Necrosis in Rat Dorsal Root Ganglion Cell Cultures by Oxidized Low Density Lipoprotein, *Neurosci. Lett. 209*, 33–36.
26. Sugawa, M., Ikeda, S., Kushima, Y., Takashima, Y., and Cynshi, O. (1997) Oxidized Low Density Lipoprotein Caused CNS Neuron Cell Death, *Brain Res. 761*, 165–172.
27. Kivatinitz, S.C., Pelsman, M.A., Alonso, A.C., Bagatolli, L., and Quiroga, S. (1997) High-Density Lipoprotein Aggregated by Oxidation Induces Degeneration of Neuronal Cells, *J. Neurochem. 69*, 2102–2114.
28. Bassett, C.N., Neely, M.D., Sidell, K.R., Markesbery, W.R.,

Swift, L.L., and Montine, T.J. (1999) Cerebrospinal Fluid Lipoproteins Are More Vulnerable to Oxidation in Alzheimer's Disease and Are Neurotoxic When Oxidized *ex vivo*, *Lipids 34*, 1273–1280.
29. Terry, R., and Wisniewski, H. (1970) The Ultrastructure of the Neurofibrillary Tangle and the Senile Plaque, in *CIBA Foundation Symposium on Alzheimer's Disease and Related Conditions* (Wolstenholme, G., and O'Connor, M., eds.) pp.145–168, J&A Churchill, London.
30. Gray, E.G., Paula-Barbosa, M., and Roher, A. (1987) Alzheimer's Disease: Paired Helical Filaments and Cytomembranes, *Neuropath. Appl. Neurobiol. 13*, 91–110.
31. Paula-Barbosa, M., Tavares, M.A., and Cadete-Leite, A. (1987) A Quantitative Study of Frontal Cortex Dendritic Microtubules in Patients with Alzheimer's Disease, *Brain Res. 417*, 139–142.
32. Metuzals, J., Robitaille, Y., Houghton, S., Gauthier, S., Kang, C.Y., and Leblanc, R. (1988) Neuronal Transformations in Alzheimer's Disease, *Cell Tissue Res. 252*, 239–248.
33. Kowall, N.W., and Kosik, K.S. (1987) Axonal Disruption and Aberrant Localization of Tau Protein Characterize the Neuropil Pathology of Alzheimer's Disease, *Ann. Neurol. 22*, 639–643.
34. Lee, V.M. (1996) Regulation of Tau Phosphorylation in Alzheimer's Disease, *Ann. NY Acad. Sci. 777*, 107–113.
35. Goedert, M. (1996) Tau Protein and the Neurofibrillary Pathology of Alzheimer's Disease, *Ann. NY Acad. Sci. 777*, 121–131.
36. Neely, M.D., Sidell, K.R., Graham, D.G., and Montine, T.J. (1999) The Lipid Peroxidation Product 4-Hydroxynonenal Inhibits Neurite Outgrowth, Disrupts Neuronal Microtubules, and Modifies Cellular Tubulin, *J. Neurochem. 72*, 2323–2333.
37. Montine, K.S., Bassett, C.N., Ou, J.J., Markesbery, W.R., Swift, L.L., and Montine, T.J. (1998) Apolipoprotein E Allelic Influence on Human Cerebrospinal Fluid Apolipoproteins, *J. Lipid Res. 39*, 2443–2451.
38. Esterbauer, H., and Ramos, P. (1995) Chemistry and Pathophysiology of Oxidation of LDL, in *Reviews of Physiology, Biochemistry and Pharmacology* (Blaustein, M.P., Grunicke, H., Habermann, E., Pette, D., Reuter, H., Sakmann, B., Schultz, G., Schweiger, M., and Weibel, E.R., eds.) Vol. 127, pp. 31–64, Springer, Berlin.
39. Laemmli, U.K. (1970) Cleavage of Structural Proteins During the Assembly of the Head of Bacteriophage T4, *Nature 227*, 680–685.
40. Swift, L.L. (1995) Assembly of Very Low Density Lipoproteins in Rat Liver: A Study of Nascent Particles Recovered from the Rough Endoplasmic Reticulum, *J. Lipid Res. 36*, 395–406.
41. Morrison, W., and Smith, L. (1964) Preparation of Fatty Acid Methyl Esters and Dimethylacetals from Lipids with Boron Fluoride-Methanol, *J. Lipid Res. 5*, 600–608.
42. Babson, A., Shapiro, P., and Phillips, G. (1962) A New Assay for Cholesterol and Cholesterol Esters in Serum Which Is Not Affected by Bilirubin, *Clin. Chim. Acta 7*, 800–804.
43. Olmsted, J.B., Carlson, K., Klebe, R., Ruddle, F., and Rosenbaum, J. (1970) Isolation of Microtubule Protein from Cultured Mouse Neuroblastoma Cells, *Proc. Natl. Acad. Sci. USA 65*, 129–136.
44. Roheim, P.S., Carey, M., Forte, T., and Vega, G.L. (1979) Apolipoproteins in Human Cerebrospinal Fluid, *Proc. Natl. Acad. Sci. USA 76*, 4646–4649.
45. Puppione, D.L., Fischer, W.H., Park, M., Gazal, O.S., and Williams, G.L. (1998) Microsequencing of Bovine Cerebrospinal Fluid Apolipoproteins: Identification of Bovine Apolipoprotein E, *Lipids 33*, 781–786.
46. Haberland, M.E., and Steinbrecher, U.P. (1992) Modified Low-Density Lipoproteins: Diversity and Biological Relevance in Atherogenesis, in *Molecular Genetics of Coronary Artery Disease: Candidate Genes and Processes in Atherosclerosis* (Lusis, A.J., Rotter, J.I., and Sparks, R.S., eds.) Vol. 14, pp. 35–61, Karger, New York.
47. Scanu, A.M., Edelstein, C., and Keim, P. (1975) Serum Lipoproteins, in *The Plasma Proteins* (Putnam, F.W., ed.) Vol. 1, pp. 317–491, Academic Press, New York.
48. Beffert, U., Danik, M., Krzywkowski, P., Ramassamy, C., Berrada, F., and Poirier, J. (1998) The Neurobiology of Apolipoproteins and Their Receptors in the CNS and Alzheimer's Disease, *Brain Res. Brain Res. Rev. 27*, 119–142.
49. Pitas, R.E., Boyles, J.K., Lee, S.H., Foss, D., and Mahley, R.W. (1987) Astrocytes Synthesize Apolipoprotein E and Metabolize Apolipoprotein E-Containing Lipoproteins, *Biochim. Biophys. Acta 917*, 148–161.
50. Zannis, V.I., Breslow, J.L., Utermann, G., Mahley, R.W., Weisgraber, K.H., Havel, R.J., Goldstein, J.L., Brown, M.S., Schonfeld, G., Hazzard, W.R., *et al.* (1982) Proposed Nomenclature of ApoE Isoproteins, ApoE Genotypes, and Phenotypes, *J. Lipid Res. 23,* 911–914.
51. Illingworth, D.R., and Glover, J. (1971) The Composition of Lipids in Cerebrospinal Fluid of Children and Adults, *J. Neurochem. 18*, 769–776.
52. Jackson, R.L., Morrisett, J.D., and Gotto, A.M., Jr. (1976) Lipoprotein Structure and Metabolism, *Physiol. Rev. 56*, 259–316.
53. Hermier, D., and Dillon, J.C. (1992) Characterization of Dietary-Induced Hypercholesterolemia in the Chicken, *Biochim. Biophys. Acta 1124*, 178–184.
54. Weisgraber, K.H., and Mahley, R.W. (1996) Human Apolipoprotein E: the Alzheimer's Disease Connection, *FASEB J. 10*, 1485–1494.
55. Dhaliwal, B.S., and Steinbrecher, U.P. (1999) Scavenger Receptors and Oxidized Low Density Lipoproteins, *Clin. Chim. Acta 286*, 191–205.
56. Borsum, T., Henriksen, T., Carlander, B., and Reisvaag, A. (1982) Injury to Human Cells in Culture Induced by Low Density Lipoprotein: An Effect Independent of Receptor Binding and Endocytotic Uptake of Low Density Lipoprotein, *Scand. J. Clin. Lab. Invest. 42*, 75–81.
57. Hessler, J.R., Morel, D.W., Lewis, L.J., and Chisolm, G.M. (1983) Lipoprotein Oxidation and Lipoprotein-Induced Cytotoxicity, *Arteriosclerosis 3*, 215–222.
58. Noble, R.C. (1978) Digestion, Absorption and Transport of Lipids in Ruminant Animals, *Prog. Lipid Res. 17*, 55–91.
59. Hoff, H.F., Chisolm, G.M. III, Morel, D.W., Juergens, G., and Esterbauer, H. (1988) Chemical and Functional Changes in LDL Following Modification by 4-Hydroxynonenal, in *Oxy-Radicals in Molecular Biology and Pathology,* (Cerutti, P.A., Fridovich, I., and Mccord, J.M., eds.) pp. 459–472, Alan R. Liss, Inc., New York.
60. Suc, I., Meilhac, O., Lajoie-Mazenc, I., Vandaele, J., Jurgens, G., Salvayre, R., and Negre-Salvayre, A. (1998) Activation of EGF Receptor by Oxidized LDL, *FASEB J. 12*, 665–671.
61. Esterbauer, H. (1982) Aldehydic Products of Lipid Peroxidation, in *Free Radicals, Lipid Peroxidation and Cancer* (McBrien, D.C.H., and Slater, T.F., eds.) pp.101–128, Academic Press, London.

[Received March 20, 2000, and in revised form July 14, 2000; revision accepted September 7, 2000]

Involvement of the Ceramide Signaling Pathway in Modulating the Differentiated State of Porcine Thyroid Cells

C. Schneider, N. Delorme, N. Buisson-Legendre, G. Bellon, H. Emonard, H. El btaouri, W. Hornebeck, B. Haye, and L. Martiny*

Université de Reims Champagne-Ardenne, UFR de Médecine et de Sciences, 51687 Reims Cedex 2, France

ABSTRACT: Neutral sphingomyelinase (Smase) is a cell membrane-associated phospholipase that hydrolyzes sphingomyelin to phosphocholine and ceramide, a lipid second messenger involved in cell differentiation and/or apoptosis. We first evidenced that porcine cultured thyroid cells could express neutral Smase activity even if thyrotropin (TSH), an essential hormone in thyroid cell differentiation, was found to induce a 1.7-fold decrease in Smase activity. Triggering the ceramide pathway by exogenous addition of neutral bacterial Smase (0.1 U/mL for 48 h), which transiently increased ceramide level by fourfold, drastically modified thyroid cell morphology. The follicle-like structures generated by TSH were disrupted, and the Smase-induced cell spreading was accompanied by a parallel loss of cell ability to iodinate proteins as well as a decrease of the adenylate cyclase system response. These inhibitory effects have been reproduced using short-chain exogenous ceramide analogs (C_2-ceramides). Overall these data showed that ceramides emerged as potential mediators of dedifferentiation in thyroid cells.

Paper no. L8446 in *Lipids 35,* 1259–1268 (November 2000).

In the presence of thyrotropin (TSH), porcine thyroid cells reconstituted follicle-like structures similar to those found *in vivo*. This polarized cell organization is closely related to the expression of thyroid cell function (1). TSH exerts its effects on cell behavior mainly *via* the cAMP cascade, since forskolin (F), a classical adenylate cyclase activator, mimicks TSH effects on cell morphology and differentiated status.

Otherwise, the absence of hormone or a long-term treatment with phorbol myristate acetate (PMA) promotes the destabilization of the follicular structures, which form a monolayer. The initial steps of signal transduction involved in the control of differentiated porcine thyroid cells cultures are the subject of the present report.

During the last decade, neutral sphingomyelinase (Smase), a cell membrane-associated phospholipase that hydrolyzes sphingomyelin (SM) to phosphocholine and ceramide, has been described in many tissues (2) including FRTL-5 cells (3); however, its presence in normal thyroid cells had never been demonstrated. It has been shown that ceramides activate different signaling pathways involved in apoptosis as well as differentiation (4,5). Ceramides appear to induce typical morphological changes in many types of cells (6–8). SM hydrolysis is induced by cytokines such as tumor necrosis factor α (TNF α), interleukin-1β (IL1β), nerve growth factor (NGF), and interferon γ (IFN γ), and by cross-linking of Fas, and also by physical stresses such as heat shock, radiation, and chemotherapeutic drugs (9).

The exact role of ceramides remains to be elucidated, but it can be suggested that ceramides act as an important regulator of antiproliferative and apoptotic pathways and as an inhibitor of protein trafficking and secretion.

In this paper we demonstrated that porcine thyroid cells in culture display Smase activity. SM hydrolysis is down regulated by TSH, which physiologically controls cell differentiation. Increasing the cellular content of ceramide, in TSH-treated cells, with exogenous Smase led to dedifferentiation of thyroid cells with a progressive loss of functional activity.

EXPERIMENTAL PROCEDURES

Primary cultures of porcine thyroid cells. The preparation of thyroid cells has been described in detail elsewhere (10). Briefly, thyroid epithelial cells were isolated from adult porcine glands by a discontinuous trypsin-EGTA treatment. Freshly isolated cells suspended at a concentration of 10^6 cells/mL in Eagle's minimum essential medium (pH 7.4), containing 10% (vol/vol) fetal calf serum, penicillin (200 U/mL), streptomycin sulfate (0.05 mg/mL), and TSH (1 mU/mL) were plated directly onto 24-well poly (L-lysine)-treated culture dishes at the density of 10^6 cells per well, and incubated at 37°C in a 95% air/5% CO_2 atmosphere. Two days after the onset of cultures, the medium was withdrawn and replaced for metabolic experiments with fresh "serum-free" medium containing either Smase, truncated ceramide (C_2-Cer 1-20 μM), or other agonists for 2 d in the presence of TSH 1 mU/mL. The morphology of cells was examined using phase contrast micrography (Olympus IMT 2, magnification × 37.5).

*To whom correspondence should be sent at Laboratoire de Biochimie, UFR Sciences, IFR 53 Biomolécules, UPRES-A CNRS 6021, BP 1039, 51687 Reims Cedex 2, France. E-mail: laurent.martiny@univ-reims.fr

Abbreviations: DAG, diacylglycerol; ECM, extracellular matrix; EGF, epidermal growth factor; F, forskolin; FITC, fluorescein isothiocyanate; ILIβ, interleukin-1β; IMBX, isomethylbutyl xanthine; IFN γ, interferon gamma; PBI, protein bound iodine; PBS, phosphate-buffered saline; PI, phosphatidylinositol; PMA, phorbol myristate acetate; PS, phosphatidylserine; SM, sphingomyelin; Smase, sphingomyelinase; TSH, thyrotropin; TNF α, tumor necrosis factor α.

Thyroid protein iodination. Cells seeded in plastic dishes were cultured as indicated above. At day 4, they were rinsed with 20 mM Earle's Hepes buffer (pH 7.2) and incubated for 45 min at 37°C in the same buffer containing 1 μCi Na [^{125}I]. Factors were added to the medium at concentrations indicated in the legends of figures. At the end of the incubation period, the cells were rinsed with Earle's Hepes buffer containing 0.1 mM KI and 5 mg/mL bovine serum albumin. Proteins were precipitated with ice-cold trichloroacetic acid [10% final (wt/vol)]. After centrifugation (5,000 × *g* for 5 min), the pellets were resuspended and washed twice with cold 10% (wt/vol) trichloroacetic acid and counted as protein-bound iodine (PB^{125}I).

cAMP assay. Cells seeded in plastic dishes were cultured as indicated above. At day 4, they were rinsed with 20 mM Earle's Hepes buffer (pH 7.2) and incubated for 5 min at 37°C in the same buffer containing 1 mM isomethylbutyl xanthine (IBMX) and TSH (10 mU/mL). Reactions were stopped by the addition of 1 M final concentration of $HClO_4$ followed by immersion into an ice bath. The cells were homogenized and their cAMP contents quantified by a radioimmunological method as described by Cailla *et al*. (11), except that bound and free ligand were separated by precipitation of bound ligand with a mixture of γ-globulin (2.5 mg/mL) in citrate buffer (pH 6.2) and polyethyleneglycol 6000 (20 g in 100 mL water).

SM quantification. For SM quantification, $8{\cdot}10^6$ thyroid cells were cultured for 48 h with TSH (1 mU/mL) and then incubated for a period of 48 h in a total volume of 4 mL of complete medium containing 0.4 μCi/mL of [methyl-^{3}H]choline (sp. act. 81.0 Ci/mmol, Dupont de Nemours NEN, Les Ulis, France). Cells were then washed and resuspended in serum-free medium with or without bacterial Smase (sp. act. 180 U/mg; BioMol®, Philadelphia, PA) for acute treatments. Cell supernatants were then withdrawn and cells were collected, resuspended in PBS (phosphate-buffered saline), and frozen. For extraction and separation of labeled SM, frozen cells were thawed and sonicated for 3 × 15 s. An aliquot was taken for protein determination (12), and the remainder was extracted with 2.5 mL of chloroform/methanol, (2:1, by vol), vortex-mixed, and centrifuged at 1,000 × *g* for 15 min. Labeled SM was isolated according to Jaffrezou *et al*. (13).

Ceramide quantification. Ceramide levels were quantified by the diacylglycerol (DAG) kinase assay (14). Briefly, monolayers of thyroid cells cultured as described above were stimulated with Smase for various periods. The medium was removed, and cells were collected in PBS by scraping and centrifugation. Total cellular lipids were then extracted using the method of Bligh and Dyer (15), and the organic phase was dried under a nitrogen stream. The resulting lipids were resuspended in 20 μL solubilization buffer (cardiolipin 5 mM, diethylenetriaminepentaacetic acid 1 mM, octylglucopyranoside 7.5% wt/vol). To the solubilized lipids, 80 μL of imidazole buffer (50 mM, pH 6.5) containing NaCl (50 mM), EGTA (1 mM), $MgCl_2$ (12.5 mM), 50 μCi [^{32}P-γ]ATP (sp. act. 3000 Ci/mmol, Dupont de Nemours NEN) and DAG kinase (10 μL/63 mU) was added. After incubation for 30 min at 25°C, the reaction was stopped by extraction with 3 mL of methanol/chloroform (2:1, vol/vol), 1.7 mL of 1% (wt/vol) $HClO_4$, and 1 mL of chloroform. The organic phase was washed twice with 2 mL of 1% (wt/vol) $HClO_4$, and an aliquot (0.5 mL) was dried under a nitrogen stream. The lipids were then resuspended in 100 μL of chloroform/methanol (100:5, vol/vol). An aliquot (20 μL) of the lipid solution was then applied to a thin-layer chromatographic plate (silica gel 60; Merck, Darmstadt, Germany) and developed in chloroform/methanol/acetic acid (65:15:5, by vol). The dried plate was autoradiographed and ceramide-1-phosphate (R_f = 0.14) spots were scraped off and counted. For ceramide levels, quantification of known amounts of commercial ceramides (0–80 pmol) was performed to generate a standard curve.

Neutral Smase assay. Membranes were prepared from thyroid cells as follows. Cells were washed with PBS and homogenized in lysis buffer (20 mM Tris-HCl pH 7.5, 2 mM EDTA, 5 mM EGTA, 1 mM phenylmethylsulfonyl fluoride, 10 μg/mL leupeptin, 10 μg/mL aprotinin, and 1 mM sodium orthovanadate) with 10 strokes in a Dounce homogenizer and centrifuged at 30,000 × *g* for 20 min. The resulting pellet was suspended in reaction buffer (150 mM NaCl, 25 mM Hepes pH 7.5, 5 mM EGTA, 1 mM EDTA, 3 mM $MgCl_2$, 40 mM β-glycerophosphate, 200 μM octylglucoside). Smase activity was quantified using 4,4-difluoro-5,7-dimethyl-4-bora-3a,4a-diaza-*S*-indacene-3-propionyl-sphingomyelin (D-3522; Molecular Probes, Eugene, OR) fluorescent substrate, essentially as described by Ella *et al*. (16).

Apoptosis assay. A fluorescein isothiocyanate (FITC) conjugate of the phosphatidylserine (PS)-binding protein, annexin V, has been used previously to detect PS externalization in apoptotic cells (17–19). The cells were washed with 0.5 mL of PBS and resuspended in 200 μL of binding buffer containing Hepes 10 mM (pH 7.4), NaCl 140 mM, $CaCl_2$ 5 mM, and propidium iodine 50 μg/mL. FITC-annexin V solution (5 μL) and phosphatidylinositol (PI) solution (5 μL at a final concentration of 0.5 μg/mL) were added. After gentle mixing, the cell suspension was stored in the dark at room temperature for 10 min and then analyzed using microscopy fluorescence (510 nm emission filter) to visualize the green FITC fluorescence and 580 nm filter to detect the red PI staining.

Statistical analysis. Statistical analysis of data was performed using Student's *t*-test. Differences were considered as statistically significant for *P* values lower than 0.05.

RESULTS

The presence of TSH in the culture medium is essential for a correct expression of thyroid function, which is related to the reorganization of isolated cells into polarized multicellular structures (Fig. 1A). A similar morphological situation is observed when thyroid cells are cultured in the presence of F (Fig. 1B) suggesting a cAMP-dependent mechanism. In contrast, the follicular structures are destabilized under stimulation by phorbol ester or in absence of TSH (Figs. 1C and 1D).

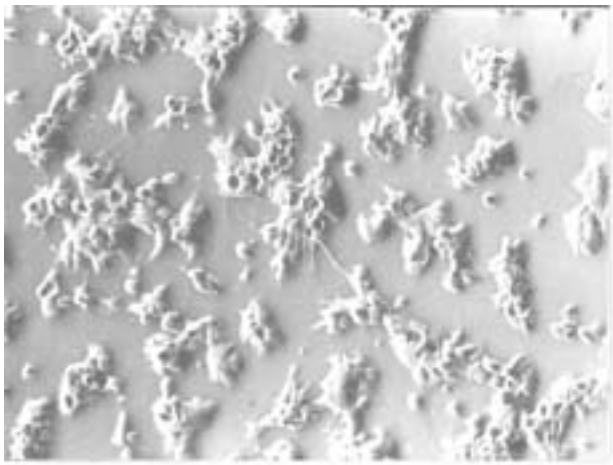

A. TSH-cells

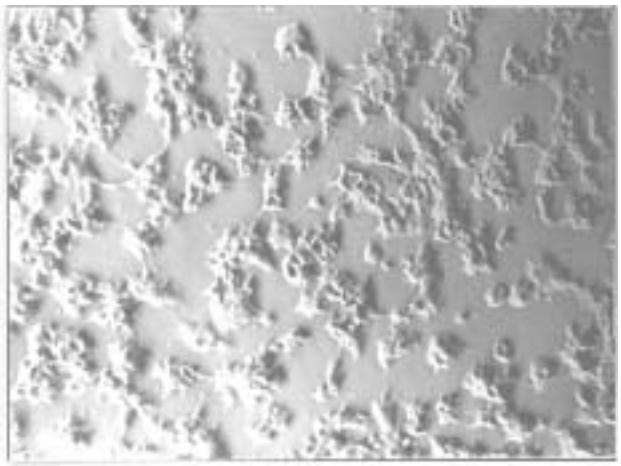

B. Forskolin-cells

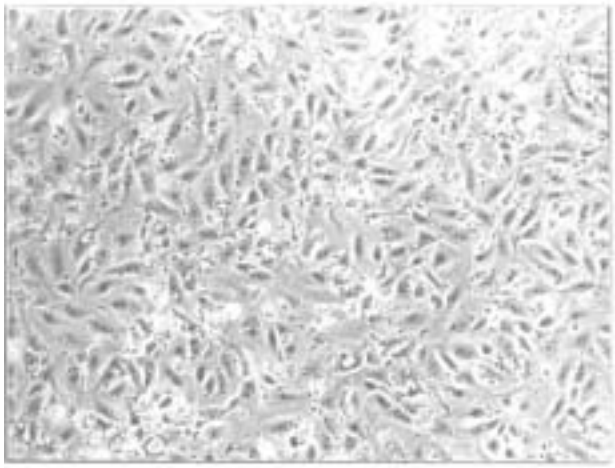

C. PMA-cells

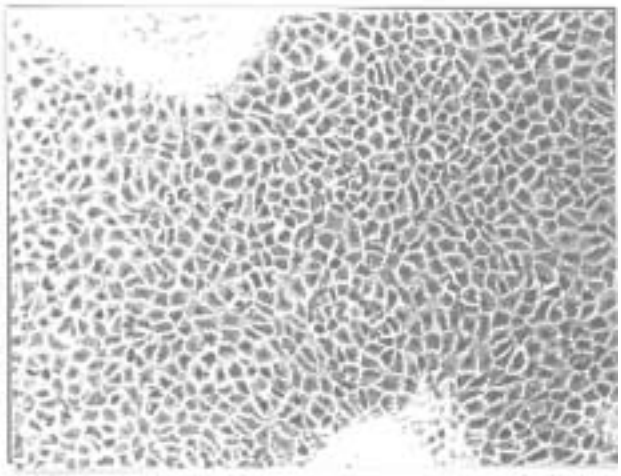

D. Control-cells

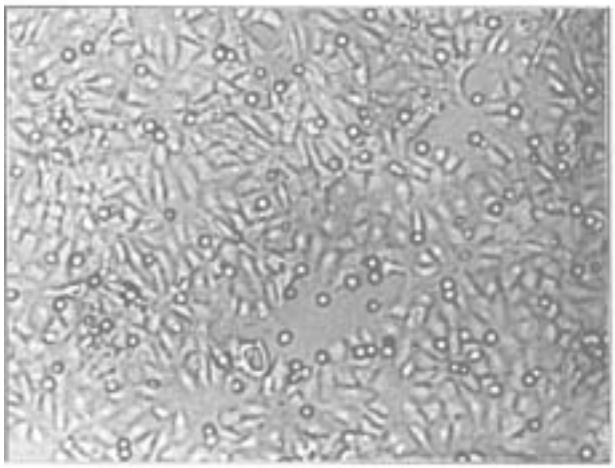

E. TSH-cells 48 hours after sphingomyelinase treatment

FIG. 1. Influence of different culture treatments on the morphology of porcine thyroid cells. Phase-contrast microscopy of living cells in presence of various agonists. (A) Cells treated with thyrotropin (TSH) (1 mU/mL). (B) Cells treated with Forskolin (F) (10^{-5} M). (C) Cells treated with phorbol myristate acetate (PMA) (10^{-7} M). (D) Cells cultured without agonist. (E) Cells treated with sphingomyelinase (Smase) 0.1 U/mL.

Follicle disruption rapidly leads to the constitution of a monolayer displaying a fibroblastic phenotype.

Increasing the intracellular levels of ceramides by addition of exogenous bacterial Smase induces conspicuous morphological changes. Treatment of thyroid cells for 48 h promotes a progressive spreading of the cells as shown on Figure 1E. This phenomenon could be attributed to a modification in extracellular matrix (ECM) remodeling, since during that time no cell proliferation was observed.

The Smase activity measured under different culture conditions allowed us to suggest a strong relationship between ceramide level and the maintenance of differentiated phenotype and thyroid function.

Therefore, neutral Smase activity of thyroid cells was found to be negatively regulated by TSH as shown in Figure 2A. Control cells and PMA-treated cells exhibited a 1.7-fold higher neutral Smase activity as compared to TSH cells or F-treated cells.

Moreover, basal ceramide levels were measured under the same culture conditions (Fig. 2B) and exhibited a pattern in

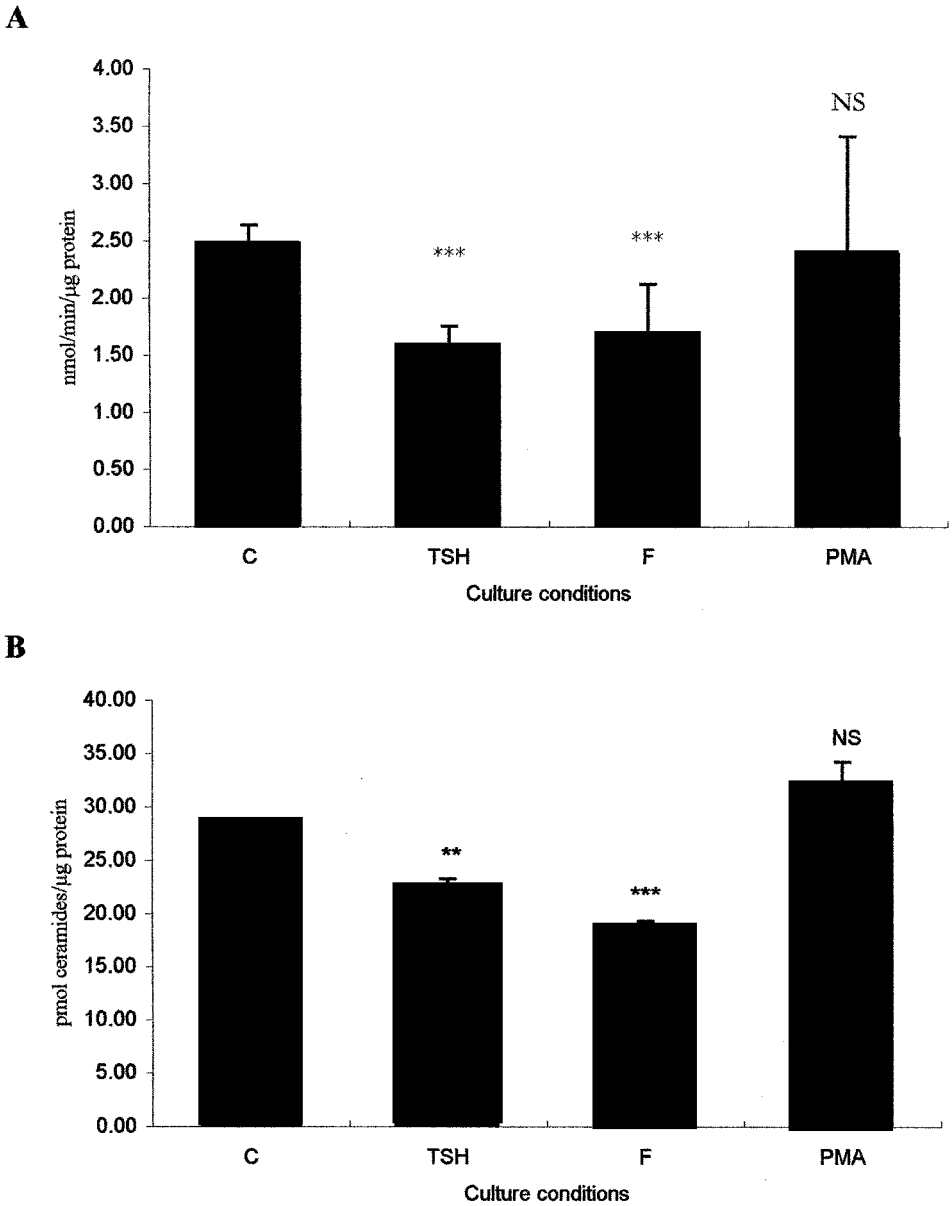

FIG. 2. Effects of culture conditions on (A) neutral Smase activity and (B) ceramides basal levels in porcine thyroid cells. Cells were treated for 96 h with TSH (1 mU/mL), F (10^{-5} M), PMA (10^{-7} M), or (C) without any agonist. (A) Membranes were prepared and Smase activity was quantified using 4,4-difluoro-5,7-dimethyl-4-bora-3a,4a-diaza-*S*-indacene-3-propionyl-sphingomyelin (SM) as substrate (as described in the Experimental Procedures section). (B) After total lipid extraction, amount of ceramide was quantified using diacylglycerol kinase method. Each data point represents the average ± SEM of triplicate. NS, nonsignificant, $^{**}P < 0.001$, $^{***}P < 0.0001$. See Figure 1 for abbreviations.

agreement with the neutral Smase activity: higher levels in control and in PMA cells compared to F and TSH cells (30 pmol vs. 20 pmol).

To analyze the existence of a ceramide signaling pathway in porcine thyroid cells, we evaluated the effect of exogenous bacterial Smase on ceramide and SM production. Figure 3 demonstrates that exogenous Smase induced a rapid increase of intracellular ceramides (3.5-fold) after 5 min of treatment, with a parallel decrease of SM (50%) level at the same time. Then, amounts of ceramides and SM progressively reached a plateau after 45 min of treatment with exogenous Smase. These results are in agreement with the existence of the SM/ceramide cycle in porcine thyroid cells since we observed a rapid and transient increase in ceramide levels coupled to the disappearance of its precursor. This increase supported the hypothesis of a putative role of second messenger for ceramides issued from SM hydrolysis.

Since DAG kinase tests are controversial (20), we have confirmed our results by metabolic labeling with [9,10-^{3}H]-palmitic acid both on ceramide production and SM degradation (data not shown).

The capacity to organify iodine reflects thyroid cells' biological activity. Figure 4 shows the dose-dependent effect of exogenous Smase on the ability of porcine thyroid cells cultured for 4 d with TSH (0.1 U/mL) to iodinate proteins; PBI was significantly inhibited by Smase with a 50% inhibition at 0.1 U/mL. To demonstrate that the effect of Smase was not simply due to any disturbing effect on membrane structure, a ceramidase inhibitor (which provokes an accumulation of intracellular ceramides by blocking their metabolism to sphingosine) was added together with Smase to cell culture medium. Under such experimental conditions, the ceramidase inhibitor also potentiated the Smase effect even though the lack of specificity of *N*-oleyl ethanolamine must be taken into consideration.

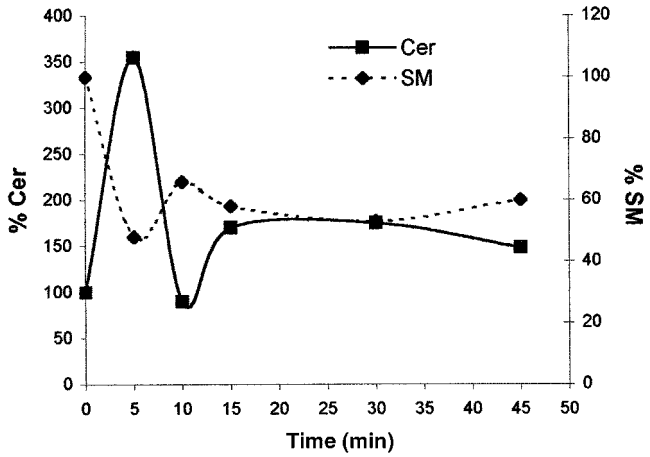

FIG. 3. Effect of exogenous bacterial Smase on ceramide (cer) and sphingomyelin (SM) levels in TSH-treated thyroid cells. Cells were treated for the indicated times with 0.1 U/mL Smase, lipids were extracted, and cer and Smase were then quantified as described in the Experimental Procedures section. One hundred percent is defined as the basal level. This experiment was repeated three or more times with identical results. See Figure 1 for other abbreviations.

An effect on adenylate cyclase activity was also evidenced (Fig. 5). Following 4 d of culture with TSH (0.1 mU/mL),

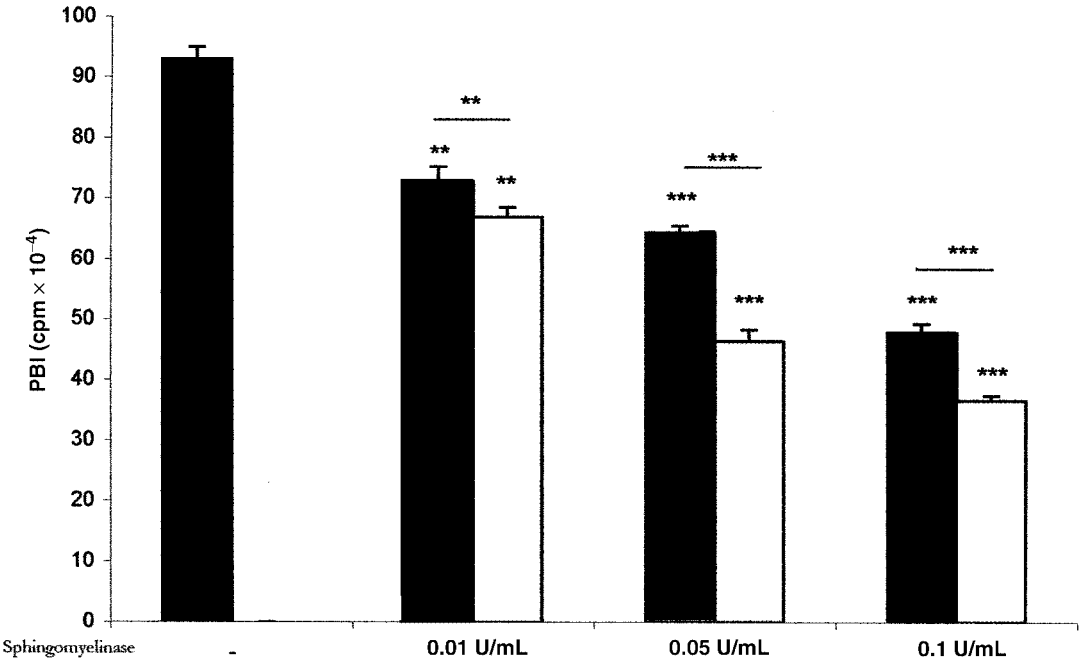

FIG. 4. Effect of exogenous Smase on protein iodination. Thyroid cells were cultured 4 d in the presence of TSH (0.1 mU/mL). After washing, aliquots of thyroid cell suspension were treated for 45 min with Smase (solid column) or Smase and ceramidase inhibitor *N*-oleoylethanolamine (1 μM: open column) at the concentration indicated. Protein-bound iodine (PBI) was measured as described in the Experimental Procedures section. Each data point represents the average ± SEM of triplicate. NS, nonsignificant, $^*P < 0.05$, $^{**}P < 0.001$, $^{***}P < 0.0001$. See Figure 1 for other abbreviations.

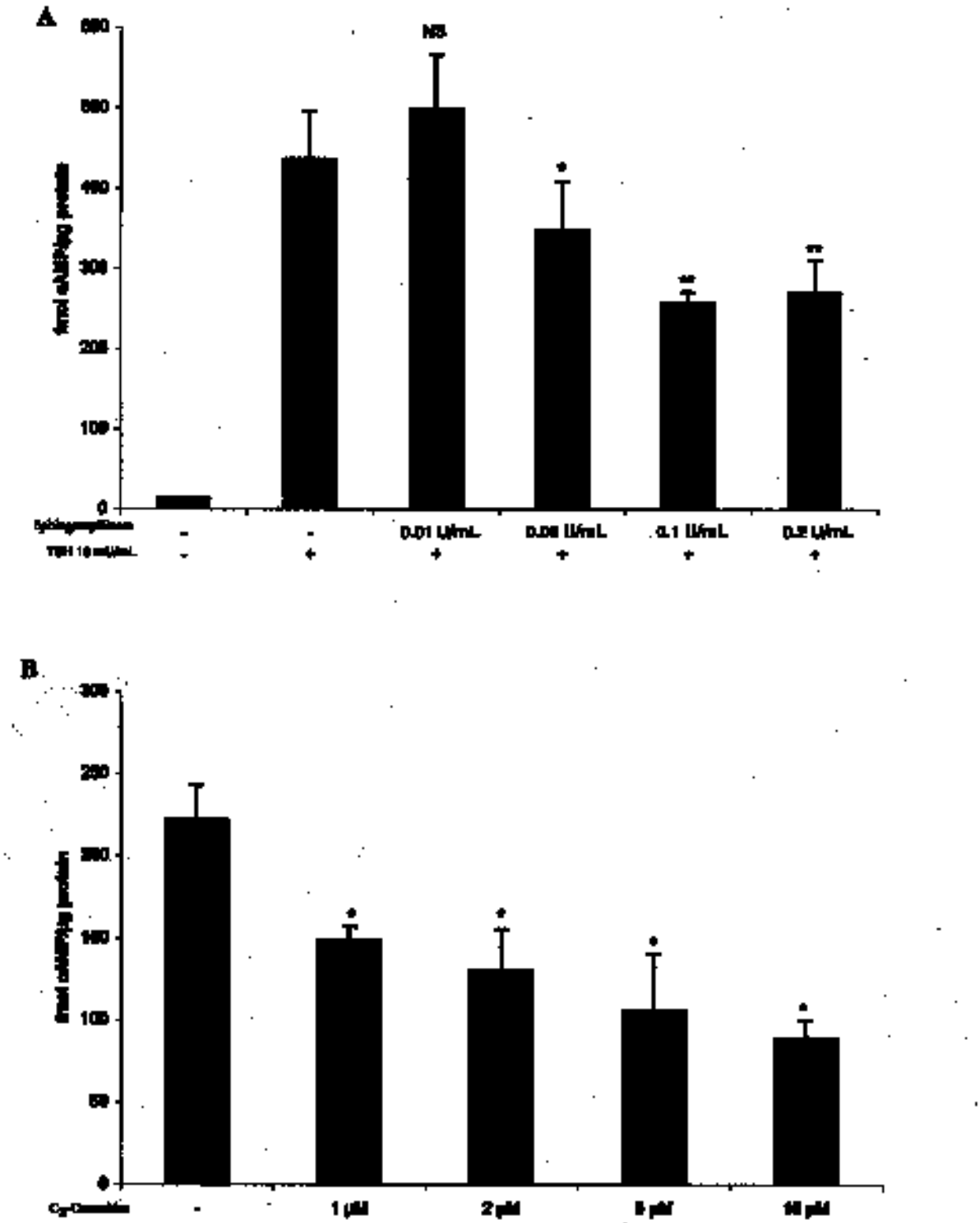

FIG. 5. Effect of exogenous Smase on cAMP accumulation. Reconstituted thyroid follicles were cultured for 4 d with TSH (0.1 mU/mL). (A) Aliquots of washed thyroid cell suspension were incubated for 5 min with TSH (10 mU/mL), IMBX (10^{-3} M), and with Smase at the concentration indicated. (B) Aliquots of washed thyroid cell suspension were incubated for 5 min with TSH (10 mU/mL), IMBX (10^{-3} M), and with C_2-ceramides in a range of 1 to 10 μM. cAMP was measured as described in the Experimental Procedures section. Each data point represents the average ± SEM of triplicate determinations. NS, nonsignificant, $*P < 0.05$, $**P < 0.001$, $***P < 0.0001$. IMBX, isomethylbutyl xanthine; for other abbreviations see Figure 1.

washed thyroid cells were incubated 5 min in the presence of TSH (10 mU/mL) and IBMX (10^{-3} M), an inhibitor of phosphodiesterases. Under these conditions, a dose-dependent inhibition of TSH-stimulated cAMP production by Smase was obtained (Fig. 5A). A 55% maximal extent of inhibition was reached using 0.1 U/mL Smase (598 fmol/μg protein vs. 270 fmol/μg protein). In parallel, we reproduced these observations using C_2-ceramides, which inhibited cAMP production in a dose-dependent manner (Fig. 5B).

The physiological relevance of the ceramide signaling pathway has been considered by studying the apoptotic process under different conditions. We measured apoptosis after a 24-h treatment period in the presence of 20 μM C_2-ceramides or in the presence of 0.5 U/mL Smase using two distinct methods. We measured either the fluorescence linked to the intercalation of bis-benzamidine intercalation in DNA in order to analyze chromatin condensation or annexin V-FITC to visualize PS flip-flop.

Figure 6 showed that addition of Smase (0.5 U/mL) for 24 h in the culture medium had no effect on these two parameters (Figs. 6A and 6C) in spite of important morphological changes as shown in Figure 1D. In contrast, permeant C_2-ceramides (20 μM) used under a similar experimental procedure induced chromatin condensation as underlined with arrows in Figure

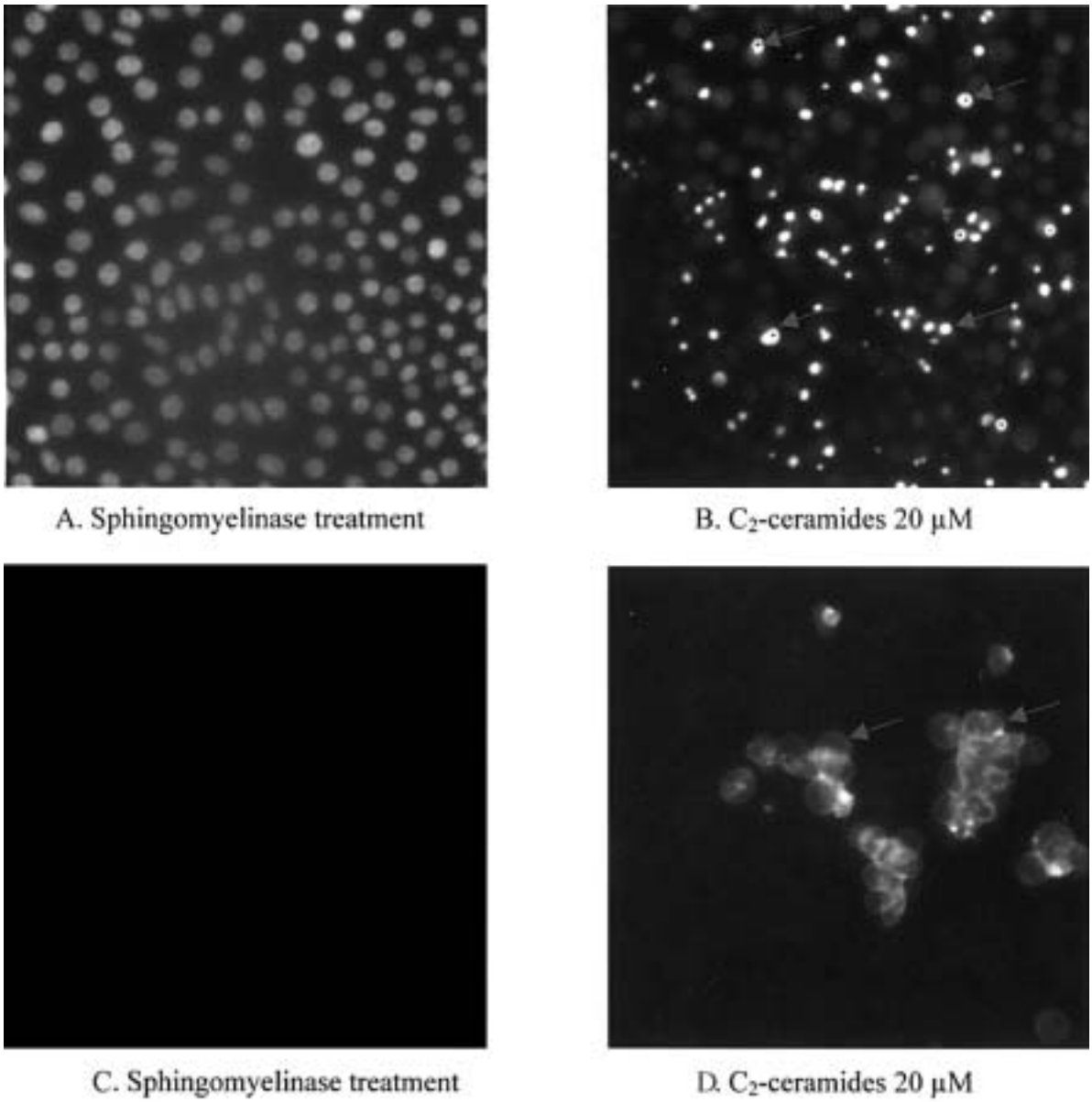

FIG. 6. Influence of exogenous Smase and C_2-ceramides on apoptosis. Porcine thyroid cells were cultured 48 h with TSH (1 mU/mL) as described in the Experimental Procedures section. After the culture period, the medium was withdrawn and replaced with medium containing Smase (0.5 U/mL) or truncated ceramides (C_2-ceramides). (A,B) Bis-benzamidine fluorescence corresponding to chromatin condensation was evaluated after 24 h of treatment. (C,D) Annexin V-fluorescein isothiocyanate (FITC) evidenced the phospholipidic flip-flop in the same conditions. See Figure 1 for other abbreviations.

6B). This effect was confirmed with annexin-FITC (Fig. 6D) insofar as annexin V tightly bound PS when this phospholipid was located at the outer leaflet of the cell membrane.

DISCUSSION

TSH can be considered as the main physiological regulator of the thyroid gland. *In vitro,* TSH induced porcine thyroid cultured cells to reconstitute follicle-like structures, which allow cells to incorporate iodine into thyroglobulin and to display adenylate cyclase responsiveness. These two parameters generally reflected a differentiated state of thyroid cells. TSH exerts its effects during the culture period, mainly *via* the cAMP cascade. However, this situation cannot be considered as exclusive, and part of the TSH effects occurred *via* cAMP-independent mechanisms. As in our previous studies, these results have demonstrated the involvement of glycosyl phosphoinositide-derived metabolites in the control of organification, iodide transport, and cAMP accumulation (21). Moreover, other factors like epidermal growth factor (EGF) (22) and transforming growth factor β (23) also contribute, through signaling pathways that involved protein phosphorylation on tyrosine or serine/threonine residues, to maintain a fine balance between proliferation and differentiation mechanisms.

During the last decade, another class of membrane lipids, the sphingolipids and their metabolites, have been shown to play an active role in complex signaling pathways including cell growth, differentiation (24), or programmed cell death (25). Several cytokines, such as TNF α, ILIβ, or IFN γ can trigger ceramide pathway, following Smase activation in different biological models (9).

In this report, we demonstrated the existence of a neutral Smase in porcine thyroid cells. This is a cell-surface associated enzyme that hydrolyzes SM to ceramide, and we clearly evidenced such a precursor-product relationship in our system. Since levels of endogenous neutral Smase activity were lower in 4 d in TSH-treated follicles as compared to control cells, it suggested that this hormone exerted a long-term negative control on intracellular ceramide amounts. TSH chronic treatment of porcine thyroid cells is essential to restore follicular morphology and thyroid functions. This control occurs through a cAMP-dependent mechanism as it was mimicked by F. In the absence of TSH in culture medium, thyroid cells progressively lose their functional characteristics and form a monolayer. The physiological relevance of this breakdown could correspond to a precise equilibrium between signaling pathways leading either to cell survival or to apoptosis. Long-term TSH treatment, *via* a cAMP mediation, triggers the positive signals for function and differentiation in porcine thyroid cells and in parallel represses Smase activity and ceramide production. On the other hand, the lack of TSH-altered cell program allowed cells to exhibit higher Smase activity and ceramide levels. In opposition, Pekary and Hershman (3) reported in FRTL-5 cells that TNF α markedly increased ceramide levels and Smase activity, but that TSH had no significant effect on ceramide release. In the same way, the Smase signaling pathway has been related to TNF α action in thyroid disorder (26).

For our part, we are unable to evidence in porcine thyroid cultured cells any effect of TNF α on Smase activity. Moreover, TNF α production in the culture medium cannot be detected. Nevertheless, it must be indicated that the FRTL-5 cell line differs from normal thyroid cells, particularly in the ability of iodide binding to proteins or in the lack of growth control by EGF (27). Alternatively, ceramide content of thyroid cells could directly modulate their differentiated state. To verify such a hypothesis, cells were treated with exogenous bacterial Smase or short-chain permeant ceramides. Such treatment altered follicular structures and, in parallel, induced loss of the functional activity of thyroid cells. Iodine organification and production of cAMP were markedly inhibited.

In contrast, other investigations using different cell types demonstrated that ceramides can positively regulate adenylate cyclase activity. Pyne *et al*. (28) showed that short-chain cells permeant ceramides (C_2 and C_6) increased the intracellular level of cAMP. Similar results were obtained by Bösel and Pfeuffer (29) using long-chain ceramides (C_{16} and $C_{18/24}$). However, it remains difficult to precisely evaluate the exact penetration and efficiency of ceramides inside the cells, and long-chain ceramides could affect the structural organization of membrane bilayers. In our study, however, C_2-ceramides were able, in a dose-dependent manner, to reproduce the effects of Smase on cAMP levels in thyroid cells.

The TSH-controlled ability to express differentiated thyroid functions is linked to the spatial reorganization of cells into follicular structures. Thyroid cells cultured in the absence of TSH form monolayers, where cells progressively lose their functional activity and exhibit a Smase activity higher than in TSH-treated cells. Otherwise, it has been reported that Smase could cause morphological changes (30) and that TNF α was able to induce the expression of cell adhesion molecules in keratinocytes and microvascular endothelial cells through a ceramide-dependent mechanism. Modification of thyroid cell morphology has been reported to be associated with not only the redistribution of the cytoskeleton network (31) and changes in the expression of junctional proteins such as E-cadherin (32) but also with modifications of extracellular matrix composition (33).

Our results suggested a crosstalk between two signaling pathways leading to distinct morphologic behaviors and functions. Elevation of cyclic adenosine monophosphate levels induced the expression of thyroid specialized genes and directed the differentiation process. In contrast, the increase in cellular ceramide content can be related to dedifferentiation according to the cell monolayer constitution and to PBI inhibition. The reciprocal control of these second messenger levels could influence downstream the balance between protein kinase A and protein kinase C activities. The determination of intracellular targets of ceramide action will provide us interesting information about the cascade of events governing cell programming. In this field of investigations, the mitogen-activated protein kinases cascade, the ceramide-activated pro-

tein phosphatase, and atypical protein kinase C zeta (9) appear to be the best candidates for mediating ceramide effects. In this field, apoptosis seems to be largely associated with ceramide generation (9). More recently, Wang *et al.* (34) postulated the existence of a balance between cell survival and programmed cell death as a function of ceramide concentration.

The spectacular morphological changes observed during long-term treatment of thyroid cells prompted us to investigate whether Smase and ceramides could induce apoptosis in these culture conditions. The analysis of chromatin condensation using bis-benzamidine and the annexin V-FITC technique for study of the PS flip-flop showed that ceramides were able to induce an apoptotic effect as early as 24 h of treatment (Fig. 1). However, the absence of programmed cell death induction under Smase treatment is questionable. Different explanations can be proposed to illuminate this point. First, the amount of intracellular ceramide released after Smase addition is not sufficient to induce apoptosis compared to the concentration of exogenous ceramides used in this set of experiments. The second point is related to the localization of the signaling pool of ceramides as described in leukemic cells (35) where exogenous Smase caused elevation of the ceramide levels without alterations of the cell viability. Further investigations are in progress to detail the mechanisms of ceramide action in governing cell death.

In conclusion, our reported data strongly supported an essential role of the ceramide signaling pathway in the control of programs that lead to the progressive conversion of functionally normal thyroid cells to a dedifferentiated phenotype.

ACKNOWLEDGMENTS

We thank Odette Legué for her excellent technical assistance. We are grateful to the Sobevir (Rethel, France) for the supply of thyroid glands. This work was supported by the Ministere Education Nationale Recherche et Technologie (MENRT), the Centre National de la Recherche Scientifique (CNRS), and by grants from Europol'agro, the region Champagne Ardenne and the Ligue contre le Cancer de l'Aube.

REFERENCES

1. Mauchamp, J., Mirrione, A., Alquier, C., and Andre, F. (1998) Follicle-like Structure and Polarized Monolayer: Role of the Extracellular Matrix on Thyroid Cell Organization in Primary Culture, *Biol. Cell 90*, 369–380.
2. Tomiuk, S., Hofmann, K., Nix, M., Zumbansen, M., and Stoffel, W. (1998) Cloned Mammalian Neutral Sphingomyelinase: Functions in Sphingolipid Signaling? *Proc. Natl. Acad. Sci. USA 95*, 3638–3643.
3. Pekary, E., and Hershman, J.N. (1998) Tumor Necrosis Factor, Ceramide, Transforming Growth Factor-beta1, and Aging Reduce Na^+/I^- Symporter Messenger Ribonucleic Acid Levels in FRTL-5 Cells, *Endocrinology 139*, 703–712.
4. Okazaki, T., Bell, R.M., and Hannun, Y.A. (1989) Sphingomyelin Turnover Induced by Vitamin D3 in HL-60 Cells. Role in Cell Differentiation, *J. Biol. Chem. 264*, 19076–19080.
5. Pena, L.A., Fuks, Z., and Kolesnick, R. (1997) Stress-Induced Apoptosis and the Sphingomyelin Pathway, *Biochem. Pharmacol. 53*, 615–621.
6. Verheij, M., Bose, R., Lin, X.H., Yao, B., Jarvis, W.D., Grant, S., Birrer, M.J., Szabo, E., Zon, L.I., Kyriakis, J.M., *et al.* (1996) Requirement for Ceramide-Initiated SAPK/JNK Signalling in Stress-Induced Apoptosis, *Nature 380*, 75–79.
7. Mathias, S., Younes, A., Kan, C.C., Orlow, I., Joseph, C., and Kolesnick, R.N. (1993) Activation of the Sphingomyelin Signaling Pathway in Intact EL4 Cells and in a Cell-Free System by IL-1 Beta, *Science 259*, 519–522.
8. Brugg, B., Michel, P.P., Agid, Y., and Ruberg, M. (1996) Ceramide Induces Apoptosis in Cultured Mesencephalic Neurons, *J. Neurochem. 66*, 733–739.
9. Hannun, Y.A. (1994) The Sphingomyelin Cycle and the Second Messenger Function of Ceramide, *J. Biol. Chem. 269*, 3125–3128.
10. Mauchamp, J., Margotat, A., Chambard, M., Charrier, B., Remy, L., and Michel-Bechet, M. (1979) Polarity of Three-Dimensional Structures Derived from Isolated Hog Thyroid Cells in Primary Culture, *Cell Tissue Res. 204*, 417–430.
11. Cailla, H.L., Racine-Weisbuch, M.S., and Delaage, M.A. (1973) Adenosine 3′,5′ Cyclic Monophosphate Assay at 10^{-15} Mole Level, *Anal. Biochem. 56*, 394–407.
12. Lowry, O.H., Rosebrough, N.J., Farr, A.L., and Randall, R.J. (1951) Proteins Measurement with the Folin Phenol Reagent, *J. Biol. Chem. 193*, 265–275.
13. Jaffrezou, J.P., Levade, T., Bettaieb, A., Andrieu, N., Bezombes, C., Maestre, N., Vermeersch, S., Rousse, A., and Laurent, G. (1996) Daunorubicin-Induced Apoptosis: Triggering of Ceramide Generation Through Sphingomyelin Hydrolysis, *EMBO J. 15*, 2417–2424
14. Preiss, J.E., Loomis, C.R., Bell, R.M., and Niedel, J.E. (1987) Quantitative Measurement of *sn*-1,2-Diacylglycerols, *Methods Enzymol. 141*, 294–300.
15. Bligh, E.G., and Dyer, W.T. (1959) A Rapid Method of Total Lipid Extraction and Purification, *Can. J. Biochem. Physiol. 37*, 911–917.
16. Ella, K.M., Qi, C., Dolan, J.W., Thompson, R.P., and Meier, K.E. (1997) Characterization of a Sphingomyelinase Activity in *Saccharomyces cerevisiae, Arch. Biochem. Biophys. 340*, 101–110.
17. Homburg, C.H., De Haas, M., Von dem Borne, A.E., Verhoeven, A.J., Reutelingsperger, C.P., and Roos, D. (1995) Human Neutrophils Lose Their Surface Fc Gamma RIII and Acquire Annexin V Binding Sites During Apoptosis *in vitro, Blood 85*, 532–540.
18. Koopamn, G., Reutlingserger, C.P., Kuitjen, G.A., Keehnen, R.M., Pals, S.T., and Van Oers, M.H. (1994) Annexin V for Flow Cytometric Detection of Phosphatidylserine Expression on B Cells Undergoing Apoptosis, *Blood 84*, 1415–1420.
19. Vermes, I., Haanen, C., Steffens-Nakken, H., and Reutlingsperger, C. (1995) A Novel Assay for Apoptosis. Flow Cytometric Detection of Phosphatidylserine Expression on Early Apoptotic Cells Using Fluorescein Labelled Annexin V, *J. Immunol. Methods 184*, 39–51.
20. Watts, J.D., Aebersold, R., Polverino, A.J., Patterson, S.D., and Gu, M. (1999) Ceramide Second Messengers and Ceramide Assays, *Trends Biochem. Sci. 24*, 228.
21. Martiny, L., Antonicelli, F., Thuilliez, B., Lambert, B., Jacquemin, C., and Haye, B. (1990) Control by Thyrotropin of the Production by Thyroid Cells of an Inositol Phosphate-glycan, *Cell. Signal. 2*, 21–27.
22. Lamy, F., Wilkin, F., Baptist, M., Posada, J., Roger, P.P., and Dumont, J.E. (1993) Phosphorylation of Mitogen-Activated Protein Kinases Is Involved in the Epidermal Growth Factor and Phorbol Ester, but Not in the Thyrotropin/cAMP, Thyroid Mitogenic Pathway, *J. Biol. Chem. 268*, 8398–8401.
23. Taton, M., Lamy, F., Roger, P.P., and Dumont, J.E. (1993) General Inhibition by Transforming Growth Factor Beta 1 of Thy-

rotropin and cAMP Responses in Human Thyroid Cells in Primary Culture, *Mol. Cell. Endocrinol. 95*, 13–21.
24. Okazaki, T., Bielawska, A., Bell, R.M., and Hannun, Y.A. (1990) Role of Ceramide as a Lipid Mediator of 1 Alpha,25-Dihydroxyvitamin D3-Induced HL-60 Cell Differentiation, *J. Biol. Chem. 265*, 15823–15831.
25. Ji, L., Zhang, G., Uematsu, S., Akahori, Y., and Hirabayashi, Y. (1995) Induction of Apoptotic DNA Fragmentation and Cell Death by Natural Ceramide, *FEBS Lett. 358*, 211–214.
26. Kimura, T., Okajima, F., Kikuchi, T., Kuwabara, A., Tomura, H., Sho, K., Kobayashi, I., and Kondo, Y. (1997) Inhibition of TSH-Induced Hydrogen Peroxide Production by TNF-Alpha Through a Sphingomyelinase Signaling Pathway, *Am. J. Physiol. 273*, E639–E643.
27. Eggo, M.C., Bachrach, L.K., Fayet, G., Errick, J.E., Kudlow, J.E., Cohen, M.F., and Burrow, G.N. (1984) The Effects of Growth Factors and Serum on DNA Synthesis and Differentiation in Thyroid Cells in Culture, *Mol. Cell. Endocrinol. 38*, 141–150.
28. Pyne, S., Tolan, D.G., Conway, A.M., and Pyne, N. (1997) Sphingolipids as Differential Regulators of Cellular Signalling Processes, *Biochem. Soc. Trans. 25*, 549–556.
29. Bösel, A., and Pfeuffer, T. (1998) Differential Effects of Ceramides upon Adenylyl Cyclase Subtypes, *FEBS Lett. 422*, 209–212
30. Spiegel, S., and Merrill, J.R. (1996) Sphingolipid Metabolism and Cell Growth Regulation, *FASEB. J. 10*, 1388–1397.
31. Roger, P.P., Christophe, D., Dumont, J.E., and Pirson, I. (1997) The Dog Thyroid Primary Culture System: A Model of the Regulation of Function, Growth and Differentiation Expression by cAMP and Other Well-Defined Signaling Cascades, *Eur. J. Endocrinol. 137*, 579–598.
32. Brabant, G., Hoang Vu, C., Behrends, J., Cetin, Y., Potter, E., and Dumont, J.E. (1995) Regulation of the Cell-Cell Adhesion Protein, E-Cadherin, in Dog and Human Thyrocytes *in vitro, Endocrinology 136*, 3113–3119.
33. Bellon, G., Chaqour, B., Antonicelli, F., Wegrowski, J., Claisse, D., Haye, B., and Borel, J.P. (1994) Differential Expression of Thrombospondin, Collagen, and Thyroglobulin by Thyroid-Stimulating Hormone and Tumor-Promoting Phorbol Ester in Cultured Porcine Thyroid Cells, *J. Cell. Physiol. 160*, 75–88.
34. Wang, Y.M., Seibenhener, M.L., Vandenplas, M.L., and Wooten, M.W. (1999) Atypical PKCζ Is Activated by Ceramide, Resulting in Coactivation of NFκB/JNK Kinase and Cell Survival, *J. Neurosci. Res. 55*, 293–302.
35. Zhang, P., Liu, B., Jenkins, G.M., Hannun, Y.A., and Obeid, L.M. (1997) Expression of Neutral Sphingomyelinase Identifies a Distinct Pool of Sphingomyelin Involved in Apoptosis, *J. Biol. Chem. 272,* 9609–9612.

[Received January 19, 2000, and in revised form July 11, 2000; revision accepted August 17, 2000]

Modulation of Arachidonate and Docosahexaenoate in *Morone chrysops* Larval Tissues and the Effect on Growth and Survival

Moti Harel*, Eric Lund, Sonja Gavasso, Ryan Herbert, and Allen R. Place

Center of Marine Biotechnology, University of Maryland, Baltimore, Maryland 21202

ABSTRACT: The extent to which extreme dietary levels of arachidonate (AA) and/or docosahexaenoate (DHA) modulate lipid composition in the body tissues and consequently affect growth and survival in freshwater *Morone* larvae species was examined. White bass, *M. chrysops,* larvae (day 24–46) were fed *Artemia* nauplii enriched with algal oils containing varying proportions of AA and DHA (from 0 to over 20% the total fatty acids). Growth was significantly reduced ($P < 0.05$) in larvae fed a DHA-deficient *Artemia* diet. Increases in dietary levels of AA also were associated with a significant growth reduction. However, the inhibitory effect of AA on larvae growth could be suppressed by the dietary addition of DHA (at a level of 21.6% of the total fatty acids in enrichment lipids). Larval brain + eyes tissue accumulated over 10 times more DHA than AA in its structural lipids (phosphatidylcholine, phosphatidylethanolamine) at any dietary ratio. In contrast, DHA accumulation, as compared to AA, in gill lipids declined considerably at higher than 10:1 DHA/AA tissue ratios. DHA and eicosapentaenoic acid (EPA) contents in brain + eyes tissue were most sensitive to competition from dietary AA, being displaced from the tissue at rates of 0.36 ± 0.07 mg DHA and 0.46 ± 0.11 mg EPA per mg increase in tissue AA, and 0.55 ± 0.14 mg AA per mg increase in tissue DHA. On the other hand, AA and EPA levels in gill tissue were most sensitive to dietary changes in DHA levels; AA was displaced at rates of 0.37 ± 0.11 mg, whereas EPA increased at rates of 0.68 ± 0.28 mg per mg increase in tissue DHA. Results suggest that balanced dietary DHA/AA ratios (that allow DHA/AA ratios of 2.5:1 in brain + eyes tissue) promote a high larval growth rate, which also correlates with maximal regulatory response in tissue essential fatty acids.

Paper no. L8399 in *Lipids 35,* 1269–1280 (November 2000).

The white bass, *Morone chrysops,* is a freshwater fish species, closely related to the striped bass, *M. saxatilis*. Adult white bass are piscivorus, occupy freshwater habitats, and as such may retain and preferentially conserve their limited dietary n-3 polyunsaturated fatty acid (PUFA) sources (1,2). *Morone* larvae, in common with many other commercially important marine larval species, are not able to elongate and desaturate n-3 and n-6 precursors into their PUFA metabolites. In fact, of the four marine teleosts including ayu, *Plecoglossus altivelis,* red sea bream, *Pagrus major,* and puffer fish, *Fugu rubripes,* members of the genus *Morone* demonstrated the lowest conversion rate of 18:n-3 precursor to its C_{20} and C_{22} fatty acid metabolites (3). Thus, larvae must be provided with or be able to preserve sufficient levels of PUFA in order to meet the nutritional requirements for optimal growth.

Because the n-6 and n-3 fatty acids share a common biosynthetic pathway, the relationship between dietary n-6 and n-3 fatty acids and their distribution in larval body tissue is of interest. In brain tissue and eye retinal tissue of mammals, docosahexaenoic acid (DHA, 22:6n-3) is the most prominent fatty acid (4–7). Rapid DHA accumulation also coincides with neuronal differentiation and development of structural phospholipids of the central nervous system (5,6,8). In addition to DHA, arachidonic acid (AA, 20:4n-6) is a critical component of membrane lipids and specifically accumulates in brain phospholipids during early development (9,10). AA plays an active role in signal transduction both through the production of eicosanoids in whole body tissues and as a second messenger in neural tissue (11–14). Recent studies have shown that dietary supplementation of AA together with DHA inhibited DHA accretion in the phospholipid fraction of tissue lipids (10). This antagonistic relationship might be detrimental to the proper function of brain and neural tissues, where DHA is believed to serve a vital function.

Conversely, the developing brain, because of its high affinity for PUFA, may be very susceptible to an excess of PUFA in the diet. The adverse effects on larval growth and survival caused by excessive essential fatty acids (EFA) in the diet have been previously reported (15–17). Furthermore, it can be deduced from (i) the established involvement of DHA and eicosapentaenoic acid (EPA, 20:5n-3) in modulating production of AA-derived eicosanoids and (ii) the low Δ-5 and Δ-6 fatty acid desaturase activities in some vertebrates that marine fish might require AA in their diet not only preformed but also in balanced ratio with other EFA. Such an absolute re-

*To whom correspondence should be addressed at Center of Marine Biotechnology, University of Maryland, 701 East Pratt St., Baltimore, MD 21202. E-mail: harel@umbi.umd.edu

Abbreviations: AA, arachidonic acid; DHA, docosahexaenoic acid; DPA, docosapentaenoic acid (22:5n-3); EFA, essential fatty acids; EPA, eicosapentaenoic acid; HUFA, highly unsaturated fatty acids; PC, phosphatidylcholine; PE, phosphatidylethanolamine; PI, phosphatidylinositol; PS, phosphatidylserine; psu, practical salinity units; PUFA, polyunsaturated fatty acids; TAG, triacylglycerols; UV, ultraviolet.

quirement for AA has been recently established for juvenile turbot, *Scophthalmus maximus* (18), and Japanese flounder, *Paralichthys olivaceus* (19); however, the combined requirement for these two EFA in both absolute and relative amounts is not known for any species.

The objectives of this study were to examine the extent to which extreme nutritional levels of DHA, AA, or a combination of the two would modulate lipid composition in larval tissues, and to establish the combined nutritional requirements for both DHA and AA. Animals used in this study were metamorphosed white bass larvae (day 24–46), which were at a sensitive developmental stage when high mortality generally occurs.

MATERIALS AND METHODS

Formulation of enrichment emulsions. A 3 × 3 factorial design (two factors, DHA and AA, at nine different combinations in duplicate blocks) was used to simultaneously study the effect of increasing dietary levels of DHA and AA on larval performances. Nine different emulsions having varying proportions of DHA-rich triacylglycerols (TAG) from heterotrophically grown algae, *Crypthecodinium* spp., and AA-rich TAG from fungi, *Mortierella* spp. (DHASCO and ARASCO, respectively, Martek Biosciences Corp., Columbia, MD) were formulated (Table 1). TAG of the algae *Crypthecodinium* spp. and the fungi *Mortierella* spp. contain 49% DHA and 54% AA of the total fatty acids, respectively, and less than 0.5% EPA. A mixture of 2% alginic acid, 2% polyoxyethylene sorbitan mono-oleate (Tween-80), 1% ascorbic acid, 1% vitamin E, 1% silicon-based anti-foaming agent (all made by Sigma Chemical Co., St. Louis, MO) and 5% soy lecithin [80% phosphatidylcholine (PC); Archer Daniels Midland Co., Decatur, IL] were added to the oils (all additions made by weight). Oil mixtures were emulsified with an equal amount of distilled water by first homogenizing at low speed (Ultra-Turrax T8; IKA Labortechnik, Staufen, Germany) for 15 s and then sonicating for an additional 15 s at one-third of the maximal sonication energy level (Sonifier 450; Branson Sonic Power Company, Danbury, CT). Fresh emulsions were prepared on a weekly base and stored at 4°C for daily use.

Enrichment of Artemia *nauplii. Artemia* cysts (premium grade; Sanders Brine Shrimp Co., Ogden, UT) were dehydrated in fresh water for 1 h and decapsulated in a 0.1 M NaOH solution containing 3% active chlorine. Hatching was carried out in 20 psu (practical salinity units) artificial seawater at 28°C with vigorous aeration. The nauplii were harvested after 16 h, separated from unhatched cysts and hatching debris, thoroughly rinsed, and kept at room temperature for an additional 6–8 h until they reached Instar-II stage (complete development of digestive system) before being transferred to the enrichment medium. Then 0.4 g/L of each enrichment emulsion (doses were based on the oil quantity in the emulsion) was fed to Instar II-stage *Artemia* nauplii (200,000 nauplii per liter) at time 0 (1700). At 0900 the following day (after 16 h), half of the nauplii were removed and fed to larvae. An additional 0.2 g/L of enrichment emulsion

TABLE 1
Lipid Mixture and Fatty Acid Composition of the Enrichment Diets[a]
(% w/w and % of total fatty acids, respectively)

	Enrichment diets (DHA/AA ratio)								
	0:0	10:0	20:0	0:13	12:13	21:13	3:26	12:26	23:26
Lipid mixture (% w/w)									
DHA-TAG	0	25	50	0	25	50	0	25	50
AA-TAG	0	0	0	25	25	25	50	50	50
Olive-oil	100	75	50	75	50	25	50	25	0
FAME									
14:0	2.8	5.3	7.1	2.4	5.0	7.6	1.7	4.4	7.5
16:0	6.3	7.0	8.2	6.6	7.6	8.9	7.0	8.5	9.8
16:1n-7	5.2	7.6	5.7	7.5	5.5	3.5	5.1	3.1	ND
18:0	1.6	1.2	0.7	3.8	3.7	3.8	6.1	6.3	6.6
18:1n-9	70.7	56.7	45.7	54.8	43.9	34.7	39.8	31.2	20.4
18:1n-7	9.0	7.0	4.4	6.6	4.4	2.6	4.4	2.6	ND
18:2n-6	3.3	4.0	3.2	5.1	4.7	4.5	6.1	5.7	5.0
18:3n-3	1.7	1.1	0.8	1.6	0.9	0.5	2.1	0.6	0.5
20:4n-6	ND	ND	ND	12.6	12.7	12.8	25.6	25.8	26.4
20:5n-3	ND	ND	ND	ND	ND	ND	ND	0.6	ND
22:6n-3	0.3	10.1	20.3	ND	11.5	21.2	2.6	11.7	23.3
Total sat	10.8	13.5	16.0	12.7	16.4	20.3	14.8	19.2	23.9
Total mono	83.9	71.3	55.8	67.9	53.8	40.8	49.2	37.4	20.4
Total diene	3.3	4.0	3.2	5.1	4.7	4.5	6.1	5.7	5.0
Total poly	2.0	11.2	21.1	14.1	25.1	34.5	29.8	37.7	50.6

[a]Total sat, percentage of saturated fatty acids in the diet; Total mono, percentage of fatty acids containing one double bond; Total diene, percentage of fatty acids containing two double bonds; Total poly, percentage of fatty acids containing three or more double bonds; ND, not detectable; FAME, fatty acid methyl ester. Docosahexaenoic acid triacylglycerols (DHA-TAG) and arachidonic acid triacylglycerols (AA-TAG) are DHA- and AA-rich TAG (49% DHA and 54% AA, respectively, obtained from Martek Biosciences, Columbia, MD); olive oil was obtained from a local market.

was added, and the remaining nauplii were fed to the larvae at 1600. A random set of samples of 16-h enriched *Artemia* nauplii were analyzed for lipid and fatty acid composition (Table 2).

Larvae rearing. Newly hatched white bass *M. chrysops* larvae were obtained from Aquafuture Inc. (Turners Falls, MA). Larvae were grown for 17 d on DHA- and AA-deficient rotifers, *Brachionus plicatilis* (2–5 rotifers/mL), which had been cultured on freshwater *Chlorella* paste (Martek Biosciences) at 0.5 g/10^6 rotifers/d. Larvae were randomly distributed in eighteen 60-L larval rearing tanks at an initial density of 160 larvae per tank. The tanks were gently aerated and the water volume was exchanged 1–2 times per day with biofiltered, ultraviolet (UV) light-treated recirculating water. A 14:10 h light/dark photoperiod was maintained using fluorescent light tubes (Daylight; 40 watts; 800–1200 lux at the water surface). Temperature was maintained at 24 ± 2°C and salinity at 2–6 psu. Water quality was monitored daily, and levels of total NH_3, un-ionized NH_3, NO_2, and pH were maintained below 0.2 ppm, 0.001 ppm, 0.3 ppm, and at 8.02, respectively, by partial replacement with fresh water. Pooled samples of forty 17-d-old larvae were taken for initial dry weight determinations (lyophilized to constant weight; balance: Mettler UMT2, Toledo, Switzerland, sensitivity = ±0.1 mg; lyophilizer: Labconco, Kansas City, MO) and fatty acid analysis.

Newly hatched *Artemia* nauplii were introduced to the larvae from day 17 until day 24 (once a day at 20–40 nauplii/L), while rotifer concentrations were gradually reduced to complete removal by day 24. Larvae were then fed twice daily with previously enriched *Artemia* nauplii, as described above, at concentrations of 50–100 nauplii/L for the next 22 d. Feeding experiments were terminated on day 46, at which time 40 larvae were sampled from each rearing tank. Samples were washed with distilled water, dried on paper towels, placed into test tubes, and lyophilized to constant weight. Muscle tissue, gill tissue, and eyes, including contiguous brain tissue, were dissected from each freeze-dried larva. The dry weight of a whole larva and the weight of a pooled sample containing 10 separated tissues were recorded to the nearest 0.1 mg (Mettler UMT2; Toledo, Switzerland). Survivorship was determined based on the initial and final counts of larvae in each rearing tank.

Lipid and fatty acid analysis. Total lipids were extracted from enriched *Artemia* nauplii, larvae muscle, gills, and brain + eye tissues according to the method of Folch *et al.* (20). Lipid weight was determined gravimetrically and expressed as a percent dry weight. The fatty acid compositions of total lipids from *Artemia* nauplii and larvae muscle, gills, and brain + eye tissues were determined following the method of Morisson and Smith (21). The lipid extracts, including internal standards (25 µg of each 19:0 and 21:0 fatty acids, Nu-Chek-Prep, Inc., Elysian, MN) were saponified with saturated KOH in methanol and transmethylated with 10% boron trifluoride in methanol (Supelco Inc., Bellefonte, PA).

Tissue lipid classes were separated on silica gel-G thin-layer chromatography taper plates (20 × 20 cm, uniplate; Analtech, Newark, DE) using a double-solvent development system (22). The plates were first developed to half-length in chloroform/methyl acetate/isopropanol/methanol/0.25% aqueous potassium chloride (25:25:25:10:9, by vol) to separate the individual polar lipid classes. Full-length development in hexane/diethyl ether/glacial acetic acid (80:20:2, by vol) was used to separate the neutral lipid classes. Spots for polar and neutral lipid classes were identified by comparison with authentic standards after visualization with 0.025% (wt/vol) 2′,7′-dichlorofluorescein in ethanol under UV light.

TABLE 2
Lipid and Fatty Acid Composition of *Artemia* Nauplii After 16 h Enrichment with Various DHA/AA Dietary Ratios[a] (mg/g dry weight)

	Enrichment diets (DHA/AA ratio)								
	0:0	10:0	20:0	0:13	12:13	21:13	3:26	12:26	23:26
Total lipids	224	244	265	251	243	267	226	251	252
FAME									
14:0	0.6	3.1	3.9	0.6	1.5	2.9	0.7	1.4	2.4
16:0	12.8	22.6	21.4	12.6	16.8	16.8	14.1	14.3	15.3
16:1n-7	1.9	2.3	2.6	1.7	2.3	2.4	1.9	2.0	2.2
18:0	8.3	10.5	9.8	8.4	11.0	10.0	10.6	10.2	10.2
18:1n-9	70.5	98.0	87.2	69.9	63.8	55.3	62.2	45.3	39.5
18:1n-7	9.2	11.4	8.8	8.8	9.8	7.7	8.7	8.0	5.8
18:2n-6	10.4	9.7	8.8	12.1	12.8	10.6	13.7	13.1	12.9
18:3n-3	23.6	31.1	23.6	20.7	31.6	26.0	26.5	28.3	24.2
20:4n-6	1.5	2.8	4.9	12.5	15.4	15.7	23.9	25.0	25.3
20:5n-3	2.9	4.4	6.0	2.1	4.7	5.5	2.4	4.1	5.2
22:5n-3	ND	ND	0.5	ND	ND	0.4	ND	ND	0.4
22:6n-3	ND	5.0	13.0	0.4	3.8	8.3	0.5	4.1	7.4
Total sat	15.3	18.0	18.4	14.4	16.9	18.4	15.4	16.6	18.5
Total mono	57.6	55.6	51.8	53.7	43.7	40.5	44.1	35.5	31.5
Total diene	7.3	4.8	4.6	8.1	7.4	6.6	8.3	8.4	8.6
Total poly	19.8	21.6	25.2	23.8	32.0	34.6	32.3	39.5	41.4

[a]See Table 1 for abbreviations.

PC, phosphatidylethanolamine (PE), phosphatidylinositol + phosphatidylserine (PI + PS), and TAG spots were scraped into tubes for transmethylation of the fatty acid components, as described above. The fatty acid methyl esters were analyzed by using a Hewlett-Packard 5890A gas chromatograph equipped with a flame-ionization detector and a 30 m × 0.25 mm i.d. capillary column with 0.25 µm film thickness (DB Wax, J&W Scientific, Folsom, CA). The carrier gas was helium at 1 mL/min flow rate. Injector and detector temperatures were 300°C, and the oven temperature was programmed from an initial temperature of 50°C, held for 2 min, to 200°C in 16 min, from 200 to 210°C in 11 min, and from 210 to 220°C in 18 min. The integrated peak areas of the fatty acid methyl esters were identified by comparison with known standards and quantified through the use of known amounts of internal standards. Fatty acid compositions of whole tissue lipids and lipid classes were expressed in mg fatty acid/g dry weight tissue.

Statistical analysis. Both *Artemia* nauplii enrichment and larvae feeding experiments were arranged in a complete block design (two blocks), including DHA and AA as treatment factors. All data are reported as means ± SEM. Analysis of variance was used (23) to determine differences between and within treatment means of survival, weight, whole tissue lipid and lipid classes content, and fatty acid composition. Percentage data were normalized by arcsine transformation prior to analysis. When significant differences between the means were detected, a Bonferroni multiple comparison test was applied. A significance level of 95% ($P < 0.05$) was used throughout.

RESULTS

Retention of lipid and fatty acids in Artemia *nauplii.* Table 2 presents the lipid and fatty acid composition in *Artemia* nauplii after enrichment for 16 h with various DHA/AA ratios. Overall, *Artemia* retained equal amounts of dietary lipids ($P > 0.05$) regardless of enrichment treatments, whereas the EFA composition reflected that of the dietary composition. AA retention by *Artemia* was almost four times higher than that of DHA retention (25.3 mg AA/g dry weight vs. 7.4 mg DHA/g dry weight). Retention efficiency of dietary AA and DHA (relative to maximum retention obtained at a minimum level of competing fatty acid) by the *Artemia* as a function of increased competition between the two fatty acids is shown in Figure 1. A reduction of over 55% of maximal DHA retention was observed in the presence of increasing levels of dietary AA, whereas reduction in AA retention as a result of increasing competition by dietary DHA was only 25% of its maximal levels. Moreover, the proportion of AA in *Artemia* lipids was generally equal to its dietary proportion, whereas the DHA proportion was almost 25% lower than its dietary proportion. As a result of retroconversion activities of the absorbed DHA, the relative proportion of the EPA metabolite in *Artemia* lipids was also increased from its basal levels of 2.1–2.9 mg/g dry weight. The net increase in *Artemia* EPA was estimated as approximately 20% of that of the corresponding DHA increase, based on the mg/g dry weight values [net percentage increase in EPA/(net increase in EPA + DHA)] as derived from the data presented in Table 2. Levels of linoleic and linolenic fatty acids (18:2n-6) in the enriched *Artemia* were nearly constant and mostly reflected their endogenous resources.

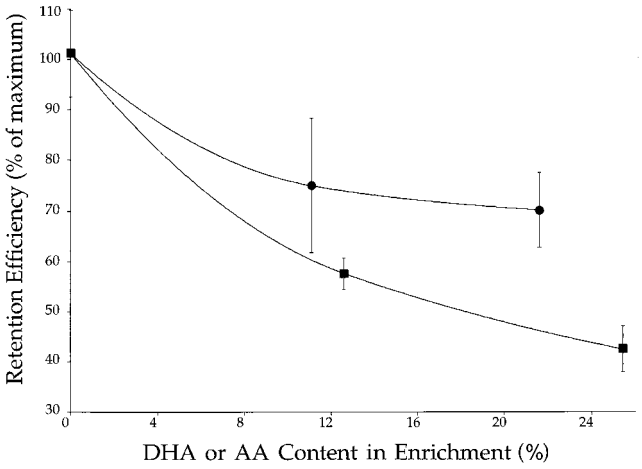

FIG. 1. Retention efficiency in *Artemia* nauplii (relative to maximum retention at zero competition) of dietary docosahexaenoic acid (DHA) (■) and arachidonic acid (AA) (●) as a function of the competition level between the two fatty acids. *Artemia* were enriched for 16 h with diets containing equal amount of DHA (21.6% of total fatty acids) but increasing levels of AA (0–26.9% of total fatty acids), or with diets containing equal amounts of AA (25.4% of total fatty acids) but increasing levels of DHA (2.6–23.3% of total fatty acids). Data are mean ± SEM values, $n = 3$.

Dietary effects on larval growth and survival. Larval growth was significantly affected after 22 d of dietary treat-

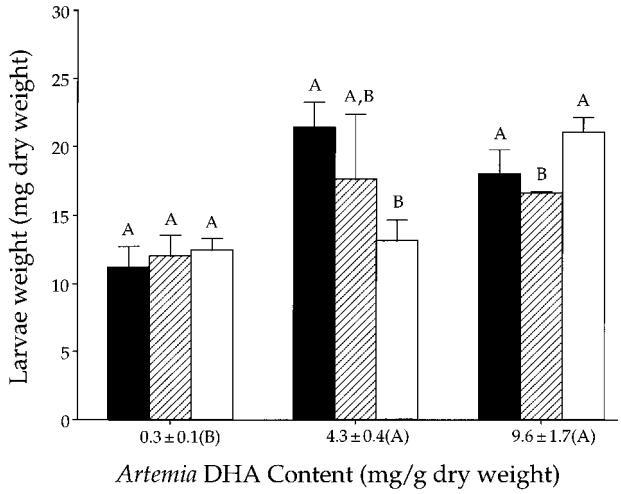

FIG. 2. Weight of white bass larvae after 22 d of feeding on enriched *Artemia* with varying DHA/AA dietary contents. AA content in enriched *Artemia* are: 3.1 ± 1.0 (solid bar), 14.5 ± 1.8 (diagonally lined bar), and 24.7 ± 0.4 mg/g dry weight (open bar). Data are means ± SEM values, $n = 3$. Bars with different letters indicate significant weight differences within dietary treatments ($P < 0.05$). *Artemia* DHA levels with different letters in parentheses indicate significant weight difference between dietary treatments ($P < 0.05$). For abbreviations see Figure 1.

TABLE 3
Fatty Acid Composition of Larvae White Bass Body Tissues at the Start of Feeding Experiment[a] (mg/g dry wt)

FAME	Muscle	Brain + eyes	Gills
14:0	0.7	2.1	0.8
16:0	6.5	16.3	14.6
16:1n-7	2.2	2.8	1.9
18:0	3.2	9.1	10.1
18:1n-9	19.9	12.3	22.4
18:1n-7	3.9	2.6	5.0
18:2n-6	3.6	2.7	5.3
18:3n-3	4.3	6.4	7.3
20:4n-6	0.8	1.9	3.1
20:4n-3	1.2	1.1	ND
20:5n-3	4.2	5.1	3.6
22:5n-6	ND	ND	0.6
22:5n-3	ND	2.4	ND
22:6n-3	2.3	7.9	1.8
Total sat	19.7	18.7	16.9
Total mono	49.2	31.7	47.7
Total diene	6.8	4.9	8.6
Total poly	24.2	44.6	26.7

[a]See Table 1 for abbreviations.

ments (Fig. 2, $P < 0.05$), but larval survival was not significantly different (64.9 ± 1.7%, $P > 0.05$). Larvae grew significantly slower ($P < 0.05$) when fed a DHA-deficient *Artemia* diet regardless of AA levels. Increasing contents of dietary AA at a moderate DHA level (4.3 ± 0.4 mg DHA/g dry weight) resulted in a significant growth inhibition, as larval growth was reduced from 21.3 ± 1.8 mg dry weight at no dietary AA to 13.1 ± 1.5 mg dry weight at 24.7 mg AA/g dry weight ($P < 0.05$). The inhibitory effect of high dietary AA on larval growth was nearly eliminated by the inclusion of high levels of DHA in the *Artemia* diet (9.6 ± 1.7 mg DHA/g dry weight). Nevertheless, increasing *Artemia* DHA levels above 4.3 mg DHA/g dry weight regardless of AA levels did not result in further improvement in larval growth.

Dietary effects on lipids and fatty acid composition of larval body tissues. Larval total lipid content was not affected by dietary treatments (17.1 ± 0.5% dry weight in all dietary groups, $n = 18$, $P > 0.05$). At the beginning of the experiment (on day 24), the lipid composition of larval tissues mainly reflected their *Chlorella*-enriched rotifer diet. Muscle and gill lipids were mostly composed of monounsaturated fatty acids (49.2 and 47.7% of all fatty acids, respectively, Table 3), while the largest proportion of PUFA was found in brain + eye tissue lipids (44.6% of all fatty acids). After 22 d of feeding, the lipid composition of all larval tissues responded to dietary changes. Most changes occurred in the proportion of monounsaturated and polyunsaturated fatty acid classes. The proportion of PUFA in brain + eye tissue lipids increased from 31.0 ± 1.1% to a maximum of 54.1 ± 0.8%. This dramatic increase in the proportion of PUFA in brain + eye lipid was at the expense of a corresponding decrease in the proportion of monounsaturated fatty acids (Table 4). The same pattern of response to dietary changes was observed in larval muscle and gill tissues, although the adjustment was not as pronounced (Tables 5 and 6). The gill tissue lipids were the most effective in increasing the proportion of PUFA over the course of the experiment (over 60% increase, Tables 3 and 6.), whereas brain + eye tissue lipids from larvae fed deficient diets lost 50% of their original proportions (Tables 3 and 4).

All three larval tissues responded to AA dietary shortage by exhibiting a selective accumulation of AA at low dietary content (Fig. 3B). Higher selectivity, especially in gill tissue,

TABLE 4
Fatty Acid Composition of Larvae White Bass Brain + Eye Tissue After 22 d of Dietary Treatment[a,b] (mg/g dry weight)

	Artemia diets (DHA/AA ratio)								
FAME	0.0:1.5	5.0:2.8	13.0:4.9	0.4:12.5	3.8:15.4	8.3:15.7	0.5:23.9	4.1:25.0	7.4:25.3
14:0	0.6 ± 0.5	0.8 ± 0.6	1.8 ± 0.1	ND	0.7 ± 0.5	1.8 ± 0.2	0.9 ± 0.5	ND	1.5 ± 0.1
16:0	23.6 ± 2.5	29.2 ± 1.4	30.5 ± 0.7	21.4 ± 0.4	26.4 ± 1.2	31.6 ± 2.7	31.7 ± 5.0	26.1 ± 0.2	29.3 ± 0.5
16:1n-7	4.1 ± 0.1	4.0 ± 0.4	3.1 ± 0.2	3.1 ± 0	3.0 ± 0.1	3.0 ± 0.3	4.6 ± 0.3	2.6 ± 0.1	2.1 ± 0.1
18:0	15.1 ± 1.3	18.0 ± 1	18.4 ± 0.4	13.8 ± 0.3	16.6 ± 0.8	19.4 ± 1.2	20.4 ± 3.1	17.1 ± 0	19.1 ± 0.7
18:1n-9	49.8 ± 6.2	43.3 ± 4.3	35.1 ± 2.9	32.7 ± 0.8	32.3 ± 1.6	31.9 ± 3.4	46.4 ± 4.7	27.9 ± 1.5	22.4 ± 3.1
18:1n-7	10.7 ± 1.6	9.5 ± 1.2	8.1 ± 1.1	4.5 ± 0.4	8.1 ± 0.7	8.5 ± 0.4	11.7 ± 1.3	7.6 ± 0.5	6.8 ± 0.2
18:2n-6	9.8 ± 1.5	7.1 ± 0.4	5.5 ± 0.5	6.1 ± 0	6.1 ± 0.2	6.2 ± 0.5	10.6 ± 1.3	6.2 ± 0.3	5.0 ± 0.6
18:3n-3	22.0 ± 1.4	15.3 ± 1.6	10.2 ± 0.3	12.6 ± 0	12.9 ± 0.1	12.2 ± 0.3	12.2 ± 0.7	12.2 ± 1.1	9.6 ± 1.0
20:4n-6	6.5 ± 0.2	4.1 ± 0.1	3.5 ± 0.3	32.4 ± 1.4	23.2 ± 0.8	20.3 ± 0.3	59.9 ± 10	30.1 ± 0.7	22.7 ± 1.6
20:4n-3	1.7 ± 0.1	ND	ND	0.6 ± 0.8	ND	0.7 ± 0.9	1.1 ± 0.1	ND	ND
20:5n-3	14.8 ± 1.0	12.4 ± 0.7	10.8 ± 1	7.1 ± 0.3	7.2 ± 0.3	8.1 ± 0.5	9.2 ± 1.3	6.8 ± 0.1	6.2 ± 0.7
22:5n-6	ND	ND	ND	5.7 ± 0.6	1.7 ± 0.3	ND	7.1 ± 1.6	3.5 ± 0.0	1.7 ± 0.2
22:5n-3	4.2 ± 0.1	3.7 ± 0.1	3.3 ± 0.1	4.9 ± 0.4	3.2 ± 0.1	3.3 ± 0	7.6 ± 1.3	3.3 ± 0.1	3.2 ± 0.2
22:6n-3	1.8 ± 0.2	62.7 ± 3.4	79.8 ± 0.5	3.2 ± 0	46.8 ± 0.9	65.7 ± 5.6	7.5 ± 1.2	37.8 ± 1	58.2 ± 0.7
Total sat	23.9 ± 0.1	22.8 ± 0.1	24.1 ± 0.3	23.8 ± 0.2	23.2 ± 0.6	24.8 ± 0.1	23.0 ± 0.4	23.8 ± 0.2	26.6 ± 0.5
Total mono	39.2 ± 0.1	27.0 ± 0.6	22.0 ± 1.1	27.2 ± 0.4	23.1 ± 0.1	20.4 ± 0.5	27.2 ± 0.8	21.4 ± 0.6	16.7 ± 1.1
Total diene	6.0 ± 0.1	3.4 ± 0.1	2.6 ± 0.1	4.1 ± 0.1	3.2 ± 0	2.9 ± 0	4.6 ± 0.1	3.4 ± 0.1	2.7 ± 0.1
Total poly	31.0 ± 1.1	46.7 ± 0.9	51.2 ± 1.1	44.9 ± 0.7	50.5 ± 0.5	51.9 ± 0.3	45.3 ± 0.6	51.7 ± 0.7	54.1 ± 0.8

[a]See Table 1 for abbreviations.
[b]Larvae were fed on *Artemia* nauplii enriched with nine different diets containing varying proportions of DHA-/AA-rich oils (detailed composition of diets and enriched *Artemia* are presented in Tables 1 and 2). Data are mean ± SEM values for two blocks.

TABLE 5
Fatty Acid Composition of Larvae White Bass Muscle Tissue After 22 d of Dietary Treatment[a] (mg/g dry weight)

	Artemia diets (DHA/AA ratio)								
FAME	0.0:1.5	5.0:2.8	13.0:4.9	0.4:12.5	3.8:15.4	8.3:15.7	0.5:23.9	4.1:25.0	7.4:25.3
14:0	0.2 ± 0.2	0.7 ± 0.1	1.1 ± 0.1	0.2 ± 0.2	0.7 ± 0.1	1.1 ± 0.2	0.3 ± 0.3	0.8 ± 0.1	1.1 ± 0.1
16:0	7.8 ± 0.1	7.5 ± 0.7	7.5 ± 0.7	7.4 ± 0.7	8.5 ± 0.4	9.1 ± 1.2	7.3 ± 1.8	9.0 ± 0.5	10.1 ± 0.3
16:1n-7	2.3 ± 0.1	2.3 ± 0.2	2.2 ± 0.2	2.0 ± 0.3	2.0 ± 0.2	1.9 ± 0.3	1.8 ± 0.5	1.8 ± 0.1	1.6 ± 0.1
18:0	4.3 ± 0.1	3.2 ± 0.1	3.4 ± 0.3	4.1 ± 0.4	4.5 ± 0.3	4.7 ± 0.6	4.2 ± 1.0	5.0 ± 0.3	5.7 ± 0.1
18:1n-9	24.2 ± 0.1	23.0 ± 1.2	21.1 ± 2.1	21.5 ± 1.9	20.6 ± 2.6	20.1 ± 1.8	18.8 ± 3.2	20.0 ± 1.1	18.5 ± 0.2
18:1n-7	4.7 ± 0.1	4.0 ± 0.7	3.8 ± 0.3	4.0 ± 0.4	4.3 ± 0.9	4.3 ± 0.3	4.1 ± 0.5	4.6 ± 0.4	4.5 ± 0.2
18:2n-6	4.6 ± 0.1	3.5 ± 0.2	3.5 ± 0.3	4.0 ± 0.5	4.1 ± 0.4	4.3 ± 0.5	4.5 ± 1.3	4.8 ± 0.3	4.8 ± 0.1
18:3n-3	11.5 ± 1.4	10.1 ± 0.7	10.1 ± 0.5	9.6 ± 1.2	10.4 ± 1.7	11.8 ± 1.1	10.6 ± 1.3	11.6 ± 0.4	12.1 ± 1.9
20:4n-6	1.9 ± 0.1	1.0 ± 0.1	1.0 ± 0.1	11.3 ± 1.2	8.8 ± 1.3	8.1 ± 0.5	14.5 ± 4.2	13.1 ± 0.5	12.1 ± 0.1
20:4n-3	1.0 ± 0.1	1.0 ± 0.0	0.9 ± 0.0	0.6 ± 0.1	ND	ND	0.8 ± 0.1	0.3 ± 0.5	0.3 ± 0.4
20:5n-3	2.7 ± 0.1	2.8 ± 0.1	2.9 ± 0.3	1.4 ± 0.2	2.4 ± 0.3	2.9 ± 0.3	1.5 ± 0.5	2.2 ± 0.1	2.8 ± 0.1
22:5n-6	0.6 ± 0.8	ND	ND	0.8 ± 1.1	1.1± 0.4	0.6± 0.9	2.5 ± 0.3	1.7 ± 0.2	0.6 ± 0.9
22:5n-3	ND	ND	ND	ND	ND	ND	ND	ND	ND
22:6n-3	0.4 ± 0.2	4.7 ± 0.1	8.1 ± 0.5	0.4 ± 0.0	5.3 ± 0.7	7.9 ± 1.1	0.7 ± 0.2	4.4 ± 0.1	7.6 ± 0.2
Total sat	18.6 ± 0.7	17.9 ± 0.2	18.3 ± 0.7	17.4 ± 0.3	18.8 ± 0.1	19.4 ± 0.1	16.5 ± 0.1	18.7 ± 0.4	20.7 ± 0.1
Total mono	47.1 ± 0.1	45.9 ± 0.6	41.3 ± 4.5	40.9 ± 0.2	37.0 ± 1.7	34.2 ± 0.3	34.9 ± 0.1	33.3 ± 0.1	30.1 ± 0.3
Total diene	6.9 ± 0.1	5.5 ± 0.1	5.3 ± 0.5	5.9 ± 0.1	5.6 ± 0.1	5.6 ± 0.1	6.3 ± 0.1	6.1 ± 0.1	5.9 ± 0.1
Total poly	27.3 ± 0.3	30.7 ± 0.3	35.1 ± 1.5	35.8 ± 0.2	38.5 ± 0.5	40.8 ± 0.3	42.7 ± 0.1	42.0 ± 0.5	43.4 ± 0.2

[a]See Tables 1and 4 for abbreviations and experimental design.

was apparent at dietary contents lower than 2.8 mg AA/g dry weight. Tissue selectivity was largely unchanged at dietary contents higher than 4.9 mg AA/g dry weight. Conversely, DHA accumulation was almost five times higher in brain + eye tissue than in gill and muscle tissue (Fig. 3A). In addition, the selective accumulation of DHA in larvae brain + eyes in response to dietary increase was twofold higher than the selective accumulation of AA. The specific accumulation of DHA in larval brain + eye lipids reached its maximal selectivity at a dietary content of about 5 mg/g dry weight, with only moderate reduction at higher dietary levels. Gill and muscle tissues exhibited only minor selectivity to DHA, mostly at lower than 5 mg/g dry weight as compared to 3–5 times higher selectivity for AA at lower dietary AA levels.

The overall preference of each individual lipid class in larval tissue for both DHA and AA over a wide range of dietary ratios is presented in Figure 4. It is apparent that the PE fraction retained the highest proportion of DHA over AA in each larval tissue at all dietary ratios, whereas PI + PS fraction retained the lowest proportion. High proportions of DHA were also retained in brain + eye tissue PC, especially at high dietary DHA/AA ratios (>1). In addition, changes in DHA/AA

TABLE 6
Fatty Acid Composition of Larvae White Bass Gill Tissue After 22 d of Dietary Treatment[a] (mg/g dry weight)

	Artemia diets (DHA/AA ratio)								
FAME	0.0:1.5	5.0:2.8	13.0:4.9	0.4:12.5	3.8:15.4	8.3:15.7	0.5:23.9	4.1:25.0	7.4:25.3
14:0	ND	0.6 ± 0.6	0.8 ± 0.8	ND	ND	0.8 ± 0.8	ND	0.6 ± 0.6	1.2 ± 0
16:0	13.9 ± 2.5	15.3 ± 0.3	10.9 ± 3.5	14.7 ± 0.4	13.0 ± 0.1	15.8 ± 1.9	14.8 ± 0.7	12.6 ± 3.7	14.6 ± 0.1
16:1n-7	3.5 ± 0.5	3.5 ± 0.3	1.4 ± 1.2	2.8 ± 0.1	2.1 ± 0.1	2.2 ± 0.3	2.5 ± 0.1	1.1 ± 1.0	ND
18:0	9.4 ± 1.3	9.7 ± 0.7	6.5 ± 1.7	9.7 ± 0.1	8.8 ± 0	9.9 ± 0.8	10.4 ± 0.5	9.2 ± 2.4	10.1 ± 0
18:1n-9	35.8 ± 3.4	37.0 ± 2.8	21.0 ± 4.3	31.1 ± 0.4	22.0 ± 1.3	23.4 ± 2.6	26.8 ± 0.5	18.7 ± 6.3	20.5 ± 0.5
18:1n-7	7.6 ± 0.7	7.4 ± 0.3	4.3 ± 1.5	6.7 ± 0.4	5.3 ± 0.8	5.9 ± 0.4	6.8 ± 0.4	4.9 ± 0.3	6.0 ± 0.4
18:2n-6	7.3 ± 1.2	6.4 ± 0.4	4.0 ± 1.5	6.2 ± 0.1	4.7 ± 0.3	5.3 ± 0.5	6.7 ± 0.1	4.8 ± 1.5	4.8 ± 0
18:3n-3	16.0 ± 0.7	12.7 ± 1.1	8.1 ± 2.0	12.5 ± 0.8	9.0 ± 3.5	10.9 ± 1.6	12.9 ± 0.9	8.5 ± 0.7	4.6 ± 3.1
20:4n-6	4.0 ± 1.3	3.1 ± 0.3	3.3 ± 0.2	23.0 ± 0.4	16.5 ± 0.1	16.6 ± 0.7	30.0 ± 1.4	18.7 ± 5.5	18.5 ± 0.1
20:4n-3	ND	ND	ND	ND	ND	ND	ND	ND	ND
20:5n-3	4.7 ± 1.1	6.5 ± 1.4	5.3 ± 1.9	2.6 ± 0.1	3.8 ± 0.1	4.9 ± 0.5	2.7 ± 0	2.7 ± 0.8	3.6 ± 0
22:5n-6	ND	ND	ND	ND	0.9 ± 1.2	0.5 ± 0.7	4.0 ± 0.6	1.5 ± 2.1	2.6 ± 0.5
22:5n-3	ND	ND	ND	ND	ND	ND	ND	ND	ND
22:6n-3	0.3 ± 0.2	9.4 ± 2.5	12.5 ± 4.3	0.7 ± 0	8.4 ± 0	13.2 ± 2.3	1.5 ± 0.2	5.4 ± 1.5	9.7 ± 0.2
Total sat	22.7 ± 0.1	22.9 ± 2.0	23.3 ± 0.7	22.2 ± 0.3	23.1 ± 0.1	24.2 ± 0.3	21.2 ± 0.5	25.3 ± 0.2	26.9 ± 0
Total mono	45.8 ± 0.1	42.9 ± 0.1	34.2 ± 0.1	36.9 ± 0.3	31.1 ± 1.2	28.8 ± 0.4	30.3 ± 0.4	27.9 ± 1.6	27.5 ± 0.3
Total diene	7.1 ± 0.1	5.7 ± 0.1	5.1 ± 0.3	5.6 ± 0.1	5.0 ± 0.1	4.8 ± 0.1	5.6 ± 0.1	5.4 ± 0.1	5.0 ± 0
Total poly	24.4 ± 0.7	28.4 ± 2.4	37.4 ± 0.6	35.3 ± 0.2	40.8 ± 0.1	42.1 ± 0.5	42.9 ± 0.8	41.5 ± 1.6	40.5 ± 1.2

[a]See Tables 1 and 4 for abbreviations and experimental design.

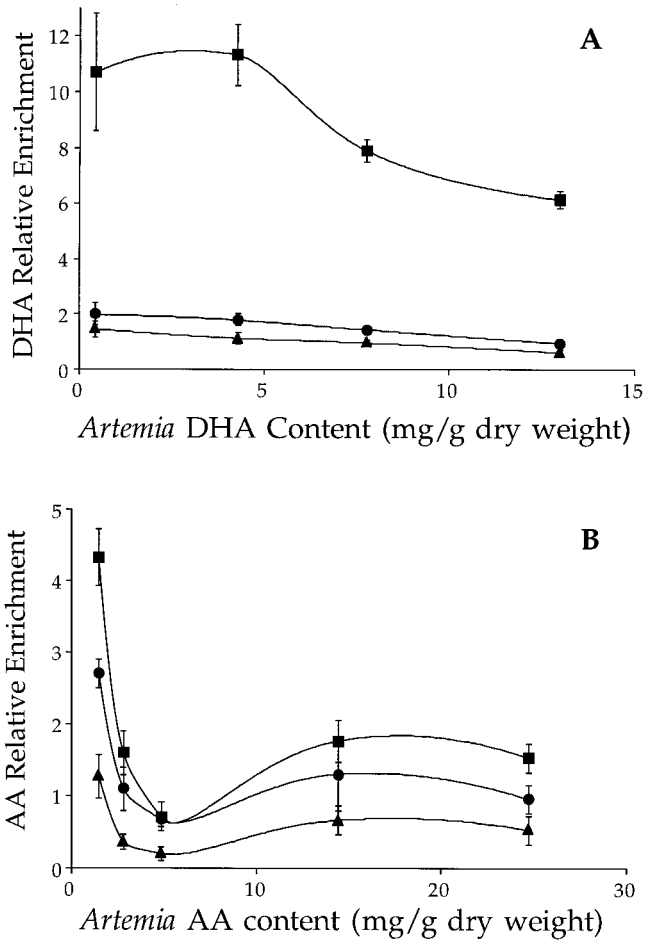

FIG. 3. Selective incorporation of DHA (A) and AA (B) in white bass larval brain + eyes (■), gills (●), and muscle (▲) tissues as a function of increasing dietary content. Larvae were fed for 22 d on *Artemia* enriched with increasing levels of DHA and AA. Values are calculated from data presented in Tables 4, 5, and 6. Data are pooled mean ± SEM values for two blocks. For abbreviations see Figure 1.

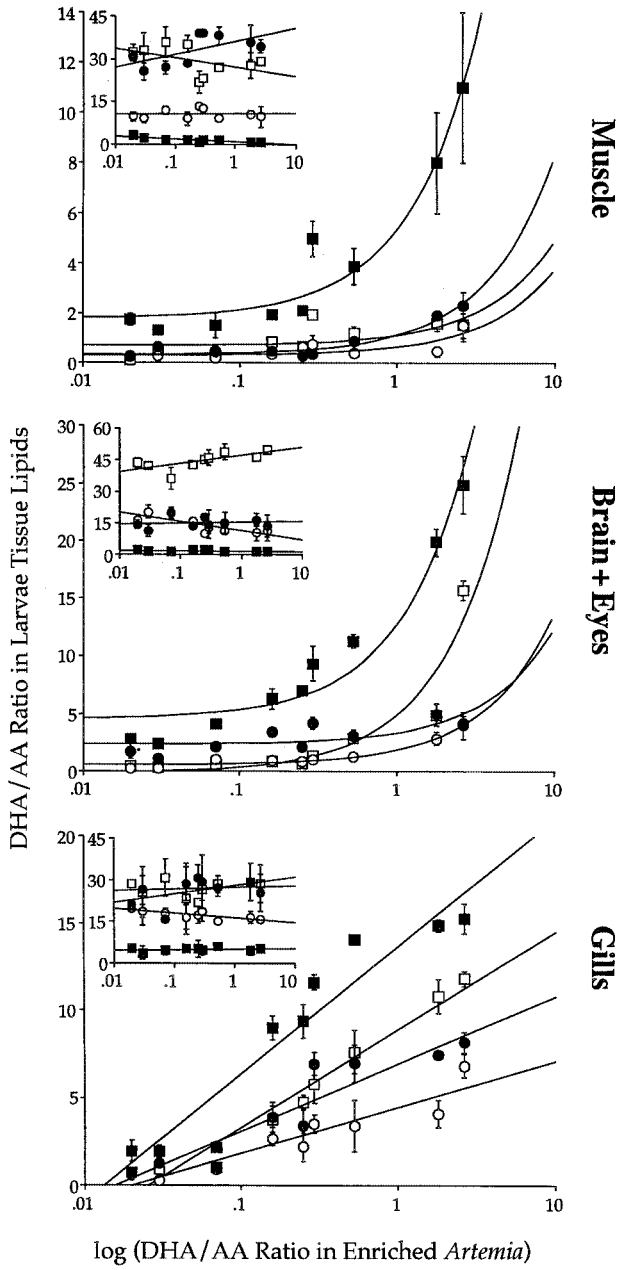

FIG. 4. Effects of enriched *Artemia* dietary DHA/AA ratio on the DHA/AA ratio of white bass larvae muscle, brain + eyes and gill phosphatidylcholine (□), phosphatidylethanolamine (■), phosphatidylinositol + phosphatidylserine (○), and triacylglycerols (●). Insets show the effect of dietary treatment DHA/AA ratio on the percentage of total fatty acids in each lipid class relative to total tissue fatty acids. White bass larvae were fed *Artemia* diets enriched with increasing DHA/AA ratio from day 24 to day 46. The best fit curvilinear lines show a linear relationship of the dietary treatments with gill lipid classes, whereas in muscle and brain + eye tissues the relationship includes a quadratic component. Data are pooled mean ± SEM values for two blocks. For abbreviations see Figure 1.

ratios in larval muscle and brain + eye tissues corresponded linearly with dietary changes, but the magnitude of the change in gill tissue was considerably smaller at higher dietary ratios. The neutral lipids in muscle and brain + eyes exhibited little change in the DHA/AA ratios with dietary changes, although the brain + eye neutral lipids DHA/AA ratio was nearly threefold higher. The gill neutral lipid stores generally reflected the saturable DHA/AA ratio of the polar classes.

Specific accumulation of linolenic acid, EPA, and docosapentaenoic acid (DPA, 22:5n-3) in brain + eye tissue of larvae fed on a diet deficient in both DHA and AA was also noticed (Table 4). Although both linolenic acid and EPA were present in the enriched *Artemia* diets, the proportion of brain + eyes and gill linolenic acid and EPA was nearly twofold higher in larvae fed a DHA- or AA-deficient diet. On the other hand, 22:5n-3 was completely absent in muscle and gill tissue lipids, whereas EPA was not as responsive to DHA or AA dietary changes. Similarly, high levels of 22:5n-6, which is the elongated/desaturated metabolite of AA also accumulated in larval tissues, particularly in brain + eye tissue of larvae fed high levels of AA. However, accumulation of this fatty acid metabolite in larval tissues could be eliminated by dietary inclusion of DHA. Figure 5 illustrates the ratios of

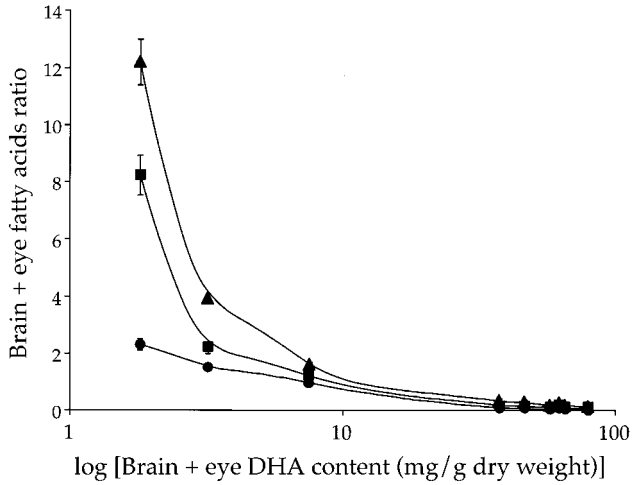

FIG. 5. Relationship between linolenic acid/DHA (▲), EPA/DHA (■), and docosapentaenoic acid (22:5n-3)/DHA (●) and DHA contents in larval white bass brain + eye tissue. Values are calculated from data presented in Table 4. Data are mean ± SEM values for two blocks. For abbreviations see Figure 1.

linolenic acid/DHA, EPA/DHA, and 22:5n-3/DHA in brain + eye tissue lipids relative to its DHA content. It clearly shows that larval brain + eye tissue compensates for its DHA shortage by dramatically increasing the proportion of both EPA and 22:5n-3 as well as linolenic acid. Compensation occurred mainly at levels lower than 10 mg DHA/g dry weight tissue, while at higher tissue DHA contents these fatty acids tended to level off.

Displacement or accumulation rates for each of the essential fatty acids, DHA, AA, EPA, linolenic acid, linoleic acid as well as oleic acid (18:1n-9), in relation with increasing uptake of DHA or AA in larval tissues are summarized in Table 7. In muscle and gill tissues, increased uptake of DHA significantly increased tissue EPA (0.53–0.68 mg increase in EPA per mg increase in tissue DHA). Brain + eye EPA content was not changed by increased uptake of DHA, but was reduced significantly with the increasing uptake of AA (at a rate of 0.46 ± 0.11 mg EPA per mg AA). Dramatic displacement rates were also found for DHA and AA. Brain + eye DHA content was the most sensitive to competition from AA, being displaced at a rate of 0.36 ± 0.07 mg DHA/mg increase in tissue AA, while muscle and gill tissue DHA was not sensitive to increasing levels of AA. On the other hand, AA content in all larval tissues was sensitive to changes in DHA levels, being displaced from brain + eyes at the highest rate of 0.55 ± 0.14 mg AA/mg DHA followed by gills (0.37 ± 0.11 mg AA/mg increase in tissue DHA) and muscle tissue (0.25 ± 0.06 mg AA/mg increase in tissue DHA). Both linolenic and linoleic acids were significantly accumulated in muscle tissue with the increasing uptake of AA (0.16 ± 0.03 and 0.29 ± 0.04 mg/mg AA, respectively), whereas oleic acid was significantly displaced (0.13 ± 0.02 mg/mg AA). Oleic acid was also rapidly displaced from brain + eye tissue with the increasing uptake of AA (0.36 ± 0.11 mg/mg AA) and from gill

TABLE 7
Displacement of Essential Fatty Acids [DHA, AA, EPA, linolenic (18:3n-3) and linoleic (18:2n-6) acids, and 18:1n-9] from Larvae White Bass Tissues by Increased Uptake of DHA or AA[a]

	Brain + eyes	Muscle	Gills
DHA vs. AA	–0.36 ± 0.07 mg/mg AA (R^2 = 0.95, P = 0.008)*	No displacement (P = 0.56)***	No displacement (P = 0.23)***
EPA vs. AA	–0.46 ± 0.11 mg/mg AA (R^2 = 0.81, P = 0.01)*	No displacement (P = 0.19)***	No displacement (P = 0.69)***
18:3n-3 vs. AA	No displacement (P = 0.72)***	+0.16 ± 0.03 mg/mg AA (R^2 = 0.87, P = 0.007)*	No displacement (P = 0.46)***
18:2n-6 vs. AA	No displacement (P = 0.90)***	+0.29 ± 0.04 mg/mg AA (R^2 = 0.97, P = 0.0003)*	No displacement (P = 0.99)***
18:1n-9 vs. AA	–0.36 ± 0.11 mg/mg AA R^2 = 0.74, P = 0.03)*	–0.13 ± 0.02 mg/mg AA (R^2 = 0.92, P = 0.002)*	No displacement (P = 0.4)***
AA vs. DHA	–0.55 ± 0.14 mg/mg DHA (R^2 = 0.80, P = 0.01)*	–0.25 ± 0.06 mg/mg DHA (R^2 = 0.82, P = 0.01)*	–0.37 ± 0.11 mg/mg DHA (R^2 = 0.73, P = 0.03)*
EPA vs. DHA	No displacement (P = 0.83)***	+0.53 ± 0.02 mg/mg DHA (R^2 = 0.99, P < 0.0001)*	+0.68 ± 0.28 mg/mg DHA (R^2 = 0.6, P = 0.07)**
18:3n-3 vs. DHA	No displacement (P = 0.40)***	+0.16 ± 0.04 mg/mg DHA (R^2 = 0.77, P = 0.02)*	No displacement (P = 0.11)***
18:2n-6 vs. DHA	No displacement (P = 0.35)***	No displacement (P = 0.46)***	No displacement (P = 0.46)***
18:1n-9 vs. DHA	No displacement (P = 0.32)***	No displacement (P = 0.46)***	–0.28 ± 0.1 mg/mg DHA (R^2 = 0.65, P = 0.05)**

[a]First-order linear regressions between each pair of fatty acids were obtained by plotting the amount of each essential fatty acid that accumulated in the tissue (in mg/g dry weight) at equal dietary levels (excluding deficient treatments) vs. increasing tissue levels of DHA or AA. A plus or minus sign represents accumulation or displacement, respectively. Rates are mean ± SE value of the slope for two blocks. Regression coefficient (R^2) and P-values indicate the significance level of interaction. *Significant degree of interaction at $P < 0.05$, **low degree of interaction ($P < 0.1$), ***no interaction between the fatty acids ($P > 0.1$). Each regression plot was based on six data point. Displacement rates were calculated based on data presented in Tables 4–6.

tissue with the increasing uptake of DHA (0.28 ± 0.1 mg/mg DHA).

DISCUSSION

Varying dietary DHA and AA ratios affect growth and tissue fatty acid composition during larval development and metamorphosis of white bass, *M. chrysops.* In addition, we observed a marked competition between EFA with both DHA and AA levels fluctuating greatly with the dietary challenges, suggesting that white bass larvae are unable to regulate their EFA composition in the face of dietary changes. These results with *M. chrysops* larvae support previous works that showed *Morone* species, including striped bass and hybrid striped bass (24,25), had PUFA requirements similar to marine fish. Unlike mammals, which can further elongate and desaturate dietary fatty acid precursors to maintain phospholipid composition (26,27), marine fish larvae require a continuous dietary supplementation in an appropriate balance of both AA and DHA. Our results demonstrate the dose-response nature of DHA and AA and their interaction in specific body tissues and lipid classes. Moreover, results specifically suggest that gill tissue AA may decrease sharply at dietary DHA/AA ratios higher than 10.

The ability to convert linolenic acid and EPA to DHA has been generally attributed to freshwater fish species (28); therefore, it was interesting to see whether white bass larvae retained such elongation/desaturation capabilities when raised under almost freshwater conditions (2–6 psu). In fact, larval brain + eye tissue retained only small amounts of DHA (as low as 1.8 ± 0.2 mg/g dry weight) when fed on both linolenic acid and EPA-rich but DHA-deficient *Artemia* diets, suggesting a very low capacity to further elongate and desaturate existing levels of EPA. High accumulation of these fatty acids in brain + eye tissue generally occurred at low DHA levels (<5 mg DHA/g dry weight, Fig. 5), with a significant reduction at increasing DHA levels. Recent studies in mammals have found only trace amounts of EPA in the brain (7), while 22:5n-3 is a product of Δ-6 desaturase systems and generally exhibits a considerable enrichment only in brain + eye tissue, and probably has a low rate of further desaturation to DHA.

The low level of desaturation observed may also be a reflection of dietary input. Tissue lipids of larvae fed DHA- and AA-deficient diets contained high levels of oleic acid, which originated from its elevated levels in the diets. This was particularly noticeable in brain + eye tissues, which doubled in their monounsaturated fatty acid levels in the case of dietary DHA and AA deficiency. Studies in mammals have shown that high dietary intake of oleic acid (18:1n-9) can be associated with a reduced Δ-6 desaturation activity, thereby further limiting the tissue capacity to produce long-chain highly unsaturated fatty acid (HUFA) metabolites from their precursors (29,30), although we are unaware of similar findings in fish larvae. Based on our results, we estimate that in order to avoid compensation by less functional fatty acids, such as oleic acid, EPA, and 22:5n-3, white bass larvae brain + eye tissue must retain a minimum of 5 mg DHA/g dry weight. Our results demonstrate that DHA is specifically incorporated into the structural lipids (mainly PC and PE) of brain + eye tissue, and also that PC containing DHA was the major component in this tissue. This observation is consistent with other works in showing that DHA-rich phospholipids, mainly PC and PE, are the largest constituents of DHA-rich lipid classes in tissues such as neural, retinal, and testicular tissues of many teleost fish (31–34).

Dietary supplementation of AA enhanced DHA accretion in larval brain + eye tissue, as well as 22:5n-6, but only when fed as part of DHA-deficient diets (an elevation from 1.8 ± 0.2 mg DHA/g dry weight at no dietary AA up to 7.5 ± 1.2 mg DHA/g dry weight at the highest content of dietary AA). By contrast, increasing levels of brain + eye DHA were associated with lower accumulation of AA (a reduction from 6.5 ± 0.2 mg AA/g dry weight at no dietary DHA to 3.5 ± 0.3 mg AA/g dry weight at the highest content of dietary DHA). This implies that uptake of AA into brain + eye tissue lipids could preserve more DHA in case of its deficiency, thereby reducing tissue requirement for dietary DHA. Studies have suggested that in a state of deficiency the metabolic conversion of 18:3n-3 and 18:2n-6 to long-chain metabolites is much more efficient than under normal conditions (35,36). Given that both n-3 and n-6 families share the same metabolic pathways of degradation and desaturation and chain elongation, and that the conversion efficiency of long-chain HUFA precursors increases in a state of dietary deficiency, it is not surprising that more DHA was accumulated at higher dietary AA. Therefore, by supplementing with n-6 long-chain metabolites (such as AA), more limiting resources of desaturation and chain elongation will be freed for the production and preservation of tissue DHA.

The question therefore has been raised whether diets rich in n-6 long-chain metabolites could offset the need for n-3 long-chain metabolites. Results show that brain + eye tissue of larvae fed a DHA-deficient but AA-rich diet accumulated, besides a significant amount of 22:5n-6, a maximum of 7.5 ± 1.2 mg DHA/g dry weight, which is slightly above the suggested minimal requirement of 5 mg/g dry weight (Fig. 3). Nonetheless, growth of these larvae was retarded almost by half relative to that of DHA-fed larvae. It is therefore more likely that the observed growth impediment in larvae fed AA-rich but DHA-deficient diets was a result of other functional disorders associated with DHA deficiency. For example, Bell *et al*. (33) found dietary PUFA-deficiency effects on visual performance and predation activity, especially at low light intensities. Other studies have found that eicosanoid production in juvenile turbot, *Scophthalmus maximus,* is dependent on dietary PUFA (37). Consequently, we have concluded that DHA could not be replaced in larvae white bass diets either by its dietary precursors or by n-6 metabolites (including EPA, AA, and 22:5n-6).

Our results clearly showed that when both DHA and AA were supplemented in the diet, DHA was more efficient in displacing AA from larvae gill tissue than AA was in displac-

ing DHA (0.37 ± 0.11 mg decrease in AA per mg increase in DHA vs. no displacement of DHA with increasing tissue AA, $P = 0.23$). On the other hand, DHA increase was associated with a significant accumulation in gill EPA. Such a dramatic reduction in AA or elevation in EPA would have a marked influence on the ability of the larval gill to osmoregulate effectively, since AA-derived prostanoids are essential for regulating fluid and electrolyte balance in fish gill and kidney (38). In fact, we obtained evidence in striped bass, a related species to white bass, that larvae fed DHA-rich diets with no addition of AA survived poorly when challenged by hypersaline water (39).

We also observed higher accumulations of AA relative to DHA in the enriched *Artemia* (Fig. 1). *Artemia* nauplii have been found to metabolize dietary lipids actively and to store them mainly as TAG (40). This would suggest that fatty acid β-oxidation in *Artemia* is more similar to animal models in which n-3 long-chain PUFA were chain-shortened more rapidly than n-6 fatty acids (41–43). This contrasts with mammals, which actively oxidize PUFA by the peroxisomal β-oxidation system. Fish oxidized PUFA mainly by the mitochondrial β-oxidation system, hence enabling them to conserve more n-3 PUFA in their tissues (44).

In contrast with the general tendency of DHA to level off in the lipids of gill tissue, that of the muscle and brain + eye lipids showed a strong linear increase with increasing dietary levels. Furthermore, there were major differences between brain + eyes, muscle, and gills tissues in response to dietary DHA/AA changes. Brain + eyes preferentially accumulating DHA over AA especially into structural lipids (PC, PE), while muscle was equally responsive to both fatty acids. Gills tissue progressively accumulated larger amounts of AA, mainly into the PI fraction, which is a likely source of eicosanoid production in fish (see recent review, Ref. 45). Gills were also the most responsive tissue to a low dietary DHA/AA ratio, but with a limited extent of increase in DHA absorption at high DHA/AA ratios. This result suggests a specific tissue response that regulates either retention or incorporation of EFA into its lipids. Such a specific regulatory response reflects distinct and separate roles that each fatty acid may play in a particular tissue. DHA accumulates particularly in brain synaptic membranes (5,6,10,46), and in the photoreceptor rod outer segments (47). In addition to DHA, AA also accumulates in brain phospholipids (10,14,48), where it actively participates in signal transduction and second messenger functions in neural cells (11,12,49). Furthermore, AA is important as a precursor of eicosanoid production throughout the body (37,50). In the gills and kidney, eicosanoids are involved in the stimulation of ionic transport that regulates the osmotic pressure in the larvae during environmental change (18). Given the antagonistic effect of DHA on AA, and the competition between both, which presumably outweighs the preferential effect in different tissues, an appropriate dietary balance between the two seems essential for the proper functioning of these sensitive tissues.

Finally, our results indicate that the maximal regulatory effect of DHA in brain + eyes was obtained at about 5 mg/g tissue content, whereas maximal regulatory effect of AA was obtained at about 2 mg/g. These estimated values suggest an optimal DHA/AA ratio of *ca*. 2:1 in *Artemia* enrichment diet for larval white bass. Similar ratios were also reported for sea bass larvae (45), of which an optimal dietary ratio of DHA/EPA of *ca.* 2:1 and EPA/AA at *ca*. 1:1 has been suggested.

These findings may be of relevance to questions concerning both the deprivation and excessive loading of long-chain EFA in larval diets. Results suggest that provision of linolenic acid, EPA, and 22:5n-3 may help to offset the decrease in DHA observed in brain + eye tissue, although at the expense of optimal growth. They also clearly support a trend toward regulatory limits on the incorporation of DHA into larval tissues, showing a maximum tissue response at DHA/AA ratio of approximately 2.5:1. At higher than 10:1 ratios, the EFA imbalance in tissue lipids could increase exponentially in favor of DHA.

ACKNOWLEDGMENTS

This research project was funded by the Northeastern Regional Aquaculture Center (Project #94-38500-0044), the Maryland Agricultural Experiment Station's Competitive Grant Program (Project Number MBI-94-78), and by a grant from the U.S.-Israel Science and Technology Foundation, U.S. Department of Commerce. This is a contribution No. 515 from the Center of Marine Biotechnology, University of Maryland Biotechnology Institute.

REFERENCES

1. Eldridge, M.B., Joseph, J.D., Taberski, K.M., and Seaborn, G.T. (1983) Lipid and Fatty Acid Composition of the Endogenous Energy Sources of Striped Bass *(Morone saxatilis)* Eggs, *Lipids 18,* 510–513.
2. Martin, R.M., Wright, D.A., and Means, J.C. (1984) Fatty Acids and Starvation in Larval Striped Bass *(Morone saxatilis)*, *Comp. Biochem. Physiol. B 77,* 785–790.
3. Kanazawa, A., Teshima, S., and Ono, K. (1979) Relationship Between Essential Fatty Acid Requirements of Aquatic Animals and the Capacity for Bioconversion of Linolenic Acid to Highly Unsaturated Fatty Acids, *Comp. Biochem. Physiol. B 63,* 295–298.
4. Neuringer, M., Anderson, G.J., and Connor, W.E. (1988) The Essentiality of n-3 Fatty Acids for the Development and Function of the Retina and Brain, *Annu. Rev. Nutr. 8,* 517–541.
5. Mourente, G., Tocher, D.R., and Sargent, J.R. (1991) Specific Accumulation of Docosahexaenoic Acid (22:6n-3) in Brain Lipids During Development of Juvenile Turbot (*Scophthalmus maximus* L.), *Lipids 26,* 871–877.
6. Arbuckle, L.D., and Innis, S.M. (1992) Docosahexaenoic Acid in Developing Brain and Retina of Piglets Fed High or Low α-Linolenate Formula With and Without Fish Oil, *Lipids 27,* 89–93.
7. Wainwright, P.E., Huang, Y.S., Bulman-Fleming, B., Dalby, D., Mills, D.E., Redden, P., and McCutcheon, D. (1992) The Effects of Dietary n-3/n-6 Ratio on Brain Development in the Mouse: A Dose Response Study with Long-chain n-3 Fatty Acids, *Lipids 27,* 98–103.
8. Brown, M.F. (1994) Modulation of Rhodopsin Function by Properties of the Membrane Bilayer, *Chem. Phys. Lipids 73,* 159–180.

9. Rehncrona, S., Westerberg, E., Akesson, B., and Siesjo, B.K. (1982) Brain Cortical Fatty Acids and Phospholipids During and Following Complete and Severe Incomplete Ischemia, *J. Neurochem. 38,* 84–93.
10. Huang, M.-C., and Craig-Schmidt, M.C. (1996) Arachidonate and Docosahexaenoate Added to Infant Formula Influence Fatty Acid Composition and Subsequent Eicosanoid Production in Neonatal Pigs, *J. Nutr. 126,* 2199–2208.
11. Shimizu, T., and Wolfe, L.S. (1990) Arachidonic Acid Cascade and Signal Transudation, *J. Neurochem. 55,* 1–15.
12. Bell, J.G., Tocher, D.R., and Sargent, J.R. (1994) Effect of Supplementation with 20:3(n-6), 20:4(n-6) and 20:5(n-3) on the Production of Prostaglandins E and F of the 1-, 2- and 3- Series in Turbot *(Scophthalmus maximus)* Brain Astroglial Cells in Primary Culture, *Biochim. Biophys. Acta 1211,* 335–342.
13. Fonlupt, P., Croset, M., and Lagarde, M. (1994) Incorporation of Arachidonic and Docosahexaenoic Acids into Phospholipids of Rat Brain Membranes, *Neurosci. Lett. 171,* 137–141.
14. Shetty, H.U., Smith, Q.R., Washizaki, K., Rapoport, S.I., and Purdon, A.D. (1996) Identification of Two Molecular Species of Rat Brain Phosphatidylcholine That Rapidly Incorporate and Turn Over Arachidonic Acid *in vivo, J. Neurochem. 67,* 1702–1710.
15. Takeuchi, T., and Watanabe, T. (1977) Requirement of Carp for Essential Fatty Acids, *Bull. Jpn. Soc. Sci. Fish. 43,* 541–551.
16. Takeuchi, T., and Watanabe, T. (1979) Requirement of Juvenile Red Sea Bream *(Pagrus major)* for Eicosapentaenoic and Docosahexaenoic Acids, *Bull. Jpn. Soc. Sci. Fish. 45,* 1517–1520.
17. Bell, J.G., and Ghioni, C. (1993) Lipid Composition of Eyes from American *(Homarus americanus)* and European *(Homarus gammarus)* Lobsters, *Comp. Biochem. Physiol. B 105,* 649–653.
18. Castell, J.D., Bell, J.G., Tocher, D.R., and Sargent, J.R. (1994) Effects of Purified Diets Containing Different Combinations of Arachidonic and Docosahexaenoic Acid on Survival, Growth and Fatty Acid Composition of Juvenile Turbot *(Scophthalmus maximus), Aquaculture 128,* 315–333.
19. Estevez, A., Ishikawa, M., and Kanazawa, A. (1997) Effects of Arachidonic Acid on Pigmentation and Fatty Acid Composition of Japanese Flounder (*Paralichthys olivaceus,* Temminck and Schlegel), *Aquacult. Res. 28,* 279–289.
20. Folch, J., Lees, M., and Sloane Stanley, G.H.S. (1957) A Simple Method for the Isolation and Purification of Total Lipids from Animal Tissues, *J. Biol. Chem. 226,* 497–509.
21. Morrison, W.R., and Smith, L.M. (1964) Preparation of Fatty Acid Methyl Esters and Dimethyl Acetyls from Lipids with Boron Fluoride-Methanol, *J. Lipid Res. 5,* 600–608.
22. Olsen, R.E., and Henderson, R.J. (1989) The Rapid Analysis of Neutral and Polar Marine Lipids Using Double-Development HPTLC and Scanning Densitometry, *J. Exp. Mar. Biol. Ecol. 129,* 189–197.
23. ANOVA, *Statview 4.5* (1992) Abacus Concepts, Inc., Berkeley, CA.
24. Douglas, F.M., Wright, D.A., and Means, J.C. (1984) Fatty Acids and Starvation in Larval Striped Bass *(Morone saxatilis), Comp. Biochem. Physiol. B 77,* 785–790.
25. Tuncer, H., and Harrell, R.M. (1992) Essential Fatty Acid Nutrition of Larval Striped Bass *(Morone saxatilis)* and Palmetto Bass (*M. saxatilis* × *M. chrysops*), *Aquaculture 101,* 1–2.
26. Bezard, J., Blond, J.P., Bernard, A., and Clouet, P. (1994) The Metabolism and Availability of Essential Fatty Acids in Animal and Human Tissues, *Reprod. Nutr. Dev. 34,* 539–568.
27. Gerster, G. (1998) Can Adults Adequately Convert Alpha-Linolenic Acid (18:3n-3) to Eicosapentaenoic Acid (20:5n-3) and Docosahexaenoic Acid (22:6n-3)? *Internat. J. Vit. Nutr. Res. 68,* 159–173.
28. Watanabe, T., Ohta, M., Kitajima, C., and Fujita, S. (1982) Improvement of Dietary Value of Brine Shrimp *Artemia salina* for Fish Larvae by Feeding Them on Omega 3 Highly Unsaturated Fatty Acids, *Bull. Jpn. Soc. Sci. Fish. 48,* 1775–1782.
29. Holman, R.T. (1964) Nutritional and Metabolic Interrelationships Between Fatty Acids, *Fed. Proc. 23,* 1062–1067.
30. Periago, J.L., Sanchez del Castillo, M.A., Caamano, G., and Suarez, M.D. (1989) Changes in Lipid Composition of Liver Microsomes and Fatty Acyl-Desaturase Activities Induced by Medium-chain Triglyceride Feeding, *Lipids 24,* 383–388.
31. Bell, M.V., and Dick, J.R. (1993) The Appearance of Rods in the Eyes of Herring and Increased Di-docosahexaenoyl Molecular Species of Phospholipids, *J. Mar. Biol. Assoc. U.K. 73,* 679–688.
32. Navarro, J.C., Batty, R.S., Bell, M.V., and Sargent, J.R. (1993) Effects of Two *Artemia* Diets with Different Contents of Polyunsaturated Fatty Acids on the Lipid Composition of Larvae of Atlantic Herring *(Clupea harengus), J. Fish Biol. 43*, 503–515.
33. Bell, M.V., Batty, R., Navarro, J.C., Sargent, J.R., and Dick, J.R. (1995) Dietary Deficiency of Docosahexaenoic Acid Impairs Vision at Low Light Intensities in Juvenile Herring (*Clupea harengus* L.), *Lipids 30,* 443–449.
34. Estevez, A., and Kanazawa, A. (1996) Fatty Acid Composition of Neural Tissues of Normally Pigmented and Unpigmented Juveniles of Japanese Flounder Using Rotifer and *Artemia* Enriched in n-3 HUFA, *Fish. Sci. 62,* 88–93.
35. Bjerve, K.S., Mostad, I.L., and Thorensen, L. (1987) Alpha-Linolenic Acid Deficiency in Patients on Long Term Gastric Tube Feeding Estimation of Linolenic Acid and Long-chain Unsaturated n-3 Fatty Acid Requirement in Man, *Am. J. Clin. Nutr. 45,* 66–77.
36. Ruyter, B., and Thomassen, M.S. (1999) Metabolism of n-3 and n-6 Fatty Acids in Atlantic Salmon Liver: Stimulation by Essential Fatty Acid Deficiency, *Lipids 34,* 1167–1176.
37. Bell, M.V., Castell, J.D., Tocher, D.R., MacDonald, F.M., and Sargent, J.R. (1995) Effects of Different Dietary Arachidonic Acid: Docosahexaenoic Acid Ratios on Phospholipid Fatty Acid Compositions and Prostaglandins Production in Juvenile Turbot *(Scophthalmus maximus), Fish Physiol. Biochem. 14,* 139–151.
38. Bell, J.G., Farndale, B.M., Dick, J.R., and Sargent, J.R. (1996) Modification of Membrane Fatty Acid Composition, Eicosanoid Production, and Phospholipase A Activity in Atlantic Salmon *(Salmo salar)* Gill and Kidney by Dietary Lipids, *Lipids 31,* 1163–1171.
39. Harel, M., Gavasso, S., Leshin, J., Gubernatis, A., and Place, A.R. (2000) Enhancing the Stress and Non-specific Immune Responses of Larval Striped Bass, *Morone saxitalis* by Dietary Modulation of n-3 and n-6 Series Fatty Acids, presented at Aqua 2000 Congress, The Annual Meeting of the World and European Aquaculture Societies, Nice, France, May 2–6, 2000.
40. Harel, M., Ozkizilcik, S., Lund, E., Behrens, P., and Place, A.R. (1999) Enhanced Absorption of Docosahexaenoic Acid (DHA, 22:6n-3) in *Artemia* Nauplii Using a Dietary Combination of DHA-rich Phospholipids and DHA-sodium Salts, *Comp. Biochem. Physiol. B 124,* 169–176.
41. Leyton, J., Drury, P.J., and Crawford, M.A. (1987) Differential Oxidation of Saturated and Unsaturated Fatty Acids *in vivo* in the Rat, *Br. J. Nutr. 57,* 383–393.
42. Nettleton, J.A. (1991) n-3 Fatty Acids: Comparison of Plant and Seafood Sources in Human Nutrition, *J. Am. Diet. Assoc. 91,* 331–337.
43. Vamecq, V., Valle, L., Lechene de la Porte, P., Fontaine, M., Craemer, D., Van den Branden, C., Lafont, H., Grataroli, R., and Nalbone, G. (1993) Effect of Various n-3/n-6 Fatty Acid Ratio Contents of High Fat Diets on Rat Liver and Heart Peroxisomal and Mitochondrial Beta-Oxidation, *Biochim. Biophys. Acta 1170,* 151–156.
44. Sargent, J.R., Henderson, R.J., and Tocher, D.R. (1989) The

Lipids, in *Fish Nutrition* (Halver, J.E., ed.) pp. 153–218, Academic Press Inc., New York.
45. Sargent, J., Bell, G., McEvoy, L., Tocher, D., and Estevez, A. (1999) Recent Development in the Essential Fatty Acid Nutrition of Fish, *Aquaculture 177,* 191–199.
46. Tocher, D.R. (1993) Effects of Growth Factors on the Metabolism of Linolenate (18:3n-3) and Eicosapentaenoate (20:5n-3) in Rainbow Trout *(Oncorhynchus mykiss)* Astrological Cells in Primary Culture, *Comp. Biochem. Physiol. B 105,* 743–748.
47. Kanazawa, A. (1991) Importance of Dietary Docosahexaenoic Acid on Growth and Survival of Fish Larvae, in *Finfish-Hatchery in Asia. Proceeding of Finfish Hatchery in Asia '91*, pp. 87–95, Tungkang Marine Laboratory, Keelung Taiwan.
48. Mourente, G., and Tocher, D.R. (1992) Effects of Weaning onto a Pelleted Diet on Docosahexaenoic Acid (22:6n-3) Levels in Brain of Developing Turbot (*Scophthalmus maximus* L.), *Aquaculture 105,* 363–377.
49. Axelrod, J., Burch, R.M., and Jelsema, C.L. (1988) Receptor-Mediated Activation of Phospholipase A_2 *via* GTP-Binding Proteins: Arachidonic Acid and Its Metabolites as Second Messengers, *Trends Neurosci. 11,* 117–123.
50. Sargent, J.R. (1995) Origin and Functions of Egg Lipids: Nutritional Implications, in *Broodstock Management and Egg and Larval Quality* (Bromage, N.R., and Roberts, R.J., eds.) pp. 353–372, Blackwell, Oxford.

[Received November 29, 1999, and in revised form August 9, 2000; revision accepted October 2, 2000]

Effects of Fructose and Troglitazone on Phospholipid Fatty Acid Composition in Rat Skeletal Muscle

John N. Clore*, Jing Li, and William B. Rizzo

Departments of Medicine and Pediatrics, Virginia Commonwealth University, Richmond, Virginia

ABSTRACT: Skeletal muscle phospholipid fatty acid (PLFA) composition is associated with insulin sensitivity in animal models and in man. However, it is not clear whether changes in insulin sensitivity cause a change in PLFA composition or vice versa. The present studies have examined the effects of agents known to increase or decrease insulin sensitivity on PLFA composition of the major phospholipids, phosphatidylcholine (PC) and phosphatidylethanolamine (PE), in soleus and extensor digitorum longus muscle. Four groups of Sprague-Dawley rats—control, 0.2% troglitazone (Tgz), 60% fructose fed, and fructose + Tgz—were treated for 3 wk. Fructose feeding was associated with a decrease in muscle membrane polyunsaturated fatty acids (PUFA) and n-3 fatty acids in both PC and PE. Administration of Tgz alone resulted in an increase in liver (3.75 ± 0.93 to 6.93 ± 1.00 μmol/min/mg tissue, $P < 0.05$) and soleus muscle (0.34 ± 0.03 to 0.67 ± 0.09 μmol/min/mg, $P < 0.01$) elongase activity, which would be expected to increase membrane PUFA. However, Tgz decreased PLFA associated with greater insulin sensitivity (e.g., PUFA and n-3 fatty acids) and increased PLFA associated with decreased insulin sensitivity (16:0 and n-6 fatty acids) in both PC and PE. Co-administration of fructose and Tgz did not reverse the decrease in PUFA observed with fructose alone. We conclude that the improvement in insulin sensitivity reported with Tgz is associated with an apparently paradoxical effect to decrease PUFA and n-3 PLFA composition in rat skeletal muscle. These studies suggest that Tgz-mediated increases in insulin sensitivity do not result in improved PLFA composition.

Paper no. L8537 in *Lipids 35*, 1281–1287 (November 2000).

Insulin sensitivity is related in part to the composition of skeletal muscle membranes. We (1) and others (2–4) have shown an inverse relationship between insulin resistance and the percentage of long-chain polyunsaturated fatty acids (PUFA) in human muscle membrane phospholipids (PL). Moreover, increased PUFA are found in membrane PL of more insulin sensitive muscle (Type I) compared to Type II fibers (2,5), suggesting that membrane PL fatty acid composition may play a significant role in the relative insulin responsiveness of muscle fiber types. Of particular interest are the PL phosphatidylcholine (PC) and phosphatidylethanolamine (PE), which together account for more than 75% of the total plasma membrane PL. It is known that the outer and inner layers of the plasma membrane bilayers contain greater proportions of PC and PE, respectively. Thus, differences in the fatty acid composition of these two PL species could have independent effects on insulin responsiveness. In support of this hypothesis, we recently demonstrated that the fatty acid composition of PC (but not PE) in Type II rat muscle was characterized by an enrichment of palmitic acid (16:0) relative to stearic acid (18:0), which suggested a defect in fatty acid elongation in the insulin-resistant muscle. In addition, studies performed in our laboratory in normal human volunteers demonstrated for the first time that the fatty acid composition of PC, but not PE, was related to insulin sensitivity.

Although considerable evidence exists for an association between PL fatty acid (PLFA) composition and insulin sensitivity, recent studies suggest that changes in insulin sensitivity are also associated with changes in fatty acid composition. In studies performed in rats, Storlein *et al.* (8) showed that diets high in fat are associated with increased insulin resistance and that alterations in the fatty acid composition of the diet could ameliorate that effect. Marked changes in skeletal muscle PLFA induced by diets low in PUFA have also been shown to reduce insulin binding and, presumably, insulin action in rats (9,10). In man, Anndersson *et al.* (11) have demonstrated that increasing exercise, which is well known to increase insulin sensitivity, is associated with a decrease in skeletal muscle membrane saturation and total n-6 fatty acids. Finally, we have recently reported that nicotinic acid, an agent known to reduce insulin sensitivity, decreases skeletal muscle membrane PUFA composition of PC but not PE (12). Despite these and other data demonstrating a relationship between changes in insulin sensitivity and PLFA composition, it is by no means clear whether changes in insulin sensitivity mediate the changes in PLFA composition or vice versa. To address this issue, we have examined the effects of (i) high fructose feeding, which is known to increase insulin resistance (13), and (ii) troglitazone, an agent known to improve insulin sensitivity (14) and to reverse the effects of fructose in animal models (15) on skeletal muscle membrane PLFA. Our studies have demonstrated adverse effects of both trogli-

*To whom correspondence should be addressed at Division of Endocrinology and Metabolism, Virginia Commonwealth University, Box 980155, Richmond, VA 23298. E-mail: clore@hsc.vcu.edu

Abbreviations: CL, cardiolipin; EDL, extensor digitorum longus; F, fructose; PC, phosphatidylcholine; PE, phosphatidylethanolamine; PI, phosphatidylinositol; PL, phospholipid; PLFA, PL fatty acid; PS, phosphatidylserine; PUFA, polyunsaturated fatty acid; SM, sphingomyelin; Tgz, troglitazone; TLC, thin-layer chromatography.

tazone and high fructose diet on fatty acid composition. These studies suggest that the improvement in insulin sensitivity known to occur with troglitazone administration is not mediated by induction of a more favorable skeletal muscle membrane fatty acid profile.

MATERIALS AND METHODS

Study design. Male Sprague Dawley rats (~120 gm) were used in all of the described studies. Animals were housed individually and had free access to food and water. After adaptation to a powdered standard chow, the animals were divided into four groups and fed *ad libitum* with the following diets for 3 wk: standard powdered chow; powdered chow supplemented with troglitazone (0.2%) as previously described (Tgz); 60% fructose (F) diet (Harlan Teklad, Madison, WI); and 60% fructose supplemented with 0.2% troglitazone (F + Tgz). Analysis of the fatty acid composition of the regular chow diet and the high fructose diet is shown in Table 1. Mean body weights of animals (170.8 ± 2.9 g, $n = 52$) were not different at sacrifice in any of the treatment groups (data not shown). Overnight-fasted male Sprague-Dawley rats were killed by cervical dislocation after undergoing ether anesthesia. Blood samples were obtained by cardiac puncture, and soleus and extensor digitorum longus (EDL) muscles were removed immediately for assessment of insulin sensitivity and/or PL analyses. All studies were approved by the Institutional Animal Care Utilization Committee of Virginia Commonwealth University.

PLFA composition. PLFA were analyzed according to Borkman *et al.* (16) with minor modifications. Hemi-muscles (50–60 mg) were homogenized and total lipids were extracted by the method of Folch *et al.* (17). The lipid extracts were dried under nitrogen, dissolved in 10 mL of hexane, and applied to 3 mL silica gel columns (J.T. Baker, Inc., Phillipsburg, NJ). After elution of less polar lipids with 20 mL hexane followed by 10 mL dichlormethane, PL were eluted with 10 mL methanol. The methanol eluates were dried under nitrogen and transmethylated with 1.5 mL 1 N methanolic HCL at 80°C overnight. Fatty acid methyl esters were extracted with 6 mL hexane and dried under nitrogen.

To determine the fatty acid composition of individual PL species, PC, PE, sphingomyelin (SM), phosphatidylinositol (PI), cardiolipin (CL), and phosphatidylserine (PS) were first separated by thin-layer chromatography (TLC) on silica gel G plates (LK6D; Whatman, Maidstone, England) using a solvent system consisting of chloroform/ethanol/triethylamine/water (30:34:30:8, by vol) for the first development and hexane/dimethyl ether (50:50, vol/vol) for the second development. PL were visualized under ultraviolet light after spraying the plate with rhodamine G. The separated PL spots were scraped and placed into glass tubes. Fatty acid methyl esters were prepared as described above by treatment with methanolic acid.

Fatty acid methyl esters from both the total PL fractions and the individual PL species were redissolved in 20 μL hexane, separated, and quantitated on a Hewlett-Packard 5890 gas chromatograph equipped with a 30 × 0.2 mm fused-silica capillary column (Omega Wax 320; Supelco, Inc., Bellefonte, PA,) and flame-ionization detector. The injection temperature was 250°C and the detector temperature was 300°C. The initial oven temperature was 140°C. After 5 min the oven temperature was increased from 140 to 200°C at a rate of 20°C/min, then to 280°C at 5°C/min. Fatty acids were identified by comparing their retention times with those of authentic standards.

Most of the gas chromatograph peaks were identified as specific fatty acid methyl esters. In the total PL and PC preparations, these fatty acid methyl esters accounted for 87 and 93% of the total integrated area, respectively, whereas they comprised only 79% of the integrated area in the PE fraction. In all samples, however, there were peaks immediately preceding 16:0 and 18:0 that were suspected to be dimethyl acetal derivatives of fatty aldehydes released from ether PL (plasmalogens). To confirm this identification, PE from bovine brain containing 60% plasmalogens (Sigma, St. Louis, MO) was chromatographed before and after mild acid fume hydrolysis (18). After mild acid fume hydrolysis and separation on TLC plates, the peaks before 16:0 and 18:0 suspected of being derived from plasmalogens completely disappeared, essentially confirming their identity.

Plasma insulin concentrations were determined by radioimmunoassay (19). In some experiments, microsomal elongase activity was determined in liver and skeletal muscle samples using 2-^{14}C-malonyl CoA as previously described (18). Concentrations of malonyl CoA were determined by the incorporation of ^{3}H-acetyl CoA into palmitic acid (20) following the addition of fatty acid synthetase isolated from rat liver (21). PL, triglyceride, cholesterol, and fatty acid standards were obtained from Sigma. High-performance precoated silica gel Hp-K plates (10 × 10 cm) were purchased from Whatman (Clifton, NJ). All other reagents and solvents were of analytical or high-performance liquid chromatography-grade from Sigma or Fisher (Pittsburgh, PA).

Statistical analysis. All analyses were performed using SPSS v10.0.5 (SPSS, Inc., Chicago, IL). Comparison of groups was performed using one-way analysis of variance and Tukey's HSD *post hoc* test. Comparison of groups to

TABLE 1
Fatty Acid Composition (%) of Regular Chow and a 60% Fructose Diet

	16:0	18:0	18:1n-6	18:2n-6	18:3n-6	18:3n-3
Regular chow	11.1	7.2	7.0	10.2	53.3	5.4
Fructose (60%)	22.8	35.0	20.0	11.6	0.15	0.5

TABLE 2
Phosphatidylcholine Fatty Acid Composition in Rat Soleus Muscle After 3 wk of Diet Composed of Standard Chow (control), Chow Plus 0.2% Troglitazone (Tgz), 60% Fructose Chow (fructose), and Fructose Plus Tgz[a]

	Control	Tgz	Fructose	Fructose + Tgz
16:0	20.5 ± 0.4	22.5 ± 0.2	22.9 ± 0.8*	23.7 ± 0.9**
18:0	18.6 ± 0.4	15.3 ± 0.2**	18.4 ± 1.0	15.5 ± 0.4**,‡
18:1n-6	8.1 ± 0.1	10.0 ± 0.2*	16.3 ± 0.9**	18.1 ± 0.4**
18:2n-6	17.3 ± 0.3	20.1 ± 0.5**	14.8 ± 0.5**	15.8 ± 0.5*
18:3n-6	0.16 ± 0.1	0.17 ± 0.01	0.1 ± 0.1**	0.1 ± 0.1**
20:4n-6	20.6 ± 0.4	19.1 ± 0.3	14.2 ± 0.6**	11.8 ± 0.5**,‡
22:4n-6	0.74 ± 0.1	0.7 ± .01	0.6 ± 0.03**	0.4 ± 0.1**,‡
22:5n-3	2.55 ± 0.1	2.1 ± 0.4**	0.73 ± 0.05**	0.5 ± 0.1**,‡
22:6n-3	5.70 ± 0.2	3.5 ± 0.2**	2.1 ± 0.15**	1.2 ± 0.1**,‡
16:0/18:0	1.1 ± 0.1	2.4 ± 0.3**	1.3 ± 0.1	1.5 ± 0.1
ΣC20–22	30.4 ± 0.4	26.2 ± 0.5**	19.0 ± 0.75**	15.5 ± 0.7**,‡
20:4/20:3	52.1 ± 8.6	47.0 ± 5.6	14.3 ± 1.8**	9.8 ± 1.5**
20:3/18:2	0.02 ± 0.01	0.02 ± 0.01	0.07 ± 0.01**	0.07 ± 0.01**

[a]Results shown are mean percentage ± SEM; $n = 6$ animals in each group. *$P < 0.05$, **$P < 0.01$ compared to control. ‡$P < 0.01$ compared to fructose alone.

control was performed by one-way analysis of variance and Dunnett's *post hoc* test. Statistical significance was assumed at the 5% level.

RESULTS

No differences in fasting plasma glucose (94.3 ± 5.4, 96.1 ± 2.9, 101.1 ± 4.2 mg/dL, ns) or insulin (0.22 ± 0.03, 0.21 ± 0.02, 0.20 ± 0.03 ng/mL, ns) concentrations were seen in animals fed F, Tgz, or control diet, respectively. However, significant effects of Tgz and a high F diet on soleus and EDL muscle PC fatty acids were observed. As shown in Table 2, treatment with Tgz increased the content of oleic (18:1) and linoleic (18:2) acids and decreased stearic (18:0), eicosapentanoic (22:5n-3), and decosahexanoic (22:6) acid as well as the total PUFA content of soleus muscle. Following 3 wk of a high F diet, the content of oleic acid in PC fatty acids obtained from soleus muscle increased from 8.1 ± 0.1 to 16.3 ± 0.9% ($P < 0.001$) whereas a broad-based reduction in the content of long-chain PUFA was observed ($P < 0.001$) compared to regular chow-fed animals. These changes likely reflect the lower content of long-chain PUFA in the F diet (Table 1) (22). Contrary to our hypothesis, supplementation with Tgz again decreased PC content of 18:0 despite greater dietary content, and total PUFA decreased further compared to F alone. Comparison of the PC fatty acid composition of the insulin sensitive soleus (Table 2) and insulin-resistant EDL (Table 3) muscle demonstrates the known striking differences in the two muscle types (7) with a greater ratio of 16:0 to 18:0 (4.0 ± 0.2 vs 1.1 ± 0.1, $P < 0.01$) and decreased PUFA (24.2 ± 0.9 vs. 30.4 ± 0.4, $P < 0.01$) in EDL compared to soleus muscle, respectively. However, nearly identical directional changes were observed in the fatty acid content of EDL muscle following Tgz administration without or with high F feeding

TABLE 3
Phosphatidylcholine Fatty Acid Composition in Rat Extensor Digitorum Longus Muscle After 3 wk of Diet Composed of Standard Chow, Chow Plus 0.2% Troglitazone (Tgz), 60% Fructose Chow, and Fructose Plus Tgz[a]

	Control	Tgz	Fructose	Fructose + Tgz
16:0	32.5 ± 0.9	34.2 ± 0.9	34.7 ± 0.5*	34.5 ± 0.4
18:0	8.1 ± 0.2	5.8 ± 0.1**	7.8 ± 0.3	6.0 ± 0.3**,‡
18:1n-6	7.0 ± 0.1	8.5 ± 0.2**	14.6 ± 0.4**	16.7 ± 0.4**,‡
18:2n-6	23.3 ± 0.7	26.1 ± 0.3**	18.9 ± 0.3**	16.5 ± 0.5**,‡
18:3n-6	0.2 ± 0.1	0.2 ± 0.1	0.1 ± 0.1**	0.1 ± 0.1**
20:4n-6	18.0 ± 0.6	15.4 ± 0.5**	12.1 ± 0.3**	11.3 ± 0.3**
22:4n-6	0.6 ± 0.1	0.5 ± 0.1	0.4 ± 0.1**	0.4 ± 0.1**
22:5n-3	1.8 ± 0.1	1.2 ± 0.1**	0.5 ± 0.1**	0.5 ± 0.1**
22:6n-3	3.1 ± 0.2	1.7 ± 0.1**	1.2 ± 0.1**	1.0 ± 0.1**
16:0/18:0	4.0 ± 0.2	5.9 ± 0.2**	4.7 ± 0.2	5.8 ± 0.3**,‡
ΣC20–22	24.2 ± 0.9	19.6 ± 0.6**	15.5 ± 0.4*	15.1 ± 0.5**
20:4/20:3	45.9 ± 7.0	40.6 ± 1.7	12.4 ± 0.7**	7.2 ± 0.5**
20:3/18:2	0.02 ± 0.01	0.01 ± 0.01	0.05 ± 0.01**	0.10 ± 0.01**,‡

[a]Results shown are mean percentage ± SEM; $n = 6$ animals in each group. *$P < 0.05$, **$P < 0.01$ compared to control. †$P < 0.05$, ‡$P < 0.01$ compared to fructose alone.

TABLE 4
Phosphatidylethanolamine Fatty Acid Composition in Rat Soleus Muscle After 3 wk of Diets Composed of Standard Chow, Chow Plus 0.2% Troglitazone (Tgz), 60% Fructose Chow, and Fructose Plus Tgz[a]

	Control	Tgz	Fructose	Fructose + Tgz
16:0	3.9 ± 0.2	5.1 ± 0.5*	4.2 ± 0.2	4.9 ± 0.2†
18:0	24.6 ± 0.3	22.7 ± 0.3*	24.5 ± 0.8	23.9 ± 0.2
18:1n-6	4.7 ± 0.1	6.2 ± 0.2*	7.4 ± 0.6**	8.9 ± 0.6
18:2n-6	6.3 ± 0.3	7.9 ± 0.1**	4.6 ± 0.2**	6.3 ± 0.4‡
18:3n-6	0.07 ± 0.01	0.08 ± 0.01	0.05 ± 0.01	0.05 ± 0.01
20:4n-6	16.4 ± 0.3	16.9 ± 0.4	19.5 ± 0.4**	19.6 ± 0.4**
22:4n-6	2.2 ± 0.1	2.5 ± 0.2	2.7 ± 0.2	2.7 ± 0.3
22:5n-3	4.3 ± 0.1	4.5 ± 0.3	2.3 ± 0.1**	2.6 ± 0.2**
22:6n-3	17.1 ± 0.7	12.8 ± 0.3	10.8 ± 0.8**	8.0 ± 0.6**,†
16:0/18:0	0.16 ± 0.01	0.23 ± 0.02**	0.17 ± 0.01	0.20 ± 0.01*
ΣC20–22	40.5 ± 0.8	37.1 ± 1.1	36.6 ± 1.4*	34.9 ± 1.4*
20:4/20:3	93.6 ± 14.5	204.6 ± 83.8	27.0 ± 3.3**	15.0 ± 0.2‡
20:3/18:2	0.03 ± 0.01	0.02 ± 0.01	0.17 ± 0.02**	0.23 ± 0.03**

[a]Results shown are mean percentage ± SEM; $n = 6$ animals in each group. *$P < 0.05$, **$P < 0.01$ compared to control. $^{\dagger}P < 0.05$, $^{\ddagger}P < 0.01$ compared to fructose alone. See Table 2 for abbreviations.

(Table 3) when compared to those in soleus muscle (Table 2).

Analysis of the fatty acid composition of PE from soleus and EDL muscles was also performed (Tables 4 and 5). Expected differences in the fatty acid composition of soleus and EDL muscle between PC and PE were observed, with greater content of saturated fatty acids in PC and greater PUFA in PE (7). Despite these differences in fatty acid composition, administration of Tgz resulted in similar changes in the proportion of fatty acids in PE to those observed in PC. As shown in Figure 1A (soleus muscle), the content of total n-6 fatty acids in PC was significantly greater than that of PE ($P < 0.001$). Alternatively, the content of n-3 fatty acids was greater in PE compared to PC ($P < 0.001$). However, the content of total n-6 fatty acids increased ($P < 0.01$) and n-3 decreased ($P < 0.01$) following Tgz administration in both PL. Similar directional changes of n-6 and n-3 fatty acids were observed in the more insulin-resistant EDL muscle following Tgz administration (data not shown). The effect of F administration on n-6 and n-3 fatty acids was also examined (Fig. 1B). Striking reductions in n-3 fatty acids were observed in PC ($P < 0.01$) and PE ($P < 0.01$) in soleus muscle. Similar reductions in n-3 fatty acids were observed in EDL muscle in PC (4.89 ± 0.0.26 to 1.67 ± 0.10%, $P < 0.01$) and PE (21.2 ± 0.3 to 13.9 ± 1.3%, $P < 0.01$). Significant increases in PE n-6 fatty acids were observed in soleus (Fig. 1B) and EDL muscle (data not shown) after F feeding compared to control animals. In contrast, no significant changes in PC n-6 fatty acids were observed with F feeding.

We did not expect that an insulin sensitizer would decrease fatty acid elongation. However, the increase in the ratio of 16:0 to 18:0 (inversely correlated with elongase activity) observed in these studies following Tgz administration suggests that elongase activity was decreased. Since increases in this marker have generally been associated with decreased insulin

TABLE 5
Phosphatidylethanolamine Fatty Acid Composition in Rat Extensor Digitorum Longus Muscle After 3 wk of Diets Composed of Standard Chow, Chow Plus 0.2% Troglitazone (Tgz), 60% Fructose Chow, and Fructose Plus Tgz[a]

	Control	Tgz	Fructose	Fructose + Tgz
16:0	5.1 ± 0.3	6.0 ± 0.9	5.3 ± 0.3	5.8 ± 0.3
18:0	26.0 ± 0.3	23.3 ± 0.3**	26.7 ± 0.6	24.1 ± 0.4**,†
18:1n-6	5.6 ± 0.1	8.0 ± 0.3	7.6 ± 0.8	9.6 ± 0.7**
18:2n-6	8.1 ± 0.2	10.0 ± 0.2**	6.9 ± 0.3*	7.1 ± 0.4
18:3n-6	0.08 ± 0.01	0.10 ± 0.01	0.05 ± 0.01	0.06 ± 0.01
20:4n-6	14.2 ± 0.4	14.9 ± 0.7	16.7 ± 0.3**	16.3 ± 0.3**
22:4n-6	2.2 ± 0.1	2.5 ± 0.3	2.3 ± 0.2	2.2 ± 0.2
22:5n-3	5.0 ± 0.2	4.8 ± 0.5	2.9 ± 0.2**	3.3 ± 0.3**
22:6n-3	16.2 ± 0.2	12.0 ± 0.6**	11.2 ± 0.9**	10.1 ± 1.0**
16:0/18:0	0.20 ± 0.01	0.27 ± 0.03*	0.20 ± 0.01	0.24 ± 0.01
ΣC20–22	38.3 ± 0.7	34.8 ± 2.1	34.1 ± 1.7	33.5 ± 1.6
20:4/20:3	63.5 ± 5.4	91.4 ± 50.2	31.4 ± 3.9	16.2 ± 1.4‡
20:3/18:2	0.03 ± 0.01	0.03 ± 0.01	0.09 ± 0.01**	0.16 ± 0.02**,†

[a]Results shown are mean percentage ± SEM; $n = 6$ animals in each group. *$P < 0.05$, **$P < 0.01$ compared to control. $^{\dagger}P < 0.05$, $^{\ddagger}P < 0.01$ compared to fructose alone. See Table 2 for abbreviations.

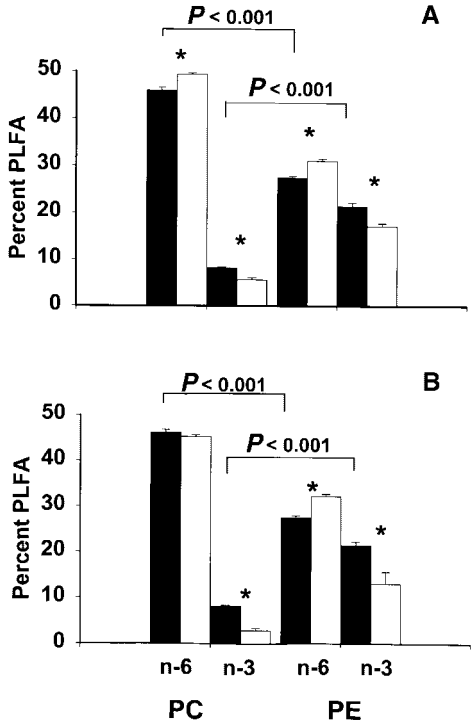

FIG. 1. Percent fatty acid composition of total n-6 and n-3 fatty acids in phosphatidylcholine (PC) and phosphatidylethanolamine (PE) from rat soleus muscle. (A) Results in the absence (■) or presence (□) of 0.2% troglitazone for 3 wk. (B) Results in animals fed standard chow (■) or 60% fructose chow (□) for 3 wk. Results shown are mean percentage ± SEM; $n = 6$ animals in each group. *$P < 0.01$.

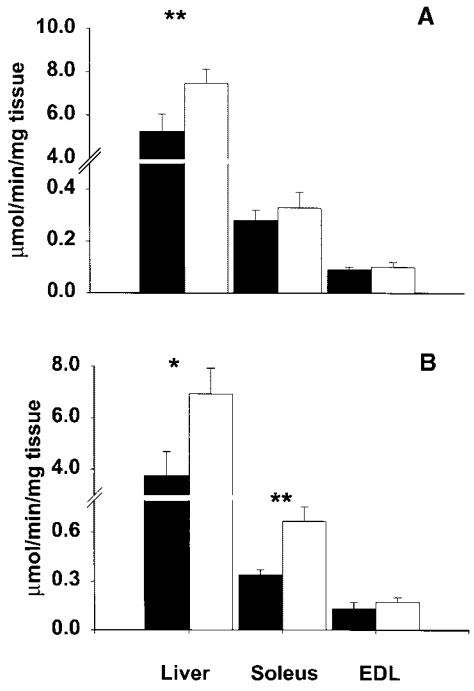

FIG. 2. Microsomal elongase activity (expressed as μmol/min/mg tissue) in liver, soleus, and extensor digitorum longus (EDL) muscle. (A) Results in animals fasted overnight (■) and in fed animals (□) ($n = 6$ in each group). (B) Results in fasted animals fed standard chow (■) or chow supplemented with 0.2% troglitazone for 3 wk (□) ($n = 4$ animals in each group). Results shown are mean ± SEM; *$P < 0.05$, **$P < 0.01$.

sensitivity, additional experiments were performed to determine the effect of Tgz on elongase activity measured directly in liver and muscle. In preliminary experiments, elongase activity was determined in liver, soleus, and EDL muscles from fed and fasted rats. As shown in Figure 2A, liver elongase activity increased in fed animals compared to fasted animals ($P < 0.01$). Skeletal muscle enzyme activity was less than 5% of that in liver, with the activity in soleus muscle threefold higher than that in EDL (0.28 ± 0.04 vs. 0.09 ± 0.01 μmol/min/mg tissue). In contrast to results obtained with liver, enzyme activity did not change with feeding in either soleus or EDL. To confirm a physiologic effect of feeding in skeletal muscle in our studies, malonyl CoA concentrations were also determined. As expected, tissue malonyl CoA levels increased in both soleus (2.2 ± 0.6 to 2.9 ± 0.6 nmol/g, $P < 0.01$) and EDL (0.6 ± 0.2 to 1.4 ± 0.4 nmol/g, $P < 0.01$) with feeding. The effects of Tgz on elongase activity were then examined. As shown in Figure 2B, liver enzyme activity increased in liver and soleus muscle following Tgz administration. No change in elongase activity was observed in EDL following Tgz administration. Thus, a decrease in elongase activity, which might explain the observed increase in the ratio of 16:0 to 18:0 and the decrease in PUFA following Tgz administration, was not found.

DISCUSSION

The present studies were designed to determine the effect of F (an agent known to induce insulin resistance) and Tgz (an agent known to improve insulin resistance) on PL fatty acids in insulin-sensitive and insulin-resistant skeletal muscle. Numerous studies have demonstrated an association between PL fatty acid content and insulin sensitivity. Increased 16:0 (7) and decreased long-chain PUFA have been described in association with reduced insulin sensitivity. In addition, strategies to increase or decrease insulin sensitivity have been shown to alter PL fatty acid composition in animals and man (4,5,23,24). Based on these data, we hypothesized that Tgz administration would be associated with improvements in PLFA composition of rat skeletal muscle (EDL in particular) and that this effect would be greater in the insulin-resistant model of F feeding. Indeed, F feeding was associated with changes in the fatty acid composition of rat skeletal muscle, which have been associated with insulin resistance. However, the expected improvement in PLFA composition following Tgz administration was not observed.

High F diets are well known to induce insulin resistance in animals. Both peripheral and hepatic insulin resistance have been shown in F-fed animals using the euglycemic

clamp technique (15,25). Two mechanisms have been proposed for the increase in insulin resistance. F feeding is known to increase plasma and tissue triglycerides in association with a reduction in insulin sensitivity (15,25,26). Particular attention has been given to the potential role for tissue triglycerides in this model of insulin resistance, with the effect attributed to the fat composition of high F diets (26). An effect of Tgz to reduce skeletal muscle tissue triglycerides in association with an increase in insulin-stimulated glucose disposal has been demonstrated (27,28). Total tissue triglycerides were not determined in the present studies.

Changes in PLFA composition of skeletal muscle membrane may also contribute to the improvement in insulin sensitivity. The higher saturated fatty acid content of the commercial high F diet used in the present studies (Table 1) and in most reported studies would be expected to alter membrane composition and skeletal muscle insulin sensitivity. Storlein *et al.* (8) have shown a 50% reduction in total body glucose disposal and an 80% reduction in skeletal muscle glucose disposal in rats fed a high saturated fat diet in association with changes in skeletal muscle PL fatty acid composition. Striking reductions in total PL long-chain n-3 fatty acids were observed in these studies. Similar reductions in long-chain n-3 fatty acids in both PC and PE were observed in animals fed the high F diet in the present studies. Administration of any of several thiazolidinediones has been shown to ameliorate the induction of insulin resistance induced by diets high in F (15) or fat (29,30). Thus, our model should have permitted us to observe an improvement in PLFA composition with Tgz administration if such a mechanism was involved in improvement of insulin sensitivity. However, an improvement in PLFA composition in the F-fed animals was not observed after Tgz administration. Rather, long-chain n-3 fatty acids (22:5n-3, 22:6n-3) as well as total PUFA fell after Tgz treatment in both muscle types. These results were virtually identical to those observed following Tgz administration in animals fed a standard chow diet, suggesting an independent effect of Tgz. The Tgz-induced changes in PL fatty acid composition observed in the present studies appear to contradict previous studies using BRL 49653, another thiazolidinedione (29). In the latter studies, BRL 49653 was shown to increase insulin sensitivity (measured using the clamp technique) in fat-fed animals without a change in PL fatty acid composition. However, these investigators examined total PL fatty acids whereas we have examined two individual PL species, namely, PC and PE, which together account for more than 75% of total PL (7). It is certainly possible that opposing changes in the fatty acid composition of PI, SM, CL, and PS to those of PC and PE might account for this discrepancy. Nevertheless, both the present studies and those of Oakes *et al.* (29) support the contention that the improvement in insulin sensitivity induced by thiazolidinediones is not mediated by changes in PL fatty acid composition.

Potential mechanisms for the changes in composition of PL fatty acids observed in the present studies following Tgz treatment are a reduction in fatty acid elongation and/or desaturation. Elongase is a ubiquitous enzyme complex, which is responsible for the addition of two-carbons from malonyl CoA to both saturated and unsaturated fatty acids in liver and muscle. The consistent increase in ratio of 16:0 to 18:0 in both PC and PE as well as the marked reduction in n-3 long-chain fatty acids in both soleus and EDL muscle after Tgz treatment is consistent with this hypothesis. However, an insulin sensitizer would be expected to increase, not decrease, elongation. To examine this possibility further, we have measured microsomal elongase activity directly in liver and muscle using palmitoyl CoA as substrate. Liver activity increased significantly following refeeding and Tgz treatment, consistent with an insulin-mediated effect. In keeping with the greater insulin sensitivity of oxidative muscle, malonyl CoA concentrations and enzyme activity were greater in soleus compared to EDL muscle. Moreover, elongase activity increased in soleus but not EDL muscle after treatment with Tgz. Moreover, elongase activity is inhibited by certain fatty acids (31), and a decrease in free fatty acid availability by Tgz (27) would also be expected to increase elongase activity. Thus, a Tgz-induced reduction in elongase activity, either *in vivo* or *in vitro,* seems unlikely. With regard to the possibility that Tgz may have decreased desaturase activity, consistent changes in Δ^5 desaturase (20:4/20:3 ratio) or Δ^6 desaturase (20:3/18:2 ratio) activity were not observed in our studies (Tables 3–6).

In conclusion, our data have shown that Tgz administration is associated with changes in PLFA composition, which have been previously linked to insulin resistance. These studies suggest that the improvement in insulin sensitivity mediated by TGZ is not the result of changes in PLFA composition.

ACKNOWLEDGMENT

These studies were supported in part by National Institute of Health grants, RO1 DK43013 and RO1 DK18903.

REFERENCES

1. Clore, J.N., Li, J., Gill, R., Gupta, S., Spencer, R., Azzam, A., Zuelzer, W., Rizzo, W.B., and Blackard, W.G. (1998) Skeletal Muscle Phosphatidylcholine Fatty Acids and Insulin Sensitivity in Normal Humans, *Am. J. Physiol. 275*, E665–E670.
2. Kriketos, A.D., Pan, D.A., Lillioja, S., Cooney, G.J., Baur, L.A., Milner, M.R., Sutton, J.R., Jenkins, A.B., Bogardus, C., and Storlien, L.H., (1996) Interrelationships Between Muscle Morphology, Insulin Action, and Adiposity, *Am. J. Physiol. 270*, R1332–R1339.
3. Pan, D.A., Hulbert, A.J., and Storlien, L.H. (1994) Dietary Fats, Membrane Phospholipids and Obesity, *J. Nutr. 124*, 1555–1565.
4. Vessby, B., Tengblad, S., and Lithell, H. (1994) Insulin Sensitivity Is Related to the Fatty Acid Composition of Serum Lipids and Skeletal Muscle Phospholipids in 70-year-old Men, *Diabetologia 37*, 1044–1050.
5. Kriketos, A.D., Pan, D.A., Sutton, J.R., Hoh, J.F., Baur, L.A., Cooney, G.J., Jenkins, A.B., and Storlien, L.H. (1995) Relationships Between Muscle Membrane Lipids, Fiber Type, and Enzyme Activities in Sedentary and Exercised Rats, *Am. J. Physiol. 269*, R1154–R1162.

6. Takagi, A. (1971) Lipid Composition of Sarcoplasmic Reticulum of Human Skeletal Muscle, *Biochim. Biophys. Acta 248*, 12–20.
7. Blackard, W.G., Li, J., Clore, J.N., and Rizzo, W.B. (1997) Phospholipid Fatty Acid Composition in Type I and Type II Rat Muscle, *Lipids 32*, 193–198.
8. Storlien, L.H., Jenkins, A.B., Chisholm, D.J., Pascoe, W.S., Khouri, S., and Kraegen, E.W. (1991) Influence of Dietary Fat Composition on Development of Insulin Resistance in Rats. Relationship to Muscle Triglyceride and Omega- 3 Fatty Acids in Muscle Phospholipid, *Diabetes 40*, 280–289.
9. Clandinin, M.T., Cheema, S., Field, C.J., and Baracos, V.E. (1993) Dietary Lipids Influence Insulin Action, *Ann. NY Acad. Sci. 683*, 151–163.
10. Liu, S., Baracos, V.E., Quinney, H.A., and Clandinin, M.T., (1994) Dietary Omega-3 and Polyunsaturated Fatty Acids Modify Fatty Acyl Composition and Insulin Binding in Skeletal-Muscle Sarcolemma, *Biochem. J. 299*, 831–837.
11. Andersson, A., Sjodin, A., Olsson, R., and Vessby, B. (1998) Effects of Physical Exercise on Phospholipid Fatty Acid Composition in Skeletal Muscle, *Am. J. Physiol. 274*, E432–E438.
12. Clore, J.N., Harris, P.A., Li, J., Azzam, A., Gill, R., Zuelzer, W., Rizzo, W.B., and Blackard, W.G. (2000) Changes in Phosphatidylcholine Fatty Acid Composition Are Associated with Altered Skeletal Muscle Insulin Responsiveness in Normal Man, *Metabolism 49*, 232–238.
13. Tobey, T.A., Mondon, C.E., Zavaroni, I., and Reaven, G.M. (1982) Mechanism of Insulin Resistance in Fructose-Fed Rats, *Metabolism 31*, 608–612.
14. Ciaraldi, T.P., Gilmore, A., Olefsky, J.M., Goldberg, M., and Heidenreich, K.A. (1990) *In vitro* Studies on the Action of CS-045, a New Antidiabetic Agent, *Metabolism 39*, 1056–1062.
15. Lee, M.K., Miles, P.D., Khoursheed, M., Gao, K.M., Moossa, A.R., and Olefsky, J.M. (1994) Metabolic Effects of Troglitazone on Fructose-Induced Insulin Resistance in the Rat, *Diabetes 43*, 1435–1439.
16. Borkman, M., Storlien, L.H., Pan, D.A., Jenkins, A.B., Chisholm, D.J., and Campbell, L.V. (1993) The Relation Between Insulin Sensitivity and the Fatty-Acid Composition of Skeletal-Muscle Phospholipids, *N. Engl. J. Med. 328*, 238–244.
17. Folch, J., Lees, M., and Sloane Stanley, G.H. (1957) A Simple Method for the Isolation and Purification of Total Lipids from Animal Tissues, *J. Biol. Chem. 226*, 497–509.
18. Alegret, M., Cerqueda, E., Ferrando, R., Vazquez, M., Sanchez, R.M., Adzet, T., Merlos, M., and Laguna, J.C. (1995) Selective Modification of Rat Hepatic Microsomal Fatty Acid Chain Elongation and Desaturation by Fibrates: Relationship with Peroxisome Proliferation, *Br. J. Pharmacol. 114*, 1351–1358.
19. Morgan, C.R., and Lazarow, A. (1963) Immunoassay of Insulin: Two Antibody System: Plasma Insulin Levels of Normal, Subdiabetic and Diabetic Rats, *Diabetes 12*, 115–126.
20. McGarry, J.D., Stark, M.J., and Foster, D.W. (1978) Hepatic Malonyl-CoA Levels of Fed, Fasted and Diabetic Rats as Measured Using a Simple Radioisotopic Assay, *J. Biol. Chem. 253*, 8291–8293.
21. Linn, T.C. (1981) Purification and Crystallization of Rat Liver Fatty Acid Synthetase, *Arch. Biochem. Biophys. 209*, 613–619.
22. Ayre, K.J., and Hulbert, A.J. (1996) Dietary Fatty Acid Profile Influences the Composition of Skeletal Muscle Phospholipids in Rats, *J. Nutr. 126*, 653–662.
23. Kraegen, E.W., Clark, P.W., Jenkins, A.B., Daley, E.A., Chisholm, D.J., and Storlien, L.H. (1991) Development of Muscle Insulin Resistance After Liver Insulin Resistance in High-Fat-Fed Rats, *Diabetes 40*, 1397–1403.
24. Pan, D.A., Lillioja, S., Milner, M.R., Kriketos, A.D., Baur, L.A., Bogardus, C., and Storlien, L.H. (1995) Skeletal Muscle Membrane Lipid Composition Is Related to Adiposity and Insulin Action, *J. Clin. Invest. 96*, 2802–2808.
25. Thorburn, A.W., Storlien, L.H., Jenkins, A.B., Khouri, S., and Kraegen, E.W. (1989) Fructose-Induced *in vivo* Insulin Resistance and Elevated Plasma Triglyceride Levels in Rats, *Am. J. Clin. Nutr. 49*, 1155–1163.
26. Storlien, L.H., Oakes, N.D., Pan, D.A., Kusunoki, M., and Jenkins, A.B. (1993) Syndromes of Insulin Resistance in the Rat. Inducement by Diet and Amelioration with Benfluorex, *Diabetes 42*, 457–462.
27. Sreenan, S., Keck, S., Fuller, T., Cockburn, B., and Burant, C.F. (1999) Effects of Troglitazone on Substrate Storage and Utilization in Insulin-Resistant Rats, *Am J. Physiol. 276*, E1119–E1129.
28. Higa, M., Zhou, Y.T., Ravazzola, M., Baetens, D., Orci, L., and Unger, R.H. (1999) Troglitazone Prevents Mitochondrial Alterations, Beta Cell Destruction, and Diabetes in Obese Prediabetic Rats, *Proc. Natl. Acad. Sci. USA 96*, 11513–11518.
29. Oakes, N.D., Kennedy, C.J., Jenkins, A.B., Laybutt, D.R, Chisholm, D.J., and Kraegen, E.W. (1994) A New Antidiabetic Agent, BRL 49653, Reduces Lipid Availability and Improves Insulin Action and Glucoregulation in the Rat, *Diabetes 43*, 1203–1210.
30. Kraegen, E.W., James, D.E., Jenkins, A.B., Chisholm, D.J., and Storlien, L.H. (1989) A Potent *in vivo* Effect of Ciglitazone on Muscle Insulin Resistance Induced by High Fat Feeding of Rats, *Metabolism 38*, 1089–1093.
31. Prasad, M.R., Nagi, M.N., Ghesquier, D., Cook, L., and Cinti, D.L. (1986) Evidence for Multiple Condensing Enzymes in Rat Hepatic Microsomes Catalyzing the Condensation of Saturated, Monounsaturated, and Polyunsaturated Acyl Coenzyme A, *J. Biol. Chem. 261*, 8213–8217.

[Received May 22, 2000 and in revised form August 18, 2000; revision accepted August 23, 2000]

Phospholipid Identification and Quantification of Membrane Vesicle Subfractions by ^{31}P-^{1}H Two-Dimensional Nuclear Magnetic Resonance

B. Larijani[a,1], D.L. Poccia[a], and L. Charles Dickinson[b,*]

[a]Department of Biology, Amherst College, Amherst, Massachusetts 01002, and [b]Conte National Center for Polymer Research, Department of Polymer Science and Engineering, University of Massachusetts at Amherst, Amherst, Massachusetts 01003

ABSTRACT: An approach to the direct quantification of phospholipids from two-dimensional ^{31}P-^{1}H nuclear magnetic resonance (NMR) spectroscopy with isotropic proton mixing has been developed as a general method for phospholipid analysis of minor membrane vesicle subfractions. Membrane vesicles were subfractionated by sedimentation to density equilibrium in a sucrose gradient, and a modified Folch method was employed to extract their phospholipids. The coefficient for the NMR detection efficiency of each phospholipid and the relative mole percentage of the phospholipids present in the membrane vesicles were calculated. We demonstrate low detection limits such that relative concentrations of phospholipids in membrane subfractions may be determined even in the submicromolar range.

Paper no. L8443 in *Lipids 35,* 1289–1297 (November 2000).

Various types of high-resolution nuclear magnetic resonance (NMR) spectroscopy have been used to analyze lipids present in biological samples (1–8). NMR spectroscopy as a tool for analysis of lipids and phospholipids has advantages over chromatographic techniques because prior separation and derivitization of components are not required (2,7). Proton and phosphorus NMR can determine exact structures of phospholipids and have been employed for the quantification of different head groups and fatty acid chains (1–3,7).

Although conventional one-dimensional (1D) proton NMR has been used to determine lipid profiles for different types of tissues (1), overlapping chemical shifts often limit precise peak assignments. One-dimensional ^{31}P NMR spectroscopy is restricted by the small chemical shift range (i.e., 1.5 ppm) and the different short relaxation times for each phospholipid (6,7). Furthermore, the phospholipid chemical shifts and line widths are significantly dependent on the lipid composition, solvent composition, pH, counterions, and water content (6,7). The chemical shift of a phosphate group is also sensitive to very slight changes in conformation, and to fatty acid chain composition and length (4,8). For example, introduction of unsaturated groups on either side of the phosphatidylcholine acyl chains causes an upfield shift, and an increase in the length of disaturated acyl chains results in the phosphorus chemical shift shifting closer to the absolute value of –0.500 ppm (8).

To acquire unambiguous peak assignments, two-dimensional (2D) heteronuclear (^{31}P-^{1}H) multiple quantum coherence NMR spectroscopy (HMQC) with isotropic proton mixing has been used as an analytical method. Previously, 1D and 2D NMR were used for the analysis of plasma membranes of whole cells, tumor cells, and tissue extracts (1,4–6). Here we extend the HMQC method to identify and directly quantify submicromolar levels of phospholipids present in individual membrane subfractions separated by buoyant density.

HMQC, an inverse correlation technique (where the protons of the lipid head group and lipid backbone are observed as edited by the phosphorus resonance to which they are coupled) is effective at lower detection limits than the usual low millimolar (mM) range. As previously shown by Edzes *et al.* (4), the incorporation of isotropic proton mixing in a 2D heteronuclear correlated NMR spectroscopy method greatly increases the clarity of assignment of head group and lipid backbone protons. Each phospholipid can be characterized by its specific "fingerprint" proton pattern. However, isotropic proton mixing causes a complication in the direct quantification of the specific phospholipids by HMQC. Unlike the case for 1D NMR, peak integrals at the same concentration of sev-

[1]Present address: Imperial Cancer Research Fund, 44 Lincoln Inn Fields, London WC2A 3PX, United Kingdom.

*To whom correspondence should be sent.
E-mail: charlie@telemann.pse. umass.edu

Abbreviations: AAPC, β-acetyl-γ-*O*-alkyl-L-α-phosphatidylcholine; 1D, one-dimensional; 2D, two-dimensional; DPPC, L-α-phosphatidylcholine, dipalmitoyl; DPPE, DL-α-phosphatidylethanolamine, dipalmitoyl; DPPS, DL-α-phosphatidyl-L-serine, dipalmitoyl; DPSM, dipalmitoyl sphingomyelin; ER, endoplasmic reticulum; GARP, globally optimized alternating phase rectangular pulse decoupling; HMQC, heteronuclear multiple quantum coherence; HMSQ, heteronuclear single quantum coherence; *K*, coefficient of efficiency of NMR detection; LB, lysis buffer; LPC, lysophosphatidylcholine; MLEV, Malcolm Levitt decoupling scheme; MV, membrane vesicle; MWB, membrane wash buffer; NMR, nuclear magnetic responance; PE, phosphatidylethanolamine; PI, L-α-phosphatidylinositol sodium salt; PMSF, phenylmethylsulfonylfluoride; TN, Tris-NaCl; TOCSY, total correlation spectroscopy.

eral phospholipids will vary according to different efficiencies of the spin mixing that are dependent on $J_{H\text{-}H}$ coupling constants as well as mobility. Therefore, the 2D peaks in different phospholipids are not detected at the same efficiency. To resolve this problem in a simple and practical way, coefficients of efficiency of NMR detection (K) of each relevant phospholipid were calculated. By determining the K values for each, the relative mole percentage of the phospholipids present in the membrane vesicles could be directly calculated from the 2D HMQC spectra.

The biological properties and functions of sea urchin egg cytoplasmic membrane vesicles (MV) have been studied, although until now there has not been a measure of their phospholipid composition. The importance of determining the phospholipid composition of these distinct MV subfractions lies in the fact that such MV populations cooperate in forming the nuclear envelope *in vitro* (9). MV are from egg cytoplasmic origin and can be resolved into four different subsets: MV1, MV2, MV3, and MV4, differing in buoyant density. MV1 and MV2 are involved directly in nuclear envelope formation, and MV1 contains vesicles crucial for the fusion of MV2 subfractions (9). Owing to the particular roles of the MV in the formation of the nuclear envelope and the unique properties of MV1 (9), we investigated the phospholipid compositions of MV1, MV2, and MV3.

This paper demonstrates that with minimal sample handling the lipid/phospholipid profile of minor membrane subfractions can be easily determined and shows how the individual phospholipids present can be directly quantified from the HMQC spectra with isotropic proton mixing.

MATERIAL AND METHODS

Materials. Lytechinus pictus (sea urchins) were obtained from Marinus, Inc. (Long Beach, CA). All phospholipid standards, [DL-α-phosphatidyl-L-serine, dipalmitoyl (DPPS), L-α-phosphatidylcholine, dipalmitoyl (DPPC), DL-α-phosphatidylethanolamine, dipalmitoyl (DPPE), L-α-phosphatidylinositol sodium salt (PI), dipalmitoyl sphingomyelin (DPSM), β-acetyl-γ-*O*-alkyl-L-α-phosphatidylcholine (AAPC)], deuterated solvents (deuterium oxide, chloroform, methanol), EDTA, and potassium hydroxide were purchased from Sigma Chemical Co. (St. Louis, MO). Porcine blood was acquired from Cleveland Scientific (Cleveland, OH). Solvents used for lipid extraction, chloroform, and methanol were high-performance liquid chromatography (HPLC) grade and purchased from Fisher Scientific (Fair Lawn, NJ). Buffers were egg lysis buffer [LB; 10 mM Hepes, 250 mM NaCl, 5 mM $MgCl_2$, 110 mM glycine, 250 mM glycerol, 1 mM phenylmethylsulfonylfluoride (PMSF), 1 mM dithiothreitol, pH 8.0], Tris-NaCl (TN; 10 mM Tris-HCl, 0.15 M NaCl at pH 7.2), and membrane wash buffer (MWB; 250 mM sucrose, 50 mM KCl, 2.5 mM $MgCl_2$, 50 mM Hepes, 1 mM dithiothreitol, 1 mM ATP, 1 mM PMSF, pH 7.5).

Methods. (i) Egg extracts: The gametes of the *L. pictus* were collected and fertilized, and sea urchin egg extracts were prepared according to Collas and Poccia (10). Briefly, fertilized eggs were washed in Millipore-filtered seawater and egg LB, resuspended in an equal volume of LB, and homogenized on ice, using a 22-gauge needle and syringe. The lysate was centrifuged at 10,000 × *g* for 10 min at 4°C in a microcentrifuge. The clear cytoplasm (S_{10}) was withdrawn and further centrifuged for 2 h at 100,000 × *g* at 4°C in a Ti50 rotor (Beckman Instruments, Carlsbad, CA). The clear cytosolic fraction (S_{100}) was recentrifuged for 1 h at 100,000 × *g* to collect the remaining pelleted membrane fractions. S_{100} was frozen in liquid nitrogen and stored at –80°C.

(ii) Membrane vesicle isolation and subfractionation. All solutions contained fresh 1m M protease inhibitor PMSF. The MV pelleted at 100,000 × *g* were washed twice by resuspension in MWB and centrifuged at 40,000 × *g* for 10 min. These membrane vesicles are referred to as (MV0). The quantity of MV0 was maintained constant in all experiments. The MV were routinely obtained from 2.5 mL of S_{10} extracts and resuspended in 200 μL of MWB. The MV0 was subfractionated by sedimentation to density equilibrium in a sucrose gradient. The 200 μL of MV0 in MWB was suspended in 0.5–1 mL of ice-cold TN buffer containing 1 mM PMSF. By using a gradient maker (Biorad, Richmond, CA), 15 mL of a 0.2–2.0 M linear sucrose gradient in TN buffer was made and slowly deposited into a 16 mL SW28 ultracentrifuge tube held on ice. The MV0 suspension was applied to the gradient and fractionated by sedimentation to density equilibrium at 150,000 × *g* for 20 h at 4°C in a SW28 rotor (Beckman, Fullerton, CA). Vesicles were fractionated into four fractions, MV1, MV2, MV3 and MV4, with respective median densities of 1.02, 1.04–1.08, 1.13, and 1.18. The fractions were collected as described by Collas and Poccia (9). Each fraction was washed with 4 vol of MWB and recentrifuged at 150,000 × *g* for 30 min. The fractions were resuspended in a minimal volume of MWB and stored at –80°C.

(iii) Lipid extraction of membrane subfractions. A modified Folch procedure, adapted by Glonek *et al.* (11), was used for the extraction of MV subfractions. Each subfraction was resuspended in 200 μL of MWB and added to 4 mL of ice-cold chloroform/methanol (2:1, vol/vol). The solvent-to-sample ratio was 20:1 (mL solvent/g sample). The homogenate was sonicated for 2 min and was allowed to settle for 1 h at room temperature. It was then filtered, and K_4-EDTA (0.2 M, pH 6.0, at 0.2 mL per mL of chloroform/methanol) was added. The mixture was agitated vigorously and allowed to separate overnight at room temperature. The lower chloroform phase was collected and evaporated under a stream of argon. The dried lipid samples either were used immediately or were stored at –80°C.

(iv) Preparation of porcine red blood cell ghosts. Erythrocyte ghosts were utilized to verify the accuracy of the quantification method. Ghost erythrocytes were prepared using the procedures in the *Current Protocols in Immunology* (12). The lipids of 1×10^{10} ghost were extracted and stored at –80°C.

(v) NMR spectroscopy. All spectra were obtained on a Bruker AMX-2 500MHz NMR spectrometer with a Bruker 5-mm broadband indirect probe tuned to 202 MHz and

500.13 MHz. The probe temperature was stabilized at 298 K, and samples were left to stabilize for 20 min at this temperature before data acquisition. The parameters for the HMQC-total correlation spectroscopy (TOCSY) 2D spectra shown in this work are as follows: ^{1}H and ^{31}P 90 degree pulses, respectively 8.0 and 9.5 μs, recycle delay 2 s, acquisition time 0.68 s, sweep width F_2 2008 Hz in 2750 real points, sweep width F_1 607Hz in 64 slices, MLEV17 mixing at 7.1 kHz power for 101 ms (45 cycles), globally optimized alternating phase rectangular pulse (GARP) ^{31}P decoupling during acquisition at 2.4 kHz power, refocus delay 0.071 s ($J_{P\text{-}H}$ = 7 Hz). Data sets were processed with zero-shifted sine-bell window functions in both directions and displayed in magnitude mode for 2D integration. The number of scans was varied to give sufficient signal. Two-hour runs with 48 scans were performed for concentrated extracts, and 20-h runs with 480 scans for submicromolar lipid extracts. Furthermore, owing to the presence of three deuterated solvents, for reproducibility the field was adjusted by systematically locking on the $CDCl_3$ signal. To confirm that the field was locked on the $CDCl_3$ signal, the proton chemical shifts were verified prior to running the HMQC.

Extracted lipids were dissolved in a ternary solvent system consisting of a mixture of $CDCl_3$/CD_3OD/K_4EDTA in D_2O (100:40:20 by vol). The K_4EDTA was at the same concentration in D_2O as explained above. The solvent system was optimized because the chemical shift and the linewidths of the phospholipid peaks (in ^{31}P NMR) vary depending on the solvent composition (6,7). The lipid sample and the solvent system were mixed in a glass vial and allowed to equilibrate for an hour prior to transfer to a 5-mm NMR tube. A small aqueous phase was formed at the top after 1 min. This layer above the sample allowed a proper equilibrium to be maintained and prevented significant organic solvent evaporation during NMR analysis. Care was taken to have a clean separation between the organic and aqueous phase. Any emulsion of water in the organic layer degraded the homogeneity of the magnetic field.

HMQC choice and parameters. To maximize sensitivity and resolution we chose from the currently available array of NMR pulse sequences an indirectly detected 2D method with its potential $(\gamma_H/\gamma_P)^{2.5}$ = 9.5-fold increase in signal over direct ^{31}P observation. (γ_H/γ_P is the gyromagnetic ratio of protons/phosphorus.) The ^{31}P-^{1}H connectivity can be established *via* either heteronuclear single quantum coherence (HSQC) (13,14) or multiple quantum coherence HMQC, which give proton resonances along the F_2 axis and a single phosphorus resonance for each phospholipid in the projection along the F_1 axis. Although the former method has been generally used for its often simpler line shape, we chose to look at both methods and, as seen below, found the HMQC slightly better for our purposes. The intensity of each correlation depends on the specific ^{31}P to ^{1}H coherence transfer, which is different for different protons in various phospholipids. To spread out the proton dimension to all protons coupled to a phosphorus spin with their range of coupling constants, the magnetism at the end of the sequence was mixed throughout the spin system with a Malcolm Levitt decoupling scheme (MLEV)17 total spin correlation sequence (TOCSY) (15). Since a large number of scans would be required for our low concentrations and our laboratory did not have a gradient probe capable of observing ^{31}P through the ^{1}H spins, we chose to use pulse programs without gradient selection. The required phase cycle of eight has the advantage of giving a square root of two benefit to signal-to-noise ratio over the same number of scans with gradient selection. The pulse programs were taken from a modern NMR handbook (16). The final HSQC-TOCSY and HMQC-TOCSY 2D sequences were made simply by splicing the TOCSY program onto the original HMQC or HSQC. Pulse sequence parameter optimization was carried out on a 4 μM DPPC sample in the standard ternary solvent system described above. The delay for coherence transfer, $1/2*J_{P\text{-}H}$ for HMQC and $1/4*J_{P\text{-}H}$ for HSQC, was varied with $J_{P\text{-}H}$ from 1 to 9 Hz and found to maximize the signal at the expected 7 Hz. The TOCSY spin lock interval was varied from 34 to 135 ms and, although some signals were still increasing and some decreasing, the compromise value was set to 101 ms.

Previous work employing 2D-NMR techniques to fingerprint phospholipids differed somewhat from our technique of choice and did not choose for optimal signal-to-noise. Edzes *et al.* (4) used an INEPT-TOCSY with WALTZ mixing thus detecting ^{31}P signals directly. Although gaining fourfold in sensitivity over simple ^{31}P detection, this technique loses the very significant additional 2.5-fold sensitivity increase accruing from indirect detection *via* the protons. Henke *et al.* (6) used gradient-enhanced HSQC-TOCSY with MLEV proton mixing. While this technique takes advantage of the full enhancement available in the indirect detection, normal gradient selection results in 41% loss in sensitivity for a comparable number of scans compared to phase cycling selection.

Phospholipid quantification. To determine the detection limit for our protocol, several different concentrations of phospholipid standards were analyzed from 4 to 0.04 μM. The 2D integration mode in XWIN-NMR (Bruker, Billerica, MA) software was used to integrate each peak. To determine the integration values of different concentrations of phospholipids, various dilutions were prepared. The first set consisted of 3.9 μM DPPC, 3.9 μM PI, 3.9 μM DPPS, and 3.9 μM DPPE, the second set 0.4 μM DPPC, 0.39 μM PI, and 0.40 μM DPPE, and the third set 0.04 μM DPPC, 0.039 μM PI, and 0.04 μM DPPE. To achieve reproducibility and optimize our system, saturated acyl chain standards were used since their chemical shifts are most stable and these standards were used previously (8). Phospholipid standards were dissolved in 700 μL of 100:40:20 (by vol) deuterated chloroform, methanol, and K_4EDTA in D_2O. The efficiency coefficients (K) of each phospholipid relative to DPPC in the standard mix were calculated so that the relative mole percentage of phospholipids in the samples could be determined. K was calculated using Equation 1:

$$K_{2/1} = \frac{[PL_1] \times A_2}{[PL_2] \times A_1} \quad [1]$$

where A_1 and A_2 are the integration values of the most intense peak per phospholipid. [PL_1] and [PL_2] are molar concentrations of the phospholipids.

K values were determined from the three sets, and the standard deviations were evaluated. The relative molarity of each particular phospholipid in the different membrane subfractions was obtained by multiplying the ratio of A_1/A_2 by its corresponding *K* value. For example the relative molarity of DPPE to DPPC was calculated as follows:

$$\left[\frac{\text{DPPE}}{\text{DPPC}}\right] = K_{\text{PC/PE}} \frac{A_{\text{PC}}}{A_{\text{PC}}} \quad [2]$$

The mole percentage of phospholipid was determined relative to the most prominent phospholipid in the 2D spectrum, where the value of the most prominent phospholipid was considered to be 1.

To verify the accuracy of this quantification method with a complex biological system, phospholipids of porcine erythrocyte ghosts were quantified and results compared to literature values. Data obtained for the composition of the MV were compared to endoplasmic reticulum and Golgi membranes.

RESULTS AND DISCUSSION

Both HMQC-TOCSY and HSQC-TOCSY 2D spectra were run on a mixture of four standard phospholipids [DPPC, L-α-phosphatidylinositol, dipalmitoyl (DPPI), DPPS, and DPPE] in order to determine the optimal method. Signal-to-noise levels were comparable, but HMQC-TOCSY spectra consistently gave approximately 20% better signal-to-noise for most peaks. To the F_1 resolution level which the experiments were run, any residual proton splitting of the HMQC peaks was not problematic, although the line shapes were not elegant. HSQC gave some clean simple peaks and some split peaks, the latter apparently due to the problematic case of $J_{\text{H-H}}$–$J_{\text{P-H}}$. In any case the resulting peaks were reproducibly integrable.

Chemical shifts and the detection limit. The 2D chemical shifts of the phospholipid standard HMQC spectra were determined from their corresponding 1D spectra. Edzes *et al.* (7) and Pearce and Komoroski (8) have demonstrated that the ^{31}P chemical shifts of various phospholipids are not comparable in different samples. Nonetheless, the order of appearance relative to a reference standard of choice remains constant. The irreproducibility of the exact resonance positions is due to the sensitivity of the chemical shift of a phosphate group to very slight changes in its conformation, environment, or the acyl chain composition (4,8). In this study DPPC, with a chemical shift of –0.510 ppm (8), was defined as a reference standard owing to its stability in all solvent systems and environments such as variations in pH (3). The 1D ^{31}P NMR spectra were calibrated by analyzing 4 μM DPPC standard under the same conditions as the sample analyses. The dipalmitoyl (16:0) saturated chain of PC has the closest value to –0.510 ppm (8). To avoid variations in 2D chemical shifts caused by chain length and saturation, the dipalmitoyl derivatives of phosphatidylserine, phosphatidylethanolamine, and sphingomyelin were utilized for optimization of the method. The 1D phosphorus chemical shifts were verified by spiking samples with DPPC, AAPC, PI, DPPS, DPSM, and DPPE.

Figures 1A and 1B show the variation in chemical shifts with different ternary solvent compositions. Comparing the high quality of resolution in Figure 1A to the lower resolution in Figure 1B, we see that an increase in the methanol/K_4EDTA portion of the ternary solvent results in narrowing the line widths of the phospholipid peaks. The 100:40:20 (by vol) solvent system chosen for our experiments promoted resolution of PE from cardiolipin and PI from lysophosphatidylcholine (LPC) and so

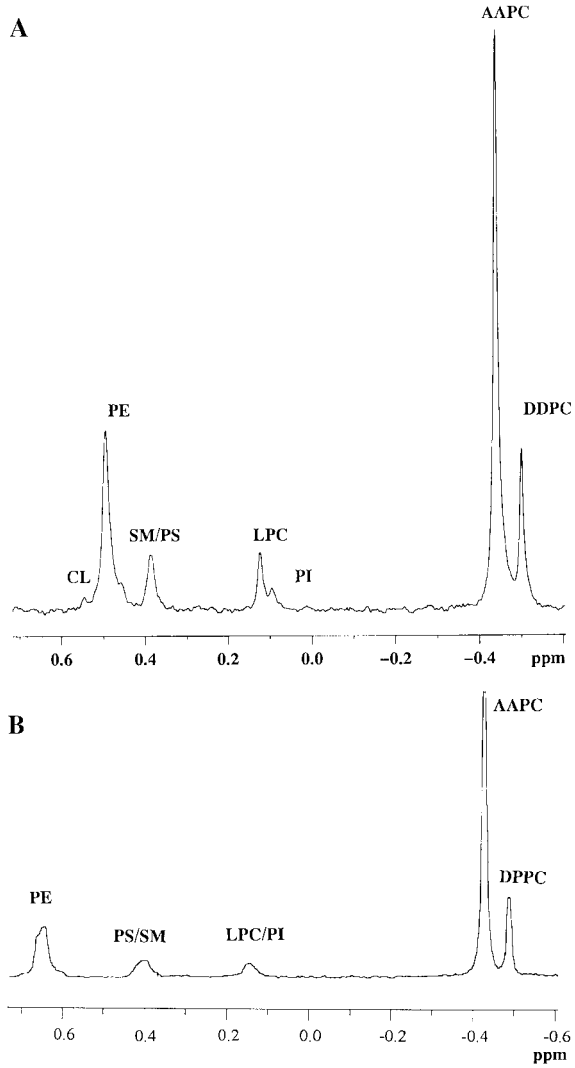

FIG. 1. Phosphorus spectrum of MV0 in a ternary solvent of chloroform/methanol/0.2 M K_4-EDTA at 298.1K. (A) Solvent ratio 100:40:20 by vol; with this methanol and K_4-EDTA ratio the phospholipid peak widths become narrower and better resolution is achieved. This solvent was chosen for all NMR spectra in this work. (B) Solvent ratio 100:16:4 by vol; in this spectrum phospholipid peaks are not so well resolved as in Figure 1A. CL, cardiolipin; PE, phosphatidylethanolamine; SM/PS, sphingomyelin/phosphatidylserine; LPC, lysophosphatidylcholine; PI, phosphatidylinositol; AAPC, β-acetyl-γ-*O*-alkyl-L-α-phosphatidylcholine; DDPC, L-α-phosphatidylcholine, dipalmitoyl; NMR, nuclear magnetic resonance.

TABLE 1
Phosphorus Chemical Shifts of Phospholipids from Literature and MV0[a] Extracts in $CDCl_3/CH_3OH/K_4EDTA$ (100:40:20, by vol)

Phospholipids	Literature[b] (ppm)	MV0 extracts (ppm)
DPPC	–0.51	–0.50
AAPC	–0.45	–0.47
PI	–0.2, 0.00	–0.1, 0.098
LPC	0.10	0.12
PS	0.25	0.40
SM	0.30	0.40
PE	0.43	0.44
PE plasmalogen	0.44	0.48
CL	0.51	0.53

[a]DDPC, L-α-phosphatidylcholine, dipalmitoyl; AAPC, β-acetyl-γ-*O*-alkyl-L-α-phosphatidylcholine; Pl, L-α-phosphatidylinositol sodium salt; LPC, lysophosphatidylcholine; PS, phosphatidylserine; SM, sphingomyelin; PE, phosphatidylethanoloamine; CL, cardiolipin; MV0, membrane vesicles treated with protease inhibitor, centrifuged, washed with membrane wash buffer, and centrifuged.
[b]From Reference 3.

this solvent was used as the optimal solvent system. Table 1 gives the 1D ^{31}P NMR chemical shifts of a variety of phospholipids from the literature (3) and of peaks observed in lipid extracts of MV0. Special note should be taken of the variations in literature and experimental values of PI chemical shifts.

Since HMQC was used to determine the fingerprint profile of each distinct membrane vesicle subfraction, the proton chemical shift region of interest was 3.0 to 5.8 ppm identity peaks, where each phospholipid head group and the glycerol backbone proton is observed. Table 2 shows the specific values of the proton identity peaks for each phospholipid.

Other chemical shifts in this region correspond mostly to protons on the glycerol backbone or to head groups that overlap one another. The common proton on the backbone of all glycerophospholipids is at 5.2 to 5.4 ppm (C**H**OCOR) (4). These identity peaks and their correlation with phosphorus in the HMQC spectra define the fingerprint profile.

Figures 2A and 2B demonstrates the fingerprint profiles of a mixture of (A) phospholipid standards at 4 μM DPPC, 3.9 μM PI, 3.9 μM DPPS, and 3.9 μM DPPE and (B) a mixture of phospholipid standards at 0.4 μM DPPC, 0.30 μM PI, and 0.4 μM DPPE. The F_1 and F_2 coordinates for DPPC, PI, DPPE, and DDPS are –0.5, 3.50 ppm; –0.17, 3.83 ppm; 0.20, 3.9 ppm; and 0.44, 3.1 ppm, respectively. Figure 2C shows that a concentration of 0.04 μM per phospholipid is the detection limit for a 20-h HMQC run with the specific parameters indicated in the previous section. In an attempt to shorten recycle time we tried a 10 mM final concentration of chromium (III) acetylacetonate [$Cr(acac)_3$] (17) in the 4 μM mixture of standards. However, this addition resulted in the disappearance of the phospholipid peaks from the 2D spectra.

For the 0.04 μM HMQC (Fig. 2C) , a 1D horizontal slice through the DPPC spectrum gives a signal-to-noise ratio of 3:1 for the DPPC identity peak. This indicates that we are near the limit for sufficient signal to characterize.

Figure 2D is the fingerprint profile of 3.9 μM PI. Unlike other phospholipids, there is a difference in the F_1 coordinate of PI alone and in a mixture of standards. This variation in the phosphorus chemical shift, due to the effect of different fatty acid chains, has also been pointed out in previous studies (7,11). Furthermore, the charged PI is highly sensitive to slight changes of pH, and thus its chemical shift varies to a greater extent than zwitterionic phospholipids such as DPPC. In a mixture of standards, F_1 and F_2 are –0.17, 3.83 ppm, respectively. The F_1 and F_2 values when PI is not in the mixture are –0.24, 3.80 ppm, respectively. It can also be seen that, unlike the phosphorus chemical shift, the proton chemical shift varies only slightly (0.03 ppm). Thus, for identifying the phospholipids in different MV, both coordinates have to be taken into consideration and specific attention has to be paid to the proton identity peak with its correlated phosphorus peak when assigning the phospholipid peaks.

Quantification of standards and determination of their efficiency coefficients K. The most intense peaks in the 2D spectra for each phospholipid, at three concentrations i.e., 4, 0.4, and 0.04 μM, were integrated. For 4 μM DPPC, PI, and DPPE these respective ^{31}P, ^{1}H peaks were –0.5, 3.5 ppm, –0.17, 5.2 ppm, and 0.44, 3.9 ppm. Even at 0.04 μM the most prominent peaks of DPPC, PI, and DPPE were still integrable and the signal-to-noise was greater than 3, as mentioned previously. The linearity of the 2D integrations with respect to the three sets of lipid concentrations is shown in Figure 3.

Since in biological membranes PC is generally more prominent than phospholipids with other head groups, it is taken to be the reference phospholipid. The *K* values of PI with respect to different concentrations of DPPC were calculated as follows:

$$K_{PI/PC} = (4.0\ \mu M/3.9\ \mu M) \times (1357_{PI}/2600_{PC}) \quad [3]$$

$$K_{PI/PC} = 0.53 \quad [4]$$

$$K_{PI/PC} = (0.04\ \mu M/0.039\ \mu M) \times (16_{PI}/25_{PC}) \quad [5]$$

$$K_{PI/PC} = 0.66 \quad [6]$$

The *K* values for PI/DPPC, DPPS/DPPC, and DPPE/DPPC are 0.71 ± 017; 0.88 ± 0.13; and 0.95 ± 0.14, respectively.

TABLE 2
Proton Chemical Shifts of the Phospholipid Head Groups: The Identity Peaks

Identity peaks	Chemical shift (ppm)	Peak profile
PC-N^+-($C\mathbf{H}_3$)$_3$	3.20[a], 3.18[b]	Singlet
PS-C**H**(OCO^-)NH_3^+	4.00[a], 3.93[b]	Multiplet
PI-**H**^{6} of inositol (IUPAC) nomenclature	3.75[a], 3.87[b]	Triple peak (not 1:2:1)
PE-C**H**^{2}N	3.16[a], 3.11[b]	Triplet

[a]From Reference 1.
[b]From Reference 4. PC, phosphatidylcholine; for other abbreviations see Table 1.

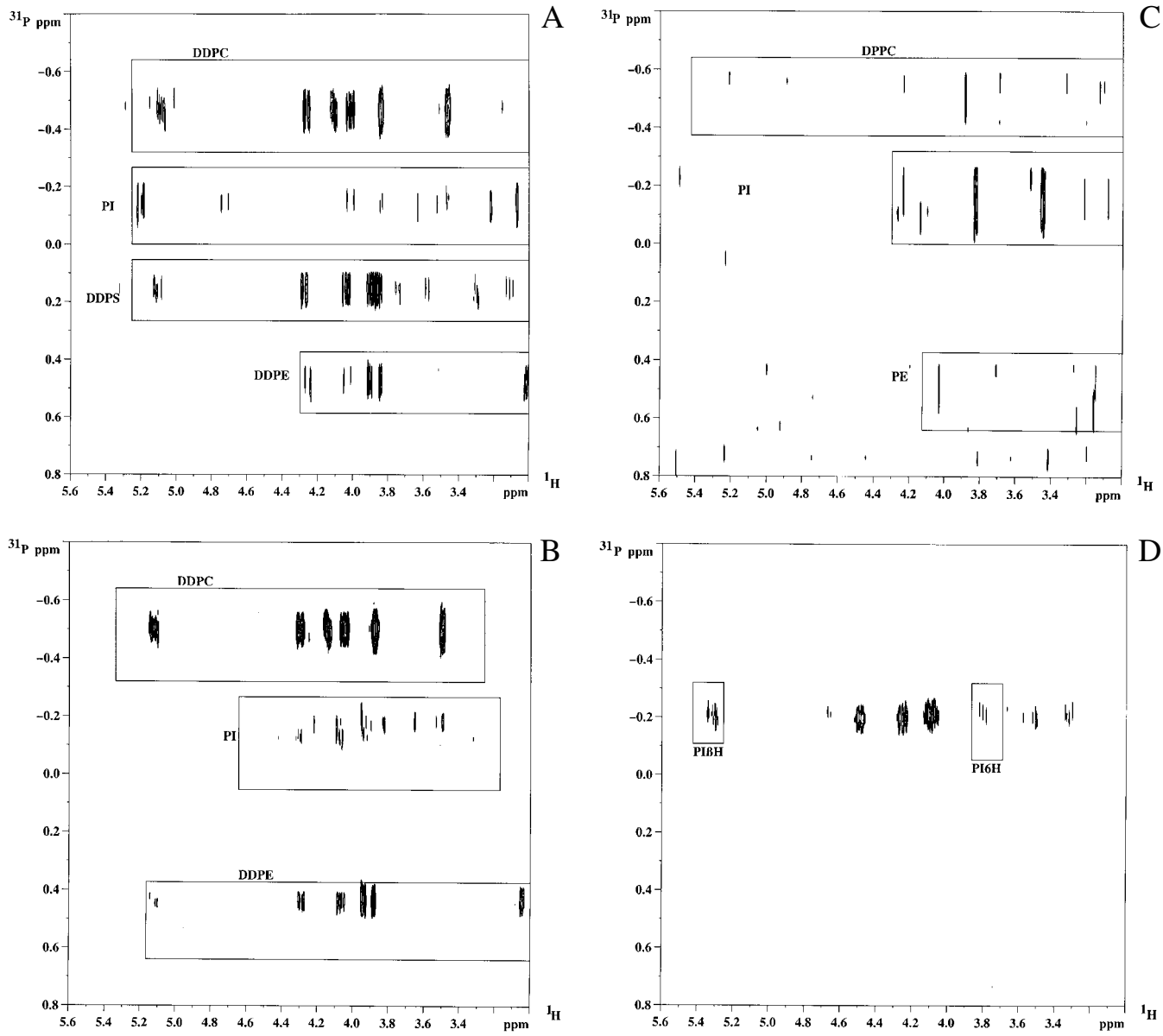

FIG. 2. Heteronuclear multiple quantum coherence (HMQC) fingerprint profiles (A, B, C), all taken at 298.1 K in 100:40:20 (by vol) chloroform/methanol/0.2 M K_4EDTA. (A) 4 μM DPPC, 3.9 μM DPPS, and 3.9 μM DPPE; (B) 0.4 μM DPPC, 0.39 μM Pl, and 0.4 μM DPPE; (C) 0.04 μM DPPC, 0.039 μM Pl, and 0.04 μM DPPE. A one-dimensional horizontal slice through the DPPC peaks gives a signal-to-noise ratio of 3:1, indicating an approach to the limits for reliable integration. (D) HMQC of 3 μM pure Pl standard in 100:40:20 (by vol) chloroform/methanol/0.2 M K_4EDTA at 298.1 K. The labeled regions indicate the identity peak of Pl (–0.2, 3.75 ppm) and the proton on the β carbon of the glycerol backbone (–0.2, 5.2 ppm) (C**H**OCOR), respectively. DPPS, DL-α-phosphatidyl-L-serine, dipalmitoyl; DPPE, DL-α-phosphatidylethanolamine, dipalmitoyl; for other abbreviations see Figure 1.

Standard deviations were calculated from integral values of the three sets of dilutions. To verify the accuracy of the *K* values, they were used to calculate the relative phospholipid molarity in porcine erythrocyte ghosts. Figure 4 shows the HMQC spectrum of the porcine erythrocyte ghosts. The relative phospholipid molarity calculated from the most intense peaks is shown in Table 3. The similarity of the experimental values to those already in the literature (19,20) illustrates that this method of quantification of HMQC spectra is reliable and accurate.

Phospholipid profile and quantification of distinct membrane vesicle subfractions. Figure 5 illustrates the 2D phospholipid profile of the MV1 fraction. MV1 fractions were obtained from three separate preparations of MV0 and analyzed to show the reproducibility of the MV1 phospholipid profile. The fingerprint profile of MV1 demonstrates a peak at –0.2, 3.77 ppm and at –0.2, 5.3 ppm. The triple peak at 3.77 ppm represents the identity peak of PI-$\mathbf{H}^6$ (IUPAC nomenclature) from the inositol head group. The –0.2 ppm chemical shift

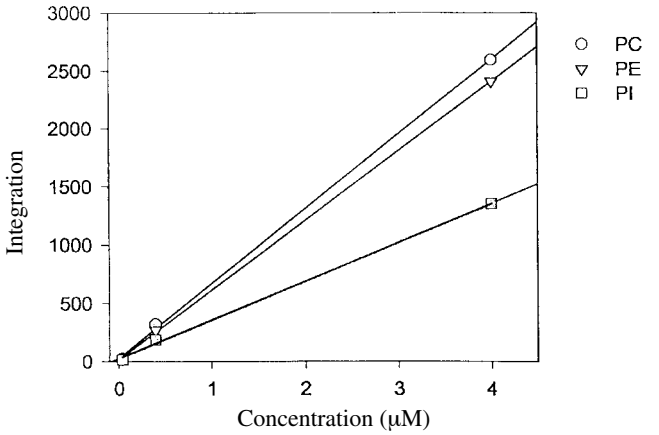

FIG. 3. Integral values from two-dimensional (2D) spectra vs. concentration for phospholipids demonstrating linearity of 2D integrations with phospholipid concentration.

TABLE 3
Phospolipid Composition of Erythrocyte Ghosts

Phospholipids (PL)	Ghost human RBC[a] PL (mol%)	Ghost porcine RBC[b] PL (mol%)	Ghost porcine RBC[c] PL (mol%)
Phosphatidylcholine	30	40	34
Phosphatidylethanolamine	25	33.5	32
Phosphatidylserine	27	7.4	9.7
Phosphatidylinositol	15	6.1	5
Sphingomyelin	—	—	15
Lysophosphatidylcholine	2	4	5

[a]From Reference 20.
[b]From Reference 19.
[c]Present work. (—) = Not detectable.

corresponds to the PI phosphorus chemical shift when PI is in a pure form and not mixed with other phospholipids. From the unique coherence of the proton triple peak at 3.77 ppm with the phosphorus peak at –0.2 ppm it can be concluded that MV1 is mainly composed of PI.

This result can be directly compared to the pure PI standard (Fig. 2D) and furthermore to the 1D F_2 slice through the characteristic PI triplet structure as shown by Casu *et al.* (1) and Henke *et al.* (6). The absence of the other peaks (–0.2, 4.01 ppm; –0.2, 4.2 ppm; and –0.2, 4.4 ppm) in the MV1 HMQC spectrum, with respect to the PI standard, may be due to the variability in the coherence transfer in a biological environment relative to the pure environment of the standard. This means that a given initial coherence follows a certain pathway in a pure sample through single and multiple quantum levels before it is transferred to a single quantum coherence that can be detected by the NMR spectrometer. Mobility is a crucial factor in coherence transfer; lower mobility may be eliminating the unobserved crosspeaks. Whatever the mechanism, because of the presence of other types of molecules in the MV1 extracts, the coherence transfer pathway and its time of evolution to be transferred to a single quantum coherence may be different from that of the pure standard. However, the –0.2, 3.77 ppm (identity peak) is consistently detected as is the –0.2, 5.3 ppm peak. The 5.3 ppm chemical

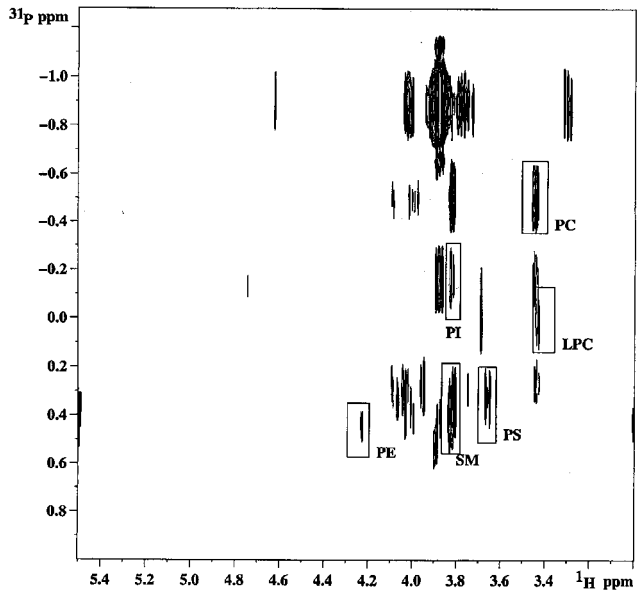

FIG. 4. HMQC of porcine erythrocyte ghosts. The most intense phospholipid peaks were used for calculating relative mol% of phosopholipids and are outlined with a square. The sample also contained tributylphosphate as a standard not used for this analysis. PC, phosphatidylcholine; for other abbreviations see Figures 1 and 2.

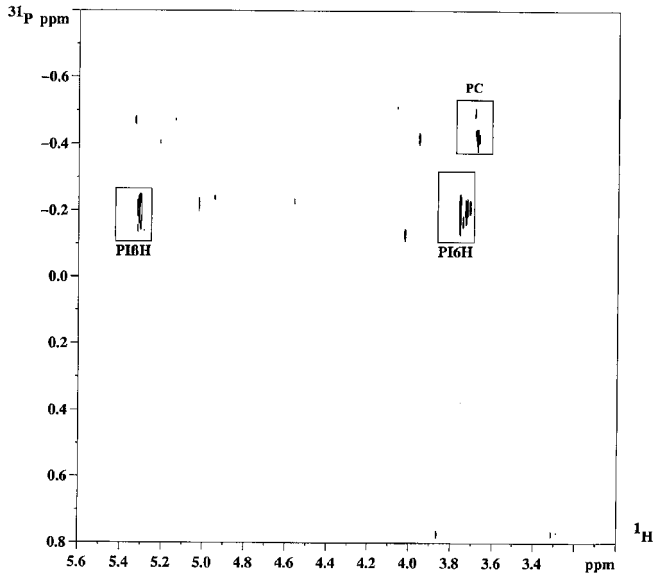

FIG. 5. HMQC fingerprint profile of MVI phospholipids showing PI is the main component. The identity peak at –0.22, 3.75 ppm illustrates the characteristic proton triplet of PI-**H**^{6} of the inositol head group and the proton on the β carbon of the glycerol backbone. The profile of this identity peak is analogous to that shown in Henke *et al.* (6) and to the PI standard in Figure 2D. PC is present as a minor fraction. For abbreviations see Figures 1 and 2.

TABLE 4
Phospholipid Composition of Egg Cytoplasmic Membrane Vesicles and Related Membranes

Phospholipids (PL)	ER rat liver[a] PL (mol%)	Golgi, rat liver[a] PL (mol%)	MV0 PL (% total)	MV1 PL (mol%)	MV2 PL (mol%)	MV3 PL (mol%)
Phosphatidylcholine	58	50	63	11 ± 5[b]	62	73
Phosphatidylethanolamine	22	20	21	—	28	13
Phosphatidylserine	3	6	7.5	—	5	4
Phosphatidylinositol	10	12	3.1	89 ± 5[b]	6	10
Cardiolipin	—	1	—	—	—	—
Lysophosphatidylglycerides	No accurate data	No accurate data	5.2	—	—	—

[a]From Reference 18.
[b]Standard deviation from three separate MV1 extractions.

shift corresponds to the proton of the β carbon on the glycerol backbone (C**H**OCOR).

The mole percentage of PC relative to PI was determined in the following way:

$$\frac{[PC]}{[PI]} = K_{PI/PC}\frac{(A_{PC})}{(A_{PI})} \quad [7]$$

$$\frac{[PC]}{[PI]} = 0.7\frac{(76)}{(563)} = 0.094 \quad [8]$$

Values from these replicates were normalized and the mole percentage for the MV1 fraction were calculated to be 89 ± 5 and 11 ± 5% for PI and PC, respectively.

Figure 6 represents the phospholipid profile of MV2. Similar spectra (not shown) are found for MV3. MV2 is composed of DPPC, PI, DPPS, and DPPE with the following identity peaks: PC (–0.56, 3.5 ppm), PI (–0.25, 3.36 ppm), PS (0.29, 4.1 ppm), and PE (0.4, 3.05 ppm). MV3 also is composed of the above phospholipids with PC at –0.53, 3.5 ppm; PI at –0.22, 3.9 ppm; PS at 0.2, 3.7–3.8 ppm, and PE at 0.44, 3.04 ppm. The order of appearance of each phospholipid relative to the reference standard, DPPC, remains constant in both MV2 and MV3. All peaks were consistently twofold greater than the noise level. The lowest integration value of the phospholipid peaks was 89 and the signal-to-noise ratio of a slice was 3:1.

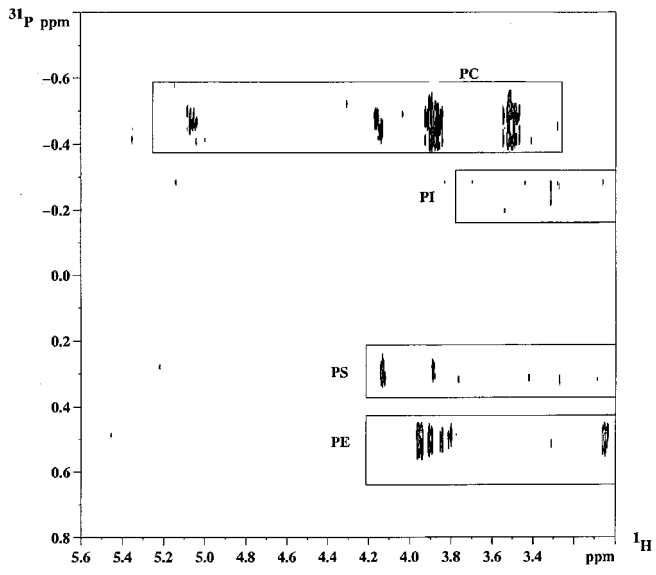

FIG. 6. Phospholipid profile of MV2 membrane vesicles, showing a completely different profile from MV1. MV2 is composed of PC, PI, PS, and PE. MV2 was extracted from the same sucrose gradient as MV1. For abbreviations see Figure1.

The *K* values were used to calculate the mole percentage phospholipid per membrane subfraction. MV2 contains enzymatic markers of the Golgi and ER (9) so results were compared to ER and Golgi from rat liver (18) (Table 4). It can be concluded that MV0, MV2, and MV3 have similar compositions typical of the ER or Golgi membranes. However, MV1 exhibits a striking difference. This membrane subfraction is mainly composed of phosphatidylinositol with PC being the minor phospholipid.

This new method of analysis may be used as a general protocol for the simultaneous identification and quantification of phospholipids in cellular membrane subfractions at a detection limit of 0.04 μM per phospholipid, with minimum sample handling.

ACKNOWLEDGMENTS

The authors are grateful to Drs. John M. Pearce and Thomas Glonek for sharing sample preparation protocols and reviewing the initial phosphorus NMR spectra. This work was supported by U.S. National Institute of Health Award GM55970 and an Amherst College Faculty Research Award to D.L.P.

REFERENCES

1. Casu, M., Anderson, G.J., Choi, G., and Gibbons, W.A (1991) NMR Lipid Profiles, Tissues and Body Fluids. *Magn. Reson. Chem. 29*, 594–602.
2. Adosraku, R.K., Smith, J.D., Nicolaou, A., and Gibbons, W.A. (1996) *Tetrahymena therophila*; Analysis of Phospholipids and Phosphonolipids by High Field ^{1}H-NMR, *Biochim. Biophys. Acta 1299*, 167–174.
3. Pearce, J.M., Shifman, M.A., Pappas, A.A., and Komoroski, R.A. (1991) Analysis of Phospholipids in Human Amniotic Fluid by ^{31}P NMR, *Magn. Reson. Med. 21*, 107–116.
4. Edzes, H.T., Teerlink, T., Valk, J. (1991) Phospholipid Identifica-

tion in Tissue Extracts by Two-Dimensional ^{32} P-^{1}H NMR Spectroscopy with Isotropic Mixing, *J. Magn. Reson. 95*, 387– 395.
5. Merchant, T.E., Diamantis, P.M., Lauwers, G., Haida. T., Kasimos, J.N., Guillem, J., Glonek, T., and Minsky, B.O. (1995) Characterization of Malignant Colon Tumors with ^{31}P Nuclear Magnetic Resonance Phospholipid and Phosphatic Metabolic Profiles, *Cancer 76*, 1715–1723.
6. Henke, J., Willker, W., Engelmann, J., and Leibfritz, D. (1996) Combined Extraction Techniques of Tumour Cells and Lipid/ Phospholipid Assignment by Two-Dimensional NMR Spectroscopy, *Anticancer Res. 16*, 1417–1427.
7. Edzes, H.T., Teerlink, T., Van Der Knapp, M.S., and Valk, J. (1992) Analysis of Phospholipids by ^{31}P-NMR at Different Compositions of the Solvent System Chloroform-Methanol-Water, *Magn. Reson. Med. 26*, 46–59.
8. Pearce, J.M., and Komoroski, R.A. (1993) Resolution of Phospholipid Molecular Species by ^{31}P-NMR, *Magn. Reson. Med.* 29, 724–731.
9. Collas, P., and Poccia, D.L. (1996) Distinct Egg Membrane Vesicles Differing in Binding and Fusion Properties Contribute to Sea Urchin Male Pronuclear Envelopes Formed *in vitro*, *J. Cell Sci. 109*, 1275–1283.
10. Collas, P., and Poccia, D.L. (1998) Methods for Studying *in vitro* Assembly of Male Pronuclei Using Oocyte Extracts from Marine Invertebrates: Sea Urchins and Surf Clams, *Methods Cell Biol. 53*, 417–452.
11. Glonek, T., and Merchant, T.E. (1996) ^{31}P Nuclear Magnetic Resonance Profiling of Phospholipids, in *Advances in Lipid Methodology—Three* (Christie, W.W., ed.) pp. 37–75, Oily Press, Dundee.
12. Coligan, J.E., Kruesbeek, A.M., Margulies, D.H., Shevach, E.M., and Strober, W. (1997) in *Current Protocols in Immunology* (Coico, R., ed.) Section 13.5.2–13.5.12, John Wiley & Sons, Inc., New York.
13. Bodenhausen, G., Ruben, D.J. (1980) natural Abundance Nitrogen-15 NMR by Enhanced Heteronuclear Spectroscopy, *Chem. Phys. Lett 69*, 185–188.
14. Bax, A., Griffey, R.H., and Hawkins, B.L. (1983) Correlation of Proton and Nitrogen-15 Chemical Shifts by Multiple Quantum NMR, *J. Magn. Reson. 55*, 301–315.
15. Bax, A., and Davis, D.G. (1985) MLEV-17 Based Two-dimensional Homonuclear Magnetization Transfer Spectroscopy, *J. Magn. Reson. 65*, 355–360.
16. Braun, S., Kalinowski, H.-O., and Berger, S. (1998) in *150 and More Basic NMR Experiments*, Experiments: HMQC,10.13, HSQC,10.17, TOCSY,10.18, Wiley-VCH, NewYork.
17. Metz, K.R., and Dunphy, K.L. (1996) Absolute Quantitation of Tissue Phospholipids Using ^{31}P NMR, *J. Lipid Res. 37*, 2251– 2265.
18. Van Meer, G. (1998) Lipids in the Golgi Membrane, *Trends Cell. Biol. 8*, 29–33.
19. Engen, R.L., and Clark, C.L. (1990) High-Performance Liquid Chromatography Determination of Erythrocyte Membrane Phospholipid Composition in Several Animal Species, *Am. J. Vet. Res. 51*, 577–580.
20. Wintrobe, M.M., Lee, G.R., Boggs, D.R., Bithell, T.C., Foerster, J., *et al.* (1981) in *Clinical Hematology,* Chapter 4, pp. 80, Lea & Febiger, Philadelphia.

[Received January 17, 2000, and in revised form September 14, 2000; revision accepted September 18, 2000]

ARTICLE

Fatty Acid Analysis of Blood Plasma of Patients with Alzheimer's Disease, Other Types of Dementia, and Cognitive Impairment

Julie A. Conquer[a,*], Mary C. Tierney[c], Julie Zecevic[a], William J. Bettger[a], and Rory H. Fisher[c]

[a]Human Nutraceutical Research Unit and Deptartment of Human Biology and Nutritional Sciences, University of Guelph, Guelph, Ontario, Canada N1G 2W1, [b]Geriatric Research, Department of Family and Community Medicine, and [c]Geriatric Medicine, Sunnybrook and Women's College Health Sciences Centre, University of Toronto, Toronto, Ontario, Canada M4N 3M5

ABSTRACT: Fatty acid differences, including docosahexaenoic acid (DHA; 22:6n-3) have been shown in the brains of Alzheimer's patients (AD) as compared with normal age-matched individuals. Furthermore, low serum DHA is a significant risk factor for the development of AD. The relative concentration of DHA and other fatty acids, however, in the plasma of AD patients compared with patients with other kinds of dementias (other dementias; OD), patients who are cognitively impaired but nondemented (CIND), or normal patients is not known. In this study we analyzed the total phospholipid, phosphatidylcholine (PC), phosphatidylethanolamine (PE), and lysophosphatidylcholine (lysoPC) fractions of plasma from patients diagnosed with AD, OD, or CIND and compared them with a group of elderly control subjects with normal cognitive functioning. Plasma phospholipid and PC levels of 20:5n-3, DHA, total n-3 fatty acids, and the n-3/n-6 ratio were lower in the AD, OD, and CIND groups. Plasma phospholipid 24:0 was lower in the AD, OD, and CIND groups as compared with the group of control patients, and total n-6 fatty acid levels were higher in the AD and CIND groups only. In the plasma PE fraction, levels of 20:5n-3, DHA, and the total n-3 fatty acid levels were significantly lower in the AD, OD, and CIND groups. DHA levels were lower in the lysoPC fraction of CIND individuals only. There were no other differences in the fatty acid compositions of the different phospholipid fractions. Therefore, in AD, OD, and CIND individuals, low levels of n-3 fatty acids in the plasma may be a risk factor for cognitive impairment and/or dementia. Interestingly, a decreased level of plasma DHA was not limited to the AD patients but appears to be common in cognitive impairment with aging.

Paper no. L8562 in *Lipids 35*, 1305–1312 (December 2000).

*To whom correspondence should be addressed at Human Nutraceutical Research Unit, University of Guelph, Guelph, Ontario, Canada N1G 2W1. E-mail: jconquer@uoguelph.ca

Abbreviations: AA, arachidonic acid; AD, Alzheimer's Disease; ANCOVA, analysis of covariance; ANOVA, analysis of variance; CIND, cognitively impaired nondemented; CNS, central nervous system; CT, computer tomography; DHA, docosahexaenoic acid; EPA, eicosapentaenoic acid; lyso PC, lysophosphatidylcholine; MUFA, monounsaturated fatty acid; N, normal; OD, other dementias; PC, phosphatidylcholine; PE, phosphatidylethanolamine; PL, phospholipid; PUFA, polyunsaturated fatty acid; SAT, saturated fatty acid; TLC, thin-layer chromatography.

Alzheimer's disease (AD) is a neurodegenerative disorder that is characterized by progressive memory loss, intellectual decline, and eventually global cognitive impairment. Major symptoms include short- and long-term memory loss, impairments of language and speech, decline of abstract reasoning, and visual-spatial perceptual changes. The incidence of dementia in Western countries, of which AD is the leading cause, is estimated to be approximately 10% of the population over the age of 65 y and 47% of the population over 80 y of age (1). Although much research has been conducted in the area of prevention and treatment of AD, the cause of AD is as yet unknown. It is most likely that a combination of factors contributes to the etiology of AD.

The diversity in the fatty acid composition of brain phospholipids (PL) may influence the biophysical properties of membrane lipids including, for example, fluidity properties and charge (2). Optimal functioning of membrane proteins of the neuron depends on membrane potential, receptor occupancy, phosphorylation-dependent intermolecular associations, and protein and lipid composition (2). In neurons, synaptosomes have the highest concentration of long-chain polyunsaturated fatty acids (PUFA), including docosahexaenoic acid (DHA) and arachidonic acid (AA) (3). The exact function of these PUFA is not clear although AA is the main substrate for synthesis of various eicosanoid mediators (4) and DHA appears to exert a role in membrane fluidity and long-term potentiation, a process that is necessary for memory function (5).

Expanding knowledge in the area of lipid biochemistry suggests that AD is associated with brain lipid defects (6–9). Decreased levels of AA and DHA have been shown in phosphatidylcholine (PC) and phosphatidylethanolamine (PE) fractions from various regions of the AD brain (frontal grey, frontal white, hippocampus, pons) by some (6,10) but not all investigators (11). Aging itself has no influence on the fatty acid composition of PC and/or PE in these fractions of the brain (6). Membrane destabilization, due to a loss of potentially important unsaturated fatty acids, may contribute to AD pathogenesis or it may facilitate the deposition of the neuro-

toxic amyloid β-protein. Other lipid defects that have been associated with the AD brain include a deficiency in the PL ethanolamine plasmalogen (12) and PE (13), and increases in phosphatidylinositol and PC (7) in various brain regions.

As yet, it is not clear whether the plasma fatty acid composition of AD patients differs from other aging patients. It is also not known whether there are plasma fatty acid differences of individuals with other types of dementia or cognitive impairment as compared with elderly controls. It is known, however, that a decreased level of at least one fatty acid in plasma, DHA, is a risk factor for the development of AD (14). Several neurological disorders, which present with altered neuronal fatty acid composition, are also associated with changes in plasma fatty acid composition, such as schizophrenia, depression, attention deficit hyperactivity disorder, and retinitis pigmentosa (15–18). Although AD is not similar to the above-mentioned neuronal disorders, it is possible that the plasma fatty acid composition of AD patients is altered relative to control subjects as well as subjects with other kinds of cognitive impairment.

In this study we examined whether the plasma fatty acid composition of various PL fractions [total PL, PC, PE, lysophosphatidylcholine (lysoPC)] of AD patients differed from those of normal elderly control subjects as well as patients with other kinds of dementias and cognitive impairments. These PL fractions were chosen as they constitute the major repository for fatty acids and are structurally important. The cognitively impaired nondemented (CIND) group was included in order to examine the cross-sectional continuum of cognitive changes in people who were aging normally to those who showed cognitive impairment with no dementia to those with dementia in order to shed light on potential developmental changes in the individual.

MATERIALS AND METHODS:

Subjects. Participants in this study included 84 people who were recruited from a large urban center, and who were screened for one of two ongoing longitudinal studies. Participants in our normal (N) control group are part of a study investigating predictors for the development of AD (19). The other study involves the identification of cognitive and other factors associated with increased risk of harm among seniors living alone in the community (20). Of 96 subjects who were eligible to participate in this study, 84 agreed to donate their blood for this investigation. Informed consent was obtained from all subjects or their legal guardians. Each individual in the study received a thorough physical examination, a computer tomography (CT) scan, and hematology, renal, liver, and metabolic function tests, as well as a detailed neuropsychological assessment by a geriatrician. For the purposes of this investigation, participants were classified as being members of one of the following four groups.

(i) Normal control group. Nineteen people were individually screened by a study physician to ensure there was no history or evidence of brain damage, psychiatric illness, chronic drug or alcohol abuse, or any medical illness likely to affect the brain. All individuals meeting medical criteria for the study were screened with a battery of neuropsychological tests to ensure normal cognitive functioning.

(ii) AD group. Nineteen individuals were diagnosed as having AD based on the consensual decisions of a board-certified geriatrician and a board-certified neuropsychologist that the person met the National Institute of Neurological and Communication Disorders-Alzheimer's Disease and Related Disorders Association criteria for probable AD (21). All individuals were medically screened to ensure that they did not have alternative causes for their cognitive impairment, including chronic alcohol or drug abuse, chronic infections, stroke, hypoxia, metabolic disorders, nutritional disorders, intracranial mass lesions, psychoses, brain trauma, or other neurological diseases. If evidence for these other causes of cognitive impairment was noted they were excluded from the AD group.

(iii) Other dementia (OD) group. Ten individuals met diagnostic criteria for dementia (DSM-IV; Ref. 22) with an etiology other than AD. Eight participants in this group were diagnosed with vascular dementia based on DSM-IV criteria and CT scan evidence of a vascular lesion, one had alcohol-induced persisting dementia, and one had dementia due to head trauma.

(iv) CIND group. Thirty-six were categorized as CIND if they did not meet the DSM-IV criteria for dementia but were found on the neuropsychological examination to score at least one standard deviation below the norm for their age group on tests of verbal and visual memory, language, apraxia, or other areas of cognitive functioning.

Measures. The following tests were used for the neuropsychological diagnostic assessment of the subjects. The Weschler Adult Intelligence Scale-Revised (WAIS-R) (23), Digit symbol, California Verbal Learning Test (24), Rey Osterrieth copy and short delay (25), the Benton Visual Naming Test (26), and the Boston Naming Test (27).

Blood collection. For each participant 10–15 mL of blood was collected by antecubital venipuncture into tubes containing the anticoagulant sodium citrate. Centrifugation (15 min, 3,000 rpm) was carried out on the samples, and 1.5 mL of plasma was removed and placed into Eppendorf tubes for storage at –70°C until analysis. Samples were analyzed for saturated fatty acid (SAT), PUFA and monounsaturated fatty acid (MUFA) composition of total PL, PC, PE, and lysoPC fractions.

Fatty acid analysis of PL, PC, PE and lysoPC. Total PL, PC, PE, and lysoPC were isolated from plasma following lipid extraction as described by Folch (28). The fatty acid analysis of the total PL, PC, PE, and lysoPC was accomplished following thin-layer chromatography (TLC), transmethylation, and gas–liquid chromatography. The individual phospholipids (PC, PE, and lysoPC) were separated by two-dimensional TLC using pre-coated Silica Gel 60 plates (20 × 20 cm, 250 μm; EM Separations Technology, Merck, Gibbstown, NY) and developed in a solution of chloroform/methanol/acetic acid/water in a ratio of 50:37.5:3.5:2. Silica bands containing these PL bands were scraped off, and 5.0 μL of 17:0 standard

was added as an internal standard. Transmethylation was as previously described (29). Gas–liquid chromatography of the fatty acid methyl esters from the total PL, PC, and PE fractions, was performed using a Varian 3800 gas chromatograph (Palo Alto, CA) equipped with a 30 m DB-23 capillary column (0.32 mm internal diameter, 0.1 μm film thickness) using hydrogen as the carrier gas (60 cm/s) with flow rates for air hydrogen, and nitrogen of 320, 35, and 25 mL/min, respectively. The initial column temperature (60°C) was held for 0.8 min and increased to 170°C at 20°C/min. Next, the column temperature was increased to 193°C at a rate of 1.5°C/min and then to 250°C at a rate of 40°C/min. The initial temperature of the injector (60°C) was held for 0.3 min and then increased to 250°C at 175°C/min and held for 25 min.

Statistical analysis. All data are reported as mean (standard error; SEM). Comparisons of demographic characteristics among groups were analyzed by analysis of variance (ANOVA), followed by least squared means only if $P < 0.05$. Significance is reported if $P < 0.05$. Fatty acid composition multifactorial data were analyzed by ANOVA (SAS 6.0, SAS Institute, Cary, NC). If $P < 0.05$, this was followed by analysis of covariance (ANCOVA) with age and education as the covariates. Least squared means analysis was performed only if $P < 0.05$ for the ANCOVA. Significance is reported if $P \leq 0.05$.

RESULTS

Table 1 shows the subject characteristics for all groups. There were more females than males in every group (AD, CIND, and N) other than the OD group, which had equal numbers of each sex. Patients with AD and CIND were significantly older than controls, but the average age of patients with OD was not significantly different from controls ($P > 0.05$). There was also a significant difference in the number of years of education (a gross indicator of socioeconomic levels) among the four groups: patients with AD, OD, and CIND had less education than controls. In order to correct for this, in statistical comparisons between the four groups, an ANCOVA, with age and education as the covariates, was done to account for possible effects of these parameters .

Multifactorial ANOVA results were $P < 0.05$ for total PL, PC, PE, and lysoPC. The fatty acid composition of the plasma total PL of individuals who were designated AD, OD, CIND, or N are given in Table 2 [mean (SEM), wt%]. The levels of most fatty acids from plasma PL were similar among the four groups. However, the amounts of 20:5n-3, 22:6n-3, 24:0, total n-3 fatty acids, and the n-3/n-6 ratio were lower in the AD, OD, and

TABLE 1
Subject Characteristics of Demented, Cognitvely Impaired, and Normal Individuals[a]

	AD	OD	CIND	N
Age (yr)	82.7 (0.3)[a]	79.4 (0.8)[a,b]	83.3 (0.2)[a]	77.5 (0.3)[b]
Sex (males/ females)	6/13	5/5	9/27	7/12
Education (yr)	10.6 (0.8)[a]	10.6 (0.7)[a]	11.2 (1.0)[a]	14.6 (0.7)[b]

[a]Values are reported as mean (SEM) for $n = 19$ (AD), 10 (OD), 36 (CIND), and 19 (N) individuals. [a,b]Significantly different as measured by analysis of covariance (ANCOVA) ($P < 0.05$) followed by least squared means. Abbreviations: AD, Alzheimer's disease; OD, other dementias; CIND, cognitively impaired nondemented; N, normal.

TABLE 2
Fatty Acid Analysis (wt% of total) of Plasma Total Phospholipid of Demented, Cognitively Impaired, and Normal Individuals

Fatty acids	AD		OD		CIND		N	
16:0	27.2	(0.4)	27.5	(0.6)	27.3	(0.3)	27.9	(0.4)
18:0	13.3	(0.3)	13.3	(0.3)	13.2	(0.2)	13.2	(0.3)
18:1	13.9	(0.4)	14.2	(0.6)	13.9	(0.3)	12.5	(0.4)
18:2n-6	19.9	(0.6)	18.5	(0.4)	20.0	(0.5)	19.0	(0.6)
20:3n-6	2.9	(0.1)	3.2	(0.3)	3.0	(0.1)	2.7	(0.2)
20:4n-6	10.1	(0.4)	9.6	(0.4)	9.4	(0.3)	9.1	(0.4)
20:5n-3	0.86	(0.06)[a]	0.87	(0.10)[a]	0.88	(0.07)[a]	1.5	(0.2)[b]
22:0	1.1	(0.0)	1.2	(0.1)	1.1	(0.0)	1.3	(0.1)
22:5n-3	1.0	(0.1)	1.0	(0.1)	1.0	(0.1)	1.1	(0.0)
22:6n-3 (DHA)	3.1	(0.2)[a]	3.8	(0.2)[a]	3.7	(0.2)[a]	4.6	(0.4)[b]
24:0	0.89	(0.04)[a]	0.96	(0.09)[a]	0.90	(0.04)[a]	1.1	(0.0)[b]
24:1	2.2	(0.1)[a]	2.5	(0.2)[a,b]	2.1	(0.1)[a]	2.5	(0.1)[b]
Total SAT	43.7	(0.4)	44.2	(0.4)	43.7	(0.3)	44.7	(0.3)
Total MUFA	17.0	(0.5)	17.6	(0.6)	16.9	(0.3)	16.1	(0.4)
Total PUFA	39.3	(0.4)	38.1	(0.8)	39.4	(0.2)	39.2	(0.5)
Total n-3	5.6	(0.2)[a]	6.0	(0.3)[a]	6.0	(0.3)[a]	7.8	(0.5)[b]
Total n-6	33.7	(0.5)[a]	32.1	(0.7)[a,b]	33.4	(0.3)[a]	31.4	(0.6)[b]
n-3/n-6	0.17	(0.01)[a]	0.19	(0.01)[a]	0.18	(0.01)[a]	0.25	(0.02)[b]
Total PL (mg/dl)	209.0	(8.4)	202.5	(7.1)	224.2	(6.4)	211.4	(6.9)

[a]Values are reported as means (SEM) for $n = 19$ (AD), 10 (OD), 36 (CIND), and 19 (N) individuals. [a,b]Significantly different as measured by ANCOVA ($P < 0.05$) followed by least squared means. Fatty acids found at less than 0.5% were not included in the table. Abbreviations: SAT, saturated fatty acid; MUFA, monounsaturated fatty acid; PUFA, polyunsaturated fatty acid; PL, phospholipid; DHA, docosahexaenoic acid; PL, phospholipid; for other abbreviations see Table 1.

CIND groups as compared with controls (N). Total n-6 fatty acids were significantly higher in the AD and CIND groups only. The levels of total SAT, MUFA, and PUFA as well as total PL (mg/dL) were similar among the four groups ($P > 0.05$).

Table 3 shows the levels of fatty acids in the plasma PC fraction of individuals designated as AD, OD, CIND, or N. The plasma PC fatty acid composition differed among the four groups. The levels of 20:5n-3, 22:6n-3, total omega-3 fatty acids, and the n-3/n-6 ratio were lower in the AD-, OD-, and CIND-designated individuals than in the controls (N). Total SAT, PUFA, and MUFA as well as total n-6 fatty acids and total PC (mg/dL) did not differ among the four groups ($P > 0.05$).

The fatty acid composition of the plasma PE fraction (AD, OD, CIND, and N) is given in Table 4. Levels of 20:5n-3 and 22:6n-3 were significantly lower in the AD, OD, and CIND groups as compared with control (N). Total n-3 fatty acids were also significantly lower in the AD, OD, and CIND groups. As in the PC fraction there were no significant differences in total SAT, MUFA, n-6 fatty acids, and total PE (mg/dL) ($P > 0.05$). There was also no difference in the n-3/n-6 fatty acid ratio among the groups ($P > 0.05$).

Table 5 shows the fatty acid composition of plasma lysoPC in individuals designated as AD, OD, CIND, and N. There were no significant differences in the fatty acid composition of lysoPC as shown ($P > 0.05$). However, DHA levels were significantly lower in individuals with CIND (0.10 %) vs. AD (0.49 %), OD (0.40 %), and N (0.48%) (data not shown).

DISCUSSION

This is the first study to compare the compositions of plasma total PL, plasma PC, plasma PE, and plasma lysoPC fractions from patients with AD, OD, and CIND with a group of normal elderly controls. Recent studies suggest that dietary intake of fish, the most important source of long-chain n-3 fatty acids such as 20:5n-3 (eicosapentaenoic acid; EPA) and DHA, is inversely correlated with the development of dementia, and in particular Alzheimer's disease, in Western countries (30–32). Furthermore, Kyle *et al.* (14) suggest that decreased DHA levels in the plasma PC of elderly individuals is predictive of the development of AD after 10 y. These results, coupled with the results of earlier studies (6,10) showing decreased levels of DHA in the brain of individuals with AD, as well as papers suggesting a link between decreased levels of DHA in serum and various neurologic pathologies (15–18), suggest that plasma levels of DHA, and possibly other n-3 fatty acids, may be lower in the plasma of AD patients as well as patients with other dementias.

Dietary n-3 fatty acids consist mainly of α-linolenic acid (18:3n-3), EPA (20:5n-3), and DHA (22:6n-3). In young, healthy individuals, it is generally accepted that total plasma PL n-3 fatty acid status (including DHA status) represents n-3 fatty acid intake (33–35). Although metabolism of α-linolenic acid to EPA and DHA occurs in humans, it is limited to approximately 5% (36). Comparison of fatty acid levels between individuals with AD, OD, and CIND and normal elderly individuals clearly suggests differences in the fatty acid composition of total PL. The decreased levels of EPA (by approximately 42%), DHA (by 17–33%) and total n-3 levels (by 23–28%) in the plasma PL of patients with AD, OD, and CIND suggest that the dietary intake of the n-3 fatty acids is lower than that of normal subjects. The possibility of increased breakdown, either before or after disease onset, cannot be ruled out. The increased levels of F_4-isoprostanes ob-

TABLE 3
Fatty Acid Analysis (wt% of total) of Plasma Phosphatidylcholine of Demented, Cognitively Impaired, and Normal Individuals

Fatty acids	AD		OD		CIND		N	
16:0	27.7	(0.5)	27.9	(0.8)	28.6	(0.4)	28.2	(0.5)
18:0	12.9	(0.3)	13.2	(0.4)	12.3	(0.4)	12.9	(0.4)
18:1	15.0	(0.5)	15.3	(0.7)	15.0	(0.3)	13.7	(0.4)
18:2n-6	22.4	(0.6)	21.4	(0.7)	22.5	(0.5)	21.7	(0.6)
20:3n-6	3.3	(0.1)	3.7	(0.3)	3.4	(0.1)	3.1	(0.2)
20:4n-6	9.9	(0.4)	9.6	(0.4)	9.3	(0.4)	9.1	(0.5)
20:4n-3	0.13	(0.02)	0.14	(0.02)	0.10	(0.01)	0.18	(0.02)
20:5n-3	1.0	(0.1)[a]	1.0	(0.1)[a]	1.0	(0.1)[a]	1.7	(0.2)[b]
22:5n-3	1.1	(0.0)	1.0	(0.1)	1.0	(0.0)	1.1	(0.0)
22:6n-3 (DHA)	3.2	(0.2)[a]	3.8	(0.3)[a]	3.6	(0.2)[a]	4.9	(0.4)[b]
24:0	0.08	(0.01)	0.08	(0.01)	0.08	(0.01)	0.10	(0.01)
24:1	0.11	(0.03)	0.13	(0.02)	0.13	(0.01)	0.13	(0.02)
Total SAT	41.6	(0.5)	41.9	(0.5)	41.9	(0.4)	42.2	(0.2)
Total MUFA	16.1	(0.5)	16.3	(0.7)	16.0	(0.3)	14.8	(0.5)
Total PUFA	42.3	(0.4)	41.8	(0.9)	42.1	(0.4)	43.0	(0.5)
Total n-3	5.7	(0.3)[a]	6.3	(0.3)[a]	6.0	(0.3)[a]	8.4	(0.6)b
Total n-6	36.5	(0.5)	35.6	(0.9)	36.1	(0.4)	34.7	(0.7)
n-3/n-6	0.16	(0.01)[a]	0.18	(0.01)[a]	0.17	(0.01)[a]	0.25	(0.02)[b]
Total PC (mg/dL)	153.0	(6.8)	147.5	(5.6)	163.3	(5.5)	158.7	(6.3)

[a]Values are reported as means (SEM) for $n = 19$ (AD), 10 (OD) 36 (CIND), and 19 (N) individuals. [a,b]Significantly different as measured by ANCOVA ($P < 0.05$) followed by least squared means. Fatty acids found at less than 0.5% were not included in this table. PC, phosphatidylcholine; for other abbreviations see Tables 1 and 2.

TABLE 4
Fatty Acid Analysis (wt% of total) of Plasma Phosphatidylethanolamine of Demented, Cognitively Impaired, and Normal Individuals

Fatty acids	AD		OD		CIND		N	
14:0	2.6	(0.3)	2.8	(0.6)	2.4	(0.2)	2.6	(0.3)
14:1	1.1	(0.1)	1.2	(0.2)	1.1	(0.1)	1.1	(0.1)
15:0	1.6	(0.2)	1.5	(0.2)	1.6	(0.2)	1.2	(0.1)
16:0	22.4	(1.3)	23.6	(2.3)	23.7	(0.8)	21.3	(0.8)
16:1	2.2	(0.5)	3.2	(0.7)	2.0	(0.3)	1.9	(0.4)
18:0	17.4	(2.6)	13.9	(2.8)	20.4	(2.1)	14.3	(1.9)
18:1	17.4	(1.7)	18.7	(2.7)	15.5	(1.2)	16.1	(1.2)
18:2n-6	12.3	(1.5)	11.3	(1.6)	11.6	(1.2)	12.8	(1.3)
20:3n-6	0.78	(0.06)	0.78	(0.10)	0.92	(0.05)	0.77	(0.06)
20:4n-6	11.4	(1.2)	11.0	(1.7)	10.3	(0.7)	12.5	(1.0)
20:5n-3	0.85	(0.09)[a]	0.92	(0.18)[a]	0.91	(0.11)[a]	2.0	(0.2)[b]
22:5n-3	1.4	(0.2)	1.7	(0.7)	1.4	(0.1)	1.6	(0.1)
22:6n-3 (DHA)	4.6	(0.4)[a]	6.1	(1.0)[a]	5.5	(0.6)[a]	8.2	(0.7)[b]
24:0	0.79	(0.09)	0.70	(0.12)	0.62	(0.07)	0.90	(0.08)
Total SAT	46.0	(3.8)	43.1	(4.6)	49.2	(2.7)	40.9	(2.4)
Total MUFA	21.4	(1.9)	23.8	(2.8)	19.1	(1.3)	19.8	(1.2)
Total PUFA	32.6	(2.4)	33.1	(3.0)	31.7	(1.7)	39.3	(1.8)
Total n-3	7.5	(0.6)[a]	9.4	(1.4)[a]	8.4	(0.7)[a]	12.6	(0.9)[b]
Total n-6	25.1	(2.0)	23.7	(2.1)	23.4	(1.4)	26.7	(1.3)
n-3/n-6	0.32	(0.02)	0.40	(0.05)	0.38	(0.03)	0.48	(0.03)
Total PE (mg/dL)	20.7	(1.6)	18.2	(1.6)	22.4	(2.2)	19.2	(1.4)

[a]Values are reported as means (SEM) for $n = 19$ (AD), 10 (OD), 36 (CIND), and 19 (N) individuals. [a,b]Significantly different as measured by ANCOVA ($P < 0.05$) followed by least squared means. Fatty acids found at less than 0.5% were not included in this table. PE, phosphatidylethanolamine; for other abbreviations see Tables 1 and 2.

served in both the brain and cerebrospinal fluid of AD patients (37,38) suggest that DHA breakdown and other oxidative damage are occurring in AD. Furthermore, results indicate that it possibly occurs early in the course of AD. Although the reason for decreased levels of n-3 fatty acids in plasma PL of AD, OD, and CIND patients is not clear, our data are in agreement with those of Kyle *et al.* (14), who suggested that decreased DHA levels were found to be a risk indicator for the development of AD, and with recent publications inversely linking fish intake to development of dementia (30–32). There is very little information on fatty acid status and actual cognitive functioning in adults. It is not clear whether DHA levels in various parts of the brain play a role in cognitive functioning of human adults, including the elderly.

Decreased levels of EPA (by 41%) and DHA (by 22–35%) were also observed in the PC fraction of individuals with AD, OD, and CIND vs. normal individuals. This resulted in decreased levels of total n-3 fatty acids (25–32%) and a decreased ratio of n-3/n-6 fatty acids (28–36%) in these groups. Since PC makes up most of the total PL in plasma (approximately 75%), these results were expected. The decreased levels of DHA in plasma PC support the results of Kyle *et al.* (14). Interestingly, although EPA (54–57%), DHA (26–44%), and total n-3 fatty acid (25–40%) levels were also decreased in the plasma PE of

TABLE 5
Fatty Acid Analysis (wt% of total) of Plasma Lysophosphatidylcholine of Demented, Cognitively Impaired, and Normal Individuals

Fatty acids	AD		OD		CIND		N	
16:0	49.2	(2.3)	54.3	(3.0)	53.2	(1.6)	51.5	(1.8)
18:0	16.9	(1.4)	17.2	(1.3)	18.5	(1.1)	19.0	(2.2)
18:1	16.1	(1.4)	13.5	(1.4)	14.3	(0.6)	13.6	(0.5)
18:2n-6	14.9	(1.8)	12.1	(1.6)	11.4	(0.7)	13.4	(1.3)
20:4n-6	1.9	(0.3)	2.2	(0.5)	1.8	(0.2)	2.7	(0.3)
Total SAT	68.1	(1.4)	69.2	(1.6)	72.1	(1.5)	70.5	(2.0)
Total MUFA	15.9	(1.4)	14.7	(1.1)	14.3	(0.7)	13.6	(0.5)
Total PUFA	15.7	(1.8)	16.0	(1.0)	13.6	(0.6)	16.1	(1.2)
Total n-3	0.64	(0.14)	0.82	(0.25)	0.54	(0.10)	1.0	(0.2)
Total n-6	16.8	(1.9)	14.3	(2.1)	13.2	(0.6)	16.1	(1.3)
n-3/n-6	0.04	(0.01)	0.05	(0.01)	0.04	(0.01)	0.06	(0.01)

[a]Values are reported as means (SEM) for $n = 8$ (AD), 5 (OD), 10 (CIND), and 10 (N) individuals. Fatty acids found at less than 0.5% are not included in this table. For abbreviations see Tables 1 and 2.

AD, OD, and CIND patients, as compared with normal individuals, there were no significant differences in the ratio of n-3/n-6 fatty acids within this faction. The decreased levels of DHA, EPA, and total n-3 fatty acids in the PE fraction of AD, OD, and CIND individuals, are consistent with the decreased levels of these fatty acids as observed in PC and total PL.

This study is the first to examine differences in the fatty acid composition of the PE and lysoPC fractions in AD, OD, and CIND individuals as compared with elderly controls. In contrast with the differences in n-3 fatty acid levels of the PL, PC, and PE fractions, there were no measurable differences in the fatty acid composition of lysoPC in AD, OD, or CIND patients as compared with the normal group.

It has been suggested that the PC pool is used as a pathway for the supply of various PUFA, including DHA, to the brain (38). Thus, decreased levels of DHA in total PL, PC, and PE in the plasma of AD patients may also be partially responsible for decreased levels of this fatty acid in the brain. It is not clear whether individuals with CIND and OD also have decreased brain levels of DHA. Although decreased brain levels of DHA could be due to a combination of decreased plasma DHA levels and increased DHA breakdown in the brain itself, there is as yet no clear indication as to whether the decreased DHA levels in plasma occur prior to or post-disease onset. The results of Kyle *et al.* (14) and others (30–32) suggest however, that plasma fatty acid compositional changes may occur prior to disease onset.

The decreased levels of EPA in the plasma of the AD, OD, and CIND patients as observed in this study can be explained by decreased consumption of EPA-containing foods, such as fish or fish oils. There are no other studies with which to compare these results, as levels of EPA have not been previously compared in plasma of AD, OD, and CIND individuals. Thus, one can hypothesize that decreased fish consumption prior to disease onset, as suggested by Kalmijn *et al.* (30,31) and Grant (32), may be at least partially responsible for both the lower levels of EPA and DHA and the initiation or potentiation of cognitive decline. One limitation of this study is that no dietary intakes or histories were done on the patients. Thus, it is not clear whether the patients presently consume, or consumed in the past, diets that were lower in n-3 fatty acids. Furthermore, socioeconomic background may have played a role in dietary choices since the patient groups were less educated than the control group, and education is a gross indicator of socioeconomic level. However, our statistical analysis indicated that differences among the groups in levels of EPA and DHA remained when education was used as a covariate in these analyses. It remains to be tested whether decreased levels of n-3 fatty acids in the plasma and/or brain of patients with AD, as well as OD and CIND, contribute to disease symptoms, or whether they were only a biochemical change that occurs alongside those other changes responsible for disease symptoms. However, data in humans suggest that neural membranes are characterized by high concentrations of DHA (approximately 31% in adult human cerebral cortex PE) (40), which suggests an important role in central nervous system (CNS) functioning. Furthermore, dietary DHA levels in infants correlate with brain levels of DHA as well as cognitive functioning (41,42). The actual role of DHA in CNS functioning is not clear, although it is likely that more than one process is involved (40).

Very few studies have investigated whether DHA, or n-3 fatty acid, supplementation reduces the occurrence and/or the symptoms of AD and the other dementias. As mentioned earlier, Kalmijn *et al.* (30,31) and Grant (32) have suggested that decreased fish consumption is correlated with cognitive impairment. Another study involving the supplementation of AD patients with SR-3 (n-3/n-6, 1:4) in a double-blind manner showed improvements in mood, cooperation, appetite, sleep, and short-term memory (43). A more recent study, by Terano *et al.* (44), suggests that supplementation of elderly people with mild to moderate dementia (of thrombotic cerebrovascular disorders) with 0.72 g DHA per day for one year resulted in improvements in both the serum fatty acid content and scores on the Mini-Mental State examination and the Hasegawa's Dementia rating scale. A study in adult rats suggests that chronic administration of DHA results in a significant improvement in the spatial learning deficit following occlusion (45). Although data on the effects of n-3 fatty acid supplementation on symptoms of dementia and cognitive decline are limited, the effort to increase fish, fish products, or other sources of omega-3 fatty acids in the diets of both the population at large and the elderly seems prudent. This may be difficult to do in groups of noninstitutionalized elderly, such as the subjects in our study, but would be feasible for the elderly in nursing homes, retirement homes, and hospitals.

In conclusion, this study suggests that the fatty acid composition of plasma total PL, as well as PC and PE, differs between individuals with AD, OD, and CIND as compared with healthy elderly men and women. In general, decreased levels of EPA, DHA, total n-3 fatty acids, and the ratio of n-3/n-6 fatty acids, were noted. It is not clear whether the decreased levels of these fatty acids are due to dietary differences between the groups, or whether the levels of these fatty acids decreased prior to or after disease onset. Furthermore, it is not clear why decreased levels of EPA, DHA, and total n-3 fatty acids were observed in the OD and CIND groups, in addition to the AD group. It is likely that some of the CIND patients had incipient AD and were showing early signs of the disease. Of the patients in the OD group, 80% had vascular dementia, and although there is no evidence to suggest that plasma DHA levels are inversely correlated with stroke, there is indirect evidence to suggest that DHA supplementation improves cognition in patients with dementia due to stroke (43). It would be interesting to answer these questions as well as to determine the effect of supplementation with DHA, or total n-3 fatty acids, in future studies. Differences in levels of various n-3 fatty acids in the plasma of AD, OD, and CIND individuals may add further information to our expanding knowledge of biochemical abnormalities that occur outside of the brain in AD and other dementias.

ACKNOWLEDGMENTS

We would like to thank the Scottish Rite Charitable Foundation for funding this investigation. In addition, special thanks go to Dr. Diana Philbrick for her input in the development of the manuscript.

REFERENCES

1. Evans, D.A., Funkenstein, H.H., Alber, M., Scherr, P.A., Cook, N.R., Chown, M., Herbert, L., Hennekens, C., and Taylor, J. (1989) Prevalence of Alzheimer's Disease in a Community Population of Older Persons: Higher Than Previously Reported, *JAMA 262*, 2551–2556.
2. Chapman, D. (1983) *Biomembrane Fluidity: the Concept and Its Development in Membrane Fluidity in Biology. Vol. 2: General Principles* (Aaloia, R.C., ed.) pp. 5–42, Academic Press, New York.
3. Martinez, M., and Mougan, I. (1998) Fatty Acid Composition of Human Brain Phospholipids During Normal Development, *J. Neurochem. 71*, 2528–2533.
4. Spector, A.A. (1999) Essentiality of Fatty Acids, *Lipids 34 (suppl.)*, S1–S3.
5. Lim, S.Y., and Suzuki, H. (2000) Intakes of Dietary Docosahexaenoic Acid Ethyl Ester and Egg Phosphatidylcholine Improve Maze-Learning Ability in Young and Old Mice, *J. Nutr. 130*, 1629–1632.
6. Söderburg, M., Edlund, C., Kristensson, K., and Dallner, G. (1991) Fatty Acid Composition of Brain Phospholipids in Aging and in Alzheimer's Disease, *Lipids 26*, 421–428.
7. Söderburg, M., Edlund, C., Kristensson, K., Alafuzoff, I., and Dallner, G. (1992) Lipid Composition in Different Regions of the Brain in Alzheimer's Disease/Senile Dementia of Alzheimer's Type, *J. Neurochem. 59*, 1646–1653.
8. Nitsch, R., Pittas, A., Blustztajn, J.K., Slock, B.E., and Growdon, J. (1991) Alterations of Phospholipid Metabolites in Post-Mortem Brains from Patients with Alzheimer's Disease, *Ann. NY Acad. Sci. 640*, 110–113.
9. Mulder, M., Ravid, R., Swaab, D.F., deLoet, E.R., Haasdijk, E.D., Julk, J., van der Bloom, J., and Havekes, L.M. (1998) Reduced Levels of Cholesterol, Phospholipids, and Fatty Acids in CSF of Alzheimer's Disease Patients Are Not Related to Apo E4, *Alz. Dis. Assoc. Dis. 12*, 198–203.
10. Prasad, M.R., Lovell, M.A., Yatin, M., Dhillon, H., and Markesbery, W.R. (1998) Regional Membrane Phospholipid Alterations in Alzheimer's Disease, *Neurochem. Res. 23*, 81–88.
11. Brooksbank, B.W.L., and Martinez, M. (1989) Lipid Abnormalities in the Brain in Adult Down's Syndrome and Alzheimer's Disease, *Mol. Chem. Neuropathol. 11*, 157–185.
12. Ginsberg, L., Rafique, S., Xuereb, J.H., Rapoport, S.I., and Gershfeld, N.L. (1995) Disease and Anatomic Specificity of Ethanolamine Plasmalogen Deficiency in Alzheimer's Disease Brain, *Brain Res. 698*, 223–226.
13. Ellison, D.W., Beal, M.F., and Martin, J.B. (1987) Phosphoethanolamine and Ethanolamine Are Decreased in Alzheimer's Disease and Huntington's Disease, *Brain Res. 417*, 389–392.
14. Kyle, D.J., Schaefer, E., Patton, G., and Beiser, A. (1999) Low Serum Docosahexaenoic Acid Is a Significant Risk Factor for Alzheimer's Dementia, *Lipids 34 (suppl.)*, S245.
15. Stevens, L.J., Zentall, S.S., Deck, J.L., Abate, M.L., Watkins, B.A., Lipp, S.R., and Burgess, J.R. (1995) Essential Fatty Acid Metabolism in Boys with Attention-Deficit Hyperactivity Disorder, *Am. J. Clin. Nutr. 62*, 761–768.
16. Laugharne, J.D.E., Mellor, J.E., and Peet, M. (1996) Fatty Acids and Schizophrenia, *Lipids 31 (suppl.)*, S163–S165.
17. Simonelli, F., Hanna, C., Romano, N., Nunziata, G., and Rinaldi, E. (1996) Evaluation of Fatty Acids in Membrane Phospholipids of Erythrocytes in Retinitis Pigmentosa Patients, *Ophthalmic Res. 28*, 93–96.
18. Peet, M., Murphy, B., Shay, J., and Horrobin, D. (1998) Depletion of Omega-3 Fatty Acid Levels in Red Blood Cell Membranes of Depressive Patients, *Biol. Psychiat. 43*, 315–319.
19. Tierney, M.C., Szalai, J.P., Snow, W.G., Fisher, R.H., Nores, A., Nadon, G., Dunn, E., and St. George-Hyslop, P.H. (1996) Prediction of Probable Alzheimer's Disease in Memory-Impaired Patients: A Prospective Longitudinal Study, *Neurology 46*, 661–665.
20. Tierney, M.C. (1997) Editorial: How Safe are Cognitively Impaired Seniors who Live Alone, *Can. J. Aging 16*, 177–189.
21. McKhann, G., Drachman, D., Folstein, M., Katzman, R., Price, D., and Stadlan, E. (1984) Clinical Diagnosis of Alzheimer's Disease: Report of the NINCDS-ADRDA Work Group Under the Auspices of Department of Health and Human Services Task Force on Alzheimer's Disease, *Neurology 34*, 939–944.
22. American Psychiatric Association (1994) *Diagnostic and Statistical Manual of Mental Disorders,* 4th edn., American Psychiatric Association, Washington, DC.
23. Wechsler, D. (1981) *Wechsler Adult Intelligence Scale-Revised*, Psychological Corporation, New York.
24. Delis, D.C., Kramer, J.H., Kaplan, E., and Ober, B.A. (1987) *CVLT: California Verbal Learning Test: Research Edition*, adult version, manual, Psychological Corporation, San Antonio.
25. Lezak, M.D. (1982) *Neuropsychological Assessment*, 2nd edn., Oxford University Press, New York.
26. Benton, A., and Hamsher, K. (1983) *Multilingual Aphasia Examination*, AJA Associates, Iowa City.
27. Kaplan, E., Goodglass, H., and Weintraub, S. (1983) Boston Naming Test, Lea & Fibiger, Philadelphia.
28. Folch, J., Lees, M., Sloan Stanley, G.H. (1957) A Simple Method for the Isolation and Purification of Total Lipids from Animal Tissue, *J. Biol. Chem. 226*, 497–509.
29. Conquer, J.A., and Holub, B.J. (1996) Supplementation with an Algae Source of Docosahexaenoic Acid Increases (n-3) Fatty Acid Status and Alters Selected Risk Factors for Heart Disease in Vegetarian Subjects, *J. Nutr. 126*, 3032–3039.
30. Kalmijn, S., Launer, L.J., Ott, A., Witteman, J.C., Hofman, A., and Breteler, M.M. (1997) Dietary Fat Intake and the Risk of Incident Dementia in the Rotterdam Study, *Ann. Neurol. 42*, 776–782.
31. Kalmijn, S., Feskens, E.J.M., Launer, L.J., and Kromhout, D. (1997) Polyunsaturated Fatty Acids, Antioxidants, and Cognitive Function in Very Old Men, *Am. J. Epidemiol. 145*, 33–41.
32. Grant, W.B. (1997) Dietary Links to Alzheimer's Disease, *Alzheimer Dis. Rev. 2*, 42–55.
33. Ma, J., Folsom, A.R., Eckfeldt, J.H., Lewis, S.L., and Chambless, L.E. (1995) Short- and Long-Term Repeatability of Fatty Acid Composition of Human Plasma Phospholipids and Cholesterol Esters, *Am. J. Clin. Nutr. 62*, 572–578.
34. Bonaa, K.H., Bjerve, K.S., and Nordoy, A. (1992) Habitual Fish Consumption, Plasma Phospholipid Fatty Acids, and Serum Lipids: The Tromso Study, *Am. J. Clin. Nutr. 55*, 1126–1134.
35. Nikkari, T., Luukkainen, P., Pietinen, P., and Buska, P. (1995) Fatty Acid Composition of Serum Lipid Fractions in Relation to Gender and Quality of Dietary Fat, *Ann. Med. 27*, 491–498.
36. Emken, E.A., Adlof, R.O., and Gulley, R.M. (1994) Dietary Linoleic Acid Influences Desaturation and Acylation of Deuterium-Labelled Linoleic Acid and Linolenic Acids in Young Adult Males, *Biochim. Biophys. Acta 1213*, 277–288.
37. Montine, T.J., Beal, M.F., Cudkowicz, M.E., O'Donnell, H., Margolin, R.A., McFarland, L., Bachrach, A.F., Zackert, W.E., Roberts, L.J., and Morrow, J.D. (1999) Increased CSF F_2-Isoprostane Concentration in Probable AD, *Neurology 52*, 562–565.

38. Nourooz-Zadeh, J., Liu, E.H.C., Yhlen, B., Anggard, E.E., and Halliwell, B. (1999) F_4-Isoprostanes as Specific Marker of Docosahexaenoic Acid Peroxidation in Alzheimer's Disease, *J. Neurochem. 72*, 724–740.
39. Magret, V., Elkhalil, L., Nazih-Sanderson, F., Martin, F., Bourre, J.M., Fruchart, J.C., and Delbart, C. (1996) Entry of Polyunsaturated Fatty Acids into the Brain: Evidence That High-Density Lipoprotein-Induced Methylation of Phosphatidylethanolamine and Phospholipase A2 Are Involved, *Biochem. J. 316*, 805–811.
40. Burdge, G.C. (1998) The Role of Docosahexaenoic Acid in Brain Development and Fetal Alcohol Syndrome, *Biochem. Soc. Trans. 26*, 246–252.
41. Jamieson, E.C., Farquharson, J., Logan, R.W., Howatson, A.G., Patrick, W.J., Weaver, L.T., and Cockburn, F. (1999) Infant Cerebellar Gray and White Matter Fatty Acids in Relation to Age and Diet, *Lipids 34*, 1065–1071.
42. Cunnane, S.C., Francescutti, V., Brenna, J.T., and Crawford, M.A. (2000) Breast-fed Infants Achieve a Higher Rate of Brain and Whole Body Docosahexaenoate Accumulation Than Formula-fed Infants Not Consuming Dietary Docosahexaenoate, *Lipids 35*, 105–111.
43. Yehuda, S., and Rabinovitz, S. (1996) Essential Fatty Acids Preparation (SR-3) Improves Alzheimer's Patients Quality of Life, *Int. J. Neurosci. 87*, 141–149.
44. Terano, T., Fujishiro, S., Ban, T., Yamamoto, K., Tanaka, T., Noguchi, Y., Tamura, Y., Yazawa, K., and Hirayama, T. (1999) Docosahexaenoic Acid Supplementation Improves the Moderately Severe Dementia from Thrombotic Cerebrovascular Diseases, *Lipids 34*, S345–S346.
45. Okada, M., Amamoto, T., Tomonaga, M., Kawachi, A., Yazawa, K., Mine, K., and Fujiwara, M. (1996) The Chronic Administration of Docosahexaenoic Acid Reduces the Spatial Cognitive Defect Following Transient Forebrain Ischemia in Rats, *Neuroscience 71*, 17–25.

[Received June 15, 2000, and in final revised form and accepted October 24, 2000]

In Vivo Evaluation of the Effects of Continuous Exercise on Skeletal Muscle Triglycerides in Trained Humans

Jesus Rico-Sanz[a], Marjan Moosavi[a], E. Louise Thomas[a], John McCarthy[b], Glyn A. Coutts[a], Nadeem Saeed[a], and Jimmy D. Bell[a,*]

[a]The Robert Steiner MRI Unit, MRC Clinical Sciences Centre, Imperial College School of Medicine, Hammersmith Hospital, and [b]The National Sports Medicine Institute of the United Kingdom, London, England

ABSTRACT: Magnetic resonance spectroscopy (^{1}H MRS) and imaging (MRI) were used to investigate the effects of a bout of moderate prolonged exercise on intra (IMCL)- and extramyocellular lipid (EMCL) utilization in the soleus, tibialis anterior, and gastrocnemius muscles of five trained human subjects. MRI and ^{1}H MRS measurements were obtained before and after a 90 min run on a calibrated treadmill at a velocity corresponding to 64 ± 1.5% of each subjects' maximal rate of oxygen consumption. There were significant decreases in IMCL following exercise in the tibialis (pre: 22.37 ± 4.33 vs. post: 15.16 ± 3.25 mmol/kg dry wt; $P < 0.01$) and soleus (pre: 36.93 ± 1.45 vs. post: 29.85 ± 2.44 mmol/kg dry wt; $P < 0.01$) muscles. There was also a decrease in the gastrocnemius muscle, although this did not reach the level of significance (pre: 33.78 ± 5.35 vs. post: 28.48 ± 5.44 mmol/kg dry weight; $P < 0.10$). No significant changes were observed in EMCL or subcutaneous fat. In conclusion, this study showed that IMCL were significantly utilized in the tibialis and soleus muscles of aerobically endurance-trained humans. The absence of significant utilization of IMCL in the gastrocnemius may reflect differences in fiber type and/or intensity of contraction for each muscle group.

Paper no. L8579 in *Lipids 35*, 1313–1318 (December 2000).

There is increasing interest in the study of intramyocellular lipid (IMCL), both because of its potential role as an energy depot and because of its possible contribution to the pathogenesis of certain diseases (1–3). IMCL accounts for approximately 2,000–3,000 kcal of stored energy, making it a greater source of potential energy than muscle glycogen, which in an average person can contribute 1,000–2,000 kcal (1).

Compared to glycogen utilization by muscle, relatively little is known about net IMCL oxidation during exercise. It has been suggested that during moderate-intensity exercise, total fat oxidation is far in excess of the rate of plasma free fatty acids and triglyceride (TG) uptake, requiring additional net fat oxidation from a pool of IMCL (4). However, several groups have investigated IMCL levels following exercise with variable results. While some groups have reported significant reductions in IMCL following exercise (1–3,5–7), other groups have reported no changes in IMCL (8–10). The reason for the discrepancy is unclear, but differences in subject population, type, intensity and duration of exercise, and variations in methodology may be important contributory factors.

A number of studies have shown that *in vivo* magnetic resonance spectroscopy (MRS) can be utilized to study muscle TG in human subjects (11–16). The advantages of this technique over muscle biopsy include its noninvasive nature and its significantly higher reproducibility of measurements (11,13). This has opened up the opportunity to assess changes in IMCL metabolism in human subjects in different regions within a muscle and in different muscle groups. In a recent study of a single subject, Boesch *et al.* (11) showed a net decrease in IMCL levels in the tibialis muscle following 3 h of cycling (11), while Krssak *et al.* (16) reported a significant decrease in IMCL in the soleus muscle following a 2–3 h treadmill run to exhaustion at 65–70% maximal rate of oxygen consumption (VO_2max). Rico-Sanz *et al.* (13) reported no net utilization of IMCL following a protocol of alternating velocity. These results, as with needle biopsy studies, suggest that IMCL utilization may be conditional to factors such as type, intensity, and duration of exercise.

In this study we have used *in vivo* ^{1}H MRS and MR imaging (MRI) to determine the extent to which IMCL and extramyocellular lipids (EMCL) are utilized during exercise, in endurance-trained athletes, during a 90-min run at 64 ± 1.5% VO_2max. The results showed that levels of IMCL were significantly reduced in the tibialis and soleus muscles after the exercise program.

METHODS

Six healthy, non-smoking Caucasian male subjects (age 35.0 ± 1.5 yr) were studied. The subjects, all distance runners, with recent half-marathon times of less than 1 h 40 min, were recruited from running clubs in London. Written informed consent was obtained from all volunteers. The research was approved by the Ethics Committee of the Royal Postgraduate

*To whom correspondence should be addressed at Robert Steiner MRI Unit, Imperial College School of Medicine, Hammersmith Hospital, Du Cane Rd., London, W12 0HS, UK. E-mail: jimmy.bell@csc.mrc.ac.uk

Abbreviations: BASES, British Association of Sports and Exercise Sciences; BMI, body mass index; Cho, choline; Cr, creatine; EMCL, extramyocellular lipid; FTa, fast twitch oxidative glycolytic fiber; HRmax, maximal heart rate; IMCL, intramyocellular lipid; MRI, magnetic resonance imaging; MRS, magnetic resonance spectroscopy; TE, echo time; TG, triglyceride; TR, repetition time; VO_2max, maximal rate of oxygen consumption.

Medical School, Hammersmith Hospital, London (REC. 96/5030). Exclusion criteria included claustrophobia, metal implants, medication, or sports supplements. One subject was not included in the final data analysis, as he struggled to complete the exercise protocol and his VO_2max during the run was considerably higher than the 64% VO_2max required in the protocol (he was running at close to 85% VO_2max). Furthermore, it was subsequently ascertained that this subject had completed a full marathon the previous day, thus invalidating his inclusion in the study.

Exercise testing. All participants were assessed for their physical fitness at the National Sports Medicine Institute of the UK (Sports and Exercise Performance Unit) prior to inclusion in the study. All tests were performed on fully rested subjects, i.e., no training in the 48 h preceding the test, and all subjects were asked to maintain their standard pre-test dietary and physical preparation. This was done to avoid potential confounding factors such as changes in dietary and physical activity influencing muscle TG content (17).

VO_2max. VO_2max measurements were made for each subject 2–7 days prior to the exercise test. The British Association of Sport and Exercise Sciences (BASES) physiological testing guidelines (1997) and protocol for middle- and long-distance runners were used to assess VO_2max (18). In brief, each subject performed an incremental velocity treadmill running test with a 1% elevation. Treadmill velocity was then incremented 1 km/h every 2 min until the runner reached a respiratory quotient of approximately 1. Following this, the treadmill elevation was increased by 1% per minute, while maintaining the same constant velocity achieved in the last 2-min stage. All subjects were encouraged to continue the test to volitional exhaustion. Oxygen consumption was measured by continuously analyzing expired air for percentage of oxygen and carbon dioxide using an on-line, breath-by-breath metabolic cart (Medgraphics CPX/D system; Medical Graphics Corporation, Minneapolis, MN). Subjects rated their perceived exertion in the last 30 s of each treadmill stage using an unmodified Borg scale (19). Subjects' heart rates were monitored continuously throughout the test (using a Hewlett- Packard 43120A combined 3-lead electrocardiogram monitor/defibrillator). Resting (seated) heart rate (HR) before the test, and recovery HR (3 min immediately posttest) were also recorded. All measurements were carried out by the same accredited (BASES) exercise physiologist (JM). The HR corresponding to VO_2max was taken as maximum HR.

MRS and MRI. Imaging and spectroscopy data were acquired with a 1.5T Picker Eclipse multinuclear system using a quadrature bird-cage coil 30 cm in diameter. In each examination, subjects lay in a supine position with the left calf placed along the axis of the coil and immobilized with firm padding. Transverse T_1-weighted MR images [repetition (TR), 600 ms; echo time (TE), 16 ms] were acquired to determine the placement of the ^{1}H MRS voxels, with a slice thickness of 5 mm, a 20-cm field of view and 192 × 256 data matrix. Spectra were obtained from the soleus, tibialis, and gastrocnemius muscles of the left leg, using a PRESS sequence, from a 2 × 2 × 2 cm^3 voxel with TE/TR = 135/1500 ms and 256 averages. The spectra were acquired without water suppression. Following the exercise bout, subjects were carefully repositioned in the magnet, ensuring correct muscle level and fiber orientation, and the above MR protocol was repeated.

MR data analysis. Spectra were analyzed as previously described (13). Briefly, the muscle spectra were analyzed by VARPRO, an iterative non-linear least square fitting method operating in the time domain. The water peak was quantified by using one exponentially decaying sinusoid (corresponding to one Lorentzian line in the frequency domain), while total creatine (Cr_{tot} = phosphocreatine + free Cr) and choline (Cho) resonances were modeled as two single Gaussian decaying sinusoids with equal damping factors. The $(–CH_2–)_n$ and $–CH_3$ resonances from IMCL and EMCL were deconvoluted and modeled as one Gaussian decaying sinusoid each. Peak areas for each signal were obtained and lipid resonances were quantified with reference to Cr_{tot} after correcting for T_1 and T_2 as previously described (13).

MR images were analyzed as previously described (20), using an image segmentation software program that employs a threshold range and a contour-following algorithm with an interactive image editing facility. The volumes (cm^3) of each compartment (subcutaneous and extramyocellular adipose tissue, bone marrow, and bone) were calculated by summing the relevant pixel counts and multiplying by the pixel volume in cm^3.

Exercise protocol. Following the first MR scan, the subjects (having restrained from exercising for 48 h prior to the examination) were given a 5-min warm-up period and permitted to stretch adequately before the test commenced. This was followed by a run at a pace corresponding to 64 ± 1.5% of each subjects VO_2max for 90 min, on a calibrated [using standardized American College of Sport Medicine guidelines (21)] Pulse treadmill, in an air-conditioned environment (17°C). Subjects were given free access to plain water during the run and levels were recorded for each subject. HR was monitored and recorded every 5 s using a Polar Accurex Plus heart rate monitor. Subjects were instructed to give an overall rating of perceived exertion using the Borg scale (19) during the last 30 s of each 5-min interval throughout the continuous 90-min run. All subjects were returned to the MR scanner within 10 min for their postexercise examination.

Statistical analysis. All data are presented as mean ± SEM (except where individual values are quoted). Possible differences before and after exercise were tested for by using the Student's paired *t*-test. Significance was taken as $P < 0.05$. Pearson product movement correlation coefficients (r) were used to assess the relationship between variables.

RESULTS

Subject characteristics. Individual VO_2max and body mass index (BMI) for each volunteer are shown in Table 1. The mean VO_2max for the volunteers was 61.2 ± 3.4 mL/kg/min (range: 54.0 to 74.3 mL/kg/min). The average BMI was 22.5 ± 1.0 kg/m^2 (range: 20.2 to 25.7 kg/m^2).

TABLE 1
Subjects' Characteristics[a]

Subject	Age (yr)	BMI (kg/m^2)	VO_2max (mL/kg/min)	HR_{max} (beats/min)
1	38	25.7	59.9	180
2	35	21.8	64.4	188
3	38	23.5	60.0	182
4	34	20.2	74.3	174
5	30	21.1	54.0	164

[a]BMI, body mass index; HR_{max}; maximal heart rate.

In vivo ^1H MRS. Typical *in vivo* ^{1}H MR spectra from the tibialis muscle before and after exercise are shown in Figure 1. Changes in IMCL were measured in the soleus, tibialis, and gastrocnemius. Comparing the group as a whole, the tibialis muscle (pre: 22.37 ± 4.33 vs. post: 15.16 ± 3.25 mmol/kg dry weight; $P < 0.01$) and the soleus (pre: 36.93 ± 1.45 vs. post: 29.85 ± 2.44 mmol/kg dry weight; $P < 0.01$) but not the gastrocnemius (pre: 33.78 ± 5.35 vs. post: 28.48 ± 5.44 mmol/kg dry weight; $P = 0.10$) showed a significant decrease in IMCL following exercise. However, considering each runner individually (Fig. 2A–C), decreases in IMCL were observed in four of five subjects in the gastrocnemius muscle.

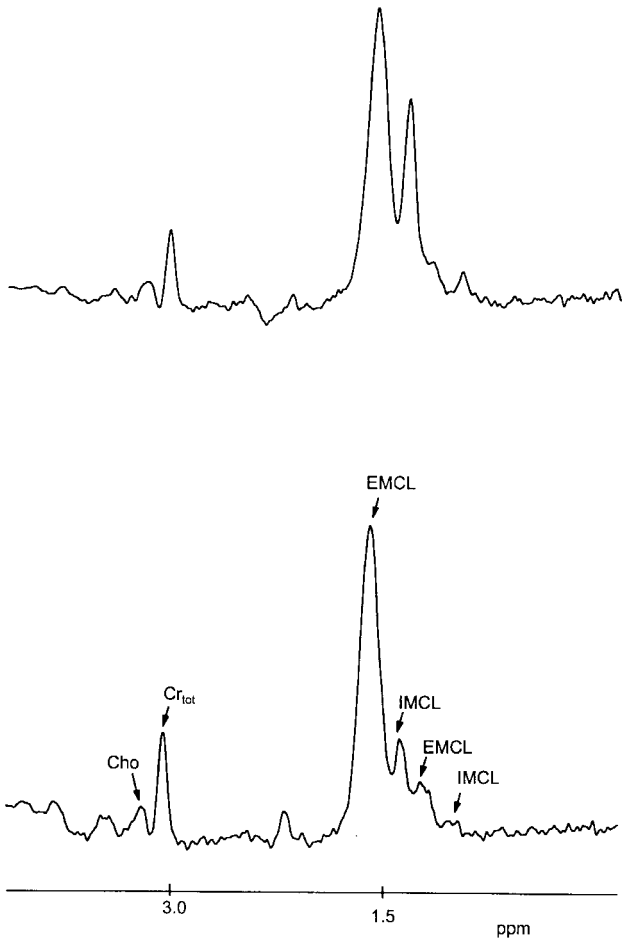

FIG. 1. Typical *in vivo* ^{1}H magnetic resonance spectra from tibialis muscle before (top) and after (bottom) exercise. Cho, choline-containing compounds (carnitine + glycerophosphocholine); Cr_{tot}, creatine + phosphocreatine; IMCL, intramyocellular lipid; EMCL, extramyocellular lipid.

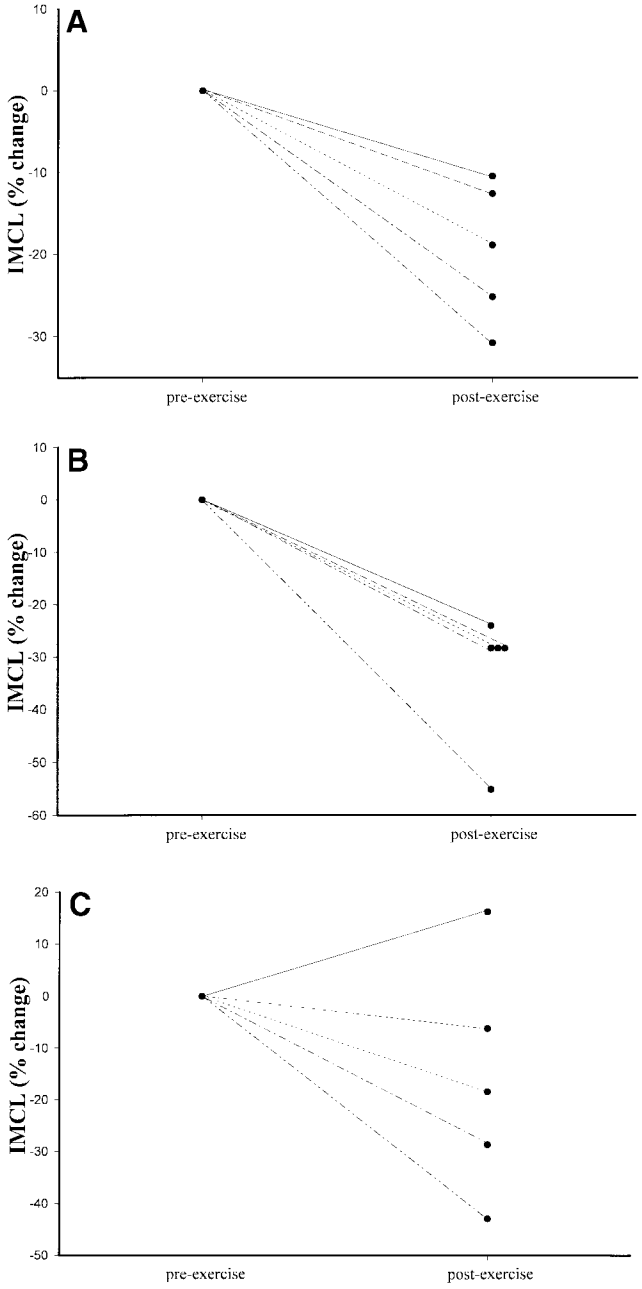

FIG. 2. Individual changes in IMCL in the (A) soleus, (B) tibialis, and (C) gastrocnemius muscles following exercise. See Figure 1 for abbreviation.

A significant decrease in Cho/Cr levels (pre: 0.67 ± 0.09; post: 0.55 ± 0.08, $P < 0.01$) was observed in the gastrocnemius after exercise. No such changes were observed in other muscle groups.

MRI. There were no significant changes in the levels of EMCL (37.08 ± 5.68 vs. 34.87 ± 5.90 cm^3, $P = 0.22$), subcutaneous fat (360.85 ± 87.59 vs. 349.15 ± 82.95 cm^3, $P = 0.47$),

bone marrow (108.22 ± 9.44 vs. 108.94 ± 9.08 cm^3, $P = 0.73$) or bone (190.00 ± 9.55 vs. 186.97 ± 8.68 cm^3, $P = 0.24$) measured by MRI following the exercise intervention.

DISCUSSION

In this study we have shown that IMCL levels are significantly decreased in the tibialis and soleus muscles following a 90-min bout of exercise at 64 ± 1.5% VO_2max. A decrease in IMCL was also observed in the gastrocnemius muscle of some subjects, but it did not reach significance for the subject population as a whole. No changes were observed in levels of EMCL in any of the muscle groups.

Assessment of IMCL content in human skeletal muscle has, to date, been carried out principally by the use of needle biopsy. However, this technique has the drawback of, besides being invasive, showing relatively poor reproducibility due to contamination from associated adipose tissue. Indeed, Wendling *et al.* (10) reported that changes in IMCL levels above 24% could be considered meaningful by this technique (10). Using needle biopsies, several groups have reported changes in IMCL between 20 and 50% following exercise (1–3,5–7), while others have reported no changes (8–10). In part, these contradictory results may arise from the high coefficient of variation associated with needle biopsies. In the present study we have partly overcome this problem by the use of *in vivo* ^{1}H MRS to evaluate muscle IMCL noninvasively. It has been previously demonstrated that ^{1}H MRS estimation of IMCL in healthy volunteers shows good agreement with published literature values (13), with good intra-examination (2%) and interexamination (*ca.*13%) coefficients of variation (13). Moreover, Boesch *et al.* (11) have reported that, using this technique, they have detected a significant decrease in IMCL in one subject after 3 h of mountain cycling, suggesting that prolonged continuous exercise may lead to a net decrease in IMCL. This is clearly confirmed by the present study. Moreover, during the preparation of this manuscript, Krssak *et al.* (16) have reported a significant decrease in IMCL in the soleus muscle following a 2–3 h treadmill run to exhaustion at 65–70% VO_2max.

The degree of IMCL utilization observed in our study varied significantly between muscle groups for any given subject. In most subjects, IMCL utilization was observed in all muscle groups, though the extent of these changes varied between muscles, with the largest changes associated with the tibialis muscle (−24 to −55%). The general trend appeared to be tibialis > gastrocnemius > soleus. The possible reasons for this variation are unclear, but may reflect differences in oxidative capacity of the muscle groups (22–24). According to the histochemical literature, the gastrocnemius and tibialis muscles are composed of relatively higher percentages of fast twitch fibers compared to the soleus (22–24). Furthermore, the metabolic and oxidative potential of these muscle groups is relatively different as a direct consequence of their muscle fiber composition and adaptation (24). We have recently shown differences in the level of IMCL in different muscle types at rest, which appear to be partly associated with the oxidative capacity of those muscles (12). Studies in animals have shown that IMCL provides a significant amount of energy for contraction in fast twitch red muscle fibers, but not in other fiber types (25). In addition, IMCL levels are affected by the ability of different muscle types to take up circulating TG. Studies with labeled chylomicron have shown that exogenous TG contributes to the turnover of IMCL in slow twitch fiber (26). Therefore, the relative levels of IMCL in a given muscle fiber will reflect the opposing effects of oxidation and TG uptake (27,28).

These results suggest that the tibialis muscles of the subjects in the present study were probably composed of more fast twitch oxidative glycolytic fibers (FTa) than the soleus and gastrocnemius, and that the metabolic capacity of IMCL resynthesis of slow twitch fibers in our subjects might be relatively high. In those subjects where IMCL degradation was also observed in the soleus and gastrocnemius muscle, it is probable that these muscle groups contained a significant proportion of the FTa fibers. Coupled with these differences in muscle fiber composition, it is also possible that the individual muscles groups may be working at different intensities. The whole body may experience an overall intensity of 64 ± 1.5%, but each muscle group might experience an intensity of 40, 70, or 90% or any other value depending on the oxidative capacity of that particular muscle. This could clearly affect the levels of IMCL utilization during the exercise in different muscle groups. Further work is therefore required to determine the relative contribution of Type I and Type II fibers to IMCL muscle content and metabolism.

The reason for the differences in IMCL utilization between subjects for a given muscle group may be due to a combination of factors including level of training and fiber type adaptation. Since exercise intensity is a major factor in determining the nature of the fuel oxidized during exercise, this may partly explain why some subjects utilized IMCL to a greater or lesser extent following exercise. As exercise intensity increases, there is an increase in carbohydrate utilization and decrease in circulating lipids (29). Indeed, it has been reported that circulating fatty acids are used as an energy substrate for exercise at intensities below 80–90% VO_2max; above this intensity, carbohydrates are the predominant substrate (30). Thus, it is possible that for each subject the combination of the overall and local (for each muscle) exercise intensity played a significant role in the recruitment of fibers, leading to significant individual differences in levels of IMCL utilization. Work is presently underway in an effort to try to unravel the possible mechanism by which different factors, including fiber type composition, levels of training, exercise intensity, genetics and diet, influence the relative rate of IMCL utilization and resynthesis during exercise.

The role of IMCL as an energy source during exercise appears to be highly dependent on the duration, type and intensity of the exercise protocol. In the present study we have shown a significant decrease in IMCL following continuous exercise at 60–70% VO_2max. However, previous studies, including our own, have shown no change in IMCL following intermittent or high-intensity exercise (8–10,13). We observed no change in IMCL following an exercise protocol of alternat-

ing intensity to fatigue, including walking, jogging, running and sprinting (13). Similar lack of effects was recently reported by Brechtel *et al.* (31) using a protocol of continuous exercise at an intensity >80% VO_2max (31). Thus, to maximize IMCL utilization during exercise, continuous exercise at an intensity of 60–70% VO_2max is necessary. Further work is, however, required to ascertain the time course of IMCL utilization during prolonged exercise.

The metabolic role of EMCL, if any, in muscle is not fully understood. This study has shown that, following 90 min of exercise, there was no significant utilization of EMCL. This finding is in agreement with previous research, which has suggested that EMCL is relatively metabolically inert and does not contribute to fat oxidation during exercise at intensities greater than 25% VO_2max (4,14). Interestingly, recent work by Goodpaster *et al.* (32) suggects that EMCL levels are altered following significant weight loss. The general level of EMCL in this study appeared to reflect each subjects overall body fat content (results not shown).

An unexpected finding in this study was the significant decrease in Cho/Cr ratio in the gastrocnemius muscle. The Cho peak (3.20 ppm) in the *in vivo* ^{1}H MR spectrum is composed primarily of carnitine and glycerophosphocholine (33). Previous studies have reported a decrease in muscle carnitine following prolonged exercise, accompanied by a corresponding increase in acetylcarnitine (34). This, however, cannot explain the results observed in the present study since signals from carnitine and acylcarnitine co-resonate (*ca.* 3.20 ppm). Therefore, the overall intensity of the Cho peak would remain unchanged. It is, however, possible that during intense lipid utilization some of these metabolites may become bound to other metabolites, leading to T_2 shortening and an apparent decrease in signal intensity. In the case of the tibialis muscle, the net levels of Cho/Cr are relatively low, so potential decreases in this ratio may be below the detection level of the technique. Further work is therefore required to elucidate the exact metabolic mechanism by which exercise may affect the intensity of the Cho-containing resonance and its physiological significance.

In summary, the results of the present study show that IMCL is significantly utilized by the tibialis and soleus muscles during prolonged continuous exercise. The lack of group significance for the gastrocnemius muscle might reflect muscle group differences in fiber type composition and capacity to oxidize and resynthesize IMCL. Finally, this study shows that *in vivo* MRS is a useful tool for noninvasively studying substrate utilization during exercise. This may in future allow us to investigate the influence of factors such as training status and exercise intensity, as well as diet and genotype, on energy substrate utilization.

ACKNOWLEDGMENTS

Financial support provided by Marconi Medical System and the Medical Research Council are gratefully acknowledged. We would also like to thank Gabby Jenkinson for her help with this work.

REFERENCES

1. Essen, B., Hagenfeldt, L., and Kaijser, L. (1977) Utilization of Blood-Borne and Intramuscular Substrates During Continuous and Intermediate Exercise in Man, *J. Physiol. Lond. 265*, 489–506.
2. Froberg, S.O., and Mossfeldt, F. (1971) Effect of Prolonged Strenuous Exercise on the Concentration of Triglycerides, Phospholipids and Glycogen in Muscle of Man, *Acta Physiol. Scand. 82*, 167–171.
3. Pan, D.A., Lillioja, S., Kriketos, A.D., Milner, M.R., Baur, L.A., Bogardus, C., Jenkins, A.B., and Storlien, L.H. (1997) Skeletal Muscle Triglyceride Levels Are Inversely Related to Insulin Action, *Diabetes 46*, 983–988.
4. Romijn, J.A., Coyle, E.F., Sidossis, L.S., Gastaldelli, A., Horowitz, J.F., Endert, E., and Wolfe, R.R. (1993) Regulation of Endogenous Fat and Carbohydrate Metabolism in Relation to Exercise Intensity and Duration, *Am. J. Physiol. 265*, E380–E391.
5. Carlson, L.A., Ekelund, L., and Froberg, S.O. (1971) Concentration of Triglycerides, Phospholipids and Glycogen in Skeletal Muscle and of Free Fatty Acids and β-Hydroxybutyric Acid in Blood in Man in Response to Exercise, *Eur. J. Clin. Invest. 1*, 248–254.
6. Costill, D.L., Gollnick, P.D., Jansson, E.D., Saltin, B., and Stein, E. (1973) Glycogen Depletion Pattern in Human Muscle Fibres During Distance Running, *Acta Physiol. Scand. 89*, 374–383.
7. Hurley, B.F., Nemeth, P.M., Martin, W.H. III, Hagberg, J.M., Dalsky, G.P., and Holloszy, J.O. (1986) Muscle Triglyceride Utilization During Exercise: Effect of Training, *J. Appl. Physiol. 60*, 562–567.
8. Kiens, B., Essen-Gustavsson, B., Christensen, N..J., and Saltin, B. (1993) Skeletal Muscle Substrate Utilization During Submaximal Exercise in Man: Effect of Endurance Training, *J. Appl. Physiol. (Lond.) 469*, 459–478.
9. Starling, R.D., Trappe, T.A., Parcell, A.C., Kerr, A.C., Fink, W.J., and Costill, D.L. (1997) Effects of Diet on Muscle Triglyceride and Endurance Performance, *J. Appl. Physiol. 82*, 1185–1189.
10. Wendling, P.S., Peters, S.J., Heigenhauser, G.J.F., and Spriet, L.L. (1996) Variability of Triacyglycerol Content in Human Skeletal Muscle Biopsy Samples, *J. Appl. Physiol. 81*, 1150–1155.
11. Boesch, C., Slotboom, J., Hoppeler, H., and Kreis, R. (1997) *In Vivo* Determination of Intra-myocellular Lipids in Human Muscle by Means of Localized ^{1}H-MR Spectroscopy, *Magn. Reson. Med. 37*, 484–493.
12. Rico-Sanz, J., Thomas, E.L., Jenkinson, G., Mierisova, S., Iles, R.A., and Bell, J.D. (1999) Diversity in Levels of Intracellular Total Creatine and Triglycerides in Human Skeletal Muscles Observed by ^{1}H MRS, *J. Appl. Physiol. 87*, 2068–2072.
13. Rico-Sanz, J., Hajnal, J.V., Thomas, E.L., Mierisova, S., Ala-Korpela, M., and Bell, J.D. (1998) Intracellular and Extracellular Skeletal Muscle Triglyceride Metabolism During Alternating Intensity Exercise in Humans, *J. Physiol. 510*, 615–622.
14. Schick, F., Eismann, B., Jung, W.L., Bongers, H., Bunse, M., and Lutz, O. (1993) Comparison of Localized Proton NMR Signals of Skeletal Muscle and Fat Tissue *In Vivo*: Two Lipid Compartment in Muscle Tissue, *Magn. Reson. Med. 29*, 158–167.
15. Szczepaniak, L.S., Babcock, E.E., Schick, F., Dobbins, R.L., Garg, A., Burns, D.K., McGarry, J.D., and Stein, D.T. (1999) Measurement of Intracellular Triglyceride Stores by ^{1}H Spectroscopy: Validation *in Vivo*, *Am. J. Physiol. 276*, E977–E989.
16. Krssak, M., Petersen, K.F., Bergeron, R., Price, T., Laurent, D., Rothman, D.L., Roden, M., and Shulman, G.I. (2000) Intramuscular Glycogen and Intramyocellular Lipid Utilization During

Prolonged Exercise and Recovery in Man: A ^{13}C and ^{1}H Nuclear Magnetic Resonance Spectroscopy Study, *J. Clin. Endocrinol. Metab. 85*, 748–754.
17. Boesch, C., Decombaz, J., Slotboom, J., and Kreis, R. (1999) Observation of Intramyocellular Lipids by Means of ^{1}H Magnetic Resonance Spectroscopy, *Proc. Nutr. Soc. 58*, 841–850.
18. Bird, S., and Davison, R. (eds.) (1997) *British Association of Sport and Exercise Sciences Guidelines for the Physiological Testing of Athletes*, pp. 59–72, Headingley, Leeds.
19. Borg, G. (1970) Perceived Exertion as an Indicator of Somatic Stress, *Scand. J. Rehab. Med. 2*, 92–98.
20. Thomas, E.L., Saeed, N., Hajnal, J.V., Brynes, A.E., Goldstone, A.P., Frost, G., and Bell, J.D. (1998) Magnetic Resonance Imaging of Total Body Fat, *J. Appl. Physiol. 85*, 1778–1785.
21. Blair, S.N., Painter, P., Pate, R.R., Smith, L.K., and Taylor, C.B. (1988) *American College of Sport Medicine College Resource Annual for Guidelines for Exercise Testing and Prescription*, pp. 408–410, Lea & Febiger, Philadelphia.
22. Henriksson-Larsen, K.B., Friden, J., and Wretling, M.L. (1985) Distribution of Fibre Sizes in Human Skeletal Muscle. An Enzyme Histochemical Study in Tibialis Anterior, *Acta Physiol. Scand. 123*, 171–177.
23. Henriksson-Larsen, K.B., Lexell, J., and Sjostrom, M. (1983) Distribution of Different Fibre Types in Human Muscles. I. Method for the Preparation and Analysis of Cross-sections of Whole Tibialis Anterior, *Histochem. J. 15*, 167–178.
24. Saltin, B., and Gollnick, P.D. (1983) Skeletal Muscle Adaptability: Significance for Metabolism and Performance, in *Handbook of Physiology—Skeletal Muscle* (Peachey, L.D., Adrian, R.H., and Geiger, S.R., eds.), pp. 555–631, American Physiological Society, Bethesda.
25. Gorski, J. (1992) Muscle Triglyceride Metabolism During Exercise, *Can. J. Physiol. Pharmacol. 70*, 123–31.
26. Mackie, B.G., Dudley, G.A., Kaciuba-Uscilko, H., and Terjung, R.L. (1980) Uptake of Chylomicron Triglycerides by Contracting Skeletal Muscle in Rats, *J. Appl. Physiol. 49*, 851–855.
27. Oscai, L.B., Essig, D.A., and Palmer, W.K. (1990) Lipase Regulation of Muscle Triglyceride Hydrolysis, *J. Appl. Physiol. 69*, 1571–1577.
28. Lithell, H., Orlander, J., Schele, R., Sjodin, B., and Karlsson, J. (1979) Changes in Lipoprotein-Lipase Activity and Lipid Stores in Human Skeletal Muscle with Prolonged Heavy Exercise, *Acta Physiol. Scand. 107*, 257–261.
29. Holloszy, J.O., Kohrt, W.M., and Hansen, P.A. (1998) The Regulation of Carbohydrate and Fat Metabolism During and After Exercise, *Front. Biosci. 3*, D1011–D1027.
30. Gollnick, P.D. (1985) Metabolism of Substrates: Energy Substrate Metabolism During Exercise and as Modified by Training, *Fed. Proc. 44*, 353–357.
31. Goodpaster, B.H., Thaete, F.L., and Kelley, D.E. (2000) Thigh Adipose Tissue Distribution Is Associated with Insulin Resistance in Obesity and in Type 2 Diabetes Mellitus, *Am. J. Clin. Nutr. 71*, 885–892.
32. Brechtel, K., Niess, A., Jacob, S., Machann, J., Haering, H.U., Dickhuth, H.H., Claussen, C.D., and Schick, F. (2000) Direct Assessment of Intramyocellular Lipids (IMCL) During Exercise in Well Trained Male Runners: A ^{1}H-MRS Study, *Proceedings of the Eight Annual Meeting of the International Society for Magnetic Resonance,* Denver, Vol. 2, 1882.
33. Chung, Y.L., Wassif, W.S., Jenkinson, G., Scott, D.L., and Bell, J.D. (1997) Correlation Between *in Vivo* and *in Vitro* ^{1}H-MRS of Human Muscle, *Proceedings of the Fifth Annual Meeting of the International Society for Magnetic Resonance,* Vancouver, Vol. 2, 1335.
34. Constantin-Teodosiu, D., Cederblad, G., and Hultman, E. (1992) PDC Activity and Acetyl Group Accumulation in Skeletal Muscle During Prolonged Exercise, *J. Appl. Physiol. 73*, 2403–2407.

[Received July 3, 2000, and in revised form October 10, 2000; revision accepted October 16, 2000]

Linoleic Acid Metabolism in the Spontaneously Diabetic Rat: Δ6-Desaturase Activity vs. Product/Precursor Ratios

J.E. Brown[a,1], R.M. Lindsay[b,2], and R.A. Riemersma[a,c]*

[a]Cardiovascular Research Unit, Departments of Cardiology and Medicine, University of Edinburgh, Edinburgh EH8 9XF, Scotland, [b]Metabolic Unit, Western General Hospital, Edinburgh EH4 2XU, Scotland, and [c]Department of Medical Physiology, University of Tromsø, Tromsø, Norway

ABSTRACT: The activity of Δ6-desaturase of linoleic acid, a rate-limiting step in the formation of arachidonic acid, is decreased in animal models of severe, uncontrolled diabetes. The aim of the study was to measure the activity of liver microsomal Δ6-desaturase of spontaneously diabetic BioBreeding/Edinburgh rats receiving subcutaneous insulin daily and of genetically related nondiabetic animals. The activity of Δ6-desaturase was then compared with indices of activity (plasma lipid fatty acid product/precursor ratios) frequently used in human studies. Diabetic rats treated with insulin had 75 ± 8% of the activity of microsomal Δ6-desaturase of nondiabetic controls ($P < 0.05$). Insulin withdrawal tended to reduce the activity further (61% of control), although the activity did not differ from insulin-treated diabetic rats. The ratio of plasma phospholipid or cholesteryl ester γ-linolenic over linoleic acid was not decreased in insulin-treated diabetic rats. By contrast, the ratio of γ-linolenic over linoleic acid of microsomes was almost threefold higher in insulin-treated diabetic rats ($P < 0.05$). The γ-linolenic over linoleic acid ratio as an index of activity gave inconsistent results in insulin-deprived rats. The ratio of γ-linolenic over linoleic acid of cholesteryl esters did not differ between control and diabetic rats, nor did it correlate with microsomal Δ6-desaturase activity. Furthermore, the index of Δ6-desaturase activity, derived from the fatty acid composition of microsomal phospholipids, did not correlate with microsomal Δ6-desaturase activity. Diabetes, even when controlled by regular insulin injections, reduces the metabolism of linoleic acid, but the effect is less than previously published. The fatty acid compositions of plasma and liver microsomal lipids are not reliable indices of Δ6-desaturase activity in diabetes.

Paper no. L8455 in *Lipids 35,* 1319–1323 (December 2000).

The ability to provide sufficient amounts of long-chain polyunsaturated fatty acids such as arachidonic acid (20:4n-6) depends greatly on the conversion of linoleic acid (18:2n-6) to γ-linolenic acid (18:3n-6) *via* the rate-limiting enzyme Δ6-desaturase. Impaired 18:2n-6 metabolism is associated with diabetic neuropathy and altered prostanoid synthesis (1–3) and has been implicated in the microvascular complications of diabetes (4). Plasma fatty acid compositions are by and large used in human studies as an index of the activity of Δ6-desaturase, since for obvious reasons enzyme activity cannot be measured in liver biopsies. Increased levels of 18:2n-6 with decreased levels of 20:4n-6 in plasma, platelet and red blood cell lipids from subjects with insulin-dependent diabetes mellitus may indicate an impairment in 18:2n-6 metabolism (5,6). However, not all studies on diabetes have revealed such fatty acid patterns (7–9). Tissue fatty acid composition can also be affected by diet. Diabetic patients consume 40% more 18:2n-6 than nondiabetic subjects (8), in accordance with World Health Organization recommendations (10). Therefore, an important question remains whether the higher tissue levels of 18:2n-6 in diabetic patients are indeed due to an impaired conversion of 18:2n-6 to other longer-chain n-6 fatty acids.

The spontaneously diabetic, insulin-dependent BioBreeding Wistar rat from Edinburgh (BB/E) is an animal model with a pathology of destructive insulitis comparable with human diabetic subjects (11,12). The aim of this study was to examine the effect of diabetes on the Δ6-desaturation of 18:2n-6 in BB/E rats stabilized with regular insulin treatment. We compared our results with an index of Δ6-desaturase activity based on fatty acid compositional analyses of plasma phospholipids (PL) and cholesterol esters (CE) under controlled dietary conditions.

MATERIALS AND METHODS

Male insulin-dependent diabetic Wistar BB/E rats ($n = 12$, 151 ± 15 d old, duration of diabetes 61 ± 7 d) and male nondiabetic rats from a related strain ($n = 6$, 152 ± 5 d old) were used (11). Diabetic rats required a daily subcutaneous insulin injection (2.9 ± 0.3 IU/d, Bovine Ultratard U40; Novo Nordisk, Bagsvaerd, Denmark). Animals had free access to water and a chow (Rat & Mouse No. 1 diet; S.D.S., Witham, United Kingdom) that contained 2.5% (w/w) fat. The fatty acid composition was: 19.1% saturates, 16.5% monounsaturates, 57.4% 18:2n-6, and 6.5% α-linolenic acid. Experiments were carried out under the Animal (Scientific Procedures) Act 1986.

[1]Present address: Food Safety Research Group, School of Biological Sciences, University of Surrey, Guildford, GU2 7XH, England.

[2]Present address: 11 Bonnylee Steadings, Colinton, Edinburgh EH13 0HA, Scotland.

*To whom correspondence should be addressed at the Cardiovascular Research Unit, University of Edinburgh, George Square, Edinburgh EH8 9XF, Scotland. E-mail: Rudolph@srvl.med.ed.ac.uk

Abbreviations: BB/E, BioBreeding/Edinburgh; CE, cholesterol esters; PL, phospholipid.

Oxidative desaturation of [1-^{14}C]18:2n-6 by liver microsomes (500 μg) was estimated by measuring the formation of radioactive 18:3n-6, dihomo-γ-linolenic acid (20:3n-6), and 20:4n-6 (13). The incubation mixture (1.2 mL) contained (in μmol): ATP, 4.0; Coenzyme A, 0.25; NADH, 1.25; $MgCl_2$, 0.5; bovine serum albumin (essentially fatty acid free), 0.01; glutathione, 1.5; potassium phosphate, 45.0 (pH 7.2), and [1-^{14}C]18:2n-6, 0.2 (~140,000 dpm; Amersham International, Amersham, United Kingdom) and were carried out in room air at 37°C. Incubations were terminated after 20 min by addition of 10% (wt/vol) potassium hydroxide in aqueous methanol containing 0.005% (wt/vol) butylated hydroxytoluene. After saponification, methyl esters formed using BF_3-methanol reagent were separated into dienes and trienes plus tetraenes by argentation thin-layer chromatography using $CHCl_3$/CH_3OH/acetic acid/H_2O (90:7.5:7.5:0.8, by vol) as the solvent mixture (14). The two fractions were scraped directly into scintillation vials and counted (1217 Rackbeta counter; Wallac Oy, Turku, Finland). The activity of Δ6-desaturase is related to the amount of microsomal protein (250–750 μg) and substrate (40–200 nmol) (15). Routinely, 500 μg protein and 200 nmol substrate were used, and under these conditions the dilution of [1-^{14}C]18:2n-6 by endogenous substrate is negligible and the protein binding of the substrate is controlled (15). Enzyme activity was expressed as pmol of products formed by 1 mg of microsomal protein per minute with a correction of the specific activity due to the presence of free 18:2n-6 in microsomes. [This is particularly important when a large amount of microsomal protein, i.e., 5 mg, is used (15).]

Plasma phospholipid fatty composition was determined by gas chromatography (16). Microsomal nonesterified linoleic acid content was determined as follows. Lipids from microsomes (10 mg in 1 mL) and heptadecanoic acid (internal standard) were extracted using Folch's mixture and separated by thin-layer chromatography using hexane/diethylether/formic acid (80:20:2, by vol) as the solvent mixture. The nonesterified fatty acid band was scraped off and methylated using diazomethane. The methyl esters were concentrated and redissolved in a small amount of $CHCl_3$ (5–10 μL) and analyzed by gas chromatography (16).

The ratio of 18:3n-6 over 18:2n-6 was used as an index of Δ6-desaturase. An overall index of 18:2n-6 desaturation was also used. This was calculated as follows:

$$(18:3n\text{-}6 + 20:3n\text{-}6 + 20:4n\text{-}6 + 20:5n\text{-}6 + 22:5n\text{-}6)/18:2n\text{-}6 \quad [1]$$

Plasma insulin was assayed by radioimmunoassay using rat insulin standards (17) (Novo Research Institute, Bagsvaerd, Denmark) and plasma glucose using the glucose oxidase method (18). Red blood cell glycosylated hemoglobin was determined by boronic acid affinity chromatography [Pierce & Warriner (UK) Ltd., Chester, United Kingdom].

Diabetic rats were divided into two groups (n = 6) and matched for age, duration of diabetes, and daily insulin dose. One group continued to receive insulin injections and was sacrificed 6 h after their last insulin dose (insulin treated). Insulin treatment of the other group was discontinued for 54 h, after which time the rats were sacrificed (insulin deprived). The dose of insulin did not differ between the two groups (3.0 ± 0.3 and 2.7 ± 0.1 IU/d). Nondiabetic rats were studied at the same time. Rats were sacrificed under anesthesia (Sagatal®; Rhône Mérieux, Dublin, Eire) between 1545 and 1615 h in view of the circadian rhythm of Δ6-desaturase, and livers were removed for microsome preparation (19).

Statistical analysis. Results are shown as mean ± SD. Statistical analyses were conducted using Minitab (CLE.COM Ltd., Birmingham, United Kingdom). The data were analyzed by one-way analysis of variance, followed by unpaired Student's *t*-test.

RESULTS

Plasma glucose levels in insulin-treated diabetic rats were reduced by more than 60 % ($P < 0.05$) compared to controls despite similar plasma insulin levels (Table 1). Insulin withdrawal for 54 h caused significant weight loss, hyperglycemia, and undetectable insulin levels in 3 of 5 rats (Table 1).

Δ6-Desaturase activity in insulin-treated diabetic rats was decreased to 75 ± 8% of control values ($P = 0.013$; Table 1). Insulin withdrawal tended to reduce the activity further (61% of control), although this does not differ from insulin-treated diabetic rats. Liver microsomal nonesterified 18:2n-6 levels were significantly raised ($P < 0.05$) in insulin-deprived diabetic rats (Table 1; the detailed fatty acid composition of plasma and microsomal lipids can be obtained from the authors), demonstrating the need to correct the specific activity of radioactive linoleic acid for this. Insulin-treated diabetic rats had significantly higher plasma PL levels, and the total

TABLE 1
Body Weight, Plasma Glucose, Insulin, Erythrocyte Glycosylated Hemoglobin, and the Effect of Diabetes and Insulin Withdrawal on Microsomal Δ6-Desaturation of 18:2n-6 and Free 18:2n-6 Content in Liver Microsomes of the Rat[a]

		Diabetic	
Measurement	Nondiabetic (n = 6)	+ Insulin (n = 6)	– Insulin (n = 5)
Body weight (g)	420 ± 24	403 ± 52	354 ± 39*
Liver/body weight ratio (%)	3.4 ± 0.3	4.0 ± 0.5*	3.5 ± 0.1
Glucose (mmol/L)	9.0 ± 1.0	3.5 ± 1.4*	28.6 ± 4.7*,†
Insulin (mU/L)	134 ± 42	173 ± 70	5‡
Glycosylated hemoglobin (%)	3.4 ± 0.1	6.1 ± 1.4*	9.2 ± 1.9*,†
Microsomes			
Δ6-desaturase activity (pmol/min·mg protein)	367 ± 53	277 ± 48*	223 ± 54*
Nonesterified 18:2n-6 (nmol/mg protein)[b]	1.9 ± 0.2	2.3 ± 1.2	7.7 ± 3.7*

[a]Significant group differences by one-way analysis of variance of all measurements. Follow-up test: *$P < 0.05$ vs. nondiabetic controls; †$P < 0.05$ vs. insulin-treated diabetic rats. ‡n = 2, three samples below level of detection (5 mU/L).
[b]The detailed fatty acid composition of plasma and microsomal lipids can be obtained from the authors.

TABLE 2
Fatty Acid Composition of Plasma Phospholipids (PL) and the Index of Δ6-Desaturation of Plasma PL and Cholesterol Esters (CE) and Hepatic Microsomal PL in Nondiabetic and Diabetic Rats[a]

Measurement	Nondiabetic (n = 6)	Diabetic + Insulin (n = 6)	Diabetic – Insulin (n = 5)
Total PL (μmol/L)	1,590 ± 180	1,890 ± 170*	3,510 ± 270*,†
n-6 PUFA (total):	1,320 ± 136	1,578 ± 151*	2,851 ± 149*,†
18:2	587 ± 41	795 ± 107*	1,528 ± 128*,†
18:3[b]	5.8 ± 1.3	7.4 ± 1.5	8.9 ± 3.2
20:3	35 ± 5	53 ± 9*	27 ± 2*,†
20:4	661 ± 94	695 ± 95*	1,268 ± 117*,†
Indices of Δ6-desaturase			
Plasma PL			
18:3/18:2 (× 1,000)	10 ± 2	9 ± 2	6 ± 2*,†
Overall index (× 10)[c]	12 ± 1	10 ± 2*	9 ± 1*,†
Plasma CE			
18:3/18:2 (× 1,000)	35 ± 2	44 ± 9	36 ± 8
Overall index (× 10)	28 ± 3	23 ± 3*	19 ± 3*
Microsomal PL			
18:3/18:2 (× 1,000)	15 ± 2	44 ± 16*	21 ± 14
Overall index (× 10)	22 ± 1	15 ± 2*	12 ± 1*,†

[a]Significant group differences by one-way analysis of variance of all measurements except 18:3n-6 and plasma CE 18:3n-6/18:2n-6 ratio. Follow-up tests: *$P < 0.05$ vs. nondiabetic controls. †$P < 0.05$ vs. insulin-treated diabetic rats.
[b]Unresolved peak, contains also 20:0.
[c]For definition of indices see the Materials and Methods section. PUFA, polyunsaturated fatty acids.

amount of n-6 fatty acids increased proportionally (Table 2). The ratio of 18:3n-6/18:2n-6, which arguably reflects the activity of Δ6-desaturation, was, however, normal. Plasma PL levels increased further after insulin deprivation, and the Δ6-desaturation index was significantly reduced ($P < 0.05$; Table 2). This plasma PL index of Δ6-desaturation was related to the activity of liver microsomal Δ6-desaturase determined *in vitro* ($r = 0.54$, $P < 0.05$; Fig. 1). The overall index of 18:2n-6 desaturation derived from plasma PL fatty acid composition was also correlated to microsomal Δ6-desaturase activity ($r = 0.55$; $P < 0.05$; Table 2).

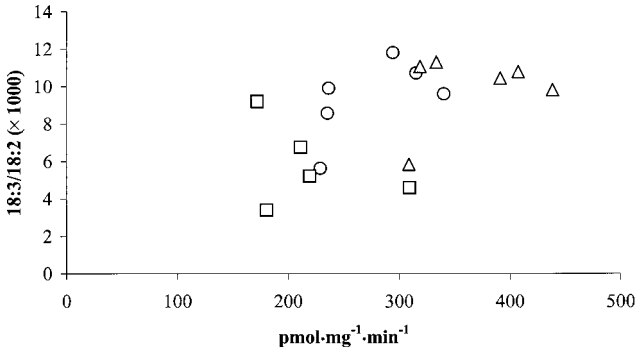

FIG. 1. The relation between microsomal Δ6-desaturation of 18:2n-6 and the index of Δ6-desaturation derived from plasma phospholipid fatty acid composition in normal and diabetic rats. The correlation coefficient is 0.54, $P < 0.05$. Control (n = 6), △; diabetic-insulin treated (n = 6), ○; diabetic-insulin withdrawn (n = 5), □.

By contrast, the 18:3n-6/18:2n-6 ratio derived from plasma CE did not differ significantly between control and diabetic rats. However, the overall index of 18:2n-6 desaturation calculated from the plasma CE composition was reduced in both groups of diabetic rats and correlated well with liver Δ6-desaturase activity ($r = 0.53$, $P < 0.05$).

The ratio of microsomal PL 18:3n-6/18:2n-6 was not related to the measured activity ($r = -0.2$, not significant), but despite this, the overall index of 18:2n-6 desaturation derived from this fatty acid pool was related to the activity of Δ6-desaturase estimated *in vitro* ($r = 0.73$, $P < 0.001$).

DISCUSSION

Δ6-Desaturase in liver microsomes of diabetic rats maintained on regular insulin injections is reduced by some 25%. Insulin withdrawal tended to cause a further small, though nonsignificant, reduction in Δ6-desaturase activity. Nevertheless, the reduction in Δ6-desaturase activity is not as large as previously observed in untreated streptozotocin-induced diabetic rats (20) or diabetic rats that did not receive insulin for 48 h (21). The reason for this apparent discrepancy is largely methodological (see below).

The activity of Δ6-desaturase in our study is much higher (200–400 vs. 40–80 pmol·min^{-1}·mg protein^{-1}) than in previous reports (21–23). These differences apply to both nondiabetic and diabetic animals and are therefore not due to different strains, severity of diabetes, etc. They are more likely explained by important methodological aspects. Microsomes from nondiabetic rats, isolated and washed at low ionic strength, lose a lipoprotein-like fraction, and associated with this is a reduction in Δ6-desaturase activity from 284 ± 9 to 72 ± 3 pmol·min^{-1}·mg protein^{-1} (24). Thus, our activity of Δ6-desaturase in nondiabetic rats is in good agreement with that of Brenner's group (19,24). It is important to note that some of the low activities were observed in the presence of cytoplasmic protein, since the microsomes were suspended in the supernatant (23). This is important, as the cytosolic protein fraction activates Δ6-desaturase of washed microsomes (24).

An additional factor must contribute to the low activity of Δ6-desaturase in microsomes from diabetic animals previously published. Plasma and microsomal nonesterified 18:2n-6 (see Table 1) increase to high levels in uncontrolled diabetes. This can lead to a significant dilution of the [1-^{14}C]-18:2n-6 in the assay, particularly when a large amount (5 mg) of microsomal protein is used. Using our data in Table 2 we calculated that the microsomal nonesterified 18:2n-6 of ~8 nmol/mg protein would reduce Δ6-desaturase activity by 30%. This problem of course is more severe if smaller amounts of substrate (40 nmol) are used (21,23). In our method a smaller amount of microsomal protein (0.5 mg) is used, containing <4 nmol free 18:2n-6 (0.5 mg × 7.7 nmol/mg protein). Thus, the dilution of the radioactive substrate (200 nmol) is less than 2%. Hence any correction has a negligible effect. Only a systematic study of Δ6-desaturase activity and of inhibitory and activating factors can resolve this method-

ological question fully. Nevertheless, our results strengthen previous suggestions that diabetes, whether controlled with daily insulin injections or not, causes a significant reduction in Δ6-desaturase activity in the BB diabetic rat model, though it is probably less than previously thought (21,23).

Plasma lipid n-6 fatty acid ratios are frequently used in human studies as an index of Δ6-desaturase activity (8,9). There was a good relationship between liver microsomal Δ6-desaturase activity determined *in vitro* and some of the indices of Δ6-desaturase based on the n-6 fatty acid composition of plasma PL. This was not the case for the 18:3n-6/18:2n-6 ratio derived from either plasma CE or liver microsomal PL, although, in each case, the overall index of 18:2n-6 desaturation did correlate with the activity of Δ6-desaturase. Clearly the type of lipid analyzed for fatty acid composition and the specific ratio used is of critical importance.

The lipid composition of plasma depends on the nutritional and hormonal state, and this is particularly relevant in diabetes, when in uncontrolled diabetes, plasma lipids (particularly triacylglycerol) increase (25,26). As the fatty acid compositions of these lipid classes are quite different, the changing lipid composition, after the induction of diabetes, would alter the Δ6-desaturase indices *per se*. The use of a defined lipid pool, such as low density lipoprotein phosphatidylcholine, may therefore be superior to monitor Δ6-desaturase activity.

Another concern about the use of n-6 fatty acid ratios as an index of Δ6-desaturase activity stems from the relatively large measurement error of the minor n-6 fatty acids that determine these ratios. Even when injecting large amounts of methyl esters during gas chromatography, the coefficient of variation for minor peaks (<1% of total fatty acids) was about 17.5% while it was less that 5% for 18:2n-6 (16). Clearly, whatever n-6 fatty acid ratio is used as an index of Δ6-desaturase, many factors will determine the precise value. Concerns about the use of fatty acid ratios as an index of Δ6-desaturase activity have been expressed previously (27).

Recent advances in the use of uniformly ^{13}C-labeled 18:2n-6 combined with high-precision combustion gas–liquid chromatography–isotope ratio mass spectrometry (28) has made it possible to demonstrate, but not to quantify, the conversion of 18:2n-6 to 20:4n-6 in man (29). An early study concentrating on Δ5-desaturation of ^{2}H-labeled dihomo-γ-linolenic acid suggested that the activity of this enzyme was impaired in newly diagnosed diabetics (30). However, even today, precise quantification of the activities of these enzymes using stable isotopes is not easy. This is because of the difficulty the differential incorporation of fatty acids into plasma lipid fractions poses. The assessment of relative activities (i.e., before and after treatment within an individual) is simpler, provided the fatty acid composition of the plasma lipid fractions does not change during the experiment. Methods to quantify the Δ6-desaturation of linoleic acid and to monitor the biological requirements for its long-chain polyunsaturated fatty acids in man need to be developed.

In summary, the activity of Δ6-desaturase is depressed in the insulin-treated BB diabetic rat, but to a smaller degree than shown previously. The apparent discrepancy is largely explained by methodological factors that led to an overestimation of the inhibition of Δ6-desaturase in earlier studies. The activity is perhaps reduced fractionally further by insulin withdrawal. The ratio of 18:3n-6 over 18:2n-6 derived from plasma lipids (CE, PL) as a marker of Δ6-desaturase yields inconsistent results, although PL 18:3n-6 over 18:2n-6 is related to the actual microsomal activity. Many factors will affect the fatty acid composition of plasma lipids, making these ratios unreliable markers to monitor the activity of 18:2n-6 conversion in humans.

ACKNOWLEDGMENTS

We acknowledge Dr. Joyce Baird for her encouragement and support. This work was supported by a Ph.D. studentship from the British Heart Foundation (90/47) and a grant from the Ministry of Agriculture, Fisheries and Food (CSA 1813).

REFERENCES

1. Cotter, M.A., and Cameron, N.E. (1997) Effects of Dietary Supplementation with Arachidonic Acid Rich Oils on Nerve Conduction and Blood Flow in Streptozotocin-Diabetic Rats, *Prostaglandins Leukotrienes Essent. Fatty Acids 56*, 337–343.
2. Cameron, N.E., Cotter, M.A., and Robertson, S. (1991) Essential Fatty Acid Diet Supplementation. Effects on Peripheral Nerve and Skeletal Muscle Function and Capillarization in Streptozocin-Induced Diabetic Rats, *Diabetes 40*, 532–539.
3. Horrobin, D.F. (1993) Fatty Acid Metabolism in Health and Disease: The Role of Δ6-Desaturase, *Am. J. Clin. Nutr. 57*, 732–737.
4. Jamal, G.A. (1994) The Use of γ-Linolenic Acid in the Prevention and Treatment of Diabetic Neuropathy, *Diabetic Med. 11*, 145–149.
5. Jones, D.B., Carter, R.D., Haitas, B., and Mann, J.I. (1983) Low Phospholipid Arachidonic Acid Values in Diabetic Platelets, *Br. Med. J. 286*, 173–175.
6. Van Doormaal, J.J., Idema, I.G., Muskiet, F.A.J., Martini, I.A., and Doorenbos, H. (1988) Effects of Short-Term High Dose Intake of Evening Primrose Oil on Plasma and Cellular Fatty Acid Compositions, α-Tocopherol Levels, and Erythropoiesis in Normal and Type 1 (insulin-dependent) Diabetic Men, *Diabetologia 31*, 576–584.
7. Kalofoutis, A., and Lekakis, J. (1981) Changes of Platelet Phospholipids in Diabetes Mellitus, *Diabetologia 21*, 540–543.
8. Tilvis, R.S., and Miettinen, T.A. (1985) Fatty Acid Compositions of Serum Lipids, Erythrocytes, and Platelets in Insulin-Dependent Diabetic Women, *J. Clin. Endocrinol. Metab. 61*, 741–745.
9. Freyberger, G., Gin, H., Heape, A., Juguelin, H., Boisseau, M.R., and Cassagne, C. (1989) Phospholipid and Fatty Acid Composition of Erythrocytes in Type I and Type II Diabetes, *Metabolism 38*, 673–678.
10. World Health Organization (1990) Diet, Nutrition and Prevention of Chronic Diseases, *Technical Report Series,* Vol. 797, pp. 171–172, World Health Organisation, Geneva.
11. Baird, J.D. (1989) Relevance of the BB Rat as a Model for Human Insulin-Dependent (Type I) Diabetes Mellitus, *Recent Adv. Endocrinol. Metab. 3*, 253–280.
12. Elias, D., Bone, A.J., Baird, J.D., Cooke, A., and Cohen, I.R. (1990) Insulin-Mimicking Anti-Idiotypic Antibodies in Development of Spontaneous Autoimmune Diabetes in BB/E Rats, *Diabetes 39*, 1467–1471.

13. Garg, M.L., Sebokova, E., Thomson, A.B.R., and Clandinin, M.T. (1988) Δ6-Desaturase Activity in Rat Liver Microsomes of Rats Fed Diets Enriched with Cholesterol and/or ω3 Fatty Acids, *Biochem. J. 249*, 351–356.
14. Gardiner, N.S., and Duncan, J.R. (1988) Enhanced Prostaglandin Synthesis as a Mechanism for Inhibition of Melanoma Cell Growth by Ascorbic Acid, *Prostaglandins Leukotrienes Essent. Fatty Acids 34*, 119–126.
15. Brown, J.E. (1995) Factors Influencing Δ6-Desaturation of Linoleic Acid, Ph.D. Thesis, University of Edinburgh, Edinburgh, Scotland.
16. Wood, D.A., Riemersma, R.A., Butler, S., Thomson, M., Macintyre, C., Elton, R.A., and Oliver, M.F. (1987) Linoleic and Eicosapentaenoic Acids in Adipose Tissue and Platelets and Risk of Coronary Heart Disease, *Lancet i*, 177–183.
17. Ashby, J.P., and Speake, R.N. (1975) Insulin and Glucagon Secretion from Isolated Islets of Langerhans, *Biochem. J. 150*, 89–96.
18. Swoboda, B.E.P., and Massey, V. (1965) Purification and Properties of the Glucose Oxidase from *Aspergillus niger*, *J. Biol. Chem. 240*, 2209–2215.
19. De Gomez Dumm, I.N.T., De Alaniz, M.J.T., and Brenner, R.R. (1984) Daily Variations of the Biosynthesis and Composition of Fatty Acids in Rats Fed on Complete and Fat-Free Diets, *Lipids 19*, 91–95.
20. Faas, F.H., and Carter, W.J. (1980) Altered Fatty Acid Desaturation and Microsomal Fatty Acid Composition in the Streptozotocin Diabetic Rat, *Lipids 15*, 953–961.
21. Mimouni, V., and Poisson, J.-P. (1990) Spontaneous Diabetes in BB Rats: Evidence for Insulin Dependent Liver Microsomal Δ6- and Δ5-Desaturase Activities, *Horm. Metab. Res. 22*, 405–407.
22. Chanussot, B., Narce, M., and Poisson, J.-P. (1989) Liver Microsomal Δ-6 and Δ-5 Linoleic-Acid Desaturation in Female BB-Rats, *Diabetologia 32,* 786–791.
23. Mimouni, V., and Poisson, J.-P. (1992) Altered Desaturase Activities and Fatty Acid Composition in Liver Microsomes of Spontaneously Diabetic Wistar BB Rat, *Biochim. Biophys. Acta 1123*, 296–302.
24. Leikin, A.I., and Brenner, R.R. (1986) Regulation of Linoleic Acid Δ6-Desaturation by a Cytosolic Lipoprotein-like Fraction in Isolated Rat Liver Microsomes, *Biochim. Biophys. Acta 876,* 300–308.
25. Murthy, V.K., and Shipp, J.C. (1979) Synthesis and Accumulation of Triglycerides in Liver of Diabetic Rats. Effect of Insulin Treatment, *Diabetes 28*, 472–478.
26. Howard, B.V. (1987) Lipoprotein Metabolism in Diabetes Mellitus, *J. Lipid Res. 28*, 613–628.
27. Poisson, J.-P., and Cunnane S.C. (1991) Long-Chain Fatty Acid Metabolism in Fasting and Diabetes: Relation Between Altered Desaturase Activity and Fatty Acid Composition, *J. Nutr. Biochem. 2*, 60–70.
28. Brenna, J.T. (1997) Use of Stable Isotopes to Study Fatty Acid and Lipoprotein Metabolism in Man, *Prostaglandins Leukotrienes Essent. Fatty Acids 57,* 467–472.
29. Cunnane, S.C., and Likhodii, S.S. (1996) ^{13}C NMR Spectroscopy and Gas Chromatograph Combustion Isotope Ratio Mass Spectrometry: Complementary Applications in Monitoring the Metabolism of ^{13}C-Labelled Polyunsaturated Fatty Acids, *Can. J. Physiol. Pharmacol. 74*, 761–768.
30. Boustani, S.E., Causse, J.E., Descomps, B., Monnier, L., Mendy, F., and de Paulet, A.C. (1989) Direct *in vivo* Characterization of Delta 5 Desaturase Activity in Humans by Deuterium Labeling: Effect of Insulin, *Metabolism 38*, 315–321.

[Received January 17, 2000, and in final revised form July 13, 2000; revision accepted October 6, 2000]

Hepatic Microsomal and Peroxisomal Docosahexaenoate Biosynthesis During Piglet Development

Zhiying Li[a], Murray L. Kaplan[a,*], and David L. Hachey[b]

[a]Department of Food Science and Human Nutrition, Iowa State University, Ames, Iowa 50011, and
[b]Department of Pharmacology, College of Medicine, Vanderbilt University, Nashville, Tennessee 37232

ABSTRACT: The roles of peroxisomes and microsomes on the biosynthetic pathway for docosahexaenoic acid (DHA) from α-linolenic acid (ALA) were investigated. Microsomes and peroxisomes were prepared from livers of fetal and neonatal piglets by a combination of differential and gradient layer centrifugation. Microsomes, peroxisomes, and combined cell fractions were incubated with [^{13}C-U]18:3n-3. The [M] and [M + 18] isotopomers of the fatty acids in the long-chain polyunsaturated fatty acid (LCPUFA) n-3 pathway were detected by gas chromatography–mass spectrometry. The quantity of each fatty acid was determined by gas chromatography, and synthesis of each fatty acid was calculated for a 30-min period. Synthesis of DHA was not detected in combined fetal liver fractions. The data suggest that DHA in the fetus is probably supplied from maternal sources through the placenta. In either singly incubated microsomal or peroxisomal preparations from neonatal livers, no DHA synthesis was detected. After combination of the microsomal and peroxisomal fractions, DHA synthesis was evident and increased rapidly between birth and 2 wk of age. This is the first demonstration of the entire biosynthetic LCPUFA n-3 pathway in subcellular organelles starting from isotopically labeled ALA to the final product, DHA, with all the intermediates present and isotopically labeled. The primary importance of the data is that it unequivocally demonstrates that peroxisomes are required for biosynthesis of DHA from ALA.

Paper no. L8580 in *Lipids 35*, 1325–1333 (December 2000).

Interest in long-chain polyunsaturated fatty acids (LCPUFA) biosynthesis has recently been renewed because impaired biosynthesis of the LCPUFA, docosahexaenoic acid (DHA), is now known to be associated with peroxisomal disorders (1–4). LCPUFA are present in all animal cell membranes and are important components of lipids unique to brain and other neural tissues. In peroxisomal disorders, LCPUFA are either absent or are present in low amounts in cells. The classic idea for the biosynthesis of LCPUFA is that it is a microsomal process (5). The classically accepted pathway for the biosynthesis of n-6 LCPUFA series is that it proceeds from linoleic acid by a microsomal system of sequential desaturation followed by elongation: 18:2n-6 → 18:3n-6 → 20:3n-6 → 20:4n-6 → 22:4n-6 → 22:5n-6. For the n-3 LCPUFA series, the classic pathway proceeds from α-linolenic acid (ALA): 18:3n-3 → 18:4n-3 → 20:4n-3 → 20:5n-3 → 22:5n-3 → 22:6n-3.

Singh *et al.* (6) reported that children with adrenoleukodystrophy accumulated long-chain saturated fatty acids due to impaired oxidation of long-chain fatty acids such as 24:0 and 26:0. Martinez (1) observed that infants with Zellweger's syndrome, total absence of peroxisomes, were unable to synthesize docosapentaenoic acid (22:5n-6) and DHA. These reports clearly indicated that peroxisomes are involved in LCPUFA biosynthesis. Sprecher and his colleagues have published several papers on the possible intracellular pathway and putative sites of synthesis of intermediates in LCPUFA biosynthesis (7–9). In isolated microsomes and peroxisomes, they studied one step at a time in the pathway and suggested that elongation of 22:4n-6 to 24:4n-6 and desaturation to 24:5n-6 occur in the microsomes followed by peroxisomal β-oxidation to 22:5n-6. In the n-3 series of LCPUFA, a similar pathway is suggested for biosynthesis of 22:6n-3. If the Sprecher hypothesis is correct, biosynthesis of 22:5n-3, but not 22:6n-3 from 18:3n-3, should be detected in microsomes. If peroxisomes are then added to the microsomal preparation, biosynthesis from 18:3n-3 to 22:6n-3 should be demonstrable. To our knowledge, no one has demonstrated the entire biosynthetic LCPUFA n-3 series in subcellular organelles from isotopically labeled ALA to the final product, DHA, with all the intermediates present and isotopically labeled.

The data reported here are the first to demonstrate in mixed microsomal and peroxisomal fractions isotopic enrichment and biosynthesis of all the intermediates in the conversion of ALA to DHA. Furthermore, the data unequivocally demonstrate that peroxisomes are required for biosynthesis of DHA from ALA.

EXPERIMENTAL PROCEDURES

Animals. The project was approved by Iowa State University (ISU) Committee on Animal Care. Four 70–72-d-old and five 110–112-d-old gestation Yorkshire fetal male piglets were ob-

*To whom correspondence should be addressed at 1127 Human Nutritional Sciences Bldg., Iowa State University, Ames, IA 50011.
E:mail: mkaplan@iastate.edu

Abbreviations: ALA, α-linolenic acid; ANOVA, analysis of variance; BSA, bovine serum albumin; DHA, docosahexaenoic acid; GC–FID; gas chromatography–flame-ionization detector; GC–MS, gas chromatography–mass spectrometry; ISU, Iowa State University; LCPUFA, long-chain polyunsaturated fatty acids; PFB, pentafluorobenzyl.

tained from the ISU Meat Laboratory. Animals were obtained only two at a time. The sows were stunned by electrocution, hung on a hoist, and killed by exsanguination by standard procedures used for U.S. Department of Agriculture-inspected slaughter houses. The uteri were dissected, weighed, and placed on ice at the slaughter facility and immediately transferred to an adjoining laboratory. After approximately 5 min, the livers of the fetuses were dissected, weighed, and placed into iced 0.9% NaCl and transferred to our laboratory within 5 min. Fifteen Yorkshire neonatal piglets were obtained from the Swine Breeding Farm, ISU. The piglets were divided into three groups: 2–3-d-old, 1-wk-old, and 2-wk-old. Each group contained five animals. Only two female piglets were in the 2–3-d-old group. The other 13 animals were males. The neonatal piglets were removed from the sows and immediately killed by a rapid blow to the head; the livers were dissected, weighed, and placed into iced 0.9% NaCl immediately at the Swine Breeding Farm. The livers were transferred to our laboratory within 15 min.

Organelle isolation. Livers were homogenized with one part liver to four parts media that contained 250 mM sucrose, 1 mM EDTA, 20 mM Tris-HCl, pH 7.4 at 4°C. Mitochondria, peroxisomes, microsomes, and cytosol were isolated by a combination of differential and gradient layer centrifugation as outlined in Scheme 1. The method was essentially a modification of the methods outlined by Ghosh and Hajra (10) and Das *et al.* (11) to increase the yield and purity of the peroxisomes and the purity of microsomes. The purity of the cell fractions was verified by assays of enzymatic markers. Succinate dehydrogenase (EC 1.3.99.1) was used as the mitochondrial membrane marker, and was assayed by the method of Singer and Kearney (12) with phenazine methosulfate and 2,6-dichloroindophenol as the artificial electron acceptors. Glutamate dehydrogenase (EC 1.4.1.2) was used as mito-

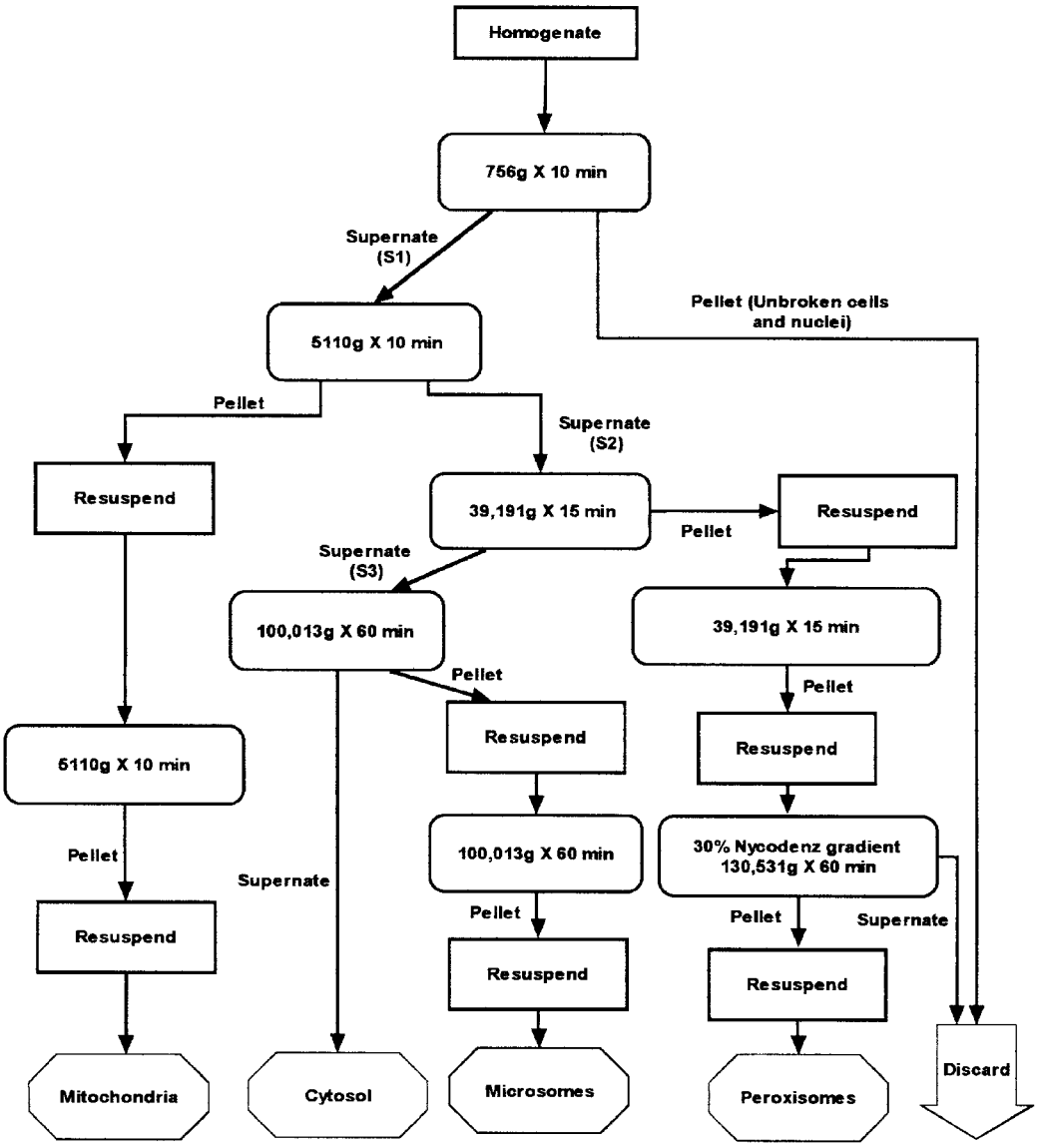

SCHEME 1

chondrial matrix marker and was assayed by the method of Fisher (13). Catalase (EC 1.11.1.6) was used as the peroxisomal marker and was assayed by the method outlined by Aebi (14), which followed the absorbance of H_2O_2 at 240 nm. Glucose-6-phosphatase (EC 3.1.3.9) was used as the microsomal marker and was assayed by the method of Nordlie and Arion (15) with determination of the inorganic phosphate released. Lactate dehydrogenase (EC 1.1.1.27) was used as the cytosolic marker and was assayed by the method of Kaplan and Fried (16).

Cell fractions were used immediately for LCPUFA synthesis as outlined below. The remainder of each of the cell fractions was rapidly frozen by immersion of the tubes into liquid nitrogen and stored at −80°C for enzyme assays and protein determination at a later time. The protein was assayed by the method of Lowry *et al.* (17).

LCPUFA biosynthesis. The procedure of LCPUFA biosynthesis was a modification of the method outlined by Voss *et al.* (9). The incubation media was made fresh on the day of use. Ten milliliters of reaction buffer that contained 150 mM KH_2PO_4, 10 mM $MgCl_2$, and 1.5 mM dithioerythritol, pH 7.4, was added to 32 mg β-NADH, 36 mg β-NADPH, 110 mg ATP, 8 mg CoASH, 7.4 mg malonyl-CoA, and 40 mg bovine serum albumin (BSA) to obtain Part 1 of the incubation media. Hexane was used to dilute [^{13}C-U]18:3n-3 (Martek, Columbia, MD) to 2 mg per mL stock solution of labeled substrate. Then 4.4 mL of the stock substrate solution was dried under N_2 and dissolved in 10 mL reaction buffer that contained 150 mM KH_2PO_4, 10 mM $MgCl_2$, and 1.5 mM dithioerythritol, pH 7.4. This was heated and shaken in a water bath at 55°C until well dissolved to obtain Part 2 of the incubation media. Incubation media Part 1 was held at 37°C, and then slowly added to incubation media Part 2 to obtain the final incubation media that was held at 37°C until promptly used. The reaction mixture consisted of 0.3 mL of a specific cell fraction to which was added 0.6 mL of the final incubation media that contained 150 mM KH_2PO_4, 10 mM $MgCl_2$, 1.5 mM dithioerythritol, 2 mg BSA/mL, 1.5 mM [^{13}C-U]18:3n-3, 2 mM β-NADH, 2 mM β-NADPH, 10 mM ATP, 0.46 mM CoASH, 0.4 mM malonyl-CoA, pH 7.4. For the combined microsomal and peroxisomal incubation, 0.15 mL of each fraction was used. The mixtures were incubated at 37°C with shaking in 16 × 100 mm tubes for 30, 60, and 120 min, and the reactions were stopped by addition of 0.1 mL 3 N HCl. The tubes were capped, frozen at −20°C, and saved for later analysis.

Analytical procedures. The lipids were extracted by the method of Radin (18) with minor modifications. Optima grade solvents (Fisher Scientific, Chicago, IL) were used. Internal standards that contained 185 nmol of heptadecanoic acid (17:0) and 0.104 nmol of pentacosanoic acid (25:0) were added to each sample. The lipids were extracted with 2 mL hexane/isoproponal (4:1, vol/vol), followed by the addition of 1.0 mL saturated NaCl solution. After shaking, the samples were centrifuged at 1000 × *g* for 10 min. The supernatant was pipetted into a clean 16 × 100 mm tube, the bottom layer was extracted three more times with 2.0 mL hexane and all the supernate fractions from the same sample were combined.

The extracted lipids were evaporated to dryness at 37°C under N_2 and then were saponified by addition of 1 mL 15% KOH in methanol, layered with N_2, sealed tightly, and heated at 80°C for 1 h. After the tubes cooled, 2 mL of H_2O was added. Nonsaponifiable lipids were extracted three times with 2 mL hexane and discarded. Small pieces of Congo red pH papers were added to the remaining lower aqueous layers followed by addition of 1 mL 12 N HCl. The samples were extracted three times with 2 mL hexane; the supernates were collected and dried under N_2.

Pentafluorobenzyl (PFB) esters were prepared as described by Hachey *et al.* (19). To each sample was added 1.0 mL 0.1 M tetrabutyl ammonium hydrogen sulfate in 0.1 M phosphate buffer, pH 9.0 followed by sonication for 5 min. Then, 500 μL of 0.13 M α-bromo-2,3,4,5,6-pentafluorotoluene (Aldrich Chemical Co., Milwaukee, WI) solution was added, and the samples were sonicated for 30 min. The PFB esters were extracted into autosampler vials twice with 1 mL hexane and evaporated to dryness under N_2, and the PFB-fatty acids were re-dissolved in 0.5 mL hexane.

The PFB esters were injected into a Fisons Trio 1000 gas chromatograph–mass spectrometer (GC–MS) (Thermoquest, San Jose, CA) tuned for negative chemical ionization with methane as the reagent gas. The GC column was a medium polar, Omegawax-320 capillary column (Supelco, Bellefonte, PA) that was 30.0 m × 320 μm × 0.25 μm film. The injector and detector temperatures were 250°C. The initial oven temperature was 150°C and increased at a rate of 5°C/min to 280°C, then held at 280°C for 9 min. Helium velocity was 10 mL/min and the split ratio was 1:25. A second splitless injection of each sample was made to detect the very low concentration of 20-, 22-, and 24-carbon fatty acids in the n-3 series. The tracer/tracee ratios were calculated from the areas of the [M] and [M + 18] isotopomers for each fatty acid. The total amount of each fatty acid was determined on a Hewlett-Packard 6890 GC equipped with a flame-ionization detector (FID). The same column, temperature program, and flow rate were used as for the GC–MS. Both 1:25 split and splitless injections were also made in the GC. The amount of enriched fatty acid was calculated by multiplying the tracer/tracee ratio by the total amount of each fatty acid determined by GC–FID.

Statistical analysis. Data were analyzed by analysis of variance (ANOVA) using the Generalized Linear Models procedure from the Statistical Analysis System (SAS, Version 6.12 SAS Institute Inc., Cary, NC). Pair-wise comparisons were made by the protected *t*-test, which uses the mean square error term from the ANOVA. Data were considered statistically significant at $P < 0.05$.

RESULTS

Body weight, liver weight, and litter size of fetal and neonatal piglets in this study are presented in Table 1. Fetal growth was very rapid between 70 and 110 d of gestation with nearly a sixfold gain in body weight and liver weight. Postnatal growth between birth and 1 wk of age was also very rapid.

TABLE 1
Body Weight, Liver Weight, and Litter Size of Fetal and Neonatal Piglets

	Fetal group 1	Fetal group 2	Pig group 1	Pig group 2	Pig group 3
Number of animals	4	5	5	5	5
Age[a] (d)	70–72	110–112	2–3	6–8	13–14
Weight[b] (g)	253.5 ± 6.9[a]	1476.2 ± 132.6[b]	1139.2 ± 187.3[a]	2526.0 ± 324.1[b]	3586.6 ± 332.1[c]
Liver weight[b] (g)	9.00 ± 0.11[a]	50.33 ± 6.96[b]	34.42 ± 5.32[a]	82.59 ± 8.98[b]	103.93 ± 15.08[c]
Litter size	12–13	8–15	10–15	8–13	10–12

[a]Age of fetuses are the days of gestation. All animals are males except two females in pig group 1.
[b]Weight and liver weight values are means ± SEM. Values in the same row for fetal groups and pig groups with different roman superscripts were significantly different at least at the $P < 0.05$ level.

Body weight and liver weight doubled during this first postnatal week. Between birth and 2 wk of age, the accretion of body weight and liver weight was a threefold increment.

Enzyme activities were assayed within 1 wk after isolation of the hepatic organelles. Five neonatal piglets and five fetal pigs were randomly selected to measure recovery of organelles by assay of enzymatic markers. Comparisons were made to activities in the 756 × *g* supernate fraction. For fetal pigs, only animals from Fetal group 2 (110–112 d gestation) were used for enzymatic assays because the amounts of each cell fraction isolated from animals in Fetal group 1 (70–72 d gestation) were very limited. The percentage recovery and specific activity of each enzymatic marker in the cell fractions of neonatal piglets are shown in Table 2. The microsomes had a low contamination by peroxisomes (1.42% catalase recovery). The peroxisomes also had a low contamination by microsomes (5.30% glucose-6-phosphatase recovery). Both fractions had a very high percentage recovery, 41.20 and 17.49%, respectively, for the microsomes and peroxisomes. Both microsomes and peroxisomes had very low contamination by mitochondria. The purities of the cytosol and mitochondria were relatively low because both fractions had high peroxisomal contamination, 22.70 and 31.58% catalase recovery, respectively. The goal of the procedure for isolation of the organelles was to obtain microsomes and peroxisomes without significant presence of mitochondria. In Table 3, the percentage recovery and specific activity of the enzymatic markers in fetal pigs are shown. The results are similar to the results from the neonatal piglets, except that the microsomes had a relatively low percentage recovery (25.54%) and relatively high contamination with mitochondria (9.58% succinate dehydrogenase recovery, 14.11% glutamate dehydrogenase recovery).

All detectable enrichments of the [M + 18] isotopomers of each fatty acid were integrated, including the precursor fatty acid, 18:3n-3. In Figure 1, typical peaks from GC–MS chromatograms of enriched key fatty acids, 20:5n-3, 22:6n-3, 24:5n-3, and 24:6n-3 are shown. Isotopic enrichment of all the fatty acids of n-3 series from 18:3n-3 to 24:6n-3 was detected.

Incubations of the cell fractions were carried out for 30, 60, and 120 min. Isotopic ratios and the amounts synthesized from [^{13}C-U]18:3n-3 were not different between these time periods. Therefore, only the data for the 30-min incubation period are reported. In Table 4, the amounts of fatty acids synthesized in the 756 × *g* supernate fractions of each group are shown. In the three neonatal piglet groups, syntheses of all the fatty acids from 18:4n-3 to 24:6n-3 were detected. In Fetal group 1, only syntheses of 18:4n-3, 20:3n-3, 20:4n-3, and 20:5n-3 were detected. In Fetal group 2, besides the 18-carbon and 20-carbon fatty acids, 22:4n-3 and 24:5n-3 syntheses were also detected. Among the five groups, Fetal group 1 had the lowest syntheses of 18:4n-3, 20:3n-3, and 20:5n-3 ($P < 0.05$). Within the three neonatal pig groups, there were no differences in syntheses of

TABLE 2
Percentage Recovery and Specific Activity of Enzymatic Markers in Organelles from Neonatal Piglet Livers[a]

	Cytosol	Mitochondria	Microsomes	Peroxisomes
Glucose-6-phosphatase				
Percentage recovery	5.28 ± 0.52	12.16 ± 0.94	41.20 ± 0.59	5.30 ± 0.34
Specific activity[b,1]	110.11 ± 14.36	708.72 ± 39.95	3,832.09 ± 446.41	2,417.73 ± 94.21
Succinate dehydrogenase				
Percentage recovery	6.99 ± 0.69	62.57 ± 3.29	5.26 ± 1.01	0.53 ± 0.06
Specific activity[b,2]	1.25 ± 0.05	30.51 ± 1.06	4.07 ± 0.46	2.02 ± 0.33
Glutamate dehydrogenase				
Percentage recovery	4.35 ± 0.34	56.85 ± 3.57	9.55 ± 0.65	1.10 ± 0.10
Specific activity[b,2]	21.34 ± 0.79	730.25 ± 9.15	190.23 ± 11.48	114.29 ± 5.44
Lactose dehydrogenase				
Percentage recovery	77.14 ± 3.72	1.66 ± 0.08	4.15 ± 0.29	0.25 ± 0.01
Specific activity[b,2]	8,114.34 ± 204.48	503.89 ± 40.30	1,704.23 ± 102.91	380.24 ± 35.29
Catalase				
Percentage recovery	22.70 ± 1.50	31.58 ± 3.41	1.42 ± 0.10	17.49 ± 1.03
Specific activity[b,3]	1.63 ± 0.43	6.15 ± 0.71	0.44 ± 0.01	36.58 ± 3.29

[a]Values are means ± SEM for five animals.
[b]Specific activities units; [1]nmol × (15 min)$^{-1}$ × mg protein^{-1}; [2]nmol × min^{-1} × mg protein^{-1}; [3]μmol × s^{-1} × mg protein^{-1}.

TABLE 3
Percentage Recovery and Specific Activity of Enzymatic Markers in Organelles from Fetal Piglet Livers[a]

	Cytosol	Mitochondria	Microsomes	Peroxisomes
Glucose-6-phosphatase				
Percentage recovery	9.68 ± 0.21	16.97 ± 1.26	25.54 ± 0.95	2.97 ± 0.15
Specific activity[b,1]	740.21 ± 44.38	1,442.33 ± 104.33	8,563.19 ± 400.86	3,970.21 ± 501.28
Succinate dehydrogenase				
Percentage recovery	6.45 ± 0.61	43.09 ± 1.03	9.58 ± 0.73	1.00 ± 0.12
Specific activity[b,2]	0.85 ± 0.14	18.28 ± 2.02	5.55 ± 0.50	2.31 ± 0.47
Glutamate dehydrogenase				
Percentage recovery	10.14 ± 1.62	42.32 ± 1.03	14.11 ± 0.35	1.05 ± 0.02
Specific activity[b,2]	35.02 ± 0.90	484.32 ± 29.31	214.17 ± 18.06	63.12 ± 5.12
Lactose dehydrogenase				
Percentage recovery	80.21 ± 3.68	1.53 ± 0.24	3.82 ± 0.10	0.21 ± 0.03
Specific activity[b,1]	4793.22 ± 417.45	280.55 ± 31.01	1,114.36 ± 148.13	330.32 ± 20.17
Catalase				
Percentage recovery	28.29 ± 2.39	19.86 ± 1.51	1.04 ± 0.16	13.95 ± 1.08
Specific activity[b,3]	3.32 ± 0.46	7.50 ± 0.90	0.54 ± 0.04	28.72 ± 1.90

[a]Values are means ± SEM for five animals.
[b]Specific activities units; [1]nmol × (15 min)$^{-1}$ × mg protein^{-1}; [2]nmol × min^{-1} × mg protein^{-1}; [3]μmol × s^{-1} × mg protein^{-1}.

18:4n-3 and 20:5n-3. Pig group 2 had the highest synthesis of 20:3n-3, and Pig group 1 had the highest synthesis of 20:4n-3 ($P < 0.05$). There were no differences in synthesis of 22:4n-3 among the four groups that had detectable synthesis of 22:4n-3. For 22:5n-3 and 22:6n-3, the amount of syntheses increased with an increase in age. Pig group 3 had highest synthesis of 22:5n-3 compared with Pig groups 1 and 2 ($P < 0.05$). Pig groups 2 and 3 had higher synthesis of 22:6n-3 than Pig group 1 ($P < 0.05$). For 24:6n-3, no differences in synthesis were detected, although Pig groups 1 and 3 had the higher synthesis of 24:5n-3 than Fetal group 2 and Pig group 2 ($P < 0.01$). The data show that, in the 756 × *g* supernate, synthesis of 22:6n-3 was detected in the neonatal pigs and rapidly increased by the first week of postnatal life. Furthermore, synthesis of 22:6n-3 was undetected in the two fetal groups.

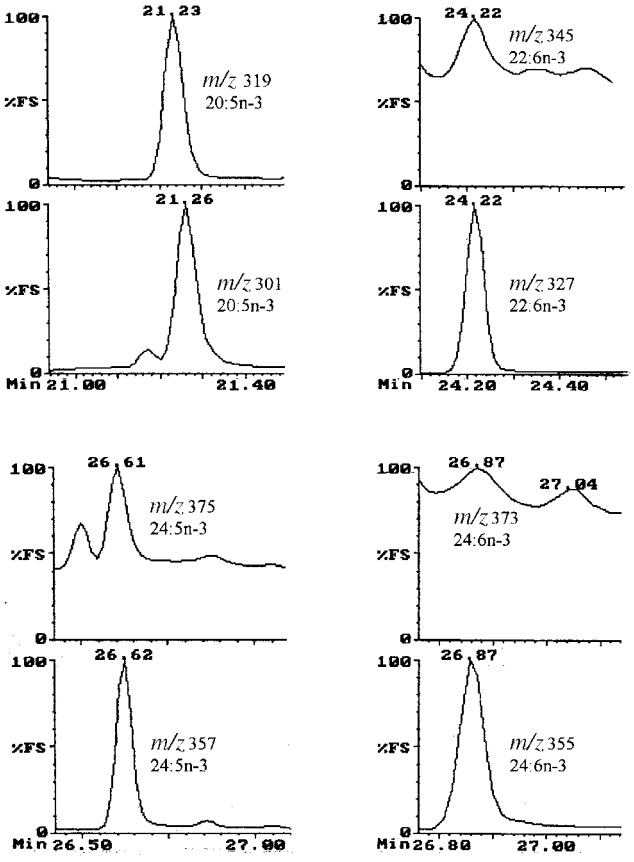

FIG. 1. Typical peaks from gas chromatography–mass spectrometry chromatograms of nonenriched [M] and enriched [M + 18] isotopomers of key fatty acids, 20:5n-3, 22:6n-3, 24:5n-3, and 24:6n-3.

Microsomal synthesis of LCPUFA in the n-3 series is presented in Table 5. The most important difference from Table 4 is that only two animals in pig group 1 had detectable 22:6n-3 enrichment (not significantly different from 0). Only syntheses of fatty acids 18:4n-3, 20:3n-3, 20:4n-3, and 20:5n-3 could be detected in Fetal group 1. In Fetal group 2, 24:5n-3 and 24:6n-3 enrichments were also detected. There were no differences among the five groups in synthesis of 18:4n-3. Synthesis of 20:3n-3 in pig groups 2 and 3 was higher than in Fetal group 1 and Pig group 1 ($P < 0.05$). Pig group 3 had the highest synthesis of 20:4n-3 ($P < 0.05$). For 20:5n-3, Fetal group 2 had the highest synthesis. For the 24-carbon fatty acids, there were no differences among the four groups that had detectable enrichments. The early Fetal group 1 had no detectable enrichment of 24-carbon fatty acids. Within the three neonatal piglet groups, there were no differences in the 22-carbon fatty acids except that Pig group 3 had the most 22:4n-3 synthesized ($P < 0.01$).

In Table 6, isotopic incorporation into peroxisomal LCPUFA is presented. For Fetal group 1, no isotopic label was detected in any n-3 LCPUFA. For Fetal group 2 and Pig group 2, only the fatty acids 18:4n-3, 20:3n-3, 20:4n-3 and 20:5n-3 had detectable ^{13}C enrichments. For Pig groups 1 and 3, although there were detectable 22-carbon LCPUFA enrichments, none of them was significantly different from 0 ($P < 0.05$).

The amounts of newly synthesized LCPUFA in mixtures of microsomes and peroxisomes are presented in Table 7. The re-

TABLE 4
Biosynthesis of LCPUFA in the 756 × *g* Supernate from Fetal and Neonatal Piglet Livers[a]

	Fetal group 1	Fetal group 2	Pig group 1	Pig group 2	Pig group 3	MSE
Age[b] (d)	70–72	110–112	2–3	6–8	13–14	
N	4	5	5	5	5	
18:4n-3	39.1957[d]	212.9525[c]	133.1251[a,c]	68.4420[a]	81.8934[a]	3319.9965
20:3n-3	1.3822[c]	11.7475[b]	4.8849[a,c]	14.4800[b]	7.0388[a]	8.8735
20:4n-3	0.6291[a,c]	0.0735[c]	2.2583[b]	1.8199[a]	1.0592[a]	0.8603
20:5n-3	0.1004[a]	1.3866[c]	0.2945[b]	0.2148[b]	0.2228[b]	0.3727
22:4n-3		0.0205[a]	0.0154[a]	0.0128[a]	0.0072[a]	0.0001
22:5n-3			0.0039[a]	0.0139[a]	0.0446[b]	0.0002
22:6n-3			0.0094[a]	0.1943[b]	0.2590[b]	0.0072
24:5n-3		0.0035[a]	0.0470[b]	0.0032[a]	0.0406[b]	0.0002
24:6n-3			0.0040[a]	0.0090[a]	0.0042[a]	0.0000

[a]The cell fractions were incubated in media that contained [^{13}C-U]18:3n-3 as described in the Experimental Procedures section. Values are the means in nmol fatty acids synthesized in 30 min per mg protein. Across a row the means with different roman superscripts were significantly different at least at the $P < 0.05$ level.
[b]Age of fetuses are in days of gestation. LCPUFA, long-chain polyunsaturated fatty acids; MSE; mean square of the error (general linear model-analysis of variance).

sults were very similar to the results from the complete system in the 756 × *g* supernate in Table 4. For the two fetal groups, Fetal group 1 had ^{13}C enrichments only in 18:4n-3, 20:3n-3, 20:4n-3, and 20:5n-3. In Fetal group 2, also detected were low syntheses of 24:5n-3 and 24:6n-3. In the three neonatal piglet groups, syntheses of all the fatty acids from 18:4n-3 to 24:6n-3 were detected except 24:4n-3. Within the five groups, Fetal group 2 and Pig group 1 had higher synthesis of 18:4n-3 than Fetal group 1 and Pig group 2 ($P < 0.05$). Pig group 3 had the highest syntheses of 20:3n-3 and 20:4n-3, and Fetal group 2 had the highest synthesis of 20:5n-3. For 22:4n-3 synthesis, there were no differences among the three neonatal piglet groups. For 22:5n-3 and 22:6n-3, syntheses in the postnatal piglets increased with increased age. Pig groups 2 and 3 had higher synthesis of 22:5n-3 than Pig group 1 ($P < 0.05$). Pig group 3 had the highest, and Pig group 1 had the lowest synthesis of 22:6n-3 ($P < 0.05$). For the 24-carbon fatty acids, synthesis also increased with increased age. For 24:5n-3, Pig groups 2 and 3 had higher syntheses than did Fetal group 2 and Pig group 1 ($P < 0.05$). For 24:6n-3, Pig group 3 had higher synthesis than did Fetal group 2 ($P < 0.01$). The most striking result from the data above is that after addition of microsomes and peroxisomes together in the system, 22:6n-3 was synthesized, but synthesis was not detected in the separate microsomal and peroxisomal incubations.

The comparisons of key products in the LCPUFA biosynthetic pathway between incubations of microsomal fractions and mixtures of microsomes and peroxisomes within the three neonatal pig groups are summarized in Figure 2. All the groups had significant differences in 22:6n-3 synthesis ($P < 0.01$) when peroxisomes were added to microsomal preparations. Pig groups 1 and 2 also had significant differences in 24:5n-3 synthesis. But in Pig group 1, microsomes alone had higher synthesis of 24:5n-3 than the mixture ($P < 0.05$) whereas in Pig group 2, the mixture had higher synthesis than microsomes alone ($P < 0.01$).

TABLE 5
Biosynthesis of LCPUFA in Microsomes from Fetal and Neonatal Piglet Livers[a]

	Fetal group 1	Fetal group 2	Pig group 1	Pig group 2	Pig group 3	MSE
Age[b] (d)	70–72	110–112	2–3	6–8	13–14	
N	4	5	5	5	5	
18:4n-3	146.1412[a]	373.9621[a]	347.8873[a]	201.9053[a]	279.1991[a]	33,670.9370
20:3n-3	4.3482[a]	8.8941[a,b]	3.9409[a]	17.3589[b]	15.6704[b]	53.1973
20:4n-3	0.4140[a]	0.3949[a]	0.6560[a]	0.9940[a]	9.0555[b]	1.1763
20:5n-3	0.1014[a]	2.2319[b]	0.3978[a]	0.4404[a]	0.3174[a]	0.1412
22:4n-3			0.0053[a]	0.0086[a]	0.0603[b]	0.0005
22:5n-3			0.0373[a]	0.4162[a]	0.0116[a]	0.2099
22:6n-3			0.0276[c]			0.0006
24:5n-3		0.0503[a]	0.0447[a]	0.1287[a]	0.2527[a]	0.0277
24:6n-3		0.0195[a]	0.0074[a]	0.0255[a]	0.0288[a]	0.0011

[a]Microsomes were incubated in media that contained [^{13}C-U]18:3n-3 as described in the Experimental Procedures section. Values are the means in nmol fatty acids synthesized in 30 min per mg protein. Across a row the means with different roman superscripts were significantly different at least at the $P < 0.05$ level.
[b]Ages of fetuses are in days of gestation.
[c]Value is not significantly different from 0. Only two animals in the group had detectable enrichment in 22:6n-3. See Table 4 for abbreviations.

TABLE 6
Biosynthesis of LCPUFA in Peroxisomes from Fetal and Neonatal Piglet Livers[a]

	Fetal group 1	Fetal group 2	Pig group 1	Pig group 2	Pig group 3	MSE
Age[b] (d)	70–72	110–112	2–3	6–8	13–14	
N	4	5	5	5	5	
18:4n-3		451.4951[a]	219.2426[b]	247.3023[b]	439.5811[a,b]	18436.0010
20:3n-3		12.6202[b]	1.0117[a]	1.7357[a]	4.6992[a]	31.5673
20:4n-3		0.7360[a]	0.6007[a,b]	1.6081[a,c]	0.3819[a,b]	0.4789
20:5n-3		3.2036[a]	0.3280[b]	0.7683[b]	0.2564[b]	1.7381
22:4n-3			0.0063[c]		0.0151[d]	0.0001
22:5n-3			0.0313[c]		0.0278[d]	0.0003
22:6n-3			0.0746[c]		0.2038[d]	0.0390
24:5n-3						
24:6n-3						

[a]Peroxisomes were incubated in media that contained [^{13}C-U]18:3n-3 as described in the Experimental Procedures section. Values are the means in nmol fatty acids synthesized in 30 min per mg protein. Across a row the means with different roman superscripts were significantly different at least at the $P < 0.05$ level.
[b]Age of fetuses are in days of gestation.
[c]Values are not significantly different from 0. Only one animal in the group had detectable enrichment in 22-carbon fatty acids.
[d]Values are not significantly different from 0. Only two animals in the group had detectable enrichment in 22-carbon fatty acids. See Table 4 for abbreviations.

DISCUSSION

The data reported above showed that fetal growth between 70 and 110 d of gestation was very rapid. Postnatal growth between birth and 1 wk of age was also very rapid. Synthesis in late fetal life is high for fatty acids at the beginning of the LCPUFA n-3 pathway with some detection of isotopic label in 24:5n-3. In late fetal life, the synthetic system may be ready to develop because EPA accumulates and there is some label in the 24-carbon fatty acids. Synthesis of EPA in Fetal group 2 was sixfold higher than in the three neonatal pig groups (Table 4). Synthesis of DHA was not detected in the combined fetal liver fractions. This probably is the only reported examination of hepatic LCPUFA synthesis in midgestational and late-gestational fetal tissue. Our data support the hypothesis that DHA in the fetus is probably supplied from maternal sources through the placenta (20). In humans, fetal DHA accumulation occurs primarily during the last intrauterine trimester (21). In human studies, a positive relationship exists between maternal ingestion of DHA during pregnancy and concentrations of DHA in infant tissues. Low concentrations of DHA in plasma phospholipids of umbilical cord arteries were detected in infants of vegetarian mothers (22). Maternal diets high in fish oils during pregnancy increased DHA concentration in newborns (23).

Our data also indicate that synthesis of DHA in the 756 × *g* supernate increased rapidly in neonatal piglets as age increased, corresponding to the rapid neonatal rate of growth. Synthesis increased 20-fold from 2–3 d of age to 1 wk of age and increased 27-fold between 2–3 d of age and 2 wk of age (Table 4). This result is consistent with the recent reports that human infants can synthesize DHA from ALA (24,25).

DHA, until recently, was thought to be synthesized directly from 22:5n-3 by the action of a microsomal acyl-CoA-

TABLE 7
Biosynthesis of LCPUFA in Mixtures of Microsomes and Peroxisomes from Fetal and Neonatal Piglet Livers[a]

	Fetal group 1	Fetal group 2	Pig group 1	Pig group 2	Pig group 3	MSE
Age[b] (d)	70–72	110–112	2–3	6–8	13–14	
N	4	5	5	5	5	
18:4n-3	168.4357[b]	512.9278[a]	437.0247[a]	228.2845[b]	341.3588[a,b]	22,239.4740
20:3n-3	6.9341[a,c]	7.5689[a]	4.3121[a,c]	13.4542[a,b]	14.4964[b]	20.1814
20:4n-3	0.4449[a]	0.0275[a,d]	1.3298[b]	1.0309[a,b]	3.1596[c]	0.2479
20:5n-3	0.4677[a]	2.0787[b]	0.4109[a]	0.7941[a]	0.4015[a]	0.4730
22:4n-3			0.0046[a]	0.0136[a]	0.0251[a]	0.0004
22:5n-3			0.0774[a]	0.1823[b]	0.2397[b]	0.0185
22:6n-3			0.0887[a]	1.2318[b]	1.6650[c]	0.0984
24:5n-3		0.0105[a]	0.0088[a]	0.3299[b]	0.1776[b]	0.0168
24:6n-3		0.0030[a]	0.0129[a,b]	0.0172[a,b]	0.0339[b]	0.0005

[a]Mixed microsomes and peroxisomes were incubated in media that contained [^{13}C-U]18:3n-3 as described in the Experimental Procedures section. Values are the means in nmol fatty acids synthesized in 30 min per mg protein. Across a row the means with different roman superscripts were significantly different at least at the $P < 0.05$ level.
[b]Ages of fetuses are in days of gestation. See Table 4 for abbreviations.

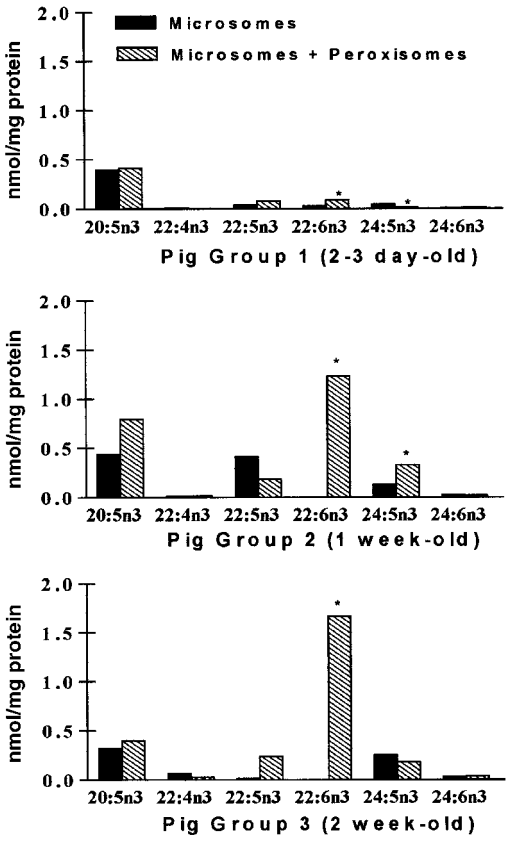

FIG. 2. Comparisons of key products in the long-chain polyunsaturated fatty acids biosynthesis pathway of neonatal piglets. These are comparisons from data in Tables 5 and 7. The cell fractions were incubated in media that contained [^{13}C-U]18:3n-3 for 30 min as described in the Experimental Procedures section. * $P < 0.05$.

dependent Δ4-desaturase (5,26). However, one recent study suggested that microsomes do not have an acyl-CoA-dependent Δ4-desaturase (9). DHA synthesis is reported to occur by β-oxidation of 24-carbon fatty acids in peroxisomes (9,27,28). Our study demonstrates that the entire biosynthetic LCPUFA n-3 pathway from ALA to DHA is evident only when microsomes and peroxisomes are mixed. The data also indicate that microsomes alone are not able to synthesize 22:6n-3 (Table 5), which is consistent with studies that show elongation from 22:5n-3 to 24:5n-3 followed by desaturation to 24:6n-3 in microsomes followed by β-oxidation in peroxisomes to 22:6n-3 (9,27,28). In peroxisomal fractions, only 18- and 20-carbon fatty acids could be synthesized (Table 6). This might be due to the 5% contamination with microsomes, which are very active (Tables 2 and 3).

Our data, to our knowledge, are the first demonstration of the entire biosynthetic LCPUFA n-3 pathway in sucellular organelles. The primary importance of the data is that it supports the Sprecher hypothesis (9) and unequivocally demonstrates that both microsomes and peroxisomes are required for biosynthesis of DHA from ALA. Furthermore, this report demonstrated that DHA synthesis in combined fetal liver fractions was not demonstrable *in vitro*.

ACKNOWLEDGMENTS

This work is Journal Paper No. J-18952 of the Iowa Agriculture and Home Economics Experiment Station, Ames, Iowa, Project No. 3542, and supported in part by Hatch Act, State of Iowa Funding, Special Research Initiation Grant from Iowa State University, and USDA contract 94-3415-0269.

The authors thank Dr. Stephen Ford for provision of fetal and neonatal piglets and Matthew Wilson for his help in euthanizing the piglets.

REFERENCES

1. Martinez, M. (1989) Polyunsaturated Fatty Acid Changes Suggesting a New Enzymatic Defect in Zellweger Syndrome, *Lipids 24*, 261–265.
2. Martinez, M. (1990) Severe Deficiency of Docosahexaenoic Acid in Peroxisomal Disorders: A Defect of Δ-4 Desaturation? *Neurology 40*, 1292–1298.
3. Martinez, M. (1992) Abnormal Profiles of Polyunsaturated Fatty Acids in the Brain, Liver, Kidney and Retina of Patients with Peroxisomal Disorders, *Brain Res. 583*, 171–182.
4. Martinez, M., Mougan, I., Roig, M., and Ballabriga, A. (1994) Blood Polyunsaturated Fatty Acids in Patients with Peroxisomal Disorders. A Multicenter Study, *Lipids 29*, 273–280.
5. Mayes, P.A. (1996) Metabolism of Unsaturated Fatty Acids and Eicosanoids, in *Harper's Biochemistry* (Murray, R.K., Granner, D.K., Mayes, P.A., and Rodwell, V.W., eds.) 24th edn., pp. 236–244, Appleton and Lange, East Norwalk.
6. Singh, I., Moser, A.B., Moser, H.W., and Kishimoto, Y. (1984) Adrenoleukodystrophy: Impaired Oxidation of Very Long Chain Fatty Acids in White Blood Cells, Cultured Skin Fibroblasts and Amniocytes, *Pediatr. Res. 18*, 286–290.
7. Mohammed, B.S., Sankarappa, S., Geiger, M., and Sprecher, H. (1995) Reevaluation of the Pathway for the Metabolism of 7,10, 13,16-Docosatetraenoic Acid to 4,7,10,13,16-Docosapentaenoic Acid in Rat Liver, *Arch. Biochem. Biophys. 317*, 179–184.
8. Geiger, M., Mohammed, B.S., Sankarappa, S., and Sprecher, H. (1993) Studies to Determine If Rat Liver Contains Chain-Length-Specific Acyl-CoA 6-Desaturases, *Biochim. Biophys. Acta 1170*, 137–142.
9. Voss, A., Reinhart, M., Sankarappa, S., and Sprecher, H. (1991) The Metabolism of 7,10,13,16,19-Docosapentaenoic Acid to 4, 7,10,13,16,19-Docosahexaenoic Acid in Rat Liver Is Independent of a 4-Desaturase, *J. Biol. Chem. 266*, 19995–20000.
10. Ghosh, M.K., and Hajra, A.K. (1986) A Rapid Method for the Isolation of Peroxisomes from Rat Liver, *Anal. Biochem. 159*, 169–174.
11. Das, A.K., Harie, S., and Hajra, A.K. (1992) Biosynthesis of Glycerolipid Precursors in Rat Liver Peroxisomes and Their Transport and Conversion to Phosphatidate in the Endoplasmic Reticulum, *J. Biol. Chem. 267*, 9724–9730.
12. Singer, T.P., and Kearney, E.B. (1974) Succinate Dehydrogenase Activity, *Methods Biochem. Anal. 4*, 307–333.
13. Fisher, H.F. (1985) L-Glutamate Dehydrogenase from Bovine Liver, in *Methods in Enzymology* (Meister, A., ed.) Vol. 113, pp. 16–27, Academic Press, Orlando.
14. Aebi, H. (1984) Catalase *in Vitro*, in *Methods in Enzymology* (Lowenstein, J.M., ed.) Vol. 105, pp. 121–126, Academic Press, New York.
15. Nordlie, R.C., and Arion, W.J. (1966) Glucose-6-phosphatase, in *Methods in Enzymology* (Lowenstein, J.M., ed.) Vol. 9, pp.

619–625, Academic Press, New York.
16. Kaplan, M.K., and Fried, G.H. (1973) Adaptive Enzyme Responses in Adipose Tissue of Obese Hyperglycemia Mice, *Arch. Biochem. Biophys. 158*, 711–719.
17. Lowry, O.J., Rosebrough, N.J., Farr, A.L., and Randall, R.J. (1951) Protein Measurement with the Folin Phenol Reagent, *J. Biol. Chem. 193*, 265–275.
18. Radin, N.S. (1981) Preparation of Lipid Extracts, in *Methods in Enzymology* (Lowenstein, J.M., ed.) Vol. 72(D), pp. 5–7, Academic Press, New York.
19. Hachey, D.L., Patterson, B.W., Elsas, L.J., II, Reeds, P.J., and Klein, P.D. (1991) Isotopic Determination of Organic Keto Acid Pentafluorobenzyl Esters in Biological Fluids by Negative Chemical Ionization Gas Chromatography/Mass Spectrometry, *Anal. Chem. 63*, 919–923.
20. Olsen, S.F., Salvig, J.D., and Secher, N. (1998) Does Dietary Docosahexaenoic Acid in Human Pregnancy Affect Offspring Brain Development: Opportunities for Research, in *Essential Fatty Acids and Eicosanoids: Invited Papers from the Fourth International Congress* (Riemersma, R.A., Armstrong, R., Kelly, R.W., and Wilson, R., eds.), pp. 128–130, AOCS Press, Champaign.
21. Carson, S.E. (1989) Polyunsaturated Fatty Acids and Infant Nutrition, in *Dietary ω3 and ω6 Fatty Acids: Biological Effects and Nutritional Essentiality* (Calli, C., and Simopoulis, A.P., eds.), pp. 147–157, Plenum Press, New York.
22. Reddy, S., Sanders, T.A.B., and Obeid, O. (1994) The Influence of Maternal Vegetarian Diet on Essential Fatty Acids Status of the Newborn, *Eur. J. Clin. Nutr. 48*, 358–368.
23. Connor, W.E., Lowensohn, R., and Hatcher, L. (1996) Increased Docosahexaenoic Acid Levels in Human Newborn Infants by Administration of Sardines and Fish Oil During Pregnancy, *Lipids 31*, 183–187.
24. Salem, N., Jr., Wegher, B., Mena, P., and Uauy, R. (1996) Arachidonic and Docosahexaenoic Acids Are Biosynthesized from Their 18-Carbon Precursors in Human Infants, *Proc. Natl. Acad. Sci. USA 93*, 49–54.
25. Sauerwald, T.U., Hachey, D.L., Jensen, C.L., Chen, H., Anderson, R.E., and Heird, W.C. (1997) Intermediates in Endogenous Synthesis of C22:6ω3 and C20:4ω6 by Term and Preterm Infants, *Pediatr. Res. 41*, 183–187.
26. Sprecher, H. (1992) Long Chain Fatty Acid Metabolism, in *Polyunsaturated Fatty Acids in Human Nutrition* (Bracco, U., and Deckelbaum, R.J., eds.) pp. 13–24, Raven Press, Ltd., New York.
27. Luthria, D.L., Mohammed, B.S., and Sprecher, H. (1996) Regulation of the Biosynthesis of 4,7,10,13,16,19-Docosahexaenoic Acid, *J. Biol. Chem. 271*, 16020–16025.
28. Moore, S.A., Hurt, E., Yoder, E., Sprecher, H., and Spector, A.A. (1995) Docosahexaenoic Acid Synthesis in Human Fibroblasts Involves Peroxisomal Retroconversion of Tetracosahexaenoic Acid, *J. Lipid Res. 36*, 2433–2443.

[Received July 6, 2000, and in revised form and accepted October 3, 2000]

Dietary Cholesterol Induces Changes in Molecular Species of Hepatic Microsomal Phosphatidylcholine

Ana M. Bernasconi, Horacio A. Garda, and Rodolfo R. Brenner*

Instituto de Investigaciones Bioquímicas de La Plata (INIBIOLP), CONICET-UNLP, Facultad de Ciencias Médicas, 1900-La Plata, Argentina

ABSTRACT: After 21 days on a diet containing 1 g% cholesterol and 0.5 g% cholic acid, rats had an increased content of cholesterol in liver microsomal lipids. In liver, both cholesterol content and Δ9 desaturase activity increased, whereas Δ6 and Δ5 desaturase activities decreased. These changes correlated with increases in oleic, palmitoleic, and linoleic acids and decreases in arachidonic and docosahexenoic acids in total microsomal lipids. Similar fatty acid changes were found in phosphatidylcholine (PC), the principal lipid of the microsomal membrane. In PC the predominant molecular fatty acid species (67% of the total) in the control rats were 18:0/20:4, 16:0/20:4, and 16:0/18:2; and they mainly determined the contribution of PC to the biophysical and biochemical properties of the phospholipid bilayer. The cholesterol diet decreased specifically the 18:0/20:4 species, and to a lesser extent, 16:0/20:4 and 18:0/22:6. The 18:1-containing species, especially 18:1/18:2 and less so 16:0/18:1 and 18:1/20:4, were increased. A new 18:1/18:1 species appeared. The independent effects of the presence of cholesterol and change of the fatty acid composition of the phospholipid bilayer of liver microsomes on the packing were studied by fluorescence methods using 6-lauroyl-2,4-dimethylaminonaphthalene, 1,6-diphenyl-1,3,5-hexatriene and 1-(4-trimethylammonium phenyl)-6-phenyl-1,3,5-hexatriene, which test different parameters and depths of the bilayer. Data showed that the increase of cholesterol in the membrane, and not the change of the fatty acid composition of phospholipids, was the main determinant of the increased bulk packing of the bilayer. The increase of fluid oleic- and linoleic-containing species almost compensated for the drop in 20:4- and 22:6-containing molecules. But the most important effect was that the general drop in essential n-6 and n-3 polyunsaturated fatty acids meant that this endogenous source for the needs of the animal decreased.

Paper no. L8499 in *Lipids 35*, 1335–1344 (December 2000).

*To whom correspondence should be addressed at Instituto de Investigaciones Bioquímicas (INIBIOLP), CONICET-UNLP, Facultad de Ciencias Médicas, calles 60 y 120, 1900 La Plata, Argentina.
E-mail: rbrenner@atlas. med.unlp.edu.ar

Abbreviations: DPH 1,6-diphenyl-1,3,5-hexatriene; ELSD, evaporative light-scattering detector; GLC, gas–liquid chomatography; GP, generalized polarization; HPLC, high-performance liquid chromatography; Laurdan, 6-lauroyl-2,4-dimethylaminonaphthalene; PC, phosphatidylcholine; r_s, steady-state fluorescence anisotropy; r_∞, limiting anisotropy; *S*, order parameter; SRE, sterol-responsive element; SREBP, SRE-binding protein; τ, lifetime; Δτ, differential polarized phase lifetime; τ_M, modulation lifetime; τ_P, phase τ_R, rotational correlation time; TMA-DPH, 1-(4-trimethylammoniumphenyl)-6-phenyl-1,3,5-hexatriene.

Cholesterol and phospholipids are obligatory and simultaneous components of many eukaryotic membranes. The cholesterol content of membranes is modified by the amount of cholesterol ingested. We (1,2) and other authors (3) have shown that the ingestion of cholesterol not only increases the cholesterol content of rat liver microsomes but also increases the Δ9 fatty acid desaturase activity that converts stearic to oleic acid and decreases the Δ6 and Δ5 desaturases that convert linoleic and α-linolenic acids to higher polyunsaturated fatty acids. These changes in desaturase activities are correlated with modifications in the percentage of fatty acid in the phospholipids of liver membrane. An increase of oleic acid and a decrease in arachidonic and docosahexaenoic acids were shown. A rise in cholesterol in the microsomes increased the overall rigidity of the microsomal membrane as measured by fluorometric methods (1).

Considering that changes in membrane fluidity produced by different factors can alter the activity or kinetics of intrinsic enzymes and lipid protein interactions (4), as shown for the UDP-glucuronyl transferase (5,6), glucose-6-phosphatase (7,8), fatty acid desaturases (7,8) and NADH-cytochrome-C-reductase (7,8), Leikin and Brenner (1,2) suggested that dietary cholesterol induced rigidity of microsomes could be a factor for the fatty acid Δ9 desaturation increase. In addition to this suggestion, which was verified in experiments in which cholesterol was incorporated *in vitro* in the microsomes (7), it was pointed out that some of this activation effect could be due to a change in desaturase synthesis (1).

This last suggestion was confirmed by Landau *et al.* (9) who showed that cholesterol feeding induced an increase of stearoyl-CoA desaturase RNA in rat liver, but no information was given on the Δ6 and Δ5 desaturase problem and on the mechanism of the changes evoked by cholesterol in microsome fluidity.

We know from preceding publications (1) that the cholesterol diet increases the proportion of oleic acid and decreases the proportions of arachidonic and docosahexaenoic acid in microsomal phospholipids, but we do not know which specific molecules are modified.

In the present work, we addressed this question and also which molecular species of microsomal phosphatidylcholine (PC), the principal phospholipid component of the membrane,

are specifically modified by the change in Δ9, Δ6, and Δ5 desaturase activity as evoked by the high-cholesterol diet.

Moreover, the preceeding publication (1) showed, as expected, that the cholesterol incorporation in the liver microsomal membrane increased the microsomal membrane overall packing. However, at that time, the extent to which the change of fatty acid composition of the bilayer phospholipids, as evoked by the modification of the Δ9, Δ6, and Δ5 desaturation activity, contributed to this effect was not investigated; nor was the cholesterol-specific effect investigated. For these reasons, the biophysical properties of a bilayer prepared only with liver microsomal membrane phospholipids were compared to one prepared with whole lipids. Special probes that tested the properties at different depths of the bilayer were used.

EXPERIMENTAL PROCEDURES

Animals and diets. International regulations for animal care were observed throughout these experiments. Male Wistar rats were separated after weaning into two groups of eight animals each. The control group was fed, as in the experiment of Leikin and Brenner (1), a diet composed of 64 g% starch, 23 g% delipidated casein, and 13 g% corn oil plus 2% vitamins and 4% minerals, as described by Rogers and Harper (10). The test group was fed the same diet as the control, with the addition of 1 g% cholesterol and 0.5 g% cholic acid. The reason for the cholic acid addition to the food was to increase cholesterol absorption in the intestine. Ingestion of a small amount of cholic acid did not alter the microsomal membrane composition (Brenner, R.R., unpublished). The animals were pair-fed, and both groups gained the same amount of weight. After an experimental period of 21 d, the animals were killed by decapitation without anesthesia and exanginated. The liver from each animal was rapidly excised and placed in an ice-cold homogenizing solution (1:3 wt/vol) composed of 0.25 M sucrose, 1 mM EDTA, and 10 mM phosphate buffer (pH 7.2). Microsomes were obtained by differential ultracentrifugation at 100,000 × *g* (Beckman Ultracentrifuge) as described elsewhere (11). They were kept stored at –80°C.

Protein concentration was measured according to the procedure of Lowry *et al.* (12).

Lipid analysis. Lipids were extracted from microsomes according to the procedure of Folch *et al.* (13). Total lipid content was measured by aliquot evaporation to constant weight. Cholesterol content was determined by the procedure of Huang *et al.* (14), and total phosphorus by the method of Chen *et al.* (15).

Total phospholipids were separated from nonpolar lipids by absorption on activated silicic acid. Between 8 and 10 mg of total lipids, dissolved in 3 mL of chloroform, was mixed with 25 times their weight of silicic acid. Nonpolar lipids were washed out twice with chloroform.

PC and other phospholipid classes were separated from total lipids by high-performance liquid chromatography (HPLC) using an evaporative light-scattering detector (ELSD) (16). An Econosil silica column of 10 μm and 250 × 4.6 mm from All-tech Associates (Deerfield, IL), was used. Elution was performed at a flow rate of 1 mL/min by a gradient of hexane/isopropanol/dichloromethane (40:48:12, by vol) to hexane/isopropanol/dichloromethane/water (40:42:8:8, by vol) for 15 min followed by additional elution with the latter solvent for 30 min. Solvents were previously sonicated to eliminate air. Lipids (300 μg) dissolved in 50 μL of mobile phase were injected.

Nebulization in the ELSD was set at 90°C drift tube temperature and 2.20 L/min of nitrogen gas flow to the nebulizer the PC peak was collected manually from the column effluent using a flow splitter. The solvent was evaporated under N_2 and redissolved in methanol/triethylamine (2:1).

PC molecular species separation. The separation of the molecular species was done by using the method of Brouwers *et al.* (17). In this case, triethylamine proved to be very efficient for the removal of specific interactions between the phospholipid headgroup and HPLC column material. Resolution of molecular species was performed on two 5 μm endcapped Lichrosphere 100-RP18 columns in series obtained from Merck (Darmstadt, Germany). Isocratic elution was applied with a solvent composed of methanol/acetonitrile-triethylamine (58:40:2, by vol) at a flux of 1 mL/min. The detection and quantification were done in an ELSD using N_2 as nebulizer gas at a flux of 1.8 L/min and a temperature of 100°C (17).

A sample of 1 mg of PC was injected; 5 parts out of 100 went to the detector, and the remaining materials of the peaks were collected and identified by gas–liquid chromatography (GLC) analysis.

Fatty acid compositions of both PC and molecular species were analyzed by GLC in a Hewlett-Packard 5840 apparatus after esterification with methanol. A 10% SP2330 column (Supelco Inc., Bellefonte, PA) packed on Chromosorb WAW was used. The temperature was programmed to obtain a linear increase of 3°C/min from 140 to 220°C. The chromatographic peaks were identified by comparison of the retention times with those of standards.

Fluorescence measurements. (i) Fluorescent probes. 1,6-Diphenyl-1,3,5-hexatriene (DPH) was purchased from Sigma Chemical Co. (St. Louis, MO). 6-Lauroyl-2,4-dimethylaminonaphthalene (Laurdan) and 1-(4-trimethylammoniumphenyl)-6-phenyl-1,3,5-hexatriene (TMA-DPH) were purchased from Molecular Probes (Eugene, OR).

(ii) Liposome preparation. Two types of liposomes were prepared, one with the total microsomal lipids and the other with the phospholipids. Lipids (0.8 mg) in $CHCl_3$ were added to a rounded-bottom glass tube. $CHCl_3$ was evaporated under a N_2 stream, and 1 mL of buffer A (Tris-HCl 0.1 M, NaCl 0.15 M, pH 8.0) was added. After 15 min at room temperature to allow hydration, samples were vigorously vortexed for 2 min. Then the lipid suspensions were extruded 11 times through a 100-nm-pore filter using a LiposoFast extruder (Avestin, Inc., Ottawa, Ontario, Canada).

(iii) Liposome labeling. Extruded liposomes (0.25 mL) were mixed with 0.25 mL of a $4 \cdot 10^{-6}$ M suspension of the fluorescent probe (DPH, TMA-DPH, or Laurdan) in buffer A and vigorously vortexed. Samples were kept at room temper-

ature for at least 30 min, and then diluted 5 times with buffer A before the fluorescent measurements were made. The final concentration of the samples was 80 μg/mL of lipids and $4 \cdot 10^{-7}$ M of the fluorescent probe.

(iv) Fluorescence measurements. All measurements were made in an SLM 4800 spectrofluorometer in 1 × 1 cm cuvettes.

DPH and TMA-DPH fluorescence. DPH or TMA-DPH steady-state fluorescence anisotropy (r_S), lifetime (τ) and differential polarized phase lifetime (Δτ) were measured using an excitation wavelength of 361 nm and observing the total emission at wavelengths >389 nm through a sharp cut-off filter (KV389) according to Lakowicz *et al.* (18,19) with some modification (20–22). For the τ and Δτ measurements, the exciting light was modulated sinusoidally in amplitude at 18 or 30 MHz with a Debye-Sears modulator and vertically polarized with a Glan-Thompson polarizer. For τ, the emission was observed through a Glan-Thompson polarizer oriented 55° to the vertical to eliminate the effect of Brownian rotation (23). The phase shift and demodulation of the emitted light were measured relative to the reference standard 1,4-bis(5-phenyloxazol-2-yl)benzene in ethanol (τ = 1.35 ns) (24) and used to compute the phase (τ_P) and modulation (τ_M) lifetimes of the samples (25). Δτ was obtained from the phase shift between the parallel and perpendicular components of the emission observed with the emission polarizer vertically or horizontally oriented, respectively. Data were interpreted according with the model of hindered wobbling rotation (26). The values obtained for r_S, τ, and Δτ were used to compute: (i) the rotational correlation time (τ_R), which is inversely related to the rotational rate and reflects the local viscous resistance to the probe rotation; and (ii) the limiting anisotropy (r_∞), which is related to the order parameter S ($S2 = r_\infty/r_o$) and reflects the limitation imposed by the local environment to the extent or range of the probe wobbling. τ_R was obtained from the positive solution of Equation 1:

$$0 = A\,\tau_R^2 + B\,\tau_R + C \qquad [1]$$

where,

$$A = \Delta\tau\,[\,\omega^2\,\tau^2\,(1 + 2\,r_o)\,(1 - r_o) + (1 + 2\,r_S)\,(1 - r_S)\,] - 3\tau\,(r_o - r_S) \qquad [2]$$

$$B = \tau\,[\,2\,\Delta\tau\,(1 + 2\,r_S)\,(1 - r_S) - 3\tau\,(r_o - r_S)\,] \qquad [3]$$

$$C = \tau^2\,\Delta\tau\,(1 + 2\,r_S)\,(1 - r_S) \qquad [4]$$

where r_o is the fundamental anisotropy (0.39 for DPH and TMA-DPH) (27) and $\omega = 2\,\pi \times F$, F being the modulation frequency in hertz. r_∞ was calculated from

$$r_\infty = r_S - (r_o - r_S)\,\tau_R/\tau \qquad [5]$$

Laurdan fluorescence. Intensity and generalized polarization spectra were taken essentially with monochromator bandpasses of 8 nm in excitation and emission as previously described (28). All spectra were corrected for background contribution by subtracting the signal of unlabeled samples. An excitation wavelength of 360 nm was used for emission intensity spectra and an emission wavelength of 430 nm was used for excitation intensity spectra. Generalized polarization (GP) spectra were obtained by measuring the excitation intensity spectra using 440 nm (I_{440}) and 490 nm (I_{490}) for the emission, and the emission intensity spectra at 340 nm (I_{340}) and 410 nm (I_{410}) excitation wavelength. GP in the excitation (exGP) and emission (emGP) bands were obtained from $exGP = (I_{440} - I_{490})/(I_{440} + I_{490})$ and $emGP = (I_{410} - I_{340})/(I_{410} + I_{340})$, respectively.

RESULTS

Effect of cholesterol on microsomal lipid composition of liver. Increased ingestion of cholesterol for 21 d produced an increased content of cholesterol in the liver microsomal lipids (Table 1), as shown by Leikin and Brenner (1). However, it did not decrease either the total phospholipid percentage (Table 1) or the relative proportion of different phospholipid classes (data not shown). The ratio of microsomal lipid to protein was not significantly different (0.56 ± 0.08 for the control animal vs. 0.58 ± 0.10 for the cholesterol-treated rats).

The relative fatty acid composition by weight of total lipids in liver microsomes from cholesterol-fed rats was very different from control animals (Table 2); these results were similar to those of Leikin and Brenner (1). A decrease in palmitic and stearic acids was shown, together with a sharp

TABLE 1
Composition of Cholesterol and Total Phospholipids in Microsomal Lipids of Rat Liver After Cholesterol Feeding[a]

	Control (wt%)	Cholesterol-fed (wt%)
Cholesterol	4.84 ± 0.57	8.25 ± 1.44[b]
Total phospholipids	58.00 ± 4.15	60.78 ± 5.40

[a]Results are the mean ± SD of six animals analyzed separately.
[b]Data on cholesterol are compared to control using the Student's *t* test $P < 0.001$.

TABLE 2
Effect of Cholesterol on Fatty Acid Composition (wt%) of Fatty Acids of Total Microsomal Lipids

Fatty acids	Control	Cholesterol	*P*
16:0	14.96 ± 2.14	12.42 ± 0.83	<0.01
16:1n-7	0.48 ± 0.40	1.10 ± 0.55	<0.05
18:0	20.19 ± 3.07	13.80 ± 1.66	<0.001
18:1n-9	9.94 ± 1.74	19.27 ± 2.27	<0.001
18:2n-6	14.46 ± 1.62	16.49 ± 1.22	<0.01
20:3n-9	1.12 ± 1.02	1.56 ± 0.51	
20:3n-6	1.07 ± 0.74	2.32 ± 0.47	<0.005
20:4n-6	24.46 ± 2.40	21.26 ± 1.86	<0.01
22:4n-6	3.27 ± 2.74	3.49 ± 0.68	
22:4n-3	4.22 ± 1.22	4.29 ± 0.57	
22:5n-3	1.27 ± 0.96	1.42 ± 0.25	
22:6n-3	4.56 ± 2.43	2.59 ± 0.63	<0.05

[a]Only principal fatty acids were considered. Data are the mean of eight animals ± SD of the mean.

increase in oleic acid that correlates with the enhancement of the Δ9 desaturase activity already shown in other works (1,9). An increase in linoleic acid and a decrease in arachidonic acid, essential n-6 fatty acids, and a decrase in docosahexaenoic acid of n-3 family would be in accordance with the experimentally determined decrease of Δ6 and Δ5 desaturase activities, which diminish their biosynthesis, as shown by Leikin and Brenner (1,2).

The effect of cholesterol diet on fatty acid composition of microsomal PC (Fig. 1) follows a similar pattern to total lipid fatty acids (Table 2). A decrease in palmitic and stearic acids, which are substrates of the Δ9 desaturase, and an increase in palmitoleic and oleic acids, their enzymatic products, were shown. Similarly to Table 2, an increase in linoleic acid and a decrease in arachidonic acid (which is the product of Δ6 and Δ5 desaturation of linoleic acid) were found along with a decrease of docosahexaenoic n-3 acid.

Effect of cholesterol on microsomal PC molecular species. The application of the method of Brouwers *et al.* (17) to separate molecular species of microsomal PC gave a very good resolution and quantification for them. Eleven major peaks were separated and identified for the control animals and 12 for the cholesterol-fed rats (Fig. 2). The distribution by weight percentage of the molecular species of PC is given in Table 3. As expected, no fully saturated species were detected. The majority of the species were constituted by saturated and unsaturated acids and even some of them by two unsaturated acids. The major species found were 18:0/20:4, 16:0/20:4, and 16:0/18:2, which are in accordance with the fatty acid composition of PC (Fig. 1). The same predominance was found in the PC of other liver and kidney organelles such as the nucleus (Ves Losada, A., Maté, S.M., and Brenner, R.R., unpublished data). Therefore, we must admit that these three molecular species, and mainly 18:0/20:4, are the ones that particularly determine the contribution of PC molecules to the biophysical properties and structure of the phospholipid bilayer in liver microsomes of animals fed a corn-oil diet. Undoubtedly, they also determine possibly important membrane points susceptible to oxidation.

The effect of cholesterol feeding, as expected produced on the PC composition (Fig. 1), an important change not only in the proportion of the different molecular species but also an indication of an interchange of the components.

The decrease of arachidonic acid biosynthesis from linoleic acid (1,2) evoked by cholesterol feeding would apparently explain the notable decrease of the 18:0/20:4 molecular species and the lesser decrease in 16:0/20:4, also favored by the decrease of 16:0 and 18:0, substrates of the increased Δ9 desaturase.

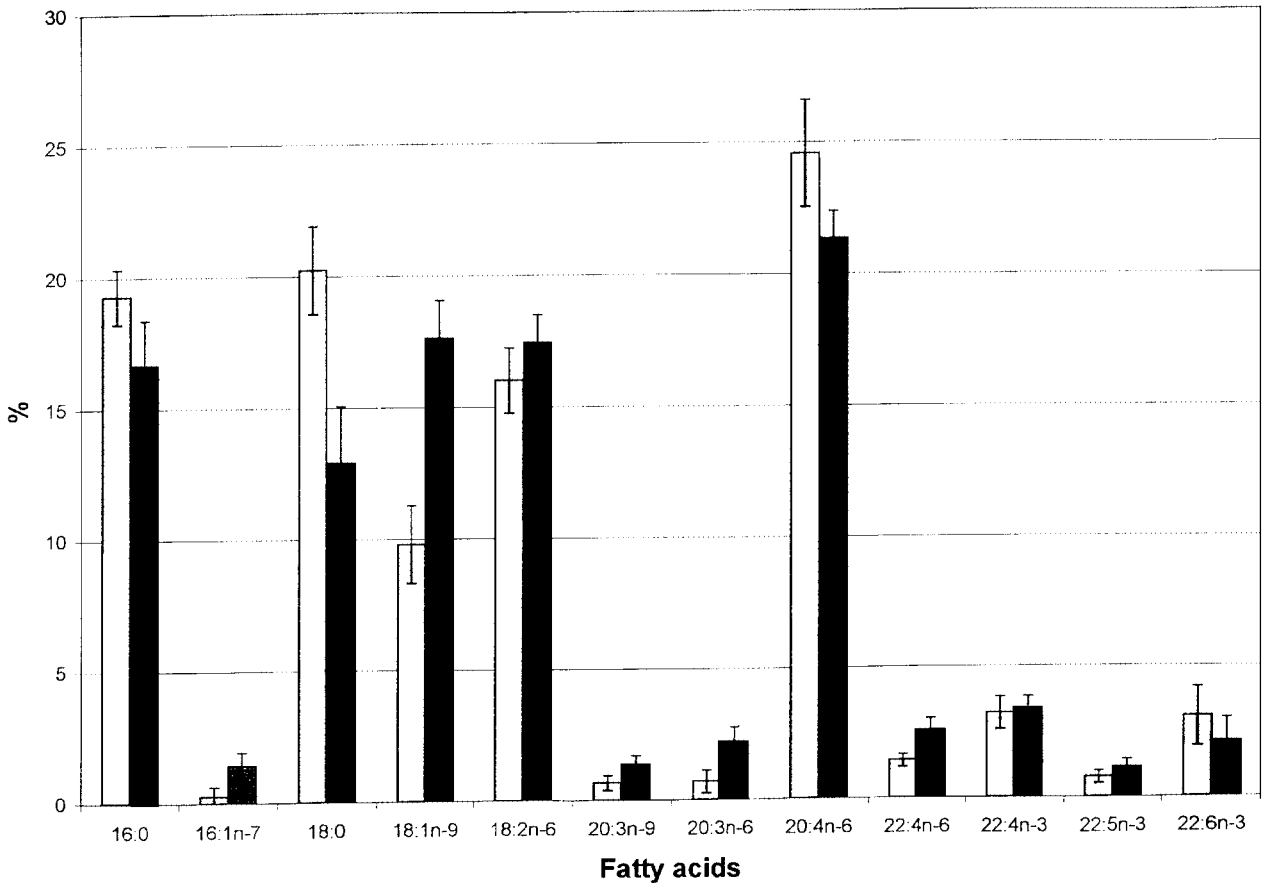

FIG. 1. Fatty acid composition (wt%) of rat liver microsomal phosphatidylcholine (PC). Results are the average of six animals analyzed individually ± SD. Open bars correspond to control animals; black bars, to cholesterol-fed rats.

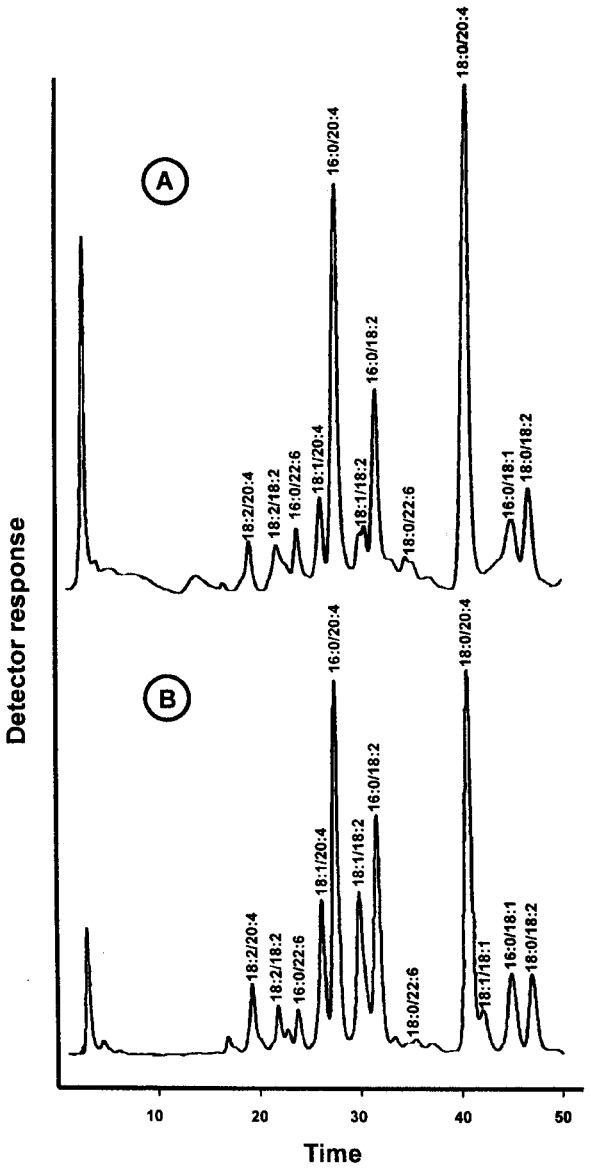

FIG. 2. High performance liquid chromatogram of PC molecular species carried out as explained in the Experimental Procedures section in two Lichrosphere 100-RP 18 columns. Peaks separated and identified by gas–liquid chromatography. (A) Control; (B) cholesterol-treated. For abbreviation see Figure 1.

However, the small increase in the minor species 18:2/20:4 and 18:1/20:4 could be due to the enhancement of 18:2 and 18:1 components as a consequence of the decrease of Δ6- and increase of Δ9-desaturase activities (1,2). It is also notable that 16:0/18:2 species did not change, probably owing to the compensatory effects of the 16:0 decrease and 18:2 increase in cholesterol-treated rats. The decrease in docosahexaenoic n-3 acid biosynthesis could be the cause of a major decrease in the 18:0/22:6 molecular species and the smaller one in 16:0/22:6.

The increase in Δ9 desaturase (1,9) evoked by the cholesterol administration enhanced not only the18:1-containing species 18:1/20:4, 18:1/18:2, and 16:0/18:1 but also the appearance of a new 18:1/18:1 molecular species. These changes produced compensation and stability of phospholipid liposome fluidity, matter that will be discussed later.

TABLE 3
Distribution by Weight Percentage of Phosphatidylcholine Molecular Species of Control and Cholesterol-Fed Rats

Molecular species	Control	Cholesterol	*P*
18:2/20:4	2.03 ± 0.81	4.31 ± 0.90	<0.001
18:2/18:2	1.58 ± 0.73	2.66 ± 0.94	<0.05
16:0/22:6	3.03 ± 1.24	2.51 ± 0.82	
18:1/20:4	3.87 ± 1.60	8.74 ± 1.41	<0.001
16:0/20:4	18.68 ± 2.36	16.41 ± 1.32	<0.05
18:1/18:2	5.13 ± 2.13	12.24 ± 1.70	<0.001
16:0/18:2	15.73 ± 2.93	15.75 ± 2.86	
18:0/22:6	3.00 ± 1.83	0.78 ± 0.72	<0.01
18:0/20:4	32.56 ± 3.53	20.11 ± 5.24	<0.001
18:1/18:1	0.00 ± 0.00	2.40 ± 1.99	<0.01
16:0/18:1	5.53 ± 0.60	7.29 ± 0.90	<0.001
18:0/18:2	8.86 ± 2.14	6.80 ± 1.14	<0.05

[a]Molecular species were separated and quantified by high-performance liquid chormatography as described in the Experimental Procedures section. Results represent the average of seven animals ± SD of the mean.

Although 18:0/20:4, 16:0/20:4, and 16:0/18:2 are still the predominant PC molecules in cholesterol-treated rats, 18:1/18:2 and to a lesser extent 18:1/20:4 and 16:0/18:1 species also play an important role in the contribution of PC to the properties and structure of the lipid bilayer.

Packing changes produced by diet in the cholesterol-containing and pure phospholipid liposomes of microsomal membranes studied by fluorometric methods. The influence of dietary cholesterol on the lipid bilayer dynamical properties was studied by measuring the dipolar relaxation of Laurdan and the rotational diffusion of DPH and TMA-DPH, which test different zones of the bilayer. With the aim of distinguishing between the specific effect of cholesterol content and that of the change in the phospholipid acyl chain composition, these measurements were made in large unilamellar vesicles composed of total microsomal lipids and in those composed of only microsomal phospholipids.

The effects of Laurdan on the fluorescence excitation and emission spectra of both types of vesicles are shown in Figure 3. No large differences were found in the excitation spectra. In contrast, the emission spectrum, which is very sensitive to the acyl chain packing, is significantly changed by the treatment in total microsomal vesicles. In these vesicles, dietary cholesterol evoked an increase in the blue-shifted unrelaxed emission at 440 nm. The blue-shifted emission, however, disappears almost completely in the vesicles made with only microsomal phospholipids, and no large effect is observed after the treatment. These Laurdan spectral changes can be quantified by the GP parameter calculated as explained in the Experimental Procedures section. GP spectra are shown in Figure 4. On the excitation band, the GP calculated between emission wavelengths of 440 and 490 nm is increased by the dietary cholesterol in the total lipid vesicles. In the cholesterol-free phospholipid vesicles, the GP values are much

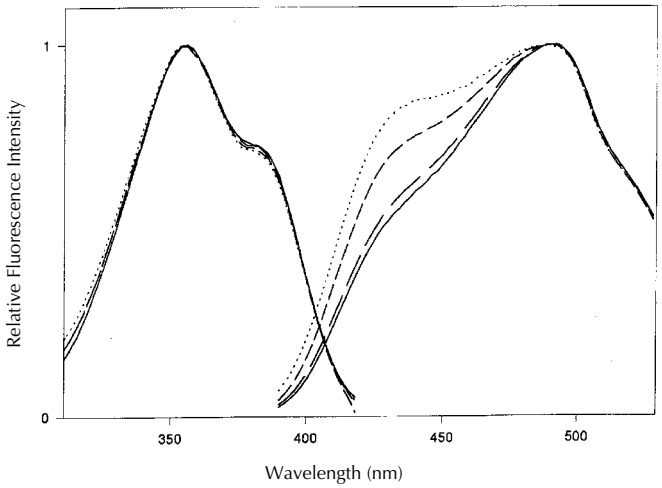

FIG. 3. Normalized excitation and emission fluorescence spectra of 6-lauroyl-2,4-dimethylaminonaphthalene (Laurdan) in unilamellar vesicles of microsomal phospholipids of control (——) and treated (— —) rats, and unilamellar vesicles of total microsomal lipids of control (– – –) and treated (·····) rats.

lower, and only a small increase in GP is observed for the phospholipid vesicles of treated microsomes with respect to the controls.

Thus, the effect of dietary cholesterol on lipid packing is mainly due to changes in the cholesterol content, and only a small effect is due to the change produced in the fatty acid composition.

Additional information on the lipid bilayer dynamical properties was obtained by studying the rotational diffusion of the neutral probe DPH, which locates deep in the bilayer, as well as of the charged TMA-DPH, which is anchored to the polar interface. These results are shown in Table 4. The steady-state anisotropy (r_s) of DPH is increased in the vesicles of total microsomal lipids of rats fed the cholesterol-rich diet. This is in accordance with previous results of Leikin and Brenner (1). Complete information on the probe rotational behavior cannot be obtained from the r_s parameter alone, since it depends on the fluorescence lifetime and is affected by both the rate and extension of the rotation. Additional lifetime and differential polarized phase measurements allow to one calculate the correlation time (τ_r), which is inversely related to the rotational rate, and the limiting anisotropy (r_∞), which is related to the wobbling extension and therefore to the membrane order. The influence of dietary cholesterol on the behavior of DPH in total lipid vesicles is mainly due to a change in the wobbling extension as indicated by marked changes in the r_∞ parameter. The rate of DPH rotation is also slowed by dietary cholesterol as shown by the change of the correlation time. DPH r_s is lower in the cholesterol-free phospholipid vesicles and in this case, on the contrary, no effect of diet is observed. The r_∞ and τ_r were also maintained in the phospholipid liposomes in spite of the change of diet.

Contrary to DPH, the r_s of the TMA-DPH probe is not changed by dietary cholesterol in other total lipid liposomes on phospholipid liposomes. The differential polarized phase measurements, however, indicated that a significant increase in TMA-DPH r_∞ is produced by the cholesterol diet only in total lipids.

Not only fluorescence lifetime is necessary to allow the calculation of the rotational parameters, but also it can inform on the probe environment polarity and water penetration into the

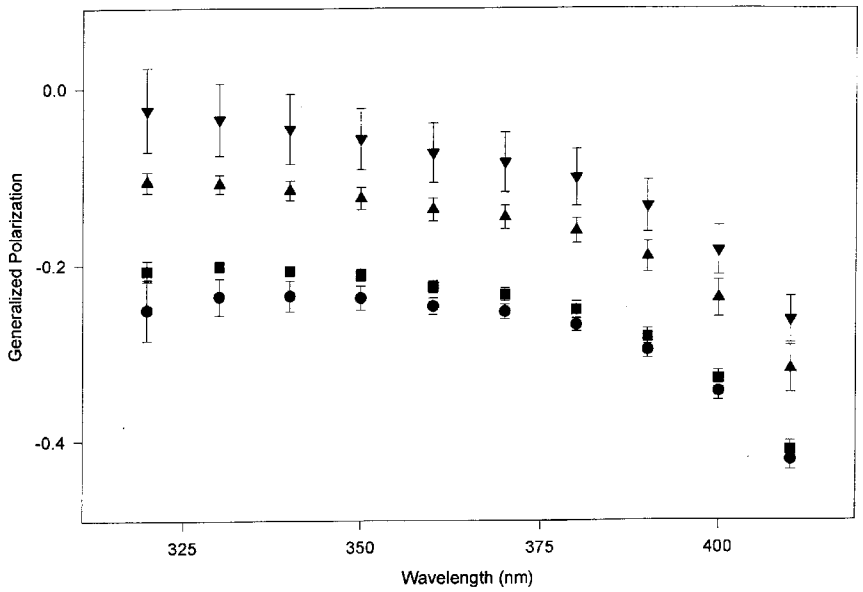

FIG. 4. Generalized polarization along the excitation band of Laurdan fluorescence in unilamellar vesicles of microsomal phospholipids of control (●) and treated (■) rats, and unilamellar vesicles of total microsomal lipids of control (▲) and treated (▼) rats. See Figure 3 for abbreviation.

TABLE 4
Effect of Dietary Cholesterol on the Lifetime and Rotational Parameters of DPH and TMA-DPH in Unilamellar Vesicles of Phospholipids and Total Lipids of Rat Liver Microsomes

		DPH				TMA-DPH			
Samples		r_S[a]	τ_P (ns)	τ_R (ns)	τ_∞	r_S[a]	τ_P (ns)	τ_R (ns)	τ_∞
Phospholipids	Controls (1)	0.066 ± 0.002	7.23 ± 0.08	1.00 ± 0.03	0.021 ± 0.002	0.192 ± 0.005	2.93 ± 0.10	1.39 ± 0.10	0.098 ± 0.012
	Treated (2)	0.069 ± 0.003	6.78 ± 0.08	1.03 ± 0.05	0.020 ± 0.002	0.197 ± 0.005	2.80 ± 0.05	1.46 ± 0.07	0.096 ± 0.008
Total lipids	Controls (3)	0.079 ± 0.005	7.27 ± 0.24	1.04 ± 0.05	0.034 ± 0.006	0.194 ± 0.008	3.49 ± 0.07	1.44 ± 0.19	0.113 ± 0.021
	Treated (4)	0.090 ± 0.003	7.02 ± 0.24	1.15 ± 0.02	0.041 ± 0.003	0.200 ± 0.008	3.40 ± 0.12	1.27 ± 0.12	0.134 ± 0.013
Statistics[b]	1 vs. 2	n.s.	$P < 0.01$	n.s.	n.s	n.s.	n.s.	n.s.	n.s.
	3 vs. 4	$P < 0.05$	n.s.	$P < 0.01$	n.s	n.s	n.s	n.s	$P < 0.05$
	1 vs. 3	$P < 0.01$	n.s.	n.s.	$P < 0.05$	n.s.	$P < 0.001$	n.s.	n.s.
	2 vs. 4	$P < 0.001$	n.s.	$P < 0.01$	n.s.	$P < 0.01$	$P < 0.05$	$P < 0.05$	$P < 0.01$

[a]Data are the mean ± standard deviation of four samples. Data were obtained from measurements at 18 MHz. Similar results were obtained at 30 MHz modulation frequency.
[b]Significance levels obtained from unpaired (1 vs. 2 and 3 vs. 4) and paired (1 vs. 3 and 2 vs. 4) Student's *t*-test. DPH, 1,6-diphenyl-1,3,5-hexatriene; TMA-DPH, 1-(4-trimethylammoniumphenyl)1-6-phenyl-1,3,5-hexatriene.

lipid bilayer. DPH lifetime is only slightly decreased by dietary cholesterol. However, after cholesterol elimination, DPH lifetime is notoriously shorter in the microsomal phospholipid vesicles of animals treated with the cholesterol-rich diet. This indicates that changes in fatty acid composition produced by treatment resulted in a more polar environment for DPH in the phospholipid vesicles. This fact may be a consequence of packing defects that allow an increased water penetration in the bilayer interior. However, when cholesterol is present, it would eliminate them by decreasing water penetration. In the case of the externally located TMA-DPH probe, the fluorescence lifetime is significantly shorter in the phospholipid vesicles than in the total lipid ones, showing the sealing effect of cholesterol against water penetration. However, in contrast to DPH, no dietary effect and therefore no molecular species change were observed on the TMA-DPH lifetime.

DISCUSSION

The ingestion by the rate of 1% dietary cholesterol evokes in the rat its incorporation into the animal's tissue including liver microsomes (Table 1), a well-documented increase in microsomal Δ9 desaturation of fatty acids, and a decrease of Δ6- and Δ5-desaturase activity (1–3,9). Whereas Leikin and Brenner (1,2) suggested the increase of Δ9 desaturation of fatty acids was the consequence of the increased packing produced by the cholesterol incorporation to the membrane, Landau *et al.* (9) presented data showing that the stearoyl-CoA desaturase RNA increases, to some extent, before the microsomal cholesterol incorporation into microsomes. This effect was investigated during short periods of time (up to 7 d), and results indicated that the enzyme synthesis was modified at the beginning of the event, in part as a result of an increase of the transcription rate as discussed by the authors (9). This result did not discard the possibility that a later viscotropic regulation of desaturase activity might be exerted by the incorporation of cholesterol to the microsomal membrane. Moreover, this fact has been shown to be produced on the Δ9 desaturase by *in vitro* incorporation of cholesterol into microsomes (7) and into other microsomal enzymes (5–8). Besides, the effect of a downward shift of temperature on membrane fluidity may be the triggering cause for the activity change in desaturase genes (29).

Ntambi (30) recently indicated that the transcriptional activation of genes containing sterol-responsive element (SRE) is under the regulation of sterols through modulation of the proteolytic maturation of the SRE-binding proteins (SREBP-1 and SREBP-2). In sterol-rich cells, proteolytic cleavage of SREBP inserted in the endoplasmic reticulum to the N-terminal mature polypeptide form does not take place. Therefore, its entrance to the nucleus, its binding to the SRE, and the activation of the Δ9 desaturase are avoided. This conclusion is deduced from cell studies (31). These interesting and important *in vitro* results do not agree with the *in vivo* results already cited (1–3,9) showing that dietary cholesterol activates the Δ9 desaturation. Therefore, more investigation on this subject is necessary to elucidate the cause for this apparent discrepancy and the possible direct or indirect effect of microsomal cholesterol on the membrane-bound Δ9 desaturase.

In fact, whichever mechanism is evoked upon Δ9-, Δ6-, and Δ5-desaturase activities by cholesterol ingestion, the fatty acid composition of the total lipids of liver microsomes is changed (Table 2) in such a way that it correlates with an increase of Δ9-desaturase activity and with a decrease in Δ6- and Δ5-desaturase activities, as shown experimentally (1–3,9). The amount of Δ9-desaturase substrates, 16:0 and 18:0, is decreased, whereas the amount of products, 18:1 and 16:1, is increased. Correspondingly, the amount of Δ6 desaturase substrate, linoleic acid, is increased whereas the amount of products of Δ6 and Δ5 desaturases, arachidonic and docosahexaenoic acids, is decreased. As expected, similar results are shown in the fatty acid composition of the microsomal PC (Fig. 1).

These effects on fatty acid composition, produced by a cholesterol-rich diet, of liver total microsomal lipids and PC

are apparently general since they have already been found by Veno and Okuyama in total liver and plasma (32). It is difficult to suppose that these changes might be due to the movement of lipids between organelles. Moreover, since the fatty acid composition of control and cholesterol-fed rats is the same from our point of view, the more plausible cause for the fatty acid changes is the modification of the desaturase activity already demonstrated (1–3,9). Of course, not all lipid classes and not all organs will show identical change. The possible effect of fatty acid capture by esterification to cholesterol as well as of specificity of enzymes involved in different phospholipid synthesis and retailoring and even fatty acid oxidation may also alter the final composition of the phospholipid species and PC molecular species.

PC is the principal phospholipid of liver endoplasmic reticulum. PC coerces other lipids into a bilayer structure and is a major determinant of the biophysical properties of phospholipid bilayers. Moreover, since the proportion of phospholipid classes was not changed in the present experiment due to the cholesterol diet, we may admit that the changes of PC composition would reflect, in some way, the biophysical changes of the phospholipidic part of the microsomal membrane.

After 21 d of the cholesterol diet, the composition of the molecular species of liver microsomal PC had reached an equilibrium, and the liver microsomal membrane had been adapted to the new situation. The following phenomena were produced in the membrane: (i) the incorporation of cholesterol increased the packing of the microsomal membrane, shown by an increase in the GP of Laurdan-labeled microsomal lipids (Fig. 4) and in the fluorescence r_∞ of DPH and TMA-DPH labeled ones (Table 4); (ii) there was a decrease in the Δ6 and Δ5 fatty acid desaturation and an increase of Δ9 desaturation, which is already well-documented (1–3,9); and (iii) there was a change of the relative ratios of palmitic, stearic, oleic, linoleic, arachidonic, and docosahexaenoic acids in phospholipid molecules like PC. These changes modified the proportion of PC molecular species. However, these changes were produced in such a way that the fluidity of the phospholipidic part of the membrane was roughly maintained, as shown by the fluorescence properties of Laurdan (Figs. 3 and 4), DPH, and TMA-DPH (Table 4).

The decrease in arachidonic acid (Fig. 1) led to a decrease mainly in the 18:0/20:4 PC molecular species, but also to a lesser extent in 16:0/20:4 that is more fluid. The 16:0/20:4 species is more fluid since it shows less rotational correlation and fluorescence anisotropy of DPH-labeled species as shown by Tricerri *et al.* (20) and Garda *et al.* (33). It also correlates with a decrease in saturated fatty acids, especially stearic acid. However, the even more fluid 18:2/20:4 species increased, along with the 18:2/18:2 species, which corresponds to an enhancement of 18:2n-6 acid (Fig. 1). Linoleic acid was fully provided by the diet, and the cholesterol diet decreased its conversion to arachidonic acid.

In this way, the effect of the decrease of highly polyunsaturated fatty acid-containing species on phospholipid membrane rigidity has been reduced to a minimum. It is even better compensated by the increase of oleic acid-containing species 18:1/20:4, 18:1/18:2, 16:0/18:1, and the appearance of a new species of 18:1/18:1 (Table 3).

As it is known, whereas saturated acids produce less fluid phospholipids with increasing chain length (20,33), polyunsaturated acids evoke only slightly more fluid liposomes than monounsaturated ones (34). Therefore, the substitution of 20:4-containing species by 18:1-containing species nearly compensates for the fluidizing effect. These results are similar to ones found in the molecular species of all phosphoglycerides of hepatic microsomal lipids of rats fed on a fat-free diet (33). Although the effect in this case was due not to cholesterol but to a dietary deficiency of fats that evoked an essential fatty acid-deficient status, the change in the availability of fatty acids to build up the membrane phospholipids was rather similar. There was an increase of oleic acid and palmitic acid and a decrease of arachidonic, stearic and obviously and differentially, linoleic acid. The eicosatrienoic n-9 acid was also enhanced by an increased biosynthesis. The distribution of the resulting molecular species was similar to the cholesterol effect, and it showed an important decrease of the 18:0/20:4n-6 species and a lesser one for 16:0/20:4n-6. Both were the major molecular species found in PC. In compensation, 16:0/18:1, 16:0/20:3n-9, and 18:0/20:3n-9 species were increased. The final result was that this molecular compensation in the phosphoglycerides in fact avoided a change in the packing of the microsomal phospholipid bilayer measured by fluorescent methods and it was similar to our actual case.

The change in the fatty acid composition found in the PC molecular species (Table 3) indicates that the type and proportion of the fatty acids at both the *sn*-1 and *sn*-2 positions had been altered. This is a consequence not only of the availability of different fatty acids but also of the changes in the specific activity of enzymes involved in PC biosynthesis. A re-tailoring process was produced; and a deacylation-reacylation at carbon *sn*-2 through a phospholipase A_2 and an acyltransferase known as Lands pathway (35) is apparent. Remodeling of PC molecular species at the *sn*-1 position of glycerol (36) also takes place. Moreover, the contribution of a *de novo* synthesis of phospholipids is also important considering especially the change in the proportion and type of fatty acids at the *sn*-1 position. The profile of PC species might also be influenced by different types of pathways of synthesis such as the phosphatidylethanolamine methylation.

In conclusion, we suggest that the re-tailoring of PC, as well as other phosphoglyceride molecular species, evoked by a high-cholesterol diet was able to nearly maintain the liquid-crystalline structure and bulk fluidity of the phospholipidic part of the microsomal membrane. However, it was unable to compensate for the striking packing effect produced by the incorporation of cholesterol molecules in the membrane.

Although the bulk average biophysical properties of the phospholipidic part of the microsomal membrane did not change, we found different molecular phospholipidic composition that un-

doubtedly alters other microscopic properties of the membrane, e.g., its chemical reactivity and possibly the interaction with proteins. The substitution, in part, of arachidonic and docosahexaenoic acid PC-containing species for oleic and linoleic-containing species evoked by cholesterol diet decreases the density of double bonds in the proximity of the membrane border, modifies the position and number of the clouds of polarizable π electrons surrounding the double bonds, and alters possible effects on membrane bound proteins. However, the most important effect produced by the fall in the amount of molecular species containing arachidonic and docosahexaenoic acids is the decrease of the endogenous source of these acids for their specific functions in brain and retina, as well as the activation of nuclear receptors, synthesis of eicosanoid, hepoxiline and lipoxine, etc.

ACKNOWLEDGEMENTS

This work was supported by grants from CONICET and CIC, Argentina. The authors are grateful to Laura Hernández for her technical assistance.

REFERENCES

1. Leikin, A.I., and Brenner, R.R. (1987) Cholesterol-Induced Microsomal Changes Modulate Desaturase Activities, *Biochim. Biophys. Acta. 922*, 294–303.
2. Leikin, A.I., and Brenner, R.R. (1988) *In vivo* Cholesterol Removal from Liver Microsomes Induces Changes in Fatty Acid Desaturase Activities, *Biochim. Biophys. Acta. 963*, 311–319.
3. Garg, M.L., Snowswell, A.M., and Sabine, J.R. (1986) Influence of Dietary Cholesterol on Desaturases Enzymes of Rat Liver Microsomes, *Prog. Lipid Res. 25*, 639–644.
4. Castuma, C.E., Brenner, R.R., De Lucca-Gattás, E., Schreier, S., and Lamy-Freund, T.M. (1991) Cholesterol Modulation of Lipid-Protein Interactions in Liver Microsomal Membrane. A Spin Label Study, *Biochemistry. 30*, 9492–9497.
5. Castuma, C.E., and Brenner, R.R. (1986) Effect of Dietary Cholesterol on Microsomal Membrane Composition, Dynamics and Kinetic Properties of UDP-Glucuronyl Transferase, *Biochim. Biophys. Acta. 855*, 231–242.
6. Castuma, C.E., and Brenner, R.R. (1989) The Influence of Fatty Acid Unsaturation and Physical Properties of Microsomal Membrane Phospholipids on UDP-Glucuronyl Transferase Activity, *Biochem. J. 258*, 723–731.
7. Garda, H.A., and Brenner, R.R. (1985) *In vitro* Modification of Cholesterol Content of Rat Liver Microsomes. Effect upon Membrane "Fluidity" and Activities of Glucose-6-phosphatase and Fatty Acid Desaturation System, *Biochim. Biophys. Acta. 819*, 45–54.
8. Garda, H.A., and Brenner, R.R. (1984) Short Chain Aliphatic Alcohols Increase Rat Liver Microsomal Membrane "Fluidity" and Affect the Activities of Some Microsomal Membrane Bound Enzymes, *Biochim. Biophys. Acta. 769,* 141–153.
9. Landau, J.M., Sekowski, A., and Hamm, M.W. (1997) Dietary Cholesterol and the Activity of Stearoyl-CoA Desaturase in Rats: Evidence for an Indirect Regulatory Effect, *Biochim. Biophys. Acta. 1345*, 349–357.
10. Rogers, G.R., and Harper, A.E. (1965) Amino Acid Diets and Maximal Growth in the Rat, *J. Nutr. 87*, 267–273.
11. Catalá, A., Nervi, A.M., and Brenner, R.R. (1975) Separation of a Protein Factor Necessary for the Oxidative Desaturation of Fatty Acids in the Rat, *J. Biol. Chem. 250*, 7481–7484.
12. Lowry, O.H., Rosebrough, N.J., Farr, A.L., and Randall, R.J. (1951) Protein Measurement with Folin Phenol Reagent, *J. Biol. Chem. 193*, 265–275.
13. Folch, J., Lees, M., and Sloane-Stanley, G.R. (1957) A Simple Method for the Isolation and Purification of Total Lipids from Animal Tissues, *J. Biol. Chem. 226*, 497–509.
14. Huang, T.C., Chen, C.P., Wefler, V., and Raftery, A. (1961) A Stable Reagent for the Lieberman-Buchard Reaction. Application to Rapid Serum Cholesterol Determination, *Anal. Chem. 33*, 1405–1406.
15. Chen, P.S., Toribara, T., and Warner, H. (1956) Microdetermination of Phosphorus, *Anal. Chem. 28*, 1756–1758.
16. Letter, W.S. (1992) A Rapid Method for Phospholipid Class Separation by HPLC Using an Evaporative Light-Scattering Detector, *J. Liq. Chromatogr. 15*, 253–266.
17. Brouwers, J.F.H.M., Gadella, B.M., Lambert, M.G., van Golde, L.M.G., and Tielens, A.G.M. (1998) Quantitative Analysis of Phosphatidylcholine Molecular Species Using HPLC and Light-Scattering Detection, *J. Lipid Res. 39*, 344–353.
18. Lakowicz, J.R., Prendergast, F.G., and Hogen, D. (1979) Differential Polarized Phase Fluorometric Investigations of Diphenylhexatriene in Lipid Bilayers. Quantitation of Hindered Depolarizing Rotations, *Biochemistry 18*, 508–519.
19. Lakowicz, J.R. (1983) *Principles of Fluorescence Spectroscopy*, pp. 51–91, Plenum Press, New York.
20. Tricerri, M.A., Garda, H.A., and Brenner, R.R. (1994) Lipid Chain Order and Dynamics at Differential Bilayer Depths in Liposomes of Several Phosphatidyl Cholines Using Differential Polarized Phase Fluorescence, *Chem. Phys. Lipids. 71*, 61–72.
21. Garda, H.A., Bernasconi, A.M., and Brenner, R.R. (1994) Possible Compensation of Structural and Viscotropic Properties in Hepatic Microsomes and Erythrocyte Membranes of Rats with Essential Fatty Acid Deficiency, *J. Lipid Res. 35*, 1367–1377.
22. Rodríguez, S., Garda, H.A., Heinzen, H., and Moyna, P. (1997) Effect of Plant Monofunctional Pentacyclic Triterpenes on the Dynamic and Structural Properties of Dipalmitoyl Phosphatidyl Choline Bilayers, *Chem. Phys. Lipids 89*, 119–130.
23. Spencer, R.D., and Weber, G. (1970) Influence of Brownian Rotations and Energy Transfer Upon the Measurements of Fluorescence Lifetime, *J. Chem. Phys. 52*, 1654–1663.
24. Lakowicz, J.R., Cherek, H., and Bevan, D.R. (1980) Demonstration of Nanosecond Dipolar Relaxation in Biopolymers by Inversion of the Apparent Fluorescence Phase Shift and Demodulation Lifetimes, *J. Biol. Chem. 255*, 4403–4406.
25. Lakowicz, J.R., and Cherek, H. (1988) Dipolar Relaxation in Proteins on the Nanosecond Timescale Observed by Wavelength Resolved Phase Fluorometry of Tryptophan Fluorescence, *J. Biol.Chem. 255*, 831–834.
26. Weber, G. (1978) Limited Rotational Motions: Recognition by Differential Phase Fluorometry, *Acta Phys. Pol. A 54*, 173–179.
27. Garda, H.A., Bernasconi, A.M., and Brenner, R.R. (1994) Influence of Membrane Proteins on Lipid Matrix Structure and Dynamics. A Differential Polarized Phase Fluorometry Study in Rat Liver Microsomes and Erythrocyte Membranes, *An. Asoc. Quím. Argent. 82*, 305–323.
28. Garda, H.A., Bernasconi, A.M., Aguilar, F., Soto, M.A., and Sotomayor, C.P. (1997) Effect of Polyunsaturated Fatty Acid Deficiency on Dipole Relaxation in the Membrane Interface of Rat Liver Microsomes, *Biochim. Biophys. Acta. 1323*, 97–104.
29. Los, B.A., and Murata, N. (1998) Structure and Expression of Fatty Acid Desaturases, *Biochim. Biophys. Acta. 1394*, 3–15.
30. Ntambi, J.M. (1999) Regulation of Stearoyl-CoA Desaturase by Polyunsaturated Fatty Acids and Cholesterol, *J. Lipid Res. 40*, 1549–1558.
31. Tabor, D.E., Kim, J.B., Spiegelman, B.M., and Edwards, P.A. (1998) Transcriptional Activation of the Stearoyl-CoA Desat-

urase-2 Gene by Sterol Regulatory Element Binding Protein/Adipocyte Determination and Differentiation Factor, *J. Biol. Chem. 273*, 22052–22058.
32. Veno, K., and Okuyama, H. (1986) A High Cholesterol/Cholate Diet Induced Fatty Liver in Spontaneously Hypertensive Rats, *Lipids 21*, 475–480.
33. Garda, H.A., Bernasconi, A.M., Tricerri, M.A., and Brenner, R.R. (1997) Molecular Species of Phosphoglycerides in Liver Microsomes of Rats Fed a Fat-Free Diet, *Lipids 32*, 507–513.
34. Stubbs, C.D., and Smith, A.D. (1984) The Modifications of Mammalian Membrane Polyunsaturated Fatty Acid Composition in Relation to Membrane Fluidity and Function, *Biochim. Biophys. Acta. 779*, 89–137.
35. Mac Donald, J.I.S., and Sprecher, H. (1991) Phospholipid Fatty Acid Remodeling in Mammalian Cells, *Biochim. Biophys. Acta 1084*, 105–121.
36. Schmid, P.C., Spimrova, I., and Schmid, H.H.O. (1997) Generation and Remodeling of Highly Polyunsaturated Molecular Species of Rat Hepatocyte Phospholipids, *Lipids 32*, 1181–1187.

[Received March 27, 2000, and in revised form October 2, 2000; revision accepted October 16, 2000]

Effect of Medium-Chain Fatty Acid Positional Distribution in Dietary Triacylglycerol on Lymphatic Lipid Transport and Chylomicron Composition in Rats

Octavio Carvajal[a], Masahiro Nakayama[a], Taiji Kishi[a], Masao Sato[a], Ikuo Ikeda[a], Michihiro Sugano[b], and Katsumi Imaizumi[a,*]

[a]Laboratory of Nutrition Chemistry, Division of Bioresource and Bioenvironmental Sciences, Graduate School, Kyushu University, Fukuoka 812-8581, Japan, and [b]Kumamoto Prefecture University, Kumamoto, Japan

ABSTRACT: The present study was carried out to examine if the positional distribution of medium-chain fatty acid (MCF) in dietary synthetic fat influences lymphatic transport of dietary fat and the chemical composition of chylomicrons in rats with permanent cannulation of thoracic duct. Four types of synthetic triacylglycerol were prepared: (i) *sn*-1(3) MCF-*sn* 2 linoleic acid, (ii) interesterified *sn*-1(3) MCF-*sn* 2 linoleic acid, (iii) *sn*-2 MCF-*sn*-1(3) linoleic acid, and (iv) interesterified *sn*-2 MCF-*sn*-1(3) linoleic acid. A purified diet composed of equal amounts of the synthetic fat and cocoa butter was given to rats with permanent lymph duct cannulation. The positional distribution of MCF in the dietary fat had no significant effect on the lymph flow, triacylglycerol output, phospholipid output, lipid composition of chylomicrons, or the particle size. The positional distribution of MCF in the synthetic triacylglycerol was maintained in the chylomicron triacylglycerol. These results showed that MCF in the dietary triacylglycerol is transported into lymphatics and the positional distribution is well preserved in chylomicron triacylglycerol.

Paper no. L8397 in *Lipids 35,* 1345–1351 (December 2000).

Octanoic and decanoic acids are representative medium-chain fatty acids (MCF) that meet a prompt demand for energy under conditions where surgical operations are carried out and pancreatic insufficiency occurs (1,2). MCF, compared with longer-chain fatty acids, are readily absorbed through the stomach as well as intestine *via* the portal route, as they have a relatively high polarity and susceptibility to β-oxidation (1,2). MCF are included to a relatively greater extent in mammalian milk and coconut oils as a form of triacylglycerol. Synthetic fats containing MCF are now used in various fields to improve the physiological properties of MCF (3–11). Absorption of MCF seems to be better than longer-chain fatty acids, but little attention has been directed to the interactive effects of MCF on longer-chain fatty acids with regard to absorption of synthetic fats and dietary fats (6,7,12). The position of longer-chain saturated fatty acids in a triacylglycerol molecule greatly influences related intestinal absorption and consequently modifies absorption rates of other longer-chain fatty acids (13–19). The importance of the position of MCF in a triacylglycerol molecule has also been advocated by us (5) and others (6,7,9–12,20,21).

Occasionally, lymphatic transport of dietary fats in rats has been measured by infusing fat-emulsion into the stomach or duodenum (22). This method has an advantage of making the interpretation of data easy since it does not need to take the interaction of lipid emulsion with other dietary components into account. Conversely, this is a drawback of this method, since the interaction of dietary components, particularly proteins, carbohydrates, and phospholipids, which influence emulsification of dietary fats from the mouth to intestine, are not taken into consideration (23). In addition, rats used for this purpose do not always recover from surgery-related stress (24). To address these problems, permanent cannulation of the thoracic duct has been done in rats (24,25), but application of this method, to characterize the lymphatic transport of dietary lipids during active dietary fat absorption, is not widespread.

In the present studies, rats were kept on diets supplemented with structure-specific fats containing MCF either in *sn*-2 or *sn*-1(3) and their interesterified fats. The lymphatic transport of dietary fats or chemical composition of lymph chylomicrons during active absorption of these dietary fats was determined in rats with a permanent lymph duct cannulation.

MATERIALS AND METHODS

Diets. All diets were prepared, based on the AIN-93G formulation (26), as described by Ni *et al.* (27). Soybean oil (7 g/100 g diet) was used for a basal diet. Cocoa butter (10.25 g/100 g diet) plus synthetic fats (10.25 g/100 g diet) was used for an experimental diet, in order to simulate a Western diet, which provides approximately 40% energy through dietary fat. Diets were prepared once a week and stored in a pow-

*To whom correspondence should be addressed.
E-mail: imaizumi@agr.kyushu-u.ac.jp

Abbreviation: MCF, medium-chain fatty acids.

TABLE 1
Total and *sn*-2 Fatty Acid Composition of Synthetic Fats[a]

	Total fatty acids (mol/100 mol)				*sn*-2 Fatty acids (mol/100 mol)			
Fatty acids	*sn*-1(3)MCF-structured	*sn*-1(3)MCF-interesterified	*sn*-2MCF-structured	*sn*-2MCF-interesterified	*sn*-1(3)MCF-structured	*sn*-1(3)MCF-interesterified	*sn*-2MCF-structured	*sn*-2MCF-interesterified
8:0	27.5	22.7	33.8	38.0	3.5	15.0	41.3	30.4
10:0	17.6	15.7	25.0	25.3	2.4	12.8	35.4	22.8
12:0	1.3	0.2	0.5	0.3	1.0	0.2	1.0	0.5
14:0	0.0	0.1	0.4	0.1	0.0	0.3	0.5	0.2
16:0	3.7	6.8	5.6	3.7	2.3	4.0	2.7	1.9
18:0	1.2	2.3	2.2	1.3	1.5	1.6	1.4	0.9
18:1	12.7	15.3	11.5	10.9	20.0	17.6	5.0	13.1
18:2n-6	32.7	32.3	19.2	17.8	58.0	43.2	5.1	25.4
18:3	4.3	4.5	2.1	2.6	12.3	5.1	5.8	4.7

[a]Values are means of duplicate analyses. MCF, medium-chain fatty acid.

dered form at 4°C until feeding.

Unilever (Vlaardingen, The Netherlands) provided four types of synthetic fats. According to the manufacturer, two types of structure-specific fats, one predominantly composed of MCF in *sn*-1(3) and linoleic acid in *sn*-2 [*sn*-1(3)MCF-structured] or MCF in *sn*-2 and linoleic acid in *sn*-1(3) [*sn*-2MCF-structured] were initially prepared and each structure-specific fat was interesterified and designated as *sn*-1(3)MCF-interesterified or *sn*-2MCF-interesterified. *sn*-1(3)MCF type fats, compared with *sn*-2MCF type fats, contained less MCF (octanoic and decanoic acid) and more linoleic and oleic acid (Table 1). *sn*-1(3)MCF-structured fats included triacylglycerols with the following total number of carbon (C): in g/100 g, 0.9 C24–C30, 10.0 C34, 13.4 C36, 5.3 C38, 24.1 C44, 15.1 C46, and 12.5 C54. Similarly, *sn*-1(3)MCF-interesterified fats included the following triacylglycerols: 3.0 C24–C30, 8.7 C34, 9.9 C36, 3.2 C38, 25.4 C44, 13.3 C46, and 18.7 C54. Accordingly, *sn*-1(3)MCF-structured fats contained molecular species with three MCF (0.9 g/100 g), two MCF and one C18 fatty acid (28.7 g/100 g), one MCF and two C18 fatty acid (39.2 g/100 g), and three C18 fatty acid (12.5 g/100 g): molecular species corresponding to *sn*-1(3)MCF-interesterified fats were three MCF (3.0 g/100 g), two MCF and one C18 fatty acid (38.7 g/100 g), and three C18 fatty acid (18.7 g/100 g). Table 2 summarizes the fatty acid composition of the experimental diet.

Animals and permanent lymph duct cannulation. Male Sprague-Dawley rats, 8 wk old, obtained from Seiwa Experimental Animals (Fukuoka, Japan) were maintained in a temperature-controlled room. Rats were trained to consume the basal diet for 1 wk and then the experimental diet for 3 wk twice a day during 1000–1100 and 1700–1800, respectively. Deionized water was freely available throughout the feeding periods. Body weight and food intake were measured daily, and feces were collected for the last 5 d and freeze-dried.

All the rats were anesthetized with Nembutal anesthesia prior to the permanent cannulation of the thoracic duct lymph, as described (25). Briefly, a cannula (Silicon tube SH, i.d. 0.5 mm and o.d. 1.0 mm; Kaneka Medics, Osaka, Japan) filled with a heparinized saline was inserted into the thoracic duct and secured within the abdominal cavity. Following closure of the abdominal wall and tunneling of the cannula to the crown of the head of the rat, an adapter made from a 1-mL plastic syringe and placed on the cannula was filled with a polyvinyl pyrrolidone solution; a flame was then used to seal the tip of the tube. The rats were returned to their cages and

TABLE 2
Total and *sn*-2 Fatty Acid Composition of Dietary Fats[a]

	Total fatty acids (mol/100 mol)				*sn*-2 Fatty acids (mol/100 mol)			
Fatty acids	*sn*-1(3)MCF-structured + cocoa butter	*sn*-1(3)MCF-interesterified + cocoa butter	*sn*-2MCF-structured + cocoa butter	*sn*-2MCF-interesterified + cocoa butter	*sn*-1(3)MCF-structured + cocoa butter	*sn*-1(3)MCF-interesterified + cocoa butter	*sn*-2MCF-structured + cocoa butter	*sn*-2MCF-interesterified + cocoa butter
8:0	15.3	12.4	19.1	23.3	1.5	8.0	22.0	14.8
10:0	9.9	8.5	14.2	15.2	1.2	6.6	18.3	12.1
12:0	0.2	0.2	0.4	0.2	0.0	0.0	0.9	0.0
14:0	0.1	0.1	0.3	0.1	0.0	0.0	0.6	0.0
16:0	14.2	16.0	14.9	13.3	3.1	4.1	4.6	3.6
18:0	15.9	16.7	15.9	14.7	3.2	3.7	4.7	3.8
18:1	21.7	23.2	20.7	19.6	46.3	46.3	36.6	41.3
18:2n-6	20.2	19.9	13.1	11.9	35.5	24.0	5.5	15.3
18:3	2.5	2.9	1.4	1.6	9.3	7.3	6.9	9.2

[a]Values are means of duplicate analyses. See Table 1 for abbreviation.

provided the experimental diet twice a day, as described above. On the third day, the rats were attached to a long PE-cannula (i.d. 0.58 and o.d. 0.97 mm; Becton Dickinson and Company, Baltimore, MD) to collect lymph. The end of the cannula was between 5–10 cm below the bottom of the cage in order to provide sufficient underpressure to allow lymph into the cannula. The lymph was collected for 15 min and the rats were then freely given access to the experimental diet for 20 min and the lymph collection was continued for another 9 h. The rats freely consumed the deionized water during the collection of lymph. After removing fibrin, ethylenediaminetetraacetic acid at a final concentration of 0.01% was added to the lymph solutions. The portion of lymph collected between 2.33 and 6.33 h was subjected to ultracentrifugation to isolate chylomicrons at $3 \times 10^6 \times g$-av. min at 10°C, using a Beckman L5-50 ultracentrifuge (Palo Alto, CA) (28).

These experiments were carried out under the guidelines for Animal Experiment in Faculty of Agriculture and the Graduate Course, Kyushu University, Fukuoka, Japan and the Law (No. 105) and Notification (No. 6) of the Government of Japan.

Determination of chylomicron particle size. Samples of lymph chylomicrons were fixed in 20 g/L osmium tetroxide (Nisshin EM, Tokyo, Japan) and examined using a JEOL JEM-2000FXII transmission electron microscope (JEOL, Tokyo, Japan) by shadow-casting with carbon-platinum pellets as described (13). Particle diameters seen on the photographic negatives (×10,000) were measured, making use of NIH Image Software (version 1.56; National Institute of Health, Bethesda, MD). The mean diameter of the chylomicrons was estimated regarding approximately 600 particles.

Biochemical analyses. The triacylglycerol structure of dietary fats and chylomicrons was analyzed by the Grignard degradation method, as described by Ikeda *et al.* (29). Dietary fats, triacylglycerols, and 2-monoacylglycerols were transmethylated with a sulfuric acid/methanol mixture (1:115, vol/vol). To prevent losses of the highly volatile methylesters of the MCF, fatty acid methyl esters were not concentrated after the hexane extraction and before injection into the gas–liquid chromatograph. Fatty acid methyl esters were analyzed by gas–liquid chromatography, as described previously (29). Analyses were performed under the following conditions: temperature program starting at 100°C followed by 5°C/min increments until the final temperature reached 220°C; detector temperature 250°C; injector temperature 250°C; flow rate of nitrogen carrier gas 15 mL/min, with a column of 10% Silar10C, Chromosorb W (AW-DMCS) 80–100 mesh (Japan Kuromato Kogyo, Tokyo, Japan). Lipids were extracted from whole lymph and chylomicrons by the method of Folch *et al*. (30). The triacylglycerols, phospholipids, and cholesterol were measured chemically (15). Lymph cholesterol was derivatized to the trimethylsilyl ether and then quantified by gas–liquid chromatography (Shimadzu, Kyoto, Japan) with an OV-17 (GL Science, Tokyo, Japan) column (29). 5-α-Cholestane (Nacalai Tesque, Kyoto, Japan) was used as an internal standard. Chylomicron-triacylglycerols were separated by thin-layer chromatography on a precoated silica gel G plate with a developing solvent (petroleum ether/diethylether/acetic acid, 82:18:1, by vol) containing *t*-butylhydroquinone as an antioxidant (29). Fecal fats were extracted according to the method of Jeejeebhoy *et al*. (31). Briefly, 1 g of freeze-dried feces was acidified with two drops of concentrated HCl to release the free fatty acids, and extracted sequentially with solvent No. 1 and solvent No. 2. The lipid extracts were dried in a vacuum desiccator and weighed, and the apparent absorption rate (%) of dietary fat was calculated as follows: 100 × [amount of daily fatty acid intake − amount of fecal fatty acids excreted]/[amount of daily fatty acid intake].

Statistics. Data were expressed as means ± SEM and analyzed by Duncans' New Multiple range test, as described previously (27).

RESULTS

Initial body weights were 305 ± 6, 304 ± 3, 308 ± 6, and 307 ± 4 g for *sn*-1(3)MCF-structured, *sn*-1(3)MCF-interesterified, *sn*-2MCF-structured, and *sn*-2MCF-interesterified group, respectively. There were no significant differences in the body weight just prior to lymph duct cannulation among the groups: 380 ± 9, 381 ± 8, 396 ± 8, and 381 ± 11 g for *sn*-1(3)MCF-structured, *sn*-1(3)MCF-interesterified, *sn*-2MCF-structured, and *sn*-2MCF-interesterifed group, respectively. Also, there were no significant differences in the food intake among the groups: 20.3 ± 1.0, 19.2 ± 0.7, 22.0 ± 0.9, and 19.8 ± 0.8 g/d for *sn*-1(3)MCF-structured, *sn*-1(3)MCF-interesterified, *sn*-2MCF-structured, and *sn*-2MCF-interesterifed group, respectively. Fecal weight was greater for rats fed the diet containing *sn*-2 MCF-structured fat than for those fed other synthetic fats: 2.09 ± 0.14^a, 2.06 ± 0.13^a, 2.70 ± 0.11^b, and 2.02 ± 0.14^a g/d for *sn*-1(3) MCF-structured group, *sn*-1(3) MCF-interesterified group, *sn*-2 MCF-structured group, and *sn*-2 MCF-interesterified group, respectively (different superscript roman letters shows significant difference at $P < 0.05$). Apparent fat absorption rate, however, was not significantly different among the groups (91.3 ± 0.9, 91.7 ± 0.8, 89.4 ± 1.6, and 92.2 ± 1.3% for *sn*-1(3) MCF-structured group, *sn*-1(3) MCF-interesterified group, *sn*-2 MCF-structured group, and *sn*-2 MCF-interesterified group, respectively).

Differences in food intake for 20 min on the day of lymph collection were not statistically significant among the groups: 4.7 ± 0.6, 4.5 ± 0.9, 4.4 ± 0.8, and 4.9 ± 0.7 g/20 min for *sn*-1(3)MCF-structured, *sn*-1(3)MCF-interesterified, *sn*-2MCF-structured, and *sn*-2MCF-interesterified, respectively. Lymph flow rates prior to, during, and after consumption of food were similar among the groups (Fig. 1). All the rats evidently increased lymph flow at 20 min and reached a maximal level 1 h after feeding and then declined to basal levels. Consumption of different synthetic fats led to no significant effect on the flow rate, at any time point.

Lymphatic lipid (triacylglycerol, phospholipid, and cholesterol) output rate prior to food consumption was similar among the groups (Fig. 2). Triacylglycerol output rate

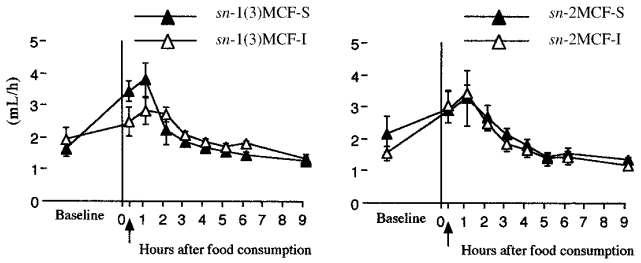

FIG. 1. Lymph flow rates in rats fed diet containing *sn*-1(3)medium-chain fatty acid (MCF)-structured plus cocoa butter [*sn*-1(3)MCF-S], *sn*-1(3)MCF-interesterified plus cocoa butter [*sn*-1(3)MCF-I], *sn*-2MCF-structured plus cocoa butter [*sn*-2MCF-S], or *sn*-2MCF-interesterified plus cocoa butter [*sn*-2MCF-I]. Arrow indicates termination of food consumption. Values are means ± SEM, $n = 6$.

reached the maximum between 2 and 4 h after food consumption, was maintained by the sixth hour, and gradually declined thereafter. There were no significant differences in triacylglycerol output rates among the four groups. Triacylglycerol mass in the lymph collected for 9.33 h after the start of food consumption did not differ significantly among the groups: 608 ± 81, 559 ± 102, 528 ± 100, and 608 ± 68 μmol/9.33 h for *sn*-1(3)MCF-structured, *sn*-1(3)MCF-interesterified, *sn*-2MCF-structured, and *sn*-2MCF-interesterified group, respectively. The pattern of phospholipid output rate was similar to that for triacylglycerol and the rate was similar among the groups. Phospholipid mass in the lymph collected for 9.33 h was also similar among the groups: 68.7 ± 4.5, 71.6 ± 7.5, 73.7 ± 8.3, and 72.7 ± 8.1 μmol/9.33 h for *sn*-1(3)MCF-structured, *sn*-1(3)MCF-interesterified, *sn*-2MCF-structured, and *sn*-2MCF-interesterified group, respectively. In contrast to these lipids, the pattern of cholesterol output rate was similar to the lymph flow. The *sn*-1(3)MCF-interesterified group maintained a higher cholesterol output rate between 2 and 6 h after food consumption than did the other groups ($P < 0.05$), hence the lymphatic cholesterol mass was greater in *sn*-1(3)MCF-interesterified group (22.5 ± 1.6 μmol/9.33 h) than in *sn*-1(3)MCF-structured group (17.4 ± 0.9 μmol/9.33 h), *sn*-2MCF-structured group (19.5 ± 0.6 μmol/9.33 h), and *sn*-2MCF-interesterified group (18.3 ± 1.6 μmol/9.33 h), which did not differ.

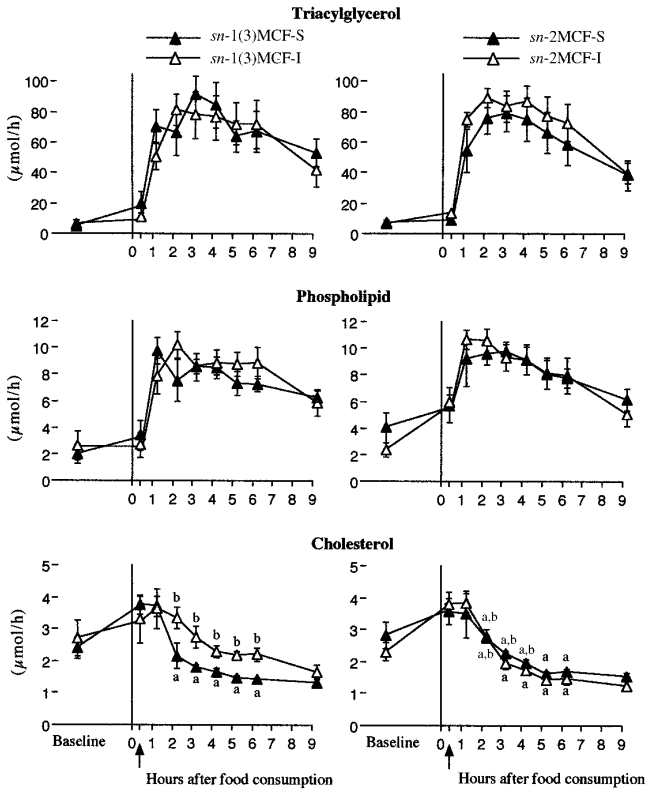

FIG. 2. Lymphatic output rates of triacylglycerol, cholesterol, and phospholipid in rats fed diets containing *sn*-1(3)MCF-structured plus cocoa butter [*sn*-1(3)MCF-S], *sn*-1(3)MCF-interesterified plus cocoa butter [*sn*-1(3)MCF-I], *sn*-2MCF-structured plus cocoa butter [*sn*-2MCF-S], or *sn*-2MCF-interesterified plus cocoa butter [*sn*-2MCF-I]. Arrow indicates termination of food consumption. Values are means ± SEM, $n = 6$. Values at each time in both panels assigned different letters are significantly different at $P < 0.05$. See Figure 1 for abbreviation.

Lymph chylomicrons were isolated from the lymph collected during 2–6 h after the food consumption and used for determinations of the chemical composition and particle size. Different structure of dietary fats did not influence the chemical composition and the particle size (Table 3). The dietary fats reflected total as well as *sn*-2 fatty acid compositions of the chylomicron triacylglycerol (Table 4). Chylomicron-triacylglycerol contained more decanoic acid than octanoic acid. Reflecting the proportion of MCF and linoleic acid in the diet, chylomicrons prepared from rats fed *sn*-2MCF type synthetic fats included more MCF than did those from the *sn*-1(3)MCF type synthetic fat-fed group and vice versa for linoleic acid. The proportion of MCF and linoleic acid in *sn*-2 position also reflected the positional specificity of these fatty acids in the diet. In contrast, the proportion of MCF in total fatty acid was not influenced by the positional distribution of MCF in the synthetic fats; there were no marked differences in the MCF proportion within *sn*-1(3)MCF type fat group and *sn*-2MCF type fat group, respectively. There were also no marked differences in the cocoa butter-derived fatty acids (palmitic, stearic, and oleic acid) in total or *sn*-2 fatty acid composition among the groups.

DISCUSSION

Evidence suggests that emulsification of dietary fat with dietary components (phospholipids, hydrophobic proteins, and carbohydrates) in the stomach and upper intestine, gastric lipolysis, stimulation of gastric hormone secretion, and fine emulsification by the lipolytic products (fatty acids and diacylglycerols) impact absorption and digestion of dietary fats (23). However, stomach or duodenum infusion of lipid emulsion was usually done to assess the transport of the emulsified lipid and composition of lymph chylomicrons (22). In this respect, our approach is particularly relevant to evaluate lymphatic transport of dietary fats in normally fed rats.

The present study showed that the positional distribution

TABLE 3
Chemical Composition and Particle Size of Lymph Chylomicrons in Rats Fed *sn*-1(3)MCF or *sn*-2MCF Type Synthetic Fats-Containing Diet[a]

	sn-1(3)MCF + cocoa butter		*sn*-2MCF + cocoa butter	
	Structured	Interesterified	Structured	Interesterified
Triacylglycerols (mol/100 mol)	85.9 ± 1.2	85.1 ± 1.4	85.0 ± 1.0	86.9 ± 0.4
Phospholipids (mol/100 mol)	11.7 ± 0.8	11.9 ± 0.9	12.4 ± 0.7	11.1 ± 0.4
Free cholesterol (mol/100 mol)	1.5 ± 0.2	2.0 ± 0.4	1.7 ± 0.1	1.3 ± 0.1
Esterified cholesterol (mol/100 mol)	0.9 ± 0.2	1.1 ± 0.3	1.0 ± 0.2	0.6 ± 0.1
Particle size (nm)	140 ± 16	121 ± 10	120 ± 7	137 ± 10

[a]Values are means ± SEM, $n = 6$. See Table 1 for abbreviation.

of MCF or the amount of MCF in the synthetic triacylglycerols exerted no significant effect on the lymphatic output rate of triacylglycerol or phospholipid, suggesting less effect of the MCF position on dietary fat absorption. These results are in agreement with apparent fat absorption in rats prior to lymph duct cannulation. However, the present results are in contrast to our previous observations (32); we found that MCF positioned in *sn*-1(3), rather than in *sn*-2, resulted in a significant increase in the absorption of dietary fats, particularly long-chain saturated fatty acids, as reflected in a lowered fecal excretion of palmitic and stearic acid, when rats were freely fed on the diets containing the synthetic fats. Although the reason for this discrepancy is not clear, it may be due to the way of feeding; in the present study, rats were restrictedly fed the diet, in contrast to the previous study in which they were fed freely. Alternatively, it may be that we failed to observe any differences between rats fed the different types of synthetic triacylglycerols due to the presence of protein or carbohydrate in the diet.

In contrast to the transport of triacylglycerol and phospholipid, the type of synthetic fats affected the pattern of cholesterol output. The *sn*-1(3) MCF-interesterified group maintained a higher cholesterol output rate than did the other groups. The reason for this remains to be determined.

Chemical compositions and particle sizes of chylomicron found in the present study were similar to those for rats to which artificial fat-emulsions were administered into the duodenum as described previously (28,33), indicating that dietary fats are transported as large chylomicrons during active fat absorption. The positions of MCF in the synthetic fats had no significant effect on the chemical composition and the sizes of chylomicrons. Despite these similarities, the type of dietary fats altered fatty acid compositions of the chylomicron-triacylglycerols. As expected, *sn*-2 positioned linoleic acid in the synthetic fats was maintained to the *sn*-2 position of the lymph chylomicron triacylglycerol because reacylation of 2-monoacylglycerol is the predominant pathway during active absorption of dietary fat (19). Interestingly, MCF was well preserved in both the *sn*-2 and *sn*-1(3) positions in the chylomicron-triacylglycerol depending on their position in the synthetic fats ingested, indicating that the MCF released from the *sn*-1(3) position of synthetic fats was also utilized in the intestine for reesterification of 2-monoacylglycerols. Therefore, these findings differ from data in previous reports that preduodenal lipases preferentially hydrolyze MCF derived from medium-chain triacylglycerols and that the resulting MCF can be absorbed predominantly through the stomach (34). It appears that MCF in 2-monoacylglycerols isomerize more rapid than do long-chain length fatty acids, thereby facilitating rapid and complete hydrolysis (35).

Positional distribution of MCF in lymph chylomicron triacylglycerol can be relevant to the catabolism of chylomicrons

TABLE 4
Fatty Acid Composition of Lymph Chylomicron Triacylglycerols in Rats Fed *sn*-1(3)MCF or *sn*-2MCF Type Synthetic Fats-Containing Diet[a]

	Total fatty acid (mol/100 mol)				*sn*-2 Fatty acids (mol/100 mol)			
Fatty acids	*sn*-1(3)MCF + cocoa butter		*sn*-2MCF + cocoa butter		*sn*-1(3)MCF + cocoa butter		*sn*-2MCF + cocoa butter	
	Structured	Interesterified	Structured	Interesterified	Structured	Interesterified	Structured	Interesterified
8:0	1.9 ± 0.2^{a}	2.3 ± 0.3^{a}	6.4 ± 0.2^{c}	4.5 ± 0.1^{b}	0.0 ± 0.0^{a}	2.2 ± 0.7^{b}	7.5 ± 0.5^{c}	3.4 ± 0.2^{b}
10:0	6.2 ± 0.3^{a}	5.4 ± 0.7^{a}	12.6 ± 0.6^{b}	11.7 ± 0.4^{b}	0.5 ± 0.2^{a}	4.1 ± 0.7^{b}	15.4 ± 0.4^{d}	8.3 ± 0.5^{c}
12:0	0.3 ± 0.0^{a}	0.3 ± 0.0^{a}	0.5 ± 0.0^{c}	0.4 ± 0.0^{b}	0.0 ± 0.0^{a}	0.1 ± 0.1^{a}	0.6 ± 0.1^{b}	0.2 ± 0.1^{a}
14:0	0.2 ± 0.0^{a}	0.3 ± 0.0^{a,b}	0.4 ± 0.0^{c}	0.3 ± 0.0^{b}	0.0 ± 0.0^{a}	0.2 ± 0.1^{a,b}	0.3 ± 0.1^{b}	0.2 ± 0.1^{a,b}
16:0	14.1 ± 0.4^{a}	16.0 ± 0.7^{b}	15.0 ± 0.7^{a,b}	14.4 ± 0.5^{a,b}	8.9 ± 0.2	9.4 ± 0.7	9.9 ± 0.4	8.7 ± 0.7
16:1	0.4 ± 0.0	0.4 ± 0.0	0.4 ± 0.1	0.5 ± 0.0	0.1 ± 0.1	0.4 ± 0.2	0.1 ± 0.1	0.1 ± 0.1
18:0	13.5 ± 0.4	13.5 ± 0.7	12.9 ± 1.1	14.0 ± 0.6	4.2 ± 0.2	4.4 ± 0.2	4.4 ± 0.3	4.5 ± 0.3
18:1	30.4 ± 0.2^{a,b}	30.4 ± 0.6^{a,b}	29.4 ± 0.8^{a}	31.4 ± 0.5^{b}	45.7 ± 0.9^{a}	46.7 ± 0.8^{a}	46.4 ± 1.1^{a}	50.2 ± 0.8^{b}
18:2n-6	28.4 ± 0.2^{c}	26.2 ± 0.6^{b}	18.7 ± 0.4^{a}	19.3 ± 0.3^{a}	36.3 ± 0.5^{d}	29.6 ± 0.5^{c}	14.4 ± 0.4^{a}	22.7 ± 0.4^{b}
18:3	3.9 ± 0.1^{b}	4.0 ± 0.1^{b}	2.7 ± 0.2^{a}	3.0 ± 0.1^{a}	3.8 ± 0.6^{d}	2.1 ± 0.1^{c}	0.5 ± 0.1^{a}	1.6 ± 0.0^{b}
20:4n-6	0.7 ± 0.1	1.2 ± 0.3	0.9 ± 0.2	0.6 ± 0.1	0.5 ± 0.1	0.7 ± 0.3	0.5 ± 0.2	0.2 ± 0.2

[a]Values are means ± SEM, $n = 6$. Values with different superscript roman letters are significantly different at $P < 0.05$. See Table 1 for abbreviation.

in blood plasma, because chylomicrons derived from the *sn*-2MCF-structured group had a longer half life in the circulation than those from the corresponding interesterified group, when they were intravenously infused into recipient rats (Carvajal, O., Kishi, T., Tomoyori, H., Sato, M., Ikeda, I., Sugano, M., and Imaizumi, K, unpublished observations).

Comparison of the proportion of octanoic and decanoic acid in the dietary fats with their proportion of the lymph chylomicron triacylglycerol allows for estimation of the transport route of these MCF into the lymphatic or portal vein circulation. More than 60% of decanoic acid in the diet seemed to be transported into the lymphatics, whereas it was less than 30% for octanoic acid. These findings are in agreement with other results that canine lymph contained more decanoic acid than octanoic acid despite a higher ratio of octanoic acid to decanoic acid in the diet (7).

In summary, our studies confirmed that MCF in the dietary triacylglycerols are transported into lymphatics and the positional distribution is well preserved in chylomicron triacylglycerol.

REFERENCES

1. Bach, A.C., Ingenbleek, Y., and Frey, A. (1996) The Usefulness of Dietary Medium-Chain Triglycerides in Body Weight Control: Fact or Fancy? *J. Lipid Res. 37,* 708–726.
2. Odle, J. (1997) New Insights into the Utilization of Medium-Chain Triglycerides by the Neonate: Observations from a Piglet Model, *J. Nutr. 127,* 1061–1067.
3. Babayan, V.K. (1987) Medium Chain Triglycerides and Structured Lipids, *Lipids 22,* 417–420.
4. Decker, E.A. (1996) The Role of Stereospecific Saturated Fatty Acid Positions on Lipid Nutrition, *Nutr. Rev. 54,* 108–110.
5. Ikeda, I., Tomari, Y., Sugano, M., Watanabe, S., and Nagata, J. (1991) Lymphatic Absorption of Structured Glycerolipids Containing Medium-Chain Fatty Acids and Linoleic Acid, and Their Effect on Cholesterol Absorption in Rats, *Lipids 26,* 369–373.
6. Jandacek, R.J., Whiteside, J.A., Holcombe, B.N., Volpenhein, R.A., and Taulbee, J.D. (1987) The Rapid Hydrolysis and Efficient Absorption of Triglycerides with Octanoic Acid in the 1 and 3 Positions and Long-Chain Fatty Acid in the 2 Position, *Am. J. Clin. Nutr. 45,* 940–945.
7. Jensen, G.L., McGarvey, N., Taraszewski, R., Wixson, S.K., Seidner, D.L., Pai, T., Yeh, Y.-Y., Lee, T.W., and DeMichele, S.J. (1994) Lymphatic Absorption of Enterally Fed Structured Triacylglycerol vs. Physical Mix in a Canine Model, *Am. J. Clin. Nutr. 60,* 518–524.
8. Lanza-Jacoby, S., Phetteplace, H., and Tripp, R. (1995) Enteral Feeding a Structured Lipid Emulsion Containing Fish Oil Prevents the Fatty Liver of Sepsis, *Lipids 30,* 707–712.
9. Lepine, A.J., Garleb, K.A., Reinhart, G.A., and Kresty, L.A. (1993) Plasma and Tissue Fatty Acid Profiles of Growing Pigs for Structured or Non-Structured Triacylglycerides Containing Medium-Chain and Marine Oil Fatty Acids, *J. Nutr. Biochem. 4,* 362–372.
10. Teo, T.C., Selleck, K.M., Wan, J.M.F., Pomposelli, J.J., Babayan, V.K., Blackburn, G.L., and Bistrian, B.R. (1991) Long-Term Feeding with Structured Lipid Composed of Medium-Chain and n-3 Fatty Acids Ameliorates Endotoxic Shock in Guinea Pigs, *Metabolism 40,* 1152–1159.
11. Tso, P., Karlstad, M.D., Bistrian, B.R., and Demichele, S.J. (1995) Intestinal Digestion, Absorption, and Transport of Structured Triglycerides and Cholesterol in Rats, *Am. J. Physiol. 268,* G568–G577.
12. Cotter, R., Johnson, R.C., Young, S.K., Lin, L.I., and Rowe, W.B. (1989) Competitive Effects of Long-Chain-Triglyceride Emulsion on the Metabolism of Medium-Chain-Triglyceride Emulsions, *Am. J. Clin. Nutr. 50,* 794–800.
13. Aoe, S., Yamamura, J., Matsuyama, H., Hase, M., Shiota, M., and Miura, S. (1997) The Positional Distribution of Dioleoylpalmitoyl Glycerol Influences Lymph Chylomicron Transport, Composition and Size in Rats, *J. Nutr. 127,* 1269–1273.
14. Brink, E.J., Haddeman, E., de Fouw, N.J., and Weststrate, J.A. (1995) Positional Distribution of Stearic Acid and Oleic Acid in a Triacylglycerol and Dietary Calcium Concentration Determines the Apparent Absorption of These Fatty Acids in Rats, *J. Nutr. 125,* 2379–2387.
15. Imaizumi, K., Abe, K., Kuroiwa, C., and Sugano, M. (1993) Fat Containing Stearic Acid Increases Fecal Neutral Steroid Excretion and Catabolism of Low Density Lipoproteins Without Affecting Plasma Cholesterol Concentration in Hamsters Fed a Cholesterol-containing Diet, *J. Nutr. 123,* 1693–1702.
16. Innis, S.M., Quinlan, P., and Diersen-Schade, D. (1993) Saturated Fatty Acid Chain Length and Positional Distribution in Infant Formula: Effects on Growth and Plasma Lipids and Ketones in Piglets, *Am. J. Clin. Nutr. 57,* 382–390.
17. Innis, S.M., and Dyer, R. (1997) Dietary Triacylglycerols with Palmitic Acid (16:0) in the 2-Position Increase 16:0 in the 2-Position of Plasma and Chylomicron Triacylglycerols, but Reduce Phospholipid Arachidonic and Docosahexaenoic Acids, and Alter Cholesteryl Ester Metabolism in Formula-Fed Piglets, *J. Nutr. 127,* 1311–1319.
18. Innis, S.M., Dyer, R.A., and Lien, E.L. (1997) Formula Containing Randomized Fats with Palmitic Acid (16:0) in the 2-Position Increases 16:0 in the 2-Position of Plasma and Chylomicron Triglycerides in Formula-Fed Piglets to Levels Approaching Those of Piglets Fed Sow's Milk, *J. Nutr. 127,* 1362–1370.
19. Small, D.M. (1991) The Effects of Glyceride Structure on Absorption and Metabolism, *Annu. Rev. Nutr. 11,* 413–434.
20. Jensen, M.M., Christensen, M.S., and Høy, C.-E. (1994) Intestinal Absorption of Octanoic, Decanoic, and Linoleic Acids: Effect of Triglyceride Structure, *Ann. Nutr. Metab. 38,* 104–116.
21. Christensen, M.S., Høy, C.-L., Becker, C.C., and Redgrave, T.G. (1995) Intestinal Absorption and Lymphatic Transport of Eicosapentaenoic (EPA), Docosahexaenoic (DHA), and Decanoic Acids: Dependence on Intramolecular Triacylglycerol Structure, *Am. J. Clin. Nutr. 61,* 56–61.
22. Tso, P. (1985) Gastrointestinal Digestion and Absorption of Lipids, *Adv. Lipid Res. 21,* 143–186.
23. Carey, M.C., and Hernell, O. (1992) Digestion and Absorption of Fat, *Semin. Gastrointest. Dis. 3,* 189–208.
24. Girardet, R.E. (1975) Surgical Techniques for Long-Term Studies of Thoracic Duct Cannulation in the Rat, *J. Applied Physiol. 39,* 682–688.
25. Remie, R., van Dongen, J.J., and Rensema, J.W. (1990) Permanent Cannulation of the Thoracic Duct, in *Manual of Microsurgery on the Laboratory Rat, Part I* (van Dongen, J.J., Remie, R., Rensema, J.W., and van Wunnik, G.H.J., eds.), Vol. 4, pp. 243–254, Elsevier, Amsterdam.
26. Reeves, P.G., Nielsen, F.H., and Fahey, G.C., Jr. (1993) AIN-93 Purified Diets for Laboratory Rodents: Final Report of the American Institute of Nutrition *ad hoc* Writing Committee on the Reformulation of the AIN-76A Rodent Diet, *J. Nutr. 123,* 1939–1951.
27. Ni, W., Tsuda, Y., Sakono, M., and Imaizumi, K. (1998) Dietary Soy Protein Isolate, Compared with Casein, Reduces Atherosclerotic Lesion Area in Apolipoprotein E-deficient Mice, *J. Nutr. 128,* 1884–1889.
28. Imaizumi, K., Fainaru, M., and Havel, R.J. (1978) Composition

of Proteins of Lymph Chylomicrons in the Rat and Alterations Produced Upon Exposure of Chylomicrons to Blood Serum Proteins, *J. Lipid Res. 19,* 712–722.
29. Ikeda, I., Yoshida, H., Tomiooka, M., Yosef, A., Imaizumi, K., Tsuji, H., and Seto, A. (1998) Effects of Long-Term Feeding of Marine Oils with Different Positional Distribution of Eicosapentaenoic and Docosahexaenoic Acids on Lipid Metabolism, Eicosanoid Production, and Platelet Aggregation in Hypercholesterolemic Rats, *Lipids 33,* 897–904.
30. Folch, J., Lees, M., and Sloane Stanley, G.H. (1957) A Simple Method for the Isolation and Purification of Total Lipids from Animal Tissue, *J. Biol. Chem. 226,* 497–509.
31. Jeejeebhoy, K.N., Ahmad, S., and Kozak, G. (1970) Determination of Fecal Fats Containing Both Medium and Long Triacylglycerides and Fatty Acids, *Clin. Biochem. 3,* 157–163.
32. Carvajal, O., Sakono, M., Sonoki, H., Nakayama, M., Kishi, T., Sato, I., Ikeda, I., Sugano, M., and Imaizumi, K. (2000) Structured Triacylglycerol Containing Medium-Chain Fatty Acids in *sn*-1(3) Facilitates the Absorption of Dietary Long-Chain Fatty Acids in Rats, *Biosci. Biotech. Biochem. 64,* 793–798.
33. Martin, I.J., Mortimer, B.-C., Miller, J., and Redgrave, T.G. (1996) Effects of Particle Size and Number on the Plasma Clearance of Chylomicrons and Remnants, *J. Lipid Res. 37,* 2696–2705.
34. Hamosh, M. (1990) *Lingual and Gastric Lipases: Their Role in Fat Digestion*, pp. 128–132, CRC Press, Boca Raton.
35. Desnuelle, P., and Savary, P. (1963) Specificity of Lipases, *J. Lipid Res. 4,* 369–384.

[Received November 24, 1999, and in revised form April 20, 2000;
revision accepted October 26, 2000]

Kinetics of 2-Monoacylglycerol Acyl Migration in Model Chylomicra

Galina Lyubachevskaya and Elizabeth Boyle-Roden*

Department of Nutrition and Food Science, University of Maryland, College Park, Maryland 20742

ABSTRACT: In the metabolism of triacylglycerol (TG)-rich lipoproteins, 2-monoacylglycerols (2-MG) are produced by lipoprotein lipase (LPL) hydrolysis of TG. The metabolic fate of 2-MG is not known with certainty. 2-MG that accumulate on the chylomicra surface have been proposed to isomerize spontaneously to 1(3)-MG, which are then hydrolyzed by LPL to free fatty acids and glycerol. In this study the rate and the effect of acyl chain saturation on the spontaneous acyl migration of 2-MG in *in vitro* model chylomicra emulsions were determined. After 1 h of incubation at 37°C, less than 20% of 2-monoolein (2-MO) or 2-monopalmitin (2-MP) spontaneously isomerized to 1(3)-MO or 1(3)-MP, respectively. Accordingly, it was concluded that spontaneous isomerization of 2-MG is not the major mechanism for 2-MG metabolism post-TG hydrolysis in chylomicra. Isomerization rates, expressed as decrease in percentage of 2-MG remaining per hour, were –5.12 and –5.86 in water, and –0.43 and –0.41 in hexane for 2-MO and 2-MP, respectively. There was no significant difference between the isomerization rates of 2-MO and 2-MP. Thus, in the present study, saturation of the MG acyl chain did not influence spontaneous acyl migration in either water or hexane, but isomerization of 2-MG was faster in water than in hexane.

Paper no. L8577 in *Lipids 35*, 1353–1358 (December 2000).

Historically, the acyl migration of 2-monoacylglycerols (2-MG) has been problematic in the characterization, isolation, and synthesis of acylglycerols, thus hindering progress in lipid metabolism research. 2-MG isomerizaton significantly interfered with the interpretation of data regarding the specificity of lipoprotein lipase (LPL) (1–3). Currently, 2-MG isomerization has proven to be a serious obstacle in the synthesis of structured lipids (4–8). However, few data on the kinetics of 2-MG acyl migration are available.

Triacylglycerol (TG) in chylomicra is hydrolyzed by LPL, which cleaves the ester bonds at the 1- and 3-TG positions, producing free fatty acids (FFA) and 2-MG. Several theories are currently proposed for the metabolic fate of 2-MG post-TG hydrolysis, including the following: 2-MG diffuse away from the site of lipolysis and fuse with cell membranes (9,10), 2-MG are bound and transported by serum albumin (11,12), 2-MG remain in chylomicra remnants or transfer to low density lipoprotein and high density lipoprotein, which are then taken up by the liver (13,14), and 2-MG spontaneously isomerize to 1(3)-MG, which are then hydrolyzed by LPL to glycerol and FFA (1–3,15). None of these theories, however, is supported by a consensus of scientific evidence.

Many investigators agree that on the surface of chylomicra, 2-MG may quickly isomerize to 1(3)-MG, which is in turn hydrolyzed by LPL. However, there are few published data that directly support this hypothesis. Nilsson-Ehle *et al.* (1–3) directly measured the degree of 2-MG isomerization that occurs during LPL hydrolysis of chylomicra-like TG emulsions; however, their data were inconsistent. Conclusions about isomerization of 2-MG in chylomicra from other studies are for the most part based on indirect methods (13, 14,16,17). Furthermore, the *in vitro* models used to investigate chylomicra lipolysis and potential 2-MG isomerization always included LPL and usually albumin, making direct interpretation of their results in regard to spontaneous 2-MG isomerization difficult. Thus, the primary goal of the present study was to determine the kinetics of spontaneous 2-MG acyl migration in chylomicra.

The degree of saturation of fatty acid acyl chains of MG may influence chylomicra lipolysis by LPL and subsequent remnant clearance by the liver (18). It has been reported that unsaturated 2-MG isomerize faster than saturated 2-MG, which suggests that differential isomerization rates of 2-MG may affect chylomicra metabolism (15). Therefore, a secondary goal of the present study was to determine the possible influence of saturation on the rate of 2-MG isomerization in model chylomicra emulsions.

An *in vitro* chylomicra emulsion model, free of other potentially complicating components such as enzymes or albumin that might induce or even catalyze 2-MG isomerization, was used. Both the 2- and 1(3)-isomers of monoolein (MO) and monopalmitin (MP) were quantified directly. Isomerization rates in water and hexane were compared to assess the effects of aqueous and organic media on the rate of acyl migration.

*To whom correspondence should be addressed at Department of Nutrition and Food Science, Marie Mount Hall, University of Maryland, College Park, MD, 20742. E-mail: eb112@umail.umd.edu

Abbreviations: ANOVA, analysis of variance; CE, cholesteryl ester; FFA, free fatty acids; GC, gas chromatography; LPL, lipoprotein lipase; MG, monoglycerine; MO, monoolein; MP, monopalmitin; PC, phosphatidylcholine; TG, triacylglycerol; TLC, thin-layer chromatography; TO, triolein.

EXPERIMENTAL PROCEDURES

Preparation of model chylomicra emulsions. 2-MO and 2-MP were purchased from Doosan Serdary Research Laboratories (Englewood Cliffs, NJ), stored at –20°C and analyzed for purity prior to use as described below. 2-MO contained 89.9% of 2-MO and 10.1% of 1(3)-MO, and 2-MP contained 90.9% of 2-MP and 9.1% of 1(3)-MP. Model chylomicra emulsion particles were prepared by a method similar to that reported by Derkson *et al.* (19). Lipids (Table 1) were combined in organic solvent in a 4-mL vial and mixed with a vortex mixer. The solvent was evaporated under nitrogen and 1 mL of aqueous Tris buffer, pH 7.4, containing 0.15 M sodium chloride and 0.008 M sodium azide, which was used as an antimicrobial agent, was added to the lipids. The mixture was sonicated for 30 min in continuous mode at power level 2 using a Heat Systems Sonicator (Plainview, NY). During sonication, samples were held in an ice-water bath to prevent heating, which can induce isomerization. Sample temperature during sonication did not exceed 15°C.

Incubations and sample analysis. Synthesized model chylomicra emulsions were held in a shaker-water bath at 37°C for 50 h. Aliquots of 25 μL were taken for thin-layer chromatography (TLC) and gas chromatography (GC) analysis at various times. There were three replicate experiments; in each, both 2-MO and 2-MP were measured in duplicate.

Particle sizing. Particles were sized using dynamic laser-light scattering to determine mean particle diameter on a number weight basis with a Nicomp Model 370 laser particle sizer (Particle Sizing Systems, Santa Barbara, CA). The size distribution of model chylomicra emulsion particles was determined to ensure that *in vitro* particles were within the biologically relevant range. Samples for particle sizing were taken at 10 min and at 24 h after preparation.

Microbial plate count. Analysis of microbial growth in the samples was necessary to ensure that isomerization of 2-MG to 1(3)-MG was not a result of microorganism metabolism. Samples for microbial plate counts were taken in duplicate after 5 and 24 h. Samples (20 μL) were plated onto nondifferentiating LB media (Lennox Broth; Sigma, St. Louis, MO) and incubated at 36°C for 24 h.

Temperature controls. The influence of temperature on the rate of 2-MG isomerization was monitored by measuring the degree of isomerization of three 10-μL aliquots of sample taken at 10 min, which were then held at –10, 10, or 25°C for 30 h.

TABLE 1
Composition of Model Chylomicra Emulsions

Lipid	Concentration (mg/mL)	Molar ratio (%)	Weight ratio (%)
Triolein	79	68.8	77.8
L-α-Phosphatidylcholine	16	16.1	15.7
Cholesterol	1	1.9	0.98
Cholesteryl laurate	0.5	0.6	0.5
2-Monoolein	3	6.4	2.9
2-Monopalmitin	3	6.4	2.9

Sonication controls. To confirm that sonication did not influence isomerization, controls were prepared as follows: the same amount and proportions of total lipid used to prepare emulsions (Table 1) were dispersed in hexane at the same time that aqueous buffer was added to emulsion samples. While samples were sonicated, the controls were kept in an ice-water bath. The 2-MG content of both sonicated and unsonicated control lipid mixtures was analyzed immediately following sonication.

Solvent controls. Solvent controls were used to determine the effect of solvent on the rate of acyl migration of 2-MG. Aqueous and hexane solvents were compared. For this purpose, the sonication controls were kept in the shaker-water bath at 37°C with the samples and were analyzed after 0, 2, 5, 9, 24, 30, and 50 h of incubation. The effect of total lipid content of model chylomicra emulsions on 2-MG isomerization was examined by comparing the percentage of 2-MG in mixtures containing 2-MG, triolein (TO), phosphatidyl choline (PC), cholesterol, and cholesteryl ester (CE) in hexane and samples containing only 2-MG and PC in hexane.

Boric acid TLC. TLC plates impregnated with 1.2% boric acid were used to separate 2-MG and 1(3)-MG (20). Samples (10 μL) containing 30 μg each of MO and MP were applied to TLC plates (silica gel 60, 250-μm layer thickness, 10 × 5 cm; Whatman, Clifton, NJ) in duplicate. The developing solvent was chloroform/methanol (98:2, vol/vol). The separated lipid bands were visualized by iodine vapors and extracted from the silica with 1 mL of benzene.

GC. MG isomers were transmethylated by addition of acetyl chloride/methanol (1:15, vol/vol). Linoleic acid (Sigma) and methyl laurate (Nu-Chek-Prep, Elysian, MN) were used as internal standards. A Hewlett-Packard 5890 series gas chromatograph equipped with a DB-23, 30-m capillary column (J&W Scientific, Folsom, CA), automatic controller, autosampler, and HP 3396A integrator was used to quantify MG isomers. For each aliquot and time point, the percentage of 2-MG remaining in the samples was calculated as 2-MG/[2-MG + 1(3)-MG] × 100.

Statistical analysis. Two statistical models, analysis of variance (ANOVA) and analysis of covariance, were used to compare rates of 2-MP and 2-MO isomerization, using the SAS software package (SAS Institute Inc., version 6.12, Cary, NC). 2-MG, time, and 2-MG vs. time were the sources of variation in the ANOVA model. Goodness of fit statistics provided in the mixed model were used to select a model that accounted for any heterogeneity associated with either time or 2-MG. The best-fitting model indicated that variances were different over time, but were homogeneous for 2-MG. Therefore, 2-MG variances were pooled to provide a more precise estimate of the random variance. In the analysis of covariance, 2-MG was a class variable, whereas time was a continuous regression variable. All nonsignificant sources of variation, except for the linear sources of variation, were removed. Linear regression effects over time were presented if all higher-order terms were not significant. Differences were considered significant at $P < 0.05$.

RESULTS AND DISCUSSION

Particle size. The particle size distribution of model chylomicra emulsions was stable over time and consistent for all experiments. The mean particle diameter on a number–weight basis ranged between 155–194 nm with a standard deviation (SD) of 34 nm and thus resembled the physiological distribution of chylomicra (19).

Microbial growth. Results of the microbial plate count indicated that all samples were free from microbial growth throughout the time course of the experiments.

Effect of temperature. The effect of temperature on the isomerization rate of 2-MG in model chylomicra emulsions is given in Table 2. In agreement with the literature, temperature was directly related to isomerization rate of 2-MG, with the rate of 2-MG migration increasing with an increase in incubation temperature. At –10°C there was no acyl migration detected at 30 h incubation in aqueous medium for either 2-MP or 2-MO.

Effect of sonication. There was no significant difference in the percentage of 2-MG remaining in the sonicated and unsonicated samples. The average percentages of 2-MP and 2-MO, with standard errors of the means, in sonicated emulsions were 91.42 ± 1.66 and 90.85 ± 1.66, respectively, and in sonication controls were 90.87 ± 1.89 and 89.90 ± 1.89, respectively. Thus, the thermal and mechanical energy resulting from sonication did not induce additional isomerization in either 2-MO or 2-MP. The initial presence of 1(3)-MG in samples is the result of acyl migration during long-term storage of 2-MG at –20°C.

Acyl migration. The acyl migration of 2-MO and 2-MP occurred slowly in model chylomicra reaching the equilibrium ratio of approximately 12:88 [2-MG/1(3)-MG] by 30 h (4,5, 15). The acyl migration of 2-MO and 2-MP, reported as means of all duplicates and experiments in model chylomicra emulsions from 0 to 5 h at 37°C and pH 7.4, is shown in Figure 1. The degree of acyl migration is presented as the percentage of 2-MG remaining at each time point based on the total amount of 2- and 1(3)-isomers in each aliquot. The results are presented as the linear regression lines because both ANOVA and analysis of covariance indicated that the best fit for the data was linear. Statistical analysis confirmed no significant difference in the variability of data among three experiments. The regression lines of 2-MO and 2-MP shown in Figure 1 overlap, showing that there was no difference between the isomerization rates of 2-MO and 2-MP as confirmed by ANOVA and analysis of covariance. There also was no effect of acyl chain saturation on isomerization rate between 2-MP and 2-MO. The only significant effect was that of time. Because 2-MG over time was not significant, change over time was not different for 2-MO or 2-MP. This suggests that saturation of acyl chain may not influence spontaneous acyl migration of 2-MG.

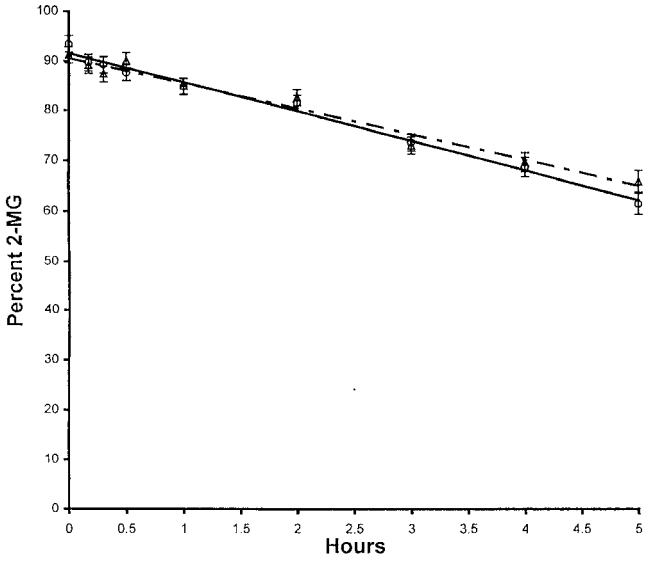

FIG. 1. Kinetics of 2-monoolein (2-MO) and 2-monopalmitin (2-MP) isomerization in model chylomicra emulsions. Values are the means ± SEM (n = 6) of the percentage of 2-MO (Δ, broken line) and 2-MP (○, solid line) remaining at different incubation times. Equations of linear regression: 2-MO, $y = -5.12x + 90.68$; and 2-MP, $y = -5.86x + 91.59$. Abbreviation: 2-MG, 2-monoacylglycerol.

The finding that saturation did not affect the 2-MG spontaneous isomerization is very important because this topic has been a subject of scientific controversy. Since the report of Mattson and Volpenhein in 1962 (15), it has been assumed that 2-MG with unsaturated acyl chains isomerize faster than 2-MG with saturated acyl chains. However, the authors admitted that their results could be erroneous due to the limited dispersability of saturated 2-MG in water. In the present study, both saturated and unsaturated 2-MG were equally dispersed in the model chylomicra emulsions.

After 1 h of incubation, less than 20% of 2-MG was isomerized to 1(3)-MG, and after 5 h, less than 40% of 2-MG was isomerized to 1(3)-MG. The rates of 2-MO and 2-MP isomerization were –5.12 and –5.86% of 2-MG/h, respectively. Thus, the rate of spontaneous isomerization of 2-MG in the model chylomicra emulsions tested in the present study was considerably less than the rate of chylomicra clearance *in vivo*. Indeed, for humans, the normal residence time of chylomicra in the circulation is less than 1 h (21). Therefore, although spontaneous isomerization of 2-MG produced from LPL hydrolysis of TG does occur, it does not appear to be the major mechanism of 2-MG metabolism in chylomicra.

TABLE 2
Temperature Controls[a]

Temperature controls (°C)	2-MO (%)	2-MP (%)
37	12.34 ± 1.90	17.07 ± 1.90
25	35.72 ± 1.66	34.24 ± 1.66
10	71.12 ± 2.34	71.69 ± 2.34
–10	89.55 ± 0.47	91.03 ± 2.47

[a]Values are the mean ± SEM (n = 6) of the percentage of 2-MG remaining at 30 h. Abbreviations: 2-MO, 2-monoolein; 2-MP, 2-monopalmitin; MG, monoacylglycerol.

A number of researchers investigating chylomicra lipolysis have commented on the potential significance of spontaneous acyl migration in lipid metabolism (1–3,10,13–17). However, their conclusions about 2-MG acyl migration were based mainly on indirect measurements of 2-MG with variable statistical significance. Most studies did not relate the rate of chylomicra clearance to the rate of 2-MG isomerization. Only Nilsson-Ehle *et al.* (1–3) directly measured the degree of 2-MG isomerization during LPL hydrolysis. However, the extent of 2-MG isomerization varied considerably for different experiments. After 20-min/incubation the amount of 2-MO recovered ranged from 95 to 36%. These variable results could be due to the fact that the objective of their studies was to investigate the specificity of LPL, not necessarily 2-MG isomerization. As a result, experimental conditions such as incubation temperature, concentrations and source of LPL, and presence or absence of albumin varied considerably. Another reason could be the difficulty in quantifying the 1(3)-isomer because of its susceptibility to further LPL hydrolysis.

The present study was designed to mimic physiological chylomicra with respect to lipid content, aqueous environment, sodium chloride concentration, particle size, pH, and temperature. Factors that might contribute to 2-MG migration, such as sonication and microbiological growth, were also controlled. Albumin and LPL were excluded so that only spontaneous chemical isomerization of 2-MG would be measured. Both 2- and 1(3)-MG isomers were quantified directly and separately. Results were reproducible, having only minimal variability among experiments as well as between duplicates. Therefore, taking into consideration the experimental design of the present study, it is likely that the spontaneous isomerization of 2-MG and their subsequent hydrolysis by LPL is not the major mechanism of 2-MG metabolism post-TG hydrolysis in chylomicra. However, direct application of these *in vitro* results to *in vivo* processes is limited because other factors may affect isomerization. Components, such as LPL or albumin, that were deliberately omitted from the model may in fact catalyze 2-MG isomerization. Scow and Olivecrona (16) reported that bovine LPL hydrolyzed chylomicra TG to mostly fatty acids and glycerol when incubations contained sufficient albumin to bind all fatty acids formed. The transient accumulation of MG under these conditions suggested that 2-MG may first isomerize to 1(3)-MG and then be hydrolyzed to fatty acid and glycerol (16). However, when albumin was either limited or added in excess, MG accumulated in the reaction mixture (16). Thus, in the presence of sufficient albumin LPL may either catalyze the isomerization of 2-MG or directly hydrolyze 2-MG.

Effect of solvent. The degree of isomerization in hexane compared to model chylomicra emulsions is shown in Figure 2. The hexane solutions of 2-MG contained the same amounts and proportions of total lipid as the emulsions (Table 1), and both were mixed and held at the same temperature for the same time. Also, the effect of total lipid content on 2-MG isom-erization was examined by comparing the rates of isomerization of 2-MG in two mixtures: 2-MG, TO, PC, cholesterol and CE, and 2-MG and PC in hexane (results not shown).

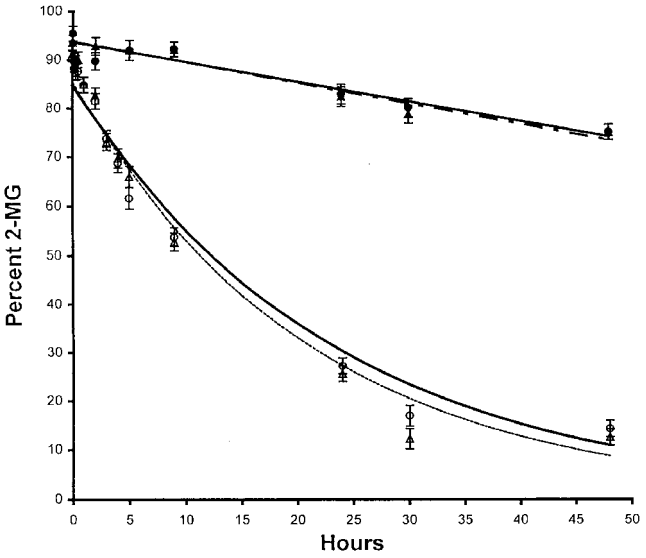

FIG. 2. Isomerization kinetics of 2-MO and 2-MP in water and hexane. Values are the means ± SEM (n = 6) of the percentage of 2-MO in water (Δ) or hexane (▲), and 2-MP in water (○) or hexane (●) remaining at different incubation times. Equations of linear regression for MG in hexane are: 2-MP, $y = -0.41x + 93.71$; and 2-MO, $y = -0.43x + 93.89$; and exponential curve fits for MG in water are: 2-MP, $y = 84.77\ e^{-0.043x}$, and 2-MO, $y = 85.61\ e^{-0.047x}$.

Both 2-MO and 2-MP isomerized more slowly in hexane than in aqueous buffer, regardless of lipid content. At 50 h of incubation, less than 30% of the 2-MG isomerized in hexane, whereas the ratio of 2-MG/1(3)-MG reached equilibrium at 30 h in water. Results presented in Figure 2 confirm that there was no difference in degree or extent of acyl migration for 2-MO and 2-MP in either water or hexane.

The literature is contradictory regarding the effects of water on 2-MG isomerization. Whereas some investigators reported that water in an organic solvent-free system is not involved in spontaneous isomerization of 2-MG (6–8,22), others suggest that water is a critical factor in promoting acyl migration (4,23–25). In the present study, isomerization of 2-MG in an aqueous environment was significantly faster than in hexane (see Fig. 2).

The presence of lipids other than MG in the emulsions did not affect the rates of 2-MG isomerization. Two different solvent controls were used. One contained 2-MG and PC in hexane and the other contained 2-MG and all other emulsion lipid components in hexane. There was no difference in isomerization rate between samples of 2-MG and PC and samples of 2-MG and all emulsion component lipids (data not shown). Thus, it can be inferred that addition of other lipid classes in proportions found in native chylomicra did not influence the rate of spontaneous acyl migration in hexane. Therefore, water is a contributing factor of 2-MG isomerization.

Several mechanisms have been proposed to explain the role of water in 2-MG acyl migration. Kodali *et al.* (25) sug-

gested that the catalytic effect of water is due to its ability to lower activation energy of formation of the 1,2-orthoester acylglycerol intermediate in isomerization of 2-MG to 1(3)-MG. Based on results of the present study, the differences between rates of isomerization in water and hexane are also proposed to be related to the physical state of 2-MG in each solvent. Currently, there is no information in the literature on the possible correlation between the physical aggregation state or mesophase of 2-MG and the rate of acyl migration. In pure organic solvent, 2-MG would be present as scattered monomers with complete freedom of rotational and translational movement in three dimensions. In organic solvent with small amounts of water, 2-MG would probably form reverse micelles with hydrophobic tails dispersed in the surrounding organic solvent, with the hydrophilic heads grouped together and with water sequestered in the center. In aqueous solvent, either lamellae or micelles would be formed, depending on the concentration of 2-MG. Molecules in lamellae are arranged in layers packed head-to-head and tail-to-tail, whereas in micelles, the tails aggregate together as the polar heads disperse in the surrounding water to form a small sphere. 2-MG in both lamellae and micelles have less freedom of movement compared to 2-MG in monomers or reverse micelles in organic solvent. Therefore, it is possible that these particular alignments are more favorable for formation of the orthoester intermediate, which would consequently increase the rate of acyl migration.

This study showed that in model chylomicra 2-MO and 2-MP spontaneously isomerized significantly more slowly than expected and that there was no difference in the rates of isomerization between the saturated and unsaturated 2-MG. In taking into account the normal plasma residence time of chylomicra *in vivo*, it can be concluded that although the spontaneous isomerization of 2-MG to 1(3)-MG may occur, it is not likely the major mechanism of 2-MG metabolism post-TG hydrolysis. Additionally, the rate of spontaneous 2-MG isomerization is significantly faster in water than in hexane. In conclusion, the differences in reported rates of 2-MG isomerization may be due to differences in the physical aggregation state of MG in the various systems studied.

ACKNOWLEDGMENTS

Dr. Larry Douglass is gratefully acknowledged for his help with statistical analysis. This work was supported by a Maryland Agriculture Experimental Station competitive grant, NFSC-99-19.

REFERENCES

1. Nilsson-Ehle, P., Belfrage, P., and Borgstrom, B. (1971) Purified Human Lipoprotein Lipase: Positional Specificity, *Biochim. Biophys. Acta 248,* 114–120.
2. Nilsson-Ehle, P., Egelrud, T., Belfrage, P., Olivecrona, T., and Borgstrom, B. (1973) Positional Specificity of Purified Milk Lipoprotein Lipase, *J. Biol. Chem. 248,* 6734–6737.
3. Nilsson-Ehle, P., Garfinkel, A.S., and Schotz, M.C. (1975) Positional Specificity of Adipose Tissue Lipoprotein Lipase, *Lipids 9,* 548–553.
4. Barton, R.H., and O'Connor, C.J. (1997) Uncatalysed Intramolecular Acyl Transfer in a Lipid Hydrolysis Product Mixture, *Aust. J. Chem. 50*, 355–361.
5. Boswinkel, G., Derksen, J.T.P., van't Riet, K., and Cuperus, F.P. (1996) Kinetics of Acyl Migration in Monoglycerides and Dependence on Acyl Chainlength, *J. Am. Oil Chem. Soc. 73*, 707–711.
6. Fureby, A.M., Adlercreutz, P., and Mattiasson, B. (1996) Acyl Migration and its Implications in Lipid Modifications, *Enzyme Eng. XIII 799*, 231–237.
7. Fureby, A.M., Virto, C., Adlercreutz, P., and Mattiasson, B. (1996) Acyl Migrations in 2-Monoolein, *Biocatal. Biotransfor. 14*, 89–111.
8. Xu, X., Skands, A.R.H., Hoy, S.-E., Mu, H., Balchen, S., and Adler-Nissen, J. (1998) Production of Specific-Structured Lipids by Enzymatic Interesterification: Elucidation of Acyl Migration by Response Surface Design, *J. Am. Oil Chem. Soc. 75*, 1179–1185.
9. Scow, R.O., Blanchette-Mackie, E.J., and Smith, L.C. (1976) Role of Capillary Endothelium in the Clearance of Chylomicrons, *Circulation Res. 39*, 149–162.
10. Fielding, P.E., and Fielding, C.J. (1991) Dynamics of Lipoprotein Transport in the Circulatory System, in *Biochemistry of Lipids*, *Lipoproteins*, and *Membranes*, (Vance, D.E., and Vance, J., eds.) Elsevier, Amsterdam, pp. 427–445.
11. Arvidsson, E.O., and Belfrange, P. (1969) Monoglyceride–Protein Interaction: The Binding of Monoolein to Native Human Serum Albumin, *Acta Chem. Scand. 23*, 232–236.
12. Thumser, A.E., Buckland, A.G., and Wilton, D.C. (1998) Monoacylglycerol Binding to Human Serum Albumin: Evidence That Monooleoylglycerol Binds at the Dansylsarcosine Site, *J. Lipid Res. 39*, 1033–1038.
13. El-Maghrabi, M.R., Waite, M., Rudel, L.L., and Sisson, P. (1978) Hydrolysis of Monoacylglycerol in Lipoprotein Remnants Catalyzed by the Liver Plasma Membrane Monoacylglycerol Acyltransferase, *J. Biol. Chem. 253*, 974–981.
14. El-Maghrabi, M.R., Waite, M., and Rudel, L.L. (1978) Monoacylglycerol Accumulation in Low and High Density Lipoproteins During the Hydrolysis of Very Low Density Lipoprotein Triacylglycerol by Lipoprotein Lipase, *Biochem. Biophys. Res. Commun. 81*, 82–88.
15. Mattson, F.H., and Volpenhein, R.A. (1962) Synthesis and Properties of Glycerides, *J. Lipid Res. 3*, 281–292.
16. Scow, R.O., and Olivecrona, T. (1977) Effect of Albumin on Products Formed from Chylomicron Triacylglycerol by Liporotein Lipase *in Vitro*, *Biochim. Biophys. Acta. 487*, 472–486.
17. Foster, D.M., and Berman, M. (1981) Hydrolysis of Rat Chylomicron Acylglycerols: A Kinetic Model, *J. Lipid Res. 22*, 506–513.
18. Mortimer, B.C., Hothouse, D.J., Martine, I.J., Stick, R.V., and Redgrave, T.G. (1994) Effects of Triacylglycerol Saturated Acyl Chains on the Clearance of Chylomicron-like Emulsions from the Plasma of the Rat, *Biochim. Biophys. Acta 1211*, 171–180.
19. Derkson, A., Ekman, S., and Small, D.M. (1989) Oleic Acid Allows more Apoprotein A1 to Bind with Higher Affinity to Large Emulsion particles Saturated with Cholesterol, *J. Biol. Chem. 264*, 6935–6940.
20. Thomas, A.E., Sharoun, J.E., and Ralston, H. (1965) Quantitative Estimation of Isomeric Monoglycerides by Thin-layer Chromatography, *J. Am. Oil Chem. Soc. 42*, 789–792.
21. Redgrave, T.G., Ly, H.L., Quintao, E.C.R., and Famberg, C.F. (1993) Clearance from Plasma of Triacylglycerol and Cholesteryl Ester after Intravenous Injection of Chylomicron-like Lipid Emulsions in Rats and Man, *Biochem J. 290*, 843–847.
22. Sjurnes, B.J., and Anthonsen, T. (1994) Acyl Migration in 1,2-Dibutyrin Dependence on Solvent and Water Activity, *Biocatalysis 9*, 285–297.

23. O'Connor, C.J., and Barton, R.H. (1998) Acyl Transfer Isomerization of Glycerol 1,2-Dibutyrate and Propane-1,2-diol 1-Butyrate, *Aust. J. Chem. 51*, 455–459.
24. Holmberg, K., and Osterberg, K. (1988) Enzymatic Preparation of Monoglycerides in Microemulsion, *J. Am. Oil Chem. Soc. 65*, 1544–1548.
25. Kodali, D.R., Tercyak, A., Fahey, D.A., and Small, D.M. (1990) Acyl Migration in 1,2-Dipalmitoyl-*sn*-glycerol, *Chem. Phys. Lipids 52*, 163–170.

[Received June 29, 2000, and in revised form September 29, 2000; revision accepted October 11, 2000]

Purification, Characterization, and Molecular Cloning of Group I Phospholipases A_2 from the Gills of the Red Sea Bream, *Pagrus major*

Noriaki Iijima*, Satoshi Uchiyama, Yukichi Fujikawa, and Muneharu Esaka

Faculty of Applied Biological Science, Hiroshima University, Higashihiroshima 739-8528, Japan

ABSTRACT: Phospholipase A_2 (PLA_2) activity was investigated in various tissues of male and female red sea bream. In both male and female fishes, the specific activity of PLA_2 in the gills was 70 times higher than that in other tissues, such as the adipose tissue, intestine, and hepatopancreas. Therefore, we tried to purify PLA_2 from the gill filaments of red sea bream to near homogeneity by sequential chromatography on Q-Sepharose Fast Flow, Butyl-Cellulofine, and DEAE-Sepharose Fast Flow columns, and by reversed-phase high-performance liquid chromatography. Two minor and one major PLA_2, tentatively named G-1, G-2 and G-3 PLA_2, were purified, and all showed a single band with an apparent molecular mass of approximately 15 kDa by sodium dodecylsulfate-polyacrylamide gel electrophoresis. The exact molecular mass values of G-1, G-2, and G-3 PLA_2 were 14,040, 14,040 and 14,005 Da, respectively. G-1, G-2, and G-3 PLA_2 had a Cys 11 and were all identical in N-terminal amino acid sequences from Ala-1 to Glu-56. A full-length cDNA encoding G-3 PLA_2 was cloned by reverse transcriptase-polymerase chain reaction and rapid amplification of cDNA ends methods, and G-3 PLA_2 was found to be classified to group IB PLA_2 from the deduced amino acid sequence. G-1, G-2, and G-3 PLA_2 had a pH optimum in an alkaline region at around pH 9–10 and required Ca^{2+} essentially for enzyme activity, using a mixed-micellar phosphatidylcholine substrate with sodium cholate. These results demonstrate that three group I PLA_2, G-1, G-2, and G-3 PLA_2, are expressed in the gill filaments of red sea bream.

Paper no. L8433 in *Lipids 35,* 1359–1370 (December 2000).

Phospholipase A_2 (phosphatide 2-acyl hydrolase, EC 3.1.1.4) (PLA_2) hydrolyzes the fatty-acyl ester bond at the *sn*-2 position of glycerophospholipids. PLA_2 has now become recognized as being a large superfamily of distinct enzymes that play a central role in diverse cellular processes including phospholipid digestion and metabolism, host defense, and signal transduction (1). New groups of Ca^{2+}-dependent low molecular mass enzymes, so-called secretory PLA_2, have recently been purified and are now classified into six groups, group I, II, III, V, IX, and X, based on their primary structures (1–3). Mammalian pancreatic type PLA_2, group IB PLA_2, was originally found in large amounts in the pancreas and was considered to function in the digestion of dietary phospholipids. However, this enzyme was later found to express in nonpancreatic tissues including the spleen, lung, kidney, and ovary (4–12). It has now been proposed to function as a kind of cytokine/growth factor in several cell lines by interacting with specific binding sites on the cell surface (13,14). Two major types of receptors, N-type and M-type receptors, have been recently identified for secretory PLA_2, including snake venom group IA PLA_2 and mammalian group IB PLA_2, and the involvement of mammalian group IB PLA_2 *via* M-type receptor in various physiological and pathophysiological responses such as cell proliferation, cell contraction, lipid mediator release, acute lung injury, and endotoxic shock has been proposed (13,15,16). These aspects indicate that the physiological importance of group I PLA_2 in the nondigestive tissues and cells is higher than considered previously.

On the other hand, there is little information about the enzymology of fish PLA_2. Attempts have been made to purify PLA_2 from liver, hepatopancreas, and muscles of fish such as rainbow trout *(Salmo gairdneri)* (17,18) and cod *(Gadus morhua)* (19,20). However, only one PLA_2 has been purified from cod muscle (19). Zambonino Infante and Cahu (21) recently analyzed the mRNA level of PLA_2 in *Dicentrarchus labrax* larvae cultured with diets containing different lipid levels but did not obtain the purified enzyme. To understand the enzymology of digestive lipolysis in fish, we purified three secretory PLA_2 from the digestive organs including the pyloric ceca and hepatopancreas of red sea bream, and two PLA_2, DE-1 and DE-2 PLA_2, purified from the hepatopancreas were found to be classified as group I PLA_2 based on

*To whom correspondence should be addressed at Faculty of Applied Biological Science, Hiroshima University, 1-4-4 Kagamiyama, Higashihiroshima 739-8528, Japan. E-mail: noriiij@hiroshima-u.ac.jp

Abbreviations: *p*-APMSF, *p*-amidinophenylmethylsulfonyl fluoride; *p*-BPB, *p*-bromophenacyl bromide; CHAPS, 3-[(3-cholamidopropyl) dimethylammonio]-1-propanesulfonate; CTAB, cetyl trimethylammonium bromide; HPLC, high-performance liquid chromatography; MALDI-TOF, matrix-assisted laser desorption ionization-time of flight; PAGE, polyacrylamide gel electrophoresis; PCR, polymerase chain reaction; PLA_2, phospholipase(s) A_2; POPC, 1-palmitoyl-2-oleoyl-*sn*-glycero-3-phosphocholine; POPE, 1-palmitoyl-2-oleoyl-*sn*-glycero-3-phosphoethanolamine; POPG, 1-palmitoyl-2-oleoyl-*sn*-glycero-3-phosphoglycerol; POPS, 1-palmitoyl-2-oleoyl-*sn*-glycero-3-phosphoserine; RACE, rapid amplification of cDNA ends; RP–HPLC, reversed-phase–HPLC; RT, reverse transcriptase; SDS, sodium lauryl sulfate; TFA, trifluoroacetic acid.

the amino acid sequence (22–24). We also found that an antiserum against *Naja naja* venom PLA_2 reacted weakly with the partially purified PLA_2 from the hepatopancreas of red sea bream and that it labeled zymogen granules of the pancreatic acinar cells and secretory materials of certain epithelial cells of epithelial crypts in the pyloric ceca of red sea bream (25). In the present report, we investigated the distribution of PLA_2 activity in the various tissues of red sea beam and found extremely high PLA_2 activity in the nondigestive tissue, gills. We further purified two minor and one major PLA_2, tentatively named G-1, G-2, and G-3 PLA_2 from the gill filaments of red sea bream. The N-terminal amino acid sequences of G-1, G-2, and G-3 PLA_2 show that they belong to group I PLA_2. Furthermore, we isolated a full-length cDNA clone of G-3 PLA_2 by polymerase chain reaction (PCR) methods and showed that G-3 PLA_2 is classified to group IB PLA_2 from the deduced amino acid sequence.

MATERIALS AND METHODS

Materials. 1-Palmitoyl-2-oleoyl-*sn*-glycero-3-phosphocholine (POPC), 1-palmitoyl-2-oleoyl-*sn*-glycero-3-phosphoethanolamine (POPE), 1-palmitoyl-2-oleoyl-*sn*-glycero-3-phosphoserine (POPS), and 1-palmitoyl-2-oleoyl-*sn*-glycero-3-phosphoglycerol (POPG) were purchased from Avanti Polar Lipids, Inc. (Birmingham, AL). Sodium cholate was purchased from Nacalai Tesque (Kyoto, Japan). 9-Anthryldiazomethane was purchased from Funakoshi Co., Ltd. (Tokyo, Japan) and *n*-heptadecanoic acid from Tokyo Kasei Organic Chemicals (Tokyo, Japan). 3-[(3-Cholamidopropyl) dimethylammonio]-1-propanesulfonate (CHAPS) and *p*-bromophenacyl bromide (*p*-BPB) were obtained from Dojindo Laboratories (Kumamoto, Japan). DEAE-Sepharose Fast Flow and Q-Sepharose Fast Flow were purchased from Pharmacia (Uppsala, Sweden). Butyl-Cellulofine was purchased from Seikagaku Kogyo (Tokyo, Japan), Asahipak ODP-50 was obtained from Showa Denko (Tokyo, Japan), YMC-Pack Protein-RP from YMC Co., Ltd. (Tokyo, Japan), and TSKgel Octadecyl-NPR from Tosoh (Tokyo, Japan). High-performance liquid chromatography (HPLC) grade CH_3CN was purchased from Nacalai Tesque, and 2-mercaptoethanol, 4-vinylpyridine, cetyl trimethylammonium bromide (CTAB), *p*-amidinophenylmethylsulfonyl fluoride (*p*-APMSF), and a silver staining kit were from Wako Pure Chemicals (Osaka, Japan). The DC Protein Assay Kit was obtained from Bio-Rad Laboratories (Richmond, CA).

Standard assay for PLA_2. PLA_2 activity was determined as described previously (23). The standard incubation systems (100 μL) for the assay of PLA_2 contained 2 mM POPC, 6 mM sodium cholate, 100 mM NaCl, 50 mM glycine-NaOH (pH 9.5), and 5 mM $CaCl_2$. One unit (U) was defined as the liberation of 1 μmol of free fatty acid/min as measured by reversed-phase (RP)–HPLC. In assays without detergent, the substrate was sonicated for 2 min in a water bath sonicator (Transsonic T460; Elma GmbH & Co. KG, Singen, Germany).

Preparation of dialyzate. Gill filaments, heart, spleen, adipose tissue, testis or ovary, hepatopancreas, stomach, pyloric ceca, and intestine were collected from five freshly killed farm-raised male and female red sea bream, *Pagrus (Chrysophrys) major* (0.8–1.0 kg), and were immediately frozen using dry ice. Frozen tissues were lyophilized, and the delipidated powder was prepared as described previously (23). Each 0.5 g of the resulting delipidated powder was solubilized in 5 mL of 5 mM Tris-HCl buffer (pH 7.4) for 1 h to yield a crude extract. The pH of the crude extract was adjusted to 4 by adding 6 N HCl, and the acidified extract was then heated at 80°C for 3 min. The cooled extract was centrifuged at 10,000 × *g* for 15 min at 4°C. The supernatant was dialyzed overnight against 5 mM Tris-HCl buffer (pH 7.4) and centrifuged at 10,000 × *g* for 15 min at 4°C. The resulting dialyzate was used for the determination of PLA_2 activity in the various red sea bream tissues.

For the purification of PLA_2, gill filaments were collected from 58 freshly killed farm-raised red sea bream (0.8–1.0 kg) and were immediately frozen using dry ice. The delipidated powder (125.5 g) of the gill filaments was solubilized in 10 vol of 5 mM Tris-HCl buffer (pH 7.4) containing 0.5 mM *p*-APMSF and a dialyzate was prepared as described above.

Purification of gill PLA_2. All steps were carried out at 4°C except for the HPLC runs, which were performed at room temperature. The dialyzate was loaded onto a Q-Sepharose Fast Flow column (5 × 5.5 cm) which was equilibrated with 5 mM Tris-HCl buffer (pH 7.4). The column was washed extensively with the same buffer, and PLA_2 activity was eluted with 5 mM Tris-HCl buffer (pH 7.4) containing 2 M NaCl at a flow rate of 5 mL/min. The active fractions were directly applied to a Butyl-Cellulofine column (2.6 × 19 cm) which was equilibrated with 5 mM Tris-HCl buffer (pH 7.4) containing 2 M NaCl. The column was washed extensively with the same buffer, followed by elution with 5 mM Tris-HCl buffer (pH 7.4) containing 0.5 M NaCl and with 5 mM Tris-HCl buffer (pH 7.4), respectively, at a flow rate of 0.6 mL/min. PLA_2 activity was eluted with 5 mM Tris-HCl buffer (pH 7.4). The active fractions were pooled, lyophilized, and dissolved in 20 mM Tris-HCl buffer (pH 8.0) containing 0.5% CHAPS. This solution was applied to a DEAE-Sepharose Fast Flow column (1.6 × 15 cm) which had been equilibrated with 20 mM Tris-HCl buffer (pH 8.0) containing 0.5% CHAPS. The PLA_2 activity was bound to the column and was eluted with a linear gradient of NaCl. The active fractions were pooled. Trifluoroacetic acid (TFA) was added to the active fractions at a final concentration of 0.1%, and the resulting solution was applied to a YMC-Pack Protein RP column (4.6 × 150 mm) which was equilibrated with 0.1% TFA/10% CH_3CN. The PLA_2 activity was bound to the HPLC column, and the column was eluted with a CH_3CN linear gradient. The active fractions were pooled. Disodium hydrogenphosphate was added to the active fractions to a final concentration of 10 mM. The resulting solution was applied to an Asahipak ODP-50 column (6 × 250 mm) that was pre-equilibrated with 10 mM Na_2HPO_4. PLA_2 activity was bound to the HPLC column. The column was then washed with 10 mM Na_2HPO_4

and eluted with a linear gradient from 10 mM Na_2HPO_4 to 0.5 mM Na_2HPO_4/60% CH_3CN. Peaks 1, 2, and 3 showing PLA_2 acivity were pooled and stored as final enzyme preparations, tentatively named G-1, G-2 and G-3 PLA_2, respectively. During the purification step, the protein concentration was measured with a DC Protein Assay Kit with bovine serum albumin as a standard. The protein concentration of G-3 PLA_2 was measured as described above. For G-1 and G-2 PLA_2, an HPLC protein determination method was devised. G-1 and G-2 PLA_2 were injected on a TSK gel Octadecyl-NPR (4.6 × 35 mm) column that had been equilibrated with 10 mM Na_2HPO_4. The column was eluted with a linear gradient from 10 mM Na_2HPO_4 to 0.5 mM Na_2HPO_4/60% CH_3CN, and the eluate was analyzed at 220 nm. G-3 PLA_2 was used for HPLC analysis as a protein standard.

Molecular weight determination of the purified enzymes. The molecular weights of purified enzymes were determined by sodium lauryl sulfate-polyacrylamide gel electrophoresis (SDS-PAGE) and a matrix-assisted laser desorption ionization time of flight (MALDI-TOF) mass spectrometer (Dynamo, Finnigan-MAT, San Jose, CA). SDS-PAGE was carried out as described by Laemmli (26) using a 16% polyacrylamide gel in the presence of 2-mercaptoethanol, and the protein bands were stained with Coomasie Brilliant Blue-R250.

For MALDI-TOF mass spectrometry, the purified enzymes were desalted by RP–HPLC with a TSKgel Octadecyl-NPR column having a linear gradient of CH_3CN from 10% CH_3CN/0.1% TFA to 70% CH_3CN/0.1% TFA, at a flow rate of 0.8 mL/min. One microliter (approximately 0.3 pmol) of the desalted enzyme solution was mixed with an equal volume of matrix solution [10 mg/mL 2,5-dihydroxybenzoic acid/10 mg/mL 5-methoxysalicylic acid (9:1, vol/vol)] on a target disk and allowed to dry. Subsequently, spectra were obtained using a MALDI-TOF mass spectrometer, with horse apomyoglobin (16,951 Da) as a calibration standard.

N-terminal amino acid sequence determination. The purified PLA_2 were reduced with 2-mercaptoethanol and were S-pyridylethylated with 4-vinylpyridine as described previously (24). The amino acid sequence of the S-pyridylethylated PLA_2 was analyzed with a Hewlett-Packard G1005A protein sequencing system (Palo Alto, CA).

Extraction of mRNA. Gill filaments were removed immediately from freshly killed red sea bream (approximately 200 g) and were stored in liquid nitrogen. Total RNA was extracted from the gill filaments using Isogen (Nippon Gene, Tokyo, Japan), and mRNA was isolated using Oligotex-dT30 <Super> (Roche Diagnostics K.K., Tokyo, Japan), according to the manufacturer's protocol.

cDNA amplification of gill G-3 PLA_2 by PCR. Primers P20 and P2a are 5′-ATCTGGCAGTTCGGCGACATGATCGAG-3′ and 5′-GC(A/G)GCCTT(C/T)CTGTCGCACTC(A/G)CA-3′, that were derived from possible cDNA sequences corresponding to parts of amino acid sequence of red sea bream gill G-3 PLA_2, IWQFGDMIE (Residues 2–10, Fig. 5), and that of conserved amino acid sequence of mammalian pancreatic PLA_2 (27) and red sea bream hepatopancreas DE-2 PLA_2 (DDBJ/EMBL, Accession No. AB009286), CECDRKAA (Residues 96–103), respectively. One microgram of red sea bream gill mRNA was used to prepare first-stranded cDNA with a RNA PCR kit (Takara, Tokyo, Japan), employing molony murine leukemia virus reverse transcriptase. An internal cDNA fragment encoding PLA_2 was generated by PCR from first-stranded cDNA of red sea bream gill using degenerated primers P20 and P2a and *Pyrococcus kodakaraensis* KOD1 (KOD dash) DNA polymerase (Toyobo, Tokyo, Japan). After an initial denaturation for 160 s at 94°C, 30 cycles of amplification were carried out, with 30 s at 94°C, 10 s at 58°C, 30 s at 74°C, followed by incubation at 74°C for 10 min. Then the PCR product was isolated from an agarose gel using Ultrafree R-MC centrifugal filter unit (0.45 μm) (Millipore, Bedford, MA) and was sequenced. From the determined nucleotide sequence of the internal cDNA, new oligomers, primers P26 (5′-CATGACGACTGCTATGGA-GCACA-3′, identical to nt 211–233) and AP22 (5′-GGTC-GCTGAGCAGGTCACCTTGCG-3′, complementary to nt 307–330) were designed for 3′- and 5′-end amplifications, respectively. A first- and second-stranded cDNA were synthesized using red sea bream gill mRNA and Marathon cDNA Amplification kit (Clontech, Palo Alto, CA) according to the manufacturer's protocol. Briefly, 1 μg of red sea bream gill mRNA was reverse-transcribed using 10 μM of cDNA synthesis primer and 20 units of avian myeloblastosis virus reverse transcriptase at 42°C for 1 h. Second-stranded cDNA synthesis was carried out using *Escherichia coli* DNA polymerase I (24 units), DNA ligase (4.8 units), and RNase H (1 unit) at 16°C for 1.5 h, followed by T4 DNA polymerase (10 units) at 16°C for 45 min. The resulting second-stranded cDNA was precipitated and ligated to Marathon cDNA Adaptor (2 μM) using 1 unit of T4 DNA ligase for 40 min at room temperature. The 5′-end amplification of PLA_2 cDNA was carried by reverse transcriptase-polymerase chain reaction (RT-PCR) with adaptor-ligated double-stranded cDNA, Adaptor primer 1 (5′-CCATCCTAATACGACTCACTATAGGGC-3′), AP22 antisense primer and KOD Dash, and 3′-end amplification of PLA_2 cDNA was with adaptor-ligated double stranded cDNA, Adaptor primer, P26 sense primer, and KOD Dash. PCR conditions of 5′- and 3′-end amplification were as follows. After an initial denaturation for 160 s at 94°C, 30 cycles of amplification were carried out, with 30 s at 94°C, 10 s at 66°C, 30 s at 74°C, followed by incubating at 74°C for 10 min. The resulting PCR products were subcloned into pGEM-T vector (Promega, Madison, WI) and were transformed into JM109 cells, and positive clones were selected on LB/ampicillin/IPTG/X-Gal plates according to the manufacturer's protocol. Plasmid DNA was purified from positive clones with QIAprep Spin Miniprep Kit (Qiagen, Tokyo, Japan) and was sequenced.

Sequencing of PCR products. Cycle sequencing reaction of PCR products was performed using Dye terminator cycle sequencing kit (PerkinElmer, Norwalk, CT), according to the manufacturer's protocol, and the sequences of PCR products

TABLE 1
Distribution of Phospholipase A_2 (PLA_2) Activity in the Various Tissues of Red Sea Bream[a]

Tissues	Specific activity (mU/mg protein)		Specific activity (mU/g tissue)	
	Male	Female	Male	Female
Gills	1000	1040	14,659	13,769
Heart	1	7	6.7	49.3
Spleen	0.4	0.4	4.3	7.1
Muscle	0.1	0.8	1.5	3.1
Adipose tissue	14.5	10	19.1	8.1
Testis	1.5	—	13.4	—
Ovary	—	0.4	—	3.9
Hepatopancreas	3	1.5	15.2	16
Stomach	0.4	0.6	2.3	11.2
Pyloric ceca	0.7	0.5	13.7	12.9
Intestine	4.2	3	69.3	34.3

[a]The reaction mixture consisted of 50 mM glycine-NaOH (pH 9.5), 2 mM 1-palmitoyl-2-oleoyl-*sn*-glycero-3-phosphocholine (POPC), 6 mM sodium cholate, 5 mM $CaCl_2$, and 0.1 M NaCl in a final volume of 0.1 mL. Data were obtained in duplicate.

were determined with an Applied Biosystems 373A DNA sequencer (Foster, CA).

RESULTS

Distribution of PLA_2 activity in the various tissues of red sea bream. The dialyzate was prepared from the various tissues of red sea bream, and PLA_2 activity in the dialyzate was measured using the mixed-micellar POPC substrate with sodium cholate. As shown in Table 1, the specific activity (mU/mg protein) of PLA_2 in the gills was extremely high, followed by adipose tissue, intestine, and hepatopancreas of male fish; PLA_2 activity of gills was over 70 times higher than that of adipose tissue and 200 times higher than that of other tissues, such as intestine, hepatopancreas and so on. Also in female fish, PLA_2 activity in the gills was exceedingly high, followed in order by adipose tissue, heart, and intestine. In comparison with PLA_2 activity per gram of tissue, specific activity of PLA_2 in the gills was 200 times higher than that in other tissues of male and female fishes.

Purification of PLA_2 from the gills of red sea bream. The purification procedure is summarized in Table 2. In starting from the crude extract, G-1, G-2, and G-3 PLA_2 were purified more than 10,000-fold, and the yields of G-1, G-2, and G-3 PLA_2 were 0.4, 0.3, and 5.5%, using mixed-micellar POPC substrate, respectively. Figure 1 documents the results obtained from a first RP–HPLC. The active fractions (fraction No. 62–70) were pooled and applied to a second RP–HPLC (Fig. 2). Three peaks of PLA_2 activity appeared in fraction No. 126–129, 133–136, and 141–148, respectively. Peaks 1, 2, and 3 (shown by the bars in Fig. 2) were pooled and were further applied to a TSKgel Octadecyl-NPR column. Peaks 1, 2, and 3 were eluted separately, and PLA_2 activity was also found in these peaks (data not shown). When peaks 1, 2, and 3 were mixed and applied to the same column, each peak eluted separately (Fig. 3). Therefore peaks 1, 2, and 3 were pooled as G-1, G-2, and G-3 PLA_2 to yield final enzyme preparations. G-1, G-2, and G-3 PLA_2 yielded a single protein band by SDS-PAGE under reducing conditions with an estimated molecular mass of approximately 15 kDa, identical to that of porcine pancreatic PLA_2 (Fig. 4). From the analysis of MALDI-TOF mass spectrometry, the exact molecular mass values of G-1, G-2, and G-3 PLA_2 were calculated to be 14,040, 14,040, and 14,005 Da, respectively. The specific activities of G-1, G-2, and G-3 PLA_2 amounted to 1294, 1143, and 1293 μmol/min/mg protein, respectively (Table 2).

N-terminal amino acid sequence of G-1, G-2, and G-3 PLA_2. The purified PLA_2 were reduced, S-pyridylethylated, and subjected to automated Edman analysis. Then, the N-terminal amino acid sequences of S-pyridylethylated G-1, G-2, and G-3 PLA_2 were determined as in the following: AIWQFGDMIECVQPGVDPINYNNYGCYCGLGGKGTPVDDLDRCCKVHDDCYGAQME.

G-1, G-2, and G-3 PLA_2 contained Cys 11 and were all identical in amino acid sequences from Ala1 to Glu56.

TABLE 2
Purification of G-1, G-2, and G-3 PLA_2 from the Gills of Red Sea Bream[a]

Purification step	Total protein (mg)	Total activity (U)	Specific activity (U/mg)	Purification (-fold)	Yield (%)
Crude extract	46,176	5,082	0.11	1	100
Dialyzate	25,111	3,570	0.14	1	70.2
Q-Sepharose Fast Flow	3,132	2,442	0.78	7	48.1
Butyl-Cellulofine	26.55	1,662	62.6	569	32.7
DEAE-Sepharose Fast Flow	8.48	1,794	211.6	1,923	35.3
YMC-Pack PROTEIN-RP	1.06	679	640.6	5,823	13.4
Asahipak ODP-50					
G-1 PLA_2	0.017	22	1,294	—	0.4
G-2 PLA_2	0.014	16	1,143	—	0.3
G-3 PLA_2	0.215	278	1,293	11,754	5.5

[a]The reaction mixture consisted of 50 mM glycine-NaOH (pH 9.5), 2 mM POPC, 6 mM sodium cholate, 5 mM $CaCl_2$, and 0.1 M NaCl, in a final volume of 0.1 mL. Data were obtained in duplicate. Protein concentration was determined with a DC Protein assay kit. For further information on purification see the Materials and Methods section. See Table 1 for abbreviations.

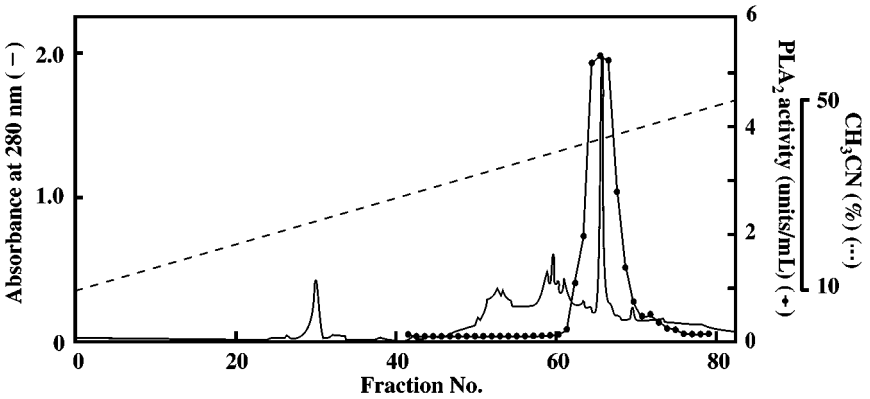

FIG. 1. Elution profile of phospholipase A_2 (PLA_2) on first reversed-phase–high-performance liquid chromatography (RP–HPLC). The pooled active fraction from the DEAE-Sepharose Fast Flow (Pharmacia, Uppsala, Sweden) column was applied to a YMC-Pack Protein RP (YMC Co. Ltd., Tokyo, Japan) column (4.6 × 250 mm) pre-equilibrated with 10% CH_3CN/0.1% trifluoroacetic acid (TFA). The elution of protein was followed by monitoring the absorbance at 280 nm (–). The dashed line indicates the linear gradient of CH_3CN. The flow rate was 1.0 mL/min. The fraction volume was 0.5 mL. The PLA_2 activity (●) of a 2 μL aliquot of each fraction was measured as described in the Materials and Methods section.

cDNA cloning of gill G-3 PLA_2. A full-length cDNA clone of gill G-3 PLA_2 was isolated by RT-PCR and rapid amplification of cDNA ends (RACE) methods. The nucleotide sequence of gill G-3 PLA_2 cDNA (1084 bp) included a 444 bp open reading frame that encoded for a signal peptide of 24 amino acids, followed by a mature protein of 124 amino acids, as shown in Figure 5. The calculated molecular mass and isoelectric point of the mature protein were 14,007 Da and 5.17, respectively. The 3′-noncoding region contained two putative polyadenylation signals located upstream of the poly A tail. An alignment of the mature amino acid sequences of bovine pancreatic PLA_2 (28), porcine pancreatic PLA_2 (29), and *N. naja kaouthia* venom PLA_2 (30) with the sequence of gill G-3 PLA_2 is presented in Figure 6. The sequence of gill G-3 PLA_2 has common characteristics with mammalian pancreatic type, group IB PLA_2, including the presence of Cys11 and the alignment of other Cys residues; residues of N-terminal helix Gln4, Phe5, and Ile9, and the presence of the absolutely conserved active-site His48, Tyr52, Tyr73 and Asp99; a "pancreatic loop" of residues 63–67 that are conserved in group IB PLA_2; the conserved sequence of the calcium-binding segment Tyr25-Gly33.

Properties of G-1, G-2, and G-3 PLA_2. Effects of pH and concentrations of Ca^{2+} and sodium cholate on the purified

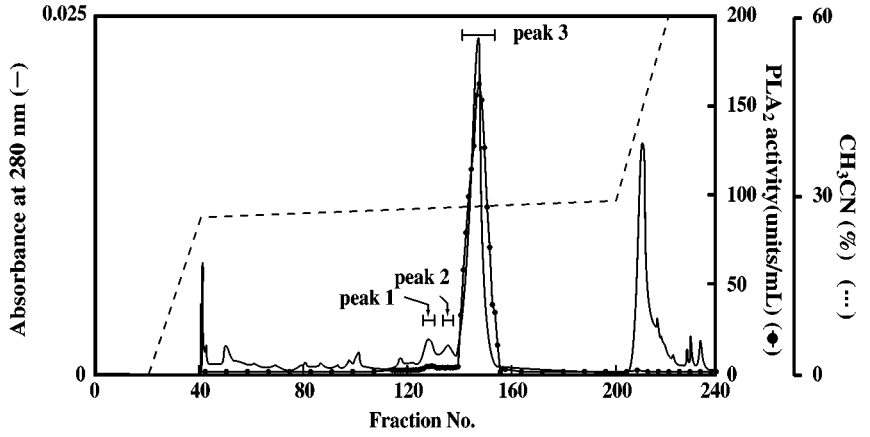

FIG. 2. Elution profile of PLA_2 on second RP–HPLC. The pooled fraction from the YMC-Pack Protein RP column was applied to an Asahipak ODP-50 (Showa Denko, Tokyo, Japan) column (6.0 × 250 mm) pre-equilibrated with 10 mM Na_2HPO_4. The elution of protein was followed by monitoring the absorbance at 280 nm (–). The dashed line indicates the linear gradient of CH_3CN. The flow rate was 1.0 mL/min. The fraction volume was 0.25 mL. Each fraction was diluted 50 times with 30% CH_3CN/0.1% TFA, and the PLA_2 activity (●) of a 2 μL aliquot of each diluent was measured as described in the Materials and Methods section. For abbreviations and other manufacturer see Figure 1.

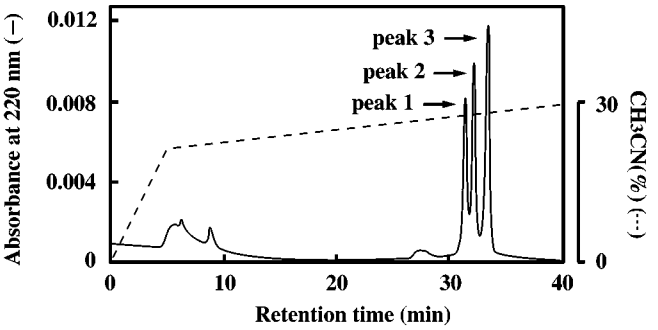

FIG. 3. Elution profile of G-1, G-2, and G-3 PLA_2 on RP–HPLC. The pooled fractions of peak 1, peak 2, and peak 3 eluted from the Asahipak ODP-50 column were mixed and were applied to a TSKgel Octadecyl-NPR (Tosoh, Tokyo, Japan) column (4.6 × 35 mm) pre-equilibrated with 10 mM Na_2HPO_4. The elution of protein was followed by monitoring the absorbance at 220 nm (–). The dashed line indicates the linear gradient of CH_3CN. The flow rate was 0.8 mL/min. For other abbreviations and manufacturer see Figures 1 and 2.

PLA_2 activity are shown in Figure 7. G-1, G-2, and G-3 PLA_2 hydrolyzed POPC efficiently in an alkaline pH region, and optimal activities for all PLA_2 were found to be at around pH 9–10 (Fig. 7A). The activities of G-1, G-2, and G-3 PLA_2 were barely detected in the presence of 1 mM EGTA (Fig. 7B). The maximal activities were observed in the presence of 2–40 mM Ca^{2+}. Activities of G-1, G-2, and G-3 PLA_2 toward POPC were not detectable in the absence of bile salts. However, they were stimulated dramatically by the addition of sodium cholate, and their optimal activities were found at cholate concentrations of about 6–8 mM (cholate/POPC molar ratio of 3–4) (Fig. 7C). The effects of various agents on the activity of purified PLA_2 were investigated using a mixed-micellar POPC substrate (Table 3). The activities of G-1, G-2, and G-3 PLA_2 toward the POPC substrate were almost completely inhibited by the addition of 1 mM EGTA or EDTA, and Mg^{2+}, Zn^{2+}, Fe^{3+}, and Cu^{2+} could not replace Ca^{2+}. CTAB and SDS greatly inhibited the activities of G-1, G-2, and G-3 PLA_2. *p*-APMSF, a serine protease inhibitor, did not inhibit the activities of G-1, G-2, or G-3 PLA_2 (data not shown). *p*-BPB, an alkylating reagent of His, inhibited all three enzymes but was less sensitive than porcine pancreatic and *N. naja kaouthia* venom PLA_2. Mixed micelles of sodium cholate and phospholipids containing various head groups (POPC, POPE and POPG) or aqueous phospholipid dispersions (without sodium cholate) were prepared and were used as substrates for examining the substrate specificity of the purified enzymes (Table 4). Porcine pancreatic PLA_2 was the most active for the micellar POPG substrate, and *N. naja kaouthia* venom PLA_2 was for micellar POPC. On the other hand, red sea bream gill G-1, G-2, and G-3 PLA_2 hydrolyzed efficiently both POPC and POPG micelles at similar rates. G-1, G-2, and G-3 PLA_2 were active for POPE and POPG liposomes, but not for POPC liposome. All PLA_2 tested were inactive for both micellar and dispersed POPS (data not shown).

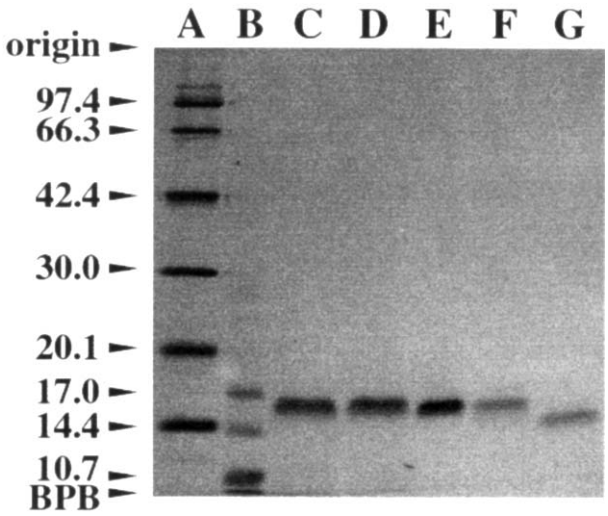

FIG. 4. Sodium lauryl sulfate-polyacrylamide gel electrophoresis of red sea bream gill G-1 (lane C), G-2 (lane D), and G-3 (lane E) PLA_2, porcine pancreatic PLA_2 (lane F), and *Naja naja kaouthia* venom PLA_2 (lane G). Molecular masses of marker proteins (lane A) from top to bottom: 97.4, 66.3, 42.4, 30.0, 20.1, and 14.4 kDa, and those of marker peptides (lane B) from top to bottom: 17.0, 14.4, and 10.7 kDa. BPB, bromophenacyl bromide; for other abbreviation see Figure 1.

DISCUSSION

We investigated the distribution of PLA_2 activity in the various tissues of red sea bream and found extremely high activity in the gills (Table 1). We had found previously that PLA_2 activity in the crude enzyme extract of pyloric ceca and hepatopancreas of red sea bream increased significantly due to dialysis (23,24). This suggests the presence of PLA_2 inhibitory materials in the crude enzyme extract. Therefore, we used a dialyzate as a sample for measuring PLA_2 activity in the present experiment. In mammals, pancreatic PLA_2 are stored as a form of proenzyme, which are converted into the active form by limited tryptic proteolysis in the intestinal lumen (31,32). Also, in red sea bream, PLA_2 activity in the hepatopancreas increased dramatically during autolysis (22). Therefore, it exists as a proenzyme in the hepatopancreas of red sea bream, similarly to porcine pancreatic PLA_2 (33). As the crude enzyme extract of hepatopancreas was not autolyzed in the present experiment, it is inappropriate to compare the PLA_2 activities of the hepatopancreas and gills. However, the specific activity of PLA_2 in a gill dialyzate (Table 1) was over 150-fold higher than that of the hepatopancreas (7 mU/mg protein) after autolysis (24). As we could not find any PLA_2 activity in the plasma of red sea bream, PLA_2 activity in the gills originated from the gills. It remains unclear whether PLA_2 exists as a proenzyme or active enzyme in other tissues in addition to hepatopancreas. However, it is thought that somewhat higher PLA_2 activity expresses in the gills of red sea bream. Therefore, we tried to purify PLA_2 from red sea bream gill filaments.

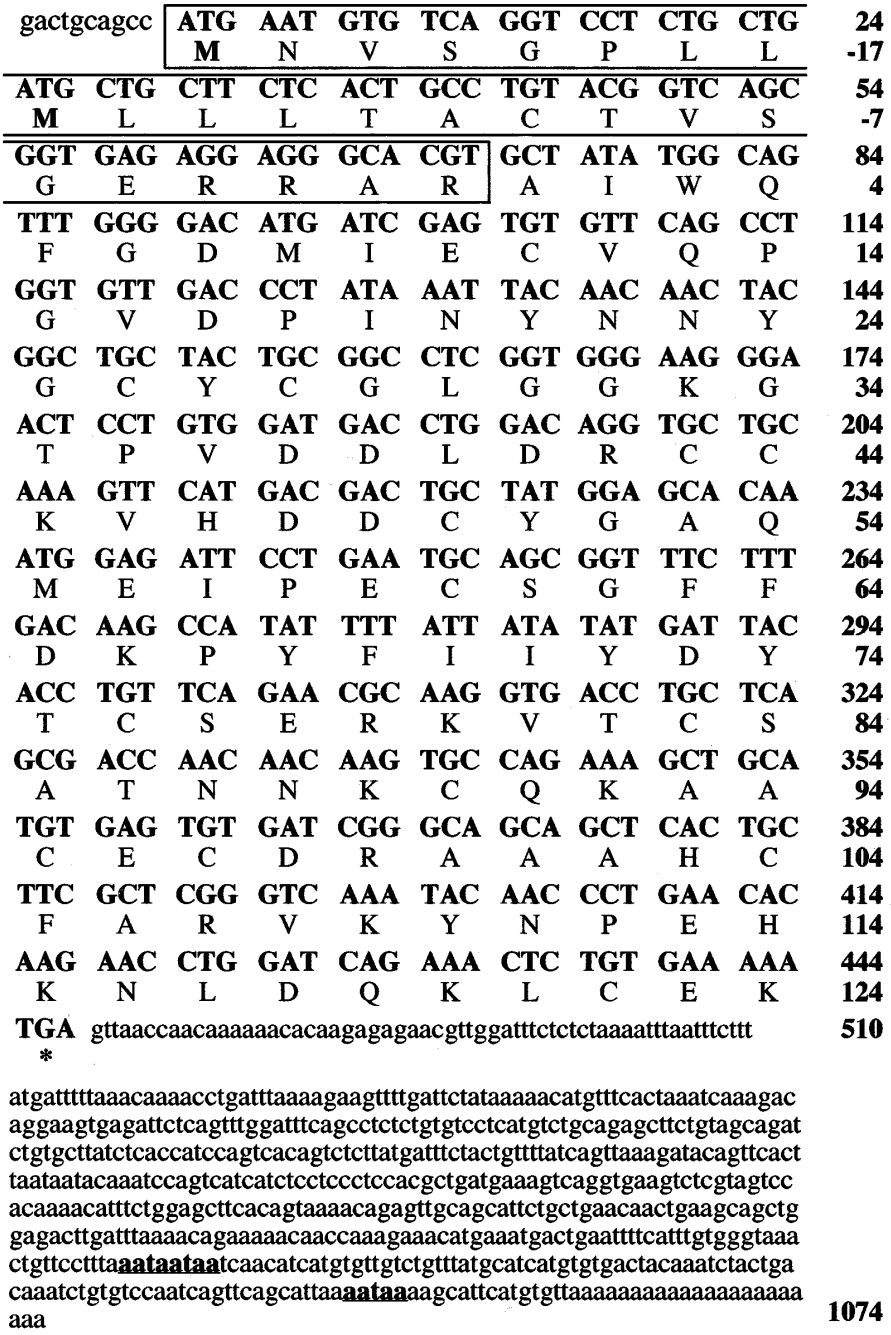

FIG. 5. Nucleotide and deduced amino acid sequences of red sea beam gill G-3 PLA_2. The predicted preprosegment is boxed and possible initiator methionines are shown in **bold**. The putative polyadenylation signal is underlined and in **bold**. Asterisk shows termination codon. For abbreviation see Figure 1.

Two minor and one major PLA_2, tentatively named G-1, G-2, and G-3 PLA_2, were finally purified with second RP–HPLC (Figs. 2 and 3) and were all identical in their N-terminal amino acid sequences from Ala1 to Glu56. A full-length cDNA clone for G-3 PLA_2 was isolated by RT-PCR and RACE methods (Fig. 5), and the molecular mass (14,005 Da) of G-3 PLA_2 obtained by time of flight mass spectrometric analysis almost coincided with that by predicted amino acid sequence of mature enzyme (14,007 Da, Fig. 6). G-3 PLA_2 contains 14 cysteines including Cys11 and Cys77 and a pancreatic loop of residues 63–67, which are commonly conserved in group IB PLA_2. In addition, G-3 PLA_2 had a pH optimum in an alkaline region at around pH 9–10 and required the presence of millimolar concentrations of Ca^{2+} for enzyme activity, using a mixed-micellar POPC substrate with sodium cholate. These results indicate that red sea bream gill G-3

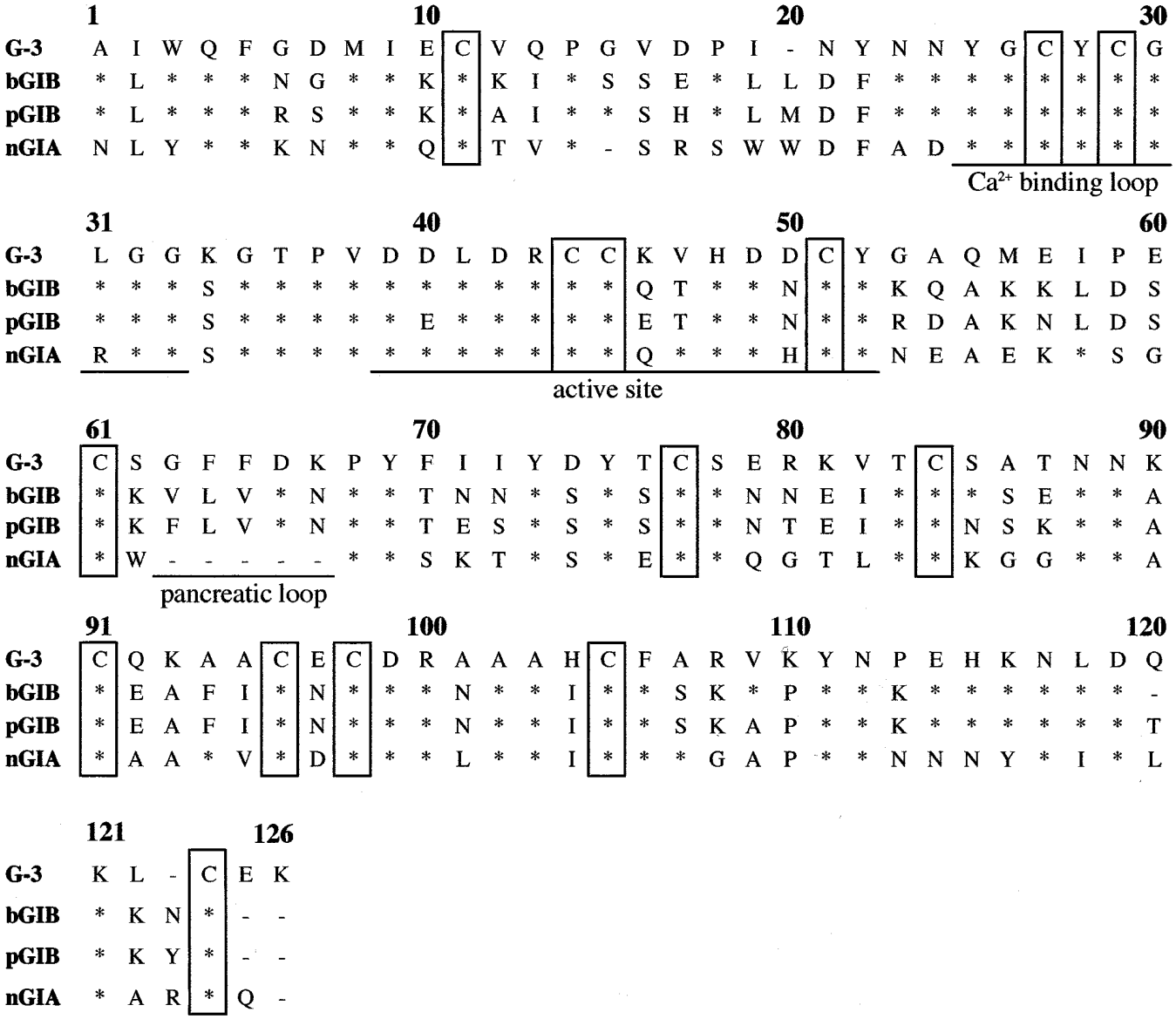

FIG. 6. Alignment of the amino acid sequences of red sea bream gill G-3 PLA_2 with other group I PLA_2. Only mature protein sequences of PLA_2 are shown. G-3, red sea bream gill G-3 PLA_2; bGIB, bovine pancreatic group IB PLA_2 (19); pGIB, porcine pancreatic group IB PLA_2 (29); nGIA, *N. naja kaouthia* venom group IA PLA_2 (30). Asterisks indicate the amino acid residues identical to those of red sea bream gill G-3 PLA_2. Cysteines that are conserved in all PLA_2 are boxed.

PLA_2 belongs to group IB PLA_2. The sequence similarity and hydropathy profiles suggest that the N-terminal 24 residues are prepropeptide sequence (Fig. 5). SignalP computer analysis (34) for the potential cleavage positions in its signal sequence suggests that the signal peptide cleavage site is present between position Gly-6 and Glu-5 preceding the mature protein. Furthermore, arginine doublet, which is the cleavage site of subtilisin-like convertase in the Golgi apparatus (35), is also included at positions –3 and –4 preceding the mature protein. Further studies are needed to understand the maturation process of gill G-3 PLA_2.

Red sea bream gill G-3 PLA_2 hydrolyzed efficiently both mixed-micellar POPG and POPC at similar rates (Table 4). It is well known that snake venom and porcine pancreatic PLA_2 show high affinity toward zwitterionic substrate POPC and negatively charged substrate POPG, respectively (31). A similar result was obtained for *N. naja kaouthia* venom and porcine pancreatic PLA_2 in the present experiment (Table 4). It has been shown that ionic residues 53 through 58 (Fig. 6) located at the end of a long α-helix loop of group IA, IB, IIA, and V PLA_2 are involved in binding to the head group of the phospholipid substrate (36–41). The cationic and anionic charges of residues 53 and 56 in mammalian pancreatic and *N. naja kaouthia* venom PLA_2 (Fig. 6) appear to be responsible for the anionic and zwitterionic phospholipid preference of these enzymes, but substitution of cationic residues 53

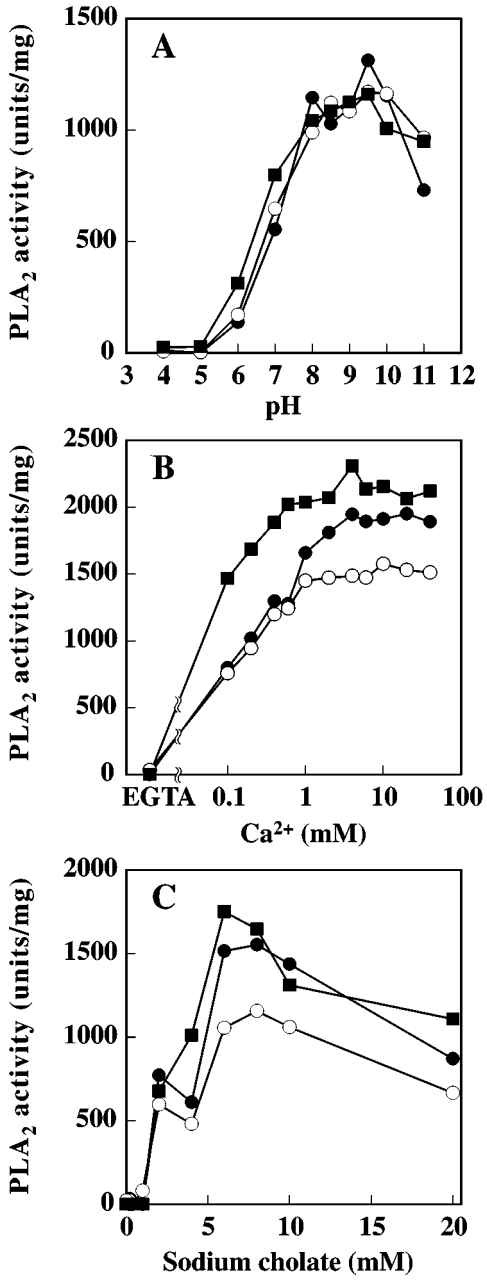

FIG. 7. Effect of pH (A), concentrations of Ca^{2+} (B) and sodium cholate (C) on the activities of red sea bream gill G-1 (●), G-2 (○), and G-3 (■) PLA_2. (A) Reaction mixtures containing purified G-1, G-2, or G-3 PLA_2, 2 mM 1-palmitoyl-2-oleoyl-*sn*-glycero-3-phosphocholine (POPC), 6 mM sodium cholate, 100 mM NaCl, and 5 mM $CaCl_2$ were incubated for 15 min at 37°C in a total volume of 100 µL. The buffers used were 50 mM acetate buffer from pH 4.0 to 5.0, 50 mM Tris-maleate buffer from pH 5.0 to 8.0, 50 mM Tris-HCl from pH 8.0 to 9.0, and 50 mM glycine-NaOH from pH 9.0 to 11.0. (B) Reaction mixtures containing purified G-1, G-2, or G-3 PLA_2, 2 mM POPC, 6 mM sodium cholate, 100 mM NaCl, 50 mM glycine-NaOH (pH 9.5), and 1 mM EGTA or 0–40 mM $CaCl_2$ were incubated, and PLA_2 activity was measured as described in the Materials and Methods section. (C) In the presence of various concentrations of sodium cholate, the activity of purified G-1, G-2, or G-3 PLA_2 was examined in a reaction mixture containing 2 mM POPC, 100 mM NaCl, 50 mM Tris-HCl (pH 8.5), and 10 mM $CaCl_2$, as described in the Materials and Methods section. Results are shown as means of two separate experiments. For abbreviation see Figure 1.

and/or 56 to nonionic residues of mammalian pancreatic PLA_2 improves higher preference for zwitterionic substrate but keeps the higher activity toward anionic substrate. In bovine and porcine pancreatic PLA_2, the methionine mutant (53M or 56M) shows a large increase in activity toward zwitterionic substrate and a slight decrease toward anionic substrate (36,39,42). Interestingly, red sea bream gill G-3 PLA_2 contains nonionic residues at residues Gly53 and Met56. As N-terminal helix Gln4, Phe5 and Ile9, Ca^{2+}-binding loop (Y25-G33) and active-site His48, Tyr52, Tyr73, and Asp99 are all conserved in red sea bream gill G-3 PLA_2 (Fig. 7), residues Gly53 and Met56 of gill G-3 PLA_2 may be interacted with choline moiety of POPC, in addition to keep the higher affinity toward POPG micelles. However, it cannot be denied that other residues of gill G-3 PLA_2 are involved in the preference for both POPC and POPG micelles, in addition to Gly53 and Met56. It is necessary to define the substrate specificity of gill G-3 PLA_2 for POPC and POPG micelles, using gill G-3 PLA_2 mutants such as G53R, M56K and G53RM56K.

In the absence of bile salts, aqueous dispersions of POPG and POPE (liposome) were appreciably hydrolyzed, whereas those of POPC were hardly hydrolyzed at all by G-3 PLA_2, similar to porcine pancreatic PLA_2 (Table 4) and rat splenic group I PLA_2 (5). The low affinity of gill PLA_2 toward POPC liposomes remains to be established.

Multiple group I PLA_2 enzymes are found in snake venom and also in the mammalian pancreas. Of 14 group I PLA_2 in the venom of the Australian king brown snake, *Pseudechis australis,* six group I PLA_2, PG-1Ga and -1Gb, Pa-3a and -3B, and Pa-15a and -15b showed microheterogeneity at the 103rd position with Thr/Ala, Thr/Pro, and Ala/Pro, respectively (43). Two group I PLA_2 isoforms exist in the porcine pancreas (44). In addition, commercially available porcine pancreatic PLA_2 consists of at least four enzymes within a range of 13,036 to 14,001 Da, and they are assumed to be genetic variants of PLA_2 (45). The N-terminal amino acid sequences of two minor PLA_2, G-1 and G-2 PLA_2, were all identical to that of G-3 PLA_2 from Ala1 to Glu56, but molecular masses of G-1 and G-2 PLA_2 (14,040 Da) were slightly higher than that of G-3 PLA_2 (14,005 Da). In addition, the enzyme properties of G-1 and G-2 PLA_2 were almost similar to that of G-3 PLA_2 (Fig. 7, Tables 3,4). Concerning the above aspects, G-1 and G-2 PLA_2 may be genetic variants of G-3 PLA_2 in which replacement or modification of amino acids occurred in the amino acid sequences from the 57th position to the carboxyl-terminus.

We recently purified two group I PLA_2 isoforms, DE-1 and DE-2 PLA_2, from the hepatopancreas of red sea bream (24). In the present report, we found one major and two minor group I PLA_2 variants in the gills of red sea bream. As we could not find a large difference in the molecular masses and amino acid sequences among three group I PLA_2 in the gills, we conclude that one group I PLA_2 isoform exists in the gills. These aspects indicate the existence of at least three structurally distinct group I PLA_2 isoforms in the hepatopancreas (DE-1 and DE-2

TABLE 3
Effect of Various Compounds on the Activities of Red Sea Bream Gill G-1, G-2, and G-3 PLA_2, Pig Pancreas PLA_2, and *Naja naja kaouthia* Venom PLA_2[a]

Compounds	Final concentration	Red sea bream gill G-1	Red sea bream gill G-2	Red sea bream gill G-3	Porcine pancreas	*N. naja kaouthia* venom
		Remaining activity (%)				
Complete		100	100	100	100	100
EGTA	1.0 mM	ND	ND	ND	ND	ND
EDTA	1.0 mM	ND	ND	ND	ND	ND
$CaCl_2$		17.8	23.3	31.9	ND	33.3
$MgCl_2$	5.0 mM	ND	ND	ND	ND	ND
$ZnCl_2$	5.0 mM	26.8	34.2	47.5	ND	16.4
$FeCl_3$	5.0 mM	ND	ND	ND	ND	ND
$CuCl_2$	5.0 mM	ND	ND	ND	ND	ND
$CuSO_4$	5.0 mM	ND	ND	ND	ND	ND
CTAB	0.01%	ND	ND	ND	ND	ND
	0.10%	2.7	ND	6.5	ND	ND
	0.20%	ND	ND	ND	ND	ND
SDS	0.01%	3.5	3.3	8.0	5.7	17.0
	0.10%	ND	ND	ND	ND	ND
	0.20%	ND	ND	ND	ND	ND
Triton X-100	0.01%	ND	ND	ND	ND	63.6
	0.10%	16.5	17.2	35.0	ND	118.9
	0.20%	26.4	23.4	46.6	ND	140.3
p-BPB	1.0 mM	63.0	74.8	76.1	24.1	15.0

[a]The activity of PLA_2 was measured in reaction mixtures containing 50 mM glycine-NaOH (pH 9.5), 2 mM POPC, 5 mM $CaCl_2$, 0.1 M NaCl, and 6 mM sodium cholate. To determine the effect of ions, $CaCl_2$ was depleted or replaced by EGTA, EDTA, $MgCl_2$, $ZnCl_2$, $FeCl_3$, $CuCl_2$, or $CuSO_4$, and the effect of detergents, sodium cholate was replaced by cetyl trimethylammonium bromide (CTAB), sodium lauryl sulfate (SDS) or Triton X-100. To determine the effect of *p*-bromophenacyl bromide (*p*-BPB), it was added to PLA_2 and incubated for 10 min at 37°C before starting the reaction. ND, not detectable; for other abbreviations see Table 1.

PLA_2) and gills (G-3 PLA_2) of red sea bream. In addition, Ca^{2+}-dependent low molecular mass PLA_2 was also found in the pyloric ceca of red sea bream (23). It is well known that multiple group I PLA_2 variants locate in the same tissue or organ such as porcine pancreas and snake venom. However, it remains unclear whether group I PLA_2 isoforms distribute in different tissues and cells of mammals and snakes. This may be the first report indicating that structurally different group I PLA_2 isoforms distribute in different tissues such as the hepatopancreas and gills of red sea bream.

TABLE 4
Comparison of Substrate Specificities of Red Sea Bream Gill G-1, G-2, and G-3 PLA_2, Porcine Pancreatic PLA_2, and *Naja naja kaouthia* Venom PLA_2 for Various Phospholipid Head Groups[a]

Origin	POPC Micelle	POPC No bile salts	POPE Micelle	POPE No bile salts	POPG Micelle	POPG No bile salts
	(units/mg protein)					
Red sea bream gill						
G-1 PLA_2	1,369	ND	170	137	1,155	128
G-2 PLA_2	1,166	ND	153	142	872	118
G-3 PLA_2	1,592	ND	357	161	1,211	119
Pig pancreas PLA_2	101	ND	278	243	1,861	250
N. naja kaouthia venom PLA_2	563	66	212	93	135	100

[a]The reaction mixture consisted of 50 mM glycine-NaOH (pH 9.5), 2 mM phospholipid, 5 mM $CaCl_2$, and 0.1 M NaCl with or without 6 mM sodium cholate in a final volume of 0.1 mL. Data were obtained in duplicate. POPE, 1-palmitoyl-2-oleoyl-*sn*-glycero-3-phosphoethanolamine; POPG, 1-palmitoyl-2-oleoyl-*sn*-glycero-3-[phospho-*rac*-(1-glycerol)]; for other abbreviations see Tables 1 and 3.

Finally, this study demonstrates that three group I PLA_2 variants exist in the gills, an organ not part of the digestive system like the hepatopancreas and pyloric ceca. Fish gills constitute a multifunctional and complex organ. The branchial epithelium consists of various cell types such as pavement cells, mucous cells, neuroepithelial cells, and ionocytes that are involved in respiratory, osmoregulatory, and excretory functions (46). We obtained monoclonal antibodies raised against purified gill PLA_2. We are now investigating the localization of PLA_2 proteins and expression of PLA_2 mRNA in the gills and other tissues of red sea bream using immunohistochemical staining and *in situ* hybridization.

ACKNOWLEDGMENTS

We would like to sincerely thank Hidetoshi Ikezawa, Application Chemist of ThermoQuest K.K. (Tokyo, Japan) for the determination of the molecular mass of PLA_2 by MALDI-TOF mass spectrometer. This work was supported in part by Grants in Aid for Scientific Research from the Ministry of Education, Science, Sports, and Culture of Japan.

REFERENCES

1. Dennis, E.A. (1997) The Growing Phospholipase A_2 Superfamily of Signal Transduction Enzymes, *Trends Biochem. Sci. 22,* 1–2.
2. Chaminade, B., Le Balle, F., Fourcade, O., Nauze, M., Delagebeaudeuf, C., Gassama-Diagne, A., Simon, M.F., Fauvel, J., and Chap, H. (1999) New Developments in Phospholipase A_2, *Lipids 34 (Suppl.),* S49–S55.
3. Tischfield, J.A. (1997) A Reassessment of the Low Molecular Weight Phospholipase A_2 Gene Family in Mammals, *J. Biol. Chem. 272,* 17247–17250.
4. Seilhamer, J.J., Randall, T.L., Yamanaka, M., and Johnson, L.K. (1986) Pancreatic Phospholipase A_2: Isolation of the Human Gene and cDNAs from Porcine Pancreas and Human Lung, *DNA 5,* 519–527.
5. Tojo, H., Ono, T., Kuramitsu, S., Kagamiyama, H., and Okamoto, M. (1988) A Phospholipase A_2 in the Supernatant Fraction of Rat Spleen, *J. Biol. Chem. 263,* 5724–5731.
6. Sakata, T., Nakamura, E., Tsuruta, Y., Tamaki, M., Teraoka, H., Tojo, H., and Ono, T. (1989) Presence of Pancreatic Type Phospholipase A_2 mRNA in Rat Gastric Mucosa and Lung, *Biochim. Biophys. Acta 1007,* 124–126.
7. Tojo, H., Ono, T., and Okamoto, M. (1991) Spleen Phospholipase A_2, *Methods Enzymol. 197,* 390–399.
8. Tojo, H., Ono, T., and Okamoto, M. (1993) Reverse-Phase High-Performance Liquid Chromatographic Assay of Phospholipases: Application of Spectrophotometric Detection to Rat Phospholipase A_2 Isozymes, *J. Lipid Res. 34,* 837–844.
9. Kortesuo, P.T., Hietaranta, A.J., Jamia, M., Hirsimaki, P., and Nevalainen, T.J. (1993) Rat Pancreatic Phospholipase A_2. Purification, Localization, and Development of an Enzyme Immunoassay, *Int. J. Pancreatol. 13,* 111–118.
10. Nevalainen, T.J., and Haapanen, T.J. (1993) Distribution of Pancreatic (Group I) and Synovial-type (Group II) Phospholipases A_2 in Human Tissues, *Inflammation 17,* 453–464.
11. Hara, S., Kudo, I., Komatani, T., Takahashi, K., Nakatani, Y., Natori, Y., Ohshima, M., and Inoue, K. (1995) Detection of Two 14 kDa Phospholipase A_2 Isoforms in Rat Kidney: Their Role in Eicosanoid Synthesis, *Biochim. Biophys. Acta 1257,* 11–17.
12. Aarsman, A.J., Schalkwijk, C.G., Neys, F.W., Iijima, N., Wherret, J.R., and van den Bosch, H. (1996) Purification and Characterization of Ca^{2+}-Dependent Phospholipase A_2 from Rat Kidney, *Arch. Biochem. Biophys. 331,* 95–103.
13. Ohara, O., Ishizaki, J., and Arita, H. (1995) Structure and Function of Phospholipase A_2 Receptor, *Prog. Lipid Res. 34,* 117–138.
14. Lambeau, G.H., Cupillard, L., and Ladzunski, M. (1997) Membrane Receptors for Venom Phospholipase A_2, in *Venom Phospholipase A_2 Enzymes: Structure, Function and Mechanism* (Kini, R.M., eds.), pp. 389–412, John Wiley & Sons, Chichester.
15. Kundu, G.C., and Mukherjee, A.B. (1997) Evidence That Porcine Pancreatic Phospholipase A_2 *via* Its High Affinity Receptor Stimulates Extracellular Matrix Invasion by Normal and Cancer Cells, *J. Biol. Chem. 272,* 2346–2353.
16. Hanasaki, K., Yokota, Y., Ishizaki, J., Itoh, T., and Arita, H. (1997) Resistance to Endotoxic Shock in Phospholipase A_2 Receptor-Deficient Mice, *J. Biol. Chem. 272,* 32792–32797.
17. Neas, N.P., and Hazel, J.R. (1984) Temperature-Dependent Deacylation of Molecular Species of Phosphatidylcholine by Microsomal Phospholipase A_2 of Thermally Acclimated Rainbow Trout, *Salmo gairdneri, Lipids 19,* 258–263.
18. Neas, N.P., and Hazel, J.R. (1985) Partial Purification and Kinetic Characterization of the Microsomal Phospholipase A_2 from Thermally Acclimated Rainbow Trout *(Salmo gairdneri), J. Comp. Physiol. 155B,* 461–469.
19. Audley, M.A., Shetty, K.J., and Kinsella, J.E. (1978) Isolation and Properties of Phospholipase A from Pollock Muscle, *J. Food Sci. 43,* 1771–1775.
20. Aaen, B., Jessen, F., and Jensen, B. (1995) Partial Purification and Characterization of a Cellular Acidic Phospholipase A_2 from Cod *(Gadus morhua), Comp. Biochem. Physiol. 110B,* 547–554.
21. Zambonino Infante, J.L., and Cahu, C.L. (1999) High Dietary Lipid Levels Enhance Digestive Tract Maturation and Improve *Dicentrarchus labrax* Larval Development, *J. Nutr. 129,* 1195–2000.
22. Iijima, N., Nakamura, M., Uematsu, K., and Kayama, M. (1990) Partial Purification and Characterization of Phospholipase A_2 from the Hepatopancreas of Red Sea Bream, *Nippon Suisan Gakkaishi 56,* 1331–1339.
23. Iijima, N., Chosa, S., Uematsu, K., Goto, T., Hoshita, T., and Kayama, M. (1997) Purification and Characterization of Phospholipase A_2 from the Pyloric Caeca of Red Sea Bream, *Pagrus major, Fish Physiol. Biochem. 16,* 487–498.
24. Ono, H., and Iijima, N. (1998) Purification and Characterization of Phospholipase A_2 Isoforms from the Hepatopancreas of Red Sea Bream, *Pagrus major, Fish Physiol. Biochem. 18,* 135–147.
25. Uematsu, K., Kitano, M., Morita, M., and Iijima, N. (1992) Presence and Ontogeny of Intestinal and Pancreatic Phospholipase A_2-like Proteins in the Red Sea Bream, *Pagrus major*. An Immunocytochemical Study, *Fish Physiol. Biochem. 9,* 427–438.
26. Laemmli, U.K. (1970) Cleavage of Structural Proteins During the Assembly of Bacteriophage T4, *Nature 227,* 680–685.
27. Heinrickson, R.L. (1991) Dissection and Sequence Analysis of Phospholipase A_2, *Methods Enzymol. 197,* 201–214.
28. Fleer, E.A.M., Verheij, H.M., and de Haas, G.H. (1978) The Primary Structure of Bovine Pancreatic Phospholipase A_2, *Eur. J. Biochem. 82,* 261–269.
29. Puijk, W.C., Verheij, H.M., and de Haas, G.H. (1977) The Primary Structure of Phospholipase A_2 from Porcine Pancreas. A Reinvestigation, *Biochim. Biophys. Acta 492,* 254–259.
30. Joubert, F.J., and Taljaard, N. (1980) Purification, Some Properties and Amino Acid Sequences of Two Phospholipase A (CM-II and CM-III) from *Naja naja kaouthia* Venom, *Eur. J. Biochem. 112,* 493–499.
31. Verheij, H.M., Slotboom, A.J., and de Haas, G.H. (1981) Structure and Function of Phospholipase A_2, *Rev. Physiol. Biochem. Pharmacol. 91,* 91–203.

32. Van den Bosch, H. (1982) Phospholipases, in *Phospholipids* (Hawthorne, J.N., and Ansell, G.B., eds.), pp. 313–357, Elsevier Biomedical, Amsterdam.
33. de Haas, G.H., Postema, N.M., Nieuwenhuizen, W., and van Deenen, L.L.M. (1967) Purification and Properties of Phospholipase A from Porcine Pancreas, *Biochim. Biophys. Acta 159,* 103–117.
34. Nielsen, H., Brunak, S., and von Heijne, G. (1999) Machine Learning Approaches for the Prediction of Signal Peptides and Other Protein Sorting Signals, *Protein Eng. 12,* 3–9.
35. Halban, P.A., and Irminger, J.C. (1994) Sorting and Processing of Secretory Proteins, *Biochem J. 299,* 1–18.
36. Noel, J.P., Deng, T., Hamilton, K.J., and Tsai, M.-D. (1990) Phospholipase A_2 Engineering. 3. Replacement of Lysine-56 by Neutral Residues Improves Catalytic Potency Significantly, Alters Substrate Specificity, and Clarifies the Mechanism of Interfacial Recognition, *J. Am. Chem. Soc. 112,* 3704–3706.
37. Noel, J.P., Bingman, C.A., Deng, T., Dupureur, C.M., Hamilton, K.J., Jiang, R.-T., Kwak, J.-G., Sekharudu, C., Sundaralingam, M., and Tsai, M.-D. (1991) Phospholipase A_2 Engineering. X-ray Structural and Functional Evidence for the Interaction of Lysine-56 with Substrates, *Biochemistry 30,* 11801–11811.
38. Lugtigheid, R.B., Otten-Kuipers, M.A., Verheij, H.M., and de Haas, G.H. (1993) Arginine 53 Is Involved in Head-Group Specificity of the Active Site of Porcine Pancreatic Phospholipase A_2, *Eur. J. Biochem. 213,* 517–522.
39. Beiboer, S.H., Franken, P.A., Cox, R.C., and Verheij, H.M. (1995) An Extended Binding Pocket Determines the Polar Head Group Specificity of Porcine Pancreatic Phospholipase A_2, *Eur. J. Biochem. 231,* 747–753.
40. Han, S.K., Yoon, E.T., Scott, D.L., Sigler, P.B., and Cho, W. (1997) Structural Aspects of Interfacial Adsorption. A Crystallographic and Site-directed Mutagenesis Study of the Phospholipase A_2 from the Venom of *Agkistrodon piscivorus piscivorus, J. Biol. Chem. 272,* 3573–3582.
41. Janssen, M.J.W., Vermeulen, L., Van der Helm, H.A., Aarsman, A.J., Slotbloom, A.J., and Egmond, M.R. (1999) Enzymatic Properties of Rat Group IIA and V Phospholipases A_2 Compared, *Biochim. Biophys. Acta 1440,* 56–72.
42. Rogers, J., Yu, B.Z., Tsai, M.D., Berg, O.G., and Jain, M.K. (1998) Cationic Residues 53 and 56 Control the Anion-induced Interfacial kcat Activation of Pancreatic Phospholipase A_2, *Biochemistry 37,* 9549–56.
43. Takasaki, C., Yutani, F., and Kajiyashiki, T. (1990) Amino Acid Sequences of Eight Phospholipases A_2 from the Venom of Australian King Brown Snake, *Pseudechis australis, Toxicon 28,* 329–339.
44. Puijk, W.C., Verheij, H.M., Wietzes, P., and de Haas, G.H. (1979) The Amino Acid Sequence of the Phospholipase A_2 Isoenzyme from Porcine Pancreas, *Biochim. Biophys. Acta 580,* 411–415.
45. Chang, T.M., Chang, C.H., Wagner, D.R., and Chey, W.Y. (1999) Porcine Pancreatic Phospholipase A_2 Stimulates Secretin Release from Secretin-Producing Cells, *J. Biol. Chem. 274,* 10758–10764.
46. Laurent, P. (1984) Gill Internal Morphology, in *Gills* (Hoar, W.S., and Randall, D.J., eds.), pp. 73–183, Academic Press,

Inc., Orlando.

[Received January 10, 2000, and in revised form July 24, 2000; revision accepted September 21, 2000]

Unusual Lipid Composition of a *Bacillus* sp. Isolated from Lake Pomorie in Bulgaria

N stor M. Carballeira[a,*], Aikomari Guzm n[a], Jordan T. Nechev[b], Kantcho Lahtchev[c], Albena Ivanova[d], and Kamen Stefanov[b]

[a]Department of Chemistry, University of Puerto Rico, San Juan, Puerto Rico 00931; Institutes of [b]Organic Chemistry with Center of Phytochemistry, [c]Microbiology, and [d]Plant Physiology, Bulgarian Academy of Sciences, Sofia 1113, Bulgaria

ABSTRACT: The lipid composition of a *Bacillus* sp., isolated from Lake Pomorie in Bulgaria, was unusual and consisted of 26 different fatty acids between C_{12} and C_{26}, with anteiso C_{15}–C_{17} saturated fatty acids predominating. The furan fatty acid, 10,13-epoxy-11-methyloctadeca-10,12-dienoic acid, was also identified, a new finding for this genus. The hydrocarbons consisted of 30 different monounsaturated hydrocarbons, between C_{25} and C_{30}, with the iso-iso, iso-anteiso, anteiso-anteiso, iso-normal, and anteiso-normal methyl branching for odd-numbered chains, and the iso-iso, iso-anteiso, iso-normal, and anteiso-normal methyl branching for even-numbered chains. The double bond positions in these hydrocarbons were determined by dimethyl disulfide derivatization followed by GC–MS, and the double-bond *cis* configuration was confirmed by infrared spectroscopy. Some previously unknown hydrocarbons in bacteria, such as (*Z*)-3,21-dimethyl-9-tricosene, (*Z*)-3,21-dimethyl-10-tricosene, (*Z*)-2,24-dimethyl-11-pentacosene, and (*Z*)-2,25-dimethyl-13-hexacosene were identified. Sterols were detected and were based on the sitosterol nucleus.

Paper no. L8285 in *Lipids 35,* 1371–1375 (December 2000).

Some microorganisms are particularly interesting for their ability either to generate or to use hydrocarbons in their metabolism (1–3). Earlier examples included bacteria capable of synthesizing monounsaturated hydrocarbons with terminal *iso-anteiso* branching distributed in either a symmetrical or unsymmetrical fashion along the terminus of the chains (4). In the case of *Sarcina lutea* ATCC 533 (*Micrococcus luteus*), a monounsaturated hydrocarbon composition of iso-anteiso C_{23}–C_{27} hydrocarbons was characterized, while *Sarcina lutea* FD 533 contained iso-anteiso C_{25}–C_{30} monounsaturated hydrocarbons (4). Further work revealed that the monounsaturation in these hydrocarbons was in or near the center of the chain, as determined by mass spectrometry (MS) on the corresponding trimethylsilyl ether derivatives (5). However, at that time no attempts were made to elucidate the double bond positions in those hydrocarbons identified in small amounts, such as the iso-anteiso 25:1 series. The accepted biosynthetic pathway to these monounsaturated hydrocarbons is that they arise from the head-to-head condensation of the appropriate combination of iso/anteiso fatty acids, with one of the fatty acids undergoing decarboxylation (5). This is consistent with the observation that only branched anteiso-anteiso hydrocarbons occur in the odd-numbered series (4).

Monounsaturated iso/anteiso hydrocarbons are not exclusive metabolites of the Micrococcaceae since they have also been reported in pseudomonads (6). For example, *Stenotrophomonas maltophilia* (previously *Pseudomonas maltophilia* and *Xanthomonas maltophilia*) biosynthesizes not only C_{27}–C_{32} monounsaturated hydrocarbons but also di- and triunsaturated hydrocarbons such as branched 30:2 (Δ9,16) and branched 30:3 (Δ8,14,21). In this particular pseudomonad, the double bond in the iso-iso and anteiso-anteiso C_{29} monounsaturated hydrocarbons occurred at C-14, but other double bond positions, for the smaller chain analogs, were not determined (6).

The fatty acid composition of this type of hydrocarbon-producing bacteria is relatively simple, inasmuch as it mainly consists of saturated C_{14}–C_{19} fatty acids with iso-anteiso methyl branching, but in all reported cases the branched even-carbon fatty acids only had the iso ramification (4,5). In most strains an 18:1 fatty acid was identified, but no double bond position was specified (5).

In this paper we report the unusual lipid composition of a *Bacillus* sp. isolated from Lake Pomorie in Bulgaria. To the best of our knowledge this is the first report of this type of iso-anteiso monounsaturated hydrocarbons for the genus *Bacillus*. The furan fatty acid 10,13-epoxy-11-methyloctadeca-10,12-dienoic acid is also reported for the first time in a *Bacillus* sp., as well as other longer-chain fatty acids.

MATERIALS AND METHODS

Instrumentation. Gas chromatography (GC)–MS data were collected at 70 eV in a Hewlett-Packard 5972A MS ChemStation (Palo Alto, CA) equipped with a 30 m × 0.25 mm special performance capillary column (HP-5MS) cross-linked

*To whom correspondence should be addressed at Department of Chemistry, University of Puerto Rico, P.O. Box 23346, San Juan, Puerto Rico 00931-3346. E-mail: ncarball@upracd.upr.clu.edu

Abbreviations: DMDS, dimethyl disulfide; ECL, equivalent chain-length; GC–MS, gas chromatography–mass spectrometry.

with 5% phenyl methylpolysiloxane. The temperature program for the analyses was as follows: 130°C for 2 min, then increased at 3°C/min to 270°C and maintained for 40 min. Infrared spectra were run in a Magna-IR 750 Nicolet (Madison, WI) spectrometer.

Bacterial isolation. Microorganisms were collected from the water of Lake Pomorie, partially connected to the Black Sea, during 1998. Samples were inoculated on 5 mL liquid YPD medium (1% wt/vol yeast extract, 2% wt/vol bactopeptone, 2% wt/vol glucose) and cultivated overnight in test tubes at 37°C. Different dilutions from each test tube were plated onto petri dishes with solid YPD medium (containing 2% wt/vol agar) and further cultivated for single colonies. Colonies with characteristic morphologies were isolated and studied. A *Bacillus* sp. was grown on liquid YPD medium supplemented with marine water in order to obtain 4% wt/vol NaCl concentration in the stationary growth phase. Cells were harvested by centrifugation and washed two times. Characterization was done by routine biochemical and antibiotic tests modified for marine bacteria. The microorganism in question was identified using the API 20E system (Analytab Products, Plainview, NY) as a *Bacillus* sp., close but not identical to *B. subtilis*.

Lipid isolation and characterization. The lipids were extracted from the bacterium (8–10 g) with chloroform/methanol (2:1, vol/vol) affording 40–45 mg of total lipids following the procedure of Bligh and Dyer (7). Hydrocarbons were isolated from the lipids by dilution in hexane followed by silica gel column chromatography utilizing only hexane as eluent. Fatty acids were identified as methyl esters, which were prepared by direct methylation of the lipid extract with 1.5 M HCl/methanol, as previously described (8).

Derivatives. The hydrocarbons and methyl esters were hydrogenated in 10 mL of absolute methanol and catalytic amounts of PtO_2. The double-bond positions in these compounds were determined by dimethyl disulfide (DMDS) derivatization following a procedure that was previously described (9). Double-bond positions and methyl branching were further confirmed by $NaIO_4/KMnO_4$ oxidation followed by acidic methanolysis. Some representative mass spectral data for the novel hydrocarbons, and their derivatives, are presented below.

(Z)-2,21-Dimethyl-(9 or 14)-tricosene. MS *m/z* (relative intensity): M^+ 350 (2), 320 (1), 292 (1), 279 (1), 270 (1), 237 (1), 225 (1), 213 (2), 199 (4), 185 (2), 171 (2), 153 (3), 143 (6), 125 (11), 111 (28), 97 (53), 83 (66), 81 (18), 70 (90), 57 (100), 55 (84).

(Z)-3,21-Dimethyl-9-tricosene. MS *m/z* (relative intensity): M^+ 350 (2), 321 (1), 320 (1), 195 (1), 181 (1), 167 (1), 153 (2), 139 (4), 125 (10), 123 (2), 112 (4), 111 (22), 97 (43), 83 (48), 71 (61), 70 (100), 57 (68), 55 (50).

3,21-Dimethyl-9,10-bis(methylthio)tricosane, 3,21-dimethyl-10,11-bis(methylthio) tricosane, and *3,21-dimethyl-11,12-bis(methylthio)tricosane*. MS *m/z* (relative intensity): M^+ 444 (7), 397 (4), 373 (6), 339 (2), 325 (7), 293 (3), 258 (6), 257 (29), 244 (2), 230 (11), 229 (57), 216 (12), 215 (65), 202 (6), 201 (12), 188 (6), 187 (40), 176 (3), 155 (6), 143 (5), 131 (7), 116 (21), 97 (44), 95 (22), 91 (14), 83 (49), 81 (33), 79 (15), 71 (44), 67 (39), 61 (60), 57 (100), 55 (95).

(Z)-2,24-Dimethyl-11-pentacosene. MS *m/z* (relative intensity): M^+ 378 (3), 322 (1), 208 (1), 195 (1), 181 (1), 167 (2), 153 (2), 140 (2), 139 (4), 126 (3), 125 (10), 112 (6), 111 (27), 97 (45), 96 (11), 85 (22), 83 (49), 82 (17), 71 (36), 69 (58), 57 (100), 55 (57).

2,24-Dimethyl-11,12-bis(methylthio)pentacosane, and *2,24-dimethyl-12,13-bis(methylthio)pentacosane*. MS *m/z* (relative intensity): M^+ 472 (6), 425 (2), 354 (2), 281 (5), 257 (15), 243 (82), 230 (19), 229 (90), 216 (5), 215 (19), 207 (16), 199 (6), 185 (3), 178 (4), 165 (3), 143 (8), 133 (7), 125 (15), 123 (11), 115 (24), 109 (14), 105 (7), 97 (54), 95 (35), 85 (34), 83 (58), 71 (50), 69 (85), 67 (42), 57 (100).

(Z)-2,25-Dimethyl-12-hexacosene. MS *m/z* (relative intensity): M^+ 392 (4), 364 (1), 336 (1), 195 (1), 182 (1), 168 (1), 167 (1), 154 (1), 153 (2), 140 (2), 139 (4), 125 (11), 111 (27), 97 (48), 96 (11), 85 (23), 83 (52), 71 (38), 69 (56), 57 (100), 55 (57).

2,25-Dimethyl-12,13-bis(methylthio)hexacosane, and *2,25-dimethyl-13,14-bis(methylthio)hexacosane*. MS *m/z* (relative intensity): M^+ 486 (5), 439 (2), 346 (2), 281 (3), 258 (8), 257 (41), 244 (16), 243 (79), 230 (12), 229 (60), 163 (5), 152 (4), 139 (5), 119 (29), 115 (28), 97 (50), 94 (35), 85 (30), 83 (58), 71 (42), 69 (69), 57 (100), 55 (88).

RESULTS

After the isolation and characterization procedure described above, at least 30 monounsaturated hydrocarbons were identified in this *Bacillus* sp. ranging in length between C_{25} and C_{30} (Table 1). All hydrocarbons displayed a similar mass spectrum, but they occurred as clusters with different molecular weights. Almost complete characterization was accomplished by further derivatization of the whole hydrocarbon mixture. Catalytic hydrogenation was used to locate methyl branching, inasmuch as the unsaturated and saturated hydrocarbon gas chromatographic profiles were practically the same, and methyl branching was easily distinguished in the saturated hydrocarbons by mass spectrometry (5). In particular, iso-iso and iso-normal saturated hydrocarbons display a significant $M^+ - 43$ peak, while anteiso-anteiso, iso-anteiso, and anteiso-normal hydrocarbons display a prominent $M^+ - 29$ peak (5). For example, 2,24-dimethylpentacosane (iso-iso) displays a strong $M^+ - 43$ fragmentation at *m/z* 337 (6%), but either 2,23-dimethylpentacosane (iso-anteiso) or 3,23-dimethylpentacosane (anteiso-anteiso) displays a strong $M^+ - 29$ fragmentation at *m/z* 351 (9–11%) upon electron impact. Plots of GC retention times vs. iso/anteiso ramifications were used to distinguish between the different branching possibilities in the hydrogenated samples, and this was extrapolated to the monounsaturated analogs. For example, it was observed that the order of elution in the C_{27} series was iso-iso, iso-anteiso, anteiso-anteiso, and iso-normal, while the elution order in the C_{28} series was iso-iso, iso-anteiso, iso-normal, and anteiso-normal (5). Further confirmation of the branch-

TABLE 1
Hydrocarbons Identified in the *Bacillus* sp. from Lake Pomorie

Hydrocarbons	Relative abundance[a] (%)
(*Z*)-2,21-Dimethyl-(9 or 14)-tricosene (i,ai-C_{25})[b,c]	0.6
(*Z*)-2,21-Dimethyl-(10 or 13)-tricosene (i,ai-C_{25})[b,c]	0.1
(*Z*)-2,21-Dimethyl-(11 or 12)-tricosene (i,ai-C_{25})[b]	1.2
(*Z*)-3,21-Dimethyl-9-tricosene (ai,ai-C_{25})[c]	2.8
(*Z*)-3,21-Dimethyl-10-tricosene (ai,ai-C_{25})[c]	0.7
(*Z*)-3,21-Dimethyl-11-tricosene (ai,ai-C_{25})	4.5
(*Z*)-2,22-Dimethyl-(10 or 14)-tetracosene (i,ai-C_{26})[b,c]	0.3
(*Z*)-2,22-Dimethyl-(11 or 13)-tetracosene (i,ai-C_{26})[b]	4.0
(*Z*)-2,22-Dimethyl-12-tetracosene (i,ai-C_{26})	2.4
(*Z*)-2,24-Dimethyl-11-pentacosene (i,i-C_{27})[c]	0.4
(*Z*)-2,24-Dimethyl-12-pentacosene (i,i-C_{27})	2.5
(*Z*)-2,23-Dimethyl-(11 or 14)-pentacosene (i,ai-C_{27})[b]	3.0
(*Z*)-2,23-Dimethyl-(12 or 13)-pentacosene (i,ai-C_{27})[b]	1.6
(*Z*)-3,23-Dimethyl-11-pentacosene (ai,ai-C_{27})	10.6
(*Z*)-3,23-Dimethyl-12-pentacosene (ai,ai-C_{27})	6.6
(*Z*)-2-Methyl-(11 or 14)-hexacosene (i-C_{27})[b]	0.6
(*Z*)-2-Methyl-(12 or 13)-hexacosene (i-C_{27})[b]	2.4
(*Z*)-2,25-Dimethyl-12-hexacosene (i,i-C_{28})	1.0
(*Z*)-2,25-Dimethyl-13-hexacosene (i,i-C_{28})[c]	1.6
(*Z*)-2,24-Dimethyl-13-hexacosene (i,ai-C_{28})	3.2
(*Z*)-2,24-Dimethyl-(12 or 14)-hexacosene (i,ai-C_{28})[b,c]	10.6
(*Z*)-2-Methyl-(12 or 14)-heptacosene (i-C_{28})[b]	0.6
(*Z*)-2-Methyl-13-heptacosene (i-C_{28})	1.8
(*Z*)-3-Methyl-(12 or 14)-heptacosene (ai-C_{28})[b]	3.2
(*Z*)-3-Methyl-13-heptacosene (ai-C_{28})	1.3
(*Z*)-2,26-Dimethyl-14-heptacosene (i,i-C_{29})	2.3
(*Z*)-2,25-Dimethyl-(13 or 14)-heptacosene (i,ai-C_{29})[b]	5.8
(*Z*)-3,25-Dimethyl-14-heptacosene (ai,ai-C_{29})	24.3

[a]The values are the percentages based on the total peak area of the hydrocarbons. Traces (0.01–0.05%) of two different kinds of C_{30} hydrocarbons were also detected. The values are the average of at least three different samples with an average error of ±0.1%.
[b]It was not possible to distinguish between these two isomers.
[c]Not identified before in bacteria.

ing was obtained *via* sodium periodate/potassium permanganate oxidation followed by acid-catalyzed methylation, which afforded the corresponding iso-anteiso and normal C_{10}–C_{15} fatty acid methyl esters. The principal cleavage product was the anteiso-15:0 acid, which mainly arose from 3,25-dimethyl-14-heptacosene.

DMDS derivatization followed by MS was used to locate the double-bond positions in the hydrocarbons. Since only monounsaturated hydrocarbons were present, the DMDS derivatives displayed a similar GC profile as the original monounsaturated hydrocarbons. Methyl branching was the key feature for the GC separation, but different double bond isomers, with the same branching, co-eluted in the same peak due to a lack of difference in polarity between the two ends of the chain. While inconvenient, this also helped in the assignment of corresponding peaks between the original hydrocarbons, the hydrogenated mixture, and the DMDS derivatives. As an example, in a single GC peak we were able to identify three isomers for the anteiso-anteiso 25:1 series, namely, the hydrocarbons 3,21-dimethyl-9-tricosene, 3,21-dimethyl-10-tricosene, and 3,21-dimethyl-11-tricosene, of which only the Δ11 isomer was previously reported in bacteria (5). The DMDS derivatives of these hydrocarbons co-eluted in a single peak. However, they were distinguishable by MS since their mass spectra displayed a M^+ at *m/z* 444 and key fragmentations at *m/z* 187 and 257 for the Δ9 isomer, at *m/z* 201 and 243 for the Δ10 isomer, and at *m/z* 215 and 229 for the Δ11 isomer. Likewise, in the iso-iso 28:1 series both 2,25-dimethyl-12-hexacosene and 2,25-dimethyl-13-hexacosene were identified in a single C_{28} iso-iso peak *via* GC–MS of their corresponding DMDS derivatives, but only the former was previously reported (5). These DMDS derivatives presented a mass spectrum with a M^+ at *m/z* 486 and key fragmentations at *m/z* 229 and 257 for the Δ12 isomer, and a single fragment at *m/z* 243 for the Δ13 isomer due to symmetry.

In the unsymmetrical hydrocarbons it was possible to narrow the possibilities to only two double-bond isomers using DMDS derivatization. However, even after $NaIO_4$/$KMnO_4$ oxidation of the whole mixture, the assignment remained ambiguous owing to the complexity of the mixture, i.e., the same fragments can arise from different hydrocarbons. For example, 2,21-dimethyl-10,11-bis(methylthio)tricosane or 2,21-dimethyl-13,14-bis(methylthio)tricosane has a M^+ at *m/z* 444 and the same fragmentations at *m/z* 201 and 243 upon electron impact (Table 1). The infrared spectrum of the monounsaturated mixture displayed no significant absorption in the 960–980 cm^{-1} region, but rather an absorption in the 760–780 cm^{-1} region, bespeaking *cis* double bonds in all of the studied monounsaturated hydrocarbons (10).

The fatty acid composition of this *Bacillus* sp. consisted of 26 different fatty acids between C_{12} and C_{26}, but the anteiso C_{15} and C_{17} saturated fatty acids were the predominant branched fatty acids in the mixture (Table 2). Saturated fatty acids accounted for 83% of the total composition. These acids were characterized by GC–MS as fatty acid methyl esters and by comparison of reference equivalent chain-length values (ECL). Noteworthy was the identification of the very long chain fatty acids tetracosanoic acid (24:0) and hexacosanoic acid (26:0). In addition, traces of 2-hydroxytetracosanoic acid (24:0) were also identified in the mixture by GC–MS. Of particular interest was the identification of 10,13-epoxy-11-methyloctadeca-10,12-dienoic acid, which was identified for the first time in a *Bacillus* sp. This acid was identified as the methyl ester by comparison of its mass spectrum with the one already reported in the literature from bacteria such as *Shewanella* or *Pseudomonas* (11,12). The mass spectrum of the methyl ester displayed a molecular ion peak (M^+) at *m/z* 322, a $M^+ - 15$ peak at *m/z* 307, a $M^+ - 31$ peak at *m/z* 291, a $M^+ - 57$ peak at *m/z* 265, a McLafferty rearrangement peak at *m/z* 74, and the most characteristic base peak at *m/z* 165 (11,12).

The sterol composition of this strain was also characterized by GC–MS, and it mainly consisted of sitosterol (79%), stigmasterol (14%), and fucosterol (7%), as judged by com-

TABLE 2
Identified Fatty Acids in the *Bacillus* sp. from Lake Pomorie

Fatty acids	Relative abundance[a] (%)
Dodecanoic (12:0)	0.9
11-Methyldodecanoic (i-13:0)	1.3
12-Methyltridecanoic (i-14:0)	3.2
Tetradecanoic (14:0)	8.1
12-Methyltetradecanoic (i-15:0)	0.7
13-Methyltetradecanoic (ai-15:0)	16.0
Pentadecanoic (15:0)	3.1
14-Methylpentadecanoic (i-16:0)	8.3
9-Hexadecenoic (16:1)	4.4
Hexadecanoic (16:0)	9.9
15-Methylhexadecanoic (i-17:0)	2.7
14-Methylhexadecanoic (ai-17:0)	11.1
Heptadecanoic (17:0)	1.1
9,12-Octadecadienoic (18:2)	1.5
9-Octadecenoic (18:1)	11.5
Octadecanoic (18:0)	10.4
17-Methyloctadecanoic (i-19:0)	0.7
16-Methyloctadecanoic (ai-19:0)	1.4
10,13-Epoxy-11-methyloctadeca-10,12-dienoic	0.2
Nonadecanoic (19:0)	0.9
Eicosanoic (20:0)	0.9
Heneicosanoic (21:0)	0.1
Docosanoic (22:0)	0.9
Tetracosanoic (24:0)	0.6
Hexacosanoic (26:0)	0.1

[a]The values are the percentages based on the total peak area of the fatty acid methyl esters, and the average of at least three different samples with an average error of ±0.1%. Traces (0.01–0.05%) of 2-OH-24:0 were also identified.

paring their mass spectra with known standards (13). Therefore, the sterols were based on the sitosterol nucleus.

DISCUSSION

The *Bacillus* sp. identified in this work has a hydrocarbon branching profile similar to that of either *S. lutea* FD 533 (*M. luteus*) or *M. lysodeikticus*, but a more complex double bond isomeric composition than either *S. lutea* ATCC 533 or *S. flava* ATCC 540 (4,5). Differences and similarities were observed for each chain length between C_{25} and C_{29}. In the 25:1 series previous findings reported the (*Z*)-3,21-dimethyl-11-tricosene as the only 25:1 anteiso-anteiso isomer, but in our *Bacillus* two additional anteiso-anteiso isomers were identified, namely, the previously unreported (*Z*)-3,21-dimethyl-9-tricosene and (*Z*)-3,21-dimethyl-10-tricosene (Table 1). The same complexity of unsaturations was also observed in the iso-anteiso 25:1 series where the three compounds (*Z*)-2,21-dimethyl-(9 or 14)-tricosene, (*Z*)-2,21-dimethyl-(10 or 13)-tricosene, and (*Z*)-2,21-dimethyl-(11 or 12)-tricosene were identified (Table 1). However, in this iso-anteiso 25:1 series it was not possible to distinguish, using DMDS derivatization, between two possible unsaturated isomers for each of the three observed combinations because of their lack of symmetry. In the 26:1 series the (*Z*)-2,22-dimethyl-(10 or 14)-tetracosene is also novel, as it has not been reported before from other bacteria (5). However, a similarity in the hydrocarbon composition of our *Bacillus* to other hydrocarbon-producing bacteria was observed inasmuch as we also identified the (*Z*)-2,22-dimethyl-(11 or 13)-tetracosene and the (*Z*)-2,22-dimethyl-12-tetracosene, both of which were reported from *S. lutea* ATCC 533 and *S. flava* ATCC 540 (5). In the 27:1 series the (*Z*)-2,24-dimethyl-11-pentacosene is unprecedented since the (*Z*)-2,24-dimethyl-12-pentacosene was the only hydrocarbon identified before in bacteria (5). Another interesting difference between the hydrocarbons of this *Bacillus* and other hydrocarbon-producing bacteria was noted with the other 27:1 isomers. For example, while *S. lutea* ATCC 533 contained only (*Z*)-3,23-dimethyl-12-pentacosene, and *S. flava* ATCC 540 only had (*Z*)-3,23-dimethyl-11-pentacosene, our *Bacillus* contained both isomers (5). This same finding, i.e., the presence of both double-bond isomers, was observed for the 27:1 iso-anteiso and 27:1 iso-normal isomers. In the 28:1 series the (*Z*)-2,25-dimethyl-13-hexacosene was not recognized in any bacteria before, inasmuch as the (*Z*)-2,25-dimethyl-12-hexacosene was the only iso-iso isomer reported in *S. flava* ATCC 540 (5). Likewise, while the (*Z*)-2,24-dimethyl-13-hexacosene was the only *iso-anteiso* isomer identified in the latter strain, the (*Z*)-2,24-dimethyl-(12 or 14)-hexacosene was not reported. However, either the 28:1 iso-iso or the 28:1 iso-anteiso series had both double-bond isomers. The remaining 28:1 iso-normal and 28:1 anteiso-normal hydrocarbons in our *Bacillus* corresponded to those previously reported in other bacteria such as the *Micrococcus* (5). The 29:1 isomers identified here also corresponded to those previously characterized in other strains (6). We also detected, in trace amounts, two C_{30} monounsaturated hydrocarbons, but the amount of material precluded any further characterization. Much of the structural data presented here also supports a biogenesis of hydrocarbons from the head-to-head condensation of two fatty acids with the concomitant decarboxylation of one of the two acids (6).

The higher abundance of anteiso fatty acids over their iso counterparts, in particular that of ai-15:0 (16%), was noteworthy in this *Bacillus*. Branched-chain fatty acids are characteristic of the genus *Bacillus*, and it has been reported that the genus can be divided into two main groups based on the ai-15:0/i-15:0 ratio (14,15). In addition, the identification of 10,13-epoxy-11-methyloctadeca-10,12-dienoic acid, although a minor component, is interesting since it was identified for the first time in a *Bacillus* sp. Much discussion has arisen as to the origin of furan fatty acids in fish, since they cannot biosynthesize these acids *de novo,* and recent findings indicate that they arise from intestinal bacteria such as *Shewanella putrefaciens* or *P. fluorescens* (12). Our findings expand the origin of these furan fatty acids to *Bacillus.* Work is in progress in our laboratories elucidating the lipid composition of unusual marine bacteria.

ACKNOWLEDGMENTS

This work was supported by grants from the National Institutes of Health (to NMC) and from the National Foundation of Scientific Research of Bulgaria under contract X-617 (to KS). A. Guzmán thanks Pfizer for an undergraduate fellowship. We thank Iraida Robledo (Department of Microbiology, University of Puerto Rico Medical Sciences campus) and Carmen Tosteson (Department of Marine Sciences, UPR-Mayagüez) for the identification of the bacterium.

REFERENCES

1. Hartmans, S., de Bont, J.A., and Harder, W. (1989) Microbial Metabolism of Short-Chain Unsaturated Hydrocarbons, *FEMS Microbiol Rev. 5*, 235–264.
2. Damste, J.S.S., Erkes, A.-M.W.E.P., Rijpstra, W.I.C., De Leeuw, J.W., and Wakeham, S.G. (1995) C32–C36 Polymethyl Alkenes in Black Sea Sediments, *Geochim. Cosmochim. Acta 59*, 347–353.
3. Hird, S.J., Evens, R., and Rowland, S.J. (1992) Isolation and Characterization of Sedimentary and Synthetic Highly Branched C20 and C25 Monoenes*, Mar. Chem. 37*, 117–129.
4. Tornabene, T.G., and Morrison, S.J. (1970) Aliphatic Hydrocarbon Contents of Various Members of the Family Micrococcaceae, *Lipids 5*, 929–937.
5. Tornabene, T.G., and Markey, S.P. (1971) Characterization of Branched Monounsaturated Hydrocarbons of *Sarcina lutea* and *Sarcina flava*, *Lipids 6*, 190–195.
6. Suen, Y., Holzer, G.U., Hubbard, J.S., and Tornabene, T.G. (1988) Biosynthesis of Acyclic Methyl Branched Polyunsaturated Hydrocarbons in *Pseudomonas maltophilia*, *J. Ind. Microbiol. 2*, 337–348.
7. Bligh, E.G., and Dyer, W.J. (1959) A Rapid Method of Total Lipid Extraction and Purification, *Can. J. Biochem. Physiol. 37*, 911–917.
8. Christie, W.W., Brechany, E.Y., Stefanov, K., and Popov, S. (1992) The Fatty Acids of the Sponge *Dysidea fragilis* from the Black Sea, *Lipids 27*, 640–644.
9. Dunkelblum, E., Tan, S.H., and Silk, R.J. (1985) Double-Bond Location in Monounsaturated Fatty Acids by Dimethyl Disulphide Derivatization and Mass Spectrometry, *J. Chem. Ecol. 11*, 265–277.
10. Doumenq, P., Guiliano, M., Bertrand, J.C., and Mille, G. (1990) GC/FT-IR Analysis of Fatty Acid Methyl Esters, *Appl. Spectrosc. 44*, 1355–1359.
11. Shirasaka, N., Nishi, K., and Shimizu, S. (1995) Occurrence of a Furan Fatty Acid in Marine Bacteria, *Biochim. Biophys. Acta 1258*, 225–227.
12. Shirasaka, N., Nishi, K., and Shimizu, S. (1997) Biosynthesis of Furan Fatty Acids (F-acids) by a Marine Bacterium, *Shewanella putrefaciens*, *Biochim. Biophys. Acta 1346*, 253–260.
13. Djerassi, C. (1978) Recent Advances in the Mass Spectrometry of Steroids, *Pure Appl. Chem. 50*, 171–184.
14. Siegel, J.P., Smith, A.R., and Novak, R.J. (1997) Comparison of the Cellular Fatty Acid Composition of a Bacterium Isolated from a Human and Alleged to Be *Bacillus sphaericus* with That of *Bacillus sphaericus* Isolated from a Mosquito Larvicide, *Appl. Environ. Microbiol. 63*, 1006–1010.

15. Klein, W., Weber, M.H.W., and Marahiel, M.A. (1999) Cold Shock Response of *Bacillus subtilis*: Isoleucine-Dependent Switch in the Fatty Acid Branching Pattern for Membrane Adaptation to Low Temperatures, *J. Bacteriol. 181*, 5341–5349.

[Received June 18, 1999, and in final revised form August 3, 2000; revision accepted August 8, 2000]

Electron Microscopy May Reveal Structure of Docosahexaenoic Acid-Rich Oil Within *Schizochytrium* sp.[1]

A. Ashford[a,*], W.R. Barclay[a], C.A. Weaver[a], T.H. Giddings[b], and S. Zeller[c]

[a]OmegaTech, Inc., Boulder, Colorado 80301-3242, [b]University of Colorado, Boulder, Colorado 80309-0347, and [c]Kelco, a Unit of Monsanto Company, San Diego, California 92123-1718

ABSTRACT: *Schizochytrium* sp. is an algae-like microorganism utilized for commercial production of docosahexaenoic acid (DHA)-rich oil and dried microalgae for use as a source of DHA in foods, feeds, and nutritional supplements. Electron microscopic analysis of whole cells of *Schizochytrium* sp. employing sample preparation by high-pressure freeze substitution suggests the presence of secondary and tertiary semicrystalline structures of triacylglycerols within the oil bodies in *Schizochytrium* sp. A fine secondary structure consisting of alternating light- and dark-staining bands was observed inside the oil bodies. Dark bands were 29 ± 1 Å in width, and light bands were 22 ± 1 Å in width. The tertiary (three-dimensional) structure may be a multilayered ribbon-like structure which appears coiled and interlaced within the oil body. In freeze-fracture photomicrographs, *Schizochytrium* oil bodies exhibited fracture planes with terraces averaging 52 ± 7 Å in height which could correspond to the combined width of two halves of two light bands and one dark band observed in the high-pressure freeze substitution photomicrographs. The results suggest that triacylglycerols within *Schizochytrium* sp. oil bodies may be organized in a triple chain-length structure. High-pressure freeze substitution electron micrographs of two other highly unsaturated oil-producing species of microalgae, *Thraustochytrium* sp. and *Isochrysis galbana,* also revealed this fine structure, whereas microalgae containing a higher proportion of saturated oil did not. The results suggest that the staining pattern is not an artifact of preparation and that the triple chain-length conformation of triacylglycerols in *Schizochytrium* sp. oil bodies may be caused by the unique fatty acid composition of the triacylglycerols.

Paper no. L8589 in *Lipids 35,* 1377–1386 (December 2000).

Schizochytrium sp., a thraustochytrid in the kingdom Stramenopila, is an algae-like microorganism that is commercially utilized to produce docosahexaenoic acid (DHA) by fermentation (1). The triacylglycerols can constitute over 70% of the weight of *Schizochytrium* sp. Additionally, *ca.* 25–45% of the fatty acids in the triacylglycerols are DHA (2), depending on culture conditions (3). Very little is known about oil-body formation in this microorganism as thraustochytrids historically are not recognized as significant oil-producing microorganisms (4).

We recently utilized electron microscopy in an attempt to identify the location of oil production in *Schizochytrium* sp. Analysis of microbial oil bodies has historically been conducted by glutaraldehyde fixation with osmium tetroxide staining wherein DHA-containing oil bodies appear as homogeneous dark-staining inclusions (5). Following normal precedent, we analyzed *Schizochytrium* sp. cells using this technique and found that the oil bodies were homogeneous and dark. In addition to this method, we utilized high-pressure freeze substitution, a relatively new type of cell preparation that is theoretically capable of preserving very fine structures within cells. Fine structures are preserved because high pressure prevents the formation of damaging ice crystals in the cells during freezing. The cells are treated with an acetone-osmium tetroxide (OsO_4) solution which removes intracellular water by successive dehydration and stains any double bonds present in organelles within the cells (6).

When electron micrographs produced using the high-pressure freeze substitution technique were observed, a fine structure was revealed within the DHA-rich oil bodies of *Schizochytrium* sp. that was organized and nonrandom. Triacylglycerols in some types of biological systems, for example milk, have been proposed to occur in semicrystalline states (7). Confirmation of these semicrystalline triacylglycerol structures has only been observed indirectly by use of freeze-fracture electron microscopy (7). In this analysis, triacylglycerol structure was also observed as a terrace-like structure in the freeze-fracture planes.

This paper describes the structures we observed within the oil bodies of *Schizochytrium* sp. using both high-pressure freeze substitution and freeze-fracture electron microscopy preparation techniques. Other types of oil-producing microalgae were also examined using high-pressure freeze substitution electron microscopy in an effort to determine whether this fine structure was an artifact of the method of preparation. A model is proposed which may describe the triacylglycerol structure of the unique DHA-rich oil in *Schizochytrium* sp.

[1]High-resolution copies of the photomicrographs used in this manuscript are available from the corresponding author.

*To whom correspondence should be addressed at OmegaTech, Inc., 4909 Nautilus Court North, Suite 208, Boulder, CO 80301-3242.
E-mail: amyashford@omegadha.com

Abbreviations: 14:0, myristic acid; 16:0, palmitic acid; 16:1, palmitoleic acid; DHA, docosahexaenoic acid (22:6n-3); DPAn-6, docosapentaenoic acid omega-6 (22:5n-6); FAME, fatty acid methyl esters; NMR, nuclear magnetic resonance; TLC, thin-layer chromatography.

MATERIALS AND METHODS

Cell culture. Schizochytrium sp. (ATCC 20888, Rockville, MD) was grown in 250-mL shake flasks in 50 mL of a 50% artificial seawater medium containing a low carbon-to-nitrogen ratio of *ca.* 10:1 (molar concentrations) to produce low oil-content cells. This medium consisted of (on a per liter basis): NaCl, 12.5 g; $MgSO_4 \cdot 7H_2O$, 2.5 g; KCl, 0.5 g; $CaCl_2$, 100 mg; glucose, 2.5 g; monosodium glutamate, 2.5 g; KH_2PO_4, 0.5 g; metals, 5 mL; and vitamin mix, 1 mL. The pH of the solution was adjusted to 7.0, and the solution was filter-sterilized. The trace metal solution contained per liter: Na_2EDTA, 6.0 g; $FeCl_3 \cdot 6H_2O$, 0.29 g; H_3BO_3, 6.84 g; $MnCl_2 \cdot 4H_2O$, 0.86; $ZnCl_2$, 0.06 g; $CoCl_2 \cdot 6H_2O$, 0.026 g; $NiSO_4 \cdot 6H_2O$, 0.052 g; $CuSO_4 \cdot 5H_2O$, 0.002 g; and $NaMoO_4 \cdot 2H_2O$, 0.005 g. The pH of the trace metals solution was adjusted to 8.0. The vitamin mix contained per liter: thiamin, 100 mg; biotin, 0.5 mg; and cyanocobalamin, 0.5 mg. The flasks were shaken at 220 rpm, maintained at 29°C, and exposed to light at an intensity of *ca.* 100 $\mu E/m^2 \cdot s$. After 24 h, a small volume from this flask was used to inoculate a separate flask containing growth medium with a high carbon-to-nitrogen ratio of *ca.* 30:1 to stimulate oil production. As described by Barclay (8), the components of this medium (per liter) were as follows: Na_2SO_4, 5 g; $MgSO_4 \cdot 7H_2O$, 1.2 g; $CaCO_3$, 0.067 g; glucose, 10.0 g; monosodium glutamate, 1.0 g; KH_2PO_4, 0.2 g; Difco yeast extract, 0.4 g; trace metals solution, 5 mL; vitamin mix, 1 mL. The culture medium was adjusted to pH 7.0, and the medium was filter-sterilized. This culture was grown for 48 h. The culture was sampled (at 0, 24, 48, and 72 h) after the inoculum of the high oil production flask for electron microscopy preparation.

Nannochloropsis occulata (UTEX LB 2164) and *Neochloris oleoabundans* (UTEX 1185) strains were obtained from the Culture Collection of Algae at the University of Texas at Austin (UTEX) and grown at 25°C with light (*ca.* 100 $\mu E/m^2 \cdot s$). *Nannochloropsis occulata* cultures were grown in f/2 medium (9) containing 60% strength sterilized seawater as well as the following additions on a per liter basis: $NaNO_2$, 0.15 g; KH_2PO_4, 0.01 g; $NaHCO_3$, 0.2 g; vitamin mix, 1 mL; soil extract, 5 mL; and f/2 trace metals mix, 5 mL. The f/2 trace metal solution contained the following per liter: Na_2EDTA, 4.36 g; $FeCl_3 \cdot 6H_2O$, 3.15 g; $MnCl_2 \cdot 4H_2O$, 180 mg; $CuSO_4 \cdot 5H_2O$, 10 mg; $ZnSO_4 \cdot 7H_2O$, 22 mg; $CoCl_2 \cdot 6H_2O$, 10 mg; $NaMoO_4 \cdot 2H_2O$, 6 mg. The medium was adjusted to pH 8.0, and the medium was autoclaved. Cultures were grown under light (*ca.* 100 $\mu E/m^2 \cdot s$) for *ca.* 4 wk.

Neochloris oleoabundans was grown in Bolds basal medium (10) containing on a per liter basis: $NaNO_3$, 250 mg; $CuCl \cdot 2H_2O$, 25 mg; $MgSO_4 \cdot 7H_2O$, 75 mg; KH_2PO_4, 250 mg; H_3BO_3, 11 mg; Bolds Basal EDTA mix, 1 mL; Bolds basal trace metals, 1 mL; and soil extract, 5 mL. Bolds Basal EDTA mix contained the following per liter: EDTA, 50 g; KOH, 31 g. Bolds Basal trace metals solution contained the following per liter: $ZnSO_4 \cdot 7H_2O$, 8.82 g; $MnCl_2 \cdot 4H_2O$, 1.44 g; MoO_3, 0.71 g; $CuSO_4 \cdot 5H_2O$, 1.57 g; $Co(NO_3)_2 \cdot 6H_2O$, 0.49 g. The medium was adjusted to pH 7.0 and autoclaved. Cultures were grown under light (*ca.* 100 $\mu E/m^2 \cdot s$) for 3–4 wk. Cells were harvested for sample preparation by gentle vacuum filtration.

Thraustochytrium sp. (ATCC 20890) was grown in 250-mL shake flasks on a rotary shaker at 220 rpm and maintained at 29°C. It was grown in a full-strength seawater culture medium with a high carbon-to-nitrogen ratio. This medium contained the following per liter: Reef Crystals™ Synthetic Sea Salts Enriched Blend made by Aquarium Systems (Mentor, OH), 40 g; glucose, 20 g; monosodium glutamate, 4 g; Difco (Detroit, MI) yeast extract, 1 g; trace metal solution, 5 mL; and vitamin mix, 1 mL. The medium was adjusted to pH 7.0 and autoclaved. Cultures were sampled at 48 h.

Crypthecodenium cohnii (ATCC 30334 sibling species G) was grown in 250-mL flasks containing 50 mL of culture medium. Cultures were grown in *Porphyridium* medium (11). This medium consisted of 50% strength seawater, 10% soil extract, and the following nutrients on a per liter basis: Difco yeast extract, 1.0 g; tryptone, 0.1 g; glucose, 3 g; biotin 0.001 mg; and thiamin 0.1 mg. The culture medium was autoclaved. Cultures were grown in the dark at room temperature. After 7 d, 100 mL of fresh *Porphyridium* medium containing one-tenth of the original concentration of yeast extract and tryptone was added to the 50 mL of culture to nitrogen-stress the culture for oil production. The *C. cohnii* culture was grown in this manner for 6 d and was then sampled for electron microscopy preparation.

Isochrysis galbana (UTEX LB 987) cultures were grown in 250-mL flasks containing 50 mL of f/2 culture medium (previously described) (10). After growing for 22 d at room temperature with light exposure, 100 mL of fresh f/2 medium lacking $NaNO_3$ was added to the 50 mL of culture to nitrogen-stress the culture and to enhance oil production. The cells were allowed to grow for six more days and were subsequently sampled for electron microscopy preparation.

Lipid analysis. Fatty acids in whole-cell *Schizochytrium* sp. and *Thraustochytrium* sp. were transesterified using 4% wt/vol sulfuric acid in methanol (100°C for 1 h). The fatty acid methyl esters (FAME) were separated and quantified on a Varian 3500 gas–liquid chromatograph (Palo Alto, CA) equipped with a flame-ionization detector and a 30 m × 0.25 mm (i.d.) Rtx 2330 fused-silica capillary column (Restek, Bellefonte, PA). Nu-Chek-Prep (Elysian, MN) fatty acid standards were employed in the analysis. Fatty acid standards were reported as percentage of total FAME.

Separation of lipid classes. Lipids were extracted from lyophilized *Schizochytrium* sp. by using the method of Bligh and Dyer (12) assisted by sonication of the cells. The total lipid extract was fractionated into the major lipid classes (phospholipid, triacylglycerols, free fatty acids, and sterols) by thin-layer chromatography (TLC) using the method outlined in St. John and Bell (13). The fractions were scraped from the TLC plates, transesterified, and analyzed by gas chromatography using the method described above.

^{13}C nuclear magnetic resonance (NMR) spectroscopy.

Quantitative ^{13}C spectra were obtained on the purified triacylglycerol fraction from *Schizochytrium* sp. microalgae (*ca.* 50–100 mg dissolved in 0.6 mL $CDCl_3$ in 5-mm tubes) at a frequency of 75 MHz with the NOE (nuclear Overhauser effect)-suppressed, inverse-gated, proton-decoupled technique. The free induction decay was acquired with a pulse delay of 40 s as described by Aursand *et al.* (14). The chemical shifts were referenced indirectly to tetramethylsilane by using the central peak of $CDCl_3$ (δ = 77.08 ppm). In this analysis, assignments of the downfield resonance at 173.2, 172.8 ppm, based on literature precedent (14), were attributed to carboxyl carbons of all fatty acids except DHA/docosapentaenoic acid (DPAn-6) (fatty acids that contain a Δ-4 unsaturation) located at positions *sn*-1,3 (α-position) and *sn*-2 (β-position) on the glycerol backbone, respectively. Assignments of the downfield resonance at 172.5 and 172.1 ppm were attributed to carboxyl carbons of DHA/DPAn-6 (fatty acids that contain a Δ-4 unsaturation) located at positions *sn*-1,3 (α) and *sn*-2 (β) on the glycerol backbone, respectively. Integration of carboxyl groups was used to estimate the amount of DPAn-6 and DHA esterified to the *sn*-2 and *sn*-1,3 positions.

High-pressure freeze substitution. Cell samples were collected and washed briefly in 15% wt/vol dextran (avg. MW 39 kD), a nonpermeating cryoprotectant, in growth medium or 5 g/L Na_2SO_4. The samples were then frozen in a BAL-TEC HPM-010 high-pressure freezer (Technotrade International, Manchester, NH) and stored under liquid nitrogen. The samples were freeze-substituted in 2% OsO_4 in acetone at −80°C following the procedures outlined by Staehelin *et al.* (15).

Freeze-fracture. Samples were collected at 48 h, and glutaraldehyde was added to the sample over 15 min to a final concentration of 1%. The cells were then washed and resuspended in a solution of 5 g Na_2SO_4/L. Glycerol, which was used as a cryoprotectant, was added over a period of 20 min to a final concentration of 30%. Samples were frozen in propane near its melting point and freeze-fractured at −113°C in a BAL-TEC BAF-060 freeze-etch system (Technotrade International). Replicas were cleaned on bleach followed by a 7.8% wt/vol potassium dichromate, 33% vol/vol sulfuric acid solution, then picked up on specimen grids for viewing by transmission electron microscopy.

Lipid-layer measurement. Crude lipid-layer widths and terrace heights were measured on resulting contact print photomicrographs using a Bausch & Lomb Stereozoom 7 (Rochester, NY) dissecting microscope with a calibrated eyepiece. Measurements were averaged and standard deviations calculated.

RESULTS AND DISCUSSION

The fatty-acid profile of *Schizochytrium* sp. is variable, depending on culture conditions which ultimately influence the ratio of triacylglycerols to phospholipids in the lipid fraction. Differences in the fatty acid composition of the triacylglycerols and phospholipids from *Schizochytrium* sp. are illustrated in Table 1. The overall fatty-acid profile of *Schizochytrium* sp. is relatively simple, consisting of five major fatty acids: DHA (22:6n-3) and DPAn-6 are the primary polyunsaturated fatty acids, and myristic (14:0), palmitic (16:0), and palmitoleic (16:1) acids are the major saturated and monounsaturated fatty acids. Together, these five fatty acids constitute over 90% of the total fatty acids in the triacylglycerols of *Schizochytrium* sp. The ratio of DHA to DPAn-6 in the triacylglycerols is *ca.* 3:1. The phospholipids are highly enriched in DHA, DPAn-6, and palmitic acid.

The results of ^{13}C NMR analysis indicated that DHA and DPAn-6 are preferentially (71–75%) esterified in the *sn*-2 position of the glycerol with the remainder (25–29%) linked in the *sn*-1,3 position (Fig. 1). Given this and the total fatty acid composition of the oil, most of the *sn*-2 positions were found to be occupied by DHA or DPAn-6. This stereospecific distribution of DHA and DPAn-6 fatty acids is similar to that reported for other highly unsaturated fatty acid-rich oils of marine, algal, and microbial origin (16). By subtraction, most of the remaining *sn*-1,3 positions would be occupied by either 14:0, 16:0, or 16:1 acids.

When the *Schizochytrium* sp. cells were prepared by high-pressure freeze substitution, patterns within the oil bodies were suggestive of both secondary and tertiary (three-dimensional) structures (Figs. 2 and 3). The fine pattern of alternating light- and dark-staining bands may be indicative of a secondary structure in the triacylglycerols. The light bands measured 22 ± 1 Å (n = 10). Larsson (7) provides a diagram drawn to scale of trilaurin as viewed along the shortest axis of the triacylglycerol unit. The length from the alpha-carbon to the end of the 12-carbon fatty acid chain is depicted as 11.7 Å. Correspondingly, Holte *et al*. (17) report that the length of palmitate should fall within the range of 13–15 Å. The width of the light bands measured approximately twice the length of crystalline myristate (14:0) and/or palmitate (16:0) as can be calculated at 11.38–12 Å and 13 Å, respectively, from the data of Larsson *et al.* (7) and Holte *et al.* (17).

OsO_4 reacted with the double bonds of unsaturated fatty acids which made them appear dark in the electron micrographs. Dark-staining bands measured 29 ± 1 Å (n = 10) in

TABLE 1
Fatty Acid Composition of Oil Extracted from *Schizochytrium* sp.

Fatty acid	Phospholipids	Triacylglycerols	Total fatty acids (%)
14:0	1.2	17.5	14.3
14:1	—	0.7	0.6
16:0	19.3	26.4	25.1
16:1	1.4	13.9	11.4
18:0	—	0.6	0.5
18:1	2.6	3.6	3.4
20:4n-6	—	0.1	0.1
20:5n-3	—	0.4	0.3
24:1	—	0.2	0.2
22:5n-6	21.3	8.8	11.0
22:5n-3	—	0.2	0.2
22:6n-3	54.2	27.6	32.9

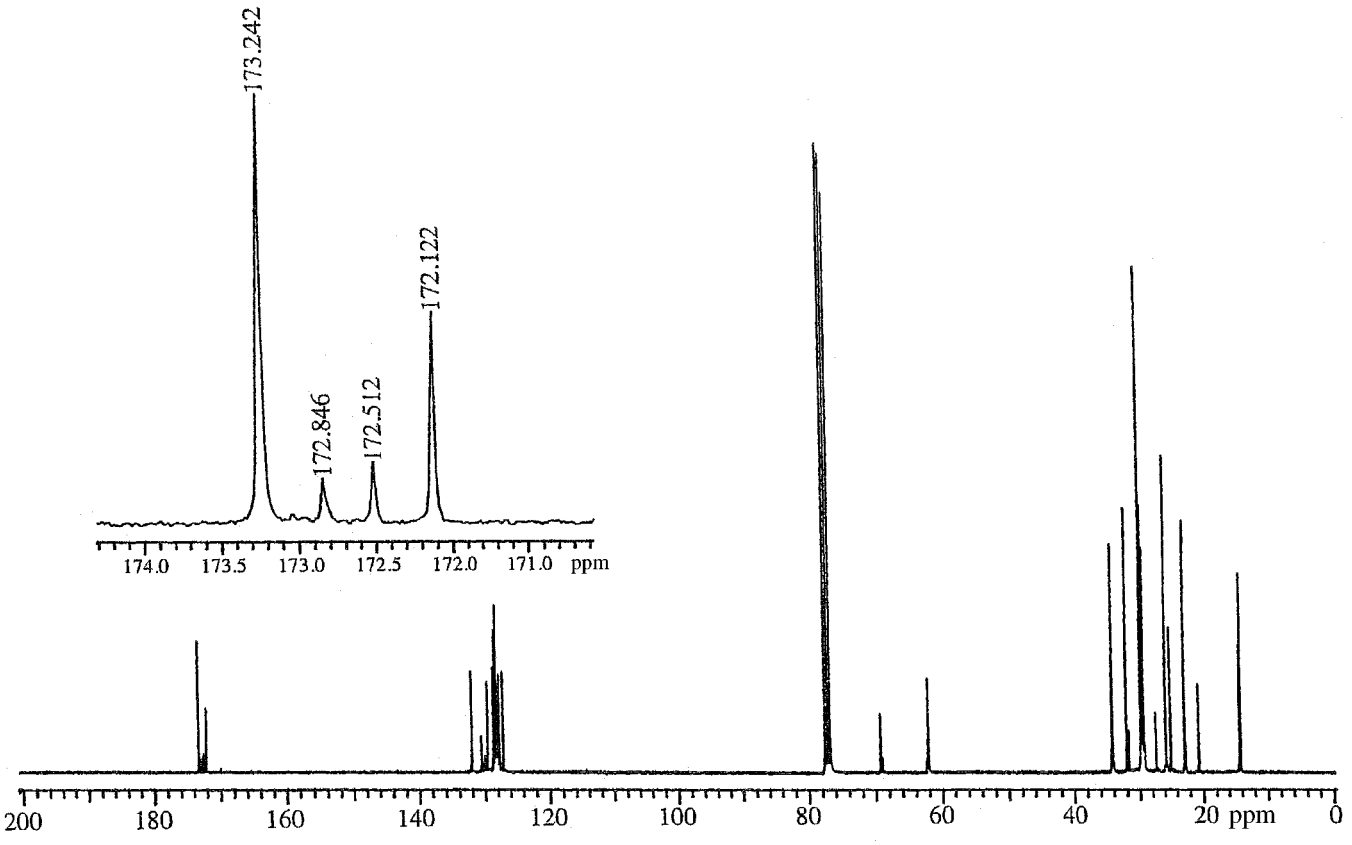

FIG. 1. ^{13}C nuclear magnetic resonance spectrum of the triacylglycerols of *Schizochytrium* sp. The data illustrate the relative amounts of docosahexaenoic acid and docosapentaenoic acid esterified to the *sn*-2 and *sn*-1,3 positions (see text for explanation).

width. The width of dark bands correspond relatively closely to the reported length of DHA in the crystalline state, 29.03 and 24.85 Å in the *sn*-1 and *sn*-2 positions of a phospholipid molecule, respectively (18). Applegate and Glomset (18), using a molecular modeling computer program (PROPHET II, BBN Systems and Technology, Cambridge, MA), have suggested that the conformational shape of the DHA molecule is a straight helical structure. In contrast, Crawford *et al.* (19), using a molecular orbital package computer program (MOPAC, Alchemy 2000 v. 20; Tripos Inc., St. Louis, MO), calculated the energy-minimized configurations of DHA and DPAn-6 and report that the molecules as being folded approximately in half. If the dark bands observed in electron photomicrographs do correspond to stained DHA and DPAn-6 molecules, a measurement of 29 ± 1 Å may provide more support for a straight helical structure of the molecules.

The fine structures within the oil bodies cannot be thylakoid membranes (which are typically associated with plastid-like organelles) because: (i) the bilayer thickness of known thylakoid membranes is thicker (*ca.* 80 Å) (20) than the thickness of the terrace heights (51 ± 7 Å) observed in freeze-fracture micrographs of *Schizochytrium*, (ii) the phospholipid content of oil in *Schizochytrium* sp. cells is less than 5% of the total lipids (Zeller, S., unpublished data), and (iii) the freeze-fracture technique revealed that there are no proteins present on the surface fracture planes of these laminar structures inside *Schizochytrium* sp. oil bodies as would normally be found on thylakoid membranes (21) (Fig. 4).

Larsson (7) previously proposed that crystalline triacylglycerol structures can occur in one of two alternative chain-layer configurations based on segregation of similar fatty acid tails. The banding pattern observed in *Schizochytrium* sp. oil bodies may best be described using Larsson's triple chain-length model, suggesting that the triacylglycerols in the oil bodies are organized in a semicrystalline state by segregation of the different fatty-acid types into separate layers. We propose that the highly unsaturated fatty-acid chains containing DHA and possibly DPAn-6 may be segregated into one interlocking dark-staining layer and the saturated and monounsaturated fatty acid chains may be segregated end-to-end to form light-staining layers. This type of arrangement may have been facilitated by the predominance of the long-chain, highly unsaturated fatty acids DHA and DPAn-6 in the *sn*-2 position of the triacylglycerol. Thus, following Larsson's triple chain-length model for mixed triacylglycerols (7), the suggested secondary structure of the triacylglycerols in *Schizochytrium* sp. may be illustrated by the model presented in Figure 5. Analysis of the freeze-fracture photomicrographs appears to confirm this layered structure in oil bodies as evidenced by terraced fracture planes (Fig. 4). Terrace heights averaged 51

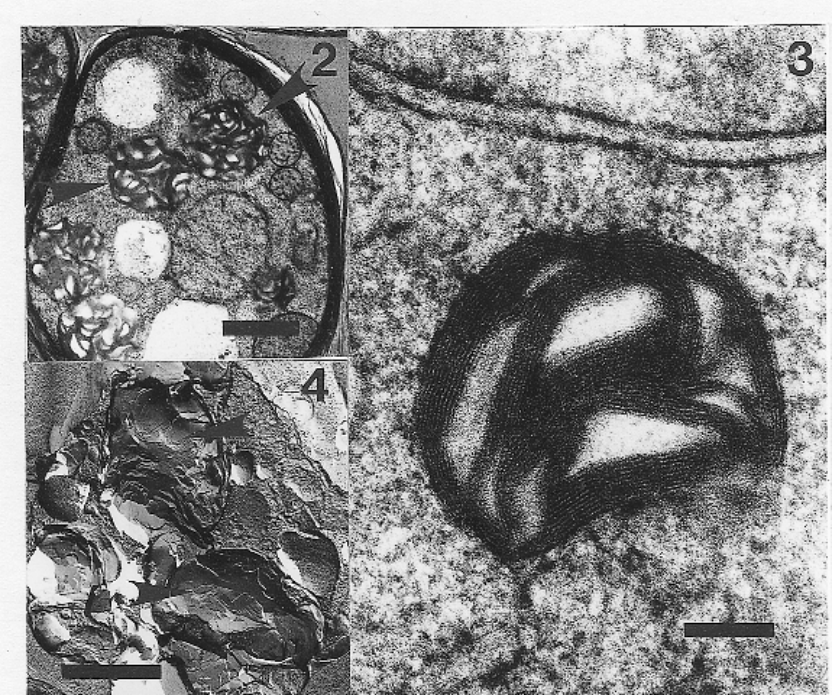

FIG. 2. Electron micrograph of a cell from an exponential culture of *Schizochytrium* sp. as preserved by high-pressure freezing and freeze-substitution. Early developing oil bodies are indicated by arrows. Bar = 1 μm.

FIG. 3. Example of the layered, fingerprint-like pattern observed inside a *Schizochytrium* sp. oil body as preserved by the high-pressure freeze substitution method. The alternating light and dark bands in the fingerprint-like structure measure 21.56 ± 1.35 Å and 28.78 ± 1.35 Å, respectively. Bar = 0.1 μm.

FIG. 4. Whole-cell *Schizochytrium* sp. as preserved by freeze fracture showing fracture planes through oil bodies. The triacylglycerol triple-layer freeze-fracture terrace shadow height averages 52.18 ± 6.8 Å. Fractured terraces inside oil bodies are indicated by arrows. Bar = 1 μm.

± 7 Å (n = 10) which, in the proposed model, may correspond to the distance from one fracture plane between two saturated lipid layers, including one interlocked dark-staining layer, to the next fracture plane between the next two end-to-end saturated lipid layers (Fig. 5).

Larsson's model (7) has been previously confirmed indirectly by freeze-fracture techniques on oil droplets in milk. This is the first time an ordered pattern has been visually observed in oil bodies of an oil-accumulating microorganism. Cell sample preparation procedures could possibly affect the conformation of the triacylglycerols within the oil bodies. However, the high-pressure freeze substitution technique rapidly freezes the cells within *ca.* 10 ms by exposure to liquid nitrogen under pressure (6). The high-pressure flash freeze should instantaneously arrest molecular movement, and subsequent segregation of the fatty-acid chains would most likely not occur (22). Thus, the triple-layer structure may be the native conformation of the triacylglycerols in the cells prior to freezing. Possibly, this secondary light- and dark-staining pattern is due to the unique fatty-acid profile of the oil produced by *Schizochytrium* sp. The composition of the oil can be generalized as containing a 2:1 ratio of saturated and monounsaturated fatty acids to highly unsaturated fatty acids.

A possible tertiary (three-dimensional) structure of the lipids in the oil bodies was revealed in the high-pressure freeze substitution photomicrographs as a ribbon-like multilayer structure of triacylglycerols coiled within the oil body (Fig. 3). These ribbon-like bands of triacylglycerols average *ca.* 500 Å in width in *Schizochytrium* sp. Their relatively constant width is surprising, and we have not yet developed a model to explain this structure.

The question has been raised of whether the light- and dark-staining pattern could merely be an artifact of electron microscopy preparation. In order to address this question, we analyzed oil-body structure in other algal and algae-like microorganisms with a variety of fatty-acid profiles. The high-pressure freeze substitution technique was used to prepare cell samples of *N. oleoabundans, N. occulata, I. galbana, C. cohnii, Thraustochytrium* sp. (ATCC 20890), and a repeat of *Schizochytrium* sp. (ATCC 20888). Electron micrographs from this experiment were compared with earlier micrographs of *Schizochytrium* sp. These specific microorganisms were selected based on prior knowledge (in the literature and from FAME analysis) of their fatty acid profiles (4,23–26). All of these algae or algae-like species of microorganisms are known

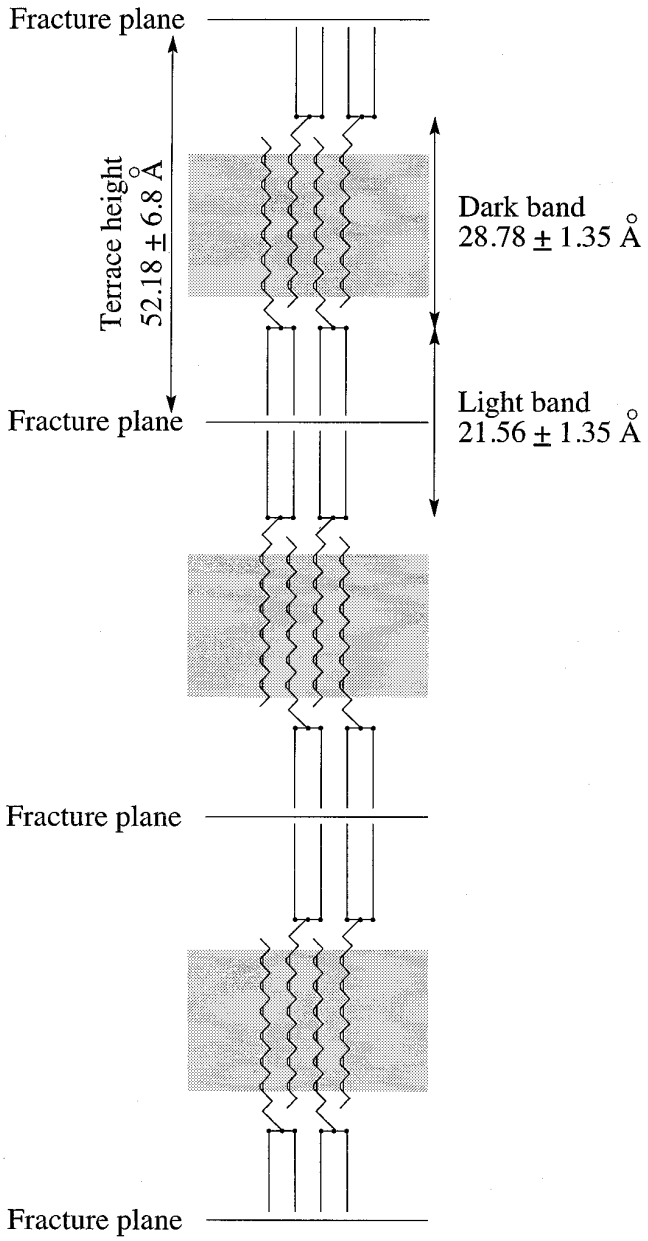

FIG. 5. Proposed model (triple-layer structure) of triacylglycerols in *Schizochytrium* sp. oil bodies which is consistent with the light- and dark-band staining pattern observed in freeze-substitution electron micrographs.

to contain significant amounts of either of the long-chain n-3 fatty acids eicosapentaenoic acid (20:5n-3) or DHA (4,24–26) except *N. oleoabundans,* which contains *ca.* 81% saturated fatty acids (23).

Electron photomicrographs did not reveal the secondary structure which has a fingerprint-like pattern in *N. oleoabundans, N. occulata*, or *C. cohnii*. Oil bodies from *N. oleoabundans* were homogeneous and did not stain (Fig. 6). This was expected because the fatty-acid profile of *N. oleoabundans* contains mostly saturated fatty acids (23) (Table 2). Oil bodies from *N. occulata* (Fig. 7) and *C. cohnii* (Figs. 8–10) were homogeneous, staining gray. The ratio of saturated and monounsaturated to highly unsaturated fatty acids in *C. cohnii* and *N. occulata* were *ca.* 6:1 and 1:1, respectively. This may not be close enough to the 2:1 ratio of saturated and monounsaturated to polyunsaturated fatty acids found in *Schizochytrium* sp. triacylglycerols, a ratio which may favor a triple chain-length formation of fatty acid tail segregation.

Electron photomicrographs of *I. galbana* exhibited oil bodies that contained the tertiary, three-dimensional interlaced pattern, but the secondary fingerprint pattern was not visible (Figs. 11–13). The tertiary ribbon-like bands measured an average of 405 ± 50 Å (n = 25). It can be confirmed that the structure inside the oil bodies differs significantly from that of the structure of thylakoid membranes seen inside chloroplasts. Figure 12 clearly shows an *I. galbana* cell containing an oil body displaying the tertiary pattern adjacent to a chloroplast containing mature thylakoid membranes. The two types of lipid structures are different with respect to shape and size. The bilayer thickness of thylakoid membranes in this organism's chloroplasts is an average of 56 ± 15 Å (n = 10), and the lumen of the granal stacks (white areas) measured 102 ± 9 Å in width. The secondary light- and dark-staining pattern was not visible within the ribbon-like bands inside oil bodies of *I. galbana*. However, the fatty-acid profile ratio of saturated and monounsaturated fatty acids to highly unsaturated fatty acids of *I. galbana* may have favored the formation of a triple-layer structure within the triacylglycerols (Fig. 13). The major saturated fatty acids 14:0 and 16:0 in addition to the major monounsaturated fatty acids (and including linoleic acid 18:2 which would most likely stain fairly lightly) add up to *ca.* 56% of the total fatty acids (24). The highly unsaturated fatty acids containing four or more double bonds add up to *ca.* 38% of total fatty acids (Table 2). These roughly correspond to the 2:1 saturated and monounsaturated to highly unsaturated fatty-acid ratio observed in *Schizochytrium* sp. The tertiary ribbon-like bands measure an average of 405 ± 50 Å (n = 25). This width is slightly different from the width of tertiary bands previously observed in *Schizochytrium* sp.

Thraustochytrium sp. electron photomicrographs exhibit both a secondary and tertiary pattern (Figs. 14,15). Tertiary ribbon-like bands measure 286 ± 74 Å. The dark bands measure 29 ± 3 Å (n = 25) in width, and the light bands measure 22 ± 3 Å (n = 25) in width. This is very similar to the measurements of the secondary dark and light bands observed within oil bodies of *Schizochytrium* sp. The fatty-acid profile of *Thraustochytrium* sp. was reported to be *ca.* 31% saturated and 68% highly unsaturated (Table 2) (4). The fatty-acid profile of *Thraustochytrium* sp. does not contain a significant amount of monounsaturated fatty acids. This fatty-acid profile produces a ratio of 1:2 saturated to highly unsaturated fatty acids. This is opposite of the fatty-acid ratios observed for *Schizochytrium* sp. Correspondingly, oil bodies of *Thraustochytrium* sp. seem to have a high percentage of dark-staining bands compared to *Schizochytrium* sp. (Fig. 16). Perhaps a different triple chain-length conformation could be hypothesized to exist in *Thraustochytrium* sp., wherein two highly

TABLE 2
Fatty Acid Composition of Various Algal and Algae-Like Microorganisms (refs. 3,23—26)

Fatty acid	*Neochloris oleoabundans*	*Nannochloropsis occulata*	*Isochrysis galbana*	*Crypthecodenium cohnii*	*Thraustochytrium* sp. ATCC 20890	*Schizochytrium* sp. ATCC 20888
12:0	—	—	—	23.4	—	—
14:0	3.8	3.8	15.1	42.1	—	14.3
14.1	—	—	—	—	—	0.6
16:0	74.6	36.4	12.4	14.1	21.4	25.1
16:1	2.2	25.8	4.0	0.7	—	11.4
18:0	3.1	3.7	—	1.4	—	0.5
18:1	13.8	7.6	20.6	4.8	—	3.4
18:2n-6	Trace	1.2	4.0	—	—	—
18:3	2.5	—	—	—	—	—
18:4	—	—	20.8	—	—	—
20:1	—	—	—	0.3	—	—
20:4n-6	—	4.6	—	—	1.4	0.1
24.1	—	—	—	—	—	0.2
20:5n-3	—	15.9	—	—	18.9	0.3
22:5n-3	—	—	—	—	5.0	0.2
22:5n-6	—	—	—	—	—	11.0
22:6n-3	—	—	17.6	13.2	43.5	32.9

unsaturated fatty-acid chains of the triacylglycerol segregate into the same layer while only one saturated fatty acid from each triacylglycerol segregates into a separate layer.

Repetition of the high-pressure freeze substitution technique with *Schizochytrium* sp. gave results essentially identical to those described above (Figs. 16,17). Ribbon-like bands measured an average of 267 ± 49 Å. These results differ from previous measurements of *ca.* 500 Å, but as can be seen by the large standard deviation of the measurements, the width of the tertiary ribbon-like bands was highly variable in pictures from the repeat experiment. Dark bands inside oil bodies measured 29 ± 2 Å, and light bands measured 22 ± 3 Å. These results are very similar to earlier measurements of dark and light bands in *Schizochytrium* sp. photomicrographs. The results of the study of other algal and algae-like microorganisms add support to the hypothesis that the staining patterns in the oil bodies of *Schizochytrium* sp. were not artifacts of the high-pressure freeze substitution preparation for electron microscopy. It also provides more evidence that the secondary light- and dark-staining pattern may be representative of the structure of triacylglycerols in their native conformation prior to freezing. The secondary staining pattern was observed in both *Schizochytrium* sp. and *Thraustochytrium* sp. It is interesting that these results were seen in two very closely related species of algae-like microorganisms (27) with fatty-acid profiles that are either 2:1 or 1:2 saturated plus monounsaturated fatty acids to highly unsaturated fatty acids. The results of this experiment suggest that the formation of a semicrystalline structure, such as the triple chain-length structure, in the microbial oil bodies may depend on the ratio of saturated and monounsaturated plus highly unsaturated fatty acids in the oil.

The tertiary ribbon-like banding pattern could be observed in two closely related species, *Schizochytrium* and *Thraustochytrium*, and in the unrelated species *I. galbana. Isochrysis galbana* is a member of the eustigmatophytes, a separate group of the heterokont algae within the stramenopiles (24,28). Although the secondary light- and dark-staining pattern could not be seen inside the tertiary, three-dimensional bands of *I. galbana*, it is encouraging that the tertiary pattern was present and that this organism had a similar fatty-acid profile of 2:1 saturated plus monounsaturated to highly unsaturated fatty acids.

In conclusion, the light- and dark-staining pattern observed in *Schizochytrium* sp. and *Thraustochytrium* sp. oil bodies may be representative of the formation of a semicrystalline structure in the triacylglycerols in the oil bodies. This interpretation is supported by: (i) the thickness of the light- and dark-staining bands corresponds to known lengths of fatty acids, (ii) freeze-fracture terrace heights in the oil bodies correspond very closely to the observed staining pattern exhibited in freeze substitution-treated oil bodies, and (iii) this pattern appears to occur in oil bodies containing triacylglycerols with a 2:1 or 1:2 ratio of saturated and monounsaturated to highly unsaturated fatty acids, a ratio which may favor the triple chain-length conformation. Further studies investigating electron micrographs of oil-producing species of microorganisms with either a 2:1 or 1:2 saturated and monounsaturated to highly unsaturated fatty acid ratio or studies of *Schizochytrium* sp. or *Thraustochytrium* sp. mutants with altered fatty-acid ratios may aid in the elucidation of factors that facilitate the unique organization of the triacylglycerols observed in *Thraustochytrium* sp. and *Schizochytrium* sp. Additionally, X-ray diffraction experiments of extracted oil samples may provide additional evidence for a triple chain-length structure in these microbial oils.

ACKNOWLEDGMENTS

We thank Dr. Ruben Abril, Patricia Abril, Andrea Egans, Dr. L. Andrew Staehelin, Dr. Klaus Gawrisch, and David Underwood for their

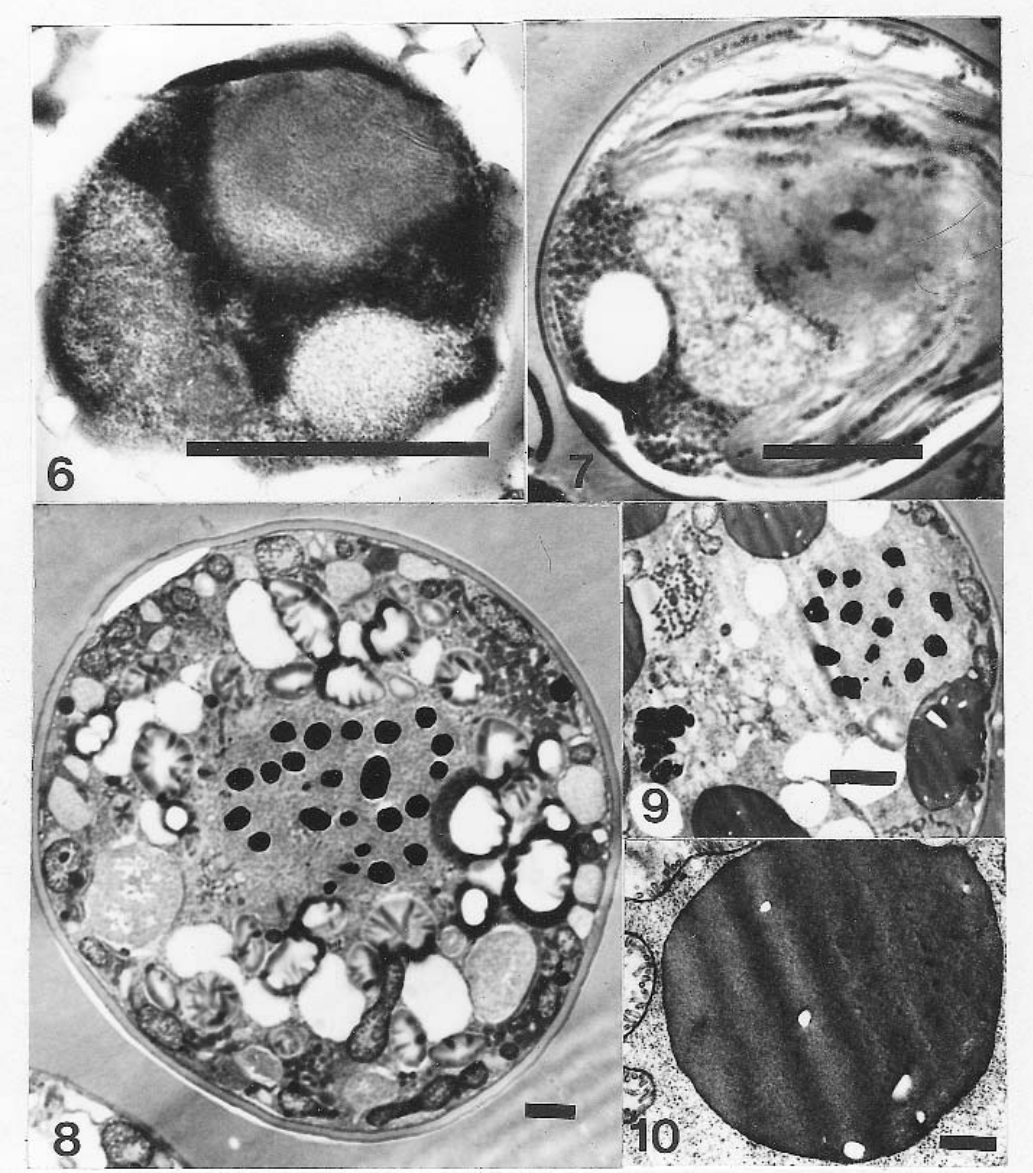

FIG. 6. *Neochloris oleoabundans* grown on Bolds basal medium. Whole cell electron photomicrograph containing light gray-staining oil bodies. Bar = 1 μm.
FIG. 7. Whole-cell electron micrograph of *Nannochloropsis occulata* grown on f/2 seawater medium. Bar = 1 μm.
FIG. 8. Whole-cell view of *Crypthecodenium cohnii* exhibiting various organelles. Bar = 1 μm.
FIG. 9. *Crypthecodenium cohnii* cell containing homogeneous dark-staining oil bodies. Bar = 1 μm.
FIG. 10. High-magnification view of an oil body from the *C. cohnii* cell displayed in Figure 9. Note the homogeneous texture of the oil body confirming that there is no light- and dark-banding pattern. Bar = 0.5 μm.

assistance in the preparation of this manuscript.

REFERENCES

1. Barclay, W.R., Meager, K.M., and Abril, J.R. (1994) Heterotrophic Production of Long-Chain Omega-3 Fatty Acids Utilizing Algae and Algae-Like Microorganisms, *J. Appl. Phycol. 6*, 123–129.
2. Barclay, W., Abril, R., Abril, P., Weaver, C., and Ashford, A. (1998) Production of Docosahexaenoic Acid from Microalgae and Its Benefits for Use in Animal Feeds, in *The Return of ω3 Fatty Acids into the Food Supply. I. Land-Based Animal Food Products and Their Health Effects* (Simopoulos, A.P., ed.), pp. 61, Karger, Basel.
3. Abril, J.R., Barclay, W.R., and Abril, P.G. (2000) Safe Use of Microalge (DHA GOLD™) in Laying Hen Feed for the Production of DHA-Enriched Eggs, in *Egg Nutrition and Biotechnology* (Sim, J.S., Nakai, S., and Guenter, W., eds.), pp. 197–202, CAB International, Wallingford.
4. Barclay, W.R. (1992) Process for the Heterotrophic Production of Microbial Products with High Concentrations of Omega-3 Highly Unsaturated Fatty Acids, U.S. Patent 5,130,242.
5. Weete, J.D., Kim, H., Gandhi, S.R., Wang, Y., and Dute, R. (1997) Lipids and Ultrastructure of *Thraustochytrium* sp. ATCC 26185, *Lipids 32*, 839–845.

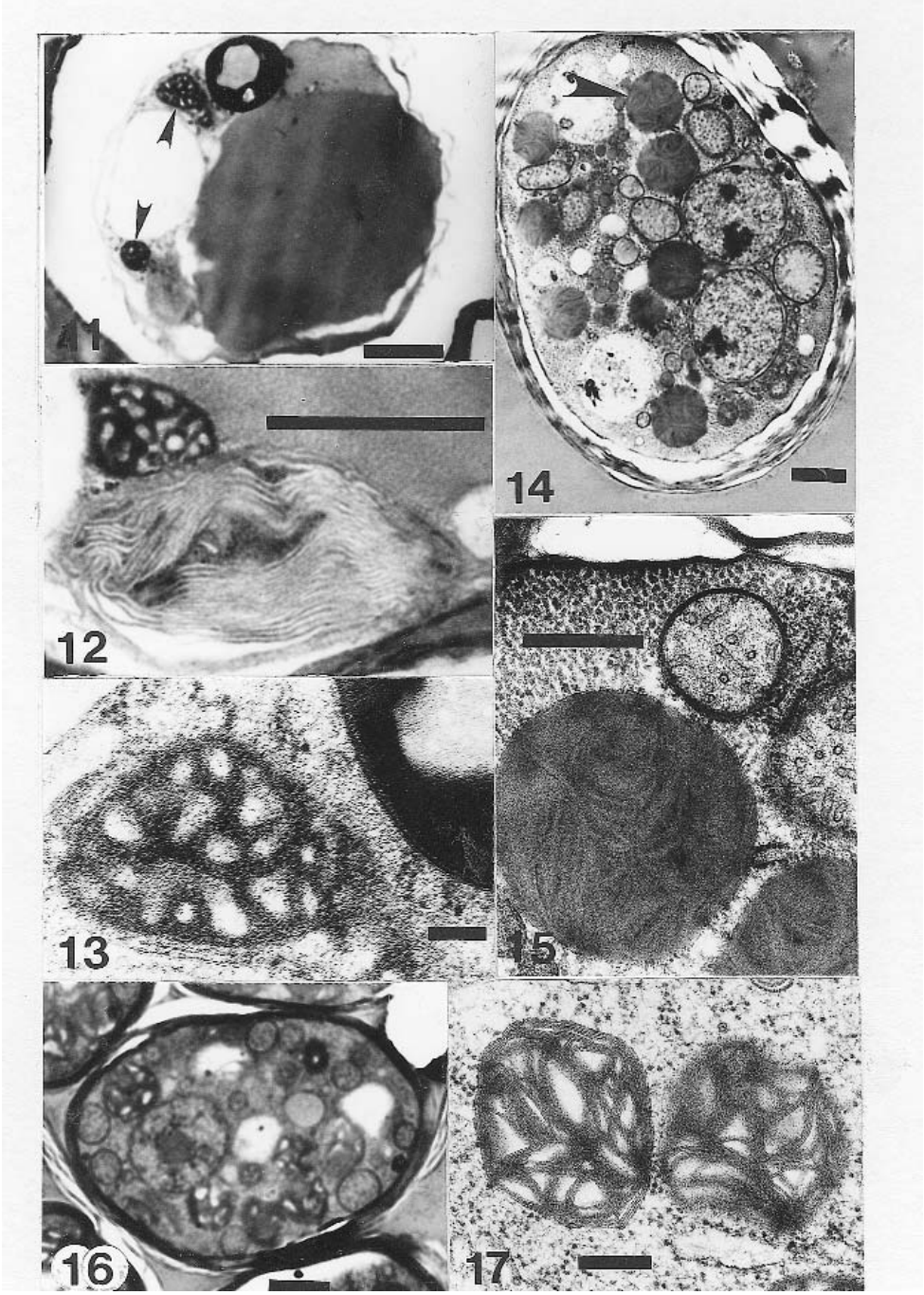

FIG. 11. Whole-cell view of *Isochrysis galbana,* displaying cytoplasm and oil bodies. Bar = 1 μm.
FIG. 12. Oil body adjacent to a chloroplast with mature thylakoid membranes in *I. galbana*. Bar = 1 μm.
FIG. 13. High-magnification view of an oil body in *I. galbana* that displayed the tertiary structure. Bar = 0.1 μm.
FIG. 14. Whole-cell electron photomicrograph of *Thraustochytrium* sp., exhibiting oil bodies with both the tertiary and secondary structure. Bar = 1 μm.
FIG. 15. Higher magnified view of an oil body from Figure 13. Note the light- and dark-banding pattern within the oil body. Bar = 0.5 μm.
FIG. 16. *Schizochytrium* sp. cell from the repeated experiment. Bar = 1 μm.
FIG. 17. High-magnification electron photomicrograph of oil bodies from *Schizochytrium* sp. Bar = 0.5 μm.

6. Staehelin, L.A., Giddings, T.H., and Moore, P.J. (1988) Structural Organization and Dynamics of the Secretory Pathway of Plant Cells, *Current Topics Plant Biochem. Physiol. 7*, 45–61.
7. Larsson, K. (1994) *Lipids—Molecular Organization, Physical Functions, and Technical Applications,* pp. 7–81, The Oily Press, Dundee.
8. Barclay, W.R. (1994) Process for Growing *Thraustochytrium* and *Schizochytrium* Using Nonchloride Salts to Produce a Microfloral Biomass Having Omega-3 Highly Unsaturated Fatty Acids, U.S. Patent 5,340,742.
9. Guillard, R.R.L., and Ryther, J.H. (1962) Studies on Marine Planktonic Diatoms. I. *Cyclotella nana* Hustedt and *Detonula confervacea* (Cleve) Gran, *Can. J. Microbiol. 8*, 229–239.
10. Bischoff, H.W., and Bold, H.C. (1963) Phycological Studies. IV. Some Algae from Enchanted Rock and Related Algae Species, The University of Texas, Austin, TX, Publication 6318, pp. 95.
11. Starr, R.C., and Zeikus, J.A. (1987) UTEX—The Culture Collection of Algae at the University of Texas at Austin, *J. Phycol. 23*, 39.
12. Bligh, E.G., and Dyer, W.J. (1959) A Rapid Method of Total Lipid Extraction and Purification, *Can. J. Biochem. Physiol. 37,* 911–917.
13. St. John, L.C., and Bell, F.D. (1989) Extraction and Fractionation of Lipids from Biological Tissues, Cells, Organelles, and Fluids, *Biotechniques 7*, 476–481.
14. Aursand, M., Rainuzzo, J.R., and Grasdalen, H. (1993) Quantitative High-Resolution ^{13}C and ^{1}H Nuclear Magnetic Resonance of ω3 Fatty Acids from White Muscle of Atlantic Salmon (*Salmo salar), J. Am. Oil Chem. Soc. 70*, 971–981.
15. Staehelin, L.A., Giddings, T.H., Kiss, J.Z., and Sack, F.D. (1990) Macromolecular Differentiation of Golgi Stacks in Root Tips of *Arabidopsis* and *Nicotiana* Seedlings as Visualized in High-Pressure Frozen and Freeze-Substituted Samples, *Protoplasma 157,* 75–91.
16. Myher, J., Kuksis, A., Geher, K., Park, P., and Diersen-Schade, D. (1996) Stereospecific Analysis of Triacylglycerols Rich in Long-Chain Polyunsaturated Acids, *Lipids 31,* 207–215.
17. Holte, L.L., Peter, S.A., Sinnwell, T.M., and Gawrisch, K. (1995) ^{2}H Nuclear Magnetic Resonance Order Parameter Profiles Suggest a Change of Molecular Shape for Phosphatidylcholines Containing a Polyunsaturated Acyl Chain, *Biophys. J. 68,* 2396–2403.
18. Applegate, K.R., and Glomset, J.A. (1991) Effect of Acyl Chain Unsaturation on the Conformation of Model Diacylglycerols: A Computer Modeling Study, *J. Lipid Res. 32,* 1635–1644.
19. Crawford, M.A., Bloom, M., Broadhurst, C.L., Schmidt, W.F., Cunnane, S.C., Galli, C., Gehbremeskel, K., Linseisen, F., Lloyd-Smith, J., and Parkington, J. (1999) Evidence for the Unique Function of Docosahexaenoic Acid During the Evolution of the Modern Hominid Brain, *Lipids 34,* S39–S47.
20. Campbell, N. (1996) *Biology*, 4th edn., pp. 140–158, The Benjamin/Cummings Publishing Company, Inc., Menlo Park.
21. Alberts, B., Bray, D., Lewis, J., Raff, M., Roberts, K., and Watson, J. (1989) *Molecular Biology of the Cell,* 2nd edn., pp. 432, Garland Publishing, Inc., New York.
22. Harris, R. (1991) *Electron Microscopy in Biology—A Practical Approach,* pp. 308, IRL Press at Oxford University Press, Oxford, New York.
23. Arredondo-Vega, B., Band-Schmidt, C., and Vasquez-Duhalt, R. (1995) Biochemical Composition of *Neochloris oleoabundans* Adapted to Marine Medium, *Cytobios 83,* 201–205.
24. Sukenik, A., and Wahnon, R. (1991) Biochemical Quality of Marine Unicellular Algae with Special Emphasis on Lipid Composition. I. *Isochrysis galbana, Aquaculture 97,* 61–72.
25. Sukenik, A., Zmora, O., and Carmeli, Y. (1993) Biochemical Quality of Marine Unicellular Algae with Special Emphasis on Lipid Composition. II. *Nannochloropsis* sp., *Aquaculture 117,* 313–326.
26. Henderson, R.J., and MacKinlay, E.E. (1991) Polyunsaturated Fatty Acid Metabolism in the Marine Dinoflagellate *Crypthecodenium cohnii, Phytochemistry 30,* 1781–1787.
27. Mannella, C., Frank, J., and Delihas, N. (1987) Interrelatedness of 5S RNA Sequences Investigated by Correspondence Analysis, *J. Mol. Evol. 24,* 228–235.
28. Leipe, D.D., Wainright, P.O., Gunderson, J.H., Porter, D., Patterson, D.J., Valois, F., Himmerich, S., and Sogin, M.L. (1994) The Stramenopiles from a Molecular Perspective: 16S-like rRNA Sequences from *Labyrinthuloides minuta* and *Cafeteria roenbergensis, Phycologia 33,* 369–377.

[Received July 19, 2000, and in final revised form and accepted September 20, 2000]

Lipid Class Composition of the Protozoan *Perkinsus marinus,* an Oyster Parasite, and Its Metabolism of a Fluorescent Phosphatidylcholine Analog

P. Soudant[a,1], F.-L.E. Chu[a,*], and Y. Marty[b]

[a]Virginia Institute of Marine Science, College of William and Mary, Gloucester Point, Virginia 23062, and
[b]UMR/CNRS 6521, Université de Bretagne Occidentale, 29285 Brest, France

ABSTRACT: *Perkinsus marinus* is one of two important protozoan parasites of the eastern oyster, *Crassostrea virginica*. The other is *Haplosporidium nelsoni*. Lipids extracted from 7-d-old *in vitro* cultured *P. marinus* meronts, incubated with fluorescent-labeled phosphatidylcholine (FL PC) and nonincubated *P. marinus* meronts, were analyzed by a high-performance liquid chromatography (HPLC) system equipped with a diol phase column, in combination with thin-layer chromatography coupled with a flame-ionization detector (TLC/FID), and high-performance thin-layer chromatography (HPTLC). Various polar and neutral lipid classes were separated by HPLC using a two-gradient solvent system. Five polar lipid classes—phosphatidylcholine (PC), phosphatidylethanolamine (PE), cardiolipin (CL), sphingomyelin (SM), and phosphatidylserine (PS)—were identified from *P. marinus* extracts. Four neutral lipid classes—triacylglycerol (TAG), steryl ester (SE), cholesterol (CHO), and fatty alcohol—were distinguished. TLC/FID analysis of meront lipids showed that the weight percentages of PC, PE, CL, SM, PS/PI, TAG, SE, and CHO were 21, 10.7, 4, 2.3, 4.3, 48.7, 7.8, and 1.2%, respectively. HPLC and HPTLC analyses revealed the presence of two SM and PS isomers in *P. marinus* extracts. *Perkinsus marinus* effectively incorporated FL PC acquired from the medium and metabolized it to various components (i.e., free fatty acid, monoacylglycerol, diacylglycerol, TAG, PE, and CL). Uptake and interconversion of FL PC in *P. marinus* meronts increased with time. After 48 h the total uptake of fluorescence (FL) was 28.9% of the FL PC added to the medium, and 43% of the incorporated FL resided in TAG.

Paper no. L8391 in *Lipids 35*, 1387–1395 (December 2000).

The protistan, *Perkinsus marinus* (Dermo), which parasitizes American (eastern) oysters (*Crassostrea virginica*) is an apicomplexan in the class Perkinsasida (1). It was originally described by Mackin *et al.* (2) as *Dermocystidium marinum*. This parasite infects eastern oyster populations along the East and Gulf Coasts of the United States and has caused severe oyster mortality from the mid-Atlantic to the Gulf since the 1950s. Presently, *P. marinus* is the most prevalent parasite of the eastern oyster in mid-Atlantic waters. The disease caused by *P. marinus* is infectious (see Ref. 3). Four life stages, meront (trophozoite), prezoosporangium, zoosporangium and biflagellate zoospore, have been identified and described (4,5). Immature meronts (merozoites), usually found in the phagosomes of hemocytes and tissues of infected oysters, are 2–4 μm and coccoid. Meronts (10–20 μm) are mature merozoites with an eccentric vacuole which often contains a refringent vacuoplast. The mature meront (schizont, 20 to 40 μm) contains 8 to 32 cells. Prezoosporangia, developed from meronts, are sometimes observed in moribund and dead oyster tissues and can enlarge to 150 μm. When tissue-associated merozoites/meronts are placed in fluid thioglycollate medium (FTM) for 4 to 5 d, they also develop into prezoosporangia (hypnospores). Prezoosporangia are characterized by having a large vacuole and an eccentric nucleus adjacent to the cell wall. Zoosporulation (production of biflagellate zoospores) usually occurs after incubating FTM-cultured prezoosporangia in estuarine or seawater (20–22 ppt) for 4–5 d. The three life stages—meront, prezoosporangia, and biflagellate zoospore—are infective (3). The merozoite/meront stage is the primary agent for disease transmission (3,5). The recent advancement in culture of meront stage of this parasite in defined media (6–8) provides the opportunity to study the biochemistry and physiology of meronts.

Host lipids play a critical role for long-term survival and life cycle completion of endogenous parasites. Investigation of host lipid utilization in parasites is thus important in understanding the disease processes and the interaction between the host and parasite. Numerous studies have been conducted and advancements have been made in understanding the processes of lipid uptake and metabolism in several mammalian parasites (e.g., *Plasmodium* sp., *Schistosoma mansoni*, *Trypanosoma brucei, Giardia lamblia*) (9–19).

[1]Present address: Université de Bretagne Occidentale, Institut Universitaire Européen de la Mer LEMAR, place Nicolas Copernic, 29280 Plouzané, France.

*To whom correspondence should be addressed. E-mail: chu@vims.edu

Abbreviations: Bodipy, 4,4-difluoro-5,7-dimethyl-4-bora-3a,4a-diaza-*s*-indacene; CER, ceramide; CHE, cholesteryl ester; CHO, cholesterol; CL, cardiolipin; DAG, diacylglycerol; FA, fatty acid; FAME, fatty acid methyl ester; FFA, free fatty acids; FH, fatty alcohol; FL, fluorescent-labeled; FTM, fluid thioglycollate medium; HPLC, high-performance liquid chromatography; HPTLC, high-performance thin-layer chromatography; LPC, lysophosphatidylcholine; MAG, monoacylglycerol; PC, phosphatidylcholine; PE, phosphatidylethanolamine; PG, phosphatidylglycerol; PI, phosphatidylinositol; PS, phosphatidylserine; SE, steryl ester; SM, sphingomyelin; TAG, triacylglycerol; TLC-FID, thin-layer chromatography coupled with a flame-ionization detector; UV, ultraviolet; YRW, York river water.

In most of the lipid metabolism studies in parasites, thin-layer chromatography (TLC) has been utilized to analyze the uptake and interconversion of fluorescent lipid analogs and/or radiolabeled lipids by parasites. Only one recent study (13) employed a high-performance liquid chromatography (HPLC) equipped with a fluorescent detector and a silica gel column to investigate the uptake and metabolism of fluorescent lipid analogs by *S. mansoni*. Polar lipid classes were separated using one solvent system (acetonitrile, methanol, phosphoric acid) in the study by Furlong *et al.* (13) and no analysis was conducted on neutral lipid components.

Several methods have been described for lipid class separation (20). Polar lipid classes are typically resolved by HPLC using columns with silica gel phases (20). Detection has normally been with either ultraviolet (UV) (200–210 nm) or light-scattering detectors (21–26). Only limited work has been done on neutral lipid class separation using the above systems (27–31).

The "diol" (1,2-dihydroxypropyl covalently bonded to silica gel) phase has not been used as extensively as silica gel alone for lipid class separation. The "diol" phase is slightly less polar than silica gel, but provides a similar resolution for polar (32–37) and neutral lipid class separation (37). The "diol" phase does have an advantage in that it is more resistant to water deactivation than silica gel phase.

Solvents such as hexane, isopropanol, methanol, acetonitrile, and water have been employed as eluents in these methods (20). By using either Silica Gel or "diol" phases, gradient elution with a mixture of hexane/isopropanol/water appeared to be the most widely used and showed satisfactory results for neutral and/or polar lipid class separation (20,25,32,37–42).

To better understand lipid metabolism in the meront stage of this parasite, we have analyzed the neutral and polar lipid class composition of meronts and of metabolites derived from the metabolism of the fluorescent lipid analog, [2-(4,4-difluoro-5,7-dimethyl-4-bora-3a,4a-diaza-*s*-indacene-3-dodecanoyl)-1-hexadecanoyl-*sn*-glycero-3-phosphocholine]. Phosphatidylcholine (PC) is the most abundant polar lipid class in both meront and prezoosporangia stages (49.8 and 75.7%, respectively) (43) and in oyster tissues (34%) (Chu, F.-L.E., and Soudant, P., unpublished data). An HPLC, equipped with photodiode array and fluorescent detectors, and a "diol" phase column, was used for lipid class analysis, in combination with TLC coupled with a flame-ionization detector (TLC/FID) and high-performance TLC (HPTLC).

EXPERIMENTAL PROCEDURES

Chemicals. (i) Lipid standards. Both fluorescent and nonlabeled lipid standards were used for identification of lipid classes. Fluorescent lipid analogs were obtained from Molecular Probe (Eugene, OR). They include: *N*-(4,4-difluoro-5,7-dimethyl-4-bora-3a,4a-diaza-*s*-indacene-3-pentanoyl) sphingosyl phosphocholine (Bodipy® FL C_5-sphingomyelin, FL SM), 2-(4,4-difluoro-5,7-dimethyl-4-bora-3a,4a-diaza-*s*-indacene-3-dodecanoyl)-1-hexadecanoyl-*sn*-glycero-3-phosphocholine (Bodipy® FL C_{12}-HPC, FL PC), 2-(4,4-difluoro-5,7-diphenyl-4-bora-3a,4a-diaza-*s*-indacene-3-dodecanoyl)-1-hexadecanoyl-*sn*-glycero-3-phosphoethanolamine (β-Bodipy® FL 530/550 C_{12}-HPE, FL PE), 4,4-difluoro-5,7-diphenyl-4-bora-3a,4a-diaza-*s*-indacene-3-hexadecanoic acid (Bodipy® FL C_{16}, FL C16), cholesteryl 4,4-difluoro-5,7-diphenyl-4-bora-3a,4a-diaza-*s*-indacene-3-dodecanoate (cholesteryl Bodipy® FL C_{12}, FL CHE).

Nonlabeled lipid standards, cholesteryl ester (CHE), free fatty acids (FFA), triacylglycerol (TAG), fatty alcohol (FH), diacylglycerol (DAG), monoacylglycerol (MAG), cholesterol (CHO), ceramide (CER), cardiolipin (CL), phosphatidylglycerol (PG), phosphatidylinositol (PI), phosphatidylserine (PS), phosphatidylethanolamine (PE), phosphatidylcholine (PC), lysophosphatidylcholine (LPC), and sphingomyelin (SM) were obtained from Sigma (St. Louis, MO). Ninhydrin was obtained from ICN Pharmaceutical (Cleveland, OH).

(ii) Solvents. Hexane, isopropanol, water, methyl acetate, chloroform, methanol, and diethyl ether were HPLC grade (Burdick and Jackson, Muskegon, MI). Carbon disulfide was ultra resi-analyzed quality (J.T. Baker, Phillipsburg, NJ). The 10% (w/w) boron trifluoride in methanol (BF_3) was obtained from Supelco (Bellefonte, PA).

Incubation with fluorescent lipid analogs and lipid extraction. Perkinsus marinus meronts were cultured in a modified Dulbecco's modified Eagle medium/Ham's F-12 medium according to Gauthier and Vasta (7) for 7 d. The lipids in the medium were derived from the 5% (vol/vol) bovine fetal serum added to the medium. Lipid analysis conducted on this medium revealed a concentration of 58.9 ± 6.0 μg lipid/mL of medium, containing 46.2 μg steryl esters (SE) and 13.9 μg phospholipids. Meront cells were harvested at 7 d postinoculation, washed, and resuspended in 0.2 μm-filtered York River Water (YRW) at a concentration of 20×10^6 cells mL^{-1}. Ten microliters of fluorescent-labeled (FL) PC dissolved in dimethylsulfoxylate at 200 μM were added to 10 mL of meront suspension and incubated at 28°C for 48 h. The optimal concentration in the medium was determined empirically. Meronts were sampled, washed three times with YRW to removed free (nonincorporated) lipid analogs, freeze-dried, and stored at –20°C for later lipid analysis after incubation with FL PC for 3, 6, 12, 24, and 48 h.

Total lipid extraction. Total lipids were extracted from FL PC-incubated and nonincubated 1-wk-old meront cells with chloroform/methanol/water mixture according to the procedure described by Bligh and Dyer (44). To prevent fading of fluorescence, all extraction steps for FL PC-incubated meronts were performed protected from light.

Fatty acid analysis. Analysis of fatty acid methyl esters (FAME) was conducted on all lipid samples to assess the biomass of meront cell used for FL PC incubation. Briefly, FL and nonlabeled lipids were transesterified with 10% (w/w) BF_3 in methanol for 10 min at 100°C (45). After cooling, the FAME were extracted with carbon disulfide (46). The organic phase was evaporated, and redissolved in hexane. Separation of FAME was carried out on a gas–liquid chromatograph

(Varian 3300) equipped with a flame-ionization detector, using a DB Wax capillary column (25 m × 0.32 mm i.d.; 0.2 μm film thickness). The column was temperature programmed from 60 to 150°C at 30°C min $^{-1}$ and 150 to 220°C at 2°C min^{-1}, injector and detector temperatures were 230 and 250°C, respectively; the flow rates of compressed air and hydrogen were 300 and 30 mL min^{-1}, respectively. Helium was used as the carrier gas (1.5 mL min^{-1}). Identification of FAME was based on the comparison of retention times with those of authentic standards.

Analysis of FL and nonlabeled lipids. (i) Analysis of lipid classes by HPLC and TLC/FID. Separation of lipid standard mixtures (FL and nonlabeled) and lipids extracted from FL PC-incubated and nonincubated *P. marinus* was carried out using a Waters HPLC system (equipped with a 717 plus autosampler, 600E multisolvent delivery system, 996 photodiode array detector, and 474 scanning fluorescence detector; Milford, MA), a Lichrosorb diol column (5 μm; 250 × 4.6 mm i.d.) (Phenomenex, Torrance, CA) and two successive solvent gradient systems. Polar lipids and FFA were separated at 30°C with a ternary gradient system: 4 min of solvent A (hexane/isopropanol, 90:10, vol/vol), 6 min of a linear gradient from solvent A to solvent B (hexane/isopropanol/water, 46:52:2, by vol), 5 min of solvent B, 15 min of a linear gradient from solvent B to solvent C (hexane/isopropanol/water, 42:52:8, by vol), and 20 min of solvent C. The column was then reactivated with solvent A for 25 min. When analysis was conducted on *P. marinus* lipid extracts, the solvent front containing all neutral lipids except FFA was collected for later separation prior to reaching the detectors, using a Rheodyne® valve (Rohmert Park, CA).

Neutral lipids were separated at 30°C with a binary gradient system: 20 min of solvent A (hexane/isopropanol, 99.7:0.3, vol/vol), 10 min of a linear gradient from solvent A to solvent B (hexane/isopropanol, 90:10, vol/vol), 30 min of solvent B. The column was reactivated with 100% hexane for 25 min.

Because of the unavailability of a light-scattering detector for lipid class quantification, nonfluorescent lipids were analyzed with HPLC using the photodiode array detector at 203 nm, in combination with TLC/FID. At a wavelength of 203 nm the absorption of fatty acids with double bonds present in lipids was maximal (20). However, the use of a UV detector has disadvantages: (i) the baseline varies with eluting solvent mixtures, and (ii) it is ineffective to quantify the lipid classes. Lipid class contents of non-FL PC-incubated *P. marinus* were thus further analyzed and quantified with TLC/FID using an Iatroscan TH-10, MK-III analyzer (Iatron Laboratories, Tokyo, Japan) (47). Briefly, after activation for 30 min at 110°C, silica gel rods were spotted, using a Hamilton syringe, with lipid samples (1–10 μL/sample). Silica gel rods were then developed using a solvent mixture containing hexane/diethyl ether/formic acid (85:15:0.04, by vol). Following development, silica gel rods were analyzed in an Iatroscan analyzer. Operating conditions were 2000 mL min^{-1} air flow, 0.73 kg cm^{-3} hydrogen pressure, and a scan speed of 3.1 mm/s. Lipid classes were identified by comparison with the co-chromatographed lipid standards. Lipid standards, CHE, FFA, TAG, DAG, MAG, CHO, FH, and PC were obtained from Sigma (St. Louis, MO). Peak area integrations were performed by computer analysis (T DataScan; RSS Inc., Bemis, TN). Standard curves were constructed for each lipid class standard (1, 2, 3, 5, and 10 μg) to determine response factors of the detector. The quantity of lipid classes was determined by comparison with an internal standard. Results are expressed as percentage of total lipids.

Fluorescent lipids were detected and quantified with the fluorescence detector (excitation, 350 nm; emission, 510 nm). The responses of the fluorescence detector to various fluorescent lipid analogs were tested. The excitation at 350 nm was used since this wavelength gave the best linear response in amounts from 0.5 pmol to 0.5 nmol for all the tested components in our study. A "Microgravimetric" correlation between μmol of fluorescent lipid analogs and fluorescent peak areas was determined, based on information provided by the supplier. Peak identification was accomplished by the comparison of retention times with FL and nonlabeled lipid standards. Incorporated FL PC and its metabolite were expressed as nmol of fluorescent lipid mg^{-1} of meront fatty acids and as a percentage of the total fluorescent lipids. The nmol of fluorescent lipid mg^{-1} of meront fatty acids were calculated by first converting the quantity of the detected fluorescent lipid to nmol using calibration curves (area vs. mass) and then dividing by the amount of total lipid (mg) present in the lipid samples.

(ii) Analysis of lipid classes by HPTLC. To further confirm the identification, components eluted from the HPLC were collected and reanalyzed by HPTLC according to Olsen and Henderson (48). Briefly, after activation for 30 min at 110°C, the plates (HPK silica gel 60, 10 × 10 cm, Whatman Laboratory Division, Clinfton, NJ) were spotted, using a Hamilton syringe, with lipid class samples collected from HPLC and analyzed in parallel with mixed lipid standards containing various lipid classes employing two solvent mixtures (polar and neutral). The polar solvent mixture consisted of methyl acetate/isopropanol/chloroform/methanol/KCl 0.25% (25:25:25:10:9, by vol) and separated the polar lipids into PI/PS, PE, PC, and SM. The neutral solvent mixture contained hexane/diethyl ether/formic acid (85:15:0.05, by vol), which separated neutral lipids into different classes (i.e., CHE/SE, MAG, TAG, and FFA). Following development, lipid classes were charred by heating the plate at 160°C for 6 min after dipping it in a cupric sulfate (3%, w/w) phosphoric acid (8%, vol/vol) solution. Free amino groups in phospholipids (e.g., PE and PS) were visualized by spraying with a solution containing 0.2% ninhydrin in butanol and incubated at 100°C for 2–3 min. Lipid classes were identified by comparison with co-chromatographed standards.

Additionally, each polar lipid component from HPLC was subjected to a mild alkaline transesterification as described by Christie (49) to test for the presence of sphingolipids which are unaffected by the procedure. The by-products were extracted with chloroform and reanalyzed in parallel with the initial polar lipid components by HPTLC using the polar sol-

vent mixture described above.

To resolve PI from PS, polar lipids were redeveloped using a solvent mixture of chloroform/methanol/acid acetic/water (25:15:4:2, by vol; 38). In order to verify the identification, two-dimensional development was also utilized for polar lipid separation using a chloroform/methanol/14 N ammonium hydroxide/water (65:30:2:2, by vol) mixture and then a mixture of chloroform/methanol/water (50:20:2, by vol).

RESULTS AND DISCUSSION

Total fatty acid contents and meront cell number. Total fatty acid contents in meront cells and cell number did not appear to change during the 48 h FL PC incubation period. These observations were expected since the FL PC incubation was conducted in nutrient-limited water (YRW). Also the fluorescent lipid analog did not appear to cause death of meronts within 48 h.

Analysis of P. marinus *lipid classes by HPLC.* The HPLC system employed in the present study separated various polar and neutral lipid standards. The elution order of polar lipid and FFA standards was: FFA, CER (peak is not shown), PE, CL, PC, SM, PI/PS, and LPC (Fig. 1A). All of these lipids eluted within 40 min. PS and PI coeluted. Inclusion of acetic acid in the mobile phase was reported to enhance separation of these two components (37). To avoid the potential degradation of Bodipy fluorescent structure by acid, acetic acid was excluded from the solvent mixture in our study. Additionally, based on the HPTLC analysis of *P. marinus* lipid classes, PI was barely detectable. The elution of neutral lipid standards was completed in 45 min and in the order of CHE, TAG, FH, DAG, CHO, MAG, and FFA (Fig. 1B).

Five polar lipids were isolated from *P. marinus* total lipid extracts, i.e. PC, PE, CL, SM, and PS (Fig. 2A). As in most parasitic protozoans, PC and PE are the two major lipid classes (9,50–52). Quantitative analysis using TLC-FID revealed that PC, PE, CL, PS/PI, and SM accounted for, respectively, 21.0,

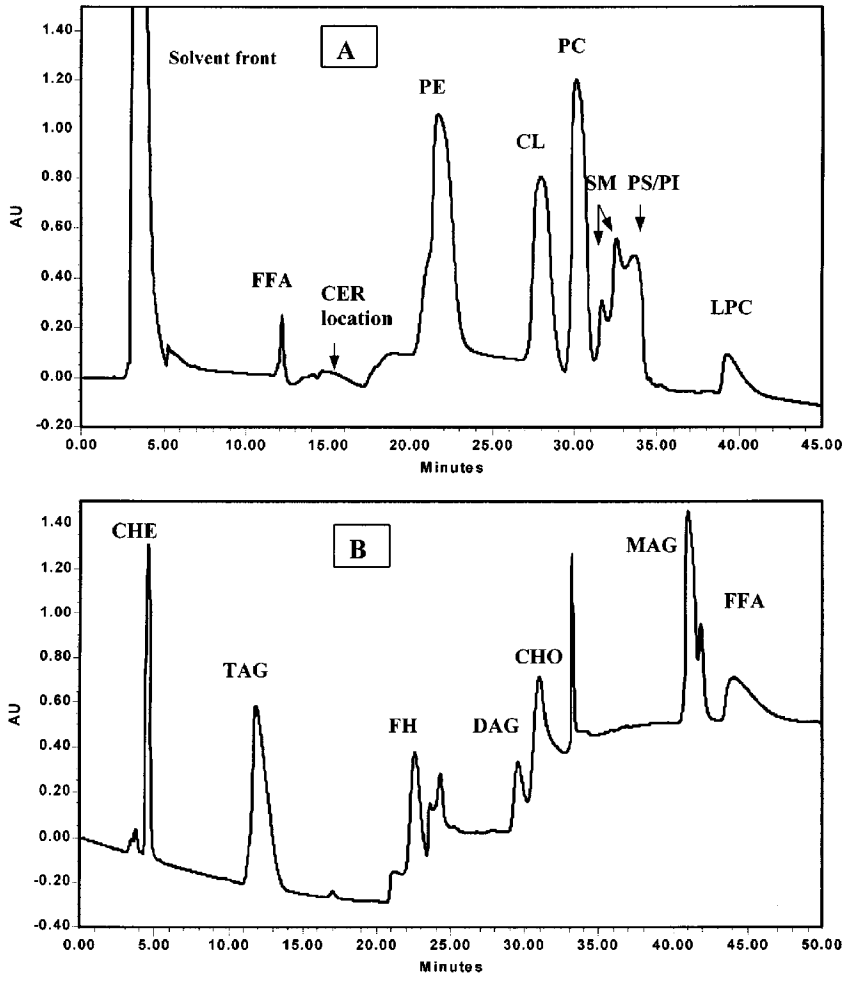

FIG. 1. High-performance liquid chromatography (HPLC) of standard lipid classes detected by ultraviolet (UV) spectrophotometry. (A) Polar lipids; (B) neutral lipids. Abbreviations: CER, ceramide; PE, phosphatidylethanolamine; CL, cardiolipin; PC, phosphatidylcholine; SM, sphingomyelin; Pl, phosphatidylinositol; PS, phosphatidylserine; LPC, lysophosphatidylcholine; CHE, cholesteryl ester; TAG, triacylglycerol; FH, fatty alcohol; DAG, diacylglycerol; CHO, cholesterol; MAG, monoacylglycerol; FFA, free fatty acid.

10.7, 4.0, 4.3, and 2.3% of the total lipids in 7-d-old meronts/merozoites (Table 1). Unlike most of the other apicomplexan species, *P. marinus* contains significant concentration of CL. CL usually locates in mitochondria, the site where it is synthesized (20,53). Numerous cytoplasmic mitochondria were noted in *P. marinus* meronts/merozoites (4,5). CL was not detected in lipids of free-living protozoans such as *Paramecium* sp., *Tetrahymena* sp., and *Entodinium* sp., and parasitic protozoans such as *Plasmodium* sp., *Toxoplasma* sp., *Giardia* sp., and *Trypanosoma* sp. (52). However, a small amount of CL (0.9% of the total complex lipids) was detected in cells of an apicomplexan species, *Crytosporidium parvum* (54). About 4% CL was also found in the polar lipids of *Leshmania tarentolae* (51). Its biosynthetic precursor, PG, in the CDP-DAG pathway (10), was also found at levels up to 10.4% in the polar lipids of trophozoites of a primitive protozoan, *G. lamblia* (55).

PS and SM coeluted into two peaks. Subsequent HPTLC analysis of these two peaks confirmed the presence of two PS and two SM isomers. The existence of these isomers in *P. marinus* was also confirmed using two-dimensional TLC. The two PS isomers were ninhyndrin positive, and the two SM isomers were unaffected by mild alkaline transesterification. Detection of two SM isomers has been reported previously (20,24–26,37). SM was reported in the protozoan parasites, *Plasmodium* sp. (9,10) and *C. parvum* (54). PS has been detected in most of the investigated protozoan species (52,56). When the two unknown components (UK1 and UK2) eluting from the HPLC column were analyzed with HPTLC, no color was developed, after dipping the plate in the cupric sulfate/phosphoric acid solution and charring at 160°C for 6 min. A group of peaks appeared near the elution time of FFA. However, when they were collected and analyzed with HPTLC, no FFA were detected. Also, no FFA was found when *P. marinus* lipid classes were analyzed by TLC-FID (Table 1).

Four neutral lipids, TAG, SE, CHO and FH, were identified in *P. marinus* lipids. (Fig. 2B). TAG was the dominant neutral lipid. This is in agreement with the results of lipid class analysis using a TLC-FID analyzer (Table 1). TAG, SE, and cholesterol (CHO) accounted for 48.7, 7.8 and 1.2% of the total lipids, respectively, in 7-d-old meront/merozoites. CHO did not appear to be an important membrane constituent of *P. marinus*, since only about 1% of CHO was detected in

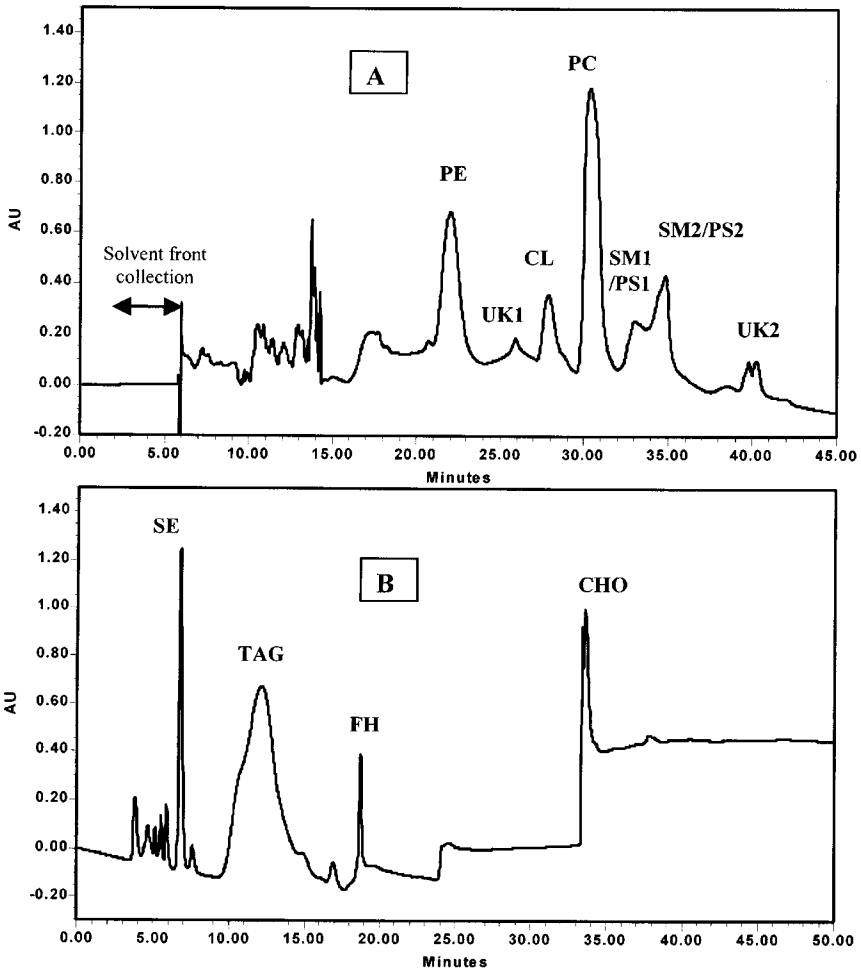

FIG. 2. HPLC chromatogram of nonfluorescent lipids from *in vitro* culture *P. marinus* cells (meronts/merozoites) detected by UV spectrophotometry. (A) Polar lipids (UK1 = unknown 1; UK2 = unknown 2); (B) neutral lipids. SE, steryl esters; for other abbreviations see Figure 1.

TABLE 1
Lipid Class Composition of 7-d-old Pellets of *in vitro Perkinsus marinus* (meronts/merozoites) Cultures[a]

Percentage of total lipids	Mean	SD
SE	7.8	0.5
TAG	48.7	1.9
FFA	ND	ND
CHO	1.2	0.1
CL	4.0	0.4
PE	10.7	0.9
PS and PI	4.3	0.5
PC	21.0	0.9
SM	2.3	1.2
µg Total lipids/10^6 cells	2.9	0.2

[a]Compositions determined by thin-layer chromatography coupled with flame-ionization detection. Results are expressed as percentage of the total lipids ($n = 3$ for mean and SD).
Abbreviations: SE, steryl ester; TAG, triacylglycerol, FFA, free fatty acids; CHO, cholesterol; PE, phosphatidylethanolamine; CL, cardiolipin; PC, phosphatidylcholine; PI, phosphatidylinositol; PS, phosphatidylserine; SM, sphingomyelin; ND, not detected.

P. marinus by TLC-FID analysis. The membrane of *Plasmodium* spp. is also deficient in CHO (9,10). Therefore, in common with most eukaryotes, TAG is the major storage lipid in *P. marinus*. Parasitic protozoans store lipids either as TAG (e.g., *Plasmodium* spp.) (57,58), as SE (e.g., *G. lamblia*) (19), or as TAG and SE (Trypanosomatidae) (51,56). In the host oyster tissues, TAG (51–67% of the total neutral lipids) is the dominant lipid class and polar (structural) lipids are predominated by PC (34%) and PE (25%) (Chu, F.-L.E., and Soudant, P., unpublished data). Sterols account for only 12% of the total neutral lipids.

Incorporation and metabolism of FL PC by P. marinus *meronts.* The UV (photodiode array) detector was ineffective to detect FL PC and its metabolites. A higher retention time was noted in fluorescent lipids compared to their nonlabeled counterparts. The increased molecular weights and polarity due to the presence of fluorescent radical in the labeled lipid may be the causes of increased retention time.

Results of HPLC analysis of FL lipids extracted from meronts/merozoites (Figs. 3A, 3B) demonstrated that *P. marinus* incorporated and modified FL PC. The detected FL PE, FL TAG, FL CL, FL MAG, FL FFA, and FL DAG are believed to be the products of FL PC metabolism and/or results of reacylation of the fluorescent acyl chain hydrolyzed off FL PC. No fluorescence was incorporated in SE. This is similar to the results obtained by Kasurinen (59) studying Bodipy 12 fatty acid incorporation by BHK (baby hamster kidney) cells.

The presence of FL DAG suggests the existence of the glycerol phosphate pathway, a common pathway for *de novo* phospholipid and TAG synthesis (53), in *P. marinus* meronts. PC and PE are synthesized *via* cytidine diphospho (CDP)-base pathway using a common precursor DAG and their respective CDP-bases. The CDP-base pathway is considered to be the most active one in synthesis of phospholipids in eukaryotes under normal conditions. The FL PE detected in meronts previously incubated with FL PC is likely synthesized *via* this pathway, using FL DAG originated from FL PC. Conversion of PC to PE has also been reported in *Plasmodium* spp. (10). However, transfer of the fluorescent acyl chain from FL PC to non-FL PE may have also taken place *via* deacylation–reacylation reactions or *de novo* synthesis of phosphatidic acid. This pathway involves the cleavage of the acyl chain by phospholipases. Our preliminary study has shown the presence of phospholipase A_2 in *P. marinus* meront. The parasite contained higher levels of this enzyme than its host hemocytes and plasma. Similarly, FL TAG was probably produced by using either FL DAG released from FL PC through the glycerol phosphate pathway, *via* reacylation of the fluorescent acyl chain, or both.

The finding of CL as one of the metabolic byproducts of FL PC implies the presence of the polyglycerophospholipid pathway in *P. marinus* mitochondria (53). The removal of the FL acyl chain from FL PC and recycling of the acyl radical for CDP-DAG synthesis is a prerequisite for this pathway. As mentioned earlier, cleavage of acyl radicals by phospholipase A_2 present in the parasite probably occurred. The intestinal protozoan parasite, *G. lamblia*, was reported to be capable of incorporating exogenous fatty acids into PG, probably *via* the CDP-DAG pathway (55). Unlike *P. marinus*, the polyglycerophospholipid pathway in *G. lamblia* appeared to end after PG synthesis.

The incorporation and interconversion of FL PC in *P. marinus* increased with time and, up to 8.5 nmol mg^{-1} FA at 48 h (Table 2). The highest uptake of FL PC from the medium was 28.9% at 48 h of postincubation. Initially (3–6 h), most of the incorporated FL PC remained as FL PC. Significant amounts of FL PE (12%), FL CL (8%), and FL TAG (18.4%) appeared after 12 h. After 48 h of incubation, a high proportion (43%) of the incorporated FL PC resided in FL TAG. These results suggest that *P. marinus* actively acquires FL PC from the nutrient-limited incubation medium (YRW) not only for membrane synthesis but also for energy reserve. Similarly, in a separate study we found that, in incubating meronts with FL palmitic acid (16:0), most of the incorporated FL 16:0 (86.9%) deposited in TAG (43).

In summary, the HPLC system employed in the present study adequately separated most polar and neutral lipid classes. An exception was that PS coeluted with PI (Fig. 1A) or SM (Fig. 2A). The oyster protozoan parasite, *P. marinus*, contains five polar lipids (PC, PE, CL, SM, and PS), with PC and PE as the two dominant lipid classes. SM and PS were characterized by the presence of two isomers. Four neutral lipids (TAG, SE, CHO, and FH) were found, with TAG as the predominant neutral lipid class. *Perkinsus marinus* metabolized FL PC to six components (i.e., FFA, MAG, DAG, PE, TAG, and CL). Incorporation and interconversion of FL PC increased with time. After 48 h of incubation, almost half

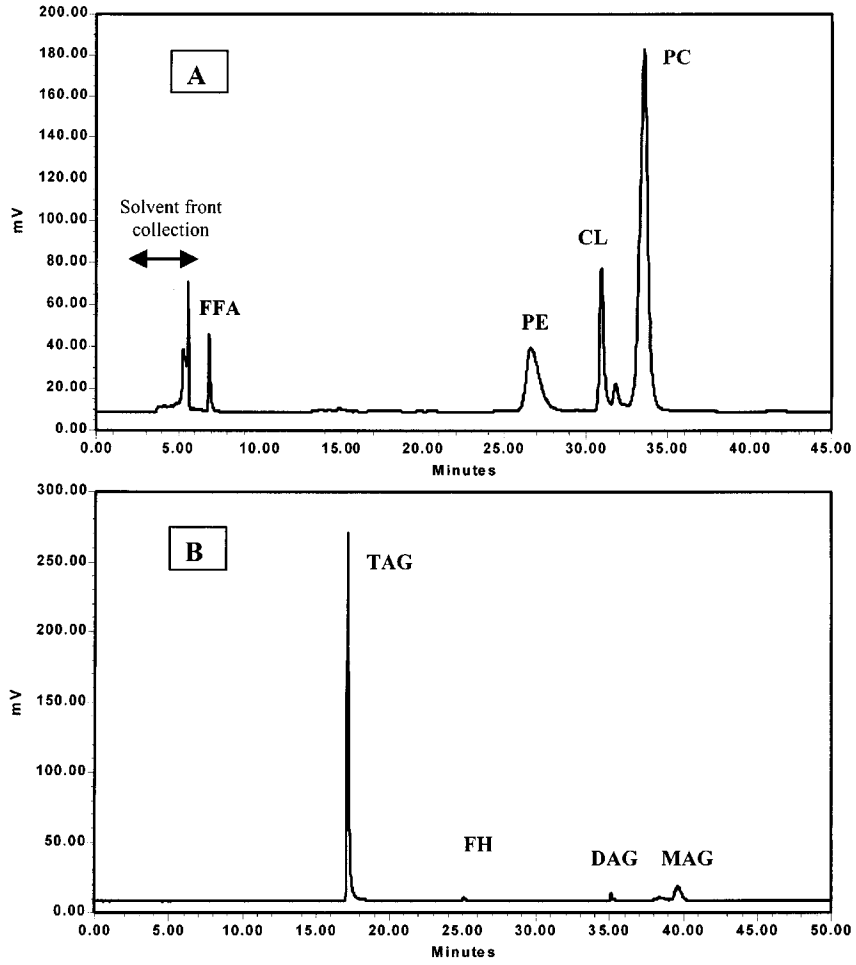

FIG. 3. HPLC separation of polar lipids + FFA and (B) neutral lipids, from *in vitro* cultures of *P. marinus* cells (meronts/merozoites) incubated 48 h with fluorescent-labeled PC and detected by a fluorescence detector. For abbreviations see Figure 1.

TABLE 2
Incorporation and Conversion of Fluorescent-Labeled PC in *in vitro* Cultured *P. marinus* Cells (meronts/merozoites) After 3, 6, 12, 24, and 48 h of Incubation[a]

	Duration of the incubation (h)									
	3		6		12		24		48	
Percentage of total incorporated fluorescent lipids	Mean	SD	Mean	SD	Mean	SD	Mean	SD	Mean	SD
SE	ND	ND	ND	ND	ND	ND	ND	ND	ND	ND
TAG	10.6	1.1	12.7	0.1	18.4	1.2	26.5	3.1	43.0	0.0
FH	0.1	0.0	0.2	0.0	0.3	0.0	0.3	0.0	0.4	0.1
DAG	1.2	0.5	0.4	0.1	0.4	0.0	0.4	0.1	0.7	0.0
MAG	2.9	1.2	2.8	0.1	4.4	0.4	4.6	0.9	3.7	0.6
FFA	2.8	0.4	3.1	0.1	3.0	0.3	3.0	0.5	3.2	0.3
PE	6.1	0.3	8.6	0.4	12.0	1.0	13.5	1.3	15.1	0.4
CL	5.4	1.7	5.8	0.0	8.2	0.4	8.9	0.8	9.6	0.2
PC	70.8	0.3	66.4	0.6	53.4	2.7	42.7	0.6	24.3	0.7
PI and PS	ND	ND	ND	ND	ND	ND	ND	ND	ND	ND
SM	ND	ND	ND	ND	ND	ND	ND	ND	ND	ND
Total of FA (mg/10 mL of culture)	0.32	0.6	0.37	0.3	0.28	0.4	0.25	0.4	0.35	0.5
Total incorporated fluorescent lipids in nmol/mg FA	0.9	0.1	1.0	0.2	1.7	0.1	3.1	0.3	8.5	1.1
Total uptake percentage of applied fluorescence (%)	2.9	0.5	3.6	0.7	4.8	0.8	7.8	2.0	28.9	1.3

[a]Abbreviations: FH, fatty alcohol; DAG, diacylglycerol; MAG, monoacylglycerol. FA, fatty acids; ND, not detected; for other abbreviations see Table 1.

(43%) of the incorporated FL PC resided in TAG.

ACKNOWLEDGMENTS

This study was supported by a grant from the Metabolic Biochemistry Program, Molecular and Cellular Bioscience Division, National Science Foundation (Grant #: MCB9728284). The authors would like to thank Georgeta Constantin, Lee Steider, and Scott M. Polk for technical assistance, and Dr. Robert C. Hale and two anonymous reviewers for the constructive review of the manuscript. Contribution number 2346 from the Virginia Institute of Marine Science, College of William and Mary.

REFERENCES

1. Levine, N.D. (1978) *Perkinsus* gen. n. and Other New Taxa in the Protozoan Phylum Apicomplexa, *J. Parasitol. 64*, 549.
2. Mackin, J.G., Owen, H.M., and Collier, A. (1950) Preliminary Note on the Occurrence of a New Protistan Parasite, *Dermocystidium marinum* n. sp., in *Crassostrea virginica* (Gmelin), *Science 111*, 328–329.
3. Chu, F.-L.E. (1996) Laboratory Investigations of Susceptibility, Infectivity and Transmission of *Perkinsus marinus* in Oysters, *J. Shellfish. Res. 15*, 57–66.
4. Perkins, F.O. (1966) Life History Studies of *Dermocystidium marinum*, an Oyster Pathogen, Ph.D. Thesis, Florida State University, Tallahassee, 273 pp.
5. Perkins, F.O. (1988) Structure of Protistan Parasites Found in Bivalve Molluscs, *Am. Fish. Soc. Spec. Publ. 18*, 93–111.
6. La Peyre, J.F., Faisal, M., and Burreson, E.M. (1993) *In vitro* Propagation of the Protozoan *Perkinsus marinu*s, a Pathogen of the Eastern Oyster, *Crassostrea virginica*, *J. Euk. Microbiol. 40*, 304–310.
7. Gauthier, J.D., and Vasta, G.R. (1993) Continuous *in vitro* Culture of the Eastern Oyster Parasite *Perkinsus marinus, J. Invert. Pathol. 62*, 321–323
8. Kleinschuster, S.J., and Swink, S.L. (1993) A Simple Method for the *in vitro* Culture of *Perkinsus marinus, Nautilus 107*, 76–78
9. Vial, H.J., and Ancelin, M.-L. (1992) Malaria Lipids, an Overview, in *Subcellular Biochemistry, Intracellular Parasites* (Avila, J.L., and Harris, J.R., eds.), Vol. 18, pp. 259–306, Plenum Press, New York.
10. Vial, H.J., and Ancelin, M.-L. (1998) Malaria Lipids, in *Malaria: Parasite Biology, Pathogenesis, and Protection* (Sherman, I.W., ed.), pp. 159–175, ASM Press, Washington, DC.
11. Smith, T.N., Brooks, T.J., and Lockard, V.G. (1970) *In Vitro* Studies on Cholesterol Metabolism in the Blood Fluke *Schistosoma mansoni, Lipids 5*, 854–856.
12. Meyer, F., Meyer, H., and Bueding, E. (1970) Lipid Metabolism in the Parasitic and Free-living Flatworms. *Schistosoma mansoni and Dugesia dorotocephala, Biochim. Biophys. Acta 210*, 257–265.
13. Furlong, S.T., Thibault, K.S., Morbelli, L.M., Quinn, J.J., and Rogers, R.A. (1995) Uptake and Compartmentalization of Fluorescent Lipid Analogs in Larval *Schistosoma mansoni, J. Lipid Res. 36*, 1–12.
14. Brouwers, J.F.H.M, Smeenk, I.M.B., van Golde, L.M.G., and Tielens, A.G.M. (1997) The Incorporation, Modification and Turnover of Fatty Acids in Adult *Schistosoma mansoni, Mol. Biochem. Parasitol. 88*, 175–185.
15. Brouwers, J.F.H.M., Van Hellemod, J.J., Van Golde, L.M.G., and Tielens, A.G.M. (1998) Ether Lipids and Their Possible Physiological Function in Adult *Schistosoma mansoni, Mol. Biochem. Parasitol. 96*, 49–58.
16. Redman, C.A., Kennington, S., Spathopoulou, T., and Kusel, J.R. (1997) Interconversion of Sphingomyelin and Ceramide in Adult *Schistosoma mansoni, Mol. Biochem. Parasitol. 90*, 145– 153.
17. Coppens, I., Levade, T., and Courtoy, P.J. (1995) Host Plasma Low Density Lipoproteins Particles as a Essential Source of Lipids for the Bloodstream Forms of *Trypanosoma brucei, J. Biol. Chem. 270*, 5736–5741.
18. Lujan, H.D., Mowatt, M.R., and Nash, T.E. (1996) Lipid Requirements and Lipid Uptake by *Giardia lamblia* Trophozoites in Culture, *J. Euk. Microbiol. 43*, 237–242.
19. Ellis, J.E., Wyder, M.A., Jarroll, E.L., and Kaneshiro, E.S. (1996) Changes in Lipid Composition During *in vitro* Encystation and Fatty Acid Desaturase Activity of *Giardia lamblia, Mol. Biochem. Parasitol. 81*, 13–25.
20. Christie, W.W. (1987) *High-Performance Liquid Chromatography and Lipids*, pp. 87–132, Pergamon Press, Oxford.
21. Christie, W.W. (1986) Separation of Lipid Classes by High-Performance Liquid Chromatography with "Mass Detector," *J. Chromatog. 361*, 396–399.
22. Breton, L., Serkiz, B., Volland, J.-P., and Lepagnol, J. (1989) A New Rapid Method for Phospholipid Separation by High-Performance Liquid Chromatography with Light-scattering Detection, *J. Chromatog. B 497*, 243–249.
23. Lutzke, B.S., and Braughler, J.M. (1990) An Improved Method for the Identification and Quantification of Biological Lipids by HPLC Using Laser Light-Scattering Detection, *J. Lipid Res. 31*, 2127–2130.
24. Juaneda, P., Rocquelin, G., and Astorg, P.O. (1990) Separation and Quantification of Heart and Liver Phospholipid Classes by High-Performance Liquid Chromatography Using a New Light-Scattering Detector, *Lipids 25*, 756–759.
25. Letter, W.S. (1992) A Rapid Method for Phospholipid Class Separation by HPLC Using an Evaporative Light-Scattering Detector, *J. Liq. Chromatogr. 15*, 253–266.
26. Bunger, H., and Pison, U. (1995) Quantitative Analysis of Pulmonary Surfactant Phospholipids by High-Performance Liquid Chromatography and Light-Scattering Detection, *J. Chromatogr. B 672*, 25–31.
27. Kiuchi, K., Ohta, T., and Ebine, H. (1975) High-Speed Liquid Chromatography Separation of Glycerides, Fatty Acids and Sterols, *J. Chromatogr. Sci. 13*, 461–466.
28. Aitzetmüller, K., and Koch, J. (1978) Liquid Chromatography Analysis of Serum Lipids and Other Lipids of Medical Interest, *J. Chromatogr. B 145*, 195–202.
29. Gillan, F.T., and Johns, R.B. (1983) Normal-Phase HPLC Analysis of Microbial Carotenoids and Neutral Lipids, *J. Chromatogr. Sci. 21*, 34–39.
30. Palmer, D.N., Anderson, M.A., and Jolly, R.D. (1984) Separation of Some Neutral Lipids by Normal-Phase High-Performance Liquid Chromatography on a Cyanopropyl Column: Ubiquinone, Dolichol, and Cholesterol Levels in Sheep Liver, *Anal. Biochem. 140*, 315–319.
31. Lapin, B.P., Pisareva, N.A., Rubtsova, T.E., and Jakevich, M.L. (1986) Separation of Lipophilic Fractions by High-Performance Liquid Chromatography, *J. Chromatogr. 365*, 229–235.
32. Carunchio, V., Nicoletti, I., Frezza, L., and Sinibaldi, M. (1984) High-Performance Liquid Chromatography Separation of Phospholipids on Chemically Bonded Silica Gel Part 1, *Ann. Chim. (Rome) 74*, 331–339.
33. Mallet, A.I., Cunningham, F.M., and Daniel, R. (1984) Rapid Isocratic High-Performance Liquid Chromatographic Purification of Platelet Activating Factor (PAF) and l Lyso-PAF from Human Skin, *J. Chromatogr. B 309*, 160–164.
34. Andrews, A.G. (1984) Estimation of Amniotic Fluid Phospho-

lipids by High-Performance Liquid Chromatography, *J. Chromatogr. B 336*, 139–150.
35. Kuhnz, W., Zimmermann, B., and Nau, H. (1985) Improved Separation of Phospholipids by High-Performance Liquid Chromatography, *J. Chromatogr. B 344*, 309–312.
36. Soudant, P., Marty, Y., Moal, J., and Samain, J.-F. (1995) Separation of Major Polar Lipids in *Pecten maximus* by High-Performance Liquid Chromatography and Subsequent Determination of Their Fatty Acids Using Gas Chromatography, *J. Chromatogr. B 673*, 15–26.
37. Silversand, C., and Haux, C. (1997) Improved High-Performance Liquid Chromatographic Method for the Separation and Quantification of Lipid Classes: Application to Fish Lipids, *J. Chromatogr. B 703*, 7–14.
38. Schlager, S.I., and Jordi, H. (1981) Separation of Cellular Phospholipid, Neutral Lipid and Cholesterol by High-Pressure Liquid Chromatography, *Biochim. Biophys. Acta 665*, 355–358.
39. Yandrasitz, J.R., Berry, G., and Segal, S. (1981) High-Performance Liquid Chromatography of Phospholipids with UV Detection: Optimization of Separations on Silica, *J. Chromatogr. B 225*, 319–328.
40. Dugan, L.L., Demediuk, L., Pendley, C.E., II, and Horrocks, L.A., (1986) Separation of Phospholipids by High-Performance Liquid Chromatography: All Major Classes, Including Ethanolamine and Choline Plasmalogens, and Most Minor Classes, Including Lysophosphatidylethanolamine. *J. Chromatogr. B 378*, 317–327.
41. Juaneda, P., and Rocquelin, G. (1986) Complete Separation of Phospholipids from Human Heart Combining two HPLC Methods, *Lipids 21*, 239–240.
42. Wiley, M.G., Pretakiewicz, M., Takahashi, M., and Lowenstein, J.M. (1992) An Extended Method for Separating and Quantitating Molecular Species of Phospholipids, *Lipids 27*, 295–301.
43. Chu, F.-L.E., Soudant, P., Volety, A.K., and Huang, Y. (2000) *Perkinsus marinus*: Uptake and Interconversion of Fluorescent Lipid Analogs in the Parasite of the Oyster, *Crassostrea virginica*, *Exp. Parasitol. 95*, 240–251.
44. Bligh, E.G., and Dyer, W.J. (1959) A Rapid Method of Total Lipid Extraction and Purification, *Can. J. Biochem. Physiol. 37*, 911–917.
45. Metcalfe, L.D., and Schmitz, A.A. (1961) The Rapid Preparation of Fatty Acid Esters for Gas Chromatography Analysis, *Anal. Chem. 33*, 363–364.
46. Marty, Y., Delaunay, F., Moal, J., and Samain, J.F. (1992) Change in the Fatty Acid Composition of *Pecten maximus* (L.), *J. Exp. Mar. Biol. Ecol. 163*, 221–234.
47. Chu, F.-L.E., and Ozkizilcik, S. (1995) Lipid and Fatty Acid Composition of Striped Bass (*Morone saxatilis*) Larvae During Development, *Comp. Biochem. Physiol. 111B*, 665–674.
48. Olsen, R.E., and Henderson, R.J. (1989) The Rapid Analysis of Neutral and Polar Marine Lipids using Double Development HPTLC and Scanning Densitometry, *J. Exp. Mar. Biol. Ecol. 129*, 189–197.
49. Christie, W.W. (1982) *Lipid Analysis*, 2nd edn., pp. 107–134, Pergamon Press, Oxford.
50. Sherman, I.W. (1979) Biochemistry of *Plasmodium* (malaria parasites), *Microbiol. Rev. 43*, 453–495.
51. Beach, D.H., Holz, G.G., Jr., and Anekwe, G.E. (1979) Lipid of *Leishmania* Promastigotes, *J. Parasitol. 65*, 203–216.
52. Smith, J.D. (1993) Phospholipid Biosynthesis in Protozoa, *Prog. Lipid Res. 32*, 47–60.
53. Gurr, M.T., and Harwood, J.L. (1991) *Lipid Biochemistry, An Introduction*, 4th edn., pp. 295–337, Chapman and Hall, New York.
54. Mitschler, R.R., Welti, R., and Upton, S.J. (1994) A Comparative Study of Lipid Composition of *Cryptosporidium parvum* (Apicomplexan) and Madin-Darby Bovine Kidneys Cells, *J. Euk. Microbiol. 41*, 8–12.
55. Stevens, T.L., Gibson, G.R., Adam, R., Maier, J., Allison-Ennis, M., and Das, S. (1997) Uptake and Cellular Localization of Exogenous Lipids by *Giardia lamblia*, a Primitive Eukaryote, *Exp. Parasitol. 86*, 133–143
56. Dixon, H., and Williamson, J. (1970) The Lipid Composition of Blood and Culture Forms of *Trypanosoma lewisi* and *Trypanosoma rhodesiense* Compared with That of Their Environment, *Comp. Biochem. Physiol. 33*, 111–128.
57. Vial, H.J., Thuet, M.J., and Philippot, J.R. (1982) Phospholipid Biosynthesis in Synchronous *Plasmodium falciparum* Cultures, *J. Protozool. 29*, 258–263.
58. Vial, H.J., Ancelin, M.-L., Thuet, M.J., and Philippot, J.R. (1989) Phospholipid Metabolism in *Plasmodium*-Infected Erythrocytes: Guidelines for Further Studies Using Radioactive Precursor Incorporations, *Parasitology 98*, 351–357.
59. Kasurinen, J. (1992) A Novel Fluorescent Fatty Acid, 5-Methyl-BDY-dodecanoic Acid, Is a Potential Probe in Lipid Transport Studies by Incorporating Selectively to Lipids of BHK cells, *Biochem. Biophys. Res. Comm. 187*, 1594–1601.

[Received November 22, 1999, and in final revised form September 25, 2000; revision accepted October 4, 2000]

Properties of a Fluorescent Bezafibrate Derivative (DNS-X). A New Tool to Study Peroxisome Proliferation and Fatty Acid β-Oxidation

Jean-Pierre Berlot, Thomas Lutz, Mustapha Cherkaoui Malki, Val rie Nicolas-Frances, Brigitte Jannin, and Norbert Latruffe*

Université de Bourgogne, Laboratorie de Biologie Moléculaire et Cellulaire, Faculté des Sciences Gabriel, 21000 Dijon, France

ABSTRACT: The first peroxisome proliferator-activated receptor (PPAR) was cloned in 1990 by Issemann and Green. Many studies have reported the importance of this receptor in the control of gene expression of enzymes involved in lipid metabolic pathways including mitochondrial and peroxisomal fatty acid β-oxidation, lipoprotein structure [apolipoprotein (apo) A2, apo CIII], and fatty acid synthase. By using radiolabeled molecules, it was shown that peroxisome proliferators bind and activate PPAR. As an alternative method, we developed a fluorescent dansyl (1-dimethylaminonaphthalene-5-sulfonyl) derivative peroxisome proliferator from bezafibrate (DNS-X), a hypolipidemic agent that exhibits an *in vitro* peroxisome proliferative activity on rat Fao-hepatic derived cultured cells. However, until now, the effect of this new compound on the liver of animals and subcellular localization was unknown. In addition to *in vivo* rat studies, we present a more efficient large-scale technique of DNS-X purification. Treating rats (DNS-X in the diet at 0.3% w/w) for 6 d leads to a hepatomegaly and a marked increase in liver peroxisomal palmitoyl-CoA oxidase activity. We also developed a method to localize and quantify DNS-X in tissues or cell compartment organelles. The primarily cytosolic distribution of DNS-X was confirmed by direct visualization using fluorescence microscopy of cultured Fao cells. Finally, transfection assay demonstrated that DNS-X enhanced the PPARα activity as well as other peroxisome proliferators do.

Paper no. L8377 in *Lipids 35*, 1397–1404 (December 2000).

Despite numerous works on the process of peroxisome proliferation as triggered by hypolipidemic agents of the fibrate family, the mechanism is not fully understood. It is now considered that induction of peroxisomal fatty acid β-oxidation enzymes by these agents involves the peroxisome proliferator-activated receptor alpha (PPARα), a member of the nuclear hormone receptor superfamily (1). Recently, the evidence of the direct binding of peroxisome proliferators (PP) to PPARα was demonstrated (2). Another possibility of the gene transcription mechanism should be the signal transduction pathway as suggested by overphosphorylation of several cellular proteins in the presence of PP (3,4). The identification of molecular complexes with an affinity for PP and of their subcellular localization will help to clarify the peroxisome proliferative process.

To elucidate these questions, we synthesized a dansylated fibrate (DNS-X: 2-[4-(*N*-dansyl-2-aminoethyl) phenoxy]-2-methylpropanoic acid) derived from bezafibrate (2-{4-[2-(4-chlorobenzamido)ethyl]phenoxy}-2-methylpropanoic acid), a hypolipidemic agent. Such fluorescent probes offer a sensitivity threshold as good as radioactively labeled compounds (5). Moreover, DNS-X was shown to be an *in vitro* PP in rat hepatic-derived Fao cells (5). This fluorescent fibrate has properties similar to those of other fibrates and is able to induce palmitoyl-CoA oxidase activity, a peroxisome proliferation marker (6). However, the effect of *in vivo* treatment of animals and the subcellular localization of this compound needs to be established.

To obtain a more efficient procedure and a better-characterized final product, in the present work we improved the DNS-X synthesis method. We also developed a high-performance liquid chromatography (HPLC) method to estimate the DNS-X purity that could be used for analytical studies as well.

To study the ability of DNS-X to be an *in vivo* PP, we treated rats with different amounts of dietary DNS-X (see the Material and Methods section). After the treatment, the peroxisomal fractions of the rat livers were isolated, the palmitoyl-CoA oxidase activity was determined in these fractions, and the *in vivo* peroxisome proliferative effect of DNS-X was observed.

Our goal was to identify the subcellular distribution of DNS-X and its concentration in blood serum and coagulate. To this end, we developed a quick and simple method to estimate the DNS-X content in biological samples. This method takes advantage of the strong fluorescence of this compound. Moreover, direct visualization of the DNS-X subcellular distribution was accomplished using fluorescence microscopy of cultured Fao cells.

Finally we tested the properties of DNS-X as a PPAR-activating molecule in transfection assays using a peroxisome pro-

*To whom correspondence should be addressed at Université de Bourgogne, LBMC, Faculté des Sciences Gabriel, 6, Bd Gabriel, 21000 Dijon, France. E-mail: latruffe@u-bourgogne.fr

Abbreviations: Bezafibrate, 2-{4-[2-(4-chlorobenzamido)ethyl]phenoxy}-2-methylpropanoic acid; DNS-Cl, 5-(dimethylamino)naphthalene-1-sulfonylchloride, or dansyl chloride; DNS-OH, 5-(dimethylamino)naphthalene-1-sulfonic acid; DNS-Phe, Dansyl phenylalanine; DNS-X, 2-[4-(*N*-dansyl-2-aminoethyl)phenoxy]-2-methylpropanoic acid; Fao cells, a rat hepatoma-derived cell line; HPLC, High-performance liquid chromatography; PBS, phosphate-buffered saline; PP, peroxisome proliferator; PPARα, peroxisome proliferator-activated receptor α; PPRE, peroxisome proliferator response element; RP-HPLC, reversed-phase HPLC; TLC, thin-layer chromatography.

liferator response element (PPRE)-driven luciferase reporter gene and a plasmid coding for PPARα.

MATERIALS AND METHODS

Chemicals. Bezafibrate was obtained from Boehringer (Ingelheim, Germany). Dansyl chloride and Nycodenz are products of Sigma (St. Louis, MO).

DNS-X chemical synthesis; new purification step. The DNS-X synthesis was carried out according to the method previously reported (5). That is, the amide group of bezafibrate was hydrolyzed in a mixture of ethanolic/aqueous 10 M KOH solution (70:30) for 5 h at 100°C. The mixture was then neutralized with 12.5 M HCl and precipitates were separated by filtration. To obtain the resulting amine in a high purity, cation exchange chromatography of the filtrate on Dowex 50 W-XS (Sigma) was used to separate it from other residues.

Then, the amine was conjugated with 5-(dimethylamino)-naphthalene-1-sulfonyl chloride (dansyl chloride, or DNS-Cl), in a solution of water/acetone (1:1) (7). In contrast to the published method (5) (in which the instructions were to dry this solution completely after the reaction), only acetone was evaporated. DNS-X was extracted three times from the remaining aqueous phase (adjusted to pH 4) with chloroform; the combined organic phases were dried over Na_2SO_4 and evaporated. The resulting product was stored at −20°C.

The amine was obtained after cationic exchange chromatography with a yield of about 40%. DNS-X was recovered after chloroform extraction with a yield of about 70%. In its high-purity form it has a translucent luminous appearance and a yellow-greenish color.

Purity analysis of the final product. The amine, DNS-X, and the residues were analyzed by thin-layer chromatography (TLC) as previously described (1) using Merck 60F-254 (20 × 20 cm; Darmstadt, Germany) plates. The developing solvents used were butanol/acetic acid/water (80:20:20), to separate compounds after cation exchange chromatography, and chloroform/ethanol/acetic acid (84:9:7), to analyze the final product.

To estimate the DNS-X purity by reversed-phase (RP)-HPLC we used the following materials and conditions: IsoChrom LC pump, Spectra-Physics (St. Albans, United Kingdom); Spectra 100 detector, Spectra-Physics; Shimadzu C-R5A Chromatopac integrator (Kyoto, Japan); Waters μBondapak C_{18} 125 Å 10 μm Guard-Pak Insert (Milford, MA); Waters μBondapak C_{18} 125 Å 10 mm, 3.9 × 300 mm column; acetonitrile/0.01 M acetate buffer, pH 4 (60:40) as mobile phase, flow rate of 1.2 mL/min. Detection was monitored at a 219 nm wavelength. Chromatography was carried out at room temperature.

Extraction of DNS-X with chloroform from the synthesis medium led to a pure final product as shown by TLC and HPLC analysis (Figs. 1 and 2). The spots of 5-(dimethylamino)naphthalene-1-sulfonic acid (DNS-OH) appeared on the TLC plate at the lowest R_f (about 0.09) with a blue fluorescence. This compound is formed by DNS-X hydrolysis and is also seen as an impurity in the DNS-Cl standard.

DNS-Cl appeared at highest R_f (about 0.97) with a yellow fluorescence, whereas DNS-X appeared at about 0.86. DNS-X showed the strongest fluorescence and was also yellow. TLC showed that the newly introduced purification step separated DNS-OH as well as DNS-Cl residues from DNS-X, since their corresponding spots on TLC disappeared after this procedure. Therefore, DNS-Cl and DNS-OH remain in the polar aqueous phase during the purification whereas DNS-X is found in the organic fraction (chloroform).

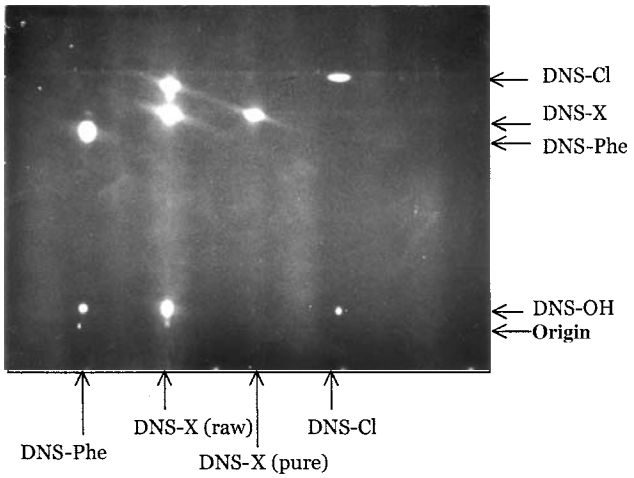

FIG. 1. Thin-layer chromatography of purifed (pure) and nonpurified (raw) DNS-X. The spots were detected under ultraviolet light at 365 nm. About 30 μg DNS-X was applied; Phe-DNS (dansyl phenylalanine) and DNS-Cl (dansyl chloride) were used as references. For further experimental conditions, see the Materials and Methods section. One can see that, after the purification, the spots of DNS-OH (dansyl hydroxyl) and DNS-Cl residues disappeared. DNS-Cl, 5-(dimethylamino)naphthalene-1-sulfonyl chloride [= dansyl chloride]; DNS-X, 2-[4-(*N*-dansyl-2-aminoethyl)phenoxy]-2-methylpropanoic acid.

The longer retention time of the ethyl ester DNS-X derivative during RP-HPLC analysis is in agreement with its higher lipophilic properties as compared to the DNS-X. The ethyl ester DNS-X derivative was probably formed during the neutralization of the ethanolic solution following hydrolysis of bezafibrate by using concentrated HCl. Indeed, this was the only step during synthesis in which ethanol was used.

The chromatogram also shows a small DNS-OH peak at 9.67 min, but it does not show either amine (no retention time) or DNS-Cl residues (generally at about 13 min). DNS-X was obtained with a purity greater than 95%. Of that 95%, 15% was present as DNS-X ethyl ester; that is, DNS-X was actually present in two forms, unesterified and esterified. This latter compound cannot be considered as contaminant since cellular esterases are known to convert the ester form into the acid form, as happens with clofibrate and fenofibrate, which are commercially available only in their ethylester forms (8).

Identification of the compounds. To assign HPLC signals to the corresponding compounds, preparative RP-HPLC and ^1H nuclear magnetic resonance (NMR) spectroscopy were used. The preparative RP-HPLC was carried out with a Waters μBondapak C_{18} 125 Å 10 μm, on a 7.8 × 300 mm column, by using acetonitrile/0.01 M acetate buffer at pH 4 (60:40) as the

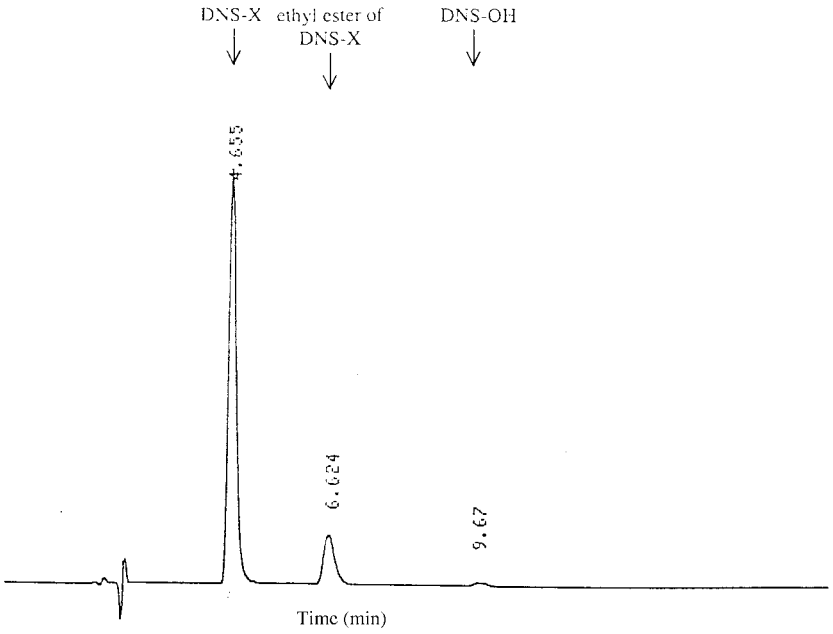

FIG. 2. Reversed-phase high-performance liquid chromatography (HPLC) of purified DNS-X. The injected quantity was about 10 nmol DNS-X per run; the compounds were detected at an absorbance wavelength of 219 nm. The main peak at 4.66 min corresponds to DNS-X, whereas the peak at 6.62 min represents the ethyl ester of DNS-X (see text and Scheme 1). The ethyl ester form of DNS-X is obtained as a by-product during synthesis. The chromatogram also shows a small peak of DNS-OH (dansyl hydroxyl) at 9.67 min, but none for either amine (which generally would elute, without retention, at about 2.5 min) or DNS-Cl residues (generally would elute at about 13 min). Thus, DNS-X was obtained with a purity of >95%; of that 95%, 15% was present as DNS-X ethyl ester. For further experimental conditions, see the Materials and Methods section. For abbreviations see Figure 1.

mobile phase at a flow rate of 3.8 mL/min. The other materials and conditions were similar to the previous analytical method (5). The RP-HPLC fractions were collected and evaporated. RP-HPLC runs were repeated in the same way to obtain at least 3 mg of each compound. ^{1}H NMR spectroscopy of the compounds was performed in $CDCl_3$ using a Bruker AC 200 machine (Karlsruhe, Germany).

Analysis of the final product by RP-HPLC (using a 3.9 × 300 mm column and a flow rate of 1.2 mL/min) showed that it yielded a main peak at 4.66 min and a small one at 6.62 min (Fig. 2). Such a resolution was not obtained by TLC analysis. By using preparative HPLC, followed by 200 MHz ^{1}H NMR analysis, the two compounds belonging to the corresponding HPLC fractions were identified, respectively, as DNS-X and its ethyl ester form (Scheme 1). In the ethyl ester fraction a triplet at $\delta = 1.19$ (t, $^3J_{HH} = 6.9$ Hz, 3 H, -CH_3) and a quadruplet at $\delta = 3.47$ (q, $^3J_{HH} = 6.9$ Hz, 2 H, -CH_2-) were seen during NMR analysis. These signals correspond to the ethyl group of the ester, and they were not present in the fraction of DNS-X. Other signals were similar to those reported before (5).

Treatment of rats. Experiments carried out with animals were in conformity with French bioethics law; our animal care facilities are approved by the Veterinary Service. Two experiments were carried out with rats (5 wk old, male Wistar rats, 120–160 g from IFFA Credo, L'Arbresle, France) having different DNS-X amounts in their diet. They were housed, three or four per cage, under conditions of controlled temperature (20 ± 2°C), humidity (30–40%), and 12 h light/12 h dark cycle. The diet was prepared by soaking the chow (standard laboratory rodent chow; UAR, Villemoisson/Orge, France) in an acetone solution of the relevant compounds (DNS-X or bezafibrate). The chow was dried at room temperature. During the treatment rats were fed exclusively with the prepared diet; drinking water was provided *ad libitum*.

In the first assay (assay 1) four rats were treated with 0.04% DNS-X (w/w) and three rats with 0.04% bezafibrate (w/w) over a 10-d period. Three nontreated rats served as controls. In the second experiment (assay 2) three rats were treated with 0.1

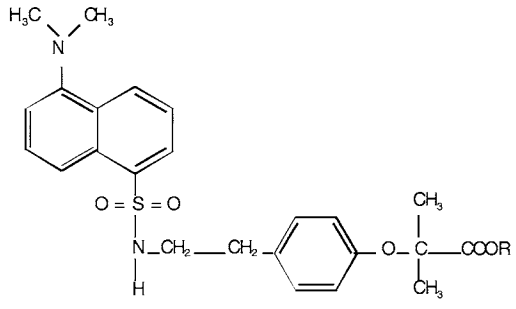

R = -H DNS-X
R = -CH_2CH_3 ethyl ester of DNS-X

SCHEME 1

and 0.3% DNS-X (w/w) for 6 d. As previously, three control rats were used. Before being sacrificed, the rats were starved overnight.

Subcellular fractionation. Rats were decapitated under ether anesthesia, and blood was collected and stored at +4°C. Then the livers were taken out, sliced, and cleaned in ice-cold isolation buffer [250 mM sucrose, 5 mM 3-(*N*-morpholino) propane sulfonic acid, 1 mM EDTA, 0.1% ethanol]. The livers were homogenized once in isolation buffer using a Potter-Elvejhem at 1,500 rpm. The homogenate was filtered through four layers of cheesecloth.

Fractionation of the liver tissue by differential centrifugation in isolation buffer was performed as described by de Duve *et al.* (9). Five fractions were isolated: nuclear fraction (N), mitochondrial fraction (M), light mitochondrial fraction (L), microsomal fraction (P), and soluble cytosolic fraction (S). Peroxisome fraction was isolated from the L fraction using 30% Nycodenz step gradient centrifugation as described by Ghosh and Hajra (10). The purity of each subcellular organelle fraction was checked as previously reported (11,12) using the following marker enzymes: cytochrome c oxidase, succinate dehydrogenase for mitochondria, catalase, α-hydroxy acid oxidase and D-amino acid oxidase for peroxisomes, lactate dehydrogenase for cytosol, cathepsin C and acid phosphatase for lysosomes, and NADPH-cytochrome c reductase for endoplasmic reticulum.

As far as possible all procedures were carried out on ice. Centrifugations were performed at 4°C. All subcellular fractions were frozen in liquid nitrogen and stored at −20°C.

Blood was separated into serum and coagulate. The coagulate was homogenized in a solution of 250 mM sucrose using an Ultra Turrax (Janke & Kunkel, Staufen, Germany) at 24,000 rpm. Both fractions were frozen and stored at −20°C.

Protein content and palmitoyl-CoA oxidase activity. Protein contents of the subcellular fractions, the serum, and the blood coagulate homogenates were determined using the method of Bradford (13).

The activities of the peroxisomal palmitoyl-CoA oxidase in the different subcellular fractions were measured by a fluorometric assay. This assay depends on H_2O_2 produced by the peroxisomal acyl-CoA oxidase, leading to a fluorescent dimer of homovanillic acid in the presence of peroxidase (6,14).

DNS-X analysis in biological samples. To show the DNS-X stability, TLC as well as spectrofluorometric assays was performed on extracts of cell liver homogenates. To estimate the DNS-X concentration in the samples the following procedure was applied for subcellular fractions, serum, or blood coagulate homogenate. To 100 µL of each sample, 900 µL acetone was added. This solution was shaken for about 5 s with a vortex and then centrifuged for 5 min at 13,000 × *g* to separate the denaturated proteins. Then the relative fluorescence of the clear supernatant was measured at 25°C using a spectrofluorimeter (Type SFM 25; Kontron Instruments, Hemile, Switzerland) and 500 µL cuvettes. The measurements were carried out at an excitation wavelength of 350 nm and an emission wavelength of 498 nm.

A calibration curve was obtained by applying the same procedure to corresponding samples from control rats. For instance, when mitochondrial fractions of treated rats were analyzed, an equal amount of mitochondrial fractions of control rats was used to obtain the calibration curve. To get the most accurate control values, mixtures of corresponding samples belonging to the three control rats were used in the ratio of 1:1:1. Thus, different volumes of DNS-X standard solutions (1,000, 500, or 100 µM DNS-X in ethanol) were added to each 100 µL of control sample.

Fluorescence microscopy. Fao cells (a rat hepatoma-derived cell line, given by Jean Dechartrette, INSERM, Hôpital Kremlin-Bicetre, Paris, France) cultured overnight (5) were washed three times with phosphate-buffered saline (PBS), then incubated for 15 min in a 0.025% DNS-X solution in PBS containing 1% vol/vol dimethylsulfoxide. Next, the cells were washed three times with PBS and fixed for 30 min with a 4% solution of paraformaldehyde in PBS. The cells were studied under a phase contrast using a Leica LB fluorescence microscope. A DAPI filter (λ excitation 340–380 nm) was used. The observed fluorescence was based on the DNS-X emission wavelength of 498 nm.

Statistics. All samples from the treated rats as well as control and calibration samples were analyzed at least three times. The mean values were taken for further calculations using Student's *t*-test.

Plasmids and transfection assays. pG.Luc BFE (-2952/2918) contains an oligonucleotide corresponding to the PPRE sequence of the bifunctional enzyme gene (8) upstream from the β-globin promoter of the luciferase expression vector pGluc. The pSG5m PPARα plasmid, a gift from Dr. S. Green (Zeneca, Macclesfield, United Kingdom), contains the mouse PPARα cDNA downstream from the SV40 promoter of pSG5.

HepG2 cells (a human hepatoblastoma cell line) were seeded in 24-well dishes at 2×10^5 cells/well in Dulbecco's modified Eagle's medium supplemented with 2 mM glutamine, 20 mM Hepes, 10% fetal calf serum, 125 µg/mL streptomycin, and 125 U/mL penicillin. After being cultured overnight, the cells were washed in serum-free medium (optiMEM; Life Technologies, Gibco BRL, Grand Island, NY) and transfected by mixing 400 ng of plasmid DNA purified on Qiagen (Studio City, CA) column [200 ng of pG.luc (-2952/-2918) containing the PPRE with or without 200 ng of pSG5m PPARα] with 2 µg of lipofectin (Gibco) in 300 µL of optiMEM which was applied to the cells. After 5 h, the transfection media were replaced by 1 mL of complete media containing, or not, Wy 14,643 (50 µM), DNS-X (50 µM), or bezafibrate (100 µM), where Wy 14,643 is 4-chloro-6-(2,3-xylidino)-2-pyrimidinylthio)acetic acid (Wyeth Laboratories, Philadelphia, PA). The media were changed after 24 h. After 48 h, the cells were washed twice with PBS and harvested in 100 µL of Reporter Lysis Buffer (Promega, Madison, WI), then centrifuged after three freeze-thaw cycles. The cleared cytosol extract (10 µL) was added to 100 µL of luciferase assay reagent (Promega) and the light emission measured for 10 s in a TLX1 luminometer (Dynatech Laboratories, McLean, VA). The luciferase values were normalized using the protein concentration values determined by Bradford (13).

RESULTS

Rat treatment. (i) Hepatosomatic index. The hepatosomatic indexes obtained after different treatments of rats show that there is only a weak increase in liver mass in rats treated with 0.04 or 0.1% DNS-X in their diet (Table I). The hepatosomatic index increased by factors of about 1.2 and 1.3, respectively, compared to the control. In contrast to this assay, rats treated either with 0.04% bezafibrate or 0.3% DNS-X showed a higher and comparable liver mass increase. The hepatosomatic indexes increased by factors of about 1.5 and 1.7, respectively. Thus, DNS-X shows a dose-dependent effect on rat liver, leading to a liver mass increase that is more marked the higher the given dose is.

Since fibrates are known to lead to both hyperplasia and hypertrophy, these data indicate that DNS-X properties are the same as those of other fibrates, although this effect is weaker than the bezafibrate effect.

(ii) Palmitoyl-CoA oxidase activity, a peroxisome marker. A strong increase in the palmitoyl-CoA oxidase activity was observed by treatment with 0.04% bezafibrate, whereas no increase was found in peroxisomes of rats treated with the same dose of DNS-X (Fig. 3A). The same results were obtained using homogenates (data not shown). The potency of DNS-X to induce palmitoyl-CoA oxidase appears weaker than that of bezafibrate. This tendency can be correlated with the small increase in hepatosomatic of rats after the treatment with DNS-X at 0.04%, compared to the one observed after bezafibrate treatment given at the same dosage.

In contrast to the assays with 0.04% DNS-X, the treatments with 0.1 and 0.3% DNS-X reveal a dose-dependent stimulation of the palmitoyl-CoA oxidase activity in the peroxisomal fraction (Fig. 3B). One can see a slight but significant increase in enzyme activity after treatment with 0.1% DNS-X in the diet. A significant increase in oxidase activity was also found in the homogenate (data not shown). Contrary to this weak effect, en zyme activity is strongly activated in peroxisomes (Fig. 3B) as well as in homogenate (data not shown) after the treatment with 0.3% DNS-X. Indeed, enzyme activity in peroxisomes increases by about 10- and in the homogenate by 12-fold (data not shown).

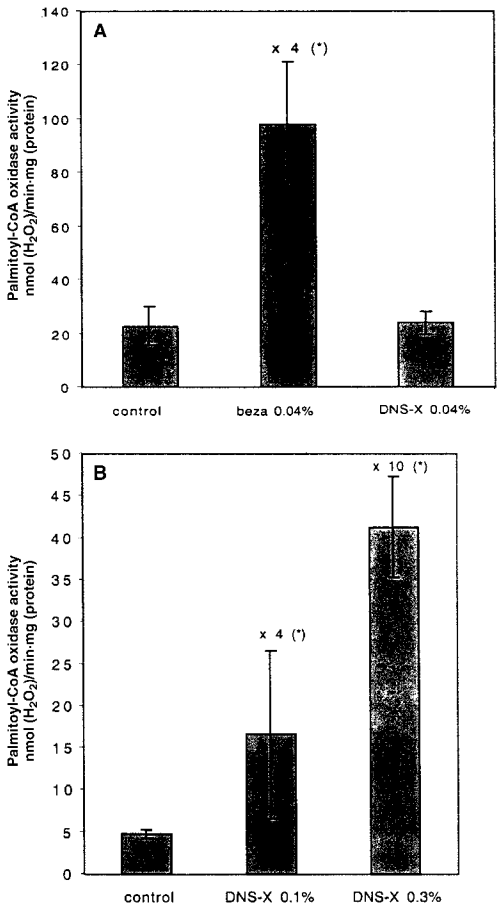

FIG. 3. Palmitoyl-CoA oxidase activity in peroxisomal fraction of rat liver. The histogram shows mean values from three or four independent treatments and error bars corresponding to the standard deviation. The factors (x ...) show an increase in enzyme activity compared to the control. (A) Over a 10-d period four rats were treated with 0.04% DNS-X (w/w) and three rats with 0.04% bezafibrate (w/w). (B) For the 6-d period there were two groups of three rats each treated with 0.1 and 0.3% DNS-X (w/w), respectively. Three nontreated control rats were used. The enzyme activity was measured by a fluorometric assay depending on oxidase-produced H_2O_2. Strong induction was obtained by bezafibrate treatment, whereas no induction was seen with DNS-X. For further experimental conditions, see the Materials and Methods section. (*) Statistically significant, $P < 0.01$. Beza, bezafibrate; for other abbreviations see Figure 1.

TABLE I
Hepatosomatic Index Obtained After Treatment of Rats with the Given Concentrations and Compounds[a]

	Hepatosomatic index (g of liver/100 g of body weight)	Factor compared to control
Control[b]	3.2 ± 0.1	—
Bezafibrate[b] 0.04%	5.0 ± 0.2 (*)	×1.5
DNS-X[b], 0.04%	3.9 ± 0.2 (*)	×1.2
DNS-X[c], 0.1%	4.4 ± 0.3 (*)	×1.3
DNS-X[a], 0.3%	5.4 ± 0.5 (*)	×1.7

[a]*Note*: Each mean value with corresponding standard deviation (±) was obtained from at least three independent assays. For further experimental conditions, see the Materials and Methods section.
[b]Indicates 10 d of treatment.
[c]Indicates 6 d of treatment. The data show only a weak liver hyperplasia in rats treated with 0.04% DNS X (40 mg of compound per 100 g of diet) and a strong and comparable liver hyperplasia in rats treated with 0.3 % DNS-X or 0.04% bezafibrate. Abbreviations: (*) Statistically significant $P < 0.01$; bezafibrate, 2-{4-[2-(chlorobenzamido)ethyl]phenoxy}-2-methylpropanoic acid; DNS-X, 2-[4-*N*-dansyl-2-aminoethyl)phenoxy]-2-methylpropanoic

Therefore, since palmitoyl-CoA oxidase activity is a marker of peroxisome proliferation (4), DNS-X can be considered as a new *in vivo* PP in rats, showing properties similar to other members of the fibrate family.

DNS-X subcellular distribution. TLC analysis of cell liver homogenate shows only one spot (not shown here) with the same R_f value as DNS-X (0.84). No trace of DNS-OH was found. This result is confirmed by spectrofluorimetric assays (Fig. 4A). Thus, DNS-X is not hydrolyzed, and the measured fluorescence is not due to scission products carrying the dansyl portion of the molecule.

Extracts of subcellular control samples followed by fluo-

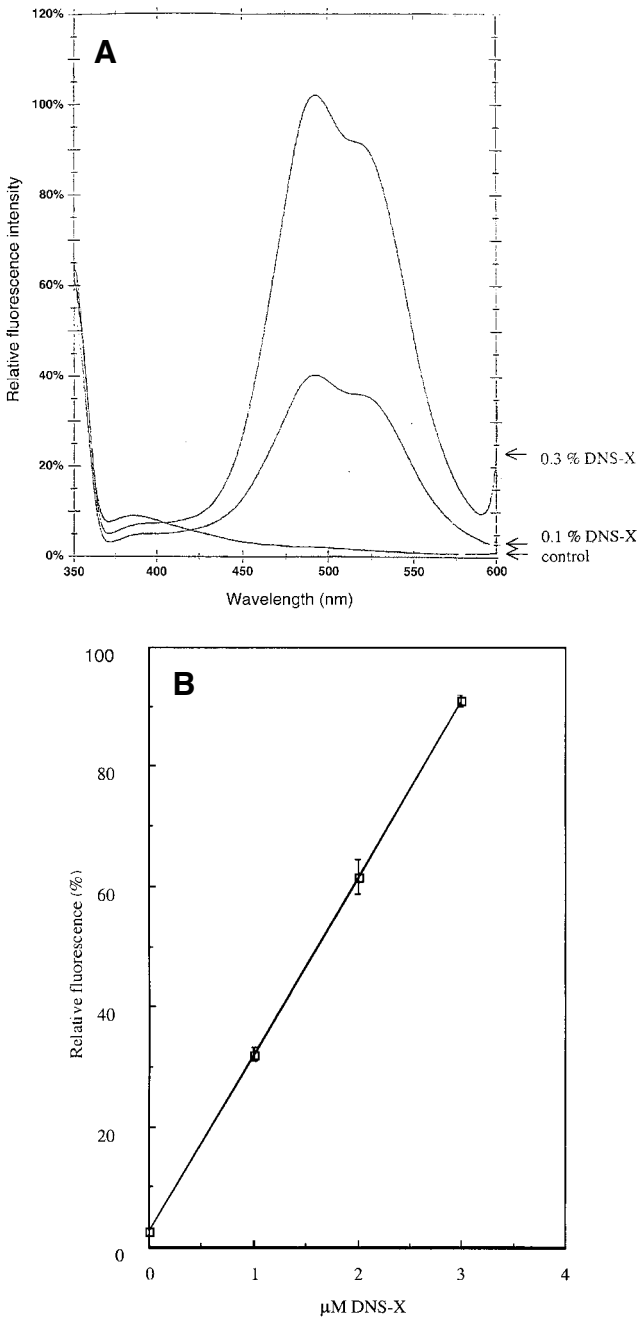

FIG. 4. Titration of DNS-X fluorescence. (A) Emission spectra of cytosolic extracts at an excitation wavelength of 350 nm are shown. The x-axis gives the emission wavelength, and the y-axis shows the relative fluorescence intensity. The extracts were obtained by taking 100 µL of a sample (in this case cytosolic fraction) and diluting to a volume of 1000 µL with acetone. After centrifugation, the spectra were measured. One can see that the fluorescence of the control is very weak. Consequently, the strong fluorescence of the other samples was dependent on the DNS-X content. Therefore, it was possible to quantify DNS-X by fluorescence measurement. (B) Calibration curve. The error bars correspond to the standard deviation of three or four independent measurements. The values were obtained by taking 100 µL of control sample (in this case cytosolic fraction), adding an appropriate volume of DNS-X standard solution, and diluting to a volume of 1000 µL with acetone. After centrifugation the relative fluorescence was measured. For experimental conditions, see the Materials and Methods section. For abbreviation see Figure 1.

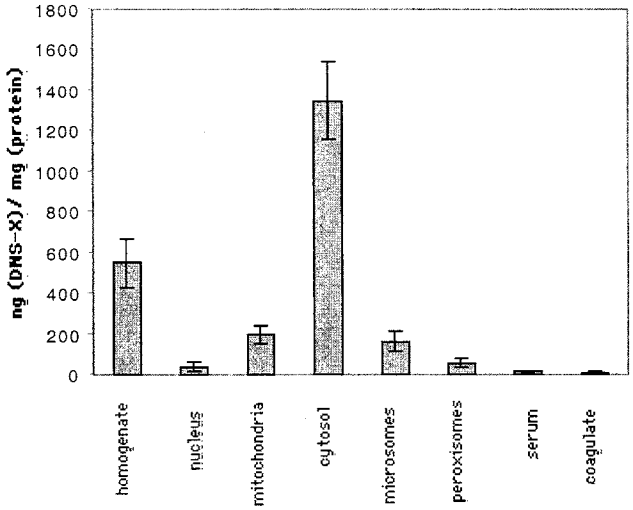

FIG. 5. Subcellular distribution of DNS-X as well as concentration in blood serum and coagulate. The histogram shows mean values from three or four independent treatments at 0.3% DNS-X. The error bars correspond to the standard deviation. The analyses were carried out as described in the text (see also Fig. 4). The results reveal a great affinity of DNS-X for cytosolic components. For further experimental conditions, see the Materials and Methods section. For abbreviation see Figure 1.

rescence measurement generally showed a weak fluorescence, compared to samples resulting from rats treated with DNS-X (Fig. 4A). Consequently, the strong fluorescence of these samples depended on the DNS-X content and therefore it was possible to develop a calibration curve by adding appropriate volumes of DNS-X standard solutions to control samples (Fig. 4B). DNS-X could be quantified for all samples obtained from 0.3%-treated rats (Fig. 5). In these samples, fluorescence was never less than the control. However, in samples obtained from rats treated with 0.1% DNS-X the fluorescence difference between sample and control was often too small to determine the DNS-X content accurately. Consequently, in these samples, DNS-X was quantified only in liver homogenate and cytosol.

For the homogenate, a content of about 210 ng of DNS-X/mg of protein was found in the samples obtained from rats treated with 0.1% DNS-X, whereas about 550 ng of DNS-X/mg of protein was found in samples from the 0.3% DNS-X assays. This represents a 2.6-fold increase in DNS-X concentration in liver homogenate for the 0.3% DNS-X assays, which is in agreement with the threefold higher concentration of this compound in the diet during treatment. The results obtained with the cytosol samples showed the same tendencies.

The DNS-X distribution in other samples obtained by the 0.3% assays showed that DNS-X was accumulated mostly in the cytosolic fraction (Fig. 5) at a concentration of about 1350 ng of DNS-X/mg of protein, much higher than in mitochondrial and microsomal fractions (~180 ng of DNS-X/mg of protein) as well as in nucleic and peroxisomal fractions (48 ng of DNS-X/mg of protein).

In serum and coagulate the concentration of DNS-X found was small (15 and 10 ng of DNS-X/mg of protein, respectively).

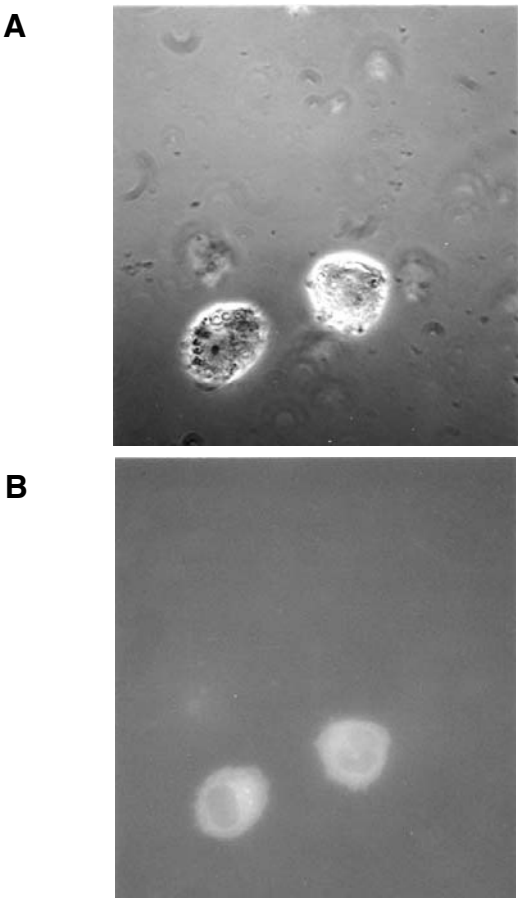

FIG. 6. Phase contrast micrograph (A) and corresponding fluorescence micrograph (B) of cultured hepatic-derived Fao cells in the presence of DNS-X (magnification × 630). Note: Although we used a 15 min incubation of DNS-X with the cells in this experiment, we also observed a rapid appearance of fluorescence for shorter time (3–5 min).

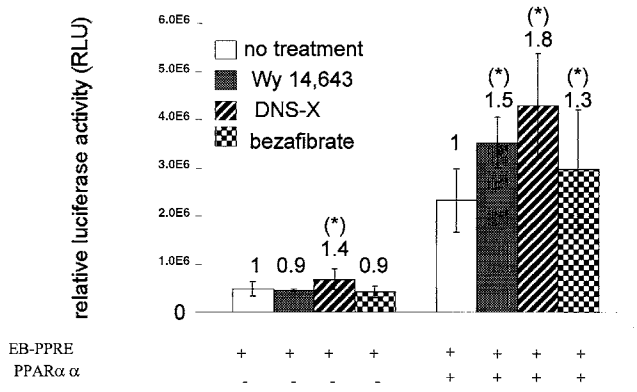

FIG. 7. Peroxisome proliferator-activated receptor α (PPARα)-activated reporter gene in transfected HepG2 cells treated with DNS-X, Wy 14,643, or bezafibrate. The histogram shows mean value of three independent transfections for each condition. The error bars correspond to the standard deviation. (*) Statistically significant, $P < 0.05$. EB:pG.luc BFE (–2952/-2918) plasmid; PPARα:pSG5m PPARα plasmid. For other abbreviations see Figure 1. The + and – signs indicate presence or absence of plasmid coding for the mouse PPARα.

This indicates a rapid plasma disappearance of DNS-X in rats, explaining the threshold concentration necessary to lead to peroxisome proliferation (see Fig. 3). Moreover, it shows that the DNS-X found in subcellular samples really belongs to intracellular components.

The estimation (data not shown) of protein content (in percentage) of each subcellular fraction compared to the total protein content (homogenate) made possible the comparison of DNS-X values obtained for the homogenate with the sum of the single values of the different subcellular fractions. For instance, if the DNS-X value per milligram of protein in homogenate is 100%, the fluorescence that is present is essentially in three subcellular compartments: 90% in the cytosol, 5% in mitochondria, 3% in endoplasmic reticulum, and only minor amounts in nuclei and peroxisomes (data not shown). Thus, the described method of analysis allows the estimation of DNS-X in biological samples.

Fluorescence microscopy. Direct observation of the subcellular distribution of DNS-X in hepatic-derived Fao cells confirms this probe accumulates mostly in the cytosolic fraction, whereas only a little penetrates the nucleus (Fig. 6A,B).

Transfection assays. It is now established that PP activate the expression of target genes having a PPRE *via* an interaction with PPAR. To evaluate if DNS-X could induce a reporter gene under control of PPARα, we transfected HepG2 cells with a luciferase gene under control of the bifunctional enzyme PPRE with or without a plasmid coding for the mouse PPARα. After transfection, cells were treated with different PP: Wy 14,643, bezafibrate (the precursor of DNS-X), or DNS-X. The results show an increase in luciferase activity in the presence of each of the three PP (Fig. 7). This increase in the presence of DNS-X is observed even in the absence of transfected PPARα plasmid suggesting that HepG2, a human hepatic-derived cell line, contains endogenous PPARα as human hepatocytes (15). Nevertheless, after transfection of the plasmid coding for PPARα, DNS-X shows a 1.8-fold increase compared to the control. These results confirm DNS-X as a PP molecule able to modulate the gene expression of enzymes involved in lipid metabolism.

DISCUSSION

With the new purification step introduced during the DNS-X synthesis, a final product with a high purity is obtained in gram quantities that is stable for months when stored under dry conditions at –20°C in the dark. Moreover, by carrying out the synthesis under the conditions described here, less time is required than for the previous method (5), e.g., from 1 or 2 d vs. a few hours. The identified ethyl ester form of DNS-X, which represents about 15%, does not interfere in assays using the final product, since fibrates are used in free or esterified form equally. Nevertheless, the formation of the ethyl ester can be avoided by performing the neutralization after the hydrolysis of bezafibrate under milder conditions.

We show here that DNS-X is a new *in vivo* PP in rats. Moreover, this PP activity is dose dependent. The property of DNS-X as an *in vivo* PP confirms and expands the results of the prelim-

inary publication (5) where DNS-X is shown as a PP only in rat cultured Fao hepatic-derived cells. To obtain comparable data on the *in vivo* effect of bezafibrate, a dose of DNS-X that was unusually high had to be given. Related to this, a possible fast pharmacokinetics of DNS-X can explain the absence of fluorescence in serum of treated rats (see Fig. 5), although DNS-X is not hydrolyzed in the liver cells of rats.

Transfection assays confirm that DNS-X can be considered as a PPARα activator since PPARα activity on PPRE-driven gene is enhanced by DNS-X as well as by other PP.

From this study we propose a fluorescent tool that exhibits PP activity *in vitro* as well as *in vivo*. In addition, this compound is not hydrolyzed in the rat liver cells, and the cell homogenates are not contamined by the external medium. This tool is useful to find out subcellular distribution of fibrates, since its fluorescence allows a low level of detection. Our findings concerning the distribution of fibrates will help elucidate the peroxisome proliferation process as triggered by hypolipidemic agents of the fibrate family (16).

The assays on DNS-X subcellular distribution obtained by quantitative analysis and by fluorescence microscopy revealed a high affinity of the molecule for cytosolic components, whereas the presence of DNS-X in other subcellular fractions was relatively weak. The fact that a high level of DNS-X was found in the cytosol is in agreement with several works where cytosolic proteins with high affinity toward fibrates were found (17–21). On the other hand, these results are in contrast with previous studies suggesting an accumulation of radioactive bezafibrate over the endoplasma reticulum (22). The weak accumulation of DNS-X in the nuclei fraction does not rule out that this compound does not bind PPARα since this nuclear receptor can be activated in the cytosol (its biosynthesis compartment) before being translocated in small amount into the nucleus.

ACKNOWLEDGMENTS

Supported by the Conseil Régional de Bourgogne and the European Erasmus program for TL (exchange with the University of Kaiserslautern). We thank Dr. Jean-Claude Leblanc and his team from the Department of Chemistry for their help in collecting NMR spectra, Dr. Marie-Claude Clemencet and Sibylle Grub for their help.

REFERENCES

1. Green, S. (1992) Receptor Mediated Mechanisms of Peroxisome Proliferators, *Biochem. Pharmacol. 43*, 393–401.
2. Latruffe, N., Vamecq, J. (1999) Medical Significance of Peroxisome Proliferators-Activated Receptors, *Lancet 354*, 141–148.
3. Passilly, P., Jannin, B. and Latruffe, N. (1995) Influence of Peroxisome Proliferators on Phosphoprotein Levels in Human and Rat Hepatic-Derived Cell Lines, *Eur. J. Biochem. 230*, 316–321.
4. Motojima, K. (1993) Peroxisome Proliferator-Activated Receptor (PPAR): Structure, Mechanisms of Activation and Diverse Functions, *Cell. Struct. Funct. 18*, 267–277.
5. Berlot, J.P., Grub, S., Duclos, C., Causeret, C., Tainturier, G., and Latruffe, N. (1997) Preparation of a Dansylated Fibrate, a New Fluorescent Tool to Study Peroxisome Proliferation. Effect on Hepatic Derived Cell Lines, *Biochimie 79*, 145–150.
6. Vamecq, J. (1990) Fluorometric Assay of Peroxisomal Oxidases, *Anal. Biochem. 186*, 340–349.
7. Gray, W.R. (1970) End-Group Analysis Using Dansyl Chloride, *Methods Enzymol. 55*, 121–138.
8. Bardot, O., Aldridge, T.C., Latruffe, N., and Green, S. (1993) PPAR-RXR Heterodimer Activates a Peroxisome Proliferator Response Element Upstream of the Bifunctional Enzyme Gene, *Biochem. Biophys. Res. Commun. 192*, 37–45.
9. de Duve, C., Pressman, B.C., Gianeto, R., Wattiaux, R., Appelmans, F. (1995) Tissue Fractionation Studies 6. Intracellular Distribution Pattern of Enzymes in Rat Liver Tissue, *Biochem. J. 60*, 604–617.
10. Ghosh, M.K., and Hajra, A.K. (1986) A Rapid Method for Isolation of Peroxisomes from Rat Liver, *Anal. Biochem. 159*, 167–174.
11. El Kebbaj, M.S., Cherkaoui Malki, M., Latruffe, N. (1996) Properties of Peroxisomes from Jerboa (*Jaculus orientalis*), *Eur. J. Cell Biol. 70*, 150–156.
12. Cherkaoui Malki, M., Bardot, O., Lhuguenot, J.C., Latruffe, N. (1990) Expression of Liver Peroxisomal Proteins as Compared to Other Organelle Marker Enzymes in Rats Treated with Hypolipidemic Agents, *Biol. Cell 69*, 83–92.
13. Bradford, M. (1976) A Rapid and Sensitive Method for the Quantitation of Microgram Quantities of Protein Utilizing the Principle of Protein Dye Binding, *Anal Biochem. 73*, 248–254.
14. Brocard, C., Ramirez, L.C., and Bournot, P. (1994) Fao Cell Line as a Model for the Study of the Effect of Peroxisome Proliferators on Cellular Functons, in *Peroxisomes* (Latruffe, N., and Bugaut, A., eds.), pp. 177–179, Springer-Verlag, Berlin.
15. Sher, T., Yi, H., McBride, W., and Gonzalez, F.J. (1993) cDNA Cloning, Chromosomal Mapping and Functional Characterization of a Human PPARα, *Biochemistry 32*, 5598–5604.
16. Motojima, K., Passilly, P., Peters, J.M., Gonzalez F.J., and Latruffe, N. (1998) Expression of Putative Fatty Acid Transporters Genes Are Regulated by PPARα and γ Activators in a Tissue- and Inducer-Specific Manner, *J. Biol. Chem. 273*, 16710–16714.
17. Bardot, O., Clemencet, M.C., Passily P., and Latruffe, N. (1995) The Analysis of Modified Peroxisome Proliferator Responsive Elements of the Peroxisomal Bifunctional Enzyme in Transfected HepG2 Reveals Two Regulatory Motifs, *FEBS Lett. 360*,183–186.
18. Lock, E.A., Mitchell, A.M., and Elcombe, C.R. (1989) Biochemical Mechanisms of Induction of Hepatic Peroxisome Proliferation, *Annu. Rev. Pharmacol. Toxicol. 29*, 145–163.
19. Lalwani, N.D., Alvares, K., Reddy, M.K., Reddy, M.N., Parikh, I., and Reddy, J.K. (1987) Peroxisome Proliferator-Binding Protein: Identification and Partial Characterization of Nanofepin-, Clofibric Acid-, and Ciprofibrate-Binding Proteins from Rat Liver, *Proc. Natl. Acad. Sci. USA 84*, 5242–5246.
20. Alvares, K., Alejandro, C., Yuan, P.M., Kawano, H., Morimoto, R.I., and Reddy, J.K. (1990) Identification of Cytosolic Peroxisome Proliferator Binding Protein as a Member of the Heat Shock Protein HSP-70 Family, *Proc. Natl. Acad. Sci. USA 87*, 5293–5297.
21. Sugiyama, H., Yamada, J., Takama, H., Kodama, Y., Watanabe, T., Taguchi, T., and Suga, T. (1997) Photoaffinity Labeling of Peroxisome Proliferator Binding Proteins in Rat Hepatocytes; Dehydroepiandrosterone Sulfate- and Bezafibrate-Binding Proteins, *Biochim. Biophys. Acta. 1339*, 321–330.
22. Momose, Y., and Nagata, T. (1993) Radioautographic Study on the Intracellular Localization of a Hypolipidemic Agent, Bezafibrate, a Peroxisome Proliferator, in Cultured Rat Hepatocytes, *Cell. Mol. Biol. 39*, 773–781.

[Received October 27, 1999, and in revised form August 17, 2000; revision accepted September 11, 2000]

Analysis of the Addition Products of α-Tocopherol with Phosphatidylcholine-Peroxyl Radicals by High-Performance Liquid Chromatography with Chemiluminescent Detection

Ryo Yamauchi[a,*], Yuji Hara[b], Hironobu Murase[c], and Koji Kato[b]

Departments of [a]Bioprocessing, and [b]Food Science, Faculty of Agriculture, Gifu University, Gifu 501-1193, and [c]CCI Corporation, Gifu 501-3923, Japan

ABSTRACT: A chemiluminescence-based high-performance liquid chromatographic method was developed for the analysis of the addition products of α-tocopherol with phosphatidylcholine-peroxyl radicals (TOO-PC). The TOO-PC eluted from a reversed-phase column was reacted with a chemiluminescent reagent consisting of a *Cypridina* luciferin analog and a lipid-soluble iron chelate in acidic methanol at 50°C, and the generated chemiluminescence was monitored. The detection limit for TOO-PC by this method was about 1 pmol. This method was applied to the detection of TOO-PC in the peroxidized membranes prepared from rabbit erythrocyte ghosts. When the erythrocyte ghosts were peroxidized by the addition of a water-soluble free radical initiator, a peak corresponding to TOO-PC was detected on the chromatogram with chemiluminescent detection. The amount of TOO-PC in the erythrocyte membranes increased with the depletion of endogenous α-tocopherol. The results indicate that this method proved useful for the detection of the TOO-PC formed by the peroxyl-radical scavenging reactions of α-tocopherol in biological systems.

Paper no. L8511 in *Lipids 35*, 1405–1410 (December 2000).

Peroxidation of lipid membranes is implicated in a variety of damaging pathological events (1–3). α-Tocopherol (vitamin E), an important natural antioxidant in both foods and biological systems, inhibits peroxidation of membrane phospholipids by trapping peroxyl radicals (4). α-Tocopherol efficiently transfers a hydrogen atom to a peroxyl radical, giving a hydroperoxide and an α-tocopheroxyl radical. The α-tocopheroxyl radical, once formed, reacts with a second peroxyl radical to form a nonradical product (4–7). The peroxyl radical-trapping reaction of α-tocopherol yields 8a-substituted tocopherones and isomeric epoxytocopherones as the primary oxidation products (8–18). The formation of these products therefore is consistent with the behavior of α-tocopherol as a chain-breaking antioxidant in biological systems. We have previously reported the isolation and characterization of 8a-(phosphatidylcholine-dioxy)-α-tocopherones (TOO-PC) as the products of the α-tocopheroxyl radical with phospholipid-peroxyl radicals during the peroxidation of 1,2-diacyl-3-*sn*-phosphatidylcholine (PC) liposomes (16–18) (Fig. 1). However, no evidence has been published on the occurrence of such TOO-PC in biological systems. In most biological membranes, the ratio of α-tocopherol to polyunsaturated fatty acids is on the order of 1:1,000 (19,20). Therefore, the research requires a highly sensitive and specific methodology to quantify the oxidation products of α-tocopherol in biological samples.

A weak chemiluminescence has been observed when lipid hydroperoxide is decomposed, and chemiluminescent probes

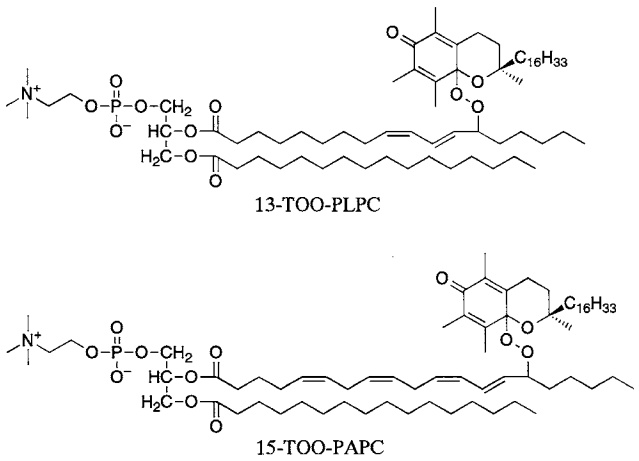

FIG. 1. Typical structures of 8a-(phosphatidylcholine-dioxy)-α-tocopherones, 1-palmitoyl-2-[(9*Z*,11*E*)-13-(8a-dioxy-α-tocopherone)-9,11-octadecadienoyl]-3-*sn*-phosphatidylcholine (13-TOO-PLPC) and 1-palmitoyl-2-[(5*Z*,8*Z*,11*Z*,13*E*)-15-(8a-dioxy-α-tocopherone)-5,8,11,13-

*To whom correspondence should be addressed at Department of Bioprocessing, Faculty of Agriculture, Gifu University, 1-1 Yanagido, Gifu City, Gifu 501-1193, Japan. E-mail: yamautir@cc.gifu-u.ac.jp

Abbreviations: AAPH, 2,2′-azobis(2-amidinopropane)dihydrochloride; Ch18:2-OOH, cholesteryl linoleate hydroperoxides; CLA, a *Cypridina* luciferin analog, 2-methyl-6-phenyl-3,7-dihydroimidazo[1,2-a]pyrazin-3-one; Fe(III)AA, iron(III) acetylacetonate; HPLC, high-performance liquid chromatography; PAPC, 1-palmitoyl-2-arachidonoyl-3-*sn*-phosphatidylcholine; PC, 1,2-diacyl-3-*sn*-phosphatidylcholine; PC-OOH, phosphatidylcholine hydroperoxides; PLPC, 1-palmitoyl-2-linoleoyl-3-*sn*-phosphatidylcholine; PLPC-OOH, 1-palmitoyl-2-linoleoyl-3-*sn*-phosphatidylcholine hydroperoxides; TOO-PC, 8a-(phosphatidylcholine-dioxy)-α-tocopherones; TOO-PAPC, 1-palmitoyl-2-[(8a-dioxy-α-tocopherone)-eicosatetraenoyl]-3-*sn*-phosphatidylcholines; TOO-PLPC, 1-palmitoyl-2-[(8a-dioxy-α-tocopherone)-octadecadienoyl]-3-*sn*-phosphatidylcholines.

are often used to amplify emission of luminescence (21). Luminol or isoluminol has usually been used as the chemiluminescent probe to detect lipid hydroperoxides (21–25). Miyazawa *et al*. (22,23) and Yamamoto *et al*. (24,25) have adapted the chemiluminescent assay of lipid hydroperoxides using high-performance liquid chromatography (HPLC) with postcolumn detection. Miyazawa *et al*. (26) have also described the hydroperoxide-specific detection of 8a-hydroperoxy-α-tocopherone, which was formed during the reaction of α-tocopherol with photochemically generated singlet oxygen, with this HPLC system. In the present study, we applied the chemiluminescence-based HPLC method for the assay of TOO-PC. We used 2-methyl-6-phenyl-3,7-dihydroimidazo[1,2-*a*]pyrazin-3-one, a *Cypridina* luciferin analog (CLA), which has been reported to be effective in amplifying the emission by superoxide anion and lipid free radicals (27,28), as a sensitive amplifier of the chemiluminescence produced by iron-induced decomposition of TOO-PC under acidic conditions.

MATERIALS AND METHODS

Chemicals. *RRR*-α-Tocopherol was purchased from Sigma Chemical Co. (St. Louis, MO) and purified by reversed-phase HPLC (16). *RRR*-γ-Tocopherol was prepared from mixed isomers of tocopherol (Hohnen Oil Co., Tokyo, Japan). α-Tocopherylquinone was prepared by the oxidation of α-tocopherol with $FeCl_3$ (17). Authentic 1-palmitoyl-2-[(8a-dioxy-α-tocopherone)-octadecadienoyl]-3-*sn*-phosphatidylcholines (TOO-PLPC) and 1-palmitoyl-2-[(8a-dioxy-α-tocopherone)-eicosatetraenoyl]-3-*sn*-phosphatidylcholines (TOO-PAPC) were prepared by reacting α-tocopherol with 1-palmitoyl-2-linoleoyl-3-*sn*-PC (PLPC) and 1-palmitoyl-2-arachidonoyl-3-*sn*-PC (PAPC), respectively (18). Authentic PLPC hydroperoxides (PLPC-OOH) were prepared by the oxidation of PLPC (18). Cholesteryl linoleate hydroperoxides (Ch18:2-OOH) were prepared by the autoxidation of cholesteryl linoleate in the presence of α-tocopherol (24). A free-radical initiator 2,2′-azobis(2-amidinopropane)dihydrochloride (AAPH) was obtained from Wako Pure Chemical Co. (Osaka, Japan). CLA was purchased from Tokyo Chemical Industry (Tokyo, Japan), and iron(III) acetylacetonate [Fe(III)AA] was from Dojindo Laboratories (Kumamoto, Japan).

Chemiluminescence-based HPLC system. The HPLC system used in the present study was essentially the same as that reported by Miyazawa *et al*. (23) and Yamamoto (25). HPLC was carried out with a Waters model 600E system (Waters, Milford, MA) connected to a Waters model 486 ultraviolet detector and a Jasco CL-925 chemiluminescence detector (Japan Spectroscopic Co., Tokyo, Japan). The mobile phase of 99% methanol containing 1 mM choline chloride was passed through an Inertsil C8 column (4.6 × 150 mm; GL Sciences Co., Tokyo, Japan) at a flow rate of 1.0 mL/min. The column eluate was monitored by an absorbance at 240 nm and subsequently passed to a reaction coil (0.76 mm × 300 cm, an inner coil volume of 1.4 mL), which was maintained at 50°C.

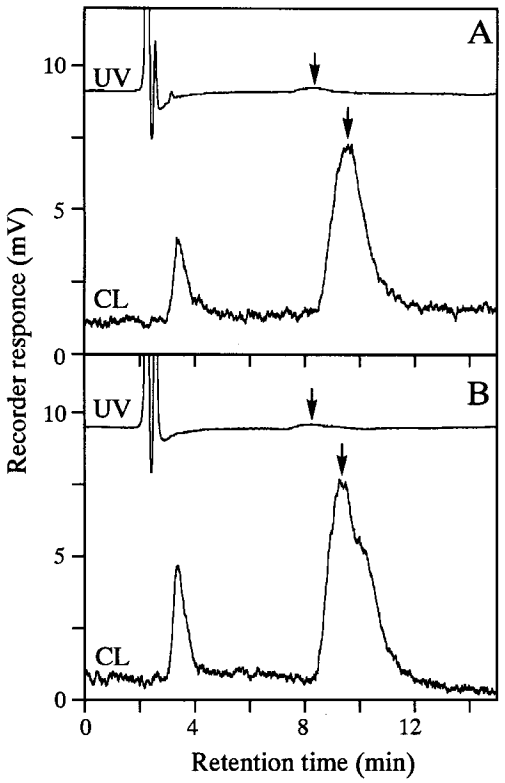

FIG. 2. High-performance liquid chromatograms (HPLC) of the standard 1-palmitoyl-2-[(8a-dioxy-α-tocopherone)-octadecadienoyl]-3-*sn*-phosphatidylcholines (TOO-PLPC) and 1-palmitoyl-2-[(8a-dioxy-α-tocopherone)-eicosatetraenoyl]-3-*sn*-phosphatidylcholines (TOO-PAPC). A solution of TOO-PLPC (13 pmol, A) or TOO-PAPC (17 pmol, B) was injected into the HPLC column. HPLC was done with an Inertsil C8 column (4.6 × 150 mm), which was developed with 1 mM choline chloride in methanol at 1.0 mL/min. After the eluate was monitored at 240 nm (UV), the chemiluminescent reagent was mixed at a flow rate of 1.0 mL/min and the resulting chemiluminescence (CL) was monitored. The arrow indicates the elution position of each 8α-(phosphatidylcholine-dioxy)-α-tocopherone (TOO-PC).

At the inlet of the reaction coil, a chemiluminescent reagent was pumped using an HPLC pump (Waters model 510) at a flow rate of 1.0 mL/min and mixed with the eluate in a T-connector. The chemiluminescent solution consisted of CLA (2 mg/L), Fe(III)AA (5 mg/L), and trifluoroacetic acid (5 mM) in methanol and was maintained at 4°C on an ice bath before mixing. The mobile phase and chemiluminescent solution were continuously sparged with helium gas. The chemiluminescence, generated by the reaction of TOO-PC with the luminescent reagent, was measured with a chemiluminescent detector. Chromatographic data were recorded by a MacLab data acquisition system with a Peaks application program (AD Instruments Pty. Ltd., Castle Hill, Australia).

Erythrocyte ghost preparation. The fresh, heparinized blood from male rabbits (JBC Inc., Gifu, Japan) was centrifuged at 1000 × *g* for 10 min to separate erythrocytes from plasma and buffy coat, and washed three times with a physiological saline. The erythrocytes were hemolyzed in 40 vol of hypotonic buffer (10 mM sodium phosphate, pH 7.4) and centrifuged at 20,000

× *g* for 40 min at 4°C. This procedure was repeated and obtained erythrocyte ghost membranes.

Peroxidation of erythrocyte ghosts. The erythrocyte ghost membranes were suspended in a 10-mM sodium phosphate buffer at pH 7.4 to give a final protein concentration of 1.0 mg/mL. After preincubating for 5 min at 37°C in a shaking water bath, AAPH (a final concentration of 0.5 mM) was added to the membrane suspensions to start lipid peroxidation (29).

Quantification. At specific intervals, a 1.0-mL aliquot of the reaction mixture was taken for lipid extraction. Total lipids were extracted by the method of Bligh and Dyer (30). The extraction solvents (methanol and chloroform) contained 0.03% butylated hydroxytoluene. The extracted lipids were evaporated to dryness under a stream of nitrogen gas, dissolved in 100 μL of ethanol, and analyzed by HPLC; α- and γ-tocopherols were quantified by reversed-phase HPLC with fluorescence detection (16). TOO-PC was quantified by the established chemiluminescence-based HPLC method described in the present study. To determine the percentage recovery of TOO-PC, authentic TOO-PLPC (130 pmol in 100 μL of ethanol) was spiked into the erythrocyte ghost sample (1.0 mL) and then extracted with chloroform/methanol as described above. PC hydroperoxides (PC-OOH) were quantified by the same conditions as the analysis of TOO-PC except for the use of an Inertsil ODS-3 column (4.6 × 150 mm; GL Sciences). A peak corresponding to PC-OOH was eluted in about 5 min under this condition. PLPC-OOH was used as the standard. α-Tocopherylquinone was analyzed by reversed-phase HPLC after the solid-phase extraction of the lipid extracts (17). In another experiment, a mixture of 3-h reaction was treated with 1 M HCl (0.1 mL) prior to extraction and the hydrolysis products were then analyzed to detect oxidized α-tocopherol present as tocopherone compounds (31).

RESULTS AND DISCUSSION

It is possible to detect TOO-PC using the method of chemiluminescence-based HPLC. Figure 2 shows typical chromatograms of authentic TOO-PLPC and TOO-PAPC monitored by an absorbance at 240 nm and the chemiluminescent detector. A very intense peak corresponding to TOO-PLPC or TOO-PAPC was observed on the chromatogram by the chemiluminescent detection, while a peak of only weak intensity was detected by ultraviolet. A mixture of CLA, Fe(III)AA, and trifluoroacetic acid in methanol as the postcolumn reagent was most suitable for this assay. Luminol has already been used in chemiluminescence-based HPLC assay for 8a-hydroperoxy-α-tocopherone under alkaline conditions (26). However, chemiluminescence was not observed when luminol was used instead for the assay of TOO-PC under acidic and alkaline conditions (data not shown). Yamamoto *et al*. (24) reported that the isoluminol assay gave a positive for all of the hydroperoxides, but not for the endoperoxide prostaglandin H_2. These results indicate that the luminol or isoluminol reagent might be unreactive with endoperoxides. On the contrary, the present assay using CLA gave positive responses for TOO-PC. Therefore, our method described here might be useful for quantification of endo-type peroxides such as TOO-PC. In addition, our chemiluminescent reagent also gave a positive response for PC-OOH and cholesteryl ester hydroperoxides. These hydroperoxides, however, did not interfere with the detection of TOO-PC under the present HPLC conditions; PLPC-OOH was eluted from the C8 column at 3.1 min of retention time and Ch18:2-OOH at 6.6 min, respectively.

We have varied the concentrations of CLA, Fe(III)AA, and trifluoroacetic acid and the length and temperature of the reaction coil in order to improve the sensitivity of chemiluminescence and to lower the detection limit of TOO-PC. CLA in solution has been reported to be relatively unstable and autoxidizable under light or in the presence of iron ions, and a chelating agent has been known to form stable complexes with these ions and inhibit the oxidation of CLA (32). Therefore, we added Fe(III)AA as a chelating agent into the chemiluminescent reagent. To decrease the chemiluminescent intensity due to autoxidation, the reagent was continuously sparged with helium gas and maintained at 4°C before mixing with the column eluate. Furthermore, the optimum generation of chemiluminescence needed 1.4 mL of the mixing coil volume and a high temperature at 50°C. The most suitable conditions were determined to be as described in the Materials and Methods section.

Standard curves for the determination of TOO-PC by this method were developed using TOO-PLPC and TOO-PAPC (Fig. 3). Each standard curve showed a good correlation between the peak area measured by chemiluminescent detection and the amount of TOO-PC ($r > 0.999$), and the two TOO-PC gave similar regression lines (TOO-PLPC, $y = 22.6x - 22.4$; TOO-PAPC, $y = 22.8x - 19.1$). The lowest detectable level of each TOO-PC as a signal-to-noise ratio of 3 was estimated to be about 1 pmol, respectively.

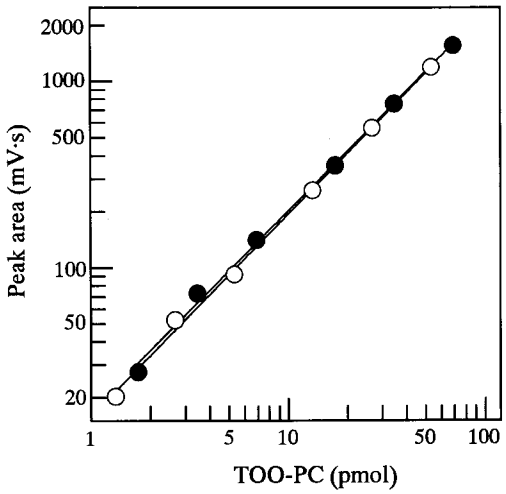

FIG. 3. Standard curve for the analysis of TOO-PLPC (○) or TOO-PAPC (●) by chemiluminescent detection. Each point represents the average value from triplicate determinations. See Figure 2 for abbreviations.

Scheme 1 shows a possible mechanism of iron-catalyzed chemiluminescent reaction of CLA with TOO-PC. Completion of the iron-catalyzed reaction of CLA with TOO-PC requires acid catalysis. The reactions might involve the hydrolysis of TOO-PC to α-tocopherone cation (T^+) and PC-OOH; that is, the 8a-(PC-dioxy) moiety is probable lost following protonation to generate PC-OOH (Eqs. 1 and 2) (12). The next reaction would be an iron-dependent free radical formation by either oxidizing PC-OOH to a peroxyl radical (PC-OO•) or reducing it to an alkoxyl radical (PC-O•) (Eqs. 3 and 4) (33). Since the acid hydrolysis preferentially occurs before the iron-dependent redox reaction, the possibility that iron ions directly catalyze hemolysis of TOO-PC is removed.

$$\text{TOO-PC} + H^+ \rightarrow \text{T}(H^+)\text{OO-PC} \quad [1]$$

$$\text{T}(H^+)\text{OO-PC} \rightarrow T^+ + \text{PC-OOH} \quad [2]$$

$$\text{PC-OOH} + Fe^{3+} \rightarrow \text{PC-OO}^{\bullet} + Fe^{2+} + H^+ \quad [3]$$

$$\text{PC-OOH} + Fe^{2+} \rightarrow \text{PC-O}^{\bullet} + Fe^{3+} + OH^- \quad [4]$$

CLA has been reported to be an effective amplifier of the chemiluminescence produced by iron-induced decomposition of lipid hydroperoxides (28). Thus, the produced free radicals (PC-OO• and PC-O•) can react with CLA, and the resulting oxidized CLA in the excited state (CLA^*_{ox}) emits chemiluminescence at 380 nm to return to its ground state (CLA_{ox}) (26,27).

We applied the chemiluminescence-based HPLC method to the detection of TOO-PC in the membranes prepared from rabbit erythrocyte ghosts. Before the detection of TOO-PC, the percentage recovery of TOO-PC in the erythrocyte ghosts was determined. In using the present method, the recovery of added TOO-PLPC was 71.4 ± 2.6% (n = 4). Liebler *et al.* (14,15) have reported that 8a-(alkyldioxy)-α-tocopherones are relatively resistant to hydrolysis in liposomal systems. Thus, TOO-PC in the erythrocyte ghosts would be relatively stable during the analytical process.

The erythrocyte ghosts suspensions were reacted with peroxyl radicals that had been generated in the aqueous phase by the thermal decomposition of AAPH. The starting reaction mixtures contained endogenous α-tocopherol (0.562 ± 0.064 μM) and γ-tocopherol (0.023 ± 0.018 μM) in the membranes (protein concentration of 1.0 mg/mL). Figure 4 shows the HPLC trace of the lipid extract from the 3-h reaction mixture. A peak corresponding to TOO-PC appeared around 9.4 min of retention time by the chemiluminescent detection, while there was no detectable peak corresponding to TOO-PC by ultraviolet detection. The identity of this peak was confirmed

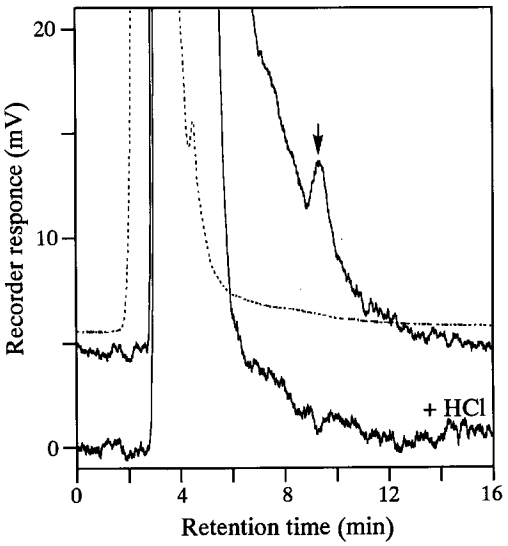

FIG. 4. HPLC of the addition products of α-tocopherol with phosphatidylcholine-peroxyl radicals from the peroxidized erythrocyte ghosts. The erythrocyte ghosts of male rabbits were suspended in 10 mM sodium phosphate buffer at pH 7.4 (a final concentration of 1.0 mg protein/mL) and incubated at 37°C for 3 h in the presence of 0.5 mM 2,2′-azobis(2-amidinopropane)dihydrochloride (AAPH). The reaction mixture was extracted with chloroform/methanol, and the total lipid fraction was injected into the HPLC. The eluate was monitored by an absorbance at 240 nm (dotted line) and by a chemiluminescence (solid line). The reaction mixture was treated with 1 M HCl prior to extraction and analyzed by HPLC with chemiluminescent detection (+ HCl). The arrow indicates the elution position of authentic TOO-PLPC. See Figure 2 for other abbreviations.

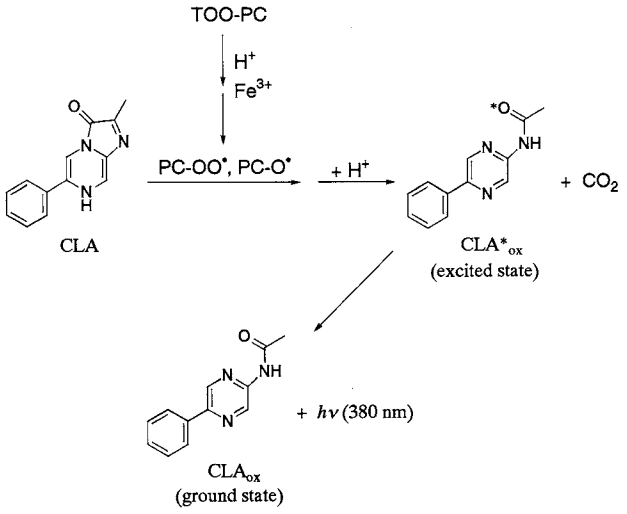

SCHEME 1

TABLE 1
Effect of the HCl Treatment on the Levels of α-Tocopherol and Its Oxidation Products[a,b]

Compound	Sample treatment	
	None (μM)	HCl[c] (μM)
α-Tocopherol	0.071 ± 0.019	0.062 ± 0.009
TOO-PC	0.021 ± 0.010	ND
α-Tocopherylquinone	0.153 ± 0.020[d]	0.296 ± 0.073[d]

[a]Erythrocyte ghost membrane was oxidized with 2,2′-azobis(2-amidinopropane)dihydrochloride for 3 h at 37°C.
[b]Each value is expressed as mean ± standard deviation of four different experiments.
[c]The sample was treated with HCl prior to extraction as described in the Materials and Methods section. This HCl treatment converts 8a-substituted α-tocopherones to α-tocopherylquinone.
[d]Significance of difference by Student's t-test ($P < 0.05$). TOO-PC, 8a-(phos-

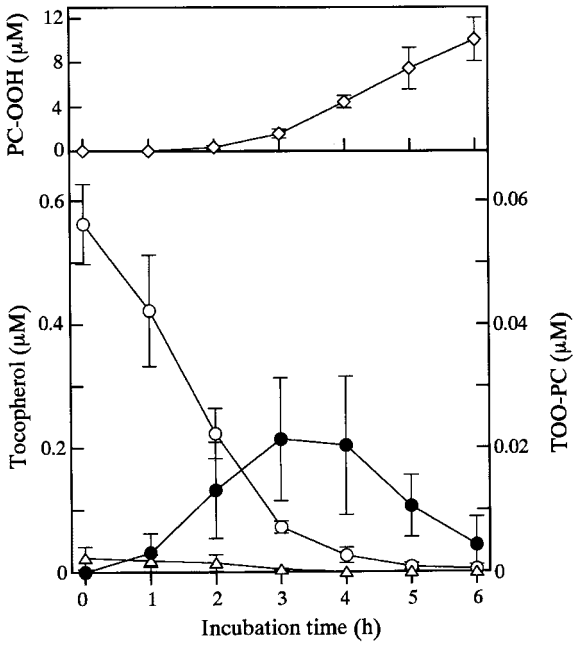

FIG. 5. Changes of endogenous tocopherols, TOO-PC, and phosphatidylcholine hydroperoxides (PC-OOH) during the AAPH-initiated peroxidation in erythrocyte ghosts. The erythrocyte ghosts of male rabbits were suspended in 10 mM sodium phosphate buffer at pH 7.4 (a final concentration of 1.0 mg protein/mL) and incubated at 37°C in air. Peroxidation was initiated by the addition of AAPH (a final concentration of 0.5 mM). The formation of PC-OOH (◇), the consumption of α- (○) and γ-tocopherols (△), and the formation of TOO-PC (●) are shown. Each value is expressed as mean ± standard deviation of four different experiments. See Figures 2 and 4 for other abbreviations.

by co-elution against the authentic standards. The peak completely disappeared when the sample extract was treated with 1 M HCl prior to analysis. This HCl treatment released additional α-tocopherylquinone (Table 1), presumably from 8a-substituted α-tocopherone precursors (31). From these results, this peak was identified to be TOO-PC although the isomeric molecular species were unknown.

The oxidation of erythrocytes and their ghost membranes serves as a model for the oxidative change of biomembranes (34). It has been found that free radicals generated in the aqueous phase attack the membrane to induce the chain oxidation of lipids and proteins and eventually cause hemolysis (29,35). Vatassery (36) reported that α-tocopherylquinone is one of the products of α-tocopherol during the peroxidation of red cell membranes. In the present study, the endogenous α-tocopherol in erythrocyte ghosts could scavenge PC-peroxyl radicals to suppress the formation of PC-OOH when the peroxidation was initiated by AAPH (Fig. 5). TOO-PC, the products of α-tocopherol with PC-peroxyl radicals, appeared with the depletion of α-tocopherol. These results indicate that the endogenous α-tocopherol in the membranes could scavenge PC-peroxyl radicals to suppress PC-OOH formations and produce TOO-PC. However, the formation of TOO-PC in the 3-h sample only accounted for 4% of the consumed α-tocopherol.

There are two pathways to scavenge peroxyl radicals by α-tocopherol (6). The first forms 8a-substituted α-tocopherones and their hydrolysis product α-tocopherylquinone, and the second involves the formation of hydroperoxyepoxy-α-tocopherones and their hydrolysis products epoxy-α-tocopherylquinones. These two pathways depend on characteristics of the experimental systems. In a polar medium or a liposomal system, both 8a-substituted tocopherones and epoxytocopherones are the major products (13–15,17,18), whereas 8a-substituted tocopherones predominate in a nonpolar medium (10,11). In the erythrocyte ghosts, only a small percentage of the total depleted α-tocopherol could be accounted for as TOO-PC (Fig. 5). This indicates that the α-tocopherol may react primarily with AAPH-derived peroxyl radicals, rather than with PC-peroxyl radicals, and form AAPH-derived tocopherones or epoxytocopherones as the major products. However, we could not detect such compounds under the present HPLC conditions.

Liebler *et al.* (37) have developed a new methodology of a stable isotope dilution capillary gas chromatography–mass spectrometry for analyzing α-tocopherol and its oxidation products. This methodology has been applied to the antioxidative reaction of α-tocopherol in a perfused rat liver model (31). The principal oxidation products of α-tocopherol in such an intact organ system were assumed to be 8a-substituted α-tocopherones rather than their hydrolyzed products. This was assumed only from the evidence that the additional release of α-tocopherylquinone was observed in the HCl-treated sample. Further studies on the identification of 8a-substituted α-tocopherones are needed to elucidate the antioxidative action of α-tocopherol *in vivo* systems.

In conclusion, the HPLC technique presented here is found advantageous for the sensitive and specific determination of TOO-PC in biological samples. We believe that such definite quantification of TOO-PC provides us with much information on the antioxidant function of α-tocopherol in biological systems. Further application of this methodology to biological materials is under study.

ACKNOWLEDGMENT

This work was supported in part by a Grant-in-Aid for Scientific Research (No. 11660124) from the Ministry of Education, Science, Sports and Culture of Japan.

REFERENCES

1. Pryor, W.A. (1973) Free Radical Reactions and Their Importance in Biological Systems, *Fed. Proc. 32*, 1862–1869.
2. Slater, T.F. (1984) Free-Radical Mechanisms in Tissue Injury, *Biochem. J. 222*, 1–15.
3. Sevanian, A., and Hochstein, P. (1985) Mechanisms and Consequences of Lipid Peroxidation in Biological Systems, *Annu. Rev. Nutr. 5*, 365–390.
4. Burton, G.W., and Traber, M.G. (1990) Vitamin E: Antioxidant Activity, Biokinetics, and Bioavailability, *Annu. Rev. Nutr. 10*, 357–382.
5. Burton, G.W., and Ingold, K.U. (1986) Vitamin E: Application of the Principles of Physical Organic Chemistry to the Explo-

ration of Its Structure and Function, *Acc. Chem. Res. 19*, 194–201.
6. Liebler, D.C. (1993) The Role of Metabolism in the Antioxidant Function of Vitamin E, *Crit. Rev. Toxicol. 23*, 147–169.
7. Kamel-Eldin, A., and Appelqvist, L.-Å. (1996) The Chemistry and Antioxidant Properties of Tocopherols and Tocotrienols, *Lipids 31*, 671–701.
8. Winterle, J., Dulin, D., and Mill, T. (1984) Products and Stoichiometry of Reaction of Vitamin E with Alkylperoxyl Radicals, *J. Org. Chem. 49*, 491–495.
9. Matsuo, M., Matsumoto, S., Iitaka, Y., and Niki, E. (1989) Radical-Scavenging Reactions of Vitamin E and Its Model Compound, 2,2,5,7,8-Pentamethylchroman-6-ol, in a *tert*-Butylperoxyl Radical-Generating System, *J. Am. Chem. Soc. 111*, 7179–7185.
10. Yamauchi, R., Matsui, T., Kato, K., and Ueno, Y. (1989) Reaction of α-Tocopherol with 2,2′-Azobis(2,4-dimethylvaleronitrile) in Benzene, *Agric. Biol. Chem. 53*, 3257–3262.
11. Yamauchi, R., Matsui, T., Kato, K., and Ueno, Y. (1990) Reaction Products of α-Tocopherol with Methyl Linoleate-Peroxyl Radicals, *Lipids 25*, 152–158.
12. Liebler, D.C., Kaysen, K.L., and Kennedy, T.A. (1989) Redox Cycles of Vitamin E: Hydrolysis and Ascorbic Acid Dependent Reduction of 8a-(Alkyldioxy)tocopherones, *Biochemistry 28*, 9772–9777.
13. Liebler, D.C., Baker, P.F., and Kaysen, K.L. (1990) Oxidation of Vitamin E: Evidence for Competing Autoxidation and Peroxyl Radical Trapping Reactions of the Tocopheroxyl Radical, *J. Am. Chem. Soc. 112*, 6995–7000.
14. Liebler, D.C., Kaysen, K.L., and Burr, J.A. (1991) Peroxyl Radical Trapping and Autoxidation Reactions of α-Tocopherol in Lipid Bilayers, *Chem. Res. Toxicol. 4*, 89–93.
15. Liebler, D.C. and Burr, J.A. (1992) Oxidation of Vitamin E During Iron-Catalyzed Lipid Peroxidation: Evidence for Electron-Transfer Reactions of the Tocopheroxyl Radical, *Biochemistry 31*, 8278–8284.
16. Yamauchi, R., Yagi, Y., and Kato, K. (1994) Isolation and Characterization of Addition Products of α-Tocopherol with Peroxyl Radicals of Dilinoleoylphosphatidylcholine in Liposomes, *Biochim. Biophys. Acta 1212*, 43–49.
17. Yamauchi, R., Yagi, Y., and Kato, K. (1996) Oxidation of α-Tocopherol During the Peroxidation of Dilinoleoylphosphatidylcholine in Liposomes, *Biosci. Biotechnol. Biochem. 60*, 616–620.
18. Yamauchi, R., Mizuno, H., and Kato, K. (1998) Preparation and Characterization of 8a-(Phosphatidylcholine-dioxy)-α-tocopherones and Their Formation During the Peroxidation of Phosphatidylcholine in Liposomes, *Biosci. Biotechnol. Biochem. 62*, 1293–1300.
19. Evarts, R.P., and Bieri, J.G. (1974) Ratios of Polyunsaturated Fatty Acids to α-Tocopherol in Tissues of Rats Fed Corn or Soybean Oils, *Lipids 9*, 860–864.
20. Kelley, E.E., Buettner, G.R., and Burns, C.P. (1995) Relative α-Tocopherol Deficiency in Cultured Cells: Free Radical-Mediated Lipid Peroxidation, Lipid Oxidizability, and Cellular Polyunsaturated Fatty Acid Content, *Arch. Biochem. Biophys. 319*, 102–109.
21. Iwaoka, T., and Tabata, F. (1984) Chemiluminescent Assay of Lipid Peroxide in Plasma Using Cytochrome *c* Heme Peptide, *FEBS Lett. 178*, 47–50.
22. Miyazawa, T., Yasuda, K., and Fujimoto, K. (1987) Chemiluminescence–High Performance Liquid Chromatography of Phosphatidylcholine Hydroperoxide, *Anal. Lett. 20*, 915–925.
23. Miyazawa, T., Fujimoto, K., Suzuki, T., and Yasuda, K. (1994) Determination of Phospholipid Hydroperoxides Using Luminol Chemiluminescence-High-Performance Liquid Chromatography, *Methods Enzymol. 233*, 324–332.
24. Yamamoto, Y., Brodsky, M.H., Baker, J.C., and Ames, B.N. (1987) Detection and Characterization of Lipid Hydroperoxides at Picomole Levels by High-Performance Liquid Chromatography, *Anal. Biochem. 160*, 7–13.
25. Yamamoto, Y. (1994) Chemiluminescence-Based High-Performance Liquid Chromatography Assay of Lipid Hydroperoxides, *Methods Enzymol. 233*, 319–324.
26. Miyazawa, T., Yamashita, T., and Fujimoto, K. (1992) Chemiluminescence Detection of 8a-Hydroperoxy-tocopherone in Photooxidized α-Tocopherol, *Lipids 27*, 289–294.
27. Nakano, M., Sugioka, K., Ushijima, Y., and Goto, T. (1986) Chemiluminescence Probe with *Cypridina* Luciferin Analog, 2-Methyl-6-phenyl-3,7-dihydroimidazo[1,2-*a*]pyrazin-3-one, for Estimating the Ability of Human Granulocytes to Generate O_2^-, *Anal. Biochem. 159*, 363–369.
28. Fukuzawa, K., Yoshimura, T., Fujii, T., Takauchi, K., Miki, M., Tamai, H., and Mino, M. (1988) Theoretical Analysis of a Site-Specific Chemiluminescence Reaction and Its Application to Quantitation of Lipid Hydroperoxides, *Chem. Phys. Lipids 48*, 197–203.
29. Miki, M., Tamai, H., Mino, M., Yamamoto, Y., and Niki, E. (1987) Free-Radical Chain Oxidation of Rat Red Blood Cells by Molecular Oxygen and Its Inhibition by α-Tocopherol, *Arch. Biochem. Biophys. 258*, 373–380.
30. Bligh, E.G., and Dyer, W.J. (1959) A Rapid Method of Total Lipid Extraction and Purification, *Can. J. Biochem. Physiol. 37*, 911–917.
31. Ham, A.J.L., and Liebler, D.C. (1997) Antioxidant Reactions of Vitamin E in the Perfused Rat Liver: Product Distribution and Effect of Dietary Vitamin E Supplementation, *Arch. Biochem. Biophys. 339*, 157–164.
32. Tawa, R., and Sakurai, H. (1997) Determination of Four Active Oxygen Species Such as H_2O_2, •OH, $•O_2^-$, and $^1O_2$ by Luminol- and CLA-Chemiluminescence Methods and Evaluation of Antioxidative Effects of Hydroxybenzoic Acids, *Anal. Lett. 30*, 2811–2825.
33. Halliwell, B., and Gutteridge, M.C. (1984) Oxygen Toxicity, Oxygen Radicals, Transition Metals and Disease, *Biochem. J. 219*, 1–14.
34. Kellogg, E.W., III, and Fridovich, I. (1977) Liposome Oxidation and Erythrocyte Lysis by Enzymically Generated Superoxide and Hydrogen Peroxide, *J. Biol. Chem. 252*, 6721–6728.
35. Niki, E., Komuro, E., Takahashi, M., Urano, S., Ito, E., and Terao, K. (1988) Oxidative Hemolysis of Erythrocytes and Its Inhibition by Free Radical Scavengers, *J. Biol. Chem. 263*, 19809–19814.
36. Vatassery, G.T. (1989) Oxidation of Vitamin E in Red Cell Membranes by Fatty Acids, Hydroperoxides and Selected Oxidants, *Lipids 24*, 299–304.
37. Liebler, D.C., Burr, J.A., Philips, L., and Ham, A.J.L. (1996) Gas Chromatography–Mass Spectrometry Analysis of Vitamin E and Its Oxidation Products, *Anal. Biochem. 236*, 27–34.

[Received April 17, 2000, and in revised form September 15, 2000; revision accepted October 3, 2000]

Protective Effect of Phytic Acid Hydrolysis Products on Iron-Induced Lipid Peroxidation of Liposomal Membranes

Sayuri Miyamoto[a], Goro Kuwata[b], Masatake Imai[b], Akihiko Nagao[c], and Junji Terao[a,*]

[a]Department of Nutrition, School of Medicine, The University of Tokushima, Tokushima 770-8503, Japan, [b]Research Institute of Morinaga & Co. Ltd., Yokohama 230-0012, Japan, and [c]National Food Research Institute, Ministry of Agriculture, Forestry and Fisheries, Tsukuba 305-0856, Japan

ABSTRACT: Beneficial effects of dietary phytic acid (*myo*-inositol hexaphosphate; IP_6) have often been explained by its strong iron ion-chelating ability, which possibly suppresses iron ion-induced oxidative damage in the gastrointestinal tract. Because phytic acid is hydrolyzed during digestion, this work aimed to know whether its hydrolysis products (IP_2, IP_3, IP_4, and IP_5) could still prevent iron ion-induced lipid peroxidation. Studies using liposomal membranes demonstrated that hydrolysis products containing three or more phosphate groups are able to inhibit iron ion-induced lipid peroxidation although their effectiveness decreased with dephosphorylation. Similarly, they also prevented iron ion-induced decomposition of phosphatidylcholine hydroperoxide. These results demonstrate that intermediate products of phytic acid hydrolysis still possess iron ion-chelating ability, and thus they can probably prevent iron ion-induced lipid peroxidation in biological systems.

Paper no. L8625 in *Lipids 35,* 1411–1413 (December 2000).

Phytic acid (*myo*-inositol hexaphosphate; IP_6) is a highly phosphorylated molecule present in cereal grains and seeds that functions as an excellent chelator of metal ions (1–3). A number of studies suggest the involvement of free iron ions in the development of gastrointestinal diseases, such as colon cancer (4–8). Dietary iron remains largely unabsorbed in the intestine, and it is hypothesized to participate in the generation of hydroxyl radical by a Fenton-type reaction in conjunction with colonic microflora (5). Therefore, inhibition of iron ion-mediated lipid peroxidation is suggested to be important for the prevention of gastrointestinal diseases. Although phytic acid has a strong inhibitory effect on iron-induced oxidative reactions, dietary phytic acid is inevitably hydrolyzed during digestion by phytase of either dietary or intestinal origin (9,10). This enzyme sequentially cleaves phosphate groups from the inositol ring, and less phosphorylated forms (IP_5, IP_4, IP_3, IP_2, and IP_1) of phytic acid are apparently present as intermediate products in the digestive tract.

The aim of this study was to clarify whether phytic hydrolysis products still have the ability to prevent iron ion-induced lipid peroxidation. For this purpose we used lower phosphorylated forms of inositol phosphate (IP_2–IP_5) derived from phytic acid hydrolysis and evaluated their protective effect against iron ion-induced lipid peroxidation in liposomal membrane.

EXPERIMENTAL PROCEDURES

Myo-inositol bis-, tris-, tetrakis- and pentakisphosphate (IP_2, IP_3, IP_4, IP_5) were prepared by the method described previously (11). Briefly, phytic acid solution (50% wt/vol, Daiichi Pharmaceutical Co., Tokyo, Japan) was adjusted to pH 6.0 with 5 N NaOH and diluted to 10%. Hydrolysis was carried out by the addition of microbial phytase (Amano Pharmaceutical Co., Nagoya, Japan), and incubated at 40°C for 24 h. Separation of phytic acid hydrolysis products was performed by anion exchange column chromatography (Dowex 1-X2, 200–400 mesh, chloride form) by stepwise gradient elution with hydrochloric acid (0.05–1.0 N). The purity of eluted fractions containing IP_2, IP_3, IP_4, and IP_5 was checked by HPLC (12).

Phytic acid and egg yolk phosphatidylcholine (EYPC; type III-E), were purchased from Sigma Chemical Co. (St. Louis, MO). EYPC was purified to remove contaminant peroxides by reversed-phase column chromatography (13). The phosphatidylcholine hydroperoxides (PC-OOH) content in the purified EYPC was lower than 0.008%. Iron(III) nitrate nonahydrate [$Fe(NO_3)_3 \cdot 9H_2O$], 3,5-di-*tert*-butyl-4-hydroxytoluene and 2-thiobarbituric acid were purchased from Nacalai Tesque Inc. (Kyoto, Japan). Ascorbic acid was from Daiichi. Desferrioxamine B methanesulfonate (Desferal) was obtained from CIBA-Geigy Japan (Tokyo, Japan). All other chemicals and solvents were of analytical grade. PC-OOH was prepared from EYPC using soybean lipoxygenase and purified by reversed-phase column chromatography by the method described previously (14).

Liposomal suspension (6.25 mM EYPC) was prepared in 10 mM Tris-HCl buffer (pH 7.4) without the addition of diethylenetriaminepentaacetic acid as previously described (15).

*To whom correspondence should be addressed at Department of Nutrition, School of Medicine, The University of Tokushima, Kuramoto-cho 3, Tokushima 770-8503, Japan. E-mail: terao@nutr.med.tokushima-u.ac.jp

Abbreviations: Desferal, Desferrioxamine B methanesulfonate; EYPC, egg yolk phosphatidylcholine; HPLC, high-performance liquid chromatography; IP_6, *myo*-inositol hexakisphosphate; IP_5, *myo*-inositol pentakisphosphate; IP_4, *myo*-inositol tetrakisphosphate; IP_3, *myo*-inositol trisphosphate; IP_2, *myo*-inositol bisphosphate; PC-OOH, phosphatidylcholine hydroperoxides; TBARS, thiobarbituric acid-reactive substances.

Aliquots of the liposomal suspension were mixed with 100 μM (final concentration) of phytic acid hydrolysis products. Lipid peroxidation was induced by the addition of $Fe(NO_3)_3$ and ascorbate (final concentrations 10 and 100 μM, respectively). Incubation was carried out at 37°C with continuous shaking, and at specific time intervals aliquots were withdrawn for the analysis of PC-OOH by high-performance liquid chromatography (HPLC) (14). At the end of incubation the amount of thiobarbituric acid-reactive substances (TBARS) was quantified by the method of Uchiyama and Mihara (16).

The ability of phytic acid hydrolysis products to chelate iron ion was estimated by measuring their inhibitory effect on iron ion-induced PC-OOH decomposition. PC-OOH solution in chloroform (0.1 μmol) was put into a test tube and the solvent completely evaporated by nitrogen stream. The residue was dispersed in 0.8 mL of Tris-HCl buffer (10 mM, pH 7.4) by vigorous mixing on a vortex mixer for 1 min and by ultrasonic irradiation for 30 s in an Astrason Ultrasonic Processor (Misonix Inc., New York). PC-OOH suspension was then mixed with phytic acid hydrolysis products or Desferal (final concentration 100 μM) and the reaction was started by the addition of $Fe(NO_3)_3$ and ascorbate solution (final concentrations 10 and 100 μM, respectively). After 10 min incubation at 37°C the residual amount of PC-OOH was quantified by HPLC as previously described (14).

Data were analyzed by one-way analysis of variance followed by the Bonferroni/Dunn *post hoc* multiple comparison test to determine statistical differences between means. A value of $P < 0.05$ was judged as statistically significant.

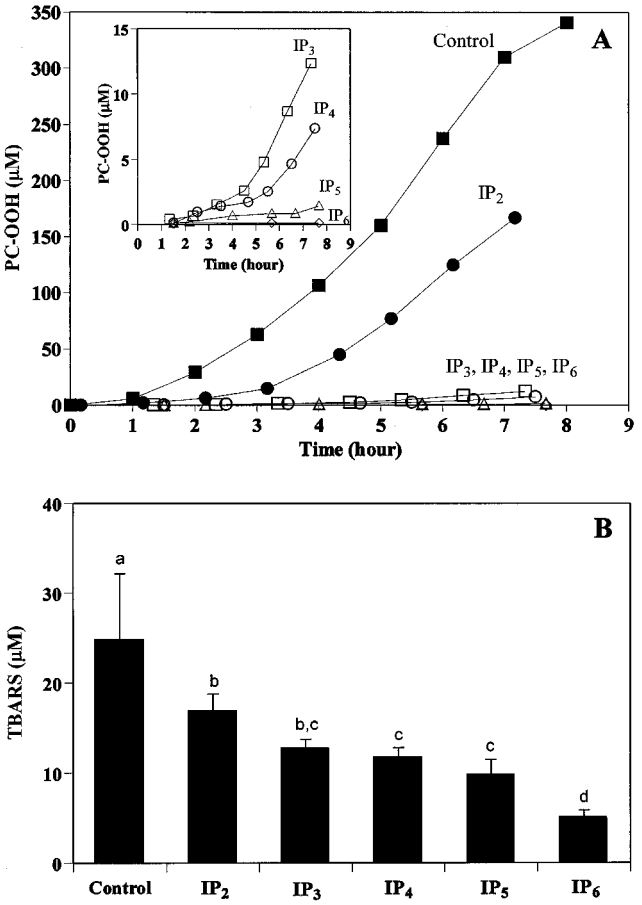

FIG. 1. Effect of phytic acid hydrolysis products on iron ion-induced lipid peroxidation of large unilamellar vesicle liposomal suspension. Liposomal suspension, consisting of 5 mM egg yolk phosphatidylcholine in Tris-HCl buffer (pH 7.4; 10 mM), was incubated with each phytic hydrolysis product (100 μM), and the oxidation was initiated by the addition of $Fe(NO_3)_3$ and ascorbic acid (10 and 100 μM, respectively). Oxidation level was determined by the measurement of phosphatidylcholine hydroperoxides (PC-OOH) and thiobarbituric acid-reactive substances (TBARS). (A) Accumulation of PC-OOH in control (■), *myo*-inositol bisphosphate (IP_2) (●), *myo*-inositol trisphosphate (IP_3) (□), *myo*-inositol tetrakisphosphate (IP_4) (○), *myo*-inositol pentakisphosphate (IP_5) (△), and *myo*-inositol hexakisphosphate (IP_6) (◇). The values shown represent the typical results of at least three experiments. (B) TBARS level after 8 h of incubation. Each value is the mean ± SD of at least four experiments. Means not sharing a common letter are significantly different ($P < 0.05$), as determined by Bonferroni/Dunn's multiple comparison test.

RESULTS AND DISCUSSION

The antioxidant effect of phytic acid hydrolysis products was evaluated in iron ion-induced large unilamellar vesicle (LUV) liposomal lipid peroxidation. Figure 1 shows the effect of phytic acid hydrolysis products on the accumulation of PC-OOH and TBARS in liposomal suspension. The accumulation of PC-OOH was slightly retarded by IP_2, whereas IP_3, IP_4, IP_5, and IP_6 suppressed PC-OOH formation (Fig. 1A); the order of suppression was $IP_3 < IP_4 < IP_5 \leq IP_6$. The amount of TBARS formed after 8 h of incubation was also significantly decreased by the addition of IP_2, IP_3, IP_4, IP_5, and IP_6 (Fig. 1B). A slight but gradual decrease in TBARS formation from IP_2–IP_6 was observed. IP_2, IP_3, IP_4, IP_5, or IP_6 by themselves had no effect on TBARS determination. Thus it is suggested that phytic acid hydrolysis products are still able to protect biological membranes against iron ion-induced lipid peroxidation.

The ability of phytic acid hydrolysis products to block iron ion-induced PC-OOH decomposition is shown in Figure 2. The strong iron chelator Desferal was used in the assay as a positive control; it inhibited the decomposition of PC-OOH almost completely. IP_2 was unable to prevent PC-OOH decomposition, whereas hydrolysis products with three or more phosphate groups significantly prevented PC-OOH decomposition ($IP_6 > IP_5 > IP_4 > IP_3$).

Antioxidant properties of phytic acid are ascribed to its strong metal ion-chelating ability (1). In this study we evaluated the antioxidant and/or chelating ability of less phosphorylated forms of inositol phosphate derived from phytic acid hydrolysis. The study using liposomal suspension as a model for biological membranes clearly demonstrated that dephosphorylation decreases the antioxidant effectiveness of IP_6 against iron ion-induced lipid peroxidation (Fig. 1). However, phytic acid hydrolysis products significantly protected liposomal membrane lipid peroxidation. It has been recognized that iron ion catalyzes the decomposition of lipid hydroperoxide with consequent generation of reactive peroxyl and/or

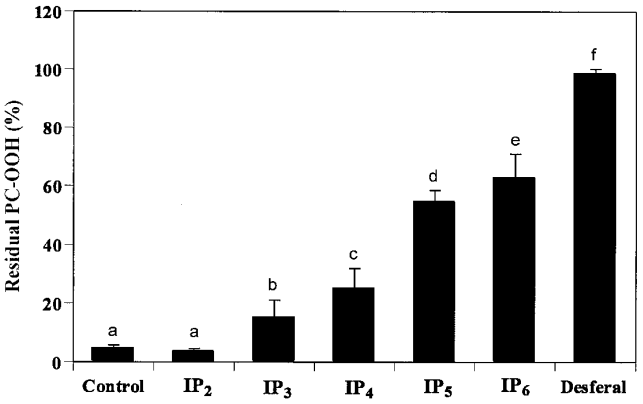

FIG. 2. Effect of phytic acid hydrolysis products on iron ion-induced decomposition of PC-OOH. Phytic acid hydrolysis product (100 μM) was added to PC-OOH suspension (100 μM) in Tris-HCl buffer (pH 7.4; 10 mM) and incubated with $Fe(NO_3)_3$ and ascorbic acid (10 and 100 μM, respectively) at 37°C for 10 min. The amount of residual PC-OOH was measured by high-performance liquid chromatography. Each value is the mean ± SD of at least four experiments. Means not sharing a common letter are significantly different ($P < 0.05$), as determined by Bonferroni/Dunn's multiple comparison test. Desferal, desferrioxamine B methanesulfonate; for other abbreviations see Figure 1.

alkoxyl radicals (4). Our results suggest that partially hydrolyzed products of phytic acid are still able to bind iron ion in a way that prevents or lowers its catalytic activity toward lipid hydroperoxides. To confirm this hypothesis, we measured their ability to prevent iron ion-induced PC-OOH decomposition (Fig. 2). In our model system IP_3, IP_4, and IP_5 significantly suppressed hydroperoxide decomposition, whereas IP_2 was unable to prevent decomposition. Graf *et al.* (2) postulated that, to have catalytic activity, iron ion requires at least one coordination site be open or occupied by a readily dissociable ligand. They have shown that phytic acid inhibits iron-mediated generation of hydroxyl radical by occupying all six iron coordination sites (2). Later studies conducted by Hawkins *et al.* (17) and Phylippy and Graf (18) demonstrated that all six phosphate groups on *myo*-inositol structure are not necessary for the inhibition of hydroxyl radical generation. Phylippy and Graf (18) proposed that 1,2,3-phosphate grouping on phytic acid structure is responsible for the inhibition of iron ion reactivity. Although we did not determine the isomers of inositol phosphate present in each product of phytic acid hydrolysis, our results demonstrate that hydrolysis of phytic acid generates compounds that are still able to prevent iron ion-induced lipid peroxidation. From the above evidences, it is probable that the hydrolysis of phytic acid in this study generated isomers containing the 1,2,3-phosphate grouping on the inositol structure.

In conclusion, hydrolysis of phytic acid generates several compounds that are still effective against iron ion-induced lipid peroxidation. It is likely that their effectiveness is modulated by the degree of hydrolysis and by the type of isomers of partially hydrolyzed inositol phosphate formed. Nevertheless, it can be expected that phytic acid hydrolysis products prevent iron ion-induced lipid peroxidation in biological system.

ACKNOWLEDGMENT

This work was partly supported by a grant-in-aid for scientific research (No. 11660127) from the Ministry of Education, Science, Sport and Culture of Japan.

REFERENCES

1. Graf, E., and Empson, K.L. (1987) Phytic Acid. A Natural Antioxidant, *J. Biol. Chem. 262,* 11647–11650.
2. Graf, E., Mahoney, J.R., Bryant, R.G., and Eaton, J.W. (1990) Iron-Catalyzed Hydroxyl Radical Formation: Stringent Requirements for Free Iron Coordination Site, *J. Biol. Chem.* 256, 3620–3624.
3. Graf, E., and Eaton, J.W. (1990) Antioxidant Functions of Phytic Acid, *Free Radical Biol. Med. 8,* 61–69.
4. Halliwell, B., and Gutteridge, J.M.C. (1990) Role of Free Radicals and Catalytic Metal Ions in Human Disease: An Overview, *Methods Enzymol. 186,* 1–85.
5. Babbs, C.F. (1990) Free Radical and the Ethiology of Colon Cancer, *Free Radical Biol. Med. 8,* 191–200.
6. Younes, M., Trepkau, H.D., and Siegers, C.P. (1990) Enhancement by Dietary Iron of Lipid Peroxidation in Mouse Colon, *Res. Commun. Chem. Path. Pharm. 70,* 349–354.
7. Nelson, R.L. (1992) Dietary Iron and Colorectal Cancer Risk, *Free Radical Biol. Med. 12,* 161–168.
8. Graf, E., and Eaton, J.W. (1993) Suppression of Colonic Cancer by Dietary Phytic Acid, *Nutr. Cancer 19,* 11–19.
9. Sandberg, A.-S., and Andersson, H. (1988) Effect of Dietary Phytase on the Digestion of Phytate in the Stomach and Small Intestine of Humans, *J. Nutr. 118,* 469–473.
10. Iqbal, T.H., Lewis, K.O., and Cooper, B.T. (1994) Phytase Activity in the Human and Rat Small Intestine, *Gut* 35, 1233–1236.
11. Shinoda, S., Kuwata, G., Iwatsuki, S., Imai, M., and Arai, S. (1995) Effect of Inositol Phosphates (products from phytate) on Mineral Availability in Rats, *J. Jpn. Soc. Nutr. Food Sci.* 48, 371–378.
12. Baba, Y., Yoza, N., and Ohashi, S. (1985) Effect of Column Temperature on High-Performance Liquid Chromatographic Behaviour of Inorganic Polyphosphates. Isocratic Ion-Exchange Chromatography, *J. Chromatogr. 348,* 27–37.
13. Arai, H., Mohri, S., Suzuki, T., Takama, K., and Terao, J. (1997) Coulometric Electrochemical Detection of Phospholipid Hydroperoxides by High-Performance Liquid Chromatography, *Biosci. Biotech. Biochem. 61,* 191–193.
14. Terao, J., Nagao, A., Park, D.-K., and Boey, P.L. (1992) Lipid Hydroperoxide Assay for Antioxidative Activity of Carotenoids, *Methods Enzymol. 213,* 454–460.
15. Terao, J., Piskula, M., and Yao, Q. (1994) Protective Effect of Epicatechin, Epicatechin Gallate, and Quercetin on Lipid Peroxidation in Phospholipid Bilayers, *Arch. Biochem. Biophys. 308,* 278–284.
16. Uchiyama, M., and Mihara, M. (1978) Determination of Malonaldehyde Precursor in Tissues by Thiobarbituric Acid Test, *Anal. Biochem. 86,* 271–278.
17. Hawkins, P.T., Poyner, D.R., Jackson, T.R., Letcher, A.J., Lander, D.A., and Irvine, R.F. (1993) Inhibition of Iron-Catalyzed Hydroxyl Radical Formation by Inositol Polyphosphates: A Possible Physiological Function for Myo-Inositol Hexakisphosphate, *Biochem. J. 294,* 929–934.
18. Phylippy, B.Q., and Graf, E. (1997) Antioxidant Functions of Inositol 1,2,3-Trisphosphate and Inositol 1,2,3,6-Tetrakisphosphate, *Free Radical Biol. Med. 22,* 939–946.

[Received September 15, 2000, and in final revised form and accepted November 10, 2000]